frontiers | Research Topics

Biostimulants in agriculture II: Towards a sustainable future

Edited by
Maurizio Ruzzi, Giuseppe Colla and Youssef Rouphael

Published in
Frontiers in Plant Science
Frontiers in Microbiology

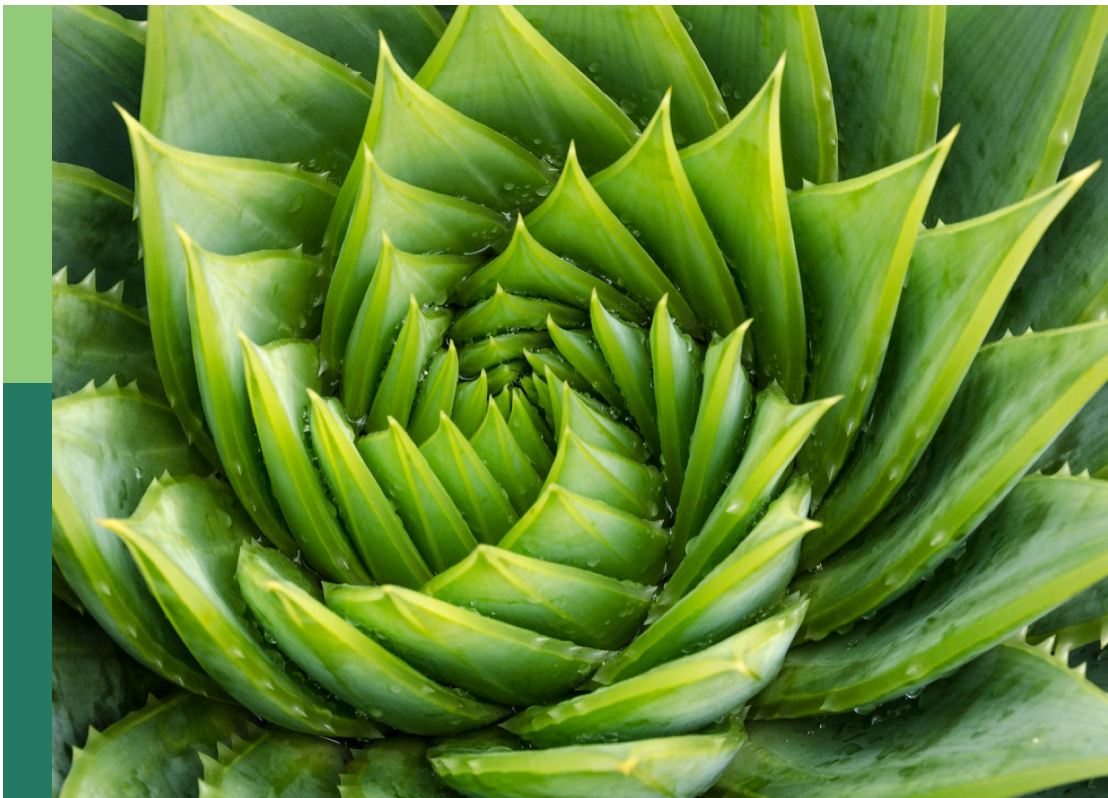

ISSN 1664-8714
ISBN 978-2-8325-5017-5
DOI 10.3389/978-2-8325-5017-5

About Frontiers

Frontiers is more than just an open access publisher of scholarly articles: it is a pioneering approach to the world of academia, radically improving the way scholarly research is managed. The grand vision of Frontiers is a world where all people have an equal opportunity to seek, share and generate knowledge. Frontiers provides immediate and permanent online open access to all its publications, but this alone is not enough to realize our grand goals.

Frontiers journal series

The Frontiers journal series is a multi-tier and interdisciplinary set of open-access, online journals, promising a paradigm shift from the current review, selection and dissemination processes in academic publishing. All Frontiers journals are driven by researchers for researchers; therefore, they constitute a service to the scholarly community. At the same time, the *Frontiers journal series* operates on a revolutionary invention, the tiered publishing system, initially addressing specific communities of scholars, and gradually climbing up to broader public understanding, thus serving the interests of the lay society, too.

Dedication to quality

Each Frontiers article is a landmark of the highest quality, thanks to genuinely collaborative interactions between authors and review editors, who include some of the world's best academicians. Research must be certified by peers before entering a stream of knowledge that may eventually reach the public - and shape society; therefore, Frontiers only applies the most rigorous and unbiased reviews. Frontiers revolutionizes research publishing by freely delivering the most outstanding research, evaluated with no bias from both the academic and social point of view. By applying the most advanced information technologies, Frontiers is catapulting scholarly publishing into a new generation.

What are Frontiers Research Topics?

Frontiers Research Topics are very popular trademarks of the *Frontiers journals series*: they are collections of at least ten articles, all centered on a particular subject. With their unique mix of varied contributions from Original Research to Review Articles, Frontiers Research Topics unify the most influential researchers, the latest key findings and historical advances in a hot research area.

Find out more on how to host your own Frontiers Research Topic or contribute to one as an author by contacting the Frontiers editorial office: frontiersin.org/about/contact

Biostimulants in agriculture II: Towards a sustainable future

Topic editors

Maurizio Ruzzi — University of Tuscia, Italy

Giuseppe Colla — University of Tuscia, Italy

Youssef Rouphael — University of Naples Federico II, Italy

Citation

Ruzzi, M., Colla, G., Rouphael, Y., eds. (2024). *Biostimulants in agriculture II: Towards a sustainable future*. Lausanne: Frontiers Media SA. doi: 10.3389/978-2-8325-5017-5

Table of contents

frontiers | Frontiers in Plant Science

TYPE Editorial
PUBLISHED 31 May 2024
DOI 10.3389/fpls.2024.1427283

OPEN ACCESS

EDITED AND REVIEWED BY
Juan A. Fernández,
Polytechnic University of Cartagena, Spain

*CORRESPONDENCE
Maurizio Ruzzi
ruzzi@unitus.it
Giuseppe Colla
giucolla@unitus.it
Youssef Rouphael
youssef.rouphael@unina.it

RECEIVED 03 May 2024
ACCEPTED 20 May 2024
PUBLISHED 31 May 2024

CITATION
Ruzzi M, Colla G and Rouphael Y (2024) Editorial: Biostimulants in agriculture II: towards a sustainable future.
Front. Plant Sci. 15:1427283.
doi: 10.3389/fpls.2024.1427283

Editorial: Biostimulants in agriculture II: towards a sustainable future

Maurizio Ruzzi[1]*, Giuseppe Colla[2]* and Youssef Rouphael[3]*

[1]Department for Innovation in Biological, Agri-food and Forestry Systems, University of Tuscia, Viterbo, Italy, [2]Department of Agriculture and Forest Sciences, University of Tuscia, Viterbo, Italy, [3]Department of Agricultural Sciences, University of Naples Federico II, Portici, Italy

KEYWORDS

non-microbial biostimulants, microbial biostimulants, European Regulation 2019/1009, abiotic stresses, nutrient use efficiency, quality

Editorial on the Research Topic
Biostimulants in agriculture II: towards a sustainable future

1 Introduction

Current socio-political scenarios are pushing the agricultural sector towards a rapid ecological transition. For this reason, modern agriculture is forced to expand its ordinary practices to achieve greater sustainability in line with the principles of economic and environmental circularity (Velasco-Muñoz et al., 2021). Nonetheless, current challenges such as the need to increase productivity and the efficiency of non-renewable resources in increasingly unfavorable contexts strain agro-ecosystems resilience. Over the last century, synthetic agrochemicals have been the only tool capable of increasing yields and ensuring satisfactory production volumes throughout the seasons (Donate and Frederico, 2019). Awareness of the weighty environmental impact associated with the disproportionate use of these chemicals has stimulated research and development of technological innovations capable of improving the sustainability of agricultural production without compromising yield and quality. In recent decades, biostimulants have represented an efficient and virtuous innovation capable of improving tolerance against a wide range of stressors, stimulating the growth and productivity of crops while efficiently utilizing nutrients (nutrient use efficiency). According to the latest European Regulation 2019/1009, plant biostimulants are defined as "*a product that stimulates the nutritional processes of plants independently of the nutrients it contains, with the sole aim of improving one or more of the following characteristics of plants or their rhizosphere: (1) the efficiency of nutrient use; (2) tolerance to abiotic stress; (3) qualitative characteristics; (4) the availability of nutrients confined in the soil or rhizosphere.*" Beneficial microorganisms and numerous natural substances and derivatives of natural and/or synthetic compounds are considered plant biostimulants; these include (1) humic substances, (2) protein hydrolysates and amino-acid based products, (3) macro- and micro-algae extracts, and plant extracts, (4) silicon; (5) Arbuscular Mycorrhizal Fungi (AMF); and (6) plant growth-promoting rhizobacteria (PGPR) belonging to the genera *Azotobacter*, *Azospirillum* and *Rhizobium* spp (EU, 2019). Although biostimulants were initially designed as a helpful tool mainly in organic farming, they are now used in all cropping systems (organic, conventional, and integrated) in the open field and protected cultivation.

Driven by the strong dependence on the agricultural sector for food, the economic size of the biostimulants market reached USD 3 billion in 2022 and is expected to grow at a compound annual growth rate (CAGR) of 10.5% over the next decade. Europe dominated the market with a revenue share of over 37.0% (GVR, 2023). This is partly attributed to the support regulations to stimulate organic food production, which are expected to drive the market in Europe and beyond in the future. The strong interest in the topic of biostimulants is confirmed by the data available on Scopus (www.scopus.com). Taking the last ten years (2013–2023) as a reference, searching for the term '*plant biostimulants*' more than 2000 scientific papers were found. These numbers are not surprising since, as reported by several authors (Jindo et al., Tripathi et al., Herrmann et al., and Li et al.), the use of substances and microorganisms with biostimulant action is of interest in all productive agricultural systems (horticulture, arboriculture and viticulture, cereal cultivation and industrial crops), even if their efficacy as underlined by the same authors varies depending on the cultivation conditions and the sensitivity of the reference species. The present topic brings together 77 scientific contributions (68 research articles and 9 reviews; Supplementary Table 1) investigating both under optimal and sub-optimal conditions, the productive and/or qualitative response of crops of agronomic interest to the application of biostimulants, as well as the use of compounds with elicitor action.

2 Biostimulants improve tolerance to abiotic stress

Due to the unpredictable and damaging effects of climatic anomalies associated with climate change, crops experience many stresses that inevitably reduce yield and final product quality, thus making it difficult to achieve food security objectives (Goud et al., 2022). Using products with biostimulant action represents one of the most innovative and promising tools to counter these stressors and reduce the gap between achievable yield and potential yield (Rouphael and Colla, 2020). Considering that plants respond to environmental stresses through adaptive cellular reprogramming, the work of Bharadwaj et al. emphasizes that during the delicate phase of seed germination, cellular sucrose levels are a very important sensor of environmental stresses that can be used to improve germination and disease detection. As discussed by Atta-Boateng and Berlyn, yield reductions are not exclusively attributable to specific stress but to a co-presence of them. Choosing cowpea (*Vigna unguiculata* (L.) Walp.), adapted to nitrogen dependence, as a model crop, Atta-Boateng and Berlyn. observed that the use of non-hormonal biostimulants (product based on antioxidants and amino acids prepared by the laboratory of the Yale School of the Environment) is an efficient tool to promote productivity when it is limited by osmotic stresses attributable to high temperatures, water limitations, and sub-optimal moisture conditions. Ambrosini et al. evaluated the ability of an animal-derived protein hydrolysate to mitigate the incidence of drought stress and root oxygen and iron deficiency conditions in hydroponically grown maize plants (*Zea mays* L.). The same authors also emphasized once again how the positive effects cannot be attributed to an exclusive mechanism of action but are instead the result of the commercial formulation's synergistic action of different components (mainly peptides). In this context, Antonucci et al., using a mixed phenotypic-omics approach, observed the mechanisms implemented following the use of a commercial glycine betaine-based biostimulant in tomato (*Solanum lycopersicum* L.) plants (during the flowering phase) subjected to water stress. The authors reported a priming effect of the biostimulant aimed at stabilizing the photosynthetic machinery, both mediated by the hyperaccumulation of carotenoids and lipids and improved water use efficiency. After foliar application of melatonin (100 μM), Zhao et al. observed an improvement in the growth and photosynthetic capacity of maize plants grown under drought conditions attributable to increased proline levels. In addition, the application of melatonin increased enzyme activities involved in nitrogen metabolism. Hernandiz et al., after optimizing the dose of putrescine (Put) and spermidine (Spd) in a growth chamber experiment, evaluated the effect of these two polyamines on maize plants grown in a protected environment under optimal irrigation and deficit irrigation conditions. Using Put and Spd with a higher meal's mineral content (Ca, Cu, and Zn) improved the saleable yield under optimal and sub-optimal conditions. Starting from the assumption that continuous states of water stress (even mild ones) negatively affect plant germination, development, and proper growth, Hameed et al. evaluated on wheat (*Triticum aestivum* L.) the effect of sodium silicate (SS) as a priming agent to reduce the effects of water stress (50% of soil water retention capacity). At plant maturity, the authors observed, under water-limited conditions, an improvement in yield parameters induced by the positive action of Si for plants previously primed with SS. Also, on wheat, Lalarukh et al. investigated the efficacy of the single or combined use of *Pseudomonas aeruginosa* (Pa) (10^8 CFU ml^{-1}) and moringa leaf extracts at different doses (MLE 1 = 1:15 v/v and MLE 2 = 1:30 v/v) under drought and nutritional stress conditions. At the end of their field trial, the authors observed for plants treated with Pa + MLE 2 a significant improvement in yield traits in stressed wheat plants. The synergy between microbial and non-microbial biostimulants is paving the way for research into biopreparations that can further improve yield performance. Considering this, Kang et al. summarized in their review the potential synergistic effects of algae and bacteria on plant production as biostimulants and biofertilizers. In this context, a commercial biostimulant based on glycine betaine (GB), distributed at a rate of 6 kg ha^{-1}, was tested. The trials were conducted on tomato plants during the flowering phase in the greenhouse. A factorial combination of two irrigation (water stress and well-watered) and two biostimulant treatments (treated and control) was adopted, along with a mixed phenotypic-omics approach. The authors demonstrated the priming effect of the biostimulant on drought tolerance, detoxification, and stabilization of the photosynthetic machinery. The metabolic profile and photosynthetic performance results suggest increased effective water utilization through lipid hyperaccumulation and leaf thickening. Also, on tomatoes subjected to combined water and nutrient deficiency, Kalozoumis et al. evaluated the possible effects of inoculating plant growth-promoting rhizobacteria (PGPR) with the agronomic practice of grafting. At the end of the experimental study, the authors emphasized the importance of the combined

selection of PGPR strains and rootstock genotypes to achieve a substantial benefit under combined stress conditions. In a similar study, Toubali et al. evaluated the single and/or combined effects of inoculating arbuscular mycorrhizal fungi and compost on the field production of quinoa (*Chenopodium quinoa* Willd.) under water stress. Microbial biostimulation and the presence of compost ensured that plants subjected to suboptimal water levels maintained high production yields due to specific morpho-physiological adaptations. The review by Etesami et al. investigates in detail the contribution of AMF, phosphate-solubilizing bacteria (PSB), and silica in improving the availability and efficacy of phosphate, a limestone-limiting macroelement, especially in calcareous and acidic soils. Wang et al. observed a significant increase in maize Bt yield, foliar contents of salicylic acid (SA) and jasmonic acid, Bt toxin content, and gene expression after inoculation of an AMF species (*Glomus caledonium*). However, even though mutualistic relationships between mycorrhizal fungi and plants are routinely 'exploited' to improve the latter's tolerance to a multitude of abiotic and other stresses, most of the scientific literature is mainly concerned with the study of arbuscular mycorrhizae. The review proposed by Wei et al. focused on describing the positive effects (increased tolerance to drought, heavy metals, soil salinity, and pathogen infections) of ericoid mycorrhizae on plants belonging to the *Ericaceae* family. Nazari et al. evaluated the interactive effects between plant and bacteriocin molecules to reduce the negative impact of low-temperature stress (5°C) on canola. Specifically, treatment with 10^{-9} thuricin 17 (Th17) significantly improved seed vigor index, germination rate, root and shoot length, and fresh weight of seeds under optimal, and low-temperature conditions. According to the study by Sun et al., the definition and characterization of vegetative attributes through leaf spectral indices could provide useful information to better understand plant-microbe relationships by optimizing bioproducts. The research by Melini et al. emphasizes that the use of selected strains of *Pantoea agglomerans* can be a promising approach for the development of new plant biostimulants for agricultural use through the fermentative production of auxin/indole 3-acetate (IAA). Similarly, through *in vitro* phenotypic analyses, Gutierrez-Albanchez et al. demonstrated the ability of a new *Pseudomonas*, designated as strain BBB001T, to produce auxins and siderophores. Subsequently, the same authors confirmed the potential of this strain by testing on olives (*Olea europaea* L.) and tomatoes (*S. lycopersicum* L.) grown under water limitation or iron deficiency, respectively. Based on the phosphate-solubilising capacity and the production of IAA, *Pseudomonas* sp. strain 1008 (isolated from the rhizosphere of wheat plants), Díaz et al. observed an increase in grain yield after inoculation of the biostimulant bacterium on wheat seeds from 2010–2017. Further genome sequencing analyses revealed the ability of strain 1008 to efficiently utilise organic and inorganic sources of phosphorus and compete for iron scavenging as well as the production of auxins and GABA. To limit the negative effects induced by iron deficiency on *Cinnamomum camphora*, Kong et al. investigated the role of *Rahnella aquatilis* (JZ-GX1) by assessing the active iron content, chlorophyll, and effects on the microbial community. The results showed that inoculation of JZ-GX1 increased chlorophyll content and enzyme activities (SOD, POD, CAT, and APX) on stressed plants. On the other hand, Macias-Benitez et al. investigated the biostimulating capacity of a rice bran enzyme extract (RBEE) used as a protective agent against oxidative damage from ozone exposure in the growth chamber. Pepper plants (*Capsicum annum* L.) treated with RBEE showed a reduction in photosynthetic limitation attributable to the oxidative action of ozone. Pot experiments conducted by Raza et al. showed that applying a vitamin B complex significantly improved the photosynthetic performance of radish plants, underlining the positive contribution of natural biostimulant products on crop productivity. Although most metals are essential trace elements for plants, their excess (often caused by human activities) is responsible for damaging effects that limit plant growth and metabolism. Considering this, the use of biostimulants to improve the effectiveness of ordinary remediation practices has been attracting increasing attention in recent years. Exploiting the synergistic effect between silicon nanoparticles and iron oxide nanoparticles, Koleva et al. observed on *Phaseolus vulgaris* plants grown on cadmium (Cd)-contaminated soil an improvement in growth and a significant reduction in electrolyte loss and malondialdehyde (MDA) content. Similarly, the foliar application of liquiritoside (liquiritin), a flavonoid complex isolated from *Glycyrrhizae radix*, proposed by Akram et al. on Chinese cabbage (*Brassica rapa* subsp. *parachinensis*) mitigated the phytotoxic effects induced by the presence of lead (Pb) through a reduction in the MDA, H_2O, and cysteine content of the treated plants. Naveed et al. evaluated the potential of compost, biochar, and co-composted biochar on *Brassica napus* plants grown on chromium (Cr)-contaminated soil. At the end of the experiment, Naveed et al. observed a significant improvement in biometric and physiological traits of Cr-stressed plants after using co-composted biochar. Mustafa et al., in a pot experiment, compared the effects of biochar obtained from agricultural waste (AB) and food waste (FWB) on key indicators of soil microbiological health with and without mineral fertilizer inputs. The results showed changes in the chemical properties of the soil after fertilization with AB and FWB, which stimulated the growth of lettuce in the growth chamber. Similarly, Hammerschmiedt et al. studied the impact of different digestates (applied at a rate of 40 t ha^{-1}) on soil chemistry and lettuce yield. At the end of the experiments, the authors observed a positive stimulation of soil microbial activity following the use of legume digestates, which could, however, accelerate nitrogen mineralization processes.

One of the environmental factors that most reduces crop growth is undoubtedly salt stress (Abdelhamid et al., 2020). Intense evapotranspiration activity stimulated by environmental warming combined with poor irrigation (often with water of poor quality) increasingly causes secondary soil salinization problems. Gao et al. evaluated the potential beneficial effects of 2-keto-L-gulonic acid (2KGA) on Chinese cabbage (*Brassica campestris* ssp. *chinensis* L.) subjected to salt stress (100 mM NaCl). The results suggest that applying 2KGA by promoting the synthesis of L-ascorbic acid can effectively alleviate the inhibitory and phytotoxic effects of NaCl salinity. Exogenous application of 5-aminolevulinic acid significantly

reduced damage caused by moderate NaCl stress (50 mmol L^{-1}) on cucumber seedlings due to increased root cytoactivity and improved Na^+ redistribution and compartmentalization (Wu et al.).

On the other hand, Sorrentino et al. observed after the application on tomato and lettuce (grown under fully controlled conditions) of a plant biostimulant based on plant-derived protein hydrolysate how the positive action of the tested product induced species-specific adaptive responses that helped to alleviate the harmful effects of NaCl salinity. Similarly, Zuluaga et al. evaluated the different sensitivity of lettuce and tomato plants to high salinity conditions (80 mM for lettuce and 120 mM for tomato) and the possible protective effects of 4 different plant-derived protein hydrolysates (C: *Malvaceae*-derived, P: *Poaceae*-derived, D: legume-derived commercial 'Trainer®' and H: legume-derived commercial 'Vegamin®'). Although lettuce had a constitutive higher sensitivity to salinity than tomato, the efficacy of biostimulants was more evident in lettuce. Regarding the positive role played by microbial biostimulants, Mellidou et al. observed on tomato plants subjected to salt stress (200 mM NaCl) an up-regulation of secondary metabolism after inoculation with *Pseudomonas oryzihabitans*, which enabled the salinized plants to respond more readily to salt-induced extremes. Also, on tomatoes, Becerril-Espinosa et al. observed how establishing an endophytic interaction with the actinobacterium *Salinispora arenicola* promotes germination and growth of roots and shoots under saline and non-saline conditions. An *in-vitro* study by Naamala et al. evaluated the stimulatory effect of cell-free supernatant (CFS) obtained from *Lactobacillus helveticus* EL2006H at different concentrations (0.2 and 1.0% *v/v*) on the germination and biometric traits of maize and soybean grown with NaCl levels of 100 and 150 mM. Although the results showed an efficacy of CFS, these were strongly influenced by the different concentrations used and the NaCl levels and plant species evaluated. In a hydroponic experiment, Tarroum et al. observed on tobacco plants an improved salt tolerance (250 mM) following the application of a nutrient solution of a cell-free supernatant obtained from a halotolerant fungal strain (A3) identified as *Penicillium olsonii*. The results obtained by Xiao et al. indicated that the application of *Bacillus cereus* G2 promoted the growth of *Glycyrrhiza uralensis* (Fisch. ex DC.) plants subjected to salt stress (75 mM NaCl) due to a significant improvement in photosynthetic efficiency and an increased in carbohydrate products from carbohydrate transformation. At different salinity levels (0, 20, 50, and 75 mM), Mhada et al. observed mitigation of the negative impact of salt stress on *Phaseolus vulgaris* plants previously primed and/or coated with a mixture of *Rhizobium tropici* and trehalose. Christakis et al. first identified endophytic bacteria of three aliphatic species: *Cakile maritima*, *Matthiola tricuspidate*, and *Crithmum maritimum*. Subsequently, they observed their ability to grow at high NaCl levels and inhibit the development of phytopathogens such as *Verticillium dahliae*, *Ralstonia solanacearum*, and *Clavibacter michiganensis*. Based on the results, the authors suggest testing halophyte endophytes as new 'bio-inoculant' agents to improve crop response to biotic and abiotic (salinity) stress conditions. Zhang et al., after identifying and isolating a new endophytic bacterium designated as *Bacillus altitudinis* strain using 16S rDNA sequencing, evaluated through bioassays the positive influence of this on the growth and development of various plant species.

3 Biostimulants increase tolerance to biotic stress

The possibility of reducing agrochemicals by developing bio-control agents would help the entire agricultural sector become more free of dependence on conventional chemical inputs, offering sustainable solutions to producers and consumers (Lahlali et al., 2022). Zhang et al., after isolating 60 actinomycetes, observed significant antifungal activity on 17 of them against *Fusarium oxysporum* f. sp. cubense tropical race 4 (TR4), a pathogen that causes one of the most common soil diseases globally. Xu et al. reported that in cucumber plants, there was a strong biocontrol activity against *F. oxysporum* sp. *cucumerinum* by a newly isolated *Bacillus subtilis* strain named YB-04. This effect was attributed to the ability of this strain to secrete amylase, cellulose, and extracellular protease, as well as produce indoleacetic acid and siderophores. After evaluating *in vitro*, the antagonistic activity of *Bacillus tequilensis* GYUN-300 (GYUN-300) against the fungal pathogen *Colletotrichum acutatum*, Kwon et al. observed on red pepper plants inoculated with GYUN-300 a reduction in the incidence of *Colletotrichum acutatum* attacks compared to untreated controls. Drobek et al. confirmed the efficacy of several microbial consortia consisting of bacteria such as: AF117AB (*Paenibacillus polymyxa*), Sp115AD (*Bacillus subtilis*), AF75AB2, Sp115AD, AF75BC (*Bacillus* sp.), AF75AA, AF75AD (*Streptomyces* sp.), JAFGU (*Lysobacter* sp.) and AF70AC (*Pseudomonas* sp.), in controlling the main microbial pathogens *(Botrytis cinerea*, *Verticillium* sp., *Phytophthora* sp. and *Colletotrichum* sp.) of strawberries, also underlining the positive impact on the final fruit quality. Seeds of two different rice varieties coated with *Trichoderma* strains inhibited the incidence of pathogens. They improved the chlorophyll content and vigor of the treated plants (Swain et al.). Valverde et al. evaluated the antifungal activity of 20 commercial macroalgae products against two post-harvest pathogens (*B. cinerea* and *Penicillium digitatum*) of fruit. Following the chemical evaluation of the tested products, the results confirmed that some specific bioactive components reduced the incidence of *B. cinerea.* At the same time, the control of *P. digitatum* was attributed to the presence of carbohydrates and polysaccharides. The application of a consortium of *Trichoderma asperellum* GDFS1009 and *Beauveria bassiana* OFDH1–5 on maize plants not only increased antioxidant enzyme activities and chlorophyll content but also decreased the survival of *Ostrinia furnacalis* (Batool et al.).

4 Biostimulants increase nutrient use efficiency

To maximize crop yields, farmers rely on large quantities of chemical fertilizers that are not always efficiently absorbed by the plant. In addition, their industrial production has an environmental

impact that is no longer sustainable. Incentivizing natural products that affect N and P utilization is necessary for present and future agriculture (Umar et al., 2020). As argued by Reis et al., among the most sustainable agricultural techniques, the use of phosphate-solubilizing microbial strains is a valuable tool. The results regarding the solubilization of calcium phosphate in a hydroponic system with *Glycine max* plants highlighted the potential of *Lysinibacillus fusiformis* (PA26), which was the most efficient due to the increased P uptake and growth promotion observed in the inoculated plants. Gong et al. point out that root space availability and P supply significantly influence phosphorus use efficiency (PUE) in maize. However, the inoculation of mycorrhizal fungi allowed plants grown in pots with small diameters (20 cm) to increase total biomass even with reduced P supply. In a similar study, Gong et al. suggest that a higher P supply could compensate for the yield loss attributable to lower density; in addition, for the same P supply, the use of single superphosphate versus mono ammonium phosphate improved the growth of maize-grown at lower planting densities. To improve PUE and growth of maize and cucumber plants grown in hydroponics, Alzate Zuluaga et al. tested the efficacy of the 15S strain of *Enterobacter* sp. Inoculation of the bacterium under P-limiting conditions induced a greater effect on cucumber plants due to an increase in P allocation in both the epigeal and hypogean parts of the plants. In connection with bacterial gene expression, Yahya et al. studied the action of phosphate solubilization by *Ochrobactrum* sp. SSR (DSM 109610). A higher P content characterized wheat plants inoculated with DSM 109610; the bacterial supplementation increased the soil availability of this macronutrient and the alkaline phosphatase activity. The review work proposed by Rizvi et al. investigates the still under-studied role of the phosphate-soluble microbiome in managing sorghum cultivation-related diseases to reduce dependence on chemical pesticides further. In line with this, Haque et al. evaluated the biofertilising action of *Enterobacter* sp. HSTU-ASh6, a rice root endophyte that mineralizes chlorpyrifos. The results of tomatoes show improved growth of treated plants after foliar application of the HSTU-ASh6 strain, even with reduced nitrogen fertilization rates. In a pot experiment on maize, Chen et al. observed an increase in PUE and yield after the combined application of humic acids (45 kg ha^{-1}) and an ammonium phosphate fertilizer compared to plants subjected to phosphorus fertilizer application alone. After extracting the humic acids (HA) in a phosphate fertilizer enhanced with HA, Jing et al. evaluated the effects on hydroponically grown maize seedlings. HA at doses of 2.5 and 5 mg C L^{-1} enhanced the average N and P uptake rates compared to untreated controls. To further investigate the effects of HA on plant growth, Wang et al. evaluated the effects of two different HAs [Aojia humic acid (AHA) and Shandong humic acid (SHA)] on maize as a model crop. After characterizing the humic acids through an ESI-HPLC-MS technology, the authors observed a different beneficial effect of AHA and SHA on maize growth (with AHA better than SHA) attributable to the significant differences in molecular compositions. Furthermore, in connection with HA, Xu et al. evaluated the effects of a root application (at 1%) on cucumber in three different hydroponic substrates (pure sand, pure cocopeat, and a mixture of sand and cocopeat). The results show that applying HA improved biometric parameters only in plants grown on pure cocopeat and cocopeat-sand mixture. Having identified, with mathematical models, the optimal doses of AMF and *Bacillus megaterium* (2.1 kg ha^{-1} for both), Ganugi et al. observed in co-inoculated maize plants an increased accumulation of N in the grain and an improved nitrogen harvest index. Through non-invasive 3D imaging of root architecture and specific biochemical assays, Mohammed et al. showed that root application of phosphite improved nitrogen assimilation and root biomass of maize seedlings. Chen et al. recorded an improvement in N, P, and K efficiency in sugarcane plants grown in China in two cultivation areas (Suixi and Wengyuan) following the application of algae extracts at different phenological states (sowing, early elongation, and early maturity). To reduce N application rates, Goñi et al. evaluated this macroelement's uptake and assimilation mechanisms by plants treated with a biostimulant based on *Ascophyllum nodosum* extracts. The results on *Arabidopsis thaliana* showed a significant increase in nitrate content 6 days after application of the biostimulant. On the other hand, subsequent field trials revealed a significant increase in nitrate use efficiency on barley plants grown with 75% N supply. Similarly, Ciriello et al. demonstrated, on hydroponic basil, that applying a plant-derived protein hydrolysate (albeit dose-dependent) can compensate for the effects of a reduced nutrient solution (1 dS m^{-1}), even improving yield and quality attributes. To improve the efficacy of synthetic fertilizers, Amaral and Brown investigated the effects of a plant-based inositol bioproduct on zinc (Zn) accumulation and mobility in wheat (*Triticum aestivum* L.) plants. Foliar application of the stimulant in combination with zinc sulfate significantly increased the concentration of this trace element in both grains and shoots compared to fertilized but not stimulated plants.

5 Biostimulants increase the qualitative characteristics of the produce

Interest in agri-food products that meet the goal of a healthy lifestyle has grown enormously in recent years. Various agronomic approaches have been proposed to enhance food products' qualitative and functional attributes, including biostimulants (Ganugi et al., 2021; Melini et al., 2023). In this respect, Godlewska et al. observed after foliar application of plant extracts from common dandelion, valerian, and giant cabbage an improvement in vitamin C, macro- and micro-nutrient content, and a variable impact on the composition of fatty acids, and low molecular weight volatile compounds. Similarly, Abd-Elkader et al. evaluated the beneficial effects of *Trichoderma viride* and *Pseudomonas fluorescens* and three plant extracts of *Eucalyptus camaldulensis* (leaf extract indicated as LE), *Citrus sinensis* (leaf extract indicated as LE) and *Ficus benghalensis* fruits (fruit extract indicated as FE) with potassium silicate (K_2SiO_3) on the biochemical composition of courgette (*Cucurbita pepo* L.) fruits. Specifically, the LE combination with K_2SiO_3 increased greenhouse-

grown zucchini fruits' total phenolic content and antioxidant activity. Wang et al. evaluated the influence of five different concentrations of methyl jasmonate (MeJA) and salicylic acid (SA) on the yield and quality characteristics of Chinese chives. Applying MeJA and SA at concentrations of 500 and 150 µM resulted in a significant increase in phenols and flavonoids, vitamin C, and volatile compounds while reducing the nitrate content. Mesa et al., to evaluate the additive and/or synergistic effects of the application of a protein hydrolysate of animal origin combined with low-N priming, observed an improvement in quality parameters (soluble sugars, acidity, and lycopene content, vitamin E and vitamin C) on greenhouse tomatoes. Also, on tomatoes, Zhang et al. studied the effects of fulvic acids (obtained from maize straw) on fruit quality. The use of fulvic acids increased the concentrations of minerals (Ca, Fe, and Zn), citric acid, malic acid, and some amino acids without affecting the concentrations of soluble sugars. A field experiment of AMF inoculation on alfalfa (*Medicago sativa* L.) intended for livestock consumption increased the yield and nutrient and fatty acid content of the forage. Pellegrino et al. observed the persistence of positive effects even two years after inoculation due to an abundance of AMF at the root level. Although AMF-released glomalin's functions are known, this molecule's exogenous application is still unknown. Liu et al. investigated the effects of easily extractable glomalin-related soil protein (EE-GRSP) and difficultly extractable glomalin (DE-GRSP) on the growth and development of orange trifoliate (*Poncirus trifoliata* L.). The application of the two extracts resulted in contrasting effects. Specifically, the exogenous application of EE-GRSP enhanced growth, while a decrease was observed for plants treated with DE-GRSP. To improve the rooting of 'Hurdal' rose cuttings, Monder et al. tested different plant origin preparations (algae extracts, organic preparation, and plant extract). The best results were obtained using algae extracts for plant cuttings at the phenological stage of closed flower buds. Finally, Łangowski et al. observed on several soybean varieties cultivated in Canada and Brazil an increase in seed yield following the application of an *Ascophyllum nodosum* extract.

7 Conclusions and challenges ahead

It is an absolute prerogative that using plant biostimulants, irrespective of origin, will increasingly contribute to a mandatory transition to more economically and ecologically sustainable production systems. Agroecosystems that are more resilient and no longer threatened by uncontrolled human activities must be an integral part of future agriculture. Although the use of natural products and/or plant biostimulants is now a complementary tool to synthetic agrochemicals, the scientific community is called upon to define the underlying genetic, molecular, and physiological mechanisms, as a better understanding of these aspects would greatly facilitate the dissemination of bio-based products in the agricultural sector. Moreover, elucidating biostimulant × plant species × environment interaction × agricultural practices are crucial, in order to select optimal combinations in terms of yield, yield components and quality, and also optimizing application parameters (e.g. timing, mode, rate). Finally, it is also urgent to understand the interactions between biostimulant products, living organisms and chemical inputs (plant protection products and/or fertilizers) to develop more sustainable production systems.

Author contributions

MR: Writing – review & editing, Writing – original draft. GC: Writing – review & editing, Writing – original draft. YR: Writing – review & editing, Writing – original draft.

Conflict of interest

The authors declare that the research was conducted in the absence of any commercial or financial relationships that could be construed as a potential conflict of interest.

The author(s) declared that they were an editorial board member of Frontiers, at the time of submission. This had no impact on the peer review process and the final decision.

Publisher's note

Supplementary material

The Supplementary Material for this article can be found online at: https://www.frontiersin.org/articles/10.3389/fpls.2024.1427283/full#supplementary-material

References

Abdelhamid, M. T., Sekara, A., Pessarakli, M., Alarcón, J., Brestic, M., El-Ramady, H., et al. (2020). "New approaches for improving salt stress tolerance in rice," in *Rice Research for Quality Improvement: Genomics and Genetic Engineering: Volume 1: Breeding Techniques and Abiotic Stress Tolerance* (Springer Nature Singapore Pte Ltd.), 247–268.

Donate, P. M., and Frederico, D. (2019). "Synthesis of New Agrochemicals," in *Sustainable Agrochemistry: A Compendium of Technologies* (Springer Nature Switzerland AG), 223–273.

EU (2019) *REGULATION OF THE EUROPEAN PARLIAMENT AND OF THE COUNCIL laying down rules on the making available on the market of EU fertilising products and amending Regulations (EC) No 1069/2009 and (EC) No 1107/2009 and repealing Regulation (EC) No 2003/2003*. Available online at: https://eur-lex.europa.eu/legal-content/EN/TXT/?uri=OJ:L:2019:170:TOC.

Ganugi, P., Martinelli, E., and Lucini, L. (2021). Microbial biostimulants as a sustainable approach to improve the functional quality in plant-based foods: A review. *Curr. Opin. Food Sci.* 41, 217–223. doi: 10.1016/j.cofs.2021.05.001

Goud, E. L., Singh, J., and Kumar, P. (2022). ""Climate change and their impact on global food production,"," in *Microbiome under changing climate* (Cambridge, MA, USA: Woodhead Publishing (Elsevier)), 415–436. doi: 10.1016/B978-0-323-90571-8.00019-5

GVR (2023). ""Biostimulants Market Size, Share & Trends Analysis Report By Active Ingredients (Acid Based, Microbial), By Crop Type, By Application (Foliar, Soil Treatment), By Region, And Segment Forecasts 2023 - 2030"," in *Market Analysis Report* (San Francisco, CA, USA: Grand View Research).

Lahlali, R., Ezrari, S., Radouane, N., Kenfaoui, J., Esmaeel, Q., El Hamss, H., et al. (2022). Biological control of plant pathogens: A global perspective. *Microorganisms* 10, 596. doi: 10.3390/microorganisms10030596

Melini, F., Melini, V., Luziatelli, F., Abou Jaoudé, R., Ficca, A. G., and Ruzzi, M. (2023). Effect of microbial plant biostimulants on fruit and vegetable quality: current research lines and future perspectives. *Front. Plant Sci.* 14, 1251544. doi: 10.3389/fpls.2023.1251544

Rouphael, Y., and Colla, G. (2020). Biostimulants in agriculture. *Front. Plant Sci.* 11, 511937. doi: 10.3389/fpls.2020.00040

Umar, W., Ayub, M. A., Rehman, M. Z. U., Ahmad, H. R., Farooqi, Z. U. R., Shahzad, A., et al. (2020). Nitrogen and phosphorus use efficiency in agroecosystems. in *Resources use efficiency in agriculture*. S. Kumar, R. S. Meena and M. K. Jhariya, editors. (Singapore: Springer). doi: 10.1007/978-981-15-6953-1_7

Velasco-Muñoz, J. F., Mendoza, J. M. F., Aznar-Sánchez, J. A., and Gallego-Schmid, A. (2021). Circular economy implementation in the agricultural sector: Definition, strategies and indicators. *Resources Conserv. Recycling* 170, 105618. doi: 10.1016/j.resconrec.2021.105618

frontiers in Plant Science

ORIGINAL RESEARCH
published: 09 February 2021
doi: 10.3389/fpls.2021.600623

Evaluation of the Potential Use of a Collagen-Based Protein Hydrolysate as a Plant Multi-Stress Protectant

*Stefano Ambrosini, Davide Sega, Chiara Santi, Anita Zamboni, Zeno Varanini and Tiziana Pandolfini**

Dipartimento di Biotecnologie, Università degli Studi di Verona, Verona, Italy

Protein hydrolysates (PHs) are a class of plant biostimulants used in the agricultural practice to improve crop performance. In this study, we have assessed the capacity of a commercial PH derived from bovine collagen to mitigate drought, hypoxic, and Fe deficiency stress in *Zea mays*. As for the drought and hypoxic stresses, hydroponically grown plants treated with the PH exhibited an increased growth and absorption area of the roots compared with those treated with inorganic nitrogen. In the case of Fe deficiency, plants supplied with the PH mixed with $FeCl_3$ showed a faster recovery from deficiency compared to plants supplied with $FeCl_3$ alone or with FeEDTA, resulting in higher SPAD values, a greater concentration of Fe in the leaves and modulation in the expression of genes related to Fe. Moreover, through the analysis of circular dichroism spectra, we assessed that the PH interacts with Fe in a dose-dependent manner. Various hypothesis about the mechanisms of action of the collagen-based PH as stress protectant particularly in Fe-deficiency, are discussed.

Keywords: protein hydrolysates, biostimulants, collagen, crop performance, Fe deprivation, abiotic stress

OPEN ACCESS

Edited by:
Youssef Rouphael,
University of Naples Federico II, Italy

Reviewed by:
Juan Parrado,
University of Seville, Spain
Diego Pizzeghello,
Università degli Studi di Padova, Italy
Francesco Sestili,
University of Tuscia, Italy

***Correspondence:**
Tiziana Pandolfini
tiziana.pandolfini@univr.it

Specialty section:
This article was submitted to Crop and Product Physiology, a section of the journal Frontiers in Plant Science

Received: *30 August 2020*
Accepted: *11 January 2021*
Published: *09 February 2021*

Citation:
Ambrosini S, Sega D, Santi C, Zamboni A, Varanini Z and Pandolfini T (2021) Evaluation of the Potential Use of a Collagen-Based Protein Hydrolysate as a Plant Multi-Stress Protectant. Front. Plant Sci. 12:600623. doi: 10.3389/fpls.2021.600623

INTRODUCTION

Ever since their appearance on land, plants had to deal with numerous abiotic stresses, including low or high temperature, deficient or excessive water, high light intensity and ultraviolet (UV) radiation, nutrient shortages or imbalances. These stresses are accountable for great crop yield loss (Wang et al., 2004; Wani et al., 2016) and are exacerbated by recent climate changes (Boyer, 1982; Rahmstorf and Coumou, 2011). The negative impact on plant growth is worsened when these stresses are combined, for instance, drought and heat stress were responsible for as much as the 40% of reduction in crops yield for maize (Daryanto et al., 2016), and up to 68% for cowpea (Farooq et al., 2017). Moreover, water shortage and soil salinity trigger oxidative, osmotic and temperature stress, representing another major challenge for productivity (Landi et al., 2017). In the future, the dramatic increase in land degradation rate is expected to result in a drastic loss of planet arable lands (Scherr, 1999). According to the data published by the European Union in the World Atlas of Desertification, the combined effects of soil degradation and climate changes will result in 10% reduction of global crop yield by 2050, with severe economic losses (Cherlet et al., 2018). The future scenarios urge scientists to search for new technologies to improve crop productivity, focusing on organic substances, which not only could replace chemical fertilizers, often responsible for environmental pollution, but could also be exploited to contrast abiotic stresses (Suhag, 2016). Nowadays, an increasingly employed resource in agriculture are plant biostimulants. This term

refers to a very broad class of substances and microorganisms that includes – as defined by the European Union – "fertilizing products the function of which is to stimulate plant nutrition processes independently of the products' nutrient content with the sole aim of improving one or more of the following characteristics of the plant or the plant rhizosphere: (i) nutrient use efficiency, (ii) tolerance to abiotic stress, (iii) quality traits, or (iv) availability of confined nutrients in the soil or rhizosphere" (European Union, 2019). Many diverse bioactive substances are catalogued as plant biostimulants based on their agricultural function claims, including: (i) humic and fulvic acids, (ii) animal and vegetal protein hydrolysates (PHs), (iii) macroalgae seaweeds extracts, and (iv) silicon, and also some beneficial microorganisms such as (i) arbuscular mycorrhizal fungi (AMF) and (ii) nitrogen-fixing bacteria of strains belonging to the genera *Rhizobium*, *Azotobacter*, and *Azospirillum*. Among the listed categories, protein hydrolysates are particularly interesting, not only because they are effective biostimulants, but especially because they are mainly produced from organic waste, well fitting into the eco-friendly scheme of circular economy (Xu and Geelen, 2018). PHs are by-products from several industrial activities and can either have animal- or plant- origins. Some of the animal matrix from which PHs can be obtained are epithelial or connective tissues, hen feathers, and bone meal (Drobek et al., 2019), while plant-derived PHs can come from carob germ proteins, alfalfa residue, wheat-condensed distiller solubles, *Nicotiana* cell wall glycoproteins and algal proteins (Calvo et al., 2014).

Most of the studies regarding PHs highlight their capacity to improve plant growth and nutrient use efficiency, proposing some mechanisms of action which might include the hormone-like activities of bioactive peptides (Santi et al., 2017; Ertani et al., 2019), the stimulation of carbon and nitrogen metabolism, as well as the regulation of nutrient uptake (Ertani et al., 2009; Colla et al., 2014). For instance, Santi et al. proved that the treatment with a bovine collagen-derived PH remarkably enhanced maize root increasing the root accumulation of K, Zn, Cu, and Mn when compared with inorganic N and amino acids treatments (Santi et al., 2017). Moreover, in the same work, the microarray analysis suggested that the treatment with the bovine collagen-derived PH to the nutrient solution caused major changes in the transcriptional profile of the roots, altering the expression of genes involved in the cell wall organization, the transport processes, the stress responses and the hormone metabolism. Recently, Paul et al. (2019b) tested eight different plant-derived protein hydrolysates on tomato plants, reporting, for some of the treatments, an increase in relative growth rate and growth performance. Moreover, metabolomic profiles of the plants treated with PHs showed that ethylene precursor 1-aminocyclopropane-1-carboxylate (ACC) and polyamines were positively modulated, and the ROS-mediated signaling pathways were affected as well (Paul et al., 2019b).

While there is a vast literature on PHs efficacy as plant growth and nutrient use efficiency enhancer, relatively few works have tried to demonstrate that these compounds are also capable to ameliorate plant performances under abiotic stress conditions. In an interesting paper, Ertani et al. proved that a plant-derived PH increased plant biomass in salt-stressed maize plants (Ertani et al., 2012), ascribing the beneficial effects to the triacontanol, a fatty acid known to act as plant growth regulator (Chen et al., 2002) and salt-stress mitigator (Çavuşoğlu et al., 2008), which is present in the PH in a noticeable amount. Another study from Lucini et al. (2015) demonstrated the beneficial effects of a plant-derived PH treatment on lettuce plants grown in pots under saline stress. The PH treatment helped the plants to better respond to saline environment compared to those treated with water only, showing an increased shoot fresh yield. In this case the authors suggested that the PH mitigated the stress by attenuating the oxidative stress, improving osmotic adjustment, and rewiring the hormone, sterol, terpene and glucosinolate profiles (Lucini et al., 2015). More recently, the work of Trevisan et al. (2019) investigated the activity of a collagen-derived PH as stress-mitigator, in maize seedlings subjected to hypoxic, saline and nutritional stress. The plants treated with this biostimulant produced longer roots in all the three stress conditions than those which did not receive the treatment. The transcription level of the superoxide dismutase *ZmSOD1a* gene was induced upon PH treatment in hypoxia, nutritional deficiency, and when saline and nutritional stress were combined. The authors therefore suggested that the PH might mitigate the effects of different stresses by regulating of the expression of genes involved in ROS scavenging (Trevisan et al., 2019). Another recent work, from Paul et al. (2019a), positively assessed the beneficial effect of a plant-derived PH as stress-mitigator on tomato plants grown under limited water availability. They suggested that PH-treated plants were able to better cope with oxidative stress thanks to major changes in phytohormones and lipid profiles (Paul et al., 2019a). Lastly, Casadesús et al. (2019, 2020) assessed the beneficial effects of a product derived from enzymatic hydrolysis of animal proteins in tomato plants grown under water, temperature or nutrient stress suggesting that the positive effects on root growth are due to the increased biosynthesis of specific phytohormones (Casadesús et al., 2019, 2020).

The aim of this work is to investigate the capacity of a collagen-based PH to act as multi-stress protectant when supplied to plant species of agricultural interest by setting up fast and reliable experimental laboratory tests. We carried out the experiments on hydroponically grown maize plants treated with a commercial PH (LMW10 – produced by SICIT group) derived from acid hydrolysis of bovine collagen. We demonstrated that the PH was able to protect the root apparatus from drought and hypoxic stresses. We also proved that the PH quickened the recovery of plants after iron (Fe) deficiency. Moreover, we provide evidence of the chemical interaction between the PH and Fe ions as a possible mechanism that could favor the micronutrient availability for root uptake in the nutrient solution.

MATERIALS AND METHODS

Plant Materials, Growth Conditions and Phenotypic Analyses

Maize seeds (P0943 Hybrid, Pioneer Italia S.p.A.) were soaked in water for 24 h and germinated in the dark on wet filter

paper for 72 h. Seedlings with similar size were then transferred in pots that can accommodate 6 plantlets, containing 2L of a 0.5 mM $CaSO_4$ solution and grown for 24 h under a 16/8 h light/dark regime at 22–26°C, 40–50% relative humidity, 125 $\mu E\ m^{-2}\ s^{-1}$ light intensity. For the experiments under drought and hypoxic conditions, seedlings were successively grown in a diluted nutrient solution containing 100 $\mu M\ MgSO_4$, 5 μM KCl, 200 $\mu M\ K_2SO_4$, 175 $\mu M\ KH_2PO_4$, 400 μM $CaSO_4$, 25 $\mu M\ NH_4H_2PO_4$, 2.5 $\mu M\ H_3BO_3$, 0.2 $\mu M\ MnSO_4$, 0.2 $\mu M\ ZnSO_4$, 0.05 $\mu M\ CuSO_4$, 0.05 $\mu M\ NaMoO_4$, 2 μM Fe-EDTA and supplemented with either protein hydrolysates (SICIT Group) or inorganic nitrogen ($NH_4H_2PO_4$) (Santi et al., 2017). The protein hydrolysate, a liquid formulation obtained from the hydrolysis of cow connective tissue, contains 32.3% (w/w) total carbon (C), 12.3% (w/w) total nitrogen (N), 10.9% (w/w) organic N of which 68.5% (w/w) total amino acids and 12.4% (w/w) free amino acids. The amino acids composition and the mineral ion concentrations are summarized in **Supplementary Tables 1, 2**. Drought stress was obtained following the method described by Han et al. (2017). The plants were grown in an aerated nutrient solution supplemented with 15% w/w of polyethylene glycol (PEG, MW6000), root growth as well as leaf fresh and dry weight (**Supplementary Figure 1**) was recorded after 9 days of treatment. To study the effects of PH under hypoxic stress, maize seedlings were grown in the above described nutrient solution interrupting air insufflation (see also Results section for detailed description of the experimental conditions). For the experiments on Fe deprivation and supply, seedlings were grown in 2L pots in a aerated Fe-deprived nutrient solution (Sega et al., 2020) containing 2 mM $Ca(NO_3)_2$, 500 $\mu M\ MgSO_4$, 100 μM KCl, 700 $\mu M\ K_2SO_4$, 100 $\mu M\ KH_2PO_4$, 10 $\mu M\ H_3BO_3$, 0.5 $\mu M\ MnSO_4$, 0.5 μM $ZnSO_4$, 0.5 $\mu M\ CuSO_4$, 0.01 $\mu M\ (NH_4)_6Mo_7O_{24}$ for 7 days. Afterwards, seedlings were transferred in the nutrient solution containing 20 μM Fe, as either FeEDTA (−Fe/+FeEDTA), or $FeCl_3$ supplemented with 0.1 mL L^{-1} PH (−Fe/+FeBio) or with the equivalent amount of N supplied (−Fe/+$FeCl_3$) as inorganic nitrogen ($NH_4H_2PO_4$). Control plants were grown in the nutrient solution containing FeEDTA 20 μM for 14 days (+FeEDTA) or in the nutrient solution deprived of Fe with the addition of 14.3 mgL^{-1} of N (−Fe/−Fe). Primary, seminal and lateral root total length and surface area were measured with WinRHIZO^{TM} scanner and automated software (Arsenault et al., 1995).

Macro- and Micro-Nutrients Quantification

The Fe concentration in the leaf samples and in the PH product was quantified by ICP-MS analysis. For the analysis dried leaf samples and the PH product (about 5 mg) were weighted and digested in a TFM micro-sampling insert using 350 µl of 69% ultrapure HNO_3. The inserts were put into a 100-ml oven vessel containing 10 ml of water (milliQ, 18.2 M cm) and 1 ml of 30% H_2O_2. As reference we digested 5 mg of NIST 1515 (apple leaves). The digestion of the samples was performed using a microwave oven (Milestone StartDR microwave). A 20-min ramping period was used to reach a digestion temperature of 180°C. The temperature was thereupon maintained for 20 min. At the end, sample were diluted with water (milliQ, 18.2 M cm) to a final concentration of 2% HNO_3. Multi-elemental analysis was carried out using the Agilent 7500cx ICP-MS (Agilent). Each macro- and micronutrient was quantified using a multi-element standard solution. For the assessment of leaf Fe concentration, we collected three biological samples, each derived from a pool of 4 leaves, and two technical replicates for each measurement. For the analysis of PH mineral content, the mean values were calculated using three technical replicates.

SPAD Measurements

A SPAD-502 Plus Chlorophyll meter® (Konica Minolta) was used to acquire SPAD values of the third fully expanded leaf of each plant. The values were distinctly taken at the top or at the mid part of the leaves. Measurements were acquired immediately before Fe was supplied in the hydroponic solution, and two, four, and 7 days after that moment. Values from nine to twelve leaves per experimental condition were sampled and averaged to a single SPAD value for each treatment.

Circular Dichroism Spectral Measurement

Circular dichroism (CD) spectra were recorded with a JASCO J-1500 spectropolarimeter (Japan Spectroscopic Co., Tokyo, Japan), using a quartz cell of 1 mm path length at 25°C. CD spectra were scanned in the far-ultraviolet range from 190 to 250 nm. Values were measured at an interval of 1 nm, and the spectra obtained were the average of 5 reads. The biostimulant was diluted in distilled water to get a total amount of nitrogen of 71.5 mg L^{-1}. $FeCl_3$ was added to the biostimulant in aqueous solutions at different concentrations [(µM) 0, 50, 100, 150, 200, 250]. Spectra of $FeCl_3$ dissolved in distilled water without the biostimulant, at different concentrations, were used as blank reference. Final spectra resulted from the subtraction of their respective blanks and subsequent smoothing. The CD data were expressed in terms of molar ellipticity, [θ], in deg $cm^2\ dmol^{-1}$ and were calculated referring to a Mean Residual Weight (MRW) fixed at 106.5 g mol^{-1}.

Quantitative RT-PCR Analysis

Total RNA was extracted from root samples, using the Spectrum^{TM} Plant Total RNA kit (Sigma-Aldrich, St. Louis, MO, United States) and quantified using NanoDrop^{TM} 1000 (Thermo Scientific, Waltham, MA, United States). For RNA extraction we used three biological samples, each consisting of the roots of four plants. DNase I treatment was carried out for each sample using one microgram of total RNA and the RQ1 RNase-Free DNase (Promega, Madison, WI, United States) according to the manufacturer's procedure. DNase-treated samples were then used to synthetized cDNA with the ImProm-II Reverse Transcription System (Promega, Madison, WI, United States). Real-time RT-PCR experiments

were performed with the Fast SYBR® Green Master Mix (Thermo Fisher Scientific) on the QuantStudio 3 Real Time-PCR (Thermo Fisher Scientific) according to the manufacturer's protocols. The reactions were carried out in a volume of 10 μL with a final primer concentration equal to 350 nM and 1 μL of a 1:3 solution of cDNA as template. The following thermal profile was set-up: 95°C for 20 s, 40 cycle of 95°C for 3 s and 60°C for 30 s. Two housekeeping transcripts were employed, one encoding an ubiquitin-conjugating enzyme (GRMZM2G027378_T01) and the other an unknown protein (GRMZM2G047204_T01), respectively. The analysis of the expression of *ZmIRT1* and *ZmYS1* was carried out with primers used by Nozoye et al. (2013) whilst for the expression of *ZmTOM1* the primers were designed accordingly to Chan-Rodriguez and Walker (2018). The sequences of all primers were reported in **Supplementary Table 3**.

The PCR reaction efficiencies were calculated with the LinRegPCR program (Ramakers et al., 2003). Mean normalized expression (MNE) (Simon, 2003) was calculated for each transcript and each sample using the two housekeeping transcripts separately. A mean MNE value was determined using a geometric mean of the two MNE values obtained for each transcript and each sample (Vandesompele et al., 2002).

Statistical Analysis

Statistical analysis was performed using GraphPad Prism version 5.03 software. Student's *t*-test for unpaired data was applied when two independent variables were compared as is the case of data shown in Figures, and a p value < 0.05 was accepted as statistically significant. Data are presented in the figures as mean and standard error of the mean.

RESULTS

The Stimulation of Root Growth Induced by PH Is Not Affected by Drought Conditions

To investigate whether the PH could mitigate drought stress, we grew maize seedlings from the emergence of the primary root in a diluted nutrient solution supplemented with the PH (Bio) or inorganic nitrogen ($NH_4H_2PO_4$; N) and 15% w/w of polyethylene glycol (PEG, MW6000) (**Figure 1A**). After 9 days of treatment, we analyzed the length and surface area of the roots. Consistently with previous results (Santi et al., 2017), the plants grown in the presence of the protein hydrolysate under normal condition had longer main and lateral roots compared to inorganic N-treated plants (**Figures 1B,C**). The improved root growth confers to Bio-treated plants also an extended absorption surface (**Figures 1D,E**). Thus, we confirmed that the PH promotes the root apparatus development when water is abundantly available. Under drought conditions obtained by using 15% PEG, plants treated with N showed a significant increase in both main and lateral root length (+37.6 and +78.1%, respectively) and area (+43.1 and +90.1%, respectively) with respect to non-stressed plants. In plants treated with Bio, drought conditions did not lead to statistically significant increase in the main root growth, while lateral roots length and area (+51.0 and +23.2%) were augmented although to a lesser extent as compared to the N-treated plants. Notably, under drought stress, plants treated with the PH maintained a significantly higher root growth compared to the plants supplied with inorganic nitrogen (main root length: +67.0%; lateral root length: +73.0%; main root area: +61.4%; lateral root area: +57.8%).

The PH Counteracts the Inhibitory Effects of Hypoxia on Root Growth

To establish whether the PH could alleviate hypoxic stress, maize seedlings were grown hydroponically in a diluted nutrient solution supplemented with the PH (Bio) or inorganic nitrogen ($NH_4H_2PO_4$; N). Control plants (N+; Bio+) were grown in pots with air insufflation, while hypoxic stress was imposed (N−; Bio−) by interrupting air flow. The plants were grown for 4 days after the emergence of the primary root, then, roots length and area were analyzed (**Figure 2A**). Under hypoxic conditions, plants treated with inorganic nitrogen (N−) showed a statistically significant reduction of main and lateral root length (−22.1 and −25.6%, respectively) (**Figures 2B,C**) and area (−24.2 and −19.5%, respectively) compared to the control (N+) (**Figures 2D,E**). The hypoxic stress in the Bio-treated plants resulted in the inhibition of lateral root growth and surface area (−35.6 and −33.7%), a bit higher than what was observed in N-treated plants. However, the PH treatment (Bio−) alleviated the effects of hypoxia on the main roots, since their length and surface area did not differ from those of Bio-treated control plants (Bio+). Overall, under hypoxic conditions, the root apparatus of Bio-treated plants (Bio−) was more developed than that of N-treated plants even when grown under sufficient oxygen supply (N+).

Further analyses were conducted to test whether the treatment with PH could favor root recovery from hypoxic stress. We therefore set up a new experiment in which plants cultivated with either the PH or inorganic nitrogen were grown hypoxically for 4 days and then supplied with air or maintained under hypoxia for further 5 days. Plants treated with inorganic nitrogen and grown for 9 days under hypoxic stress (N−−) grew stunted compared to those treated with the PH (Bio−−) (Bio−− vs. N−−: main root length: +80.1%; lateral root length: +108.1%; main root area: +65.6%; lateral root area: +136.8%; $p < 0.001$ for all the comparisons) (**Figures 3A–D**). When plants treated with inorganic nitrogen were supplied with air (N−+), the root growth did not ameliorate significantly compared to that of the oxygen depleted plants (N−−). Conversely, plants treated with the PH and supplied with air (Bio−+) showed a statistically significant increase (+24.4%) in lateral root length compared to those maintained in hypoxia (Bio−−). As for the other growth parameters, the trend observed was similar (Bio−+ vs. Bio−− seminal root length: +14.5%; seminal root area: +16.9%; lateral root area: +19.6%). Thus, the treatment with the PH showed beneficial effects on root growth under hypoxic stress and

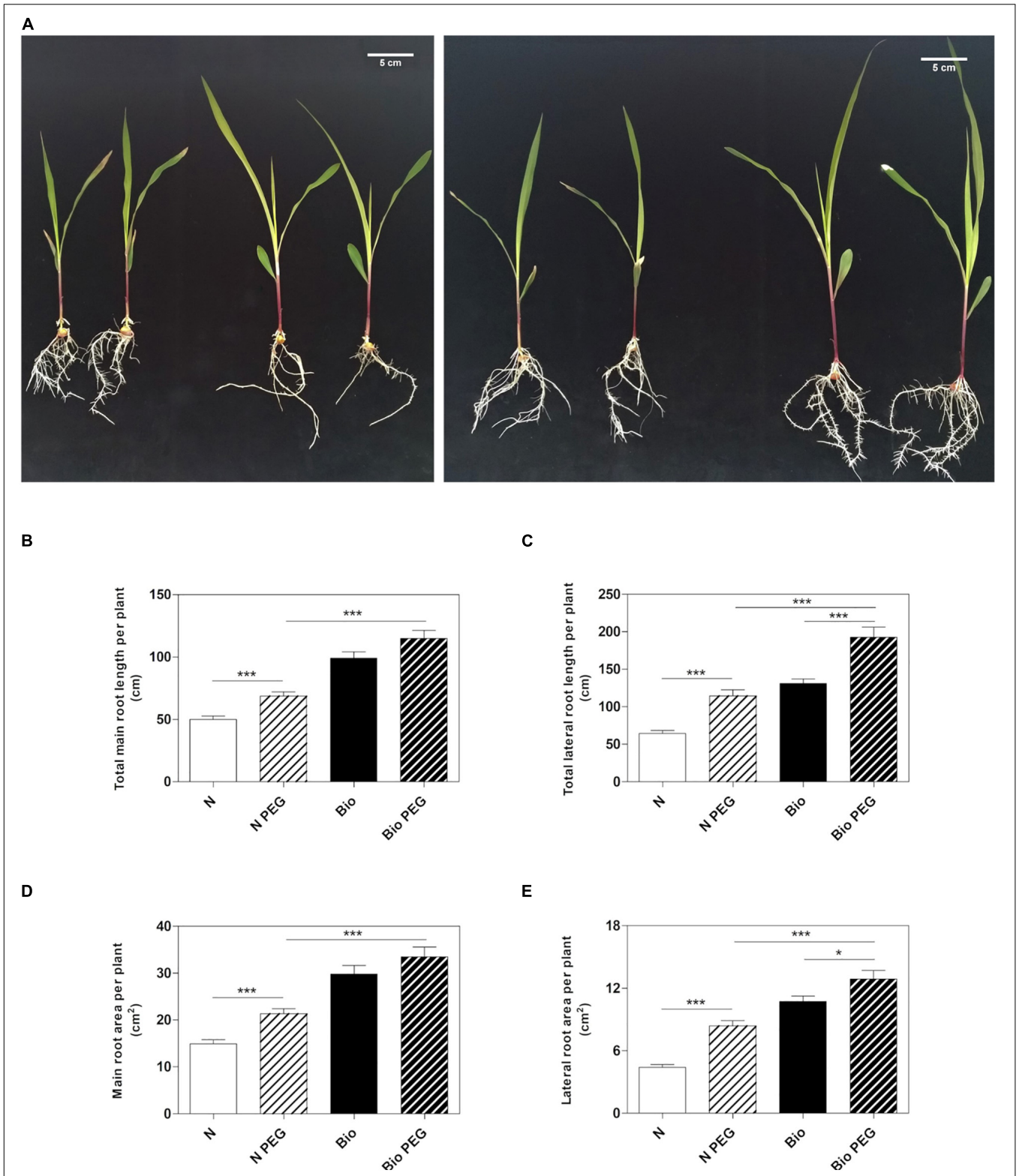

FIGURE 1 | Effects of the PH on root growth of maize plants subjected to drought stress. Maize plantlets grown with or without 15% PEG in the nutrient solution after 9 days of treatment with either 0.1 mL L^{-1} PH (Bio) or with the equivalent amount of total N (14.3 mg L^{-1}), supplied as inorganic nitrogen (N) **(A)**. Total seminal and primary root length **(B)**, total lateral root length **(C)**, total seminal and primary root area **(D)** and lateral root area of the maize plantlets treated as described above **(E)**. Root length and root area were measured with WinRHIZO^{TM} software. Mean values per plant are reported. Bars represent the standard error (SEM) ($n = 21$), Student's t-test was applied, $^{*}p < 0.05$; $^{***}p < 0.001$.

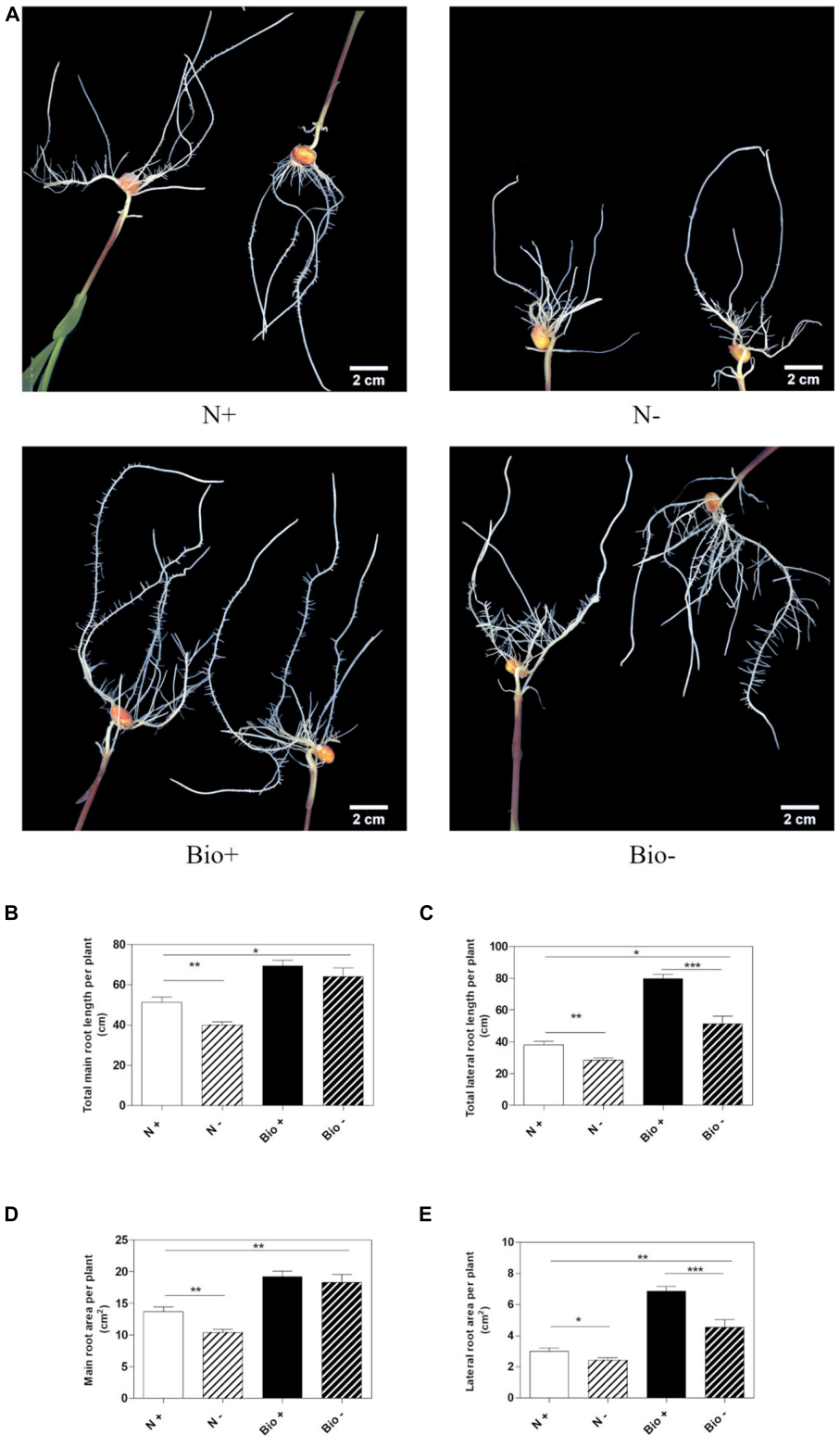

FIGURE 2 | Effects of the PH on root growth of maize plants subjected to hypoxic stress. Maize plantlets grown with (+) or without (–) air insufflation in the nutrient solution after 4 days of treatment with either 0.1 mL L^{-1} PH (Bio) or with the equivalent amount of total N (14.3 mg L^{-1}), supplied as inorganic nitrogen (N) **(A)**. Total seminal and primary root length **(B)**, total lateral root length **(C)**, total seminal and primary root area **(D)**, and lateral root area **(E)**, of the maize plantlets treated as described above. Root length and root area were measured with WinRHIZO^{TM} software. Mean values per plant are reported. Bars represent the standard error (SEM) ($n \geq 22$), Student's *t*-test was applied, $^{*}p < 0.05$; $^{**}p < 0.01$; $^{***}p < 0.001$.

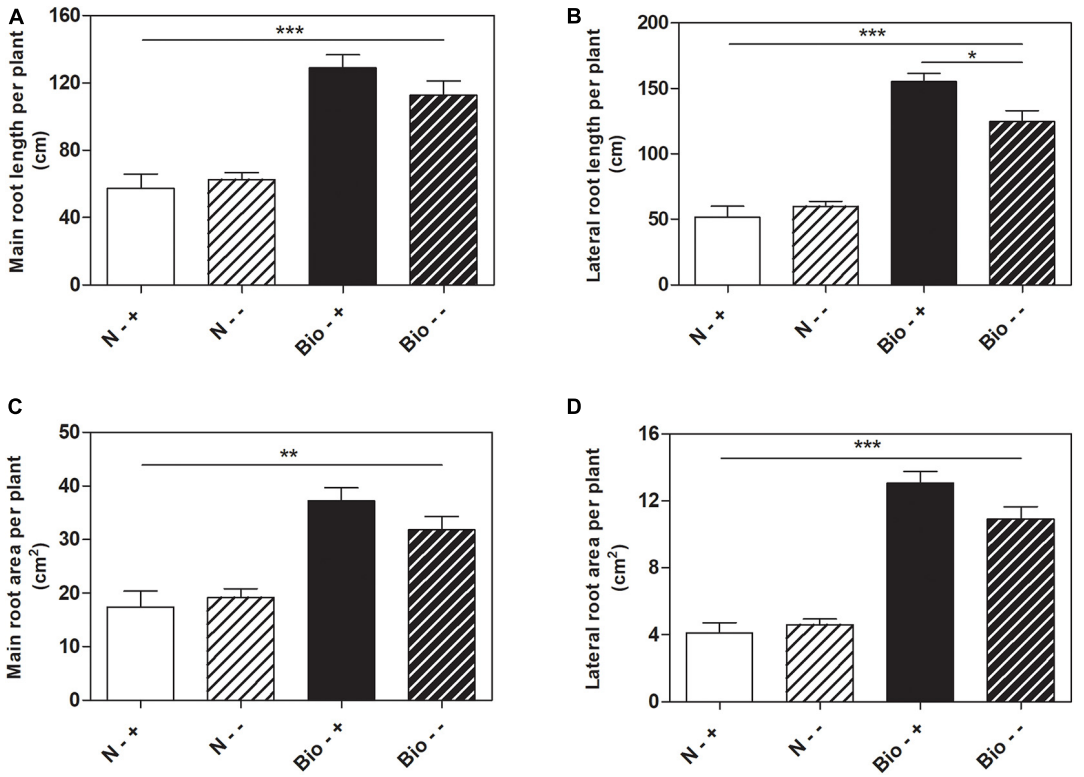

FIGURE 3 | Effects of the PH on root growth of maize plants after recovery from hypoxic stress. Total seminal and primary root length **(A)**, lateral root length **(B)**, total seminal and primary root area **(C)**, lateral root area **(D)**, of maize seedlings treated with 0.1 mL L^{-1} PH (Bio) and seedlings treated with equivalent amounts of total N (14.3 mg L^{-1}), supplied as inorganic nitrogen (N). The seedlings were hydroponically grown under hypoxia for 5 days, and then kept under normal air flow or hypoxic stress for further 4 days. Root length and root area were measured with WinRHIZO^{TM} software. Mean values per plant are reported. Bars represent the standard error (SEM) ($n \geq 7$), Student's *t*-test was applied, $^{*}p < 0.05$; $^{**}p < 0.01$; $^{***}p < 0.001$.

most probably facilitate the recovery once the plants return to normal oxygen regimen.

The Presence of PH in the Growing Solution Favors the Recovery From Fe Deficiency

To investigate whether the PH can favor plant Fe uptake after starvation, maize seedlings were grown in an Fe-depleted solution for 7 days, and then Fe was supplied to a concentration of 20 μM as Fe chelated with EDTA, $FeCl_3$, or $FeCl_3$ previously mixed with the PH (**Figures 4A–C**). Control plants were grown in a nutrient solution containing 20 μM FeEDTA (+FeEDTA), or in the absence of Fe throughout the experiment (−Fe/−Fe). We monitored the pH of the different nutrient solutions every day during Fe supply. In all the treatments the pH was favorable for Fe uptake and showed little variation among the different solutions, ranging from 5.2 to 5.3 at first day of supply to 5.9–6.2 at the end of the experiment.

At the 2nd day after the Fe supply, plants treated with the PH performed as well as the plants treated with FeEDTA (−/+FeEDTA), and significantly better than those grown in the solution containing the Fe salt only (+56.9%) if we consider the SPAD values detected in the middle part of the leaf, while no significant differences were observed in the top part (**Figures 4B,C** and **Table 1**). On the 4th day, SPAD values of plants supplied with Fe mixed with the PH were significantly higher than those of plants treated with $FeCl_3$ alone (TOP leaf: +42.0%, MID leaf: +37.5%) and similar to those of plants supplied with FeEDTA (**Figures 4A–C**). At the 7th day, maize grown with $FeCl_3$ reached mid-leaf SPAD values comparable to those of $FeCl_3$ plus protein PH, while the top-leaf values were still higher for those treated with the PH (+18.7%). Overall, during the supply, the plants treated with the mix of Fe and the PH were the fastest to overcome foliar chlorosis, reaching in only 4 days similar top-leaf SPAD values than those of the plants which did not undergo Fe starvation. Furthermore, these values were even increased in the mid-leaf (+32.3%). Similarly, the plants supplied with FeEDTA were able to recover from the chlorosis at the 4th day on the mid-leaf (+24.6%). However, they reached top-leaf SPAD values similar to the positive control just at the 7th day of supply. The worst performing plants were those supplied with $FeCl_3$: although able to reach the mid-leaf SPAD values of the positive control at the 4th day, they did not show an increase conversely to the other two theses; moreover, they could not equal the performance of the control plants at the top of the leaf (−17.5%). The analysis of the plants maintained in FeEDTA for the entire length of the experiment revealed a progressive

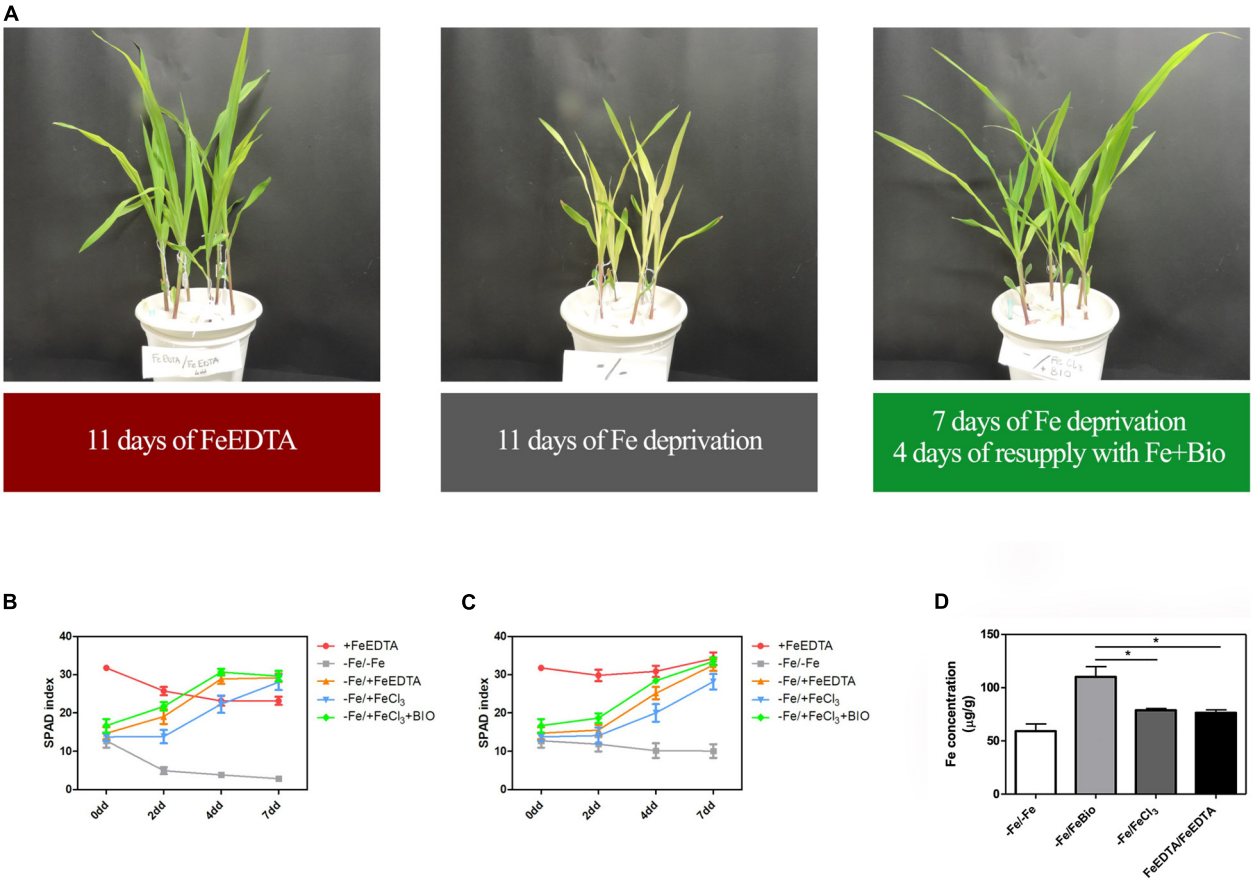

FIGURE 4 | Effects of PH on recovery from Fe deprivation. Maize plantlets grown in nutrient solutions with FeEDTA for 11 days, without any Fe source for 11 days, or without Fe for 7 days and then supplied with $FeCl_3$ mixed with the biostimulant for further 4 days **(A)**. SPAD values progression in leaves of maize seedlings treated with the PH (Bio) during recovery from Fe deprivation. Maize plantlets were grown in a nutrient solution containing FeEDTA 20 µM for 14 days (+ FeEDTA), or in an Fe-depleted nutrient solution (-Fe) for 7 days, and supplied with 20 µM Fe as either FeEDTA (–Fe/ + FeEDTA), $FeCl_3$ (–Fe/ + $FeCl_3$) or $FeCl_3$ supplemented with 0.1 mL L^{-1} PH (–Fe/ + FeBio). A group of plants were maintained in the nutrient solution deprived of Fe with the addition of 14.3 mg L^{-1} of N supplied as inorganic nitrogen (–Fe/–Fe). SPAD values were taken at the top **(B)** and mid **(C)** part of the leaf. Mean values are reported. Bars represent the standard error (SEM) ($n \geq 9$). Fe concentration in maize leaves subjected to different treatments during recovery from Fe deprivation **(D)**. Values of Fe concentration assessed via ICP-MS in maize leaves harvested after 7 days of Fe supply. Mean values are reported. Bars represent the standard error (SEM) ($n = 3$), Student's *t*-test was applied, $^*p < 0.05$.

TABLE 1 | Comparison of SPAD values in maize seedling subjected to different treatments during recovery from Fe deprivation.

Vs.		MID			TOP		
		FeEDTA/FeEDTA	**−Fe/FeEDTA**	**−Fe/$FeCl_3$**	**FeEDTA/FeE DTA**	**−Fe/FeEDTA**	**−Fe/$FeCl_3$**
2°day	−Fe/FeEDTA	−25.9%(**)			−47.9% (***)		
	−Fe/$FeCl_3$	−46.2%(***)	−27.3%n.s.		−52.7%(***)	−9.3%n.s.	
	−Fe/FeBio	−15.5%(*)	14.0%n.s.	56.9%(**)	−37.4%(***)	20.1%n.s.	32.4%n.s.
4°day	−Fe/FeEDTA	24.6%(**)			−18.5%(*)		
	−Fe/$FeCl_3$	−3.8%n.s.	−22.8%(*)		−35.1%(***)	−20.4%n.s.	
	−Fe/FeBio	32.3%(***)	6.2%n.s.	37.5%(**)	−7.9%n.s.	13.0%n.s.	42.0%(***)
7°day	−Fe/FeEDTA	26.0%(***)			−4.9%n.s.		
	−Fe/$FeCl_3$	21.0%(*)	−4.0%n.s.		−17.5%(*)	−13.3%n.s.	
	−Fe/FeBio	28.0%(**)	1.5%n.s.	5.8%n.s.	−2.1%n.s.	2.9%n.s.	18.7%(*)

Percentage variations of SPAD values recorded at mid-leaf (MID) and top-leaf (TOP) after 2, 4 or 7 days of Fe supply. Student's t-test was applied, $^*p < 0.05$; $^{**}p < 0.01$; $^{***}p < 0.001$.

decrease in the mid leaf SPAD values which was probably due to the rapid growth of the plants under optimal Fe conditions.

The positive effect of PH on Fe-deprivation recovery was confirmed by the analyses of Fe concentration in maize leaves (**Figure 4D**). In fact, in plants supplied with Fe together with the PH for 7 days the concentration of Fe was higher than that of plants grown with FeEDTA or those supplied with $FeCl_3$. These latter plants were able to reach a concentration comparable to that of the positive control plants, but significantly lower than those grown with Fe and the PH (−25.34%).

To exclude any direct contribution of the PH on plant Fe uptake, we grew Fe-deprived plants in the nutrient solution with the addition of the PH (0.1 mL L^{-1}) alone. We have compared the SPAD values measured for seven consecutively days in the leaves of plants grown without Fe and plants grown without Fe but with the addition of PH. The values recorded were similar in both treatments (−Fe and −Fe + PH) ranging from 3.5 to 10, which are typical of chlorotic maize leaves. In addition, we assessed the concentration of Fe in the product (**Supplementary Table 2**). At our experimental condition (1:10,000 PH dilution) the Fe supplied by PH was calculated to be at a concentration of 0.032 μM, therefore irrelevant compared to that presents in the nutrient solution.

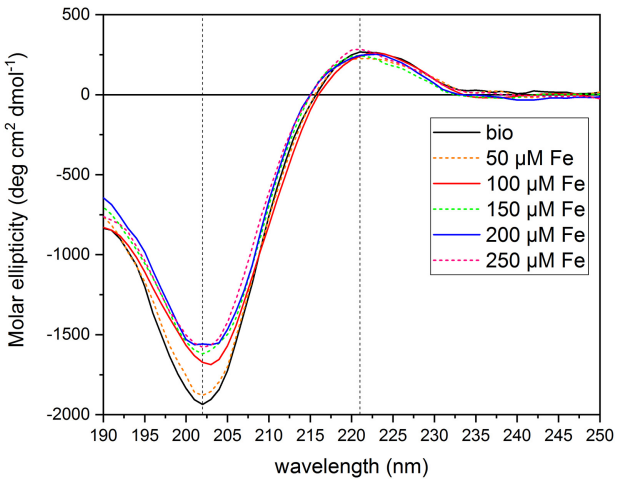

FIGURE 5 | Circular dichroism spectra of protein hydrolysate dissolved in aqueous solutions with $FeCl_3$ at different concentrations. The figure shows the CD spectra of the PH diluted in aqueous solutions ([N] = 71.5 mg L^{-1}) with different $FeCl_3$ concentrations [(μM) 0, 50, 100, 150, 200, 250]. Dashed lines mark 202 and 221 nm wavelengths. Molar ellipticity was calculated referring to a Mean Residual Weight (MRW) fixed at 106.5 g moL^{-1}.

The PH Interacts With Fe Ions

To test the hypothesis that the PH under study can act as an Fe chelator, we evaluated the interaction of the PH with Fe ions by circular dichroism. We collected the CD spectrum of the PH itself dissolved in water ([N] = 71.5 mg L^{-1}), and then the spectra of the PH mixed with $FeCl_3$ at six different concentrations [(μM) 0, 50, 100, 150, 200, 250)]. We set the PH concentration to a total amount of N of 71.75 mg L^{-1} and the $FeCl_3$ central concentration of the range to 100 μM, in order to obtain the same ratio between the Fe and the PH concentrations used in the hydroponic system for the Fe supply experiments. The PH CD spectrum obtained (**Figure 5**) is an intermediate between the typical soluble type II collagen spectrum, which features two characteristic peaks, a large negative one at 197 nm, and a small positive one at 220 nm, and the polyproline spectrum, which displays the large negative peak shifted at 206 nm, and the small positive one at 228 nm (Lopes et al., 2014). For instance, the CD spectrum of the PH presents two peaks one at 202 nm and the other at 221 nm, implying that for this product the chemical hydrolysis does not alter considerably the capability of the matrix to form polyproline II (PPII)-type structures. The CD spectra of the PH mixed with Fe showed a dose-dependent reduction of the peak at 202 nm compared to the reference spectrum of the PH alone (**Supplementary Table 4**), while the peak at 221 nm did not show major alterations when Fe is added (data not shown). At the lowest Fe concentration, 50 μM, a slight increase of the molar ellipticity value at 202 nm was observed; adding 100 μM Fe we found a greater increase; for concentrations higher than 150 μM, the molar ellipticity value remained almost unaltered, suggesting that the interaction between the PH and the Fe ions was saturated at 150 μM. These findings suggest that the PH PPII-type structure undergoes a slight conformational change in the secondary structure when Fe ions are present in the solutions. The helix is able to interact with the Fe ions, that are therefore responsible for the increase in the molar ellipticity values, although they do not destabilize the structure to the extent of denaturation (Lopes et al., 2014).

The PH Induces Transcriptional Changes in Maize Roots During Recovery From Fe Deficiency

We carried out a transcriptional analysis on the effects of the PH in maize roots during Fe supply in order to shed light on the mechanisms of action that favors recovery from Fe deficiency. We studied the expression of key genes involved in Fe uptake (*ZmTOM1*, *ZmYS1*, and *ZmIRT1*) and in peptide transport (*ZmOPT ids.* GRMZM2G152555_T01, Zm00001d031287_T001) in roots subjected for 7 days to Fe-deprivation (−Fe) and supplied for 24 h with either 20 μM $FeCl_3$ (−Fe/+$FeCl_3$) or $FeCl_3$ plus PH (−Fe/+FeBio) in comparison to roots of plants always grown under Fe deficiency (7 days plus 24 h; −Fe/−Fe) (**Figure 6**). *ZmTOM1* codes for an efflux transporter of mugineic acid family phytosiderophores and ZmYS1 codes for a proton-coupled symporter of metals chelated to phytosiderophore and to nicotianamine (Schaaf et al., 2004) and both play a key role in Strategy II of Fe acquisition employed by the graminaceous species such as maize (Kobayashi and Nishizawa, 2012). On the other hand, ZmIRT1 protein is a Fe(II) transporter involved in the Strategy I (reduction strategy). These three proteins (ZmTOM1 ZmYS1, ZmIRT1) have been shown to increase their expression level in maize roots under Fe deficiency (Li et al., 2013; Nozoye et al., 2013; Wairich et al., 2019). We clearly observed this effect after 24 h of $FeCl_3$ supply (**Figures 6A–C**). In fact, Fe supply caused a strong reduction of the transcript levels of *ZmTOM1*, *ZmYS1*, and *ZmIRT1* with respect to the roots of maize

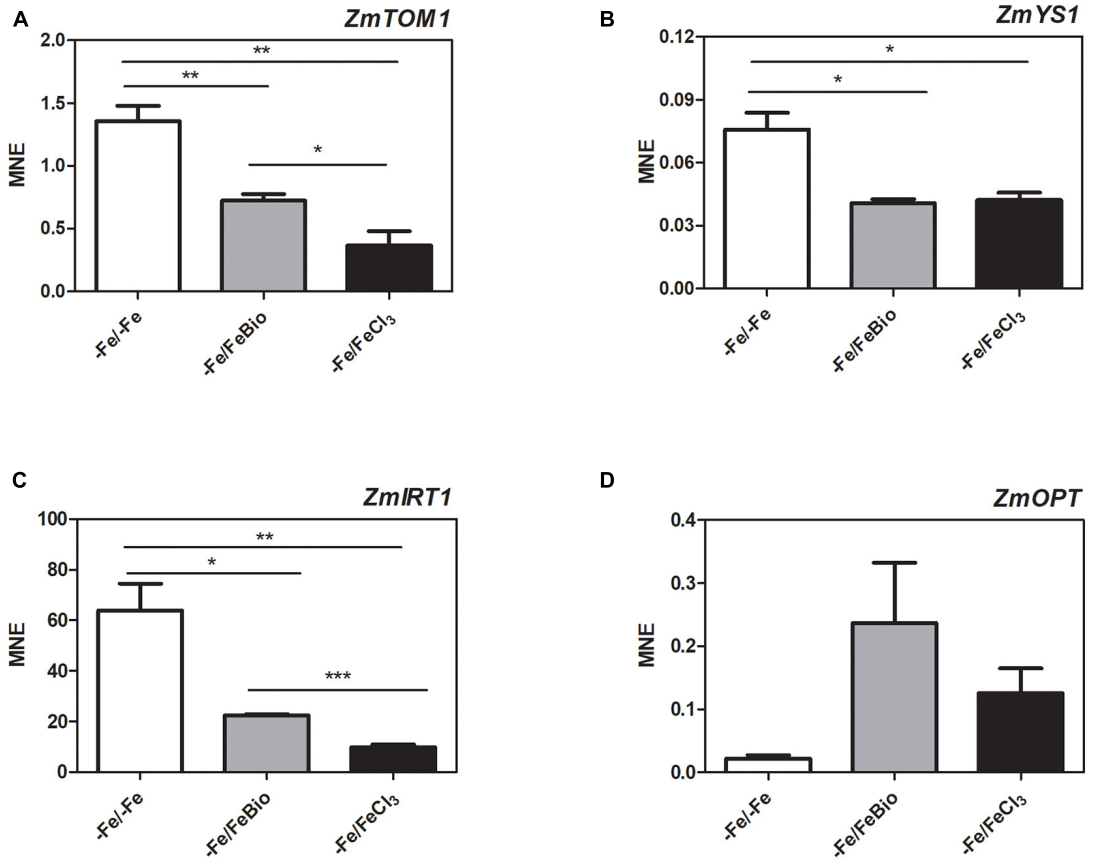

FIGURE 6 | Quantitative RT-PCR analysis of genes involved in Fe uptake in maize roots. Relative transcript level, calculated as Mean normalized expression (MNE) of *ZmTOM1* **(A)**, *ZmYS1* **(B)**, *ZmIRT1* **(C)** and *ZmOPT* **(D)** was assayed in roots of plants grown under Fe-deprivation conditions (–Fe/–Fe) and after 24 h Fe-resupply either as $FeCl_3$ (–Fe/ + $FeCl_3$) or $FeCl_3$ plus PH (–Fe/FeBio). The values are the mean of three biological replicates. Bars represent the standard error (SEM). Student's *t*-test was applied, $^*p < 0.05$; $^{**}p < 0.01$; $^{***}p < 0.001$.

plants continuously grown under Fe deficiency. In the roots supplied with $FeCl_3$ in the presence of the PH, the expression level of *ZmTOM1* and *ZmIRT1* was significantly higher than the expression measured with $FeCl_3$ alone, but still lower than the transcript levels of Fe-deprived roots (**Figures 6A,C**). We did not observe any significant difference in the expression level of *ZmYS1* between roots supplied with $FeCl_3$ in presence and absence of PH (**Figure 6B**).

In order to investigate the involvement of peptide transporters in the mechanisms that favors Fe recovery in plants treated with the PH, we analyzed the expression of the *ZmOPT*, a gene found to be responsive to the PH treatment (Santi et al., 2017). ZmOPT might be involved in mediating the uptake of Fe bound to peptides. The expression of *ZmOPT* showed an increasing tendency in both roots treated with $FeCl_3$ and $FeCl_3$ plus the PH, this trend appears more pronounced in the presence of the PH (**Figure 6D**).

Overall, concerning the modulation of genes involved in response to Fe deficiency, these results indicate that the roots supplied with $FeCl_3$ plus the PH displayed an intermediate behavior between Fe-deprived roots and roots supplied with $FeCl_3$ alone.

DISCUSSION

Biostimulants represent a vast category of products used in the agricultural practice to increase crop productivity, nutrient acquisition and stress resistance. They include natural products of animal and plant origin as well as microorganisms. Due to the generally complex nature of the biostimulants, often composed by a mixture of different molecules, it is very difficult to identify the active components responsible for the beneficial effects on crops (Yakhin et al., 2017). On the other hand, the presence of different active biomolecules in a single product can widen the physiological processes that can be targeted. This can explain the various beneficial effects that can be obtained by a single biostimulants.

The scientific research on biostimulants should be focused on two main targets: (i) to identify the bioactive components of a product (ii) to test the activity of the product on different physiological processes and under different environmental conditions. Concerning the first point, the possibility to find out the main active molecules can allow, on one hand to use a reductionist approach for studying the mechanism of action of the biostimulant, and, on the other hand, to optimize

the products at the industrial level. This approach appears feasible only with certain categories of biostimulants (e.g., protein hydrolysate obtained from a tissue with few abundant proteins), whereas quite difficult for biostimulants originated from complex matrix (e.g., seaweed extracts). The second goal is important for defining the product claims. The claims are usually based on the results from experiments conducted under green house or field conditions monitoring a single plant trait, principally crop growth or product quality. It is possible therefore that in many cases other beneficial effects can be disregarded. Experiments carried out under laboratory conditions can be used to easily test the effects of biostimulants on a great variety of physiological parameters and under different environmental conditions to obtain information on the potential uses of a product. The set-up of the experiments must be carefully planned to assure reproducibility, for instance the assessment of the biological variability and the choice of proper controls appear crucial. In this work, we have planned a series of laboratory experiments to test whether a collagen-based PH has the capacity to exert beneficial effects on plants subjected to different types of stress. The crop used was maize because in a previous work we demonstrated the positive effects of the collagen-based PH on maize root growth and mineral ion uptake after few days of application (Santi et al., 2017). The plants were grown hydroponically in an aerated nutrient solution supplied with the PH. The use of hydroponic culture has several advantages; for instance, it permits the precise control of the medium composition, the possibility to study the response to deprivation or excess of a single mineral nutrient and also the simulation of various stress conditions. A very critical issue in evaluating the effects of a biostimulant is also the choice of a proper control, in our case as the biostimulant object of the study was a PH, we added to the control nutrient solution NH_4^+ to reach the same amount of total N supplied with the PH. In this way we also proved that the effects of the biostimulant are not due to N fertilization. We chose to assess the potential activity of the collagen-based PH as multi-stress protectant against three different types of abiotic stresses: drought, hypoxia and Fe starvation and we analyzed the effects on growth during the first days after germination, a phase that can be critical for the plant emergence after sowing.

Our results confirmed the observations made by Trevisan et al. (2019) about the capacity of the PH to protect the root apparatus under hypoxic conditions and extended the analysis to the advantages that the presence of PH supplied in the medium can bring during the recovery from the stress (Trevisan et al., 2019). Indeed, when after 4 days of hypoxia the plants returned to the normal air insufflation, the presence of the PH in the medium rapidly stimulated the resumption of root growth whereas untreated roots did not seem to recover.

To our knowledge, the effects of collagen-derived PH on plants subjected to water stresses has not previously been investigated. To apply water stress conditions, we follow a method described by Han et al. (2017) to generate osmotic stress in maize plants under hydroponic cultivation by adding 15% PEG to the nutrient solution (Han et al., 2017). The response to osmotic stress was similar in N− and PH-treated plants. In both cases we observed a slight decrease in shoot fresh biomass (**Supplementary Figure 1** and **Figure 1A**) and an increase in root growth – mainly in the lateral roots for what concerns the PH-treated plants- leading to a change in shoot/root ratio which is a typical response of plants to water deficit. Although the plant species and the PEG concentration used are different, our results are in accordance with those of Ji et al. (2014), who showed that one of the effects of PEG-mediated osmotic stress in wheat is the induction of lateral root development (Ji et al., 2014). Overall, we showed that the water stress did not alter the positive effects of PH on root growth most probably allowing under longer term a better acquisition of water and nutrients in the PH- treated plants compared to the control ones.

The positive effects of PH on abiotic stress resistance has often been ascribed to its capacity to counteract the oxidative stress (Lucini et al., 2015) mainly through the induction of genes involved in antioxidant defense (Caruso et al., 2019). In this regard, we previously observed that the collagen-based PH compared to other biostimulants such as free amino acids, produces only a moderate alteration of genes related to oxidative stress under normal conditions (Santi et al., 2017) suggesting that it is not itself an oxidative stress elicitor. Interestingly, the collagen-based PH acts on phytohormone homeostasis and signaling, modifying the expression of genes involved in metabolism, transport and signal transduction of gibberellin, cytokinins and auxin (Santi et al., 2017). It is presumable that the effects of the collagen-based PH on the hormone functions could be responsible for the positive effects on root growth also under stress conditions.

Concerning the experiments of recovery after Fe-starvation, we obtained several lines of evidence about the positive effects of the collagen-based PH. The SPAD measurements and Fe concentrations in the leaves clearly demonstrated that the administration of PH mixed to $FeCl_3$ confers a faster recovery from deprivation as compared with treatments with $FeCl_3$ or FeEDTA. We can hypothesize that the positive role of the PH on Fe accumulation in starved plants is linked to both biological and chemical proprieties of the PH itself. Some interesting insights concerning the structural features of the PH under study and on its interaction with Fe were discovered thanks to the CD spectra analyses. CD has been widely used as a reliable source to study the interactions among biomolecules (Greenfield, 2007), especially proteins, and some works had already highlighted the diagnostic features of collagen, collagen peptides and poly-proline type II (PPII) structures spectra (Piez, 1968; Piez and Sherman, 1970; Adzhubei et al., 2013; Lopes et al., 2014). The PH spectra obtained was extremely reproducible and had the typical shape of the collagen peptides and PPII (type II polyproline helices) reference spectra (Lopes et al., 2014). The similarities between these CD spectra were striking and we can therefore assume that the acid hydrolysis process produces a mixture of short peptides that maintains the PPII secondary structure. Furthermore, CD spectra showed that the collagen-based PH can interact with Fe in a dose-dependent manner suggesting the formation of Fe-PH complexes. Results previously reported by Santi et al. (2017) hinted that the collagen-based PH could improve Fe uptake through a transcriptional reprogramming of genes playing a role in the metal transport processes. With the exception of

ZmYS1, here we show that the molecular components involved in maize root Fe acquisition (e.g., solubilization and uptake, *ZmTOM1* and *ZmIRT1*, respectively) (Li et al., 2013, 2018; Nozoye et al., 2013; Wairich et al., 2019) are more expressed in PH-treated roots during the $FeCl_3$ supply (**Figures 6A–C**), possibly indicating that the mechanisms of Fe sensing by maize roots are, in this condition, less susceptible to the restored cellular Fe accumulation. Interestingly, a similar behavior was described in Fe-deficient tomato plants supplied with Fe chelated to fulvic acid like water-extractable humic substances, another category of plant biostimulant (Zamboni et al., 2016). Furthermore, we cannot exclude a role of *ZmOPT* in the uptake of Fe-PH complexes, since it showed the highest expression in PH-treated roots although not statistically significant (**Figure 6D**).

We propose that the PH role as Fe deficiency stress mitigator might be explained with a combination of possibly synergic chemical and molecular mechanisms leading to an increased uptake and distribution of Fe when Fe is supplied after shortage. In particular, these mechanisms seem to be based on: (1) an enhanced stimulation of phytosiderophore (PS) efflux leading to a higher solubilization of Fe(III); (2) an increased uptake of the reduced form of Fe since the presence of *ZmFRO2* in maize genome has been ascertained (Li et al., 2018); (3) an easier uptake of Fe as a chelated complex with the PH; (4) an increased Fe solubilization due to the presence of PH and an effective ligand exchange process involving Fe-PH and PSs making more efficient the action of these chelators (**Figure 7**).

In conclusion, we demonstrated that the collagen-based PH under study, not only is a plant growth promoting agent, but it might also be used effectively as hypoxic, drought, and nutrient stress mitigator.

The protective effects cannot be related to a single mechanism of action, but most probably are the result of different activities of the peptides both in the external medium and inside the cells. A further characterization of this matrix could help to shed light on the role of its peptides at the cellular level, considering that many works have showed how small peptides are crucial for plant signaling (Gancheva et al., 2019). For instance, IRON MAN (IMA), CLV3/ESR-RELATE D

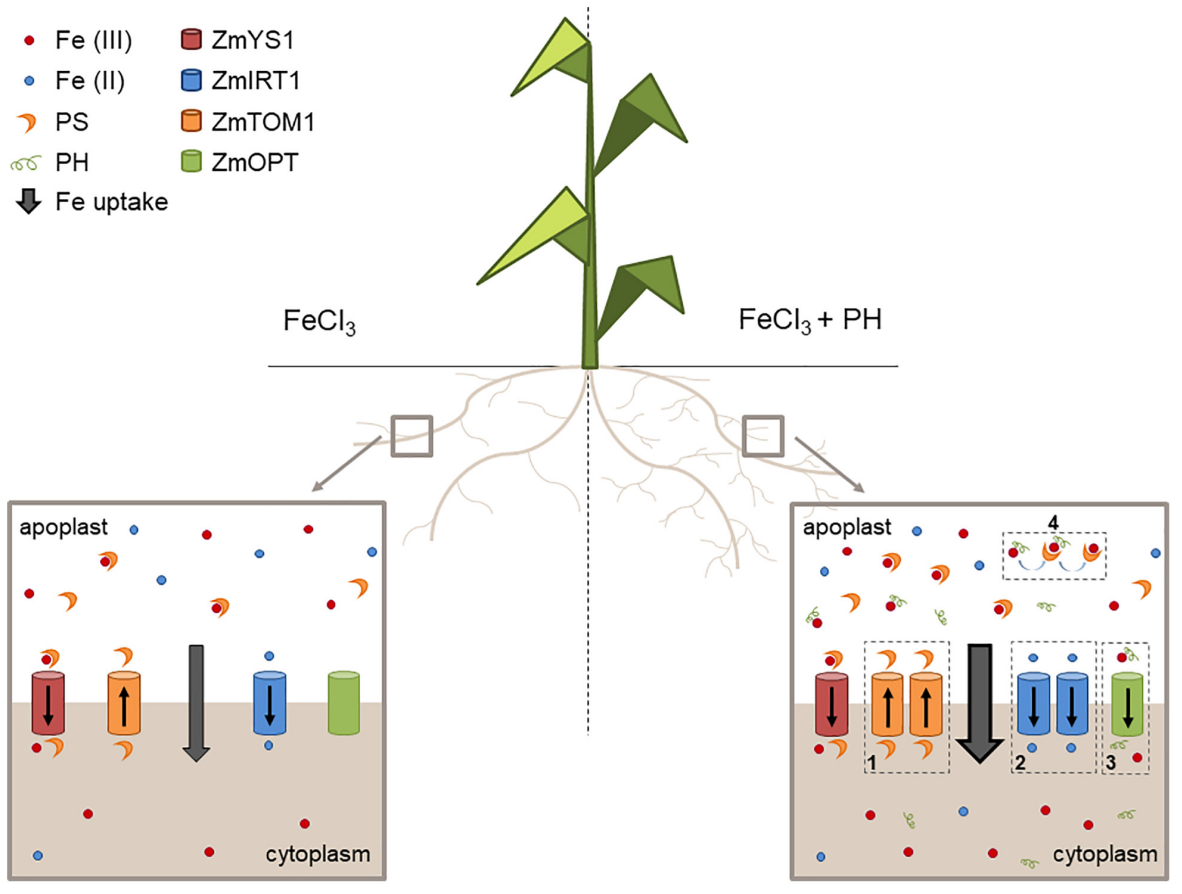

FIGURE 7 | Mechanisms of action of the PH as Fe-deficiency stress mitigator. Schematic representation of the maize root apparatus after the administration of Fe in the absence (left) or presence (right) of the PH. We show that PH increases the lateral root length (Santi et al., 2017) thus favoring soil exploration for nutrients. In addition, PH treatment maintains a higher expression of genes encoding (1) the transporter involved in PS efflux (ZmTOM1) and (2) the transporter of Fe(II) (ZmIRT1), possibly reduced by plasma membrane Fe reductase activities (not shown in the scheme). The PH tends to increase the expression of (3) putative Fe-peptide transporter (ZmOPT). The PH can also chelate Fe and facilitate the exchange of Fe to the PSs (4).

(CLE) and HYDROXYPROLINE-RICH GLYCOPEPTIDE SYSTEMINS (HypSys) are three important families of peptides, on the range of 5–20 amino acids, involved in very different processes. The members of the former family control iron transport in plants (Grillet et al., 2018), those of the second one are involved in the differentiation of shoot and root meristems (Leasure and He, 2012), while those of the third one are plant protective signal peptides, participating in plant defense reactions (Pearce, 2011).

DATA AVAILABILITY STATEMENT

The original contributions presented in the study are included in the article/**Supplementary Material**, further inquiries can be directed to the corresponding author.

AUTHOR CONTRIBUTIONS

ZV, TP, and AZ contributed to the conception and design of the study. SA, CS, and DS performed the experiments. SA, DS, AZ, ZV, and TP carried out the analysis of the data. SA and TP draft the manuscript. All authors approved the manuscript.

FUNDING

This work was supported by a Joint Project grant of the University of Verona and SICIT Group.

ACKNOWLEDGMENTS

We thank SICIT Group for the effective collaboration and scientific support. We are grateful to Fabio Piccinelli and Serena Zanzoni for the support in CD data analysis. We thank the Centro Piattaforme Tecnologiche of the University of Verona for providing access to the CD spectropolarimeter. We also thank Valentina Dusi, Angelo Betto, and Leonardo De Monte for their help with preliminary plant growth experiments.

SUPPLEMENTARY MATERIAL

The Supplementary Material for this article can be found online at: https://www.frontiersin.org/articles/10.3389/fpls.2021.600623/full#supplementary-material

REFERENCES

Adzhubei, A. A., Sternberg, M. J. E., and Makarov, A. A. (2013). Polyproline-II helix in proteins: structure and function. *J. Mol. Biol.* 425, 2100–2132. doi: 10.1016/j.jmb.2013.03.018

Arsenault, J., Pouleur, S., Messier, C., and Guay, R. (1995). WinRHIZOTM, a root-measuring system with a unique overlap correction method. *HortScience* 30:906.

Boyer, J. S. (1982). Plant productivity and environment. *Science* 218, 443–448. doi: 10.1126/science.218.4571.443

Calvo, P., Nelson, L., and Kloepper, J. W. (2014). Agricultural uses of plant biostimulants. *Plant Soil* 383, 3–41. doi: 10.1007/s11104-014-2131-8

Caruso, G., De Pascale, S., Cozzolino, E., Giordano, M., El-Nakhel, C., Cuciniello, A., et al. (2019). Protein hydrolysate or plant extract-based biostimulants enhanced yield and quality performances of greenhouse perennial wall rocket grown in different seasons. *Plants* 8:208. doi: 10.3390/plants8070208

Casadesús, A., Munne, S., and Pe, M. (2020). An enzymatically hydrolyzed animal protein-based biostimulant (Pepton) increases salicylic acid and promotes growth of tomato roots under temperature and nutrient stress. *Front. Plant Sci.* 11:953.

Casadesús, A., Polo, J., and Munné-Bosch, S. (2019). Hormonal effects of an enzymatically hydrolyzed animal protein-based biostimulant (pepton) in water-stressed tomato plants. *Front. Plant Sci.* 10:758.

Çavuşoğlu, K., Kiliç, S., and Kabar, K. (2008). Effects of some plant growth regulators on stem anatomy of radish seedlings grown under saline (NaCl) conditions. *Plant Soil Environ.* 54, 428–433. doi: 10.17221/405-pse

Chan-Rodriguez, D., and Walker, E. L. (2018). Analysis of yellow striped mutants of zea mays reveals novel loci contributing to iron deficiency chlorosis. *Front. Plant Sci.* 9:157.

Chen, S.-K., Subler, S., and Edwards, C. A. (2002). Effects of agricultural biostimulants on soil microbial activity and nitrogen dynamics. *Appl. Soil Ecol.* 19, 249–259. doi: 10.1016/s0929-1393(02)00002-1

Cherlet, M., Hutchinson, C., Reynolds, J., Hill, J., Sommer, S., and von Maltitz, G. (2018). *World Atlas of Desertification*. Luxembourg: Publication Office of the European Union.

Colla, G., Rouphael, Y., Canaguier, R., Svecova, E., and Cardarelli, M. (2014). Biostimulant action of a plant-derived protein hydrolysate produced through enzymatic hydrolysis. *Front. Plant Sci.* 5:448.

Daryanto, S., Wang, L., and Jacinthe, P. A. (2016). Global synthesis of drought effects on maize and wheat production. *PLoS One* 11:e0156362. doi: 10.1371/journal.pone.0156362

Drobek, M., Frąc, M., and Cybulska, J. (2019). Plant biostimulants: importance of the quality and yield of horticultural crops and the improvement of plant tolerance to abiotic stress-a review. *Agronomy* 9:335. doi: 10.3390/agronomy9060335

Ertani, A., Cavani, L., Pizzeghello, D., Brandellero, E., Altissimo, A., Ciavatta, C., et al. (2009). Biostimulant activity of two protein hydrolyzates in the growth and nitrogen metabolism of maize seedlings. *J. Plant Nutr. Soil Sci.* 172, 237–244. doi: 10.1002/jpln.200800174

Ertani, A., Nardi, S., Francioso, O., Sanchez-Cortes, S., Di Foggia, M., and Schiavon, M. (2019). Effects of two protein hydrolysates obtained from Chickpea (*Cicer arietinum* L.) and *Spirulina platensis* on zea mays (L.) plants. *Front. Plant Sci.* 10:954.

Ertani, A., Schiavon, M., Muscolo, A., and Nardi, S. (2012). Alfalfa plant-derived biostimulant stimulate short-term growth of salt stressed Zea mays L. plants. *Plant Soil* 364, 145–158. doi: 10.1007/s11104-012-1335-z

European Union (2019). *Regulation (EU) 2019/1009 of the European Parliament and of the Council of 5 June 2019 Laying Down Rules on the Making available on the Market of EU Fertilising Products and Amending Regulations (EC) No 1069/2009 and (EC) No 1107/2009 and Repealing Regula*. Luxembourg: Publication Office of the European Union.

Farooq, M., Gogoi, N., Barthakur, S., Baroowa, B., Bharadwaj, N., Alghamdi, S. S., et al. (2017). Drought stress in grain legumes during reproduction and grain filling. *J. Agron. Crop Sci.* 203, 81–102. doi: 10.1111/jac.12169

Gancheva, M. S., Malovichko, Y. V., Poliushkevich, L. O., Dodueva, I. E., and Lutova, L. A. (2019). Plant peptide hormones. *Russ. J. Plant Physiol.* 66, 83–103.

Greenfield, N. J. (2007). Using circular dichroism spectra to estimate protein secondary structure. *Nat. Protoc.* 1, 2876–2890. doi: 10.1038/nprot.2006.202

Grillet, L., Lan, P., Li, W., Mokkapati, G., and Schmidt, W. (2018). IRON MAN is a ubiquitous family of peptides that control iron transport in plants. *Nat. Plants* 4, 953–963. doi: 10.1038/s41477-018-0266-y

Han, B., Duan, X., Wang, Y., Zhu, K., Zhang, J., Wang, R., et al. (2017). Methane protects against polyethylene glycol-induced osmotic stress in maize by improving sugar and ascorbic acid metabolism. *Sci. Rep.* 7:46185.

Ji, H., Liu, L., Li, K., Xie, Q., Wang, Z., Zhao, X., et al. (2014). PEG-mediated osmotic stress induces premature differentiation of the root apical meristem and outgrowth of lateral roots in wheat. *J. Exp. Bot.* 65, 4863–4872. doi: 10.1093/jxb/eru255

Kobayashi, T., and Nishizawa, N. K. (2012). Iron uptake, translocation, and regulation in higher plants. *Annu. Rev. Plant Biol.* 63, 131–152. doi: 10.1146/annurev-arplant-042811-105522

Landi, S., Hausman, J. F., Guerriero, G., and Esposito, S. (2017). Poaceae vs. abiotic stress: focus on drought and salt stress, recent insights and perspectives. *Front. Plant Sci.* 8:1214.

Leasure, C. D., and He, Z. H. (2012). CLE and RGF family peptide hormone signaling in plant development. *Mol. Plant* 5, 1173–1175. doi: 10.1093/mp/sss082

Li, S., Zhou, X., Chen, J., and Chen, R. (2018). Is there a strategy I iron uptake mechanism in maize? *Plant Signal. Behav.* 13:e1161877. doi: 10.1080/15592324.2016.1161877

Li, S., Zhou, X., Huang, Y., Zhu, L., Zhang, S., Zhao, Y., et al. (2013). Identification and characterization of the zinc-regulated transporters, iron-regulated transporter-like protein (ZIP) gene family in maize. *BMC Plant Biol.* 13:114. doi: 10.1186/1471-2229-13-114

Lopes, J. L. S., Miles, A. J., Whitmore, L., and Wallace, B. A. (2014). Distinct circular dichroism spectroscopic signatures of polyproline II and unordered secondary structures: applications in secondary structure analyses. *Protein Sci.* 23, 1765–1772. doi: 10.1002/pro.2558

Lucini, L., Rouphael, Y., Cardarelli, M., Canaguier, R., Kumar, P., and Colla, G. (2015). The effect of a plant-derived biostimulant on metabolic profiling and crop performance of lettuce grown under saline conditions. *Sci. Hortic.* 182, 124–133. doi: 10.1016/j.scienta.2014.11.022

Nozoye, T., Nakanishi, H., and Nishizawa, N. K. (2013). Characterizing the crucial components of iron homeostasis in the maize mutants ys1 and ys3. *PLoS One* 8:e62567. doi: 10.1371/journal.pone.0062567

Paul, K., Sorrentino, M., Lucini, L., Rouphael, Y., Cardarelli, M., Bonini, P., et al. (2019a). A combined phenotypic and metabolomic approach for elucidating the biostimulant action of a plant-derived protein hydrolysate on tomato grown under limited water availability. *Front. Plant Sci.* 10:493.

Paul, K., Sorrentino, M., Lucini, L., Rouphael, Y., Cardarelli, M., Bonini, P., et al. (2019b). Understanding the biostimulant action of vegetal-derived protein hydrolysates by high-throughput plant phenotyping and metabolomics: a case study on tomato. *Front. Plant Sci.* 10:47.

Pearce, G. (2011). Systemin, hydroxyproline-rich systemin and the induction of protease inhibitors. *Curr. Protein Pept. Sci.* 12, 399–408. doi: 10.2174/138920311796391106

Piez, K. A. (1968). Molecular weight determination of random coil polypetides from collagen by molecular sieve chromatography. *Anal. Biochem.* 312, 305–312. doi: 10.1016/0003-2697(68)90342-4

Piez, K. A., and Sherman, M. R. (1970). Characterization of the product formed by renaturation of α1-cb2, a small peptide from collagen. *Biochemistry* 9, 4129–4133. doi: 10.1021/bi00823a015

Rahmstorf, S., and Coumou, D. (2011). Increase of extreme events in a warming world. *Proc. Natl. Acad. Sci. U. S. A.* 108, 17905–17909. doi: 10.1073/pnas.1101766108

Ramakers, C., Ruijter, J. M., Deprez, R. H. L., and Moorman, A. F. M. (2003). Assumption-free analysis of quantitative real-time polymerase chain reaction (PCR) data. *Neurosci. Lett.* 339, 62–66. doi: 10.1016/s0304-3940(02)01423-4

Santi, C., Zamboni, A., Varanini, Z., and Pandolfini, T. (2017). Growth stimulatory effects and genome-wide transcriptional changes produced by protein hydrolysates in maize seedlings. *Front. Plant Sci.* 8:433.

Schaaf, G., Ludewig, U., Erenoglu, B. E., Mori, S., Kitahara, T., and Von Wirén, N. (2004). ZmYS1 functions as a proton-coupled symporter for phytosiderophore- and nicotianamine-chelated Metals. *J. Biol. Chem.* 279, 9091–9096. doi: 10.1074/jbc.m311799200

Scherr, S. J. (1999). *Soil Degradation: a Threat to Developing Country Food Security by 2020?*. Washington, DC: International Food Policy Research Institute.

Sega, D., Baldan, B., Zamboni, A., and Varanini, Z. (2020). FePO4 NPs are an efficient nutritional source for plants: combination of nano-material properties and metabolic responses to nutritional deficiencies. *Front. Plant Sci.* 11:586470.

Simon, P. (2003). Q-Gene: processing quantitative real-time RT–PCR data. *Bioinformatics* 19, 1439–1440. doi: 10.1093/bioinformatics/btg157

Suhag, M. (2016). Potential of biofertilizers to replace chemical fertilizers. *Int. Adv. Res. J. Sci. Eng. Technol.* 3, 163–166.

Trevisan, S., Manoli, A., and Quaggiotti, S. (2019). A novel biostimulant, belonging to protein hydrolysates, mitigates abiotic stress effects on maize seedlings grown in hydroponics. *Agronomy* 9:28. doi: 10.3390/agronomy9010028

Vandesompele, J., De Preter, K., Pattyn, F., Poppe, B., Van Roy, N., De Paepe, A., et al. (2002). Accurate normalization of real-time quantitative RT-PCR data by geometric averaging of multiple internal control genes. *Genome Biol.* 3:RESEARCH0034.

Wairich, A., de Oliveira, B. H. N., Arend, E. B., Duarte, G. L., Ponte, L. R., Sperotto, R. A., et al. (2019). The combined strategy for iron uptake is not exclusive to domesticated rice (Oryza sativa). *Sci. Rep.* 9:16144.

Wang, W., Vinocur, B., Shoseyov, O., and Altman, A. (2004). Role of plant heat-shock proteins and molecular chaperones in the abiotic stress response. *Trends Plant Sci.* 9, 244–252. doi: 10.1016/j.tplants.2004.03.006

Wani, S. H., Kumar, V., Shriram, V., and Sah, S. K. (2016). Phytohormones and their metabolic engineering for abiotic stress tolerance in crop plants. *Crop J.* 4, 162–176. doi: 10.1016/j.cj.2016.01.010

Xu, L., and Geelen, D. (2018). Developing biostimulants from agro-food and industrial by-products. *Front. Plant Sci.* 871:1567.

Yakhin, O. I., Lubyanov, A. A., Yakhin, I. A., and Brown, P. H. (2017). Biostimulants in plant science: a global perspective. *Front. Plant Sci.* 7:2049.

Zamboni, A., Zanin, L., Tomasi, N., Avesani, L., Pinton, R., Varanini, Z., et al. (2016). Early transcriptomic response to Fe supply in Fe-deficient tomato plants is strongly influenced by the nature of the chelating agent. *BMC Genomics* 17:35.

Conflict of Interest: The authors declare that the research was conducted in the absence of any commercial or financial relationships that could be construed as a potential conflict of interest.

frontiers in Plant Science

ORIGINAL RESEARCH
published: 19 February 2021
doi: 10.3389/fpls.2021.625541

Silicon-Mediated Priming Induces Acclimation to Mild Water-Deficit Stress by Altering Physio-Biochemical Attributes in Wheat Plants

Arruje Hameed[1], Tahir Farooq[2], Amjad Hameed[3] and Munir Ahmad Sheikh[4]*

[1] Department of Biochemistry, Government College University Faisalabad, Faisalabad, Pakistan, [2] Department of Applied Chemistry, Government College University Faisalabad, Faisalabad, Pakistan, [3] Nuclear Institute for Agriculture and Biology (NIAB), Faisalabad, Pakistan, [4] Institute of Molecular Biology and Biotechnology (IMBB), The University of Lahore, Lahore, Pakistan

OPEN ACCESS

Edited by:
Youssef Rouphael, University of Naples Federico II, Italy

Reviewed by:
Xiangnan Li, Northeast Institute of Geography and Agroecology (CAS), China
Vasileios Fotopoulos, Cyprus University of Technology, Cyprus

***Correspondence:**
Arruje Hameed
arrujetahirfsd@gmail.com; arrujeh@yahoo.com

Specialty section:
This article was submitted to Plant Abiotic Stress, a section of the journal Frontiers in Plant Science

Received: *03 November 2020*
Accepted: *18 January 2021*
Published: *19 February 2021*

Citation:
Hameed A, Farooq T, Hameed A and Sheikh MA (2021) Silicon-Mediated Priming Induces Acclimation to Mild Water-Deficit Stress by Altering Physio-Biochemical Attributes in Wheat Plants. Front. Plant Sci. 12:625541. doi: 10.3389/fpls.2021.625541

Water-deficit stress negatively affects seed germination, seedling development, and plant growth by disrupting cellular and metabolic functions, reducing the productivity and yield of field crops. In this study, sodium silicate (SS) has been employed as a seed priming agent for acclimation to mild water-deficit stress by invoking priming memory in wheat plants. In pot experiments, the SS-primed (20, 40, and 60 mM) and non-primed control seeds were allowed to grow under normal and mild water-deficit conditions. Subsequently, known methods were followed for physiological and biochemical studies using flag leaves of 98-day mature wheat plants. The antioxidant and hydrolytic enzymes were upregulated, while proteins, reducing sugars, total sugars, and glycine betaine increased significantly in the flag leaves of wheat plants originated from SS-treated seeds compared to the control under mild water-deficit stress. Significant decreases in the malondialdehyde (MDA) and proline contents suggested a controlled production of reactive oxygen species, which resulted in enhanced cell membrane stability. The SS priming induced a significant enhancement in yield, plant biomass, and 100-grain weight of wheat plants under water-deficit stress. The improvement in the yield parameters indicated the induction of Si-mediated stress acclimation in SS-primed seeds that elicited water-deficit tolerance until the maturity of plants, ensuring sustainable productivity of climate-smart plants.

Keywords: seed priming, sustainable productivity, water-deficit stress tolerance, wheat, silicon

INTRODUCTION

Around the world, sustainable agriculture is facing severe threats from ecotoxicological conditions, climate change, and environmental stresses that pose serious challenges to global food security. Plants growing in a dynamic environment are heavily influenced by the aforesaid stress factors and exhibit a significant reduction in growth, development, and final yield, although they try to counterbalance the negative impacts through certain adaptive mechanisms, such as changing the osmotic potential, plant structure, and growth pattern, boosting the antioxidant defense potential

and regulating physiological and biochemical processes (Teh and Koh, 2016). Over the years, drought or water deficit has been recognized as the most brutal environmental stress that retards the growth and development of plants by having negative impacts on the physiological, biochemical, and morphological traits. It hampers the normal metabolic, antioxidant, and photosynthetic activation and nutrient movement in plants. The disrupted processes at the subcellular level impair the growth-promoting parameters and lead to reduced plant growth and biomass and to yield losses (Wang et al., 2018; Easwar Rao and Viswanatha Chaitanya, 2020). Wheat is a major staple food, and its seed germination, seedling growth, and plant development also experience the drought-induced negative impacts, which ultimately result in low yield (Amirjani and Mahdiyeh, 2013; Guo et al., 2017). Wheat plants experience negative changes in protein contents, antioxidant potential, and hormone composition at the vegetative and reproductive stages under drought. It also influences the chlorophyll content, cuticle thickness, and opening and closing of the stomata (Bano et al., 2012; Guan et al., 2015; Li et al., 2020). In fact, water limitations severely reduce the uptake and translocation of macro- and micronutrients, which affect leaf–water relations, photosynthesis, and chlorophyll fluorescence, resulting in reduced plant growth, early senescence, and low wheat productivity (Zlatev, 2009; Karim et al., 2012; Wang et al., 2017).

Seed germination is one of the major phases in the life of higher plants in which all well-regulated metabolic, biochemical, and physiological processes ensure the rapid and uniform emergence of seedlings and plant development. Priming is a seed pre-conditioning technique that modulates the biochemical and physiological processes for the acceleration of germination and alleviation of stress, and for higher crop yields. In fact, it programs the seeds for the tolerance of abiotic stresses by regulating metabolism, antioxidant enzymes, and protein synthesis and readjusting the underlying subcellular pathways (Wojtyla et al., 2016; Hameed et al., 2019). Over the last few decades, a range of physical, chemical, and biological treatments have been well explored for hydropriming, chemopriming, biopriming, and thermoprining for pre-germinative metabolic modulations in seeds in order to withstand abiotic and biotic stress conditions at germination, seedling growth, and plant development. Various natural and synthetic priming agents (inorganic salts, organic molecules, and natural metabolites) have been reported to boost the antioxidant potential as a stress-responsive strategy for the alleviation of drought-induced damages in germinating seeds (Aranega-Bou et al., 2014; Savvides et al., 2016; Singh et al., 2020). Various studies have reported the applications of salicylic acid, abscisic acid, jasmonic acid, hydrogen peroxide, ascorbic acid, sodium nitroprusside, sodium chloride, sodium glutamate, etc., as wheat seed priming agents to induce tolerance against drought and to mitigate the above-mentioned negative impacts (Hameed and Iqbal, 2014; Bhardwaj et al., 2017; Habib et al., 2020).

Over the last few decades, several authors have reported the ability of silicon (Si) to induce tolerance against biotic and abiotic stresses, including salinity, high temperature, chilling, drought, etc. It accelerates seed germination and enhances plant growth and crop yield. It acts as a plant protectant and biostimulant under a range of stress conditions. It also improves the water status and water use efficiency of plants and reduces lipid peroxidation under drought stress (Hasanuzzaman et al., 2018; Liu et al., 2019). It could regulate osmolyte accumulation and readjust osmotic potential under water-deficit conditions. Si provision improved the yield of rice by increasing the mobilization of photoassimilates and amino acids from vegetative tissues to grain and nitrogen use efficiency. It redirected the primary metabolism by acting as a signaling factor under unstressed conditions (Pang et al., 2019; Mohanty et al., 2020).

Keeping the above facts in mind, this study was planned to employ Si as a wheat seed priming agent to induce acclimation to mild water-deficit stress until the maturity of plants.

MATERIALS AND METHODS

In this study, spring wheat (*Triticum aestivum* L. cv. AARI-2011) seeds (100 g for each treatment) were primed with 20, 40, and 60 mM sodium silicate (SS) solution, the Si donor, for 8 h. Then, they were washed and dried at 26 ± 2°C under shade. On the other hand, some wheat seeds were soaked only in water to achieve hydro-primed seeds for comparative study. Pot experiments with a completely randomized design were conducted in three replicates (five pots per replicate with five seeds per pot) to investigate the effects of silicon-induced priming on mature wheat plants produced from SS-primed seeds under normal and mild water-deficit conditions. Each pot was filled with 1.4 g cm^{-3} sandy clay loam soil containing 22% clay, 33% silt, and 45% sand. Normal growth conditions were maintained by providing water at soil water-holding capacity. On parallel, the drought stress was induced by maintaining water at 50% soil water-holding capacity. Physiological and biochemical analyses were performed using flag leaf samples collected from 98-day matured plants originated from SS-primed, hydro-primed, and non-primed control seeds grown under normal and mild drought conditions.

Physiological Analyses

A known conductometric method was employed for the measurement of cell membrane stability (CMS) (Blum and Ebercon, 1981). The samples were autoclaved for 24 h before and after conductivity reading from the control (C) and stressed (T) leaf samples.

$$\text{CMS \%} = [(1 - (T_1/T_2))/(1 - (C_1/C_2))] \times 100$$

where T_1 is the stress sample conductance before autoclaving, T_2 is the stress sample conductance after autoclaving, C_1 is the control sample conductance before autoclaving, and C_2 control sample conductance after autoclaving.

The water status parameters (turgor, osmotic, and water potential) were measured using the youngest leaf samples according to known procedures. The difference between the water potential (Ψ_w) and osmotic potential (Ψ_s) values provided the leaf turgor potential (Ψ_p).

$$(\Psi_p = \Psi_w - \Psi_s)$$

Biochemical Analyses

Biomolecules

Total soluble proteins (TSPs) were estimated by the method of Bradford using bovine serum albumin (BSA) as the standard (Bradford, 1976). Reducing sugars were determined using a well-known dinitrosalicylic acid method (Miller, 1959) and the total sugar content estimated using the phenol sulfuric acid reagent method (Dubois et al., 1951). The reducing and total sugar contents were determined from a standard curve prepared by using glucose as the standard. Non-reducing sugars were calculated by subtracting the reducing sugars from the total sugars.

Enzymatic and Non-enzymatic Antioxidants

For the different biochemical analyses, leaf samples (0.5 g) were ground in specific extraction buffer and centrifuged at 15,000 × *g* for 20 min at 4°C for different biomolecules and enzymes. Subsequently, the separated supernatant was employed for the below given biochemical analyses according to well-established methods. Spectroscopic analyses were performed using a spectrophotometer (Hitachi, U2800).

Specific extraction buffers were used to homogenize the leaf samples (0.5 g) as in a known procedure. The activity of superoxide dismutase (SOD) was assayed by measuring its ability to inhibit the photochemical reduction of nitroblue tetrazolium (NBT) following a known method (Giannopolitis and Ries, 1977). One unit of SOD activity was defined as the amount of enzyme which caused 50% inhibition of photochemical reduction of NBT. The activities of peroxidase (POD) and catalase (CAT) were also measured using a well-established method (Chance and Maehly, 1955). For POD activity, we noted an increase in the absorbance of the reaction solution at 470 nm. In the case of CAT activity, we recorded a decrease in the absorbance of the reaction solution at 240 nm. An absorbance variation of 0.01 U/min was taken as one unit of CAT and POD activities. Further, the activities of enzymes were expressed on seed weight basis.

The level of lipid peroxidation was measured in terms of malondialdehyde (MDA, a product of lipid peroxidation) content determined by a known method which involves thiobarbituric acid (TBA) reaction (Heath and Packer, 1968). An extinction coefficient of 155 mM^{-1} cm^{-1} was used for the calculation of MDA content. The Folin–Ciocalteu reagent was employed according to a known micro-colorimetric method for the determination of the total phenolic content (TPC) (Ainsworth and Gillespie, 2007). A linear regression equation was used for the measurement of TPC after preparing the standard curve with different concentrations of gallic acid.

Hydrolytic Enzymes

Protease activity was determined by a known casein digestion assay (Drapeau, 1976). The absorbance of the filtrate was measured at 280 nm. By this method, 1 U is the amount of enzyme that releases acid-soluble fragments equivalent to 0.001 A_{280} per minute at 37°C and pH 7.8. Enzyme activity was expressed on a protein basis. The α-amylase activity was determined by following a reported method (Varavinit et al., 2002). Accordingly, maltose was used for the construction of the standard curve to measure enzyme activity.

Osmolytes

The known acid ninhydrin method was employed for the measurement of proline content at 520 nm and expressed as micrograms proline per gram fresh weight (FW) (Bates et al., 1973). A known spectroscopic method was adopted for the determination of glycine betaine (GB) (Grieve and Grattan, 1983). Warm distilled water was used to prepare an aqueous extract of dry leaves, which was mixed with 0.2 ml of potassium triiodide solution and 0.25 ml of 2 N HCl. After keeping this solution in an ice bath for 90 min, 20 ml of dichloromethane and 2 ml of water were added for the extraction of GB. The optical density of the organic phase was determined at 365 nm, and the GB concentrations were measured on a fresh weight basis.

Pigment Contents

A known spectrophotometric-based method was followed to measure chlorophyll a (chl a), chlorophyll b (chl b), total chlorophyll (total chl), and carotenoids in leaf samples (Arnon, 1949; Peters and Noble, 2014). The pigments were extracted in 85% acetone and centrifuged at 4,000 rpm for 15 min; subsequently, the supernatant was used for the absorbance of the recorded values at 645, 663, and 480 nm. Afterward, the pigment contents were calculated as follows:

$$\text{Chl a (mg/g FW)} = [12.7(OD_{663}) - 2.69(OD_{645}) \times V/1,000 \times W]$$

$$\text{Chl b (mg/g FW)} = [22.9(OD_{645}) - 4.68(OD_{663}) \times V/1,000 \times W]$$

$$\text{Carotenoids (mg/g FW)} = [A_{car}/\text{EM}] \times 1,000A_{car} = OD_{480} + 0.114(OD_{663}) - 0.638(OD_{645})$$

Where, OD represents optical density, V is the volume of the sample, W is the weight of fresh tissue taken for extraction, and EM is 2,500.

Yield Attributes

The mature wheat plants were used to calculate the plant biomass, 100-grain weight yield, and the grain yield per plant under stress and non-stress conditions.

Statistical Analyses

Finally, significance of the data was tested using variance and Tukey's (honestly significant difference, HSD) test at $p < 0.05$ and, where applicable, at $p < 0.01$. Thus, the mean ± SD values are presented in graphs.

RESULTS

The SS-treated and non-treated wheat seeds were allowed to germinate in pots under normal and mild drought stress conditions. Later, the flag leaf samples of 98-day mature plants were used for biochemical, physiological, and yield responses and compared with the control under stress and non-stress conditions.

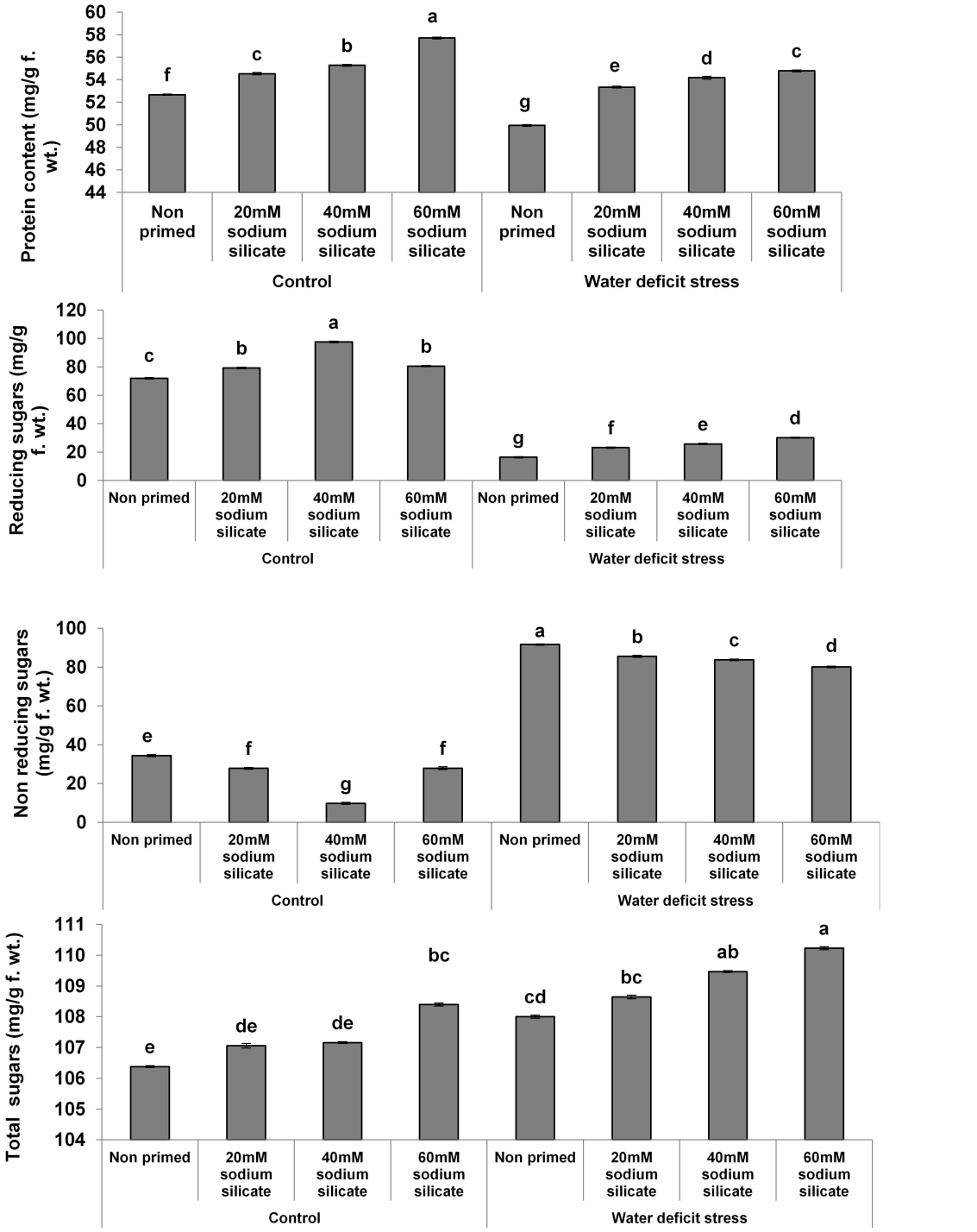

FIGURE 1 | Contents of biomolecules in the flag leaf of wheat plants grown after sodium silicate seed priming under non-stress and water-deficit stress conditions. Each data point represents the mean of three samples ± SD. Bars with different alphabet are significantly different ($p < 0.05$ and $P > 0.01$) according to Tukey's (HSD).

Biochemical Parameters

The protein contents increased significantly with increasing concentrations of the priming agent under normal as well as stress conditions compared to the control (**Figure 1**). There was a significant increase in reducing sugars with increasing concentrations of the applied sodium silicate priming solution under both conditions. However, the increasing effect was more pronounced in the flag leaves of plants originated from prime seeds under normal conditions. Interestingly, an entirely opposite effect was observed in the case of non-reducing sugars. The

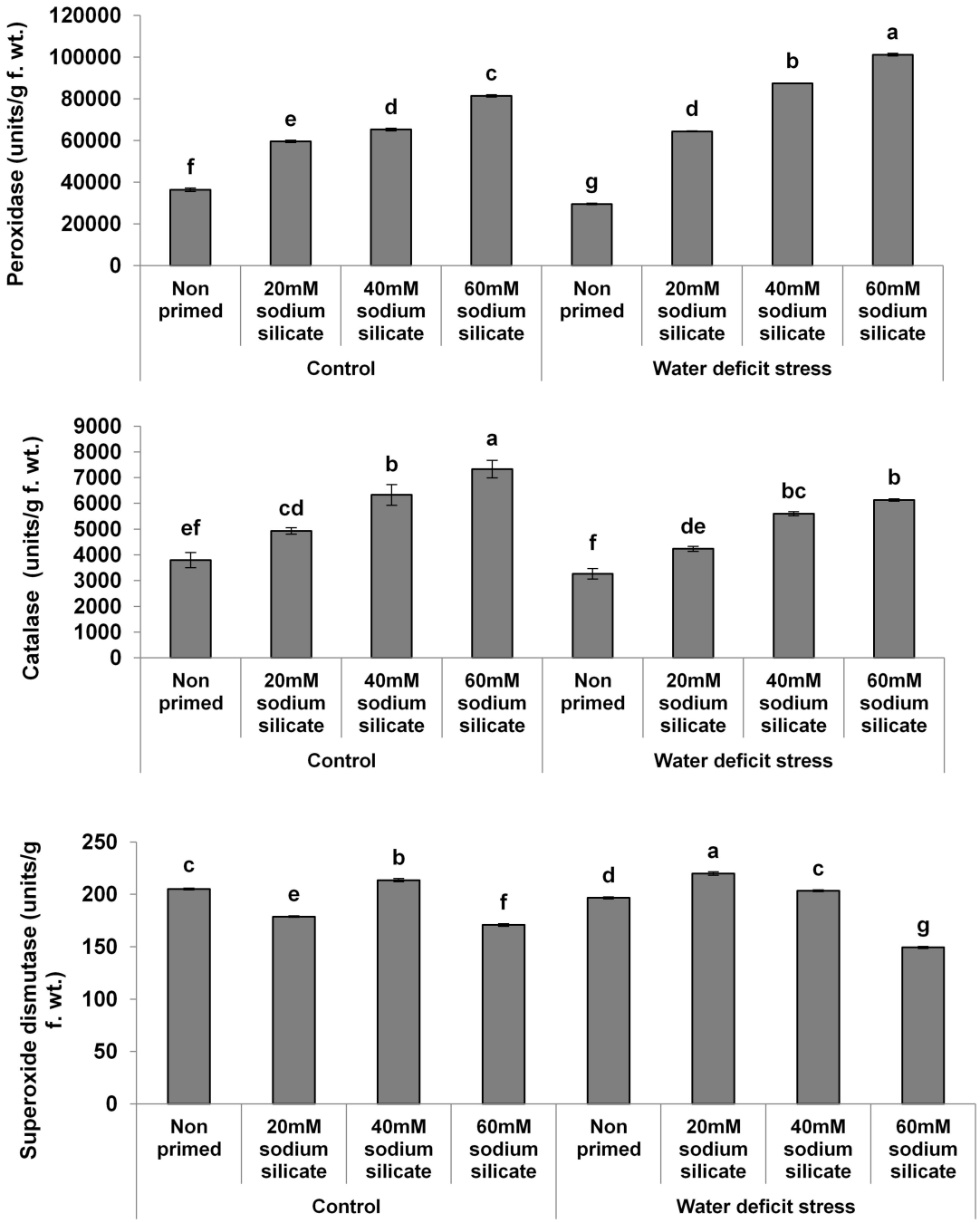

FIGURE 2 | Antioxidant enzyme activities in the flag leaf of wheat plants grown after sodium silicate seed priming under non-stress and water-deficit stress conditions. Each data point represents the mean of three samples ± SD. Bars with different alphabet are significantly different ($p < 0.05$ and $P > 0.01$) according to Tukey's (HSD).

total sugars increased with increasing concentrations of the priming agent under drought, while under normal conditions, only priming with 60 mM SS treatment induced a significant increase in total sugars.

In the case of the antioxidant enzymes, both POD and CAT activities were upregulated significantly with increasing priming concentrations under both conditions. However, a more pronounced effect was observed in POD and CAT under the mild drought and normal conditions, respectively. Priming with 20 and 40 mM SS induced a significant increase in SOD activity under drought. Under normal conditions, only 40 mM SS treatment caused a significant increase in SOD. The maximum upregulation of SOD was observed as a result of priming with 20 mM SS under stress (**Figure 2**).

The MDA contents exhibited a significant decreasing trend with increasing priming concentrations. The maximum MDA

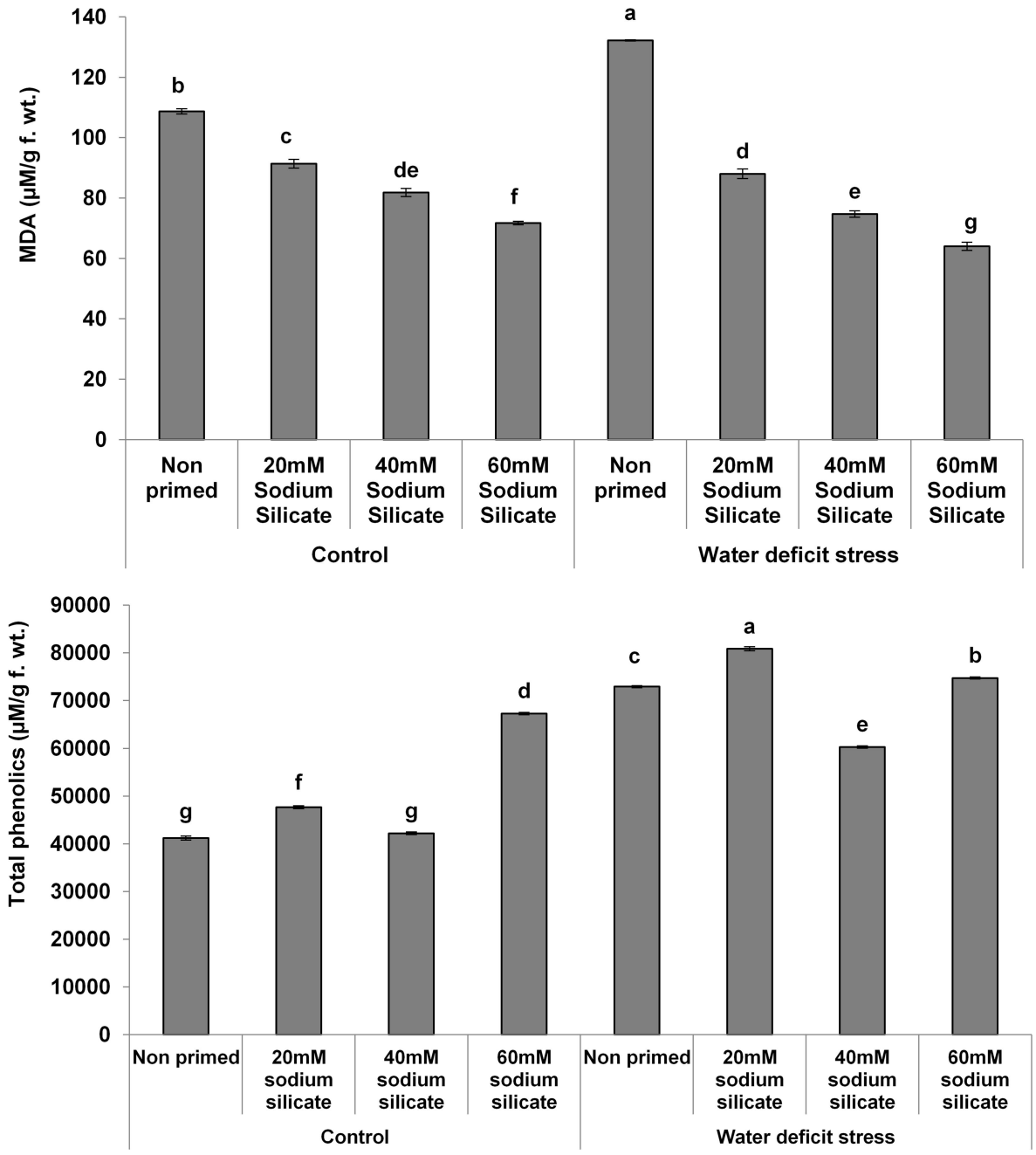

FIGURE 3 | Malondialdehyde (MDA) contents and total phenolics in the flag leaf of wheat plants grown after sodium silicate seed priming under non-stress and water-deficit stress conditions. Each data point represents the mean of three samples ± SD. Bars with different alphabet are significantly different ($p < 0.05$ and $P > 0.01$) according to Tukey's (HSD).

was observed in the flag leaves of plants originated from non-primed seeds grown under drought. Treatment with 40 mM SS induced a significant decrease, while the other treatments caused an increment in the non-enzymatic antioxidant, the TPC, under both conditions compared to the control (**Figure 3**). In the case of the hydrolytic enzymes, the protease and α-amylase activities

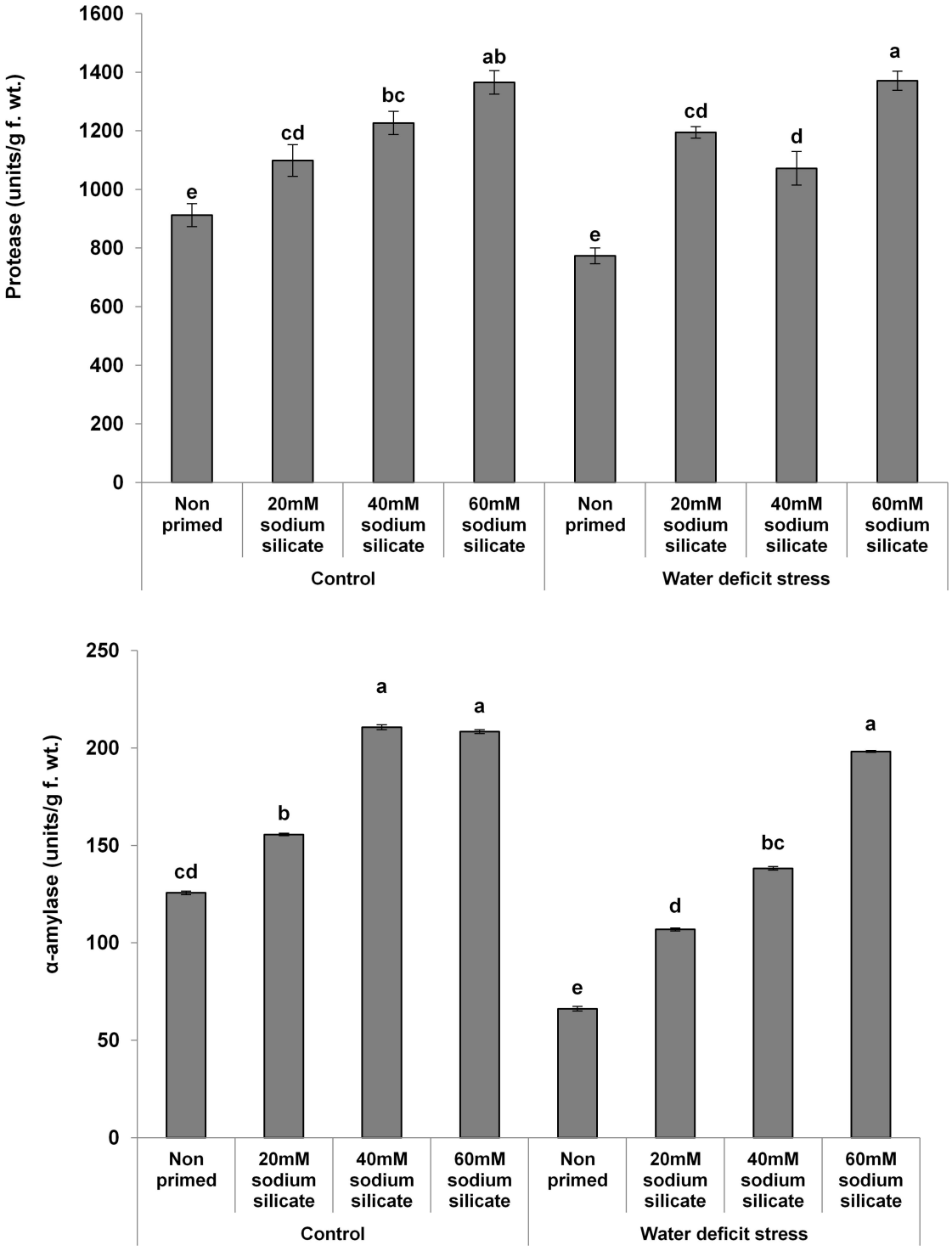

FIGURE 4 | Hydrolytic enzyme activities in the flag leaf of wheat plants grown after sodium silicate seed priming under non-stress and water-deficit stress conditions. Each data point represents the mean of three samples ± SD. Bars with different alphabet are significantly different ($p < 0.05$ and $P > 0.01$) according to Tukey's (HSD).

were significantly upregulated due to the priming treatments under normal as well as stress conditions (**Figure 4**).

The proline contents decreased significantly and linearly with increasing SS priming concentrations, while a significantly linear increase was observed in GB under both conditions (**Figure 5**).

Priming with 40 mM SS only caused a significant increase in chl a under normal conditions. The priming treatments induced a significant decrease in chl b and total chl under normal conditions. Under drought, priming with 20 and 60 mM SS caused a significant increase in chl a and chl b, respectively. Priming with 60 mM SS also increased the total chl significantly under stress. A significant increase in total carotenoids was observed as a result of priming with 20 and 40 mM SS under normal conditions. Meanwhile, priming with 60 mM induced a significant increase in total carotenoids under stress (**Table 1**).

Physiological Parameters

There was a significant and linear decrease in the water potential of flag leaves with increasing SS priming concentrations under both conditions. The osmotic potential exhibited a similar trend under stress. However, a significant increasing effect was induced by 60 mM treatment under normal conditions. A significant increase in turgor potential was observed with increasing priming concentrations under both conditions (**Table 2**). CMS increased significantly with increasing SS priming concentrations (**Figure 6**).

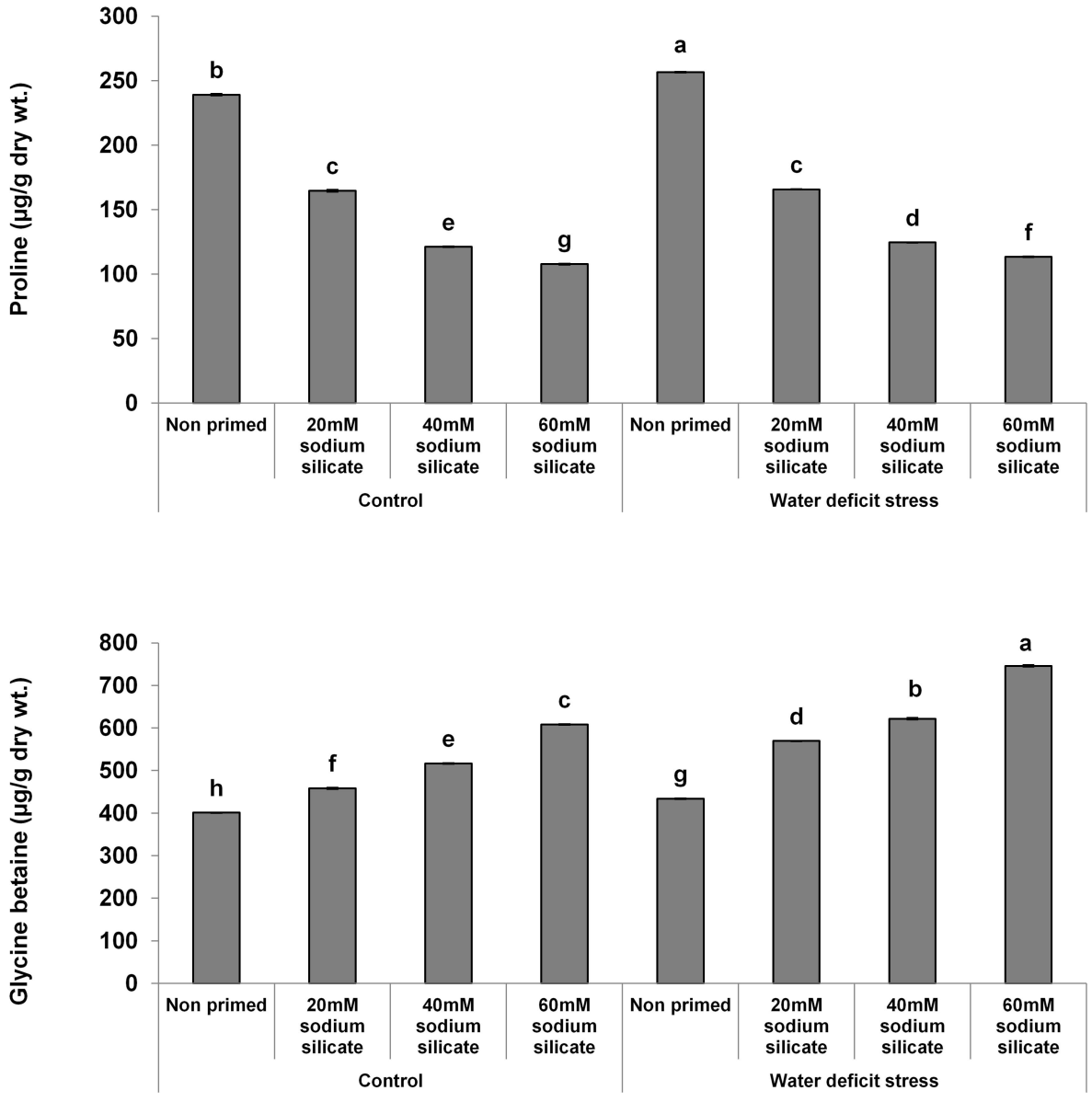

FIGURE 5 | Osmolyte contents in the flag leaf of wheat plants grown after sodium silicate seed priming under non-stress and water-deficit stress conditions. Each data point represents the mean of three samples ± SD. Bars with different alphabet are significantly different ($p < 0.05$ and $P > 0.01$) according to Tukey's (HSD).

TABLE 1 | Effect of sodium silicate priming treatments on pigments.

Pigments	Treatments							
	Non-stress				Under water-deficit stress			
	Control	20 mM sodium silicate	40 mM sodium silicate	60 mM sodium silicate	Control	20 mM sodium silicate	40 mM sodium silicate	60 mM sodium silicate
Chlorophyll a (µg/g FW)	335.611 ± 0.714d	334.837 ± 0.571d	356.237 ± 0.209a	335.090 ± 0.375d	335.274 ± 0.395d	342.317 ± 0.293b	330.613 ± 0.721e	339.277 ± 0.656c
Chlorophyll b (µg/g FW)	524.006 ± 0.827d	513.068 ± 0.855e	408.125 ± 0.730g	504.110 ± 0.628f	540.714 ± 0.781b	534.777 ± 0.311c	536.184 ± 0.522c	545.009 ± 0.575a
Total chlorophyll (µg/g FW)	859.617 ± 1.224d	847.905 ± 0.625e	764.362 ± 0.523g	839.200 ± 0.253f	875.988 ± 0.391b	877.094 ± 0.381b	866.796 ± 0.387c	884.287 ± 1.121a
Total carotenoids (mg/g FW)	32.529 ± 0.012e	32.783 ± 0.011d	32.995 ± 0.034c	32.207 ± 0.033f	33.129 ± 0.042b	32.516 ± 0.049e	33.180 ± 0.026ab	33.241 ± 0.017a

FW, fresh weight. Mean values of three replicates are presented. Within a column, means sharing the same letters are non-significantly different ($p > 0.05$ and $p > 0.01$) according to Tukey's HSD test.

Yield Attributes

The yield of plants increased significantly with priming treatments under both conditions; however, the effect was more pronounced under stress-free conditions. A significant increase in 100-grain weight was observed only as a result of priming with 20 mM SS under normal and stress conditions, while the other treatments were unable to induce any perceptible change in it. The priming treatments induced a significant increase in plant biomass under both conditions (**Table 2**).

DISCUSSION

Applications of SS as a wheat seed priming agent induced a significant increase in TSP in the flag leaves of plants under both conditions. Proteins provide energy and amino acids to germinating seeds and developing seedlings and execute a number of physiological and biochemical processes in plants, being vital enzymes in various subcellular metabolic and signaling pathways. Drought stress induces severe negative impacts on such pathways due to their high dependence on water availability (Ali and Elozeiri, 2017). As a stress-mitigating strategy, plants produce drought-responsive proteins for biochemical readjustments to counterbalance the deleterious impacts and provision of resistance against stress (Al-Jebory, 2012). Silicon applications are known to enhance the expressions of drought-related proteins in rice plants under drought (Khattab et al., 2014). Accordingly, in our study, the Si-induced marked increment in TSP has been considered as a mechanistic response to water-deficit conditions. Hence, the significant improvement of the TSP content with increasing SS concentrations suggested the facilitating role of Si in protein synthesis under normal as well as stress conditions. The produced proteins could have assisted in the regulation of metabolic pathways and provided energy and nutrients for the induction of stress tolerance.

There were significant increases in the reducing and total sugars with increasing SS concentrations under stress and stress-free conditions. Plants increase their sugar content as a part of their stress-insulating mechanism because they could provide energy for metabolic processes and assist in the regulation of stress responses. Sugars do act as osmoprotectants and provide membrane stability, especially under water-deficit conditions (O'Hara et al., 2013; Poonam et al., 2016). Maize plants produced from Si-primed seeds were reported to show higher contents of soluble sugars under alkaline and water-deficit stress (Abdel Latef and Tran, 2016; Parveen et al., 2019). Hence, a Si-mediated increase in the reducing and total sugars has been considered as a positive factor for drought tolerance in this study. However, SS priming induced a significant decrease in non-reducing sugars, which suggested their lesser requirements in water-deficit management in this study.

In our case, the Si priming treatments significantly increased the POD and CAT activities in the flag leaves of wheat plants under normal and stress conditions. Priming with 20 and 40 mM SS caused a significant increase in SOD activity under stress and normal conditions, respectively, while all the other

TABLE 2 | Effect of sodium silicate priming treatments on water status and yield parameters.

Water status/yield parameters	Treatments							
	Non-stress				Under water-deficit stress			
	Control	20 mM sodium silicate	40 mM sodium silicate	60 mM sodium silicate	Control	20 mM sodium silicate	40 mM sodium silicate	60 mM sodium silicate
Water potential (MPa)	0.540 ± 0.008e	0.511 ± 0.002f	0.494 ± 0.002fg	0.475 ± 0.004g	0.967 ± 0.017a	0.875 ± 0.004b	0.705 ± 0.004c	0.566 ± 0.004d
Osmotic potential (MPa)	1.110 ± 0.002g	1.114 ± 0.002g	1.127 ± 0.001f	1.1338 ± 0.002e	1.343 ± 0.004a	1.295 ± 0.003b	1.218 ± 0.003c	1.176 ± 0.005d
Turgor potential (MPa)	0.570 ± 0.007d	0.603 ± 0.004c	0.633 ± 0.001b	0.664 ± 0.002a	0.376 ± 0.013g	0.420 ± 0.006f	0.513 ± 0.001e	0.611 ± 0.005c
Plant biomass (g)	4.011 ± 0.094e	5.111 ± 0.075c	5.833 ± 0.110ab	5,923 ± 0.019a	3.560 ± 0.143f	5.142 ± 0.048c	4.564 ± 0,030d	5.504 ± 0.171b
100-grain weight (g)	2.962 ± 0.028b	3.764 ± 0.104a	3.419 ± 0.084ab	3.286 ± 0.054ab	2.223 ± 0.096c	3.387 ± 0.106ab	2.819 ± 0.104bc	2.869 ± 0.104bc
Yield/ plant (g)	1.217 ± 0.022ef	2.415 ± 0.068b	2.654 ± 0.098a	2.693 ± 0.033a	1.097 ± 0.023f	1.352 ± 0.003de	1.417 ± 0.011d	1.898 ± 0.089c

Mean values of three replicates are presented. Within a column, means sharing the same letters are non-significantly different ($p > 0.05$ and $p > 0.01$) according to Tukey's HSD test.

priming treatments induced a significant decrease in SOD under both conditions. In general, plants utilize non-enzymatic and enzymatic antioxidants for real-time detoxification of stress-induced reactive oxygen species (ROS). Therefore, upregulated antioxidant enzymes have been considered as a major stress-responsive strategy for counterbalancing excessive ROS (Sofo et al., 2015). The exogenous as well as priming applications of Si have been known to boost antioxidant enzymes in late-sown wheat and maize plants under drought (Sattar et al., 2017; Parveen et al., 2019). Thus, in our case, the elevated activities of the antioxidant enzymes represented an increased antioxidant potential for the provision of water-deficit tolerance in wheat plants.

The overexpression of the antioxidant enzymes along with the readjustment of biomolecules might have mitigated the negative impacts of water-deficit and helped to detoxify the excessive generation of ROS. It has been signified by the significant reduction of MDA contents with increasing priming concentrations prominently under mild water-deficit conditions. Under both conditions, two priming treatments induced a significant increase in TPC, a non-enzymatic antioxidant. The elevated antioxidant potential with reduced MDA contents suggested acclimation to water deficit in wheat plants induced as priming memory in primed seeds.

In our study, the activities of both hydrolytic (protease and α-amylase) enzymes increased significantly and almost linearly with increasing concentrations of SS under both conditions. Usually, plants show an upregulation of hydrolytic enzymes as a mechanistic approach for the mitigation of abiotic stresses including water deficit (Wang et al., 2016). They re-mobilize stored proteins and soluble sugars for the regulation of various metabolic and physiological functions vital for seed germination, seedling development, and plant growth (Adda et al., 2014; Martinez et al., 2019). In this perspective, the upregulation of the hydrolytic enzymes has been considered as a positive factor to elicit water-deficit tolerance in wheat plants.

Proline accumulation appears as one of the major stress-combating strategies in plants against a number of abiotic stresses, including water-deficit conditions. It helps the plants in osmotic readjustments for the development of water-deficit resistance. Further, it has been suggested as the biomarker of osmotic stress injury (Heuer, 2010; Chun et al., 2018). In our case, the proline contents were decreased significantly in the flag leaf of wheat plants with increasing priming concentrations compared to the control under both conditions. Accordingly, it represented that SS priming provided water-deficit acclimation in wheat plants, thus reducing the chances of osmotic injury and the requirement of proline. Glycine betaine is also produced in plants as an adaptive mechanism to counter abiotic stresses, including drought or water-deficit conditions. It is a known osmolyte that helps in stress-related osmotic readjustments for buffering of the redox potential, membrane stability, and higher ROS scavenging capacity. It interacts with the hydrophobic and hydrophilic domains of protein complexes and membranes, protects them from ROS, and maintains their structural and functional integrity. Thus, it offers counteracting mechanisms to settle the stress-related metabolic dysfunctions, ensuring

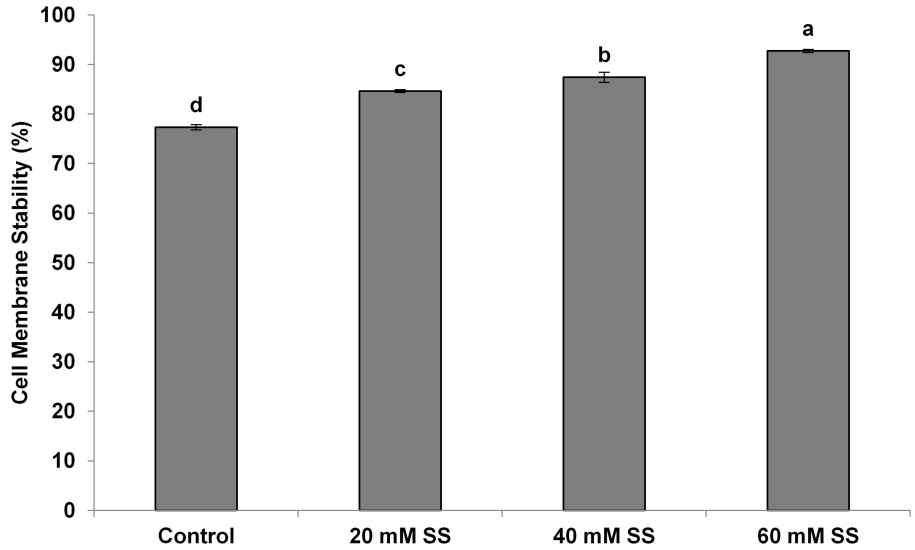

FIGURE 6 | Effect of sodium silicate seed priming on cell membrane stability. Each data point represents the mean of three samples ±SD. Bars with different alphabet are significantly different ($p < 0.05$ and $P > 0.01$) according to Tukey's (HSD).

improved growth and survival of plants (Xu et al., 2018; Annunziata et al., 2019). Silicon applications have regulated the osmolytes as a mechanistic approach to induce drought tolerance in different species of plants (Yang et al., 2017; Hasanuzzaman et al., 2018). In our case, there was a significant and linear increase in GB with increasing SS priming concentrations compared to the control under water-deficit and normal conditions. Therefore, the SS-mediated increase of GB in flag leaves has been suggested as a positive factor that elicits water-deficit tolerance in wheat plants.

Water-deficit conditions generally induce negative impacts on the chlorophyll content, resulting in a reduced photosynthetic activity (Chen et al., 2016; Hussain et al., 2019). In our case, SS priming produced significant increases in chl a, chl b, and total chl in flag leaves, suggesting the stress-mitigating role of Si under mild water-deficit conditions. Further, treatment with 60 mM SS caused a significant increase in total carotenoids under stress. In general, drought caused a significant reduction in carotenoid content in plants. They have been suggested as important precursors of plant hormones and accessory pigments for photosynthesis (Mibei et al., 2017). Foliar applications of Si also increased the photosynthetic pigments, including carotenoids, in wheat under normal and drought conditions (Maghsoudi et al., 2016). In a very recent study, silicon fertilization improved chlorophyll and carotenoids in sugarcane cultivars grown under water-deficit conditions (De Camargo et al., 2019). Thus, in our study, the silicon-mediated increase in photosynthetic pigments and carotenoids has been correlated to its stress alleviatory role for sustainable productivity.

In our case, the priming treatments resisted the negative impacts of mild water-deficit conditions and exhibited a significant increase in CMS in flag leaves. The increase in CMS has also been justified by a low MDA, a higher antioxidant potential, and higher amounts of osmolytes owing to the Si-regulated metabolic, biochemical, and signaling processes under mild water-deficit conditions. The increased CMS and the higher content of osmolytes developed osmoregulation, which significantly improved the relative water contents in flag leaves. Exogenous applications of Si have also been known to improve the CMS and water status in a variety of plants under different stress conditions (Bybordi, 2015; Maghsoudi et al., 2016; Altuntas et al., 2018).

All SS priming treatments induced biochemical alterations, consequently improving yield, plant biomass, and the 100-grain weight of wheat plants grown under mild water-deficit and normal conditions. The improvement of the yield parameters at the whole plant stage indicates the induction of priming memory in SS-primed seeds, which elicited water-deficit tolerance until the maturity of plants. Therefore, silicon-mediated priming memory in primed seeds enabled them to tolerate water deficit at the seed germination, seedling growth, and plant development stages, thus ensuring sustainable productivity with long-lasting stress acclimation.

CONCLUSION

The silicon-mediated priming effects elicited water-deficit resistance in wheat plants by upregulating the antioxidant and hydrolytic enzymes with an increased level of osmoprotectants. Further, it induced a significant reduction in proline and MDA contents, representing a lesser ROS production that resulted in enhanced cell membrane stability. The improvement in the yield parameters at the whole plant stage indicated the induction of priming-mediated biochemical alterations in SS-primed seeds that invoked water-deficit acclimation until the maturity of plants, ensuring climate-smart growth of wheat.

DATA AVAILABILITY STATEMENT

The original contributions presented in the study are included in the article/**Supplementary Material**, further inquiries can be directed to the corresponding author/s.

AUTHOR CONTRIBUTIONS

ArH conducted the experiments and analysis of data, and performed the priming, growth, germination studies, and biochemical analyses. TF contributed to the data interpretation and manuscript writing. AmH supervised the priming, growth, germination studies, and biochemical analyses. MS proposed the research plan and supervised the priming, growth, germination studies, and biochemical analyses. All authors contributed to the article and approved the submitted version.

ACKNOWLEDGMENTS

This article is a part of the Ph.D. thesis of the corresponding author entitled "Biochemical Aspects of Drought Tolerance Induced by Seed Priming in Wheat."

SUPPLEMENTARY MATERIAL

The Supplementary Material for this article can be found online at: https://www.frontiersin.org/articles/10.3389/fpls.2021.625541/full#supplementary-material

REFERENCES

Abdel Latef, A. A., and Tran, L.-S. P. (2016). Impacts of priming with silicon on the growth and tolerance of maize plants to alkaline stress. *Front. Plant Sci.* 7:243. doi: 10.3389/fpls.2016.00243

Adda, A., Regagba, Z., Latigui, A., and Merah, O. (2014). Effect of salt stress on [Alpha]-amylase activity, sugars mobilization and osmotic potential of *Phaseolus vulgaris* L. Seeds Var.'Cocorose'and'Djadida'during germination. *J. Biol. Sci.* 14, 370–375. doi: 10.3923/jbs.2014.370.375

Ainsworth, E. A., and Gillespie, K. M. (2007). Estimation of total phenolic content and other oxidation substrates in plant tissues using Folin–Ciocalteu reagent. *Nat. Protoc.* 2:875. doi: 10.1038/nprot.2007.102

Ali, A. S., and Elozeiri, A. A. (2017). "Metabolic processes during seed germination," in *Advances in Seed Biology*, ed. J. C. Jimenez-Lopez (London: IntechOpen), 141.

Al-Jebory, E. I. (2012). Effect of water stress on carbohydrate metabolism during *Pisum sativum* seedlings growth. *Euphrates J. Agric. Sci.* 4, 1–12.

Altuntas, O., Dasgan, H. Y., and Akhoundnejad, Y. (2018). Silicon-induced salinity tolerance improves photosynthesis, leaf water status, membrane stability, and growth in pepper (*Capsicum annuum* L.). *HortScience* 53, 1820–1826. doi: 10.21273/hortsci13411-18

Amirjani, M., and Mahdiyeh, M. (2013). Antioxidative and biochemical responses of wheat to drought stress. *J. Agric. Biol. Sci.* 8, 291–301.

Annunziata, M. G., Ciarmiello, L. F., Woodrow, P., Dell'Aversana, E., and Carillo, P. (2019). Spatial and temporal profile of Glycine Betaine accumulation in plants under Abiotic stresses. *Front. Plant Sci.* 10:230. doi: 10.3389/fpls.2019.00230

Aranega-Bou, P., de la O Leyva, M., Finiti, I., García-Agustín, P., and González-Bosch, C. (2014). Priming of plant resistance by natural compounds. Hexanoic acid as a model. *Front. Plant Sci.* 5:488. doi: 10.3389/fpls.2014.00488

Arnon, D. I. (1949). Copper enzymes in isolated chloroplasts. Polyphenoloxidase in Beta vulgaris. *Plant Physiol.* 24, 1–15. doi: 10.1104/pp.24.1.1

Bano, A., Ullah, F., and Nosheen, A. (2012). Role of abscisic acid and drought stress on the activities of antioxidant enzymes in wheat. *Plant Soil Environ.* 58, 181–185. doi: 10.17221/210/2011-pse

Bates, L. S., Waldren, R. P., and Teare, I. (1973). Rapid determination of free proline for water-stress studies. *Plant Soil* 39, 205–207. doi: 10.1007/bf00018060

Bhardwaj, R. D., Kaur, L., and Srivastava, P. (2017). Comparative evaluation of different phenolic acids as priming agents for mitigating drought stress in wheat seedlings. *Proc. Natl. Acad. Sci. India B Biol. Sci.* 87, 1133–1142. doi: 10.1007/s40011-015-0690-y

Blum, A., and Ebercon, A. (1981). Cell membrane stability as a measure of drought and heat tolerance in wheat 1. *Crop Sci.* 21, 43–47. doi: 10.2135/cropsci1981.0011183x002100010013x

Bradford, M. M. (1976). A rapid and sensitive method for the quantitation of microgram quantities of protein utilizing the principle of protein-dye binding. *Anal. Biochem.* 72, 248–254. doi: 10.1016/0003-2697(76)90527-3

Bybordi, A. (2015). Influence of exogenous application of silicon and potassium on physiological responses, yield, and yield components of salt-stressed wheat. *Commun. Soil Sci. Plant Anal.* 46, 109–122. doi: 10.1080/00103624.2014.956936

Chance, B., and Maehly, A. (1955). Assay of catalases and peroxidases. *Methods Biochem. Anal.* 1, 357–424. doi: 10.1002/9780470110171.ch14

Chen, D., Wang, S., Cao, B., Cao, D., Leng, G., Li, H., et al. (2016). Genotypic variation in growth and physiological response to drought stress and Re-Watering reveals the critical role of recovery in drought adaptation in maize seedlings. *Front. Plant Sci.* 6:1241. doi: 10.3389/fpls.2015.01241

Chun, S. C., Paramasivan, M., and Chandrasekaran, M. (2018). Proline accumulation influenced by Osmotic stress in Arbuscular Mycorrhizal symbiotic plants. *Front. Microbiol.* 9:2525. doi: 10.3389/fmicb.2018.02525

De Camargo, M., Bezerra, B., Holanda, L., Oliveira, A., Vitti, A., and Silva, M. (2019). Silicon fertilization improves physiological responses in sugarcane cultivars grown under water deficit. *J. Soil Sci. Plant Nutr.* 19, 81–91. doi: 10.1007/s42729-019-0012-1

Drapeau, G. R. (1976). "Protease from Staphyloccus aureus," in *Methods in Enzymology*, Vol. 45, eds J. Abelson, M. Simon, G. Verdine, and A. Pyle (Amsterdam: Elsevier), 469–475. doi: 10.1016/s0076-6879(76)45041-3

Dubois, M., Gilles, K., Hamilton, J., Rebers, P., and Smith, F. (1951). A colorimetric method for the determination of sugars. *Nature* 168, 167–167.

Easwar Rao, D., and Viswanatha Chaitanya, K. (2020). Changes in the antioxidant intensities of seven different soybean (*Glycine max* (L.) Merr.) cultivars during drought. *J. Food Biochem.* 44:e13118.

Giannopolitis, C. N., and Ries, S. K. (1977). Superoxide dismutases: I. Occurrence in higher plants. *Plant Physiol.* 59, 309–314. doi: 10.1104/pp.59.2.309

Grieve, C., and Grattan, S. (1983). Rapid assay for determination of water soluble quaternary ammonium compounds. *Plant Soil* 70, 303–307. doi: 10.1007/bf02374789

Guan, X. K., Song, L., Wang, T. C., Turner, N., and Li, F. M. (2015). Effect of drought on the gas exchange, chlorophyll fluorescence and yield of six different−era spring wheat cultivars. *J. Agron. Crop Sci.* 201, 253–266. doi: 10.1111/jac.12103

Guo, Q., Wang, Y., Zhang, H., Qu, G., Wang, T., Sun, Q., et al. (2017). Alleviation of adverse effects of drought stress on wheat seed germination using atmospheric dielectric barrier discharge plasma treatment. *Sci. Rep.* 7:16680.

Habib, N., Ali, Q., Ali, S., Javed, M. T., Haider, M. Z., Perveen, R., et al. (2020). Use of nitric oxide and hydrogen peroxide for better yield of wheat (*Triticum aestivum* L.) under water deficit conditions: growth, osmoregulation, and Antioxidative defense mechanism. *Plants* 9:285. doi: 10.3390/plants9020285

Hameed, A., Hameed, A., Farooq, T., Noreen, R., Javed, S., Batool, S., et al. (2019). Evaluation of structurally different benzimidazoles as priming agents, plant defence activators and growth enhancers in wheat. *BMC Chem.* 13:29. doi: 10.1186/s13065-019-0546-2

Hameed, A., and Iqbal, N. (2014). Chemo-priming with mannose, mannitol and H 2 O 2 mitigate drought stress in wheat. *Cereal Res. Commun.* 42, 450–462. doi: 10.1556/crc.2013.0066

Hasanuzzaman, M., Nahar, K., Anee, T., Khan, M., and Fujita, M. (2018). Silicon-mediated regulation of antioxidant defense and glyoxalase systems confers drought stress tolerance in *Brassica napus* L. *S. Afr. J. Bot.* 115, 50–57. doi: 10.1016/j.sajb.2017.12.006

Heath, R. L., and Packer, L. (1968). Photoperoxidation in isolated chloroplasts: I. kinetics and stoichiometry of fatty acid peroxidation. *Arch. Biochem. Biophys.* 125, 189–198. doi: 10.1016/0003-9861(68)90654-1

Heuer, B. (2010). "Role of proline in plant response to drought and salinity," in *Handbook of Plant and Crop Stress*, ed. M. Pessarakli (Boca Raton: CRC Press).

Hussain, H. A., Men, S., Hussain, S., Chen, Y., Ali, S., Zhang, S., et al. (2019). Interactive effects of drought and heat stresses on morpho-physiological attributes, yield, nutrient uptake and oxidative status in maize hybrids. *Sci. Rep.* 9:3890. doi: 10.1038/s41598-019-40362-7

Karim, M. R., Zhang, Y. Q., Zhao, R. R., Chen, X. P., Zhang, F. S., and Zou, C. Q. (2012). Alleviation of drought stress in winter wheat by late foliar application of zinc, boron, and manganese. *J. Plant Nutr. Soil Sci.* 175, 142–151. doi: 10.1002/jpln.201100141

Khattab, H., Emam, M., Emam, M., Helal, N., and Mohamed, M. (2014). Effect of selenium and silicon on transcription factors NAC5 and DREB2A involved in drought-responsive gene expression in rice. *Biol. Plant.* 58, 265–273. doi: 10.1007/s10535-014-0391-z

Li, S., Li, X., Wei, Z., and Liu, F. (2020). ABA-mediated modulation of elevated CO2 on stomatal response to drought. *Curr. Opin. Plant Biol.* 56, 174–180. doi: 10.1016/j.pbi.2019.12.002

Liu, B., Soundararajan, P., and Manivannan, A. (2019). Mechanisms of silicon-mediated amelioration of salt stress in plants. *Plants* 8:307. doi: 10.3390/plants8090307

Maghsoudi, K., Emam, Y., and Pessarakli, M. (2016). Effect of silicon on photosynthetic gas exchange, photosynthetic pigments, cell membrane stability and relative water content of different wheat cultivars under drought stress conditions. *J. Plant Nutr.* 39, 1001–1015. doi: 10.1080/01904167.2015.1109108

Martinez, M., Gómez-Cabellos, S., Giménez, M. J., Barro, F., Diaz, I., and Diaz-Mendoza, M. (2019). Plant Proteases: from key enzymes in germination to allies for fighting human gluten-related disorders. *Front. Plant Sci.* 10:721. doi: 10.3389/fpls.2019.00721

Mibei, E. K., Ambuko, J., Giovannoni, J. J., Onyango, A. N., and Owino, W. O. (2017). Carotenoid profiling of the leaves of selected African eggplant accessions subjected to drought stress. *Food Sci. Nutr.* 5, 113–122. doi: 10.1002/fsn3.370

Miller, G. L. (1959). Use of dinitrosalicylic acid reagent for determination of reducing sugar. *Anal. Chem.* 31, 426–428. doi: 10.1021/ac60147a030

Mohanty, S., Nayak, A. K., Swain, C. K., Dhal, B., Kumar, A., Tripathi, R., et al. (2020). Silicon enhances yield and nitrogen use efficiency of tropical low land rice. *Agron. J.* 112, 758–771. doi: 10.1002/agj2.20087

O'Hara, L. E., Paul, M. J., and Wingler, A. (2013). How do sugars regulate plant growth and development? New insight into the role of trehalose-6-phosphate. *Mol. Plant* 6, 261–274. doi: 10.1093/mp/sss120

Pang, Z., Tayyab, M., Islam, W., Tarin, M. W. K., Sarfraz, R., Naveed, H., et al. (2019). Silicon mediated improvement in tolerance of economically important crops under drought stress. *Appl. Ecol. Environ. Res.* 17, 6151–6170.

Parveen, A., Liu, W., Hussain, S., Asghar, J., Perveen, S., and Xiong, Y. (2019). Silicon priming regulates morpho-physiological growth and oxidative metabolism in Maize under drought stress. *Plants* 8:431. doi: 10.3390/plants8100431

Peters, R. D., and Noble, S. D. (2014). Spectrographic measurement of plant pigments from 300 to 800 nm. *Remote Sens. Environ.* 148, 119–123. doi: 10.1016/j.rse.2014.03.020

Poonam, R. B., Handa, N., Kaur, H., Rattan, A., and Bali, S. (2016). "Sugar signalling in plants: a novel mechanism for drought stress management," in *Water Stress and Crop Plants*, ed. P. Ahmad (Hoboken, NJ: Wiley), 287–302. doi: 10.1002/9781119054450.ch19

Sattar, A., Cheema, M., Abbas, T., Sher, A., Ijaz, M., Wahid, M., et al. (2017). Physiological response of late sown wheat to exogenous application of silicon. *Cereal Res. Commun.* 45, 202–213. doi: 10.1556/0806.45.2017.005

Savvides, A., Ali, S., Tester, M., and Fotopoulos, V. (2016). Chemical priming of plants against multiple abiotic stresses: mission possible? *Trends Plant Sci.* 21, 329–340. doi: 10.1016/j.tplants.2015.11.003

Singh, V. K., Singh, R., Tripathi, S., Devi, R. S., Srivastava, P., Singh, P., et al. (2020). "Seed priming: state of the art and new perspectives in the era of climate change," in *Climate Change and Soil Interactions*, eds M. N. V. Prasad and M. Pietrzykowski (Amsterdam: Elsevier), 143–170. doi: 10.1016/b978-0-12-818032-7.00006-0

Sofo, A., Scopa, A., Nuzzaci, M., and Vitti, A. (2015). Ascorbate peroxidase and catalase activities and their genetic regulation in plants subjected to drought and salinity stresses. *Int. J. Mol. Sci.* 16, 13561–13578. doi: 10.3390/ijms160613561

Teh, S. Y., and Koh, H. L. (2016). Climate change and soil salinization: impact on agriculture, water and food security. *Int. J. Agric. For. Plant.* 2, 1–9. doi: 10.1002/9781119180661.ch1

Varavinit, S., Chaokasem, N., and Shobsngob, S. (2002). Immobilization of a thermostable alpha-amylase. *Sci. Asia* 28, 247–251.

Wang, J. Y., Turner, N. C., Liu, Y. X., Siddique, K. H., and Xiong, Y. C. (2017). Effects of drought stress on morphological, physiological and biochemical characteristics of wheat species differing in ploidy level. *Funct. Plant Biol.* 44, 219–234. doi: 10.1071/fp16082

Wang, X., Cai, X., Xu, C., Wang, Q., and Dai, S. (2016). Drought-responsive mechanisms in plant leaves revealed by proteomics. *Int. J. Mol. Sci.* 17:1706. doi: 10.3390/ijms17101706

Wang, Z., Li, G., Sun, H., Ma, L., Guo, Y., Zhao, Z., et al. (2018). Effects of drought stress on photosynthesis and photosynthetic electron transport chain in young apple tree leaves. *Biol. Open* 7:bio035279. doi: 10.1242/bio.035279

Wojtyla, Ł, Lechowska, K., Kubala, S., and Garnczarska, M. (2016). Molecular processes induced in primed seeds—increasing the potential to stabilize crop yields under drought conditions. *J. Plant Physiol.* 203, 116–126. doi: 10.1016/j.jplph.2016.04.008

Xu, Z., Sun, M., Jiang, X., Sun, H., Dang, X., Cong, H., et al. (2018). Glycinebetaine biosynthesis in response to osmotic stress depends on Jasmonate signaling in watermelon suspension cells. *Front. Plant Sci.* 9:1469. doi: 10.3389/fpls.2018.01469

Yang, L., Han, Y., Li, P., Li, F., Ali, S., and Hou, M. (2017). Silicon amendment is involved in the induction of plant defense responses to a phloem feeder. *Sci. Rep.* 7:4232.

Zlatev, Z. (2009). Drought-induced changes in chlorophyll fluorescence of young wheat plants. *Biotechnol. Biotechnol. Equip.* 23, 438–441. doi: 10.1080/13102818.2009.10818458

Conflict of Interest: The authors declare that the research was conducted in the absence of any commercial or financial relationships that could be construed as a potential conflict of interest.

frontiers in Plant Science

ORIGINAL RESEARCH
published: 24 February 2021
doi: 10.3389/fpls.2021.631768

Ascophyllum nodosum Extract (Sealicit™) Boosts Soybean Yield Through Reduction of Pod Shattering-Related Seed Loss and Enhanced Seed Production

*Łukasz Łangowski[1], Oscar Goñi[2], Fabio Serafim Marques[3], Osvaldo Toshiyuki Hamawaki[3], Carolina Oliveira da Silva[3], Ana Paula Oliveira Nogueira[4], Morgana Aparecida Justino Teixeira[3], Jacqueline Siqueira Glasenapp[3], Marcio Pereira[5] and Shane O'Connell[2]**

[1] Brandon Bioscience, Tralee, Ireland, [2] Plant Biostimulant Group, Shannon Applied Biotechnology Centre, Munster Technological University Kerry, Tralee, Ireland, [3] Instituto de Ciências Agrárias, Universidade Federal de Uberlândia/UFU, Uberlândia, Brazil, [4] Instituto de Biotecnologia, Universidade Federal de Uberlândia/UFU, Uberlândia, Brazil, [5] Fundação Educacional de Ituverava FAFRAM, Faculdade Agronomia, Ituverava, Brazil

OPEN ACCESS

Edited by:
Youssef Rouphael,
University of Naples Federico II, Italy

Reviewed by:
Alan T. Critchley,
Cape Breton University, Canada
Tommaso Frioni,
Catholic University of the Sacred Heart, Piacenza, Italy

***Correspondence:**
Shane O'Connell
shane.oconnell@staff.ittralee.ie

Specialty section:
This article was submitted to Crop and Product Physiology, a section of the journal Frontiers in Plant Science

Received: 20 November 2020
Accepted: 25 January 2021
Published: 24 February 2021

Citation:
Łangowski Ł, Goñi O, Marques FS, Hamawaki OT, da Silva CO, Nogueira APO, Teixeira MAJ, Glasenapp JS, Pereira M and O'Connell S (2021) *Ascophyllum nodosum* Extract (Sealicit™) Boosts Soybean Yield Through Reduction of Pod Shattering-Related Seed Loss and Enhanced Seed Production. Front. Plant Sci. 12:631768. doi: 10.3389/fpls.2021.631768

Soybean is one of the most valuable commercial crops because of its high protein, carbohydrate, and oil content. The land area cultivated with soybean in subtropical regions, such as Brazil, is continuously expanding, in some instances at the expense of carbon storing natural habitats. Strategies to decrease yield/seed losses and increase production efficiency are urgently required to meet global demand for soybean in a sustainable manner. Here, we evaluated the effectiveness of an *Ascophyllum nodosum* extract (ANE), Sealicit™, in increasing yields of different soybean varieties, in two geographical regions (Canada and Brazil). In addition, we investigated the potential of Sealicit™ to reduce pod shattering at the trials in Brazil. Three different concentrations of Sealicit™ were applied to pod shatter-susceptible (SS) UFUS 6901 and shatter-resistant (SR) UFUS 7415 varieties to assess their impact on pod firmness. SS variety demonstrated a significant decrease in pod shattering, which coincided with deregulation of *GmPDH1.1* and *GmSHAT1–5* expression, genes that determine pod dehiscence, and higher seed weight per pod. Sealicit™ application to the SR variety did not significantly alter its inherent pod shatter resistance, but provided higher increases in seed yield at harvest. This yield increase maybe associated with to other yield components stimulated by the biostimulant. This work demonstrates that Sealicit™, which has previously been shown to improve pod firmness in *Arabidopsis* and selected commercial oilseed rape varieties through *IND* gene down-regulation, also has the potential to improve pod resistance and seed productivity in soybean, a member of the legume family sharing a similar strategy for seed dispersal.

Keywords: seaweed, *Ascophyllum nodosum* extract, pod shattering, soybean (*Glycine max*), seed loss, sustainable agriculture, plant biostimulants

INTRODUCTION

The increased food production requirement, in the context of limited availability of arable land and a climate emergency driven by greenhouse gas emissions, makes the development of more efficient agricultural production a necessity. At the same time, consumer trends for consumption of more plant protein and less meat result in surging demand for plant proteins and oils that are very efficiently produced by legumes, especially soybean. Since 1961, the world production of soybean has increased 13-fold through the rapid expansion of the production area (from 23.8 to 124.9 Mha) and a significant boost of average harvested seed yield (from 1,128 to 2,791 kg/ha). In 2018, United States (35%), Brazil (34%), and Argentina (11%) produced approximately 80% of the world's harvested soybean, which is equivalent to almost 350 Mt (FAO, 2018) and steadily growing.

Soybean (*Glycine max*) is a relatively young crop; it is estimated that it was domesticated only 3,000–5,000 years ago in China (Prince et al., 2020), with subsequent cultivation spreading to other Asian regions. It is believed that during that time soybean acquired a number of shatter-resistant genes to impair an evolutionary-conserved seed dispersal mechanism (Dong et al., 2014). Current crops have been optimized for desired traits, starting from the selection by first farmers (Meng et al., 2013), through genome-wide association analysis (GWAS) combined with bioinformatics (Moreira et al., 2019). Independently of the method, the decrease of seed loss by dispersal and maximization of seed production was always the main goal. The major discoveries revealing the mechanism of seed dispersal are mostly attributed to the acquisition of *Arabidopsis thaliana* as a model plant system for fundamental research. *Arabidopsis*, a member of the Brassicaceae, develops a characteristic dry dehiscent fruit composed of two fused carpels that shatter the seeds through breaking of the dehiscence zones, along the silique, after maturity (Ferrándiz, 2002; Łangowski et al., 2016). Apart from *Arabidopsis*, several important genes involved in pod shattering, namely, *IND*, *ALC*, *SHP1*, *SHP2*, and *FUL*, and their complex regulatory network involved in pod dehiscence, were identified in a number of other members of the *brassicas* (Liljegren et al., 2000, 2004; Rajani and Sundaresan, 2001; Lewis et al., 2006; Girin et al., 2011; Pabón-Mora et al., 2014; Balanzà et al., 2016) such as *Capsella rubella* (Eldridge et al., 2016; Dong et al., 2019) and *Brassica juncea* (Østergaard et al., 2006), *rapa* (Mongkolporn et al., 2003), or *napus* (Raman et al., 2014), as well as in rice and soybean (Konishi et al., 2006; Li et al., 2006; Suzuki et al., 2010; Funatsuki et al., 2014; Yoon et al., 2014; Dong and Wang, 2015). In contrast to the bicarpellate silique of crucifers, legumes (including soybean) develop a fruit consisting of a single carpel fused on both sides. The pod walls, composed of several layers and cell types, are connected along the ventral and dorsal sutures. The opening of the soybean pod is triggered by the tension built inside the senescing pod and starts on the dorsal side (Tiwari and Bhatia, 1995; Zhang et al., 2018). Dong et al. (2014) found that excessive lignification of fiber cap cells (FCC) conferred the shatter-resistant phenotype. This process is controlled by SHATTERING1–5 (SHAT1–5), homologs to AtNST1/2, which is known to promote secondary wall biosynthesis. The same study compared gene expression between the wild allele and domesticated soybean, revealing that *SHAT1–5* was 15-fold higher expressed than its wild counterpart. In parallel, Funatsuki et al. (2014) reported another major QTL (quantitative trait locus) involved in soybean pod shattering. Complementation assays showed that *POD DEHISCENCE1* (*GmPDH1.1*) was found to be highly expressed in inner sclerenchyma, which correlated with lignin deposition. *GmPDH1.1* encodes a dirigent-like protein involved in lignin biosynthesis (Suzuki et al., 2010) and pod dehiscence by increasing the twisting force in the pod wall (Dong and Wang, 2015). Therefore, the loss-of-function of *Gmpdh1* has been widely used as a shattering-resistant gene in soybean breeding (Funatsuki et al., 2014). Additionally, more than half of Chinese landraces and most of South Asian landraces were shown to possess *PDH1* and its shatter-resistant *pdh1* allele, which suggested that *pdh1* was indispensable to effectively grow soybean in a dry climate (Kaga et al., 2012; Funatsuki et al., 2014). The soybean pod is designed to withstand the natural fluctuations of humidity and temperature; however, the longer it stays in the field and the more cycles of wetting/drying occur, the higher the chance the pods will burst open with loss of the seeds to the soil. Unfortunately, because of rapidly changing weather conditions, with unexpectedly long periods of drought or rainfall and therefore delayed harvest, soybean shattering in the field, or during harvest, are becoming more frequent. These factors have been directly correlated to higher losses (Menezes et al., 2018; Zhang et al., 2018; Silveira et al., 2019), averaging 120 kg/ha in Brazil (Schanoski et al., 2011), or up to 319 kg/ha in the Southeastern United States (Philbrook and Oplinger, 1989).

In the last decade, a class of crop inputs known as plant biostimulants has gained significant attention for improving plant productivity. Plant biostimulants, especially those extracted from the brown alga *Ascophyllum nodosum*, have been reported to deliver a number of benefits to plants/crops (Craigie, 2011; Vera et al., 2011; Sharma et al., 2013; Ali et al., 2016; Goñi et al., 2016, 2018; Shukla et al., 2018, 2019; Carmody et al., 2020). Previously, we reported the efficacy of a specialty *A. nodosum* extract (ANE) biostimulant, namely, Sealicit™, and explored the mode of action (MOA) in reducing pod dehiscence in *A. thaliana* and winter oilseed rape (WOSR) (Łangowski et al., 2019). Sealicit™ is a novel ANE containing PSI-759 biomolecule complex, produced using a targeted plant signal induction (PSI) approach to formulation development. In this study, the goal was to test the efficacy of Sealicit™ in increasing yield and conferring pod shattering resistance in another major podded crop, soybean. The impact of Sealicit™ on soybean yield was assessed using a randomized block field trial design at two distinct geographical locations (Canada and Brazil) with four different varieties. Employing multiple experimental approaches, the impact of Sealicit™ on plant and pod phenotypic traits and pod firmness were assessed for two Brazilian soybean varieties UFUS 6901 [shattering-susceptible (SS)] and UFUS 7415 [shattering-resistant (SR)] (Bicalho et al., 2019). In order to decipher the MOA at the molecular level, the expression of soybean pod shattering genes, *GmPDH1.1* and *GmSHAT1–5* were also evaluated. Overall, the current studies aimed to further support the efficacy of a specialty biostimulant from

A. nodosum, with a defined composition, to reduce seed loss and increase yields in crops producing dry pods, bringing exciting opportunities for sustainable agriculture.

MATERIALS AND METHODS

Study Site, Experimental Conditions, and Treatment Application

The field trials in Canada were conducted in 2017 on two commercial glyphosate herbicide-resistant varieties (McLeod R2 referred to as V1 and NSC Austin RR2Y referred to as V2 throughout the manuscript). V1 and V2 varieties were evaluated in Minto midwestern Ontario (located at 49°24′26″ N, 100°01′26″ W and 474-m altitude) and Elm Creek, Manitoba (located at 49°40′34″ N, 97°59′32″ W and 252-m altitude), respectively. V1 was seeded on May 17, 2017, and harvested on September 28, 2017. V2 variety was seeded on May 11, 2017, and harvested on September 29, 2017. The climate for both locations is classified as humid continental climate (Dfa) according the Köppen climate classification. A mean temperature of 15.8°C, ranging from 4.6 to 25.8°C, and a mean accumulated precipitation of 262.8 mm was recorded during the trial with V1 in Minto. The V2 trial was characterized by a mean temperature of 22.5°C, ranging from 5.2 to 27.5°C, and a mean accumulated precipitation of 284.5 mm. The soil type for clay loam and loamy sand for V1 and V2 field trials, respectively, and the previous crop in both sites was flax. V1 variety has an early cycle (124 days until harvest) with average *Sclerotinia* resistance and high seed yield potential (3.3 Mt/ha). V2 has an early cycle (124 days until harvest), superior white mold resistance, and high seed yield potential (3.2 Mt/ha). Soybeans were sown by mechanical drilling with a row space of 20 cm, at a seed rate of 140 and 100 kg/ha for V1 and V2, respectively. The pest management program consisted of the application of the herbicide Round-up (900 g/ha, Bayer) and the insecticide Matador (83 mL/ha; Syngenta).

Sealicit^{TM} is a proprietary PSI-759 ANE produced under high temperatures and alkaline conditions through a targeted PSI approach to formulation development and was provided by Brandon Bioscience (Tralee, Ireland). Sealicit^{TM} was applied at 1.5 L/ha by single foliar spray at vegetative stage V2–V3, which corresponds to the stage 14–16 according to the soybean BBCH scale (SoyBase, 2020). This system is used for uniform coding for phenologically similar growth stages of all monocotyledonous and dicotyledonous plant species (Hack et al., 1992). A portable CO_2 spraying system at a constant pressure of 2.76 bars was used to apply an equivalent volume of 100 L/ha. Control plants were sprayed with an equal volume of water. The experimental design was a randomized block design with four replicates per condition and each plot was 9 m^2.

The field experiments in Brazil were conducted at the FAFRAM experimental station located in the city of Ituverava-SP (20°00′00″ S, 47°47′20″ W and 631-m altitude) between December 2, 2019, and March 25, 2020. The climate is classified as a tropical wet and dry climate (*Aw*) according the Köppen climate classification. A mean temperature of 25.2°C, ranging from 13.6°C to 34.9°C, and a mean accumulated precipitation of 250.7 mm were recorded during the field trial period in the weather observing station INM759 of Ituverava [20°36′00″ S, 47°77′00″ W and 613-m altitude (Agritempo, 2020)]. The soil type was red clay latosol, and the previous crop grown in the field trial site was soybean. Both tested commercial soybean varieties were provided by the Soybean Improvement Program of the Federal University of Uberlândia (UFU, 2020). SS variety (UFUS 6901) has a very early cycle (108 days until harvest) with resistance to the nematode *Pratylenchus brachyurus* and high seed potential yield (3.9 Mt/ha). SR variety (UFUS 7415) has an early cycle (110 days until harvest) and is highly resistant to Asian soybean rust (*Phakopsora pachyrhizi*) with tolerance to drought stress and high seed potential yield (4.3 Mt/ha) (Hamawaki et al., 2018). Soybeans were sown by mechanical drilling with a row space of 50 cm, at a seed rate of 65.3 kg/ha, on December 2, 2019, with the fertilizer application of 340 kg/ha of formulated 04-14-08 (NPK). The pest management program consisted of the application of the broad-spectrum insecticide Kaiso (100 mL/ha; Nufarm), the post emergent herbicide Dribble (400 mL/ha; Sumitomo), and the systemic fungicide Fox (500 mL/ha; Bayer). Sealicit^{TM} was applied by single foliar spray at vegetative stage V5–V7, before the emergence of the inflorescence, which corresponds to stages 16–18 according to the soybean BBCH scale. Dosage rates were 0.75, 1.5, and 3.0 L/ha of Sealicit^{TM}. A portable CO_2 spraying system at a constant pressure of 2.1 bars was used to apply an equivalent volume of 200 L/ha. Control plants were sprayed with an equal volume of water. The distance between the spray lance and the plants was 50 cm, promoting a better cover of the sprayed biostimulant on the leaf tissue. The experimental design was a randomized block design in a 4 × 2 factorial design (number of treatments × number of varieties) with 13 replicates per condition (156 plots per field trial). The plots measured 2 m wide by 5 m long (10 m^2) and had four rows. These rows were spaced 0.5 m; 0.5-m buffer zones were established for each plot, and only a central 4 m^2 was used for phenotypic determinations or sampling purposes. The final plant stand per plot averaged 43 for both soybean varieties.

Plant and Yield Measurements

In the Canadian trials, harvesting was performed using a calibrated plot combine, and final harvested plot yields were recorded for at least four independent biological replicates per variety and treatment with soybean seed yield extrapolated to kg/ha. In Brazil, plant and yield measurements were taken in at least eight independent biological replicates per variety and treatment. Three independent biological pod samples were collected per variety and treatment and pooled for further analysis. Plant height was measured from the surface of the soil to the end of the main stem (hypocotyl) at the stages of early flowering (R1; BBCH60) and full maturity (R8; BBCH89). Plant lodging was assessed visually according to the following scale (1–5); 1: almost all plants standing, 2: less than 25% plants show stem lodging, 3: 25–50% of plants show stem lodging, 4: 50–80% of plants show stem lodging, 5: 100% plants show stem lodging. The presence of Asian soybean rust disease pressure caused by the fungus *P. pachyrhizi* was assessed visually according a scale of one to five (1: no disease symptoms; 2: 25% plants

with disease symptoms; 3: 50% plants with disease symptoms; 4: 75% plants with disease symptoms; 5: 100% plants with disease symptoms). Soybean plants at stage R8 were harvested manually and processed by a soybean threshing machine. The seed yield was determined from the central 4-m^2 area of each plot. After weighing, the seed weight per plot was extrapolated to kg/ha.

Evaluation of Pod Shattering Resistance and Pod Phenotypic Traits

Soybean plants from the trials in Brazil were used for determination of pod firmness and evaluation of phenotypic traits. Before harvesting (114 days after sowing), five plants at full maturity (R8 stage or BBCH89 when the fruit ripening is complete) were picked randomly from each plot. Pods were collected randomly from these plants. In contrast to *Arabidopsis* and oilseed rape, where a mechanical test is the most common technique to measure pod firmness (Morgan et al., 2001), the oven drying method is the most convenient and widely accepted assessment of pod shattering resistance in soybean. The test implemented during the course of these field trials was based on peer-reviewed published methods with minor modifications (Funatsuki et al., 2014; Krisnawati and Adie, 2017; Krisnawatiorcid et al., 2020). First, harvested pod samples were allowed to equilibrate their moisture levels at room temperature. After this acclimatization period, pod length was measured using ImageJ software (available at[1]) with a minimum of 60 biological replicates (pods) per variety and treatment. Evaluation of pod shattering resistance and seed weight per pod was performed on five biological replicates with 20 pods per replicate. Pod shattering resistance was analyzed after incubating pod samples at 65°C for the time required to open ≥ 50% of the control pods (**Figure 2**). This time period was calibrated for both SS and SR varieties. Pod shattering was calculated as the percentage of open pods versus total number of pods. After completing the pod shattering resistance test, the same dried soybean pods were used to determine the average seed weight per pod.

RNA Isolation and qRT-PCR

RNA was obtained from soybean pods at stage R5 (BBCH 75–79), which corresponds to the stage 17b according to fruit developmental scale for the model plant *A. thaliana* (Smyth et al., 1990; Roeder and Yanofsky, 2006). Four green fruits per plant were collected from at least five plants per plot and immediately frozen in liquid nitrogen, ground, and stored in −80°C to prevent RNA degradation. All pods collected per plot were considered a single biological replicate. All samples were collected within 2 h of midday. For quantitative reverse transcriptase–polymerase chain reaction (qRT-PCR) analysis, at least three biological replicates of each treatment and variety were analyzed. Three technical replicates per biological replicate were analyzed. Expression analyses were performed by real-time PCR using a Roche LightCycler 96 System (Roche, United Kingdom). Quantitative PCR was performed using the LightCycler RNA Master SYBR Green I one-step kit (Roche, United Kingdom) according to the manufacturer's instructions. The expression level of genes of interest was expressed in n-fold change and calculated according $2^{-\Delta\Delta CT}$ (Livak and Schmittgen, 2001). Primers used for qRT-PCR reactions are as follows: *GmPDH1* FW: 5′-GAGGGAGGCGTTTTACGAC-3′; REV: 5′-GACGTGGCAACCATGACTC-3′ (Funatsuki et al., 2014); *GmSHAT1–5* FW: 5′-GGAGAACCACCACAACACCA-3′; REV: 5′-GTCCGTGCCCATCTCTACTG-3′ (AHJ81058.1); *GmCYP2* FW: 5′-CGGGACCAGTGTGCTTCTTCA-3′; REV: 5′-CCCCTCCACTACAAAGGCTCG-3′ (Jian et al., 2008). *GmCYP2* was used as the reference gene for normalization.

Statistical Analysis

Statistics were evaluated with Sigma Plot 12 and Statgraphics Centurion XVI software. The seed yield differences between control and Sealicit™ treatment for V1 and V2 were analyzed using *t* test at $p \leq 0.05$. The effects of Sealicit™ on pod shattering, *GmPDH1* and *GmSHAT1–5* gene expression was analyzed with one-way analysis of variance (ANOVA) by Tukey honestly significant difference (HSD) test at $p \leq 0.05$. The rest of plant data were compared by using two-way ANOVA, with Tukey's HSD test at $p \leq 0.05$. Where the interaction between the two factors, variety (SS and SR) and Sealicit™ treatment (0, 0.75, 1.5, and 3 L/ha) (V × S), was significant, data were subjected to one-way ANOVA, comparing all Sealicit™ treatments with each other within the same soybean variety. Where V × S interaction was not significant, the effects of variety and Sealicit™ treatments were evaluated separately, comparing the respective means through *t* test (variety) or one-way ANOVA Tukey's HSD test (Sealicit™ treatment) at $p \leq 0.05$. The application of all parametric tests was performed after checking the normality of the data (Shapiro–Wilk test) and equal variance assumptions. Unless stated otherwise, all data are expressed as average ± standard error (SE). Details of the individual sample size for each analysis are mentioned in the tables and figure legends.

RESULTS

Effects of Sealicit™ on Soybean Seed Yield

The Canadian trial seed yields for control plots of both tested varieties (V1: 3,241 kg/ha; V2: 3,388 kg/ha) were similar to average values obtained by Canadian growers in the same growing season (V1: 3,256 kg/ha; V2: 3,188 kg/ha) (Manitoba Pulse Soybean Growers, 2017). The application of Sealicit™ in V1 at vegetative stage did produce a small statistically nonsignificant yield increase (+1.08%; $p = 0.796$). However, the V2 variety had a larger increase in yield of 4.91% ($p = 0.207$), producing 164 kg/ha more than control plots (**Figure 1**). The impact of Sealicit™ on yield in the Brazilian trials was also evaluated. A two-way ANOVA analysis demonstrated that Sealicit™ treatment had a statistically significant effect on seed yield ($p = 0.026$). This parameter was also highly affected by the interaction variety x Sealicit™ ($p = 0.047$) (**Table 1**). The SS variety had increased seed yield of 6.6% ($p = 0.078$) and

[1]https://imagej.net/Welcome

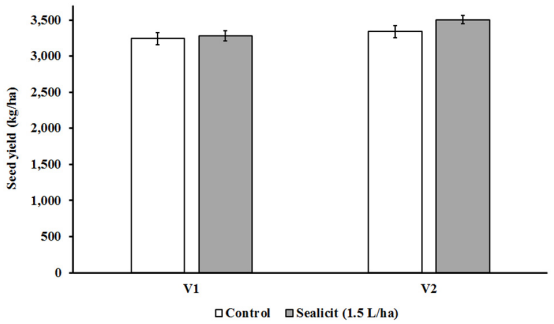

FIGURE 1 | Effects of Sealicit™ on seed yield in two commercial soybean varieties with glyphosate herbicide resistance. Sealicit™ was applied by foliar spray (1.5 L/ha) at vegetative stage (V2–V3), and its performance was benchmarked against untreated plants. Field trials with V1 and V2 were carried out in Minto (ON, Canada) and Elm Creek (MB, Canada) in 2017 under standard grower practice, respectively. Each bar represents seed yield (kg/ha). Number of biological replicates (n = 4).

6.2% (p = 0.154) at low (0.75 L/ha) and high (3 L/ha) doses, respectively. Only a minor increase of 2.2% (p = 0.555) was recorded at the 1.5 L/ha rate for the SS variety. Sealicit™ provided a more pronounced positive yield effect on the SR variety when it was applied at low (13.1%; p = 0.047) and medium (17.9%, p = 0.016) doses, respectively. However, only a small increase was recorded for the high Sealicit™ dose (1.9%; p = 0.774).

The Effects of Sealicit™ Treatment on Soybean Plant Development

The impact of soybean variety and Sealicit™ treatment on a number of plant phenotypic parameters including height, degree of lodging, and the prevalence of Asian soybean rust was assessed in both Brazilian varieties. A two-way ANOVA test revealed that in conjunction both parameters (variety × Sealicit™) had no significant effect on height or lodging parameters (**Table 2**). The SS plants showed an overall statistically significant increase of plant height at flowering (+9.2%; p = 0.006) and full maturity (+9.8%; $p \leq 0.001$) stage compared to SR plants. SS plants had increased their lodging degree 1.6 times compared to SR plants ($p \leq 0.001$); however, the absolute values of this parameter confirmed that less than 25% of the soybean plants were not erect. The effect of Sealicit™ on plant height and the degree of lodging were not statistically significant with respect to the control. Finally, soybean plants did not show any symptoms of Asian rust disease indicating the quality of the field trial (**Table 2**).

Effects of Sealicit™ on Pod Morphology

In order to assess whether Sealicit™ had any impacts on soybean pod growth and development, as reported previously for *Arabidopsis* and WOSR (Łangowski et al., 2019), the average fresh seed weight per pod and pod length were measured in SS and SR varieties. A two-way ANOVA revealed that Sealicit™ had a significant effect on the average fresh seed weight per pod (p = 0.024) (**Table 1**). In comparison to the control, the average fresh seed weight was the highest at 0.75 L/ha with the 3 L/ha application rate (7.1 and 9.5%), followed by a lower yet significant increase at the 1.5-L/ha application rate (2.4%). The two-way ANOVA test did not show any significant interactions across varieties and Sealicit™ treatments on pod length (p = 0.060). However, there was a significant increase in pod length in the SR, when compared to the SS variety ($p \leq 0.001$). When these differences were examined in detail, there were also significant differences between the treated and untreated plants ($p \leq 0.001$). Similarly, to seed weight per pod, the low and higher application rates, for both tested varieties, positively affected the pod length, which was longer by 2.5 and 3.4% as compared to control, respectively (**Table 1**).

TABLE 1 | Analysis of variance and mean comparisons for fresh seed weight per pod, pod length, and harvested seed yield at full maturity stage (R8) with two commercial soybean varieties treated with water and three concentrations of Sealicit™.

Source of variance	Seed weight/pod (g)	Pod length (cm)	Seed yield (kg/ha)
Variety (V)	NS	***	NS
Sealicit™ (S)	*	***	*
V × S	NS	NS	*
Variety			
SS	0.44 ± 0.01	4.04 ± 0.02 a	3, 691.4 ± 63.6
SR	0.44 ± 0.01	4.14 ± 0.02 b	3, 773.3 ± 66.3
Sealicit™			
Control	0.42 ± 0.01 a	4.03 ± 0.02 a	3, 522.2 ± 93.8 *a*
0.75 L/ha	0.45 ± 0.01 b	4.13 ± 0.02 b	3, 867.1 ± 86.9 *b*
1.5 L/ha	0.43 ± 0.01 ab	4.03 ± 0.02 a	3, 873.7 ± 86.9 *b*
3 L/ha	0.46 ± 0.01 b	4.18 ± 0.02 b	3, 666.4 ± 99.5 *a*
V × S			
SS + control	0.40 ± 0.02	3.98 ± 0.03	3, 558.4 ± 63.7 a
SS + 0.75 L/ha	0.46 ± 0.01	4.13 ± 0.04	3, 792.0 ± 79.4 ab
SS + 1.5 L/ha	0.43 ± 0.01	3.94 ± 0.03	3, 636.3 ± 59.8 a
SS + 3 L/ha	0.47 ± 0.02	4.13 ± 0.03	3, 779.0 ± 147.0 a
SR + control	0.43 ± 0.01	4.09 ± 0.03	3, 486.0 ± 169.9 a
SR + 0.75 L/ha	0.44 ± 0.01	4.12 ± 0.04	3, 942.2 ± 170.6 b
SR + 1.5 L/ha	0.43 ± 0.01	4.11 ± 0.03	4, 111.2 ± 111.4 b
SR + 3 L/ha	0.45 ± 0.00	4.23 ± 0.03	3, 553.8 ± 125.0 *a*

*NS, *, and ***, nonsignificant or significant at $p \leq 0.05$, and $p \leq 0.001$, respectively. Different letters indicate statistical differences for $p \leq 0.05$ based on t test (V) or one-way ANOVA Tukey's HSD test (S or V × S). Number of biological replicates (seed weight, n = 5; pod length, n ≥ 60; seed yield, n ≥ 8). ±represents standard error (SE).*

Effects of Sealicit™ on Pod Shattering Resistance

The effect of Sealicit™ and control treatments on the shatter resistance of harvested pods from the Brazilian field trial was assessed. As expected, the SS variety required a shorter calibration time (4 h) compared to the SR variety (48 h), demonstrating the sensitivity of the method used. Interestingly, when applying the same incubation times for the treated samples, we observed a strong effect of Sealicit™ on SS with very few pods bursting compared to the controls across all treatments ($p \leq 0.001$). This suggested that the lowest dose (0.75 L/ha) was sufficient to confer

TABLE 2 | Analysis of variance and mean comparisons for plant height at flowering (R1) and full maturity (R8) stage, lodging degree, and degree of Asian rust disease with two commercial soybean varieties, treated with water and three concentrations of Sealicit™.

Source of variance	Plant height flowering (cm)	Plant height maturity (cm)	Lodging degree (1–5)	Asian rust disease degree (1–5)
Variety (V)	**	***	***	NS
Sealicit™ (S)	NS	NS	NS	NS
V × S	NS	NS	NS	NS
Variety				
SS	84.2 ± 1.8b	95.1 ± 1.8b	2.2 ± 0.2b	1.0 ± 0.0
SR	77.1 ± 1.8a	86.6 ± 1.5a	1.4 ± 0.1a	1.0 ± 0.0
Sealicit™				
Control	81.4 ± 2.3	91.4 ± 2.5	1.7 ± 0.2	1.0 ± 0.0
0.75 L/ha	80.8 ± 2.8	91.2 ± 2.8	1.8 ± 0.3	1.0 ± 0.0
1.5 L/ha	81.6 ± 2.2	91.5 ± 2.3	1.8 ± 0.3	1.0 ± 0.0
3 L/ha	78.8 ± 2.7	89.3 ± 2.8	1.8 ± 0.2	1.0 ± 0.0
V × S				
SS + control	82.0 ± 2.8	93.3 ± 2.8	2.0 ± 0.4	1.0 ± 0.0
SS + 0.75 L/ha	82.6 ± 4.6	92.6 ± 4.5	2.1 ± 0.4	1.0 ± 0.0
SS + 1.5 L/ha	87.6 ± 2.5	98.4 ± 2.5	2.4 ± 0.4	1.0 ± 0.0
SS + 3 L/ha	82.4 ± 3.7	93.7 ± 3.7	2.0 ± 0.4	1.0 ± 0.0
SR + control	80.8 ± 3.7	89.6 ± 3.9	1.4 ± 0.2	1.0 ± 0.0
SR + 0.75 L/ha	76.9 ± 2.3	87.4 ± 2.2	1.3 ± 0.2	1.0 ± 0.0
SR + 1.5 L/ha	75.7 ± 2.4	84.6 ± 1.8	1.2 ± 0.1	1.0 ± 0.0
SR + 3 L/ha	75.1 ± 3.6	85.0 ± 3.6	1.7 ± 0.2	1.0 ± 0.0

*NS, **, and ***, nonsignificant or significant at $p \leq 0.01$, and $pp \leq 0.001$, respectively. Different letters indicate statistical differences for $p \leq 0.05$ based on t test (V) or one-way ANOVA Tukey's HSD test (S or V × S). Number of biological replicates ($n \geq 8$). ± represents standard error (SE).*

shattering resistance to the susceptible variety by decreasing pod opening by nearly fivefold. The SR samples showed minor decreases in shatter at low and high doses, but a slight increase at 1.5 L/ha dose; however, these fluctuations were not statistically significant (**Figure 2**).

Sealicit™ Affects the Development of Dehiscence Zone

To further assess the impact of Sealicit™ on pod shatter, the expression level of two major genes regulating pod dehiscence, *GmPDH1.1* (active in inner sclerenchyma) and *GmSHAT1–5* (active in FCCs), was examined (Funatsuki et al., 2014). The relative gene expression change was measured in reference to the housekeeping gene *CYCLOPHILIN2* (*CYP2*) (Jian et al., 2008). Funatsuki et al. (2014) showed that the transcript level of *GmPDH1.1*, which is involved in secondary wall biosynthesis and lignin deposition, decreased due to an early stop codon mutation, which is characteristic for pod-shatter resistant varieties. In our current studies, we observed that Sealicit™ significantly and gradually decreased *GmPDH1.1* expression in a concentration-dependent manner, in the variety SS (**Figure 3**). However, the expression analysis performed in the SR variety showed the opposite trend, which supports a variety-dependent effect. Next, the expression level of *GmSHAT1–5*, which similarly to *GmPDH1* is involved in secondary wall biosynthesis, was examined. Interestingly, the transcript level in pods collected from treated plants was increased in both varieties (**Figure 4**). The SR variety had a small increase that was statistically significant at the highest dose. On the other hand, a significant increase (1.6-fold) was observed for the SS variety, which is in agreement with *GmPDH1* expression level and the pod firmness test (**Figure 3**).

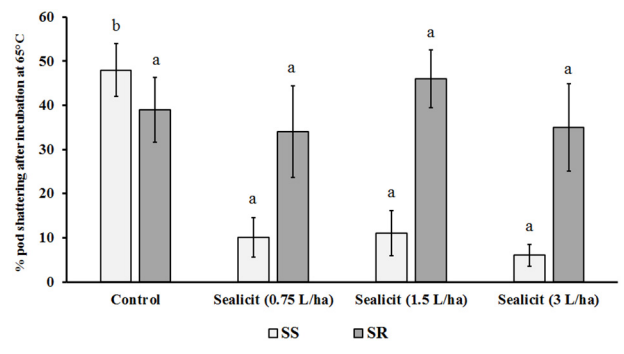

FIGURE 2 | Effects of Sealicit™ rate on soybean pod shattering. Each bar represents the percentage of open pods versus total number of pods. Different letters within the same soybean variety indicate statistically significant differences between the treatments based on one-way ANOVA Tukey's HSD test at $p \leq 0.05$. Number of biological replicates ($n = 5$).

DISCUSSION

Soybean (*G. max*) is one of the most important global crops because of its high protein and fat content. Its broad use for the production of food, oil, and fodder creates a continuously growing demand, having serious implications for the natural environment (Kocira et al., 2019). In order to reduce the

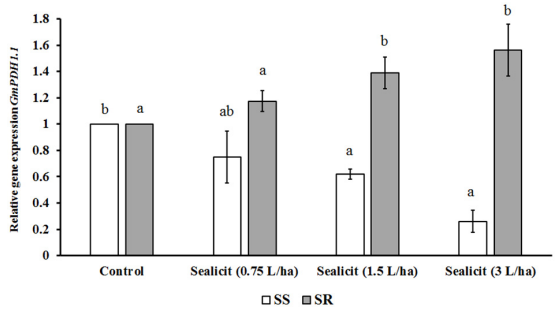

FIGURE 3 | Relative expression of *GmPDH1.1* in soybean pods treated with Sealicit™. Different letters within the same soybean variety indicate statistically significant differences between the treatments based on one-way ANOVA Tukey's HSD test at $p \leq 0.05$. Number of biological replicates ($n = 3$).

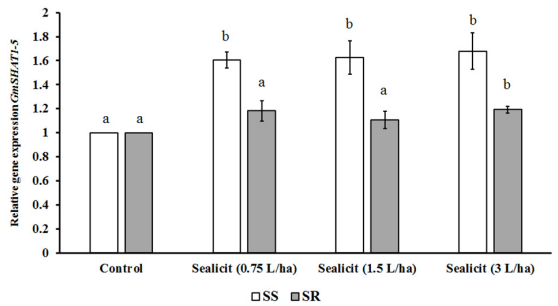

FIGURE 4 | Relative expression of *GmSHAT1–5* in soybean pods treated with Sealicit™. Different letters within the same soybean variety indicate statistically significant differences between the treatments based on one-way ANOVA Tukey's HSD test at $p \leq 0.05$. Number of biological replicates ($n = 3$).

impact of agricultural-related deforestation and pollution, new solutions for more efficient and sustainable soybean production are urgently needed. In our previous work, we have shown that ANE biostimulant Sealicit™ is capable of reducing pod shattering, influencing fruit development and yield in the model plant system *Arabidopsis*, as well as selected varieties of WOSR (Łangowski et al., 2019). Following on from the previous detailed analysis of Sealicit™ action, we have tested whether similar effects can be observed in soybean grown in field conditions. In this study, the impact of Sealicit™ on soybean productivity and pod shattering, as assessed by (i) testing pod-shatter in low humidity conditions and (ii) analyzing the expression level of major genes determining pod shattering, was determined. Productivity parameters were complemented with morphological analysis of plant height, seed weight per pod, pod length, and finally seed yield assessment. Here, we demonstrated that the same biostimulant can be successfully utilized not only in the Brassicaceae family species but also legumes, providing a new solution for a pressing problem.

Soybean Yield Evaluation

Sealicit™ field testing in Canada and Brazil using a randomized block field trial design showed consistent and agronomically sound yield results (**Table 1** and **Figure 1**). V1 and V2 seed yield values in control plots were very similar to average values obtained by Canadian growers in the same growing season (V1: 3,256 kg/ha; V2: 3,188 kg/ha, respectively) (Manitoba Pulse Soybean Growers, 2017). The effect of Sealicit™ appears to be variety specific, which is similar to that previously observed for WOSR. The yield increase for V2 was 4.91% with a $p = 0.207$. Although the p value did not meet the typical 0.05 scientific threshold, the magnitude of the yield increase was agronomically interesting, and it provided a basis for running additional trials with a larger number of replicates to reduce the p value. It should be noted that little information is available on the susceptibility of these short-cycle Canadian varieties to pod shatter, so additional trials were performed with soybean varieties with known shatter susceptibility to investigate the potential of Sealicit™ in this crop. The harvested seed yields at full maturity for the Brazilian varieties SS and SR were in the range expected in previous field trials developed in four consecutive sowing seasons in Uberlândia-MG (Bicalho et al., 2019). All treated soybean varieties with Sealicit™ produced increased yield with respect to their untreated counterparts. Yield increases were statistically significant with $p \leq 0.05$ for treatments, likely due to the higher replicate numbers versus the Canadian trials. It is evident that there was a significant interaction between the dose (0.75 and 1.5 L/ha) and the yield for the SR variety, which was not the case for the SS variety. Therefore, dose optimization on specific varieties may be important to gain maximum benefit from Sealicit™ in soybean crops.

Impact of Sealicit™ Treatments on Soybean Architecture and Pod Phenotype

While the SS variety was significantly taller than the SR variety, Sealicit™ did not demonstrate an ability to influence plant height. From published work on ANEs in soybean and tomato plants, we have learned that this class of plant biostimulants did not have a statistically significant effect on plant height despite yield increase (Guerreiro et al., 2017; Carmody et al., 2020). It indicates that this phenotypic trait may not be sufficient to predict yield benefits provided by ANE biostimulants. We have previously reported that Sealicit™ is able to increase the pod weight in *Arabidopsis* and seed weight of some WOSR varieties (Łangowski et al., 2019). Here we observed a substantial seed weight increase in both soybean varieties tested. This result is contrary to data published by Kocira et al. (2019), which presents a 1,000-soybean-seed weight decrease after foliar spray with a nonspecialty seaweed extract from *Ecklonia maxima*. This finding highlights the importance of the seaweed specie and the process used for extraction on bioactivity-related parameters of seaweed extract biostimulants (Goñi et al., 2016, 2018; Shukla et al., 2019; Carmody et al., 2020). Moreover, both soybean varieties showed an increased pod length, which is in agreement with Sealicit™ ability to dysregulate *FUL*, *RPL*, and *IND* expression and pod length in *Arabidopsis* and some WOSR varieties (Łangowski et al., 2019), suggesting that this specialized ANE biostimulant may also modulate soybean

pod auxin homeostasis and signaling, crucial for fruit growth and development (Liljegren et al., 2004; Sorefan et al., 2009; Dong et al., 2019).

Sealicit™ Impact on Pod Shattering Resistance and Pod Dehiscence Genes

Data derived from multiple trials in commercial WOSR varieties demonstrated a positive association between pod firmness and yield (Łangowski et al., 2019). Soybean pod architecture and dehiscence mechanism show significant differences in relation to Brassicaceae fruits, yet the principle of seed dispersal is still relying on lignin deposition that determines physical resistance (Dong et al., 2014; Funatsuki et al., 2014). Pod shattering resistance tests performed on soybean control pods showed variability in treated varieties, ranging from 4 h for SS to 48 h for SR, proving the robustness and sensitivity of the method. The difference in calibration time was to be expected as both varieties are genetically diverse (Bicalho et al., 2019). On the other hand, the SR variety, classified as resistant to shatter, showed no statistically significant improvement after Sealicit™ treatments, whereas the SS variety, classified as susceptible to pod shattering, showed a very significant fruit firmness increase across all the doses applied. In addition, Sealicit™ decreased *GmPDH1.1* and increased *GmSHAT1–5* expression in the SS variety, which is consistent with a reduction in shatter. Moreover, *GmPDH1.1* transcript levels were decreasing with increasing Sealicit™ concentration in SS variety, yet increasing in SR, indicating that the effect is dose and genome/variety dependent. It is important to note that the SR variety, despite showing insignificant increase in *GmPDH1.1* transcript level, also showed slight increase in *GmSHAT1–5*. Taking into account that the transcript levels of both might be extremely different, a small increase in SR *GmSHAT1–5* transcript could not only counteract the insignificant increase of *GmPDH1*, but also account for a small increase of SR in pod firmness test (**Figure 2**). Therefore, it is tempting to speculate that pod firmness in soybean fruit is a balance between the amount of the lignin deposited in the FCCs and inner sclerenchyma, which may be determined by multiple genes that ultimately regulate the dorsoventral tension. In order to gain an in-depth understanding of the mechanism and critical signaling pathways, transcriptome and proteome analysis of multiple genes involved in fruit development (i.e., *FUL*, *RPL*, *IND*, *SHP*, and *ALC*) (Ferrándiz, 2002), their mutants, and complementation lines are necessary (Dong and Wang, 2015). Most importantly, the enhanced productivity of SS was positively associated with *GmPDH1.1* and *GmSHAT1–5* gene expression, increased pod shattering resistance, and higher seed weight per pod. However, the seed yield increase in treated SR soybean plants was not clearly associated with any of the parameters evaluated in this study, being likely due to additional effects promoted by Sealicit™ that have not been the subject of investigation. As observed previously by Guerreiro et al. (2017), foliar applications of ANE biostimulant can stimulate additional yield-related parameters in soybean such as increased number of pods per plant, which could be one of the contributing factors. Briglia et al. (2019) also showed an improvement in soybean biovolume and green area after foliar spray treatment with different combinations of seaweed and plant extracts. Those additional benefits of ANE application could potentially account for increased seed weight and fresh seed yield in the SR variety.

Agronomical and Environmental Implications

The gradually increasing soybean production (by 4–5% annually) in Brazil means it will become the biggest world producer with an estimated 129 Mt in season 2020/2021. The harvested area is forecasted at a record 36.8 Mha, up by 1.7 Mha from last season's record (USDA, 2020). While soybean production in Brazil is growing, losses due to adverse weather conditions become more frequent (Rowntree et al., 2013; Van Roekel et al., 2015; Zhang et al., 2018). The Brazilian Agricultural Research Corporation (EMBRAPA) has established that one 60-kilo bag per hectare is an acceptable loss threshold value (Silveira et al., 2019). However, in the last 30 years, a wide range of yield losses (54–561 kg/ha) has been recorded in different regions of Brazil due to adverse weather events and delayed and/or inadequate mechanical harvesting (Chioderoli et al., 2012; Barbosa and Schmitz, 2015; Bandeira, 2017), averaging 120 kg/ha loss at a national level (Schanoski et al., 2011). In this study, we have demonstrated that this lost yield can be recovered and safeguarded using the ANE biostimulant Sealicit™ at a low dose rate (0.75 L/ha), increasing seed yield by an average of 9.8% in two commercial soybean varieties (+344.9 kg/ha). The use of the biostimulant would allow production output to grow in a sustainable manner contrary to expanding crop area. It is important to note that the yield uplift that can be obtained with Sealicit™ application provides a compelling return on investment for the grower (>3:1). According to the current average market price of soybean, growers will be able to obtain added revenues of $135/ha by applying Sealicit™ in the Brazilian market, which creates a strong financial incentive for the growers to switch to a more environment-friendly and sustainable agriculture.

Conclusions and Future Perspectives

ANE-based biostimulants are a rapidly growing crop input, because of their efficacy in a number of applications in modern agriculture. The investigations reported were undertaken to determine if Sealicit™ has an impact on pod development in soybean. The data generated suggest that Sealicit™ has a strong antishattering effect in a non–shatter-resistant soybean variety. It is also increasingly evident that Sealicit™ treatments, despite impacting on pod dehiscence, may have in some species and varieties accompanying effects stimulating average seed weight per pod and pod length, which ultimately reflects on yield. In order to gain a better understanding of Sealicit™'s MOA in soybean, lignin staining and transversal sections presenting fruit morphology and lignin deposition could be further analyzed. Pod shattering is determined by multiple contributing genes, which makes their identification challenging even by GWAS. Therefore, a lack of sufficient understanding of physiological and genetic mechanisms hinders improvements of such traits by intensive

breeding or genome editing (Verdugo et al., 2010; Korte and Farlow, 2013). Sealicit™ appears to provide a solution for a yield reducing concealed developmental trait that is pod shattering, not only in oilseed rape but also in soybean and possibly other species relying on similar, conserved, seed dispersal mechanisms. Biostimulants that mobilize genetic plant potential to achieve high-quality crop with maximum yield represent an attractive tool to currently applied methods for efficient food production.

DATA AVAILABILITY STATEMENT

The original contributions presented in the study are included in the article.

AUTHOR CONTRIBUTIONS

ŁŁ, OG, JG, OH, and SO'C conceived and designed the experiments. ŁŁ, FM, MT, MP, CS, and AN performed the experiments. ŁŁ, OG, OH, FM, and SO'C analyzed the data. ŁŁ, OG, and SO'C wrote the article. All authors contributed to the article and approved the submitted version.

FUNDING

This research has been conducted with the assistance of funding from the INNOWIDE call of the EU-Horizon 2020 Program under grant agreement No. 2019-1591 (SUSBEAN project).

ACKNOWLEDGMENTS

The authors would like to acknowledge the support of Luiz Ricardo Goulart's research group in the Nanobiotechnology Laboratory of the Federal University of Uberlândia-UFU for providing the equipment necessary for isolating RNA. The authors would also like to thank Brandon Bioscience for the gift of the ANE-based biostimulant Sealicit™ used in this study.

REFERENCES

Agritempo (2020). *Agromteorological Monitoring Sytem*. Available online at: http://www.agritempo.gov.br/agritempo/index.jsp (accessed May 17, 2017).

Ali, N., Farrell, A., Ramsubhag, A., and Jayaraman, J. (2016). The effect of *Ascophyllum nodosum* extract on the growth, yield and fruit quality of tomato grown under tropical conditions. *J. Appl. Phycol.* 28, 1353–1362. doi: 10.1007/s10811-015-0608-3

Balanzà, V., Roig-Villanova, I., Di Marzo, M., Masiero, S., and Colombo, L. (2016). Seed abscission and fruit dehiscence required for seed dispersal rely on similar genetic networks. *Development* 143, 3372–3381. doi: 10.1242/dev.135202

Bandeira, G. J. (2017). Perdas na Colheita da Soja em Diferentes Velocidades de Deslocamento da Colhedora.

Barbosa, E. J. A., and Schmitz, R. (2015). *Avaliação de Perdas na Colheita da Cultura da Soja na Região Noroeste do rio Grande do sul*. Available online at: https://docplayer.com.br/31039598-Avaliacao-de-perdas-na-colheita-dacultura-da-soja-na-regiao-noroeste-do-rio-grande-do-sul-erlei-jose-alessiobrabosa-1-ricardo-schmitz-2.html (accessed November 17, 2020).

Bicalho, T. F., Nogueira, A. P. O., Hamawaki, O. T., Costa, S. C., Júnior, I. J. D. M., Silva, N. S., et al. (2019). Adaptability and stability of soybean cultivars in four sowing seasons. *Biosci. J.* 35, 1450–1462. doi: 10.14393/BJ-v35n5a2019-42351

Briglia, N., Petrozza, A., Hoeberichts, F. A., Verhoef, N., and Povero, G. (2019). Investigating the impact of biostimulants on the row crops corn and soybean using high-efficiency phenotyping and next generation sequencing. *Agronomy*, 9:761. doi: 10.3390/agronomy9110761

Carmody, N., Goñi, O., Łangowski, Ł, and O'connell, S. (2020). Ascophyllum nodosum extract biostimulant processing and its impact on enhancing heat stress tolerance during tomato fruit set. *Front. Plant Sci.* 11:807. doi: 10.3389/fpls.2020.00807

Chioderoli, C. A., Silva, R. P. D., Noronha, R. H. D. F., Cassia, M. T., and Santos, E. P. D. (2012). Perdas de grãos e distribuição de palha na colheita mecanizada de soja. *Bragantia* 71, 112–121. doi: 10.1590/s0006-87052012005000003

Craigie, J. S. (2011). Seaweed extract stimuli in plant science and agriculture. *J. Appl. Phycol.* 23, 371–393. doi: 10.1007/s10811-010-9560-4

Dong, Y., Jantzen, F., Stacey, N., Łangowski, Ł, Moubayidin, L., Šimura, J., et al. (2019). Regulatory diversification of indehiscent in the capsella genus directs variation in fruit morphology. *Curr. Biol.* 29, 1038–1046.e4. doi: 10.1016/j.cub.2019.01.057

Dong, Y., and Wang, Y. Z. (2015). Seed shattering: from models to crops. *Front. Plant Sci.* 6:476. doi: 10.3389/fpls.2015.00476

Dong, Y., Yang, X., Liu, J., Wang, B. H., Liu, B. L., and Wang, Y. Z. (2014). Pod shattering resistance associated with domestication is mediated by a nac gene in soybean. *Nat. Commun.* 5:3352. doi: 10.1038/ncomms4352

Eldridge, T., Langowski, L., Stacey, N., Jantzen, F., Moubayidin, L., Sicard, A., et al. (2016). Fruit shape diversity in the brassicaceae is generated by varying patterns of anisotropy. *Development* 143, 3394–3406. doi: 10.1242/dev.135327

FAO (2018). *Food and Agriculture Organisation of United Nations*. Available online at: http://www.fao.org/faostat/en/#data/QC (accessed November 11, 2020)

Ferrándiz, C. (2002). Regulation of fruit dehiscence in arabidopsis. *J. Exp. Bot.* 53, 2031–2038. doi: 10.1093/jxb/erf082

Funatsuki, H., Suzuki, M., Hirose, A., Inaba, H., Yamada, T., Hajika, M., et al. (2014). Molecular basis of a shattering resistance boosting global dissemination of soybean. *Proc. Natl. Acad. Sci. U.S.A.* 111, 17797–17802.

Girin, T., Paicu, T., Stephenson, P., Fuentes, S., Körner, E., O'brien, M., et al. (2011). Indehiscent and spatula interact to specify carpel and valve margin tissue and thus promote seed dispersal in arabidopsis. *Plant Cell* 23, 3641–3653. doi: 10.1105/tpc.111.090944

Goñi, O., Fort, A., Quille, P., Mckeown, P. C., Spillane, C., and O'connell, S. (2016). Comparative transcriptome analysis of two ascophyllum nodosum extract biostimulants: same seaweed but different. *J. Agric. Food Chem.* 64, 2980–2989. doi: 10.1021/acs.jafc.6b00621

Goñi, O., Quille, P., and O'connell, S. (2018). *Ascophyllum nodosum* extract biostimulants and their role in enhancing tolerance to drought stress in tomato plants. *Plant Physiol. Biochem.* 126, 63–73. doi: 10.1016/j.plaphy.2018.02.024

Guerreiro, J. C., Blainski, E., da Silva, D. L., Caramelo, J. P., Pascutti, T. M., de Oliveira, N. C., et al. (2017). Effect of the seaweed extract applied on seeds and/or foliar sprays on soybean development and productivity. *J. Food Agric. Environ.* 15, 18–21.

Hack, H., Bleiholder, H., Buhr, L., Meier, U., Schnock-Fricke, U., Stauss, R., et al. (1992). Einheitliche codierung der phänologischen entwicklungsstadien mono- und dikotyler pflanzen. – erweiterte bbch-skala, allgemein Nachrichtenbl. *Deut. Pflanzenschutzd.* 44, 265–270.

Hamawaki, O. T., Hamawaki, R. L., Nogueira, A. P. O., Glasenapp, J. S., Hamawaki, C. D. L., Juliatti, F. C., et al. (2018). Development of brazilian soybean cultivars well adapted to cerrado and rust-tolerant. *Int. J. Adv. Eng. Res. Sci.* 5, 130–136.

Jian, B., Liu, B., Bi, Y., Hou, W., Wu, C., and Han, T. (2008). Validation of internal control for gene expression study in soybean by quantitative real-time pcr. *BMC Mol. Biol.* 9:59. doi: 10.1186/1471-2199-9-59

Kaga, A., Shimizu, T., Watanabe, S., Tsubokura, Y., Katayose, Y., Harada, K., et al. (2012). Evaluation of soybean germplasm conserved in nias genebank and

development of mini core collections. *Breed. Sci.* 61, 566–592. doi: 10.1270/jsbbs.61.566

Kocira, S., Szparaga, A., Kuboñ, M., Czerwińska, E., and Piskier, T. (2019). Morphological and biochemical responses of glycine max (l.) merr. To the use of seaweed extract. *Agronomy* 9:93. doi: 10.3390/agronomy9020093

Konishi, S., Izawa, T., Lin, S. Y., Ebana, K., Fukuta, Y., Sasaki, T., et al. (2006). An snp caused loss of seed shattering during rice domestication. *Science* 312, 1392–1396. doi: 10.1126/science.1126410

Korte, A., and Farlow, A. (2013). The advantages and limitations of trait analysis with gwas: a review. *Plant Methods* 9:29. doi: 10.1186/1746-4811-9-29

Krisnawati, A., and Adie, M. M. (2017). Identification of soybean genotypes for pod shattering resistance associated with agronomical and morphological characters. *Biosaintifika J. Biol. Biol. Educ.* 9:8. doi: 10.15294/biosaintifika.v9i2.8722

Krisnawatiorcid, A., Soegianto, A., Waluyo, B., and Kuswanto, K. (2020). The pod shattering resistance of soybean lines based on the shattering incidence and severity. *Czech J. Genet. Plant Breed.* 56, 111–122. doi: 10.17221/20/2020-CJGPB

Łangowski, Ł, Goñi, O., Quille, P., Stephenson, P., Carmody, N., Feeney, E., et al. (2019). A plant biostimulant from the seaweed ascophyllum nodosum (sealicit) reduces podshatter and yield loss in oilseed rape through modulation of ind expression. *Sci. Rep.* 9:16644. doi: 10.1038/s41598-019-52958-0

Łangowski, Ł, Stacey, N., and Ostergaard, L. (2016). Diversification of fruit shape in the brassicaceae family. *Plant Reprod.* 29, 149–163. doi: 10.1007/s00497-016-0278-6

Lewis, M. W., Leslie, M. E., and Liljegren, S. J. (2006). Plant separation: 50 ways to leave your mother. *Curr. Opin. Plant Biol.* 9, 59–65. doi: 10.1016/j.pbi.2005.11.009

Li, C., Zhou, A., and Sang, T. (2006). Rice domestication by reducing shattering. *Science* 311, 1936–1939. doi: 10.1126/science.1123604

Liljegren, S. J., Ditta, G. S., Eshed, Y., Savidge, B., Bowman, J. L., and Yanofsky, M. F. (2000). Shatterproof mads-box genes control seed dispersal in arabidopsis. *Nature* 404, 766–770. doi: 10.1038/35008089

Liljegren, S. J., Roeder, A. H., Kempin, S. A., Gremski, K., Østergaard, L., Guimil, S., et al. (2004). Control of fruit patterning in arabidopsis by indehiscent. *Cell* 116, 843–853. doi: 10.1016/s0092-8674(04)00217-x

Livak, K. J., and Schmittgen, T. D. (2001). Analysis of relative gene expression data using real-time quantitative pcr and the 2(-delta delta c(t)) method. *Methods* 25, 402–408. doi: 10.1006/meth.2001.1262

Manitoba Pulse Soybean Growers (2017). *Soybean Variety Guide*. Available online at: https://www.manitobapulse.ca/wp-content/uploads/2017/11/2017-Soybean-Variety-Guide-FINAL_WR.pdf (accessed May 17, 2017).

Menezes, P. C. D., Silva, R. P. D., Carneiro, F. M., Girio, L. A. D. S., Oliveira, M. F. D., and And Voltarelli, M. A. (2018). Can combine headers and travel speeds affect the quality of soybean harvesting operations? *Revist. Bras. Engenharia Agríc. Ambiental.* 20, 732–738. doi: 10.1590/1807-1929/agriambi.v22n10p732-738

Meng, Q., Hou, P., Wu, L., Chen, X., Cui, Z., and Zhang, F. (2013). Understanding production potentials and yield gaps in intensive maize production in china. *Field Crops Res.* 143, 91–97. doi: 10.1016/j.fcr.2012.09.023

Mongkolporn, O., Kadkol, G. P., Pang, E. C. K., and Taylor, P. W. J. (2003). Identification of rapd markers linked to recessive genes conferring siliqua shatter resistance in brassica rapa. *Plant Breed.* 122, 479–484. doi: 10.1046/j.0179-9541.2003.00910.x

Moreira, F. F., Hearst, A. A., Cherkauer, K. A., and Rainey, K. M. (2019). Improving the efficiency of soybean breeding with high-throughput canopy phenotyping. *Plant Methods* 15:139. doi: 10.1186/s13007-019-0519-4

Morgan, C. L., Ladbrooke, Z. L., Bruce, D. M., Child, R., and Arthur, A. E. (2001). Breeding oilseed rape for pod shattering resistance. *J. Agric. Sci.* 135, 347–359. doi: 10.1017/S0021859699008424

Østergaard, L., Kempin, S. A., Bies, D., Klee, H. J., and Yanofsky, M. F. (2006). Pod shatter-resistant brassica fruit produced by ectopic expression of the fruitfull gene. *Plant Biotechnol. J.* 4, 45–51. doi: 10.1111/j.1467-7652.2005.00156.x

Pabón-Mora, N., Wong, G. K.-S., and Ambrose, B. A. (2014). Evolution of fruit development genes in flowering plants. *Front. Plant Sci.* 5:300. doi: 10.3389/fpls.2014.00300

Philbrook, B. D., and Oplinger, E. S. (1989). Soybean field losses as influenced by harvest delays. *Agron. J.* 81, 251–258. doi: 10.2134/agronj1989.00021962008100020023x

Prince, S. J., Vuong, T. D., Wu, X., Bai, Y., Lu, F., Kumpatla, S. P., et al. (2020). Mapping quantitative trait loci for soybean seedling shoot and root architecture traits in an inter-specific genetic population. *Front. Plant Sci.* 11:1284. doi: 10.3389/fpls.2020.01284

Rajani, S., and Sundaresan, V. (2001). The arabidopsis myc/bhlh gene alcatraz enables cell separation in fruit dehiscence. *Curr. Biol.* 11, 1914–1922. doi: 10.1016/s0960-9822(01)00593-0

Raman, H., Raman, R., Kilian, A., Detering, F., Carling, J., Coombes, N., et al. (2014). Genome-wide delineation of natural variation for pod shatter resistance in brassica napus. *PLoS One* 9:e101673. doi: 10.1371/journal.pone.0101673

Roeder, A. H., and Yanofsky, M. F. (2006). Fruit development in arabidopsis. *Arabidopsis Book* 4:e0075. doi: 10.1199/tab.0075

Rowntree, S. C., Suhre, J. J., Weidenbenner, N. H., Wilson, E. W., Davis, V. M., Naeve, S. L., et al. (2013). Genetic gain × management interactions in soybean: I. Planting date. *Crop Sci.* 53, 1128–1138. doi: 10.2135/cropsci2012.03.0157

Schanoski, R., Righi, E. Z., and Werner, V. (2011). Perdas na colheita mecanizada de soja (glycine max) no município de maripá-pr. *Revist. Bras. Engenharia Agríc. Ambiental.* 15, 1206–1211. doi: 10.1590/s1415-43662011001100015

Sharma, S., Fleming, C., Selby, C., Rao, J., and Martin, T. (2013). Plant biostimulants: a review on the processing of macroalgae and use of extracts for crop management to reduce abiotic and biotic stresses. *J. Appl. Phycol.* 26, 465–490. doi: 10.1007/s10811-013-0101-9

Shukla, P. S., Borza, T., Critchley, A. T., Hiltz, D., Norrie, J., and Prithiviraj, B. (2018). Ascophyllum nodosum extract mitigates salinity stress in *Arabidopsis thaliana* by modulating the expression of mirna involved in stress tolerance and nutrient acquisition. *PLoS One* 13:e0206221. doi: 10.1371/journal.pone.0206221

Shukla, P. S., Mantin, E. G., Adil, M., Bajpai, S., Critchley, A. T., and Prithiviraj, B. (2019). *Ascophyllum nodosum*-based biostimulants: sustainable applications in agriculture for the stimulation of plant growth, stress tolerance, and disease management. *Front. Plant Sci.* 10:655.

Silveira, J., Conte, O., and Mesquita, C. D. M. (2019). *Determinação de Perdas de Grãos na Colheita de soja: Copo Medidor da Embrapa*. Available online at: https://www.infoteca.cnptia.embrapa.br/infoteca/handle/doc/979883?mode=full (accessed November 17, 2020).

Smyth, D. R., Bowman, J. L., and Meyerowitz, E. M. (1990). Early flower development in arabidopsis. *Plant Cell* 2, 755–767. doi: 10.1105/tpc.2.8.755

Sorefan, K., Girin, T., Liljegren, S. J., Ljung, K., Robles, P., Galvan-Ampudia, C. S., et al. (2009). A regulated auxin minimum is required for seed dispersal in arabidopsis. *Nature* 459, 583–586. doi: 10.1038/nature07875

SoyBase (2020). *Soybase Soybean Growth Stages Conversion Page*. Available online at: https://www.soybase.org/OntologyConversion.php (accessed May 17, 2017).

Suzuki, M., Fujino, K., Nakamoto, Y., Ishimoto, M., and Funatsuki, H. (2010). Fine mapping and development of DNA markers for the qpdh1 locus associated with pod dehiscence in soybean. *Mol. Breed.* 25, 407–418. doi: 10.1007/s11032-009-9340-5

Tiwari, S. P., and Bhatia, V. S. (1995). Characters of pod anatomy associated with resistance to pod-shattering in soybean. *Ann. Bot.* 76, 483–485. doi: 10.1006/anbo.1995.1123

UFU (2020). *Uberland Federal University Soybean Improvement Program. Soybean cultivars*. Available online at: http://www.pmsoja.iciag.ufu.br/ (accessed November 2020)

USDA (2020). *Oilseeds and Products Annual-Brazil*. Washington, DC: United States Department of Agriculture.

Van Roekel, R. J., Purcell, L. C., and Salmerón, M. (2015). Physiological and management factors contributing to soybean potential yield. *Field Crops Res.* 182, 86–97. doi: 10.1016/j.fcr.2015.05.018

Vera, J., Castro, J., Gonzalez, A., and Moenne, A. (2011). Seaweed polysaccharides and derived oligosaccharides stimulate defense responses

and protection against pathogens in plants. *Mar. Drugs* 9, 2514–2525. doi: 10.3390/md9122514

Verdugo, R. A., Farber, C. R., Warden, C. H., and Medrano, J. F. (2010). Serious limitations of the qtl/microarray approach for qtl gene discovery. *BMC Biol.* 8:96. doi: 10.1186/1741-7007-8-96

Yoon, J., Cho, L.-H., Kim, S. L., Choi, H., Koh, H.-J., and An, G. (2014). The bel1-type homeobox gene sh5 induces seed shattering by enhancing abscission-zone development and inhibiting lignin biosynthesis. *Plant J.* 79, 717–728.

Zhang, Q., Tu, B., Liu, C., and Liu, X. (2018). Pod anatomy, morphology and dehiscing forces in pod dehiscence of soybean (*Glycine max* (l.) merrill). *Flora* 248, 48–53. doi: 10.1016/j.flora.2018.08.014

Conflict of Interest: The authors declare that the research was conducted in the absence of any commercial or financial relationships that could be construed as a potential conflict of interest.

frontiers in Microbiology

ORIGINAL RESEARCH
published: 26 February 2021
doi: 10.3389/fmicb.2021.633881

Seed Biopriming With *Trichoderma* Strains Isolated From Tree Bark Improves Plant Growth, Antioxidative Defense System in Rice and Enhance Straw Degradation Capacity

Harekrushna Swain[1,2], Totan Adak[1], Arup K. Mukherjee[1], Sarmistha Sarangi[1], Pankajini Samal[3], Ansuman Khandual[1], Rupalin Jena[1], Pratap Bhattacharyya[4], Soumendra K. Naik[2], Sayaji T. Mehetre[5], Mathew S. Baite[1], Sunil Kumar M[6] and Najam Waris Zaidi[6]*

[1] Crop Protection Division, ICAR-National Rice Research Institute, Cuttack, India, [2] Department of Botany and Biotechnology, Ravenshaw University, Cuttack, India, [3] Crop Improvement Division, ICAR-National Rice Research Institute, Cuttack, India, [4] Division of Crop Production, ICAR-National Rice Research Institute, Cuttack, India, [5] Nuclear Agriculture and Biotechnology Division, Bhabha Atomic Research Centre, Trombay, India, [6] International Rice Research Institute, New Delhi, India

OPEN ACCESS

Edited by:
Giuseppe Colla,
University of Tuscia, Italy

Reviewed by:
Birinchi Kumar Sarma,
Banaras Hindu University, India
Orlando Borras-Hidalgo,
Qilu University of Technology, China

***Correspondence:**
Arup K. Mukherjee
titirtua@gmail.com;
arupmukherjee@yahoo.com

Specialty section:
This article was submitted to Microbe and Virus Interactions with Plants, a section of the journal Frontiers in Microbiology

Received: 26 November 2020
Accepted: 25 January 2021
Published: 26 February 2021

Citation:
Swain H, Adak T, Mukherjee AK, Sarangi S, Samal P, Khandual A, Jena R, Bhattacharyya P, Naik SK, Mehetre ST, Baite MS, Kumar M S and Zaidi NW (2021) Seed Biopriming With Trichoderma Strains Isolated From Tree Bark Improves Plant Growth, Antioxidative Defense System in Rice and Enhance Straw Degradation Capacity. Front. Microbiol. 12:633881. doi: 10.3389/fmicb.2021.633881

This study is a unique report of the utilization of *Trichoderma* strains collected from even tree barks for rice plant growth, its health management, and paddy straw degradation. Seven different spp. of *Trichoderma* were characterized according to morphological and molecular tools. Two of the isolated strains, namely *Trichoderma hebeiensis* and *Trichoderma erinaceum*, outperformed the other strains. Both of the strains controlled four important rice pathogens, i.e., *Rhizoctonia solani* (100%), *Sclerotium oryzae* (84.17%), *Sclerotium rolfsii* (66.67%), and *Sclerotium delphinii* (76.25%). Seed bio-priming with respective *Trichoderma* strains reduced the mean germination time, enhanced the seedling vigor and total chlorophyll content which could be related to the higher yield observed in two rice varieties; Annapurna and Satabdi. All the seven strains accelerated the decomposition of rice straw by producing higher straw degrading enzymes like total cellulase (0.97–2.59 IU/mL), endoglucanase (0.53–0.75 IU/mL), xylanase (145.35–201.35 nkat/mL), and laccase (2.48–12.60 IU/mL). They also produced higher quantities of indole acetic acid (19.19–46.28 μg/mL), soluble phosphate (297.49–435.42 μg/mL), and prussic acid (0.01–0.37 μg/mL) which are responsible for plant growth promotion and the inhibition of rice pathogen populations. Higher expression of defense enzymes like catalase (≥250% both in shoot and root), peroxidase (≥150% in root and ≥100% in shoot), superoxide dismutase (≥ 150% in root and ≥100% in shoot), polyphenol oxidase (≥160% in shoot and ≥120% in shoot), and total phenolics (≥200% in root and ≥250% in shoot) as compared to the control indicates stress tolerance ability to rice crop. The expression of the aforementioned enzymes were confirmed by the expression of corresponding defense genes like PAL

(>3-fold), DEFENSIN (>1-fold), POX (>1.5-fold), LOX (>1-fold), and PR-3 (>2-fold) as compared to the non-treated control plants. This investigation demonstrates that *Trichoderma* strains obtained from tree bark could be considered to be utilized for the sustainable health management of rice crop.

Keywords: *Trichoderma hebeiensis*, indole acetic acid, prussic acid, straw degrading enzyme, vigor index, stress responsive enzyme, antioxidant genes, biofertilizer

INTRODUCTION

The population of the world is increasing rapidly and it is expected that the world population will be around 9.6 billion in 2050. To attain food security for all, the production of food must be increased to 70% by 2050. Crops should be protected from biotic stresses in order to achieve this goal. This should be done in a more eco-friendly and sustainable way, potentially by using certain biocontrol agents (BCA).

Different BCA like bacteria, fungi, and viruses are being used frequently for the management of diseases in different crops (Abraham et al., 2013). Fungal biocontrol agents are popular as they may be reproduced easily in an artificial nutrient media and are suitable for commercial multiplication (Singh et al., 2013). Genus *Trichoderma* is compelling as a biocontrol operator against various pathogens (Parmar et al., 2015). The primary natural habitat of *Trichoderma* is traditionally seen as soil or plant rhizosphere, even though maximum diversity of these species happens over-the-ground (Druzhinina et al., 2011). With the expanding dangers to nature and to our food security, determination of *Trichoderma* spp. as a BCA has been expecting centrality in giving security for plant protection and development (Swain and Mukherjee, 2020). *Trichoderma* spp. also induces plant growth by the creation of various phytohormones and activates plant supplements for better boost. *Trichoderma* spp. is not only marketed as a biopesticide, biofertilizer, and growth promoter, but also used as a nutrient solubilizer and organic matter decomposer (Woo et al., 2014). There are just a couple of reports on the assessment of *Trichoderma* as a biocontrol specialist obtained from above the ground territories (Jahagirdar et al., 2019). As per Whipps and Lumsden (2001), almost 60% of fungal BCA market is shared by *Trichoderma* spp. and there are significant challenges to investigate. The activity or mode of action of *Trichoderma* spp. is as per the following:

1. Generation of trichodermin, trichothecenes, trichorzianins, or gliotoxins (Mukherjee et al., 2013).
2. Seeking sustenance and space (Celar, 2003).
3. Antibiosis (Swain and Mukherjee, 2020).
4. Mycoparasitic capacities—a relationship in which one living fungus goes about as a supplement hotspot for another (Punja and Utkhede, 2003).

Trichoderma spp. produces auxins that are chargeable for plant bloom and root improvement in each symbiotic and pathogenic communication with plants (Swain et al., 2018). An amazing effect on plant improvement has been demonstrated for several *Trichoderma* secondary metabolites. Koninginins, 6-pentyl-α-pyrone, trichocaranes A–D, harzianopyridone, cyclonerodiol, harzianolide, and harzianic acid are instances of exacerbates that affect plant development in a considerably subordinate way (Swain and Mukherjee, 2020). To understand the plant growth promotion activity, rice seeds were bioprimed with the *Trichoderma* strains. Biopriming will help in increase in colonization, proliferation, and establishment of BCA on the seed surface. Consequently, it will boost seedling vigor and will be able to induce systemic resistance to biotic and abiotic stresses (Singh D. P. et al., 2020). Plant-microbe interactions setup by distant, distinct, and assorted microbial associations tend to instigate various common beneficial systemic changes in the expression level of plant genes that encode for proteins to detoxify reactive oxygen species (ROS). The beneficial microorganisms because of their presence in the plant rhizosphere help plants in easing biotic and abiotic stresses (Singh P. et al., 2020).

Faster decomposition of rice straw can be achieved by inoculating microorganisms, like ligno-cellulolytic microbes. *Trichoderma* produces high levels of several biomass degrading enzymes like cellulase and xylanase (Juturu and Wu, 2014). These enzymes degrade cellulose and hemicellulose, respectively. Lignin was degraded by ligninolytic enzymes into simpler phenyl rings (Sancez, 2009). In this investigation, we analyzed seven distinctive spp. of *Trichoderm*a segregated from the bark of various trees in the Odisha province of India to consider biocontrol properties and rice straw decomposition capacity alongside their growth promotion activity in rice by the production of various enzymes and the expression of genes related to this.

MATERIALS AND METHODS

Isolation, Characterization, Growth Condition and Biocontrol Potential of *Trichoderma* spp.

Seven *Trichoderma* strains were collected from the bark of various trees. The isolation and purification of all the strains were made according to standard techniques described by Mukherjee et al. (2014). *Trichoderma* species were identified by using the typical conidiophores structure (Gams and Bissett, 1998) and according to ISTH guidelines. Molecular characterization, identification, and construction of the phylogenetic tree of all the fungal isolates were done according to Swain et al. (2018). Total genomic DNA from the young mycelia was secluded by utilizing standard SDS (sodium dodecyl sulfate) technique

(Mukherjee et al., 2014). The molecular characterization of all the fungal segregates were based on the sequences of Internal Transcribed Spacer (ITS) regions, Translation Elongation Factor 1 (TEF1) regions and RNA Polymerase B-larger subunit-II (RPB-II) regions according to standard strategies[1]. The species were recognized by BLASTN search on the NCBI site and the character was affirmed by contrasting the sequences and with authentic sequences from GenBank, and a phylogenetic tree constructed on http://www.phylogeny.fr. Biocontrol potential of isolated *Trichoderma* strains was evaluated against above *Rhizoctonia solani* CRRI-RS-8 (MTCC-12232) causing sheath blight of rice, *Sclerotium oryzae* CRRI-S.O (MTCC-12230) causing seedling blight of rice, *Sclerotium rolfsii* causing foot rot of rice and *Sclerotium delphinii* (MTCC11568) causing seedling rot of rice.

The confrontation assay was carried out by concurrent inoculation of both *Trichoderma* and the pathogen close to the edge of the plate, put opposite to one another. Plates inoculated with pathogens only were utilized as control. The percentage of mycelial growth inhibition was determined by Swain et al. (2018)

$$\text{Percentage of inhibition} = [(R1 - R2)/R1] \times 100$$

where, R1, radial growth of the pathogen in control plate; R2, radial growth of the pathogen in test plate.

Quantification of Production of Indole Acetic Acid, Prussic Acid, and Solubilization of Inorganic Phosphate by *Trichoderma* spp.

The indole acetic acid (IAA) produced by different strains of *Trichoderma* was quantified as per Sureshrao et al. (2016). For the quantitative estimation of IAA, agar plugs (5 mm) from the edge of actively growing colonies of *Trichoderma* were inoculated to 20 ml DF (Dworkin and Foster) salts minimal media and incubated for 3 days at 28°C. The medium was supplemented with L-tryptophan at a concentration of 1.02 g l^{-1}. After incubation for 72 h, the mycelia were removed from the culture medium by centrifugation at 5,000 rpm for 5 min. One ml aliquot of the supernatant was mixed vigorously with 4 ml of Salkowski's reagent and allowed to stand at room temperature for 20 min. The absorbance at 535 nm was measured. The concentration of IAA in each culture supernatant was determined by using an IAA (Himedia) as standard curve.

For prussic acid production, *Trichoderma* spp. was grown on Tryptic Soya Agar (TSA) supplemented with 4.4 g L^{-1} of glycine for 2 days. White filter paper discs were cut in the same size and soaked in picric acid solution. The sheets of filter papers were placed on the upper lid of each plate. The plates were sealed with Parafilm and incubated for 7 days at 28°C. After incubation, prussic acid production was observed by the color changes of the filter paper from yellow to light brown or reddish brown (Meera and Balabaskar, 2012). The colored filter paper was then eluted by placing the filter paper in a clean test tube containing 10 mL distilled water and the absorbance was measured at 625 nm by using a spectrophotometer (Manwar et al., 2011).

Quantitative estimation of phosphate solubilization was performed in Pikovskaya broth (Himedia) containing tricalcium phosphate as a phosphate source. Freshly grown *Trichoderma* isolates were inoculated to 50 ml of Pikovskaya's broth and incubated at 28°C and allowed to shake at 100 rpm. After 5 days the broth culture was centrifuged at 10,000 rpm for 10 min. To the 0.5 ml of the culture supernatant, 5 ml of chloromolybdic acid was added and mixed thoroughly. Volume was made up to 10 ml with distilled water and 125 µl chlorostannous acid was added to it. Immediately, the final volume was made-up to 25 ml with distilled water and mixed thoroughly. The absorbance was measured at 610 nm by using a spectrophotometer. The corresponding amount of soluble phosphorous was calculated from a standard curve of potassium dihydrogen phosphate (KH_2PO_4). Phosphate solubilizing activity was expressed in terms of tricalcium phosphate solubilization which in turn was measured by µg ml^{-1} of available orthophosphate as calibrated from the standard curve of KH_2PO_4 (Jackson, 1973).

Qualitative and Quantitative Screening of Straw Degrading Enzymes Produced by *Trichoderma* spp.

Seven *Trichoderma* strains were screened for cellulase activity on carboxy-methyl cellulose (CMC) (Analytical Reagent grade, Himedia, India) and xylanase activity on xylan agar medium containing 1% beech wood xylan (Molecular biology grade, Himedia, India) as the substrate (Teather and Wood, 1982). The *Trichoderma* isolates were cultured on petriplates (90 mm × 15 mm, Himedia, India) containing 1% CMC agar media or 1% beech wood xylan media at 26°C. After 5 days' incubation, plates were stained with 1% solution of Congo red and followed by destained with 1N NaOH solution on a Gyrotory Shaker (Model G2, New Brunswick Scientific Co., Inc., Edison, NJ, United States) at 50 rpm for 15 min to detect clear distinct zone (Saczi et al., 1986). The Enzymatic Index (EI) was calculated for the above two enzymes by measuring the clearance zone as per Florencio et al. (2012).

The qualitative screening for laccase activity of the *Trichoderma* strains were examined by culturing the respective isolates on PDA media supplemented with 0.04% guaiacol (Extra Pure, Himedia, India) and 0.01% (w/v) chloramphenicol with pH 5.5. They were examined for the development of a mixture of red-brown colored zone around the fungal colonies after incubation at 28°C for 72 h (Kalra et al., 2013). Here; three independent experiments were performed with three imitates per isolate. For each isolate the average EI of the three analyses was determined alongside the standard deviation.

The quantitative enzymatic screening of seven *Trichoderma* strains was carried out. Assay of four major enzymes, i.e., total cellulase, endoglucanase, xylanase, and laccase were carried out. The extraction of the crude enzyme was done using rice straw (Variety, Swarna sub-1, *Indica type*) as the base material as per Pathak et al. (2014) with minor modifications. *Trichoderma*

[1]http://www.isth.info/tools/blast/markers.php

grown on PDA plates (2 days' culture) were sub-cultured and grown on rice bran (4%) agar media for a period of 5 days at 27°C. After completion of the incubated period, 10 mL of sterile double distilled water having 0.1% polyoxyethylene (20) sorbitan monooleate was added to the plates to collect the fungal spores. Fungal spores (2×10^6 CFU/mL) were inoculated in 250 mL flask containing grinded sterilized rice straw of 5 g and 15 mL of Mandel and Reese nutrient salt solution (NSS). After 5 days of incubation, crude enzyme extraction was done by using citrate buffer (pH 4.8) in NSS: extraction buffer (1:2: V/V). The fermented matter was shaken for 15 min at room temperature. Multilayered cheese cloth was used for the filtration of the fermented product and the centrifugation of the filtrate was done at 10,000 rpm for 15 min at 4°C (Hermel, Labortechnik GmbH, Type-Z36HK, Nr-580901000). The clear supernatant was used as a crude enzyme sample.

The total cellulase activity and endo-β-1,4-glucanase of the above *Trichoderma* strains was determined as units per milliliter (IU/mL) by Dinitro Salicylic Acid (DNS) method using Whatman No.1 filter paper and 2% CMC as substrates, respectively (Ghosh, 1987). The activity of xylanase and laccase enzyme produced by the *Trichoderma* isolates were measured by using 1% xylan (Bailey et al., 1992) and guaiacol (Monssef et al., 2016) as substrates, respectively. The activity of xylanase and laccase was expressed in nkat/mL and IU/mL, respectively.

In vitro Preparation of Rice Straw Compost by *Trichoderma* spp.

The *in vitro* preparation of rice straw compost was carried out by all the strains of *Trichoderma*. The moisture content in rice straw was measured. Inoculums of seven different isolates (10^7 cfu mL^{-1}) were poured into different conical flasks (250 mL) containing 25 gm of straw (Variety, Swarna sub-1, *Indica type*) and kept at ambient temperature. The weight of the flask was measured at regular intervals along with control until 60 days after inoculation. The C/N ration of the decomposed rice straw was determined. Total carbon and nitrogen content was measured according to the methods given by Walkley and Black (1934) and Keeney and Bremner (1965), respectively.

Measurement of Plant Growth Promoting Parameters, Vigor Index, and Chlorophyll Content Under Greenhouse Conditions

Biocontrol potential and growth promotion property of *Trichoderma* strains were confirmed under controlled conditions. Rice seeds (Annapurna, *Indica* type and Satabdi, *Indica* type) were bio-primed with respective *Trichoderma* formulations (1×10^7 cfu g^{-1}) and set in soils (double autoclaved) filled in 30 cm × 30 cm pots. Soapstone (a mix of Talcum powder, hydrous magnesium silicate, and Talc) was used to prepare the respective *Trichoderma* formulation as per Indian Patent File no. 1240/KOL/2015. Seeds not primed with *Trichoderma* formulation were treated as control. Germination capacity and vigor index of the seeds sown in the pot were examined as per Abdul-Baki and Anderson (1973) and Swain et al. (2018). For the assessment of vigor index germination percentage, seedling length and dry weight of seedling was taken into consideration. The effect of *Trichoderma* on the plant chlorophyll content of the leaf was evaluated as per Porra (2002).

Measurement of Plant Growth Promoting Parameters Under Field Conditions

For the assessment of growth promotion under *in vivo* conditions two direct seeded rice varieties ("Annapurna" and "Satabdi") were used. Seeds dressed with respective *Trichoderma* formulations were treated as treatments. The experiment was conducted in completely randomized design with four replications. The agronomical parameters (root length, shoot length, dry root weight, dry shoot weight, no of tiller/hill, and yield/hill) were recorded. Expression of plant stress responsive enzymes like peroxidase (PER), catalase (CAT), superoxide dismutase (SOD), polyphenol oxidase (PPO), and total phenolics (TP) conveyed by the plants treated with *Trichoderma* were investigated at active tillering stage (Arnon, 1949; Sadasivam and Manickum, 2011; Swain et al., 2018).

Extraction of RNA, cDNA Synthesis and Examination of Gene Articulation by Real-Time-PCR

Total RNA was extracted from the fresh plant leaves by utilizing RNeasy Plant Mini Kit (Qiagen, Germany). RNA concentration was quantified by using Nano Drop 2000 (Thermo Fisher Scientific). cDNA synthesis was carried out by using Maxima H minus first strand cDNA synthesis Kit with dsDNase (Thermo Fisher Scientific) as per the manufacturer's guidelines. Quantitative real-time (RT-PCR) reaction was performed in the Insta-Q96 RT-PCR system (Himedia Laboratories, Mumbai, India) using Maxima SYBRGreen/ROX qPCR master mix (Thermo Fisher Scientific) for five growth promotion and antioxidant genes, i.e., POX (peroxidase), LOX (lipoxigenase), PAL (phenylalanine ammonia lyase), DEFENSIN, PR-3 (PR protein). Act (actin) was utilized as housekeeping genes for normalization of relative gene articulation level. All primers were designed by IDT programming. All the treatments were in sets of three for each primer pair in a similar plate. The PCR reactions were set by convention formulated by Singh P. et al. (2020) with minor adjustments.

Statistical Analysis

Statistical analysis was performed by utilizing the Statistical Analysis Software (SAS) of ICAR-IASRI, New Delhi[2] was used for statistical analysis. All the investigations were replicated three times. Seed germination rate was ARCSINE transformed. The other seed quality boundaries were examined with no change. All the information was exposed to single way characterized analysis of variance (ANOVA) and means of treatments were compared based on Tukey's honestly significant difference test (HSD) at 0.05 probability level using SAS.

[2]www.iasri.res.in/sscnars/-

RESULTS AND DISCUSSION

Identification of *Trichoderma* Strains

Based on morphological characteristics and molecular identification, the isolates were identified as *Trichoderma harzianum* (CRRI-T1), *Trichoderma erinaceum* (CRRI-T2), *Trichoderma atroviride* (CRRI-T3), *Trichoderma hebeiensis* (CRRI-T15), *Trichoderma parareesei* (CRRI-T16), *Trichoderma longibrachiatum* (CRRI-T22), and *Trichoderma reesei* (CRRI-T27) (**Figure 1** and **Supplementary Figure 1**). The ITS sequence data from CRRI-T1, CRRI-T2, CRRI-T3, CRRI-T22, CRRI-T27, and TEF sequence data from CRRI-T15, CRRI-T16 have been deposited with NCBI (**Table 1**). Out of these 7 isolates 4 are rarely found in India (i.e., *T. erinaceum, T. hebeiensis, T. parareesei,* and *T. reesei*). This provides the evidence for the maximum diversity of this genus occurring above ground. This may be the first time in India, we are reporting *T. hebeiensis, T. parareesei,* and *T. reesei* from the above ground. *T. reesei* reported earlier were isolated from soil and obtained from the mutation of other species of *Trichoderma* (Kar et al., 2006; Saravanan et al., 2008).

Biocontrol Capability of *Trichoderma* Strains and Its Mechanism

Mycelial growth of *R. solani, S. oryzae, S. rolfsii,* and *S. delphinii* were inhibited by 98.33–100.00, 18.75–84.17, 14.17–66.67, and 56.67–76.25%, respectively. CRRIT-2, CRRIT-3, CRRIT-15, CRRIT-16 overgrew *R. solani* within 3 days. Similarly, these isolates grew quicker in dual culture against *S. oryzae* and covered minimum of 70% of the medium surface within 3 days (**Table 1**). In case of *S. delphinii*, CRRIT-15, CRRIT-2 exhibited more than 70% inhibitory effect whereas all other strains were able to colonize in between 58 and 63% of the medium surface. Among the seven strains, *T. hebeiensis* (CRRIT-15) and *T. erinaceum* (CRRIT-2) was superior antagonist against four rice pathogens **(Supplementary Figure 2**). Biocontrol potential of these isolates can be correlated with prussic acid (HCN) production. The highest quantity of HCN was produced by CRRI-T15 (0.37 μg/mL) which was significantly higher as compared to other isolates. Other isolates such as CRRI-T1, CRRI-T2, CRRI-T3, CRRI-T16, and CRRI-T27 produced 0.03, 0.02, 0.05, 0.02, and 0.03 μg/mL HCN (**Table 2**).

Many species of *Trichoderma* were accounted for as biocontrol specialists for a wide range of plant pathogens (Abdollahi et al., 2012; Kumar et al., 2012; Swain et al., 2018). Mycoparasitism is clearly one of the mechanisms for biocontrol action of *Trichoderma* (Mukherjee et al., 2013). Besides mycoparasitism, release of prussic acid has been proposed as a significant antifungal component. Cyanide produced by microbes may act as an inhibitor to soil borne pathogens without any harm to the host plant (Noori and Saud, 2012). Hence, for the management of soil borne pathogens, the prussic acid produced by *Trichoderma* spp. played a vital role. Biocontrol potential of *Trichoderma* spp. mainly depends on the host plant, agro climatic conditions and nutrient availability (Mukherjee et al., 2013). To the best of our knowledge, *T. hebeiensis* and *T. parareesei* from the above ground part have been explored as potential biocontrol for the first time.

Trichoderma as a Decomposer

Cellulase activity of fungal isolates with EI values of more than 1.5 were considered to be potential cellulase producers (Florencio et al., 2012; Saroj et al., 2018). All the seven strains were potential

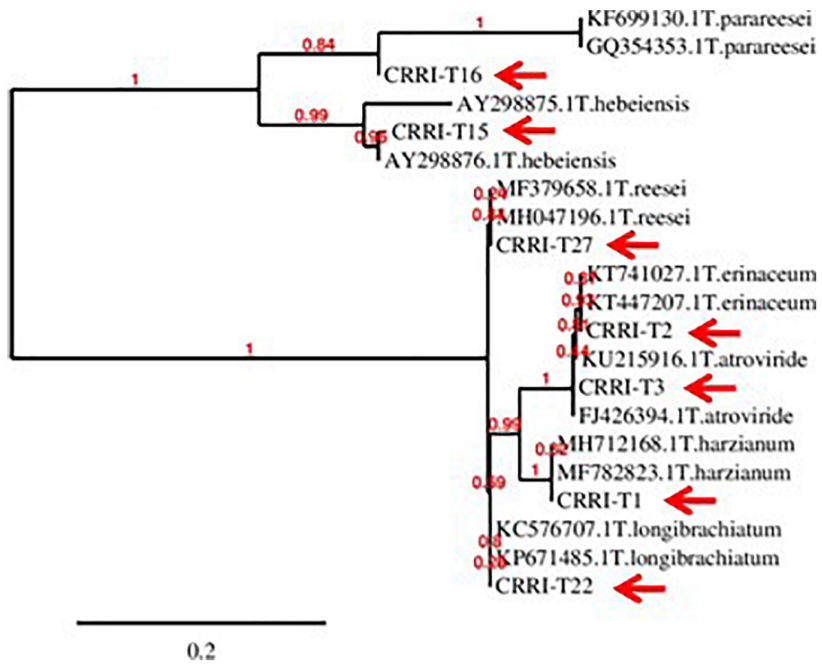

FIGURE 1 | Phylogeny of the isolated *Trichoderma* spp. (CRRI-T1 to CRRI-T27) used for the recent study.

TABLE 1 | Details of *Trichoderma* isolates and confrontation assay showing the inhibition of pathogen growth by different *Trichoderma* isolates on PDA medium.

Strain designation	Source of collection	Place of collection	GPS location	Species identified	NCBI accession Nos.	Percentage of inhibition			
						Rhizoctonia solani	***Sclerotium oryzae***	***Sclerotium rolfsii***	***Sclerotium delphinii***
CRRI-T1	Bark of a *Litchi chinensis*	NRRI, Cuttack	85°92′E, 20°45′N	*Trichoderma harzianum*	KX853519.1	98.75^{A}	67.50^{C}	40.83^{D}	63.33^{B}
CRRI-T2	Bark of a *Cassia tora*	42-Mouza (Barala), Cuttack	86°92′E, 20°44′N	*Trichoderma erinaceum*	KR014407.1	100.00^{A}	73.33^{B}	49.58^{C}	75.00^{A}
CRRI-T3	Bark of a *Cassia tora*	42-Mouza (Barala), Cuttack	86°58′E, 20°45′N	*Trichoderma atroviride*	KR014408.1	100.00^{A}	70.83^{BC}	47.50^{C}	56.67^{C}
CRRI-T15	Bark of a *Samanea saman*	42-Mouza (Barala), Cuttack	86°52′E, 20°45′N	*Trichoderma hebeiensis*	MK247223.1	100.00^{A}	84.17^{A}	66.67^{A}	76.25^{A}
CRRI-T16	Bark of a *Samanea saman*	42-Mouza (Barala), Cuttack	86°12′E, 20°44′N	*Trichoderma parareesei*	MK247224.1	100.00^{A}	69.58^{BC}	57.50^{B}	58.75^{BC}
CRRI-T22	Decomposed wood of *Dalbergia sissoo*	NRRI, Cuttack	85°92′E, 20°45′N	*Trichoderma longibrachiatum*	MH894348.1	98.33^{A}	18.75^{E}	14.17^{E}	59.58^{BC}
CRRI-T27	Bark of a *Samanea saman*	Fakirpada, Cuttack	86°92′E, 20°45′N	*Trichoderma reesei*	MK163352.1	99.58^{A}	31.67^{D}	45.42^{CD}	59.17^{BC}
					CV (%)	0.65	3.05	5.01	1.585
					Tukey's HSD at 5%	1.855	5.1802	6.5756	5.5483

Means with same letter are not significantly different at $p \leq 0.05$.

TABLE 2 | Quantitative enzyme assay of selected *Trichoderma* isolates.

Treatment name	IAA (in μ g/mL)	HCN (in μ g/mL)	Inorganic phosphate (in μ g/mL)	Endoglucanase (in IU/mL)	Total cellulase (in IU/mL)	Xylanase (in nkat/mL)	Laccase (in IU/mL)
CRRIT-1	31.37^{C}	0.03^{C}	318.20^{D}	0.67^{C}	0.99^{E}	145.35^{E}	2.64^{C}
CRRIT-2	42.38^{B}	0.27^{B}	412.30^{B}	0.70^{BC}	0.87^{F}	195.89^{B}	11.74^{A}
CRRIT-3	30.39^{C}	0.05^{C}	339.30^{C}	0.68^{C}	2.13^{B}	192.99^{B}	9.85^{B}
CRRIT-15	46.28^{A}	0.37^{A}	435.42^{A}	0.75^{A}	2.59^{A}	201.35^{A}	12.60^{A}
CRRIT-16	22.42^{D}	0.02^{C}	303.70^{DE}	0.59^{D}	1.09^{D}	152.43^{D}	3.35^{C}
CRRIT-22	19.19^{E}	0.01^{C}	297.49^{E}	0.53^{E}	0.97^{E}	149.29^{DE}	2.48^{C}
CRRIT-27	32.01^{C}	0.03^{C}	320.20^{D}	0.74^{AB}	1.28^{C}	164.40^{C}	2.87^{C}
CV (%)	3.48	18.93	1.74	2.38	1.64	0.85	6.99
Tukey's HSD at 5%	3.1823	0.0601	17.2	0.0453	0.0665	4.1534	1.2982

Means with same letter are not significantly different at $p \leq 0.05$.

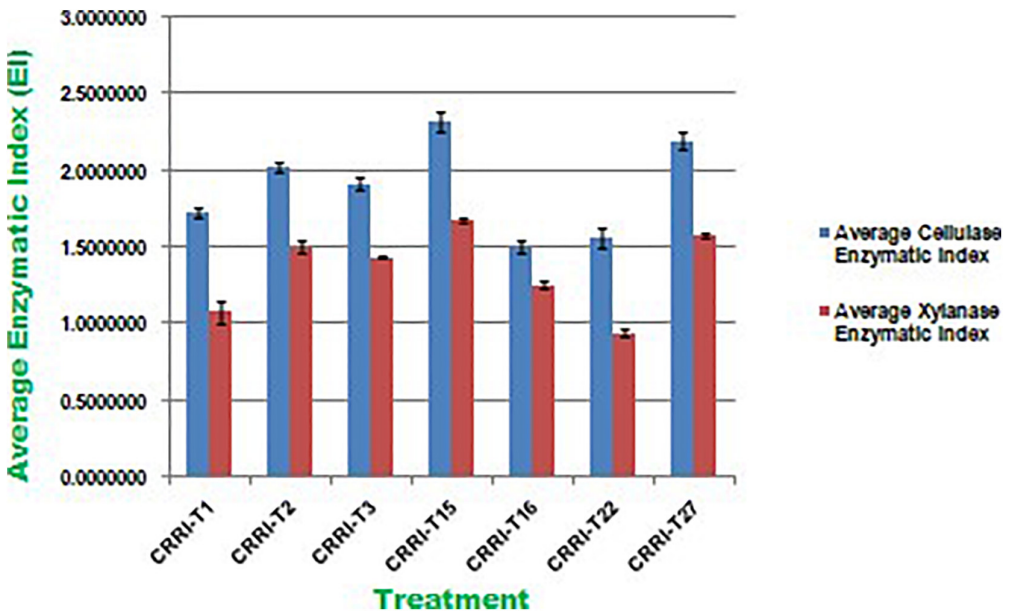

FIGURE 2 | Enzymatic Index of cellulase and xylanase activity of Trichoderma isolates used in the present study.

cellulase producers as the EI value was more than 1.5. Earlier Saroj et al. (2018) reported thermophilic fungi isolated from soil, i.e., *Aspergillus fumigatus JCM 10253* and *Aspergillus terreus* with highest EI values of 1.50 and 1.24 for cellulase activity, respectively. Florencio et al. (2012) reported *T. harzianum* CEN 139, *T.* sp. 104 NH and *T. harzianum* CEN 155 exhibited 1.74, 1.72, and 1.61 EI value for cellulase activity, respectively. Similarly, EI values of xylanase activity of *Trichoderma* isolates ranged from 0.50 to 1.33. CRRIT-15 exhibited the highest xylanase activity, i.e., 1.68 EI value followed by CRRIT-27 and CRRIT-2. The strains reported by Saroj et al. (2018) exhibited range 1.01–1.13 of EI value for xylanase activity. However, CRRIT-26, CRRIT-2, and CRRIT-27 had better cellulase and xylanase activities in comparison to others as reported earlier. All the strains exhibited positive reddish-brown zones around the fungal colonies indicating laccase activity. Monssef et al. (2016) examined 24 fungal isolates for the production laccase enzyme and found only *T. harzianum* could produce the enzyme. These results are in line with Gochev and Krastanov (2007) who found that many of *Trichoderma* spp. with cellulase activity could also be a good source of laccase (**Figure 2**).

All the isolates were examined for endoglucanase, total cellulase, xylanase, and laccase activity. CRRIT-15 showed maximum endoglucanase activities, i.e., 0.75 IU/mL whereas CRRIT-22 isolate showed lowest endoglucanase activities (i.e., 0.53 IU/mL). Similarly, CRRIT-15 and CRRIT-3 showed maximum total cellulase activities, i.e., 2.59 and 2.13 IU/mL, respectively. Similarly, CRRIT-15 released maximum xylanase activity of 201.35 nkat/mL followed by CRRIT-2 195.89 nkat/mL. Among four isolates, CRRIT-15 showed 12.60 IU/mL of laccase activity followed by CRRIT-3 9.85 IU/mL of activity (**Table 2**).

Earlier Druzhinina et al. (2011) reported that *T. reesei* is a major source of hydrolytic enzymes like cellulase and hemicellulase. *T. harzianum* CEN 139, *T.* sp. 104 NH, and *T. harzianum* CEN 155 exhibited 1.74, 1.72, and 1.61 EI value and 0.27, 0.23, and 0.22 IU/mL of endoglucanase activity, respectively

TABLE 3 | Characteristics of *Trichoderma* mediated-rice straw-compost.

Treatment name	Gravimetric weight loss of decomposed rice straw after 30 days (in percentage)	Gravimetric weight loss of decomposed rice straw after 60 days (in percentage)	C/N (in percentage)
Control	4.48^{G}	12.52^{E}	67.40^{A}
CRRIT-1	7.97^{F}	10.49^{F}	35.33^{B}
CRRIT-2	17.46^{B}	18.27^{B}	18.27^{B}
CRRIT-3	10.76^{E}	12.53^{E}	34.01^{B}
CRRIT-15	18.60^{A}	20.95^{A}	24.78^{F}
CRRIT-16	14.61^{C}	15.35^{C}	29.72^{CD}
CRRIT-22	12.65^{D}	13.55^{D}	30.39^{C}
CRRIT-27	16.81^{B}	18.57^{B}	28.54^{DE}
CV (%)	2.34	1.27	1.38
Tukey's HSD at 5%	0.8724	0.5605	1.3851

Means with same letter are not significantly different at $p \leq 0.05$.

TABLE 4 | Effect of *Trichoderma* application on seedling vigor index of different rice varieties.

Treatment name	Seedling length (cm)		Seedling dry weight (g)		Vigor index-1		Vigor index-2	
	Annapurna	Satabdi	Annapurna	Satabdi	Annapurna	Satabdi	Annapurna	Satabdi
Control	20.10^{C}	21.67^{D}	0.09^{D}	0.11^{F}	2210.00^{D}	2166.67^{D}	9.67^{D}	11.00^{D}
CRRIT1	24.70^{B}	29.03^{BC}	0.11^{C}	0.14^{E}	2470.00^{C}	3036.67^{ABC}	11.33^{C}	14.00^{C}
CRRIT2	27.40^{AB}	33.03^{AB}	0.14^{A}	0.19^{B}	2740.00^{AB}	3336.67^{AB}	14.00^{A}	17.33^{AB}
CRRIT3	26.53^{AB}	31.30^{ABC}	0.14^{AB}	0.16^{CD}	2653.33^{BC}	2996.67^{BC}	13.67^{AB}	16.00^{BC}
CRRIT15	28.57^{A}	35.47^{A}	0.15^{A}	0.21^{A}	2923.33^{A}	3413.33^{A}	14.00^{A}	18.33^{A}
CRRIT16	26.03^{AB}	33.53^{AB}	0.12^{BC}	0.18^{BC}	2603.33^{BC}	3153.33^{ABC}	12.33^{BC}	16.00^{BC}
CRRIT22	25.03^{B}	28.23^{C}	0.12^{C}	0.16^{DE}	2530.00^{BC}	2823.33^{C}	12.00^{C}	15.33^{BC}
CRRIT27	24.97^{B}	28.03^{C}	0.12^{C}	0.16^{DE}	2436.67^{BC}	3257.67^{AB}	11.67^{C}	15.67^{BC}
CV (%)	3.92	5.33	4.27	4.96	3.39	4.46	3.87	5.21
Tukey's HSD at 5%	2.8722	4.6085	0.0152	0.0232	250.76	388.66	1.3881	2.3207

Means with same letter are not significantly different at $p \leq 0.05$.

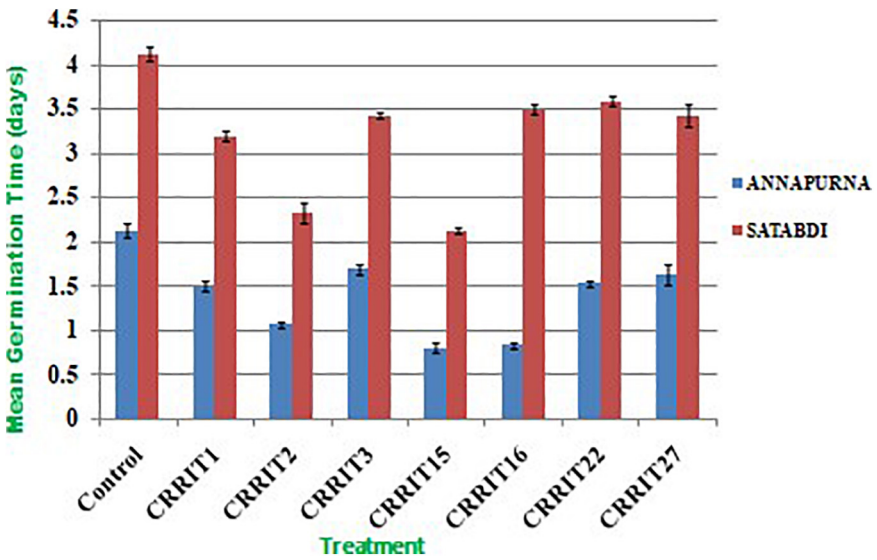

FIGURE 3 | Mean germination time in rice varieties treated with *Trichoderma* and control condition.

TABLE 5 | Chlorophyll content in different rice varieties due to the application of different *Trichoderma* isolates.

Treatment name	Chl*a* (mg/g of fresh leaf)		Chl*b* (mg/g of fresh leaf)		Chl*a*/Chl*b* (mg/g of fresh leaf)		Total chlorophyll (mg/g of fresh leaf)	
	Annapurna	**Satabdi**	**Annapurna**	**Satabdi**	**Annapurna**	**Satabdi**	**Annapurna**	**Satabdi**
Control	3.73^{E}	1.18^{F}	0.87^{D}	0.11^{F}	4.28^{A}	10.78^{A}	4.61^{E}	1.29^{F}
CRRIT1	8.70^{D}	8.43^{E}	2.38^{C}	3.04^{E}	3.66^{B}	2.77^{D}	11.09^{D}	11.47^{E}
CRRIT2	14.43^{A}	15.60^{C}	4.35^{AB}	4.38^{CD}	3.33^{EC}	3.57^{B}	18.78^{A}	19.98^{C}
CRRIT3	12.71^{C}	14.63^{D}	4.04^{AB}	4.36^{D}	3.14^{C}	3.36^{B}	16.76^{C}	18.99^{D}
CRRIT15	13.37^{BC}	20.55^{A}	4.52^{A}	6.98^{A}	2.98^{C}	2.95^{CD}	17.89^{AB}	27.54^{A}
CRRIT16	14.35^{A}	15.35^{CD}	4.34^{AB}	4.84^{C}	3.31^{EC}	3.17^{BCD}	18.69^{A}	20.19^{C}
CRRIT22	13.36^{BC}	19.51^{B}	3.97^{B}	5.60^{B}	3.36^{EC}	3.49^{B}	17.34^{BC}	25.11^{B}
CRRIT27	13.87^{AB}	15.43^{C}	4.06^{AB}	4.71^{CD}	3.42^{EC}	3.28^{BC}	17.93^{AB}	20.14^{C}
CV (%)	2.22	1.90	5.06	3.86	4.79	3.33	2.08	1.78
Tukey's HSD at 5%	0.7542	0.7586	05197	0.4724	0.4736	0.3999	0.9223	0.9277

Means with same letter are not significantly different at $p \leq 0.05$.

(Florencio et al., 2012). Lee et al. (2011) reported *T. harzianum* isolated from post-harvest rice straw possesses 0.095 IU/mL of endoglucanase activity and 0.222 IU/mL of total cellulase activity. Similarly, Pathak et al. (2014) reported *T. harzianum* isolated from soil, rotting wood, and manure from different locales of northern India possesses 1.28 IU/mL endoglucanase and 0.37 IU/mL of total cellulase activity. So, both the isolates NRRIT-26 and NRRIT-27 seem to be a very good potential cellulase and xylanase producer and they may be used as a better option for the preparation of rice straw compost as compared to the previous reports. According to Pathak et al. (2014) 100.2 IU/mL of xylanase activity was observed in the case of *T. harzianum* collected from various location of northern India. NRRIT-26, i.e., *T. reesei* showed highest xylanase activity as compared to the other three isolates that can be considered as the best candidate for rice straw compost. The other three strains, i.e., NRRIT-27, CRRIT-13, and CRRIT-5 also showed higher xylanase activity in comparison to isolates reported by Lee et al. (2011) and Pathak et al. (2014).

Moreover, *T. harzianum* and *T. longibrachiatum* are the wellsprings of laccase production as portrayed by Holker et al. (2002) and Velazquez-Cedeno et al. (2004), respectively. We reported here the creation of laccase enzyme in all the *Trichoderma* isolates isolated from tree bark. *Trichoderma* are adapted well to rice straw and they could be utilized to degrade straw as reported by previous researchers (Kang et al., 2004). Overall, the isolate, CRRIT-15 released the highest number of enzymes as compared to other isolates. Hence, it may be used as a candidate for the preparation of rice straw compost in an economically way.

The *Trichoderma* inoculated straw was decomposed at a faster rate as compared to the non-inoculated one. Among the seven *Trichoderma* strains, NRRIT-15, CRRIT-2, and NRRIT-27 could be able to produce compost from rice straw at a faster rate. There was 18.60, 17.46, and 16.81% of weight loss of the rice straw with NRRIT-15, CRRIT-2, and NRRIT-27 treatments, respectively, after 30 days (**Table 3**). The loss of weight of the rice straw was 20.95, 18.27, and 18.57%, respectively, after 60 days when treated with NRRIT-15, CRRIT-2, and NRRIT-27. The above mentioned three isolates had also secreted higher quantities of ligno-cellulolytic enzymes as stated above. These enzymes decomposed the rice straw at a faster rate. There were insignificant changes in weight loss after 60 days of incubation as compared to 30 days of incubation. Similarly, the C/N ratio did not vary between 30 and 60 days. So based on these data, we can conclude the compost is generally stable after 30 days of incubation. As *Trichoderma* mediated rice straw compost has a low C/N ratio in *in vitro* condition, the technique can be extended to field conditions which will improve organic matter along with fertility of the soil.

Trichoderma as a Plant Growth Promoter

Auxins play a critical role for both the plant growth and root development. The quantity of IAA synthesized by various *Trichoderma* strains in the broth was ranged from 19.19 to 46.28 μg/mL (**Table 4**). The highest IAA was produced by CRRI-T15 (46.28 μg/mL) which was significantly higher followed by CRRI-T2 (42.38 μ g/mL).

Quantitative assessment of soluble phosphate concentrations in Pikovskaya's broth was varied from 297.49 to 435.42 μg/mL (**Table 2**). CRRI-T15 may be treated as the best inducer of phosphate mobilization as it exhibited higher phosphate solubilization capacity in Pikovaskaya's broth. The amount of inorganic phosphate solubilized was 435.42 μg/mL. Other *Trichoderma* strains, i.e., CRRI-T1, CRRI-T2, CRRI-T3, CRRI-T16, CRRI-T22, and CRRI-T27 were also good phosphate solubilizers.

Parameters related to seed vigor and seed germination of different *Trichoderma* dressed seeds varied from 2.13–4.13 days (Mean germination time), 2166.67–3413.33 (Vigor index-I) and 11.00–18.33 (Vigor index-II), respectively in variety Satabdi (**Figure 3**). A similar trend was also found in the case of the Annapurna rice variety. Physiological parameters among the treatments were significantly varied in both the varieties. Absolute chlorophyll content went from 4.61 to 18.78 mg/g in the Annapurna rice variety. Seeds inoculated with *T. hebeiensis* (CRRIT-15), *T. parareese*i (CRRIT-16), *T. erinaceum* (CRRIT-2), and *T. longibrachiatum* (CRRIT-22) had significantly higher chlorophyll parameters when contrasted with other isolates depicted in the current examination (**Table 5**). Seed biopriming

TABLE 6 | Growth promotion in different rice varieties due to *Trichoderma* application as indicated by various agronomical parameters.

Treatment name	Dry root weight (g)		Dry shoot weight (g)		Fresh root weight (g)		Fresh shoot weight (g)		Root length (cm)		Shoot length (cm)		Number of tiller/hill		Yield/hill (g)	
	Annapurna	Satabdi	Annapurna	Satabdi	Annapurna	Satabdi	Annapurna	Satabdi	Annapurna	Satabdi	Annapurna	Satabdi	Annapurna	Satabdi	Annapurna	Satabdi
Control	0.13^{G}	0.20^{E}	0.28^{C}	0.57^{D}	0.32^{E}	0.52^{F}	1.35^{F}	1.30^{E}	2.60^{D}	1.80^{F}	9.54^{E}	8.33^{D}	12.00^{D}	11.00^{E}	19.59^{F}	22.20^{D}
CRRIT1	0.24^{F}	0.49^{DE}	0.62^{C}	1.14^{D}	0.46^{E}	1.40^{E}	1.94^{E}	2.62^{D}	3.13^{D}	2.67^{E}	11.41^{E}	9.30^{D}	14.33^{CD}	18.33^{CD}	23.46^{DE}	33.60^{C}
CRRIT2	0.35^{E}	1.16^{AB}	2.63^{B}	2.66^{ABC}	1.67^{B}	2.42^{BC}	7.67^{B}	6.43^{A}	6.57^{B}	5.47^{BC}	17.37^{AB}	17.60^{A}	16.67^{BC}	23.67^{AB}	26.96^{BC}	41.38^{AB}
CRRIT3	0.79^{CD}	0.79^{CD}	2.64^{B}	2.33^{BC}	1.20^{D}	1.93^{D}	6.77^{CD}	5.86^{B}	6.13^{BC}	5.20^{C}	16.32^{BCD}	16.33^{B}	18.00^{AB}	19.67^{C}	29.23^{AB}	39.46^{B}
CRRIT15	0.96^{A}	1.34^{A}	3.79^{A}	3.05^{A}	1.91^{A}	2.98^{A}	8.72^{A}	6.80^{A}	7.33^{A}	6.17^{A}	19.00^{A}	18.37^{A}	20.33^{A}	24.67^{A}	31.14^{A}	43.53^{A}
CRRIT16	0.73^{B}	1.00^{ABC}	2.32^{B}	2.95^{AB}	1.65^{B}	2.23^{C}	7.45^{BC}	6.30^{AB}	6.63^{B}	5.70^{B}	17.32^{ABC}	16.00^{B}	20.00^{A}	21.00^{BC}	30.54^{A}	40.80^{B}
CRRIT22	0.67^{C}	0.91^{BC}	2.48^{B}	2.33^{C}	1.38^{C}	1.77^{D}	6.32^{DE}	3.37^{C}	5.80^{C}	4.47^{D}	14.45^{D}	14.67^{C}	15.00^{C}	16.00^{D}	22.73^{E}	36.15^{C}
CRRIT27	0.62^{D}	1.01^{ABC}	2.27^{B}	2.53^{ABC}	1.22^{CD}	2.61^{B}	5.91^{E}	6.66^{A}	6.73^{AB}	5.20^{C}	15.33^{CD}	16.10^{B}	19.33^{A}	20.67^{C}	25.60^{CD}	40.38^{B}
CV (%)	2.59	13.82	9.42	9.79	5.08	5.08	4.33	3.59	3.76	3.28	4.57	2.84	5.36	4.79	3.17	2.45
Tukey's HSD at 5%	0.0402	0.3431	0.5777	0.6191	0.1794	0.2905	07198	0.5089	0.6083	0.4327	1.9868	1.2063	2.6206	2.6766	2.391	2.629

Means with same letter are not significantly different at $p \leq 0.05$.

TABLE 7 | Expression of defense enzymes related to stress in the rice varieties.

Treatment name	Expression of catalase (in unit/min/gm)				Expression of peroxidase (in unit/min/gm)				Expression of superoxide dismutase (in unit/min/gm)				Expression of polyphenol oxidase (in unit/min/gm)				Expression of total phenolics (in unit/min/gm)			
	Annapurna		Satabdi		Annapurna		Satabdi		Annapurna		Satabdi		Annapurna		Satabdi		Annapurna		Satabdi	
	ROOT	SHOOT	ROOT	SHOOT	ROOT	SHOOT	ROOT	SHOOT	ROOT	SHOOT	ROOT	SHOOT	ROOT	SHOOT	ROOT	SHOOT	ROOT	SHOOT	ROOT	SHOOT
Control	5.00^{E}	7.00^{E}	5.00^{F}	5.67^{E}	0.51^{F}	0.39^{E}	0.52^{D}	0.42^{H}	3.56^{E}	5.98^{E}	4.39^{G}	3.63^{G}	20.49^{D}	24.99^{D}	19.23^{D}	27.55^{D}	0.11^{G}	3.48^{G}	0.10^{G}	3.73^{G}
CRRIT1	9.00^{D}	18.33^{D}	10.67^{E}	10.33^{D}	0.72^{E}	0.84^{D}	0.66^{D}	0.67^{G}	7.78^{CD}	8.50^{D}	5.57^{F}	5.43^{F}	25.85^{C}	30.35^{C}	24.60^{C}	32.92^{C}	0.87^{F}	4.37^{F}	0.86^{F}	4.62^{F}
CRRIT2	20.67^{A}	27.67^{AB}	20.33^{B}	24.67^{AB}	1.28^{AB}	1.89^{A}	2.11^{A}	1.49^{C}	10.58^{A}	12.42^{A}	10.31^{B}	11.64^{B}	58.78^{A}	63.28^{A}	57.53^{A}	65.85^{A}	4.20^{B}	7.70^{B}	4.19^{B}	7.95^{B}
CRRIT3	18.33^{B}	26.00^{BC}	19.67^{BC}	23.33^{B}	1.07^{C}	1.46^{B}	1.66^{C}	1.13^{E}	9.59^{B}	10.27^{C}	9.76^{C}	10.44^{C}	41.15^{B}	45.65^{B}	39.90^{B}	48.21^{B}	2.90^{D}	6.40^{D}	2.89^{D}	6.66^{D}
CRRIT15	21.67^{A}	28.67^{A}	22.33^{A}	26.33^{A}	1.33^{A}	1.98^{A}	2.18^{A}	1.92^{A}	11.14^{A}	12.82^{A}	12.62^{A}	12.51^{A}	60.02^{A}	64.52^{A}	58.76^{A}	67.08^{A}	4.73^{A}	8.23^{A}	4.72^{A}	8.49^{A}
CRRIT16	18.33^{B}	24.33^{C}	18.67^{CD}	23.33^{B}	1.14^{BC}	1.03^{C}	1.82^{B}	1.25^{D}	8.12^{C}	10.45^{C}	8.65^{D}	9.69^{D}	41.95^{B}	46.45^{B}	40.70^{B}	49.01^{B}	3.04^{D}	6.54^{CD}	3.03^{D}	6.79^{CD}
CRRIT22	16.33^{C}	20.67^{D}	17.67^{D}	19.67^{C}	0.86^{DE}	1.10^{C}	1.55^{C}	0.98^{F}	7.19^{D}	9.99^{C}	7.55^{E}	8.51^{E}	27.97^{C}	32.47^{C}	26.72^{C}	35.04^{C}	2.01^{E}	5.51^{E}	1.99^{E}	5.76^{E}
CRRIT27	18.67^{B}	26.33^{ABC}	19.33^{BC}	25.33^{A}	1.02^{CD}	1.61^{B}	1.87^{B}	1.62^{B}	9.73^{B}	11.45^{B}	9.89^{BC}	10.44^{C}	43.47^{B}	47.97^{B}	42.21^{B}	50.53^{B}	3.43^{C}	6.93^{C}	3.42^{C}	7.19^{C}
CV (%)	3.23	3.73	3.11	3.09	6.03	4.64	3.30	3.17	3.18	3.14	2.08	2.01	2.47	2.22	2.55	2.10	4.63	2.29	4.65	2.19
Tukey's HSD at 5%	1.4911	2.4043	1.4952	1.7643	0.1721	0.1721	0.1468	0.1081	0.7743	0.9249	0.5144	0.5233	2.8383	2.8383	2.8383	2.8383	0.3549	0.4046	0.3549	0.4046

Means with same letter are not significantly different at $p \leq 0.05$.

with beneficial microbes have been reported by several workers for their ability to mitigate biotic stress in an efficient way (Singh P. et al., 2020). During biopriming, antagonistic PGPR increases on the seed surface, thereby defending the plant from pathogen attack and enabling it to be sustained under various stress conditions (Rajput et al., 2019).

In the field study, all the strains of *Trichoderma* controlled the plant growth along with various agronomical parameters. The highest yield (31.14 g/hill) was recorded from CRRIT-15 followed by CRRIT-16 and CRRIT-13. Similar trends were observed in the case of the Satabdi rice variety (**Table 6**). As an overall study, all the isolates performed better than the control one **(Supplementary Figures 3**, **4**). Previously Swain et al. (2018) reported higher total chlorophyll content, plant vigor in direct seeded rice treated with *Trichoderma*. Previously Mukherjee et al. (2013) and Mukherjee et al. (2018) explained the role of *Trichoderma* as a plant growth promoter. The enhancement of seed vigor parameters may be due to the production of phenolic compounds and secondary metabolite namely harzianolide by *Trichoderma* spp. (Cai et al., 2013). This result was also found in case of chickpea and wheat (Zhang et al., 2019). All these positive impacts of vigor property helped the plant in uptake and mobilization of nutrients for a longer time, which leads to a better yield.

Among the secondary metabolites, IAA (auxin) helps in plant growth and potentially increases the root length as well. Laboratory studies have emphasized the role of plant growth promoting fungi as auxin producers and biocontrol operators (Hossain et al., 2007; Contreras-Cornejo et al., 2009) in plant development. This key hormone was synthesized by the fungus *Trichoderma* in symbiotic as well as in pathogenic interactions (Gravel et al., 2007). Similarly, plants can only uptake and mobilize essential micronutrients if they are solubilized by microbes (Rudresh et al., 2005). As indicated by Dunaitsev et al. (2008) *Trichoderma* spp. can deliver phosphate from mineral crude materials as plant accessible structures. It was seen that *Trichoderma* isolates a demonstrated higher capacity to solubilize the phosphate as they additionally displayed great reactions to plant growth promotion action after direct seed treatments. *Trichoderma* as plant symbionts for updated supplement take-up, extended root and shoot advancement, improved plant influence and biotic/abiotic stress flexibility have been widely discussed (Harman, 2011).

Improvement of Plant Resistance by the Articulation of Stress Responsive Enzymes

Inside and out higher verbalization of the enzymes related to stress was seen in *Trichoderma* seed treated plants when appeared differently in relation to untreated plants against both the rice assortments. Correspondingly, CRRIT-15, and CRRIT-2 treated root and shoots of rice assortment Annapurna and Satabdi had exceptionally higher PER, SOD, PPO, and TP activity contrasted with other treatment. Also, catalase action was higher in CRRIT-15 and CRRIT-2 treatment in both root and shoot. Comparative examples were found in peroxidase action in root and shoot of both the rice assortments (**Table 7**).

In blend with their immediate impact on the pathogen structure and action, *Trichoderma* spp. has additionally been found to invigorate plant resistance mechanisms (Yedidia et al., 2001). Successful *Trichoderma* strains can instigate a more grounded reaction in the plant contrasted with pathogen-triggered immunity by creating an assortment of microorganisms related molecular patterns (MAMPs), for example, hydrophobins, expansin-like proteins, metabolites, and catalysts like catalase, peroxidase, and superoxide dismutage, having a direct antimicrobial movement (Vargas et al., 2008). *Trichoderma* can likewise improve ETI by causing a quicker reaction (preparing), or initiate it by discharging exacerbates that, similarly as with some pathogen molecules, are explicitly perceived by plant cell receptors (Bailey et al., 1993). In the present exploration, the stress enzymes expressed in a higher amount in *Trichoderma* treatments rather than the control group. Mohapatra and Mittra (2017) and Swain et al. (2018) documented that *Trichoderma* spp. triggered the fabrication of antioxidant enzymes in wheat and rice seedlings, respectively. *Trichoderma* isolates were accounted to help fundamental defense reactions through different catalysts (Małolepsza et al., 2017). PPO is engaged with the plant guard system against pathogens by catalyzing the oxidation of phenols to quinines in an oxygen-subordinate way (Daw et al., 2008). An increase in defense enzymes activity (Mandal et al., 2013) and TP content (Mandal et al., 2013) in plants with a reaction to pathogen assault has also been previously reported.

Trichoderma Seed Biopriming Induces Antioxidant Gene Expression in Rice Plants

Plants have created solid cell antioxidant molecular systems because of the utilization of biocontrol specialists like *Trichoderma* (Rejeb et al., 2014; Swain et al., 2018), however the initiation and articulation of these genes change under plant organism communication conditions (Singh D. P. et al., 2020). Albeit, both organism-treated and non-treated plants were developed under typical development conditions. We investigated the plant molecular reactions as far as the outflow of prominent defense (PAL and DEFENSIN) and antioxidant (POX, LOX, and PR-3) genes following microbial inoculation (**Table 8**). We observe multifold over expression of genes in both the strains. However, *Trichoderma* seed biopriming caused >2-fold up regulation of every gene in both the rice varieties. Besides, CRRIT-15 exhibited the highest level of fold expression (i.e., >3) of all the genes as compared to control one. CRRIT-16 and CRRIT-2 treatment performed the second highest level of fold expression (i.e., >2.5) by following CRRIT-15 (**Figures 4**, **5**).

Seed biopriming with beneficial microbes have been accounted for their capacity to relieve biotic stress in an effective way. During the process of seed biopriming, antagonistic plant growth promotive activity increases on the seed surface, hence not only defending the plant from pathogen attack but also promoting the plant growth (Swain et al., 2018;

TABLE 8 | Details of primers used in antioxidant and defense related gene expression study.

Serial No.	Primer name	Gene name	Primer sequence 5′-3′
1	Rice (Actin)F	Actin	CTGCTGGAATGTGCTGAGAGAT
	Rice (Actin)R		CGTCTGCGATAATGGAACTGG
2	Rice (POX)F	Peroxidase	CATGCTACTGCTCACCTTTGA
	Rice (POX)R		TCACTCTAGGTGGGATATACT
3	Rice (LOX)F	Lipoxygenase	AGATGAGGCGCGTGATGAC
	Rice (LOX)R		CATGGAAGTCGAGCATGAACA
4	Rice (PAL)F	Phenylalanine ammonia lyase	GGTGTTCTGCGAGGTGATGA
	Rice (PAL)R		AGGGTGGTGCTTCAGCTTGT
5	Rice (Defensin)F	Defense Enzyme	CCGGCGAACTGCGTGTAC
	Rice (Defensin)R		GGCGTCGAGCAGAATTGG
6	Rice (PR-3)F	PR Protein	TACTGTGTCCAGAGCTCGCAGTGG
	Rice (PR-3)R		TCTGGTTGTAGCAGTCCAAGTTGG

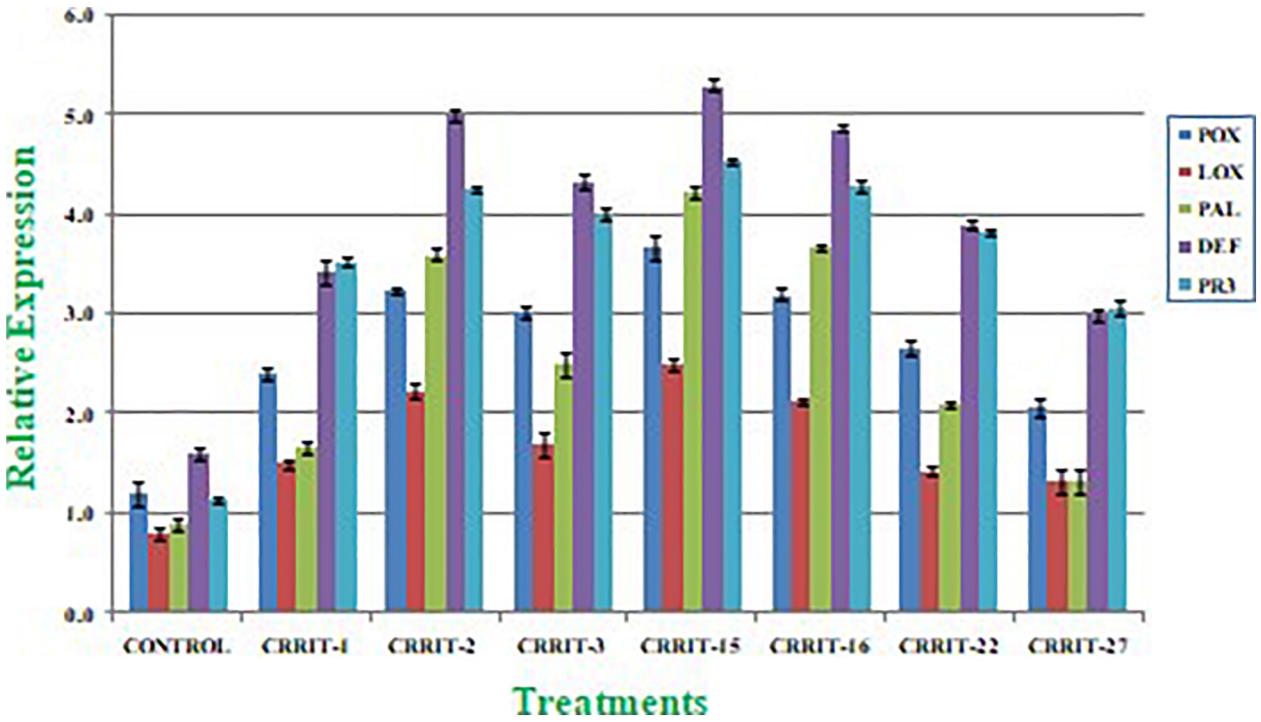

FIGURE 4 | Expression of antioxidant and defense related genes in rice variety (Annapurna). Results are expressed as means of three replicates and vertical bars indicate the standard deviation of the means.

Rajput et al., 2019). Co-vaccination of *Paenibacillus polymyxa* and *Rhizobium tropici* mitigated drought in common bean (*Phaseolus vulgaris* L.) (Figueiredo et al., 2008). In the present study it was found that *Trichoderma* treated plants exhibited an increase in total phenol content catalase content, peroxidase content superoxide dismutase content and expression of defense gene (POX, LOX, PAL, DFENSIN, and PR-3) as compared to control one. This further authenticates the induction of growth responses and defense response in rice up on application of *Trichoderma* in rice seeds. Plant phenolics are normally framed in light of both biotic and abiotic stress through enactment of phenyl propanoid pathway and include in cellulase, lignin, xylanase, and biosynthesis. Thus, PPO catalyzes phenolics, exacerbating the production of quinines through a secondary reaction, which further prompts the arrangement of an earthy colored complex polymer, melanin; a physical hindrance to microbe ingression (Taranto et al., 2017). In this study all the *Trichoderma* strains exhibited higher total phenol content, PPO activity as compared to the control one. Besides, CRRIT-15, CRIT-16, and CRRIT-2 out-perform the others. This suggests a synergistic effect of *Trichoderma* in induction of plant growth and defense in rice varieties. Notwithstanding these, acceptance of different development promotive genes and antioxidant agent responsive genes mitigates oxidative stress in plant

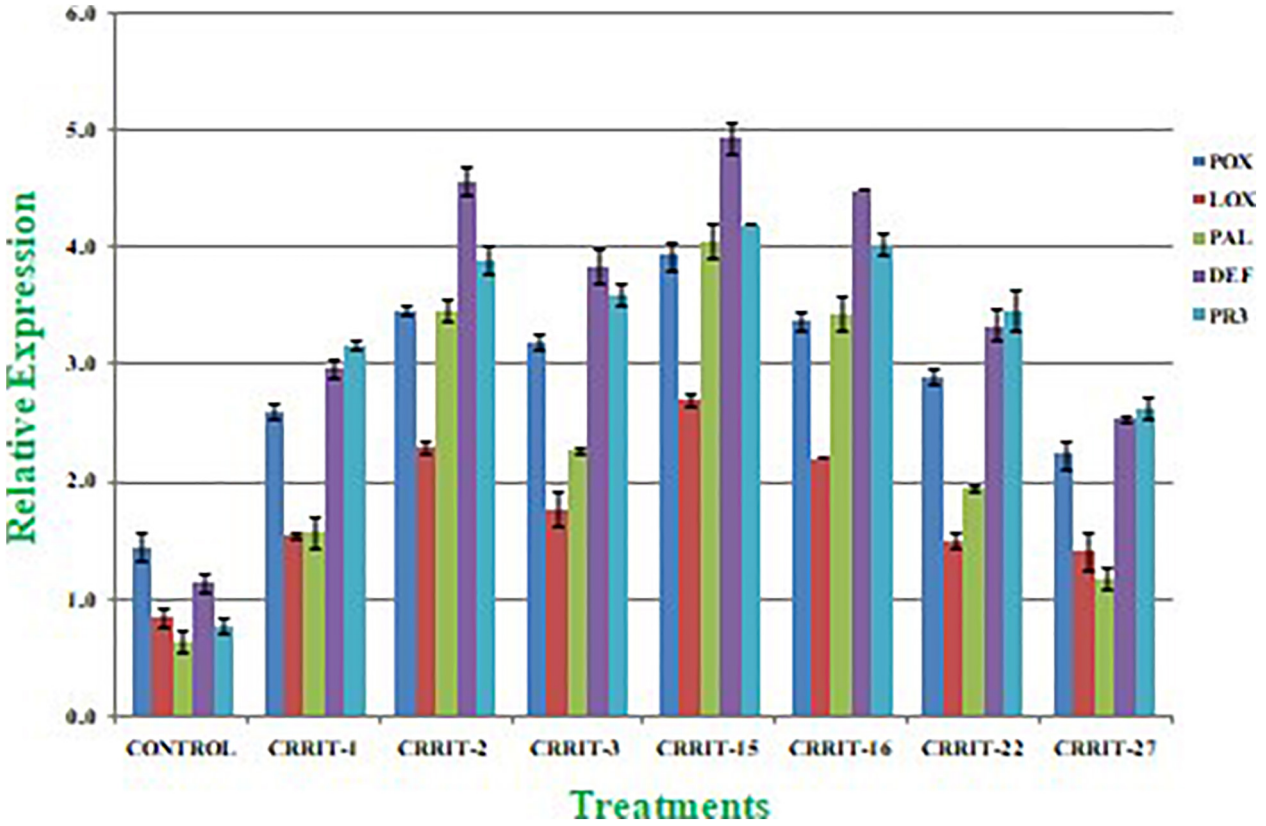

FIGURE 5 | Expression of antioxidant and defense related genes in rice variety (Satabdi). Results are expressed as means of three replicates and vertical bars indicate the standard deviation of the means.

cells. Our outcomes are validated with Singh et al. (2013) in which they revealed improved movement of PAL, PPO, PO, and SOD content in chickpea treated with *Pseudomonas*, *Trichoderma*, and *Rhizobium*. Contrasting these discoveries and our outcomes prompts the presumption that stronghold of rice with microbial inoculants characteristically balanced molecular components to give resilience against ROS scavenging in a manner to making plants fortified against stress difficulties. Rice seed biopriming of *Trichoderma* could, accordingly, become a proficient methodology for raising yield for better profitability and resistance against stress conditions.

CONCLUSION

In India alone, an excess of 250 commercial formulations are available, however, a large portion of them are from a solitary strain, i.e., *Trichoderma viride* (presently renamed as *Trichoderma asperelloides*). Most of the *Trichoderma* strains defined in literature were isolated from the soil or rhizosphere, but very few are isolated from the above ground aerial parts. In the present study we evaluated both the biocontrol and growth promotion activity of seven different *Trichoderma* strains isolated from above ground parts. The rice seed treatment with *Trichoderma* strains not only promoted germination, seedling vigor, and growth of the plant, but also increase the level of gene expression related to plant defense. Apart from growth promotion these strains imparted intrinsic stress tolerance to rice by producing a higher amount of defense enzymes like catalase, peroxidase, superoxide dismutase, polyphenol oxidase, and total phenolics content as evidenced by the expression of their respective genes. Our recent investigation tries to fill the gap by isolating and identifying above ground *Trichoderma* strains for rice health management. Two strains, namely *T. hebeiensis* and *T. erinaceum* may be promoted in sustainable crop management for their beneficial role.

DATA AVAILABILITY STATEMENT

The raw data supporting the conclusions of this article will be made available by the authors, without undue reservation.

AUTHOR CONTRIBUTIONS

HS: investigation, statistical analysis, and writing – original draft. TA: conceptualization and writing – review and editing. AM: conceptualization, writing – review and editing, project administration, resources, and supervision. PS, SS, AK, and RJ:

investigation. PB: methodology. SN: writing – review and editing, and project administration. SM: project administration. MB: statistical analysis. SKM and NZ: conducted the field trials and recorded the data. All authors contributed to the article and approved the submitted version.

ACKNOWLEDGMENTS

Authors are immensely thankful to Department of Science and Technology (DST), Govt. of India, for providing DST-INSPIRE Fellowship to Harekrushna Swain having Fellowship No. IF140749 (NRRI EAP-195). Authors duly acknowledge the Board of Research in Nuclear Science (BRNS), Department of Atomic Energy, and Govt. of India SANCTION No. 35/14/35/2016-BRNS/35159, dated on December 1, 2016 (NRRI EAP-233) and International Rice Research Institute, New Delhi, India (NRRI EAP-186) for providing funds. Authors are also thankful to Director, ICAR-NRRI, Cuttack-753006 and HOD, Department of Botany and Biotechnology, Ravenshaw University, Cuttack-753003 for providing necessary technical support.

SUPPLEMENTARY MATERIAL

The Supplementary Material for this article can be found online at: https://www.frontiersin.org/articles/10.3389/fmicb.2021.633881/full#supplementary-material

REFERENCES

Abdollahi, M., Rahnama, K., Marabadi, M., Ommati, F., and Zaker, M. (2012). The in vitro efficacy of Trichoderma isolates against *Pythium aphanidermatum*, the causal agent of sugar beet root rot. *J. Res. Agric. Sci.* 8, 79–87.

Abdul-Baki, A., and Anderson, J. D. (1973). Vigor determination in Soybean seed by multiple criteria. *Crop Sci.* 13, 630–633. doi: 10.2135/cropsci1973.0011183x001300060013x

Abraham, A., Philip, S., Jacob, C. K., and Jayachandran, K. (2013). Novel bacterial endophytes from *Hevea brasiliensis* as biocontrol agent against *Phytophthora* leaf fall disease. *Biocontrol* 58, 675–684. doi: 10.1007/s10526-013-9516-0

Arnon, D. I. (1949). Copper enzymes in isolated chloroplast: polyphenol oxidase in *Beta vulgaris*. *Plant Physiol.* 24, 1–15. doi: 10.1104/pp.24.1.1

Bailey, B. A., Korcak, R. F., and Anderson, J. D. (1993). Sensitivity to an ethylene biosynthesis-inducing endoxylanase in *Nicotiana tabacum*-L cv xanthi is controlled by a single dominant gene. *Plant Physiol.* 101, 1081–1088. doi: 10.1104/pp.101.3.1081

Bailey, M. J., Biely, P., and Poutanen, K. (1992). Inter-laboratory testing of methods for assay of xylanase activity. *J. Biotechnol.* 23, 257–270. doi: 10.1016/0168-1656(92)90074-j

Cai, F., Yu, G., Wang, P., Wei, Z., Fu, L., Shen, Q., et al. (2013). Harzianolide, a novel plant growth regulator and systemic resistance elicitor from *Trichoderma harzianum*. *Plant Physiol. Biochem.* 73, 106–113. doi: 10.1016/j.plaphy.2013.08.011

Celar, F. (2003). Competition for ammonium and nitrate forms of nitrogen between some phytopathogenic and antagonistic soil fungi. *Biol. Control* 28, 19–24. doi: 10.1016/s1049-9644(03)00049-5

Contreras-Cornejo, H. A., Macias-Rodríguez, L., Cortés-Penagos, C., and López-Bucio, J. (2009). Trichoderma virens, a plant beneficial fungus, enhances biomass production and promotes lateral root growth through an auxin-dependent mechanism in *Arabidopsis*. *Plant Physiol.* 149, 1579–1592. doi: 10.1104/pp.108.130369

Daw, B. D., Zhang, L. H., and Wang, Z. Z. (2008). Salicylic acid enhances antifungal resistance to *Magnaporthe grisea* in rice plants. *Austral. Plant Pathol.* 37, 637–644. doi: 10.1071/ap08054

Druzhinina, I. S., Seidl-Seiboth, V., Herrera-Estrella, A., Horwitz, B. A., Kenerley, C. M., Monte, E., et al. (2011). Trichoderma: the genomics of opportunistic success. *Nat. Rev. Microbiol.* 9, 749–759. doi: 10.1038/nrmicro2637

Dunaitsev, I. A., Kolombet, L. V., Zhigletsova, S. K., Bystrova, E. V., Besaeva, S. G., Klykova, M. V., et al. (2008). Phosphate releasing microorganisms with antagonistic activity against phytopathogenic microorganisms. *Mikol. Fitopatol.* 42, 264–269.

Figueiredo, M. V. B., Buritya, H. A., Martínez, C. R., and Chanway, C. P. (2008). Alleviation of drought stress in the common bean (*Phaseolus vulgaris* L.) by co-inoculation with *Paenibacillus polymyxa* and *Rhizobium tropici*. *Appl. Soil Ecol.* 40, 182–188. doi: 10.1016/j.apsoil.2008.04.005

Florencio, C., Couri, S., and Farinas, C. S. (2012). Correlation between agar plate screening and solid state fermentation for the prediction of cellulase production by Trichoderma strains. *Enzyme Res.* 2012:793708. doi: 10.1155/2012/793708

Gams, W., and Bissett, J. (1998). "Morphology and identification of Trichoderma," in *Trichoderma and Gliocladium*, Vol. 1, eds C. P. Kubicek and G. E. Harman (London: Taylor and Francis), 1–34.

Ghosh, T. K. (1987). Measurement of cellulase activities. *Pure Appl. Chem.* 59, 257–268. doi: 10.1351/pac198759020257

Gochev, V. K., and Krastanov, A. I. (2007). Isolation of laccase producing trichoderma species. *Bulgarian J. Agric. Sci.* 13, 171–176.

Gravel, V., Antoun, H., and Tweddell, R. J. (2007). Growth stimulation and fruit yield improvement of greenhouse tomato plants by inoculation with *Pseudomonas putida* or *Trichoderma atroviride*: possible role of indole acetic acid (IAA). *Soil Biol. Biochem.* 39, 1968–1977. doi: 10.1016/j.soilbio.2007.02.015

Harman, G. E. (2011). Multifunctional fungal plant symbionts: new tools to enhance plant growth and productivity. *New Phytol.* 189, 647–649. doi: 10.1111/j.1469-8137.2010.03614.x

Holker, U., Dohse, J., and Hofer, M. (2002). Extracellular Laccase in ascomycetes *Trichoderma atroviridae* and *Trichoderma harzianum*. *Folia Microbiol.* 47, 423–427.

Hossain, M., Sultana, F., Kubota, M., Koyama, H., and Hyakumachi, M. (2007). The plant growth-promoting fungus *Penicillium simplicissimum* GP17-2 induces resistance in *Arabidopsis thaliana* by activation of multiple defense signals. *Plant Cell Physiol.* 48, 1724–1736. doi: 10.1093/pcp/pcm144

Jackson, M. L. (1973). *Soil Chemical Analysis*. New Delhi: Printice hall of India, 392.

Jahagirdar, S., Kambrekar, D. N., Navi, S. S., and Kunta, M. (2019). "Plant growth-promoting fungi: diversity and classification," in *Bioactive Molecules in Plant Defense*, eds S. Jogaiah and M. Abdelrahman (Cham: Springer).

Juturu, V., and Wu, J. C. (2014). Microbial cellulases: engineering production and applications. *Renew. Sustain. Energy Rev.* 33, 188–203. doi: 10.1016/j.rser.2014.01.077

Kalra, K., Chauhan, R., Shavez, M., and And Sachdeva, S. (2013). Isolation of laccase producing Trichoderma species and effect of pH and temperature on its activity. *Int. J. ChemTech Res.* 5, 2229–2235.

Kang, S. W., Park, Y. S., Lee, J. S., Hong, S. I., and Kim, S. W. (2004). Production of cellulases and hemicellulases by *Aspergillus niger* KK2 from lignocellulosic biomass. *Bioresour. Technol.* 91, 153–156. doi: 10.1016/s0960-8524(03)00172-x

Kar, S., Mandal, A., Das Mohapatra, P. K., Mondal, K. C., and Pati, B. R. (2006). Production of cellulase free xylanase by *Trichoderma reesei* SAF3. *Braz. J. Microbiol.* 37, 462–464. doi: 10.1590/s1517-83822006000400011

Keeney, D. R., and Bremner, J. M. (1965). Steam distillation methods for determining of ammonium, nitrate and nitrite. *Anal. Chim. Acta* 32, 485–497. doi: 10.1016/s0003-2670(00)88973-4

Kumar, K., Amaresan, N., Bhagat, S., Madhuri, K., and Srivastava, R. C. (2012). Isolation and characterization of *Trichoderma* spp. for antagonistic activity against root rot and foliar pathogens. *Indian J. Microbiol.* 52, 137–144. doi: 10.1007/s12088-011-0205-3

Lee, S., Jang, Y., Lee, Y. M., Lee, J., Lee, H., Kim, G. H., et al. (2011). Rice straw-decomposing fungi and their cellulolytic and Xylanolytic enzymes. *J. Microbiol. Biotechnol.* 21, 1322–1329. doi: 10.4014/jmb.1107.07022

Małolepsza, U., Nawrocka, J., and Szczech, M. (2017). Trichoderma virens 106 inoculation stimulates defense enzyme activities and enhances phenolics levels in tomato plants leading to lowered Rhizoctonia solani infection. *Biocontrol Sci. Technol.* 27, 180–199. doi: 10.1080/09583157.2016.1264570

Mandal, S., Kar, I., Mukherjee, A. K., and Acharya, P. (2013). Elicitor-induced defense responses in *Solanum lycopersicum* against *Ralstonia solanacearum*. *Sci. World J.* 2013:561056. doi: 10.1155/2013/561056

Manwar, A. V., Rakh, R. R., Raut, L. S., and Dalvi, S. M. (2011). Biological control of Sclerotium rolfsii, causing stem rot of groundnut by *Pseudomonas* cf. monteilii. *Recent Res. Sci. Technol.* 3, 26–34.

Meera, T., and Balabaskar, P. (2012). Isolation and characterization of *Pseudomonas* fluorescens from rice fields. *Int. J. Food Agric. Vet. Sci.* 2, 113–120.

Mohapatra, S., and Mittra, B. (2017). Alleviation of *Fusarium oxysporum* induced oxidative stress in wheat by *Trichoderma viride*. *Arch. Phytopathol. Plant Protect.* 50, 84–96. doi: 10.1080/03235408.2016.1263052

Monssef, R., Abd Hassan, A., Enas, A., and Ramadan, M. E. (2016). Production of Laccase enzyme for their potential application to decolorize fungal pigments on aging and paper parchment. *Ann. Agric. Sci.* 61, 145–154. doi: 10.1016/j.aoas.2015.11.007

Mukherjee, A. K., Sampath, Kumar, A., Kranthi, S., and Mukherjee, P. K. (2014). Biocontrol potential of three novel *Trichoderma* strains: isolation, evaluation and formulation. *3Biotech* 4, 275–281. doi: 10.1007/s13205-013-0150-4

Mukherjee, A. K., Swain, H., Adak, T., and Chattopadhyaya, K. (2018). Evaluation of Trichoderma based product 'RiceVit' in farmers field of Chandol, Kendrapada, Odisha. *NRRI Newslett.* 39, 20–21.

Mukherjee, P. K., Horwitz, B. A., Singh, U. Shankar, Mukherjee, M., and Schmoll, M. (2013). *Trichoderma: Biology and Applications*. London: CAB International.

Noori, M. S. S., and Saud, H. M. (2012). Potential plant growth-promoting activity of *Pseudomonas* spp. isolated from paddy soil in Malaysia as biocontrol agent. *J. Plant Pathol. Microbiol.* 3:2. doi: 10.4172/2157-7471.1000120

Parmar, H. J., Bodar, N. P., Lakhani, H. N., Patel, S. V., Umrania, V. V., and Hassan, M. M. (2015). Production of lytic enzymes by Trichoderma strains during in vitro antagonism with Sclerotium rolfsii, the causal agent of stem rot of groundnut. *Afr. J. Microbiol. Res.* 9, 365–372. doi: 10.5897/ajmr2014.7330

Pathak, P., Bharadwaj, N., and Singh, A. K. (2014). Production of crude cellulase and xylanase from Trichoderma harzianum PPDDN10NFCCI-2925 and its application in photocopier waste paper recycling. *Appl. Biochem. Biotechnol.* 172, 3776–3797. doi: 10.1007/s12010-014-0758-9

Porra, R. J. (2002). The chequered history of the development and use of simultaneous equations for the accurate determination of chlorophylls a and b. *Photosynth. Res.* 73, 149–156. doi: 10.4324/9781351187596-10

Punja, Z. K., and Utkhede, R. S. (2003). Using fungi and yeasts to manage vegetable crop diseases. *Trends Biotechnol.* 21, 400–407. doi: 10.1016/s0167-7799(03)00193-8

Rajput, R. S., Singh, P., Singh, J., Vaishnav, A., Ray, S., and Singh, H. B. (2019). Trichoderma mediated seed biopriming augments antioxidant and phenylpropanoid activities in tomato plant against *Sclerotium rolfsii*. *J. Pharmacogn. Phytochem.* 8, 2641–2647.

Rejeb, I. B., Pastor, V., and Mauch-Mani, B. (2014). Plant responses to simultaneous biotic and abiotic stress: molecular mechanisms. *Plants* 3, 458–475. doi: 10.3390/plants3040458

Rudresh, D. L., Shivaprakash, M. K., and Prasad, R. D. (2005). Tricalcium phosphate solubilizing abilities of *Trichoderma* spp. in relation to P uptake and growth and yield parameters of chickpea (*Cicer arietinum* L.). *Can. J. Microbiol.* 51, 217–222. doi: 10.1139/w04-127

Saczi, A., Radford, A., and Erenler, K. (1986). Detection of cellulolytic fungi by using congo red as an indicator: a comparative study with the dinitrosalicylic acid reagent method. *J. Appl. Microbiol.* 61, 559–562. doi: 10.1111/j.1365-2672.1986.tb01729.x

Sadasivam, S., and Manickum, A. (2011). *Biochemical Methods*, third Edn. New Delhi: New Age International (P) Limited Publishers, 203–204.

Sancez, C. (2009). Lignocellulosic residues: biodegradation and bioconversion by fungi. *Biotechnol. Adv.* 27, 185–194. doi: 10.1016/j.biotechadv.2008.11.001

Saravanan, D., Dinesh, C., Kartikeyan, S., Vivekanandan, A., Nalankilli, G., and Ramachandran, T. (2008). Biopolishing of cotton fabrics with total cellulase of *Trichoderma reesei* and optimization using Taguchi methods. *J. Appl. Polym. Sci.* 112, 3402–3409. doi: 10.1002/app.29826

Saroj, P., Manasa, P., and Narasimhulu, K. (2018). Characterization of thermophilic fungi producing extracellular lignocellulolytic enzymes for lignocellulosic hydrolysis under solid state fermentation. *Bioresour. Bioprocess* 5:31. doi: 10.1186/s40643-018-0216-6

Singh, A., Sarma, B. K., Upadhyay, R. S., and Singh, H. B. (2013). Compatible rhizosphere microbes mediated alleviation of biotic stress in chickpea through enhanced antioxidant and phenylpropanoid activities. *Microbiol. Res.* 168, 33–40. doi: 10.1016/j.micres.2012.07.001

Singh, D. P., Singh, V., Shukla, R., Sahu, P., Prabha, R., Gupta, A., et al. (2020). Stage-dependent concomitant microbial fortification improves soil nutrient status, plant growth, antioxidative defense system and gene expression in rice. *Microbiol. Res.* 239:126538. doi: 10.1016/j.micres.2020.126538

Singh, P., Singh, J., Ray, S., Rajput, R. S., Vaishnav, A., Singh, R. K., et al. (2020). Seed biopriming with antagonistic microbes and ascorbic acid induce resistance in tomato against *Fusarium* wilt. *Microbiol. Res.* 237:126482. doi: 10.1016/j.micres.2020.126482

Sureshrao, K. S., Pradeeprao, K. V., Dnyanobarao, G. S., Agrawal, T., and Kotasthane, A. S. (2016). Efficiency of different trichoderma isolates on plant growth promoting activity in rice (*Oryza sativa* L.). *Int. J. Bio Resour. Stress Manag.* 7, 489–500.

Swain, H., Adak, T., Mukherjee, A. K., Mukherjee, P. K., Bhattacharyya, P., Behera, S., et al. (2018). Novel Trichoderma strains. isolated from tree barks as potential biocontrol agents and biofertilizers for direct seeded rice. *Microbiol. Res.* 214, 83–90. doi: 10.1016/j.micres.2018.05.015

Swain, H., and Mukherjee, A. K. (2020). "Host–pathogen–trichoderma interaction," in *Trichoderma*, eds A. Sharma and P. Sharma (Singapore: Springer), 149–165. doi: 10.1007/978-981-15-3321-1_8

Taranto, F., Pasqualone, A., Mangini, G., Tripodi, P., Miazzi, M., Pavan, S., et al. (2017). Polyphenol oxidases in crops: biochemical, physiological and genetic aspects. *Int. J. Mol. Sci.* 18:377. doi: 10.3390/ijms18020377

Teather, R. M., and Wood, P. J. (1982). Use of Congo red-polysaccharide interactions in enumeration and characterization of cellulolytic bacteria from the bovine rumen. *Appl. Environ. Microbiol.* 43, 777–780. doi: 10.1128/aem.43.4.777-780.1982

Vargas, W. A., Djonovic, S., Sukno, S. A., and Kenerley, C. M. (2008). Dimerization controls the activity of fungal elicitors that trigger systemic resistance in plants. *J. Biochem. Chem.* 283, 19804–19815. doi: 10.1074/jbc.m802724200

Velazquez-Cedeno, M. A., Farnet, A. M., Ferre, E., and Savoie, J. M. (2004). Variations of lignocellulosic activities in dual cultures of *Pleurotuso streatus* and *Trichoderma longibrachiatum* on unsterilized wheat straw. *Mycologia* 96, 712–719. doi: 10.2307/3762105

Walkley, A., and Black, I. A. (1934). An examination of the Degtareff method for determining soil organic matter, and a proposed modification of the chromic acid titration method. *Soil Sci.* 37, 29–38. doi: 10.1097/00010694-193401000-00003

Whipps, J. M., and Lumsden, R. D. (2001). "Commercial use of fungi as plant disease biological control agents: status and prospects," in *Fungi as Biocontrol Agents: Progress, Problems and Potential*, eds T. M. Butt, C. Jackson, and N. Magan (Wallingford: CABI Publishing), 9–22. doi: 10.1079/9780851993560.0009

Woo, S. L., Ruoco, M. F., and Vinale, F. (2014). Trichoderma-based products and their widespread use in agriculture. *Open Mycol. J.* 8(Suppl. 1, M4), 71–126. doi: 10.2174/1874437001408010071

Yedidia, I., Srivastva, A. K., Kapulnik, Y., and Chet, I. (2001). Effect of Trichoderma harzianum on microelement concentrations and increased growth of cucumber plants. *Plant Soil* 235, 235–242.

Zhang, S., Xu, B., and Gan, Y. (2019). Seed treatment with *Trichoderma longibrachiatum* T6 promotes wheat seedling growth under Nacl stress through activating the enzymatic and non-enzymatic antioxidant defense system. *Int. J. Mol. Sci.* 20:3729. doi: 10.3390/ijms20153729

Conflict of Interest: The authors declare that the research was conducted in the absence of any commercial or financial relationships that could be construed as a potential conflict of interest.

frontiers in Plant Science

ORIGINAL RESEARCH
published: 18 March 2021
doi: 10.3389/fpls.2021.636121

5-Aminolevulinic Acid Improves Morphogenesis and Na^+ Subcellular Distribution in the Apical Cells of *Cucumis sativus* L. Under Salinity Stress

*Yue Wu[1], Na Liu[1], Linli Hu[1], Weibiao Liao[1], Zhongqi Tang[1], Xuemei Xiao[1], Jian Lyu[1], Jianming Xie[1], Alejandro Calderón-Urrea[2,3] and Jihua Yu[1,4]**

[1]College of Horticulture, Gansu Agricultural University, Lanzhou, China, [2]Department of Biology, College of Science and Mathematics, California State University, Fresno, Fresno, CA, United States, [3]College of Plant Protection, Gansu Agricultural University, Lanzhou, China, [4]Gansu Provincial Key Laboratory of Arid Land Crop Science, Gansu Agricultural University, Lanzhou, China

OPEN ACCESS

Edited by:
Youssef Rouphael,
University of Naples Federico II, Italy

Reviewed by:
Jin Sun,
Nanjing Agricultural University, China
Mohsin Tanveer,
University of Tasmania, Australia

***Correspondence:**
Jihua Yu
yujihuagg@163.com
orcid.org/0000-0001-5849-7636

Specialty section:
This article was submitted to Plant Abiotic Stress, a section of the journal Frontiers in Plant Science

Received: 30 November 2020
Accepted: 22 February 2021
Published: 18 March 2021

Citation:
Wu Y, Liu N, Hu L, Liao W, Tang Z, Xiao X, Lyu J, Xie J, Calderón-Urrea A and Yu J (2021) 5-Aminolevulinic Acid Improves Morphogenesis and Na^+ Subcellular Distribution in the Apical Cells of Cucumis sativus L. Under Salinity Stress. Front. Plant Sci. 12:636121. doi: 10.3389/fpls.2021.636121

Soil salinity causes damage to plants and a reduction in output. A natural plant growth regulator, 5-aminolevulinic acid (ALA), has been shown to promote plant growth under abiotic stress conditions. In the present study, we assessed the effects of exogenously applied ALA (25 mg L^{-1}) on the root architecture and Na^+ distribution of cucumber (*Cucumis sativus* L.) seedlings under moderate NaCl stress (50 mmol L^{-1}). The results showed that exogenous ALA improved root length, root volume, root surface area, and cell activity in the root tips, which were inhibited under salt stress. In addition, although salinity stress increased the subcellular Na^+ contents, such as those of the cell wall, nucleus, plastid, and mitochondria, ALA treatment reduced these Na^+ contents, except the soluble fraction. Molecular biological analysis revealed that ALA application upregulated both the SOS1 and HA3 transcriptional and translational levels, which suggested that the excretion of Na^+ into the cytoplasm cloud was promoted by exogenous ALA. Meanwhile, exogenously applied ALA also upregulated the gene and protein expression of NHX1 and VHA-A under salinity stress, which suggested that the compartmentalization of Na^+ to the vacuole was enhanced. Overall, exogenous ALA mitigated the damage caused by NaCl in cucumber by enhancing Na^+ redistribution and increasing the cytoactivity of root cells.

Keywords: salinity, 5-aminolevulinic acid, Na^+ distribution, proton pump, Na^+/H^+ antiporter, root architecture

INTRODUCTION

High salinity levels in cultivated fields are caused by a combination of factors, such as excessive chemical fertilizer application, prolonged cultivation, or the effects of global climate change. Globally, almost 30 plant species provide 90% of the food consumed by the human population (Zörb et al., 2019). However, most of these species are salt-sensitive, and more than 20% of crops are affected by soil salinity (Negrão et al., 2016). Therefore, ways to improve the salt tolerance of crops has received a recent increase in research attention among agricultural scientists.

The imbalance of the K^+/Na^+ ratio under salt stress conditions adversely affects plant growth (Shah et al., 2021). Specifically, the harmful effects of high Na^+ concentration in the cytoplasm leads to ion toxicity, which can be observed at the whole-plant level, as lower growth rates and leaf and root damage. Under saline conditions, extracellular Na^+ competes with the K^+ transport in cells because Na^+ and K^+ have a similar hydrated radius (Gong et al., 2010). The flow of Na^+ into cells is a passive process, which requires a negative electric potential difference across the plasma membrane. However, the displacement of Na^+ is an active process that involves Na^+/H^+ antiporters located on the plasma membrane and tonoplast, which regulate the compartmentation and efflux of Na^+ (Yamaguchi et al., 2013). The Na^+/H^+ antiporters on the plasma membrane and tonoplast are encoded by *salt overly sensitive 1* (*SOS1*) and Na^+/H^+ exchanger (*NHX1*), respectively (Zhang et al., 2017; Tanveer, 2020). The cytoplasmic enzymes of halophytes are as sensitive to salinity levels as the enzymes of glycophytes (Wakeel et al., 2011). Therefore, to alleviate the ion toxicity, Na^+ can be compartmentalized into vacuole or excreted out of protoplast. The adaption of halophilous plants in saline conditions is due to their active and efficient reduction of cytoplasmic Na^+ levels, and their ability to maintain relatively lower Na^+ concentrations and higher K^+/Na^+ ratios in the cytoplasm (Cuin et al., 2011).

Ion imbalance induced by salinity directly affects plant growth in the rhizosphere environment. Under saline conditions, the Na^+ and K^+ contents have been shown to sharply increase and decrease in root cells, respectively (Zhang et al., 2018; Huo et al., 2020). Additionally, salt stress negatively affects the lateral root number and total root length, which leads to an incomplete root system architecture (Julkowska et al., 2017). Meanwhile, H^+-pumps and Na^+/K^+ transporters, which contribute to cell ion exchange and homeostasis, respond (i.e., are up- or downregulated) to high Na^+ conditions as physiological adaptations (Zhao et al., 2016; Yan et al., 2020). In addition, lipid peroxidation occurs in root cells; thus causing increases in reactive oxygen species (Nath et al., 2019) and a reduction in root cell activity (Wang et al., 2020).

5-Aminolevulinic acid (ALA) is a metabolic intermediate in plants, animals, and bacteria. The downstream metabolic pathway of ALA provides chlorophyll, heme, siroheme, vitamin B_{12}, and phytochromobilin in higher plants (Wu et al., 2019b). ALA has been considered to play a promotive role in plants under abiotic stress and normal conditions (Ali et al., 2013a,b). Under saline conditions, the gene expression levels of proline synthesis can be upregulated by ALA in *Brassica napus* L. seedlings (Xiong et al., 2018). Moreover, exogenous ALA was shown to regulate the accumulation of H_2O_2 in roots to activate the relative gene expression of Na^+ transporters, which mitigated the harmful effect of salt on the shoots (Wu et al., 2019a). Our previous study showed that exogenous ALA enhanced the photosynthesis of cucumber leaves under NaCl stress by upregulating chlorophyll biosynthesis (Wu et al., 2018). In this study, we conducted physiological and molecular level investigations to explore the promotive role of ALA on cucumber roots under saline (NaCl) rhizospheric conditions. Further, we also investigated the root architecture, ultrastructure of apical cells, and Na^+ distribution of cucumber root cells, and the mechanism by which ALA application impacted these factors.

MATERIALS AND METHODS

Plant Material and Growth Conditions

Cucumber (*Cucumis sativus* L. 'Xinchun No. 4') seedlings were used as the plant material. Healthy plump seeds were selected and sterilized with 0.03% potassium permanganate solution for 10 min. After soaking for 6 h in distilled water, seeds were placed on wet filter paper under dark conditions (28 ± 1°C). After germination, seedlings were grown in a climatic cabinet for 5 days, with a light intensity of 350–450 μmol m^{-2} s^{-1}, photoperiod 12/12 h, temperature of 28/18°C (day/night), and relative humidity of 50–60%. Seedlings with fully spread cotyledons, of uniform size, and with healthy roots were selected and transferred to opaque plastic containers for hydroponic culturing. Each container contained four cucumber seedlings. During plant cultivation, the half-strength Yamasaki cucumber nutrient solution was used [$Ca(NO_3)_2$ 1.75 mmol L^{-1}, KNO_3 3 mmol L^{-1}, $NH_4H_2PO_4$ 0.5 mmol L^{-1}, and $MgSO_4{\cdot}7H_2O$ 1 mmol L^{-1}]. The nutrient solution was changed at 2-day intervals. The experimental treatments were executed using seedlings that had been grown for 30 days.

Experimental Design

Cucumber seedlings with three fully expanded true leaves, uniform size, and healthy roots were selected for the treatments. Four treatments were used in this study: (1) Control: normal nutrient solution; (2) NaCl: 50 mmol L^{-1} NaCl in nutrient solution; (3) NaCl + ALA: 50 mmol L^{-1} NaCl in nutrient solution + 25 mg L^{-1} foliar sprayed ALA, and (4) ALA: normal nutrient solution + 25 mg L^{-1} foliar sprayed ALA. The concentrations of moderate NaCl stress and optimal ALA application were selected based on the findings of our previous study (Wu et al., 2018). ALA (Sigma Aldrich, United States) applications were applied by thoroughly spraying the prepared solution on both the upper and lower surfaces of leaves with a hand sprayer (200 ml per treatment). Moreover, ALA applications involved two treatments, i.e., at 0 and 24 h. In the treatments that did not receive ALA applications, distilled water was sprayed in the same manner. Each replication comprised 10 containers, and each treatment was replicated three times. Experimental treatments were arranged in a completely randomized design. The nutrient solution was changed at 2-day intervals and aerated continuously with an air pump. All indexes were measured at 10 days after treatment application.

Root Morphology Indexes

The roots were removed from the seedlings and rinsed with distilled water. The root architecture was photographed using a root scanner (STD 4800, Canada), and the root morphology indexes (including total root length, root volume, root surface

area, and number of root tips) were analyzed using Win RHIZO 5.0 (Regent Instruments, Inc., Canada).

Root Activity and Cell Viability Staining

For fluorescence microscopy, fluorescein diacetate (FDA; 5 mg; Sigma Aldrich, United States) was dissolved in 1 ml acetone. The FDA solution (0.4 ml) was then made up to volume (5 ml) with 0.65 mmol L^{-1} mannitol. Propidium iodide (PI; 2 mg; Sigma Aldrich, United States) was dissolved in 0.65 mmol L^{-1} mannitol, and made up to volume of 5 ml. The FDA and PI solutions were mixed in equal volumes, and the root tips were soaked in the mixed solution for 40 min in the dark, and then washed three times with deionized water for 5 min each. Red and green fluorescence and concurrent images were obtained with a fluorescent microscope (Leica DM600 400×, Germany) at 485 and 530 nm, excitation and emission, respectively. The fluorescence densities of the FDA and PI solutions were analyzed using ImageJ software.

Root activity was determined according to the method of Zhang et al. (2013). Root tip samples (0.5 g) were soaked in a solution containing 5 ml 0.4% (w/v) triphenyl tetrazolium chloride (TTC) and 5 ml PBS (pH 7.0) under dark conditions for 1 h at 37°C. Sulfuric acid (2 ml, 1 mol L^{-1}) was then added to end the reduction of TTC. Root samples were ground with 5 ml of acetic ether and quartz sand. The extracted solution from the root was fixed to 10 ml with acetic ether. Absorbance was measured at 485 nm, and the root activity was calculated according to the standard curve.

Contents of Na^+, K^+ in Root Subcellular Fraction

The subcellular fractions of cucumber roots were separated according to the method described by Jabeen et al. (2014). Root samples were fully homogenized with 5 ml extracting solution (0.25 mol L^{-1} sucrose, 50 mmol L^{-1}, pH 7.5 Tris-HCl, and 1 mmol L^{-1} dithioerythritol), and then filtered through a filter cloth (80 μm). The filter residue was the cell wall fraction. The filtrate was made up to volume (40 ml) with the extraction solution mentioned previously. The solution was centrifuged at 1,500 × *g* for 10 min to obtain the sediment (the plastid fraction). The supernatant was then centrifuged at 5,000 × *g* for 20 min to obtain the nucleus fraction, and again at 15,000 × *g* for 30 min to obtain the mitochondrial fraction. The final supernatant represented the soluble fraction of the root cell. Every subcellular fraction was dried in an oven, and the Na^+ and K^+ contents were determined using an atomic absorption spectrometer (ZEEnit 700P, Analytik Jena, Germany).

Fluorescence Microscopy of Na^+ on Root Tip and Hypocotyl

The fluorescence of Na^+ was observed according to the method of Bonales-Alatorre et al. (2013). Coro-Na™-Green AM (Invitrogen, Thermo Fisher Scientific, United States) was assisting dissolved by 0.2 ml dimethyl sulfoxide. Samples with four repetitions in each treatment were stained with 15 μmol L^{-1} CoroNa™-Green AM, which was dissolved by Ca^{2+}-MES (pH 6.1). Root tip and hypocotyl of seedlings were length cut and stained in dark condition for 1 h and then washed three times with deionized water for 5 min each. The green fluorescence of Na^+ and images were obtained with a fluorescent microscope (Leica DM600 400×, Germany) at 488 and 525 nm, excitation and emission, respectively. The relative green fluorescence intensity of Na^+ revealed in root or hypocotyl was analyzed using ImageJ software, which indicated the light intensity of in unit area of each sample.

Western Blot Analysis

The protein expression levels of Na^+/H^+ antiporter in plasma membrane (SOS1), Na^+/H^+ antiporter in tonoplast (NHX1), H^+-ATPase in plasma membrane (HA3), and H^+-ATPase in tonoplast were analyzed by Western blotting. The membrane protein of cucumber plants was extracted using the TCA/acetone method. The concentration of protein samples was measured using the bicinchoninic acid (BCA) method and a BCA Protein Assay Kit (Beyotime Biotechnology, P.R. China). Membrane protein samples were separated by SDS-PAGE. The separated proteins were transferred onto a polyvinylidene difluoride (PVDF) membrane, and the nonspecific binding of antibodies was blocked with 5% non-fat dried milk in PBS for 1 h at 25 ± 1°C. Membranes were then incubated overnight at 4°C with polyclonal antibodies at the appropriate dilution against SOS1 (1:2500; Agrisera, Vännäs, Sweden), NHX1 (1:2500; Agrisera, Vännäs, Sweden), HA3 (1:2500; Agrisera, Vännäs, Sweden), and VHA-A (1:5000; Abcam, Shanghai, China). The PVDF membrane was then incubated with goat anti-rabbit IgG (H&L) and HRP-conjugated secondary antibody (diluted 1:3000) for 1 h at room temperature. The color was developed using an electrochemiluminescence (ECL) substrate (BioRad, United States). Finally, the developed films were scanned and precisely quantified using Amersham Imager 600 (General Electric, United States).

Real-Time qPCR Analysis

The gene transcriptional levels of *SOS1*, *NHX1*, *HA3*, and *VHA-A* were determined by q-PCR. The cucumber *U6* gene was used as an internal control. The gene bank accession numbers of the sequences used to design the primers are shown in **Table 1**. Treatment samples were randomly obtained from three roots, and each treatment was replicated three times. The TaKaRa MiniBEST Plant RNA Extraction Kit (TaKaRa Biomedicals, Japan) was used to extract the total RNA from cucumber roots. The cDNA was synthesized using the Revert Aid First Strand cDNA Synthesis Kit (Thermo Scientific, United States). The reaction system of the PCR test consisted of 2 μl cDNA, 0.8 μl forward primer, 0.8 μl reverse primer, 10 μl 2 × Tli RNaseH Plus, and 6.4 μl RNase Free dH_2O. The PCR procedure was executed for three technical replications per biological sample. The PCR reaction conditions were as follows: first, 95°C for 30 s for the initial denaturation, and then 95°C for 5 s, 60°C for 30 s for the cycle steps (40 cycles), 95°C for 5 s, 60°C for 60 s for the melting curve, and, finally, 50°C for 30 s for the cooling step. Quantification analyses were conducted using the comparative CT value method, following Livak and Schmittgen (2001).

Ultrastructure Observation

Fresh root tip samples (0.5 cm) were fixed in 3% glutaraldehyde in 0.1 mol L^{-1} phosphate buffer (pH 7.4) for 48 h at 4°C, and then fixed in 1% H_2OsO_4 solution for 5 h. Samples were then dehydrated using a graded ethanol series (70, 80, 90, and 100%) and then embedded in Epon812 epoxy resin. Ultrathin slices were cut using a microtome (Leica EM UC6 ultra-microtome, Japan), and the tissue slices were stained with uranyl acetate and lead citrate for 15 min. Ultrathin tissue slices of cucumber roots were observed and photographed using a transmission electron microscope (TEM, Joel JEM-1230, Japan).

Statistical Analysis

Analyses of variance were performed using SPSS 22.0 (SPSS Institute Inc., United States) software, and the treatment means were compared using Tukey's test, at a 0.05 level of probability. The results are expressed as means ± SEs. All figures were prepared using OriginPro2017 (OriginLab Institute Inc., United States) software.

RESULTS

ALA Treatment Restored Root Morphology Changes Associated With Salt Stress

Under salt stress, the total root length, number of root tips, root volume, and root surface area decreased by 33.96, 46.13, 58.17, and 47.46%, respectively (**Table 2** and **Figure 1**). However, exogenous application of ALA restored root growth to the level observed in the control group. Furthermore, the total root length was significantly improved by ALA under conditions without salt stress.

ALA Treatment Abrogated Root Cell Activity Changes Associated With Salt Stress

The results of the living-dead fluorescence analysis of root cells are shown in **Figures 2A–D**. The control group root cells showed relatively higher green fluorescence. Red fluorescence was enhanced on the root tip under NaCl stress, especially in the apical elongation zone, which was wilted. The root

TABLE 1 | Primer sequences and Genbank accession numbers of *SOS1*, *NHX1*, *HA3*, *VHA-A*, and *U6* gene.

Gene symbol	Accession number	Forward primer	Reverse primer
SOS1	JQ655747.1	5'-AGGAAGGTTCAAAGCCTAGTG-3'	5'-CATGAGTAAATGTGGGGTGCA-3'
NHX1	FJ843078.1	5'-TGCTTTTGCCACCCTTTCA-3'	5'-TTCCAACCAGAACCAATCCC-3'
HA3	EF375892.2	5'-TGGAAAACAAGACCGCCTTT-3'	5'-GGTTGGAGGCCATGTAAGGTT-3'
VHA-A	AY580162.1	5'-CATTCCTGGAGCGTTTGGTT-3'	5'-CATTTCATTTCCTCTCTCTCCACAA-3'
U6	JW929310.1	5'-ACAGAGAAGATTAGCATGGCC-3'	5'-GACCAATTCTCGATTTGTGCG-3'

TABLE 2 | Effects of exogenous 5-aminolevulinic acid (ALA) on root morphology parameters of cucumber seedlings under salt stress.

Treatment	Total root length (cm $plant^{-1}$)	Root tips number (# $plant^{-1}$)	Root volume (cm^3 $plant^{-1}$)	Root surface area (cm^2 $plant^{-1}$)
Control	2067.72 ± 130 b	1,589 ± 117 a	4.59 ± 0.43 a	345.38 ± 27 a
NaCl	1365.53 ± 3 c	856 ± 62 b	1.92 ± 0.09 b	181.45 ± 4 b
NaCl+ALA	1989.07 ± 98 b	1,616 ± 239 a	4.64 ± 0.96 a	337.54 ± 42 a
ALA	2426.27 ± 64 a	1,116 ± 106 ab	6.09 ± 0.33 a	430.46 ± 10 a

Value (mean ± SE) was the mean of three independent experiments, and significant differences ($p < 0.05$) among different treatments were indicated by different letters.

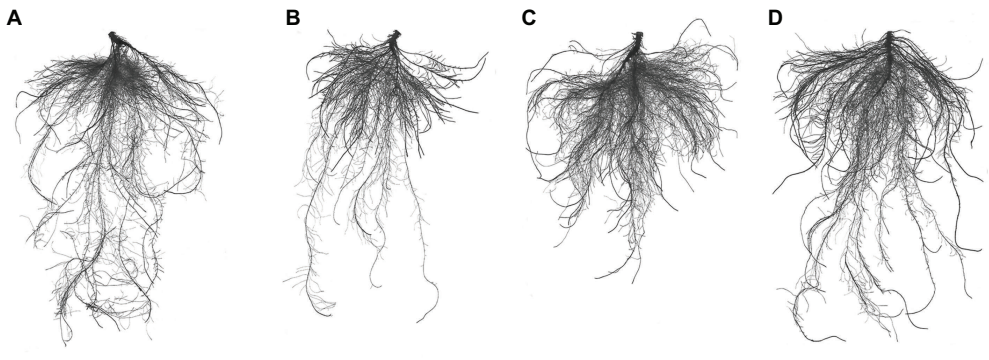

FIGURE 1 | Root architecture characteristics of cucumber seedlings. **(A)** Normal growth condition. **(B)** Treatment with 50 mmol L^{-1} NaCl. **(C)** Treatment with 50 mmol L^{-1} NaCl + 25 mg L^{-1} ALA. **(D)** Treatment with 25 mg L^{-1} ALA under normal growth condition.

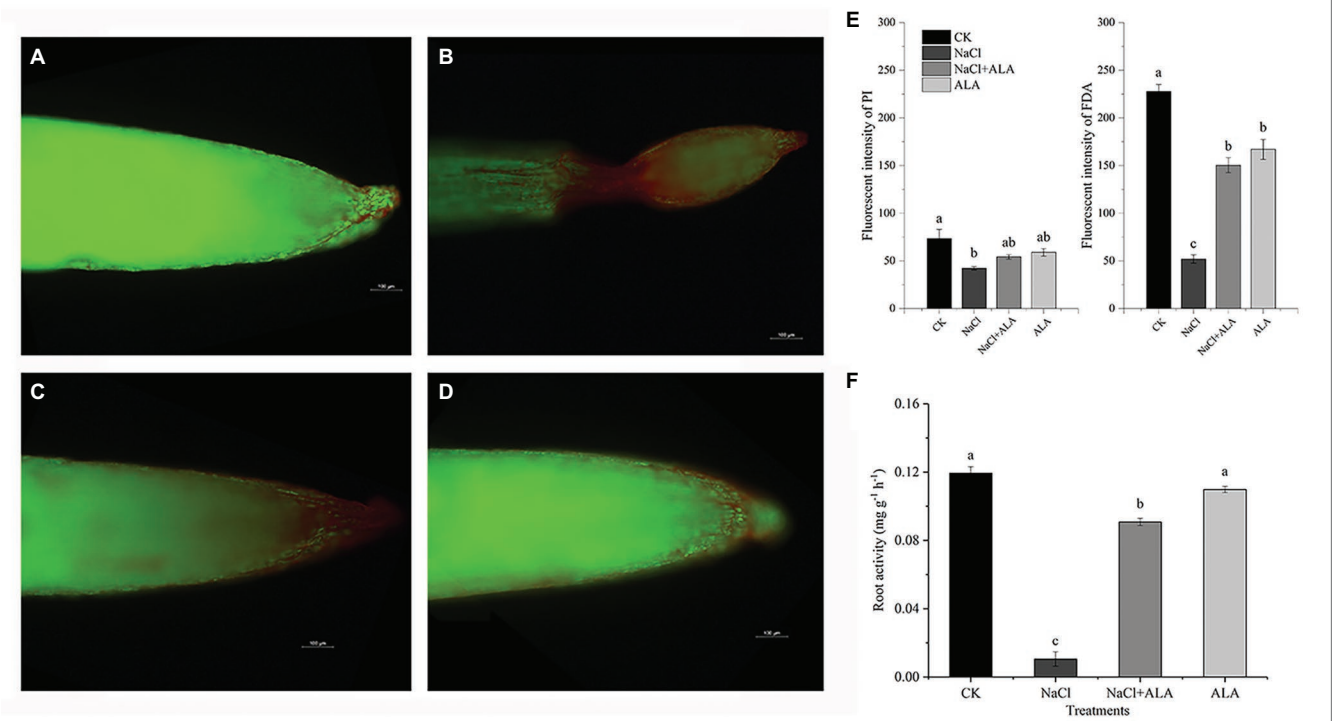

FIGURE 2 | The living-death cell fluorescence and activity of apical cells of cucumber seedlings. **(A–D)** Viable cells show green fouorescence while non-viable cells show red. **(E)** Fluorescence intensities of green and red fouorescence. **(F)** Root tip activities of cucumber seedlings. Data represent means of three replicates. Bars indicate the SE. Significant differences ($p < 0.05$) between treatments are indicated by different letters.

tips of seedlings treated with ALA under salt stress showed normal apical morphology; however, the green fluorescence was enhanced. NaCl stress significantly decreased the intensities of FDA and PI. However, application of ALA markedly increased the fluorescence of living cells (**Figure 2E**). The root cell activity was suppressed under saline conditions; however, the application of ALA reversed the inhibitory effect of NaCl and significantly enhanced the root tip activity (**Figure 2F**).

ALA Treatment Ameliorated Root Subcellular Na^+, K^+ Changes Associated With Salt Stress

After treatment with NaCl, the Na^+ contents in the root cells increased significantly (**Figure 3**). The Na^+ concentrations in the cell wall, nucleus, plastid, mitochondria, and soluble fractions of roots were 1.6-, 2.1-, 8.4-, 13.0-, and 3.3-fold higher than those of control group. Moreover, the K^+ concentration was significantly decreased in the mitochondrial and soluble fractions. After the foliar spray of ALA, the Na^+ contents in each of the root cell fractions were reduced significantly, except for the cell wall. Meanwhile, the K^+ contents of the soluble fractions were markedly increased by exogenous ALA application under salt stress. Under normal growth conditions, the application of ALA increased the K^+ content in the nucleus, but decreased its content in mitochondria, compared with the control.

ALA Treatment Suppressed Na^+ Fluorescence Changes Associated With Salt Stress

The Na^+ absorption of cucumber root tips and hypocotyls were determined by staining with CoroNa™-Green AM (**Figure 4**). Under NaCl stress, the Na^+ intensity in the root tips and hypocotyls increased by 102.39 and 62.41%, respectively, compared with the control (**Figures 4A,B**). The Na^+ fluorescence in the root tissue was obviously enhanced, especially in the epidermis and stele. However, the fluorescence intensity in both the roots and hypocotyls decreased to the level of the control after exogenous application of ALA on the leaves. At the same time, the green fluorescence in the stele of the roots and hypocotyls was weakened (**Figures 4C–J**).

ALA Treatment Upregulated Ion Transporters Levels Associated With Salt Stress

The expression of SOS1 protein was downregulated under saline conditions but was significantly enhanced by exogenous ALA (**Figure 5A**). Meanwhile, the protein expression of SOS1 was also upregulated by ALA alone. Under salt stress, the relative expression level of *SOS1* was downregulated, but not significantly, compared to the control. The application of ALA significantly upregulated the transcriptional level of *SOS1* under salt stress conditions, i.e., to 7.8 times that of the control. The protein expression level of the tonoplast Na^+/H^+ transporter, NHX1,

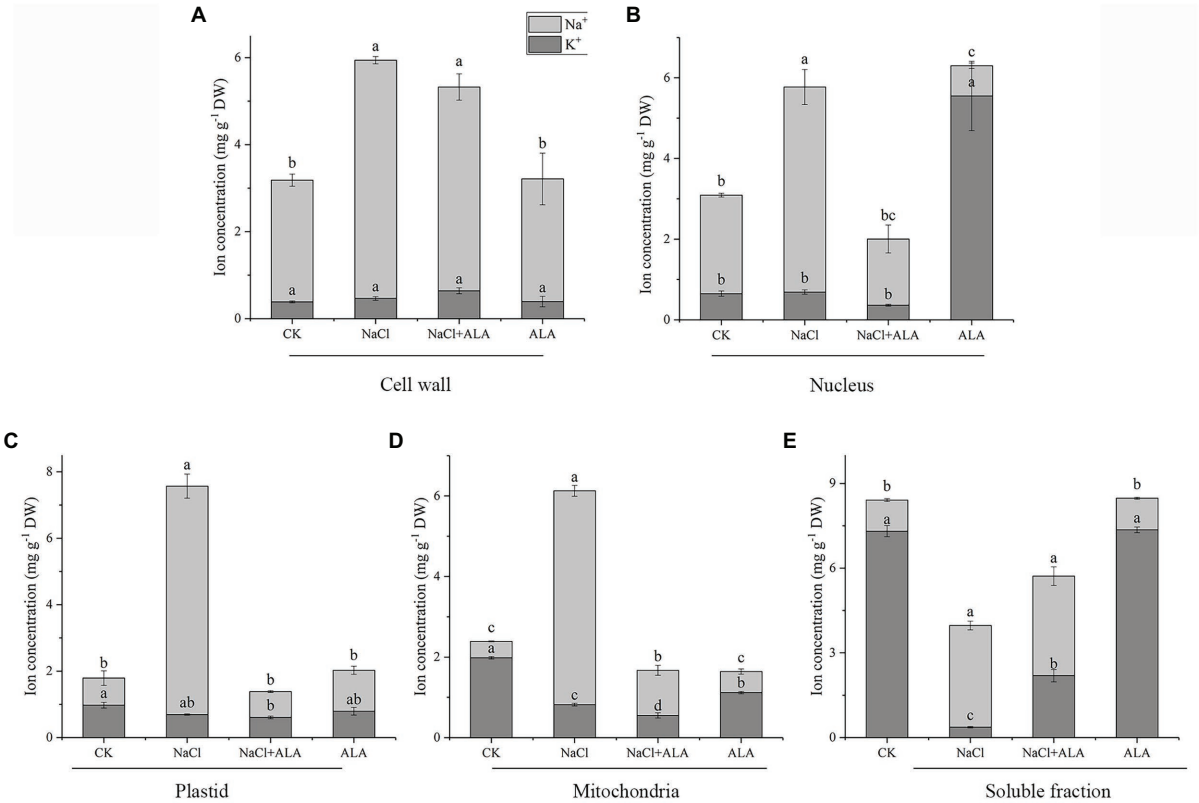

FIGURE 3 | Subcellular Na^+, K^+ concentration in apical cells of cucumber seedlings. **(A)** Na^+, K^+ concentration in cell wall. **(B)** Na^+, K^+ concentration in nucleus. **(C)** Na^+, K^+ concentration in plastid. **(D)** Na^+, K^+ concentration in mitochondria. **(E)** Na^+, K^+ concentration in soluble fraction of cucumber root cells. Data represent means of three replicates. Bars indicate the SE. Significant differences ($p < 0.05$) between treatments are indicated by different letters.

remained stable under NaCl conditions; however, exogenous ALA stimulated its expression to increase by 3-fold, compared to the control (**Figure 5B**). Moreover, the expression of *NHX1* was upregulated by ALA under normal conditions and under NaCl stress conditions (i.e., by 4.5-fold compared to the control). However, the results of the other treatments did not differ significantly from those of the control. The investigation of the proton pump in cucumber root cells revealed that the protein expression levels of HA3 and VHA-A remained stable under salt stress. However, exogenous ALA significantly upregulated their expression under stressful and non-stressful conditions (**Figures 5C,D**). Similar to *SOS1*, exogenous ALA enhanced the *HA3* gene expression level to 15 times under NaCl conditions when compared with the control (**Figure 5C**). However, the relative expression of the *VHA-A* gene was significantly upregulated by exogenous ALA under both salt stress and non-stress conditions; i.e., were 13 and 17 times that of the control, respectively (**Figure 5D**).

ALA Treatment Improved Apical Cells Ultrastructure Changes Associated With Salt Stress

The ultrastructure of the apical cell was observed by transmission electron microscopy. In the control group, the apical cells showed a regular morphology, with a clear central vacuole, a normal number of plastids, and sufficient starch granules. The mitochondrial morphology was regular, with a clear intimal structure and they gathered near the plastids (**Figures 6A–D**). However, under NaCl stress the cell morphology of root cells was obviously altered (**Figures 6E–H**). The cell wall became thicker and had a wave shape, and the number of plastids and starch decreased; however, the number of mitochondria increased. In addition, dark ion deposition increased in the cytoplasm. Exogenous application of ALA under salt stress reduced the ion deposition in the cytoplasm of apical cells, and the central vacuole was clearly visible (**Figures 6I–L**). However, the cell morphology was not obviously improved, the intercellular space was enlarged, the plastids and starch granules were rare, and the number of mitochondria increased. Moreover, when ALA was applied under control conditions, the cell morphology was regular; the mitochondria gathered near the plastids, and clear rough endoplasmic reticuli were visible (**Figures 6M–P**).

DISCUSSION

Physiological damage occurs when plants suffer under saline conditions in the rhizosphere environment. Salt stress inhibits

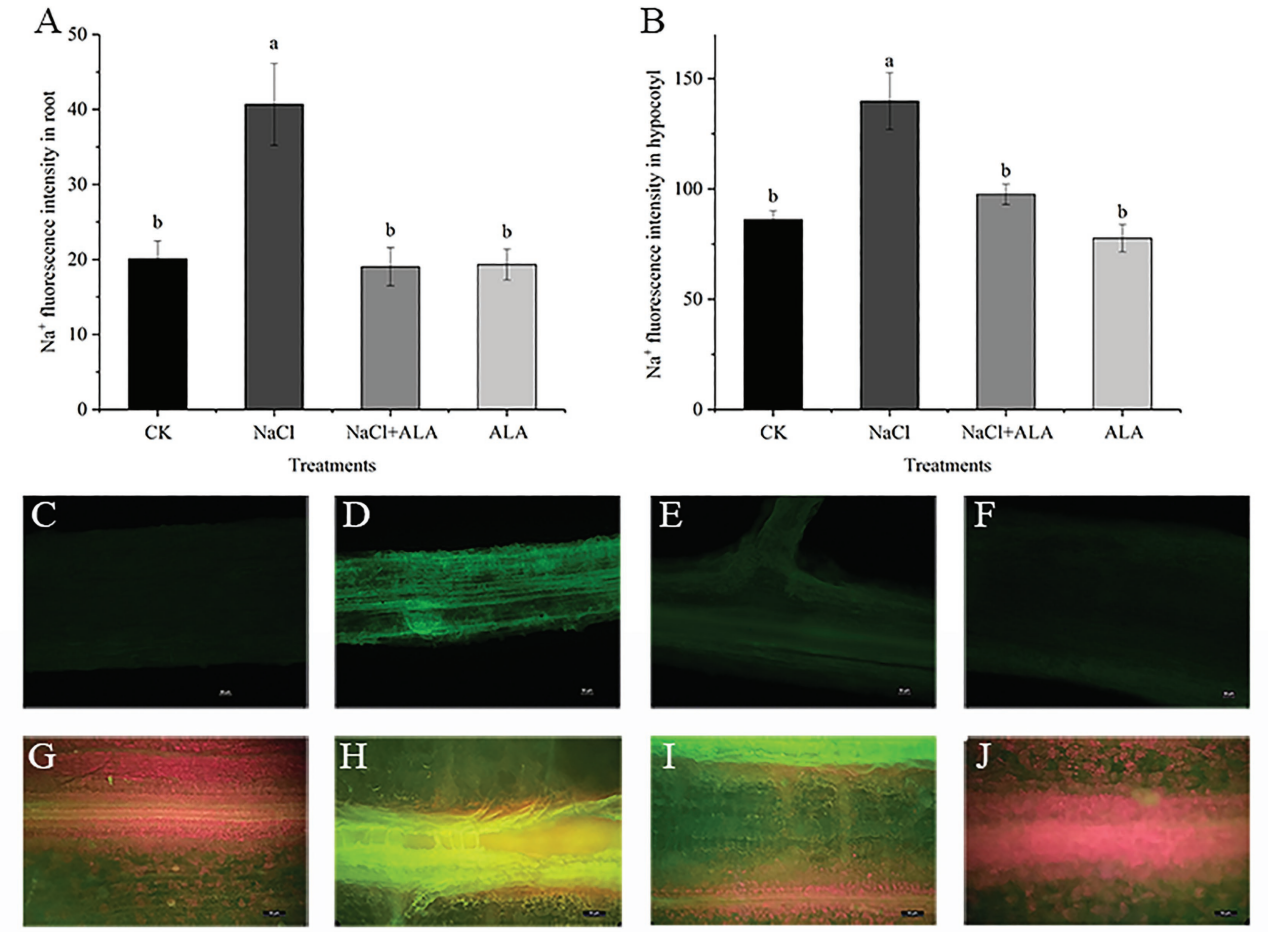

FIGURE 4 | The fluorescence images of Na^+ in root and hypocotyl of cucumber seedlings. **(A)** Fluorescence intensities of Na^+ in root. **(B)** Fluorescence intensities of Na^+ in hypocotyl. Data represent means of four replicates. Bars indicate the SE. Significant differences ($p < 0.05$) between treatments are indicated by different letters. **(C–F)** The Na^+ fluorescence images in root of seedlings. Scale bar = 50 μm. **(G–J)** The Na^+ fluorescence images in hypocotyl of seedlings. Scale bar = 50 μm.

many physiological and biochemical responses, including the anatomical morphology of leaves, physiological function of cells, photosynthesis reactions, water transport, protein synthesis, and energy production (Khan et al., 2020). In recent years, a natural plant growth regulator, ALA, has frequently been reported to improve plant resistance to environmental stress (see Akram and Ashraf, 2013 for a review). In the present study, NaCl stress inhibited the growth of cucumber roots. Moreover, all root morphological parameters showed significant decreases, the lateral roots were sparse, and the length of the roots decreased significantly. Moreover, NaCl caused apoptosis and wilting and a significant reduction in the living cells of roots, especially in the apical elongation area of seedlings under salt stress. These findings are consistent with those of a study on *Arabidopsis thaliana* L., in which the activity of *Arabidopsis* apical cells decreased gradually after exposure to low pH conditions, and the area of dead cells expanded gradually. The apical elongation region of *A. thaliana* was completely apoptotic after 2 h of low pH stress (Koyama et al., 2001). However, exogenous ALA has been shown to positively affect the root inhibition caused by various abiotic stresses. For example, medium Cd stress was previously shown to inhibit the root growth of *B. napus*, but 25 mg L^{-1} exogenous ALA application significantly improved the root average diameter, total volume, and total superficial area (Ali et al., 2013b). Additionally, in the present study, ALA application significantly increased root cell activity and the number of living cells in the apical elongation zone. Similarly, in alfalfa (*Medicago sativa* L.) plants, hydrogen-rich water (10%, v/v) was shown to relieve the harmful effects of Cd stress and decrease the number of dead root cells (Cui et al., 2013).

A relatively higher rhizospheric salt condition can cause osmotic stress in plants. In the present study, Na^+ was mainly enriched in the cell wall under normal growth conditions, while high K^+ and low Na^+ environments were found in plastids, mitochondria, and the soluble fractions of root cells. In contrast, a reduction in K^+ has been observed in the plastids, mitochondria, and the soluble fractions of root cells under

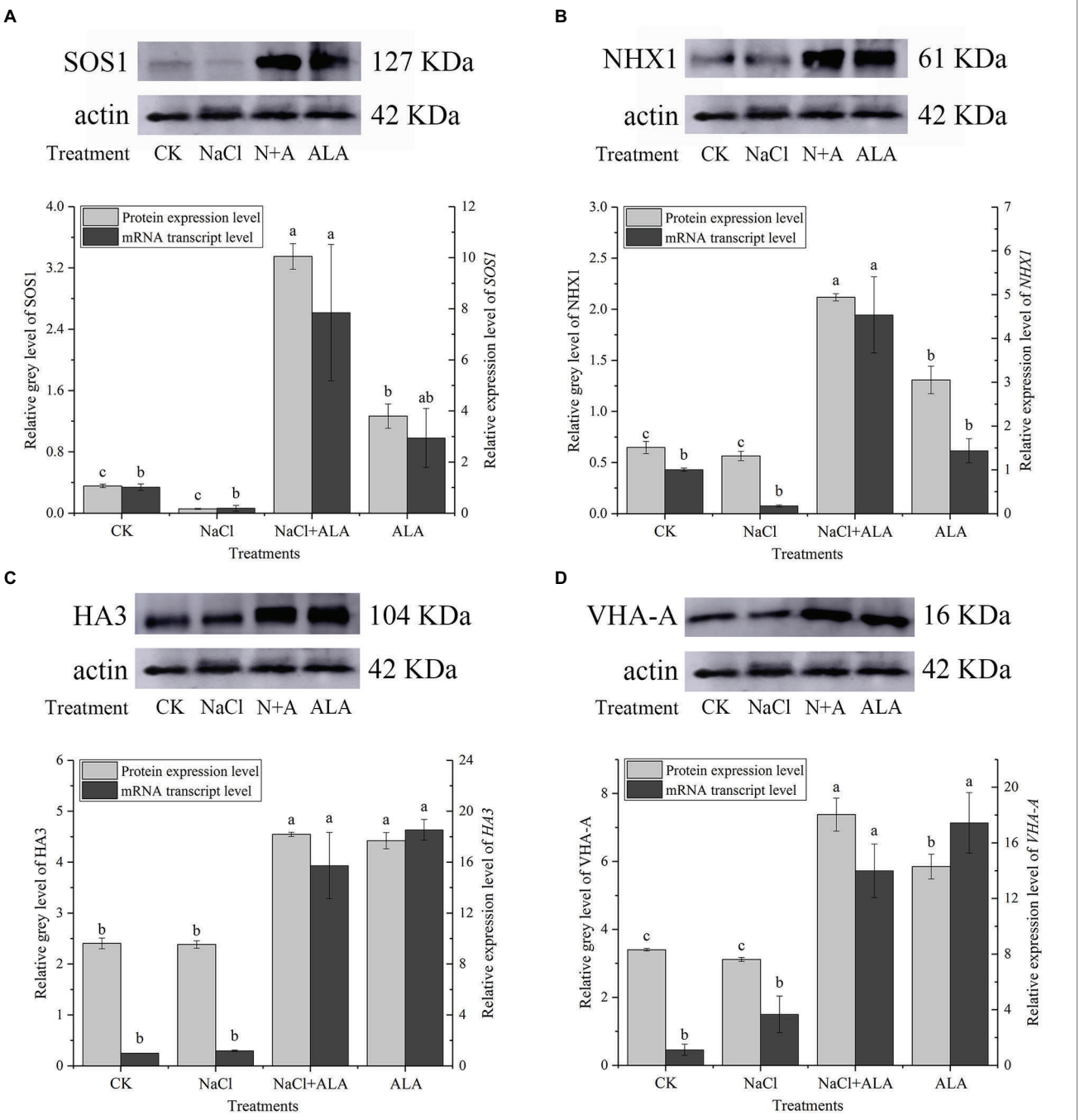

FIGURE 5 | The protein and gene expression levels of ion transporters in cucumber root. **(A)** Protein/gene expression of Na^+/H^+ antiporter in plasma membrane (*SOS1*). **(B)** Protein/gene expression of Na^+/H^+ antiporter in tonoplast (*NHX1*). **(C)** Protein/gene expression of H^+-ATPase in plasma membrane (*HA3*). **(D)** Protein/gene expression of H^+-ATPase in tonoplast (*VHA-A*). The bands are the protein expression bands of each transporter protein, and the histograms showing the ratio of gray level to actin gray level of ion transport protein expression. Data represent means of three replicates. Bars indicate the SE. Significant differences ($p < 0.05$) between treatments are indicated by different letters.

saline conditions. Moreover, in the present study, Na^+ increased significantly in each fraction of the root cells under salt stress. Similarly, the Na^+ concentration reportedly increased and the K^+ concentration decreased in barley (*Hordeum vulgare* L.) under 300 mmol L^{-1} NaCl (Jabeen et al., 2014). Rhizospheric salt stress is considered to affect the ion balance in root cells and increase the Na^+/K^+ ratio. This imbalance occurs because Na^+ and K^+ have similar ionic radius, and excessive Na^+ in

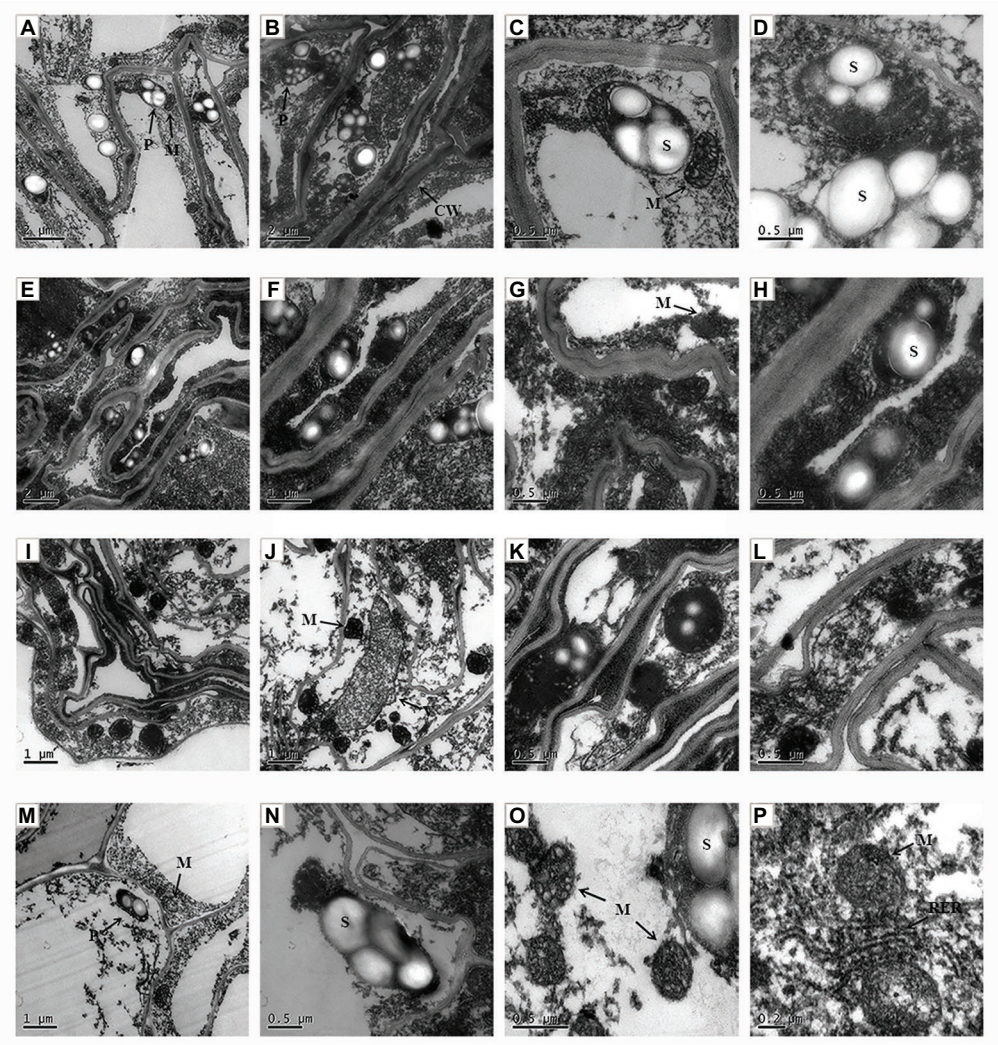

FIGURE 6 | The ultrastructural observation of root tip cell of cucumber seedlings. **(A–D)** Seedlings grown in control condition. **(E–H)** Fifty millimole per liter NaCl treated seedlings. **(I–L)** Seedlings treated with 50 mmol L^{-1} NaCl and 25 mg L^{-1} ALA simultaneously. **(M–P)** Seedlings sprayed 25 mg L^{-1} ALA only. CW, cell wall; P, plastid; S, starch; M, mitochondria; V, vacuole; RER, rough surfaced endoplasmic reticulum.

the apoplast competes with the potassium channel. Furthermore, Na^+ in trophoplasts disturbs the function of K^+ and destroys the stability of the cell wall and cell membrane structure (Yamaguchi et al., 2013). In addition, excessive Na^+ can cause damage to cell microtubules and ribosomes, and accelerate cell senescence (Munns, 1993). Therefore, maintaining the intracellular K^+ content above a certain threshold and maintaining a high ratio of cell fluid K^+/Na^+ (i.e., retaining a higher K^+ content, or preventing the accumulation of Na^+ in leaves) is the key to normal growth and salt tolerance in plants under salt stress. Moreover, in this study, exogenous ALA reduced the accumulation of Na^+ in cucumber root cells under salt stress and significantly lowered the Na^+ level in organelles.

5-Aminolevulinic acid application was also shown to upregulate the transcriptional level under salt stress and the protein expression level of the Na^+/H^+ antiporter (SOS1) as well as the proton pump (HA3) on the plasma membrane. On the plasma membrane, the proton-motive force is mainly formed by a proton pump, and the proton-motive force is the major driving force for the transmembrane active transport of mineral elements in plant cells. The plasma membrane Na^+/H^+ antiporter is an electrically neutral Na^+/H^+ (1:1) transmembrane transporter that is dependent on the transmembrane H^+ concentration gradient. Generally, the potential difference in the plasma membrane could be enhanced by increasing the salt concentration in the extracellular environment. At this time, the H^+-ATPase on the plasma membrane could utilize the energy generated by the hydrolyzed ATP to pump H^+ out of the cells to produce an electrochemical potential gradient. This force has the ability to activate the Na^+/H^+ antiporter, which can transport Na^+ out of the cell against the electrochemical potential gradient (Allakhverdiev et al., 1999). The gene encoding the Na^+/H^+

antiporter was first investigated and cloned in *A. thaliana* and has been shown to be associated with the salt tolerance of plants (Shi et al., 2000). Compared with wild type plants, *Arabidopsis* plants with an overexpression of *SOS1* showed significantly decreased Na^+ contents in the transpirational flow of xylem under saline conditions. Moreover, the calluses regenerated from transgenic plants also showed a strong tolerance to salt, and the concentration of Na^+ in the cells was lower than that in wild type plants (Shi et al., 2002). In addition, transgenic *Arabidopsis* plants with the soybean *GmsSOS1* gene showed improved salt tolerance and reduced reactive oxygen species contents under salt stress, and the yeast cells expressing *GmsSOS1* showed a decrease in Na^+ accumulation under NaCl conditions (Zhao et al., 2016). These research results suggest that the enhancement of the plasma membrane Na^+/H^+ antiporter and H^+-ATPase to exude Na^+ out of the cell are prerequisites for improving plant salt tolerance. Moreover, the Na^+/H^+ antiporter and H^+-ATPase were enhanced by exogenous ALA in cucumber root cells under NaCl stress. In fact, the SOS1 protein functions through the SOS signal pathway, which is involved with two other proteins: SOS2 and SOS3, i.e., a protein kinase and a Ca^{2+}-binding protein, respectively. Reportedly, Ca^{2+} can rapidly accumulate in the cytoplasm under high Na^+ conditions, and a higher concentration of Ca^{2+} will activate SOS3. The activated SOS3 then binds SOS2 to form a SOS2-SOS3 calcium-dependent protein kinase complex, which can deactivate the self-inhibitory sites at the C terminal of the SOS1 protein by phosphorylation, and finally increase the activity of SOS1 (Liu and Zhu, 1998; Quintero et al., 2011).

Under saline conditions, Na^+ is usually excreted out of the cells of glycophytes, but accumulates in the vacuoles of halophytes (Blumwald, 2000). Mineral ions in the cytoplasm, such as Na^+, can be compartmentalized into vacuoles by ion transporters located on the tonoplast. There are two kinds of tonoplast proton pumps in plants: V-H^+-ATPase and V-H^+-PPase. These pumps hydrolyze ATP and PPi to pump H^+ into the vacuole and develop proton-motive force across the vacuolar membrane, which stimulates the Na^+/H^+ antiporter on the tonoplast. For example, salt stress was shown to upregulate the proton pump and Na^+/H^+ antiporter on the tonoplast of *Suaeda salsa* L. leaves at the transcriptional level and transferred more Na^+ into vacuoles (Qiu et al., 2007). Previously, transgenic *Arabidopsis* plants with the gene encoding the subunit B of the tonoplast H^+-ATPase (*HcVHA-B*) of *Halostachys caspica* had significantly higher Na^+ contents but an improved morphology and salt tolerance compared to the wild type plants, because of a substantial Na^+ enrichment of the vacuoles (Hu et al., 2012). In the present study, the transcriptional and translational levels of the subunit A of V-H^+-ATPase under NaCl stress did not show any significant difference compared to the control; however, exogenous ALA upregulated the gene and protein expression levels of VHA-A. This indicated that ALA application can improve the compartmentation of Na^+ into vacuoles and enhance the salt resistance of cucumber seedlings. In fact, the tonoplast H^+-ATPase is a multisubunit complex. Similarly, it was found that the subunit E of V-H^+-ATPase, in *Broussonetia papyrifera* L., responded to relatively high salt conditions, and its mRNA and protein levels were upregulated under 150 mmol L^{-1} NaCl stress (Zhang et al., 2012). Overexpression of the subunits of V-H^+-ATPase of salt-resistant wheat in *Arabidopsis* plants, including a, A, c, C, d, D, F, I, G, and H, was found to enhance the salt tolerance of transgenic plants. Among them, the most salt-tolerant was the transgenic *A. thaliana* with the c subunit (He et al., 2014).

The tonoplast Na^+/H^+ antiporter is a structural or constitutive protein whose activity is regulated by the Na^+ content in halophytes (Apse and Blumwald, 2007). The activity of the tonoplast Na^+/H^+ antiporter can be affected rapidly by NaCl stress. In the presence of an NHX protein synthesis inhibitor, its activity can still be rapidly stimulated by NaCl, which might be due to the presence of NHX proteins rather than resynthesized proteins (Blumwald, 2000). Moreover, when salt-treated plants were transferred to Na-deficient conditions, the Na^+/H^+ antiporter was inactivated (Garbarino and DuPont, 1989). Interestingly, in *Plantago* species, the activity of the tonoplast Na^+/H^+ antiporter was only found in salt-tolerant *Plantago maritima* L., but not in salt-sensitive *Plantago media* L. (Staal et al., 1991). In this study, the seedlings treated with exogenous ALA showed higher mRNA and protein levels of NHX1, indicating that the capacity of Na^+ compartments in cells can be improved with ALA application. The Na^+, compared to the tonoplast Na^+/H^+ antiporter from the cytoplasm to the vacuole, can be used as an osmotic agent to maintain the cell osmotic potential and contribute to water absorption. In addition, in transgenic tomato plants expressing *SbNHX* of *Sorghum bicolor*, the tonoplast Na^+/H^+ antiporter was found to have an interactive relationship with the gene family of the cation/proton antiporter (*CPA*), such as *SOS*. This suggests that NHX proteins might assist the cation antiporters on the plasma membrane to excrete Na^+ from cells and, thus, enhance the salt resistance of plants; however, the mechanism of their interaction remains unclear (Palavalasa et al., 2017). Besides, decrease of Na^+ in cytoplasm could lead to cut down of ROS and alleviate of stress damages. For example, overexpressing transcriptional activator *NAC1* could significantly reduce Na^+ content in shoot and root of *Panicum virgatum* L., and enhance the enzymatic activities of SOD, POD, and CAT (Wang et al., 2019). Inhibiting ascorbic acid synthesis regulation gene *VTC1-3* by RNA interfering technology could increase ROS production and aggravate salt damages in rice roots (Wang et al., 2018).

In the present study, rhizosphere salt stress caused root cell damage and irregular cell morphology at the subcellular level. Exogenous ALA application *via* leaf spraying repaired the cell wall and alleviated the degree of its thickening. These results are consistent with those of a study on *B. napus* L., where ALA application repaired the morphological disorders of root cells caused by Cd stress (Ali et al., 2013a). In addition, the number of mitochondria in apical cells under salt stress can be increased by exogenous ALA. On the other hand, the number of mitochondria in the root tip cells increased under excessive KNO_3 stress (Čiamporová and Mistrík, 1993). Mitochondria are the energy-producing organs in plant cells. The increase in mitochondria can reveal a "mitochondrial pump" function, and develop the intracellular energy regulating

mechanism, which ensures energy supply during the adaptation to salt stress. Therefore, the increase in the mitochondrial number is an adaptation mechanism of root cells to stress conditions. Exogenous ALA promotes an increase in the mitochondrial number and function in apical cells to produce more energy to and thus further adapt to salt stress. In addition, the ion concentration in the cytoplasm increased under salt stress, which led to deposition; however, exogenous ALA reduced the cytosolic concentration. Furthermore, after ALA treatment, the ion deposition in vacuoles was more obvious under NaCl, which verified that exogenous ALA application enhanced the ion compartmentalization capacity of root tip cells in cucumber seedlings.

CONCLUSION

Salt stress significantly inhibited the root architecture and activity of cucumber seedlings. However, the adverse effects caused by NaCl were shown to be abrogated by exogenous ALA application. On the one hand, the application of ALA improved the excretion of Na^+ from the cytoplasm by upregulating the H^+-ATPase and Na^+/H^+ antiporter on the plasma membrane. On the other hand, the H^+-ATPase and Na^+/H^+ antiporter on the tonoplast could also be enhanced at both the transcriptional and translational levels to compartmentalize Na^+ into the vacuoles. Therefore, the ultrastructure of apical cells and the biochemical reactions in the cytoplasm could be ameliorated by exogenous ALA, to effectively alleviate the effects and damage caused by salt stress in cucumber roots and shoots.

DATA AVAILABILITY STATEMENT

The original contributions presented in the study are included in the article/supplementary material; further inquiries can be directed to the corresponding author.

AUTHOR CONTRIBUTIONS

YW, ZT, and JY conceived and designed the research. YW, XX, and NL conducted the experiments. YW, LH, and JL analyzed the data and prepared the figures and illustrations. YW wrote the main body of the manuscript. WL, AC-U, and JX read the manuscript and made valuable inputs. All authors contributed to the article and approved the submitted version.

FUNDING

This work was supported by the Special Fund for Talent of Gansu Agricultural University (GAU-KYQD-2018-34), National Natural Science Foundation of China (31660584), Agriculture Research System of China (CARS-23-C-07), and Gansu Province Science and Technology Project (17ZD2NA015-03).

ACKNOWLEDGMENTS

We are grateful to Basharat Ali (Department of Agronomy, University of Agriculture Faisalabad, Pakistan) who critically read the manuscript and made valuable suggestions for its improvement.

REFERENCES

Akram, N. A., and Ashraf, M. (2013). Regulation in plant stress tolerance by a potential plant growth regulator, 5-aminolevulinic acid. *J. Plant Growth Regul.* 32, 663–679. doi: 10.1007/s00344-013-9325-9

Ali, B., Huang, C. R., Qi, Z. Y., Ali, S., Daud, M. K., Geng, X. X., et al. (2013a). 5-Aminolevulinic acid ameliorates cadmium-induced morphological, biochemical, and ultrastructural changes in seedlings of oilseed rape. *Environ. Sci. Pollut. Res.* 20, 7256–7267. doi: 10.1007/s11356-013-1735-5

Ali, B., Tao, Q., Zhou, Y., Gill, R. A., Ali, S., Rafiq, M. T., et al. (2013b). 5-Aminolevolinic acid mitigates the cadmium-induced changes in *Brassica napus* as revealed by the biochemical and ultra-structural evaluation of roots. *Ecotoxicol. Environ. Saf.* 92, 271–280. doi: 10.1016/j.ecoenv.2013.02.006

Allakhverdiev, S. I., Nishiyama, Y., Suzuki, I., Tasaka, Y., and Murata, N. (1999). Genetic engineering of the unsaturation of fatty acids in membrane lipids alters the tolerance of *Synechocystis* to salt stress. *Proc. Natl. Acad. Sci. U. S. A.* 96, 5862–5867. doi: 10.1073/pnas.96.10.5862

Apse, M. P., and Blumwald, E. (2007). Na^+ transport in plants. *FEBS Lett.* 581, 2247–2254. doi: 10.1016/j.febslet.2007.04.014

Blumwald, E. (2000). Sodium transport and salt tolerance in plants. *Curr. Opin. Cell Biol.* 12, 431–434. doi: 10.1016/S0955-0674(00)00112-5

Bonales-Alatorre, E., Shabala, S., Chen, Z. -H., and Pottosin, I. (2013). Reduced tonoplast fast-activating and slow-activating channel activity is essential for conferring salinity tolerance in a facultative halophyte, quinoa. *Plant Physiol.* 162, 940–952. doi: 10.1104/pp.113.216572

Čiamporová, M., and Mistrík, I. (1993). The ultrastructural response of root cells to stressful conditions. *Environ. Exp. Bot.* 33, 11–26. doi: 10.1016/0098-8472(93)90052-H

Cui, W., Gao, C., Fang, P., Lin, G., and Shen, W. (2013). Alleviation of cadmium toxicity in *Medicago sativa* by hydrogen-rich water. *J. Hazard. Mater.* 260, 715–724. doi: 10.1016/j.jhazmat.2013.06.032

Cuin, T. A., Bose, J., Stefano, G., Jha, D., Tester, M., Mancuso, S., et al. (2011). Assessing the role of root plasma membrane and tonoplast Na^+/H^+ exchangers in salinity tolerance in wheat: in planta quantification methods. *Plant Cell Environ.* 34, 947–961. doi: 10.1111/j.1365-3040.2011.02296.x

Garbarino, J., and DuPont, F. M. (1989). Rapid induction of Na^+/H^+ exchange activity in barley root tonoplast. *Plant Physiol.* 89, 1–4. doi: 10.1104/pp.89.1.1

Gong, X., Li, J., Xu, K., Wang, J., and Yang, H. (2010). A controllable molecular sieve for Na^+ and K^+ ions. *J. Am. Chem. Soc.* 132, 1873–1877. doi: 10.1021/ja905753p

He, X., Huang, X., Shen, Y., and Huang, Z. (2014). Wheat V-H^+-ATPase subunit genes significantly affect salt tolerance in *Arabidopsis thaliana*. *PLoS One* 9:e86982. doi: 10.1371/journal.pone.0086982

Hu, Y. -Z., Zeng, Y. -L., Guan, B., and Zhang, F. -C. (2012). Overexpression of a vacuolar H^+-pyrophosphatase and a B subunit of H^+-ATPase cloned from the halophyte *Halostachys caspica* improves salt tolerance in *Arabidopsis thaliana*. *Plant Cell Tissue Organ Cult.* 108, 63–71. doi: 10.1007/s11240-011-0013-9

Huo, L., Guo, Z., Jia, X., Sun, X., Wang, P., Gong, X., et al. (2020). Increased autophagic activity in roots caused by overexpression of the autophagy-related gene *MdATG10* in apple enhances salt tolerance. *Plant Sci.* 294:110444. doi: 10.1016/j.plantsci.2020.110444

Jabeen, Z., Hussain, N., Han, Y., Shah, M. J., Zeng, F., Zeng, J., et al. (2014). The differences in physiological responses, ultrastructure changes, and Na^+ subcellular distribution under salt stress among the barley genotypes differing in salt tolerance. *Acta Physiol. Plant.* 36, 2397–2407. doi: 10.1007/s11738-014-1613-x

Julkowska, M. M., Koevoets, I. T., Mol, S., Hoefsloot, H., Feron, R., Tester, M. A., et al. (2017). Genetic components of root architecture remodeling in response to salt stress. *Plant Cell* 29, 3198–3213. doi: 10.1105/tpc.16.00680

Khan, W. D., Tanveer, M., Shaukat, R., Ali, M., and Pirdad, F. (2020). "An overview of salinity tolerance mechanism in plants" in *Salt and drought stress tolerance in plants*. *Signaling and communication in plants*. eds. M. Hasanuzzaman and M. Tanveer (Cham: Springer), 1–16.

Koyama, H., Toda, T., and Hara, T. (2001). Brief exposure to low-pH stress causes irreversible damage to the growing root in *Arabidopsis thaliana*: pectin–Ca interaction may play an important role in proton rhizotoxicity. *J. Exp. Bot.* 52, 361–368. doi: 10.1093/jexbot/52.355.361

Liu, J., and Zhu, J. K. (1998). A calcium sensor homolog required for plant salt tolerance. *Science* 280, 1943–1945. doi: 10.1126/science.280.5371.1943

Livak, K. J., and Schmittgen, T. D. (2001). Analysis of relative gene expression data using real-time quantitative PCR and the $2^{-\Delta\Delta CT}$ method. *Methods* 25, 402–408. doi: 10.1006/meth.2001.1262

Munns, R. (1993). Physiological processes limiting plant growth in saline soils: some dogmas and hypotheses. *Plant Cell Environ.* 16, 15–24. doi: 10.1111/j.1365-3040.1993.tb00840.x

Nath, M., Bhatt, D., Jain, A., Saxena, S. C., Saifi, S. K., Yadav, S., et al. (2019). Salt stress triggers augmented levels of Na^+, Ca^{2+} and ROS and alter stress-responsive gene expression in roots of CBL9 and CIPK23 knockout mutants of *Arabidopsis thaliana*. *Environ. Exp. Bot.* 161, 265–276. doi: 10.1016/j.envexpbot.2018.10.005

Negrão, S., Schmöckel, S. M., and Tester, M. (2016). Evaluating physiological responses of plants to salinity stress. *Ann. Bot.* 119, 1–11. doi: 10.1093/aob/mcw191

Palavalasa, H., Narasu, L., Varshney, R., and KaviKishor, P. (2017). Genome wide analysis of sodium transporters and expression of Na^+/H^+-antiporter-like protein (*SbNHXLP*) gene in tomato for salt tolerance. *Front. Plant Sci.* 11:604690. doi: 10.3389/fpls.2020.604690

Qiu, N., Chen, M., Guo, J., Bao, H., Ma, X., and Wang, B. (2007). Coordinate up-regulation of V-H^+-ATPase and vacuolar Na^+/H^+ antiporter as a response to NaCl treatment in a C3 halophyte *Suaeda salsa*. *Plant Sci.* 172, 1218–1225. doi: 10.1016/j.plantsci.2007.02.013

Quintero, F. J., Martinez-Atienza, J., Villalta, I., Jiang, X., Kim, W. -Y., Ali, Z., et al. (2011). Activation of the plasma membrane Na^+/H^+ antiporter Salt-Overly-Sensitive 1 (SOS1) by phosphorylation of an auto-inhibitory C-terminal domain. *Proc. Natl. Acad. Sci. U. S. A.* 108, 2611–2616. doi: 10.1073/pnas.1018921108

Shah, A. N., Tanveer, M., Abbas, A., Fahad, S., Baloch, M. S., Ahmad, M. I., et al. (2021). Targeting salt stress coping mechanisms for stress tolerance in *Brassica*: a research perspective. *Plant Physiol. Biochem.* 158, 53–64. doi: 10.1016/j.plaphy.2020.11.044

Shi, H., Ishitani, M., Kim, C., and Zhu, J. K. (2000). The *Arabidopsis thaliana* salt tolerance gene *SOS1* encodes a putative Na^+/H^+ antiporter. *Proc. Natl. Acad. Sci. U. S. A.* 97, 6896–6901. doi: 10.1073/pnas.120170197

Shi, H., Lee, B. H., Wu, S. J., and Zhu, J. K. (2002). Overexpression of a plasma membrane Na^+/H^+ antiporter gene improves salt tolerance in *Arabidopsis thaliana*. *Nat. Biotechnol.* 21, 81–85. doi: 10.1038/nbt766

Staal, M., Maathuis, F. J. M., Elzenga, J. T. M., Overbeek, J. H. M., and Prins, H. B. A. (1991). Na^+/H^+ antiport activity in tonoplast vesicles from roots of the salt-tolerant *Plantago maritima* and the salt-sensitive *Plantago media*. *Physiol. Plant.* 82, 179–184. doi: 10.1111/j.1399-3054.1991.tb00078.x

Tanveer, M. (2020). Tissue-specific reactive oxygen species signalling and ionic homeostasis in *Chenopodium quinoa* and *Spinacia oleracea* in the context of salinity stress tolerance. doctoral dissertation. University of Tasmania.

Wakeel, A., Asif, A. R., Pitann, B., and Schubert, S. (2011). Proteome analysis of sugar beet (*Beta vulgaris* L.) elucidates constitutive adaptation during the first phase of salt stress. *J. Plant Physiol.* 168, 519–526. doi: 10.1016/j.jplph.2010.08.016

Wang, H., Liang, L., Liu, S., An, T., Fang, Y., Xu, B., et al. (2020). Maize genotypes with deep root systems tolerate salt stress better than those with shallow root systems during early growth. *J. Agron. Crop Sci.* 206, 711–721. doi: 10.1111/jac.12437

Wang, J., Zhang, L., Wang, X., Liu, L., Lin, X., Wang, W., et al. (2019). *PvNAC1* increases biomass and enhances salt tolerance by decreasing Na^+ accumulation and promoting ROS scavenging in switchgrass (*Panicum virgatum* L.). *Plant Sci.* 280, 66–76. doi: 10.1016/j.plantsci.2018.11.007

Wang, Y., Zhao, H., Qin, H., Li, Z., Liu, H., Wang, J., et al. (2018). The synthesis of ascorbic acid in rice roots plays an important role in the salt tolerance of rice by scavenging ROS. *Int. J. Mol. Sci.* 19:3347. doi: 10.3390/ijms19113347

Wu, W. W., He, S. S., An, Y. Y., Cao, R. X., Sun, Y. P., Tang, Q., et al. (2019a). Hydrogen peroxide as a mediator of 5-aminolevulinic acid-induced Na^+ retention in roots for improving salt tolerance of strawberries. *Physiol. Plant.* 167, 5–20. doi: 10.1111/ppl.12967

Wu, Y., Jin, X., Liao, W., Hu, L., Dawuda, M. M., Zhao, X., et al. (2018). 5-Aminolevulinic acid (ALA) alleviated salinity stress in cucumber seedlings by enhancing chlorophyll synthesis pathway. *Front. Plant Sci.* 9:635. doi: 10.3389/fpls.2018.00635

Wu, Y., Liao, W., Dawuda, M. M., Hu, L., and Yu, J. (2019b). 5-Aminolevulinic acid (ALA) biosynthetic and metabolic pathways and its role in higher plants: a review. *Plant Growth Regul.* 87, 357–374. doi: 10.1007/s10725-018-0463-8

Xiong, J. L., Wang, H. C., Tan, X. Y., Zhang, C. L., and Naeem, M. S. (2018). 5-aminolevulinic acid improves salt tolerance mediated by regulation of tetrapyrrole and proline metabolism in *Brassica napus* L. seedlings under NaCl stress. *Plant Physiol. Biochem.* 124, 88–99. doi: 10.1016/j.plaphy.2018.01.001

Yamaguchi, T., Hamamoto, S., and Uozumi, N. (2013). Sodium transport system in plant cells. *Front. Plant Sci.* 4:410. doi: 10.3389/fpls.2013.00410

Yan, F., Wei, H., Ding, Y., Li, W., Chen, L., Ding, C., et al. (2020). Melatonin enhances Na^+/K^+ homeostasis in rice seedlings under salt stress through increasing the root H^+-pump activity and Na^+/K^+ transporters sensitivity to ROS/RNS. *Environ. Exp. Bot.* 182:104328. doi: 10.1016/j.envexpbot.2020.104328

Zhang, M., Fang, Y., Liang, Z., and Huang, L. (2012). Enhanced expression of vacuolar H^+-ATPase subunit E in the roots is associated with the adaptation of *Broussonetia papyrifera* to salt stress. *PLoS One* 7:e48183. doi: 10.1371/journal.pone.0048183

Zhang, X., Huang, G., Bian, X., and Zhao, Q. (2013). Effects of root interaction and nitrogen fertilization on the chlorophyll content, root activity, photosynthetic characteristics of intercropped soybean and microbial quantity in the rhizosphere. *Plant Soil Environ.* 59, 80–88. doi: 10.17221/613/2012-PSE

Zhang, H., Li, X., Zhang, S., Yin, Z., Zhu, W., Li, J., et al. (2018). Rootstock alleviates salt stress in grafted mulberry seedlings: physiological and PSII function responses. *Front. Plant Sci.* 9:1806. doi: 10.3389/fpls.2018.01806

Zhang, W. D., Wang, P., Bao, Z., Ma, Q., Duan, L. J., Bao, A. K., et al. (2017). SOS1, HKT1;5, and NHX1 synergistically modulate Na^+ homeostasis in the halophytic grass *Puccinellia tenuiflora*. *Front. Plant Sci.* 8:576. doi: 10.3389/fpls.2017.00576

Zhao, X., Wei, P., Liu, Z., Yu, B., and Shi, H. (2016). Soybean Na^+/H^+ antiporter *GmsSOS1* enhances antioxidant enzyme activity and reduces Na^+ accumulation in *Arabidopsis* and yeast cells under salt stress. *Acta Physiol. Plant.* 39:19. doi: 10.1007/s11738-016-2323-3

Zörb, C., Geilfus, C. M., and Dietz, K. J. (2019). Salinity and crop yield. *Plant Biol.* 21, 31–38. doi: 10.1111/plb.12884

Conflict of Interest: The authors declare that the research was conducted in the absence of any commercial or financial relationships that could be construed as a potential conflict of interest.

frontiers in Plant Science

REVIEW
published: 12 April 2021
doi: 10.3389/fpls.2021.656662

Potential of Algae–Bacteria Synergistic Effects on Vegetable Production

*Yeeun Kang[1], Minjeong Kim[2], Changki Shim[2], Suyea Bae[1] and Seonghoe Jang[1]**

[1] World Vegetable Center Korea Office, Wanju-gun, Jeollabuk-do, South Korea, [2] Organic Agricultural Division, National Institute of Agricultural Sciences, RDA, Wanju-gun, Jeollabuk-do, South Korea

Modern agriculture has become heavily dependent on chemical fertilizers, which have caused environmental pollution and the loss of soil fertility and sustainability. Microalgae and plant growth-promoting bacteria (PGPB) have been identified as alternatives to chemical fertilizers for improving soil fertility. This is because of their biofertilizing properties, through the production of bioactive compounds (e.g., phytohormones, amino acids, and carotenoids) and their ability to inhibit plant pathogens. Although treatment based on a single species of microalgae or bacteria is commonly used in agriculture, there is growing experimental evidence suggesting that a symbiotic relationship between microalgae and bacteria synergistically affects each other's physiological and metabolomic processes. Moreover, the co-culture/combination treatment of microalgae and bacteria is considered a promising approach in biotechnology for wastewater treatment and efficient biomass production, based on the advantage of the resulting synergistic effects. However, much remains unexplored regarding the microalgal–bacterial interactions for agricultural applications. In this review, we summarize the effects of microalgae and PGPB as biofertilizing agents on vegetable cultivation. Furthermore, we present the potential of the microalgae–PGPB co-culture/combination system for the environmentally compatible production of vegetables with improved quality.

Keywords: biofertilizers, combinational application, microalgae, mixed cultures, plant growth-promoting bacteria, vegetables

OPEN ACCESS

Edited by:
Maurizio Ruzzi, University of Tuscia, Italy

Reviewed by:
Narendra Singh, Southern University of Science and Technology, China
Ana L. Gonçalves, University of Porto, Portugal

***Correspondence:**
Seonghoe Jang
seonghoe.jang@worldveg.org

Specialty section:
This article was submitted to Crop and Product Physiology, a section of the journal Frontiers in Plant Science

Received: *21 January 2021*
Accepted: *12 March 2021*
Published: *12 April 2021*

Citation:
Kang Y, Kim M, Shim C, Bae S and Jang S (2021) Potential of Algae–Bacteria Synergistic Effects on Vegetable Production. Front. Plant Sci. 12:656662. doi: 10.3389/fpls.2021.656662

INTRODUCTION

Ecological Problems Caused by Chemical Fertilizers in Agriculture

High amounts of chemical fertilizers have been used to obtain high product yields with increased cultivation efficiency in agriculture. However, the excessive use of chemical fertilizers frequently causes severe environmental damage, such as water, soil, and air pollution (Savci, 2012). Moreover, the excessive use of chemical fertilizers leads to soil acidification and hardening, which decrease root vigor with reduced respiration. The population of beneficial microorganisms is also reduced by this practice, resulting in a loss of soil fertility and a high incidence of root diseases (Chandini et al., 2019). In particular, nitrogen (N) fertilizers are absorbed by crops in reactive forms

such as nitrate (NO_3), ammonia (NH_3), and nitrogen oxides (NOx). These reactive forms can be sustainably produced by soil microbes, but with chemical fertilizers, excessive amounts remain in the soil, flow to the groundwater, and even contribute to the production of greenhouse gases such as nitrous oxide (N_2O) (Choudhury and Kennedy, 2005; Giles, 2005).

The Advantage of Biofertilizers in Agriculture

Biofertilizers have been recommended as an alternative to chemical fertilizers in order to avoid the problems caused by chemical fertilizers in agriculture (Mahanty et al., 2017). Biofertilizers are preparations containing living or dormant cells, which have the advantage of growth-promoting functions in crops. This is performed through the production of phytohormones and/or useful substances/biochemicals, thereby enabling the development of ecofriendly and sustainable agriculture (Kumar, 2018). In general, biofertilizers play a significant role in the decomposition of organic matter, which aids mineralization within the soil, consequently increasing the availability of nutrients for plants and improving crop yield (Rodrìguez and Fraga, 1999).

Moreover, the application of biofertilizers can increase the quantity and biodiversity of useful bacteria, such as plant growth-promoting rhizobacteria (PGPR) belonging to *Azotobacter*, *Bacillus*, *Burkholderia*, *Pantoea*, *Pseudomonas*, *Serratia*, and *Streptomyces* (Verma et al., 2019; Gou et al., 2020). Currently, it is believed that the co-evolution of plant–microbe interactions has allowed some of the bacteria to be facultative intracellular endophytes (Bulgarelli et al., 2013), among which are PGPR that have beneficial effects on plants through direct or indirect pathways. For example, some PGPR strains affect plant growth by synthesizing phytohormones, metabolizing them, and/or acting on hormone biosynthesis in plants, while others produce substances that work against soil-borne pathogens (Beneduzi et al., 2012). In the last few decades, as the interest of consumers toward safe agricultural products grew, it became important to exploit beneficial microbes as biofertilizers for use in food safety practices and sustainable crop production (Shi et al., 2011).

The Role of Microorganisms in Plant Growth

Different microbial species coexist in the soil and have a variety of beneficial effects on plant growth promotion and biological control. These microbes usually improve soil fertility by providing nutrients, such as carbon, nitrogen, phosphorus, potassium, trace elements, vitamins, and amino acids, and making them accessible for plants. In doing so, they promote growth by mediating various activities, such as nitrogen fixation and phosphate and potassium solubilization (Güneş et al., 2014; Bagyalakshmi et al., 2017). These microbes are able to release plant growth-regulating substances, such as phytohormones, and also have a suppressive effect on plant diseases by producing/secreting antibiotics and/or secondary metabolites that work against pathogens (Yoshihisa et al., 1989; Sessitsch et al., 2004; Jung et al., 2006). These microorganisms are known as plant growth-promoting bacteria (PGPB), which generally belong to *Pseudomonas*, *Azospirillum*, *Rhizobium*, and *Bacillus* (Walsh et al., 2001; Esitken et al., 2010; Ahemad and Kibret, 2014).

Characteristics of Microalgae

In addition to PGPB, some microalgae species have also been used to promote plant growth, yield, and fruit quality (Guo et al., 2020). Microalgae are typically microscopic algae, which range in sizes between micrometers and tens of micrometers, depending on the species. It has been estimated that 200,000–800,000 species exist (Ebenezer et al., 2011), but only around 40,000–50,000 species have been described thus far (Suganya et al., 2016). They are photosynthetic eukaryotes, which do not have roots, stems, or leaves, unlike higher plants, and range from unicellular to multicellular species (Singh and Saxena, 2015). Many species of microalgae have been utilized for the removal of contaminants from wastewater or sewage, as well as the conversion of said sewage into an effluent that can be reused for various purposes. This is because of their ability to absorb and metabolize nutrients and heavy metals in the water such as cadmium, lead, zinc, and copper (Rajamani et al., 2007). Under certain growth conditions, microalgae produce and accumulate large amounts of lipids, proteins, and carbohydrates in the cell. The lipid content of microalgae is higher than that of other biofuels, usually between 20% and 50% of the cell's dry weight but can reach up to 70% (Duan et al., 2012; Sun et al., 2018). Because of this, they have also been regarded as a suitable candidate for third-generation biofuel feedstock. A variety of studies have been conducted to maximize the potential of microalgae as biofuels, including the applications of genetically modified microalgae; high-density mass culturing; and efficient processes for cultivation, harvest, and extraction (Ghasemi et al., 2012).

In recent years, an increasing amount of research has been conducted to study the effects of microalgal–bacterial co-culture/combination systems for wastewater treatment and biomass production (Ramanan et al., 2016; Qi et al., 2018). However, investigations into microalgal–bacterial co-culture/combination systems for crop production remain largely unexplored. Hence, the current review describes the effects of microalgae and bacteria as biofertilizer agents in vegetable cultivation. Furthermore, it aims to propose the potential of the microalgae–PGPB co-culture/combination system to improve the production and the quality of vegetables.

EVALUATION OF MICROALGAE AS BIOFERTILIZERS FOR VEGETABLE PRODUCTION

Effect of Microalgae as Biofertilizers on Crop Cultivation

Many studies have indicated that microalgae are increasingly being employed, not only in bioremediation and biofuel

production but also in agriculture. This is because a wide range of bioactive compounds, including plant growth-promoting substances (such as phytohormones), amino acids, carotenoids, and phycobilins, can be produced from microalgae. These compounds contribute to high productivity in agricultural crops by promoting plant growth and conferring resistance against pathogens with minimal environmental costs (Stirk et al., 2013b; Michalak and Chojnacka, 2014).

Microalgal extracts contain phytohormones such as auxin, cytokinin, abscisic acid, ethylene, and gibberellin, which play key roles in the regulation of growth and development. Accordingly, microalgal extracts can be used as renewable sources of plant biostimulation (Stirk et al., 2013a; Romanenko et al., 2015). Auxin is an essential regulator of various plant developmental processes, such as cell division and elongation. Indole-3-acetic acid (IAA) and indole-3-butanoic acid (IBA), the two dominant types of auxins in microalgae, can both stimulate and inhibit the growth and metabolism of higher plants (Hashtroudi et al., 2013). Cytokinins are involved in many physiological processes in plants, including root and shoot development, leaf senescence, nutrient mobilization, and seed germination (Ha et al., 2012), while gibberellins are able to promote cell division, trigger the accumulation of pigments and proteins, and stimulate cell elongation and expansion (Sponsel and Hedden, 2010). Ethylene is a gaseous plant hormone that renders tolerance to abiotic stresses such as drought, low temperatures, and high salinity, as well as biotic stresses such as the penetration of pathogens (Pierik et al., 2006). Thus, phytohormones not only affect plant growth and development but also activate plant defense systems against plant pathogens via interacting/cross-talking networks among them (Checker et al., 2018).

Various Microalgae Species Used for Important Vegetable Cultivation

Based on the increasing number of studies demonstrating that microalgae have the ability to promote plant growth and defend against plant pathogens, several microalgae species are being used in the cultivation of important vegetables (**Table 1**). In general, *Chlorella vulgaris*, *Chlorella fusca*, and *Spirulina platensis* have been used for tomato, cucumber, onion, lettuce, and pepper cultivation with a view to promote their production with marketable quality (Kim et al., 2018; Bumandalai, 2019; Rachidi et al., 2020).

Tomato (*Solanum lycopersicum* L.)

Tomato is the most popular home garden vegetable. It is a rich source of vitamins, minerals, and flavonoids such as quercetin (Nicola et al., 2009). Strategies for improving the productivity and nutritional quality of tomatoes are of great interest to producers (Dorais et al., 2008). In tomato fruits, treatment with *Nannochloropsis oculata* has been found to induce 33% and 36% higher levels of sugar and carotenoid content, respectively, compared to those treated with inorganic fertilizer under greenhouse conditions (Coppens et al., 2016). It was also found that among young tomato plants grown in phytotrons, the number of nodes, dry weight, and length of shoots had significantly increased from treatment with polysaccharide extracts from *Arthrospira platensis*, *Dunaliella salina*, and *Porphyridium* sp. when compared to the untreated control. Tomato plants treated with polysaccharide extracts also showed an increase in the activities of nitrate reductase (NR) and NAD-glutamate dehydrogenase (NAD-GDH), key enzymes for nitrogen assimilation and amino acid synthesis, as well as

TABLE 1 | Typical cases of microalgal effects on vegetable production.

Vegetable	Microalgae species	Application	References
Tomato	*Nannochloropsis oculata*	Increased contents of sugar and carotenoid in fruits	Coppens et al. (2016)
	Chlorella vulgaris	Improved growth of shoot and root	Bumandalai (2019)
	Arthrospira platensis, *Dunaliella salina*, and *Porphyridium* sp.	Improved activities of nitrate reductase (NR) and NAD-glutamate dehydrogenase (NAD-GDH) related to nitrogen assimilation and amino acid synthesis in leaves	Rachidi et al. (2020)
	Chlorella vulgaris and *Chlorella sorokiniana*	Increased activities of β-1,3-glucanase and phenylalanine ammonia lyase (PAL) linked to defense mechanisms in leaves	Farid et al. (2019)
	Acutodesmus dimorphus	Increased number of branches and flowers in plants	Garcia-Gonzalez and Sommerfeld (2016)
Onion	*Spirulina platensis* + cow dung	Improved growth, yield, and content of pigments in leaves and elevated levels of biochemicals and minerals	Dineshkumar et al. (2020)
	Scenedesmus subspicatus + humic acid	Promoted root growth at the early developmental stages and increased contents of sugars and proteins in bulbs	Gemin et al. (2019)
Cucumber	*Chlorella vulgaris*	Promoted root growth	Bumandalai (2019)
	Anabaena vaginicola and *Nostoc calcicola*	Improved rooting abilities likely affected by indole-3-butyric acid (IBA) and indole-3-acetic acid (IAA)	Shariatmadari et al. (2013)
Eggplant	*Spirulina platensis*	Increased fruit production without significant alterations in the levels of N, P, K, and Na in the leaves, when treated with low concentrations	Dias et al. (2016)
Pepper	*Dunaliella salina* and *Phaeodactylum tricornutum*	Improved salt tolerance during germination by reducing superoxide radicals and lipid peroxidation	Guzmán-Murillo et al. (2013)
Lettuce	*Chlorella vulgaris*	Reduced mineral fertilizer consumption up to 60% by adding living *Chlorella vulgaris* in the nutrient solution	Ergun et al. (2020)
	Scenedesmus quadricauda	Increased plant growth and protein content in leaves by activating key enzymes related to N, C, and secondary metabolisms (i.e., phenylalanine ammonia lyase; PAL)	Puglisi et al. (2020)

phenylalanine ammonia lyase (PAL) and β-1,3-glucanase, which activate plant defenses against pathogens (Kobayashi et al., 1995; Vera et al., 2011; Chen et al., 2017; Farid et al., 2019; Rachidi et al., 2020). Microalgal polysaccharides can elevate the activity of NADPH-synthesizing enzymes, shifting conditions to be more conducive to reduction in the intracellular redox state, which may favor photosynthesis and cell division. In addition, the levels of ascorbate (AsA) content and ascorbate peroxidase (APX) activity, which play central roles in photosynthesis and abiotic stress tolerance, have been shown to increase in polysaccharide-treated plants (Castro et al., 2012; Smirnoff, 2018; Chanda et al., 2019; **Figure 1**). Moreover, Garcia-Gonzalez and Sommerfeld (2016) assessed the properties of the microalgae *Acutodesmus dimorphus* as a biofertilizer and/or biostimulant. Under greenhouse conditions, foliar application of the algal extract at a concentration of 3.75 g ml^{-1} on tomato plants caused an increase in the number of branches and flowers per plant (Garcia-Gonzalez and Sommerfeld, 2016).

Onion (*Allium cepa* L.)

Onion is one of the most economically important vegetable crops consumed primarily because of its ability to enhance the flavor of other foods (Kandoliya et al., 2015). Field experiments were performed at the experimental farm of Annamalai University, India, in 2016–2017 to determine the efficacy of microalgae, such as *C. vulgaris* and *S. platensis*, as biofertilizers on onion plants. Treatment comprising of cow dung with *S. platensis* on onion plants resulted in higher amounts of micro- and macronutrients available in the soil, including nitrogen, phosphate, potassium, zinc, and manganese. There was also an increase in the levels of biochemicals in the onion, such as total soluble sugars, total phenols, and free amino acids, along with improved growth parameters, when compared to the untreated control. In addition to this, higher amounts of minerals were observed in onion plants treated with "cow dung + *S. platensis*" and "cow dung + *C. vulgaris*" (Dineshkumar et al., 2020). Furthermore, compared to the untreated control, treatment with a mixture of *Scenedesmus subspicatus* and humic acid synergistically increased the onion root length by 39% and the concentration of soluble proteins by 37% (Gemin et al., 2019).

Cucumber (*Cucumis sativus* L.)

Cucumber is also an important vegetable crop (Huang et al., 2009) that is cultivated in many countries within both temperate

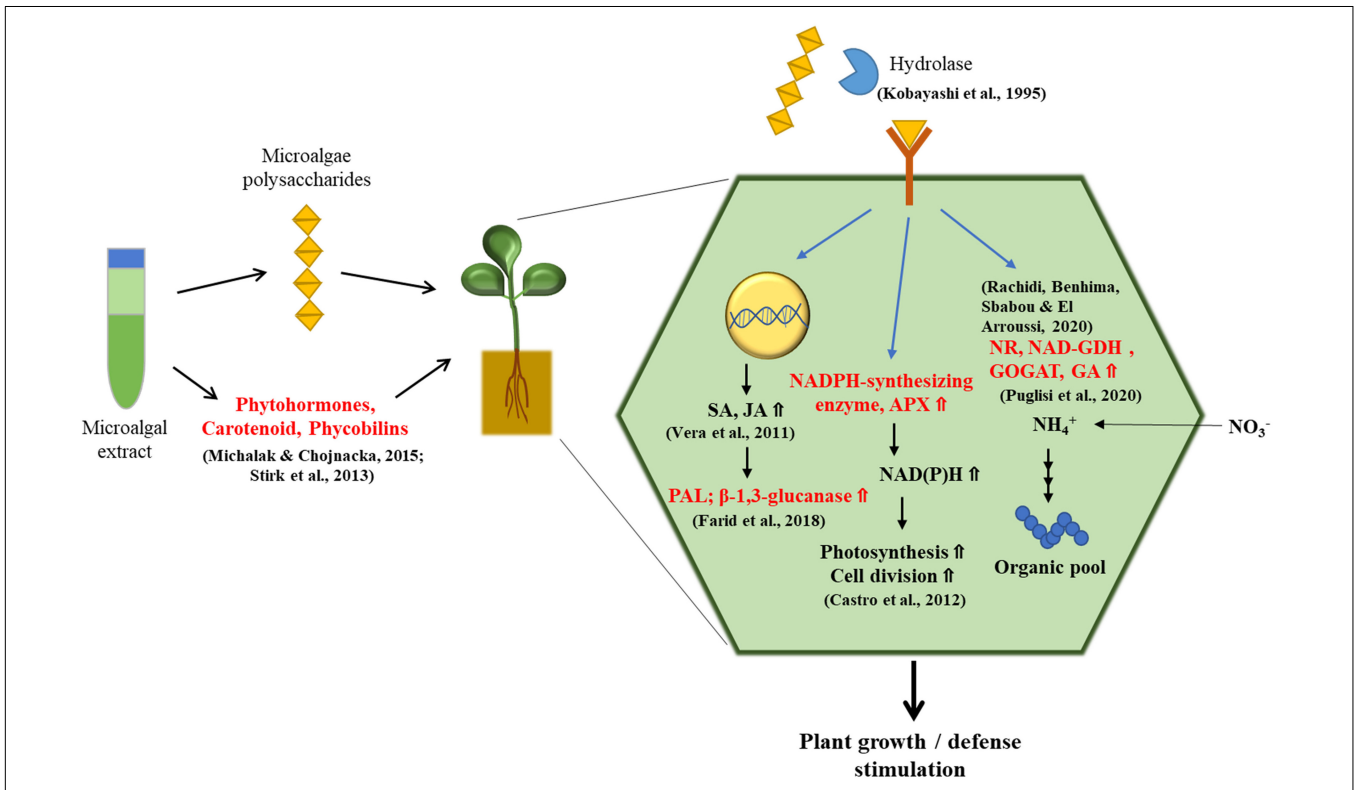

FIGURE 1 | The treatment of microalgae extracts stimulates plant growth and defense system. Microalgal extracts contain many plant growth-promoting compounds such as polysaccharides, phytohormones, carotenoids, and phycobilins, which have the ability to stimulate the plant growth and defense system. Large polysaccharides from microalgal extracts are broken down into smaller fragments of oligosaccharides by hydrolytic enzymes. Oligosaccharides are perceived by plant's membrane receptor and have a significant stimulatory effect on the plant growth by regulating activities of enzymes such as nitrate reductase (NR) and NAD-glutamate dehydrogenase (NAD-GDH) related with nitrate assimilation. Moreover, polysaccharides can increase activity of NADPH-synthesizing enzymes, ascorbate peroxidase (APX), and the amount of ascorbate (AsA), which are associated with photosynthesis, fundamental cellular metabolism, and cell cycle. Defense pathways are also stimulated by polysaccharides in plant cells: polysaccharide treatment upregulates the expression of genes involved in salicylic acid (SA) and jasmonic acid (JA) signaling pathways, resulting in increased activities of β-1,3-glucanase and phenylalanine ammonia lyase (PAL) linked to plant defense system.

and tropical zones (Tatlioglu, 1993). When vegetable crops such as cucumber, tomato, and squash were treated with *Anabaena vaginicola* and *Nostoc calcicola*, they showed increased growth factors when compared to the untreated control. These growth factors included root length, fresh and dry weight of roots, and plant height. Auxins such as IBA, which are involved in root development in plants, were also shown to be available with this treatment in the range of 1.275–2.958 $\mu g\ g^{-1}$ dry weight with a trace amount of IAA in microalgal cells (Shariatmadari et al., 2013).

Eggplant (*Solanum melongena* L.)

Eggplant is ranked among the top 10 vegetables in terms of oxygen radical absorbance capacity due to its high content of total phenolics (Cao et al., 1996). Dias et al. (2016) conducted field and laboratory experiments to evaluate the growth, yield, and postharvest quality of eggplants with different concentrations of *S. platensis* solutions for foliar application at the Centro de Ciências e Tecnologia de Alimentos (CCTA), Brazil. This experiment was performed between October 2014 and January 2015. The results revealed that the number of fruits significantly increased in plants treated with low concentrations of this treatment (10, 15, 25, and 35 $g\ l^{-1}$). This is likely due to the greater abundance of polypeptides, amino acids, and hormones in the microalgal species acting as plant growth promoters when compared to the levels in the untreated control (Dias et al., 2016).

Pepper (*Capsicum annuum* L.)

Pepper is a popular commercial vegetable and spice crop that is valued for its fruit color, flavor, pungency, and nutrient content (Kumar et al., 2006). Treatment with extracts of *D. salina* increased the germination rate by 69% and the root length of bell peppers by 24% in 25 mM NaCl. Meanwhile, *Phaeodactylum tricornutum* treatment was found to reduce the production of superoxide radicals and lipid peroxidation triggered by salt stress, when compared to the untreated control (Guzmán-Murillo et al., 2013).

Lettuce (*Lactuca sativa* L.)

Treatment of lettuce seedlings with *Scenedesmus quadricauda* extract promoted plant growth and induced the accumulation of chlorophyll, carotenoids, and total protein content in the plant cell. In addition, the leaf dry weights were positively affected by the treatment with *S. quadricauda* extract, reaching an increase of approximately 26% when compared to the untreated control. From a metabolic point of view, the treated leaves revealed increased enzyme activity levels of glutamate synthase (GOGAT), glutamine synthase (GS), citrate synthase (CS), malate dehydrogenase (MDH), and PAL, which are key enzymes associated with nitrogen (Gupta et al., 2012), carbon (Schiavon et al., 2008), and phenylpropanoid metabolism (Hyun et al., 2011). This suggested that the positive effect on the growth of lettuce most likely occurs through the stimulation of the metabolic pathways of carbon, nitrogen, and phenylpropanoid (Puglisi et al., 2020).

EVALUATION OF BACTERIA AS BIOFERTILIZERS FOR VEGETABLE PRODUCTION

The Effect of Bacteria as Biofertilizers on Crop Cultivation

Bacteria are a major class of microorganisms that function as decomposers and recyclers in the soil. In doing so, these microbes contribute to the processes of nutrient cycling, energy flow, and bioconversion in the ecosystem. Most agricultural production systems are dependent on soil bacterial biomass pools, which facilitate quick responses to diverse environmental changes (Pankhurst et al., 1996). Microbial inoculums called effective microorganisms (EM), containing mixed cultures of beneficial and naturally occurring microorganisms, can increase the microbial diversity of the soil ecosystem. They consist mainly of lactic acid bacteria, photosynthetic bacteria, yeast, *Actinomyces*, and fermenting fungi (Balogun et al., 2016). Among these effective microorganisms, PGPB form specific symbiotic relationships with plants and directly promote plant growth by facilitating resource acquisition and/or modulating plant hormone levels (Glick, 1995). The application of PGPB to vegetable cultivations can prevent the excessive use of chemical fertilizers by up to 30%, thereby reducing production costs and pollution (Geries and Elsadany, 2021). PGPB treatments also have the ability to improve host plant defenses against soil-borne pathogens by producing antibiotics such as 2,4-diacetylphloroglucinol (2,4-DAPG), pyoluteorin (PLT), pyrrolnitrin, and phenazine-1-carboxylate (Bangera and Thomashow, 1999; Duffy and Défago, 1999).

Various Bacterial Species Used for Vegetable Cultivation

It has been adequately demonstrated that many species of bacteria are able to promote the growth and development of vegetables and control pathogens through various mechanisms, one of which include the production/release of inhibitory substances, allowing target crops to be disease resistant (**Table 2**). Representative commercially available bacterial strains are of the genus *Bacillus* spp.; these include *B. amyloliquefaciens*, *B. subtilis*, *B. cereus*, *B. licheniformis*, and *B. pumilus*, which produce various compounds for the biocontrol of plant pathogens and the growth promotion of vegetables such as tomato, cucumber, onion, lettuce, and pepper (Gutiérrez-Mañero et al., 2001; Compant et al., 2005; Cawoy et al., 2011; Yuan et al., 2012; Nie et al., 2017). Silo-Suh et al. (1994) reported that *B. cereus* UW85 suppresses the damping-off disease caused by *Phytophthora medicaginis* in alfalfa through the production of two fungistatic antibiotics, zwittermicin A and kanosamine (Silo-Suh et al., 1994).

In addition, *Serratia liquefaciens* and *Pseudomonas putida* are known to generate *N-acyl*-L-homoserine lactone (AHL) signaling molecules, which enhance the systemic resistance of tomato plants against the leaf fungal pathogen, *Alternaria alternata* (Schuhegger et al., 2006). Recently, it was shown that two

TABLE 2 | Typical cases of bacterial effects on vegetable production.

Vegetable	Bacteria species	Application	References
Tomato	*Serratia liquefaciens* and *Pseudomonas putida*	Induced systemic resistance against the fungal leaf pathogen *Alternaria alternata* in tomato by producing *N-acyl*-L-homoserine (AHL) lactone	Schuhegger et al. (2006)
	Pantoea agglomerans and *Burkholderia anthina*	Increased plant height, root length, shoot and root dry weight, phosphorous uptake level, and the available phosphorus content of soil	Walpola and Yoon (2013)
	Bacillus amyloliquefaciens	Suppressed bacterial wilt disease by reducing the population of *Ralstonia solanacearum*	Huang et al. (2014)
	Bacillus circulans	Stimulated seedling growth by increasing nutrient uptake parameters	Mehta et al. (2015)
Onion	*Azotobacter chroococcum*, *Bacillus subtilis*, and *Pseudomonas fluorescens*	Produced indole-3-acetic acid (IAA) and siderophores and improved growth and yield with higher solubilization of tricalcium phosphate (TCP)	Čolo et al. (2014)
	Bacillus subtilis	Inhibited the growth of *Setophoma terrestris*, a causal agent of pink root disease	Albarracín Orio et al. (2016)
Cucumber	*Pseudomonas corrugate* and *Pseudomonas aureofaciens*	Inhibited root and crown rot caused by *Pythium aphanidermatum* by stimulating the activities of defense enzymes in the root tissue	Chen et al. (2000)
	Bacillus subtilis	Improved growth and yield by reducing losses caused by *Pythium* root rot	Utkhede and Koch (1999)
Lettuce	*Bacillus amyloliquefaciens*	Alleviated the disease severity of bottom rot caused by *Rhizoctonia solani*.	Chowdhury et al. (2013)
Pepper	*Bacillus licheniformis* and *Bacillus subtilis*	Produced auxins, antifungal β-glucanases, and siderophores; stimulated seed germination; and promoted the growth of vegetative organs such as root, stem, and leaf	Lim and Kim (2009)

phosphate-solubilizing bacteria (PSB), *Pantoea agglomerans* and *Burkholderia anthina*, contributed to improved growth traits of tomato plants with a higher level of phosphorous content in the soil, when compared to the untreated control, under greenhouse conditions (Walpola and Yoon, 2013). The ability of *Azotobacter chroococcum* and *Pseudomonas fluorescens* to improve vegetative growth and yield in onion production through the production of IAA, siderophores, and the solubilization of tricalcium phosphate (TCP) has also been demonstrated (Tarakhovskaya et al., 2007; Čolo et al., 2014).

RELATIONSHIP BETWEEN MICROALGAE AND BACTERIA

Microalgae–Bacteria Interactions

In natural environments, microalgae and bacteria coexist and interact with each other. As a result, they demonstrate both beneficial (Unnithan et al., 2014) and harmful/toxic relationships (Doucette, 1995). The relationship between microalgae and bacteria is greatly dependent on the species and the environmental conditions (Doucette, 1995; Croft et al., 2005; Mujtaba and Lee, 2016). In actuality, both microalgae and bacteria can produce growth factors, and/or exotoxins, that promote and/or inhibit growth and development. In the beneficial relationship, microalgae enhance bacterial growth by providing photosynthetic oxygen and dissolved organic matter such as organic carbon, calcium carbonate, and 2,3-dihydroxypropane-1-sulfonate (DHPS) (Wolfaardt et al., 1994; Borde et al., 2003; Cooper and Smith, 2015). Generally speaking, the photosynthetic oxygen produced by microalgae or cyanobacteria (blue-green algae) is used as an electron acceptor in the bacterial degradation of organic matter. In turn, bacteria support photoautotrophic growth of their partners by providing carbon dioxide and other stimulatory means (Subashchandrabose et al., 2011). In a similar way, bacteria are also able to offer a selective advantage to microalgae for enhanced growth by providing micronutrients such as B-vitamins. These vitamins act as co-factors that are required for enzyme activity in the central cellular metabolism (Croft et al., 2005). Moreover, microalgae can acquire nutrients such as inorganic carbon, nitrogen, phosphorus, and sulfate generated from organic matter, through the activities of extracellular bacterial enzymes. However, in harmful/toxic relationships, microalgae can inhibit bacterial activity by releasing antibacterial metabolites and increasing the pH, the dissolved oxygen concentration, and the temperature of the culture medium (Naviner et al., 1999; Schumacher et al., 2003; Ribalet et al., 2008).

Both microalgae and PGPB have the ability to promote plant growth by producing polysaccharides and phytohormones, such as auxin and cytokinin. Furthermore, they can prevent plant diseases by stimulating defense systems and secreting antifungal enzymes and antibiotics (**Figure 2**; Najdenski et al., 2013; Stirk et al., 2013b; Walpola and Yoon, 2013; Michalak and Chojnacka, 2014; Cordero et al., 2016).

Reciprocal Influence During the Co-culture/Combination of Microalgae and Bacteria

As microalgae have been widely used in various industries, extensive studies have shown that when microalgae and bacteria are co-cultured, there is an increase in microalgal productivity in the production of useful substances such as total lipids, carbohydrates, and chlorophylls (**Table 3**).

Amavizca et al. (2017) demonstrated that two PGPB strains, *Azospirillum brasilense* Cd and *B. pumilus* ES4, have similar effects on the growth of the green microalga *Chlorella sorokiniana* UTEX 2714, without any form of physical contact between them. The two PGPB remotely enhanced the growth rate of microalgae up to six-fold and induced an increase in the total

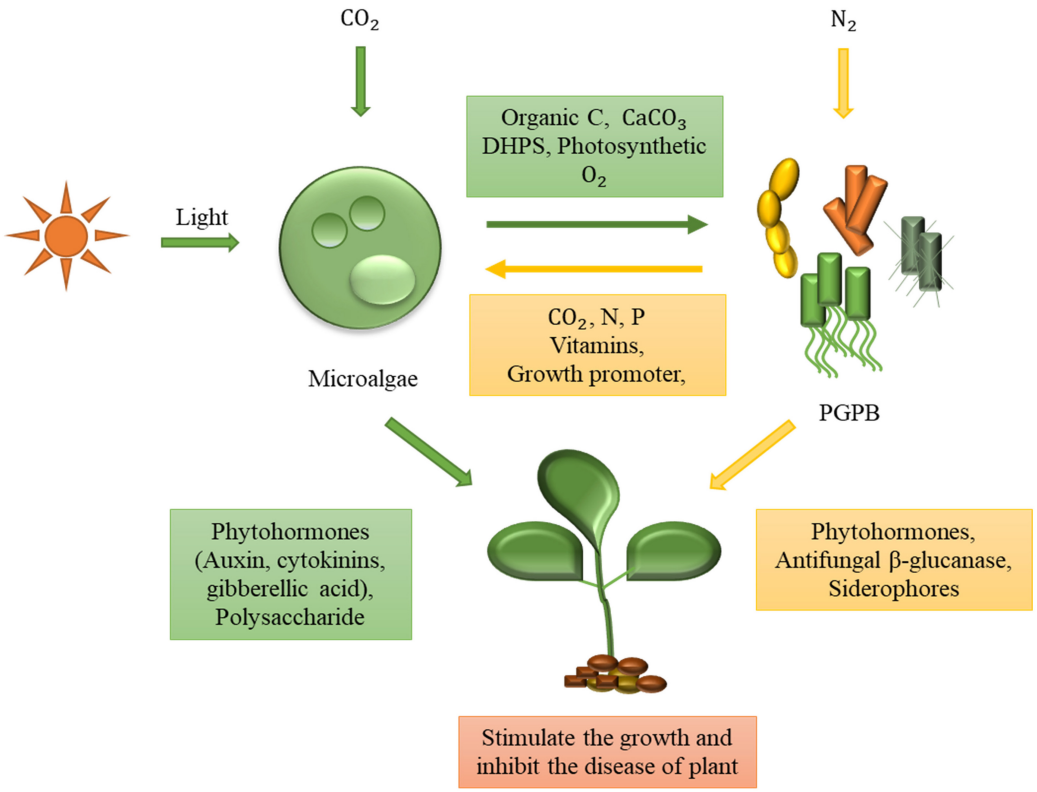

FIGURE 2 | Symbiotic interactions between microalgae and plant growth-promoting bacteria (PGPB) for sustainable cultivation of plants. Microalgae and PGPB in the symbiotic relationship cooperate with each other by efficient exchange of nutrients. Microalgae supply photosynthetic oxygen, organic carbon, calcium carbonate, and 2 3-dihydroxypropane-1-sulfonate (DHPS) to bacteria in exchange for micronutrients (i.e., vitamins) and macronutrients (i.e., nitrogen and phosphorus). Both microalgae and bacteria can enhance plant growth by producing phytohormones and other growth stimulants. Moreover, they are also able to inhibit plant diseases by using their distinct disease-suppressive mechanisms.

TABLE 3 | Examples of microalgae–bacteria interactions in co-culture/combination.

Microalgae	Bacteria	Comments	References
Chlorella sorokiniana	*Azospirillum brasilense* and *Bacilus pumilus*	Two plant growth-promoting bacteria (PGPB) remotely enhanced the growth of the microalgae with elevated amounts of total lipids, carbohydrates, and chlorophyll a in the microalgal cells	Amavizca et al. (2017)
	Bacterial strain CSSB-3 (98.6% identical to the 16S rDNA gene sequence of *Microbacterium trichotecenolyticum*)	Promoted the growth of *C. sorokiniana* in the mixed culture with CSSB-3 under a photoautotrophic condition	Watanabe et al. (2005)
	Azospirillum brasilense	*Azospirillum brasilense* increased *C. sorokiniana* growth through a variety of mechanisms, including the production of IAA	Peng et al. (2020)
Chlorella vulgaris	*Azospirillum brasilense*	Increased pigment and lipid contents, lipid variety, and cell and population size of the microalgae *Chlorella* spp.	de-Bashan et al. (2002)
Amphidinium operculatum	*Halomonas* sp.	*Amphidinium* acquires vitamin B_{12} through a direct interaction with *Halomonas* sp.	Croft et al. (2005)
Tetraselmis chuii	*Muricauda* sp.	*Muricauda* significantly promoted the growth of *T. chuii* and *C. fusiformis*, but drastically inhibited the growth of *N. gaditana*.	Han et al. (2016)
Cylindrotheca fusiformis			
Nannochloropsis gaditana			

amounts of lipids, carbohydrates, and chlorophyll *a* in the microalgal cells. These beneficial effects have been ascribed to the volatile compounds produced by the bacteria, which include CO_2 (Amavizca et al., 2017). In addition, plant growth-promoting bacteria, such as *A. brasilense*, have the potential to significantly increase *C. sorokiniana* growth rates through a variety of mechanisms, including the production of IAA (Peng et al., 2020). Croft et al. (2005) reported that bacterial strains of

Halomonas sp. have a growth-enhancing effect on the microalga *Amphidinium operculatum* through the provision of vitamin B_{12}. In addition to this, the presence of algal extracts also leads to the promotion of bacterial growth with upregulated vitamin B_{12} biosynthesis, displaying positive reciprocity (Croft et al., 2005). Sometimes, a single bacterial strain can induce different effects on the growth and proliferation of distinct microalgae. For example, *Muricauda* sp. was found to promote the growth of *Tetraselmis chuii* and *Cylindrotheca fusiformis*, but drastically inhibited the growth of *Nannochloropsis gaditana* (Han et al., 2016).

CO-CULTURING/COMBINATION OF MICROALGAE–BACTERIA

Microalgae–Bacteria Co-culture for Wastewater Treatment and Biomass Production

The co-culture system of bacteria and microalgae has been mainly used for wastewater treatment and biomass production. Mujtaba et al. (2017) investigated the efficiency of nutrient removal (i.e., ammonium, phosphate, etc.) and the reduction of chemical oxygen demand (COD) from wastewater, using the symbiotic co-culture of *P. putida* and immobilized *C. vulgaris*. In general, symbiotic co-culture systems facilitate the simultaneous removal of a greater variety of nutrients from wastewater compared to monocultures (Mujtaba et al., 2017). Ogbonna et al. (2000) found that it is impossible to remove all nutrients such as acetate, propionate, ammonia, nitrate, and phosphorus from wastewater at once using monocultures of *Rhodobacter sphaeroides*, *C. sorokiniana*, and *S. platensis*, whereas these nutrients can all be removed simultaneously by using the co-culture system (Ogbonna et al., 2000). Moreover, the symbiotic co-culture of *A. brasilense* and *Scenedesmus* sp. has been successfully applied to biofuel production with higher biomass volume. This indicates that the symbiotic co-culture has the potential to increase microalgal colony size, and the fatty acid content inside biofuels, in nitrogen-deficient media (Contreras et al., 2019). The combination of cyanobacteria/microalgae and bacteria can more efficiently detoxify organic and inorganic pollutants and remove nutrients from wastewater compared to using either of them alone.

Soils and aquatic systems contaminated by heavy metals have also become a serious issue in crop production because of the risks associated with food contamination. Microalgae have the ability to detoxify and volatilize heavy metals via microalgal metabolism and high levels of metal binding (Yu et al., 1999). Microalgae form metal-binding peptides (organometallic complexes) such as class III metallothionein (MtIII) (Perales-Vela et al., 2006), which facilitate appropriate control of the cytoplasmic concentration of heavy metals, thereby preventing or neutralizing the potential toxicity caused by heavy metals (Kaplan, 2013; Priya et al., 2014). The application of microalgae, which can bioabsorb and biotransform arsenate (As) in rice fields, reduces the availability of As to plants, thereby rendering the food grains safe for human consumption (Debnath and Bhadury, 2016). In the case of the algal–bacterial synergistic interactions, a higher removal efficiency of heavy metals was achieved with the addition of bacterial inoculum, which enhanced algal growth with additional CO_2 and organic compounds provided by the bacteria (Unnithan et al., 2014; Mubashar et al., 2020). Furthermore, algae can also be recycled as biofertilizing agents (Guo et al., 2020).

Potential of Microalgae–Bacteria Co-cultures/Combination for Vegetable Cultivation

There are two distinct application methods for the simultaneous use of microalgae and bacteria, one is co-culturing the microbes from the beginning and the other is preparing a mixture containing microalgae/microalgal extract and bacteria gained from each pure culture (combination).

The combined application of specific bacteria, which are growth promoters in plants and/or biocontrol agents against plant pathogens, can lead to the synergy necessary for ideal vegetable cultivation. When *Pantoea ananatis* and *P. fluorescens* (CPP-2) were co-cultured, IAA production and phosphate solubilization were higher than those from either strain alone. Additionally, the co-culture of CPP-2 showed promotion effects on root and shoot elongation of pea (*Pisum sativum*) plants when compared to the culture of an individual strain (Anwar et al., 2019). Moreover, the combination of *P. putida* WCS358 and RE8 was shown to enhance the suppression of *Fusarium* wilt in radish by approximately 50%, when compared to the untreated control, while that of the single-strain treatments was reduced by 30%. Even when one strain failed to suppress disease with a single application, the combination treatment still exhibited a suppressive effect against the disease. This implies that the reinforced resistance, brought on the combination application, is likely due to the additive/combinational effect of different disease-suppressive mechanisms (Boer et al., 2003).

Even though the application of microorganisms, via co-culture/combination treatment, is more effective for vegetable production (Minuto et al., 1993; Raupach and Kloepper, 1998), the use of a single microbial species for vegetable cultivation is commonly observed in practical situations. Although the activity of one microbial species is relatively narrow in scope from a practical point of view, it is easier to obtain related patents and/or safety certificates for the use of a single microbial species in agricultural and commercial sectors with obvious effects in a short period of time. In addition to this, the application of a single microbial species makes the processes of cultivation, harvesting, and extraction simpler and easier (Sylvia et al., 2005). However, in the case of co-culture/combination, the ability to suppress plant pathogens and promote plant growth is much more effective than that of the monoculture system because the microbes in the co-culture/combination system promote the growth of plants and/or prevent pathogens by different mechanisms (Spadaro and Gullino, 2005).

Several important practical examples of mixed treatments of cyanobacteria/microalgae–bacteria have been reported for crop cultivation (**Table 4**).

TABLE 4 | Examples of co-inoculation of microalgae–bacteria in agriculture.

Crop	Microalgae/cyanobacteria	Bacteria	Application	References
Rice	*Anabaena laxa*, *Anabaena* sp., and *Anabaena oscillarioides*	*Providencia* sp., *Brevundimonas* sp., and *Ochrobactrum* sp.	Enhanced carbon sequestration and plant growth in treatments involving a combination of bacterial and microalgal strains	Prasanna et al. (2012)
Lettuce	*Chlorella vulgaris*	*Bacillus licheniformis*, *Bacillus megatherium*, *Azotobacter* sp., *Azospirillum* sp., and *Herbaspirillum* sp.	Increased the plant weight and total carotenoid content especially under stress conditions during summer	Kopta et al. (2018)
Common bean	*Anabaena cylindrica*	*Rhizobium tropici*, *Rhizobium freirei*, and *Azospirillum brasilense*	Promoted plant growth parameters and grain production by 84% in plants inoculated with *Rhizobium* + *Azospirillum* + *Anabaena*	Horácio et al. (2020)
Maize	*Anabaena cylindrica*	*Azospirillum brasilense*	Increased yield performance of maize hybrid in Londrina and Faxinal	Gavilanes et al. (2020)
Onion	*Spirulina platensis*	*Pseudomonas stutzeri*	Enhanced plant growth, productivity, and bulb quality and reduced the production cost in treatments involving the combined treatment of *S. platensis* extract and nitrogen-fixing *P. stutzeri*	Geries and Elsadany (2021)

In 2012, the effects of combined treatments of cyanobacterial strains—CR1, CR2, and CR3 (*Anabaena laxa*, *Anabaena* sp., and *Anabaena oscillarioides*)—and bacterial strains—PR3, PR7, and PR10 (*Providencia* sp., *Brevundimonas* sp., and *Ochrobactrum* sp.)—on rice crop yield and C-N sequestration in soil were first reported in a pot experiment (Prasanna et al., 2012).

The synergistic efficacy of the combination of freshwater algae (*C. vulgaris*) and plant growth-promoting bacteria (*B. licheniformis*, *Bacillus megatherium*, *Azotobacter* sp., *Azospirillum* sp., and *Herbaspirillum* sp.) on yields and nutritional values of leaf and romaine lettuces has also been observed. The combined application of microalgal–bacterial preparation led to a significant increase of the romaine and leaf lettuce weight by 12.9% and 22.7%, respectively. Of note, total carotenoids in amounts 26.7% higher than in the controls were detected in the treated romaine lettuce under stress conditions during summer (Kopta et al., 2018).

Recently, Horácio et al. (2020) evaluated the effects of co-inoculation with a diazotrophic cyanobacterium (*Anabaena cylindrica*, Ana), *Rhizobium* (*R. tropici* + *R. freirei*, Riz), and *A. brasilense* (Azo) on the development of the common bean under greenhouse conditions. Grain production in the plants co-inoculated with Ana + Riz + Azo and fertilized with N (100 kg N ha^{-1}) was 84.4% and 86.3% higher than that of untreated controls, respectively. This indicates that N fertilization can be replaced by co-inoculation with selected cyanobacterial–bacterial strains (Horácio et al., 2020). In addition, Gavilanes et al. (2020) conducted two field experiments to assess the efficacy of co-inoculation of *A. cylindrica* with *A. brasilense* on the yield performance of four maize cultivars in two locations (Londrina and Faxinal in Paraná, Brazil). They found that the co-inoculation of *A. cylindrica* and *A. brasilense* resulted in a yield that increased by 9% (967 kg ha^{-1}) in Londrina and 23% (1,744 kg ha^{-1}) in Faxinal, compared to the uninoculated control (Gavilanes et al., 2020).

It was also found that the growth and productivity of onion plants with the combination treatment were promoted when compared to those with either single-agent treatment. This supports the result of biochemical analyses that state that extracts of both *S. platensis* and *Pseudomonas stutzeri* possess bioactive compounds such as HCN, NH_3, IAA, and amino acids that have stimulatory effects on plant growth and quality (Geries and Elsadany, 2021).

Additionally, after culturing *C. fusca* and *B. amyloliquefaciens* cc178 separately, they were combined in a ratio of 2:1 and used to irrigate tomato roots. It was found that rooting of fine roots was promoted and the plant growth, yield, and soluble liquid sugar content in fruits had significantly increased with the combination treatment when compared to each single treatment (unpublished data). Therefore, the combined application of microalgae and PGPB can exert beneficial effects on the yield and quality of vegetable crops.

CONCLUSION AND FUTURE DIRECTIONS

Microalgae and bacteria have received great interest as biofertilizers in ecofriendly vegetable production. Until now, monoculture systems using certain agricultural microorganisms have been highlighted to improve the yield and quality of agricultural products. However, co-culture/combination systems of microorganisms can be more effective in enhancing microbial diversity in the soil, resistance to plant diseases, and productivity of vegetable crops. Therefore, further investigations to uncover the molecular mechanisms underlying the effect of microalgae–bacteria co-culture/combination on vegetable growth, and/or plant disease suppression, will be necessary for the extension of sustainable agriculture.

AUTHOR CONTRIBUTIONS

All authors listed have made a substantial, direct and intellectual contribution to the work, and approved the final version of the manuscript for publication.

FUNDING

This research was financially supported in part by the World Vegetable Center Korea Office budget (WKO #10000379) and the long-term strategic donors to the World Vegetable Center: Republic of China (Taiwan), UK aid from the United Kingdom Government, United States Agency for International Development (USAID), Australian Centre for International Agricultural Research (ACIAR), Germany, Thailand, Philippines, South Korea, and Japan.

ACKNOWLEDGMENTS

The authors are grateful to Dr. Srinivasan Ramasamy for careful reading of the manuscript.

REFERENCES

Ahemad, M., and Kibret, M. (2014). Mechanisms and applications of plant growth promoting rhizobacteria: current perspective. *J. King Saud Univ. Sci.* 26, 1–20. doi: 10.1016/j.jksus.2013.05.001

Albarracín Orio, A. G., Brücher, E., and Ducasse, D. A. (2016). A strain of *Bacillus subtilis* subsp. subtilis shows a specific antagonistic activity against the soil-borne pathogen of onion *Setophoma terrestris*. *Eur. J. Plant Pathol.* 144, 217–223. doi: 10.1007/s10658-015-0762-0

Amavizca, E., Bashan, Y., Ryu, C.-M., Farag, M. A., Bebout, B. M., and de-Bashan, L. E. (2017). Enhanced performance of the microalga *Chlorella sorokiniana* remotely induced by the plant growth-promoting bacteria *Azospirillum brasilense* and *Bacillus pumilus*. *Sci. Rep.* 7:41310. doi: 10.1038/srep41310

Anwar, M. S., Paliwal, A., Firdous, N., Verma, A., Kumar, A., and Pande, V. (2019). Co-culture development and bioformulation efficacy of psychrotrophic PGPRs to promote growth and development of Pea (*Pisum sativum*) plant. *J. Gen. Appl. Microbiol.* 65, 88–95. doi: 10.2323/jgam.2018.05.007

Bagyalakshmi, B., Ponmurugan, P., and Balamurugan, A. (2017). Potassium solubilization, plant growth promoting substances by potassium solubilizing bacteria (KSB) from southern Indian Tea plantation soil. *Biocatal. Agricult. Biotechnol.* 12, 116–124. doi: 10.1016/j.bcab.2017.09.011

Balogun, R. B., Ogbu, J. U., Umeokechukwu, E. C., and Kalejaiye-Matti, R. B. (2016). "Effective micro-organisms (EM) as sustainable components in organic farming: principles, applications and validity," in *Organic Farming for Sustainable Agriculture*, ed. D. Nandwani (Cham: Springer), 259–291. doi: 10.1007/978-3-319-26803-3_12

Bangera, M. G., and Thomashow, L. S. (1999). Identification and characterization of a gene cluster for synthesis of the polyketide antibiotic 2,4-diacetylphloroglucinol from *Pseudomonas* fluorescens Q2-87. *J. Bacteriol.* 181, 3155–3163. doi: 10.1128/jb.181.10.3155-3163.1999

Beneduzi, A., Ambrosini, A., and Passaglia, L. M. (2012). Plant growth-promoting rhizobacteria (PGPR): their potential as antagonists and biocontrol agents. *Genet. Mol. Biol.* 35, 1044–1051. doi: 10.1590/s1415-47572012000600020

Boer, M., Bom, P., Kindt, F., Keurentjes, J., Sluis, I., Loon, L., et al. (2003). Control of Fusarium wilt of radish by combining *Pseudomonas* putida strains that have different disease-suppressive mechanisms. *Phytopathology* 93, 626–632. doi: 10.1094/PHYTO.2003.93.5.626

Borde, X., Guieysse, B., Delgado, O., Muñoz, R., Hatti-Kaul, R., Nugier-Chauvin, C., et al. (2003). Synergistic relationships in algal–bacterial microcosms for the treatment of aromatic pollutants. *Bioresource Technol.* 86, 293–300. doi: 10.1016/S0960-8524(02)00074-3

Bulgarelli, D., Schlaeppi, K., Spaepen, S., Van Themaat, E. V. L., and Schulze-Lefert, P. (2013). Structure and functions of the bacterial microbiota of plants. *Annu. Rev. Plant Biol.* 64, 807–838. doi: 10.1146/annurev-arplant-050312-120106

Bumandalai, O. (2019). Effect of *Chlorella vulgaris* as a biofertilizer on germination of tomato and cucumber seeds. *Int. J. Aquat. Biol.* 7, 95–99. doi: 10.22034/ijab.v7i2.582

Cao, G., Sofic, E., and Prior, R. L. (1996). Antioxidant capacity of tea and common vegetables. *J. Agricult. Food Chem.* 44, 3426–3431. doi: 10.1021/jf9602535

Castro, J., Vera, J., González, A., and Moenne, A. (2012). Oligo-carrageenans stimulate growth by enhancing photosynthesis, basal metabolism, and Cell Cycle in Tobacco Plants (var. Burley). *J. Plant Growth Regulat.* 31, 173–185. doi: 10.1007/s00344-011-9229-5

Cawoy, H., Bettiol, W., Fickers, P., and Ongena, M. (2011). "*Bacillus*-based biological control of plant diseases," in *Pesticides in the Modern World – Pesticides Use and Management*, ed. M. Stoytcheva (Rijeka: InTech), 273–302. doi: 10.5772/17184

Chanda, M.-J., Merghoub, N., and El Arroussi, H. (2019). Microalgae polysaccharides: the new sustainable bioactive products for the development of plant bio-stimulants? *World J. Microbiol. Biotechnol.* 35:177. doi: 10.1007/s11274-019-2745-3

Chandini, Kumar, R., Kumar, R., and Prakash, O. (2019). "The impact of chemical fertilizers on our environment and ecosystem," in *Research Trends in Environmental Sciences*, ed. P. Sharma (New Delhi: AkiNik Publications), 69–86.

Checker, V. G., Kushwaha, H. R., Kumari, P., and Yadav, S. (2018). "Role of phytohormones in plant defense: signaling and cross talk," in *Molecular Aspects of Plant-Pathogen Interaction*, eds A. Singh and I. Singh (Singapore: Springer), 159–184. doi: 10.1007/978-981-10-7371-7_7

Chen, C., BÉLanger, R. R., Benhamou, N., and Paulitz, T. C. (2000). Defense enzymes induced in cucumber roots by treatment with plant growth-promoting rhizobacteria (PGPR) and *Pythium aphanidermatum*. *Physiol. Mol. Plant Pathol.* 56, 13–23. doi: 10.1006/pmpp.1999.0243

Chen, Y., Li, F., Tian, L., Huang, M., Deng, R., Li, X., et al. (2017). The phenylalanine ammonia lyase gene LjPAL1 is involved in plant defense responses to pathogens and plays diverse roles in lotus japonicus-rhizobium symbioses. *Mol. Plant Microbe Interact.* 30, 739–753. doi: 10.1094/mpmi-04-17-0080-r

Choudhury, A. T. M. A., and Kennedy, I. R. (2005). Nitrogen fertilizer losses from rice soils and control of environmental pollution problems. *Commun. Soil Sci. Plant Anal.* 36, 1625–1639. doi: 10.1081/CSS-200059104

Chowdhury, S. P., Dietel, K., Rändler, M., Schmid, M., Junge, H., Borriss, R., et al. (2013). Effects of *Bacillus amyloliquefaciens* FZB42 on lettuce growth and health under pathogen pressure and its impact on the rhizosphere bacterial community. *PLoS One* 8:e68818. doi: 10.1371/journal.pone.0068818

Èolo, J., Hajnal-Jafari, T., Duri, S., Stamenov, D., and Hamidovi, S. (2014). Plant growth promotion rhizobacteria in onion production. *Polish J. Microbiol.* 63, 83–88. doi: 10.33073/PJM-2014-012

Compant, S., Duffy, B., Nowak, J., Clément, C., and Barka, E. A. (2005). Use of plant growth-promoting bacteria for biocontrol of plant diseases: principles. *Mech. Action Fut. Prospect.* 71, 4951–4959. doi: 10.1128/AEM.71.9.4951-4959.2005

Contreras, J., Mata, T., Bermúdez, S., Caetano, N., Chandra, R., García, S., et al. (2019). Symbiotic co-culture of *Scenedesmus* sp. and *Azospirillum brasilense* on N-deficient media with biomass production for biofuels. *Sustainability* 11:707. doi: 10.3390/su11030707

Cooper, M. B., and Smith, A. G. (2015). Exploring mutualistic interactions between microalgae and bacteria in the omics age. *Curr. Opin. Plant Biol.* 26, 147–153. doi: 10.1016/j.pbi.2015.07.003

Coppens, J., Grunert, O., Van Den Hende, S., Vanhoutte, I., Boon, N., Haesaert, G., et al. (2016). The use of microalgae as a high-value organic slow-release fertilizer results in tomatoes with increased carotenoid and sugar levels. *J. Appl. Phycol.* 28, 2367–2377. doi: 10.1007/s10811-015-0775-2

Cordero, J., Garbayo, I., Cuaresma, M., Montero Lobato, Z., González-delValle, M. A., and Vílchez, C. (2016). Impact of microalgae-bacteria interactions on the production of algal biomass and associated compounds. *Mar. Drugs* 14:100. doi: 10.3390/md14050100

Croft, M. T., Lawrence, A. D., Raux-Deery, E., Warren, M. J., and Smith, A. G. (2005). Algae acquire vitamin B12 through a symbiotic relationship with bacteria. *Nature* 438, 90–93. doi: 10.1038/nature04056

de-Bashan, L. E., Bashan, Y., Moreno, M., Lebsky, V. K., and Bustillos, J. J. (2002). Increased pigment and lipid content, lipid variety, and cell and population size of the microalgae *Chlorella* spp. when co-immobilized in alginate beads with the microalgae-growth-promoting bacterium *Azospirillum brasilense*. *Can. J. Microbiol.* 48, 514–521. doi: 10.1139/w02-051

Debnath, M., and Bhadury, P. (2016). Adaptive responses and arsenic transformation potential of diazotrophic Cyanobacteria isolated from rice fields of arsenic affected Bengal Delta Plain. *J. Appl. Phycol.* 28, 2777–2792. doi: 10.1007/s10811-016-0820-9

Dias, G. A., Rocha, R. H. C., Araújo, J. L., Lima, J. F., and Guedes, W. A. (2016). Growth, yield, and postharvest quality in eggplant produced under different foliar fertilizer (*Spirulina platensis*) treatments. *Semina Ciênc. Agrár.* 37, 3893–3902. doi: 10.5433/1679-0359.2016v37n6p3893

Dineshkumar, R., Subramanian, J., Arumugam, A., Ahamed Rasheeq, A., and Sampathkumar, P. (2020). Exploring the microalgae biofertilizer effect on onion cultivation by field experiment. *Waste Biomas. Valorizat.* 11, 77–87. doi: 10.1007/s12649-018-0466-8

Dorais, M., Ehret, D., and Papadopoulos, A. (2008). Tomato (*Solanum lycopersicum*) health components: from the seed to the consumer. *Phytochem. Rev.* 7, 231–250. doi: 10.1007/s11101-007-9085-x

Doucette, G. J. (1995). Interactions between bacteria and harmful algae: a review. *Nat. Tox.* 3, 65–74. doi: 10.1002/nt.2620030202

Duan, X., Ren, G. Y., Liu, L. L., and Zhu, W. X. (2012). Salt-induced osmotic stress for lipid overproduction in batch culture of *Chlorella vulgaris*. *Afr. J. Biotechnol.* 11, 7072–7078. doi: 10.5897/AJB11.3670

Duffy, B. K., and Défago, G. (1999). Environmental factors modulating antibiotic and siderophore biosynthesis by *Pseudomonas* fluorescens biocontrol strains. *Appl. Environ. Microbiol.* 65, 2429–2438. doi: 10.1128/AEM.65.6.2429-2438.1999

Ebenezer, V., Medlin, L., and Ki, J.-S. (2011). Molecular detection quantification and diversity evaluation of microalgae. *Mar. Biotechnol.* 14, 129–142. doi: 10.1007/s10126-011-9427-y

Ergun, O., Dasgan, H., and Isık, O. (2020). Effects of microalgae *Chlorella vulgaris* on hydroponically grown lettuce. *Acta Horticult.* 2, 169–176. doi: 10.17660/ActaHortic.2020.1273.23

Esitken, A., Yildiz, H. E., Ercisli, S., Figen Donmez, M., Turan, M., and Gunes, A. (2010). Effects of plant growth promoting bacteria (PGPB) on yield, growth and nutrient contents of organically grown strawberry. *Sci. Horticult.* 124, 62–66. doi: 10.1016/j.scienta.2009.12.012

Farid, R., Mutale-Joan, C., Redouane, B., Mernissi Najib, E. L., Abderahime, A., Laila, S., et al. (2019). Effect of microalgae polysaccharides on biochemical and metabolomics pathways related to plant defense in *Solanum lycopersicum*. *Appl. Biochem. Biotechnol.* 188, 225–240. doi: 10.1007/s12010-018-2916-y

Garcia-Gonzalez, J., and Sommerfeld, M. (2016). Biofertilizer and biostimulant properties of the microalga *Acutodesmus dimorphus*. *J. Appl. Phycol.* 28, 1051–1061. doi: 10.1007/s10811-015-0625-2

Gavilanes, F. Z., Souza Andrade, D., Zucareli, C., Horácio, E. H., Sarkis Yunes, J., Barbosa, A. P., et al. (2020). Co-inoculation of Anabaena cylindrica with *Azospirillum brasilense* increases grain yield of maize hybrids. *Rhizosphere* 15:100224. doi: 10.1016/j.rhisph.2020.100224

Gemin, L. G., Mógor, ÁF., De Oliveira Amatussi, J., and Mógor, G. (2019). Microalgae associated to humic acid as a novel biostimulant improving onion growth and yield. *Sci. Horticult.* 256:108560. doi: 10.1016/j.scienta.2019.108560

Geries, L., and Elsadany, A. (2021). Maximizing growth and productivity of onion (*Allium cepa* L.) by *Spirulina platensis* extract and nitrogen-fixing endophyte *Pseudomonas stutzeri*. *Arch. Microbiol.* 203, 169–181. doi: 10.1007/s00203-020-01991-z

Ghasemi, Y., Rasoul-Amini, S., Naseri, A. T., Montazeri-Najafabady, N., Mobasher, M. A., and Dabbagh, F. (2012). Microalgae biofuel potentials (Review). *Appl. Biochem. Microbiol.* 48, 126–144. doi: 10.1134/S0003683812020068

Giles, J. (2005). Nitrogen study fertilizes fears of pollution. *Nature* 433:791. doi: 10.1038/433791a

Glick, B. R. (1995). The enhancement of plant growth by free-living bacteria. *Canad. J. Microbiol.* 41, 109–117. doi: 10.1139/m95-015

Gou, J.-Y., Suo, S.-Z., Shao, K.-Z., Zhao, Q., Yao, D., Li, H.-P., et al. (2020). Biofertilizers with beneficial rhizobacteria improved plant growth and yield in chili (*Capsicum annuum* L.). *World J. Microbiol. Biotechnol.* 36:86. doi: 10.1007/s11274-020-02863-w

Güneş, A., Turan, M., Güllüce, M., and Şahin, F. (2014). Nutritional content analysis of plant growth-promoting rhizobacteria species. *Eur. J. Soil Biol.* 60, 88–97. doi: 10.1016/j.ejsobi.2013.10.010

Guo, S., Wang, P., Wang, X., Zou, M., Liu, C., and Hao, J. (2020). "Microalgae as biofertilizer in modern agriculture," in *Microalgae Biotechnology for Food, Health and High Value Products*, eds M. Alam, J. L. Xu, and Z. Wang (Singapore: Springer), 397–411. doi: 10.1007/978-981-15-0169-2_12

Gupta, N., Gupta, A. K., Gaur, V. S., and Kumar, A. (2012). Relationship of nitrogen use efficiency with the activities of enzymes involved in nitrogen uptake and assimilation of finger millet genotypes grown under different nitrogen inputs. *ScientificWorldJournal* 2012, 625731. doi: 10.1100/2012/625731

Gutiérrez-Mañero, F. J., Ramos-Solano, B., Probanza, A., Mehouachi, J., Tadeo, F., and Talon, M. (2001). The plant-growth-promoting rhizobacteria *Bacillus pumilus* and *Bacillus licheniformis* produce high amounts of physiologically active gibberellins. *Physiol. Plant.* 111, 206–211. doi: 10.1034/j.1399-3054.2001.1110211.x

Guzmán-Murillo, M. A., Ascencio, F., and Larrinaga-Mayoral, J. A. (2013). Germination and ROS detoxification in bell pepper (*Capsicum annuum* L.) under NaCl stress and treatment with microalgae extracts. *Protoplasma* 250, 33–42. doi: 10.1007/s00709-011-0369-z

Ha, S., Vanková, R., Yamaguchi-Shinozaki, K., Shinozaki, K., and Tran, L.-S. (2012). Cytokinins: metabolism and function in plant adaptation to environmental stresses. *Trends Plant Sci.* 17, 172–179. doi: 10.1016/j.tplants.2011.12.005

Han, J., Zhang, L., Wang, S., Yang, G., Zhao, L., and Pan, K. (2016). Co-culturing bacteria and microalgae in organic carbon containing medium. *J. Biol. Res.* 23:8. doi: 10.1186/s40709-016-0047-6

Hashtroudi, M. S., Ghassempour, A., Riahi, H., Shariatmadari, Z., and Khanjir, M. (2013). Endogenous auxins in plant growth-promoting Cyanobacteria—Anabaena vaginicola and Nostoc calcicola. *J. Appl. Phycol.* 25, 379–386. doi: 10.1007/s10811-012-9872-7

Horácio, E. H., Zucareli, C., Gavilanes, F. Z., Yunes, J. S., dos Santos, Sanzovo, A. W., et al. (2020). Co-inoculation of rhizobia, azospirilla and cyanobacteria for increasing common bean production Co-inoculação de rizobio, azospirillum e cianobactérias no aumento da produção de feijão comum Semina: Ciências Agrárias. *Londrina* 41, 2015–2028. doi: 10.5433/1679-0359.2020v41n5Supl1p2015

Huang, J., Wei, Z., Tan, S., Mei, X., Shen, Q., and Xu, Y. (2014). Suppression of bacterial wilt of tomato by bioorganic fertilizer made from the antibacterial compound producing strain *Bacillus amyloliquefaciens* HR62. *J. Agricult. Food Chem.* 62, 10708–10716. doi: 10.1021/jf503136a

Huang, S., Li, R., Zhang, Z., Li, L., Gu, X., Fan, W., et al. (2009). The genome of the cucumber *Cucumis sativus* L. *Nat. Genet.* 41, 1275–1281. doi: 10.1016/B978-0-08-040826-2.50017-5

Hyun, M. W., Yun, Y. H., Kim, J. Y., and Kim, S. H. (2011). Fungal and plant phenylalanine ammonia-lyase. *Mycobiology* 39, 257–265. doi: 10.5941/myco.2011.39.4.257

Jung, H. K., Kim, J. R., Woo, S. M., and Kim, S. D. (2006). An auxin producing plant growth promoting rhizobacterium *Bacillus subtilis* AH18 which has siderophore-producing biocontol activity. *Kor. J. Microbiol. Biotechnol.* 34, 94–100.

Kandoliya, U., Bodar, N., Bajaniya, V., Bhadja, N., and Golakiya, B. (2015). Determination of nutritional value and antioxidant from bulbs of different onion (Allium cepa) variety: a comparative study. *Int. J. Curr. Microbiol. App. Sci* 4, 635–641.

Kaplan, D. (2013). "Absorption and adsorption of heavy metals by microalgae," in *Handbook of Microalgal Culture*, eds. A. Richmond and Q. Hu (Chichester, UK: John Wiley & Sons, Ltd), 602–611. doi: 10.1002/9781118567166.ch32

Kim, M.-J., Shim, C.-K., Kim, Y.-K., Ko, B.-G., Park, J.-H., Hwang, S.-G., et al. (2018). Effect of biostimulator *Chlorella fusca* on improving growth and qualities of chinese chives and spinach in organic farm. *Plant Pathol. J.* 34, 567–574. doi: 10.5423/PPJ.FT.11.2018.0254

Kobayashi, A., Tai, A., and Kawazu, K. (1995). Structural elucidation of an elicitor-active oligosaccharide, LN-3, prepared from Algal laminaran. *J. Carbohydr. Chem.* 14, 819–832. doi: 10.1080/07328309508005378

Kopta, T., Pavlikova, M., Sêkara, A., Pokluda, R., and Maršálek, B. (2018). Effect of bacterial-algal biostimulant on the yield and internal quality of lettuce (*Lactuca sativa* L.) produced for spring and summer crop. *Not. Botan. Horti. Agrobot. Cluj Napoc.* 46, 615–621. doi: 10.15835/nbha46211110

Kumar, S., Kumar, R., and Singh, J. (2006). "16 - Cayenne/American pepper," in *Handbook of Herbs and Spices*, ed. K. V. Peter (Abington, PA: Woodhead Publishing), 299–312. doi: 10.1533/9781845691717.3.299

Kumar, V. V. (2018). "Biofertilizers and biopesticides in sustainable agriculture," in *Role of Rhizospheric Microbes in Soil*, ed. V. Meena (Singapore: Springer), 377–398.

Lim, J.-H., and Kim, S.-D. (2009). Synergistic plant growth promotion by the indigenous auxins-producing PGPR *Bacillus subtilis* AH18 and Bacillus licheniforims K11. *J. Kor. Soc. Appl. Biol. Chem.* 52, 531–538. doi: 10.3839/jksabc.2009.090

Mahanty, T., Bhattacharjee, S., Goswami, M., Bhattacharyya, P., Das, B., Ghosh, A., et al. (2017). Biofertilizers: a potential approach for sustainable agriculture development. *Environ. Sci. Pollut. Res.* 24, 3315–3335. doi: 10.1007/s11356-016-8104-0

Mehta, P., Walia, A., Kulshrestha, S., Chauhan, A., and Shirkot, C. K. (2015). Efficiency of plant growth-promoting P-solubilizing *Bacillus circulans* CB7 for enhancement of tomato growth under net house conditions. *J. Basic Microbiol.* 55, 33–44. doi: 10.1002/jobm.201300562

Michalak, I., and Chojnacka, K. (2014). Algae as production systems of bioactive compounds. *Eng. Life Sci.* 15:191. doi: 10.1002/elsc.201400191

Minuto, A., Migheli, Q., and Garibaldi, A. (1993). "Integrated control of soil-borne plant pathogens by solar heating and antagonistic microorganisms," in *Proceedings of the IV International Symposium on Soil and Substrate Infestation and Disinfestation*, Vol. 382, Leuven, 138–144. doi: 10.17660/actahortic.1995.382.14

Mubashar, M., Naveed, M., Mustafa, A., Ashraf, S., Shehzad Baig, K., Alamri, S., et al. (2020). Experimental investigation of chlorella vulgaris and *Enterobacter* sp. MN17 for decolorization and removal of heavy metals from textile wastewater. *Water* 12:3034. doi: 10.3390/w12113034

Mujtaba, G., and Lee, K. (2016). Advanced treatment of wastewater using symbiotic co-culture of microalgae and bacteria. *Appl. Chem. Eng* 27, 1–9. doi: 10.14478/ace.2016.1002

Mujtaba, G., Rizwan, M., and Lee, K. (2017). Removal of nutrients and COD from wastewater using symbiotic co-culture of bacterium *Pseudomonas* putida and immobilized microalga Chlorella vulgaris. *J. Industr. Eng. Chem.* 49, 145–151. doi: 10.1016/j.jiec.2017.01.021

Najdenski, H. M., Gigova, L. G., Iliev, I. I., Pilarski, P. S., Lukavský, J., Tsvetkova, I. V., et al. (2013). Antibacterial and antifungal activities of selected microalgae and cyanobacteria. *Int. J. Food Sci. Technol.* 48, 1533–1540. doi: 10.1111/ijfs.12122

Naviner, M., Bergé, J. P., Durand, P., and Le Bris, H. (1999). Antibacterial activity of the marine diatom *Skeletonema costatum* against aquacultural pathogens. *Aquaculture* 174, 15–24. doi: 10.1016/S0044-8486(98)00513-4

Nicola, S., Tibaldi, G., Fontana, E., Crops, A.-V., and Plants, A. (2009). Tomato production systems and their application to the tropics. *Acta Horticult.* 821, 27–34. doi: 10.17660/ActaHortic.2009.821.1

Nie, P., Li, X., Wang, S., Guo, J., Zhao, H., and Niu, D. (2017). Induced systemic resistance against *Botrytis cinerea* by *Bacillus cereus* AR156 through a JA/ET- and NPR1-dependent signaling pathway and activates PAMP-triggered immunity in *Arabidopsis*. *Front. Plant Sci.* 8:238. doi: 10.3389/fpls.2017.00238

Ogbonna, J. C., Yoshizawa, H., and Tanaka, H. (2000). Treatment of high strength organic wastewater by a mixed culture of photosynthetic microorganisms. *J. Appl. Phycol.* 12, 277–284. doi: 10.1023/A:1008188311681

Pankhurst, C. E., Ophel-Keller, K., Doube, B. M., and Gupta, V. V. S. R. (1996). Biodiversity of soil microbial communities in agricultural systems. *Biodiver. Conserv.* 5, 197–209. doi: 10.1007/BF00055830

Peng, H., de-Bashan, L. E., Bashan, Y., and Higgins, B. T. (2020). Indole-3-acetic acid from *Azosprillum brasilense* promotes growth in green algae at the expense of energy storage products. *Algal Res.* 47:101845. doi: 10.1016/j.algal.2020.101845

Perales-Vela, H. V., Peña-Castro, J. M., and Cañizares-Villanueva, R. O. (2006). Heavy metal detoxification in eukaryotic microalgae. *Chemosphere* 64, 1–10. doi: 10.1016/j.chemosphere.2005.11.024

Pierik, R., Tholen, D., Poorter, H., Visser, E. J. W., and Voesenek, L. A. C. J. (2006). The Janus face of ethylene: growth inhibition and stimulation. *Trends Plant Sci.* 11, 176–183. doi: 10.1016/j.tplants.2006.02.006

Prasanna, R., Joshi, M., Rana, A., Shivay, Y. S., and Nain, L. (2012). Influence of co-inoculation of bacteria-cyanobacteria on crop yield and C–N sequestration in soil under rice crop. *World J. Microbiol. Biotechnol.* 28, 1223–1235. doi: 10.1007/s11274-011-0926-9

Priya, M., Gurung, N., Mukherjee, K., and Bose, S. (2014). "23 – Microalgae in removal of heavy metal and organic pollutants from soil," in *Microbial Biodegradation and Bioremediation*, ed. S. Das (Oxford: Elsevier), 519–537. doi: 10.1016/b978-0-12-800021-2.00023-6

Puglisi, I., La Bella, E., Rovetto, E. I., Lo Piero, A. R., and Baglieri, A. (2020). Biostimulant effect and biochemical response in lettuce seedlings treated with A *Scenedesmus quadricauda* extract. *Plants (Basel Switzerland)* 9:123. doi: 10.3390/plants9010123

Qi, W., Mei, S., Yuan, Y., Li, X., Tang, T., Zhao, Q., et al. (2018). Enhancing fermentation wastewater treatment by co-culture of microalgae with volatile fatty acid- and alcohol-degrading bacteria. *Algal Res.* 31, 31–39. doi: 10.1016/j.algal.2018.01.012

Rachidi, F., Benhima, R., Sbabou, L., and El Arroussi, H. (2020). Microalgae polysaccharides bio-stimulating effect on tomato plants: growth and metabolic distribution. *Biotechnol. Rep.* 25:e00426. doi: 10.1016/j.btre.2020.e00426

Rajamani, S., Siripornadulsil, S., Falcao, V., Torres, M., Colepicolo, P., and Sayre, R. (2007). "Phycoremediation of heavy metals using transgenic microalgae," in *Transgenic Microalgae as Green Cell Factories*, eds R. León, A. Galván, and E. Fernández (New York, NY: Springer), 99–109. doi: 10.1007/978-0-387-75532-8_9

Ramanan, R., Kim, B.-H., Cho, D.-H., Oh, H.-M., and Kim, H.-S. (2016). Algae–bacteria interactions: evolution, ecology and emerging applications. *Biotechnol. Adv.* 34, 14–29. doi: 10.1016/j.biotechadv.2015.12.003

Raupach, G. S., and Kloepper, J. W. (1998). Mixtures of plant growth-promoting rhizobacteria enhance biological control of multiple cucumber pathogens. *Phytopathology* 88, 1158–1164. doi: 10.1094/PHYTO.1998.88.11.1158

Ribalet, F., Intertaglia, L., Lebaron, P., and Casotti, R. (2008). Differential effect of three polyunsaturated aldehydes on marine bacterial isolates. *Aquat Toxicol.* 86, 249–255. doi: 10.1016/j.aquatox.2007.11.005

Rodrìguez, H., and Fraga, R. (1999). Phosphate solubilizing bacteria and their role in plant growth promotion. *Biotechnol. Adv.* 17, 319–339. doi: 10.1016/S0734-9750(99)00014-2

Romanenko, E., Kosakovskaya, I., and Romanenko, P. (2015). Phytohormones of microalgae: biological role and involvement in the regulation of physiological processes. Pt I. auxins, abscisic acid, ethylene. *Int. J. Algae* 17, 179–201. doi: 10.1615/InterJAlgae.v18.i2.70

Savci, S. (2012). Investigation of effect of chemical fertilizers on environment. *APCBEE Proc.* 1, 287–292. doi: 10.1016/j.apcbee.2012.03.047

Schiavon, M., Ertani, A., and Nardi, S. (2008). Effects of an alfalfa protein hydrolysate on the gene expression and activity of enzymes of the tricarboxylic acid (TCA) cycle and nitrogen metabolism in *Zea mays* L. *J. Agric. Food Chem.* 56, 11800–11808. doi: 10.1021/jf802362g

Schuhegger, R., Ihring, A., Gantner, S., Bahnweg, G., Knappe, C., Vogg, G., et al. (2006). Induction of systemic resistance in tomato by N-acyl-L-homoserine lactone-producing rhizosphere bacteria. *Plant Cell Environ.* 29, 909–918. doi: 10.1111/j.1365-3040.2005.01471.x

Schumacher, G., Blume, T., and Sekoulov, I. (2003). Bacteria reduction and nutrient removal in small wastewater treatment plants by an algal biofilm. *Water Sci. Technol.* 47, 195–202. doi: 10.2166/wst.2003.0605

Sessitsch, A., Reiter, B., and Berg, G. (2004). Endophytic bacterial communities of field-grown potato plants and their plant-growth-promoting and antagonistic abilities. *Can. J. Microbiol.* 50, 239–249. doi: 10.1139/w03-118

Shariatmadari, Z., Riahi, H., Mehri, S., Seyed Hashtroudi, M., Ghassempour, A., and Aghashariatmadary, Z. (2013). Plant growth promoting cyanobacteria and their distribution in terrestrial habitats of Iran. *Soil Sci. Plant Nutr.* 59, 535–547. doi: 10.1080/00380768.2013.782253

Shi, Y., Cheng, C., Lei, P., Wen, T., and Merrifield, C. J. (2011). Safe food, green food, good food: chinese community supported agriculture and the rising middle class. *Int. J. Agric. Sustain.* 9, 551–558. doi: 10.1080/14735903.2011.619327

Silo-Suh, L. A., Lethbridge, B. J., Raffel, S. J., He, H., Clardy, J., and Handelsman, J. (1994). Biological activities of two fungistatic antibiotics produced by *Bacillus cereus* UW85. *Appl. Environ. Microbiol.* 60, 2023–2030. doi: 10.1128/AEM.60.6.2023-2030.1994

Singh, J., and Saxena, R. (2015). "An introduction to microalgae: diversity and significance. diversity and significance," in *Handbook of Marine Microalgae: Biotechnology Advances*, ed. S. K. Kim (Amsterdam: Academic Press), 11–24. doi: 10.1016/B978-0-12-800776-1.00002-9

Smirnoff, N. (2018). Ascorbic acid metabolism and functions: a comparison of plants and mammals. *Free Radic. Biol. Med.* 122, 116–129. doi: 10.1016/j.freeradbiomed.2018.03.033

Spadaro, D., and Gullino, M. L. (2005). Improving the efficacy of biocontrol agents against soilborne pathogens. *Crop Protect.* 24, 601–613. doi: 10.1016/j.cropro.2004.11.003

Sponsel, V. M., and Hedden, P. (2010). "Gibberellin biosynthesis and inactivation," in *Plant Hormones*, ed. P. J. Davies (Dordrecht: Springer), 63–94. doi: 10.1007/978-1-4020-2686-7_4

Stirk, W. A., Bálint, P., Tarkowská, D., Novák, O., Strnad, M., Ördög, V., et al. (2013a). Hormone profiles in microalgae: gibberellins and brassinosteroids. *Plant Physiol. Biochem.* 70, 348–353. doi: 10.1016/j.plaphy.2013.05.037

Stirk, W. A., Ördög, V., Novák, O., Rolčík, J., Strnad, M., Bálint, P., et al. (2013b). Auxin and cytokinin relationships in 24 microalgal strains(1). *J. Phycol.* 49, 459–467. doi: 10.1111/jpy.12061-

Subashchandrabose, S. R., Ramakrishnan, B., Megharaj, M., Venkateswarlu, K., and Naidu, R. (2011). Consortia of cyanobacteria/microalgae and bacteria: biotechnological potential. *Biotechnol. Adv.* 29, 896–907. doi: 10.1016/j.biotechadv.2011.07.009

Suganya, T., Varman, M., Masjuki, H. H., and Renganathan, S. (2016). Macroalgae and microalgae as a potential source for commercial applications along with biofuels production: a biorefinery approach. *Renew. Sustain. Ener. Rev.* 55, 909–941. doi: 10.1016/j.rser.2015.11.026

Sun, X.-M., Ren, L.-J., Zhao, Q.-Y., Ji, X.-J., and Huang, H. (2018). Microalgae for the production of lipid and carotenoids: a review with focus on stress regulation and adaptation. *Biotechnol. Biof.* 11, 272–272. doi: 10.1186/s13068-018-1275-9

Sylvia, D., Fuhrmann, J., Hartel, P., and Zuberer, D. (2005). *Principles and Applications of Soil Microbiology*. Upper Saddle River, NJ: Prentice Hall. 550.

Tarakhovskaya, E. R., Maslov, Y. I., and Shishova, M. F. (2007). Phytohormones in algae. *Rus. J. Plant Physiol.* 54, 163–170. doi: 10.1134/S1021443707020021

Tatlioglu, T. (1993). "13 – cucumber: *Cucumis sativus* L," in *Genetic Improvement of Vegetable Crops*, eds G. Kalloo and B. O. Bergh (Amsterdam: Pergamon), 197–234.

Unnithan, V. V., Unc, A., and Smith, G. B. (2014). Mini-review: a priori considerations for bacteria–algae interactions in algal biofuel systems receiving municipal wastewaters. *Algal Res.* 4, 35–40. doi: 10.1016/j.algal.2013.11.009

Utkhede, R. S., and Koch, C. A. (1999). Rhizobacterial growth and yield promotion of cucumber plants inoculated with *Pythium aphanidermatum*. *Can. J. Plant Pathol.* 21, 265–271. doi: 10.1080/07060669909501189

Vera, J., Castro, J., Gonzalez, A., and Moenne, A. (2011). Seaweed polysaccharides and derived oligosaccharides stimulate defense responses and protection against pathogens in plants. *Mar. Drugs* 9, 2514–2525. doi: 10.3390/md9122514

Verma, M., Mishra, J., and Arora, N. (2019). "Plant growth-promoting rhizobacteria: diversity and applications," in *Environmental Biotechnology: For Sustainable Future*, eds R. Sobti, N. Arora, and R. Kothari (Singapore: Springer), 129–173. doi: 10.1007/978-981-10-7284-0_6

Walpola, B. C., and Yoon, M.-H. (2013). Isolation and characterization of phosphate solubilizing bacteria and their co-inoculation efficiency on tomato plant growth and phosphorous uptake. *Afr. J. Microbiol. Res.* 7, 266–275. doi: 10.5897/AJMR12.2282

Walsh, U. F., Morrissey, J. P., and O'Gara, F. (2001). *Pseudomonas* for biocontrol of phytopathogens: from functional genomics to commercial exploitation. *Curr. Opin. Biotechnol.* 12, 289–295. doi: 10.1016/s0958-1669(00)00212-3

Watanabe, K., Takihana, N., Aoyagi, H., Hanada, S., Watanabe, Y., Ohmura, N., et al. (2005). Symbiotic association in *Chlorella* culture. *FEMS Microbiol. Ecol.* 51, 187–196. doi: 10.1016/j.femsec.2004.08.004

Wolfaardt, G. M., Lawrence, J. R., Robarts, R. D., and Caldwell, D. E. (1994). The role of interactions, sessile growth and nutrient amendments on the degradative efficiency of a microbial consortium. *Can. J. Microbiol.* 40, 331–340. doi: 10.1139/m94-055

Yoshihisa, H., Zenji, S., Fukushi, H., Katsuhiro, K., Haruhisa, S., and Takahito, S. (1989). Production of antibiotics by *Pseudomonas* cepacia as an agent for biological control of soilborne plant pathogens. *Soil Biol. Biochem.* 21, 723–728. doi: 10.1016/0038-0717(89)90070-9

Yu, Q., Matheickal, J. T., Yin, P., and Kaewsarn, P. (1999). Heavy metal uptake capacities of common marine macro algal biomass. *Water Res.* 33, 1534–1537. doi: 10.1016/S0043-1354(98)00363-7

Yuan, J., Li, B., Zhang, N., Waseem, R., Shen, Q., and Huang, Q. (2012). Production of bacillomycin- and macrolactin-type antibiotics by *Bacillus amyloliquefaciens* NJN-6 for suppressing soilborne plant pathogens. *J. Agricult. Food Chem.* 60, 2976–2981. doi: 10.1021/jf204868z

Conflict of Interest: The authors declare that the research was conducted in the absence of any commercial or financial relationships that could be construed as a potential conflict of interest.

frontiers in Microbiology

ORIGINAL RESEARCH
published: 04 May 2021
doi: 10.3389/fmicb.2021.681567

Endophytic Bacterial Isolates From Halophytes Demonstrate Phytopathogen Biocontrol and Plant Growth Promotion Under High Salinity

*Christos A. Christakis[1], Georgia Daskalogiannis[2], Anastasia Chatzaki[3], Emmanouil A. Markakis[3], Glykeria Mermigka[1], Angeliki Sagia[2], Giulio Flavio Rizzo[4], Vittoria Catara[4], Ilias Lagkouvardos[5], David J. Studholme[6] and Panagiotis F. Sarris[1,2,6]**

[1] Institute of Molecular Biology and Biotechnology, Foundation for Research and Technology – Hellas, Heraklion, Greece, [2] Department of Biology, University of Crete, Heraklion, Greece, [3] Laboratory of Mycology, Department of Viticulture, Vegetable Crops, Floriculture and Plant Protection, Institute of Olive Tree, Subtropical Crops and Viticulture, Hellenic Agricultural Organization DIMITRA, Heraklion, Greece, [4] Department of Agriculture, Food and Environment, University of Catania, Catania, Italy, [5] ZIEL–Institute for Food and Health, Technical University of Munich, Freising, Germany, [6] Biosciences, University of Exeter, Exeter, United Kingdom

Halophytic endophytes potentially contribute to the host's adaptation to adverse environments, improving its tolerance against various biotic and abiotic stresses. Here, we identified the culturable endophytic bacteria of three crop wild relative (CWR) halophytes: *Cakile maritima*, *Matthiola tricuspidata,* and *Crithmum maritimum*. In the present study, the potential of these isolates to improve crop adaptations to various stresses was investigated, using both *in vitro* and *in-planta* approaches. Endophytic isolates were identified by their 16S rRNA gene sequence and evaluated for their ability to: grow *in vitro* in high levels of NaCl; inhibit the growth of the economically important phytopathogens *Verticillium dahliae*, *Ralstonia solanacearum,* and *Clavibacter michiganensis* and the human pathogen *Aspergillus fumigatus;* provide salt tolerance *in-planta*; and provide growth promoting effect *in-planta*. Genomes of selected isolates were sequenced. In total, 115 endophytic isolates were identified. At least 16 isolates demonstrated growth under increased salinity, plant growth promotion and phytopathogen antagonistic activity. Three showed *in-planta* suppression of *Verticillium* growth. Furthermore, representatives of three novel species were identified: two *Pseudomonas* species and one *Arthrobacter*. This study provides proof-of-concept that the endophytes from CWR halophytes can be used as "bio-inoculants," for the enhancement of growth and stress tolerance in crops, including the high-salinity stress.

Keywords: halophytes, endophytes, stress tolerance, salinity tolerance, biofertilizers, biocontrol, bio-inoculants, growth-promotion

OPEN ACCESS

Edited by:
Maurizio Ruzzi,
University of Tuscia, Italy

Reviewed by:
Divjot Kour,
Eternal University, India
Mariana Reginato,
National University of Río Cuarto, Argentina

***Correspondence:**
Panagiotis F. Sarris
p.sarris@imbb.forth.gr;
p.sarris2@exeter.ac.uk

Specialty section:
This article was submitted to Microbe and Virus Interactions with Plants, a section of the journal Frontiers in Microbiology

Received: *16 March 2021*
Accepted: *07 April 2021*
Published: *04 May 2021*

Citation:
Christakis CA, Daskalogiannis G, Chatzaki A, Markakis EA, Mermigka G, Sagia A, Rizzo GF, Catara V, Lagkouvardos I, Studholme DJ and Sarris PF (2021) Endophytic Bacterial Isolates From Halophytes Demonstrate Phytopathogen Biocontrol and Plant Growth Promotion Under High Salinity. Front. Microbiol. 12:681567. doi: 10.3389/fmicb.2021.681567

INTRODUCTION

Bacterial endophytes are widespread among plants and colonize intercellular and intracellular spaces of all host compartments. Each individual plant is a host to bacterial and fungal endophytes that colonize its tissues for all or part of its life cycle without causing any apparent pathogenesis (Ryan et al., 2008). Various studies have shown how microbial communities contribute to plant defense and the substantial beneficial effects they have on host plants, including improved nutrient acquisition, accelerated growth, resilience against pathogens and improved resistance against abiotic stress such as heat, drought, and salinity (Rodriguez et al., 2019).

The diversity and structure of endophytic microbiomes are dynamic and directly affected by ecological characteristics of the host plant and soil such as geographic location, environmental factors and interactions within the host plant (Edwards et al., 2015). Most characterized members of bacterial endophytic communities belong to the *Actinobacteria*, *Bacteroidetes*, *Firmicutes*, and *Proteobacteria* (Bulgarelli et al., 2013, 2015; Edwards et al., 2015). However, endophytic microbiome structure can be affected by the host-plant species' genotype, plant organ or tissue type, developmental stage, growing season, geographic, and field conditions, soil type, nutrient status of the host species and cultivation practices (Rodríguez-Blanco et al., 2015; Liu et al., 2017; Rodriguez et al., 2019).

Endophytic microbes hold enormous potential to increase plant health. Interestingly, endophytic bacteria can be used to overcome the effect of salinity stress, promote plant growth and nutrient uptake; these approaches can provide beneficial and environmentally friendly solutions for a sustainable global food security (Glick, 2014; Tkacz and Poole, 2015; Vaishnav et al., 2019). For successful exploitation of endophytes, we need a deeper understanding of endophytic community composition and the mechanisms that underlie their plant growth promotion, in order to successfully select the most efficient bacterial isolates.

Members of endophytic bacterial communities influence each other with antagonistic, competitive, and mutualistic interactions (Toju et al., 2018). This results from nutritional competition, exchange and even metabolic interdependence. This, in turn can influence microbiome composition and its effect on the host-plant (Rodriguez et al., 2019). Host-plant genotype can also have a dramatic impact on microbial members; individual cultivars can influence the microbial community structure and the beneficial effects of endophytic bacteria (Haney et al., 2015; Marques et al., 2015; Pérez-Jaramillo et al., 2016; Rodriguez et al., 2019). Thus, for the utilization of endophytic bacterial isolates, an optimum approach is to isolate key bacterial strains from crop wild relatives (CWRs) (Mendes et al., 2013).

Halophytes could be valuable sources of novel endophytic isolates that can be used to overcome various biotic and abiotic stresses (Ruppel et al., 2013; Shabala, 2013; Yuan et al., 2016; Etesami and Beattie, 2018). High salinity in plants results in ionic and osmotic stress due increased extracellular hypertonic conditions and accumulation of Na^+ and Cl^- intracellularly (Vaishnav et al., 2019). The resulting stress affects intracellular water balance, rate of cell division, hormonal imbalance, changes in photosynthesis, nutrient translocation, processes that decrease plant growth (Munns, 2002). Plant-associated microorganism can contribute to plant health impeded by salinity stress, by influencing phytohormonal levels and signaling, contributing to homeostasis maintenance of toxic ions under salinity stress, enhancing photosynthesis, and contributing to biomass production and allocation (Dodd and Pérez-Alfocea, 2012). Since soil salinity disrupts the physiological and morphological plant processes and increases pathogen susceptibility (Etesami and Beattie, 2018), the use of plant growth promoting endophytes in crops can be a more eco-friendly approach than agricultural chemicals.

Here, we tested the hypothesis that cultivated endophytic bacteria isolated from three CWR halophytic plant species have properties of salinity stress tolerance, plant growth promotion and phytopathogen growth inhibition. These species included two members of the *Brassicaceae* family (*Matthiola tricuspidata* and *Cakile maritima*), and one of the *Apiaceae* family (*Crithmum maritimum*). To test this hypothesis, we cultured and identified 115 different bacterial isolates and functionally characterized them in *in vitro* and *in-planta* assays. The bacterial isolates were tested *in vitro* for their ability to grow on salinity levels up to 17.5%, their biocontrol of the economically important plant phytopathogens *Verticillium dahliae*, *Ralstonia solanacearum,* and *Clavibacter michiganensis* ssp. *michiganensis.* Subsequently, isolates with demonstrated *in vitro* salt tolerance, were tested *in-planta* to demonstrate whether they promoted plant growth under no stress conditions and under high salinity. Furthermore, bacterial isolates were tested *in-planta* to check their biocontrol properties against *Verticillium dahliae*. This is the first study of bacterial endophytes obtained from *M. tricuspidata*, *Cr. maritimum,* and *Ca. maritima*, and identifies their potential as bacterial bio-inoculants in commercial crops to overcome salinity stress and plant diseases caused by the economically important pathogens.

MATERIALS AND METHODS

Site Description and Plant Sample Collection

Samples were collected during summer 2018 in three distinct sites in Crete, Greece: site 1 (S1: N35°25′. E24°41′), site 2 (S2: N35°06, E25°48), and site 3 (S3: N35°00, E25°44) (**Supplementary Figure 1**). At S1, a natural beach area favoring salt-marsh vegetation, three *Matthiola tricuspidata* individuals were collected. At S2, a beach area close to Pachia Ammos village, three *Crithmum maritimum* individuals were collected. At S3, a popular beach area located in the town of Ierapetra, three individuals of *Cakile maritima* were collected. Each sample was collected with sterile gloves, forceps and gloves, placed in separate plastic bags to avoid cross contamination and immediately transported to the laboratory for processing.

Plant Surface Sterilization and Endophytic Cell Isolation

Leaf and root materials from each species were cut and processed individually. Plant material was gently washed with sterile distilled water repeatedly to remove soil and dust particles. For surface sterilization, plant roots and leaves were placed into sterile Erlenmeyer flasks containing ethanol 75% v/v for 60 s with shaking and then in sterile Erlenmeyer flasks containing sodium hypochlorite solution 3% w/v^{-1} (NaClO) for 10 min. The plant materials were then placed again in ethanol 75% v/v for 60 s. To remove any remaining NaClO, plant materials were rinsed 10 times with sterile distilled water (dH_2O). The sterilization and transfer procedures were carried out in a type II laminar flow hood. About 100 μL of the last rinse (for each analyzed sample) was plated on Nutrient Agar (NA) medium and monitored for microbial growth to evaluated surface sterilization efficiency. Only successfully sterilized root material was used further. Approximately 500 mg of leaves and roots per each species were weighed and slashed to small parts for further processing using a sterile scalpel and further grounded into a slurry with an autoclaved pestle and mortar. The slurry was transferred into sterile petri dishes and 30 mL of autoclaved dH_2O was added. The petri dishes were sealed and placed onto a rotary shaker (150 rpm) at 25°C for 2 h. After shaking, 100 μl of the material in triplicate were inoculated on NA plates and incubated at 28°C. Colony forming units (cfus) were chosen from each plate based on their color, texture and morphology. Pure bacterial colonies were grown in Nutrient Broth (NB) and cells stocks were stored in 50% v/v glycerol at −80°C. A total of 115 isolates were identified.

Bacterial Isolation and Identification of Isolates

To identify the 115 bacterial isolates, 16S rRNA gene Sanger sequencing method was employed. To extract crude genomic DNA, 1 mL of liquid bacterial culture in NB was placed in liquid nitrogen for 15 s. After room temperature incubation, the lysate was centrifuged at 10,000 × g for 1 min. Two microliter of the lysate were used to amplify the 16S rRNA gene using primers 27F: 5′-AGAGTTTGATCCTGGCTCAG-3′ (White et al., 1990) and 1492R: 5′-GTTTACCTTGTTACGACTT-3′ (Lane, 1991). PCR reactions of 20 μL were amplified in a BioRad T-100 Thermocycler with initial denaturation at 94°C for 2 min, followed by 35 cycles of 5 s at 94°C, 30 s annealing at 47°C, 2 min primer extension at 72°C, and a final extension at 72°C for 5 min. Apart from the lysate, each tube contained, Bac-Free PCR Buffer, 250 nM of each primer, 0.2 mM of each deoxy- ribonucleotide triphosphate and 0.1 U BAC-Free HotStart Taq polymerase (Nippon Genetics, Europe). PCR products were purified using Nucleo Spin Gel and PCR Clean up (Macherey-Nagel, Germany). Cleaned-up PCR products were sent to Macrogen (Europe) for sequencing with primer 27F.

The resulting chromatograms were quality inspected using MEGA 5 (Kumar et al., 2018) and the start/end regions of low quality were manually trimmed off. Cleaned-up fasta files were aligned in SILVA (Quast et al., 2013). The resulting sequences of the 16S rRNA gene were queried against ezBioCloud (Yoon et al., 2017) reference database for identification and documentation of the described bacterial isolate with the closest sequence similarity.

Bacterial Salt Tolerance Assay

The salt tolerance of all bacterial isolates was estimated on the basis of the population density of these isolates at different concentrations of NaCl (ranging from 0.5, 5, 10, 15, and 17.5% (w/v) in NA. Ten microliter drops of freshly prepared NB cultures of each isolate were inoculated on sterilized petri plates, containing 25 mL NA with increasing NaCl concentrations and incubated at 28°C. For each NaCl concentration, an *Escherichia coli* laboratory isolate was inoculated as a negative control. After 24 h of incubation, the growth of each isolate was estimated compared to *E. coli* growth.

In vitro Growth Inhibition of Phytopathogens

Antibacterial activity of the bacterial isolates against the phytopathogenic bacteria *Ralstonia solanacearum,* and *Clavibacter michiganensis* was evaluated by co-culturing each of the bacterial isolates on NA lawn covered by *R. solanacearum* or *C. michiganensis*. The inhibition zone indicating inhibition by bacterial growth was recorded as the antibacterial effect. Antifungal activity of the isolates against *Verticillium dahliae* was investigated. Potato dextrose agar (PDA) was inoculated with each bacterial isolate for 24 h at 28°C and then *V. dahliae* was inoculated at room temperature for 3–4 weeks. Fungal growth inhibition was determined by measuring the inhibition zone of *V. dahliae* hyphae on the media.

In vitro Hemolysis Screening Assay

In order to assay the bacterial isolates for hemolytic activity, each isolate was grown on blood agar plates. The bacterial isolates were inoculated with the spot test method and were incubated at room temperature for 48 h. The known non-mammalian-pathogenic species *Ensifer meliloti* was employed as a negative control (**Supplementary Figure 2B**).

In vitro Growth Inhibition of Fungal Human Pathogen

Antifungal activity of specific isolates against anthropopathogenic fungus A*spergillus fumigatus* was evaluated by co-culturing 11 bacterial isolates on NA plate lawn covered by *A. fumigatus* for 72 h at room temperature under absence of light. The following isolates were tested: CML04, CMR11, CMR22, CMR25, CrR12, CrR25, MTR12, MTR17a, MTR17b, MTR17c, MTR17d. Fungal growth inhibition was determined by the growth inhibition zone of the A. *fumigatus* hyphae on the media.

In-planta Salt Tolerance Assays

Twelve of the bacterial isolates were selected, according to their ability to grow in high salinity conditions (up to 17.5% w/v NaCl), in order to test their plant growth promotion capacity of the model plant *Arabidopsis thaliana*. Firstly, the experiment was performed with no abiotic stress conditions. Bacterial isolates

were cultured in NB for 46 h at 25°C with stirring. NB cultures were centrifuged at 224 × g for 15 min, the supernatant was discarded and the cells were resuspended in 50 mL sterilized dH_2O. Seeds of *A. thaliana* ecotype Columbia (Col-0) were grown in plastic pots (6 × 6 × 7 cm) filled with vermiculite: soil (1:1), at 25°C (16 h light/8 h dark). For each isolate and the corresponding control, 5 individual plants were grown in each pot. *A. thaliana* plants were watered with dH_2O for 10 days. Then, plants were watered with 10 mL suspensions of the 12 bacterial isolate liquid cultures, and were left for 7 days to let the bacterial isolates adapt. Subsequently, for a 30 day span, plants were watered every 2–3 days with dH_2O. At the end of the experiment, the fresh weight of the leaves from each plant was measured. The leaves were then dried at 65–70°C for 2 days and their dry weight was measured.

The same experiment was performed under salt treatment. Specifically, after the 7 day period of bacterial isolate inoculation, instead of dH_2O, the plants were watered with 10 mL of 250 mM NaCl. Fresh and dry weight of the leaves was measured.

For both experiments, mock samples were employed where no bacterial isolates were inoculated and control plants were inoculated with the isolate *Escherichia coli* (Control-*E. coli*), to check that the plants would not use the bacteria as a fertilizer.

Confrontation and Volatile Tests of Selected Bacterial Isolates Against *Verticillium dahliae*

A total of 16 isolates were selected for direct *in vitro* antagonism of *V. dahliae*. Fourteen of these isolates were selected due to their strong inhibition of V. dahliae in initial tests (**Supplementary Table 1**; CrR14, CrR18, MTR18, CMR01, CMR03, CML04, CMR25, MTR17a, MTR17d, MTR17f, MTR17g, MTR17h, and MTR17b, MTR17c). Two additional isolates were selected (CrR04 and MTR12) with medium inhibition in initial tests (**Supplementary Table 1**) for comparison. Direct *in vitro* antagonism of *V. dahliae* was evaluated by dual-culture assays (confrontation test) on PDA (Lahlali et al., 2007). In particular, a 6 mm diameter mycelial disc taken from the periphery of a 2 week-old PDA fungal culture was placed on a new PDA plate (90 mm in diameter) at approximately 25 mm-distance from the center of the plate. Then, a 30 mm-long line from each bacterial isolate (taken from a 48 h-old tripticasein soy broth (TSB) liquid culture with an inoculation loop) was streaked on the opposite site of the plate at equal distance from the center (one isolate per plate). Moreover, *Trichoderma harzianum* strain T22 was isolated from the commercial biofungicide TRIANUM-P (Koppert B.V. Hellas) and included in *in vitro* bioassays for comparison. Plates inoculated only with *V. dahliae* agar discs were served as controls. Plates (three per bacterial isolate plus controls) were incubated at 24°C in the dark. The radius of fungal colonies toward the direction of the test isolate and that of controls was measured 5, 7, 9, and 12 days post inoculation (d.p.i.) and radial growth rates were expressed in mm/day. At the end of the bioassays (12 d.p.i.) the underside of the plates was scanned using a Samsung Xpress SL-M2875ND Laser Multifunction Printer at 1200 dpi and microsclerotial (black) area on each plate image was determined manually using the image processing software ImageJ 1.46r (National Institutes of Health, United States). Then, the number of spores was estimated by transferring a 6 mm-diameter disc taken from the periphery of each culture into a 1.5 mL Eppendorf tube with 1 mL of water, and vortexed for 30 s. The number of spores was measured using a haematocytometer under a light microscope. Moreover, actively growing mycelia from cultures' periphery (located closer to test isolate) were prepared and microscopic observations (30 readings per culture) were carried out to estimate hyphae width.

To evaluate the capacity of bacterial isolates to affect *V. dahliae* growth via the production of volatile compounds, dual-plate assays (Chaurasia et al., 2005) were conducted (volatile test). In brief, one 6 mm-diameter agar disc of actively growing mycelium of the fungus was placed in the center of a new PDA plate (90 mm in diameter), whilst each bacterial isolate (taken from a 48 h-old TSB liquid culture) was streaked on another PDA plate. The covers of the two plates were removed and resultant plates were adjusted together (bacterial culture was upturned) and sealed with cellophane membrane so the two microbes would share the same headspace without coming in contact with each other. Dual plates (upright and upturned) inoculated only with *V. dahliae* served as controls. Similarly, in dual-culture assays, dual-plates (three per bacterial isolate) were incubated at 24°C in the dark and the growth, microclerotial area, sporulation and hyphae width of fungal colonies were measured as described above.

Radial growth inhibition (RGI), microsclerotia formation inhibition (MFI), sporulation inhibition (SI) and hyphae thinning (HT) were calculated according to the formula: [(Vc-Vt)/Vc] × 100 where Vc = the microscopic value of *V. dahliae* in control plates and Vt = the respective value of *V. dahliae* against the antagonistic isolate in dual-culture or dual-plate assays.

Bacterial Isolates and Fungal Inoculum Preparation for *in-planta* Bioassays

The 16 selected (see above) bacterial isolates (CrR14, CrR18, CrR04, MTR12, MTR18, CMR01, CMR03, CML04, CMR25, MTR17a, MTR17d, MTR17f, MTR17g, MTR17h, and MTR17b, MTR17c) were used in *in-planta* bioassays. The isolates were grown in Erlenmeyer flasks with 200 mL liquid TSB, in an orbital incubator at 180 rpm and 28°C for 48 h in the dark. Bacterial suspensions were centrifuged at 3,000 × g for 10 min and cells were re-suspended in water reaching a final concentration of 10^8 cfu mL^{-1} (measured by dilution plating).

The highly virulent *V. dahliae* isolate 999-1 (Markakis et al., 2016), which originated from symptomatic eggplants (*Solanum melongena* L.), was used. *V. dahliae* conidial suspension for eggplant—*V. dahliae* bioassays was prepared as previously described (Markakis et al., 2016). In brief, conidia were produced by growing each *V. dahliae* strain in potato dextrose broth (PDB) at 160 rpm and 25°C in the dark for 5 days. Then, conidia were harvested by filtrating through three layers of cheesecloth and the suspensions centrifuged at 3,000 × g for 10 min. Spores were re-suspended in sterilized dH_2O and their concentration was adjusted to 5×10^6 conidia mL^{-1}.

In-planta Verticillium Wilt Suppression Bioassays

Eggplant seedlings (cv. Black Beauty) were used in the *in-planta* bioassays. Plants at the one-true-leaf stage, grown in 100 mL-capacity pots containing soil substrate (HuminSubstrat, Klasmann-3 Deilmann GmbH, Germany) were root-drenched with bacterial suspension (20 mL of 10^8 cfu mL^{-1} of each isolate per plant), whereas plants that served as controls (negative = no bacterium/no fungus assigned as "C−" and positive = no bacterium/plus pathogen assigned as "V.D.") were treated with 20 mL of water. One week later, eggplants (at the second-true-leaf stage) were inoculated with *V. dahliae* by drenching the soil substrate in each pot with conidial suspension (20 mL of 5×10^6 conidia mL^{-1} per pot). Negative control plants (C−) were treated with 20 mL of water. Eggplants were maintained under controlled conditions at 23 ± 2°C with a 12 h light and dark cycle.

Two independent experiments (experiments I and II) were conducted to evaluate the suppressive effect of the aforementioned bacterial isolates against *V. dahliae*. In experiment I, 11 treatments (C−, V.d., V.d. + CrR14, V.d. + CrR18, V.d. + CrR04, V.d. + MTR12, V.d. + MTR18, V.d. + CMR01, V.d. + CMR03, V.d. + CML04 and V.d. + CMR25) were applied; whereas in experiment II, 10 treatments were conducted (C−, V.d., V.d. + MTR17a, V.d. + MTR17d, V.d. + BMTR17f, V.d. + MTR17g, V.d. + MTR17h, V.d. + MTR17b, V.d. + MTR17c, and V.d. + TRIANUM-P). The commercial biofungicide TRIANUM-P was included in experiment II (assigned as V.d. + TRIANUM-P) and applied according to manufacturer's instruction (20 mL of 3×10^7 cfu mL^{-1} per plant). TRIANUM-P was served as a *V. dahliae*-suppressive reference treatment. Within each experiment, each treatment consisted of seven plants and experiments were replicated three times.

Disease Assessment

Verticillium wilt symptoms on eggplant were recorded at 2-, 3-, and 4- day intervals from 12 to 30 d.p.i with *V. dahliae*. Bioassays were evaluated by estimating disease severity, disease incidence, mortality and relative area under disease progress curve (RAUDPC). Disease parameters were recorded as previously described (Markakis et al., 2016). Briefly, disease severity at each observation was calculated from the number of wilting leaves, as a percentage of total number of leaves per each plant. Disease ratings were plotted over time to generate disease progress curves. Subsequently the area under disease progress curve (AUDPC) was calculated by the trapezoidal integration method (Campbell and Madden, 1990). Disease was expressed as a percentage of the maximum possible area with reference to the maximum value potential reached over the whole period of each experiment and is referred to as RAUDPC. Disease incidence was estimated as the percentage of infected plants. Only plants with a final disease severity of ≥20% were considered infected, to discriminate between *V. dahliae*-associated disease symptoms and other weak symptoms occasionally observed (**Supplementary Table 2**). Mortality was estimated as the percentage of dead plants.

Plant Growth

Growth parameters were evaluated at the end of bioassays (at 24 and 30 d.p.i. for experiments I and II, respectively). To estimate the effect of the aforementioned treatments on plant growth, all plants were clipped off at the soil surface level and their height, fresh weight and leaf number were measured.

Fungal Pathogen Re-isolation

To verify the presence of the applied *V. dahliae* strain in plant tissues, five plants per treatment in each experiment were randomly selected. Eggplant leaves which had been cut above soil level previously were removed and their stems were surface-disinfected by spraying with 95% ethyl alcohol and by quickly passing them through flame three times. For each plant, 3 xylem chips taken from different sites along the stem (base, middle and upper part of the stem) and aseptically placed onto acidified PDA after removing the phloem. Plates were then incubated at 24°C in the dark for 14 days. The emerging fungi that grew out of tissue excisions were examined visually and under a light microscope and identified according to their morphological characteristics (Pegg and Brady, 2002). Pathogen isolation ratio was expressed as the frequency of positive *V. dahliae* isolations of each plant.

Statistics

Analysis of variance (ANOVA) was employed to determine the effects of replication (1, 2, or 3), treatment (C−, V.d., V.d. + CrR14, V.d. + CrR18, V.d. + CrR04, V.d. + MTR12, V.d. + MTR18, V.d. + CMR01, V.d. + CMR03, V.d. + CML04, V.d. + CMR25 in Experiment I and C−, V.d., V.d. + MTR17a, V.d. + MTR17d, V.d. + BMTR17f, V.d. + MTR17g, V.d. + MTR17h, V.d. + MTR17b, V.d. + MTR17c, V.d. + TRIANUM-P in experiment II) and their interaction on disease incidence (DI), final disease severity (FDS), mortality (M), RAUDPC and isolation ratio (IR), and on plant height, fresh weight and total number of leaves (**Supplementary Tables 2**, **3**). Prior to ANOVA, normality of data and homogeneity of variance across treatments was evaluated and an arcsine transformation was applied to normalize variance. When a significant *F* test was obtained for treatments ($P \leq 0.05$), the data were subjected to means separation by Tukey's honestly significant difference test. Morphological and physiological characteristics of *V. dahliae* in dual-culture and dual-plate assays were also analyzed by Tukey's test ($P \leq 0.05$). Moreover, standard errors of means were calculated.

Bacterial Genome Sequencing and Annotation

Twelve bacterial isolates were selected for whole genome sequencing (CrR16, CMR16, CrR07, CMR13, CrR06, CrR18, CrR14, CMR27, CMR25, CML04, CMR29, CrR25). The isolates were selected when they met more than two of the following criteria: (a) the 16S rRNA gene sequence of the isolates being 99.6% similar to their closest relative or lower, (b) exhibiting salt tolerance higher than the 5% threshold, (c) exhibiting medium or strong inhibition against the growth of at least 2 of the 3 tested phytopathogens *Verticillium dahliae*, *Ralstonia*

solanacearum, and *Clavibacter michiganensis* ssp. *michiganensis* (**Supplementary Table 1**). For each isolate a 250 bp paired-end library was produced for use with the Illumina MiSeq sequencing system (University of Exeter Sequencing Service, Exeter, United Kingdom). Reads were assembled using SPAdes 3.12.0 (Bankevich et al., 2012) and the assembled sequence was annotated using the NCBI Prokaryotic Genome Annotation Pipeline (PGAP). Raw sequence reads and assembled genomes were uploaded to the Sequence Read Archive (Leinonen et al., 2011) and GenBank (Dennis Benson et al., 2017) and are available under BioProject accession number PRJNA634334. RAST (Rapid Annotation using Subsystem Technology) (Overbeek et al., 2014) was employed for genome analysis and annotation.

Sequence Alignment and Phylogenetic Tree Construction

Selected gene sequences were aligned with ClustalX v2.0 (Larkin et al., 2007) and subsequently manually corrected. Sequence relationships were inferred using the maximum-likelihood (ML) method. ML phylogenies were constructed using MEGA 5.2 (Tamura et al., 2011). Phylogenetic trees were constructed using the concatenated *recA* and *gyrB* genes and assuming the bootstrap value derived from 1,500 replicates to represent the evolutionary history of the included taxa.

The evolutionary history of *Arthrobacter recA-gyrB* genes were inferred by using the Maximum Likelihood method based on the Tamura-Nei model (Tamura and Nei, 1993). The bootstrap consensus tree inferred from 500 replicates (Felsenstein, 1985) was taken to represent the evolutionary history of the taxa analyzed (Felsenstein, 1985). Branches corresponding to partitions reproduced in less than 50% bootstrap replicates are collapsed. Initial tree(s) for the heuristic search were obtained automatically as follows. When the number of common sites was <100 or less than one fourth of the total number of sites, the maximum parsimony method was used; otherwise BIONJ method with MCL distance matrix was used. Trees were drawn to scale, with branch lengths measured in the number of substitutions per site. The analysis involved 25 nucleotide sequences. Codon positions included were 1st + 2nd + 3rd + Non-coding. All positions with less than 95% site coverage were eliminated. That is, fewer than 5% alignment gaps, missing data, and ambiguous bases were allowed at any position. Evolutionary analyses were conducted in MEGA5 (Tamura et al., 2011).

The evolutionary history *Arthrobacter recA-gyrB* genes was inferred with the Maximum Likelihood method as above. The tree with the highest log likelihood (−7831.6808) was selected. Initial tree(s) for the heuristic search were obtained automatically as follows. When the number of common sites was <100 or less than one fourth of the total number of sites,

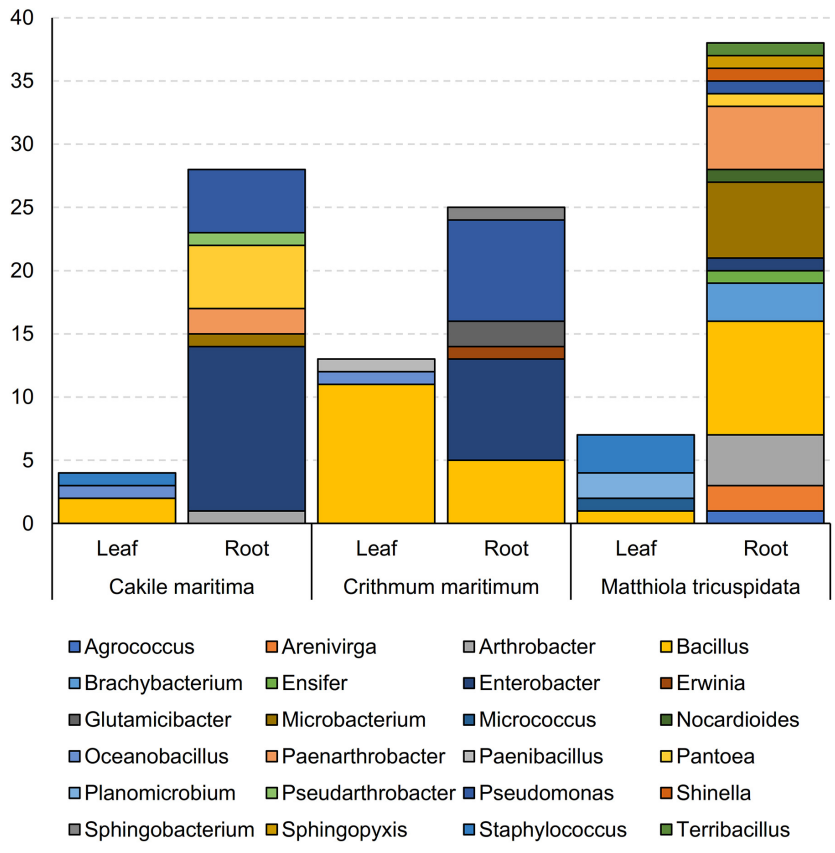

FIGURE 1 | Abundance of genera of bacterial isolates obtained from leaves and roots of *Matthiola tricuspidata*, *Crithmum maritimuma,* and *Cakile maritima* plants.

the maximum parsimony method was used; otherwise BIONJ method with MCL distance matrix was used. The bootstrap consensus tree inferred from 500 replicates (Felsenstein, 1985) is taken to represent the evolutionary history of the taxa analyzed (Felsenstein, 1985). The tree was drawn to scale, with branch lengths measured in the number of substitutions per site. The analysis involved 22 nucleotide sequences. Codon positions included were 1st + 2nd + 3rd + Non-coding. All positions with less than 95% site coverage were eliminated as described above. Evolutionary analyses conducted in MEGA5 as described above.

RESULTS

Identification and Abundance of Culturable Endophytic Bacteria

Endophytic bacteria were cultivated from different surface-sterilized tissue samples from all three halophytes. A total of 115 pure bacterial cultures showing different colony morphology (from root or leaf) were obtained; 91 were retrieved from roots and 24 from leaves. In detail, 45, 31, and 39 isolates were obtained from *M. tricuspidate, Ca. maritima,* and *Cr. Maritimum*, respectively (**Supplementary Table 1**).

For all 115 isolates, total 16S rRNA gene sequencing allowed for taxonomic analysis (**Figure 1** and **Supplementary Table 1**). Bacterial isolates were assigned to 5 different classes (**Supplementary Table 1**) and 24 genera (**Figure 1** and **Supplementary Table 1**). The most prevalent genus was *Bacillus*, accounting for 24% of the isolates, followed by *Enterobacter* (19%) and *Pseudomonas* (12%). The highest number of bacteria were isolated from roots of *M. tricuspidata* (38), followed by *Ca. maritima* roots (28) and *Cr. maritimum* roots (25), in contrast to the number of bacteria isolated from leaf samples (*M. tricuspidata*: 7, *Ca. maritima*: 4 and *Cr. maritimum*: 13). Isolates of genus *Bacillus* were isolated from all plants and tissues except the roots of *Cr. maritimum,* while *Pseudomonas* isolates were only isolated from root samples.

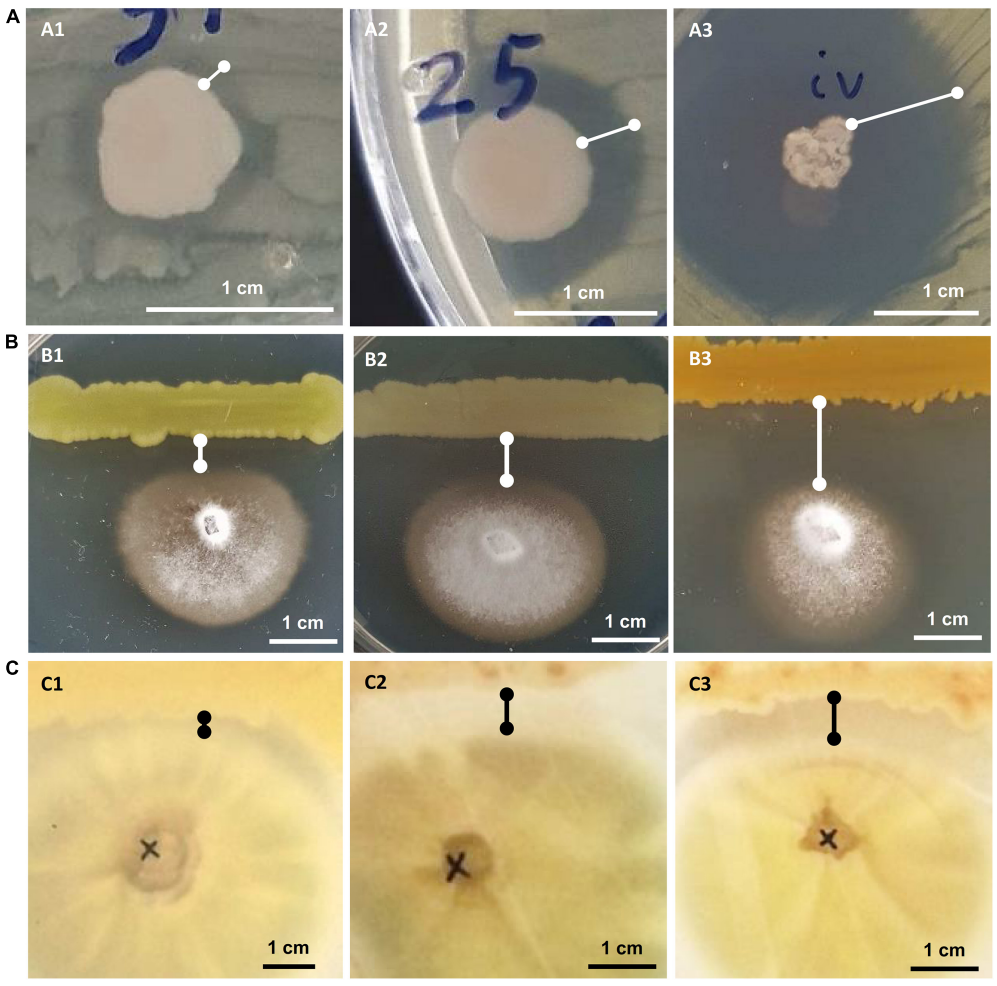

FIGURE 2 | *In vitro* growth inhibition experiments: against phytopathogenic bacteria *Ralstonia solanacearum* or *Clavibacter michiganensis* **(A)**, against phytopathogenic fungus *Verticillium dahliae* **(B)** and against human pathogenic fungus *Aspergillus fumigatus* **(C)**. Representative experiments are shown to display their "weak" (A1–C1), "medium" (A2–C2), or "strong" (A3–C3) inhibitory activity.

TABLE 1 | *In-planta* plant growth promotion and salt tolerance assays in *Arabidopsis thaliana* plants. For the salt tolerance assays plants were watered with and without NaCl solution every 2-3 days and fresh and dry plant weight was measured.

		Plant growth promotion assay#1 (sampling at 29 days)		***Plant growth promotion assay#2 (sampling at 34 days)***		***Salinity stress assay assay#1 (sampling at 39 days)***		***Salinity stress assay assay#2 (sampling at 39 days)***	
Host Plant	**Isolate**	**Fresh weight**	**Dry weight**	**Fresh weight**	**Dry weight**	**Fresh weight**	**Dry weight**	**Fresh weight**	**Dry weight**
Cakile maritima	CML12	0.410	0.029	1.500	0.109	0.246	0.034	0.307	0.038
Cakile maritima	CML15	0.204	0.025	1.240	0.135	0.309	0.052	0.347	0.060
Cakile maritima	CMR13	0.144	0.022	1.134	0.170	0.239	0.032	0.252	0.034
Crithmum maritimum	CrL01	0.541	0.053	1.761	0.168	0.147	0.031	0.186	0.041
Crithmum maritimum	CrL04	0.149	0.019	1.169	0.137	0.197	0.031	0.203	0.032
Crithmum maritimum	CrL11	0.242	0.026	1.244	0.130	0.236	0.034	0.217	0.030
Crithmum maritimum	CrR16	0.277	0.026	1.307	0.123	0.165	0.031	0.194	0.035
Crithmum maritimum	CrR22	0.094	0.016	1.003	0.150	0.275	0.042	0.297	0.045
Crithmum maritimum	CrR23	0.170	0.023	1.173	0.148	0.103	0.026	0.127	0.030
Matthiola tricuspidata	MTL01	0.113	0.017	1.132	0.145	0.202	0.037	0.213	0.038
Matthiola tricuspidata	MTR05	0.169	0.028	1.139	0.184	0.322	0.056	0.364	0.062
Matthiola tricuspidata	MTR27	0.114	0.015	1.119	0.150	0.213	0.033	0.209	0.033
	Control *E. coli*	0.110	0.017	1.111	0.171	0.235	0.034	0.216	0.031
	Control H2O	0.156	0.023	1.056	0.089	1.266	0.094	1.212	0.088
	Control Salt	*N/A*	*N/A*	*N/A*	*N/A*	0.250	0.034	0.221	0.029

Apart from *Bacillus*, which was isolated from both roots and leaves, the rest of the genera were isolated only from roots or leaves (**Supplementary Table 1**). Similarly, all isolates from the genera *Enterobacter, Pseudomonas, Microbacterium, Paenarthrobacter, Pantoea, Arthrobacter, Brachybacterium, Arenivirga,* and *Glutamicibacter* were isolated from root samples, whereas the isolates *Oceanobacillus, Planomicrobium,* and *Staphylococcus* were isolated only from leaf samples (**Supplementary Table 1**).

The most frequently isolated genera were hosted in at least two of the three halophyte species. *M. tricuspidata* hosted the largest number of genera (18). *Ca. maritima* hosted the largest number of *Enterobacter* (13 out of 22) and the smallest number of *Bacillus* (2 out of 28). Members of the genera *Brachybacterium* and *Arenivirga* were isolated only from *M. tricuspidata* plants, whilst *Glutamicibacter* were isolated only from *Cr. maritimum* and the *Planomicrobium* from *Ca. maritima*.

Bacterial Growth Under Salinity Stress

Bacterial isolates were tested for their ability to grow in elevated NaCl concentrations (5, 7.5, 10, 15, and 17.5%) (**Supplementary Figure 2A**). Most isolates showed growth at 5% NaCl (96 isolates). From the 28 isolates from *Ca. maritima* roots, 26 isolates (92.9% of the total) showed ability to grow at 5% salinity, and 14 of these (50%) showed growth at 7.5% salinity; all four isolates from the leaves of the same plant showed growth at 10% salinity and two of these could grow at 17.5%. 21 out of 25 isolates (84%) of the roots of *Cr. maritimum* could grow at 5% salt and 16 (64%) could grow at 10% salinity. 12 out of 13 (92.3%) isolates from the leaves of *Cr. maritimum* could grow at the 5% level and eight (61.5%) could grow at 10% salt. From the 38 isolates obtained from the root of *M. triscupidata*, 27 (71%) could grow at the 5% salt threshold and three could grow in 10% salt.

Of the six isolates that managed to grow at 17.5% salinity, four were isolated from leaf tissues (**Supplementary Table 1**): *Staphylococcus saprophyticus* (CML12) and *Oceanobacillus picturae* (CML15) isolated from *Ca. maritima* leaves, *Oceanobacillus picturae* (CrL11) from *Cr. maritimum* leaves, and *Micrococcus aloeverae* (MTL04) from *M. triscupidata* leaves (**Supplementary Table 1** and **Supplementary Figure 2A**). The two isolates from root tissues that could grow on 17.5% are *Enterobacter hormaechei* subsp. *hoffmannii* (CMR13) isolated from *Ca. maritima* and *Bacillus hwajinpoensis* (CrR23) isolated from *Cr. maritimum* (**Supplementary Table 1** and **Supplementary Figure 2A**). Another three *Bacilli* isolates (CrR16: *Bacillus haikouensis*, CrR22: *Bacillus haikouensis*, MTR05: *Terribacillus saccharophilus*) showed

TABLE 2 | Values of fungal parameters of *Verticillium dahliae* treated with 16 different bacterial isolates (CrR14, CrR18, CrR04, MTR12, MTR18, CM0R1, CMR03, CML04, CMR25, MTR17a, MTR17d, MTR17f, MTR17g, MTR17h, MTR17b, MTR17c) and *Trichoderma harzianum* strain T22 in dual-culture and dual-plate assays. Values were estimated as the percentage of inhibition compared to control (V.d.).

Treatment	Fungal parameters[a]							
	Dual-culture assays (confrontation test)				Dual-plate assays (volatile test)			
	RGI (%)	SI (%)	HWT (%)[b]	MFI (%)	RGI (%)[c]	SI (%)[d]	HWT (%)[e]	MFI (%)[f]
V.d.	0.00 h	0.00 e	0.00 d	0.00 f	0.00 cde	0.00 b	0.00 de	0.00 cde
V.d. + CrR14	52.92 c	70.87 cd	25.21 abc	68.98 ab	8.75 c	83.08 a	18.46 abcd	13.56 bcd
V.d. + CrR18	76.78 b	57.11 d	33.53 a	52.41 bcde	−1.97 cde	79.68 a	22.33 ab	24.99 cde
V.d. + CrR04	45.73 cd	74.30 bc	20.56 abcd	47.88 bcde	4.66 cd	21.84 ab	21.09 abc	71.91 ab
V.d. + MTR12	23.97 ef	92.94 a	22.92 abc	26.65 cdef	−3.83 cde	82.75 a	25.99 a	−20.10 cde
V.d. + MTR18	33.95 de	89.36 bc	23.49 abc	34.23 bcdef	−2.78 cde	83.13 a	30.95 a	−1.86 cde
V.d. + CMR01	21.91 ef	81.46 abc	30.26 ab	60.41 abcd	−1.54 cde	84.81 a	30.72 a	−25.08 cde
V.d. + CMR03	27.22 ef	88.34 abc	17.56 abcd	47.42 bcde	7.70 c	56.63 ab	21.45 abc	42.98 abc
V.d. + CML04	59.69 c	70.31 cd	18.10 abcd	65.11 abc	−1.10 cde	78.68 a	28.22 a	−32.44 de
V.d. + CMR25	23.15 ef	79.00 abc	13.67 abcd	23.94 def	−3.58 cde	70.63 ab	17.55 abcd	−12.64 cde
V.d. + MTR17a	45.22 cd	82.66 abc	6.89 cd	22.63 def	−8.86 de	−100.42 c	−5.11 e	−43.35 cd
V.d. + MTR17d	45.85 cd	83.99 abc	5.56 ab	32.93 bcdef	3.31 cd	74.61 ab	−3.78 e	−2.18 de
V.d. + MTR17f	51.46 c	74.21 bc	10.89 bcd	18.77 ab	−16.21 e	77.33 ab	1.56 de	−60.99 e
V.d. + MTR17g	16.75 fg	5.29 e	21.33 abc	62.41 abcd	−4.50 cde	38.33 ab	3.00 cde	−2.99 cde
V.d. + MTR17h	2.86 gh	70.53 cd	5.59 cd	−67.79 g	55.99 b	−116.97 c	5.59 bcde	−298.98 f
V.d. + MTR17b	49.02 cd	81.79 abc	0.58 d	22.91 def	74.57 a	−120.55 c	0.58 de	97.83 a
V.d. + MTR17c	60.21 c	91.26 a	7.60 cd	24.02 def	69.06 ab	−88.87 c	6.35 bcde	99.28 a
V.d. + TRIANUM-P	95.79 a	79.46 abc	nm	98.91 a	ne	ne	ne	ne

[a] *Fungal parameters were calculated according to the formula: [(Vc-Vt)/Vc] × 100 where Vc = the microscopic value of V. dahliae in control and Vt = the respective value of V. dahliae toward the antagonistic isolate in dual-culture or dual-plate assays. Each value represents the mean of 3 replicates. RGI, (radial growth inhibition; SI, (sporulation (spore production) inhibition; HWT, (hyphae width thinning; MFI, (microsclerotia formation inhibition. Within columns, values followed by the same letter are not significantly different according to Tukey's HSD test at P ≤ 0.05.*

[b] *"nm" indicates that HWT values were not measured since T. harzianum overgrown V. dahliae in dual-culture assays and pathogen hyphae could not be identified.*

[c, d, e, f] *"ne" indicates that RGI, SI, HWT and MFI were not estimated since T. harzianum could reach directly V. dahliae even in dual-plate assays.*

growth on 15% salinity (**Supplementary Table 1** and **Supplementary Figure 2A**).

Phytopathogens Growth Inhibition Ability

All bacterial isolates were subjected to *in vitro* inhibition assays against three known phytopathogens: the bacteria *Ralstonia solanacearum* and *Clavibacter michiganensis* subsp. *michiganensis* and the fungus *Verticillium dahliae*. In the assays against the phytopathogenic bacteria, the bacterial isolates that showed any kind of inhibition were characterized as having "weak," "medium" or "strong" inhibitory activity based on the size of the inhibition zone around the bacterial colony (**Figure 2**). In the *in vitro* assay against *Verticillium* the inhibitory activity was similarly judged as "weak," "medium" or "strong" based on the linear distance between the bacterial and the fungal colonies (**Figure 2**).

Twenty-five (21.7%) out of 115 bacterial isolates demonstrated inhibition of the *Ralstonia solanacearum* growth (**Supplementary Table 1**). These 25 isolates belong to six genera: *Bacillus, Enterobacter, Erwinia, Glutamicibacter, Paenarthrobacter,* and *Pseudomonas*. Isolate CML04 (*Bacillus altitudinis*), obtained from leaf tissues of *Ca. maritima,* was the only leaf-derived isolate that showed antagonistic activity against all 3 tested phytopathogens (**Supplementary Table 1**). Of the 45 isolates isolated from *M. triscupidata*, three isolates showed a weak inhibitory zone against *Ralstonia*. A total of 10 isolates belonging to the genera *Enterobacter* and *Pseudomonas* (**Supplementary Table 1**) showed a strong inhibition (**Figure 2**).

A lower number of isolates showed any kind of inhibition against the phytopathogenic *Clavibacter michiganensis* subsp. *michiganensis*: 17 isolates out of 115 (14.8%). All 9 isolates from *M. triscupidata* (*Bacillus licheniformis* or *Bacillus sonorensis* isolates) demonstrated a strong inhibition zone (**Figure 2**). Similarly, two isolates from *Cr. maritimum* roots (both *Pseudomonas glareae*, CrR12 and CrR13) showed a strong inhibition zone (**Supplementary Table 1**). An additional two and four isolates showed weak and medium inhibition zone against *Clavibacter*, respectively (**Supplementary Table 1**).

The majority (76.5%) of the bacterial isolates demonstrated inhibition of the phytopathogenic fungus *Verticillium dahliae* (**Supplementary Table 1**). These isolates originate from both leaf and root tissues from all three halophytes. A strong inhibition zone was demonstrated by 34 of these 88 isolates, all of which except one, were isolated from halophytic plant roots (**Supplementary Table 1**). From these 34, 11 isolates belong to the genus *Bacillus*, another 11 to *Pseudomonas* and five to *Enterobacter* (**Supplementary Table 1**).

Eleven isolates were tested for inhibition against the human pathogenic fungus *Aspergillus fumigatus*. Interestingly, five isolates were able to inhibit the growth of *A. fumigatus* (**Figure 2**). Isolate CML04 (*Bacillus altitudinis*) isolated from *Ca. maritima* was the only isolate from leaf tissues able to show inhibitory effect,

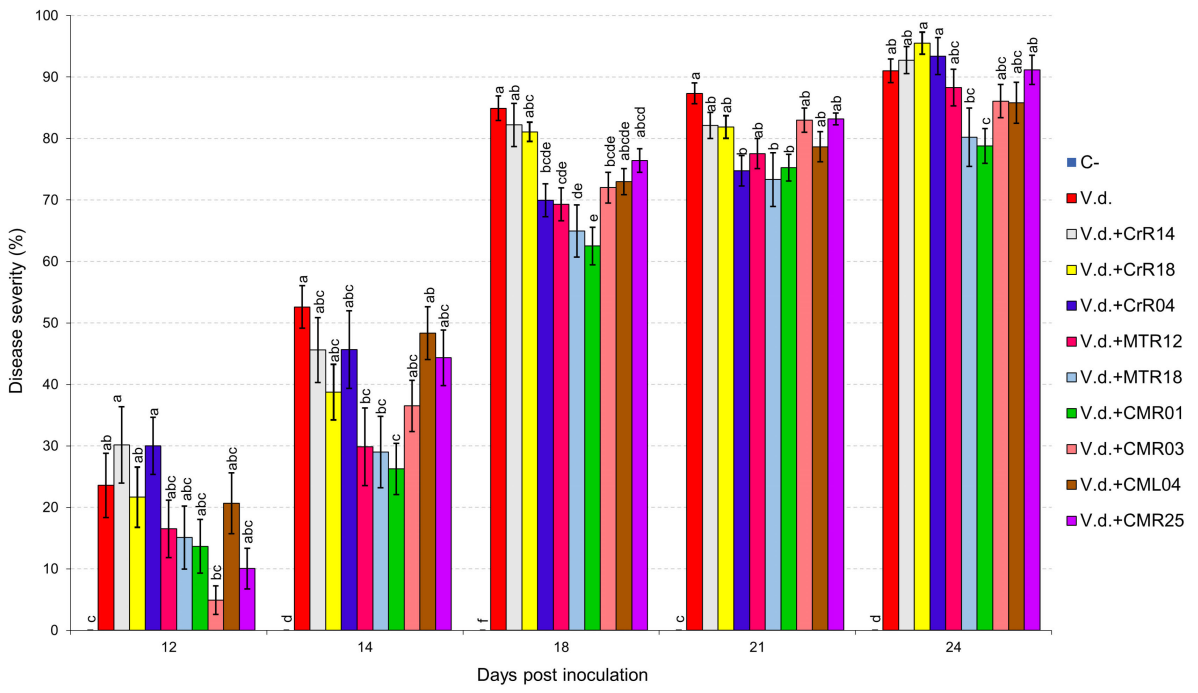

FIGURE 3 | Verticillium wilt disease severity index on eggplant treated with various bacterial isolates at 12, 14, 18, 21, and 24 days post inoculation with *Verticillium dahliae* conidial suspension (20 mL of 5 × 10^6 conidia mL^{-1}). Each column represents the mean of 21 plants after combining the results of 3 replicated experiments (experiment I). Columns at each observation time point followed by the same letter are not significantly different according to Tukey's HSD test at $P \leq 0.05$. Vertical bars indicate standard errors.

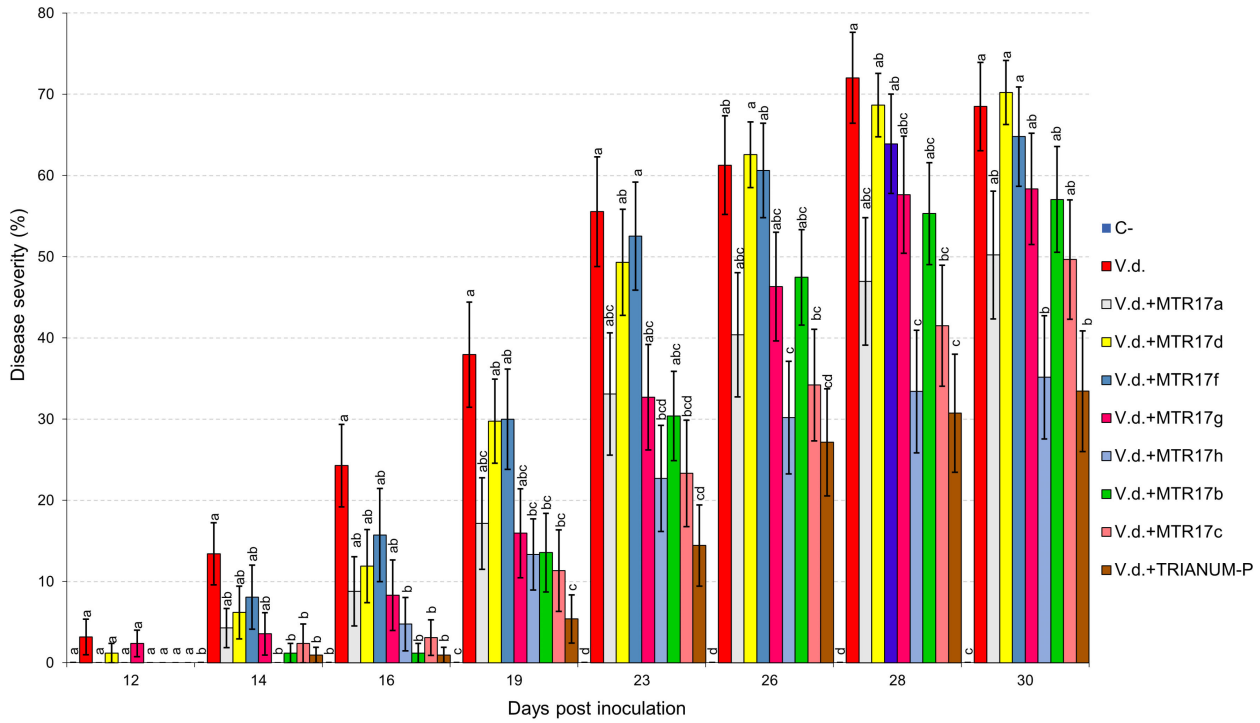

FIGURE 4 | Verticillium wilt disease severity index on eggplant treated with various bacterial isolates and the commercial biofungicide TRIANUM-P (Koppert B.V. Hellas) at 12, 14, 16, 19, 23, 26, 28, and 30 days post inoculation with *Verticillium dahliae* conidial suspension (20 mL of 5×10^6 conidia mL^{-1}). Each column represents the mean of 21 plants after combining the results of 3 replicated experiments (experiment II). Columns at each observation time point followed by the same letter are not significantly different according to Tukey's HSD test at $P \leq 0.05$. Vertical bars indicate standard errors.

while the remaining isolates were isolated from *M. triscupidata* roots (**Supplementary Table 1**). Two isolates MTR17d (*Bacillus sonorensis*) and MTR17b (*Bacillus licheniformis*) showed a strong inhibition zone (**Figure 2** and **Supplementary Table 1**).

In-planta Assay for Plant Growth Promotion and Salt Tolerance

Bacterial isolates with *in vitro* 10% and 17.5% NaCl salt tolerance were selected for the *in-planta* assays to demonstrate potential plant growth promotion under "no stress." *Arabidopsis thaliana* plants were imbued with bacterial cultures and left for 7 days for the bacteria to adapt. Then, after watering the plants for a month, fresh and dry leaf weight were calculated (**Table 1**). The same experiment was repeated where after the 7 day mark, the plants were watered with 10 mL of 250 mM NaCl solution every 2–3 days for 30 days.

Under no stress conditions, plants inoculated with isolates CML12, CML15, CrL01, CrL11, CrR16, CrR23, MTR05 showed an increase in fresh leaf weight between 1.1 and 2.6 times to the non-inoculated plants and between 1.0 and 2.3 times increase in dry leaf weight (**Table 1**). Under salt stress, the growth promotion effect was less accentuated, since plants imbued with isolates CML15, CrR22, MTR05 had less increased fresh and dry leaf (**Table 1**).

Isolates CML15 and MTR05 conferred an increase in fresh and dry leaf weight both under no stress and under salt stress whereas isolate CrR22 had a positive affect only under salt stress condition (**Table 1**). On the other hand, isolates CML12, CrL01, CrL11, CrR16, and CrR23 had a positive effect on fresh and dry weight under no stress condition (**Table 1**).

Direct and Indirect *in vitro* Effects of *Verticillium dahliae* Growth

The selected 16 bacterial isolates with the exception of MTR17h inhibited significantly *V. dahliae* growth rate in dual-culture assays. However, only MTR17h, MTR17b, and MTR17c could suppress fungal growth by means of volatile compounds (**Table 2**). Likewise, nearly all isolates were capable of inhibiting fungal sporulation (except of MTR17g) in dual-culture assays. Most isolates significantly inhibited spore production in dual-plate assays. Interestingly, three isolates caused a significant induction of *V. dahliae* sporulation in such assays (MTR17h, MTR17b, and MTR17c), indicating that fungal growth suppression induces fungal sporulation (**Table 2**). Moreover, six out of 16 isolates could significantly reduce hyphae width in direct culture conditions, whereas seven out of 16 were capable of hyphae width reduction by the mean of volatiles. Additionally, nine isolates significantly inhibited microsclerotia formation in dual-culture assays; however, only three isolates significantly reduced microsclerotia formation in dual-plate assays (**Table 2**). MTR17h caused significant induction in

microsclerotia formation both in dual-culture and in dual-plate assays.

Suppression of *Verticillium* Wilt Symptoms *in-planta*

For the suppression of *Verticillium dahliae* wilt symptoms *in-planta* we used a well-established fungus/plant system, the *Verticillium*/eggplant system. We selected 16 bacterial isolates that showed promising *in vitro* growth inhibition effect to *Verticillium*.

Two distinct assays were performed (hereafter known as "experiment I" and "experiment II"). *V. dahliae* wilt symptoms on eggplant started 12 days after inoculation (d.p.i.), with *V. dahliae* conidial suspension and were recorded periodically for another 12 days in experiment I. Isolates CrR4, MTR12, MTR18, and CMR01 suppressed significantly disease severity at 18 and 21 d.p.i. whereas MTR18 and CM1 treatments caused significant reduction of disease severity at most observation time points (**Table 2** and **Figures 3**, **4**). Considering all disease parameters, CMR01 was the most effective isolate in terms of disease suppression (**Table 2**, **Figure 3**, and **Supplementary Tables 2**, **3**). First disease symptoms in experiment II were also observed on 12 d.p.i. and recorded until 30 d.p.i. Disease severity progressed rapidly in the control (*V.d.*) and the non-suppressive treatments (MTR17d, MTR17f, and MTR17g), whereas MTR17a-, MTR17h-, MTR17b-, and MTR17c-treated plants showed less prominent symptoms and slower disease development (**Table 2** and **Supplementary Figure 3**). Disease parameters indicated that isolate MTR17h, is comparable to the positive control (fungus *Trichoderma harzianum* isolate + TRIANUM-P), as the most effective in symptom suppression (**Table 2** and **Figure 4**). While observed decrease in symptom severity in MTR17h-treated plants was associated with significantly lower *V. dahliae* re-isolation ratio compared to positive control (*V.d.*) plants, MTR17h isolate did not show strong growth inhibition effect on *V. dahliae* in *in vitro* assays (**Figure 4**), indicating less active growth of the pathogen into the xylem vessels. This finding could suggest that the plant innate immunity activation/reinforcement effect by MTR17h, needs to be further investigated in the future. Neither symptoms nor positive isolations were observed in negative control plants.

TABLE 3 | Values (± standard errors) of disease parameters for eggplants inoculated with *V. dahliae* and treated with different bacterial isolates and TRIANUM-P (CrR14, CrR18, CrR04, MTR12, MTR18, CMR01, CMR03, CML04, CMR25 in experiment I, and MTR17a, MTR17d, MTR17f, MTR17g, MTR17h, MTR17b, MTR17c, TRIANUM-P in experiment II) or not (C−, V.d.).

Experiment	Treatment	Disease parameters[a]				
		DI (%)	FDS (%)	M (%)	RAUDPC (%)	IR
Experiment I	C−	0.00 ± 0.00b	0.00 ± 0.00c	0.00 ± 0.00c	0.00 ± 0.00c	0.00 ± 0.00b
	V.d.	100.00 ± 0.00a	91.00 ± 1.91ab	100.00 ± 0.00a	42.36 ± 2.08a	0.55 ± 0.07ab
	V.d. + CrR14	100.00 ± 0.00a	92.74 ± 2.21ab	95.24 ± 4.76a	42.54 ± 2.62a	0.65 ± 0.05a
	V.d. + CrR18	100.00 ± 0.00a	95.50 ± 1.80a	90.48 ± 6.15ab	39.19 ± 1.99ab	0.55 ± 0.08ab
	V.d. + CrR04	100.00 ± 0.00a	93.40 ± 2.99a	78.57 ± 7.70ab	39.84 ± 2.18ab	0.60 ± 0.05ab
	V.d. + MTR12	100.00 ± 0.00a	88.29 ± 2.74abc	80.95 ± 9.91ab	33.86 ± 2.59ab	0.80 ± 0.07a
	V.d. + MTR18	100.00 ± 0.00a	80.19 ± 4.75bc	71.43 ± 8.69ab	31.67 ± 3.02b	0.55 ± 0.05ab
	V.d. + CMR01	100.00 ± 0.00a	78.79 ± 2.85c	52.38 ± 14.29b	30.72 ± 2.18b	0.55 ± 0.08ab
	V.d. + CMR03	100.00 ± 0.00a	86.07 ± 2.71abc	66.67 ± 14.55ab	32.25 ± 1.47b	0.65 ± 0.08a
	V.d. + CML04	100.00 ± 0.00a	85.82 ± 3.34abc	69.05 ± 5.67ab	37.91 ± 2.00ab	0.65 ± 0.05a
	V.d. + CMR25	100.00 ± 0.00a	91.17 ± 2.37ab	80.95 ± 9.91ab	35.71 ± 1.46ab	0.85 ± 0.03a
Experiment II	C−	0.00 ± 0.00c	0.00 ± 0.00c	0.00 ± 0.00b	0.00 ± 0.00*d*	0.00 ± 0.00b
	V.d.	90.48 ± 6.15ab	68.49 ± 5.43a	47.62 ± 9.91a	26.76 ± 2.95a	0.53 ± 0.05a
	V.d. + MTR17a	71.43 ± 15.31ab	50.21 ± 7.88ab	33.33 ± 10.29ab	15.05 ± 2.81bc	0.20 ± 0.09ab
	V.d. + MTR17d	95.24 ± 4.76a	70.22 ± 3.93a	23.81 ± 14.02ab	23.04 ± 2.20ab	0.40 ± 0.20ab
	V.d. + MTR17f	85.71 ± 9.91ab	64.79 ± 6.12a	33.33 ± 14.51ab	22.95 ± 2.67ab	0.38 ± 0.17ab
	V.d. + MTR17g	80.95 ± 6.73ab	58.36 ± 6.85ab	38.10 ± 11.34ab	16.81 ± 2.84abc	0.27 ± 0.12ab
	V.d. + MTR17h	52.38 ± 12.30b	35.15 ± 7.58b	4.76 ± 4.76b	10.51 ± 2.58 *cd*	0.10 ± 0.04b
	V.d. + MTR17b	80.95 ± 9.91ab	57.05 ± 6.52ab	19.05 ± 6.73ab	14.85 ± 2.03bc	0.40 ± 0.18ab
	V.d. + MTR17c	76.19 ± 9.52ab	49.66 ± 7.35ab	23.81 ± 6.15ab	11.73 ± 2.35c	0.13 ± 0.06ab
	V.d. + TRIANUM-P	52.38 ± 6.74b	33.45 ± 7.44b	4.76 ± 4.76b	7.88 ± 1.94 *cd*	0.20 ± 0.09ab

[a] *Disease parameters were evaluated periodically on the basis of external symptoms during a period of 24 days (in Experiment I) and 30 days (in Experiment II) after root drenching with Verticillium dahliae conidial suspension (20 mL of 5 × 10^6 conidia mL^{-1} per plant). One week prior to inoculation with V. dahliae, plants were root-drenched with bacterial suspension (20 mL of 10^8 cfu mL^{-1} of each isolate per plant); whereas TRIANUM-P was also included in experiment* II *and applied by root drenching (20 mL of 3 × 10^7 cfu mL^{-1} per plant). DI, (final disease incidence; FDS, (final disease severity; M, (mortality; RAUDPC, (relative area under the disease progress curve with reference to the maximum value potentially reached over each assessment period; IR, (isolation ratio. Each value represents the mean of 21 plants after combining the results of 3 replicated experiments (except from IR that represents the mean of 5 plants in total). Within experiments, values in columns followed by the same letter are not significantly different according to Tukey's HSD test at $P \leq 0.05$.*

Effects of Treatments in Plant Growth

Growth parameters of eggplant inoculated with *V. dahliae* and treated with the 16 isolates and the *T. harzianum* isolate TRIANUM-P or not (C−), are shown on **Table 3**. *V. dahliae*-inoculated plants treated with MTR17c and *T. harzianum* TRIANUM-P developed significantly higher fresh weight compared with the *V. dahliae*-inoculated controls, whereas most of the plant growth parameters in non-inoculated plants were significantly higher than the inoculated ones.

Whole-Genome Sequencing and Analysis of Selected Endophytic Bacterial Isolates

Whole-genome sequencing (WGS) was performed on 12 selected isolates. Genomes were annotated using RAST (**Supplementary Figure 5**). All genes related to the virulence, disease and defense that were predicted are presented in **Table 4** and **Supplementary Table 2**.

Genome-wide average nucleotide identity (ANI) calculations against all bacterial genome assemblies in GenBank pointed to the existence of three previously unknown bacterial species; their genomes showed less than 95% ANI with any previously sequenced genomes. Phylogenetic analysis of the *recA* and *gyrB* gene sequences extracted from the genomes (**Figures 5**, **6**) had indicated that two isolates belong to *Pseudomonadaceae*, while the third was a member of *Arthrobacter* genus. Isolates CMR25 and CMR27 belonged to an unidentified species of the *P. putida* group (**Figure 6**) and isolate CrR25 was an undefined species of the *P. mendocina* group (**Figure 6**). Consistent with these results, 16S rRNA gene sequences of CMR25 and CMR27 were 99.8% identical to that of *Pseudomonas plecoglossicida* and CrR25 was 98.75% identical to that of *Pseudomonas benzenivorans*. WGS analysis places CMR16 as an unidentified *Arthrobacter* species (**Figure 5**), while its 16S rRNA gene sequence assigns the isolate to *Paenarthrobacter nitroguajacolicus* (Kotoučková et al., 2004) with 98.78% identity. This species has been previously isolated from leaves of maize (Pisarska and Pietr, 2012) and promoted growth of wheat under salt stress (Safdarian et al., 2019). Unfortunately, no genome sequence is available for the type strain of this species; however, the ANI between CMR16

TABLE 4 | Number of genes related to Virulence, Disease and Defense features of the three new bacterial species identified in this study. The genome analysis and the annotation was performed using the RAST genome annotation software.

Virulence, disease and defense	*Arthrobacter* sp. CMR16	*Pseudomonas* sp. CrR25	*Pseudomonas* sp. CMR27	*Pseudomonas* sp. CMR25
Resistance to antibiotics and toxic compounds	**19**	**56**	**42**	**45**
Mercury resistance operon	1	0	0	0
Copper homeostasis	6	25	18	18
Cobalt-zinc-cadmium resistance	4	12	17	16
Resistance to fluoroquinolones	2	5	2	5
Copper homeostasis: copper tolerance	2	2	2	2
Beta-lactamase	1	0	2	1
Mercuric reductase	3	3	0	0
Multidrug Resistance Efflux Pumps	0	7	0	0
Resistance to chromium compounds	0	1	1	3
Invasion and intracellular resistance	**19**	**21**	**14**	**17**
Mycobacterium virulence operon involved in protein synthesis (SSU ribosomal proteins)	6	9	6	7
Mycobacterium virulence operon involved in DNA transcription	3	6	2	4
Mycobacterium virulence operon possibly involved in quinolinate biosynthesis	3	3	3	3
Listeria surface proteins: Internalin-like proteins	4	0	0	0
Mycobacterium virulence operon involved in protein synthesis (LSU ribosomal proteins)	3	3	3	3
Bacteriocins, ribosomally synthesized antibacterial peptides	**0**	**2**	**2**	**2**
Tolerance to colicin E2	0	2	2	2
Membrane Transport	**14**	**77**	**86**	**83**
Protein secretion system, Type II (Widespread colonization island)	11	14	10	10
Protein secretion system, Type II (General Secretion Pathway)	0	15	0	0
Protein secretion system, Type V (Two partner secretion pathway–TPS)	0	4	0	0
Protein secretion system, Type I	0	0	29	22
Protein secretion system, Type III	0	0	0	0
Protein secretion system, Type VI	0	0	0	0
Protein and nucleoprotein secretion system, Type IV (Type IV pilus)	0	28	22	20
Protein and nucleoprotein secretion system, Type IV (Conjugative transfer)	0	12	0	0
Protein secretion system, Type VII (Chaperone/Usher pathway, CU)	0	0	13	12
Twin-arginine translocation system	3	4	7	7
Protein secretion system, Type VIII (Extracellular nucleation/precipitation pathway, ENP)	0	0	5	12

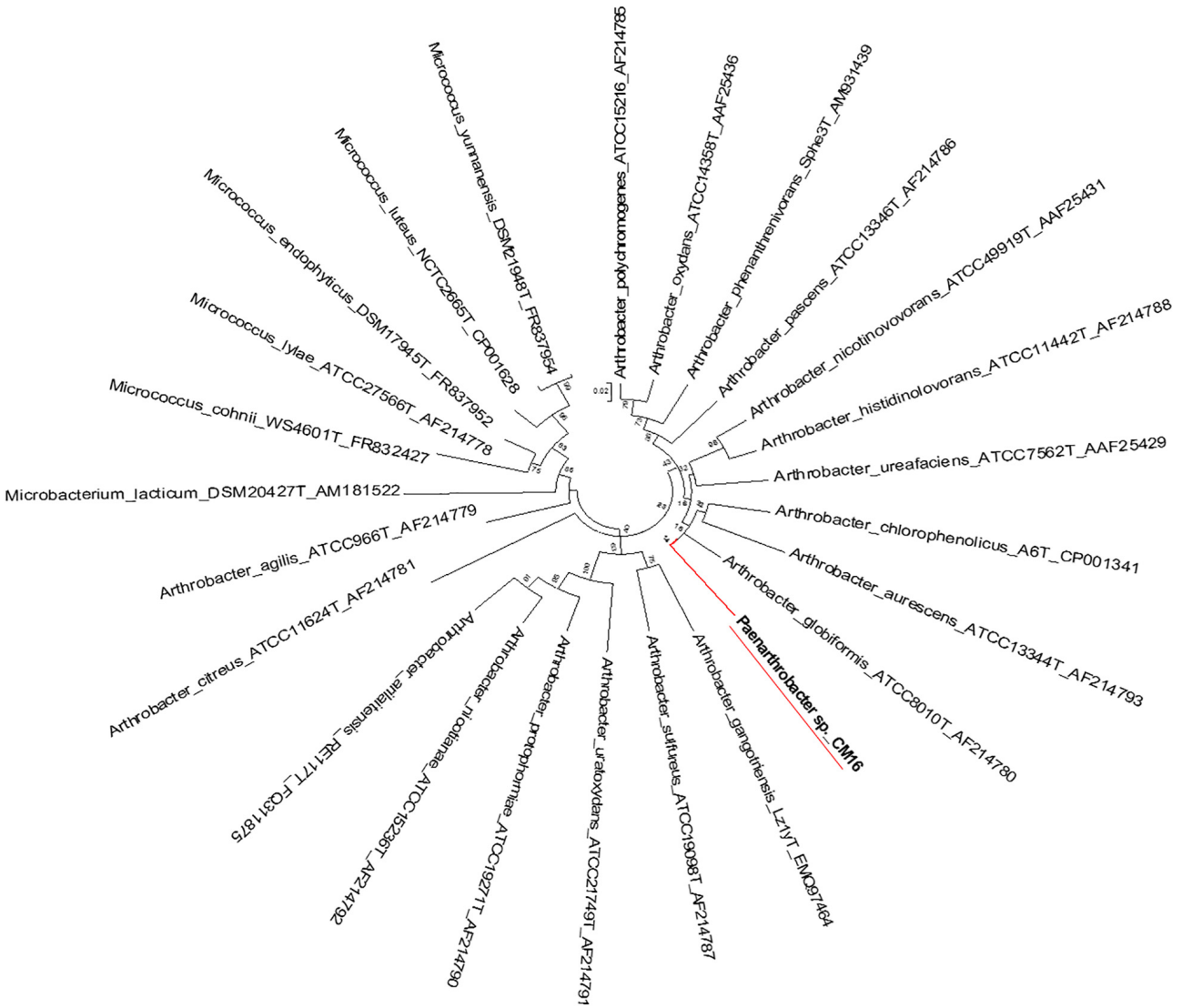

FIGURE 5 | Molecular phylogenetic analysis of *Arthrobacter recA-gyrB* genes by Maximum Likelihood method. Phylogenetic tree is drawn to scale, with branch lengths measured in the number of substitutions per site.

genome and previously sequenced genomes (Yao et al., 2015) of *Paenarthrobacter nitroguajacolicus* (Kotoučková et al., 2004) range between 86.08 and 86.76%, well below the widely used threshold of 96% for species membership.

DISCUSSION

Utilization of endophytic microorganisms for the control of biotic/abiotic stresses is a relatively unexplored area of research. Endophytes have been studied for over two decades (Saikkonen et al., 1998; Hasegawa et al., 2006; Kaul et al., 2016), however, our understanding about their role in plant defense against biotic/abiotic stresses is still limited (Liu et al., 2020; Pascale et al., 2020). Isolation, identification and the study of endophytes from plants that undergo continued abiotic stress could be essential for the development of proper biocontrol strategy for sustainable agriculture and food security.

Here, we investigated the abundance of taxa of the culturable bacterial endophytes of three halophytic plants, endemic in Crete island, Greece, using culture-dependent techniques (**Figure 7**). We also investigated the proof-of-concept of using the halophytes as a valuable source of beneficial microbes that can potentially be used in agriculture, by testing our initial hypothesis that these endophytes have plant growth promotion and biocontrol properties.

Taxonomically, 24 different genera were identified, the three most abundant ones were *Bacillus*, *Enterobacter,* and *Pseudomonas,* all of which have been previously observed in

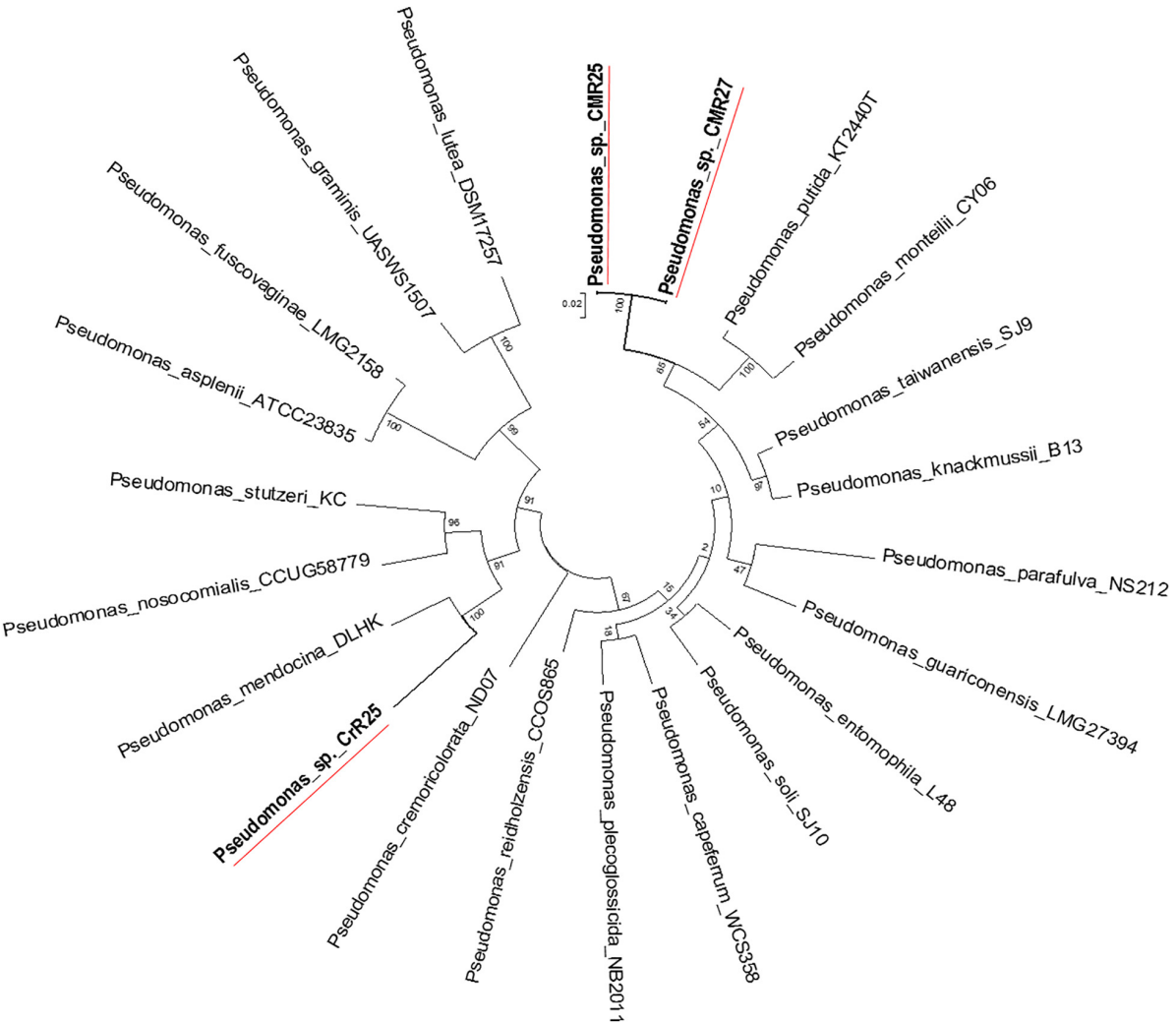

FIGURE 6 | Molecular Phylogenetic analysis of the *recA-gyrB* genes from Pseudomonads belonging to *P. putida* and *P. mendocina* groups by Maximum Likelihood method. The tree with the highest log likelihood (–7831.6808) is shown. The tree is drawn to scale, with branch lengths measured in the number of substitutions per site.

studies of the endophytic microbiome of halophytes (Shabala, 2013; Qin et al., 2014; Mora-Ruiz et al., 2016; Yuan et al., 2016).

In-planta testing of *Oceanobacillus picturae* (CML15), *Terribacillus saccharophilus* (MTR05), and *Bacillus haikouensis* (CrR22) demonstrated an increase in both dry and fresh leaf weight in *Arabidopsis thaliana* plant under salinity stress. These isolates are promising biofertilizers, since other isolates of the same species have also been shown to have plant growth promotion properties; *Terribacillus saccharophilus*, firstly reported at 2007, is a known halophilic bacterium able to grow on 0–16% NaCl (An et al., 2007; Liu et al., 2010). This species is a known endophytic bacterium (Han et al., 2011), shown to trigger an increase on monoterpenes, sesquiterpenes, tocopherols, and membrane sterols, compounds engaged in antioxidant capacity in leaf tissues of grape resulting in stress tolerance (Salomon et al., 2016). *Bacillus haikouensis* is halotolerant bacterium isolated from paddy soil, able to grow on up to 17% NaCl (Li et al., 2014). *Oceanobacillus picturae* is a halophilic phosphate-solubilizing species with demonstrated siderophore production potential, isolated from saline environments and shown to promote plant growth in mangroves and confer salinity stress tolerance in barley (El-Tarabily and Youssef, 2010; Mapelli et al., 2013; Orhan and Demirci, 2020). Many of our isolates were able to grow at high concentrations of salt (5–17% NaCl).

Isolates belonging to the species *Bacillus licheniformis, Bacillus sonorensis, Pseudomonas glareae, Enterobacter hormaechei, Pseudomonas benzenivorans, Pseudomonas monteilii, Pseudomonas plecoglossicida* were shown to have strong antagonistic activity against the phytopathogenic bacteria *Ralstonia solanacearum* and *Clavibacter michiganensis* subsp. *michiganensis*, two very important plant pathogens with high economic impact on agriculture (Gartemann et al., 2003; Peeters et al., 2013). Both are very important phytopathogens, since *Ralstonia* has a large host range able to infect more than 200 plant

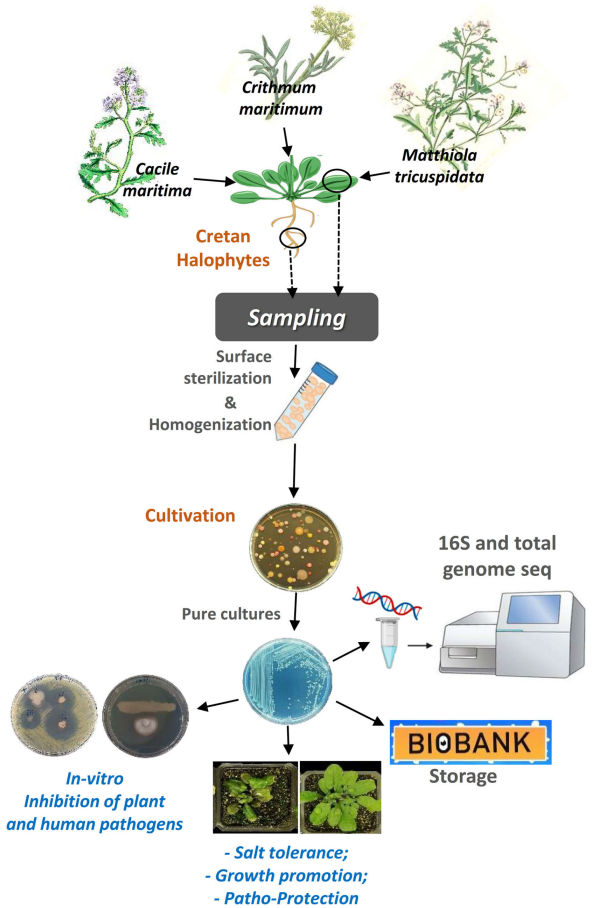

FIGURE 7 | A graphical abstract describing the steps of the procedure we followed to accomplish this work.

species easily adaptable in varying environmental conditions whereas *C. michiganensis* subsp. *michiganensis* is able to infect wheat, maize, potatoes, and red and green peppers, despite its main host being tomatoes (Eichenlaub and Gartemann, 2011; Peeters et al., 2013; Hwang et al., 2018). Moreover, specific isolates with *in vitro* growth inhibition effect against *V. dahliae*, were tested for their ability to inhibit *V. dahliae in-planta*. Several isolates demonstrated an *in-planta* suppression effect of the polyphagous pathogen *V. dahliae*. Interestingly, isolates with strong *in vitro* effect did not manage to inhibit *V. dahliae in-planta,* but other isolates with medium or low *in vitro* effect inhibited *in-planta V. dahliae* growth strongly. These data provide the proof of concept for our study but also indicate that in future studies all resulting isolates need to be investigated for their *in-planta* antifungal and/or antibacterial growth inhibition capacity.

Furthermore, the whole-genome sequencing (WGS) of selected isolates revealed three new previously unidentified bacterial species. The identification of three new species in a very small number isolates indicates the high potential of the wild halophytic endophytome in terms of identifying new microbial species with novel capabilities, that could be beneficial for both agriculture (stress tolerance, growth promotion, etc.) and potentially in clinical practice (identification of new antibiotics, antifungal compounds, etc.).

The results from the study of the microbial collection we generated, could be the basis for the future development of various synthetic "bio-inoculants," as the isolates possess all of the following attributes for such usage: (a) they are not pathogenic and do not induce plant disease; (b) are able to colonize plants, and (c) are culturable, so they can be used in modern agriculture. Furthermore, these isolates can be the basis for future studies, including the investigation of the colonization strategies that these microbes use, as well as, the elucidation of the molecular dialogs that take place during host-root colonization; the growth promotion; the salt tolerance and the immunity activation, by unique beneficial endophytes or artificial endophytic communities.

DATA AVAILABILITY STATEMENT

The datasets presented in this study can be found in online repositories. The names of the repository/repositories and accession number(s) can be found in the article/**Supplementary Material**.

AUTHOR CONTRIBUTIONS

PS designed the research. CC, GD, AC, EM, AS, GM, and GR performed the research. CC, IL, DS, VC, EM, and PS analyzed the data. CC, EM, DS, VC, and PS wrote the manuscript. All authors have read and approved the manuscript.

FUNDING

This project utilized equipment funded by the Wellcome Trust Institutional Strategic Support Fund (WT097835MF), the Wellcome Trust Multi-User Equipment Award (WT101650MA) and BBSRC LOLA award (BB/K003240/1). This work benefitted from the support of the University of Exeter's High-Performance Computing (HPC) facility. The project was partially supported by the Emblematic Action of the Greek General Secretariat for Research and Technology, "Agro4Crete," Protocol Number: SAE 013, Operational Program: SAE 013.

ACKNOWLEDGMENTS

We acknowledge Dr. Karen Moore, Audrey Farbos, Georgina Morris of the Exeter Sequencing Service at University of Exeter, for DNA library preparation and genome sequencing.

SUPPLEMENTARY MATERIAL

The Supplementary Material for this article can be found online at: https://www.frontiersin.org/articles/10.3389/fmicb.2021.681567/full#supplementary-material

REFERENCES

An, S.-Y., Asahara, M., Goto, K., Kasai, H., and Yokota, A. (2007). *Terribacillus saccharophilus* gen. nov., sp. nov. and *Terribacillus halophilus* sp. nov., spore-forming bacteria isolated from field soil in Japan. *Int. J. Syst. Evol. Microbiol.* 57, 51–55. doi: 10.1099/ijs.0.64340-0

Bankevich, A., Nurk, S., Antipov, D., Gurevich, A. A., Dvorkin, M., Kulikov, A. S., et al. (2012). SPAdes: a new genome assembly algorithm and its applications to single-cell sequencing. *J. Comput. Biol.* 19, 455–477. doi: 10.1089/cmb.2012.0021

Bulgarelli, D., Garrido-Oter, R., Münch, P. C., Weiman, A., Dröge, J., Pan, Y., et al. (2015). Structure and function of the bacterial root microbiota in wild and domesticated barley. *Cell Host Microb.* 17, 392–403. doi: 10.1016/j.chom.2015.01.011

Bulgarelli, D., Spaepen, S., Schlaeppi, K., Schulze-Lefert, P., and van Themaat, E. V. L. (2013). Structure and functions of the bacterial microbiota of plants. *Annu. Rev. Plant Biol.* 64, 807–838. doi: 10.1146/annurev-arplant-050312-120106

Campbell, C., and Madden, L. (1990). *Introduction to Plant Disease Epidemiology*. Hoboken, NJ: John Wiley & Sons.

Chaurasia, B., Pandey, A., Palni, L. M. S., Trivedi, P., Kumar, B., and Colvin, N. (2005). Diffusible and volatile compounds produced by an antagonistic *Bacillus subtilis* strain cause structural deformations in pathogenic fungi in vitro. *Microbiol. Res.* 160, 75–81. doi: 10.1016/j.micres.2004.09.013

Dennis Benson, G. A., Cavanaugh, M., Clark, K., Karsch-Mizrachi, I., Ostell, J., Pruitt, K. D., et al. (2017). GenBank. *Nucleic Acids Res.* 46, D41–D47. doi: 10.1093/nar/gkx1094

Dodd, I. C., and Pérez-Alfocea, F. (2012). Microbial amelioration of crop salinity stress. *J. Exp. Bot.* 63, 3415–3428. doi: 10.1093/jxb/ers033

Edwards, J., Johnson, C., Santos-Medellín, C., Lurie, E., Podishetty, N. K., Bhatnagar, S., et al. (2015). Structure, variation, and assembly of the root-associated microbiomes of rice. *Proc. Natl. Acad. Sci. U.S.A.* 112, E911–E920. doi: 10.1073/pnas.1414592112

Eichenlaub, R., and Gartemann, K.-H. (2011). The *Clavibacter michiganensis* subspecies: molecular investigation of gram-positive bacterial plant pathogens. *Annu. Rev. Phytopathol.* 49, 445–464. doi: 10.1146/annurev-phyto-072910-095258

El-Tarabily, K. A., and Youssef, T. (2010). Enhancement of morphological, anatomical and physiological characteristics of seedlings of the mangrove Avicennia marina inoculated with a native phosphate-solubilizing isolate of *Oceanobacillus picturae* under greenhouse conditions. *Plant Soil* 332, 147–162. doi: 10.1007/s11104-010-0280-y

Etesami, H., and Beattie, G. A. (2018). Mining halophytes for plant growth-promoting halotolerant bacteria to enhance the salinity tolerance of non-halophytic crops. *Front. Microbiol.* 9:148. doi: 10.3389/fmicb.2018.00148

Felsenstein, J. (1985). Confidence limits on phylogenies: an approach using the bootstrap. *Evolution* 39:783. doi: 10.2307/2408678

Gartemann, K.-H., Kirchner, O., Engemann, J., Gräfen, I., Eichenlaub, R., and Burger, A. (2003). *Clavibacter michiganensis* subsp. michiganensis: first steps in the understanding of virulence of a Gram-positive phytopathogenic bacterium. *J. Biotechnol.* 106, 179–191. doi: 10.1016/j.jbiotec.2003.07.011

Glick, B. R. (2014). Bacteria with ACC deaminase can promote plant growth and help to feed the world. *Microbiol. Res.* 169, 30–39. doi: 10.1016/j.micres.2013.09.009

Han, J., Song, Y., Liu, Z., and Hu, Y. (2011). Culturable bacterial community analysis in the root domains of two varieties of tree peony (*Paeonia ostii*). *FEMS Microbiol. Lett.* 322, 15–24. doi: 10.1111/j.1574-6968.2011.02319.x

Haney, C. H., Samuel, B. S., Bush, J., and Ausubel, F. M. (2015). Associations with rhizosphere bacteria can confer an adaptive advantage to plants. *Nat. Plants* 1:15051. doi: 10.1038/nplants.2015.51

Hasegawa, S., Meguro, A., Shimizu, M., Nishimura, T., and Kunoh, H. (2006). Endophytic actinomycetes and their interactions with host plants. *Actinomycetologica* 20, 72–81. doi: 10.3209/saj.20.72

Hwang, I. S., Oh, E.-J., Kim, D., and Oh, C.-S. (2018). Multiple plasmid-borne virulence genes of *Clavibacter michiganensis* ssp. capsici critical for disease development in pepper. *New Phytol.* 217, 1177–1189. doi: 10.1111/nph.14896

Kaul, S., Sharma, T., and Dhar, K. M. (2016). "Omics" tools for better understanding the plant-endophyte interactions. *Front. Plant Sci.* 7:955. doi: 10.3389/fpls.2016.00955

Kotoučková, L., Schumann, P., Durnová, E., Spröer, C., Sedláček, I., Neča, J., et al. (2004). *Arthrobacter nitroguajacolicus* sp. nov., a novel 4-nitroguaiacol-degrading actinobacterium. *Int. J. Syst. Evol. Microbiol.* 54, 773–777. doi: 10.1099/ijs.0.02923-0

Kumar, S., Stecher, G., Li, M., Knyaz, C., and Tamura, K. (2018). MEGA X: molecular evolutionary genetics analysis across computing platforms. *Mol. Biol. Evol.* 35, 1547–1549. doi: 10.1093/molbev/msy096

Lahlali, R., Bajii, M., and Jijakli, M. H. (2007). Isolation and evaluation of bacteria and fungi as biological control agents against *Rhizoctonia solani*. *Commun. Agric. Appl. Biol. Sci.* 72, 973–982.

Lane, J. D. (1991). "16S/23S rRNA sequencing," in *Nucleic Acid Techniques in Bacterial Systematics*, eds E. Stackebrandt and M. Goodfellow (Hoboken, NJ: John Wiley & Sons Ltd), 115–175.

Larkin, M. A., Blackshields, G., Brown, N. P., Chenna, R., McGettigan, P. A., McWilliam, H., et al. (2007). Clustal W and Clustal X version 2.0. *Bioinformatics* 23, 2947–2948. doi: 10.1093/bioinformatics/btm404

Leinonen, R., Sugawara, H., and Shumway, M. (2011). The sequence read archive. *Nucleic Acids Res.* 39, D19–D21. doi: 10.1093/nar/gkq1019

Li, J., Yang, G., Lu, Q., Zhao, Y., and Zhou, S. (2014). *Bacillus haikouensis* sp. nov., a facultatively anaerobic halotolerant bacterium isolated from a paddy soil. *Antonie van Leeuwenhoek Int. J. Gen. Mol. Microbiol.* 106, 789–794. doi: 10.1007/s10482-014-0248-7

Liu, H., Brettell, L. E., Qiu, Z., and Singh, B. K. (2020). Microbiome-mediated stress resistance in plants. *Trends Plant Sci.* 25, 733–743. doi: 10.1016/j.tplants.2020.03.014

Liu, H., Carvalhais, L. C., Crawford, M., Singh, E., Dennis, P. G., Pieterse, C. M. J., et al. (2017). Inner plant values: diversity, colonization and benefits from endophytic bacteria. *Front. Microbiol.* 8:2552. doi: 10.3389/fmicb.2017.02552

Liu, W., Jiang, L., Guo, C., and Yang, S. S. (2010). *Terribacillus aidingensis* sp. nov., a moderately *Halophilic bacterium*. *Int. J. Syst. Evol. Microbiol.* 60, 2940–2945. doi: 10.1099/ijs.0.017228-0

Mapelli, F., Marasco, R., Rolli, E., Barbato, M., Cherif, H., Guesmi, A., et al. (2013). Potential for plant growth promotion of Rhizobacteria associated with salicornia growing in tunisian hypersaline soils. *Biomed Res. Int.* 2013, 1–13. doi: 10.1155/2013/248078

Markakis, E. A., Fountoulakis, M. S., Daskalakis, G. C., Kokkinis, M., and Ligoxigakis, E. K. (2016). The suppressive effect of compost amendments on *Fusarium oxysporum* f.sp. radicis-cucumerinum in cucumber and *Verticillium dahliae* in eggplant. *Crop Prot.* 79, 70–79. doi: 10.1016/j.cropro.2015.10.015

Marques, J. M., da Silva, T. F., Vollú, R. E., de Lacerda, J. R. M., Blank, A. F., Smalla, K., et al. (2015). Bacterial endophytes of sweet potato tuberous roots affected by the plant genotype and growth stage. *Appl. Soil Ecol.* 96, 273–281. doi: 10.1016/j.apsoil.2015.08.020

Mendes, R., Garbeva, P., and Raaijmakers, J. M. (2013). The rhizosphere microbiome: Significance of plant beneficial, plant pathogenic, and human pathogenic microorganisms. *FEMS Microbiol. Rev.* 37, 634–663. doi: 10.1111/1574-6976.12028

Mora-Ruiz, M. D. R., Font-Verdera, F., Orfila, A., Rita, J., and Rosselló-Móra, R. (2016). Endophytic microbial diversity of the halophyte *Arthrocnemum macrostachyum* across plant compartments. *FEMS Microbiol. Ecol.* 92:fiw145. doi: 10.1093/femsec/fiw145

Munns, R. (2002). Comparative physiology of salt and water stress. *Plant. Cell Environ.* 25, 239–250. doi: 10.1046/j.0016-8025.2001.00808.x

Orhan, F., and Demirci, A. (2020). Salt stress mitigating potential of Halotolerant/Halophilic plant growth promoting. *Geomicrobiol. J.* 37, 663–669. doi: 10.1080/01490451.2020.1761911

Overbeek, R., Olson, R., Pusch, G. D., Olsen, G. J., Davis, J. J., Disz, T., et al. (2014). The SEED and the rapid annotation of microbial genomes using subsystems technology (RAST). *Nucleic Acids Res.* 42, D206–D214. doi: 10.1093/nar/gkt1226

Pascale, A., Proietti, S., Pantelides, I. S., and Stringlis, I. A. (2020). Modulation of the root microbiome by plant molecules: the basis for targeted disease suppression and plant growth promotion. *Front. Plant Sci.* 10:1741. doi: 10.3389/fpls.2019.01741

Peeters, N., Guidot, A., Vailleau, F., and Valls, M. (2013). *Ralstonia solanacearum*, a widespread bacterial plant pathogen in the post-genomic era. *Mol. Plant Pathol.* 14, 651–662. doi: 10.1111/mpp.12038

Pegg, G. G. F., and Brady, B. L. B. (2002). *Verticillium Wilts*. New York, NY: CABI.

Pérez-Jaramillo, J. E., Mendes, R., and Raaijmakers, J. M. (2016). Impact of plant domestication on rhizosphere microbiome assembly and functions. *Plant Mol. Biol.* 90, 635–644. doi: 10.1007/s11103-015-0337-7

Pisarska, K., and Pietr, S. J. (2012). Isolation and partial characterization of culturable endophytic *Arthrobacter* spp. from leaves of maize (*Zea mays* L.). *Commun. Agric. Appl. Biol. Sci.* 77, 225–233.

Qin, S., Zhang, Y. J., Yuan, B., Xu, P. Y., Xing, K., Wang, J., et al. (2014). Isolation of ACC deaminase-producing habitat-adapted symbiotic bacteria associated with halophyte *Limonium sinense* (Girard) Kuntze and evaluating their plant growth-promoting activity under salt stress. *Plant Soil* 374, 753–766. doi: 10.1007/s11104-013-1918-3

Quast, C., Pruesse, E., Yilmaz, P., Gerken, J., Schweer, T., Yarza, P., et al. (2013). The SILVA ribosomal RNA gene database project: improved data processing and web-based tools. *Nucleic Acids Res.* 41, D590–D596. doi: 10.1093/nar/gks1219

Rodriguez, P. A., Rothballer, M., Chowdhury, S. P., Nussbaumer, T., Gutjahr, C., and Falter-Braun, P. (2019). Systems biology of plant-microbiome interactions. *Mol. Plant* 12, 804–821. doi: 10.1016/j.molp.2019.05.006

Rodríguez-Blanco, A., Sicardi, M., and Frioni, L. (2015). Plant genotype and nitrogen fertilization effects on abundance and diversity of diazotrophic bacteria associated with maize (*Zea mays* L.). *Biol. Fertil. Soils* 51, 391–402. doi: 10.1007/s00374-014-0986-8

Ruppel, S., Franken, P., and Witzel, K. (2013). Properties of the halophyte microbiome and their implications for plant salt tolerance. *Funct. Plant Biol.* 40:940. doi: 10.1071/FP12355

Ryan, R. P., Germaine, K., Franks, A., Ryan, D. J., and Dowling, D. N. (2008). Bacterial endophytes: recent developments and applications. *FEMS Microbiol. Lett.* 278, 1–9. doi: 10.1111/j.1574-6968.2007.00918.x

Safdarian, M., Askari, H., Shariati, J. V., and Nematzadeh, G. (2019). Transcriptional responses of wheat roots inoculated with *Arthrobacter nitroguajacolicus* to salt stress. *Sci. Rep.* 9:1792. doi: 10.1038/s41598-018-38398-2

Saikkonen, K., Faeth, S. H., Helander, M., and Sullivan, T. J. (1998). FUNGAL ENDOPHYTES: a continuum of interactions with host plants. *Annu. Rev. Ecol. Syst.* 29, 319–343. doi: 10.1146/annurev.ecolsys.29.1.319

Salomon, M. V., Purpora, R., Bottini, R., and Piccoli, P. (2016). Rhizosphere associated bacteria trigger accumulation of terpenes in leaves of *Vitis vinifera* L. cv. Malbec that protect cells against reactive oxygen species. *Plant Physiol. Biochem.* 106, 295–304. doi: 10.1016/j.plaphy.2016.05.007

Shabala, S. (2013). Learning from halophytes: physiological basis and strategies to improve abiotic stress tolerance in crops. *Ann. Bot.* 112, 1209–1221. doi: 10.1093/aob/mct205

Tamura, K., and Nei, M. (1993). Estimation of the number of nucleotide substitutions in the control region of mitochondrial DNA in humans and chimpanzees. *Mol. Biol. Evol.* 10, 512–526. doi: 10.1093/oxfordjournals.molbev.a040023

Tamura, K., Peterson, D., Peterson, N., Stecher, G., Nei, M., and Kumar, S. (2011). MEGA5: molecular evolutionary genetics analysis using maximum likelihood, evolutionary distance, and maximum parsimony methods. *Mol. Biol. Evol.* 28, 2731–2739. doi: 10.1093/molbev/msr121

Tkacz, A., and Poole, P. (2015). Role of root microbiota in plant productivity. *J. Exp. Bot.* 66, 2167–2175. doi: 10.1093/jxb/erv157

Toju, H., Peay, K. G., Yamamichi, M., Narisawa, K., Hiruma, K., Naito, K., et al. (2018). Core microbiomes for sustainable agroecosystems. *Nat. Plants* 4, 247–257. doi: 10.1038/s41477-018-0139-4

Vaishnav, A., Shukla, A. K., Sharma, A., Kumar, R., and Choudhary, D. K. (2019). Endophytic bacteria in plant salt stress tolerance: current and future prospects. *J. Plant Growth Regul.* 38, 650–668. doi: 10.1007/s00344-018-9880-1

White, T. J., Bruns, T., Lee, S., and Taylor, J. (1990). "Amplification and direct sequencing of fungal ribosomal RNA genes for phylogenetics," in *PCR Protocols*, eds M. A. Innis, D. H. Gelfand, J. J. Sninsky, and T. J. White (San Diego: Academic Press), 315–322. doi: 10.1016/B978-0-12-372180-8.50042-1

Yao, Y., Tang, H., Su, F., and Xu, P. (2015). Comparative genome analysis reveals the molecular basis of nicotine degradation and survival capacities of *Arthrobacter*. *Sci. Rep.* 5:8642. doi: 10.1038/srep08642

Yoon, S.-H., Ha, S.-M., Kwon, S., Lim, J., Kim, Y., Seo, H., et al. (2017). Introducing EzBioCloud: a taxonomically united database of 16S rRNA gene sequences and whole-genome assemblies. *Int. J. Syst. Evol. Microbiol.* 67, 1613–1617. doi: 10.1099/ijsem.0.001755

Yuan, Z., Druzhinina, I. S., Labbé, J., Redman, R., Qin, Y., Rodriguez, R., et al. (2016). Specialized microbiome of a halophyte and its role in helping non-host plants to withstand salinity. *Sci. Rep.* 6:32467. doi: 10.1038/srep32467

Conflict of Interest: The authors declare that the research was conducted in the absence of any commercial or financial relationships that could be construed as a potential conflict of interest.

frontiers in Plant Science

ORIGINAL RESEARCH
published: 05 May 2021
doi: 10.3389/fpls.2021.664682

Reducing Nitrogen Input in Barley Crops While Maintaining Yields Using an Engineered Biostimulant Derived From *Ascophyllum nodosum* to Enhance Nitrogen Use Efficiency

*Oscar Goñi[1,2], Łukasz Łangowski[2], Ewan Feeney[2], Patrick Quille[1] and Shane O'Connell[1,2]**

[1] Plant Biostimulant Group, Shannon Applied Biotechnology Centre, Munster Technological University-Tralee, Tralee, Ireland, [2] Brandon Bioscience, Tralee, Ireland

OPEN ACCESS

Edited by:
Petronia Carillo, University of Campania Luigi Vanvitelli, Italy

Reviewed by:
Pradeep Kumar, Central Arid Zone Research Institute (ICAR), India
Luigi Lucini, Catholic University of the Sacred Heart, Italy

***Correspondence:**
Shane O'Connell
shane.oconnell@staff.ittralee.ie

Specialty section:
This article was submitted to Crop and Product Physiology, a section of the journal Frontiers in Plant Science

Received: 05 February 2021
Accepted: 08 April 2021
Published: 05 May 2021

Citation:
Goñi O, Łangowski Ł, Feeney E, Quille P and O'Connell S (2021) Reducing Nitrogen Input in Barley Crops While Maintaining Yields Using an Engineered Biostimulant Derived From Ascophyllum nodosum to Enhance Nitrogen Use Efficiency. Front. Plant Sci. 12:664682. doi: 10.3389/fpls.2021.664682

Intensive agricultural production utilizes large amounts of nitrogen (N) mineral fertilizers that are applied to the soil to secure high crop yields. Unfortunately, up to 65% of this N fertilizer is not taken up by crops and is lost to the environment. To compensate these issues, growers usually apply more fertilizer than crops actually need, contributing significantly to N pollution and to GHG emissions. In order to combat the need for such large N inputs, a better understanding of nitrogen use efficiency (NUE) and agronomic solutions that increase NUE within crops is required. The application of biostimulants derived from extracts of the brown seaweed *Ascophyllum nodosum* has long been accepted by growers as a sustainable crop production input. However, little is known on how *Ascophyllum nodosum* extracts (ANEs) can influence mechanisms of N uptake and assimilation in crops to allow reduced N application. In this work, a significant increase in nitrate accumulation in *Arabidopsis thaliana* 6 days after applying the novel proprietary biostimulant PSI-362 was observed. Follow-up studies in barley crops revealed that PSI-362 increases NUE by 29.85–60.26% under 75% N input in multi-year field trials. When PSI-362 was incorporated as a coating to the granular N fertilizer calcium ammonium nitrate and applied to barley crop, a coordinated stimulation of N uptake and assimilation markers was observed. A key indicator of biostimulant performance was increased nitrate content in barley shoot tissue 22 days after N fertilizer application (+17.9–72.2%), that was associated with gene upregulation of root nitrate transporters (*NRT1.1*, *NRT2.1,* and *NRT1.5*). Simultaneously, PSI-362 coated fertilizer enhanced nitrate reductase and glutamine synthase activities, while higher content of free amino acids, soluble protein and photosynthetic pigments was measured. These biological changes at stem elongation stage were later translated into enhanced NUE traits in harvested grain. Overall, our results support the agronomic use of this engineered ANE

that allowed a reduction in N fertilizer usage while maintaining or increasing crop yield. The data suggests that it can be part of the solution for the successful implementation of mitigation policies for water quality and GHG emissions from N fertilizer usage.

Keywords: biostimulant, *Ascophyllum nodosum* extract, nitrogen use efficiency, barley, yield, sustainability, GHG emissions

INTRODUCTION

Nitrogen (N) is a critical nutrient to provide optimal growth and yield of all agricultural crops. The invention of the Haber–Bosch process for the production of N and its role in the green revolution during the nineteen sixties led to transformative improvements in crop yields, allowing sustained population growth worldwide. Large amounts of N fertilizer are currently intensively supplemented by growers every season in the form of nitrate (NO_3^-), ammonium (NH_4^+) or urea. The annual global demand for N chemical fertilizers is continuously increasing and is driven by population growth and a global shift toward a more protein-rich diet in developing countries (Lassaletta et al., 2016). Estimated global N containing fertilizer use in 2020 was 110 Mt (IFA, 2019). However, it is also estimated that the energy demanding Haber–Bosch process for the production of N chemical fertilizers consumes 2% of the world's energy supply as fossil fuels, making N fertilizer expensive to produce and representing a relevant cost source for growers (Pfromm, 2017).

Nitrate is the predominant form of N taken up by plants from the soil due to its negative charge and high soil mobility, however most plants also benefit from inclusion of N in the form of ammonium in order to boost their N content (Hachiya and Sakakibara, 2017; Vidal et al., 2020). Crop plants are intrinsically inefficient at accessing applied N. Depending on the crop, agronomy practices and soil type, more than half of the supplemented N fertilizer can be lost to the environment (Raun and Johnson, 1999; White and Brown, 2010; Gutiérrez, 2012; Yan et al., 2020). These losses are not only increasing the cost of production but most importantly are increasing environmental pollution. Nitrogen fertilizers that are not retained in the soil, are washed out and leached to waterways and into groundwater. Nitrogen is an important contributor to eutrophication and water quality (Ascott et al., 2017; Wang et al., 2019). Furthermore, high amounts of greenhouse gas (GHG) emissions are associated with N use, either directly through N fertilizer production (mainly CO_2 and N_2O) or indirectly via emission of nitrous oxide gas (N_2O) by denitrification processes in the soil (Schaufler et al., 2010). Therefore, maintaining high crop yields while decreasing N fertilizer requirements by improving N use efficiency (NUE) in crops is essential to produce sustainable and environment friendly food. The potential economic benefits to growers of using N more efficiently is compelling, an improvement of NUE in crops by 1% could save approximately $1.1 billion annually (Kant et al., 2011; Kanter et al., 2015).

As a phenotypic trait, NUE is frequently defined by crop breeders/plant scientists as the rate of conversion of N input (e.g., N- fertilizer applied and/or soil N) into total plant biomass or specific plant organ biomass (e.g., grain yield). NUE is an inherently complex trait because it involves interaction between genetic, environmental and agronomy factors. NUE can be broken down into two different components for a crop: N uptake efficiency (Nupeff) and N utilization efficiency (Nuteff) (Moll et al., 1982; Anbessa and Juskiw, 2012; Hawkesford and Riche, 2020). Nupeff is the ratio of N taken up by the crop compared to what N is available from the soil and/or applied as fertilizer. Nuteff can be calculated as the amount of crop produced per unit of N taken up by the crop. The plant biological processes responsible for NUE include: N uptake, N transport, N assimilation, N translocation and recycling when the plant or its organs are aging. Each step is tightly controlled at gene transcriptional, translational, and post-translational level and includes low and high-affinity N transporters (Noguero and Lacombe, 2016; Hachiya and Sakakibara, 2017; Wang et al., 2018; Vidal et al., 2020) along with enzymes related to N assimilation pathways such as nitrate reductase (NR), glutamate synthase (GOGAT), and glutamine synthetase (GS) (Tischner, 2000; Masclaux-Daubresse et al., 2010; Pratelli and Pilot, 2014; Hirel and Krapp, 2020).

Approaches for increasing NUE for crops includes selective plant breeding, genetic modification, soil management and fertilizer technologies/management. Breeding programs to obtain high grain yielding varieties growing under contrasting/reduced N regimes have focused on traits such as bigger root length or surface area, larger above-ground biomass, higher grain harvest index or enhanced photosynthetic capacity (Anbessa and Juskiw, 2012; Prey et al., 2019; Vicente et al., 2019; Voss-Fels et al., 2019). Genetic modification techniques have produced new varieties of some crops able to increase biomass and seed yield under reduced N inputs through manipulation of genes for N uptake and transport (Fang et al., 2013; Han et al., 2016; Wang et al., 2018; Li et al., 2020), N assimilation (Perchlik and Tegeder, 2017; James et al., 2018; Gao et al., 2019) and N remobilization (Chen et al., 2020). However, it is important to note that these new varieties have been mainly developed in pot or hydroponic systems and have not been validated in field conditions (Masclaux-Daubresse et al., 2010; Wang et al., 2018). The potential impact of novel fertilizer technologies such as urease and nitrification inhibitors or slow-release fertilizer coatings to enhance NUE and/or mitigate GHG emissions have been intensively studied over the last years, showing promising results. However, specific NUE data is limited and should be interpreted cautiously as only a few studies included reduced N rates in the trial designs (Snyder, 2017; Rose et al., 2018; Dimkpa et al., 2020).

The new EU Fertilising Products Regulation, which entered into force on 15 July 2019, establishes plant biostimulants as a separate category of fertilizers that are defined by their ability to

improve nutrient use efficiency, tolerance to abiotic stress and/or quality traits regardless of their nutrient content (EU Regulation 2019/1009, 2019). Plant biostimulants have gained significant attention from scientists, the agroindustry, and growers over recent years as more sustainable solutions for crop production are sought (Du Jardin, 2015; Rouphael and Colla, 2020). Globally, the biostimulant market accounted for $3.19 billion in 2019 and is expected to reach $9.22 billion by 2027, growing at a CAGR of 14.2% during the forecast period (Research and Markets, 2020). Biostimulants made using extracts from the brown seaweed *Ascophyllum nodosum* (ANE) are accepted as effective and robust products (Yakhin et al., 2017; Shukla et al., 2019). A number of publications have demonstrated that ANE biostimulants improve fruit quality (Frioni et al., 2018), reduce pod shattering (Łangowski et al., 2019), enhance tolerance to abiotic stresses (Goñi et al., 2018; Carmody et al., 2020) and improve nutrient uptake in diverse crops (Turan and Köse, 2004; Jannin et al., 2013; Billard et al., 2014; Sabir, 2014; Stamatiadis et al., 2015; Frioni et al., 2018; Laurent et al., 2020). However, little is known on how ANEs can influence mechanisms of N uptake and assimilation in crops under reduced N conditions. The integration of biostimulants with current crop husbandry practices to enhance NUE may present challenges (i.e., method of application, timing, rates, etc.) in some production systems. These challenges can be overcome with a consistent and positive yield response trend in field conditions, economic/environmental justification for their use and acceptance by relevant stakeholders of the supporting scientific evidence on the effectiveness of the technology.

In this study, we investigated the potential of an ANE based biostimulant, PSI-362, to increase NUE in barley crops under reduced N input in multi year field trials. The method of application of the biostimulant as a foliar spray or top dressing was also investigated. In order to assess the impact on NUE, well-established N uptake and assimilation plant parameters at phenotypical, metabolic, enzymatic, and molecular level were evaluated in the model plant *Arabidopsis thaliana* and barley crop. Overall, the results support the agronomic use of this engineered ANE that allowed a 25% reduction in N fertilizer usage while maintaining or increasing crop yield.

MATERIALS AND METHODS

Materials

ANE biostimulant containing the PSI-362 biomolecule complex was provided by Brandon Bioscience (Tralee, Ireland). The compositional characterization of PSI-362 was performed according to Carmody et al. (2020) and consisted of ash (43.7% w/w dry), carbohydrates (26.0% w/w dry), polyphenols (12.3% w/w dry) and other organic components (18% w/w dry). The N:P:K macronutrient content of PSI-362 was 0.4:0.1:8.0% w/v. Commercially available granular CAN + S (27% w/w N; 4% w/w S) was kindly provided by Target Fertilisers (Enniscorthy, Ireland). CAN + S was coated with PSI-362 biomolecule complex using standard fertilizer coating technology. All chemical reagents used for the biochemical assays were purchased from Sigma-Aldrich (Arklow, Ireland) and Bio-Rad (Watford, United Kingdom). Phytostrip tubes were purchased from 4titude Ltd. (Wotton, United Kingdom). The primers were purchased from Eurofins Genomics (Ebersberg, Germany).

Evaluation of PSI-362 in *Arabidopsis thaliana* Seedlings

An initial evaluation of the ability of PSI-362 to improve NUE and nitrate content was carried out using *Arabidopsis thaliana* (Col-0) seedlings. This experiment was based on a high throughput root microphenotyping platform published previously (Vasilieva et al., 2021). Arabidopsis seeds were sterilized and grown on Phytostrip tubes filled with a sterile solid medium and inserted into 96-well plates (six seeds per tube). This medium contained Phytagel, sucrose, ammonium nitrate as N source, magnesium chloride and calcium chloride. Once Arabidopsis seeds germinated, a liquid nutrient medium based on Gamborg's B-5 (B5) medium was added to the wells. Seedlings were subjected to two different N conditions by the selective addition of ammonium nitrate to this liquid medium (2.66 and 13.33 mM, respectively). PSI-362 was applied as biostimulant treatment to the same liquid medium under low and high N conditions at 0.04% w/v per well. Distilled water was applied as an untreated control. Arabidopsis seedlings grew for 6 days at a temperature of 22/21°C (day/night; 16/8 h) and 70% relative humidity (RH) under a light intensity of 100 $\mu mol \cdot m^{-2} \cdot s^{-1}$. After this time period, Arabidopsis seedling tissue was collected to determine nitrate content as described in Section "Measurement of N Metabolites, Free Amino Acids, and Soluble Protein."

Experimental Design of Barley Pot Trial

The pot experiments were performed in a cultivation room under controlled conditions (19/14°C with 16 h of light and 8 h of darkness and 80 ± 5% RH under a light intensity of 120 $\mu mol \cdot m^{-2} \cdot s^{-1}$). Winter barley plants (cv. Towers; **Supplementary Table 1**) were grown in pots with a capacity of 2 L filled with a model soil prepared by mixing one part of sand and two parts of coarse loamy soil from field trials area described in Section "Experimental Design of Field Trials With PSI-362 Applied as Foliar Spray" (bulk density 1.41 $g \cdot cm^{-3}$, pH 6.1, 33.60 $g \cdot kg^{-1}$ DW organic matter, 2.50 $g \cdot kg^{-1}$ DW total N, 230.77 $g \cdot kg^{-1}$ amino sugar-N, 2.59 $mg \cdot kg^{-1}$ DW available P, and 63.36 $mg \cdot kg^{-1}$ DW available K). Soil N, P, and K index was defined as 1, 1, and 2, respectively (Teagasc, 2015). Experiments were performed in three independent pots per treatment, with 20 plants per pot. Barley seeds were sown at a depth of 3 cm and plants were irrigated with 1 liter of water per pot every 3 days in order to create equal soil moisture conditions in all pots. Temperature and relative moisture content were recorded regularly with a portable USB data logger (EBI300 TH, Ebro Electronic). The experiment was completed for three different treatments: (1) untreated control fertilized with CAN + S; (2) treated with PSI-362 foliar spray and fertilized with CAN + S; (3) treated with CAN coated with PSI-362. Granular N fertilizer addition (CAN or coated CAN with PSI-362) was added to 7-day-old plants (growth stage GS12-14) on the soil surface at a rate

of 67 kg N·ha^{-1} (75% of recommended N at this growth stage). Treated plants with foliar spray received the same amount of PSI-362 as those that were treated with the coated fertilizer. The barley plants were harvested 14 days after receiving treatments (growth stage GS22-23). The root and the above ground parts of the plants were washed and dried at 100°C for 24 h to determine both fresh weight (FW) and dry weight (DW). The efficiency of the conversion of added inorganic N into total plant dry matter (DM) was calculated per independent pot:

$$NUE_{plant} = DM_{plant}/N_{fertilized}$$

Experimental Design of Field Trials With PSI-362 Applied as Foliar Spray

We initially investigated the effect of PSI-362 applied by foliar spray on grain yield and NUE in recommended spring and winter barley varieties (**Supplementary Table 1**) growing under reduced N fertilizer rate (75%) and compared to standard grower practice (100% N). These open-field experiments were conducted in Tralee, Co. Kerry, Ireland (52° 16′ N, 9° 41′ W and 16 m altitude) during the 2016, 2017, and 2018 growing seasons. The climate is classified as temperate oceanic (Cfb) according the Köppen climate classification. The average minimum, maximum and mean temperatures of 9.9°C, 18.2°C, and 14.1°C, and a mean monthly accumulated precipitation of 63.0 mm was recorded during the field trial period. The soil type was coarse loamy, and the previous crop grown in the field trial site was grass. Soil characteristics were evaluated every season and representative samples were collected in a W shaped pattern across the sampling area. Soil bulk density was measured with a volumetric cylinder, soil pH was measured in buffer pH 4–10 to also estimate the lime requirements, organic matter content was determined gravimetrically after burning the sample at 440°C for 12 h, total N evaluation was carried out using the Kjeldahl method, amino sugar quantification was performed using the Illinois test, and available K and P were extracted through the Morgan method and quantified by ICP-MS and spectrophotometry, respectively. The obtained values for these trials were: bulk density 1.22 g·cm^{-3}, pH 5.6–6.1, 43.10–49.50 g·kg^{-1} DW organic matter, 3.40–4.10 g·kg^{-1} DW total N, 305–388 g·kg^{-1} amino sugar-N, 2.98–3.92 mg·kg^{-1} DW available P, and 78.20–92.50 mg·kg^{-1} DW available K. Soil N, P, and K index was defined as 1, 2, and 2, respectively (Teagasc, 2015). Every year, the field trials area was rotated to overcome any carryover effects from the previous year.

Two spring and one winter barley varieties (cv. KWS Irina, cv. Mickle, and cv. KWS Towers; **Supplementary Table 1**) were sown by mechanic drilling at a seed rate of 180–190 and 150–160 kg·ha^{-1} between March-April and October, respectively. The experimental design was the same for all field trials sites: a randomized complete block with five replicates and experimental units (plots) measuring 3 m × 5 m (15 m^2). N fertilization was designed to follow conventional farming practices in Ireland according to the Agriculture and Food Development Authority (Teagasc) recommendations (Teagasc, 2015). A quantity of 155 and 117 kg N·ha^{-1} was supplied in two applications for spring barley growing under 100% N rate and 75% N rate, respectively. 200 and 150 kg N·ha^{-1} was supplied in four applications for winter barley growing under 100% and 75% N rate, respectively. Barley crops were treated three times by foliar spray with PSI-362 (1 L·ha^{-1}) at mid tillering stage (GS22-27), at early stem elongation stage (GS30-31), and at the start of the booting stage (GS41-43). Water was sprayed as a control in the untreated plants. A central 1 m^2 area from the plots was harvested manually at barley maturity (GS92) and processed by a cereal threshing machine. Grain yield was measured for each plot and corrected to a standard moisture of 20%. Additional information of the grower program for spring and winter barley trials can be found in **Supplementary Tables 2, 3**, respectively.

Experimental Design of Field Trials With PSI-362 Coated Fertilizer

In the 2019 growing season, the effect of PSI-362 coated CAN + S fertilizer on spring barley (cv. Gangway) was evaluated in two independent open-field trials under different reduced N fertilizer rates (73% and 88%) and compared to standard grower practice (100% N). Field 1 was laid out in Ardfert, Co. Kerry, Ireland (52° 22′ N, 9° 45′ W and 16 m altitude) from April 2 to August 28, 2019. Field 2 was conducted in Courtnacuddy, Co. Wexford, Ireland (52° 28′ N, 6° 42′ W and 82 m altitude) from April 1 to August 19, 2019. The climate for both locations is classified as temperate oceanic (Cfb) according the Köppen climate classification. The average minimum, maximum, and mean temperatures of 7.9°C, 15.4°C, and 11.7°C, and a mean monthly accumulated precipitation of 78.21 mm was recorded during the field 1 trial period. The field 2 trial period was characterized by an average minimum, maximum and mean temperatures of 6.7°C, 14.6°C, and 10.8°C, and a mean monthly accumulated precipitation of 90.73 mm. The field 1 soil type was coarse loamy, and the previous crop rotation was potato. The field 2 soil type was clay loam, and spring barley was grown in the previous rotation. Soil chemical characteristics for both fields were evaluated before sowing and after harvesting according to the same methodology described in Section "Experimental Design of Barley Pot Trial" (**Supplementary Tables 4, 5**). For both fields, soil N, P, and K index was defined as 1, 4, and 4, respectively (Teagasc, 2015).

Barley was sown at the beginning of April by mechanical drilling at a seed rate of 190 and 140 kg·ha^{-1} for field 1 and 2, respectively. Split plot design was used for both field trials and the average area of each condition (control 100% N or PSI-362 treated reduced N fertilizer) was 1.25 and 6.10 ha for field 1 and field 2, respectively. A quantity of 140.6 and 102.8 kg N·ha^{-1} was supplied in two applications for field 1 under untreated 100% N rate and PSI-362 treated 73% N rate, respectively. A common first application of NPK 10-10-20 (380 kg·ha^{-1}) was added first to both conditions on sowing. A second application with CAN + S (380 kg·ha^{-1}) and PSI-362 coated CAN + S (240 kg·ha^{-1}) was applied on untreated and treated plants at mid tillering stage (GS22-27), respectively. Regarding field 2, 158.1 and 140.5 kg N·ha^{-1} was supplied in two applications for untreated 100% N rate and PSI-362 treated 88% N rate, respectively. An

initial application of NPK 22-8-0 (375 kg·ha^{-1}) added in the seedbed to both conditions was followed by a second application with CAN + S (280 kg·ha^{-1}) and PSI-362 coated CAN + S (215 kg·ha^{-1}) to untreated and treated plants at mid tillering stage (GS22-27), respectively. Additional information of the grower program for both trials can be found in **Supplementary Table 6**.

Shoot and root tissue from untreated and treated fields were sampled and phenotypically evaluated 22 days after the second fertilizer application in plants at early stem elongation stage (GS30-31). The samples were snap-frozen in liquid nitrogen, ground and kept in −80°C until further biochemical, enzymatic and gene expression analysis. Field 1 was manually harvested at growth stage GS92 using at least six independent 1 m^2 plots and grain was processed through a cereal trashing machine. Field 2 was harvested at the same maturity stage using a combine harvester. Before grain harvest from each plot, whole plant samples were collected for further phenotypical determination.

Plant and Grain Measurements of Field Trials With PSI-362 Coated Fertilizer

Barley plants were harvested at 22 days after second fertilizer application (stage GS30-31) and at grain maturity (GS92). The number of plant tillers was also counted. Plants at early stem elongation stage (GS30-31) were divided into roots and shoots and FW was measured. Plant DW was determined by drying these fresh samples in a convection oven for 24 h at 100°C. Plants harvested at maturity stage (GS92) were divided into roots, grains, remaining ears (glumes and beards), and remaining shoots (stems and leaves) and dried for 72 h at 50°C before biomass determination. Obtained values were expressed at 20% moisture. The harvest index was calculated as the grain biomass divided by the above-ground plant biomass. Grain yield was determined from the harvested and trashed plots, corrected to a to a standard moisture of 20%, and extrapolated t·ha^{-1}. A random grain subsample from each plot was used to determine the thousand-grain weight (TGW). N content was determined in grain samples at 20% moisture through the Kjeldahl method and grain protein content was calculated by multiplying the N content by the barley-specific protein factor of 5.83 (Mariotti et al., 2008). Total P content was determined from the same grain digest samples of the Kjeldhal method through the molybdovanadate method. Total K content was determined in grain after nitric acid extraction and further evaluation by atomic emission spectroscopy.

Calculation of NUE and Its Components for Field Trials

NUE_{grain} was calculated as the yield of grain produced per unit of N fertilizer and expressed as kg grain per kg N fertilizer:

$$NUE_{grain} = Grain\ yield/N_{fertilized}$$

Grain N uptake efficiency ($Nupeff_{grain}$) was calculated as the grain N uptake (Nup_{grain}) in relation to the quantity of fertilizer and expressed as kg N available in grain per kg N fertilizer. Nup_{grain} was calculated by multiplying its nitrogen content ($N\%$) by grain yield at 20% moisture:

$$Nupeff_{grain} = Nup_{grain}/N_{fertilized} = (Grain\ yield \times (N\%)_{grain})/N_{fertilized}$$

Grain N utilization efficiency ($Nuteff_{grain}$) was calculated as the amount of grain produced per Nup_{grain} and expressed as kg grain per kg N available in grain:

$$Nuteff_{grain} = Grain\ yield/Nup_{grain} = Grain\ yield/(Grain\ yield \times (N\%)_{grain})$$

The soil N component was not considered for the calculation of NUE traits as per the methodology suggested by Prey et al. (2019).

Greenhouse gas emissions from field trials with PSI-362 coated fertilizer were estimated using a carbon footprint decision support tool for spring barley (AHDB, 2012) and expressed as kilograms of carbon dioxide equivalent ($kgCO_2e$) per hectare. The information required to calculate this carbon footprint was taken from field trial records (crop and soil type, grain yield and moisture, fertilizer rate, crop protection inputs, crop residue management, field energy use, and grain drying). PSI-362 manufacture carbon footprint was also included in the estimation for treated crops.

Measurement of N Metabolites, Free Amino Acids, and Soluble Protein

Nitrate content was determined in Arabidopsis seedlings and barley shoot tissue according to nitration of salicylic acid under acidic conditions as described by Hachiya and Okamoto (2017) and quantified as mg·g^{-1} DW. Free amino acids and ammonium extraction was performed by mixing 40 mg of barley shoot tissue with 800 µl of ethanol 70% (v/v), kept overnight at 4°C under dark and centrifuged at 20,000 × g for 10 min at 4°C. These supernatants were first used for the estimation of total free amino acids content using ninhydrin reagent. 100 µl of supernatant was mixed with 75 µl of reaction mixture [8% (w/v) ninhydrin in acetone] and incubated for 30 min at 80°C. After cooling at room temperature, 100 µl of ethanol 50% (v/v) was added and the absorbance was measured at 570 nm. After preparing a calibration standard curve with glutamic acid, total free amino acids content was expressed as mg·g^{-1} DW. Individual free amino acids and ammonium content was evaluated in the same extracts through a reversed phase high performance liquid chromatography (RP-HPLC) and UV detection at 280 and 300 nm of the aminoenones formed by the reaction of amino acids and ammonia with the derivatization reagent diethyl ethoxymethylenemalonate (DEEMM) (Gómez-Alonso et al., 2007). Compounds were identified by comparison of retention time to that of commercial standards, quantified by peak integration and expressed as mg·g^{-1} DW. Soluble protein content was measured from the extracts used for the NR and GS enzymatic assays (see section "NR and GS Activity Assays") through the modified version of the Bradford method in a 96

well plate using a protein-dye reagent (Bio-Rad) and expressed as $mg \cdot g^{-1}$ DW.

Measurement of Photosynthetic Pigments

Photosynthetic pigments from collected barley shoot tissue (chlorophyll a, chlorophyll b and carotenoids) were extracted by homogenizing 40 mg of shoot tissue with 1 ml of acetone 80% (v/v). After incubation for 5 h at 4°C, samples were centrifuged at 20,000 × *g* for 10 min at 4°C. The supernatants were collected and diluted with acetone 80% (v/v) before measuring the absorbance at 470, 647 and 663 nm. Empirical equations described by Lichtenthaler and Buschmann (2001) for total chlorophylls (chlorophyll a + chlorophyll b) and carotenoids concentrations were used and results were expressed as $mg \cdot g^{-1}$ DW.

NR and GS Activity Assays

For the extraction of NR and GS, frozen ground barley shoot tissue was homogenized in the extraction buffer [50 mM HEPES-KOH (pH 7.5), 10% glycerol (v/v), 2% (w/v) PVPP, 2 mM DTT, 1/300 dilution protease inhibitor cocktail P9599 (Sigma-Aldrich)] for 2 h at 4°C, followed by centrifugation at 20,000 × *g* for 20 min at 4°C. NR activity was measured in the obtained protein extracts in the absence of $MgCl_2$ (total activity) and in the presence of $MgCl_2$ (actual activity). The reaction was incubated for 45 min at 30°C after the addition of 60 µl of protein extract to 340 µl of reaction buffer containing 50 mM HEPES-KOH (pH 7.5), 10 mM KNO_3, 5 mM EDTA (total activity) or 5 mM $MgCl_2$ (actual activity), 10 mM FAD, 1 mM DTT, and 0.2 mM NADH. The reaction was stopped by adding 120 µl of 0.6 M zinc acetate and the samples were centrifuged at 25,000 × *g* for 5 min. The amount of produced nitrite was determined spectrophotometrically at 540 nm according Hachiya and Okamoto (2017) and NR activity was expressed as nmol $NO_2^- \cdot h^{-1} \cdot mg^{-1}$ protein. The activation state of NR was defined as the activity measured in the presence of 5 mM $MgCl_2$ divided by the activity measured in the presence of 5 mM EDTA (expressed as a percentage). GS was determined by incubating 60 µl of protein extract with 120 µl of reaction buffer (50 mM Tris-HCl (pH 7.5), 20 mM $MgSO_4$, 4 mM EDTA, 80 mM sodium glutamate, 6 mM hydroxylamine, and 8 mM ATP) for 60 min at 30°C. The reaction was stopped by adding 180 µl of 0.122 M $FeCl_3$, 0.5 M TCA, and 2 M HCl and the samples were centrifuged at 16,000 × *g* for 10 min at 4°C. The absorbance of γ-glutamylmonohydroxamate (γ-GHM) in the supernatant was measured at 560 nm, with γ-GHM used as the standard for the calibration curve. GS activity was expressed as µmol γ-GHM$\cdot h^{-1} \cdot mg^{-1}$ protein.

RNA Extraction and RT-qPCR

Total RNA was isolated from frozen ground barley root tissue harvested in field 1 by Plant/Fungi Total RNA Purification Kit (Norgen Biotek, Canada) following the manufacturer's instructions. RNA was treated with RNase-Free DNase I Kit (Norgen Biotek, Canada) in order to remove efficiently genomic DNA contamination. RNA concentration and purity was measured using Qubit (Thermo Fisher Scientific). Expression analysis of *HvNRT1.1* (*HORVU7Hr1G071600*), *HvNRT2.1* (*HORVU6Hr1G005590.1*), and *HvNRT1.5* (*HORVU6Hr1G070450.3*) genes was performed by RT-qPCR using a Roche LightCycler® 96 System (Roche, United Kingdom) and a LightCycler® RNA Master SYBR Green I one-step kit (Roche, United Kingdom) according to the manufacturer's instructions. The expression level of the barley *HvUBC9* (*HORVU5Hr1G088270*) gene was used as the reference. The $2^{-\Delta\Delta CT}$ method was used to quantify relative normalized gene expression levels. The primers sequences used are shown in **Supplementary Table 7**.

Statistical Analysis

Nitrate assessment in Arabidopsis seedlings was performed in at least four independent biological replicates per treatment and N condition (12 technical replicates per biological replicate). Phenotypic and NUE assessment of the barley pot trial was done in three independent pots, with 20 plants per pot. Grain yield, TGW, grain N content measurement, calculation of NUE derived traits, and GHG emissions was done in at least four independent biological replicates per treatment and variety. Soil characterization was performed in three independent replicates. Phenotype assessment in barley plants from field trials was carried out in at least 60 independent biological replicates. Shoot samples collected from barley plants at stage GS30-32 were pooled for further analysis. For biochemical and enzymatic analysis, at least four biological replicates of each treatment were performed, using three technical replicates per biological replicate. For gene expression analysis, at least three biological replicates of each treatment were performed, using three technical replicates per biological replicate. Statistics were evaluated with Sigma Plot 12 and Statgraphics Centurion XVI software. The differences between control and PSI-362 treatment for every field trial were analyzed using *t*-test at $p \leq 0.05$. The effect of different treatments on the barley pot trial was analyzed with the one-way analysis of variance (ANOVA) by Tukey's HSD test at $p \leq 0.05$. Arabidopsis nitrate data were compared by using two-way ANOVA, with Tukey's HSD test at $p \leq 0.05$. The application of all parametric tests was performed after checking the data normality (Shapiro–Wilk's test) and equal variance assumptions. Unless stated otherwise, all data are expressed as average ± standard error (SE). Details of the individual sample size for each analysis and statistical test used is mentioned in the tables and figure legends.

RESULTS

Effect of PSI-362 in Nitrate Content of Arabidopsis Seedlings Under Different N Levels

The effect of PSI-362 was first evaluated in seedlings of the model plant *Arabidopsis thaliana* using a high throughput root microphenotyping platform. When a two-way ANOVA test was

run, it was found that all three parameters (N level, PSI-362 treatment and N level × PSI-362 treatment) were statistically significant for nitrate content (**Figure 1**). Therefore, all data were subjected to *t*-test, comparing PSI-362 versus control effect under low and high N levels (2.66 and 13.33 mM of ammonium nitrate, respectively). While the different N amount added to untreated seedlings had a remarkable effect on nitrate content (low N: 2.69 $mg{\cdot}g^{-1}$ DW vs. high N: 26.46 $mg{\cdot}g^{-1}$ DW), our results also showed that PSI-362 applied through the root significantly increased this parameter by 11.92% ($p = 0.049$) and 6.85% ($p = 0.420$) compared to the low and high N control, respectively (**Figure 1**). It would suggest that PSI-362 can improve capacity for nitrate uptake in Arabidopsis under controlled conditions in the N range tested, but with the best performance at the lowest N rate.

Effect of PSI-362 Mode of Application on Pot Experiments in Barley

Granular CAN + S fertilizer was coated with PSI-362 and its biostimulant effect on plant biomass and NUE_{plant} was compared with the same amount of PSI-362 applied by a single foliar spray in a winter barley pot trial. As can be observed in **Figure 2**, regardless of the method of application, both PSI-362 treatments significantly increased plant biomass between 13.88 and 16.67% compared to untreated plants fertilized with the same amount of N ($p \leq 0.05$). The measured phenotypic change also demonstrated a superior NUE_{plant} for barley plants treated with either PSI-362 coated fertilizer (+15.03%) or foliar PSI-362 (+17.19%), indicating that bioactive molecules from PSI-362 can be easily released from CAN + S granules and stimulate the plants through their root system to utilize N fertilizer more efficiently.

Effect of PSI-362 Applied by Foliar Spray on Barley Yield and NUE

Three 1L/Ha foliar applications of PSI-362 (at tillering, stem elongation and booting stage) on recommended spring and winter barley varieties growing under reduced N fertilizer rate (75%) resulted in no difference or significantly higher grain yield for 5 out 5 field trials performed during 2016 to 2018 compared to plants growing under the recommended rate in standard agricultural practice ($p \leq 0.05$) (**Figure 3**). Overall, PSI-362 treated barley varieties showed a statistically significant 3-year average yield increase of 5.57% ($p = 0.011$) using 25% less N. Similarly, the NUE_{grain} of the PSI-362 treatments was 29.85–60.26% higher than those of the control conditions ($p \leq 0.05$) (**Supplementary Table 8**). The data demonstrates the ability of PSI-362 to deliver yield with a 25% reduction of N mineral fertilizer, significantly enhancing the amount of barley grain per unit of N supplied under field conditions.

Effect of PSI-362 Coated Fertilizer on Vegetative Parameters at Early Stem Elongation Stage

In order to explore the effect of PSI-362 coated fertilizer on vegetative traits in spring barley, a comparative phenotypical analysis was performed on plants harvested at 22 days after the second fertilizer application (stage GS30-31). This analysis was performed on two independent field trials characterized by a different reduction of N fertilizer rate. Barley plants treated with PSI-362 coated fertilizer from field 1 (73% N) increased their shoot FW, root FW, root DW and number of tillers per plant by 6.91, 10.79, 21.05% and 9.45% compared to 100% N control, but these changes were not statistically significant ($p > 0.05$). While the effect of PSI-362 coated fertilizer in field 2 (88% N) was not statistically significant either, the mean values of shoot DW, root FW and root DW showed a similar increasing trend compared to the untreated plants (+14.11, +6.56, and +16.43%, respectively) (**Table 1**).

Effect of PSI-362 Coated Fertilizer on N Uptake, Metabolic and Molecular Parameters

The PSI-362 coated fertilizer was applied at mid tillering stage (GS22-27), just before the stem elongation phase (GS30-39), which is the most important timing on spring barley for N uptake (Teagasc, 2015). In order to assess the long term impact of the biostimulant on N uptake and assimilation parameters, a metabolic analysis of shoot samples collected 22 days after application was performed. N uptake in control and treated plants at stage GS30-31 was evaluated through the measurement of shoot nitrate content. Plants treated with PSI-362 coated fertilizer significantly increased this parameter in field 1 (+17.87%, $p = 0.046$) and field 2 (+72.23%, $p \leq 0.001$) compared to control plants growing under 100% N rate (**Table 2**). To provide some insights on the effect of PSI-362 coated fertilizer on N uptake mechanisms, the relative gene expression levels of three major nitrate transporters, namely *NRT1.1* and *NRT2.1*, both expressed in epidermal and cortical cells, and *NRT1.5*, expressed in root pericycle cells were measured (Vidal et al., 2020). The root tissue of barley plants at stage GS30-31 was collected from plants of field 1, which had a similar N fertilizer program as the field trials performed between 2016 and 2018. The application of PSI-362 coated fertilizer caused a significant upregulation within *NRT1.1*, *NRT2.1*, and *NRT1.5* expression levels by 1. 77-, 1. 72-, and 1.21-fold with respect to the 100% N control ($p \leq 0.001$), suggesting increased root capacity for nitrate uptake and transport in barley crop under field conditions (**Figure 4**).

Effect of PSI-362 Coated Fertilizer on N Assimilation Metabolic Parameters

In order to assess the impact of PSI-362 coated fertilizer 22 days after application on well-known N assimilation parameters, a metabolic analysis of shoot samples from control and treated plants at early stem elongation stage (GS31-32) was performed. While reduced N fertilizer levels decreased shoot ammonium content in treated plants from field 1 (−15.56%, $p = 0.044$) and field 2 (−20.89%, $p = 0.015$), an opposite trend was observed in the content of total free amino acids. The effect of PSI-362 coated fertilizer on this N-assimilation parameter was consistent. Treated plants from field 1 and field 2 growing under 73 and 88% N fertilization levels, respectively, had significantly increased total free amino acid content in shoot tissue by 23.25% ($p = 0.021$)

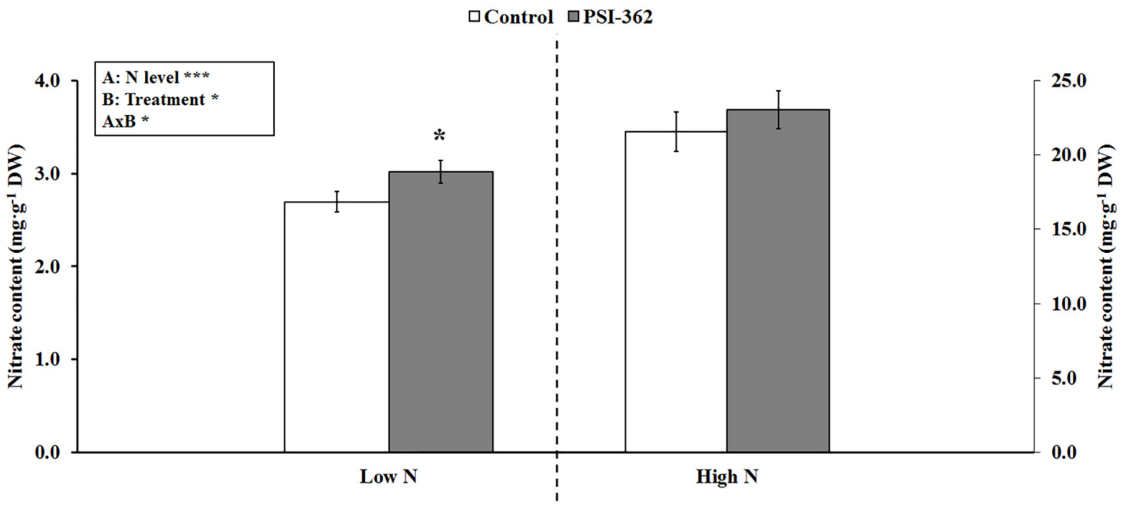

FIGURE 1 | Nitrate content in Arabidopsis seedlings. The effect of PSI-362 added by root application to Arabidopsis seedlings growing under low and high N levels (2.66 and 13.33 mM ammonium nitrate, respectively) was evaluated 6 days after application. Since interaction AxB was significant (***$p \leq 0.001$), data were subjected to *t*-test, comparing PSI-362 treatment versus control within the same N level. In this case, means followed by asterisk indicate statistically significant differences between control and PSI-362 treatment within the same N level (*$p \leq 0.05$). Number of biological replicates ($n \geq 4$).

	Control	PSI-362 foliar	PSI-362 coated CAN+S
Biomass (g FW·plant^{-1})	**0.72 ± 0.02** a	**0.84 ± 0.02** b	**0.82 ± 0.02** b
NUE_{plant} (g DW·g^{-1}N)	**12.04 ± 0.42** a	**14.11 ± 0.57** b	**13.85 ± 0.48** b

FIGURE 2 | Effect of PSI-362 treatment applied by foliar spray or coated with CAN + S fertilizer on plant biomass and NUE of winter barley (cv. Towers). A pot trial was performed to evaluate if the application mode of PSI-362 (foliar spray or coated with N mineral fertilizer) affected differently to barley growth and compared with an untreated control. Fertilizer (CAN + S) and PSI-362 biostimulant were added to plants at 2–3 leaf stage (GS12–13) at the same time. The dose of PSI-362 applied by foliar spray or coating was exactly the same and control plants were sprayed with distilled water. The phenotypical assessment was performed 14 days after fertilizer/PSI-362 treatment application. Means followed by different small letter within the same row indicate significant differences between treatments based on one-way ANOVA Tukey's HSD test at $p \leq 0.05$. Number of biological replicates (plant biomass, $n = 60$; NUE, $n = 3$).

and 22.71% ($p = 0.050$) compared to the untreated shoots (**Table 2**). Glutamate was the major component of the free amino acids pool, together with glutamine, aspartate, asparagine, alanine, and serine. PSI-362 coated fertilizer strongly affected glutamate, increasing it to 18.95% ($p = 0.006$) and 46.84% ($p \leq 0.001$) of the control values in shoot tissue of field 1 and field 2, respectively. This biostimulant treatment had a similar effect on glutamine, another key N metabolite that has an important role as amino group donor to form other amino acids, with a significant increase of 29.33 and 153.30% ($p \leq 0.001$) in PSI-362 treated plants. Aspartate increased by 28.04% ($p = 0.005$) and 112.87% ($p \leq 0.001$) in treated shoots from field 1 and field 2, respectively; while asparagine only showed a significant 4.3-fold increase ($p \leq 0.001$) in treated plants from field 2. The results in **Table 2** also demonstrated that in barley plants treated with PSI-362 coated fertilizer the endogenous proline content increased significantly in both fields compared to 100% N control (+16.41–20.16%; $p \leq 0.05$). This same stimulating

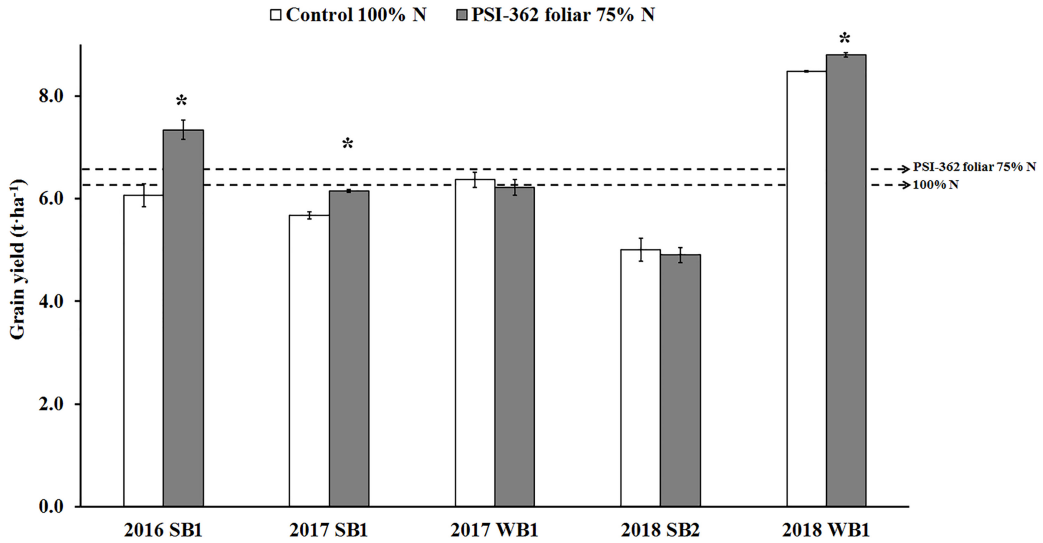

FIGURE 3 | Effect of foliar PSI-362 treatment on grain yield of spring and winter barley varieties growing under 75% N fertilizer rate in 3 consecutive seasons (2016–2018). PSI-362 was applied three times by foliar spray at mid tillering stage (GS22-27), early stem elongation stage (GS30-31), and at the start of the booting stage (GS41-43), and its performance was benchmarked against untreated plants growing under 100% N fertilizer rate. SB1, spring barely cv. KWS Irina; WB1, winter barley cv. KWS Towers; SB2, spring barley cv. Mickle. Chart represents grain yield (t·ha^{-1}) expressed at 20% moisture. Means followed by asterisk indicate statistically significant differences between control and PSI-362 treatment within the same field trial based on *t*-test at $p \leq 0.05$. The horizontal dashed lines represent the average yield value for untreated 100% N (6.24 t·ha^{-1}) and foliar PSI-362 75% N (6.57 t·ha^{-1}). Number of plots harvested per field trial ($n \geq 5$).

TABLE 1 | Effect of PSI-362 coated CAN + S fertilizer on phenotypic parameters in barley crop (cv. Gangway) 22 days after application.

Parameter[1]	Field 1		Field 2	
	Control 100% N	PSI-362 coated 73% N	Control 100% N	PSI-362 coated 88% N
Shoot FW (g plant^{-1})	5.26 ± 0.26	5.62 ± 0.76	5.74 ± 0.32	6.55 ± 0.08
Shoot DW (g plant^{-1})	0.57 ± 0.03	0.54 ± 0.07	0.54 ± 0.02	0.57 ± 0.01
Root FW (g plant^{-1})	0.64 ± 0.06	0.71 ± 0.10	0.41 ± 0.02	0.43 ± 0.02
Root DW (g plant^{-1})	0.13 ± 0.01	0.16 ± 0.02	0.08 ± 0.01	0.10 ± 0.01
Number tillers per plant	4.23 ± 0.47	4.63 ± 0.68	4.83 ± 0.16	4.84 ± 0.24

[1] *Data are the means ± SE. Number of biological replicates (n = 30). No statistically significant differences between control and treated sample at p ≤ 0.05 were observed (t-test).*

effect by coated PSI-362 fertilizer under reduced N rate was also observed for alanine (+12.83–14.61%), serine (+2.94–18.12%), glycine (+7.70–55.15%), and essential amino acids such as methionine (+8.07−37.90%), lysine (+12.19−19.20%), and threonine (+14.27–80.48%) content.

The ability of PSI-362 coated fertilizer to influence N assimilation early in the stem elongation stage was also evaluated through the measurement of soluble protein and photosynthetic pigments content in shoot tissue (**Table 2**). Higher protein content in shoot tissue relative to 100% N control were observed for barley plants fertilized with PSI-362 coated CAN + S at 73% N (+24.86, $p \leq 0.001$) and 88% N (+21.84, $p \leq 0.001$) rate. Accumulation of both chlorophylls (a + b) was similarly affected in treated plants, increasing by 36.24% ($p = 0.003$) and 30.28% ($p = 0.050$) in field 1 and field 2, respectively. Finally, this ANE biostimulant also induced a statistically significant accumulation of carotenoids in the shoots of barley plants growing with reduced N (+40.50–60.92%).

Effect of PSI-362 Coated Fertilizer on NR and GS Activity

Total NR activity in barley shoots of control plants growing under 100% N rate was very similar for both field 1 and field 2 (15.69 and 17.94 nmol $NO_2^- \cdot h^{-1} \cdot mg^{-1}$ protein, respectively) (**Figure 5**). As expected, actual NR activity in presence of $MgCl_2$ was lower and the calculated activation state for untreated plants ranged between 60.91% (field 1) and 50.92% (field 2). While the application of PSI-362 coated fertilizer led to a significant increase in NR activity in shoot tissue of plants at stage GS31-32, the magnitude of this variation differed between field 1 and field 2, being directly correlated to nitrate content measured in the same tissue (**Table 2**). Treated plants growing under 73% N increased their total NR activity in shoot tissue by 24.82% ($p = 0.019$) compared to control (**Figure 5A**). However, this activity was 4.7-fold higher in shoots of treated plants growing in field 2 (**Figure 5B**). Interestingly, the NR activation state also increased

TABLE 2 | Effect of PSI-362 coated CAN + S fertilizer on N forms (nitrate and ammonia), free amino acids, soluble protein, and photosynthetic pigments in barley shoot tissue (cv. Gangway) at 22 days after application.

Metabolite[1]	Field 1		Field 2	
	Control 100% N	PSI-362 coated 73% N	Control 100% N	PSI-362 coated 88% N
Nitrate (mg·g^{-1} DW)	12.72 ± 0.45	14.99 ± 0.66*	14.15 ± 1.57	24.37 ± 0.39***
Ammonia (mg·g^{-1} DW)	0.16 ± 0.01	0.13 ± 0.01*	0.21 ± 0.01	0.16 ± 0.01*
Free total amino acids (mg·g^{-1} DW)	36.40 ± 1.62	44.86 ± 1.21*	36.80 ± 2.42	45.16 ± 1.69*
Glutamate (mg·g^{-1} DW)	7.29 ± 0.29	8.68 ± 0.26**	6.91 ± 0.35	10.15 ± 0.55***
Glutamine (mg·g^{-1} DW)	1.38 ± 0.04	1.78 ± 0.05***	1.02 ± 0.08	2.58 ± 0.12***
Aspartate (mg·g^{-1} DW)	2.26 ± 0.10	2.89 ± 0.14**	1.36 ± 0.09	2.89 ± 0.14***
Asparagine (mg·g^{-1} DW)	0.94 ± 0.19	1.11 ± 0.18	0.43 ± 0.05	2.30 ± 0.13***
Proline (mg·g^{-1} DW)	0.66 ± 0.01	0.77 ± 0.01*	0.47 ± 0.02	0.57 ± 0.02*
Alanine (mg·g^{-1} DW)	1.25 ± 0.03	1.41 ± 0.04*	1.38 ± 0.11	1.59 ± 0.19
Serine (mg·g^{-1} DW)	0.96 ± 0.05	0.98 ± 0.04	0.74 ± 0.02	0.87 ± 0.03*
Glycine (mg·g^{-1} DW)	0.11 ± 0.01	0.12 ± 0.01	0.16 ± 0.01	0.26 ± 0.01***
Methionine (mg·g^{-1} DW)	0.20 ± 0.01	0.28 ± 0.03*	0.25 ± 0.01	0.27 ± 0.01
Lysine (mg·g^{-1} DW)	0.45 ± 0.02	0.50 ± 0.02	0.40 ± 0.01	0.47 ± 0.03*
Threonine (mg·g^{-1} DW)	0.33 ± 0.02	0.37 ± 0.02	0.27 ± 0.02	0.48 ± 0.05***
Soluble protein (mg·g^{-1} DW)	115.61 ± 4.34	144.35 ± 6.10***	136.04 ± 4.12	165.75 ± 4.58***
Total chlorophyll (a + b) (mg·g^{-1} DW)	8.63 ± 0.32	11.75 ± 0.22**	6.55 ± 0.23	10.17 ± 0.20***
Carotenoids (mg·g^{-1} DW)	1.79 ± 0.08	2.34 ± 0.14*	1.52 ± 0.05	2.10 ± 0.03***

[1]*Data are the means ± SE. Number of biological replicates ($n \geq 4$).*
*Difference between control and treated sample within the same field was significant at *$p \leq 0.05$, **$p \leq 0.01$, and ***$p \leq 0.001$, respectively (t-test).*

significantly with PSI-362 coated fertilizer treatment ($p \leq 0.001$), reaching values of 70.53 and 65.63% for plants from field 1 and field 2, respectively.

GS activity was also assayed in shoots of barley plants 22 days after the second N fertilizer application. Similarly to NR activity, control plants growing under 100% N rate showed comparable GS activity values in field 1 and field 2 (3.22 and 3.80 μmol γ-GHM·h^{-1}·mg^{-1} protein, respectively). GS activity was also significantly stimulated by PSI-362 coated fertilizer, increasing its γ-glutamyl transferase activity in plants from field 1 (+30.63%, $p = 0.014$) and field 2 (+7.39%, $p = 0.035$) (**Figure 6**).

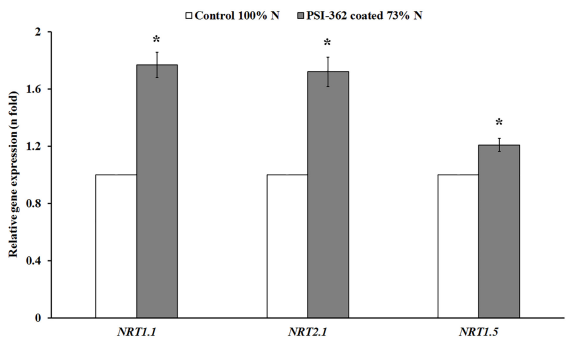

FIGURE 4 | Relative expression of major nitrate transporter genes in spring barley root tissue (cv. Gangway). The effect of PSI-362 coated CAN + S fertilizer on the relative expression of *HvNRT1.1*, *HvNRT2.1*, and *HvNRT1.5* in root tissue 22 days after application in field 1 (73% N fertilizer rate). Results are expressed as the relative $\log_2$ fold-change with respect to the *HvUBC9* gene expression level and benchmarked against untreated plants growing under 100% N fertilizer rate. The error bars represent SE and means followed by asterisk within the same gene and field indicate significant differences between control and the PSI-362 treatment based on *t*-test at $p \leq 0.05$. Number of biological replicates ($n = 3$).

Effect of PSI-362 Coated Fertilizer on Plant and Grain Parameters at Harvest

The results presented in **Table 3** indicate that the application of PSI-362 coated fertilizer in barley grown under reduced N fertilizer rate did not have a statistically significant effect on total plant biomass at harvest compared to control crop fertilized at 100% N rate. While a reduction of 27% N in field 1 was translated in a higher biomass in treated plants (+8.14%, $p = 0.319$), no significant difference was recorded in field 2 (−0.94%, $p = 0.957$). Barley plants from field 1 fertilized with PSI-362 coated CAN + S were characterized as having a significantly higher number of tillers at maturity stage (+23.30%, $p = 0.030$), but this effect was not observed in field 2 (**Table 3**). Interestingly, the application of PSI-362 coated fertilizer was characterized by a higher harvest index in both fields (11.31–18.37%), and this increase in dry matter partitioned to the grain was statistically significant for treated barley plants growing with 88% N ($p = 0.044$).

Harvested grain yield differences between control plants grown under 100% N and those treated with PSI-362 coated fertilizer at reduced N rate showed a similar trend to that observed in barley trials developed from 2016 to 2018: either these differences were significantly higher in treated plants growing under 73% N rate (+3.70%, $p = 0.042$) or PSI-362 coated fertilizer led to no statistically significant difference in grain yield compared to control in field 2 ($p = 0.780$). An opposite trend was observed for the thousand grain weight (TGW) and protein

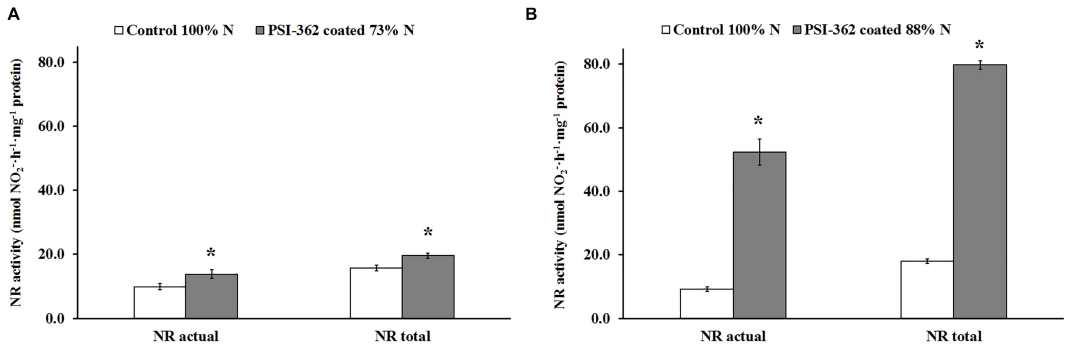

FIGURE 5 | NR activity in spring barley shoot tissue (cv. Gangway). The effect of PSI-362 coated CAN + S fertilizer on actual NR (in presence of $MgCl_2$) and total NR (in absence of $MgCl_2$) activity was evaluated in shoot tissue 22 days after application. **(A)** Barley crop grown in the field 1 under 73% N recommended fertilizer rate; **(B)** barley crop grown in the field 2 under 88% N recommended fertilizer rate. Results in treated plants were benchmarked against untreated plants growing under 100% N fertilizer rate. Means followed by asterisk within the same NR activity type and field indicate significant differences between control and the PSI-362 treatment based on *t*-test at $p \leq 0.05$. Number of biological replicates ($n \geq 4$).

content in both fields. While there were minimal differences in both parameters between treated and control crop in field 1, a significant increase of grain protein content (+12.50%, $p \leq 0.001$) and higher TGW (3.68%, $p = 0.095$) was observed in barley treated with PSI-362 fertilizer at 88% N rate compared to untreated crop grown under 100% N rate. Concerning other macronutrients such as P and K, there were no statistically significant differences in their content between grain harvested from treated and untreated plants (**Table 3**).

Effect of PSI-362 Coated Fertilizer on NUE and Environmental Parameters

The process of conversion of N fertilizer into grain biomass was evaluated through the amount of grain yield harvested per amount of N supplied to plants (NUE_{grain}). There was a consistent increase of this parameter for treated crop in field 1 (+41.83%, $p \leq 0.001$) and field 2 (+9.13%, $p = 0.225$), which agrees with the observed results in previous trials with PSI-362 applied as foliar spray (**Supplementary Table 7**). Because NUE_{grain} is mathematically the product of $Nupeff_{grain} \times Nuteff_{grain}$, both second level traits were also calculated. The plant capacity to take up soil available N by the plant and allocate it to the grain was measured through $Nupeff_{grain}$ trait. Overall, barley crop treated with PSI-362 coated fertilizer significantly enhanced this parameter in both field 1 (+40.95%, $p \leq 0.001$) and field 2 (+21.92%, $p = 0.011$), being the main contribution to the observed variation between treated and control NUE_{grain} and confirming the ability of PSI-362 to recover N more efficiently (**Table 4**). However, we did not observe statistically significant differences between treated and untreated plants in the $Nuteff_{grain}$, remaining similar in field 1 (+0.36%, $p = 0.942$) or decreasing in field 2 (−10.49%, $p = 0.355$). Therefore, it indicates that this trait was not substantially impacting on NUE_{grain} variation (**Table 4**).

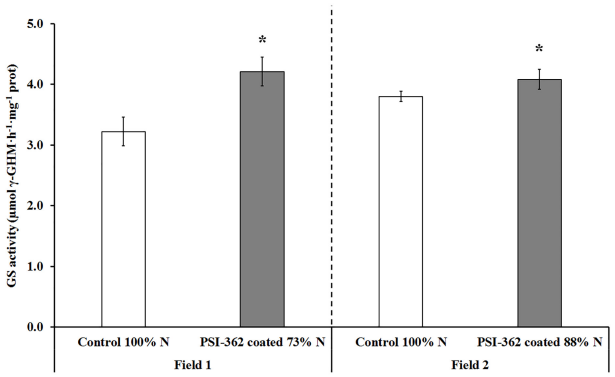

FIGURE 6 | GS activity in spring barley shoot tissue (cv. Gangway). The effect of PSI-362 coated CAN + S fertilizer on GS activity was evaluated in shoot tissue 22 days after application. **Field 1:** Barley crop grown in the field 1 under 73% N recommended fertilizer rate. **Field 2**: barley crop grown in the field 2 under 88% N recommended fertilizer rate. Results in treated plants were benchmarked against untreated plants growing under 100% N fertilizer rate. Means followed by asterisk within the same field indicate significant differences between control and the PSI-362 treatment based on *t*-test at $p \leq 0.05$. Number of biological replicates ($n \geq 4$).

Despite these differences on N uptake efficiency, there were no statistically significant differences in the soil total N between control and treated plots after harvesting the crop (**Supplementary Tables 4, 5**). In addition, there were also no statistically significant differences in the content of available P and K before sowing and after harvesting in either field 1 or field 2. A higher content of amino sugar determined through the Illinois test in the organic fraction of soils treated with PSI-362 coated fertilizer after harvesting in field 1 (+30.21%, $p = 0.085$) and field 2 (+20.83%, $p = 0.096$) was recorded.

Estimated GHG emission calculations show that the application of PSI-362 led to a reduction in GHG emissions per hectare of cultivated area. The carbon equivalent emission estimate decreased nearly 22% for the treated crop growing under 73% N in field 1 (-483.52 $kgCO_2e \cdot ha^{-1}$), whereas this reduction was closer to 9% (-224.49 $kgCO_2e \cdot ha^{-1}$) with the application of PSI-362 coated fertilizer at 88% N rate in field 2 (**Table 4**).

TABLE 3 | Effect of PSI-362 coated CAN + S fertilizer on plant and grain derived parameters in barley crop (cv. Gangway) at harvest.

Parameter[1]	Field 1		Field 2	
	Control 100% N	PSI-362 coated 73% N	Control 100% N	PSI-362 coated 88% N
Plant biomass[2] (g plant^{-1})	7.15 ± 0.04	7.74 ± 0.25	6.53 ± 0.73	6.47 ± 0.48
Number tillers per plant	3.17 ± 0.14	3.90 ± 0.17*	3.32 ± 0.13	3.19 ± 0.12
Harvest index (g·g^{-1})	0.57 ± 0.05	0.67 ± 0.04	0.53 ± 0.02	0.60 ± 0.01*
Grain yield[2] (T·ha^{-1})	6.36 ± 0.15	6.60 ± 0.11*	9.93 ± 0.60	9.63 ± 0.28
TGW (g)	52.58 ± 0.28	52.49 ± 0.26	48.24 ± 0.80	50.02 ± 0.50
Grain protein concentration (%w/w)	8.36 ± 0.39	8.31 ± 0.13	9.60 ± 0.09	10.80 ± 0.01***
Grain P content(%w/w)	0.28 ± 0.02	0.28 ± 0.03	0.28 ± 0.02	0.26 ± 0.02
Grain K content(%w/w)	0.44 ± 0.02	0.42 ± 0.03	0.44 ± 0.04	0.43 ± 0.02

[1]Data are the means ± SE. Number of biological replicates (n ≥ 4).
[2]Plant biomass, grain yield and grain characterization were expressed at 20% moisture.
*Difference between control and treated sample within the same field was significant at *p ≤ 0.05, and ***p ≤ 0.001, respectively (t-test).*

TABLE 4 | Effect of PSI-362 coated CAN + S fertilizer on NUE and environmentally derived parameters in barley crop (cv. Gangway) at harvest.

Parameter[1]	Field 1		Field 2	
	Control 100% N	PSI-362 coated 73% N	Control 100% N	PSI-362 coated 88% N
NUE_{grain} (kg grain·kg^{-1} N fertilizer)	45.25 ± 1.31	64.18 ± 1.06***	62.81 ± 4.89	68.54 ± 1.96
$Nupeff_{grain}$ (kg N grain·kg^{-1} N fertilizer)	0.65 ± 0.06	0.91 ± 0.01***	1.04 ± 0.05	1.27 ± 0.01*
$Nuteff_{grain}$ (kg grain·kg^{-1} N grain)	69.76 ± 2.26	69.97 ± 1.38	60.31 ± 4.70	53.98 ± 1.55
GHG emissions (tCO_2e·ha^{-1})	2.23 ± 0.07	1.74 ± 0.05***	2.54 ± 0.19	2.31 ± 0.07

[1]Data are the means ± SE. Number of biological replicates (n ≥ 4).
*Difference between control and treated sample within the same field was significant at *p ≤ 0.05, and ***p ≤ 0.001, respectively (t-test).*

DISCUSSION

Nitrogen fertilizer application rates are currently unsustainable, both environmentally (e.g., N pollution of soil, water and GHG emissions) and economically (e.g., reduced grower margins). A recent data compilation from 230 studies has reported that cereal crops only take up between 36% and 42% of applied N fertilizer (Yan et al., 2020), confirming previous low NUE estimations for cereal production (Raun and Johnson, 1999; Omara et al., 2019). Therefore, enhancing NUE is a necessity for developing sustainable agricultural production to feed a growing world population. The ability of ANE biostimulants to influence N uptake and assimilation mechanisms have been previously investigated in controlled conditions in the model plant *A. thaliana* (Durand et al., 2003), and crop plants such as oilseed rape (Jannin et al., 2013; Billard et al., 2014) and durum wheat (Laurent et al., 2020). In this study, it has been demonstrated under field conditions that an engineered biostimulant derived from *Ascophyllum nodosum*, PSI-362, is capable of increasing NUE_{grain} in barley by 29.85–60.26% when compared to current standard grower practices without compromising yields. Two methods of application of the biostimulant to barley were evaluated; foliar spray and top dressing via biostimulant coated granular fertilizer, with the effectiveness of the biostimulant evident for both methods in pot and field trials. Along with several enhanced N assimilation markers, a key indicator of biostimulant performance was increased nitrate content in barley shoot tissue 22 days after N fertilizer application. Additional plant phenotype, metabolic, enzymatic, and genetic analysis was performed on top dressed PSI–362 coated CAN + S barley crops to further support its role in enhancing NUE.

Impact of PSI-362 on Phenotypic and Yield Markers

Current knowledge shows that NUE is a highly complex trait derived from diverse molecular, metabolic, physiological, developmental, and environmental interactions over the entire life cycle of the crop. Field experiments using a randomized block trial design for the ANE PSI-362 applied by foliar spray at three critical growth stages of barley provided agronomically relevant results during three consecutive growing seasons. While tested varieties showed fluctuations on harvested grain yield on their response to PSI-362, the measured values were in the range expected for spring (5.6–7.3 t·ha^{-1}) and winter (8.6–9.1 t·ha^{-1}) barley in Ireland between 2016 and 2018 (CSO, 2019). Most importantly, the field experiments demonstrated that the foliar application of an engineered ANE biostimulant was able to maintain or increase grain yield in barley grown with 25% less N fertilizer.

In order to expand the applicability and facilitate the implementation of PSI-362 in standard grower programs, PSI-362 was co-formulated with a N mineral granular fertilizer (CAN + S). Granular CAN based fertilizer is an efficient source

of N with both nitrate and ammonium forms to maximize plant growth (Hachiya and Sakakibara, 2017). This N fertilizer is widely used by growers in Western Europe (2.16 Mt N·year^{-1}), representing 51% of total worldwide consumption in 2019 (IFASTAT, 2019). Synchronizing N fertilizer application with the crop demand is critical for increasing NUE and reducing fertilizer losses. The co-formulation of CAN + S and PSI-362 is in-keeping with the 4R nutrient framework for increasing crop NUE: right rate, right source, right timing, and right placement. Previous research has shown that the critical period to positively influence spring barley yield and grain quality is the tillering and early stem elongation growth stages (Křen et al., 2015). These growth stages are characterized by a significant increase of N uptake, dry matter accumulation and responsiveness to N fertilization in terms of further grain yield (Baethgen et al., 1995; McTaggart and Smith, 1995; Hauggaard-Nielsen et al., 1998; Chatskikh and Olesen, 2007). Therefore, increasing uptake with PSI-362 at this growth stage was targeted based on the observed benefits of foliar applied PSI-362 enhancing NUE. Application of PSI-362 directly to the soil at the same time as the main N fertilizer application at the mid tillering stage was anticipated to provide similar benefits by stimulating N uptake, transport and assimilation mechanisms from root and shoot tissues before the stem elongation growth stage, compensating for the decreased N rate. The pot experiments revealed that the same dose of PSI-362 delivered by either foliar spray or coating of CAN + S granules enhanced plant biomass and NUE in an equivalent way.

Environmental conditions during the trials in field 1 and field 2 were favorable for spring barley production. The average Irish grain yield from the 2019 season was 8.0 t·ha^{-1} (CSO, 2020), which was 11% higher than the average yield recorded for the period 2014–2018 (Teagasc, 2018). While variations below and above this average grain yield value from field 1 and field 2 were likely related to differences in the grower program, soil chemical characteristics or crops grown in the previous season, our current results demonstrated that a moderate (i.e., 11–27%) reduction in N rate, combined with a single application of PSI-362 coated fertilizer, can maintain or increase grain yield, confirming the previous trend observed with three foliar applications of this biostimulant. Previous research about the effects of breeding on west European and Argentinean spring barley varieties from 1931 have demonstrated that overall improvements in grain yield can be achieved via different phenotypic routes (Abeledo et al., 2008; Bingham et al., 2012). Interestingly, this biostimulant treatment was able to improve important yield components such as plant biomass and harvest index, with no effect on grain size.

PSI-362 Coated Fertilizer and N Uptake Mechanisms

The ability to take up and transport more nitrate from roots to shoots under reduced N fertilizer conditions has been observed as an adaptative response in wild barley genotypes to cope with low N field conditions (Quan et al., 2016). The top-dressing application of PSI-362 coated CAN + S to barley plants at mid-tillering stage (GS22-27) was also translated into a substantial stimulation of nitrate uptake and transport processes 22 days after application despite the reduction of N fertilizer rate, providing a significantly higher nitrate content in shoot tissue at stage GS30-31. These results were consistent with the proof of concept nitrate accumulation results in the model plant *Arabidopsis thaliana* 6 days after applying PSI-362 through the root under two different N levels. Although previous studies have highlighted the positive impact of ANEs on N uptake of oilseed rape and durum wheat growing under optimum nutrient conditions (Jannin et al., 2013; Billard et al., 2014; Laurent et al., 2020), no research to date has demonstrated the effect of ANEs on nitrate accumulation under reduced N fertilizer rate in real field conditions. PSI-362 ANE biostimulant did not possess any relevant N content to explain this nitrate accumulation effect in barley. The ability of specific biomolecules within commercial ANEs to induce plant growth and abiotic stress defense responses has been recently reviewed (Shukla et al., 2019; Goñi et al., 2020), with some of these studies reporting that ANEs can significantly dysregulate relevant genetic markers (Gonñi et al., 2016; Goñi et al., 2018; Shukla et al., 2018; Łangowski et al., 2019; Carmody et al., 2020). To elucidate PSI-362 mode of action at the molecular level, the expression of three nitrate plasma membrane carriers (NRT1.1, NRT1.5, and NRT2.1) was tested. A strong increase of expression of these genetic markers in roots of treated barley plants growing under 73% N rate was found, indicating that they could have a prominent role in facilitating N accumulation in shoot tissue. *NRT1.1* is an extensively studied gene that codes a dual affinity nitrate transporter and can also act as a nitrate transceptor. *NRT1.1* expression is known to be highly responsive to the amount of nitrate available in the environment as well as phosphorylation events under hormonal control (Lay-Pruitt and Takahashi, 2020). NRT2.1 is another crucial component controlling high affinity nitrate transport and predominantly localizes to the plasma membrane of root cells (Vidal et al., 2020). The long-distance nitrate transport between root and shoot is regulated by the gene *NRT1.5*, coding a low-affinity bidirectional nitrate transporter (Lin et al., 2008). Enhanced expression of *NRT1.5* gene in root tissue and increased nitrate transport from root to shoot through the xylem vascular tissues has been observed previously in a high NUE oilseed rape genotype (Han et al., 2016). Increased *NRT1.1* transceptor expression along with high-affinity transporter *NRT2.1* and long-distance transporter *NRT1.5* have implications for auxin biosynthesis and root architecture. Analysis of auxin signaling reporter lines combined with analysis of auxin biosynthesis and transport would be necessary to fully understand PSI-362 effect on plant development and physiology and what is the role of NRT1.1 as integrator. The observed nitrate accumulation in shoot tissue suggests that this biostimulant application could also increase the nitrate transport capacity in multiple ways. For example, through phosphorylation/dephosphorylation events controlled by CIPK23 kinase (Vidal et al., 2020), which can switch NRT transporters to high-affinity mode and facilitate the nutrients flow. Although it is tempting to speculate, nitrate uptake is a complex process, therefore detailed analysis of short- and long-term effects on root and shoot transcriptome need to be performed to fully comprehend the intricacy of this ANE biostimulant effect on NUE.

PSI-362 Coated Fertilizer and Enzymes Involved in N Assimilation Mechanisms

Nitrate assimilation occurs first via NR enzyme to nitrite and then via nitrite reductase (NiR) to ammonium (Tischner, 2000; Masclaux-Daubresse et al., 2010). PSI-362 coated fertilizer did enhance nitrate assimilation at stage GS30-31 through a direct effect on increased NR enzymatic activity in shoot tissue, this change being positively correlated to nitrate accumulation. Gene expression, protein translation and enzymatic activity of NR is positively regulated by nitrate, light, and carbohydrates (Kaiser et al., 2002; Lillo, 2008; Yanagisawa, 2014; Huarancca Reyes et al., 2018). However, this regulation does not necessarily happen simultaneously at these three levels (Carillo et al., 2005). NR enzyme from PSI-362 treated plants was also found to be in a higher constitutively active state compared to untreated plants, regardless of N reduction rate in field 1 and field 2. This enhancement of the NR activation state indicates that PSI-362 may modulate the phosphorylation state of this enzyme 22 days after application, improving shoot nitrate reducing capacities under more adverse growth conditions. At the post-translational level, NR undergoes a partial kinase-dependent reversible inhibition, due to a phosphorylation of a serine residue in hinge 1 followed by a binding to 14-3-3 proteins in presence of divalent cations or polyamines. Therefore, NR activity in the presence of $MgCl_2$ usually reflects the activity of dephosphorylated NR forms versus the activity of all NR forms in presence of EDTA (Athwal and Huber, 2002; Yanagisawa, 2014).

PSI-362 Coated Fertilizer and N Assimilation to Amino Acids

The ammonium produced from reduced nitrate is fixed into the amino acid glutamine through the enzyme GS, constituting the first step in the biosynthesis of organic N compounds and serving as the cornerstone of N assimilation along with GOGAT enzyme (Hirel and Krapp, 2020). The current results showed that GS activity was significantly higher in plants treated with PSI-362 coated fertilizer, enhancing the nitrate assimilation pathway under reduced N rate, which in turn was associated to a lower content of ammonium and an accumulation of glutamine, both substrate and end-product of this enzyme. While GS has been proposed as an interesting target for genetic modification for NUE, attempts to overexpress GS have yielded inconsistent results (James et al., 2018). A recent cisgenic strategy to increase expression of native cytosolic GS1 in barley provided an enhanced enzymatic activity and did increase grain yield and NUE (Gao et al., 2019). Moreover, correlation studies performed in several wheat varieties suggested the presence of a strong relationship between GS activity and different N metabolic markers such as amino acids, soluble protein, and chlorophyll (Kichey et al., 2006, 2007). The increased glutamine assimilation occurred in a coordinated manner with the accumulation of asparagine, glutamate and other amino acids derived from glutamate through transamination reactions such as alanine, aspartate or proline, or essential amino acids derived from aspartate (e.g., methionine, lysine, and threonine) (Pratelli and Pilot, 2014). Therefore, it seems that PSI-362 coated fertilizer had a positive influence on stimulating barley shoots ability to acquire inorganic N and assimilate it into glutamine, favoring other amino acid biosynthetic processes simultaneously.

PSI-362 Coated Fertilizer and Additional Plant Metabolic Parameters

As recently reviewed by Fernie et al. (2020), any attempt to improve crop production and plant NUE through modification of N transport and metabolism pathways will only be effective if all processes are synchronized because unbalanced changes in internal N metabolite pools can generate end-product inhibition or substrate limitations of the respective amino acid synthesis pathways. Thus, the significant accumulation of total free amino acids in barley plants treated with PSI-362 coated fertilizer was also linked to a higher content of macromolecules derived from them such as soluble proteins or chlorophylls. An increased soluble protein content in barley shoot may be associated to a stimulated carbon fixation capacity because the majority of leaf soluble protein content in leaves of C3 plants is present as ribulose-1-5 bis-phosphate carboxylase-oxygenase (Rubisco), the key enzyme of the Calvin cycle (Feller et al., 2008). Together with this factor, the higher photosynthetic pigments content observed in shoot tissue could support this improvement of canopy photosynthesis at stage GS30-31 according to the model established by Cabrera-Bosquet et al. (2009). Overall, stimulating N uptake and assimilation mechanisms before the reproductive stage could facilitate subsequent N absorption during the grain filling process thereby compensating any detrimental effect associated with lower N fertilizer rate. Previous studies in winter wheat and barley have demonstrated that grain filling is mainly fueled with N remobilized from pre-anthesis biomass accumulation (Egle et al., 2008; Zhou et al., 2018).

Impact of PSI-362 Coated Fertilizer on NUE, Soil, and Environmentally Derived Parameters

This research demonstrates that the intrinsically low barley NUE_{grain} can be enhanced consistently through the application of PSI-362, with this improvement being achieved through better $Nupeff_{grain}$. Increasing $Nupeff_{grain}$ trait as a way to further improve NUE has been suggested in previous breeding studies that evaluate barley and wheat varieties (Bingham et al., 2012; Thorwarth et al., 2018). However, unlike breeding programs that can take several years (Garnett et al., 2015), the application of PSI-362 coated fertilizer represents a more convenient, quicker, and profitable solution for growers to recover more N provided by reduced rates of N mineral fertilizer. The soil nitrogen analysis post-harvest suggests that soil N depletion is not occurring in the field trials performed with PSI-362. This finding is in agreement with previous observations over a wide range of N application, with similar amounts of residual N remaining in the soil after harvesting treated and untreated crops (Makowski et al., 1999; Bingham et al., 2012; Venterea et al., 2016). GHG

emissions from the use of N mineral fertilizers are usually split into two parts: emissions from the energy-intensive manufacture process (mainly CO_2 and N_2O) and the emission of N_2O from the fertilized soil (AHDB, 2012). The estimated results determined through the inputs and outputs recorded in the trials developed with PSI-362 coated fertilizer revealed a significant reduction of carbon footprint compared with current practice. Assuming savings of 483 $kgCO_2e{\cdot}ha^{-1}$ as obtained with PSI-362 coated fertilizer under 73% N rate, a reduction of 27.5 $MtCO_2e$ can be expected per season if this agronomic input is implemented in the whole EU cereal production area (56.9 MHa; FAOSTAT, 2019).

Summary and Perspectives

The data presented demonstrates that an engineered biostimulant, PSI-362, derived from *Ascophyllum nodosum*, is capable of increasing NUE in barley under field conditions. The targeted application of PSI-362 as a coating on a granular N mineral fertilizer enhanced N uptake, transport and assimilation markers at phenotypic, metabolic, enzymatic and genetic levels in a coordinated manner. The efficient uptake of more nitrate by the crop when it needs it, results in enhanced NUE derived traits in harvested grain. These results support the agronomic use of this biostimulant with its effect delivered through a defined physiological mode of action that allows up to 27% reduction in N fertilizer usage while maintaining or increasing crop yield. The magnitude of the nitrogen reduction achieved with PSI-362 without compromising yield suggests it can have a role in delivering the European Union (EU) target of a 20% reduction in nitrogen use in agriculture. However, in order to expand the applicability and impact of PSI-362 within agriculture, additional data supporting its efficacy in other important crops (e.g., grass, wheat, maize, etc.) may be beneficial. Further investigation of the mode of action at a basic plant science level to understand the optimal conditions for efficacy will be important to facilitate adoption of this NUE biostimulant technology. The availability of biostimulant innovations in the market to enhanced NUE are going to be critical for achieving more profitable, sustainable and environmentally acceptable agricultural practices.

DATA AVAILABILITY STATEMENT

The original contributions presented in the study are included in the article/**Supplementary Material**, further inquiries can be directed to the corresponding author.

AUTHOR CONTRIBUTIONS

OG, ŁŁ, EF, PQ, and SO'C conceived and designed the experiments. OG, ŁŁ, EF, and PQ performed the experiments and analyzed the data. OG, ŁŁ, EF, and SO'C wrote the article. All authors reviewed and approved the article. All authors contributed to the article and approved the submitted version.

FUNDING

This project was supported partly by the European Union through the European Regional Development Fund and the Development & Innovation (RD&I) Fund of Enterprise Ireland (Project No. 164475).

ACKNOWLEDGMENTS

The authors would like to thank Brandon Bioscience and Target Fertilisers for the gift of the ANE-based biostimulant (PSI-362) and mineral fertilizer (CAN + S) used in this study, respectively. The authors would like to thank the late Philip Reck for his vision, ingenuity and outstanding contribution to sustainable crop management, which was key in developing the coated CAN + S and performing field trials in this research. The authors thank Clifford's Farm for access to crops and assistance with crop agronomy.

SUPPLEMENTARY MATERIAL

The Supplementary Material for this article can be found online at: https://www.frontiersin.org/articles/10.3389/fpls.2021.664682/full#supplementary-material

REFERENCES

Abeledo, L. G., Calderini, D. F., and Slafer, G. A. (2008). Nitrogen economy in old and modern malting barleys. *Field Crops Res.* 106, 171–178. doi: 10.1016/j.fcr.2007.11.006

AHDB (2012). *Understanding Carbon Footprinting for Cereals and Oilseeds*. Available online at: https://ahdb.org.uk/carbon-footprint-decision-tool (accessed on 1 December 2020).

Anbessa, Y., and Juskiw, P. (2012). Strategies to increase nitrogen use efficiency of spring barley. *Can. J. Plant Sci.* 92, 617–625. doi: 10.4141/cjps2011-207

Ascott, M. J., Gooddy, D. C., Wang, L., Stuart, M. E., Lewis, M. A., Ward, R. S., et al. (2017). Global patterns of nitrate storage in the vadose zone. *Nat. Commun.* 8, 1–7. doi: 10.1038/s41467-017-01321-w

Athwal, G. S., and Huber, S. C. (2002). Divalent cations and polyamines bind to loop 8 of 14−3−3 proteins, modulating their interaction with phosphorylated nitrate reductase. *Plant J.* 29, 119–129. doi: 10.1046/j.0960-7412.2001.01200.x

Baethgen, W. E., Christianson, C. B., and Lamothe, A. G. (1995). Nitrogen fertiliser effects on growth, grain yield, and yield components of malting barley. *Field Crops Res.* 43, 87–99. doi: 10.1016/0378-4290(95)00034-N

Billard, V., Etienne, P., Jannin, L., Garnica, M., Cruz, F., Garcia-Mina, J. M., et al. (2014). Two biostimulants derived from algae or humic acid induce similar responses in the mineral content and gene expression of winter oilseed rape (*Brassica napus* L.). *J. Plant Growth Regul.* 33, 305–316. doi: 10.1007/s00344-013-9372-2

Bingham, I. J., Karley, A. J., White, P. J., Thomas, W. T. B., and Russell, J. R. (2012). Analysis of improvements in nitrogen use efficiency associated with 75 years of spring barley breeding. *Eur. J. Agron.* 42, 49–58. doi: 10.1016/j.eja.2011.10.003

Cabrera-Bosquet, L., Albrizio, R., Araus, J. L., and Nogués, S. (2009). Photosynthetic capacity of field-grown durum wheat under different N

availabilities: a comparative study from leaf to canopy. *Environ. Exp. Bot.* 67, 145–152. doi: 10.1016/j.envexpbot.2009.06.004

Carillo, P., Mastrolonardo, G., Nacca, F., and Fuggi, A. (2005). Nitrate reductase in durum wheat seedlings as affected by nitrate nutrition and salinity. *Funct. Plant Biol.* 32, 209–219. doi: 10.1071/FP04184

Carmody, N., Goñi, O., Łangowski, Ł, and O'Connell, S. (2020). *Ascophyllum nodosum* extract biostimulant processing and its impact on enhancing heat stress tolerance during tomato fruit set. *Front. Plant Sci.* 11:807. doi: 10.3389/fpls.2020.00807

Chatskikh, D., and Olesen, J. E. (2007). Soil tillage enhanced CO_2 and N_2O emissions from loamy sand soil under spring barley. *Soil Till. Res.* 97, 5–18. doi: 10.1016/j.still.2007.08.004

Chen, K. E., Chen, H. Y., Tseng, C. S., and Tsay, Y. F. (2020). Improving nitrogen use efficiency by manipulating nitrate remobilization in plants. *Nat. Plants* 6, 1126–1135. doi: 10.1038/s41477-020-00758-0

CSO (2019). *Area, Yield and Production of Crops 2018*. New Delhi: CSO.

CSO (2020). *Area, Yield and Production of Crops 2019*. New Delhi: CSO.

Dimkpa, C. O., Fugice, J., Singh, U., and Lewis, T. D. (2020). Development of fertilisers for enhanced nitrogen use efficiency–trends and perspectives. *Sci. Total Environ.* 731:139113. doi: 10.1016/j.scitotenv.2020.139113

Du Jardin, P. (2015). Plant biostimulants: definition, concept, main categories and regulation. *Sci. Horticult.* 196, 3–14. doi: 10.1016/j.scienta.2015.09.021

Durand, N., Briand, X., and Meyer, C. (2003). The effect of marine bioactive substances (N PRO) and exogenous cytokinins on nitrate reductase activity in *Arabidopsis thaliana*. *Physiol. Plant.* 119, 489–493. doi: 10.1046/j.1399-3054.2003.00207.x

Egle, K., Beschow, H., and Merbach, W. (2008). Assessing post-anthesis nitrogen uptake, distribution and utilisation in grain protein synthesis in barley (*Hordeum vulgare* L.) using 15N fertiliser and 15N proteinogenic and non-proteinogenic amino acids. *Ann. Appl. Biol.* 152, 209–221. doi: 10.1111/j.1744-7348.2007.00207.x

EU Regulation 2019/1009 (2019). Regulation (EU) 2019/1009 of the European Parliament and of the Council of 5 June 2019 Laying Down Rules on the Making Available on the Market of EU Fertilising Products and Amending Regulations (EC) No 1069/2009 and (EC) No 1107/2009 and Repealing Regulation (EC) No 2003/2003 (Text with EEA relevance). Available online at: https://eur-lex.europa.eu/eli/reg/2019/1009/oj (accessed December 1, 2020).

Fang, Z., Xia, K., Yang, X., Grotemeyer, M. S., Meier, S., Rentsch, D., et al. (2013). Altered expression of the PTR/NRT 1 homologue Os PTR 9 affects nitrogen utilization efficiency, growth and grain yield in rice. *Plant Biotechnol. J.* 11, 446–458. doi: 10.1111/pbi.12031

FAOSTAT (2019). Available online at: http://www.fao.org/faostat/en/#data/QC (accessed on 24 January 2021).

Feller, U., Anders, I., and Mae, T. (2008). Rubiscolytics: fate of Rubisco after its enzymatic function in a cell is terminated. *J. Exp. Bot.* 59, 1615–1624. doi: 10.1093/jxb/erm242

Fernie, A. R., Bachem, C. W., Helariutta, Y., Neuhaus, H. E., Prat, S., Ruan, Y. L., et al. (2020). Synchronization of developmental, molecular and metabolic aspects of source–sink interactions. *Nat. Plants* 6, 55–66. doi: 10.1038/s41477-020-0590-x

Frioni, T., Sabbatini, P., Tombesi, S., Norrie, J., Poni, S., Gatti, M., et al. (2018). Effects of a biostimulant derived from the brown seaweed *Ascophyllum nodosum* on ripening dynamics and fruit quality of grapevines. *Sci. Hortic.* 232, 97–106. doi: 10.1016/j.scienta.2017.12.054

Gao, Y., de Bang, T. C., and Schjoerring, J. K. (2019). Cisgenic overexpression of cytosolic glutamine synthetase improves nitrogen utilization efficiency in barley and prevents grain protein decline under elevated CO_2. *Plant Biotechnol. J.* 17, 1209–1221. doi: 10.1111/pbi.13046

Garnett, T., Plett, D., Heuer, S., and Okamoto, M. (2015). Genetic approaches to enhancing nitrogen-use efficiency (NUE) in cereals: challenges and future directions. *Funct. Plant Biol.* 42, 921–941. doi: 10.1071/FP15025

Gómez-Alonso, S., Hermosín-Gutiérrez, I., and García-Romero, E. (2007). Simultaneous HPLC analysis of biogenic amines, amino acids, and ammonium ion as aminoenone derivatives in wine and beer samples. *J. Agric. Food Chem.* 55, 608–613. doi: 10.1021/jf062820m

Goñi, O., Quille, P., and O'Connell, S. (2018). *Ascophyllum nodosum* extract biostimulants and their role in enhancing tolerance to drought stress in tomato plants. *Plant Physiol. Biochem.* 126, 63–73. doi: 10.1016/j.plaphy.2018.02.024

Goñi, O., Quille, P., and O'Connell, S. (2020). "Seaweed carbohydrates," in *The Chemical Biology of Plant Biostimulants*, eds D. Geelen and L. Xu (Hoboken, NJ: John Wiley & Sons), 57–95.

Gonñi, O., Fort, A., Quille, P., McKeown, P. C., Spillane, C., and O'Connell, S. (2016). Comparative transcriptome analysis of two *Ascophyllum nodosum* extract biostimulants: same seaweed but different. *J. Agric. Food Chem.* 64, 2980–2989. doi: 10.1021/acs.jafc.6b00621

Gutiérrez, R. A. (2012). Systems biology for enhanced plant nitrogen nutrition. *Science* 336, 1673–1675. doi: 10.1126/science.1217620

Hachiya, T., and Okamoto, Y. (2017). Simple spectroscopic determination of nitrate, nitrite, and ammonium in *Arabidopsis thaliana*. *Bio-Protocol* 7:e2280. doi: 10.21769/BioProtoc.2280

Hachiya, T., and Sakakibara, H. (2017). Interactions between nitrate and ammonium in their uptake, allocation, assimilation, and signaling in plants. *J. Exp. Bot.* 68, 2501–2512. doi: 10.1093/jxb/erw449

Han, Y. L., Song, H. X., Liao, Q., Yu, Y., Jian, S. F., Lepo, J. E., et al. (2016). Nitrogen use efficiency is mediated by vacuolar nitrate sequestration capacity in roots of *Brassica napus*. *Plant Physiol.* 170, 1684–1698. doi: 10.1104/pp.15.01377

Hauggaard-Nielsen, H., de Neergaard, A., Jensen, L. S., Høgh-Jensen, H., and Magid, J. (1998). A field study of nitrogen dynamics and spring barley growth as affected by the quality of incorporated residues from white clover and ryegrass. *Plant Soil.* 203, 91–101. doi: 10.1023/A:1004350215467

Hawkesford, M. J., and Riche, A. B. (2020). Impacts of G × E × M on nitrogen use efficiency in wheat and future prospects. *Front. Plant Sci.* 11:1157. doi: 10.3389/fpls.2020.01157

Hirel, B., and Krapp, A. (2020). *Nitrogen Utilization in Plants I Biological and Agronomic Importance. Encyclopedia of Biochemistry*, 3rd Edn. Amsterdam: Elsevier.

Huarancca Reyes, T., Scartazza, A., Pompeiano, A., Ciurli, A., Lu, Y., Guglielminetti, L., et al. (2018). Nitrate reductase modulation in response to changes in C/N balance and nitrogen source in Arabidopsis. *Plant Cell Physiol.* 59, 1248–1254. doi: 10.1093/pcp/pcy065

IFA (2019). *Executive Summary Fertiliser Outlook 2019 – 2023*. Kolkata: IFA.

IFASTAT (2019). *Preliminary IFA 2019 Global Nitrogen Fertiliser Market Assessment*. Available online at: https://www.ifastat.org/supply/Nitrogen%20Products/AN%20and%20CAN (accessed on 17 December 2020)

James, D., Borphukan, B., Fartyal, D., Achary, V. M. M., and Reddy, M. K. (2018). "Transgenic manipulation of glutamine synthetase: a target with untapped potential in various aspects of crop improvement," in *Biotechnologies of Crop Improvement*, Vol. 2, eds S. S. Gosal and S. H. Wani (Cham: Springer), 367–416.

Jannin, L., Arkoun, M., Etienne, P., Laîné, P., Goux, D., Garnica, M., et al. (2013). *Brassica napus* growth is promoted by *Ascophyllum nodosum* (L.) Le Jol. seaweed extract: microarray analysis and physiological characterisation of N, C, and S metabolisms. *J. Plant Growth Regul.* 32, 31–52. doi: 10.1007/s00344-012-9273-9

Kaiser, W. M., Weiner, H., Kandlbinder, A., Tsai, C. B., Rockel, P., Sonoda, M., et al. (2002). Modulation of nitrate reductase: some new insights, an unusual case and a potentially important side reaction. *J. Exp. Bot.* 53, 875–882. doi: 10.1093/jexbot/53.370.875

Kant, S., Bi, Y.-M., and Rothstein, S. J. (2011). Understanding plant response to nitrogen limitation for the improvement of crop nitrogen use efficiency. *J. Exp. Bot.* 62, 1499–1509. doi: 10.1093/jxb/erq297

Kanter, D. R., Zhang, X., and Mauzerall, D. L. (2015). Reducing nitrogen pollution while decreasing farmers' costs and increasing fertiliser industry profits. *J. Environ. Qual.* 44, 325–335. doi: 10.2134/jeq2014.04.0173

Kichey, T., Heumez, E., Pocholle, D., Pageau, K., Vanacker, H., Dubois, F., et al. (2006). Combined agronomic and physiological aspects of nitrogen management in wheat highlight a central role for glutamine synthetase. *New Phytol.* 169, 265–278. doi: 10.1111/j.1469-8137.2005.01606.x

Kichey, T., Hirel, B., Heumez, E., Dubois, F., and Le Gouis, J. (2007). In winter wheat (*Triticum aestivum* L.), post-anthesis nitrogen uptake and remobilisation to the grain correlates with agronomic traits and nitrogen physiological markers. *Field Crops Res.* 102, 22–32.

Křen, J., Klem, K., Svobodová, I., Míša, P., and Neudert, L. (2015). Yield and grain quality of spring barley as affected by biomass formation at early growth stages. *Plant Soil Environ*. 60, 221–227.

Łangowski, Ł, Goñi, O., Quille, P., Stephenson, P., Carmody, N., Feeney, E., et al. (2019). A plant biostimulant from the seaweed *Ascophyllum nodosum* (Sealicit) reduces podshatter and yield loss in oilseed rape through modulation of *IND* expression. *Sci. Rep*. 9, 1–11. doi: 10.1038/s41598-019-52958-0

Lassaletta, L., Billen, G., Garnier, J., Bouwman, L., Velazquez, E., Mueller, N. D., et al. (2016). Nitrogen use in the global food system: past trends and future trajectories of agronomic performance, pollution, trade, and dietary demand. *Environ. Res. Lett*. 11:095007. doi: 10.1088/1748-9326/11/9/095007

Laurent, E. A., Ahmed, N., Durieu, C., Grieu, P., and Lamaze, T. (2020). Marine and fungal biostimulants improve grain yield, nitrogen absorption and allocation in durum wheat plants. *J. Agric. Sci*. 158, 279–287. doi: 10.1017/S0021859620000660

Lay-Pruitt, K. S., and Takahashi, H. (2020). Integrating N signals and root growth: the role of nitrate transceptor NRT1.1 in auxin-mediated lateral root development. *J. Exp. Bot*. 71, 4365–4368. doi: 10.1093/jxb/eraa243

Li, M., Xu, J., Gao, Z., Tian, H., Gao, Y., and Kariman, K. (2020). Genetically modified crops are superior in their nitrogen use efficiency-a meta-analysis of three major cereals. *Sci. Rep*. 10:8568. doi: 10.1038/s41598-020-65684-9

Lichtenthaler, H. K., and Buschmann, C. (2001). Chlorophylls and carotenoids: measurement and characterisation by UV-VIS spectroscopy. *Curr. Protoc. Food Anal. Chem*. 1, F4–F3. doi: 10.1002/0471142913.faf0403s01

Lillo, C. (2008). Signalling cascades integrating light-enhanced nitrate metabolism. *Biochem. J*. 415, 11–19. doi: 10.1042/BJ20081115

Lin, S. H., Kuo, H. F., Canivenc, G., Lin, C. S., Lepetit, M., Hsu, P. K., et al. (2008). Mutation of the *Arabidopsis* NRT1.5 nitrate transporter causes defective root-to-shoot nitrate transport. *Plant Cell* 20, 2514–2528. doi: 10.1105/tpc.108.060244

Makowski, D., Wallach, D., and Meynard, J. M. (1999). Models of yield, grain protein, and residual mineral nitrogen responses to applied nitrogen for winter wheat. *Agron. J*. 91, 377–385. doi: 10.2134/agronj1999.00021962009100030005x

Mariotti, F., Tomé, D., and Mirand, P. P. (2008). Converting nitrogen into protein—beyond 6.25 and Jones' factors. *Crit. Rev. Food Sci. Nutr*. 48, 177–184. doi: 10.1080/10408390701279749

Masclaux-Daubresse, C., Daniel-Vedele, F., Dechorgnat, J., Chardon, F., Gaufichon, L., and Suzuki, A. (2010). Nitrogen uptake, assimilation, and remobilization in plants: challenges for sustainable and productive agriculture. *Ann. Bot*. 105, 1141–1157. doi: 10.1093/aob/mcq028

McTaggart, I. P., and Smith, K. A. (1995). The effect of rate, form and timing of fertiliser N on nitrogen uptake and grain N content in spring malting barley. *J. Agric. Sci*. 125, 341–353. doi: 10.1017/S0021859600084847

Moll, R. H., Kamprath, E. J., and Jackson, W. A. (1982). Analysis and interpretation of factors which contribute to efficiency of nitrogen utilization 1. *Agron. J*. 74, 562–564. doi: 10.2134/agronj1982.00021962007400030037x

Noguero, M., and Lacombe, B. (2016). Transporters involved in root nitrate uptake and sensing by *Arabidopsis*. *Front. Plant Sci*. 7:1391. doi: 10.3389/fpls.2016.01391

Omara, P., Aula, L., Oyebiyi, F., and Raun, W. R. (2019). World cereal nitrogen use efficiency trends: review and current knowledge. *Agrosyst. Geosci. Environ*. 2, 1–8. doi: 10.2134/age2018.10.0045

Perchlik, M., and Tegeder, M. (2017). Improving plant nitrogen use efficiency through alteration of amino acid transport processes. *Plant Physiol*. 175, 235–247. doi: 10.1104/pp.17.00608

Pfromm, P. H. (2017). Towards sustainable agriculture: fossil-free ammonia. *J. Renew. Sustain. Energy* 9:034702. doi: 10.1063/1.4985090

Pratelli, R., and Pilot, G. (2014). Regulation of amino acid metabolic enzymes and transporters in plants. *J. Exp. Bot*. 65, 5535–5556. doi: 10.1093/jxb/eru320

Prey, L., Kipp, S., Hu, Y., and Schmidhalter, U. (2019). Nitrogen use efficiency and carbon traits of high-yielding european hybrid vs. line winter wheat cultivars: potentials and limitations. *Front. Plant Sci*. 9:1988. doi: 10.3389/fpls.2018.01988

Quan, X., Zeng, J., Ye, L., Chen, G., Han, Z., Shah, J. M., et al. (2016). Transcriptome profiling analysis for two Tibetan wild barley genotypes in responses to low nitrogen. *BMC Plant Biol*. 16:30. doi: 10.1186/s12870-016-0721-8

Raun, W. R., and Johnson, G. V. (1999). Improving nitrogen use efficiency for cereal production. *Agron. J*. 91, 357–363. doi: 10.2134/agronj1999.00021962009100030001x

Research and Markets (2020). *Agriculture Biostimulant - Global Market Outlook (2019-2027)*. European Union: Research and Markets.

Rose, T. J., Wood, R. H., Rose, M. T., and Van Zwieten, L. (2018). A re-evaluation of the agronomic effectiveness of the nitrification inhibitors DCD and DMPP and the urease inhibitor NBPT. *Agricult. Ecosyst. Environ*. 252, 69–73. doi: 10.1016/j.agee.2017.10.008

Rouphael, Y., and Colla, G. (2020). Biostimulants in agriculture. *Front. Plant Sci*. 11:40. doi: 10.3389/fpls.2020.00040

Sabir, A. (2014). Vine growth, yield, berry quality attributes and leaf nutrient content of grapevines as influenced by seaweed extract (*Ascophyllum nodosum*) and nanosize fertiliser pulverizations. *Sci. Hortic*. 175, 1–8. doi: 10.1016/j.scienta.2014.05.021

Schaufler, G., Kitzler, B., Schindlbacher, A., Skiba, U., Sutton, M. A., and Zechmeister-Boltenstern, S. (2010). Greenhouse gas emissions from European soils under different land use: effects of soil moisture and temperature. *Eur. J. Soil Sci*. 61, 683–696. doi: 10.1111/j.1365-2389.2010.01277.x

Shukla, P. S., Borza, T., Critchley, A. T., Hiltz, D., Norrie, J., and Prithiviraj, B. (2018). *Ascophyllum nodosum* extract mitigates salinity stress in *Arabidopsis thaliana* by modulating the expression of miRNA involved in stress tolerance and nutrient acquisition. *PLoS One* 13:e0206221. doi: 10.1371/journal.pone.0206221

Shukla, P. S., Mantin, E. G., Adil, M., Bajpai, S., Critchley, A. T., and Prithiviraj, B. (2019). *Ascophyllum nodosum*-based biostimulants: sustainable applications in agriculture for the stimulation of plant growth, stress tolerance, and disease management. *Front. Plant Sci*. 10:655. doi: 10.3389/fpls.2019.00655

Snyder, C. S. (2017). Enhanced nitrogen fertiliser technologies support the '4R'concept to optimise crop production and minimise environmental losses. *Soil Res*. 55, 463–472. doi: 10.1071/SR16335

Stamatiadis, S., Evangelou, L., Yvin, J. C., Tsadilas, C., Mina, J. M. G., and Cruz, F. (2015). Responses of winter wheat to *Ascophyllum nodosum* (L.) Le Jol. extract application under the effect of N fertilization and water supply. *J. Appl. Phycol*. 27, 589–600. doi: 10.1007/s10811-014-0344-0

Teagasc (2015). *The Spring Barley Guide. Teagasc-Agriculture and Food Development Authority*. Available online at: https://www.teagasc.ie/media/website/publications/2015/The-Spring-Barley-Guide.pdf (accessed December 10, 2020).

Teagasc (2018). *Cereal Crops*. Available online at: https://www.teagasc.ie/crops/crops/cereal-crops/\relax$\@@underline{\hbox{\setbox\tw@\hbox{\begingroup\pdfcolorstack\main@pdfcolorstackpush{0001k0001K}\aftergroup\pdfcolorstack\main@pdfcolorstackpop\relax\endgraf\endgroup}\dp\tw@\z@\box\tw@}}\mathsurround\z@$\relax (accessed on 10 December 2020)

Thorwarth, P., Piepho, H. P., Zhao, Y., Ebmeyer, E., Schacht, J., Schachschneider, R., et al. (2018). Higher grain yield and higher grain protein deviation underline the potential of hybrid wheat for a sustainable agriculture. *Plant Breed*. 137, 326–337. doi: 10.1111/pbr.12588

Tischner, R. (2000). Nitrate uptake and reduction in higher and lower plants. *Plant Cell Environ*. 23, 1005–1024. doi: 10.1046/j.1365-3040.2000.00595.x

Turan, M., and Köse, C. (2004). Seaweed extracts improve copper uptake of grapevine. *Acta Agric. Scand. Sect. B-Soil Plant Sci*. 54, 213–220. doi: 10.1080/09064710410030311

Vasilieva, T., Goñi, O., Quille, P., O'Connell, S., Kosyakov, D., Shestakov, S., et al. (2021). Chitosan plasma chemical processing in beam-plasma reactors as a way of environmentally friendly phytostimulants production. *Processes* 9:103. doi: 10.3390/pr9010103

Venterea, R. T., Coulter, J. A., and Dolan, M. S. (2016). Evaluation of intensive "4R" strategies for decreasing nitrous oxide emissions and nitrogen surplus in rainfed corn. *J. Environ. Qual*. 45, 1186–1195. doi: 10.2134/jeq2016.01.0024

Vicente, R., Vergara-Díaz, O., Kerfal, S., López, A., Melichar, J., Bort, J., et al. (2019). Identification of traits associated with barley yield performance using contrasting nitrogen fertilizations and genotypes. *Plant Sci*. 282, 83–94. doi: 10.1016/j.plantsci.2018.10.002

Vidal, E. A., Alvarez, J. M., Araus, V., Riveras, E., Brooks, M., Krouk, G., et al. (2020). Nitrate 2020: thirty years from transport to signaling networks. *Plant Cell* 32, 2094–2119. doi: 10.1105/tpc.19.00748

Voss-Fels, K. P., Stahl, A., Wittkop, B., Lichthardt, C., Nagler, S., Rose, T., et al. (2019). Breeding improves wheat productivity under contrasting agrochemical input levels. *Nature Plants* 5, 706–714. doi: 10.1038/s41477-019-0445-5

Wang, R., Min, J., Kronzucker, H. J., Li, Y., and Shi, W. (2019). N and P runoff losses in China's vegetable production systems: loss characteristics, impact, and management practices. *Sci. Total Environ.* 663, 971–979. doi: 10.1016/j.scitotenv.2019.01.368

Wang, Y. Y., Cheng, Y. H., Chen, K. E., and Tsay, Y. F. (2018). Nitrate transport, signaling, and use efficiency. *Annu. Rev. Plant Biol.* 69, 85–122. doi: 10.1146/annurev-arplant-042817-040056

White, P. J., and Brown, P. H. (2010). Plant nutrition for sustainable development and global health. *Ann. Bot*. 105, 1073–1080. doi: 10.1093/aob/mcq085

Yakhin, O. I., Lubyanov, A. A., Yakhin, I. A., and Brown, P. H. (2017). Biostimulants in plant science: a global perspective. *Front. Plant Sci*. 7:2049. doi: 10.3389/fpls.2016.02049

Yan, M., Pan, G., Lavallee, J. M., and Conant, R. T. (2020). Rethinking sources of nitrogen to cereal crops. *Glob. Change Biol*. 26, 191–199. doi: 10.1111/gcb.14908

Yanagisawa, S. (2014). Transcription factors involved in controlling the expression of nitrate reductase genes in higher plants. *Plant Sci*. 229, 167–171. doi: 10.1016/j.plantsci.2014.09.006

Zhou, B., Serret, M. D., Pie, J. B., Shah, S. S., and Li, Z. (2018). Relative contribution of nitrogen absorption, remobilization, and partitioning to the ear during grain filling in chinese winter wheat. *Front. Plant Sci*. 9:1351. doi: 10.3389/fpls.2018.01351

Conflict of Interest: Brandon Bioscience manufactures PSI-362. Third party growers performed field trials and provided the yield results. This project was supported partly by Enterprise Ireland. The funder provided support in the form of consumables and salary for authors (ŁŁ, OG, and EF), but did not have any additional role in the study design, data collection and analysis, decision to publish, or preparation of the manuscript. ŁŁ, OG, EF, and SO'C are employed by Brandon Bioscience.

The remaining author declares that the research was conducted in the absence of any commercial or financial relationships that could be construed as a potential conflict of interest.

frontiers in Plant Science

ORIGINAL RESEARCH
published: 26 May 2021
doi: 10.3389/fpls.2021.659130

Effects of Seaweed Extracts on the Growth, Physiological Activity, Cane Yield and Sucrose Content of Sugarcane in China

Diwen Chen[1,2,3], Wenling Zhou[3], Jin Yang[1,2], Junhua Ao[3], Ying Huang[3], Dachun Shen[3], Yong Jiang[3], Zhenrui Huang[4,5] and Hong Shen[1,2]**

[1] College of Natural Resources and Environment, South China Agricultural University, Guangzhou, China, [2] Guangdong Provincial Key Laboratory of Eco-Circular Agriculture, Guangzhou, China, [3] Institute of Bioengineering, Guangdong Academy of Sciences, Guangzhou, China, [4] Crops Research Institute, Guangdong Academy of Agricultural Sciences, Guangzhou, China, [5] Guangdong Provincial Key Laboratory of Crop Genetics and Improvement, Guangzhou, China

Seaweed extracts (SEs) have been widely used as biostimulants in crop management due to their growth-promoting and stress-resistant effects. To date, there are few reports of the effect of SEs on sucrose content and cane yield. Here, we conducted field experiments for three consecutive growth seasons (2017∼2019) in two areas (Suixi and Wengyuan) of China, to investigate the yield and sugar content of sugarcane in response to SE treatment at different growth stages. The results showed that spraying SEs once at seedling (S), early elongation (E), and early mature (M) stages, respectively, once at S and E stages, respectively, or once at the S stage increased the cane yield by 9.23, 9.01, and 3.33%, respectively, implying that SEs application at the early elongation stage played a vital role in promoting sugarcane growth. Photosynthetic parameters and nutrient efficiency analysis showed that spraying SEs at S and E stages enhanced the net photosynthetic rate, transpiration rate, and water use efficiency, and increased N, P, or K utilization efficiency, compared with those of the control. Notably, cane yield increasing rate of SEs in 2017 and 2018 were higher than those in 2019 in Wengyuan but lower than those in 2019 in Suixi. Interestingly, the total rainfall and monthly average rainfall in 2017 and 2018 were lower than those in 2019 in Wengyuan but higher than those in 2019 in Suixi. The results suggested that the yield increasing rate of SEs on sugarcane was better in less rainfall years. The sucrose content of sugarcane showed no difference between spraying SEs at the M stage alone or at the three growth stages but was higher than those of SE treatments at S and/or E stages. Enzyme activity analysis showed that spraying SEs at the M stage increased the activity of sucrose phosphate synthase activity by 9.14% in leaves and 15.16% in stems, and decreased soluble acid invertase activity in stems by 16.52%, which contributed to the sucrose increase of 5.00%. The above results suggested that SEs could increase cane yield and promote sucrose accumulation in sugarcane. The yield increasing effect was more obvious under conditions of drought stress.

Keywords: seaweed extracts, foliar application, sugarcane (*Saccharum officinarum* L.), photosynthesis, sucrose

OPEN ACCESS

Edited by:
Youssef Rouphael, University of Naples Federico II, Italy

Reviewed by:
Catello Di Martino, University of Molise, Italy
Larissa Anatolyevna Ivanova, Tyumen State University, Russia

****Correspondence:***
Zhenrui Huang
fjsi@163.com
Hong Shen
hshen@scau.edu.cn

Specialty section:
This article was submitted to Crop and Product Physiology, a section of the journal Frontiers in Plant Science

Received: *27 January 2021*
Accepted: *19 April 2021*
Published: *26 May 2021*

Citation:
Chen D, Zhou W, Yang J, Ao J, Huang Y, Shen D, Jiang Y, Huang Z and Shen H (2021) Effects of Seaweed Extracts on the Growth, Physiological Activity, Cane Yield and Sucrose Content of Sugarcane in China. Front. Plant Sci. 12:659130. doi: 10.3389/fpls.2021.659130

INTRODUCTION

Sugarcane is the most important sugar crop and is also an important renewable energy crop (Commodity Bureau, 2015). China is the third largest sugarcane producer in the world after Brazil and India (Faostat, 2016). In recent years, periods of drought have become more frequent and serious due to global climate change (Hoover et al., 2017). Some climate models predict that the occurrence frequency of drought and extreme drought in subtropical and tropical regions will increase in the future, and the impact scope will be larger (Burke et al., 2006). Drought directly causes serious damage to various crops, such as sugarcane. Drought could lead to the reduction of sugarcane yield and have a serious impact on sugarcane agricultural production and the sugar industry (Vasantha et al., 2005). The arid slope areas of Guangxi, Guangdong, and Yunnan are the main sugarcane-growing areas in China. The water source of most sugarcane fields basically depends on rainfall, and there were almost no irrigation measures. Unfortunately, the uneven rainfall in these areas was prone to seasonal drought, which seriously affects the normal growth of sugarcane. How to effectively improve the drought resistance of sugarcane and ensure the yield of sugarcane and sugar has become an important topic in the field of sugarcane research (Kumar et al., 2014; Liu et al., 2016; Pereira et al., 2019; Singh et al., 2019). Thus far, there have been some studies to achieve high-efficiency irrigation management of sugarcane by changing the field application measures (Singh A.K. et al., 2018). Others use soil water retaining agents to improve the soil water holding capacity, promote root water absorption, and improve sugarcane drought resistance to ensure sugarcane yield and sugar content (Marcos et al., 2018; Singh et al., 2018a; Silveira et al., 2019). Nowadays, more and more scholars are interested in improving the stress ability of sugarcane under biological and abiotic stress, by applying exogenous growth stimulating substances (Pereira et al., 2019; Watanabe et al., 2019).

Seaweed extracts (SEs) are a kind of biostimulant extracted from seaweed (especially brown algae) that can promote crop growth, improve crop quality, and enhance crop stress resistance. SE mainly contain natural hormones, such as auxin, cytokinin, gibberellin, abscisic acid, and other active substances such as seaweed polysaccharide, sugar alcohol, betaine, and phenolic compounds (Crouch and van Staden, 1993; Jardin, 2012; Battacharyya et al., 2015), which have been used in agriculture for many years (Friedlander and Ben-Amotz, 1990; Mukherjee and Patel, 2020). The studies have shown that SEs were beneficial to soil improvement and crop growth. The colony counts in the soil and metabolic activities of soil microbes were found to increase following SEs applications, which contributed to increase plant root and shoot growth (Alam et al., 2013). SEs increased the absorption of soil nutrients by plants, stimulated the growth of crops, increased yield (Renaut et al., 2019; Boukhari et al., 2020), and enhanced plant resistance to biotic (Machado et al., 2014; Ben Salah et al., 2018) and abiotic stress (Bradáčová et al., 2016; Cabo et al., 2019; Khompatara et al., 2019). For example, SEs sprayed on onion grown under water stress significantly increased N, P, and K uptake by 116, 113, and 93% compared to the unsprayed plants (Almaroai and Eissa, 2020). Another study found that SEs increased chlorophyll content by increasing the biogenesis of chloroplasts and reducing chlorophyll degradation, which was due to the up-regulated genes associated with photosynthesis, cell metabolism, stress response and S and N metabolism in *Brassica napus* L. (Jannin et al., 2013). Researchers postulated that the stimulatory effect of seaweed extracts on plant growth was due to the complex of active substance, which act directly or by influencing gene regulation in the plant (Arioli et al., 2015). There was a significantly higher expression levels of the PinII and ETR-1 marker genes with SEs application than controls. This was coupled with a marked increase in gene transcripts involved in auxin (IAA), gibberellin (Ga2Ox) and cytokinin (IPT) biosynthesis, which provides possible evidence for induced growth in plants treated with SEs (Ali et al., 2019).

Seaweed extracts have been shown to be effective in improving stress resistance in many other crops, such as spinach (Xu and Leskovar, 2015), maize (Trivedi et al., 2018a,b), sweet orange (Spann and Little, 2011), zucchini squash (Rouphael et al., 2016), and cucumber (Spann and Little, 2011). There are almost no reports on the application of SEs in sugarcane, especially in arid areas without irrigation. Indian researchers have conducted field experiments in western and southern India, which showed that the application of SEs could improve the yield and sugar content of sugarcane (Deshmaukh and Phonde, 2013; Karthikeyan and Shanmugam, 2017). In addition, other reports in India showed that the application of SEs could reduce fertilizer input and increase sugar yield (Deshmaukh and Phonde, 2013; Karthikeyan and Shanmugam, 2017). Meanwhile, it is believed that the application of SEs in sugarcane could reduce carbon dioxide emission and encourage the use of biostimulants, such as SE, under the background of adverse effects of global climate change (Singh et al., 2018b). However, the soil, climate, and cultivation measures between China and India are different. It is necessary to carry out tests to investigate the application effects of SEs on sugarcane in China. Specifically, in conditions without irrigation, the effects of SEs on sugarcane growth, yield, and sucrose content are not clear. We, therefore, conducted a series of field experiments for three consecutive years (1-year planting and 2-year ratoons) in the main sugarcane producing areas of China to investigate the effects of SEs on sugarcane growth, yield, and sugar content in terms of yield components, photosynthetic parameters, nutrient utilization rate, sucrose content, and sugar-related enzyme activities.

MATERIALS AND METHODS

Trial Sites and Weather Data

Wengyuan (113.94E, 24.27N) and Suixi counties (110.28E, 21.35N), which both have subtropical climates, were selected as the trial sites. **Figure 1** shows the monthly precipitation and monthly average temperature of the two sites from 2017 to 2019. In winter, the temperature in Wengyuan was 3–6°C lower than that of Suixi. The 3-year average temperature in Wengyuan was 22.3°C and that in Suixi was 24.4°C. The rainfall in Wengyuan from 2017 to 2019 was 1,498, 1,674, and 2,183 mm, respectively, and the rainfall in Suixi from 2017 to 2019 was 1,805, 2,098, and

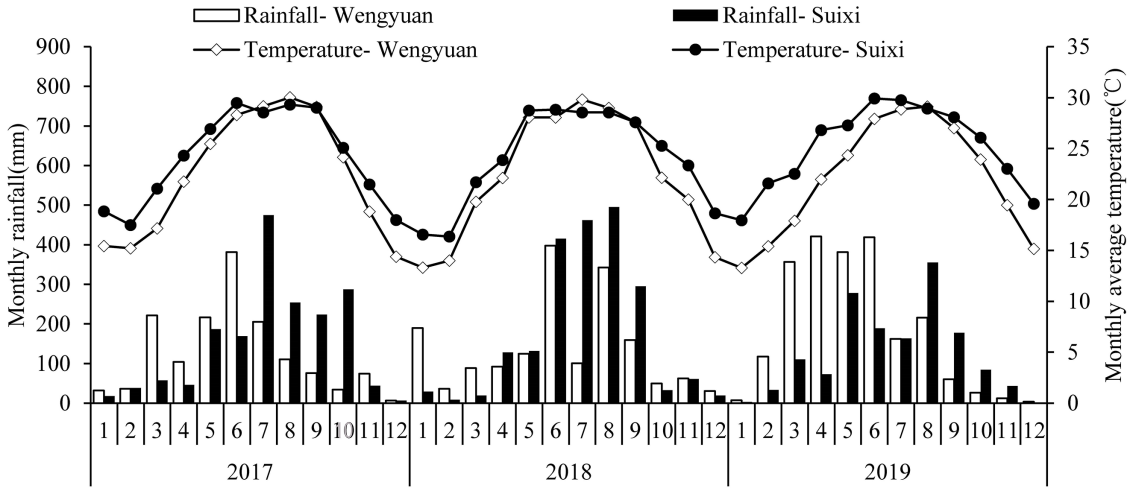

FIGURE 1 | Monthly total rainfall and average temperature during experimental year (2017–2019) in two sites. Numbers in the X axis represent the months in 3 years.

1,514 mm, respectively. The soil in the sugarcane field was latosol at Suixi and red soil at Wengyuan. Soil properties are listed in **Table 1**.

Plant Materials and SE

The sugarcane variety used in Suixi was "ROC22" and in Wengyuan, it was "Yuetang60." These two varieties were the main local cultivated varieties.

The raw material of SEs was obtained from cultured kelp in the coastal waters of southeast China. The SEs was a kind of liquid product obtained by complex enzymatic hydrolysis. The content of the main nutrients and active substances in the SE were pH 6.85, EC value 14.35 mS/cm, N 0.56 g/L, P_2O_5 0.28 g/L, K_2O 12.06 g/L, Ca 3.32 g/L, Mg 2.65 g/L, S 1.68 g/L, organic matter 25.10 g/L, alginic acid 20.16 g/L, seaweed polyphenol 205.56 mg/L, effective seaweed oligosaccharide 4.00 g/L, total sugar 13.00 g/L, mannitol 12.10 g/L, and free amino acid 5.00 g/L.

Treatments and Cultural Practices

A total of five treatments were set up in the field experiments, and each treatment was repeated four times. Treatments were randomly distributed including: (1) spraying water without SE as a control (CK); (2) spraying SEs once at the seedling stage (SE1); (3) spraying SEs both at seedling and early elongation stages (SE2); (4) spraying SEs at seedling, early elongation, and early mature stages (SE3); and (5) spraying SEs once at the early mature stage (SE4). The purpose of SE5 was only to study the effect of SE on the sugar content of sugarcane. The application amount of SE remained constant at 3 L/ha, which was diluted 100 times with clear water and sprayed by an unmanned aerial vehicle. The application time at the seedling, early elongation, and early mature stages were in late March, mid-June, and early November every year, respectively. There was a slight difference in dates between different years (within 10 days).

Both sites were newly planted in 2017 and ratoons in 2018–2019. The former crops planted at these sites were sugarcane. The planting time of Suixi and Wengyuan was December 27, 2016 and December 10, 2016, respectively. Plot sizes were 168 m^2 (7 rows × 20 m) and 126 m^2 (7 rows × 15 m) at Suixi and Wengyuan, respectively. Both sites had a row-spacing of 1.2 m. All experiments had 3–5 guard rows to minimize cross influence. Total fertilization amounts were 483 kg N, 240 kg P_2O_5, and 450 kg K_2O, and the fertilization amount in ratoon (2018/2019) was 432 kg N, 225 kg P_2O_5, and 405 kg K_2O. Cane in all of the experiments was planted and cultivated following local cultivation practices and was harvested after approximately 12 months of growth.

TABLE 1 | Physical and chemical properties of experimental soils.

Trial site	pH	Organic matter ($g \cdot kg^{-1}$)	Total-N ($g \cdot kg^{-1}$)	Available P ($mg \cdot kg^{-1}$)	Available K ($mg \cdot kg^{-1}$)
Suixi	4.80	14.97	0.92	65.35	140.13
Wengyuan	4.73	20.83	1.17	21.93	66.83

Measurements

Cane Yield and Its Components

On the 15th day after the second spraying treatment in 2017–2018, plant height was measured with a special ruler for measuring the plant height of sugarcane, and 30 plants were randomly measured in each plot to take the average of a sample. Every year (2017–2019) from December 15–20, the diameter of the central stem of sugarcane was measured with a vernier caliper, and 30 plants were randomly measured in each plot to take the average of a sample. The millable cane numbers in the area of 36 m^2 (3 rows in the middle × 10 m length) were counted in each plot and converted into the millable cane number per hectare. The cane yield (fresh cane weight) was converted into yield per hectare by weighing an area of 36 m^2 in each plot.

SPAD (Soil and Plant Analyzer Development) Value and Photosynthetic Parameters of Leaves

In 2017 and 2018, SPAD value measurements of sugarcane leaves were taken 3 times at 2 weeks after each SE application. A chlorophyll meter (SPAD-502) was used to measure the middle part of the fully expanded leaves at the top of the sugarcane plant, and the average value of 10 plants was taken as a measured value.

In sunny weather, from 9:00 a.m. to 11:00 a.m., using a LI-6400 portable photosynthetic system, the photosynthetic parameters of the middle part of the leaves of sugarcane with red and blue light sources were measured, and 10 plants were measured repeatedly to obtain the average value. The following measurements were recorded: CO_2 concentration 390.5 μmol/mol, light intensity 800 μ mol/(m^2s), net photosynthetic rate (*Pn*), and transpiration rate (*Tr*). The ratio of *Pn*/*Tr* was calculated as instant water use efficiency (WUEI).

Nutrient Utilization Efficiency (NUE) and Partial Factor Productivity (PFP)

When sugarcane was harvested, 10 sugarcane plants were randomly selected from each plot, and the sugarcane stems and leaves were collected, and fresh weight were weighed, then killed at 105 °C for 30 min and dried to constant weight at 70°C, and dry weight were weighed, and water contents of stems and leaves were calculated. The drying sample was crushed through a 0.15-mm sieve, treated with H_2SO_4-H_2O_2 followed by wet digestion (Bao, 2000), and the nutrient content of nitrogen (N) and phosphorus (P) contents were analyzed by an Automatic Flow Injection Analyzer (Proxima, Alliance, France), and potassium (K) content was measured with a Flame Emission Spectrophotometer (M425, Sherwood, United Kingdom). The Nutrient content per plant was the sum of the nutrient content of stem and leaf. The nutrient utilization efficiency (NUE) of N, P, and K were calculated as follows:

$NUE_{N/P/K}$ = Nutrient content per plant (*N*/*P*/*K*) × millable cane number per hectare /the amount of *N*/*P*/*K* fertilizer applied ($F_{N/P/K}$) per hectare

$PFP_{N/P/K}$ = Cane yield/$F_{N/P/K}$

Contents of Sucrose and Reducing Sugar in Sugarcane, and Theoretical Sugar Yield

The sugar parameters of cane were sampled and tested at each harvest time in 2017–2019. The content of sucrose, glucose, and fructose were determined by HPLC. A total of 10 canes were randomly selected from each plot, and the tenth node (counting from bottom to top) was peeled and cut into small pieces, which were ground into a uniform powder with liquid nitrogen. The powder (2.5 g) was weighed and placed in a 50 mL centrifuge tube, and 10 mL ethanol with a volume fraction of 80% was added. For extraction, the samples were incubated in an 80°C water bath for 30 min, shaken once every 5 min, and centrifuged at 12,000 r·min^{-1} for 15 min to collect the supernatant. The extraction was repeated twice with 80% ethanol, and the supernatants of the three extractions were combined in a 50 mL centrifuge tube, which were soaked in a water bath at 90°C for about 3 h, volatilized to about 2 mL, and the supernatant was fixed to 10 mL. The supernatant was filtered with a 0.22 μm microporous membrane to remove impurities and obtain the sugar extract. Chromatographic conditions were as follows: YMC-Pack NH_2 carbohydrate column (250 mm × 4.6 mm, 5 μm), column temperature 40°C, flow rate 1 mL·min^{-1}, injection volume 20 μL, and time 20 min. According to the peak area and concentration of the standard sample, the sugar content in the sample was calculated by using the formula: standard sample peak area/standard sample concentration = sample peak area/sample concentration. The content of reducing sugar was the sum of the glucose and fructose content. Theoretical sugar yield was calculated by cane yield per unit area multiplied by sucrose content. Sucrose content, reducing sugar content, and theoretical sugar yield were all based on fresh weight of cane.

SAI and SPS Enzyme Activities

In 2018, 10–12 days after spraying SEs at the mature stage, the leaves (completely unfolded at the top of sugarcane) and stems (peeled from the tenth node, counting from bottom to top, and cut into small pieces) were sampled. After picking, they were put into liquid nitrogen until analysis and detection in the laboratory. The sample powder (2 g) was ground with liquid nitrogen, weighed, and put into a 10 mL centrifuge tube, and 8 mL of enzyme extract (50 mM Hepes (pH 7.5), 12 mM MgCl, 1 mM EDTA, 1 mM EGTA, 10 mM DTT, 2 mM benzamidine, 2 mM N-aminocapronate, and 10 mM diethyldithiocarbamate) was added and extracted by shaking on ice for 30 min. Samples were centrifuged at 4°C at 15,000 rpm for 10 min. The supernatant (4 mL) was placed into a 2 mL centrifuge tube. The extraction and enzyme activity of SAI and SPS were determined according to the methods of Zhu et al. (1997) and Gutiérrez-Miceli et al. (2002).

Statistical Analyses

We used Microsoft Excel 2013 and SPSS 19.0 to analyze the data. The results were expressed as the mean value and standard error. Analysis of variance and average comparison were based on the least significant difference (LSD) test of 5% probability level in the same place and year.

RESULTS

Effects of SEs on Photosynthetic Physiology of Leaves

SPAD

The SPAD value of leaves increased significantly after spraying SEs at the seedling stage (**Figure 2A**). Similarly, after the second spraying (SE2/SE3) in the elongation period, SPAD values in plants treated with SEs were significantly higher than that without SE application (**Figure 2B**), but there was no significant difference between the treatment sprayed with SE only once at the seedling stage and the control treatment. Spraying for the third time at the early mature stage did not affect the SPAD value of leaves (**Figure 2C**). However, there were differences between different years at the same test site.

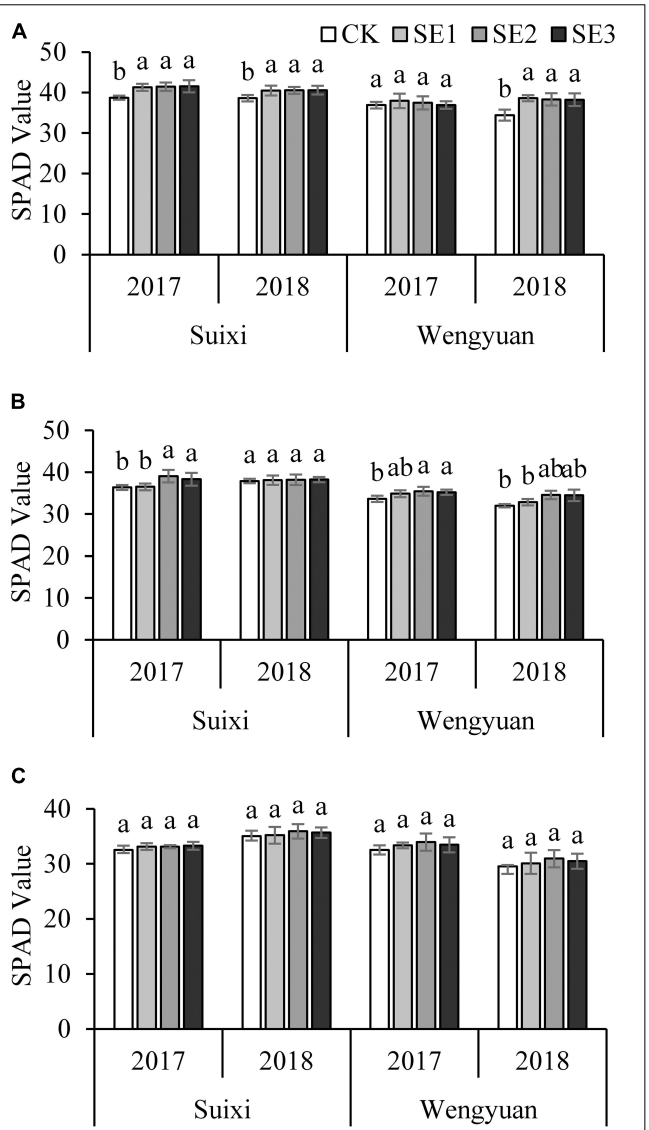

FIGURE 2 | SPAD value of the fully expended top leaf in the seeding **(A)**, Elongation **(B)**, and early maturity **(C)** stages under different SE treatments. ANOVA analysis was conducted among different treatments at the same trial site in the same year and bars with different letters indicate the significance at the 0.05 level.

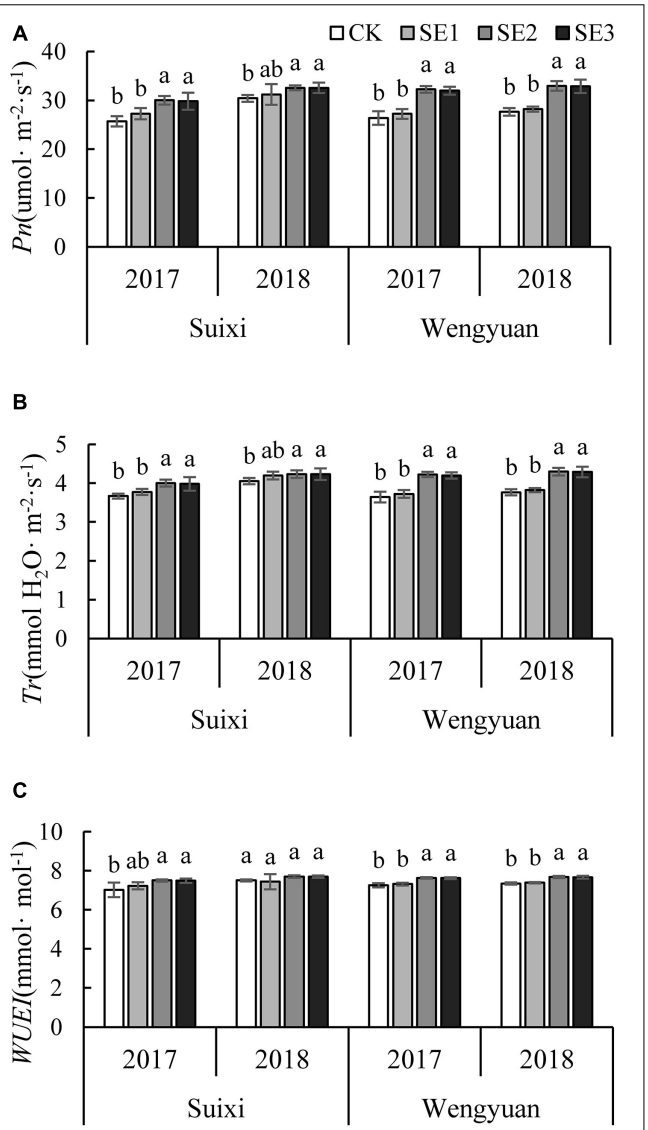

FIGURE 3 | The *Pn*, *Tr*, and *WUEI* of the fully expended top leaf in the Elongation stages under different SE treatments **(A)** *Pn*, **(B)** *Tr*, and **(C)** *WUEI*. ANOVA analysis was conducted among different treatments at the same trial site in the same year and different years and bars with different letters indicate the significance at the 0.05 level.

Pn, Tr, and WUEI

SE application at the early elongation period (SE2 and SE3) made *Pn* significantly higher than that of the no SE treatment, with an average increase of 14.52%. All four experiments had the same performance (**Figure 3A**). However, treatment of SE application only once at the seedling stage (SE1) did not have the same effect. Furthermore, the *Pn* of SE2 and SE3 treatments were significantly higher than that of SE1 in three trials (Suixi in 2017, Wengyuan in 2017 and 2018).

The results of *Tr* were similar to *Pn*. The *Tr* of sugarcane sprayed with SEs during the elongation period was significantly higher than that of the control, with an average increase of 10.62%. All experimental results were consistent (**Figure 3B**). In addition, *Tr* of SE2 and SE3 were significantly higher than that of SE1 in 3 trials (Suixi in 2017, Wengyuan in 2017 and 2018).

The *WUEI* of SE2 and SE3 was significantly higher than that of the control in the elongation period, with an average increase of 4.70% (**Figure 3C**). Furthermore, WUEI in SE2 and SE3 was significantly higher than that of SE1 in Wengyuan.

Effects of SEs on Nutrient Utilization Efficiency (NUE) of N, P, and K

The data shown in **Table 2** comprise the NUE of N, P, and K of sugarcane, which are the average of six experimental results in

TABLE 2 | N, P, K utilization efficiency and partial productivity of sugarcane under different treatments.

Treatment	Utilization efficiency (%)			Partial productivity (kg/kg)		
	N	P	K	N	P	K
CK	32.87 ± 2.23ab	7.96 ± 0.62c	42.75 ± 2.86b	216.08 ± 18.06*a*	421.32 ± 33.32*a*	230.95 ± 19.08*a*
SE1	36.12 ± 4.00ab	8.22 ± 0.91bc	45.09 ± 4.67*ab*	223.36 ± 20.89a	435.46 ± 37.87a	238.73 ± 22.04a
SE2	38.67 ± 2.43a	9.02 ± 0.87ab	48.61 ± 4.09a	235.55 ± 22.08a	459.28 ± 40.85a	251.76 ± 23.35a
SE3	39.03 ± 5.01a	9.1 ± 0.5a	48.95 ± 3.95a	236.01 ± 20.72a	460.2 ± 38.52a	252.25 ± 21.91a

[a] *Data presented as mean ± SE, n = 4. Different letters in each column show significant difference at p <0.05, according to LSD.*

two sites for 3 years. The results showed that the NUE of N, P, and K sprayed with SEs were all improved to a certain extent compared with the control. In SE1, SE2, and SE3, the NUE of N increased by 9.88, 17.64, and 18.74%, respectively, of P by 3.26, 13.31, and 14.31%, respectively, and of K by 5.48, 13.70, and 14.49%, respectively. In addition, the N, P, and K PFP of the two treatments (average of SE2 and SE3) were increased by 19.71, 38.42, and 21.06 kg/kg, respectively, compared with the control but the differences were not significant.

Effects of SEs on Yield Components of Sugarcane

The plant height of sugarcane sprayed with SEs in April was significantly higher than that of CK, and there were significant differences in 4 of 6 experiments (**Table 3**). After spraying SEs for the second time in the elongation period (SE2/SE3), the plant height of sugarcane in August was significantly higher than that of the control, and this effect was also shown in four experiments. However, spraying SEs for the third time had no significant effect on plant height. According to the results of 3 years of experiments at two sites, compared with the non-SE application, SE3, SE2, and SE1 increased the height of sugarcane by 4.81, 4.66, and 2.04%, respectively. In addition, SE application had no significant effect on the millable cane per unit area (**Table 3**). Therefore, the promotion effect of SEs on sugarcane growth was mainly reflected in the increase of sugarcane plant height.

Effects of Different Treatments on Sugarcane Yield

Spraying SEs both at seedling and elongation stages improved sugarcane yield significantly, and the yields of SE2 and SE3 were increased by 9.01 and 9.23%, respectively, compared with those of sugarcane without SE, while the yield of sugarcane sprayed with SEs once at the seedling stage was not significantly different from the control (with a 3.33% yield increase).

The effect of SEs on yield varied with different years and sites. SE treatment (SE3, SE2, and SE1) increased the yield by 6.17, 6.96, and 7.80%, respectively, in Suixi and by 7.59, 9.71, and 4.69%, respectively, in Wengyuan from 2017 to 2019 compared with the control. The 3-year average yield of SE2 and SE3 treatments significantly increased 9.17 and 8.95%, respectively, in Suixi and by 8.83 and 9.53%, respectively, in Wengyuan. However, the yields showed no significant difference between SE2 and SE3 treatments. Similarly, there was no difference in yield between SE4 treatment and CK, which indicated that spraying SEs at the mature stage had no significant effect on yield.

Sucrose Content, Reducing Sugar Content, and Sugar Yield of Sugarcane in Harvest Period

Sucrose Content

Regardless of whether SEs were sprayed in both seedling and elongation stages, the sucrose content of cane with SE application in the mature stage (SE3/SE4) was significantly higher than that of cane without SE application, and the sucrose content of SE3 and SE4 in Suixi in 3 years was 5.71 and 5.49% higher, respectively, than that of the control (**Table 8**). Furthermore, the increase in Wengyuan was 4.72 and 4.11%, respectively. The average in 3 years at the two sites of SE3 and SE4 treatments significantly increased by 5.21 and 4.79%, respectively (total average 5.00%), compared with those of the control ($P < 0.05$). Notably, SE3 and SE4 treatments were also significantly higher than SE1 and SE2 treatments.

Reducing Sugar

Spraying SEs at the mature stage significantly decreased the reducing sugar content of sugarcane by 32.56 and 34.32% (average 33.44%) than that of SE1 and SE2, respectively (**Table 4**). However, there was no significant difference in reducing sugar content between SE1 and SE2 treatments and those without SE treatment.

Theoretical Sugar Yield

The 3-year average of sugar content per unit area in Suixi and Wengyuan was significantly higher than that in non-SE treatments, and SE3 was the highest in every year and each place, which was significantly higher than all other treatments. Compared with the control, the sugar content per unit area of SE3 treatment in Suixi and Wengyuan was significantly increased by 15.31 and 16.56%, respectively ($P < 0.05$) and the comprehensive average was increased by 15.92%. In addition, SE1, SE2, and SE4 treatments increased by 5.43, 12.60, and 7.83%, respectively, compared with those of the control (**Table 5**).

Effects of SEs on the Activity of Sucrose Phosphate Synthase (SPS) and Soluble Acid Invertase (SAI)

Compared with the treatment without SE, the activity of SPS in leaves of SE3 and SE4 treatments increased by 9.34 and

TABLE 3 | Agronomic characters of sugarcane under different treatments.

Site/Year	Treatment	Plant height (cm)			Stalk diameter (mm)	Millable stalks (plant·hm^{-2})
		Apr.	Aug.	Dec.	Dec.	Dec.
Suixi/2017	CK	60.97 ± 1.92b[a]	212.25 ± 1.79c	285.85 ± 3.63b	32.79 ± 0.64a	54058 ± 1355a
	SE1	67.5 ± 1.39a	217.02 ± 1.01b	290.45 ± 1.1ab	32.61 ± 0.45a	54390 ± 633a
	SE2	68.65 ± 0.88a	236.65 ± 1.77a	298.52 ± 3.74a	33.07 ± 0.33a	54896 ± 599a
	SE3	67.25 ± 2.17a	238.22 ± 3.29a	301.4 ± 1.39a	33.21 ± 0.54a	54087 ± 967a
Suixi/2018	CK	72.67 ± 0.35b	216.1 ± 1.05a	284.05 ± 1.61b	32.11 ± 0.27a	55498 ± 974a
	SE1	77.35 ± 1.6a	220.87 ± 2.01a	289 ± 2.61ab	32.51 ± 0.66a	55229 ± 1280a
	SE2	79.57 ± 1.13a	225.9 ± 4.34a	293.85 ± 2.02a	32.89 ± 0.29a	55641 ± 885a
	SE3	77.17 ± 2.26a	223.85 ± 5.39a	291.52 ± 2.24a	32.93 ± 0.96a	55223 ± 787a
Suixi/2019	CK	70.21 ± 1.02b	206.43 ± 2.47b	268.28 ± 1.24b	31.56 ± 0.20a	52720 ± 736a
	SE1	78.17 ± 4.45a	212.75 ± 1.9a	273.36 ± 2.4ab	31.66 ± 0.28a	52751 ± 545a
	SE2	77.92 ± 1.02a	217.76 ± 1.41a	283 ± 2.45a	32.07 ± 0.17a	52937 ± 614a
	SE3	80.26 ± 4.48a	217.13 ± 1.44a	284.27 ± 1a	32.16 ± 0.49a	52604 ± 732a
Wengyuan/2017	CK	50.47 ± 2.77b	209.77 ± 2.91b	275.95 ± 3.34b	32.07 ± 0.62a	52926 ± 1328a
	SE1	57.97 ± 1.53a	214.55 ± 2.97ab	281.5 ± 3.31b	32.17 ± 0.40a	53116 ± 865a
	SE2	57.9 ± 2.27a	222.5 ± 4.02a	291.7 ± 2.68a	32.56 ± 0.53a	52672 ± 746a
	SE3	57.55 ± 1.28a	224.95 ± 3.27a	292 ± 1.81a	32.68 ± 0.37a	52641 ± 521a
Wengyuan/2018	CK	63.57 ± 1.18b	207.72 ± 4.07b	276.82 ± 3.02b	32.64 ± 0.27a	53519 ± 1417a
	SE1	70.07 ± 0.63a	213.27 ± 1.93ab	285.32 ± 4.91ab	32.93 ± 0.45a	54009 ± 420a
	SE2	69.55 ± 1.21a	218.17 ± 2.77a	291.35 ± 3.41a	33.46 ± 0.16a	53549 ± 1440a
	SE3	69.8 ± 1.58a	222.32 ± 2.55a	292.15 ± 2a	33.42 ± 0.12a	53715 ± 960a
Wengyuan/2019	CK	66.67 ± 2.57a	200.28 ± 2.04b	262.61 ± 2.02b	31.67 ± 0.39a	51326 ± 1107a
	SE1	67.24 ± 0.96a	204.46 ± 1.59ab	267.57 ± 1.37ab	31.66 ± 0.33a	51663 ± 522a
	SE2	68.35 ± 0.84a	209.07 ± 1.42a	272.13 ± 1.1a	31.76 ± 0.36a	51714 ± 622a
	SE3	67.89 ± 1.34a	208.77 ± 1.33a	271.69 ± 1.2a	31.90 ± 0.47a	51781 ± 816a

[a]*Data presented as mean ± SE, n = 4. Different letters in each column show significant difference in the same year, the same site at p <0.05, according to LSD.*

TABLE 4 | Reducing sugar content of sugarcane with different treatments at harvest.

Treatments	Suixi (%)				Wengyuan (%)				Total average (%)
	2017	2018	2019	AVERAGE	2017	2018	2019	Average	
CK	0.47 ± 0.06a[a]	0.37 ± 0.1a	0.32 ± 0.01a	0.39 ± 0.05a	0.4 ± 0.05a	0.46 ± 0.06a	0.32 ± 0.01a	0.43 ± 0.05a	0.41 ± 0.05a
SE1	0.43 ± 0.08a	0.37 ± 0.06a	0.3 ± 0.01a	0.37 ± 0.02ab	0.41 ± 0.04a	0.43 ± 0.03a	0.3 ± 0.01a	0.43 ± 0.02a	0.4 ± 0.03a
SE2	0.46 ± 0.08a	0.34 ± 0.05a	0.3 ± 0.01a	0.37 ± 0.01b	0.38 ± 0.05a	0.42 ± 0.01a	0.3 ± 0.01a	0.42 ± 0.02a	0.39 ± 0.03a
SE3	0.31 ± 0.07b	0.24 ± 0.05b	0.21 ± 0b	0.25 ± 0.01c	0.28 ± 0.03b	0.31 ± 0.01b	0.21 ± 0b	0.3 ± 0.01b	0.28 ± 0.02b
SE4	0.29 ± 0.02b	0.25 ± 0.05b	0.21 ± 0.03b	0.25 ± 0.03c	0.28 ± 0.04b	0.28 ± 0.04b	0.21 ± 0.03b	0.29 ± 0.02b	0.27 ± 0.03b

[a]*Data presented as mean ± SE, n = 4. Different letters in each column show significant difference in the same year, the same site at p <0.05, according to LSD.*

TABLE 5 | Theoretical sugar yield of sugarcane with different treatments at harvest time.

Treatment	Suixi (t·hm^{-2})				Wengyuan (t·hm^{-2})				Total average (t hm^{-2})
	2017	2018	2019	Average	2017	2018	2019	Average	
CK	17.00 ± 1.01c[a]	16.71 ± 0.16c	14.46 ± 0.53d	16.05 ± 0.55e	15.15 ± 0.72d	16.48 ± 0.77c	13.94 ± 0.20c	15.19 ± 0.37d	15.62 ± 0.42e
SE1	17.15 ± 1.00c	17.65 ± 0.76c	15.41 ± 0.4c	16.74 ± 0.42d	16.09 ± 0.53c	17.73 ± 0.38bc	14.80 ± 0.47bc	16.21 ± 0.42c	16.47 ± 0.41d
SE2	18.61 ± 0.74b	18.75 ± 0.60a	16.69 ± 0.58a	18.01 ± 0.32b	17.44 ± 0.54b	18.69 ± 0.72a	15.37 ± 0.34a	17.17 ± 0.26b	17.59 ± 0.27b
SE3	19.35 ± 0.66a	18.99 ± 1.02a	17.20 ± 0.56a	18.51 ± 0.51a	17.86 ± 0.43a	19.38 ± 0.42a	15.88 ± 0.5a	17.71 ± 0.21a	18.11 ± 0.33a
SE4	18.18 ± 1.10b	17.80 ± 0.58b	15.70 ± 0.33b	17.23 ± 0.53c	16.90 ± 0.56c	17.52 ± 0.60b	14.98 ± 0.39b	16.47 ± 0.45c	16.85 ± 0.09c

[a]*Data presented as mean ± SE, n = 4. Different letters in each column show significant difference in the same year, the same site at p <0.05, according to LSD.*

8.95% (average 9.14%), respectively, and the SPS enzyme activity in stalks increased significantly by 15.56 and 14.76% (average 15.16%), respectively ($P < 0.05$). However, the activities of SPS in leaves and stems of sugarcane treated with SE1 and SE2 did not change significantly. The SAI enzyme activity in stalks of SE3 and SE4 treatments significantly decreased by 15.20 and 17.84%, respectively (average 16.52%, $p < 0.05$), and was also significantly lower than that of the SE1 treatment (**Table 6**).

Correlation Analysis Between Annual Rainfall and Plant Height, Sucrose Content, Cane Yield and Cane Yield Increase

We used the data of SE2 and SE3 treatments in which SEs had the best effects on sugarcane yield to analyze the correlation of plant height, sucrose content, cane yield and cane yield increase (relative to the treatment without SEs) with annual rainfall. The results showed that plant height, sucrose content and cane yield had no significant correlations with annual rainfall, but the increase of cane yield had a significant negative correlation with rainfall (**Figure 4**), that means the lower the annual rainfall, the greater the increase in sugarcane yield from SEs application.

DISCUSSION

Effects of SEs on Sugarcane Growth and Cane Yield

Biostimulatory activities of SEs were evident throughout the experiments, shown by significant increases in plant height and cane yield. The results of this study are also in agreement with reports on other crops, including strawberry, maize, and tomato (Alam et al., 2013; Ali et al., 2016; Trivedi et al., 2018a,b). The yields of the treatments with SE application (SE1, SE2, and SE3) were higher than those without SE application, with the average increase range of 2.67–9.17% in Suixi and 4.04–9.53% in Wengyuan (**Table 7**). It has been reported that the application of SE had a better effect on the increase of cane yield. One study showed that SE application both in the soil and on the leaves increased the yield of sugarcane by 14.1% (Deshmaukh and Phonde, 2013), and another experiment showed that spraying SEs on sugarcane three times could achieve a yield increase of 20.47–28.79% (Karthikeyan and Shanmugam, 2017). In terms of yield components, seaweed extract had the greatest effect on plant height, but had no significant effect on stem diameter and millable cane number. The growth promoting properties observed may be a result of the effects of growth regulatory substances present in SE, including low molecular weight biostimulants (seaweed oligosaccharides) that can promote crop growth and high molecular weight biostimulants (algal polysaccharides) that can improve crop stress resistance. These substances induced the biosynthesis of hormones such as phytohormones abscisic acid, cytokinin, and auxin in treated plants (Khan et al., 2009; Aremu et al., 2016; Patel et al., 2018; Ali et al., 2019; Renaut et al., 2019; Mukherjee and Patel, 2020). It has been reported that the yield increasing with SEs applications was associated with improved chlorophyll biosynthesis (higher SPAD index) (Youssef et al., 2018). Our results determined at seedling and elongation stages showed that spraying SEs could significantly increase the SPAD value of sugarcane leaves, which indicated that the application of SEs increased chlorophyll content in leaves (**Figure 2**), which is also supported by other reports (Lingakumar et al., 2004; Ali et al., 2016, 2019). This might be due to the existence of betaine, amino acids, and other active substances in SEs that inhibit the degradation of chlorophyll (Blunden et al., 1996), Seaweed extracts also contain magnesium, which is necessary for chlorophyll synthesis (Almaroai and Eissa, 2020). Our results showed that spraying SEs had a significant effect on the photosynthetic rate of sugarcane leaves which were consistent with those of SPAD, and these resulted in a stronger ability of plants to maintain a better photosynthetic performance (Santaniello et al., 2017).

Nutrient absorption is an important factor for high yield of crops, and more nutrient absorption leads to higher cane

TABLE 6 | Activities of SPS and SAI in leaves and stems of different treatments at mature stage.

	Treatment	SPS (μmol Suc g^{-1}Fw h^{-1})		SAI (μmol Glu g^{-1}Fw h^{-1})	
		Suixi	Wengyuan	Suixi	Wengyuan
Leaf	CK	453.65 ± 20.36*b*[a]	462.36 ± 34.68b	870.63 ± 44.44a	972.5 ± 81.75a
	SE1	455.45 ± 20.99b	469.05 ± 20.94b	894.81 ± 25.68a	936.16 ± 85.06a
	SE2	449.75 ± 22.23b	472.31 ± 10.83b	905.42 ± 20.50a	959.75 ± 86.07a
	SE3	489.42 ± 7.96a	512.25 ± 15.79a	888.87 ± 45.17a	946.25 ± 94.7a
	SE4	481.50 ± 13.17a	516.75 ± 13.04a	922.25 ± 51.69a	953.55 ± 66.26
Stalk	CK	228.56 ± 11.89b	255.85 ± 20.01b	359.14 ± 29.94a	332.89 ± 14.47a
	SE1	244.06 ± 26.83b	259.80 ± 13.68b	336.85 ± 20.43a	345.85 ± 13.09a
	SE2	247.30 ± 22.71b	254.60 ± 5.10b	363.31 ± 24.99a	343.33 ± 11.84a
	SE3	274.61 ± 7.46a	283.92 ± 10.67a	289.60 ± 31.12b	296.14 ± 23.90b
	SE4	271.35 ± 16.85a	287.85 ± 9.77a	283.99 ± 8.21b	294.81 ± 5.11b

[a]*Data presented as mean ± SE, n = 4. Different letters in each column show significant difference in the same organ, the same site at p <0.05, according to LSD.*

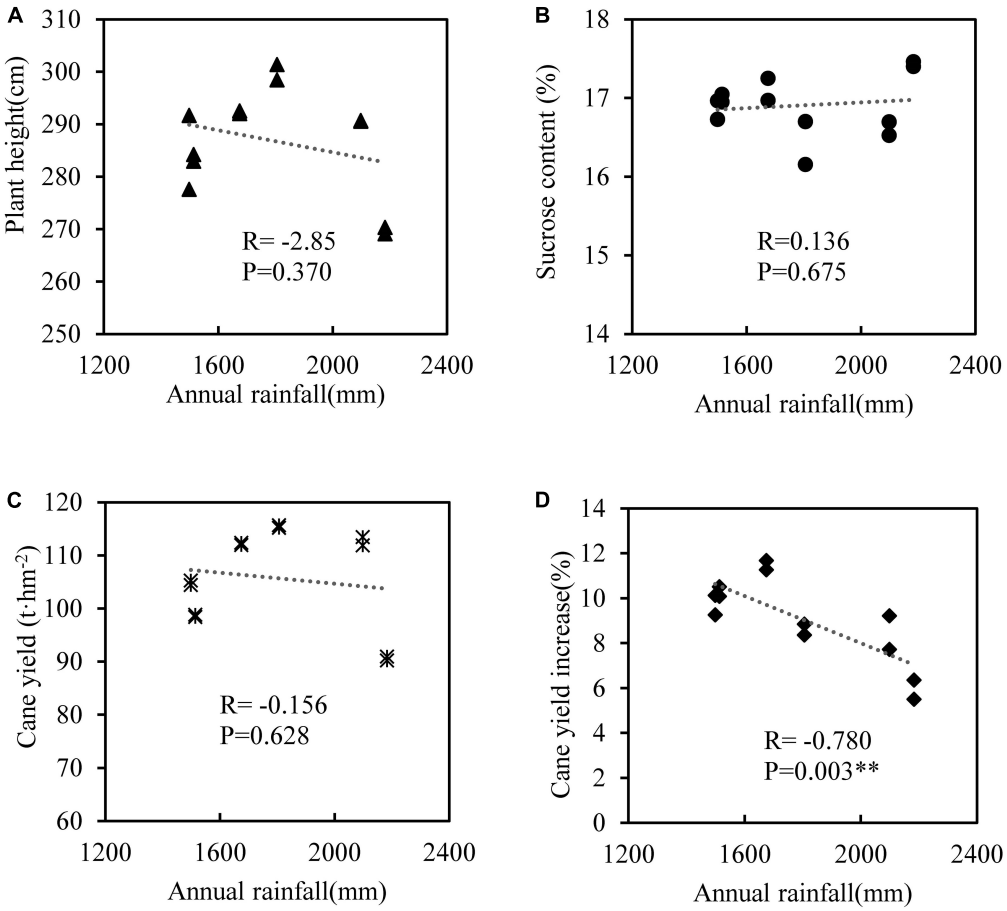

FIGURE 4 | Correlation analysis between annual rainfall and plant height **(A)**, sucrose content **(B)**, cane yield **(C),** and cane yield increase **(D)** with SE2 and SE3 treatments. $n = 12$, **denotes $p < 0.01$.

TABLE 7 | Cane yield under different treatments.

Site	Treatment	2017 (t·hm^{-2})	2018 (t·hm^{-2})	2019 (t·hm^{-2})	Average (t·hm^{-2})
Suixi	CK	106.30 ± 6.36*b*[a]	103.88 ± 1.68b	89.44 ± 2.25b	99.87 ± 2.98b
	SE1	107.69 ± 3.27b	107.97 ± 3.29b	91.96 ± 1.00b	102.54 ± 1.75b
	SE2	115.19 ± 2.01a	113.45 ± 1.79a	98.46 ± 2.42a	109.03 ± 1.61a
	SE3	115.70 ± 5.38a	111.9 ± 5.35ab	98.84 ± 2.63a	108.82 ± 2.98a
	SE4	107.21 ± 7.33b	104.73 ± 1.39b	90.19 ± 3.14b	100.71 ± 3.79b
Wengyuan	CK	95.60 ± 2.65b	100.62 ± 4.99b	85.54 ± 1.88c	93.92 ± 1.72b
	SE1	98.84 ± 4.10b	106.86 ± 2.57ab	87.44 ± 2.49bc	97.71 ± 2.92b
	SE2	104.45 ± 4.28a	111.94 ± 2.83a	90.24 ± 2.36ab	102.21 ± 1.24a
	SE3	105.29 ± 3.21a	112.36 ± 3.32a	90.97 ± 1.60a	102.87 ± 0.93a
	SE4	99.07 ± 3.19b	102.82 ± 2.31b	86.54 ± 1.34c	96.14 ± 1.40b

[a]*Data presented as mean ± SE, n = 4. Different letters in each column show significant difference in the same year, the same site at p<0.05, according to LSD.*

yields (Rhodes et al., 2018). The results showed that the utilization efficiency of nitrogen, phosphorus and potassium in sugarcane sprayed with SEs was significantly higher than that in the treatment without SEs. Previous studies have shown that the application of SEs can promote the growth of crop roots, improve the ability of roots to absorb macroelement nutrients and transfer them to the aboveground (Crouch et al., 1990), which is related to the hormones substances in SE (Finnie and van Staden, 1985; Jeannin et al., 1991), and the hormones substances may promote up-regulated expression of nutrient transport genes, thus improving root uptake and transport of nutrients (Krouk et al., 2010; Rathore et al., 2009). Further studies in the promotion mechanism for SEs regulating plant root growth confirmed

TABLE 8 | Sucrose content of sugarcane with different treatments at harvest time.

Treatment	Suixi(%)				Wengyuan (%)				Total average (%)
	2017	2018	2019	Average	2017	2018	2019	Average	
CK	15.99 ± 0.08c[a]	16.10 ± 0.38b	16.95 ± 0.40b	16.08 ± 0.12b	16.09 ± 0.37b	16.52 ± 0.30b	16.95 ± 0.40b	16.52 ± 0.30b	16.13 ± 0.11b
SE1	15.91 ± 0.55c	16.34 ± 0.35b	16.93 ± 0.35b	16.34 ± 0.22b	16.28 ± 0.30b	16.59 ± 0.18b	16.93 ± 0.35b	16.60 ± 0.26b	16.47 ± 0.26b
SE2	16.16 ± 0.77bc	16.53 ± 0.32ab	17.12 ± 0.56ab	16.54 ± 0.28b	16.37 ± 0.34b	16.7 ± 0.64ab	17.12 ± 0.56ab	16.73 ± 0.42b	16.68 ± 0.35b
SE3	16.73 ± 0.29ab	16.97 ± 0.24a	17.69 ± 0.19a	17.03 ± 0.24a	16.96 ± 0.22a	17.25 ± 0.14a	17.69 ± 0.19a	17.30 ± 0.10a	17.13 ± 0.21a
SE4	16.96 ± 0.2a	17.25 ± 0.21a	17.51 ± 0.29a	17.06 ± 0.14a	17.06 ± 0.09a	17.04 ± 0.32a	17.51 ± 0.29a	17.20 ± 0.17a	17.10 ± 0.18a

[a]*Data presented as mean ± SE, n = 4. Different letters in each column show significant difference in the same year, the same site at p<0.05, according to LSD.*

that SEs could up-regulated the gene expression and enzyme activity of nitrate reductase at the post-transcriptional level (Zhang et al., 2013).

Effects of SEs on Sugar Accumulation of Sugarcane

Sucrose content is the most important quality index of sugarcane. All over the world, the sugarcane industry has tried to find ways to improve the sucrose content of sugarcane or accelerate the ripening of sugarcane, among which growth regulator substances are the most frequently used (Rossetto et al., 2003; Li, 2004; Van Heerden et al., 2015; Cunha et al., 2017). In the management of sugarcane, sugar increasers or ripening agents can be applied at the early mature period to advance the harvest period or increase the sucrose content. SEs are a kind of biostimulant that contains a variety of plant hormones, which could regulate the growth and development of plants (Khan et al., 2009; Craigie, 2011; Ali et al., 2016). Therefore, our experiment also set the third application time at the early mature period (from the end of October to November) to evaluate its effects on the sucrose content of sugarcane. Furthermore, we set the treatment of spraying SEs alone in the early mature period (SE4) and compared it with SE3. The results showed that the sucrose content of canes with SE treatment (SE3 and SE4) were significantly increased in comparison with that of non-SE and the SE1 treatment at the early stage of maturity. It was even higher than that of the SE2 treatment in some experiments, and there was no significant difference between SE3 and SE4. These results indicated that the increase of sucrose was mainly due to the SE application at the mature stage, rather than at the seedling and elongation stages.

Sugar conversion and accumulation in sugarcane is regulated by many enzymes, including sucrose synthase (SS), sucrose phosphate synthase (SPS), and invertase (INV) (Sturm, 1999; Winter and Huber, 2000). SPS is a key regulatory enzyme in the distribution of photosynthetic products to sucrose and starch in plants and is positively correlated with sucrose accumulation (Grof et al., 2007). INV is one of the key enzymes controlling sucrose metabolism in plants, which irreversibly catalyzes the conversion of sucrose + H_2O into fructose + glucose. SAI is a kind of INV, which mainly exists in vacuoles and plays a role in regulating sucrose and hexose levels (Tian et al., 2009), and cane sugar is negatively correlated with SAI activity. In this study, SPS in the direction of sucrose synthesis and SAI in the direction of decomposition and transformation were selected as representatives for analysis. The results showed that spraying SEs at the early stage of maturity significantly increased the activity of SPS enzymes in leaves and stems, which was beneficial to the synthesis and accumulation of sucrose. For stems, SE application significantly reduced the activity of the SAI enzyme, which reduced the decomposition of sucrose in sugarcane stems. Therefore, it could be speculated that SEs regulated related enzymes in sugarcane, promoted the synthesis and accumulation of sucrose, and reduced the transformation to reducing sugar, thus, improving the sucrose content of sugarcane. Reports have shown the elicitation of various plant enzymes and the increasing in the activity of these enzymes by SEs (El Modafar et al., 2012; Ali et al., 2019). The regulation of enzymes activity observed may be as a result of the effects of phytohormones and growth regulatory substances present in the SEs and induced the biosynthesis of hormones by treated plants (Kang et al., 2014; Ramkissoon et al., 2017).

Sucrose accumulation related to biosynthesis of plant hormone signal transduction, which are consistent with the physiological effects elicited by exogenous hormone substances application on sugarcane. While the hormone in signal transduction at the maturation stage are great different from other stage in sugarcane (Cunha et al., 2017). Therefore, the ideal effect can be obtained only when it is applied at mature stage.

Importance of Applying Seaweed Fertilizer in Rain-Fed Agricultural Areas

Cane yield is closely related to climate factors (Inman-Bamber and Smith, 2005; Liu et al., 2016). In this study, the cane yield of the two experimental sites were different in different years, and the effect of seaweed extract on the yield was also different in different years. In this study, the annual rainfall of the two sites were different (**Figure 1** and **Table 1**). Sugarcane has a great demand for water during the period of rapid growth (May to August every year) in China. The growth of sugarcane is severely inhibited if there was no rainfall and irrigation, resulting in a decline in yield. The uneven seasonal rainfall was also different in the two places. Specifically, the rainfall at Wengyuan in 2017 and 2019 was mainly distributed in March to July and less in the later months, while in June to September 2018, it was less distributed in the early months (**Figure 1**). In Wengyuan, the highest yield of the 3 years was in 2018 (**Table 7**), which might be related to the high coincidence between the rainy season and rapid growth of sugarcane in that year. However, the yield in 2019 was lowest,

and there were two reasons for this. First, the rainfall decreased significantly after July in that year compared with previous years, which affected sugarcane growth; second, as the second year of ratoon, the emergence of sugarcane generally decreased with the increase of ratoon years, which led to the decrease of millable cane number per unit area (one of the yield components) (**Table 3**). The rainfall in Suixi from 2017 to 2019 was less in January to May, and more in June to September, especially in 2019. There was no significant difference in sugarcane production between 2017 and 2018 because the rainy season in these 2 years basically coincided with the rapid growth stage of sugarcane. The lowest output in 2019 was due to similar reasons as that of Wengyuan. The effects of SE application on yield also had year-to-year differences. SE treatments had different improvement on sugarcane yield in different years and places, among which Suixi had the largest improvement (>9%) in 2019, which had the least annual total rainfall (1513.72 mm) and monthly average rainfall (126.14 mm). The increase of yield at Wengyuan in 2017 and 2018 was > 10% and < 6% in 2019. Correspondingly, the total rainfall (1498.66 mm/1674.83 mm) and monthly rainfall average (124.89 mm/139.57 mm) in 2017 and 2018 were lower than those in 2019 (rainfall values were not shown in **Figure 1**). The yield increase rates of SE1, SE2, and SE3 treatments in Suixi were 2.67, 9.17, and 8.95%, respectively, and those of Wengyuan were 4.04, 8.83, and 9.53%, respectively. These results indicated that spraying SEs only once at the seedling stage was not enough to improve yield but spraying SEs two or three times at different growth stages was better.

In addition, the WUEI analysis could also well correspond with this result. The results showed that the WUEI of plants sprayed with SEs in the early elongation stage was significantly higher than that without SEs application, which indicated that SEs could improve the water use efficiency and drought resistance of crops (Neily et al., 2010; Trivedi et al., 2018a,b). Research showed that SEs induced a partial stomatal closure, associated with changes in the expression levels of genes involved in ABA-responsive and antioxidant system pathways under drought stress conditions (Santaniello et al., 2017), and SEs was able to mitigate the drought stress by regulating the expression of genes involved in ABA biosynthesis and ROS detoxification (Shukla et al., 2018).

Based on the above analysis, the effect of SEs on sugarcane yield was more obvious under drought conditions, which could be due to the fact that the SEs contained many active substances which were conducive to improving the drought tolerance of sugarcane (Spann and Little, 2011; Martynenko et al., 2016; Shukla et al., 2018). Therefore, it is suggested that SEs should be sprayed once both at seedling and early elongation stages in sugarcane management in rain-fed agricultural areas.

CONCLUSION

In this study, spraying SEs on sugarcane leaves at seedling and early elongation stages promoted sugarcane growth in rainfed areas without irrigation. SE application promoted photosynthesis and transpiration, improved WUEI and utilization efficiency of nitrogen, phosphorus, and potassium, and increased the height of sugarcane, thus, increasing the yield and economic benefits. Moreover, in drought years, SEs had more significant effects on alleviating sugarcane yield decline caused by drought.

Furthermore, we found that spraying SEs at the early mature stage of sugarcane could regulate the activities of enzymes related to sugar accumulation in sugarcane leaves and stems, increase the activities of sucrose phosphate synthase in leaves and stems, and reduce the activities of soluble acid invertase in stems, which was conducive to promoting sucrose accumulation in sugarcane stems.

Due to the improvement effect of SEs on sugarcane yield and sucrose content in this research, we suggest that SEs should be sprayed at different growth stages in sugarcane production. It is better to spray three times at seedling, elongation, and early mature stages. These provide a theoretical basis for the application of SE in agricultural areas.

DATA AVAILABILITY STATEMENT

The original contributions presented in the study are included in the article/supplementary material, further inquiries can be directed to the corresponding author/s.

AUTHOR CONTRIBUTIONS

DC conceived and designed the experiments with the help of HS. DC, WZ, JA, DS, and YJ performed the field trials and agronomy study. DC analyzed the data and wrote many parts of the manuscript. YH performed the enzyme study and analyzed the data. WZ and JY performed and wrote the statistical analyses. DS, YH, and YJ performed sucrose and nutrient analysis. ZH prepared the figures. DC wrote the first draft of the manuscript with the help of JY, WZ, and HS. ZH and DC prepared the final manuscript with the help of HS. All authors contributed to the article and approved the submitted version.

FUNDING

This study was financed by the China Agricultural Research System (CARS-170203), Guangdong Provincial Science and Technology Plan (2019B030301007), the National Key Research and Development Program of China (2017YFD0200208 and 2016YFD0200405-5), and Central Public-interest Scientific Institution Basal Research Fund for Chinese Academy of Tropical Agricultural Sciences (1630052019001).

ACKNOWLEDGMENTS

We would like to thank Mingfu Wen, Qingwen Luo, Junxian Yang, and Zhonghua Chen very much for helping us to manage sugarcane cultivation for the 3 years. We would also like to thank the LetPub (www.letpub.com) for its linguistic assistance during the preparation of this manuscript and reviewers for their valuable comments.

REFERENCES

Alam, M. Z., Braun, G., Norrie, J., and Hodges, D. M. (2013). Effect of A*scophyllum* extract application on plant growth, fruit yield and soil microbial communities of strawberry. *Can. J. Plant Sci.* 93, 23–36. doi: 10.4141/cjps2011-260

Ali, N., Farrell, A., Ramsubhag, A., and Jayaraman, J. (2016). The effect of ascophyllum nodosum extract on the growth, yield and fruit quality of tomato grown under tropical conditions. *J. Appl. Phycol.* 28, 1353–1362. doi: 10.1007/s10811-015-0608-3

Ali, O., Ramsubhag, A., and Jayaraman, J. (2019). Biostimulatory activities of ascophyllum nodosum extract in tomato and sweet pepper crops in a tropical environment. *Plos One* 14:216710. doi: 10.1371/journal.pone.0216710

Almaroai, Y. A., and Eissa, M. A. (2020). Role of marine algae extracts in water stress resistance of onion under semiarid conditions. *J. Soil Sci. Plant Nutr.* 20, 1092–1101. doi: 10.1007/s42729-020-00195-0

Aremu, A. O., Plaèková, L., Gruz, J., Bíba, O., Novák, O., Stirk, W. A., et al. (2016). Seaweed-derived biostimulant (Kelpak§) influences endogenous cytokinins and bioactive compounds in hydroponically grown eucomis autumnalis. *J. Plant Growth Regul.* 35, 151–162. doi: 10.1007/s00344-015-9515-8

Arioli, T., Mattner, S. W., and Winberg, P. C. (2015). Applications of seaweed extracts in australian agriculture: past, present and future. *J. Appl. Phycol.* 27, 2007–2015. doi: 10.1007/s10811-015-0574-9

Bao, S. D. (2000). *Soil Agrochemical Analysis*. Beijing: Chinese Agriculture Press.

Battacharyya, D., Babgohari, M. Z., Rathor, P., and Prithiviraj, B. (2015). Seaweed extracts as biostimulants in horticulture. *Sci. Hortic.-Amsterdam* 196, 39–48. doi: 10.1016/j.scienta.2015.09.012

Ben Salah, I., Aghrouss, S., Douira, A., Aissam, S., El Alaoui-Talibi, Z., Filali-Maltouf, A., et al. (2018). Seaweed polysaccharides as bio-elicitors of natural defenses in olive trees against verticillium wilt of olive. *J. Plant Interact.* 13, 248–255. doi: 10.1080/17429145.2018.1471528

Blunden, G., Jenkins, T., and Liu, Y. W. (1996). Enhanced leaf chlorophyll levels in plants treated with seaweed extract. *J. Appl. Phycol.* 8, 535–543. doi: 10.1007/BF02186333

Boukhari, M. E. M. E., Barakate, M., Bouhia, Y., and Lyamlouli, K. (2020). Trends in seaweed extract based biostimulants: manufacturing process and beneficial effect on soil-plant systems. *Plants* 9:359. doi: 10.3390/plants9030359

Bradáčová, K., Weber, N. F., Morad-Talab, N., Asim, M., Imran, M., Weinmann, M., et al. (2016). Micronutrients (Zn/Mn), seaweed extracts, and plant growth-promoting bacteria as cold-stress protectants in maize. *Chem. Biol. Technol. Agric.* 3:19. doi: 10.1186/s40538-016-0069-1

Burke, E. J., Brown, S. J., and Christidis, N. (2006). Modeling the recent evolution of global drought and projections for the twenty-first century with the hadley centre climate model. *J. Hydrometeorol.* 7:1113. doi: 10.1175/JHM544.1

Cabo, S., Morais, M. C., Aires, A., Carvalho, R., Pascual Seva, N., Silva, A. P., et al. (2019). Kaolin and seaweed-based extracts can be used as middle and long-term strategy to mitigate negative effects of climate change in physiological performance of hazelnut tree. *J. Agron. Crop. Sci.* 206, 28–42. doi: 10.1111/jac.12369

Commodity Bureau, R. (2015). *CRB commodity yearbook*. Chicago, IL: Commodity Research Bureau.

Craigie, J. S. (2011). Seaweed extract stimuli in plant science and agriculture. *J. Appl. Phycol.* 23, 371–393. doi: 10.1007/s10811-010-9560-4

Crouch, I. J., Beckett, R. P., and van Staden, J. (1990). Effect of seaweed concentrate on the growth and mineral nutrition of nutrient-stressed lettuce. *J. Appl. Phycol.* 2, 269–272.

Crouch, I. J., and van Staden, J. (1993). Evidence for the presence of plant growth regulators in commercial seaweed products. *Plant Growth Regul.* 13, 21–29. doi: 10.1007/BF00207588

Cunha, C. P., Roberto, G. G., Vicentini, R., Lembke, C. G., Souza, G. M., Ribeiro, R. V., et al. (2017). Ethylene-induced transcriptional and hormonal responses at the onset of sugarcane ripening. *Sci. Rep.* 7:43364. doi: 10.1038/srep43364

Deshmaukh, P. S., and Phonde, D. B. (2013). Effect of seaweed extract on growth, yield and quality of sugarcane. *Int. J. Agric. Sci.* 9, 750–753.

El Modafar, C., Elgadda, M., El Boutachfaiti, R., Abouraicha, E., Zehhar, N., Petit, E., et al. (2012). Induction of natural defence accompanied by salicylic acid-dependant systemic acquired resistance in tomato seedlings in response to bioelicitors isolated from green algae. *Sci. Hortic.* 138, 55–63. doi: 10.1016/j.scienta.2012.02.011

Faostat. (2016). *Food and Agriculture Organization of the United Nations*. Rome: FAOSTAT.

Finnie, J. F., and van Staden, J. (1985). Effect of seaweed concentrate and applied hormones on in vitro cultured tomato roots. *Plant Physiol.* 120, 215–222.

Friedlander, M., and Ben-Amotz, A. (1990). Acclimation of brown seaweeds in an outdoor cultivation system and their cytokinin-like activity. *J. Appl. Phycol.* 2, 145–154. doi: 10.1007/BF00023376

Grof, C. P. L., Albertson, P. L., Bursle, J., Perroux, J. M., Bonnett, G. D., and Manners, J. M. (2007). Sucrose-phosphate synthase, a biochemical marker of high sucrose accumulation in sugarcane. *Crop Sci.* 47, 1530–1539. doi: 10.2135/cropsci2006.12.0825

Gutiérrez-Miceli, F. A., Rodríguez-Mendiola, M. A., Ochoa-Alejo, N., Méndez-Salas, R., Dendooven, L., and Arias-Castro, C. (2002). Relationship between sucrose accumulation and activities of sucrose-phosphatase, sucrose synthase, neutral invertase and soluble acid invertase in micropropagated sugarcane plants. *Acta Physiol. Plant* 24, 441–446. doi: 10.1007/s11738-002-0041-5

Hoover, D. L., Knapp, A. K., and Smith, M. D. (2017). Photosynthetic responses of a dominant C4 grass to an experimental heat wave are mediated by soil moisture. *Oecologia* 183, 303–313. doi: 10.1007/s00442-016-3755-6

Inman-Bamber, N. G., and Smith, D. M. (2005). Water relations in sugarcane and response to water deficits. *Field Crop Res.* 92, 185–202. doi: 10.1016/j.fcr.2005.01.023

Jannin, L., Arkoun, M., Etienne, P., Laîné, P., Goux, D., Garnica, M., et al. (2013). Brassica napus growth is promoted by ascophyllum nodosum (L.) Le Jol. seaweed extract: microarray analysis and physiological characterization of N, C, and S metabolisms. *J. Plant Growth Regul.* 32, 31–52. doi: 10.1007/s00344-012-9273-9

Jardin, P. D. (2012). *The Science of Plant Biostimulants-A bibliographic analysis, Ad hoc study report*. Brussels: European Commission.

Jeannin, I., Lescure, J., and Morot-Gaudry, J. (1991). The effects of aqueous seaweed sprays on the growth of maize. *Botanica Marina* 34, 469–474.

Kang, O. L., Ghani, M., Hassan, O., Rahmati, S., and Ramli, N. (2014). Novel agaro-oligosaccharide production through enzymatic hydrolysis: physicochemical properties and antioxidant activities. *Food Hydrocolloids* 42, 304–308. doi: 10.1016/j.foodhyd.2014.04.031

Karthikeyan, K., and Shanmugam, M. (2017). The effect of potassium-rich biostimulant from seaweed kappaphycus alvarezii on yield and quality of cane and cane juice of sugarcane var. Co 86032 under plantation and ratoon crops. *J. Appl. Phycol.* 29:3245. doi: 10.1007/s10811-017-1211-6

Khan, W., Rayirath, U. P., Subramanian, S., Jithesh, M. N., Rayorath, P., Hodges, D. M., et al. (2009). Seaweed extracts as biostimulants of plant growth and development. *J. Plant Growth Regul.* 28, 386–399. doi: 10.1007/s00344-009-9103-x

Khompatara, K., Pettongkhao, S., Kuyyogsuy, A., Deenamo, N., and Churngchow, N. (2019). Enhanced resistance to leaf fall disease caused by phytophthora palmivora in rubber tree seedling by sargassum polycystum extract. *Plants* 8:168. doi: 10.3390/plants8060168

Krouk, G., Lacombe, B., Bielach, A., Perrine-Walker, F., Malinska, K., Mounier, E., et al. (2010). Nitrate-regulated auxin transport by NRT1. 1 defines a mechanism for nutrient sensing in plants. *Dev. Cell* 18, 927–937.

Kumar, T., Kumar, T., Uzma, Khan, M. R., Khan, M. R., Abbas, Z., et al. (2014). Genetic improvement of sugarcane for drought and salinity stress tolerance using arabidopsis vacuolar pyrophosphatase (AVP1) gene. *Mol. Biotechnol.* 56, 199–209. doi: 10.1007/s12033-013-9695-z

Li, Y. (2004). Beneficial effects of ethephon application on sugarcane under sub-tropical climate of china. *Sugar Tech.* 6, 235–240. doi: 10.1007/BF02942503

Lingakumar, K., Jeyaprakash, R., Manimuthu, C., and Haribaskar, A. (2004). Influence of Sargassum sp. crude extract on vegetative growth and biochemical characteristics in Zea mays and Phaseolus mungo. *Seaweed Res. Utiln.* 26, 155–160.

Liu, J., Basnayake, J., Jackson, P. A., Chen, X., Zhao, J., Zhao, P., et al. (2016). Growth and yield of sugarcane genotypes are strongly correlated across irrigated and rainfed environments. *Field Crop Res.* 196, 418–425. doi: 10.1016/j.fcr.2016.07.022

Machado, L. P., Matsumoto, S. T., Jamal, C. M., Da Silva, M. B., Da Cruz Centeno, D., Neto, P. C., et al. (2014). Chemical analysis and toxicity of seaweed extracts with inhibitory activity against tropical fruit anthracnose fungi. *J. Sci. Food Agr.* 94, 1739–1744. doi: 10.1002/jsfa.6483

Marcos, F. C. C., Silveira, N. M., Marchiori, P. E. R., Machado, E. C., Souza, G. M., Landell, M. G. A., et al. (2018). Drought tolerance of sugarcane propagules is improved when origin material faces water deficit. *Plos One* 13:e206716. doi: 10.1371/journal.pone.0206716

Martynenko, A., Shotton, K., Astatkie, T., Petrash, G., Fowler, C., Neily, W., et al. (2016). Thermal imaging of soybean response to drought stress: the effect of ascophyllum nodosum seaweed extract. *SpringerPlus* 5:1393. doi: 10.1186/s40064-016-3019-2

Mukherjee, A., and Patel, J. S. (2020). Seaweed extract: biostimulator of plant defense and plant productivity. *Int. J. Environ. Sci. Tech.* 17, 553–558. doi: 10.1007/s13762-019-02442-z

Neily, W., Shishkov, L., Nickerson, S., Titus, D., and Norrie, J. (2010). *Commercial Extract From the Brown Seaweed Ascophyllum Nodosum (Acadian) Improves Early Establishment and Helps Resist Water Stress in Vegetable and Flower Seedlings*. Florida: 2010 ASHS Annual Conference.

Patel, K., Agarwal, P., and Agarwal, P. K. (2018). Kappaphycus alvarezii sap mitigates abiotic-induced stress in triticum durum by modulating metabolic coordination and improves growth and yield. *J. Appl. Phycol.* 30, 2659–2673. doi: 10.1007/s10811-018-1423-4

Pereira, L. B., Andrade, G. S., Meneghin, S. P., Vicentini, R., and Ottoboni, L. M. M. (2019). Prospecting plant growth-promoting bacteria isolated from the rhizosphere of sugarcane under drought stress. *Curr. Microbiol.* 76, 1345–1354. doi: 10.1007/s00284-019-01749-x

Ramkissoon, A., Ramsubhag, A., and Jayaraman, J. (2017). Phytoelicitor activity of three caribbean seaweed species on suppression of pathogenic infections in tomato plants. *J. Appl. Phycol.* 34, 123–129. doi: 10.1007/s10811-017-1160-0

Rathore, S. S., Chaudhary, D. R., Boricha, G. N., Ghosh, A., Bhatt, B. P., Zodape, S. T., et al. (2009). Effect of seaweed extract on the growth, yield and nutrient uptake of soybean (*Glycine max*) under rainfed conditions. *South African J. Bot.* 75, 351–355.

Renaut, S., Masse, J., Norrie, J. P., Blal, B., and Hijri, M. (2019). A commercial seaweed extract structured microbial communities associated with tomato and pepper roots and significantly increased crop yield. *Microb. Biotechnol.* 12, 1346–1358.

Rhodes, R., Miles, N., and Hughes, J. C. (2018). Interactions between potassium, calcium and magnesium in sugarcane grown on two contrasting soils in south africa. *Field Crop Res.* 223, 1–11. doi: 10.1016/j.fcr.2018.01.001

Rossetto, M. R. M., Purgatto, E., Do Nascimento, J. R. O., Lajolo, F. M., and Cordenunsi, B. R. (2003). Effects of gibberellic acid on sucrose accumulation and sucrose biosynthesizing enzymes activity during banana ripening. *Plant Growth Regul.* 41, 207–214. doi: 10.1023/B:GROW.0000007508.91064.8c

Rouphael, Y., Micco, V. D., Arena, C., Raimondi, G., and Pascale, S. D. (2016). Effect of ecklonia maxima seaweed extract on yield, mineral composition, gas exchange, and leaf anatomy of zucchini squash grown under saline conditions. *J. Appl. Phycol.* 29, 459–470. doi: 10.1007/s10811-016-0937-x

Santaniello, A., Scartazza, A., Gresta, F., Loreti, E., Biasone, A., Di Tommaso, D., et al. (2017). Ascophyllum nodosum seaweed extract alleviates drought stress in arabidopsis by affecting photosynthetic performance and related gene expression. *Front. Plant Sci.* 8:1362. doi: 10.3389/fpls.2017.01362

Shukla, P. S., Shotton, K., Norman, E., Neily, W., Critchley, A. T., and Prithiviraj, B. (2018). Seaweed extract improve drought tolerance of soybean by regulating stress-response genes. *AoB plants* 10:plx51. doi: 10.1093/aobpla/plx051

Silveira, N. M., Seabra, A. B., Marcos, F., Pelegrino, M. T., Machado, E. C., and Ribeiro, R. V. (2019). Encapsulation of S-nitrosoglutathione into chitosan nanoparticles improves drought tolerance of sugarcane plants. *Nitric Oxide* 84, 38–44. doi: 10.1016/j.niox.2019.01.004

Singh, A. K., Visha Kumari, V., Gupta, R., Singh, P., and Solomon, S. (2018). Efficient irrigation water management in sugarcane through alteration of field application parameters under subtropical india. *Sugar Tech.* 20, 21–28. doi: 10.1007/s12355-017-0514-x

Singh, I., Anand, K. G. V., Solomon, S., Shukla, S. K., Rai, R., Zodape, S. T., et al. (2018b). Can we not mitigate climate change using seaweed based biostimulant: a case study with sugarcane cultivation in India. *J. Clean Prod.* 204, 992–1003. doi: 10.1016/j.jclepro.2018.09.070

Singh, I., Verma, R. R., and Srivastava, T. K. (2018a). Growth, yield, irrigation water use efficiency, juice quality and economics of sugarcane in pusa hydrogel application under different irrigation scheduling. *Sugar Tech.* 20, 29–35. doi: 10.1007/s12355-017-0515-9

Singh, P., Singh, S. N., Tiwari, A. K., Pathak, S. K., Singh, A. K., Srivastava, S., et al. (2019). Integration of sugarcane production technologies for enhanced cane and sugar productivity targeting to increase farmers' income: strategies and prospects. *3 Biotech* 9:48. doi: 10.1007/s13205-019-1568-0

Spann, T. M., and Little, H. A. (2011). Applications of a commercial extract of the brown seaweed ascophyllum nodosum increases drought tolerance in container-grown 'hamlin' sweet orange nursery trees. *Hortscience* 46, 577–582. doi: 10.21273/HORTSCI.46.4.577

Sturm, A. (1999). Invertases. primary structures, functions, and roles in plant development and sucrose partitioning. *Plant Physiol.* 121, 1–8. doi: 10.1104/pp.121.1.1

Tian, H., Kong, Q., Feng, Y., and Yu, X. (2009). Cloning and characterization of a soluble acid invertase-encoding gene from muskmelon. *Mol Biol. Rep.* 36, 611–617. doi: 10.1007/s11033-008-9219-2

Trivedi, K., Vijay Anand, K. G., Kubavat, D., Patidar, R., and Ghosh, A. (2018a). Drought alleviatory potential of kappaphycus seaweed extract and the role of the quaternary ammonium compounds as its constituents towards imparting drought tolerance in zea mays L. *J. Appl. Phycol.* 30, 2001–2015. doi: 10.1007/s10811-017-1375-0

Trivedi, K., Vijay Anand, K. G., Vaghela, P., and Ghosh, A. (2018b). Differential growth, yield and biochemical responses of maize to the exogenous application of kappaphycus alvarezii seaweed extract, at grain-filling stage under normal and drought conditions. *Algal Res.* 35, 236–244. doi: 10.1016/j.algal.2018.08.027

Van Heerden, P. D. R., Mbatha, T. P., and Ngxaliwe, S. (2015). Chemical ripening of sugarcane with trinexapac-ethyl (Moddus§) — mode of action and comparative efficacy. *Field Crop Res.* 181, 69–75. doi: 10.1016/j.fcr.2015.06.013

Vasantha, S., Alarmelu, S., and Hemaprabha, G. (2005). Evaluation of promising sugarcane genotypes for drought. *Sugar Tech.* 7, 82–83. doi: 10.1007/BF02942536

Watanabe, K., Saensupo, S., Na-iam, Y., Klomsa-ard, P., and Sriroth, K. (2019). Effects of superabsorbent polymer on soil water content and sugarcane germination and early growth in sandy soil conditions. *Sugar Tech.* 21, 444–450. doi: 10.1007/s12355-018-0672-5

Winter, H., and Huber, S. C. (2000). Regulation of sucrose metabolism in higher plants: localization and regulation of activity of key enzymes. *Crit. Rev. Biochem. Mol. Biol.* 35, 253–289. doi: 10.1080/07352680091139178

Xu, C., and Leskovar, D. I., (2015). Effects of *A. nodosum* seaweed extracts on spinach growth, physiology and nutrition value under drought stress [J]. *Sci. Hortic.* 183, 39–47. doi: 10.1016/j.scienta.2014.12.004

Youssef, R., Maria, G., Mariateresa, C., Eugenio, C., Mauro, M., Marios, K., et al. (2018). Plant- and seaweed-based extracts increase yield but differentially modulate nutritional quality of greenhouse spinach through biostimulant action. *Agronomy* 8:126. doi: 10.3390/agronomy8070126

Zhang, Y., Liu, H., Yin, H., Wang, W., Zhao, X., and Du, Y. (2013). Nitric oxide mediates alginate oligosaccharides-induced root development in wheat (*triticum aestivum* L.). *Plant Physiol. Biochem.* 71, 49–56. doi: 10.1016/j.plaphy.2013.06.023

Zhu, Y. J., Komor, E., and Moore, P. H. (1997). Sucrose accumulation in the sugarcane stem is regulated by the difference between the activities of soluble acid invertase and sucrose phosphate synthase. *Plant Physiol.* 115, 609–616. doi: 10.1104/pp.115.2.609

Conflict of Interest: The authors declare that the research was conducted in the absence of any commercial or financial relationships that could be construed as a potential conflict of interest.

frontiers in Plant Science

ORIGINAL RESEARCH
published: 01 June 2021
doi: 10.3389/fpls.2021.678925

Integration of Gas Exchange With Metabolomics: High-Throughput Phenotyping Methods for Screening Biostimulant-Elicited Beneficial Responses to Short-Term Water Deficit

Giulia Antonucci[1]*, *Michele Croci*[1], *Begoña Miras-Moreno*[2], *Alessandra Fracasso*[1] and *Stefano Amaducci*[1]

[1] Department of Sustainable Crop Production, Università Cattolica del Sacro Cuore (UCSC), Piacenza, Italy, [2] Department for Sustainable Food Process, Research Centre for Nutrigenomics and Proteomics, Università Cattolica del Sacro Cuore, Piacenza, Italy

OPEN ACCESS

Edited by:
Maurizio Ruzzi,
University of Tuscia, Italy

Reviewed by:
Mirza Hasanuzzaman,
Sher-e-Bangla Agricultural University, Bangladesh
Yi Xu,
Texas A&M University, United States

***Correspondence:**
Giulia Antonucci
giulia.antonucci@unicatt.it

Specialty section:
This article was submitted to Plant Abiotic Stress, a section of the journal Frontiers in Plant Science

Received: 10 March 2021
Accepted: 04 May 2021
Published: 01 June 2021

Citation:
Antonucci G, Croci M, Miras-Moreno B, Fracasso A and Amaducci S (2021) Integration of Gas Exchange With Metabolomics: High-Throughput Phenotyping Methods for Screening Biostimulant-Elicited Beneficial Responses to Short-Term Water Deficit. Front. Plant Sci. 12:678925. doi: 10.3389/fpls.2021.678925

Biostimulants are emerging as a feasible tool for counteracting reduction in climate change-related yield and quality under water scarcity. As they are gaining attention, the necessity for accurately assessing phenotypic variables in their evaluation is emerging as a critical issue. In light of this, high-throughput phenotyping techniques have been more widely adopted. The main bottleneck of these techniques is represented by data management, which needs to be tailored to the complex, often multifactorial, data. This calls for the adoption of non-linear regression models capable of capturing dynamic data and also the interaction and effects between multiple factors. In this framework, a commercial glycinebetaine- (GB-) based biostimulant (Vegetal B60, ED&F Man) was tested and distributed at a rate of 6 kg/ha. Exogenous application of GB, a widely accumulated and documented stress adaptor molecule in plants, has been demonstrated to enhance the plant abiotic stress tolerance, including drought. Trials were conducted on tomato plants during the flowering stage in a greenhouse. The experiment was designed as a factorial combination of irrigation (water-stressed and well-watered) and biostimulant treatment (treated and control) and adopted a mixed phenotyping-omics approach. The efficacy of a continuous whole-canopy multichamber system coupled with generalized additive mixed modeling (GAMM) was evaluated to discriminate between water-stressed plants under the biostimulant treatment. Photosynthetic performance was evaluated by using GAMM, and was then correlated to metabolic profile. The results confirmed a higher photosynthetic efficiency of the treated plants, which is correlated to biostimulant-mediated drought tolerance. Furthermore, metabolomic analyses demonstrated the priming effect of the biostimulant for stress tolerance and detoxification and stabilization of photosynthetic machinery. In support of this, the overaccumulation of carotenoids was particularly relevant, given their photoprotective role in preventing the overexcitation of photosystem II. Metabolic profile

and photosynthetic performance findings suggest an increased effective use of water (EUW) through the overaccumulation of lipids and leaf thickening. The positive effect of GB on water stress resistance could be attributed to both the delayed onset of stress and the elicitation of stress priming through the induction of H_2O_2-mediated antioxidant mechanisms. Overall, the mixed approach supported by a GAMM analysis could prove a valuable contribution to high-throughput biostimulant testing.

Keywords: water stress, biostimulant, GAMM, metabolomics, tomato, gas exchange, glycinebetaine, climate change

INTRODUCTION

Adaptation to climate change is becoming central to the conversation about water management for agriculture (Iglesias and Garrote, 2015). Among the suggestions to improve resiliency and adaptive capacity, the most cited approach is the introduction of drought-resistant crops. While this can be achieved through classical breeding and biotechnology, such efforts have so far produced little results (Nuccio et al., 2018). Moreover, in the second case, even when plants are successfully genetically modified (GM), resistant plants typically represent a restricted number of crops. In this sense, a technology applicable to multiple crops in multiple locations would represent a desirable alternative: as pointed out by Del Buono (2020), biostimulants could represent a sustainable measure to foster the resilience of cropping systems under limited water conditions. The earliest response of plants to drought is represented by stomatal closure, which results in the inhibition of photosynthesis (Michaletti et al., 2018), and therefore leads to CO_2 uptake and concentration reduction (Medrano et al., 2002). Multiple osmolytes can be found among biostimulant constituents targeting water stress resistance in plants, such as glycinebetaine (GB). GB not only acts as an osmoregulator but also stabilizes the structures and activities of enzymes and protein complexes *via* detoxification of reactive oxygen species (Papageorgiou et al., 1991; Papageorgiou and Murata, 1995), while maintaining the integrity of membranes against the damaging effects of excessive salt (Tang et al., 2014, Tian et al., 2017, Yang and Lu, 2005; Mbarki et al., 2018), cold (Quan et al., 2004), heat (Yang et al., 2006; Allakhverdiev et al., 2007), freezing (Razavi et al., 2018; Wang et al., 2019), and also drought (Ma et al., 2006). The role of GB in plant resistance to abiotic stress has been widely investigated and documented (Gorham, 1995; Sakamoto and Murata, 2002; Ashraf and Foolad, 2007; Chen and Murata, 2010; Huang et al., 2020), ranging from exogenous application to genetic engineering (Fariduddin et al., 2013), to its biosynthesis and the underlying molecular mechanisms behind in planta accumulation under stress (Annunziata et al., 2019). While it has been argued that the osmolyte accumulation does not entail positive effects on yield under drought conditions (Serraj and Sinclair, 2002), many reports demonstrate the positive effect of osmolyte accumulation generally (notably Blum, 2016) and GB specifically on plant growth and final yield. Among drought resistance mechanisms activated by GB, osmotic adjustment has been observed to enhance soil moisture extraction and, therefore, transpiration (Blum, 2016). At the same time, higher yielding plants are characterized by high stomatal conductance over time and higher transpiration (Blum, 2009). Indeed, Mäkelä et al. (1999) found that GB could enhance photosynthetic efficiency by reducing photorespiration and enhancing stomatal conductance in tomato plants grown under drought and salinity. This resulted in increased net photosynthesis of stressed plants. This is of particular relevance since tomato plants (*Solanum lycopersicum* L.) do not naturally accumulate GB (Wyn Jones and Storey, 1981). GB foliar application was also found to increase the yield of tomato plants under saline or heat stress (Mäkelä et al., 1998). Likewise, Agboma et al. (1997a,b) found that exogenous application of GB was indeed involved in the maintenance of a higher yield in maize and sorghum grains and tobacco leaves and resulted in improved water-use efficiency. GB was found to have a positive effect on yield also on soybean (Agboma et al., 1997b), common beans (Xing and Rajashekar, 1999), wheat (Agboma et al., 1997a), sunflower (Hussain et al., 2008), and cotton (Ahmad et al., 2014). Moreover, Park et al. found that genetically engineered GB (2004) and exogenously applied GB (2006) increased the tolerance of tomato plants to chilling stress. Interestingly, they suggest that, in addition to its macromolecule and membrane protecting action, GB-enhanced chilling tolerance might imply stress priming through the induction of H_2O_2-mediated antioxidant mechanisms.

According to Fleming et al. (2019), scientific recognition of the potential of biostimulants has not grown as fast as the interest from industry. This has been due to limited fundamental research of their modes of action and the speed at which new multi-compound products have entered the market. In the investigation of biostimulant activity, the necessity of accurate assessment of phenotypic variables is emerging as a critical issue (Rouphael et al., 2018) while at the same time the combined phenotypic-omic approach is gaining momentum. In recent years, emerging digital technologies such as sensors, automatic image acquisition, and the connected algorithms and models have seen an increasing adoption, resulting in increasing volumes and complexity of data. Large-scale acquisition of data has allowed data interpretation to shift from a model-based to a data-based paradigm, by improving the possibility to generalize the data acquired and consequently allowing for an increase in model accuracy. On the flip side of the coin, the main challenge lies in data management: the huge amount of data generated needs to be handled both at the acquisition and analysis stage through proper, often custom, tools (Coppens et al., 2017). In this context,

non-destructive phenotyping techniques characterized by high accuracy (high-throughput techniques) have gained popularity in the scientific community and have been successfully employed in plant breeding (Araus and Cairns, 2014; Halperin et al., 2017; Tardieu et al., 2017; Campbell et al., 2018; Mir et al., 2019), precision agriculture (Chawade et al., 2019), and biostimulant activity testing (Petrozza et al., 2014; Rouphael et al., 2018; Paul et al., 2019a,b). High-throughput phenotyping technologies have attracted attention for their potential in: (1) screening and monitoring multiple morpho-physiological traits; (2) time-series measurements, crucial in the acquisition and interpretation of high spatial and temporal resolution data; and (3) labor automation, time, and cost efficiency (Rouphael et al., 2018). Halperin et al. (2017) have proposed a platform, which uses a custom algorithm to select genotypes based on their abiotic stress resistance characteristics. The system coupled with single-leaf gas exchange acquisition provides high-resolution whole plant transpiration, biomass gain, stomatal conductance, and root flux. As pointed out by Teklić et al. (2020), in addition to the investigation of the effect of biostimulants on plant stress response, there is a growing necessity to elucidate stress and interactions of biostimulants in terms of metabolic changes. To further explore the variation in physiological traits, the integration of phenotyping data and omics data represents the next frontier and a promising tool to bridge the phenotype–genotype gap (Coppens et al., 2017) and to understand dynamic plant stress responses in a changing environment (Gosa et al., 2019). Specifically, high-throughput phenotyping data in combination with metabolomics have already been successfully applied to biostimulant testing (Lucini et al., 2015; Paul et al., 2019a,b; Rouphael et al., 2020). In metabolomics, two commonly used analytical strategies can be distinguished: untargeted and targeted strategies. Untargeted metabolomics, by aiming to detect as many metabolites as possible in a biological sample, is particularly suited to identifying metabolite abundance variations connected to either environmental stimuli or genetic variations (Cheng et al., 2018). Metabolomics has a recognized potential to provide significant insights into the mechanisms of the stress response (Shulaev et al., 2008; Arbona et al., 2013) by identifying different compounds, such as the molecules involved in stress acclimation (e.g., secondary metabolites) and by-products of stress metabolism, and has been successfully applied to the investigation of biostimulant action in general (Lucini et al., 2015, 2018; Paul et al., 2019a,b) and especially under abiotic stresses (Nephali et al., 2020). Lastly, responding to the necessity to analyze the volumes and complexity of data produced through high-throughput phenotyping, non-linear regression models are emerging. These models need to be capable of capturing dynamic data, often time series, as well as the interaction and effects between multiple factors (Ohana-Levi et al., 2020). Among these, generalized additive mixed models (GAMMs) have been successfully featured in several applied science fields (Murase et al., 2009; Zuur et al., 2009; Pedersen et al., 2019; Boswijk et al., 2020; Ohana-Levi et al., 2020) including ecology at large and plant ecophysiology. In particular, Ohana-Levi et al. (2020) highlighted the potential of GAMs to model non-linear relationships between evapotranspiration (ETc) drivers and evaluating their impacts on grapevine transpiration.

In light of this, GB is particularly fit to test the suitability and accuracy of GAMMs in modeling dynamic plant response to drought: widely investigated, its protective action on the photosystem is documented for several abiotic stresses (Huang et al., 2020). At the same time, while available research concentrates mostly on the effect of GB application on yield traits and cell-level effects (Annunziata et al., 2019), a correlation between GB treatment and modifications in photosynthetic rates has received little attention: published research mainly concerns enhanced photosynthetic performance under salt stress (Yang and Lu, 2015; Hamani et al., 2020) and drought (Nawaz and Wang, 2020). Likewise, the effects of GB on water-use efficiency (WUE) have been scarcely investigated (Ahmed et al., 2019) and although both of its abundance (natural or GM) in plant tissues and its exogenous application have been widely linked to stress response, the effects of exogenous application of GB on the metabolomic profile of leaves are yet to be investigated.

Based on the current literature, the hypothesis tested here was whether a biostimulant (GB-based) treatment can be efficiently modeled through GAMM and whether the treatment would result in tangibly different metabolite expression profiles, thereby completing the information derived from GAMM. In order to achieve this, the duration and dynamics of the effect on photosynthesis, transpiration, and WUE were investigated, jointly with a snapshot analysis of metabolic profile.

MATERIALS AND METHODS

Plant Material and Growing Conditions

The experiments were conducted in a greenhouse and the metabolomics analysis in the laboratory of the Department of Sustainable Crop Production of the Università Cattolica del Sacro Cuore, Piacenza. Tomato seeds (H1281 variety, Heinz) were directly sown in a greenhouse at 20°C at 2 cm in a seeding tray (35-ml cell plug) containing a commercial complete mixture of sand—blonde peat—humus. Seeds were kept in dark conditions for 5 days until germination, thereafter they were provided with a PPFD of 800 μmol m^{-2} s^{-1} through light-emitting diode (LED) lighting. Seven days after emergence (DAE), 50 uniformly developed seedlings, at second true leaf unfolded (BBCH 12), were transplanted in 2.3-L pots filled with a commercial complete mixture of sand—blonde peat—humus (1,000 $\pm$ 1 g). Plants were fertilized at a transplant with 40 ml of a complete commercial solution (COMPO, Concime Liquido Universale, Bologna, Italy) at 1.05% w/v (7% N; 5% P; 6% K; 0.01% B; 0.004% Cu; 0.04% Fe; 0.02% Mn; 0.001% Mo; and 0.002% Zn). Fertilization was provided every 2 weeks. The pots were placed under LED lamps to provide a PPFD of 800 μmol m^{-2} s^{-1} to the top canopy with a photoperiod of 16 h light and 8 h dark. Pots were watered to field capacity (FC) every second day. The temperature was not controlled and in the range between 35°C during the day and 8°C during the night (19.5°C average). Of the 50 plants, 32 homogeneously developed plants were selected, of which 12 plants were destined for gas exchange analysis and 20 for metabolomics analysis, while the rest was discarded.

The experiment was designed as a factorial combination of irrigation (water-stressed and well-watered) and biostimulant treatment (treated and control). The water-stressed plants were allowed to dry down for three consecutive days by the withdrawal of irrigation. Thereafter, all plants were irrigated. Gas exchange analysis was carried out on three replicates for each treatment, for a total of 12 plants while metabolomics analyses were carried out on five replicates per each treatment, totaling 20 plants. Plants dedicated to gas exchange analyses were kept in the gas exchange acquisition system for 9 days until the end of the experiment (3 initial days to adapt to the ventilation and lighting, followed by dry down) while plants dedicated to metabolomics analysis were kept in the greenhouse under a tunnel replicating the conditions of the gas exchange acquisition system (same air inlet and LED lighting).

Biostimulant Characteristics and Treatment

The day before the beginning of the gas exchange analysis, the pots were irrigated to saturation and allowed to drain overnight. The treatment with the biostimulant was carried out on 36 DAE on one half of the plant while the other half was sprayed with distilled water. Biostimulant was sprayed at a rate of 6 kg/ha, with a dilution of 300 L/ha to a total of 10 g/plant. Dose and dilution were chosen based on commercial use of the product (Vegetal B60®, ED&F MAN Liquid Products Italia, Bologna, Italy). Vegetal B60® is an organic product extracted exclusively from sugar beet without any added chemical additives. It contains 30% of GB and 5% of L–amino acids, 5% of total organic nitrogen, and 12% of organic carbon.

All pots were sealed in plastic bags fitted around the base of each plant stem to prevent soil evaporation. Well-watered plants were kept at 80% FC throughout the experiment, while for water -stressed plants irrigation was interrupted 3 days after the treatment (on 39 DAE). About 200 g of water were reintegrated to WS plants on 41 DAE, 2 days after irrigation was stopped, to contrast the high rate of soil drying and allow for a longer dry-down period and a more gradual onset of drought stress (a transpiration exceeding 200 g d^{-1} would have brought the plant at wilting point on DAE 41). Leaf area (LA) of each plant was calculated every 3 days from the start of stress imposition (39 DAE). Leaves were placed on squared paper (square of side 0.5 cm, used as the reference of known size) reinforced with a rigid base and photographed with a phone camera, taking care that no leaves overlapped. Images were then processed by using ImageJ (Schneider et al., 2012) to extract LA and compute the total LA of each plant.

Gas Exchange Analysis

Gas exchange was evaluated through a semiautomated multichamber whole-canopy system [slightly modified from the system previously described in Fracasso et al. (2017)]. In particular, the system computes net photosynthetic rate (*Pn*), transpiration rate (E), and WUE. Every pot was measured every 12 min for a total of 120 measurements per day. *Pn* (μmol s^{-1} m^{-2}) and E (mmol s^{-1} m^{-2}) were calculated based on flow rates and CO_2 and water vapor differentials by using the formula provided in Long and Hallgren (1985). Data were acquired 24 h per day at intervals of 1 min. The semiautomated multichamber system is composed of 12 adjustable open chambers connected to a CIRAS-DC double channel absolute CO_2/H_2O IR gas analyser (PP-System, Amesbury, MA, USA). Air drawn at 3 m above ground from outside the greenhouse is collected in a buffer tank (0.44 m^3 capacity) to ensure the stability of inlet CO_2 concentration and then, forced by one centrifugal blower (Vorticent C25/2M Vortice, Milan, Italy), to distribute air to the chambers through 50-mm-diameter rigid plastic pipes. The air flow rate of each chamber is controlled by a baffle and is constantly measured at least 50 cm downstream of the baffle itself with digital flowmeters (50 Pa D6F-PH0026AD1, OMRON, Kyoto, Japan) according to a flow-restriction method (Osborne, 1977). Each chamber is connected to a set of 12 solenoid valves in series (model 177 B04/Z610, Sirai, Bussero, Italy) through a sampling tube (Ø 10 mm). Air sampling is switched from one chamber to another at programmed time intervals (Raspberry Pi B+, Raspberry Pi Foundation, Northants, UK). In order to ensure air flushing inside the sampling tubes and the complete air exchange inside CIRAS-DC, rotary vane pumps (model G 6/01-K-LCL; Gardner, Denver Thomas, Pucheim, Germany) with 33.3 cm^3 s^{-1} of flow rate were added before CIRAS-DC. Both the inlet air temperature and the air temperature of each chamber (outlet) were measured by using digital temperature sensors (Dallas DS18B20, Dallas Semiconductor Corp., Dallas, TX, USA).

On 36 DAE, 12 plants were transferred under the gas exchange acquisition system and were kept in the system for 9 days until the end of the experiment (as mentioned above) while 20 plants were kept under a tunnel replicating the conditions of the gas exchange acquisition system and were sampled for metabolomics analyses. Both the tunnel and the gas acquisition system were provided with the same air inlet, namely forced air collected from outside (as described above), and the same LED lighting, namely 800 μmol m^{-2} s^{-1} PPFD.

Sample Harvest and Metabolomic Analysis

Gas exchange was measured throughout the duration of the stress: as soon as the *Pn* of stressed plants started decreasing, plants were sampled for metabolomics. Sampling of the 20 plants kept under the tunnel replicating the conditions of the gas acquisition system was carried out on 42 DAE. The second and third fully expanded leaves from the top of each plant were excised and dipped into liquid nitrogen. Samples were kept at −20°C and subsequently analyzed. Plant samples were homogenized in pestle and mortar by using liquid nitrogen and extracted as previously reported (Paul et al., 2019b). Briefly, an aliquot (1.0 g) was extracted in 10 ml of 0.1% HCOOH in 80% aqueous methanol by using an Ultra-Turrax (Ika T-25, Staufen, Germany). The extracts were centrifuged (12,000 g) and filtered into amber vials through a 0.22-μm cellulose membrane for analysis. Thereafter, metabolomic analysis was carried out by ultra-high performance liquid chromatograph (UHPLC) coupled to a quadrupole-time-of-flight mass spectrometer (UHPLC/QTOF-MS). The metabolomic facility included a 1,290 ultra-high-performance liquid chromatograph, a G6550

iFunnel Q-TOF mass spectrometer, and a JetStream Dual Electrospray ionization source (all from Agilent Technologies, Santa Clara, CA, USA). The untargeted analysis was carried out as previously described (Rouphael et al., 2016). Briefly, reverse-phase chromatography was carried out on an Agilent PFP column (2.0 × 100 mm, 3 μm) and by using a 33-min linear elution gradient (6–94% acetonitrile water, with a flow of 200 μl min^{-1} at 35°C). The mass spectrometric acquisition was done in SCAN (100–1,000 m/z) and positive polarity (Pretali et al., 2016). Quality controls (QCs) were analyzed in data-dependent MS/MS mode by using 12 precursors per cycle (1 Hz, 50–1,200 m/z, positive polarity, active exclusion after 2 spectra), with collision energies of 10, 20, and 40 eV for collision-induced decomposition.

Raw spectral data were processed by using Agilent Profinder B.07 software, (Santa Clara, CA, USA) as described in Miras-Moreno et al. (2020). The PlantCyc 12.6 database (Plant Metabolic Network; Release: April 2018) was used to putatively annotate compounds according to Level 2 with reference to the COSMOS Metabolomics Standards Initiative (Salek et al., 2015). QCs were analyzed by using the MS-DIAL 3.98 (RIKEN Center for Sustainable Resource Science: Metabolome Informatics Research, Yokohama, Japan) to compare the MS/MS spectra to the publicly available MS/MS experimental spectra built in the software (e.g., MoNA) (Tsugawa et al., 2015).

Data Analysis

Gas Exchange Curve Fitting Using GAM(M)

The experiment was evaluated from the day prior to stress imposition (38 DAE) for three consecutive days of water stress (DAE 39-41) until the start of stress recovery (42 DAE). Statistical analyses on gas exchange data were carried out *via* GAMMs. GAMMs are regression models, which allow for modeling non-linear regressions (Wieling, 2018). Unlike linear models (1), which feature a sum of linear terms, GAMMs (2) are characterized by a sum of smooth functions. GAMMs are used to estimate smooth functional relationships between predictor variables and the response. GAMM data fitting is characterized by a penalized fit: the fit of the data is balanced with the complexity of the model by penalizing wiggliness, namely the deviation from total smoothness, and thus avoiding overfitting (Pedersen et al., 2019).

$$Y_{ij=}\ \beta_0 + \sum \beta_j x_i + \ \in_{ij} \quad (1)$$

$$Y_{ij=}\ \beta_0 + \sum f_j(x_i) + \ \in_{ij} \quad (2)$$

Among the multiple advantages of this approach is the possibility to handle the complexity of the data without oversimplifying them, the determination of the relationship between the dependent variable and the predictors as a function of the algorithm, which can be linear but is not necessarily linear, the inclusion of multiple numeric predictors and the possibility to include autoregressive AR(1) error model for Gaussian models in order to handle the autocorrelation component of the error (van Rij et al., 2019). The inclusion of autocorrelation is particularly relevant in time-series data sets, where each datapoint is clearly correlated to (and therefore dependent on) the previous and the next datapoints. Therefore, this analysis is particularly useful to data sets characterized by dynamic and time-series data (Boswijk et al., 2020).

After Wieling (2018), the analysis started from a simple generalized additive model, the sophistication of which was progressively increased and extended step-by-step. While one would normally directly choose the model reflecting the hypothesis, this approach was chosen to shed light on the process using generalized additive modeling.

Net photosynthesis (*Pn*), transpiration rate (E), and WUE were used as the response variable for the following series of GAM(M)s:

a. Sole irrigation as a fixed factor, including a smooth for day-of-treatment and hour in the day, based on treatment.
b. Irrigation treatment and biostimulant treatment as fixed factors, no interaction between the factors. Including a smooth for day-of-treatment and hour in the day, based on both treatments.
c. Irrigation treatment and biostimulant treatment as fixed factors, interaction between the factors. Including a smooth for day-of-treatment and hour in the day, based on both treatments.
d. Introduction of tensor product-based smooths between hour and day.
e. Inclusion of a smooth for day-of-treatment and hour in the day, based on both treatments, and allowing for random effect per individual.
f. Addition of non-linear random effects per individual for day-of-treatment.
g. Introduction of individual-based autocorrelation.

Models d:g are nested within model c, allowing for comparison of methods using log-likelihood/F tests. This allowed us to evaluate Akaike information criterion (AIC) changes among models and, thus, to find the model with the most explanatory power given the degrees of freedom, while at the same time assessing whether better or worse models explained significantly different amounts of the deviance in the data. Statistical tests were performed by using the software R version 4.0.2 (R Core Team, 2020). GAMM models were fitted in R by using a cubic regression spline smoother, with the package itsadug (van Rij et al., 2020). Mixed model selection, fitting, and validation followed (Zuur et al., 2009). Biostimulant and stress treatment factors were used in mixed linear models for hypothesis testing.

Chemometric Interpretation of Metabolites

Chemometric interpretation of metabolites was performed by using Mass Profiler Professional B.12.06 from Agilent (Santa Clara, CA, USA) as previously described (Corrado et al., 2020). The unsupervised hierarchical cluster analysis (HCA—distance measure: Euclidean; clustering algorithm: Ward's) was produced based on the normalized molecular features. The supervised orthogonal partial least squares-discriminant analysis (OPLS-DA) was carried out with SIMCA 16 (Umetrics, Umeå, Sweden)

TABLE 1 | Characteristics of the nine compared models of influence on photosynthesis.

Model	Resid. Df	Resid. Dev	AIC	dAIC	Dev. Expl (%)
a	3391.454	11624.1257	13974.67	5006.285	61.5
b	3378.586	10206.6696	13552.31	4583.922	66.2
c	3377.564	9648.388	13361.94	4393.553	68
d	3265.717	7618.79372	12724.36	3755.977	74.7
e	3231.964	4454.29886	10950.84	1982.455	85.2
f	3182.686	3307.85823	10024.21	1055.83	89
g	3214.175	3679.9617	8968.384	0	87.8

Model names as in the text: a is the sole irrigation as a fixed factor, including a smooth for day-of-treatment and hour in the day, based on treatment. b has both irrigation and biostimulant treatment as fixed factors. c adds the interaction between the factors and includes a smooth for day-of-treatment and hour in the day, based on both treatments. d introduces tensor product-based smooths between hour and day. e includes a smooth for day-of-treatment and hour in the day, based on both treatments, and allowing for random effect per individual. f adds non-linear random effects per individual for day-of-treatment. g introduces individual-based autocorrelation. Resid.Df, residual degrees of freedom; Resid.Dev, residual deviance; dAIC, difference in AIC based on model g. Dev. Expl. (%) = deviance explained.

at default parameters. CV-ANOVA ($p < 0.01$) and permutation testing ($n = 100$) were also applied to validate and to exclude overfitting. Goodness-of-fit R2Y and goodness-of-prediction Q2Y were also calculated from the OPLS-DA model. Outliers were investigated according to Hotelling's T2 (95 and 99% confidence limit for the suspect and strong outliers, respectively). The most discriminant compounds in separation were selected by performing the variables importance in projection (VIP) analysis.

Thereafter, differential compounds were investigated through Volcano plot analysis, combining fold-change (FC > 2) and ANOVA ($p < 0.0$, 1, Bonferroni multiple testing correction) and were then uploaded into the Omic Viewer Pathway Tool of PlantCyc (Stanford, CA, USA) to identify pathways affected by the treatments as in Caspi et al. (2013).

RESULTS

Gas Exchange Analysis

On 36 DAE, 12 plants were transferred under the gas exchange acquisition system and were kept in the system for 9 days until the end of the experiment. Plants were treated with a factorial combination of irrigation (well-watered and water-stressed) and biostimulant treatment (treated and control). Water-stressed plants were allowed to dry down for three consecutive days by the withdrawal of irrigation. Gas exchange data were processed *via* GAMMs. GAMMs are non-linear regression models which are characterized by a sum of smooth functions. Data were analyzed by building models of growing complexity (**Table 1**, model a–g), as previously explained. The regression models allowed to explore the dynamics of the influence of the biostimulant and water treatments on photosynthetic performance.

Among the candidate GAMMs, the optimal model was model g, including Photosynthesis ∼ irrigation treatment * biostimulant treatment and non-linear interactions between both treatments and the duration of the experiment (expressed in days) and the time of the day (expressed in hours), smooths for the duration of the experiment and the time of the day on both treatments and non-linear variability of the individuals over the duration of the experiment. Moreover, model g included autocorrelation for time over the individual. The model explained 87.8% of the total deviance with an Adj.R^2 of 0.872. While the next best model, which did not include autocorrelation (model f), explained 89% of the deviance (Adj.R^2 0.883), when the models were confronted *via* AIC (Akaike, 1974), and model g scored consistently lower in terms of AIC score although bearing more degrees of freedom (**Table 1**).

The inclusion of the sole irrigation treatment factor (model a) explained 61.5% of the deviance in the data. The addition of the biostimulant treatment factor (model b) increased the deviance explained by 4.7%. The addition of further information increased the deviance explained as follows: the inclusion of the interaction between the fixed factors (model c) resulted in an additional 1.8%. The further introduction of tensor product-based smooths between hour and day (model d) added 6.7% deviance explained, while allowing for random effect per individual (model e) further added 10.5% to it. Lastly, the addition of non-linear random effects per individual for day-of-treatment (model f) resulted in 1.8% more deviance explained.

Under water-stressed conditions, model g highlighted statistically higher *Pn* (**Figure 1**) in plants treated with biostimulant compared to control plants starting shortly before 39 DAE and lasting throughout the experiment until 42 DAE. Conversely, under well-watered conditions, there was no significant difference between treatments. When considering biostimulant-treated (BT) plants, the difference between water-stressed and well-watered plants was significantly lower for water-stressed plants starting half 40 DAE to half 41 DAE. Lastly, well-watered and water-stressed untreated plants displayed a significant negative difference from mid-39 DAE to mid-42 DAE.

The influence of day-of-treatment (38–42 DAE), starting from the day prior to stress imposition, and hour was evaluated separately for each treatment (biostimulant and water treatment). Through the use of GAMMs, the significance of the effect of day and hour on biostimulant and water treatment was further investigated singularly for each dimension of both factors (biostimulant treated/control treated and water-stressed/well-watered) (**Table 2**). The results show that all the partial correlations were statistically significant for at least one of the two levels of the factors at the value of $p < 0.001$ level, except for the effect of hour and day of week on biostimulant treatment, which was significant at the value of $p < 0.05$. While the significance of the smooth terms does not provide information on whether the patterns are statistically significant, this suggests that each individual variable has a statistically significant influence on modeling the wiggliness of *Pn*, which in turn confirms the distance of *Pn* from a linear function.

The partial effect (referred solely to biostimulant treatment) of biostimulant treatment on *Pn* observed for each day-of-treatment is of particular interest (**Figure 2**): while no effect can be detected for the control treatment (which is represented by a linear function), the biostimulant treatment has a detectable effect on the wiggliness of the *Pn* curve.

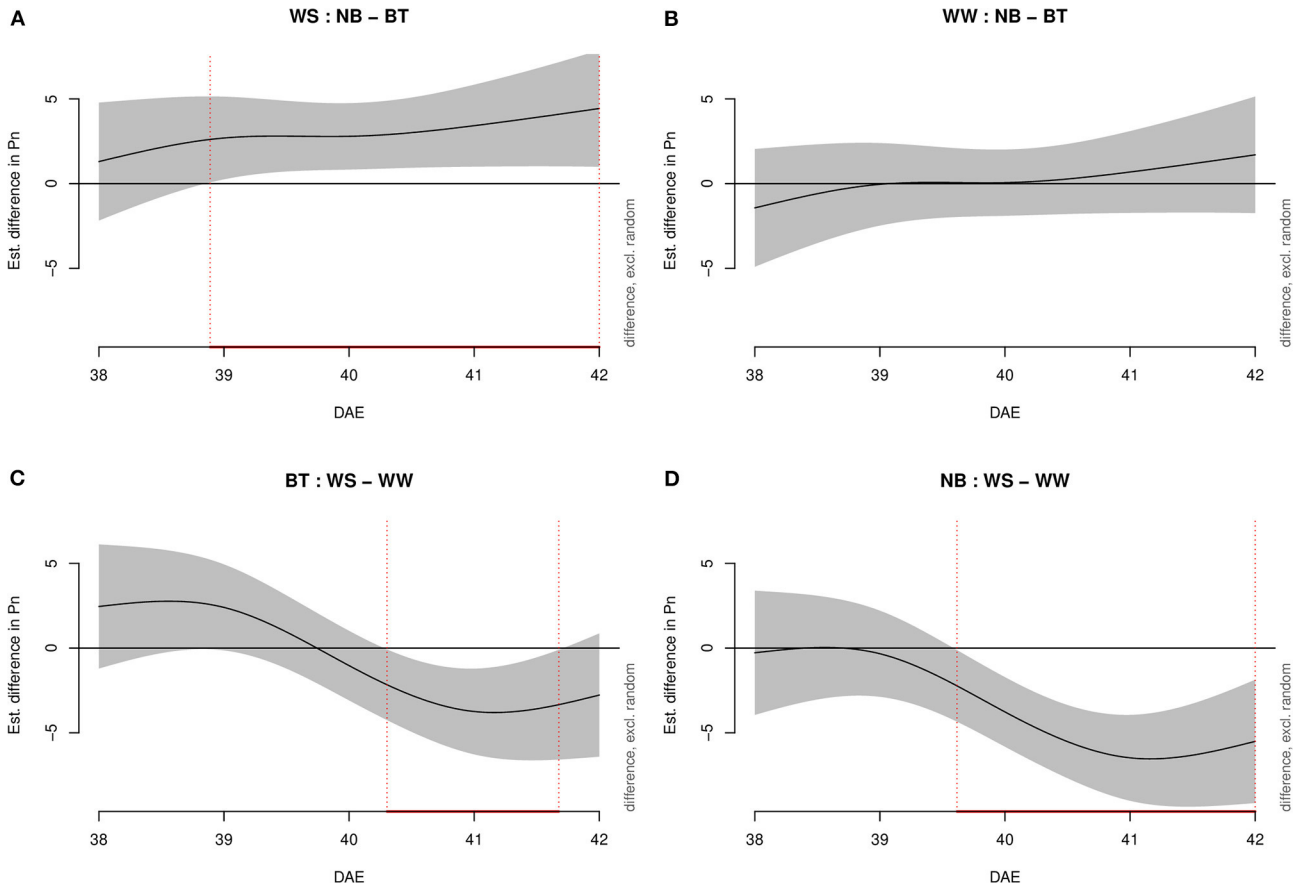

FIGURE 1 | Graphs showing differences in *Pn* according to model g among all combinations of treatments (irrigation and biostimulant). Random effects were excluded. The baseline is represented by untreated plants above and by watered (control) plants below. The pointwise 95% CI is shown by a shaded band. When the shaded confidence band does not overlap with the *x*-axis (i.e., the value is significantly different from zero), this is indicated by a red line on the *x*-axis (and vertical dotted lines). **(A)** Water-stressed (WS), comparison between no biostimulant (NB) and biostimulant treatment (BT). **(B)** Well-watered (WW), comparison between NB and BT. **(C)** BT, comparison between WS and WW. **(D)** NB, comparison between WS and WW.

Transpiration (E, mmol m^{-2} s^{-1}) was evaluated through increasingly complex models, as *Pn*. Model g was once more the best fitting model, with 88.2% of deviance explained and 0.875 Adj.R^2. As for *Pn*, water-stressed BT plants performed significantly better than untreated plants (**Figure 3**). In particular, the performance of BT plants was significantly higher from mid-38 DAE to mid-40 DAE. Conversely, non-stressed plants (biostimulant treated/untreated) did not show any significant difference in transpiration. Water-stressed BT plants had a higher E than well-watered plants from mid-41 DAE until mid-42 DAE. Untreated plants differed from late 39 DAE throughout the end of the experiment.

As for *Pn* and E, WUE was evaluated through increasingly complex models (**Figure 4**). Model g was confirmed as the best model, with 85.3% deviance explained and 0.843 Adj.R^2.: As for *Pn* and E, no significant difference was highlighted among well-watered plants (both biostimulant treated and not). The difference in WUE between treated and untreated plants spanned from shortly before the day of stress imposition (39 DAE) to the third day (41 DAE). The duration of the difference among BT plants (well-watered/water-stressed) extended from early 40 DAE to 42 DAE while the difference among untreated well-watered and water-stressed plants went from 40 DAE to 42 DAE.

Untargeted Metabolomics

In this study, the untargeted metabolomics approach was able to reveal more than 3,400 molecular features. The annotated compounds and composite mass spectra (mass and abundance combinations), together with compounds confirmed by MS/MS, are listed in **Supplementary Table 1**. The data set was first interpreted through an unsupervised hierarchical clustering. This unsupervised clustering approach enabled the description of similarities/dissimilarities among treatments, as shown in **Figure 5A**.

Two main clusters were generated—one including the BT water-stressed treatment and the other including both irrigated and stressed untreated treatments and the treated irrigated one. Two distinct subclusters, one including the untreated water stressed (WS) and the other both the treated and untreated irrigated treatments, could be identified. The

TABLE 2 | Influence of partial effects on *Pn* using generalized additive mixed modeling (GAMM) multivariate analysis.

Partial effect	Edf	*F*	*p*-value
te(day_of_treatment, hour):WellWatered	1.819e+01	0.481	0.000509***
te(day_of_treatment, hour):WaterStressed	3.084e+01	5.554	<2e−16***
te(day_of_treatment, hour):NoBiostimulant	6.220e+00	0.219	0.000288***
te(day_of_treatment, hour):BiostimulantTreated	2.847e+01	1.636	<2e−16***
s(day_of_treatment): WellWatered	1.000e+00	2.872	0.090207
s(day_of_treatment): WaterStressed	3.803e+00	17.018	8.28e−12***
s(day_of_treatment): NoBiostimulant	9.612e−05	0.666	0.993127
s(day_of_treatment): BiostimulantTreated	3.415e+00	3.049	0.010673*
s(hour): WellWatered	1.632e+01	11.215	<2e−16***
s(hour): WaterStressed	6.051e+00	3.626	0.000573***
s(hour): NoBiostimulant	1.000e+00	1.258	0.262130
s(hour): BiostimulantTreated	5.880e+00	2.523	0.012176*
s(day_of_treatment, ID_plant)	3.805e+01	26.618	<2e−16***

**significant difference at P < 0.05, ***significant difference at P < 0.001.*

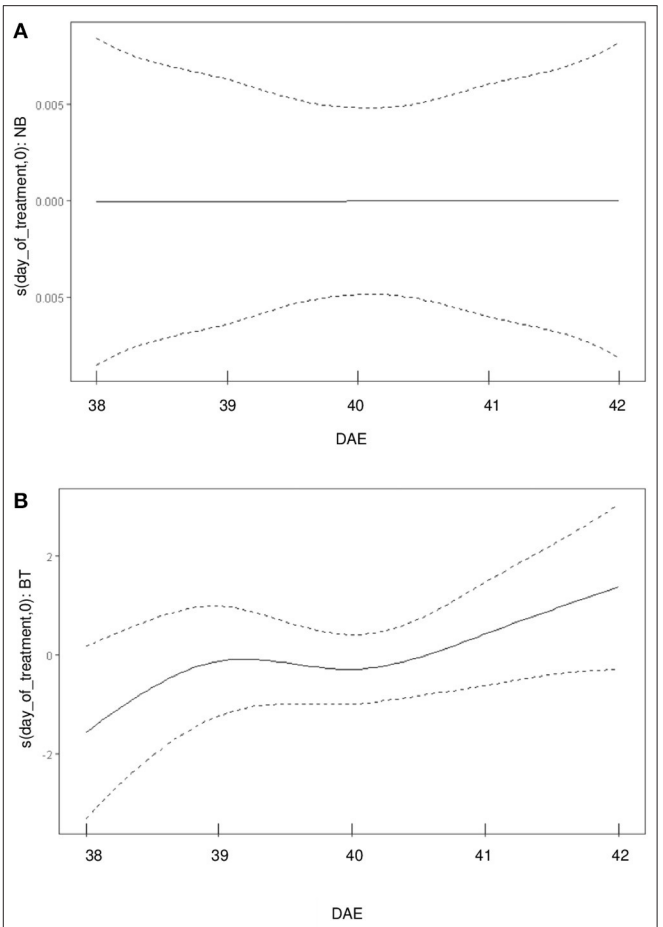

FIGURE 2 | Uncoupling of the partial effects of BT/control treatment on the wiggliness of *Pn* curve. **(A)** partial effects of control treatment (NB) over the day of treatment [in days after emergence (DAE)] on *Pn*. **(B)** partial effects of BT over the day-of-treatment (in DAE) on *Pn*.

WS, BT profile differed starkly from the others: the naive (unsupervised) hierarchical clustering of metabolomic signatures revealed distinctive profiles in tomato leaves under limited water availability, which is the result of the application of the biostimulant.

OPLS-DA analysis allowed separating predictive and orthogonal components (i.e., the components ascribable to technical and biological variation) of variance. The subsequent supervised statistics were used to discriminate the tomato samples according to the treatment. The OPLS-DA (**Figure 5B**) effectively separated the stressed from the non-stressed plants and pointed out irrigation as the main separation factor. Among the stressed plants, treated plants presented the most distinct profile as suggested by the HCA, and were clearly separated from the non-treated ones. Similar metabolic profiles were found for non-stressed plants regardless of the treatment. The model parameters of the OPLS-DA regression were R2Y = 0.89 and Q2Y = 0.73, respectively. The model was validated (CV-ANOVA $p = 1.50 \times 10^{-5}$) and overfitting was excluded through permutation testing ($N = 100$). Given the validated model outcomes, the VIP variable selection method was used to identify compounds explaining the observed differences. The discriminating compounds with a VIP score >1.3 were considered as discriminants. About 147 compounds resulted from this selection and are summarized in **Supplementary Table 2**. Thereafter, a Volcano analysis ($p < 0.01$; FC > 2) was performed and the significant compounds were then uploaded into the Omics Dashboard tool from PlantCyc to facilitate the discussion of results (**Supplementary Table 3**).

Notably, relatively few biochemical classes included most of the discriminant metabolites (**Figure 6**).

The metabolic profile of water-stressed BT plants sharply differs from the others. The most affected classes of compounds were secondary metabolites, particularly in their biosynthesis, followed by cellular structure synthase and fatty acid and lipid synthesis. Regarding secondary metabolite biosynthesis, terpenoid biosynthesis, nitrogen-containing secondary compound biosynthesis, and phenylpropanoid derivative biosynthesis were the most affected. Compounds related to terpenoid biosynthesis were strongly over-accumulated, mostly represented by triterpenoids and tetraterpenoids, with a high abundance of carotenoids: this is particularly relevant considering the role of carotenoids in photosynthetic organisms.

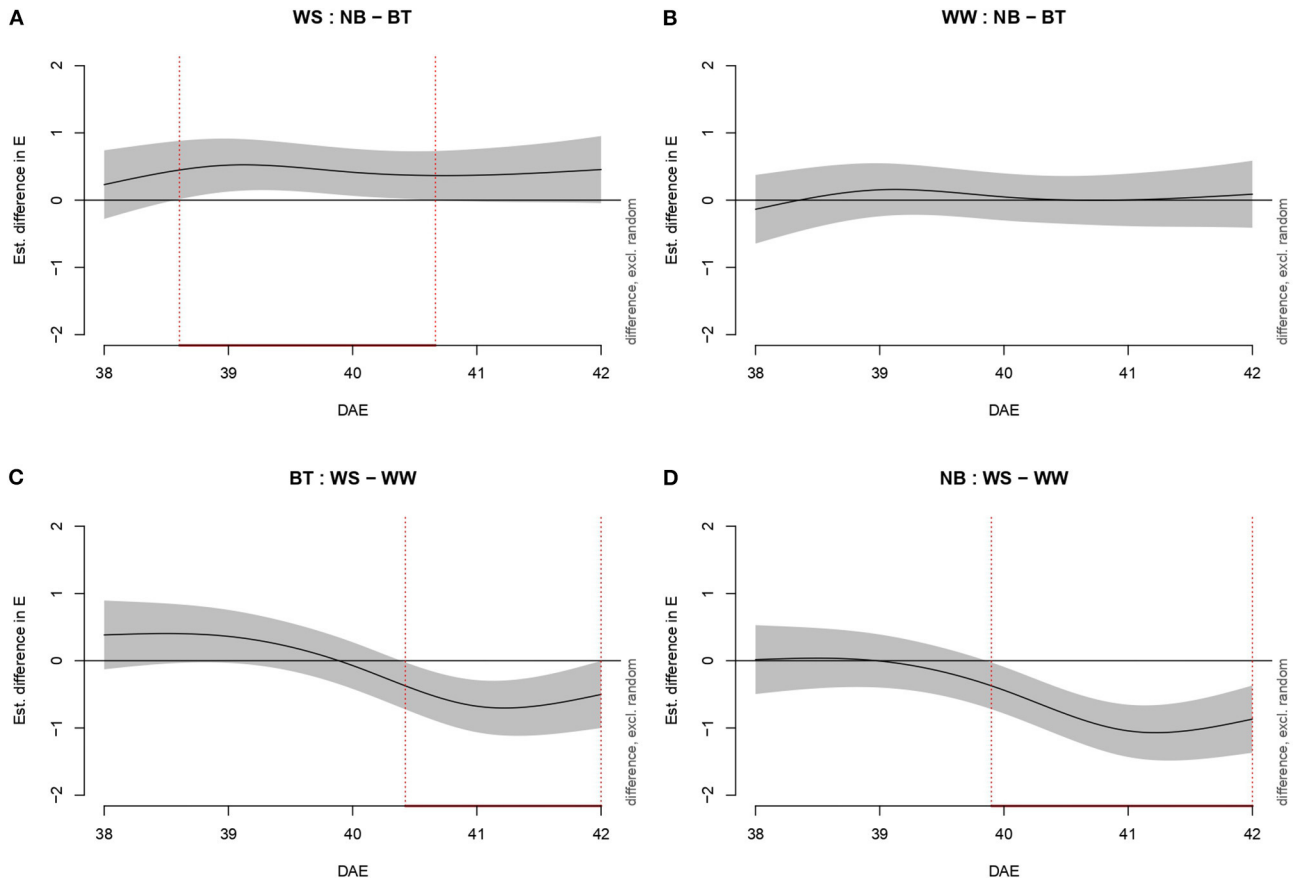

FIGURE 3 | Graphs showing differences in transpiration (mmol m^{-2} s^{-1}) according to model g among all combinations of treatments (irrigation and biostimulant). Random effects are excluded. The baseline above is represented by untreated plants, below by watered (control) plants. The pointwise 95% CI is shown by a shaded band. When the shaded confidence band does not overlap with the *x*-axis (i.e., the value is significantly different from zero), this is indicated by a red line on the *x*-axis (and vertical dotted lines). **(A)** WS, comparison between NB and BT. **(B)** WW, comparison between NB and BT. **(C)** BT, comparison between WS and WW. **(D)** NB, comparison between WS and WW.

At the same time, compounds responsible for terpenoid degradation were significantly underaccumulated. Interestingly, phytoalexins were also found to be over-accumulated. Cell structure synthase metabolites, among which stearate and oleate, were strongly over-accumulated. Concerning vitamin biosynthesis, molecules responsible for thiamine biosynthesis were sharply over-accumulated. Among fatty acids and lipids, cutin synthase metabolites were strongly over-accumulated, together with epoxylated and hydroxylated fatty acids, stearate, and unsaturated fatty acids. Sphingolipids were also found to be over-accumulated. Concerning degradation, amino acids degrading molecules showed a generalized under-accumulation, for instance regarding glutamate, lysine, and tryptophan. Lastly, interestingly gibberellin degrading pathways were under-accumulated in BT plants, but differences could be detected among water treatments: the control group showed a sharp under-accumulation of molecules involved in epoxidation, while the stressed group showed a sharp decrease in succinate content, involved in the hydroxylation of gibberellins.

DISCUSSION

One of the primary adverse effects of water deficit stress is the inhibition of photosynthesis triggered by stomatal closure, which represents the earliest response to drought (Michaletti et al., 2018). As a result, CO_2 uptake and concentration in leaves are reduced (Medrano et al., 2002). In view of this, the results from the GAMM analysis confirmed that BT plants performed better in terms of *Pn*, E, and WUE compared to untreated plants under water stress. The use of generalized additive modeling enabled the analysis of the full set of dynamic data, without the need to reduce time resolution (i.e., average overtime or select specific time points). Moreover, with this analysis, the effect of treatments (i.e., drought and biostimulant application) on the patterns (i.e., wiggliness) of gas exchange data was accurately modeled and discriminated, also considering data autocorrelation. The use of GAMM allowed for the extraction of information on the effect of the biostimulant devoid of temporal correlation and random errors due to individual replicates, non-linear interactions between both treatments and the duration of the experiment

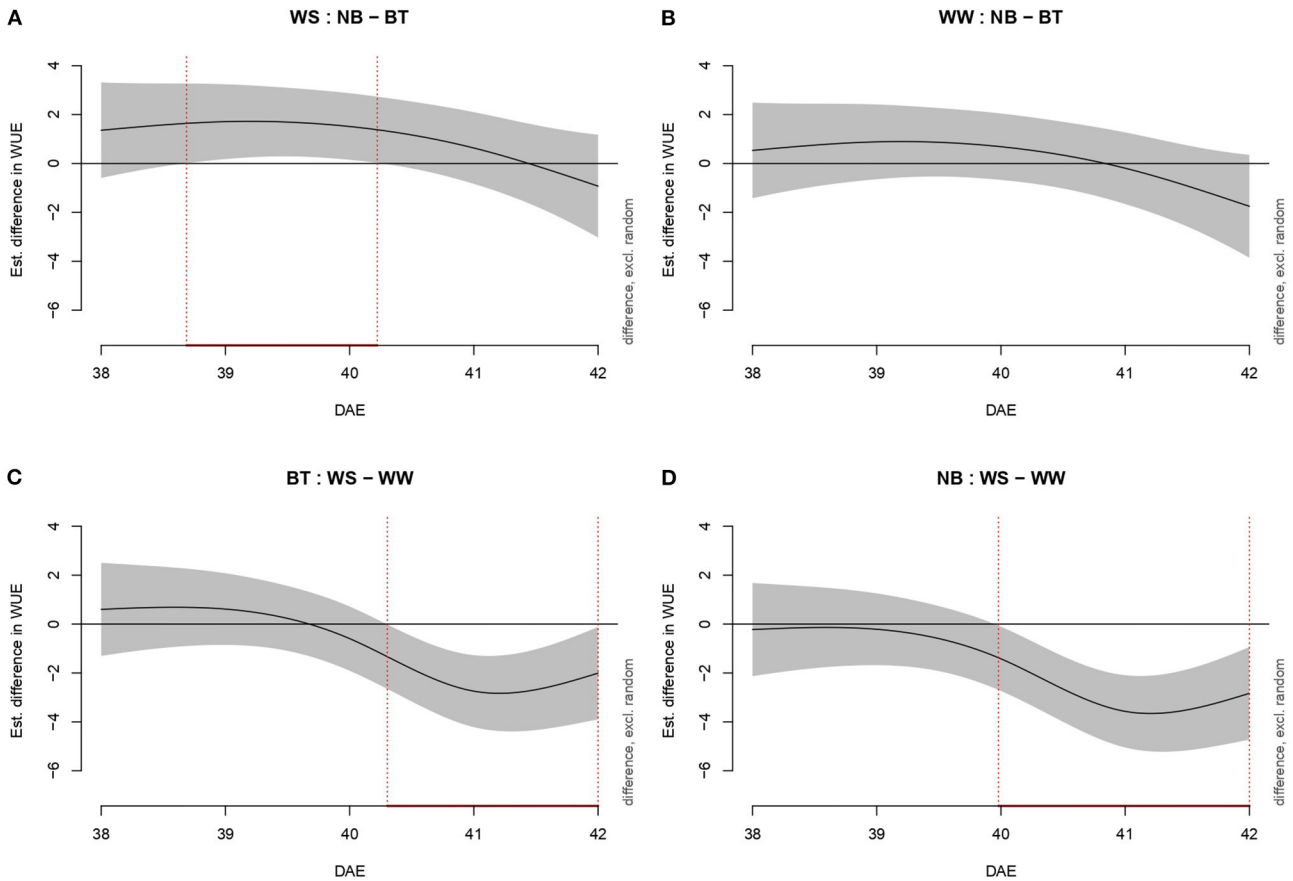

FIGURE 4 | Graphs showing differences in water-use efficiency (WUE) among all combination of treatments (irrigation and biostimulant). Random effects are excluded. The baseline above is represented by untreated plants, below by watered (control) plants. The pointwise 95% CI is shown by a shaded band. When the shaded confidence band does not overlap with the *x*-axis (i.e., the value is significantly different from zero), this is indicated by a red line on the *x*-axis (and vertical dotted lines). **(A)** WS, comparison between NB and BT. **(B)** WW, comparison between NB and BT. **(C)** BT, comparison between WS and WW. **(D)** NB, comparison between WS and WW.

(expressed in days) and the time of the day (expressed in hours). At the same time, GAMM analysis allowed to consider different smooths for a day (duration of the experiment) and hour (time of the day) for both factors (water and biostimulant). Lastly, the use of GAMM allowed for the inclusion of non-linear variability of the individuals over the duration of the experiment. While the significance of the smooth terms does not provide information on the statistical significance between patterns, each individual variable has a statistically significant influence on modeling the wiggliness of *Pn*, which in turn confirms the distance of *Pn* from a linear function. This resulted in a model explaining 87.8% of the deviance. Further, the use of GAMMs enabled the comparison between the curves of stressed and well-watered plants, both with and without biostimulant, thereby providing both a visual screening tool and a statistical tool to further confirm or disprove the effect of biostimulant treatment. The positive effect of the biostimulant treatment observed through GAMM analysis is in line with literature findings on the potential of GB to increase photosynthetic performance under water stress (Yang and Lu, 2005; Hamani et al., 2020; Nawaz and Wang, 2020), especially in tomato (Mäkelä et al., 1999). Differences in the length of significance windows among *Pn*, E, and WUE were detected. While the photosynthetic rate was constantly higher for treated plants compared to the untreated ones, from stress imposition (39 DAE) to the end of stress (42 DAE), the positive effect in the BT water-stressed plants for transpiration rate, and consequently WUE, was shorter compared to *Pn*. Specifically, under water-stressed conditions, the positive effect of the biostimulant treatment on E was reduced in duration, indicating that higher transpiration could only be supported until late, on 40 DAE (second day of water stress) and efficacy on WUE was further reduced to early on 40 DAE. This indicates that the increased photosynthetic rate after the first day of water stress imposition is followed by increased transpiration, resulting in the reduction of the WUE advantage. WUE is a largely diffused performance indicator for crop yield and water consumption. Water-stressed plants typically exhibit a higher WUE due to a more conservative use of water, resulting in improved resource utilization efficiency under conditions of water scarcity (Zhao et al., 2020). Nevertheless, high stomatal conductance over

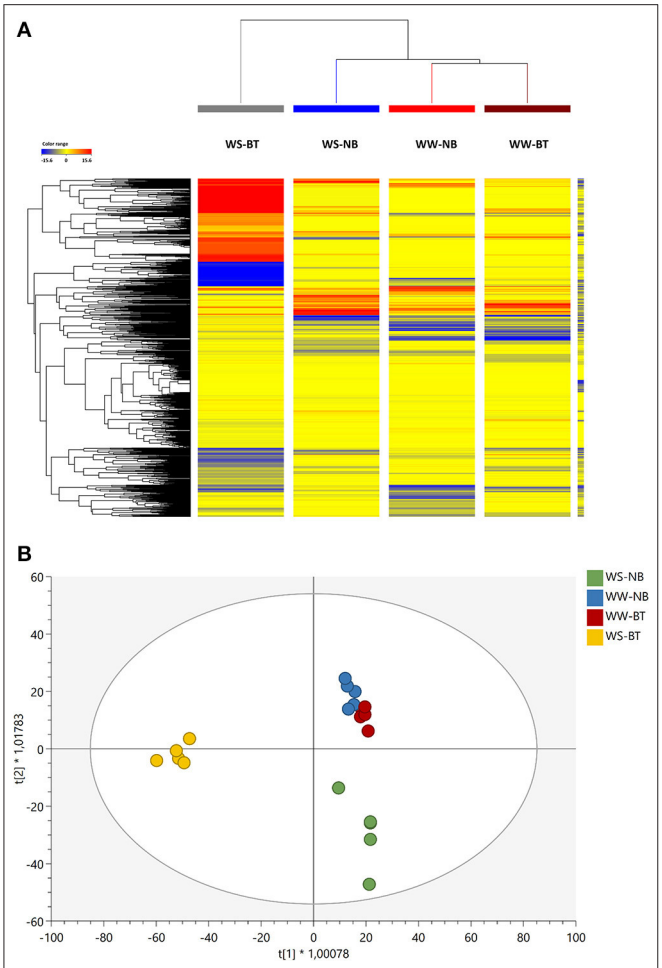

FIGURE 5 | (A) Unsupervised hierarchical cluster analysis (HCA, Euclidean similarity; linkage rule: Ward's). The analysis was carried out from metabolite profiles in tomato leaves from the factorial combination of BT and water treatment as gained from ultra-high performance liquid chromatograph (UHPLC) coupled to a quadrupole-time-of-flight mass spectrometer (QTOF-MS) untargeted metabolomics. Compound intensity was used to produce fold-change-based heat maps, on which clustering was based. **(B)** Score plot of Orthogonal Projection to Latent Structures Discriminant Analysis (OPLS-DA) unsupervised analysis carried out from metabolite profiles in tomato leaves treated or untreated plants, as gained from UHPLC/QTOF-MS untargeted metabolomics.

time is essential to high plant production, translating into maximized soil water-use for transpiration, or effective use of water (EUW) for transpiration. It is therefore evident that, under drought conditions, higher stomatal conductance over time will result in lower WUE (Blum, 2009). Indeed, drought-resistant plants display the minimization of leaf permeability, for example, by means of higher epicuticular wax deposition, in order to maximize soil water capture while diverting water to stomatal transpiration (Blum, 2009). Besides, Blum indicates the EUW as the key objective in maximizing biomass production under a limited water regime.

The increased photosynthetic rate was in line with the protective role of GB in terms of cellular osmotic adjustment, detoxification of reactive oxygen species, and protection and stabilization of membrane integrity (Ashraf and Foolad, 2007) and is further supported by the sharp separation of the metabolic profile of the water-stressed BT thesis. At the same time, the smaller reduction in net photosynthesis in leaves subjected to water stress can be attributed to an increased stomatal conductance, as well as the maintenance of chloroplast ultrastructure (Ma et al., 2006) and Rubisco activity (Yang et al., 2005). Indeed, the overaccumulation of carotenoids is of particular interest, given their photoprotective role in preventing the overexcitation of photosystem II (Uarrota et al., 2018), while at the same time acting as toxic oxygen species scavengers, structure stabilizators, and excess energy dissipators (Griffiths et al., 1955; Frank and Cogdell, 1996; Polívka and Sundström, 2004). GB has indeed been found to have a strong protective effect on the structure and function of the oxygen-evolving complex of PSII *in vitro* against multiple abiotic stresses (Mamedov et al., 1991, 1993; Papageorgiou et al., 1991; Papageorgiou and Murata, 1995; Allakhverdiev et al., 2003). Wang et al. (2010) found that drought stress can interfere with the state of the lipids in thylakoid membrane, which, if damaged, might cause PSII to be impaired. Concurrently, cell membrane stability depends on the absence of lipid peroxidation, caused by reactive oxygen species (ROS) accumulation. Moreover, they found that carotenoid concentrations in water stressed, GB-treated plants were consistently higher compared to untreated plants. They also demonstrated that the ability of GB to decrease ROS levels is not direct, but rather indirect. These findings imply that GB acts as an elicitor to other scavenger molecules, thereby strongly supporting our findings on carotenoid concentration. Indeed, Wang et al. (2010) correlated GB accumulation to xanthophyll cycle-dependent nonradiative energy dissipation, thereby drawing a strong connection between the protective action derived from GB overaccumulation and carotenoid synthesis. In addition, GB-synthetizing transgenic plants have been found to display higher activity of ROS-detoxifying enzymes (Yang et al., 2006; Ahmad et al., 2010). Supporting these arguments, Xu et al. (2018) hypothesized that GB may act both as an osmotic stress hardening molecule and as a signaling molecule in acclimation, rather than only *via* a direct action. Concerning energy supply, it is particularly interesting to notice the sharp accumulation of thiamine precursors, as thiamine plays a pivotal role in carbon metabolism and is essential for cell energy supply in all organisms. Moreover, it is essential in carbon fixation through the Calvin cycle and the non-mevalonate isoprenoid biosynthesis pathway, from which thousands of metabolites are derived including chlorophyll, phytols, and carotenoids, and also several phytohormones (Noordally et al., 2020). Thiamine has also been linked to plant adaptation responses to persistent abiotic stress conditions, including drought (Wong et al., 2006), and oxidative stress (Rapala-Kozik et al., 2008; Tunc-Ozdemir et al., 2009). In addition, the overaccumulation of specific secondary metabolites suggests a stress priming activity induced by the biostimulant treatment: phytoalexins have been associated with increased drought tolerance in multiple species (Kuc, 1995; Hatmi et al., 2014; Vaughan et al., 2015); phenylpropanoid biosynthetic pathway is activated under abiotic stress conditions,

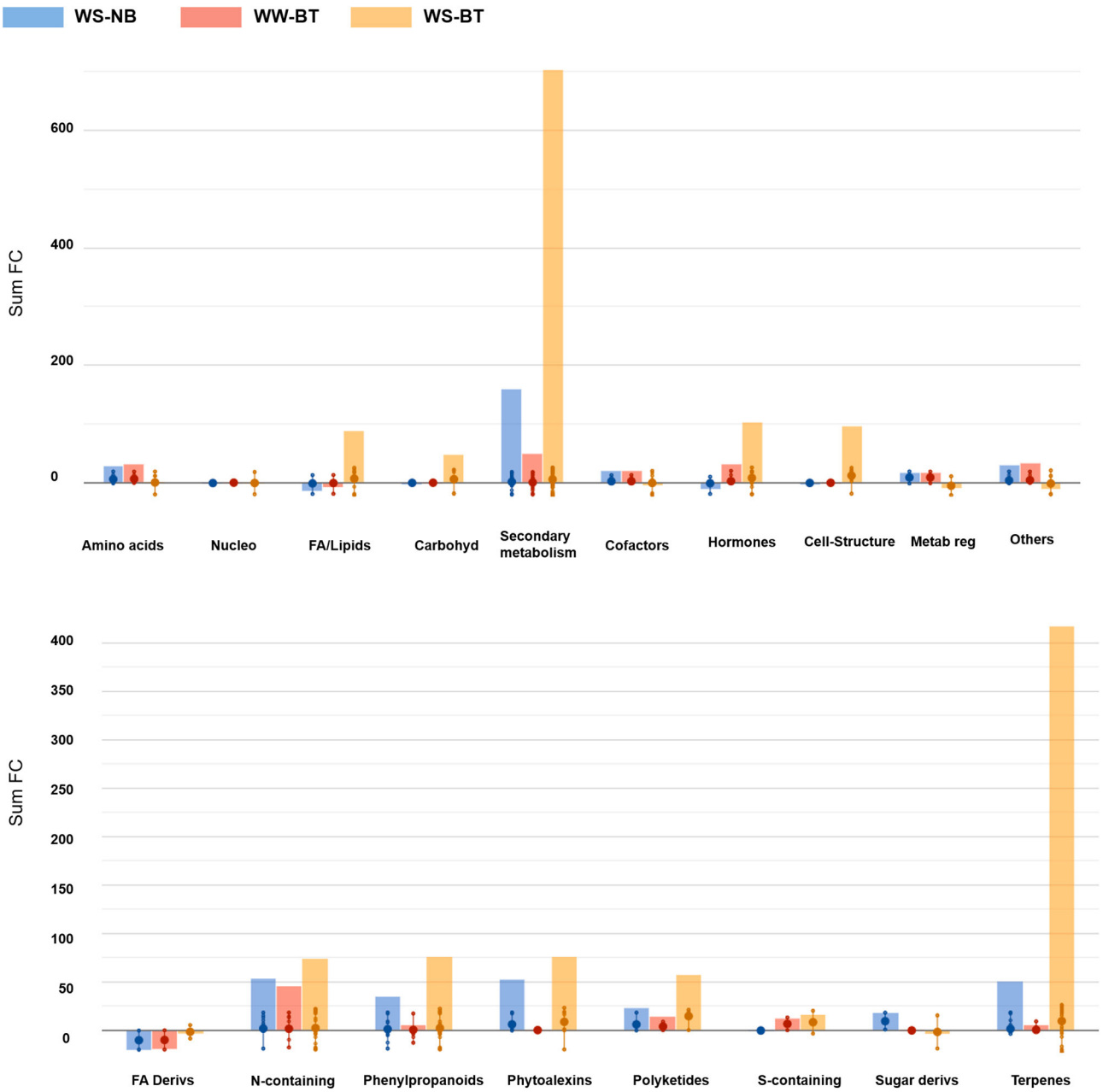

FIGURE 6 | Bar graphs resulting from the import of volcano analysis data [$p < 0.01$; field capacity (FC) > 2] on the Omics Dashboard tool from PlantCyc. The treatments FC difference is calculated based on WW, control treatment (WW–NB). The first bar (in blue) depicts WS–BT results, the second (in red) depicts WW–BT results, the last (in yellow) depicts WS–BT results. The abbreviated subcategory names on the *x*-axis correspond to: Nucleo: nucleosides and nucleotides; FA/Lipids: fatty acids and lipids; Amines: amines and polyamines; Carbohyd: carbohydrates; Cofactors: cofactors, prosthetic groups, electron carriers, and vitamins; Metab reg: Metabolic Regulators.

resulting in stimulated biosynthesis of phenolic compounds with strong antioxidative potential (Sharma et al., 2019). Lastly, the overaccumulation of lipids and specifically cutin synthase metabolites supports the maximization of stomatal transpiration (Kerstiens, 1997, 2006). All things considered, the positive effect of GB on water stress resistance could be attributed both to the delayed onset of stress, and consequently the enhanced natural response of tomato plants, and the elicitation of stress priming through the induction of H_2O_2-mediated antioxidant mechanisms, as Park et al. (2004, 2006) suggested, and molecules with strong antioxidant potential (such as xanthophylls).

In conclusion, the study demonstrated the potential of the GAMM method to describe and discriminate biostimulant action

(GB, in this case) to improve photosynthetic performance under water stress conditions. In this, the GAMM method was crucial in extracting the effect of biostimulant treatment under dynamic gas exchange acquisition. GAMM analysis effectively improved the interpretation of time series data, enabling both the description of the dynamics of water stress onset and the isolation of the effect related to the biostimulant treatment. Moreover, compared to the other treatments, water-stressed BT plants displayed a starkly different and stress tolerance-related metabolic profile, in agreement with the findings on photosynthetic performance. The metabolites accumulated suggest a priming effect for stress tolerance, *via* detoxification and stabilization of the photosynthetic machinery. The duration and dynamics of the positive effect of the biostimulant treatment under water stress differed for photosynthesis, transpiration, and WUE, the last two being limited in time. This could depend on an increased transpiration efficiency, translating into maximized soil water use for transpiration, or the EUW for transpiration. At the same time, minimization of leaf permeability through increased leaf wax content is one of the main strategies that plants employ to divert water to stomatal transpiration. Indeed, the metabolic profile findings support the increased EUW through the overaccumulation of lipids and cutine synthase metabolites. The present research brought further evidence that GB protective action on photosystem II is not only direct but also strongly connected to the production of other scavenger molecules (e.g., carotenoids and phytoalexins), making the case that GB acts both as an osmotic stress hardening molecule and as a signaling molecule in acclimation. Nonetheless, further research is needed to deepen the connection between exogenous GB treatment and metabolic response.

DATA AVAILABILITY STATEMENT

The original contributions presented in the study are included in the article/**Supplementary Material**, further inquiries can be directed to the corresponding author/s.

AUTHOR CONTRIBUTIONS

GA designed and performed the experiment, analyzed, and interpreted the data, created the figures for gas exchange, and wrote the manuscript. GA and MC optimized experimental techniques and analyzed gas exchange data. BM-M performed statistical analysis of the metabolome and data interpretation, created the figures for metabolomics, and participated in methods writing. AF was involved in experimental design and participated in data acquisition. SA supervised the design of the experiment, provided intellectual contributions, oversaw data analysis and interpretation, and corrected the manuscript.

ACKNOWLEDGMENTS

The authors gratefully acknowledge financial support from ED&F Man Liquid products ITALIA SRL (Bologna, Italy). One of the authors (BM-M, Grant Number: 21252/PD/19) would like to acknowledge support from the Consejería de Empleo, Universidades, Empresa y Medio Ambiente of the CARM, through the Fundación Séneca-Agencia de Ciencia y Tecnología de la Región de Murcia (Spain).

SUPPLEMENTARY MATERIAL

The Supplementary Material for this article can be found online at: https://www.frontiersin.org/articles/10.3389/fpls.2021.678925/full#supplementary-material

Supplementary Table 1 | Untargeted metabolomics data set containing the annotated compounds in both ***MS-only and MS/MS following the ultra-high performance liquid chromatography coupled to a quadrupole-time-of-flight mass spectrometer (UHPLC-QTOF-MS) analysis.

Supplementary Table 2 | Discriminant metabolites identified by the variables importance in projection (VIP) analysis in leaves following biostimulant application. Compounds were selected as discriminant by possessing a VIP score >1.3.

Supplementary Table 3 | Differential metabolites as derived from Volcano analysis [value of $p < 0.01$; field capacity (FC) > 2] and uploaded to the PlantCyc pathway Tool software for the subsequent analysis.

REFERENCES

Agboma, P. C., Jones, M. G. K., Peltonen-Sainio, P., Rita, H., and Pehu, E. (1997a). Exogenous glycinebetaine enhances grain yield of maize, sorghum and wheat grown under two supplementary watering regimes. *J. Agron. Crop Sci.* 178, 29–37. doi: 10.1111/j.1439-037X.1997.tb00348.x

Agboma, P. C., Sinclair, T., Jokinen, K., Peltonen-Sainio, P., and Pehu, E. (1997b). An evaluation of the effect of exogenous glycinebetaine on the growth and yield of soybean: timing of application, watering regimes and cultivars. *Field Crops Res.* 54, 51–64. doi: 10.1016/S0378-4290(97)00040-3

Ahmad, R., Kim, Y. H., Kim, M. D., Kwon, S. Y., Cho, K., Lee, H. S., et al. (2010). Simultaneous expression of choline oxidase, superoxide dismutase and ascorbate peroxidase in potato plant chloroplasts provides synergistically enhanced protection against various abiotic stresses. *Physiol. Plantarum* 138, 520–533. doi: 10.1111/j.1399-3054.2010.01348.x

Ahmad, S., Raza, I., Ali, H., Shahzad, A. N., Atiq-ur-Rehman, and Sarwar, N. (2014). Response of cotton crop to exogenous application of glycinebetaine under sufficient and scarce water conditions. *Brazilian J. Botany* 37, 407–415. doi: 10.1007/s40415-014-0092-z

Ahmed, N., Zhang, Y., Li, K., Zhou, Y., Zhang, M., and Li, Z. (2019). Exogenous application of glycine betaine improved water use efficiency in winter wheat (*Triticum aestivum* L.) via modulating photosynthetic efficiency and antioxidative capacity under conventional and limited irrigation conditions. *Crop J.* 7, 635–650. doi: 10.1016/j.cj.2019.03.004

Akaike, H. (1974). A new look at the statistical model identification. *IEEE T. Automat. Contr.* 19, 716–723. doi: 10.1109/TAC.1974.1100705

Allakhverdiev, S. I., Hayashi, H., Nishiyama, Y., Ivanov, A. G., Aliev, J. A., Klimov, V. V., et al. (2003). Glycinebetaine protects the D1/D2/Cytb559 complex of photosystem II against photo-induced and heat-induced inactivation. *J. Plant Physiol.* 160, 41–49. doi: 10.1078/0176-1617-00845

Allakhverdiev, S. I., Los, D. A., Mohanty, P., Nishiyama, Y., and Murata, N. (2007). Glycinebetaine alleviates the inhibitory effect of moderate heat stress on the repair of photosystem II during photoinhibition. *Biochim. Biophys. Acta* 1767, 1363–1371. doi: 10.1016/j.bbabio.2007.10.005

Annunziata, M. G., Ciarmiello, L. F., Woodrow, P., Dell'Aversana, E., and Carillo, P. (2019). Spatial and temporal profile of glycine betaine accumulation in plants under abiotic stresses. *Front. Plant Sci.* 10:230. doi: 10.3389/fpls.2019.00230

Araus, J. L., and Cairns, J. E. (2014). Field high-throughput phenotyping: the new crop breeding frontier. *Trends Plant Sci.* 19, 52–61. doi: 10.1016/j.tplants.2013.09.008

Arbona, V., Manzi, M., Ollas, C., and Gómez-Cadenas, A. (2013). Metabolomics as a tool to investigate abiotic stress tolerance in plants. *Int. J. Mol. Sci.* 14, 4885–4911. doi: 10.3390/ijms14034885

Ashraf, M., and Foolad, M. (2007). Roles of glycine betaine and proline in improving plant abiotic stress resistance. *Environ. Exp. Bot.* 59, 206–216. doi: 10.1016/j.envexpbot.2005.12.006

Blum, A. (2009). Effective use of water (EUW) and not water-use efficiency (WUE) is the target of crop yield improvement under drought stress. *Field Crops Res.* 112, 119–123. doi: 10.1016/j.fcr.2009.03.009

Blum, A. (2016). Osmotic adjustment is a prime drought stress adaptive engine in support of plant production. *Plant Cell Environ.* 40, 4–10. doi: 10.1111/pce.12800

Boswijk, V., Loerts, H., and Hilton, N. H. (2020). Salience is in the eye of the beholder: increased pupil size reflects acoustically salient variables. *Ampersand* 7:100061. doi: 10.1016/j.amper.2020.100061

Campbell, Z. C., Acosta-Gamboa, L. M., Nepal, N., and Lorence, A. (2018). Engineering plants for tomorrow: how high-throughput phenotyping is contributing to the development of better crops. *Phytochem. Rev.* 17, 1329–1343. doi: 10.1007/s11101-018-9585-x

Caspi, R., Dreher, K., and Karp, P. D. (2013). The challenge of constructing, classifying, and representing metabolic pathways. *FEMS Microbiol. Letters* 345, 85–93. doi: 10.1111/1574-6968.12194

Chawade, A., van Ham, J., Blomquist, H., Bagge, O., Alexandersson, E., and Ortiz, R. (2019). High-throughput field-phenotyping tools for plant breeding and precision agriculture. *Agronomy* 9:258. doi: 10.3390/agronomy9050258

Chen, T. H., and Murata, N. (2010). Glycinebetaine protects plants against abiotic stress: mechanisms and biotechnological applications. *Plant Cell Environ.* 34, 1–20. doi: 10.1111/j.1365-3040.2010.02232.x

Cheng, J., Lan, W., Zheng, G., and Gao, X. (2018). Metabolomics: a high-throughput platform for metabolite profile exploration. *Methods Mol. Biol.* 265–292. doi: 10.1007/978-1-4939-7717-8_16

Coppens, F., Wuyts, N., Inzé, D., and Dhondt, S. (2017). Unlocking the potential of plant phenotyping data through integration and data-driven approaches. *Current Opinion Systems Biol.* 4, 58–63. doi: 10.1016/j.coisb.2017.07.002

Corrado, G., Lucini, L., Miras-Moreno, B., Chiaiese, P., Colla, G., De Pascale, S., et al. (2020). Metabolic insights into the anion-anion antagonism in sweet basil: effects of different nitrate/chloride ratios in the nutrient solution. *Int. J. Mol. Sci.* 21:2482. doi: 10.3390/ijms21072482

Del Buono, D. (2020). Can biostimulants be used to mitigate the effect of anthropogenic climate change on agriculture? It is time to respond. *Sci. Total Environ.* 751:141763. doi: 10.1016/j.scitotenv.2020.141763

Fariduddin, Q., Varshney, P., Yusuf, M., Ali, A., and Ahmad, A. (2013). Dissecting the role of glycine betaine in plants under abiotic stress. *Plant Stress* 7, 8–18. doi: 10.1080/17429145.2012.716455

Fleming, T. R., Fleming, C. C., Levy, C. C. B., Repiso, C., Hennequart, F., Nolasco, J. B., et al. (2019). Biostimulants enhance growth and drought tolerance inArabidopsis thalianaand exhibit chemical priming action. *Annals Appl. Biol.* 174, 153–165. doi: 10.1111/aab.12482

Fracasso, A., Magnanini, E., Marocco, A., and Amaducci, S. (2017). Real-time determination of photosynthesis, transpiration, water-use efficiency and gene expression of two sorghum bicolor (moench) genotypes subjected to dry-down. *Front. Plant Sci.* 8:3. doi: 10.3389/fpls.2017.00932

Frank, H. A., and Cogdell, R. J. (1996). Carotenoids in photosynthesis. *Photochem. Photobiol.* 63, 257–264. doi: 10.1111/j.1751-1097.1996.tb03022.x

Gorham, J. (1995). "Betaines in higher plants – biosynthesis and role in stress metabolism," in *Amino Acids and Their Derivatives in Higher Plants,* Wallsgroves, R.M., ed (Cambridge: Cambridge University Press), 171–203. doi: 10.1017/CBO9780511721809.013

Gosa, S. C., Lupo, Y., and Moshelion, M. (2019). Quantitative and comparative analysis of whole-plant performance for functional physiological traits phenotyping: new tools to support pre-breeding and plant stress physiology studies. *Plant Sci.* 282, 49–59. doi: 10.1016/j.plantsci.2018.05.008

Griffiths, M., Sistrom, W., Cohen-Bazire, G., and Stanier, R. (1955). Function of carotenoids in photosynthesis. *Nature* 176, 1211–1214. doi: 10.1038/1761211a0

Halperin, O., Gebremedhin, A., Wallach, R., and Moshelion, M. (2017). High-throughput physiological phenotyping and screening system for the characterization of plant-environment interactions. *Plant J.* 89, 839–850. doi: 10.1111/tpj.13425

Hamani, A. K. M., Wang, G., Soothar, M. K., Shen, X., Gao, Y., Qiu, R., et al. (2020). Responses of leaf gas exchange attributes, photosynthetic pigments and antioxidant enzymes in NaCl-stressed cotton (Gossypium hirsutum L.) seedlings to exogenous glycine betaine and salicylic acid. *BMC Plant Biol.* 20:434. doi: 10.1186/s12870-020-02624-9

Hatmi, S., Gruau, C., Trotel-Aziz, P., Villaume, S., Rabenoelina, F., and Baillieul, F., et al. (2014). Drought stress tolerance in grapevine involves activation of polyamine oxidation contributing to improved immune response and low susceptibility to *Botrytis cinerea*. *J. Exp. Botany* 66, 775–787. doi: 10.1093/jxb/eru436

Huang, S., Zuo, T., and Ni, W. (2020). Important roles of glycinebetaine in stabilizing the structure and function of the photosystem II complex under abiotic stresses. *Planta* 251:63. doi: 10.1007/s00425-019-03330-z

Hussain, M., Malik, M. A., Farooq, M., Ashraf, M. Y., and Cheema, M. A. (2008). Improving drought tolerance by exogenous application of glycinebetaine and salicylic acid in sunflower. *J. Agron. Crop Sci.* 194, 193–199. doi: 10.1111/j.1439-037x.2008.00305.x

Iglesias, A., and Garrote, L. (2015). Adaptation strategies for agricultural water management under climate change in Europe. *Agric. Water Manag.* 155, 113–124. doi: 10.1016/j.agwat.2015.03.014

Kerstiens, G. (1997). *In vivo* manipulation of cuticular water permeance and its effect on stomatal response to air humidity. *N. Phytol.* 137, 473–480. doi: 10.1046/j.1469-8137.1997.00847.x

Kerstiens, G. (2006). Water transport in plant cuticles, an update. *J. Exp. Bot.* 57, 2493–2499. doi: 10.1093/jxb/erl017

Kuc, J. (1995). Phytoalexins, stress metabolism, and disease resistance in plants. *Ann. Rev. Phytopathol.* 33, 275–297. doi: 10.1146/annurev.py.33.090195.001423

Long, S. P., and Hallgren, J. E. (1985). "Measurement of CO_2 assimilation by plants in the field and the laboratory," in *Techniques in Bioproductivity and Photosynthesis*, eds J. Coombs, D.O. Hall, S.P. Long and J.M.O. Scurlock, 2nd edn, (Oxford: Pergamon Press), 62–94. doi: 10.1016/B978-0-08-031999-5.50016-9

Lucini, L., Rouphael, Y., Cardarelli, M., Bonini, P., Baffi, C., and Colla, G. (2018). A vegetal biopolymer-based biostimulant promoted root growth in melon while triggering brassinosteroids and stress-related compounds. *Front. Plant Sci.* 9, 1–10. doi: 10.3389/fpls.2018.00472

Lucini, L., Rouphael, Y., Cardarelli, M., Canaguier, R., Kumar, P., and Colla, G. (2015). The effect of a plant-derived biostimulant on metabolic profiling and crop performance of lettuce grown under saline conditions. *Sci. Hortic.* 182, 124–133. doi: 10.1016/j.scienta.2014.11.022

Ma, Q. Q., Wang, W., Li, Y. H., Li, D. Q., and Zou, Q. (2006). Alleviation of photoinhibition in drought-stressed wheat (Triticum aestivum) by foliar-applied glycinebetaine. *J. Plant Physiol.* 163, 165–175. doi: 10.1016/j.jplph.2005.04.023

Mäkelä, P., Jokinen, K., Kontturi, M., Peltonen-Sainio, P., Pehu, E., and Somersalo, S. (1998). Foliar application of glycinebetaine—a novel product from sugar beet—as an approach to increase tomato yield. *Industrial Crops Products* 7, 139–148. doi: 10.1016/S0926-6690(97)00042-3

Mäkelä, P., Kontturi, M., Pehu, E., and Somersalo, S. (1999). Photosynthetic response of drought- and salt-stressed tomato and turnip rape plants to foliar-applied glycinebetaine. *Physiol. Plantarum* 105, 45–50. doi: 10.1034/j.1399-3054.1999.105108.x

Mamedov, M., Hayashi, H., and Murata, N. (1993). Effects of glycinebetaine and unsaturation of membrane lipids on heat stability of photosynthetic electron-transport and phosphorylation reactions in Synechocystis PCC6803. *Biochim. Biophys. Acta* 1142, 1–5. doi: 10.1016/0005-2728(93)90077-S

Mamedov, M., Hayashi, H., Wada, H., Mohanty, P., Papageorgiou, G., and Murata, N. (1991). Glycinebetaine enhances and stabilizes the evolution of oxygen and the synthesis of ATP by cyanobacterial thylakoid membranes. *FEBS Lett.* 294, 271–274. doi: 10.1016/0014-5793(91)81446-F

Mbarki, S., Sytar, O., Cerda, A., Zivcak, M., Rastogi, A., He, X., et al. (2018). "Strategies to mitigate the salt stress effects on photosynthetic apparatus and productivity of crop plants," in *Salinity Responses and Tolerance in Plants*, vol 1. (Berlin: Springer), 85–136.

Medrano, H., Escalona, J. M., Bota, J., Giulias, J., and Flexas, J. (2002). Regulation of photosynthesis of C3 plants in response to progressive drought: stomatal conductance as a reference parameter. *Ann. Bot.* 89, 895–905. doi: 10.1093/aob/mcf079

Michaletti, A., Naghavi, M. R., Toorchi, M., Zolla, L., and Rinalducci, S. (2018). Metabolomics and proteomics reveal drought-stress responses of leaf tissues from spring-wheat. *Sci. Rep.* 8:5710. doi: 10.1038/s41598-018-24012-y

Mir, R. R., Reynolds, M., Pinto, F., Khan, M. A., and Bhat, M. A. (2019). High-throughput phenotyping for crop improvement in the genomics era. *Plant Sci.* 282, 60–72. doi: 10.1016/j.plantsci.2019.01.007

Miras-Moreno, B., Corrado, G., Zhang, L., Senizza, B., Righetti, L., Bruni, R., et al. (2020). The metabolic reprogramming induced by sub-optimal nutritional and light inputs in soilless cultivated green and red butterhead lettuce. *Int. J. Mol. Sci.* 21:6381. doi: 10.3390/ijms21176381

Murase, H., Nagashima, H., Yonezaki, S., Matsukura, R., and Kitakado, T. (2009). Application of a generalized additive model (GAM) to reveal relationships between environmental factors and distributions of pelagic fish and krill: a case study in Sendai Bay, Japan. *ICES J. Marine Sci.* 66, 1417–1424. doi: 10.1093/icesjms/fsp105

Nawaz, M., and Wang, Z. (2020). Abscisic acid and glycine betaine mediated tolerance mechanisms under drought stress and recovery in *Axonopus compressus*: a new insight. *Sci. Rep.* 10:6942. doi: 10.1038/s41598-020-63447-0

Nephali, L., Piater, L. A., Dubery, I. A., Patterson, V., Huyser, J., Burgess, K., et al. (2020). Biostimulants for plant growth and mitigation of abiotic stresses: a metabolomics perspective. *Metabolites* 10:505. doi: 10.3390/metabo10120505

Noordally, Z. B., Trichtinger, C., Dalvit, I., Hofmann, M., Roux, C., Zamboni, N., et al. (2020). The coenzyme thiamine diphosphate displays a daily rhythm in the Arabidopsis nucleus. *Commun. Biol.* 3:209. doi: 10.1038/s42003-020-0927-z

Nuccio, M., Paul, M., Bate, N., Cohn, J., and Cutler, S. (2018). Where are the drought tolerant crops? An assessment of more than two decades of plant biotechnology effort in crop improvement. *Plant Sci.* 273, 110–119. doi: 10.1016/j.plantsci.2018.01.020

Ohana-Levi, N., Munitz, S., Ben-Gal, A., and Netzer, Y. (2020). Evaluation of within-season grapevine evapotranspiration patterns and drivers using generalized additive models. *Agric. Water Manag.* 228:105808. doi: 10.1016/j.agwat.2019.105808

Osborne, W. C. (1977). *Fans, 2nd Edn*. Oxford: Pergamon Press.

Papageorgiou, G. C., Fujimura, Y., and Murata, N. (1991). Protection of the oxygen-evolving photosystem II complex by glycinebetaine. *Biochim. Biophy. Acta* 1057, 361–366. doi: 10.1016/S0005-2728(05)80148-3

Papageorgiou, G. C., and Murata, N. (1995). The unusually strong stabilizing effects of glycine betaine on the structure and function of the oxygen-evolving Photosystem II complex. *Photosyn. Res.* 44, 243–252. doi: 10.1007/BF000 48597

Park, E.-J., Jeknić, Z., and Chen, T. H. H. (2006). Exogenous application of glycinebetaine increases chilling tolerance in tomato plants. *Plant Cell Physiol.* 47, 706–714. doi: 10.1093/pcp/pcj041

Park, E. J., Jeknić, Z., Sakamoto, A., DeNoma, J., Yuwansiri, R., Murata, N., et al. (2004). Genetic engineering of glycinebetaine synthesis in tomato protects seeds, plants, and flowers from chilling damage. *Plant J.* 40, 474–487. doi: 10.1111/j.1365-313x.2004.02237.x

Paul, K., Sorrentino, M., Lucini, L., Rouphael, Y., Cardarelli, M., Bonini, P., et al. (2019a). Understanding the biostimulant action of vegetal-derived protein hydrolysates by high-throughput plant phenotyping and metabolomics: a case study on tomato. *Front. Plant Sci.* 10, 1–14. doi: 10.3389/fpls.2019.00047

Paul, K., Sorrentino, M., Lucini, L., Rouphael, Y., Cardarelli, M., Bonini, P., et al. (2019b). A combined phenotypic and metabolomic approach for elucidating the biostimulant action of a plant-derived protein hydrolysate on tomato grown under limited water availability. *Front. Plant Sci.* 10, 1–15. doi: 10.3389/fpls.2019.00493

Pedersen, E. J., Miller, D. L., Simpson, G. L., and Ross, N. (2019). Hierarchical generalized additive models in ecology: an introduction with mgcv. *PeerJ* 7:e6876. doi: 10.7717/peerj.6876

Petrozza, A., Santaniello, A., Summerer, S., Di Tommaso, G., Di Tommaso, D., Paparelli, E., et al. (2014). Physiological responses to Megafol® treatments in tomato plants under drought stress: a phenomic and molecular approach. *Sci. Hortic.* 174, 185–192. doi: 10.1016/j.scienta.2014.05.023

Polívka, T. š., and Sundström, V. (2004). Ultrafast dynamics of carotenoid excited states–from solution to natural and artificial systems. *Chem. Rev.* 104, 2021–2072. doi: 10.1021/cr020674n

Pretali, L., Bernardo, L., Butterfield, T. S., Trevisan, M., and Lucini, L. (2016). Botanical and biological pesticides elicit a similar induced systemic response in tomato (*Solanum lycopersicum*) secondary metabolism. *Phytochemistry* 130, 56–63. doi: 10.1016/j.phytochem.2016.04.002

Quan, R., Shang, M., Zhang, H., Zhao, Y., and Zhang, J. (2004). Improved chilling tolerance by transformation with betA gene for the enhancement of glycinebetaine synthesis in maize. *Plant Sci.* 166, 141–149. doi: 10.1016/j.plantsci.2003.08.018

R Core Team (2020). R: A language and environment for statistical computing. R Foundation for Statistical Computing, Vienna, Austria. Available online at: https://www.R-project.org/

Rapala-Kozik, M., Kowalska, E., and Ostrowska, K. (2008). Modulation of thiamine metabolism in Zea mays seedlings under conditions of abiotic stress. *J. Exp. Bot.* 59, 4133–4143. doi: 10.1093/jxb/ern253

Razavi, F., Mahmoudi, R., Rabiei, V., Aghdam, M. S., and Soleimani, A. (2018). Glycine betaine treatment attenuates chilling injury and maintains nutritional quality of hawthorn fruit during storage at low temperature. *Sci. Hortic.* 233, 188–194. doi: 10.1016/j.scienta.2018.01.053

Rouphael, Y., Colla, G., Bernardo, L., Kane, D., Trevisan, M., and Lucini, L. (2016). Zinc excess triggered polyamines accumulation in lettuce root metabolome, as compared to osmotic stress under high salinity. *Front. Plant Sci.* 7, 1–9. doi: 10.3389/fpls.2016.00842

Rouphael, Y., Lucini, L., Miras-Moreno, B., Colla, G., Bonini, P., and Cardarelli, M. (2020). Metabolomic responses of maize shoots and roots elicited by combinatorial seed treatments with microbial and non-microbial biostimulants. *Front. Microbiol.* 11, 1–11. doi: 10.3389/fmicb.2020.00664

Rouphael, Y., Spíchal, L., Panzarová, K., Casa, R., and Colla, G. (2018). High-throughput plant phenotyping for developing novel biostimulants: from lab to field or from field to lab? *Front. Plant Sci.* 9, 1–5. doi: 10.3389/fpls.2018.01197

Sakamoto, A., and Murata, N. (2002). The role of glycine betaine in the protection of plants from stress: clues from transgenic plants. *Plant Cell Environ.* 25, 163–171. doi: 10.1046/j.0016-8025.2001.00790.x

Salek, R. M., Neumann, S., Schober, D., Hummel, J., Billiau, K., Kopka, J., et al. (2015). COordination of Standards in MetabOlomicS (COSMOS): facilitating integrated metabolomics data access. *Metabolomics* 11, 1587–1597. doi: 10.1007/s11306-015-0810-y

Schneider, C. A., Rasband, W. S., and Eliceiri, K. W. (2012). NIH Image to ImageJ: 25 years of image analysis. *Nat. Methods* 9, 671–675. doi: 10.1038/nmeth.2089

Serraj, R., and Sinclair, T. (2002). Osmolyte accumulation: can it really help increase crop yield under drought conditions?. *Plant Cell Environ.* 25, 333–341. doi: 10.1046/j.1365-3040.2002.00754.x

Sharma, A., Shahzad, B., Rehman, A., Bhardwaj, R., Landi, M., and Zheng, B. (2019). Response of phenylpropanoid pathway and the role of polyphenols in plants under abiotic stress. *Molecules*. 24:2452. doi: 10.3390/molecules24132452

Shulaev, V., Cortes, D., Miller, G., and Mittler, R. (2008). Metabolomics for plant stress response. *Physiol. Plantarum* 132, 199–208. doi: 10.1111/j.1399-3054.2007.01025.x

Tang, X., Mu, X., Shao, H., Wang, H., and Brestic, M. (2014). Global plant-responding mechanisms to salt stress: physiological and molecular levels and implications in biotechnology. *Crit. Rev. Biotechnol.* 35, 425–437. doi: 10.3109/07388551.2014.889080

Tardieu, F., Cabrera-Bosquet, L., Pridmore, T., and Bennett, M. (2017). Plant phenomics, from sensors to knowledge. *Current Biol.* 27, R770–R783. doi: 10.1016/j.cub.2017.05.055

Teklić, T., Paradiković, N., Špoljarević, M., Zeljković, S., Lončarić, Z., and Lisjak, M. (2020). Linking abiotic stress, plant metabolites, biostimulants and functional food. *Ann. Appl. Biol.* 178, 169–191. doi: 10.1111/aab.12651

Tian, F., Wang, W., Liang, C., Wang, X., Wang, G., and Wang, W. (2017). Overaccumulation of glycine betaine makes the function of the thylakoid membrane better in wheat under salt stress. *Crop J.* 5, 73–82. doi: 10.1016/j.cj.2016.05.008

Tsugawa, H., Cajka, T., Kind, T., Ma, Y., Higgins, B., Ikeda, K., et al. (2015). MS-DIAL: data-independent MS/MS deconvolution for comprehensive metabolome analysis. *Nat. Methods* 12, 523–526. doi: 10.1038/nmeth.3393

Tunc-Ozdemir, M., Miller, G., Song, L., Kim, J., Sodek, A., Koussevitzky, S., et al. (2009). Thiamin confers enhanced tolerance to oxidative stress in arabidopsis. *Plant Physiol.* 151, 421–432. doi: 10.1104/pp.109.140046

Uarrota, V., Stefen, D., Leolato, L., Gindri, D., and Nerling, D. (2018). "Revisiting carotenoids and their role in plant stress responses: from biosynthesis to plant signaling mechanisms during stress," in *Antioxidants and Antioxidant Enzymes in Higher Plants*, Springer, 207–232. doi: 10.1007/978-3-319-75088-0_10

van Rij, J., Hendriks, P., van Rijn, H., Baayen, R. H., and Wood, S. N. (2019). Analyzing the time course of pupillometric data. *Trends Hearing* 23:233121651983248. doi: 10.1177/2331216519832483

van Rij, J., Wieling, M., Baayen, R., and van Rijn, H. (2020). itsadug: Interpreting Time Series and Autocorrelated Data Using GAMMs. *R* package version 2.4

Vaughan, M. M., Christensen, S., Schmelz, E. A., Huffaker, A., Mcauslane, H. J., Alborn, H. T., et al. (2015). Accumulation of terpenoid phytoalexins in maize roots is associated with drought tolerance. *Plant Cell Environ.* 38, 2195–2207. doi: 10.1111/pce.12482

Wang, G. P., Zhang, X. Y., Li, F., Luo, Y., and Wang, W. (2010). Overaccumulation of glycine betaine enhances tolerance to drought and heat stress in wheat leaves in the protection of photosynthesis. *Photosynthetica* 48, 117–126. doi: 10.1007/s11099-010-0016-5

Wang, L., Shan, T., Xie, B., Ling, C., Shao, S., Jin, P., et al. (2019). Glycine betaine reduces chilling injury in peach fruit by enhancing phenolic and sugar metabolisms. *Food Chem.* 272, 530–538. doi: 10.1016/j.foodchem.2018.08.085

Wieling, M. (2018). Analyzing dynamic phonetic data using generalized additive mixed modeling: a tutorial focusing on articulatory differences between L1 and L2 speakers of English. *J. Phonetics* 70, 86–116. doi: 10.1016/j.wocn.2018.03.002

Wong, C. E., Li, Y., Labbe, A., Guevara, D., Nuin, P., Whitty, B., et al. (2006). Transcriptional profiling implicates novel interactions between abiotic stress and hormonal responses in thellungiella, a close relative of arabidopsis. *Plant Physiol.* 140, 1437–1450. doi: 10.1104/pp.105.070508

Wyn Jones, G. R., and Storey, R. (1981). "Betaines," in *The Physiology and Biochemistry of Drought Resistance in Plants*, eds. L. G. Paleg, D. Aspinall (Sydney: Academic Press), 171–204.

Xing, W., and Rajashekar, C. B. (1999). Alleviation of water stress in beans by exogenous glycine betaine. *Plant Sci.* 148, 185–192. doi: 10.1016/S0168-9452(99)00137-5

Xu, Z., Sun, M., Jiang, X., Sun, H., Dang, X., Cong, H., et al. (2018). Glycinebetaine biosynthesis in response to osmotic stress depends on jasmonate signaling in watermelon suspension cells. *Front. Plant Sci.* 9, 8–11. doi: 10.3389/fpls.2018.01469

Yang, X., Liang, Z., and Lu, C. (2005). Genetic engineering of the biosynthesis of glycinebetaine enhances photosynthesis against high temperature stress in transgenic tobacco plants. *Plant Physiol.* 138, 2299–2309. doi: 10.1104/pp.105.063164

Yang, X., and Lu, C. (2005). Photosynthesis is improved by exogenous glycinebetaine in salt-stressed maize plants. *Physiol. Plantarum* 124, 343–352. doi: 10.1111/j.1399-3054.2005.00518.x

Yang, X., Wen, X., Gong, H., Lu, Q., Yang, Z., Tang, Y., et al. (2006). Genetic engineering of the biosynthesis of glycinebetaine enhances thermotolerance of photosystem II in tobacco plants. *Planta* 225, 719–733. doi: 10.1007/s00425-006-0380-3

Zhao, W., Liu, L., Shen, Q., Yang, J., Han, X., Tian, F., et al. (2020). Effects of water stress on photosynthesis, yield, and water use efficiency in winter wheat. *Water* 12:2127. doi: 10.3390/w12082127

Zuur, A., Ieno, E. N., Walker, N., Saveliev, A. A., and Smith, G. M. (2009). *Mixed Effects Models and Extensions in Ecology with R*. New York, NY: Springer. doi: 10.1007/978-0-387-87458-6

Conflict of Interest: The authors declare that the research was conducted in the absence of any commercial or financial relationships that could be construed as a potential conflict of interest.

frontiers in Plant Science

ORIGINAL RESEARCH
published: 04 June 2021
doi: 10.3389/fpls.2021.670236

Impact of Plant Growth-Promoting Rhizobacteria Inoculation and Grafting on Tolerance of Tomato to Combined Water and Nutrient Stress Assessed via Metabolomics Analysis

Panagiotis Kalozoumis[1], Dimitrios Savvas[1], Konstantinos Aliferis[2,3], Georgia Ntatsi[1], George Marakis[1], Evridiki Simou[1], Anastasia Tampakaki[4] and Ioannis Karapanos[1]*

[1] Department of Crop Science, Laboratory of Vegetable Production, Agricultural University of Athens, Athens, Greece, [2] Department of Crop Science, Laboratory of Pesticide Science, Agricultural University of Athens, Athens, Greece, [3] Department of Plant Science, McGill University, Macdonald Campus, Sainte-Anne-de-Bellevue, QC, Canada, [4] Department of Crop Science, Laboratory of General and Agricultural Microbiology, Agricultural University of Athens, Athens, Greece

OPEN ACCESS

Edited by:
Maurizio Ruzzi, University of Tuscia, Italy

Reviewed by:
Paolo Bonini, Ngalab (Spain), Spain
Luigi Lucini, Catholic University of the Sacred Heart, Italy

***Correspondence:**
Dimitrios Savvas
dsavvas@aua.gr

Specialty section:
This article was submitted to Plant Abiotic Stress, a section of the journal Frontiers in Plant Science

Received: *20 February 2021*
Accepted: *12 April 2021*
Published: *04 June 2021*

Citation:
Kalozoumis P, Savvas D, Aliferis K, Ntatsi G, Marakis G, Simou E, Tampakaki A and Karapanos I (2021) Impact of Plant Growth-Promoting Rhizobacteria Inoculation and Grafting on Tolerance of Tomato to Combined Water and Nutrient Stress Assessed via Metabolomics Analysis. Front. Plant Sci. 12:670236. doi: 10.3389/fpls.2021.670236

In the current study, inoculation with plant growth-promoting rhizobacteria (PGPR) and grafting were tested as possible cultural practices that may enhance resilience of tomato to stress induced by combined water and nutrient shortage. The roots of tomato grown on perlite were either inoculated or not with PGPR, applying four different treatments. These were PGPR-T1, a mix of two *Enterobacter* sp. strains (C1.2 and C1.5); PGPR-T2, *Paenibacillus* sp. strain DN1.2; PGPR-T3, *Enterobacter mori* strain C3.1; and PGPR-T4, *Lelliottia* sp. strain D2.4. PGPR-treated plants were either self-grafted or grafted onto *Solanum lycopersicum* cv. M82 and received either full or 50% of their standard water, nitrogen, and phosphorus needs. The vegetative biomass of plants subjected to PGPR-T1 was not reduced when plants were cultivated under combined stress, while it was reduced by stress to the rest of the PGPR treatments. However, PGPR-T3 increased considerably plant biomass of non-stressed tomato plants than did all other treatments. PGPR application had no impact on fruit biomass, while grafting onto 'M82' increased fruit production than did self-grafting. Metabolomics analysis in tomato leaves revealed that combined stress affects several metabolites, most of them already described as stress-related, including trehalose, myo-inositol, and monopalmitin. PGPR inoculation with *E. mori* strain C3.1 affected metabolites, which are important for plant/microbe symbiosis (myo-inositol and monopalmitin). The rootstock M82 did not affect many metabolites in plant leaves, but it clearly decreased the levels of malate and D-fructose and imposed an accumulation of oleic acid. In conclusion, PGPR are capable of increasing tomato tolerance to combined stress. However, further research is required to evaluate more strains and refine protocols for their application. Metabolites that were discovered as biomarkers could be used to accelerate the screening process for traits such as stress tolerance to abiotic and/or abiotic stresses. Finally, 'M82' is a suitable rootstock for tomato, as it is capable of increasing fruit biomass production.

Keywords: biostimulant, hydroponics, grafting, metabolomics, M82, PGPR, tomato, water stress

INTRODUCTION

The Mediterranean region, where tomato is widely cultivated, is expected to be strongly affected by the climate change in the following years (Giorgi, 2006; Giorgi and Lionello, 2008). One of the consequences of climate change in the Mediterranean area is the decrease of the average yearly precipitation, which leads to water scarcity, a situation already familiar to many Mediterranean countries (Saadi et al., 2015). Tomato is a water-demanding crop (Ngouajio et al., 2007), and, consequently, water deficit can result in severe yield decreases compared with cultivation under fully irrigated conditions (Kuşçu et al., 2014). Additionally, irrigation along with other parameters, including fertilization, affects the nutritional composition of tomato fruits (Smith and Hui, 2004). To cope with this situation, it is crucial to develop new cropping approaches contributing to reduced water consumption. Deficit irrigation has been postulated as an alternative irrigation strategy that might save water without or with minimal consequences on crop yield, but conclusions as to whether the concomitant yield losses are affordable do not converge (Giuliani et al., 2016).

In addition to water deficit, excessive fertilizer application in intensive agriculture and horticulture also raises environmental concerns, especially in developed countries, but also in developing countries where an increased phosphorus demand is recorded (Desmidt et al., 2015). The initial fears about the availability of P resources are currently revised, and many studies suggest that natural P reserves will not be depleted in the next 100 years (Günther, 1997; Cisse and Mrabet, 2004; Van Vuuren et al., 2010). However, if the plant-available P in the Earth's crust is depleted, access to discrete global reserves is politically sensitive, energy demanding, and economically challenging (Godfray et al., 2010; Neset and Cordell, 2012; Desmidt et al., 2015). Similarly, the use of N fertilizers is associated with increased greenhouse gas emissions, thereby contributing to climate change, firstly because their production through industrial N_2 fixation entails extensive consumption of fossil fuels (Chen et al., 2018) and secondly because part of the soil NO_3–N is converted into N_2O in the soil (Smith and Zimmerman, 1981). Thus, crop fertilization strategies associated with reduced application of N and P fertilizers are strongly supported by current European policies (EU Directive 889/2008).

Plant growth-promoting rhizobacteria (PGPR) application is considered an effective strategy to stimulate plant growth, while modulating abiotic stress responses via a multitude of mechanisms (Patakioutas et al., 2015; Ruzzi and Aroca, 2015; Backer et al., 2018; Rouphael and Colla, 2020). Plant growth promotion by PGPR is the outcome of different mechanisms, such as biological nitrogen fixation, ethylene levels reduction, siderophore production, phytohormone production, induction of pathogen resistance, nutrient solubilization, mycorrhizal functioning, and decreasing pollutant toxicity (Glick et al., 1999; Rouphael and Colla, 2020). Nutrient solubilization can lead to production of biofertilizers, particularly for solubilizing phosphorus (De Pascale et al., 2018) where resources are limited (Bhattacharyya and Jha, 2012). Induced systemic resistance can also provide an effective pathogen protection even in organic agriculture (Ramamoorthy et al., 2001). Thus, inoculation of plant roots with a mix of different growth-promoting bacteria strains is considered a very promising technique to protect plants from diseases and simultaneously enhance plant growth (Murphy et al., 2003).

Many different PGPR strains have been already tested in tomato crops under different soil or soilless conditions (De Brito et al., 1995; Yan et al., 2003). Colonization of tomato roots with PGPR is performed by inoculating the seeds or by applying the bacteria suspension thoroughly into the soil/soilless medium with no need of sterilization (Yan et al., 2003). Many studies with tomato showed that PGPR inoculation increases yield (Gagné et al., 1993), lycopene, antioxidants, and potassium in tomato fruits (Ordookhani et al., 2010). Furthermore, PGPR increased P levels in tomato shoots (Hariprasad and Niranjana, 2009) and contributed to more efficient control of nematode and pathogen infections (Seleim et al., 2011; Shanmugam and Kanoujia, 2011; Almaghrabi et al., 2013).

Grafting is an alternative technique that can confer enhanced tolerance to tomato under both biotic and abiotic stress conditions (Lee and Oda, 2003; Rouphael et al., 2017). Amelioration of abiotic stress imposed by shortage of nutrients or water has been reported by several scientists, including Rouphael et al. (2008a,b), Savvas et al. (2010), Schwarz et al. (2010), Colla et al. (2011), and Rouphael et al. (2017). Some rootstocks proved to be capable of mitigating nutrient shortage stress by increasing the nutrient-to-water uptake ratio, thereby resulting in enhanced nutrient translocation to the shoot (Savvas et al., 2017). Nevertheless, for some other nutrients, increased nutrient-to-water uptake ratios occur merely because of their enhanced deposition to the rootstock.

Stress due to shortage of water also restricts plant growth and crop yield due to impairment of the plant metabolism. Drought stress imposes generation of reactive oxygen species during several metabolic processes (Sánchez-Rodríguez et al., 2011). Other important metabolites affected by water deficit are sugar and sugar derivatives (Dumville and Fry, 2002; Semel et al., 2007) and amino acids (Semel et al., 2007), where changes in proline and glutamate content have been recognized as responses to drought stress (Zhu, 2000; Bartels and Sunkar, 2005; Semel et al., 2007). Fatty and organic acids generally increase as a response to drought stress, especially those occurring as intermediates of the tricarboxylic acid (TCA) cycle.

Scarcity of good-quality irrigation water and high demand of energy in fertilizer production, combined with reduced availability of plant nutrient resources, impose increasing pressure to horticulture to adopt water- and nutrient-saving cultural practices with no or minimal yield losses. To address this challenge, inoculation with PGPR and grafting onto suitable rootstocks were tested in the current study as possible cultural practices that may enhance resilience of greenhouse tomato to stress induced by combined water and nutrient (N and P) shortage. To contribute to the discovery of potential biomarkers that might accelerate the progress of screening new effective biostimulants and rootstocks, the impact on plant metabolism

was studied by applying metabolomics analysis, in addition to growth and yield responses.

MATERIALS AND METHODS

Plant Material, Growth Conditions, and Treatments

The experiment was conducted during the winter of 2017 in a glasshouse at the Agricultural University of Athens (N 37°59′10″, E 23°42′29″, altitude 24 m). Tomato (*Solanum lycopersicum*) cv. Belladonna F1 was grown in an open hydroponic system using perlite as growing medium, placed in pots. Plants were either self-grafted (Belladonna/Belladonna) or grafted onto tomato *S. lycopersicum* Mill. cv. M82. The tomato cultivar M82, which has been previously studied under water deficit conditions (Rigano et al., 2016; Illouz-Eliaz et al., 2020), was selected because it has been used for backcrossing with *Solanum pennelli* aiming to produce water-stress-tolerant tomato rootstocks (Lippman et al., 2007; Ofner et al., 2016).

Tomato seedlings were transplanted into the greenhouse on November 23, 2018, at the stage of five true leaves. Before being transplanted, the growing medium around the roots of the seedlings was removed, and the roots were placed for 1 min into a PGPR suspension containing 10^9 CFU ml^{-1}, which was diluted 10-fold before use. The inoculation of tomato seedlings was repeated 5 days later by drenching the growing medium with the same PGPR suspension using a 5-ml pipette. Five PGPR strains were used to establish the following four PGPR treatments: PGPR-T1, a mix of two *Enterobacter* sp. strains (C1.2 and C1.5); PGPR-T2, *Paenibacillus* sp. strain DN1.2; PGPR-T3, *Enterobacter mori* strain C3.1; and PGPR-T4, *Lelliottia* sp. strain D2.4. These PGPR treatments were complemented with a control treatment in which no PGPR was applied to the tomato roots. The bacterial strains used in the present study belong to bacterial genera or species known to exhibit PGP traits according to the literature (Jha et al., 2011; Amaresan et al., 2020; Orozco-Mosqueda and Gustavo, 2020). Moreover, the strains showed tolerance in the presence of 8% (w/v) NaCl (Tampakaki et al., unpublished results), and for this reason, they were considered suitable for testing under drought conditions.

Plant density was 2.4 plants m^{-2} at the beginning of the experiment. The experiment was set up as a three-factorial (2 rootstocks × 5 PGPR × 2 stress treatments), completely randomized block design with three replicates per treatment and three plants per replicate. A bumblebee hive was placed into the glasshouse on December 19, 2017, to secure optimal pollination. On January 8, 2018, i.e., 6 weeks after transplanting, one plant per replicate was sampled and used to estimate the root and the aboveground biomass production. After removal of these plants, the plant density decreased to 1.6 plants m^{-2}. Harvest commenced on February 9, 2018; and the experiment was terminated on March 30, 2018. Air temperature was always maintained to levels above 13°C during the night and above 18°C during the day.

Combined stress was applied by reducing water and nutrient (N and P) supply to 50% of the standard supply in the non-stress treatment. The daily amount of supplied nutrient solution (NS) differed among stressed and non-stressed treatments. Non-stressed treatments were fertigated using a solar meter to control irrigation frequency aiming to obtain a drainage fraction of 20% of the total NS amount supplied to plants. The irrigation frequency in the stressed plants was similar with that applied to the non-stress plants, but the amount of NS provided at each irrigation event was half as much as that provided to the non-stressed plants. Additionally, concentrations of nitrogen and phosphorus in the NS supplied to the stressed plants were half as high as in the standard NS for tomato (Savvas et al., 2013) provided to the non-stressed plants. Nutrient concentrations in the NS are provided in **Supplementary Table 1**.

Biomass and Total Yield Determination

Aboveground biomass samples were obtained 6 weeks after transplanting and at the end of the cultivation, by harvesting the entire shoot. Root fresh biomass was also measured at the first sampling. After the tomato shoot was harvested, fresh weight was recorded, and samples were oven-dried at 65°C for at least 72 h, until constant weight was achieved, and used to determine their dry weight and mineral composition. The impact of the experimental treatments on fruit yield was assessed by manually harvesting three times a week all commercially ripe fruits commencing on February 9, 2018, and terminating on March 30, 2018. Fruits were also classified into four classes (Extra Class, Class I, Class II, and non-marketable) as described in the Eu Regulation (543/2011).

Mineral Analysis

The dried samples of tomato leaves were powdered using a blade mill and passed through a 40-mesh sieve. Plant tissue samples were used for chemical analysis to determine total N, P, and K concentrations. Total N was determined applying the Kjeldahl method. To estimate P and K, leaf samples were milled and dry ashed at 550°C for 5 h, and the ash was dissolved in 1 M of HCl. Phosphorus was measured photometrically as phosphomolybdate blue complex at 880 nm using a 96-position microplate spectrophotometer (Anthos Zenyth 200; Biochrom, United States). Potassium was determined using a flame photometer (Sherwood Model 410, Cambridge, United Kingdom).

Gas Chromatography/Electron Impact/Mass Spectrometry Metabolomics Analysis of Tomato Leaves

Chemicals and Reagents

For the derivatization of samples for gas chromatography/electron impact/mass spectrometry (GC/EI/MS) analysis, the reagents ribitol, methoxylamine hydrochloride, *N*-methyl-*N*-(trimethyl-silyl)trifluoroacetamide (MSTFA), and pyridine were used (Sigma-Aldrich Ltd., Steinheim, Germany). The organic

solvents methanol and ethyl acetate (Carlo Erba Reagents, Val de Reuil, France) were used for the extraction of leaf tissues.

Plant Material and Sample Preparation

Entire young, fully expanded, and healthy tomato leaves were collected and placed directly in liquid nitrogen for quenching and then were stored at −80°C until further processing. Samples were collected from plants 55 days following transplantation. Metabolomics was applied to non-stressed and stressed plants and to self-grafted and grafted M82 plants. Furthermore, based on the results of early plant biomass measurements, only samples of plants from the PGPR-T3 and non-inoculated plants were subjected to metabolomics.

Metabolite Extraction for Gas Chromatography/Electron Impact/Mass Spectrometry Analysis

Tomato leaves were pulverized using pestle and mortar in liquid nitrogen, and the pulverized tissues were placed in Eppendorf tubes (2 ml) and stored in −80°C. For metabolomics, 50 mg was transferred into Eppendorf tubes (2 ml); and 1 ml of a solution of methanol:ethyl acetate (50:50 v/v) and 20 μl of ribitol (0.2 mg ml^{-1} methanol), serving as internal standard, were added. A previously described protocol was used (Kostopoulou et al., 2020), with minor modifications. Samples that were obtained by pooling portions of the biological replications of each treatment served as the quality-control samples. The resulting suspensions were sonicated for 20 min in an ultrasonic bath (Branson 1210, Danbury, United States) and then agitated using a horizontal rotary shaker (GFL 3006, Gesellschaft für Labortechnik mbH, Burfwedel, Germany) at 150 rpm for 2 h. The suspensions were filtered using PSTFA filters (0.2-μm pore diameter, Macherey-Nagel, Duren, Germany). Derivatization of samples for GC/EI/MS analysis was performed in a two-step process using methoxylamine hydrochloride in pyridine (20 mg ml^{-1}) for methoxymation and MSTFA for silylation. The derivatized samples were finally transferred to microinserters (180 μl, Macherey-Nagel).

Gas Chromatography–Mass Spectrometry Analyses

The derivatized samples were analyzed by GC/EI/MS (GC/EI/MS Agilent 6890n, Agilent Technologies Inc.) equipped with an inert mass-selective detector 5973 (MSD) and a 7683 autosampler. The electron ionization was set to 70 eV, and full scan mass spectra were acquired at 50–800 Da in a rate of 4 scans per second with a 10-min solvent delay. The temperature for the ion source was set to 150°C and for the transfer line to 230°C. An HP-5MS capillary column (30 m, i.d. 0.25 mm, and film thickness 0.25 μm; Agilent Technologies Inc.) was used, and helium (He 6.0) was the carrier gas. Samples were injected in completely randomized order on column, and the injector split ratio was set to 5:1. The initial temperature of the oven was 70°C, stable for 5 min, followed by an increase of 5°C per min to 295°C.

Statistical Analysis

The experiment was set as a complete randomized block design with three factors (2 × 5 × 2) and three replications per treatment. Data were analyzed by applying three-way analysis of variance (ANOVA) to assess main effects [rootstocks (R), PGPR, and stress conditions (S)], three first-order interactions (R × PGPR, R × S, and PRPR × S), and one second-order interaction (R × PGPR × S). Multiple comparisons of means were performed by applying the Duncan multiple range test ($p < 0.05$) after performing three-way ANOVA. The data were statistically analyzed using STATISTICA, version 8.0 (StatSoft, Inc., Tulsa, OK, United States).

For the metabolomics analyses, all experimental events were controlled using the software MSD Chemstation (Agilent). The deconvolution of the acquired total ion chromatograms was performed using the software AMDIS v.2.66 [National Institute of Standards and Technology (NIST); Gaithersburg, MD, United States], and the MS database of the NIST '08 (NIST; Gaithersburg, MD, United States). The absolute identification for selected metabolites was performed by matching their retention times and mass fragmentation patterns to those of analytical standards, which had been analyzed employing the same method and analyzer, as recommended by the Metabolomics Standards Initiative (MSI) (Sansone et al., 2007). The tentative annotation of features was performed based on the similarities of their fragmentation patterns to those of entries of the NIST library (>90%). Based on the deconvolution of the data, features present also in the experimental blank samples or features that correspond to column artifacts were excluded from analyses. The data pre-processing, including feature alignment and gap filling, was performed using the software MS-Dial v.3.70, applying the recommended settings for GC/EI/MS (Tsugawa et al., 2015). The discovery of trends and biomarkers was on based on the values of scaled and centered orthogonal partial least square (OPLS) regression coefficients (CoeffCS) ($p < 0.05$). OPLS-discriminant analysis (OPLS-DA) was applied, since it provides optimal model interpretability and transparency (Aliferis and Chrysayi-Tokousbalides, 2011), using the software SIMCA-P v.13.0.3 (Umetrics, Sartorius Stedim Data Analytics AB, Umeå, Sweden), as previously described (Chatzigianni et al., 2020; Karamanou and Aliferis, 2020; Kostopoulou et al., 2020). The hierarchical cluster analysis (HCA) of the data was performed by the Ward linkage method.

RESULTS

Biomass Production

Six weeks after transplanting, the exposure of tomato to combined nutrient (N and P) and water stress reduced significantly the aboveground fresh biomass compared with non-stressed plants (**Figure 1i**). Inoculation of tomato with PGPR exerted a positive influence on plant biomass than did non-inoculated plants regardless of the applied PGPR treatment. Among the different PGPR treatments, PGPR-T3 had the highest biomass under both non-stress and combined stress conditions. Plants inoculated with PGPR-T3 exhibited also significantly higher root biomass than did the rest of the PGPR treatments and the non-inoculated plants under both no stress and combined stress conditions (**Figure 1ii**). Grafting 'Belladonna' onto 'M82'

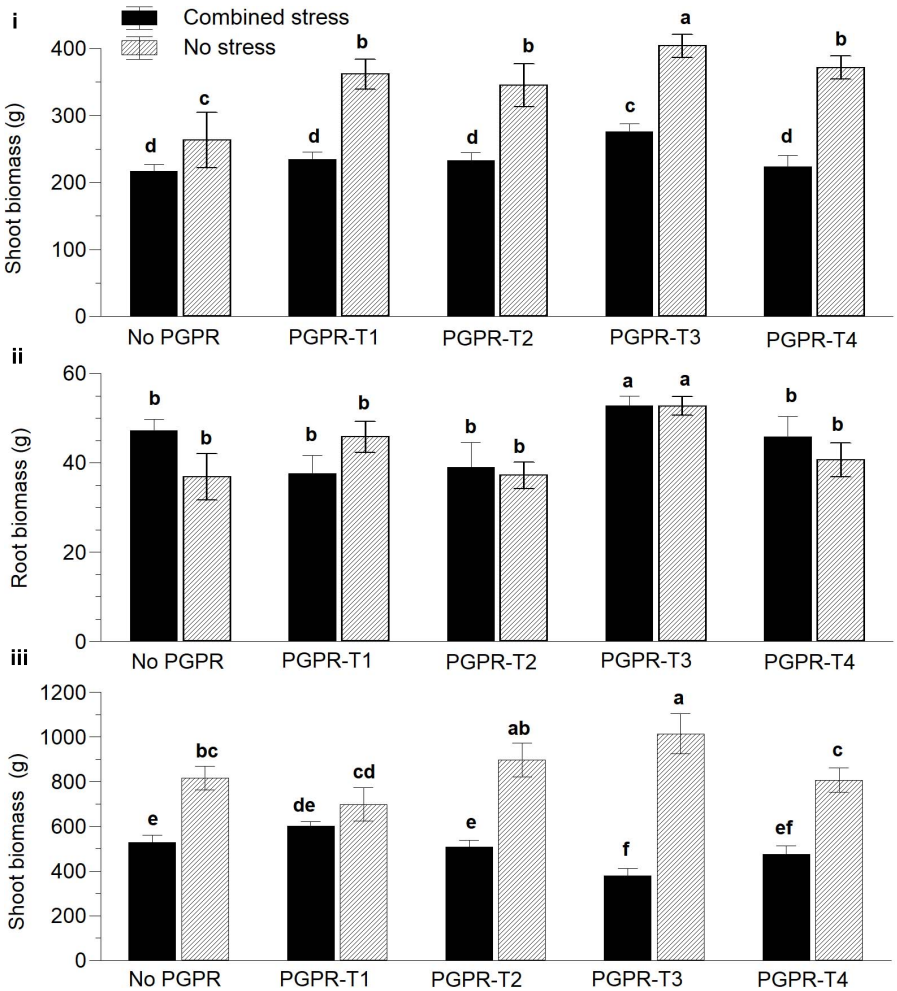

FIGURE 1 | Effects of combined water and nutrient stress (restriction of water, N, and P supply by 50%), and plant growth-promoting rhizobacteria (PGPR) inoculation on aboveground vegetative biomass **(i)** and root biomass **(ii)** 45 days after transplanting and aboveground biomass at the end of the cultivation period **(iii)**. PGPR-T1, a mix of *Enterobacter* sp. strains C1.2 and C1.5; PGPR-T2, *Paenibacillus* sp. strain DN1.2; PGPR-T3, *Enterobacter mori* strain C3.1; and PGPR-T4, *Lelliottia* sp. strain D2.4. Data are means of three replications. Means followed by different letters indicate significant differences according to the Duncan multiple range test ($p < 0.05$).

had no impact on the fresh plant biomass 6 weeks after transplanting (data not presented).

At the end of the experiment, clear differences were again observed between non-stressed plants and plants exposed to combined water and N/P stress, regarding the aboveground fresh biomass. More specifically, non-stressed plants resulted in higher aboveground biomass than did stressed plants (**Figure 1iii**). The PGPR application also affected the aboveground vegetative biomass, but its impact interacted with the combined water and nutrient stress. Under non-stress conditions, PGPR-T3 resulted in the highest aboveground vegetative biomass, and the difference was significant in comparison not only with the treatment without PGPR application but also with PGPR-T1 and PGPR-T4. However, under combined water and nutrient stress conditions, PGPR-T3 resulted in the lowest aboveground vegetative biomass. Furthermore, the aboveground vegetative biomass was not reduced by combined water and nutrient stress in plants of the PGPR-T1, while it was reduced in all other PGPR treatments.

Plants grafted onto the rootstock M82 exhibited 30% higher aboveground fresh biomass than did self-grafted plants under non-stress conditions. However, under stress conditions imposed by combined nutrient and water shortage, grafting had no impact on the aboveground vegetative biomass (data not presented).

Tomato Yield

Plants cultivated under combined water and N–P deficit produced fewer fresh fruits by 34.8% than did plants with optimal fertigation (**Table 1**). The reduction of yield by combined water and nutrient stress originated from decreases in both the mean fruit weight by 15.7% and the number of fruits per plant by 22.7%. Moreover, combined stress restricted also the total weight of fruit graded Extra Class and Class I by 37.9%. Inoculation of tomato roots with PGPR had no impact on total fruit yield and

TABLE 1 | Effects of combined restriction of water, N, and P supply by 50%, PGPR inoculation (PGPR-T1, a mix of *Enterobacter* sp. strains C1.2 and C1.5; PGPR-T2, *Paenibacillus* sp. strain DN1.2; PGPR-T3, *Enterobacter mori* strain C3.1; and PGPR-T4, *Lelliottia* sp. strain D2.4) and grafting (self-grafted plants and grafted plants onto M82) on tomato total fruit production, fruit number, fruit mean weight, and weight of fruits graded Extra Class and Class I.

Treatment	Total fruit production (kg m^{-2})	Number of fruits m^{-2}	Mean fruit weight (g)	Extra class and class I (kg m^{-2})
No stress	4.20 a	26.4 a	159.2 a	3.99 a
Stress	2.74 b	20.4 b	134.2 b	2.48 b
No PGPR	3.33	23.3	142.7	3.09
PGPR-T1	3.55	24.4	145.3	3.28
PGPR-T2	3.54	23.7	149.2	3.30
PGPR-T3	3.49	23.5	148.2	3.31
PGPR-T4	3.43	23.2	148.1	1.18
Self-grafted	3.28 b	22.1 b	148.4	3.04 b
Grafted onto M82	3.66 a	25.2 a	145.0	3.43 a
Significant interactions				
No stress × self-grafted				3.65 b
No stress × grafted onto M82				4.34 a
Stress × self-grafted				2.43 c
Stress × grafted onto M82				2.53 c
Statistical significance				
Stress	***	***	***	***
PGPR treatment	ns	ns	ns	ns
Grafting	*	*	ns	*
Stress × PGPR	ns	ns	ns	ns
Stress × grafting	ns	ns	ns	**
PGPR × grafting	ns	ns	ns	ns
Stress × PGPR × grafting	ns	ns	ns	ns

*Means (n = 3) followed by different letters indicate significant differences according to the Duncan multiple range test ($p < 0.05$), at $p < 0.05$, $p < 0.01$, and $p < 0.001$, denoted by *, **, and ***, respectively; ns, not significant.*
PGPR, plant growth-promoting rhizobacteria.

TABLE 2 | Effects of combined restriction of water, N, and P supply by 50%, PGPR inoculation (PGPR-T1, a mix of *Enterobacter* sp. strains C1.2 and C1.5; PGPR-T2, *Paenibacillus* sp. strain DN1.2; PGPR-T3, *Enterobacter mori* strain C3.1; and PGPR-T4, *Lelliottia* sp. strain D2.4) and grafting (self-grafted plants and grafted plants onto M82) on total N (g kg^{-1} DM) and P (g kg^{-1} DM) in tomato leaves.

Treatment	N (g kg^{-1} DM)	P (g kg^{-1} DM)
No stress	35.2 a	7.30 a
Stress	32.1 b	2.60 b
No PGPR	32.3 b	5.36
PGPR-T1	31.2 b	4.69
PGPR-T2	37.0 a	4.57
PGPR-T3	33.2 b	5.17
PGPR-T4	34.5 ab	4.99
Self-grafted	34.6	5.33 a
Grafted onto M82	32.7	4.58 b
Significant interactions		
No stress × no PGPR	37.0 a	
No stress × PGPR-T1	34.3 a	
No stress × PGPR-T2	36.5 a	
No stress × PGPR-T3	33.6 a	
No stress × PGPR-T4	34.7 a	
Stress × no PGPR	27.0 b	
Stress × PGPR-T1	28.0 b	
Stress × PGPR-T2	37.6 a	
Stress × PGPR-T3	32.9 ab	
Stress × PGPR-T4	34.3 a	
Statistical significance		
Stress	**	***
PGPR treatment	*	ns
Grafting	ns	**
Stress × PGPR	*	ns
Stress × grafting	ns	ns
PGPR × grafting	ns	ns
Stress × PGPR × grafting	ns	ns

*Means (n = 3) followed by different letters indicate significant differences according to the Duncan multiple range test at $p < 0.05$, $p < 0.01$, and $p < 0.001$, denoted by *, **, and ***, respectively; ns, not significant.*
PGPR, plant growth-promoting rhizobacteria.

yield components, as well as quality grading. Grafting onto the rootstock M82 did not affect fruit mean weight but significantly increased the number of fruits per plant resulting in 11.6% more total fruit production and a significant increase in Extra Class fruits compared with self-grafting. The effect of grafting on total fruit yield and number of fruits per plant did not interact with the combined water and nutrient stress, while the production of Extra and Class I fruits was enhanced by grafting only under non-stress conditions.

Leaf Nutrient Concentrations

Combined reduction of water, N, and P supply by 50% decreased significantly the total N concentrations in leaves when the roots were not inoculated, or inoculated with PGPR-T1 or PGPR-T3, but had no impact on leaf total-N when inoculated with PGPR-T2 and PGPR-T4 (**Table 2**). Grafting had no significant impact on the leaf total N concentration. Under non-stress conditions, PGPR inoculation did not affect the leaf total N level, while under combined water and nutrient stress conditions, PGPR-T2 and PGPR-T4 resulted in significantly higher leaf total N levels compared with PGPR-T1.

The leaf P concentration was significantly reduced by combined water and nutrient stress conditions regardless of grafting and PGPR application (**Table 2**). Grafting onto M82 reduced slightly but significantly the leaf P concentration from 5.3 to 4.6 mg g^{-1}. The leaf K concentration was significantly reduced from 51.4 to 45.2 mg g^{-1} when plants were exposed to combined water and nutrient stress, while grafting and PGPR application had no significant impact on the leaf K (data not presented).

Metabolomics Analysis

Fluctuations in tomato leaf metabolome in response to combined water and nutrient stress, PGPR inoculation, and grafting were recorded using bioinformatics software and metabolite species-specific databases. A representative raw GC/EI/MS data set

[*S. lycopersicum* L. (Tomato) (PMG-01-21)] can be found at the repository of the Pesticide Metabolomics Group of the Agricultural University of Athens[1]. In total, 167 metabolite features were discovered, and the annotated ones belonging to various chemical groups are presented in **Supplementary Data Set 1**. The application of OPLS-DA revealed tight groups with no outliers at $p < 0.05$ (**Figure 2**). The leaf metabolome of tomato plants treated with *E. mori* strain C3.1 (PGPR-T3) was clearly discriminated from that of non-inoculated plants, except for plants grafted onto M82 under combined stress conditions. Non-stressed plants were also clearly discriminated from plants exposed to combined water and nutrient stress, except for stressed plants, which were self-grafted and inoculated with *E. mori* strain C3.1 (**Figure 3**). The examination of the hierarchical manner of the treatments metabolism generally revealed that PGPR inoculation had the greatest cluster distance from the non-inoculated treatment except of plants inoculated with PGPR-T3, grafted onto 'M82' and cultivated under combined stress, which was discriminated from the rest of the PGPR treatments.

Based on the values of the corresponding CoeffCS, the metabolites exhibiting the most marked accumulation, which exceeded a 10-fold increase in plants exposed to combined water, N, and P stress, were ethylene glycol, L-lactic acid, ethyl phosphoric acid, phosphoric acid, glycine, malate, pyroglutaminic acid, oleic acid, and α-α-trehalose, while succinic acid, glyceric acid, citric acid, D-fructose, myo-inositol, stearic acid, and 1-monopalmitin were reduced 10-fold (**Figure 4**). The PGPR inoculation with PGPR-T3 increased over 10-fold D-fructose and α-α-trehalose levels but decreased ethanolamine, glycerol, malate, myo-inositol, oleic acid, 2-*O*-glycerol-α-D-galactopyranoside, and 1-monopalmitin in tomato leaves (**Figure 5**). Finally, grafting 'Belladona' onto the rootstock 'M82' resulted in a more than 10-fold higher relative abundance of stearic acid, oleic acid, 2-*O*-glycerol-α-D-galactopyranoside, and 1-monopalmitin but lower than 10-fold relative abundance of malate, D-fructose, and myo-inositol than in self-grafted 'Belladonna' (**Figure 6**).

[1]https://www.aua.gr/pesticide-metabolomicsgroup/Resources/default.html

DISCUSSION

Biomass Production

Plant growth-promoting rhizobacteria can stimulate plant growth through a range of mechanisms, including excretion of substances acting as plant growth regulators or stimulation of their biosynthesis by plants, improved nutrient acquisition, and inhibition of fungal plant pathogens (Raaijmakers et al., 2009; Choudhary et al., 2011). Furthermore, PGPR can induce systemic tolerance to abiotic stress (Yang et al., 2009). In a study with tomato and pepper cultivated under optimal or water stress conditions, inoculation of the roots with PGPR increased biomass production compared with no application of PGPR under both optimal and water stress conditions (Mayak et al., 2004). On the other hand, in an experiment with tomato inoculated with different PGPR strains, Shen et al. (2012) found that PGPR-induced growth promotion occurred only under stress conditions imposed by simulated seawater irrigation. These contradictory results indicate that the impact of PGPR application on cultivated plants is species- and strain-specific, as different bacteria possess different growth stimulation mechanisms, as also suggested by Dey et al. (2004).

Although the use of PGPR on tomato cultivation has been already addressed in several studies, the PGPR strains applied in the current study have never been tested in the past as PGPR. All PGPR treatments applied in the current study enhanced the root

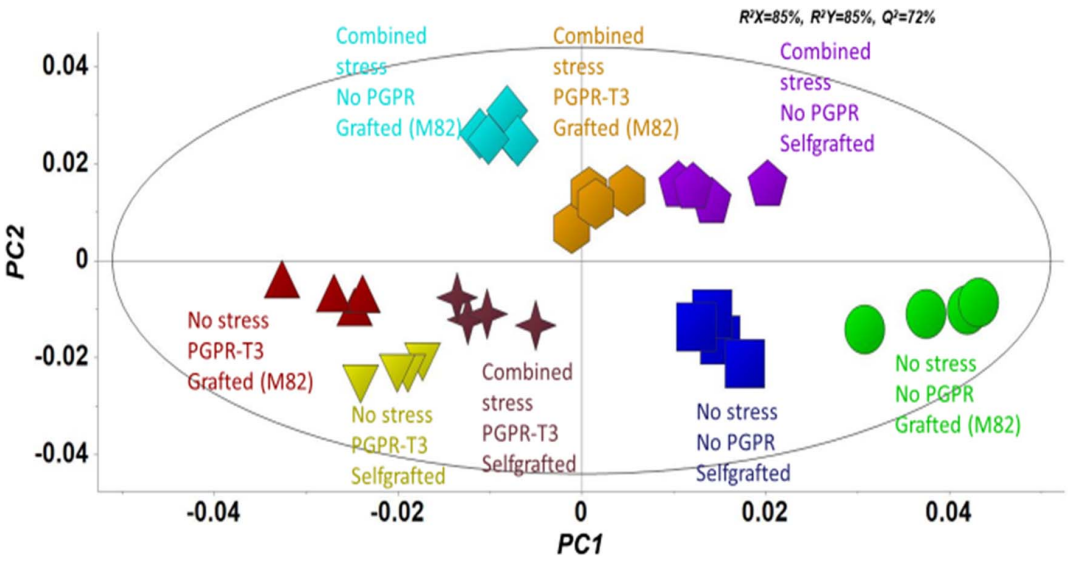

FIGURE 2 | Orthogonal partial least squares-discriminant analysis (OPLS-DA) PC1/PC2 score plot for the gas chromatography/electron impact/mass spectrometry (GC/EI/MS) metabolite profiles of tomato leaves [principal component (PC)]. The ellipse represents the Hotelling T^2 with 95% confidence interval.

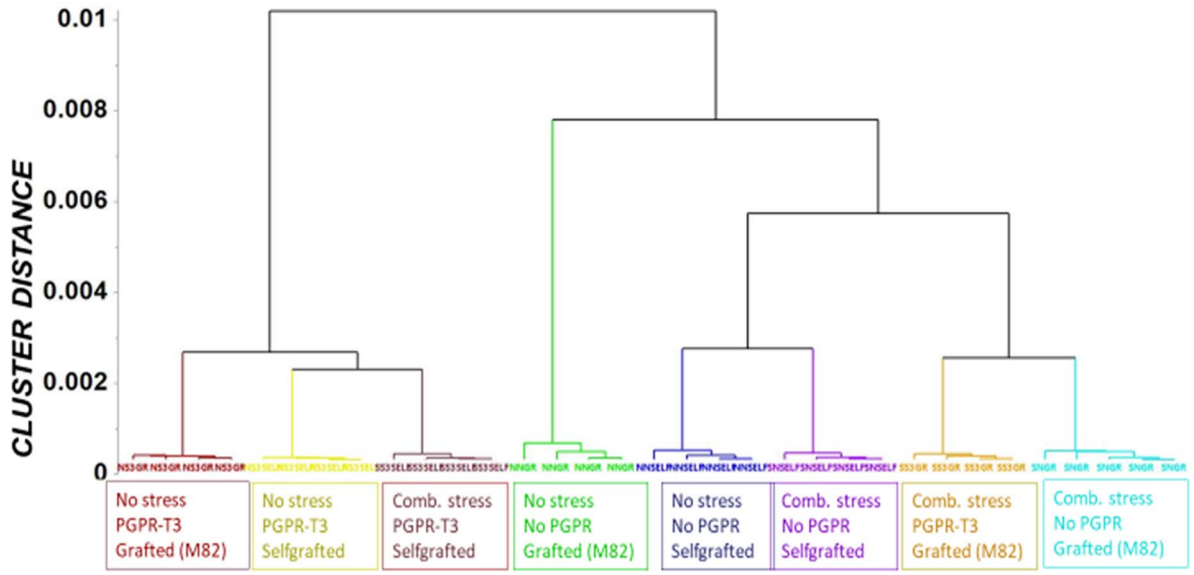

FIGURE 3 | Orthogonal partial least square (OPLS) dendrogram for the recorded gas chromatography/electron impact/mass spectrometry (GC/EI/MS) metabolite profiles of tomato leaves. Cluster distances were calculated using the Ward linkage method.

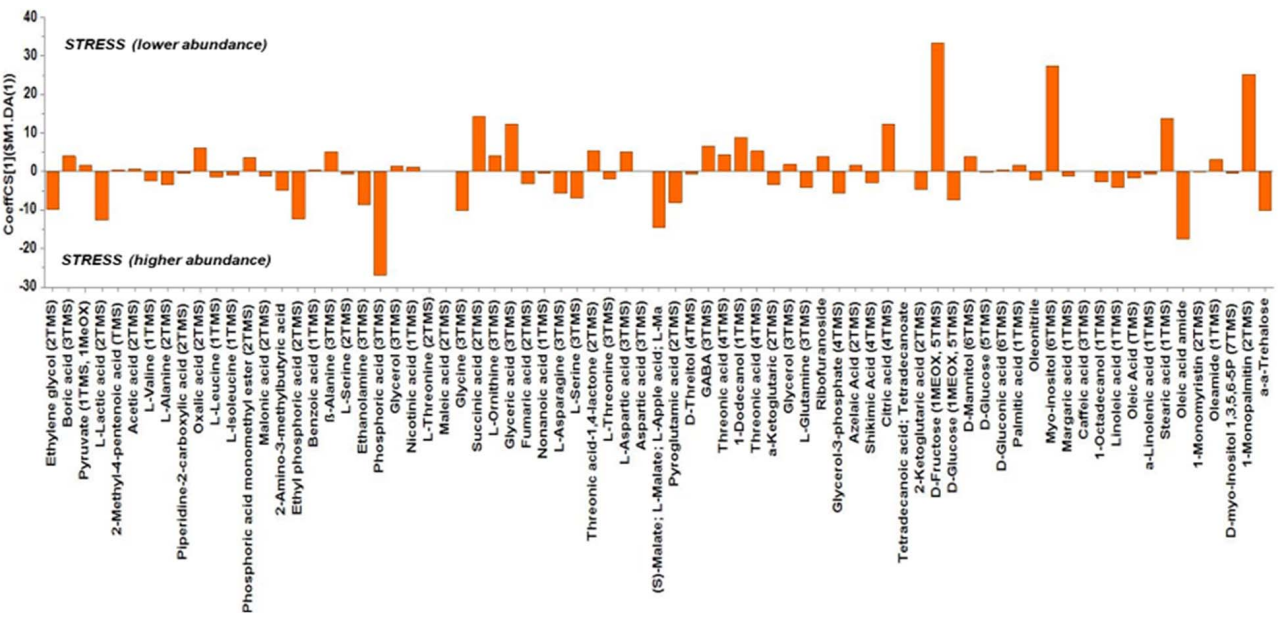

FIGURE 4 | Orthogonal partial least square (OPLS) coefficient plots for the gas chromatography/mass spectrometry (GC/MS) metabolic profiles of tomato leaves performing pairwise comparisons between non-stressed plants and combined stressed plants. The values of scaled and centered OPLS regression coefficients (CoeffCS) are displayed. Influential metabolites for the observed discriminations between the metabolomes of non-stressed and combined stress plants are displayed with jackknifed confidence intervals ($p < 0.05$). Negative values of CoeffCS denote metabolites with higher concentration in combined stressed plants, whereas positive values are those with higher concentration in non-stressed plants.

and shoot growth of tomato under non-stress conditions during the early vegetative developmental stage. However, *E. mori* strain C3.1 (PGPR-T3) increased more markedly the root and shoot biomass than the other three PGPR treatments, compared with no application of PGPR. Furthermore, both the root and shoot biomass of plants treated with *E. mori* strain C3.1 were not reduced by application of combined nutrient/water stress for 6 weeks, compared with those of plants not treated with PGPR.

Despite the protective role of PGPR-T3 on tomato growth during the early cultivation stage, PGPR-T3 resulted in the lowest shoot biomass under combined nutrient and water stress conditions at crop termination. These results indicate that the

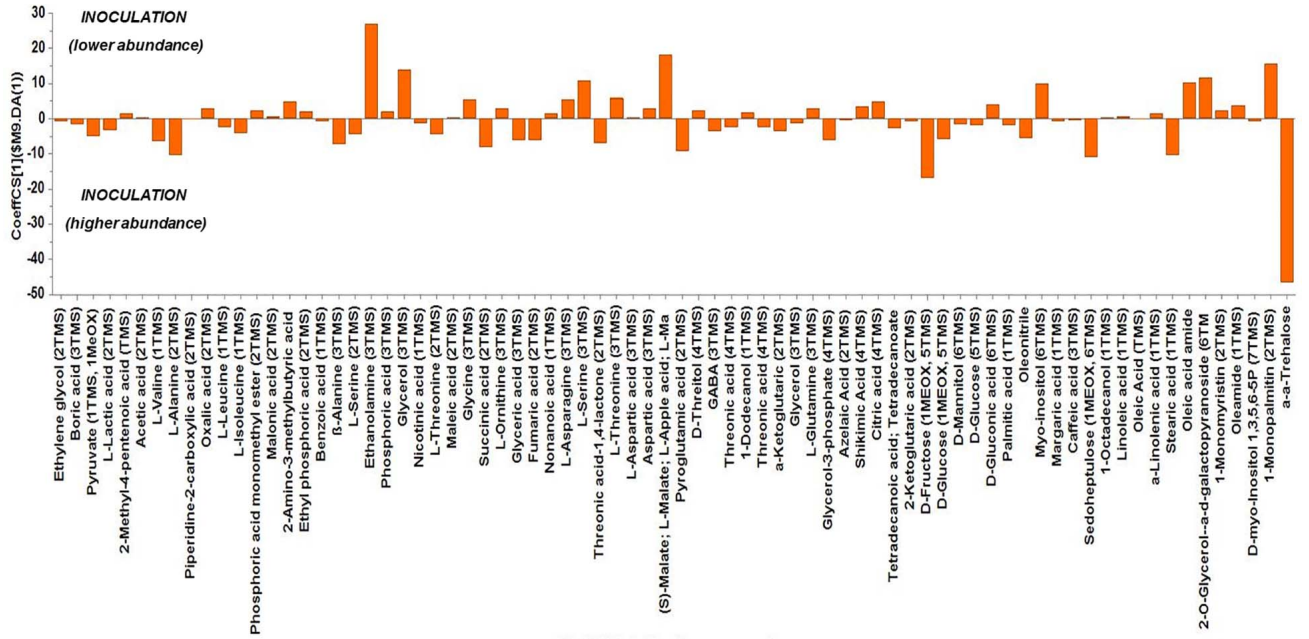

FIGURE 5 | Orthogonal partial least square (OPLS) coefficient plots for the gas chromatography/mass spectrometry (GC/MS) metabolic profiles of tomato leaves performing pairwise comparisons between non-inoculated plants [No plant growth-promoting rhizobacteria (PGPR)] and plants inoculated with PGPR-T3. The values of scaled and centered OPLS regression coefficients (CoeffCS) are displayed. Influential metabolites for the observed discriminations between the metabolomes of non-inoculated plants and plants inoculated with PGPR-T3 are displayed with jackknifed confidence intervals ($p < 0.05$). Negative values of CoeffCS denote metabolites with higher concentration in plants inoculated with PGPR-T3, whereas positive values are those with higher concentration in non-inoculated plants.

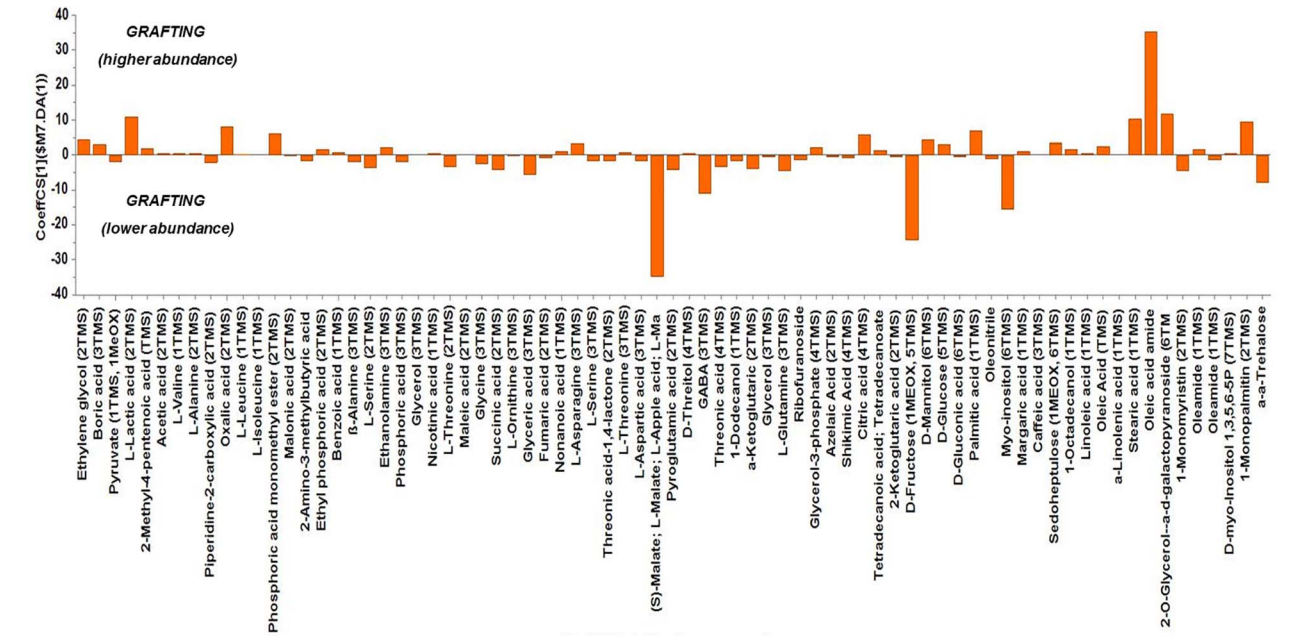

FIGURE 6 | Orthogonal partial least square (OPLS) coefficient plots for the gas chromatography/mass spectrometry (GC/MS) metabolic profiles of tomato leaves performing pairwise comparisons between self-grafted tomato plants ('Belladonna' F1) and plants grafted onto the rootstock M82. The values of scaled and centered OPLS regression coefficients (CoeffCS) are displayed. Influential metabolites for the observed discriminations between the metabolomes of self-grafted and grafted plants are displayed with jackknifed confidence intervals ($p < 0.05$). Negative values of CoeffCS denote metabolites with higher concentration in self-grafted plants, whereas positive values are those with higher concentration in plants grafted onto 'M82'.

protective effect of *E. mori* strain C3.1 was attenuated during the cropping period. Since PGPR was applied only once at crop establishment, a possible explanation for the different responses of stressed tomato to PGPR-T3 at the early growth stage and at crop termination is that the stress conditions might have decreased the population density of PGPR in the long term. In agreement with this consideration, Patakioutas et al. (2015) reported an appreciable reduction in the population density of *Bacillus amyloliquefaciens* in a hydroponic greenhouse tomato crop after about 30 weeks of cultivation. This finding indicates that inoculation with some PGPR strains may need repetition one or more times in long-term greenhouse crops exposed to stress conditions to maintain an effective density of PGPR population in the root zone. However, this has to be confirmed experimentally. On the other hand, PGPR-T1 had no protective effect against combined nutrient/water stress during the early vegetative period of growth but maintained shoot growth to similar levels with non-inoculated non-stressed plants at crop termination. This response indicates that the mix of the *Enterobacter* sp. strains C1.2 and C1.5 deploys a different protective mechanism against stress than the rest of the PGPR treatments tested in the current study, which is adaptive and operates only under long-term stress conditions.

Grafting onto 'M82' did not protect plants against combined nutrient and water stress, in agreement with Rigano et al. (2016), who found that this rootstock is not tolerant to water deficit, although it is a vigorous rootstock. However, under non-stress conditions, grafting onto 'M82' boosted shoot growth, in agreement with Ntatsi et al. (2014) and Rouphael et al. (2017), who stated that grafting tomato onto vigorous rootstocks increases tomato growth.

Tomato Yield

Several studies have shown that PGPR can increase tomato fruit production, an effect that in most cases is ascribed to enhanced protection against plant diseases. For instance, Gravel et al. (2007) reported yield increases in hydroponic tomato inoculated with *Pseudomonas brevicompactum*, *Pseudomonas marginalis*, *Pseudomonas putida*, and *Trichoderma atroviride*. In other studies, PGPR enhanced tomato fruit yield only under stress conditions. Thus, Gagné et al. (1993) reported yield increases in an autumn crop of tomato inoculated with a *Pseudomonas* fluorescence strain under suboptimal natural light conditions. However, in spring, under more favorable light conditions, the tomato fruit biomass was not influenced by inoculation with *Pseudomonas*. In the current study, combined water and nutrient stress decreased significantly tomato fruit biomass, whereas PGPR inoculation under the conditions of the current experiment was incapable of eliminating or mitigating the stress effects on fruit production. The lack of any benefit from PGPR application concerning fruit yield supports the previously stated notion that the population density of PGPR in the roots decays with time under real growing conditions, and re-inoculation during a long-term cropping period is required. This suggestion is in line with a previous report of Yan et al. (2003), who found that the population density of *Pseudomonas* strains used as PGPR in the roots followed a decreasing pattern with time.

Grafting onto M82 increased total fruit yield, regardless of stress conditions, whereas the Extra Class and Class I fruit yield was increased by grafting only under non-stress conditions. These results show that the fruit biomass production in tomato grafted onto 'M82' is less susceptible to combined nutrient/water stress than the vegetative growth. However, these results also corroborate previous results of Rigano et al. (2016), suggesting that 'M82' is not tolerant to water stress.

Leaf Nutrient Status

The reduction of the total N concentration in leaves of tomato exposed to combined nutrient and water stress is fully anticipated since one of the stress factors was the reduction of the N supply by 50%. However, under combined stress conditions, PGPR-T2, PGPR-T3, and PGPR-T4 managed to sustain the leaf N concentrations to similar levels with those measured in non-stressed plants. These results show that the PGPR strains DN1.2 of *Paenibacillus* sp., C3.1 of *E. mori*, and D2.4 of *Lelliottia* sp. are capable of maintaining normal nitrogen uptake under conditions of restricted N supply up to 50% of the standard levels. In a previous study, Adesemoye et al. (2010) found that enhanced N uptake by plants was due to increased plant uptake of N originating from fertilizer and not from enhanced mobilization of organic N reserves in the soil. The current results are in line with those findings, since in the current study the plants were cultivated on an inert medium in which only inorganic N was supplied. Cordero et al. (2018) also reported increased N concentration in tomato leaves following root inoculation with PGPR. According to these researchers, increased N acquisition by plants treated with PGPR results from increased root surface, stimulation of metabolic processes contributing to nutrient mobilization, and utilization of N reserves from the microbial biomass turnover. Nevertheless, the maintenance of normal leaf N in tomato plants inoculated with PGPR-T2, PGPR-T3, and PGPR-T4 under combined stress conditions did not prevent stress-induced fruit yield restrictions in these treatments. These results indicate that the yield reduction in tomato exposed to combined nutrient and water stress was not due to shortage of N.

Unlike the leaf N, the leaf P concentrations were not affected by PGPR, presumably because, in the current study, tomato was cultivated hydroponically on an inert medium and not in the soil. The P concentrations in NSs supplied to hydroponic crops (usually 1–1.5 mmol L^{-1}, Savvas and Gruda, 2018) may be 100-fold higher than the Pi concentrations encountered by plants in the soil solution (Schachtman et al., 1998), while the inert porous media used in hydroponics do not contain any P reserves. Thus, PGPR could not provide a benefit by mobilizing P reserves under conditions of limited P availability in the root environment. In agreement with this consideration, Gravel et al. (2007) reported that inoculation of tomato roots with PGPR had no impact on the leaf nutrient status in tomato plants grown on rockwool, whereas the same microorganisms increased the available P in plants cultivated on an organic medium. Furthermore, the same

researchers did not find any beneficial effect of PGPR on plant K status, in agreement with the current study.

Metabolomics Analysis

The metabolomics analysis in tomato leaves revealed a clear discrimination between the different treatments, which indicates that they all had an impact on leaf metabolism. PGPR-T3 exerted the strongest impact on leaf metabolism, as all PGPR-T3 treatments, irrespective of grafting and stress exposure, were clearly discriminated from the treatments without PGPR inoculation (**Figures 2**, **3**). The only exception was the treatment combining PGPR-T3 inoculation with grafting onto 'M82' under water/nutrient stress, which exhibited a similar metabolic profile with that of the non-inoculated treatments, thus questioning the successful symbiosis of PGPR-T3 with the roots of M82.

Plants are complex organisms, and it is difficult to study and understand the exact role of each of the identified metabolites. In general, the metabolic roles of most sugars, proline, α-α-trehalose, monopalmitin, and GABA have been extensively studied. Other metabolites, for example, those participating in the TCA cycle, have also been studied extensively, but the exact function of most of them is poorly understood (Semel et al., 2007). Although many studies corroborate previous findings concerning metabolic pathways, the role of many metabolites remains contentious among researchers (Van Der Merwe et al., 2009).

The metabolic responses of plants differ when they are exposed only to water, N, or P shortage, compared with cultivation under stress caused by combined shortage. In the present study, glycine, for example, increased in plants exposed to combined water, N, and P shortage. Sung et al. (2015), who studied the impact of N, P, and K deficiencies on leaf and root metabolism in tomato, found that glycine decreases in tomato leaves exposed to partial N starvation but increases in plants exposed to P deficiency. Combined consideration of the current results and those of Sung et al. (2015) leads to the conclusion that, in the current study, the impact of P stress on glycine overwhelmed that of N stress. In contrast, citrate decreased in the present study under combined N and P stress, similarly to what Sung et al. (2015) reported under N stress, but diverged from the results under P shortage, indicating that the dominant factor for citrate in the current study was the N availability. Glycerate and fructose were reduced by combined stress in the present study, similarly to the reduction found by the same authors under only N or P stress. The observed accumulation of malate and trehalose under combined stress could be ascribed to their well-documented protective role under osmotic and oxidative stress (Cortina and Culiáñez-Macià, 2005; Semel et al., 2007). Finally, myo-inositol can be a protective compound under salt stress conditions, with a dual role. On the one hand, it can affect metabolism as a signal or a key metabolite (Hu et al., 2018). On the other hand, according to previous studies, under salinity stress, myo-inositol can balance osmotically the cytosol (Zhang et al., 2001), while its derivatives participate in plant stress responses such as programmed cell death (Kaur et al., 2013). However, in the present study, the levels of myo-inositol decreased in plants exposed to combined water, N, and P stress compared with non-stress conditions. This response may indicate that myo-inositol has a protective role only against salt stress, while the genes regulating its biosynthesis are downregulated under nutrient or water shortage conditions.

The phosphoric acid determined as a metabolite represents all forms of phosphates participating in cell metabolism. As reported by Wasaki et al. (2003), P deficiency imposes upregulation of many genes related to P metabolism and concomitantly enhances the biosynthesis of metabolites involved in P metabolism, such as pyruvate kinase and the accompanying phosphoenolpyruvate phosphatase, glucose-6-phosphate isomerase, inorganic pyrophosphatase, purple acid phosphatase, and inorganic phosphate transporters. Nevertheless, P deficiency also downregulates genes related to P metabolism, such as acid phosphatase (Wasaki et al., 2003). Under stress conditions, the needs for energy transport aiming to mobilize defense mechanisms entail increased biosynthesis of phosphorylated intermediates (Latz et al., 2013). As a result, upregulation of genes involved in the biosynthesis of phosphate containing metabolites exceeds downregulation, and concomitantly, the level of metabolically related phosphates increases, although the total P concentration in plant tissues may decrease, as was the case in the current study (**Table 2**). In agreement with this consideration, Wasaki et al. (2003) stated that P deficiency stress stimulates upregulation of genes that control the biosynthesis of metabolites substituting phospholipids in cell membrane, thereby increasing the levels of phosphates available for metabolic functions that contribute to energy transport. Phospholipids count for 17% of P in leaves (Lambers et al., 2012). Thus, their substitution with non-phosphorus lipids in cell membranes in response to stress conditions (Tawaraya et al., 2018) could maintain the levels of P-containing metabolites.

Colonization of tomato roots by PGPR clearly affected tomato metabolism, but only few metabolites exhibited a substantial fluctuation. The strongest impact of PGPR was on trehalose biosynthesis. Trehalose, which serves primarily as a storehouse of glucose for energy and/or for synthesis of cellular components, is also involved in functions protecting membranes and proteins against stress (Elbein et al., 2003). Furthermore, trehalose is involved in interactions between plants and microorganisms, including both symbiosis (Müller et al., 1994) and pathogenesis (Brodmann et al., 2002). More specifically, trehalose is present at relatively high concentrations in nodules, indicating a positive relationship between trehalose and nodulation (Streeter and Gomez, 2006), while the suppression of trehalose metabolism is associated with reduced pathogenicity (Tournu et al., 2013). These results indicate that trehalose promotes colonization of plants by bacterial microorganisms through alteration of the carbohydrate metabolism to their favor, regardless of whether the plant–microbe relationship is beneficial or destructive to plants. Hence, the accumulation of trehalose in plants treated with PGPR-T3 in the current study, compared with non-treated plants, is presumably part of a mechanism contributing to successful establishment of a plant/PGPR symbiosis.

Rudrappa et al. (2008) have reported that malic acid/malate is a metabolite-promoting plant–PGPR communication in roots. Rudrappa et al. (2008) performed experiments with knockout

Arabidopsis mutants for malic acid transporter and observed that the plants were unable to recruit PGPR for symbiosis. The recorded downregulation of malate in leaves of tomato inoculated with PGPR may be a result of malate translocation from leaves to roots aiming to facilitate colonization by PGPR. However, the metabolic profile of roots was not determined in the current study, and thus this hypothesis, although reasonable, is not adequately supported by the current experimental data.

Monopalmitin is a carbon source for plants, plant-related microbiome, and legume plants to sustain symbiosis with arbuscular mycorrhizal fungi, which is found in root exudates of several plant species (Feng et al., 2019). In sugarcane leaves, 2-monopalmitin content increased when inoculation with PGPR (*Gluconacetobacter diazotrophicus* and *Herbaspirillum seropedicae*) was combined with humic acid addition, whereas PGPR inoculation itself had no effect on monopalmitin accumulation (Aguiar et al., 2018). However, little is known on the exact role of monopalmitin, and although it was reduced in the leaves of plants colonized by PGPR, this metabolite in roots might be involved in plant/PGPR symbiosis.

Grafting onto the rootstock 'M82' had either a very weak or no impact on most metabolites. However, the levels of three metabolites were clearly reduced by grafting onto 'M82' (malate, D-fructose, and myo-inositol), while one metabolite (oleic acid) accumulated. According to Van Der Merwe et al. (2009), transgenic tomato exhibiting decreased expression of the mitochondrial malate dehydrogenase, and concomitantly increased malate levels, imposed a clear reduction in root biomass. In the current study, the increased root biomass of grafted plants was associated with reduced malate levels, corroborating an inverse relationship between malate levels and root biomass. The reduction of the D-fructose levels in leaves of tomato grafted onto 'M82' compared with self-grafted plants may point to an increased sink activity in roots, as many tomato rootstocks form a more vigorous root system than self-rooted plants (Rouphael et al., 2017). Oleic acid is one of the three fatty acids (along with palmitic and linoleic acid) present, as free fatty acids in tomato fruits, melons, and cucumbers and are strongly responsible for the flavor of many vegetables, as they act as precursors in the biosynthesis of most straight-chain esters in aromatic volatile compounds (Hao et al., 2018). Having a profile different than that of fruits, tomato leaf fatty acids are responsible for leaf flavor, producing aroma volatiles through the lipoxygenase/hydroperoxide lyase enzyme pathway. Thus, changes in fatty acid composition in tomato leaves can lead to altered composition of lipid-derived flavor compounds (Wang et al., 2001). The results obtained from the current study do not reveal how the genotypic difference between root and leaves in grafted plants mediates a change in the level of oleic acid in tomato leaves. Furthermore, the current study does not show if the levels of fatty acids associated with flavor were influenced also in fruit of grafted tomato. However, Hao et al. (2018) reported that the levels of free fatty acids in fruit of grafted melons were lower than in fruits from non-grafted plants, and this was associated with reduced fruit aroma. Further research is required to test the fatty acid profile in fruit of grafted tomato and relate it to possible changes in volatile compounds and concomitantly in fruit flavor.

CONCLUSION

The improved vegetative growth of plants inoculated with all PGPR strains tested in this study, but especially with *E. mori* strain C3.1, corroborates previous studies, which showed that application of appropriate PGPR strains may improve tomato growth. On the other hand, the lack of any beneficial effect of PGPR on fruit yield, but also on the vegetative growth at the end of the crop under combined stress conditions, indicate that a single PGPR inoculation at crop establishment may be not sufficient, especially under stress conditions. Selection of appropriate PGPR strains, tolerant to multiple stress, and repetition of PGPR application during the cropping period, are key factors to obtain benefits from PGPR application, especially under stress conditions.

The improved growth and yield of non-stressed tomato plants grafted onto 'M82,' compared with non-grafted plants and the absence of any yield benefit from grafting onto this rootstock under stress conditions, corroborate previous reports suggesting that grafting onto suitable rootstocks enhances tomato fruit yield. However, on the other hand, the results of the current study show that 'M82' is not a suitable rootstock for plants grown under conditions of restricted water supply and points to the need to screen for tolerant rootstock genotypes to water and nutrient limitations.

The metabolomics analysis showed that water/nutrient stress and PGPR inoculation have a strong impact of the leaf metabolism, whereas grafting has a weaker but non-negligible impact. Combined nutrient and water stress enhanced by 10% or more the biosynthesis of L-lactic acid, ethyl phosphoric acid, phosphoric acid, glycine, malate, oleic acid, and α-α-trehalose, while it reduced by 10% or more the levels of succinic acid, glyceric acid, citric acid, D-fructose, myo-inositol, stearic acid, and 1-monopalmitin. Similarly, the application of PGPR enhanced by 10% or more D-fructose and α-α-trehalose, while it reduced by 10% or more the biosynthesis of ethanolamine, glycerol, L-serine, malate, myo-inositol, and 1-monopalmitin. Finally, grafting onto M82 enhanced by 10% or more the biosynthesis of oleic acid, while reducing by 10% or more the biosynthesis of malate, D-fructose, and myo-inositol compared with self-grafting.

As a general conclusion, this study showed that both PGPR and grafting are promising tools for improvement of tomato performance. However, to obtain a benefit under combined stress conditions, selection of appropriate PGPR strains and rootstock genotypes, and establishment of suitable protocols regarding method, time, and number of PGPR applications are crucial factors for success. The current study contributes to a better understanding of changes imposed to plant metabolism by combined water/nutrient stress, PGPR, and grafting. This new insight concerning metabolites influenced by stress, PGPR, and grafting can be useful in rapid screening of PGPR strains and rootstock genotypes with resilience to multiple stress conditions,

which may increasingly appear in commercial tomato crops in view of the climate change.

DATA AVAILABILITY STATEMENT

The raw data supporting the conclusions of this article will be made available by the authors, without undue reservation.

AUTHOR CONTRIBUTIONS

DS and PK conceived and designed the experiments. PK, GN, GM, ES, and IK performed the experiments and the mineral analyses. KA and PK performed the metabolomics analysis. AT provided the PGPR strains and performed the inoculation. PK, DS, and KA analyzed the data and wrote the manuscript. DS, KA, GN, AT, and IK reviewed the manuscript. All authors have read and approved the manuscript.

FUNDING

This research was funded by the European Commission within the HORIZON2020 project "TOMRES – A novel and integrated approach to increase multiple combined stress tolerance in plants using tomato as a model" (Grant Agreement 727929).

ACKNOWLEDGMENTS

We thank Danny Zamir from the Hebrew University of Jerusalem for providing the seeds of M82.

SUPPLEMENTARY MATERIAL

The Supplementary Material for this article can be found online at: https://www.frontiersin.org/articles/10.3389/fpls.2021.670236/full#supplementary-material

Supplementary Figure 1 | Orthogonal partial least squares-discriminant analysis (OPLS-DA) PC1/PC2 score plot of metabolomic profiles of non-stressed and exposed to combined stress tomato plants **(i)**, non-inoculated plants (No PGPR) and plants inoculated with PGPR-T3 **(ii)**, and self-grafted tomato plants ('Belladonna' F1) and plants grafted onto 'M82' **(iii)**. The ellipse represents the Hotelling T2 with 95% confidence interval.

Supplementary Data set 1 | Annotated metabolite features in the GC/EI/MS profiles of *Solanum lycopersicum* L. leaves.

REFERENCES

Adesemoye, A. O., Torbert, H. A., and Kloepper, J. W. (2010). Increased plant uptake of nitrogen from ^{15}N-depleted fertilizer using plant growth-promoting rhizobacteria. *Appl. Soil Ecol.* 46, 54–58. doi: 10.1016/j.apsoil.2010.06.010

Aguiar, N. O., Olivares, F. L., Novotny, E. H., and Canellas, L. P. (2018). Changes in metabolic profiling of sugarcane leaves induced by endophytic diazotrophic bacteria and humic acids. *PeerJ* 6:e5445. doi: 10.7717/peerj.5445

Aliferis, K. A., and Chrysayi-Tokousbalides, M. (2011). Metabolomics in pesticide research and development: review and future perspectives. *Metabolomics* 7, 35–53. doi: 10.1007/s11306-010-0231-x

Almaghrabi, O. A., Massoud, S. I., and Abdelmoneim, T. S. (2013). Influence of inoculation with plant growth promoting rhizobacteria (PGPR) on tomato plant growth and nematode reproduction under greenhouse conditions. *Saudi J. Biol. Sci.* 20, 57–61. doi: 10.1016/j.sjbs.2012.10.004

Amaresan, N., Kumar, M. S., Annapurna, K., Kumar, K., and Sankaranarayanan, A. (eds) (2020). *Beneficial Microbes in Agro-Ecology: Bacteria and Fungi*. Florida, FL: Academic Press.

Backer, R., Rokem, J. S., Ilangumaran, G., Lamont, J., Praslickova, D., Ricci, E., et al. (2018). Plant growth-promoting rhizobacteria: context, mechanisms of action, and roadmap to commercialization of biostimulants for sustainable agriculture. *Front. Plant Sci.* 9:1473. doi: 10.3389/fpls.2018.01473

Bartels, D., and Sunkar, R. (2005). Drought and salt tolerance in plants. *Crit. Rev. Plant Sci.* 24, 23–58.

Bhattacharyya, P. N., and Jha, D. K. (2012). Plant growth-promoting rhizobacteria (PGPR): emergence in agriculture. *World J. Microb. Biotechn.* 28, 1327–1350. doi: 10.1007/s11274-011-0979-9

Brodmann, D., Schuller, A., Ludwig-Müller, J., Aeschbacher, R. A., Wiemken, A., Boller, T., et al. (2002). Induction of trehalase in *Arabidopsis* plants infected with the trehalose-producing pathogen *Plasmodiophora brassicae*. *Mol. Plant Microbe Int.* 15, 693–700. doi: 10.1094/mpmi.2002.15.7.693

Chatzigianni, M., Aliferis, K. A., Ntatsi, G., and Savvas, D. (2020). Effect of N supply level and N source ratio on *Cichorium spinosum* L. metabolism. *Agron* 10:952. doi: 10.3390/agronomy10070952

Chen, J. G., Crooks, R. M., Seefeldt, L. C., Bren, K. L., Bullock, R. M., Darensbourg, M. Y., et al. (2018). Beyond fossil fuel–driven nitrogen transformations. *Science* 360:6391.

Choudhary, D. K., Sharma, K. P., and Gaur, R. K. (2011). Biotechnological perspectives ofmicrobes in agro-ecosystems. *Biotechnol. Lett.* 33, 1905–1910. doi: 10.1007/s10529-011-0662-0

Cisse, L., and Mrabet, T. (2004). World phosphate production: overview and prospects. *Phosphorus Res. Bullet.* 15, 21–25. doi: 10.3363/prb1992.15.0_21

Colla, G., Rouphael, Y., Mirabelli, C., and Cardarelli, M. (2011). Nitrogen-use efficiency traits of mini-watermelon in response to grafting and nitrogen-fertilization doses. *J. Plant Nutr. Soil Sci.* 174, 933–941. doi: 10.1002/jpln.201000325

Cordero, I., Balaguer, L., Rincón, A., and Pueyo, J. J. (2018). Inoculation of tomato plants with selected PGPR represents a feasible alternative to chemical fertilization under salt stress. *J. Plant Nutr. Soil Sci.* 181, 694–703. doi: 10.1002/jpln.201700480

Cortina, C., and Culiáñez-Macià, F. A. (2005). Tomato abiotic stress enhanced tolerance by trehalose biosynthesis. *Plant Sci.* 169, 75–82. doi: 10.1016/j.plantsci.2005.02.026

De Brito, A. M., Gagne, S., and Antoun, H. (1995). Effect of compost on rhizosphere microflora of the tomato and on the incidence of plant growth-promoting rhizobacteria. *Appl. Environ. Microb.* 61, 194–199. doi: 10.1128/aem.61.1.194-199.1995

De Pascale, S., Rouphael, Y., and Colla, G. (2018). Plant biostimulants: Innovative tool for enhancing plant nutrition in organic farming. *Eur. J. Hort. Sci.* 82, 277–285. doi: 10.17660/ejhs.2017/82.6.2

Desmidt, E., Ghyselbrecht, K., Zhang, Y., Pinoy, L., Van der Bruggen, B., Verstraete, W., et al. (2015). Global phosphorus scarcity and full-scale P-recovery techniques: a review. *Crit. Rev. Environ. Sci. Technol.* 45, 336–384. doi: 10.1080/10643389.2013.866531

Dey, R., Pal, K. K., Bhatt, D. M., and Chauhan, S. M. (2004). Growth promotion and yield enhancement of peanut (*Arachis hypogeal* L.) by application of plant growth promoting rhizobacteria. *Microbiol. Res.* 159, 371–394. doi: 10.1016/j.micres.2004.08.004

Dumville, J. C., and Fry, S. C. (2002). Gentiobiose: a novel oligosaccharin in ripening tomato fruit. *Planta* 216, 484–495. doi: 10.1007/s00425-002-0869-3

Elbein, A. D., Pan, Y. T., Pastuszak, I., and Carroll, D. (2003). Review. New insights on trehalose: a multifunctional molecule. *Glycobiol* 13, 17R–27R.

Eu Regulation (543/2011). *EN 15.6.2011 Official Journal of the European Union L 157/109*. Brussels: European Union.

Feng, H., Zhang, N., Fu, R., Liu, Y., Krell, T., Du, W., et al. (2019). Recognition of dominant attractants by key chemoreceptors mediates recruitment of plant growth-promoting rhizobacteria. *Environ. Microb.* 21, 402–415. doi: 10.1111/1462-2920.14472

Gagné, S., Dehbi, L., Le Quéré, D., Cayer, F., Morin, J. L., Lemay, R., et al. (1993). Increase of greenhouse tomato fruit yields by plant growth-promoting rhizobacteria (PGPR) inoculated into the peat-based growing media. *Soil Biol. Biochem.* 25, 269–272. doi: 10.1016/0038-0717(93)90038-d

Giorgi, F. (2006). Climate change hot-spots. *Geophysical Res. Lett.* 33:8.

Giorgi, F., and Lionello, P. (2008). Climate change projections for the Mediterranean region. *Glob. Planet. Change* 63, 90–104. doi: 10.1016/j.gloplacha.2007.09.005

Giuliani, M. M., Gatta, G., Nardella, E., and Tarantino, E. (2016). Water saving strategies assessment on processing tomato cultivated in Mediterranean region. *Ital. J. Agron.* 11, 69–76. doi: 10.4081/ija.2016.738

Glick, B. R., Patten, C. L., Holguin, G., and Penrose, D. M. (1999). *Biochemical and genetic mechanisms used by plant growth-promoting bacteria*. London: Imperial College Press.

Godfray, H. C. J., Beddington, J. R., Crute, I. R., Haddad, L., Lawrence, D., Muir, J. F., et al. (2010). Food security: the challenge of feeding 9 billion people. *Sci.* 327, 812–881.

Gravel, V., Antoun, H., and Tweddell, R. J. (2007). Growth stimulation and fruit yield improvement of greenhouse tomato plants by inoculation with *Pseudomonas putida* or *Trichoderma atroviride*: possible role of indole acetic acid (IAA). *Soil Biol. Biochem.* 39, 1968–1977. doi: 10.1016/j.soilbio.2007.02.015

Günther, F. (1997). Hampered effluent accumulation process: phosphorus management and societal structure. *Ecol. Econ.* 21, 159–174. doi: 10.1016/s0921-8009(96)00100-0

Hao, J. H., Qi, Z. Y., Li, J. R., Liu, C. J., Wang, L., Jin, W. T., et al. (2018). Effects of grafting on free fatty acid contents and related synthetic enzyme activities in peel and flesh tissues of oriental sweet melon during the different development period. *Earth Environ. Sci.* 185:012009. doi: 10.1088/1755-1315/185/1/012009

Hariprasad, P., and Niranjana, S. R. (2009). Isolation and characterization of phosphate solubilizing rhizobacteria to improve plant health of tomato. *Plant Soil* 316, 13–24. doi: 10.1007/s11104-008-9754-6

Hu, L., Zhou, K., Li, Y., Chen, X., Liu, B., Li, C., et al. (2018). Exogenous myo-inositol alleviates salinity-induced stress in *Malus hupehensis* Rehd. *Plant Physiol. Biochem.* 133, 116–126. doi: 10.1016/j.plaphy.2018.10.037

Illouz-Eliaz, N., Nissan, I., Nir, I., Ramon, U., Shohat, H., and Weiss, D. (2020). Mutations in the tomato gibberellin receptors suppress xylem proliferation and reduce water loss under water-deficit conditions. *J. Exp. Bot.* 71, 3603–3612. doi: 10.1093/jxb/eraa137

Jha, C. K., Aeron, A., Patel, B. V., Maheshwari, D. K., and Saraf, M. (2011). "*Enterobacter*: role in plant growth promotion," in *Bacteria in agrobiology: plant growth responses*, ed. D. K. Maheshwari (Heidelberg: Springer), 159–182. doi: 10.1007/978-3-642-20332-9_8

Karamanou, D. A., and Aliferis, K. A. (2020). The yeast (*Saccharomyces cerevisiae*) YCF1 vacuole transporter: Evidence on its implication into the yeast resistance to flusilazole as revealed by GC/EI/MS metabolomics. *Pestic. Biochem. Physiol.* 165:104475. doi: 10.1016/j.pestbp.2019.09.013

Kaur, H., Verma, P., Petla, B. P., Rao, V., Saxena, S. C., and Majee, M. (2013). Ectopic expression of the ABA-inducible dehydration-responsive chickpea L-myo-inositol 1-phosphate synthase 2 (CaMIPS2) in *Arabidopsis* enhances tolerance to salinity and dehydration stress. *Planta* 237, 321–335. doi: 10.1007/s00425-012-1781-0

Kostopoulou, S., Ntatsi, G., Arapis, G., and Aliferis, K. A. (2020). Assessment of the effects of metribuzin, glyphosate, and their mixtures on the metabolism of the model plant *Lemna minor* L. applying metabolomics. *Chemosphere* 239:124582. doi: 10.1016/j.chemosphere.2019.124582

Kuşçu, H., Turhan, A., and Demir, A. O. (2014). The response of processing tomato to deficit irrigation at various phenological stages in a sub-humid environment. *Agric. Water Manage.* 133, 92–103. doi: 10.1016/j.agwat.2013.11.008

Lambers, H., Cawthray, G. R., Giavalisco, P., Kuo, J., Laliberté, E., Pearse, S. J., et al. (2012). Proteaceae from severely phosphorus-impoverished soils extensively replace phospholipids with galactolipids and sulfolipids during leaf development to achieve a high photosynthetic phosphorus-use-efficiency. *New Phytol.* 196, 1098–1108. doi: 10.1111/j.1469-8137.2012.04285.x

Latz, A., Mehlmer, N., Zapf, S., Mueller, T. D., Wurzinger, B., Pfister, B., et al. (2013). Salt stress triggers phosphorylation of the *Arabidopsis* vacuolar K^+ channel TPK1 by calcium-dependent protein kinases (CDPKs). *Mol. Plant* 6, 1274–1289. doi: 10.1093/mp/sss158

Lee, J. M., and Oda, M. (2003). Grafting of herbaceous vegetable and ornamental crops. *Hortic. Rev.* 28, 61–124. doi: 10.1002/9780470650851.ch2

Lippman, Z. B., Semel, Y., and Zamir, D. (2007). An integrated view of quantitative trait variation using tomato interspecific introgression lines. *Curr. Opin. Genet. Dev.* 17, 545–552. doi: 10.1016/j.gde.2007.07.007

Mayak, S., Tirosh, T., and Glick, B. R. (2004). Plant growth-promoting bacteria that confer resistance to water stress in tomatoes and peppers. *Plant Sci.* 166, 525–530. doi: 10.1016/j.plantsci.2003.10.025

Müller, J., Xie, Z. P., Staehelin, C., Mellor, R. B., Boller, T., and Wiemken, A. (1994). Trehalose and trehalase in root nodules from various legumes. *Physiol. Plant.* 90, 86–92. doi: 10.1034/j.1399-3054.1994.900113.x

Murphy, J. F., Reddy, M. S., Ryu, C. M., Kloepper, J. W., and Li, R. (2003). Rhizobacteria-mediated growth promotion of tomato leads to protection against Cucumber mosaic virus. *Phytopath* 93, 1301–1307. doi: 10.1094/phyto.2003.93.10.1301

Neset, T. S. S., and Cordell, D. (2012). Global phosphorus scarcity: identifying synergies for a sustainable future. *J. Sci. Food Agric.* 92, 2–6. doi: 10.1002/jsfa.4650

Ngouajio, M., Wang, G., and Goldy, R. (2007). Withholding of drip irrigation between trans-planting and flowering increases the yield of field-grown tomato under plastic mulch. *Agric. Water Manage.* 87, 285–291. doi: 10.1016/j.agwat.2006.07.007

Ntatsi, G., Savvas, D., Kläring, H. P., and Schwarz, D. (2014). Growth, yield and metabolic responses of temperature-stressed tomato to grafting onto rootstocks differing in cold tolerance. *J. Amer. Soc. Hort. Sci.* 139, 230–243. doi: 10.21273/jashs.139.2.230

Ofner, I., Lashbrooke, J., Pleban, T., Aharoni, A., and Zamir, D. (2016). *Solanum pennellii* backcross inbred lines (BILs) link small genomic bins with tomato traits. *Plant J.* 87, 151–160. doi: 10.1111/tpj.13194

Ordookhani, K., Khavazi, K., Moezzi, A., and Rejali, F. (2010). Influence of PGPR and AMF on antioxidant activity, lycopene and potassium contents in tomato. *Afr. J. Agric. Res.* 5, 1108–1116.

Orozco-Mosqueda, M., and Gustavo, S. (2020). Plant-microbial endophytes interactions: scrutinizing their beneficial mechanisms from genomic explorations. *Curr. Plant Biol.* 25:100189. doi: 10.1016/j.cpb.2020.100189

Patakioutas, G., Dimou, D., Yfanti, P., Karras, G., Ntatsi, G., and Savvas, D. (2015). Root inoculation with beneficial micro-organisms as a means to control *Fusarium oxysporum* f. sp. lycopersici in two Greek landraces of tomato grown on perlite. *Acta Hortic.* 1107, 277–286. doi: 10.17660/actahortic.2017.1168.36

Raaijmakers, M. J., Paulitz, C. T., Steinberg, C., Alabouvette, C., and Moënne-Loccoz, Y. (2009). The rhizosphere: a playground and battlefield for soilborne pathogens and beneficial microorganisms. *Plant Soil* 321, 341–361. doi: 10.1007/s11104-008-9568-6

Ramamoorthy, V., Viswanathan, R., Raguchander, T., Prakasam, V., and Samiyappan, R. (2001). Induction of systemic resistance by plant growth promoting rhizobacteria in crop plants against pests and diseases. *Crop Protect.* 20, 1–11. doi: 10.1016/s0261-2194(00)00056-9

Rigano, M. M., Arena, C., Di Matteo, A., Sellitto, S., Frusciante, L., and Barone, A. (2016). Eco-physiological response to water stress of drought-tolerant and drought-sensitive tomato genotypes. *Plant Biosyst.* 150, 682–691. doi: 10.1080/11263504.2014.989286

Rouphael, Y., and Colla, G. (2020). Toward a sustainable agriculture through plant biostimulants: from experimental data to practical applications. *Agronomy* 10:1461. doi: 10.3390/agronomy10101461

Rouphael, Y., Cardarelli, M., Rea, E., and Colla, G. (2008a). Grafting of cucumber as a means to minimize copper toxicity. *Environ. Exp. Bot.* 63, 49–58. doi: 10.1016/j.envexpbot.2007.10.015

Rouphael, Y., Cardarelli, M., Colla, G., and Rea, E. (2008b). Yield mineral composition, water relations, and water use efficiency of grafted mini-watermelon plants under deficit irrigation. *HortSci* 43, 730–736. doi: 10.21273/hortsci.43.3.730

Rouphael, Y., Venema, J. H., Edelstein, M., Savvas, D., Colla, G., Ntatsi, G., et al. (2017). "Grafting as a Tool for Toletance of Abiotic Stress," in *Vegetable*

Grafting: Principles and Practices, eds G. Colla, F. Pérez-Alfocea, and D. Schwarz (Oxfordshire: CABI), 171–215. doi: 10.1079/9781780648972.0171

Rudrappa, T., Czymmek, K. J., Paré, P. W., and Bais, H. P. (2008). Root-secreted malic acid recruits beneficial soil bacteria. *Plant Physiol.* 148, 1547–1556. doi: 10.1104/pp.108.127613

Ruzzi, M., and Aroca, R. (2015). Plant growth-promoting rhizobacteria act as biostimulants inhorticulture. *Sci. Hort.* 196, 124–134. doi: 10.1016/j.scienta.2015.08.042

Saadi, S., Todorovic, M., Tanasijevic, L., Pereira, L. S., Pizzigalli, C., and Lionello, P. (2015). Climate change and Mediterranean agriculture: impacts on winter wheat and tomato crop evapotranspiration, irrigation requirements and yield. *Agric. Water Manag.* 147, 103–115. doi: 10.1016/j.agwat.2014.05.008

Sánchez-Rodríguez, E., Moreno, D. A., Ferreres, F., del Mar, Rubio-Wilhelmi, M., and Ruiz, J. M. (2011). Differential responses of five cherry tomato varieties to water stress: changes on phenolic metabolites and related enzymes. *Phytochemistry* 72, 723–729. doi: 10.1016/j.phytochem.2011.02.011

Sansone, S.-A., Fan, T., Goodacre, R., Griffin, J. L., Hardy, N. W., Kaddurah-Daouk, R., et al. (2007). The metabolomics standards initiative. *Nat. Biotechnol.* 25:846. doi: 10.1038/nbt0807-846b

Savvas, D., and Gruda, N. (2018). Application of soilless culture technologies in the modern greenhouse industry—A review. *Eur. J. Hort. Sci.* 83, 280–293. doi: 10.17660/ejhs.2018/83.5.2

Savvas, D., Colla, G., Rouphael, Y., and Schwarz, D. (2010). Amelioration of heavy metal and nutrient stress in fruit vegetables by grafting. *Sci. Hort.* 127, 156–161. doi: 10.1016/j.scienta.2010.09.011

Savvas, D., Gianquinto, G., Tuzel, Y., and Gruda, N. (2013). Soilless culture. *FAO Plant Prod. Protect. Paper* 217, 303–354.

Savvas, D., Öztekin, G. B., Tepecik, M., Ropokis, A., Tüzel, Y., Ntatsi, G., et al. (2017). Impact of grafting and rootstock on nutrient-to-water uptake ratios during the first month after planting of hydroponically grown tomato. *J. Hort. Sci. Biot.* 92, 294–302. doi: 10.1080/14620316.2016.1265903

Schachtman, D. P., Reid, R. J., and Ayling, S. M. (1998). Phosphorus uptake by plants: from soil to cell. *Plant Physiol.* 116, 447–453. doi: 10.1104/pp.116.2.447

Schwarz, D., Rouphael, Y., Colla, G., and Venema, J. H. (2010). Grafting as a tool to improve tolerance of vegetables to abiotic stresses. Thermal stress, water stress and organic pollutants. *Sci. Hort.* 127, 162–171. doi: 10.1016/j.scienta.2010.09.016

Seleim, M. A. A., Saead, F. A., Abd-El-Moneem, K. M. H., and Abo-ELyousr, K. A. M. (2011). Biological control of bacterial wilt of tomato by plant growth promoting rhizobacteria. *Plant Pathol. J.* 10, 146–153. doi: 10.3923/ppj.2011.146.153

Semel, Y., Schauer, N., Roessner, U., Zamir, D., and Fernie, A. R. (2007). Metabolite analysis for the comparison of irrigated and non-irrigated field grown tomato of varying genotype. *Metabolomics* 3, 289–295. doi: 10.1007/s11306-007-0055-5

Shanmugam, V., and Kanoujia, N. (2011). Biological management of vascular wilt of tomato caused by *Fusarium oxysporum* f. sp. lycospersici by plant growth-promoting rhizobacterial mixture. *Biol. Control* 57, 85–93. doi: 10.1016/j.biocontrol.2011.02.001

Shen, M., Kang, Y. J., Wang, H. L., Zhang, X. S., and Zhao, Q. X. (2012). Effect of plant growth-promoting rhizobacteria (PGPRs) on plant growth, yield, and quality of tomato (*Lycopersicon esculentum* Mill.) under simulated seawater irrigation. *J. General Appl. Microbiol.* 58, 253–262. doi: 10.2323/jgam.58.253

Smith, J. S., and Hui, Y. H. (2004). *Food processing: principles and applications*. New Jersey,NJ: John Wiley Sons.

Smith, M. S., and Zimmerman, K. (1981). Nitrous oxide production by nondenitrifying soil nitrate reducers. *Soil Sci. Soc. Am. J.* 45, 865–871. doi: 10.2136/sssaj1981.03615995004500050008x

Streeter, J. G., and Gomez, M. L. (2006). Three enzymes for trehalose synthesis in *Bradyrhizobium* cultured bacteria and in bacteroids from soybean nodules. *Appl. Environ. Microbiol.* 72, 4250–4255. doi: 10.1128/aem.00256-06

Sung, J., Lee, S., Lee, Y., Ha, S., Song, B., Kim, T., et al. (2015). Metabolomic profiling from leaves and roots of tomato (*Solanum lycopersicum* L.) plants grown under nitrogen, phosphorus or potassium-deficient condition. *Plant Sci.* 241, 55–64. doi: 10.1016/j.plantsci.2015.09.027

Tawaraya, K., Honda, S., Cheng, W., Chuba, M., Okazaki, Y., Saito, K., et al. (2018). Ancient rice cultivar extensively replaces phospholipids with non-phosphorus glycolipid under phosphorus deficiency. *Physiol. Plant.* 163, 297–305. doi: 10.1111/ppl.12699

Tournu, H., Fiori, A., and van Dijck, P. (2013). Relevance of trehalose in pathogenicity: some general rules, yet many exceptions. *PLoS Pathog.* 9:e1003447. doi: 10.1371/journal.ppat.1003447

Tsugawa, H., Cajka, T., Kind, T., Ma, Y., Higgins, B., Ikeda, K., et al. (2015). MS-DIAL: Data-independent MS/MS deconvolution for comprehensive metabolome analysis. *Nat. Methods* 12, 523–526. doi: 10.1038/nmeth.3393

Van Der Merwe, M. J., Osorio, S., Moritz, T., Nunes-Nesi, A., and Fernie, A. R. (2009). Decreased mitochondrial activities of malate dehydrogenase and fumarase in tomato lead to altered root growth and architecture via diverse mechanisms. *Plant Physiol.* 149, 653–669. doi: 10.1104/pp.108.130518

Van Vuuren, D. P., Bouwman, A. F., and Beusen, A. H. (2010). Phosphorus demand for the 1970–2100 period: a scenario analysis of resource depletion. *Glob. Environ. Change* 20, 428–439. doi: 10.1016/j.gloenvcha.2010.04.004

Wang, C., Xing, J., Chin, C.-K., Ho, C.-T., and Martin, C. E. (2001). Modification of fatty acids changes the flavor volatiles in tomato leaves. *Phytochem* 58, 227–232. doi: 10.1016/s0031-9422(01)00233-3

Wasaki, J., Yonetani, R., Kuroda, S., Shinano, T., Yazaki, J., Fujii, F., et al. (2003). Transcriptomic analysis of metabolic changes by phosphorus stress in rice plant roots. *Plant Cell Env.* 26, 1515–1523. doi: 10.1046/j.1365-3040.2003.01074.x

Yan, Z., Reddy, M. S., and Kloepper, J. W. (2003). Survival and colonization of rhizobacteria in a tomato transplant system. *Canad. J. Microb.* 49, 383–389. doi: 10.1139/w03-051

Yang, J., Kloepper, W. J., and Ryu, C.-M. (2009). Rhizosphere bacteria help plants tolerate abiotic stress. *Trends Plant Sci.* 14, 1–4. doi: 10.1016/j.tplants.2008.10.004

Zhang, L., Ma, X. L., Zhang, Q., Ma, C. L., Wang, P. P., Sun, Y. F., et al. (2001). Expressed sequence tags from a NaCl-treated Suaeda salsa cDNA library. *Gene* 267, 193–200. doi: 10.1016/s0378-1119(01)00403-6

Zhu, J. K. (2000). Genetic analysis of plant salt tolerance using Arabidopsis. *Plant Physiol.* 124, 941–948. doi: 10.1104/pp.124.3.941

Conflict of Interest: The authors declare that the research was conducted in the absence of any commercial or financial relationships that could be construed as a potential conflict of interest.

frontiers in Plant Science

ORIGINAL RESEARCH
published: 08 June 2021
doi: 10.3389/fpls.2021.655060

AMF Inoculation Can Enhance Yield of Transgenic *Bt* Maize and Its Control Efficiency Against *Mythimna separata* Especially Under Elevated CO_2

Long Wang[1,2], *Xiaohui Wang*[1], *Fanqi Gao*[3], *Changning Lv*[1], *Likun Li*[1], *Tong Han*[4] *and Fajun Chen*[1]*

[1] *Department of Entomology, College of Plant Protection, Nanjing Agricultural University, Nanjing, China,* [2] *Department of Landscape Architecture, College of Biological and Agricultural Engineering, Weifang University, Weifang, China,* [3] *Jinshanbao Experimental Class, College of Agriculture, Nanjing Agricultural University, Nanjing, China,* [4] *Department of Phytology, College of Life Sciences, Nanjing Agricultural University, Nanjing, China*

OPEN ACCESS

Edited by:
Youssef Rouphael, University of Naples Federico II, Italy

Reviewed by:
Philipp Franken, Friedrich Schiller University Jena, Germany
Elisa Pellegrino, Sant'Anna School of Advanced Studies, Italy

***Correspondence:**
Fajun Chen
fajunchen@njau.edu.cn

Specialty section:
This article was submitted to Plant Symbiotic Interactions, a section of the journal Frontiers in Plant Science

Received: *18 January 2021*
Accepted: *10 May 2021*
Published: *08 June 2021*

Citation:
Wang L, Wang X, Gao F, Lv C, Li L, Han T and Chen F (2021) AMF Inoculation Can Enhance Yield of Transgenic Bt Maize and Its Control Efficiency Against Mythimna separata Especially Under Elevated CO_2. Front. Plant Sci. 12:655060. doi: 10.3389/fpls.2021.655060

The promotion and application of transgenic *Bt* crops provides an approach for the prevention and control of target lepidopteran pests and effectively relieves the environmental pressure caused by the massive usage of chemical pesticides in fields. However, studies have shown that *Bt* crops will face a new risk due to a decrease in exogenous toxin content under elevated carbon dioxide (CO_2) concentration, thus negatively affecting the ecological sustainability of *Bt* crops. Arbuscular mycorrhizal fungi (AMF) are important beneficial microorganisms that can effectively improve the nutrient status of host plants and are expected to relieve the ecological risk of *Bt* crops under increasing CO_2 due to global climate change. In this study, the *Bt* maize and its parental line of non-transgenic *Bt* maize were selected and inoculated with a species of AMF (*Funneliformis caledonium*, synonyms: *Glomus caledonium*), in order to study the secondary defensive chemicals and yield of maize, and to explore the effects of *F. caledonium* inoculation on the growth, development, and reproduction of the pest *Mythimna separata* fed on *Bt* maize and non-*Bt* maize under ambient carbon dioxide concentration (aCO_2) and elevated carbon dioxide concentration (eCO_2). The results showed that eCO_2 increased the AM fungal colonization, maize yield, and foliar contents of jasmonic acid (JA) and salicylic acid (SA), but decreased foliar Bt toxin content and *Bt* gene expression in *Bt* maize leaves. *F. caledonium* inoculation increased maize yield, foliar JA, SA contents, *Bt* toxin contents, and *Bt* gene expression in *Bt* maize leaves, and positively improved the growth, development, reproduction, and food utilization of the *M. separata* fed on non-*Bt* maize. However, *F. caledonium* inoculation was unfavorable for the fitness of *M. separata* fed on *Bt* maize, and the effect was intensified when combined with eCO_2. It is indicated that *F. caledonium* inoculation had adverse effects on the production of non-*Bt* maize due to the high potential risk of population occurrence of *M. separata*, while it was just the opposite for *Bt* maize. Therefore, this study confirms that the AMF can increase the yield and promote the expression levels of its endogenous (JA,

SA) and exogenous (Bt toxin) secondary defense substances of *Bt* maize under eCO_2, and finally can enhance the insect resistance capacity of *Bt* crops, which will help ensure the sustainable utilization and safety of *Bt* crops under climate change.

Keywords: elevated CO_2, transgenic *Bt* maize, arbuscular mycorrhizal fungi, *Mythimna separata*, control efficiency, yield

INTRODUCTION

In recent years, many transgenic *Bt* crops, such as *Bt* maize and *Bt* cotton, have been grown around the world and have shown high resistance to specific target pests, mainly Lepidoptera insects (Wu et al., 2008; Liu et al., 2016). As a result, *Bt* crops have been used to control a wider range of pests, such as *Helicoverpa armigera* (Hübner), *Heliothis virescens*, and *Mythimna separata* (Riddick et al., 1998; Chen F. J. et al., 2011; Chang et al., 2013). Meanwhile, human activities, specifically fossil fuel burning and land-use change, are rapidly increasing the level of carbon dioxide (CO_2) in the atmosphere (Yu and Chen, 2019; Yao et al., 2020). Specifically, it has been reported that the atmospheric CO_2 concentration increased from 288 to 405 ppm from 1800 to 2018 (www.esrl.noaa.gov/gmd/ccgg/trends/). With the acceleration of industrialization, it is estimated that the concentration of CO_2 in the atmosphere will increase from 800 to 1,000 ppm by the end of the twenty-first century (Pachauri and Reisinger, 2014).

Plant productivity is fundamentally tied to atmospheric CO_2 by photosynthesis, and the increase in atmospheric CO_2 concentration can improve the photosynthetic capacity of plants and undoubtedly affect the plant physiology with profound impacts on all aspects, including the increase in photosynthetic rate, biomass, and seed production (Dietterich et al., 2015; Johnson and Hartley, 2018; Zhu et al., 2018). Most studies reported that elevated CO_2 (eCO_2) increased the C/N ratio in plant tissues; thus, the content of carbohydrates in plant tissues increased and the content of N-containing compounds decreased (Chen et al., 2005a; Xu et al., 2015; Dai et al., 2018). All these changes in turn affect the production of plant secondary metabolites (Stiling and Cornelissen, 2007). Elevated CO_2 may enhance or weaken plant defense against herbivorous insects, at least partly due to the changes in C- and N-based defensive metabolites, as well as plant nutrients, especially protein content (Kretzschmar et al., 2009). Some studies have shown that jasmonic acid (JA), ethylene (ET), and salicylic acid (SA) are secondary defense substances of plants against aphids under eCO_2 (Sun et al., 2013; Guo et al., 2014), and reported that eCO_2 caused a significant reduction of N-based compounds (i.e., *Bt* toxin proteins) in *Bt* crops (Chen et al., 2005b; Wu et al., 2011a; Liu et al., 2019). Hence, it is speculated that under the condition of climate change, transgenic *Bt* crops will face a new risk that the effective control of the target pests will be reduced.

Arbuscular mycorrhizal fungi (AMF) can form associations with the roots of about 80% of terrestrial plant species (Smith and Read, 2008) and exchange soil-derived nutrients (Marschner and Dell, 1994) for plant-derived hexoses and lipids (Helber et al., 2011; Keymer and Lankau, 2017). AMF improve the supply of inorganic nutrients, especially phosphate (Rillig and Mummey, 2006). However, since AMF can also enhance the nitrogen uptake and utilization of plants (Hawkins et al., 2000) and improve their resistance to external biotic and abiotic stresses (Jung et al., 2012; Frew and Price, 2019), we hypothesize that they can be used to alleviate the problems of *Bt* toxin protein decline under eCO_2, and reduce the risk of *Bt* crops under future climate change. In order to test this hypothesis, we inoculated *Bt* maize with AMF (*Funneliformis caledonium*) under elevated CO_2 concentration to explore the interaction between eCO_2 and AM fungal inoculation on plant growth and secondary defense metabolites of *Bt* maize, and the effects on the growth and development and food utilization of the main maize pest armyworm from 2017 to 2018. We further hypothesize that *F. caledonium* inoculation under eCO_2 could (a) increase the biomass and yield of maize; (b) promote the expression of endogenous (JA, SA) and exogenous (Bt toxin) secondary defense substances in *Bt* maize leaves; and (c) decrease indices of growth, development, and reproduction of *M. separata*.

MATERIALS AND METHODS

CO_2 Setting

A 2-year experiment (2017–2018) was conducted in six open-top chambers (OTCs) in Ningjin County, Shandong Province of China (37.64° N, 116.8° E). OTCs are 2.5 m in height × 3.2 m in diameter. Two concentration levels of CO_2 are applied successively, namely, the ambient level (aCO_2, 375 μl/l) and the elevated level (eCO_2, 750 μl/l). Each CO_2 treatment uses three OTCs. During the experiment, OTCs were continuously filled with CO_2. The average CO_2 concentration is shown in **Supplementary Table 1**.

Arbuscular Mycorrhizal Fungi and *Bt* Maize

Funneliformis caledonium (strain number 90036, referred to as FC, synonyms: *Glomus caledonium*) was provided by the State Key Laboratory of Soil & Sustainable Agriculture, Institute of Soil Science, the Chinese Academy of Sciences. The inoculum consisted of spores, mycelium, maize root fragments, and soil (storage: under normal temperature, keep in dry, cool place). The *Bt* maize cultivar (line IE09S034 with *Cry1Ie*, namely, *Bt*) and the parental line of non-transgenic *Bt* maize (cv. Xianyu 335, namely, Xy) were provided by The Institute of Crop Sciences of the Chinese Academy of Agricultural Science. *Bt* maize and non-*Bt* maize were planted in plastic barrels (the height of 45 cm and the diameter of 30 cm) filled with 20 kg soils and 10 g compound fertilizer (N: P: K = 18: 15: 12), respectively. Soil pH was 7.2, organic carbon 11.7 g/kg, total nitrogen 2.27 g/kg, and total phosphorus 0.56 g/kg. On June 10 of each sampling year, 100 g inoculum of *F. caledonium* (namely, FC in figure) and 100 g

sterilized strain (namely, CK in figure) were evenly spread at 4 cm under maize seed as control; three maize seeds were sown in each barrel with a sowing depth of 2 cm, and two maize were reserved after emergence. Maize were irrigated every two to three days to ensure the water demand for maize growth.

There were eight treatments [two CO_2 concentration (aCO_2 and eCO_2), two maize treatments (*Bt* and Xy), and two AMF inoculations (*F. caledonium* and CK)]. Each treatment included three OTCs; each OTC included four planting patterns (*Bt* + AMF, *Bt* + CK, Xy + AMF, and Xy + CK); each planting pattern included five repeats; that is, each treatment contained a total of 15 repeats.

Arbuscular Mycorrhizal Fungi Colonization and AMF Phospholipid Fatty Acid (PLFA) Content

In two sampling years, AMF colonization was determined on heading stage (BBCH-59), and it was determined by the method of trypan blue staining and grid counting (Phillips and Hayman, 1970). The fresh plant roots were washed with distilled water and then blotted dry with absorbent paper. One hundred one centimeter roots were randomly cut and placed in a 10% KOH solution at 30°C for 30 min, and then, the KOH was discarded and rinsed with distilled water. After acidification in 2% HCl for 60 min, the HCl was discarded, rinsed with distilled water, and stained in 5% trypan blue dye solution (w/v, lactic acid: glycerol: water = 1: 1: 1). Then, the dye solution was discarded, and the roots were rinsed with distilled water and transferred to a square with a grid at the bottom. We observed the number of infected and uninfected root segments under the microscope. Colonization (%) = number of infected root segments/total root segments (Mcgonigle et al., 1990). The improved Bligh-Dyer method was used to extract microbial PLFA from soil (Bossio and Scow, 1998; Ruess and Chamberlain, 2010). About 8.0 g of the freeze-dried soil sample was weighed into a Teflon tube, and the lipids from soil were extracted by multiple oscillation centrifugation with a Bligh-Dyer mixed extract prepared in a ratio of 1: 2: 0.8 with chloroform: methanol: citrate buffer. The aqueous phase and the organic phase were separated by keeping away from light overnight, and the lower organic-phase supernatant containing the phospholipid was taken up and then dried with nitrogen in a water bath. The sample was dissolved and dried with a small amount of chloroform and acetone several times and passed through a SPE silica gel column to remove neutral lipids and glycolipids from the sample, followed by separation and purification with methanol to collect PLFA, and dried with nitrogen again. The separated PLFA is methylated by a liquid (methanol: toluene 1:1 mixture) and a liquid of KOH–methanol solution, and then the reaction was terminated with acetic acid. Finally, it was extracted with n-hexane and dried with nitrogen to obtain PLFA methyl ester. With C19: 0 as the internal standard, the content of methyl ester of characteristic fatty acids was analyzed by MIDI identification system, and the soil PLFA content was expressed in nmol/g through peak area and internal standard curve.

Foliar Bt Toxin Content and *Bt* Gene Expression in the Leaves of *Bt* Maize

During the heading stage (BBCH-59) of maize, the foliar content of Bt toxin protein was measured by using plant *Bt-Cry1Ie* protein ELISA Kit (mlbio, China). Moreover, the real-time quantitative reverse transcription PCR was performed on a 7500 real-time PCR system (Applied Biosystems Inc.) for *Bt* gene expression analysis. Total RNA was extracted from the leaf tissues by using TRIzol® reagent (Invitrogen). The concentration and quality of samples were determined by NanoDrop™ spectrophotometer (Thermo Scientific) and 1.5% agarose gel electrophoresis. The cDNA synthesis was carried out with 100 ng of total RNA by using PrimeScript™ RT reagent Kit with gDNA Eraser (Takara, Japan). Reverse transcriptase reactions were performed in a reaction volume of 20 μl. Quantitative real-time PCR was performed with a 7500 real-time PCR detection system (Applied Biosystems) using 1 × SYBR® *Premix Ex Taq*™ (TaKaRa, Japan), 2 μl cDNA products (diluted from 20 to 200 μl with RNase-free water), and 0.2 μM primers in a final volume of 20 μl. Reaction conditions are 95°C, 30 s pre-denaturation; 95°C, 5 s, 60°C, 34 s, 40 cycles. The cDNA was amplified by PCR using the primers shown in **Supplementary Table 2**. Quantification of the transcript levels of target genes was conducted by following the $2^{-\Delta\Delta Ct}$ normalization method. The relative expression level was represented as the fold change by comparing three treatments (aCO_2 + AMF, aCO_2 +CK, and eCO_2 +AMF) and the treatment of eCO_2 + CK, respectively. Three technical replicates were performed on each sample of cDNA.

Jasmonic Acid and Salicylic Acid Contents in Maize Leaves

During the heading stage (BBCH-59) of maize, the foliar contents of JA and SA were measured in our laboratory by using plant JA ELISA Kit (YaJi Biological, China) and plant SA ELISA Kit (YaJi Biological, China).

Insect Development and Food Utilization

The colony of armyworm, *M. separata*, was collected in maize fields in Kangbao County, Hebei (China), and continuously reared on artificial diet for more than 15 generations in growth chamber (GDN-400D-4; Ningbo Southeast Instrument CO., LTD, Ningbo, China) (Song et al., 2020). The third-instar larvae with uniform size were randomly selected and were individually fed on fresh maize leaves, which were selected from each treatment at the heading stage (BBCH-59). The feeding trials were conducted in a plastic dish (6 cm in diameter) in 2017 and 2018. Each treatment consisted of five replicates (a total of 20 larvae per replicate).

The initial weights of third-instar larvae were individually measured with an electronic balance (AL104; METTLER-TOLEDO, Greifensee). Larvae feces, pupal weight, and the remaining parts of leaves were also carefully weighed. At the same time, dry weight of larvae and maize leaves was calculated during the experiment. Moreover, the food utilization indices, including relative consumption rate (RCR), relative growth rate (RGR), efficiency of conversion of digested food (ECD), and efficiency

of conversion of ingested food (ECI), were measured (Chen et al., 2005b).

$$RCR = I/(B^*T);\ RGR = G/(B^*T);$$

$$ECD\ (\%) = G/(I\text{-}F)^*100\%;\ ECI\ (\%) = G/I^*100\%$$

where I is the feeding amount (the weight of maize leaves before feeding minus the weight of maize leaves before feeding and after feeding); B is the average larval weight during the experiment (the average larval weight before feeding and after feeding); T is the experiment time (d); G is the added larval weight (the larval weight after feeding minus the larval weight before feeding); and F is the weight of total feces.

The larval lifespan, pupation rate/duration, and emergence of *M. separata* fed on leaves of *Bt* and non-*Bt* maize inoculated with and without *F. caledonium* were recorded every 12 h. Pairs of novel moths, including female: male ratio of 1: 1, were transferred to metal screen cages for oviposition and fed on 10% honey. The survivorship and fecundity of *M. separata* were observed every day until death.

Data Analysis

Data were analyzed using IBM-SPSS v.20.0 software (IBM, Armonk, NY). Three-way ANOVAs were used to test the effects of sampling years (2017 vs. 2018), CO_2 levels (elevated vs. ambient), AMF inoculation (*F. caledonium* vs. CK), transgenic treatment (*Bt* maize vs. non-*Bt* maize), and their interactions on the indices of Bt toxin and *Bt* gene expression in the leaves of *Bt* maize. Four-way ANOVAs were used to test the effects of sampling years (2017 vs. 2018), CO_2 levels (elevated vs. ambient), AMF inoculation (*F. caledonium* vs. CK), transgenic treatment (*Bt* maize vs. non-*Bt* maize), and their interactions on the indices of AMF colonization and AMF-PLFA content, foliar contents of JA and SA, and growth, development, and reproduction of *M. separata*. Significant differences between or among treatments were analyzed by Tukey's test at $P < 0.05$.

RESULTS

Arbuscular Mycorrhizal Fungi Colonization and AMF-PLFA Content of *Bt* and Non-*Bt* Maize Influenced by CO_2 Levels and *F. caledonium* Inoculation

Four-way ANOVAs showed that AMF inoculation, CO_2 level, and sampling years, and the interactions between AMF inoculation and CO_2 level ($F \geq 4.47$, $P \leq 0.042 < 0.05$) significantly affected the AMF colonization on *Bt* and non-*Bt* maize (**Supplementary Table 3**). Compared with control, AMF inoculation significantly increased the AMF colonization of *Bt* and non-*Bt* maize in two sample years no matter under aCO_2 or eCO_2 (**Figures 1A,C**). Compared with aCO_2, eCO_2 significantly increased the AMF colonization of non-*Bt* maize inoculated with *F. caledonium* in 2017 and 2018, that of *Bt* maize inoculated with *F. caledonium* in 2017, and that of *Bt* maize not inoculated in 2018 ($P < 0.05$; **Figures 1A,C**).

Moreover, four-way ANOVAs also showed that AMF inoculation ($F = 3385.14$, $P < 0.001$), CO_2 level ($F = 52.68$, $P < 0.001$), and sampling years ($F = 17.27$, $P < 0.001$) significantly affected the AMF-PLFA content of *Bt* and non-*Bt* maize (**Supplementary Table 3**). Compared with control, AMF inoculation significantly increased the AMF-PLFA content of *Bt* and non-*Bt* maize in two sample years no matter under aCO_2 or eCO_2 (**Figures 1B,D**). Compared with aCO_2, eCO_2 significantly increased the AMF-PLFA content of *Bt* maize inoculated with *F. caledonium* in 2017 and 2018, and also significantly increased the AMF-PLFA content of non-*Bt* maize inoculated with *F. caledonium* in 2018 and non-*Bt* maize not inoculated in 2017 ($P < 0.05$; **Figures 1B,D**).

Foliar Bt Protein Content and *Bt* Gene Relative Expression Level in Leaves of *Bt* Maize Influenced by CO_2 Levels and *F. caledonium* Inoculation

Three-way ANOVAs showed that AMF inoculation ($F \geq 275.07$, $P < 0.001$), CO_2 level ($F \geq 5.89$, $P \leq 0.027$), and their interaction ($F \geq 18.88$, $P < 0.001$) significantly affected the foliar Bt protein content and *Bt* gene relative expression level in the leaves of *Bt* maize (**Supplementary Table 4**).

For the foliar Bt protein content, compared with aCO_2, eCO_2 significantly decreased the foliar Bt protein content of *Bt* maize without *F. caledonium* inoculation, but significantly increased the foliar Bt protein content of *Bt* maize inoculated with *F. caledonium* (**Figures 2A,C**). Compared with control, AMF inoculation significantly increased the foliar Bt protein content of *Bt* maize under aCO_2 and eCO_2 ($P < 0.05$; **Figures 2A,C**).

For the *Bt* gene relative expression level, compared with aCO_2, eCO_2 significantly decreased the *Bt* gene relative expression level in the leaves of *Bt* maize without *F. caledonium* inoculation (**Figures 2B,D**). Compared with control, AMF inoculation significantly increased the *Bt* gene relative expression level of *Bt* maize under aCO_2 and eCO_2 ($P < 0.05$; **Figures 2B,D**).

Foliar JA and SA Contents in Leaves of *Bt* and Non-*Bt* Maize Influenced by CO_2 Levels and *F. caledonium* Inoculation

Four-way ANOVAs showed that AMF inoculation ($F \geq 216.16$, $P < 0.001$) and CO_2 level ($F \geq 99.02$, $P < 0.001$) significantly affected the foliar JA and SA contents of *Bt* and non-*Bt* maize (**Supplementary Table 4**).

For the foliar JA content, compared with control, AMF inoculation significantly increased the foliar JA content of *Bt* and non-*Bt* maize in two sample years no matter under aCO_2 or eCO_2 (**Figures 3A,C**). Compared with aCO_2, eCO_2 significantly increased the foliar JA content of *Bt* and non-*Bt* maize without *F. caledonium* inoculation in 2017 and 2018, and *Bt* maize inoculated with *F. caledonium* in 2017 and non-*Bt* maize inoculated with *F. caledonium* in 2018 ($P < 0.05$; **Figures 3A,C**).

For the foliar SA content, compared with control, AMF inoculation significantly increased the foliar SA content of *Bt* and non-*Bt* maize in two sample years no matter under aCO_2 or eCO_2 (**Figures 3B,D**). Compared with aCO_2, eCO_2 significantly

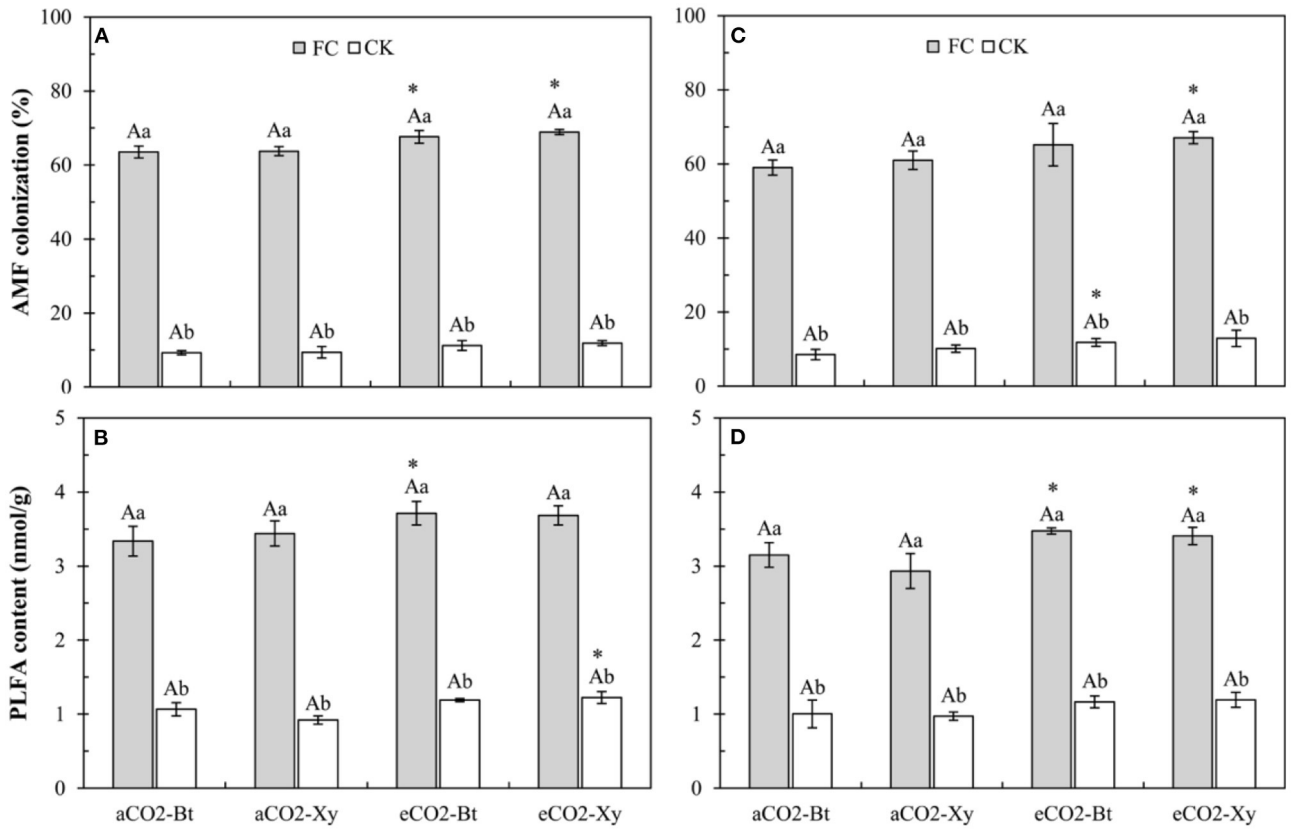

FIGURE 1 | Effects of the inoculation with arbuscular mycorrhizal fungi (AMF), *F. caledonium,* on the AMF colonization and AMF-PLFA content of *Bt* maize (Bt) and its parental line of non-*Bt* maize (Xy) under ambient CO_2 (aCO_2) and elevated CO_2 (eCO_2) at the heading stage (BBCH-59) in 2017 **(A,B)** and 2018 **(C,D)**. (FC, *F. caledonium* inoculation; CK, the control without *F. caledonium* inoculation; aCO_2-Bt, *Bt* maize under aCO_2; aCO_2-Xy, non-*Bt* maize under aCO_2; eCO_2-Bt, *Bt* maize under eCO_2; eCO_2-Xy, non-*Bt* maize under eCO_2; different uppercase, lowercase letters, and * indicate significant difference between *Bt* maize and non-*Bt* maize, between *F. caledonium* inoculation and non-inoculation of *F. caledonium,* and between aCO_2 and eCO_2 under the same other conditions as revealed by Tukey's test) ($P < 0.05$; $n = 15$).

increased the foliar SA content of *Bt* and non-*Bt* maize in two sample years regardless of *F. caledonium* inoculation or not (**Figures 3B,D**).

Food Utilization of *M. separata* Larvae Fed on *Bt* and Non-*Bt* Maize Influenced by CO_2 Levels and *F. caledonium* Inoculation

Four-way ANOVAs showed that AMF inoculation ($F \geq 4.20$, $P \leq 0.048$), CO_2 level ($F \geq 4.24$, $P \leq 0.047$), transgenic treatment ($F \geq 36.98$, $P < 0.001$), and their interactions ($F \geq 12.19$, $P < 0.0014$) significantly affected all the food utilization indices of *M. separata* larvae, except for the interaction between CO_2 level and AMF inoculation on RGR ($F = 0.72$, $P = 0.40 > 0.05$; **Supplementary Table 5**). Moreover, the interaction between CO_2 level, AMF inoculation, and transgenic treatment also significantly affected the ECD ($F = 32.63$, $P < 0.001$) and ECI ($F = 9.78$, $P = 0.004 < 0.01$) of *M. separata* larvae (**Supplementary Table 5**).

Compared with non-*Bt* maize, the ECD of *M. separata* larvae fed on *Bt* maize inoculated with and without *F. caledonium* was significantly decreased in two sample years no matter under aCO_2 or eCO_2. Compared with control, AMF inoculation significantly increased the ECD of *M. separata* larvae fed on non-*Bt* maize under eCO_2 in 2017 and 2018. Compared with aCO_2, eCO_2 significantly decreased the ECD of *M. separata* larvae fed on *Bt* maize inoculated with and without *F. caledonium* in two sample years, while significantly increased the ECD of *M. separata* larvae fed on non-*Bt* maize inoculated with *F. caledonium* in 2017 and 2018, and significantly decreased the ECD of *M. separata* larvae fed on non-*Bt* maize without *F. caledonium* inoculation in 2018 ($P < 0.05$; **Figures 4A,E**).

Compared with non-*Bt* maize, the ECI of *M. separata* larvae fed on *Bt* maize inoculated with and without *F. caledonium* was significantly decreased in two sample years no matter under aCO_2 or eCO_2. Compared with control, AMF inoculation significantly increased the ECI of *M. separata* larvae fed on non-*Bt* maize under aCO_2 and eCO_2 in two sample years, while significantly decreased the ECI of *M. separata* larvae fed on *Bt* maize under aCO_2 in 2017 and 2018. Compared with aCO_2, eCO_2 significantly decreased the ECI of *M. separata* larvae fed on *Bt* and non-*Bt* maize without *F. caledonium* inoculation in 2017

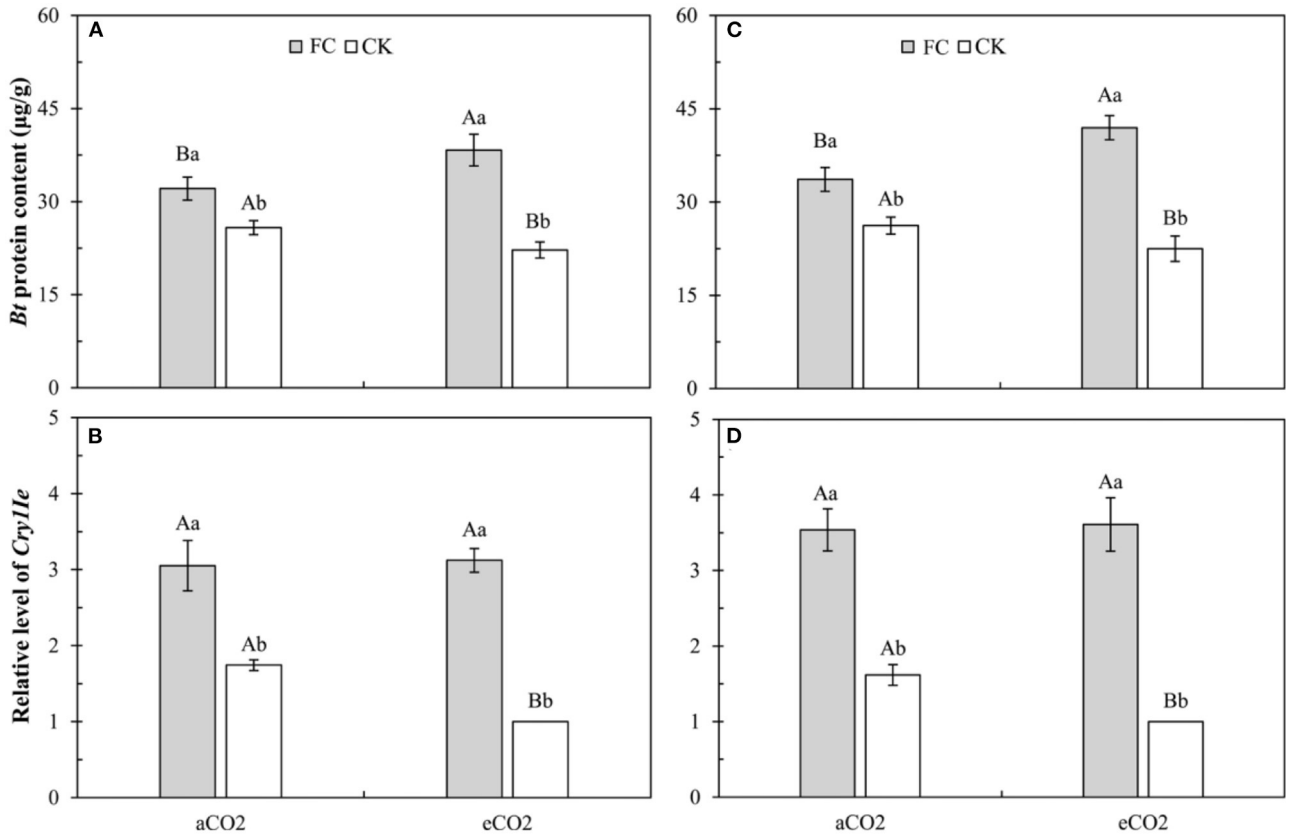

FIGURE 2 | Effects of the inoculation with arbuscular mycorrhizal fungi (AMF), *F. caledonium*, on foliar Bt protein content and *Bt* gene relative expression level in leaves of *Bt* maize under ambient CO_2 (aCO_2) and elevated CO_2 (eCO_2) at the heading stage (BBCH-59) in 2017 **(A,B)** and 2018 **(C,D)**. (Note: Different uppercase and lowercase letters indicate a significant difference between aCO_2 and eCO_2, and between *F. caledonium* inoculation and non-inoculation of *F. caledonium* under the same other conditions as revealed by Tukey's test) ($P < 0.05$; $n = 15$).

and 2018, while significantly increased the ECI of *M. separata* larvae fed on non-*Bt* maize with *F. caledonium* inoculation in 2017 and significantly decreased the ECI of *M. separata* larvae fed on *Bt* maize with *F. caledonium* inoculation in 2018 ($P < 0.05$; **Figures 4B,F**).

Compared with non-*Bt* maize, the RGR of *M. separata* larvae fed on *Bt* maize inoculated with and without *F. caledonium* was significantly decreased in two sample years no matter under aCO_2 or eCO_2. Compared with control, AMF inoculation significantly increased the RGR of *M. separata* larvae fed on non-*Bt* maize under aCO_2 and eCO_2 in 2017 and 2018, while significantly decreased the RGR of *M. separata* larvae fed on *Bt* maize under aCO_2 and eCO_2 in two sample years. Compared with aCO_2, eCO_2 significantly decreased the RGR of *M. separata* larvae fed on non-*Bt* maize without *F. caledonium* inoculation in 2017 and 2018, and that of *M. separata* larvae fed on non-*Bt* maize with *F. caledonium* inoculation in 2017 ($P < 0.05$; **Figures 4C,G**).

Compared with non-*Bt* maize, the RCR of *M. separata* larvae fed on *Bt* maize inoculated with and without *F. caledonium* was significantly decreased under aCO_2 in 2017 and 2018, while the RCR of *M. separata* larvae fed on *Bt* maize without *F. caledonium* inoculation significantly increased under eCO_2 in two sample years. Compared with control, AMF inoculation significantly decreased the RCR of *M. separata* larvae fed on *Bt* maize in two sample years no matter under aCO_2 or eCO_2, while significantly increased the RCR of *M. separata* larvae fed on non-*Bt* maize under aCO_2 in 2017 and 2018. Compared with aCO_2, eCO_2 significantly decreased the RCR of *M. separata* larvae fed on non-*Bt* maize inoculated with *F. caledonium* in 2017 and 2018, while significantly increased the RCR of *M. separata* larvae fed on *Bt* maize without *F. caledonium* inoculation in two sample years ($P < 0.05$; **Figures 4D,H**).

Growth, Development, and Reproduction of *M. separata* Fed on *Bt* and Non-*Bt* Maize Influenced by CO_2 Levels and *F. caledonium* Inoculation

Four-way ANOVAs showed that sampling year ($F \geq 7.97$, $P \leq 0.008$), CO_2 level ($F \geq 24.20$, $P < 0.001$), transgenic treatment ($F \geq 164.88$, $P < 0.001$), and the interaction between transgenic treatment and AMF inoculation ($F \geq 4.23$, $P \leq 0.047$) significantly affected all measured indices of *M. separata*,

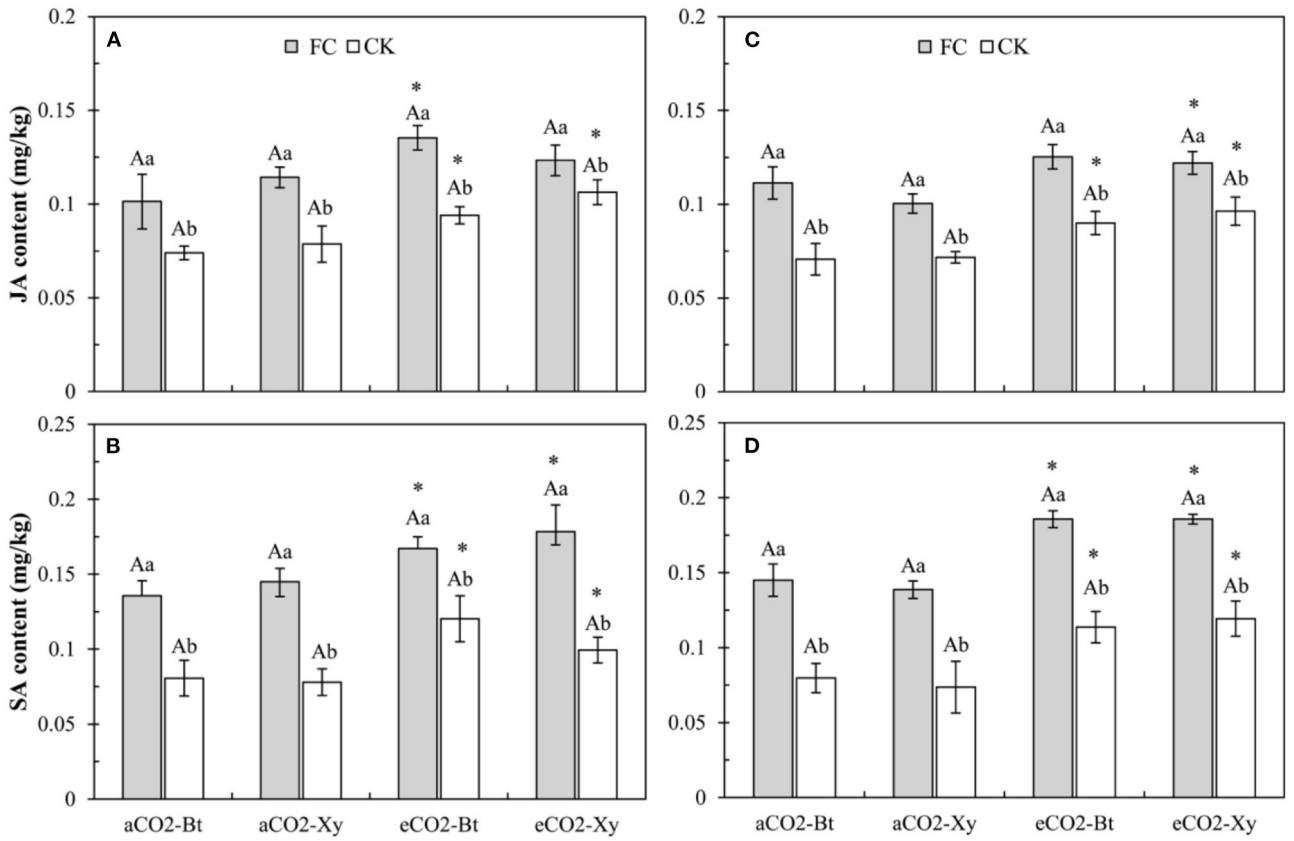

FIGURE 3 | Effects of the inoculation with arbuscular mycorrhizal fungi (AMF), *F. caledonium,* on the foliar JA and SA contents of *Bt* maize (Bt) and its parental line of non-*Bt* maize (Xy) under ambient CO_2 (aCO_2) and elevated CO_2 (eCO_2) at the heading stage (BBCH-59) in 2017 **(A,B)** and 2018 **(C,D)**. (Note: FC, *F. caledonium* inoculation; CK, the control without *F. caledonium* inoculation; aCO_2-Bt, *Bt* maize under aCO_2; aCO_2-Xy, non-*Bt* maize under aCO_2; eCO_2-Bt, *Bt* maize under eCO_2; eCO_2-Xy, non-*Bt* maize under eCO_2; Different uppercase, lowercase letters and * indicate significant difference between *Bt* maize and non-*Bt* maize, between *F. caledonium* inoculation and non-inoculation of *F. caledonium,* and between aCO_2 and eCO_2 under the same other conditions as revealed by Tukey's test, the same in the following figures) ($P < 0.05$; $n = 15$).

except the interaction between transgenic treatment and AMF inoculation on pupation rate of *M. separata* ($F = 0.23$, $P = 0.63$; **Supplementary Table 6**). Moreover, AMF inoculation significantly affected pupal weight and pupal duration of *M. separata* ($F \geq 15.07$, $P < 0.001$), the interaction between CO_2 level and transgenic treatment significantly affected larval lifespan of *M. separata* ($F = 89.64$, $P < 0.001$), and the interactions between CO_2 level and AMF inoculation affected fecundity of *M. separata* ($F = 12.65$, $P = 0.001$) (**Supplementary Table 6**).

Compared with non-*Bt* maize, the larval lifespan of *M. separata* larvae fed on *Bt* maize inoculated with and without *F. caledonium* was significantly extended in two sample years no matter under aCO_2 or eCO_2. Compared with control, AMF inoculation significantly shortened the larval lifespan of *M. separata* fed on non-*Bt* maize under aCO_2 and eCO_2 in 2017 and 2018, while significantly prolonged the larval lifespan of *M. separata* fed on *Bt* maize under aCO_2 and eCO_2 in 2017 and 2018. Compared with aCO_2, eCO_2 significantly extended the larval lifespan of *M. separata* larvae fed on *Bt* maize inoculated with and without *F. caledonium* in two sample years ($P < 0.05$; **Figures 5A,E**).

Compared with non-*Bt* maize, the pupation rate of *M. separata* fed on *Bt* maize inoculated with and without *F. caledonium* was significantly decreased under aCO_2 in two sample years no matter under aCO_2 or eCO_2 ($P < 0.05$; **Figures 5B,F**).

Compared with non-*Bt* maize, the pupal weight of *M. separata* fed on *Bt* maize inoculated with and without *F. caledonium* was significantly decreased in two sample years no matter under aCO_2 or eCO_2. Compared with control, AMF inoculation significantly increased the pupal weight of *M. separata* fed on non-*Bt* maize under aCO_2 and eCO_2 in 2017 and 2018, while significantly decreased the pupal weight of *M. separata* fed on *Bt* maize under aCO_2 and eCO_2 in two sample years. Compared with aCO_2, eCO_2 significantly decreased the pupal weight of *M. separata* fed on *Bt* and non-*Bt* maize in two sample years regardless of *F. caledonium* inoculation or not ($P < 0.05$; **Figures 5C,G**), respectively.

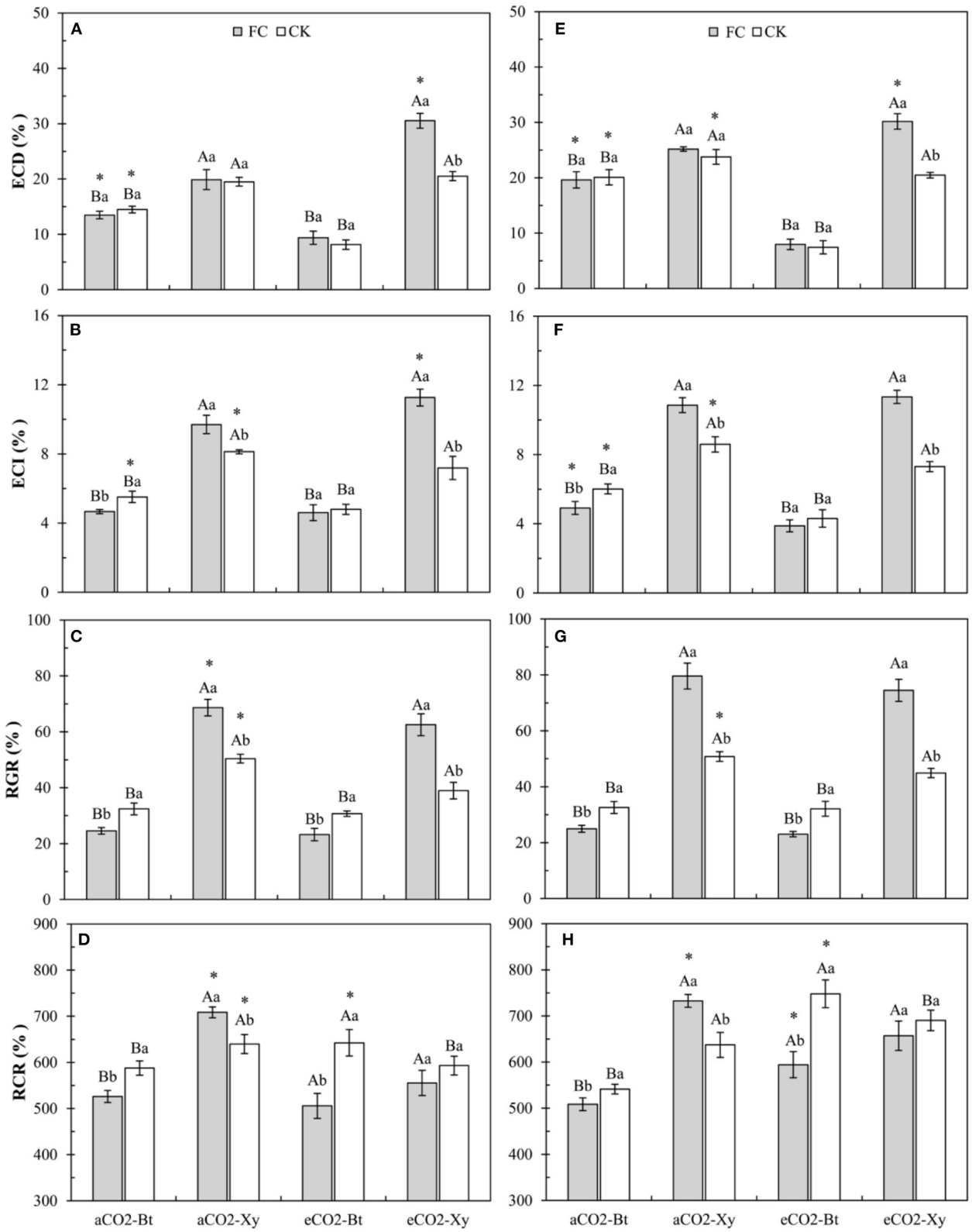

FIGURE 4 | Effects of the inoculation with arbuscular mycorrhizal fungi (AMF), *F. caledonium*, on the food utilization of *M. separata* larvae fed on *Bt* maize (Bt) and its parental line of non-*Bt* maize (Xy) under ambient CO_2 (aCO_2) and elevated CO_2 (eCO_2) at the heading stage (BBCH-59) in 2017 **(A–D)** and 2018 **(E–H)**. (Note: the same as **Figure 3**) ($P < 0.05$; $n = 5$).

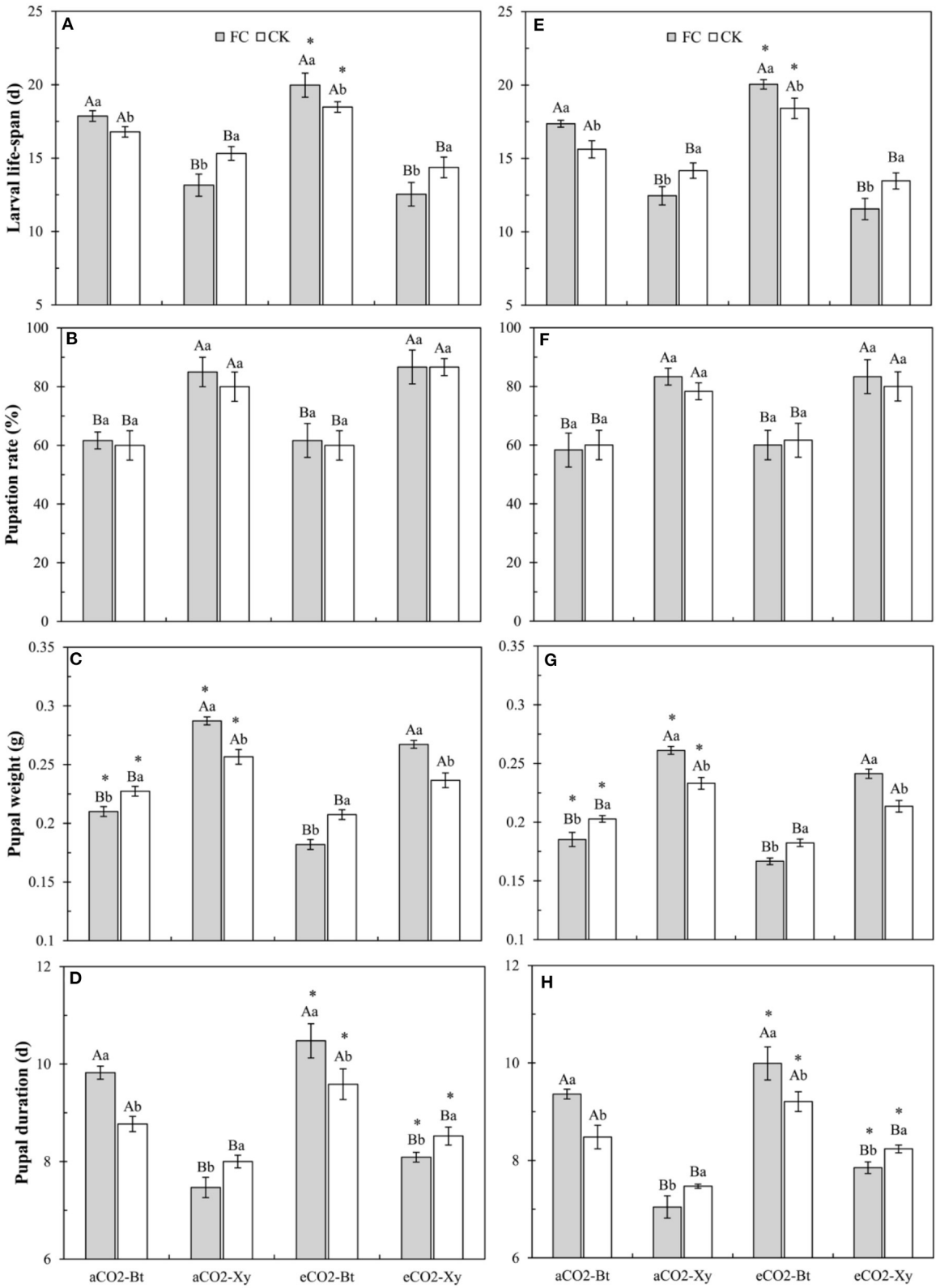

FIGURE 5 | Effects of the inoculation with arbuscular mycorrhizal fungi (AMF), *F. caledonium,* on the growth and development of *M. separata* larvae fed on *Bt* maize (Bt) and its parental line of non-*Bt* maize (Xy) under ambient CO_2 (aCO_2) and elevated CO_2 (eCO_2) at the heading stage (BBCH-59) in 2017 **(A–D)** and 2018 **(E–H)**. (Note: the same as **Figure 3**) ($P < 0.05$; $n = 5$).

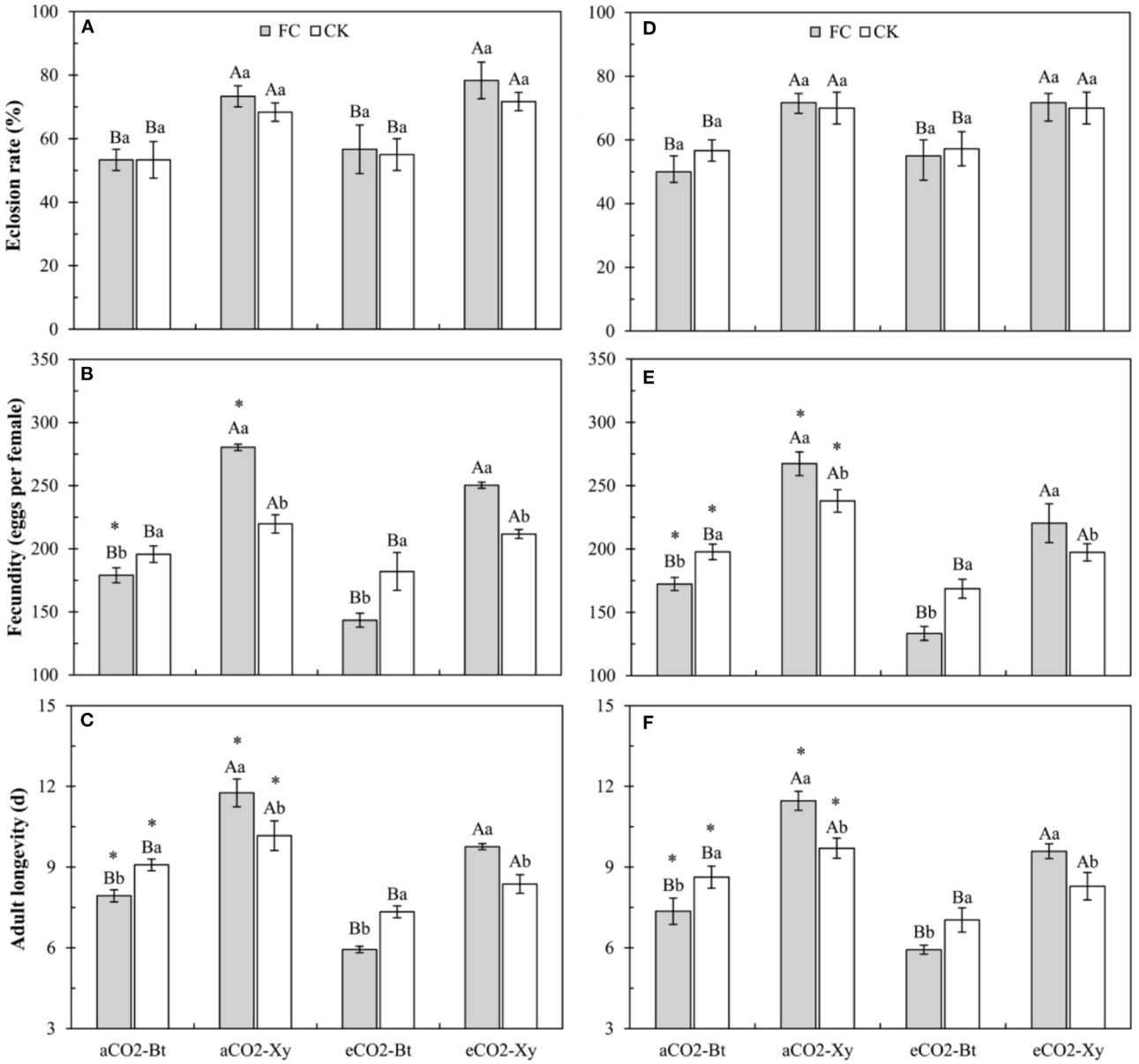

FIGURE 6 | Effects of the inoculation with arbuscular mycorrhizal fungi (AMF), *F. caledonium*, on the growth and development of *M. separata* adults fed on *Bt* maize (Bt) and its parental line of non-*Bt* maize (Xy) under ambient CO_2 (aCO_2) and elevated CO_2 (eCO_2) at the heading stage (BBCH-59) in 2017 **(A–C)** and 2018 **(D–F)**. (Note: the same as **Figure 3**) ($P < 0.05$; $n = 5$).

Compared with non-*Bt* maize, the pupal duration of *M. separata* fed on *Bt* maize inoculated with and without *F. caledonium* was significantly extended in two sample years no matter under aCO_2 or eCO_2. Compared with control, AMF inoculation significantly shortened the pupal duration of *M. separata* fed on non-*Bt* maize under aCO_2 and eCO_2 in 2017 and 2018, while significantly extended the pupal duration of *M. separata* fed on *Bt* maize under aCO_2 and eCO_2 in two sample years. Compared with aCO_2, eCO_2 significantly extended the pupal duration of *M. separata* fed on *Bt* and non-*Bt* maize in two sample years regardless of *F. caledonium* inoculation or not ($P < 0.05$; **Figures 5D,H**).

Compared with non-*Bt* maize, the eclosion rate of *M. separata* fed on *Bt* maize inoculated with and without *F. caledonium* was significantly decreased in two sample years no matter under aCO_2 or eCO_2 ($P < 0.05$; **Figures 6A,D**).

Compared with non-*Bt* maize, the fecundity of *M. separata* fed on *Bt* maize inoculated with and without *F. caledonium* was significantly decreased in two sample years no matter under aCO_2 or eCO_2. Compared with control, AMF inoculation

significantly increased the fecundity of *M. separata* fed on non-*Bt* maize under aCO_2 and eCO_2 in 2017 and 2018, while significantly decreased the fecundity of *M. separata* fed on *Bt* maize under aCO_2 and eCO_2 in two sample years. Compared with aCO_2, eCO_2 significantly decreased the fecundity of *M. separata* fed on *Bt* and non-*Bt* maize in two sample years regardless of *F. caledonium* inoculation or not ($P < 0.05$; **Figures 6B,E**).

Compared with non-*Bt* maize, the adult longevity of *M. separata* fed on *Bt* maize inoculated with and without *F. caledonium* was significantly shortened in two sample years no matter under aCO_2 or eCO_2. Compared with control, AMF inoculation significantly extended the adult longevity of *M. separata* fed on non-*Bt* maize under aCO_2 and eCO_2 in 2017 and 2018, while significantly shortened the adult longevity of *M. separata* fed on *Bt* maize under aCO_2 and eCO_2 in two sample years. Compared with aCO_2, eCO_2 significantly shortened the adult longevity of *M. separata* fed on *Bt* and non-*Bt* maize in two sample years regardless of *F. caledonium* inoculation or not ($P < 0.05$; **Figures 6C,F**).

Yield of *Bt* and Non-*Bt* Maize Influenced by CO_2 Levels and *F. caledonium* Inoculation

Four-way ANOVAs showed that AMF inoculation significantly affected all indices of maize yield ($F \geq 10.23$, $P \leq 0.003$), CO_2 level significantly affected ear weight per plant and grain weight per ear (CO_2 level: $F \geq 45.24$, $P < 0.001$), transgenic treatment significantly affected ear weight per plant ($F = 10.89$, $P = 0.002$), and the interaction between CO_2 level and AMF inoculation significantly affected the grain weight per ear ($F = 4.48$, $P = 0.042 < 0.05$) (**Supplementary Table 3**).

Compared with non-*Bt* maize, the dry ear weight per plant of *Bt* maize without *F. caledonium* inoculation was significantly enhanced under eCO_2 in 2017, and that with *F. caledonium* inoculation was significantly increased under aCO_2 in 2018. Compared with control, AMF inoculation significantly increased the dry ear weight per plant of *Bt* and non-*Bt* maize in two sample years no matter under aCO_2 or eCO_2. Compared with aCO_2, eCO_2 significantly increased the dry ear weight per plant of *Bt* and non-*Bt* maize in two sample years regardless of *F. caledonium* inoculation or not ($P < 0.05$; **Figures 7A,D**).

Compared with control, AMF inoculation significantly increased the grain weight per ear of *Bt* and non-*Bt* maize in two sample years no matter under aCO_2 or eCO_2. Compared with aCO_2, eCO_2 significantly increased the grain weight per ear of *Bt* and non-*Bt* maize inoculated with *F. caledonium* in two sample years, and significantly increased that of *Bt* maize without *F. caledonium* inoculation in 2017 and that of non-*Bt* maize without *F. caledonium* inoculation in 2018 ($P < 0.05$; **Figures 7B,E**). Compared with control, AMF inoculation significantly increased the 100-grain weight of non-*Bt* maize under aCO_2 in 2017, and that of *Bt* and non-*Bt* maize under eCO_2 in 2018 ($P < 0.05$; **Figures 7C,F**).

DISCUSSION

The values of AMF colonization and AMF-PLFA content indicate the colonization efficiency of AMF on maize. In this experiment, *F. caledonium* inoculation significantly increased the AMF colonization and AMF-PLFA content no matter what maize variety or CO_2 level, and this ensured the validity of the following research work. Meanwhile, elevated CO_2 can increase photosynthesis of plants, improve plant growth, and promote the transfer of carbon source substances from host plants to the root-symbiotic AMF, which is beneficial for AMF colonization and growth (Diaz et al., 1993; Cheng et al., 2012). The colonization was increased by ∼10% in *Medicago truncatula* and by as much as 50% in *Brachypodium distachyon* (Jakobsen et al., 2016). Treseder (2004) also reported that the AMF colonization reflected an increased colonization speed under eCO_2. Alberton et al. (2005) found that mycorrhizal fungi and mycorrhizal plants to elevated CO_2 were significantly positive, and the response ratio for AM fungi was 1.21 (an increase of 21%), indicating a significantly different response, and AM colonization percentage also had a certain degree of improvement. In this study, the AMF colonization and the AMF-PLFA content of *Bt* and non-*Bt* maize under eCO_2 were generally higher than those under aCO_2; therefore, it is presumed that elevated CO_2 did have a positive facilitation on the colonization of *F. caledonium* on maize (Diaz et al., 1993; Drigo et al., 2013; Becklin et al., 2016). Besides, there were no differences in the AMF colonization and AMF-PLFA content between *Bt* maize and its parental line of non-*Bt* maize; the results showed that the presence of the cry1Ie protein in maize did not affect the colonization of the AMF community, and it is consistent with the research report of Cheeke et al.; Cheeke et al. (2014; 2015; Zeng et al., 2018).

Overall, the plant biomass and grain yield increased with the increasing level (200–400 ppm) of atmospheric CO_2 for most crops (Chen M. et al., 2011; Wang et al., 2018). In this study, the results showed that eCO_2 significantly increased maize ear weight per plant and grain weight per ear, while it did not significantly affect the 100-grain weight. It is mainly because eCO_2 can enhance photosynthesis and in turn, has a positive effect on crop biomass and production (Guo et al., 2016; Liu et al., 2019). Although the maize yield was improved, the comprehensive nutritional quality of maize grain (100-grain weight) could not be improved; it may be due to the decreased nitrogen content at high CO_2 levels. Moreover, *F. caledonium* inoculation significantly increased all the yield indices (ear weight per plant, grain weight per ear, and 100-grain weight). The main function of AMF is to enhance the uptake of nutrient elements (e.g., N, P, K, Ca, Mg, Zn, and Fe) by host plants, improve the nutrient metabolism capacity and nutrient level of plant tissues, and then promote the growth and fruiting of plants (Sharifi et al., 2007; Terrer et al., 2016; Turrini et al., 2017). In addition, under the combined effects of eCO_2 and *F. caledonium* inoculation, the ear weight per plant and grain weight per ear of *Bt* and non-*Bt* maize showed a further significant increase, which benefit from the improvement of AMF colonization under eCO_2.

Insects are sensitive to environmental variations, and environmental stresses can cause changes in their growth,

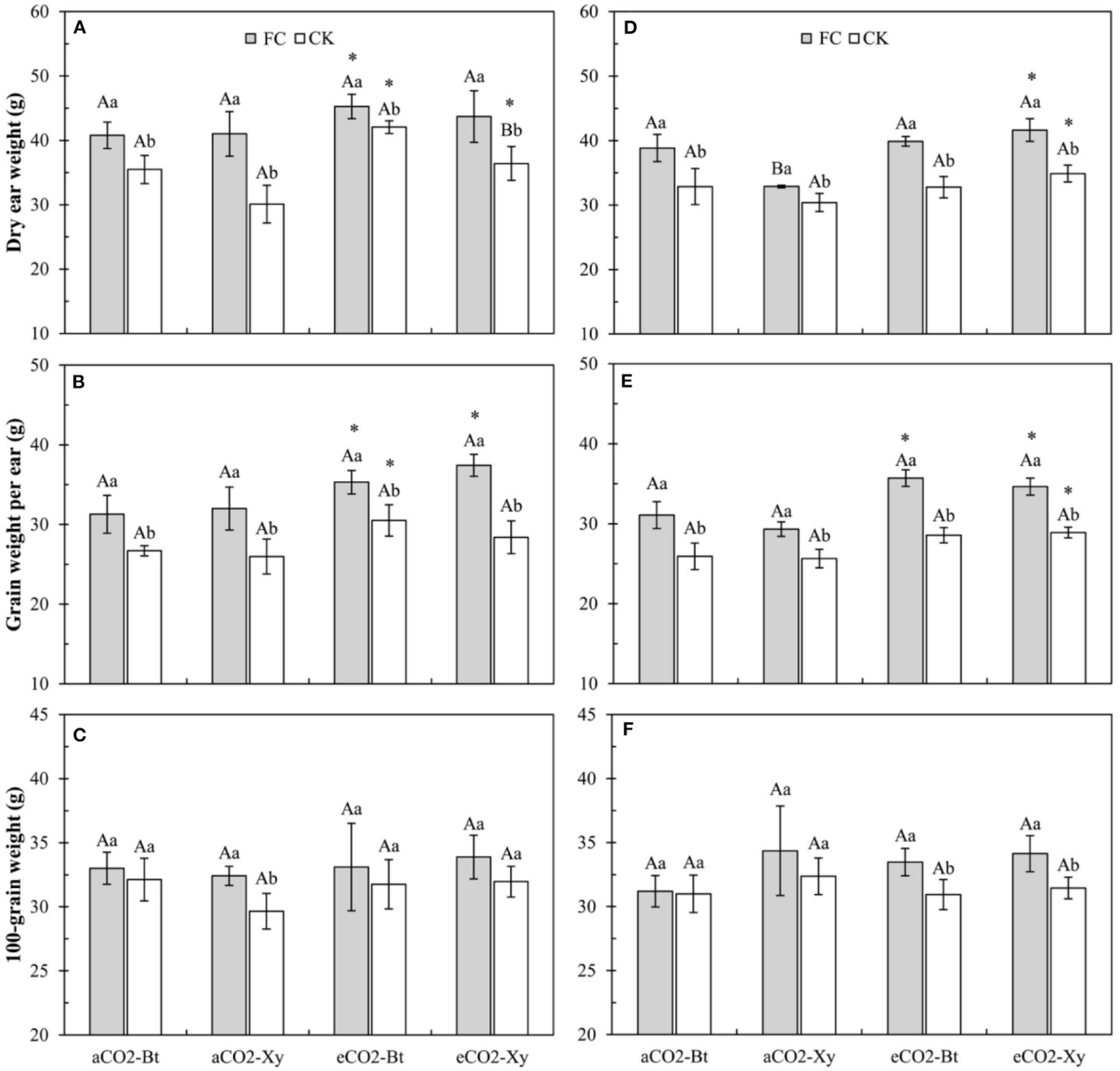

FIGURE 7 | Effects of the inoculation with arbuscular mycorrhizal fungi (AMF), *F. caledonium*, on the yield of *Bt* maize (Bt) and its parental line of non-*Bt* maize (Xy) under ambient CO_2 (aCO_2) and elevated CO_2 (eCO_2) in 2017 **(A–C)** and 2018 **(D–F)**. (Note: the same as **Figure 3**) ($P < 0.05$; $n = 15$).

development, fecundity, food utilization, and the occurrence and distribution of populations as a result of metabolic rate fluctuation (Bloom et al., 2010). Usually, endogenously secondary defensive chemicals (e.g., JA and SA) and nutrient components (e.g., C, N, P, and K) are the two main factors that affect the population fitness of pests; the balance between secondary defensive chemicals and nutrient components determines the development trend of pests after feeding. If the pests feed on transgenic *Bt* plants, in addition to the above-mentioned two influencing factors, the Bt toxin protein will also have a significant adverse effect on the growth and food utilization of pests and occupy the dominant position among the three. Prutz and Dettner (2005) reported that the transgenic *Bt* maize decreased the growth rate and increased the mortality of *Chilo partellus*, which might be attributed to the termination of larval metamorphosis fed on *Bt* maize. Most studies showed adverse effects of *Cry* proteins on lifetable parameters of different herbivores (Lawo et al., 2010), which might be due to the interaction of feeding inhibitors and growth inhibitors. In this study, we found that *Bt* maize obviously decreased almost all measured indices of food utilization (ECD, ECI, and RGR), and it showed that the ability of food digestion and absorption

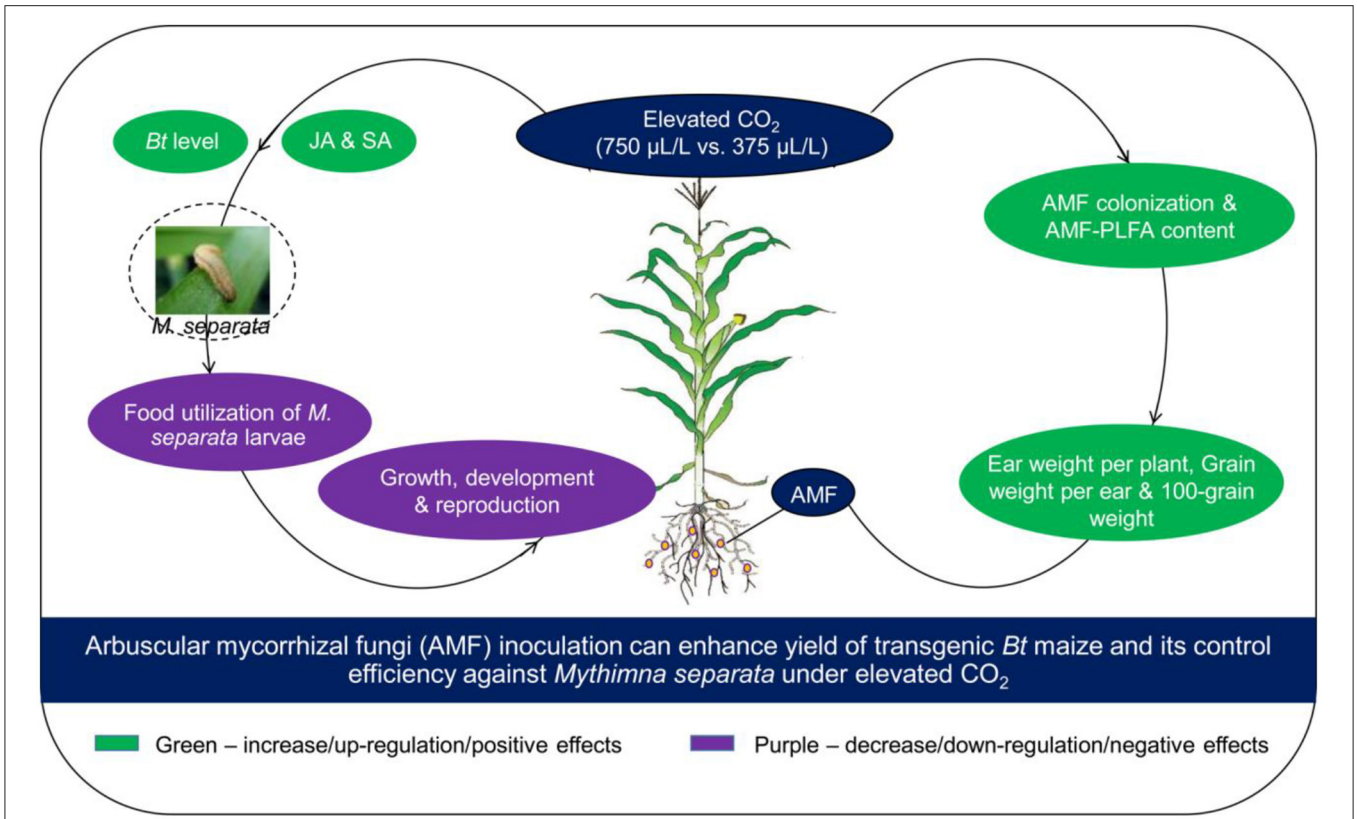

FIGURE 8 | A schematic model that AMF inoculation can enhance the yield of transgenic *Bt* maize and its control efficiency against *M. separata* under elevated CO_2.

of pests has caused serious damage by Bt toxin. Meanwhile, lifetable parameters (growth, development, and reproduction of *M. separata* larvae; pupation rate, pupal weight, eclosion rate, and fecundity of *M. separata* adult) markedly decreased feeding on *Bt* maize, and Bt toxin also prolonged the larval lifespan and shortened the adult longevity of *M. separata* regardless of the CO_2 level and *F. caledonium* inoculation or not in 2017 and 2018. These results showed that *Bt* maize obviously retarded the growth and development of *M. separata* and were similar to those of previous studies.

Previous studies have examined that in most plants, elevated CO_2 tends to promote plant photosynthesis and also leads to a decrease in foliar nitrogen content and an increase in C: N ratio (Johns et al., 2003; Li et al., 2018). Meanwhile, nitrogen is the main component of exogenous *Bt* protein in *Bt* crops. Plant nitrogen uptake, nitrogen-level status, and C: N ratio could affect the production of exogenous Bt toxins for *Bt* crops (Gao et al., 2009; Jiang et al., 2013). Numerous studies have shown that eCO_2 can significantly reduce the exogenous Bt protein content of *Bt* cotton and *Bt* rice, while increasing their yield (Coviella et al., 2000, 2002; Chen et al., 2005b; Wu et al., 2011a,b), and also found the "dilution effect" on exogenous Bt protein or inhibition on *Bt*-transgene expression (Chen F. J. et al., 2011; Jiang et al., 2017; Liu et al., 2019). Moreover, elevated CO_2 also affected the production of primary and secondary metabolites, and the defense mechanisms of crop plants (e.g., JA and SA) (Stiling and Cornelissen, 2007; Sun et al., 2016). In this study, eCO_2 significantly decreased the ECI and RGR of *M. separata* larvae fed on non-*Bt* maize without *F. caledonium* inoculation, and was almost adverse to all the measured indices of growth and development of *M. separata*; it is mainly due to the increased secondary defense substances (i.e., JA and SA) in plants and the declined food nutrient level (e.g., fewer N) under elevated CO_2 (Armstrong et al., 1995; Coviella et al., 2002; Liu et al., 2019). Many studies found that elevated CO_2 had adverse effects on the developmental duration, pupation, and eclosion of cotton bollworm, *H. armigera* (Akbar et al., 2016), and reduced the oviposition number of borers and semilooper (Stange, 1997; Rao et al., 2013). On the other hand, elevated CO_2 decreased the RGR of the *Spodoptera litura* and *H. armigera* (Hattenschwiler and Schafellner, 2004), and also significantly reduced the ECD and ECI of *H. armigera* (Yin et al., 2010). Meanwhile, eCO_2 also significantly reduced the ECD, ECI, pupal weight, fecundity, and adult longevity, and significantly extended the development duration of *M. separata* fed on *Bt* maize with and without *F. caledonium* inoculation. This shows that despite the decrease in exogenous Bt toxin content, the increase in secondary defense substances and the decline in nutrient quality can also make a relatively adverse effect on *M. separata*.

The effect of *F. caledonium* inoculation on *M. separata* fed on *Bt* maize and non-*Bt* maize was just the opposite; that is, *F. caledonium* inoculation significantly reduced the ECI, RGR, and RCR of *M. separata* larvae fed on *Bt* maize under aCO_2 and eCO_2, while significantly increased the ECI and RGR of *M. separata* larvae fed non-*Bt* maize under aCO_2 and eCO_2, and RCR of *M. separata* larvae fed on non-*Bt* maize under aCO_2, and ECD of *M. separata* larvae fed on non-*Bt* maize under eCO_2. In addition, *F. caledonium* inoculation and transgenic treatment had a significant interaction on the growth, development, and reproduction of *M. separata*. Specifically, as fed on *Bt* maize, *F. caledonium* inoculation significantly extended the developmental duration of larvae and pupae of *M. separata* under aCO_2 and eCO_2, significantly reduced the pupal weight and fecundity, and significantly shortened the adult longevity of *M. separata*. On the contrary, as fed on non-*Bt* maize, *F. caledonium* inoculation significantly shortened the developmental duration of larvae and pupae of *M. separata* under aCO_2 and eCO_2, and significantly increased the pupal weight of *M. separata* under aCO_2 and eCO_2. Thus, it was observed that *F. caledonium* inoculation had diametrically opposite effects on the growth, development, and food utilization of *M. separata* fed on *Bt* maize and non-*Bt* maize; that is, *F. caledonium* inoculation reduced the food utilization efficiency and had adverse effects on the growth, development, and reproduction of *M. separata* fed on *Bt* maize, while it improved the food utilization efficiency and had positive effects on the growth, development, and reproduction of *M. separata* fed on non-*Bt* maize. This is mainly due to the promotion of the absorption and utilization of soil nutrients in maize plants by *F. caledonium* inoculation, thus improving the nutrient level of maize plant tissues (Sharifi et al., 2007; Rodriguez and Sanders, 2015). So it is concluded that *M. separata* larvae can get more plant nutrition when fed on non-*Bt* maize inoculated with *F. caledonium*. When fed on *Bt* maize inoculated with *F. caledonium*, *M. separata* larvae not only obtained more plant nutrients, but also ingested more doses of exogenous *Bt* toxin, which improved the target resistance ability of *Bt* crops based on the exogenous Bt toxin, and further reduced the food utilization efficiency, growth, development, and reproduction of *M. separata*, and at the same time, the promotion of AMF colonization by eCO_2 further enhanced the target resistance level of *Bt* maize to *M. separata*.

Overall, our research showed that eCO_2 was beneficial for AMF colonization on roots, and maize yield, but it had negative effects on the growth, development, reproduction, and food utilization of *M. separata*. *F. caledonium* inoculation was positive for maize yield and nutrient quality, and in favor of the growth, development, reproduction, and food utilization of the *M. separata* fed on non-*Bt* maize. However, *F. caledonium* inoculation was unfavorable for the population fitness of *M. separata* fed on *Bt* maize. Namely, regardless of the CO_2 level, inoculation of *F. caledonium* had a detrimental effect on the production of non-*Bt* maize as the result of a high potential risk of *M. separata* production hazard, while its effects on *Bt* maize were just the opposite; that is, *F. caledonium* inoculation had positive effects on the production of *Bt* maize especially under eCO_2 due to the lower potential risk of population occurrence of *M. separata*. Ultimately, the results proved that all of our hypotheses were confirmed: It showed that the AMF inoculation of *F. caledonium* under eCO_2 was more effective in improving the control efficiency of *Bt* maize on the target insect pest, *M. separata*, promoted the expression of endogenous (JA, SA) and exogenous (Bt toxin) secondary defense substances in *Bt* maize leaves, and also increased the biomass and yield of maize (**Figure 8**). We have reason to expect this friendly and effective biological way serving for mitigating the ecological risk of *Bt* maize and improving its ecological sustainable utilization capacity under global climate change.

DATA AVAILABILITY STATEMENT

The original contributions presented in the study are included in the article/**Supplementary Materials**, further inquiries can be directed to the corresponding author/s.

AUTHOR CONTRIBUTIONS

LW and FC conceived research. LW, XW, and TH conducted the experiments. LW, FG, CL, and LL analyzed data and conducted statistical analysis. LW and FC wrote the manuscript. FC secured funding. All authors read and approved the manuscript.

FUNDING

This study was supported by the National Nature Science Foundation of China (NSFC) (31871963), the National Key Research and Development Program of China (2017YFD0200400), the Fundamental Research Funds for the Central Universities (KYZ201818), the Qing-Lan Project of Jiangsu Province of China, and the Postgraduate Research and Practice Innovation Program of Jiangsu Province (KYCX17_0574).

SUPPLEMENTARY MATERIAL

The Supplementary Material for this article can be found online at: https://www.frontiersin.org/articles/10.3389/fpls.2021.655060/full#supplementary-material

REFERENCES

Akbar, S. M., Pavani, T., Nagaraja, T., and Sharma, H. C. (2016). Influence of CO_2 and temperature on metabolism and development of *Helicoverpa armigera* (Noctuidae: Lepidoptera). *Environ. Entomol.* 45, 229–236. doi: 10.1093/ee/nvv144

Alberton, O., Kuyper, T. W., and Gorissen, A. (2005). Taking mycocentrism seriously: mycorrhizal fungal and plant responses to elevated CO_2. *New Phytol.* 167, 859–868. doi: 10.1111/j.1469-8137.2005.01458.x

Armstrong, C. L., Parker, G. B., and Pershing, J. C. (1995). Field evaluation of European corn borer control in progeny of 173 transgenic corn events

expressing an insecticidal protein from *Bacillus thuringiensis*. *Crop Sci.* 35, 550–557. doi: 10.2135/cropsci1995.0011183X003500020045x

Becklin, K. M., Mullinix, G. W. R., and Ward, J. K. (2016). Host plant physiology and mycorrhizal functioning shift across a glacial through future CO_2 gradient. *Plant Physiol.* 172, 789–801. doi: 10.1104/pp.16.00837

Bloom, A. J., Burger, M., Asensio, J. S. R., and Cousins, A. B. (2010). Carbon dioxide enrichment inhibits nitrate assimilation in wheat and Arabidopsis. *Science* 328, 899–903. doi: 10.1126/science.1186440

Bossio, D. A., and Scow, K. M. (1998). Impacts of carbon and flooding on soil microbial communities: phospholipid fatty acid profiles and substrate utilization patterns. *Microb. Ecol.* 35, 265–278. doi: 10.1007/s002489900082

Chang, X., Liu, G. G., He, K. L., Shen, Z. C., Peng, Y. F., and Ye, G. Y. (2013). Efficacy evaluation of two transgenic maize events expressing fused proteins to *CrylAb*-susceptible and -resistant *Ostrinia furnacalis* (Lepidoptera: Crambidae). *J. Econ. Entomol.* 106, 2548–2556. doi: 10.1603/EC13100

Cheeke, T. E., Darby, H., Rosenstiel, T. N., Bever, J. D., and Cruzan, M. B. (2014). Effect of *Bacillus thuringiensis* (*Bt*) maize cultivation history on arbuscular mycorrhizal fungal colonization, spore abundance and diversity, and plant growth. *Agric. Ecosyst. Environ.* 195, 29–35. doi: 10.1016/j.agee.2014.05.019

Cheeke, T. E., Schütte, U. M., Hemmerich, C. M., Cruzan, M. B., Rosenstiel, T. N., and Bever, J. D. (2015). Spatial soil heterogeneity has a greater effect on symbiotic arbuscular mycorrhizal fungal communities and plant growth than genetic modification with *Bacillus thuringiensis* toxin genes. *Mol. Ecol.* 24, 2580–2593. doi: 10.1111/mec.13178

Chen, F. J., Ge, F., and Parajulee, M. N. (2005a). Impact of elevated CO_2 on tri-trophic interaction of *Gossypium hirsutum*, *Aphis gossypii*, and *Leis axyridis*. *Environ. Entomol.* 34, 37–46. doi: 10.1603/0046-225X-34.1.37

Chen, F. J., Wu, G., Ge, F., and Parajulee, M. N. (2011). Relationships between exogenous-toxin quantity and increased biomass of transgenic *Bt* crops under elevated carbon dioxide. *Ecotoxicol. Environ. Saf.* 74, 1074–1080. doi: 10.1016/j.ecoenv.2011.02.001

Chen, F. J., Wu, G., Ge, F., Parajulee, M. N., and Shrestha, R. B. (2005b). Effects of elevated CO_2 and transgenic *Bt* cotton on plant chemistry, performance, and feeding of an insect herbivore, the cotton bollworm. *Entomol. Exp. Appl.* 115, 341–350. doi: 10.1111/j.1570-7458.2005.00258.x

Chen, M., Shelton, A., and Ye, G. Y. (2011). Insect-resistant genetically modified rice in China: from research to commercialization. *Annu. Rev. Entomol.* 56, 81–101. doi: 10.1146/annurev-ento-120709-144810

Cheng, L., Booker, F. L., Tu, C., Burkey, K. O., Zhou, L. S., Shew, H. D., et al. (2012). Arbuscular mycorrhizal fungi increase organic carbon decomposition under elevated CO_2. *Science* 337, 1084–1087. doi: 10.1126/science.1224304

Coviella, C. E., Morgan, D. J. W., and Trumble, J. T. (2000). Interactions of elevated CO_2 and nitrogen fertilization: effects on production of *Bacillus thuringiensis* toxins in transgenic plants. *Environ. Entomol.* 29, 781–787. doi: 10.1603/0046-225x-29.4.781

Coviella, C. E., Stipanovic, R. D., and Trumble, J. T. (2002). Plant allocation to defensive compounds: interactions between elevated CO_2 and nitrogen in transgenic cotton plants. *J. Exp. Bot.* 53, 323–331. doi: 10.1093/jexbot/53.367.323

Dai, Y., Wang, M. F., Jiang, S. L., Zhang, Y. F., Parajulee, M. N., and Chen, F. J. (2018). Host-selection behavior and physiological mechanisms of the cotton aphid, *Aphis gossypii*, in response to rising atmospheric carbon dioxide levels. *J. Insect Physiol.* 109, 149–156. doi: 10.1016/j.jinsphys.2018.05.011

Diaz, S., Grime, J. P., Harris, J., and McPherson, E. (1993). Evidence of a feedback mechanism limiting plant response to elevated carbon dioxide. *Nature* 354, 616–617. doi: 10.1038/364616a0

Dietterich, L. H., Zanobetti, A., Kloog, I., Huybers, P., Leakey, A. D., Bloom, A. J., et al. (2015). Impacts of elevated atmospheric CO_2 on nutrient content of important food crops. *Sci. Data* 2:150036. doi: 10.1038/sdata.2015.36

Drigo, B., Kowalchuk, G. A., Knapp, B. A., Pijl, A. S., Boschker, H. T. S., and Veen, J. A. (2013). Impacts of 3 years of elevated atmospheric CO_2 on rhizosphere carbon flow and microbial community dynamics. *GCB Bioenergy* 19, 621–636. doi: 10.1111/gcb.12045

Frew, A., and Price, J. N. (2019). Mycorrhizal-mediated plant-herbivore interactions in a high CO_2 world. *Funct. Ecol.* 33, 1376–1385. doi: 10.1111/1365-2435.13347

Gao, H. J., Xiao, N. W., Li, J. S., Chen, F. J., and Zhai, B. P. (2009). Effects of double atmospheric CO_2 concentration on nitrogen metabolism of transgenic *Bt* cotton under different nitrogen fertilization levels. *Chinese J. Ecol.* 28, 2213–2219.

Guo, H., Huang, L., Sun, Y., and Gou, H. G. (2016). The contrasting effects of elevated CO_2 on TYLCV infection of tomato genotypes with and without the resistance gene, *Mi-1.2*. *Front. Recent Dev. Plant Sci.* 7:1680. doi: 10.3389/fpls.2016.01680

Guo, H. J., Sun, Y. C., Li, Y. F., Liu, X. H., Wang, P. Y., Zhu-Salzman, K., et al. (2014). Elevated CO_2 alters the feeding behaviour of the pea aphid by modifying the physical and chemical resistance of *Medicago truncatula*. *Plant Cell Environ.* 37, 2158–2168. doi: 10.1111/pce.12306

Hattenschwiler, S., and Schafellner, C. (2004). Gypsy moth feeding in the canopy of a CO_2-enriched mature forest. *GCB Bioenergy* 10, 1899–1908. doi: 10.1111/j.1365-2486.2004.00856.x

Hawkins, H. J., Johansen, A., and George, E. (2000). Uptake and transport of organic and inorganic nitrogen by arbuscular mycorrhizal fungi. *Plant Soil* 226, 275–285. doi: 10.1023/A:1026500810385

Helber, N., Wippel, K., Sauer, N., Schaarschmidt, S., Hause, B., and Requena, N. (2011). A versatile monosaccharide transporter that operates in the arbuscular mycorrhizal fungus Glomus sp is crucial for the symbiotic relationship with plants. *Plant Cell* 23, 3812–3823. doi: 10.1105/tpc.111.089813

Jakobsen, I., Smith, S. E., Smith, F. A., Watts-Williams, S. J., Clausen, S. S., and Gronlund, M. (2016). Plant growth responses to elevated atmospheric CO_2 are increased by phosphorus sufficiency but not by arbuscular mycorrhizas. *J. Exp. Bot.* 67, 6173–6186. doi: 10.1093/jxb/erw383

Jiang, S. L., Lu, Y. Q., Dai, Y., Qian, L., Muhuammd, A. B., Li, T., et al. (2017). Impacts of elevated CO_2 on exogenous *Bacillus thuringiensis* toxins and transgene expression in transgenic rice under different levels of nitrogen. *Sci. Rep.* 7:14716. doi: 10.1038/s41598-017-15321-9

Jiang, Y., Huang, S., Cai, M., Li, C., Kong, X., Zhang, F., et al. (2013). Yield changes of *Bt*-MH63 with Cry1C∗ or *Cry2A*∗ genes compared with MH63 (*Oryza sativa*) under different nitrogen levels. *Field Crop Res.* 151, 101–106. doi: 10.1016/j.fcr.2013.06.017

Johns, C. V., Beaumont, L. J., and Hughes, L. (2003). Effects of elevated CO_2 and temperature on development and consumption rates of *Octotoma championi* and *O. scabripennis* feeding on *Lantana camara*. *Entomol. Exp. Appl.* 108, 169–178. doi: 10.1046/j.1570-7458.2003.00076.x

Johnson, S. N., and Hartley, S. E. (2018). Elevated carbon dioxide and warming impact silicon and phenolic-based defences *differently* in native and exotic grasses. *Glob. Change Biol.* 24, 3886–3896. doi: 10.1111/gcb.13971

Jung, S. C., Martinez-Medina, A., Lopez-Raez, J. A., and Pozo, M. J. (2012). Mycorrhiza-induced resistance and priming of plant defenses. *J. Chem. Ecol.* 38, 651–664. doi: 10.1007/s10886-012-0134-6

Keymer, D. P., and Lankau, R. A. (2017). Disruption of plant-soil-microbial relationships influences plant growth. *J. Ecol.* 105, 816–827. doi: 10.1111/1365-2745.12716

Kretzschmar, F. D. S., Aidar, M. P. M., Salgado, I., and Braga, M. R. (2009). Elevated CO_2 atmosphere enhances production of defense-related flavonoids in soybean elicited by no and a fungal elicitor. *Environ. Exp. Bot.* 65, 319–329. doi: 10.1016/j.envexpbot.2008.10.001

Lawo, N. C., Wäckers, F. L., and Romeis, J. (2010). Characterizing indirect prey-quality mediated effects of a *Bt* crop on predatory larvae of the green lacewing, *Chrysoperla carnea*. *J. Insect Physiol.* 56, 1702–1710. doi: 10.1016/j.jinsphys.2010.06.012

Li, Z., Parajulee, M. N., and Chen, F. J. (2018). Influence of elevated CO_2 on development and food utilization of armyworm *Mythimna separata* fed on transgenic *Bt* maize infected by nitrogen-fixing bacteria. *PeerJ* 6:5138. doi: 10.7717/peerj.5138

Liu, Q. S., Hallerman, E., Peng, Y. F., and Li, Y. H. (2016). Development of *Bt* rice and *Bt* maize in China and their efficacy in *target* pest control. *Int. J. Mol. Sci.* 17:1561. doi: 10.3390/ijms17101561

Liu, Y. M., Dang, Z. H., Parajulee, M. N., and Chen, F. J. (2019). Interactive effects of [CO_2] and temperature on plant *chemistry* of transgenic *Bt* rice and population dynamics of a non-target planthopper, *Nilaparvata lugens* (Stål) under different levels of soil nitrogen. *Toxins* 11:261. doi: 10.3390/toxins11050261

Marschner, H., and Dell, B. (1994). Nutrient uptake in mycorrhizal symbiosis. *Plant Soil* 159, 89–102. doi: 10.1007/BF00000098

Mcgonigle, T. P., Evans, D. G., and Miller, M. H. (1990). Effect of degree of soil disturbance on mycorrhizal colonization and phosphorus absorption by maize in growth chamber and field experiments. *New Phytol.* 116, 629–636. doi: 10.1111/j.1469-8137.1990.tb00548.x

Pachauri, R. K., and Reisinger, A. (2014). *Climate Change 2014: Synthesis Report*. Contribution of Working Groups I, II and III to the fifth assessment report of the Intergovernmental Panel on Climate Change. IPCC.

Phillips, J. M., and Hayman, D. S. (1970). Improved procedures for clearing roots and staining parasitic and vesicular-arbuscular mycorrhizal fungi for rapid assessment of infection. *Q. Rev. Biol.* 55, 158–161. doi: 10.1016/S0007-1536(70)80110-3

Prutz, G., and Dettner, K. (2005). Effects of transgenic *Bacillus thuringiensis*-maize on larval food consumption, utilization and growth in the grass-moth species *Chilo partellus* under laboratory conditions (Lepidoptera: Crambidae). *Entomol. Gen*. 28, 161–172. doi: 10.1111/j.0013-8703.2005.00229.x

Rao, M. S., Srinivas, K., Vanaja, M., Manimanjari, D., Rama Rao, C. A., and Venkateswarlu, B. (2013). Response of multiple generations of semilooper, *Achaea janata* feeding on castor to elevated CO_2. *J. Environ. Biol.* 34, 877–883. doi: 10.1177/1363459312465973

Riddick, E. W., Dively, G., and Barbosa, P. (1998). Effect of a seed-mix deployment of *Cry3A*-transgenic and nontransgenic potato on the abundance of *Lebia grandis* (Coleoptera: Carabidae) and *Coleomegilla maculata* (Coleoptera: Coccinellidae). *Ann. Entomol. Soc. Am.* 91, 647–653. doi: 10.1093/aesa/91.5.647

Rillig, M. C., and Mummey, D. L. (2006). Mycorrhizas and soil structure. *New phytol.* 171, 41–53. doi: 10.2307/3694482

Rodriguez, A., and Sanders, I. R. (2015). The role of community and population ecology in applying mycorrhizal fungi for improved food security. *ISME J.* 9, 1053–1061. doi: 10.1038/ismej.2014.207

Ruess, L., and Chamberlain, P. M. (2010). The fat that matters: soil food web analysis using fatty acids and their carbon stable isotope signature. *Soil Biol. Biochem*. 42, 1898–1910. doi: 10.1016/j.soilbio.2010.07.020

Sharifi, M., Ghorbanli, M., and Ebrahimzadeh, H. (2007). Improved growth of salinity-stressed soybean after inoculation with salt pre-treated mycorrhizal fungi. *J. Plant Physiol.* 164, 1144–1156. doi: 10.1016/j.jplph.2006.06.016

Smith, S. E., and Read, D. J. (2008). Mycorrhizal symbiosis. *Q. Rev. Biol.* 3, 273–281. doi: 10.1016/B978-012370526-6.50018-0

Song, Y. Y., Liu, J. W., and Chen, F. J. (2020). Azotobacter chroococcum inoculation can improve plant growth and resistance of maize to armyworm, *Mythimna separata* even under reduced nitrogen fertilizer application. *Pest Manag. Sci.* 76, 4131–4140. doi: 10.1002/ps.5969

Stange, G. (1997). Effects of changes in atmospheric carbon dioxide on the location of hosts by the moth, *Cactoblastis cactorum*. *Oecologia* 110, 539–545. doi: 10.2307/4221642

Stiling, P., and Cornelissen, T. (2007). How does elevated carbon dioxide (CO_2) affect plant–herbivore interactions? A field experiment and meta-analysis of CO_2-mediated changes on plant chemistry and herbivore performance. *Glob. Change Biol.* 13, 1823–1842. doi: 10.1111/j.1365-2486.2007.01392.x

Sun, Y. C., Guo, H. J., and Ge, F. (2016). Plant–aphid interactions under elevated CO_2: some cues from aphid feeding behavior. *Front Plant Sci.* 7:502. doi: 10.3389/fpls.2016.00502

Sun, Y. C., Guo, H. J., Zhu-Salzman, K., and Ge, F. (2013). Elevated CO_2 increases the abundance of the peach aphid on Arabidopsis by reducing jasmonic acid defenses. *Plant Sci*. 210, 128–140. doi: 10.1016/j.plantsci.2013.05.014

Terrer, C., Vicca, S., Hungate, B. A., Phillips, R. P., and Prentice, I. C. (2016). Mycorrhizal association as a primary control of the CO_2 fertilization effect. *Science* 353, 72–74. doi: 10.1126/science.aaf4610

Treseder, K. K. (2004). A meta-analysis of mycorrhizal responses to nitrogen, phosphorus, and atmospheric CO_2 in field studies. *New Phytol*. 164, 347–355. doi: 10.1111/j.1469-8137.2004.01159.x

Turrini, A., Bedini, A., Loor, M. B., Santini, G., Sbrana, C., Giovannetti, M., et al. (2017). Local diversity of native arbuscular mycorrhizal symbionts differentially affects growth and nutrition of three crop plant species. *Biol. Fert. Soils* 54, 203–217. doi: 10.1007/s00374-017-1254-5

Wang, L., Li, L. K., Song, Y. Y., Han, T., Li, Z., Wan, G. J., et al. (2018). Elevated CO_2 and temperature alter *specific*-species population dynamic and interspecific competition of three wheat aphids. *J. Appl. Entomol*. 142, 863–872. doi: 10.1111/jen.12536

Wu, G., Chen, F. J., Ge, F., and Xiao, N. W. (2011a). Impacts of elevated CO_2 on expression of plant defensive compounds in *Bt*-transgenic cotton in response to infestation by cotton bollworm. *Agric. For. Entomol*. 13, 77–82. doi: 10.1111/j.1461-9563.2010.00508.x

Wu, G., Chen, F. J., Xiao, N. W., and Ge, F. (2011b). Influences of elevated CO_2 and pest damage on the allocation of plant defense compounds in *Bt*-transgenic cotton and enzymatic activity of cotton aphid. *Insect Sci*. 18, 401–408. doi: 10.1111/j.1744-7917.2011.01429.x

Wu, K. M., Lu, Y. H., Feng, H. Q., Jiang, Y. Y., and Zhao, J. Z. (2008). Suppression of cotton bollworm in multiple crops in china in areas with Bt toxin-containing cotton. *Science* 321, 1676–1678. doi: 10.1126/science.1160550

Xu, Z. Z., Jiang, Y. L., and Zhou, G. S. (2015). Response and adaptation of photosynthesis, respiration, and antioxidant systems to elevated CO_2 with environmental stress in plants. *Front. Plant Sci.* 6:701. doi: 10.3389/fpls.2015.00701

Yao, Z. S., Wang, R., Zheng, X. H., Mei, B. L., Zhou, Z. X., Xie, B. H., et al. (2020). Elevated atmospheric CO_2 reduces yield-scaled N_2O fluxes from subtropical rice systems: six site-years field experiments. *Glob. Change Biol.* 27, 327–339. doi: 10.1111/gcb.15410

Yin, J., Sun, Y. C., and Wu, G. (2010). Effects of elevated CO_2 associated with maize on multiple generations of the cotton bollworm, *Helicoverpa armigera*. *Entomol. Exp. Appl.* 136, 12–20. doi: 10.1111/j.1570-7458.2010.00998.x

Yu, T., and Chen, Y. (2019). Effects of elevated carbon dioxide on environmental microbes and its mechanisms: a review. *Sci. Total Environ*. 655, 865–879. doi: 10.1016/j.scitotenv.2018.11.301

Zeng, H., Zhong, W., Tan, F., Shu, Y., Feng, Y., and Wang, J. (2018). The influence of Bt maize cultivation on communities of arbuscular mycorrhizal fungi revealed by MiSeq sequencing. *Front Microbiol*. 9:3275. doi: 10.3389/fmicb.2018.03275

Zhu, C. W., Kobayashi, K., Loladze, I., Zhu, J. G., Jiang, Q., Xu, X., et al. (2018). Carbon dioxide (CO_2) levels this century will alter the protein, micronutrients, and vitamin content of rice grains with potential health consequences for the poorest rice-dependent countries. *Sci. Adv.* 4:eaaq1012. doi: 10.1126/sciadv.aaq1012

Conflict of Interest: The authors declare that the research was conducted in the absence of any commercial or financial relationships that could be construed as a potential conflict of interest.

frontiers in Plant Science

ORIGINAL RESEARCH
published: 17 June 2021
doi: 10.3389/fpls.2021.651152

Systematic Investigation of the Effects of Seven Plant Extracts on the Physiological Parameters, Yield, and Nutritional Quality of Radish (*Raphanus sativus* var. *sativus*)

Katarzyna Godlewska[1], Paweł Pacyga[2], Izabela Michalak[3], Anita Biesiada[1], Antoni Szumny[4], Natalia Pachura[4] and Urszula Piszcz[5]*

[1] Department of Horticulture, Faculty of Life Sciences and Technology, Wrocław University of Environmental and Life Sciences, Wrocław, Poland, [2] Department of Energy Technologies, Turbines, and Modeling of Heat-Flow Processes, Faculty of Mechanical and Power Engineering, Wrocław University of Science and Technology, Wrocław, Poland, [3] Department of Advanced Material Technologies, Faculty of Chemistry, Wrocław University of Science and Technology, Wrocław, Poland, [4] Department of Chemistry, Faculty of Biotechnology and Food Science, Wrocław University of Environmental and Life Sciences, Wrocław, Poland, [5] Department of Plant Nutrition, The Faculty of Life Sciences and Technology, Wrocław University of Environmental and Life Sciences, Wrocław, Poland

OPEN ACCESS

Edited by:
Youssef Rouphael, University of Naples Federico II, Italy

Reviewed by:
Petronia Carillo, University of Campania Luigi Vanvitelli, Italy
Spyridon Alexandros Petropoulos, University of Thessaly, Greece

***Correspondence:**
Katarzyna Godlewska
katarzyna.godlewska@upwr.edu.pl

Specialty section:
This article was submitted to Crop and Product Physiology, a section of the journal Frontiers in Plant Science

Received: *11 January 2021*
Accepted: *17 May 2021*
Published: *17 June 2021*

Citation:
Godlewska K, Pacyga P, Michalak I, Biesiada A, Szumny A, Pachura N and Piszcz U (2021) Systematic Investigation of the Effects of Seven Plant Extracts on the Physiological Parameters, Yield, and Nutritional Quality of Radish (Raphanus sativus var. sativus). Front. Plant Sci. 12:651152. doi: 10.3389/fpls.2021.651152

The modern agricultural sector faces the challenge of addressing the needs of the fast-growing global population. This process should be both high-yielding and sustainable, without creating risks for the environment and human health. Therefore, natural products are gaining attention in the production of safe and nutritious food. In a systematic effort to develop affordable and effective biostimulants, we examined the impact of botanical extracts on the growth and physiological parameters of radish plants under field conditions. Ultrasound-assisted extraction, mechanical homogenization, and water were used for the production of potential plant-based biostimulants. Foliar applications of the bio-products, developed and used in our study, have led to an increase in the examined parameters (total yield, dry weight, photosynthetic pigments, vitamin C, nitrates, and micro- and macroelements). A decrease in the total phenolic compounds content was also noted, as well as a varied impact on the steam volatile compounds, fatty acids, sterol, and glucosinolates composition. The most beneficial effects on radish, in terms of physiological and biochemical properties, were found in groups treated with extracts based on the common dandelion, valerian, and giant goldenrod. This innovative approach presented in our study could provide a valuable tool for sustainable horticultural production.

Keywords: higher plants, extraction, bioactive compounds, radish, yield, nutritional quality, sustainable food production

INTRODUCTION

Globally, agriculture and horticulture constitute a multitrillion dollar industry. This sector provides a wide variety of crops for food, feed, and ornamental purposes (Zulfiqar et al., 2019). Due to the exponentially growing population, limited available farmland, genetic potential of crops, depletion of natural resources, and climate change, agribusiness is facing the challenge of devising more

effective and sustainable solutions to facilitate the reduction of malnutrition, poverty, starvation, and energy and water usage while concurrently increasing the yield and the quality of crops (Campos et al., 2019; Pereira et al., 2019; Szparaga et al., 2019; Zulfiqar et al., 2019; Kamble et al., 2020). The Green Revolution implemented in the 1960s was characterized by large increases in crop yields due to the extensive use of pesticides and fertilizers (Pereira et al., 2019; Rose et al., 2019). The long-standing excess usage of these products has led to serious threats to human health and the environment worldwide (e.g., ground water and air pollution, water eutrophication, and soil quality degradation) (Ertani et al., 2014; Vejan et al., 2016; Campos et al., 2019; Costa et al., 2019; Ekin, 2019; Pereira et al., 2019; Shang et al., 2019; Shukla et al., 2019; Zulfiqar et al., 2019). On the other hand, these products have been necessary to satisfy the growing human demand for food. Furthermore, the overuse of fertilizers has increased the cost of production and reduced the profit margins for farmers (Zulfiqar et al., 2019). Climate change and unfavorable growing conditions can increase plant susceptibility to pathogens (Shukla et al., 2019). Consequently, the establishment of sustainable principles, strategies, technological advancements, and innovations (Pereira et al., 2019; Shang et al., 2019) is crucial to enhance the effectiveness of fertilizers, to meet the requirements of environmentally friendly crop management practices, and to cope with high productivity demands (Bulgari et al., 2015; Paradiković et al., 2018; Ekin, 2019; Shang et al., 2019; Shukla et al., 2019). Crop resistance to diseases, soil salinity, drought, heavy metals, as well as their increased nutritional value are getting highly desirable (Vejan et al., 2016; Bulgari et al., 2019).

Bio-based products (including crop residues, plants, and seaweed), applied at low doses, may be a promising solution to diminish fertilizer rates and simultaneously exert beneficial effects on plant growth (Ertani et al., 2014). Biostimulants have become more popular in sustainable agriculture in recent years because of their beneficial properties. They stimulate various physiological processes that promote nutrient acquisition and utilization by plants; enhance the root development (the length and number of root hairs), shoot development, yield, and nutritional quality of plants; counteract the effects of biotic and abiotic stresses; improve the activity of soil microbiota; and reduce the use of fertilizers and the content of undesirable compounds (e.g., nitrates and heavy metals) in cultivated plants (Ertani et al., 2014; Bulgari et al., 2015; Paradiković et al., 2018; Rouphael et al., 2018; Szparaga et al., 2018; Carillo et al., 2019a,b; Ekin, 2019; Shukla et al., 2019; Cozzolino et al., 2020). The effects of biostimulants may differ, depending on the plant species (e.g., different leaf permeability levels), cultivar, physiological stages, type of product, dose, concentration, time, and application method (e.g., foliar, soil drench, or seed treatment), as well as environmental conditions (Ertani et al., 2014; Bulgari et al., 2015; Paradiković et al., 2018; Szparaga et al., 2018). In the European Union, the countries of France, Italy, and Spain are the primary producers of biostimulants. As reported by Grand View Research, Inc., the market size of these products is projected to be worth approximately USD 4.14 billion by 2025 (Bulgari et al., 2019). According to the new European Union Regulation, 2019/1009, plant biostimulants are defined on the basis of their agricultural impacts on crops. They may contain protein hydrolysates, humic substances, algal and botanical extracts, inorganic compounds (e.g., Si), growth-promoting bacteria, mycorrhizal fungi (D'Addabbo et al., 2019; Cozzolino et al., 2020), amino acids, chitin, chitosan, vitamins, and poly- and oligosaccharides (Bulgari et al., 2015). The beneficial effects of biostimulants are not associated with their macro– and micronutrient composition but rather with their content of activating compounds, like endogenous hormones, small peptides, free amino acids, phenolics, and triacontanol (Ertani et al., 2014; Yakhin et al., 2017), which may affect plant metabolisms by triggering glycolysis enzyme activities, the Krebs cycle, and nitrate assimilation (Ertani et al., 2009; Colla et al., 2015, 2017; Yakhin et al., 2017; Palumbo et al., 2018; Sandhu et al., 2018; Alfosea-Simón et al., 2020; Cozzolino et al., 2020; Francesca et al., 2020). On the other hand, if their biological activity depends on the presence of natural plant hormones, they ought to be classified as plant growth regulators (Bulgari et al., 2015). The hormonal activity of plants can alter the electrochemical gradient of protons formed across the cell membrane through proton pump modulation (Paradiković et al., 2018). By virtue of the complexity of biostimulants' composition, it is difficult to assign their beneficial effects on plants to a particular compound, especially when that compound may interact with other molecules in a synergistic way (Bulgari et al., 2015, 2019). Hence, their mechanism of action is still not well-understood, and these types of products should be categorized based on the physiological responses of plants (Bulgari et al., 2015).

In recent years, numerous reports have highlighted the beneficial effects of biostimulants applications in the worldwide cultivation of various crops, especially for achieving higher yields. New research should focus not only on short-term studies of young seedlings but also on real field conditions with mature plants (Ertani et al., 2014). Nevertheless, the impact of the application of bio-products on the nutritional value and health-promoting potential of plants is not well-documented but has been observed in several crops (Kocira, 2019; Cocetta and Ferrante, 2020). Many of these compounds exhibit a favorable impact on the health-related characteristics of vegetables and fruits (Cocetta and Ferrante, 2020)—for example, the presence of antioxidants imparts nutraceutical properties to plant products (Kocira, 2019). Presently, fruits, vegetables, and edible flowers rich in phytonutrients (plant-derived substances; neither vitamins nor minerals) are gaining more attention both among scientists and consumers. These are usually plant secondary metabolites (synthesized from primary metabolites) and are involved in various mechanisms, e.g., in plant interaction with the environment, defense responses to stresses (by serving as phytoalexins, antioxidants, and signal molecules), as well as to deter animals or, conversely, to attract them to spread seeds or pollinate flowers (due to their anthocyanin content). These compounds often function as antioxidants; they increase the antioxidant potential of fruits, vegetables, and flowers, and they obstruct oxidative reactions under stress conditions (Bulgari et al., 2015). A diet low in fruits and vegetables is associated with an increased risk of various debilitating nutritional diseases. As

reported by the Global Burden of Disease Study, a low intake of fruits can be attributed to 3.4 million deaths, while low vegetable consumption was estimated to cause 1.8 million demises globally (Bulgari et al., 2019). Presently, healthy lifestyles and high-quality foods are piquing a growing interest among consumers. Therefore, there is a need to develop new, cheaper products for use in organic agriculture to enable greater access to more affordable and eco-friendly food (Kowalski and Kaniszewski, 2017).

Radish (*Raphanus sativus* var. *sativus*) was chosen as a model plant in the present study. There are numerous radish cultivars differing in shape (round, oval, icicle, half long, long, conical, cylindrical, spindle), color (white, pink, red, purple, black), flavor, and growing conditions (Paul et al., 2016; Dhaliwal, 2017). Radish is widely cultivated due to its taste and low content of calories but high nutrients (e.g., K, Fe, Ca, Na, Zn, Mn, P, vitamins C and B, folic acid, fiber) (Paul et al., 2016; Banihani, 2017; Dhaliwal, 2017; Kowalski and Kaniszewski, 2017). This root vegetable is valued for the presence of phytochemicals, especially glucosinolates, which are hydrolyzed into bioactive compounds (e.g., isothiocyanates, nitriles, thiocyanates, epithionitriles, and oxazolidinethiones) that are of use to plants (e.g., for defense) and human health. The consumption of radish has been shown to lower the risk of different types of cancers (e.g., breast, colon, lung, stomach, prostate, pancreas, and rectal cancer), as well as supports the prevention of constipation, stone formation, and jaundice (Paul et al., 2016; Banihani, 2017; Dhaliwal, 2017; Manivannan et al., 2019). Radish also exhibits antimicrobial, anticancer, antioxidant, and anxiety-reducing properties (Manivannan et al., 2019). In Poland, the cultivation area of radish is estimated at 700 ha and field cultivation accounts for one-third of the whole area (Chohura and Kołota, 2011). Due to the low light in the autumn–spring period, the overaccumulation of nitrates in plant tissues may sometimes be a problem (Kowalski and Kaniszewski, 2017).

Hence, our current study aimed to determine the possibility of transforming higher plants that are widely found in Europe (herbs of St. John's wort, leaves of giant goldenrod, flowers and leaves of common dandelion, flowers of red clover, leaves of nettle, and roots of valerian) into low-cost products that are rich in bioactive compounds for use in modern horticulture to achieve higher yield, quality, and profitability. Ultrasound-assisted extraction (UAE) and mechanical homogenization (MH) were used for the production of potential water-based biostimulants. The selected raw materials were not previously used for these purposes.

MATERIALS AND METHODS

All analyses were carried out according to the methodology provided by Godlewska et al. (2020b). Brief descriptions of our methodology are presented below.

Raw Materials for the Botanical Extract Production

This study assessed the potential of using higher plants for the production of plant-based extracts. The raw materials collection date depended on the plant part used for the extraction and the plant developmental stage. They were collected/purchased once in 2017 in the amount needed to carry out all planned research. The extraction of biologically active compounds from St. John's wort (*Hypericum perforatum* L.; herb) (marked as: Hp H), giant goldenrod (*Solidago gigantean* Ait.; leaf) (Sg L), common dandelion (*Taraxacum officinale* (L.) Weber ex F.H. Wigg; flower, leaf) (To F, To L), red clover (*Trifolium pretense* L.; flower) (Tp F), nettle (*Urtica dioica* L.; leaf) (Ur L), and valerian (*Valeriana officinalis* L.; root) (Vo R) was performed using ultrasound-assisted extraction (UAE) and mechanical shearing combined with sonic energy (MH). For the first method, the dried and ground biomass was mixed with deionized water (1:20 *w*/*v*), soaked (30 min), subsequently sonicated (30 min), and then centrifuged (10 min, 4,500 rpm). For the second method (MH), the mixture was homogenized (1 min, 28,000 rpm) and centrifuged (10 min, 4,500 rpm). The final bioactive formulations were composed of an active ingredient (extract, 0.5% *w*/*v*), an antioxidant agent (L-ascorbic acid, 0.15% *w*/*v*), an adjuvant (Protector, 0.02% *w*/*v*), a preservative (potassium sorbate, 0.1% *w*/*v*), and water (up to 100%).

The Field Trials

The radish (*Raphanus sativus* var. *sativus*) was grown in the field under a temperate climate in Poland (**Supplementary Figure 1**). Hydrocomplex Yara Mila (250 $kg{\cdot}ha^{-1}$) and ammonium saltpetre (330 $kg{\cdot}ha^{-1}$) were used for the fertilization of the fine clay soil (pH 7.05, EC 144.3 $\mu S{\cdot}cm^{-1}$, 1.8% humus, 35.1 mg P, 89.5 mg K, and 44 mg Mg in 1 dm^3). The experiments were performed in randomized complete blocks. Seeds (cultivar "Carmen," PlantiCo) were sown on August 20, 2018, with spacing of 20 cm × 4 cm (plot size: 1 m^2; 125 plants per plot; 3 plots per treatment). The spraying, at a dose of 300 $L{\cdot}ha^{-1}$, was performed three times in the morning on sunny and windless days (September 5, September 12, and September 19, 2018). Plants were harvested on September 24, 2018. During the growing season, regular mechanical weeding and irrigation were conducted. Moreover, the insecticide (Karate Zeon 050 CS) was applied in accordance with the manufacturer's recommendations. Plant samples were collected twice: 7 days after the second spraying (the first term of leaves of rosette collection) and after harvesting (the second term of leaves of rosette and root collection) to perform chemical analyses. As the control groups, we used plants sprayed with water (C), a formulation with water without an active ingredient (CF), and a commercial biostimulant (CB).

Chemicals

Acetone, calcium carbonate, ethanol, potassium persulphate, sodium acetate, and sodium carbonate were purchased from IDALIA (Radom, Poland); azino-bis-3-ethylbenzthiazoline-6-sulphonic acid (ABTS), diphenyl-2-picrylhydrazyl (DPPH), ferric-reducing antioxidant power (FRAP), Folin–Ciocalteu's phenol reagent, gallic acid, tripyridyl-S-triazine (TPTZ), and Trolox were purchased from Archem (Łany, Poland); acetic acid, activated carbon, ammonium metavanadate, ammonium molybdate tetrahydrate, ascorbic acid, barium chloride dihydrate, cyclohexane, magnesium nitrate, 65% nitric

acid, oxalic acid, sodium bicarbonate, and sodium sulfate were purchased from CHEMPUR (Piekary Śląskie, Poland); 2,6-dichlorophenolindophenol sodium salt hydrate was purchased from ACROS ORGANICS (ARGENTA; Poznań, Poland); chloroform, hydrochloric acid (38%), and methanol were purchased from STANLAB (Lublin, Poland); standard solutions and Tween TM 80 were purchased from Merck (Darmnstadt, Germany); 2-undecanone and BF_3/MeOH were purchased from Sigma-Aldrich (Saint Louis, MO, USA); hexane and sodium bicarbonate were purchased from UQF (Wrocław, Poland); n-hexane (99%) was purchased from POCH Basic (Gliwice, Poland); helium was purchased from Air Products (Warsaw, Poland); and potassium hydroxide was purchased from Avantor (Gliwice, Poland).

The Photosynthetic Pigments, Greenness Index of the Leaves, and Leaf Color

The contents of chlorophyll $a + b$ and carotenoids were determined in fresh leaves. Samples (0.4 g) were disintegrated, using a mortar and a pestle with the addition of a few drops of acetone (80%), a pinch of sand, and calcium carbonate. The obtained mixture was filtered, transferred to a volumetric flask (50 ml) and filled with acetone. The absorbances were measured in four replicates at 663, 645, and 470 nm with the use of a spectrophotometer (HACH DR1900, Berlin, Germany). The greenness indexes of the leaves were evaluated, using an SPAD 502 Plus Chlorophyll Meter (Konica Minolta, Osaka, Japan), and the colors of the leaves were measured, using MiniScan (Hunter Lab EZ, Reston, Virginia, USA) (in 10 replicates).

Vitamin C

For determination of the vitamin C content, the fresh leaves (∼10 g) and roots (∼15 g) were homogenized in oxalic acid (200 ml, 2%) and filtrated. Solutions (10 ml) were titrated (in four replicates) with Tillmans' reagent as long as a light pinkish color appeared and was maintained for at least 30 s.

Total Phenolic Compounds

The total phenolic compound (TPC) content was evaluated in fresh, comminuted shoots and roots (∼2 g). The biomasses were placed in tubes, mixed with aqueous methanol (20 ml, 80%), sonicated (15 min), and centrifuged (10 min, 4,500 rpm). To the obtained supernatants (0.1 ml), the Folin–Ciocalteu's phenol reagent (0.2 ml) and distilled water (2 ml) were added, and the mixtures were kept in the dark (3 min). Next, sodium carbonate (1 ml, 20%) was added to the reaction mixtures and left in the dark for 1 h. The absorbance (765 nm) was then assessed (in four replicates).

The Antioxidant Activity (DPPH, ABTS, and FRAP Assays)

The antioxidant activities were assessed in ten-fold diluted supernatants prepared for TPC analyses. The absorbance measurements were made in four replicates.

For the DPPH assay, supernatants (0.5 ml), ethanol (1.5 ml), and DPPH solution (0.5 ml) were mixed and incubated at room temperature without access to light (10 min). The radical stock solution of DPPH was freshly prepared by dissolving in ethanol.

For the ABTS assay, a diluted ABTS solution (3 ml) was added to the supernatants (30 μl) and kept in the dark (6 min). The $ABTS^{\bullet+}$ solution was prepared by the reaction of aqueous ABTS solution (5 ml, 7 mM) with potassium persulfate solution (88 μl, 140 mM). The mixture was incubated in the dark at 29°C for more than 14 h.

For the FRAP assay, supernatants (1 ml) and FRAP reagent (3 ml) were left to react (10 min). The FRAP reagent was prepared by mixing the acetate buffer (300 mM), TPTZ (10 ml in 40 mM HCl) and $FeCl_3 \cdot 6H_2O$ (20 mM) in a ratio of 10:1:1.

For the DPPH assay, the absorbance was measured at 517 nm; for the ABTS assay, the absorbance was measured at 734 nm; and for the FRAP assay, the absorbance was measured at 593 nm.

Nitrates

For the assessment of nitrates, the dried and ground samples (0.4 g) were mixed with acetic acid (100 ml, 2%) and activated carbon (0.5–1 g), shaken (30 min, 150 rpm), and filtrated (the first drops were not collected). An ionometer (Thermo 5 Star Orion, Beverly, MA, USA) with an ion-selective electrode was used for the measurements.

Macroelements, Microelements, and Heavy Metals

For the macroelement (Ca, K, Mg, P), microelement (Cu, Fe, Mn, Zn), and heavy metal (Ni, Cd, Pb) content evaluations, the dried and ground samples were mineralized (450°C, 8 h) in the oven (CZYLOK, Jastrzębie-Zdrój, Poland); then, the ash was digested (65% HNO_3) and evaporated on a heating plate (110°C, 6 h), dissolved (1 M HNO_3), and transferred to a flask. The phosphorus content of P was determined colorimetrically at 400 nm after a reaction with molybdate and ammonium metavanadate (Cecil CE 2011 photometer; Cambridge, UK). Atomic absorption spectrophotometry (ASA) (Varian Spectra AA 220/FS, Mulgrave, Australia) was used for the determination of the K, Ca, Mg, Mn, Fe, Cu, Zn, Cd, Pb, and Ni content. The S content was examined according to the oxidation of sulfur-based on the turbidity of the solution of sulfate content precipitating as barium sulfate (Cecil CE 2011 photometer; Cambridge, UK). The N content was examined by the Kjeldahl method. The samples were mineralized in concentrated H_2SO_4 with the addition of Se and H_2O_2. The cooled solution was mixed with a strong base solution, and the emitted ammonia was distilled into a saturated boric acids solution with the addition of a mixed indicator (methyl red and bromocresol green). The solution of ammonia in boric acid was determined by titration with a standard hydrochloric acid solution (0.01 M) until an initial color was obtained.

Steam Volatile Compounds

For the steam volatile compounds analyses (the amount of a single component calculated as a percentage (%) of the whole GC-MS chromatogram area), the frozen leaves (30 g) were placed in flasks and boiled with distilled water (100 ml) in a

heating mantle. The cyclohexane (1 ml), containing 1 mg of 2-undecanone, was used as an internal standard. A distillation process (50 min) was performed, using a Deryng apparatus (Szczepanik et al., 2018). The chromatographic analyses (GCMS QP 2020, Shimadzu, Kyoto, Japan) were carried out in three replicates.

Fatty Acids

For the preparation of the lipid fraction (the amount of a single component calculated as a percentage (%) of the whole GC-MS chromatogram area), the dried roots (350 mg) were macerated with chloroform (5 ml), filtered, and evaporated. The extracted non-polar lipid fraction (25 mg) was saponified (5 min at 65°C) with 0.5 M KOH/MeOH solution (2 ml), and subjected to methylation (10 min at 65°C) by adding 14% (*v*/*v*) BF_3/MeOH (2 ml). In the next step, distilled water (5 ml) was added, and the methyl esters of fatty acids were extracted with hexane (10 ml). The mixture was then washed with 10% sodium bicarbonate (10 ml) and dried over anhydrous sodium sulfate. The organic phase was evaporated under reduced pressure and dissolved in hexane (200 μl). The gas chromatograph coupled with a mass spectrometer (Shimadzu GCMS QP 2020) was used to analyze the profiles of fatty acid methyl esters (in three replicates).

Sterols

A dried radish root (300 mg) was macerated with chloroform (5 ml). The sterol profile was evaluated, using the method of derivatization with N, O-Bis(trimethylsilyl)trifluoroacetamide (BSTFA) silylation via GC-MS (Shimadzu QP 2020, Shimadzu, Kyoto, Japan). The solution was filtered and then evaporated on a vacuum evaporator under reduced pressure. Next, pyridine (500 μl) and BSTFA (50 μl) were added to the sample. The mixture was then transferred to a vial and heated for 15 min at 70°C. Separation was achieved using a Zebron ZB-5 capillary column (30 m, 0.25 mm, 0.25 μm; Phenomenex, Torrance, CA, USA). The parameters of the GC-MS analysis were as follows: a scan mode with a mass range from 40 to 1,050 *m*/*z* in the electronic impact (EI) mode at 70 eV with the 10 scan s^{-1} mode. Helium was used as a carrier gas at a flow rate of 1 ml·min^{-1} in a split ratio of 1:20, along with the following program: (a) 100°C for 1 min; (b) a rate of 2°C min^{-1} from 100 to 190°C; and (c) a rate of 5°C min^{-1} from 190 to 300°C. The injector was maintained at 280°C. Identification of the compounds was performed, using two different analytical methods to compare the retention times with those of authentic chemicals (Supelco C7–C40 Saturated Alkanes Standard), and the mass spectra were obtained with the available library data (Willey NIST 17, match index > 90%).

Glucosinolates

Freeze-dried samples of radish roots (0.5 g) were extracted with 90% methanol (10 ml, 30 min, 70°C, shaken every 5 min). After this process, the samples were filtered and centrifuged (10 min, 15,000 rpm). The supernatants were separated; methanol was evaporated from the mixtures. Then, the samples were dissolved in water (1 ml), and the LC-MS analyses were carried out by means of reversed-phase high-performance liquid chromatography (HPLC Shimadzu Prominence-i LC-2030C, Kyoto, Japan), equipped with a PDA detector coupled to a triple quadrupole mass spectrometer (Shimadzu LCMS-8045). Glucosinolates present in the radish roots were semi-quantified, using the LC-MS-tq apparatus in the MRMs mode (**Table 1**). The separation of the desired compounds was performed, using the following mobile phase: water with 0.1% TFA (eluent A) and acetonitrile with 0.1% TFA (eluent B). The flow rate was set at 0.25 ml·min^{-1}, and the gradient was as follows: starting at 1% solvent B for 3 min, then reaching 20% up to 20 min, 30% up to 23 min, and 0.1% B at 35 min. The Kinetex C18 100A column (100 × 3 mm, 2.6 μm particle size, Phenomenex, Germany) was used. Singrin was used as an external standard (Ciska et al., 2000; Ediage et al., 2011; Maldini et al., 2017).

Statistical Analyses

The STATISTICA program ver. 13.3 (TIBCO Software Inc., Tulsa, OK, USA) was used for the statistical analyses of the results. The normality of the distribution was assessed, using the Shapiro–Wilk test and homogeneity of variances by the Brown–Forsythe test. For the normal distribution and homogeneity of variances, differences were evaluated, using the Tukey's Honest Significant Difference (HSD) test. The data were significantly different for $p < 0.05$. For distributions other than normal, the Kruskal–Wallis test was used. An "a" was used to indicate statistically significant differences between the botanical extracts and water (C), "b" indicates a significant difference between the botanical extracts and the formulation (CF), and "c" indicates a significant difference between the botanical extracts and the commercial biostimulant (CB).

RESULTS

Total Yield, Fresh, and Dry Weight of Leaves of Rosette and Roots

In our experimental design, the first control group contained plants that were sprayed with water (C), the second one included plants sprayed with the formulation in water (without an active ingredient—extract) (CF), and the third one included plants sprayed with the commercial biostimulant (CB).

The application of all botanical extracts significantly increased the total yield of radish (**Table 2**). The highest root yield was achieved in the groups treated with To L MH and Sg L MH (81.2 and 80.6% more than in C and 24.9 and 24.5% more than in CB, respectively), while the lowest yield was found with Ur L MH and Ur L UAE (44 and 44.2% more than in C; 0.7 and 0.6% less than in CB). The largest yield of leaves of rosette was observed after the application of Sg L MH and Hp H MH (31.3 and 27.6% more than in C; 15.4 and 12.2% more than in CB), and the smallest was found for To F UAE and Ur L MH (2.7 and 7.2% more than in C; 9.7 and 5.4% less than in CB). Bio-products also promoted the growth of radish roots with diameters >4 cm (e.g., Tp F UAE: 10.2% more than in CB), as well as the aboveground parts (e.g., Hp H MH and Sg L UAE: 32.8 and 34% more than in CB). There were no plants of the aforementioned size in the control group (C). The least stimulating activity in this root range was noted after the use of Hp H UAE for roots (35.7% less than in CB) and Vo R UAE for leaves of rosette (8.2% less than in CB). The

TABLE 1 | A list of multiple reaction monitoring (MRM) transitions and mass spectrometric conditions used for the identification of glucosinolates in radish roots.

	RT, min	MRM transition *m/z* (Q1 → Q3)	Q1, V	CE, V	Q3, V
Glucoerucin	3.84	420.3 → 357.1	20.0	12.0	25.0
		420.3 → 330.0	20.0	17.0	15.0
		420.3 → 258.0	20.0	25.0	26.0
Gluconapin	4.27	372.3 → 354.1	18.0	14.0	24.0
		372.3 → 130.1	18.0	25.0	25.0
		372.3 → 127.9	18.0	22.0	24.0
Progoitrin	10.73	388.3 → 342.3	19.0	12.0	22.0
		388.3 → 128.5	19.0	22.0	25.0
		388.3 → 62.0	18.0	14.0	14.0
Glucoraphenin	11.76	434.3 → 388.2	15.0	11.0	26.0
		434.3 → 371.1	20.0	13.0	27.0
		434.3 → 344.0	21.0	18.0	24.0
4-metoxyglucobrassicin	15.56	476.5 → 386.2	23.0	18.0	26.0
		476.5 → 325.1	16.0	14.0	11.0
		476.5 → 313.9	23.0	25.0	21.0
Glucobrassicin	17.16	446.5 → 400.2	12.0	12.0	18.0
		446.5 → 428.2	21.0	13.0	15.0
		446.5 → 358.0	12.0	20.0	24.0
Glucoraphanin	18.25	435.5 → 399.2	21.0	13.0	27.0
		435.5 → 372.1	15.0	12.0	18.0
		435.5 → 273.2	15.0	24.0	17.0
Gluconasturtiin	18.41	421.6 → 358.1	20.0	12.0	24.0
		421.6 → 277.5	11.0	14.0	29.0
		421.6 → 146.1	19.0	30.0	28.0
Glucobrassicanapin	28.25	385.6 → 349.1	14.0	15.0	23.0
		385.6 → 233.1	18.0	21.0	22.0
		385.6 → 327.2	10.0	19.0	21.0

RT, retention time; Q1, parent ion; Q3, fragment ion; CE, collision energy.

heaviest average root weight with a diameter between 2 and 4 cm was found in the groups treated with To L MH (50.7 and 24.4% more than in C and CB) and Sg L MH (42.7 and 17.9% more than in C and CB), and the heaviest leaves were found for Hp H MH (35 and 14.9% more than in C and CB), Sg L MH (34.6 and 14.5% more than in C and CB), and Vo R MH (31.4 and 11.8% more than in C and CB). Decreased fresh weight was observed only in the leaves of rosette after the application of To F UAE (4.3 and 18.5% less than in C and CB). The highest average weight of the root with a diameter smaller than 2 cm was observed after spraying radish with Vo R MH (4.8% less than in C and 67% more than in CB) and Sg L MH (8.8% less than in C and 60% more than in CB), while the lowest was found with Ur L UAE (40.5% less than in C and 4.4% more than in CB). The heaviest weight of the aboveground parts within this root diameter was achieved after radish treatment with To F UAE (2.4% less than in C and 20.4% more than in CB) and Vo R MH (3.9% less than in C and 18.5% more than in CB), and the lowest was found with To L MH (30.4 and 14.1% less than in C and CB) and Ur L UAE (29.4 and 13% less than in C and CB). The application of Ur L UAE increased the dry weight of leaves of rosette (**Table 2**) in both the first and the second terms of the plant collection (7.5 and 8.3% more than in C; 17.2 and 10.9% more than in CB), while To L MH decreased the examined parameter (12.7 and 13.9% less than in C; 4.8 and 11.9% less than in CB). In the case of roots (**Table 2**), Ur L UAE increased the dry weight the most (37.9 and 51.8% more than in C and CB), and Sg L MH increased dry weight the least (7.3% less than in C and 2.1% more than in CB).

Photosynthetic Pigments, Greenness Index of the Leaves, and Leaf Color

An increase in the content of photosynthetic pigments in the cultivated plants treated with botanical extracts was observed in the first term of the sample collection but showed varying impacts in the second term. In the first term, the bio-product Vo R UAE particularly increased the chlorophyll content (**Table 3**) (31.5 and 26.3% more than in C and CB), whereas To L MH decreased its content (16.4 and 19.7% less than in C and CB). In the second term (**Table 3**), the application of Vo R UAE, Sg L MH, and Ur L MH resulted in a slightly higher amount of a green pigment in leaves (4.5, 4.5, and 3% more than in C; 16.7, 16.7, and 15% more than in CB). The use of To L UAE, To F MH, and Sg L UAE caused a significant reduction in its content (19.4, 19.4, and 17.9% less than in C; 10, 10, and 8.3% less than in CB). In the first

TABLE 2 | Effect of the foliar application of the botanical extracts on the fresh weight of leaves of rosette and root (after harvest), the total yield of radish ($N = 3^*$, mean ± SD), and dry weight of radish leaves of rosette (after second spraying and after harvest) and root (after harvest) ($N = 3$, mean ± SD).

Group	Root diameter <2 cm		Root diameter 2–4 cm		Root diameter >4 cm		Total yield		Total yield minus non-marketable yield	Dry weight		
	Leaves of rosette	Root	Leaves of rosette	Root	Leaves of rosette	Root	Leaves of rosette	Root		Leaves of rosette after 2nd spraying	Leaves of rosette	Roots
	g						$t \cdot ha^{-1}$		%	%		
C	8.46 ± 0.88b,c	7.93 ± 1.52b,c	9.14 ± 1.12c	17.67 ± 1.70b,c	0b,c	0b,c	11.04 ± 0.99c	15.76 ± 2.59b,c	97.64	8.55 ± 0.34	8.54 ± 0.41	3.72 ± 0.37
CF	6.52 ± 0.54a	5.59 ± 0.47a,c	10.57 ± 1.14	22.91 ± 3.10a	29.5 ± 03.27a,c	53.00 ± 5.72a,c	12.24 ± 1.34	24.35 ± 3.22a	98.51	8.37 ± 0.31	8.04 ± 0.25	3.87 ± 0.30
CB	6.86 ± 0.54a	4.52 ± 0.52a,b	10.74 ± 0.49a	21.40 ± 1.52a	17.39 ± 2.56a,b	61.54 ± 8.83a,b	12.56 ± 1.49a	22.86 ± 3.22a	94.93	7.84 ± 0.19	8.34 ± 0.39	3.38 ± 0.40
Hp H UAE	6.30 ± 0.85a	7.09 ± 1.60b,c	11.42 ± 0.51a	24.87 ± 1.00a,c	19.15 ± 2.00a,b	39.60 ± 6.52a,b,c	12.41 ± 1.27a	24.24 ± 3.05a	95.10	8.25 ± 0.29	8.72 ± 0.40	4.06 ± 0.07
Hp H MH	7.18 ± 1.53a	5.68 ± 0.36a,c	12.34 ± 2.41a,b,c	24.16 ± 3.35a,c	23.10 ± 2.20a,b,c	55.40 ± 2.78a,c	14.09 ± 1.93a,b,c	25.28 ± 2.80a	98.26	8.59 ± 0.18	8.06 ± 0.46	4.10 ± 0.38
Sg L UAE	6.76 ± 0.98a	5.53 ± 0.68a,c	10.96 ± 1.63a	22.19 ± 1.72a	23.30 ± 3.92a,b,c	60.45 ± 8.61a,b	12.74 ± 1.87a	23.96 ± 3.03a	98.06	7.72 ± 0.10	8.86 ± 0.43	3.64 ± 0.14
Sg L MH	7.85 ± 1.69b,c	7.23 ± 1.70b,c	12.30 ± 2.97a,b,c	25.22 ± 2.68a,c	18.94 ± 3.74a,b	59.35 ± 2.20a,b	14.49 ± 2.75a,b,c	28.46 ± 4.15a,b,c	97.70	7.88 ± 0.18	8.30 ± 0.33	3.45 ± 0.32
To F UAE	8.26 ± 1.14b,c	6.28 ± 1.29a,c	8.75 ± 1.43b,c	21.58 ± 3.37a	16.26 ± 0.71a,b	47.43 ± 5.55a,b,c	11.34 ± 1.63	23.58 ± 3.93a	98.38	8.27 ± 0.22	7.68 ± 0.49	4.25 ± 0.35
To F MH	7.83 ± 0.19b,c	6.72 ± 1.48a,b,c	11.76 ± 0.54a	23.39 ± 2.81a	20.65 ± 4.67a,b,c	47.63 ± 8.95a,b,c	13.84 ± 1.70a,b	25.31 ± 4.90a	94.89	8.36 ± 0.28	8.26 ± 0.26	3.83 ± 0.05
To L UAE	7.20 ± 0.79a	5.38 ± 0.30a	11.72 ± 0.68a	23.49 ± 2.98a	20.75 ± 2.25a,b,c	58.25 ± 5.19a,b	13.65 ± 1.25a,b	25.77 ± 2.93a,c	95.58	8.07 ± 0.22	8.85 ± 0.28	3.75 ± 0.23
To L MH	5.89 ± 0.69a,c	4.97 ± 0.49a	11.35 ± 2.37a	26.63 ± 5.39a,b,c	19.10 ± 2.78a,b	53.57 ± 5.25a,c	13.09 ± 1.83a	28.55 ± 4.11a,b,c	94.59	7.46 ± 0.38a	7.35 ± 0.32	3.62 ± 0.13
Tp F UAE	7.01 ± 1.33a	5.35 ± 0.87a	11.84 ± 1.46a	23.48 ± 2.73a	22.05 ± 2.90a,b,c	67.80 ± 4.74a,b,c	13.22 ± 1.80a	23.65 ± 3.60a	97.80	7.88 ± 0.40	8.56 ± 0.43	4.13 ± 0.33
Tp F MH	6.66 ± 1.23a	6.10 ± 0.16a,c	11.42 ± 1.31a	23.31 ± 1.96a	19.29 ± 4.91a,b	51.10 ± 0.99a,c	13.30 ± 2.21a	25.45 ± 1.58a,c	98.17	8.31 ± 0.25	8.38 ± 0.23	3.90 ± 0.19
Ur L UAE	5.97 ± 1.03a	4.72 ± 1.09a	10.55 ± 1.60	20.36 ± 1.42a,b	19.72 ± 3.57a,b	54.17 ± 2.43a,c	12.09 ± 1.91	22.73 ± 2.98a	94.47	9.19 ± 0.16 c	9.25 ± 0.36	5.13 ± 0.33a,b,c
Ur L MH	6.29 ± 0.78a	5.19 ± 0.62a	10.04 ± 0.07	20.60 ± 1.77a	20.26 ± 3.79a,b,c	54.06 ± 7.59a,c	11.84 ± 1.22	22.69 ± 2.59a	96.52	8.58 ± 0.27	8.68 ± 0.44	3.57 ± 0.40
Vo R UAE	6.36 ± 0.94a	5.31 ± 0.53a	11.35 ± 1.37a	24.61 ± 2.95a,c	15.97 ± 2.22a,b	57.63 ± 5.41a	12.69 ± 1.39a	25.48 ± 3.31a,c	97.44	8.43 ± 0.13	7.99 ± 0.39	4.02 ± 0.22
Vo R MH	8.13 ± 1.46b,c	7.55 ± 1.43b,c	12.01 ± 2.29a,b	23.83 ± 2.51a	17.23 ± 3.37a,b	48.57 ± 3.13a,c	13.97 ± 2.38a,b,c	26.35 ± 3.42a,c	95.52	8.23 ± 0.19	8.04 ± 0.40	4.42 ± 0.30

*(a) Statistically significant differences ($p < 0.05$) between the control group (C) and the botanical extracts. (b) Statistically significant differences ($p < 0.05$) between the formulation (CF) and the botanical extracts. (c) Statistically significant differences ($p < 0.05$) between commercial biostimulant (CB) and the botanical extracts. UAE, ultrasound-assisted extraction; MH, mechanical homogenization; Hp H, Hypericum perforatum L. (St. John's wort, herb); Sg L, Solidago gigantea Ait. (giant goldenrod, leaf); To F, To L, Taraxacum officinale (L.) Weber ex F.H. Wigg (common dandelion, flower, leaf); Tp F, Trifolium pratense L. (red clover, flower); Ur L, Urtica dioica L. (nettle, leaf); Vo R, Valeriana officinalis L. (valerian, root). *Three replications (plots)—each consisted of 125 plants.*

TABLE 3 | Effect of the foliar application of the botanical extracts on the chlorophyll *a* + *b* content (*N* = 4, mean ± SD), the carotenoids content (*N* = 4, mean ± SD), the *L*, *a*, *b* values (*N* = 10, mean ± SD), and the SPAD values (*N* = 10, mean ± SD) of radish leaves of rosette (after second spraying and after harvest).

Group	Chlorophyll *a* + *b*		Carotenoids		Color						Greenness indexes	
	After 2nd spraying	After harvest	After 2nd spraying	After harvest	After 2nd spraying			After harvest			After 2nd spraying	After harvest
	mg·g^{-1} FW		μg·g^{-1} FW		*L*	*a*	*b*	*L*	*a*	*b*	SPAD values	
C	0.73 ± 0.06	1.34 ± 0.03	16.94 ± 1.15	28.47 ± 1.19	42.05 ± 2.71	−9.36 ± 0.65	21.04 ± 2.01	42.23 ± 0.49	−8.66 ± 0.25	18.25 ± 0.76	36.53 ± 1.28	34.72 ± 1.23
CF	0.82 ± 0.03	1.23 ± 0.04	20.01 ± 1.31	25.33 ± 0.69	43.77 ± 0.79	−8.40 ± 0.34	19.12 ± 0.50	41.18 ± 1.10	−8.78 ± 0.23	18.25 ± 0.87	35.95 ± 1.80	35.72 ± 1.53
CB	0.76 ± 0.02	1.20 ± 0.05	18.55 ± 0.92	25.20 ± 0.71	43.53 ± 0.77	−9.18 ± 0.44	21.72 ± 0.91	43.17 ± 0.19	−8.01 ± 0.43	15.87 ± 1.45	35.60 ± 1.08	36.63 ± 0.56
Hp H UAE	0.83 ± 0.06	1.22 ± 0.04	19.04 ± 0.88	25.09 ± 0.59	41.74 ± 0.10	−7.99 ± 0.18a,c	17.82 ± 0.43a,c	41.58 ± 0.61	−8.27 ± 0.17	16.85 ± 0.23	40.82 ± 1.42a,b,c	41.25 ± 2.22a,b,c
Hp H MH	0.75 ± 0.04	1.21 ± 0.05	18.89 ± 0.93	26.74 ± 1.10	41.38 ± 0.73	−8.15 ± 0.04a,c	15.26 ± 0.13a,b,c	40.88 ± 0.26 c	−8.64 ± 0.01	17.38 ± 0.18	45.48 ± 2.02a,b,c	39.65 ± 1.44a,b
Sg L UAE	0.83 ± 0.06	1.10 ± 0.03a	18.05 ± 0.67	24.02 ± 0.98a	40.51 ± 0.38	−8.35 ± 0.03a	17.06 ± 0.27a,c	40.16 ± 0.56 c	−8.52 ± 0.05	18.25 ± 0.35	40.73 ± 2.11a,b,c	40.45 ± 0.63a,b
Sg L MH	0.84 ± 0.08	1.40 ± 0.07	16.58 ± 0.88b	27.95 ± 0.63	41.77 ± 0.34	−9.33 ± 0.05	19.45 ± 0.28	43.01 ± 0.22	−8.91 ± 0.15	17.38 ± 0.43	40.13 ± 1.30a,b,c	39.43 ± 0.79a
To F UAE	0.74 ± 0.04	1.24 ± 0.05	19.67 ± 0.56	26.75 ± 0.85	39.95 ± 1.68	−7.80 ± 0.22a,c	18.80 ± 0.47 c	42.24 ± 0.25	−8.65 ± 0.11	18.85 ± 0.59	38.72 ± 1.12	39.58 ± 1.45a,b
To F MH	0.81 ± 0.04	1.08 ± 0.02a	20.72 ± 0.85a	22.85 ± 1.13a	42.65 ± 0.10	−8.47 ± 0.24	17.34 ± 0.38a,c	40.48 ± 0.51 c	−8.27 ± 0.49	15.43 ± 0.68	41.12 ± 1.21a,b,c	43.72 ± 2.33a,b,c
To L UAE	0.90 ± 0.03	1.08 ± 0.06	19.71 ± 0.75	23.39 ± 0.64a	42.89 ± 0.95	−8.89 ± 0.17	18.62 ± 0.19 c	43.91 ± 0.92b	−8.77 ± 0.54	19.42 ± 1.18 c	39.33 ± 1.88 c	38.85 ± 1.66a
To L MH	0.61 ± 0.05b	1.25 ± 0.07	12.07 ± 0.34a,b,c	24.96 ± 0.90a	40.50 ± 0.84	−9.39 ± 0.14b	19.42 ± 0.34	42.58 ± 0.30	−8.03 ± 0.13	17.54 ± 0.09	40.28 ± 1.15a,b,c	40.18 ± 0.95a,b
Tp F UAE	0.78 ± 0.04	1.36 ± 0.08	17.36 ± 0.75	28.40 ± 1.18	41.24 ± 0.41	−9.14 ± 0.28	19.95 ± 0.56	43.30 ± 0.57	−7.87 ± 0.53	17.03 ± 0.77	38.67 ± 1.03	44.12 ± 2.01a,b,c
Tp F MH	0.82 ± 0.06	1.28 ± 0.05	19.62 ± 1.15	26.42 ± 0.68	40.57 ± 0.53	−9.51 ± 0.10b	19.67 ± 0.52	42.29 ± 0.74	−7.05 ± 0.21a,b	15.94 ± 0.20	38.35 ± 1.69	41.82 ± 2.24a,b,c
Ur L UAE	0.80 ± 0.03	1.16 ± 0.07	19.35 ± 0.72	23.36 ± 0.88a	39.76 ± 0.13b	−7.50 ± 0.07a,c	15.72 ± 0.29a,b,c	40.47 ± 1.13 c	−8.05 ± 0.36	17.31 ± 1.12	41.13 ± 2.22a,b,c	43.60 ± 2.57a,b,c
Ur L MH	0.71 ± 0.03	1.38 ± 0.08	16.98 ± 1.00	28.74 ± 1.15c	40.95 ± 0.46	−8.30 ± 0.20a	19.63 ± 1.26	40.10 ± 0.09 c	−8.77 ± 0.12	17.61 ± 0.09	38.70 ± 0.93	39.35 ± 1.94a
Vo R UAE	0.96 ± 0.04a,c	1.40 ± 0.09	22.25 ± 0.96a,c	28.82 ± 1.11c	42.67 ± 2.06	−8.83 ± 0.28	18.84 ± 1.10 c	39.52 ± 0.17a,c	−6.56 ± 0.16a,b,c	13.94 ± 0.25a,b	39.23 ± 0.62 c	44.47 ± 2.09a,b,c
Vo R MH	0.67 ± 0.04	1.32 ± 0.06	14.10 ± 0.85b,c	26.86 ± 1.16	42.10 ± 0.29	−9.55 ± 0.05b	20.05 ± 0.17	41.26 ± 0.25	−7.86 ± 0.75	16.80 ± 1.70	38.88 ± 1.53	41.08 ± 1.44b,c

(a) Statistically significant differences ($p < 0.05$) between the control group (C) and the botanical extracts. (b) Statistically significant differences ($p < 0.05$) between the formulation (CF) and the botanical extracts. (c) Statistically significant differences ($p < 0.05$) between commercial biostimulant (CB) and the botanical extracts. UAE, ultrasound-assisted extraction; MH, mechanical homogenization; Hp H, Hypericum perforatum L. (St. John's wort, herb); Sg L, Solidago gigantea Ait. (giant goldenrod, leaf); To F, To L, Taraxacum officinale (L.) Weber ex F.H. Wigg (common dandelion, flower, leaf); Tp F, Trifolium pratense L. (red clover, flower); Ur L, Urtica dioica L. (nettle, leaf); Vo R, Valeriana officinalis L. (valerian, root). * *Three replications (plots)—each consisted of 125 plants.*

term, the highest content of carotenoids (**Table 3**) was observed after the application of Vo R UAE (31.3 and 19.9% more than in C and CB), like in the case of chlorophyll content. In the second term, this extract showed the most stimulating activity, but the difference was nonsignificant in comparison to the control group (1.2 and 14.4% more than in C and CB). The lowest carotenoid content was observed for To L MH (in the first term: 28.7 and 34.9% less than in C and CB) and for To F MH (in the second term: 19.7 and 9.3% less than in C and CB).

Most bio-products did not significantly increase the leaf color, expressed as the *L*, *a*, *b* values presented in **Table 3**. The level of light or dark is described by the *L* value, redness or greenness is indicated by the *a* value, and yellowness or blueness is represented by the *b* value. These values are necessary to depict the leaf color.

The SPAD measurements demonstrated that all obtained bio-products increased the greenness index of the leaves (**Table 3**). In the first term, the greatest enhancement of the SPAD index was noted in the group treated with Hp H MH (24.5 and 27.8% more than in C and CB), while the smallest was found for Tp F MH (5 and 7.7% more than in C and CB). In the second term, the highest stimulating activity was observed for Vo R UAE (28.1 and 21.4% more than in C and CB), which corresponds to the results obtained for chlorophyll, with the lowest observed for To L UAE (11.9 and 6.1% more than in C and CB).

Vitamin C

In the majority of cases, the novel extracts raised the level of vitamin C in the leaves of rosette and in the roots (**Table 4**). For instance, in both terms of the samples collection, Vo R MH increased its content (in the first term: 29.9 and 10.5% more than in C and CB; in the second term: 116 and 44.4% more than in C and CB), while To L MH decreased its content (in the first term: 6.9 and 20.7% less than in C and CB; in the second term: 25.8% more than in C and 15.7% less than in CB). However, for the roots, Tp F MH increased the content of vitamin C (46.3 and 33.8% more than in C and CB), while Vo R MH reduced it (10.5 and 18.2% less than in C and CB).

Total Phenolic Compounds and Antioxidant Activity (DPPH, ABTS, and FRAP Assays)

In general, the content of total phenolic compounds (TPC) in radish (**Table 4**) was not intensified by the application of botanical extracts in relation to the control groups. The largest amount of TPC in the leaves of rosette, in both terms, was observed in the groups treated with Sg L MH (in the first term: 1.1% less than in C but 23.8% more than in CB; in the second term: 10.7 and 2.9% more than in C and CB) and To F UAE (in the first term: 0.1 and 25.3% more than in C and CB; in the second term: 7.2% more than in C and 0.4% less than in CB). In the roots (**Table 4**), the most elevated amount of TPC was noted after the application of To F MH (13.2 and 50.5% more than in C and CB), and the lowest was observed for Tp F UAE (37.2 and 16.5% less than in C and CB).

The DPPH assay revealed that the bio-products mainly lowered the antioxidant activity in the leaves but increased it in the roots (**Table 5**). The natural preparations based on To F (UAE) and Vo R (MH) increased the activity by 76.5 and 79.8% in comparison to C and by 147 and 152% in comparison to CB in the leaves collected during the first term. The lowest activity was caused by the application of To L MH and Tp F MH (35.3 and 33.6% less than in C and 9.4 and 7.1% less than in CB). In the leaves from the second term of the plant collection, the extract Sg L UAE enhanced the activity by 28.6 and 51.8% in comparison to C and CB, while To F MH and Ur L MH diminished this activity by 40.8 and 39.8% when compared with C and by 30.1 and 28.9% when compared with CB. The antioxidant activity assessed in the roots was mostly increased after the foliar spraying with To F MH (158 and 170% more than in C and CB) but decreased with Sg L UAE (26.7 and 23.3% less than in C and CB) and To L UAE (33.3 and 30.2% less than in C and CB).

The antioxidant activity measured with the ABTS assay in the aboveground parts (in both terms) was not increased after the application of all examined bio-products, whereas, in the roots, in all cases, the activity was significantly higher with reference to the control group (**Table 5**). In the leaves collected in the first term, the most elevated activity was found after the use of Vo R MH (25% less than in C and 104% more than in CB), and the least was found for To F MH (65.9 and 7% less than in C and CB) and Sg L UAE (65.7 and 6.5% less than in C and CB). In the second term of the samples collection, the highest level was noted for Tp F UAE (21.8% less than in C and 228% more than in CB), and the lowest was found for Ur L UAE (73.4% less than in C and 11.5% more than in CB). The foliar spraying with To L UAE increased the antioxidant activity the most (178 and 10.7% more than in C and CB), while Tp F MH showed the least impact (24.1% more than in C and 36.8% less than in CB).

The opposite trend was observed in the case of antioxidant activity measured with the FRAP assay. In general, this activity was increased in leaves of rosette but decreased in the roots (**Table 5**). For example, the highest activity was noted in the group treated with Sg L MH (53.4 and 20.2% more than in C and CB), and the lowest was observed for Hp H UAE (5.7 and 26.1% less than in C and CB) and Vo R UAE (6.1 and 26.4% less than in C and CB) in the leaves from the first collection, whereas for the aboveground parts from the second term, Sg L UAE enhanced the activity (73.8 and 76.8% more than in C and CB), while Sg L MH reduced it (18.9 and 17.5% less than in C and CB). In the roots, the formulation based on Sg L (UAE) increased the activity (4.2 and 16.2% more than in C and CB), while the one based on Hp H (MH) decreased it (43.6 and 37.2% less than in C and CB).

Nitrates

In most instances, the application of the obtained bio-products resulted in a higher content of nitrates in all parts of the model plant (**Table 6**). The foliar spraying with Vo R MH increased the amount of examined ions in the leaves of rosette collected in the first term (57.5 and 39% more than in C and CB), while Vo R UAE and Ur L UAE (21.9 and 31.1% less than in C and CB for both extracts) decreased its content. In the harvested leaves of rosette and roots, the highest amount was observed in the groups treated with Ur L UAE (in leaves: 52.7 and 51.1% more than in C and CB; in the roots: 73.7 and 125% more than in C and CB), and the lowest was found for Vo R UAE and To F UAE

TABLE 4 | The effect of the foliar application of the botanical extracts on the vitamin C content ($N = 4$, mean ± SD) and the total phenolic compounds content ($N = 4$, mean ± SD) of radish leaves (after second spraying and after harvest) and roots (after harvest).

Group	Vitamin C			Total phenolic compounds		
	Leaves of rosette after 2nd spraying	Leaves of rosette after harvest	Roots after harvest	Leaves of rosette after 2nd spraying	Leaves of rosette after harvest	Roots after harvest
	mg·100 g^{-1} FW			mg GAE·100 g^{-1} FW		
C	105.33 ± 3.76b,c	52.23 ± 1.31b,c	26.33 ± 1.25b	105.24 ± 4.28c	131.89 ± 3.86	36.73 ± 1.11c
CF	124.70 ± 4.94a	78.53 ± 1.72a	35.53 ± 1.88a,c	108.85 ± 4.60c	129.92 ± 4.31	35.37 ± 1.93c
CB	123.77 ± 5.36a	77.97 ± 2.67a	28.80 ± 1.02b	84.07 ± 3.14a,b	141.91 ± 4.68	27.63 ± 0.87a,b
Hp H UAE	126.77 ± 2.86a	94.47 ± 2.68aa,b,c	29.83 ± 1.08b	76.54 ± 4.67a,b	109.01 ± 3.11a,b,c	23.99 ± 1.18a,b
Hp H MH	99.00 ± 2.16b,c	75.53 ± 2.62a	35.23 ± 0.84a,c	90.03 ± 3.56a,b	125.60 ± 3.69c	24.12 ± 0.86a,b
Sg L UAE	125.77 ± 4.34a	90.53 ± 2.70a	30.37 ± 1.21b	82.02 ± 3.27a,b	117.92 ± 3.77c	38.34 ± 1.46c
Sg L MH	133.27 ± 3.68a	110.73 ± 4.45a,b,c	26.13 ± 1.18b	104.07 ± 3.77c	145.99 ± 3.02b	29.67 ± 0.93a,b
To F UAE	123.93 ± 3.91a	79.80 ± 2.53a	30.37 ± 1.62b	105.33 ± 3.08c	141.37 ± 5.91	28.73 ± 1.39a,b
To F MH	112.83 ± 2.45	81.70 ± 3.85a	31.97 ± 0.66a	92.06 ± 3.19b	129.02 ± 4.18	41.57 ± 1.52b,c
To L UAE	109.60 ± 4.91	92.30 ± 4.66a,b,c	27.73 ± 1.11b	83.99 ± 3.77a,b	128.29 ± 4.49	33.70 ± 2.00c
To L MH	98.10 ± 2.50b,c	65.73 ± 2.93a	27.33 ± 0.91b	95.43 ± 4.91	136.28 ± 3.30	23.76 ± 1.13a,b
Tp F UAE	99.67 ± 4.13b,c	93.73 ± 3.62a,b,c	37.10 ± 1.70a,c	91.80 ± 4.13b	115.56 ± 4.27a,c	23.08 ± 0.55a,b
Tp F MH	130.30 ± 4.21a	98.03 ± 4.11a,b,c	38.53 ± 1.75a,c	81.32 ± 2.76a,b	133.77 ± 3.15	31.18 ± 0.95a
Ur L UAE	115.70 ± 4.65	86.40 ± 3.51a	34.13 ± 1.36a,c	91.76 ± 4.69b	124.78 ± 4.53c	27.78 ± 0.92a,b
Ur L MH	121.10 ± 3.31a	81.27 ± 1.81a	33.53 ± 1.63a	86.63 ± 2.52a,b	131.07 ± 3.17	33.50 ± 1.71c
Vo R UAE	126.60 ± 4.56a	112.20 ± 5.23a,b,c	37.50 ± 1.06a,c	95.63 ± 2.45	111.30 ± 3.15a,b,c	26.90 ± 1.31a,b
Vo R MH	136.80 ± 6.78a	112.57 ± 5.33a,b,c	23.57 ± 1.07b,c	88.81 ± 3.83a,b	114.26 ± 4.84a,b,c	34.19 ± 1.79c

(a) Statistically significant differences ($p < 0.05$) between the control group (C) and the botanical extracts. (b) Statistically significant differences ($p < 0.05$) between the formulation (CF) and the botanical extracts. (c) Statistically significant differences ($p < 0.05$) between commercial biostimulant (CB) and the botanical extracts. UAE, ultrasound-assisted extraction; MH, mechanical homogenization; Hp H, Hypericum perforatum L. (St. John's wort, herb); Sg L, Solidago gigantea Ait. (giant goldenrod, leaf); To F, To L, Taraxacum officinale (L.) Weber ex F.H. Wigg (common dandelion, flower, leaf); Tp F, Trifolium pratense L. (red clover, flower); Ur L, Urtica dioica L. (nettle, leaf); Vo R, Valeriana officinalis L. (valerian, root).

in both leaves (20.3 and 21.1% less than in C and CB for both extracts) and roots (20.2% less than in C and 3.2% more than in CB; 17.5% less than in C and 6.8% more than in CB). Notably, the amount of nitrates in radish was lower than the maximum allowable levels established for vegetables, e.g., fresh spinach (3,500 mg·kg^{-1}), lettuce (3,000–5,000 mg·kg^{-1}), iceberg lettuce (2,000–2,500 mg·kg^{-1}), and wild rocket (6,000–7,000 mg·kg^{-1}) (European Communities, 2006).

Macroelements, Microelements, and Heavy Metals

In the case of radish leaves, generally, P, K, Mg, and S were increased in the biomass, and N and Ca decreased. The highest content of P was observed in the group treated with To F MH and Vo R MH (higher by 25.8% than in the control group–C), and the highest content of K was observed in the groups treated with Ur L UAE (higher by 29.7% than in C), Vo R MH (higher by 27.2% than in C), and Hp H UAE (higher by 24.5% than in C). The greatest amount of Mg was found in the group treated with Sg L UAE (higher by only 3.1% than in C), and Vo R MH (higher by only 1.5% than in C), and the highest content of S was found in the groups treated with To L MH (higher by 18.4% than in C), Vo R UAE (higher by 13.2% than in C), and Ur L UAE (higher by 11.4% than in C). The extracts produced from nettle (*Urtica dioica* L.) and valerian (*Valeriana officinalis* L.) ensured an increase in the content of macronutrients. The amount of nitrogen was comparable in all tested groups, but, for botanical extracts, it was slightly lower than in the control group (C), from 2.7% for Ur L UAE to 8.1% for Sg L UAE. The same was observed for the content of Ca in the leaves. In all experimental groups, this content was lower than in the control group (from 18.5% for Tp F UAE to 2.5% for To L MH) (**Table 7A**).

The results showed that the tested macroelements were better accumulated in the roots, as more statistically significant differences were demonstrated (**Table 7A**). The content of N was highest in the groups treated with Hp H UAE (by 5.7% higher than in C), P for Ur L UAE (by 20.4% higher), K for Vo R MH (by 6.8% higher), Ca for Vo R MH (by 25.4% higher), and Mg for Vo R MH (by 75.1% higher). The content of S was comparable in all experimental groups but was slightly lower than that in the control group. This analysis showed that the extract from valerian (*Valeriana officinalis* L.) was the most effective in increasing the macronutrient content in the roots. In most cases, the production method did not affect the macronutrient content in the tested biomass.

The examined botanical extracts, applied foliarly, increased the level of some microelements (**Table 7B**), especially Zn in the leaves (in all experimental groups). In other cases, the micronutrient composition of the leaves was comparable to that in the control group. Higher contents of the examined elements were reported for Fe (for To L UAE, higher by 24.3% than in the control group) and Zn (for Sg L UAE, higher by 24.8% than in

TABLE 5 | The effect of the foliar application of the botanical extracts on the antioxidant activities (DPPH assay, ABTS assay, FRAP assay) ($N = 4$, mean ± SD) of radish leaves (after second spraying and after harvest) and roots (after harvest).

Group	DPPH assay			ABTS assay			FRAP assay		
	Leaves of rosette after 2nd spraying	Leaves of rosette after harvest	Roots after harvest	Leaves of rosette after 2nd spraying	Leaves of rosette after harvest	Roots after harvest	Leaves of rosette after 2nd spraying	Leaves of rosette after harvest	Roots after harvest
	μM Trolox·g^{-1} FW								
C	1.19 ± 0.04c	0.98 ± 0.08b	0.45 ± 0.04	10.44 ± 0.49b,c	17.90 ± 0.74b,c	2.32 ± 0.21b,c	2.64 ± 0.12b	3.55 ± 0.18	3.30 ± 0.32
CF	1.09 ± 0.10c	0.61 ± 0.07a,c	0.46 ± 0.07	8.02 ± 0.40a,c	4.97 ± 0.34a	4.81 ± 0.48a	4.23 ± 0.46a,c	3.18 ± 0.19	2.94 ± 0.16
CB	0.85 ± 0.07a,b	0.83 ± 0.05 b	0.43 ± 0.10	3.83 ± 0.27a,b	4.27 ± 0.19a	4.56 ± 0.29a	3.37 ± 0.22 b	3.49 ± 0.19	2.96 ± 0.21
Hp H UAE	0.95 ± 0.02a	0.63 ± 0.06a	0.69 ± 0.04a,b,c	4.59 ± 0.27a,b	9.99 ± 0.48a,b,c	4.05 ± 0.38a	2.49 ± 0.22 b,c	3.72 ± 0.20	2.82 ± 0.24
Hp H MH	0.93 ± 0.04a	0.61 ± 0.05a,c	0.76 ± 0.05a,b,c	4.56 ± 0.32a,b	9.78 ± 0.54a,b,c	3.08 ± 0.31 b	3.13 ± 0.22 b	3.93 ± 0.37 b	1.86 ± 0.16a,b,c
Sg L UAE	0.91 ± 0.04a	1.26 ± 0.05a,b,c	0.33 ± 0.02	3.58 ± 0.22a,b	12.92 ± 0.80a,b,c	4.68 ± 0.50a	2.64 ± 0.26 b	6.17 ± 0.38a,b,c	3.44 ± 0.28
Sg L MH	1.68 ± 0.10a,b,c	0.93 ± 0.10 b	0.80 ± 0.04a,b,c	3.80 ± 0.43a,b	7.25 ± 0.31a,b,c	3.48 ± 0.49	4.05 ± 0.35a	2.88 ± 0.18	2.80 ± 0.19
To F UAE	2.10 ± 0.07a,b,c	0.85 ± 0.04 b	0.80 ± 0.09a,b,c	4.43 ± 0.31a,b	8.02 ± 0.35a,b,c	2.90 ± 0.20a,c	3.58 ± 0.25a	2.96 ± 0.20	3.04 ± 0.31
To F MH	0.98 ± 0.06	0.58 ± 0.06a,c	1.16 ± 0.08a,b,c	3.56 ± 0.34a,b	6.14 ± 0.40a	4.46 ± 0.45a	3.53 ± 0.20a	3.03 ± 0.23	3.07 ± 0.15
To L UAE	1.06 ± 0.10	1.07 ± 0.09 b,c	0.30 ± 0.09	4.53 ± 0.48a,b	8.91 ± 0.45a,b,c	5.05 ± 0.48a	2.66 ± 0.16 b	3.74 ± 0.21	2.78 ± 0.22
To L MH	0.77 ± 0.09a,b	0.98 ± 0.08 b	0.90 ± 0.07a,b,c	5.67 ± 0.46a,b,c	11.30 ± 0.48a,b,c	2.98 ± 0.42 b,c	2.84 ± 0.14 b	4.23 ± 0.23 b,c	2.40 ± 0.13a
Tp F UAE	1.01 ± 0.09	1.11 ± 0.09 b,c	0.56 ± 0.07	6.46 ± 0.51a,b,c	14.00 ± 0.86a,b,c	3.10 ± 0.43 b	2.98 ± 0.28 b	3.19 ± 0.15	2.85 ± 0.30
Tp F MH	0.79 ± 0.06a,b	0.70 ± 0.05a	1.04 ± 0.06a,b,c	6.83 ± 0.40a,c	5.85 ± 0.46a	2.88 ± 0.42 b,c	2.63 ± 0.19 b	3.81 ± 0.27	2.65 ± 0.23
Ur L UAE	1.78 ± 0.04a,b,c	0.64 ± 0.07a	0.53 ± 0.06	5.37 ± 0.46a,b,c	4.76 ± 0.42a	4.66 ± 0.29a	3.19 ± 0.26 b	3.39 ± 0.19	2.39 ± 0.16a
Ur L MH	0.83 ± 0.08a,b	0.59 ± 0.07a,c	1.00 ± 0.09a,b,c	5.07 ± 0.67a,b	5.51 ± 0.49a	4.21 ± 0.32a	3.13 ± 0.19 b	4.45 ± 0.23a,b,c	2.33 ± 0.14a
Vo R UAE	1.07 ± 0.07c	0.94 ± 0.08 b	0.64 ± 0.04c	6.08 ± 0.31a,b,c	13.16 ± 0.71a,b,c	3.55 ± 0.49	2.48 ± 0.19 b,c	3.80 ± 0.23	2.48 ± 0.21
Vo R MH	2.14 ± 0.09a,b,c	0.76 ± 0.08a	0.37 ± 0.06	7.83 ± 0.44a,c	5.96 ± 0.36a	3.89 ± 0.37a	3.40 ± 0.31a,c	4.56 ± 0.24a,b,c	3.22 ± 0.32

(a) Statistically significant differences ($p < 0.05$) between the control group (C) and the botanical extracts. (b) Statistically significant differences ($p < 0.05$) between the formulation (CF) and the botanical extracts. (c) Statistically significant differences ($p < 0.05$) between commercial biostimulant (CB) and the botanical extracts. UAE, ultrasound-assisted extraction; MH, mechanical homogenization; Hp H, Hypericum perforatum L. (St. John's wort, herb); Sg L, Solidago gigantea Ait. (giant goldenrod, leaf); To F, To L, Taraxacum officinale (L.) Weber ex F.H. Wigg (common dandelion, flower, leaf); Tp F, Trifolium pratense L. (red clover, flower); Ur L, Urtica dioica L. (nettle, leaf); Vo R, Valeriana officinalis L. (valerian, root).

TABLE 6 | The effect of the foliar application of the botanical extracts on the nitrates content ($N = 3$, mean ± SD) of leaves of rosette (after second spraying and after harvest) and roots (after harvest).

Group	Leaves of rosette after 2nd spraying	Leaves of rosette after harvest	Roots after harvest
		mg·kg^{-1} FW	
C	1,177.15 ± 190.05	1,746.36 ± 139.59	414.11 ± 44.66
CF	664.27 ± 85.93c	1,181.64 ± 180.38	315.39 ± 23.00
CB	1,334.60 ± 106.97b	1,763.92 ± 197.94	319.99 ± 30.41
Hp H UAE	1,510.87 ± 186.91b	2,236.21 ± 165.57b	424.66 ± 32.47
Hp H MH	1,507.07 ± 233.45b	2,132.94 ± 270.27b	533.84 ± 54.92b,c
Sg L UAE	1,255.07 ± 111.46	1,594.48 ± 173.79	413.09 ± 46.42
Sg L MH	1,704.77 ± 168.77b	1,562.54 ± 239.96	366.48 ± 38.78
To F UAE	1,510.21 ± 119.35b	1,391.79 ± 175.11	341.82 ± 43.19
To F MH	1,471.21 ± 167.65b	2,046.52 ± 245.82b	505.01 ± 66.71b,c
To L UAE	1,268.90 ± 166.77	2,096.39 ± 307.57b	502.94 ± 43.35b,c
To L MH	1,744.36 ± 166.43b	1,572.90 ± 160.38	434.47 ± 43.31
Tp F UAE	1,625.58 ± 199.79b	2,653.45 ± 193.48a,b,c	410.24 ± 30.35
Tp F MH	1,674.76 ± 243.29b	2,202.20 ± 180.58b	455.91 ± 43.67
Ur L UAE	919.44 ± 85.57	2,666.06 ± 336.20a,b,c	719.16 ± 75.47a,b,c
Ur L MH	1,502.30 ± 134.73b	2,043.16 ± 243.12b	386.01 ± 44.79
Vo R UAE	919.02 ± 86.86	1,391.77 ± 108.09	330.25 ± 26.94
Vo R MH	1,854.43 ± 289.14a,b	1,455.10 ± 120.74	429.47 ± 40.77

(a) Statistically significant differences ($p < 0.05$) between the control group (C) and the botanical extracts. (b) Statistically significant differences ($p < 0.05$) between the formulation (CF) and the botanical extracts. (c) Statistically significant differences ($p < 0.05$) between commercial biostimulant (CB) and the botanical extracts. UAE, ultrasound-assisted extraction; MH, mechanical homogenization; Hp H, Hypericum perforatum L. (St. John's wort, herb); Sg L, Solidago gigantea Ait. (giant goldenrod, leaf); To F, To L, Taraxacum officinale (L.) Weber ex F.H. Wigg (common dandelion, flower, leaf); Tp F, Trifolium pratense L. (red clover, flower); Ur L, Urtica dioica L. (nettle, leaf); Vo R, Valeriana officinalis L. (valerian, root).

the control group). As with macronutrients, the micronutrients (Fe, Cu, Zn, Mn) were more strongly accumulated in the roots (**Table 7B**). Again, the most significant results were obtained for the extract from valerian, whose Fe, Cu, and Mn contents were, respectively, 27.9, 45.5, and 29.3% higher than those in the control group.

The content of heavy metals (Ni, Cd, and Pb) was generally lower in the leaves and roots of radish in the experimental groups compared with the control, with the exception of the Ni content in the roots, which was higher than in the control group (**Table 7B**). The obtained levels of Cd and Pb were comparable with the results presented in other studies, where the content of Cd was at a level between 1 and 2.8 mg·kg^{-1}, and Pb was found at 6.4–10.98 mg·kg^{-1} (Varalakshmi and Ganeshamurthy, 2008; Veissi et al., 2015; Rolli et al., 2016). The tolerable levels in agricultural crops are 3 mg·kg^{-1} for Cd and 10 mg·kg^{-1} for Pb (Rolli et al., 2016), whereas, according to the EC Commission Regulations, the threshold content is 0.05–0.2 and 0.1–0.3 mg·kg^{-1}, respectively [(EC) Commission Regulation No. 2006.364.5 of 19 December 2006, setting maximum levels for certain contaminants in foodstuffs].

Steam Volatile Compounds

GC–MS analyses of the distilled essential oil from the radish leaves revealed 38 peaks, which were found to represent steam volatile compounds (SVCs) (**Supplementary Table 1**). The following components constituted the main parts of the SVCs: limonene, myrcene, phytol, and cis-β-ocimene. However, p-Cymene, β-pinene, ionone epoxide, nonanal, hexahydrofarnesyl acetone, and hex-(2*E*)-enal were present in smaller quantities. In most cases, the examined extracts did not increase the content of limonene, except for Vo R UAE (11.3 and 9.5% more than in C and CB), To L UAE (4.8 and 3.1% more than in C and CB), and Hp H UAE (3.2 and 1.5% more than in C and CB). The lowest increment was observed after treatment with Tp F MH (25.4 and 26.6% less than in C and CB). The amount of myrcene was mostly lower than that in the control group (C), but an increase was noted after the application of the aforementioned bio-products, Vo R UAE (7.4 and 25.9% more than in C and CB), To L UAE (2.3 and 19.9% more than in C and CB), and Hp H UAE (1.1 and 18.5% more than in C and CB). The foliar spraying with Tp F MH decreased the content of myrcene (33.4 and 21.9% less than in C and CB). A great diversity was observed among the examined groups in terms of phytol content. Extracts based on e.g., Tp F MH significantly increased the phytol amount (329 and 468% more than in C and CB), along with Sg L UAE (175 and 234% more than in C and CB), To L MH (132 and 207% more than in C and CB), Sg L MH (120 and 192% more than in C and CB), and To F UAE (110 and 178% more than in C and CB). On the other hand, extracts obtained from Vo R UAE (64.4 and 52.9% less than in C and CB) and To L UAE (56.9 and 42.9% less than in C and CB) significantly reduced the phytol amount. In most cases, the content of cis-β-ocimene was also decreased compared with the control group (C). The highest increment was noted in the groups sprayed with Hp H UAE (7.3 and 21% more than in

TABLE 7A | The effect of the foliar application of the botanical extracts on the content of macroelements ($N = 3$, mean ± SD) in radish leaves of rosette and roots (after harvest).

Group	N		P		K		Ca		Mg		S	
	Leaves	Roots	Leaves	Roots	Leaves	Roots	Leaves	Roots	Leaves	Roots	Leaves	Roots
	g·kg^{-1} DW											
C	37.00 ± 1.85	32.75 ± 1.64	1.94 ± 0.10	4.41 ± 0.22	32.22 ± 1.61b,c	80.44 ± 4.02	11.13 ± 0.56	9.63 ± 0.48b,c	2.59 ± 0.13	2.13 ± 0.11	7.19 ± 0.36	7.05 ± 0.35
CF	34.50 ± 1.73	31.75 ± 1.59	2.19 ± 0.11	4.47 ± 0.22c	41.47 ± 2.07a	71.58 ± 3.58	10.08 ± 0.50	7.68 ± 0.38a	2.56 ± 0.13	1.86 ± 0.09	8.30 ± 0.42	6.15 ± 0.31
CB	35.00 ± 1.75	33.25 ± 1.66	2.16 ± 0.11	3.72 ± 0.19b	38.39 ± 1.92a	77.05 ± 3.85	10.49 ± 0.52	7.71 ± 0.39a	2.71 ± 0.14	1.90 ± 0.10	7.98 ± 0.40	6.20 ± 0.31
Hp H UAE	35.75 ± 1.79	34.63 ± 1.73	2.13 ± 0.11	5.16 ± 0.26a,c	40.10 ± 2.01a	81.83 ± 4.09	10.44 ± 0.52	7.55 ± 0.38a	2.61 ± 0.13	1.84 ± 0.09	8.00 ± 0.40	7.08 ± 0.35
Hp H MH	35.25 ± 1.76	34.00 ± 1.70	1.88 ± 0.09	5.16 ± 0.26a,c	36.72 ± 1.84	79.36 ± 3.97	10.60 ± 0.53	8.29 ± 0.41a	2.58 ± 0.13	2.09 ± 0.10	7.29 ± 0.36	6.58 ± 0.33
Sg L UAE	34.00 ± 1.70	32.13 ± 1.61	2.06 ± 0.10	5.28 ± 0.26a,b,c	37.76 ± 1.89	83.34 ± 4.17b	9.88 ± 0.49	7.87 ± 0.39a	2.67 ± 0.13	2.02 ± 0.10	7.53 ± 0.38	7.04 ± 0.35
Sg L MH	34.75 ± 1.74	33.50 ± 1.68	1.97 ± 0.10	4.59 ± 0.23c	35.06 ± 1.75b	74.92 ± 3.75	10.77 ± 0.54	7.59 ± 0.38a	2.58 ± 0.13	1.82 ± 0.09	7.61 ± 0.38	6.33 ± 0.32
To F UAE	35.25 ± 1.76	33.75 ± 1.69	2.16 ± 0.11	5.25 ± 0.26a,b,c	38.26 ± 1.91a	80.14 ± 4.01	9.70 ± 0.48	8.30 ± 0.42a	2.45 ± 0.12	2.16 ± 0.11	7.06 ± 0.35b	6.50 ± 0.33
To F MH	34.75 ± 1.74	33.75 ± 1.69	2.44 ± 0.12a	4.72 ± 0.24c	33.69 ± 1.68b	78.30 ± 3.91	10.22 ± 0.51	7.91 ± 0.40a	2.48 ± 0.12	1.95 ± 0.10	7.13 ± 0.36b	6.50 ± 0.33
To L UAE	35.00 ± 1.75	32.88 ± 1.64	2.09 ± 0.10	4.75 ± 0.24c	36.69 ± 1.83	84.30 ± 4.21b	10.22 ± 0.51	7.63 ± 0.38a	2.65 ± 0.13	1.85 ± 0.09	7.24 ± 0.36	7.03 ± 0.35
To L MH	35.25 ± 1.76	33.50 ± 1.68	1.28 ± 0.06a,b,c	4.75 ± 0.24c	37.78 ± 1.89	81.63 ± 4.08	10.85 ± 0.54	8.40 ± 0.42	2.52 ± 0.13	2.02 ± 0.10	8.51 ± 0.43a	6.68 ± 0.33
Tp F UAE	35.75 ± 1.79	34.00 ± 1.70	2.13 ± 0.11	5.09 ± 0.25c	39.16 ± 1.96a	82.03 ± 4.10	9.02 ± 0.45a	8.04 ± 0.40a	2.58 ± 0.13	2.01 ± 0.10	7.50 ± 0.38	6.86 ± 0.34
Tp F MH	35.50 ± 1.78	34.00 ± 1.70	2.00 ± 0.10	2.13 ± 0.11a,b,c	39.46 ± 1.97a	37.24 ± 1.86a,b,c	10.70 ± 0.54	10.09 ± 0.50b,c	2.56 ± 0.13	2.48 ± 0.12a,b,c	7.40 ± 0.37	6.71 ± 0.34
Ur L UAE	36.00 ± 1.80	33.50 ± 1.68	2.03 ± 0.10	5.31 ± 0.27a,b,c	41.78 ± 2.09a	82.45 ± 4.12	10.01 ± 0.50	7.96 ± 0.40a	2.52 ± 0.13	2.01 ± 0.10	8.01 ± 0.40	6.70 ± 0.34
Ur L MH	35.00 ± 1.75	33.75 ± 1.69	2.03 ± 0.10	2.06 ± 0.10a,b,c	37.43 ± 1.87	34.40 ± 1.72a,b,c	10.32 ± 0.52	10.40 ± 0.52b,c	2.53 ± 0.13	2.48 ± 0.12a,b,c	7.41 ± 0.37	6.74 ± 0.34
Vo R UAE	34.50 ± 1.73	32.75 ± 1.64	2.16 ± 0.11	5.06 ± 0.25c	37.65 ± 1.88	83.81 ± 4.19b	10.15 ± 0.51	8.26 ± 0.41a	2.34 ± 0.12	1.98 ± 0.10	8.14 ± 0.41	6.90 ± 0.35
Vo R MH	34.75 ± 1.74	34.25 ± 1.71	2.44 ± 0.12a	5.16 ± 0.26a,c	40.98 ± 2.05a	85.91 ± 4.30b	10.49 ± 0.52	12.08 ± 0.60a,b,c	2.63 ± 0.13	3.73 ± 0.19a,b,c	7.09 ± 0.35b	6.81 ± 0.34

(a)Statistically significant differences ($p < 0.05$) between the control group (C) and the botanical extracts. (b) Statistically significant differences ($p < 0.05$) between the formulation (CF) and the botanical extracts. (c) Statistically significant differences ($p < 0.05$) between commercial biostimulant (CB) and the botanical extracts. UAE, ultrasound-assisted extraction; MH, mechanical homogenization; Hp H, Hypericum perforatum L. (St. John's wort, herb); Sg L, Solidago gigantea Ait. (giant goldenrod, leaf); To F, To L, Taraxacum officinale (L.) Weber ex F.H. Wigg (common dandelion, flower, leaf); Tp F, Trifolium pratense L. (red clover, flower); Ur L, Urtica dioica L. (nettle, leaf); Vo R, Valeriana officinalis L. (valerian, root).

TABLE 7B | The effect of the foliar application of the botanical extracts on the content of microelements and toxic elements ($N = 3$, mean ± SD) in radish leaves of rosette and roots (after harvest).

Group	Fe		Cu		Zn		Mn		Ni		Cd		Pb	
	Leaves	Roots	Leaves	Roots	Leaves	Roots	Leaves	Roots	Leaves	Roots	Leaves	Roots	Leaves	Roots
	mg·kg^{-1} DW													
C	1,503.75 ± 75.19b	426.75 ± 21.34b	5.68 ± 0.28	1.54 ± 0.08b	37.49 ± 1.87	45.16 ± 2.26b	85.13 ± 4.26b	25.63 ± 1.28c	10.44 ± 0.52c	5.33 ± 0.27b	1.66 ± 0.08	0.66 ± 0.03b,c	10.05 ± 0.50	5.49 ± 0.27b,c
CF	1,100.00 ± 55.00a,c	337.88 ± 16.89a	6.08 ± 0.30	1.95 ± 0.10a,c	41.71 ± 2.09	30.19 ± 1.51a,c	72.00 ± 3.60a	28.00 ± 1.40	10.05 ± 0.50	3.94 ± 0.20a,c	1.58 ± 0.08	0.51 ± 0.03a	9.17 ± 0.46	3.21 ± 0.16a
CB	1,412.50 ± 70.63b	380.88 ± 19.04	6.26 ± 0.31	1.41 ± 0.07b	41.03 ± 2.05	43.34 ± 2.17b	83.00 ± 4.15	30.50 ± 1.53a	8.76 ± 0.44a	5.63 ± 0.28b	1.61 ± 0.08	0.50 ± 0.03a	9.55 ± 0.48	3.61 ± 0.18a
Hp H UAE	1,631.25 ± 81.56b,c	446.63 ± 22.33b	4.46 ± 0.22a,b,c	1.53 ± 0.08b	43.95 ± 2.20a	43.93 ± 2.20b	83.75 ± 4.19	23.25 ± 1.16b,c	8.40 ± 0.42a,b	6.41 ± 0.32a,b	1.60 ± 0.08	0.65 ± 0.03b,c	10.66 ± 0.53b	5.04 ± 0.25b,c
Hp H MH	1,298.75 ± 64.94	519.00 ± 25.95a,b,c	4.50 ± 0.23a,b,c	1.61 ± 0.08b	43.20 ± 2.16	43.54 ± 2.18b	79.13 ± 3.96	33.50 ± 1.68a,b	8.69 ± 0.43a	7.33 ± 0.37a,b,c	1.68 ± 0.08	0.58 ± 0.03	9.28 ± 0.46	4.39 ± 0.22a,b,c
Sg L UAE	1,567.50 ± 78.38b	420.38 ± 21.02b	5.50 ± 0.28	1.69 ± 0.08b,c	46.80 ± 2.34a	45.98 ± 2.30b	86.50 ± 4.33b	22.25 ± 1.11b,c	11.11 ± 0.56c	5.03 ± 0.25b	1.54 ± 0.08	0.66 ± 0.03b,c	9.93 ± 0.50	5.03 ± 0.25b,c
Sg L MH	1,107.50 ± 55.38a,c	313.88 ± 15.69a	5.26 ± 0.26b,c	1.81 ± 0.09a,c	40.55 ± 2.03	39.84 ± 1.99b	77.25 ± 3.86	26.75 ± 1.34	8.59 ± 0.43a,b	5.00 ± 0.25b	1.68 ± 0.08	0.53 ± 0.03a	9.34 ± 0.47	3.79 ± 0.19a
To F UAE	1380.00 ± 69.00b	494.38 ± 24.72b,c	4.95 ± 0.25b,c	1.89 ± 0.09a,c	40.01 ± 2.00	46.60 ± 2.33b	86.50 ± 4.33b	32.25 ± 1.61a	10.24 ± 0.51c	5.78 ± 0.29b	1.55 ± 0.08	0.68 ± 0.03b,c	9.51 ± 0.48	5.14 ± 0.26b,c
To F MH	1,496.25 ± 74.81b	462.38 ± 23.12b,c	5.29 ± 0.26c	1.70 ± 0.09c	37.74 ± 1.89	41.86 ± 2.09b	81.88 ± 4.09	31.25 ± 1.56a	10.40 ± 0.52c	11.04 ± 0.55a,b,c	1.59 ± 0.08	0.58 ± 0.03	9.41 ± 0.47	3.68 ± 0.18a
To L UAE	1,868.75 ± 93.44a,b,c	543.25 ± 27.16a,b,c	5.93 ± 0.30	1.45 ± 0.07b	41.98 ± 2.10	43.61 ± 2.18b	86.75 ± 4.34b	23.88 ± 1.19c	9.19 ± 0.46	6.00 ± 0.30b	1.54 ± 0.08	0.65 ± 0.03b,c	10.42 ± 0.52	5.10 ± 0.26b,c
To L MH	1,162.50 ± 58.13a,c	379.38 ± 18.97	4.88 ± 0.24a,b,c	1.54 ± 0.08b	43.00 ± 2.15	42.10 ± 2.11b	88.38 ± 4.42b	31.25 ± 1.56a	8.51 ± 0.43a,b	6.84 ± 0.34a,b,c	1.65 ± 0.08	0.59 ± 0.03	9.93 ± 0.50	4.06 ± 0.20a,b
Tp F UAE	1,318.75 ± 65.94b	433.00 ± 21.65b	4.66 ± 0.23a,b,c	1.38 ± 0.07b	39.18 ± 1.96	42.35 ± 2.12b	82.00 ± 4.10	24.00 ± 1.20c	8.49 ± 0.42a,b	5.54 ± 0.28b	1.63 ± 0.08	0.68 ± 0.03b,c	9.85 ± 0.49	4.84 ± 0.24b,c
Tp F MH	1,360.00 ± 68.00b	365.88 ± 18.29	4.51 ± 0.23a,b,c	1.65 ± 0.08b	40.55 ± 2.03	40.68 ± 2.03b	84.38 ± 4.22	29.13 ± 1.46	8.03 ± 0.40a,b	5.73 ± 0.29b	1.68 ± 0.08	0.55 ± 0.03a	9.58 ± 0.48	3.95 ± 0.20a,b
Ur L UAE	1,185.00 ± 59.25a,c	517.13 ± 25.86a,b,c	4.85 ± 0.24a,b,c	1.50 ± 0.08b	38.38 ± 1.92	44.41 ± 2.22b	74.50 ± 3.73	30.63 ± 1.53a	8.81 ± 0.44a	6.44 ± 0.32a,b	1.58 ± 0.08	0.63 ± 0.03b,c	9.46 ± 0.47	5.11 ± 0.26b,c
Ur L MH	1,156.25 ± 57.81a,c	390.38 ± 19.52	4.69 ± 0.23a,b,c	1.54 ± 0.08b	37.71 ± 1.89	41.95 ± 2.10b	72.63 ± 3.63a	29.75 ± 1.49	8.63 ± 0.43a,b	9.34 ± 0.47a,b,c	1.61 ± 0.08	0.54 ± 0.03a	8.61 ± 0.43	4.39 ± 0.22a,b,c
Vo R UAE	1,582.50 ± 79.13b	541.75 ± 27.09a,b,c	5.73 ± 0.29	1.81 ± 0.09a,c	41.88 ± 2.09	45.41 ± 2.27b	81.75 ± 4.09	27.75 ± 1.39	9.76 ± 0.49	5.65 ± 0.28b	1.50 ± 0.08	0.71 ± 0.04b,c	9.84 ± 0.49	5.60 ± 0.28b,c
Vo R MH	1,201.25 ± 60.06a	545.88 ± 27.29a,b,c	4.35 ± 0.22a,b,c	2.24 ± 0.11a,b,c	41.55 ± 2.08	46.11 ± 2.31b	82.63 ± 4.13	33.13 ± 1.66a,b	8.09 ± 0.40a,b	7.24 ± 0.36a,b,c	1.61 ± 0.08	0.64 ± 0.03b,c	9.31 ± 0.47	4.11 ± 0.21a,b

(a) Statistically significant differences ($p < 0.05$) between the control group (C) and the botanical extracts. (b) Statistically significant differences ($p < 0.05$) between the formulation (CF) and the botanical extracts. (c) Statistically significant differences ($p < 0.05$) between commercial biostimulant (CB) and the botanical extracts. UAE, ultrasound-assisted extraction; MH, mechanical homogenization; Hp H, Hypericum perforatum L. (St. John's wort, herb); Sg L, Solidago gigantea Ait. (giant goldenrod, leaf); To F, To L, Taraxacum officinale (L.) Weber ex F.H. Wigg (common dandelion, flower, leaf); Tp F, Trifolium pratense L. (red clover, flower); Ur L, Urtica dioica L. (nettle, leaf); Vo R, Valeriana officinalis L. (valerian, root).

C and CB) and Vo R UAE (3.4 and 16.6% more than in C and CB), and the lowest was found with Tp F MH (31.4 and 22.6% less than in C and CB).

Fatty Acids

The largest percentage share of fatty acids (**Supplementary Table 2**) accounted for linolenic acid (methyl ester) and hexadecanoic acid (methyl ester), followed by 9,12-hexadecadienoic acid (methyl ester), 9*Z*-9-octadecenoic acid (ethyl ester), 11-octadecenoic acid (methyl ester), and octadecanoic acid (methyl ester). The content of linolenic acid was the highest in the groups treated with Ur L UAE (14.7 and 19.3% more than in C and CB) and Sg L MH (14.3 and 18.8% more than in C and CB) and the lowest after the application of Ur L MH (27.2 and 24.3% less than in C and CB) and Tp F MH (24.8 and 21.8% less than in C and CB). The tested botanical extracts did not increase the amount of the second acid in comparison with the control group. The highest value was achieved for Sg L MH (13.2% less than in C and 9% more than in CB), and the lowest was achieved for To F MH (34.7 and 18% less than in C and CB). The application of Sg L MH resulted in the highest amount of 9,12-hexadecadienoic acid (6.4 and 23.7% more than in C and CB) and 11-octadecenoic acid (1% less than in C and 19.3% more than in CB) in comparison to the other examined extracts, while the lowest was observed in groups treated with Ur L MH: 38.7 and 28.7% less than in C and CB for 9,12-hexadecadienoic acid and 35.1 and 21.8% less than in C and CB for 11-octadecenoic acid, respectively. On the other hand, the largest percentage share of 9*Z*-9-octadecenoic acid was noted after the foliar spraying with Ur L UAE (29.5 and 16% less than in C and CB). The greatest stimulation of octadecanoic acid content was observed in the group treated with To F UAE (39.3% less than in C and 10% more than in CB). The application of To F MH caused the smallest increase in 9*Z*-9-octadecenoic acid (53 and 43.9% less than in C and CB) and octadecanoic acid (53.3 and 15.4% less than in C and CB) content. It can be seen that, of all used extracts, To F UAE increased to the greatest extent the content of tetradecanoic acid (ethyl ester) (no change in the control group and 225% more than in CB), tetradecanoic acid (12-methyl-, methyl ester) (8.4 and 177% more than in C and CB), and pentadecanoic acid (14-methyl-, methyl ester) (4.1 and 181% more than in C and CB), while Tp F UAE had the greatest content of *Z*-9-Hexadecenoic acid (methyl ester) (3.4 and 29.5% more than in C and CB). The treatment with Tp F MH decreased the amount of tetradecanoic acid (ethyl ester) (65% less than in C and 13.7% more than in CB) and pentadecanoic acid (14-methyl-, methyl ester) (63.2 and 0.8% less than in C and CB). The lowest content of tetradecanoic acid (12-methyl-, methyl ester) was observed for Hp H MH (59% less than in C and 4.6% more than in CB), while the lowest content of *Z*-9-hexadecenoic acid (methyl ester) was observed for To L UAE (62.1 and 52.6% less than in C and CB).

Sterols

Only two sterols were observed in the dried radish roots (**Table 8**). It can be seen that the botanical extracts mostly lowered the content of β-sitosterol (TMS derivative), for instance, after treatment with To L MH (8.9 and 8.4% less than in C and CB). Only the foliar application of Tp F UAE (1.9 and 2.5% more than in C and CB) and Sg L UAE (0.1 and 0.7% more than in C and CB) led to an increase of the previously mentioned content. The opposite trend was observed in the amount of campesterol (TMS derivative); in most of the cases, this content was enhanced, e.g., in the group sprayed with To L MH (15.7 and 14.5% more than in C and CB), while only two bio-products diminished it: Tp F UAE (3.3 and 4.3% less than in C and CB) and Sg L UAE (0.2 and 1.3% less than in C and CB).

TABLE 8 | The effect of the foliar application of the botanical extracts on the sterols composition [the amount of a single component calculated as a percentage (%) of the whole GC-MS chromatogram area] ($N = 3$, mean ± SD) of radish roots (after harvest).

	Campesterol, TMS derivative	β-Sitosterol, TMS derivative
RT, min	26.592	27.975
RI_exp	2,683	2,784
RI_lit	2,689	2,789
C	36.17 ± 0.23	63.83 ± 0.23
CF	36.37 ± 0.07	63.63 ± 0.07
CB	36.56 ± 0.09	63.44 ± 0.09
Hp H UAE	36.93 ± 0.06a,b	63.07 ± 0.06a,b
Hp H MH	37.96 ± 0.08a,b,c	62.04 ± 0.08a,b,c
Sg L UAE	36.09 ± 0.10c	63.91 ± 0.10c
Sg L MH	36.26 ± 0.08	63.74 ± 0.08
To F UAE	36.34 ± 0.07	63.66 ± 0.07
To F MH	36.82 ± 0.10a	63.18 ± 0.10a
To L UAE	39.00 ± 0.04a,b,c	61.00 ± 0.04a,b,c
To L MH	41.86 ± 0.10a,b,c	58.14 ± 0.10a,b,c
Tp F UAE	34.97 ± 0.05a,b,c	65.03 ± 0.05a,b,c
Tp F MH	36.42 ± 0.15	63.58 ± 0.15
Ur L UAE	39.87 ± 0.11a,b,c	60.13 ± 0.11a,b,c
Ur L MH	37.82 ± 0.15a,b,c	62.18 ± 0.15a,b,c
Vo R UAE	37.93 ± 0.15a,b,c	62.07 ± 0.15a,b,c
Vo R MH	37.55 ± 0.23a,b,c	62.45 ± 0.23a,b,c

(a) Statistically significant differences ($p < 0.05$) between the control group (C) and the botanical extracts. (b) Statistically significant differences ($p < 0.05$) between the formulation (CF) and the botanical extracts. (c) Statistically significant differences ($p < 0.05$) between commercial biostimulant (CB) and the botanical extracts. RT, retention time; RI, retention indices; RI_lit, retention indices according to NIST (The NIST Mass Spectral Search Program for the NIST/EPA/NIH EI and NIST Tandem Spectral Library, 2017); RI_exp, retention indices based on experiments; UAE, ultrasound-assisted extraction; MH, mechanical homogenization; Hp H, Hypericum perforatum L. (St. John's wort, herb); Sg L, Solidago gigantea Ait. (giant goldenrod, leaf); To F, To L, Taraxacum officinale (L.) Weber ex F.H. Wigg (common dandelion, flower, leaf); Tp F, Trifolium pratense L. (red clover, flower); Ur L, Urtica dioica L. (nettle, leaf); Vo R, Valeriana officinalis L. (valerian, root).

Glucosinolates

The detected glucosinolates in the radish roots are presented in **Table 9**. It can be noted that the foliar treatment with the botanical extracts had a statistically significant impact on the glucosinolates composition. The chromatographic analyses revealed that the roots consisted mostly of glucoerucin and glucobrassicanapin, followed by gluconasturtiin, and then gluconapin. The content of glucoerucin was the most increased in the groups treated with Sg L UAE (9.8 and 8.5% more than in

C and CB), Hp H UAE (7.2 and 5.9% more than in C and CB), Hp H MH (6.6 and 5.3% more than in C and CB), and the least with Vo R MH (8.6 and 9.8% less than in C and CB), To F UAE (8.3 and 9.4% less than in C and CB), and Ur L UAE (8.2 and 9.3% less than in C and CB). In the case of glucobrassicanapin, the highest amounts were observed in the groups treated with To L UAE (7 and 8.5% more than in C and CB) and Ur L MH (5.9 and 7.4% more than in C and CB), while the lowest with Hp H MH (1% less than in C and 0.3% more than in CB), Sg L MH (0.5% less than in C and 0.8% more than in CB), and Hp H UAE (0.5% less than in C and 0.9% more than in CB). The concentration of gluconasturtiin was the most increased after the treatment with Sg L MH (2.9 and 10.6% more than in C and CB), Vo R MH (2.2 and 9.8% more than in C and CB), and Tp F UAE (1.1 and 8.7% more than in C and CB), while the most decreased with To L UAE (10.6 and 4% less than in C and CB), Ur L MH (10.1 and 3.4% less than in C and CB), and Sg L UAE (9.8 and 3.1% less than in C and CB). The content of gluconapin was the most elevated in the groups sprayed with Sg L MH (39.2 and 18.7% more than in C and CB) and Vo R MH (38.4 and 18% more than in C and CB), whereas the utilization of To F MH (0.4 and 15.1% less than in C and CB) and Tp F MH (2.3% more than in C and 12.8% less than in CB) led to the lowest values this parameter.

DISCUSSION

About 33% of global organic farming is located in Europe, and 6.4% of this farming is situated in Poland, where the interest in sustainable agricultural techniques and technologies is constantly growing and has been especially strong in the recent years of 1999–2013. During this period, the number of Polish producers of organic food increased from 27 to 26,499, and the crop area increased from 300 to 674,694 ha (Pylak et al., 2019). Thus, there is clearly a need to develop new, sustainable products to provide high-quality yields and support the future of organic farming (Röös et al., 2018). The lower yield (by 5–32%) in organic horticulture, in relation to conventional farming, is mostly caused by nutrient availability (mainly N and P) but is also linked to fungal or bacteria pathogens (Fess and Benedito, 2018; Pylak et al., 2019). Therefore, the application of biostimulants to increase crop productivity, soil nutrient availability, water use efficiency, plant nutrient uptake, and assimilation has emerged as a promising eco-friendly approach. These factors could contribute to a decrease in the use of fertilizers (in particular, rich in nitrogen) and an increase in crop tolerance to abiotic and biotic stresses (Bulgari et al., 2015, 2019; Paradiković et al., 2018; Drobek et al., 2019; Pylak et al., 2019; Rouphael and Colla, 2020). The broad modes of action of biostimulants range from triggering N metabolism or P release from soil to stimulating root growth and improving plant establishment (Madende and Hayes, 2020), which are advantageous activities from both an economic and environmental perspective (Rouphael and Colla, 2020). Furthermore, these products have not shown negative or harmful impacts on people and animals. The positive effects resulting from their use are influenced by many factors, including the type of bio-product, the dose, the application method, and the plant cultivar (Drobek et al., 2019).

The types of raw materials, solvents, and extraction methods have a significant influence on the final composition of biostimulants of plant growth (Pylak et al., 2019; Madende and Hayes, 2020). For biostimulant production, fresh (when unstable compounds are present) or dry materials, grounded into small particles, can be used. Water is the most popular solvent, but the use of organic ones (e.g., ethanol, methanol) allows to extract more substances (aromatic or saturated organic compounds), exhibiting better activity (e.g., antimicrobial) (Pylak et al., 2019). Biostimulants consist of various bioactive compounds, such as amino acids, peptides, proteins, nucleotides, nucleosides, lipids, phenols, phenolic acids, quinones, flavones, flavonoids, flavonols, tannins and coumarins, terpenoids/isoprenoids, alkaloids, glucosinolates, plant hormones (abscisic acid, auxins, cytokinins, gibberellins, ethylene), plant growth regulators (brassinosteroids), betaines, sugars (carbohydrates, oligo-, and polysaccharides), aminopolysaccharides, vitamins, humic substances, beneficial elements, furostanol glycosides, and sterols (Baghel et al., 2019; Pylak et al., 2019; Madende and Hayes, 2020). Because these chemical substances exhibit diverse effects, the modes of their action remain mostly unidentified (Paradiković et al., 2018; Bulgari et al., 2019; Caradonia et al., 2019; Drobek et al., 2019; Kim et al., 2019; Madende and Hayes, 2020). Furthermore, the composition of various biostimulants has still not been fully characterized (Pylak et al., 2019; Madende and Hayes, 2020), and biostimulants usually consist of complex multicomponents whose activities depend on the synergistic action of different bioactive molecules rather than individual compounds (Bulgari et al., 2019; Caradonia et al., 2019). Transcriptome analyses will allow us to scrutinize gene expression and thus provide greater knowledge of the biostimulant targets in plants, the affected physiological pathways, and the activated receptors. This information will improve our understanding of the effects and functions of their components (identified and unidentified) and may be used in the classification of new products and assessment of their effectiveness (Bulgari et al., 2015).

The current state of knowledge shows that different mechanisms may participate in the stimulating properties of biostimulants. Their positive effects on the yield and the quality of crops may result from the use of a single bio-product, as well as a combination of several products, allowing them to provide even better results. It is still necessary to undertake detailed wide-scale research on the impact of specific biostimulants on various species, treatments (e.g., doses and application methods), growth stages, etc. (Paradiković et al., 2018). We have conducted a series of experiments on various plant species, including radish (present study, field conditions), celeriac (field conditions) (Godlewska et al., 2020b), cabbage seedlings (laboratory tests) (Godlewska et al., 2019, 2020a), and white head cabbage (field conditions) (Godlewska et al., 2021), using botanical extracts (produced from St. John's wort, giant goldenrod, common dandelion, red clover, nettle, and valerian). Significant differences were observed in the plant responses to these bioproducts. The plant-based extracts that exerted the highest (↑) and lowest (↓) biostimulating activity of the examined parameters are summarized in **Tables 10A**,**B**. This comparison indicates the importance of precise planning

TABLE 9 | The effect of the foliar application of the botanical extracts on the glucosinolates content ($\mu g \cdot g^{-1}$) ($N = 3$, mean ± SD) of radish roots (after harvest).

Group	Glucoerucin	Gluconapin	Progoitrin	Glucoraphenin	4-metoxyglucobrassicin	Glucobrassicin	Glucoraphanin	Gluconasturtiin	Glucobrassicanapin
C	241.29 ± 15.27	48.69 ± 5.59	7.73 ± 0.90	21.38 ± 1.53	26.45 ± 0.79	17.39 ± 0.90	8.82 ± 0.49	135.73 ± 3.49c	218.58 ± 4.17b
CF	245.59 ± 0.81	43.28 ± 2.41c	9.00 ± 0.16	21.51 ± 0.42	25.06 ± 0.58c	17.53 ± 0.20	8.68 ± 0.33	130.81 ± 0.38	227.91 ± 0.80a,c
CB	244.30 ± 7.34	57.12 ± 2.55b	7.47 ± 0.26	22.47 ± 0.30	28.17 ± 0.38b	16.94 ± 0.40	8.47 ± 0.17	126.27 ± 0.90a	215.61 ± 0.88b
Hp H UAE	258.70 ± 4.76	60.51 ± 0.86a,c	7.61 ± 0.50	25.20 ± 0.57a,b	29.46 ± 0.49a,b	17.65 ± 0.65	8.69 ± 0.23	135.75 ± 1.80c	217.55 ± 1.08b
Hp H MH	257.29 ± 7.61	55.02 ± 2.54b	8.53 ± 0.61	20.82 ± 0.61	27.85 ± 0.17b	17.98 ± 0.29	10.80 ± 0.32a,b,c	124.66 ± 0.22a,b	216.35 ± 0.49b
Sg L UAE	265.00 ± 8.20	62.58 ± 2.81a,b	7.96 ± 0.33	22.69 ± 0.85	25.39 ± 0.41c	17.05 ± 0.47	10.29 ± 0.35a,b,c	122.40 ± 3.25a,b	227.69 ± 1.81a,c
Sg L MH	238.56 ± 3.11	67.78 ± 1.29a,b	7.37 ± 0.42	23.30 ± 0.53	25.45 ± 0.78c	17.87 ± 0.53	9.40 ± 0.50	139.62 ± 0.61b,c	217.40 ± 1.19b
To F UAE	221.23 ± 1.34	64.79 ± 1.59a,b	7.75 ± 0.39	23.13 ± 1.43	28.97 ± 0.67a,b	18.24 ± 0.85	8.95 ± 0.65	132.77 ± 0.61c	228.17 ± 1.47a,c
To F MH	234.64 ± 3.79	48.47 ± 4.62	8.43 ± 0.24	19.36 ± 0.35	26.27 ± 0.75	17.75 ± 0.85	9.74 ± 0.41	130.73 ± 0.07	218.49 ± 0.88b
To L UAE	235.09 ± 5.09	63.24 ± 3.72a,b	7.59 ± 0.31	24.12 ± 1.98	28.67 ± 0.74b	17.11 ± 0.31	9.02 ± 0.32	121.28 ± 1.41a,b	233.98 ± 3.08a,c
To L MH	249.64 ± 2.97	55.02 ± 4.85b	7.09 ± 0.63b	21.60 ± 0.20	24.37 ± 0.48c	16.66 ± 0.25	8.82 ± 0.11	129.65 ± 1.59a	224.23 ± 0.44c
Tp F UAE	239.82 ± 4.13	61.56 ± 0.88a,b	7.86 ± 0.45	22.45 ± 0.46	28.91 ± 0.64a,b	17.93 ± 0.69	9.10 ± 0.26	137.21 ± 1.05b,c	220.62 ± 1.09b
Tp F MH	231.04 ± 2.72	49.79 ± 2.01	6.89 ± 0.51b	20.66 ± 1.48	25.61 ± 0.27c	18.75 ± 0.38	9.69 ± 0.24	128.14 ± 0.38a	218.46 ± 0.26b
Ur L UAE	221.61 ± 1.23	61.99 ± 1.45a,b	8.02 ± 0.28	23.27 ± 0.48	28.44 ± 1.03b	17.60 ± 0.47	8.90 ± 0.33	132.36 ± 1.78c	224.03 ± 1.33c
Ur L MH	243.87 ± 9.45	56.67 ± 2.47b	8.03 ± 0.50	21.77 ± 0.99	25.91 ± 0.78	16.75 ± 0.31	11.06 ± 0.19a,b,c	121.96 ± 0.82a,b	231.58 ± 0.32a,c
Vo R UAE	247.13 ± 18.65	62.21 ± 2.54a,b	7.87 ± 0.48	21.46 ± 1.01	25.91 ± 0.67	17.08 ± 0.90	9.27 ± 0.24	132.03 ± 2.25	223.87 ± 2.24c
Vo R MH	220.44 ± 1.74	67.40 ± 0.92a,b	7.51 ± 0.40	22.95 ± 0.67	27.52 ± 0.34b	17.91 ± 0.47	9.67 ± 0.44	138.66 ± 0.95b,c	224.97 ± 1.35a,c

(a) Statistically significant differences ($p < 0.05$) between the control group (C) and the botanical extracts. (b) Statistically significant differences ($p < 0.05$) between the formulation (CF) and the botanical extracts. (c) Statistically significant differences ($p < 0.05$) between commercial biostimulant (CB) and the botanical extracts. UAE, ultrasound-assisted extraction; MH, mechanical homogenization; Hp H, Hypericum perforatum L. (St. John's wort, herb); Sg L, Solidago gigantea Ait. (giant goldenrod, leaf); To F, To L, Taraxacum officinale (L.) Weber ex F.H. Wigg (common dandelion, flower, leaf); Tp F, Trifolium pratense L. (red clover, flower); Ur L, Urtica dioica L. (nettle, leaf); Vo R, Valeriana officinalis L. (valerian, root).

of research, as well as studying the impact of the obtained products on various plant species. In general, extracts based on the common dandelion, valerian, nettle, and giant goldenrod could be considered in the cultivation of cabbage; those based on St. John's wort, common dandelion, and giant goldenrod could be used to cultivate celeriac; and those based on the common dandelion, valerian, giant goldenrod could be used for growing radish.

The application of plant-derived biostimulants has continued to rise by virtue of their favorable impact on the growth, yield, vigor, quality, and shelf life of some horticultural plants (e.g., due to the content of bioactive peptides that activate signaling pathways involving phytohormone biosynthesis) (Baghel et al., 2019; Caradonia et al., 2019; Jindo et al., 2020; Rouphael and Colla, 2020; Zulfiqar et al., 2020). Peptides are also engaged in the cell differentiation, induction of protease inhibitors, cell division, and pollen self-incompatibility responses (Kim et al., 2019). A higher content of proteins may be associated with an increase in the carbohydrate content in leaves. In turn, a greater amount of sugars generally accelerates nitrogen inclusions through the nitrate assimilation pathway. This increased growth can be also ascribed to sugars that serve as an energy source and stimulate nitrogen uptake. Carbohydrates provide the skeleton for the incorporation of reduced nitrate (ammonia) in amino acids and increased protein biosynthesis. The enhancement of sugar biosynthesis in plants is also linked to the higher content of chlorophyll, net photosynthesis, and quantum efficiency of photosystem II (Bulgari et al., 2015). Polysaccharides and a combination of diverse amino acids and short peptides (protein hydrolysates) exhibit a beneficial impact on plant growth and protection against abiotic and/or biotic stresses (Bulgari et al., 2019).

Biostimulants act in numerous stages of plant growth, from increasing the accessibility of nutrients in the soil to improving the postharvest quality of crops (even during stress conditions) (Zulfiqar et al., 2020). Their mechanisms, founded upon enhanced physiological, biochemical, and molecular processes, can be attributed to (a) the stimulation of essential enzymatic activities that correlate with the metabolism of nitrogen and the elicitation of target hormone-like activity (auxin and gibberellin; direct mechanism) and (b) the increase in the nutritional status of crops through the alteration of root development (biomass, density, and lateral root branching), which increases the absorption and translocation of macro and micro-nutrients (Caruso et al., 2019; Pylak et al., 2019; Zulfiqar et al., 2020). Higher nutrient availability can be affected by several factors, such as the presence of compounds in biostimulants (e.g., nutrients, amino acids, peptides, peptones, or proteins), improved microbial activity, or the content of chelating agents, thereby increasing nutrient solubility in soil. Biostimulants can also enhance nutrient uptake by upregulating the genes involved in their transport (Pylak et al., 2019), ameliorate the microbial and enzymatic activity of the soil, modify the solubility and transportability of micronutrients, increase soil cation exchange via nitrogen provision, and create more available complexes with insoluble elements (e.g., Fe) (Bulgari et al., 2019; Madende and Hayes, 2020). An improved photosynthesis process and carbon metabolism may also be observed (Zulfiqar et al., 2020). Studies showed that improved root growth is not necessarily associated with the presence of auxins due to their low concentrations but, instead, with organic compounds (e.g., amino acids, linear carboxylic acids, and aromatic carboxylic acids) that show auxin-like activity (Pylak et al., 2019).

The use of biostimulants can be particularly advantageous in poor soil conditions and in horticultural crops with low inputs (Bulgari et al., 2019). The inhibition of pathogen growth, antimicrobial activity, and defense mechanisms can be triggered by the presence of compounds that have phenolic structures, e.g., carvacrol, eugenol, or thymol (Pylak et al., 2019). Various antioxidants and elicitors, due to their synthesis in plants, can help deal with adverse growth conditions (e.g., temperature extremes, drought, and reduced nutrient absorption) (Paradiković et al., 2018). Biostimulants can alter the activity of enzymes and influence the antioxidant properties of compounds, such as lycopene, ascorbic acid, and phenolic compounds (Drobek et al., 2019).

The present study showed that extracts based on higher plants had a significant impact on the growth and physiological parameters of radish. The foliar application of the obtained formulations increased the yield of leaves of rosette (e.g., Sg L MH, Hp H MH), as well as the roots (e.g., To L MH, Sg L MH), dry weight (e.g., Ur L UAE), the content of photosynthetic pigments (e.g., Vo R UAE) and vitamin C (e.g., Vo R MH, Tp F MH). In the majority of cases, the tested extracts did not enhance the amount of total phenolic compounds (excluding, e.g., To F MH). The antioxidant activity (measured using the DPPH and ABTS assays) was mainly decreased in the leaves and increased in the roots after the application of the botanical extracts. The opposite trend was observed in the antioxidant activity measured using the FRAP assay. We also observed macronutrient enrichment in the leaves of rosette (e.g., Ur L UAE, Vo R MH, To L MH) and the roots (e.g., Hp H UAE, Vo R MH, Sg L UAE, To L UAE), alongside enrichment of micronutrients in the leaves of rosette (e.g., To L UAE, Hp H UAE, Vo R UAE, Sg L UAE) and the roots (e.g., Vo R MH, To F UAE). In most cases, the obtained bio-products lowered the content of heavy metals in the radish leaves and roots. The foliar application of the extracts exerted a varied impact on the composition of steam volatile compounds, fatty acids, sterols, and glucosinolates. The application of the bio-products resulted in higher content of nitrates in all parts of the model plant (e.g., Vo R MH, Ur L UAE).

The tested plant-based extracts are products that can be used in agriculture as potential biostimulants to reduce the cost of food production and achieve better quality yields. The raw materials (plants commonly found in the natural environment) constitute a rich source of biologically active compounds that exhibit a beneficial effect on the growth and chemical composition of crop plants. The final effect of their action depends on numerous factors (e.g., the raw material type, the extraction method, the application method, the plant variety, and the growth conditions). It is still necessary to conduct further research to gain a better understanding of their mechanisms. To understand the multiple effects of biostimulants, the development of appropriately designed experiments is crucial. Considering their positive effects on plants and various novel research possibilities, these biostimulants are attracting

TABLE 10A | Effect of the foliar application of the examined botanical extracts on the growth and development of different model plants under controlled conditions (laboratory tests) and real environmental conditions (field trials).

Examined parameter		Laboratory tests – cabbage seedlings (Godlewska et al., 2019, 2020a)	Field tests – cabbage (Godlewska et al., 2021)	Field tests – celeriac (Godlewska et al., 2020b)	Field tests – radish (current study)
Fresh weight	↑	Shoots – Ur L UAE (98.8 and 106.1% more than in C and CB) – To F UAE (91.8 and 98.8% more than in C and CB) Roots – Vo R UAE (215.4 and 115.8% more than in C and CB) – Sg L UAE (184.6 and 94.7% more than in C and CB) – To F UAE (161.5 and 78.9% more than in C and CB) – To L UAE (176.9 and 89.5% more than in C and CB) – Hp H UAE (153.8 and 73.7% more than in C and CB) – Ur L UAE (146.2 and 68.4% more than in C and CB)	Head weight < 1.2 kg – Tp F UAE (50 and 106% more than in C and CB) – Vo R UAE (37.9 and 89.6% more than in C and CB) – Hp H MH (36.4 and 87.5% more than in C and CB) – To L UAE (36.4 and 87.5% more than in C and CB) – Ur L UAE (33.3 and 83.3% more than in C and CB) Outer leaves of head weight < 1.2 kg – Vo R UAE (37.5 and 49.4% more than in C and CB) – Ur L UAE (35.2 and 46.9% more than in C and CB) – Hp H MH (23.9 and 34.6% more than in C and CB) Head weight > 1.2 kg – Hp H UAE (8.8 and 3.6% more than in C and CB) – Ur L MH (2.3 more than in C and 2.6% less than in CB) – To F MH (1.5 more than in C and 3.3% less than in CB) Outer leaves of head weight > 1.2 kg – Sg L UAE (17.9 and 11.3% more than in C and CB) – Tp F MH (10.6 and 4.4% more than in C and CB) – Sg L MH (9.3 and 3.1% more than in C and CB) – Hp H UAE (7.9 and 1.9% more than in C and CB)	Root diameter < 5 cm Leaves of rosette – To F UAE (152.4 and 104.9% more than in C and CB) Roots – Tp F UAE (29.9 and 86.6% more than in C and CB) Root diameter 5–9 cm Leaves of rosette – To L MH (12.2% less than in C and 11.8% more than in CB) Roots – To L MH (5.3 less than in C and 11.9% more than in CB) Root diameter 9–13 cm Leaves of rosette – Hp H MH (no plants in C and 104.7% more than in CB) Roots – Hp H MH (no plants in C and 77.1% more than in CB)	Root diameter < 2 cm Leaves of rosette – To F UAE (2.4% less than in C and 20.4% more than in CB) – Vo R MH (3.9% less than in C and 18.5% more than in CB) Roots – Vo R MH (4.8% less than in C and 67.0% more than in CB) – Sg L MH (8.8% less than in C and 60.0% more than in CB) Root diameter 2–4 cm Leaves of rosette – Hp H MH (35.0 and 14.9% more than in C and CB) – Sg L MH (34.6 and 14.5% more than in C and CB) – Vo R MH (31.4 and 11.8% more than in C and CB) Roots – To L MH (50.7 and 24.4% more than in C and CB) – Sg L MH (42.7 and 17.9% more than in C and CB) Root diameter > 4 cm Leaves of rosette – Hp H MH (no plants in C; 32.8% more than in CB) – Sg L UAE (no plants in C; 34.0% more than in CB) Roots – Tp F UAE (no plants in C; 10.2% more than in CB)

(Continued)

TABLE 10A | Continued

Examined parameter		Laboratory tests – cabbage seedlings (Godlewska et al., 2019, 2020a)	Field tests – cabbage (Godlewska et al., 2021)	Field tests – celeriac (Godlewska et al., 2020b)	Field tests – radish (current study)
	↓	Shoots – Hp H UAE (0 and 3.7% more than in C and CB) Roots – Tp F UAE (84.6 and 26.3% more than in C and CB)	Head weight < 1.2 kg – Vo R MH (33.3 and 8.3% less than in C and CB) Outer leaves of head < 1.2 kg – To L UAE (26.1 and 19.8% less than in C and CB) – To F MH (23.9 and 17.3% less than in C and CB) Head weight > 1.2 kg – Sg L MH (14.6 and 18.6% less than in C and CB) – To F UAE (11.5 and 15.7% less than in C and CB) – Ur L UAE (10.0 and 14.2% less than in C and CB) Outer leaves of head weight > 1.2 kg – Ur L UAE (13.2 and 18.1% less than in C and CB) – To F UAE (8.6 and 13.8% less than in C and CB)	Root diameter < 5 cm Leaves of rosette – Sg L MH (2.8 and 21.2% less than in C and CB) Roots – Sg L MH (48.4 and 25.9% less than in C and CB) Root diameter 5–9 cm Leaves of rosette – Tp F UAE (39.6 and 23.1% less than in C and CB) Roots – Vo R MH (31.4 and 18.9% less than in C and CB) Root diameter 9–13 cm Leaves of rosette – To F MH (no plants in C; 3.0% less than in CB) Roots – Tp F MH (no plants in C; 7.5% less than in CB)	Root diameter < 2 cm Leaves of rosette – To L MH (30.4 and 14.1% less than in C and CB) – Ur L UAE (29.4 and 13.0% less than in C and CB) Roots – Ur L UAE (40.5% less than in C and 4.4% more than in CB) Root diameter 2–4 cm Leaves of rosette – To F UAE (4.3 and 18.5% less than in C and CB) Roots – Ur L UAE (15.2% more than in C and 4.9% less than in CB) – Ur L MH (16.6% more than in C and 3.7% less than in CB) Root diameter > 4 cm Leaves of rosette – Vo R UAE (no plants in C; 8.2% less than in CB) Roots – Hp H UAE (no plants in C; 35.7% less than in CB)
Dry weight	↑	Shoots – To F UAE (60.7 and 61.6% more than in C and CB) – Ur L UAE (60.2 and 61.0% more than in C and CB) Roots – Vo R UAE (53.3 and 33.3% more than in C and CB) – Sg L UAE (48.3 and 29.0% more than in C and CB) – To L UAE (48.3 and 29.0% more than in C and CB)	Leaves after the second spraying – To F MH (10.2 and 7.8% more than in C and CB) – Ur L UAE (7.5 and 5.2% more than in C and CB) Heads after harvest – Hp H UAE (3.7 and 7.1% more than in C and CB) – Vo R UAE (4.3 and 7.7% more than in C and CB)	The first term of leaves of rosette collection – Sg L UAE (0.4 and 1.3% more than in C and CB) The second term of leaves of rosette collection – Tp F MH (20.8 and 12.8% more than in C and CB) Roots – To F MH (28.7% more than in C and 2.2% less than in CB) – To L MH (28.7% more than in C and 2.2% less than in CB) – Tp F UAE (30.2% more than in C and 1.0% less than in CB) – Vo R MH (29.3% more than in C and 1.7% less than in CB)	The first term of leaves of rosette collection – Ur L UAE (7.5 and 17.2% more than in C and CB) The second term of leaves of rosette collection – Ur L UAE (8.3 and 10.9% more than in C and CB) Roots – Ur L UAE (37.9 and 51.8% more than in C and CB)

(Continued)

TABLE 10A | Continued

Examined parameter		Laboratory tests – cabbage seedlings (Godlewska et al., 2019, 2020a)	Field tests – cabbage (Godlewska et al., 2021)	Field tests – celeriac (Godlewska et al., 2020b)	Field tests – radish (current study)
	↓	Shoots – Hp H UAE (1.3 and 1.8% more than in C and CB) Roots – Tp F UAE (27.0 and 10.4% more than in C and CB)	Leaves after the second spraying – Hp H UAE (7.6 and 9.6% less than in C and CB) Heads after harvest – Ur L MH (9.7 and 6.8% less than in C and CB)	The first term of leaves of rosette collection – Sg L MH (6.4 and 5.5% less than in C and CB) The second term of leaves of rosette collection – Vo R UAE (0.4% more than in C and 6.2% less than in CB) Roots – Ur L UAE (9.6% more than in C and 16.7% less than in CB)	The first trm of leaves of rosette collection – To L MH (12.7 and 4.8% less than in C and CB) The second term of leaves of rosette collection – To L MH (13.9 and 11.9% less than in C and CB) Roots – Sg L MH (7.3% less than in C and 2.1% more than in CB)
Chlorophyll *a* + *b*	↑	Leaves – To L UAE (109.6 and 1.0% more than in C and CB) – Hp H UAE (106.2% more than in C and 1.7% less than in CB) Roots n/a	Leaves after the second spraying – To L MH (46.0 and 24.0% more than in C and CB) – To F MH (31.5 and 11.6% more than in C and CB) – Hp H MH (30.6 and 11.0% more than in C and CB) – To L UAE (28.2 and 8.9% more than in C and CB) – Sg L UAE (25.8 and 6.8% more than in C and CB) – Sg L MH (25.0 and 6.2% more than in C and CB)	The first term of leaves of rosette collection – Ur L MH (17.6 and 2.2% more than in C and CB) – Sg L MH (16.7 and 1.2% more than in C and CB) – Hp H MH (16.7 and 1.2% more than in C and CB) The second term of leaves of rosette collection – To F UAE (11.4 and 34.7% more than in C and CB) – To F MH (5.9 and 28.1% more than in C and CB) Roots n/a	The first term of leaves of rosette collection – Vo R UAE (31.5 and 26.3% more than in C and CB) The second term of leaves of rosette collection – Vo R UAE (4.5 and 16.7% more than in C and CB) – Sg L MH (4.5 and 16.7% more than in C and CB) – Ur L MH (3.0 and 15.0% more than in C and CB) Roots n/a
	↓	Leaves – Vo R UAE (1.9% more than in C and 51.4% less than in CB) – To F UAE (7.7% more than in C and 48.6% less than in CB) Roots n/a	Leaves after the second spraying – To F UAE (6.5% more than in C and 9.6% less than in CB) – Vo R MH (9.7% more than in C and 6.8% less than in CB)	The first term of leaves of rosette collection – To L UAE (2.9 and 15.7% less than in C and CB) – Tp F UAE (0.5 and 13.6% less than in C and CB) The second term of leaves of rosette collection – Ur L UAE (9.3% less than in C and 9.7% more than in CB) – Vo R MH (8.9% less than in C and 10.2% more than in CB) Roots n/a	The first term of leaves of rosette collection – To L MH (16.4 and 19.7% less than in C and CB) The second term of leaves of rosette collection – To L UAE (19.4 and 10.0% less than in C and CB) – To F MH (19.4 and 10.0% less than in C and CB) – Sg L UAE (17.9 and 8.3% less than in C and CB) Roots n/a

(Continued)

TABLE 10A | Continued

Examined parameter		Laboratory tests – cabbage seedlings (Godlewska et al., 2019, 2020a)	Field tests – cabbage (Godlewska et al., 2021)	Field tests – celeriac (Godlewska et al., 2020b)	Field tests – radish (current study)
SPAD	↑	Leaves – To L UAE (31.1 and 1.6% more than in C and CB) – Hp H UAE (31.7 and 2.1% more than in C and CB) Roots n/a	Leaves after the second spraying – To F MH (12.4 and 21.8% more than in C and CB) – Sg L MH (10.0 and 19.2% more than in C and CB) – Ur L MH (7.7 and 16.7% more than in C and CB) – Vo R MH (7.6 and 16.6% more than in C and CB) – To L UAE (7.4 and 16.4% more than in C and CB)	The first term of leaves of rosette collection – Hp H MH (10.7 and 10.9% more than in C and CB) The second term of leaves of rosette collection – To L MH (15.3 and 9.8% more than in C and CB) Roots n/a	The first term of leaves of rosette collection – Hp H MH (24.5 and 27.8% more than in C and CB) The second term of leaves of rosette collection – Vo R UAE (28.1 and 21.4% more than in C and CB) Roots n/a
	↓	Leaves – To F UAE (3.1% more than in C and 20.1% less than in CB) – Vo R UAE (6.2% more than in C and 17.6% less than in CB) Roots n/a	Leaves after the second spraying – Sg L UAE (0.8% less than in C and 7.6% more than in CB) – To F UAE (0.5 and 8.9% more than in C and CB)	The first term of leaves of rosette collection – Tp F MH (2.0 and 1.8% less than in C and CB) – Vo R UAE (0.7 and 0.5% less than in C and CB) The second term of leaves of rosette collection – Hp H MH (1.6 and 6.4% less than in C and CB) Roots n/a	The first term of leaves of rosette collection – Tp F MH (5.0 and 7.7% more than in C and CB) The second term of leaves of rosette collection – To L UAE (11.9 and 6.1% more than in C and CB) Roots n/a
Carotenoids	↑	Leaves – Hp H UAE (67.3% more than in C and 8.1% less than in CB) – Tp F UAE (67.2% more than in C and 8.1% less than in CB) – Vo R UAE (67.9% more than in C and 7.7% less than in CB) Roots n/a	Leaves after the second spraying – To L MH (21.8 and 19.2% more than in C and CB) – To L UAE (13.5 and 11.1% more than in C and CB)	The first term of leaves of rosette collection – To L MH (8.9 and 1.4% more than in C and CB) – Vo R UAE (9.4 and 1.9% more than in C and CB) The second term of leaves of rosette collection – To F UAE (7.1 and 30.8% more than in C and CB) Roots n/a	The first term of leaves of rosette collection – Vo R UAE (31.3 and 19.9% more than in C and CB) The second term of leaves of rosette collection – Vo R UAE (1.2 and 14.4% more than in C and CB) – Ur L MH (0.9 and 14.0% more than in C and CB) Roots n/a

(Continued)

TABLE 10A | Continued

Examined parameter		Laboratory tests – cabbage seedlings (Godlewska et al., 2019, 2020a)	Field tests – cabbage (Godlewska et al., 2021)	Field tests – celeriac (Godlewska et al., 2020b)	Field tests – radish (current study)
Total phenolic compounds	↓	Leaves – To F UAE (0.9% more than in C and 44.6% less than in CB) Roots n/a	Leaves after the second spraying – Vo R MH (4.4 and 6.4% less than in C and CB) – Ur L MH (2.5 and 4.5% less than in C and CB) – Tp F MH (2.4 and 4.5% less than in C and CB) – To F UAE (2.3 and 4.4% less than in C and CB)	The first term of leaves of rosette collection – Sg L UAE (14.0 and 19.9% less than in C and CB) The second term of leaves of rosette collection – Ur L UAE (14.2% less than in C and 4.7% more than in CB) Roots n/a	The first term of leaves of rosette collection – To L MH (28.7 and 34.9% less than in C and CB) The second term of leaves of rosette collection – and for To F MH (19.7 and 9.3% less than in C and CB) Roots n/a
	↑	Shoots – Ur L UAE (23.3 and 7.5% more than in C and CB) Roots n/a	Leaves after the second spraying – Vo R UAE (39.7 and 136% more than in C and CB) – Sg L UAE (6.1 and 79.7% more than in C and CB) Heads after harvest – Vo R UAE (34.6 and 60.3% more than in C and CB) – Sg L UAE (6.9 and 27.4% more than in C and CB)	The first term of leaves of rosette collection – Hp H MH (30.8 and 50.2% more than in C and CB) The second term of leaves of rosette collection – Tp F MH (23.1% more than in C and 14.5% less than in CB) Roots – Hp H UAE (6.7 and 5.3 times more than in C and CB)	The first term of leaves of rosette collection – Sg L MH (1.1% less than in C but 23.8% more than in CB) – To F UAE (0.1 and 25.3% more than in C and CB) The second term of leaves of rosette collection – Sg L MH (10.7 and 2.9% more than in C and CB) – To F UAE (7.2% more than in C and 0.4% less than in CB) Roots – To F MH (13.2 and 50.5% more than in C and CB) – Sg L UAE (4.4 and 38.8% more than in C and CB)
	↓	Shoots – Vo R UAE (41.4 and 48.9% less than in C and CB) – Tp F UAE (32.8 and 41.4% less than in C and CB) Roots n/a	Leaves after the second spraying – Ur L MH (47.7 and 11.5% less than in C and CB) Heads after harvest – Ur L MH (29.7 and 16.3% less than in C and CB) – Hp H UAE (30.2 and 17.3% less than in C and CB)	The first term of leaves of rosette collection – Tp F UAE (43.7 and 35.4% less than in C and CB) The second term of leaves of rosette collection – Sg L UAE (28.6 and 50.4% less than in C and CB) Roots – Vo R UAE (14.0 and 31.1% less than in C and CB)	The first term of leaves of rosette collection – Tp F MH (22.7 and 3.3% less than in C and CB) – Sg L UAE (22.1 and 2.4% less than in C and CB) The second term of leaves of rosette collection – Hp H UAE (17.3 and 23.2% less than in C and CB) Roots – Tp F UAE (37.2 and 16.5% less than in C and CB) – To L MH (35.3 and 14.0% less than in C and CB) – Hp H UAE (34.7 and 13.2% less than in C and CB)

(Continued)

TABLE 10A | Continued

Examined parameter		Laboratory tests – cabbage seedlings (Godlewska et al., 2019, 2020a)	Field tests – cabbage (Godlewska et al., 2021)	Field tests – celeriac (Godlewska et al., 2020b)	Field tests – radish (current study)
Antioxidant activity – DPPH	↑	Shoots – Ur L UAE (2.5 and 12.4% less than in C and CB) Roots n/a	Leaves after the second spraying – To L UAE (21.2 and 12.9% more than in C and CB) – Vo R UAE (16.8 and 8.8% more than in C and CB) – Sg L UAE (10.2 and 2.7% more than in C and CB) – Hp H UAE (5.1% more than in C and 2.0% less than in CB) – Vo R MH (2.9% more than in C and 4.1% less than in CB) Heads after harvest – Vo R MH (48.9 and 379% more than in C and CB) – Sg L UAE (40 and 350% more than in C and CB) – Hp H UAE (15.6 and 271% more than in C and CB)	The first term of leaves of rosette collection – Hp H MH (2.6 and 2.0 times more than in C and CB) – Sg L MH (2.6 and 2.0 times more than in C and CB) The second term of leaves of rosette collection – Sg L MH (21.3 and 62.2% more than in C and CB) Roots – Tp F UAE (5.2 and 3.2 times more than in C and CB)	The first term of leaves of rosette collection – To F UAE (76.5 and 147.1% more than in C and CB) – Vo R MH (79.8 and 151.8% more than in C and CB) The second term of leaves of rosette collection – Sg L UAE (28.6 and 51.8% more than in C and CB) Roots – To F MH (157.8 and 169.8% more than in C and CB)
	↓	Shoots – Sg L UAE (56.6 and 61.0% less than in C and CB) Roots n/a	Leaves after the second spraying – Tp F UAE (30.7 and 35.4% less than in C and CB) – Ur L UAE (31.4 and 36.1% less than in C and CB) – Tp F MH (33.6 and 38.1% less than in C and CB) Heads after harvest – Tp F UAE (37.8% less than in C and 100% more than in CB) – Tp F MH (51.1% less than in C and 57.1% more than in CB) – Vo R UAE (57.8% less than in C and 35.7% more than in CB)	The first term of leaves of rosette collection – Vo R UAE (31.8 and 47.6% less than in C and CB) The second term of leaves of rosette collection – Ur L MH (45.2 and 26.7% less than in C and CB) Roots – Ur L MH (27.8 and 55.2% less than in C and CB)	The first term of leaves of rosette collection – To L MH (35.3 and 9.4% less than in C and CB) – Tp F MH (33.6 and 7.1% less than in C and CB) The second term of leaves of rosette collection – To F MH (40.8 and 30.1% less than in C and CB) – Ur L MH (39.8 and 28.9% less than in C and CB) Roots – Sg L UAE (26.7 and 23.3% less than in C and CB) – To L UAE (33.3 and 30.2% less than in C and CB)

(Continued)

TABLE 10A | Continued

Examined parameter		Laboratory tests – cabbage seedlings (Godlewska et al., 2019, 2020a)	Field tests – cabbage (Godlewska et al., 2021)	Field tests – celeriac (Godlewska et al., 2020b)	Field tests – radish (current study)
Antioxidant activity – ABTS	↑	Shoots – To F UAE (4.4 times and 40.3% more than in C and CB) – Ur L UAE (5.4 times and 73.9% more than in C and CB) Roots n/a	Leaves after the second spraying – Sg L MH (67.4 and 39.2% more than in C and CB) – Ur L UAE (56.6 and 30.2% more than in C and CB) – Hp H MH (48.5 and 23.5% more than in C and CB) – Hp H UAE (45.6 and 21.2% more than in C and CB) Heads after harvest – Hp H MH (47.7 and 121% more than in C and CB)	The first term of leaves of rosette collection – Vo R MH (73.7 and 44.9% more than in C and CB) – Hp H MH (50.8 and 25.8% more than in C and CB) The second term of leaves of rosette collection – Tp F UAE (10.7% less than in C and 7.7% more than in CB) Roots – To L UAE (127.9 and 132.3% more than in C and CB)	The first term of leaves of rosette collection – Vo R MH (25.0% less than in C and 104.4% more than in CB) The second term of leaves of rosette collection – Tp F UAE (21.8% less than in C and 227.9% more than in CB) – Vo R UAE (26.5% less than in C and 208.2% more than in CB) – Sg L UAE (27.8% less than in C and 202.6% more than in CB) Roots – To L UAE (177.7 and 10.7% more than in C and CB) – Sg L UAE (101.7 and 2.6% more than in C and CB) – Ur L UAE (100.9 and 2.2% more than in C and CB)
	↓	Shoots – Tp F UAE (138% more than in C and 23.6% less than in CB) – Vo R UAE (198% more than in C and 4.5% less than in CB) Roots n/a	Leaves after the second spraying – To F UAE (15.8% more than in C and 3.7% less than in CB) – Vo R UAE (18.7% more than in C and 1.3% less than in CB) Heads after harvest – To F UAE (72.1 and 58.2% less than in C and CB)	The first term of leaves of rosette collection – Vo R UAE (29.0 and 40.8% less than in C and CB) The second term of leaves of rosette collection – To L UAE (55.2 and 45.9% less than in C and CB) Roots – Sg L UAE (1.1 and 2.9% more than in C and CB)	The first term of leaves of rosette collection – To F MH (65.9 and 7.0% less than in C and CB) – Sg L UAE (65.7 and 6.5% less than in C and CB) The second term of leaves of rosette collection – Ur L UAE (73.4% less than in C and 11.5% more than in CB) Roots – Tp F MH (24.1% more than in C and 36.8% less than in CB) – To F UAE (25.0% more than in C and 36.4% less than in CB) – To L MH (28.4% more than in C and 34.6% less than in CB)

(Continued)

TABLE 10A | Continued

Examined parameter		Laboratory tests – cabbage seedlings (Godlewska et al., 2019, 2020a)	Field tests – cabbage (Godlewska et al., 2021)	Field tests – celeriac (Godlewska et al., 2020b)	Field tests – radish (current study)
Antioxidant activity – FRAP	↑	Shoots – Ur L UAE (50.7 and 31.5% more than in C and CB) Roots n/a	Leaves after the second spraying – Hp H UAE (33.9 and 62.0% more than in C and CB) – Tp F UAE (28.3 and 55.3% more than in C and CB) – Sg L UAE (27.3 and 54.0% more than in C and CB) – Sg L MH (26.0 and 52.2% more than in C and CB) Heads after harvest – Tp F UAE (37.4 and 10.5% more than in C and CB) – Vo R MH (36.6 and 9.8% more than in C and CB)	The first term of leaves of rosette collection – Sg L MH (60.6 and 53.0% more than in C and CB) The second term of leaves of rosette collection – Sg L MH (0% more than in C and 13.3% less than in CB) Roots – To F MH (42.6 and 3.6% more than in C and CB)	The first term of leaves of rosette collection – Sg L MH (53.4 and 20.2% more than in C and CB) The second term of leaves of rosette collection – Sg L UAE (73.8 and 76.8% more than in C and CB) Roots – Sg L UAE (4.2 and 16.2% more than in C and CB) – Vo R MH (2.4% less than in C and 8.8% more than in CB)
	↓	Shoots – To L UAE (32.9 and 41.4% less than in C and CB) Roots n/a	Leaves after the second spraying – Ur L MH (16.1% less than in C and 1.5% more than in CB) – Hp H MH (14.5% less than in C and 3.5% more than in CB) – To L MH (13.8% less than in C and 4.3% more than in CB) Heads after harvest – To L MH (26.0 and 40.5% less than in C and CB)	The first term of leaves of rosette collection – To L MH (18.5 and 22.3% less than in C and CB) The second term of leaves of rosette collection – To L MH (29.3 and 38.7% less than in C and CB) Roots – Vo R UAE (3.0% more than in C and 25.2% less than in CB) – Tp F UAE (4.0% more than in C and 24.5% less than in CB) – Sg L UAE (5.9% more than in C and 23.0% less than in CB)	The first term of leaves of rosette collection – Hp H UAE (5.7 and 26.1% less than in C and CB) – Vo R UAE (6.1 and 26.4% less than in C and CB) The second term of leaves of rosette collection – Sg L MH (18.9 and 17.5% less than in C and CB) – To F UAE (16.6 and 15.2% less than in C and CB) Roots – Hp H MH (43.6 and 37.2% less than in C and CB)

UAE, ultrasound-assisted extraction; MH, mechanical homogenisation; 1st term—samples of leaves of rosette taken for analyses 7 days after the second spraying; 2nd term—samples of leaves of rosette taken for analyses after harvesting; n/a, not analysed; C, control; CB, commercial biostimulant; Hp H, Hypericum perforatum L. (St. John's wort, herb); Sg L, Solidago gigantea Ait. (giant goldenrod, leaf); To F, To L, Taraxacum officinale (L.); Weber ex F. H. Wigg (common dandelion, flower, leaf); Tp F, Trifolium pratense L. (red clover, flower); Ur L, Urtica dioica L. (nettle, leaf); Vo R, Valeriana officinalis L. (valerian, root).

TABLE 10B | Effect of the foliar application of the examined botanical extracts on the growth and development of different model plants during real environment conditions (field trials).

Examined parameter		Field tests – cabbage (Godlewska et al., 2021)	Field tests – celeriac (Godlewska et al., 2020b)	Field tests – radish (current study)
Vitamin C	↑	Leaves after the second spraying – Tp F MH (52.1 and 25.9% more than in C and CB) – Sg L MH (31.0 and 8.4% more than in C and CB) – To F MH (29.2 and 6.9% more than in C and CB) – To F UAE (30.0 and 7.3% more than in C and CB) Heads after harvest – To L UAE (28.2 and 69.7% more than in C and CB)	The first term of leaves of rosette collection – Vo R UAE (57.6 and 41.6% more than in C and CB) The second term of leaves of rosette collection – Hp H MH (22.3 and 36.5% more than in C and CB) Roots – Ur L UAE (22.9 and 21.2% more than in C and CB)	The first term of leaves of rosette collection – Vo R MH (29.9 and 10.5% more than in C and CB) The second term of leaves of rosette collection – Vo R MH (115.5 and 44.4% more than in C and CB) Roots – Tp F MH (46.3 and 33.8% more than in C and CB) – Vo R UAE (42.2 and 30.2% more than in C and CB)
	↓	Leaves after the second spraying – Vo R UAE (0.8 and 17.9% less than in C and CB) – Sg L UAE (0.3 and 17.5% less than in C and CB) Heads after harvest – Ur L UAE (23.3% less than in C and 1.5% more than in CB) – To F MH (20.7% less than in C and 5.0% more than in CB)	The first term of leaves of rosette collection – To L MH (2.8 and 12.2% less than in C and CB) The second term of leaves of rosette collection – To F MH (24.7 and 15.8% less than in C and CB) Roots – Vo R UAE (13.9 and 15.1% less than in C and CB)	The first term of leaves of rosette collection – To L MH (6.9 and 20.7% less than in C and CB) The second term of leaves of rosette collection – To L MH (25.8% more than in C and 15.7% less than in CB) Roots – Vo R MH (10.5 and 18.2% less than in C and CB)
Nitrates	↑	Leaves after the second spraying – To L UAE (0.3% less than in C and 76.5% more than in CB) – Sg L UAE (16.7% less than in C and 47.4% more than in CB) – Ur L MH (19.5% less than in C and 42.5% more than in CB) – Tp F UAE (20.6% less than in C and 40.5% more than in CB) Heads after harvest – Tp F MH (186 and 115% more than in C and CB) – To F UAE (89.9 and 42.7% more than in C and CB) – Sg L MH (84.9 and 38.9% more than in C and CB) – To L MH (75.1 and 31.6% more than in C and CB) – To L UAE (73.0 and 30.0% more than in C and CB)	The first term of leaves of rosette collection – Ur L UAE (44.5 and 34.4% more than in C and CB) The second term of leaves of rosette collection – To L MH (140 and 52.8% more than in C and CB) Roots – Tp F UAE (15.8% less than in C and 22.2% more than in CB) – Ur L UAE (16.2% less than in C and 21.6% more than in CB)	The first term of leaves of rosette collection – Vo R MH (57.5 and 39.0% more than in C and CB) – To L MH (48.2 and 30.7% more than in C and CB) The second term of leaves of rosette collection – Ur L UAE (in leaves: 52.7 and 51.1% more than in C and CB) – Tp F UAE (51.9 and 50.4% more than in C and CB) Roots – Ur L UAE (73.7 and 124.7% more than in C and CB)

(Continued)

TABLE 10B | Continued

Examined parameter			Field tests – cabbage (Godlewska et al., 2021)	Field tests – celeriac (Godlewska et al., 2020b)	Field tests – radish (current study)
	↓		Leaves after the second spraying – Sg L MH (58.0 and 25.6% less than in C and CB) – To L MH (53.4 and 17.6% less than in C and CB) – Vo R MH (50.0 and 11.4% less than in C and CB) Heads after harvest – Vo R UAE (2.4% more than in C and 23.0% less than in CB) – Ur L MH (22.0% more than in C and 8.4% less than in CB) – Sg L UAE (26.4% more than in C and 5.1% less than in CB)	The first term of leaves of rosette collection – Tp F UAE (8.9 and 1.4% more than in C and CB) – Sg L MH (9.4 and 1.8% more than in C and CB) The second term of leaves of rosette collection – Vo R MH (27.5% more than in C and 18.8% less than in CB) Roots – Ur L MH (49.4 and 26.5% less than in C and CB) – Tp F MH (45.9 and 21.5% less than in C and CB)	The first term of leaves of rosette collection – Vo R UAE (21.9 and 31.1% less than in C and CB) – Ur L UAE (21.9 and 31.1% less than in C and CB) The second term of leaves of rosette collection – Vo R UAE (20.3 and 21.1% less than in C and CB, for both extracts) – To F UAE (20.3 and 21.1% less than in C and CB) Roots – Vo R UAE (20.2% less than in C and 3.2% more than in CB) – To F UAE (17.5% less than in C and 6.8% more than in CB) – Sg L MH (11.5% less than in C and 14.5% more than in CB)
Macroelements	↑	N	Heads after harvest – Sg L UAE (12.3 and 0.2% more than in C and CB) – To L MH (12.3 and 0.2% more than in C and CB)	Leaves of rosette – Vo R UAE (4.8 and 0.4% more than in C and CB) – Vo R MH (3.2% more than in C and 1.2% less than in CB) Roots – Hp H MH (4.8 and 1.8% more than in C and CB) – Vo R UAE (4.6 and 1.7% more than in C and CB) – Tp F MH (4.4 and 1.5% more than in C and CB)	Leaves of rosette – Ur L UAE (2.7% less than in C and 2.9% more than in CB) – Tp F UAE (3.4% less than in C and 2.1% more than in CB) Roots – Hp H UAE (5.7 and 4.2% more than in C and CB) – Vo R MH (4.6 and 3.0% more than in C and CB)
		P	Heads after harvest – Ur L MH (20.9% less than in C and 3.1% more than in CB) – Tp F MH (20.9% less than in C and 3.1% more than in CB)	Leaves of rosette – Ur L MH (6.9% less than in C and 26.8% more than in CB) Roots – Tp F MH (27.2 and 27.2% more than in C and CB) – Sg L UAE (23.1 and 23.1% more than in C and CB)	Leaves of rosette – To F MH (25.8 and 13.0% more than in C and CB) – Vo R MH (25.8 and 13.0% more than in C and CB) Roots – Ur L UAE (20.4 and 42.7% more than in C and CB) – Sg L UAE (19.7 and 41.9% more than in C and CB) – To F UAE (19.0 and 41.1% more than in C and CB)
		K	Heads after harvest – Sg L UAE (1.1% less than in C and 0.7% more than in CB)	Leaves of rosette – Vo R UAE (7.8% less than in C and 36.5% more than in CB) – Vo R MH (15.5% less than in C and 25.0% more than in CB) – Ur L MH (16.1% less than in C and 24.1% more than in CB) Roots – Sg L UAE (26.6 and 50.1% more than in C and CB) – Ur L UAE (20.6 and 43.0% more than in C and CB)	Leaves of rosette – Ur L UAE (29.7 and 8.8% more than in C and CB) – Vo R MH (27.2 and 6.7% more than in C and CB) Roots – Vo R MH (6.8 and 11.5% more than in C and CB) – To L UAE (4.8 and 9.4% more than in C and CB)

(Continued)

TABLE 10B | Continued

Examined parameter			Field tests – cabbage (Godlewska et al., 2021)	Field tests – celeriac (Godlewska et al., 2020b)	Field tests – radish (current study)
		Ca	Heads after harvest – To L UAE (36.1 and 27% higher than in C and CB) – Tp F MH (36.1 and 27% higher than in C and CB) – Sg L MH (28.6 and 20% higher than in C and CB) – To L MH (27.1 and 18.7% higher than in C and CB) – Vo R MH (26.6 and 18.2% higher than in C and CB)	Leaves of rosette – To F UAE (40.9 and 287% more than in C and CB) – Sg L MH (40.4 and 286% more than in C and CB) – Ur L MH (28.3 and 252% more than in C and CB) – Vo R MH (23.7 and 240% more than in C and CB) Roots – Ur L UAE (8.7 and 16.3% more than in C and CB)	Leaves of rosette – To L MH (2.5% less than in C and 3.4 more than in CB) – Sg L MH (3.2% less than in C and 2.7% more than in CB) Roots – Vo R MH (25.4 and 56.7% more than in C and CB) – Ur L MH (8.0 and 34.9% more than in C and CB) – Tp F MH (4.8 and 30.9% more than in C and CB)
		Mg	Heads after harvest – Tp F MH (17.9 and 9.8% higher than in C and CB) – Ur L UAE (13.7 and 5.9% higher than in C and CB) – To L MH (12.6 and 4.9% higher than in C and CB) – Sg L MH (12.6 and 4.9% higher than in C and CB) – To L UAE (11.6 and 3.9% higher than in C and CB)	Leaves of rosette – Vo R UAE (4.7 and 2.0% more than in C and CB) Roots – Sg L UAE (33.3 and 39.7% more than in C and CB) – Tp F UAE (31.3 and 37.6% more than in C and CB)	Leaves of rosette – Sg L UAE (3.1% more than in C and 1.5% less than in CB) – To L UAE (2.3% more than in C and 2.2% less than in CB) – Vo R MH (1.5% more than in C and 3.0% less than in CB) Roots – Vo R MH (75.1 and 96.3% more than in C and CB)
		S	Heads after harvest – Sg L MH (12.7 and 2.7% higher than in C and CB) – Hp H MH (10.9 and 1.0% higher than in C and CB) – To L MH (11.2 and 1.3% higher than in C and CB)	Leaves of rosette – To L MH (49.5 and 82.7% more than in C and CB) – Tp F MH (34.7 and 64.5% more than in C and CB) Roots – To L MH (36.4 and 76.0% more than in C and CB) – Hp H MH (36.4 and 76.0% more than in C and CB)	Leaves of rosette – To L MH (18.4 and 6.6% more than in C and CB) – Vo R UAE (13.2 and 2.0% more than in C and CB) Roots – Hp H UAE (0.4 and 14.2% more than in C and CB) – Sg L UAE (0.1% less than in C and 13.5% more than in CB) – To L UAE (0.3% less than in C and 13.4% more than in CB)
	↓	N	Heads after harvest – To L UAE (4.4 and 14.7% lower than in C and CB) – Sg L MH (3.4 and 13.7% lower than in C and CB) – Tp F MH (2.9 and 13.4% lower than in C and CB)	Leaves of rosette – To L MH (11.7 and 15.4% less than in C and CB) Roots – Ur L MH (7.1 and 9.7% less than in C and CB)	Leaves of rosette – Sg L UAE (8.1 and 2.9% less than in C and CB) – Vo R UAE (6.8 and 1.4% less than in C and CB) Roots – Sg L UAE (1.9 and 3.4% less than in C and CB) – Vo R UAE (0.0 and 1.5% less than in C and CB)
		P	Heads after harvest – Sg L MH (49.4 and 34.0% lower than in C and CB) – Vo R MH (45.5 and 28.9% lower than in C and CB)	Leaves of rosette – Hp H UAE (48.4 and 29.7% less than in C and CB) Roots – Vo R MH (1.8 and 1.8% less than in C and CB) – Vo R UAE (1.3 and 1.3% less than in C and CB)	Leaves of rosette – To L MH (34.0 and 40.7% less than in C and CB) – Hp H MH (3.1 and 13.0% less than in C and CB) Roots – Ur L MH (53.3 and 44.6% less than in C and CB) – Tp F MH (51.7 and 42.7% less than in C and CB)
		K	Heads after harvest – Sg L MH (14.6 and 13.1% lower than in C and CB) – Ur L MH (10.9 and 9.3% lower than in C and CB)	Leaves of rosette – To L MH (40.8 and 12.4% less than in C and CB) – Tp F MH (38.9 and 9.6% less than in C and CB) Roots – Hp H UAE (6.3% less than in C and 11.1% more than in CB) – To F MH (6.1% less than in C and 11.3% more than in CB)	Leaves of rosette – To F MH (4.6% more than in C and 12.2% less than in CB) Roots – Ur L MH (57.2 and 55.4% less than in C and CB) – Tp F MH (53.7 and 51.7% less than in C and CB)

(Continued)

TABLE 10B | Continued

Examined parameter			Field tests – cabbage (Godlewska et al., 2021)	Field tests – celeriac (Godlewska et al., 2020b)	Field tests – radish (current study)
		Ca	Heads after harvest – Ur L MH (4.8% higher than in C and 2.2% lower than in CB) – Vo R UAE (6.8% higher than in C and 0.3% lower than in CB)	Leaves of rosette – Ur L UAE (67.3 and 10.2% less than in C and CB) – Vo R UAE (65.9 and 6.4% less than in C and CB) Roots – To F UAE (3.9% less than in C and 2.8% more than in CB) – Vo R MH (2.9% less than in C and 3.8% more than in CB)	Leaves of rosette – Tp F UAE (19.0 and 14.0% less than in C and CB) Roots – Hp H UAE (21.6 and 2.1% less than in C and CB) – Sg L MH (21.2 and 1.6% less than in C and CB) – To L UAE (20.8 and 1.0% less than in C and CB)
		Mg	Heads after harvest – Hp H MH (1.1% higher than in C and 5.9% lower than in CB) – Vo R UAE (2.1% higher than in C and 4.9% lower than in CB) – Ur L MH (3.2% higher than in C and 3.9% lower than in CB) – To F UAE (4.2% higher than in C and 2.9% lower than in CB)	Leaves of rosette – Hp H UAE (17.7 and 19.8% less than in C and CB) Roots – To F MH (2.5% less than in C and 2.1% more than in CB) – Vo R MH (1.0% less than in C and 3.7% more than in CB) – To F UAE (0.5 and 5.3% more than in C and CB)	Leaves of rosette – Vo R UAE (9.7 and 13.7% less than in C and CB) Roots – Sg L MH (14.6 and 4.2% less than in C and CB) – Hp H UAE (13.6 and 3.2% less than in C and CB) – To L UAE (13.1 and 2.6% less than in C and CB)
		S	Heads after harvest – Vo R UAE (0.8% higher than in C and 8.2% lower than in CB) – Vo R MH (1.5% higher than in C and 7.5% lower than in CB) – Ur L MH (2.2% higher than in C and 6.9% lower than in CB)	Leaves of rosette – Vo R UAE (13.4% less than in C and 5.9% more than in CB) Roots – Tp F MH (10.9% less than in C and 15.0% more than in CB)	Leaves of rosette – To F UAE (1.8 and 11.5% less than in C and CB) – Vo R MH (1.4 and 11.2% less than in C and CB) Roots – Sg L MH (10.2% less than in C and 2.1% more than in CB)
Microelements and toxic elements	↑	Fe	Heads after harvest – Vo R MH (14.3 and 0.8% higher than in C and CB) – To L MH (12.2% higher than in C and 1.1% lower than in CB) – Sg L UAE (7.8% higher than in C and 5.0% lower than in CB)	Leaves of rosette – To F MH (2.4 times higher and 31.2% more than in C and CB) Roots – To L UAE (1.5 times and 70.7% more than in C and CB)	Leaves of rosette – To L UAE (24.3 and 32.3% more than in C and CB) – Hp H UAE (8.5%and 15.5% more than in C and CB) Roots – Vo R MH (27.9 and 43.3% more than in C and CB) – To L UAE (27.3 and 42.6% more than in C and CB) – Vo R UAE (26.9 and 42.2% more than in C and CB)
		Cu	Heads after harvest – To F UAE (1.5% higher than in C and 6.5% lower than in CB)	Leaves of rosette – Vo R UAE (9.8 and 9.5% more than in C and CB) Roots – To F UAE (3.2 and 30.5% more than in C and CB) – Hp H MH (0.3 and 26.7% more than in C and CB)	Leaves of rosette – To L UAE (4.4% more than in C and 5.3% less than in CB) – Vo R UAE (0.9% more than in C and 8.5% less than in CB) Roots – Vo R MH (45.5 and 58.9% more than in C and CB) – To F UAE (22.7 and 34.0% more than in C and CB)

(Continued)

TABLE 10B | Continued

Examined parameter		Field tests – cabbage (Godlewska et al., 2021)	Field tests – celeriac (Godlewska et al., 2020b)	Field tests – radish (current study)
	Zn	Heads after harvest – Sg L UAE (5.3% higher than in C and 3.6% lower than in CB)	Leaves of rosette – Vo R UAE (23.3 and 9.1% more than in C and CB) – Vo R MH (19.4 and 5.6% more than in C and CB) Roots – Sg L UAE (30.9 and 60.0% more than in C and CB)	Leaves of rosette – Sg L UAE (24.8 and 14.1% more than in C and CB) – Hp H UAE (17.2 and 7.1% more than in C and CB) Roots – To F UAE (3.2 and 7.5% more than in C and CB) – Vo R MH (2.1 and 6.4% more than in C and CB)
	Mn	Heads after harvest – Hp H MH (the same content as in C and CB)	Leaves of rosette – To L MH (61.4 and 30.3% more than in C and CB) – Tp F MH (54.8 and 25.0% more than in C and CB) Roots – Tp F UAE (33.5 and 34.4% more than in C and CB) – To L UAE (32.4 and 33.3% more than in C and CB)	Leaves of rosette – To L MH (3.8 and 6.5% more than in C and CB) – To L UAE (1.9 and 4.5% more than in C and CB) Roots – Hp H MH (30.7 and 9.8% more than in C and CB) – Vo R MH (29.3 and 8.6% more than in C and CB)
	Ni	Heads after harvest – To F MH (43.5% higher than in C and 16.9% lower than in CB) – To L MH (40.6% higher than in C and 18.6% lower than in CB)	Leaves of rosette – Sg L MH (3 times and 36.8% more than in C and CB) – Vo R MH (3 times and 36.8% more than in C and CB) Roots – Ur L MH (2 and 2.5 times more than in C and CB)	Leaves of rosette – Sg L UAE (6.4 and 26.8% more than in C and CB) – To F MH (0.4% less than in C and 18.7% more than in CB) – To F UAE (1.9% less than in C and 16.9% more than in CB) Roots – To F MH (107.1 and 96.1% more than in C and CB)
	Cd	Heads after harvest – Tp F UAE (77.8 and 77.8% higher than in C and CB) – Hp H UAE (66.7 and 66.7% higher than in C and CB) – Sg L MH (66.7 and 66.7% higher than in C and CB) – To F UAE (66.7 and 66.7% higher than in C and CB) – To L UAE (66.7 and 66.7% higher than in C and CB)	Leaves of rosette – To L MH (69.0 and 96.0% more than in C and CB) – Hp H UAE (58.6 and 84.0% more than in C and CB) Roots – Sg L UAE (40.7 and 123.5% more than in C and CB) – To L UAE (20.4 and 91.2% more than in C and CB) – Hp H UAE (18.5 and 88.2% more than in C and CB)	Leaves of rosette – Hp H MH (1.2 and 4.3% more than in C and CB) – Sg L MH (1.2 and 4.3% more than in C and CB) – Tp F MH (1.2 and 4.3% more than in C and CB) Roots – Vo R UAE (7.6 and 42.0% more than in C and CB) – To F UAE (3.0 and 36.0% more than in C and CB) – Tp F UAE (3.0 and 36.0% more than in C and CB)
	Pb	Heads after harvest – To L UAE (30.5 and 29.0% higher than in C and CB) – Hp H UAE (28.4 and 27.0% higher than in C and CB) – Sg L UAE (24.0 and 22.6% higher than in C and CB)	Leaves of rosette – Sg L UAE (26.2 and 131.1% more than in C and CB) – Vo R UAE (19.1 and 118.1% more than in C and CB) – To L UAE (17.3 and 114.7% more than in C and CB) Roots – To L UAE (13.9 and 190.3% more than in C and CB) – Vo R UAE (5.9 and 169.9% more than in C and CB)	Leaves of rosette – Hp H UAE (6.1 and 11.6% more than in C and CB) – To L UAE (3.7 and 9.1% more than in C and CB) Roots – Vo R UAE (2.0 and 55.1% more than in C and CB)
↓	Fe	Heads after harvest – Tp F UAE (20.0 and 29.5% lower than in C and CB) – Tp F MH (18.5 and 28.1% lower than in C and CB)	Leaves of rosette – Vo R MH (15.2% more than in C and 36.5% less than in CB) Roots – Vo R MH (9.7% less than in C and 1.5% more than in CB)	Leaves of rosette – Sg L MH (26.4 and 21.6% less than in C and CB) – Ur L MH (23.1 and 18.1% less than in C and CB) – To L MH (22.7 and 17.7% less than in C and CB) Roots – Sg L MH (26.4 and 7.6% less than in C and CB)

(Continued)

TABLE 10B | Continued

Examined parameter		Field tests – cabbage (Godlewska et al., 2021)	Field tests – celeriac (Godlewska et al., 2020b)	Field tests – radish (current study)
	Cu	Heads after harvest – Tp F MH (19.1 and 25.5% lower than in C and CB) – Sg L MH (16.6 and 23.2% lower than in C and CB)	Leaves of rosette – Sg L MH (5.3 and 5.5% less than in C and CB) – Sg L UAE (4.7 and 5.0% less than in C and CB) Roots – Vo R UAE (21.6 and 1.0% less than in C and CB)	Leaves of rosette – Vo R MH (23.4 and 30.5% less than in C and CB) – Hp H UAE (21.5 and 28.8% less than in C and CB) Roots – Tp F UAE (10.4 and 2.1% less than in C and CB) – To L UAE (5.8% less than in C and 2.8% more than in CB)
	Zn	Heads after harvest – Tp F UAE (13.0 and 20.3% lower than in C and CB) – Hp H UAE (9.7 and 17.3% lower than in C and CB) – To L UAE (9.6 and 17.2% lower than in C and CB)	Leaves of rosette – Sg L MH (3.6 and 14.8% less than in C and CB) Roots – Sg L MH (12.6% less than in C and 6.9% more than in CB)	Leaves of rosette – Ur L MH (0.6% more than in C and 8.1% less than in CB) – To F MH (0.7% more than in C and 8.0% less than in CB) Roots – Sg L MH (11.8 and 8.1% less than in C and CB) – Tp F MH (9.9 and 6.1% less than in C and CB)
	Mn	Heads after harvest – Tp F MH (18.0 and 18.0% lower than in C and CB) – Hp H UAE (16.6 and 16.6% lower than in C and CB)	Leaves of rosette – Ur L MH (1.3 and 20.3% less than in C and CB) Roots – Hp H MH (9.2 and 8.5% less than in C and CB)	Leaves of rosette – Ur L MH (14.7 and 12.5% less than in C and CB) – Ur L UAE (12.5 and 10.2% less than in C and CB) Roots – Sg L UAE (13.2 and 27.0% less than in C and CB) – Hp H UAE (9.3 and 23.8% less than in C and CB)
	Ni	Heads after harvest – Vo R UAE (0.0% higher than in C and 42.1% lower than in CB) – Tp F UAE (4.2% higher than in C and 39.7% lower than in CB)	Leaves of rosette – Ur L UAE (15.9 and 62.2% less than in C and CB) Roots – Sg L MH (41.3 and 26.7% less than in C and CB)	Leaves of rosette – Tp F MH (23.1 and 8.3% less than in C and CB) – Vo R MH (22.5 and 7.6% less than in C and CB) Roots – Sg L MH (6.2 and 11.2% less than in C and CB) – Sg L UAE (5.6 and 10.7% less than in C and CB)
	Cd	Heads after harvest – To F MH (the same content as in C and CB) – Vo R UAE (the same content as in C and CB)	Leaves of rosette – Ur L MH (31.0 and 20.0% less than in C and CB) – To F UAE (3.4% less than in C and 12.0% more than in CB) Roots – Tp F MH (39.6% less than in C and 11.8% more than in CB) – To L MH (25.9% less than in C and 17.6% more than in CB) – Ur L MH (24.1% less than in C and 20.6% more than in CB)	Leaves of rosette – Sg L UAE (7.2 and 4.3% less than in C and CB) – To L UAE (7.2 and 4.3% less than in C and CB) – To F UAE (6.6 and 3.7% less than in C and CB) Roots – Sg L MH (19.7% less than in C and 6.0% more than in CB) – Ur L MH (18.2% less than in C and 8.0% more than in CB) – Tp F MH (16.7% less than in C and 10.0% more than in CB)

(Continued)

TABLE 10B | Continued

Examined parameter			Field tests – cabbage (Godlewska et al., 2021)	Field tests – celeriac (Godlewska et al., 2020b)	Field tests – radish (current study)
		Pb	Heads after harvest – Ur L MH (0.9 and 2.0% lower than in C and CB) – Hp H MH (2.3 and 1.2% higher than in C and CB)	Leaves of rosette – Tp F MH (60.8 and 28.2% less than in C and CB) – Ur L MH (59.9 and 26.6% less than in C and CB) Roots – Hp H MH (65.3 and 11.5% less than in C and CB) – To F MH (62.5 and 4.4% less than in C and CB)	Leaves of rosette – Ur L MH (14.3 and 9.8% less than in C and CB) Roots – To F MH (33.0% less than in C and 1.9% more than in CB) – Sg L MH (31.0% less than in C and 5.0% more than in CB)
Steam volatile compounds	↑		Heads after harvest e.g., 2-undecanone: – Sg L UAE (6.7 and 15.4% more than in C and CB) – To L UAE (6.0 and 14.6% more than in C and CB) e.g., trisulfide (dimethyl-): – To F UAE (11.6 and 11.1% more than in C and CB) – Vo R MH (10.5 and 10.0% more than in C and CB) – Tp F UAE (9.5 and 9.0% more than in C and CB) e.g., tetrasulfide (dimethyl-): – Hp H MH (28.3 and 16.0% more than in C and CB)	Leaves of rosette e.g., β-myrcene: – Sg L MH (57.7 and 31.0% more than in C and CB) e.g., limonene: – Ur L UAE (15.3 and 11.8% more than in C and CB)	Leaves of rosette e.g., β -myrcene: – Vo R UAE (7.4 and 25.9% more than in C and CB) – To L UAE (2.3 and 19.9% more than in C and CB) – Hp H UAE (1.1 and 18.5% more than in C and CB) e.g., limonene: – Vo R UAE (11.3 and 9.5% more than in C and CB) – To L UAE (4.8 and 3.1% more than in C and CB) – Hp H UAE (3.2 and 1.5% more than in C and CB)
	↓		Heads after harvest e.g., 2-undecanone: – To F UAE (25.1 and 19.0% less than in C and CB) – Hp H MH (24.5 and 18.4% less than in C and CB) e.g., trisulfide (dimethyl-): – Sg L UAE (15.1 and 15.5% less than in C and CB) – Tp F MH (13.7 and 14.1% less than in C and CB) – To L UAE (12.0 and 12.4% less than in C and CB) e.g., tetrasulfide (dimethyl-): – –Tp F MH (24.9 and 32.1% less than in C and CB)	Leaves of rosette e.g., β -myrcene: – Ur L UAE (8.2 and 23.8% less than in C and CB) e.g., limonene: – Tp F UAE (18.1 and 20.5% less than in C and CB)	Leaves of rosette e.g., β -myrcene: – Tp F MH (33.4 and 21.9% less than in C and CB) e.g., limonene: – Tp F MH (25.4 and 26.6% less than in C and CB)
Fatty acids	↑		Heads after harvest e.g., hexadecanoic acid: – To L MH (34.7 and 11.3% more than in C and CB) – To F MH (27.9 and 5.7% more than in C and CB) – Tp F MH (22.7 and 1.3% more than in C and CB) e.g., linolenic acid: – Vo R UAE (66.0 and 90.2% more than in C and CB) – To L UAE (55.3 and 78.0% more than in C and CB) – Sg L UAE (39.2 and 59.5% more than in C and CB) e.g., linoleic acid: – Vo R UAE (14.1 and 22.3% more than in C and CB) – Sg L UAE (13.5 and 21.7% more than in C and CB) – Ur L UAE (10.9 and 18.8% more than in C and CB) e.g., 9Z-9-octadecenoic acid (ethyl ester): – To L MH (43.6 and 50.2% more than in C and CB) – Vo R MH (39.5 and 46.0% more than in C and CB) e.g., octadecanoic acid: – To F MH (14.0 and 54.8% more than in C and CB) – Hp H UAE (7.1 and 45.4% more than in C and CB)	Roots e.g., 9,12-hexadecadienoic acid (methyl ester): – Hp H MH (21.6% more than in C and 2.0% less than in CB) – Tp F MH (21.6% more than in C and 2.0% less than in CB) e.g., hexadecanoic acid, methyl ester: – To F UAE (9.4 and 0.2% less than in C and CB)	Roots e.g., linolenic acid (methyl ester): – Ur L UAE (14.7 and 19.3% more than in C and CB) – Sg L MH (14.3 and 18.8% more than in C and CB) e.g., hexadecanoic acid (methyl ester): – Sg L MH (13.2% less than in C and 9.0% more than in CB) e.g., 9,12-hexadecadienoic acid (methyl ester): – Sg L MH (6.4 and 23.7% more than in C and CB)

(Continued)

TABLE 10B | Continued

Examined parameter		Field tests – cabbage (Godlewska et al., 2021)	Field tests – celeriac (Godlewska et al., 2020b)	Field tests – radish (current study)
	↓	Heads after harvest e.g., hexadecanoic acid: – Vo R UAE (21.4 and 35.1% less than in C and CB) – Sg L UAE (12.9 and 28.0% less than in C and CB) e.g., linolenic acid: – To L MH (49.8 and 42.5% less than in C and CB) – Vo R MH (31.3 and 21.3% less than in C and CB) e.g., linoleic acid: – To L MH (32.3 and 27.4% less than in C and CB) – Vo R MH (22.7 and 17.2% less than in C and CB) e.g., 9Z-9-octadecenoic acid (ethyl ester): – Vo R UAE (40.8 and 38.0% less than in C and CB) – To L UAE (31.0 and 27.8% less than in C and CB) e.g., octadecanoic acid: – Vo R UAE (65.0 and 52.5% less than in C and CB) – To L UAE (60.2 and 45.9% less than in C and CB)	Roots e.g., 9,12-hexadecadienoic acid (methyl ester): – To L MH (13.0% more than in C and 8.9% less than in CB) e.g., hexadecanoic acid, methyl ester: – Vo R UAE (35.7 and 29.2% less than in C and CB)	Roots e.g., linolenic acid (methyl ester): – Ur L MH (27.2 and 24.3% less than in C and CB) – Tp F MH (24.8 and 21.8% less than in C and CB) e.g., hexadecanoic acid (methyl ester): – To F MH (34.7 and 18.0% less than in C and CB) e.g., 9,12-hexadecadienoic acid (methyl ester): – Ur L MH (38.7 and 28.7% less than in C and CB)
Sterols	↑	Heads after harvest campesterol: – Vo R MH (10.1 and 11.1% more than in C and CB) – To F UAE (9.9 and 10.9% more than in C and CB) β-sitosterol: – Tp F MH (0.3 and 0.5% less than in C and CB) – Sg L UAE (0.3 and 0.5% less than in C and CB) – Hp H UAE (0.4 and 0.6% less than in C and CB)	n/a	Roots campesterol (TMS derivative): – To L MH (15.7 and 14.5% more than in C and CB) β-sitosterol (TMS derivative): – Tp F UAE (1.9 and 2.5% more than in C and CB) – Sg L UAE (0.1 and 0.7% more than in C and CB).
	↓	Heads after harvest campesterol: – Tp F MH (1.2 and 2.2% more than in C and CB) – Sg L UAE (1.4 and 2.3% more than in C and CB) β-sitosterol: – Vo R MH (2.3 and 2.5% less than in C and CB) – To F UAE (2.3 and 2.5% less than in C and CB)	n/a	Roots campesterol (TMS derivative): – Tp F UAE (3.3 and 4.3% less than in C and CB) – Sg L UAE (0.2 and 1.3% less than in C and CB) β-sitosterol (TMS derivative): – To L MH (8.9 and 8.4% less than in C and CB)

UAE, ultrasound-assisted extraction; MH, mechanical homogenisation; na, not analysed; C, control; CB, commercial biostimulant; Hp H, Hypericum perforatum L. (St. John's wort, herb); Sg L, Solidago gigantea Ait. (giant goldenrod, leaf); To F, To L, Taraxacum officinale (L.) Weber ex F. H. Wigg (common dandelion, flower, leaf); Tp F, Trifolium pratense L. (red clover, flower); Ur L, Urtica dioica L. (nettle, leaf); Vo R, Valeriana officinalis L. (valerian, root).

increasing attention every year among scientists, producers, and possible consumers. Appropriately prepared, characterized, and tested bio-products could be an integral component of sustainable agriculture in the foreseeable future.

DATA AVAILABILITY STATEMENT

The original contributions presented in the study are included in the article/**Supplementary Material**, further inquiries can be directed to the corresponding author.

AUTHOR CONTRIBUTIONS

KG designed and conducted all the research, analyzed the obtained data, and wrote the paper. PP participated in the field experiments, reviewed, and edited the paper. IM analyzed the obtained data and reviewed and edited the paper. AB supervised the work and reviewed and edited the paper. AS participated in the analyses of essential oils and fatty acids. NP participated in the analyses of essential oils and fatty acids. UP conducted the analyses of elements. All authors have read and agreed to the published version of the manuscript.

FUNDING

This work was supported by The Wrocław University of Environmental and Life Sciences (Poland) as the Ph.D., research program Innowacyjny Doktorat, Grant No. D220/0008/18 and financed in the framework of the grant entitled Mechanism of Action of Novel Plant-Derived Extracts and Their Impact on Stress Resilience of *Arabidopsis thaliana* (2018/29/N/NZ9/02430) attributed by The National Science Center in Poland.

SUPPLEMENTARY MATERIAL

The Supplementary Material for this article can be found online at: https://www.frontiersin.org/articles/10.3389/fpls.2021.651152/full#supplementary-material

Supplementary Figure 1 | The weather conditions during the field experiments.

Supplementary Table 1 | The effect of the foliar application of the botanical extracts on the profile of steam volatile compounds (the amount of a single component calculated as a percentage (%) of the whole GC-MS chromatogram area) ($N = 3$, mean ± SD) of radish leaves of rosette (after harvest). Statistically significant differences ($p < 0.05$) between the control group (C) and the botanical extracts. (b) Statistically significant differences ($p < 0.05$) between the formulation (CF) and the botanical extracts. (c) Statistically significant differences ($p < 0.05$) between commercial biostimulant (CB) and the botanical extracts. RT, retention time; RI, retention indices; RI_lit, retention indices according to NIST (The NIST Mass Spectral Search Program for the NIST/EPA/NIH EI and NIST Tandem Spectral Library, 2017), FFNSC (Mondello, 2015), Adams (Adams, 2017); RI_exp, retention indices based on experiments; UAE, ultrasound-assisted extraction; MH, mechanical homogenization; Hp H, *Hypericum perforatum* L. (St. John's wort, herb); Sg L, *Solidago gigantea* Ait. (giant goldenrod, leaf); To F, To L, *Taraxacum officinale* (L.) Weber ex F.H. Wigg (common dandelion, flower, leaf); Tp F, *Trifolium pratense* L. (red clover, flower); Ur L, *Urtica dioica* L. (nettle, leaf); Vo R, *Valeriana officinalis* L. (valerian, root).

Supplementary Table 2 | The effect of the foliar application of the botanical extracts on the fatty acids composition [the amount of a single component calculated as a percentage (%) of the whole GC-MS chromatogram area] ($N = 3$, mean ± SD) of radish roots (after harvest). Statistically significant differences ($p < 0.05$) between the control group (C) and the botanical extracts. (b) Statistically significant differences ($p < 0.05$) between the formulation (CF) and the botanical extracts. (c) Statistically significant differences ($p < 0.05$) between commercial biostimulant (CB) and the botanical extracts. Abbreviations: RT, retention time; RI, retention indices; RI_lit, retention indices according to FFNSC (Mondello, 2015); RI_exp, retention indices based on experiments; UAE, ultrasound-assisted extraction; MH, mechanical homogenization; Hp H, *Hypericum perforatum* L. (St. John's wort, herb); Sg L, *Solidago gigantea* Ait. (giant goldenrod, leaf); To F, To L, *Taraxacum officinale* (L.) Weber ex F.H. Wigg (common dandelion, flower, leaf); Tp F, *Trifolium pratense* L. (red clover, flower); Ur L, *Urtica dioica* L. (nettle, leaf); Vo R, *Valeriana officinalis* L. (valerian, root).

REFERENCES

Adams, R. P. (2017). *Identification of Essential Oil Components by Gas Chromatography/Mass Spectrometry, 4th Edn.* Allured Pub Corp: Carol Stream.

Alfosea-Simón, M., Simón-Grao, S., Zavala-Gonzalez, E. A., Cámara-Zapata, J. M., Simón, I., Martínez-Nicolás, J. J., et al. (2020). Application of biostimulants containing amino acids to tomatoes could favor sustainable cultivation: implication for tyrosine, lysine, and methionine. *Sustainability* 12:9729. doi: 10.3390/su12229729

Baghel, M., Nagaraja, A., Srivastav, M., Meena, N. K., Senthil Kumar, M., Kumar, A., et al. (2019). Pleiotropic influences of brassinosteroids on fruit crops: a review. *Plant Growth Regul.* 87, 375–388. doi: 10.1007/s10725-018-0471-8

Banihani, S. A. (2017). Radish (*Raphanus sativus*) and diabetes. *Nutrients* 9:1014. doi: 10.3390/nu9091014

Bulgari, R., Cocetta, G., Trivellini, A., Vernieri, P., and Ferrante, A. (2015). Biostimulants and crop responses: a review. *Biol. Agric. Hortic.* 31, 1–17. doi: 10.1080/01448765.2014.964649

Bulgari, R., Franzoni, G., and Ferrante, A. (2019). Biostimulants application in horticultural crops under abiotic stress conditions. *Agronomy* 9:306. doi: 10.3390/agronomy9060306

Campos, E. V. R., Proença, P. L. F., Oliveira, J. L., Bakshi, M., Abhilash, P. C., and Fraceto, L. F. (2019). Use of botanical insecticides for sustainable agriculture: future perspectives. *Ecol. Indic.* 105, 483–495. doi: 10.1016/j.ecolind.2018.04.038

Caradonia, F., Battaglia, V., Righi, L., Pascali, G., and La Torre, A. (2019). Plant biostimulant regulatory framework: prospects in Europe and current situation at international level. *J. Plant Growth Regul.* 38, 438–448. doi: 10.1007/s00344-018-9853-4

Carillo, P., Colla, G., El-Nakhel, C., Bonini, P., D'Amelia, L., Dell'Aversana, E., et al. (2019a). Biostimulant application with a tropical plant extract enhances *Corchorus olitorius* adaptation to sub-optimal nutrient regimes by improving physiological parameters. *Agronomy* 9:249. doi: 10.3390/agronomy9050249

Carillo, P., Colla, G., Fusco, G. M., Dell'Aversana, E., El-Nakhel, C., Giordano, M., et al. (2019b). Morphological and physiological responses induced by protein hydrolysate-based biostimulant and nitrogen rates in greenhouse spinach. *Agronomy* 9:450. doi: 10.3390/agronomy9080450

Caruso, G., De Pascale, S., Cozzolino, E., Giordano, M., El-Nakhel, C., Cuciniello, A., et al. (2019). Protein hydrolysate or plant extract-based biostimulants enhanced yield and quality performances of greenhouse perennial wall rocket grown in different seasons. *Plants* 8:208. doi: 10.3390/plants8070208

Chohura, P., and Kołota, E. (2011). The effect of nitrogen fertilization on radish yielding. *Acta Sci. Pol. Hortorum Cultus* 10, 23–30.

Ciska, E., Martyniak-Przybyszewska, B., and Kozlowska, H. (2000). Content of glucosinolates in cruciferous vegetables grown at the same site for two years under different climatic conditions. *J. Agric. Food Chem.* 48, 2862–2867. doi: 10.1021/jf981373a

Cocetta, G., and Ferrante, A. (2020). Nutritional and nutraceutical value of vegetable crops as affected by biostimulants application. *eLS* 1–8. doi: 10.1002/9780470015902.a0028906

Colla, G., Cardarelli, M., Bonini, P., and Rouphael, Y. (2017). Foliar application of protein hydrolysate, plant and seaweed extracts increase yield but differentially modulate fruit quality of greenhouse tomato. *Hort. Sci.* 52, 1214–1220. doi: 10.21273/HORTSCI12200-17

Colla, G., Nardi, S., Cardarelli, M., Ertani, A., Lucini, L., Canaguier, R., et al. (2015). Protein hydrolysates as biostimulants in horticulture. *Sci. Hortic.* 196, 28–38. doi: 10.1016/j.scienta.2015.08.037

Costa, J. A. V., Freitas, B. C. B., Cruz, C. G., Silveira, J., and Morais, M. G. (2019). Potential of microalgae as biopesticides to contribute to sustainable agriculture and environmental development. *J. Environ. Sci. Health Part B Pestic. Food Contam. Agric. Wastes* 54, 366–375. doi: 10.1080/03601234.2019.1571366

Cozzolino, E., Giordano, M., Fiorentino, N., El-Nakhel, C., Pannico, A., Di Mola, I., et al. (2020). Appraisal of biodegradable mulching films and vegetal-derived biostimulant application as eco-sustainable practices for enhancing lettuce crop performance and nutritive value. *Agronomy* 10:427. doi: 10.3390/agronomy10030427

D'Addabbo, T., Laquale, S., Perniola, M., and Candido, V. (2019). Biostimulants for plant growth promotion and sustainable management of phytoparasitic nematodes in vegetable crops. *Agronomy* 9:616. doi: 10.3390/agronomy9100616

Dhaliwal, M. S. (2017). *Handbook of Vegetable Crops, 3rd Edn.* New Delhi: Kalyani Publishers.

Drobek, M., Frac, M., and Cybulska, J. (2019). Plant biostimulants: Importance of the quality and yield of horticultural crops and the improvement of plant tolerance to abiotic stress-a review. *Agronomy* 9:335. doi: 10.3390/agronomy9060335

Ediage, E. N., Di Mavungu, J. D., Scippo, M. L., Schneider, Y. J., Larondelle, Y., Callebaut, A., et al. (2011). Screening, identification and quantification of glucosinolates in black radish (*Raphanus sativus* L. *niger*) based dietary supplements using liquid chromatography coupled with a photodiode array and liquid chromatography-mass spectrometry. *J Chromatogr A* 1218, 4395–4405. doi: 10.1016/j.chroma.2011.05.012

Ekin, Z. (2019). Integrated use of humic acid and plant growth promoting rhizobacteria to ensure higher potato productivity in sustainable agriculture. *Sustainability* 11:3417. doi: 10.3390/su11123417

Ertani, A., Cavani, L., Pizzeghello, D., Brandellero, E., Altissimo, A., Ciavatta, C., et al. (2009). Biostimulant activity of two protein hydrolyzates in the growth and nitrogen metabolism of maize seedlings. *J. Plant Nutr. Soil Sci.* 172, 237–244. doi: 10.1002/jpln.200800174

Ertani, A., Pizzeghello, D., Francioso, O., Sambo, P., Sanchez-Cortes, S., and Nardi, S. (2014). *Capsicum chinensis* L. growth and nutraceutical properties are enhanced by biostimulants in a long-term period: chemical and metabolomic approaches. *Front. Plant Sci.* 5:375. doi: 10.3389/fpls.2014.00375

European Communities (2006). *Commission Regulation No. 2006.364.5 of 19 December 2006 Setting Maximum Levels for Certain Contaminants in Foodstuffs*. Brussels: European Communities.

Fess, T. L., and Benedito, V. A. (2018). Organic versus conventional cropping sustainability: A comparative system analysis. *Sustainability* 10:272. doi: 10.3390/su10010272

Francesca, S., Arena, C., Mele, B. H., Schettini, C., Ambrosino, P., Barone, A., and Rigano, M. M. (2020). The use of a plant-based biostimulant improves plant performances and fruit quality in tomato plants grown at elevated temperatures. *Agronomy* 10:363. doi: 10.3390/agronomy10030363

Godlewska, K., Biesiada, A., Michalak, I., and Pacyga, P. (2019). The effect of plant-derived biostimulants on white head cabbage seedlings grown under controlled conditions. *Sustainability* 11:5317. doi: 10.3390/su11195317

Godlewska, K., Biesiada, A., Michalak, I., and Pacyga, P. (2020a). The effect of botanical extracts obtained through ultrasound-assisted extraction on white head cabbage (*Brassica oleracea* L. *var. capitata L.*) seedlings grown under controlled conditions. *Sustainability* 12:1871. doi: 10.3390/su12051871

Godlewska, K., Pacyga, P., Michalak, I., Biesiada, A., Szumny, A., Pachura, N., et al. (2020b). Field-scale evaluation of botanical extracts effect on the yield, chemical composition and antioxidant activity of celeriac (*Apium graveolens* L. var. *rapaceum*). *Molecules* 25:4212. doi: 10.3390/molecules25184212

Godlewska, K., Pacyga, P., Michalak, I., Biesiada, A., Szumny, A., Pachura, N., et al. (2021). Effect of botanical extracts on the growth and nutritional quality of field-grown white head cabbage (*Brassica oleracea* var. *capitata*). *Molecules* 26:1992. doi: 10.3390/molecules26071992

Jindo, K., Olivares, F. L., Malcher, D. J., da Paixão Malcher, D. J., Sánchez-Monedero, M. A., Kempenaar, C., et al. (2020). From lab to field: Role of humic substances under open-field and greenhouse conditions as biostimulant and biocontrol agent. *Front. Plant Sci.* 11:426. doi: 10.3389/fpls.2020.00426

Kamble, S. S., Gunasekaran, A., and Gawankar, S. A. (2020). Achieving sustainable performance in a data-driven agriculture supply chain: a review for research and applications. *Int. J. Prod. Econ.* 219, 179–194. doi: 10.1016/j.ijpe.2019.05.022

Kim, H. J., Ku, K. M., Choi, S., and Cardarelli, M. (2019). Vegetal-derived biostimulant enhances adventitious rooting in cuttings of basil, tomato, and chrysanthemum via brassinosteroid-mediated processes. *Agronomy* 9:74. doi: 10.3390/agronomy9020074

Kocira, S. (2019). Effect of amino acid biostimulant on the yield and nutraceutical potential of soybean. *Chil. J. Agric. Res.* 79, 17–25. doi: 10.4067/S0718-58392019000100017

Kowalski, A., and Kaniszewski, S. (2017). Effect of organic fertilization on the quality and yield of two radish cultivars in greenhouse organic cultivation. *Acta Hortic.* 1164, 189–194. doi: 10.17660/ActaHortic.2017.1164.24

Madende, M., and Hayes, M. (2020). Fish by-product use as biostimulants: An overview of the current state of the art, including relevant legislation and regulations within the EU and USA. *Molecules* 25:1122. doi: 10.3390/molecules25051122

Maldini, M., Foddai, M., Natella, F., Petretto, G. L., Rourke, J. P., Chessa, M., and Pintore, G. (2017). Identification and quantification of glucosinolates in different tissues of *Raphanus raphanistrum* by liquid chromatography tandem-mass spectrometry. *J. Food Compos. Anal.* 61, 20–27. doi: 10.1016/j.jfca.2016.06.002

Manivannan, A., Kim, J. H., Kim, D. S., Lee, E. S., and Lee, H. E. (2019). Deciphering the nutraceutical potential of *Raphanus sativus*—a comprehensive overview. *Nutrients* 11:402. doi: 10.3390/nu11020402

Mondello, L. (2015). *Mass Spectra of Flavors and Fragrances of Natural and Synthetic Compounds, 3rd Edn.* Hoboken, NJ: Wiley.

Palumbo, G., Schiavon, M., Nardi, S., Ertani, A., Celano, G., and Colombo, C. M. (2018). Biostimulant potential of humic acids extracted from an amendment obtained via combination of olive mill wastewaters (OMW) and a pre-treated organic material derived from municipal solid waste (MSW). *Front. Plant Sci.* 9:1028. doi: 10.3389/fpls.2018.01028

Paradiković, N., Teklić, T., Zeljković, S., Lisjak, M., and Špoljarević, M. (2018). Biostimulants research in some horticultural plant species—a review. *Food Energy Secur.* 8, 1–17. doi: 10.1002/fes3.162

Paul, D. D. S., Harini, P., Assvitha, S., Kalairasi, A., Ganesh, S., and Umamaheswari, A. (2016). Phytochemical investigation and anticancer activity of leaf extract of *Raphanus sativus* var. *sativus. Int. J. Res. Pharmacol. Pharmacother.* 39–45.

Pereira, A. D. E. S., Oliveira, H. C., and Fraceto, L. F. (2019). Polymeric nanoparticles as an alternative for application of gibberellic acid in sustainable agriculture: a field study. *Sci. Rep.* 9:7135. doi: 10.1038/s41598-019-43494-y

Pylak, M., Oszust, K., and Frac, M. (2019). Review report on the role of bioproducts, biopreparations, biostimulants and microbial inoculants in organic production of fruit. *Rev. Environ. Sci. Biotechnol.* 18, 597–616. doi: 10.1007/s11157-019-09500-5

Rolli, N. M., Gadi, S. B., Giraddi, T. P., Paramanna, D., and Giddannavar, H. S. (2016). Accumulation of xenobiotics in vegetables and itd impact on health. *Int. J. Curr. Res.* 8, 24906–24912.

Röös, E., Mie, A., Wivstad, M., Salomon, E., Johansson, B., Gunnarsson, S., et al. (2018). Risks and opportunities of increasing yields in organic farming. A review. *Agron. Sustain. Dev.* 38:14. doi: 10.1007/s13593-018-0489-3

Rose, D. C., Sutherland, W. J., Barnes, A. P., Borthwick, F., Ffoulkes, C., Hall, C., et al. (2019). Integrated farm management for sustainable agriculture: lessons for knowledge exchange and policy. *Land Policy* 81, 834–842. doi: 10.1016/j.landusepol.2018.11.001

Rouphael, Y., and Colla, G. (2020). Editorial: Biostimulants in agriculture. *Front. Plant Sci.* 11:40. doi: 10.3389/fpls.2020.00040

Rouphael, Y., Giordano, M., Cardarelli, M., Cozzolino, E., Mori, M., Kyriacou, M. C., et al. (2018). Plant- and seaweed-based extracts increase yield but

differentially modulate nutritional quality of greenhouse spinach through biostimulant action. *Agronomy* 8:216. doi: 10.3390/agronomy8070126

Sandhu, R. K., Nandwani, D., and Nwosisi, S. (2018). Assessing seaweed extract as a biostimulant on the yield of organic leafy greens in Tennessee. *J. Agric. Univ.* 102, 53–64. doi: 10.46429/jaupr.v102i1-2.17531

Shang, Y., Kamrul Hasan, M., Ahammed, G. J., Li, M., Yin, H., and Zhou, J. (2019). Applications of nanotechnology in plant growth and crop protection: a review. *Molecules* 24:2558. doi: 10.3390/molecules24142558

Shukla, P. S., Mantin, E. G., Adil, M., Bajpai, S., Critchley, A. T., and Prithiviraj, B. (2019). *Ascophyllum nodosum*-based biostimulants: sustainable applications in agriculture for the stimulation of plant growth, stress tolerance, and disease management. *Front. Plant Sci.* 10:655. doi: 10.3389/fpls.2019.00655

Szczepanik, M., Walczak, M., Zawitowska, B., Michalska-Sionkowska, M., Szumny, A., Wawrzeńczyk, C., et al. (2018). Chemical composition, antimicromicrobial activity and insecticidal activity against the lesser mealworm *Alphitobius diaperinus* (Panzer) (*Coleoptera: Tenebrionidae*) of *Origanum vulgare* L. ssp. *hirtum* (Link) and *Artemisia dracunculus L.* essential oils. *J. Sci. Food Agric.* 98, 767–774. doi: 10.1002/jsfa.8524

Szparaga, A., Kocira, S., Kocira, A., Czerwińska, E., Swieca, M., Lorencowicz, E., et al. (2018). Modification of growth, yield, and the nutraceutical and antioxidative potential of soybean through the use of synthetic biostimulants. *Front. Plant Sci.* 871:1401. doi: 10.3389/fpls.2018.01401

Szparaga, A., Kubo,ń, M., Kocira, S., Czerwińska, E., Pawłowska, A., Hara, P., et al. (2019). Towards sustainable agriculture-agronomic and economic effects of biostimulant use in common bean cultivation. *Sustainability* 11:4575. doi: 10.3390/su11174575

The NIST Mass Spectral Search Program for the NIST/EPA/NIH EI and NIST Tandem Spectral Library. Gaithersburg, MD: Standard Reference Data Program of the National Institute of Standards and Technology (2017).

Varalakshmi, L. R., and Ganeshamurthy, A. N. (2008). A market survey of vegetables in Bangalore for heavy metal contamination in relation to human health. *J. Hortic. Sci.* 3, 75–78.

Veissi, M., Meighani, N., and Latifi, M. (2015). Evaluation of heavy metals (lead, cadmium and chromium) and nitrates in some vegetables cultivated in Ahvaz, Iran. *Curr. Top. Toxicol.* 11, 29–34.

Vejan, P., Abdullah, R., Khadiran, T., Ismail, S., and Nasrulhaq Boyce, A. (2016). Role of plant growth promoting rhizobacteria in agricultural sustainability-a review. *Molecules* 21:573. doi: 10.3390/molecules21050573

Yakhin, O., Lubyanov, A. A., Yakhin, I. A., and Brown, P. H. (2017). Biostimulants in plant science: a global perspective. *Front. Plant Sci.* 7:2049. doi: 10.3389/fpls.2016.02049

Zulfiqar, F., Casadesús, A., Brockman, H., and Munné-Bosch, S. (2020). An overview of plant-based natural biostimulants for sustainable horticulture with a particular focus on moringa leaf extracts. *Plant Sci.* 295:110194. doi: 10.1016/j.plantsci.2019.110194

Zulfiqar, F., Navarro, M., Ashraf, M., Akram, N. A., and Munné-Bosch, S. (2019). Nanofertilizer use for sustainable agriculture: advantages and limitations. *Plant Sci.* 289:110270. doi: 10.1016/j.plantsci.2019.110270

Conflict of Interest: The authors declare that the research was conducted in the absence of any commercial or financial relationships that could be construed as a potential conflict of interest.

frontiers in Microbiology

ORIGINAL RESEARCH
published: 25 June 2021
doi: 10.3389/fmicb.2021.692313

Endophytic *Bacillus altitudinis* Strain Uses Different Novelty Molecular Pathways to Enhance Plant Growth

*Dening Zhang[1], Hongli Xu[1], Jingyao Gao[1], Roxana Portieles[1], Lihua Du[1], Xiangyou Gao[1], Carlos Borroto Nordelo[2] and Orlando Borrás-Hidalgo[1,3]**

[1] Joint R&D Center of Biotechnology, Retda, Yota Bio-Engineering Co., Ltd., Rizhao, China, [2] VBS Biotec SA, Mexico, Mexico, [3] State Key Laboratory of Biobased Material and Green Papermaking, Shandong Provincial Key Lab of Microbial Engineering, Qilu University of Technology (Shandong Academy of Science), Jinan, China

The identification and use of endophytic bacteria capable of triggering plant growth is an important aim in sustainable agriculture. In nature, plants live in alliance with multiple plant growth-promoting endophytic microorganisms. In the current study, we isolated and identified a new endophytic bacterium from a wild plant species *Glyceria chinensis* (Keng). The bacterium was designated as a *Bacillus altitudinis* strain using 16S rDNA sequencing. The endophytic *B. altitudinis* had a notable influence on plant growth. The results of our assays revealed that the endophytic *B. altitudinis* raised the growth of different plant species. Remarkably, we found transcriptional changes in plants treated with the bacterium. Genes such as maturase K, tetratricopeptide repeat-like superfamily protein, LOB domain-containing protein, and BTB/POZ/TAZ domain-containing protein were highly expressed. In addition, we identified for the first time an induction in the endophytic bacterium of the major facilitator superfamily transporter and DNA gyrase subunit B genes during interaction with the plant. These new findings show that endophytic *B. altitudinis* could be used as a favourable candidate source to enhance plant growth in sustainable agriculture.

Keywords: endophytic bacteria, *Bacillus altitudinis*, plant growth, transcriptome, *Glyceria chinensis*

OPEN ACCESS

Edited by:
Maurizio Ruzzi,
University of Tuscia, Italy

Reviewed by:
Tyler Helmann,
United States Department of Agriculture (USDA), United States
Sergio de los Santos Villalobos,
Instituto Tecnológico de Sonora (ITSON), Mexico

***Correspondence:**
Orlando Borrás-Hidalgo
borrasorlando@yahoo.com

Specialty section:
This article was submitted to Microbe and Virus Interactions with Plants, a section of the journal Frontiers in Microbiology

Received: *08 April 2021*
Accepted: *26 May 2021*
Published: *25 June 2021*

Citation:
Zhang D, Xu H, Gao J, Portieles R, Du L, Gao X, Borroto Nordelo C and Borrás-Hidalgo O (2021) Endophytic Bacillus altitudinis Strain Uses Different Novelty Molecular Pathways to Enhance Plant Growth. Front. Microbiol. 12:692313. doi: 10.3389/fmicb.2021.692313

INTRODUCTION

The use of fertilisers in agricultural practice to increase yields has had harmful effects on the environment and quality of the soil for a long time (Worlanyo and Jiangfeng, 2021). To minimise these negative impacts, the use of microorganisms located in the rhizosphere and in endophytic environments, such as bio-fertilisers, has received increased attention (Atieno et al., 2020). Beneficial plant–bacteria communities have been studied for many years (Pieterse et al., 2012; Zipfel and Oldroyd, 2017; Afzal et al., 2019; Ke et al., 2021; Song et al., 2021; Zhang et al., 2021). There are different bacteria in a direct interconnection with the plant cells; therefore, they might produce a direct beneficial effect (Hallmann et al., 1997). Different plant species are colonised by a great diversity of endophytic bacteria, such as *Pseudomonas*, *Bacillus*, *Enterobacter*, *Burkholderia*, and *Azospirillum* (Lodewyckx et al., 2002; Weyens et al., 2009).

The range of endophytic bacteria depends on the plant species and crop conditions (Zinniel et al., 2002; Ulrich et al., 2008). Endophytic bacteria colonise the intracellular and intercellular

spaces of plant tissues and promote plant growth (Ulrich et al., 2008; Lugtenberg and Kamilova, 2009; Vacheron et al., 2013; Hardoim et al., 2015; Santoyo et al., 2016; Gouda et al., 2018). The procedures used by endophytic bacteria to boost plant growth constitute an essential step in the endophytic bacteria applications (Wani et al., 2015). However, the process by which endophytic bacteria enhance plant growth are not well understood (Hardoim et al., 2008; Marasco et al., 2012; Rashid et al., 2012; Bruto et al., 2014). Important evidence suggests that there is a relationship between genes involved in beneficial features (Bruto et al., 2014). The useful functions comprise the bacterial ability to enhance nutrient acquisition, fix nitrogen, acquire iron, and produce siderophores in plant species (Zhang et al., 2009; Hardoim et al., 2015; Zhou et al., 2016).

Furthermore, endophytic bacteria enhance plant growth through the production of different phytohormones. Phytohormones produced during endophytic colonisation process improved plant nutrient absorption and biomass (Gravel et al., 2007; Phetcharat and Duangpaeng, 2012; Shi et al., 2014). Plant growth regulators such as cytokines, ethylene, abscisic acid (ABA), gibberellins, and indole-3-acetic acid (IAA) are produced by endophytic bacteria during interactions with plants (Vacheron et al., 2013). Interestingly, IAA showed a crucial effect on plant growth and development processes. Modulating IAA is a notable hallmark through which the endophytic bacteria might strengthen plant growth. In addition, ethylene constitutes an essential plant hormone involved in different developmental and physiological processes (Sun et al., 2016). The enzyme 1-aminocyclopropane-1-carboxylate (ACC) deaminase precursor of ethylene is produced by endophytic bacteria (Sun et al., 2009). The hydrolysis of ACC improved plant growth under stress conditions (Santoyo et al., 2016). Plant growth-promoting endophytic bacteria displayed ACC deaminase activity (Nikolic et al., 2011; Zhang et al., 2011; Rashid et al., 2012). These bacteria can produce ACC deaminase to enhance plant growth. Mutation of the ACC deaminase gene compromised the canola growth (Sun et al., 2009). Moreover, diverse endophytic bacterial strains have the ability to release volatile organic compounds such as acetoin, pentadecane, 2,3-butanediol, 1 hexanol, and indole, which enhance plant growth (Ryu et al., 2003; Gutiérrez-Luna et al., 2010; Blom et al., 2011; Hernández-Calderón et al., 2018).

Plant endophytic bacteria have great potential to be used as bio-fertilisers. Although different types of bacterial species were identified from a broad plant species range, the action of these bacteria is commonly unstable under field conditions (Afzal et al., 2019). The poor understanding of the tricky events that control this alliance at the molecular level might be the reason. However, it is possible to obtain a better understanding through the evaluation of the both bacterial and plant genes expressed during the interaction (Afzal et al., 2019). The development of RNA-sequencing techniques has allowed the identification of transcripts involved in plant growth. However, few studies have investigated the endophytic bacterial diversity in unexplored wild plant species. Wild plant species survive in different environments and under diverse stress conditions. Identification of endophytic bacteria isolated from these species might allow the use of diverse mechanisms in these bacteria to promote plant growth (Afzal et al., 2019). The present study aimed to isolate, identify, and characterise endophytic bacteria from wild plant species and characterise their plant growth-promoting properties and the main molecular events involved in endophytic bacteria–plant interactions.

MATERIALS AND METHODS

Isolation of Endophytic Bacterium

The samples were collected from wild plant species *Glyceria chinensis* (Keng) localised along the margin of the Fu Tuan River (35°20′17″N, 119°26′8″E) within 5 km[1] of the coastal region of Rizhao City in Shandong Province (People's Republic of China). The wild plant species was classified according to data on morphological traits from the Flora of China.[2] This experimental study complies with Chinese national and local laws, and sample collection has been permitted by the Rizhao administration and Municipal Sciences and Technology Department [Collection information: South China Botanical Garden (IBSC) of the Chinese Academy of Sciences. Source: China Digital Plant Specimens Museum. Identifier: 0114164. Collector: Zhang Zhisong Acquisition number: 401467]. A total of 100 samples were collected randomly during the spring season. Firstly, the plant material (stems and roots) was rinsed with water. The samples were cut into small pieces under aseptic conditions. Each sample was surface sterilised with 70% ethanol for 1 min and immersed in a sodium hypochlorite solution (5%) during 1 min. Subsequently, the samples were washed in sterile distilled water during 1 min and dried on filter paper. After proper drying, pieces of plant parts were physically treated in a TissueLyser (Qiagen, Hilden, Germany) during 5 min in 1 ml of sterile water. The debris was decanted and 100 μl of the remaining water was incubated in Luria–Bertani (LB) agar medium (yeast extract, 5 g/L: peptone, 10 g/L; sodium chloride, 5 g/L; agar, 12 g/L; pH 7) at 37°C for 3 days. Parallel to the samples, the final wash solution of the surface sterilisation procedure was also spread plated onto the MS medium plate which served as a control. The bacteria were only isolated from processed samples internally. This was the criteria to classify as endophytes and not the surface contaminates. Bacterial colonies were selected based on growth rate, colony morphology, and pigmentation. Bacterial isolates were selected and purified by streaking procedure. These were incubated at 37°C. Pure cultures of the bacterial strains were maintained in 30% glycerol at −80°C.

Plant Materials and Growth Conditions

Arabidopsis thaliana ecotype Columbia plants were used in the experiments. First, surface-sterilised seeds were plated on Murashige and Skoog (0.5 × MS) basal media (Sigma Aldrich, St. Louis, MO, United States) supplemented with 1% w/v sucrose. The seeds were stored at 4°C in the dark for 2 days and transferred to a controlled growth room under a 16-h light/8-h dark photoperiod at 22°C. Small plants were transplanted to a

[1] https://www.ezbiocloud.net

[2] http://www.iplant.cn/foc/

mixture of soil composed of peat plugs and vermiculite in a 1:1 ratio during 14 days. In addition, *Nicotiana tabacum*, corn, and soybean seeds were germinated and the plants grown in pots (6") containing sterilised black turf and rice husk (4:1) substrate and maintained in a controlled growth room at 23°C.

Identification of Endophytic Bacterium

The DNA from endophytic bacterium was extracted according to Sambrook et al. (1989). The 16S rRNA gene was used for molecular identification. A fragment of 16S rRNA gene was amplified by polymerase chain reaction (PCR) using the forward primer 27F 5′-AGAGTTTGATCCTGGCTCAG-3′ and reverse primer 1492R 5′-GGTTACCTTGTTACGACTT-3′. The amplification process was conducted in a Thermal Cycler T100 machine (Bio-Rad Life Science Research, Shanghai, People's Republic of China) using a Taq PCR Master Mix Kit (Qiagen, Hilden, Germany). The PCR reaction was as follows: 95°C for 10 min; 35 cycles of 95°C for 30 s, 55°C for 1 min, and 72°C for 1.5 min; and final extension at 72°C for 10 min. The purified PCR fragment was sequenced using an ABI 3730 DNA sequencer (Applied Biosystems, ThermoFisher Scientific, Chino, CA, United States). The 16S rRNA gene fragment sequence (1,147 bp) was identified using BLASTN homology searches (Altschul et al., 1997). The National Center for Biotechnology Information (NCBI) GenBank, European Molecular Biology Laboratory–European Bioinformatics Institute (EMBL–EBI), and taxonomically united database of 16S rRNA EzBioCloud[2] were used as databases (Yoon et al., 2017; De Los Santos Villalobos et al., 2019; Ha et al., 2019). Additionally, the full 16S rRNA gene (1,544 bp), glycosyl hydrolase lipoprotein, and SDR family oxidoreductase genes sequenced through RNA sequencing were used to an accurate identification. The phylogenetic tree was done using the neighbour-joining method and the full 16S rRNA (Saitou and Nei, 1987).

Greenhouse Experiments

Seeds pre-germinated from *A. thaliana*, *N. tabacum*, corn, and soybean were treated with endophytic bacterial fermentation twice weekly for 1 month. The selected bacterial strain was incubated in 100 ml of LB broth medium in a 250-ml Erlenmeyer flask with shaking (200 rpm) for 1 day at 37°C in the dark. The optical density (OD) from endophytic bacterial fermentation was adjusted to 1.0 (4.77×10^9 CFU/ml), and 30 ml of the fermentation was applied per pot. Each plastic pot received three pre-germinated seeds, and the plants were grown in a controlled growth room at 25°C and irrigated with water without any fertilisers. A completely randomised pot experiment with five replicates for each treatment was done to analyse the influence of the endophytic bacterium on the growing of different plant species. The substrate contained black turf and rice husks (4:1). The substrate was sterilised at 120°C during 20 min. Additionally, the roots of the plants inoculated with the endophytic bacterium used in the experiments were processed, and the bacterium was again isolated and classified as the original strain using the same protocol mentioned above. In *Arabidopsis* plants, the rosette diameter, leaf size, root size, and fresh weight parameters were evaluated after 1 month of treatment with endophytic bacterial fermentation. In addition, colony-forming units from endophytic bacteria were determined after 1 month of treatment. Plant size and fresh weight were evaluated in *N. tabacum*, corn, and soybean plants after 1 month of treatment. Data were analysed using GraphPad Prism software (La Jolla, CA, United States). Significant differences among the mean values were determined using *t*-test at $p < 0.05$. Five replicates were used for each treatment. The experiments were replicated twice.

Identification of New Genes Using RNA Sequencing

The *Arabidopsis* plants were treated with aliquots of 30 ml (4.77×10^9 CFU/ml) of endophytic bacterium. The bacterium was inoculated in the sterilised substrate around the plants (5-day-old). The colonisation of bacterium in the roots was verified using the same protocol used in the isolation of this strain from wild plant species on LB plates at different time points. The endophytic bacterium was well established 72 h post-inoculation. Leaves, stems, and roots from five plants were collected 72 h post-inoculation. Plants treated with water were used as control. Treatments and controls were repeated three times per group. The total RNA was extracted using the Qiagen RNeasy Midi Kit (Hilden, Germany), and the concentration of the total RNA was determined using spectrometry. The treatment and control samples were repeated three times per group. After extracting the total RNA, eukaryotic mRNA was enriched using oligo(dT) beads. The samples were sequenced using Illumina HiSeq™ 2000 (Personalbio Co., Shanghai, People's Republic of China). High-quality reads were processed using the Perl script, and the differentially expressed genes were identified using the edgeR package.[3] Genes with a fold change ≥ 2 were considered significant differentially expressed genes. Gene ontology (GO) and the Kyoto Encyclopedia of Genes and Genomes (KEGG) pathway enrichment analysis were used to characterise the differentially expressed genes. GO functional annotations were obtained from the non-redundant annotation results. In addition, the GO annotations were analysed using the Blast2GO software[4] (Conesa et al., 2005). The RNA sequencing was done following these steps: (1) total RNA extraction; (2) total RNA quality test; (3) rRNA removal; (4) RNA fragmentation between 200 and 300 bp by ion disruption; (5) PCR: the first chain of cDNA was synthesised by random primers and reverse transcriptase; when the second chain of cDNA was synthesised, the library of chain-specific components was constructed, and dTTP was replaced by dUTP, which greatly improved the accuracy of the results. (6) PCR enrichment of library fragments: the size of the library ranged from 300 to 400 bp. (7) Library quality inspection: the size of the library was detected by Agilent 2100 Bioanalyzer, and the total concentration of the library was detected by fluorescence quantitative analysis. (8) Illumina sequencing: the best amount of sample was selected for PCR amplification. (9) Annealing of sequencing at the same time of synthesis: the prokaryote genetic analysis process firstly filtered the raw off-machine data to obtain a high-quality sequence, comparing the

[3] www.r-project.org/

[4] www.blast2go.com

TABLE 1 | Total bacterial population at harvest.

Samples	Root endosphere (10^2 CFU/cm fresh root)[a]
SB001	9.40 ± 0.75
SB002	0.10 ± 0.01
SB003	2.50 ± 0.02
SB004	1.10 ± 0.04
SB005	0.20 ± 0.01
SB006	0.50 ± 0.02

[a]*Means of five replicates.*

filtered sequence with the species reference genome. Based on the results of the comparison, the amount of expression of each gene was calculated. On this basis, the expression difference analysis, enrichment analysis, and cluster analysis of the sample were further carried out. The transcription structure of the sample was analysed and the manipulative substructure of the sample gene obtained. UTR, SNP, and InDel were obtained. HTSeq 0.6.1p2[5] was used to compare the read count values from each gene as the original expression of the gene. To make gene expression levels comparable between different genes and samples, we normalised the sequencing depth and gene length using fragments per kilobase of transcript per million (FPKM). FPKM calculates the number of fragments that two reads can compare to the same transcript. In the reference transcription group, we generally took into account the FPKM >1 when the gene was expressed. Pearson correlation coefficients were used to indicate the level of expression correlation between genes in the sample to test the reliability of the experiments and whether sample selection was reasonable. The level correlation of gene expression between samples was an important index to test the reliability of the experiments and whether sample selection was reasonable. The log2 fold change was calculated by dividing the FPKM values from the bacterium during interaction with *Arabidopsis* (SB001) and the bacterium without interaction with *Arabidopsis* (B001).

RESULTS

Isolation and Identification of the Endophytic Bacterium *Bacillus altitudinis*

Six endophytic bacteria strains were isolated from wild plant species. The ability of the six isolated endophytic bacteria to colonise and persist in wild plant species was tested. Of these six, only one isolate (SB001) colonised this plant species at levels ranging from 9.40×10^2 CFU/cm fresh root compared with the other five strains, where the level was lower (**Table 1**). Based on the levels of colonisation, the isolated endophytic strain SB001 was selected for further assays.

The isolate SB001 showed a small rod-shaped structure and Gram-positive spore-forming bacterium distinctive of the genus *Bacillus*. The bacterium strain was identified using the partial (1,147 bp) and full (1,544 bp) 16S rRNA gene. Using the taxonomically united database of 16S rRNA in EzBioCloud, the full 16S rRNA was definitively identified as a top hit with *Bacillus altitudinis* with 100% similarity. Partial 16S rRNA sequences had an ambiguous 96.94% of similarity with *B. altitudinis*. Additionally, glycosyl hydrolase lipoprotein and SDR family oxidoreductase genes confirmed the identification of *B. altitudinis* (**Supplementary Table 1**). Considering the identification, the phylogenetic tree was constructed by comparing the full 16S rRNA gene sequences of the isolate SB001 with the reference strain sequences from the NCBI GenBank public database. Molecular analysis indicated that the isolated strain SB001 belongs to the genus *Bacillus* showing an identity percentage of 100% and *E*-value of 0.0 with *B. altitudinis* strain W3 (**Figure 1**).

Bacillus altitudinis Strain Promotes the Growth of Different Plant Species

The endophytic strain was also evaluated for plant growth promotion in different plant species. There was significant growth in *Arabidopsis* plants treated with the endophytic bacterium *B. altitudinis* (**Figure 2A**). The rosette diameter (**Figure 2B**), leaf size (**Figure 2C**), and fresh weight (**Figure 2E**) were considerably increased by inoculation with the *B. altitudinis* strain compared with the control in *Arabidopsis* plants at 20 days. However, endophytic bacteria did not influence root size (**Figure 2D**). Nevertheless, endophytic bacteria were suitably established in *Arabidopsis* roots (**Figure 2F**).

The *B. altitudinis* strain significantly stimulated the growth of *N. tabacum* plants (**Figure 3A**) and showed a substantial influence on plant size (**Figure 3B**) and fresh weight (**Figure 3C**) in *N. tabacum* plants. Inoculation with the *B. altitudinis* strain considerably enhanced the growth of maize plants with respect to non-inoculated plants (**Figure 4A**). Compared with the non-inoculated plants, the endophytic strain increased the plant size (**Figure 4B**) and fresh weight (**Figure 4C**) in inoculated plants. However, the endophytic strain had no significant influence on soybean plant growth (**Figure 5**). Overall, these results revealed that *B. altitudinis* improved the vegetative growth of different plant species following inoculation.

Bacillus altitudinis Induces Transcriptional Changes in Genes Involved in Plant Growth

RNA-seq was used to evaluate the interactions between *B. altitudinis* and *Arabidopsis*. To generate RNA-seq data sets, we prepared cDNA libraries from mock-inoculated and inoculated with the endophytic bacterium *B. altitudinis* from *Arabidopsis* plant RNA and sequenced them on two separate flow cells. The range of gene expression during the *B. altitudinis–Arabidopsis* interaction was determined. During the interaction, 27,628 transcripts were identified and annotated (**Supplementary Table 2**). From this, 7,379 new transcripts were annotated (**Supplementary Table 3**). The highest number of transcripts (33.57%) showed an expression level change of between 1- and 10-fold. The lowest number of transcripts was distributed at the highest expression level

[5]http://htseq.readthedocs.io

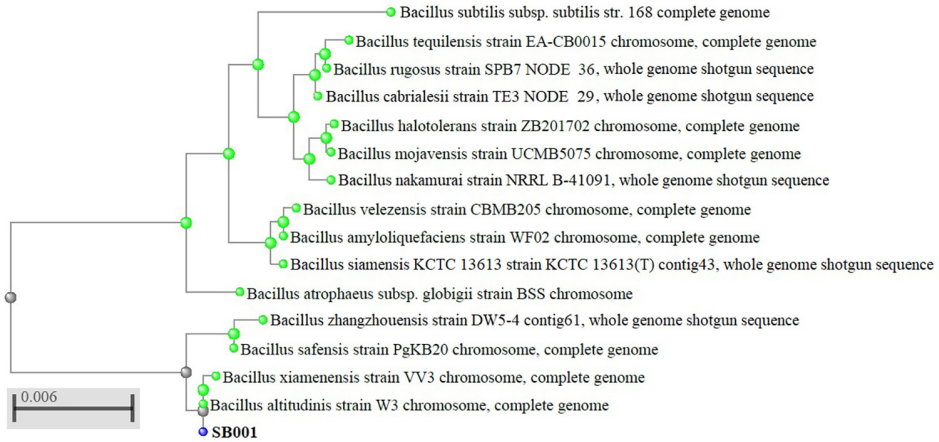

FIGURE 1 | Phylogenetic tree of 16S rRNA sequences from endophytic bacterium strain (SB001) compared with representative members of *Bacillus* genus with more than 98% of identity.

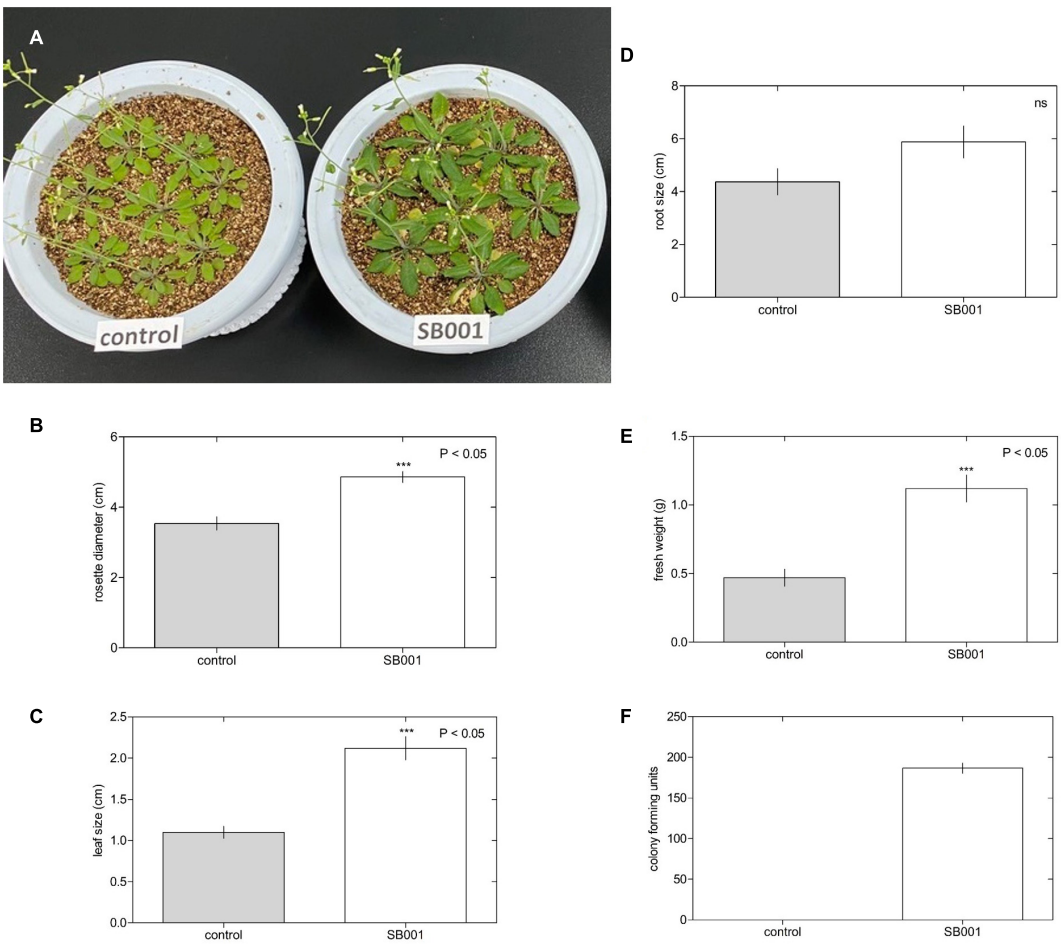

FIGURE 2 | Endophytic bacterium *B. altitudinis* induces significant *Arabidopsis* plant growth. Plants (5-day-old) were mock-treated (control) or inoculated with 30 ml of *B. altitudinis* at 4.77 × 10^9 CFU/ml. **(A)** Phenotype of *Arabidopsis* plants mock-treated (control) and treated with *B. altitudinis* fermentations (SB001) at 20 days post-inoculation. Effect on the rosette diameter **(B)**, leaf size **(C)**, root size **(D)**, and fresh weight **(E)** of *Arabidopsis* plants treated with *B. altitudinis* fermentations (SB001). **(F)** Colony-forming units were determined in *Arabidopsis* plants mock-treated (control) and treated with *B. altitudinis* fermentations (SB001). Each bar represents mean values with standard errors of two independent experiments (n = 10). ***$P \leq 0.001$.

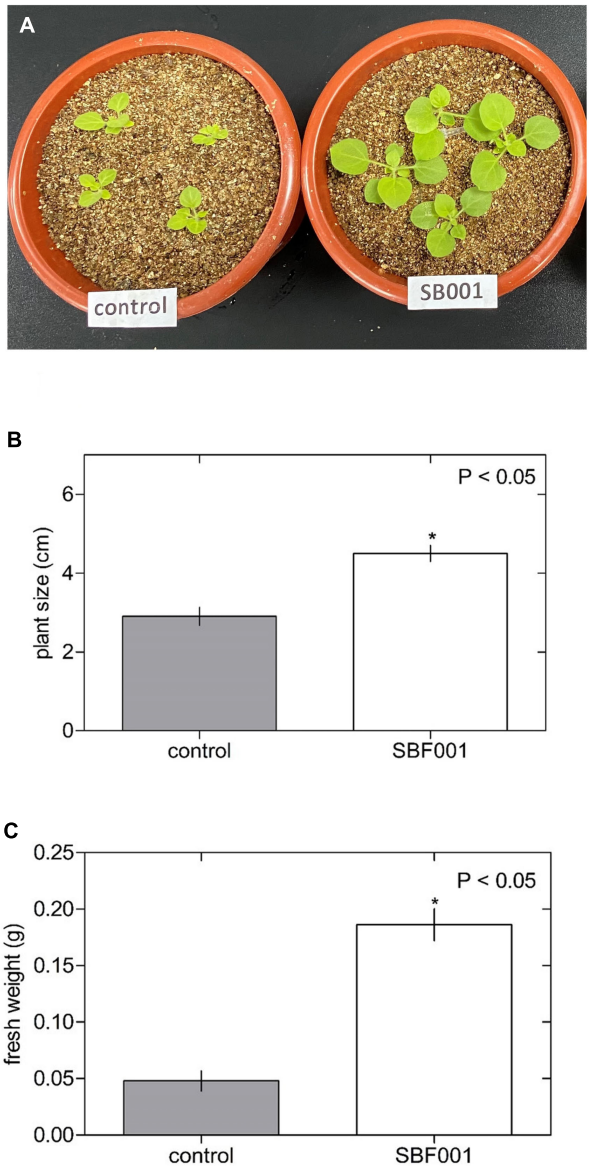

FIGURE 3 | Endophytic bacterium *B. altitudinis* induces significant *Nicotiana tabacum* plant growth. Plants (5-day-old) were mock-treated (control) or inoculated with 30 ml of *B. altitudinis* at 4.77 × 10^9 CFU/ml. **(A)** Phenotype of *N. tabacum* plants mock-treated (control) and treated with *B. altitudinis* fermentations (SB001) at 20 days post-inoculation. Effect on plant size **(B)** and fresh weight **(C)** of *N. tabacum* plants mock-treated (control) and treated with *B. altitudinis* fermentations (SB001). Each bar represents mean values with standard errors of two independent experiments (n = 10). *$P \leq 0.05$.

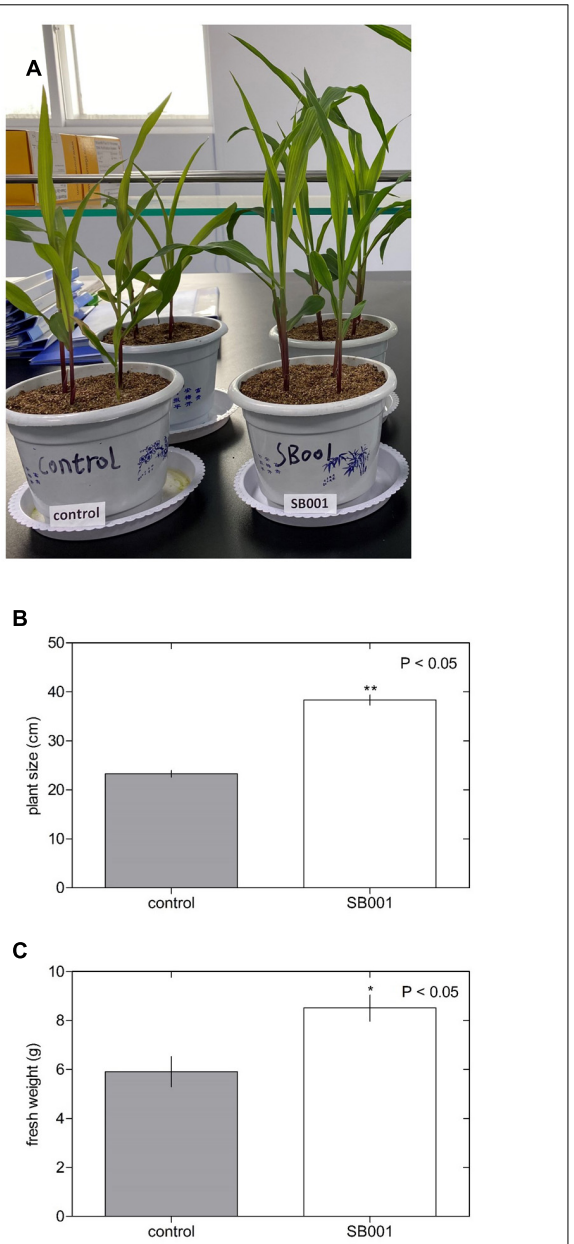

FIGURE 4 | Endophytic bacterium *B. altitudinis* induces significant maize plant growth. Plants (5-day-old) were mock-treated (control) or inoculated with 30 ml of *B. altitudinis* at 4.77 × 10^9 CFU/ml. **(A)** Phenotype of maize plants mock-treated (control) and treated with *B. altitudinis* fermentations (SB001) at 20 days post-inoculation. Effect on plant size **(B)** and fresh weight **(C)** of maize plants mock-treated (control) and treated with *B. altitudinis* fermentations (SB001). Each bar represents mean values with standard errors of two independent experiments (n = 10). *$P \leq 0.05$; **$P \leq 0.01$.

between >100-fold change (**Figure 6**). Analysis of RNA-seq data during the interaction revealed 368 differentially expressed transcripts, which included 256 upregulated and 112 downregulated transcripts (**Figure 7**). Among them, maturase K, tetratricopeptide repeat (TPR)-like superfamily protein, LOB domain-containing protein, and BTB/POZ and TAZ domain-containing proteins showed the highest gene differential expression during *B. altitudinis–Arabidopsis* interaction. Trihelix transcription factor (TF) ASR3, TF MYB90, and *O*-methyltransferase family proteins were significantly repressed during the interaction (**Table 2** and **Supplementary Table 4**).

Differentially expressed transcripts were subjected to functional analyses. GO enrichment analysis was performed using the annotated difference gene to calculate the list

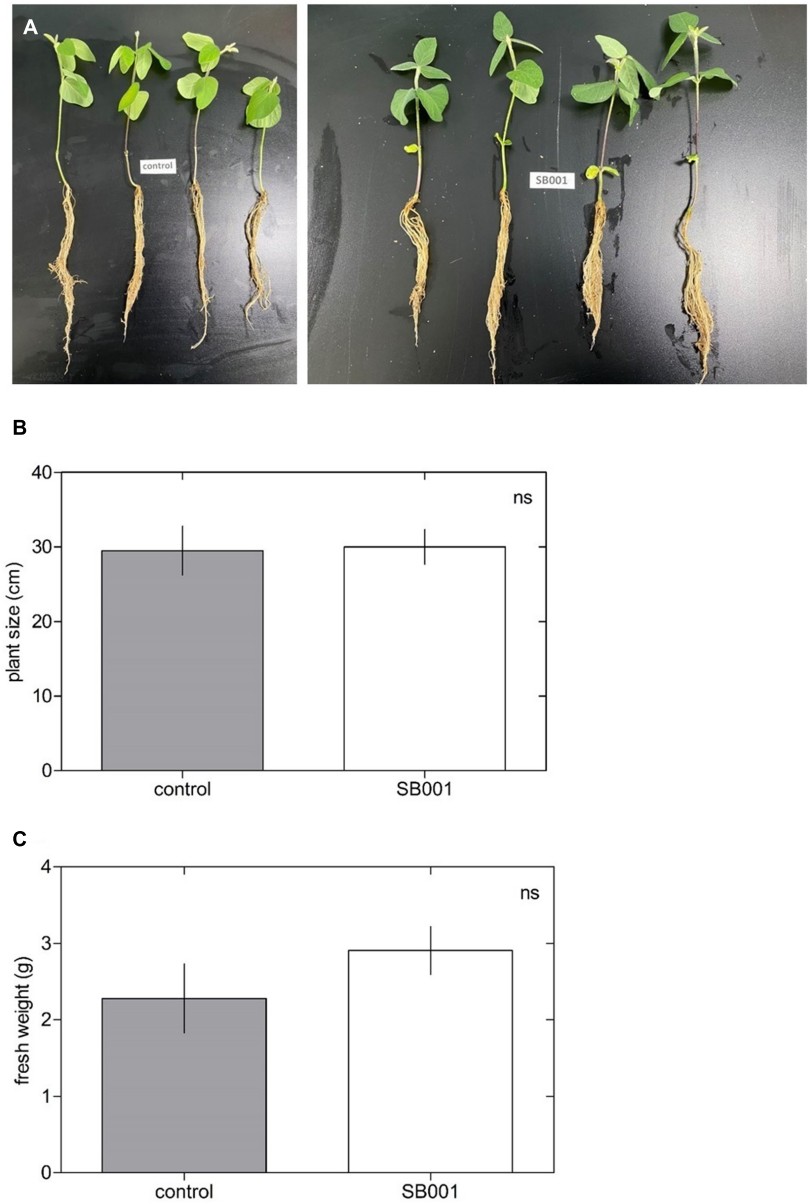

FIGURE 5 | Endophytic bacterium *B. altitudinis* does not induce soybean plant growth. Plants (5-day-old) were mock-treated (control) or inoculated with 30 ml of *B. altitudinis* at 4.77 × 10^9 CFU/ml. **(A)** Phenotype of soybean plants mock-treated (control) and treated with *B. altitudinis* fermentations (SB001) at 20 days post-inoculation. Effect on plant size **(B)** and fresh weight **(C)** of soybean plants mock-treated (control) and treated with *B. altitudinis* fermentations (SB001). Each bar represents mean values with standard errors of two independent experiments (n = 10).

of genes and the number of genes for each term. The transcripts with the largest increases in expression were NADH dehydrogenase (quinone), NADH dehydrogenase (ubiquinone) activity, NADH dehydrogenase, and oxidoreductase (**Figure 8A**). Based on the KEGG pathway, we categorised the most significant transcripts into nitrogen metabolism and oxidative phosphorylation pathways (**Figure 8B** and **Supplementary Table 5**). The expression profile of TF genes displays the upcoming transcription actions regulated by these genes. To determine their important roles, the TFs involved in the *B. altitudinis–Arabidopsis* interaction were analysed. The largest TF families detected in our study were basic helix-loop-helix (bHLH) DNA-binding superfamily protein, TF MYB13 (MYB), ethylene responsive factor (ERF), NAC domain-containing protein 1 (NAC), and zinc finger protein ZAT1 (C2H2), respectively (**Figure 9**).

During the interaction, a total of 3,413 genes were annotated from *B. altitudinis*. From these, genes with a log2 fold change between −1.2 and 5.3 were analysed. Twenty-two and 8 *B. altitudinis* genes were up- and down-regulated

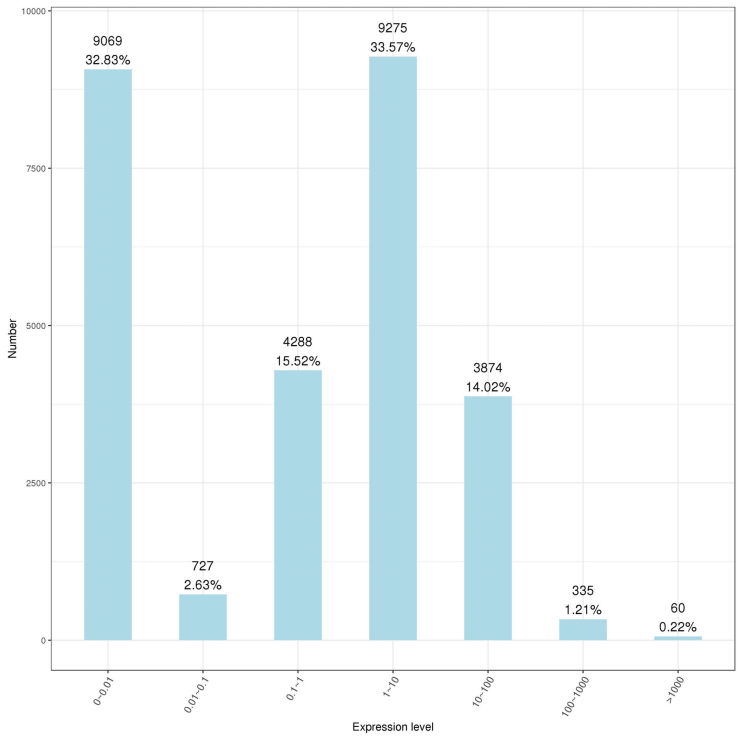

FIGURE 6 | Statistics showing the range of plant gene expressions during the *B. altitudinis–Arabidopsis* interaction. Horizontal coordinates represent the range of expression measures, and ordinates represent the number of genes in each expression interval.

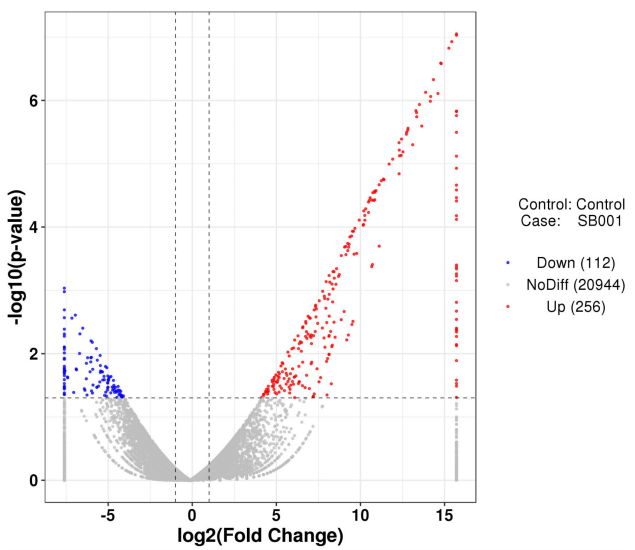

FIGURE 7 | Volcanic diagrams of differential expression genes. The horizontal coordinates are log2 (fold change) and the ordinates are -log10 (*p*-value). The two vertical dashed lines are 2 times the difference threshold, and the horizontal dashed lines are *p*-value 0.05 thresholds. A red dot indicates the upregulated genes group, a blue dot indicates the downregulated genes group, and a grey dot represents a non-significant difference in the expression of the genes group. The scale was fixed considering the minimum and maximum log2 values (between -7.60 and 15.70) included in the **Supplementary Table 4**.

during the interaction with *Arabidopsis* plants, respectively. The rest of these genes were undefined, repeated, low significant fold change, or involved in the primary metabolism of the bacterium. The major facilitator superfamily (MFS) transporter, sucrose-6-phosphate hydrolase, phosphate ABC transporter, DNA gyrase subunit B, polysaccharide biosynthesis protein, serine phosphatase, and flagellar biosynthesis protein had the highest expression levels in *B. altitudinis* during the interaction with *Arabidopsis* plants. Moreover, elongation factors G, 2,3-butanediol dehydrogenase, dihydrolipoamide succinyltransferase, and proline dehydrogenase were highly downregulated in bacteria (**Table 3** and **Supplementary Table 6**).

DISCUSSION

Different classes of microorganism have the potential to promote plant growth. The favourable effects of endophytic bacteria derived from the roots have been demonstrated. The significant reaction of these endophytic bacteria on plant growth has been achieved by both direct and indirect processes. Direct effects comprise the production of molecules that encourage plant growth (Goswami et al., 2016). In the current study, different endophytic bacteria strains were isolated from wild plant species. The SB001 strain was the most abundant in the inner tissues of the wild plant species. The strain was identified as *B. altitudinis* through morphological and molecular analyses.

TABLE 2 | Most important differentially expressed genes in *Arabidopsis* plants inoculated with *B. altitudinis*.

ID	Log2 fold change	Description
Upregulated genes		
ATCG00040	12.8	Maturase K
ATCG00360	12.3	Tetratricopeptide repeat (TPR)-like superfamily protein
AT4G37540	11.1	LOB domain-containing protein
AT3G48360	10.7	BTB/POZ and TAZ domain-containing protein
AT5G50915	9.5	Transcription factor bHLH137
AT4G28040	9.2	WAT1-related protein
AT5G09730	9.1	Beta-D-xylosidase
AT4G37390	8.9	Auxin-responsive GH3 family protein
AT4G16590	8.7	Cellulose synthase-like A01
AT4G15210	8.4	Beta-amylase
AT3G45140	8.1	Lipoxygenase 2
AT5G44050	8.1	Protein DETOXIFICATION 28
AT1G54020	8.0	GDSL esterase/lipase At1g54020
AT1G52400	8.0	Beta-D-glucopyranosyl abscisate beta-glucosidase
AT3G47340	7.9	DIN6
AT2G39030	7.9	*L*-ornithine N5-acetyltransferase NATA1
AT1G01480	7.8	1-Aminocyclopropane-1-carboxylate synthase
AT5G20630	7.5	Germin-like protein subfamily
AT4G36850	7.4	PQ-loop repeat family protein
AT4G22755	7.3	SMO1–3
AT3G44300	7.2	NIT2
AT1G73260	7.2	Kunitz trypsin inhibitor 1
AT4G21680	7.1	Protein NRT1/PTR family
AT1G02205	7.1	Fatty acid hydroxylase superfamily
ATMG00570	7.0	Sec-independent periplasmic protein translocase
ATCG00190	6.6	DNA-directed RNA polymerase subunit beta
AT2G43620	6.6	Endochitinase At2g43620
AT4G37150	6.1	MES9
AT2G25900	6.0	Zinc finger CCCH domain-containing protein
AT3G16240	5.9	Aquaporin TIP2-1
AT5G12940	5.9	Leucine-rich repeat (LRR) family protein
AT5G03260	5.8	Laccase
AT4G23600	5.7	Cystine lyase CORI3
AT1G09350	5.6	Hexosyltransferase
AT1G76930	5.6	Extensin
AT1G54010	5.5	Inactive GDSL esterase/lipase-like protein
AT1G03220	5.4	Eukaryotic aspartyl protease family protein
AT1G52040	5.4	Myrosinase-binding protein
AT2G39800	5.3	Delta-1-pyrroline-5-carboxylate synthase A
AT4G01870	5.1	TolB protein-related
AT2G05790	5.1	*O*-glycosyl hydrolases family 17 protein
AT2G07715	5.1	Nucleic acid-binding, OB-fold-like protein
AT1G05680	5.0	Glycosyltransferase
AT2G23130	5.0	Lysine-rich arabinogalactan protein
AT5G20250	5.0	Raffinose synthase family protein
AT5G40890	4.9	Chloride channel protein CLC-a
AT2G06850	4.9	Xyloglucan endotransglucosylase/hydrolase protein
AT1G78850	4.9	EP1-like glycoprotein
AT2G29350	4.8	SAG13
AT4G12420	4.8	Monocopper oxidase-like protein SKU5
AT5G25980	4.7	Myrosinase
AT3G01500	4.5	Beta carbonic anhydrase 1, chloroplastic
AT1G44350	4.5	IAA-amino acid hydrolase
AT4G34710	4.4	Arginine decarboxylase
AT1G77760	4.3	Nitrate reductase
AT1G45201	4.1	Triacylglycerol lipase-like 1
Downregulated genes		
AT2G33550	−7.4	Trihelix transcription factor ASR3
AT1G66390	−7.1	Transcription factor MYB90
AT1G21120	−7.0	*O*-methyltransferase family protein
AT2G28720	−6.3	Histone
AT1G56250	−6.2	F-box protein VBF
AT2G16600	−6.0	Peptidyl-prolyl cis–trans isomerase
AT5G23750	−5.6	Remorin family protein
AT3G52280	−5.5	General transcription factor group E6
AT1G68790	−5.4	Protein CROWDED NUCLEI
AT2G40880	−5.3	Cysteine proteinase inhibitor
AT3G51920	−5.1	Calmodulin-like protein
AT5G05410	−5.1	Dehydration-responsive element-binding protein 2A
AT5G52740	−5.1	Heavy metal-associated isoprenylated plant protein 12
AT3G51910	−5.0	Heat stress transcription factor A-7a
AT5G16570	−5.0	Glutamine synthetase
AT5G16470	−5.0	Protein METHYLENE BLUE SENSITIVITY 2
AT1G76720	−4.9	Eukaryotic translation initiation factor 2 (eIF-2)
AT5G40340	−4.9	Tudor/PWWP/MBT superfamily protein
AT1G22160	−4.9	FCS-like zinc finger 5
AT5G39950	−4.8	Thioredoxin H2
AT5G55660	−4.3	DEK domain-containing chromatin associated protein
AT5G52640	−4.3	Heat shock protein 90
AT4G19840	−4.3	Protein PHLOEM PROTEIN 2-LIKE A1
AT4G29160	−4.2	Vacuolar protein sorting-associated protein
AT3G25230	−4.2	Peptidylprolyl isomerase
AT3G52400	−4.0	Syntaxin
AT2G33550	−7.4	Trihelix transcription factor ASR3

(Continued)

Several plant growth promotion assays were conducted to determine whether SB001 could promote plant growth in different plant species under greenhouse conditions. Inoculated *A. thaliana*, *N. tabacum*, and maize plants exhibited growth improvement, and significant increases were observed for several growth variables, such as fresh weight and plant size, between the inoculated and non-inoculated control plants. However, this strain did not influence soybean growth. It is likely that the internal tissue environment of soybean roots is not suitable for the correct setting of the bacterium. Interestingly, *B. altitudinis* strain was well established in *Arabidopsis* roots,

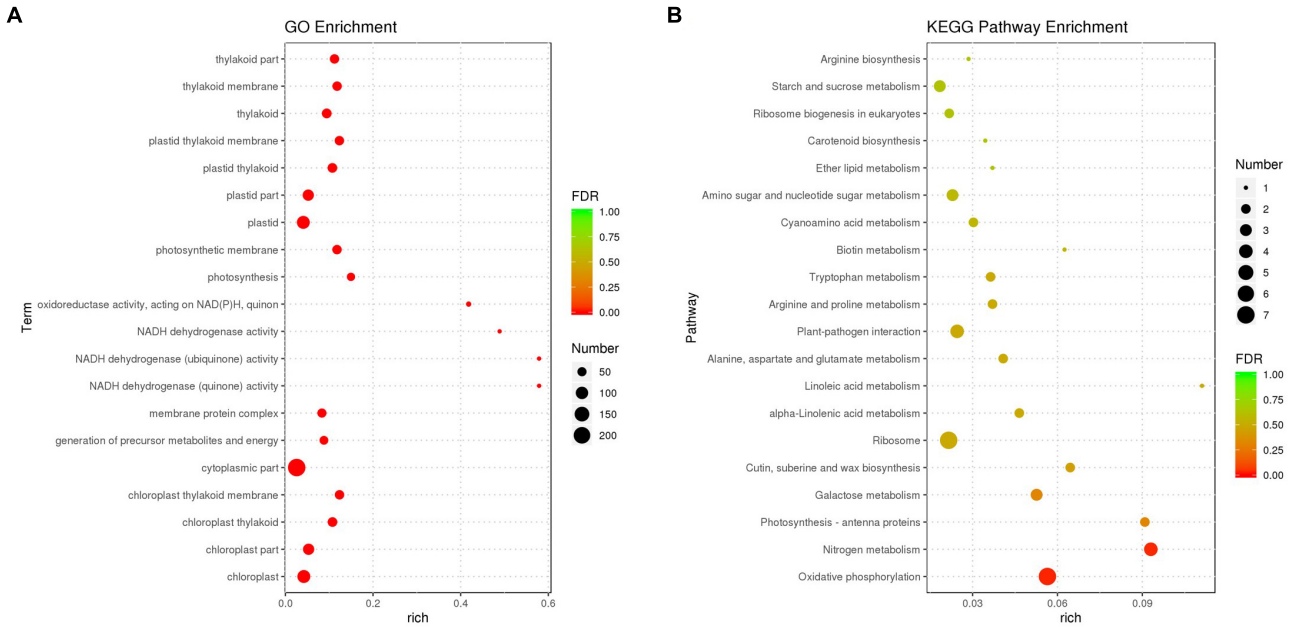

FIGURE 8 | Gene ontology (GO) **(A)** and KEGG pathway-rich analysis **(B)**. Based on the GO-rich and KEGG results, the extent of richness is measured by the rich factor, false discovery rate (FDR) values, and the number of genes that were collected into this GO term or KEGG pathway. Rich factor refers to the ratio of the number of different genes collected in the GO term or KEGG pathway to the number of genes annotated.

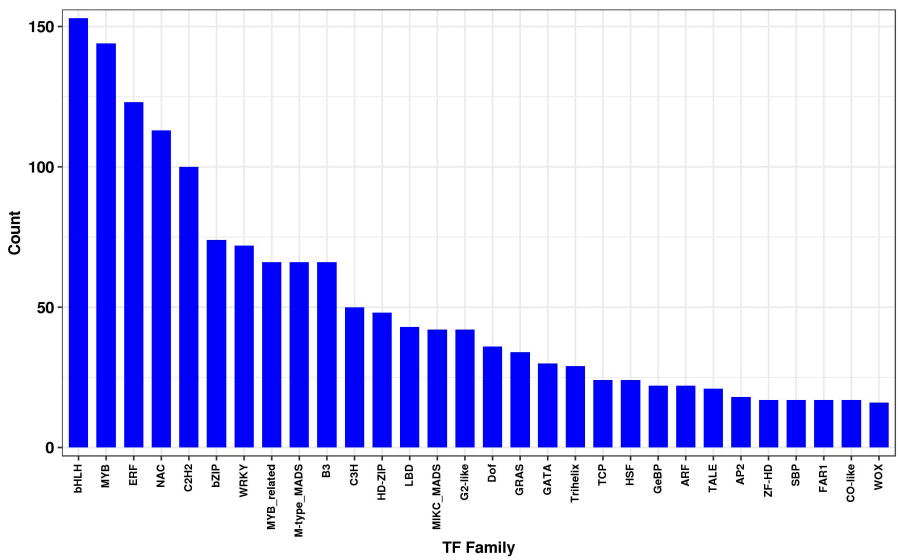

FIGURE 9 | Transcription factor family. The horizontal coordinates are different transcription factor families, and the ordinates are the number of genes that fall into that transcription factor family.

which constitutes important evidence of the ability of this strain to colonise internal tissues. Remarkably, this endophytic strain displayed vigorous plant growth-promoting effects in non-host plants. This result proposes that SB001 has the ability to efficiently enhance the growth of a broad range of plant species, and consequently, this might be used in applications under field conditions.

Earlier studies showed that several *Bacillus* species isolated from various hosts promote plant growth (Ashraf et al., 2004; Xie et al., 2014; Kuan et al., 2016; Pourbabaee et al., 2016; Radhakrishnan and Lee, 2016; Fouda et al., 2021). For example, *B. insolitus*, *B. subtilis*, and *B. methylotrophicus* increased the size and weight of shoots, leaves, and roots from diverse plant species (Ashraf et al., 2004; Radhakrishnan and Lee, 2016).

TABLE 3 | Most important differentially expressed genes in *B. altitudinis* during the interaction with *Arabidopsis* plants.

ID	Log2 fold change	Swiss-Prot
Upregulated genes		
Gene2967	5.3	MFS transporter
Gene2185	4.5	Sucrose-6-phosphate hydrolase
Gene1412	4.0	Phosphate ABC transporter
Gene3573	3.5	DNA gyrase subunit B
Gene1888	3.3	Polysaccharide biosynthesis protein
Gene3614	3.3	Serine phosphatase
Gene273	3.3	Flagellar biosynthesis protein
Gene1747	2.7	Electron transfer flavoprotein subunit beta
Gene3085	2.5	Phosphoribosylaminoimidazole synthetase
Gene1805	2.3	Bifunctional oligoribonuclease/PAP phosphatase NrnA
Gene3086	2.3	Phosphoribosylglycinamide formyltransferase
Gene1799	2.2	Acetyl-carboxylase subunit beta
Gene1627	2.0	Rod shape-determining protein
Gene1555	1.7	Uridine kinase
Gene388	1.6	Cell division protein
Gene459	1.5	Branched-chain alpha-keto acid dehydrogenase subunit E2
Gene2681	1.4	3-Hydroxyacyl-CoA dehydrogenase
Gene1634	1.2	Valyl-tRNA synthetase
Gene2803	1.1	Alpha-mannosidase
Gene369	1.0	Isoleucine
Gene284	1.0	Flagellar basal body rod protein
Gene389	1.0	Cell division protein
Downregulated genes		
Gene3695	−3.8	Elongation factor G
Gene1531	−2.7	2,3-Butanediol dehydrogenase
Gene1048	−2.6	Dihydrolipoamide succinyltransferase succinyl transferase
Gene2911	−2.6	Proline dehydrogenase
Gene3548	−1.9	Single-stranded DNA-binding protein
Gene668	−1.7	Flagellin
Gene3183	−1.4	Crp/Fnr family transcriptional regulator
Gene3475	−1.2	Flotillin

Furthermore, *B. subtilis* and *B. methylotrophicus* induced the production of hormones such as IAA, cytokinins, gibberellic acid (GA), and spermidines to stimulate plant growth (Xie et al., 2014; Radhakrishnan and Lee, 2016; Fouda et al., 2021), whereas *B. megaterium* and *B. methylotrophicus* boosted endogenous proteins, amino acids, and minerals in plants (Kang et al., 2014; Radhakrishnan and Lee, 2016). Strain SB001 exhibited different plant growth-promoting properties, which were reflected in the enhanced vegetative growth of different plant species, although these properties under soil conditions need to be investigated. Due to its beneficial plant growth-promoting activities, the *B. altitudinis* strain may be used as a source of bio-fertiliser in sustainable agriculture.

Plant–harmless bacteria interactions have been studied for many years. However, the molecular events used and involved during the interaction are not well understood, which makes it difficult to use the advantages of these complex interactions under natural conditions. Endophytic bacteria positively impact plant growth and select beneficial bacterial colonisers (Hardoim et al., 2008; Marasco et al., 2012; Rashid et al., 2012). In this study, we conducted transcriptome sequencing of *Arabidopsis–B. altitudinis* interactions to identify and quantify the expression grades of transcripts. A large number of novel candidate genes related with primary and secondary metabolite biosynthesis were identified in our expressed sequence tag (EST) data set. The results show new understandings in the expression data of this endophytic bacterium, as well as a first insight into the gene expression patterns during *Arabidopsis–B. altitudinis* interaction. Moreover, the transcriptome information obtained in this study provides a significant contribution to gaining a suitable understanding of the molecular events implicated in the interaction.

Remarkably, GO and KEGG analyses showed significant changes, suggesting that the *B. altitudinis* strain had a considerable effect on the plant. Our data indicated that SB001 induces important pathways involved in plant growth. All the information about the molecular interactions in known metabolic and regulatory pathways are contained in the KEGG pathway database (Kanehisa and Goto, 2000). Interestingly, the maturase K (chloroplast-encoded splicing factor), TPR-like superfamily protein, LOB domain-containing protein, and BTB/POZ and TAZ domain-containing protein genes were highly induced for the first time during the *Arabidopsis–B. altitudinis* interaction.

Previously, maturase K gene expression was associated with developmental stage, etiolation, and regulation processes related with development and photosynthesis (Barthet and Hilu, 2007). Maturase K has influence in gene expression in plants and interferes with the proper expression of the photosynthetic mechanism (Qu et al., 2018). Indeed, the induction of the maturase K gene might have an effect on plant growth during the interaction, through an enhancing photosynthetic process. TPR proteins are important in plant hormone signalling, such as GA, cytokinin, and ethylene (Jacobsen et al., 1996; Wang et al., 2004; Greenboim-Wainberg et al., 2005; Yoshida et al., 2005). In addition, the TPR gene was a key positive regulator of ABA during *Arabidopsis* seedling development (Rosado et al., 2006).

Conversely, LOB domain-containing protein genes constitute a gene family that encodes plant-specific TFs that play key functions during plant growth (Zhang et al., 2020). These proteins are essential TFs that regulate plant organ development, photomorphogenesis (Mangeon et al., 2011), petiole development (Ge et al., 2014), hormone response (Zentella et al., 2007), and metabolism regulation (Rubin et al., 2009). Additionally, BTB/POZ and TAZ domain-containing protein genes are required during gametophyte development (Robert et al., 2009). This is an essential element of a signalling network that recognises and responds to diverse stimuli (Mandadi et al., 2009). Furthermore, the TF MYB90 is repressed during the interaction. Previously, it was found

that heterologous expression of the TF AtMYB90 increased the anthocyanin production and inhibited the tomato plant growth (Li et al., 2018). The endophytic bacterium SB001 was capable of promoting growth through activation of important pathways implicated in plant growth, including the synthesis of phytohormones and TFs.

The TFs constitute crucial functional factors involved in the regulation of gene expression (Jiao et al., 2003). Numerous processes such as brassinosteroid signalling, ABA signalling, and axillary meristem formation are regulated by bHLH family members during seedling development (Zhao et al., 2012). A total of 153 transcripts were identified as bHLH TF proteins, and these constituted the largest TF family during the interaction. In addition, the bHLH proteins are a phytochrome interacting factor (Toledo-Ortiz et al., 2003).

The MYB proteins were involved in regulatory networks controlling development and metabolism of a diversity of plant species (Dubos et al., 2010). MYB115 and MYB118 had a key part in embryogenesis in *Arabidopsis* plants (Wang et al., 2009). Also, MYB38 and MYB18 regulate hypocotyl elongation in response to blue (Hong et al., 2008) and far-red light, respectively (Yang et al., 2009). Other MYB proteins, such as MYB58, MYB63, MYB85, MYB68, and MYB46, were related in the regulation of cell wall biosynthesis (Zhou et al., 2009). In this study, 144 putative MYB genes were detected during *Arabidopsis* seedling development.

The large NAC TF family was involved in a diversity of developmental events in *Arabidopsis* and soybean (Shamimuzzaman and Vodkin, 2013). This NAC TF family has the capacity to permit crosstalk between different pathways (Olsen et al., 2005). Furthermore, C2H2 zinc finger protein genes play a significant part in the development and differentiation (Razin et al., 2012). During the interaction, 100 putative C2H2 zinc finger genes were identified. In addition, ethylene responsive factor (ERF) TFs belong to the Apetala2/ERF) TF family involved in plant growth.

Interestingly, the MFS transporter and DNA gyrase subunit B protein genes were highly expressed in *B. altitudinis* during the interaction with the plant, which constitutes the first evidence of the expression of these types of genes in this species. The MFS transporter facilitates the transport of diverse molecules such as sugars, vitamins, amino acids, and hormones across cell membranes. These proteins are in different prokaryote and eukaryote organisms (Pao et al., 1998). It is likely that the high expression of this gene allows the transport of important hormones involved in plant growth. Silencing of the *A. thaliana* gyrase-A gene was embryo-lethal, whereas silencing of gyrase-B genes led to severely affected growth and development (Wall et al., 2004). We speculate that the overexpression of the gyrase gene in *B. altitudinis* might enhance plant growth.

CONCLUSION

Here, we report a new *B. altitudinis* endophytic strain isolated from wild plant species. Our finding revealed that the endophytic bacterium induced a key group of genes associated with plant growth-promoting traits. We demonstrated that this strain has a favourable reaction on plant growth. Remarkably, our results suggest that maturase K, TPR-like superfamily protein, LOB domain-containing protein, and BTB/POZ/TAZ domain-containing protein might be involved for the first time in this process. Furthermore, the MFS transporter and DNA gyrase subunit B genes expressed in *B. altitudinis* may be implicated in the observed effects. Future studies should evaluate the direct functions of these genes in plant growth during interactions. In addition, the potential beneficial effects of *B. altitudinis* strain under natural conditions need to be further investigated. In the long term, the new finding would allow the development of suitable and effective strategies in sustainable agriculture.

DATA AVAILABILITY STATEMENT

The data presented in the study are deposited in the (SRX11022601) repository, accession number (PRJNA733570).

AUTHOR CONTRIBUTIONS

OB-H, HX, and XG conceived the study. OB-H and DZ designed the experiments. DZ, HX, JG, RP, LD, XG, CB, and OB-H did the experiments. DZ and OB-H assisted in the data analysis. OB-H wrote the manuscript. All authors contributed to the article and approved the submitted version.

FUNDING

This study was supported by the Special Funds for Guiding Local Science and Technology Development of Central Government of Shandong Province (No. YDZX20193700004362).

SUPPLEMENTARY MATERIAL

The Supplementary Material for this article can be found online at: https://www.frontiersin.org/articles/10.3389/fmicb.2021.692313/full#supplementary-material

Supplementary Table 1 | Identification of endophytic bacterium.

Supplementary Table 2 | Annotation *Arabidopsis–B. altitudinis* interaction.

Supplementary Table 3 | New transcript annotation *Arabidopsis*-SB001 interaction.

Supplementary Table 4 | *Arabidopsis* vs. *B. altitudinis* up and down regulated genes during the interaction.

Supplementary Table 5 | KEGG enrichment *Arabidopsis–B. altitudinis* interaction.

Supplementary Table 6 | *B. altitudinis* bacterium.

REFERENCES

Afzal, I., Shinwari, Z. K., Sikandar, S., and Shahzad, S. (2019). Plant beneficial endophytic bacteria: mechanisms, diversity, host range and genetic determinants. *Microbiol. Res.* 221, 36–49. doi: 10.1016/j.micres.2019.02.001

Altschul, S. F., Madden, T. L., Schaffer, A. A., Zhang, J., Zhang, Z., Miller, W., et al. (1997). Gapped BLAST and PSIBLAST: a new generation of protein database search programs. *Nucleic Acids Res.* 25, 3389–3402. doi: 10.1093/nar/25.17.3389

Ashraf, M., Hasnain, S., Berge, O., and Mahmood, T. (2004). Inoculating wheat seedlings with exopolysaccharide-producing bacteria restricts sodium uptake and stimulates plant growth under salt stress. *Biol. Fertil. Soils* 40, 157–162. doi: 10.1007/s00374-004-0766-y

Atieno, M., Herrmann, L., Nguyen, H. T., Phan, H. T., Nguyen, N. K., Srean, P., et al. (2020). Assessment of biofertilizer use for sustainable agriculture in the Great Mekong Region. *J. Environ. Manag.* 275:111300. doi: 10.1016/j.jenvman.2020.111300

Barthet, M. M., and Hilu, K. W. (2007). Expression of matK: functional and evolutionary implications. *Am. J. Bot.* 94, 1402–1412. doi: 10.3732/ajb.94.8.1402

Blom, D., Fabbri, C., Connor, E. C., Schiestl, F. P., Klauser, D. R., Boller, T., et al. (2011). Production of plant growth modulating volatiles is widespread among rhizosphere bacteria and strongly depends on culture conditions. *Environ. Microbiol.* 13, 3047–3058. doi: 10.1111/j.1462-2920.2011.02582.x

Bruto, M., Prigent-Combaret, C., Muller, D., and Moenne-Loccoz, Y. (2014). Analysis of genes contributing to plant-beneficial functions in plant growth-promoting rhizobacteria and related *proteobacteria*. *Sci. Rep.* 4:6261. doi: 10.1038/srep06261

Conesa, A., Götz, S., García-Gómez, J. M., Terol, J., Talón, M., and Robles, M. (2005). Blast2GO: a universal tool for annotation, visualization and analysis in functional genomics research. *Bioinformatics* 2, 3674–3676. doi: 10.1093/bioinformatics/bti610

De Los Santos Villalobos, S., Robles, R. I., Parra Cota, F. I., Larsen, J., Lozano, P., and Tiedje, J. M. (2019). *Bacillus cabrialesii* sp. nov., an endophytic plant growth promoting bacterium isolated from wheat (*Triticum turgidum* subsp. durum) in the Yaqui Valley. *Mexico Int. J. Syst. Evol. Microbiol.* 69, 3939–3945. doi: 10.1099/ijsem.0.003711

Dubos, C., Stracke, R., Grotewold, E., Weisshaar, B., Martin, C., Lepiniec, L., et al. (2010). MYB transcription factors in *Arabidopsis*. *Trends Plant Sci.* 15, 573–581.

Fouda, A., Eid, A. M., Elsaied, A., El-Belely, E. F., Barghoth, M. G., Azab, E., et al. (2021). Plant growth-promoting endophytic bacterial community inhabiting the leaves of *Pulicaria incisa* (Lam.) DC inherent to arid regions. *Plants* 10:76. doi: 10.3390/plants10010076

Ge, L., Peng, J., Berbel, A., Madueño, F., and Chen, R. (2014). Regulation of compound leaf development by PHANTASTICA in *Medicago truncatula*. *Plant Physiol.* 164, 216–228. doi: 10.1104/pp.113.229914

Goswami, D., Thakker, J. N., and Dhandhukia, P. C. (2016). Portraying mechanics of plant growth promoting rhizobacteria (PGPR). *Cogent Food Agric.* 2, 1–19. doi: 10.1080/23311932.2015.1127500

Gouda, S., Kerry, R. G., Das, G., Paramithiotis, S., Shin, H. S., and Patra, J. K. (2018). Revitalization of plant growth promoting rhizobacteria for sustainable development in agriculture. *Microbiol. Res.* 206, 131–140. doi: 10.1016/j.micres.2017.08.016

Gravel, V., Antoun, H., and Tweddell, R. J. (2007). Growth stimulation and fruit yield improvement of greenhouse tomato plants by inoculation with *Pseudomonas* putida or *Trichoderma atroviride*: possible role of indole acetic acid (IAA). *Soil Biol. Biochem.* 39, 1968–1977. doi: 10.1016/j.soilbio.2007.02.015

Greenboim-Wainberg, Y., Maymon, I., Borochov, R., Alvarez, J., Olszewski, N., Ori, N., et al. (2005). Cross talk between gibberellin and cytokinin: the *Arabidopsis* GA response inhibitor SPINDLY plays a positive role in cytokinin signaling. *Plant Cell* 7, 92–102. doi: 10.1105/tpc.104.028472

Gutiérrez-Luna, F. M., López-Bucio, J., Altamirano-Hernández, J., Valencia-Cantero, E., Reyes de la Cruz, H., and Macías-Rodríguez, L. (2010). Plant growth-promoting rhizobacteria modulate root-system architecture in *Arabidopsis thaliana* through volatile organic compound emission. *Symbiosis* 51, 75–83. doi: 10.1007/s13199-010-0066-2

Ha, S. M., Kim, C. K., Roh, J., Byun, J. H., Yang, S. J., Choi, S. B., et al. (2019). Application of the whole genome-based bacterial identification system, TrueBac ID, in clinical isolates which were not identified with three MALDI-TOF M/S systems. *Ann. Lab Med.* 39, 530–536. doi: 10.3343/alm.2019.39.6.530

Hallmann, J., Quadt-Hallmann, A., Mahaffee, W. F., and Kloepper, J. W. (1997). Bacterial endophytes in agricultural crops. *Can. J. Microbiol.* 43, 895–914. doi: 10.1139/m97-131

Hardoim, P. R., Van Overbeek, L. S., Berg, G., Pirttila, A. M., Compant, S., Campisano, A., et al. (2015). The hidden world within plants: ecological and evolutionary considerations for defining functioning of microbial endophytes. *Microbiol. Mol. Biol. Rev.* 79, 293–320. doi: 10.1128/MMBR.00050-14

Hardoim, P. R., van Overbeek, L. S., and van Elsas, J. D. (2008). Properties of bacterial endophytes and their proposed role in plant growth. *Trends Microbiol.* 16, 463–471. doi: 10.1016/j.tim.2008.07.008

Hernández-Calderón, E., Aviles-Garcia, M. E., Castulo-Rubio, D. Y., Macías-Rodríguez, L., Ramírez, V. M., Santoyo, G., et al. (2018). Volatile compounds from beneficial or pathogenic bacteria differentially regulate root exudation, transcription of iron transporters, and defense signaling pathways in Sorghum bicolor. *Plant Mol. Biol.* 96, 291–304. doi: 10.1007/s11103-017-0694-5

Hong, S. H., Kim, H. J., Ryu, J. S., Choi, H., Jeong, S., Shin, J., et al. (2008). CRY1 inhibits COP1-mediated degradation of BIT1, a MYB transcription factor, to activate blue light-dependent gene expression in Arabidopsis. *Plant J.* 55, 361–371. doi: 10.1111/j.1365-313x.2008.03508.x

Jacobsen, S. E., Binkowski, K. A., and Olszewski, N. E. (1996). SPINDLY, a tetratricopeptide repeat protein involved in gibberellin signal transduction in *Arabidopsis*. *Proc. Natl. Acad. Sci. U.S.A.* 93, 9292–9296. doi: 10.1073/pnas.93.17.9292

Jiao, Y., Yang, H., Ma, L., and Sun, N. (2003). A genome-wide analysis of blue-light regulation of *Arabidopsis* transcription factor gene expression during seedling development. *Plant Physiol.* 133, 1480–1493. doi: 10.1104/pp.103.029439

Kanehisa, M., and Goto, S. (2000). KEGG: kyoto encyclopedia of genes and genomes. *Nucleic Acids Res.* 28, 27–30.

Kang, S. M., Radhakrishnan, R., You, Y. H., Joo, G. J., Lee, I. J., Lee, K. E., et al. (2014). Phosphate solubilizing Bacillus megaterium mj1212 regulates endogenous plant carbohydrates and amino acids contents to promote mustard plant growth. *Indian J. Microbiol.* 54, 427–433. doi: 10.1007/s12088-014-0476-6

Ke, J., Wang, B., and Yoshikuni, Y. (2021). Microbiome engineering: synthetic biology of plant-associated microbiomes in sustainable agriculture. *Trends Biotechnol.* 39, 244–261. doi: 10.1016/j.tibtech.2020.07.008

Kuan, K. B., Othman, R., Rahim, K. A., and Shamsuddin, Z. H. (2016). Plant growth-promoting rhizobacteria inoculation to enhance vegetative growth, nitrogen fixation and nitrogen remobilization of maize under greenhouse conditions. *PLoS One* 11:e0152478. doi: 10.1371/journal.pone.0152478

Li, N., Wu, H., Ding, Q., Li, H., Li, Z., Ding, J., et al. (2018). The heterologous expression of Arabidopsis PAP2 induces anthocyanin accumulation and inhibits plant growth in tomato. *Funct. Integr. Genom.* 18, 341–353. doi: 10.1007/s10142-018-0590-3

Lodewyckx, C., Vangronsveld, J., Porteous, F., Moore, E. R. B., and Taghavi, S. (2002). Endophytic bacteria and their potential applications. *Crit. Rev. Plant Sci.* 21, 583–606.

Lugtenberg, B., and Kamilova, F. (2009). Plant growth-promoting rhizobacteria. *Annu. Rev. Microbiol.* 63, 541–556. doi: 10.1146/annurev.micro.62.081307.162918

Mandadi, K. K., Misra, A., Ren, S., and McKnight, T. D. (2009). BT2, a BTB protein, mediates multiple responses to nutrients, stresses, and hormones in *Arabidopsis*. *Plant Physiol.* 150, 1930–1939. doi: 10.1104/pp.109.139220

Mangeon, A., Bell, E. M., Lin, W. C., Jablonska, B., and Springer, P. S. (2011). Misregulation of the LOB domain gene DDA1 suggests possible functions in auxin signalling and photomorphogenesis. *J. Exp. Bot.* 62, 221–233. doi: 10.1093/jxb/erq259

Marasco, R., Rolli, E., Ettoumi, B., Vigani, G., Mapelli, F., Borin, S., et al. (2012). A drought resistance-promoting microbiome is selected by root system under desert farming. *PLoS One.* 7:e48479. doi: 10.1371/journal.pone.0048479

Nikolic, B., Schwab, H., and Sessitsch, A. (2011). Meta genomic analysis of the 1-aminocyclopropane- 1-carboxylate deaminase gene (acdS) operon of

an uncultured bacterial endophyte colonizing Solanum tuberosum L. *Arch. Microbiol.* 193, 665–676. doi: 10.1007/s00203-011-0703-z

Olsen, A. N., Ernst, H. A., Leggio, L. L., and Skriver, K. (2005). NAC transcription factors: structurally distinct, functionally diverse. *Trends Plant Sci.* 10, 79–87. doi: 10.1016/j.tplants.2004.12.010

Pao, S. S., Paulsen, T. I, and Saier, M. H. Jr. (1998). Major facilitator superfamily. *Microbiol. Mol. Biol. Rev.* 62, 1–34.

Phetcharat, P., and Duangpaeng, A. (2012). Screening of endophytic bacteria from organic rice tissue for indole acetic acid production. *Proc. Eng.* 32, 177–183. doi: 10.1016/j.proeng.2012.01.1254

Pieterse, C. M., Van der Does, D., Zamioudis, C., León-Reyes, A., and Van Wees, S. C. (2012). Hormonal modulation of plant immunity. *Annu. Rev. Cell Dev. Biol.* 28, 489–521. doi: 10.1146/annurev-cellbio-092910-154055

Pourbabaee, A. A., Bahmani, E., Alikhani, H. A., and Emami, S. (2016). Promotion of wheat growth under salt stress by halotolerant bacteria containing ACC deaminase. *J. Agric. Sci. Technol.* 18, 855–864.

Qu, Y., Legen, J., Arndt, J., Henkel, S., Hoppe, G., Thieme, C., et al. (2018). Ectopic transplastomic expression of a synthetic MatK gene leads to cotyledon-specific leaf variegation. *Front. Plant Sci.* 4:1453. doi: 10.3389/fpls.2018.01453

Radhakrishnan, R., and Lee, I. J. (2016). Gibberellins producing Bacillus methylotrophicus KE2 supports plant growth and enhances nutritional metabolites and food values of lettuce. *Plant Physiol. Biochem.* 109, 181–189. doi: 10.1016/j.plaphy.2016.09.018

Rashid, S., Charles, T. C., and Glick, B. R. (2012). Isolation and characterization of new plant growth-promoting bacterial endophytes. *Appl. Soil Ecol.* 61, 217–224. doi: 10.1016/j.apsoil.2011.09.011

Razin, S. V., Borunova, V. V., Maksimenko, O. G., and Kantidze, O. L. (2012). Cys2His2 zinc finger protein family: classification, functions, and major members. *Biochemistry.* 77, 217–226. doi: 10.1134/s0006297912030017

Robert, H. S., Quint, A., Brand, D., Vivian-Smith, A., and Offringa, R. (2009). BTB and TAZ domain scaffold proteins perform a crucial function in *Arabidopsis* development. *Plant J.* 58, 109–121. doi: 10.1111/j.1365-313X.2008.03764.x

Rosado, A., Schapire, A. L., Bressan, R. A., Harfouche, A. L., Hasegawa, P. M., Valpuesta, V., et al. (2006). The *Arabidopsis* tetratricopeptide repeat-containing protein TTL1 is required for osmotic stress responses and abscisic acid sensitivity. *Plant Physiol.* 142, 1113–1126. doi: 10.1104/pp.106.085191

Rubin, G., Tohge, T., Matsuda, F., Saito, K., and Scheible, W. R. (2009). Members of the LBD family of transcription factors repress anthocyanin synthesis and affect additional nitrogen responses in *Arabidopsis*. *Plant Cell* 21, 3567–3584. doi: 10.1105/tpc.109.067041

Ryu, C. M., Farag, M. A., Hu, C. H., Reddy, M. S., Wei, H. X., Pare, P. W., et al. (2003). Bacterial volatiles promote growth in *Arabidopsis*. *Proc. Natl. Acad. Sci. U.S.A* 100, 4927–4932. doi: 10.1073/pnas.0730845100

Saitou, N., and Nei, M. (1987). The neighbor-joining method: a new method for reconstructing phylogenetic trees. *Mol. Biol. Evol.* 4, 406–425.

Sambrook, J., Fritschi, E. F., and Maniatis, T. (1989). *Molecular Cloning: A Laboratory Manual*. New York, NY: Cold Spring Harbor Laboratory Press.

Santoyo, G., Moreno-Hagelsieb, G., Orozco-Mosqueda Mdel, C., and Glick, B. R. (2016). Plant growth-promoting bacterial endophytes. *Microbiol. Res.* 183, 92–99. doi: 10.1016/j.micres.2015.11.008

Shamimuzzaman, M., and Vodkin, L. (2013). Genome-wide identification of binding sites for NAC and YABBY transcription factors and co-regulated genes during soybean seedling development by ChIP-Seq and RNA-Seq. *BMC Genomics* 14:77. doi: 10.1186/1471-2164-14-477

Shi, Y., Yang, H., Zhang, T., Sun, J., and Lou, K. (2014). Illumina-based analysis of endophytic bacterial diversity and space-time dynamics in sugar beet on the north slope of Tianshan Mountain. *Appl. Microbiol. Biotechnol.* 98, 6375–6385. doi: 10.1007/s00253-014-5720-9

Song, S., Liu, Y., Wang, N. R., and Haney, C. H. (2021). Mechanisms in plant-microbiome interactions: lessons from model systems. *Curr. Opin. Plant Biol.* 2:102003. doi: 10.1016/j.pbi.2021.102003

Sun, L., Wang, X., and Li, Y. (2016). Increased plant growth and copper uptake of host and nonhost plants by metal-resistant and plant growth-promoting endophytic bacteria. *Int. J. Phytoremed.* 18, 494–501. doi: 10.1080/15226514.2015.1115962

Sun, Y., Cheng, Z., and Glick, B. R. (2009). The presence of a1-aminocyclopropane-1-carboxylate (ACC) deaminase deletion mutation alters the physiology of the endophytic plant growth-promoting bacterium Burkholderia phytofirmans PsJN. *FEMS Microbiol. Lett.* 296, 131–136. doi: 10.1111/j.1574-6968.2009.01625.x

Toledo-Ortiz, G., Huq, E., and Quail, P. H. (2003). The *Arabidopsis* basic/helix-loop-helix transcription factor family. *Plant Cell.* 15, 1749–1770. doi: 10.1105/tpc.013839

Ulrich, K., Ulrich, A., and Ewald, D. (2008). Diversity of endophytic bacterial communities in poplar grown under field conditions. *FEMS Microbiol. Ecol.* 63, 169–180. doi: 10.1111/j.1574-6941.2007.00419.x

Vacheron, J., Desbrosses, G., Bouffaud, M. L., Touraine, B., Moenne-Loccoz, Y., Muller, D., et al. (2013). Plant growth-promoting rhizobacteria and root system functioning. *Front. Plant Sci.* 4:356. doi: 10.3389/fpls.2013.00356

Wall, M. K., Mitchenall, L. A., and Maxwell, A. (2004). *Arabidopsis thaliana* DNA gyrase is targeted to chloroplasts and mitochondria. *Proc. Natl. Acad. Sci. U.S.A.* 101, 7821–7826. doi: 10.1073/pnas.0400836101

Wang, K. L., Yoshida, H., Lurin, C., and Ecker, J. R. (2004). Regulation of ethylene gas biosynthesis by the *Arabidopsis* ETO1 protein. *Nature* 428, 945–950. doi: 10.1038/nature02516

Wang, X., Niu, Q. W., Teng, C., Li, C., Mu, J., Chua, N. H., et al. (2009). Overexpression of PGA37/MYB118 and MYB115 promotes vegetative-to-embryonic transition in *Arabidopsis*. *Cell Res.* 19, 224–235. doi: 10.1038/cr.2008.276

Wani, Z. A., Ashraf, N., Mohiuddin, T., and Riyaz-Ul-Hassan, S. (2015). Plant-endophyte symbiosis, an ecological perspective. *Appl. Microbiol. Biotechnol.* 99, 2955–2965. doi: 10.1007/s00253-015-6487-3

Weyens, N., van der Lelie, D., Taghavi, S., and Vangronsveld, J. (2009). Phytoremediation: Plant-endophyte partnerships take the challenge. *Curr. Opin. Biotech.* 20, 248–254. doi: 10.1016/j.copbio.2009.02.012

Worlanyo, A. S., and Jiangfeng, L. (2021). Evaluating the environmental and economic impact of mining for post-mined land restoration and land-use. *J. Environ. Manag.* 279, 111623. doi: 10.1016/j.jenvman.2020.111623

Xie, S., Wu, H. J., Zang, H., Wu, L., Zhu, Q., and Gao, X. (2014). Plant growth promotion by spermidine-producing Bacillus subtilis OKB105. *Mol. Plant Microbe Interact.* 27:6556663. doi: 10.1094/MPMI-01-14-0010-R

Yang, S. W., Jang, I. C., Henriques, R., and Chua, N. H. (2009). FAR-RED ELONGATED HYPOCOTYL1 and FHY1-LIKE associate with the *Arabidopsis* transcription factors LAF1 and HFR1 to transmit phytochrome A signals for inhibition of hypocotyl elongation. *Plant Cell* 21, 1341–1359. doi: 10.1105/tpc.109.067215

Yoon, S. H., Ha, S. M., Kwon, S., Lim, J., Kim, Y., Seo, H., et al. (2017). Introducing EzBioCloud: a taxonomically united database of 16S rRNA and whole genome assemblies. *Int. J. Syst. Evol. Microbiol.* 67, 1613–1617. doi: 10.1099/ijsem.0.001755

Yoshida, H., Nagata, M., Saito, K., Wang, K. L., and Ecker, J. R. (2005). *Arabidopsis* ETO1 specifically interacts with and negatively regulates type 2 1-aminocyclopropane-1-carboxylate synthases. *BMC Plant Biol.* 5:14. doi: 10.1186/1471-2229-5-14

Zentella, R., Zhang, Z. L., Park, M., Thomas, S. G., Endo, A., Murase, K., et al. (2007). Global analysis of DELLA direct targets in early gibberellin signaling in *Arabidopsis*. *Plant Cell* 19, 3037–3057. doi: 10.1105/tpc.107.054999

Zhang, H., Sun, Y., Xie, X., Kim, M. S., Dowd, S. E., and Pare, P. W. (2009). A soil bacterium regulates plant acquisition of iron via deficiency inducible mechanisms. *Plant J.* 58, 568–577. doi: 10.1111/j.1365-313x.2009.03803.x

Zhang, J., Cook, J., Nearing, J. T., Zhang, J., Raudonis, R., Glick, B. R., et al. (2021). Harnessing the plant microbiome to promote the growth of agricultural crops. *Microbiol. Res.* 245:126690. doi: 10.1016/j.micres.2020.126690

Zhang, Y., Li, Z., Ma, B., Hou, Q., and Wan, X. (2020). Phylogeny and functions of LOB domain proteins in plants. *Int. J. Mol. Sci.* 21:2278. doi: 10.3390/ijms21072278

Zhang, Y. F., He, L. Y., Chen, Z. J., Wang, Q. Y., Qian, M., and Sheng, X. F. (2011). Characterization of ACC deaminase-producing endophytic bacteria isolated from copper-tolerant plants and their potential in promoting the growth and copper accumulation of *Brassica napus*. *Chemosphere* 83, 57–62. doi: 10.1016/j.chemosphere.2011.01.041

Zhao, H., Li, X., and Ma, L. (2012). Basic helix-loop-helix transcription factors and epidermal cell fate determination in *Arabidopsis*. *Plant Signal Behav.* 7, 1556–1560. doi: 10.4161/psb.22404

Zhou, C., Guo, J., Zhu, L., Xiao, X., Xie, Y., Zhu, J., et al. (2016). *Paenibacillus polymyxa* BFKC01 enhances plant iron absorption via improved root systems and activated iron acquisition mechanisms. *Plant Physiol. Biochem* 105, 162–173. doi: 10.1016/j.plaphy.2016.04.025

Zhou, J., Lee, C., Zhong, R., and Ye, Z. H. (2009). MYB58 and MYB63 are transcriptional activators of the lignin biosynthetic pathway during secondary cell wall formation in *Arabidopsis*. *Plant Cell* 21, 248–266. doi: 10.1105/tpc.108.063321

Zinniel, D. K., Lambrecht, P., Harris, N. B., Feng, Z., Kuczmarski, D., Higley, P., et al. (2002). Isolation and characterization of endophytic colonizing bacteria from agronomic crops and prairie plants. *Appl. Environ. Microbiol.* 68, 2198–2208. doi: 10.1128/aem.68.5.2198-2208.2002

Zipfel, C., and Oldroyd, G. E. (2017). Plant signalling in symbiosis and immunity. *Nature* 543, 328–336. doi: 10.1038/nature22009

Conflict of Interest: DZ, HX, JG, RP, LD, XG, and OB-H were employed by the company Yota Bio-Engineering Co., Ltd. CB was employed by the company VBS Biotec SA, Mexico.

The remaining author declare that the research was conducted in the absence of any commercial or financial relationships that could be construed as a potential conflict of interest.

frontiers in Plant Science

REVIEW
published: 01 July 2021
doi: 10.3389/fpls.2021.699618

Contribution of Arbuscular Mycorrhizal Fungi, Phosphate–Solubilizing Bacteria, and Silicon to P Uptake by Plant

Hassan Etesami[1], Byoung Ryong Jeong[2] and Bernard R. Glick[3]*

[1] Department of Soil Science, University of Tehran, Tehran, Iran, [2] Department of Horticulture, Division of Applied Life Science (BK21+ Program), Graduate School, Gyeongsang National University, Jinju, South Korea, [3] Department of Biology, University of Waterloo, Waterloo, ON, Canada

Phosphorus (P) availability is usually low in soils around the globe. Most soils have a deficiency of available P; if they are not fertilized, they will not be able to satisfy the P requirement of plants. P fertilization is generally recommended to manage soil P deficiency; however, the low efficacy of P fertilizers in acidic and in calcareous soils restricts P availability. Moreover, the overuse of P fertilizers is a cause of significant environmental concerns. However, the use of arbuscular mycorrhizal fungi (AMF), phosphate–solubilizing bacteria (PSB), and the addition of silicon (Si) are effective and economical ways to improve the availability and efficacy of P. In this review the contributions of Si, PSB, and AMF in improving the P availability is discussed. Based on what is known about them, the combined strategy of using Si along with AMF and PSB may be highly useful in improving the P availability and as a result, its uptake by plants compared to using either of them alone. A better understanding how the two microorganism groups and Si interact is crucial to preserving soil fertility and improving the economic and environmental sustainability of crop production in P deficient soils. This review summarizes and discusses the current knowledge concerning the interactions among AMF, PSB, and Si in enhancing P availability and its uptake by plants in sustainable agriculture.

Keywords: phosphorus availability, silicon fertilizer, silicate solubilization, silicate-solubilizing bacteria, synergistic interactions

OPEN ACCESS

Edited by:
Maurizio Ruzzi, University of Tuscia, Italy

Reviewed by:
Manuela Giovannetti, University of Pisa, Italy
Katsuharu Saito, Shinshu University, Japan

****Correspondence:***
Hassan Etesami
hassanetesami@ut.ac.ir

Specialty section:
This article was submitted to Plant Nutrition, a section of the journal Frontiers in Plant Science

Received: *23 April 2021*
Accepted: *10 June 2021*
Published: *01 July 2021*

Citation:
Etesami H, Jeong BR and Glick BR (2021) Contribution of Arbuscular Mycorrhizal Fungi, Phosphate–Solubilizing Bacteria, and Silicon to P Uptake by Plant. Front. Plant Sci. 12:699618. doi: 10.3389/fpls.2021.699618

INTRODUCTION

There is a growing need to improve food production to meet the requirements of the increasing world population. This may be done in either of two ways: increasing the area under cultivation or enhancing the yield per unit area. The former is not possible in many countries of the world due to a number of restrictions including the availability of water or soil resources, climate change, drought, and soil salinization (Etesami and Noori, 2019). On the other hand, one of the ways to increase the yield per unit area is to improve the nutritional properties of the soil. As an essential plant nutrient, P is required for carbon metabolism, energy generation, energy transfer, enzyme

activation, membrane formation, and nitrogen (N_2) fixation (Schachtman et al., 1998). P also forms key biological molecules like ATP, nucleic acids, and phospholipids (Marschner, 1995). P deficiency is a significant limiting factor for the growth and yield of crops that affects approximately 50% of all agricultural ecosystems around the world (Lynch, 2011; Ringeval et al., 2017; Etesami, 2020). To address this issue, there has been an enormous worldwide increase in the use of P fertilizers. The high agricultural P demand has put the sustainability of P mining for fertilizer production into question (Elser, 2012). P fertilizers often lead to the addition of a large excess of P in agricultural soils. Unfortunately, >80% of the P fertilizers applied to the soil is lost due to adsorption and fixation processes (de La Vega et al., 2000; Vance et al., 2003) or it is transformed into organic forms (Holford, 1997), which represent 40–80% of total soil P (Bünemann et al., 2010), with phytates as the most common form (Menezes-Blackburn et al., 2014). Therefore, the availability of this added P to plants is limited (about 0.1% of the total P).

P is usually absorbed by the plant in a limited range of soil conditions, i.e., pH 6.5–7 as $H_2PO_4^-$ and HPO_4^{2-}. When the soil pH exceeds 7.0, inorganic phosphate (Pi) is predominantly mineralized and immobilized as calcium phosphates. At lower soil pH levels, P is usually bound/adsorbed by soluble aluminum (Al), iron (Fe), manganese (Mn), or the associated hydrous oxides (Brady and Weil, 1999). At neutral pH, Pi adsorbs to weathered silicates such as clay minerals (Rajan, 1975). Thus, the P concentration in soils with pH < 6.5 or pH > 7 is suboptimal, and is generally about 1–10 μM (Schachtman et al., 1998), which can result in crop yield depressions of 5–15% (Shenoy and Kalagudi, 2005).

The theoretical increase in plant growth efficiency from adding chemical P fertilizers has peaked so that additional chemical P fertilization cannot be expected to significantly increase plant yield (Etesami, 2020). Twenty-two million tons of P (3–4% of the total P demand) are annually extracted from natural sources (i.e., non-renewable phosphate rocks), according to the US geological survey (Gaxiola et al., 2011), which puts the natural P sources in risk of depletion (Cordell et al., 2009). Therefore, a more efficient use of P is needed, including maximizing P acquisition and utilization efficiencies (Veneklaas et al., 2012).

Some plants can efficiently acquire and/or use P to maintain metabolism and growth (Lambers et al., 2010; Aziz et al., 2014). Some plant mechanisms for improving P acquisition efficiency include (Ramaekers et al., 2010; Johri et al., 2015): (i) increased expression of high affinity P transporters; (ii) soil exploration at a minimal metabolic cost; (iii) topsoil foraging; (iv) stimulation of root hair growth; (v) redistribution of growth among root types; (vi) increase of the root-to-shoot ratio; (vii) the secretion of organic acids (e.g., citrate, malate, or oxalate) from roots to the soil; (viii) the activation of an advanced bio-molecular system; and (xi) enhanced acid phosphatase (rAPase) or phytase secretion.

Plants have also developed some biotic interactions with diverse soil microorganisms that promote plant growth. Arbuscular mycorrhizal fungi (AMF) and plant growth-promoting bacteria (PGPB) are the most common such microorganisms. AMF and PGPB, and especially the phosphate-solubilizing bacteria subgroup (PSB), are known to help overcome P deficiency in plants. PSB and AMF are a part of the key biogeochemical cycling processes (Sharma et al., 2013; Etesami, 2020).

Phosphate–solubilizing bacteria exist in most soils (Rodrìguez and Fraga, 1999). In *in vitro* conditions, they can improve P bioavailability by lowering the soil pH, solubilizing Pi, activating synthesized phosphatases, mineralizing organic P, and/or chelating P from Al^{3+}, Ca^{2+}, and Fe^{3+} (Rodrìguez and Fraga, 1999; Browne et al., 2009; Sharma et al., 2013; Etesami, 2020). Nearly all soils also contain AMF, which associate with approximately 80% of all plant roots (Smith and Read, 2008; Brundrett and Tedersoo, 2018). The ability of AMF to promote plant growth and yield and enhance P uptake has been well documented (Miransari, 2010; Jansa et al., 2011; Smith et al., 2011; Smith and Smith, 2011; Nadeem et al., 2014; Brundrett and Tedersoo, 2018; Etesami, 2020).

As a consequence of variable soil conditions, microorganisms may change crop productivity. Climate change also has a substantial impact on the effectiveness of microorganisms. One way to increase the efficiency of microorganisms under adverse environmental conditions is the co–inoculation of microorganisms (Nadeem et al., 2014; Etesami et al., 2015b; Etesami and Maheshwari, 2018; Ghorchiani et al., 2018) that stimulates plant growth through various mechanisms (Bashan et al., 2004). AMF and PGPB can work together to yield sustainable plant growth in malnourished environments (Zarei et al., 2006; Mohamed et al., 2014; Nadeem et al., 2014; Lee et al., 2015; Xun et al., 2015). Combinations of AMF and PGPB are commonly used to increase crop yields (Mäder et al., 2011; Ghorchiani et al., 2018), improve fruit quality (Ordookhani et al., 2010; Bona et al., 2016), boost phytoremediation, enhance the fertilizer nutrient use efficiency (Xun et al., 2015), lower chemical fertilization application requirements (Adesemoye et al., 2009), and increase salinity tolerance (Gamalero et al., 2009).

The use of silicon (Si) fertilizer has also been proposed as an environmentally friendly, ecologically compatible method of improving plant growth and the resistance to multiple environmental stresses including nutritional imbalances (Etesami and Jeong, 2018, 2020; Etesami et al., 2020). Previous studies have reported that Si increases plant uptake of P (Kostic et al., 2017; Neu et al., 2017; Rezakhani et al., 2019a,b; Schaller et al., 2019). Combining Si and microorganism applications has been proposed to effectively induce improved plant growth and nutrition (Etesami, 2018; Etesami and Adl, 2020). Previous studies have observed that AMF and Si work together to improve plant growth regardless of the stress conditions (Hajiboland et al., 2018; Moradtalab et al., 2019), and that PSB and Si synergistically help plants better uptake P (Rezakhani et al., 2019a,b). However, how AMF, PSB and Si interact to affect P availability for plants is poorly understood. Thus, a better understanding of the interactions of AMF, PSB and Si would allow growers to rely less on chemical P fertilizers and instead utilize biological processes to maintain fertility and enhance plant growth. Hence, this review discusses the mechanisms which AMF, PSB, and Si, individually and together, use to

increase plant uptake of P in agricultural systems where proper nutrition might otherwise suggest heavy use of P fertilizers. This review also highlights future research needs regarding how to improve plant uptake of P using AMF, PSB, and Si. In addition, the role of silicate-solubilizing bacteria (SSB), which convert insoluble silicate forms to available forms for the plant, in increasing P and Si availability and their uptake by plants is discussed.

PLANT RESPONSES TO P SCARCITY

Plants exhibit a complex array of biochemical, morphological, and physiological adaptations to deal with P deficiency, which are generally known as "P starvation responses" (Plaxton, 2004) and endeavor to increase P acquisition capacity and to preserve plant vitality (Pang et al., 2015). Some P deficiency responses are as follows. A preferential carbohydrate allocation toward the roots, higher density of root hairs, greater root surface area and length, as well as root cluster formations alter the root structure and lead to reduced plant growth and increased root-to-shoot ratio (Gilroy and Jones, 2000; Liao et al., 2001; Sánchez-Calderón et al., 2006; Lynch, 2007; Niu et al., 2013; Aziz et al., 2014; Lambers and Plaxton, 2015). The greater surface area provided by the larger root system allows for better absorption of nutrients, including P, through increased contact with the soil (Römer and Schenk, 1998; López-Bucio et al., 2003; Lynch, 2007). Another important response to P deficiency is an increase in the root organic acid exudations, i.e., carboxylates (mainly citrate and malate) to the rhizosphere to increase the rhizospheric inorganic P availability (Neumann and Römheld, 1999; Vance et al., 2003; Raghothama and Karthikeyan, 2005; Johnson and Loeppert, 2006; Pang et al., 2015). Plants also exhibit an increased efficiency of cellular P uptake. Inorganic P in soils is generally very immobile, so that the uptake of rhizospheric Pi is affected by the high–affinity Pi/H^+ symporters associated to the plasma membranes that belong to the *PHT1* gene family (Gu et al., 2016). Previous studies observed that P deficiency induced the expression of Pi transporters in wheat (Gilroy and Jones, 2000; Tittarelli et al., 2007; Miao et al., 2009; Jia et al., 2011; Kostic et al., 2015; Kostic et al., 2017). Plants also induce enzymes that scavenge and recycle Pi, such as acid phosphatase, which catalyzes Pi hydrolysis from Pi–monoesters; nuclease, which degrades extracellular DNA and RNA; and phosphodiesterase, which liberates Pi from nucleic acids (Duff et al., 1994; Plaxton and Carswell, 1999; Gaume et al., 2001; Plaxton, 2004). Plants may also induce alternate cytosolic glycolysis pathways (Plaxton and Carswell, 1999), tonoplast pyrophosphatase that pumps H^+, and different respiratory electron transport pathways (Gonzàlez-Meler et al., 2001; Plaxton, 2004). Plants also remobilize the internal P from one plant part to another (Gill and Ahmad, 2003). Plants modify the carbohydrate partitioning between source and sink, photosynthesis, sugar metabolism in response to P deficiency (Sánchez-Calderón et al., 2006), the cations in carbon metabolism and alternate respiratory pathways (Uhde-Stone et al., 2003), and/or membrane biosynthesis to require lower amounts of P (Uhde-Stone et al., 2003; Lambers et al., 2006). Moreover, plants establish mycorrhizal symbioses, beneficial associations between soil fungi and plant roots (Smith and Read, 2008).

AMF AND THEIR MECHANISMS OF P UPTAKE/MOBILIZATION

Arbuscular mycorrhizae are endomycorrhiza where the fungal hyphae penetrate the root cell walls and get in touch with the plasmalemma. AMF are commonly found in all of earth's ecosystems with plants (Redecker et al., 2013). The formation of arbuscular mycorrhiza has allowed plants to survive and grow in natural habitats for millions of years without fertilizers, pesticides and irrigation. AMF belong to the subphylum Glomeromycotina (Bruns et al., 2018), encompassing 340 described species[1].

Having evolved 400–450 million years ago, this symbiosis is likely the oldest type of mycorrhiza, and it involves a wide variety of plants (Smith and Read, 2008). AMF are obligate symbionts and acquire all of their organic carbon requirements from their plant partners. The symbiosis is often mutualistic based largely on carbon exchange from the plant (4–20% of photosynthetically fixed carbon) and P delivered by the fungi (Wright et al., 1998; Smith and Smith, 2011). More than 80% of earth's plant species are estimated to be able to form this mycorrhizal symbiosis (Wang and Qiu, 2006). The benefits of the arbuscular mycorrhizae in various plants (mostly in crops) have been proven (Smith and Read, 2008). AMF increase plant resistance to abiotic stresses, improve mineral uptake (particularly of P), enhance water relations, and provide protection against soil-borne pathogens to promote plant growth (Smith and Read, 2008). On top of significantly aiding the P supply to plants, AMF can help plants acquire macronutrients and micronutrients like Cu, K, Mg, N, and Zn, especially when they're present in less soluble forms in soils (Meding and Zasoski, 2008; Smith and Read, 2008). These fungi penetrate the root cortical cell walls and establish arbuscules, which are haustoria–like structures, that mediate the metabolite exchanges between the host cell and the fungi (Oueslati, 2003). AMF enhance the root zone absorption area by 10–100% and improve the plant ability to utilize more soil resources. Mycorrhizal roots are able to reach a greater soil volume than non-mycorrhizal ones, thanks to the extraradical hyphae that facilitate the nutrient absorption and translocation (Smith and Read, 2008). AMF increase the nutrient absorption by increasing the absorption area of the roots, and also release chemicals such as glomalin, a glycoprotein secreted by hyphae and spores of AMF. Glomalin in the soil aids the uptake of nutrients such as Fe and P that are difficult to dissolve (Smith and Read, 2008; Miransari, 2010; Emran et al., 2017; Begum et al., 2019). P is easily absorbed from soil particles and therefore Pi-free zones are readily formed around the roots. Extraradical hyphae of the mycorrhizal roots extend beyond these P-depleted zones, taking up the bio-available Pi that is otherwise inaccessible to plants.

[1]http://www.amf-phylogeny.com

The roots of arbuscular mycorrhizal plants have two pathways to absorb P. The first pathway is common to both arbuscular mycorrhizal plants and non-arbuscular mycorrhizal plants, where P is directly absorbed from the root epidermis and hairs. The second pathway involves P entering the root cortical cells (intraradical mycelium) (Smith and Smith, 2011), where symbiotic interfaces are provided by arbuscules or hyphal coils, through the fungal hyphae (P uptake from the interfacial apoplast by cell-specific Pi transporter gene expression in the mycorrhizal roots) (Benedetto et al., 2005; Balestrini et al., 2007; Gomez-Ariza et al., 2009; Tisserant et al., 2012; Fiorilli et al., 2013). This is a rapid P translocation over many centimeters. New physiological and molecular evidence suggests that for P, regardless of plant growth responses, the mycorrhizal pathway is operational (Smith and Smith, 2011). The function of the transporters and the translocation of Pi in the fungi and the transfer of Pi to the host plants have been well reviewed (Johri et al., 2015; Ezawa and Saito, 2018).

As mentioned above, the low solubility of P in acidic and alkaline soils (e.g., lower than 10 μM) results in a very low mobility (Schachtman et al., 1998). Therefore, when P is absorbed by the roots, its replacement from bulk soil is very slow, which leads to the establishment of P-depletion zones, where all the available P has been utilized quickly from around the roots, thereby reducing P uptake by the root epidermis hairs (the first pathway of P absorption) (Schachtman et al., 1998; Smith and Smith, 2011). Therefore, for improved P acquisition, plants must overcome these depletion areas and display root activities in other parts of the soil. The result of this effort for P (and other relatively immobile soil resources) acquisition is determined by the root system surface area. The most important role of the hyphae in mycorrhizal fungi is the increase of the root surface area (depletion is lower around small–diameter arbuscular mycorrhizal fungal hyphae) (Smith and Smith, 2011). In addition, mycorrhizal plants are able to exude organic acids such as citrate and malate that chelate Al^{3+} (Klugh and Cumming, 2007; Klugh-Stewart and Cumming, 2009) and Ca^{2+} and dissolve aluminum and calcium phosphates. By enhancing the soil contact area through AMF hyphae, plants are granted improved access to Pi and orthophosphates in the soil solution (Bouhraoua et al., 2015), as the roots are able to directly take up the released Pi with the help of arbuscular mycorrhizal fungal hyphae. Arbuscular mycorrhizal roots do not establish a fungal sheath, and theoretically are able to use both of the nutrient uptake pathways. It has been proposed that the two nutrient uptake pathways act additively in the arbuscular mycorrhizal symbiosis (Bücking et al., 2012). However, approximately 80% of P uptake in a mycorrhizal plant is estimated to be supplied by the fungi (Marschner and Dell, 1994). AMF also increase the ability of legumes to fix N_2 and reduce the amount of inorganic N that leaches (Veresoglou et al., 2012). Nitrogen is a component of chlorophyll and thus is important for photosynthesis. The transfer of photosynthetic materials to the roots results, in turn, in increased activity of soil microorganisms including AMF and PSB.

In general, AMF can increase P uptake in P-deficient soils by (i) increasing the P uptake rate (P influx) per unit of arbuscular mycorrhizal root. This increased P uptake rate with AMF is due to the high effectiveness with which hyphal surfaces absorb P from the soil, compared to the cylindrical root surfaces (Sharif and Claassen, 2011); (ii) expanding the mycorrhizal hyphal network to reach beyond the rhizosphere, absorbing Pi by AMF hyphae via fungal Pi transporters up to 25 cm around the roots, translocating the Pi to intracellular fungal structures in the root cortical cells (Smith et al., 2011; Garg and Pandey, 2015); (iii) storing P in the form of polyphosphates, such that the fungi can keep the internal Pi levels relatively low, effectively transferring P from soil to plant-based hyphae through appressoria and from the extraradical mycelium to the intraradical mycelium (Pepe et al., 2020); (iv) having hyphae with a small diameter (2–20 μm) that allow the fungi to access small soil cores for P, and achieve greater P influx rates for a given surface area (Jakobsen et al., 1992; Jakobsen et al., 2001); and (v) decreasing the depletion zone around the roots or hyphae (decreasing the impact of rhizospheric Pi depletion) (Smith et al., 2011; Garg and Pandey, 2015). In one study, P depletion around the roots of *Capsicum annuum* L. plants or the hyphae of *Glomus mossea* only extended to about 0.06 cm and thus only ∼7% of the soil P was positionally available to the roots. But for the hyphae it was ∼100%, of the soil was positionally available because the half distance between neighboring hyphae was only 0.01 cm (Sharif and Claassen, 2011). As a general conclusion, the high effectiveness of hyphal surfaces to absorb P from soils may be enough in most cases to explain how AMF improve the uptake of available P from the soil.

PSB AND THEIR MECHANISMS OF P UPTAKE/MOBILIZATION

Rhizospheric P mineralization and solubilization are important mechanisms by which PSB increase the nutrient availability for plants (Glick, 2012). PSB play a major role in all three main parts of the soil P cycle (dissolution–precipitation, mineralization–immobilization, and sorption–desorption). There are various mechanisms by which PSB can change the insoluble phosphates into available forms (Gyaneshwar et al., 2002; Khan et al., 2007; Sharma et al., 2013; Etesami and Maheshwari, 2018; Etesami, 2020). PSB strains belong to various genera (e.g., *Achromobacter*, *Actinomadura*, *Aerobactor*, *Agrobacterium*, *Alcaligenes*, *Arthrobacter,* *Azotobacter*, *Azospirillum*, *Bacillus*, *Chryseobacterium*, *Delftia*, *Enterobacter*, *Gordonia*, *Klebsiella*, *Pantoea*, *Phyllobacterium*, *Pseudomonas*, *Rhizobium*, *Rhodococcus*, *Serratia*, *Streptomyces,* *Thiobacillus*, *Xanthobacter*, *Xanthomonas*) (Sharma et al., 2013; Etesami, 2020) and can solubilize insoluble Pi compounds including dicalcium phosphate, hydroxyapatite, tricalcium phosphate, and rock phosphate, and mineralize organic phosphate compounds to forms that can be absorbed by plants (i.e., $H_2PO_4^-$ and HPO_4^{2-}) (Khan et al., 2009; Ramaekers et al., 2010; Alori et al., 2017; Etesami, 2020). Each phosphate–solubilizing bacterium may employ multiple mechanisms to solubilize insoluble P. Some of the most significant bacterial mechanisms that increases P availability for plants are briefly discussed in the following sections.

Production of Organic Acids

Most P uptake occurs in the pH range 6.5–7. However, because of equilibrium reactions such as sorption/desorption and the dissolution of P-bearing minerals are pH-dependent, PSB solubilize Pi in neutral to alkaline soils by excreting protons and producing organic and inorganic acids (Farhat et al., 2009; Jones and Oburger, 2011). NH_4^+ assimilation by plants and PSB leads to hydrogen ion (H^+) excretion to maintain electroneutrality (Parks et al., 1990; Wu et al., 2008). Organic acids (e.g., 2–ketogluconic, aspartic, citric, gluconic, lactic, malic, malonic, oxalic, succinic, and tartaric acid) are produced by bacterial metabolism, mainly due to oxidative respiration or carbon source fermentations, such as periplasmic glucose oxidizing into gluconic acid and being released into the soil solution, or the oxidation of organic matter or animal fertilizers added to the soil (Gyaneshwar et al., 2002; Trolove et al., 2003; Goldstein, 2007; Jones and Oburger, 2011). Organic acids can solubilize P from mineral surfaces via ligand-promoted dissolution or ligand exchange (Jones and Oburger, 2011; Oburger et al., 2011). In addition, PSB can indirectly reduce the pH of the rhizosphere and increase P levels by affecting the root system and, consequently, increasing the root exudates. Since root exudates contain different chelating agents and organic acids, they can increase the rhizospheric P availability. Organic acids (or organic anions) can enhance the rhizospheric P levels by lowering the pH, as PSB generally release the dissociated organic acids with protons, which allows them to preserve electroneutrality (Whitelaw et al., 1999; Castagno et al., 2011; Jones and Oburger, 2011). Organic acids compete with phosphates for fixation sites, or even replace the adsorbed phosphates on the soil clays surfaces, such as amorphous aluminum oxides, goethite, kaolinite, and montmorillonite. Chelating agents present in the root exudates (e.g., siderophores) can improve P availability to plants by promoting the chelation of P-bound Al^{3+}, Ca^{2+}, and Fe^{3+}, or establishing soluble complexes with metal ions associated with insoluble P, which circumvents Pi precipitation (**Figure 1**) (Whitelaw, 1999; Rashid et al., 2004; Osorio Vega, 2007). On the other hand, root exudates come from different carbon sources (e.g., amino acids, mucilage, nucleotides, organic acids, phyto–siderophores, sugars, and vitamins) and have different signals, which lead to the attraction of microbial flora at the root level, including PSB. Increases in the microbial population result in the production of more rhizospheric organic acid production and subsequently decreases the rhizospheric pH (Khan et al., 2007; Pothier et al., 2007; Badri and Vivanco, 2009; Drogue et al., 2013; Sharma et al., 2013; Etesami et al., 2015b; Etesami, 2020; **Figure 1**).

Production of Inorganic Acids

Mineral acids like carbonic acid (H_2CO_3), hydrochloric acid (HCl), nitric acid (HNO_3), and sulfuric acid (H_2SO_4), in addition to organic acids, have been reported to contribute to solubilizing insoluble Pi (Sharma et al., 2013). Sulfur–oxidizing bacteria (SOB) such as those belonging to the genus *Thiobacillus* and nitrifying bacteria (NB) like those belonging to the genera *Nitrosomonas* and *Nitrobacter*, oxidize sulfur and ammonia and lead to the formation of inorganic acids and, consequently, reduce the pH, which ultimately increases the rhizospheric P availability (Stamford et al., 2003). SOB oxidize reduced sulfur compounds to produce sulfuric acid in the presence of oxygen to obtain energy while NB get their energy by oxidizing inorganic nitrogen compounds. Carbon dioxide (CO_2) resulting from microbial respiration and organic matter decomposition, after combining with water, becomes carbonic acid which can also reduce the rhizospheric pH and lead to increased P availability (**Figure 1**). In general, the role of inorganic acids in the solubilization of P is lower than that of organic acids and is less frequently reported. Since the ability of PSB to lower the pH in certain instances is not always associated with Pi solubilization ability, acidification cannot be the only mechanism for dissolving insoluble Pi (Bashan et al., 2013).

Siderophore Production

Plants and microorganisms in low-iron conditions produce siderophores which are low molecular weight (200–2000 Da) organic compounds with an iron–chelating ability (Ahmed and Holmström, 2014). The primary role of siderophores is to chelate Fe(III) under various environmental conditions making the element available to plants and microorganisms. Siderophores can bind to a variety of metals besides Fe(III) including Al, Ca, Cd, Co, Cu, Mn, Mo, Ni, Pb, and Zn, albeit with a lower affinity (Ahmed and Holmström, 2014). PSB have also been shown to be capable of producing siderophores (Vassilev et al., 2006; Caballero-Mellado et al., 2007; Hamdali et al., 2008; Karimzadeh et al., 2020) which can promote the dissolution of insoluble mineral P (Sharma et al., 2013). Siderophores can improve P availability for plants by ligand exchange and chelating the elements (e.g., Al^{3+}, Ca^{2+}, and Fe^{3+}) that form a complex with P (**Figure 1**).

Indole–3–Acetic Acid (IAA) and ACC-Deaminase Production

One mechanism that plants employ to deal with P deficiency is to allocate a large portion of the photosynthetic substrates to root growth, to develop fine roots with small diameters with greater surface area. Fine roots, especially root hairs, are associated with scavenging soil P with their high surface area (Rengel and Marschner, 2005). PGPB, including PSB, can improve a plant's P capturing capacity by promoting root growth through branching, hormonal stimulation, or root hair development (phytostimulation; e.g., production of IAA or enzymes that modify plant ethylene precursors, like 1-aminocyclopropane 1-carboxylic acid (ACC) deaminase) (Richardson et al., 2009; Hayat et al., 2010; Emami et al., 2019). A plant's response to P starvation stress can result in a decrease in the number of root hairs (Borch et al., 1999). The ACC deaminase enzyme can degrade the precursor for the ethylene production and influences how P affects the root growth; ethylene can adjust the root architectural response to soil P availability (Etesami and Maheshwari, 2018).

The abundance and length of the root hairs are positively correlated with the immobile element uptake. Modified root

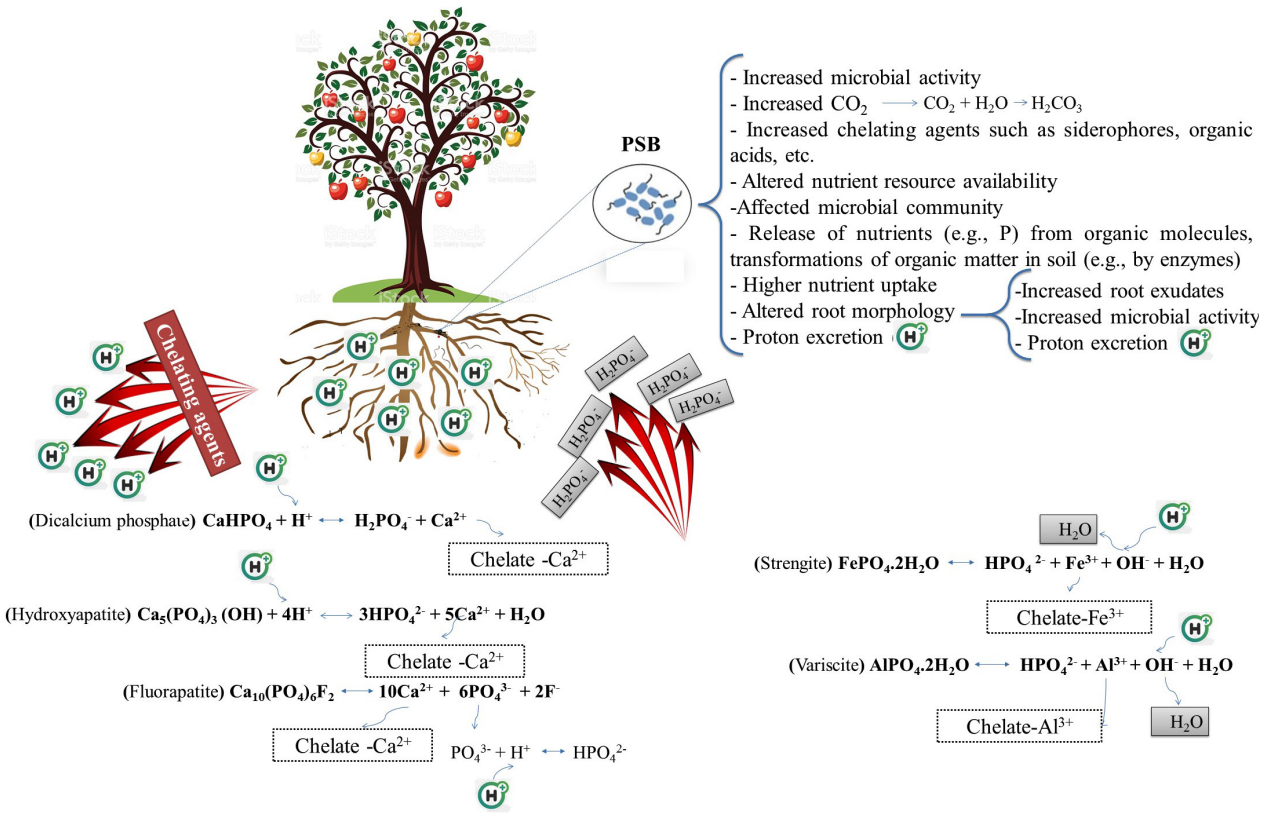

FIGURE 1 | The part that phosphate solubilizing bacteria (PSB) play to improve plant's ability to acquire the soil phosphorus by altering the sorption equilibria that may increase the net orthophosphate ion transfer into the soil solution. Protons and metal chelating agents are especially effective in solubilizing precipitated phosphorus forms (aluminum phosphates and iron phosphates in acidic conditions, and calcium phosphates in alkaline conditions). Le Chatelier's principle states that increasing a certain substance's concentration leads to the balance shifting such that consumption of that substance increases, and lowering the concentration of a material promotes the balance toward the production of the said material. Chelating agents (organic anions, siderophores, etc.) remove Al^{3+}, and Ca^{2+}, and Fe^{3+} ions from the reaction and cause the balance to shift such that more $H_2PO_4^-$ and HPO_4^{2-} are produced. The addition of H^+ ion also causes the balance to be adjusted to encourage the reduction of H^+ ions, leading to more $H_2PO_4^-$ and HPO_4^{2-} to be produced.

morphology of inoculated plants may enhance P uptake (Rengel and Marschner, 2005). Many PSB genera in soils are known to secrete IAA (Ahemad and Khan, 2010; He et al., 2010; Ahemad, 2012; Misra et al., 2012; Oves et al., 2013; Etesami and Alikhani, 2016a,b; Etesami and Maheshwari, 2018; Emami et al., 2019; Karimzadeh et al., 2020) that plant roots absorb, leading to increased endogenous pool of IAA in plants (Glick et al., 2007). In addition, many PSB are also reported to produce ACC deaminase (Iqbal et al., 2012; Sarathambal and Ilamurugu, 2013; Etesami et al., 2014; Shahzad et al., 2014; Etesami and Alikhani, 2016a; Karimzadeh et al., 2020).

Bacterial IAA can promote the development (architecture, branching, etc.) of the root system and increase root exudation. Organic acids in root exudates lead to rhizosphere acidification (Dakora and Phillips, 2002; Amir and Pineau, 2003; Jones et al., 2003) and also play an important part in forming and increasing the mobility of complexes with essential ions for plant uptake (**Figure 1**; Etesami et al., 2015a). For example, Hinsinger (2001) reported the role of exuded carboxylates in solubilizing various P complexes. Exuded organic acid anions may also be the growth substrates for microorganisms. Root exudates are a more effective nutrient source than soil organic matter that are easily degradable for microorganisms in the rhizosphere (Rengel and Marschner, 2005).

The increase in CO_2 production from respiration of the rhizosphere microbial population leads to acidification of the rhizospheric environment. This can also lead to enhanced P availability, by increasing the release of new root extracts. Rhizospheric acidification also results from the H^+ pump from plant and microbe nutrient uptake, N_2 fixation by the symbiosis between *Rhizobium* and legume, and organic matter decomposition (Marschner and Rimmington, 1988). Certain microorganisms may indirectly enhance P nutrition for plants by enhancing root growth or root hair elongation, which allows for a greater degree of soil exploration instead of directly increasing soil P availability. IAA–producing PSB can also solubilize insoluble Pi in a manner similar to PSB by increasing the root surface area and subsequently increasing the root exudates (Dobbelaere et al., 1999; Lambrecht et al., 2000; Steenhoudt and Vanderleyden, 2000; Etesami and Maheshwari, 2018; Emami et al., 2019). In general, plant growth regulators influence root architecture and can increase P acquisition efficiency, especially

from unavailable forms, and for this purpose root traits are a key factor (Campos et al., 2018).

Organic P Mineralization

Organic P forms a significant part (40–80%) of the total soil P. Plants encountering P deficiency increase the exudation of P–hydrolyzing enzymes. In addition to dissolving phosphates affected by organic acids, the reactions of the phosphatase group of enzymes in the soil are also important. Phosphatases play a significant part in the organic P mineralization in soils. PSB can mineralize organic P by secreting phosphatases (Khan et al., 2009; Sharma et al., 2013; Etesami, 2020). Microbial–derived phosphatases are more likely to be combined with phosphate compounds than plant phosphatases are, and they help release orthophosphates from soil organic P (Tarafdar et al., 2001). Phytate (inositol hexaphosphate) is one of main soil organic P forms, accounting for over 50% of the total soil P (Osborne and Rengel, 2002). Phosphatases are not effective in mineralizing phytate. Phytase secreted by microorganisms converts phytate into P esters that can be broken down into Pi by phosphatases (Rengel and Marschner, 2005). Inorganic P immobilization by PSB can indirectly help P solubilization. PSB remove and assimilate P from the liquid culture medium according to the sink theory, activating the indirect dissolution of apatite or $Ca_3(PO_4)_2$ (Illmer et al., 1995; Guidry and Mackenzie, 2003). This can be explained according to Le Chatelier's principle, which states that lowering the concentration of Pi in soil solution promotes the balance toward the production of the Pi (e.g., release of Pi from calcium phosphates). Over a long period of time, all of the microbial P can potentially become available to plants. P immobilization in the biomass has been suggested to be an important mechanism for regulating P supply in a soil solution (Seeling and Zasoski, 1993), and for keeping labile P forms protected from reactions with the soil (Olander and Vitousek, 2004).

Si AND ITS ROLE IN P UPTAKE/MOBILIZATION

Elemental Si is the second most abundant element in the lithosphere (approximately 28%). Si dioxide (SiO_2) is the most common form of Si in soils. The main Si components in most soils includes amorphous silica, feldspars, kaolin, orthoclase, plagioclase, quartz, smectite, and vermiculite (Sahebi et al., 2015). Most Si contained in silicate minerals, and only a very small portion of the Si found in nature is available for use by plants (Struyf et al., 2010). The soluble Si is dependent on the pH and redox potential of the soil (Ma and Takahashi, 2002). In soils, Si is found as amorphous Si (minerogenic silica nodules, biogenic phytoliths, etc.), dissolved Si (adsorbed to aluminum or iron oxides/hydroxides or free in the soil solution), crystalline Si (primary silicates like feldspars, mica, quartz and secondary silicates like clay minerals), and poorly crystalline Si (e.g., secondary quartz) (Sauer et al., 2006). The soil soluble Si levels in ecosystems can differ up to two orders of magnitude (0.01–2.0 mM) (Haynes, 2014), and is mainly dependent on the parent material, soil diagenesis stage, and vegetation type (Derry et al., 2005; Struyf and Conley, 2009).

Si is not identified as an essential nutrient for plant growth and development. However, an increasing number of studies indicate that Si is a quasi-essential nutrient and is beneficial to plants, especially when under different stresses such as drought, heavy metal toxicity, nutritional imbalance, plant pathogens, and salinity; Si is also known to play an important part in plant ecology and evolution (Etesami and Jeong, 2018). Plant roots absorb the Si present as silicic acid [$Si(OH)_4$] at levels of 0.1–0.6 mM in the soil solution, and pass it through the plasma membrane via two Si transporters, *Lsi1* and *Lsi2*, that respectively function as the influx and efflux transporters and have been identified in barley, pumpkin, rice, and wheat (Ma et al., 2006, 2007; Chiba et al., 2009; Mitani-Ueno et al., 2011; Montpetit et al., 2012). Si is polymerized to silica gel ($SiO_2 \cdot nH_2O$) in plants, generally referred to as silica bodies or phytoliths, which are released back into the soil as dead plant materials that decay and then may be taken up by plants (Carey and Fulweiler, 2012). Si is customarily found as hydrogen-bound bound organic Si complexes in plant tissues (Carlisle et al., 1977) and saturates the walls of the epidermis and vessels (Kaufmian et al., 1969) where it strengthens plant tissues and reduces water transpiration.

Si levels in the aboveground plant parts differ greatly depending on the plant species, accounting for 0.1–10.0% of the dry weight, and are often at concentrations similar to that of essential macronutrients such as K, N, and P (Epstein, 1999). Plants take up Si actively via metabolically–driven transporters, or passively or rejectively, with water (Mitani and Ma, 2005). The disparity in the Si accumulation of different crop species is due to the difference in the Si absorbing capacity of the roots. Generally, monocots are considered good Si accumulators, where Si concentrations are greater than 1% of the dry weight, whereas most dicots accumulate Si at levels lower than 0.1% of the total biomass and are considered excluders (Guntzer et al., 2012).

Si also influences the uptake of micronutrients and macronutrients in plants (Etesami and Jeong, 2018; Greger et al., 2018). Si fertilization increases P levels in different crops and improves plant growth by enhancing P availability for plants (Gladkova, 1982; Jianfeng and Takahashi, 1991; Singh and Sarkar, 1992; Owino-Gerroh and Gascho, 2005; Kostic et al., 2017; Neu et al., 2017; Reithmaier et al., 2017; Etesami and Jeong, 2018; Rezakhani et al., 2019a,b; Schaller et al., 2019). For example, Greger et al. (2018) found that Si increased the soil P availability by up to 50%. Kostic et al. (2017) also observed that Si supplied as Na_2SiO_3 increased P levels in the shoots of wheat grown in low P acid soil (available $P < 4$ mg kg^{-1} and pH 4.0) to an adequate level (>0.3%) in the range of P-fertilized wheat under greenhouse conditions. In this study, Si application increased the root organic acid exudation, such as malate and citrate that mobilize the rhizospheric Pi and up-regulate expression of Pi transporters (*TaPHT1.1* and *TaPHT1.2*). This organic acid exudation by the wheat roots was many times higher than without Si application, and the P uptake was doubled. There is insufficient data regarding the effect of exogenous Si on organic acid production in plants. In a recent study, it was found that Si can alter organic acid production in plants by increasing carbon

fluxes into TCA cycle and the activity of TCA cycle enzymes (Das et al., 2019). However, further work is needed to elucidate how Si modulates organic acid metabolism in plants under P deficit conditions.

Much remains to be investigated on how Si interferes with soil P mobilization. Some mechanisms by which Si improves soil P availability and plant P uptake are as follows: (i) competitive exchange and sorptive interaction of P and Si (Smyth and Sanchez, 1980; Koski-Vähälä et al., 2001; Owino-Gerroh and Gascho, 2005; Konhauser et al., 2007; Planavsky et al., 2010). P binding to soil minerals was observed to be the lowest with silicate minerals (Rajan, 1975; Brady and Weil, 1999); (ii) increasing the soil pH to enhance soil P availability in acidic soils (Owino-Gerroh and Gascho, 2005); (iii) indirectly improving P utilization by plants by decreasing the uptake and availability of metals (Hingston, 1972; Sigg and Stumm, 1981; Schwertmann and Fechter, 1982; Ma and Takahashi, 1990). P availability is controlled by levels of other metals such as Fe and Mn under P deficiency. A large proportion of soil Pi is strongly bound/adsorbed to aluminum, iron and manganese hydroxides in the soil (Beauchemin et al., 2003). Si decreases the iron and manganese availability in soil by affecting the element binding to the soil particles (Schaller et al., 2019) and reducing the pool of hydroxides (Treder and Cieslinski, 2005; Meharg and Meharg, 2015) and can therefore indirectly increase P availability (Ma, 2004; Greger et al., 2018). Si may increase P availability for plants even in high P conditions by mobilizing P from such mineral surfaces (e.g., aluminum, iron and manganese hydroxides) (Cross and Schlesinger, 1995; Yang and Post, 2011); (iv) modifying the C:N:P stoichiometry and improving the nutrient use efficiency (Neu et al., 2017); (v) increasing the root organic anion efflux to mobilize the rhizospheric Pi (Kostic et al., 2017; Etesami and Jeong, 2018). Si significantly increased the exudation rates of citrate and malate to directly stimulate inorganic P acquisition by the roots (Kostic et al., 2017). Organic anions such as acetic, aconitic, citric, malic, fumaric, lactic, oxalic, and succinic acids compete with Pi to form complexes with aluminum, calcium, and iron and may hydrolyze organic P (Grierson, 1992; Gerke et al., 2000; Hinsinger, 2001; Kihara et al., 2003; Aziz et al., 2011; Etesami and Jeong, 2018). Organic acids like malic and citric acids were observed to reduce the pH and result in a substantially increased P mobilization from calcium compounds (Dinkelaker and Marschner, 1992) and effectively enhanced P uptake from sparingly soluble rock phosphates (Aziz et al., 2011); (*vi*) enhancing the gene expressions related to Pi uptake under P deficiency, which is key to improving the Pi absorption in different plant species (Leggewie et al., 1997; Karthikeyan et al., 2002; Tittarelli et al., 2007; Miao et al., 2009; Kostic et al., 2017). The P use efficiency of plants under P deficiency could be improved with manipulation of gene expressions related to Pi uptake (Aziz et al., 2014). A number of genes are involved with plant adaptation to P deficiency, associated with regulating the acquisition, internal remobilization of P, and changing the metabolism as well as signaling transduction (Fang et al., 2009). Si has been observed to modulate the expression of stress-related genes and alter plant metabolism in response to various plant stresses (Pavlovic et al., 2013; Ye et al., 2013; Kim et al., 2014; Kostic et al., 2017); and (vii) mobilizing or desorbing of organic carbon from soil particles or mineral binding sites (e.g., goethite) (Tipping, 1981; Reithmaier et al., 2017). Si has a strong bonding affinity to minerals in the soil comparable with carbon and P, and may mobilize the two elements and make them more available for microbial decomposition (Schaller et al., 2019). The released carbon can supply the microorganisms, including PSB, with energy for their growth in soils. The carbon dioxide produced by microbial respiration results in the production of carbonic acid, leading to increased P availability. Microbial respiration was observed to lower the soil pH by producing carbonic acid, and thus led to dissolution of apatite as Pi (Guidry and Mackenzie, 2003). How the Si availability in soils interacts with P availability in soils is generally poorly understood and requires further research.

SYNERGISTIC EFFECTS OF AMF, PSB, AND Si ON P AVAILABILITY

Synergistic Effects of AMF and PSB on P Availability

In mycorrhizal association, the plant and fungi interact both in the soil around the root (rhizosphere) and in soil around the fungal hyphae (mycorrhizosphere) (Johansson et al., 2004). The fungi interact with other microorganisms in the mycorrhizosphere whose synergistic effects increase plant growth and also populations of both (Artursson et al., 2006; Agnolucci et al., 2015). The presence of different bacterial taxa that colonized the surface of AM extraradical hyphae and spores that form biofilm–like structures on them has been reported in natural ecosystems (Scheublin et al., 2010; Lecomte et al., 2011; Cruz and Ishii, 2012; Agnolucci et al., 2015; Iffis et al., 2016). There may exist cooperation between AMF and the associated bacteria, such as PSB (Zhang et al., 2016). PSB may provide the hyphae with Pi and rely on the carbon released by AMF. Earlier research demonstrated that AMF and PSB may enhance P acqusition of the AM host plant through their interactactions (Kim et al., 1997; Toro et al., 1997; Sharma et al., 2013; Calvo et al., 2014; **Figure 2**). However, the mechanisms by which this nutritional improvement is brought about remain unclear (Artursson et al., 2006). In the following sections, what is currently known of how AMF and PSB influence each other and, consequently, increase P availability, are discussed separately.

Effects of PSB on AMF and AMF-Mediated P Availability

Effect of PSB on solubilizing insoluble phosphates

The phosphate-solubilizing activities of AMF are still controversial although AM plants have generally been shown to increase the uptake of insoluble Pi (Yao et al., 2001; Klugh-Stewart and Cumming, 2009; Campos et al., 2018). In many studies, mycorrhizal inoculants were observed to alter the composition and/or amount of total low molecular weight organic acids (LMWOAAs) exuded by AM plants (Klugh and Cumming, 2007; Klugh-Stewart and Cumming, 2009). However,

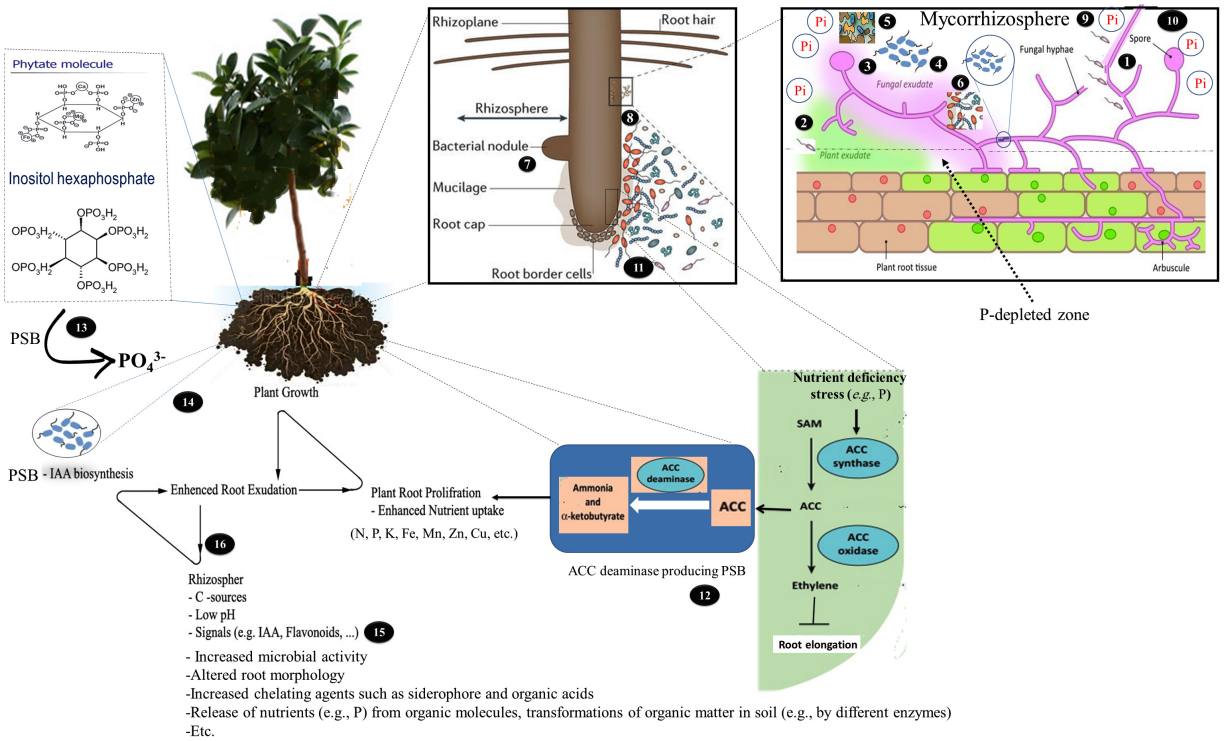

FIGURE 2 | A schematic representation of how the interaction between arbuscular mycorrhizal fungi (AMF) and phosphate-solubilizing bacterium (PSB) affect the host plant's utilization of the organic and inorganic phosphorus (P). **(1)** PSB use the hyphae to access greater soil volumes further away, which can benefit the fungi as phosphorus solubilizers may grow into insoluble-phosphorus-containing patches away from the route along the AMF hyphae; **(2)** PSB can colonize the rhizosphere (potentially rich with resources from plant exudates) by using the AMF hyphae to allow growth in other directions towards the plant; **(3)** AMF can supply energy-rich carbohydrates (C) via the extraradical hyphae for PSB; **(4)** the fungal exudates can change the rhizospheric pH, influence the chemical composition of the root exudates, and increase microbial activity; **(5)** AM hyphae and mycelial exudates can improve soil structure by binding to soil particles and through glomalin production, which may glue soil particles together and subsequently affect soil moisture retention; **(6)** AMF colonization can influence the bacterial community compositions in the mycorrhizosphere; **(7)** AMF can increase the ability of legumes to fix N_2 and reduce the amount of inorganic nitrogen that leaches, increasing plant growth and subsequently enhancing root exudates; **(8)** PSB can stimulate the AMF colonization; **(9)** AMF, unlike root hairs, can extend much farther away from the root surfaces. In other words, the extraradical hyphae extend beyond the phosphorus depletion zone, to absorb the bioavailable phosphates that are otherwise inaccessible for plants. In addition, AMF-solubilized phosphates and bacteria are more efficiently taken up by plants through a mycorrhizal-mediated channel between the plant roots and the surrounding soil; **(10)** AMF can take up and transfer inorganic phosphorus to the roots by their effective mycorrhizal mycelium, reaching microhabitats where orthophosphates are made available with phosphorus-mobilizing microorganisms and preventing quick immobilization of orthophosphates by microbial biomass; **(11)** PSB can improve the nitrogen and phosphorus availability for AMF and plants through organic matter decomposition; **(12)** PSB (ACC deaminase positive), by synthesizing ACC deaminase, can lower the stress ethylene levels, which is involved in stimulating the growth of AMF; **(13)** PSB can increase the AMF hyphal growth by hydrolyzing organic phosphorus with secretion of enzyme phosphatases and phytases and providing mineral phosphorus for the fungi; **(14)** PSB (IAA positive) can increase the IAA levels, resulting in more lateral roots that form the preferred penetration sites for AM hyphae. In addition, AMF can use the IAA the related compounds as a part of their colonization strategy to interact with plants, which leads to stimulated plant growth and modified basal plant defense mechanisms; **(15)** PSB can promote the induce flavonoid release from plants to promote mycorrhiza formations, thus facilitating root colonization; and **(16)** PSB (IAA positive) can loosen plant cell walls to promote root exudation to provide additional nutrients that support the microbial growth of microbes.

direct evidence for solubilization of P by AM fungi has not been obtained to date. Despite the fact that AM fungi might not exude LMWOAAs by themselves, they can, however, improve P solubilization and/or mineralization indirectly by stimulating the surrounding soil microbes via the exudation of labile C, thus increasing local nutrient availability in the hyphosphere and in soil patches beyond the root hairs (Hodge et al., 2009; Cheng et al., 2012; Jansa et al., 2013).

PSB solubilize phosphates and release Pi ions from the sparingly soluble organic/inorganic P compounds found in nature into a form that AMF can acquire and deliver to the plant (Toro et al., 1997, 1998; Ordoñez et al., 2016). ^{32}P-Labeling studies have shown that mycorrhiza increase the absorptive root surface areas to facilitate P uptake, but do not help in P solubilization (Gaur, 2003). In another ^{32}P-labeling study, seven bacterial strains isolated from AMF spores facilitated P uptake by promoting the development of AM extraradical mycelium (Battini et al., 2017).

Arbuscular mycorrhizal fungi cannot extract P on their own from indigenous less-available forms of P sources, such as rock phosphates, and can only absorb Pi ions from the soil solution (Antunes et al., 2007). However, with the help of certain bacteria (Villegas and Fortin, 2001) AMF can acquire P from rock phosphates and translocate it to the host plant.

AMF were able to acquire P from sources that were otherwise inaccessible with the help of PSB (Toro et al., 1997). These interactions can also indirectly benefit plants; *Medicago sativa* shoot P concentrations were observed to be improved (Zhang et al., 2016). The interaction between the two microorganism groups may lead to synergistic effects. It has been found that the AMF–PSB interactions only benefit plants when additional P was also supplied (Zhang et al., 2016). Zhang et al. (2014a) showed that P concentrations available in the soil regulate P mobilization and immobilization to determine the bacterial P contribution to plants. In general, when the available P level is low in soils, AMF and PSB compete for the P, and this competition is not stimulated by the fungi. With additional P supply, PSB improved the AMF hyphal growth, and the PSB activities were stimulated by the fungi (Zhang et al., 2016).

Effect of PSB on mineralizing organic P

During evolution with plants, AMF have lost the genes encoding proteins involved in saprotrophic function (Tisserant et al., 2013), which means that they cannot directly breakdown soil organic matter (Leigh et al., 2011; Zhang et al., 2014b). PSB can increase the AMF hyphal growth by hydrolyzing organic P with secretion of the phosphatases and phytases and providing mineral P to the fungi (Dobbelaere et al., 2003; Wang et al., 2016; Zhang et al., 2016). It has been reported that AMF cannot secrete phosphatases (Tisserant et al., 2013) and directly decompose organic nutrients (Smith and Read, 2008; Tisserant et al., 2013). AM fungi possess many genes encoding acid phosphatases in their genomes, with at least seven genes expressed in *Rhizophagus clarus* (Sato et al., 2015). However, secretion of phosphatases is mostly associated with the cell wall (Olsson et al., 2002) and their presence in the rhizosphere has been demonstrated only in limited cases (Tarafdar and Marschner, 1994; Koide and Kabir, 2000). The magnitude of these processes is questioned as it is difficult to isolate the effects of plants, fungi and others microorganisms present in the experiments under non-sterile conditions (Joner and Jakobsen, 1995; Joner et al., 2000). In an *in vitro* monoxenic culture, Sato et al. (2015) provided evidence that the acid phosphatase activity originated from *R. clarus*. Nevertheless, the interaction of AM association with the phosphatase activity and the subsequent P acquisition by efficient genotypes is still unclear (Campos et al., 2018).

Because AMF are unable to release phosphatases outside the hyphae, AMF's organic P utilization appears to depend on the recruitment of other soil microbes (Tisserant et al., 2013; Zhang et al., 2016). The microbiome associated with the hyphae may play a key role in AMF's utilization of organic P. AMF may shift the microbiome composition to influence organic P mineralization (Zhang et al., 2016, 2018b). Importantly, AMF hyphae seem to specifically recruit bacteria that produce alkaline phosphatase which can mineralize organic P; these species are not found when AMF is excluded (Zhang et al., 2018b). Despite the fact that a major AMF function is to increase P availability to plants (Smith and Read, 2008), AMF cannot release phosphatases into the soil (Tisserant et al., 2013; Zhang et al., 2016). In a study under controlled, sterile conditions, the AMF *Rhizophagus irregularis* DAOM 197198 released carbon-rich compounds to stimulate PSB functions, but did not directly influence the phosphatase activities (Zhang et al., 2016). Thus, AMF cannot directly utilize organic P, which limits its contribution to plant uptake of P. PSB accounts for up to 40% of all culturable bacteria (Jorquera et al., 2008) and can make up for this defect in AMF. This suggests that AMF and PSB need to interact to help plants uptake P (Zhang et al., 2018b). Recent results demonstrate that the AMF hyphal surfaces are colonized by PSB and the hyphal exudates are utilized as a carbon source (Wang et al., 2016). In other words, AMF can attract PSB and help them multiply to improve the organic P utilization by releasing hyphal exudates and providing a carbon source (Zhang et al., 2014b, 2016; Wang et al., 2016). PSB can then colonize the AMF hyphal surfaces (Wang et al., 2016). This enhances the activities of the phosphatases released by the PSB, and stimulates the organic P mineralization (Zhang et al., 2016). The extraradical AMF hyphae can then access Pi released from organic P sources (Tarafdar and Marschner, 1994; Feng et al., 2003). In addition, AMF hyphae-associated PSB in the soil play an important role in phytate P mineralization and that the AMF primes the mineralization and turnover of the organic P (organic P utilization affected by the AMF-bacteria interaction) (Zhang et al., 2014b). For example, in a recent study Zhang et al. (2018a) observed that fructose exuded by an arbuscular mycorrhizal fungus, *Rhizophagus irregularis*, stimulated the expression of phosphatase genes in a phosphate solubilizing bacterium, *Rahnella aquatilis*, as well as the rate of phosphatase release into the growth medium by regulating its protein secretory system. The phosphatase activity was also subsequently increased, promoting the mineralization of organic P (i.e., phytate) into Pi, stimulating simultaneously the processes involved in P uptake by *Rh. irregularis*. In general, PSB can increase P availability for AMF, especially from organic P sources, which may increase the expression of Pi transporter genes in the AMF hyphae (Zhang et al., 2016; **Figure 3**).

Effect of PSB on arbuscular mycorrhizal symbiosis

Bacteria are known to influence AMF fitness (Frey-Klett et al., 2007; Scheublin et al., 2010; Nuccio et al., 2013) and ecological functions (Hodge et al., 2001; Feng et al., 2003; Cheng et al., 2012; Zhang et al., 2014b). PSB can lead to increased plant growth parameters by stimulating the native AMF's establishment, growth rate, multiplication, and spore germination (Barea et al., 2002; Bianciotto and Bonfante, 2002; Artursson et al., 2006; Frey-Klett et al., 2007; Berta et al., 2014). PSB can promote AMF extraradical hyphal growth and allow PSB to explore a greater volume of the mycorrhizosphere and AMF hyphae to gain access to new solubilized P sources (Ordoñez et al., 2016). Increased mycelial growth of *Glomus mosseae* spores, for example, was reported to be caused by an unidentified PGP rhizobacterium (Azcón, 1987). These bacteria also helped mycorrhiza by promoting root colonization by indigenous and introduced AMF (Toro et al., 1997). Bacteria can promote hyphal growth and facilitate root penetration by AMF via producing compounds that increase cell penetrability and result in increased root exudation rates (Hildebrandt et al., 2002; Jeffries et al., 2003; Jäderlund et al., 2008). Following hyphal growth, the rates of root colonization and AMF development also increase

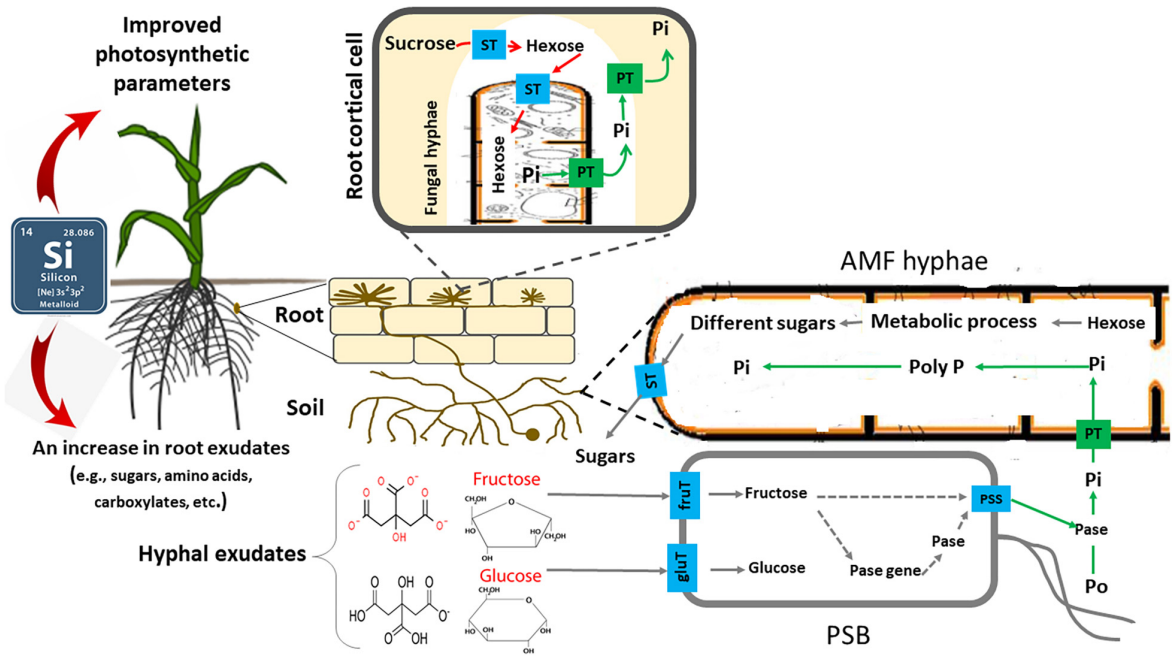

FIGURE 3 | Schematic representation of role of silicon (Si), arbuscular mycorrhizal fungi (AMF), and phosphate-solubilizing bacteria (PSB) in mineralizing organic phosphorus (Po). Si increases photosynthetic products in root and rhizosphere by improving photosynthetic parameters of plant. The fructose exuded by AMF stimulates the expression of phosphatase genes in PSB as well as the rate of phosphatase release into the growth medium by regulating their protein secretory system. The phosphatase activity is subsequently increased, promoting the mineralization of Po (i.e., phytate) into Pi, stimulating simultaneously the processes involved in P uptake by the AMF. ST, sugar transporter; fruT, fructose transporter; glut, glucose transporter; PT, phosphate transporter; PSS, protein secretory system; Pase, phosphatase; Pi, inorganic P; and Po, organic P. For more details, see Zhang et al. (2018a).

(Barea et al., 2005; Richardson et al., 2009). Bacterial IAA is known to be able to loosen plant cell walls and therefore promote root exudation which supplies additional nutrition that can support microbial growth (Chaintreuil et al., 2000; Sevilla et al., 2001; James et al., 2002; Chi et al., 2005). One of components of root exudates is enzymes such as amylase, DNase, phosphatase, polygalacturonase, protease, RNase, sucrase, urease, and xylanase that can play a role in organic P mineralization, decomposition of other organic compounds, and release of mineral elements (Ahemad and Kibret, 2014; Canarini et al., 2019), and, therefore, provide mineral P and other elements for the AMF. It is well established that bacterial IAA increases the ability of plants to convert nutrients from non–available forms to available forms by increasing the root system, root discharge and microbial flora (Etesami et al., 2015b). Bacteria IAA–mediated release of root exudates can enhance P mobility for plants and AMF by releasing protons (H^+) or by forming amino/organic acid mineral complexes (by chelation of cations accompanying P e.g., Fe^{3+}, Al^{3+}, and Ca^{2+}), and indirectly (as a source of nutrients for microorganisms) by stimulating the microbial activities in the rhizosphere (functioning, growth, propagation, survival) (Etesami et al., 2015b). The increased soil saprobiotic microbial populations mediated by root exudates can, in turn, improve N availability for AMF through organic matter decomposition (Leigh et al., 2011; Herman et al., 2012; Nuccio et al., 2013). Other microorganisms attracted to root exudates stimulate hyphal growth, mycorrhizal colonization, and spore production, thereby increasing AMF fitness (Frey-Klett et al., 2007). Flavonoids are the main signaling compounds that are isolated from plant root exudates, and it's been suggested that they play a distinct role in the AM development. Different flavonoids affect the growth and differentiation of the hyphae as well as root colonization in a structure–specific manner. Flavonoids also influence presymbiotic growth differently according to the genus and species. Furthermore, it has also been proposed that some of the so-called mycorrhiza helper bacteria that promote mycorrhiza formation induce flavonoid release from plants, and facilitate root colonization by mycorrhizal plants (Schrey et al., 2014). A number of studies have demonstrated that the IAA-secretion induced stimulation of root hair growth and lateral root elongation supplies more active sites and access for symbiotic AMF and PSB associations (Aarab et al., 2015; Etesami et al., 2015b). Therefore, it seems that PSB (IAA positive) stimulate root hair elongation to improve root weight and architecture, and therefore potentially improve mycorrhizal formation. Previous studies have shown that PGPB modify hormonal signaling in plants to influence root architecture, stimulate the growth of the shoots and roots, and increase essential nutrient uptake (Appanna, 2007; Bhattacharyya and Jha, 2012). AMF-induced plant growth is in part attributed to modified plant hormone level (Bi et al., 2019; Wang et al., 2021).

The relationship between the AMF and host roots is complex and requires a continuous exchange of signals which leads to a developmental coexistence (Gianinazzi-Pearson, 1996;

Hause and Fester, 2005). Phytohormones are the signals that regulate various plant growth processes and can therefore manage colonization and AM symbiosis formation (Barker and Tagu, 2000; Ludwig-Müller and Güther, 2007; Foo et al., 2013; Gutjahr, 2014). For example, bacterial IAA may increase the number of lateral roots for fungi to colonize in early growth stages to facilitate host colonization (Kaldorf and Ludwig-Müller, 2000). Increased IAA levels and IAA–induced gene expressions have been suggested to contribute to phenotypic changes during mycorrhizal colonization (Ludwig-Müller and Güther, 2007). Fungi may use IAA and the related compounds as a colonization strategy to interact with plants, stimulating plant growth and modifying basal plant defense mechanisms (Prusty et al., 2004; Contreras-Cornejo et al., 2009). Generally, the increased levels of IAA result in more lateral roots that form the preferred penetration sites for the AM hyphae.

Abscisic acid (ABA) is a sesquiterpenoid hormone, derived from carotenoids, which functions at multiple levels to regulate AM symbiosis (Ludwig-Müller, 2010). ABA deficiency also results in the induction of ethylene production, which adversely affects mycorrhizal interaction with plants (Herrera-Medina et al., 2007; Martín-Rodríguez et al., 2011). The synthesis of ACC deaminase produced by PSB lowers the stress ethylene levels associated with stimulating AMF growth (Gamalero et al., 2008; Etesami et al., 2015b).

In addition, gibberellins (GAs), key regulators of plant growth and development, play a role during arbuscular mycorrhizal (AM) formation (Foo et al., 2013; Martín-Rodríguez et al., 2015, 2016; Foo et al., 2016; Pons et al., 2020). GAs inhibit arbuscular mycorrhizal symbioses (McGuiness et al., 2019) by altering GA response changes in the expression of genes associated with mycorrhizal colonization (Martín-Rodríguez et al., 2015), inhibiting AM hyphal entry into the host root, and suppressing the expression of reduced arbuscular mycorrhization1 (RAM1) and RAM2 homologs that function in hyphal entry and arbuscule formation (Takeda et al., 2015). The balance between ABA and GAs is also essential for AM formation in plant roots (Martín-Rodríguez et al., 2016; McGuiness et al., 2019) as the imbalance in the ABA/GAs ratio can reduce arbuscule abundance in mycorrhizal roots (Martín-Rodríguez et al., 2015). In addition, GA signaling also positively interacts with symbiotic responses and promotes AM colonization of the host root. For example, in one study (Takeda et al., 2015), low GA conditions suppressed arbuscular mycorrhiza-induced subtilisin-like serine protease1 (SbtM1) expression, which is required for AM fungal colonization and reduced hyphal branching in the host root. In this study, the reduced hyphal branching and SbtM1 expression due to the inhibition of GA biosynthesis were recovered by GA treatment, supporting the theory that insufficient GA signaling causes inhibitory effects on arbuscular mycorrhiza development. Accordingly, it seems that PSB positive for ABA and GA-producing traits can regulate the level of production of these hormones in the plant and lead to improved arbuscular mycorrhizal symbioses. The ability to produce GAs in some bacteria has been reported (Hamayun et al., 2010; Kang et al., 2012; Tatsukami and Ueda, 2016; Etesami and Glick, 2020). However, it is not yet clear if mycorrhizal fungi produce GA. Therefore, the presence of such bacteria is necessary to improve mycorrhizal symbioses.

Effects of AMF on PSB and PSB-Mediated P Availability

Mycorrhizae affect both the composition and number of the rhizospheric and hyphospheric bacterial communities (Offre et al., 2007; Agnolucci et al., 2015; Taktek et al., 2015), as well as bacterial communities of the surface of the AMF hyphae or mycelium closely attached to the soil (Zhang et al., 2014b; Turrini et al., 2018). AMF result in the establishment of an extensive soil hyphal network, creating a dedicated niche for bacteria (Bianciotto and Bonfante, 2002; Agnolucci et al., 2015). In the cytoplasm of some AMF isolates belonging to the Gigasporaceae family endophytic bacteria are found, which is a case where bacteria coexist with fungi (Turrini et al., 2018). The bacterial colonization of the AMF hyphal and spore surfaces has been confirmed with molecular and microscopic analyses and illustrates the existence of a close relationship between the two microorganism groups (Toljander et al., 2006; Bharadwaj et al., 2008; Scheublin et al., 2010; Agnolucci et al., 2015). Similar to roots, AMF hyphae are rapid channels for photosynthates and release carbon-rich compounds into the soil (Toljander et al., 2007; Bharadwaj et al., 2012) and can stimulate microbial growth and function (Drigo et al., 2010; Leigh et al., 2011; Blagodatskaya and Kuzyakov, 2013; Kaiser et al., 2015; Zhang et al., 2016). The root exudates are a major nutrient source for the rhizospheric PSB, and its chemical composition may be influenced by the AMF (Artursson et al., 2006). Furthermore, the extensive extraradical AMF hyphae and the exudates create conditions that can influence bacterial activities and growth (Toljander et al., 2007; Bharadwaj et al., 2012; Gahan and Schmalenberger, 2015) including PSB (Taktek et al., 2015; Ordoñez et al., 2016; Wang et al., 2016; Turrini et al., 2018). The changes in the soil bacterial community composition induced by AMF are described, both under *in vivo* and controlled conditions (Marschner et al., 2001; Toljander et al., 2006, 2007).

Arbuscular mycorrhizal fungi enhance the chlorophyll content, PSII photochemical efficiency, and net photosynthetic rate of plants (Wu and Xia, 2006; Zhu et al., 2014; Augé et al., 2016; Shi-Chu et al., 2019) and also transfer plant photosynthates underground, which can stimulate PSB activity and growth (Zhang et al., 2016) as most PSB are heterotrophic and depend on nutrient substrates that can be easily decomposed. AMF hyphae are also rapid channels for the recently produced photosynthates, which can attract PSB and promote their growth (Kaiser et al., 2015). In addition, it has been found that the availability of easily decomposable organic compounds limits microbial P solubilization in soil extracts from phosphate minerals (Brucker and Spohn, 2019; Brucker et al., 2020). Saprotrophic phosphate solubilizing microorganisms in mineral soils generally lack sufficient carbon (Demoling et al., 2007; Heuck et al., 2015) because most organic carbon in soils is protected from sorptive or recalcitrant microbial decomposition or is simply spatially inaccessible (De Nobili et al., 2001; Dungait et al., 2012). Accordingly, increased microbial P solubilization rates are

reported when carbon sources become available (Hameeda et al., 2006; Patel et al., 2008).

Arbuscular mycorrhizal fungi generate a vast extraradical hyphae in the soil that microorganisms can inhabit (Gahan and Schmalenberger, 2015). PSB can grow alongside AMF hyphae in and out of the root, in sterile conditions as well as with an indigenous microbial community (Ordoñez et al., 2016), demonstrating the close relationship of AMF and PSB (Scheublin et al., 2010; Agnolucci et al., 2015). This may help PSB to use the hyphae to access areas further away in the soil to acquire insoluble P. By developing an external mycelium, AMF, upon root colonization, connect the root with the surrounding soil microhabitats and can contribute to nutrient capture and supply (Toro et al., 1997). The PSB can also use the AMF hyphae to allow growth in the direction toward the plant, colonize the rhizosphere, and use more plant exudates (Ordoñez et al., 2016).

Phosphate–solubilizing bacteria attachment to the extraradical AMF hyphae can ensure that P solubilization would occur in locations where it is the most beneficial for fungi to access the additional soluble P. The phosphate solubilized by AMF and PSB is effectively absorbed by plants through a channel formed by the mycorrhiza between plant roots and the surrounding soil (Artursson et al., 2006).

Since the mobilized orthophosphates can quickly be immobilized by microbial biomass, AMF can absorb and transfer the nutrients to the roots through their effective mycorrhizal mycelium, and reach microhabitats where orthophosphates are made available by P-mobilizing microorganisms (Richardson et al., 2009). AMF cannot directly decompose organic nutrients, as they have no known saprotrophic capabilities (Smith and Read, 2008; Tisserant et al., 2013). AMF can also increase the soil saprobiotic microbe activities, including those of PSB. These bacteria can decompose organic matter and in turn also improve the N and P availability for AMF and plants (Leigh et al., 2011; Herman et al., 2012; Nuccio et al., 2013). Previously, Linderman (1992) reported that AMF enhance the activity of nitrogen–fixing bacteria (NFB) and PSB and thus promote plant growth. PSB can also release diffrent enzymes to decompose the organic matter, and can provide mineral nutrients for the AMF hyphae (Hodge and Fitter, 2010; Hodge, 2014; Zhang et al., 2014b). Therefore, in exchange for using the carbon released by the AMF, these microbes can provide additional benefits to the fungi. AMF and PSB may obtain their required nutrients from their partners and enhance their own fitness through cooperation. By increasing the root surface areas for nutrient acquisition, or through more specific mechanisms, AMF can also help plants resist abiotic and biotic stresses (Artursson et al., 2006; Miransari, 2010; Sikes, 2010; Mohammad and Mittra, 2013). PSB solubilize phosphates into forms that are usable by the AMF, and AMF can absorb the P and transport it to the plant using a range of mechanisms. AMF may also help spread PSB to neighboring rhizospheres. Therefore, AMF and PSB interact synergistically.

AMF Increase Si Uptake by Plants

The benefits of Si nutrition, although significant, are limited due to its restricted uptake by plant (Anda et al., 2016). However, AMF such as *Glomus etunicatum*, *G. versiform, G. coronatum*, *Rhizophagus clarus* (=*Glomus clarum*), *Rhizophagus irregularis* (=*Glomus intraradices*), and *Funneliformis mosseae* (= *Glomus mosseae*) were observed to increase Si uptake in the roots and shoots of mycorrhizal plants (i.e., *Saccharum* spp., *Glycine max* L., *Zea mays* L., *Cajanus cajan* L., *Cicer arietinum* L., strawberry, and banana) compared to non–mycorrhizal plants (Yost and Fox, 1982; Kothari et al., 1990; Clark and Zeto, 1996; Clark and Zeto, 2000; Nogueira et al., 2002; Hammer et al., 2011; Garg and Singla, 2015; Anda et al., 2016; Garg and Bhandari, 2016a,b; Frew et al., 2017; Garg and Singh, 2018; Hajiboland et al., 2018; Gbongue et al., 2019; Moradtalab et al., 2019). AMF play a substantial role in Si uptake, translocation from the external solution to the intraradical mycelium, and transfer from the fungal cells to the root cells. The mechanisms remain unclear but it is not excluded that active transport is involved via transporters located within the extraradical hyphae at the soil-fungus interface for the uptake of Si and at the plant–fungal interface (i.e., arbuscule) for its transfer across the peri–arbuscular interface in the plant cells (Yost and Fox, 1982; Hammer et al., 2011; Anda et al., 2016; Garg and Bhandari, 2016b). These studies highlight the importance of AMF inoculation as tools to effectively enhance Si uptake by plants. Therefore, it would be of great interest to investigate how AM symbiosis enhances the host plant uptake of Si and how AM symbiosis and Si uptake help to improve P nutrition and plant growth.

Si Increases Mycorrhizal Effectiveness in Plants

Mycorrhizal effectiveness (or responsiveness of plants to mycorrhizae) is defined as the difference in the growth of plants with and without mycorrhizae (Janos, 2007). Mycorrhizal effectiveness is influenced by different factors like fungal species, plant species and genotype, and soil conditions (Tawaraya, 2003). Compared to the studies widely performed on the effects of P availability as a soil chemical factor on the mycorrhizal effectiveness, research on how Si affects mycorrhizal effectiveness are lacking. However, in two recent studies (Hajiboland et al., 2018; Moradtalab et al., 2019), mycorrhizal effectiveness was increased with Si treatments in strawberry plants inoculated with AMF *Rhizophagus clarus*, *Rhizophagus intraradices*, and *Glomus versiform* compared to AMF plants not treated with Si. Some known mechanisms by which Si benefits the AMF effectiveness include: (i) enhancing the uptake and transfer of nutrients for plants and stimulating the root growth in AMF plants, which can lead to promoted AMF colonization (Hajiboland et al., 2018); (ii) increasing the photosynthetic rate such that the fungal partner is able to receive a greater carbon supply, for example, by increasing the leaf chlorophyll levels, photosynthetic enzyme activities, and stomatal conductance (Guntzer et al., 2012; Hajiboland, 2012) (**Figure 3**) and improving the leaf stability so that leaves are oriented more horizontally (Botta et al., 2014). Since 4–20% of the fixed carbon from photosynthesis is transferred to the AMF, the mycorrhizal association relies on the organic carbon supplied from their photosynthetic partners (Smith and Read, 2008). Furthermore, the photosynthetic rate (organic carbon supply) is positively correlated with the hyphal absorption capacity and

arbuscule formation (Smith and Read, 2008; Anda et al., 2016; Moradtalab et al., 2019); (iii) modifying the phenolic metabolic pathways in AMF host plants and/or reducing polymerization and lignin synthesis (Rodrigues et al., 2004; Mandal et al., 2010; Hajiboland et al., 2018), which can affect how AMF interact with the host plant. Studies have investigated how Si affects the metabolism of phenolic compounds in plants (Dragišić Maksimović et al., 2007; Hajiboland et al., 2017). Phenolic compounds, such as flavonoids, are known to potentially help facilitate AMF to interact with their host plants (Vierheilig, 2004; Mandal et al., 2010), improve fungal growth parameters such as branching, hyphal growth, spore germination (Steinkellner et al., 2007) and secondary spore formation, and contribute to the fungal invasion and root arbuscule formation (Hassan and Mathesius, 2012); and (*iv*) increasing the pool of soluble sugars in the roots, which is crucial for the entry and further establishment in the roots, of AMF (Moradtalab et al., 2019). Future research should investigate the metabolic and molecular mechanisms that are associated with the synergistic relationship of Si and AMF.

PSB Increase the Availability and Uptake of Si for Plants

Phosphate–solubilizing bacteria generally have the ability to weather silicates, likely because basic metabolic activities like organic acid production and respiration can cause the weathering of minerals (Brucker et al., 2020). PSB mainly solubilize insoluble Pi by acidifying the microenvironment (Etesami, 2020). In addition to increasing P availability for plants, there are some reports that PSB are also able to increase Si availability and uptake. Lee et al. (2019) observed that the PSB strain *Enterobacter ludwigii* GAK2, isolated from paddy soils, was able to significantly increase P and Si levels in rice plant tissues grown on insoluble Pi [$Ca_3(PO_4)_2$] and insoluble silicate ($Mg_2O_8Si_3$) based soils. This bacterial strain also increased rice plant growth indices (chlrophyll content, fresh biomass, root and shoot lengths). In another study, the PSB strains *Bacillus simplex* UT1 and *Pseudomonas* sp. FA1 significantly increased the shoot Si levels in sorghum (*Sorghum bicolor* L.) (Rezakhani et al., 2019a) and wheat (*Triticum aestivum* L.) (Rezakhani et al., 2019b). Given the role of Si in increasing soil P availability, one question that arises here is whether the Si-mediated increase in soil P availability has an inhibitory effect on bacterial solubilization of P from insoluble Pi sources. It is noteworthy that microbial P solubilization is not influenced by the soil P availability. For example, in a study (Brucker et al., 2020), adding P (100 mg of ground apatite) to soil extracts from soils with various P fractions (bioavailable P between 0.6 to 38 mg kg^{-1} and total P between 0.42 to 1.23 g kg^{-1}) and degree of weathering, which had been incubated 28 days, did not substantially reduce P solubilization rates, which indicates that the P availability does not affect the microbial soil P solubilization. It is probable that microbial P solubilization is not driven by the microbial P demand but rather is a side effect of microbial metabolism. It was also observed that P fertilization over several years did not influence PSB abundance in the grassland soils of different continents (Widdig et al., 2019). Generally, PSB can benefit plants by accelerating the weathering of silicates and increasing the rhizospheric concentration of available Si.

Si Increases the Population of PSB

The potential effect of Si on the soil microbial community has attracted only a limited amount of attention. However, there are some reports showing that Si can significantly influences some soil microbial community components (e.g., it increased beneficial bacterial population and reduced soil fungi/bacteria ratio) (Wainwright et al., 2003; Hordiienko et al., 2010; Karunakaran et al., 2013; Wang et al., 2013; Lin et al., 2020). It is reported that bacteria use Si-based autotrophy as a source of energy to support CO_2 fixation (Das et al., 1992). It is also proposed that the first bacteria may have evolved on earth because of Si (Wainwright et al., 2003). A number of bacteria and fungi are able to grow on nutrient-free silica gel and distilled water (Wainwright et al., 1991). According to a study (Wainwright et al., 2003), silicic acid increases the number of both aerobic and facultative anaerobic bacteria in ultra-pure water incubated under strict oligotrophic conditions. In addition, organisms use silica through silicification, a process by which silica is utilized and deposited by bacteria (Perry, 2003) and also Si-based compounds stimulate the population of oligotrophic bacteria in soil (Ai-Falih, 2003). In a previous study (Karunakaran et al., 2013), it was shown that the microbial population increased with an increase in concentration of nanosilica. In addition, silica content in biomass also increased with an increase in the concentration of nanosilica. It is known that nanosilica is not toxic to the soil bacterial community (Karunakaran et al., 2013). The reason behind the interaction between nanosilica and bacteria may reflect a hydration property of the nanosilica surface, which could facilitate the attraction of silica to the microbial surface (Gordienko and Kurdish, 2007).

There are a few studies that have focused on the effect of Si application on the activity and population of PSB. In one study, the efficiency of nanosilica (0.5 g kg^{-1} of soil) was evaluated in terms of its effects on beneficial microbial population such as PSB in the rhizosphere soil of maize (Rangaraj et al., 2014). When compared with the control (2.0×10^4 CFU g^{-1}), the silica-treated rhizosphere soils revealed an increase in the PSB population (4.4×10^4 CFU g^{-1}). This shows that the addition of silica may act as a substrate for P uptake systems in soil as well as in plants. An increase in the population of PSB of nanosilica-amended soil indicates enhanced soil fertility and enhanced available nutrients to the plants. The increased population of PSB in nanosilica-treated rhizosphere soil may be due to the availability of more P to plants, as the Si competes for P in a plant system. Because both P and Si influence the P content and the population of PSB, the uptake of either source increases the populations of PSB. Hence, silica may act as a substrate for PSB, which results in an increase in the population of PSB and availability of P. The changes in soil inorganic nutrients with respect to silica fertilization may also be due to the production of organic compounds by increased microbial activity and desorption of inorganic nutrients from soil mineral compounds (Karunakaran et al., 2013). It is also reported that the bacteria use silica from soil and hence, there is a decrease in the silica content in the soil (Wainwright et al., 2003). Thus,

nanosilica can be included for fertilizer formulations to make the soil more fertile and to improve soil phosphate-solubilizing bacterial community for improving plant P nutrition.

SSB INCREASE AVAILABILITY OF P AND Si AND THEIR UPTAKE BY PLANTS

Plants are not able to absorb Si until monosilicic acid (H_4SiO_4) is released into the soil solution through weathering or dissolution (Kang et al., 2017). Monosilicic acid generally originates from the weathering of soil minerals that contain Si, desorption from the soil matrix, irrigation water, and Si fertilizers (Klotzbücher et al., 2015). Si fertilizers, unlike conventional fertilizers, have a limited availability and are often not affordable for many farmers (Meena et al., 2014). Therefore, they are rarely used in many countries, especially in developing countries. Silicate fertilizers are usually composed of (*i*) industrial byproducts or slags rich in Si, whose application may lead to metal contamination of soils, (*ii*) bentonite, diatomaceous earth, feldspars, and micas, which are biologically/minerally derived Si fertilizers with low Si bioavailability and high application rates and (*iii*) highly soluble, but very expensive, potassium silicates (Datnoff et al., 2001). Si-rich crop residues, construction/demolition wastes that contain aluminum, calcium, and potassium silicates, mineral/metal mining wastes, and silicate rocks may be recycled to affordable silicate fertilizers. The solubility of the primary and secondary minerals in soils is the main factor that influences the soil Si concentration (Sommer et al., 2006). The primary and secondary minerals can be subjected to physico-chemical and biochemical interventions that accelerate the solubility for soil applications (Bin et al., 2008), but biochemical action via microbial activities is considered most important for this process (Vasanthi et al., 2018). Many studies have observed that microbes isolated from the surface of silicate minerals weather different silicates (Sheng et al., 2008; Lapanje et al., 2012; Wang et al., 2015).

Plants and their associated microflora are known to also influence silicate weathering (the dissolution and mobilization of silicate minerals in soil) by altering the physical soil properties, modifying the soil pH, and producing chelating ligands (Cornelis et al., 2011). It has been reported that among microorganisms, plant associated bacteria accelerate the dissolution of silicates and release Si to the plant–soil system (Savant et al., 1996; Hutchens et al., 2003; Sheng and He, 2006; Uroz et al., 2009; Chandrakala et al., 2019) through bio-weathering processes (Klotzbücher et al., 2015). With an increase in knowledge of how Si benefits plants, rhizospheric soils have been explored in search of new bacteria that solubilize silicates (Kang et al., 2017; Vasanthi et al., 2018). SSB have been gathering increasing interest, as rhizospheric silicate solubilization leads to increased potassium and Si uptake, which reduces the need for potash fertilizers.

The ability to solubilize silicates (to depolymerize crystalline silicate) has been reported in various Gram-positive and Gram-negative bacteria (*Burkholderia eburnea* CS4-2, *Bacillus* sp., *Bacillus flexus, Bacillus globisporus, B. mucilaginosus, B. megaterium* and *Pseudomonas fluorescens, Burkholderia susongensis* sp., *Rhizobium* sp., *Rhizobium yantingense*, *Rhizobium tropici*, and *Pseudomonas stutzeri*) (Malinovskaya et al., 1990; Lin et al., 2002; Liu et al., 2006; Vasanthi et al., 2013, 2018; Chen et al., 2015; Gu et al., 2015; Wang et al., 2015; Umamaheswari et al., 2016; Kang et al., 2017; Chandrakala et al., 2019).

Silicate-solubilizing bacteria can potentially release soluble silica from biogenic materials such as diatomaceous earth, rice husks, rice straw, and siliceous earth, as well as from insoluble, inorganic (Al, Ca, K, and Mg) silicates and silicate minerals such as feldspar and biotite (Wang et al., 2015; Chandrakala et al., 2019). These bacteria have been isolated from different habitats, such as rice plant rhizospheres (Kang et al., 2017; Chandrakala et al., 2019), from rice field soil samples (Vasanthi et al., 2013), weathered feldspar surfaces (Sheng and He, 2006), weathered rock surfaces (Gu et al., 2015), weathered rock (purple siltstone) surfaces (Chen et al., 2015), pond sediments, river water, soils, and talc minerals (Umamaheswari et al., 2016), potassium mine tailings (Huang et al., 2013), quercus petreae oak mycorrhizal roots surroundings (Calvaruso et al., 2010), and weathered rocks (Wang et al., 2015).

Some mechanisms which SSB could utilize to release soluble silica from insoluble silicates include: (i) production of organic acids including citric, tartaric, acetic, gluconic, hexadecanoic, malic, oxalic, phthalic, oleic, heptadecanoic, and hydroxypropionic acids (Vassilev et al., 2006; Vasanthi et al., 2018), which have metal complexing properties that may bind with aluminum and iron silicates and render silicates soluble, also provide protons (H^+) for protonation for silicate hydrolysis (Duff and Webley, 1959; Avakyan et al., 1986; Drever and Stillings, 1997); (ii) inorganic acid production (i.e., oxidation of sulfur, reduction of sulfides to sulfuric acid, oxidation of ammonia to nitrates, and conversion of nitrates to nitric acid, which can act on silicates); (iii) synthesis and discharge of carbonic anhydrase that catalyzes the interconversion between carbon dioxide produced by soil microbes and water, and the dissociated ions of carbonic acid (Brucker et al., 2020), which promotes the microbial conversion of silicate minerals as observed in orthoclase degradation to kaolinite (Waksman and Starkey, 1924). In addition, CO_2 sequestration in basaltic acquifers and the associated carbonate mineralization might maintain an environment suitable for silicate mineral dissolution (Pokrovsky et al., 2011); (iv) production of siderophores, which bind and transport iron(III) which can play a part in silicate solubilization by scavenging iron from silicate minerals as observed in hornblende degradation (Kalinowski et al., 2000); (v) the reduction of sulfates and production of H_2S, which reacts with cations like Ca and Fe of silicate minerals forming sulfides and thus rendering silicate solubilization (Ehrlich et al., 2015); (vi) absorption and binding of the inorganic silicate ions on bacterial surfaces, due to having ionizable carboxylates and phosphates of lipopolysaccharides in Gram-negative bacteria and peptidoglycan, teichoic acids and teichoic acids in Gram-positive bacteria and their high reactivity to the ions, rendering dissolution (Urrutia and Beveridge, 1994); (vii) extracellular polysaccharide production (Xiao et al., 2016; Kang et al., 2017), which is implicated in weathering of rocks and breakdown of silicates due to their wetting and drying

properties and acting as a sorbent of metal ions (binding silicates and affecting the equilibrium between the fluid and mineral phases, rendering them soluble) during this vital activity. The biofilm formation also solubilizes silicates in their microenvironment (Malinovskaya et al., 1990); and (viii) alkali production (Kutuzova, 1969). It is known that SSB can solubilize silicates by shifting the pH of the environment toward alkalinity by decomposing the organic matter and fixing nitrogen, to subsequently form ammonia and amines (Vasanthi et al., 2018); and acidolysis, the most commonly found mechanism of silicate mineral weathering (Jongmans et al., 1997; Chandrakala et al., 2019). Future research should focus on the yet unknown mineral weathering mechanisms of these bacteria (Kang et al., 2017).

These bacteria, isolated from both plant roots and soil minerals, could also increase the plant Si uptake and therefore Si levels in plants (Peera et al., 2016; Kang et al., 2017; Vasanthi et al., 2018; Chandrakala et al., 2019). In one study (Kang et al., 2017), it was found that inoculation of japonica rice plants with the SSB strain *Burkholderia eburnea* CS4-2 increased the Si content in the plants grown on the plant growth substrate including insoluble silicates. In addition, the plant growth attributes (chlorophyll levels, root and shoot lengths, root and shoot fresh weights, etc.) were also improved compared to those of the control and of plants grown on insoluble silica. CS4-2, when applied together with insoluble silica, significantly promoted the growth of rice plants (Kang et al., 2017). Chandrakala et al. (2019) found that the SSB strain *Rhizobium* sp. IIRR-1 isolated from the rhizospheric soil around rice plants could colonize and grow on all insoluble silicates, which resulted in increased silica release into the culture media (12.45–60.15% over that of the control). This strain also successfully colonized the roots of rice seedlings and improved their vigor by 29.18% compared to that of the control.

In addition to providing plants with Si, SSB can also solubilize P and other nutrients like Ca, Fe, K, Mg, and Zn, bound to the silicate minerals from insoluble sources and provide plants with P (Lin et al., 2002; Liu et al., 2006; Vasanthi et al., 2018; Chandrakala et al., 2019; Lee et al., 2019). The mechanisms for P solubilization are also responsible for the biogenic silicate weathering; namely, the release of extracellular polysaccharides, organic acids, protons, and siderophores (Vassilev et al., 2006; Gorbushina and Broughton, 2009; Uroz et al., 2009; Etesami, 2020). Silicate weathering provides access to minerals that contain P, such as apatite, which are calcium phosphates, and therefore is also related to P solubilization (Gorbushina and Broughton, 2009; Uroz et al., 2009). For example, studies have reported that SSB produce organic acids such as acetic, formic, and gluconic acids during the solubilization of insoluble tri-calcium silicates and other insoluble nutrient sources (Park et al., 2009). The aforementioned studies show that SSB utilization may improve the solubilization of insoluble P and Si, which could ultimately increase the plant P and Si uptake and to substantially improve the plant growth and health. Compared to the studies performed on PSB and other PGPB, very few studies have been conducted to isolate SSB with plant growth-promoting activities from plant-associated soils (Kang et al., 2017; Vasanthi et al., 2018), likely because SSB only accounts for a low proportion of the total bacteria that exist in soils and silicate minerals (Vasanthi et al., 2018).

The outcome of this review paper may widen research scope for use of Si/nanosilica (or SSB) in combination with AMF and PSB in improving P use efficiency in sustainable agriculture (**Figure 4**).

FUTURE PROSPECTS

Arbuscular mycorrhizal fungi provide their host plants with P and other nutrients in exchange for photosynthates, by effectively increasing the volume of the soil solution that host plants can acquire minerals from via the hyphae that develop from the roots. AMF prevent the available P from re-precipitating before plants have access, and their capacity to transport P to plants can account for up to 80% of a plant's total P uptake. However, much of the soil P exists in an insoluble form, and some AMF can only exploit soluble P sources. PSB can solubilize these insoluble P forms and potentially make them available for absorption by AMF hyphae and plants. PSB also increase the AMF hyphal expression Pi transporter genes. In addition to increasing P availability in soils, Si also enhances the expression of plant genes associated with inorganic P absorption under P-deficient conditions. Previous studies, indicate that AMF and PSB, Si and AMF, and Si and PSB synergistically act to more effectively increase the plant uptake of P, improving the growth of different plants more than when each was applied on its own. Accordingly, the use of Si along with these two microbial groups may increase P availability in the rhizosphere.

Several suggestions and avenues of research would move us closer to adopting this strategy for developing environment-friendly P-biofertilizer to be used as supplements and/or alternatives to chemical P fertilizers:

(i) It is known that AMF and PSB cooperate, in addition to having synergistic effects (Zhang et al., 2016). According to Zhang et al. (2016) AMF and free–living PSB cooperated for mutual benefit by supplying the required carbon or P for each microorganism, though these interactions were dependent on the environmental P availability. This indicates that when using co–inoculation of AMF and PSB, the amount of available P in the soil should be considered;

(ii) AMF hyphae, by secreting certain metabolites such as carbohydrates (Hooker et al., 2007; Toljander et al., 2007) (e.g., sugars such as galactose, fructose, glucose, and trehalose) (Zhang et al., 2018a,b), carboxylates (e.g., aconitate, citrate, and succinate) (Tawaraya et al., 2006; Zhang et al., 2018b), and amino acids (Bharadwaj et al., 2012), only benefit specific microorganisms and inhibit others (Nuccio et al., 2013; Bender et al., 2014). The exact mechanisms of these interactions remains to be investigated, although previous research has made suggestions: physical interactions such as the capacity to attach to the hyphae of the AMF (Scheublin et al., 2010), niche competition for nutrients (Veresoglou et al., 2011), and AMF hyphal exudation directly and indirectly

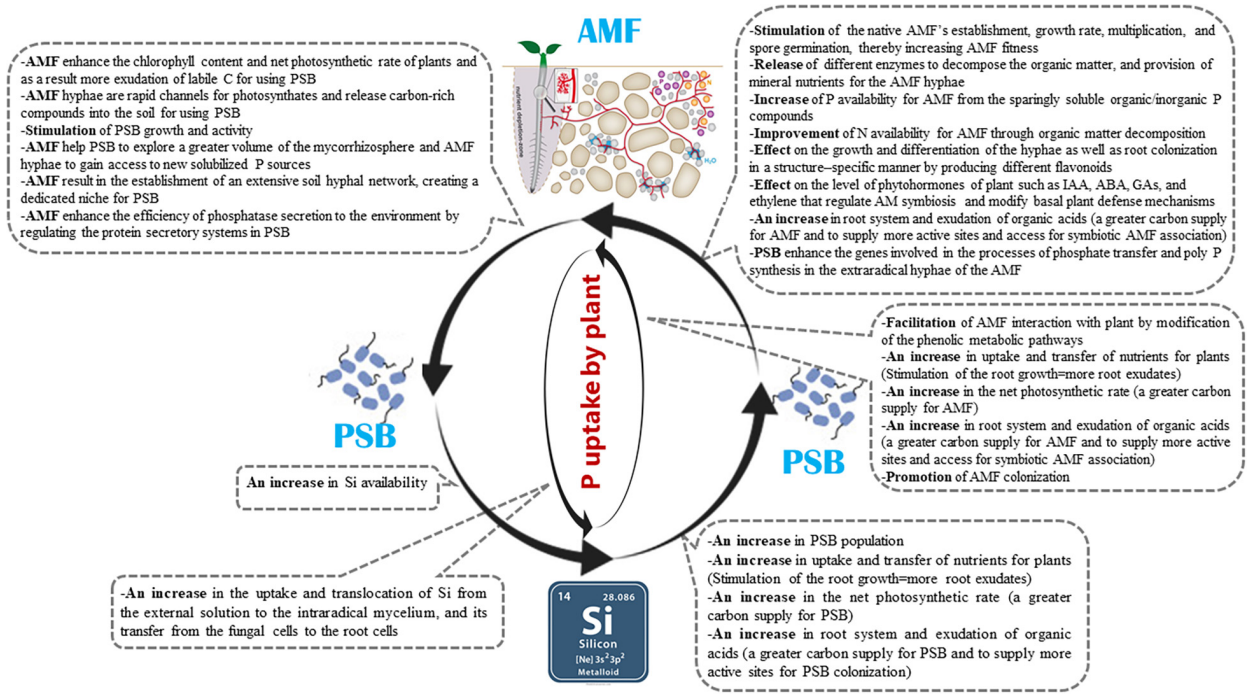

FIGURE 4 | Synergistic effects of among arbuscular mycorrhizal fungi (AMF), phosphate-solubilizing bacterium (PSB), and silicon (Si) on P Availability and its uptake by plant.

manipulating the community (Toljander et al., 2007). In addition, it is important to note that the stimulated microbes positively affect AMF fitness in general (Scheublin et al., 2010; Nuccio et al., 2013);

(iii) It has also been found that relative to other PSB strains, the different bacteria may positively or negatively influence the AMF hyphal growth. Future research should investigate which combination and plant-growth-promoting characteristics are the most affected by fungal secretions, as the knowledge is yet unclear. Furthermore, it should be investigated which soil conditions (available P content, pH, organic matter composition, etc.) lead to the best results in plants when the co–inoculation of AMF and PSB with Si is provided;

(iv) Further research is necessary to identify the different mechanisms with which spore- and AMF hyphae-associated PSB affect plant growth with and without AMF in non-sterile conditions in the field. Evidence to date is still inconsistent regarding significant organic P mineralization by AMF. Continuous monitoring of the characteristics of the different AMF mycelial exudates, and how they interact with the biotic and abiotic environments *in situ* will also help further the understanding AMF's ecological roles (Toljander, 2006);

(v) The relationship between certain soil bacteria and mycorrhizal fungi provides new insights into the design of mixed inoculation, while identifying fungal strains that contain plant growth-promoting endosymbiotic bacteria and mycorrhiza helper bacteria (bacterial communities living strictly associated with AMF spores extraradical mycelium and mycorrhizal roots, in the mycorrhizosphere) evidenced by ACC deaminase activities, IAA production, siderophore production, Pi solubilization, and N_2 fixation ability enables new strategies for AMF use (Turrini et al., 2018). A better understanding of such relationships between certain bacteria and fungi should lead to substantial ecological benefits and contribute to sustainable agriculture;

(vi) To make optimal use of soil microorganisms to maximize the benefits for plant growth and development, future research should investigate how the soil bacteria and fungi interact. Calcareous soils with a high pH and low P availability could benefit greatly from making use of such microorganism interactions;

(vii) Since the coexistence of AMF and PSB in the rhizosphere spans millions of years, numerous interactions should have evolved between the two microorganism groups. The exact mechanisms between AMF and PSB should be identified. It is not clear whether the phosphate-solubilizing ability of any bacteria allows them to attach to the extraradical AMF hyphae (Scheublin et al., 2010);

(viii) Most research has been done using culturable bacteria. Since most bacteria are unculturable, more research is needed dealing with unculturable bacteria in the mycorrhizosphere, which will lead to an improved knowledge of the microbial community and the associated mycorrhizospheric interactions (Toljander, 2006);

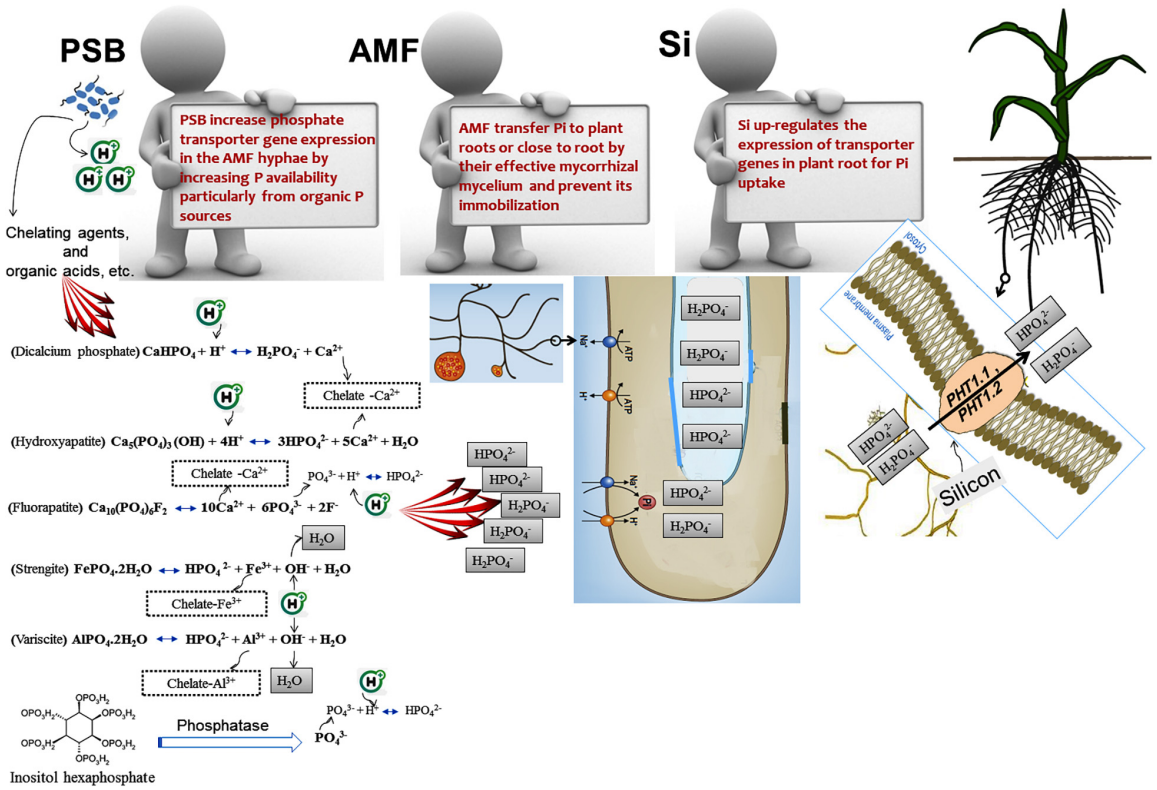

FIGURE 5 | Synergetic role of among arbuscular mycorrhizal fungi (AMF), phosphate-solubilizing bacterium (PSB), and silicon (Si) in improving phosphorus (P) uptake by plant.

(ix) Further research to evaluate the application and the efficacy of AMF, PSB, and SSB (or Si fertilizers) as co–inoculants or as independent inoculants under various environmental stresses on crops fertilized with different low-solubility P sources in real world conditions is necessary, where the survival of AMF, PSB, and SSB, as well as how the mechanisms with which they promote plant growth is affected by competition with the endemic microorganisms, environmental stresses, and soil conditions;

(x) Further research is necessary to validate the AMF and PSB performance in conjunction with SSB or suitable insoluble silicate sources, as silica itself is considered as agronomically beneficial and its mobilization is always accompanied by the release of other macronutrients and macronutrients that are bound to silicate minerals, under various field conditions and different ecosystems; and

(xi) Because AMF are unable to release phosphatases outside the hyphae, organic P utilization by AMF seems to depend on the presence of other soil microbes. Since different bacterial genera possess different organic P mineralization abilities (Rodrìguez and Fraga, 1999) and multiple plant-growth-promoting characteristics, bacteria are expected to promote plant growth more effectively in comparison to microorganisms that only possess a single plant growth-promoting trait (Shahi et al., 2011; Etesami and Maheshwari, 2018); manipulation of the bacterial community associated with the AMF hyphae (i.e., introduction of superior PSB and SSB into the hyphae) may influence the organic P mineralization and Si uptake processes in plants.

CONCLUSION

P is a vital element in crop nutrition. Adverse environmental effects of chemical-based P fertilizers have compelled us to find a sustainable approach for efficient P availability in agriculture to meet the ever-increasing global demand of food. According to the review paper, the use of AMF, PSB, and the addition of Si can be an effective and economical way to improve the availability and efficacy of P. Based on what is known about them, the combination of AMF, PSB, and Si (or SSB) may be utilized as a strategy for improving plant growth in P-deficient soils and minimizing chemical fertilization to exercise sustainable agriculture (**Figure 5**). The combination can help plants effectively utilize the low-solubility P sources by solubilizing them into utilizable forms that are later absorbed by plants. This may assist in solving problems encountered with the crop production economy and food shortages, which also make the co-inoculation with Si or SSB a promising technique for use in commercial inoculant formulations.

AUTHOR CONTRIBUTIONS

HE wrote the manuscript. BJ checked and edited the sections related to silicon in this manuscript. BG revised and approved the final version to be published. All the authors contributed to the article and approved the submitted version.

ACKNOWLEDGMENTS

We express our gratitude to the University of Tehran for providing the facilities necessary for this research.

REFERENCES

Aarab, S., Ollero, F. J., Megías, M., Laglaoui, A., Bakkali, M., and Arakrak, A. (2015). Isolation and screening of bacteria from rhizospheric soils of rice fields in Northwestern Morocco for different plant growth promotion (PGP) activities: an in vitro study. *Int. J. Curr. Microbiol. Appl. Sci.* 4, 260–269.

Adesemoye, A. O., Torbert, H. A., and Kloepper, J. W. (2009). Plant growth-promoting rhizobacteria allow reduced application rates of chemical fertilizers. *Microb. Ecol.* 58, 921–929. doi: 10.1007/s00248-009-9531-y

Agnolucci, M., Battini, F., Cristani, C., and Giovannetti, M. (2015). Diverse bacterial communities are recruited on spores of different arbuscular mycorrhizal fungal isolates. *Biol. Fertility Soils* 51, 379–389. doi: 10.1007/s00374-014-0989-5

Ahemad, M. (2012). Implications of bacterial resistance against heavy metals in bioremediation: a review. *J. Institute Integrative Omics Appl. Biotechnol (IIOAB)* 3, 39–46.

Ahemad, M., and Khan, M. (2010). Phosphate solubilizing *Enterobacter* asburiae strain PS2. *Afr. J. Microbiol. Res.* 5, 849–857.

Ahemad, M., and Kibret, M. (2014). Mechanisms and applications of plant growth promoting rhizobacteria: current perspective. *J. King Saud University-science* 26, 1–20. doi: 10.1016/j.jksus.2013.05.001

Ahmed, E., and Holmström, S. J. M. (2014). Siderophores in environmental research: roles and applications. *Microbial Biotechnol.* 7, 196–208. doi: 10.1111/1751-7915.12117

Ai-Falih, A. M. (2003). Effect of silicon compounds on oligotrophic soil bacteria. *Saudi. J. Biol. Sci.* 10, 131–137.

Alori, E. T., Glick, B. R., and Babalola, O. O. (2017). Microbial phosphorus solubilization and its potential for use in sustainable agriculture. *Front. Microbiol.* 8:971. doi: 10.3389/fmicb.2017.00971

Amir, H., and Pineau, R. (2003). Release of Ni and Co by microbial activity in New Caledonian ultramafic soils. *Can. J. Microbiol.* 49, 288–293. doi: 10.1139/w03-039

Anda, C. C. O., Opfergelt, S., and Declerck, S. (2016). Silicon acquisition by bananas (cV Grande Naine) is increased in presence of the arbuscular mycorrhizal fungus Rhizophagus irregularis MUCL 41833. *Plant Soil* 409, 77–85. doi: 10.1007/s11104-016-2954-6

Antunes, P. M., Schneider, K., Hillis, D., and Klironomos, J. N. (2007). Can the arbuscular mycorrhizal fungus Glomus intraradices actively mobilize P from rock phosphates? Pedobiologia 51, 281–286. doi: 10.1016/j.pedobi.2007.04.007

Appanna, V. (2007). Efficacy of phosphate solubilizing bacteria isolated from vertisols on growth and yield parameters of sorghum. *Res. J. Microbiol.* 2, 550–559. doi: 10.3923/jm.2007.550.559

Artursson, V., Finlay, R. D., and Jansson, J. K. (2006). Interactions between arbuscular mycorrhizal fungi and bacteria and their potential for stimulating plant growth. *Environ. Microbiol.* 8, 1–10. doi: 10.1111/j.1462-2920.2005.00942.x

Augé, R. M., Toler, H. D., and Saxton, A. M. (2016). Mycorrhizal stimulation of leaf gas exchange in relation to root colonization, shoot size, leaf phosphorus and nitrogen: a quantitative analysis of the literature using meta-regression. *Front. Plant Sci.* 7:1084. doi: 10.3389/fpls.2016.01084

Avakyan, Z. A., Pivovarova, T. A., and Karavaiko, G. I. (1986). Properties of a new species, bacillus-mucilaginosus. *Microbiology* 55, 369–374.

Azcón, R. (1987). Germination and hyphal growth of Glomus mosseae in vitro: effects of rhizosphere bacteria and cell-free culture media. *Soil Biol. Biochem.* 19, 417–419. doi: 10.1016/0038-0717(87)90032-0

Aziz, T., Ahmed, I., Farooq, M., Maqsood, M. A., and Sabir, M. (2011). Variation in phosphorus efficiency among Brassica cultivars I: internal utilization and phosphorus remobilization. *J. Plant Nutrition* 34, 2006–2017. doi: 10.1080/01904167.2011.610487

Aziz, T., Sabir, M., Farooq, M., Maqsood, M. A., Ahmad, H. R., and Warraich, E. A. (2014). "Phosphorus deficiency in plants: responses, adaptive mechanisms, and signaling," in *Plant signaling: Understanding the Molecular Crosstalk*. K. R. Hakeem, R. U. Rehman, I. Tahir eds (Springer: Berlin), 133–148. doi: 10.1007/978-81-322-1542-4_7

Badri, D. V., and Vivanco, J. M. (2009). Regulation and function of root exudates. *Plant Cell Environ.* 32, 666–681. doi: 10.1111/j.1365-3040.2009.01926.x

Balestrini, R., Gómez-Ariza, J., Lanfranco, L., and Bonfante, P. (2007). Laser microdissection reveals that transcripts for five plant and one fungal phosphate transporter genes are contemporaneously present in arbusculated cells. *Mol. Plant Microbe Interact.* 20, 1055–1062. doi: 10.1094/mpmi-20-9-1055

Barea, J. -M., Pozo, M. J., Azcon, R., and Azcon-Aguilar, C. (2005). Microbial co-operation in the rhizosphere. *J. Exp. Bot.* 56, 1761–1778. doi: 10.1093/jxb/eri197

Barea, J. M., Toro, M., Orozco, M. O., Campos, E., and Azcón, R. (2002). The application of isotopic (32P and 15N) dilution techniques to evaluate the interactive effect of phosphate-solubilizing rhizobacteria, mycorrhizal fungi and Rhizobium to improve the agronomic efficiency of rock phosphate for legume crops. *Nutrient Cycling Agroecosystems* 63, 35–42.

Barker, S. J., and Tagu, D. (2000). The roles of auxins and cytokinins in mycorrhizal symbioses. *J. Plant Growth Regulat.* 19, 144–154. doi: 10.1007/s003440000021

Bashan, Y., Holguin, G., and De-Bashan, L. E. (2004). Azospirillum-plant relationships: physiological, molecular, agricultural, and environmental advances (1997-2003). *Can. J. Microbiol.* 50, 521–577. doi: 10.1139/w04-035

Bashan, Y., Kamnev, A. A., and De-Bashan, L. E. (2013). Tricalcium phosphate is inappropriate as a universal selection factor for isolating and testing phosphate-solubilizing bacteria that enhance plant growth: a proposal for an alternative procedure. *Biol. Fertility Soils* 49, 465–479. doi: 10.1007/s00374-012-0737-7

Battini, F., Grønlund, M., Agnolucci, M., Giovannetti, M., and Jakobsen, I. (2017). Facilitation of phosphorus uptake in maize plants by mycorrhizosphere bacteria. *Sci. Rep.* 7:4686.

Beauchemin, S., Hesterberg, D., Chou, J., Beauchemin, M., Simard, R. R., and Sayers, D. E. (2003). Speciation of phosphorus in phosphorus-enriched agricultural soils using X-ray absorption near-edge structure spectroscopy and chemical fractionation. *J. Environ. Qual.* 32, 1809–1819. doi: 10.2134/jeq2003.1809

Begum, N., Qin, C., Ahanger, M. A., Raza, S., Khan, M. I., Ashraf, M., et al. (2019). Role of arbuscular mycorrhizal fungi in plant growth regulation: implications in abiotic stress tolerance. *Front. Plant Sci.* 10:1068. doi: 10.3389/fpls.2019.01068

Bender, S. F., Plantenga, F., Neftel, A., Jocher, M., Oberholzer, H. -R., Köhl, L., et al. (2014). Symbiotic relationships between soil fungi and plants reduce N2O emissions from soil. *ISME J.* 8, 1336–1345. doi: 10.1038/ismej.2013.224

Benedetto, A., Magurno, F., Bonfante, P., and Lanfranco, L. (2005). Expression profiles of a phosphate transporter gene (GmosPT) from the endomycorrhizal fungus *Glomus mosseae*. *Mycorrhiza* 15, 620–627. doi: 10.1007/s00572-005-0006-9

Berta, G., Copetta, A., Gamalero, E., Bona, E., Cesaro, P., Scarafoni, A., et al. (2014). Maize development and grain quality are differentially affected by mycorrhizal fungi and a growth-promoting pseudomonad in the field. *Mycorrhiza* 24, 161–170. doi: 10.1007/s00572-013-0523-x

Bharadwaj, D. P., Alström, S., and Lundquist, P. -O. (2012). Interactions among Glomus irregulare, arbuscular mycorrhizal spore-associated bacteria, and plant pathogens under in vitro conditions. *Mycorrhiza* 22, 437–447. doi: 10.1007/s00572-011-0418-7

Bharadwaj, D. P., Lundquist, P. -O., and Alström, S. (2008). Arbuscular mycorrhizal fungal spore-associated bacteria affect mycorrhizal colonization, plant growth and potato pathogens. *Soil Biol. Biochem.* 40, 2494–2501. doi: 10.1016/j.soilbio.2008.06.012

Bhattacharyya, P. N., and Jha, D. K. (2012). Plant growth-promoting rhizobacteria (PGPR): emergence in agriculture. *World J. Microbiol. Biotechnol.* 28, 1327–1350. doi: 10.1007/s11274-011-0979-9

Bi, Y., Xiao, L., and Sun, J. (2019). An arbuscular mycorrhizal fungus ameliorates plant growth and hormones after moderate root damage due to simulated coal mining subsidence: a microcosm study. *Environ. Sci. Poll. Res.* 26, 11053–11061. doi: 10.1007/s11356-019-04559-7

Bianciotto, V., and Bonfante, P. (2002). Arbuscular mycorrhizal fungi: a specialised niche for rhizospheric and endocellular bacteria. *Antonie Van Leeuwenhoek* 81, 365–371.

Bin, L., Ye, C., Lijun, Z. H. U., and Ruidong, Y. (2008). Effect of microbial weathering on carbonate rocks. *Earth Sci. Front.* 15, 90–99. doi: 10.1016/S1872-5791(09)60009-9

Blagodatskaya, E., and Kuzyakov, Y. (2013). Active microorganisms in soil: critical review of estimation criteria and approaches. *Soil Biol. Biochem.* 67, 192–211. doi: 10.1016/j.soilbio.2013.08.024

Bona, E., Cantamessa, S., Massa, N., Manassero, P., Marsano, F., Copetta, A., et al. (2016). Arbuscular mycorrhizal fungi and plant growth-promoting pseudomonads improve yield, quality and nutritional value of tomato: a field study. *Mycorrhiza* 27, 1–11. doi: 10.1007/s00572-016-0727-y

Borch, K., Bouma, T., Lynch, J., and Brown, K. (1999). Ethylene: a regulator of root architectural responses to soil phosphorus availability. *Plant Cell Environ.* 22, 425–431. doi: 10.1046/j.1365-3040.1999.00405.x

Botta, A., Rodrigues, F. A., Sierras, N., Marin, C., Cerda, J. M., and Brossa, R. (2014). "Evaluation of Armurox® (complex of peptides with soluble silicon) on mechanical and biotic stresses in gramineae," in *Proceedings of the 6th International Conference on Silicon in Agriculture*, Stockholm, Sweden, 26–30.

Bouhraoua, D., Aarab, S., Laglaoui, A., Bakkali, M., and Arakrak, A. (2015). Phosphate solubilizing bacteria efficiency on mycorrhization and growth of peanut in the northwest of Morocco. *Am. J. Microbiol. Res.* 3, 176–180.

Brady, N. C., and Weil, R. R. (1999). *The Nature and Properties of Soil* 12th edn. New York, NY: Mac. Pub. Com. 625–640.

Browne, P., Rice, O., Miller, S. H., Burke, J., Dowling, D. N., Morrissey, J. P., et al. (2009). Superior inorganic phosphate solubilization is linked to phylogeny within the *Pseudomonas fluorescens* complex. *Appl. Soil Ecol.* 43, 131–138. doi: 10.1016/j.apsoil.2009.06.010

Brucker, E., and Spohn, M. (2019). Formation of soil phosphorus fractions along a climate and vegetation gradient in the Coastal Cordillera of Chile. *Catena* 180, 203–211. doi: 10.1016/j.catena.2019.04.022

Brucker, E., Kernchen, S., and Spohn, M. (2020). Release of phosphorus and silicon from minerals by soil microorganisms depends on the availability of organic carbon. *Soil Biol. Biochem.* 143:107737. doi: 10.1016/j.soilbio.2020.107737

Brundrett, M. C., and Tedersoo, L. (2018). Evolutionary history of mycorrhizal symbioses and global host plant diversity. *New Phytol.* 220, 1108–1115. doi: 10.1111/nph.14976

Bruns, T. D., Corradi, N., Redecker, D., Taylor, J. W., and Öpik, M. (2018). Glomeromycotina: what is a species and why should we care? *New Phytol.* 220, 963–967. doi: 10.1111/nph.14913

Bücking, H., Liepold, E., and Ambilwade, P. (2012). The role of the mycorrhizal symbiosis in nutrient uptake of plants and the regulatory mechanisms underlying these transport processes. *Plant Sci.* 4, 108–132.

Bünemann, E. K., Oberson, A., and Frossard, E. (2010). *Phosphorus in Action: Biological Processes in Soil Phosphorus Cycling*. Berlin: Springer Science & Business Media.

Caballero-Mellado, J., Onofre-Lemus, J., Estrada-De Los Santos, P., and Martínez-Aguilar, L. (2007). The tomato rhizosphere, an environment rich in nitrogen-fixing *Burkholderia species* with capabilities of interest for agriculture and bioremediation. *Appl. Environ. Microbiol.* 73, 5308–5319. doi: 10.1128/aem.00324-07

Calvaruso, C., Turpault, M. -P., Leclerc, E., Ranger, J., Garbaye, J., Uroz, S., et al. (2010). Influence of forest trees on the distribution of mineral weathering-associated bacterial communities of the *Scleroderma citrinum* mycorrhizosphere. *Appl. Environ. Microbiol.* 76, 4780–4787. doi: 10.1128/aem.03040-09

Calvo, P., Nelson, L., and Kloepper, J. W. (2014). Agricultural uses of plant biostimulants. *Plant Soil* 383, 3–41. doi: 10.1007/s11104-014-2131-8

Campos, P., Borie, F., Cornejo, P., López-Ráez, J. A., López-García, Á., and Seguel, A. (2018). Phosphorus acquisition efficiency related to root traits: is mycorrhizal symbiosis a key factor to wheat and barley cropping? *Front. Plant Sci.* 9:752. doi: 10.3389/fpls.2018.00752

Canarini, A., Kaiser, C., Merchant, A., Richter, A., and Wanek, W. (2019). Root exudation of primary metabolites: mechanisms and their roles in plant responses to environmental stimuli. *Front. Plant Sci.* 10:157. doi: 10.3389/fpls.2019.00157

Carey, J. C., and Fulweiler, R. W. (2012). The terrestrial silica pump. *PLoS One* 7:e52932. doi: 10.1371/journal.pone.0052932

Carlisle, E. M., Mckeague, J. A., Siever, R., and Van Soest, P. J. (1977). "Silicon," in *Geochemistry and the Environment*. Elsevier: Washington, DC, 54–115.

Castagno, L., Estrella, M., Sannazzaro, A., Grassano, A., and Ruiz, O. (2011). Phosphate-solubilization mechanism and in vitro plant growth promotion activity mediated by *Pantoea eucalypti* isolated from *Lotus tenuis* rhizosphere in the Salado River Basin (Argentina). *J. Appl. Microbiol.* 110, 1151–1165. doi: 10.1111/j.1365-2672.2011.04968.x

Chaintreuil, C., Giraud, E., Prin, Y., Lorquin, J., Ba, A., Gillis, M., et al. (2000). Photosynthetic bradyrhizobia are natural endophytes of the African wild rice *Oryza breviligulata*. *Appl. Environ. Microbiol.* 66, 5437–5447. doi: 10.1128/aem.66.12.5437-5447.2000

Chandrakala, C., Voleti, S. R., Bandeppa, S., Kumar, N. S., and Latha, P. C. (2019). Silicate solubilization and plant growth promoting potential of *Rhizobium sp*. isolated from rice rhizosphere. *Silicon* 11, 2895–2906. doi: 10.1007/s12633-019-0079-2

Chen, W., Sheng, X. -F., He, L. -Y., and Huang, Z. (2015). Rhizobium yantingense sp. nov., a mineral-weathering bacterium. *Int. J. Systematic Evol. Microbiol.* 65, 412–417. doi: 10.1099/ijs.0.064428-0

Cheng, L., Booker, F. L., Tu, C., Burkey, K. O., Zhou, L., Shew, H. D., et al. (2012). Arbuscular mycorrhizal fungi increase organic carbon decomposition under elevated CO2. *Science* 337, 1084–1087. doi: 10.1126/science.1224304

Chi, F., Shen, S. H., Cheng, H. P., Jing, Y. X., Yanni, Y. G., and Dazzo, F. B. (2005). Ascending migration of endophytic rhizobia, from roots to leaves, inside rice plants and assessment of benefits to rice growth physiology. *Appl. Environ. Microbiol.* 71, 7271–7278. doi: 10.1128/aem.71.11.7271-7278.2005

Chiba, Y., Mitani, N., Yamaji, N., and Ma, J. F. (2009). HvLsi1 is a silicon influx transporter in barley. *Plant J.* 57, 810–818. doi: 10.1111/j.1365-313x.2008.03728.x

Clark, R. Á., and Zeto, S. K. (2000). Mineral acquisition by arbuscular mycorrhizal plants. *J. Plant Nutrition* 23, 867–902. doi: 10.1080/01904160009382068

Clark, R. B., and Zeto, S. K. (1996). Mineral acquisition by mycorrhizal maize grown on acid and alkaline soil. *Soil Biol. Biochem.* 28, 1495–1503. doi: 10.1016/s0038-0717(96)00163-0

Contreras-Cornejo, H. A., Macías-Rodríguez, L., Cortés-Penagos, C., and López-Bucio, J. (2009). Trichoderma virens, a plant beneficial fungus, enhances biomass production and promotes lateral root growth through an auxin-dependent mechanism in *Arabidopsis*. *Plant Physiol.* 149, 1579–1592. doi: 10.1104/pp.108.130369

Cordell, D., Drangert, J. -O., and White, S. (2009). The story of phosphorus: global food security and food for thought. *Global Environ. Change* 19, 292–305. doi: 10.1016/j.gloenvcha.2008.10.009

Cornelis, J.-T., Delvaux, B., Georg, R., Lucas, Y., Ranger, J., and Opfergelt, S. (2011). Tracing the origin of dissolved silicon transferred from various soil-plant systems towards rivers: a review. *Biogeosciences* 8, 89–112.

Cross, A. F., and Schlesinger, W. H. (1995). A literature review and evaluation of the. *Hedley fractionation*: applications to the biogeochemical cycle of soil phosphorus in natural ecosystems. *Geoderma* 64, 197–214. doi: 10.1016/0016-7061(94)00023-4

Cruz, A. F., and Ishii, T. (2012). Arbuscular mycorrhizal fungal spores host bacteria that affect nutrient biodynamics and biocontrol of soil-borne plant pathogens. *Biol. Open* 1, 52–57. doi: 10.1242/bio.2011014

Dakora, F. D., and Phillips, D. A. (2002). Root exudates as mediators of mineral acquisition in low-nutrient environments. *Plant Soil* 245, 35–47.

Das, P., Manna, I., Sil, P., Bandyopadhyay, M., and Biswas, A. K. (2019). Exogenous silicon alters organic acid production and enzymatic activity of TCA cycle in two NaCl stressed indica rice cultivars. *Plant Physiol. Biochem.* 136, 76–91. doi: 10.1016/j.plaphy.2018.12.026

Das, S., Mandal, S., Chakrabarty, A. N., and Dastidar, S. G. (1992). Metabolism of silicon as a probable pathogenicity factor for Mycobacterium & *Nocardia spp*. *Indian J. Med. Res.* 95, 59–65.

Datnoff, L. E., Snyder, G. H., and Korndörfer, G. H. (2001). *Silicon in Agriculture*. Amsterdam: Elsevier.

de La Vega, O. M., Guevara-Garcia, A., and Herrera-Estrella, L. (2000). Enhanced phosphorus uptake in transgenic tobacco plants that overproduce citrate. *Nat. Biotechnol.* 18, 450–453. doi: 10.1038/74531

De Nobili, M., Contin, M., Mondini, C., and Brookes, P. (2001). Soil microbial biomass is triggered into activity by trace amounts of substrate. *Soil Biol. Biochem.* 33, 1163–1170. doi: 10.1016/s0038-0717(01)00020-7

Demoling, F., Figueroa, D., and Bååth, E. (2007). Comparison of factors limiting bacterial growth in different soils. *Soil Biol. Biochem.* 39, 2485–2495. doi: 10.1016/j.soilbio.2007.05.002

Derry, L. A., Kurtz, A. C., Ziegler, K., and Chadwick, O. A. (2005). Biological control of terrestrial silica cycling and export fluxes to watersheds. *Nature* 433, 728–731. doi: 10.1038/nature03299

Dinkelaker, B., and Marschner, H. (1992). In vivo demonstration of acid phosphatase activity in the rhizosphere of soil-grown plants. *Plant Soil* 144, 199–205. doi: 10.1007/bf00012876

Dobbelaere, S., Croonenborghs, A., Thys, A., Broek, A. V., and Vanderleyden, J. (1999). Phytostimulatory effect of *Azospirillum brasilense* wild type and mutant strains altered in IAA production on wheat. *Plant Soil* 212, 153–162.

Dobbelaere, S., Vanderleyden, J., and Okon, Y. (2003). Plant growth-promoting effects of diazotrophs in the rhizosphere. *Crit. Rev. Plant Sci.* 22, 107–149. doi: 10.1080/713610853

Dragišić Maksimović, J., Bogdanović, J., Maksimović, V., and Nikolic, M. (2007). Silicon modulates the metabolism and utilization of phenolic compounds in cucumber (*Cucumis sativus* L.) grown at excess manganese. *J. Plant Nutrition Soil Sci.* 170, 739–744. doi: 10.1002/jpln.200700101

Drever, J. I., and Stillings, L. L. (1997). The role of organic acids in mineral weathering. *Colloids Surf. A: Physicochem. Eng. Aspects* 120, 167–181. doi: 10.1016/s0927-7757(96)03720-x

Drigo, B., Pijl, A. S., Duyts, H., Kielak, A. M., Gamper, H. A., Houtekamer, M. J., et al. (2010). Shifting carbon flow from roots into associated microbial communities in response to elevated atmospheric CO2. *Proc. Natl. Acad. Sci. U S A.* 107, 10938–10942. doi: 10.1073/pnas.0912421107

Drogue, B., Combes-Meynet, E., Moënne-Loccoz, Y., Wisniewski-Dyé, F., and Prigent-Combaret, C. (2013). Control of the cooperation between plant growth-promoting rhizobacteria and crops by rhizosphere signals. *Mol. Microbial Ecol. Rhizosphere* 1-2, 279–293. doi: 10.1002/9781118297674.ch27

Duff, R. B., and Webley, D. M. (1959). 2-Ketogluconic acid as a natural chelator produced by soil bacteria. *Chem. Industry* 1329, 1376–1377.

Duff, S. M. G., Sarath, G., and Plaxton, W. C. (1994). The role of acid phosphatases in plant phosphorus metabolism. *Physiol. Plant.* 90, 791–800. doi: 10.1111/j.1399-3054.1994.tb02539.x

Dungait, J. A. J., Hopkins, D. W., Gregory, A. S., and Whitmore, A. P. (2012). Soil organic matter turnover is governed by accessibility not recalcitrance. *Global Change Biol.* 18, 1781–1796. doi: 10.1111/j.1365-2486.2012.02665.x

Ehrlich, H. L., Newman, D. K., and Kappler, A. (2015). *Ehrlich's Geomicrobiology*. Boca Raton, FL: CRC press.

Elser, J. J. (2012). Phosphorus: a limiting nutrient for humanity? *Curr. Opin. Biotechnol.* 23, 833–838. doi: 10.1016/j.copbio.2012.03.001

Emami, S., Alikhani, H. A., Pourbabaei, A. A., Etesami, H., Sarmadian, F., and Motessharezadeh, B. (2019). Effect of rhizospheric and endophytic bacteria with multiple plant growth promoting traits on wheat growth. *Environ. Sci. Pollution Res.* 26, 19804–19813. doi: 10.1007/s11356-019-05284-x

Emran, M., Rashad, M., Gispert, M., and Pardini, G. (2017). Increasing soil nutrients availability and sustainability by glomalin in alkaline soils. *Agricul. Biosystems Eng.* 2, 74–84.

Epstein, E. (1999). Silicon. *Annu. Rev. Plant Biol.* 50, 641–664.

Etesami, H. (2018). Can interaction between silicon and plant growth promoting rhizobacteria benefit in alleviating abiotic and biotic stresses in crop plants? *Agricul. Ecosystems Environ.* 253, 98–112. doi: 10.1016/j.agee.2017.11.007

Etesami, H. (2020). "Enhanced phosphorus fertilizer use efficiency with microorganisms," in *Nutrient Dynamics for Sustainable Crop Production*. R. Meena (eds) Singapore: Springer, 215–245. doi: 10.1007/978-981-13-8660-2_8

Etesami, H., Alikhani, H. A., and Hosseini, H. M. (2015a). Indole-3-acetic acid (IAA) production trait, a useful screening to select endophytic and rhizosphere competent bacteria for rice growth promoting agents. *MethodsX* 2, 72–78. doi: 10.1016/j.mex.2015.02.008

Etesami, H., Alikhani, H.A., and Mirseyed Hosseini, H. (2015b). "Indole-3-acetic acid and 1-Aminocyclopropane-1-Carboxylate deaminase: bacterial traits required in rhizosphere, rhizoplane and/or endophytic competence by beneficial bacteria," in *Bacterial Metabolites in Sustainable Agroecosystem*, ed. D.K. Maheshwari. (Cham: Springer International Publishing), 183-258.

Etesami, H., and Adl, S. M. (2020). Can interaction between silicon and non–rhizobial bacteria benefit in improving nodulation and nitrogen fixation in salinity–stressed legumes? a review. *Rhizosphere* 15:100229. doi: 10.1016/j.rhisph.2020.100229

Etesami, H., and Alikhani, H. A. (2016a). Co-inoculation with endophytic and rhizosphere bacteria allows reduced application rates of N-fertilizer for rice plant. *Rhizosphere* 2, 5–12. doi: 10.1016/j.rhisph.2016.09.003

Etesami, H., and Alikhani, H. A. (2016b). Rhizosphere and endorhiza of oilseed rape (*Brassica napus* L.) plant harbor bacteria with multifaceted beneficial effects. *Biol. Control* 94, 11–24. doi: 10.1016/j.biocontrol.2015.12.003

Etesami, H., and Glick, B. R. (2020). Halotolerant plant growth–promoting bacteria: prospects for alleviating salinity stress in plants. *Environ. Exp. Bot.* 178:104124. doi: 10.1016/j.envexpbot.2020.104124

Etesami, H., and Jeong, B. R. (2018). Silicon (Si): review and future prospects on the action mechanisms in alleviating biotic and abiotic stresses in plants. *Ecotoxicol. Environ. Saf* 147, 881–896. doi: 10.1016/j.ecoenv.2017.09.063

Etesami, H., and Jeong, B. R. (2020). Importance of silicon in fruit nutrition: agronomic and physiological implications. *Fruit Crops* 2020, 255–277. doi: 10.1016/b978-0-12-818732-6.00019-8

Etesami, H., and Maheshwari, D. K. (2018). Use of plant growth promoting rhizobacteria (PGPRs) with multiple plant growth promoting traits in stress agriculture: action mechanisms and future prospects. *Ecotoxicol. Environ. Saf.* 156, 225–246. doi: 10.1016/j.ecoenv.2018.03.013

Etesami, H., and Noori, F. (2019). "Soil salinity as a challenge for sustainable agriculture and bacterial-mediated alleviation of salinity stress in crop plants," in *Saline Soil-based Agriculture by Halotolerant Microorganisms*. (eds) M. Kumar, H. Etesami, V. Kumar (Singapore: Springer).

Etesami, H., Hosseini, H. M., Alikhani, H. A., and Mohammadi, L. (2014). Bacterial biosynthesis of 1-aminocyclopropane-1-carboxylate (ACC) deaminase and indole-3-acetic acid (IAA) as endophytic preferential selection traits by rice plant seedlings. *J. Plant Growth Regulat.* 33, 654–670. doi: 10.1007/s00344-014-9415-3

Etesami, H., Jeong, B. R., and Rizwan, M. (2020). The use of silicon in stressed agriculture management: action mechanisms and future prospects. *Metalloids Plants: Adv. Future Prospects*, 381–431. doi: 10.1002/9781119487210.ch19

Ezawa, T., and Saito, K. (2018). How do arbuscular mycorrhizal fungi handle phosphate? new insight into fine-tuning of phosphate metabolism. *New Phytol.* 220, 1116–1121.

Fang, Z., Shao, C., Meng, Y., Wu, P., and Chen, M. (2009). Phosphate signaling in *Arabidopsis* and *Oryza sativa*. *Plant Sci.* 176, 170–180.

Farhat, M. B., Farhat, A., Bejar, W., Kammoun, R., Bouchaala, K., Fourati, A., et al. (2009). Characterization of the mineral phosphate solubilizing activity of *Serratia marcescens* CTM 50650 isolated from the phosphate mine of Gafsa. *Arch. Microbiol.* 191, 815–824. doi: 10.1007/s00203-009-0513-8

Feng, G., Song, Y. C., Li, X. L., and Christie, P. (2003). Contribution of arbuscular mycorrhizal fungi to utilization of organic sources of phosphorus by red clover in a calcareous soil. *Appl. Soil Ecol.* 22, 139–148. doi: 10.1016/s0929-1393(02)00133-6

Fiorilli, V., Lanfranco, L., and Bonfante, P. (2013). The expression of GintPT, the phosphate transporter of *Rhizophagus irregularis*, depends on the symbiotic status and phosphate availability. *Planta* 237, 1267–1277. doi: 10.1007/s00425-013-1842-z

Foo, E., Mcadam, E. L., Weller, J. L., and Reid, J. B. (2016). Interactions between ethylene, gibberellins, and brassinosteroids in the development of rhizobial and mycorrhizal symbioses of pea. *J. Exp. Bot.* 67, 2413–2424. doi: 10.1093/jxb/erw047

Foo, E., Ross, J. J., Jones, W. T., and Reid, J. B. (2013). Plant hormones in arbuscular mycorrhizal symbioses: an emerging role for gibberellins. *Ann. Bot.* 111, 769–779. doi: 10.1093/aob/mct041

Frew, A., Powell, J. R., Allsopp, P. G., Sallam, N., and Johnson, S. N. (2017). Arbuscular mycorrhizal fungi promote silicon accumulation in plant roots, reducing the impacts of root herbivory. *Plant Soil* 419, 423–433. doi: 10.1007/s11104-017-3357-z

Frey-Klett, P., Garbaye, J.A., and Tarkka, M. (2007). The mycorrhiza helper bacteria revisited. *New Phytol.* 176, 22–36. doi: 10.1111/j.1469-8137.2007.02191.x

Gahan, J., and Schmalenberger, A. (2015). Arbuscular mycorrhizal hyphae in grassland select for a diverse and abundant hyphospheric bacterial community involved in sulfonate desulfurization. *Appl. Soil Ecol.* 89, 113–121. doi: 10.1016/j.apsoil.2014.12.008

Gamalero, E., Berta, G., Massa, N., Glick, B. R., and Lingua, G. (2008). Synergistic interactions between the ACC deaminase-producing bacterium *Pseudomonas putida* UW4 and the AM fungus *Gigaspora rosea* positively affect cucumber plant growth. *FEMS Microbiol. Ecol.* 64, 459–467. doi: 10.1111/j.1574-6941.2008.00485.x

Gamalero, E., Lingua, G., Berta, G., and Glick, B. R. (2009). Beneficial role of plant growth promoting bacteria and arbuscular mycorrhizal fungi on plant responses to heavy metal stress. *Can. J. Microbiol.* 55, 501–514. doi: 10.1139/w09-010

Garg, N., and Bhandari, P. (2016a). Interactive effects of silicon and arbuscular mycorrhiza in modulating ascorbate-glutathione cycle and antioxidant scavenging capacity in differentially salt-tolerant *Cicer arietinum* L. genotypes subjected to long-term salinity. *Protoplasma* 253, 1325–1345. doi: 10.1007/s00709-015-0892-4

Garg, N., and Bhandari, P. (2016b). Silicon nutrition and mycorrhizal inoculations improve growth, nutrient status, K+/Na+ ratio and yield of *Cicer arietinum* L. genotypes under salinity stress. *Plant Growth Regulat.* 78, 371–387. doi: 10.1007/s10725-015-0099-x

Garg, N., and Pandey, R. (2015). Effectiveness of native and exotic arbuscular mycorrhizal fungi on nutrient uptake and ion homeostasis in salt-stressed *Cajanus cajan* L.(Millsp.) genotypes. *Mycorrhiza* 25, 165–180. doi: 10.1007/s00572-014-0600-9

Garg, N., and Singh, S. (2018). Arbuscular mycorrhiza rhizophagus irregularis and silicon modulate growth, proline biosynthesis and yield in *Cajanus cajan* L. Millsp. (pigeonpea) genotypes under cadmium and zinc stress. *J. Plant Growth Regulat.* 37, 46–63. doi: 10.1007/s00344-017-9708-4

Garg, N., and Singla, P. (2015). Naringenin-and Funneliformis mosseae-mediated alterations in redox state synchronize antioxidant network to alleviate oxidative stress in *Cicer arietinum* L. genotypes under salt stress. *J. Plant Growth Regulat.* 34, 595–610. doi: 10.1007/s00344-015-9494-9

Gaume, A., Mächler, F., De León, C., Narro, L., and Frossard, E. (2001). Low-P tolerance by maize (*Zea mays* L.) genotypes: significance of root growth, and organic acids and acid phosphatase root exudation. *Plant Soil* 228, 253–264.

Gaur, A. C. (2003). "Microbial mineral phosphate solubilization-an over view," in *National Symposium On Mineral Phosphate Solubilization*, Vol. 1, 1–3.

Gaxiola, R. A., Edwards, M., and Elser, J. J. (2011). A transgenic approach to enhance phosphorus use efficiency in crops as part of a comprehensive strategy for sustainable agriculture. *Chemosphere* 84, 840–845. doi: 10.1016/j.chemosphere.2011.01.062

Gbongue, L. -R., Lalaymia, I., Zeze, A., Delvaux, B., and Declerck, S. (2019). Increased silicon acquisition in bananas colonized by *Rhizophagus irregularis* MUCL 41833 reduces the incidence of *Pseudocercospora fijiensis*. *Front. Plant Sci.* 9:1977. doi: 10.3389/fpls.2018.01977

Gerke, J., Beißner, L., and Römer, W. (2000). The quantitative effect of chemical phosphate mobilization by carboxylate anions on P uptake by a single root. I. the basic concept and determination of soil parameters. *J. Plant Nutrition Soil Sci.* 163, 207–212. doi: 10.1002/(sici)1522-2624(200004)163:2<207::aid-jpln207>3.0.co;2-p

Ghorchiani, M., Etesami, H., and Alikhani, H. A. (2018). Improvement of growth and yield of maize under water stress by co-inoculating an arbuscular mycorrhizal fungus and a plant growth promoting rhizobacterium together with phosphate fertilizers. *Agricul. Ecosystems Environ.* 258, 59–70. doi: 10.1016/j.agee.2018.02.016

Gianinazzi-Pearson, V. (1996). Plant cell responses to arbuscular mycorrhizal fungi: getting to the roots of the symbiosis. *Plant Cell* 8:1871. doi: 10.2307/3870236

Gill, M. A., and Ahmad, Z. (2003). Inter-varietal differences of absorbed-phosphorus utilization in cotton exposed to P-free nutrition: part II. P-absorption and remobilization in plant. *Pakistan J. Sci. Res. (Pakistan)* 55, 10–14

Gilroy, S., and Jones, D. L. (2000). Through form to function: root hair development and nutrient uptake. *Trends Plant Sci.* 5, 56–60. doi: 10.1016/s1360-1385(99)01551-4

Gladkova, K. F. (1982). The role of silicon in phosphate plant nutrition. *Agrochemistry* 2:133.

Glick, B. R. (2012). Plant growth-promoting bacteria: mechanisms and applications. *Scientifica* 2012:963401.

Glick, B. R., Cheng, Z., Czarny, J., and Duan, J. (2007). Promotion of plant growth by ACC deaminase-producing soil bacteria. *Eur. J. Plant Pathol.* 119, 329–339. doi: 10.1007/978-1-4020-6776-1_8

Goldstein, A. H. (2007). "Future trends in research on microbial phosphate solubilization: one hundred years of insolubility", in: *First International Meeting on Microbial Phosphate Solubilization* eds E. Velázquez, C. Rodríguez-Barrueco (Dordrecht: Springer), 91–96. doi: 10.1007/978-1-4020-5765-6_11

Gomez-Ariza, J., Balestrini, R., Novero, M., and Bonfante, P. (2009). Cell-specific gene expression of phosphate transporters in mycorrhizal tomato roots. *Biol. Fertility Soils* 45, 845–853. doi: 10.1007/s00374-009-0399-2

Gonzàlez-Meler, M. A., Giles, L., Thomas, R. B., and Siedow, J. N. (2001). Metabolic regulation of leaf respiration and alternative pathway activity in response to phosphate supply. *Plant Cell Environ.* 24, 205–215. doi: 10.1111/j.1365-3040.2001.00674.x

Gorbushina, A. A., and Broughton, W. J. (2009). Microbiology of the atmosphere-rock interface: how biological interactions and physical stresses modulate a sophisticated microbial ecosystem. *Annu. Rev. Microbiol.* 63, 431–450. doi: 10.1146/annurev.micro.091208.073349

Gordienko, A. S., and Kurdish, I. K. (2007). Surface electrical properties of *Bacillus subtilis* cells and the effect of interaction with silicon dioxide particles. *Biophysics* 52, 217–219. doi: 10.1134/s0006350907020121

Greger, M., Landberg, T., and Vaculík, M. (2018). Silicon influences soil availability and accumulation of mineral nutrients in various plant species. *Plants* 7:41. doi: 10.3390/plants7020041

Grierson, P. F. (1992). Organic acids in the rhizosphere of Banksia integrifolia Lf. *Plant Soil* 144, 259–265. doi: 10.1007/bf00012883

Gu, J. -Y., Zang, S. -G., Sheng, X. -F., He, L. -Y., Huang, Z., and Wang, Q. (2015). Burkholderia susongensis sp. nov., a mineral-weathering bacterium isolated from weathered rock surface. *Int. J. Systematic Evol. Microbiol.* 65, 1031–1037. doi: 10.1099/ijs.0.000059

Gu, M., Chen, A., Sun, S., and Xu, G. (2016). Complex regulation of plant phosphate transporters and the gap between molecular mechanisms and practical application: what is missing? *Mol. Plant* 9, 396–416. doi: 10.1016/j.molp.2015.12.012

Guidry, M. W., and Mackenzie, F. T. (2003). Experimental study of igneous and sedimentary apatite dissolution: control of pH, distance from equilibrium, and temperature on dissolution rates. *Geochimica et Cosmochimica Acta* 67, 2949–2963. doi: 10.1016/s0016-7037(03)00265-5

Guntzer, F., Keller, C., and Meunier, J. -D. (2012). Benefits of plant silicon for crops: a review. *Agronomy Sustainable Dev.* 32, 201–213. doi: 10.1007/s13593-011-0039-8

Gutjahr, C. (2014). Phytohormone signaling in arbuscular mycorhiza development. *Curr. Opin. Plant Biol.* 20, 26–34. doi: 10.1016/j.pbi.2014.04.003

Gyaneshwar, P., Kumar, G. N., Parekh, L. J., and Poole, P. S. (2002). Role of soil microorganisms in improving P nutrition of plants. *Plant Soil* 245, 83–93.

Hajiboland, R. (2012). "Effect of micronutrient deficiencies on plants stress responses," in *Abiotic Stress Responses in Plants*. eds P. Ahmad, M. Prasad (New York, NY: Springer), 283–329. doi: 10.1007/978-1-4614-0634-1_16

Hajiboland, R., Bahrami-Rad, S., and Poschenrieder, C. (2017). Silicon modifies both a local response and a systemic response to mechanical stress in tobacco leaves. *Biol. Plantarum* 61, 187–191. doi: 10.1007/s10535-016-0633-3

Hajiboland, R., Moradtalab, N., Aliasgharzad, N., Eshaghi, Z., and Feizy, J. (2018). Silicon influences growth and mycorrhizal responsiveness in strawberry plants. *Physiol. Mol. Biol. Plants* 24, 1103–1115. doi: 10.1007/s12298-018-0533-4

Hamayun, M., Khan, S. A., Khan, A. L., Rehman, G., Kim, Y. -H., Iqbal, I., et al. (2010). Gibberellin production and plant growth promotion from pure cultures of *Cladosporium sp*. MH-6 isolated from cucumber (*Cucumis sativus* L.). *Mycologia* 102, 989–995. doi: 10.3852/09-261

Hamdali, H., Bouizgarne, B., Hafidi, M., Lebrihi, A., Virolle, M. J., and Ouhdouch, Y. (2008). Screening for rock phosphate solubilizing actinomycetes from moroccan phosphate mines. *Appl. Soil Ecol.* 38, 12–19. doi: 10.1016/j.apsoil.2007.08.007

Hameeda, B., Reddy, Y. H. K., Rupela, O. P., Kumar, G. N., and Reddy, G. (2006). Effect of carbon substrates on rock phosphate solubilization by bacteria from composts and macrofauna. *Curr. Microbiol.* 53, 298–302. doi: 10.1007/s00284-006-0004-y

Hammer, E. C., Nasr, H., Pallon, J., Olsson, P. A., and Wallander, H. (2011). Elemental composition of arbuscular mycorrhizal fungi at high salinity. *Mycorrhiza* 21, 117–129. doi: 10.1007/s00572-010-0316-4

Hassan, S., and Mathesius, U. (2012). The role of flavonoids in root–rhizosphere signalling: opportunities and challenges for improving plant–microbe interactions. *J. Exp. Bot.* 63, 3429–3444. doi: 10.1093/jxb/err430

Hause, B., and Fester, T. (2005). Molecular and cell biology of arbuscular mycorrhizal symbiosis. *Planta* 221, 184–196. doi: 10.1007/s00425-004-1436-x

Hayat, R., Ali, S., Amara, U., Khalid, R., and Ahmed, I. (2010). Soil beneficial bacteria and their role in plant growth promotion: a review. *Annals Microbiol.* 60, 579–598. doi: 10.1007/s13213-010-0117-1

Haynes, R. J. (2014). A contemporary overview of silicon availability in agricultural soils. *J. Plant Nutrition Soil Sci.* 177, 831–844. doi: 10.1002/jpln.201400202

He, L. Y., Zhang, Y. F., Ma, H. Y., Chen, Z. J., Wang, Q. Y., Qian, M., et al. (2010). Characterization of copper-resistant bacteria and assessment of bacterial communities in rhizosphere soils of copper-tolerant plants. *Appl. Soil Ecol.* 44, 49–55. doi: 10.1016/j.apsoil.2009.09.004

Herman, D. J., Firestone, M. K., Nuccio, E., and Hodge, A. (2012). Interactions between an arbuscular mycorrhizal fungus and a soil microbial community mediating litter decomposition. *FEMS Microbiol. Ecol.* 80, 236–247. doi: 10.1111/j.1574-6941.2011.01292.x

Herrera-Medina, M. J., Steinkellner, S., Vierheilig, H., Ocampo Bote, J. A., and García Garrido, J. M. (2007). Abscisic acid determines arbuscule development and functionality in the tomato arbuscular mycorrhiza. *New Phytol.* 175, 554–564. doi: 10.1111/j.1469-8137.2007.02107.x

Heuck, C., Weig, A., and Spohn, M. (2015). Soil microbial biomass C: N: P stoichiometry and microbial use of organic phosphorus. *Soil Biol. Biochem.* 85, 119–129. doi: 10.1016/j.soilbio.2015.02.029

Hildebrandt, U., Janetta, K., and Bothe, H. (2002). Towards growth of arbuscular mycorrhizal fungi independent of a plant host. *Appl. Environ. Microbiol.* 68, 1919–1924. doi: 10.1128/aem.68.4.1919-1924.2002

Hingston, F. (1972). The role of the proton in determining adsorption envelopes. *J. Soil Sci.* 23, 175–191.

Hinsinger, P. (2001). Bioavailability of soil inorganic P in the rhizosphere as affected by root-induced chemical changes: a review. *Plant Soil* 237, 173–195.

Hodge, A. (2014). Interactions between arbuscular mycorrhizal fungi and organic material substrates. *Adv. Appl. Microbiol.* 89, 47–99. doi: 10.1016/b978-0-12-800259-9.00002-0

Hodge, A., and Fitter, A. H. (2010). Substantial nitrogen acquisition by arbuscular mycorrhizal fungi from organic material has implications for N cycling. *Proc. Natl. Acad. Sci. U S A.* 107, 13754–13759. doi: 10.1073/pnas.1005874107

Hodge, A., Berta, G., Doussan, C., Merchan, F., and Crespi, M. (2009). Plant root growth, architecture and function. *Plant Soil* 321, 153–187. doi: 10.1007/s11104-009-9929-9

Hodge, A., Campbell, C. D., and Fitter, A. H. (2001). An arbuscular mycorrhizal fungus accelerates decomposition and acquires nitrogen directly from organic material. *Nature* 413, 297–299. doi: 10.1038/35095041

Holford, I. C. R. (1997). Soil phosphorus: its measurement, and its uptake by plants. *Soil Res.* 35, 227–240. doi: 10.1071/s96047

Hooker, J. E., Piatti, P., Cheshire, M. V., and Watson, C. A. (2007). Polysaccharides and monosaccharides in the hyphosphere of the arbuscular mycorrhizal fungi Glomus E3 and Glomus tenue. *Soil Biol. Biochem.* 39, 680–683. doi: 10.1016/j.soilbio.2006.08.006

Hordiienko, A. S., Samchuk, A. I., and Kurdysh, I. K. (2010). Influence of silicon dioxide and saponite on growth of *Bacillus subtilis* IMV B-7023. *Mikrobiolohichnyi Zhurnal* 72, 33–39.

Huang, Z., He, L., Sheng, X., and He, Z. (2013). Weathering of potash feldspar by *Bacillus sp*. L11. *Wei sheng wu xue bao* 53, 1172–1178.

Hutchens, E., Valsami-Jones, E., Mceldowney, S., Gaze, W., and Mclean, J. (2003). The role of heterotrophic bacteria in feldspar dissolution–an experimental approach. *Mineral. Magazine* 67, 1157–1170. doi: 10.1180/0026461036760155

Iffis, B., St-Arnaud, M., and Hijri, M. (2016). Petroleum hydrocarbon contamination, plant identity and arbuscular mycorrhizal fungal (AMF) community determine assemblages of the AMF spore-associated microbes. *Environ. Microbiol.* 18, 2689–2704. doi: 10.1111/1462-2920.13438

Illmer, P., Barbato, A., and Schinner, F. (1995). Solubilization of hardly-soluble AlPO 4 with P-solubilizing microorganisms. *Soil Biol. Biochem.* 27, 265–270. doi: 10.1016/0038-0717(94)00205-f

Iqbal, M. A., Khalid, M., Shahzad, S. M., Ahmad, M., Soleman, N., and Akhtar, N. (2012). Integrated use of Rhizobium leguminosarum, plant growth promoting rhizobacteria and enriched compost for improving growth, nodulation and yield of lentil (*Lens culinaris* Medik.). *Chilean J. Agricul. Res.* 72:104. doi: 10.4067/s0718-58392012000100017

Jäderlund, L., Arthurson, V., Granhall, U., and Jansson, J. K. (2008). Specific interactions between arbuscular mycorrhizal fungi and plant growth-promoting bacteria: as revealed by different combinations. *FEMS Microbiol. Lett.* 287, 174–180. doi: 10.1111/j.1574-6968.2008.01318.x

Jakobsen, I., Abbott, L. K., and Robson, A. D. (1992). External hyphae of vesicular-arbuscular mycorrhizal fungi associated with *Trifolium subterraneum* L. 1. spread of hyphae and phosphorus inflow into roots. *New Phytol.* 120, 371–380. doi: 10.1111/j.1469-8137.1992.tb01077.x

Jakobsen, I., Gazey, C., and Abbott, L. K. (2001). Phosphate transport by communities of arbuscular mycorrhizal fungi in intact soil cores. *New Phytol.* 149, 95–103. doi: 10.1046/j.1469-8137.2001.00006.x

James, E. K., Gyaneshwar, P., Mathan, N., Barraquio, W. L., Reddy, P. M., Iannetta, P. P. M., et al. (2002)). Infection and colonization of rice seedlings by the plant growth-promoting bacterium *Herbaspirillum seropedicae* Z 67. *Mol. Plant Microbiol. Interact* 15, 894–906. doi: 10.1094/mpmi.2002.15.9.894

Janos, D. P. (2007). Plant responsiveness to mycorrhizas differs from dependence upon mycorrhizas. *Mycorrhiza* 17, 75–91. doi: 10.1007/s00572-006-0094-1

Jansa, J., Bukovská, P., and Gryndler, M. (2013). Mycorrhizal hyphae as ecological niche for highly specialized hypersymbionts – or just soil free-riders? *Front. Plant Sci.* 4:134. doi: 10.3389/fpls.2013.00134

Jansa, J., Finlay, R., Wallander, H., Smith, F. A., and Smith, S. E. (2011). "Role of mycorrhizal symbioses in phosphorus cycling," in *Phosphorus in Action*. eds E. Bünemann, A. Oberson, and E. Frossard (Berlin: Springer), 137–168. doi: 10.1007/978-3-642-15271-9_6

Jeffries, P., Gianinazzi, S., Perotto, S., Turnau, K., and Barea, J. -M. (2003). The contribution of arbuscular mycorrhizal fungi in sustainable maintenance of plant health and soil fertility. *Biol. Fertility Soils* 37, 1–16. doi: 10.1007/s00374-002-0546-5

Jia, H., Ren, H., Gu, M., Zhao, J., Sun, S., Zhang, X., et al. (2011). The phosphate transporter gene OsPht1; 8 is involved in phosphate homeostasis in rice. *Plant Physiol.* 156, 1164–1175. doi: 10.1104/pp.111.175240

Jianfeng, M. A., and Takahashi, E. (1991). Effect of silicate on phosphate availability for rice in a P-deficient soil. *Plant Soil* 133, 151–155. doi: 10.1007/bf00009187

Johansson, J. F., Paul, L. R., and Finlay, R. D. (2004). Microbial interactions in the mycorrhizosphere and their significance for sustainable agriculture. *FEMS Microbiol. Ecol.* 48, 1–13. doi: 10.1016/j.femsec.2003.11.012

Johnson, S. E., and Loeppert, R. H. (2006). Role of organic acids in phosphate mobilization from iron oxide. *Soil Sci. Soc. Am. J.* 70, 222–234. doi: 10.2136/sssaj2005.0012

Johri, A. K., Oelmüller, R., Dua, M., Yadav, V., Kumar, M., Tuteja, N., et al. (2015). Fungal association and utilization of phosphate by plants: success, limitations, and future prospects. *Front. Microbiol.* 6:984. doi: 10.3389/fmicb.2015.00984

Joner, E. J., and Jakobsen, I. (1995). Growth and extracellular phosphatase activity of arbuscular mycorrhizal hyphae as influenced by soil organic matter. *Soil Biol. Biochem.* 27, 1153–1159. doi: 10.1016/0038-0717(95)00047-i

Joner, E. J., Van Aarle, I. M., and Vosatka, M. (2000). Phosphatase activity of extra-radical arbuscular mycorrhizal hyphae: a review. *Plant Soil* 226, 199–210.

Jones, D. L., and Oburger, E. (2011). "Solubilization of phosphorus by soil microorganisms," in *Phosphorus in Action*. Eds E. K. Bunemann, A. Oberson, E. Frossard (Berlin: Springer), 169–198. doi: 10.1007/978-3-642-15271-9_7

Jones, D., Dennis, P., Owen, A., and Van Hees, P. (2003). Organic acid behavior in soils–misconceptions and knowledge gaps. *Plant Soil* 248, 31–41. doi: 10.1007/978-94-010-0243-1_3

Jongmans, A. G., Van Breemen, N., Lundström, U., Van Hees, P. A. W., Finlay, R. D., Srinivasan, M., et al. (1997). Rock-eating fungi. *Nature* 389, 682–683.

Jorquera, M. A., Hernández, M. T., Rengel, Z., Marschner, P., and De La Luz Mora, M. (2008). Isolation of culturable phosphobacteria with both phytate-mineralization and phosphate-solubilization activity from the rhizosphere of plants grown in a volcanic soil. *Biol. Fertility Soils* 44:1025. doi: 10.1007/s00374-008-0288-0

Kaiser, C., Kilburn, M. R., Clode, P. L., Fuchslueger, L., Koranda, M., Cliff, J. B., et al. (2015). Exploring the transfer of recent plant photosynthates to soil microbes: mycorrhizal pathway vs direct root exudation. *New Phytol.* 205, 1537–1551. doi: 10.1111/nph.13138

Kaldorf, M., and Ludwig-Müller, J. (2000). AM fungi might affect the root morphology of maize by increasing indole-3-butyric acid biosynthesis. *Physiol. Plant* 109, 58–67. doi: 10.1034/j.1399-3054.2000.100109.x

Kalinowski, B. E., Liermann, L. J., Brantley, S. L., Barnes, A., and Pantano, C. G. (2000). X-ray photoelectron evidence for bacteria-enhanced dissolution of hornblende. *Geochim. Cosmochimica Acta* 64, 1331–1343. doi: 10.1016/s0016-7037(99)00371-3

Kang, S. -M., Khan, A. L., Hamayun, M., Hussain, J., Joo, G. -J., You, Y. -H., et al. (2012). Gibberellin-producing Promicromonospora sp. SE188 improves *Solanum lycopersicum* plant growth and influences endogenous plant hormones. *J. Microbiol.* 50, 902–909. doi: 10.1007/s12275-012-2273-4

Kang, S. -M., Waqas, M., Shahzad, R., You, Y. -H., Asaf, S., Khan, M. A., et al. (2017). Isolation and characterization of a novel silicate-solubilizing bacterial strain Burkholderia eburnea CS4-2 that promotes growth of japonica rice (*Oryza sativa* L. cv. Dongjin). *Soil Sci. Plant Nutrition* 63, 233–241.

Karimzadeh, J., Alikhani, H. A., Etesami, H., and Pourbabaei, A. A. (2020). Improved phosphorus uptake by wheat plant (*Triticum aestivum* L.) with rhizosphere fluorescent pseudomonads strains under water-deficit stress. *J. Plant Growth Regulation* 40, 162–178 doi: 10.1007/s00344-020-10087-3

Karthikeyan, A. S., Varadarajan, D. K., Mukatira, U. T., D'urzo, M. P., Damsz, B., and Raghothama, K. G. (2002). Regulated expression of *Arabidopsis* phosphate transporters. *Plant Physiol.* 130, 221–233. doi: 10.1104/pp.020007

Karunakaran, G., Suriyaprabha, R., Manivasakan, P., Yuvakkumar, R., Rajendran, V., Prabu, P., et al. (2013). Effect of nanosilica and silicon sources on plant growth promoting rhizobacteria, soil nutrients and maize seed germination. *IET Nanobiotechnol.* 7, 70–77. doi: 10.1049/iet-nbt.2012.0048

Kaufmian, P. B., Bigelow, W. C., Petering, L. B., and Drogosz, F. B. (1969). Silica in developing epidermal cells of Avena internodes: electron microprobe analysis. *Science* 166, 1015–1017. doi: 10.1126/science.166.3908.1015

Khan, M. S., Zaidi, A., and Wani, P. A. (2007). Role of phosphate-solubilizing microorganisms in sustainable agriculture—a review. *Agronomy Sustainable Dev.* 27, 29–43. doi: 10.1051/agro:2006011

Khan, M. S., Zaidi, A., Wani, P. A., and Oves, M. (2009). Role of plant growth promoting rhizobacteria in the remediation of metal contaminated soils. *Environ. Chem. Lett.* 7, 1–19. doi: 10.1007/s10311-008-0155-0

Kihara, T., Wada, T., Suzuki, Y., Hara, T., and Koyama, H. (2003). Alteration of citrate metabolism in cluster roots of white lupin. *Plant Cell Physiol.* 44, 901–908. doi: 10.1093/pcp/pcg115

Kim, K. Y., Jordan, D., and Mcdonald, G. A. (1997). Effect of phosphate-solubilizing bacteria and vesicular-arbuscular mycorrhizae on tomato growth and soil microbial activity. *Biol. Fertility Soils* 26, 79–87. doi: 10.1007/s003740050347

Kim, Y. H., Khan, A. L., Waqas, M., Shim, J. K., Kim, D. H., Lee, K. Y., et al. (2014). Silicon application to rice root zone influenced the phytohormonal and antioxidant responses under salinity stress. *J. Plant Growth Regulation* 33, 137–149. doi: 10.1007/s00344-013-9356-2

Klotzbücher, T., Marxen, A., Vetterlein, D., Schneiker, J., Türke, M., Van Sinh, N., et al. (2015). Plant-available silicon in paddy soils as a key factor for sustainable rice production in Southeast Asia. *Basic Appl. Ecol.* 16, 665–673. doi: 10.1016/j.baae.2014.08.002

Klugh, K. R., and Cumming, J. R. (2007). Variations in organic acid exudation and aluminum resistance among arbuscular mycorrhizal species colonizing *Liriodendron tulipifera*. *Tree Physiol.* 27, 1103–1112. doi: 10.1093/treephys/27.8.1103

Klugh-Stewart, K., and Cumming, J. R. (2009). Organic acid exudation by mycorrhizal *Andropogon virginicus* L.(broomsedge) roots in response to aluminum. *Soil Biol. Biochem.* 41, 367–373. doi: 10.1016/j.soilbio.2008.11.013

Koide, R. T., and Kabir, Z. (2000). Extraradical hyphae of the mycorrhizal fungus Glomus intraradices can hydrolyse organic phosphate. *New Phytol.* 148, 511–517. doi: 10.1046/j.1469-8137.2000.00776.x

Konhauser, K. O., Lalonde, S. V., Amskold, L., and Holland, H. D. (2007). Was there really an archean phosphate crisis? *Science* 315, 1234–1234. doi: 10.1126/science.1136328

Koski-Vähälä, J., Hartikainen, H., and Tallberg, P. (2001). Phosphorus mobilization from various sediment pools in response to increased pH and silicate concentration. *J. Environ. Qual.* 30, 546–552. doi: 10.2134/jeq2001.302546x

Kostic, L., Nikolic, N., Bosnic, D., Samardzic, J., and Nikolic, M. (2017). Silicon increases phosphorus (P) uptake by wheat under low P acid soil conditions. *Plant Soil* 419, 447–455. doi: 10.1007/s11104-017-3364-0

Kostic, L., Nikolic, N., Samardzic, J., Milisavljevic, M., Maksimović, V., Cakmak, D., et al. (2015). Liming of anthropogenically acidified soil promotes phosphorus acquisition in the rhizosphere of wheat. *Biol. Fertility Soils* 51, 289–298. doi: 10.1007/s00374-014-0975-y

Kothari, S. K., Marschner, H., and Römheld, V. (1990). Direct and indirect effects of VA mycorrhizal fungi and rhizosphere microorganisms on acquisition of mineral nutrients by maize (*Zea mays* L.) in a calcareous soil. *New Phytol.* 116, 637–645. doi: 10.1111/j.1469-8137.1990.tb00549.x

Kutuzova, R. S. (1969). Release of silica from minerals as a result of microbial activity. *Mikrobiologiya* 38, 596–602.

Lambers, H., and Plaxton, W. C. (2015). Phosphorus: back to the roots. *Annual Plant Rev.* 48, 3–22.

Lambers, H., Brundrett, M. C., Raven, J. A., Hopper, S. D. (2010). Plant mineral nutrition in ancient landscapes: high plant species diversity on infertile soils is linked to functional diversity for nutritional strategies. *Plant Soil* 334, 11–31. doi: 10.1007/s11104-010-0444-9

Lambers, H., Shane, M. W., Cramer, M. D., Pearse, S. J., and Veneklaas, E. J. (2006). Root structure and functioning for efficient acquisition of phosphorus: matching morphological and physiological traits. *Ann. Bot.* 98, 693–713. doi: 10.1093/aob/mcl114

Lambrecht, M., Okon, Y., Broek, A. V., and Vanderleyden, J. (2000). Indole-3-acetic acid: a reciprocal signalling molecule in bacteria–plant interactions. *Trends Microbiol.* 8, 298–300. doi: 10.1016/s0966-842x(00)01732-7

Lapanje, A., Wimmersberger, C., Furrer, G., Brunner, I., and Frey, B. (2012). Pattern of elemental release during the granite dissolution can be changed by aerobic heterotrophic bacterial strains isolated from Damma Glacier (central Alps) deglaciated granite sand. *Microb. Ecol.* 63, 865–882. doi: 10.1007/s00248-011-9976-7

Lecomte, J., St-Arnaud, M., and Hijri, M. (2011). Isolation and identification of soil bacteria growing at the expense of arbuscular mycorrhizal fungi. *FEMS Microbiol. Lett.* 317, 43–51. doi: 10.1111/j.1574-6968.2011.02209.x

Lee, K. -E., Adhikari, A., Kang, S. -M., You, Y. -H., Joo, G. -J., Kim, J. -H., et al. (2019). Isolation and characterization of the high silicate and phosphate solubilizing novel strain *Enterobacter ludwigii* GAK2 that promotes growth in rice plants. *Agronomy* 9:144. doi: 10.3390/agronomy9030144

Lee, Y., Krishnamoorthy, R., Selvakumar, G., Kim, K., and Sa, T. (2015). Alleviation of salt stress in maize plant by co-inoculation of arbuscular mycorrhizal fungi and *Methylobacterium oryzae* CBMB20. *J. Korean Soc. Appl. Biol. Chem.* 58, 533–540. doi: 10.1007/s13765-015-0072-4

Leggewie, G., Willmitzer, L., and Riesmeier, J. W. (1997). Two cDNAs from potato are able to complement a phosphate uptake-deficient yeast mutant: identification of phosphate transporters from higher plants. *Plant Cell* 9, 381–392. doi: 10.2307/3870489

Leigh, J., Fitter, A. H., and Hodge, A. (2011). Growth and symbiotic effectiveness of an arbuscular mycorrhizal fungus in organic matter in competition with soil bacteria. *FEMS Microbiol. Ecol.* 76, 428–438. doi: 10.1111/j.1574-6941.2011.01066.x

Liao, H., Rubio, G., Yan, X., Cao, A., Brown, K. M., and Lynch, J. P. (2001). Effect of phosphorus availability on basal root shallowness in common bean. *Plant Soil* 232, 69–79. doi: 10.1007/978-94-010-0566-1_7

Lin, Q. -M., Rao, Z. -H., Sun, Y. -X., Yao, J., and Xing, L. -J. (2002). Identification and practical application of silicate-dissolving bacteria. *Agricultural Sci. China* 1, 81–85.

Lin, W. -P., Jiang, N. -H., Peng, L., Fan, X. -Y., Gao, Y., Wang, G. -P., et al. (2020). Silicon impacts on soil microflora under *Ralstonia solanacearum* inoculation. *J. Int. Agricul.* 19, 251–264. doi: 10.1016/s2095-3119(18)62122-7

Linderman, R. G. (1992). Vesicular-arbuscular mycorrhizae and soil microbial interactions. *Mycorrhizae Sustainable Agricul.* 54, 45–70. doi: 10.2134/asaspecpub54.c3

Liu, W., Xu, X., Wu, X., Yang, Q., Luo, Y., and Christie, P. (2006). Decomposition of silicate minerals by Bacillus mucilaginosus in liquid culture. *Environ. Geochem. Health* 28, 133–140. doi: 10.1007/s10653-005-9022-0

López-Bucio, J., Cruz-Ramırez, A., and Herrera-Estrella, L. (2003). The role of nutrient availability in regulating root architecture. *Curr. Opin. Plant Biol.* 6, 280–287. doi: 10.1016/s1369-5266(03)00035-9

Ludwig-Müller, J. (2010). "Hormonal responses in host plants triggered by arbuscular mycorrhizal fungi," in *Arbuscular Mycorrhizas: Physiology and Function*, H. Koltai and Y. Kapulnik (Berlin: Springer), 169–190.

Ludwig-Müller, J., and Güther, M. (2007). Auxins as signals in arbuscular mycorrhiza formation. *Plant Signal. Behav.* 2, 194–196. doi: 10.4161/psb.2.3.4152

Lynch, J. P. (2007). Roots of the second green revolution. *Aus. J. Botany* 55, 493–512. doi: 10.1071/bt06118

Lynch, J. P. (2011). Root phenes for enhanced soil exploration and phosphorus acquisition: tools for future crops. *Plant Physiol.* 156, 1041–1049. doi: 10.1104/pp.111.175414

Ma, J. F. (2004). Role of silicon in enhancing the resistance of plants to biotic and abiotic stresses. *Soil Sci. Plant Nutrition* 50, 11–18. doi: 10.1080/00380768.2004.10408447

Ma, J. F., and Takahashi, E. (2002). *Soil, Fertilizer, and Plant Silicon Research in Japan*. Elsevier: Amsterdam.

Ma, J. F., Tamai, K., Yamaji, N., Mitani, N., Konishi, S., Katsuhara, M., et al. (2006). A silicon transporter in rice. *Nature* 440, 688–691.

Ma, J. F., Yamaji, N., Mitani, N., Tamai, K., Konishi, S., Fujiwara, T., et al. (2007). An efflux transporter of silicon in rice. *Nature* 448, 209–212. doi: 10.1038/nature05964

Ma, J., and Takahashi, E. (1990). Effect of silicon on the growth and phosphorus uptake of rice. *Plant Soil* 126, 115–119. doi: 10.1007/bf00041376

Mäder, P., Kaiser, F., Adholeya, A., Singh, R., Uppal, H. S., Sharma, A. K., et al. (2011). Inoculation of root microorganisms for sustainable wheat–rice and wheat–black gram rotations in India. *Soil Biol. Biochem.* 43, 609–619. doi: 10.1016/j.soilbio.2010.11.031

Malinovskaya, I. M., Kosenko, L. V., Votselko, S. K., and Podgorskii, V. S. (1990). Role of *Bacillus mucilaginosus* polysaccharide in degradation of silicate minerals. *Microbiology* 59, 49–55.

Mandal, S. M., Chakraborty, D., and Dey, S. (2010). Phenolic acids act as signaling molecules in plant-microbe symbioses. *Plant Signal. Behav.* 5, 359–368. doi: 10.4161/psb.5.4.10871

Marschner, H. (1995). *Mineral Nutrition of Higher Plants* 2nd edition. Great Britain: Academic press.

Marschner, H., and Dell, B. (1994). Nutrient uptake in mycorrhizal symbiosis. *Plant Soil* 159, 89–102. doi: 10.1007/bf00000098

Marschner, H., and Rimmington, G. (1988). Mineral nutrition of higher plants. *Plant Cell Environ.* 11, 147–148.

Marschner, P., Crowley, D., and Lieberei, R. (2001). Arbuscular mycorrhizal infection changes the bacterial 16 S rDNA community composition in the rhizosphere of maize. *Mycorrhiza* 11, 297–302. doi: 10.1007/s00572-001-0136-7

Martín-Rodríguez, J. A., Huertas, R., Ho-Plágaro, T., Ocampo, J. A., Turečková, V., Tarkowská, D., et al. (2016). Gibberellin–abscisic acid balances during arbuscular mycorrhiza formation in tomato. *Front. Plant Sci.* 7:1273. doi: 10.3389/fpls.2016.01273

Martín-Rodríguez, J. Á., León-Morcillo, R., Vierheilig, H., Ocampo, J. A., Ludwig-Müller, J., and García-Garrido, J. M. (2011). Ethylene-dependent/ethylene-independent ABA regulation of tomato plants colonized by arbuscular mycorrhiza fungi. *New Phytol.* 190, 193–205. doi: 10.1111/j.1469-8137.2010.03610.x

Martín-Rodríguez, J. Á., Ocampo, J. A., Molinero-Rosales, N., Tarkowská, D., Ruíz-Rivero, O., and García-Garrido, J. M. (2015). Role of gibberellins during arbuscular mycorrhizal formation in tomato: new insights revealed by endogenous quantification and genetic analysis of their metabolism in mycorrhizal roots. *Physiol. Plant.* 154, 66–81. doi: 10.1111/ppl.12274

McGuiness, P. N., Reid, J. B., and Foo, E. (2019). The role of gibberellins and brassinosteroids in nodulation and arbuscular mycorrhizal associations. *Front. Plant Sci.* 10:269. doi: 10.3389/fpls.2019.00269

Meding, S. M., and Zasoski, R. J. (2008). Hyphal-mediated transfer of nitrate, arsenic, cesium, rubidium, and strontium between arbuscular mycorrhizal forbs and grasses from a California oak woodland. *Soil Biol. Biochem.* 40, 126–134. doi: 10.1016/j.soilbio.2007.07.019

Meena, V. D., Dotaniya, M. L., Coumar, V., Rajendiran, S., Kundu, S., and Rao, A. S. (2014). A case for silicon fertilization to improve crop yields in tropical soils. *Proc. Natl. Acad. Sci. U S A. India Section B: Biol. Sci.* 84, 505–518. doi: 10.1007/s40011-013-0270-y

Meharg, C., and Meharg, A. A. (2015). Silicon, the silver bullet for mitigating biotic and abiotic stress, and improving grain quality, in rice? *Environ. Exp. Botany* 120, 8–17. doi: 10.1016/j.envexpbot.2015.07.001

Menezes-Blackburn, D., Jorquera, M. A., Gianfreda, L., Greiner, R., and De La Luz Mora, M. (2014). A novel phosphorus biofertilization strategy using cattle manure treated with phytase–nanoclay complexes. *Biol. Fertility Soils* 50, 583–592.

Miao, J., Sun, J., Liu, D., Li, B., Zhang, A., Li, Z., et al. (2009). Characterization of the promoter of phosphate transporter TaPHT1. 2 differentially expressed in wheat varieties. *J. Genet. Genom.* 36, 455–466. doi: 10.1016/s1673-8527(08)60135-6

Miransari, M. (2010). Contribution of arbuscular mycorrhizal symbiosis to plant growth under different types of soil stress. *Plant Biol.* 12, 563–569.

Misra, N., Gupta, G., and Jha, P. N. (2012). Assessment of mineral phosphate-solubilizing properties and molecular characterization of zinc-tolerant bacteria. *J. Basic Microbiol.* 52, 549–558. doi: 10.1002/jobm.201100257

Mitani, N., and Ma, J. F. (2005). Uptake system of silicon in different plant species. *J. Exp. Bot.* 56, 1255–1261. doi: 10.1093/jxb/eri121

Mitani-Ueno, N., Yamaji, N., and Ma, J. F. (2011). Silicon efflux transporters isolated from two pumpkin cultivars contrasting in Si uptake. *Plant Signal. Behav.* 6, 991–994. doi: 10.4161/psb.6.7.15462

Mohamed, A. A., Eweda, W. E. E., Heggo, A. M., and Hassan, E. A. (2014). Effect of dual inoculation with arbuscular mycorrhizal fungi and sulphur-oxidising bacteria on onion (*Allium cepa* L.) and maize (*Zea mays* L.) grown in sandy soil under green house conditions. *Annals Agricul. Sci.* 59, 109–118. doi: 10.1016/j.aoas.2014.06.015

Mohammad, A., and Mittra, B. (2013). Effects of inoculation with stress-adapted arbuscular mycorrhizal fungus Glomus deserticola on growth of *Solanum melogena* L. and *Sorghum sudanese* Staph. seedlings under salinity and heavy metal stress conditions. *Arch. Agronomy Soil Sci.* 59, 173–183. doi: 10.1080/03650340.2011.610029

Montpetit, J., Vivancos, J., Mitani-Ueno, N., Yamaji, N., Rémus-Borel, W., Belzile, F., et al. (2012). Cloning, functional characterization and heterologous expression of TaLsi1, a wheat silicon transporter gene. *Plant Mol. Biol.* 79, 35–46. doi: 10.1007/s11103-012-9892-3

Moradtalab, N., Hajiboland, R., Aliasgharzad, N., Hartmann, T. E., and Neumann, G. (2019). Silicon and the association with an arbuscular-mycorrhizal fungus (*Rhizophagus clarus*) mitigate the adverse effects of drought stress on strawberry. *Agronomy* 9:41. doi: 10.3390/agronomy9010041

Nadeem, S. M., Ahmad, M., Zahir, Z. A., Javaid, A., and Ashraf, M. (2014). The role of mycorrhizae and plant growth promoting rhizobacteria (PGPR) in improving crop productivity under stressful environments. *Biotechnol. Adv.* 32, 429–448. doi: 10.1016/j.biotechadv.2013.12.005

Neu, S., Schaller, J., and Dudel, E. G. (2017). Silicon availability modifies nutrient use efficiency and content, C: N: P stoichiometry, and productivity of winter wheat (*Triticum aestivum* L.). *Sci. Rep.* 7:40829.

Neumann, G., and Römheld, V. (1999). Root excretion of carboxylic acids and protons in phosphorus-deficient plants. *Plant Soil* 211, 121–130.

Niu, Y. F., Chai, R. S., Jin, G. L., Wang, H., Tang, C. X., and Zhang, Y. S. (2013). Responses of root architecture development to low phosphorus availability: a review. *Ann. Bot.* 112, 391–408. doi: 10.1093/aob/mcs285

Nogueira, M. A., Cardoso, E., and Hampp, R. (2002). Manganese toxicity and callose deposition in leaves are attenuated in mycorrhizal soybean. *Plant Soil* 246, 1–10. doi: 10.1111/j.1365-313x.2010.04399.x

Nuccio, E. E., Hodge, A., Pett-Ridge, J., Herman, D. J., Weber, P. K., and Firestone, M. K. (2013). An arbuscular mycorrhizal fungus significantly modifies the soil

bacterial community and nitrogen cycling during litter decomposition. *Environ. Microbiol.* 15, 1870–1881. doi: 10.1111/1462-2920.12081

Oburger, E., Jones, D. L., and Wenzel, W. W. (2011). Phosphorus saturation and pH differentially regulate the efficiency of organic acid anion-mediated P solubilization mechanisms in soil. *Plant Soil* 341, 363–382. doi: 10.1007/s11104-010-0650-5

Offre, P., Pivato, B., Siblot, S., Gamalero, E., Corberand, T., Lemanceau, P., et al. (2007). Identification of bacterial groups preferentially associated with mycorrhizal roots of *Medicago truncatula*. *Appl. Environ. Microbiol.* 73, 913–921. doi: 10.1128/aem.02042-06

Olander, L. P., and Vitousek, P. M. (2004). Biological and geochemical sinks for phosphorus in soil from a wet tropical forest. *Ecosystems* 7, 404–419.

Olsson, P. A., Van Aarle, I. M., Allaway, W. G., Ashford, A. E., and Rouhier, H. (2002). Phosphorus effects on metabolic processes in monoxenic arbuscular mycorrhiza cultures. *Plant Physiol.* 130, 1162–1171. doi: 10.1104/pp.009639

Ordoñez, Y. M., Fernandez, B. R., Lara, L. S., Rodriguez, A., Uribe-Vélez, D., and Sanders, I. R. (2016). Bacteria with phosphate solubilizing capacity alter mycorrhizal fungal growth both inside and outside the root and in the presence of native microbial communities. *PLoS One* 11:e0154438. doi: 10.1371/journal.pone.0154438

Ordookhani, K., Khavazi, K., Moezzi, A., and Rejali, F. (2010). Influence of PGPR and AMF on antioxidant activity, lycopene and potassium contents in tomato. *African J. Agricul. Res.* 5, 1108–1116.

Osborne, L. D., and Rengel, Z. (2002). Growth and P uptake by wheat genotypes supplied with phytate as the only P source. *Australian J. Agricul. Res.* 53, 845–850. doi: 10.1071/ar01102

Osorio Vega, N. W. (2007). A review on beneficial effects of rhizosphere bacteria on soil nutrient availability and plant nutrient uptake. *Revista Facultad Nacional de Agronomia Medellin* 60, 3621–3643.

Oueslati, O. (2003). Allelopathy in two durum wheat (*Triticum durum* L.) varieties. *Agricult. Ecosystems Environ.* 96, 161–163. doi: 10.1016/s0167-8809(02)00201-3

Oves, M., Khan, M. S., and Zaidi, A. (2013). Chromium reducing and plant growth promoting novel strain *Pseudomonas aeruginosa* OSG41 enhance chickpea growth in chromium amended soils. *Eur. J. Soil Biol.* 56, 72–83. doi: 10.1016/j.ejsobi.2013.02.002

Owino-Gerroh, C., and Gascho, G. J. (2005). Effect of silicon on low pH soil phosphorus sorption and on uptake and growth of maize. *Commun. Soil Sci. Plant Anal.* 35, 2369–2378. doi: 10.1081/lcss-200030686

Pang, J., Yang, J., Lambers, H., Tibbett, M., Siddique, K. H. M., and Ryan, M. H. (2015). Physiological and morphological adaptations of herbaceous perennial legumes allow differential access to sources of varyingly soluble phosphate. *Physiol. Plant.* 154, 511–525. doi: 10.1111/ppl.12297

Park, K. H., Lee, C. Y., and Son, H. J. (2009). Mechanism of insoluble phosphate solubilization by *Pseudomonas fluorescens* RAF15 isolated from ginseng rhizosphere and its plant growth-promoting activities. *Lett. Appl. Microbiol.* 49, 222–228. doi: 10.1111/j.1472-765x.2009.02642.x

Parks, E. J., Olson, G. J., Brinckman, F. E., and Baldi, F. (1990). Characterization by high performance liquid chromatography (HPLC) of the solubilization of phosphorus in iron ore by a fungus. *J. Industrial Microbiol.* 5, 183–189. doi: 10.1007/bf01573868

Patel, D. K., Archana, G., and Kumar, G. N. (2008). Variation in the nature of organic acid secretion and mineral phosphate solubilization by Citrobacter sp. DHRSS in the presence of different sugars. *Curr. Microbiol.* 56, 168–174. doi: 10.1007/s00284-007-9053-0

Pavlovic, J., Samardzic, J., Maksimović, V., Timotijevic, G., Stevic, N., Laursen, K. H., et al. (2013). Silicon alleviates iron deficiency in cucumber by promoting mobilization of iron in the root apoplast. *New Phytol.* 198, 1096–1107. doi: 10.1111/nph.12213

Peera, S. K. P. G., Balasubramaniam, P., and Mahendran, P. P. (2016). Effect of fly ash and silicate solubilizing bacteria on yield and silicon uptake of rice in Cauvery Delta Zone. *Environ. Ecol.* 34, 1966–1971.

Pepe, A., Giovannetti, M., and Sbrana, C. (2020). Appressoria and phosphorus fluxes in mycorrhizal plants: connections between soil-and plant-based hyphae. *Mycorrhiza* 30, 589–600. doi: 10.1007/s00572-020-00972-w

Perry, C. C. (2003). Silicification: the processes by which organisms capture and mineralize silica. *Rev. Mineral. Geochem.* 54, 291–327. doi: 10.1515/9781501509346-015

Planavsky, N. J., Rouxel, O. J., Bekker, A., Lalonde, S. V., Konhauser, K. O., Reinhard, C. T., et al. (2010). The evolution of the marine phosphate reservoir. *Nature* 467, 1088–1090. doi: 10.1038/nature09485

Plaxton, W. C. (2004). *Plant Response to Stress: Biochemical Adaptations to Phosphate Deficiency. Encyclopedia of Plant and Crop Science*. Marcel Dekker, New York, 976–980.

Plaxton, W. C., and Carswell, M. C. (1999). "Metabolic aspects of the phosphate starvation response in plants," in *Plant Responses to Environmental Stresses: from Phytohormones to Genome Reorganization* ed H. R. Lerner (New York, NY: Marcel Dekker), 349–372. doi: 10.1201/9780203743157-16

Pokrovsky, O., Shirokova, L., Stockman, G., Zabelina, S., Bénézeth, P., Gerard, E., et al. (2011). Quantifying the role of microorganisms in silicate mineral dissolution at the conditions of CO2 storage in basalts. *Geophys. Res. Abstracts* 13:13904.

Pons, S., Fournier, S., Chervin, C., Bécard, G., Rochange, S., Frei Dit Frey, N., et al. (2020). Phytohormone production by the arbuscular mycorrhizal fungus *Rhizophagus irregularis*. *PLoS One* 15:e0240886. doi: 10.1371/journal.pone.0240886

Pothier, J. F., Wisniewski-Dye, F., Weiss-Gayet, M., Moenne-Loccoz, Y., and Prigent-Combaret, C. (2007). Promoter-trap identification of wheat seed extract-induced genes in the plant-growth-promoting rhizobacterium *Azospirillum brasilense* Sp245. *Microbiology* 153, 3608–3622. doi: 10.1099/mic.0.2007/009381-0

Prusty, R., Grisafi, P., and Fink, G. R. (2004). The plant hormone indoleacetic acid induces invasive growth in *Saccharomyces cerevisiae*. *Proc. Natl. Acad. Sci. U S A.* 101, 4153–4157. doi: 10.1073/pnas.0400659101

Raghothama, K. G., and Karthikeyan, A. S. (2005). Phosphate acquisition. *Plant Soil* 274:37.

Rajan, S. S. S. (1975). Phosphate adsorption and the displacement of structural silicon in an allophane clay. *J. Soil Sci.* 26, 250–256. doi: 10.1111/j.1365-2389.1975.tb01949.x

Ramaekers, L., Remans, R., Rao, I. M., Blair, M. W., and Vanderleyden, J. (2010). Strategies for improving phosphorus acquisition efficiency of crop plants. *Field Crops Res.* 117, 169–176. doi: 10.1016/j.fcr.2010.03.001

Rangaraj, S., Gopalu, K., Rathinam, Y., Periasamy, P., Venkatachalam, R., and Narayanasamy, K. (2014). Effect of silica nanoparticles on microbial biomass and silica availability in maize rhizosphere. *Biotechnol. Appl. Biochem.* 61, 668–675. doi: 10.1002/bab.1191

Rashid, M., Khalil, S., Ayub, N., Alam, S., and Latif, F. (2004). Organic acids production and phosphate solubilization by phosphate solubilizing microorganisms (PSM) under in vitro conditions. *Pak. J. Biol. Sci.* 7, 187–196. doi: 10.3923/pjbs.2004.187.196

Redecker, D., Schüßler, A., Stockinger, H., Stürmer, S. L., Morton, J. B., and Walker, C. (2013). An evidence-based consensus for the classification of arbuscular mycorrhizal fungi (Glomeromycota). *Mycorrhiza* 23, 515–531. doi: 10.1007/s00572-013-0486-y

Reithmaier, G. -M. S., Knorr, K. -H., Arnhold, S., Planer-Friedrich, B., and Schaller, J. (2017). Enhanced silicon availability leads to increased methane production, nutrient and toxicant mobility in peatlands. *Sci. Rep.* 7: 8728.

Rengel, Z., and Marschner, P. (2005). Nutrient availability and management in the rhizosphere: exploiting genotypic differences. *New Phytol.* 168, 305–312. doi: 10.1111/j.1469-8137.2005.01558.x

Rezakhani, L., Motesharezadeh, B., Tehrani, M. M., Etesami, H., and Hosseini, H. M. (2019a). Effect of silicon and phosphate-solubilizing bacteria on improved phosphorus (P) uptake is not specific to insoluble P-fertilized sorghum (*Sorghum bicolor* L.) Plants. *J. Plant Growth Regulat.* 39, 239–253. doi: 10.1007/s00344-019-09978-x

Rezakhani, L., Motesharezadeh, B., Tehrani, M. M., Etesami, H., and Hosseini, H. M. (2019b). Phosphate–solubilizing bacteria and silicon synergistically augment phosphorus (P) uptake by wheat (*Triticum aestivum* L.) plant fertilized with soluble or insoluble P source. *Ecotoxicol. Environ. Safety* 173, 504–513. doi: 10.1016/j.ecoenv.2019.02.060

Richardson, A. E., Barea, J. -M., Mcneill, A. M., and Prigent-Combaret, C. (2009). Acquisition of phosphorus and nitrogen in the rhizosphere and plant growth promotion by microorganisms. *Plant Soil* 321, 305–339. doi: 10.1007/s11104-009-9895-2

Ringeval, B., Augusto, L., Monod, H., Apeldoorn, D., Bouwman, L., Yang, X., et al. (2017). Phosphorus in agricultural soils: drivers of its distribution at the global scale. *Global Change Biol.* 23, 3418–3432 doi: 10.1111/gcb.13618

Rodrigues, F. Á., Mcnally, D. J., Datnoff, L. E., Jones, J. B., Labbé, C., Benhamou, N., et al. (2004). Silicon enhances the accumulation of diterpenoid phytoalexins in rice: a potential mechanism for blast resistance. *Phytopathology* 94, 177–183.

Rodrìguez, H., and Fraga, R. (1999). Phosphate solubilizing bacteria and their role in plant growth promotion. *Biotechnol. Adv.* 17, 319–339. doi: 10.1016/s0734-9750(99)00014-2

Römer, W., and Schenk, H. (1998). Influence of genotype on phosphate uptake and utilization efficiencies in spring barley. *Eur. J. Agronomy* 8, 215–224. doi: 10.1016/s1161-0301(97)00061-0

Sahebi, M., Hanafi, M. M., Siti nor Akmar, A., Rafii, M. Y., Azizi, P., Tengoua, F. F., et al. (2015). Importance of silicon and mechanisms of biosilica formation in plants. *BioMed Res. Int.* 2015:396010.

Sánchez-Calderón, L., López-Bucio, J., Chacón-López, A., Gutiérrez-Ortega, A., Hernández-Abreu, E., and Herrera-Estrella, L. (2006). Characterization of low phosphorus insensitive mutants reveals a crosstalk between low phosphorus-induced determinate root development and the activation of genes involved in the adaptation of *Arabidopsis* to phosphorus deficiency. *Plant Physiol.* 140, 879–889. doi: 10.1104/pp.105.073825

Sarathambal, C., and Ilamurugu, K. (2013). Saline tolerant plant growth promoting diazotrophs from rhizosphere of *Bermuda grass* and their effect on rice. *Indian J. Weed Sci.* 45, 80–85.

Sato, T., Ezawa, T., Cheng, W., and Tawaraya, K. (2015). Release of acid phosphatase from extraradical hyphae of arbuscular mycorrhizal fungus *Rhizophagus clarus*. *Soil Sci. Plant Nutrition* 61, 269–274. doi: 10.1080/00380768.2014.993298

Sauer, D., Saccone, L., Conley, D. J., Herrmann, L., and Sommer, M. (2006). Review of methodologies for extracting plant-available and amorphous Si from soils and aquatic sediments. *Biogeochemistry* 80, 89–108. doi: 10.1007/s10533-005-5879-3

Savant, N. K., Snyder, G. H., and Datnoff, L. E. (1996). Silicon management and sustainable rice production. *Adv. Agronomy* 58, 151–199. doi: 10.1016/s0065-2113(08)60255-2

Schachtman, D. P., Reid, R. J., and Ayling, S. M. (1998). Phosphorus uptake by plants: from soil to cell. *Plant Physiol.* 116, 447–453. doi: 10.1104/pp.116.2.447

Schaller, J., Faucherre, S., Joss, H., Obst, M., Goeckede, M., Planer-Friedrich, B., et al. (2019). Silicon increases the phosphorus availability of Arctic soils. *Sci. Rep.* 9:449.

Scheublin, T. R., Sanders, I. R., Keel, C., and Van Der Meer, J. R. (2010). Characterisation of microbial communities colonising the hyphal surfaces of arbuscular mycorrhizal fungi. *ISME J.* 4, 752–763. doi: 10.1038/ismej.2010.5

Schrey, S., Hartmann, A., and Hampp, R. (2014). "Rhizosphere interactions," in *Ecological Biochemistry: Environmental and Interspecies Interactions*, eds G.-J. Krauss and D. H. Nies (New Jersey, USA: John Wiley & Sons, Inc.), 292–311. doi: 10.1002/9783527686063.ch15

Schwertmann, U., and Fechter, H. (1982). The point of zero charge of natural and synthetic ferrihydrites and its relation to adsorbed silicate. *Clay Minerals* 17, 471–476. doi: 10.1180/claymin.1982.017.4.10

Seeling, B., and Zasoski, R. J. (1993). Microbial effects in maintaining organic and inorganic solution phosphorus concentrations in a grassland topsoil. *Plant Soil* 148, 277–284. doi: 10.1007/bf00012865

Sevilla, M., Gunapala, N., Burris, R., and Kennedy, C. (2001). Comparison of benefit to sugarcane plant growth and 15N2 incorporation following inoculation of sterile plants with *Acetobacter diazotrophicus* wild-type and nif- mutant strains. *Mol. Plant–Microbe Interact.* 14, 358–366. doi: 10.1094/mpmi.2001.14.3.358

Shahi, S. K., Rai, A. K., Tyagi, M. B., Sinha, R. P., and Kumar, A. (2011). Rhizosphere of rice plants harbor bacteria with multiple plant growth promoting features. *Afr. J. Biotechnol.* 10, 8296–8305. doi: 10.5897/ajb11.602

Shahzad, S. M., Khalid, A., Arif, M. S., Riaz, M., Ashraf, M., Iqbal, Z., et al. (2014). Co-inoculation integrated with P-enriched compost improved nodulation and growth of Chickpea (*Cicer arietinum* L.) under irrigated and rainfed farming systems. *Biol. Fertility Soils* 50, 1–12. doi: 10.1007/s00374-013-0826-2

Sharif, M., and Claassen, N. (2011). Action mechanisms of arbuscular mycorrhizal fungi in phosphorus uptake by *Capsicum annuum* L. *Pedosphere* 21, 502–511. doi: 10.1016/s1002-0160(11)60152-5

Sharma, S. B., Sayyed, R. Z., Trivedi, M. H., and Gobi, T. A. (2013). Phosphate solubilizing microbes: sustainable approach for managing phosphorus deficiency in agricultural soils. *SpringerPlus* 2:587.

Sheng, X. F., and He, L. Y. (2006). Solubilization of potassium-bearing minerals by a wild-type strain of *Bacillus edaphicus* and its mutants and increased potassium uptake by wheat. *Can. J. Microbiol.* 52, 66–72. doi: 10.1139/w05-117

Sheng, X. F., Zhao, F., He, L. Y., Qiu, G., and Chen, L. (2008). Isolation and characterization of silicate mineral-solubilizing *Bacillus globisporus* Q12 from the surfaces of weathered feldspar. *Can. J. Microbiol.* 54, 1064–1068. doi: 10.1139/w08-089

Shenoy, V. V., and Kalagudi, G. M. (2005). Enhancing plant phosphorus use efficiency for sustainable cropping. *Biotechnol. Adv.* 23, 501–513. doi: 10.1016/j.biotechadv.2005.01.004

Shi-Chu, L., Yong, J., Ma-Bo, L., Wen-Xu, Z., Nan, X., and Hui-Hui, Z. (2019). Improving plant growth and alleviating photosynthetic inhibition from salt stress using AMF in alfalfa seedlings. *J. Plant Interact.* 14, 482–491. doi: 10.1080/17429145.2019.1662101

Sigg, L., and Stumm, W. (1981). The interaction of anions and weak acids with the hydrous goethite (α-FeOOH) surface. *Colloids Surf.* 2, 101–117. doi: 10.1016/0166-6622(81)80001-7

Sikes, B. A. (2010). When do arbuscular mycorrhizal fungi protect plant roots from pathogens? *Plant Signal. Behav.* 5, 763–765. doi: 10.4161/psb.5.6.11776

Singh, K. P., and Sarkar, M. C. (1992). Phosphorus availability in soils as affected by fertilizer phosphorus, sodium silicate and farmyard manure. *J. Ind. Soc. Soil Sci.* 40, 762–767.

Smith, S. E., and Read, D. J. (2008). *Mycorrhizal Symbiosis*. London: Academic Press.

Smith, S. E., and Smith, F. A. (2011). Roles of arbuscular mycorrhizas in plant nutrition and growth: new paradigms from cellular to ecosystem scales. *Annu. Rev. Plant Biol.* 62, 227–250. doi: 10.1146/annurev-arplant-042110-103846

Smith, S. E., Jakobsen, I., Grønlund, M., and Smith, F. A. (2011). Roles of arbuscular mycorrhizas in plant phosphorus nutrition: interactions between pathways of phosphorus uptake in arbuscular mycorrhizal roots have important implications for understanding and manipulating plant phosphorus acquisition. *Plant Physiol.* 156, 1050–1057. doi: 10.1104/pp.111.174581

Smyth, T. J., and Sanchez, P. A. (1980). Effects of lime, silicate, and phosphorus applications to an *Oxisol* on phosphorus sorption and ion retention. *Soil Sci. Soc. Am. J.* 44, 500–505. doi: 10.2136/sssaj1980.03615995004400030012x

Sommer, M., Kaczorek, D., Kuzyakov, Y., and Breuer, J. (2006). Silicon pools and fluxes in soils and landscapes—a review. *J. Plant Nutrition Soil Sci.* 169, 310–329. doi: 10.1002/jpln.200521981

Stamford, N. P., Santos, P. R. D., Moura, A. M. M. F. D., and Freitas, A. D. S. D. (2003). Biofertilzers with natural phosphate, sulphur and *Acidithiobacillus* in a siol with low available-P. *Sci. Agricola* 60, 767–773. doi: 10.1590/s0103-90162003000400024

Steenhoudt, O., and Vanderleyden, J. (2000). Azospirillum, a free-living nitrogen-fixing bacterium closely associated with grasses: genetic, biochemical and ecological aspects. *FEMS Microbiol. Rev.* 24, 487–506. doi: 10.1111/j.1574-6976.2000.tb00552.x

Steinkellner, S., Lendzemo, V., Langer, I., Schweiger, P., Khaosaad, T., Toussaint, J. -P., et al. (2007). Flavonoids and strigolactones in root exudates as signals in symbiotic and pathogenic plant-fungus interactions. *Molecules* 12, 1290–1306. doi: 10.3390/12071290

Struyf, E., and Conley, D. J. (2009). Silica: an essential nutrient in wetland biogeochemistry. *Front. Ecol. Environ.* 7, 88–94. doi: 10.1890/070126

Struyf, E., Smis, A., Van Damme, S., Garnier, J., Govers, G., Van Wesemael, B., et al. (2010). Historical land use change has lowered terrestrial silica mobilization. *Nat. Commun.* 1:129.

Takeda, N., Handa, Y., Tsuzuki, S., Kojima, M., Sakakibara, H., and Kawaguchi, M. (2015). Gibberellins interfere with symbiosis signaling and gene expression and alter colonization by arbuscular mycorrhizal fungi in *Lotus japonicus*. *Plant Physiol.* 167, 545–557. doi: 10.1104/pp.114.247700

Taktek, S., Trépanier, M., Servin, P. M., St-Arnaud, M., Piché, Y., Fortin, J. A., et al. (2015). Trapping of phosphate solubilizing bacteria on hyphae of the arbuscular mycorrhizal fungus *Rhizophagus irregularis* DAOM 197198. *Soil Biol. Biochem.* 90, 1–9. doi: 10.1016/j.soilbio.2015.07.016

Tarafdar, J. C., and Marschner, H. (1994). Phosphatase activity in the rhizosphere and hyphosphere of VA mycorrhizal wheat supplied with inorganic and organic phosphorus. *Soil Biol. Biochem.* 26, 387–395. doi: 10.1016/0038-0717(94)90288-7

Tarafdar, J. C., Yadav, R. S., and Meena, S. C. (2001). Comparative efficiency of acid phosphatase originated from plant and fungal sources. *J. Plant Nutrition Soil Sci.* 164, 279–282. doi: 10.1002/1522-2624(200106)164:3<279::aid-jpln279>3.0.co;2-l

Tatsukami, Y., and Ueda, M. (2016). Rhizobial gibberellin negatively regulates host nodule number. *Sci. Rep.* 6:27998.

Tawaraya, K. (2003). Arbuscular mycorrhizal dependency of different plant species and cultivars. *Soil Sci. Plant Nutrition* 49, 655–668. doi: 10.1080/00380768.2003.10410323

Tawaraya, K., Naito, M., and Wagatsuma, T. (2006). Solubilization of insoluble inorganic phosphate by hyphal exudates of arbuscular mycorrhizal fungi. *J. Plant Nutrition* 29, 657–665. doi: 10.1080/01904160600564428

Tipping, E. (1981). The adsorption of aquatic humic substances by iron oxides. *Geochimica et Cosmochimica Acta* 45, 191–199. doi: 10.1016/0016-7037(81)90162-9

Tisserant, E., Kohler, A., Dozolme-Seddas, P., Balestrini, R., Benabdellah, K., Colard, A., et al. (2012). The transcriptome of the arbuscular mycorrhizal fungus Glomus intraradices (DAOM 197198) reveals functional tradeoffs in an obligate symbiont. *New Phytol.* 193, 755–769. doi: 10.1111/j.1469-8137.2011.03948.x

Tisserant, E., Malbreil, M., Kuo, A., Kohler, A., Symeonidi, A., Balestrini, R., et al. (2013). Genome of an arbuscular mycorrhizal fungus provides insight into the oldest plant symbiosis. *Proc. Natl. Acad. Sci. U S A.* 110, 20117–20122.

Tittarelli, A., Milla, L., Vargas, F., Morales, A., Neupert, C., Meisel, L., et al. (2007). Isolation and comparative analysis of the wheat TaPT2 promoter: identification in silico of new putative regulatory motifs conserved between monocots and dicots. *J. Exp. Bot.* 58, 2573–2582. doi: 10.1093/jxb/erm123

Toljander, J. (2006). *Interactions Between Soil Bacteria and Arbuscular Mycorrhizal Fungi*. Disseration Uppsala : Sveriges lantbruksuniv

Toljander, J. F., Artursson, V., Paul, L. R., Jansson, J. K., and Finlay, R. D. (2006). Attachment of different soil bacteria to arbuscular mycorrhizal fungal extraradical hyphae is determined by hyphal vitality and fungal species. *FEMS Microbiol. Lett.* 254, 34–40. doi: 10.1111/j.1574-6968.2005.00003.x

Toljander, J. F., Lindahl, B. D., Paul, L. R., Elfstrand, M., and Finlay, R. D. (2007). Influence of arbuscular mycorrhizal mycelial exudates on soil bacterial growth and community structure. *FEMS Microbiol. Ecol.* 61, 295–304. doi: 10.1111/j.1574-6941.2007.00337.x

Toro, M., Azcon, R., and Barea, J. (1997). Improvement of arbuscular mycorrhiza development by inoculation of soil with phosphate-solubilizing rhizobacteria to improve rock phosphate bioavailability ((sup32) P) and nutrient cycling. *Appl. Environ. Microbiol.* 63, 4408–4412. doi: 10.1128/aem.63.11.4408-4412.1997

Toro, M., Azcón, R., and Barea, J. M. (1998). The use of isotopic dilution techniques to evaluate the interactive effects of Rhizobium genotype, mycorrhizal fungi, phosphate-solubilizing rhizobacteria and rock phosphate on nitrogen and phosphorus acquisition by *Medicago sativa*. *New Phytol.* 138, 265–273. doi: 10.1046/j.1469-8137.1998.00108.x

Treder, W., and Cieslinski, G. (2005). Effect of silicon application on cadmium uptake and distribution in strawberry plants grown on contaminated soils. *J. Plant Nutrition* 28, 917–929. doi: 10.1081/pln-200058877

Trolove, S., Hedley, M., Kirk, G., Bolan, N., and Loganathan, P. (2003). Progress in selected areas of rhizosphere research on P acquisition. *Soil Res.* 41, 471–499. doi: 10.1071/sr02130

Turrini, A., Avio, L., Giovannetti, M., and Agnolucci, M. (2018). Functional complementarity of arbuscular mycorrhizal fungi and associated microbiota: the challenge of translational research. *Front. Plant Sci.* 9:1407. doi: 10.3389/fpls.2018.01407

Uhde-Stone, C., Zinn, K. E., Ramirez-Yáñez, M., Li, A., Vance, C. P., and Allan, D. L. (2003). Nylon filter arrays reveal differential gene expression in proteoid roots of white lupin in response to phosphorus deficiency. *Plant Physiol.* 131, 1064–1079. doi: 10.1104/pp.102.016881

Umamaheswari, T., Srimeena, N., Vasanthi, N., Cibichakravarthy, B., Anthoniraj, S., and Karthikeyan, S. (2016). Silica as biologically transmutated source for bacterial growth similar to carbon. *Matt. Arch.* 2:e201511000005.

Uroz, S., Calvaruso, C., Turpault, M. -P., and Frey-Klett, P. (2009). Mineral weathering by bacteria: ecology, actors and mechanisms. *Trends Microbiol.* 17, 378–387. doi: 10.1016/j.tim.2009.05.004

Urrutia, M. M., and Beveridge, T. J. (1994). Formation of fine grained silicate minerals and metal precipitates by a bacterial surface and the implications on the global cycling of silicon. *Chem. Geol.* 116, 261–280. doi: 10.1016/0009-2541(94)90018-3

Vance, C. P., Uhde-Stone, C., and Allan, D. L. (2003). Phosphorus acquisition and use: critical adaptations by plants for securing a nonrenewable resource. *New Phytol.* 157, 423–447. doi: 10.1046/j.1469-8137.2003.00695.x

Vasanthi, N., Saleena, L. M., and Anthoni, A. R. (2013). Evaluation of media for isolation and screening of silicate solubilising bacteria. *Int. J. Curr. Res.* 5, 406–408.

Vasanthi, N., Saleena, L. M., and Raj, S. A. (2018). Silica solubilization potential of certain bacterial species in the presence of different silicate minerals. *Silicon* 10, 267–275. doi: 10.1007/s12633-016-9438-4

Vassilev, N., Vassileva, M., and Nikolaeva, I. (2006). Simultaneous P-solubilizing and biocontrol activity of microorganisms: potentials and future trends. *Appl. Microbiol. Biotechnol.* 71, 137–144. doi: 10.1007/s00253-006-0380-z

Veneklaas, E. J., Lambers, H., Bragg, J., Finnegan, P. M., Lovelock, C. E., Plaxton, W. C., et al. (2012). Opportunities for improving phosphorus-use efficiency in crop plants. *New Phytol.* 195, 306–320. doi: 10.1111/j.1469-8137.2012.04190.x

Veresoglou, S. D., Chen, B., and Rillig, M. C. (2012). Arbuscular mycorrhiza and soil nitrogen cycling. *Soil Biol. Biochem.* 46, 53–62. doi: 10.1016/j.soilbio.2011.11.018

Veresoglou, S. D., Sen, R., Mamolos, A. P., and Veresoglou, D. S. (2011). Plant species identity and arbuscular mycorrhizal status modulate potential nitrification rates in nitrogen-limited grassland soils. *J. Ecol.* 99, 1339–1349. doi: 10.1111/j.1365-2745.2011.01863.x

Vierheilig, H. (2004). Regulatory mechanisms during the plant arbuscular mycorrhizal fungus interaction. *Can. J. Botany* 82, 1166–1176. doi: 10.1139/b04-015

Villegas, J., and Fortin, J. A. (2001). Phosphorus solubilization and pH changes as a result of the interactions between soil bacteria and arbuscular mycorrhizal fungi on a medium containing NH4+ as nitrogen source. *Can. J. Botany* 79, 865–870. doi: 10.1139/b01-069

Wainwright, M., Al-Wajeeh, K., Wickramasinghe, N. C., and Narlikar, J. V. (2003). Did silicon aid in the establishment of the first bacterium? *Int. J. Astrobiol.* 2, 227–229. doi: 10.1017/s1473550403001587

Wainwright, M., Barakah, F., Al-Turk, I., and Ali, T. A. (1991). Oligotrophic micro-organisms in industry, medicine and the environment. *Sci. Prog.* 75, 313–322.

Waksman, S. A., and Starkey, R. L. (1924). Microbiological analysis of soil as an index of soil fertility: VII. carbon dioxide evolution1. Soil Science 17, 141–162. doi: 10.1097/00010694-192402000-00004

Wang, B., and Qiu, Y. L. (2006). Phylogenetic distribution and evolution of mycorrhizas in land plants. *Mycorrhiza* 16, 299–363. doi: 10.1007/s00572-005-0033-6

Wang, F., Shi, N., Jiang, R., Zhang, F., and Feng, G. (2016). In situ stable isotope probing of phosphate-solubilizing bacteria in the hyphosphere. *J. Exp. Botany* 67, 1689–1701. doi: 10.1093/jxb/erv561

Wang, L., Cai, K., Chen, Y., and Wang, G. (2013). Silicon-mediated tomato resistance against *Ralstonia solanacearum* is associated with modification of soil microbial community structure and activity. *Biol. Trace Elem. Res.* 152, 275–283. doi: 10.1007/s12011-013-9611-1

Wang, R. R., Wang, Q., He, L. Y., Qiu, G., and Sheng, X. F. (2015). Isolation and the interaction between a mineral-weathering *Rhizobium tropici* Q34 and silicate minerals. *World J. Microbiol. Biotechnol.* 31, 747–753. doi: 10.1007/s11274-015-1827-0

Wang, Y., Zhang, W., Liu, W., Ahammed, G. J., Wen, W., Guo, S., et al. (2021). Auxin is involved in arbuscular mycorrhizal fungi-promoted tomato growth and NADP-malic enzymes expression in continuous cropping substrates. *BMC Plant Biol.* 21:48. doi: 10.1186/s12870-020-02817-2

Whitelaw, M. A. (1999). Growth promotion of plants inoculated with phosphate-solubilizing fungi. *Adv. Agronomy* 69, 99–151. doi: 10.1016/s0065-2113(08)60948-7

Whitelaw, M. A., Harden, T. J., and Helyar, K. R. (1999). Phosphate solubilisation in solution culture by the soil fungus *Penicillium radicum*. *Soil Biol. Biochem.* 31, 655–665. doi: 10.1016/s0038-0717(98)00130-8

Widdig, M., Schleuss, P. M., Weig, A. R., Guhr, A., Biederman, L. A., Borer, E. T., et al. (2019). Nitrogen and phosphorus additions alter the abundance of phosphorus-solubilizing bacteria and phosphatase activity in grassland soils. *Front. Environ. Sci.* 7:185. doi: 10.3389/fenvs.2019.00185

Wright, D. P., Read, D. J., and Scholes, J. D. (1998). Mycorrhizal sink strength influences whole plant carbon balance of *Trifolium repens* L. *Plant Cell Environ.* 21, 881–891. doi: 10.1046/j.1365-3040.1998.00351.x

Wu, L., Jacobson, A. D., and Hausner, M. (2008). Characterization of elemental release during microbe–granite interactions at T= 28 C. *Geochimica et Cosmochimica Acta* 72, 1076–1095. doi: 10.1016/j.gca.2007.11.025

Wu, Q. -S., and Xia, R. -X. (2006). Arbuscular mycorrhizal fungi influence growth, osmotic adjustment and photosynthesis of citrus under well-watered and water stress conditions. *J. Plant Physiol.* 163, 417–425. doi: 10.1016/j.jplph.2005.04.024

Xiao, B., Sun, Y. -F., Lian, B., and Chen, T. -M. (2016). Complete genome sequence and comparative genome analysis of the *Paenibacillus mucilaginosus* K02. *Microb. Pathog.* 93, 194–203. doi: 10.1016/j.micpath.2016.01.016

Xun, F., Xie, B., Liu, S., and Guo, C. (2015). Effect of plant growth-promoting bacteria (PGPR) and arbuscular mycorrhizal fungi (AMF) inoculation on oats in saline-alkali soil contaminated by petroleum to enhance phytoremediation. *Environ. Sci. Pollut. Res.* 22, 598–608. doi: 10.1007/s11356-014-3396-4

Yang, X., and Post, W. M. (2011). Phosphorus transformations as a function of pedogenesis: a synthesis of soil phosphorus data using Hedley fractionation method. *Biogeosciences* 8, 2907–2916. doi: 10.5194/bg-8-2907-2011

Yao, Q., Li, X., Feng, G., and Christie, P. (2001). Mobilization of sparingly soluble inorganic phosphates by the external mycelium of an abuscular mycorrhizal fungus. *Plant Soil* 230, 279–285.

Ye, M., Song, Y., Long, J., Wang, R., Baerson, S. R., Pan, Z., et al. (2013). Priming of jasmonate-mediated antiherbivore defense responses in rice by silicon. *Proc. Natl. Acad. Sci. U S A.* 110, E3631–E3639.

Yost, R. S., and Fox, R. L. (1982). Influence of mycorrhizae on the mineral contents of cowpea and soybean grown in an Oxisol 1. *Agronomy J.* 74, 475–481. doi: 10.2134/agronj1982.00021962007400030018x

Zarei, M., Saleh-Rastin, N., Alikhani, H. A., and Aliasgharzadeh, N. (2006). Responses of lentil to co-inoculation with phosphate-solubilizing rhizobial strains and arbuscular mycorrhizal fungi. *J. Plant Nutrition* 29, 1509–1522. doi: 10.1080/01904160600837667

Zhang, L., Ding, X., Chen, S., He, X., Zhang, F., and Feng, G. (2014a). Reducing carbon: phosphorus ratio can enhance microbial phytin mineralization and lessen competition with maize for phosphorus. *J. Plant Interact.* 9, 850–856. doi: 10.1080/17429145.2014.977831

Zhang, L., Fan, J., Ding, X., He, X., Zhang, F., and Feng, G. (2014b). Hyphosphere interactions between an arbuscular mycorrhizal fungus and a phosphate solubilizing bacterium promote phytate mineralization in soil. *Soil Biol. Biochem.* 74, 177–183. doi: 10.1016/j.soilbio.2014.03.004

Zhang, L., Feng, G., and Declerck, S. (2018a). Signal beyond nutrient, fructose, exuded by an arbuscular mycorrhizal fungus triggers phytate mineralization by a phosphate solubilizing bacterium. *ISME J.* 12, 2339–2351. doi: 10.1038/s41396-018-0171-4

Zhang, L., Shi, N., Fan, J., Wang, F., George, T. S., and Feng, G. (2018b). Arbuscular mycorrhizal fungi stimulate organic phosphate mobilization associated with changing bacterial community structure under field conditions. *Environ. Microbiol.* 20, 2639–2651. doi: 10.1111/1462-2920.14289

Zhang, L., Xu, M., Liu, Y., Zhang, F., Hodge, A., and Feng, G. (2016). Carbon and phosphorus exchange may enable cooperation between an arbuscular mycorrhizal fungus and a phosphate-solubilizing bacterium. *New Phytol.* 210, 1022–1032. doi: 10.1111/nph.13838

Zhu, X. Q., Wang, C. Y., Chen, H., and Tang, M. (2014). Effects of arbuscular mycorrhizal fungi on photosynthesis, carbon content, and calorific value of black locust seedlings. *Photosynthetica* 52, 247–252. doi: 10.1007/s11099-014-0031-z

Conflict of Interest: The authors declare that the research was conducted in the absence of any commercial or financial relationships that could be construed as a potential conflict of interest.

frontiers in Plant Science

ORIGINAL RESEARCH
published: 26 July 2021
doi: 10.3389/fpls.2021.644229

Effect of Humic Acid Addition on Buffering Capacity and Nutrient Storage Capacity of Soilless Substrates

Jingcheng Xu[1,2†], Esraa Mohamed[1†], Qiang Li[1], Tao Lu[1], Hongjun Yu[1] and Weijie Jiang[1*]*

[1] *Key Laboratory of Horticultural Crops Genetic Improvement (Ministry of Agriculture), Institute of Vegetables and Flowers, Chinese Academy of Agricultural Sciences, Beijing, China,* [2] *Taizhou Academy of Agricultural Sciences, Taizhou, China*

Excessive application of fertilizers has become a major issue in croplands of intensive agricultural systems in China, resulting in severe non-point source pollution; thus, reduction in the use of chemical fertilizers has received significant attention. Improving the nutrient storage capacity of soils or substrates is an effective approach for solving this problem. Humic acids (HA) are excellent soil conditioners. Thus, in the present study, their ability to improve the physico-chemical properties of three substrates with different textures was evaluated. HA treatments included 1% HA root application in three different types of substrates, including pure sand, pure cocopeat, and a mixture of sand:cocopeat (1:1, v/v) and their relative controls. We examined the morphological parameters of cucumber seedlings as well as pH buffering capacity (pHBC), total organic carbon (TOC), organic matter (OM), cation exchange capacity (CEC), and nutrient storage capacity of the three substrates. The results show that HA application improved the morphological parameters of cucumber seedlings (plant height, stem diameter, and biomass) in pure cocopeat and cocopeat-sand mixture treatments. On the contrary, HA addition had harmful effects on the cucumber seedlings cultivated in sand due to the low pHBC of sand. The seedlings cultivated in pure cocopeat showed the best morphological parameter performances among the seedlings grown in the three substrates. Furthermore, pHBC, TOC, OM, and CEC were enhanced by HA application. Incorporation of HA improved ammonium (NH_4^+) and potassium (K^+) storage capacity while decreasing phosphorus (P) storage. Pure cocopeat had the highest pHBC, TOC, OM, CEC, and nutrient storage capacity among the three substrates. In conclusion, mixing 1% HA into substrates promoted cucumber growth, improved substrate properties, and enhanced fertilizer use efficiency. Pure cocopeat is a suitable substrate for cucumber cultivation, and mixing cocopeat with sand amends the substrate properties and consequently improves plant growth.

Keywords: humic acid, substrate properties, cucumber, pH buffering capacity, storage capacity

OPEN ACCESS

Edited by:
Youssef Rouphael, University of Naples Federico II, Italy

Reviewed by:
Vitor L. Nascimento, Universidade Federal de Lavras, Brazil
Luciano Pasqualoto Canellas, State University of the North Fluminense Darcy Ribeiro, Brazil

****Correspondence:***
Weijie Jiang
email@uni.edu;
jiangweijie@caas.cn
Hongjun Yu
yuhongjun@caas.cn

† These authors have contributed equally to this work

Specialty section:
This article was submitted to Plant Nutrition, a section of the journal Frontiers in Plant Science

Received: *20 December 2020*
Accepted: *06 April 2021*
Published: *26 July 2021*

Citation:
Xu J, Mohamed E, Li Q, Lu T, Yu H and Jiang W (2021) Effect of Humic Acid Addition on Buffering Capacity and Nutrient Storage Capacity of Soilless Substrates. Front. Plant Sci. 12:644229. doi: 10.3389/fpls.2021.644229

Abbreviations: CEC, Cation exchange capacity; HA, humic acid; OM, Organic carbon; pHBC, pH buffering capacity; TOC, Total organic carbon.

INTRODUCTION

Chemical fertilizers are one of the most important factors in the agricultural production of modern civilization, and they can dramatically enhance crop yield. In China, the unprecedented population boom is threatening food production self-sufficiency (Wei et al., 2015). In an attempt to make the most of the limited productive arable land and achieve high food production sustainably, farmers tend to cultivate high-yielding varieties which have a high demand for nutrients. Therefore, substantial quantities of synthetic fertilizers are chronically input into fields (Cai et al., 2002; Chen et al., 2004; Cui et al., 2008; He et al., 2009; Yan et al., 2012). However, irrational agricultural practices lead to low fertilizer use efficiency and severe agricultural non-point source pollution (Sun et al., 2012; Fan et al., 2014). Compared with developed countries, China lost more nutrients in agricultural production, and fertilizer use efficiency of nitrogen (N), phosphorus (P), and potassium (K) was less than 35, 20, and 50%, respectively (Li et al., 2010); thus, taking a deep look into the improvement of fertilizer use efficiency is of great significance and necessity.

In general, after fertilization, some nutrients are absorbed by the soil, and others are lost, such as leaching and volatilization loss (Ahmad et al., 1982; Dong et al., 2009). The storage capacity of nutrients (mainly N, P, and K) is considered a crucial index of soil productivity evaluation. Nutrient absorption and release play a vital role in fertilizer use efficiency as they affect soil nutrient supplies, which are important for crop nutrient uptake (Anderson and Magdoff, 2005; Simonsson et al., 2009; Nieder et al., 2011). With the current concerns regarding environmental protection and the demand for production of more food with less fertilizer application, the focus is directed toward enhancing soil nutrient storage capacity, which could be a way to improve fertilizer use efficiency to minimize fertilizer loss and leaching into the environment.

Humic acids (HA) are a new type of biostimulant that have become popular in recent years and are mainly derived from the decomposition of animal and plant remains by microbes under aerobic and anaerobic conditions and during various geochemical processes (Dogan et al., 2014). HA perform various functions in agricultural production; for instance, HA could be used as growth regulators to alter hormone levels in plants and to alleviate the deleterious effects of abiotic stress on plants (Mora et al., 2012; Bijanzadeh et al., 2019). A previous study shows that soil properties, such as aggregation, aeration, and permeability, could be greatly improved by HA application in saline-sodic soils (Nan et al., 2016). K fixation was significantly reduced by incorporation of HA in brown soils (Liang et al., 2005; Lan et al., 2016). In addition, previous studies demonstrate that the addition of HA significantly improved P availability in inceptisol (Cimrin and Yilmaz, 2005). In general, previous studies mainly focus on the effects of HA application on natural soil types with similar physico-chemical properties. For example, the bulk density of saline-sodic soils and brown soils is about 1.40 $g \cdot cm^{-3}$, and the organic matter (OM) content of saline-sodic soils, brown soils, and inceptisol is about 10 $g \cdot kg^{-1}$. Soilless substrates have proper pH value, lighter bulk density and no soil-borne disease, which can replace soil to provide a good growth environment for plants (Vaughn et al., 2011; Banitalebi et al., 2021). Nowadays, more and more farmers are inclined to use soilless substrates for vegetable cultivation in protected fields (Gao et al., 2018). Limited studies have been carried out on the effects of HA application on soilless substrates with significantly different bulk density, porosity, OM, pH buffering capacity (pHBC), and nutrient storage capacity. Cocopeat is an organic soilless substrate made of coir, which is suitable for use as a growing substrate due to its excellent physical properties, such as high water-holding capacity and porosity (Abad et al., 2005). Cucumber is widely cultivated in China on account of its delicious taste, short nutritional cycle and high economic benefits (Zhao et al., 2019). According to the results of preliminary experiments, the addition of HA to cocopeat at a rate of 1% (HA:water, w/w) significantly improved cucumber yield under 15% fertilizer reduction (unpublished). Seedling quality has a significant effect on the yield of plants (Markovic et al., 1997). Thus, in the present study, our primary aim was to investigate the effects of 1% HA application to substrates with significantly different physico-chemical properties on cucumber seedling growth and substrate properties, especially on the pHBC and nutrient storage capacity.

MATERIALS AND METHODS

Growth Conditions and Experimental Materials

The experiment was conducted in a glasshouse at the Soilless Culture Department, Institute of Vegetables and Flowers (IVF), Chinese Academy of Agricultural Sciences (CAAS), Beijing, China, in the period from February to April 2019. Cucumber (*Cucumis sativus* L.) (cv. Zhongnong No. 26) was selected as the plant material. Cucumber seedlings were kept in a glasshouse under natural light intensity and a natural photoperiod. Cocopeat and sand were provided by the Beijing Yinong Agricultural Technology Company (Beijing, China). Characteristics of the three different substrates used in the study are shown in **Table 1**. Humic acid (pH: 5.74, fulvic acid: 43.94%, organic matter: 47.3%, total N: 5.98%, total K: 2.25%, total P: 0.04%, SiO_2: 0.18%) was obtained from Shandong Quanlinjiayou Humic Acid Technology Company (Shandong, China) and was extracted from wheat straw, and there is no hormone in this humic acid.

Experimental Design

The trial consisted of two treatments [no HA application and 1% HA (HA:water, w/w) root application], using three types of substrates: pure sand, pure cocopeat, and a mixture of sand:cocopeat (1:1, v/v), for a total of six treatment combinations [T1: pure sand without HA, T2: pure sand with 1% HA, T3: pure cocopeat without HA, T4: pure cocopeat with 1% HA, T5: mixture of sand: cocopeat (1:1, v/v) without HA, T6: mixture of sand: cocopeat (1:1, v/v) with 1% HA]. The treatments were organized in a randomized complete block design with three replicates for each treatment, and each treatment included 18 plants. The addition rate of HA, 1% (HA:water, w/w), was determined according to previous experiments (unpublished).

TABLE 1 | Basic physico-chemical properties of three different substrates.

Substrates	pH	Total N (g kg^{-1})	Total P (g kg^{-1})	Total K (g kg^{-1})	Bulk density (g cm^{-3})	Total porosity (%)	Water-holding porosity (%)	Air-filled porosity (%)
Pure sand	8.17	0.47	0.02	0.24	1.34	36.57	9.53	27.04
Pure cocopeat	6.50	6.35	0.60	8.28	0.13	76.66	57.96	18.70
Mixture of sand and cocopeat (1:1, v/v)	7.00	3.19	0.24	4.17	0.52	55.29	33.22	22.07

TABLE 2 | Composition of nutrient solution for cucumber proposed by Yamazaki.

Macronutrients	Final concentration (mg/L)	Micronutrients	Final concentration (mg/L)
KNO_3	607	H_3BO_3	2.86
$Ca(NO_3)_2{\cdot}4H_2O$	826	$MnSO_4{\cdot}4H_2O$	2.13
$NH_4H_2PO_4$	115	$ZnSO_4{\cdot}7H_2O$	0.22
$MgSO_4{\cdot}7H_2O$	483	$CuSO_4{\cdot}5H_2O$	0.08
		$(NH_4)_6Mo_7O_{24}{\cdot}4H_2O$	0.02
		Na-Fe-EDTA	30

Cucumber seeds were germinated and sown in the trays filled with peat until the seedlings developed three true leaves. Before transplanting, HA was thoroughly mixed with different substrates [pure sand, pure cocopeat, and a mixture of sand:cocopeat (1:1, v/v)]. The seedlings were then transplanted into plastic pots containing 1.2 L of substrate [T1: pure sand without HA, T2: pure sand with 1% HA, T3: pure cocopeat without HA, T4: pure cocopeat with 1% HA, T5: mixture of sand: cocopeat (1:1, v/v) without HA, T6: mixture of sand: cocopeat (1:1, v/v) with 1% HA]. The same management practices were applied across all treatments. The nutrient solution used in the experiment was a special Yamazaki cucumber cultivation formula as shown in **Table 2**. The pots were watered with this nutrient solution once or twice a week, depending on substrate humidity, and the same quantity of nutrient solution was applied to all treatments.

Morphological Measurements

At the end of the experiment, 18 plants were randomly sampled from each treatment to measure plant height and stem diameter using a ruler and an electronic vernier caliper, respectively. Thereafter, the roots and shoots of these plants were separated. Fresh weights of shoots and roots were measured immediately after harvesting using an electronic balance. The plant materials were then dried in a ventilated oven at 70°C for 4–5 days until the dry weights were constant, and their dry weight was determined by an electronic balance.

Substrate Properties

Substrate samples were air-dried, ground, and sieved through a 2-mm sieve to attain homogeneity in their properties.

The pH buffering capacity (pHBC) was determined using acid-base titration techniques (Xu et al., 2012).

Substrate samples were analyzed for TOC using the dry combustion method. OM was calculated as OM (g/kg) = TOC (g/kg) × 1.724 (Gao et al., 2018). CEC of the substrates was measured using the ammonium acetate compulsory displacement method (Xu et al., 2012).

The storage capacity of NH_4^+ of different substrates was measured by a modified method (Nieder et al., 2011). In detail, 1 g of substrate was weighed into each of three 50-mL polyethylene tubes, and 30 mL of different concentration NH_4Cl solutions were added, whose concentrations were 0.001, 0.005, 0.01, 0.05, 0.1, 0.3, 0.5, and, 1 M (standardized), respectively. The suspensions were shaken for 24 h at 25°C and equilibrated for 1 day at 25°C, after that collected 10 mL of supernatant. The residual NH_4^+ in supernatants were determined by Kjeldahl procedure. Due to the addition amount of NH_4^+ was known, which could be calculated, combined with the data of the residual NH_4^+ in supernatants, and the total adsorption quantity of NH_4^+ of substrates treated by different concentration NH_4Cl solutions were calculated. According to the above-mentioned data, the curves of NH_4^+ concentration and total adsorption quantity of NH_4^+ of treated substrates were fitted by Excel, absorption saturation point of different substrates were known. The treated substrates corresponding to the absorption saturation point were then dried at 50°C for 72 h prior to fixed NH_4^+ measurement. The method for the determination of fixed NH_4^+ is that 0.5 g of dried substrate was weighed into each of three 50 mL polyethylene tubes, and 20 mL of alkaline KOBr solution was added into each tube; the suspensions were shaken for 30 min and equilibrated for 2 h and then heated in a water bath and boiled for 5 min. After that, it was cooled and equilibrated the suspension overnight. The next day, the supernatants were discarded and the residues were washed by 40 mL of 0.5 M KCl three times, then 20 mL 5 N HF:1 N HCl was added into each tube and shaken for 24 h; all fixed NH_4^+ of substrates were released into the suspensions after the above procedure. Finally, the NH_4^+ released was determined by steam distillation of the substrate-sulfuric acid mixture after adding 1M NaOH by Kjeldahl procedure.

The storage capacity of P of different substrates was measured by a modified method (Butegwa et al., 1995). In detail, 1 g of substrate was weighed into each of three 50-mL polyethylene tubes, and 30 mL of different concentration KH_2PO_4 solutions were added, whose concentrations of P were 100, 300, 500, 1,000, 1,500, 2,000, 3,000, 4,000, 5,000, and 6,000 mg/L (standardized), respectively. The suspensions were shaken for 24 h at 25°C and equilibrated for 1 day at 25°C; after that were collected 10 mL of supernatant, the residual P in supernatants were determined by ICP-AES (ICP6300, Britain). Due to the additional amount of P being known, which could be calculated, combined with the data of residual P in supernatants, the total adsorption quantity of P of substrates treated by different

concentration KH_2PO_4 solutions were calculated. According to the above-mentioned data, the curves of P concentration and total adsorption quantity of P of treated substrates was fitted by Excel, and absorption saturation point of different substrates were known. The treated substrates corresponding to the absorption saturation point were then dried at 50°C for 72 h prior to fixed phosphorus measurement. Exchangeable P was determined by extractions in 1% NH_4HCO_3 (pH 7.0) and analysis of the extracts with ICP-AES (ICP6300, Britain) following filtration through filter paper. Fixed P was calculated by subtracting the amount of exchangeable P from the total adsorption quantity of P.

The storage capacity of K^+ of different substrates was measured by a modified method (Simonsson et al., 2009). In detail, 1 g of substrate was weighed into each of three 50 mL polyethylene tubes, and 30 mL of different concentration KCl solutions were added, whose concentrations of K^+ were 100, 200, 400, 1,000, 1,500, 2,000, 3,000, 4,000, 6,000, and 8,000 mg/L (standardized), respectively. The suspensions were shaken for 24 h at 25°C and equilibrated for 1 day at 25°C; after that was collected 10 mL of supernatant, the residual K^+ in supernatants was determined by ICP-AES (ICP6300, Britain). Due to the additional amount of K^+ being known, which could be calculated, combined with the data of residual K^+ in supernatants, the total adsorption quantity of K^+ of substrates treated by different concentration KCl solutions was calculated. According to the above-mentioned data, the curves of K^+ concentration and total adsorption quantity of K^+ of treated substrates was fitted by Excel, and the absorption saturation point of different substrates were known. The treated substrates corresponding to the absorption saturation point underwent two additional wetting-drying cycles, which each involved shaking with 5 mL distilled water for 6 h and drying at 105°C for 16 h prior to fixed K^+ measurement. Exchangeable K^+ was determined by repeated extractions in 1 M NH_4Ac (pH 7.0) and analysis of the extracts with ICP-AES (ICP6300, Britain) following centrifugation (2,000 rpm × 10 min) and filtration through a filter paper. Fixed K^+ was calculated by subtracting the amount of exchangeable K^+ from the total adsorption quantity of K^+.

Statistical Analysis

All data were analyzed using Excel 2019 and SPSS 17.0 software, and the statistical significance of the differences between treatments was determined by Duncan's multiple range test (significance level $P < 0.05$).

RESULTS

Morphological Parameters

There was a difference in plant height among the six treatments (**Table 3**). HA application increased the height of cucumber seedlings cultivated in pure cocopeat and the mixture of sand:cocopeat (1:1, v/v) by 17.59 and 20.02%, respectively, whereas the pure sand treatments showed an opposite trend when HA was applied, indicating that the three substrates responded differently to the application of HA. HA application to cocopeat or the mixture of sand:cocopeat (1:1, v/v) did not have effect on the stem diameter, whereas it decreased the stem diameter of cucumber seedlings grown in sand (by 16.29%) compared with that of cucumber seedlings grown in sand without HA addition. To investigate whether HA utilization affected cucumber biomass, we analyzed the fresh and dry weights of shoots and roots at the end of the trial period. Incorporation of 1% HA to the cocopeat increased the fresh and dry weight of roots by 26.37 and 17.86%, respectively, compared with that of roots of plants grown in cocopeat without HA application. HA addition to the mixture of sand:cocopeat (1:1, v/v) significantly increased the fresh and dry weight of shoots and roots compared with those of the groups without HA application. In contrast, there was a decrease in the fresh and dry weight of cucumber shoots and roots when 1% HA was applied to sand compared with that without HA addition.

pH Buffering Capacity

The pH buffering capacity (pHBC) was defined as the number of moles of H^+ or OH^- necessary to increase and decrease the pH of 1 kg of soil by 1 pH unit (Mowbray and Schlesinger, 1988). The acid and alkali buffering curves for the six treatments are presented in **Figures 1, 2**, respectively, and all correlation coefficients of the quadratic regression curve (R^2) were > 0.95. The pHBC values for the six treatments were calculated using the corresponding regression equations of the buffering curves. In the case when the same amount of acid was added, the faster the pH value decreased, the lower the acid buffering capacity of the substrate, whereas in the case when the same amount of alkali was added, the faster the pH value increased, the lower the alkali buffering capacity of the substrate. The substrates with poor acid or alkali buffering capacity showed a more dramatic change in the acid or alkali buffering curve. As shown in **Figures 1**, **2**, the pHBC of the groups without HA addition fluctuated more sharply after acid or alkali addition than that of the groups to which HA was applied. As shown in **Figure 3**, there was a great variation in pHBC among the different groups. The presence of HA contributed to an increase in acid and alkali pHBC compared with those in groups without HA application. In addition, among the three types of substrates, the greatest acid and alkali pHBC were observed in the cocopeat groups, whereas the groups with the mixture of sand:cocopeat (1:1, v/v) showed better performance of acid and alkali pHBC than that of the sand groups.

TOC, OM, and CEC

As shown in **Table 4**, higher TOC and OM were observed in the substrates with 1% HA application than those in the substrates without HA application, and CEC was consistently influenced by HA application. Moreover, in comparison to sand and the mixture of sand:cocopeat (1:1, v/v) treatments, the cocopeat treatment performed better with respect to TOC, OM, and CEC.

TABLE 3 | Effects of 1% HA addition on the morphological parameters of cucumber seedlings.

Treatments	Plant height (cm)	Stem diameter (mm)	Fresh weight of shoots (g)	Dry weight of shoots (g)	Fresh of roots (g)	Dry weight of roots (g)
T1	15.22 ± 1.01 e	3.50 ± 0.18 c	11.89 ± 0.42 d	2.52 ± 0.26 d	4.27 ± 0.13 e	0.88 ± 0.02 e
T2	12.33 ± 0.66 f	2.93 ± 0.29 d	9.59 ± 0.14 e	2.12 ± 0.07 e	2.35 ± 0.06 f	0.42 ± 0.07 f
T3	29.67 ± 1.45 b	4.31 ± 0.31 ab	18.77 ± 0.74 a	7.34 ± 0.92 a	7.62 ± 0.46 b	1.40 ± 0.18 b
T4	34.89 ± 2.71 a	4.77 ± 0.18 a	19.99 ± 1.68 a	7.70 ± 1.08 a	9.63 ± 0.39 a	1.65 ± 0.12 a
T5	18.33 ± 1.15 d	3.99 ± 0.19 b	14.16 ± 0.42 c	6.10 ± 0.48 c	6.41 ± 0.32 d	1.10 ± 0.04 d
T6	22.00 ± 0.33 c	4.31 ± 0.12 ab	16.14 ± 0.20 b	6.67 ± 0.31 b	6.88 ± 0.10 c	1.21 ± 0.05 c

T1, sand; T2, sand + 1% HA; T3, cocopeat; T4, cocopeat + 1% HA; T5, 1:1 sand:cocopeat; T6, 1:1 sand:cocopeat + 1% HA. Data represents the average of three replicates ± SE. Different letters indicate significant differences at $P < 0.05$.

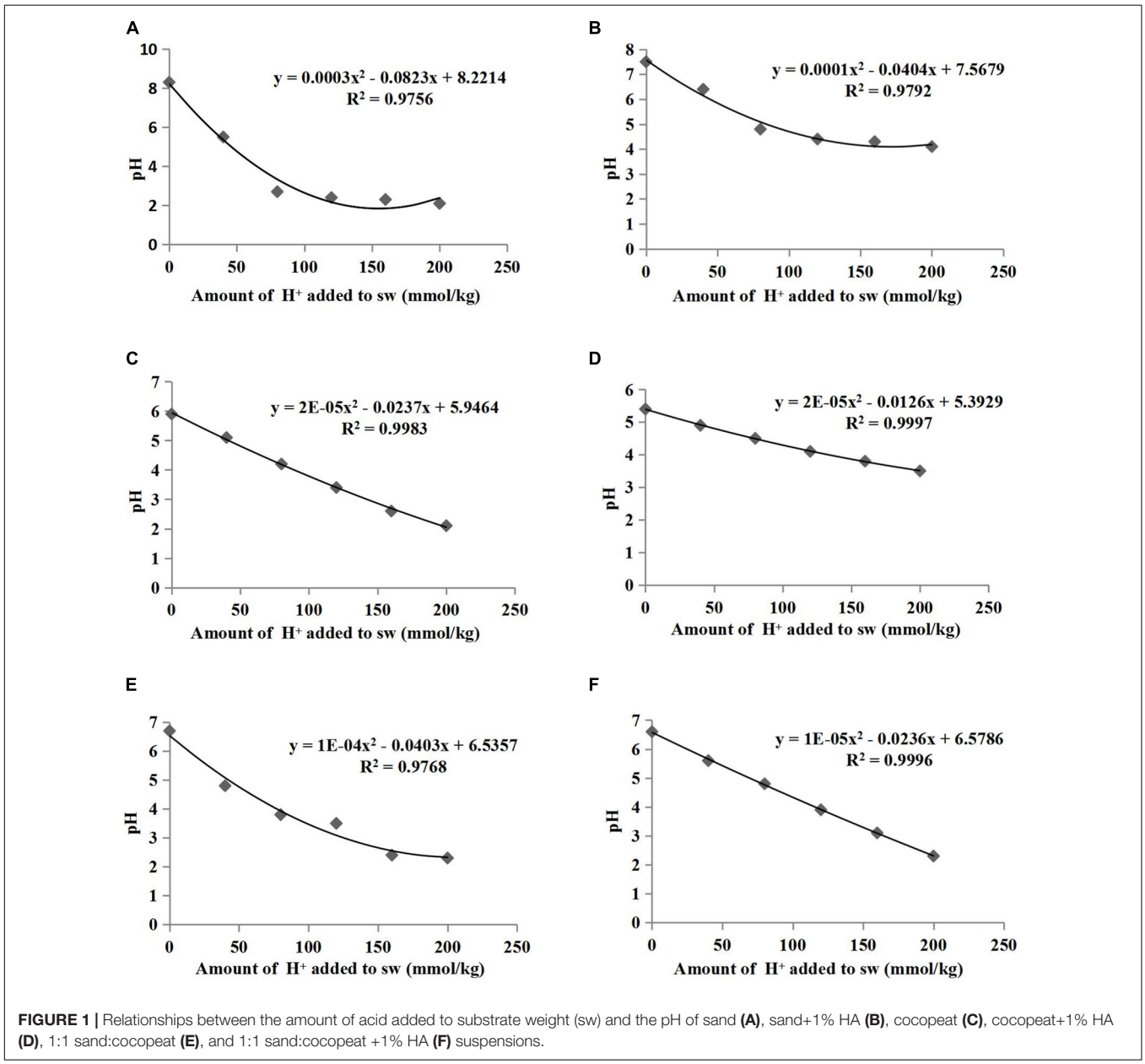

FIGURE 1 | Relationships between the amount of acid added to substrate weight (sw) and the pH of sand **(A)**, sand+1% HA **(B)**, cocopeat **(C)**, cocopeat+1% HA **(D)**, 1:1 sand:cocopeat **(E)**, and 1:1 sand:cocopeat +1% HA **(F)** suspensions.

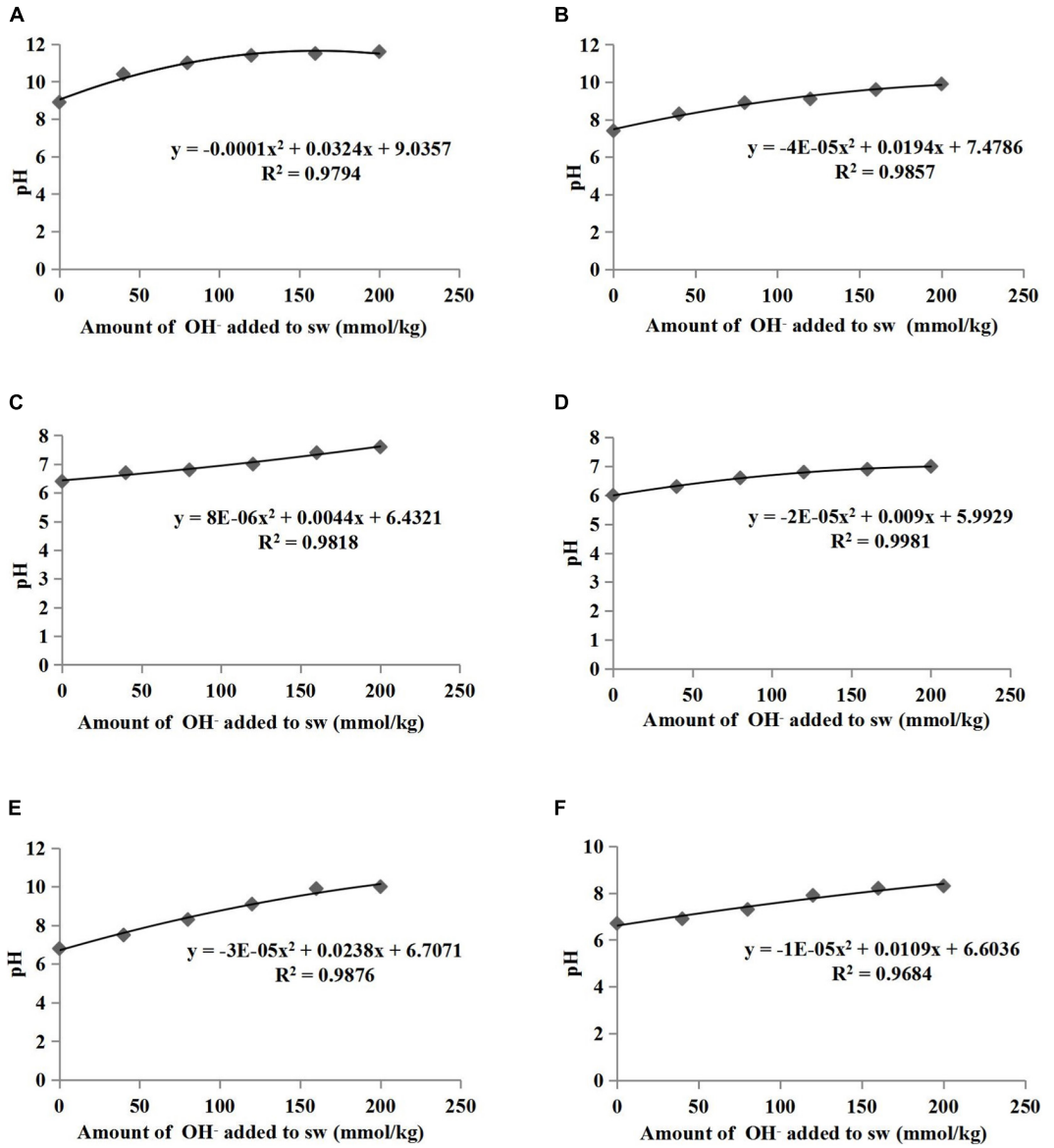

FIGURE 2 | Relationships between the amount of alkali added to substrate weight (sw) and the pH of sand **(A)**, sand+1% HA **(B)**, cocopeat **(C)**, cocopeat+1% HA **(D)**, 1:1 sand:cocopeat **(E)**, and 1:1 sand:cocopeat +1% HA **(F)** suspensions.

Storage Capacity of NH_4^+ in Different Substrates

As shown in **Figure 4**, it could be clearly noted that the adsorption saturation points varied among the substrates. In the case of pure sand and pure cocopeat groups, total NH_4^+ absorption tended to be saturated when the concentration of NH_4Cl solution reached 0.3 and 0.5 M, respectively. The total NH_4^+ adsorption curves of all treatments could be divided into two distinct parts. In the first part, NH_4Cl solution concentrations were below the saturation point, and the total NH_4^+ adsorption quantity increased greatly with increasing solution concentrations. The second part of the curve was associated with the NH_4Cl solution concentrations beyond the saturation point, at which all absorption curves became relatively flat, which indicated that they were almost saturated. Furthermore, all substrates were already saturated with 1.0 M NH_4Cl solution. In relation to the abovementioned results, we calculated the storage capacity of NH_4^+ at the complete saturation point (the corresponding concentration of NH_4Cl solution was 1.0 M). The storage capacity of NH_4^+ was related to three parameters, including total NH_4^+, fixed NH_4^+, and exchangeable NH_4^+ adsorption quantities. Among the three types of substrates, the storage capacity of NH_4^+ in cocopeat and in sand were the highest and the lowest, respectively. As shown in **Table 5**, HA application seemed to be an important factor that influenced the NH_4^+

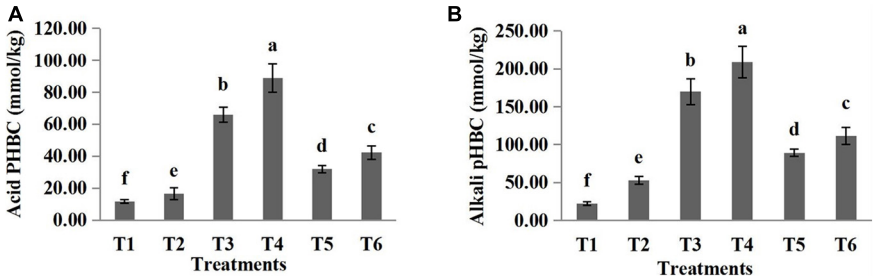

FIGURE 3 | Acid **(A)** and alkali **(B)** buffering capacity of different substrates. Bars represent standard errors. T1, sand; T2, sand + 1% HA; T3, cocopeat; T4, cocopeat + 1% HA; T5, 1:1 sand:cocopeat; T6, 1:1 sand:cocopeat + 1% HA. Different letters above the bars indicate significant differences at $P < 0.05$ according to Duncan's multiple range test.

TABLE 4 | Effects of 1% HA addition on total organic carbon (TOC), organic matter (OM), and cation exchange capacity (CEC) of different substrates.

Treatments	TOC (g/kg)	OM (g/kg)	CEC (cmol/kg)
T1	2.40 ± 0.60 f	4.14 ± 1.03 f	1.37 ± 0.29 f
T2	10.20 ± 0.60 e	17.58 ± 1.03 e	4.77 ± 0.25 e
T3	67.20 ± 1.59 b	115.85 ± 2.74 b	17.33 ± 0.86 b
T4	76.80 ± 1.59 a	131.89 ± 2.74 a	27.43 ± 0.58 a
T5	21.40 ± 1.83 d	36.89 ± 3.16 d	9.37 ± 0.76 d
T6	41.80 ± 0.92 c	72.06 ± 1.58 c	12.47 ± 0.46 c

T1, sand; T2, sand + 1% HA; T3, cocopeat; T4, cocopeat + 1% HA; T5, 1:1 sand:cocopeat; T6, 1:1 sand:cocopeat + 1% HA. Data represents the average of three replicates ± SE. Different letters indicate significant differences at P < 0.05.

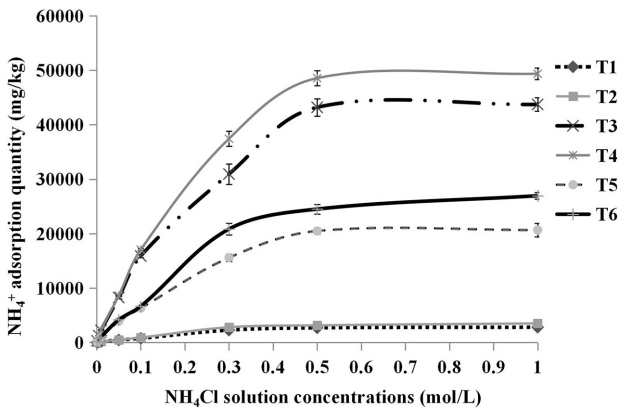

FIGURE 4 | Relationships between the concentrations of NH_4Cl solution added and the total NH_4^+ adsorption quantity. T1, sand; T2, sand + 1% HA; T3, cocopeat; T4, cocopeat + 1% HA; T5, 1:1 sand:cocopeat; T6, 1:1 sand:cocopeat + 1% HA.

adsorption of substrates due to the significantly higher total NH_4^+, fixed NH_4^+, and exchangeable NH_4^+ adsorption in the substrates to which 1% HA was applied. Additionally, most of the adsorbed NH_4^+ was present in the exchangeable form, which could easily be released from substrates and used by crops when needed.

TABLE 5 | Effects of 1% HA addition on NH_4^+ storage capacity of different substrates.

Treatments	Total NH_4^+ adsorption quantity (mg/kg)	Exchangeable NH_4^+ adsorption quantity (mg/kg)	Fixed NH_4^+ adsorption quantity(mg/kg)
T1	2800.00 ± 396.76 f	2798.94 ± 306.15 f	1.07 ± 0.12 f
T2	3500.00 ± 401.22 e	3498.76 ± 298.11 e	1.64 ± 0.11 e
T3	43715.00 ± 1243.85 b	43702.46 ± 1243.69 b	12.54 ± 0.51 b
T4	49350.00 ± 1050.00 a	49335.45 ± 1049.78 a	16.55 ± 0.43 a
T5	20650.00 ± 1212.44 d	20643.91 ± 1212.84 d	6.09 ± 0.43 d
T6	26950.00 ± 613.25 c	26942.23 ± 606.36 c	7.77 ± 0.18 c

T1, sand; T2, sand + 1% HA; T3, cocopeat; T4, cocopeat + 1% HA; T5, 1:1 sand:cocopeat; T6, 1:1 sand:cocopeat + 1% HA. Data represents the average of three replicates ± SE. Different letters indicate significant differences at P < 0.05.

Storage Capacity of P in Different Substrates

The relationships between the concentrations of KH_2PO_4 solution added and the total phosphorus adsorption quantities of different substrates are shown in **Figure 5**. The total P adsorption quantity increased with increasing solution concentrations until the substrates were completely saturated with P. The absorption saturation points of pure sand, pure cocopeat, and the mixture of sand:cocopeat (1:1, v/v) were approximately 2,000, 3,000, and 2,000 mg/L, respectively. To ensure that all substrates were in a state of complete saturation and to obtain accurate results, we selected the 6,000 mg/L point to calculate the storage capacity of P for different types of substrates, and the corresponding results are presented in **Table 6**. Cocopeat treatments absorbed the greatest amount of P, whereas sand treatments absorbed the least, which was in accordance with the results of the NH_4^+ absorption measurement. According to the analysis of the variance, no significant difference in exchangeable P was detected between HA application and no HA application treatments, whereas the treatments without HA addition were higher than those with HA addition on both total and fixed P adsorption quantity for three types of substrates.

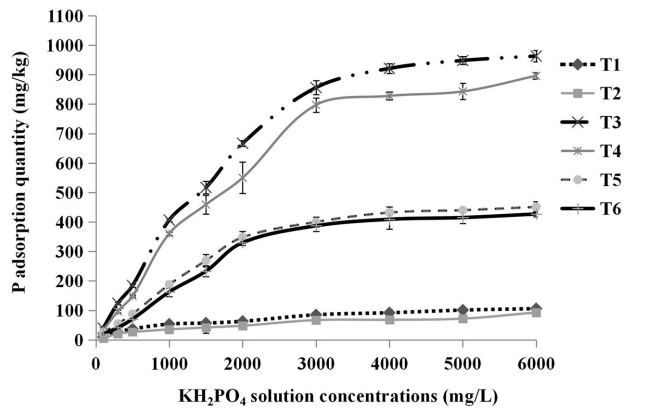

FIGURE 5 | Relationships between the concentrations of KH_2PO_4 solution added and the total P adsorption quantity. T1, sand; T2, sand + 1% HA; T3, cocopeat; T4, cocopeat + 1% HA; T5, 1:1 sand: cocopeat; T6, 1:1 sand: cocopeat + 1% HA.

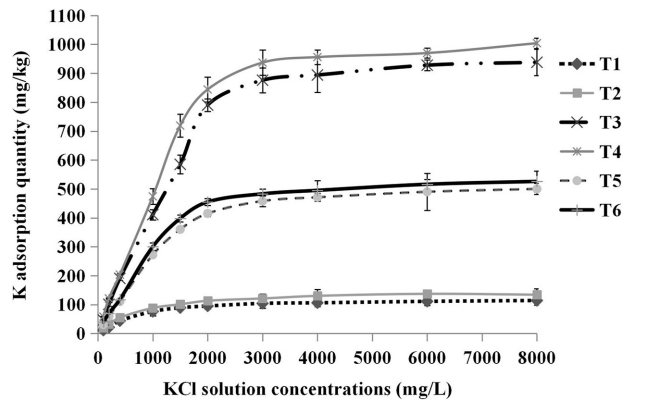

FIGURE 6 | Relationships between the concentrations of KCl solution added and the total K adsorption quantity. T1, sand; T2, sand + 1% HA; T3, cocopeat; T4, cocopeat + 1% HA; T5, 1:1 sand: cocopeat; T6, 1:1 sand: cocopeat + 1% HA.

TABLE 6 | Effects of 1% HA addition on phosphorus storage capacity of different substrates.

Treatments	Total P adsorption quantity (mg/kg)	Exchangeable P adsorption quantity (mg/kg)	Fixed P adsorption quantity (mg/kg)
T1	106.00 ± 4.58 e	89.90 ± 5.25 c	16.10 ± 1.91 c
T2	93.00 ± 3.00 f	86.03 ± 2.72 c	6.97 ± 0.39 d
T3	953.00 ± 12.12 a	889.71 ± 15.37 a	63.29 ± 8.71 a
T4	896.00 ± 10.54 b	874.04 ± 13.35 a	21.96 ± 3.88 b
T5	451.00 ± 8.08 c	424.67 ± 16.71 b	26.33 ± 4.98 b
T6	427.00 ± 9.17 d	412.24 ± 10.48 b	14.76 ± 2.39 c

T1, sand; T2, sand + 1% HA; T3, cocopeat; T4, cocopeat + 1% HA; T5, 1:1 sand: cocopeat; T6, 1:1 sand: cocopeat + 1% HA. Data represents the average of three replicates ± SE. Different letters indicate significant difference at $P < 0.05$.

TABLE 7 | Effects of 1% HA addition on potassium storage capacity of different substrates.

Treatments	Total K^+ adsorption quantity (mg/kg)	Exchangeable K^+ adsorption quantity (mg/kg)	Fixed K^+ adsorption quantity (mg/kg)
T1	104.00 ± 6.39 f	81.67 ± 5.80 f	22.33 ± 2.31 d
T2	132.00 ± 9.17 e	103.87 ± 7.41 e	28.13 ± 2.92 c
T3	938.00 ± 25.43 b	698.53 ± 37.04 b	239.47 ± 21.37 a
T4	1004.00 ± 18.33 a	782.93 ± 15.03 a	221.07 ± 33.35 a
T5	500.00 ± 9.29 d	397.48 ± 15.90 d	102.52 ± 12.57 b
T6	526.00 ± 9.17 c	426.59 ± 4.81 c	99.41 ± 11.38 b

T1, sand; T2, sand + 1% HA; T3, cocopeat; T4, cocopeat + 1% HA; T5, 1:1 sand: cocopeat; T6, 1:1 sand: cocopeat + 1% HA. Data represents the average of three replicates ± SE. Different letters indicate significant difference at $P < 0.05$.

Storage Capacity of K^+ in Different Substrates

We found that there was a difference in the K adsorption saturation point among different substrates. Pure sand, pure cocopeat, and the mixture of both were nearly saturated when the concentration of KCl solution was 2,000, 3,000, and 2,000 mg/L, respectively. The shapes of the total K adsorption curves were similar to those of the NH_4^+ adsorption curves, and the substrates were completely saturated when they were treated with the 8,000 mg/L KCl solution. Based on these results, we calculated the storage capacity of K at the saturation point (the concentration of the corresponding KCl solution was 8,000 mg/L). The storage capacity parameters of K included total K, fixed K, and exchangeable K adsorption quantities. It was apparent that the storage capacity parameters of K in cocopeat were the highest among the three substrate types (**Figure 6**). As shown in **Table 7**, for the three types of substrates, the total K, fixed K, and exchangeable K adsorption quantities were enhanced by HA addition compared with those without HA addition. Moreover, we also observed that exchangeable K played a key role in the amount of total adsorbed K, and this was consistent with the results of NH_4^+ absorption.

DISCUSSION

Effects of HA Addition to Different Substrates on Plant Morphological Parameters

We comparatively evaluated the effects of HA addition on three differently textured substrates and found that the effects varied. The results revealed that the addition of 1% HA to the pure cocopeat substrate and to a mixture of sand:cocopeat (1:1, v/v) had a positive effect on the morphological characteristics of cucumber plants, which was consistent with previous results related to soil measurements (Dobbss et al., 2007). The reason for this may be that HA benefits various biochemical processes. Several studies indicate that HA has auxin-like activity, stimulating root development through a significant proliferation of lateral roots and activation of H^+-ATPases and H^+-PPase in vacuoles as well as in the plasmalemma (Zandonadi et al., 2007).

Roots are the main plant organ for the absorption of nutrients and water, and an optimal root system is one of the requirements for yield formation (Liu et al., 2015). In the present study, the root biomass of cucumber seedlings with HA addition was higher than that of cucumber seedlings without HA addition in the pure cocopeat and in the mixture of sand:cocopeat (1:1, v/v) treatments. In addition, HA can also increase the water-holding capacity of the substrate to alleviate water stress, which may explain why HA benefits plants (García et al., 2014). HA addition achieved favorable results in pure cocopeat and in the mixture of sand:cocopeat (1:1, v/v), whereas the results were completely opposite in the pure sand groups. This may be attributed to the poor acid pHBC of sand as shown in **Figure 3A**. There were differences in acid pHBC between sand and the other substrates. HA is an acidic substance, and pH is one of the most representative indicators of substrate chemical properties (Gao et al., 2018). When HA was added to sand, pH decreased dramatically, owing to the poor acidic pHBC, and improper rhizospheric pH led to physiological disorder of roots, thereby severely affecting plant uptake of water and nutrients, which consequently resulted in low plant biomass (Wang et al., 2016).

Morphological plant parameters can indirectly reflect substrate quality. In the present study, all morphological parameters of cucumber seedlings differed among the three substrates, and seedlings in the cocopeat groups showed the best performance. Previous studies demonstrate that cocopeat is suitable for use as a growing substrate because of its excellent physical properties, such as high water-holding capacity and porosity, which are beneficial to root development (Zhu et al., 2019). In addition, the root system releases some CO_2 during root respiration that must dissipate from the root environment (Li et al., 2018), and because cocopeat has high porosity, CO_2 could rapidly dissipate from the rhizosphere. Compared with cocopeat, sand was more compact and had a lower water retention capacity, which led to a severe restriction of root growth (Liu et al., 2015). Therefore, significant differences were observed in the morphological parameters of plants grown in pure cocopeat and those grown in pure sand.

Effects of HA Addition to Different Substrates on pHBC, TOC, OM, and CEC

Soil pHBC refers to the ability of soil to mitigate the change in pH after the addition of acidic or alkaline substances, and it includes acid and alkali buffering capacity (Lieb et al., 2011). In general, the application of chemical fertilizers greatly affects soil pH; for instance, NH_4^+ application results in acidification because plants absorb more cations than anions and consequently release protons to the soil, whereas excess nitrates lead to soil alkalization (Schaller, 1987). Logically, soils with low pHBC are sensitive to acidification or alkalization, which greatly influences their nutrient availability and thereby the acquisition of nutrients by plants (Shi et al., 2017). Therefore, substrates with high pHBC are beneficial for cultivation. In the present study, the incorporation of HA resulted in stronger pH buffering behavior of the three substrates (**Figure 3**), indicating that HA addition is beneficial for stabilizing the rhizosphere pH, and consequently promoting plant growth.

As shown in **Table 4**, compared with the treatments without HA addition, the treatments with HA addition increased TOC and OM in the three different substrates. HA is a macromolecular organic substance rich in organic carbon (Saidimoradi et al., 2019), which is why mixing HA into substrates enhanced TOC and OM in the three substrates (**Table 4**). A previous study reported that the content of OM in the soil was positively correlated with soil pHBC (Xu et al., 2012). This is because there is an ample amount of oxygen-containing functional groups, such as carboxyl and phenolic hydroxyl groups, on the surface of OM (Liang et al., 2011). These groups accept protons when pH decreases and provide protons when pH increases (Kida et al., 2005), making a great contribution to pHBC improvement. Furthermore, we found that in the HA application treatments, the alkali buffering capacity of the three substrates was greater than their acid buffering capacity. The reason for this was because HA carries abundant acidic functional groups which can effectively neutralize alkaline components.

Cation exchange capacity (CEC) is a crucial index for assessing substrate quality, and it describes the potential of a substrate to absorb and release nutrients. High CEC can reduce fluctuations in ion concentrations (Pincus et al., 2017). As shown in **Table 4**, there was a difference in CEC between the treatments with and without HA addition. Previous studies have demonstrated that there was a positive correlation between CEC and OM. The reason for this positive correlation is that OM possesses a large number of functional groups which can be hydrolyzed to produce negative charges; these negative charges are able to adsorb a high amount of exchangeable cations and consequently improve CEC (Shekofteh et al., 2017).

Our results show that the TOC and OM of cocopeat groups were higher than those of the other groups (**Table 4**). Cocopeat is an agricultural by-product manufactured after the selection of fiber from coconut husks (Hongpakdee and Ruamrungsri, 2017); thus, it is rich in OM. On the other hand, sand is an inorganic substrate; therefore, TOC and OM differed significantly among the three substrates. In addition, it could be clearly observed that pHBC of cocopeat was significantly higher than that of the other two substrates (**Figure 3**), which was consistent with the high OM content of cocopeat. Furthermore, the CEC results coincided with OM measurements as shown in **Table 4**. The CEC of the cocopeat was significantly higher than that of the other two substrates. Additionally, in the mixture of sand:cocopeat (1:1, v/v), cocopeat addition compensated for the deficiency of OM in sand and consequently improved the CEC.

Effects of HA Addition to Different Substrates on N, P, and K Storage Capacities

The results show that the presence of HA increased the NH_4^+ storage capacity in the three different substrates (**Table 5**). CEC affects the soil storage capacity for nutrients (Wang et al., 2019); therefore, a difference in CEC between HA groups and no HA groups might lead to differences in NH_4^+ storage capacity.

Additionally, the chemical reaction of NH_4^+ with HA is closely linked to NH_4^+ storage because these two substances frequently form NH_4^+ humate, which has higher stability than other NH_4^+ salts. NH_4^+ volatilization loss was reduced by this process, and this ultimately increased the storage capacity of NH_4^+ (Dong et al., 2009). Furthermore, NH_4^+ could be incorporated into HA through covalent bonding, and the majority of NH_4^+ appears to be in the form of indole and pyrrole N (Thorn and Mikita, 1992). This may also explain why HA addition actively modified NH_4^+ storage capacity. Moreover, a previous study showed that HA could easily bind with NH_4^+ owing to its strong complexation and absorption capabilities. In the present study, HA showed significant slow-release effects on N release and utilization, which consequently increased fertilizer use efficiency (Chen et al., 2017). Fixed NH_4^+ and exchangeable NH_4^+ are the main constituents of adsorbed NH_4^+ in the soil (Egashira et al., 1998). Exchangeable NH_4^+ can be directly used by plants (Beuters et al., 2014), and this accounted for the majority of absorbed NH_4^+ in the present study (**Table 5**), implying that the adsorption of NH_4^+ by the three substrates was temporary and easily taken up by plants. Compared with that in the groups without HA addition, higher exchangeable NH_4^+ was observed in the HA addition groups, indicating that HA could improve the exchangeable NH_4^+ storage capacity in the three substrates.

P is an essential nutrient for plant growth, and phosphate deficiency can disrupt plant metabolism (Yang et al., 2004); therefore, the availability of phosphates is an important agricultural issue. Once phosphate fertilizers are applied to soils, a series of complex reactions that decrease phosphate availability may gradually occur. The main reactions include phosphate adsorption into soil and precipitation in the form of calcium phosphate minerals (Parfitt et al., 2010; Perassi and Borgnino, 2014), which can adversely affect the uptake of phosphorus by plant roots. In our experiment, the results showed that HA addition decreased total P adsorption, indicating that it has a desirable impact on the improvement of phosphate availability. It is generally accepted that HA is rich in anions, such as hydroxyl and carboxyl ions (Liang et al., 2011), and that it can reduce the adsorption of soil minerals to phosphates because of the strong competition of both anions for the same adsorption sites on the surface of soil minerals. In addition, HA can bind with Ca^{2+} in the soil and interact with Ca-P to inhibit the formation of Ca-P precipitates. These effects improved the mobility of P and ultimately enhanced P availability in the soil (Cimrin and Yilmaz, 2005; Antelo et al., 2007; Perassi and Borgnino, 2014; Zhou et al., 2015). The results of our study were in accordance with those of previous studies as shown in **Table 6**. HA addition could suppress phosphate fixation in the three different substrates; in other words, the availability of phosphates was increased.

The release of absorbed K^+ in the soil occurred in the rhizosphere when K^+ concentration in the rhizosphere solution decreased below the threshold (Hinsinger and Jaillard, 2010). HA exerts a regulatory effect on nutrient forms in fertilizers, and it could react with K^+ in fertilizers to form K^+ humate, which is not easily lost with water, and the presence of potassium humate can provide the ability to slowly release potassium (Liu et al., 2006). This means that HA application directly enhances the storage capacity of K^+ in the soil and modifies the potassium supply pattern. Our results are in accordance with the results of earlier research as shown in **Table 7**. The total K^+ adsorption of the three different substrates with HA application was significantly higher than that of the three groups without HA application. The total adsorbed K^+ comprises exchangeable K^+ and fixed K^+ (Askegaard et al., 2003). In the present study, exchangeable K^+ accounted for the majority of adsorbed K^+. Exchangeable K^+ in the rhizosphere serves as the main source of K for plants (Madaras and Koubová, 2016). In our experiment, the amount of absorbed exchangeable K^+ in the HA addition groups was significantly higher than that in the groups without HA addition, and the difference in this indicator might explain the difference in plant growth between the treatments with and without HA addition. Furthermore, a previous study demonstrated that HA could enhance the proportion of exchangeable K^+ in adsorbed K^+ (Olk and Cassman, 1995). In the present study, the presence of HA increased the proportion of exchangeable K^+ in adsorbed K^+.

CONCLUSION

Incorporation of HA to different texture substrates had different effects on plant growth parameters (plant height, stem diameter, and biomass). In pure cocopeat and the mixture of sand: cocopeat (1:1, v/v), HA application improved the growth of cucumber seedlings, whereas in sand, HA addition was harmful to plant growth. The comprehensive evaluation showed that pHBC, organic matter content, and CEC in the HA groups were higher than those in the groups without HA. Treatments with HA addition resulted in higher NH_4^+ and K^+ storage capacity, while decreasing P fixation, thus increasing P availability, indicating that HA application enhanced fertilizer efficiency. Among the three substrates, cocopeat was the best substrate for cultivation, and incorporating cocopeat into sand was beneficial to plant growth. Overall, cocopeat with 1% HA was the best treatment in this study.

DATA AVAILABILITY STATEMENT

The original contributions presented in the study are included in the article/**Supplementary Material**, further inquiries can be directed to the corresponding author/s.

AUTHOR CONTRIBUTIONS

WJ, HY, QL, and TL contributed to the conception and design of the study. JX and EM conducted the experiments, collected the data, and performed the statistical analysis. JX wrote the first draft of the manuscript. WJ, HY, and TL contributed to the writing and revision of the manuscript. All authors have given final approval for the publication of the manuscript.

FUNDING

This research work was financially supported by the National key R&D program of China (2019YFD1001901), the National Key R&D Program of China (2018YFD0800401), and National Key R&D Program of China (2017YFE0118500).

ACKNOWLEDGMENTS

We are grateful to Heng Wang, Lin Chai, Peng Liu, and Xue Zhang for their constructive advice on the experiments, Yangfan Song and Cong Wang for the management of greenhouse. We would like to thank all our colleagues for their helpful discussions and assistance.

SUPPLEMENTARY MATERIAL

The Supplementary Material for this article can be found online at: https://www.frontiersin.org/articles/10.3389/fpls.2021.644229/full#supplementary-material

REFERENCES

Abad, M., Fornes, F., Carrion, C., Noguera, V., Noguera, P., Maquieira, A., et al. (2005). Physical properties of various coconut coir dusts compared to peat. *HortScience* 40, 2138–2144. doi: 10.21273/HORTSCI.40.7.213

Ahmad, N., Reid, E. D., Nkrumah, M., Griffith, S. M., and Gabriel, L. (1982). Crop utilization and fixation of added ammonium in soils of the West Indies. *Plant Soil* 67, 167–186. doi: 10.1007/BF02182765

Anderson, B. H., and Magdoff, F. R. (2005). Relative movement and soil fixation of soluble organic and inorganic phosphorus. *J. Environ. Qual.* 34:2228. doi: 10.2134/jeq2005.0025

Antelo, J., Arce, F., Avena, M., Fiol, S., López, R., and Macias-Vázquez, I. F. (2007). Adsorption of a soil humic acid at the surface of goethite and its competitive interaction with phosphate. *Geoderma* 138, 12–19. doi: 10.1016/j.geoderma.2006.10.011

Askegaard, M., Eriksen, J., and Olesen, J. E. (2003). Exchangeable potassium and potassium balances in organic crop rotations on a coarse sand. *Soil Use Manag.* 19, 96–103. doi: 10.1079/SUM2002173

Banitalebi, G., Mosaddeghi, M. R., and Shariatmadari, H. (2021). Evaluation of physico-chemical properties of biochar-based mixtures for soilless growth media. *J. Mater. Cycles Waste Manag.* 23, 950–964. doi: 10.1007/s10163-021-01181-z

Beuters, P., Eichert, T., and Hw, S. (2014). Influence of pre-crop and root architecture on the mobilization of non-exchangeable NH4. *Plant Soil Environ.* 60, 372–378. doi: 10.17221/260/2014-PSE

Bijanzadeh, E., Naderi, R., and Egan, T. P. (2019). Exogenous application of humic acid and salicylic acid to alleviate seedling drought stress in two corn (*Zea mays* L.) hybrids. *J. Plant Nutr.* 42, 1483–1495. doi: 10.1080/01904167.2019.1617312

Butegwa, C. N., Mullins, G. L., and Chien, S. H. (1995). Induced phosphorus fixation and the effectiveness of phosphate fertilizers derived from Sukulu Hills phosphate rock. *Fert. Res.* 44, 231–240. doi: 10.1007/BF00750930

Cai, G. X., Chen, D. L., Ding, H., Pacholski, A., Fan, X. H., and Zhu, Z. L. (2002). Nitrogen losses from fertilizers applied to maize, wheat and rice in the North China Plain. *Nutr. Cycl. Agroecosyst.* 63, 187–195. doi: 10.1023/A:1021198724250

Chen, Q., Zhang, X., Zhang, H., Christie, P., Li, X., Horlacher, D., et al. (2004). Evaluation of current fertilizer practice and soil fertility in vegetable production in the Beijing region. *Nutr. Cycl. Agroecosyst.* 69, 51–58. doi: 10.1023/B:FRES.0000025293.99199.ff

Chen, X., Kou, M., Tang, Z., Zhang, A., Li, H., and Wei, M. (2017). Responses of root physiological characteristics and yield of sweet potato to humic acid urea fertilizer. *PLoS One* 12:e189715. doi: 10.1371/journal.pone.0189715

Cimrin, K. M., and Yilmaz, I. (2005). Humic acid applications to lettuce do not improve yield but do improve phosphorus availability. *Acta Agric. Scand. Section B Soil Plant Sci.* 55, 58–63. doi: 10.1080/09064710510008559

Cui, Z., Chen, X., Miao, Y., Zhang, F., Sun, Q., Schroder, J., et al. (2008). On-Farm evaluation of the improved soil n–based nitrogen management for summer maize in north china plain. *Agron. J.* 100:517. doi: 10.2134/agronj2007.0194

Dobbss, L. B., Medici, L. O., Peres, L. E. P., Pino-Nunes, L. E., Rumjanek, V. M., Façanha, A. R., et al. (2007). Changes in root development of *Arabidopsis* promoted by organic matter from oxisols. *Ann. Appl. Biol.* 151, 199–211. doi: 10.1111/j.1744-7348.2007.00166.x

Dogan, Y., Togay, Y., Togay, N., and Kulaz, H. (2014). Effect of humic acid and phosphorus applications on the yield and yield components in lentil (*Lens culinaris* medic.). *Legume Res.* 37:316. doi: 10.5958/j.0976-0571.37.3.048

Dong, L., Córdova-Kreylos, A. L., Yang, J., Yuan, H., and Scow, K. M. (2009). Humic acids buffer the effects of urea on soil ammonia oxidizers and potential nitrification. *Soil Biol. Biochem.* 41, 1612–1621. doi: 10.1016/j.soilbio.2009.04.023

Egashira, K., Hagimine, M., and Moslehuddin, A. Z. M. (1998). Fixed ammonium in some Bangladesh soils. *Soil Sci. Plant Nutr.* 44, 269–272. doi: 10.1080/00380768.1998.10414449

Fan, Z., Lin, S., Zhang, X., Jiang, Z., Yang, K., Jian, D., et al. (2014). Conventional flooding irrigation causes an overuse of nitrogen fertilizer and low nitrogen use efficiency in intensively used solar greenhouse vegetable production. *Agric. Water Manag.* 144, 11–19. doi: 10.1016/j.agwat.2014.05.010

Gao, Y., Yu, H., Liu, P., Ma, C., Li, Q., and Jiang, W. (2018). Ending composting during the thermophilic phase improves cultivation substrate properties and increasing winter cucumber yield. *Waste Manag.* 79, 260–272. doi: 10.1016/j.wasman.2018.07.048

García, A. C., Santos, L. A., Izquierdo, F. G., Rumjanek, V. M., Castro, R. N., dos Santos, F. S., et al. (2014). Potentialities of vermicompost humic acids to alleviate water stress in rice plants (*Oryza sativa* L.). *J. Geochem. Explor.* 136, 48–54. doi: 10.1016/j.gexplo.2013.10.005

He, F., Jiang, R., Chen, Q., Zhang, F., and Su, F. (2009). Nitrous oxide emissions from an intensively managed greenhouse vegetable cropping system in Northern China. *Environ. Pollut.* 157, 1666–1672. doi: 10.1016/j.envpol.2008.12.017

Hinsinger, P., and Jaillard, B. (2010). Root-induced release of interlayer potassium and vermiculitization of phlogopite as related to potassium depletion in the rhizosphere of ryegrass. *J. Soil Sci.* 44, 525–534. doi: 10.1111/j.1365-2389.1993.tb00474.x

Hongpakdee, P., and Ruamrungsri, S. (2017). Coconut coir dust ratio affecting growth and flowering of potted petunia hybrids. *Acta Hortic.* 1167, 369–374. doi: 10.17660/ActaHortic.2017.1167.53

Kida, Y., Mita, Y., Fukushi, K., and Sato, T. (2005). Mechanisms of alkaline buffering by peat and quantitative estimation of its buffering capacity. *Landsc. Ecol. Eng.* 1, 127–134. doi: 10.1007/s11355-005-0016-y

Lan, X., Xia, X., Han, Y., Wu, Y., Liang, C., and Du, L. (2016). The effect of humus acids on fixation and release of potassium in meadow soil. *Chin. J. Soil Sci.* 47, 949–953. doi: 10.19336/j.cnki.trtb.2016.04.27

Li, X., Guo, D., Zhang, C., Niu, D., Fu, H., and Wan, C. (2018). Contribution of root respiration to total soil respiration in a semi-arid grassland on the Loess Plateau. *China. Sci. Total Environ.* 627, 1209–1217. doi: 10.1016/j.scitotenv.2018.01.313

Li, X., Zhu, J., Gu, X., and Zhu, J. (2010). Current situation and control of agricultural non-point source pollution. *China Popul. Resour. Environ.* 20, 81–84. doi: 10.1111/j.1752-1688.1984.tb04790.x

Liang, C., Luo, L., Du, L., and Pan, D. (2005). Effect of humic acids on fixation and release of potassium in cultivated brown soil. *Acta Pedol. Sin.* 42, 468–472. doi: 10.3321/j.issn:0564-3929.2005.03.018

Liang, L., Lv, J., Luo, L., Zhang, J., and Zhang, S. (2011). Influences of surface-coated fulvic and humic acids on the adsorption of metal cations to SiO2 nanoparticles. *Colloids Surf, A Physicochem. Eng. Asp.* 389, 27–32. doi: 10.1016/j.colsurfa.2011.09.002

Lieb, A. M., Darrouzet-Nardi, A., and Bowman, W. D. (2011). Nitrogen deposition decreases acid buffering capacity of alpine soils in the southern Rocky Mountains. *Geoderma* 164, 220–224. doi: 10.1016/j.geoderma.2011.06.013

Liu, F., Xing, S., Liu, C., Du, Z., and Duan, C. (2006). Characteristics of adsorption of K+ on humic acid extracted from brown coal. *Trans. Chin. Soc. Agric. Eng.* 8, 27–31. doi: 10.11674/zwyf.2005.0414

Liu, X., Zhang, X., Chen, S., Sun, H., and Shao, L. (2015). Subsoil compaction and irrigation regimes affect the root–shoot relation and grain yield of winter wheat. *Agric. Water Manag.* 154, 59–67. doi: 10.1016/j.agwat.2015.03.004

Madaras, M., and Koubová, M. (2016). Potassium availability and soil extraction tests in agricultural soils with low exchangeable potassium content. *Plan, Soil Environ.* 61, 234–239. doi: 10.17221/171/2015-PSE

Markovic, V., Djurovka, M., and Ilin, Z. (1997). The effect of seedling quality on tomato yield, plant and fruit characteristics. *Acta Hortic.* 462, 163–170. doi: 10.17660/ActaHortic.1997.462.21

Mora, V., Baigorri, R., Bacaicoa, E., Zamarreño, A. M., and García-Mina, J. M. (2012). The humic acid-induced changes in the root concentration of nitric oxide, IAA and ethylene do not explain the changes in root architecture caused by humic acid in cucumber. *Environ. Exp. Bot.* 76, 24–32. doi: 10.1016/j.envexpbot.2011.10.001

Mowbray, T., and Schlesinger, W. H. (1988). The buffer capacity of organic soils of the bluff mountain fen, north carolina. *Soil Sci.* 146, 73–79. doi: 10.1097/00010694-198808000-00003

Nan, J., Chen, X., Chen, C., Lashari, M. S., Deng, J., and Du, Z. (2016). Impact of flue gas desulfurization gypsum and lignite humic acid application on soil organic matter and physical properties of a saline-sodic farmland soil in Eastern China. *J. Soils Sediments* 16, 2175–2185. doi: 10.1007/s11368-016-1419-0

Nieder, R., Benbi, D. K., and Scherer, H. W. (2011). Fixation and defixation of ammonium in soils: a review. *Biol. Fert. Soils* 47, 1–14. doi: 10.1007/s00374-010-0506-4

Olk, D. C., and Cassman, K. G. (1995). Reduction of potassium fixation by two humic acid fractions in vermiculitic soils. *Soil Sci. Soc. Am. J.* 59:1250. doi: 10.2136/sssaj1995.03615995005900050007x

Parfitt, R. L., Hume, L. J., and Sparling, G. P. (2010). Loss of availability of phosphate in New Zealand soils. *Eur. J. Soil Sci.* 40, 371–382. doi: 10.1111/j.1365-2389.1989.tb01281.x

Perassi, I., and Borgnino, L. (2014). Adsorption and surface precipitation of phosphate onto CaCO3–montmorillonite: effect of pH, ionic strength and competition with humic acid. *Geoderma* 23, 600–608. doi: 10.1016/j.geoderma.2014.06.017

Pincus, L. N., Ryan, P. C., Huertas, F. J., and Alvarado, G. E. (2017). The influence of soil age and regional climate on clay mineralogy and cation exchange capacity of moist tropical soils: a case study from Late Quaternary chronosequences in Costa Rica. *Geoderma* 308, 130–148. doi: 10.1016/j.geoderma.2017.08.033

Saidimoradi, D., Ghaderi, N., and Javadi, T. (2019). Salinity stress mitigation by humic acid application in strawberry (*Fragaria x ananassa Duch.*). *Sci. Hortic.* 256:108594. doi: 10.1016/j.scienta.2019.108594

Schaller, G. (1987). PH changes in the rhizosphere in relation to the pH-buffering of soils. *Plant Soil* 97, 439–444. doi: 10.1007/BF02383234

Shekofteh, H., Ramazani, F., and Shirani, H. (2017). Optimal feature selection for predicting soil CEC: comparing the hybrid of ant colony organization algorithm and adaptive network-based fuzzy system with multiple linear regression. *Geofis. Int.* 298, 27–34. doi: 10.1016/j.geoderma.2017.03.010

Shi, R., Hong, Z., Li, J., Jiang, J., Baquy, M. A., Xu, R. K., et al. (2017). Mechanisms for increasing the pH buffering capacity of an acidic ultisol by crop Residue-Derived biochars. *J. Agric. Food Chem.* 65, 8111–8119. doi: 10.1021/acs.jafc.7b02266

Simonsson, M., Hillier, S., and Öborn, I. (2009). Changes in clay minerals and potassium fixation capacity as a result of release and fixation of potassium in long-term field experiments. *Geoderma* 151, 109–120. doi: 10.1016/j.geoderma.2009.03.018

Sun, B., Zhang, L., Yang, L., Zhang, F., Norse, D., and Zhu, Z. (2012). Agricultural Non-Point source pollution in china: causes and mitigation measures. *Ambio* 41, 370–379. doi: 10.1007/s13280-012-0249-6

Thorn, K. A., and Mikita, M. A. (1992). Ammonia fixation by humic substances: a nitrogen-15 and carbon-13 NMR study. *Sci. Total Environ.* 113, 67–87. doi: 10.1016/0048-9697(92)90017-M

Vaughn, S. F., Deppe, N. A., Palmquist, D. E., and Berhow, M. A. (2011). Extracted sweet corn tassels as a renewable alternative to peat in greenhouse substrates. *Indust. Crops Prod.* 33, 514–517. doi: 10.1016/j.indcrop.2010.10.034

Wang, H., Xu, J., Liu, X., Zhang, D., Li, L., Li, W., et al. (2019). Effects of long-term application of organic fertilizer on improving organic matter content and retarding acidity in red soil from China. *Soil Tillage Res.* 195:104382. doi: 10.1016/j.still.2019.104382

Wang, X., Tang, C., Severi, J., Butterly, C. R., and Baldock, J. A. (2016). Rhizosphere priming effect on soil organic carbon decomposition under plant species differing in soil acidification and root exudation. *New Phytol.* 211, 864–873. doi: 10.1111/nph.13966

Wei, X., Zhang, Z., Shi, P., Wang, P., Chen, Y., Song, X., et al. (2015). Is yield increase sufficient to achieve food security in china? *PLoS One* 10:e116430. doi: 10.1371/journal.pone.0116430

Xu, R., Zhao, A., Yuan, J., and Jiang, J. (2012). PH buffering capacity of acid soils from tropical and subtropical regions of China as influenced by incorporation of crop straw biochars. *J. Soils Sediments* 12, 494–502. doi: 10.1007/s11368-012-0483-3

Yan, Y., Tian, J., Fan, M., Zhang, F., Li, X., Christie, P., et al. (2012). Soil organic carbon and total nitrogen in intensively managed arable soils. *Agric. Ecosyst. Environ.* 150, 102–110. doi: 10.1016/j.agee.2012.01.024

Yang, W., Liu, S., Feng, F., Hou, H., Jiang, G., Xu, Y., et al. (2004). Effects of phosphate deficiency on the lipid composition in cucumber thylakoid membranes and PSII particles. *Plant Sci.* 166, 1575–1579. doi: 10.1016/j.plantsci.2004.02.010

Zandonadi, D. B., Canellas, L. P., and Façanha, A. R. (2007). Indolacetic and humic acids induce lateral root development through a concerted plasmalemma and tonoplast H+ pumps activation. *Planta* 225, 1583–1595. doi: 10.1007/s00425-006-0454-2

Zhao, H., Zhai, X., Guo, L., Yang, Y., Li, J., Ren, C., et al. (2019). Comparing protected cucumber and field cucumber production systems in China based on emergy analysis. *J. Clean. Prod.* 236, 117641–117648.

Zhou, S., Limoge, Q., Tan, J., Xing, W., and Chen, Q. (2015). Strategies in efficient utilization of soil NPK nutrients with humic acid amendments. *Humic. Acid* 2, 1–8. doi: 10.19451/j.cnki.issn1671-9212.2015.02.003

Zhu, Y., Dyck, M., Cai, H., Song, L., and Chen, H. (2019). The effects of aerated irrigation on soil respiration, oxygen, and porosity. *J. Integr. Agric.* 18, 2854–2868. doi: 10.1016/S2095-3119(19)62618-3

Conflict of Interest: The authors declare that the research was conducted in the absence of any commercial or financial relationships that could be construed as a potential conflict of interest.

Publisher's Note: All claims expressed in this article are solely those of the authors and do not necessarily represent those of their affiliated organizations, or those of the publisher, the editors and the reviewers. Any product that may be evaluated in this article, or claim that may be made by its manufacturer, is not guaranteed or endorsed by the publisher.

frontiers in Plant Science

ORIGINAL RESEARCH
published: 02 August 2021
doi: 10.3389/fpls.2021.700273

Bioformulation of Silk-Based Coating to Preserve and Deliver *Rhizobium tropici* to *Phaseolus vulgaris* Under Saline Environments

Manal Mhada[1], Augustine T. Zvinavashe[2], Zakaria Hazzoumi[3], Youssef Zeroual[4], Benedetto Marelli[2] and Lamfeddal Kouisni[5]*

[1] African Integrated Plant and Soil Research Group, AgroBioSciences, Mohammed VI Polytechnic University (UM6P), Benguerir, Morocco, [2] Department of Civil and Environmental Engineering, Massachusetts Institute of Technology, Cambridge, MA, United States, [3] Green Biotechnology Laboratory, Moroccan Foundation for Advanced Science Innovation and Research (MAScIR), Rabat, Morocco, [4] Situation Innovation—OCP Group, Casablanca, Morocco, [5] African Sustainable Agriculture Research Institute (ASARI–UM6P), Laayoune, Morocco

OPEN ACCESS

Edited by:
Maurizio Ruzzi, University of Tuscia, Italy

Reviewed by:
Debojyoti Moulick, Assam University, India
Salma Mukhtar, University of the Punjab, Pakistan

***Correspondence:**
Manal Mhada
manal.mhada@um6p.ma

Specialty section:
This article was submitted to Plant Abiotic Stress, a section of the journal Frontiers in Plant Science

Received: *25 April 2021*
Accepted: *31 May 2021*
Published: *02 August 2021*

Citation:
Mhada M, Zvinavashe AT, Hazzoumi Z, Zeroual Y, Marelli B and Kouisni L (2021) Bioformulation of Silk-Based Coating to Preserve and Deliver Rhizobium tropici to Phaseolus vulgaris Under Saline Environments. Front. Plant Sci. 12:700273. doi: 10.3389/fpls.2021.700273

Seed priming has been for a long time an efficient application method of biofertilizers and biocontrol agents. Due to the quick degradation of the priming agents, this technique has been limited to specific immediate uses. With the increase of awareness of the importance of sustainable use of biofertilizers, seed coating has presented a competitive advantage regarding its ability to adhere easily to the seed, preserve the inoculant, and decompose in the soil. This study compared primed *Phaseolus vulgaris* seeds with *Rhizobium tropici* and trehalose with coated seeds using a silk solution mixed with *R. tropici* and trehalose. We represented the effect of priming and seed coating on seed germination and the development of seedlings by evaluating physiological and morphological parameters under different salinity levels (0, 20, 50, and 75 mM). Results showed that germination and morphological parameters have been significantly enhanced by applying *R. tropici* and trehalose. Seedlings of coated seeds show higher root density than the freshly primed seeds and the control. The physiological response has been evaluated through the stomatal conductance, the chlorophyll content, and the total phenolic compounds. The stability of these physiological traits indicated the role of trehalose in the protection of the photosystems of the plant under low and medium salinity levels. *R. tropici* and trehalose helped the plant mitigate the negative impact of salt stress on all traits. These findings represent an essential contribution to our understanding of stress responses in coated and primed seeds. This knowledge is essential to the design of coating materials optimized for stressed environments. However, further progress in this area of research must anticipate the development of coatings adapted to different stresses using micro and macro elements, bacteria, and fungi with a significant focus on biopolymers for sustainable agriculture and soil microbiome preservation.

Keywords: biomaterial in agriculture, sustainable agriculture, food security, soil salinity, seed coating

INTRODUCTION

Seed production is one of the critical agri-businesses that relies not only on exploiting potential genetic resources of the crop-seed itself but also on advances in multiple technologies that enable efficient use of different biological resources such as beneficial microorganisms.

Seed priming or pretreatment was used in agriculture a century ago. However, the use of bioagents was first reported by Callan et al. (1990). The method implies seed inoculation with beneficial microorganisms. According to Bisen et al. (2015), the biopriming with beneficial microbes offers an innovative crop protection tool by improving the seed quality, germination rate, seedling vigor and uniformity, and plant ability to withstand harsh growth conditions, thus ensuring sustainable crop production (Bisen et al., 2015). Another use of biopriming has sprung by understanding plant growth promoting bacteria functions and mechanisms. The discovery of phosphate solubilizing bacteria has led to its use in agriculture as a potential biofertilizer. For example, it has been reported that phosphate solubilizing rhizobacteria strongly influences wheat root traits and aboveground physiology (Elhaissoufi et al., 2020). Although seed priming is facing many challenges related to the conservation of bioformulation, storage, and difficulties in upscaling management. We can overcome challenges by coating seeds using biofertilizers embodied within films synthesized from biomaterials (Zvinavashe et al., 2021).

Among the most important features that a germinating seed may exhibit would be a coating agent that preserves seed health, guarantees a high germination rate, tolerates stresses, delivers beneficial microorganisms, and contributes to sustainable agriculture (Pedrini et al., 2017; Rocha et al., 2019). Thus, the importance of biopolymers designed for agriculture and inspired by nature. Silk was one of the most promising biopolymers due to its natural properties. The combination of beta-sheet structures with inter-and intra-molecular hydrogen bonds that provides high flexibility in the natural fiber also guarantees extreme conformability in regenerated film format (Marelli et al., 2016).

Many research activities are conducted to develop a good coating agent and components that could play a role in crucial stages in plant growth in stressed environments (Maity et al., 2019; Soumare et al., 2020; Meftah Kadmiri et al., 2021). To develop new strategies to enhance abiotic stress tolerance of crop plants (Iordachescu and Imai, 2008), bioinspired coating using silk was developed (Zvinavashe et al., 2019), combining trehalose and *R. tropici*. Both have been known for their effect on different stages of the crop cycle and their ability to promote growth.

Trehalose has been identified as an osmoprotectant and signaling molecule controlling various processes ranging from seed development and germination to guard cell movement and overall plant growth (Gómez et al., 2010). Trehalose is biosynthesized through different pathways in different living organisms except for mammals (Elbein et al., 2003). The catabolism enzymes are trehalase, trehalose phosphorylase, trehalose-6-phosphate phosphorylase, and trehalose-6-phosphate hydrolase which are widespread in living cells and may be of considerable importance in regulating the level of trehalose in the cell and managing the trehalose/sugar ratio in the demanding sink (Chen and Haddad, 2004). The level of trehalose is significantly increased in various cells when exposed to various environmental stresses, reflecting that abiotic stresses differentially regulate trehalose biosynthesis genes in higher plants (Bae et al., 2005).

The second component of the newly designed coating called "Silk Coating" is *R. tropici*. Besides its ability to promote growth and increase stress tolerance in legumes, trehalose accumulation has also been described in *Rhizobium* in response to several stressful conditions such as high external osmolarity, low oxygen concentrations, or desiccation (McIntyre et al., 2007). Trehalose also acts as an osmoprotectant when exogenously supplied to *R. leguminosarum* (Gouffi et al., 1999). It is also a common disaccharide in the root nodules of legumes and is present in bacteroids serving as molecular signals during biological nitrogen fixation (Gómez et al., 2010; Zvinavashe et al., 2019), which could reflect an important role for this molecule in symbiosis. It was also demonstrated by Müller et al. (1998) that the addition of exogenous trehalose to the growth medium increased sucrose synthase and alkaline invertase activities in soybean. Besides, the inoculation of common bean (*Phaseolus vulgaris*) with the symbiotic bacterium *R. etli*, which was engineered to overexpress the *Escherichia coli* trehalose-6-phosphate synthase (otsA), resulted in more trehalose production and formation of more nodules with higher nitrogenase activity (Suárez et al., 2008). In agreement with this, deletion of the endogenous otsA gene in *R. etli* reduced the number of nodules, nitrogenase activity, and plant biomass.

Due to the well-known stress-protecting properties of trehalose in microorganisms and plants, "trehalose/bacteria" could be a valuable mixture to target to improve abiotic stress tolerance in crop plants.

The objectives of this study were (1) to investigate the effect of exogenous application of trehalose and *R. tropici* in two different methods (Priming and coating) on different parameters; (2) to compare the freshly primed *P. vulgaris* seeds with trehalose and *R. tropici* with seeds coated with trehalose and *R. tropici* using silk as a coating agent; and (3) and to explore the potential of silk as a coating agent.

MATERIALS AND METHODS

Plant Material

Seeds of common bean (*P. vulgaris*) commercial variety White Kidney, with an initial germination rate above 95% and initial seed moisture content below 10% (on a dry weight basis), were used in this study. To minimize fungal contamination during the experiment, seeds were surface sterilized with 2% NaOCl solution (household bleach diluted with sterile water) for 15 min and rinsed three times with sterile water.

Before seed preparation, the coating solution was prepared using the protocol developed by Zvinavashe et al. A 6% silk solution was prepared based on Rockwood et al. (2011) protocol to which we added trehalose at 6% and *R. tropici* grown in Lysogeny broth (LB) media at 28°C until achieving an OD_{600}

value of 2. The bacterial solution was centrifuged for 5 min. The pellet was rinsed two times using sterile water, as shown in **Figure 1**. Before usage, seeds were stored at cool temperature (4°C) for 70 days.

Experimental Details

In addition to seeds coated with silk, trehalose, and *R. tropici* (named: Coating) previously described, healthy seeds were primed at the laboratory using sterile water for the negative control and Trehalose 6% and *R. tropici* (cultivated at LB media and watched and centrifuged twice with distilled and sterilized water) as a positive control with constant gentle agitation for 30 min (**Figure 1**). To ensure that the priming solution covered all the seed surfaces, a volume of 1:5 is used for negative and positive control treatments. This methodology was inspired by *On-farm* seed priming described by Harris et al. (2001).

To assess the effect of each treatment on common bean germination, 15 healthy seeds from each treatment were evenly germinated on two layers of filter paper in 10 cm diameter Petri dishes. After adding 10 mL of NaCl solutions ($S0 = 0$, $S1 = 15$, $S2 = 25$, and $S3 = 50$ mM) to each replicate, Petri dishes were covered with lids and placed in the dark. An equal volume of distilled water was applied to all Petri dishes when their moisture content declined. All the treatments were laid out in a randomized complete block design, replicated three times, and kept recording physiological attributes.

To ascertain the role of seed priming in alleviating salinity, the pots experiment was conducted using large pots (20/30 cm) filled with local soil without any physical treatment. The four previous seed treatments were applied to determine the effect of salinity on the plant establishment and behavior along the growth cycle. Five salinity levels (0, 25, 50, 75, and 100 mM) were applied.

Morphological and Physiological Response of the Seed and Plant

During the experiment, different levels of analysis were conducted to dissociate the components of the combined effects of the treatment. At the seed level: (1) daily germination and (2) germination rate. At the shoot level: (1) shoot length; (2) stomatal conductance using an SC-1 Leaf Porometer (Decagon Devices, Inc., Pullman, WA); and (3) chlorophyll content using the CL-01 Chlorophyll Content System. Moreover, at the root level, (1) root density; (2) primary root length; and (3) lateral root length were measured using the root scanner WinRhizo (Regent Instruments Inc., Quebec, Canada).

Biochemical Response

Extraction of Total Phenolic Compounds (TPC)

Fragments of leaves and roots (0.5 g FM) were ground in a mortar containing a specific volume, usually 5 mL, of ethanol 50% (water-alcohol solution). The extracts were collected in tubes with lids and well-numbered, then left overnight at 4°C to let ethanol extracting the maximum amount of phenol present in the leaves extract as described by Singleton and Rossi (1965). In the tubes containing the leaf extracts, there was a risk of the existence of chlorophylls, eliminated by adding 3 mL of the extract on 0.5 mL of chloroforms. Tubes were vortexed and centrifuged for 5 min at 5 × 1,000 mtp; two phases were separated, supernatant was added, and pellet.

Determination of TPC

We followed the method based on the Folin–Ciocalteu reagent, described by Singleton and Rossi (1965) and Hazzoumi et al. (2017). The following mixture was prepared in test tubes: 0.5 mL of extract, 3 mL of distilled water, 0.5 mL of Na2CO3 (20%), to which 0.5 mL of Folin–Ciocalteu reagent was added after 3 min. The tubes were agitated and then placed for 30 min at 40°C. After that, the absorbance was read at 760 nm. The content of phenolic compounds was calculated using gallic acid for the standard curve and expressed in milligrams per gram of fresh leaf matter.

Statistical Analysis

A two-way ANOVA was performed using the general linear model to compare seed treatments and saline levels. Descriptive statistics and ANOVA were carried out using the software R version 3.6.0 with the Agricolae, followed by Tukey's multiple comparison test ($p < 0.05$) to discriminate statistically different values. Graphs were generated using the ggplot2 in R version 4.0.5 version.

RESULTS

Germination and Seedlings Development

Seed germination is a critical phase that impacts crop establishment and yield. It is considered a bottleneck, and once surpassed, the plant can use other strategies to tolerate an excess of salt in the environment. To evaluate the effect of salinity on seed germination and seedlings, a daily record was conducted. ANOVA test (**Table 1**) shows that seed treatment and salinity significantly affect germination throughout the experiment. A highly significant interaction was observed between the treatments.

Table 2 illustrates the effect of increasing salt (0 mM to 50 mM) on the percent of germinating seeds. It was observed that the percentage of germination decreases with increasing salt concentrations for the control seeds. However, a significant increase happens when applying a seed treatment. The ANOVA (**Table 1**) showed that coated seeds behave better at a high salinity level than the freshly treated seeds because the silk preserves the bacteria and the trehalose in its fibroins.

Besides germination rate, ANOVA analysis showed that hypocotyl diameter (HD) varies significantly between seed treatments and saline levels (**Table 1**). Presented data showed that salinity stress distinctly decreases hypocotyl diameter (**Figure 2**). However, the seed treatment affects the behavior of the seedling and induces an increase in hypocotyl diameter. At a low salinity level (S1), the Silk Coating presents the largest diameter with 0.67 cm, followed by trehalose and bacteria (0.50 and 0.46 cm, respectively). The same trend is observed at 15, 25, and 50 mM of salinity levels.

At S2 (25 mM), the common bean is intensely influenced by salinity, and seed treatments reinforce the seedling by

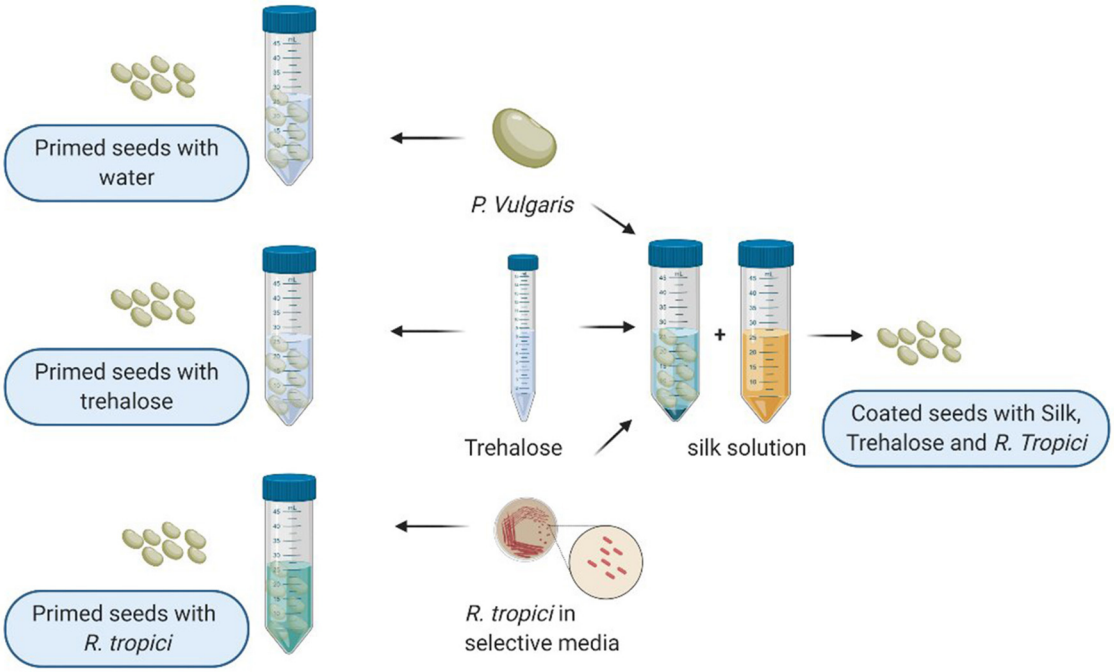

FIGURE 1 | Illustration of seed priming and seed coating protocol created with BioRender.com.

TABLE 1 | ANOVA table of the evolution of germination throughout the experience, germination rate (GR), and hypocotyl diameter (HD) in early germination test.

	df	Day 2	Day 3	Day 4	Day 5	GR	HD
Seed Treatment	5	0.090·	0.046*	0.0436*	0.130	0.0240*	5.41e-08***
Salinity level	3	0.009**	0.020*	0.0128*	0.001**	0.0018**	7.84e-07***
Seed Trt: Salinity	15	0.174	0.002**	0.0009***	0.003**	0.0002***	0.0265*
Residual	48						

*Signif. codes: 0 '***' 0.001 '**' 0.01 '*' 0.05 '.' 0.1 ' ' 1.*

TABLE 2 | Means and SD of *Phaseolus vulgaris* germination rate (GR) in percent under different seed treatments and salinity levels.

Salinity levels	Control	*R. tropici*	Trehalose	Coating	Means
S0	87 ± 9^{a}	87 ± 9^{abc}	80 ± 16^{cd}	87 ± 9^{abc}	85 ± 12
S1	87 ± 9^{abc}	80 ± 0^{cd}	93 ± 9^{ab}	87 ± 9^{abc}	87 ± 9
S2	67 ± 9^{cd}	87 ± 9^{abc}	87 ± 9^{abc}	93 ± 9^{ab}	83 ± 14
S3	53 ± 9^{d}	73 ± 9^{cd}	87 ± 9^{abc}	93 ± 9^{a}	77 ± 18
Means	73 ± 17	82 ± 10	87 ± 12	90 ± 10	83 ± 14

$^{a-d}$Different letters indicate significant statistical differences ($p < 0.05$, Tukey's test).

increasing the hypocotyl diameter. At S3, the highest salinity level (50 mM), the inoculated seed with *R. Tropici*, presented a diameter equivalent to the control seeds. The Silk Coating and trehalose remained higher with 0.45 and 0.44 cm. Nevertheless, the control presents the lowest diameter in all salinity levels. At 15 mM, salinity concentration stimulates the growth for the control, indicating that salt at low concentration can be used as a priming agent even for glycophytes.

Physiological Activity

The ANOVA for different physiological parameters showed that the effects of seed treatments and salinity on common bean plants are significant (**Table 3**).

Stomatal Conductance

The effects of salinity on stomatal conductance are shown in **Figure 2**. Stomatal conductance always declines with increasing salinity concentration. The effect of salinity was more dramatic

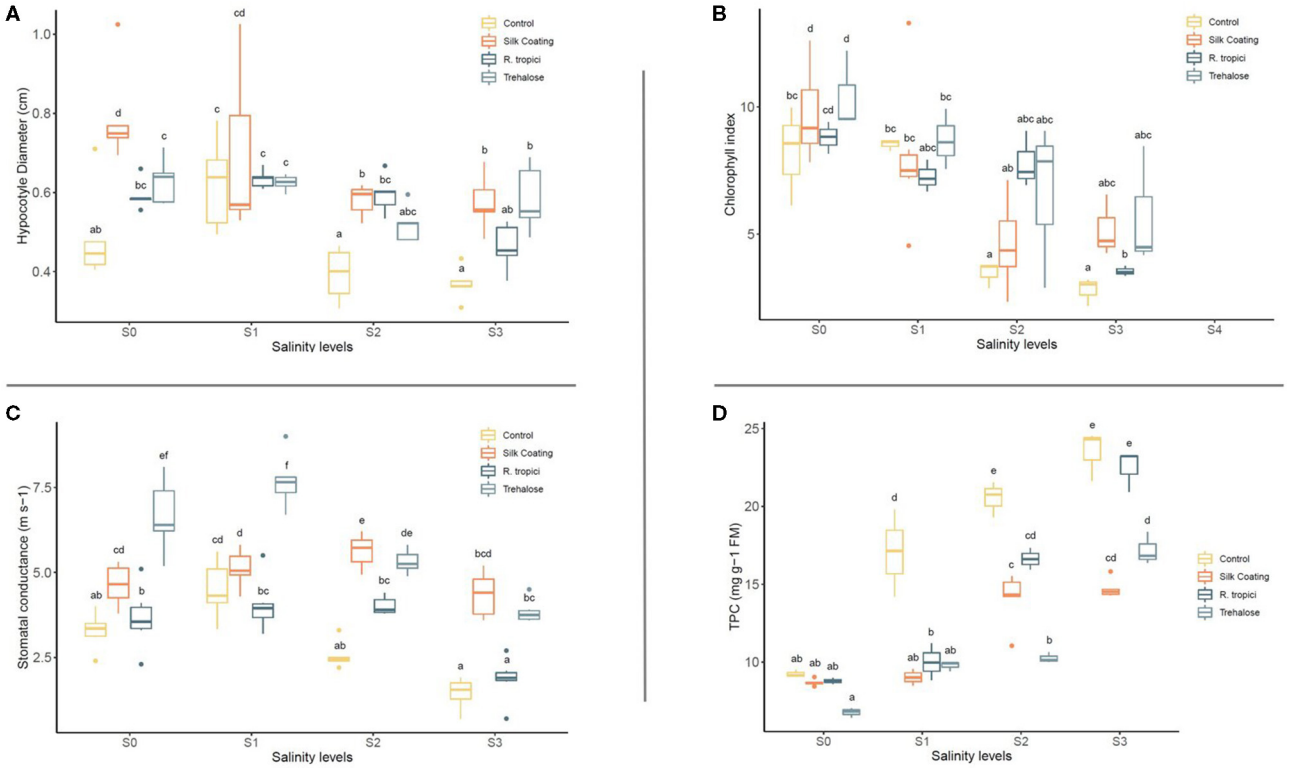

FIGURE 2 | Effect of seed treatments on hypocotyl diameter **(A)**, stomatal conductance **(B)**, chlorophyll content **(C)**, and total phenolic compounds [TPC, **(D)**], under different salinity levels (*S0* = 0 mM, *S1* = 25 mM, *S2* = 50 mM, and *S3* = 75 mM).

TABLE 3 | ANOVA table of physiological parameters measured from pot experiment.

	df	SEm	StC	Chll	TPC
Seed Trt	3	0.0102*	1.64e-14***	0.0001***	0.0073**
Salinity level	3	3.54e-16***	1.84e-12***	< 2e-16***	4.53e-06***
Seed Trt:Salinity	9	0.0301*	3.14e-07***	0.0003***	0.1214
Residual	80				

*Signif. codes: 0 '***' 0.001 '**' 0.01 '*' 0.05 '.' 0.1 ' ' 1.*
SEm, seed emergence; Chll, chlorophyll content; StC, stomatal conductance; TPC, total phenolic compounds.

in control seeds than in the other treatments. At S3 (50 mM), Silk Coating performs better than seeds treated with trehalose and the bacteria, while the control remains at the last position, indicating that plant reaction to salinity relies on the seed treatments.

Chlorophyll Content

Data for stomatal conductance as a gas exchange characteristic and a level of plant control showed that, upon exposure to saline stress, the plant significantly reduces its photosynthetic activity through the control of the stomata. Damages caused by salinity are felt at the photosynthesis machinery. Data presented in **Figure 2** shows that the application of saline stress significantly reduced the photosynthetic activity at the branching and vegetative growth stage of the common bean. This decrease in the chlorophyll index was more intense for the control as compared with the other treatments. However, freshly treated seeds presented a high photosynthetic activity in comparison with the coated seeds.

At S0, seeds soaked in trehalose showed the highest photosynthetic activity, followed equally by the seeds soaked in the bacteria, the Silk Coating, and the control. By increasing the salinity level to 25 mM, the plant activity decreases slightly compared with 50 mM salinity level where the control reduces its photosynthetic activity to half, while the treated seeds with *R. tropici* and trehalose maintain their activity. Silk Coating and trehalose treated seeds showed a different reaction compared to the control and the bacteria in 75 mM because of the existing charge of bacteria and trehalose that could be preserved in the silk fibroins.

TABLE 4 | ANOVA table of *Phaseolus vulgaris* morphological parameters measured from pot experiment.

	Df	SFL	RD	FRL-P	FRL-L
Seed Trt	3	0.00898**	4.81e-11***	2.01e-15***	< 2e-16***
Salinity level	3	<2e-16***	7.15e-07***	7.76e-08***	< 2e-16***
Seed Trt:Salinity	9	0.65123	0.0553·	0.987	2.31e-15***
Residual	80				

*Signif. Codes: 0 '***' 0.001 '**' 0.01 '*' 0.05 '.' 0.1 ' ' 1.*
SFL, shoot final length; RD, roots density; FRL, root final length; P, primary; L, lateral.

TPCs

Content of TPC changes with the coating application, trehalose, and salinity level. According to **Figure 2**, the quantity of phenolic compounds in the control plant increases progressively with salinity levels, reflecting a natural response of the plant against the ions of the salt in the medium. However, the seeds soaked in the trehalose reflect a significant reduction of the TPC level. The soaked seeds with bacteria presented the best response against salts in the medium. By recording the most significant decrease of TPC, the content of this latter was less than the control, which means that the plant did not need to synthesize more TPC to tolerate salt stress.

The biosynthesis of phenolic compounds is proportionally linked to salts concentration in the plant microenvironment, whatever the treatment is. About 0 mM showed one-third <75 mM; this variation keeps the same trend in *R. tropici* and Silk Coating, but the trehalose showed a different reaction for 25 mM and 50 mM salinity levels. These treatments reflect almost the same TPC content, highlighting the ability of the trehalose ability to mitigate the negative impact of salt stress on the plant up to an optimal concentration (50 mM in this case).

Using a formulation based on Silk material enriched by *R. tropici* helped the plant to tolerate salt stress, especially in the lowest and highest concentrations; however, the trehalose showed a significant effect in the medium salt stress concentration (50 mM).

Morphology of the Plant

Length of the Shoot

Application of salt stress significantly reduced the plant length for all seed treatments (**Table 4**). A similar decreasing trend was observed due to salt stress. However, this decrease was not the same in all seed treatments. The control seeds were more severely affected by salinity than were the primed and coated seeds. The trehalose and the bacteria significantly increased the length under stress and non-stress conditions (**Figure 3**).

Architecture of the Root

Density of the Root

At different salinity levels, seed treatments have increased the root density compared to the untreated control (**Figure 4**). Nevertheless, data indicate that gradually increasing salinity levels from 0 to 75 mM NaCl has decreased root density. The application of trehalose induces an additive stimulatory effect on roots. The same growth pattern was observed for seeds freshly inoculated with *R. tropici*. However, the effect is reduced with increased salinity level testifying to the impact of salinity on the bacterial development in soil. In addition, it was noticed that the Silk Coating has a more pronounced and significant increase of roots than the control. At 75 mM of NaCl, the uncoated control and the seed treated with the bacteria did not tolerate the high salinity level and died after 35 days. In contrast, seeds treated with trehalose and coated seeds are behaving well and produce mature plants. This salt concentration is a threshold concentration for common bean; the cultivar used in this experiment does not survive beyond it. The plant viability at this salt concentration may be due to trehalose that promotes roots formation and growth at an early stage. The coated seeds with silk also showed viable plants, and this could be evidence of the role of the silk-based coating on the protection of the bacteria in a high salinity environment.

Primary and Lateral Roots

After 90 days of growth, it was observed that common bean seedlings produce a highly branched root system with abundant lateral roots and a short primary root. Changes in root parameters of common bean under three seed treatments are presented in **Figure 5**. Response to seed treatments did not differ significantly for primary root length under stress and non-stress conditions. However, they are significantly higher than the control.

Irrigation of common bean plants with saline water caused significant decreases in root development relative to control plants. On the other hand, plants from treated seeds enhanced lateral root length under unstressed and salinity-stressed environments. At a low salinity level, inoculation with *R. tropici* was more effective, followed by trehalose. Coated seeds have presented the same principal root length but less lateral root length. Even though it has better performance than the control at unstressed and salinity-stressed conditions, these results suggest that, in *P. vulgaris*, Silk Coating, trehalose, and *R. tropici* may play a crucial role in changing root architecture under saline stress.

DISCUSSION

Germination and Seedlings Development

Germination is a critical stage in the crop cycle. It has been demonstrated that this stage is susceptible to all stresses. In this study, the effect on germination rate induced by seed treatment underlines the importance of priming and biopriming in seed production to improve plant behavior under stressed environments. To alleviate saline stress, a seed coating was developed using Silk as a binding agent, trehalose for its ability to stimulate germination and growth in saline stress and *R. tropici* for its ability to colonize common bean roots and produce nodules for an efficient Nitrogen fixation (Zvinavashe et al., 2019).

Seed priming is one of the universal methods used in fertilizers application. Freshly primed seeds usually contain a high concentration of the priming agents, but it is susceptible to degradation or leaching after irrigation. Results are proof of

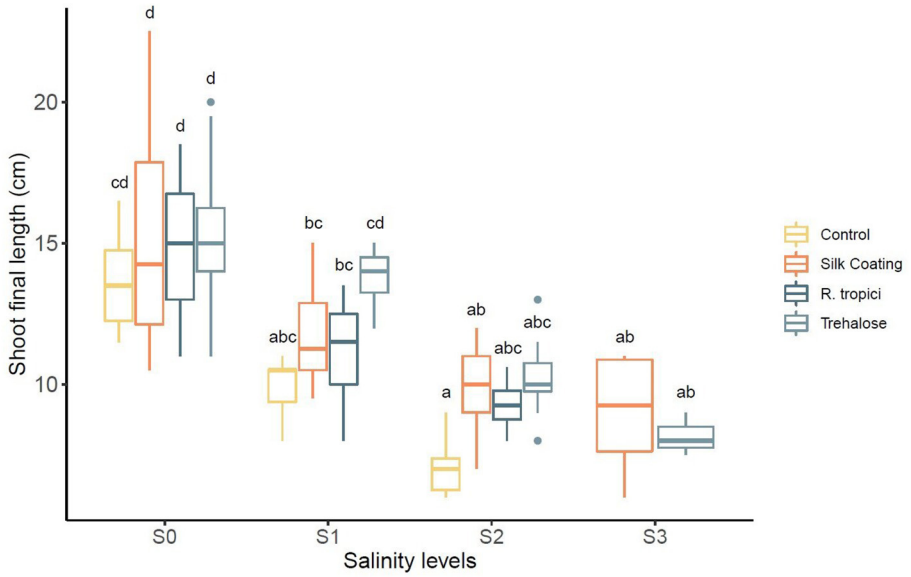

FIGURE 3 | Effect of different salinity levels (*S0* = 0 mM, *S1* = 25 mM, *S2* = 50 mM, and *S3* = 75 mM) on *Phaseolus vulgaris* shoot length in centimeters.

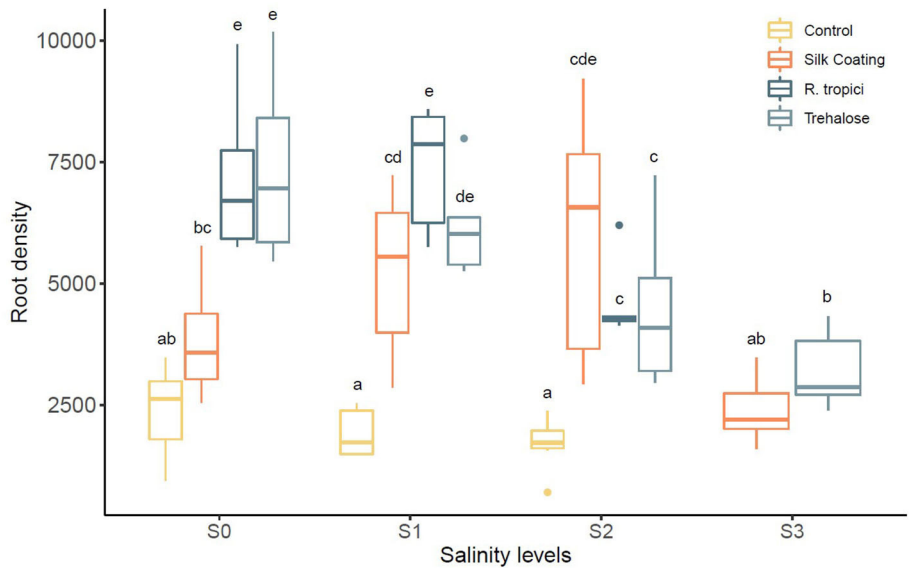

FIGURE 4 | Effect of different salinity levels (*S0* = 0 mM, *S1* = 25 mM, *S2* = 50 mM, and *S3* = 75 mM) on *Phaseolus vulgaris* root density.

the efficiency of the Silk Coating since it exceeds all the seed treatments, mainly in the high salinity levels by maintaining the trehalose and the bacteria in the seed microenvironment. It has also shown a high germination rate and high seedlings diameter at the highest salinity level, supporting the hypothesis of the conservation of the formulation elements by the Silk fibroins in saline conditions.

To further understand the priming effect on germination, independent experimentation was conducted *in vitro* using a Petri dish to evaluate the germination rate and the seedling vigor under saline treatments. The same trend was observed, and the coated seeds performed better than the other treatments for inducing germination in saline treatments. Besides, it confers to the seedling a significant vigor, explaining the plant strength during the growth cycle. The observed effects are mainly due to the combined action of trehalose and *R. Tropici*, both of which promote growth through different mechanisms. Trehalose, a disaccharide, is an essential signal metabolite in plants

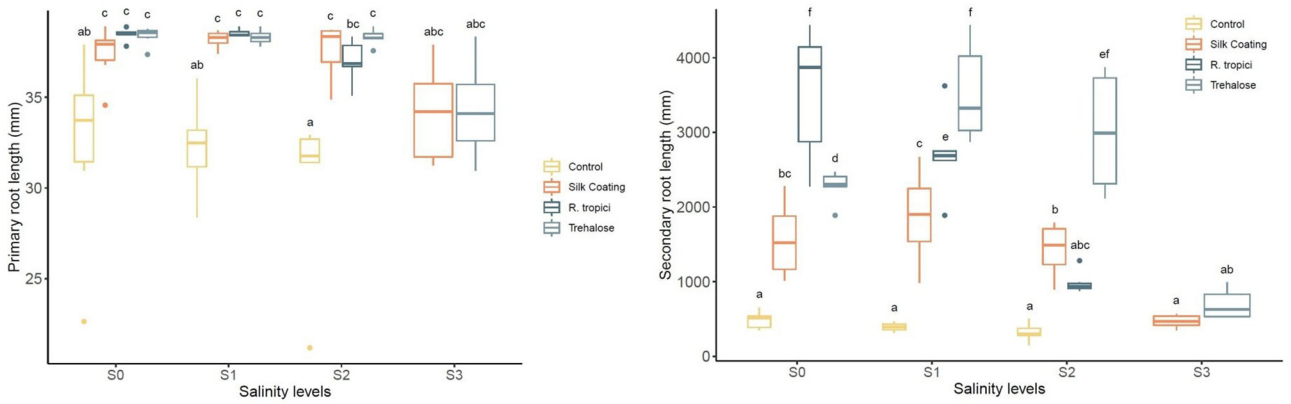

FIGURE 5 | *Phaseolus vulgaris* primary roots length (left) and lateral root length (right) under different seed treatments and salinity levels.

and an essential regulator of many physiological processes, including seed germination and stress response. Within the seed germination process, trehalose plays an essential role in regulating the growth of vegetative and embryogenic tissue in a mechanism involving ABA and sugar metabolism (Gómez et al., 2010). It also plays a vital role as an osmolyte, stress signaling, and stress protectant of the membrane and proteins against the adverse effects of stress (Crowe et al., 1984).

Trehalose regulates many genes, among them the transcription factor bZIP11, which affects the regulation of carbohydrate metabolism, inducing a regulation of the developmental phase transitions (like germination and flowering), carbohydrate, and amino acid metabolisms (Gazzarrini and Tsai, 2014). Accordingly, it has been reported that, in rice, the [trehalose:sucrose] ratio in germinating tissues leads to a regulation of amylase activation for increased starch mobilization and contributes through its regulators OsTPP7 to anaerobic germination tolerance (Kretzschmar et al., 2015). Trehalose hydrolysis is a major reaction during early germination. Presumably, it serves as a source of carbon for synthesis and glucose for energy, and its use in seed coating has been efficient.

R. tropici was added to the silk and trehalose to increase the efficiency of the coating formulation. This bacterium has been widely studied and has proven its ability to increase yield components during the crop cycle, even in areas with medium salinity where untreated seeds do not perform very well. However, it has been observed that it is sensitive to high salinity. Therefore, an exogenous application of trehalose may also help the bacteria tolerate abiotic stress (Cardoso et al., 2007), which supports our results showing the performance of the coated seeds with a mixture of trehalose, *R. tropici,* and silk in high salinity levels.

Physiological Response

Salt stress presents one of the most limiting abiotic factors that affect plant growth and production by altering physiological and biochemical activities (Rockwood et al., 2011; Hazzoumi et al., 2017). Protection of the photosynthetic machinery significantly contributes to the ability of the plant to withstand stress and reactive oxygen species (ROS) produced upon exposure to saline stress. This study demonstrated that the coated and primed seeds maintained several physiological processes under saline treatments, including photosynthesis through stomatal conductance and chlorophyll content. Many studies highlighted the effect of salinity on photosynthetic activity due to the sensitivity of Photosystem II to NaCl as a non-stomatal regulation (Brugnoli and Lauteri, 1991; Taïbi et al., 2016). While there is stomatal regulation that has also been reported for several plant species, both halophytes and non-halophytes, which refers to stomatal conductance, correlated with photosynthetic capacity (Wong et al., 1979). In this study, and to attenuate the effect of salinity on photosynthetic activity, seeds were treated with trehalose and *R. tropici*. Both directly affect photosynthesis by allocating and metabolizing carbohydrates (Gazzarrini and Tsai, 2014) and contributing to a higher N2 fixation rate (Bethlenfalvay et al., 1978), respectively.

Previous studies have shown that supplementation of trehalose in saline medium protects *Catharanthus roseus* from the inhibitory effects of salt on growth and photosynthesis (Crowe et al., 1984; Gazzarrini and Tsai, 2014; Hazzoumi et al., 2017). Trehalose accumulation was correlated with higher soluble carbohydrate levels, and a high photosynthesis capacity under stress and non-stress conditions, supporting the increase observed in non-saline treatment. In this study, variation in stomatal conductance and chlorophyll content were strongly expressed in high salinity levels, where coated seeds performed better than the treated seeds and the control, showing that combining trehalose and *R. tropici* helps to maintain a high photosynthetic activity. These increments probably may be attributed to the protective effects of trehalose on photosynthetic systems (Abdallah et al., 2016). Besides, it has been discovered that trehalose plays an important role in plant-microorganism interactions through a higher number of nodules and nitrogenase activity, greater biomass, and an increase in grain yield in inoculated plants under normal or stress conditions (Iturriaga et al., 2009). Photosynthetic and chlorophyll parameters in our

study indicated that trehalose helps the plant mitigate the adverse effects of salinity and increase *R. tropici* performance under saline stress.

To tolerate salt ions, the plant accumulates polyphenols which are involved in the defense mechanism. The role of TPCs in the stimulation of plant resistance was provided in many species and for different biotic and abiotic stress situations (Benhamou et al., 2000). Phenolic compounds are directly involved in scavenging free radicals and protect plants against the damaging effects of increased ROS levels (Petridis et al., 2012). The negative impact of salinity was mainly attributed to water deficit due to lowered water potential in the root zone, specific ion toxicity arising from a higher concentration of sodium and chloride, and the nutritional imbalance.

The osmotic adjustment is a central part of the physiological mechanisms by which plants respond to salinity stress. The salinity generates water stress by disturbance of plant water balance (caused by ions disequilibrium). The accumulation of specific osmotic adjustment solutes (e.g., proline, soluble sugars, and soluble protein) in the cytosol and organelles helps in the osmotic adjustment and improving the growth and development of plants. We note that salt stress causes an increase in TPC accumulation. Increasing polyphenols content in tissue is reported to be a plant response to salinity and indicates the induction of synthesis of secondary metabolism to defend against salt stress. This considerable accumulation is confirmed in *Anethum graveolens* L. (Mehr et al., 2012) and *Vetiveria zizanioides* L. (Manebr et al., 2011). However, the plants treated with trehalose presents better performance in stressful environments. According to Sadak et al. (2019), trehalose foliar application in different concentrations (0,1 mM and 0,5 mM) improves the antioxidant defense system of the quinoa plant against reactive oxygen species (Sadak et al., 2019). The impact of trehalose was accompanied by a significant decrease in lipid peroxidation, hydrogen peroxide contents, and LOX (Lipoxygenase) activity. These decreases were correlated with significant increases in total phenolic contents as compared with untreated plants. A similar positive impact of trehalose was recorded in maize plants exposed to salt stress by increasing the growth parameters and photosynthetic activity of the plant (Rohman et al., 2019).

The antioxidant activity of phenolic compounds was principally due to their role as electron and hydrogen donors, which stabilize the unpaired electron (Huang et al., 2005). The stimulation of TPC by trehalose might be due to the role of this latter as signaling function and their implication in different metabolic pathways in stress conditions by inducing the synthesis of TPC (Alam et al., 2014; Sadak et al., 2019).

Shoots and Root Development Under Salinity Stress

The present study includes the effect of seed treatments on photosynthetic activity through the regulation of stomata. Previous studies demonstrate that the effect of salinity on the CO_2 assimilation rate was mainly due to the reduction of stomatal conductance (Brugnoli and Lauteri, 1991). Evidence of the impact on biomass production.

Exogenous trehalose application was effective in mitigating the harmful effects of saline stress conditions on gas exchange attributes. The ameliorative effect of trehalose on photosynthesis indicates that it plays a role in protecting the photosynthetic system, as already reported, through trehalose signaling mechanisms that can enhance this capacity. Furthermore, trehalose induces an ameliorative effect in plant biomass when carbon supply is not a limiting factor (Rady et al., 2011).

Such effects of exogenously applied trehalose might have been due to its contribution to lowering the cell osmotic potential, which helps plants absorb water from the soil. Plant length is one of the biomass components in addition to the total leaf area and dry biomass. This study demonstrated that seed treatments, under saline and normal conditions, help to maintain and improve plant biomass relative to the control. Other studies emphasized the role of trehalose in the regulation of Na^+ in plant tissues, including leaves (Garcia et al., 1997), indicating that it may play a direct or indirect role in determining ion selectivity by controlling cellular exclusion of Na^+. A hypothesis was supported by Joshi et al. (2020), where transgenic lines had higher K^+/Na^+ ratios than the wild type under salinity stress

Our studies showed that coated and primed seeds and seedlings were less affected by saline stress in comparison to the control, as evidenced by their higher germination rates and better subsequent growth under these stress conditions due to efficient sequestration of sodium that has been considered as one of the critical components differentiating between control and treated seeds. Moreover, the degree of damage increases with stress intensity.

Based on the present results, it could be concluded that salinity stress adversely affected growth and physiological parameters compared with control plants. Trehalose can neutralize the effect of salinity stress and result in a significant improvement of morphological traits, physiological parameters, and phytochemical activity (Ding et al., 2018). Trehalose pretreatment alleviated damages through efficient stimulation of the antioxidant defense. Exogenous application of trehalose enhanced the level of internal trehalose, which mainly stimulated the protective activities for the plants (Abdallah et al., 2016).

The *P. vulgaris* root system undergoes significant architectural changes in root density and lateral root length due to the exogenous seed treatments. Those modifications in the root architecture may determine the capacity of the plant to acquire available water and nutrient. Analysis of plants from treated seeds showed that trehalose and *R. tropici* increase the root density. It also promotes the principal and lateral root formation under saline treatments. The same result was observed for coated seeds, indicating the effect of trehalose and the bacteria after 3 months of conservation at 4°C. Lateral root development has been suggested to be under the control of polar auxin transport (Casimiro et al., 2001). Many studies have confirmed that trehalose is an essential signal metabolite in plants, linking growth and development to carbon metabolism (Figueroa and Lunn, 2016). A recent study suggests that auxin acts downstream of trehalose 6 Phosphate to promote seed filling, thereby providing an

outstanding example of how a metabolic signal governs the hormonal control in a critical phase transition in a crop plant (Meitzel et al., 2021).

CONCLUSION

Exogenous application of trehalose and *R. tropici*, ingredients of the seed coating, impacts plant growth under non-stressed and stressed environments. The roots readily absorb trehalose and are easily transported to the aerial parts to function as a major defensive response to several abiotic stresses. This experiment is evidence of the role of trehalose in seed priming. This sugar induces osmotic stress that stimulates the growth of shoots and roots. This study proves that fresh soaking seems to be more productive. Using silk-based coating can be more efficient for preserving the formulation in stored seeds and delivering it to seedlings. This study shines a new light on the role of trehalose in the biofertilizers preservation, plant survival under osmotic stress conditions, and the development of new functional seed coatings that integrate Rhizobium preservation with precise delivery in the soil.

DATA AVAILABILITY STATEMENT

The raw data supporting the conclusions of this article will be made available by the authors, without undue reservation.

AUTHOR CONTRIBUTIONS

BM and ATZ contributed to the coating design and formulation at MIT. LK managed the project at the UM6P. YZ contributed by funding and scientific follow-up from OCP. MM and ZH contributed in the physiological and agronomic evaluation of the seed coating at the UM6P. All authors contributed to the article and approved the submitted version.

FUNDING

OCP Group supported this work under the UM6P and MIT Research Program (UMRP) within the framework of Project AS12 (2017-2021) granted to Benedetto Marelli at the Massachusetts Institute of Technology (MIT).

ACKNOWLEDGMENTS

We are grateful for the support of the UM6P research facilities and experimental farm staff and the Université Mohammed VI Polytechique–MIT Research Program (UMRP).

SUPPLEMENTARY MATERIAL

The Supplementary Material for this article can be found online at: https://www.frontiersin.org/articles/10.3389/fpls.2021.700273/full#supplementary-material

REFERENCES

Abdallah, M. M.-S., Abdelgawad, Z. A., and El-Bassiouny, H. M. S. (2016). Alleviation of the adverse effects of salinity stress using trehalose in two rice varieties. *S. Afr. J. Bot.* 103, 275–282. doi: 10.1016/j.sajb.2015.09.019

Alam, M. M., Nahar, K., Hasanuzzaman, M., and Fujita, M. (2014). Trehalose-induced drought stress tolerance: a comparative study among different Brassica species. *Plant Omics* 7, 271.

Bae, H., Herman, E., Bailey, B., Bae, H.-J., and Sicher, R. (2005). Exogenous trehalose alters Arabidopsis transcripts involved in cell wall modification, abiotic stress, nitrogen metabolism, and plant defense. *Physiologia Plantarum* 125, 114–126. doi: 10.1111/j.1399-3054.2005.00537.x

Benhamou, N., Gagn,é, S., Le Quér,é, D., and Dehbi, L. (2000). Bacterial-mediated induced resistance in cucumber: beneficial effect of the endophytic bacterium Serratia plymuthica on the protection against infection by Pythium ultimum. *Phytopathology*® 90, 45–56. doi: 10.1094/PHYTO.2000.90.1.45

Bethlenfalvay, G. J., Abu-Shakra, S. S., and Phillips, D. A. (1978). Interdependence of nitrogen nutrition and photosynthesis in *Pisum sativum* L: II. Host Plant Response to Nitrogen Fixation by Rhizobium Strains. *Plant Physiol.* 62, 131–133. doi: 10.1104/pp.62.1.131

Bisen, K., Keswani, C., Mishra, S., Saxena, A., Rakshit, A., and Singh, H. B. (2015). "Unrealized potential of seed biopriming for versatile agriculture," in *Nutrient Use Efficiency: From Basics to Advances*, eds Rakshit, A., Singh, Harikesh Bahadur, Sen, A. New Delhi, India: Springer, 193–206. doi: 10.1007/978-81-322-2169-2_13

Brugnoli, E., and Lauteri, M. (1991). Effects of salinity on stomatal conductance, photosynthetic capacity, and carbon isotope discrimination of salt-tolerant (*Gossypium hirsutum L.*) and salt-sensitive (*Phaseolus vulgaris L.*) C3 non-halophytes. *Plant Physiol.* 95, 628–635. doi: 10.1104/pp.95.2.628

Callan, N. W., Mathre, D., and Miller, J. B. (1990). Bio-priming seed treatment for biological control of pythium ultimum preemergence damping-off in SH-2 sweet corn. *Plant Dis.* 74, 368–372. doi: 10.1094/PD-74-0368

Cardoso, F. S., Castro, R. F., Borges, N., and Santos, H. (2007). Biochemical and genetic characterization of the pathways for trehalose metabolism in *Propionibacterium freudenreichii*, and their role in stress response. *Microbiology* 153, 270–280. doi: 10.1099/mic.0.29262-0

Casimiro, I., Marchant, A., Bhalerao, R. P., Beeckman, T., Dhooge, S., Swarup, R., et al. (2001). Auxin transport promotes arabidopsis lateral root initiation. *Plant Cell* 13, 843–852. doi: 10.1105/tpc.13.4.843

Chen, Q., and Haddad, G. G. (2004). Role of trehalose phosphate synthase and trehalose during hypoxia: from flies to mammals. *J. Exp. Biol.* 207, 3125–3129. doi: 10.1242/jeb.01133

Crowe, J. H., Crowe, L. M., and Chapman, D. (1984). Preservation of membranes in anhydrobiotic organisms: the role of trehalose. *Science* 223, 701–703. doi: 10.1126/science.223.4637.701

Ding, F., Wang, R., and Wang, T. (2018). Enhancement of germination, seedling growth, and oxidative metabolism of barley under simulated acid rain stress by exogenous trehalose. *Crop Sci.* 58, 783–791. doi: 10.2135/cropsci2017.08.0491

Elbein, A. D., Pan, Y. T., Pastuszak, I., and Carroll, D. (2003). New insights on trehalose: a multifunctional molecule. *Glucobiology* 13, 17R−27R. doi: 10.1093/glycob/cwg047

Elhaissoufi, W., Khourchi, S., Ibnyasser, A., Ghoulam, C., Rchiad, Z., Zeroual, Y., et al. (2020). Phosphate solubilizing rhizobacteria could have a stronger influence on wheat root traits and aboveground physiology than rhizosphere p solubilization. *Front. Plant Sci.* 11:979. doi: 10.3389/fpls.2020.00979

Figueroa, C. M., and Lunn, J. E. (2016). A tale of two sugars: trehalose 6-phosphate and sucrose. *Plant Physiol.* 172, 7–27. doi: 10.1104/pp.16.00417

Garcia, A. B., Engler, J., Iyer, S., Gerats, T., Montagu, M. V., and Caplan, A. B. (1997). Effects of osmoprotectants upon NaCl stress in rice. *Plant Physiol.* 115, 159–169. doi: 10.1104/pp.115.1.159

Gazzarrini, S., and Tsai, A. Y.-L. (2014). Trehalose-6-phosphate and SnRK1 kinases in plant development and signaling: the emerging picture. *Front. Plant Sci.* 5:119. doi: 10.3389/fpls.2014.00119

Gómez, L. D., Gilday, A., Feil, R., Lunn, J. E., and Graham, I. A. (2010). AtTPS1-mediated trehalose 6-phosphate synthesis is essential for embryogenic and vegetative growth and responsiveness to ABA in germinating seeds and stomatal guard cells. *The Plant Journal* 64, 1–13. doi: 10.1111/j.1365-313X.2010.04312.x

Gouffi, K., Pica, N., Pichereau, V., and Blanco, C. (1999). Disaccharides as a new class of nonaccumulated osmoprotectants for Sinorhizobium meliloti. *Appl. Environ. Microbiol.* 65, 1491–1500. doi: 10.1128/AEM.65.4.1491-1500.1999

Harris, D., Pathan, A. K., Gothkar, P., Joshi, A., Chivasa, W., and Nyamudeza, P. (2001). On-farm seed priming: using participatory methods to revive and refine a key technology. *Agric. Syst*. 69, 151–164. doi: 10.1016/S0308-521X(01)00023-3

Hazzoumi, Z., Moustakime, Y., and Joutei, K. A. (2017). Effect of arbuscular mycorrhizal fungi and water stress on ultrastructural change of glandular hairs and essential oil compositions in *Ocimum gratissimum*. *Chem. Biol. Technol. Agric*. 4:20. doi: 10.1186/s40538-017-0102-z

Huang, C., He, W., Guo, J., Chang, X., Su, P., and Zhang, L. (2005). Increased sensitivity to salt stress in an ascorbate-deficient Arabidopsis mutant. *J. Exp. Bot*. 56, 3041–3049. doi: 10.1093/jxb/eri301

Iordachescu, M., and Imai, R. (2008). Trehalose biosynthesis in response to abiotic stresses. *J. Integr. Plant Biol*. 50, 1223–1229. doi: 10.1111/j.1744-7909.2008.00736.x

Iturriaga, G., Suárez, R., and Nova-Franco, B. (2009). Trehalose metabolism: from osmoprotection to signaling. *Int. J. Mol. Sci*. 10, 3793–3810. doi: 10.3390/ijms10093793

Joshi, R., Sahoo, K. K., Singh, A. K., Anwar, K., Pundir, P., Gautam, R. K., et al. (2020). Enhancing trehalose biosynthesis improves yield potential in marker-free transgenic rice under drought, saline, and sodic conditions. *J. Exp. Bot*. 71, 653–668. doi: 10.1093/jxb/erz462

Kretzschmar, T., Pelayo, M. A. F., Trijatmiko, K. R., Gabunada, L. F. M., Alam, R., Jimenez, R., et al. (2015). A trehalose-6-phosphate phosphatase enhances anaerobic germination tolerance in rice. *Nat. Plants* 1, 1–5. doi: 10.1038/nplants.2015.124

Maity, A., Sharma, J., and Pal, R. K. (2019). Novel potassium solubilizing bio-formulation improves nutrient availability, fruit yield and quality of pomegranate (*Punica granatum* L.) in semi-arid ecosystem. *Scientia Horticulturae* 255, 14–20. doi: 10.1016/j.scienta.2019.05.009

Manebr, A., Saratale, G., and Samant, B. (2011). Studies on the effects of salinity on growth, polyphenol content andphotosynthetic response in *Vetiveria zizanioides* (L.) Nash. *Emir. J. Food Agric*. 23:59. doi: 10.9755/ejfa.v23i1.5313

Marelli, B., Brenckle, M. A., Kaplan, D. L., and Omenetto, F. G. (2016). Silk fibroin as edible coating for perishable food preservation. *Sci. Rep*. 6:25263. doi: 10.1038/srep25263

McIntyre, H. J., Davies, H., Hore, T. A., Miller, S. H., Dufour, J.-P., and Ronson, C. W. (2007). Trehalose biosynthesis in *Rhizobium leguminosarum* bv. trifolii and its role in desiccation tolerance. *Appl. Environ. Microbiol*. 73, 3984–3992. doi: 10.1128/AEM.00412-07

Meftah Kadmiri, I., El Mernissi, N., Azaroual, S. E., Mekhzoum, M. E. M., Qaiss, A. E. K., and Bouhfid, R. (2021). Bioformulation of microbial fertilizer based on clay and alginate encapsulation. *Curr. Microbiol*. 78, 86–94. doi: 10.1007/s00284-020-02262-2

Mehr, Z. S., Khajeh, H., Bahabadi, S. E., and Sabbagh, S. K. (2012). Changes on proline, phenolic compounds and activity of antioxidant enzymes in *Anethum graveolens* L. under salt stress. *Int. J. Agron. Plant Prod*. 3, 710–715. https://www.cabdirect.org/cabdirect/abstract/20143088424

Meitzel, T., Radchuk, R., McAdam, E. L., Thormählen, I., Feil, R., Munz, E., Hilo, A., Geigenberger, P., Ross, J. J., Lunn, J. E., and Borisjuk, L. (2021). Trehalose 6-phosphate promotes seed filling by activating auxin biosynthesis. *New Phytol*. 229, 1553–1565. doi: 10.1111/nph.16956

Müller, J., Boller, T., and Wiemken, A. (1998). Trehalose affects sucrose synthase and invertase activities in soybean (*Glycine max* [L.] Merr.) roots. *J. Plant Physiol*. 153, 255–257. doi: 10.1016/S0176-1617(98)80078-3

Pedrini, S., Merritt, D. J., Stevens, J., and Dixon, K. (2017). Seed coating: science or marketing spin? *Trends Plant Sci*. 22, 106–116. doi: 10.1016/j.tplants.2016.11.002

Petridis, A., Therios, I., Samouris, G., and Tananaki, C. (2012). Salinity-induced changes in phenolic compounds in leaves and roots of four olive cultivars (*Olea europaea* L.) and their relationship to antioxidant activity. *Environ. Exp. Bot*. 79, 37–43. doi: 10.1016/j.envexpbot.2012.01.007

Rady, M. M., Sadak, M. S., El-Bassiouny, H. M. S., and El-Monem, A. A. A. (2011). Alleviation the adverse effects of salinity stress in sunflower cultivars using nicotinamide and α-tocopherol. *Aust. J. Basic Appl. Sci*. 5, 342–355. https://www.cabdirect.org/cabdirect/abstract/20113396379

Rocha, I., Ma, Y., Souza-Alonso, P., Vosátka, M., Freitas, H., and Oliveira, R. S. (2019). Seed coating: a tool for delivering beneficial microbes to agricultural crops. *Front. Plant Sci*. 10:1357. doi: 10.3389/fpls.2019.01357

Rockwood, D. N., Preda, R. C., Yücel, T., Wang, X., Lovett, M. L., and Kaplan, D. L. (2011). Materials fabrication from Bombyx mori silk fibroin. *Nat. Protoc*. 6, 1612–1631. doi: 10.1038/nprot.2011.379

Rohman, M. M., Islam, M. R., Monsur, M. B., Amiruzzaman, M., Fujita, M., and Hasanuzzaman, M. (2019). Trehalose protects maize plants from salt stress and phosphorus deficiency. *Plants* 8:568. doi: 10.3390/plants8120568

Sadak, M. S., El-Bassiouny, H. M. S., and Dawood, M. G. (2019). Role of trehalose on antioxidant defense system and some osmolytes of quinoa plants under water deficit. *Bull. Natl. Res. Cent*. 43:5. doi: 10.1186/s42269-018-0039-9

Singleton, V. L., and Rossi, J. A. (1965). Colorimetry of total phenolics with phosphomolybdic-phosphotungstic acid reagents. *Am. J. Enol. Vitic*. 16, 144–158.

Soumare, A., Boubekri, K., Lyamlouli, K., Hafidi, M., Ouhdouch, Y., and Kouisni, L. (2020). From isolation of phosphate solubilizing microbes to their formulation and use as biofertilizers: status and needs. *Front. Bioeng. Biotechnol*. 7:425. doi: 10.3389/fbioe.2019.00425

Suárez, R., Wong, A., Ramírez, M., Barraza, A., Orozco, M., del, C., et al. (2008). Improvement of drought tolerance and grain yield in common bean by overexpressing trehalose-6-phosphate synthase in rhizobia. *MPMI* 21, 958–966. doi: 10.1094/MPMI-21-7-0958

Taïbi, K., Taïbi, F., Ait Abderrahim, L., Ennajah, A., Belkhodja, M., and Mulet, J. M. (2016). Effect of salt stress on growth, chlorophyll content, lipid peroxidation and antioxidant defence systems in *Phaseolus vulgaris* L. *S. Afr. J. Bot*. 105, 306–312. doi: 10.1016/j.sajb.2016.03.011

Wong, S. C., Cowan, I. R., and Farquhar, G. D. (1979). Stomatal conductance correlates with photosynthetic capacity. *Nature* 282, 424–426. doi: 10.1038/282424a0

Zvinavashe, A. T., Lim, E., Sun, H., and Marelli, B. (2019). A bioinspired approach to engineer seed microenvironment to boost germination and mitigate soil salinity. *PNAS* 116, 25555–25561. doi: 10.1073/pnas.1915902116

Zvinavashe, A. T., Mardad, I., Mhada, M., Kouisni, L., and Marelli, B. (2021). Engineering the plant microenvironment to facilitate plant-growth-promoting microbe association. *J. Agric. Food Chem*. doi: 10.1021/acs.jafc.1c00138

Conflict of Interest: YZ was employed by the company OCP Group.

The remaining authors declare that the research was conducted in the absence of any commercial or financial relationships that could be construed as a potential conflict of interest.

Publisher's Note: All claims expressed in this article are solely those of the authors and do not necessarily represent those of their affiliated organizations, or those of the publisher, the editors and the reviewers. Any product that may be evaluated in this article, or claim that may be made by its manufacturer, is not guaranteed or endorsed by the publisher.

frontiers in Plant Science

ORIGINAL RESEARCH
published: 17 August 2021
doi: 10.3389/fpls.2021.713984

Comparative Transcriptomics and Metabolomics Reveal an Intricate Priming Mechanism Involved in PGPR-Mediated Salt Tolerance in Tomato

Ifigeneia Mellidou[1], Aggeliki Ainalidou[2], Anastasia Papadopoulou[2], Kleopatra Leontidou[2], Savvas Genitsaris[3], Evangelos Karagiannis[4], Bram Van de Poel[5] and Katerina Karamanoli[2]**

[1] Institute of Plant Breeding and Genetic Resources, Hellenic Agricultural Organization DEMETER (ex NAGREF), Thermi, Greece, [2] Laboratory of Agricultural Chemistry, School of Agriculture, Aristotle University of Thessaloniki, Thessaloniki, Greece, [3] Section of Ecology and Taxonomy, School of Biology, National and Kapodistrian University of Athens, Athens, Greece, [4] Laboratory of Pomology, Department of Horticulture, Aristotle University of Thessaloniki, Thessaloniki, Greece, [5] Division of Crop Biotechnics, Department of Biosystems, University of Leuven, Leuven, Belgium

OPEN ACCESS

Edited by:
Maurizio Ruzzi,
University of Tuscia, Italy

Reviewed by:
Jos Thomas Puthur,
University of Calicut, India
Abdul Latif Khan,
University of Nizwa, Oman

***Correspondence:**
Ifigeneia Mellidou
imellidou@agro.auth.gr
Katerina Karamanoli
katkar@agro.auth.gr

Specialty section:
This article was submitted to Plant Abiotic Stress, a section of the journal Frontiers in Plant Science

Received: 24 May 2021
Accepted: 01 July 2021
Published: 17 August 2021

Citation:
Mellidou I, Ainalidou A, Papadopoulou A, Leontidou K, Genitsaris S, Karagiannis E, Van de Poel B and Karamanoli K (2021) Comparative Transcriptomics and Metabolomics Reveal an Intricate Priming Mechanism Involved in PGPR-Mediated Salt Tolerance in Tomato. Front. Plant Sci. 12:713984. doi: 10.3389/fpls.2021.713984

Plant-associated beneficial strains inhabiting plants grown under harsh ecosystems can help them cope with abiotic stress factors by positively influencing plant physiology, development, and environmental adaptation. Previously, we isolated a potential plant growth promoting strain (AXSa06) identified as *Pseudomonas oryzihabitans*, possessing 1-aminocyclopropane-1-carboxylate deaminase activity, producing indole-3-acetic acid and siderophores, as well as solubilizing inorganic phosphorus. In this study, we aimed to further evaluate the effects of AXSa06 seed inoculation on the growth of tomato seedlings under excess salt (200 mM NaCl) by deciphering their transcriptomic and metabolomic profiles. Differences in transcript levels and metabolites following AXSa06 inoculation seem likely to have contributed to the observed difference in salt adaptation of inoculated plants. In particular, inoculations exerted a positive effect on plant growth and photosynthetic parameters, imposing plants to a primed state, at which they were able to respond more robustly to salt stress probably by efficiently activating antioxidant metabolism, by dampening stress signals, by detoxifying Na^+, as well as by effectively assimilating carbon and nitrogen. The primed state of AXSa06-inoculated plants is supported by the increased leaf lipid peroxidation, ascorbate content, as well as the enhanced activities of antioxidant enzymes, prior to stress treatment. The identified signatory molecules of AXSa06-mediated salt tolerance included the amino acids aspartate, threonine, serine, and glutamate, as well as key genes related to ethylene or abscisic acid homeostasis and perception, and ion antiporters. Our findings represent a promising sustainable solution to improve agricultural production under the forthcoming climate change conditions.

Keywords: abiotic tolerance, ACC-deaminase, antioxidant metabolism, bio-stimulants, priming state, *Pseudomonas oryzihabitans*

INTRODUCTION

In the forthcoming years, global challenges due to climate change and environmental stresses, including soil salinity, are expected to significantly alter soil properties, causing detrimental effects not only on plant growth and crop production, but also on cultivable area worldwide due to salinization (Liu et al., 2017; Kozminska et al., 2018; Corwin, 2021). Apart from disrupting ion balance and cellular homeostasis, high Na^+ concentrations in the soil trigger osmotic stress that impairs water usage, photosynthesis, and biosynthesis of proteins and lipids, as well as cell redox state by over-accumulating reactive oxygen species (ROS) (Liu et al., 2017). Excess salt may activate a wide range of physiological and biochemical adjustments to support plant growth and cellular functions. These include the effective compartmentalization of Na^+ in vacuoles by specific transporters, long-distance ion transport from roots to leaves and stems, alterations in leaf or root morpho-anatomical structures, as well as the production of osmotically active compounds and the accumulation of plant hormones and other signaling molecules (Shabala, 2013; Mellidou et al., 2016; Devkar et al., 2020).

Among the effective strategies to cope with soil salinity, the use of improved management practices in highly saline regions, as well as the implication of conventional or molecular technologies toward the development of salt tolerant crop species are of outmost importance. However, these strategies are often time consuming and cost-demanding. The application of beneficial microbes represents an alternative environmental-friendly strategy to address this issue (Chauhan et al., 2019). The plant rhizosphere represents a delicate and dynamic ecosystem that hosts a variety of microorganisms with diverse and multifaceted functions in plant growth and development, or survival under unfavorable environmental conditions (Kearl et al., 2019; Genitsaris et al., 2020). Plant Growth Promoting Rhizobacteria (PGPR) can provide cross-protection against multiple stress factors by facilitating the growth of their plant symbionts in many different ways (Bruto et al., 2014). Among others, they supply atmospheric nitrogen, synthesize siderophore and phytohormones, solubilize inorganic phosphorus (P), release volatiles, form biofilm, or produce stress alleviating enzymes, such as the 1-aminocyclopropane-1-carboxylate (ACC) deaminase, and cell-wall degrading enzymes (Mayak et al., 2004; Yang et al., 2009; Shariati et al., 2017; Leontidou et al., 2020; Jiao et al., 2021). PGPR-mediated salt tolerance may be achieved via modifications in Na^+, K^+, and Ca^{+2} homeostasis thereby allowing plants to sustain a higher K^+/Na^+ within cells (Bharti et al., 2016; Safdarian et al., 2019). At the molecular level, salt stress regulates the expression of several genes coding for late embryogenesis (LEA) proteins, osmoregulatory proteins, redox-regulated proteins, transcription factors (TFs) such as WRKY, transporters/antiporters, and salt overly sensitive (SOS) proteins (Safdarian et al., 2019).

In an attempt to investigate plant microbiomes and the co-evolutionary signature of host-microorganism interactions, a large number of emblematic PGPR model strains have been isolated, characterized and applied as "biostimulants" to enhance plant abiotic stress tolerance (Liu et al., 2017; Olanrewaju et al., 2017; Leontidou et al., 2020; Yadav et al., 2020). The physiological, transcriptomic, and metabolomic profiles of PGPR-mediated salt tolerance have been explored in differed crops including *Arabidopsis* (Liu et al., 2017), rice (Chauhan et al., 2019), and wheat (Safdarian et al., 2019), suggesting intricate metabolic and hormonal signaling events implicated in plant responses against salt stress.

Plant-associated beneficial strains inhabiting arid and harsh ecosystems may help plants survive under abiotic and biotic stress factors, as these microbes have developed complex adaptive traits in co-evolution with their plant hosts, in contrast to those found in frequently cultivated areas (Fierer, 2017). Previously, we were able to isolate a potential PGPR strain (AXSa06), identified as *Pseudomonas oryzihabitans*, from the National Park of Delta Axios (Leontidou et al., 2020), a highly diverse ecosystem which includes the estuaries of four rivers and has been included in the Natura 2000 network of European ecological regions with code GR122000268 (Vokou et al., 2016). *In vitro* experiments showed that AXSa06 possessed ACC deaminase activity, produced a considerable amount of IAA and siderophores, as well as solubilized inorganic P (Leontidou et al., 2020). PGPR strains containing ACC deaminase activity may help plants ameliorate stress injury by promoting plant and root growth, through scavenging plant ACC, thereby reducing ethylene production (Orozco-Mosqueda et al., 2020). Although this strain has been isolated from a perennial *Sarcocornia* sp. grown in highly saline soils, it could efficiently colonize the rhizosphere of tomato plants (Leontidou et al., 2020).

Due to its interesting phyto-beneficial traits, we aimed to further evaluate the effects of AXSa06 seed inoculation on the growth of tomato seedlings under excess salt (200 mM NaCl). Deciphering transcriptomic and metabolomic changes of inoculated plants exposed to salt stress provided important insights into the complicated mechanism that allowed our novel strain to induce salt tolerance in plants. The proposed model suggests that AXSa06 forced plants to a "primed" state. This state is related to specific metabolite accumulation, repressed stress-inducing signals through a dampened ethylene and abscisic acid (ABA) metabolism, and eventually in effective trade-off between growth and defense responses. The identified signatory molecules including AsA, and the amino acids aspartate, threonine, serine, and glutamate, may serve as possible biomarkers for PGPR priming in tomato.

MATERIALS AND METHODS

Plant Material, Growth Conditions, and Salt Treatment

Tomato seeds of cv "ACE 55" were used to explore plant responses to salt stress upon AXSa06 inoculation. The strain has been previously isolated from an adverse—highly saline—ecosystem (National Park of Delta Axios, Greece) and genetically characterized as *Pseudomonas oryzihabitans* using a Whole Genome Sequencing approach (Leontidou et al., 2020). Seeds were surface sterilized in 70% ethanol (v/v) and subsequently in

2.4% (v/v) sodium hypochlorite. Prior sterilization, seeds were kept in the dark for 24 h at 4°C and then incubated for 72 h in PNS agar plates (1.8% agar) at 25°C to ensure synchronization in growth.

For inoculation with the selected bacteria, called AXSa06, spontaneous rifampicin-resistant mutants were prepared as described earlier (Karamanoli et al., 2005) in order to easily monitor bacterial dynamics in the rhizosphere during experimentation. Seeds were "bacterized" for 30 min in a mixture of the bacterial suspension and 2% methyl cellulose (MC) solution (w/v) (Sigma, Germany) in a 1:1 (v/v) ratio, as previously described (Leontidou et al., 2020). The control seeds were immersed in a mixture of Phosphate Buffer Saline (PBS) and MC (1:1). In turn, seeds of both treatments were placed in pots filled with sterilized peat and perlite (3:1 v/v) in a growth chamber (Snijders Microclima 1,750, Snijders Scientific BV, Netherlands) for 3 weeks at 16/8 h and 25/22°C, receiving plant nutrient medium containing 0.5% (w/v) sucrose (PNS). Salt stress was applied to 21-day old seedlings by the addition of 200 mM NaCl for 7 days based on our preliminary experiments in tobacco (Mellidou et al., 2016) and tomato (Leontidou et al., 2020). Plants received equal volume of 200 mM NaCl solution or tap water (control plants), without leaching. The concentration of NaCl in the pots was regularly monitored by measuring the Electrical Conductivity (EC) after the completion of the irrigation, and values had to be in the range of 3.0–3.5 dS m^{-1}. In total, there were four treatments, (1) non-inoculated non-stressed (0 mM NaCl), (2) non-inoculated salt-stressed (200 mM NaCl), (3) AXSa06-inoculated non-stressed, and (4) AXSa06-inoculated salt-stressed, each consisted of 20 plants (**Supplementary Figure 1**). At the end of the stress period, plant growth-related and physiological parameters were evaluated, while leaf and root tissues were frozen in liquid nitrogen and kept at −80°C until further analysis.

Plant Growth and Physiological Measurements

Shoot length and total leaf number were recorded for all plants exposed to 200 mM NaCl for 7 days, while above the ground biomass (stems and leaves), on a fresh weight basis, was evaluated for 10 plants per treatment, at the end of stress treatment. Among the physiological parameters, net photosynthetic rate (A_{net}, mmol m^{-2} s^{-1}), and chlorophyll content index [CCI = (% transmittance at 931 nm)/(% transmittance at 653 nm)] were assessed in 10 plants per treatment using a portable photosynthesis meter (LCPROT-001/BW, ADC BiosScientific Ltd., UK), and an Opti-Sciences CCM-200 chlorophyll content meter (OptiSciences Inc.), respectively. Measurements were taken on the second fully expanded leaf (counting from the apex) as described earlier (Mellidou et al., 2016, 2017).

Salt Stress Markers Evaluation

The accumulation of Na^+ in tomato leaves inoculated with AXSa06 following treatments with 200 mM NaCl for 7 days was determined as previously described (Mellidou et al., 2016).

Briefly, leaf samples (0.5 g) were heated in a muffle furnace at 500°C for at least 4 h, and the residue was dissolved in a 3.6 M HCl/1.4 M HNO_3 aqueous solution. In turn, Na^+ content was determined in a flame photometer (Jenway PFP 7, Gransmore Green, Felsted England).

Malonyldialdehyde (MDA) content was determined in leaf samples to estimate the degree of lipid peroxidation using the thiobarbituric acid (TBA) test (Heath and Packer, 1968), with a few modifications (Mellidou et al., 2020). Briefly, frozen leaf powder (200 mg) was homogenized in 600 mL 0.1% (w/v) trichloroacetic acid (TCA) solution, and centrifuged at 14,000 rpm for 15 min at 4°C. In turn, 0.5 mL of the supernatant was added to 1.5 mL 0.5% (w/v) TBA in 20% TCA, the mixture was boiled for 25 min, and the reaction was completed by immersing the reaction tubes on ice. The MDA content was calculated by measuring the absorbance of supernatant at 532 nm, after subtracting the value for non-specific absorption at 600 nm, using an extinction coefficient of 155 mM^{-1} cm^{-1}.

REL was determined essentially as previously described (McKay, 1998). Briefly, at the end of stress treatment, roots were thoroughly rinsed with tap water, immersed in glass tubes containing 15 ml of deionized water with known EC and vortexed vigorously. After 24 h in dark, EC was measured before and after boiling at 110°C for 20 min using the electrical conductivity meter ConductoMeter (Metrohm, Herisau, Switzerland). The injury index was estimated from the formula: REL (%) = [(EC before/EC after boiling) ×100]/initial root weight. Measurements were performed using five replicates per treatment.

Proline content was also assayed in leaf tissues according to Bates (1976). Briefly, 100 mg of leaf powder was homogenized in 5 ml of 3% (w/v) aqueous sulfosalicylic acid and then centrifuged at 14,000 rpm for 10 min at 4°C. One ml acid-nynhydrin reagent and 1 ml glacial acetic acid was added to 1 ml of supernatant, and the mixture was heated at 100°C for 1 h. After terminating the reaction in an ice bath, the reaction mixture was extracted with 2 ml toluene, vortexed vigorously, and left at room temperature for 30 min. Proline content was determined by measuring the absorbance of the fraction with toluene at 520 nm, based on a standard curve with pure proline of known concentrations.

For all measurements, five biological replications per treatment were used, corresponding to five individual plants.

Determination of Non-enzymatic and Enzymatic Antioxidants

Ascorbic acid (AsA) was determined spectrophotometrically using the ascorbate oxidase (AO) enzyme as previously described (Pateraki et al., 2004). Calculations were based upon the difference in absorbance at 265 nm before and 3 min after the addition of AO (1 U/μl) to a 200 μL aliquot of extract in 200 mM sodium phosphate buffer (pH 5.6). Total AsA (totAsA) content was determined by measuring absorbance 10 min after adding 10 mM DTT to a separate extract aliquot. Measurements were performed using five biological and two technical replicates per treatment.

For enzyme activities, total proteins were extracted from 500 mg of leaf tissues, and purified using ion-exclusion Sephadex G-25 column (PD 10, GE Healthcare) essentially as previously described (Mellidou et al., 2012). Bovine serum albumin (Sigma)

was used as standard for the quantification of protein content of the extracts according to Bradford method (Bradford, 1976). The activities of catalase (EC 1.11.1.6, CAT), superoxide dismutase (SOD; EC 1.15.1.1), pyrogallol-based peroxidase (EC 1.11.1.7, POX), and ascorbate peroxidase (EC 1.11.1.11, APX) were determined based on optimized "in-house" protocols (Mellidou et al., 2012, 2017). All technical measurements were conducted in duplicates for each of the five biological replicates per treatment.

Quantification of ACC and MACC Content in Leaves and Roots

As AXSa06 strain possesses ACC deaminase gene, as well as *in vitro* ACC activity (Leontidou et al., 2020), metabolites from the ethylene biosynthetic pathway (ACC and MACC) were quantified in leaves and roots of the plants at exposure to 200 mM NaCl, essentially as previously described (Bulens et al., 2011; Van de Poel et al., 2014). Enzyme activities of ACC synthase and ACC oxidase were below the threshold of detection limit, and thus not able to be quantified.

Ethylene Quantification in Excised Tomato Leaves

Ethylene production was quantified in excised non-inoculated and AXSa06-inoculated tomato leaves upon salt stress as previously described (Kim et al., 2013, 2016). Briefly, leaves were excised, weighted, and placed in a glass tube. After 30 min without sealing, the glass tubes were capped with a septa stopper, and incubated for an hour at room temperature. One ml gas sample was removed from the tube using a syringe and injected into a gas chromatograph (GC-2014ATF Shimadzu), equipped with a flame ionization detector (FID) and a stainless-steel column (filled with Porapak P, Q, R, S), to quantify ethylene gas levels. Measurements were performed using five individual biological replicates per treatment.

RNA Isolation, Library Construction, and Sequencing

Leaf tissues were used for total RNA extraction using RNeasy Plant Mini Kit (QIAGEN) according to the manufacturer's instructions. Three biological replicates were employed per treatment. Quantification and qualification of the extracted RNA was checked using the RNA Nano 6000 Assay Kit of the Agilent Bioanalyzer 2100 system (Agilent, CA, USA) to ensure that the RNA Integrity Number (RIN) values were above 7. In total, 12 RNA-Seq libraries were prepared and purified using QIAseq Stranded mRNA Select Kit (QIAGEN) following manufacturer's instructions. After generating the index-coded samples, each cDNA library was sequenced in a single lane of Illumina platforms (Novaseq 6000 System) with 150 bp paired-end reads, obtaining above 24 M raw reads per sample. Raw data obtained from sequencing were converted to Fastq format and deposited to the European Nucleotide Archive, under PRJEB42497.

Analysis of Sequencing Data

Raw sequences were processed with fastp (Chen et al., 2018) to remove reads containing adapter bases, poly-N sequences, and reads with low quality. After quality control, high quality paired-end reads were aligned to the tomato reference genome (Hosmani et al., 2019) using HISAT2 (Kim et al., 2015). The Stringtie (Kovaka et al., 2019) was used to assemble the set of transcript isoforms obtained in the mapping step, and gffcompare (Pertea and Pertea, 2020) was used to compare the assemblies to reference annotation files and sort out new genes from known ones. The read counts mapped for each gene, including known and novel genes, were produced using Featurecounts (Liao et al., 2014), and fragments per kilobase for exon model (FPKM) was calculated for each gene. Differential gene expression levels between treatments (consisted of three biological replicates) were determined using DESeq2 R package. *P*-values were corrected with the Benjamini-Hochberg adjustment within the R *p*.adjust function and the FDR (False Discovery Rate) was also calculated among the genes. Genes adjusted $P \leq 0.01$ and $\log_2$ (fold-change) ≥ 1.5 were considered as up-regulated, and those with $\log_2$ (fold-change) ≤ 1.5 as down-regulated. Gene ontology (GO) and KEGG enrichment analysis of DEGs was accomplished using clusterProfiler (Yu et al., 2012).

Metabolite Extraction and Derivatization

Analysis of polar metabolites was performed as previously described (Ainalidou et al., 2016). Leaf tissues (500 mg) were homogenized in liquid nitrogen and transferred to 2 mL screw cap tubes with 1,400 μL of 100% methanol. Adonitol (100 μL of 0.2 mg mL^{-1} aqueous solution) was added as internal quantitative standard and vortexed, following incubation at 70°C for 10 min. Samples were then centrifuged at 11,000 × g (4°C) for 10 min and the supernatants were transferred to glass vials. Subsequently, 750 μL of chloroform and 1,500 μLl of cold distilled H_2O were added. The mixtures were centrifuged at 2,200 g (4°C) for 15 min and 150 μL from the upper phase (polar phase) were transferred into new 1.5 mL glass vials. The vials were placed in a vacuum desiccator for overnight drying. For the derivatization, dried residues were re-dissolved in 40 μL of 20 mg mL^{-1} methoxyamine hydrochloride in pyridine, and were shaken at 37°C for 2 h. For the completion of derivatization, samples were treating with 70 μL of N-Methyl-N-(trimethylsilyl)-trifluoroacetamide (MSTFA) reagent and incubated at 37°C for 30 min. The aliquots were stored at −20°C, until further analysis by a GC–MS system.

Gas Chromatography–Mass Spectrometry (GC–MS)–Based Metabolite Profiling

GC–MS analysis was performed in Thermo Trace Ultra GC equipped with ISQ MS and TriPlus RSH autosampler (Switzerland). One microliter sample volumes were injected with a split ratio of 70:1. Separations were carried out on a TR-5MS capillary column 30 m × 0.25 mm × 0.25 μm. Injector temperature was set at 220°C, ion source at 230°C, and the interface at 250°C, while a constant flow rate of the carrier gas (He) was set at 1 mL min^{-1}. The GC temperature program was held at 70°C for 5 min, then increased to 240°C at a rate of 8°C min^{-1}, and held at 240°C for 15 min. After 5 min solvent delay, mass range of m/z 50–600 was recorded. The mass spectra were acquired in electron impact ionization (EI) mode. The peak area integration and chromatogram visualization were performed

using Xcalibur processing program. For peak identification and mass spectra tick evaluation was performed and NIST11 database were used. Mass spectra were cross referenced with those of authentic standards in the GOLM metabolome database (Kopka et al., 2005; Ainalidou et al., 2016). Quantification of the detected metabolites was assessed based on the relative response compared to adonitol as the internal standard, and expressed as relative abundance.

Statistical Analysis

All data were analyzed by SPSS (Version 25. Chicago, SPSS Inc.). Duncan multiple-range tests were performed to determine significant differences between inoculated vs. non-inoculated seedlings under control or salt stress conditions.

RESULTS

AXSa06 Inoculation Improved Morpho-Physiological and Biochemical Traits in Tomato During Salt Stress

In order to easily monitor strain population throughout the experiment, rifampicin resistant mutants were employed. Under the selected experimental growth conditions, the AXSa06 strain was well-established in the rhizosphere of inoculated plants prior to stress application, while it was also able to grow at highly saline soil conditions (Leontidou et al., 2020). To confirm that AXSa06, identified as *Pseudomonas oryzihabitans*, was able to alleviate salt stress in tomato seedlings, plant-growth, and physiological traits were recorded in treatments with or without 200 mM NaCl. At control conditions (0 mM NaCl), no particular differences related to growth or photosynthesis were recorded between non-inoculated and AXSa06-inoculated plants (**Figures 1A–D**). Treatments with 200 mM NaCl led to a significant decrease in both shoot length (**Figure 1A**) and leaf number (**Figure 1B**) only in non-inoculated plants compared to non-stressed plants. Inoculated plants, not only maintained their growth-related traits at non-stressed levels, but also had higher shoot length (14.2%; **Figure 1A**) and more leaves (8.7%; **Figure 1B**) compared to non-inoculated stressed plants. Salt stress caused a significant decrease in A_{net} (50.5% **Figure 1C**) and CCI (50.2%; **Figure 1D**), respectively, in non-inoculated plants compared to control conditions. By contrast, the negative effect of 200 mM NaCl in AXSa06-inoculated plants was less prominent, with a 33.9 and 3.9% reduction in A_{net} and CCI, respectively. Both A_{net} and CCI were higher in inoculated plants compared to non-inoculated ones (33.4 and 52.3%, respectively) under salt stress. These results support the positive effect of inoculation with AXSa06 on plant growth and physiological parameters of tomato seedlings exposed to 200 mM NaCl.

The accumulation of leaf Na^+ and proline contents was dramatically enhanced at exposure of plants to 200 mM NaCl (**Figures 1E,F**). Nonetheless, leaves of non-inoculated plants contained significantly higher amount (54.0%) of Na^+ compared to inoculated ones, while inoculated plants accumulated slightly more proline (12.4%) in leaves than non-inoculated ones, yet not significant. Interestingly, in the absence of NaCl, inoculation with AXSa06 resulted in enhanced leaf MDA content (68.6% higher compared to non-inoculated plants), suggesting that inoculation with the strain probably imitated the effect of mild oxidative stress (**Figure 2A**). With regard to REL, it was significantly enhanced at exposure to 200 mM NaCl, regardless the presence of AXSa06 (**Figure 2B**). Nonetheless, REL of AXSa06-inoculated plants at exposure to salt stress was lower (80.23% on average) compared to non-inoculated plants (91.83%), although not significant due to the large scale of values, indicating that there was probably less negative impact of salt in the roots at the presence of the strain. At the same time, the fact that REL of unstressed inoculated plants was also lower (35.5%) compared to non-inoculated plants (44.6%) suggested that the potential oxidative boost at control conditions, as highlighted by the enhanced MDA content, was not harmful with regard to electrolyte leakage from roots.

This mild oxidative boost in AXSa06-inoculated plants was further supported by the increased activities of antioxidant enzymes, POX (**Figure 2C**) and CAT (**Figure 2D**), at control conditions. In particular, POX and CAT specific activities were 73.0 or 68.4% higher in inoculated plants compared to non-inoculated ones, respectively. When 200 mM NaCl was applied, no further induction in MDA content or POX activity was observed in inoculated plants, likewise in non-inoculated plants, in which both traits were remarkably enhanced. By contrast, CAT activity decreased in inoculated plants at exposure to salt stress, nearly at control levels of non-inoculated plants. Upon salt stress, SOD activity was significantly increased in inoculated plants, but remained unaltered in non-inoculated ones (**Figure 2E**). The activity of APX, the first enzyme in the AsA-GSH (glutathione) cycle responsible for the oxidation of AsA to monodehydroascorbate (MDHA) with the parallel detoxification of H_2O_2, was increased in non-inoculated plants at exposure to stress. Notwithstanding, APX activity remained at low levels in inoculated plants (**Figure 2F**), probable due to the lower H_2O_2 accumulation within the cell owing to its better detoxification by other peroxidases (**Figure 2C**).

Inoculation With AXSa06 Altered Root and Leaf ACC Levels Under Salinity Stress

In this study, the application of 200 mM NaCl enhanced ACC and reduced MACC levels in the roots of non-inoculated plants (**Figures 3A,B**). By contrast, inoculation with the ACC-deaminase possessing strain, AXSa06, maintained root ACC content under salt stress similar to control levels, probably due to the ACC deaminase activity of the strain. Intriguingly though, a remarkable increase in root MACC content was observed after inoculation owing to salt stress, probably indicative of a AXSa06-mediated feedback regulation on redirecting plant ethylene synthesis. The opposite trend was evident in the leaves of salt-stressed plants (**Figures 3C,D**). In particular, at the absence of inoculum, leaf ACC content decreased, probably to support the ethylene production owing to stress, as indicated in the excised leaves of the same plants (**Supplementary Figure 2**). However, in inoculated plants, ACC levels remained unaltered upon salt stress (**Figure 3C**), whilst a significant decrease in

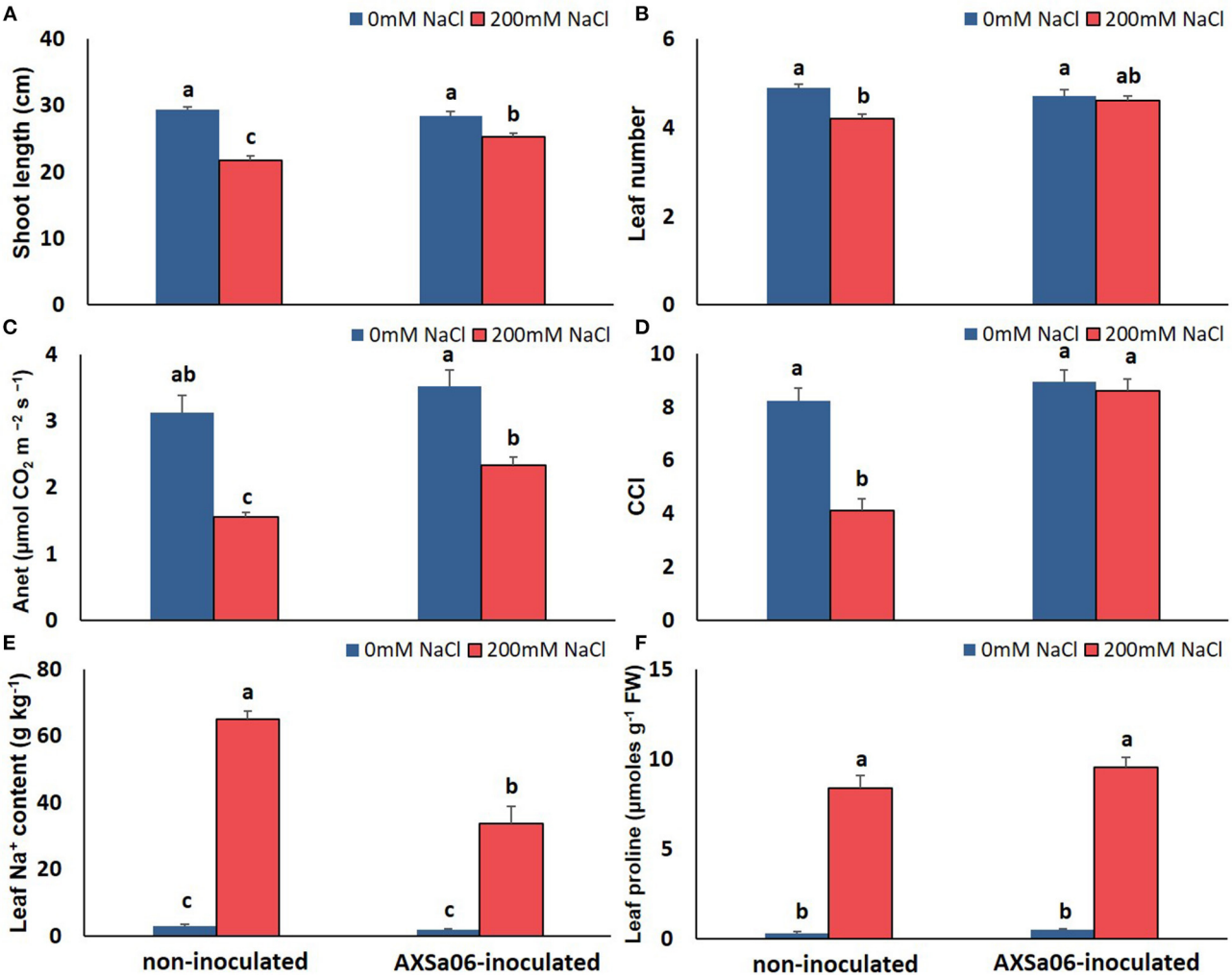

FIGURE 1 | Effect of AXSa06 (*Pseudomonas oryzihabitans*) seed inoculation on tomato seedlings treated with 200 mM NaCl for 7 days: **(A)** shoot length (cm); **(B)** leaf number; **(C)** net photosynthesis (Anet, μmol CO_2 m^{-2} s^{-1}); **(D)** chlorophyll content index; **(E)** leaf Na^+ content (g kg^{-1}); **(F)** leaf proline content (μmols g^{-1} FW). Data are means ± standard error. Different letters indicate statistically significant differences between treatments based on Duncan's multiple range test ($P < 0.05$).

ethylene production was evident in excised leaves at exposure to 200 mM NaCl (**Supplementary Figure 2**). Although no *in vivo* ethylene measurements were performed, ethylene determination in excised leaves of plants inoculated with AXSa06 highlighted the capacity of these plants to produce ethylene upon salt stress. Leaf MACC levels remained largely unchanged by both the salinity or inoculation treatment (**Figure 3D**). These observations suggested that at the presence of AXSa06, the above-the-ground tissues may accumulate lower ACC levels, that could lead to reduced ethylene-related stress signals as a result of ACC deaminase activity below the ground, compared to non-inoculated plants.

Overview of Transcriptome Analysis and Read Assembly

To unravel the mechanism of AXSa06-mediated salt tolerance in tomato plants, transcriptome profiling was carried out using an RNA-Seq approach. After removing adapter sequences and low-quality reads, a total of 677.6 M with an average of 56.5 M clean reads and a Q30 percentage ≥95% were generated for the 12 cDNA libraries (**Supplementary Table 1**). No remarkable differences were observed in read number between inoculated vs. non-inoculated plants, or between control and salt stress conditions. The clean reads were mapped to the tomato reference genome, cv Heinz 1706 version 4.0 (Hosmani et al., 2019), with an average total mapping ratio around 97%, and uniquely mapping ratio at 94.6%. After averaging replicate values, total transcripts with FPKM >1 for each treatment varied from 17,873 to 18,153, of which the novel transcripts ranged from 249 to 274 (**Supplementary Tables 2–5**).

The expression of these transcripts was subjected to a Principal component analysis (PCA) (**Figure 4A**). The first two components, which explained 61% of the variation, were able to distinguish the four different groups of treatments,

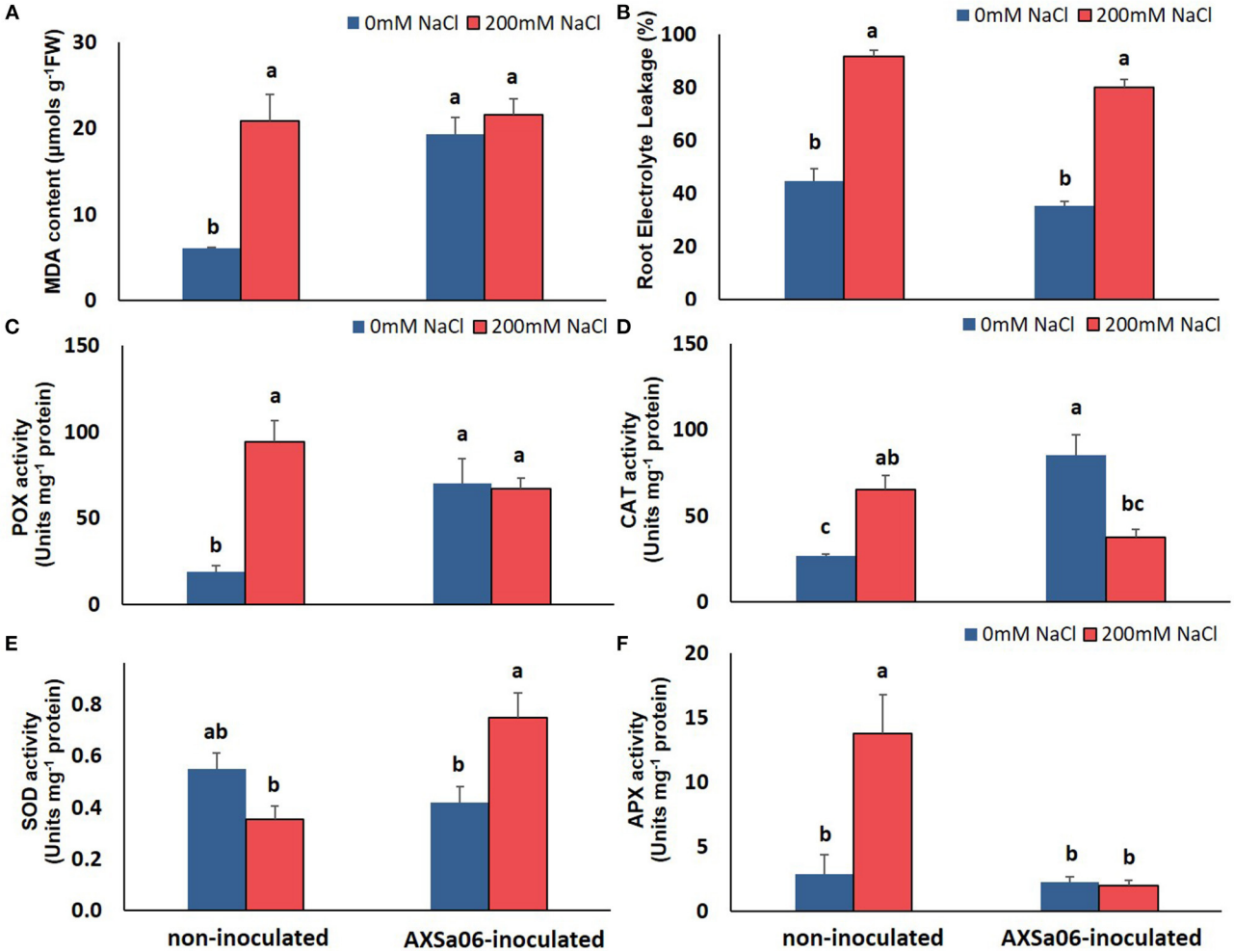

FIGURE 2 | Oxidative-related effect of AXSa06 (*Pseudomonas oryzihabitans*) seed inoculation on tomato seedlings treated with 200 mM NaCl for 7 days: **(A)** MDA content (μmols g^{-1} FW); **(B)** Root Electrolyte Leakage (%); **(C)** POX specific activity (Units mg^{-1} protein); **(D)** CAT specific activity (Units mg^{-1} protein); **(E)** SOD specific activity (Units mg^{-1} protein); **(F)** APX specific activity (Units mg^{-1} protein). Data are means of five biological replicates ± standard error. Different letters indicate statistically significant differences between treatments based on Duncan's multiple range test ($P < 0.05$).

with three biological replicates clustering together, and each group having certain differences in their gene expression profiles. Furthermore, at total number of 17,263 transcripts (on average 96% of total expressed genes) were expressed in all treatments, with the uniquely expressed transcripts ranging from 110 (AXSa06-inoculated at 0 mM) to 213 (non-inoculated at 200 mM) (**Figure 4B**). Differentially Expressed Genes (DEGs) between treatments were defined using $|\log_2(\text{fold change}) > 1.5|$, and corrected ($p \leq 0.01$). In total, 264 and 108 DEGs were identified between control and salt stress, in non-inoculated or inoculated plants, respectively (**Figure 4C** and **Supplementary Tables 6, 7**). Among them, 159 and 83 genes were significantly up-regulated in salt-treated plants in non-inoculated and inoculated plants, respectively, whilst 105 and 25 were down-regulated, suggesting that transcriptomic profiles of non-inoculated plants were more disturbed by NaCl, compared to those of inoculated plants. Although gene expression profiles altered significantly as a response to salt stress to a different extent, there were 43 overlapping DEGs that were regulated by salt stress, regardless inoculations with AXSa06. Among them, the most interesting DEGs up-regulated due to stress involved in central metabolic pathways were alcohol dehydrogenase (ID544074), chitinase (ID544149), $_L$-ascorbate oxidase (ID101252861), and proline dehydrogenase (ID778202). In the same regard, 3-ketoacyl-CoA synthase 11 (ID101268510), indole-3-acetic acid-amino synthetase (ID101258277), inositol 2-dehydrogenase (ID101260461), and indole-3-pyruvate monooxygenase YUCCA5 (ID101267265) were significantly down-regulated in both non-inoculated and inoculated plants owing to NaCl treatment. By contrast, there were also two inositol oxygenase genes (ID 101263222 and 101254427) that were up-regulated in inoculated plants but down-regulated in non-inoculated plants.

Gene ontology (GO) annotation analysis of DEGs between stressed and non-stressed plants returned 170 GO terms, classified into the two GO classes (BP, Biological Process;

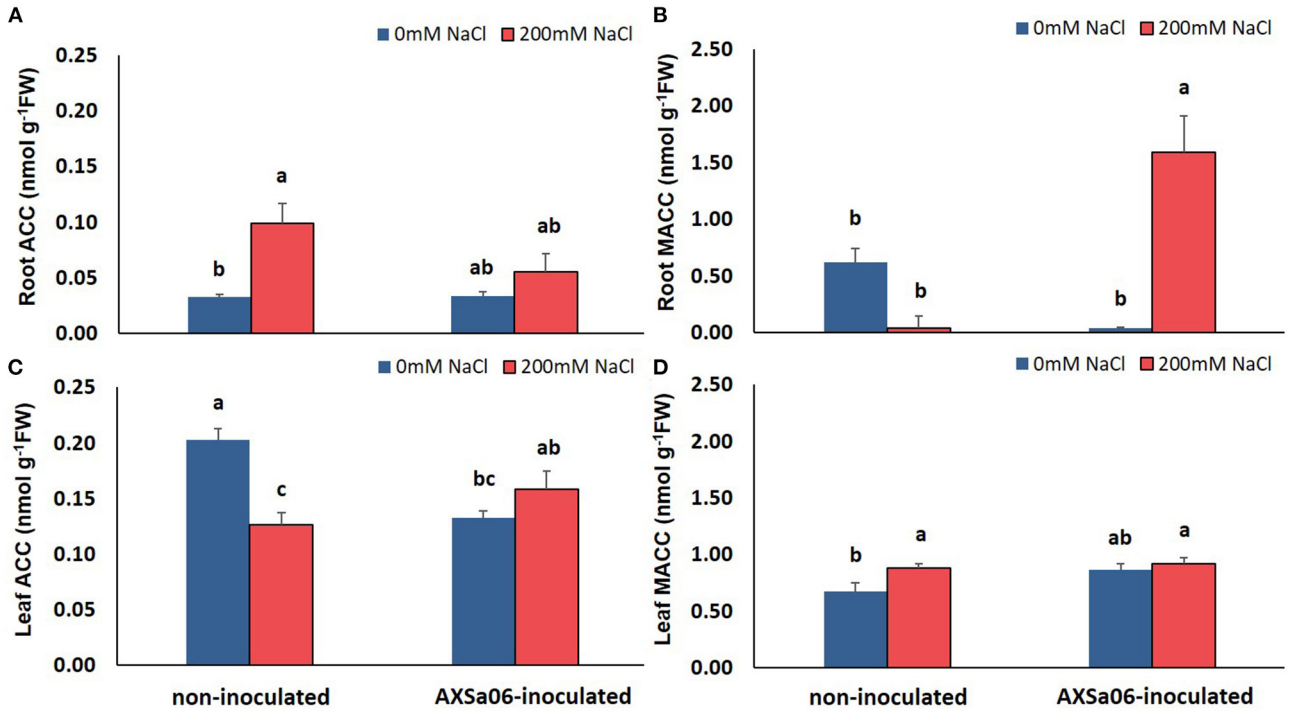

FIGURE 3 | Contents of ACC and MACC in roots **(A,B)** and leaves **(C,D)** of tomato seedlings inoculated or not with AXSa06 (*Pseudomonas oryzihabitans*) at exposure to 200 mM NaCl for 7 days. Data are means of five biological replicates ± standard error. Different letters indicate statistically significant differences between treatments based on Duncan's multiple range test ($P < 0.05$).

MF, Molecular Function). Among them, 20 or 30 significant GO terms were enriched for non-inoculated and AXSa06-inoculated plants, respectively (**Supplementary Table 8** and **Supplementary Figure 3**). At the absence of inoculum, the most significant (corrected $p < 0.05$) enrichment terms of up-regulated genes due to NaCl treatments in the BP category were response to wounding (GO:0009611), and amine metabolic process (GO:0009308), whilst in the MF, there were endopeptidase inhibitor (GO:0004866) and regulator (GO:0061135) activity, peptidase regulator (GO:0061134), and inhibitor (GO:0030414), as well as enzyme inhibitor (GO:0004857), and regulator (GO:0030234) activity (**Supplementary Figure 3A**). By contrast, at inoculations with AXSa06, GO terms of the BP category such as response to stress (GO:0006950), defense response (GO:0006952), and response to biotic stimulus (GO:0009607) were significantly enriched under salt stress (**Supplementary Figure 3B**). Among the most significant down-regulated GO terms at the absence of inoculum, there were small molecular metabolic process (GO:0006950), cellular carbohydrate metabolic process (GO:0044262), single organism carbohydrate metabolic (GO:0044723), and catabolic (GO:0044724) processes (**Supplementary Figure 3C**). Interestingly, the majority of up-regulated GO terms significantly enriched in non-inoculated plants exposed to stress, were identified as significantly down-regulated in inoculated plants (**Supplementary Figures 3A,D**), suggesting that *Pseudomonas oryzihabitans* AXSa06 strain was able to reverse—to some extent—the modifications stimulated by salt treatment.

As a further step, the DEGs were also examined against KEGG database to identify active biological pathways in tomato seedlings at exposure to salt and AXSa06 treatments (**Supplementary Figure 4** and **Supplementary Table 9**). Assignments of significant DEGs between stressed and non-stressed plants into KEGG pathways showed that the most significant induced pathways were protein processing in endoplasmic reticulum (sly04141), phenylpropanoid biosynthesis (sly00940), plant-pathogen interaction (sly04626), and arginine-proline metabolism (sly00330) in non-inoculated plants (**Supplementary Figure 4A**), while in AXSa06-plants, pathways of phenylpropanoid biosynthesis (sly00940), as well as starch and sucrose metabolism (sly00500) were up-regulated (**Supplementary Figure 4B**). The phenylpropanoid metabolic pathway that was induced regardless the presence of the PGP strain, contributes to lignin biosynthesis, including several lignin-forming peroxidases and cell-wall related proteins that were found to be over-expressed upon salt treatment (**Supplementary Tables 6, 7**). Plant hormone signal transduction pathway (sly04075) was significant down-regulated as a response to stress, regardless inoculation with AXSa06 (**Supplementary Figures 4C,D**), but in a very different way, as it will be discussed below. By contrast, photosynthetic-related pathways (sly00195 and sly00196), as well as those related to carbon (sly00710, sly 01200), glyoxylate and dicarboxylate

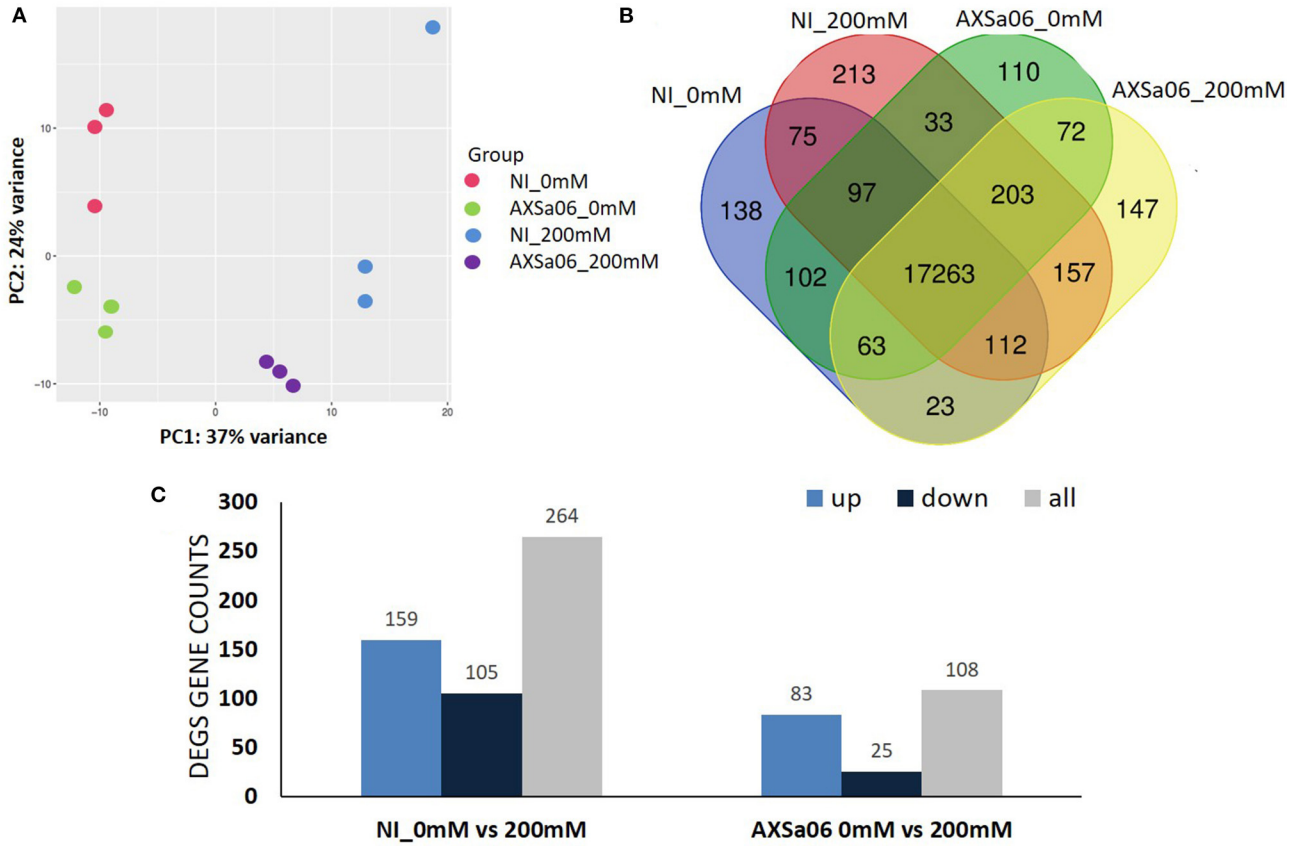

FIGURE 4 | (A) Principal Component analysis of all the expressed transcripts with FPKM >1 in non-inoculated (NI) and AXSa06-inoculated plants treated with 0 mM or 200 mM NaCl. **(B)** Venn diagram of the expressed transcripts with FPKM >1 highlighting commonly and uniquely expressed genes between different treatments. **(C)** The number of Differentially Expressed Genes (DEGs) representing up- and down-regulated transcripts in non-inoculated and inoculated plants due to NaCl treatment.

(sly00630), or nitrogen metabolism (sly00910), were only repressed at the absence of inoculum in response to salt stress (**Supplementary Figure 4B**), indicating the notable salt-mediated handicap in primary metabolism. Intriguingly, amino acid biosynthesis (sly01230) was significantly down-regulated in AXSa06-inoculated plants exposed to 200 mM NaCl.

Transcript abundance of DEGs in non-inoculated and inoculated plants in response to 200 mM NaCl, is also presented using heat maps (**Supplementary Figures 5, 6**), highlighting a series of changes in gene expression profiles when plants subjected to stress, whilst the entire list of DEGs between stressed and non-stressed plants is also displayed (**Supplementary Tables 6, 7**). The highest up-regulated genes in non-inoculated plants as a response to salt stress were ferredoxin (ID101248335) and a small heat shock protein (ID544205), whilst the top down-regulated DEGs included a spermidine hydroxycinnamoyl transferase-like (ID101254821), and the MYB transcription factor RADIALIS-like 6 protein (ID101244580) (**Supplementary Table 6**). By contrast, among the highest up-regulated genes in AXSa06-inoculated plants as a response to salt stress, there were abscisic acid 8'-hydroxylase 3 (ID101254720), and a non-specific lipid-transfer protein 1-like (ID101265675), while among the highest down-regulated genes, there were the MYB transcription factor RADIALIS-like 3 (ID101246530), and gamma-glutamyl peptidase 3-like (ID101254399) (**Supplementary Table 7**). Below, we explored manually a broad number of genes of particular interest that were modulated by AXSa06-inoculation by focusing on transcripts related to photosynthesis, amino acid metabolism, plant growth and development, stress responses, hormone synthesis and signaling, transcription factors, and other salt-responsive proteins (**Figure 5**). Genes with FPKM >1 in at least one treatment were considered as expressed (**Supplementary Table 10**).

Energy Metabolism

Some genes of the central metabolism such as phosphoenolpyruvate carboxylase (ID101245149) and O-acyltransferase WSD1 (ID101246264) were significantly up-regulated, and some others including 3-ketoacyl-CoA synthase 11 (ID101268510) were down-regulated, in non-inoculated plants as a response to salt stress (**Supplementary Table 6**). Others related to lipid-metabolism were down-regulated when non-inoculated plants were exposed to 200 mM NaCl.

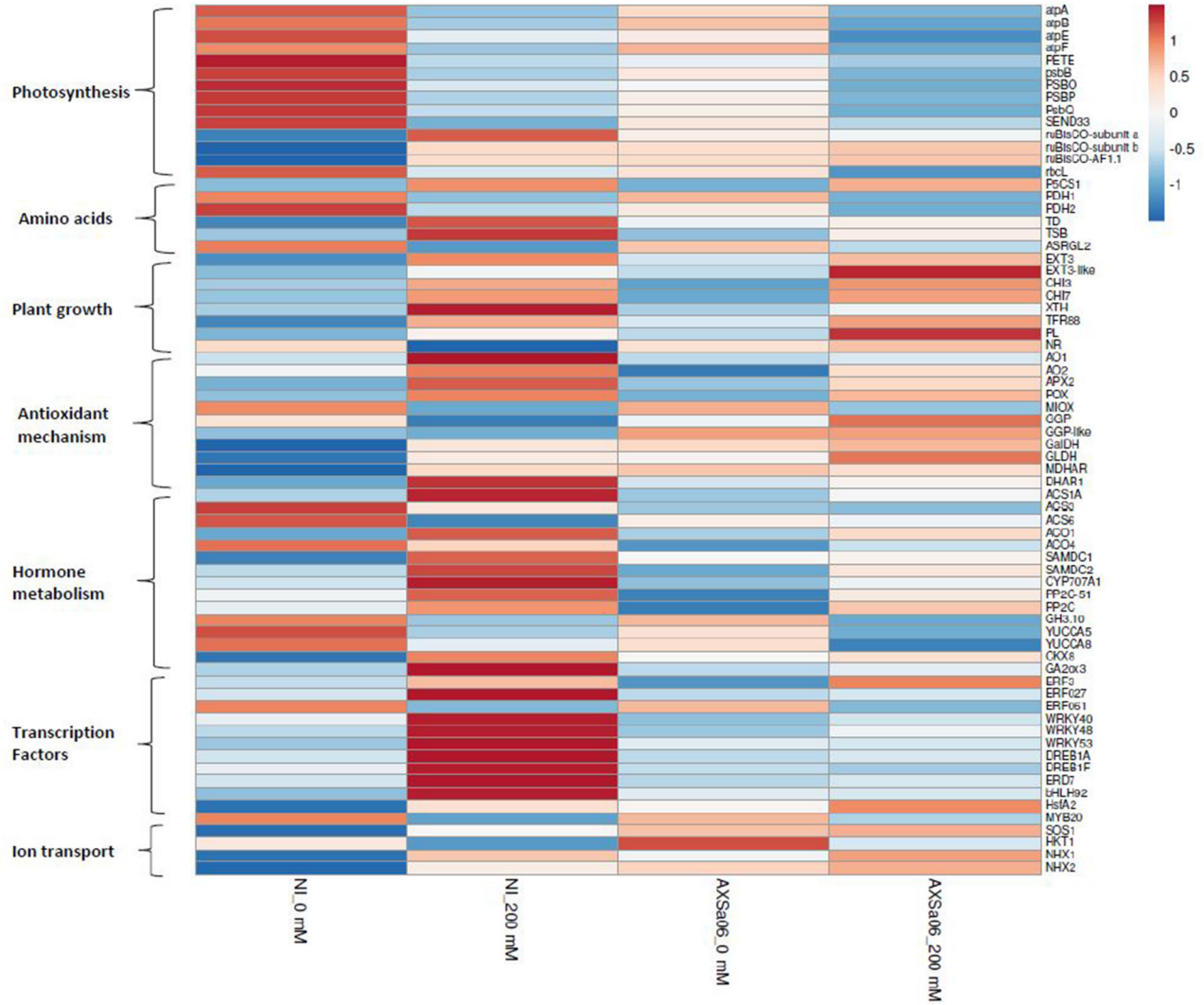

FIGURE 5 | Heatmap of selected genes of interest related to photosynthesis, amino acids, plant growth, antioxidant mechanism, hormone metabolism, transcription factors and ion transport, in the leaves of tomato seedlings inoculated with AXSa06 (*Pseudomonas oryzihabitans*) at exposure to 200 mM NaCl, based on $\log_2$ transformed FPKM values. The entire list of these genes followed by FPKM values is provided in **Supplementary Table 10**. NI, non-inoculated.

These included glycerophosphodiester phosphodiesterase (ID101261081), palmitoyl-monogalactosyldiacylglycerol delta-7 desaturase (ID101250586), GDSL esterase/lipase 1 (ID101268445), and 3-ketodihydrosphingosine reductase (ID101248253). Similarly, the expression of several genes involved in these pathways were also induced [O-acyltransferase WSD1 (ID101251623) and GDSL esterase/lipase (ID101250696)] or repressed [glycerophosphodiester phosphodiesterase (ID101261081), 3-ketoacyl-CoA synthase 11 (ID101268510)] under salt condition in AXSa06-inoculated plants (**Supplementary Table 7**).

Compared to 0 mM NaCl, a wide number of genes related to light reaction in photosynthesis and ATP synthesis were found to be down-regulated upon salt stress in the absence of inoculum (**Figure 5** and **Supplementary Table 10**), as further suggested by KEGG enrichment (**Supplementary Table 9**). These included the ATP synthases CF1 alpha (*atpA*), beta (*atpB*), epsilon (*atpE*), and CF0 (*atpF*), chloroplastic plastocyanin (*PETE*), photosystem II 23 protein (*PSBP*), photosystem II CP47 apoprotein (*psbB*), chloroplastic oxygen-evolving enhancer protein 1 (*PSBO*), photosystem II oxygen-evolving complex protein 3 (*PsbQ*), and ferredoxin-I (SEND33) (**Figure 5**). Down-regulation of the above-mentioned photosynthesis-related genes occurred to a lesser extent in AXSa06-inoculated plants upon salt stress, suggesting that the energy metabolism related to photosynthetic apparatus was less disturbed compared to non-inoculated plants. This is in line with the enhanced net photosynthesis in inoculated plants compared to non-inoculated plants at exposure to 200 mM NaCl (**Figures 1C,D**). Interestingly, transcript levels of the chloroplastic *ruBisCO* large subunit-binding protein

subunit alpha (ID101265242), subunit beta (ID101253117) and accumulation factor 1.1 (ID101251433) were also higher in inoculated plants compared to non-inoculated ones at control conditions, suggesting a probable better carbon assimilation due to the inoculum.

Amino Acid Metabolism

Several pathways related to the metabolism of amino acids were also modulated in response to salt stress regardless inoculation with AXSa06 (**Figure 5** and **Supplementary Table 10**). Proline is an important osmoprotectant synthesized in plant cells to alleviate salt stress conditions, over-accumulated in stressed plants regardless inoculation with AXSa06 (**Figure 1E**). In line with this observation, the key gene in the proline biosynthesis, delta-1-pyrroline-5-carboxylate synthase (*P5CS1*; ID101244293), was significantly up-regulated in the presence of salt, probably to help plants survive unfavorable abiotic conditions. Furthermore, the negative regulation of proline dehydrogenase (*PDH*), the enzyme that converts L-proline to L-glutamate, was conductive to the accumulation of proline in both non-inoculated (ID778202, ID101268445) and inoculated (ID778202) plants in response to NaCl treatment. Intriguingly, at the absence of inoculum, threonine dehydratase (*TD*; ID543983) responsible for the synthesis of L-isoleucine from L-threonine, and tryptophan synthase beta chain (*TSB*; ID101256422), responsible for the synthesis of L–tryptophan from indole and L-serine, were significantly up-regulated in stressed plants. By contrast, isoaspartyl peptidase/L-asparaginase 2 (*ASRGL2*; ID101245157) from the asparagine catabolic pathway was down-regulated.

Plant Growth and Development

The transcript levels of several genes involved in plant growth-related processes were also induced at 200 mM NaCl, regardless PGPR inoculation. These included extensins (*EXT*; ID544158, ID101249726) and chitinases (*CHI*; ID544149, ID544147) (**Figure 5** and **Supplementary Table 10**). In addition, cell-wall modification enzymes such as xyloglucan endotransglucosylase/hydrolase (*XTH*; ID101258345) that participates in cell-wall loosening and might benefit cell wall extension, or the plant cell wall protein *SlTFR88* (ID778266) were upregulated by salt stress at the absence of inoculum. By contrast, a pectate lyase (*PL*; ID778293), involved in cell-wall composition, was up-regulated by AXSa06-inoculation in response to salt stress. These changes in transcript levels of genes related to cell-wall modification alterations may be necessary for plant survival under unfavorable conditions, and were probably triggered by ethylene. On the other hand, nitrate reductase (*NR*; ID100736473), encoding the enzyme catalyzing the NAD(P)H-mediated conversion of nitrate to nitrite, which is the rate-limiting step of nitrogen assimilation pathway in higher plants, was significantly down-regulated only in non-inoculated plants due to salt stress. This finding may indicate a transition of metabolism from developmental processes to defense mechanisms. Thus, the inhibition of nitrogen assimilation pathway driven via NR activity, and occurred at high salinity conditions, may be prevented by AXSa06-inoculation.

Antioxidant-Related Genes

Several stress-responsive transcripts were detected among DEGs between control and salt stress treatments. At the absence of inoculum, transcripts related to ROS detoxification and homeostasis including ferredoxin (ID101248335), *AO* (ID101252344), L-ascorbate peroxidase (*APX*; ID101258987), and lignin-forming anionic peroxidase (*LPOX*; ID101261260), showed higher expression in stressed plants compared to control ones (**Figure 5** and **Supplementary Tables 6, 10**). By contrast, others such as *myo*-inositol oxygenase (*MIOX*; ID100316875 and ID101254427) and peroxidase 51 (*POX51*; ID101244162) or peroxidase 3 (*POX3*; ID101244376) exhibited lower expression. Similarly, the transcript levels of several stress-induced genes were up-regulated in AXSa06-inoculated plants at exposure to 200 mM NaCl. These included lignin-forming anionic peroxidase (*LPOX*; ID101261260), suberization-associated anionic peroxidase 2 (ID101245316), ferredoxin (ID101266472), *AO* (ID101252861), and inositol oxygenase 1 (ID101263222) (**Figure 5** and **Supplementary Tables 7, 10, 11**). Heat-shock proteins (HSPs) the molecular chaperones that inhibit the stress-mediated denaturation of proteins, were also up-regulated in this study. In particular, five HSPs (ID544024, ID544205, ID101254946, ID101264936, and ID101255223) were induced after salt stress only in non-inoculated plants (**Supplementary Table 6**). An up-regulation of key ascorbate (AsA) biosynthetic genes including GDP-L-galactose phosphorylase (*GGP*, ID101255942), L-galactose dehydrogenase (*GalDH*; ID101254135), and L-galactono-1,4-lactone dehydrogenase (*GLDH*; ID544206), as well as monodehydroascorbate reductase (*MDHAR*; ID101264360) from the AsA recycling pathway, was also evident in AXSa06-inoculated plants at control conditions compared to non-inoculated ones, supporting an enhancement of AsA-mediated antioxidant defense mechanism in these plants (**Figure 5** and **Supplementary Table 10**). This is also in agreement with an enhanced AsA pool due to inoculation as well be discussed below (**Figure 6**).

Since phenylpropanoids contribute to plant abiotic stress responses, genes encoding for key enzymes of their biosynthetic pathways were searched in a query to the KEGG database (**Supplementary Tables 9, 11**). Transcripts coding for 24 genes were found to be up-regulated in response to NaCl treatments in both non-inoculated and inoculated plants (**Supplementary Figure 7**). The identified genes have diverse functions related to phenylpropanoid-related pathways, being involved in key steps such as L-phenylalanine conversion in cinnamic acid [phenylalanine ammonia lyase (PAL2)], or catalysis of the final branches for lignin production (i.e., lignin-forming anionic peroxidase, ID101261260) or suberization (suberization-associated peroxidases, *TMP1*, *TAP2*, and ID101265511). Interestingly, although several β-glucosidase genes (ID101247513, ID101263519, and ID100191127) were up-regulated due to salt stress in both non-inoculated and inoculated plants, their transcript levels were higher at the absence of NaCl in inoculated compared to non-inoculated plants, suggesting

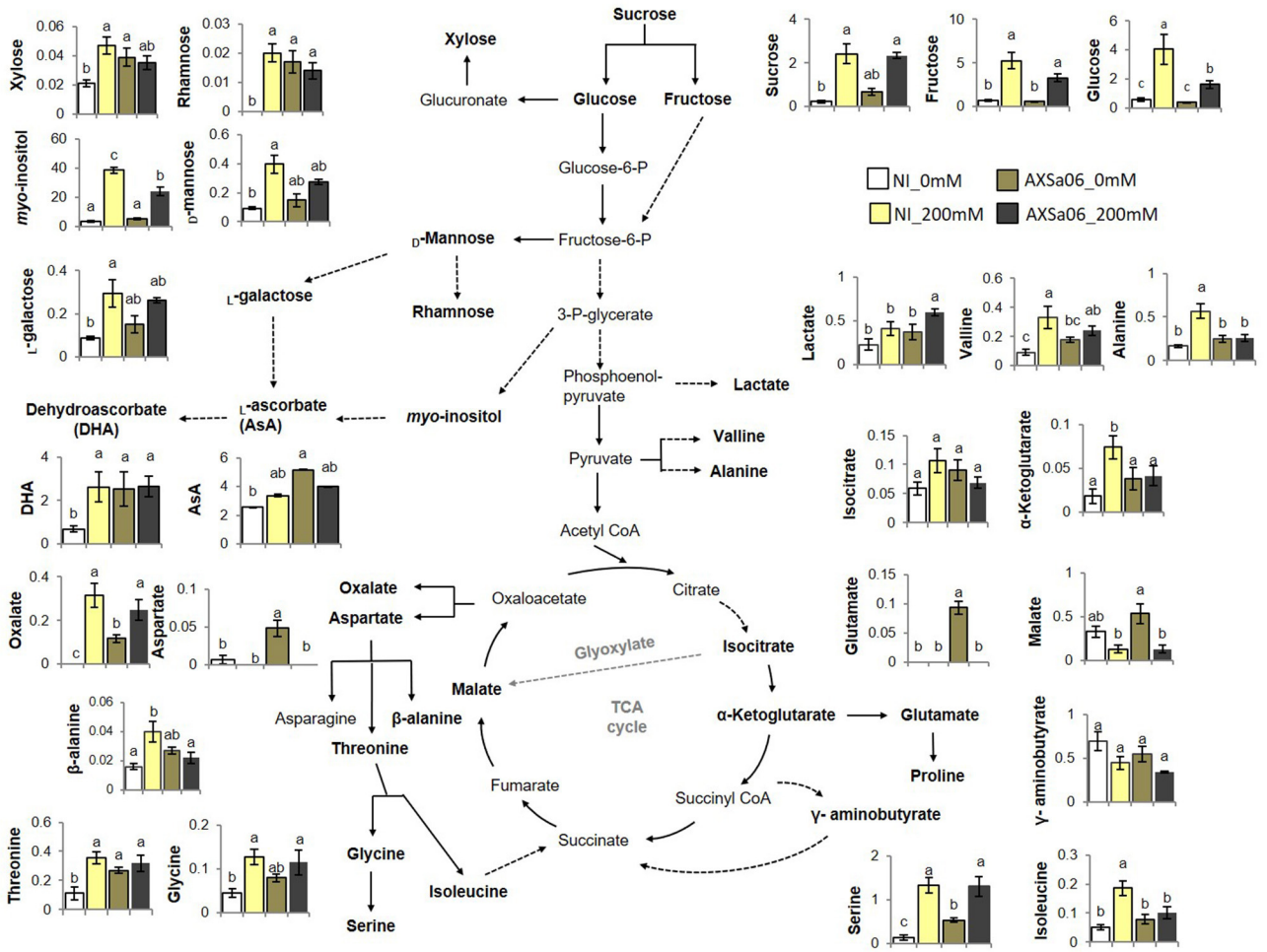

FIGURE 6 | Selected metabolomic profiles of leaves from tomato seedlings inoculated or not with AXSa06 (*Pseudomonas oryzihabitans*) at exposure to 200 mM NaCl. Amounts were expressed as relative abundance based on the relative response compared to internal standard adonitol and are provided in **Supplementary Table 12**. Ascorbic acid (AsA) and its oxidized form (dehydroascorbate, DHA) were determined spectrophotometrically based on the AO enzyme method. Data are means of five biological replicates ± standard error. Different letters indicate statistically significant differences between treatments based on Duncan's multiple range test ($P < 0.05$). NI, non-inoculated.

that AXSa06 inoculation has also affected and remodeled phenylpropanoid pathway.

Hormone-Related Pathways

The expression levels of hormone-related genes were also differentially regulated by both AXSa06-inoculation and treatment with 200 mM NaCl (**Figure 5** and **Supplementary Table 10**). At the absence of inoculum, salt stress enhanced ethylene biosynthesis as indicated by the significant up-regulation of ACC-synthase 1A (*ACS1A*; ID544028). At the same time S-adenosylmethionine decarboxylase (*SAMDC2*, ID101260400), a key enzyme linking ethylene metabolism and polyamine (spermine and spermidine biosynthesis), previously associated with modified salt responses in tobacco plants (Mellidou et al., 2016, 2020), was also over-expressed under salt stress. The remarkable up-regulation of ethylene biosynthesis through transcription of *ACS1* and *ACO1* due to NaCl treatments was evident at the absence of inoculum (**Figure 5**). Notably, AXSa06-inoculated plants showed no particular alteration in the expression of ethylene biosynthetic genes upon exposure to salt stress. This is in line with results on ACC accumulation in the leaves (**Figure 3C**), supporting the impact of the ACC deaminase strain, AXSa06, in inhibiting ethylene synthesis either due to limited precursor availability or ethylene signaling.

Three ABA receptors PYL4 (ID101250944, ID101258963, and ID101256856), required for ABA-mediated responses such as stomatal closure, were significantly down-regulated in non-inoculated plants in response to salt stress (**Supplementary Table 6**), whilst only one ABA receptor PYL4 (ID101258963) was repressed in inoculated plants (**Supplementary Table 7**). On the other hand, although the expression levels of some ABA-signaling genes such as protein

phosphatase 2C (*PP2C*; ID101249794, ID101258071) that act as negative regulators of ABA-mediated responses, or ABA 8′-hydroxylase (*CYP707A1*; ID101254720), the key enzyme in ABA oxidation/catabolism, were induced upon salt stress regardless the presence of the inoculum (**Figure 5** and **Supplementary Table 10**), but the induction was more drastic in AXSa06-inoculated plants. In particular, these three genes were detected among the top DEGs in AXSa06-inoculated plants in response to 200 mM NaCl (**Supplementary Table 7**), suggesting a more stunning suppression of ABA signaling due to the PGP strain. Notably however, considering expression levels of these negative regulators of ABA signaling, inoculated plants showed lower expression regardless stress treatment compared to non-inoculated plants. Genes related to other hormone catabolism, such as cytokinin oxidation (cytokinin dehydrogenase; *CKX8*; ID101055579) or gibberellin oxidation (gibberellin 2-oxidase; *GA2ox3*; ID100134888) were up-regulated only in stressed non-inoculated plants, suggesting that these plants probably perceive more stress signals than inoculated ones (**Figure 5**). Another gene involved in auxin metabolism (indole-3-acetic acid-amido synthetase; *GH3.10*; ID101258277) was significantly down-regulated due to NaCl treatment regardless inoculation with AXSa06.

Transcription Factors

Several transcription factor (TFs) families such as WRKY, MYB, and bHLH exert pivotal roles in plant responses to abiotic stress factors. In non-inoculated plants, a broad number of TFs were induced by salt stress, including dehydration-responsive element-binding protein 1A (*DREB1A*; ID109119806 and ID101248897), ethylene-responsive *ERF027* (ID101246746), *WRKY* (ID101264826, ID101246812, ID101261141), *EARLY-RESPONIVE TO DEHYDRATION* protein (*ERD7*; ID101263355), *bHLH92* (ID101245202), and heat stress TF *HsfA2* (ID101255223) (**Figure 5** and **Supplementary Table 10**). A few TFs were also down-regulated in non-inoculated plants treated with NaCl. These included *ERF061* (ID10125880) and *MYB20* (ID101264349). By contrast, only one abiotic stress-responsive TF, *ERF3*-like (ID606713) was up-regulated in inoculated plants under salt stress conditions. Since TFs act downstream the hormonal signals, this finding further supports the previous hypothesis that inoculated plants may receive less stress signals than non-inoculated ones due to the suppression of ABA- and ethylene-activated responses.

Other Salt-Responsive Genes

The broad number of secondary structures enables LEA proteins to play multiple roles in abiotic stress, constituting an essential footprint of plant tolerance against irreversible damage (Artur et al., 2019). Homologs of this large protein family were found to be over-expressed at 200 mM NaCl in both non-inoculated (ID544157; **Supplementary Table 6**) and AXSa06-inoculated plants (ID100750252; **Supplementary Table 7**). Laccases are also widely present in plants, and have been related to disease resistance and lignin biosynthesis, while their involvement in abiotic stress tolerance is less clear (Liu et al., 2017). In this study, two different laccases (ID101251693 and ID101253711) were positively regulated by salt stress, regardless the presence of inoculum (**Supplementary Tables 6, 7**). By contrast, galactinol synthase (ID101261450), the key enzyme in the biosynthesis of raffinose, was only up-regulated in AXSa06-inoculated plants exposed to 200 mM NaCl (**Supplementary Table 7**).

An interesting observation of this study is that the SOS1 protein (ID778208), a putative plasmalemma Na^+/H^+ antiporter essential in maintaining ion homeostasis under salinity, through partitioning Na^+ between plant organs (Olías et al., 2009), was significantly higher (1.4-fold) in AXSa06-inoculated plants compared to non-inoculated plants at control conditions (0 mM NaCl) (**Figure 5** and **Supplementary Table 10**). At salt stress, transcript levels of *SOS1* were induced in non-inoculated plants, while remained at very high levels in inoculated ones. Similarly, the Na^+ transporter *HKT1*, as well as the Na^+/H^+ antiporters (*NHX1* and *NHX2*), were up-regulated due to AXSa06 inoculation at control conditions. These findings indicated a putative improved mechanism of preventing the accumulation of excess Na^+ in photosynthetic tissues, thus supporting a role of AXSa06 as a priming agent that facilitated plants to tolerate abiotic stress factors.

Metabolome Reprogramming Under Salt Treatment

In an attempt to generate a comprehensive picture of metabolite reprogramming occurring in AXSa06-inoculated plants at exposure to 200 mM NaCl, we evaluated the abundance of 46 metabolites using GC-MS (**Figure 6** and **Supplementary Table 12**). In total, 25 metabolites showed differential accumulation at the absence of inoculum in plants exposed to salt stress compared to control, whilst at the presence of inoculum, only 14 metabolites differed significantly between stressed and un-stressed plants. Among them, 24 and seven were increased, while one and seven were decreased, in non-inoculated or inoculated plants, respectively.

Of the metabolites with differential accumulation during salt stress, most of them belonged to sugars or amino acids, indicating that their metabolic pathways were predominantly affected by NaCl treatments. In particular, accumulation of sucrose, fructose, glucose, *myo*-inositol, and xylitol, were significantly increased due to salt treatment in both non-inoculated and inoculated plants, but to a greater extent at the absence of inoculum (**Figure 6**). By contrast, xylose, rhamnose, $_D$-mannose, $_L$-galactose, allose, sedoheptulose, erythrose, and 2-deoxy-$_D$-erythro-pentitol, showed higher accumulation due to salt stress only in non-inoculated plants. As for organic acids identified in this study, oxalate and 2-ketoglutarate increased in non-inoculated plants exposed to stress, whilst lactate and oxalate increased in AXSa06-inoculated ones. However, the accumulation of two other organic acids, malate, and galactarate decreased in inoculated plants. A broad number of amino acids increased as a response to salt stress at the absence of inoculum, including alanine, valine, isoleucine, glycine, serine, threonine, and cystathionine. Among them, only serine was induced in AXSa06 plants, while two other

amino acids, aspartate and glutamate decreased at exposure to 200 mM NaCl. No particular changes in AsA contents due to NaCl application were recorded, but inoculated plants had significantly higher AsA levels at control conditions (**Figure 6**). Furthermore, similar to the majority of sugars, DHA, the oxidized form of AsA representing an indicator of cellular redox homeostasis was enhanced at NaCl treatment of non-inoculated plants, but remained unaltered when the inoculum was applied.

Collectively, these metabolomic findings suggest that salt stress imposed far less metabolomic reprogramming when plants were inoculated with AXSa06. The metabolomic profile of non-inoculated compared to inoculated plants at control conditions (0 mM NaCl) revealed a vast number of metabolites over-accumulated in AXSa06 treatments (**Figure 6** and **Supplementary Table 12**). In particular, the sugars 2-desoxy-inosose, 2-deoxy ribose and the cell-wall related xylose and rhamnose, the sugar alcohols erythritol and 2-deoxy ribitol, the amino acids aspartate, threonine, serine and glutamate, as well as the acids 2-deoxy ribonate, oxalate and AsA, were all increased owing to AXSa06 inoculation, indicating a probably reprogramming of metabolism that may support plant adaptation against salt. This pattern was further supported by results concerning sucrose, mannose, valine, glycine, and malate, although differences were not statistically significant.

DISCUSSION

Plants have evolved symbiotic interactions with soil microbes that can alter plant phenotypic plasticity in a broad range of traits during plant growth or in response to changing environment (Goh et al., 2013). PGPR can enhance plant growth via direct or indirect mechanisms, including nutrient mobilization, solubilization and bio-availability, phyto-hormone biosynthesis, and induced systemic resistance (Yang et al., 2009; Pérez-Jaramillo et al., 2018; Gamez et al., 2019). Along with their plant-growth-promoting properties, and their ability to protect from phytopathogenic infections, some PGPR are also capable of enhancing tolerance to abiotic stresses such as salinity and drought (Yang et al., 2009). The exact mode of action by which PGPR affect plant growth under adverse environmental conditions may be both plant species- and strain-specific, as highlighted by the vast number of studies in different plants (Liu et al., 2017; Chauhan et al., 2019; Gamez et al., 2019; Safdarian et al., 2019). The present study demonstrated that AXSa06, a *Pseudomonas oryzihabitans* strain previously isolated from extreme saline ecosystem, able to consume ACC, to produce IAA and siderophores, as well as to solubilize inorganic P (Leontidou et al., 2020), efficiently colonized the rhizosphere of tomato seedlings and promoted plant growth under salt stress. Inoculations with the strain seem to impose plants to a primed state, at which they are able to respond more robustly to abiotic stress owing to the earlier increased and more efficient activation of the defense response, as previously reported (Conrath, 2011). The investigation of key genes and metabolic pathways further supported the primed state of AXSa06-inoculated plants prior to NaCl treatments that probably has led to a less disturbed metabolism after exposure to stress, by dampening stress signals, contributing to AXSa06-mediated tolerance. This is further supported by the GO enrichment analysis demonstrating that *Pseudomonas oryzihabitans* AXSa06 strain was able to down-regulate transcripts related to peptidase regulator or inhibitor activity that were otherwise found to be stimulated by salt treatment in non-inoculated plants due to protein degradation and synthesis of defensive proteins.

AXSa06 Stimulated Antioxidant Mechanism

As a primary stress response to NaCl treatments, a burst in ROS production is expected, resulting in extensive cellular damage if not tightly regulated by the antioxidant scavenging systems in plants (Gémes et al., 2016; Noctor et al., 2016). Several antioxidant enzymes, including CAT, SOD, APX, and POX are known to increase in response to salt stress in order to mitigate salt-induced damage as has been reported in many plant species, including tobacco (Mellidou et al., 2016) and cotton (Hamani et al., 2020). Previous studies also reported an up-regulation of ROS scavenging activities and of antioxidant components accumulation due to bacteria inoculation under salt conditions (Bharti et al., 2016; Chen et al., 2016). Nevertheless, in this study, the prior-to-stress stimulation of antioxidant machinery (enzymatic and non-enzymatic) in AXSA06 plants may account for the improved salt adaptation, without any additional energy cost to support the protection of cellular redox homeostasis when stress is applied. In other words, strain inoculation may have imitated the effect of mild oxidative stress, similar to what is expected during salt stress. This primed state of AXSa06-inoculated plants is supported by the increased content of AsA and its oxidized form, DHA, as well as the enhanced activities of antioxidant enzymes, including POX and CAT that scavenge H_2O_2, compared to non-inoculated ones at control conditions. Within this context, the induction of antioxidant defense mechanism probably has occurred to limit down lipid peroxidation due to inoculation in non-stressed plants, which, however, did not show any visual symptom of oxidative stress. Although MDA content has been mostly considered as an oxidative stress marker triggering a wide range of other developmental signals, it can be also beneficial for plants in a number of ways participating in the induction of antioxidant defense or membrane repair (Tounekti et al., 2011; Kurutas, 2016; Morales and Munné-Bosch, 2019). Since photosynthetic process was not inhibited, plant growth was vigor, and ROS were probably efficiently removed in the inoculated plants, these plants may experience a mild oxidative boost just enough to increase their alertness, for amplified defense responses upon the onset of stress treatment. In other words, lipid peroxidation in inoculated plants may be beneficial—to a certain extent—to stimulate their alertness prior to stress. Tounekti et al. (2011) also reported that when MDA accumulation is elevated, rosemary plants can withstand salt-induced oxidative stress, by activating the xanthophyll cycle-dependent dissipation of excess excitation energy in leaves.

Due to their non-specific reactions with different ROS, POX enzymes participate in a broad number of physiological functions, including auxin catabolism, suberization, lignifications, cell wall elongation, and pathogen attack (Malviya et al., 2020). Previously, homologs of different *POX* genes have been implicated in lignin and xylan accumulation in *Arabidopsis* through ROS signaling (Cosio et al., 2017), as well as in salt tolerance in soybean (Jin et al., 2019). Herein, a lignin-related *POX* was up-regulated at exposure to 200 mM NaCl regardless inoculation, but a suberization-associated *POX* only at the presence of the PGPR strain. Although suberization primary occurs in the roots, this adaptive anatomical process is important for the prevention of apoplastic flow of toxic Na^+ under salt stress (Shabala et al., 2012).

In response to abiotic stress, plants synthesize a broad number of secondary metabolites possessing or inducing antioxidant properties to alleviate the over-accumulation of ROS and inhibit cell membrane peroxidation (Baba et al., 2017; Sharma et al., 2019). In particular, upon stress treatments, the phenylpropanoid pathways are commonly activated through the up-regulation of the transcript levels of genes encoding key biosynthetic enzymes like *PAL*, chalcone synthase and isomerase (Perin et al., 2019). In line with previous reports, several phenylpropanoid-related genes were up-regulated upon salt treatment, but this occurred regardless the presence of AXSa06. Although phenolic compounds were not determined in this study, the slightly increased transcript levels of the related genes at control conditions due to AXSa06 compared to non-inoculated plants, suggested that plants employed these metabolites as a communication tool to attract desirable symbiotic rhizobacteria, as have already been demonstrated between legumes and nitrogen fixing bacteria (Biała and Jasiński, 2018). On the other hand, β-glucosidases have an interesting role in abiotic stresses, particularly dehydration through ABA, by hydrolyzing secondary metabolites that are stored in inactive glycosylated forms (Baba et al., 2017). These enzymes have crucial functions in plants in response to altered environmental cues, including the glycosylation of secondary metabolites that are stored in inactive glycosylated forms and the activation of lignin precursors (Rouyi et al., 2014). The higher transcript levels of various β-glucosidase genes due to AXSa06 may contribute to the enhanced stress tolerance of inoculated plants, by releasing glucose which could serve as an alternative source of energy during insufficient photosynthesis.

AsA has numerous functions linked to oxidative relief under stress conditions, including the cellular scavenging of H_2O_2 via APX, or the apoplastic regulation of the AsA redox state via AO, which is important for stress perception and orchestration of defense responses (Mellidou and Kanellis, 2017). Therefore, AsA pool size and homeostasis may act as the signal of the oxidative injury occurring under stress, and play a pivotal role in controlling plant responses to environmental changes (Pignocchi et al., 2003). Transcript levels of *APX* were up-regulated at the absence of inoculum as a response to salinity, contributing to the significant increase in DHA accumulation in these plants, but no similar pattern was observed in AXSa06 treatments, indicated that these plants may sense less oxidative stress. If these oxidized forms cannot be regenerated by monodehydroascorbate reductase (MDHAR) and dehydroascorbate reductases (DHAR) in the AsA-GSH cycle, then AsA is permanently lost (Noctor et al., 2016). The increased transcript levels of AsA biosynthetic and recycling genes, combined with the accumulation of AsA itself and its precursor, L-galactose at control conditions, indicated that inoculations with AXSa06 enhanced the AsA-mediated capacity of plants to scavenge ROS, further supporting the role of this strain as a priming agent against stress. This is in line with previous studies demonstrating that the regulation of antioxidant enzyme activities by PGPR exert a pivotal role in stimulating strain-mediated salt tolerance of plants (Safdarian et al., 2019).

AXSa06 Altered Amino Acid and Sugar Metabolism Imitating Salt Stress Responses

Although the phenomenon has been known for decades, the molecular basis of PGPR-mediated priming against abiotic stresses is far from being clearly elucidated. The over-accumulation of osmoprotectants such as proline is considered as the most usual mechanism of osmotic stress avoidance. Indeed, at exposure to salt stress, proline levels highly increased in both inoculated and non-inoculated plants, and similar to results from others (Kim et al., 2014; Liu et al., 2017), transcript levels of *P5CS1*, a key gene from proline biosynthetic pathway leading to osmoregulation, was also stimulated, independently of inoculation. These findings indicated that AXSa06-mediated stress tolerance is probably not related to a more efficient osmoregulatory activity in inoculated plants, at least due to proline.

Carbohydrates, including hexoses (fructose and glucose), disaccharides (sucrose and trehalose), and oligosaccharides (raffinose), are well-known to control ionic balance, maintaining cell turgor, while some of them are also considered as signaling molecules or even as ROS detoxification molecules in response to salt stress (Keunen et al., 2013; Patel et al., 2020). In this study, inoculated plants showed enhanced accumulation of certain sugars prior to stress application (erythrose, xylose, 2-deoxy -ribose, and 2-desoxy-inosose), or displayed no particular induction of some other sugars (sucrose and galactose) in exposure to salt stress similar to those observed in non-inoculated plants. These results support the notion that the metabolism of AXSa06-inoculated plants was less disturbed due to salt. The synthesis of other compatible solutes, such as raffinose family oligosaccharides (RFOs), represents an additional mechanism used by plants to adapt during the adverse effects of stressful conditions (Liu et al., 2021). Their mode of action involves the protection of membranes from hydroxyl radicals, as they are found between the head groups of lipids. The formation of galactinol from *myo*-inositol is catalyzed by galactinol synthase, representing the first enzyme that commits carbon toward RFO formation (Vinson et al., 2020). Transcript levels of this gene were only significantly induced in AXSa06-inoculated plants exposed to 200 mM NaCl, indicating an additional role of galactinols as osmoprotectants

and stabilizers of cellular membranes, but also as scavengers of ROS under excess salt (Nishizawa et al., 2008). Although none of these compounds were quantified in this study, the decreased levels of *myo*-inositol—the substrate of galactinol synthase—upon AXSa06 inoculation due to stress, may reflect the better adaptation of inoculated plants through this pathway.

Notably, the level of four amino acids (aspartate, threonine, serine, and glutamate) all increased owing to AXSa06 inoculation under control conditions indicating prominent changes in amino acids metabolism. Previously, the accumulation of free amino acids in combination with the higher transcript levels of related biosynthesis genes have been linked with salt tolerance, suggesting a crucial role of amino acid metabolism in stress tolerance (Zhang et al., 2017; Liu et al., 2020). Among these amino acids, the higher abundance of aspartate and glutamate mediated by AXSa06 inoculation at the absence of stress is of particular interest. Both molecules are involved in asparagine biosynthesis that is a major part of amino acid and nitrogen metabolism in plants (Curtis et al., 2018), strongly regulated by salt stress (Rashmi et al., 2019), and may operate as a pool of precursors for this metabolic branch, when plants exposed to NaCl. Asparagine has been also implicated in the early responses against salt stress in sugar beet (Liu et al., 2020), and can be further used as precursor in methionine and glutathione biosynthesis, that are able to scavenge ROS (Noctor et al., 2012). On the other hand, glutamate can be used to produce proline and gamma-aminobutyric acid (GABA) (Liu et al., 2020). In *Arabidopsis*, knockout mutants with T-DNA insertion in asparagine synthetase 2 gene exhibited limited salt tolerance and impaired nitrogen assimilation and translocation by the NaCl treatment relative to the wild-type (Maaroufi-Dguimi et al., 2011). In spite of the fact that GABA has been reported to alleviate salt stress injury in tomato seedlings by modifications in ion flux, amino acid synthesis and key enzyme expression (Wu et al., 2020), no similar relation was found in this study. Moreover, the increased levels of threonine and serine after AXSa06 inoculation revealed the modification of "glycine, serine, and threonine metabolism" pathway in response to inoculum at control conditions. Similarly, in non-inoculated plants exposed to salt stress, genes related to this pathway, such as *TD* and *TSB* were significantly up-regulated, with a concomitant increase in metabolic fluxes, whilst *ASRGL2* involved in asparagine metabolic pathway was down-regulated in non-inoculated plants, probably to support fluxes toward threonine and serine that were enhanced. These findings further support the notion that at control conditions AXSa06 exerted a similar response of primary metabolism related to amino acids as non-inoculated plants at the presence of NaCl, suggesting a kind of mild stress due to the inoculum that primed plants prior stress exposure.

No particular changes in tricarboxylic acid cycle were observed between non-inoculated and AXSa06-inoculated plants at metabolic or transcriptomic level in response to salt stress. This could be probably explained by an earlier induction of this pathway during the first days of stress application, as previously reported in sugar beet (Liu et al., 2020), that we were not able to detect at long-term (7 days) salt stress. An early down-regulation of pathways related to energy metabolism could serve as the signal for the transition from plant growth to the enhancement of defense mechanisms to cope with the stress factor (Bandehagh and Taylor, 2020). On the basis of these considerations, future studies should focus on discriminating early and late responses to salt stress, as well as providing clues on their importance in alleviating stress injury.

AXSa06 Regulates Hormone Production and Signaling

Ethylene and ABA are considered as key phytohormones, acting in concert as double-edged swords to coordinate stress responses to various abiotic factors (Müller, 2021). Several lines of evidence over the last decades suggest that salt stress stimulates ethylene production in plants, ultimately inhibiting plant growth and development (Riyazuddin et al., 2020). In this regard, PGPR that possess ACC deaminase activity are considered to increase salt tolerance of plants through inhibiting ethylene production by consuming ACC, and thus enhancing plant growth (Liu et al., 2017; Safdarian et al., 2019), although this is not their sole mode of action accounting for salt tolerance. In this study, root ACC content decreased in inoculated plants compared to non-inoculated ones exposed to salt stress, highlighting the positive effect of inoculation with the ACC deaminase-containing strain on inhibiting the ACC flux toward ethylene biosynthesis. Nonetheless, its effect in the above-the-ground parts is less clear. Under salt stress, the reduction in ACC content at the absence of inoculum may be attributed to its consumption to produce ethylene due to NaCl treatments, whilst no particular changes were observed at the presence of inoculum, probably because the ethylene signal from the roots is inhibited due to the consumption of ACC from the strain. During salt stress, *ACS3* and *ACO4* displayed no particular up-regulation, while *ACS1A* and *ACO1* were upregulated, but to a lesser extent when plants were inoculated with ASXa06. This data suggests that ethylene production, and in turn, ethylene signaling, are probably inhibited by the AXSa06 inoculum. Although the ethylene production has not been measured *in vivo*, ethylene determination in the excised leaves of AXSa06-inoculated plants further confirmed that there was less ethylene signaling-sensitivity during salt stress, and consequently less feedback of ethylene on its own biosynthesis, as highlighted by the lack of major modifications in the expression of ethylene-biosynthetic genes. The reduced ethylene production could also account for the observed higher ACC accumulation under salt stress compared to non-inoculated plants, suggesting that ACC was not consumed for ethylene production in inoculated plants. All these findings need to be further confirmed to elucidate the exact role of ethylene in PGPR-mediating tolerance. Previously, it has been demonstrated that ethylene signaling and homeostasis is linked with certain PGPR-mediated responses in modulating plant stress tolerance (Chen et al., 2013; Poupin et al., 2016; Liu et al., 2017). The dramatic increase in root MACC content of inoculated plants exposed to 200 mM NaCl indicated that the major part of ACC was used for MACC formation rather than ethylene biosynthesis, thus evidencing that the ethylene accumulation in the roots is inhibited resulting to lower levels

of ethylene signaling in the above-the ground-parts. MACC is an end product, providing a potential mechanism to control ethylene biosynthesis (Van de Poel et al., 2014), while its exact mode of action under salt stress requires further investigation.

ABA and ethylene have antagonistic relations in the control of stomatal opening and closure (Müller, 2021). In this study, the expression of some ABA signaling components such as protein phosphatases 2C that act as negative regulators of ABA-mediated responses, or ABA 8′-hydroxylase, the key enzyme in ABA oxidation/catabolism, were more drastically induced under salt stress conditions owing to AXSa06 inoculation compared to non-inoculated plants, suggesting a more vivid suppression of ABA signaling and accumulation. The up-regulation of these genes has been previously correlated to enhanced salt tolerance, as ABA regulates the integration of stress signals, especially the ethylene-mediated ones (Campobenedetto et al., 2020). At the same time, the lower absolute expression of these ABA-related genes at both control and stress conditions in the presence of AXSa06 may be related to the lower accumulation of ABA, that could have otherwise led to stomata closure, disturbing photosynthesis (Jakab et al., 2005; Vishwakarma et al., 2017). Previously, the ABA-signaling components have been found to regulate both fast and slow ABA-mediated responses to tackle dehydration under salinity (Vishwakarma et al., 2017). Therefore, the beneficial impact of AXSa06 inoculations in plant salt tolerance could be possibly due to the more rapid and efficient suppression of both ethylene- and ABA-mediated stress signals.

Several TF families, including WRKY, bHLH, and DREB, have been previously demonstrated to orchestrate plant stress reactions against abiotic stress (Golldack et al., 2011; Liu et al., 2017). In the present study, non-inoculated plants showed an induction of these TFs when exposed to salt stress, which may be regarded as a defense reaction to ameliorate stress damage, by modulating osmotic and ROS homeostasis. In contrast to other studies on PGPR stains (Liu et al., 2017; Safdarian et al., 2019), these stress-responsive TFs, similar to ERFs that are located downstream the genes of the ethylene signaling pathway, were not upregulated in AXSa06-inoculated plants exposed to stress compared to non-stress conditions. These observations suggest that AXSa06 prevented the induction of the stress-induced ethylene biosynthesis, and further damped ABA synthesis and signaling during salt stress. In other words, AXSa06 minimizes the activity of two major abiotic stress hormones, and thus inoculated plants displayed less hormone-mediated responses due to salt stress.

As AXSa06 is able to produce IAA *in vitro* (Leontidou et al., 2020), the probable enhanced strain-mediated IAA production may serve as an important signal for plants to cope with salt stress. Although salt stress imposed IAA modifications at the transcript level regardless AXSa06 inoculation, there was no clear link between the PGP strain and IAA homeostasis. In particular, an indole-3-acetic acid-amino synthetase, responsible for the inhibition of free IAA accumulation (Ding et al., 2008), was down-regulated regardless the presence of the strain. Genes of the *GH3* (Gretchen Hagen 3) family are involved in IAA homeostasis through catalysis of auxin conjugation and by binding free IAA to amino acids (Liu et al., 2016). In rice, some *GH3* genes were found to be related to stress responses, i.e., by decreasing the endogenous IAA content enhancing drought tolerance (Zhang et al., 2009), or through modulating ABA levels under drought and freezing stress (Du et al., 2012). One of the key genes in the tryptophan-dependent pathway of auxin biosynthesis is indole-3-pyruvate monooxygenase *YUCCA*, which convert indole-3-pyruvic acid to bioactive IAA (Zhao et al., 2001). Its transcript levels were also found to be down-regulated regardless the presence of the PGP strain, further supporting the disruption of IAA homeostasis predominantly due to salt stress, and not owing to AXSa06. Taken together, it is evident that AXSa06 did not have a direct impact on IAA metabolism, while the intriguing crosstalk between IAA, ethylene and ABA metabolism, as well as other signal networks, needs to be further elucidated using hormone-deficient mutants.

AXSa06 Alleviates Ion Toxicity

On the other hand, salt stress evokes ion toxicity due to the higher Na^+ accumulation within plant tissues. Several ion transporters have been shown to regulate Na^+ influxes into plant cells, by inducing Na^+ circulation and sequestration (Liu et al., 2017). For instance, overexpression of *NHX* encoding a tonoplast Na^+/H^+ antiporter enhanced salt tolerance of *Arabidopsis* plants (Zhang and Blumwald, 2001), while its expression can be induced by inoculations with *Bacillus amyloliquefaciens* in maize (Chen et al., 2016) and *Arabidopsis* (Liu et al., 2017), but not in rice (Nautiyal et al., 2013), indicating that transcriptome responses are species-dependent. Another Na^+ transporter with high affinity for K^+, the sodium transporter *HKT1*, is also known to be induced in plants due to inoculations with *Bacillus* species, thereby limiting Na^+ accumulation and toxicity in plant cells (Chen et al., 2016; Liu et al., 2017). In this study, the lower Na^+ contents measured in leaves of AXSa06-inoculated plants may be due to the induction of *NHX1*, *NHX2,* and *HKT1* transcript levels due to bacterial inoculation prior to stress application that enabled an efficient mechanism of Na^+ detoxification for coping with salt stress in tomato seedlings (Bharti et al., 2016; Chen et al., 2016). Furthermore, the SOS signaling pathway has been proposed to mediate cellular signaling under salt stress, in order to maintain ion homeostasis (Ji et al., 2013). The expression pattern of *SOS1* was induced both at control and NaCl treatments at inoculations with the *Pseudomonas oryzihabitans* strain, further contributing to the observed salt tolerance of inoculated plants. Taking into consideration that the ABA signaling pathway was not enhanced in the presence of bacterium, it is evident that this SOS-mediated pathway acts independent of ABA to help plants withstand Na^+ toxicity during salt stress through an intricate mechanism that needs to be further explored.

AXSa06 Mitigates the Negative Effect of Salt Stress on Photosynthesis

The increased net photosynthetic rate and chlorophyll content of the AXSa06-inoculated plants compared to non-inoculated plants under salt stress can be attributed to the ACC-deaminase activity due to the presence of inoculum in the rhizosphere that can mitigate the effect of salt on photosynthesis, as previously reported (Chauhan et al., 2019). In tomato, ethylene levels can

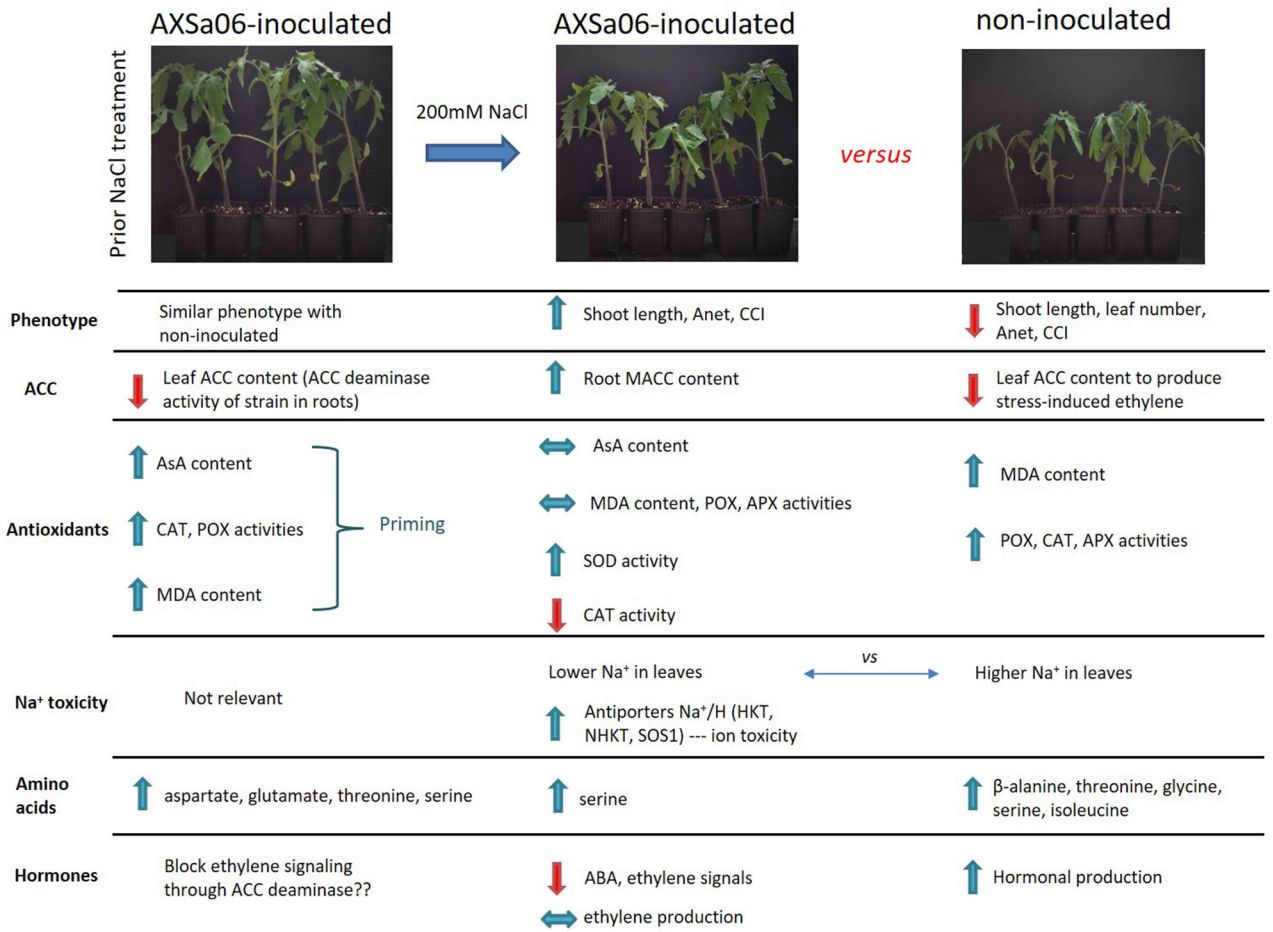

FIGURE 7 | Proposed model for AXSa06-mediated salt tolerance in tomato seedlings exposed to 200 mM NaCl. Inoculation with AXSa06 imposed plants at a pre-conditioned state prior to stress application, by stimulating their antioxidant defense response, by blocking ethylene signals through the activity of ACC deaminase, as well as by enhancing amino acid synthesis. Upon salt stress exposure, AXSa06-inoculated plants showed improved growth and photosynthetic traits, as well as a reduced tendency for Na^+ uptake which is accompanied by enhanced transcript levels of Na^+/H^+ antiporters. Furthermore, AXSa06 represses stress-inducing signals through a dampened ethylene and ABA metabolism, as well as reduced activation of downstream transcription.

have a negative impact on plant photosynthesis (Ceusters and Van de Poel, 2018), which is probably ameliorated by the ASXa06 inoculum. Furthermore, the enhanced net photosynthesis upon salt stress in the presence of the PGP strain may be related to the suppression of ABA signals that would otherwise had led to stomatal closure and photosynthesis suppression (Yu et al., 2020). This is in accordance with the down-regulation of the photosynthetic KEGG pathway, as well as the transcript levels of *NR*, at the absence of inoculum under salt stress. *NR* is the key enzyme for the reduction of NO_3^- to NO_2^- in nitrogen assimilation in plants cells, which coordinates with the rate of photosynthesis and the availability of C skeletons. It can also function as a key enzymatic source of nitric oxide, which then regulates plant growth and resistance to abiotic stresses (Fu et al., 2018). Thus, a better assimilation of both N and C may be evident at the presence of AXSa06, as further illustrated by the more active ruBisCO.

CONCLUSION

Collectively, our results reinforce the hypothesis that inoculations with the *Pseudomonas oryzihabitans* strain (AXSa06) significantly increased the alertness of inoculated plants, imposing them on a pre-conditioned state prior to stress application that render them primed for amplified defense responses. The primed state resulted from an enhancement of antioxidant adaptive mechanism, accompanied by a reduced tendency for Na^+ uptake (**Figure 7**). Furthermore, AXSa06 represses stress-inducing signals through a dampened ethylene and ABA metabolism and a reduced activation of downstream transcription factors when stress is applied. The differential modulation of the identified metabolites and transcripts is dependent on the perceived stimuli originated from AXSa06 inoculation that enables plants to fine-tune their defense responses. The identified signatory molecules including AsA,

and the amino acids aspartate, threonine, serine, and glutamate, may serve as possible biomarkers for PGPR priming in tomato. Furthermore, inoculations with AXSa06 alleviate the negative impact of salinity on photosynthetic machinery and carbon assimilation, through a more active *ruBisCO* and *NR*, involving an efficient mechanism of Na^+ detoxification. The molecular mechanism that links microbial signals with plant phenotypic plasticity and fitness merits further investigation to identify possible links between PGPR-priming and epigenetic memory to enhance plant tolerance under diverse environmental cues.

DATA AVAILABILITY STATEMENT

The original contributions presented in the study are publicly available. This data can be found here: NCBI repository, accession number: PRJEB42497.

AUTHOR CONTRIBUTIONS

This study was designed and conceived by IM and KK. Stress experiments, plant growth, physiological, and biochemical evaluation was conducted by IM and AP. Determination of Na^+ was conducted by AP. Ethylene-metabolite related work was carried out by BVP, while ethylene determination by EK. Transcriptomic analyses were performed by IM, KL, and SG. Metabolomic analyses were undertaken by AA and AP. Data interpretation and manuscript preparation were done by IM. This whole project was supervised by IM and KK. All authors interpreted the results, read, and approved the final manuscript.

FUNDING

This project was funded by the Hellenic Foundation for Research and Innovation (HFRI) and the General Secretariat for Research and Innovation (GSRI), under the grant agreement no. 705, awarded to IM.

ACKNOWLEDGMENTS

We would like to thank Prof. Theodora Matsi (AUTH) for her contribution in determination of Na^+ contents, and Eleni Zimvrakaki (AUTH) for technical assistance in metabolomic analyses. We acknowledge support by Veerle Verdoodt (KULeuven) for help with the ACC/MACC analysis.

SUPPLEMENTARY MATERIAL

The Supplementary Material for this article can be found online at: https://www.frontiersin.org/articles/10.3389/fpls.2021.713984/full#supplementary-material

REFERENCES

Ainalidou, A., Tanou, G., Belghazi, M., Samiotaki, M., Diamantidis, G., Molassiotis, A., et al. (2016). Integrated analysis of metabolites and proteins reveal aspects of the tissue-specific function of synthetic cytokinin in kiwifruit development and ripening. *J. Proteomics* 143, 318–333. doi: 10.1016/j.jprot.2016.02.013

Artur, M. A. S., Rienstra, J., Dennis, T. J., Farrant, J. M., Ligterink, W., and Hilhorst, H. (2019). Structural plasticity of intrinsically disordered LEA proteins from *Xerophyta schlechteri* provides protection *in vitro* and *in vivo*. *Front. Plant Sci.* 10:1272. doi: 10.3389/fpls.2019.01272

Baba, S. A., Vishwakarma, R. A., and Ashraf, N. (2017). Functional characterization of CsBGlu12, a β-glucosidase from crocus sativus, provides insights into its role in abiotic stress through accumulation of antioxidant flavonols. *J. Biol. Chem.* 292, 4700–4713. doi: 10.1074/jbc.M116.762161

Bandehagh, A., and Taylor, N. L. (2020). Can alternative metabolic pathways and shunts overcome salinity induced inhibition of central carbon metabolism in crops? *Front. Plant Sci.* 11:1072. doi: 10.3389/fpls.2020.01072

Bates, C. J. (1976). Prolyl hydroxylase in platelets. *FEBS Lett.* 72, 235–237. doi: 10.1016/0014-5793(76)80976-3

Bharti, N., Pandey, S. S., Barnawal, D., Patel, V. K., and Kalra, A. (2016). Plant growth promoting rhizobacteria *Dietzia natronolimnaea* modulates the expression of stress responsive genes providing protection of wheat from salinity stress. *Sci. Rep.* 6:34768. doi: 10.1038/srep34768

Biała, W., and Jasiński, M. (2018). The phenylpropanoid case – it is transport that matters. *Front. Plant Sci.* 9:1610. doi: 10.3389/fpls.2018.01610

Bradford, M. M. (1976). A rapid and sensitive method for the quantitation of microgram quantities of protein utilizing the principle of protein-dye binding. *Anal. Biochem.* 72, 248–254.

Bruto, M., Prigent-Combaret, C., Muller, D., and Moënne-Loccoz, Y. (2014). Analysis of genes contributing to plant-beneficial functions in plant growth-promoting rhizobacteria and related Proteobacteria. *Sci. Rep.* 4:6261. doi: 10.1038/srep06261

Bulens, I., Van de Poel, B., Hertog, M. L. A. T. M., De Proft, M. P., Geeraerd, A. H., and Nicolai, B. M. (2011). Protocol: an updated integrated methodology for analysis of metabolites and enzyme activities of ethylene biosynthesis. *Plant Methods* 7:17. doi: 10.1186/1746-4811-7-17

Campobenedetto, C., Grange, E., Mannino, G., van Arkel, J., Beekwilder, J., Karlova, R., et al. (2020). A biostimulant seed treatment improved heat stress tolerance during cucumber seed germination by acting on the antioxidant system and glyoxylate cycle. *Front. Plant Sci.* 11:836. doi: 10.3389/fpls.2020.00836

Ceusters, J., and Van de Poel, B. (2018). Update: ethylene exerts species-specific and age-dependent control of photosynthesis. *Plant Physiol.* 176, 2601–2612. doi: 10.1104/pp.17.01706

Chauhan, P. S., Lata, C., Tiwari, S., Chauhan, A. S., Mishra, S. K., Agrawal, L., et al. (2019). Transcriptional alterations reveal *Bacillus amyloliquefaciens*-rice cooperation under salt stress. *Sci. Rep.* 9:11912. doi: 10.1038/s41598-019-48309-8

Chen, L., Dodd, I. C., Theobald, J. C., Belimov, A. A., and Davies, W. J. (2013). The rhizobacterium *Variovorax paradoxus* 5C-2, containing ACC deaminase, promotes growth and development of *Arabidopsis thaliana* via an ethylene-dependent pathway. *J. Exp. Bot.* 64, 1565–1573. doi: 10.1093/jxb/ert031

Chen, L., Liu, Y., Wu, G., Veronican Njeri, K., Shen, Q., Zhang, N., et al. (2016). Induced maize salt tolerance by rhizosphere inoculation of *Bacillus amyloliquefaciens* SQR9. *Physiol. Plant.* 158, 34–44. doi: 10.1111/ppl.12441

Chen, S., Zhou, Y., Chen, Y., and Gu, J. (2018). fastp: an ultra-fast all-in-one FASTQ preprocessor. *Bioinformatics* 34, i884–i890. doi: 10.1093/bioinformatics/bty560

Conrath, U. (2011). Molecular aspects of defence priming. *Trends Plant Sci.* 16, 524–531. doi: 10.1016/j.tplants.2011.06.004

Corwin, D. L. (2021). Climate change impacts on soil salinity in agricultural areas. *Eur. J. Soil Sci.* 72, 842–862. doi: 10.1111/ejss.13010

Cosio, C., Ranocha, P., Francoz, E., Burlat, V., Zheng, Y., Perry, S. E., et al. (2017). The class III peroxidase PRX17 is a direct target of the MADS-box transcription factor AGAMOUS-LIKE15 (AGL15) and participates in lignified tissue formation. *New Phytol.* 213, 250–263. doi: 10.1111/nph.14127

Curtis, T. Y., Bo, V., Tucker, A., and Halford, N. G. (2018). Construction of a network describing asparagine metabolism in plants and its application to the

identification of genes affecting asparagine metabolism in wheat under drought and nutritional stress. *Food Energy Secur*. 7:e00126. doi: 10.1002/fes3.126

Devkar, V., Thirumalaikumar, V. P., Xue, G. P., Vallarino, J. G., Turečkov,á, V., Strnad, M., et al. (2020). Multifaceted regulatory function of tomato SlTAF1 in the response to salinity stress. *New Phytol*. 225, 1681–1698. doi: 10.1111/nph.16247

Ding, X., Cao, Y., Huang, L., Zhao, J., Xu, C., Li, X., et al. (2008). Activation of the indole-3-acetic acid–amido synthetase GH3-8 suppresses expansin expression and promotes salicylate- and jasmonate-independent basal immunity in rice. *Plant Cell* 20, 228 LP—240 LP. doi: 10.1105/tpc.107.055657

Du, H., Wu, N., Fu, J., Wang, S., Li, X., Xiao, J., et al. (2012). A GH3 family member, OsGH3-2, modulates auxin and abscisic acid levels and differentially affects drought and cold tolerance in rice. *J. Exp. Bot*. 63, 6467–6480. doi: 10.1093/jxb/ers300

Fierer, N. (2017). Embracing the unknown: disentangling the complexities of the soil microbiome. *Nat. Rev. Microbiol*. 15, 579–590. doi: 10.1038/nrmicro.2017.87

Fu, Y.-F., Zhang, Z.-W., and Yuan, S. (2018). Putative connections between nitrate reductase S-nitrosylation and NO synthesis under pathogen attacks and abiotic stresses. *Front. Plant Sci*. 9:474. doi: 10.3389/fpls.2018.00474

Gamez, R. M., Rodríguez, F., Vidal, N. M., Ramirez, S., Vera Alvarez, R., Landsman, D., et al. (2019). Banana (*Musa acuminata*) transcriptome profiling in response to rhizobacteria: *Bacillus amyloliquefaciens* Bs006 and *Pseudomonas fluorescens* Ps006. *BMC Genomics* 20:378. doi: 10.1186/s12864-019-5763-5

Gémes, K., Jung Kim, Y., Park, K. Y., Moschou, P. N., Andronis, E., Valassakis, C., et al. (2016). An NADPH-oxidase/polyamine oxidase feedback loop controls oxidative burst under salinity. *Plant Physiol*. 172, 1418–1431. doi: 10.1104/pp.16.01118

Genitsaris, S., Stefanidou, N., Leontidou, K., Matsi, T., Karamanoli, K., and Mellidou, I. (2020). Bacterial communities in the rhizosphere and phyllosphere of halophytes and drought-tolerant plants in mediterranean ecosystems. *Microorganisms* 8:1708. doi: 10.3390/microorganisms8111708

Goh, C.-H., Veliz Vallejos, D. F., Nicotra, A. B., and Mathesius, U. (2013). The impact of beneficial plant-associated microbes on plant phenotypic plasticity. *J. Chem. Ecol*. 39, 826–839. doi: 10.1007/s10886-013-0326-8

Golldack, D., Lüking, I., and Yang, O. (2011). Plant tolerance to drought and salinity: stress regulating transcription factors and their functional significance in the cellular transcriptional network. *Plant Cell Rep*. 30, 1383–1391. doi: 10.1007/s00299-011-1068-0

Hamani, A. K. M., Wang, G., Soothar, M. K., Shen, X., Gao, Y., Qiu, R., et al. (2020). Responses of leaf gas exchange attributes, photosynthetic pigments and antioxidant enzymes in NaCl-stressed cotton (*Gossypium hirsutum* L.) seedlings to exogenous glycine betaine and salicylic acid. *BMC Plant Biol*. 20:434. doi: 10.1186/s12870-020-02624-9

Heath, R. L., and Packer, L. (1968). Photoperoxidation in isolated chloroplasts: I. Kinetics and stoichiometry of fatty acid peroxidation. *Arch. Biochem. Biophys*. 125, 189–198. doi: 10.1016/0003-9861(68)90654-1

Hosmani, P. S., Flores-Gonzalez, M., van de Geest, H., Maumus, F., Bakker, L. V., Schijlen, E., et al. (2019). An improved *de novo* assembly and annotation of the tomato reference genome using single-molecule sequencing, Hi-C proximity ligation and optical maps. *bioRxiv* 767764. doi: 10.1101/767764

Jakab, G., Ton, J., Flors, V., Zimmerli, L., Métraux, J. P., and Mauch-Mani, B. (2005). Enhancing *Arabidopsis* salt and drought stress tolerance by chemical priming for its abscisic acid responses. *Plant Physiol*. 139, 267–274. doi: 10.1104/pp.105.065698

Ji, H., Pardo, J. M., Batelli, G., Van Oosten, M. J., Bressan, R. A., and Li, X. (2013). The salt overly sensitive (SOS) pathway: established and emerging roles. *Mol. Plant* 6, 275–286. doi: 10.1093/mp/sst017

Jiao, X., Takishita, Y., Zhou, G., and Smith, D. L. (2021). Plant associated rhizobacteria for biocontrol and plant growth enhancement. *Front. Plant Sci*. 12:634796. doi: 10.3389/fpls.2021.634796

Jin, T., Sun, Y., Zhao, R., Shan, Z., Gai, J., and Li, Y. (2019). Overexpression of peroxidase gene GsPRX9 confers salt tolerance in soybean. *Int. J. Mol. Sci*. 20. doi: 10.3390/ijms20153745

Karamanoli, K., Menkissoglu-Spiroudi, U., Bosabalidis, A. M., Vokou, D., and Constantinidou, H. I. A. (2005). Bacterial colonization of the phyllosphere of nineteen plant species and antimicrobial activity of their leaf secondary metabolites against leaf associated bacteria. *Chemoecology* 15, 59–67. doi: 10.1007/s00049-005-0297-5

Kearl, J., McNary, C., Lowman, J. S., Mei, C., Aanderud, Z. T., Smith, S. T., et al. (2019). Salt-tolerant halophyte rhizosphere bacteria stimulate growth of alfalfa in salty soil. *Front. Microbiol*. 10:1849. doi: 10.3389/fmicb.2019.01849

Keunen, E., Peshev, D., Vangronsveld, J., Van Den Ende, W., and Cuypers, A. (2013). Sugars and abiotic stress. *Plant Cell Environ*. 36, 1242–1255. doi: 10.1111/pce.12061

Kim, D., Langmead, B., and Salzberg, S. L. (2015). HISAT: a fast spliced aligner with low memory requirements. *Nat. Methods* 12, 357–360. doi: 10.1038/nmeth.3317

Kim, J.-G., Stork, W., and Mudgett, M. B. (2016). Quantification of ethylene production in tomato leaves infected by *Xanthomonas euvesicatoria*. *Bio-protocol* 6:e1723. doi: 10.21769/bioprotoc.1723

Kim, J. G., Stork, W., and Mudgett, M. B. (2013). *Xanthomonas* type III effector XopD desumoylates tomato transcription factor SlERF4 to suppress ethylene responses and promote pathogen growth. *Cell Host Microbe* 13, 143–154. doi: 10.1016/j.chom.2013.01.006

Kim, K., Jang, Y.-J., Lee, S.-M., Oh, B.-T., Chae, J.-C., and Lee, K.-J. (2014). Alleviation of salt stress by enterobacter sp. EJ01 in tomato and *Arabidopsis* is accompanied by up-regulation of conserved salinity responsive factors in plants. *Mol. Cells* 37, 109–117. doi: 10.14348/molcells.2014.2239

Kopka, J., Schauer, N., Krueger, S., Birkemeyer, C., Usadel, B., Bergmüller, E., et al. (2005). GMD@CSB.DB: the golm metabolome database. *Bioinformatics* 21, 1635–1638. doi: 10.1093/bioinformatics/bti236

Kovaka, S., Zimin, A. V., Pertea, G. M., Razaghi, R., Salzberg, S. L., and Pertea, M. (2019). Transcriptome assembly from long-read RNA-seq alignments with StringTie2. *Genome Biol.* 20:278. doi: 10.1186/s13059-019-1910-1

Kozminska, A., Al Hassan, M., Hanus-Fajerska, E., Naranjo, M. A., Boscaiu, M., and Vicente, O. (2018). Comparative analysis of water deficit and salt tolerance mechanisms in silene. *South African J. Bot*. 117, 193–206. doi: 10.1016/j.sajb.2018.05.022

Kurutas, E. B. (2016). The importance of antioxidants which play the role in cellular response against oxidative/nitrosative stress: current state. *Nutr. J*. 15, 71. doi: 10.1186/s12937-016-0186-5

Leontidou, K., Genitsaris, S., Papadopoulou, A., Kamou, N., Bosmali, I., Matsi, T., et al. (2020). Plant growth promoting rhizobacteria isolated from halophytes and drought-tolerant plants: genomic characterisation and exploration of phyto-beneficial traits. *Sci. Rep*. 10:14857. doi: 10.1038/s41598-020-71652-0

Liao, Y., Smyth, G. K., and Shi, W. (2014). featureCounts: an efficient general purpose program for assigning sequence reads to genomic features. *Bioinformatics* 30, 923–930. doi: 10.1093/bioinformatics/btt656

Liu, K., Wang, J., Li, H., Zhong, J., Feng, S., Pan, Y., et al. (2016). Identification, expression and IAA-amide synthetase activity analysis of gretchen hagen 3 in papaya fruit (*Carica papaya* L.) during postharvest process. *Front. Plant Sci*. 7:1555. doi: 10.3389/fpls.2016.01555

Liu, L., Wang, B., Liu, D., Zou, C., Wu, P., Wang, Z., et al. (2020). Transcriptomic and metabolomic analyses reveal mechanisms of adaptation to salinity in which carbon and nitrogen metabolism is altered in sugar beet roots. *BMC Plant Biol*. 20:138. doi: 10.1186/s12870-020-02349-9

Liu, L., Wu, X., Sun, W., Yu, X., Demura, T., Li, D., et al. (2021). Galactinol synthase confers salt-stress tolerance by regulating the synthesis of galactinol and raffinose family oligosaccharides in poplar. *Ind. Crops Prod*. 165:113432. doi: 10.1016/j.indcrop.2021.113432

Liu, S., Hao, H., Lu, X., Zhao, X., Wang, Y., Zhang, Y., et al. (2017). Transcriptome profiling of genes involved in induced systemic salt tolerance conferred by *Bacillus amyloliquefaciens* FZB42 in Arabidopsis thaliana. *Sci. Rep*. 7:10795. doi: 10.1038/s41598-017-11308-8

Maaroufi-Dguimi, H., Debouba, M., Gaufichon, L., Clément, G., Gouia, H., Hajjaji, A., et al. (2011). An *Arabidopsis* mutant disrupted in ASN2 encoding asparagine synthetase 2 exhibits low salt stress tolerance. *Plant Physiol. Biochem*. 49, 623–628. doi: 10.1016/j.plaphy.2011.03.010

Malviya, M. K., Li, C.-N., Solanki, M. K., Singh, R. K., Htun, R., Singh, P., et al. (2020). Comparative analysis of sugarcane root transcriptome in response to the plant growth-promoting *Burkholderia anthina* MYSP113. *PLoS ONE* 15:e0231206. doi: 10.1371/journal.pone.0231206

Mayak, S., Tirosh, T., and Glick, B. R. (2004). Plant growth-promoting bacteria that confer resistance to water stress in tomatoes and peppers. *Plant Sci*. 166, 525–530. doi: 10.1016/j.plantsci.2003.10.025

McKay, H. (1998). Root electrolyte leakage and root growth potential as indicators of spruce and larch establishment. *Silva Fenn.* 32, 241–252.

Mellidou, I., and Kanellis, A. K. (2017). Genetic control of ascorbic acid biosynthesis and recycling in horticultural crops. *Front. Chem*. 5:50. doi: 10.3389/fchem.2017.00050

Mellidou, I., Karamanoli, K., Beris, D., Haralampidis, K., Constantinidou, H.-I. A., and Roubelakis-Angelakis, K. A. (2017). Underexpression of apoplastic polyamine oxidase improves thermotolerance in *Nicotiana tabacum*. *J. Plant Physiol*. 218, 171–174. doi: 10.1016/j.jplph.2017.08.006

Mellidou, I., Karamanoli, K., Constantinidou, H.-I. A., and Roubelakis-Angelakis, K. A. (2020). Antisense-mediated S-adenosyl-L-methionine decarboxylase silencing affects heat stress responses of tobacco plants. *Funct. Plant Biol*. 47, 651–658. doi: 10.1071/FP19350

Mellidou, I., Keulemans, J., and Kanellis, A. K. (2012). Regulation of fruit ascorbic acid concentrations during ripening in high and low vitamin C tomato cultivars. *BMC Plant Biol*. 12:239. doi: 10.1186/1471-2229-12-239

Mellidou, I., Moschou, P. N., Ioannidis, N. E., Pankou, C., Gemes, K., Valassakis, C., et al. (2016). Silencing S-adenosyl-L-methionine decarboxylase (SAMDC) in *Nicotiana tabacum* points at a polyamine-dependent trade-off between growth and tolerance responses. *Front. Plant Sci*. 7:379. doi: 10.3389/fpls.2016.00379

Morales, M., and Munné-Bosch, S. (2019). Malondialdehyde: facts and artifacts. *Plant Physiol.* 180, 1246–1250. doi: 10.1104/pp.19.00405

Müller, M. (2021). Foes or friends: ABA and ethylene interaction under abiotic stress. *Plants* 10:448. doi: 10.3390/plants10030448

Nautiyal, C. S., Srivastava, S., Chauhan, P. S., Seem, K., Mishra, A., and Sopory, S. K. (2013). Plant growth-promoting bacteria *Bacillus amyloliquefaciens* NBRISN13 modulates gene expression profile of leaf and rhizosphere community in rice during salt stress. *Plant Physiol. Biochem*. 66, 1–9. doi: 10.1016/j.plaphy.2013.01.020

Nishizawa, A., Yabuta, Y., and Shigeoka, S. (2008). Galactinol and raffinose constitute a novel function to protect plants from oxidative damage. *Plant Physiol.* 147, 1251–1263. doi: 10.1104/pp.108.122465

Noctor, G., Mhamdi, A., Chaouch, S., Han, Y., Neukermans, J., Marquez-Garcia, B., et al. (2012). Glutathione in plants: an integrated overview. *Plant Cell Environ.* 35, 454–484. doi: 10.1111/j.1365-3040.2011.02400.x

Noctor, G., Mhamdi, A., and Foyer, C. H. (2016). Oxidative stress and antioxidative systems: recipes for successful data collection and interpretation. *Plant Cell Environ*. 39, 1140–1160. doi: 10.1111/pce.12726

Olanrewaju, O. S., Glick, B. R., and Babalola, O. O. (2017). Mechanisms of action of plant growth promoting bacteria. *World J. Microbiol. Biotechnol*. 33:197. doi: 10.1007/s11274-017-2364-9

Olías, R., Eljakaoui, Z., Li, J. U. N., De Morales, P. A. Z. A., Marín-Manzano, M. C., Pardo, J. M., et al. (2009). The plasma membrane Na+/H+ antiporter SOS1 is essential for salt tolerance in tomato and affects the partitioning of Na^+ between plant organs. *Plant Cell Environ*. 32, 904–916. doi: 10.1111/j.1365-3040.2009.01971.x

Orozco-Mosqueda, M. D. C., Glick, B. R., and Santoyo, G. (2020). ACC deaminase in plant growth-promoting bacteria (PGPB): an efficient mechanism to counter salt stress in crops. *Microbiol. Res*. 235:126439. doi: 10.1016/j.micres.2020.126439

Patel, M. K., Kumar, M., Li, W., Luo, Y., Burritt, D. J., Alkan, N., et al. (2020). Enhancing salt tolerance of plants: from metabolic reprogramming to exogenous chemical treatments and molecular approaches. *Cells* 9, 1–26. doi: 10.3390/cells9112492

Pateraki, I., Sanmartin, M., Kalamaki, M. S., Gerasopoulos, D., and Kanellis, A. K. (2004). Molecular characterization and expression studies during melon fruit development and ripening of L-galactono-1,4-lactone dehydrogenase. *J. Exp. Bot*. 55, 1623–1633. doi: 10.1093/jxb/erh186

Pérez-Jaramillo, J. E., Carrión, V. J., de Hollander, M., and Raaijmakers, J. M. (2018). The wild side of plant microbiomes. *Microbiome* 6, 4–9. doi: 10.1186/s40168-018-0519-z

Perin, E. C., da Silva Messias, R., Borowski, J. M., Crizel, R. L., Schott, I. B., Carvalho, I. R., et al. (2019). ABA-dependent salt and drought stress improve strawberry fruit quality. *Food Chem*. 271, 516–526. doi: 10.1016/j.foodchem.2018.07.213

Pertea, G., and Pertea, M. (2020). GFF utilities: GffRead and GffCompare. *F1000Research* 9:304. doi: 10.12688/f1000research.23297.2)

Pignocchi, C., Fletcher, J. M., Wilkinson, J. E., Barnes, J. D., and Foyer, C. H. (2003). The function of ascorbate oxidase in tobacco. *Plant Physiol.* 132, 1631–1641. doi: 10.1104/pp.103.022798

Poupin, M. J., Greve, M., Carmona, V., and Pinedo, I. (2016). A complex molecular interplay of auxin and ethylene signaling pathways is involved in *Arabidopsis* growth promotion by *Burkholderia phytofirmans* PsJN. *Front. Plant Sci*. 7:492. doi: 10.3389/fpls.2016.00492

Rashmi, D., Barvkar, V. T., Nadaf, A., Mundhe, S., and Kadoo, N. Y. (2019). Integrative omics analysis in *Pandanus odorifer* (Forssk.) Kuntze reveals the role of Asparagine synthetase in salinity tolerance. *Sci. Rep*. 9:932. doi: 10.1038/s41598-018-37039-y

Riyazuddin, R., Verma, R., Singh, K., Nisha, N., Keisham, M., Bhati, K. K., et al. (2020). Ethylene: a master regulator of salinity stress tolerance in plants. *Biomolecules* 10:959. doi: 10.3390/biom10060959

Rouyi, C., Baiya, S., Lee, S. K., Mahong, B., Jeon, J. S., Ketudat- Cairns, J. R., et al. (2014). Recombinant expression and characterization of the cytoplasmic rice β-glucosidase Os1BGlu4. *PLoS ONE* 9:e96712. doi: 10.1371/journal.pone.0096712

Safdarian, M., Askari, H., Shariati, J., V., and Nematzadeh, G. (2019). Transcriptional responses of wheat roots inoculated with *Arthrobacter nitroguajacolicus* to salt stress. *Sci. Rep*. 9:1792. doi: 10.1038/s41598-018-38398-2

Shabala, L., Mackay, A., Tian, Y., Jacobsen, S.-E., Zhou, D., and Shabala, S. (2012). Oxidative stress protection and stomatal patterning as components of salinity tolerance mechanism in quinoa (*Chenopodium quinoa*). *Physiol. Plant*. 146, 26–38. doi: 10.1111/j.1399-3054.2012.01599.x

Shabala, S. (2013). Learning from halophytes: physiological basis and strategies to improve abiotic stress tolerance in crops. *Ann. Bot*. 112, 1209–1221. doi: 10.1093/aob/mct205

Shariati, V. J., Malboobi, M. A., Tabrizi, Z., Tavakol, E., Owilia, P., and Safari, M. (2017). Comprehensive genomic analysis of a plant growth-promoting rhizobacterium *Pantoea agglomerans* strain P5. *Sci. Rep*. 7:15610. doi: 10.1038/s41598-017-15820-9

Sharma, A., Shahzad, B., Rehman, A., Bhardwaj, R., Landi, M., and Zheng, B. (2019). Response of phenylpropanoid pathway and the role of polyphenols in plants under abiotic stress. *Molecules* 24:2452. doi: 10.3390/molecules24132452

Tounekti, T., Vadel, A., Oñate, M., Khemira, H., and Munné-Bosch, S. (2011). Salt-induced oxidative stress in rosemary plants: damage or protection? *Environ. Exper. Bot*. 71, 298–305. doi: 10.1016/j.envexpbot.2010.12.016

Van de Poel, B., Vandenzavel, N., Smet, C., Nicolay, T., Bulens, I., Mellidou, I., et al. (2014). Tissue specific analysis reveals a differential organization and regulation of both ethylene biosynthesis and E8 during climacteric ripening of tomato. *BMC Plant Biol*. 14:11. doi: 10.1186/1471-2229-14-11

Vinson, C. C., Mota, A. P. Z., Porto, B. N., Oliveira, T. N., Sampaio, I., Lacerda, A. L., et al. (2020). Characterization of raffinose metabolism genes uncovers a wild Arachis galactinol synthase conferring tolerance to abiotic stresses. *Sci. Rep*. 10:15258. doi: 10.1038/s41598-020-72191-4

Vishwakarma, K., Upadhyay, N., Kumar, N., Yadav, G., Singh, J., Mishra, R. K., et al. (2017). Abscisic acid signaling and abiotic stress tolerance in plants: a review on current knowledge and future prospects. *Front. Plant Sci.* 8:161. doi: 10.3389/fpls.2017.00161

Vokou, D., Giannakou, U., Kontaxi, C., and Vareltzidou, S. (2016). "Axios, aliakmon, and gallikos delta complex (Northern Greece)," in *The Wetland Book*, eds C. Finlayson, G. Milton, R. Prentice, and N. Davidson (Dordrecht: Springer). doi: 10.1007/978-94-007-4001-3_253

Wu, X., Jia, Q., Ji, S., Gong, B., Li, J., Lü, G., et al. (2020). Gamma-aminobutyric acid (GABA) alleviates salt damage in tomato by modulating Na^+ uptake, the GAD gene, amino acid synthesis and reactive oxygen species metabolism. *BMC Plant Biol*. 20:465. doi: 10.1186/s12870-020-02669-w

Yadav, V. K., Raghav, M., Sharma, S. K., and Bhagat, N. (2020). Rhizobacteriome: promising candidate for conferring drought tolerance in crops. *J. Pure Appl. Microbiol*. 14, 73–92. doi: 10.22207/JPAM.14.1.10

Yang, J., Kloepper, J. W., and Ryu, C. M. (2009). Rhizosphere bacteria help plants tolerate abiotic stress. *Trends Plant Sci*. 14, 1–4. doi: 10.1016/j.tplants.2008.10.004

Yu, G., Wang, L. G., Han, Y., and He, Q. Y. (2012). ClusterProfiler: an R package for comparing biological themes among gene clusters. *Omi. A J. Integr. Biol*. 16, 284–287. doi: 10.1089/omi.2011.0118

Yu, Z., Duan, X., Luo, L., Dai, S., Ding, Z., and Xia, G. (2020). How plant hormones mediate salt stress responses. *Trends Plant Sci*. 25, 1117–1130. doi: 10.1016/j.tplants.2020.06.008

Zhang, H.-X., and Blumwald, E. (2001). Transgenic salt-tolerant tomato plants accumulate salt in foliage but not in fruit. *Nat. Biotechnol*. 19, 765–768. doi: 10.1038/90824

Zhang, S.-W., Li, C.-H., Cao, J., Zhang, Y.-C., Zhang, S.-Q., Xia, Y.-F., et al. (2009). Altered architecture and enhanced drought tolerance in rice via the down-regulation of indole-3-acetic acid by TLD1/OsGH3.13 activation. *Plant Physiol*. 151, 1889–1901. doi: 10.1104/pp.109.146803

Zhang, Z., Mao, C., Shi, Z., and Kou, X. (2017). The amino acid metabolic and carbohydrate metabolic pathway play important roles during salt-stress response in tomato. *Front. Plant Sci*. 8:1231. doi: 10.3389/fpls.2017.01231

Zhao, Y., Christensen, S. K., Fankhauser, C., Cashman, J. R., Cohen, J. D., Weigel, D., et al. (2001). A role for flavin monooxygenase-like enzymes in auxin biosynthesis. *Science* 291, 306–309. doi: 10.1126/science.291.5502.306

Conflict of Interest: The authors declare that the research was conducted in the absence of any commercial or financial relationships that could be construed as a potential conflict of interest.

Publisher's Note: All claims expressed in this article are solely those of the authors and do not necessarily represent those of their affiliated organizations, or those of the publisher, the editors and the reviewers. Any product that may be evaluated in this article, or claim that may be made by its manufacturer, is not guaranteed or endorsed by the publisher.

frontiers in Plant Science

ORIGINAL RESEARCH
published: 20 August 2021
doi: 10.3389/fpls.2021.732279

Limiting-Stress-Elimination Hypothesis: Using Non-hormonal Biostimulant to Reduce Stress and Increase Savanna Cowpea [*Vigna unguiculata* (L.) Walp.] Productivity

Acheampong Atta-Boateng and Graeme P. Berlyn*

School of the Environment, Yale University, New Haven, CT, United States

An alternative decision axiom to guide in determining the optimal intervention strategy to maximize cowpea production is proposed. According to the decrement from the maximum concept of Mitscherlich, the decrement from the maximum for each stressor must be minimized to produce the absolute maximum production. In crop production, this means all deficient nutrients must be supplemented to ensure maximum yield and laid the foundation in fertilizer formulation. However, its implementation is not economically feasible in many situations, particularly where multiple environmental factors impact crop productivity as in the case of low resource conditions. We propose and test the hypothesis that yield allocation will increase when the most limiting stressor among prevailing stressors is eliminated at least until the next limiting stressor impacts productivity. We selected drought limiting savanna conditions and cowpea (*Vigna unguiculata*), adapted to nitrogen dependence. To determine the limiting condition, we measured the response of cowpea to D-sorbitol, nitrogen, and non-hormonal biostimulant (nhB) treatments. The nhB treatment increased total biomass by 45% compared to nitrogen, 13%, and D-sorbitol, 17%, suggesting osmotic stress is more limiting in the observed savanna conditions. The effect of the biostimulant is due to antioxidants and key amino acids that stimulate metabolism and stress resistance. Where nitrogen becomes the next constraining factor, biostimulants can contribute organic nitrogen. The study supports the use of biostimulants as candidate intervention under conditions where crop productivity is limited by multiple or alternating constraints during crop growth.

Keywords: biostimulant, cowpea, osmotic stress, nitrogen, fertilizer, sprengel-liebig law, sustainable agriculture

OPEN ACCESS

Edited by:
Maurizio Ruzzi,
University of Tuscia, Italy

Reviewed by:
Lydia Ndinelao Horn,
University of Namibia, Namibia
Frank Oroka,
Delta State University, Nigeria

****Correspondence:***
Acheampong Atta-Boateng
acheampong.atta-boateng@ouce.ox.ac.uk
orcid.org/0000-0002-3355-5286

Specialty section:
This article was submitted to Crop and Product Physiology, a section of the journal Frontiers in Plant Science

Received: *28 June 2021*
Accepted: *26 July 2021*
Published: *20 August 2021*

Citation:
Atta-Boateng A and Berlyn GP (2021) Limiting-Stress-Elimination Hypothesis: Using Non-hormonal Biostimulant to Reduce Stress and Increase Savanna Cowpea [Vigna unguiculata (L.) Walp.] Productivity. Front. Plant Sci. 12:732279. doi: 10.3389/fpls.2021.732279

INTRODUCTION

The plant stress–response–feedback continuum is an important physiological process that shapes plant plasticity. Factors that account for stress in plants are broadly categorized into abiotic and biotic stressors. Biotic stressors, such as herbivory, pest attack, and disease-causing pathogens, and abiotic stressors, such as drought, salinity, heavy metals, floods, and extreme temperatures, account for major crop losses globally (Gull et al., 2019). To understand how plants respond and cope

with stress, a stressor, such as heat or drought, is introduced to the living plant specimen under controlled conditions to observe the response (Arbona et al., 2016; Atta-Boateng et al., 2019). However, under field conditions, crops are exposed to multiple environmental factors (Chapin et al., 1987). In addition, the relative impact of all the possible prevailing stressors on yield is difficult to detect. Furthermore, the intensity of the stress effect does not stay constant throughout the growing season. The centralized system of stress response concept suggests that all plants respond to different stress types in the same basic way, particularly those adapted to low-resourced environments or adjusted to low resource supply (Chapin, 1991). This framework has implications on the implementation of agricultural advances and oversimplifies interventions, especially under marginal conditions where crops, such as legumes, are adopted to low soil nutrients or drought.

Cowpea is the most cultivated legume in West Africa, and its production benefits human and livestock nutrition in addition to long-term soil amendment that sustains cropping systems on marginal lands in low-income economies (Dakora and Keya, 1997; Duranti and Gius, 1997; FAO, 2004; IITA, 2010; Foyer et al., 2016). Cowpea is suggested to originate from West and Central Africa, which currently has most of the germplasm (Boukar et al., 2019b). The biotic constraints of cowpea include parasitic weeds, insect pests particularly aphids, fungal, viral, and bacterial diseases, whereas high temperature, drought, and erratic rainfalls during the growing season constitute major abiotic constraints (Boukar et al., 2019a,b; Horn and Shimelis, 2020). Biotic and abiotic interventions in the past few decades include the introduction of drought-resistant and disease-tolerance cowpea varieties and supporting genetic breeding research programs across Sub-Saharan Africa (SSA) (Boukar et al., 2019a,b). These are essential for managing long-term biotic and abiotic growth conditions. However, major gaps exist for inputs required to manage short-term in-season growth conditions.

Early work by Carl Sprengel and Justus von Liebig's Law of the Minimum revolutionized plant mineral nutrition, where the scarcest nutrient was found to govern growth (Liebig, 1840; van der Ploeg et al., 1999). Later, Mitscherlich (1909), based on Liebig's Law further showed that marginal productivity decreased as levels of limiting growth factor increased. Meaning, when all other factors of growth are kept constant at optimum levels, increase in the levels of the limiting factor increases yield until no further increment affects yield. As all other growth factors cannot be optimal and constant under field conditions, this implies in practice that all stress factors must be eliminated to attain maximum yield. Harmsen (2000) acknowledged the limitations of the Mitscherlich equation in rainfed semi-arid conditions and proposed a modified theory (Equation 1):

$$Y = Y_\theta - Y_\theta \, e^{-\epsilon_{nt}} N_t {Y_\theta}^{n-1} \quad (1)$$

where Y is the total dry matter, Y_θ, potential yield as a function of available moisture (θ), ϵ_{nt}, activity coefficient, N_t, total nutrient content, and n is a constant. The model (Equation 1) describes crop response to nutrient availability under rainfed semi-arid conditions and can predict the nutrient requirement for a specified yield level. Nonetheless, the model assumptions restrict practical interventions to mineral nutrient input, given seasonal rainfall availability. The yield impact of limiting factors that alternates during the growing season and the difficulty of its prediction require alternatives frameworks that allow the design of inputs that are pliable to manage dynamic field conditions.

Although SSA contributes more than 70% of global cowpea output, cowpea cultivation is under-produced and concentrated in low-productive regions, which are particularly vulnerable to climate risks (Timko et al., 2008; IITA, 2010; Muñoz-Amatriaín et al., 2017). In the Guinea savanna ecological biome, high temperature, low soil nitrogen, and soil structure exacerbate threats the peak rainy and the dry season conditions cause to agricultural production (Runge-Metzger and Diehl, 1993; Gyasi, 1995). Interventions that can address specific production constraint is currently lacking.

Policy directives on interventions, especially for smallholder farmers in savanna regions continue to focus narrowly on increasing fertilizer inputs (FAO, 2005, 2011; Martey et al., 2014). However, it is unclear whether N fertilizer for instance is the ideal intervention for increasing legume production in the savanna. N fertilization has been shown to decrease N-fixing rates in legumes (McAuliffe et al., 1958; Salvagiotti et al., 2008). Although the application of inoculants in combination with fertilizers on cowpea showed a promising yield effect (Kyei-Boahen et al., 2017), the treatment was beneficial only at specific nutrient deficiency levels. Meanwhile, besides the complexity of the socioeconomic factors that limit fertilizer access in the least productive regions (Erisman et al., 2008; Brown, 2014), the negative environmental impact of misapplied fertilizers is overlooked (Ann and Socolow, 1994; Vitousek et al., 1997). The Ceres2030 report investigated the impact of scientific productivity toward eradicating global hunger (Laborde et al., 2020). The study found that more than 95% of global research interventions toward food security was less relevant toward addressing key need gaps (Laborde et al., 2020). Others have highlighted the need for strategic interventions through sustainable crop production to overcome food insecurity amid climate threats and the rising global population (Tilman et al., 2002; Bita and Gerats, 2013).

In our study, we propose and report a preliminary test of an alternative approach to increase cowpea production under savanna conditions. We hypothesize that productivity, such as growth (total biomass allocation) increases when a relatively more limiting constraint among existing growth constraints is relieved until the next limiting constraint impacts productivity. We formulate a non-hormonal biostimulant (nhB) that treats multiple stressors and tests its effect on nodulation, biomass, and leaf physiological responses in cowpea in comparison with inorganic N fertilizer and exogenous compatible osmolyte.

MATERIALS AND METHODS

Study Area

The study site was located in the Northern region and covers 40% of (92,456 mile^{-2}; latitudes 4°-12°N) land cover by area of Ghana. Two major ecological zones characterize the region:

the sub-humid to semi-arid Guinea savanna and the arid Sudan savanna zones (Gyasi, 1995). The Inter-Tropical Conversion Zone controls rainfall seasons in Ghana, with one wet season in the north and two wet seasons in the south. Low, erratic rainfall ranging between 150 and 250 mm/month in a single dry season to 1,100–1,200 mm month^{-1} in a single wet season characterizes the study area. Mean monthly temperature during the growing season ranges between 26 and 30°C (Buah and Mwinkaara, 2009). During the study period, the total rainfall (daily mean) recorded was 203.8 (6.6 mm day^{-1}); average sunshine was 5.8 h; the mean temperature was 26.7°C (ranging from 29.7°C$_{max}$ to 23.6°C$_{min}$); and the mean relative humidity recorded was 84% (ranging from 93 to 75% min). The soil at the study site constituted 55.8% sand, 41.96% silt, and 2.2% loam. Weather and soil analysis data were obtained from the Savanna Agriculture Research Institute, Council for Scientific and Industrial Research, Ghana.

Plant Preparation and Treatments

Three experimental blocks, each containing four distinct raised soil beds of dimension 2 × 8 m each and interspaced by a meter gap, were prepared across a slope in a series-like fashion. Each bed in a block represented a treatment group based on a Randomized Complete Block Design. Each soil bed was seeded with cowpea, the common African cultivar Songotra-IT97K-499-35, which is *Striga gesnerioide*s resistant (Asare et al., 2011; Muñoz-Amatriaín et al., 2017).

Germinated seedlings were thinned at 10 cm height to 40 plants for each growing bed of size 80 × 40 cm. Treatments were assigned randomly within and between blocks.

Given the conditions of Guinea savanna, we will use the term osmotic stress to represent the likelihood of both drought and heat stress incidence as they occur in tandem (Dwivedi et al., 2018) or specifically to represent conditions, such as low soil moisture, atmospheric vapor pressure deficit, and salinity, for their similarity in physiological responses (Munns, 2002; Chaves et al., 2009). Three treatments were prepared to treat osmotic stress. First, 0.25 g L^{-1} (coded *sorbL*), and second, 0.5 g L^{-1} (coded *sorbH*) compatible osmolyte, D-Sorbitol (Hexane 1, 2, 3, 4, 5, 6-Hexol) of molecular weight 182.17 g mol^{-1} obtained from Sigma-Aldrich, USA. The third osmotic treatment was an antioxidant and amino acid-based nhB (coded *nhB*), prepared from the laboratory at the Yale School of the Environment. The active components of nhB include 2-amino-5-guanidinopentanoic acid, L-ascorbic acid, thiamine mononitrate, and *cis*-1, 2, 3, 5-*trans*-4, 6-cyclohexanehexol. To arrive at the final treatment formulation, different iterations of nhB beta were evaluated in root-shoot allocation experimental trials in a glasshouse using *Raphinus sativus* (cherry belle variety) as a model plant. The satisfactory formulation was attained when *R. sativus* maintained a fresh root: shoot biomass ratio of ∼1:1 and yields over 100%. By this approach, we assumed that the overall yield output of nhB treatment will vary by species type and allocation cost to stress response depending on field conditions.

Furthermore, 5 g L^{-1} nitrogen was prepared from 98% ammonium nitrate (NH_4NO_3) as inorganic nitrogen treatment (coded *Nfert*). All control groups were treated with equal volumes of distilled water, which was used to prepare treatment solutions. Each plant replicate received 50 ml of treatment dose biweekly until the onset of pod formation. Nitrogen was applied directly to the soil around the stem of plants while *sorbL, sorbH, nhB,* and controls were applied to both foliage and soil.

Plant Sampling and Measurement

Out of 40 plant without growth defects, 15 plants were tagged for repeated measurements throughout the growth stages. Leaf measurements were conducted during the active photosynthetic period in the morning (PPDF ranged from 900 to 1,200 mmol m^{-2}s^{-1}). Leaf temperature, chlorophyll fluorescence, and chlorophyll content of the youngest fully expanded leaf of each tagged plant were measured 2 weeks after each treatment time during the vegetative, flowering, and pod growth stages of cowpea. We used common plant biophysical markers (Ernst, 1999) and traits in our assessment to allow reliable reproducibility and convenience in the study sites.

Biomass and Nitrogen-Fixing Traits

The root zones were softened by inundating with water to allow the whole plant to be removed from the soil bed with intact roots. The soil debris was brushed off, and the root nodules per plant were carefully removed, counted, weighed, and re-weighed after oven drying to a constant weight at 60°C to obtain the total weight of nodule per plant and the total number of nodules formed per plant. Furthermore, whole plants with intact pods were oven-dried to constant weight to obtain total biomass, then followed by separate measurements of pods.

Leaf Physiological Measurement

Leaf temperature, T_l was measured as an indicator of plant stress (Udompetaikul et al., 2011; Rodríguez et al., 2015; Carroll et al., 2017). Variations in moisture stresses are known to significantly alter leaf temperature, causing it to deviate from ambient temperature (Wiegand and Namken, 1966). T_l was measured by a laser-guided infrared thermometer (ST60 ProPlus™ Raytec, Santa Cruz, CA, USA). The laser was pointed to the adaxial surface of the leaf, where the device collects optically emitted, reflected, and transmitted energy by the leaf surface on a detector as an ambient temperature reading in °C (±0.07°C).

The stress manifested in plants can be determined by observing the leaf photosystem II (PSII), which is a protein complex in the light-dependent reactions of plant photosynthesis. PSII damage is the first manifestation of stress in plant leaves (Maxwell and Johnson, 2000), and the efficiency of this state is referred to as photochemical efficiency. Maximum quantum yield at PSII is determined based on the chlorophyll fluorescence ratio, $F_vF_m{}^{-1}$, a well-studied phenomenon in the plant physiology (Rodríguez et al., 2015) and a well-established physiological indicator of plant tolerance to the environmental stress, including drought and heat (Méthy et al., 1994; Maxwell and Johnson, 2000; Dwivedi et al., 2018). Plant stress that affects the PSII is determined based on a calculated variable fluorescence(F_v) to maximal fluorescence (F_m) ratio using a chlorophyll fluorescence device (model OS-30p, Opti-Sciences,

Inc. Hudson, New Hamshire, USA). To measure $F_vF_m^{-1}$, leaf samples were dark-adapted by placing leaves inside plastic cuvettes to block the incident light on the selected portion of the leaf blade for 30 min. Then a weak modulated light is immediately irradiated from a fluorometer on dark-adapted leaf blade to excite a pre-photosynthetic antenna. Upon light saturation at maximum light exposure, the maximum fluorescence, F_m, is determined and $F_vF_m^{-1}$ computed and recorded by the fluorometer. Chlorophyll fluorescence is one of the most frequently used plant measurement techniques (Schreiber and Bilger, 1993) and has been used extensively in stress studies in several legumes (Georgieva and Yordanov, 1993; Stoddard et al., 2006). The leaf chlorophyll content is a physiological trait associated with drought and heat stress (Dwivedi et al., 2018). A handheld chlorophyll-detecting device, SPAD-502 (Minolta Camera Co., Osaka, Japan), was used to measure the leaf chlorophyll content. The sample leaf was placed in between a receptor window and a measuring head. By pressing the measuring head, the chlorophyll content was determined at 650 and 940 nm in SPAD units at ±1.0 accuracy (see Richardson et al., 2002).

Statistical Analysis

The Lme4 package in R (Bates et al., 2015) was used to perform mixed-effect modeling (MEM) by restricted maximum likelihood *t*-tests. MEM performs ANOVA on repeatedly measured variables and estimates fixed and random sources of variation. To know where significant differences occurred, we tested general linear hypotheses by multiple pairwise comparisons of means based on Tukey's honestly significant difference (HSD) tests on normally distributed data. All statistical analyses were conducted using the R programming language and environment (R Core Team). The null hypothesis (H_0) assume no differences in population means such that: T_1 (control), $= T_2 = T_3 = \ldots T_x$; where $\alpha \leq 0.05$ and T_x indicates x treatment type. Furthermore, the alternative hypothesis (H_a) assumes differences in population means such that: $T_1 \neq T_2$, or $T_3, = \ldots T_x$; at least at a significance level of $p < 0.05$.

RESULTS

Effect of Treatments on Biomass, Pod Capacity, and Root Nodulation

The mean biomass of cowpea was significantly different between nhB and all other treatments ($p < 0.001$, **Table 1**). nhB had the highest biomass output, 45% followed by sorbL (17%), sorbH (13.3%), Nfert (13.1%), and controls. Nodulation capacity determined by the means of the total number of nodules formed per cowpea was significantly different ($p < 0.01$) among treatment groups.

N-treated cowpea relatively formed the highest number of nodules per root and nodule weight (**Figures 1C,D**). Thus, we refuse to accept the null hypothesis that there is no difference in the mean effect of treatment interventions on cowpea growth with respect to biomass and nodulation capacity. The effect of blocking was significant on biomass response ($p < 0.01$), number of pods ($p < 0.05$), and mean number and oven-dry weight of nodules ($p < 0.0001$). This indicates that measured responses to treatments are independent of the significant variations in site conditions. This is of statistical importance to emphasize the reliability of the study outcome.

TABLE 1 | Summary ANOVA of mean response of treatment groups.

Parameter variables		DF	*F*-Value	(Pr > F)
Biomass	Treatment	4	6.1889	<0.0001***
	Blocks	2	4.907	0.0082**
No. of pods	Treatment	4	1.598	0.1759^{ns}
	Blocks	2	4.207	0.016*
Nodule mass	Treatment	4	0.414	0.798^{ns}
	Blocks	2	83.59	<0.0001***
No. of nodules	Treatment	4	3.413	0.009**
	Blocks	2	55.2	<0.0001***

*Superscript stars indicate the levels of significance, where *(0.05), **(0.01), ***(0.001), and ^{ns}(not significant).*

The treatment effects on both the mean number of pods formed per cowpea and the mean nodule mass per cowpea root were not significant (**Table 1**). Nevertheless, pod yield per plant was relatively highest in nhB-treated cowpea (**Figure 1B**).

Effect of Treatments on Leaf Physiological Responses

The mean effect of treatments on leaf chlorophyll content in cowpea did not differ significantly; however, the difference ($p = 0.05$) in leaf chlorophyll responses to sorbL and sorbH (which vary by D-sorbitol concentration) indicates that the concentration of exogenous D-sorbitol application on cowpea leaves might be important to chlorophyll response under savanna conditions. Leaf fluorescence in nitrogen-fertilized cowpea differed significantly from cowpeas treated with nhB, sorbL, and sorbH (**Table 2**).

Treatment effect on leaf temperature, T_l response was significantly different in fertilizer-treated cowpea and the rest of treatment groups (**Table 2**). Although stress variables are weakly correlated (**Supplementary Figure 1**), the correlation plot shows the general relation of leaf physiological indicators to aid in the interpretation of leaf treatment responses. Higher leaf temperature does not necessarily indicate a healthy status as in controls. A relatively higher T_l, lower leaf chlorophyll content, and fluorescence should indicate a relatively stressful condition.

DISCUSSION

Biomass and Physiological Responses of Cowpea to Osmotic and N Treatments

Low soil fertility and drought constitute abiotic factors that constrain cowpea production (Roberts, 2013). Although legumes are adapted to low nitrogen conditions, N-fixation may come at a cost. Nodulation has been used to evaluate stress in legumes (Rai and Singh, 1999). Under savanna conditions, other competing abiotic factors further constrain the biological N-fixing capacity of nodulating legumes and consequently may limit

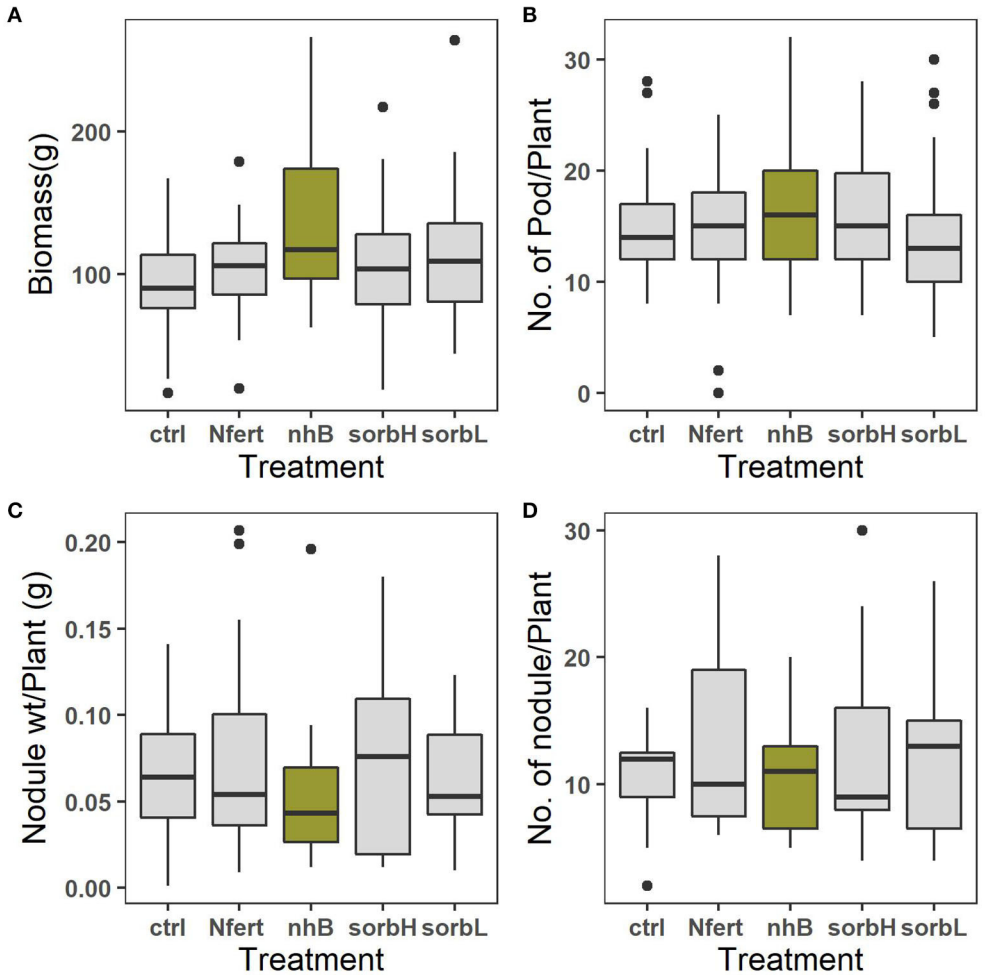

FIGURE 1 | Means of total biomass, grams per plant **(A)**, mean number of pods per plant **(B)**, mean weight of root nodule per plant **(C)**, and mean number of root nodules formed by roots per plant **(D)** in response to cowpea treatments; control, N fertilizer (Nfert), sorbitol (sorbL and sorbH), and non-hormonal biostimulant (nhB).

nitrogen contribution to productivity. We hypothesized that where cowpea is constrained by multiple factors, an intervention that alleviates the relatively more limiting factor may lower the physiological cost of mitigating the constraining factor, allowing allocation toward yield. Total biomass and pod yield are used in the study as proxies for productivity or yield allocation. Biomass is a common measure of plant productivity in ecological studies (Roberts et al., 1993; Tilman et al., 1997; Klironomos et al., 2000; van Grunsven et al., 2007; TerHorst and Munguia, 2008; Fraser et al., 2015), and stress evaluation in legume crops (Ashraf and Chishti, 1993; Ashraf and Zafar, 1997; O'Toole et al., 2001). Based on the relatively higher biomass, pod yield, and lower investment in the root nodules in nhB, sorbL, and sorbH cowpea treatments (**Figures 1A–D**), we conjecture that osmotic stress is more limiting than soil nitrogen need in cowpea in the study area. The additional higher yield in nhB may be due to the combined effect of antioxidants and amino acids used in the formulation. More nodules were formed in untreated controls than biostimulant, nitrogen, and sorbitol treatments and may indicate the reduced need for nitrogen.

TABLE 2 | Significant pairs from multiple mean comparisons based on Tukey's honestly significant difference (HSD) test from a linear mixed-effect model fit.

Parameter variables	Treatments	Estimate (error)	*Z*-value	(Pr >|z|)
Chlorophyll fluorescence, $FvFm^{-1}$	Nfert-nhB	0.0368 (0.0128)	2.859	0.033*
	Nfert-sorbL	−0.0333 (0.0113)	−2.926	0.028*
	Nfert-sorbH	−0.0399 (0.0113)	−3.506	0.004**
Chlorophyll content	sorbL-sorbH	−2.5979 (1.0300)	−2.522	0.05
Leaf temperature, T_l	Nfert-nhB	−1.1436 (0.2867)	−3.989	<0.001***
	Nfert-cntl	−1.3616 (0.2554)	−5.345	<0.001***
	Nfert-sorbL	0.7694 (0.2548)	3.020	0.021*
	Nfert-sorbH	0.9004 (0.2548)	3.534	0.003***

*Except reported, all other possible mean pairs were not significant. Superscript stars indicate the levels of significance, where *(0.05), **(0.01), and ***(0.001).*

Nitrogen, biostimulant, and sorbitol treatments reduced cowpea stress in contrast with controls (**Figure 2**). While we expected higher N-fixing capacity and $F_vF_m^{-1}$ to increase

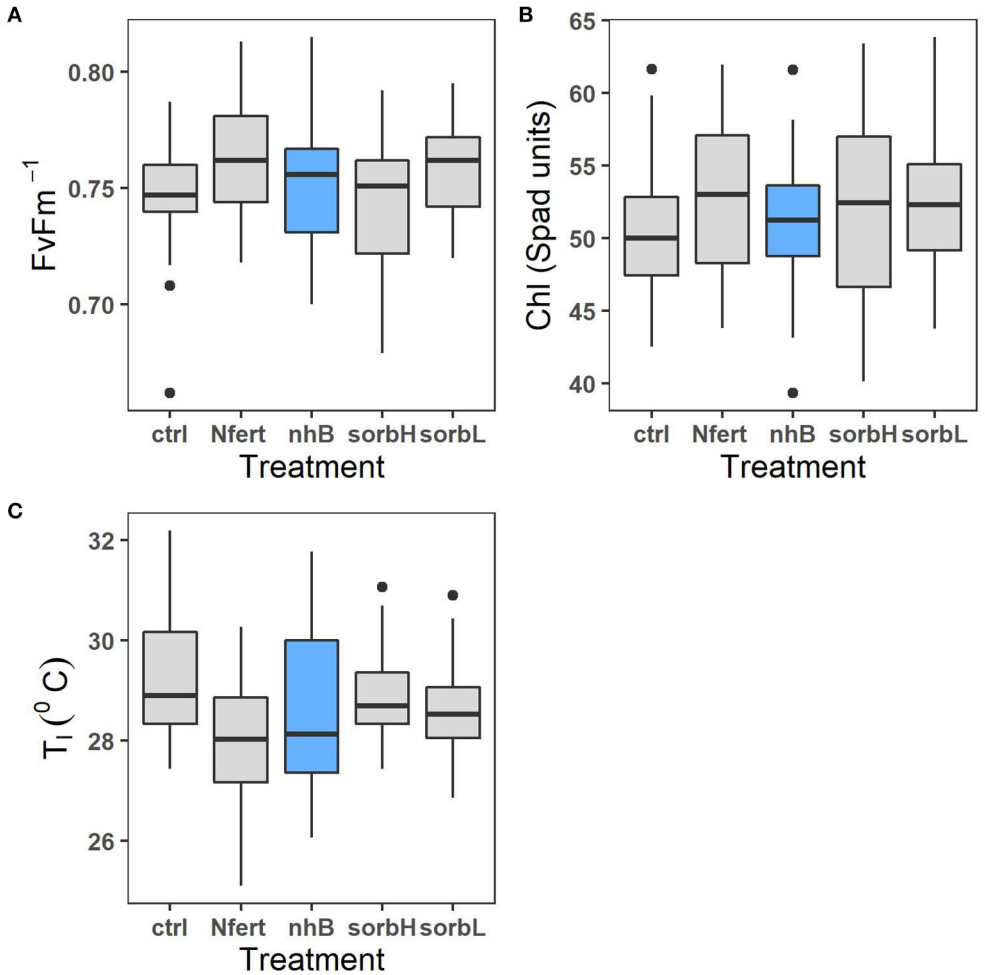

FIGURE 2 | Leaf physiological response of cowpea to osmotic treatments (sorbL, sorbH, and nhB) and N fertilizer treatment (Nfert). Plots represent chlorophyll fluorescence ratio **(A)**, leaf chlorophyll content **(B)**, and leaf temperature **(C)**.

productivity, the response was relatively lower in N treatment than in biostimulant and sorbitol treatments. Maintaining leaf moisture while fixing carbon may be the more efficient strategic role of the osmoprotection compared to N-fertilized cowpea, which showed higher proxy-photosynthetic activity (**Figures 2A,B**), yet seemingly more leaf water loss, resulting from a cooling effect and lower leaf temperature. The relatively lower biomass and increased nodulation response to N treatment suggest a plausible trade-off to increased investment toward a need for physiological response and N-fixation (**Figures 1C,D**). Contrary, higher biomass and leaf stress responses to osmotic treatments support the conjecture that exogenous osmolytes alleviate the need and the cost of metabolic response, thereby directing more allocation toward whole-plant biomass output.

Effect of Non-hormonal Biostimulant and D-Sorbitol on Cowpea

Biostimulants, since their origination, definition, and development over the past four decades, have been shown to improve stress resistance and promote plant development (Russo and Berlyn, 1991). Although drought avoidance by hydraulic controls (Hall and Schulze, 1980; Turk and Hall, 1980) and leaf paraheliotropism (Schakel and Hall, 1979) (also observed in this study) persists in cowpea, osmoadaptation through metabolite accumulation is reported as a more conservative strategy in cowpea (Goufo et al., 2017). The relative increase in biomass, following sorbitol and biostimulant treatments supports osmoadaptation as an important drought response strategy in cowpea. From our results, we conjecture that external application of osmolyte-containing compounds may prevent the inherent metabolic need and cost for cowpeas to initiate osmoadaptation, thereby making readily available more resources for biomass allocation.

In a study of 88 cowpea metabolites, *myo*inositol and arginine were reported to have no beneficial effect on cowpea yield (Goufo et al., 2017). Contrary to our findings, *myo*inositol and arginine, both active constituents of the nhB formulation improved biomass allocation in cowpea. The contrasting findings may result from differences between the metabolite concentration in naturally occurring cowpea leaves and the concentrations used

in the nhB formula. Further, our study reports the first yield effects of exogenous D-sorbitol on savanna cowpea. Although D-sorbitol does not constitute the reported metabolites expressed in drought-stressed cowpea, its effect on yield in our study suggests that metabolite–yield relations may be non-species specific. In that, the metabolites expressed by plants under stressful conditions may not represent the only possible strategy but a choice, perhaps governed by adoptive mechanisms peculiar to the species or based on inherent biochemical resources available to initiate the metabolic response process.

Implication of the Limiting-Stress-Elimination Hypothesis in Savanna Legume Production

According to the proposed limiting-stress-elimination hypothesis (LSEH), when the limiting stress is eliminated, stress impact is relieved (**Figures 3A,B**), until the next available stress becomes most limiting. The scope of this study here is not to establish the most limiting stressor in cowpea.

Instead, we have demonstrated which, among identifiable constraints relatively limits cowpea productivity most by showing whose "elimination" (by treatment) relatively increased cowpea biomass. This makes the study application relevant to ongoing field situations where stressors may be short-lived yet damaging to yield. Contrary to the law of minimum and diminishing soil productivity (Mitscherlich, 1909) whereby maximum productivity requires relieving all decrements from the optimal level for each nutrient, intervention by the LSEH focuses on the predominant limiting stressor given prevailing conditions and not a host of stressors. In the Guinea savanna of West Africa, where leguminous crops are predominantly constrained by limited soil nitrogen and osmotic stress, the simultaneous treatment to eliminate multiple abiotic stressors may increase farming costs beyond economic practicality.

Increasing legume production constitutes a long-term food security initiative and ecological restoration strategy whereby legumes improve soil N, increase the availability of percent arable lands, and the possible recruitment or cultivation of less competitive but essential non-legume plants or crop species in the savanna. In our study, we measured N-fixation indirectly by the number of nodules formed per plant and dry mass. While N treatment relatively increased nodulation capacity significantly, the effect of inorganic N, the biostimulant, and sorbitol on mean nodule dry mass did not vary significantly. Thus, exogenous osmotic stress treatment constitutes a promising alternative for increasing cowpea production without impairing their biological N-fixing capacity. N-fixation may be an important agroecological tool for improving long-term savanna ecosystem productivity. Where necessary, the use of N fertilizers to maximize legume yield should depend on whether additional inorganic N supplement addresses the yield gap in the specific growing area. Evidence exists to question the relevance of N fertilization in cowpea. For instance, in a study by Martins et al. (2003), bacteria inoculated cowpea improved grain productivity more than N-fertilized cowpea through increased biological N-fixation. In this instance, regardless of N supplement, increased biological N-fixation through bacterial inoculation accounted for higher yield. Essentially, the metabolic cost of microbial-aided N-fixation may be lower than the metabolic cost of converting inorganic N fertilizers to readily available forms to impact yield. Similarly, in our study, minimizing the cost of stress allocation may have enhanced yield in which amino acid in nhB contributes organic nitrogen. Besides direct plant growth, biostimulants can be designed to supplement the resource needs of N-fixing bacteria to indirectly improve yield.

It can be inferred from biomass responses that a less productive outcome may ensue when an intervention targets a lesser limiting factor, while the relatively more limiting factor persists, as in the common practice of fertilizer use in crop production in arid landscapes. Hence, it becomes imperative for the agronomist to determine what constitutes the measurable limiting factor for a crop, given its growth conditions. When that is determined, management techniques and tools that improve resource use efficiency become the next relevant agronomic asset (Chaves et al., 2009). The LSEH utilizes a cost–benefit utility that should inform decisions and potential innovations entrenched in the principle of efficiency and sustainability in agricultural practices, particularly in regions challenged by both limited economic and environmental constraints. In the search for sustainable agroecological solutions, LSEH can assist agronomists to decipher appropriate interventions optimal for improving productivity.

The yield effect of biostimulant on N-fixing crops and trees and as a low input for sustainable agriculture has been discussed (Berlyn and Russo, 1990; Russo and Berlyn, 1991, 1992). The goal of this study was to demonstrate the potential of nhB as an input specifically in conditions where fluctuating diurnal or within-season temporal biophysical stressors can impact yield. Although the study satisfies statistical assumptions, it is a test of hypothesis limited to a single species as such, further inquiry can be useful to expand the scope and limitations of the hypothesis. However, from years of experience in biostimulant formulation, there is a remarkable advantage, especially when adopting core formula to other crops and often require small adjustment in the constituent compounds and or their concentrations. Further, our study does not report on the potential implementation cost. Earlier developments, including ROOT 1™ and ROOT 2™ that constituted mycorrhiza were successfully commercialized and available at low cost, and we assume that recent developments based on more available resources will likewise make nhB accessible at low cost.

CONCLUSIONS

Crops growing in the Guinea savanna sub-biome are constrained by a myriad of factors including low soil N, high temperature, and drought. Eliminating each constraint as proposed by the decrement from the maximum concept can be impractical, especially in low-income economies that depend on rainfed

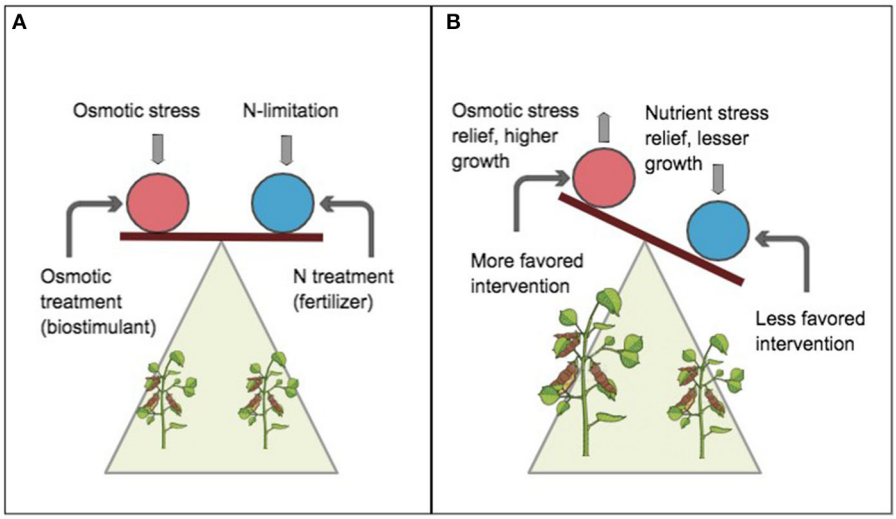

FIGURE 3 | A schematic of the limiting-stress-elimination hypothesis (LSEH). Circles represent whole-plant organisms. Balanced plane implies a notion of significance or pedigree of stress impact. Vertical arrows indicate stressors (osmotic and nitrogen limitation), downward arrow implies stress impact, and upward arrow implies relived stress. Curved arrows indicate applied intervention (exogenous biostimulant and nitrogen deposition). At equilibrium **(A)**, the stressor impact on productivity is assumed similar. Without any intervention, the impact of multiple stressors can be assumed to be synergetic and difficult to detect. However, when defined interventions are simultaneously applied, a shift in slope or tilt **(B)** distinguishes the relative magnitude of the impact of a conjected stressor and how much it limits plant productivity. The favored intervention **(B)** in the red circle shows sensitivity to stress response by plant and eliminates or alleviates the impact of the stressor. This results in increased productivity indicated by an upward tilt (analogous to a "lighter weighing effect").

agriculture. Although fertilizer input remains the predominant approach to crop nutrient enrichment, it is beneficial where soil nutrient deficit mostly limits crop productivity. The study hypothesized that productivity is relatively maximized when a relatively more limiting stress factor to growth is relieved among other possible stressors. In a case study with cowpea growing in the savanna conditions, osmotic stress treatment increased yield more than N treatment. However, non-hormonal biostimulant treatment, which constitutes both osmolyte and organic nitrogen sources impacted yield most. We conjecture that biostimulants can better manage crop production where productivity may be limited by alternating factors across the growing cycle or by multiple constraints.

DATA AVAILABILITY STATEMENT

The original contributions presented in the study are included in the article/**Supplementary Materials**, further inquiries can be directed to the corresponding author/s.

AUTHOR CONTRIBUTIONS

AA-B and GB conceived the idea, interpreted the results, and wrote the manuscript. AA-B conducted experiments, collected data, and performed the statistical analysis.

FUNDING

The work was funded by a Carpenter Sperry Internship and Research Fund (grant# 20140505151359455), a Yale Institute of Biospheric Studies' (YIBS) Masters Research Grant, and a Tropical Resource Institute Endowment Fellowship.

ACKNOWLEDGMENTS

AA-B would like to thank research and study support for master thesis work at the Yale School of Environment. The authors are grateful for weather and soil analysis data from the Savanna Agriculture Research Institute, Council for Scientific and Industrial Research, Ghana. They also thank Dr. Isaac K. Addai and Dr. Adu-Gyamfi for technical advice, facilitating field experimental site, laboratory, and voluntary field technician support. The authors are grateful to Kwadwo Asamoah Atta-Boateng and Alexander N. Adjei for field assistance. The content of this paper (re-written and expanded but same data) was previously submitted in preprint (Atta-Boateng and Berlyn, 2019).

SUPPLEMENTARY MATERIAL

The Supplementary Material for this article can be found online at: https://www.frontiersin.org/articles/10.3389/fpls.2021.732279/full#supplementary-material

REFERENCES

Ann, K. P., and Socolow, R. H. (1994). *Physics Today*. New York, NY: American Institute of Physics.

Arbona, V., Manzi, M., Zandalinas, S. I., Vives-Peris, V., Pérez-Clemente, R. M., and Gómez-Cadenas, A. (2016). "Physiological, metabolic, and molecular responses of plants to abiotic stress," in *Stress Signaling in Plants: Genomics and Proteomics Perspective, Vol. 2*, eds M. Sarwat, A. Ahmad, M. Z. Abdin, M. M. Ibrahim (Cham: Springer International Publishing), 1–35. doi: 10.1007/978-3-319-42183-4_1

Asare, A. T., Akrong, C. K., Gowda, B. S., Galyuon, I. K. A., Aboagye, L. M., Takrama, J. F., et al. (2011). Evaluation of agro-morphological diversity in some segregating lines of cowpea (*Vigna unguiculata* L. Walp). *J. Ghana Sci. Assoc.* 13:11. Available online at: http://www.ghanascience.org.gh/wp-content/uploads/2018/04/1-11-Asare-1.pdf (accessed July 24, 2019).

Ashraf, M., and Chishti, S. N. (1993). Waterlogging tolerance of some accessions of lentil (*Lens culinaris Medic.*). *Trop. Agric.* 70. Available online at: https://journals.sta.uwi.edu/ojs/index.php/ta/article/view/7067 (Accessed June 7, 2021).

Ashraf, M., and Zafar, Z. U. (1997). Effect of potassium deficiency on growth and some biochemical characteristics in two lines of lentil (*Lens culinaris* Medic.). *Acta Physiol. Plant.* 19, 9–15. doi: 10.1007/s11738-997-0016-7

Atta-Boateng, A., and Berlyn, G. P. (2019). Limiting-stress-elimination hypothesis: approach to increase savanna cowpea productivity by stress reduction. *bioRxiv* 594754. doi: 10.1101/594754

Atta-Boateng, A., Berlyn, G. P., O'Hern, C. S., and Felson, A. J. (2019). Suitability of wetland macrophyte in green cooling tower performance. *Ecol. Eng.* 127, 487–493. doi: 10.1016/j.ecoleng.2018.08.002

Bates, D., Mächler, M., Bolker, B., and Walker, S. (2015). Fitting Linear Mixed-Effects models using lme4. *J. Stat. Softw.* 67, 1–48. doi: 10.18637/jss.v067.i01

Berlyn, G. P., and Russo, R. O. (1990). The use of organic biostimulants in nitrogen fixing trees. *NIFTRR* 8, 1–2.

Bita, C. E., and Gerats, T. (2013). Plant tolerance to high temperature in a changing environment: scientific fundamentals and production of heat stress-tolerant crops. *Front. Plant Sci.* 4:273. doi: 10.3389/fpls.2013.00273

Boukar, O., Belko, N., Chamarthi, S., Togola, A., Batieno, J., Owusu, E., et al. (2019a). Cowpea (*Vigna unguiculata*): genetics, genomics and breeding. *Plant Breed.* 138, 415–424. doi: 10.1111/pbr.12589

Boukar, O., Togola, A., Chamarthi, S., Belko, N., Ishikawa, H., Suzuki, K., et al. (2019b). "Cowpea [*Vigna unguiculata* (L.) Walp.] breeding," in *Advances in Plant Breeding Strategies: Legumes*, eds J. M. Al-Khayri, S. M. Jain, D. V. Johnson (Cham: Springer International Publishing), 201–243. doi: 10.1007/978-3-030-23400-3_6

Brown, A. (2014). Limits of eco-intensification. *Nat. Clim. Chang.* 4, 326–326. doi: 10.1038/nclimate2230

Buah, S. S. J., and Mwinkaara, S. (2009). Response of Sorghum to nitrogen fertilizer and plant density in the guinea savanna zone. *J. Agron.* 8, 124–130. doi: 10.3923/ja.2009.124.130

Carroll, D. A., Hansen, N. C., Hopkins, B. G., and DeJonge, K. C. (2017). Leaf temperature of maize and crop water stress index with variable irrigation and nitrogen supply. *Irrigat. Sci.* 35, 549–560. doi: 10.1007/s00271-017-0558-4

Chapin, F. S. (1991). Integrated responses of plants to stress. *Bioscience* 41, 29–36. doi: 10.2307/1311538

Chapin, F. S., Bloom, A. J., Field, C. B., and Waring, R. H. (1987). Plant responses to multiple environmental factors. *Bioscience* 37, 49–57. doi: 10.2307/1310177

Chaves, M. M., Flexas, J., and Pinheiro, C. (2009). Photosynthesis under drought and salt stress: regulation mechanisms from whole plant to cell. *Ann. Bot.* 103, 551–560. doi: 10.1093/aob/mcn125

Dakora, F. D., and Keya, S. O. (1997). Contribution of legume nitrogen fixation to sustainable agriculture in Sub-Saharan Africa. *Soil Biol. Biochem.* 29, 809–817. doi: 10.1016/S0038-0717(96)00225-8

Duranti, M., and Gius, C. (1997). Legume seeds: protein content and nutritional value. *Field Crops Res.* 53, 31–45. doi: 10.1016/S0378-4290(97)00021-X

Dwivedi, S. L., Siddique, K. H. M., Farooq, M., Thornton, P. K., and Ortiz, R. (2018). Using biotechnology-led approaches to uplift cereal and food legume yields in dryland environments. *Front. Plant Sci.* 9:1249. doi: 10.3389/fpls.2018.01249

Erisman, J. W., Sutton, M. A., Galloway, J., Klimont, Z., and Winiwarter, W. (2008). How a century of ammonia synthesis changed the world. *Nat. Geosci.* 1, 636–639. doi: 10.1038/ngeo325

Ernst, W. H. O. (1999). "Biomarkers in Plants," in *Biomarkers: A Pragmatic Basis for Remediation of Severe Pollution in Eastern Europe*, eds D. B. Peakall, C. H. Walker, and P. Migula (Dordrecht: Springer Netherlands). doi: 10.1007/978-94-011-4550-3_10

FAO (2004). *COWPEA Post-harvest Operations-Post-harvest Compendium COWPEA: Post-Harvest Operations Organisation: Food and Agriculture Organization of the United Nations*. Available online at: http://www.fao.org/3/a-au994e.pdf (accessed July 24, 2019).

FAO (2005). *Fertilizer Use by Crop in Ghana*. Rome: Food and Agriculture Organization of the United Nations Land and Plant Nutrition Management Service Land and Water Development Division.

FAO (2011). *Food Insecurity in the World How Does International Price Volatility Affect Domestic Economies and Food Security?* Rome: Food Insecurity in the World.

Foyer, C. H., Lam, H.-M., Nguyen, H. T., Siddique, K. H. M., Varshney, R. K., Colmer, T. D., et al. (2016). Neglecting legumes has compromised human health and sustainable food production. *Nat. Plants* 2:16112. doi: 10.1038/nplants.2016.112

Fraser, L. H., Pither, J., Jentsch, A., Sternberg, M., Zobel, M., Askarizadeh, D., et al. (2015). Worldwide evidence of a unimodal relationship between productivity and plant species richness. *Science* 349, 302–305. doi: 10.1126/science.aab3916

Georgieva, K., and Yordanov, I. (1993). Temperature dependence of chlorophyll fluorescence parameters of pea seedlings. *J. Plant Physiol.* 142, 151–155. doi: 10.1016/S0176-1617(11)80955-7

Goufo, P., Moutinho-Pereira, J. M., Jorge, T. F., Correia, C. M., Oliveira, M. R., Rosa, E. A. S., et al. (2017). Cowpea (*Vigna unguiculata* L. Walp.) metabolomics: osmoprotection as a physiological strategy for drought stress resistance and improved yield. *Front. Plant Sci.* 8:586. doi: 10.3389/fpls.2017.00586

Gull, A., Ahmad Lone, A., and Ul Islam Wani, N. (2019). "Biotic and Abiotic Stresses in Plants," in *Abiotic and Biotic Stress in Plants*, ed A. B. De Oliveira (London: IntechOpen). doi: 10.5772/intechopen.85832

Gyasi, E. A. (1995). Farming in Northern Ghana. *ILEIA Newslett.* 11:23.

Hall, A., and Schulze, E. (1980). Drought effects on transpiration and leaf water status of cowpea in controlled environments. *Aust. J. Plant Physiol.* 7:141. doi: 10.1071/PP9800141

Harmsen, K. (2000). A modified mitscherlich equation for rainfed crop production in semi-arid areas: 1. Theory. *Netherl. J. Agric. Sci.* 48, 237–250. doi: 10.1016/S1573-5214(00)80016-0

Horn, L. N., and Shimelis, H. (2020). Production constraints and breeding approaches for cowpea improvement for drought prone agro-ecologies in Sub-Saharan Africa. *Ann. Agric. Sci.* 65, 83–91. doi: 10.1016/j.aoas.2020.03.002

IITA (2010). *Annual Report 2009/10*. Croydon. Available online at: http://annualreport.iita.org/wp-content/uploads/2010/04/iita-annual-report-2009-10.pdf (accessed July 24, 2019).

Klironomos, J. N., McCune, J., Hart, M., and Neville, J. (2000). The influence of arbuscular mycorrhizae on the relationship between plant diversity and productivity. *Ecol. Lett.* 3, 137–141. doi: 10.1046/j.1461-0248.2000.00131.x

Kyei-Boahen, S., Savala, C. E. N., Chikoye, D., and Abaidoo, R. (2017). Growth and yield responses of cowpea to inoculation and phosphorus fertilization in different environments. *Front. Plant Sci.* 8:646. doi: 10.3389/fpls.2017.00646

Laborde, D., Murphy, S., Parent, M., Porciello, J., and Smaller, C. (2020). *Ceres2030: Sustainable Solutions to end Hunger Summary Report*. Winnepeg: International Institute for Sustainable Development (IISD).

Liebig, J. (1840). *Organic Chemistry in Ites Applications to Agriculture and Physiology, 1st Edn.* London: Taylor & Walton.

Martey, E., Wiredu, A. N., Etwire, P. M., Fosu, M., Buah, S. S. J., Bidzakin, J., et al. (2014). Fertilizer adoption and use intensity among smallholder farmers in northern Ghana: a case study of the AGRA soil health project. *Sustain. Agric. Res.* 3:24. doi: 10.22004/ag.econ.230530

Martins, L. M. V., Xavier, G. R., Rangel, F. W., Ribeiro, J. R. A., Neves, M. C. P., Morgado, L. B., et al. (2003). Contribution of biological nitrogen fixation to cowpea: a strategy for improving grain yield in the semi-arid region of Brazil. *Biol. Fertil. Soils* 38, 333–339. doi: 10.1007/s00374-003-0668-4

Maxwell, K., and Johnson, G. N. (2000). Chlorophyll fluorescence—a practical guide. *J. Exp. Bot.* 51, 659–668. doi: 10.1093/jexbot/51.345.659

McAuliffe, C., Chamblee, D. S., Uribe-Arango, H., and Woodhouse, W. W. (1958). Influence of inorganic nitrogen on nitrogen fixation by legumes as revealed by N151. *Agron. J.* 50, 334–337. doi: 10.2134/agronj1958.00021962005000060014x

Méthy, M., Olioso, A., and Trabaud, L. (1994). Chlorophyll fluorescence as a tool for management of plant resources. *Remote Sens. Environ.* 47, 2–9. doi: 10.1016/0034-4257(94)90121-X

Mitscherlich, E. A. (1909). Das gesetz des minimums und das gesetz des abnehmenden bodenertrages. *Landwirtschaft. Jahrb.* 38, 537–552.

Munns, R. (2002). Comparative physiology of salt and water stress. *Plant Cell Environ.* 25, 239–250. doi: 10.1046/j.0016-8025.2001.00808.x

Muñoz-Amatriaín, M., Mirebrahim, H., Xu, P., Wanamaker, S. I., Luo, M., Alhakami, H., et al. (2017). Genome resources for climate-resilient cowpea, an essential crop for food security. *Plant J.* 89, 1042–1054. doi: 10.1111/tpj.13404

O'Toole, N., Stoddard, F. L., and O'Brien, L. (2001). Screening of chickpeas for adaptation to autumn sowing. *J. Agron. Crop Sci.* 186, 193–207. doi: 10.1046/j.1439-037X.2001.00475.x

R Core Team. (2014). *R: The R Project for Statistical Computing*. Vienna: R Core Team.

Rai, R., and Singh, R. P. (1999). Effect of salt stress on interaction between lentil (*Lens culinaris*) genotypes and *Rhizobium spp*. strains: symbiotic N2 fixation in normal and sodic soils. *Biol. Fertil. Soils* 29, 187–195. doi: 10.1007/s003740050543

Richardson, A. D., Duigan, S. P., and Berlyn, G. P. (2002). An evaluation of noninvasive methods to estimate foliar chlorophyll content. *New Phytol.* 153, 185–194. doi: 10.1046/j.0028-646X.2001.00289.x

Roberts, M. J., Long, S. P., Tieszen, L. L., and Beadle, C. L. (1993). "Measurement of plant biomass and net primary production of herbaceous vegetation," in *Photosynthesis and Production in a Changing Environment*, eds D. O. Hall, J. M. O. Scurlock, H. R. Bolhár-Nordenkampf, R. C. Leegood, S. P. Long (Dordrecht: Springer Netherlands), 1–21. doi: 10.1007/978-94-010-9626-3_1

Roberts, P. A. (2013). *Genetic Improvements of Cowpea to Overcome Biotic Stress and Drought Constraints to Grain Productivity*.

Rodríguez, V. M., Soengas, P., Alonso-Villaverde, V., Sotelo, T., Cartea, M. E., and Velasco, P. (2015). Effect of temperature stress on the early vegetative development of *Brassica oleracea* L. *BMC Plant Biol.* 15:145. doi: 10.1186/s12870-015-0535-0

Runge-Metzger, A., and Diehl, L. (1993). Farm household systems in northern Ghana : a case study in farming systems oriented research for the development of improved crop production systems. *J. Margraf. Sci. Books*.

Russo, R., and Berlyn, G. (1992). Vitamin-Humic-algal root biostimulant increases yield of green bean. *Hort. Sci.* 27:847. doi: 10.21273/HORTSCI.27.7.847

Russo, R. O., and Berlyn, G. P. (1991). The use of organic biostimulants to help low input sustainable agriculture. *J. Sustain. Agric.* 1, 19–42. doi: 10.1300/J064v01n02_04

Salvagiotti, F., Cassman, K. G., Specht, J. E., Walters, D. T., Weiss, A., and Dobermann, A. (2008). Nitrogen uptake, fixation and response to fertilizer N in soybeans: a review. *Field Crops Res.* 108, 1–13. doi: 10.1016/j.fcr.2008.03.001

Schakel, K., and Hall, A. (1979). Reversible leaflet movements in relation to drought adaptation of cowpeas, *Vigna unguiculata* (L.) Walp. *Aust. J. Plant Physiol.* 6, 265–276. doi: 10.1071/PP9790265

Schreiber, U., and Bilger, W. (1993). "Progress in chlorophyll fluorescence research: major developments during the past years in retrospect," in *Progress in Botany/Fortschritte der Botanik*, eds H.-D. Behnke, U. Lüttge, K. Esser, J. W. Kadereit, M. Runge (Berlin: Springer), 151–173. doi: 10.1007/978-3-642-78020-2_8

Stoddard, F. L., Balko, C., Erskine, W., Khan, H. R., Link, W., and Sarker, A. (2006). Screening techniques and sources of resistance to abiotic stresses in cool-season food legumes. *Euphytica* 147, 167–186. doi: 10.1007/s10681-006-4723-8

TerHorst, C. P., and Munguia, P. (2008). Measuring ecosystem function: Consequences arising from variation in biomass-productivity relationships. *Commu. Ecol.* 9, 39–44. doi: 10.1556/ComEc.9.2008.1.5

Tilman, D., Cassman, K. G., Matson, P. A., Naylor, R., and Polasky, S. (2002). Agricultural sustainability and intensive production practices. *Nature* 418, 671–677. doi: 10.1038/nature01014

Tilman, D., Lehman, C. L., and Thomson, K. T. (1997). Plant diversity and ecosystem productivity: theoretical considerations. *Proc. Natl. Acad. Sci. U.S.A.* 94, 1857–1861. doi: 10.1073/pnas.94.5.1857

Timko, M. P., Rushton, P. J., Laudeman, T. W., Bokowiec, M. T., Chipumuro, E., Cheung, F., et al. (2008). Sequencing and analysis of the gene-rich space of cowpea. *BMC Genomics* 9:103. doi: 10.1186/1471-2164-9-103

Turk, K. J., and Hall, A. E. (1980). Drought adaptation of cowpea. II. Influence of drought on plant water status and relations with seed yield1. *Agron. J.* 72:421. doi: 10.2134/agronj1980.00021962007200030005x

Udompetaikul, V., Upadhyaya, S. K., Slaughter, D., Lampinen, B., Shackel, K., and House Louisville, G. (2011). "Plant water stress detection using leaf temperature and microclimatic information written for presentation at the 2011 ASABE annual international meeting sponsored by ASABE," in *ASABE Annual International Meeting* (Louisville). doi: 10.13031/2013.39304

van der Ploeg, R. R., Böhm, W., and Kirkham, M. B. (1999). On the origin of the theory of mineral nutrition of plants and the law of the minimum. *Soil Sci. Soc. Am. J.* 63:1055. doi: 10.2136/sssaj1999.6351055x

van Grunsven, R. H. A., van der Putten, W. H., Bezemer, T. M., Tamis, W. L. M., Berendse, F., and Veenendaal, E. M. (2007). Reduced plant-soil feedback of plant species expanding their range as compared to natives. *J. Ecol.* 95, 1050–1057. doi: 10.1111/j.1365-2745.2007.01282.x

Vitousek, P. M., Aber, J. D., Howarth, R. W., Likens, G. E., Matson, P. A., Schindler, D. W., et al. (1997). Human alteration of the global nitrogen cylcle: sources and consequences. *Ecol. Applic.* 7, 737–750. doi: 10.1890/1051-0761(1997)007[0737:HAOTGN]2.0.CO;2

Wiegand, C. L., and Namken, L. N. (1966). Influences of plant moisture stress, solar radiation, and air temperature on cotton leaf temperature1. *Agron. J.* 58, 582. doi: 10.2134/agronj1966.00021962005800060009x

Conflict of Interest: The authors declare that the research was conducted in the absence of any commercial or financial relationships that could be construed as a potential conflict of interest.

Publisher's Note: All claims expressed in this article are solely those of the authors and do not necessarily represent those of their affiliated organizations, or those of the publisher, the editors and the reviewers. Any product that may be evaluated in this article, or claim that may be made by its manufacturer, is not guaranteed or endorsed by the publisher.

frontiers in Microbiology

ORIGINAL RESEARCH
published: 20 August 2021
doi: 10.3389/fmicb.2021.672751

Pseudomonas *palmensis* sp. nov., a Novel Bacterium Isolated From *Nicotiana glauca* Microbiome: Draft Genome Analysis and Biological Potential for Agriculture

Enrique Gutierrez-Albanchez[1,2], Ana García-Villaraco[2], José A. Lucas[2], Ignacio Horche[1], Beatriz Ramos-Solano[2] and F. J. Gutierrez-Mañero[2]*

[1] Biobab R&D S. L., Madrid, Spain, [2] Plant Physiology, Pharmaceutical and Health Sciences Department, Faculty of Pharmacy, Universidad San Pablo-CEU Universities, Boadilla del Monte, Spain

A novel *Pseudomonas*, designated strain BBB001^T, an aerobic, rod-shaped bacterium, was isolated from the rhizosphere of *Nicotiana glauca* in Las Palmas Gran Canaria, Spain. Genomic analysis revealed that it could not be assigned to any known species of *Pseudomonas*, so the name *Pseudomonas palmensis* sp. nov. was proposed. A 16S rRNA gene phylogenetic analysis suggested affiliation to the *Pseudomonas brassicae* group, being *P. brassicae* MAFF212427 ^{T} the closest related type strain. Upon genomic comparisons of both strains, all values were below thresholds established for differentiation: average nucleotide identity (ANI, 88.29%), average amino acid identity (AAI, 84.53%), digital DNA-DNA hybridization (dDDH, 35.4%), and TETRA values (0.98). When comparing complete genomes, a total of 96 genes present exclusively in BBB001^T were identified, 80 of which appear associated with specific subsystems. Phenotypic analysis has shown its ability to assimilate glucose, potassium gluconate, capric acid malate, trisodium citrate, and phenylacetic acid; it was oxidase positive. It is able to produce auxins and siderophores *in vitro*; its metabolic profile based on BIOLOG Eco has shown a high catabolic capacity. The major fatty acids accounting for 81.17% of the total fatty acids were as follows: $C_{16:0}$ (33.29%), summed feature 3 (22.80%) comprising $C_{16:1}$ ω7*c* and C $_{16:1}$ ω6*c*, summed feature 8 (13.66%) comprising $C_{18:1}$ ω7*c*, and $C_{18:1}$ω6*c* and $C_{17:0}$ cyclo (11.42%). The ability of this strain to improve plant fitness was tested on tomato and olive trees, demonstrating a great potential for agriculture as it is able to trigger herbaceous and woody species. First, it was able to improve iron nutrition and growth on iron-starved tomatoes, demonstrating its nutrient mobilization capacity; this effect is related to its unique genes related to iron metabolism. Second, it increased olive and oil yield up to 30% on intensive olive orchards under water-limiting conditions, demonstrating its capacity to improve adaptation to adverse conditions. Results from genomic analysis together with differences in phenotypic features and chemotaxonomic analysis support the proposal of strain BBB001^T (=LMG 31775^T = NCTC 14418^T) as the type strain of a novel species for which the name *P. palmensis* sp. nov is proposed.

Keywords: *Pseudomonas palmensis*, rhizobacteria, *Nicotiana glauca*, PGPB, iron mobilization, plant adaptation, drought, biostimulant

OPEN ACCESS

Edited by:
Maurizio Ruzzi,
University of Tuscia, Italy

Reviewed by:
Javier Pascual,
Darwin Bioprospecting Excellence, Spain
Munusamy Madhaiyan,
Temasek Life Sciences Laboratory, Singapore

****Correspondence:***
Beatriz Ramos-Solano
bramsol@ceu.es

Specialty section:
This article was submitted to Microbe and Virus Interactions with Plants, a section of the journal Frontiers in Microbiology

Received: *26 February 2021*
Accepted: *20 July 2021*
Published: *20 August 2021*

Citation:
Gutierrez-Albanchez E, García-Villaraco A, Lucas JA, Horche I, Ramos-Solano B and Gutierrez-Mañero FJ (2021) Pseudomonas palmensis sp. nov., a Novel Bacterium Isolated From Nicotiana glauca Microbiome: Draft Genome Analysis and Biological Potential for Agriculture. Front. Microbiol. 12:672751. doi: 10.3389/fmicb.2021.672751

INTRODUCTION

Plant growth–promoting bacteria (PGPBs) are bacteria that colonize plant roots and promote plant growth. These bacteria live in the rhizosphere and play a very important role in plant fitness; in some species, they live in symbiosis with the plant, whereas in most of them, they establish a loose relationship colonizing the root surface. Plants often depend on these PGPBs to acquire nutrients, whereas in other cases, PGPB provides protection against certain pathogens, produces phytohormones such as auxins improving plant development, or helps the plant to get adapted to biotic and abiotic stresses such as herbivores, pathogenic microorganisms, or salinity (Barriuso et al., 2005; Delfin et al., 2015; Bano and Muqarab, 2017).

Nicotiana glauca is a plant species from the *Solanaceae* family, native from South America and naturalized in the Mediterranean area and in the Canary Islands. Able to colonize poor soils, *N. glauca* contains anabasine, an alkaloid that confers some toxicity, and indicates the existence of a complex secondary metabolism, inducible and probably related to defense and plant adaptation (Sinclair et al., 2004; DeBoer et al., 2009). Therefore, wild populations of *N. glauca* colonizing harsh environments will select the best candidates for adaptation and would be a good source for putative PGPBs (Ramos-Solano et al., 2010). Many different bacterial genera have been reported to be PGPBs, and among them, *Pseudomonas* strains are very abundant. They are Gram-negative flagellated bacteria, often known because of the pigment production; they play crucial roles in soil health and plant development (Kloepper, 1992) and affect plant growth (Van Loon, 2007). Among the mechanisms frequently used by *Pseudomonas* species to benefit plant growth are siderophore production (Mavrodi et al., 2001; Rasouli-Sadaghiani et al., 2014), phosphate solubilization (Anzuay et al., 2013), or stimulation of plant protection triggering induced systemic resistance (Bakker et al., 2007; Fatima and Anjum, 2017).

As part of an ongoing research, bacteria from the rhizosphere of *N. glauca* were isolated, and strain BBB001^T was characterized. In this study, a full genetic analysis was conducted to investigate the phylogenetic relationship of strain BBB001^T within the *Pseudomonas* genus by sequencing the whole genome and comparing with those of the most similar genomes within this genus. A polyphasic characterization was also carried out. In addition, two biological assays were performed to support its potential for agriculture, one to demonstrate its ability to improve iron nutrition in tomato and another one to increase olive production under water-limiting conditions.

RESULTS

Phenotypic Characterization

Strain BBB001^T isolated from the rhizosphere of *N. glauca* was classed as a Gram-negative, non–endospore-forming rod. Strain BBB001^T grows on plate count agar (PCA) at 28°C forming circular colonies < 1 mm Ø, with smooth borders, opaque, yellowish, and creamy texture. In liquid culture (nutrient broth), color changes from pale yellow in the exponential growth phase to intense yellow on the stationary phase after 24 h at 28°C.

Temperature growth test shows that the strain BBB001^T grows in 24 h from 4 to 40°C, although at low temperatures (4°C) it takes up to 72 h. As regards pH, strain BBB001^T grows in a pH range from 6 to 10 and with a salt concentration from 2 to 6%. The optimal temperature, pH, and salinity of growth for strain BBB001^T are as follows: 28°C, pH 8, and 0% salinity.

The API20 NE reveals its ability to assimilate several substrates, namely, glucose, potassium gluconate, capric acid, malate, trisodium citrate, and phenylacetic acid; it is oxidase positive (**Table 1**). Compared to *Pseudomonas brassicae* MAFF212427^T and *Pseudomonas laurentiana* GSL-010^T, strain BBB001^T is able to degrade CAP, whereas *P. brassicae*^{T} cannot, and it is oxidase positive, whereas *P. laurentiana*^{T} is not, sharing all other metabolic capabilities with the two type strains.

According to BIOLOG ECO, strain BBB001^T is able to degrade several carboxylic acids, among which it is worth noting malic acid, hydroxybutyric acid and glucosaminic acid, the latter can also be consumed as a source of nitrogen. Among sugars, glucose-1-phosphate, cellobiose, lactose, and *N*-acetyl glucosamine stand out. As a nitrogen source, strain BBB001^T catabolizes the two amines (putrescine and phenyl ethylamine), although the consumption of some amino acids, such as serine and glycol-L-glutamic acid, is also remarkable (**Supplementary Table 2**).

The major fatty acids (>81.17% of the total fatty acids) are $C_{16:0}$ (33.29%), summed feature 3 (22.80%) comprising $C_{16:1}$ ω7*c* and $C_{16:1}$ ω6*c*, summed feature 8 (13.66%) comprising $C_{18:1}$ ω7*c*, and $C_{18:1}$ ω6*c* and $C_{17:0}$ cyclo (11.42%).

In addition, this strain resulted positive for auxins as for siderophores synthesis and negative for chitinases production.

In addition to API20 information, **Table 1** summarizes available information from the most closely related *Pseudomonas* species, confirming differences for strain BBB001^T. Interestingly, and different from BBB001^T, "*Pseudomonas qingdaonensis*" strain JJ3^T was not able to degrade D-galacturonic acid, and its temperature range runs from 4 to 37°C, whereas BBB001^T runs from 4 to 40°C (Sawada et al., 2020).

Phylogenetic Analysis

The genome of the BBB001^T strain was analyzed with the tools available at EzBioCloud. First, EzBioCloud's identification service provides proven similarity-based searches against quality-controlled databases of 16S rRNA sequences. After that, the ANI (average nucleotide identity), AAI (average amino acid identity), dDDH, and TETRA analysis were performed. Type (Strain) Genome Server (TYGS) was used to analyze the complete genome.

Estimates of the Degree of Similarity Between Genomes

(a) Phylogenetic analysis and delimitation of species based on the analysis of 16S. The size of 16S rRNA gene was 1,541 bp (MW009702). The analysis based on 16S rRNA gene indicated that the strain BBB001^T shared the highest similarity with *P. qingdaonensis* JJ3^T (100%, non-validated taxon), *P. brassicae* MAFF212427^T (99.85%), and *Pseudomonas*

TABLE 1 | Characteristics that differentiate *Pseudomonas palmensis* sp. nov. from the type strains of the most closely related *Pseudomonas* species: *Pseudomonas brassicae* MAFF212427 ^{T} (Sawada et al., 2020) and *Pseudomonas laurentiana* GSL-010 ^{T} (Wright et al., 2018).

	Strain BBB001^{T}	***Pseudomonas brassicae* MAFF 212427^{T}**	***Pseudomonas laurentiana* GSL-010^{T}**
Cell size (μm)	0.5–0.8 × 1.5–3.8	2.1 ± 0.4 × 1.2 ± 0.1	1.75–2.2 × 0.5–0.7
Isolation source	Rhizosphere (Spain)	Diseased broccoli	Seawater (Canada)
Temperature range (optimal) (°C)	4–40 (28)	4–35 (27)	10–37 (30)
NaCl optimal (%, w/v)	0	ND	0.5
Maximum NaCl (%, w/v)	6	ND	3
pH range	6–10	ND	5–10
pH optimum	8	ND	7–7.5
API20 NE			
[CAP]	+	–	+
OX	+	+	–
Saturated fatty acid			
$C_{10:0}$	–	–	0.11
$C_{12:0}$	4.02	4.00	2.66
$C_{14:0}$	0.94	–	1.76
$C_{15:0}$	–	–	0.42
$C_{16:0}$	33.29	28.10	32.29
$C_{17:0}$	–	–	0.13
$C_{18:0}$	0.52	–	0.18
Unsaturated fatty acid			
$C_{16:1}$ ω 5*c*	–	–	0.11
$C_{17:1}$, ω 8*c*	–	–	0.10
$C_{18:1}$, ω 7*c*	–	–	8.30
Branched fatty acid			
$C_{17:0}$ cyclo	11.42	7.80	1.13
$C_{18:1}$ 11 methyl ω7c	–	–	0.35
$C_{19:0}$ cyclo ω8*c*	0.81	–	–
Hydroxy fatty acid			
$C_{8:0}$ 3-OH	–	–	–
$C_{10:0}$ 3-OH	9.96	4.00	3.83
$C_{11:0}$ 3-OH	–	–	–
$C_{12:0}$ 2-OH	4.23	2.60	4.18
$C_{12:0}$ 3-OH	4.35	3.90	3.66
$C_{12:1}$ 3-OH	–	–	0.07
Summed Features*			
2	–	–	–
3	22.80	29.00	40.43
7	–	–	0.17
8	13.66	17.5	0
Utilization of:			
L-Phenylalanine	+	Unkown	–

For API20 NE results obtained in this study, all three strains were negative for NO3, TRP, GLU, ADH, URE, ESC, GEL, PNPG, GLU, ARA, MNE, MAN, NAG, MAL, GNT, and ADI and positive for GNT, GLU, MLT, CIT, and PAC. Characteristics for API20 NE and biolog plates are scored as follows: – negative reaction; + positive reaction. Fatty acid profile expressed as% (FAME): – indicates absence of the fatty acid. Summed feature represents two or three fatty acids that cannot be separated using the MIDI system. Summed feature 3 comprises $C_{16:1}$ ω7c/$C_{16:1}$ ω 6c; summed feature 8 comprises $C_{18:1}$ ω 7c/$C_{18:1}$ ω 6c.*

defluvii WCHP16^{T} (99.31%), whereas *P. laurentiana* GSL-010^{T}, *Pseudomonas japonica* NBRC 103040^{T}, and *Pseudomonas huaxiensis* WCHPS060044^{T} were between 99.00 and 99.1% (**Table 2**). A phylogenetic tree was constructed based on comparison of the most similar 16S rRNA gene sequences available in the TYGS database (**Figure 1**). Three different groups appeared in the tree: group 1 in which *Pseudomonas japonica* NBRC 103040^{T}, *Pseudomonas sinwaenesis* WCHPs060039^{T}, and *Pseudomonas ineficax* JV551A3^{T} were located; group 2, represented by *Pseudomonas alkylphenolica* KL28^{T}, *Pseudomonas huaxinesis* WCHPs060044^{T}, *Pseudomonas vranoviensis* CCM 7279^{T}, *Pseudomonas donghuensis* HYS^{T}, *Pseudomonas wandersilveriensis* CCOS 864^{T}, and *Pseudomonas tructae* SNU WT1^{T}; finally group 3, involving *P. qingdaonensis* JJ3(T), strain BBB001, *P. brassicae* MAFF212427^{T}, *P. laurentiana* GSL-010^{T}, and *Pseudomonas akapagensis* PS24^{T}. In the third group, *P. laurentiana* GSL-010^{T} and *P. akapagensis* PS24^{T} separated from the other three, showing that

TABLE 2 | Similarity of the 16S rRNA of the 30 taxa with valid names and strain BBB001^T.

Rank	Name	Type Strain (T)	Accession	Pairwise Similarity(%)	Authors
1	Pseudomonas qingdaonensis'	JJ3	PHTD01000020	100.0	Wang et al., 2019
2	*Pseudomonas brassicae*	MAFF 212427	LC514379	99.9	Sawada et al., 2020
3	*Pseudomonas defluvii*	WCHP16	KY979145	99.3	Qin et al., 2020
4	*Pseudomonas laurentiana*	GSL-010	KY471137	99.1	Wright et al., 2018
5	*Pseudomonas japonica*	NBRC 103040	BBIR01000146	99.0	Pungrasmi et al., 2008
6	*Pseudomonas huaxiensis*	WCHPs060044	MH428812	99.0	Qin et al., 2019a
7	*Pseudomonas alkylphenolica*	KL28	CP009048	98.9	Mulet et al., 2015
8	*Pseudomonas graminis*	DSM 11363	Y11150	98.8	Behrendt et al., 1999
9	*Pseudomonas donghuensis*	HYS	AJJP01000212	98.8	Gao et al., 2015
10	*Pseudomonas sichuanensis*	WCHPs060039	QKVM01000121	98.8	Qin et al., 2019b
11	*Pseudomonas rhizosphaerae*	DSM 16299	CP009533	98.6	Peix et al., 2003
12	*Pseudomonas wadenswilerensi*	CCOS 864	LT009706	98.6	Frasson et al., 2017
13	*Pseudomonas plecoglossicida*	NBRC 103162	BBIV01000080	98.6	Nishimori et al., 2000
14	*Pseudomonas wanovensis*	CCM 7279	AY970951	98.6	Tvrzova et al., 2006
15	*Pseudomonas asiatica*	RYU5	MH517510	98.6	Tohya et al., 2019a
16	*Pseudomonas taiwanensis*	BCRC 17751	EU103629	98.6	Wang et al., 2010
17	*Pseudomonas putida*	NBRC 14164	AP013070	98.5	Trevisan, 1889; Migula, 1895
18	*Pseudomonas inefficax*	JV551A3	OPYN01000008	98.5	Keshavarz-Tohid et al., 2019
19	*Pseudomonas asplenni*	ATCC 23835	LT629777	98.4	Ark and Tompkins, 1946; Savulescu, 1947
20	*Pseudomonas monteilii*	NBRC 103158	BBIS01000088	98.4	Elomari et al., 1997
21	*Pseudomonas tructae*	SNU WT1	CP035952	98.4	Oh et al., 2019
22	*Pseudomonas coleopterorum*	Esc2Am	KM888184	98.4	Menéndez et al., 2015
23	*Pseudomonas reidholzensis*	CCOS 865	LT009707	98.4	Frasson et al., 2017
24	*Pseudomonas juntendi*	BML3	MK680061	98.4	Tohya et al., 2019b
25	*Pseudomonas cremoricolorata*	1AM 1541	AB060137	98.3	Uchino et al., 2001
26	*Pseudomonas entomophila*	L48	CT573326	98.3	Mulet et al., 2012
27	*Pseudomonas mosselii*	CIP 105259	AF072688	98.3	Dabboussi et al., 2002
28	*Pseudomonas moorei*	RW10	AM293566	98.3	Cámara et al., 2007
29	*Pseudomonas lutea*	DSM 17257	JRMB01000004	98.2	Peix et al., 2004
30	*Pseudomonas helmanticensis*	OHA11	HG940537	98.2	Ramírez-Bahena et al., 2014
31	*Pseudomonas baetica*	a390	FM201274	98.2	López et al., 2012

In column 1, accession number is indicated after the species name.

P. qingdaonensis JJ3(T) and strain BBB001 grouped together, separate from *P. brassicae* MAFF212427^T, which is the closest phylogenetically related strain.

(b) The highest values of ANI and AAI (88.29 and 84.83%, respectively) were obtained with the genome of the species *P. brassicae* MAFF212427^T. The highest value of dDDH (35.4%) and the lower intergenomic distance (0.11) was obtained when comparing strain BBB001^T and *P. brassicae* MAFF212427^T (**Table 1**). G + C content shows a difference of 0.65% between genomes of these two strains. TETRA values were between 0.86 and 0.988, not showing a significant resemblance between the genome of strain BBB001^T and the other 24 genomes (**Table 3**). Comparison with the genome of *P. qingdaonensis* JJ3(T) (non-validated taxon) showed the highest values (**Table 3**).

Phylogenetic Analyses Based on Complete Genome Sequences

The genome of strain BBB001^T [1] (WGS: JAFKEC000000000) was compared against all type strain genomes available in the TYGS database *via* the MASH algorithm, a fast approximation of intergenomic relatedness (Ondov et al., 2016), and the 10 type strains with the smallest MASH distances chosen per user genome resulting in a phylogenetic tree (**Figure 2**).

The comparative analysis of the complete genomes identified a total of 79 genes present exclusively in strain BBB001^T (**Supplementary Table 2**). Among these genes (**Figure 3**), transcription-related genes were the most abundant (18) representing 23% or these unique genes; 16 genes were not associated with specific subsystems (20%); 6 were associated with cell wall, membrane, and envelope synthesis (8%); and 6 (8%) were related to inorganic transport and metabolism (eggnog-emapper). Further analysis was carried out on genes related to inorganic transport and metabolism, and two genes related to the uptake and iron metabolism were identified by blast in antiSMASH 5.0[2] secondary metabolism database; this is consistent with data from phenotypic characterization.

Biological Assays

The biological assay on iron-starved tomato was conducted to proof the biological effect associated with iron absorption

[1]https://www.ncbi.nlm.nih.gov/bioproject/PRJNA705568

[2]https://antismash.secondarymetabolites.org/#!/start

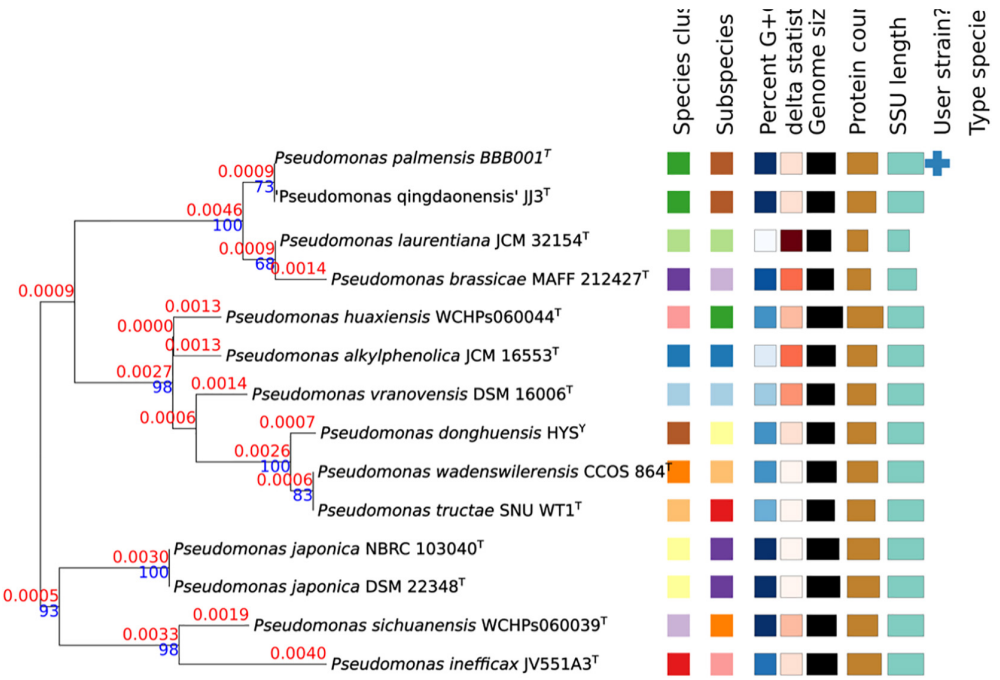

FIGURE 1 | Tree inferred with FastME 2.1.6.1 (Lefort et al., 2015) from GBDP distances calculated from 16s rRNA gene sequences. The branch lengths are scaled in terms of GBDP distance formula d5. The blue numbers are GBDP pseudo-bootstrap support values > 60% from 100 replications, with an average branch support of 80.9%. The branch length values (in red) represent the evolutionary time between two nodes. Unit: substitutions per sequence site. The tree was rooted at the midpoint (Farris, 1972).

(Fe^{3+}) and metabolism unique genes of this strain (**Figure 3**). Data showed that both strain BBB001^T and its culture media free of bacteria (chelate) supplemented with non-soluble iron were able to revert chlorosis due to iron deficiency, according to visual evaluation (data not shown). Strain BBB001^T significantly increased dry weight (**Figure 4A**), Fe concentration (**Figure 4B**), and photosynthetic pigments (chlorophylls and carotenes, **Figure 4C**), against the positive control (Fe-EDTA) and the negative control. The chelate produced by the bacteria significantly increased all parameters, except the increase in dry weight, which was non-significant; increases were not as marked as with the bacteria (**Figure 4**).

The biological assay in the intensive olive orchard was conducted aiming to demonstrate the ability of the strain to improve plant adaptation to stress situations, decreasing water input by 25% of regular watering. Results showed a statistically significant increase in olive yield up to 30% (kg/ha), as well as in oil production (**Figure 5**). Interestingly, the production achieved with strain BBB001^T under water-limiting conditions (12,000 kg/ha) reached similar values to controls under regular water regime (data not shown).

DISCUSSION

Strain BBB001^T isolated from the rhizosphere of *N. glauca* is able to improve plant yield in olive trees under water-limiting conditions and to efficiently supply iron to tomato under iron-limiting conditions, demonstrating its good potential for agriculture. Although the beneficial effects in plants have been described before for other *Pseudomonas* (Kloepper, 1992; Mavrodi et al., 2001; Bakker et al., 2007; Van Loon, 2007; Anzuay et al., 2013; Rasouli-Sadaghiani et al., 2014; Fatima and Anjum, 2017), the multiphasic genomic analysis has evidenced that this is a new strain with beneficial properties for agriculture, for which the name *Pseudomonas palmensis* sp. nov. has been proposed.

The ability of *N. glauca* to select the best strains to improve adaptation to harsh environments has been evidenced consistent with previous studies (Ramos-Solano et al., 2010). Its complex secondary metabolism, inducible and probably related to defense and plant adaptation (Sinclair et al., 2004; DeBoer et al., 2009), together with scarcity of nutrients, is key to select strains that play crucial roles in soil health and plant development. In line with this statement, strain BBB001^T was positive for auxins and for siderophore production. The ability to produce auxins is very common and is related to increases in root surface, which provide plants with an enhanced capacity to absorb water and nutrients and therefore increased growth potential (Gutierrez Mañero et al., 1996).

The carbon source utilization fingerprint characteristic of strain BBB001^T indicates a great adaptive capacity to survive in the rhizosphere of plants, quickly metabolizing organic acids and carbohydrates released by roots, which makes this strain a good root colonizer, one of the traits necessary for effective PGPBs (Posada et al., 2018). This is consistent with bioassay results, as

TABLE 3 | Similarity of the 24 genomes with strain BBB001^T genome.

Rank	Name	genome accesion number	ANI%	AAI%	dDDH	Intergenomic distance	Difference G + C (%)	TETRA
1	Pseudomonas qingdaonensis' JJ3(T)	PHTD00000000.1	99.2	95.0	93.4	0.0855	0.14	0.9998
2	*Pseudomonas brassicae* MAFF 212427(T)	LC514391.1	88.3	84.5	35.4	0.1167	0.65	0.9880
3	*Pseudomonas laurentiana* JCM 32154(T)	JAAHBT000000000.1	81.6	81.0	25.1	0.1732	4.35	0.8680
4	*Pseudomonas japonica* NBRC 103040(T)	NZ BBIR00000000.1	83.6	78.0	26.7	0.1618	0.10	0.9600
5	*Pseudomonas alkylphenolica* KL28(T)	NZ CP009048.1	83.4	80.0	27.1	0.1597	3.43	0.9384
6	*Pseudomonas graminis* DSM 11363(T)	NZ FOHW00000000.1	77.9	72.5	22.5	0.1951	3.8	0.9040
7	*Pseudomonas donghuensis* HYS(T)	NZ AJJP00000000.1	84.2	78.0	27.7	0.1554	1.64	0.9699
8	*Pseudomonas sichuanensis* WCHPs060039(T)	NZ QKVM00000000.1	82.0	76.8	25.3	0.1716	0.29	0.9840
9	*Pseudomonas rhizosphaerae* DSM 16299 (T)	CP009533.1	79.7	72.6	23.5	0.1859	2.06	0.9550
10	*Pseudomonas wadenswilerensis* CCOS 864(T)	NZ UIDD00000000.1	84.1	78.8	27.7	0.1556	1.67	0.9680
11	*Pseudomonas plecoglossicida* NBRC 103162(T)	NZ BBIV00000000.1	81.9	74.9	25.1	0.1732	1.26	0.9820
12	*Pseudomonas vranovensis* CCM 7279(T)	NZ AUED00000000.1	83.3	81.1	26.6	0.1630	2.53	0.9610
13	*Pseudomonas asiatica* RYU5(T)	NZ BUF01000001.1	81.9	77.0	25.3	0.1718	1.24	0.9760
14	*Pseudomonas taiwanensis* BCRC 17751(T)	NZ AUEC00000000.1	81.0	77.9	24,00	0.1823	2.19	0.9610
15	*Pseudomonas putida* NBRC 14164(T)	NC 021505.1	81.4	76.3	25,00	0.1745	1.72	0.9700
16	*Pseudomonas inefficax* JV551A3(T)	OPYN00000000.1	81.8	75.8	25.5	0.1706	1.21	0.9718
17	*Pseudomonas monteilii* NBRC 103158(T)	NZ BBIS00000000.1	81.5	77.1	24.7	0.1768	2.37	0.9670
18	*Pseudomonas coleopterorum* LMG 28558(T)	FNTZ00000000.1	79.6	74.3	23.4	0.1866	2.17	0.9542
19	*Pseudomonas reidholzensis* CCOS 865(T)	UNOZ00000000	82.1	76.2	25,00	0.1741	0.03	0.9700
20	*Pseudomonas cremoricolorata* 1AM 1541(T)	NZ AUEA00000000.1	80.7	73.9	23.6	0.1856	0.55	0.9531
21	*Pseudomonas mosselii* CIP 105259(T)	NZ MRVJ00000000.1	82.3	77.4	25.4	0.1715	0.38	0.9810
22	*Pseudomonas moorei* DSM 12647(T)	NZ FNKJ01000003.1	79.4	72.8	23.6	0.1850	4.40	0.9120
23	*Pseudomonas lutea* DSM 17257(T)	JRMB00000000.1	77.4	74.4	22.5	0.1946	3.91	0.8920
24	*Pseudomonas baetica* a390(T)	PKLC00000000.1	78.8	73.4	22.9	0.1916	5.30	0.8681

For each genome, its length [in base pairs (bp)], number of annotated genes, and the values of ANI, AAI, dDDH, intergenomic distance, G + C difference, and TETRA index estimated in the comparison with the genome of Pseudomonas BBB001^T. In column 1, the genome accession number is indicated after the species name in RefSeq.

field-grown olives evidence an increase in yield due to bacterial effects, probably due to an efficient colonization.

As there is an increasing number of PGPBs being described, many of which belong to *Pseudomonas*, a multiphasic approach to study its genome was taken to unravel the hidden information of this strain with such a good performance. First, analysis of the 16S rRNA revealed a high similarity (>99%) to five species with validated names. Sequencing of the 16S ribosomal gene (16S rRNA) is the basic tool in the current system classification of bacterial species. Generally, similarity values for the 16S rRNA gene less than 98.65 to 99% are accepted for different species (Kim et al., 2014). However, the 16S rRNA gene may offer limited resolution power as it shows a low capacity for discrimination between closely related species. Furthermore, some species may show very similar sequences of 16S rRNA (>99%), despite being clearly different according to DDH values (Ash et al., 1991; Rosselló-Móra and Amann, 2001). Consistently, ANI and AAI values confirmed differences to existing validated genomes. The values of ANI and AAI represent a robust measure of the evolutionary distance between genomes, as it has been empirically verified that ANI and AAI values of 95 to 96% equals a DDH value (DNA–DNA hybridization) of 70%, commonly used to delimit prokaryotic species (Konstantinidis and Tiedje, 2005; Richter and Rosselló-Móra, 2009; Kim et al., 2014). The closer related strain genomes will show similar frequencies of tetranucleotide use, with correlation indexes (TETRA) equal to or greater than 0.99 (Teeling et al., 2004; Richter and Rosselló-Móra, 2009). The highest values of ANI and AAI obtained in the comparison with the genome of the species *P. brassicae* were well below the 95% threshold established for considering that both genomes belong to the same species. The highest value of dDDH and the lower intergenomic distance were obtained when comparing strain BBB001^T and *P. brassicae* MAFF212427^T (**Table 3**), being the value of dDDH much lower than the 70% necessary to be able to assign strain BBB001^T to this species. This result is also corroborated by TETRA values, which did not show a significant resemblance between the genome of strain BBB001^T and the other genomes with values less than 0.99%. In the phylogenetic tree constructed in TYGS with complete genome data (**Figure 2**), strain BBB001^T is closely related with *P. brassicae* MAFF212427^T and *P. qingdaonensis* JJ3^T. In this case, the analysis establishes a closer relationship between strain BBB001^T and *P. qingdaonensis* JJ3^T, which taxonomic name is not validated yet[3]. It is likely therefore that the repertoire of accessory genes of strain BBB001^T is more like that of *P. qingdaonensis* JJ3^T than that of *P. brassicae* MAFF212427^T.

Comparison of the most similar complete genomes at Pan-seq revealed novel regions of this strain, a total of 96 genes were present exclusively in strain BBB001^T, and 80 of these genes appear associated with specific subsystems. Among these genes

[3]https://lpsn.dsmz.de/species/pseudomonas-qingdaonensis

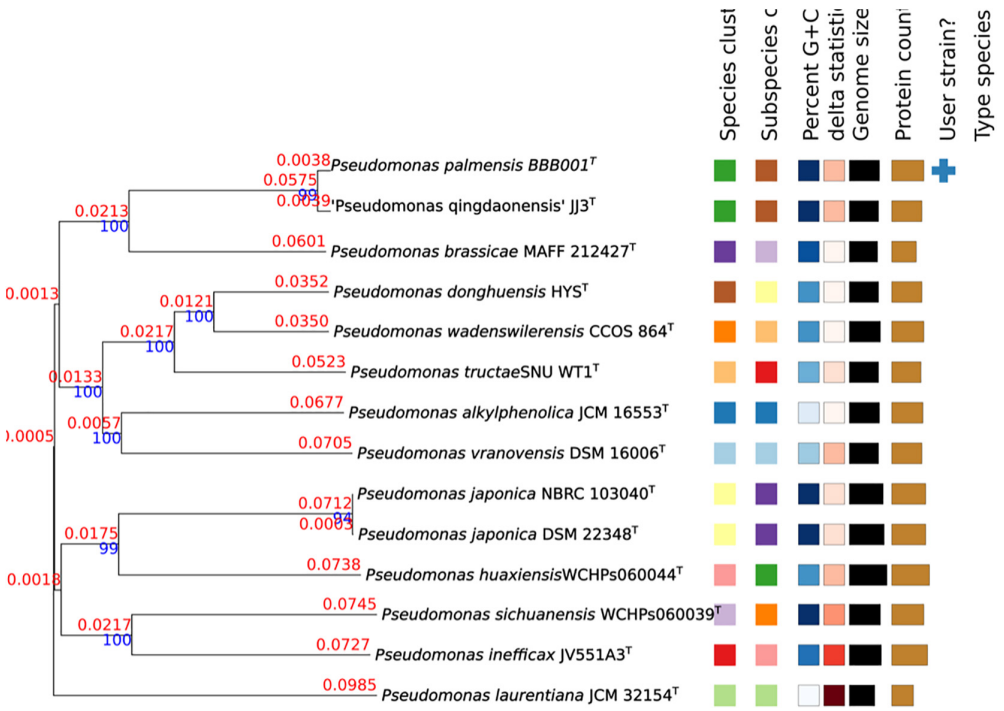

FIGURE 2 | Phylogenetic tree constructed in TYGS. Tree inferred with FastME 2.1.6.1 (Lefort et al., 2015) from GBDP distances calculated from genome sequences. The branch lengths are scaled in terms of GBDP distance formula d5. The numbers above the branches are GBDP pseudo-bootstrap support values > 60% from 100 replications, with an average branch support of 94.3%. The branch length values represent the evolutionary time between two nodes. Unit: substitutions per sequence site. The tree was rooted at the midpoint (Farris, 1972).

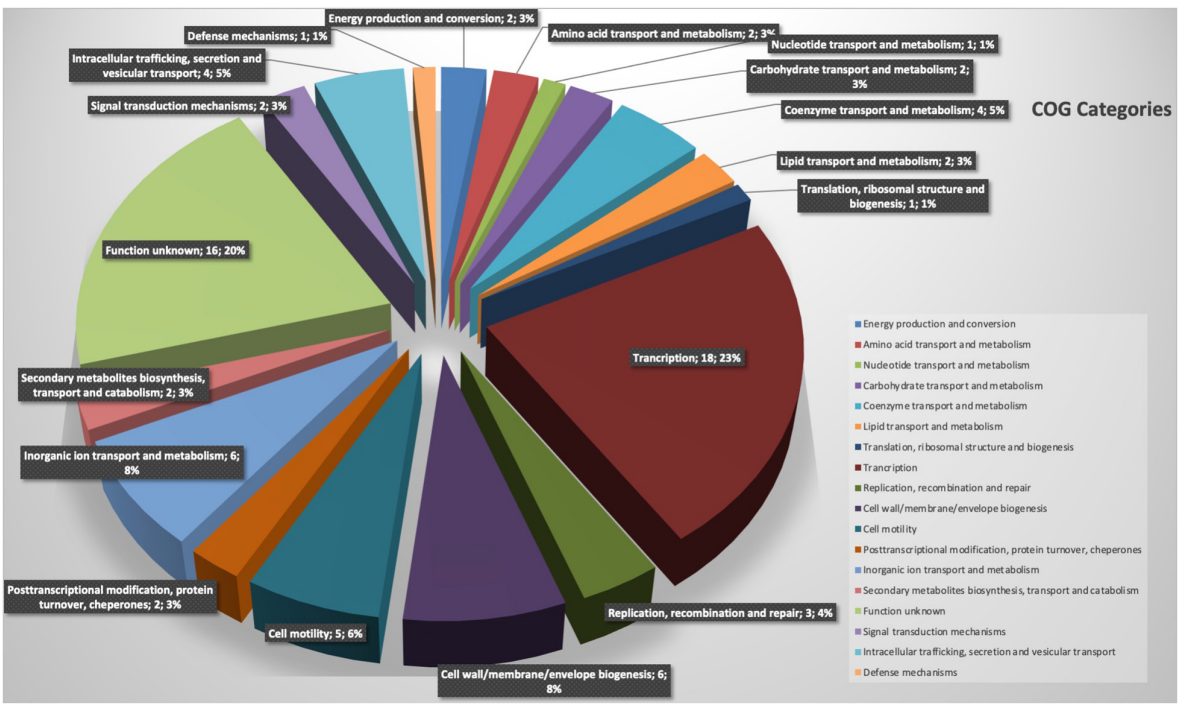

FIGURE 3 | Representation of functional categories of novel regions of *strain* BBB001T.

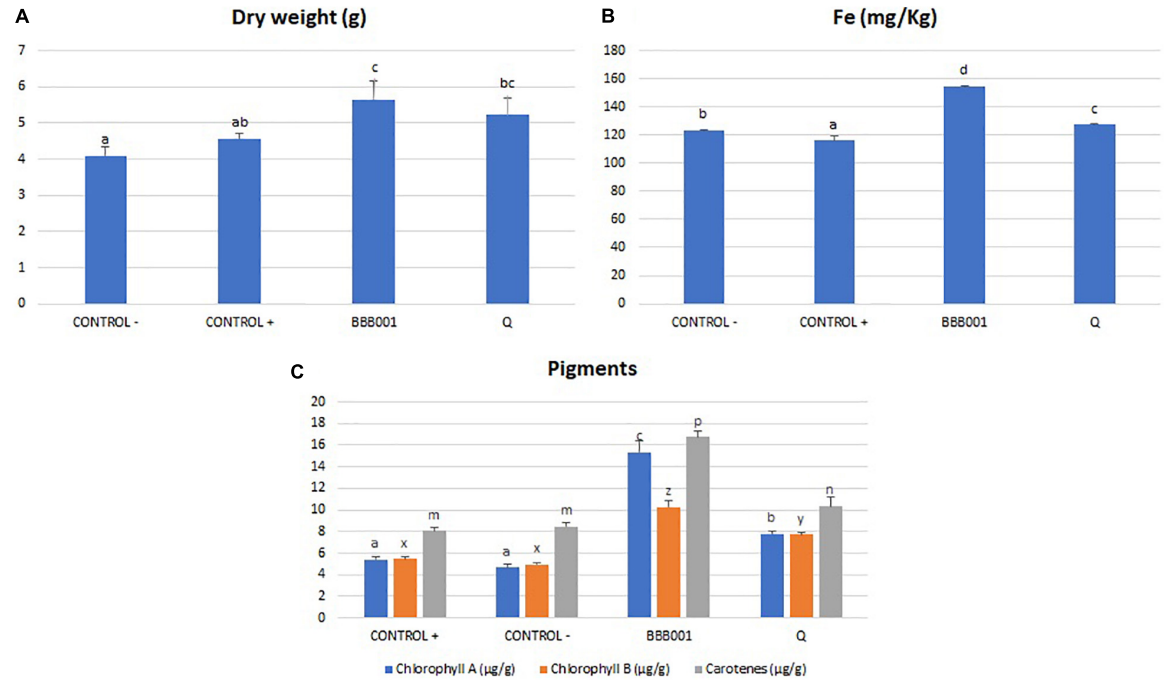

FIGURE 4 | (A) Dry weight of tomato plants (g). **(B)** Iron plant content (mg/kg). **(C)** Pigment concentration (mg/g) on tomato leaves. Different letters denote statistically significant differences according to LSD test ($p < 0.05$) for chlorophyl a (a, b, and c), chlorophyl b (x, y, and z), and carotenes (m, n, and p).

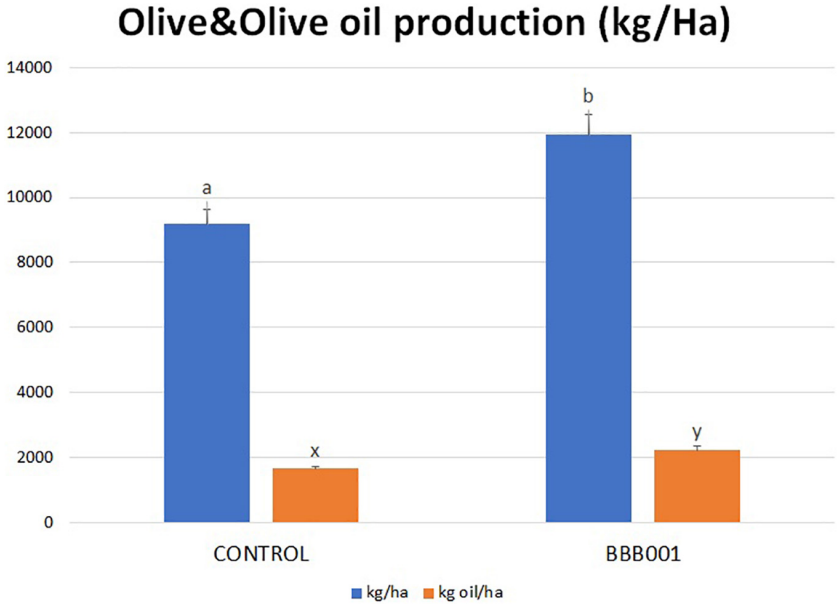

FIGURE 5 | Olive and olive oil production of *Olea europaea* trees (kg/ha). Different letters denote statistically significant differences according to LSD test ($p < 0.05$) for olive yield (a, b), oil yield (x, y).

(**Figure 3**), those related to the uptake and iron metabolism were found (Coulton et al., 1983; Braun, 2003; Miethke and Marahiel, 2007) and correlate with data from phenotypic characterization.

Biological assays were designed to evidence the potential of the strain for agriculture based on its unique genes related to iron metabolism on the one hand and of its general performance. The biological assay on iron-starved tomato was conducted based on information about unique genes of this strain related to iron absorption (Fe^{3+}) and metabolism (**Figure 3**). Data showed that both BBB001^T and its culture media free of bacteria

(chelate) supplemented with non-soluble iron were able to revert chlorosis due to iron deficiency, according to visual evaluation, significantly increasing dry weight, iron concentration and photosynthetic pigments in iron-starved tomatoes, being the bacteria much more efficient than the chelate (**Figure 4**).

The differences between the bacteria and the culture media suggest that the increased iron mobilization is strongly improved when the bacteria are present, consistent with the multitarget response proposed for beneficial bacteria (Ilangumaran and Smith, 2017). In this type of response, bacteria improve iron mobilization probably supported by an increased root development that allows an increase in absorption surface (Gutierrez Mañero et al., 1996), a response attributed to auxin concentration, also present in the unique gene set of the strain. The beneficial effect on iron nutrition also shows an increase of photosynthetic pigments on the shoot, being especially striking the increase on chlorophyll a, the key player on light reactions as it is mainly located on photosystems. The increase in photosynthetic potential is evidenced on growth (dry weight), with the highest increase in dry weight on the bacteria treated plants, confirming that not only iron limits plant growth and supporting the better performance of bacteria in agriculture, where many environmental factors change along plant growth cycle.

The biological assay in the intensive olive orchard was conducted aiming to demonstrate the ability of the strain to improve plant adaptation to stress situations, especially the lack of water, as this situation becomes more and more frequent nowadays. The mechanisms involved in plant adaptation to stress are common to many other stressful situations such as salinity or biotic stress, through common signaling pathways (Martin-Rivilla et al., 2020). Plant adaptive mechanisms involve ionic homeostasis and modulation of redox balance among others (Kangasjärvi et al., 2014; Kollist et al., 2019). Olive yield (kg/ha) and oil production increased significantly (up to 30%) despite the 25% decrease of water input (**Figure 4**). The registered increase in oil was due to two factors: the increment in olive production and the increase in fat yield, reaching similar values to controls under regular water regimen (data not shown).

These results support the suitability of this strain to activate adaptive mechanisms in different plant species, from herbaceous to woody plant species, as well as its versatility to different environmental stress factors, evidencing its multitarget power (Ilangumaran and Smith, 2017).

Genomic analysis on strain BBB001 revealed that it could not be assigned to any known species of *Pseudomonas*, so the name *P. palmensis* sp. nov. was proposed for strain BBB001^T. A 16S rRNA gene sequence–based phylogenetic analysis suggested that the strain BBB001^T was affiliated with the *P. brassicae* group with *P. brassicae* MAFF212427^T as the most closely related type strain (99.85% similarity). Genomic comparisons of strain BBB001^T with the type strain species *P. brassicae* MAFF212427^T were all below thresholds established for differentiation. In the comparative analysis of complete genomes, a total of 96 genes present exclusively in strain BBB001^T were identified, 80 of which appear associated with specific subsystems.

Also, the novel taxon possesses several phenotypic traits related to beneficial plant traits, like auxin production or iron mobilization. Results obtained in iron-starved tomato and water-limited olive orchards confirm the potential of this strain for agriculture. On the one hand, it is efficient for iron mobilization under nutrient stress and adverse conditions, consistent with the specific and unique set of genes associated with iron metabolism, so it can be used to develop organic Fe supplies for sustainable agriculture, both the strain and its metabolites. On the other hand, it can improve adaptation to water-limiting conditions while keeping high productivity, so it is an excellent candidate to develop biotechnological products for agriculture under harsh conditions. Finally, the effects recorded in herbaceous species such as tomato, as well as in a woody species such as olive, confirm its wide scope capability to succeed in most agronomic crops, as this strain can trigger plant metabolism in different species.

In summary, all phenotypic and genomic characterization of the novel strain BBB001^T reveals a distinct and well-differentiated species from all *Pseudomonas* species with validated reference taxons and, more precisely, different from *P. brassicae* MAFF212427^T.

Thus, based on the polyphasic approach, we describe a novel *Pseudomonas* species, for which the name *P. palmensis* sp. nov. is proposed, based on the geographical origin of isolation, Las Palmas de Gran Canarias (Islas Canarias, Spain). The type strain is strain BBB001^T (= LMG 31775 = NCTC 14418).

Description of *Pseudomonas palmensis* sp. nov

Pseudomonas palmensis (palm.en'sis), N.L. masc./fem. adj. palmensis, belonging to Las Palmas de Gran Canaria, Spain, from which the type strain was isolated.

Cells are Gram-reaction negative, aerobic, rod-shaped bacteria ranging between 0.5 and 0.8 μm × 1.5–3.8 μm long, non–endospore-forming rods. Colonies grow on PCA at 28°C forming circular colonies < 1 mm Ø, with smooth borders, opaque, yellowish, and creamy texture. In liquid culture (nutrient broth), color changes from pale yellow in the exponential growth phase to intense yellow on the stationary phase after 24 h at 28°C. Growth occurs at 4 to 40°C in 24 h but not at 42°C. As regards pH, strain BBB001^T grows in a pH range from 6 to 10 and with a salt concentration from 2 to 6%. The optimal temperature, pH, and salinity of growth for BBB001^T are 28°C, pH 8, and 0% salinity. It is able to assimilate glucose, potassium gluconate, capric acid malate, trisodium citrate, and phenylacetic acid; it is oxidase positive. Its metabolic profile based on BIOLOG Eco shows a high catabolic capacity. It is able to produce auxins and siderophores, but not chitinases. The major fatty acids (> 81.17% of the total fatty acids) are $C_{16:0}$ > summed feature 3 ($C_{16:1}\omega7c/C_{16:1}$ $\omega6c$), > summed feature 8 ($C_{18:1}\omega7c/C_{18:1}\omega6c$) > $C_{17:0}$ cyclo.

The strain BBB001^T was isolated form the rhizosphere of *N. glauca* L. in Las Palmas de Gran Canaria Spain, in 2017. The genomic DNA G + C content of the type strain is 64.05%. The draft genome and 16S rRNA gene

sequences of the strain BBB001^T have been deposited at the NCBI GenBank under accession numbers MW009702 and JAFKEC000000000, respectively. The type strain is BBB001^T (= LMG 31775 = NCTC 14418).

MATERIALS AND METHODS

Origin of Bacteria

The bacterial screening was carried out over the rhizosphere of wild populations of *N. glauca* in Las Palmas de Gran Canaria (Islas Canarias, Spain; Coordinates UTM: 28°01′36.8″ N 15°23′19.7W) in December 2017. The soil intimately adhered to roots, and the thinner roots (diameter 1–2 mm) of four plants were pooled at random and constituted a replicate; four replicates were sampled. All materials were brought to the laboratory in plastic bags at 4°C. One gram of rhizosphere soil and thinner roots were suspended in 10 mL sterile distilled water and homogenized for 1 min in an Omni Mixer. One hundred microliters of the soil suspension was used to prepare serial 10-fold dilutions in a final volume of 1 mL; 100 μL was plated on Standard Methods Agar (Pronadisa Spain) and incubated for 4 days at 28°C. Individual colonies were selected after 36 h. To avoid duplication, isolated colonies were marked on the plate after selection. Eighty colony-forming units (cfu) were selected from each serial-dilution series, that is, from each replicate (four), constituting 320 cfu. All were isolated and grouped according to Gram staining, morphological characteristics, and sporulating capacity into four parataxonomic groups: Gram-positive endospore-forming bacilli, Gram-positive non–endospore-forming bacilli, Gram-negative bacilli, and other morphologies were grouped under "Others." All isolates were kept at −20°C on glycerol: water (1:4) (Ramos-Solano et al., 2010). Our bacterium was isolated from these dilutions and was kept at −20°C on glycerol: water (1:4).

Phenotypic Characterization

Our bacterium was tested for *in vitro* production of auxins, (Benizri et al., 1998), siderophores (Alexander and Zuberer, 1991), and chitinases (Rodríguez-Kábana et al., 1983; Frändberg and Schnürer, 1998) using specific culture media in which a color change reveals the biochemical trait.

To test pH and salt tolerance rates of BBB001^T, the following procedure was followed. Growth was tested in presence of 0 to 8% (wt/vol) NaCl (at intervals of 1%) and at pH 4 to 10 (at intervals of 0.5 pH units) by supplementing TSB with appropriate buffer systems (pH 4–5.5, 0.1 M citric acid/0.1 M sodium citrate; pH 6–9, 0.1 M KH_2PO_4/0.1 M NaOH; pH 8.5–10, 0.1 M $NaHCO_3$/0.1 M Na_2CO_3 (Xu et al., 2005). After autoclaving, pH medium was adjusted by the addition of NaOH/HCl 1 M before sterile filtration (pore size 0.22 μm). Analyses were carried out at 28°C for 48 h by shaking at 140 revolutions/min (rpm) in an orbital shaker and measuring OD_{600} nm every 2 h. Each well contained 200 μL of the selected medium and was inoculated at a dilution of 1:1,000 with an overnight culture of cells grown in unmodified TSB at 28°C for 24 h. Periphery pH and NaCl growth conditions previously obtained were also studied, using 5-mL tubes at 28°C for 1 week. Growth at 4 to 42°C was tested in tubes containing 7 mL TSB with shaking at 140 rpm for 8 days. All strains were precultured overnight at 28°C with TSB before suspending one loop of cells in 1 mL TSB as inoculation culture. The 7-mL test tubes were inoculated with 10 μL of the inoculation culture. The optimal growth temperature was determined using the SPECTROstar nano (BMG Labtech) and TSB under the same conditions as used for testing growth at different NaCl concentrations and pH. The range for optimal growth was determined by the length of the lag phase until the cultures achieved an increase in OD_{600} of 0.2.

The metabolic capabilities were evaluated by API 20NE and BIOLOG ECO according to manufacturer instructions. The bacterial suspension was prepared from bacterial biomass grown for 24 h in PCA resuspended in $MgSO_4$ 10 mM to achieve 95% of transmittance at 620 nm. Biolog ECO plates were then inoculated with 150 μL per well. Plates were incubated at 25°C in darkness. Each well contained a substrate and tetrazolium salts, which turn violet when reduced by the activity of microorganisms. Three replicates per treatment and sampling time were performed. Kinetics of average well color development (AWCD) were used to perform a curve and to determine bacterial speed using the 31 provided substrates. From this curve, 7-day incubation time was chosen to represent the catabolic profile of the strain.

Fatty acid composition was determined according to MIDI microbial identification system (Sasser, 1990) on an Agilent 6850 gas chromatograph, provided with the MIDI microbial identification system with method TSBA6 (MIDI, 2008). This fatty acid profile was obtained from strain BBB001 grown in nutrient agar, at 28°C, for 24 h.

Phylogenetic Analysis

To investigate the phylogenetic relationship of strain BBB001^T with other species of *Pseudomonas* genus and define the taxonomic allocation, three main strategies were used:

- Estimate the similarity between genomes: (a) phylogenetic analysis and delimitation of species based on the analysis of 16S rRNA and (b) ANI, AAI, hybridization DNA–DNA *in silico* or dDDH (digital DNA–DNA hybridization), difference in the content of guanine-cytosine (G + C), and frequency of tetranucleotide use.
- Phylogenetic analysis at complete genome level.
- Characterization of novel regions.

Libraries Preparation

The DNA extraction from the lyophilized culture was performed with the REAL MicroSpin DNA Isolation kit (Durviz), strictly following the manufacturer's instructions. A sample that did not contain a bacterial culture was processed in parallel with the other samples to verify the absence of cross contamination during DNA extraction. DNA was quantified using fluorometric methods (Qubit, Thermo Fisher Scientific).

Nextera XT Library Prep kit (Illumina) was used to prepare the library, following the manufacturer's instructions. The fragment size distribution was then checked on an Agilent 2100

Bioanalyzer, using the Agilent DNA 1000 kit. Qubit dsDNA HS kit was used to check library concentration.

Based on these concentration data, the library was equimolarly mixed and loaded in a fraction of a MiSeq Paired-End 300 (Illumina) run.

Quality Analysis and Sequencing Data

The FastQC 0.11.3 program was used to analyze the quality of the sequencing. Trimmomatic 0.36 (Bolger et al., 2014) was used to remove the adapters (ILLUMINACLIP option) and poor-quality regions (SLIDINGWINDOW: 5: 30). All sequences smaller than 80 base pairs were also discarded.

De novo Assembly and Quality Analysis

Short sequences were assembled *de novo* using SPAdes 3.10 (Bankevich et al., 2012). SPAdes is based on the creation of graphs using the algorithm known as de Bruijin using different kmers. As recommended in the manual, kmers 21, 33, 55, 77, 99, and 127 were used; the –cov-cutoff option was set to auto and the –careful option was enabled. SPAdes use the information from the two pairs of files generated in the sequencing to transform contigs into scaffolds by introducing Ns between the contigs that can be joined.

The quality of the assemblies was analyzed using the QUAST 4.4 program (Gurevich et al., 2013).

The sequences of each sample were mapped in the assembly generated by SPAdes, to determine the coverage of each genomic region using BWA 0.7.12 (Li and Durbin, 2010). SAMtools 0.1.19 (Li et al., 2009) was used to determine the depth of sequencing and eliminate secondary or poor-quality mappings.

Qualimap 2.2.1 (Okonechnikov et al., 2015) was used to observe how the coverage is distributed throughout the genome and, in addition, to extract the specific coverage of each scaffold. To avoid possible inconsistencies or the presence of contaminating sequences, those scaffolds with less than 10 X coverage were discarded from the successive analyses. In addition, those scaffolds with a length less than 1,000 base pairs were also eliminated.

The sequencing of the complete genome on the Illumina platform MiSeq PE300 generated 986,724 sequences and a total of 290 megabases (Mb). The sequences obtained after applying the quality filters were assembled *de novo* to create larger sequences (scaffolds). Strain BBB001^T genome assembly generated 128 scaffolds with a total length of 5.91 Mb. The mapping of the sequences against the assembled genome confirmed that 99.94% of the sequences obtained for strain BBB001^T could be used for the generation of the assembly.

Estimates of the Degree of Similarity Between Genomes

Phylogenetic Analysis and Delimitation of Species Based on the Analysis of 16S

16S rRNA sequences were BLAST-queried against all strains with a validated name in the reference database at the Ezbiocloud website.

ANI and AAI

The first stage of this analysis consists in the comparison at the nucleotide (ANI) and amino acid (AAI) level of strain BBB001^T genome with all complete genomes available in the EzBiocloud database for similar genomes according to the 16S analysis previously performed. The estimates of the nucleotide identity index (ANI) were calculated using[4]. The amino acid content (AAI) was calculated at http://enve-omics.ce.gatech.edu/aai/. Values below 95% indicate a new species (Richter and Rosselló-Móra, 2009; Kim et al., 2014).

dDDH and Content in G + C

Based on the results of the previous section, the 26 genomes located in the fourth quartile of the distribution of the ANI values were selected (i.e., predictably, the most closely related to strain BBB001^T), to calculate the intergenomic distances and the dDDH indexes, using the GGDC web server (Genome-to-Genome Distance Calculator). This server also calculates the difference in G + C content of genomes analyzed. Values less than 70% are indicative of significant differences (Richter and Rosselló-Móra, 2009; Kim et al., 2014).

Frequencies of Use of Tetranucleotides

The JSpecies software (Richter and Rosselló-Móra, 2009) was used to calculate the differences in tetranucleotide usage profiles between the genome of strain BBB001^T and the 26 most related genomes. Values greater than 99% are indicative of significant differences (Teeling et al., 2004; Richter and Rosselló-Móra, 2009).

Phylogenetic Analyses Based on Complete Genome Sequences

The genome sequence of BB001 was uploaded to the TYGS, a free bioinformatics platform available under https://tygs.dsmz.de, for a whole genome-based taxonomic analysis (Meier Kolthoff and Göker, 2019).

First, BB001 genome was compared against all type strain genomes available in the TYGS database *via* the MASH algorithm, a fast approximation of intergenomic relatedness (Ondov et al., 2016), and the 10 type strains with the smallest MASH distances chosen per user genome. This was used as a proxy to find the best 50 matching type strains (according to the bitscore) for each user genome and to subsequently calculate precise distances using the Genome BLAST Distance Phylogeny (GBDP) approach under the algorithm "coverage" and distance formula d5 (Meier-Kolthoff et al., 2013). These distances were finally used to determine the 10 closest type strain genomes for each of the user genomes.

For the phylogenomic inference, all pairwise comparisons among the set of genomes were conducted using GBDP and accurate intergenomic distances inferred under the algorithm "trimming" and distance formula d5 (Meier-Kolthoff et al., 2013). One hundred distance replicates were calculated each. Digital DDH values and confidence intervals were calculated using the recommended settings of the GGDC 2.1 (Meier-Kolthoff et al., 2013).

[4]https://www.ezbiocloud.net/tools/ani

The resulting intergenomic distances were used to infer a balanced minimum evolution tree with branch support *via* FASTME 2.1.6.1 including SPR postprocessing (Lefort et al., 2015). Branch support was inferred from 100 pseudo-bootstrap replicates each. The trees were rooted at the midpoint (Farris, 1972) and visualized with PhyD3 (Kreft et al., 2017).

Characterization of *Pseudomonas* BBB001^T Novel Regions

The novel regions were determined using the web server Pan-seq[5]. The Novel Region Finder of this software currently identifies any genomic regions present in any of the "Selected Query" sequences (genomes of the 26 species closer in EzBiocloud) that are not present in any of the "Selected Reference" sequences (genome of BB001) and returns these regions in multi-fasta format. These comparisons are done using the nucmer program from MUMmer v3. Annotations of novel sequences were computed using eggnog-mapper (Huerta-Cepas et al., 2017) based on eggNOG 4.5 orthology data (Huerta-Cepas et al., 2018).

Biological Assays Experimental Set Up

Iron Mobilization on Tomato

Tomato (*Solanum lycopersicum* L.) seeds were germinated in cocopeat with 24°C/19°C (day/night), and 15-h/9-h light–dark and kept in the greenhouse under controlled conditions throughout the 12 weeks of the experiment. Four treatments were used in this experiment: (1) control + (Fe-EDTA), (2) control− (no iron, no bacterial treatment), (3) strain BBB001^T, and (4) the culture media free of bacteria [chelate (Q) produced by BBB001^T]; to obtain treatments 3 and 4, strain was inoculated on nutrient broth and was grown for 24 h at 28°C under shaking, and then the culture media was centrifuged at 4,000 rpm, and the supernatant was treatment 4 (chelate), and treatment 3 was made by resuspending cells in the same volume of $MgSO_4$ 10 mM solution. A total of 96 plants arranged in three replicates with eight plants each per treatment. Plants were grown under iron deficiency conditions achieved by washing substrate with bicarbonate buffer pH 8.5 to bring substrate to basic pH preventing iron absorption. After sowing, plants were watered twice a week with bicarbonate buffer pH 8.5 to maintain a high pH and with Hoagland without iron once a week. When chlorosis appeared (6 weeks after sowing), bacteria were delivered to plant roots by soil drench supplemented with iron ($FeCl_3$). Three doses were delivered every 2 weeks; each dose consisted of 10 mL of strain BBB001^T (or chelate), at 1×10^8 cfu/mL per plant supplemented with $FeCl_3$ in an equivalent concentration of iron per plant to even that of Fe-EDTA. Two days after the last inoculation, plants were harvested to analyze dry weight, iron content, and photosynthetic pigments.

After 12 weeks of experiment, plants were harvested and dried, and plant weight was recorded. Leaves from plants in a replicate were pooled, and chlorophylls and carotenes were analyzed according to Lichtenthaler and Hartmut (1987), and iron was determined by atomic absorption spectrometry (method PNT.08.01).

[5]https://lfz.corefacility.ca/panseq/page/index.html

Olea europaea Production in Intensive Orchards Under Water Limitation

A 12-year-old intensive orchard of *O. europaea* var. Arbequina in Toledo (Spain) (Coordinates UTM 393782–4343510) was used for this experiment. Two lines of 100 m each were selected, and treatments were marked within the two lines on a random block design. Treatments consisted in three replicates of seven trees; BBB001^T treatment was root inoculated (500 mL per tree with a bacterial concentration 1×10^8 cfu/mL) every 2 weeks from April to October, and controls were mock inoculated with water. Regular watering consists of four times a week, each 2 L/h for 3 h; in experimental trees, one time was skipped to decrease water input by 25%. Olives were harvested at the end of October, collecting all olives from the seven trees in the replicate, which were weighed, and fat content determined with Soxhlet. Production (kg/ha) was estimated calculating production per plant and considering orchard's plant density (1,600/ha).

Statistical Analysis

To evaluate treatment effects on all variables, one-way analysis of variance was performed. When significant differences appeared ($p < 0.05$), LSD test (least significant difference) Fisher was used. Statgraphics Plus for Windows was the program used.

DATA AVAILABILITY STATEMENT

The datasets presented in this study can be found in online repositories. The names of the repository/repositories and accession number(s) can be found below: https://www.ncbi.nlm.nih.gov/bioproject/PRJNA705568.

AUTHOR CONTRIBUTIONS

FJGM conceptualized the manuscript. EG-A and IH carried on the bacterial isolation. EG-A analyzed the genomic data. JL, AG-V, and EG-A developed tomato bioassay and drafted the manuscript. EG-A, BR-S, and FJGM developed olive assay. FJGM and BR-S wrote and supervised the final version. All authors contributed to the article and approved the submitted version.

ACKNOWLEDGMENTS

The authors would like to thank Antonio Marin for providing olive orchards and manipulation.

SUPPLEMENTARY MATERIAL

The Supplementary Material for this article can be found online at: https://www.frontiersin.org/articles/10.3389/fmicb.2021.672751/full#supplementary-material

REFERENCES

Alexander, D. B., and Zuberer, D. A. (1991). Use of chrome azurol S reagents to evaluate siderophore production by rhizosphere bacteria. *Biol. Fertil. Soils* 12, 39–45. doi: 10.1007/bf00369386

Anzuay, M. S., Frola, O., Angelini, J. G., Ludueña, L. M., Fabra, A., and Taurian, T. (2013). Genetic diversity of phosphate-solubilizing peanut (*Arachis Hypogaea* L.) associated bacteria and mechanisms involved in this ability. *Symbiosis* 60, 143–154. doi: 10.1007/s13199-013-0250-2

Ark, P. A., and Tompkins, C. M. (1946). Bacterial leaf blight of bird's-nest fern. *Phytopathology* 36, 758–761.

Ash, C., Farrow, J. A. E., Dorsch, M., Stackebrandt, E., and Collins, M. D. (1991). Comparative analysis of *Bacillus anthracis, Bacillus cereus*, and related species on the basis of reverse transcriptase sequencing of 16s Rrna. *Int. J. Syst. Evol. Microbiol*. 41, 343–346. doi: 10.1099/00207713-41-3-343

Bakker, P. A. H. M., Pieterse, C. M. J., and Van Loon, L. C. (2007). Induced systemic resistance by fluorescent *Pseudomonas* spp. *Phytopathol* 97, 239–243. doi: 10.1094/phyto-97-2-0239

Bankevich, A., Nurk, S., Antipov, D., Gurevich, A. A., Dvorkin, M., Kulikov, A. S., et al. (2012). SPAdes: a new genome assembly algorithm and its applications to single-cell sequencing. *J. Comp. Biol.* 19, 455–477. doi: 10.1089/cmb.2012.0021

Bano, A., and Muqarab, R. (2017). Plant defence induced by PGPR against *Spodoptera litura* in tomato (*Solanum lycopersicum* L.). *Plant Biol*. 19, 406–412. doi: 10.1111/plb.12535

Barriuso, J., Pereyra, M. T., Lucas, J. A., Megias, M., Manero, F. J. G., and Ramos, B. (2005). Screening for putative PGPR to improve establishment of the symbiosis *Lactarius deliciosus-Pinus* Sp. *Microb. Ecol*. 50, 82–89. doi: 10.1007/s00248-004-0112-9

Behrendt, U., Ulrich, A., Schumann, P., Erler, W., Burghardt, J., and Seyfarth, W. (1999). A taxonomic study of bacteria isolated from grasses: a proposed new species *Pseudomonas graminis* sp. nov. *Int. J. Syst. Bacteriol.* 49, 297–308.

Benizri, E., Courtade, A., Picard, C., and Guckert, A. (1998). Role of maize root exudates in the production of auxins by *Pseudomonas fluorescens* M.3.1. *Soil. Biol. Biochem* 30, 1481–1484. doi: 10.1016/s0038-0717(98)00006-6

Bolger, A. M., Lohse, M., and Usadel, B. (2014). PHYLUCE is a software package for the analysis of conserved genomic loci. *Bioinformatics* 30, 2114–2120.

Braun, V. (2003). Iron uptake by *Escherichia coli*. *Front. Biosci.* 8:1409–1421. doi: 10.2741/1232

Cámara, B., Strömpl, C., Verbarg, S., Spröer, C., Pieper, D. H., and Tindall, B. J. (2007). *Pseudomonas reinekei* sp. nov., *Pseudomonas moorei* sp. nov. and *Pseudomonas mohnii* sp. nov., novel species capable of degrading chlorosalicylates or isopimaric acid. *Int. J. Syst. Evol. Microbiol.* 57, 923–931.

Coulton, J. W., Mason, P., and Dubow, M. S. (1983). Molecular cloning of the ferrichrome-iron receptor of *Escherichia coli* K-12. *J. Bacteriol.* 156, 1315–1321. doi: 10.1128/jb.156.3.1315-1321.1983

Dabboussi, F., Hamze, M., Singer, E., Geoffroy, V., Meyer, J. M., and Izard, D. (2002). *Pseudomonas mosselii* sp. nov., a novel species isolated from clinical specimens. *Int. J. Syst. Evol. Microbiol.* 52(Pt 2), 363–376.

DeBoer, K. D., Lye, J. C., Campbell, D., Aitken, A., Su, K.-K., and Hamill, J. D. (2009). The A622 gene in *Nicotiana glauca* (Tree Tobacco): evidence for a functional role in pyridine alkaloid synthesis. *Plant Molec. Biol.* 69:299. doi: 10.1007/s11103-008-9425-2

Delfin, E. F., Rodriguez, F. M., and Paterno, E. S. (2015). Biomass partitioning, yield, nitrogen and phosphorus uptake of PGPR inoculated tomato (*Lycopersicum esculentum* L) under field condition. *Philipp. J. Crop. Sci*. 40, 59–65.

Elomari, M., Coroler, L., Verhille, S., Izard, D., and Leclerc, H. (1997). *Pseudomonas monteilii* sp. nov., isolated from clinical specimens. *Int. J. Syst. Bacteriol.* 47, 846–852.

Farris, J. S. (1972). Estimating phylogenetic trees from distance matrices. *Am. Nat.* 106, 645–667. doi: 10.1086/282802

Frasson, D., Opoku, M., Picozzi, T., Torossi, T., Balada, S., Smits, T. H. M., et al. (2017). *Pseudomonas wadenswilerensis* sp. nov. and *Pseudomonas reidholzensis* sp. nov., two novel species within the *Pseudomonas putida* group isolated from forest soil. *Int. J. Syst. Evol. Microbiol.* 67, 2853–2861.

Fatima, S., and Anjum, T. (2017). Identification of a potential ISR determinant from *Pseudomonas aeruginosa* pm12 against fusarium wilt in tomato. *Front. Plant Sci.* 8:848. doi: 10.3389/fpls.2017.00848

Frändberg, E., and Schnürer, J. (1998). Antifungal activity of chitinolytic bacteria isolated from airtight stored cereal grain. *Can. J. Microbiol.* 44, 121–127. doi: 10.1139/w97-141

Gao, J., Xie, G., Peng, F., and Xie, Z. (2015). *Pseudomonas donghuensis* sp. nov., exhibiting high-yields of siderophore. *Antonie Van Leeuwenhoek* 107, 83–94.

Gurevich, A., Saveliev, V., Vyahhi, N., and Tesleret, G. (2013). QUAST: quality assessment tool for genome assemblies. *Bioinformatics* 29, 1072–1075. doi: 10.1093/bioinformatics/btt086

Gutierrez Mañero, F. J., Acero, N., Lucas, J. A., and Probanza, A. (1996). The influence of native rhizobacteria on European alder [*Alnus glutinosa* (L.) Gaertn.] growth. II. Characterization and biological assays of metabolites from growth promoting and growth inhibiting bacteria. *Plant Soil* 182, 67–74. doi: 10.1007/BF00010996

Huerta-Cepas, J., Forslund, K., Coelho, L. P., Szklarczyk, D., Jensen, L. J., von Mering, C., et al. (2017). Fast genome-wide functional annotation through orthology assignment by eggNOG-mapper. *Mol. Biol. Evol.* 34, 2115–2122. doi: 10.1093/molbev/msx148

Huerta-Cepas, J., Szklarczyk, D., Heller, D., Hernandez-Plaza, A., Forslund, S. M. K., Cook, H., et al. (2018). EggNOG 5.0: A hierarchical, functionally and phylogenetically annotated orthology prediction resource based on 5090 organisms and 2502 viruses. *Nucleic Acids Res.* 47, D309–D314.

Ilangumaran, G., and Smith, D. L. (2017). Plant growth promoting rhizobacteria in amelioration of salinity stress: a systems biology perspective. *Front. Plant Sci*. 8:1768. doi: 10.3389/fpls.2017.01768

Kangasjärvi, S., Tikkanen, M., Durian, G., and Aro, E. M. (2014). Photosynthetic light reactions. An adjustable hub in basic production and plant immunity signaling. *Plant Physiol. Biochem*. 81, 128–134. doi: 10.1016/j.plaphy.2013.12.004

Keshavarz-Tohid, V., Vacheron, J., Dubost, A., Prigent-Combaret, C., Taheri, P., Tarighi, S., et al. (2019). Genomic, phylogenetic and catabolic re-assessment of the *Pseudomonas putida* clade supports the delineation of *Pseudomonas alloputida* sp. nov., *Pseudomonas inefficax* sp. nov., *Pseudomonas persica* sp. nov., and *Pseudomonas shirazica* sp. nov. *Syst. Appl. Microbiol.* 42, 468–480.

Kim, M., Oh, S. H., Park, S. C., and Chun, J. (2014). Towards a taxonomic coherence between average nucleotide identity and 16s Rrna gene sequence similarity for species demarcation of Prokaryotes. *Intl. J. System. Evol. Microbiol.* 64, 346–351. doi: 10.1099/ijs.0.059774-0

Kloepper, J. W. (1992). Plant growth-promoting rhizobacteria as biological control agents. *Soil microbial ecology applications in agricultural and environmental management. pp.255-274 ref.6 pp. ISBN : 0824787374* ed F.B.METTING JUNIOR. *Publisher*.Newyork, NY: Marcel Dekker Inc.

Kollist, H., Zandalinas, S. I., Sengupta, S., Nuhkat, M., Kangasjärvi, J., and Mittler, R. (2019). Rapid responses to abiotic stress: Priming the landscape for the signal transduction network. *Trends Plant. Sci*. 24, 25–37. doi: 10.1016/j.tplants.2018.10.003

Konstantinidis, K. T., and Tiedje, J. M. (2005). Genomic insights that advance the species definition for prokaryotes. *Proc. Nat. Acad. Sci.* 102, 2567–2572. doi: 10.1073/pnas.0409727102

Kreft, L., Botzki, A., Coppens, F., Vandepoele, K., and Van Bel, M. (2017). PhyD3: A phylogenetic tree viewer with extended phyloXML support for functional genomics data visualization. *Bioinformatics*. 33, 2946–2947. doi: 10.1093/bioinformatics/btx324

Lefort, V., Desper, R., and Gascuel, O. (2015). FastME 2.0: A comprehensive, accurate, and fast distance-based phylogeny inference program. *Mol. Biol. Evol.* 32, 2798–2800. doi: 10.1093/molbev/msv150

Li, H., and Durbin, R. (2010). Fast and accurate long-read alignment with burrows–wheeler transform. *Bioinformatics* 26, 589–595. doi: 10.1093/bioinformatics/btp698

Li, H., Handsaker, B., Wysoker, A., Fennell, T., Ruan, J., Homer, N., et al. (2009). The sequence alignment/map format and SAMtools. *Bioinformatics* 25, 2078–2079. doi: 10.1093/bioinformatics/btp352

Lichtenthaler and Hartmut, K. (1987). Chlorophylls and carotenoids: pigments of photosynthetic biomembranes. *Met. Enzymol*. 148, 350–382. doi: 10.1016/0076-6879(87)48036-1

López, J. R., Diéguez, A. L., Doce, A., De la Roca, E., De la Herran, R., Navas, J. I., et al. (2012). *Pseudomonas baetica* sp. nov., a fish pathogen isolated from wedge sole, *Dicologlossa cuneata* (Moreau). *Int. J. Syst. Evol. Microbiol.* 62, 874–882.

Martin-Rivilla, H., Garcia-Villaraco, A., Ramos-Solano, B., Gutierrez-Mañero, F. J., and Lucas, J. A. (2020). Bioeffectors as biotechnological tools to boost plant innate immunity: signal transduction pathways involved. *Plants* 9:1731. doi: 10.3390/plants9121731

Mavrodi, D. V., Bonsall, R. F., Delaney, S. M., Soule, M. J., Phillips, G., and Thomashow, L. S. (2001). Functional analysis of genes for biosynthesis of pyocyanin and phenazine-1-carboxamide from *Pseudomonas aeruginosa* Pao1. *J. Bacteriol*. 183, 6454–6465. doi: 10.1128/jb.183.21.6454-6465.2001

Meier Kolthoff, J. P., and Göker, M. (2019). TYGS is an automated high-throughput platform for state-of-the-art genome- based taxonomy. *Nat. Commun.* 10:2182.

Meier-Kolthoff, J. P., Auch, A. F., Klenk, H. P., and Goker, M. (2013). Genome sequence-based species delimitation with confidence intervals and improved distance functions. *BMC Bioinformatics* 14:60. doi: 10.1186/1471-2105-14-60

Menéndez, E., Ramírez-Bahena, M. H., Fabryová, A., Igual, J. M., Benada, O., Mateos, P. F., et al. (2015). *Pseudomonas coleopterorum* sp. nov., a cellulase-producing bacterium isolated from the bark beetle *Hylesinus fraxini*. *Int. J. Syst. Evol. Microbiol.* 65, 2852–2858.

MIDI (2008). *Sherlock microbial identification system operating manual, version 6.1*. Newark, DE: MIDI Inc.

Miethke, M., and Marahiel, M. A. (2007). Siderophore-based iron acquisition and pathogen control. *Microbiol. Mol. Biol. Rev.* 71, 413–451. doi: 10.1128/mmbr.00012-07

Migula, W. (1895). "Schizomycetes (Bacteria, Bacterien)," in *Die Natürlichen Pfanzenfamilien Teil I, Abteilung Ia,* eds A. Engler and K. Prantl (Leipzig: Wilhelm Engelmann), 1–44.

Mulet, M., Gomila, M., Lemaitre, B., Lalucat, J., and García-Valdés, E. (2012). Taxonomic characterisation of *Pseudomonas* strain L48 and formal proposal of *Pseudomonas entomophila* sp. nov. Syst. *Appl. Microbiol.* 35, 145–149.

Mulet, M., Sánchez, D., Lalucat, J., Lee, K., and García-Valdés, E. (2015). *Pseudomonas alkylphenolica* sp. nov., a bacterial species able to form special aerial structures when grown on p-cresol. *Int. J. Syst. Evol. Microbiol.* 65, 4013–4018.

Nishimori, E., Kita-Tsukamoto, K., and Wakabayashi, H. (2000). *Pseudomonas plecoglossicida* sp. nov., the causative agent of bacterial haemorrhagic ascites of ayu, *Plecoglossus altivelis*. *Int. J. Syst. Evol. Microbiol.* 50, 83–89.

Oh, W. T., Jun, J. W., Giri, S. S., Yun, S., Kim, H. J., Kim, S. G., et al. (2019). *Pseudomonas tructae* sp. nov., novel species isolated from rainbow trout kidney. *Int. J. Syst. Evol. Microbiol.* 69, 3851–3856.

Okonechnikov, K., Conesa, A., and García-Alcalde, F. (2015). Qualimap 2:advanced multi-sample quality control for high-throughput sequencing data. *Bioinformatics* 32, 292–294. doi: 10.1093/bioinformatics/btv566

Ondov, B. D., Treangen, T. J., and Melsted, P. (2016). Mash: Fast genome and metagenome distance estimation using MinHash. *Genome. Biol*. 17, 1–14.

Peix, A., Rivas, R., Mateos, P. F., Martínez-Molina, E., Rodríguez-Barrueco, C., and Velázquez, E. (2003). *Pseudomonas rhizosphaerae* sp. nov., a novel species that actively solubilizes phosphate *in vitro*. *Int. J. Syst. Evol. Microbiol.* 53, 2067–2072.

Peix, A., Rivas, R., Santa-Regina, I., Mateos, P. F., Martínez-Molina, E., Rodríguez-Barrueco, C., et al. (2004). *Pseudomonas lutea* sp. nov., a novel phosphate-solubilizing bacterium isolated from the rhizosphere of grasses. *Int. J. Syst. Evol. Microbiol.* 54, 847–850.

Posada, L., Álvarez, J. C., Romero-Tabarez, M., Luz de-Bashan, and Villegas-Escobar, V. (2018). Enhanced molecular visualization of root colonization and growth promotion by *Bacillus subtilis* Ea-Cb0575 in different growth systems. *Microbiol. Res.* 217, 69–80. doi: 10.1016/j.micres.2018.08.017

Pungrasmi, W., Lee, H. S., Yokota, A., and Ohta, A. (2008). *Pseudomonas japonica* sp. nov., a novel species that assimilates straight chain alkylphenols. *J. Gen. Appl. Microbiol.* 54, 61–69.

Qin, J., Feng, Y., Lü, X., and Zong, Z. (2019a). *Pseudomonas huaxiensis* sp. nov., isolated from hospital sewage. *Int. J. Syst. Evol. Microbiol.* 69, 3281–3286.

Qin, J., Hu, Y., Feng, Y., Xaioju, L., and Zong, Z. (2019b). *Pseudomonas sichuanensis* sp. nov., isolated from hospital sewage. *Int. J. Syst. Evol. Microbiol.* 69, 517–522.

Qin, J., Hu, Y., Wu, W., Feng, Y., and Zong, Z. (2020). *Pseudomonas defluvii* sp. nov., isolated from hospital sewage. *Int. J. Syst. Evol. Microbiol.* 70, 4199–4203.

Ramírez-Bahena, M. H., Cuesta, M. J., Flores-Félix, J. D., Mulas, R., Rivas, R., Castro-Pinto, J., et al. (2014). *Pseudomonas helmanticensis* sp. nov., isolated from forest soil. *Int. J. Syst. Evol. Microbiol.* 64, 2338–2345.

Ramos-Solano, B., Lucas Garcia, J. A., Garcia-Villaraco, A., Algar, E., Garcia-Cristobal, J., and Gutierrez Manero, F. J. (2010). Siderophore and chitinase producing isolates from the rhizosphere of *Nicotiana glauca* graham enhance growth and induce systemic resistance in *Solanum lycopersicum* L. *Plant Soil* 334, 189–197. doi: 10.1007/s11104-010-0371-9

Rasouli-Sadaghiani, M. H., Malakouti, M. J., Khavazi, K., and Miransari, M. (2014). "Siderophore efficacy of fluorescent Pseudomonades affecting labeled iron (59 Fe) uptake by wheat (*Triticum aestivum* L.) genotypes differing in Fe efficiency". In: *Use of Microbes for the Alleviation of Soil Stresses*. ed M. Miransari. Springer: New York, NY.

Richter, M., and Rosselló-Móra, R. (2009). Shifting the genomic gold standard for the prokaryotic species definition. *Proc. Nat. Acad. Sci.* 106, 19126–19131. doi: 10.1073/pnas.0906412106

Rodríguez-Kábana, R., Godoy, G., Morgan-Jones, G., and Shelby, R. A. (1983). The determination of soil chitinase activity: conditions for assay and ecological studies. *Plant Soil*. 75, 95–106. doi: 10.1007/BF02178617

Rosselló-Móra, R., and Amann, R. (2001). The species concept for prokaryotes. *FEMS Microbiol. Rev*. 25, 39–67. doi: 10.1016/s0168-6445(00)00040-1

Sasser, M. (1990). *Identification of bacteria by gas chromatography of cellular fatty acids, MIDI. Technical note 101*. Newark, DE: MIDI.

Savulescu, T. (1947). Contribution a la classification des bacteriacees phytopathogenes. *Anal. Acad. Romane Ser. III Tom 22. Memoire* 4, 1–26.

Sawada, H., Fujikawa, T., and Horita, H. (2020). *Pseudomonas brassicae* sp. nov., a pathogen causing head rot of broccoli in Japan. *Int. J. Syst. Evol. Microbiol*. 70, 5319–5329. doi: 10.1099/ijsem.0.004412

Sinclair, S. J., Johnson, R., and Hamill, J. D. (2004). Analysis of wound-induced gene expression in nicotiana species with contrasting alkaloid profiles. *Funct. Plant Biol*. 31, 721–729. doi: 10.1071/fp03242

Teeling, H., Meyerdierks, A., Bauer, M., Amann, R., and Glöckner, F. O. (2004). Application of tetranucleotide frequencies for the assignment of genomic fragments. *Environ. Microbiol*. 6, 938–947. doi: 10.1111/j.1462-2920.2004.00624.x

Tohya, M., Watanabe, S., Teramoto, K., Uechi, K., Tada, T., Kuwahara-Arai, K., et al. (2019a). *Pseudomonas asiatica* sp. nov., isolated from hospitalized patients in Japan and Myanmar. *Int. J. Syst. Evol. Microbiol.* 69, 1361–1368.

Tohya, M., Watanabe, S., Teramoto, K., Shimojima, M., Tada, T., Kuwahara-Arai, K., et al. (2019b). *Pseudomonas juntendi* sp. nov., isolated from patients in Japan and Myanmar. *Int. J. Syst. Evol. Microbiol.* 69, 3377–3384.

Trevisan, V. B. (1889). *I Generi e le Specie delle Batteriacee. L. Zanaboni e Gabuzzi*. Available online at: http://scholar.google.com/scholar?cluster=12213764842208350008&hl=en&oi=scholarr

Tvrzova, L., Schumann, P., Sproer, C., Sedlacek, I., Pacova, Z., Sedo, O., et al. (2006). *Pseudomonas moraviensis* sp. nov. and *Pseudomonas vranovensis* sp. nov., soil bacteria isolated on nitroaromatic compounds, and emended description of *Pseudomonas asplenii*. *Int. J. Syst. Evol. Microbiol.* 56, 2657–2663.

Uchino, M., Shida, O., Uchimura, T., and Komagata, K. (2001). Recharacterization of *Pseudomonas fulva* Iizuka and Komagata 1963, and proposals of *Pseudomonas parafulva* sp. nov. and *Pseudomonas cremoricolorata* sp. nov. *J. Gen. Appl. Microbiol.* 46, 247–261.

Van Loon, L. C. (2007). "Plant responses to plant growth-promoting rhizobacteria". In: *New Perspectives and Approaches in Plant Growth-Promoting Rhizobacteria*

Research, eds P. A. H. M. Raaijmakers, G. Bloemberh, M. Hofte, P. Lemanceau, and B.M Cooke New York, NY: Springer

Wang, M. Q., Wang, Z., Yu, L. N., Zhang, C. S., Bi, J., and Sun, J. (2019). *Pseudomonas qingdaonensis* sp. nov., an aflatoxin-degrading bacterium, isolated from peanut rhizospheric soil. *Arch. Microbiol.* 201, 673–678.

Wang, L. T., Tai, C. J., Wu, Y. C., Chen, Y. B., Lee, F. L., and Wang, S. L. (2010). *Pseudomonas taiwanensis* sp. nov., isolated from soil. *Int. J. Syst. Evol. Microbiol.* 60, 2094–2098.

Wright, M. H., Hanna, J. G., Ii, D. A., and Tebo, B. M. (2018). *Pseudomonas laurentiana* sp. nov., an Mn(III)-oxidizing Bacterium Isolated from the St. Lawrence Estuary. *Pharmacogn. Commn.* 8, 153–157. doi: 10.5530/pc.2018.4.32

Xu, P., Li, W. J., Tang, S. K., Zhang, Y. Q., Chen, G. Z., Chen, H. H., et al. (2005). *Naxibacter alkalitolerans* gen. nov., sp. nov., a novel member of the family 'Oxalobacteraceae' isolated from China. *Int. J. Sys. Evo. Microbiol.* 55, 1149–1153. doi: 10.1099/ijs.0.63407-0

Conflict of Interest: The authors declare that the research was conducted in the absence of any commercial or financial relationships that could be construed as a potential conflict of interest.

Publisher's Note: All claims expressed in this article are solely those of the authors and do not necessarily represent those of their affiliated organizations, or those of the publisher, the editors and the reviewers. Any product that may be evaluated in this article, or claim that may be made by its manufacturer, is not guaranteed or endorsed by the publisher.

frontiers in Plant Science

ORIGINAL RESEARCH
published: 24 August 2021
doi: 10.3389/fpls.2021.719873

Can Inoculation With the Bacterial Biostimulant *Enterobacter* sp. Strain 15S Be an Approach for the Smarter P Fertilization of Maize and Cucumber Plants?

Mónica Yorlady Alzate Zuluaga[1,2]*, *André Luiz Martinez de Oliveira*[2], *Fabio Valentinuzzi*[1], *Raphael Tiziani*[1], *Youry Pii*[1]*, *Tanja Mimmo*[1] *and Stefano Cesco*[1]

[1] Faculty of Science and Technology, Free University of Bolzano, Bolzano, Italy, [2] Department of Biochemistry and Biotechnology, State University of Londrina, Londrina, Brazil

Phosphorus (P) is an essential nutrient for plants. The use of plant growth-promoting bacteria (PGPB) may also improve plant development and enhance nutrient availability, thus providing a promising alternative or supplement to chemical fertilizers. This study aimed to evaluate the effectiveness of *Enterobacter* sp. strain 15S in improving the growth and P acquisition of maize (monocot) and cucumber (dicot) plants under P-deficient hydroponic conditions, either by itself or by solubilizing an external source of inorganic phosphate (Pi) [$Ca_3(PO_4)_2$]. The inoculation with *Enterobacter* 15S elicited different effects on the root architecture and biomass of cucumber and maize depending on the P supply. Under sufficient P, the bacterium induced a positive effect on the whole root system architecture of both plants. However, under P deficiency, the bacterium in combination with $Ca_3(PO_4)_2$ induced a more remarkable effect on cucumber, while the bacterium alone was better in improving the root system of maize compared to non-inoculated plants. In P-deficient plants, bacterial inoculation also led to a chlorophyll content [soil-plant analysis development (SPAD) index] like that in P-sufficient plants ($p < 0.05$). Regarding P nutrition, the ionomic analysis indicated that inoculation with *Enterobacter* 15S increased the allocation of P in roots (+31%) and shoots (+53%) of cucumber plants grown in a P-free nutrient solution (NS) supplemented with the external insoluble phosphate, whereas maize plants inoculated with the bacterium alone showed a higher content of P only in roots (36%) but not in shoots. Furthermore, in P-deficient cucumber plants, all Pi transporter genes (*CsPT1.3*, *CsPT1.4*, *CsPT1.9*, and *Cucsa383630.1*) were upregulated by the bacterium inoculation, whereas, in P-deficient maize plants, the expression of *ZmPT1* and *ZmPT5* was downregulated by the bacterial inoculation. Taken together, these results suggest that, in its interaction with P-deficient cucumber plants, *Enterobacter* strain 15S might have solubilized the $Ca_3(PO_4)_2$ to help the plants overcome P deficiency, while the association of maize plants with the bacterium might have triggered a different mechanism affecting plant metabolism. Thus, the mechanisms by which *Enterobacter* 15S improves plant growth and P nutrition are dependent on crop and nutrient status.

Keywords: ***Zea mays, Cucumis sativus,*** **plant growth promoting bacteria, root exudation, P-solubilisation, phosphorus transporter, gene expression**

OPEN ACCESS

Edited by:
Maurizio Ruzzi,
University of Tuscia, Italy

Reviewed by:
Mazhar Rafique,
The University of Haripur, Pakistan
Muhammad Rizwan,
Nuclear Institute of Agriculture, Pakistan

***Correspondence:**
Mónica Yorlady Alzate Zuluaga
monicayorlady.alzatezuluaga@unibz.it
Youry Pii
youry.pii@unibz.it

Specialty section:
This article was submitted to Plant Nutrition, a section of the journal Frontiers in Plant Science

Received: *03 June 2021*
Accepted: *27 July 2021*
Published: *24 August 2021*

Citation:
Alzate Zuluaga MY, Martinez de Oliveira AL, Valentinuzzi F, Tiziani R, Pii Y, Mimmo T and Cesco S (2021) Can Inoculation With the Bacterial Biostimulant Enterobacter sp. Strain 15S Be an Approach for the Smarter P Fertilization of Maize and Cucumber Plants? Front. Plant Sci. 12:719873. doi: 10.3389/fpls.2021.719873

INTRODUCTION

Crops cultivated around the world, belonging to both monocot and dicot clades, can be very diverse; nevertheless, their growth and development are strongly influenced by the state and the availability of nutrients in the soil. Consequently, the yield levels and the overall performance of a crop can considerably vary both spatially and temporally, depending on both soil characteristics and agricultural practices. In this context, phosphorus (P) is known to play a crucial role in plant nutrition; thus helping to achieve optimal growth and productivity. Plants take up P as inorganic phosphate (Pi); however, due to its low solubility and mobility, P is sparingly available in the soil solution, as its concentration is often rather limited ($<10\,\mu M$) (Wang et al., 2017). To cope with this issue, plants have evolved morphological, biochemical, and metabolic strategies, which include: (i) the enhancement of root density and length, (ii) the release of organic acids and phosphatases, (iii) an increase in the expression of high-affinity Pi transporters, and (iv) the establishment of a symbiotic association with mycorrhizal fungi (López-Arredondo et al., 2014).

In addition to the genetic improvement of crops achieved through breeding programs, the exogenous root-inoculation with plant growth-promoting bacteria (PGPB) could prove itself to be an interesting and promising agricultural approach to the amelioration of the mineral nutrition of plants (Ramaekers et al., 2010). Indeed, beneficial bacteria colonize the root surface in the rhizosphere, where they can exert positive effects on a wide range of plant species *via* direct and indirect mechanisms (Dakora et al., 2015; Backer et al., 2018). The direct effects of PGPB inoculation can be related to either activity aimed at ameliorating the mineral nutrition of plants [e.g., nitrogen (N) fixation, P solubilization, the release of siderophores, and the enhancement of mineral nutrients uptake] (Pii et al., 2015b) or the release of hormone-like compounds that can modulate the growth of plants (Glick, 2012; Goswami et al., 2016). On the other hand, indirect effects are related to the ability of PGPB to protect plants from both abiotic (e.g., drought and salinity) and biotic (e.g., pathogens) stresses (Glick, 2012; Goswami et al., 2016).

Focusing on the biogeochemical cycle of P in soil, it has been well-demonstrated that PGPB can enhance the available fraction of this nutrient *via* an augmented secretion in the rhizosphere of organic acids and phosphatases (Billah et al., 2019). Although examples of improved plant acquisition of P have been well-described as a consequence of root inoculation with different PGPB strains, the mechanisms underlying the phenomenon remain unknown. The understanding of these interactions can be further complicated by the co-occurrence of processes underpinning P acquisition by plants; for instance, the increased nutrient bioavailability at the root-soil interface on the one hand, and the enhanced capacity of plants to transport Pi across the plasma membrane on the other hand (Pii et al., 2015b). Moreover, the ability of the roots to reacquire a wide range of small organic molecules belonging to root exudates, recently demonstrated in P-deficient tomato plants, further complicates the biochemical P cycle in the rhizosphere (Tiziani et al., 2020). Collectively, deeper comprehension of all these processes through the application of multidisciplinary approaches appears to be crucial to better exploit the properties of the PGPB strains at the field scale for the more efficient use of the endogenous P sources in soil within the context of more sustainable agriculture.

With respect to Pi-uptake mechanisms in roots, there are diverse experiences in literature aimed at the identification of the genes encoding the specific transporters and the characterization of the regulation of the entire Pi-uptake process in the roots (López-Arredondo et al., 2014). Considering the first aspect, among the genes identified, the *PHT1* gene family has the largest number of members expressed in roots, is well-recognized as mediators of Pi uptake from the external medium, and is predominantly overexpressed under P starvation (Wang et al., 2018). Considering crops and in particular monocots, 13 *PHT1* members have been identified in rice (*Oryza sativa*) (Paszkowski et al., 2002) and maize (*Zea mays*) (Liu et al., 2016), 16 in wheat (*Triticum aestivum*) (Grün et al., 2018), and nine in sorghum (*Sorghum bicolor*) (Tavares de Oliveira Melo, 2016). On the other hand, in dicots, 15 genes have been identified in the soybean (*Glycine max*) genome (Fan et al., 2013), eight in tomato (*Solanum lycopersicum*) (Chen et al., 2014) and potato (*Solanum tuberosum*) (Liu et al., 2017), and five in tobacco (*Nicotiana tabacum*) and pepper (*Capsicum frutescens*) (Chen et al., 2007). In this respect, it is interesting to note that studies aimed at characterizing the expression levels of these genes in inoculated plants (and, thence, the functionality of the Pi transporters) have been mainly conducted in plants colonized with arbuscular mycorrhizal fungi (AMF), while only a few of them considered inoculation with PGPB (Duan et al., 2015; Liu et al., 2018; Zhang et al., 2019). Therefore, the regulatory effects of PGPB on these transporters are still quite unknown. Additionally, considering that the effects of PGPB on plants significantly depend on specific interactions between plant genotypes and bacterial strains (Pii et al., 2015b; Crecchio et al., 2018), deeper knowledge about the PGPB strains (already isolated and belonging to the microbial collection banks in several research centers but not yet thoroughly investigated and characterized) appears to be fundamental.

Considering the possibility of improving P nutrition in crops using PGPB, it is worth mentioning that, in the context of previous research, the bacterium *Enterobacter* sp. strain 15S has been isolated and characterized for its particular ability to solubilize P *in vitro*, thus making it a promising tool for sustainable fertilization strategies (Zuluaga et al., 2020). Nevertheless, considering the abovementioned specificity in the PGPB-host interplay, it is mandatory to characterize the interaction of *Enterobacter* sp. strain 15S with model crops belonging to both monocots and dicots to unravel whether this bacterial strain might find a useful application at the field scale.

Based on these observations, the present research aimed to investigate the effect of *Enterobacter* sp. strain 15S inoculation on the development and P nutrition of cucumber and maize plants, which were chosen as representatives of the clades dicots and monocots, respectively. Considering the strong ability of P solubilization featured by *Enterobacter* sp. strain 15S, the bacterium effects on root P uptake of plants fed with an inorganic Pi source [$Ca_3(PO_4)_2$] were also monitored. Plants were grown

in hydroponic conditions, either in the presence (P+) or in the absence (P-) of the macronutrient P; plants were also either inoculated or not inoculated with *Enterobacter* sp. strain 15S. In addition, considering the strong P solubilization ability featured by *Enterobacter* sp. strain 15S, a set of plants were also fed an insoluble inorganic Pi source [$Ca_3(PO_4)_2$] and monitored for their growth and mineral nutrient accumulation. After a cultivation period of 21 days, the plants were sampled and assessed for their growth, the concentration of mineral elements in their tissues, biological activities of their roots (i.e., release of exudates), and the molecular modulation of Pi transporters at the root level.

MATERIALS AND METHODS

Experimental Design and Plant Growth Conditions

Cucumber (*Cucumis sativus* L. cv. Chinese Long) and maize (*Z. mays* L. – hybrid P0423, Pioneer Hi-Bred Italia S.r.l) plants were hydroponically grown under controlled environmental conditions in a climatic chamber with a 14/10-h light/dark period, 24/19°C, 250 μmol m^{-2} s^{-1} light intensity, and 70% relative humidity. Seeds were germinated for 5 days in the dark at 22°C on filter paper moistened with 0.5 mM $CaSO_4$. Five-day-old seedlings were then transferred into 2-L plastic pots filled with 1.5 L of a full-strength nutrient solution (NS), either not supplemented (P-) or P-supplemented (P+) using the soluble phosphate 0.1 mM KH_2PO_4. The NS had the following composition: 2 mM Ca $(NO_3)_2$, 0.5 mM $MgSO_4$, 0.7 mM K_2SO_4, 0.1 mM KCl, 10 μM H_3BO_3, 0.5 μM $MnSO_4$, 0.2 μM $CuSO_4$, 0.5 μM $ZnSO_4$, 0.01 μM $(NH_4)_6Mo_7O_{24}$, and 80 μM Fe-EDTA. The solution was continuously aerated and changed two times per week. After 7 days of hydroponic culture, plants were set in a 2 × 4 factorial experimental design completely randomized with two P conditions (P+ and P–) and two biostimulant treatments with the PGPB *Enterobacter* 15S, with or without insoluble $Ca_3(PO_4)_2$, provided with a dialysis tube (named 15S and 15SIP, respectively), plus two inoculated controls (named C and CIP, respectively) (**Figure 1**). Three biological replicates, with 10 (cucumber) or eight (maize) seedlings per replicate, were performed for each treatment. After 21 days of cultivation, the plants were harvested and assessed as described below.

Bacterial Biostimulant

Enterobacter sp. 15S strain (KX884932.1) was originally isolated from bulk soil under conventional horticultural management in the Laboratory of Molecular Biochemistry of the State University of Londrina (Paraná, Brazil) (Zuluaga et al., 2020). The bacterial strain was grown in Luria-Bertani (LB) medium (10 g L^{-1} tryptone, 5 g L^{-1} yeast extract, and 10 g L^{-1} NaCl) under orbital shaking at 180 rpm, 28°C, for 24 h. After that period, the cells were harvested, washed three times, and resuspended in a sterile saline solution (0.85% w/v NaCl). Bacterial biostimulant suspension was used to inoculate the hydroponic NS to a final concentration of 10^6 cell ml^{-1} (**Figure 1**). Control treatments were treated with the same amount of sterile saline solution.

Plant Analysis

Morpho-Physiological Parameters

SPAD Values

After 15 days of hydroponic culture, the plants were harvested and the changes in chlorophyll concentration of the youngest fully expanded leaves were determined using a portable chlorophyll meter (SPAD-502, Minolta, Osaka, Japan) and presented as soil-plant analysis development (SPAD) units. Measurements were performed on three plants per pot of each of the three biological replicates and at least two readings per plant were taken and averaged.

Plant Biomass

At harvest, three biological replicates of the shoots and roots were separated and dried at 65°C until constant weight. The dry weight (DW) of the roots and shoots was recorded.

Root Morphological Characteristics

For the analysis of root morphology, fresh roots were scanned using a root scanner system (EPSON Perfection V800, Regent Instruments Inc., Quebec, Canada) and data were then analyzed with the WinRHIZO software (EPSON 1680, WinRHIZO Pro2003b) to determine the root characteristics, including length, surface area, diameter, volume, and the number of tips. All determinations were made in triplicates.

Element Analysis

The plant tissue of the shoots and roots were dried at 65°C and acid digested with 68% ultrapure HNO_3 (Carlo Erba, Milano, Italy) in a single reaction chamber microwave digestion system (UltraWAVE, Milestone, Shelton, CT, USA). Concentrations of macro and micronutrients were determined using an inductively coupled plasma–optical emission spectrometer (ICP-OES Spectro CirosCCD, Spectro, Germany). Element quantification was carried out using certified multi-element standards (CPI International, https://cpiinternational.com). Tomato leaves (SRM 1573a) and spinach leaves (SRM 1547) were used as the external certified reference materials. Determinations were carried out in triplicates.

Root Exudation of Phenolics and Flavonoids

Root exudates were collected at the end of the hydroponic cultivation period. One plant of each biological replicate was removed from the NS and their roots were washed with distilled water. Plants were then transferred separately into smaller pots containing 20 ml of H_2O MQ (18.2 MΩ cm^3) as a trap solution. Pots were covered with aluminum foil to keep the roots in the dark, with the trap solution being continuously aerated. Root exudates were collected after 24 h, filtered at 0.45 μm, frozen at −80°C, freeze-dried, and resuspended in methanol 60%. The total phenolic content in the root exudates was determined using the Folin-Ciocalteau method (Folin and Ciocalteau, 1927) and was expressed as the nmol equivalent of gallic acid per gram of root fresh weight (RFW). Total flavonoid content was measured with the aluminum chloride colorimetric method (Miliauskas

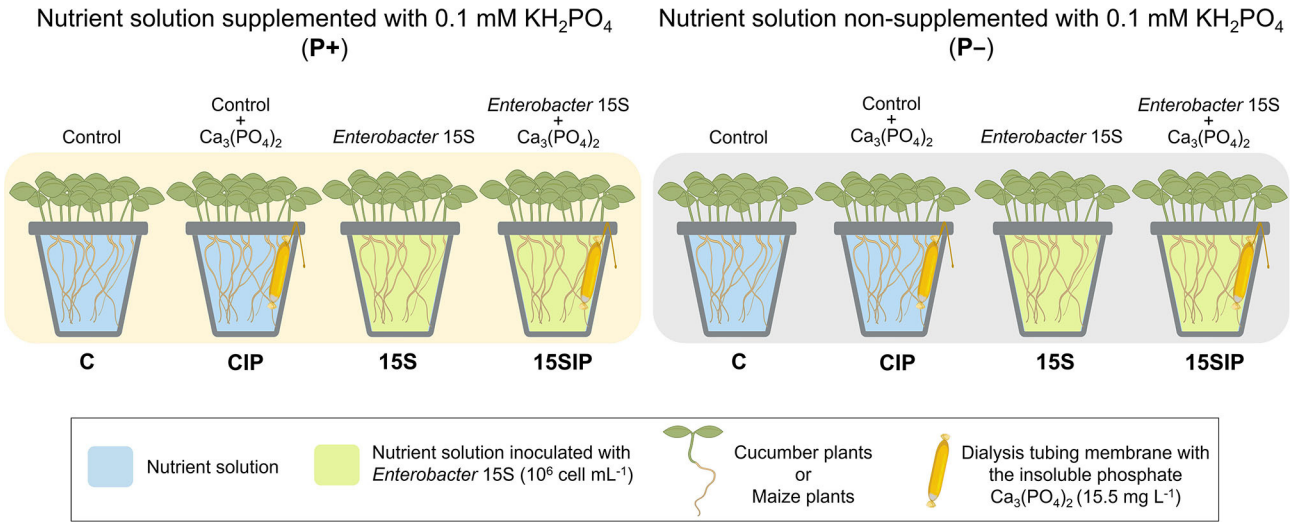

FIGURE 1 | The experimental design of the present study. Seedlings of cucumber or maize were grown on nutrient solutions (NSs) supplemented (P+) or non-supplemented (P–) with 0.1 of mM KH_2PO_4. The bacterial biostimulant with *Enterobacter* 15S was used to inoculate the hydroponic NS to a final concentration of 10^6 cell ml^{-1} (15S) and the NS in pots containing the insoluble phosphate $Ca_3(PO_4)_2$ (15SIP). Two uninoculated controls, with the insoluble phosphate $Ca_3(PO_4)_2$ (CIP) or without it (C), were also evaluated (Refer text in detail). The dialysis membrane used was a MEMBRA-CEL MD34 14 × 100, MWCO: 14000, Pore size: 50Å (Viskase Companies Inc., Willowbrook, IL, USA).

et al., 2004) and expressed as the nmol equivalent of rutin per gram of root fresh weight.

Gene Expression Analysis

Root tissues from two plants of each biological replicate were collected. The harvested roots were frozen in liquid N and stored at −80°C until use. Total RNA was extracted from frozen roots using the Spectrum Plant Total RNA Kit (Sigma-Aldrich, St. Louis, MO, USA) according to the instructions of the manufacturer. The total RNA (1 μg) was treated with 10 U of DNAse RQ1 and used for cDNA synthesis using the ImProm-II Reverse Transcription System (Promega, Madison, WI, USA) and oligo $(dT)_{15}$ primer as per the recommendations of the manufacturer. The cDNA obtained was used as a template for the quantitative real-time reverse transcription PCR (qRT-PCR) performed using the SsoFast EvaGreen Supermix (Bio-Rad, Hercules, CA, USA) and the Bio-Rad iCycler MyiQ real-time PCR system (Bio-Rad). Gene-specific primers were designed for the target genes and the housekeeping gene, the elongation factor 1α (**Supplementary Table 1**). Experiments were carried out in triplicates with the following conditions: 5 min at 95°C, followed by 40 cycles at 95°C for 30 s, and 55°C for 30 s, as described previously (Pii et al., 2016, 2019). The amplification efficiency was calculated from raw data using the LinRegPCR software (Ramakers et al., 2003). For each transcript, the mean normalized expression value (MNE; Simon, 2003) was calculated using the housekeeping transcript and the relative expression ratio values were calculated by the $2^{-\Delta\Delta Ct}$ method according to Livak and Schmittgen (2001).

Data Analysis

All experimental data for both plant species (*C. sativus* and *Z. mays*) were statistically subjected to two-way ANOVA using the software IBM SPSS Statistics 20. The mean values were separated according to Tukey's HSD test with $p < 0.05$ and *P* levels effects were compared using the *t*-test. A heatmap summarizing the morpho-physiological parameters, ionomic analysis, and root exudation responses of both plant species to the biostimulant treatments and P fertilization levels were also generated using the R software (https://www.r-project.org, performing "pheatmap," "ggplot2," and "RColorBrewer" packages). Hierarchical clustering based on standardized data was performed with Complete linkage and Manhattan distance was used as the similarity measure.

RESULTS

Plant Growth and Morpho-Physiological Parameters

At the end of the growing period, P deficiency in plants was visually and more identified in cucumber plants when compared with maize plants, since they showed typical symptoms like the dark green color of the leaves and higher expansion of the root system (**Figure 2**). However, for both plant species, the ANOVA results showed that most of the measured morpho-physiological parameters were significantly affected by P fertilization levels (P) and biostimulant treatments (I), except for the root diameter, which was not affected by the biostimulant treatments (**Supplementary Table 2**). The P × I interaction effects were also significant for both plant species, influencing most of the parameters (**Supplementary Table 2**). This interaction was better noted when comparing the mean values, as shown in **Table 1**. For instance, in cucumber plants, the SPAD index values were significantly higher in P-deficient plants (P–) when compared with P-fed plants (P+). As expected, P-deficient cucumber plants appeared darker in color (**Figure 2**) with the

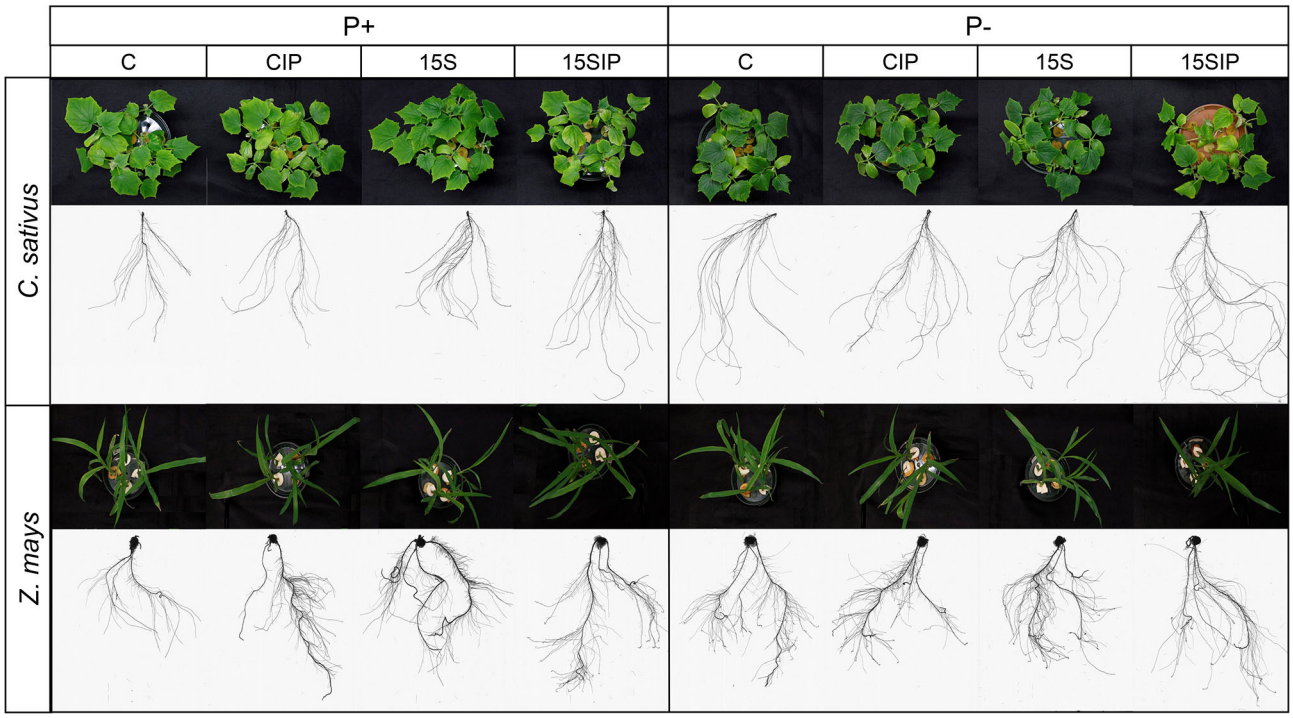

FIGURE 2 | Shoot and root apparatus of cucumber (*C. sativus*) and maize (*Z. mays*) plants in response to a factorial experiment with two P fertilization levels (P+, NS supplemented with 0.1 mM of KH_2PO_4; P–, NS non-supplemented with KH_2PO_4) and four biostimulant treatments [C, uninoculated control; CIP, uninoculated control with the insoluble phosphate $Ca_3(PO_4)_2$; 15S, inoculated with the PGPB *Enterobacter* 15S; 15SIP, inoculated with the PGPB *Enterobacter* 15S plus the insoluble phosphate $Ca_3(PO_4)_2$].

exception of the 15SIP treatment. In the latter, the plants did not exhibit darker green leaves with average values not different from those measured in plants grown in P-full condition (P+: 15SIP) (**Table 1**). Similarly, in maize plants, the highest SPAD index values were recorded under P deficiency with no visible symptoms of pigmentation on the leaves. However, in both inoculation treatments, maize plants presented lower SPAD values, which were no different from those recorded in plants grown under full P (**Table 1**). It is interesting to note that, for P-fed maize plants, the effect of the bacterial inoculation on the levels of chlorophyll contents was not significant when compared to the control. Nevertheless, a more evident effect was noted in P-deficient maize plants, suggesting the involvement of the bacteria in the amelioration of photosynthetic rates during P starvation.

In both plant species, the biomass and the architecture of the root systems were also affected by both P levels and inoculation treatments. For instance, in cucumber, the mean values recorded for root DW, total root length, surface area, volume, tips, and the root/shoot (R/S) ratio were significantly higher under P deficiency when compared with plants grown with full P; on the contrary, the shoot DW was higher under complete P (**Table 1**). Furthermore, when inoculated with *Enterobacter* 15S, P-deficient cucumber plants showed a significant decrease in the root length and surface area with respect to the uninoculated control, whereas supplementation with the insoluble $Ca_3(PO_4)_2$ (treatment P–: 15SIP) produced a significant increase in these parameters, albeit not significant when compared to the control. Additionally, root and shoot biomass were unaffected by the inoculation, whereas the R/S ratio was highly increased in both inoculant treatments (**Table 1**). A different response to the inoculation was observed in P+ cucumber plants. In particular, the length, surface area, and volume of roots were significantly increased with the use of *Enterobacter* 15S alone or in combination with the insoluble phosphate (P+: 15S and 15SIP). However, the root and shoot biomass of the cucumber plants inoculated with *Enterobacter* alone were not significantly different from control plants; instead, its combination with $Ca_3(PO_4)_2$ produced a reduction in plant biomass accumulation, while the R/S ratio was not affected.

In contrast with cucumber, P fertilization levels did not affect the root architecture of maize plants. Nonetheless, the root and shoot biomass were significantly higher under the P-full condition, while the R/S ratio increased in P-deficient plants (**Table 1**). Moreover, P– maize plants inoculated with *Enterobacter* 15S did not show significant changes in length, diameter, volume, and root biomass as compared to control plants. On the other hand, the surface area and root tips were significantly increased in plants treated with the bacteria alone (P–: 15S), albeit a reduction of 37% in the shoot biomass was observed. In P+ maize plants, the inoculation

TABLE 1 | Mean values for the morpho-physiological parameters in cucumber and maize grown hydroponically under different P-fertilization levels and different inoculation treatments with *Enterobacter* 15S.

Parameters[a]	P level[b]	Cucumber					Maize				
		Biostimulant treatments[c]					Biostimulant treatments[c]				
		C	CIP	15S	15SIP	P level effect	C	CIP	15S	15SIP	P level effect
SPAD	P+	29.97 Ba	29.93 Ba	29.17 Bab	28.80 b	29.47 B	29.47 B	31.20 B	31.40	30.97	30.76 B
	P-	43.63 Aa	41.07 Aa	43.57 Aa	30.20 b	39.62 A	38.03 Aa	38.07 Aa	32.90 b	30.63 b	34.91 A
Treatment effect		36.80 a	35.50 a	36.37 a	29.50 b		33.75 ab	34.63 a	32.15 bc	30.80 c	
Length	P+	194.15 Bb	218.40 Bab	232.52 Bab	285.17 Ba	232.56 B	229.42 Bb	522.94 a	541.27 a	456.97 Ba	437.65
	P-	424.07 Aa	305.37 Ac	330.57 Abc	374.56 Aab	358.64 A	503.23 A	500.49	519.83	522.16 A	511.43
Treatment effect		309.11 ab	261.88 c	281.54 bc	329.87 a		366.33 b	511.72 a	530.55 a	489.57 a	
Surface area	P+	17.62 Bb	19.70 Bb	22.71 Bab	28.21 Ba	22.06 B	24.53 Bd	61.88 Aa	54.94 b	47.76 c	47.28
	P-	41.26 Aa	29.08 Ab	31.81 Ab	40.16 Aa	35.58 A	46.80 Ab	47.55 Bb	53.01 a	50.40 ab	49.44
Treatment effect		29.44 b	24.39 c	27.26 bc	34.18 a		35.67 c	54.72 a	53.98 a	49.08 b	
Diameter	P+	0.29 B	0.30	0.30	0.30	0.30 B	0.32	0.34 A	0.33	0.33	0.33 A
	P-	0.34 Aa	0.30 b	0.32 ab	0.32 ab	0.32 A	0.32	0.31 B	0.33	0.31	0.32 B
Treatment effect		0.32	0.30	0.31	0.31		0.32	0.33	0.33	0.32	
Volume	P+	0.13 Bb	0.15 Bb	0.18 Bab	0.22 Ba	0.17 B	0.24 Bc	0.54 Aa	0.49 ab	0.39 b	0.42
	P-	0.26 Aab	0.22 Ab	0.24 Aab	0.32 Aa	0.26 A	0.37 A	0.36 B	0.43	0.39	0.39
Treatment effect		0.20 b	0.18 b	0.21 b	0.27 a		0.31 c	0.45 a	0.46 a	0.39 b	
Tips	P+	231.00 Bab	214.67 Bab	198.00 Bb	306.67 Ba	237.58 B	374.67 Bb	613.67 a	691.33 a	704.00 a	595.92
	P-	445.67 Aa	304.67 Ab	350.00 Aab	405.33 Aab	376.42 A	672.00 Aab	574.00 b	745.33 a	669.33 ab	665.17
Treatment effect		338.33 a	259.67 b	274.00 b	356.00 a		523.33 b	593.83 b	718.33 a	686.67 a	
RDW	P+	15.03 ab	10.50 Bc	17.00 a	11.90 Bbc	13.61 B	25.43 Aa	30.97 Aa	27.63 Aa	14.97 b	24.75
	P-	14.27	15.93 A	17.83	15.70 A	15.93 A	19.83 B	25.17 B	20.33 B	19.17	21.13
Treatment effect		14.65 b	13.22 b	17.42 a	13.8 b		22.63 b	28.07 a	23.98 ab	17.07 c	
SDW	P+	86.97 Aa	89.13 a	82.67 Aa	61.70 b	80.12	146.70 Aa	133.00 Aa	95.93 Ab	100.33 b	118.99 A
	P-	66.37 Bab	85.53 a	66.17 Bab	62.27 b	70.08	94.27 Ba	71.10 Bb	59.43 Bb	93.3 a	79.53 B
Treatment effect		76.67 ab	87.33 a	74.42 ab	61.98 b		120.48 a	102.05 b	77.68 c	96.82 b	
R/S ratio	P+	0.17 Ba	0.12 Bb	0.21 Ba	0.19 Ba	0.17 B	0.17 b	0.23 Ba	0.29 Ba	0.15 Bb	0.21 B
	P-	0.22 Ab	0.19 Ab	0.27 Aa	0.25 Aa	0.23 A	0.21 b	0.35 Aa	0.34 Aa	0.21 Ab	0.28 A
Treatment effect		0.20 ab	0.15 b	0.24 a	0.22 a		0.19 b	0.29 a	0.31 a	0.18 b	

Phosphorus level effects were compared using t-tests. Differences between means were determined using Tukey's HSD test. Significant differences ($p < 0.05$) according to Tukey's test are indicated by different capital letters when comparing contrasts in columns and different lowercase letters when comparing contrasts in rows. No significant differences are indicated by omitting notation letters.

[a] soil-plant analysis development (SPAD), SPAD units; Length, total root length (cm); Surf. area, root surface area (cm^2); Diameter, root diameter (cm); Volume, total root volume (cm^3); Tips, Number of root tips; RDW, root dry weight (mg); SDW, shoot dry weight (mg); R/S, root-to-shoot ratio.

[b] P levels: P+ [nutrient solution (NS) supplemented with 0.1 mM of KH_2PO_4]; P– (NS non-supplemented with KH_2PO_4).

[c] Biostimulant treatments: C, uninoculated control; CIP, uninoculated control with the insoluble phosphate $Ca_3(PO_4)_2$; 15S, inoculated treatment with the PGPB Enterobacter 15S; 15SIP, inoculated treatment with the PGPB Enterobacter 15S plus the insoluble phosphate $Ca_3(PO_4)_2$.

with the *Enterobacter* alone (P+: 15S) significantly increased the architecture of the root system as compared to control plants, albeit the root biomass was not affected; on the other hand, a decrease in the shoot biomass was recorded.

Evaluation of Element Composition in the Roots and Shoots of Cucumber and Maize

A suite of 10 mineral elements, among which were macronutrients (P, calcium - Ca, magnesium – Mg, and sulfur - S), micronutrients (iron - Fe, zinc - Zn, manganese - Mn, and copper - Cu), and beneficial nonessential elements (barium - Ba and sodium - Na), were analyzed in the roots and shoots of both plant species (**Figure 3** and **Supplementary Table 3**). In cucumber, regardless of P fertilization and PGPB inoculation, foliar concentrations of P, Ca, Mg, and Mn exceeded those in the roots, while Fe and Cu concentrations were higher in the roots. On the other hand, the concentrations of Ba, Zn, S, and Na were dependent on both P fertilization and PGPB inoculation. For instance, the elements mentioned were higher in roots of P+ cucumber plants as compared to shoots but displayed higher concentrations in the shoots of P– plants (**Figure 3**). In maize, the concentration of all the mineral elements was higher in roots, regardless of the P levels and inoculant treatments, except for P concentration, which was higher in aboveground tissues.

Nevertheless, P fertilization level and biostimulant treatments caused the imbalanced nutrient distribution in the roots and shoots of both plant species. As expected, P deficiency led to a decreased P concentration in the roots and shoots of both plants (**Figure 3A**). However, in cucumber, the inoculation with *Enterobacter* 15S in combination with $Ca_3(PO4)_2$ (treatment P–: 15SIP) significantly increased the content of P in the roots and shoots by about 31 and 53%, respectively, as compared to the P– uninoculated samples (P–: C). In contrast, in maize, P-deficient plants inoculated with the bacteria alone (P–: 15S) led to the enhancement of P concentration in the roots (+36%) as compared to uninoculated plants (P–: C); however, P concentration in the shoots was not affected (**Supplementary Table 3**). In the P+ condition, the P concentration values in the roots of the cucumber plants were unaffected by the treatments imposed, whereas inoculation with PGPB induced a slight decrease of this mineral in the shoots. On the contrary, in maize plants, inoculation with *Enterobacter* caused a higher accumulation of P in both the roots and shoots (**Figure 3A**).

The accumulation of Ca and Mg in the roots and shoots of both cucumber and maize grown in P deficiency was decreased when compared to plants grown in P+ conditions (**Figures 3B,C**). An exception to this trend is represented by maize roots, in which the inoculation with *Enterobacter* 15S (treatment P–: 15S) induced a higher accumulation of Mg compared to P+ plants. On the contrary, in P+ cucumber plants, treatments with the inoculants caused a significant decrease in Mg concentration (**Supplementary Table 3**). Calcium concentration was, in both P+ and P– plants, significantly increased in the roots of both 15SIP cucumber and maize, although the same treatment induced the opposite effect in cucumber shoots and no effects in maize shoot when compared to the control. Additionally, the treatment with the bacterium (i.e., 15S) resulted in the highest content of Ca in the shoots of all the maize plants.

Under P deficiency, S concentration in the roots of cucumber was increased by the 15SIP treatment as compared to P+ conditions, whereas, in the case of maize, only inoculated P-deficient plants (i.e., P–: 15S and 15SIP) showed higher S content in the roots with respect to the plants grown under P+ conditions (**Figure 3D**). The inoculation with *Enterobacter* significantly increased the concentration of S by more than 45% in the roots of both P-full and P-deficient cucumber plants compared to the control alone, while the highest content in shoots was observed in control plants combined with $Ca_3(PO_4)_2$ (treatment CIP). In contrast, the different treatments did not affect the accumulation of S in maize shoots.

Concerning the micronutrients (**Figures 3E–H**) and non-essential elements (**Figures 3I,J**), the P deprivation in the NS led to a decreasing trend in all the elements in the roots of cucumber plants, except for Mn, but caused an increase in the concentration of Fe, Mn, and Ba in the aboveground tissues. In maize plants, P deficiency induced the increase in Fe and Ba concentration at the shoot level, as well Zn and Mn in the roots. Furthermore, under P deficiency conditions, the inoculation of cucumber with *Enterobacter* 15S in combination with the insoluble phosphate (P–: 15SIP) had a significant promoting effect on the accumulation of all micronutrients in the roots when compared to the uninoculated control, whereas the same treatment had no significant effects on Fe and Mn concentration in the shoots. However, under P-sufficient conditions, a decrease in the content of all micronutrients in the shoots of cucumber was associated with *Enterobacter* 15S inoculation. Besides, the supplementation with $Ca_3(PO_4)_2$ (treatment P+: CIP) induced the highest Fe, Zn, and Ba concentrations in cucumber roots (**Figure 3** and **Supplementary Table 3**). On the other hand, P-deficient maize plants treated with the bacterium plus $Ca_3(PO_4)_2$ (treatment P–: 15SIP) showed a significant increase in the concentration of Mn and Zn in the roots and a decrease in that of Na; no changes were observed for Fe and Cu. When the bacterial inoculant was used alone, the highest concentrations of Zn, Mn, and Cu were detected in the leaves of maize as compared with uninoculated plants. In contrast, the inoculation treatments did not induce remarkable changes in the accumulation of micronutrients in the roots and shoots of maize plants grown under the full-P NS (**Figures 3E,J**). Additionally, under P+ conditions, the inoculated maize and cucumber plants showed a decreased content of Na in the roots when compared to the uninoculated plants (**Figure 3J**, treatments P+: 15S and 15SIP).

Release of Phenolics and Flavonoids

The root exudate concentration released by both plant species was determined spectrophotometrically in terms of phenolic compounds and flavonoids. **Figure 4A** shows the total content of phenolic compounds released by the cucumber and maize plants in the different conditions considered in the study. In cucumber, the amount of phenolics was higher in P-deficient conditions (ranging from 5 to 7 nmol g^{-1} RFW) compared to P+ plants (ranging from 2 to 4 nmol g^{-1} RFW). Any

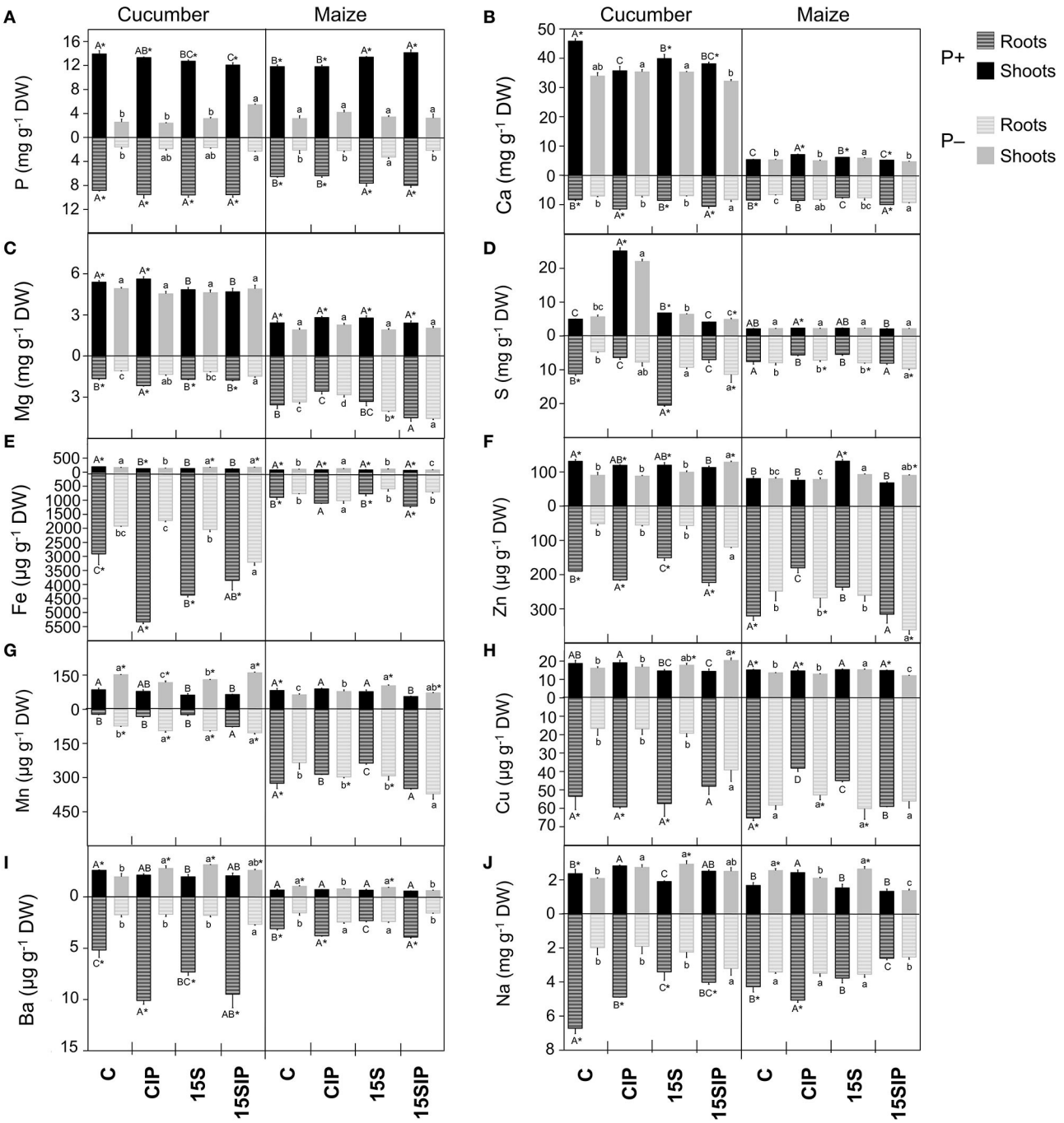

FIGURE 3 | Ionomic profile of cucumber and maize plants tissues. **(A)** Phosphorus, P; **(B)** Calcium, Ca; **(C)** Magnesium, Mg; **(D)** Sulfur, S; **(E)** Iron, Fe; **(F)** Zinc, Zn; **(G)** Manganese, Mn; **(H)** Copper, Cu; **(I)** Barium, Ba; **(J)** Sodium, Na concentrations in roots and shoots of cucumber and maize grown hydroponically under different P-fertilization levels (P+ and P–) and different biostimulant treatments with *Enterobacter* 15S (C, CIP, 15S, 15SIP). Values are means ± SE; $n = 3$. Uppercase letters compare treatments under P+, and lowercase letters compare treatments under P–. An asterisk is present when there is a difference in the same treatment between P+ and P–. Equal letters correspond to average values that do not differ according to Tukey's test ($p < 0.05$).

statistically significant difference was recorded between the different treatments. Under the P+ conditions, the content of phenolics was significantly higher in the control treatment, while inoculation with *Enterobacter* 15S induced a smaller release of phenolic compounds (**Figure 4A**). In maize plants, the root exudation of phenolics was higher as compared to cucumber. In the P+ condition, inoculation with the bacterium (P+: 15S and 15SIP treatments) induced a higher exudation of phenolics

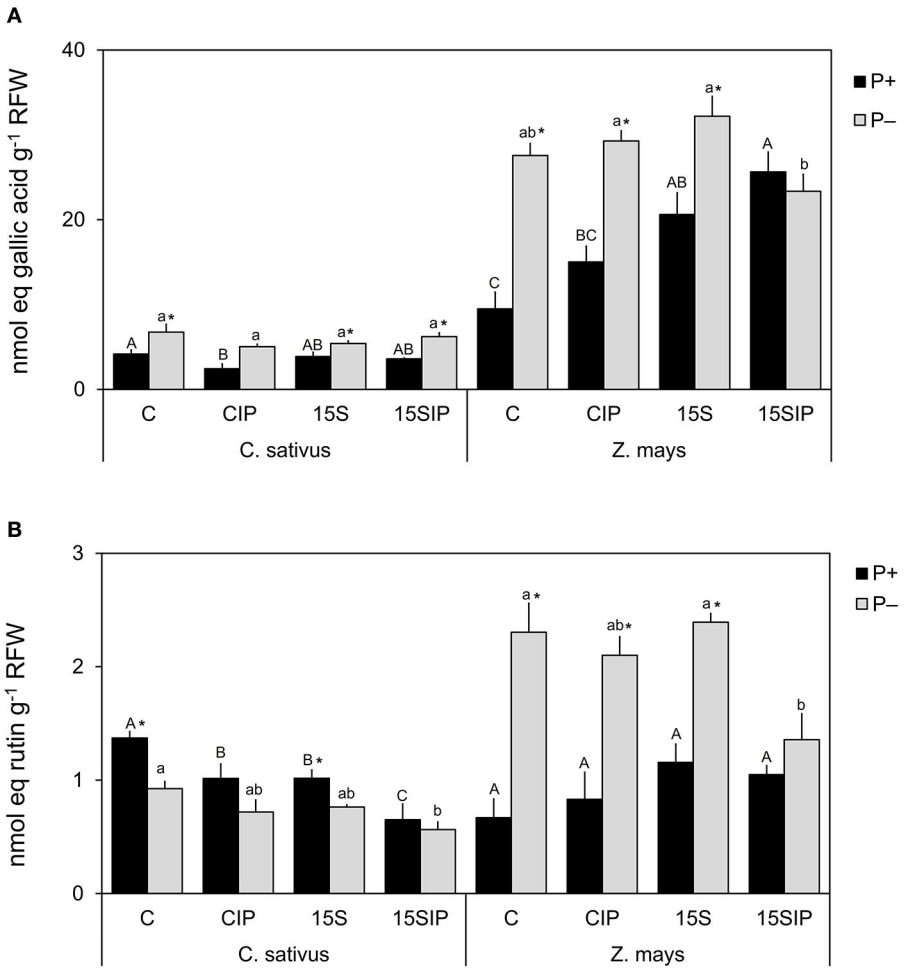

FIGURE 4 | Total phenolic compounds content **(A)** and total flavonoid content **(B)** determined in the root exudates of cucumber and maize collected at the end of the cultivation period. Values are means ± SE; $n = 3$. Capital letters compare treatments under P+, and lowercase letters compare treatments under P–. An asterisk is present when there is a difference in the same treatment between P+ and P–. Equal letters correspond to average values that do not differ according to Tukey's test ($p < 0.05$). Two-way ANOVA results: Phenolic compounds: cucumber, P ($p < 0.001$), I ($p < 0.01$), P × I (NS); maize, P ($p < 0.001$), I ($p < 0.001$), P × I ($p < 0.001$). Flavonoids: cucumber, P ($p < 0.001$), I ($p < 0.001$), P × I (NS); maize, P ($p < 0.01$), I (NS), P × I ($p < 0.01$).

compared to the uninoculated controls. On the other hand, the release of phenolics by maize plants grown in P deficiency was significantly higher (23–32 nmol g^{-1} RFW) than that observed in P+ conditions (9–26 nmol g^{-1} RFW), except for the treatment P–: 15SIP. In the latter, the bacterial inoculation and supplementation with $Ca_3(PO4)_2$ induced a decrease in the exuded phenolics, presenting levels significantly lower than that measured in control plants (**Figure 4A**).

The root exudation of flavonoids by both plant species is shown in **Figure 4B**. In cucumber, the total flavonoid content was significantly reduced by the bacterial inoculation in both P fertilization levels. However, in P+ conditions, a significantly higher production was observed for C and 15S treatments (1 and 1.4 nmol g^{-1} RFW, respectively), compared with the same treatments under P deficiency (0.8 and.9 nmol g^{-1} RFW, respectively); any remarkable effects were observed for CIP and 15SIP in both P+ and P– conditions (**Figure 4B**). On the other hand, P deficiency induced a higher exudation of flavonoids in maize (ranging from 2.1 to 2.4 nmol g^{-1} RFW) with respect to P+ plants (ranging from 0.7 to 1.2 nmol g^{-1} RFW), except for the 15SIP treatment. No significant effects were observed within P+ plants subjected to different treatments.

Phosphate Transporters Gene Expression Analysis

In plants, Pi transporter genes belonging to the *Pht1* family are strongly expressed in roots and play important roles in the transmembrane transport of Pi for its acquisition and allocation within the plants and the single cell. Most of these genes have been reported to be highly induced by P deficiency (Wang et al., 2018). In cucumber, six genes involved in the phosphate uptake have been identified, namely, *CsPT1.3*, *CsPT1.4*, *CsPT1.7*, *CsPT1.9*, *CsPT1.11*, and *Cucsa383630.1* (Naureen et al., 2018; Feil et al., 2020). However, under the conditions, the expression of

CsPT1.7 and *CsPT1.11* was not detectable under P starvation (data not shown). In maize, 13 *PhT1s* genes have been identified (Liu et al., 2016), but in this work, six of these genes were reported by Nagy et al. (2006), namely, *ZmPT1*, *ZmPT2*, *ZmPT3*, *ZmPT4*, *ZmPT5*, and *ZmPT6* were analyzed. Nonetheless, four genes (*ZmPT2*, *ZmPT3*, *ZmPT4*, and *ZmPT6*) were poorly induced by P deficiency in our experimental conditions (data not shown).

Figure 5 shows the relative expression levels of the *CsPTs* and *ZmPTs* genes under P deficiency. Results indicate that, in both plants, all the analyzed genes were expressed under the P+ condition but were highly upregulated in P-deficiency. For instance, in cucumber, *CsPT1.4* was highly induced in P- (>160-fold up to 270-fold), followed by *CsPT1.9* (>50-fold up to 150-fold) and *Cucsa383630.1* (>4-fold up to 15-fold), while *CsPT1.3* was less expressed (>2-fold) when compared to control plants under complete P fertilization. Additionally, in cucumber plants grown under a P-full NS, the expression of all *CsPTs* genes was not significantly affected by the treatments (**Figure 5**). On the other hand, inoculation with *Enterobacter* 15S induced transcriptional changes for all *CsPTs* genes under P starvation. For instance, *CsPT1.3* and *CsPT1.4* were induced by both inoculant treatments (P–: 15S and 15SIP) in comparison to uninoculated plants (P–: C and CIP). On the contrary, inoculation with the bacterium (P-: 15S) induced a significantly higher expression of the *CsPT1.9* and *Cucsa383630.1* genes as compared with the other three treatments.

In maize plants grown under P deficiency, *ZmPT5* was expressed more (>14-fold up to 127-fold) than *ZmPT1* (>2-fold up to 7-fold), compared with P-sufficient control plants. However, the inoculation induced different relative transcript levels in both genes. For instance, in maize plants grown in either P-full or P-deprived NSs, inoculation with *Enterobacter* 15S downregulated the expression of *ZmPT5* in roots when compared to uninoculated control plants under the same conditions (**Figure 5**). Nonetheless, the relative transcript levels of *ZmPT1* were significantly lower in P-deficient plants inoculated with the bacterium alone (P–: 15S), while the inoculant treatment supplemented with the insoluble phosphate (P–: 15SIP) induced the expression of a higher amount of transcript, yet not much higher than the uninoculated controls (**Figure 5**). No significant differences were observed in the expression of *ZmPT1* in maize plants under P-full conditions.

DISCUSSION

Plant Growth and Morpho-Physiological Responses to Bacterial Biostimulant Inoculation and/or P Supply

The inoculation with PGPB has been shown to improve plant growth in both favorable and unfavorable conditions, including low-nutrient availability (Oleńska et al., 2020). In the specific case of P) shortage, it has been broadly described that physiological, morphological, and molecular changes are induced in plants as a specific response to this nutritional stress (López-Arredondo et al., 2014; Elanchezhian et al., 2015). Results reported in this study show that both P availability in the NS and the bacterial biostimulant *Enterobacter* 15S were able to influence the plant biomass accumulation and the development of morpho-physiological traits in cucumber and maize plants, although to a different extent. The cucumber plants exhibited a more remarkable response to P starvation, in particular, showing a more developed root system with respect to the maize plants. Indeed, the root system is very responsive to low-P availability in the growth medium; thus, in the majority of plant species, increasing root length root surface area, and enhancing the growth of root hairs are described as common strategies to explore larger soil surfaces and intercept nutrients (Ramaekers et al., 2010). Despite the root system architecture being different between monocots and dicots, the signaling pathways underpinning P-acquisition mechanisms are conserved (Shahzad and Amtmann, 2017). The low-P availability induces an increase in the R/S ratio that is generally ascribable to a limitation in shoot biomass accumulation, an increase in root production, or both (Campos et al., 2019). However, in our experimental conditions, the biomass allocations among the two plant species resulted quite differently. While the root biomass in maize plants was reduced under P starvation, it was significantly increased in the cucumbers. In this regard, it is worth mentioning that, from a nutrient availability perspective, plants have to balance the biomass allocation to leaves and/or roots to an extent that matches the physiological activities and functions performed by these organs (Poorter et al., 2012), including those related to plant responses to nutritional disorders.

The inoculation with the bacterial biostimulant *Enterobacter* 15S affected the root architecture and biomass of both plants differently depending on P supply. Overall, the data suggest that *Enterobacter* 15S led to the improved growth of the root system in both plant species grown in P-sufficient conditions. Under P deficiency, the bacterium in combination with $Ca_3(PO_4)_2$ (P–: 15SIP) induced a remarkable effect on the whole cucumber plant, whilst the bacterium alone (P–: 15S) was more effective in improving the root system of maize plants. *Enterobacter* strains have been described to enhance the plant growth of different plant species, including monocot and dicot types (Naveed et al., 2013; Gupta et al., 2020; Ji et al., 2020). The biostimulant strain 15S used in this work was previously reported by Zuluaga et al. (2020) to have the ability to produce auxins and solubilize Pi. Bacteria-derived auxins are well-known for promoting morphological and physiological processes in plants, leading to increased growth of the root system in terms of root length and surface area; thus enhancing nutrient and water uptake (Hakim et al., 2021). Under stressful conditions (e.g., P deficiency), plants can stimulate bacteria to produce auxins (Kudoyarova et al., 2019). However, when produced in high concentrations, bacteria-derived auxins can inhibit root elongation in dicots, whereas monocots resulted in less sensitivity to such inhibition (Kudoyarova et al., 2019). In this context, it is also worth mentioning that a particular plant nutritional state (e.g., P sufficiency or P deficiency) may influence the interaction mechanisms between PGPB and host plants (Pii et al., 2016), thus explaining the contrasting results observed in this study for cucumber and maize plants. Moreover, it is important to highlight that, in a specific edaphic condition, PGPB may also

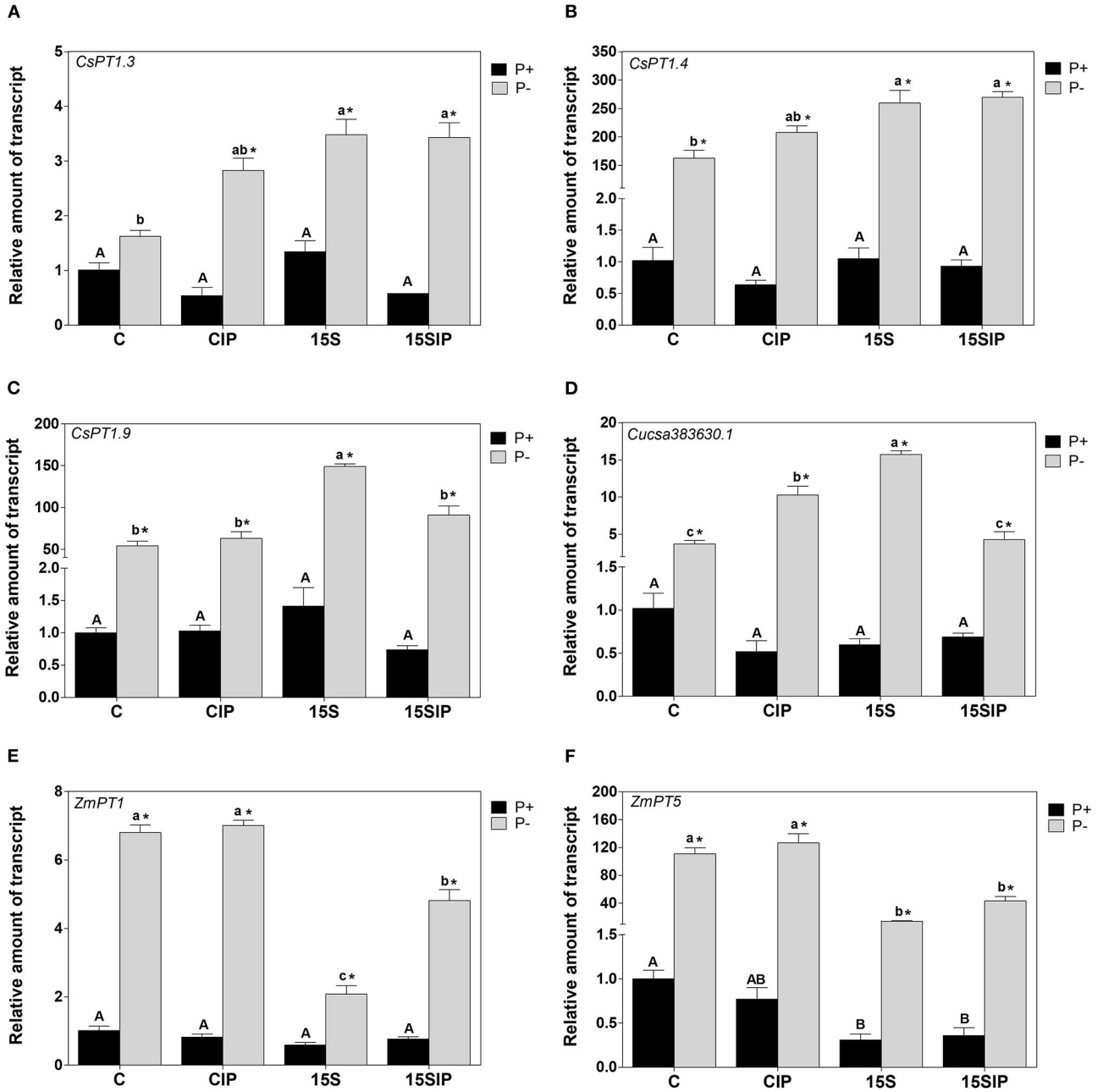

FIGURE 5 | Gene expression analysis of **(A)** *CsPT1.3*, **(B)** *CsPT1.4*, **(C)** *CsPT1.9,* and **(D)** *Cusca383630.1* in the roots of the cucumbers, and **(E)** *ZmPT1* and **(F)** *ZmPT5* in the roots of maize grown hydroponically under different P-fertilization levels (P+ and P–) and different biostimulant treatments with *Enterobacter* 15S (C, CIP, 15S, 15SIP). The expression level of each gene was normalized to the expression level of the elongation factor isoform 1-alpha (EF-1α). The relative expression ratios were calculated using the uninoculated control under complete P (P+: C) as a calibrator sample. Values are means ± SE; $n = 3$. Uppercase letters compare treatments under P+ and lowercase letters compare treatments under P–. An asterisk is present when there is a difference in the same treatment between P+ and P–. Equal letters correspond to average values that do not differ according to Tukey's test ($p < 0.05$).

display a differential preference for one particular plant species over another (Glick, 2005). The effects of this interaction rely on a set of adaptation mechanisms by both the inoculated bacteria and the host plant (Drogue et al., 2012).

Concerning chlorophyll content, a significant increase in both plant species grown under P starvation has been recorded, is particularly pronounced in cucumber leaves manifesting a particular dark green color. A similar trend has also been described in strawberry and apple plants (Valentinuzzi et al., 2015, 2019; Delaporte-Quintana et al., 2017). Moreover, a more severe or prolonged P deficiency may result in the accumulation of anthocyanins, consequently increasing the pigmentation

of the newest leaves and chlorophyll concentrations (Veazie et al., 2020). However, the inoculation of P-deficient maize plants with *Enterobacter* 15S (i.e., 15S and 15SIP) reduced the levels of chlorophyll content to the same values of the inoculated P-sufficient plants. In contrast, in cucumber plants, only the treatment with the bacterium in combination with the insoluble phosphate (15SIP) was able to induce chlorophyll contents similar to those measured in P-sufficient plants. In this respect, Delaporte-Quintana et al. (2017) already reported that the SPAD values of P-deficient strawberry plants inoculated with *Gluconacetobacter diazotrophicus* PAL5 were similar to those obtained in plants grown under sufficient P, indicating the contribution of this strain to plant P nutrition and photosynthesis.

Effects of Bacterial Biostimulant and P Supply on Mineral Nutrient Content

Several agronomic conditions such as physical-chemical properties of the growth substrate, fertilization regimes, and inoculation with PGPB have been described to induce changes in the elemental composition of crops, regardless of the clade considered (Pii et al., 2015a,b). In the present study, P deficiency led to a reduction of P content in the roots and shoots of both plants, while inoculation with the bacterial biostimulant with *Enterobacter* 15S induced a differential allocation of this element. For instance, in P-deficient cucumber plants, the inoculation in combination with $Ca_3(PO_4)_2$ (P–: 15SIP) induced a higher allocation of P in roots and shoots, whereas maize plants inoculated with the bacterial biostimulant alone showed a higher content of P only in roots. Recent study showed that the inoculation of tomato plants grown under P-deficiency and salt stress conditions with different strains of *Arthrobacter* and *Bacillus* induced an increased P concentration in roots and shoots (Tchakounté et al., 2020) and the shoots of *Brachypodium* plants (Schillaci et al., 2021). On the contrary, the inoculation of wheat plants with beneficial bacteria led to a reduced P content in roots (Talboys et al., 2014). Interestingly, under P-sufficient conditions, *Enterobacter* 15S induced opposite effects on the P concentration in the shoots of the two plant species, showing a decrease in cucumber and an increase in maize plants. The results suggest that the mechanisms by which *Enterobacter* 15S improves P acquisition and its translocation within the plant can be dependent on both plant species and nutritional status. It was observed in cultivated monocots grown at different P levels that the inoculation with PGPB can increase the adaptation of these grasses to the low-P availability through an improvement in P-use efficiency, with the functionality of the P-uptake mechanism still not being affected (Pereira et al., 2020; Schillaci et al., 2021). Moreover, in dicots grown under different P states, it has been described that plant development stimulation *via* PGPB inoculation was not accompanied by an increase in nutrient uptake by the roots and the P content in shoots that, on the contrary, appeared to be rather decreased (Belimov et al., 2002).

Regarding micronutrients (i.e., Fe, Zn, Mn, and Cu) and non-essential beneficial elements (i.e., Ba and Na), inoculation with *Enterobacter* 15S promoted their accumulation at the root level only in cucumber plants supplemented with the insoluble phosphate grown under P-deficient conditions. The same trend was also observed at the shoot level, except for Fe and Mn. In maize plants, under the same condition described for cucumber, only Mn and Zn were increased in roots, while inoculation with the bacterium alone improved the allocation of Zn, Mn, and Cu to shoots. The biochemical mechanisms underlying the nutritional processes in plants and nutrient availability can be altered by PGPB as a strategy to improve plant nutrient uptake, which, in turn, is influenced by microbial strains and plant species (Pii et al., 2015b). Additionally, under equilibrate P availability, bacterial inoculation induced a decrease in the concentrations of all micronutrients in the subaerial part of cucumber plants, whilst no significant changes were induced in maize plants. Under a specific nutritional shortage, plants can also trigger physiological modulations to maintain the ionic equilibrium of the tissues (Marschner, 1995). Thus, changes in the concentration of a mineral element might induce modulations (positive or negative) of the concentration levels of one (or more than a single) essential or non-essential nutrient. It is worth noting that, under sufficient P conditions, the accumulation of Na in the roots of both plants was reduced by inoculation with *Enterobacter* 15S. Decreased concentrations of Na have been reported in plants inoculated with PGPB and AMF as a mechanism to protect plant cells against oxidative stress by maintaining intracellular ionic homeostasis (Giri and Mukerji, 2004; Panwar et al., 2016).

A Differential Root Exudation Pattern Was Induced by P Deficiency and Bacterial Biostimulant

In specific nutritional conditions, plants can change their qualitative and quantitative composition of root exudates to increase the availability of nutrients (Badri and Vivanco, 2009) and/or to influence the microbial populations colonizing the roots (Cesco et al., 2012). Phenolic acids and flavonoids have been reported as the major secondary metabolites exudated by plant roots and are significant in diverse biological processes (Mandal et al., 2010; Cesco et al., 2012). Root exudation and regulation of these compounds seems to be an important strategy for plants to overcome P deficiency (Malus et al., 2006). Regardless of P supply, the total content of phenolic acids exuded by roots was plant species-dependent, whereas the release of flavonoids was similar in both plants hereby evaluated. In general terms, the amount and diversity of secondary metabolites released by roots are highly species-specific (Zwetsloot et al., 2018). P deficiency induced an increase in the content of phenolic acids exuded by the roots of both plants, which is in accordance with other works. For instance, under P deficiency, the amount of exuded phenolics from bean roots was five times higher (Juszczuk et al., 2004) and *Stylosanthes* roots had more than 10-fold in exudates (Luo et al., 2020), as compared to their respective controls. However, both the accumulation and exudation of phenolic compounds can also be modified in response to microbial inoculation (Vacheron et al., 2013). The inoculation of P-sufficient maize plants with *Enterobacter* 15S (treatment P+: 15SIP) induced a higher

production of phenolic compounds, while the same treatment under P deficiency elicited a lower release. No effects were induced by the inoculation in cucumber plants. These results suggest that plants interacted with the bacterial biostimulant in different ways. The exudation of phenolic compounds is induced by PGPG inoculation also in plants subjected to other nutrients deficiencies. For instance, under N scarcity, peanut plants inoculated with *Stenotrophomonas maltophilia* modified their metabolism in response to the inoculum by producing a higher amount of total phenolic compounds, thus resulting in increased antioxidants and free radical scavenging activities (Alexander et al., 2019).

In the present study, we observed that the root exudation of flavonoids was lower in both plant species when compared with the total release of phenolics. P deficiency induced an increase in the flavonoids released by maize plants, while a decreased exudation of these compounds was observed in cucumber plants. Flavonoids are known for assisting plants in tolerating and overcoming biotic and abiotic stresses generated by the external environment (Shah and Smith, 2020). It has been suggested that flavonoids released from the roots of P-deficient plants can facilitate the mobilization of P-insoluble complexes (e.g., Fe-P) and also reduce the microbial degradation of organic acids (Tomasi et al., 2008). Furthermore, inoculation with PGPB can alter not only the content but also the profile of flavonoids in root exudates (Garcia-Seco et al., 2015). In this study, regardless of P supply, the inoculation with the bacterial biostimulant significantly reduced flavonoid content in the root exudates of cucumber plants, while their concentration in maize exudates was not affected, except for the treatment 15SIP (P–); in this case, a reduction of flavonoids was induced as also observed for phenolic compounds. A differential accumulation of flavonoids was described by Zuluaga et al. (2021) in root exudates of tomato plants inoculated with the same *Enterobacter* 15S strain used in the present study. In some cases, the down-accumulation of flavonoids in PGPB-inoculated plants may indicate its consumption as a C source or a blocking in their biosynthesis (Dardanelli et al., 2010; Wu et al., 2018). In this respect, it is interesting to note that the reacquisition of a fair range of exudates by roots of intact plants as recently demonstrated by Tiziani et al. (2020) makes this assessment rather complicated.

Differential Regulation of Phosphate Transporters Was Elicited by P Starvation and the Inoculation With *Enterobacter* 15S

Members of the *PHT1* family are the most intensively studied Pi transporters genes in plants. They are known for exhibiting strong expression in the roots of both monocots and dicots (Nussaume et al., 2011). Most of these genes are strongly induced under P-limiting conditions and have been reported to be involved in the root uptake of Pi from soil solutions and then its translocation within the plant (Wang et al., 2018). Consistently, all the Pi transporters genes herein evaluated were greatly expressed in the roots of both P-starved plant species compared to P-sufficient ones. Since bacterial inoculation in P-deficient cucumber plants supplemented with $Ca_3(PO_4)_2$ increased the P accumulation in roots and shoots, a reduction in the expression of the *CsPTs* genes compared to uninoculated controls can reasonably be expected. However, in P deficiency, all Pi transporter genes were over-expressed in cucumber plants inoculated with *Enterobacter* 15S. Moreover, *CsPT1.3* and *CsPT1.4* were also upregulated in the inoculation treatment combined with the insoluble phosphate. Indeed, the downregulation of Pi transporters by microbial inoculants has not been observed for all *PHT1* Pi transporters (Duan et al., 2015). Accordingly, the results might suggest that *Enterobacter* 15S in association with cucumber plants supplemented with $Ca_3(PO_4)_2$ would have induced a greater P-uptake capacity. Similar behavior was also reported by Cataldi et al. (2020) in the expression levels of *TaPHT6* during the interaction of wheat plants with *Bacillus* strain 12A under P starvation. Concerning the inoculation with the bacteria alone, the results might suggest that *Enterobacter* 15S could have triggered the different gene regulation, including the modulation of molecular entities other than *PHT1* members. Indeed, although few works have studied the effects of PGPB on the regulation of Pi transporters, it is well-known that Pi acquisition and homeostasis can also be controlled by members of the *PHT2*, *PHT3*, *PHT4*, and *PHT5* families (Wang et al., 2017). Moreover, in plant-microbe interactions, in particular, in the case of AMF, AM-specific Pi transporters and AM-inducible Pi transporters identified in monocot and dicot species are essential to Pi transport (Zhang et al., 2019). Additionally, it cannot be excluded that the increased P accumulation observed in cucumber roots could also be a direct effect of the bacterium on plant metabolism, as previously reported by Saia et al. (2015) in wheat plants inoculated with the PGPB *Bacillus* species. Interestingly, in cucumber plants grown under P sufficient conditions, the expression of Pi transporters was not altered by the inoculant treatments. These findings might suggest that *Enterobacter* 15S has a better performance in dicots growing under a nutritional shortage.

On the other hand, in P-deficient maize plants, the expression of *ZmPT1* and *ZmPT5* was inhibited by inoculation with the bacterial biostimulant compared to the uninoculated controls. A similar result has been described by Liu et al. (2018) in the transcript level of *TaPT4* in wheat roots inoculated with *Pseudomonas* strain P34-L. The authors suggested that a better P nutritional state was induced by the bacterium colonizing the wheat rhizosphere (Liu et al., 2018). However, considering all the results described in the previous sections, we cannot state that the downregulation of maize Pi transporters in the inoculated P-deficient plants is due to a change in P nutrition due to PGPB interaction. However, the repression of maize Pi transporters might be triggered by the plant in response to the association with the bacterium, which could likely produce a direct effect on plant metabolism. Indeed, the fact that in inoculated maize plants under P-sufficient conditions, the *ZmPT5* gene was also downregulated might support this hypothesis. Nonetheless, since few studies have been focused on P transport in plant–PGPB interactions in P-deficiency, the mechanisms by which a specific PGPB alters the expression of Pi transporters remain unclear. Furthermore, some P transporters are also transcriptionally

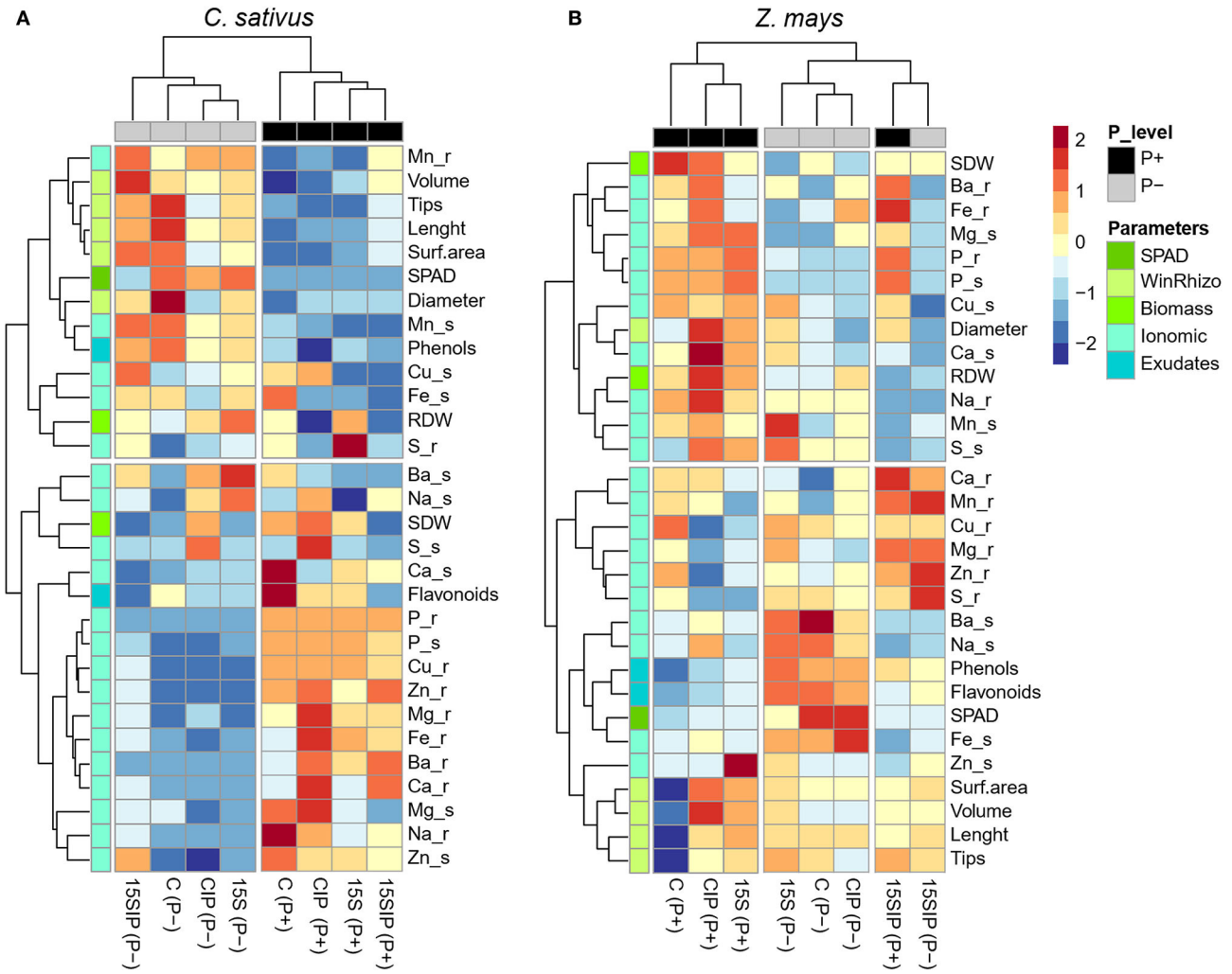

FIGURE 6 | Heatmap analysis summarizing the responses of the cucumber **(A)** and maize **(B)** plants to a factorial experiment with two P-fertilization levels (P+ and P) and four biostimulant treatments (15S; 15SIP; C, uninoculated control; CIP). The heatmap was generated using the R software (https://www.r-project.org, using the "pheatmap," "ggplot2," and "RColorBrewer" packages). Hierarchical clustering was performed with Complete linkage and Manhattan distance was used as the similarity measure. Dark red color indicates higher relative values, while a dark-blue color reflects lower relative values. Yellow color denotes values close or equal to zero, i.e., close or equal to the mean for each parameter.

regulated by stimuli other than P deficiencies or microbial associations, suggesting a more complex regulatory mechanism (Gu et al., 2016).

Clustered Heatmap of Plant Responses to Bacterial Biostimulant and P Supply

To present a visual comparison regarding the effect of inoculation with the bacterial biostimulant and levels of P supply on the growth and nutrition of cucumber and maize plants, a heatmap analysis condensing all the measured morpho-physiological, ionomic, and root exudation data was performed for each plant species (**Figure 6**). Both cucumber and maize plants showed different responses to the evaluated parameters. In cucumber plants, the main clustering factor responsible for different effects was P nutrition, albeit a clear effect of the bacterial biostimulant within the P levels was also observed (**Figure 6A**). It is expected that, under P deficiency, plants undergo various morphological, physiological, and biochemical adaptations. Intense and significant effects have been observed in cucumber plants at the levels of root system architecture, root exudation, photosynthetic rates, and nutrients under P-deficient conditions when compared to P-sufficient plants (Ciereszko et al., 2002; Zhang et al., 2012; Naureen et al., 2018). Nonetheless, the inoculation of cucumber plants with PGPB in different P states has also shown a positive contribution to the improvement of plant growth and nutrition and the abilities of the plants to deal with P deficiency (Han et al., 2006; García-López et al., 2016). The results also revealed that *Enterobacter* 15S in combination with the insoluble phosphate (15SIP) showed positive effects in alleviating the stress produced by P deprivation in cucumber plants. Since neither non-inoculated plants (CIP) nor the bacterium alone (15S) under the same conditions did not

show significant effects on P nutrition, it is possible to suggest that *Enterobacter* 15S might have solubilized the $Ca_3(PO_4)_2$ available in the dialysis tube, thus allowing cucumber plants to cope with the P limitation. Consistently, previous studies have already described the ability of *Enterobacter* strains to solubilize insoluble phosphates and promote the growth of several plant species (Ramesh et al., 2014; Bendaha and Belaouni, 2020; Zuluaga et al., 2020).

In maize plants, both P fertilization levels and biostimulant treatments affected the parameters assessed. In combination with the insoluble phosphate, *Enterobacter* 15S induced similar effects on the plant growth and nutritional state of maize plants in both P levels. However, stronger effects were induced by the bacterium alone under P-limited conditions (**Figure 6B**). These results suggest that, in the interaction with P-deficient maize plants, the bacterial strain *Enterobacter* 15S might have triggered different mechanisms than those activated in cucumber plants to help plants coping with P deficiency. Although all plant species can establish a relationship with some PGPB, inoculation with a specific bacterium has shown differential responses in the plant stimulation between monocots and dicots (Hall et al., 1996). However, more comparative studies between plant types and bacterial strains are still lacking. Furthermore, most existing studies are focused on PGPB and its role in improving N nutrition in plants, whereas only few pieces of literature are concerned with the effects of PGPB inoculation on plants grown in different P-supply conditions. For this reason, it has been suggested that the P-solubilization trait could be acknowledged as the forgotten child of PGP bacteria (Granada et al., 2018).

CONCLUSION

The results of the present study underline those plant growth responses to inoculation with the bacterial biostimulant with *Enterobacter* 15S under specific P supplies vary between maize (a representative for monocots) and cucumber (a dicot) plants. The bacterial strain 15S induced cucumber plants to cope with P shortage by solubilizing the external source of insoluble P, which led to the modulation of root architecture, mineral nutrient uptake, root exudation of phenolics, and flavonoids, and the upregulation of P starvation-inducible Pi transporter genes. On the other hand, the ability of *Enterobacter* 15S to ameliorate the P deficiency of maize plants was less remarkable than in cucumbers, albeit the strain showed better performance under P sufficiency. These results suggest that the bacterial biostimulant strain herein evaluated has an enhanced ability to alleviate P shortage in dicots. Nonetheless, its efficiency under normal P conditions can also be extended to cultivated monocots. Still, further studies are needed to evaluate the efficacy of *Enterobacter* 15S in alleviating P nutritional shortage under different soil conditions. The need for a rapid transition of agriculture toward sustainability makes the comprehension of these phenomena even more urgent, for their use as soon as possible in the field in favor of a better use of endogenous soil resources of nutrients by crops.

DATA AVAILABILITY STATEMENT

The original contributions presented in the study are included in the article/**Supplementary Material**, further inquiries can be directed to the corresponding author/s.

AUTHOR CONTRIBUTIONS

MA, AM, YP, TM, and SC conceived the work and designed the experiment. MA, FV, and RT carried out the experiments and generated the data. MA and YP analyzed the data. MA wrote the first draft of the manuscript, which was intensively edited by all authors. YP, SC, TM, and AM reviewed the manuscript and carried out the English edition. All authors contributed to the article and approved the submitted version.

FUNDING

Funding for this research was provided by the Ministero dell'Istruzione, dell'Università e della Ricerca (MIUR) through the project PHOBOS coded 2017FYBLPP. This work was supported by the Open Access Publishing Fund of the Free University of Bozen-Bolzano.

SUPPLEMENTARY MATERIAL

The Supplementary Material for this article can be found online at: https://www.frontiersin.org/articles/10.3389/fpls.2021.719873/full#supplementary-material

REFERENCES

Alexander, A., Singh, V. K., Mishra, A., and Jha, B. (2019). Plant growth promoting rhizobacterium *Stenotrophomonas maltophilia* BJ01 augments endurance against N_2 starvation by modulating physiology and biochemical activities of *Arachis hypogea*. *PLoS ONE* 14:222405. doi: 10.1371/journal.pone.0222405

Backer, R., Rokem, J. S., Ilangumaran, G., Lamont, J., Praslickova, D., Ricci, E., et al. (2018). Plant growth-promoting rhizobacteria: context, mechanisms of action, and roadmap to commercialization of biostimulants for sustainable agriculture. *Front. Plant Sci.* 9:1473. doi: 10.3389/fpls.2018.01473

Badri, D. V., and Vivanco, J. M. (2009). Regulation and function of root exudates. *Plant. Cell Environ.* 32, 666–681. doi: 10.1111/j.1365-3040.2009.01926.x

Belimov, A. A., Safronova, V. I., and Mimura, T. (2002). Response of spring rape (*Brassica napus* var. *oleifera* L.) to inoculation with plant growth promoting rhizobacteria containing 1-aminocyclopropane-1-carboxylate deaminase depends on nutrient status of the plant. *Can. J. Microbiol.* 48, 189–199. doi: 10.1139/w02-007

Bendaha, M. E. A., and Belaouni, H. A. (2020). Effect of the endophytic plant growth promoting *Enterobacter ludwigii* EB4B on tomato growth. *Hell. Plant Prot. J.* 13, 54–65. doi: 10.2478/hppj-2020-0006

Billah, M., Khan, M., Bano, A., Hassan, T. U., Munir, A., and Gurmani, A. R. (2019). Phosphorus and phosphate solubilizing bacteria: keys for sustainable agriculture. *Geomicrobiol. J.* 36, 904–916. doi: 10.1080/01490451.2019.1654043

Campos, P. M., Cornejo, P., Rial, C., Borie, F., Varela, R. M., Seguel, A., et al. (2019). Phosphate acquisition efficiency in wheat is related to root:shoot ratio, strigolactone levels, and PHO2 regulation. *J. Exp. Bot.* 70, 5631–5642. doi: 10.1093/jxb/erz349

Cataldi, M. P., Heuer, S., Mauchline, T. H., Wilkinson, M. D., Masters-Clark, E., Di Benedetto, N. A., et al. (2020). Effect of plant growth promoting bacteria on the growth of wheat seedlings subjected to phosphate starvation. *Agronomy* 10, 1–13. doi: 10.3390/agronomy10070978

Cesco, S., Mimmo, T., Tonon, G., Tomasi, N., Pinton, R., Terzano, R., et al. (2012). Plant-borne flavonoids released into the rhizosphere: impact on soil bio-activities related to plant nutrition. *A review. Biol. Fertil. Soils* 48, 123–149. doi: 10.1007/s00374-011-0653-2

Chen, A., Chen, X., Wang, H., Liao, D., Gu, M., Qu, H., et al. (2014). Genome-wide investigation and expression analysis suggest diverse roles and genetic redundancy of *Pht1* family genes in response to Pi deficiency in tomato. *BMC Plant Biol.* 14, 1–15. doi: 10.1186/1471-2229-14-61

Chen, A., Hu, J., Sun, S., and Xu, G. (2007). Conservation and divergence of both phosphate- and mycorrhiza-regulated physiological responses and expression patterns of phosphate transporters in solanaceous species. *New Phytol.* 173, 817–831. doi: 10.1111/j.1469-8137.2006.01962.x

Ciereszko, I., Janonis, A., and Kociakowska, M. (2002). Growth and metabolism of cucumber in phosphate-deficient conditions. *J. Plant Nutr.* 25, 1115–1127. doi: 10.1081/pln-120003943

Crecchio, C., Mimmo, T., Bulgarelli, D., Pertot, I., Pii, Y., Perazzolli, M., et al. (2018). "Beneficial soil microbiome for sustainable agriculture production," in ed E. Lichtfouse (Cham: Springer International Publishing), 443–481. doi: 10.1007/978-3-319-94232-2_9

Dakora, F. D., Matiru, V. N., and Kanu, A. S. (2015). Rhizosphere ecology of lumichrome and riboflavin, two bacterial signal molecules eliciting developmental changes in plants. *Front. Plant Sci.* 6:700. doi: 10.3389/fpls.2015.00700

Dardanelli, M. S., Manyani, H., González-Barroso, S., Rodríguez-Carvajal, M. A., Gil-Serrano, A. M., Espuny, M. R., et al. (2010). Effect of the presence of the plant growth promoting rhizobacterium (PGPR) *Chryseobacterium balustinum* Aur9 and salt stress in the pattern of flavonoids exuded by soybean roots. *Plant Soil* 328, 483–493. doi: 10.1007/s11104-009-0127-6

Delaporte-Quintana, P., Grillo-Puertas, M., Lovaisa, N. C., Teixeira, K. R., Rapisarda, V. A., and Pedraza, R. O. (2017). Contribution of *Gluconacetobacter diazotrophicus* to phosphorus nutrition in strawberry plants. *Plant Soil* 419, 335–347. doi: 10.1007/s11104-017-3349-z

Drogue, B., Doré, H., Borland, S., Wisniewski-Dyé, F., and Prigent-Combaret, C. (2012). Which specificity in cooperation between phytostimulating rhizobacteria and plants? *Res. Microbiol.* 163, 500–510. doi: 10.1016/j.resmic.2012.08.006

Duan, J., Tian, H., Drijber, R. A., and Gao, Y. (2015). Systemic and local regulation of phosphate and nitrogen transporter genes by arbuscular mycorrhizal fungi in roots of winter wheat (*Triticum aestivum* L.). *Plant Physiol. Biochem.* 96, 199–208. doi: 10.1016/j.plaphy.2015.08.006

Elanchezhian, R., Krishnapriya, V., Pandey, R., Rao, A. S., and Abrol, Y. P. (2015). Physiological and molecular approaches for improving phosphorus uptake efficiency of crops. *Curr. Sci.* 108, 1271–1279. doi: 10.18520/cs/v108/i7/1271-1279

Fan, C., Wang, X., Hu, R., Wang, Y., Xiao, C., Jiang, Y., et al. (2013). The pattern of *Phosphate transporter 1* genes evolutionary divergence in *Glycine max* L. *BMC Plant Biol.* 13, 1–16. doi: 10.1186/1471-2229-13-48

Feil, S. B., Pii, Y., Valentinuzzi, F., Tiziani, R., Mimmo, T., and Cesco, S. (2020). Copper toxicity affects phosphorus uptake mechanisms at molecular and physiological levels in *Cucumis sativus* plants. *Plant Physiol. Biochem.* 157, 138–147. doi: 10.1016/j.plaphy.2020.10.023

Folin, O., and Ciocalteau, V. (1927). On tyrosine and tryptophane in proteins. *J. Biol. Chem.* 73, 627–648.

García-López, A. M., Avilés, M., and Delgado, A. (2016). Effect of various microorganisms on phosphorus uptake from insoluble Ca-phosphates by cucumber plants. *J. Plant Nutr. Soil Sci.* 179, 454–465. doi: 10.1002/jpln.201500024

Garcia-Seco, D., Zhang, Y., Gutierrez-Mañero, F. J., Martin, C., and Ramos-Solano, B. (2015). Application of *Pseudomonas fluorescens* to blackberry under field conditions improves fruit quality by modifying flavonoid metabolism. *PLoS ONE* 10:142639. doi: 10.1371/journal.pone.0142639

Giri, B., and Mukerji, K. G. (2004). Mycorrhizal inoculant alleviates salt stress in *Sesbania aegyptiaca* and *Sesbania grandiflora* under field conditions: Evidence for reduced sodium and improved magnesium uptake. *Mycorrhiza* 14, 307–312. doi: 10.1007/s00572-003-0274-1

Glick, B. R. (2005). Modulation of plant ethylene levels by the bacterial enzyme ACC deaminase. *FEMS Microbiol. Lett.* 251, 1–7. doi: 10.1016/j.femsle.2005.07.030

Glick, B. R. (2012). Plant growth-promoting bacteria: mechanisms and applications. *Scientifica* 2012, 1–15. doi: 10.6064/2012/963401

Goswami, D., Thakker, J. N., and Dhandhukia, P. C. (2016). Portraying mechanics of plant growth promoting rhizobacteria (PGPR): a review. *Cogent Food Agric.* 2, 1–19. doi: 10.1080/23311932.2015.1127500

Granada, C. E., Passaglia, L. M. P., de Souza, E. M., and Sperotto, R. A. (2018). Is phosphate solubilization the forgotten child of plant growth-promoting rhizobacteria? *Front. Microbiol.* 9:2054. doi: 10.3389/fmicb.2018.02054

Grün, A., Buchner, P., Broadley, M. R., and Hawkesford, M. J. (2018). Identification and expression profiling of *Pht1* phosphate transporters in wheat in controlled environments and in the field. *Plant Biol.* 20, 374–389. doi: 10.1111/plb.12668

Gu, M., Chen, A., Sun, S., and Xu, G. (2016). Complex regulation of plant phosphate transporters and the gap between molecular mechanisms and practical application: What is missing? *Mol. Plant* 9, 396–416. doi: 10.1016/j.molp.2015.12.012

Gupta, P., Kumar, V., Usmani, Z., Rani, R., Chandra, A., and Gupta, V. K. (2020). Implications of plant growth promoting *Klebsiella* sp. CPSB4 and *Enterobacter* sp. CPSB49 in luxuriant growth of tomato plants under chromium stress. *Chemosphere* 240:124944. doi: 10.1016/j.chemosphere.2019.124944

Hakim, S., Naqqash, T., Nawaz, M. S., Laraib, I., Siddique, M. J., Zia, R., et al. (2021). Rhizosphere engineering with plant growth-promoting microorganisms for agriculture and ecological sustainability. *Front. Sustain. Food Syst.* 5, 1–23. doi: 10.3389/fsufs.2021.617157

Hall, J. A., Peirson, D., Ghosh, S., and Glick, B. R. (1996). Root elongation in various agronomic crops by the plant growth promoting rhizobacterium *Pseudomonas putida* Gr12–2. *Isr. J. Plant Sci.* 44, 37–42. doi: 10.1080/07929978.1996.10676631

Han, H. S., Supanjani, and Lee, K. D. (2006). Effect of co-inoculation with phosphate and potassium. *Plant, Soil Environ.* 52, 130–136. doi: 10.17221/3356-PSE

Ji, C., Liu, Z., Hao, L., Song, X., Wang, C., Liu, Y., et al. (2020). Effects of *Enterobacter cloacae* HG-1 on the Nitrogen-fixing community structure of wheat rhizosphere soil and on salt tolerance. *Front. Plant Sci.* 11:1094. doi: 10.3389/fpls.2020.01094

Juszczuk, I. M., Wiktorowska, A., Malusá, E., and Rychter, A. M. (2004). Changes in the concentration of phenolic compounds and exudation induced by phosphate deficiency in bean plants (*Phaseolus vulgaris* L.). *Plant Soil* 267, 41–49. doi: 10.1007/s11104-005-2569-9

Kudoyarova, G., Arkhipova, T., Korshunova, T., Bakaeva, M., Loginov, O., and Dodd, I. C. (2019). Phytohormone mediation of interactions between plants and non-symbiotic growth promoting bacteria under edaphic stresses. *Front. Plant Sci.* 10:1368. doi: 10.3389/fpls.2019.01368

Liu, B., Zhao, S., Wu, X., Wang, X., Nan, Y., Wang, D., et al. (2017). Identification and characterization of phosphate transporter genes in potato. *J. Biotechnol.* 264, 17–28. doi: 10.1016/j.jbiotec.2017.10.012

Liu, F., Xu, Y., Jiang, H., Jiang, C., Du, Y., Gong, C., et al. (2016). Systematic identification, evolution and expression analysis of the *Zea mays PHT1* gene family reveals several new members involved in root colonization by arbuscular mycorrhizal fungi. *Int. J. Mol. Sci.* 17, 1–18. doi: 10.3390/ijms17060930

Liu, X., Jiang, X., Zhao, W., Cao, Y., Guo, T., He, X., et al. (2018). Colonization of phosphate-solubilizing *Pseudomonas* sp. strain P34-L in the wheat rhizosphere and its effects on wheat growth and the expression of phosphate transporter gene *TaPT4* in wheat. *bioRxiv* 38:294736. doi: 10.1101/294736

Livak, K. J., and Schmittgen, T. D. (2001). Analysis of relative gene expression data using real-time quantitative PCR and the 2-ΔΔCT method. *Methods* 25, 402–408. doi: 10.1006/meth.2001.1262

López-Arredondo, D. L., Leyva-González, M. A., González-Morales, S. I., López-Bucio, J., and Herrera-Estrella, L. (2014). Phosphate nutrition: Improving low-phosphate tolerance in crops. *Annu. Rev. Plant Biol.* 65, 95–123. doi: 10.1146/annurev-arplant-050213-035949

Luo, J., Liu, Y., Zhang, H., Wang, J., Chen, Z., Luo, L., et al. (2020). Metabolic alterations provide insights into Stylosanthes roots responding to

phosphorus deficiency. *BMC Plant Biol.* 20, 1–16. doi: 10.1186/s12870-020-2283-z

Malus,à, E., Russo, M. A., Mozzetti, C., and Belligno, A. (2006). Modification of secondary metabolism and flavonoid biosynthesis under phosphate deficiency in bean roots. *J. Plant Nutr.* 29, 245–258. doi: 10.1080/01904160500474090

Mandal, S. M., Chakraborty, D., and Dey, S. (2010). Phenolic acids act as signaling molecules in plant-microbe symbioses. *Plant Signal. Behav.* 5, 359–368. doi: 10.4161/psb.5.4.10871

Marschner, H. (1995). *Mineral Nutrition of Higher Plants.*, ed. 2nd. London: A. Press.

Miliauskas, G., Venskutonis, P. R., and van Beek, T. A. (2004). Screening of radical scavenging activity of some medicinal and aromatic plant extracts. *Food Chem.* 85, 231–237. doi: 10.1016/j.foodchem.2003.05.007

Nagy, R., Vasconcelos, M. J. V., Zhao, S., McElver, J., Bruce, W., Amrhein, N., et al. (2006). Differential regulation of five *Pht1* phosphate transporters from maize (*Zea mays* L.). *Plant Biol.* 8, 186–197. doi: 10.1055/s-2005-873052

Naureen, Z., Sham, A., Al Ashram, H., Gilani, S. A., Al Gheilani, S., Mabood, F., et al. (2018). Effect of phosphate nutrition on growth, physiology and phosphate transporter expression of cucumber seedlings. *Plant Physiol. Biochem.* 127, 211–222. doi: 10.1016/j.plaphy.2018.03.028

Naveed, M., Mitter, B., Yousaf, S., Pastar, M., Afzal, M., and Sessitsch, A. (2013). The endophyte *Enterobacter* sp. FD17: A maize growth enhancer selected based on rigorous testing of plant beneficial traits and colonization characteristics. *Biol. Fertil. Soils* 50, 249–262. doi: 10.1007/s00374-013-0854-y

Nussaume, L., Kanno, S., Javot, H., Marin, E., Pochon, N., Ayadi, A., et al. (2011). Phosphate import in plants: focus on the PHT1 transporters. *Front. Plant Sci.* 2:83. doi: 10.3389/fpls.2011.00083

Oleńska, E., Małek, W., Wójcik, M., Swiecicka, I., Thijs, S., and Vangronsveld, J. (2020). Beneficial features of plant growth-promoting rhizobacteria for improving plant growth and health in challenging conditions: a methodical review. *Sci. Total Environ.* 743, 1–21. doi: 10.1016/j.scitotenv.2020.140682

Panwar, M., Tewari, R., and Nayyar, H. (2016). Native halo-tolerant plant growth promoting rhizobacteria Enterococcus and Pantoea sp. improve seed yield of Mungbean (*Vigna radiata* L.) under soil salinity by reducing sodium uptake and stress injury. *Physiol. Mol. Biol. Plants* 22, 445–459. doi: 10.1007/s12298-016-0376-9

Paszkowski, U., Kroken, S., Roux, C., and Briggs, S. P. (2002). Rice phosphate transporters include an evolutionarily divergent gene specifically activated in arbuscular mycorrhizal symbiosis. *Proc. Natl. Acad. Sci. USA.* 99, 13324–13329. doi: 10.1073/pnas.202474599

Pereira, N. C. M., Galindo, F. S., Gazola, R. P. D., Dupas, E., Rosa, P. A. L., Mortinho, E. S., et al. (2020). Corn yield and phosphorus use efficiency response to phosphorus rates associated with plant growth promoting bacteria. *Front. Environ. Sci.* 8:40. doi: 10.3389/fenvs.2020.00040

Pii, Y., Aldrighetti, A., Valentinuzzi, F., Mimmo, T., and Cesco, S. (2019). *Azospirillum brasilense* inoculation counteracts the induction of nitrate uptake in maize plants. *J. Exp. Bot.* 70, 1313–1324. doi: 10.1093/jxb/ery433

Pii, Y., Cesco, S., and Mimmo, T. (2015a). Shoot ionome to predict the synergism and antagonism between nutrients as affected by substrate and physiological status. *Plant Physiol. Biochem.* 94, 48–56. doi: 10.1016/j.plaphy.2015.05.002

Pii, Y., Marastoni, L., Springeth, C., Fontanella, M. C., Beone, G. M., Cesco, S., et al. (2016). Modulation of Fe acquisition process by *Azospirillum brasilense* in cucumber plants. *Environ. Exp. Bot.* 130, 216–225. doi: 10.1016/j.envexpbot.2016.06.011

Pii, Y., Mimmo, T., Tomasi, N., Terzano, R., Cesco, S., and Crecchio, C. (2015b). Microbial interactions in the rhizosphere: beneficial influences of plant growth-promoting rhizobacteria on nutrient acquisition process. A review. *Biol. Fertil. Soils* 51, 403–415. doi: 10.1007/s00374-015-0996-1

Poorter, H., Niklas, K. J., Reich, P. B., Oleksyn, J., Poot, P., and Mommer, L. (2012). Biomass allocation to leaves, stems and roots: meta-analyses of interspecific variation and environmental control. *New Phytol.* 193, 30–50. doi: 10.1111/j.1469-8137.2011.03952.x

Ramaekers, L., Remans, R., Rao, I. M., Blair, M. W., and Vanderleyden, J. (2010). Strategies for improving phosphorus acquisition efficiency of crop plants. *F. Crop. Res.* 117, 169–176. doi: 10.1016/j.fcr.2010.03.001

Ramakers, C., Ruijter, J. M., Deprez, R. H. L., and Moorman, A. F. M. (2003). Assumption-free analysis of quantitative real-time polymerase chain reaction (PCR) data. *Neurosci. Lett.* 339, 62–66. doi: 10.1016/S0304-3940(02)01423-4

Ramesh, A., Sharma, S. K., Sharma, M. P., Yadav, N., and Joshi, O. P. (2014). Plant Growth-Promoting traits in *Enterobacter cloacae* subsp. *dissolvens* MDSR9 isolated from soybean rhizosphere and its impact on growth and nutrition of soybean and wheat upon inoculation. *Agric. Res.* 3, 53–66. doi: 10.1007/s40003-014-0100-3

Saia, S., Rappa, V., Ruisi, P., Abenavoli, M. R., Sunseri, F., Giambalvo, D., et al. (2015). Soil inoculation with symbiotic microorganisms promotes plant growth and nutrient transporter genes expression in durum wheat. *Front. Plant Sci.* 6:815. doi: 10.3389/fpls.2015.00815

Schillaci, M., Arsova, B., Walker, R., Smith, P. M. C., Nagel, K. A., Roessner, U., et al. (2021). Time-resolution of the shoot and root growth of the model cereal *Brachypodium* in response to inoculation with *Azospirillum* bacteria at low phosphorus and temperature. *Plant Growth Regul.* 93, 149–162. doi: 10.1007/s10725-020-00675-4

Shah, A., and Smith, D. L. (2020). Flavonoids in agriculture: chemistry and roles in biotic and abiotic stress responses and microbial associations. *Agronomy* 10, 1–26. doi: 10.3390/agronomy10081209

Shahzad, Z., and Amtmann, A. (2017). Food for thought: how nutrients regulate root system architecture. *Curr. Opin. Plant Biol.* 39, 80–87. doi: 10.1016/j.pbi.2017.06.008

Simon, P. (2003). Q-Gene: processing quantitative real-time RT-PCR data. *Bioinformatics* 19, 1439–1440. doi: 10.1093/bioinformatics/btg157

Talboys, P. J., Owen, D. W., Healey, J. R., Withers, P. J. A., and Jones, D. L. (2014). Auxin secretion by *Bacillus amyloliquefaciens* FZB42 both stimulates root exudation and limits phosphorus uptake in *Triticum aestivium*. *BMC Plant Biol.* 14, 1–9. doi: 10.1186/1471-2229-14-51

Tavares de Oliveira Melo, A. (2016). Exploring genomic databases for in silico discovery of *Pht1* genes in high syntenic close related grass species with focus in sugarcane (*Saccharum* spp.). *Curr. Plant Biol.* 6, 11–18. doi: 10.1016/j.cpb.2016.10.004

Tchakounté, G. V. T., Berger, B., Patz, S., Becker, M., Fankem, H., Taffouo, V. D., et al. (2020). Selected rhizosphere bacteria help tomato plants cope with combined phosphorus and salt stresses. *Microorganisms* 8, 1–16. doi: 10.3390/microorganisms8111844

Tiziani, R., Pii, Y., Celletti, S., Cesco, S., and Mimmo, T. (2020). Phosphorus deficiency changes carbon isotope fractionation and triggers exudate reacquisition in tomato plants. *Sci. Rep.* 10, 1–12. doi: 10.1038/s41598-020-72904-9

Tomasi, N., Weisskopf, L., Renella, G., Landi, L., Pinton, R., Varanini, Z., et al. (2008). Flavonoids of white lupin roots participate in phosphorus mobilization from soil. *Soil Biol. Biochem.* 40, 1971–1974. doi: 10.1016/j.soilbio.2008.02.017

Vacheron, J., Desbrosses, G., Bouffaud, M.-L., Touraine, B., Moënne-Loccoz, Y., Muller, D., et al. (2013). Plant growth-promoting rhizobacteria and root system functioning. *Front. Plant Sci.* 4:356. doi: 10.3389/fpls.2013.00356

Valentinuzzi, F., Pii, Y., Vigani, G., Lehmann, M., Cesco, S., and Mimmo, T. (2015). Phosphorus and iron defciencies induce a metabolic reprogramming and affect the exudation traits of the woody plant *Fragaria* × *ananassa*. *J. Exp. Bot.* 66, 6483–6495. doi: 10.1093/jxb/erv364

Valentinuzzi, F., Venuti, S., Pii, Y., Marroni, F., Cesco, S., Hartmann, F., et al. (2019). Common and specific responses to iron and phosphorus deficiencies in roots of apple tree (*Malus* × *domestica*). *Plant Mol. Biol.* 101, 129–148. doi: 10.1007/s11103-019-00896-w

Veazie, P., Cockson, P., Henry, J., Perkins-Veazie, P., and Whipker, B. (2020). Characterization of nutrient disorders and impacts on chlorophyll and anthocyanin concentration of *Brassica rapa* var. *Chinensis. Agric.* 10, 1–16. doi: 10.3390/agriculture10100461

Wang, D., Lv, S., Jiang, P., and Li, Y. (2017). Roles, regulation, and agricultural application of plant phosphate transporters. *Front. Plant Sci.* 8:817. doi: 10.3389/fpls.2017.00817

Wang, F., Deng, M., Xu, J., Zhu, X., and Mao, C. (2018). Molecular mechanisms of phosphate transport and signaling in higher plants. *Semin. Cell Dev. Biol.* 74, 114–122. doi: 10.1016/j.semcdb.2017.06.013

Wu, Q., Ni, M., Liu, W. C., Ren, J. H., Rao, Y. H., Chen, J., et al. (2018). Omics for understanding the mechanisms of *Streptomyces lydicus* A01 promoting the growth of tomato seedlings. *Plant Soil* 431, 129–141. doi: 10.1007/s11104-018-3750-2

Zhang, B. G., Chen, Q. X., Luo, S. B., Zhang, C. Y., Yang, Q., and Liu, K. D. (2012). Effects of NPK deficiencies on root architecture and growth of cucumber. *Int.*

J. Agric. Biol. 14, 145–148. Available online at: http://www.fspublishers.org/published_papers/25808_..pdf

Zhang, Y., Hu, L., Yu, D., Xu, K., Zhang, J., Li, X., et al. (2019). Integrative analysis of the wheat *PHT1* gene family reveals a novel member involved in arbuscular mycorrhizal phosphate transport and immunity. *Cells* 8:490. doi: 10.3390/cells8050490

Zuluaga, M., Milani, K., Gonçalces, L., and Oliveira, A. L. M. (2020). Diversity and plant growth-promoting functions of diazotrophic/N-scavenging bacteria isolated from the soils and rhizospheres of two species of *Solanum*. *PLoS ONE* 15:227422. doi: 10.1371/journal.pone.0227422

Zuluaga, M., Milani, K., Miras-moreno, B., Lucini, L., Valentinuzzi, F., Mimmo, T., et al. (2021). Inoculation with plant growth-promoting bacteria alters the rhizosphere functioning of tomato plants. *Appl. Soil Ecol.* 158:103784. doi: 10.1016/j.apsoil.2020.103784

Zwetsloot, M. J., Kessler, A., and Bauerle, T. L. (2018). Phenolic root exudate and tissue compounds vary widely among temperate forest tree species and have contrasting effects on soil microbial respiration. *New Phytol.* 218, 530–541. doi: 10.1111/nph.15041

Conflict of Interest: The authors declare that the research was conducted in the absence of any commercial or financial relationships that could be construed as a potential conflict of interest.

Publisher's Note: All claims expressed in this article are solely those of the authors and do not necessarily represent those of their affiliated organizations, or those of the publisher, the editors and the reviewers. Any product that may be evaluated in this article, or claim that may be made by its manufacturer, is not guaranteed or endorsed by the publisher.

frontiers in Plant Science

ORIGINAL RESEARCH
published: 26 August 2021
doi: 10.3389/fpls.2021.722498

Liquiritoside Alleviated Pb Induced Stress in *Brassica rapa* subsp. *Parachinensis*: Modulations in Glucosinolate Content and Some Physiochemical Attributes

Waheed Akram[1], Waheed Ullah Khan[2], Anis Ali Shah[3], Nasim Ahmad Yasin[4] and Guihua Li[1]**

[1] Guangdong Key Laboratory for New Technology Research of Vegetables/Vegetable Research Institute, Guangdong Academy of Agricultural Sciences, Guangzhou, China, [2] Department of Environmental Science, The Islamia University of Bahawalpur, Bahawalpur, Pakistan, [3] Department of Botany, University of Narowal, Narowal, Pakistan, [4] RO-II Office, University of the Punjab, Lahore, Pakistan

OPEN ACCESS

Edited by:
Youssef Rouphael, University of Naples Federico II, Italy

Reviewed by:
Arafat Abdel Hamed Abdel Latef, South Valley University, Egypt
Reyes Rodenas, UMR 5546 Laboratoire de Recherche en Sciences Vegetales (LRSV), France

***Correspondence:**
Nasim Ahmad Yasin
nasimhort@gmail.com
Guihua Li
liguihua@gdaas.cn

Specialty section:
This article was submitted to Plant Abiotic Stress, a section of the journal Frontiers in Plant Science

Received: *08 June 2021*
Accepted: *30 July 2021*
Published: *26 August 2021*

Citation:
Akram W, Khan WU, Shah AA, Yasin NA and Li G (2021) Liquiritoside Alleviated Pb Induced Stress in Brassica rapa subsp. Parachinensis: Modulations in Glucosinolate Content and Some Physiochemical Attributes. Front. Plant Sci. 12:722498. doi: 10.3389/fpls.2021.722498

Current research was conducted to explore the effects of liquiritoside on the growth and physiochemical features of Chinese flowering cabbage (*Brassica rapa* subsp. *parachinensis*) under lead (Pb) stress. Lead stressed *B. rapa* plants exhibited decreased growth parameters, chlorophyll, and carotenoid contents. Moreover, Pb toxicity escalated the synthesis of malondialdehyde (MDA), hydrogen peroxide (H_2O_2), flavonoids, phenolics, and proline in treated plants. Nevertheless, foliar application of liquiritoside mitigated Pb toxicity by decreasing oxidative stress by reducing cysteine, H_2O_2, and MDA contents in applied plants. Liquiritoside significantly increased plant height, shoot fresh weight and dry weight, number of leaves, and marketable value of Chinese flowering cabbage plants exposed to Pb toxicity. This biotic elicitor also enhanced the proline, glutathione, total phenolics, and flavonoid contents in Chinese flowering cabbage plants exposed to Pb stress compared with the control. Additionally, total glucosinolate content, phytochelatins (PCs), and non-protein thiols were effectively increased in plants grown under Pb regimes compared with the control plants. Overall, foliar application of liquiritoside can markedly alleviate Pb stress by restricting Pb translocation in Chinese flowering cabbage.

Keywords: Chinese flowering cabbage, flavonoids, glucosinolates, liquiritoside, lead

INTRODUCTION

Vegetables belonging to the Brassicaceae family show cherished health remunerations effects owing to the existence of biologically active and robust antioxidative ingredients. Chinese flowering cabbage (*Brassica rapa* subsp. *parachinensis*) is an annual cole crop belonging to the Brassicaceae family. The germination to harvest period of this vegetable is less than 60 days (Peng et al., 2015). Chinese flowering cabbage has valuable biological and nutritional properties (Aixia et al., 2015). Its above-ground parts, including leaves, stem, and inflorescence, can be cooked or consumed raw as salads. Its leaves contain adequate amounts of glucosinolates and polyphenolic compounds

(Chen et al., 2008). This rich chemical composition and scientifically proven biological activity has made Chinese flowering cabbage a famous culinary plant (Chung et al., 2016).

Glucosinolates (GLs) are primarily found in plants of the genus *Brassica*, which include crops of economical and nutritional importance. GLs are rich in sulfur and anionic secondary metabolites (Johnson, 2002). GLs have been extensively studied for their protective effect against herbivory in plants and chemotherapeutic activity in humans (Barba et al., 2016). The consumption of vegetables containing glucosinolates may confer protection against cancer in humans (Johnson, 2002). The hydrolytic breakdown products of glucosinolates have beneficial effects on human health, including cytotoxic and apoptotic effects in damaged cells, and reducing risks of degenerative diseases (Barba et al., 2021).

Lead contamination in soil has rapidly increased during the last decades (Sidhu et al., 2016). Metal pollution severely affects the growth and development of metal-affected plants (Borges et al., 2019). Pesticides, fertilizers, and automobile fuel are the major sources of Pb contamination. This non-essential toxic metal impedes appropriate plant nutrition (Lamhamdi et al., 2013). The edible parts of plants may uptake higher levels of metal contaminant from polluted soils and hence become a health risk for human beings and livestock consumers (Baghaie and Fereydoni, 2019). Metal toxicity enhances oxidative injury by intensifying the synthesis of reactive oxygen species (ROS) (Malar et al., 2014). Metal stressed plants increase the antioxidative system to detoxify ROS and maintain their ionic homeostasis (Fayez et al., 2014). Lead stress also affects photosynthesis, transpiration, and ionic homeostasis in stressed plants (Devi et al., 2013). As well, the plants subjected to Pb toxicity demonstrate a higher level of lipid peroxidation and ROS (Tauqeer et al., 2016). Phenolics are secondary metabolites deposited in plants facing stress and play a defensive role against a higher level of ROS synthesized in these plants (Fayez et al., 2017).

Lethal effects of synthetics pharmaceuticals have augmented the discovery and large-scale production of natural bioactive molecules. But, the resources of natural bioactive compounds are inadequate for various reasons. Conversely, the consumer entreaty for these compounds is growing gradually. Hence, the application of novel approaches to fulfill the current growing demand for natural bioactive compounds is of immense relevance. The use of conventional approaches to accelerate natural biosynthetic pathways in plants is shown to produce high levels of bio-active compounds, without the need of genetic engineering applications (Trejo-Téllez et al., 2019). Further, advances in technology have augmented the discovery of new biotic elicitors capable of increasing the production of secondary metabolites in plants.

Glycyrrhiza uralensis Fisch (Fabaceae), commonly known as licorice, is a traditional plant recognized through the ages for its multiple health benefits and medicinal uses (Kondo et al., 2007; Tanemoto et al., 2015). The roots of this plant are used to treat influenza, coughs, and liver damage in traditional medicinal formulations (Kondo et al., 2007). Liquiritoside also known as liquiritin, is the biologically active component of licorice. This study was designed to investigate the influence of liquiritoside as a foliar spray to increase plant growth and concentration of specific biologically active substances such as proline, glucosinolates, phenolics, and flavonoids in Chinese flowering cabbage plants. In addition, Pb affects the growth of crop plants (Figlioli et al., 2019). However, there is a dearth of research work demonstrating the effect of Pb stress on *B. rapa* subsp. *parachinensis*. According to our information, the effect of Pb toxicity and the ameliorative role of liquiritoside in the mitigation of subsequent stress has never been studied before.

In the course of our study, foliar application of liquiritoside showed positive effects on the growth of Chinese flowering cabbage plants (data yet not published). Additionally, we observed that liquiritoside mitigated abiotic stress, improved biosynthesis of, glucosinolates besides, flavonoids and phenolics in treated plants (Akram et al., 2020). Yet, the application of exogenously applied liquiritoside in the mitigation of plant stress has never been inspected. Therefore, it was hypothesized that liquiritoside might also modulate the antioxidative system of plants to alleviate Pb toxicity. Henceforth, the fundamental purpose of the present study was to elucidate the impact of liquiritoside spray on the physiology and growth of the plants under Pb stress. The results of current research will help to identify the differences in physiochemical process in the liquiritoside applied Pb stressed plants, which will perhaps the valuable crop producers planning to use liquiritoside plants growing in Pb contaminated soils.

MATERIALS AND METHODS

Plant Material

A preliminary study was performed to optimize the dose of liquiritoside. Plants of Chinese flowering cabbage (*Brassica rapa* subsp. *parachinensis*) were raised in plastic pots (12-inch) containing sterilized commercial potting mix. The greenhouse experiment conducted in the present study entailed growing plants in pots containing sterilized Tref Jiffy (United States) media, which were placed in greenhouse at 20/25 ± 3°C (night/day) under a 16-h photoperiod. Commercial-grade liquiritoside of 99% purity was obtained from Riotto Botanicals, Shaanxi, China. Foliar formulations of the elicitor were prepared at different concentrations including 0, 0.15, 0.25, 0.50, 0.75 and 1 g/L. Control plants were sprayed with distilled water. The application was performed at the trifoliate stage. The relative growth rate (RGR) was calculated over 5 d time spans, after 1 week of elicitor application using the formula:

$$RGR = \frac{InW2 - InW1}{t2 - t1}$$

Where W1 = initial shoot dry weight, W2 = final shoot dry weight, t2-t1 = growth period.

Greenhouse Experiment

Based on RGR, an experimental set up was designed (**Figure 1**) under the same greenhouse conditions. Details of treatments are provided in **Table 1**. Seeds of Chinese flowering cabbage were

sown in sterilized pots. An equal amount of water was supplied along with the recommended dose of fertilizers during the trial. The trial was carried out in a RCBD design containing 5 technical replicates of each treatment. Two independent greenhouse trials were conducted. No less than 10 plants were included in each treatment. Pb was added in the potting mix (75 mg/kg of potting mix) for artificial establishment of heavy metal stress according to the experiment design.

The elicitor was applied as a foliar application starting at the four-leaf stage and repeated on a fortnight basis. Plant growth parameters such as root/shoot length, root/shoot biomass, and the number of leaves were evaluated after 2 months of first foliar spray. The marketable value of plants was calculated using the following formula:

$$\text{Marketable value (\%)} = 100 - (100 \times \text{Percentage of injured or diseased plants/Percentage of healthy plants}).$$

A minimum of 20 plants was harvested from each treatment and was used for morphological and metabolomic analysis. Plant samples intended for metabolomics analysis were frozen in liquid nitrogen and kept at –80°C till examined.

Assessment of Total Phenolic, and Flavonoids and Photosynthetic Pigments

Chlorophyll and carotenoids content was determined by using a spectrophotometer according to Metzner et al. (1965). The total phenolic contents were analyzed by employing the standard Folin-Ciocalteau method (Pavel et al., 2006) and expressed as milligrams gallic acid equivalent per gram of dry weight tissue. The total flavonoid content was estimated using the aluminum chloride colorimetric method of Chang et al. (2002).

Analysis of the Nutritional Values of Leaves

Leaf samples for nutritional analysis were prepared as described by Mahmoud et al. (2019). Leaf samples were washed, stretched on paper towels, and air-dried for 60 min at room temperature. Thereafter, leaf samples were oven-dried at 70°C to ensure persistent weight. These dried samples were ground in a stainless-steel grinder and the following nutritional analyses were performed.

Estimation of H_2O_2 and MDA

The amount of H_2O_2 content was estimated with the help of a spectrophotometer as described by Jana and Choudhuri (1981). The MDA level, a product of lipid peroxidation was quantified according to Heath and Packer (1968), with slight alterations as suggested by Zhang and Kirkham (1994).

Assessment of Antioxidative Enzymes

The enzymatic activities of POD, SOD, and CAT were analyzed as described by Gao et al. (2005).

Estimation of Phytochelatins (PCs), Non-protein Thiols (NPT), Cysteine, and Glutathione (GSH)

The cysteine content in the plant sample was measured according to the methodology of Gaitonde (1967). The amount of non-protein thiols content was estimated by employing the technique of Ellmann (1959). The quantity of sulfur-assimilating compounds was analyzed by adopting the technique of Nagalakshmi and Prasad (2001).

The amount of phytochelatins in treated plants was assessed according to Bhargava et al. (2005) by eliminating the quantity of GSH from the amount of NPTs as follows:

$$\text{PCs} = \text{NPTs - GSH}$$

Quantification of Proline Content

The technique of Bates et al. (1973) was used for the estimation of proline content.

Estimation of Lead

The quantity of Pb from digested plant samples was evaluated according to Khan et al. (2017) by using Atomic Absorption Spectrophotometer.

Quantification of Glucosinolate Content

We used our recently devised method (Akram et al., 2020) for the identification and quantification of different types of glucosinolates from the leaves of Chinese flowering cabbage plants. Leaves from 10 plants were taken from each treatment and pooled together. Analysis was performed on an API 4000 QTrap mass spectrometer equipped with a TurboIonSpray probe (AB Sciex; Foster City, CA, United States) connected to a Shimadzu UFLC (Shimadzu, Kyoto, Japan). The mass spectrometer worked with triple quadrupole analyzer in the Multiple Reaction Monitoring (MRM) mode. Sinigrin does not exist in *B. rapa* and *B. napus* (Rangkadilok et al., 2002). In this study, it was used as an internal standard for quantitative analysis of glucosinolates (Jacobo-Velázquez et al., 2011).

Statistical Analysis

The data obtained were analyzed by taking variance with the help of DSAASTAT software. The Duncan's new multiple range test was employed for evaluation of the significant difference between means of all treatments. The study trials having three replicates were repeated twice, and values of means acquired are exhibited.

RESULTS

Influence of Liquiritoside on Plant Height, Number of Leaves, Root Biomass, Shoot Biomass, and Marketable Value of Chinese Flowering Cabbage Subjected to Pb Stress

In the absence of Pb, the liquiritoside (1 g/L) treatment significantly increased the plant height, the number of leaves,

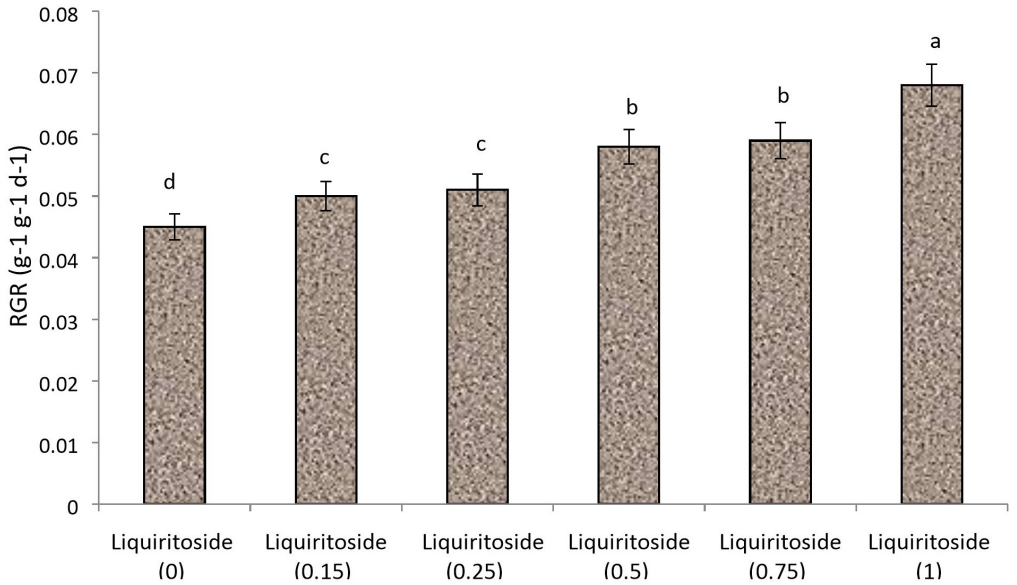

FIGURE 1 | Effect of various doses of liquiritoside (g/L) on the relative growth rate (RGR) of Chinese flowering cabbage. Mean values of two independent experiments are presented. Vertical bars show standard error between different replicates of the same treatment. Data marked by different letters are significantly different at $p < 0.05$.

marketable value, dry weight of the roots and shoots by 26, 34, 3, 27, and 20%, respectively, as compared to untreated control (**Table 1**). Liquiritoside (0.5 g/L) treatment had no significant effect on plant height, the number of leaves, marketable value, shoot, and root biomass after and before Pb exposure. In the presence of Pb, liquiritoside (1 g/L) application remarkably increased plant length, number of leaves, marketable value, the dry weight of the shoots and roots of Chinese flowering cabbage in comparison with Pb control (**Table 1**).

Effects of Liquiritoside on Chlorophyll and Carotenoid Contents, Flavonoids, and Total Phenolics in Chinese Flowering Cabbage Under Pb Stress

As shown in **Table 2**, the contents of chlorophyll *a*, chlorophyll *b*, and carotenoids in plant tissues of the control treatment were 1.17, 0.47, and 2.78 mg g^{-1}, respectively. The Pb treatment decreased the chlorophyll *a* and *b* and carotenoids contents in Chinese flowering cabbage by 27, 28, and 24%, respectively, than that of the untreated control. On the other hand, liquiritoside (1 g/L) supplementation significantly improved the chlorophyll *a* and *b* and carotenoids levels of plants exposed to Pb stress compared with relevant control.

The results showed that Pb toxicity markedly augmented the level of both flavonoids, and phenolics by 32 and 38%, respectively, in Chinese flowering cabbage plants as compared to untreated controls. However, liquiritoside supplementation further boosted the magnitude of both flavonoids, and phenolics in the subject plants under Pb toxic and nontoxic conditions (**Table 2**). The Pb+liquiritoside (1 g/L) treatment accelerated the quantities of both flavonoids, and phenolics by 17 and 31%, respectively, in Chinese flowering cabbage with respect to only Pb treated plants.

Impact of Added Liquiritoside on Antioxidant Enzyme Activities in Chinese Flowering Cabbage Under Pb Treatment

Lead stress attenuated the activities of antioxidant enzymes like SOD, CAT, and POD in Chinese flowering cabbage plants when compared with untreated control. While supplementation of liquiritoside at different concentrations further modulated the level of these antioxidant enzymes (SOD, CAT, and POD) in plants subjected to Pb stressed and non-stressed regimes. The Pb+liquiritoside (0.5 g/L) exhibited remarkable increment in the level of SOD, CAT, and POD by 24, 16, and 37, respectively, in Chinese flowering cabbage plants in contrast with only Pb treated ones (**Figure 2**).

Implications of Liquiritoside in the Modulation of GSH, PCs, Cysteine, and NPT Contents in Chinese Flowering Cabbage Exposed to Pb Toxicity

In the absence of Pb treatments, no obvious changes were observed in the GSH contents of plants with increased liquiritoside application, but the GSH contents were meaningfully different in plants raised under various liquiritoside treatments during Pb stressed conditions (**Table 3**). The pre-incubation of liquiritoside at the dose of 0.25, 0.50, and 1 g/L increased glutathione contents by 11, 14, and 18%, respectively, in Chinese cabbage plants raised under Pb regimes with respect to relevant controls. In the presence of Pb toxicity, sufficient and

TABLE 1 | Effect of liquiritoside on growth attributes of Chinese flowering cabbage plants under lead (Pb) stress.

Treatments	Plant Height	Number of leaves	Root FW	Shoot FW	Root DW	Shoot DW	Marketable value
	cm	–	g	g	g	g	(%age)
C	26.32 ± 1.78b	8.25 ± 0.35bc	15.5 ± 0.83b	81.29 ± 6.15b	6.56 ± 0.23b	54.75 ± 4.03bc	91.5 ± 5.41ab
Liquiritoside (0.25 g/L)	31.7 ± 2.19ab	9.57 ± 0.42ab	17.8 ± 0.92ab	87 ± 7.37ab	7.87 ± 0.24ab	58.08 ± 3.52b	92.4 ± 6.83a
Liquiritoside (0.50 g/L)	33.57 ± 2.38ab	10.38 ± 0.57ab	20 ± 1.25ab	95 ± 8.24ab	8.52 ± 0.27ab	61.31 ± 3.72ab	92.8 ± 6.91a
Liquiritoside (1 g/L)	35.62 ± 2.81a	12.43 ± 0.65a	22 ± 1.09a	98 ± 7.96a	8.93 ± 0.36a	68.26 ± 4.21a	93.3 ± 5.82a
Pb	18.3 ± 0.85c	6.38 ± 0.21c	9.37 ± 0.58c	64 ± 4.19c	4.15 ± 0.16c	31.17 ± 1.73d	60.4 ± 4.29c
Pb+ liquiritoside (0.25 g/L)	20.6 ± 0.93c	7.29 ± 0.26bc	12.98 ± 0.89bc	71 ± 5.73bc	6.31 ± 0.21bc	35.18 ± 2.87cd	67.8 ± 3.69bc
Pb+liquiritoside (0.50 g/L)	23.58 ± 1.15bc	8.26 ± 0.28bc	14.74 ± 0.76bc	76 ± 4.82bc	7.18 ± 0.29b	38.14 ± 2.43cd	72 ± 5.24b
Pb+liquiritoside (1 g/L)	25.16 ± 1.27b	8.91 ± 0.32b	15.63 ± 1.02b	82 ± 5.72b	8.43 ± 0.32ab	40.37 ± 2.84c	74 ± 4.82b

Values presented are mean ± standard error of two independent experiments. Data marked by the different letters in the same column are significantly different at $p < 0.05$, C = Control, Pb = Lead (75 mg/kg soil).

TABLE 2 | Effect of liquiritoside on chlorophyll, carotenoids, flavonoids, and phenolics levels of Chinese flowering cabbage plants under lead (Pb) stress.

Treatments	Chlorophyll *a*	Chlorophyll *b*	Total Chl.	Carotenoids	Flavonoids	Total phenolics
	mg g^{-1} FW	mg g^{-1} FW	mg g^{-1} FW	mg g^{-1} FW	mg of quercetin g^{-1}	mg of GAE g^{-1}
C	1.17 ± 0.052bc	0.47 ± 0.021b	1.64 ± 0.058bc	2.78 ± 0.13c	5.54 ± 0.25d	138 ± 6.17e
Liquiritoside (0.25 g/L)	1.32 ± 0.038b	0.53 ± 0.023ab	1.85 ± 0.072b	3.21 ± 0.18bc	6.62 ± 0.31c	145 ± 6.32de
Liquiritoside (0.50 g/L)	1.54 ± 0.073ab	0.61 ± 0.025ab	2.15 ± 0.085ab	3.48 ± 0.21b	7.34 ± 0.34bc	154 ± 7.24de
Liquiritoside (1 g/L)	1.65 ± 0.081a	0.64 ± 0.028a	2.29 ± 0.089a	4.36 ± 0.25a	7.86 ± 0.38bc	164 ± 7.4d
Pb	0.86 ± 0.042d	0.34 ± 0.016c	1.20 ± 0.036d	2.12 ± 0.09d	8.13 ± 0.42b	201 ± 9.6c
Pb+ liquiritoside (0.25 g/L)	0.95 ± 0.046cd	0.39 ± 0.015bc	1.34 ± 0.038cd	2.56 ± 0.13cd	9.24 ± 0.47ab	228 ± 12b
Pb+liquiritoside (0.50 g/L)	0.98 ± 0.056cd	0.42 ± 0.018bc	1.40 ± 0.041cd	2.76 ± 0.15c	9.06 ± 0.52ab	253 ± 13ab
Pb+liquiritoside (1 g/L)	1.12 ± 0.062c	0.45 ± 0.023b	1.57 ± 0.045c	2.94 ± 0.16bc	9.75 ± 0.58a	269 ± 15a

Values presented are mean ± standard error of two independent experiments. Data marked by the different letters in the same column are significantly different at $p < 0.05$, C = Control, Pb = Lead (75 mg/kg soil).

excessive liquiritoside treatment obviously increased the PCs and NPT contents in Chinese flowering cabbage plants compared with those plants in the liquiritoside deficiency treatment group. The, Pb+liquiritoside (1 g/L) treatment significantly enhanced the level of PCs and NPT in subjected plants by 14 and 17%, respectively, with respect to only Pb treated ones (**Table 3**). These findings signposted that the biosynthesis of thiol metabolic compounds (NPT, GSH, and PCs) enhanced with increased liquiritoside application in Chinese flowering cabbage to alleviate Pb stress. During the current study, liquiritoside (1 g/L) treatment noticeably attenuated the cysteine contents of Chinese flowering cabbage under nontoxic and toxic regimes (**Table 3**).

Role of Liquiritoside on Total Glucosinolates and Proline Contents of Chinese Flowering Cabbage

Lead toxicity reduced the total glucosinolates by 26% in Chinese flowering cabbage plants than that of the untreated control. However, liquiritoside supplementation augmented the level of total glucosinolates during stressed and non-stressed conditions. The application of liquiritoside at the concentration of 0.5 and 1 g/L increased the value of total glucosinolates by 23 and 29%, respectively, in plants grown under metal regimes with respect to Pb control (**Table 3**). Present results depicted that lead stress remarkably declined the level of glucosinolate contents including Progoitrin, Glucoalyssin, Gluconapin, Glucobrassicin, Neoglucobrassin, 4-Hydroxyglucobrassicin and, 4-Methoxyglucobrassicin in Chinese flowering cabbage plants with respect to analogous untreated controls, respectively. Nevertheless, liquiritoside application enhanced the values of these glucosinolate contents in Chinese flowering cabbage plants under stressed and non-stressed regimes (**Table 4**).

During the present research, proline content was enhanced by 57% in Chinese flowering cabbage exposed to Pb stress when compared with untreated control. While, differential liquiritoside (0.25, 0.5, and 1 g/L) supplementation further increased the level of proline by 26, 32, and 39%, respectively, in the subject plants under contaminated regimes than that of Pb control treatment (**Table 3**).

Effect of Liquiritoside on MDA and H_2O_2 Concentrations in Chinese Flowering Cabbage Under Pb Stress

During the present investigation, Pb toxicity considerably augmented the contents of MDA and H_2O_2 in Chinese flowering cabbage with respect to untreated control. Nevertheless, excessive liquiritoside supplementation meaningfully declined the level of both MDA and H_2O_2 in plants during toxic and nontoxic circumstances. The Pb+ liquiritoside (1 g/L) treatment

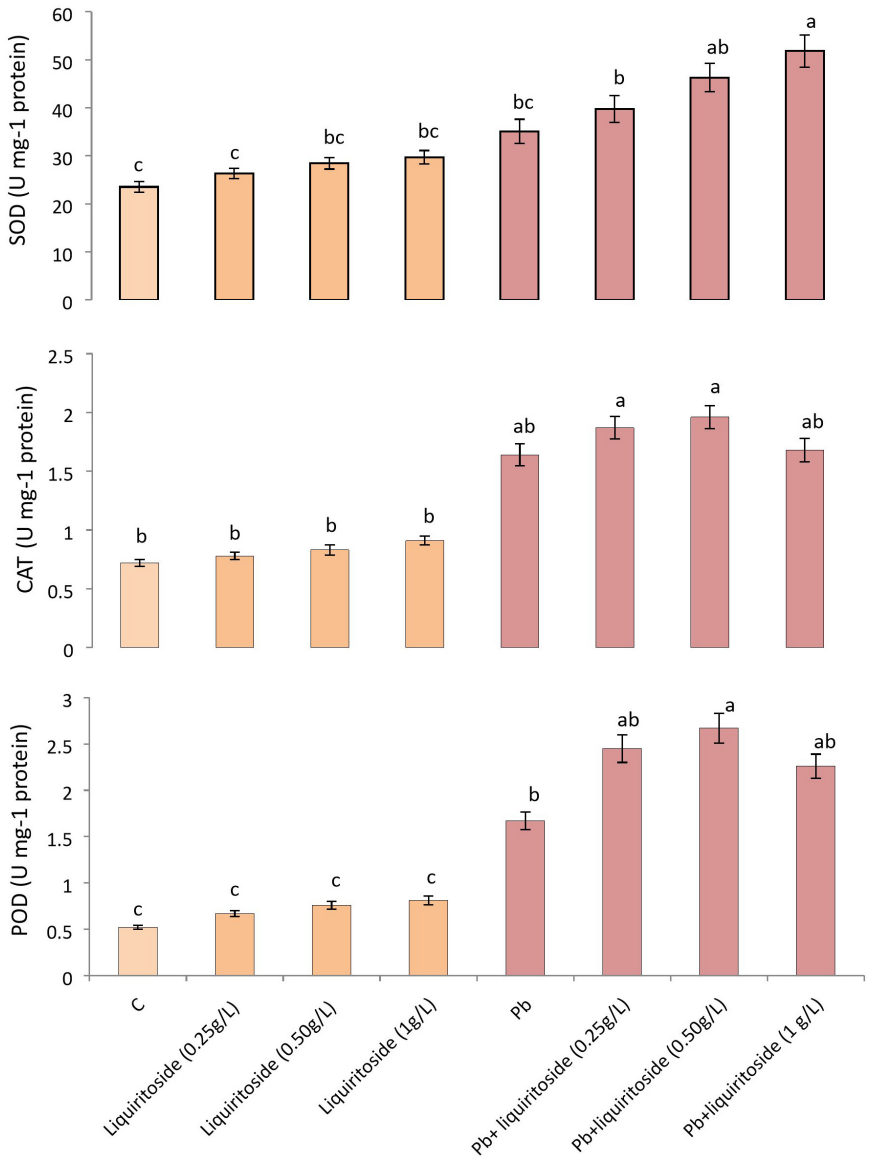

FIGURE 2 | Effect of liquiritoside on the magnitudes of antioxidant enzymes such as SOD, POD, and CAT in Chinese flowering cabbage plants under lead stress. Mean values of two independent experiments are presented. Vertical bars show standard error between different replicates of the same treatment. Data marked by different letters are significantly different at $p < 0.05$. Pb, lead; C, Control.

diminished the quantities of both H_2O_2 and MDA in Chinese flowering cabbage by 38 and 29%, respectively, as compared to concerned Pb treated groups (**Figure 3**).

Role of Liquiritoside on Pb Uptake in Roots and Shoots of Chinese Flowering Cabbage

The findings of the current study depicted that root tissues showed more Pb uptake compared with shoot tissues of Chinese flowering cabbage (**Table 5**). The higher Pb accumulation was noticed in roots and shoots of plants grown under only Pb treatment. The liquiritoside supplementation exhibited a reduction of Pb uptake in the root and the shoot tissues of Chinese flowering cabbage as compared to only the Pb treatment group (**Table 5**). With the increase in liquiritoside doses (0.25, 0.5, and 1 g/L), a Pb uptake reduction was recorded in analyzed root and shoot tissues. The excessive dose liquiritoside (1 g/L) caused 28 and 43% decline of Pb uptake in root and shoot organs of Chinese flowering cabbage in contrast with non - supplemented stressed plants. The application of liquiritoside (1 g/L) significantly reduced the translocation factor and bio-concentration factor of Pb in subjected plants than that of non-supplemented ones. The plants grown under Pb regimes exhibited decreased value flowering cabbage plants in a dose dependent manner.

TABLE 3 | Effect of liquiritoside on the levels of phytochelatins (PCs), cysteine, non-protein thiols (NPT), glucosinolates, glutathione (GSH) and proline in Chinese flowering cabbage plants under lead (Pb) stress.

Treatments	PCs	Cysteine	NPT	Total glucosinolates	GSH	Proline
	nmol-SH mg^{-1} protein	nmol-SH mg^{-1} protein	nmol-SH mg^{-1} protein	μmol g^{-1} DW	μmol g^{-1} FW	μmol g^{-1} FW
C	294.51 ± 14.16cd	115.72 ± 6.18c	490.52 ± 21d	16.45 ± 0.73b	195.38 ± 9.34cd	18.65 ± 1.45e
Liquiritoside (0.25 g/L)	301.32 ± 16.27c	112.78 ± 6.41cd	483.67 ± 19de	18.19 ± 0.87ab	182.61 ± 8.71d	20.31 ± 1.53e
Liquiritoside (0.50 g/L)	289.42 ± 15.28cd	106.83 ± 5.23cd	476.76 ± 23de	21.62 ± 1.28ab	187.23 ± 9.28d	24.86 ± 2.54de
Liquiritoside (1 g/L)	272.74 ± 13.39d	94.91 ± 4.57d	465.81 ± 24e	25.24 ± 1.36a	193.92 ± 10.26cd	31.92 ± 2.65d
Pb	304.09 ± 17.53c	151.64 ± 7.83a	543.67 ± 25c	12.25 ± 0.71c	241.72 ± 12.75c	43.42 ± 3.83c
Pb+ liquiritoside (0.25g/L)	328.74 ± 18.79b	117.87 ± 8.75c	597.45 ± 28b	16.17 ± 1.23b	269.63 ± 13.68b	58.27 ± 2.71b
Pb+liquiritoside (0.50 g/L)	335.28 ± 21.94ab	128.96 ± 7.87bc	613.67 ± 32ab	15.94 ± 0.78b	278.17 ± 14.56ab	64.16 ± 3.62ab
Pb+liquiritoside (1 g/L)	351.83 ± 19.37a	134.68 ± 8.13b	642.26 ± 34a	17.39 ± 0.98ab	291.29 ± 16.46a	71.35 ± 4.39a

Values presented are mean ± standard error of two independent experiments. Data marked by the different letters in the same column are significantly different at $p < 0.05$, C = Control, Pb = Lead (75 mg/kg soil).

DISCUSSION

In the past few years, several studies have shown that exogenous elicitors can mediate plant growth and productivity (Bibi et al., 2016; Brockman and Brennan, 2017; Colla et al., 2017). To the best of our knowledge, the present study is the first to report the positive effects of liquiritoside on the growth and health-promoting elements of Chinese flowering cabbage grown under Pb stress. The application of genistein, a flavonoid improved growth and production of salted soya bean plants (Miransari and Smith, 2007). Likewise, coumarin, a phenolic compound enhanced the growth of wheat plants exposed to salt stress. Similarly, apigenin also enhanced biomass production and the growth of paddy plants under salt stress (Mekawy et al., 2018). Similarly, it was revealed that liquiritoside enhanced growth-related attributes and marketable value of Chinese flowering cabbage exposed to Pb regimes.

The increased growth rate of Chinese flowering cabbage plants observed under the influence of the foliar elicitor could be attributed to the capability of liquiritoside to modulate phytohormones, soluble sugars, amino acids, and mineral elements in applied plants. The liquiritoside may improve the yield and quality of Chinese flowering cabbage by affecting cellular metabolism. For example, it is known that sugars act as signaling molecules and improve plant growth and development (Smeekens et al., 2010). Amino acids provide improved stress tolerance in plants (Karabudak et al., 2014). Some organic acids present in plant extracts can chelate metal ions to stimulates root growth (Battacharyya et al., 2015). All these together could supply nutrition for cell growth, with a resulting increase in growth and vigor.

Chinese flowering cabbage plants under Pb stress exhibited a reduced level of photosynthetic pigments. Several other studies have revealed that Pb deteriorated chlorophyll structure and decreased chlorophyll synthesis by replacing Fe, Mg, and Cu (Akinci et al., 2010; Ashraf et al., 2016). Foliar application of liquiritoside positively affected total chlorophyll and carotenoids content in a dose-dependent manner (**Table 2**). The positive effect of liquiritoside on leaf pigment content could be attributed to the delay in leaf senescence or enhancement in leaf pigment biosynthesis (Fan et al., 2013; Jannin et al., 2013). These beneficial effects are possibly due to the effect of liquiritoside on phytohormones. The physiological parameter of leaf pigment content also acts as indicators of improved quality of Chinese flowering cabbage that can be obtained by the application of exogenous elicitors. Analogous to our results, it was observed that apigenin-treated plants showed increased biosynthesis of photosynthetic pigments which improved the growth of paddy plants subjected to salinity stress (Mekawy et al., 2018). Moreover, the cinnamic acid applied plants also exhibited an increased amount of photosynthetic pigments besides increased growth of maize plants exposed to salt toxicity (Araniti et al., 2018).

The enzymatic and non-enzymatic antioxidants enable plants to thrive under abiotic stress conditions (Usman et al., 2020). The antioxidative compounds perform the role of sacrificial agents through their activity on ROS, thus defending plant biomolecules. Rutin as an antioxidative flavonoid, scavenge ROS, and enhance the growth of leguminous plants (Ismail et al., 2016). Quercetin synthesized by rutin has ROS scavenging capability because it acts as a substrate of guaiacol peroxidase (Amako et al., 1994). The detoxification of ROS in quercitin applied plants mitigated salt-induced stress and improved the growth of plants. The antioxidant enzymes such as POD, CAT, and SOD consume phenolics, including cinnamate, ellagate and ferulate to alleviate plant stress (Abu Taleb et al., 2013; Singh et al., 2013). Similarly, our finding also exhibited obvious modulations in the activities of POD, CAT, and SOD for dilution of Pb toxicity in liquiritoside supplemented Chinese flowering cabbage plants.

Fayez et al. (2014) demonstrated that abiotic stress modulates physiochemical attributes of plants. Plants synthesize an elevated level of MDA and H_2O_2 under stress (Noctor et al., 2015). Lead stress enhanced the biosynthesis of ROS, leading to increased oxidative injury in plants (Hattab et al., 2016). Other studies also showed that Pb enhanced lipid peroxidation in plants causing oxidative injuries (Li et al., 2013). Plants engage the antioxidant system to mitigate metal-triggered oxidative stress (Shahid et al., 2014). Phenolics and flavonoids may reduce the biosynthesis of ROS, EL H_2O_2, and MDA to alleviate plant stress (Mekawy et al., 2018). The reduced level of ROS helps in the mitigation of

TABLE 4 | Effect of liquiritoside on glucosinolate contents in Chinese flowering cabbage plants under lead (Pb) stress.

Treatments	Progoitrin	Glucoalyssin	Gluconapin	Glucobrassicin	Neoglucobrassin	4– Hydroxyglucobrassicin	4–Methoxyglucobrassicin
	μmol g^{-1} DW Sinigrin eqv.	μmol g^{-1} DW Sinigrin eqv.	μmol g^{-1} DW Sinigrin eqv.	μmol g^{-1} DW Sinigrin eqv.	μmol g^{-1} DW Sinigrin eqv.	μmol g^{-1} DW Sinigrin eqv.	μmol g^{-1} DW Sinigrin eqv.
C	0.58 ± 0.031ab	0.143 ± 0.0081ab	1.62 ± 0.051b	0.128 ± 0.0057ab	4.38 ± 0.24b	0.072 ± 0.0038e	2.46 ± 0.12b
Liquiritoside (0.25 g/L)	0.62 ± 0.032ab	0.152 ± 0.0086ab	1.67 ± 0.069ab	0.129 ± 0.0059ab	5.61 ± 0.31ab	0.078 ± 0.0043e	2.92 ± 0.14ab
Liquiritoside (0.50 g/L)	0.64 ± 0.035ab	0.163 ± 0.0092ab	1.76 ± 0.072ab	0.132 ± 0. 62ab	6.03 ± 0.42ab	0. 086 ± 0.0049e	3.37 ± 0.17ab
Liquiritoside (1 g/L)	0.67 ± 0.039a	0.174 ± 0.0091a	1.81 ± 0.084a	0.134 ± 0.0065a	6.34 ± 0.46a	0.092 ± 0.0052d	3.75 ± 0.19a
Pb	0.32 ± 0.021c	0.086 ± 0.0053b	0.97 ± 0.035d	0.075 ± 0.0027b	2.84 ± 0.14d	0.042 ± 0.0024c	1.58 ± 0.095d
Pb+ liquiritoside (0.25 g/L)	0.35 ± 0.024bc	0.091 ± 0.0061b	1.045 ± 0.042cd	0.079 ± 0.0029b	3.13 ± 0.16cd	0.049 ± 0.0027b	1.69 ± 0.098cd
Pb+liquiritoside (0.50 g/L)	0.39 ± 0.025bc	0.095 ± 0.0064b	1.167 ± 0.043cd	0.086 ± 0.0032b	3.27 ± 0.19cd	0.056 ± 0.0032ab	1.74 ± 0.10cd
Pb+liquiritoside (1 g/L)	0.42 ± 0.027b	0.098 ± 0.0068b	1.26 ± 0.048c	0.091 ± 0.0037b	3.49 ± 0.21c	0.063 ± 0.0034a	1.82 ± 0.11c

Values presented are mean ± standard error of two independent experiments. Data marked by the different letters in the same column are significantly different at $p < 0.05$, C = Control, Pb = Lead (75 mg/kg soil).

oxidative injury (Hossain et al., 2019). The improved synthesis of phenolics and flavonoids as well as antioxidant enzymes detoxify ROS and mitigate stress in gallic acid, and rutin treated plants under stress. Pheomphun et al. (2019) observed that reduced H_2O_2, MDA, and enhanced activity of antioxidant enzymes in catechin supplemented plants for the alleviation of stress.

Higher proline has been observed in plants facing stress (Ahmad et al., 2018). However, exogenously applied quercetin and coumarin improve proline content, and LRWC in plants to mitigate stress (Saleh and Madany, 2015). The increased proline biosynthesis was attributed to reduced activity of proline dehydrogenase and increased activity of pyrroline-5-carboxylate synthase in coumarin supplemented plants (Pérez-Arellano et al., 2010; Szabados and Savoure, 2010). Hence, it is assumed that liquiritoside may mitigate metal stress in applied Chinese flowering cabbage plants in the same manner.

Phenolics scavenge ROS to reduce oxidative injury in plants (Soares et al., 2019). Our results showed that liquiritoside enhanced phenolic contents and triggered the activity of antioxidant enzymes. Phenolics detoxify ROS and metal toxicity by making metal complex in plants (Tolrà et al., 2009). The results of this study are in agreement with the findings of Ashraf et al. (2016), who observed that the foliar application of plant extracts increased the total phenolics and flavonoid content of *Raphanus sativus* plants. Baenas et al. (2014) showed that the nutritional quality of sprouts of brassica vegetables was improved by foliar application of biotic elicitors. Agati and Tattini (2010) reported that flavonoids decline in ROS levels in plants affected by abiotic stress. Similarly, other researchers have described the importance of GSH, flavonoids, and ascorbic acid in mitigation of plant stress through reducing ROS synthesis (Liang et al., 2018). The augmented synthesis of flavonoid alleviates drought stress in plants (Varela et al., 2016).

Current results showed that the levels of total GLS in Chinese flowering cabbage plants exposed to Pb toxicity were significantly increased under the influence of the foliar elicitor (1 g/L) (**Table 3**). Same types of increments of GLSs have been reported in Chinese flowering cabbage in previous studies (Bhandari et al., 2015; Liang et al., 2018). Metal stressed plants modulate the synthesis of thiol ligands, including phytochelatins (PCs), non-protein thiols, cysteine, and GSH for detoxification and chelation of metal (Kumar et al., 2016; Ahmad et al., 2020). Higher synthesis of thiols in root tissues compared to foliage of plants declines uptake and translocation of injurious metals from roots to shoots (Hasan et al., 2015). The thiol-containing groups of plants such as cysteine, NPT and PCs, have a higher affinity for metals and hence assist in homeostasis and detoxification of metals (Rabêlo et al., 2018). Similarly, cysteine, NPT, GSH, and PCs may have played their part reducing Pb translocation and subsequent detoxification in Chinese cabbage flowering plants.

Plant roots immediately come in contact with metals and hence exhibit relatively more metal content as compared to above-ground parts of plants. The increased demethylation and pectin level help in reduced translocation besides the

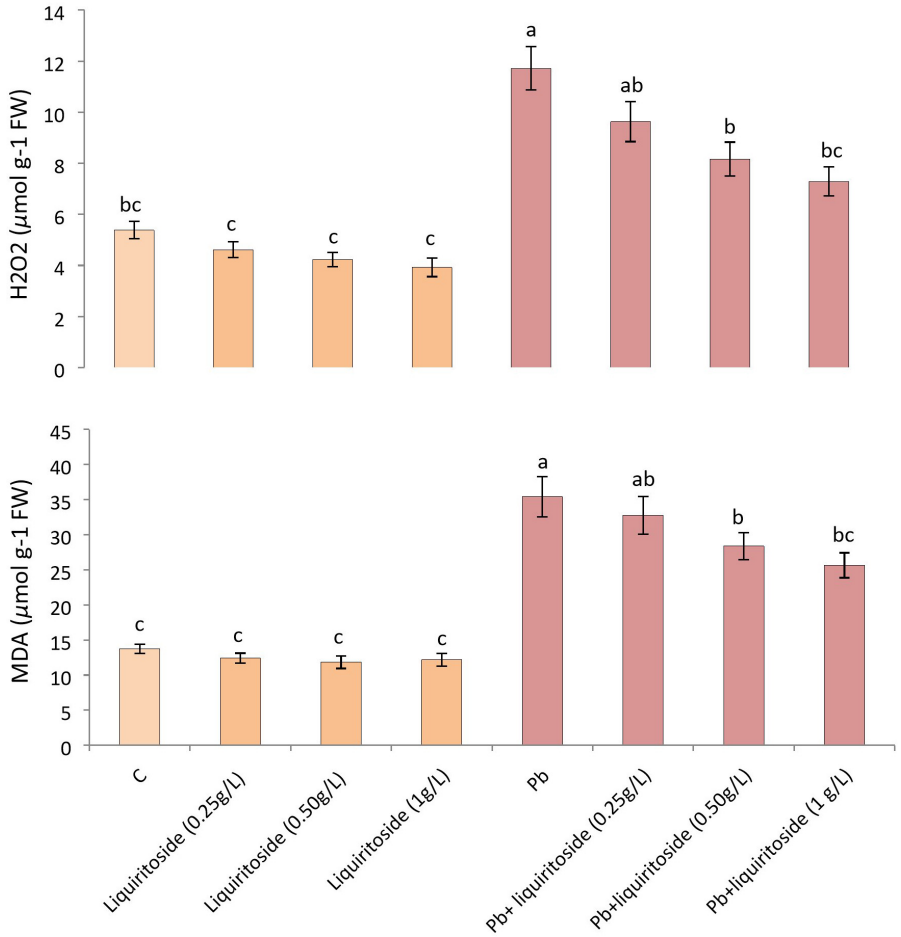

FIGURE 3 | Effect of liquiritoside on the amounts of malondialdehyde (MDA) and hydrogen peroxide (H_2O_2) in Chinese flowering cabbage plants under lead stress. Mean values of two independent experiments are presented. Vertical bars show standard error between different replicates of the same treatment. Data marked by the different letters in the same column are significantly different at $p < 0.05$. Pb, lead; C, Control.

TABLE 5 | Role of liquiritoside on Pb uptake in root and shoot tissues, bio-concentration factor (BCF), translocation factor (TF) and tolerance index (TI) of Chinese flowering cabbage plants under lead (Pb) stress.

Treatments	Root Pb uptake	Shoot Pb uptake	BCF	TF	TI
	mg kg^{-1}	mg kg^{-1}	–	–	%
C	0.86 ± 0.052c	0.52 ± 0.028c	0.55 ± 0.021c	0.60 ± 0.035a	–
Liquiritoside (0.25 g/L)	0.72 ± 0.045c	0.43 ± 0.021c	0.46 ± 0.024cd	0.59 ± 0.027a	1.21 ± 0.057ab
Liquiritoside (0.50 g/L)	0.58 ± 0.028c	0.31 ± 0.019c	0.35 ± 0.017cd	0.53 ± 0.024ab	1.27 ± 0.073ab
Liquiritoside (1 g/L)	0.47 ± 0.031b	0.23 ± 0.012c	0.28 ± 0.016c	0.48 ± 0.022b	1.35 ± 0.083a
Pb	41.09 ± 2.53a	25.64 ± 1.06a	0.87 ± 0.051a	0.62 ± 0.034a	0.69 ± 0.025c
Pb+ liquiritoside (0.25 g/L)	39.74 ± 2.62ab	18.87 ± 0.85ab	0.78 ± 0.042ab	0.47 ± 0.026bc	0.78 ± 0.038bc
Pb+liquiritoside (0.50 g/L)	36.28 ± 2.54ab	15.96 ± 0.79b	0.69 ± 0.034b	0.43 ± 0.021c	0.89 ± 0.056bc
Pb+liquiritoside (1 g/L)	29.83 ± 1.97b	14.68 ± 0.64b	0.59 ± 0.035bc	0.49 ± 0.025b	0.95 ± 0.047b

Values presented are mean ± standard error of two independent experiments. Data marked by the different letters in the same column are significantly different at $p < 0.05$, C = Control, Pb = Lead (75 mg/kg soil).

fixation of metal within the root cell walls (Liu et al., 2019). Perhaps, this strategy reduced Pb translocation from root to shoot of the plants and should be explored in further studies (Bharwana et al., 2013).

CONCLUSION

This study demonstrates that liquiritoside could be used as an effective plant growth bio-stimulant. Our findings indicate that

the nutritional and medicinal contents in leaves of Chinese flowering cabbage plants can be augmented by foliar application of liquiritoside at a rate of 0.5 g/L. The supplementation of liquiritoside alleviated Pb stress of plants by improving growth/photosynthetic pigments, glucosinolates, antioxidants, and reducing MDA, H_2O_2, cysteine, and Pb uptake. Further studies are required to understand the mechanism underlying the crop's growth effect, promoting biotic elicitor's use in organic agriculture.

DATA AVAILABILITY STATEMENT

The original contributions presented in the study are included in the article/supplementary material, further inquiries can be directed to the corresponding author/s.

AUTHOR CONTRIBUTIONS

WA: suggest the idea and perform the experiments. WUK: carry out statistical analysis. NAY: writing manuscript. AS: data analysis and manuscript drafting. GL: research designing and supervision. All authors contributed to the article and approved the submitted version.

FUNDING

This study was supported by the Science and Technology Foundation of Guangdong Province (Project No. 2020B0202090002) and Guangdong Agriculture Department of China (Project No. 2021KJ122).

REFERENCES

Abu Taleb, A., Tharwat, N., and El-Mohamedy, R. (2013). Induction of resistance in tomato plants against fusarium crown and root rot disease by *Trichoderma harzianum* and chitosan. *Egypt. J. Phytopathol.* 41, 13–26. doi: 10.21608/ejp.2013.101965

Agati, G., and Tattini, M. (2010). Multiple functional roles of flavonoids in photoprotection. *New Phytol.* 186, 786–793. doi: 10.1111/j.1469-8137.2010.03269.x

Ahmad, A., Khan, W. U., Shah, A. A., Yasin, N. A., Ali, A., Rizwan, M., et al. (2020). Dopamine alleviates hydrocarbon stress in *Brassica oleracea* through modulation of physio-biochemical attributes and antioxidant defense systems. *Chemosphere* 270:128633. doi: 10.1016/j.chemosphere.2020.128633

Ahmad, P., Abass Ahanger, M., Nasser Alyemeni, M., Wijaya, L., Alam, P., and Ashraf, M. (2018). Mitigation of sodium chloride toxicity in *Solanum lycopersicum* L. by supplementation of jasmonic acid and nitric oxide. *J. Plant Interact.* 13, 64–72. doi: 10.1080/17429145.2017.1420830

Aixia, G., Jianjun, Z., Yanhua, W., Xiaofeng, L., Shuxin, X., and Shuxing, S. (2015). Glucosinolates in self-crossed progenies of monosomic cabbage alien addition lines in Chinese cabbage. *Hortic. Plant J.* 1, 86–92.

Akinci, I. E., Akinci, S., and Yilmaz, K. (2010). Response of tomato (*Solanum lycopersicum* L.) to lead toxicity: growth, element uptake, chlorophyll and water content. *Afr. J. Agric. Res.* 5, 416–423.

Akram, W., Saeed, T., Ahmad, A., Yasin, N. A., Akbar, M., Khan, W. U., et al. (2020). Liquiritin elicitation can increase the content of medicinally important glucosinolates and phenolic compounds in Chinese kale plants. *J. Sci. Food Agric.* 100, 1616–1624. doi: 10.1002/jsfa.10170

Amako, K., Chen, G.-X., and Asada, K. (1994). Separate assays specific for ascorbate peroxidase and guaiacol peroxidase and for the chloroplastic and cytosolic isozymes of ascorbate peroxidase in plants. *Plant Cell Physiol.* 35, 497–504.

Araniti, F., Lupini, A., Mauceri, A., Zumbo, A., Sunseri, F., and Abenavoli, M. R. (2018). The allelochemical trans-cinnamic acid stimulates salicylic acid production and galactose pathway in maize leaves: a potential mechanism of stress tolerance. *Plant Physiol. Biochem.* 128, 32–40. doi: 10.1016/j.plaphy.2018.05.006

Ashraf, R., Sultana, B., Iqbal, M., and Mushtaq, M. (2016). Variation in biochemical and antioxidant attributes of *Raphanus sativus* in response to foliar application of plant leaf extracts as plant growth regulator. *J. Genetic Eng. Biotechnol.* 14, 1–8. doi: 10.1016/j.jgeb.2016.08.003

Baenas, N., García-Viguera, C., and Moreno, D. A. (2014). Biotic elicitors effectively increase the glucosinolates content in *Brassicaceae sprouts*. *J. Agric. Food Chem.* 62, 1881–1889. doi: 10.1021/jf404876z

Baghaie, A. H., and Fereydoni, M. (2019). The potential risk of heavy metals on human health due to the daily consumption of vegetables. *Environ. Health Eng. Manag.* 6, 11–16. doi: 10.15171/ehem.2019.02

Barba, F. J., Nikmaram, N., Roohinejad, S., Khelfa, A., Zhu, Z., and Koubaa, M. (2016). Bioavailability of glucosinolates and their breakdown products: impact of processing. *Front. Nutr.* 3:24. doi: 10.3389/fnut.2016.00024

Barba, F., Cravotto, G., and Munekata, P. E. S. (2021). *Design and Optimization of Innovative Food Processing Techniques Assisted by Ultrasound*. New York, NY: Elsevier Science.

Bates, L. S., Waldren, R. P., and Teare, I. D. (1973). Rapid determination of free proline for water-stress studies. *Plant Soil* 39, 205–207. doi: 10.1007/bf00018060

Battacharyya, D., Babgohari, M. Z., Rathor, P., and Prithiviraj, B. (2015). Seaweed extracts as biostimulants in horticulture. *Sci. Hortic.* 196, 39–48. doi: 10.1016/j.scienta.2015.09.012

Bhandari, S. R., Jo, J. S., and Lee, J. G. (2015). Comparison of glucosinolate profiles in different tissues of nine brassica crops. *Molecules* 20, 15827–15841. doi: 10.3390/molecules200915827

Bhargava, P., Srivastava, A. K., Urmil, S., and Rai, L. C. (2005). Phytochelatin plays a role in UV-B tolerance in N2-fixing cyanobacterium *Anabaena doliolum*. *J. Plant Physiol.* 162, 1220–1225. doi: 10.1016/j.jplph.2004.12.006

Bharwana, S. A., Ali, S., Farooq, M. A., Iqbal, N., Abbas, F., and Ahmad, M. S. A. (2013). Alleviation of lead toxicity by silicon is related to elevated photosynthesis, antioxidant enzymes suppressed lead uptake and oxidative stress in cotton. *J. Bioremed. Biodeg.* 4:187.

Bibi, A., Ullah, F., Mehmood, S., Bibi, K., Khan, S. U., Khattak, A., et al. (2016). *Moringa oleifera* Lam. leaf extract as bioregulator for improving growth of maize under mercuric chloride stress. *Acta Agric. Scand. Sec. B Soil Plant Sci.* 66, 469–475. doi: 10.1080/09064710.2016.1173225

Borges, K. L. R., Hippler, F. W. R., Carvalho, M. E. A., Nalin, R. S., Matias, F. I., and Azevedo, R. A. (2019). Nutritional status and root morphology of tomato under Cd-induced stress: comparing contrasting genotypes for metal-tolerance. *Sci. Hortic.* 246, 518–527. doi: 10.1016/j.scienta.2018.11.023

Brockman, H. G., and Brennan, R. F. (2017). The effect of foliar application of *Moringa* leaf extract on biomass, grain yield of wheat and applied nutrient efficiency. *J. Plant Nutr.* 40, 2728–2736. doi: 10.1080/01904167.2017.1381723

Chang, C. C., Yang, M. H., Wen, H. M., and Chern, J. C. (2002). Estimation of total flavonoid content in propolis by two complementary colorimetric methods. *J. Food Drug Anal.* 10, 178–182.

Chen, X., Zhu, J., Gerendás, J., and Zimmermann, N. (2008). Glucosinolates in Chinese *Brassica campestris* vegetables: Chinese cabbage, purple cai-tai, choysum, pakchoi, and turnip. *HortScience* 43, 571–574. doi: 10.21273/hortsci.43.2.571

Chung, I. M., Rekha, K., Rajakumar, G., and Thiruvengadam, M. (2016). Production of glucosinolates, phenolic compounds and associated gene expression profiles of hairy root cultures in turnip (*Brassica rapa* ssp. rapa). *3 Biotech* 6:175.

Colla, G., Cardarelli, M., Bonini, P., and Rouphael, Y. (2017). Foliar applications of protein hydrolysate, plant and seaweed extracts increase yield but differentially

modulate fruit quality of greenhouse tomato. *HortScience* 52, 1214–1220. doi: 10.21273/hortsci12200-17

Devi, R., Munjral, N., Gupta, A. K., and Kaur, N. (2013). Effect of exogenous lead on growth and carbon metabolism of pea (*Pisum sativum* L) seedlings. *Physiol. Mol. Biol. Plants.* 19, 81–89. doi: 10.1007/s12298-012-0143-5

Ellmann, G. L. (1959). Tissue sulfhydryl groups. *Arch Biochem. Biophys.* 82, 70–77. doi: 10.1016/0003-9861(59)90090-6

Fan, D., Hodges, D., Critchley, A., and Prithiviraj, B. (2013). A commercial extract of brown macroalga (*Ascophyllum nodosum*) affects yield and the nutritional quality of spinach in vitro. *Commun. Soil Sci. Plant Anal.* 44, 1873–1884. doi: 10.1080/00103624.2013.790404

Fayez, K. A., El-Deeb, B. A., and Mostafa, N. Y. (2017). Toxicity of biosynthetic silver nanoparticles on the growth, cell ultrastructure and physiological activities of barley plant. *Acta Physiol. Plant.* 39:155.

Fayez, K. A., Radwan, D. E. M., Mohamed, A. K., and Abdelrahman, A. M. (2014). Fusilade herbicide causes alterations in chloroplast ultrastructure, pigment content and physiological activities of peanut leaves. *Photosynthetica* 52, 548–554. doi: 10.1007/s11099-014-0062-5

Figlioli, F., Sorrentino, M. C., Memoli, V., Arena, C., Maisto, G., Giordano, S., et al. (2019). Overall plant responses to Cd and Pb metal stress in maize: growth pattern, ultrastructure, and photosynthetic activity. *Environ. Sci. Pollut. Res.* 26, 1781–1790. doi: 10.1007/s11356-018-3743-y

Gaitonde, M. K. (1967). A spectrophotometric method for the direct determination of cysteine in the presence of other naturally occurring amino acids. *Biochem. J.* 104, 627–633. doi: 10.1042/bj1040627

Gao, H., Chen, G., Han, L., and Lin, H. (2005). Calcium influence on chilling resistance of grafting eggplant seedlings. *J. Plant Nutr.* 27, 1327–1339. doi: 10.1081/pln-200025833

Hasan, M., Ahammed, G. J., Yin, L., Shi, K., Xia, X., Zhou, Y., et al. (2015). Melatonin mitigates cadmium phytotoxicity through modulation of phytochelatins biosynthesis, vacuolar sequestration, and antioxidant potential in *Solanum lycopersicum* L. *Front. Plant Sci.* 6:601. doi: 10.3389/fpls.2015.00601

Hattab, S., Hattab, S., Flores-Casseres, M. L., Boussetta, H., Doumas, P., Hernandez, L. E., et al. (2016). Characterisation of lead-induced stress molecular biomarkers in Medicago sativa plants. *Environ. Exp. Bot.* 123, 1–12. doi: 10.1016/j.envexpbot.2015.10.005

Heath, R. L., and Packer, L. (1968). Photoperoxidation in isolated chloroplasts: I. Kinetics and stoichiometry of fatty acid peroxidation. *Arch. Biochem. Biophys.* 125, 189–198. doi: 10.1016/0003-9861(68)90654-1

Hossain, M. S., Hasanuzzaman, M., Sohag, M. M. H., Bhuyan, M. B., and Fujita, M. (2019). Acetate-induced modulation of ascorbate: glutathione cycle and restriction of sodium accumulation in shoot confer salt tolerance in *Lens culinaris* Medik. *Physiol. Mol. Biol. Plants* 25, 443–455. doi: 10.1007/s12298-018-00640-6

Ismail, H., Maksimoviý, J. D., Maksimoviý, V., Shabala, L., Živanoviý, B. D., Tian, Y., et al. (2016). Rutin, a flavonoid with antioxidant activity, improves plant salinity tolerance by regulating K+ retention and Na+ exclusion from leaf mesophyll in quinoa and broad beans. *Funct. Plant Biol.* 43, 75–86. doi: 10.1071/fp15312

Jacobo-Velázquez, D. A., Martínez-Hernández, G. B., del, C., Rodríguez, S., Cao, C.-M., and Cisneros-Zevallos, L. (2011). Plants as biofactories: physiological role of reactive oxygen species on the accumulation of phenolic antioxidants in carrot tissue under wounding and hyperoxia stress. *J. Agric. Food Chem.* 59, 6583–6593. doi: 10.1021/jf2006529

Jana, S., and Choudhuri, M. A. (1981). Glycolate metabolism of three submersed aquatic angiosperms: effect of heavy metals. *Aquat. Bot.* 11, 67–77. doi: 10.1016/0304-3770(81)90047-4

Jannin, L., Arkoun, M., Etienne, P., Laîné, P., Goux, D., Garnica, M., et al. (2013). *Brassica napus* growth is promoted by *Ascophyllum nodosum* (L.) Le Jol. seaweed extract: microarray analysis and physiological characterization of N, C, and S metabolisms. *J. Plant Growth Regul.* 32, 31–52. doi: 10.1007/s00344-012-9273-9

Johnson, I. T. (2002). Glucosinolates: bioavailability and importance to health. *Int. J. Vit. Nutr. Res.* 72, 26–31. doi: 10.1024/0300-9831.72.1.26

Karabudak, T., Bor, M., Ozdemir, F., and Turkan, I. (2014). Glycine betaine protects tomato (*Solanum lycopersicum*) plants at low temperature by inducing fatty acid desaturase7 and lipoxygenase gene expression. *Mol. Biol. Rep.* 41, 1401–1410. doi: 10.1007/s11033-013-2984-6

Khan, W. U., Ahmad, S. R., Yasin, N. A., Ali, A., and Ahmad, A. (2017). Effect of *Pseudomonas* fluorescens RB4 and Bacillus subtilis 189 on the phytoremediation potential of Catharanthus roseus (L.) in Cu and Pb-contaminated soils. *Int. J. Phytoremed.* 19, 514–521. doi: 10.1080/15226514.2016.1254154

Kondo, K., Shiba, M., Nakamura, R., Morota, T., and Shoyama, Y. (2007). Constituent properties of licorices derived from *Glycyrrhiza uralensis*, *G. glabra*, or *G. inflata* identified by genetic information. *Biol. Pharm. Bull.* 30, 1271–1277. doi: 10.1248/bpb.30.1271

Kumar, A., Dixit, G., Singh, A. P., Dwivedi, S., Srivastava, S., Mishra, K., et al. (2016). Selenate mitigates arsenite toxicity in rice (*Oryza sativa* L.) by reducing arsenic uptake and ameliorates amino acid content and thiol metabolism. *Ecotoxicol. Environ. Safety* 133, 350–359. doi: 10.1016/j.ecoenv.2016.06.037

Lamhamdi, M., El Galiou, O., Bakrim, A., Nóvoa-Muñoz, J. C., Arias-Estévez, M., Aarab, A., et al. (2013). Effect of lead stress on mineral content and growth of wheat (*Triticum aestivum*) and spinach (*Spinacia oleracea*) seedlings. *Saudi J. Biol. Sci.* 20, 29–36. doi: 10.1016/j.sjbs.2012.09.001

Li, D. M., Nie, Y. X., Zhang, J., Yin, J. S., Li, Q., Wang, X. J., et al. (2013). Ferulic acid pretreatment enhances dehydration-stress tolerance of cucumber seedlings. *Biol. Plant.* 57, 711–717. doi: 10.1007/s10535-013-0326-0

Liang, X., Lee, H. W., Li, Z., Lu, Y., Zou, L., and Ong, C. N. (2018). Simultaneous quantification of 22 glucosinolates in 12 brassicaceae vegetables by hydrophilic interaction chromatography-tandem mass spectrometry. *ACS Omega* 3, 15546–15553. doi: 10.1021/acsomega.8b01668

Liu, Z., Pi, F., Guo, X., Guo, X., and Yu, S. (2019). Characterization of the structural and emulsifying properties of sugar beet pectins obtained by sequential extraction. *Food Hydrocoll.* 88, 31–42. doi: 10.1016/j.foodhyd.2018.09.036

Mahmoud, S. H., Salama, D. M., El-Tanahy, A. M. M., and Abd El-Samad, E. H. (2019). Utilization of seaweed (*Sargassum vulgare*) extract to enhance growth, yield and nutritional quality of red radish plants. *Ann. Agricult. Sci.* 64, 167–175. doi: 10.1016/j.aoas.2019.11.002

Malar, S., Manikandan, R., Favas, P. J. C., Sahi, S. V., and Venkatachalam, P. (2014). Effect of lead on phytotoxicity, growth, biochemical alterations and its role on genomic template stability in Sesbania grandiflora: a potential plant for phytoremediation. *Ecotoxicol. Environ. Safety* 108, 249–257. doi: 10.1016/j.ecoenv.2014.05.018

Mekawy, A. M. M., Abdelaziz, M. N., and Ueda, A. (2018). Apigenin pretreatment enhances growth and salinity tolerance of rice seedlings. *Plant Physiol. Biochem.* 130, 94–104. doi: 10.1016/j.plaphy.2018.06.036

Metzner, H., Rau, H., and Senger, H. (1965). Untersuchungen zur synchronisierbarkeit einzelner pigmentmangel-mutanten von Chlorella. *Planta* 65, 186–194. doi: 10.1007/bf00384998

Miransari, M., and Smith, D. L. (2007). Overcoming the stressful effects of salinity and acidity on soybean nodulation and yields using signal molecule genistein under field conditions. *J. Plant Nutr.* 30, 1967–1992. doi: 10.1080/01904160701700384

Nagalakshmi, N., and Prasad, M. N. V. (2001). Responses of glutathione cycle enzymes and glutathione metabolism to copper stress in *Scenedesmus bijugatus*. *Plant Sci.* 160, 291–299. doi: 10.1016/s0168-9452(00)00392-7

Noctor, G., Lelarge-Trouverie, C., and Mhamdi, A. (2015). The metabolomics of oxidative stress. *Phytochemistry* 112, 33–53. doi: 10.1016/j.phytochem.2014.09.002

Pavel, S., Klejdus, B., and Kubáò, V. (2006). Determination of total content of phenolic compounds and their antioxidant activity in vegetablesevaluation of spectrophotometric methods. *J. Agric. Food Chem.* 54, 607–616. doi: 10.1021/jf052334j

Peng, Y., Shi, D., Zhang, T., Li, X., Fu, T., Xu, Y., et al. (2015). Development and utilization of an efficient cytoplasmic male sterile system for Cai-xin (*Brassica rapa* L.). *Sci. Hortic.* 190, 36–42. doi: 10.1016/j.scienta.2015.04.002

Pérez-Arellano, I., Carmona-Álvarez, F., Martínez, A. I., Rodríguez-Díaz, J., and Cervera, J. (2010). Pyrroline-5-carboxylate synthase and proline biosynthesis: from osmotolerance to rare metabolic disease. *Protein Sci.* 19, 372–382. doi: 10.1002/pro.340

Pheomphun, P., Treesubsuntorn, C., and Thiravetyan, P. (2019). Effect of exogenous catechin on alleviating O3 stress: the role of catechin-quinone in lipid peroxidation, salicylic acid, chlorophyll content, and antioxidant enzymes of *Zamioculcas zamiifolia*. *Ecotoxicol. Environ. Safety* 180, 374–383. doi: 10.1016/j.ecoenv.2019.05.002

Rabêlo, F. H. S., Fernie, A. R., Navazas, A., Borgo, L., Keunen, E., da Silva, B. K. D. A., et al. (2018). A glimpse into the effect of sulfur supply on metabolite profiling, glutathione and phytochelatins in Panicum maximum cv. Massai exposed to cadmium. *Environ. Exp. Bot.* 151, 76–88. doi: 10.1016/j.envexpbot.2018.04.003

Rangkadilok, N., Nicolas, M. E., Bennett, R. N., Premier, R. R., Eagling, D. R., and Taylor, P. W. J. (2002). Determination of sinigrin and glucoraphanin in *Brassica* species using a simple extraction method combined with ion-pair HPLC analysis. *Sci. Hortic.* 96, 27–41. doi: 10.1016/s0304-4238(02)00119-x

Saleh, A. M., and Madany, M. M. Y. (2015). Coumarin pretreatment alleviates salinity stress in wheat seedlings. *Plant Physiol. Biochem.* 88, 27–35. doi: 10.1016/j.plaphy.2015.01.005

Shahid, M., Pourrut, B., Dumat, C., Nadeem, M., Aslam, M., and Pinelli, E. (2014). Heavy-metal-induced reactive oxygen species: phytotoxicity and physicochemical changes in plants. *Rev. Environ. Contam. Toxicol.* 232, 1–44. doi: 10.1007/978-3-319-06746-9_1

Sidhu, G. P. S., Singh, H. P., Batish, D. R., and Kohli, R. K. (2016). Effect of lead on oxidative status, antioxidative response and metal accumulation in *Coronopus didymus*. *Plant Physiol. Biochem.* 105, 290–296. doi: 10.1016/j.plaphy.2016.05.019

Singh, P. K., Singh, R., and Singh, S. (2013). Cinnamic acid induced changes in reactive oxygen species scavenging enzymes and protein profile in maize (*Zea mays* L.) plants grown under salt stress. *Physiol. Mol. Biol. Plants* 19, 53–59. doi: 10.1007/s12298-012-0126-6

Smeekens, S., Ma, J., Hanson, J., and Rolland, F. (2010). Sugar signals and molecular networks controlling plant growth. *Curr. Opin. Plant Biol.* 13, 274–279.

Soares, C., Carvalho, M. E. A., Azevedo, R. A., and Fidalgo, F. (2019). Plants facing oxidative challenges—A little help from the antioxidant networks. *Environ. Exp. Bot.* 161, 4–25. doi: 10.1016/j.envexpbot.2018.12.009

Szabados, L., and Savoure, A. (2010). Proline: a multifunctional amino acid. *Trends Plant Sci.* 15, 89–97. doi: 10.1016/j.tplants.2009.11.009

Tanemoto, R., Okuyama, T., Matsuo, H., Okumura, T., Ikeya, Y., and Nishizawa, M. (2015). The constituents of licorice (*Glycyrrhiza uralensis*) differentially suppress nitric oxide production in interleukin-1β-treated hepatocytes. *Biochem. Biophys. Rep.* 2, 153–159. doi: 10.1016/j.bbrep.2015.06.004

Tauqeer, H. M., Ali, S., Rizwan, M., Ali, Q., Saeed, R., Iftikhar, U., et al. (2016). Phytoremediation of heavy metals by *Alternanthera bettzickiana*: growth and physiological response. *Ecotoxicol. Environ. Safety.* 126, 138–146. doi: 10.1016/j.ecoenv.2015.12.031

Tolrà, R., Barceló, J., and Poschenrieder, C. (2009). Constitutive and aluminium-induced patterns of phenolic compounds in two maize varieties differing in aluminium tolerance. *J. Inorgan. Biochem.* 103, 1486–1490. doi: 10.1016/j.jinorgbio.2009.06.013

Trejo-Téllez, L. I., Estrada-Ortiz, E., Gómez-Merino, F. C., Becker, C., Krumbein, A., and Schwarz, D. (2019). Flavonoid, nitrate and glucosinolate concentrations in *Brassica* species are differentially affected by photosynthetically active radiation, phosphate and phosphite. *Front. Plant Sci.* 10:371. doi: 10.3389/fpls.2019.00371

Usman, K., Abu-Dieyeh, M. H., Zouari, N., and Al-Ghouti, M. A. (2020). Lead (Pb) bioaccumulation and antioxidative responses in *Tetraena qataranse*. *Sci. Rep.* 10:17070.

Varela, M. C., Arslan, I., Reginato, M. A., Cenzano, A. M., and Luna, M. V. (2016). Phenolic compounds as indicators of drought resistance in shrubs from *Patagonian shrublands* (Argentina). *Plant Physiol. Biochem.* 104, 81–91. doi: 10.1016/j.plaphy.2016.03.014

Zhang, J., and Kirkham, M. B. (1994). Drought-stress-induced changes in activities of superoxide dismutase, catalase, and peroxidase in wheat species. *Plant Cell Physiol.* 35, 785–791. doi: 10.1093/oxfordjournals.pcp.a078658

Conflict of Interest: The authors declare that the research was conducted in the absence of any commercial or financial relationships that could be construed as a potential conflict of interest.

Publisher's Note: All claims expressed in this article are solely those of the authors and do not necessarily represent those of their affiliated organizations, or those of the publisher, the editors and the reviewers. Any product that may be evaluated in this article, or claim that may be made by its manufacturer, is not guaranteed or endorsed by the publisher.

frontiers in Plant Science

ORIGINAL RESEARCH
published: 07 September 2021
doi: 10.3389/fpls.2021.696998

The Role of Plant Origin Preparations and Phenological Stage in Anatomy Structure Changes in the Rhizogenesis of *Rosa* "Hurdal"

Marta Joanna Monder[1]*, *Paweł Kozakiewicz*[2] and *Agnieszka Jankowska*[2]

[1] Department of Dendrological Collections, Polish Academy of Sciences Botanical Garden—Center for Biological Diversity Conservation in Powsin, Warsaw, Poland, [2] Department of Wood Science and Wood Preservation, Institute of Wood Sciences and Furniture, Warsaw University of Life Sciences—SGGW, Warsaw, Poland

Most old roses are difficult to root when propagated by cuttings. This research focused on the response of stem cuttings of *Rosa* "Hurdal" to plant origin preparations used as rhizogenesis enhancers through changes to the anatomical structure of the basal part of the stem. Cuttings derived from shoots in four phenological stages were prepared for the experiment: flower buds closed (H1); fully flowering (H2); immediately after petals have fallen (H3); 7–14 days after petals have fallen (H4). The cuttings were treated with 0.4% indole butyric acid (IBA; Ukorzeniacz A_{aqua}) or 0.2% naphthalene acetic acid (NAA; Ukorzeniacz B_{aqua}), and with plant origin preparations: Algae extract (Bio Rhizotonic), Organic preparation (Root Juice^{TM}), and Plant extract (Bio Roots). A high rooting percentage in comparison to the control (27.5%) was obtained after treatments of the H1 cuttings with Algae extract (90%), Organic preparation (80%), and Plant extract (75%). The H4 cuttings did not root, probably as a result of an overgrowing callus and limited xylem formation. The anatomical structure of the shoot differed in subsequent phenological stages during the period of rooting in various ways, depending on the rooting enhancer used for treatment. Numerous correlations between rooting percentage and anatomical structure were proved, including the key role of vascular bundles in increasing rooting percentage by widening the vessel diameter.

Keywords: adventitious roots, biostimulant, root enhancer, tracheids, vessel, xylem

OPEN ACCESS

Edited by:
Youssef Rouphael, University of Naples Federico II, Italy

Reviewed by:
Giancarlo Fascella, Council for Agricultural and Economics Research (CREA), Italy
Catello Di Martino, University of Molise, Italy

***Correspondence:**
Marta Joanna Monder
mondermarta@gmail.com

Specialty section:
This article was submitted to Crop and Product Physiology, a section of the journal Frontiers in Plant Science

Received: *18 April 2021*
Accepted: *23 July 2021*
Published: *07 September 2021*

Citation:
Monder MJ, Kozakiewicz P and Jankowska A (2021) The Role of Plant Origin Preparations and Phenological Stage in Anatomy Structure Changes in the Rhizogenesis of Rosa "Hurdal". Front. Plant Sci. 12:696998. doi: 10.3389/fpls.2021.696998

INTRODUCTION

Roses belong to the oldest and most important cultivated ornamental plants (Smulders et al., 2019), and have been significant in many fields of human life for thousands of years (Gustavsson, 1999). The majority of once-blooming old roses are valued for their winter hardiness (Gustavsson, 1999; Monder, 2014) and high resistance to pests and disease. The majority of old roses can also be successfully cultivated in the temperate zone in a climate with harsher winters on their own roots without budding on the rootstock (Gustavsson, 1999). Their maintenance in cultivation is important for biodiversity conservation and the preservation of the heritage of garden plants, and so for the implementation of the provisions of the Convention on Biological Diversity (CBD) made in Rio de Janeiro on 5 June 1992. Although old roses are commonly cultivated, they should, nevertheless, be used more often to revitalize historical

properties and urban greeneries (Gustavsson, 1999; Monder, 2021). "Hurdal" is a valuable old rose and, originally, an Alba or Villosa Hybrid. This cultivar has been more widely known since it was brought to Norway in the second half of the nineteenth century. The shrubs are ca 3-m high, with long, almost thornless stems, and big grayish leaves. The flowers are deep pink, with 15–25 petals and a mild fragrance (**Figure 1A**). The hips are oval, ca 2-cm diameter, and red-orange. The shrubs exhibit great frost hardiness and are appropriate for cultivation in a hard Scandian climate (Gustavsson, 1999).

The use of single-node leafy stem cuttings is easy and economical, and it is the most common method of rose propagation used to grow shrubs on their own roots. However, the forming of adventitious roots in the cuttings of vascular plants is a very complicated process connected with exogenous and endogenous factors (Hartmann et al., 2011), whereby rhizogenezis in cuttings of wild (Hoşafçi et al., 2005) and old roses is believed to be especially difficult (Hoşafçi et al., 2005; Ginova et al., 2012), time-consuming, and often resulting in failure (Ginova et al., 2012; Monder et al., 2016). The process of rhizogenezis, prolonged to 12 weeks, exposes the cuttings to many stress factors, and their success is also strictly connected with the content of bioactive components in stock plants (Monder et al., 2016). The anatomical structure of the shoot (Amissah et al., 2008; Bryant and Trueman, 2015) is a crucial endogenous factor in adventitious root formation for the majority of vascular plants, including roses (Monder et al., 2017).

The growth and the development of plants in the growing season are connected with many changes in their biology. Phenology is a visible effect and a source of knowledge of periodic changes in plants (Meier et al., 2009) affected by additional environmental factors (Zheng et al., 2016), including roses (Monder, 2014, 2021). The crucial role of the phenological stage of shoots in roses harvested for the preparation of cuttings has been shown a few times (Pihlajaniemi et al., 2005; Monder et al., 2016, 2019; Monder and Pacholczak, 2018). The flowering time in once-blooming roses is followed by changes in carbohydrates, soluble proteins, chlorophyll a/b, and carotenoids content (Monder et al., 2016) as well as changes in the anatomical structure (Monder et al., 2017).

Various rooting enhancers, including plant hormones (Pihlajaniemi et al., 2005; Ginova et al., 2012) and biostimulants (Monder and Pacholczak, 2019; Monder et al., 2020) were used to encourage the natural ability of cuttings to undergo rhizogenesis and also to improve the quality and physiological parameters of rooted cuttings. Some of the preparations important in nursery production contained indole butyric acid (IBA) or naphthalene acetic acid (NAA) as standard rooting enhancers in the procedure of rooting cuttings (Hartmann et al., 2011). Previous research has proven the influence of a few substances used as rooting enhancers on anatomical structure, e.g., benzyladenine and naphthalene-1-acetic acid in Fuchsias (Wróblewska, 2013), Dogwood (Pacholczak et al., 2012), and Euphorbia hybrids (Fascella and Zizzo, 2009) or carbon dioxide (Costa et al., 2007), IBA, and NAA in roses (Dawa et al., 2018; Monder et al., 2019). However, the abovementioned research did not establish which changes in anatomy had an influence on the effectiveness of the process of rhizogenesis.

Synthetic chemicals used for plant production, protection, and cultivation are often replaced, or their usage is reduced, by preparations of natural origin that includes humic acids, seaweed, and Plant extracts. Their use provides a number of benefits in stimulating growth and protecting against biotic and abiotic stresses (Oosten et al., 2017). Preparations of natural origin are preferred in sustainable eco-friendly agriculture and recommended by the Official Journal of the European Union (OJEU, 2009a,b), the National Organic Program USDA (USDA, 2017), and the Organic Materials Review Institute (OMRI, 2021). The effect of their use depends on their composition and, especially, on phytohormones (Oosten et al., 2017). Three commercial plant origin preparations recommended by their manufacturers for rooting and replanting were used in the present research and named for the purposes of this work: Bio Rhizotonic—Algae extract (Canna Continental, Los Angeles, USA, 2021), Root Juice™–Organic preparation (BioBizz Worldwide B.V., Groningen, The Netherlands, 2017), and Bio Roots—Plant extract (General Hydroponics Europe/T.A. Terra Aquatica, Fleurance, France). More detailed information on these preparations is presented in **Table 1**. These preparations were produced with Plant extract as their base and contain many biologically active substances. The content of humic substances could lead to higher nutrient content in the tissues of the cuttings as well as positive metabolic changes (Nardi et al., 2015). The above preparations affected the content of chlorophyll a, b, carotenoids, soluble proteins (Monder et al., 2020), and carbohydrates in roses (Monder and Pacholczak, 2018) and can indirectly influence the effectiveness of rhizogenesis.

The aims of this research were to recognize the response of cuttings *Rosa* "Hurdal" in anatomical structure to the plant origin preparations during the process of rhizogenesis. Moreover, we hypothesized that the response of cuttings prepared from shoots in four phenological stages may be different. Consistently, the various anatomical changes occurring in stock plants during the flowering period can affect rooting effectiveness and the quality of rooted cuttings. Analysis of changes in anatomical structure before and after the rooting process could reveal the reason for difficulties in the rooting of some rose cuttings.

MATERIALS AND METHODS

Plant Material and Experimental Conditions

The plant material of *R.* "Hurdal" (Germany–Norway; origin unknown, *Rosa* × *alba* × *Rosa villosa*, **Figure 1A**) was obtained from shrubs growing in the National Collection of Rose Cultivars in the Polish Academy of Sciences Botanical Garden Center for Biological Diversity Conservation in Powsin, Warsaw, Poland.

The single-node leafy semi-hardwood shoot cuttings of *Rosa* "Hurdals" (Gustavsson, 1999) with an original leaf (leaf area 24–27 cm^2) (**Figure 1B**) were taken from the middle part of flowering shoots (three to five buds) in four phenological stages (**Figure 1C**) according to BBCH scale in roses (Meier et al., 2009). In the present study, the letter H, accompanied by a subsequent number, was used to designate

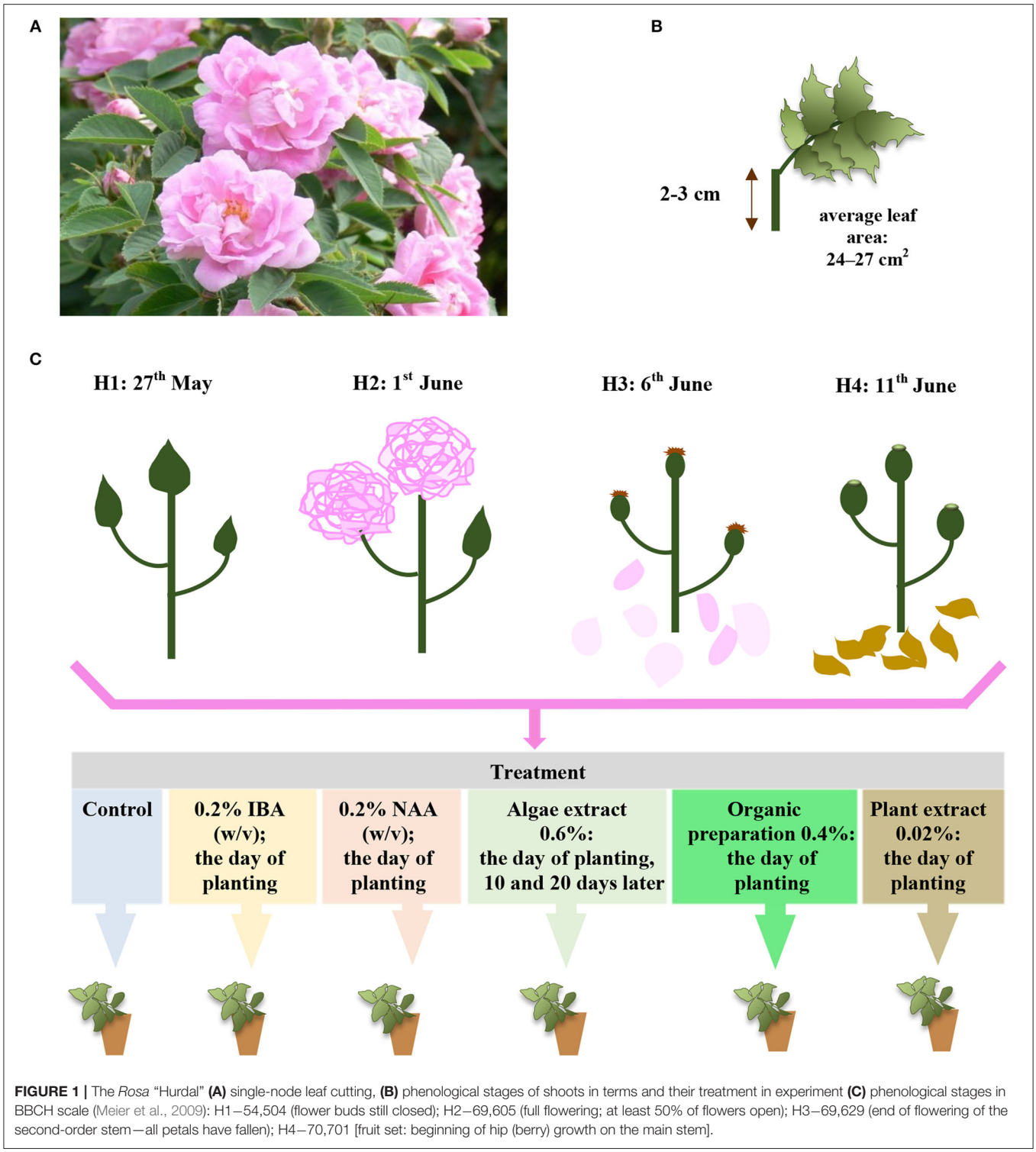

FIGURE 1 | The *Rosa* "Hurdal" **(A)** single-node leaf cutting, **(B)** phenological stages of shoots in terms and their treatment in experiment **(C)** phenological stages in BBCH scale (Meier et al., 2009): H1−54,504 (flower buds still closed); H2−69,605 (full flowering; at least 50% of flowers open); H3−69,629 (end of flowering of the second-order stem−all petals have fallen); H4−70,701 [fruit set: beginning of hip (berry) growth on the main stem].

the phenological stage of shoots harvested for the experiment in four periods: H1—May 27, 54 504 (flower buds still closed), H2—June 1, 69 605 (full flowering; at least 50% of flowers open), H3—June 6, 69 629 (end of flowering of the second-order stem: all petals fallen), H4—June 11, 70 701 (fruit set: beginning of hip growth on the main stem) (**Figure 1C**). The shoots all had similar diameters, ranging from 5 to 6 mm.

TABLE 1 | Rooting enhancers used in the rooting of *Rosa* "Hurdal."

Name in work	Preparation and producer	Characteristic	Certificate
IBA	Ukorzeniacz A_{aqua} (Himal, Poland)	0.4% IBA (indolebutyricacid)	
NAA	Ukorzeniacz B_{aqua} (Himal, Poland)	0.2% NAA (naphthaleneaceticacid)	
Algae extract	Bio Rhizotonic (Canna Continental, Los Angeles, USA, 2021)	Seaweed-based, 100% organic, N 0.6%, P 0.2%, K 0.6% vitamins such as B_1, B_2, and other biologically active substances	Organic Materials Review Institute (OMRI)
Organic preparation	Root Juice™ (BioBizz Worldwide B.V., Groningen, The Netherlands, 2017)	Combination of humic acid and seaweed extracts, N 0.1%, P_2O_5 0.1%, K_2O 0.1%, Mg 0.03%, Fe 0.013%, Mn 0.002%, Zn 0.004%, B 0.025%, Cu 0.001%	National Organic Program (NOP); Control Union Certified EU; Good Soil Quality Mark; Point Vert; Organic Materials Review Institute (OMRI), Clean Green Certified
Plant extract	Bio Roots (GHE, France/T.A. Terra Aquatica, 2021)	Amino acids and oligosaccharins, fruit oil up to 1%; humic acids 1%; pectinate 1%; sodium alginate 3%; seaweed species 10%, organic matter 84%	European regulation EC No 834/2007 on organic agriculture (Certificaat Bio Roots, 2014)

The cuttings were inserted into multipot trays (6.6 × 6.6 cm) in peat (Karaska, Poland) sand (Vistula river) medium (mixture v:v 1:1; pH 6–6.5). The cuttings were treated with 0.4% IBA (Ukorzeniacz A_{aqua}) or 0.2% NAA (Ukorzeniacz B_{aqua}), and with plant origin preparations: Algae extract (Bio Rhizotonic), Organic preparation (Root Juice™), and Plant extract (Bio Roots). The treatment and watering process is presented in detail in **Figure 1C**. Before planting, the basal parts (1 cm) of the stem were dipped in commercial rooting powder, containing 0.4% IBA or 0.2% NAA. The remaining cuttings were watered with plant origin preparations or, in the case of the control, water. The watering was performed with 10 cm^3 per pot (98 cm^3) according to the schema of the experiment. During the 10th and 20th days of rooting, the cuttings were watered with 10 cm^3 water or Algae extract per pot (98 cm^3) (**Figure 1C**). The rooting enhancers used in the experiment were purchased from companies in the sector (**Table 1**).

The experiment on rooting cuttings was conducted in the commercial nursery of M&M Kryt in Wola Prażmowska (51.56°N, 20.28°E), Poland. The rose cuttings were rooted in a foil tunnel with an electronically controlled misting system that maintained optimal climatic conditions (air temperature, 23–25°C; ambient relative humidity, 80–90%). The shading material limited the photosynthetic photon flux density to 130 $\mu mol \cdot m^{-2} \cdot s^{-1}$. To prevent fungal diseases, the following fungicides were applied to the cuttings regularly every 7–9 days starting from the day of planting: Previcur Energy 840 SL (propamocarb, 47.28%; fosetyl, 27.65%; Bayer, Poland), Amistar® 250 SC (azoxystrobin, 250 $g \cdot dm^{-3}$; Syngenta, Poland), and Score 250 SC (difenoconazole, 250 $g \cdot dm^{-3}$; Syngenta, Poland).

The Data Set of the Growth Parameters of the Cuttings

After 12 weeks, in the first days of August, the cuttings were dug out and cleaned from the medium. The rooted cuttings were earmarked for further evaluation.

The rooting percentage and the percentage of cuttings with a callus only were calculated (%) in relation to the number of planted cuttings.

The fresh weight (g) of the root system and the aboveground part were estimated for rooted cuttings, using an analytical balance (PS 6000/C/2, RADWAG, Poland). The root length (cm) was measured with a caliper from the origin of the root to the apical meristem of the primary and longest root.

Anatomical Evaluation

Samples of shoots from cuttings were retrieved for anatomical research two times for every treatment in each phenological stage: before being planted in the rooting medium and on the 25th day of the rooting process. Moreover, the samples were harvested and observed separately after 12 weeks of rhizogenesis. The shoot fragments were protected and stabilized in a mixture of anhydrous glycerine and 96% ethyl alcohol (v/v 1:1) in PAS Botanical Garden CBDC in Powsin, Warsaw, Poland. Slides were cut with a sledge microtome (pfm SLIDE 4003E, pfm medical AG, Germany) into slices 15- to 30 μm thick with cross- and longitudinal sections from the basal parts of shoots, in which rhizogenesis would have taken place. The scraps were cross-dyed with a solution of safranine. The studies were carried out using the light Olympus BX41 microscope (Olympus America Inc., New York, USA) with the Olympus DP25 digital camera connected to a computer with specialist Cell*B software (The Institute of Wood Sciences and Furniture, Warsaw University of Life Sciences—WULS, Warsaw, Poland) and an Olympus Vanox AHBT3 (Olympus America Inc., New York, USA) microscope. The measurements of cells and tissue elements were conducted with the specialist Cell*B software and cellsSens Standard 1.7.1. software in PAS Botanical Garden CBDC in Powsin, Warsaw, Poland. The width of the xylem, phloem, pith rays, and cortex, and, additionally, the early- and late-wood vessel diameter, were measured before and after 25 days of rooting cuttings and, in the shoots of the stock plant, cut on 5 August. The width of tissues between xylem and cortex was noted and observed after 25 days of rooting cuttings. All the observations were carried out on the basal part of the cuttings: 2–2.5 cm below buds in shoots.

Statistical Analysis

The experiments were constructed as randomized complete block design (RCBD) for each maturity phase and involved 24 combinations altogether for two variables (treatment, phenological stage). Each combination of treatment in four phenological stages of shoots (**Figure 1**) included four replicas of 10 cuttings. A total of 960 cuttings were planted. Additional 10 cuttings earmarked for anatomical research were planted in each combination. Moreover, the anatomical research data were collected for each phenology stage of shoots before rooting them, also from the 10 cuttings.

The values in percentage were transformed by using the function ARCSIN$(x)^{1/2}$ according to Bliss or $y = x^2 + (x^2 + 1)^2$ to compare the means and carry out analyses. The data of anatomical parameters were analyzed by using two-factorial analysis of variance (ANOVA), and Duncan's honest significant difference test was used to determine the significance of differences between the means ($\alpha = 0.05$) for two variables—the phenological stage and the rooting enhancer. For data of growth parameters, two-way analysis of variance (ANOVA) and Tukey's HSD were used ($\alpha = 0.05$) for the same variables, respectively. Correlations between the data parameters of growth and anatomical structure in cuttings were carried out for each phenological phase and treatment together and separately.

The STATISTICA 10 software package (StatsoftPolska, Cracow, Poland) was used for statistical analysis.

RESULTS

The Anatomy of the Shoots of *Rosa* "Hurdal" Stock Plants Changes Across the Different Phenological Stages That Cuttings Were Prepared in

The periderm consisted in (i) a cork cambium with undifferentiated cells (phellogen), (ii) an outer layer (epidermis) with cells in regular rows and thick walls, and (iii) living cells with thickening walls in an inner layer arranged in three to four rows. The cortical parenchyma had a similar width to the vascular bundle ring visible on cross sections of all four phenological stages of shoots. The parenchyma consisted of large cells, uneven in size, and tightly arranged along the circumference of the shoot (**Figure 2**). The width of the cortex decreased from H1 to H4 (**Figure 3**).

The vascular bundles were separated from the cortex sclerenchyma layer by irregularly arranged cells with very thickened walls and were different widths. Moreover, the ring of vascular bundles was partially irregular and with a few vascular bundles located outside. These irregular bundles were observed, especially in shoots H1 and H2. The structure visible on cross- and longitudinal sections of shoots in subsequent stages showed a progression of the lignification process (**Figure 2**). Stems collected from shoots in stages H3 and H4 had a wider wood region (**Figure 4**) where thick-walled fibers dominated, providing mechanical strength.

The width of xylem tissue increased with each fallow phenological stage. The vessels and tracheids of the xylem were located radially on the cross section in regular rows. No significant differences were found between the mean vessel diameter of early- and late-wood in H1, H2, and H3, while the means in H4 were significantly higher. There were a few cells of latewood in H1, mostly tracheids with thick walls. The layers of latewood were much wider in fallow phenological stages, and the vessels of latewood were significantly larger in diameter in H4 shoots. The width of xylem tissue increased in the shoots of stock plants until August, however without any increase to the diameter of the vessels. The last cells of visible latewood were mainly tracheids, with only a few large vessels (**Figure 4**).

The cambium layer in shoots before rooting consisted in three to four cells in H1, four to five in H3, and three to four in H4 (**Figure 2**). The cambium of stock plants in August was made up of five to six cells.

The pith rays were narrow, made up of three to five rows of the cells. Numerous starch grains were visible in pith rays in comparison with their smaller number of companion cells of phloem, xylem fibers, and cortical parenchyma (**Figure 2**). The pith rays widths were similar throughout the four phenological stages (**Figure 5**).

The pith consisted of big living irregular cells, loosely stacked in starred form around small cells, with starch grains in cross sections and in rows on longitudinal sections (**Figure 2**).

Rooting Enhancers Have a Varied Effect on Changes to the Anatomy of Stem Cuttings Harvested in Four Phenological Stages

Visible callus tissues appeared in the rhizogenesis process at the basal part of cuttings in the place of wounding after 10–14 days, and the first visible roots were spotted in week 4 near these places. On the cross sections, the roots most often appeared on the cambial zone near the pith rays and phloem. The forming roots were growing in outside, omitting the phloem and sclerenchyma layers. At the same time, numerous callus cells appeared, intensively filling the space between the first ring of xylem and sclerenchyma, and consequently growing outside through the cortex layer. The callus cells were also observed in the cambium zone and as a product of phellogen differentiation (**Figure 6**). The overgrowing of callus cells was also visible in the place of the pith on the base of the cutting (**Figure 7**). The roots probably also formed in the region of the phloem and pericycle, as was also observed after 12 weeks, without omitting the basal part of cuttings covered by a callus (**Figure 8**).

The width of the xylem tissue in control cuttings derived from shoots H1 was small compared to cuttings on which NAA preparation, Algae extract, or Organic preparation was used, and the width was even smaller in cuttings treated with Plant extract. This variable was also higher in control cuttings from shoots H2 for which Organic preparation or Plant extract was used as well as for cuttings obtained from shoots H3 treated with NAA, Organic preparation, and Plant extract. The width of xylem tissue in cuttings H4 was similar when using IBA and NAA preparations and Algae extract. The use of Organic preparation and Plant extract resulted in an increase in the width of xylem tissue. Xylem was dominated by large, thin-walled vessel elements of

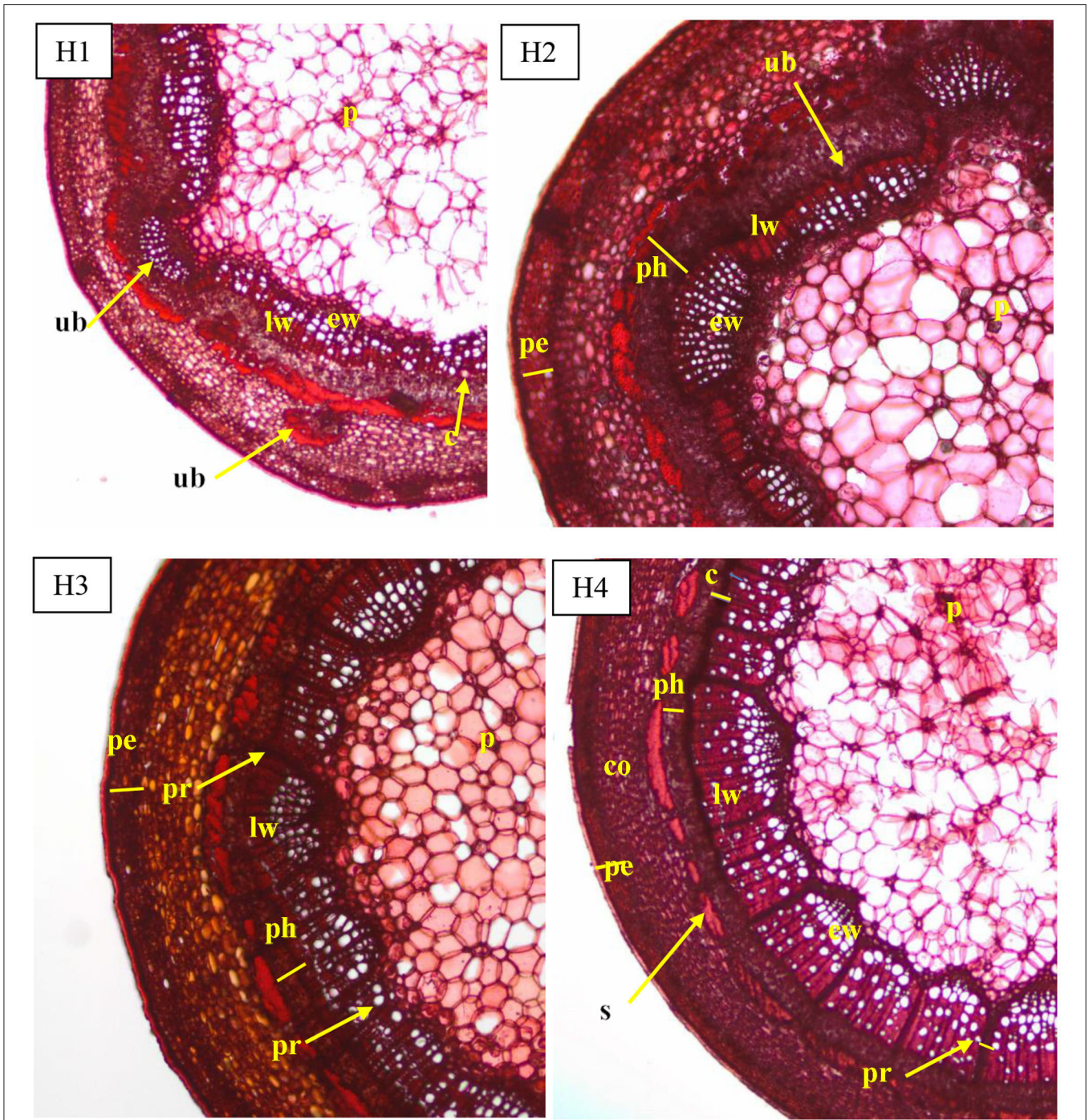

FIGURE 2 | Transverse sections of the shoots before rooting in *Rosa* "Hurdal" in four phenological stages in BBCH scale (Meier et al., 2009): H1—54,504 (flower buds still closed); H2—69,605 (full flowering; at least 50% of flowers open); H3—69,629 (end of flowering of the second-order stem—all petals have fallen); H4—70,701 [fruit set: beginning of hip (berry) growth on the main stem]. Designation of signs: ub, unregular vascular bundles; c, cambium; co, cortex; pe, periderm; ph, phloem; p, pith; pr, pith rays; s, sclerenchyma; ew, earlywood; lw, latewood.

earlywood. However, with time, the wood cells became more regular in shape, smaller, thick-walled tracheids, with a tendency for the size of vessels to decrease in diameter in the cross section due to the use of rooting enhancers (**Figure 4**).

The diameter of the vessels of early- and late-wood in H1 cuttings was higher in the control and after use of Algae extract as compared with other enhancers. In the case of H2 and H3 cuttings, the diameter of earlywood vessels was similar for all

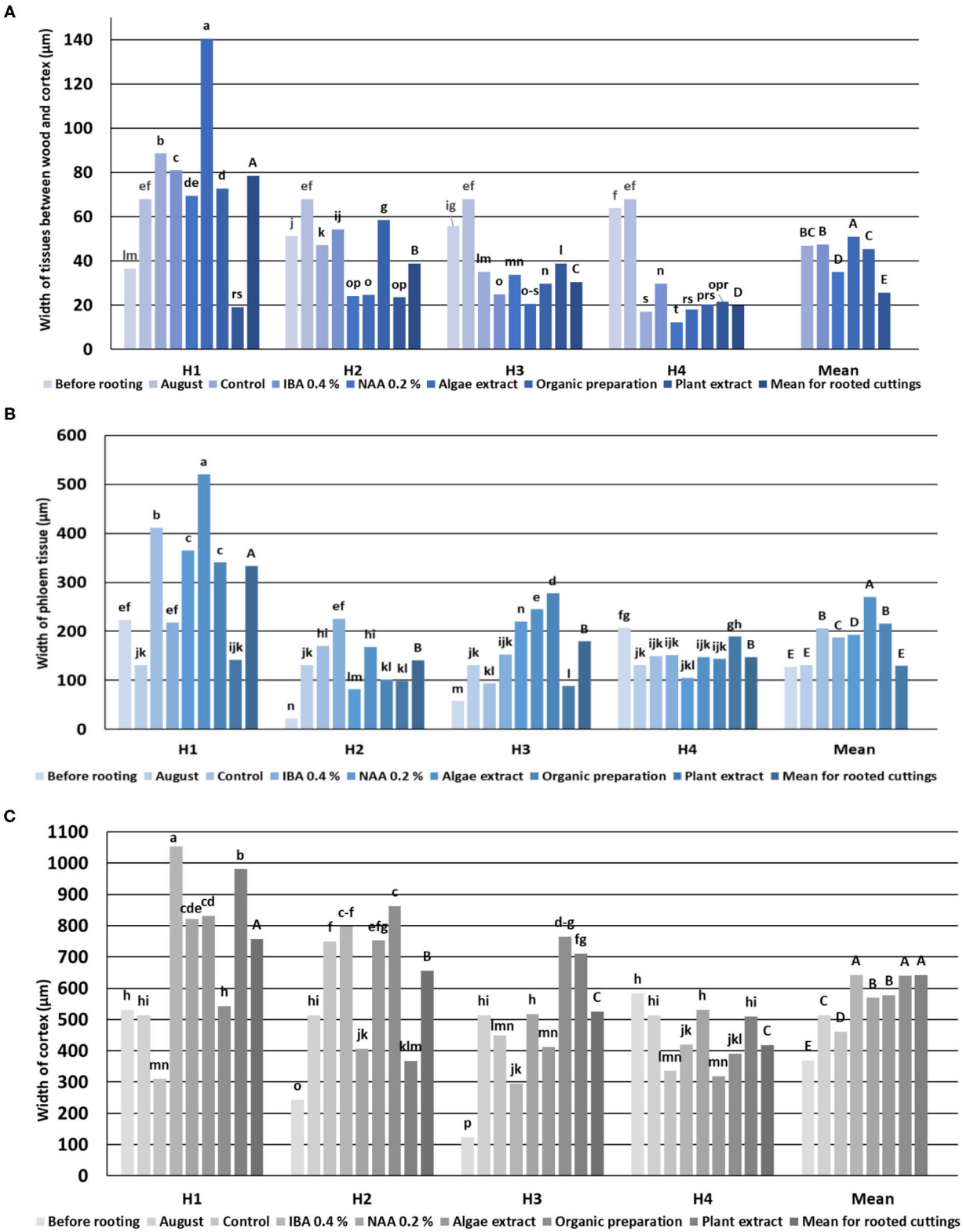

FIGURE 3 | Width of *Rosa* "Hurdal" tissues between wood and cortex **(A)**, phloem **(B)**, and cortex tissue **(C)** in stems before rooting; cuttings after 24 days of the rhizogenesis process; and stems of stock plants cut in first days of August. Control—control cuttings without rooting enhancers; IBA 0.4%—Ukorzeniacz A_{aqua} (0.4% IBA); NAA, 0.2%—Ukorzeniacz B_{aqua} (0.2% NAA); Algae extract—watering with 0.6% Bio Rhizotonic (10 ml) after planting and 10 and 20 days later; Organic

(Continued)

FIGURE 3 | preparation—watering with 0.4% Root Juice™ (10 ml) after planting; Plant extract—watering with 0.02% Bio Roots (10 ml) after planting. H1—54 504 (flower buds still closed); H2—69 605 (full flowering; at least 50% of flowers open); H3—69 629 (end of flowering of the second-order stem—all petals have fallen); H4—70 701 [fruit set: beginning of hip (berry) growth on the main stem]. Different small letters indicate significant interactions between the phenological stage and treatment (two-way ANOVA). Different capital letters indicate significant differences between phenological stages. Duncan's test ($\alpha = 0.05$) was used.

treatments. The diameter of latewood vessels of H2 after the use of Organic preparation was smaller than in the control cuttings. Compared to the control, H3 latewood vessels were larger in diameter after the use of an Organic preparation and Plant extract, and lower when using IBA and Algae extract. In the case of H4 cuttings, only the Plant extract affected the increase of earlywood diameter, while no latewood vessels were determined at this stage. The differentiation in new vessels and new ring had probably also inhibited (**Figures 4**, **9**, **10**).

The above results were compared with measurements of the xylem tissue in stock plants in August—the mean was higher than obtained by rhizogenezis in all stages H1–H4 (**Figure 4**). The cause for such results was the strong expansion of callus tissue compressing the xylem tissues of the first ring in rooted cuttings. This phenomenon probably also caused the separation of individual vascular bundles outside the first ring. A fragmentary new second ring with rows of vessels and tracheid cells was visible around and above the first ring (**Figure 7**).

The cambium zone in rooted cuttings was difficult to identify (**Figures 6–10**).

The process of rhizogenesis is characterized by intensive growth of the layer between the xylem and the cortex, especially high means were obtained for the cuttings H1, excluding those treated with Plant extract, for which the means were lowest. The growth of this layer decreased in control cuttings, following phenological stages from H2 up to H4, in which it was lowest. The preparations in H2–H4 cuttings had a different effect, with the tendency for NAA to decrease means (**Figure 4**).

The mean width of phloem tissue for rooted cuttings was highest in H1. The width of phloem tissue in H1 control-rooted cuttings was lower than after the use of rooting enhancers, excluding Plant extract. In the case of H4 rooted cuttings, the results were similar in all treatments, excluding Plant extract, for which the mean was higher (**Figure 4**).

The cortex grew intensively in H1 cuttings after the use of all rooting enhancers, and their widths were greater compared with the control. In the case of H2 cuttings, a higher mean as compared to the control was noticed as a result of the use of Plant extract only. In the case of H3 cuttings, the means after treatment by Organic preparation, Plant extract, and NAA were higher compared to the control. The use of IBA, NAA, and plant preparation affected the increase of the mean of the width of cortex tissue in H4 cuttings (**Figure 4**).

The widths of pith rays changed in the process of rhizogenesis, depending on the phenological stage and treatment. However, the means obtained for all cuttings indicated that the rooting enhancers caused a decrease in the width of pith rays compared to control cuttings (**Figure 5**).

The growth of cortex tissue and tissues between the cortex and the xylem was connected with the growth of callus tissue and auxiliary root formation visible on cross and longitudinal sections of the basal part of shoots (**Figures 6–8**).

The Essential Role of the Phenological Stage of the Shoot and Plant Origin Preparations in Rooting the Cuttings of *Rosa* "Hurdal"

The highest natural ability to root was shown for cuttings H3, and was lower for cuttings cut from shoots H1 and H2. The cuttings from shoots H4 did not root, and none of the rooting enhancers increased rooting ability (**Figure 11**).

In the case of cuttings H1, a 2- to 3-fold increase of rooting percentage was obtained through the use of IBA and preparations of plant origin compared to the control cuttings and treated NAA. The lower (control, IBA, and plant origin preparations) or similar (NAA) percentage of cuttings with a callus only was noticed. The use of rooting enhancers for cutting H2 decreased the percentage of cuttings with the callus only. The rooting percentage increased after the use of plant origin preparations compared to the control cuttings. Organic preparation and Plant extract had a similar effect on H3 cuttings (**Figure 11**).

The rooting enhancers did not affect the root length, the weight of the root system, or the aboveground part of cuttings H1. In the case of H2 stage cuttings, the use of NAA preparation and all the preparation of plant origin increased the weight of the aboveground part of the plants, while the Algae extract and Plant extract affected the weight of the root systems. The use of IBA and all preparation of plant origin increased the root length. The use of an Organic preparation resulted in higher root length, weight of the aboveground part as compared to the remaining combination of rooted H3-stage cuttings. In the case of cuttings derived from shoots at this phenological stage, none of the rooting enhancers affected the weight of the root system (**Figure 12**).

Changes in Anatomy Structure Contra Rooting Percentage Results in the Propagation of *Rosa* "Hurdal"

Correlation analysis for the rooted cuttings in all phenological stages (H1–H3) showed that an increase in rooting percentage was only strictly connected to a decrease of the percentage of cuttings with a callus only. Moreover, a higher percentage of rooted cuttings correlated positively with a higher root length, weight of the root system, and aboveground part of cuttings, and also higher mean width of tissues between the xylem and cortex, a greater diameter of early- and late-wood vessels, and wider phloem and cortex layers. In the case of the percentage of cuttings with a callus only, higher results were obtained when the root length, weight of the root system of cuttings, width of

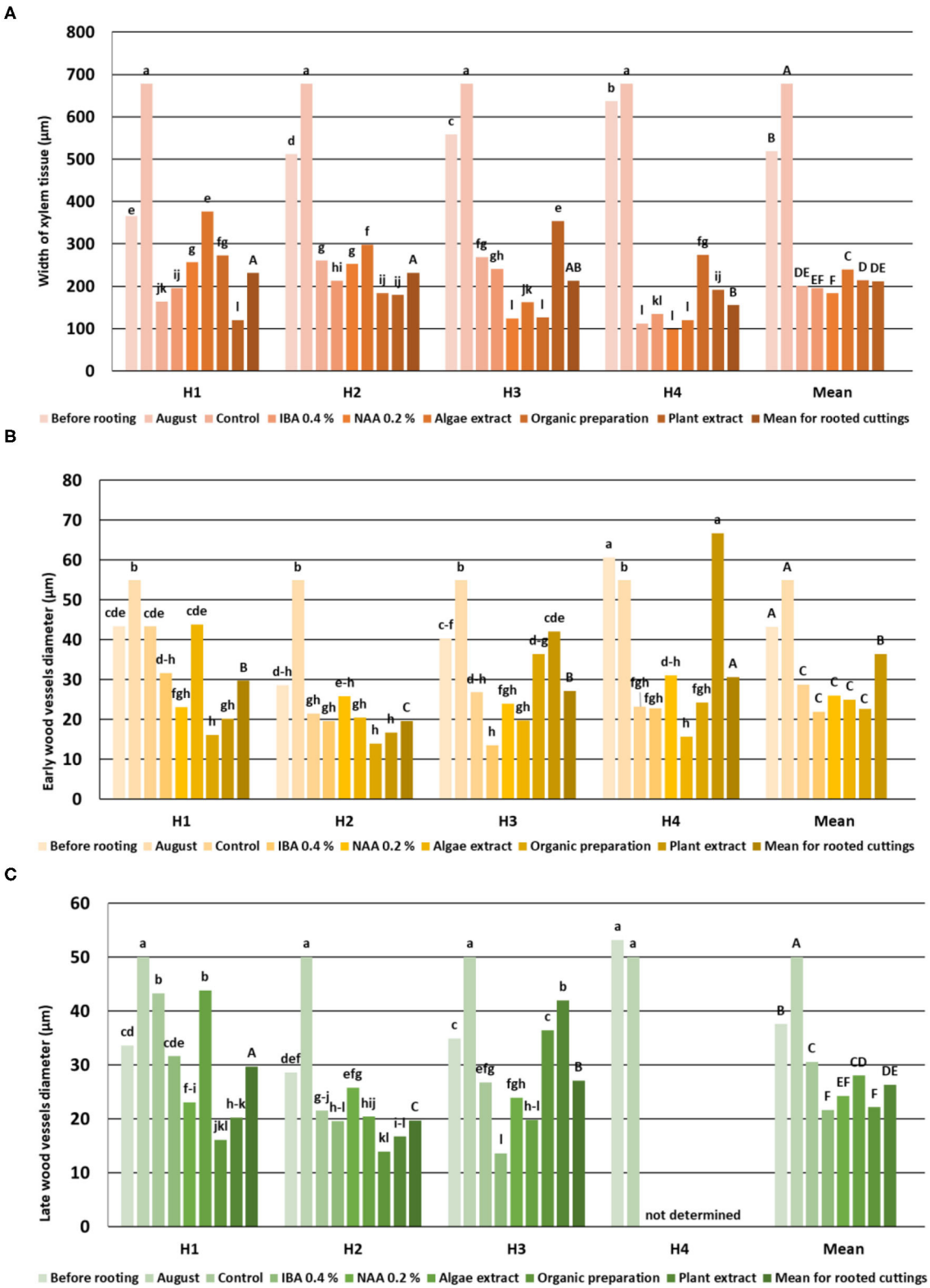

FIGURE 4 | Width of *Rosa* "Hurdal" xylem tissue **(A)**, early- **(B)**, and late-wood **(C)** vessels in stems before rooting, cuttings after 24 days of the rhizogenesis process and in stems of stock plants cut in the first days of August. Control—the control cuttings; IBA 0.4%—Ukorzeniacz A_{aqua} (0.4% IBA); NAA, 0.2%—Ukorzeniacz B_{aqua} (0.2% NAA); Algae extract—watering with 0.6% Bio Rhizotonic (10 ml) after planting and 10 and 20 days later; Organic preparation—watering with 0.4% Root Juice™

(Continued)

FIGURE 4 | (10 ml) after planting; Plant extract—watering with 0.02% Bio Roots (10 ml) after planting. H1–54 504 (flower buds still closed); H2–69 605 (full flowering; at least 50% of flowers open); H3–69 629 (end of flowering of the second-order stem—all petals have fallen); H4–70 701 [fruit set: beginning of hip (berry) growth on the main stem]. Different small letters indicate significant interactions between the phenological stage and treatment (two-way ANOVA). Different capital letters indicate significant differences between phenological stages. Duncan's test ($\alpha = 0.05$) was used.

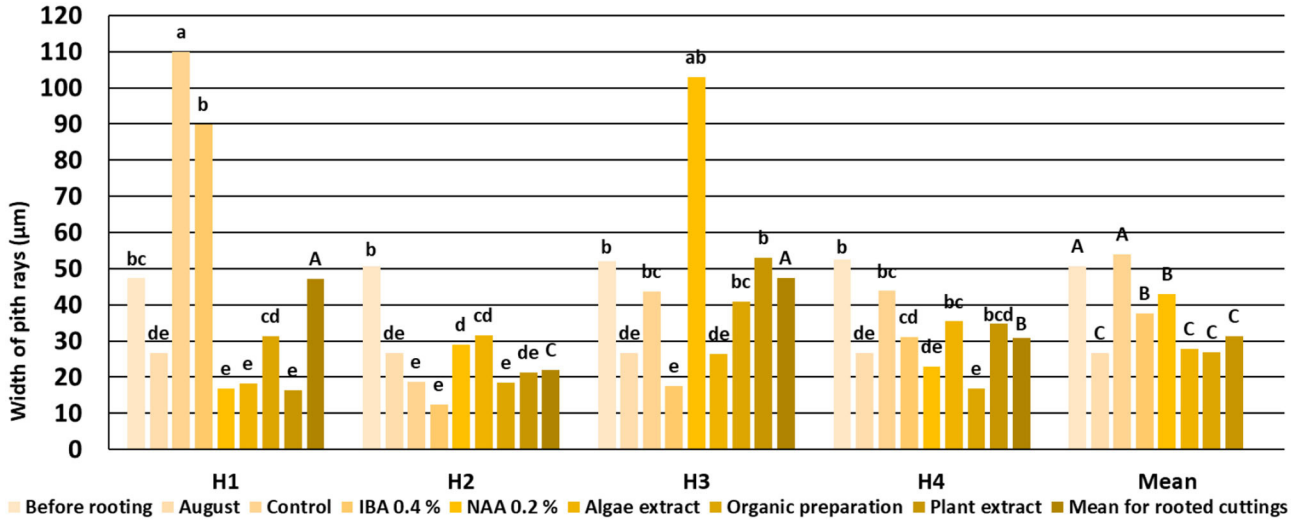

FIGURE 5 | Width of *Rosa* "Hurdal" pith rays in stems before rooting; cuttings after 24 days of the rhizogenesis process; and stems of stock plants cut in first days of August. Control—the control cuttings; IBA, 0.4%—Ukorzeniacz A_{aqua} (0.4% IBA); NAA, 0.2%—Ukorzeniacz B_{aqua} (0.2% NAA); Algae extract—watering with 0.6% Bio Rhizotonic (10 ml) after planting and 10 and 20 days later; Organic preparation—watering with 0.4% Root Juice™ (10 ml) after planting; Plant extract—watering with 0.02% Bio Roots (10 ml) after planting. H1–54 504 (flower buds still closed); H2–69 605 (full flowering; at least 50% of flowers open); H3–69 629 (end of flowering of the second-order stem—all petals have fallen); H4–70 701 [fruit set: beginning of hip (berry) growth on the main stem]. Different small letters indicate significant interactions between the phenological stage and treatment (two-way ANOVA). Different capital letters indicate significant differences between phenological stages. Duncan's test ($\alpha = 0.05$) was used.

tissues between xylem and cortex, and the diameter of early- and late-wood vessels were decreased and the phloem layer was getting narrower. The increase in length root correlated with the increase in diameter of early- and late-wood vessels, and the wider phloem layer. Correlation analysis showed a positive relationship between the weight of the root system and the aboveground part of cuttings. The anatomy parameters were also interconnected (**Table 2**).

Correlation analysis for cuttings derived from shoots with flower bud closed H1 showed a relationship between rooting percentage and estimated parameters in subsequent treatments. A larger diameter of latewood vessels in shoots before rooting was correlated with rising rooting percentage in control cuttings, treated with Algae extract, and Organic preparation, and decreasing rooting percentage with the use of NAA and Plant extract. A higher rooting percentage correlated with increase in early- and late-wood vessel diameters in cuttings 25 days after rooting, treated with Algae extract, and Organic preparation, while decreasing these parameters and the width of phloem tissue in control cuttings. The increase in rooting percentage was correlated with an increase in the percentage of cuttings with a callus only in the control, while with a decrease in this parameter when IBA, NAA, Algae extract, and Plant extract was used. An increase in rooting percentage was connected with an increase in fresh weight of the aboveground part and root system of cuttings after the use of Algae extract, while a decrease was associated with the use of Organic preparation. The higher rooting percentage was correlated with an increase in weight of the root system after the use of IBA and of the aboveground part in control cuttings. Moreover, the increase of rooting percentage correlated with the increase of root length in control and, after the use of all rooting enhancers, excluding Algae extract (**Table 3**).

The rooting percentage of H2 stage cuttings was correlated with the anatomical structure parameters of the shoots before rooting. A higher rooting percentage of control cuttings correlated with an increase in the width of xylem tissue and in the diameter of early- and late-wood vessels, but with a decrease in the width of phloem tissue in shoots before rooting cuttings. The increase in rooting percentage by the use of NAA and plant origin preparations correlated with a decrease in the width of xylem tissue in shoots before rooting. The increase in rooting percentage by the use of IBA was correlated with the increase in the diameter of early- and late-wood vessels, but a decrease in the width of phloem and cortex tissue before rooting. In the case of the use of Organic preparation and Plant extract, the increase of the width of phloem and cortex tissue and the decrease of the diameter of early- and late-wood vessels before rooting positively correlated with rooting percentage. After 25 days of

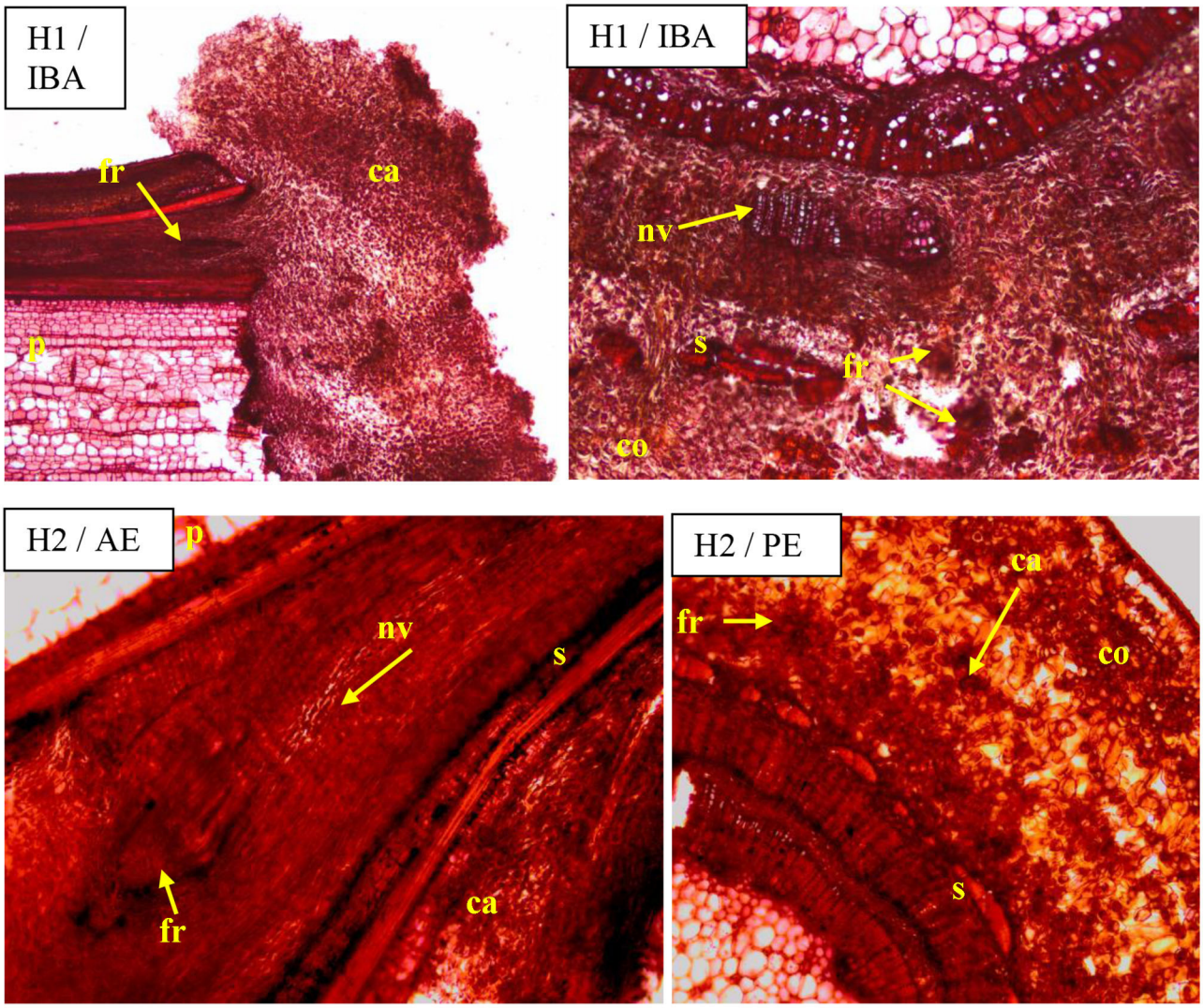

FIGURE 6 | Transverse and longitudinal sections of the shoots after 25 days of rhizogenesis rooting in *Rosa* "Hurdal" in four phenological stages in BBCH scale (Meier et al., 2009): H1—54 504 (flower buds still closed); H2—69 605 (full flowering; at least 50% of flowers open). IBA—Ukorzeniacz A_{aqua} (0.4% IBA); AE—Algae extract—watering with 0.6% Bio Rhizotonic (10 ml) after planting, 10 and 20 days later; PE—Plant extract—watering with 0.02% Bio Roots (10 ml) after planting. Designation of signs: ca, callus; co, cortex; ph, phloem; p, pith; s, sclerenchyma; nv, new vascular bundles; fr, forming roots.

rooting, an increase in the early- and late-wood vessel diameter and a decrease in the width of phloem tissue through the use of Organic preparations were correlated with the increase of rooting percentage. Correlation analysis for H2 cuttings showed a relationship between the increase of rooting percentage and the decrease of the percentage of cuttings with a callus only in control cuttings and after the use of NAA preparation, but with the increase by the use of Organic preparation and Plant extract. An increase in rooting percentage was correlated with an increase in the fresh weight of the root system and aboveground part of the rooted cuttings in the case of control cuttings and after the use of IBA. A decrease of the weight of the root system by the use of NAA caused the rooting percentage to increase. The increase in rooting percentage was correlated with an increase in the root length in the case of control cuttings and after the use of IBA, NAA, Algae, and Plant extract (**Table 4**).

In the case of cuttings derived from shoots immediately after petals had fallen (H3), correlations between rooting percentage and parameters of growth, as well as anatomical structure, were proved. Increasing rooting percentage was shown to correlate with the width of xylem tissue in shoots before rooting, where increase in the case of control cuttings and decrease in rooting enhancers were used. The larger diameter of earlywood in shoots before rooting correlated with rising rooting percentage for control cuttings and cuttings treated with Plant extract and decreasing in the case of treatment with NAA and Organic preparations. A decrease in the width of

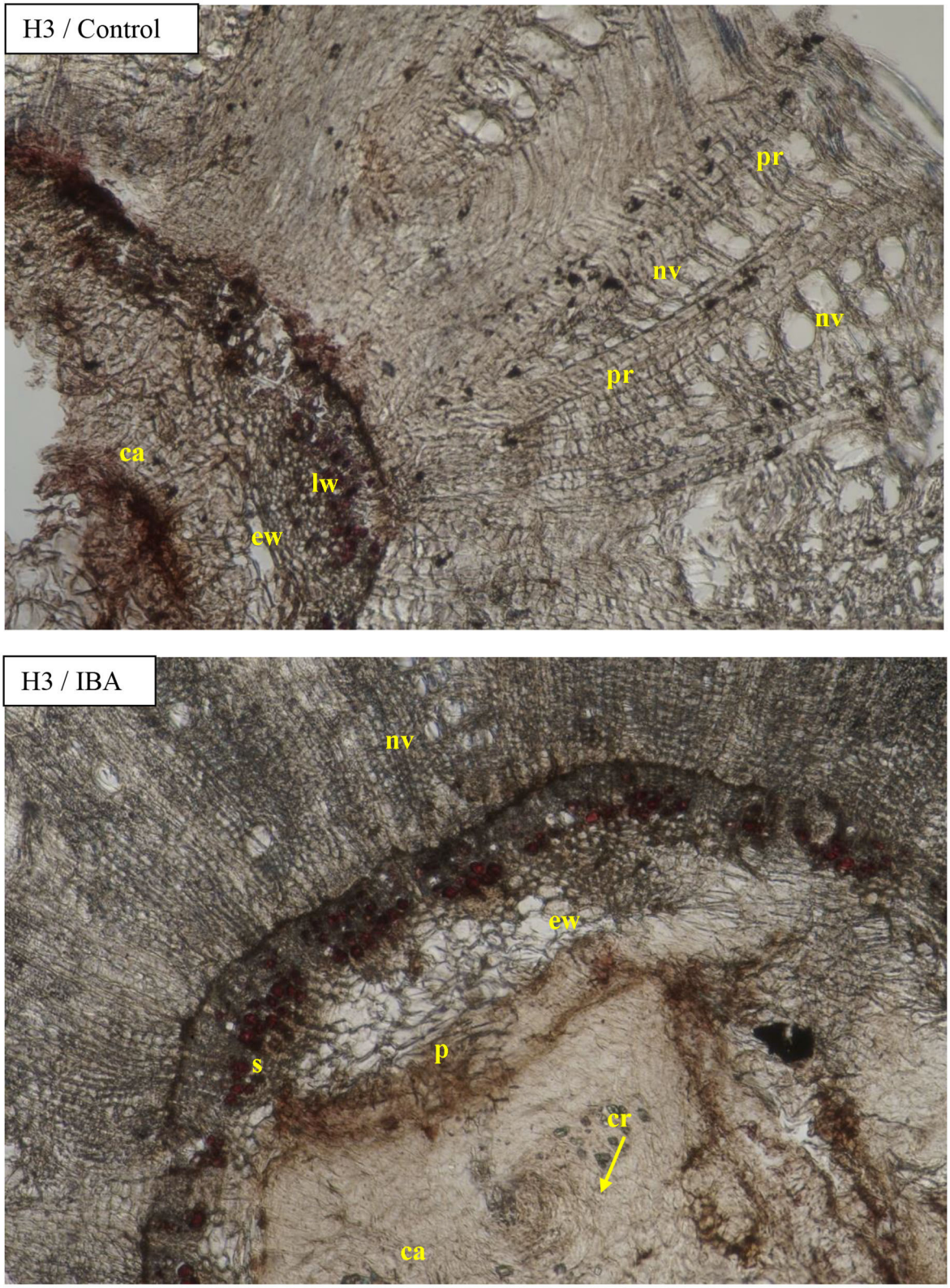

FIGURE 7 | Transverse sections of the shoots after 25 days of the process of rhizogenesis rooting in *Rosa* "Hurdal" in phenological stages in BBCH scale (Meier et al., 2009) H3–69 629 (end of flowering of the second-order stem—all petals have fallen) in control—the control cuttings without rooting enhancers and after treatment IBA—Ukorzeniacz A_{aqua} (0.4% IBA). Designation of signs: ca, callus; c, cambium; co, cortex; cr, crystals; p, pith; pr, pith rays; s, sclerenchyma; nv, new vessels/vascular bundles; ew, earlywood; lw, latewood; fr, forming root.

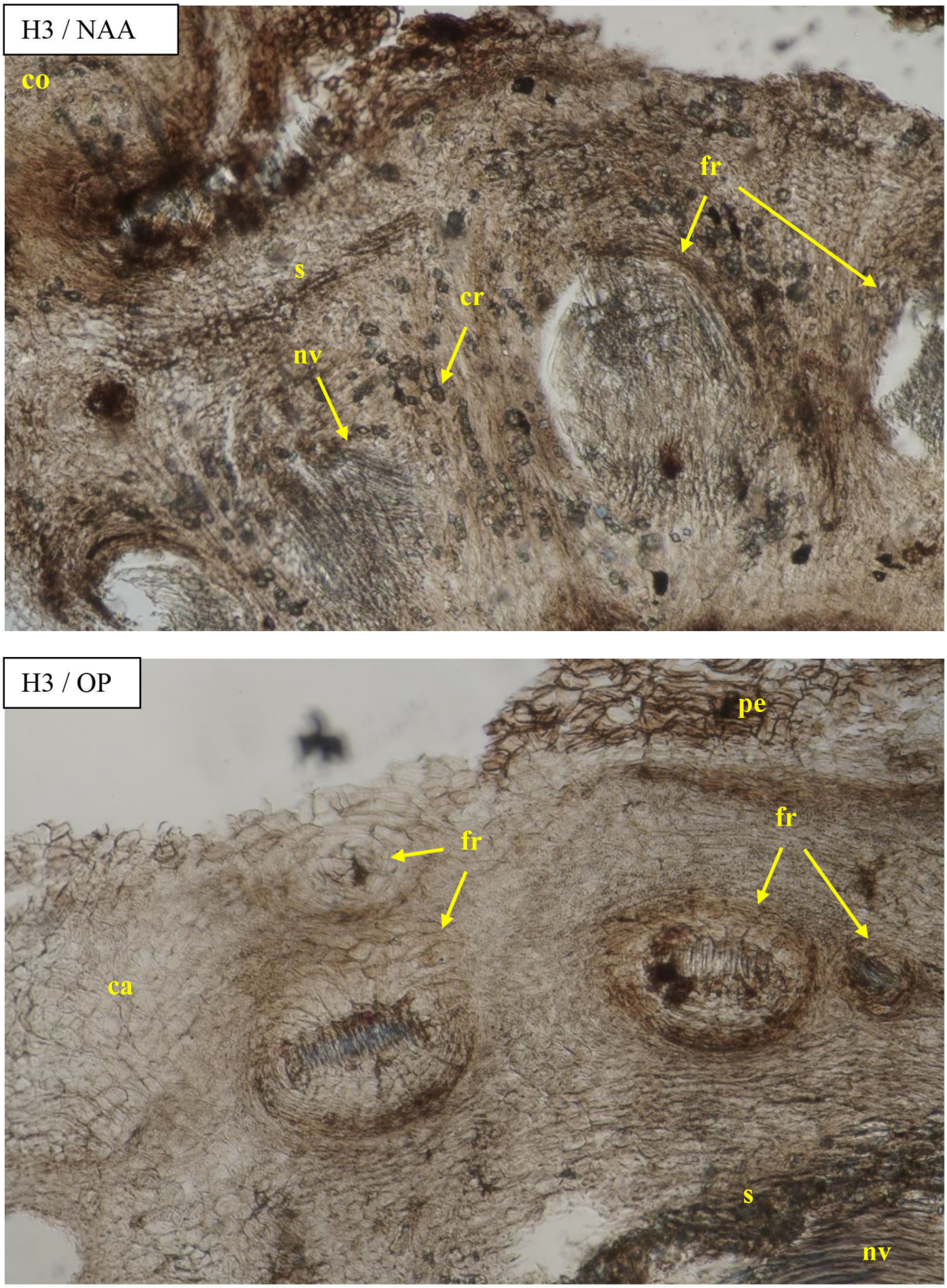

FIGURE 8 | Transverse sections of the shoots after 25 days of the process of rhizogenesis rooting in *Rosa* "Hurdal" in the phenological stage in BBCH scale (Meier et al., 2009) H3–69 629 (end of flowering of the second-order stem—all petals fallen) in control—the cuttings after treatment of NAA—Ukorzeniacz B_{aqua} (0.2% NAA) and OP—Organic preparation—watering with 0.4% Root Juice™ (10 ml) after planting. Designation of signs: ca, callus; co, cortex; cr, crystals; pe, periderm; s, sclerenchyma; nv, new vessels/vascular bundles; fr, forming root.

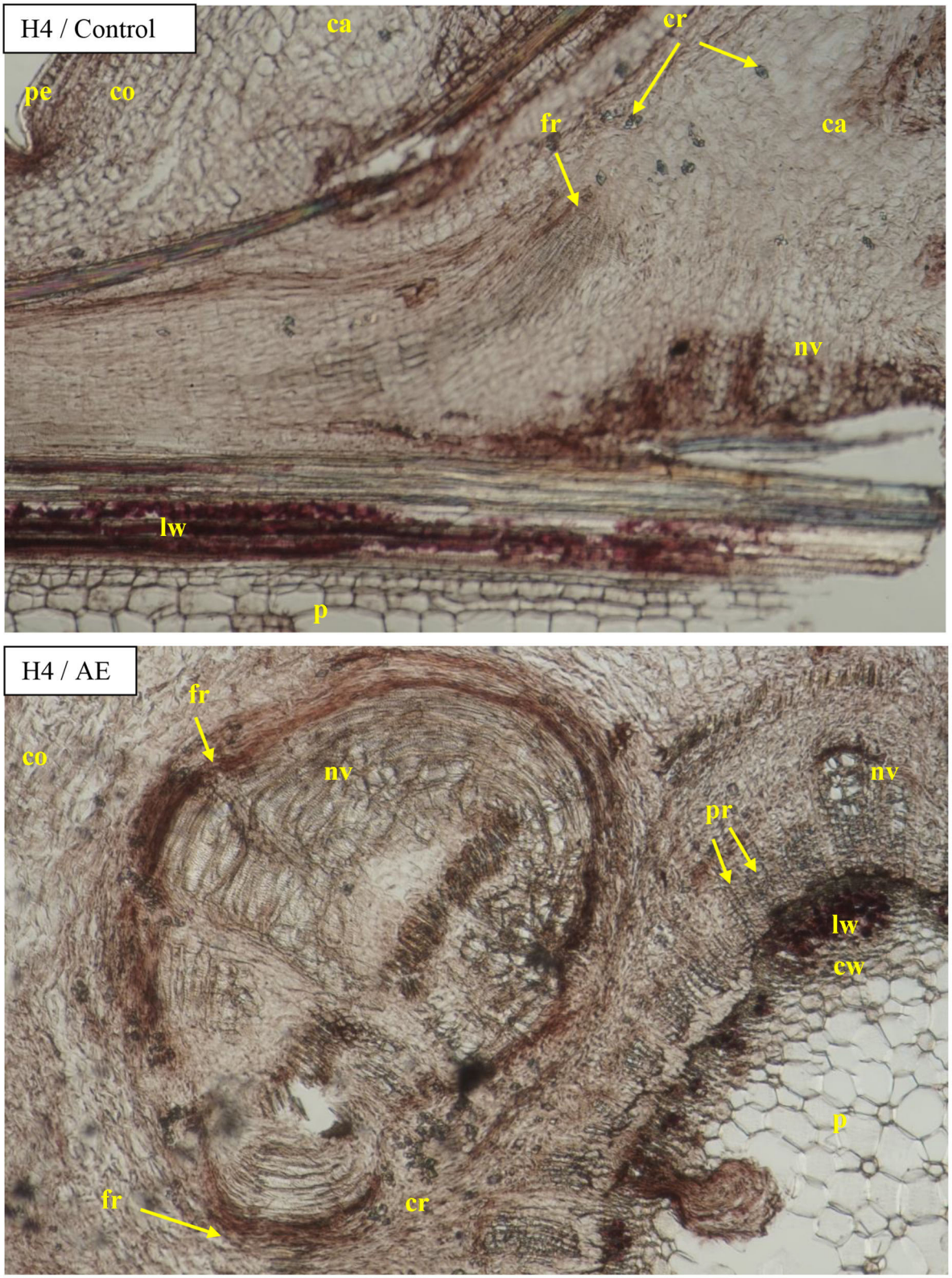

FIGURE 9 | Transverse and longitudinal sections of the shoots after 25 days of the process of rhizogenesis rooting in *Rosa* "Hurdal" in the phenological stage in BBCH scale (Meier et al., 2009) H4—70 701 [fruit set: beginning of hip (berry) growth on the main stem] in control cutting and after treatment of AE—Algae extract—watering with 0.6% Bio Rhizotonic (10 ml) after planting, 10 and 20 days later. Designation of signs: pe, periderm; ca, callus; co, cortex; cr, crystals; p, pith; pr, pith rays; nv, new vessels/vascular bundles; ew, earlywood; lw, latewood; fr, forming root.

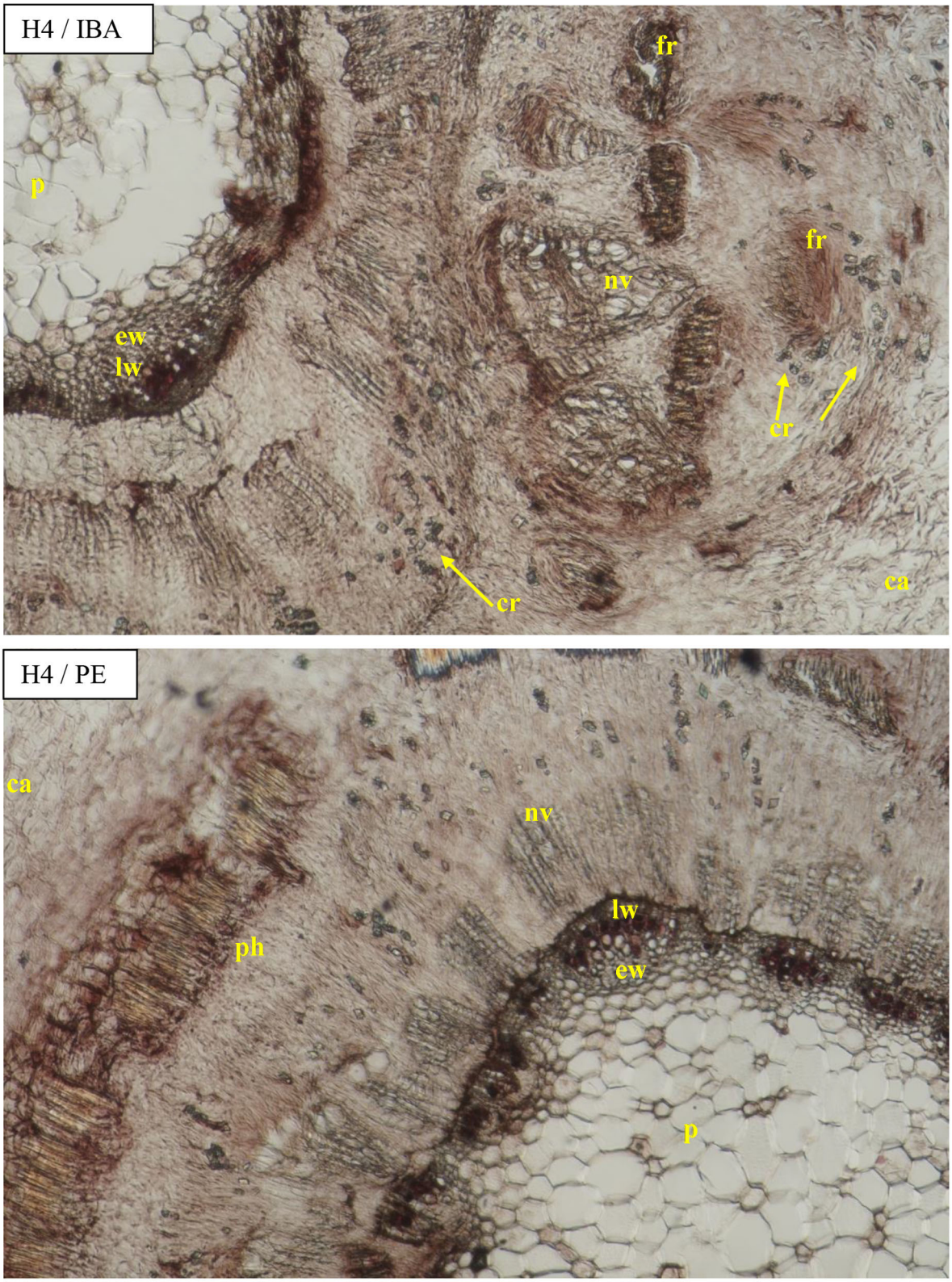

FIGURE 10 | Transverse sections of the shoots after 25 days of the process of rhizogenesis rooting in *Rosa* "Hurdal" in the phenological stage in BBCH scale (Meier et al., 2009) H4—70 701 [fruit set: beginning of hip (berry) growth on the main stem] cutting after treatment of IBA—Ukorzeniacz A_{aqua} (0.4% IBA) and PE—Plant extract—watering with 0.02% Bio Roots (10 ml) after planting. Designation of signs: ca, callus; co, cortex; cr, crystals; p, pith; pr, pith rays; ph, phloem; nv, new vessels/vascular bundles; ew, earlywood; lw, latewood; fr, forming root.

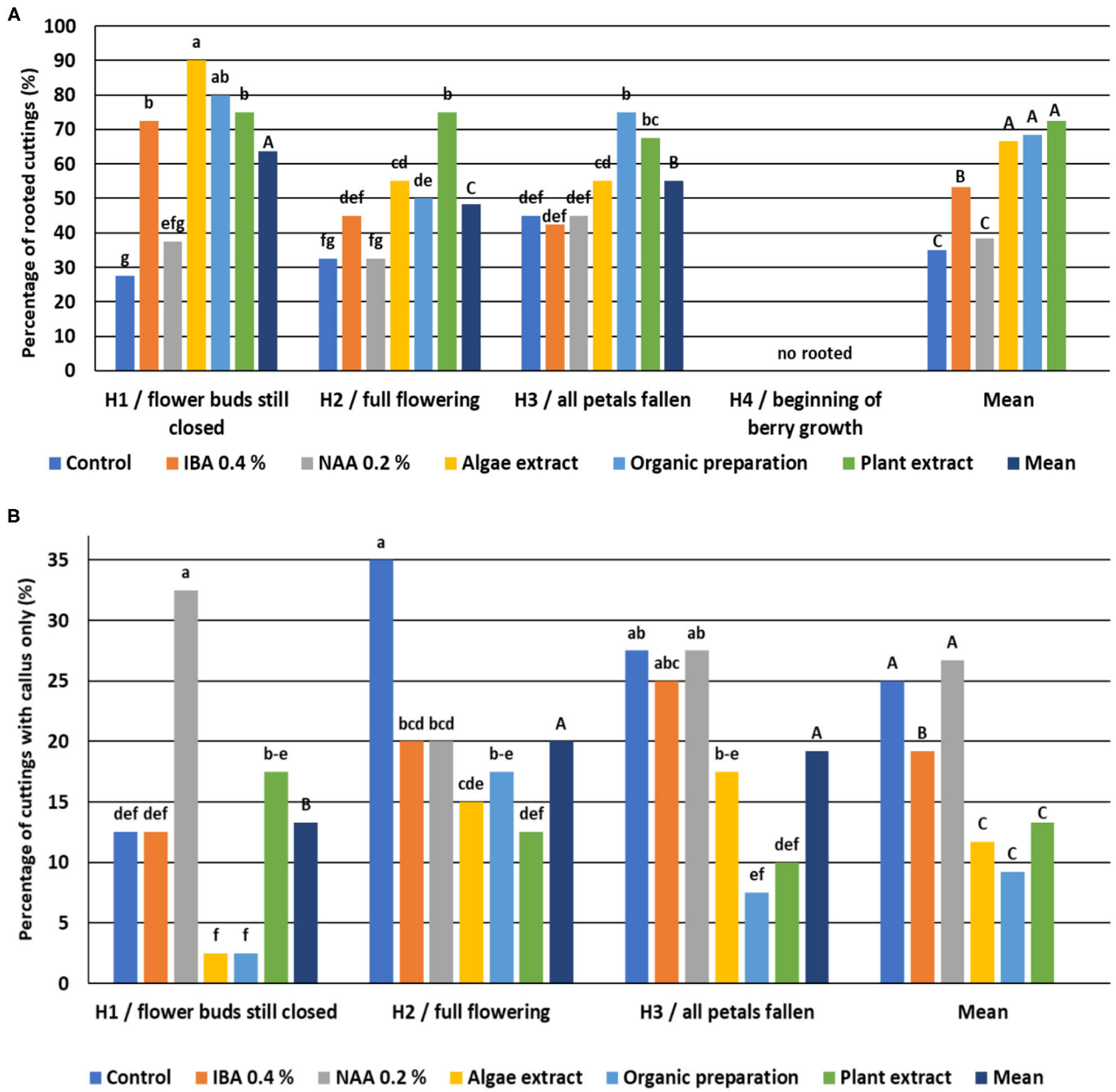

FIGURE 11 | Percentage of rooted *Rosa* "Hurdal" cuttings **(A)** and cuttings with a callus only **(B)**. Control—the control cuttings; IBA, 0.4%—Ukorzeniacz A_{aqua} (0.4% IBA); NAA, 0.2%—Ukorzeniacz B_{aqua} (0.2% NAA); Algae extract—watering with 0.6% Bio Rhizotonic (10 ml) after planting and 10 and 20 days later; Organic preparation—watering with 0.4% Root Juice™ (10 ml) after planting; Plant extract—watering with 0.02% Bio Roots (10 ml) after planting. H1—54 504 (flower buds still closed); H2—69 605 (full flowering; at least 50% of flowers open); H3—69 629 (end of flowering of the second-order stem—all petals have fallen); H4—70 701 [fruit set: beginning of hip (berry) growth on the main stem]. Different small letters indicate significant interactions between the phenological stage and treatment (two-way ANOVA). Different capital letters indicate significant differences between phenological stages. Tukey's test ($\alpha = 0.05$) was used.

cortex tissue in control cuttings and in the latewood vessel diameter in shoots before rooting correlated with an increase in rooting percentage for cuttings treated with IBA, NAA, and Algae extract. The increasing of width of the cortex layer in shoots before rooting was positively connected with rooting percentage where NAA, Algae extract, and Organic preparations were used. The increasing of width of the xylem tissue, early- and late-wood diameters, and phloem tissue after 25 days of rooting was correlated with higher rooting percentage in the case of control cuttings. Moreover, the rise in the diameter of early- and latewood vessels after 25 days in cuttings treated with Algae extract and Organic preparation correlated positively with

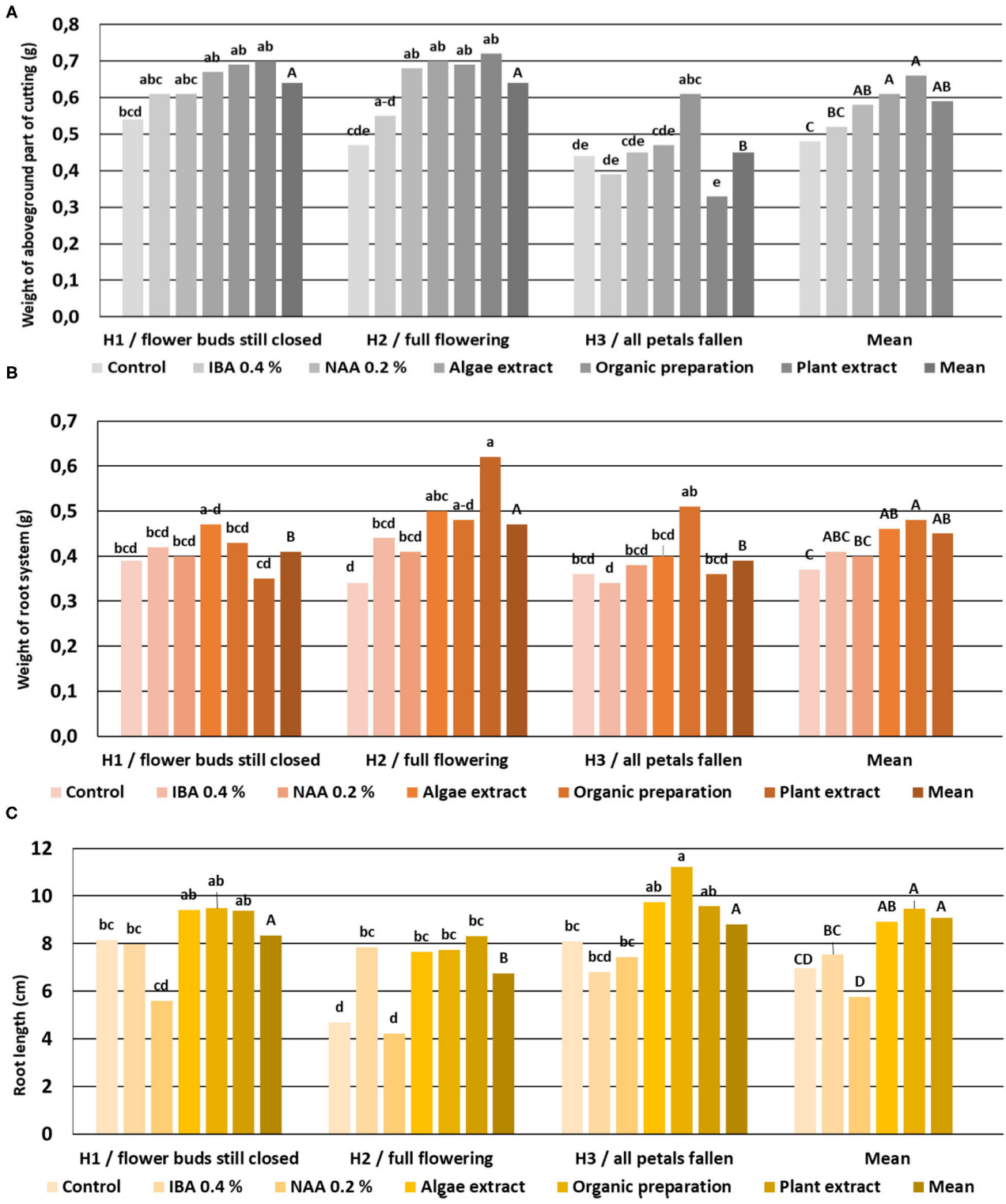

FIGURE 12 | The root length **(C)**, weight of the aboveground part **(A)**, and root system **(B)** in rooted cuttings of *Rosa* "Hurdal." Control—the control cuttings; IBA, 0.4%—Ukorzeniacz A_{aqua} (0.4% IBA); NAA, 0.2%—Ukorzeniacz B_{aqua} (0.2% NAA); Algae extract—watering with 0.6% Bio Rhizotonic (10 ml) after planting, 10 and 20 days later; Organic preparation—watering with 0.4% Root Juice^{TM} (10 ml) after planting; Plant extract—watering with 0.02% Bio Roots (10 ml) after planting. H1—54 504 (flower buds still closed); H2—69 605 (full flowering; at least 50% of flowers open); H3—69 629 (end of flowering of the second-order stem—all petals have fallen); H4—70 701 [fruit set: beginning of hip (berry) growth on the main stem]. Different small letters indicate significant interactions between the phenological stage and treatment (two-way ANOVA). Different capital letters indicate significant differences between phenological stages. Tukey's test (α =0.05) was used.

TABLE 2 | Effect correlations between measured parameters of growth and anatomical structure in *Rosa* "Hurdal" after 25 days of rooting cuttings in all phases taken together.

Variable	Rooting percentage	Percentage of cuttings with callus only	Root length	Fresh weight of root system	Fresh weight of above ground part	Width of xylem tissue	Width of tissues between xylem and cortex	Early wood vessel diameter	Late wood vessel diameter	Width of pith rays	Width of phloem tissue	Width of cortex tissue
	1	2	3	4	5	6	7	8	9	10	11	12
1	1.00											
2	−0.63***	1.00										
3	0.44**	−0.49**	1.00									
4	0.10*	−0.07	0.03	1.00								
5	0.15*	−0.11*	−0.01	0.48**	1.00							
6	0.07	−0.06	−0.06	0.02	−0.03	1.00						
7	0.17*	−0.21*	0.05	0.02	0.08*	0.30**	1.00					
8	0.10*	−0.17*	0.12*	−0.03	−0.06	0.14*	0.34**	1.00				
9	0.10*	−0.17*	0.12*	−0.03	−0.06	0.14**	0.34**	0.99*****	1.00			
10	−0.22*	−0.07	0.03	−0.05	−0.05	−0.15**	0.24*	0.33**	0.33**	1.00		
11	0.25*	−0.25*	0.14*	0.02	0.09*	0.26**	0.76****	0.35**	0.35**	0.12*	1.00	
12	0.23*	−0.05	0.07	−0.02	0.09*	0.03	0.25*	0.07	0.07	−0.15*	0.14*	1.00

*Marked correlations are significant at $p < 0.05$. Correlation significance: *0.08–0.29—very low; **0.30–0.49—low; ***0.50–0.69—restrained; ****0.70–0.89—high; ***** >0.90—very high.*

rooting percentage. In the case of cuttings rooted with the use of a Plant extract, a correlation was found between the increase of rooting percentage and the decrease of the early- and late-wood vessel diameter and width of pith rays and cortex tissue in cuttings after 25 days of rooting. The increase of rooting percentage was strictly correlated with a decrease in percentage of cuttings with a callus only both in control cuttings and after the use of any rooting enhancer. Moreover, the increase of rooting percentage correlated with the decrease of fresh weight of the root system for the control cuttings and treated auxins, while with the increase of the weight of the aboveground parts of cuttings treated with the NAA. Additionally, the rooting percentage increased with increase in the root length in the case of control cuttings and after the use of IBA, NAA, Algae, and Plant extract (**Table 5**).

DISCUSSION

Changes in the seasonal cambial activity and morphophysiological status of stock plants affected the adventitious root formation of cuttings of *Artemisia arborescens* (Fascella et al., 2012), *Ficus infectoria* (Anand and Heberlein, 1975), *Juniperus* L. (Torchik, 2015), olive (Abousalim et al., 1993), and roses (Monder et al., 2017). The different periods of delivery and rooting of cuttings suggested changes in various groups of roses (Hoşafçi et al., 2005; Pihlajaniemi et al., 2005; Monder et al., 2016).

The 1-year shoots of *R.* "Hurdal" used for cuttings in all phenological stages before and after rhizogenesis were characterized by an anatomical structure typical for woody plants of *Rosaceae* and the genus *Rosa* (Zhang, 1992). The diameters of the vessels measured by Zhang (1992) were 70–400 (mostly 114–192) μm, 40–96% solitary, round to oval, or angular, whereby the tangential diameter of earlywood vessels was 35–155 (40–250) μm and tangential latewood vessels—19–52 (15–130) μm. The means of this parameter were low for *R.* "Hurdal." The mean diameter of the earlywood vessel before rooting depends on the phenological stage and reaches a mean from 28.66 μm in H2 to 60.59 μm in H4. The latewood vessel diameter showed a tendency to increase and reach a mean from 28.86 μm in H2 to 53.2 μm in H4. Low values of the diameter can limit the transport of water (Rosell et al., 2017), and, additionally, single-node leafy stem cuttings have limited storage capacity due to the small size of the shoot, which hinders the survival of the cuttings (Costa et al., 2007). However, the vessel diameter in woody plants is affected by many factors (Rosell et al., 2017). Moreover, the tracheids of *R.* "Hurdals" had thick walls and a very small diameter. However,

TABLE 3 | Effect correlations between percentage of rooted cuttings and measured parameters of growth and anatomical structure in *Rosa* "Hurdal" before and after 25 days of rooting cuttings derived from shoots H1, with flower buds closed (BBCH 54 504).

Variable	Percentage of rooted cuttings					
	Control	IBA 0.4%	NAA 0.2%	Algae extract 3 × 0.6%	Organic preparation 0.4%	Plant extract 0.02%
SD	33.31	18.08	8.40	12.40	7.16	23.20
Percentage of cuttings with callus only	0.29*	−0.88****	−1.00*****	−0.94*****	0.00	−1.00*****
Root length	0.24*	0.44**	0.88****	−0.28*	0.22*	0.65***
Fresh weight of root system	0.02	0.33**	0.07	0.15*	−0.49**	−0.01
Fresh weight of aboveground part	0.33**	−0.02	0.01	0.17*	−0.42**	0.01
Width of xylem tissue	−0.04	−0.01	0.01	0.01	−0.05	−0.10
Width of tissues between xylem and cortex	0.00	0.00	0.00	0.00	0.00	0.00
Earlywood vessels diameter	−0.12*	0.00	0.00	0.25*	0.17*	0.00
Latewood vessels diameter	−0.12*	0.00	0.00	0.25*	0.17*	0.00
Width of pith rays	0.00	0.00	0.00	0.00	0.00	0.00
Width of phloem tissue	−0.11*	0.02	0.03	−0.03	0.04	0.00
Width of cortex	0.00	0.00	0.00	0.00	0.00	0.00
Before rooting						
Width of xylem tissue	0.00	0.00	0.00	0.00	0.00	0.00
Earlywood vessel diameter	−0.03	0.01	0.02	−0.03	−0.06	0.02
Latewood vessel diameter	0.14*	−0.05	−0.11*	0.15*	0.25*	−0.08*
Width of pith rays	0.00	0.00	0.00	0.00	0.00	0.00
Width of phloem tissue	0.04	−0.01	−0.03	0.04	0.07	−0.02
Width of cortex	−0.04	0.01	0.03	−0.04	−0.07	0.02
Width of early wood tissue	0.00	0.00	0.00	0.00	0.00	0.00
Width of late wood tissue	0.00	0.00	0.00	0.00	0.00	0.00

*Marked correlations are significant at $p < 0.05$. Correlation significance: *0.08–0.29—very low; **0.30–0.49—low; ***0.50–0.69—restrained; ****0.70–0.89—high; ***** >0.90—very high.*

the callus in *Rosa* Madelon® had differentiated vessels that can contribute to water transport before new roots take over this function (Costa et al., 2007).

The natural reaction of a cambium to wounding caused by cutting is a callus formation at the base, both in woody (Strzelecka, 2017) and herbaceous plants (Wróblewska, 2013). The callus proliferation precedes root initiation. The proliferation of parenchyma or phloem tissue (callus) is crucial to root formation and better rooting of shoot cuttings. The new parenchyma tissue (callus) can grow rapidly through cambial meristematic activity before forming adventitious roots, as in the stem cuttings of *Rosa* Madelon® (Costa et al., 2007). The adventitious roots formed by *Rosa rugosa* stem cuttings are preceded by callus tissue at the cut surface of the stem base (Fouda and Schmidt, 1994). A callus can prevent the entry of pathogenic organisms at the wound (Cline and Neely, 1983), affect positively the hydration of a cutting (Scagel, 2004), and reduce susceptibility to stem rot (Howard and Harrison-Murray, 1995). However, callus overgrowth could be an unfavorable phenomenon in *R.* "Hurdal," and result in a high percentage of cuttings with calluses only. Vessel measurement after 25 days suggested a decrease in such cuttings, probably because their tissues had been squeezed by growing callus cells; however, the vessel diameter of latewood in H4 was not determined due to the lack of unambiguous differentiation between the cells. The effects of preparations were different and depended on the phenological stage in *R.* "Hurdal" as in *Rosa beggeriana* "Polstjårnan" and *Rosa helenae* "Semiplena" (Monder et al., 2019). The IBA and NAA preparations decreased the width of xylem tissue, probably because of overgrowth of callus cells.

The shoots of *R.* "Hurdals" grew intensively up to the appearance of flower buds and harvest time for cuttings. The lignifying process of the shoots progressed and stem lignification and regular tissue arrangement were characteristics in rooted cuttings during all of the H1–H4 phases. The same observations were also visible on both once-flowering *R.* "Polstjårnan" and *R.* "Semiplena" (Monder et al., 2019).

The experiment conducted on *R.* "Hurdals" show the crucial role of the phenological stage of shoots of the stock plant in which the cuttings were prepared, both in terms of propagation and anatomical changes. The changes to anatomical structure in subsequent phenological stages of flowering before the cuttings were prepared affected the response to rooting enhancers and consequently the effectiveness of rhizogenesis.

The experiment also shows that the changes in anatomical structure before rooting cuttings affected the changes in anatomy structure in response to IBA, NAA, and plant origin preparations in the process of rhizogenesis. It suggested that the specific anatomic structure of shoots before rooting led to favorable or unfavorable changes caused by rooting enhancers, including

TABLE 4 | Effect correlations between percentage of rooted cuttings and measured parameters of growth and anatomical structure in *Rosa* "Hurdal" before and after 25 days of rooting cuttings derived from shoots H2, in full flowering; at least 50% of flowers open (BBCH 69 605).

Variable	Percentage of rooted cuttings					
	Control	IBA 0.4%	NAA 0.2%	Algae extract 3 × 0.6%	Organic preparation 0.4%	Plant extract 0.02%
SD	13.56	5.06	23.07	5.06	7.16	11.32
Percentage of cuttings with callus only	−0.75****	0.00	−0.62***	0.00	0.43**	−0.94*****
Root length	0.20*	0.50**	0.50**	0.70****	0.04	0.28*
Fresh weight of root system	0.08*	0.34**	−0.13*	−0.04	−0.05	−0.14
Fresh weight of aboveground part	0.09*	0.16*	0.08*	−0.07	0.05	0.04
Width of xylem tissue	−0.11*	0.03	0.04	0.02	0.06	−0.08
Width of tissues between xylem and cortex	0.00	0.00	0.00	0.00	0.00	0.00
Earlywood vessels diameter	−0.07	−0.10	0.04	0.00	0.18*	−0.09*
Latewood vessels diameter	−0.07	−0.10	0.04	0.00	0.18*	−0.09*
Width of pith rays	0.00	0.00	0.00	0.00	0.04	0.00
Width of phloem tissue	−0.02	−0.26	0.00	0.00	−0.20*	0.02
Width of cortex	0.00	0.00	0.00	0.00	0.00	0.00
Before rooting						
Width of xylem tissue	0.18*	0.02	−0.18*	−0.19*	−0.15*	−0.11*
Earlywood vessel diameter	0.09*	0.45**	0.05	0.00	−0.32**	−0.40**
Latewood vessel diameter	0.09*	0.45**	0.05	0.00	−0.32**	−0.40**
Width of pith rays	0.00	0.00	0.00	0.00	0.00	0.00
Width of phloem tissue	−0.08*	−0.42**	−0.05	0.00	0.29*	0.37**
Width of cortex	−0.05	−0.24*	−0.03	0.00	0.17*	0.22*
Width of early wood tissue	0.00	0.00	0.00	0.00	0.00	0.00
Width of late wood tissue	0.00	0.00	0.00	0.00	0.00	0.00

*Marked correlations are significant at $p < 0.05$. Correlation significance: *0.08–0.29—very low; **0.30–0.49—low; ***0.50–0.69—restrained; ****0.70–0.89—high; ***** >0.90—very high.*

plant origin preparations. Changes in the structure of the cambium zone, where the cells differentiate, are of particular importance. Changes to cortex tissues, where the cells of phellogen can also differentiate, are equally significant.

The overgrowth of a callus may squeeze the first ring of xylem tissue, consequently decreasing the vessel diameter and causing new irregular bundles to appear in the zone between the sclerenchyma and late-wood xylem after 25 days and new ring vascular bundles to form in 12 weeks. These phenomena were not observed either in *R. beggeriana* "Polstjårnan" or *R. helenae* "Semiplena", which had a high rooting percentage (Monder et al., 2019) compared with *R.* "Hurdal." Callus overgrowth was not observed in both cultivars. Neither of the rooting enhancers under study (excluding the NAA preparation of *R.* "Semiplena") stimulated callus proliferation (Monder et al., 2019).

In contrast to *R.* "Hurdal," both *R.* "Polstjårnan" and "Semiplena" had a tendency for adventitious root formation along the stem, omitting its calloused basal part (Monder et al., 2019). "Hurdal" has a high tendency to an overgrowing callus, with a high percentage of cuttings developing a callus only. The use of plant origin preparations decreased the percentage of cuttings with a callus only, while the use of IBA increased it for H1 cuttings. However, none of the rooting enhancers caused an increase in the rooting ability on the internode or along the stem of *R.* "Hurdal." The roots in "Hurdal" appeared at the base only and were obstructed by callus overgrowth. The roots of the *Rosa* "Semiplena" and "Polstjarnan" also started appearing on the basal part after the 3–4 weeks of rooting, and, later, after 6–8 weeks, they appeared in the node ("Polstjårnan") and along the internode ("Semiplena") (Monder et al., 2019). These phenomena were not noted for the "Hurdal" rooted cuttings, and roots were observed only at the basal part of cuttings independent of rooting enhancers.

Despite the above, the research on *R.* "Hurdal" confirmed previous observations concerning *R.* "Polstjårnan" and "Semiplena" (Monder et al., 2019). The adventitious roots omitted the sclerenchyma layer, which did not form the regular ring in any of the abovementioned roses (Monder et al., 2019). The role of sclerenchyma in difficulties in root formation has not been sufficiently proven. Pericyclic sclerenchyma can be correlated with difficulty in the rooting of some woody species (Beakbane, 1969); however, rooting capabilities are connected more with the natural ability to root easily, as in *Ficus pumila*, than with the presence of sclerenchyma tissue (Davies and Joiner, 1982).

Callus overgrowth was probably one of the main reasons for the low percentage of rooted cuttings *R.* "Hurdals." The callus formation at the basal part of the shoot of cuttings is one of the first histological reactions occurring in response to wounding caused by severance in woody plant species (Costa et al., 2007, Amissah et al., 2008). The high percentage of cuttings with a callus only, calculated after 12 weeks, resulted in a high ratio

TABLE 5 | Effect correlations between percentage of rooted cuttings and measured parameters of growth and anatomical structure in *Rosa* "Hurdal" before and after 25 days of rooting cuttings derived from shoots H3, immediately after petals have fallen (BBCH 69 629).

Variable	Percentage of rooted cuttings					
	Control	IBA 0.4%	NAA 0.2%	Algae extract 3 × 0.6%	Organic preparation 0.4%	Plant extract 0.02%
SD	16.74	24.15	16.79	15.19	15.19	13.16
Percentage of cuttings with callus only	−0.64***	−0.99*****	−0.98*****	−0.51***	−0.70****	−0.19*
Root length	0.29*	0.53***	0.40**	0.12*	0.07	0.10*
Fresh weight of root system	−0.12*	−0.17*	−0.16*	−0.01	0.05	−0.04
Fresh weight of aboveground part	−0.04	−0.01	0.22*	0.06	0.06	0.03
Width of xylem tissue	0.15*	0.07	−0.15*	−0.06	0.01	0.00
Width of tissues between xylem and cortex	0.00	0.00	0.00	0.00	0.00	0.00
Earlywood vessels diameter	0.13*	0.00	−0.04	0.08*	0.09*	−0.26*
Latewood vessels diameter	0.13*	0.00	−0.04	0.08*	0.09*	−0.26*
Width of pith rays	0.00	0.00	0.00	0.00	0.00	−0.96*****
Width of phloem tissue	0.18*	0.00	0.04	0.00	0.00	0.00
Width of cortex	−0.10	0.00	0.00	0.00	0.00	−0.15*
Before rooting						
Width of xylem tissue	0.33**	−0.09*	−0.26*	−0.24*	−0.17*	−0.10*
Earlywood vessel diameter	0.15*	−0.05	−0.15*	0.00	−0.33**	0.48**
Latewood vessel diameter	0.05	−0.13*	−0.13*	−0.13*	−0.07	0.07
Width of pith rays	0.00	0.00	0.00	0.00	0.00	0.00
Width of phloem tissue	0.00	0.00	0.00	0.00	0.00	0.00
Width of cortex	−0.71****	0.05	0.46**	0.32**	0.47**	−0.01
Width of early wood tissue	0.00	0.00	0.00	0.00	0.00	0.00
Width of late wood tissue	0.00	0.00	0.00	0.00	0.00	0.00

*Marked correlations are significant at $p < 0.05$. Correlation significance: *0.08–0.29—very low; **0.30–0.49—low; ***0.50–0.69—restrained; ****0.70–0.89—high; ***** >0.90—very high.*

compared with the rooting percentage in the same combination. Simultaneously, the strong growth of callus cells caused a high percentage of cuttings to develop a callus only, especially after treatments with IBA and NAA preparations and in the case of control cuttings, with a high ratio to rooted cuttings. The overgrowing callus also filled the place of the pith and broke the vascular bundles of the first ring, which were visible on cross sections after 12 weeks. The numerous callus cells may have caused compression of the first ring of wood tissue and, probably, quickly established the second ring, enabling the maintenance of wood vessel function in a changed anatomical structure. Vessels wide in diameter and wide pith rays were noted. The mean width of the pith rays for all the phenological stages of cuttings was higher for control cuttings and those treated with IBA and NAA preparations than preparations of the plant origin. In the case of H4 stage cuttings of "Hurdal," a decrease of formation was observed in latewood. These cuttings did not root, and none of the rooting enhancers increased rooting ability.

According to previous research, the cambium has a crucial role in adventitious root formation; however, it is still not known whether new parenchyma tissues are a part of the cambium, phloem, or xylem (Fouda and Schmidt, 1994; Costa et al., 2007), also in *Rosa* "Hurdals." Roots primordia have appeared in the cambium zone in *Rosa* "Semiplena" and "Polstjarnan" (Monder et al., 2019). Roots in woody plants can be also formed in the phloem and the pericycle zone (Haissig, 1974), as was observed in *R.* "Hurdal" 25 days after cutting and after 12 weeks of rooting.

In the present study, each of the rooting enhancers had a different influence on anatomy structure. These results are contrary to research on *Rhododendron ponticum*, where rooting powders with IBA and NAA did not affect anatomical changes in the structure of cuttings, or did so only slightly (Strzelecka, 2017). However, the results do confirm previous research on "Polstjårnan" and "Semiplena." The application of NAA preparation caused a decrease in the wood cell diameter and the width of xylem, cambium, and phloem tissue in "Polstjårnan" cuttings as well as of the wood cell diameter and width of xylem tissue in "Semiplena." The use of NAA, IBA, and plant origin preparations in "Semiplena" cuttings caused phloem tissue to widen (Monder et al., 2019).

The plant origin preparations positively affected the rooting percentage of *R.* "Hurdal" as well as the quality (the weight of the root system and the aboveground part) of rooted cuttings. Moreover, by the use of the aforementioned preparations, a lower percentage of cuttings with a callus only was noted. These results have certainly indicated the possibility for use of these preparations in the rooting of "Hurdal" rose cuttings and may be recommended as alternative preparations of natural origin in the ecological propagation (91/414/EEC, 2009/128/WE; OJEU), compared to the classic synthetic stimulators. Plant

origin preparations could positively influence changes in the condition of cuttings and the content of bioactive components in roses (Monder and Pacholczak, 2018, 2019; Monder et al., 2020) due to supplementation with nutritive substances or unknown rooting cofactors and IAA-like substances present in the bio preparations (Nardi et al., 2015; Oosten et al., 2017). Most bio preparations of plant origin contain different substances similar to auxins in various concentrations (Crouch and Van Staden, 1993; Thorsen et al., 2010; Pacholczak et al., 2016).

DATA AVAILABILITY STATEMENT

The raw data supporting the conclusions of this article will be made available by the authors, without undue reservation.

AUTHOR CONTRIBUTIONS

MM designed the experiment, analyzed the data, and wrote the manuscript with contribution and revision from all the authors. MM made the growth analyses. PK and AJ performed the sample preparations and observations. AJ and MM contributed to anatomy measurements and data analyses. All authors contributed to the article and approved the submitted version.

FUNDING

The experiments were supported by the National Science Center, research project No. NN 310008240.

REFERENCES

Abousalim, A., Walali, L. D. M., and Slaoui, K. (1993). Effect of phenological stage on rooting of semi-hardwood olive cuttings in heated frames. *Olivae* 46, 30–37.

Amissah, J. N., Paolillo, D. J. Jr., and Bassuk, N. (2008). Adventitious root formation in stem cuttings of *Quercus biocolor* and *Quercus macrocarpa* and its relationship to stem anatomy. *J. Amer. Soc. Horticult. Sci.* 133, 479–486. doi: 10.21273/JASHS.133.4.479

Anand, V. K., and Heberlein, G. T. (1975). Seasonal changes in the effects of auxin on rooting in stem cuttings of *Ficus infectoria*. *Physiol. Plant.* 34, 330–334. doi: 10.1111/j.1399-3054.1975.tb03848.x

Beakbane, B. (1969). Relationships between structure and adventitious rooting. *Proc. Int. Plant Prop. Soc.* 19, 192–201.

BioBizz Worldwide B.V., Groningen, The Netherlands (2017). *Root Juice^{TM}*. Available online at: http://www.biobizz.com/products/#root%c2%b7juice (cited January 19, 2017).

Bryant, P. H., and Trueman, S. J. (2015). Stem anatomy and adventitious rot formation in cuttings of *Angophora,Corymbia* and *Eucalyptus*. *Forests* 6, 1337–1238. doi: 10.3390/f6041227

Canna Continental, Los Angeles, USA (2021). *Bio Rhizotonic.* Available online at: https://www.canna.ca/biorhizotonic (cited July, 2021).

Certificaat Bio Roots (2014). *No: C8008445INP-01.2013.* Available online at: http://www.eurohydro.com/pdf/certif-bioboosters.pdf/ (cited January 19, 2017).

Cline, M. N., and Neely, D. (1983). The histology and histochemistry of the wound-healing process in Geranium cuttings. *J. Amer. Soc. Horticult. Sci.* 108, 496–502.

Costa, J. M., Heuvelink, E., Pol, P. A., and Put, H. M. C. (2007). Anatomy and morphology of rooting in leafy rose stem cuttings and starch dynamics following severance. *Acta Hortic.* 751, 495–502. doi: 10.17660/ActaHortic.2007.751.63

Crouch, I. J., and Van Staden, J. (1993). Evidence for the presence of plant growth regulators in commercial seaweed products. *Plant Growth Regul.* 13, 21–29. doi: 10.1007/BF00207588

Davies, F. T. Jr, Lazarte, J. E., and Joiner, J. N. (1982). Initiation and development of roots in juvenile and mature leaf bud cuttings of *Ficuspumila* L. *Amer. J. Bot.* 69, 804–811. doi: 10.2307/2442971

Dawa, S., Rather, Z. A., Stobgais, T., Angdus, T., Lakdan, S., and Tundup, P. (2018). Effect of growth regulators and growth media on the rhizogenesis of some genotypes of rose through stem cuttings. *Int. J. Curr. Microbiol. Appl. Sci.* 7, 1138–1147. doi: 10.20546/ijcmas.2018.701.138

Fascella, G., Militello, M., and Carrubba, A. (2012). Propagation of *Artemisia arborescens* L. by stem-cutting: adventitious root formation under different conditions. *Prop. Ornament. Plants* 12, 171–177. Available online at: https://iris.unipa.it/handle/10447/78600#.YQrrI4gzaUk

Fascella, G., and Zizzo, G. V. (2009). Efficient propagation technique of *Euphorbia x lomi* Thai hybrids. *HortScience* 44, 495–498. doi: 10.21273/HORTSCI.44.2.495

Fouda, R. A., and Schmidt, G. (1994). Histological changes in the stems of some *Rosa* species propagated by leafy cuttings as affected by IBA treatments. *Acta Agron. Hungar.* 43, 265–275.

Ginova, A., Tsvetkov, I., and Kondakova, V. (2012). *Rosa damascena* Mill. – an overview for evaluation of propagation methods. *Bulg. J. Agric. Sci.* 18, 514–556. Available online at: https://www.agrojournal.org/18/04-11-12.pdf

Gustavsson, L. A. (1999). *Rosen Leksikon*. Kopenhaga: RosinanteForlag A/S.

Haissig, B. E. (1974). Origins of adventitious roots. *N. Z. J. For. Sci.* 4, 299–310.

Hartmann, H. T., Kester, D. E., Davies, F. T., and Geneve, R. L. (2011). *Plant Propagation, Principles and Practices*. Prentice-Hall, NJ: Englewood Cliffs.

Hoşafçi, H., Arslan, N., and Sarihan, E. O. (2005). Propagation of dog rose (*Rosa canina* L.) plants by softwood cuttings. *Acta Hortic.* 690, 139–142. doi: 10.17660/ActaHortic.2005.690.20

Howard, B. H., and Harrison-Murray, R. S. (1995). Responses of dark-pre conditioned and normal light grown cuttings of *Syringa vulgaris* 'Madame Lemoine' to light and wetnessgradients in the propagation environment. *J. Hort. Res.* 70, 989–1001. doi: 10.1080/14620316.1995.11515375

Meier, U., Bleiholder, H., Brumme, H., Bruns, E., Mehring, B., Proll, T., et al. (2009). Phenological growth stages of roses (*Rosa* sp.): codification and description according to the BBCH scale. *Ann. Appl. Biol.* 154, 231–238. doi: 10.1111/j.1744-7348.2008.00287.x

Monder, M. J. (2014). Evaluation of growth and flowering of historical cultivars of *Rosa gallica* L. growing in the National Collection of Rose Cultivars in the Polish Academy of Sciences Botanical Garden in Powsin. *Acta Agrobot.* 67, 39–52. doi: 10.5586/aa.2014.036

Monder, M. J. (2021). Response of rambler roses to changing climate conditions in urbanized areas of the european lowlands. *Plants* 10:457. doi: 10.3390/plants10030457

Monder, M. J., Kozakiewicz, P., and Jankowska, A. (2017). Effect of anatomical structure of shoots in different flowering phase on rhizogenesis of once-blooming roses. *Notul. Botan. Hort. Agrobot. Cluj Nap.* 45, 408–416. doi: 10.15835/nbha45210854

Monder, M. J., Kozakiewicz, P., and Jankowska, A. (2019). Anatomical structure changes in stem cuttings of rambler roses induced with plant origin preparations. *Sci. Hortic.* 255, 242–254. doi: 10.1016/j.scienta.2019.05.034

Monder, M. J., Niedzielski, M., and Woliński, K. (2020). Effect of phenological stage and rooting enhancers on physiological parameters in stem cuttings in the process of rhizogenesis of *Rosa* × *alba* 'Maiden's Blush'. *Agriculture* 10:572. doi: 10.3390/agriculture10110572

Monder, M. J., Niedzielski, M., Woliński, K., and Pacholczak, A. (2016). The impact of seasonal changes in plant tissue on rhizogenesis of stem cuttings of the once flowering roses. *Notul. Botan. Hort. Agrobot. Cluj Nap.* 44, 92–99. doi: 10.15835/nbha44110244

Monder, M. J., and Pacholczak, A. (2018). Preparations of plant origin enhance carbohydrate content in plant tissues of rooted cuttings of rambler roses: *Rosa beggeriana* 'Polstjärnan' and *Rosa helenae* 'Semiplena'. *Acta Agric. Scand. B Soil Plant Sci.* 68, 189–198. doi: 10.1080/09064710.2017.1378365

Monder, M. J., and Pacholczak, A. (2019). Rhizogenesis and concentration of carbohydrates in cuttings harvested at different phenological stages of once-blooming rose shrubs and treated with rooting stimulants. *Biol. Agric. Horticult.* 36, 53–70. doi: 10.1080/01448765.2019.1685407

Nardi, S., Pizzeghello, D., Schaivon, M., and Ertani, A. (2015). Plant biostimulants: physiological responses induced by protein hydrolyzed-based products and humic substances in plant metabolism. *Sci. Agricult.* 73, 18–23. doi: 10.1590/0103-9016-2015-0006

OJEU (2009a). *Regulation (EC) No 1107/2009 of the European Parliament and of the Council of 21 October 2009 Concerning the Placing of Plant Protection Products on the Market and Repealing Council Directives 79/117/EEC and 91/414/EEC. L 309/1-50*. Official Journal of the European Union 2009.

OJEU (2009b). *Directive 2009/128/EC of the European Parliament and of the Council of 21 October 2009 Establishing a Framework for Community Action to Achieve the Sustainable Use of Pesticides. L 309/71–86*. Official Journal of the European Union.

OMRI (2021). *OMRI Products List, Web Edition*. Organic Materials Review Institute. Available online at: https://www.omri.org/omri-lists (cited July, 2021).

Oosten, M. J., Pepe, O., Pascale, S., Silletti, S., and Maggio, A. (2017). The role of biostimulants and bioeffectors as alleviators of abiotic stress in crop plants. *Chem. Biol. Technol. Agric.* 4:5. doi: 10.1186/s40538-017-0089-5

Pacholczak, A., Nowakowska, K., and Pietkiewicz, S. (2016). The effects of synthetic auxin and a seaweed-based biostimulator on physiological aspects of rhizogenesis in ninebark stem cuttings. *Notul. Botan. Hort. Agrobot. Cluj Nap.* 44, 85–91. doi: 10.15835/nbha44110061

Pacholczak, A., Szydło, W., Jacygrad, E., and Federowicz, M. (2012). Effect of auxins and the biostimulator Algamino Plant on rhizogenesis in stem cuttings of two dogwood cultivars (*Cornus alba* 'Aurea'and 'Elegantissima'). *Acta Sci. Polon. Hort. Cult.* 11, 93–103. Available online at: https://czasopisma.up.lublin.pl/index.php/asphc/article/view/3042

Pihlajaniemi, H., Siurainen, M., Rautio, P., Laine, K., Peteri, S. L., and Huttunen, S. (2005). Field evaluation of phenology and success of hardy, micropropagated old shrub roses in northern Finland. *Acta Agric. Scand. B Soil Plant Sci.* 55, 275–286. doi: 10.1080/09064710500217128

Rosell, J. A., Olson, M. E., and Anfodillo, T. (2017). Scaling of xylem vessel diameter with plant size: causes, predictions, and outstanding question. *Curr. For. Rep.* 3, 46–59. doi: 10.1007/s40725-017-0049-0

Scagel, C. F. (2004). Changes in cutting composition during early stage of adventitious rooting of miniature rose altered by inoculation of mycorrhizal arbuscular fungi. *J. Amer. Soc. Horticult. Sci.* 129,624–634. doi: 10.21273/JASHS.129.5.0624

Smulders, M. J. M., Arens, P., Bourke, P. M., Debener, T., Linde, M., Riek, J., et al. (2019). In the name of the rose: a roadmap for rose research in the genome era. *Horticul. Res.* 6:65. doi: 10.1038/s41438-019-0156-0

Strzelecka, K. (2017). Anatomical structure and adventitious root formation in *Rhododendron ponticum* L. cuttings. *Acta Scient. Polon. Hort. Cult.* 6, 15–22. Available online at: https://czasopisma.up.lublin.pl/index.php/asphc/article/view/4208

T.A. Terra Aquatica (2021). *Pro Roots. Homepage General Hydroponics Europe / T.A. Terra Aquatica*. Available online at: https://www.eurohydro.com/pro-roots (cited July, 2021).

Thorsen, M. K., Woodward, M., and McKenzie, B. M. (2010). Kelp (*Laminaria digitata*) increases germination and affects rooting and plant vigour in crops and native plants from an arable grassland in the Outer Hebrides, Scotland. *J. Coast. Conserv.* 14, 239–247. doi: 10.1007/s11852-010-0091-6

Torchik, V. (2015). Effect of donor plant phenological phase on root formation of stem cuttings of ornamental *Juniperus* L. cultivars. *Prop. Ornam. Plants* 5, 51–55. Available online at: https://www.journal-pop.org/2005_5_1_51-55.html

USDA (2017). *National Organic Program*. United States Department of Agriculture Available online at: https://www.ams.usda.gov/about-ams/programs-offices/national-organic-program (cited March 16, 2017).

Wróblewska, K. (2013). The influence of benzyladenine and naphthalene-1-acetic acid on rooting and growth of *Fuchsia hybrida* cuttings. *Acta Scient. Polon. Hort. Cult.* 12, 101–113. doi: 10.5586/aa.2012.026

Zhang, S.-Y. (1992). Systematic wood anatomy of the *Rosaceae*. *Blumea* 3, 81–158.

Zheng, F., Tao, Z., Liu, Y., Xu, Y., Dai, J., and Ge, Q. (2016). Variation of main phenophases in phenological calendar in East China and their response to climate change. *Adv. Meteorol.* 2016:9546380. doi: 10.1155/2016/9546380

Conflict of Interest: The authors declare that the research was conducted in the absence of any commercial or financial relationships that could be construed as a potential conflict of interest.

Publisher's Note: All claims expressed in this article are solely those of the authors and do not necessarily represent those of their affiliated organizations, or those of the publisher, the editors and the reviewers. Any product that may be evaluated in this article, or claim that may be made by its manufacturer, is not guaranteed or endorsed by the publisher.

frontiers in Plant Science

ORIGINAL RESEARCH
published: 20 September 2021
doi: 10.3389/fpls.2021.745402

Differential Effects of Exogenous Glomalin-Related Soil Proteins on Plant Growth of Trifoliate Orange Through Regulating Auxin Changes

*Rui-Cheng Liu[1], Wei-Qin Gao[1], Anoop Kumar Srivastava[2], Ying-Ning Zou[1], Kamil Kuča[3], Abeer Hashem[4], Elsayed Fathi Abd_Allah[5] and Qiang-Sheng Wu[1,3]**

[1] College of Horticulture and Gardening, Yangtze University, Jingzhou, China, [2] ICAR-Central Citrus Research Institute, Nagpur, India, [3] Department of Chemistry, Faculty of Science, University of Hradec Kralove, Hradec Kralove, Czechia, [4] Botany and Microbiology Department, College of Science, King Saud University, Riyadh, Saudi Arabia, [5] Plant Production Department, College of Food and Agricultural Sciences, King Saud University, Riyadh, Saudi Arabia

Multiple functions of glomalin released by arbuscular mycorrhizal fungi are well-recognized, whereas the role of exogenous glomalins including easily extractable glomalin-related soil protein (EE-GRSP) and difficultly extractable glomalin-related soil protein (DE-GRSP) is unexplored for plant responses. Our study was carried out to assess the effects of exogenous EE-GRSP and DE-GRSP at varying strengths on plant growth and chlorophyll concentration of trifoliate orange (*Poncirus trifoliata*) seedlings, along with changes in root nutrient acquisition, auxin content, auxin-related enzyme and transporter protein gene expression, and element contents of purified GRSP. Sixteen weeks later, exogenous GRSP displayed differential effects on plant growth (height, stem diameter, leaf number, and biomass production): the increase by EE-GRSP and the decrease by DE-GRSP. The best positive effect on plant growth occurred at exogenous EE-GRSP at ½ strength. Similarly, the GRSP application also differently affected total chlorophyll content, root morphology (total length, surface area, and volume), and root N, P, and K content: positive effect by EE-GRSP and negative effect by DE-GRSP. Exogenous EE-GRSP accumulated more indoleacetic acid (IAA) in roots, which was associated with the upregulated expression of root auxin synthetic enzyme genes (*PtTAA1*, *PtYUC3*, and *PtYUC4*) and auxin influx transporter protein genes (*PtLAX1*, *PtLAX2*, and *PtLAX3*). On the other hand, exogenous DE-GRSP inhibited root IAA and indolebutyric acid (IBA) content, associated with the downregulated expression of root *PtTAA1*, *PtLAX1*, and *PtLAX3*. Root IAA positively correlated with root *PtTAA1*, *PtYUC3*, *PtYUC4*, *PtLAX1*, and *PtLAX3* expression. Purified EE-GRSP and DE-GRSP showed similar element composition but varied in part element (C, O, P, Ca, Cu, Mn, Zn, Fe, and Mo) concentration. It concluded that exogenous GRSP triggered differential effects on growth response, and the effect was associated with the element content of pure GRSP and the change in auxins and root morphology. EE-GRSP displays a promise as a plant growth biostimulant in citriculture.

Keywords: auxin, carrier protein, citrus, glomalin, mycorrhiza, IAA, transporter protein

OPEN ACCESS

Edited by:
Maurizio Ruzzi,
University of Tuscia, Italy

Reviewed by:
Qing Yao,
South China Agricultural University, China
Qingjiang Wei,
Jiangxi Agricultural University, China

***Correspondence:**
Qiang-Sheng Wu
wuqiangsh@163.com

Specialty section:
This article was submitted to Plant Nutrition, a section of the journal Frontiers in Plant Science

Received: *22 July 2021*
Accepted: *17 August 2021*
Published: *20 September 2021*

Citation:
Liu R-C, Gao W-Q, Srivastava AK, Zou Y-N, Kuča K, Hashem A, Abd_Allah EF and Wu Q-S (2021) Differential Effects of Exogenous Glomalin-Related Soil Proteins on Plant Growth of Trifoliate Orange Through Regulating Auxin Changes. Front. Plant Sci. 12:745402. doi: 10.3389/fpls.2021.745402

INTRODUCTION

Arbuscular mycorrhizal fungi (AMF) in the soil are extensively reported to colonize the roots of roughly 80% of terrestrial plants, forming arbuscular mycorrhizas (AMs). AMs help the host plant to absorb water and nutrients, whereas the host delivers the photoassimilates to the mycorrhizal fungi in the root for their growth (Huang et al., 2021a). Such mycorrhizal symbiosis represents important functions on promoting plant growth, improving stress resistance, enriching rhizospheric microbial diversity, and stabilizing ecosystems (Zhao et al., 2015; Wang et al., 2018). Spores and mycelium of AMF release an N-linked glycoprotein (glomalin) into the soil, popularly known as glomalin-related soil protein (GRSP) according to the Bradford assay (Rillig, 2004; Rillig and Mummey, 2010). GRSP is primarily divided into two fractions, viz., easily extractable GRSP (EE-GRSP) and difficultly extractable GRSP (DE-GRSP) (Koide and Peoples, 2013; Wu et al., 2014). EE-GRSP is considered to be newly produced by AMF and relatively more labile, whereas DE-GRSP originates from the turnover of EE-GRSP and thus represents a comparatively older glomalin of an inactive nature (Koide and Peoples, 2013; Wu et al., 2015a). Earlier studies indicated that GRSP promoted the storage of soil organic carbon (SOC), improved the distribution and stability of soil water-stable aggregate (WSA), enhanced the drought tolerance of plants, and reduced the metal toxicity of soil (Zou et al., 2014; Gao et al., 2019; He et al., 2020; Meng et al., 2020). The direct contribution of GRSP on WSA stability was much stronger than mycorrhizal extraradical hyphae or root mycorrhizal colonization (Rillig et al., 2001; Wu et al., 2014).

Studies have shown that GRSP was composed of 3–5% N, 36–59% C, 4–6% H, 33–49% O, 0.03–0.1% P, 0.8–8.8% Fe, and other cations (e.g., K, Ca, Si, Cu, and Mg), depending upon soil properties (Rillig et al., 2001; Lovelock et al., 2004; Nichols, 2008; Zhang et al., 2017a). Schindler et al. (2007) observed that the GRSP of peat soil contained aromatic hydrocarbons (42–49%), carboxyl groups (24–30%), and carbohydrates (4–16%) evident from the analysis of nuclear magnetic resonance (NMR). GRSP is, thus, a mixture, rich in various elements, essential to plant growth and development. Based on the mineral elements in GRSP, it is reasonable to hypothesize that GRSP as a biostimulant potentially improves plant growth responses. To confirm this hypothesis, Wang et al. (2015) firstly observed that the concentration of exogenous EE-GRSP was curvilinearly related with plant biomass yield in potted trifoliate orange (*Poncirus trifoliata* L. Raf.), with ½ strength of EE-GRSP exhibiting the highest magnitude of growth responses. Wu et al. (2015b) through a field study proved that exogenous EE-GRSP treatment produced a significant increase in SOC and soil phosphatase activity in 27-year-old Satsuma mandarin grafted on trifoliate orange. Chi et al. (2018) reported that ½ strength of exogenous EE-GRSP improved leaf gas exchange, iron-superoxide dismutase activity, abscisic acid, indole-acetic acid (IAA), and methyl jasmonate concentrations in leaves of potted trifoliate orange seedlings exposed to soil drought stress. These studies demonstrated the ability of exogenous EE-GRSP in improving plant growth response (Zou et al., 2015).

Although these experiments have shown an improved effect of exogenous EE-GRSP on plants, the underlying mechanisms remain still unclear. It is also unknown whether DE-GRSP, another fraction of GRSP, has a similar beneficial response on plant growth. Therefore, the present work aimed at evaluating the response of exogenous EE-GRSP and DE-GRSP at varying strengths on the growth of trifoliate orange seedlings, and at revealing the mechanism of GRSP affecting plant growth by analyzing the changes of auxins, gene expression, and mineral elements of purified GRSP fractions.

MATERIALS AND METHODS

Preparation of Exogenous EE-GRSP and DE-GRSP

Soil samples were collected from a citrus orchard (located at the campus of Yangtze University), air-dried, sieved through 4-mm nylon, incubated with 20 mmol/L citrate buffer (pH 7.0) (m:v = 1:8) at 121°C and 0.11 MPa for 30 min and centrifuged at 10,000 × *g*/min for 5 min. The supernatant was collected as an exogenous full-strength EE-GRSP solution. The residues of EE-GRSP extraction in the centrifugal tube was continued to incubate with the same volume of 50 mmol/L sodium citrate buffer (pH 8.0) at 121°C and 0.11 MPa for 60 min, and centrifuged at 10,000 × *g*/min for 10 min (Wu et al., 2015a). The second supernatant was collected as a full-strength DE-GRSP solution. The soluble protein concentration was 0.24 and 0.36 mg/L in full-strength EE-GRSP and DE-GRSP solution, as put forward by the Bradford (1976) assay. A total of about 12 L of full-strength EE-GRSP and DE-GRSP solution were collected, respectively, along with 1.5 kg of the soil used.

Experimental Design

In a completely randomized design, the experiment consisted of seven treatments: (i) control with 20 mmol/L citrate buffer (pH 7.0) (0 GRSP), (ii) quarter-strength EE-GRSP (¼ EE-GRSP), (iii) half-strength EE-GRSP (½ EE-GRSP), (iv) full-strength EE-GRSP (1 EE-GRSP), (v) quarter-strength DE-GRSP (¼ DE-GRSP), (vi) half-strength DE-GRSP (½ DE-GRSP), and (vii) full-strength DE-GRSP (1 DE-GRSP). The ½ and ¼ EE-GRSP was diluted with the full-strength EE-GRSP with 20 mmol/L citrate buffers (pH 7.0), and the ½ and ¼ DE-GRSP was prepared using the full-strength DE-GRSP by diluting with 50 mmol/L citrate buffers (pH 8.0). Each treatment was replicated four times, and each replicate consisted of two pots, resulting in a total of 56 pots (corresponding to 168 seedlings).

Plant Setup

Three four-leaf-old trifoliate orange seedlings grown in autoclaved sand were transplanted into a plastic pot (2.1-L), in which 1.6 kg of autoclaved (121°C, 0.11 MPa, 2 h) soil sieved with 4-mm-size nylon was supplied. After 2 weeks of plant acclimatization, exogenous GRSP treatments were initiated. A 50 ml of exogenous EE-GRSP or DE-GRSP solution as per the proposed strength was applied into the corresponding pot at weekly intervals, for a total of 16 times. The experiment was carried out in an intelligent artificial climate chamber (AGC-P,

Zhejiang QiuShi Artificial Environment Co., Ltd., Hangzhou, China) from March 22 to July 21, 2018, where the photon? ux density was 900 μmol/m^2/s, day/night temperature 28/20°C, and relative air humidity 68% during the experiment.

Determination of Plant Growth and Chlorophyll Concentrations

Plant height, stem diameter, and leaf number were recorded before harvest. The seedlings were divided into shoots and roots. The intact roots were scanned using the Epson Perfection V700 Photo Dual Lens System (J221A, Seiko Epson Corporation, Jakarta Selatan, Indonesia). The scanned root images were analyzed using the WinRHIZO software (Regent Instruments Inc., Montreal, QC, Canada) to obtain root morphological variables including total length, surface area, and volume. Subsequently, shoot and root biomass was weighed after drying at 75°C for 48 h. The total chlorophyll concentration was determined by the procedure suggested by Arnon (1949).

Determination of Root Nutrient Acquisition

Root samples were digested in H_2SO_4 and H_2O_2. Subsequently, N content was determined by a chemical analyzer (Smartchem 200, Scientific Instruments Limited, Weston, FL, USA), and other mineral elements were assayed with the help of the ICP-Spectrometer (IRIS Advantage, Thermo Fisher Scientific Inc., Waltham, MA, USA).

Determination of Root Auxins

Root IAA and indolebutyric acid (IBA) were extracted according to the method outlined by Dobrev and Kamínek (2002) with minor modification. The 0.2 g of root samples was ground in liquid nitrogen, extracted by adding 1 ml of pre-cooled extracting solution (methanol, distilled water, and formic acid, 15/4/1, v/v/v) for 12 h at 4°C, and centrifuged at 8,000 × *g*/min for 10 min. The centrifuged residue was re-extracted with 0.5 ml of the extracting solution for 2 h at 4°C. After centrifugation, two supernatants were combined, evaporated at 40°C under reduced pressure to near dryness (∼0.5 ml), and decolorized three times with 0.5 ml of petroleum ether. After discarding the upper ether phase, the down phase was evaporated to the dryness at 40°C under reduced pressure, and 0.5-ml mobile phase (methanol and ddH_2O in a ratio of 2:3) was added to dissolve. The content of IAA and IBA was determined with the help of high-performance liquid chromatography (HPLC; LC-100, Shanghai Wufeng Scientific Instrument Co., Ltd., Shanghai, China). The injection volume was 10 μl, the flow rate was 0.8 ml/min, the column temperature was 35°C, the sampling time was 40 min, and the detection wavelength was 254 nm.

Expression Levels of Genes Associated With IAA

The extraction of total RNA from the roots and the reverse transcription of RNA were carried out according to the protocol previously described by Liu et al. (2018a). Four genes associated with IAA synthesis (*PtTAA1*, *PtTAR2*, *PtYUC3,* and *PtYUC4*) and four influx transporter protein genes of auxins (*PtAUX1*, *PtLAX1*, *PtLAX2,* and *PtLAX3*) were associated with the IAA synthesis and transport in trifoliate orange (Liu et al., 2018b) and selected according to the genome database of trifoliate orange (http://citrus.hzau.edu.cn/orange/index.php) (Huang et al., 2021b). The primers (**Table 1**) of these selected genes were designed with Primer 5. The *β-actin* was used as the housekeeping gene. The quantitative reverse transcription (qRT)-PCR was carried out using the conditions described by Liu et al. (2018a). The relative quantitative expression of genes was calculated by the $2^{-\Delta\Delta CT}$ method as suggested by Livak and Schmittgen (2001).

Determination of Nutrient Elements in Purified EE-GRSP and DE-GRSP

We chose to purify the full-strength GRSP solution in order to study the difference in nutrient composition between exogenous EE-GRSP and DE-GRSP. The purification of EE-GRSP and DE-GRSP was performed according to the method described by He et al. (2020). The extracted full-strength GRSP solution was precipitated with HCl solution, dissolved with NaOH solution, dialyzated in a dialysis bag (MD 44-1000) with ddH_2O, centrifuged at 5,000 × *g*/min for 5 min, and then freeze-dried. The nutrient elements, viz., C, H, O, S, and N contents of purified EE-GRSP and DE-GRSP, were analyzed by the Automatic Element Analyzer (Euro Vector EA3000, Shanghai Woolong Instrument Co., Ltd, Shanghai, China), whereas other elements were determined as per the ICP-Spectrometer (Optima 8000, PerkinElmer, Melville, NY, USA).

Statistical Analysis

The generated data were statistically analyzed by ANOVA through the SAS software (v8.1; SAS Institute Inc., Cary, NC, USA). The significant difference between treatments was compared with Duncan's multiple range test at 0.05 levels. Pearson's correlation coefficient was calculated with the help of the SAS software.

RESULTS

Changes in Growth Performance

Compared with the control (0 GRSP), exogenous EE-GRSP significantly increased plant height, leaf number, stem diameter, and shoot and root biomass of trifoliate orange seedlings, with ½ EE-GRSP treatment having the most significant effect, increasing 17, 19, 22, 52, and 38%, respectively (**Figure 1** and **Table 2**). By contrast, the growth response of DE-GRSP treatment was completely different from that of exogenous EE-GRSP, resulting in a significant inhibition in these plant growth parameters. The inhibiting effect of DE-GRSP on growth increased with the increase of DE-GRSP concentrations. Compared with 0 GRSP, 1 DE-GRSP significantly reduced plant height, leaf number, stem diameter, and shoot and root biomass by 61, 52, 50, 71, and 41%, respectively.

Changes in Chlorophyll Concentration

Application of exogenous EE-GRSP significantly increased leaf total chlorophyll concentration, independent of the concentrations, with ½ EE-GRSP treatment displaying the

TABLE 1 | Specific primer sequences of genes used in this study for quantitative reverse transcription (qRT)-PCR.

Genes	Accession number	Forward primer (5′ → 3′)	Reverse primer (5′ → 3′)
PtTAA1	Pt4g006620	TTTGAGGCGTTTTGGAGGAA	TTGTTGATTGCTTCAGCGAGTT
PtTAR2	Pt3g005090	CACACACGGCACACCCCTA	GCCTCCCACTCCCCAGATC
PtYUC3	Pt9g009520	CCTTCAGGTTTAGCCGTTGC	GGAAGTTTGGAAGTTGGCAGA
PtYUC4	Pt1g005780	GACCATCTGGGTTAGCCGTTT	GTATTTTGGGAAGTTTTCAGGGA
PtAUX1	Pt6g013420	CTTGACTCTGCCCTATTCATTCTC	TGGACCCAGTAACCCATCAAGC
PtLAX1	Pt4g022040	TTGGCGGACATGCAGTGAC	CAGCGGCAGCAGAAGGAAT
PtLAX2	Pt8g001790	TGTGGGAAGATGGGTAGGGAC	TAGTVATGCTCGCCCACCC
PtLAX3	Pt5g008650	ATCACTTTCGCTCCTGCTGC	CAAACCCAAATCCCACCACTA
β-Actin	Pt7g003560	CCGACCGTATGAGCAAGGAAA	TTCCTGTGGACAATGGATGGA

Gene accession number is from the genome database of trifoliate orange.

FIGURE 1 | Growth performance of trifoliate orange by exogenous EE-GRSP and DE-GRSP at varying strength. DE-GRSP, difficultly extractable glomalin-related soil protein; EE-GRSP, easily extractable glomalin-related soil protein.

highest magnitude of response (**Figure 2**). Nevertheless, all the DE-GRSP treatments significantly reduced total chlorophyll concentration compared with 0 GRSP treatment. In a regression analysis between chlorophyll concentration and EE-GRSP and DE-GRSP concentration, a quadratic relationship was observed with exogenous EE-GRSP treatments, showing the highest total chlorophyll concentration occurring between 0.012 and 0.018 mg protein/ml (**Figure 3A**). And with exogenous DE-GRSP treatment conditions, total chlorophyll concentration was negatively and linearly correlated with DE-GRSP concentration (**Figure 3B**).

Changes in Root Mineral Element Contents

Application of exogenous GRSP influenced the root nutrient acquisition to varying proportions. Compared with the control (0 GRSP), ¼ EE-GRSP treatment significantly increased root N, P, K, Ca, Mg, Zn, and Fe content by 7, 43, 42, 342, 8, 32, and 5%, respectively; ½ EE-GRSP treatment dramatically increased root N, P, K, Ca, Mg, Cu, and Fe content by 21, 23, 60, 314, 84, 50, and 12%, respectively; 1 EE-GRSP significantly increased root N, P, K, and Zn content by 12, 84, 12, and 35%, respectively (**Table 3**). However, compared with 0 GRSP, ¼ DE-GRSP treatment significantly reduced root N, P, K, Mg, Cu, Zn, and Fe content by 22, 31, 23, 17, 27, 22, and 78%, respectively; ½ DE-GRSP decreased root N, P, K, Mg, Cu, Zn, and Fe content by 21, 15, 34, 19, 3, 32, and 70%, respectively; and 1 DE-GRSP treatment reduced root N, P, K, Mg, Cu, Zn, and Fe content by 20, 29, 31, 25, 46, 32, and 59%, respectively. However, EE-GRSP and DE-GRSP displayed no significant effect on root Mn content.

Changes in Root Morphology

Compared with the control, ¼ EE-GRSP treatment had no significant effect on root total length, root surface area, and root volume, whereas ½ EE-GRSP treatment significantly increased root total length, surface area, and volume by 25, 35, and 43%, respectively (**Figures 4A–C**). Application of 1 EE-GRSP distinctly increased root total length and surface area by 27 and 17%, respectively, with no significant effect on root volume. Exogenous application of DE-GRSP, however, almost significantly decreased root total length, surface area, and volume compared to the control, with increasing DE-GRSP strength, except that there was no difference in root volume between ¼ DE-GRSP and the control.

Changes in Element Composition of Purified GRSP

From the purified EE-GRSP and DE-GRSP, we collectively detected C, H, O, N, P, K, Ca, Mg, Cu, Al, Mn, Mo, Zn, and Fe, and some elements were below a detection concentration (**Figures 5A–C**). A significant difference in element content

TABLE 2 | Effects of exogenous GRSP on plant growth performance of potted trifoliate orange seedlings.

Treatments	Plant height (cm)	Leaf number (#/plant)	Stem diameter (mm)	Biomass (g DW/plant)	
				Shoot	Root
0 GRSP	19.68 ± 0.22c	17.55 ± 0.19d	2.01 ± 0.08c	0.96 ± 0.07c	0.68 ± 0.04c
¼ EE-GRSP	21.83 ± 0.33b	19.13 ± 0.15b	2.59 ± 0.06a	1.02 ± 0.08c	0.73 ± 0.05b
½ EE-GRSP	23.06 ± 0.44a	20.85 ± 0.17a	2.45 ± 0.13a	1.46 ± 0.10a	0.94 ± 0.08a
1 EE-GRSP	21.47 ± 0.19b	18.58 ± 0.34c	2.22 ± ± 0.14b	1.10 ± 0.11b	0.73 ± 0.07b
¼ DE-GRSP	10.63 ± 0.34d	9.93 ± 0.15e	1.51 ± 0.04e	0.37 ± 0.03d	0.53 ± 0.05d
½ DE-GRSP	8.83 ± 0.14e	9.00 ± 0.24f	1.77 ± 0.07d	0.32 ± 0.03d	0.49 ± 0.05d
1 DE-GRSP	7.67 ± 0.11f	8.50 ± 0.16f	1.00 ± 0.06f	0.28 ± 0.03e	0.40 ± 0.03e

Data (mean ± SD, n = 4) followed by the different letters among treatments indicate significant differences at $p < 0.05$.
DE-GRSP, difficultly extractable glomalin-related soil protein; EE-GRSP, easily extractable glomalin-related soil protein.

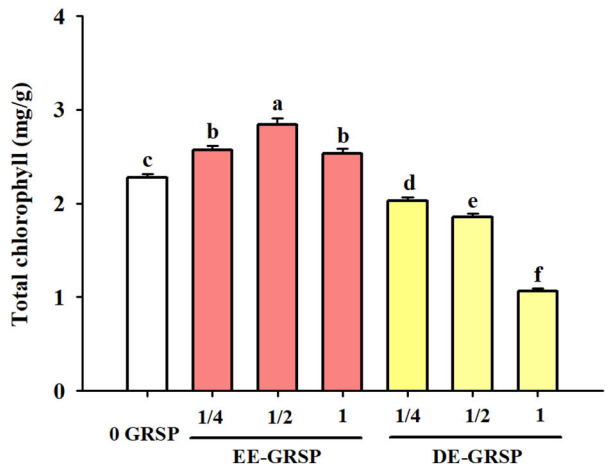

FIGURE 2 | Effects of exogenous EE-GRSP and DE-GRSP on total chlorophyll concentration in leaves of trifoliate orange seedlings. Data (mean ± SD, $n = 4$) followed by different letters above the bars indicate significant differences ($p < 0.05$). DE-GRSP: difficultly extractable glomalin-related soil protein; EE-GRSP: easily extractable glomalin-related soil protein.

between purified EE-GRSP and purified DE-GRSP was observed. H, N, K, Al, and Mg content were not significantly different between two GRSP fractions. Purified DE-GRSP showed higher C, Ca, Cu, Mn, Zn, and Fe content than purified EE-GRSP by 52, 41, 43, 45, 38, and 55%, respectively. Purified EE-GRSP, however, had 9, 40, and 334% significantly higher O, P, and Mo content, respectively, than purified DE-GRSP.

Changes in Root Auxins

Compared with the control treatment, ¼ EE-GRSP treatment significantly reduced root IAA and IBA content by 25 and 23%, respectively (**Figure 6**); ½ EE-GRSP treatment registered an increase in root IAA and IBA content by 121 and 87%, respectively; and 1 EE-GRSP treatment recorded the increase in root IAA content by 40%, but decreased root IBA content by 10%. On the other hand, exogenous DE-GRSP application showed a decreasing trend on root IAA and IBA content. Compared with 0 GRSP treatment, ¼ DE-GRSP, ½ DE-GRSP, and 1 DE-GRSP treatment reduced root IAA content by 51, 40, and 33%, respectively, with the corresponding reduction in root IBA content by 52, 41, and 30%, respectively.

Changes in Expression of Root Genes Associated With Auxin Synthesis

Compared with the control, root *PtTAA1* expression was induced by exogenous ¼ EE-GRSP and ½ EE-GRSP, whereas it was inhibited by exogenous DE-GRSP with full strength (**Figure 7A**). Root *PtTAR2* expression was not affected by exogenous EE-GRSP, whereas it was downregulated by ¼ and 1 DE-GRSP application, accompanied by upregulated expression of *PtTAR2* by ½ DE-GRSP (**Figure 7B**). The *PtYUC3* expression was upregulated by exogenous EE-GRSP, along with increased expression with an increase in the concentration of EE-GRSP, but the *PtYUC3* expression remained unaffected by exogenous DE-GRSP, independent of its concentration (**Figure 7C**). The *PtYUC4* expression was increased by exogenous ¼ EE-GRSP but inhibited by ¼ DE-GRSP (**Figure 7D**).

Changes in Expression Levels of Root Auxin Influx Transporter Protein Genes

Application of ¼ and ½ EE-GRSP treatment upregulated *PtLAX1* and *PtLAX2* expression, coupled with downregulated expression of *PtLAX1* with ¼ DE-GRSP and *PtLAX2* with 1 DE-GRSP, compared with the control (**Figures 7E,F**). Root *PtLAX3* expression was increased by ½ EE-GRSP while reduced by ½ DE-GRSP (**Figure 7G**). Root *PtAUX1* expression was induced by 1 DE-GRSP, whereas inhibited by ¼ and ½ DE-GRSP (**Figure 7H**).

Correlation Between Root IAA Concentration and Gene Expression Levels

Root IAA was significantly and positively correlation with *PtTAA1* ($p < 0.01$), *PtYUC3* ($p < 0.01$), *PtYUC4* ($p < 0.05$), *PtLAX1* ($p < 0.01$), and *PtLAX3* ($p < 0.01$), respectively (**Table 4**). However, there was no any significant correlation of root IAA with *PtTAR2*, *PtLAX2*, and *PtAUX1*.

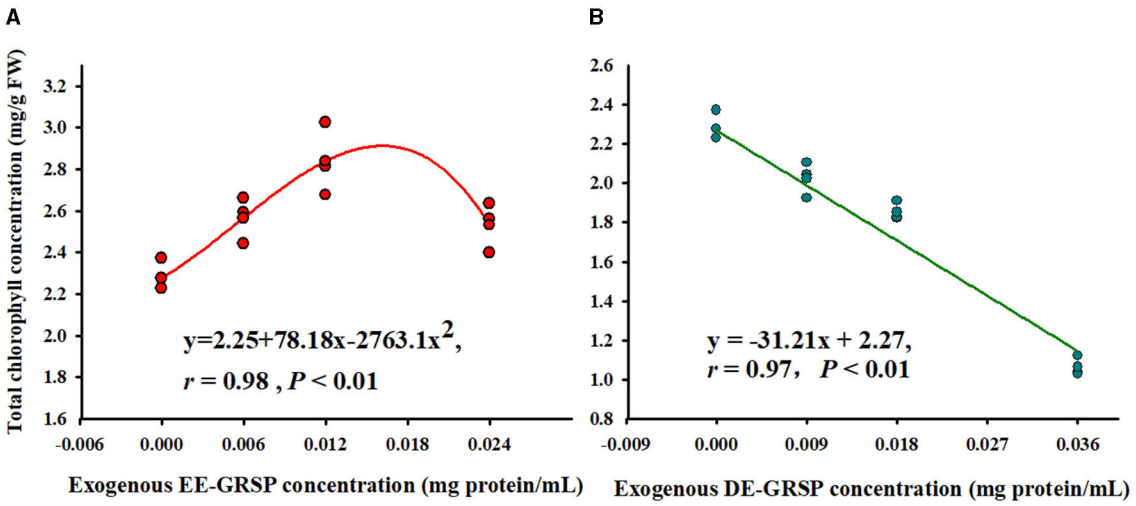

FIGURE 3 | Correlation between exogenous EE-GRSP **(A)** and exogenous DE-GRSP **(B)** and total chlorophyll concentration ($n = 16$). DE-GRSP, difficultly extractable glomalin-related soil protein; EE-GRSP, easily extractable glomalin-related soil protein.

TABLE 3 | Effects of exogenous EE-GRSP and DE-GRSP on nutrient acquisition in roots of trifoliate orange seedlings.

Treatments	N (%)	P (g/kg)	K (g/kg)	Ca (g/kg)	Mg (g/kg)	Cu (mg/kg)	Zn (mg/kg)	Mn (mg/kg)	Fe (mg/kg)
0 GRSP	1.07 ± 0.02d	2.03 ± 0.02d	9.60 ± 0.42d	6.11 ± 0.25cd	3.09 ± 0.09c	14.14 ± 0.82b	11.68 ± 0.54b	47.68 ± 6.64a	1720.49 ± 31.61c
¼ EE-GRSP	1.14 ± 0.03c	2.90 ± 0.03b	13.66 ± 0.59b	27.03 ± 1.09a	3.35 ± 0.08b	16.35 ± 0.37b	15.38 ± 0.72a	46.73 ± 7.00a	1804.40 ± 32.99b
½ EE-GRSP	1.29 ± 0.03a	2.50 ± 0.03c	15.33 ± 0.66a	25.28 ± 1.04b	5.69 ± 0.14a	21.22 ± 5.67a	10.21 ± 0.48c	44.90 ± 6.73a	1927.29 ± 35.33a
1 EE-GRSP	1.20 ± 0.03b	3.73 ± 0.04a	10.76 ± 0.47c	6.20 ± 0.25cd	2.75 ± 0.07d	17.14 ± 3.31b	15.82 ± 0.74a	45.66 ± 6.83a	1752.08 ± 32.12c
¼ DE-GRSP	0.83 ± 0.01e	1.40 ± 0.02f	7.39 ± 0.32e	6.44 ± 0.26cd	2.56 ± 0.06e	10.27 ± 0.59c	9.07 ± 1.82c	46.80 ± 2.90a	380.40 ± 6.97f
½ DE-GRSP	0.85 ± 0.02e	1.72 ± 0.02e	6.38 ± 0.28f	7.02 ± 0.28c	2.49 ± 0.06e	9.95 ± 1.15c	7.99 ± 0.37d	42.78 ± 3.38a	520.82 ± 9.67e
1 DE-GRSP	0.86 ± 0.02e	1.44 ± 0.02f	6.59 ± 0.29f	5.83 ± 0.24d	2.32 ± 0.06f	7.63 ± 0.44d	7.97 ± 0.37d	44.25 ± 6.32a	703.47 ± 12.86d

Data (mean ± SD, n = 4) followed by the different letters among treatments indicate significant differences at $p < 0.05$.
DE-GRSP, difficultly extractable glomalin-related soil protein; EE-GRSP, easily extractable glomalin-related soil protein.

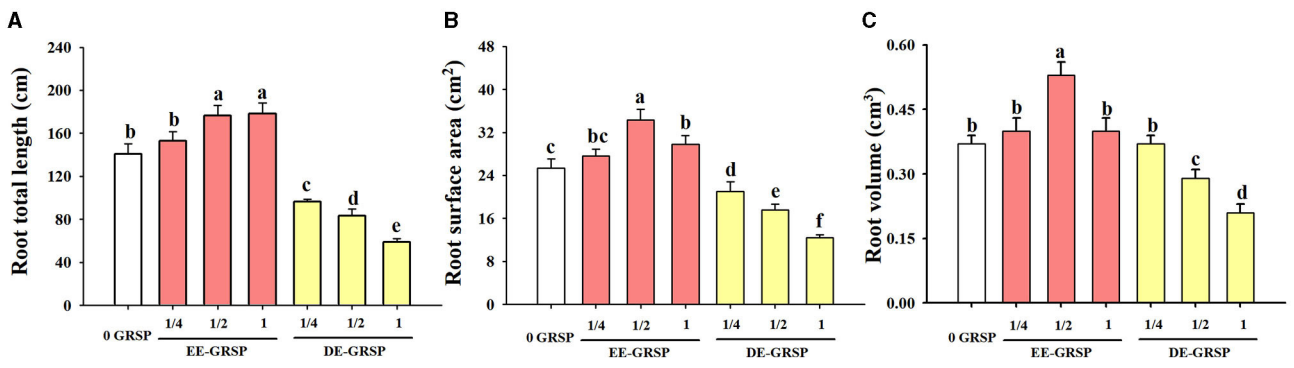

FIGURE 4 | Effects of exogenous EE-GRSP and DE-GRSP on root total length **(A)**, root surface area **(B)**, and root volume **(C)** of trifoliate orange. Data (mean ± SD, $n = 4$) followed by different letters above the bars indicate significant differences ($p < 0.05$). DE-GRSP, difficultly extractable glomalin-related soil protein; EE-GRSP, easily extractable glomalin-related soil protein.

DISCUSSION

In this study, we firstly observed a difference in plant growth response of trifoliate orange with exogenous application of two GRSP fractions. Exogenous EE-GRSP strongly promoted plant growth, whereas exogenous DE-GRSP distinctly inhibited plant growth. Such results provide important clues in favor of EE-GRSP functioning as a growth promoter of trifoliate

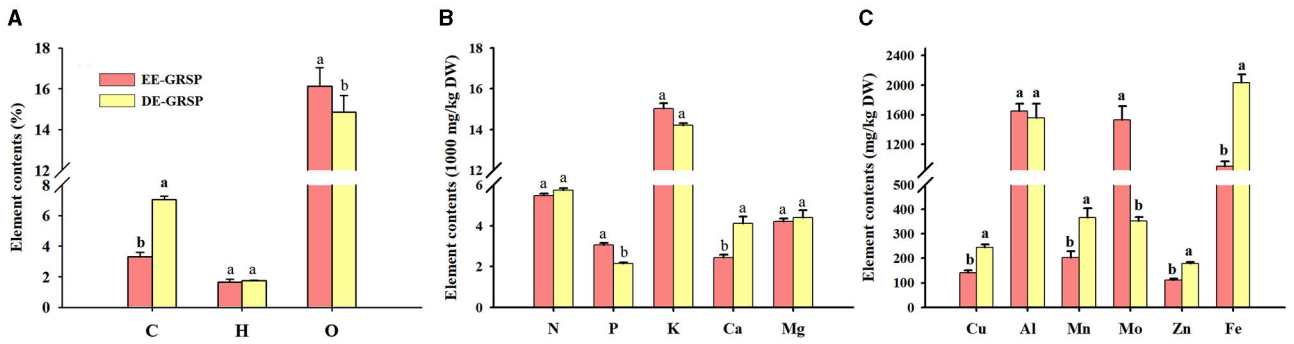

FIGURE 5 | Differences in the element content [**(A)**: C, H, and O; **(B)**: N, P, K, Ca, and Mg; **(C)**: Cu, Al, Mn, Mo, Zn, and Fe] in purified EE-GRSP and DE-GRSP. Data (mean ± SD, $n = 4$) followed by different letters above the bars indicate significant differences ($p < 0.05$). DE-GRSP, difficultly extractable glomalin-related soil protein; EE-GRSP, easily extractable glomalin-related soil protein.

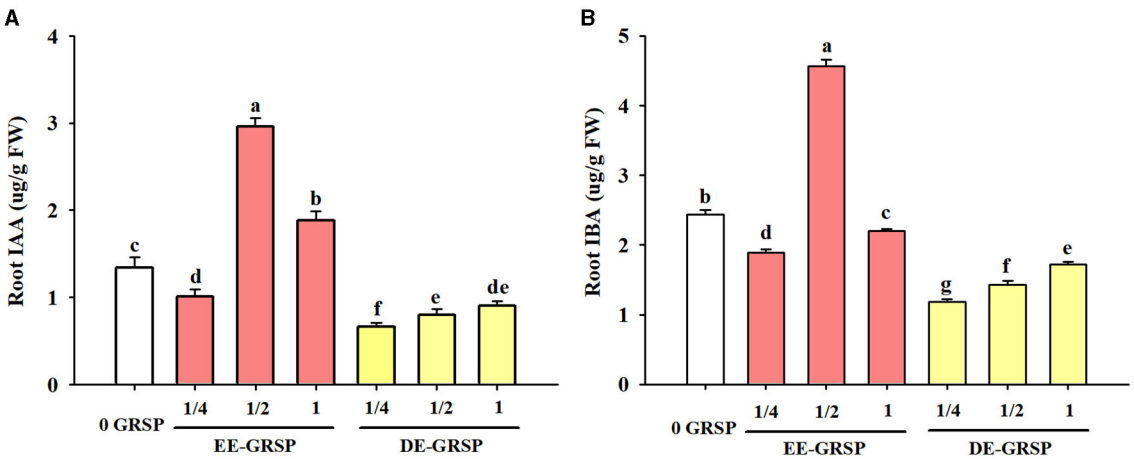

FIGURE 6 | Effects of exogenous EE-GRSP and DE-GRSP on root IAA **(A)** and IBA **(B)** concentrations of trifoliate orange seedlings. Data (mean ± SD, $n = 4$) followed by different letters above the bars indicate significant differences ($p < 0.05$). DE-GRSP, difficultly extractable glomalin-related soil protein; EE-GRSP, easily extractable glomalin-related soil protein; IAA, indoleacetic acid; IBA, indolebutyric acid.

orange. The increase in plant growth response to EE-GRSP treatments was consistent with the findings of Wang et al. (2015). It is well-known that GRSP contained an amount of humic acid (Gadkar and Rillig, 2006), similar to NMR spectrum-based humic acid (Schindler et al., 2007). Humic acid as an important component of humic substance, a part of natural organic matter, could improve the growth performance of various plants (Spohn and Giani, 2010; Mora et al., 2012; Xu et al., 2012; Duan, 2014; Dong et al., 2016). It is believed that EE-GRSP having a parallel NMR spectrum-based humic acid-like substance, functions in increasing plant growth. On the other hand, plant height, stem diameter, leaf number, and biomass production decreased significantly after the application of DE-GRSP, and the inhibitory effect increased with the increase of exogenous DE-GRSP concentration. Perhaps DE-GRSP contains some impurities (Gillespie et al., 2011) that are detrimental to plant growth, but it is not clear about the nature of those impurities responsible for such undesirable plant responses. EE-GRSP, an active form of newly produced glomalin, and DE-GRSP, a recalcitrant and older glomalin (Wu et al., 2015a), also contribute primarily toward difference in magnitude of plant response. More studies have to be conducted to analyze the difference in molecular structure and relevant properties between EE-GRSP and DE-GRSP.

In the present study, leaf total chlorophyll content was differentially affected by EE-GRSP and DE-GRSP. Exogenous EE-GRSP significantly increased total chlorophyll content, and the most significant effect was observed with ½ EE-GRSP. In contrast, exogenous DE-GRSP caused a significant decrease in total chlorophyll content. Our study also revealed that GRSP contained many mineral elements, such as Fe and Mg, which are part of chlorophyll (Schindler et al., 2007). In addition, EE-GRSP as a heat-shock protein-like substance could keep the stability of PSII complexes and thylakoid membrane, which plays

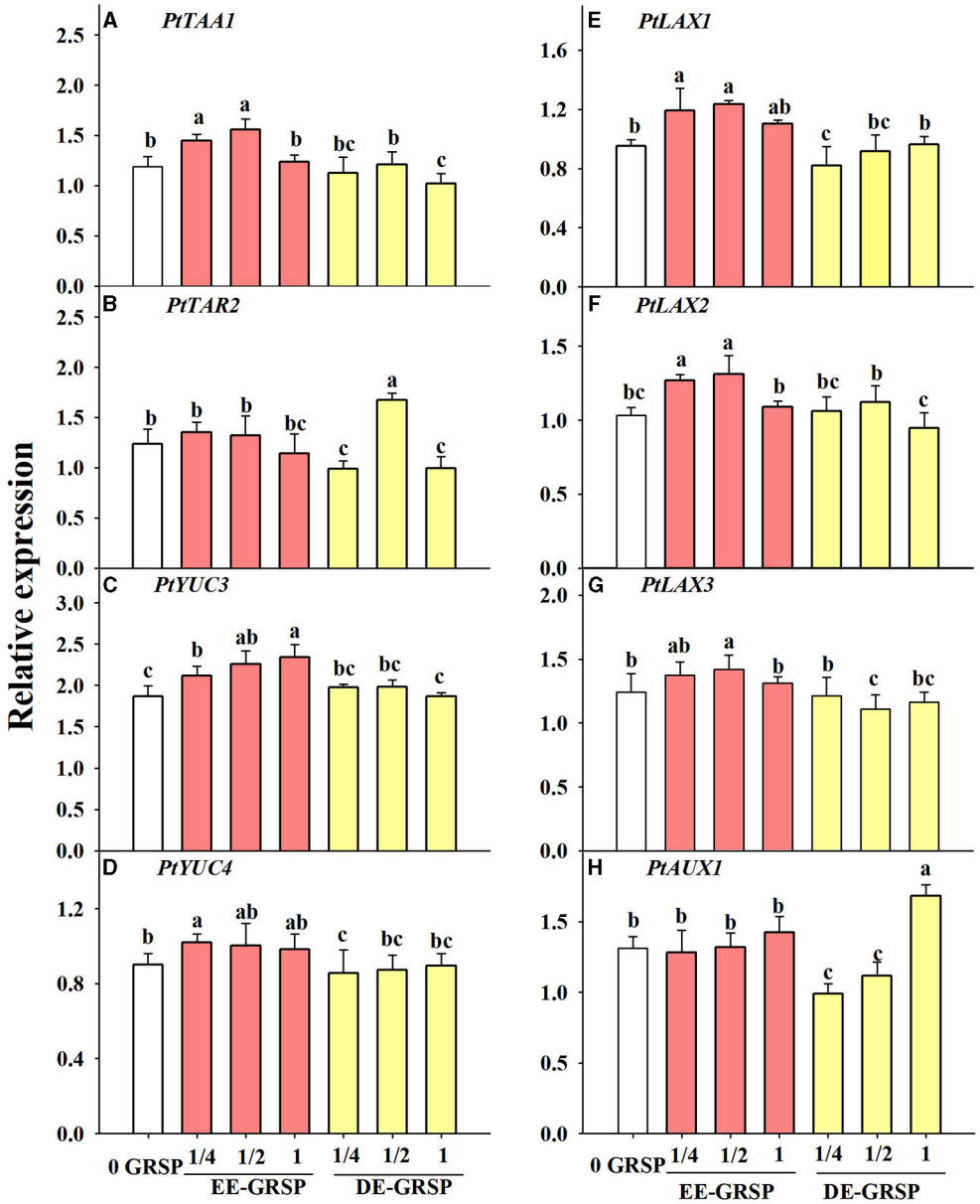

FIGURE 7 | Effects of exogenous EE-GRSP and DE-GRSP on relative expression levels of auxin synthetase genes **(A–D)** and transporter protein genes **(E–H)** in roots of trifoliate orange seedlings. Data (mean ± SD, $n = 4$) followed by different letters above the bars indicate significant differences ($p < 0.05$). DE-GRSP, difficultly extractable glomalin-related soil protein; EE-GRSP, easily extractable glomalin-related soil protein.

an important role in chlorophyll functioning. Chi et al. (2018) proposed that EE-GRSP as a molecular chaperone improved plant photosynthetic efficiency. On the contrary, DE-GRSP is an inert substance recalcitrant in the soil, which possibly induced a disadvantageous influence on chlorophyll production. The content of Fe in purified DE-GRSP was significantly higher than that in purified EE-GRSP. Nevertheless, it still showed that exogenous DE-GRSP inhibited the chlorophyll content, hinting toward another unknown mechanism to be perused as future research.

We investigated the elemental composition alongside their concentrations of purified GRSP, revealing the presence of as many 14 elements, of which P, K, Mo, and O were higher in purified EE-GRSP than in purified DE-GRSP. Other nutrients, viz., C, Ca, Cu, Mn, Zn, and Fe, displayed higher concentrations in purified DE-GRSP than in purified EE-GRSP. The variation in element contents of two GRSP fractions constituted different organic substances (e.g., tyrosine, tryptophan, fulvic acid, humic acid, nitrobenzoxadiazole, and calcofluor) (Zhang et al., 2017b), thus presenting such contrasting growth responses.

TABLE 4 | The Pearson's correlation coefficient between root IAA and expressions of auxin synthetase genes and carrier genes ($n = 28$).

	Genes associated with auxin synthesis				Auxin influx carrier genes			
	PtTAA1	***PtTAR2***	***PtYUC3***	***PtYUC4***	***PtLAX1***	***PtLAX2***	***PtLAX3***	***PtAUX1***
Root IAA	0.62**	0.07	0.61**	0.40*	0.63**	0.47	0.53**	0.21

IAA, indoleacetic acid.
*$p < 0.05$; **$p < 0.01$.*

The root nutrient acquisition of trifoliate orange was differentially regulated by exogenous GRSP: an increase in N, P, K, Ca, and Fe under EE-GRSP application conditions and a reduction in N, P, K, Mg, Cu, Zn, and Fe under DE-GRSP application conditions. As reported by Chi et al. (2018), ½ EE-GRSP improved the morphological establishment of trifoliate orange roots under normal water and drought stress. Exogenous EE-GRSP also improved soil aggregate stability and soil enzyme activity (Wang et al., 2015), both of which are beneficial to plant growth and nutrient acquisition. Root Fe was elevated by exogenous EE-GRSP, amounting to 1.8–4.9%, and inhibited by exogenous DE-GRSP, amounting to 59.1–77.9%. However, purified DE-GRSP possessed 55% higher Fe than purified EE-GRSP, gluing more Fe into an organic state to render Fe into inaccessible form to be absorbed by plant roots. Our study also showed that EE-GRSP-applied plants maintained a relatively higher root total length, surface area, and volume than the control plants, with ½ EE-GRSP presenting the best effect. However, DE-GRSP dramatically inhibited the root morphology, and the root morphology declined with the increasing concentration of DE-GRSP. The changed trend of root morphology was surprisingly consistent with the plant growth performance and chlorophyll changes triggered by GRSP application. As a result, it was concluded that changes in plant growth response and root nutrient acquisition under GRSP application are associated with root morphology triggered after GRSP application.

Plant growth response is closely linked to endogenous auxins (Zheng et al., 2013; Chen et al., 2016). In the present study, exogenous ½ and 1 EE-GRSP significantly increased root IAA and IBA contents, due to the presence of tryptophan (the precursor of auxins) in purified EE-GRSP (Zhang et al., 2017b), accelerating the synthesis of auxins. Chi et al. (2018) also observed an increase of IAA in trifoliate orange under soil water deficit conditions, following the application of exogenous EE-GRSP. However, exogenous application of DE-GRSP deteriorated the soil environment for roots to absorb nutrients (Zhang, 2009), thus hampering the bidirectional transport of IAA in the phloem.

The synthesis of IAA in plants starts with the conversion of L-tryptophan into 3-indole pyruvic acid (IPyA) in the presence of tryptophan transcarbamylase (tryptophan aminotransferase related, TAA1/TAR), which is then converted into IAA under the influence of flavin monooxygenase-like enzymes (YUCs) (Brumos et al., 2014). In the present study, exogenous application of EE-GRSP induced root *PtTAA1*, *PtYUC3,* and *PtYUC4* expression, depending upon the concentration of EE-GRSP used, whereas exogenous DE-GRSP inhibited the relative expression of *PtTAA1* and *PtYUC4*. The GRSP-regulated IAA change was related to the expression of GRSP-induced auxin-related synthase genes (*PtTAA1*, *PtYUC3*, and *PtYUC4*), based on the correlation analysis. TAA is involved in the conversion of tryptophan into IpyA, and then YUCs convert IpyA into IAA (Brumos et al., 2014). It indicates that the two processes were regulated by exogenous GRSP. Indeed, the IAA synthesis process is regulated by various transcription factors, such as the phytochrome-interacting factor 4 (*PIF4*) for direct regulation of *TAA1* gene expression and the *PIF7* for regulation of *YUCs* (Li et al., 2012; Sun et al., 2012), implying that exogenous GRSP regulated *PIF* transcription factors to modulate the expression of *TAA* and *YUCs*. However, the evidence of direct involvement is lacking in our study, and further research is needed in this direction.

In plants, IAA enters into cells in the form of anion under the influence of endocytosis carrier genes (Delbarre et al., 1996). *Auxin residue 1/like AUX1* (*Aux*/*LAX*) genes play an important role in auxin influx (Yoshihiro and Keiichirou, 2012). The results of our study showed that the application of exogenous EE-GRSP with quarter and half strength upregulated the expression of *PtLAX1* and *PtLAX2* and did not affect the expression of *PtAUX1*, suggesting *LAX* genes could be induced by EE-GRSP. However, exogenous DE-GRSP, to some extent, decreased the expression of *PtLAX* genes, dependent on the combination of DE-GRSP concentration and gene species, likely to reduce the flow of IAA from shoot parts to roots. A positive correlation of root IAA with *PtLAX1* and *PtLAX3* suggested the stimulating effect of GRSP on the expression of IAA influx carrier genes. The *AtLAX1* in *Arabidopsis thaliana* was expressed in the vascular system of the primary root maturation zone but weakly expressed at the root tip (Peret et al., 2012). The expression of *AtLAX3* at the cortex of the newly lateral root primordia mediated auxin transport during lateral root primordia development, making the formation and development of lateral roots easier (Swarup et al., 2008). Higher expression of *PtLAX1* and *PtLAX3* in EE-GRSP-treated plants indicated better polar auxin transport and lateral root formation, as seen in greater root morphology in EE-GRSP-treated plants. Such results also showed that the change of root IAA in response to the GRSP application is associated with regulation of IAA in polar transport from shoots to roots, besides aiding in the formation of lateral roots.

CONCLUSION

Exogenous GRSP triggered differential effects on plant growth response of trifoliate orange: the increase by exogenous EE-GRSP and the reduction by exogenous DE-GRSP. The change in

plant growth under GRSP application conditions was associated with the element content of pure GRSP, the auxin content of the plant, and root morphology. GRSP-regulated IAA changes were associated with the GRSP regulation of *TAA* and *YUC* gene expression in the IAA synthesis pathway and polarity transport of IAA. These results provide the future possibility of using EE-GRSP as a plant growth promoter for citrus production. However, more field studies coupled with elaboration on the physiological basis of GRSP functioning and mechanism of growth response by GRSP are mandatory before such efforts become an accepted field practice as a technological novelty.

DATA AVAILABILITY STATEMENT

The original contributions presented in the study are included in the article/supplementary material, further inquiries can be directed to the corresponding author.

AUTHOR CONTRIBUTIONS

R-CL, W-QG, and Q-SW designed the experiment. W-QG prepared the materials for the experiment. R-CL, Y-NZ, KK, and Q-SW analyzed the data. R-CL wrote the manuscript. AS, AH, EA, Q-SW, and KK revised the manuscript. All authors have read and agreed to the published version of the manuscript.

FUNDING

This study was supported by the National Natural Science Foundation of China (31372017) and the 2020 Joint Projects between Chinese and CEECs' Universities (202019). This work was also supported by the UHK project VT2019-2021. The authors would like to extend their sincere appreciation to the Researchers Supporting Project Number (RSP-2021/134), King Saud University, Riyadh, Saudi Arabia.

REFERENCES

Arnon, D. I. (1949). Copper enzymes in isolated chloroplasts. Polyphenoloxidase in *Beta vulgaris*. *Plant Physiol*. 24, 1–15. doi: 10.1104/pp.24.1.1

Bradford, M. M. (1976). A rapid and sensitive method for the quantitation of microgram quantities of protein utilizing the principle of protein-dye binding. *Anal. Biochem*. 72, 248–254. doi: 10.1016/0003-2697(76)90527-3

Brumos, J., Alonso, J. M., and Stepanova, A. N. (2014). Genetic aspects of auxin biosynthesis and its regulation. *Physiol. Plant*. 151, 3–12. doi: 10.1111/ppl.12098

Chen, D., Wang, W. A., Yue, Q. Q., and Zhao, Q. (2016). Research progress of plant auxin as a regulator of cold stress response. *J. Plant Physiol*. 7, 989–997. doi: 10.13592/j.cnki.ppj.2016.0042

Chi, G. G., Srivastava, A. K., and Wu, Q. S. (2018). Exogenous easily extractable glomalin-related soil protein improves drought tolerance of trifoliate orange. *Arch. Agron. Soil Sci*. 64, 1341–1350. doi: 10.1080/03650340.2018.1432854

Delbarre, A., Muller, P., and Guern, I. J. (1996). Comparison of mechanisms controlling uptake and accumulation of 2,4-dichlorophenoxy acetic acid, naphthalene-1-acetic acid, and indole-3-acetic acid in suspension-cultured tobacco cells. *Planta* 198, 532–541. doi: 10.1007/BF00262639

Dobrev, P. I., and Kamínek, M. (2002). Fast and efficient separation of cytokinins from auxin and abscisic acid and their purification using mixed-mode solid-phase extraction. *J. Chromatogr. A* 950, 21–29. doi: 10.1016/S0021-9673(02)00024-9

Dong, S. S., Dou, S., Lin, C. M., Li, L. B., and Tan, C. (2016). Decomposition rate of corn straw in soil and its effects on soil humus composition. *J. Jilin Agric. Univ*. 38, 579–586. doi: 10.13327/j.jjlau.2016.3373

Duan, D. C. (2014). *Regulation Mechanism of Humic Acid on the Pb Bioavailability and Toxicity to Tea Plant (Cameilia sinensis L.)*. [Doctor's thesis]. [Hangzhou]: Zhejiang University.

Gadkar, V., and Rillig, M. C. (2006). The arbuscular mycorrhizal fungal protein glomalin is a putative homolog of heat shock protein 60. *FEMS Microbiol. Lett*. 263, 93–101. doi: 10.1111/j.1574-6968.2006.00412.x

Gao, W. Q., Wang, P., and Wu, Q. S. (2019). Functions and application of glomalin-related soil proteins: a review. *Sains Malays*. 48, 111–119. doi: 10.17576/jsm-2019-4801-13

Gillespie, A. W., Farrell, R. E., Walley, F. L., Ross, A. R. S., Leinweber, P., and Eckhardt, K. U. (2011). Glomalin-related soil protein contains non-mycorrhizal related heat-stable proteins, lipids and humic materials. *Soli Biol. Biochem*. 43, 766–777. doi: 10.1016/j.soilbio.2010.12.010

He, J. D., Chi, G. G., Zou, Y. N., Shu, B., Wu, Q. S., Srivastava, A. K., et al. (2020). Contribution of glomalin-related soil proteins to soil organic carbon in trifoliate orange. *Agric. Ecosyst. Environ,. Appl. Soil Ecol*. 154:103592. doi: 10.1016/j.apsoil.2020.103592

Huang, G. M., Srivastava, A. K., Zou, Y. N., Wu, Q. S., and Kuča, K. (2021a). Exploring arbuscular mycorrhizal symbiosis in wetland plants with a focus on human impacts. *Symbiosis*. doi: 10.1007/s13199-021-00770-8.

Huang, Y., Xu, Y. T., Jiang, X. L., Yu, H. W., Jia, H. H., Tan, C. M., et al. (2021b). Genome of a citrus rootstock and global DNA demethylation caused by heterografting. *Hortic. Res*. 8:69. doi: 10.1038/s41438-021-00505-2

Koide, R. T., and Peoples, M. S. (2013). Behavior of Bradford-reactive substances is consistent with predictions for glomalin. *Agric. Ecosyst. Environ. Appl. Soil Ecol*. 63, 8–14. doi: 10.1016/j.apsoil.2012.09.015

Li, L., Ljung, K., Breton, G., Schmitz, R. J., Pruneda-Paz, J., Cowing-Zitron, C., et al. (2012). Linking photoreceptor excitation to changes in plant architecture. *Gene Dev*. 26, 785–790. doi: 10.1101/gad.187849.112

Liu, C. Y., Wang, P., Zhang, D. J., Zou, Y. N., Kuča, K., and Wu, Q. S. (2018a). Mycorrhiza-induced change in root hair growth is associated with IAA accumulation and expression of *EXPs* in trifoliate orange under two P levels. *Sci. Hortic*. 234, 227–235. doi: 10.1016/j.scienta.2018.02.052

Liu, C. Y., Zhang, F., Zhang, D. J., Srivastava, A. K., Wu, Q. S., and Zou, Y. N. (2018b). Mycorrhiza stimulates root-hair growth and IAA synthesis and transport in trifoliate orange under drought stress. *Sci. Rep*. 8:1978. doi: 10.1038/s41598-018-20456-4

Livak, K. J., and Schmittgen, T. D. (2001). Analysis of relative gene expression data using real-time quantitative PCR and the $2^{-\Delta\Delta CT}$. *Methods* 25, 402–408. doi: 10.1006/meth.2001.1262

Lovelock, C. E., Wright, S. F., Clark, D. A., and Ruess, R. W. (2004). Soil stocks of glomalin produced by arbuscular mycorrhizal fungi across a tropical rain forest landscape. *J. Ecol*. 92, 278–287. doi: 10.1111/j.0022-0477.2004.00855.x

Meng, L. L., He, J. D., Zou, Y. N., Wu, Q. S., and Kuča, K. (2020). Mycorrhiza-released glomalin-related soil protein fractions contribute to soil total nitrogen in trifoliate orange. *Plant Soil Environ*. 66, 183–189. doi: 10.17221/100/2020-PSE

Mora, V., Bacaicoa, E., Zamarreño, A. M., Aguirre, E., and Garcia-Mina, J. M. (2012). Action of humic acid on promotion of cucumber shoot growth involves nitrate-related changes associated with the root-to-shoot distribution of cytokinins, polyamines and mineral nutrients. *J. Plant Physiol*. 167, 633–642. doi: 10.1016/j.jplph.2009.11.018

Nichols, K. A. (2008). "Indirect contributions of AM fungi and soil aggregation to plant growth and protection," in *Sustainable Agriculture and Forestry*, eds Z. A. Siddiqui (Berlin: Springer), 177–194. doi: 10.1007/978-1-4020-8770-7_7

Peret, B., Swarup, K., Ferguson, A., Seth, M., Yang, Y. D., Dhondt, S., et al. (2012). *AUX/LAX* genes encode a family of auxin influx transporters that perform

distinct functions during *Arabidopsis* development. *Plant Cell* 24, 2874–2885. doi: 10.1105/tpc.112.097766

Rillig, M. C. (2004). Arbuscular mycorrhizae, glomalin and soil aggregation. *Can. J. Soil Sci.* 84, 355–363. doi: 10.4141/S04-003

Rillig, M. C., and Mummey, D. L. (2010). Mycorrhizas and soil structure. *New Phytol.* 171, 41–53. doi: 10.1111/j.1469-8137.2006.01750.x

Rillig, M. C., Wright, S. F., Nichols, K. A., Schmidt, W. F., and Torn, M. S. (2001). Unusually large contribution of arbuscular mycorrhizal fungi to soil organic matter pools in tropical forest soils. *Plant Soil* 233, 167–177. doi: 10.1023/A:1010364221169

Schindler, F. V., Mercer, E. J., and Rice, J. A. (2007). Chemical characteristics of glomalin-related soil protein (GRSP) extracted from soils of varying organic matter content. *Soil Biol. Biochem.* 39, 320–329. doi: 10.1016/j.soilbio.2006.08.017

Spohn, M., and Giani, L. (2010). Water-stable aggregates, glomalin-related soil protein, and carbohydrates in a chronosequence of sandy hydromorphic soils. *Soil Biol. Biochem.* 42, 1505–1511. doi: 10.1016/j.soilbio.2010.05.015

Sun, J. Q., Qi, L. L., Li, Y. N., Chu, J. F., and Li, C. Y. (2012). PIF4-mediated activation of *YUCCA8* expression integrates temperature into the auxin pathway in regulating *Arabidopsis* hypocotyl growth. *PLoS Genet.* 8:e1002594. doi: 10.1371/journal.pgen.1002594

Swarup, K., Benkova, E., Swarup, R., Casimiro, I., Peret, B., Yang, Y. D., et al. (2008). The auxin influx carrier LAX3 promotes lateral root emergence. *Nat. Cell Biol.* 10, 946–954. doi: 10.1038/ncb1754

Wang, S., Wu, Q. S., and He, X. H. (2015). Exogenous easily extractable glomalin-related soil protein promotes soil aggregation, relevant soil enzyme activities and plant growth in trifoliate orange. *Plant Soil Environ.* 61, 66–71. doi: 10.17221/833/2014-PSE

Wang, Y., Wang, M., Li, Y., Wu, A., and Huang, J. (2018). Effects of arbuscular mycorrhizal fungi on growth and nitrogen uptake of *Chrysanthemum morifolium* under salt stress. *PLoS ONE* 7:12181. doi: 10.1371/journal.pone.0196408

Wu, Q. S., Cao, M. Q., Zou, Y. N., and He, X. H. (2014). Direct and indirect effects of glomalin, mycorrhizal hyphae, and roots on aggregate stability in rhizosphere of trifoliate orange. *Sci. Rep.* 4:5823. doi: 10.1038/srep05823

Wu, Q. S., Li, Y., Zou, Y. N., and He, X. H. (2015a). Arbuscular mycorrhiza mediates glomalin-related soil protein production and soil enzyme activities in the rhizosphere of trifoliate orange grown under different P levels. *Mycorrhiza* 25, 121–130. doi: 10.1007/s00572-014-0594-3

Wu, Q. S., Srivastava, A. K., Wang, S., and Zeng, J. X. (2015b). Exogenous application of EE-GRSP and changes in citrus rhizosphere properties. *Ind. J. Agric. Sci.* 85, 58–62.

Xu, D. B., Wang, Q. J., Wu, Y. C., Yu, G. H., Shen, Q. R., and Huang, Q. W. (2012). Humic-like substances from different compost extracts could significantly promote cucumber growth. *Pedosphere* 22, 815–824. doi: 10.1016/S1002-0160(12)60067-8

Yoshihiro, M., and Keiichirou, N. (2012). The pathway of auxin biosynthesis in plants. *J. Exp. Bot.* 8, 2853–2872. doi: 10.1093/jxb/ers091

Zhang, B. (2009). *Effects of MAG2 Gene on the Germination and the Growth of Seedling in Arabidopsis thaliana Under the Stress Condition*. [Master's thesis]. [Lanzhou]: Lanzhou University.

Zhang, Z. H., Wang, Q., Wang, H., Nie, S. M., and Liang, Z. W. (2017a). Effects of soil salinity on the content, composition, and ion binding capacity of glomalin-related soil protein. *Sci. Total Environ.* 581, 657–665. doi: 10.1016/j.scitotenv.2016.12.176

Zhang, Z. L., Wang, W. J., Wang, Q., Wu, Y., Wang, H. M., and Pei, Z. X. (2017b). Glomalin amount and compositional variation, and their associations with soil properties in farmland, northeastern China. *J. Plant Nutr. Soil Sci.* 180, 563–575. doi: 10.1002/jpln.201600579

Zhao, R. X., Guo, W., Bi, N., Guo, J. Y., Wang, L. X., Zhao, J., et al. (2015). Arbuscular mycorrhizal fungi affect the growth, nutrient uptake and water status of maize (*Zea mays* L.) grown in two types of coal mine spoils under drought stress. *Agric. Ecosyst. Environ. Appl. Soil Ecol.* 88, 41–49. doi: 10.1016/j.apsoil.2014.11.016

Zheng, Y., Zhou, A. P., Liu, Y. K., and He, C. Z. (2013). The polar transport and regulatory mechanism of auxin in plant. *J. Yunnan Agric. Univ.* 6, 122–128. doi: 10.3969/j.issn.1004-390X(n).2013.06.020

Zou, Y. N., Srivastava, A. K., and Wu, Q. S. (2015). Glomalin: a potential soil conditioner for perennial fruits. *Int. J. Agric. Biol.* 18, 293–297. doi: 10.17957/IJAB/15.0085

Zou, Y. N., Srivastava, A. K., Wu, Q. S., and Huang, Y. M. (2014). Glomalin-related soil protein and water relations in mycorrhizal citrus (*Citrus tangerina*) during soil water deficit. *Arch. Agron. Soil Sci.* 60, 1103–1114. doi: 10.1080/03650340.2013.867950

Conflict of Interest: The authors declare that the research was conducted in the absence of any commercial or financial relationships that could be construed as a potential conflict of interest.

Publisher's Note: All claims expressed in this article are solely those of the authors and do not necessarily represent those of their affiliated organizations, or those of the publisher, the editors and the reviewers. Any product that may be evaluated in this article, or claim that may be made by its manufacturer, is not guaranteed or endorsed by the publisher.

frontiers in Plant Science

ORIGINAL RESEARCH
published: 27 September 2021
doi: 10.3389/fpls.2021.728527

Phosphorus-Use Efficiency Modified by Complementary Effects of P Supply Intensity With Limited Root Growth Space

*Haiqing Gong, Bilisuma Kabeto Wako, Yue Xiang and Xiaoqiang Jiao**

Department of Plant Nutrition, Key Laboratory of Plant-Soil Interactions, Ministry of Education, National Academy of Agriculture Green Development, China Agricultural University, Beijing, China

Space availability and the maintenance of adequate phosphorus (P) supply in the root zone are essential for achieving high yield and P-use efficiency in maize production by manipulating the root morphology and arbuscular mycorrhizal (AM) fungi colonization. A major trade-off exists between root growth and AM colonization that is influenced by soil P supply intensity and space availability. However, how soil P manipulates the root morphological characteristics and AM colonization to compensate for the limitation of root-growth space induced by high-planting density is not clear. Therefore, pot experiments were conducted to investigate interactions between the root growth and AM fungi by optimizing soil P supply to compensate for limited root growth space induced by high-planting density. Similar shoot biomass and P uptake values were obtained in P200 (200 mg P kg^{-1} soil) under D = 40 (i.e., diameter of the pot is 40 cm) and P400 under D = 30, and similar values were obtained for root length, tap root length, root angle, lateral root density, and AM colonization. However, the improvement in P supply in the root zone, shoot biomass, and P uptake in P400 under D = 20 were lower than in P200 under D = 30, and there were no significant differences in the root parameters between P200 and P400 under D = 20; similarly, the root growth and AM colonization exhibited similar trends. These results suggest that optimizing P supply in the root zone to regulate the interaction between root morphological traits and AM colonization can compensate for limited root-growth space. Although P supply in the root zone increased after the root-growth space was compressed, it could not meet the P demand of maize; thus, to achieve the most efficient use of P under intensive high-density maize production, it is necessary to optimally coordinate root growth space and P supply in the root zone.

Keywords: AM colonization, maize, phosphorus supply intensity, space availability, trade-off

OPEN ACCESS

Edited by:
Maurizio Ruzzi,
University of Tuscia, Italy

Reviewed by:
Gabriela Quiroga,
Consejo Superior de Investigaciones Científicas (CSIC), Spain
Tao Zhang,
Northeast Normal University, China

****Correspondence:***
Xiaoqiang Jiao
xqjiao526@126.com

Specialty section:
This article was submitted to Plant Nutrition, a section of the journal Frontiers in Plant Science

Received: *21 June 2021*
Accepted: *27 August 2021*
Published: *27 September 2021*

Citation:
Gong H, Kabeto Wako B, Xiang Y and Jiao X (2021) Phosphorus-Use Efficiency Modified by Complementary Effects of P Supply Intensity With Limited Root Growth Space. Front. Plant Sci. 12:728527. doi: 10.3389/fpls.2021.728527

INTRODUCTION

The sustainable use of phosphorus (P) is a major challenge in agricultural production, especially in high-density planting systems (Testa et al., 2016). High planting density reduces the growth space of maize roots per plant; such conditions are often accompanied by smaller roots per plant, reduced soil volume occupied by the root system, and decreased the total root length (Wang et al., 2020). Maize plants primarily depend on the root morphological traits to enhance P acquisition in

the soil (Lambers et al., 2015; Wang et al., 2020). The low root growth spaces are induced by high planting density, which results in difficulty in acquiring P from the soil (Shao et al., 2018). Artificially increasing P supply is an effective method of regulating the P absorption capacity of plants to meet the P demand of high-density populations (Poorter et al., 2012). In intensive agriculture, smallholders often employ the insurance approach, that is, large amounts of mineral P fertilizer are applied in excess to increase the P availability to crop plants, resulting in low P-use efficiency (PUE) (Dhillon et al., 2017; Zhang et al., 2019), with considerable adverse environmental impacts, such as non-point source pollution of surface waters (Ni et al., 2015). Therefore, both the P supply and root growth space availability should be considered when attempting to increase the PUE under intensive high-density planting maize systems.

The P-supply intensity and root-growth-space availability often affect the root morphology and arbuscular mycorrhizal (AM) colonization (Zhang et al., 2017; Shao et al., 2018; Wang et al., 2020), and in turn, impact PUE under maize production. Lyu et al. (2016) showed that at the root soil interface, available P could be enhanced by altering the root morphology. Moreover, P has been shown to stimulate root development and subsequent P uptake (Ma et al., 2020). In addition, P availability can profoundly influence the plant responses to AM colonization (Campos et al., 2018). The high level of P can inhibit AM colonization, reducing P uptake, and the benefits of AM colonization (Breuillin et al., 2010). Furthermore, increasing evidence demonstrates that high plant density can affect the plant root morphology and AM colonization (Schroeder and Janos, 2004; Niu et al., 2020). Space availability decreases with the increasing plant density, and the root growth is subsequently inhibited. In maize, the high plant density reduces the root to shoot ratio, root biomass, and root length (Shao et al., 2018); however, root length density increases with high-density planting, which increases the chances of roots crossing and overlapping, and could easily lead to P deficiency in the rhizosphere (Postma et al., 2014; Li et al., 2019). In contrast, AM colonization increases with an increase in the planting density, as AM fungi can partially alleviate P deficiency stress (Abdel-Fattah and Asrar, 2012). Hence, a trade-off exists between the root morphological traits and AM colonization to enhance P acquisition under intensive P supply and space availability; however, the mechanism of interactive effects of root morphological traits and AM colonization on maize P uptake is not fully understood. A deeper understanding of the mechanisms of root and AM interactive effects on the root growth space exploitation and maize P uptake is key to fostering high PUE.

The high plasticity of root system architecture and AM fungi responses to P supply intensity and space availability have indicated a high potential to improve PUE in maize production (Postma et al., 2014; Li et al., 2019; Shao et al., 2019). For example, PUE in maize production can be improved by manipulating the root morphology and AM colonization to maintain an appropriate P supply intensity in the root zone (Deng et al., 2017; Kobae, 2019; Chu et al., 2020). Similarly, maintaining space for proper root growth in intensive high-plant-density maize production systems could modify the root morphology and AM colonization to enhance maize yield (Yu et al., 2019; Hou et al., 2021). However, most of the previous studies in high-density planting systems have focused on the regulation of root morphology. Our understanding of how AM colonization in high-density planting systems responds to P supply is poor (Ma et al., 2013; Teng et al., 2013; Testa et al., 2016), in addition to how altered P supply affects the root growth and AM colonization to compensate for limited root growth space. To simultaneously achieve high maize yield and PUE in high-density planting systems, it is necessary to comprehensively consider P supply in the root zone and root-growth space by modifying root morphology and AM colonization. An improved understanding of the compensatory effects of maize root expansion on the root growth space, under P supply intensity regulation, would further enhance our understanding of the biological potential for efficient P use in maize.

Here, a pot experiment was carried out with maize to determine the compensation mechanisms of soil P supply intensity on the maize root morphology, AM colonization, and P uptake under different space availability scenarios. The present study specifically aimed: (1) to investigate maize growth and P uptake under different P intensities and root-growth space treatments; and (2) to examine the compensatory effects of soil P supply on root-growth space to determine environments that enhance PUE in maize.

MATERIALS AND METHODS

Experimental Site

A greenhouse pot experiment was conducted from June to August 2020 at the Quzhou Experimental Station of China Agricultural University (36° 51′ 57″ N, 150° 0′ 37″ E), Quzhou County, Hebei province, China. Calcareous loamy soil was collected from the Quzhou Long-Term Fertilizer Station (36° 52′ 0″ N, 115° 02′ 0″ E) of China Agricultural University, Hebei province, China. The basic soil properties were as followed: pH, 8.13; soil organic carbon (SOC), 7.3 g kg^{-1}; Olsen-P, 2.40 mg kg^{-1}; soil total nitrogen (TN), 0.91 g kg^{-1}; and available potassium (AK), 183 mg kg^{-1}. The soil was air-dried and passed through a 2-mm sieve prior to experimentation. The soil pH was measured in a 1:2.5 (w/v) soil/water slurry. SOC was determined with 0.25-mm sieved soil as explained by Cambardella et al. (2001). Soil TN was determined using the Kjeldahl method (Carter and Gregorich, 2007). Soil Olsen-P was determined in 0.5 M $NaHCO_3$ extracts using Mo-Sb colorimetry (Olsen et al., 1954).

Experimental Design and Management

The experiment consisted of a 3 × 3 complete factorial design. There were three P levels (0, 200, and 400 mg P kg^{-1} soil as CaH_2PO_4, hereafter referred to as P0, P200, and P400, respectively) and three pot sizes (20 cm diameter × 50 cm height, 30 cm diameter × 50 cm height, and 40 cm diameter × 50 cm height, hereafter referred to as D = 20, D = 30, and D = 40, respectively). Each of the nine treatment combinations was replicated four times to yield a total of 36 pots.

Urea and muriate of potash were applied to all the treatments at a rate of 150 kg ha^{-1} to supply nitrogen (N) and potassium (K),

TABLE 1 | Two-way ANOVA of the effects of phosphorous (P) supply, space availability, and their interaction on P supply and space availability.

Parameters	P supply		Space availability		P supply × Space availability	
	F-value	*P*-value	*F*-value	*P*-value	*F*-value	*P*-value
Shoot biomass	148.9	<0.0001	87.28	<0.0001	16.17	<0.0001
Shoot P content	149.01	<0.0001	92.01	<0.0001	<0.0001	<0.0001
Root biomass	133.3	<0.0001	73.05	<0.0001	10.74	<0.0001
Root length	156.3	<0.0001	115.5	<0.0001	18.05	<0.0001
Tap root length	103.3	<0.0001	115.0	<0.0001	7.921	0.0002
Root angle	1.5712	0.2022	146.1	<0.0001	6.137	0.0012
Lateral root density	92.04	<0.0001	13.87	<0.0001	4.115	0.0099
AM colonization	1128	<0.0001	235.8	<0.0001	61.90	<0.0001
Bulk soil Olsen P	654.3	<0.0001	1.280	0.0701	1.618	0.2129
Rhizosphere soil Olsen P	1,128	<0.0001	235.8	<0.0001	61.90	<0.0001

which are often limiting factors in the calcareous loamy soils. All fertilizers were incorporated and thoroughly mixed with the soil at the time of planting.

Maize seeds (*Zea mays* L. cv. Zhengdan958) were surface sterilized in 10% v/v H_2O_2 for 30 min, washed with deionized water, and placed in a dish containing aerated saturated $CaSO_4$ solution at 25°C in the dark until a radicle emerged. Then, four germinated seeds of uniform size were sown in each pot. Each pot was watered daily to 80% field capacity as measured by weight. The temperature ranged from a minimum of 22°C at night to a maximum of 30°C during the day.

Plant Harvest and Measurements

The plants were harvested 55 days after sowing. The shoots were cut at the soil surface, oven-dried at 105°C for 30 min and then, at 75°C for 3 days until they reached constant weight and weighed to record the biomass. Afterward, the shoots were crushed and homogenized. Shoot P concentration was determined using the vanadomolybdate method (Johnson and Ulrich, 1959) after wet digestion with a mixture of 5 ml of 98% H_2SO_4 and 8 ml of 30% H_2O_2.

Soil Sampling and Measurements

Bulk soil sample was obtained 20 cm from the soil surface using a soil auger. Rhizosphere soil was obtained by brushing off the soil adhering to the whole roots with a sterile brush. Visible roots were removed manually before the samples were ground to pass through a 2-mm sieve and dried naturally. Soil Olsen-P was determined in 0.5 M NaHCO3 extracts using Mo-Sb colorimetry (Olsen et al., 1954).

Root Sampling and Root Parameter Measurements

After cutting off the shoots, the excavated roots were shaken briefly to remove a large fraction of the soil adhering to the root crown. The root angle was assessed using the method outlined by Hecht et al. (2019). Afterward, all the visible roots in each pot were collected from the soil on a 2 mm-diameter mesh and washed clean with running water in the lab. Total root length was analyzed using Win-RHIZO software (Pro2004b, version 5.0, Regent Instruments Inc., QC, Canada). Lateral root density was the number of lateral roots per unit length of primary root, which was calculated by dividing the number of lateral roots per 5 cm of primary root by the 5 cm length of the root.

The fine roots were cut to 1 cm segments and thoroughly mixed. The root samples were cleaned with 10% (w:v) potassium hydroxide and placed in a water bath (90°C) for 2 h. The cooled root samples were cleaned in 2% HCl for 5 min and then stained with Trypan blue solution. For each sample, 15 root segments were used to evaluate AM colonization by scoring based on the findings of Trouvelot et al. (1986) and calculated using MYCOCALC program (http://www.dijon.inra.fr/mychintec/Mycocalc-prg/ download.html). AM colonization (%) = number of intersections colonized (hyphae, arbuscules, vesicles, and hyphal coils)/total number of intersections examined × 100% (Zhang et al., 2014).

All roots were collected and dried at 75°C for 72 h and weighed to determine the biomass.

Statistical Analysis

IBM SPSS Statistics 20.0 (IBM Corp., Armonk, NY, USA) was used to compute one-way or two-way ANOVA. The mean differences among the means were determined by the least significant difference (LSD) at $P \leq 0.05$ probability level. The data were presented as graphs prepared by Sigmaplot version 10.0 (Systat Software Inc., San Jose, CA, USA).

RESULTS

Shoot Biomass and P Content

Shoot biomass was significantly affected by soil P supply and space availability ($P < 0.01$, **Table 1**; **Figures 1A,B**; **Supplementary Figures 1A,B**). Shoot biomass increased as the soil P supply increased, and the highest shoot biomass was obtained in the P400 treatment groups, followed by in the P200 and P0 treatments. The effect of space availability on shoot biomass was more prominent when more P was added

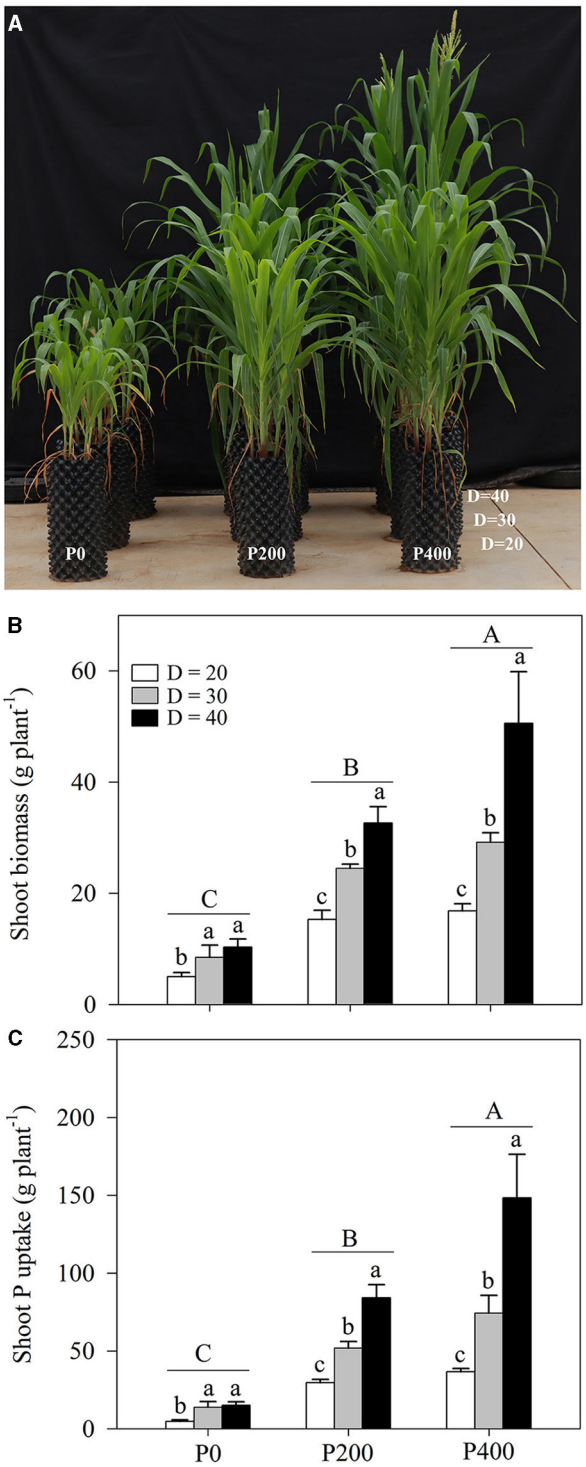

FIGURE 1 | Plant growth performance **(A)**, shoot biomass **(B)**, and shoot phosphorous (P) content **(C)**, under different P supply gradients and space availability conditions. Each value represents the mean of four replicates (+SD). Different lower-case letters indicate a significant difference among different space availability levels, and different capital letters indicate a significant among different P levels. P0, 0 mg P kg^{-1} soil; P200, 200 mg P kg^{-1} soil; and P400, 400 mg P kg^{-1} soil; D = 20, D = 30, and D = 40 represent diameter of pot is 20, 30, and 40 cm, respectively.

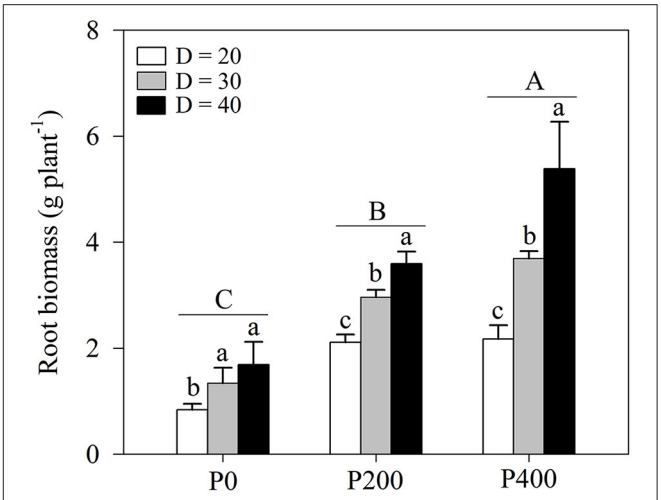

FIGURE 2 | Root biomass under different phosphorous (P) supply gradients and space availability conditions. Each value represents the mean of four replicates (+SD). Different lower-case letters indicate a significant difference among different space availability levels, and different capital letters indicate a significant among different P levels ($P < 0.05$). P0, 0 mg P kg^{-1} soil; P200, 200 mg P kg^{-1} soil; and P400, 400 mg P kg^{-1} soil; D = 20, D = 30, and D = 40 represent diameter of pot is 20, 30, and 40 cm, respectively.

to the soil (P200 and P400 treatments); however, the limited space availability could restrict the growth of shoot biomass. Lower shoot biomass was obtained with the D = 20 treatment among all the P supply treatments (**Figures 1A,B**). However, the reduction in shoot biomass due to space limitation was compensated by soil P supply with certain space availability treatments. Higher shoot biomass was obtained in P400 under D = 30, which was equivalent to the shoot biomass observed in P200 under D = 40; the shoot biomass in P200 under D = 30 was significantly higher than that in P0 under D = 40. Furthermore, the shoot biomass in P400 under D = 20 was significantly lower than in P200 under D = 30. In addition, the shoot biomass did not tend to increase under the improving P supply conditions at lower space availability treatments. Under D = 30 and D = 40, the shoot biomass significantly increased as soil P supply increased, while there was no significant difference in the shoot biomass between P200 and P400 under D = 20, indicating that the shoot biomass was restricted by the amount of space and could not be compensated by soil P supply.

The shoot P content in maize among the treatments was also significantly affected by soil P supply and space availability ($P < 0.01$, **Table 1**; **Figure 1C**; **Supplementary Figure 1C**). The shoot P content increased as soil P supply increased, and the lower rates of shoot P uptake were obtained with the D = 20 treatment across different P supply rates, when compared with D = 30 and D = 40. Similar complementary effects of soil P supply and space availability on the shoot P content were obtained under some circumstances. When compared with that in P200 under D = 20 and D = 30, higher P content was obtained under D = 40. Further, the shoot P content in P200

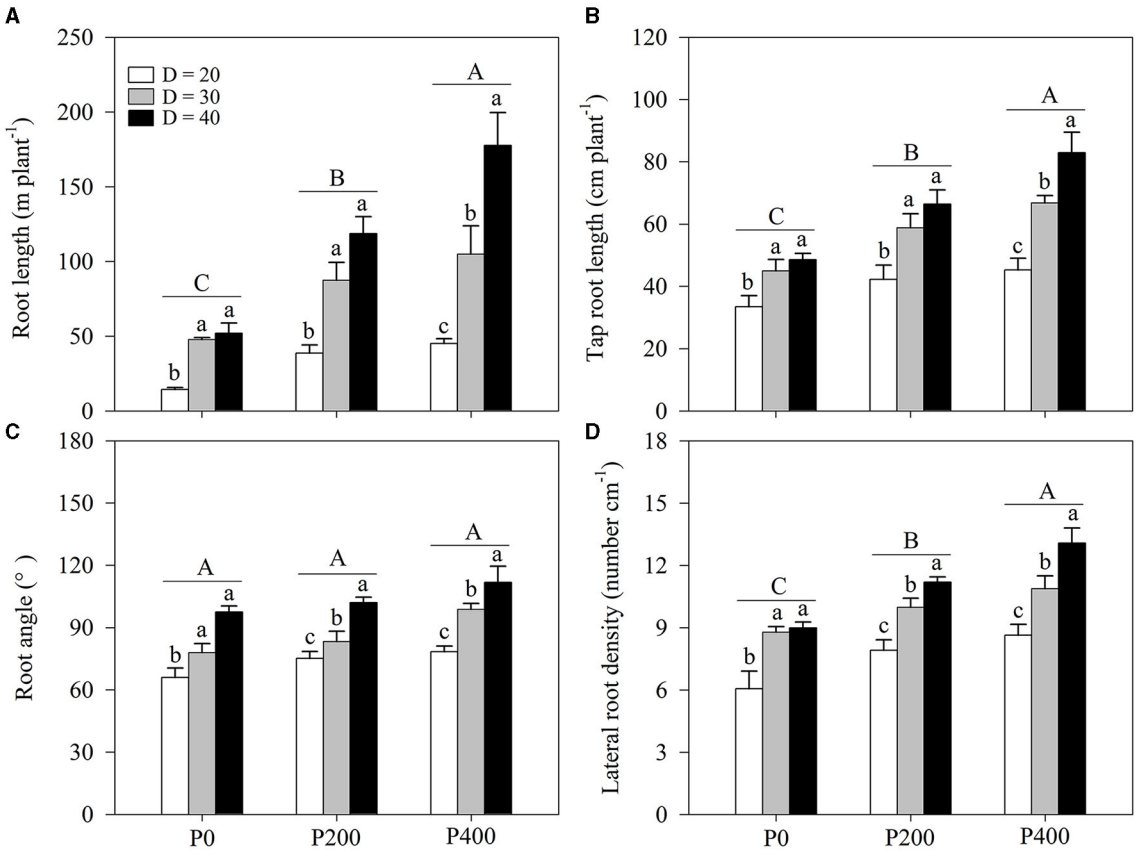

FIGURE 3 | (A) Root length, **(B)** tap root length, **(C)** root angle, and **(D)** lateral root density under different phosphorous (P) supply gradients and space availability conditions. Each value represents the mean of four replicates (+SD). Different lower-case letters indicate a significant difference among different space availability levels, and different capital letters indicate a significant among different P levels ($P < 0.05$). P0, 0 mg P kg^{-1} soil; P200, 200 mg P kg^{-1} soil; and P400, 400 mg P kg^{-1} soil; D = 20, D = 30, and D = 40 represent diameter of pot is 20, 30, and 40 cm, respectively.

under D = 30 was significantly higher than in P0 under D = 40. In contrast, the shoot P content obtained in P200 under D = 30 was significantly higher than in P400 under D = 20. There was no significant difference in the shoot P content as P supply increased from P200 to P400 under D = 20 due to the space limitation.

Root Biomass

Root biomass was significantly influenced by soil P supply and space availability ($P < 0.01$, **Table 1**; **Figure 2**; **Supplementary Figure 2**). Root biomass increased as soil P supply increased, and the effect of space availability on root biomass was stronger under higher P supply (P200 and P400), while no significant difference was observed in P0 between D = 30 and D = 40. There was a strong complementary effect of soil P supply and space availability on root growth. Similar root biomass levels were observed in P200 under D = 40 and P400 under D = 30; root biomass in P200 under D = 30 was significantly higher than in P0 under D = 40. However, a higher root biomass was observed in P200 under D = 30 than in P400 under D = 20. In addition, root biomass increased as soil P supply increased under higher space availability (D = 30 and D = 40).

Root Morphological Traits

The root length was strongly influenced by soil P supply ($P < 0.01$) and space availability ($P < 0.01$) (**Table 1**; **Figure 3A**; **Supplementary Figure 3A**). The effect of root length increased as soil P supply increased. The effect of space availability on the root length was stronger at higher P supply levels (P400). The complementary effects of soil P supply and space availability on root length were obtained; root length obtained in P200 under D = 40 was equivalent to the root length obtained in P400 under D =30. Furthermore, the root length obtained in P200 under D = 30 was significantly higher than in P0 under D = 40; however, the root length did not increase as space availability decreased: there was no significant difference in the root length between P200 and P400 under D = 20. Finally, the root length in P400 under D = 20 was lower than that in P200 under D = 30.

Tap root length was also affected by soil P supply and space availability (**Table 1**; **Figure 3B**; **Supplementary Figure 3B**). Tap root length increased as space availability increased. Similar tap

root length was obtained in P400 under D = 30 and P200 under D = 40 and tap root length in P200 under D = 30 was significantly higher than that in P0 under D = 40. However, there was no significant difference in tap root length between P200 and P400 under D = 20. Furthermore, tap root length in P400 under D = 20 was lower than that in P200 under D = 30.

The root angle was strongly affected by space availability, with little relationship to soil P supply (**Table 1**; **Figure 3C**; **Supplementary Figure 3C**). Significantly higher root angles were observed in D = 40 compared with that in D = 20 and D = 30 among all P supply treatments; however, there was no significant difference in the root angle between P400 under D = 30 and P200 under D = 40. The effect of soil P supply on the root angle was negligible under low space availability (D = 20).

Soil P supply and space availability significantly influenced the lateral root density. The lateral root density significantly increased as P supply increased, while the effect of space availability on the lateral root density was considerable when more P was added to the soil (P200 and P400). Notably, the lateral root density obtained in P400 under D = 30 was equivalent to the lateral root density in P200 under D = 40. Significantly higher lateral root density was obtained in P200 under D = 30 than in P0 under D = 40. Similar to root angle, the effect of soil P supply on lateral root density was negligible under lower space availability (D = 20). The lateral root density in P400 under D = 20 was lower than that in P200 under D = 30.

AM Colonization

Arbuscular mycorrhizal colonization was significantly affected by soil P supply and space availability (**Table 1**; **Figure 4**; **Supplementary Figure 4**); AM colonization decreased with increasing P supply from P0 to P400, regardless of space availability. Furthermore, the effect of AM colonization decreased as the space availability increased in all P treatments; P supply in the root zone and intraspecific density altered plant responses to AM colonization. Higher levels of AM colonization were observed under D = 20 compared with under D = 30 and D = 40. No significant differences were found between AM colonization in P200 under D = 40 and P400 under D = 30, while AM colonization in P0 under D = 40 was significantly higher than that in P200 under D = 30. AM colonization decreased significantly as P supply increased under D = 30 and D = 40, whereas there was no significant difference between AM colonization under conditions of higher P supply (P200 and P400) under D = 20. In addition, AM colonization decreased as space availability increased. The findings imply that the absorption of P by maize is most dependent on AM fungi at the limit of space availability, especially under P0.

Soil Olsen-P Concentration

Bulk soil Olsen-P concentration was strongly affected by soil P supply, with little correlation with space availability (**Table 1**; **Figure 5A**; **Supplementary Figure 5A**). In contrast, the rhizosphere soil Olsen-P concentration was greatly influenced by both soil P supply and space availability (**Table 1**; **Figure 5B**; **Supplementary Figure 5B**). Soil Olsen-P concentration in the bulk and rhizosphere soils increased as soil P supply increased.

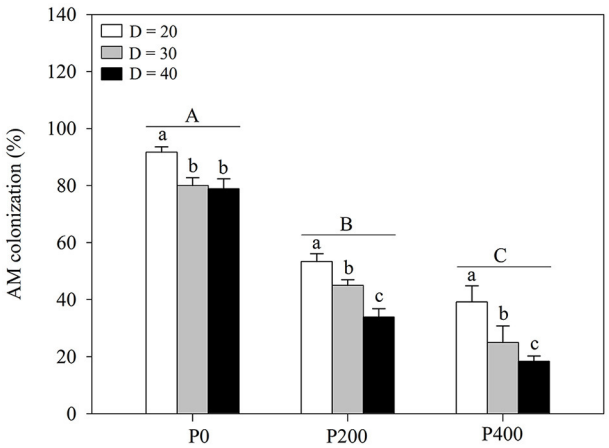

FIGURE 4 | Arbuscular mycorrhizal (AM) colonization under different phosphorous (P) supply gradients and space availability conditions. Each value represents the mean of four replicates (+SD). Different lower-case letters indicate a significant difference among different space availability levels, and different capital letters indicate a significant among different P levels ($P < 0.05$). P0, 0 mg P kg^{-1} soil; P200, 200 mg P kg^{-1} soil; and P400, 400 mg P kg^{-1} soil; D = 20, D = 30, and D = 40 represent diameter of pot is 20, 30, and 40 cm, respectively.

The highest soil Olsen-P concentration was observed in P400 followed by in P200 and then P0. Higher rhizosphere soil-Olsen P concentrations were obtained in P200 under D = 40 and P400 under D = 30.

DISCUSSION

Plants have evolved a series of mechanisms to acquire P from the soil (Lynch, 2011). In maize, the root morphology is a major pathway for obtaining P from soils (Liu et al., 2016; Lugli et al., 2020). Therefore, in addition to P supply in the root zone, space availability for root growth is critical for optimal maize production (Lynch, 2013; Poorter et al., 2016); however, in the maize plants grown at high density, root growth space can be limited, and whether additional soil P supply can compensate for such limitation and the underlying mechanisms are not fully understood. Understanding such interactions is crucial for improving the PUE of under high maize planting density production. In the present study, similar shoot biomass and P uptake were observed in P200 under D = 40 and P400 under D = 30 (**Figure 1**). Furthermore, the shoot biomass and P uptake in P400 under D = 30 were significantly higher than those in P200 under D = 40. Under insufficient space for root growth, the increasing P supply in the root zone could satisfy crop P demands to a certain extent (Poorter et al., 2012). The findings suggest that the negative effects of low space availability on shoot biomass and shoot P uptake could be counteracted by the improved soil P supply for enhanced maize growth.

With reduced space availability, the photoassimilates are less frequently allocated to the roots (Poorter et al., 2012; Shah et al., 2017). The findings of the previous studies have suggested

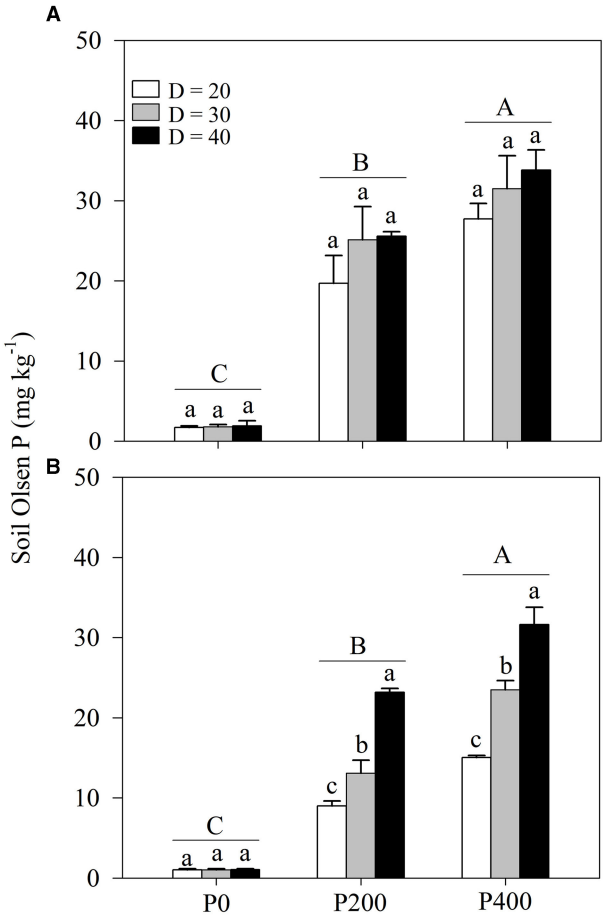

FIGURE 5 | (A) Bulk soil Olsen phosphorous (P) and **(B)** rhizosphere soil Olsen P under different P supply gradients and space availability conditions. Each value represents the mean of four replicates (+SD). Different lower-case letters indicate a significant difference among different space availability levels, and different capital letters indicate a significant among different P levels ($P < 0.05$). P0, 0 mg P kg^{-1} soil; P200, 200 mg P kg^{-1} soil; and P400, 400 mg P kg^{-1} soil; D = 20, D = 30, and D = 40 represent diameter of pot is 20, 30, and 40 cm, respectively.

that root growth is more inhibited under high plant density than shoot growth, which may be a factor limiting nutrient uptake, especially immobilized soil P (Shao et al., 2018). In addition, under P deficiency, the plants may allocate more carbon to the belowground parts; in maize, the root to shoot ratio can increase along with the enhanced root length and lateral root density to increase the exploration of more areas (Postma and Lynch, 2011; Niu et al., 2020). Over the long-term, low P input is usually accompanied by low productivity. As P is immobilized, increasing mineral P input into the soil is a common agronomy practice used to improve productivity (Zhang et al., 2019). In the present study, both bulk and rhizosphere soil Olsen-P concentrations increased as P supply increased (**Figure 5**; **Supplementary Figure 5**), which is similar to the findings observed when alfalfa was grown in a loessial soil (Peng et al., 2020). P is a nutrient that stimulates shoot biomass production and more importantly, acts as a regulatory signal mediating changes in root architecture (López-Bucio et al., 2003; Pongrac et al., 2020). Therefore, under lower space availability, a plant requires greater P supply to build a more efficient root system with a sufficient capacity to absorb P. In the present study, root dry weight in P400 under D = 30 was similar to that in P200 under D = 40, and root dry weight in P400 under D = 30 was significantly higher than that in P200 under D = 40 (**Figure 2**; **Supplementary Figure 2**). Root growth regulation by soil P supply and space availability could explain the complementary effects of the two factors on shoot biomass and P uptake.

Changes in space availability led to the plant responses that alter the root architecture (Ramireddy et al., 2018). The reduced space availability inhibits root length, tap root elongation, and the development of lateral roots (**Figures 3A,B,D**; **Supplementary Figures 3A,B,D**). In maize, the root architecture, such as root length, root surface area, root volume, and root diameter, can decrease under high plant density (Mi et al., 2016; Shao et al., 2018). In addition, the steeper root angles were obtained in treatments with lower space availability (**Figure 3C**; **Supplementary Figure 3C**), increasing the risks of rhizosphere P deficiency (**Figure 5B**). However, improved AM colonization was observed with lower space availability, suggesting that the soil P acquisition predominantly relies on root-associated AM fungi under high-planting density, where the formation of a sizeable hyphal network structure in the soil benefits P uptake (Deng et al., 2017). However, the regulation of root growth through P supply intensity is closely related to crop productivity through the exploitation of the biological potential for nutrient-use efficiency enhancement (Shen et al., 2013; McNickle, 2020). Root morphology exhibits high plasticity under varying P supply levels (Wang et al., 2020); increasing P supply induces root length growth, tap root elongation, and development of lateral roots and facilitates the acquisition of P through expansion into a greater soil volume, thereby increasing the absorptive surfaces of the roots (Williamson et al., 2001). In contrast, according to the results of the present study, AM colonization decreases as P supply increased. As expected, the root length, tap root length, and lateral root density increased as soil P supply increased through increased root-soil contact, subsequently enhancing P uptake (**Figures 3A,B,D**; **Supplementary Figures 3A,B,D**), while AM colonization decreased. Notably, this study results indicated similar root length, root angle, and lateral root density values in P200 under D = 40 and in P400 under D = 30. This finding suggests that P supply intensity may compensate for the limitation of growth space through the exploitation of the biological potential of maize to enhance P uptake through the root morphological changes.

At higher planting densities, plant growth and development can be limited by soil nutrients in the root zone (Dong et al., 2015). When the nutrient content is adequate for plant growth, increases in growth space may improve productivity (Fageria and Moreira, 2011). In the present study, shoot biomass and P uptake significantly increased with an increase in space availability under P200 and P400 (**Figure 1**; **Supplementary Figure 1**). In contrast, higher P supply (P200 and P400) did not improve shoot biomass and P uptake under D = 20 (**Figure 1**; **Supplementary Figure 1**).

Due to the existence of a threshold value for the efficient uptake of P by maize roots, maize cannot absorb more P than the threshold value, even if the amount of P supply is increased in a P-limited area (Santner et al., 2012). There are two plant P uptake pathways in the soil that include P uptake from soil: P uptake by roots and the AM fungal pathway (Watts-Williams et al., 2015). Root development and AM colonization are hindered under lower space availability considering that the plant density can lead to growth factor competition (Schroeder and Janos, 2004). The potential of root biology may not be fully exploited by P supply through the regulation of root morphology and AM colonization; therefore, only by matching P supply and space availability can root growth be regulated and the plant PUE can then be improved.

Collectively, the findings of the present study provide an important scientific basis for an enhanced understanding of the mechanisms *via* which soil P supply intensity could be used to counteract the adverse effects of high maize planting density on root morphology, P uptake, and PUE improvement, for sustainable crop production with high yields and high nutrient-use efficiency. Whether the advantages of soil P supply can compensate for the limited root growth spaces induced by high planting density under field conditions still requires further comprehensive studies.

CONCLUSIONS

Both P supply in the root zone and space availability influence the PUE in maize by influencing the root morphology and AM colonization dynamics. Similar shoot biomass and P uptake were observed in the conditions with high P supply and low space availability, and in the conditions with low P supply and high space availability. The lower maize biomass observed in conditions with relatively low space availability was fully counteracted by the relatively high P supply through the modification of root morphology and AM colonization activities. Furthermore, shoot biomass and P uptake did not increase with increased P supply in the root zone after root-growth space was reduced; here, the lower maize biomass obtained under low space availability was not fully counteracted by the relatively high P supply. The findings highlight the need to optimally coordinate the root growth space and P supply in the root zone, specifically to achieve optimal PUE under the intensive high-density maize production. The results of the present study highlight that understanding the optimal P supply in the root zone and space availability are essential for high PUE under the intensive high-density maize production system.

DATA AVAILABILITY STATEMENT

The original contributions presented in the study are included in the article/**Supplementary Material**, further inquiries can be directed to the corresponding author/s.

AUTHOR CONTRIBUTIONS

XJ supervised the experiments. HG performed most of the experiments and drafted the manuscript. BK and YX contributed reagents, materials, and analysis tools. All authors discussed the results and commented on the manuscript.

FUNDING

This study was supported by the National Natural Science Foundation of China (NSFC) (32172675, 31701999) and the Deutsche Forschungsgemeinschaft (DFG, German Research Foundation)-328017493/GRK 2366 (Sino-German International Research Training Group AMAIZE-P).

SUPPLEMENTARY MATERIAL

The Supplementary Material for this article can be found online at: https://www.frontiersin.org/articles/10.3389/fpls.2021.728527/full#supplementary-material

REFERENCES

Abdel-Fattah, G. M., and Asrar, A. W. A. (2012). Arbuscular mycorrhizal fungal application to improve growth and tolerance of wheat (Triticum aestivum L.) plants grown in saline soil. *Acta Physiol. Plant.* 34, 267–277. doi: 10.1007/s11738-011-0825-6

Breuillin, F., Schramm, J., Hajirezaei, M., Ahkami, A., Favre, P., Druege, U., et al. (2010). Phosphate systemically inhibits development of arbuscular mycorrhiza in Petunia hybrida and represses genes involved in mycorrhizal functioning. *Plant J.* 64, 1002–1017. doi: 10.1111/j.1365-313X.2010.04385.x

Cambardella, C. A., Gajda, A. M., Doran, J. W., Wienhold, B. J., and Kettler, T. A. (2001). "Estimation of particulate and total organic matter by weight loss on ignition," in *Assessment Methods for Soil Carbon*, eds R. Lal, J. M. Kimble, R. F. Follett, and B. A. Stewart (Boca Raton, FL: Lewis), 349–359.

Campos, P., Borie, F., Cornejo, P., López-Ráez, J. A., López-García, Á., and Seguel, A. (2018). Phosphorus acquisition efficiency related to root traits: Is mycorrhizal symbiosis a key factor to wheat and barley cropping? *Front. Plant Sci.* 9:752. doi: 10.3389/fpls.2018.00752

Carter, M., and Gregorich, E. (2007). *Soil Sampling and Methods of Analysis. 2nd Edn*. Boca Raton, FL: CRC Press, 15–24. doi: 10.1201/9781420005271

Chu, Q., Zhang, L., Zhou, J., Yuan, L., Chen, F., Zhang, F., et al. (2020). Soil plant-available phosphorus levels and maize genotypes determine the phosphorus acquisition efficiency and contribution of mycorrhizal pathway. *Plant Soil* 449, 357–371. doi: 10.1007/s11104-020-04494-4

Deng, Y., Feng, G., Chen, X., and Zou, C. (2017). Arbuscular mycorrhizal fungal colonization is considerable at optimal Olsen-P levels for maximized yields in an intensive wheat-maize cropping system. *F. Crop. Res.* 209, 1–9. doi: 10.1016/j.fcr.2017.04.004

Dhillon, J., Torres, G., Driver, E., Figueiredo, B., and Raun, W. R. (2017). World phosphorus use efficiency in cereal crops. *Agron. J.* 109, 1670–1677. doi: 10.2134/agronj2016.08.0483

Dong, T., Zhang, Y., Zhang, Y., and Zhang, S. (2015). Continuous planting under a high density enhances the competition for nutrients among young *Cunninghamia lanceolata* saplings. *Ann. For. Sci.* 73, 331–339. doi: 10.1007/s13595-015-0518-1

Fageria, N. K., and Moreira, A. (2011). The role of mineral nutrition on root growth of crop plants. *Adv. Agron.* 80, 63–152. doi: 10.1016/B978-0-12-385531-2.00004-9

Hecht, V. L., Temperton, V. M., Nagel, K. A., Rascher, U., Pude, R., and Postma, J. A. (2019). Plant density modifies root system architecture in spring barley (*Hordeum vulgare* L.) through a change in nodal root number. *Plant Soil* 439, 179–200. doi: 10.1007/s11104-018-3764-9

Hou, L., Zhang, X., Feng, G., Li, Z., Zhang, Y., and Cao, N. (2021). Arbuscular mycorrhizal enhancement of phosphorus uptake and yields of maize under high planting density in the black soil region of China. *Sci. Rep.* 11:1100. doi: 10.1038/s41598-020-80074-x

Johnson, C. M., and Ulrich, A. (1959). *Analytical Methods for Use in Plant Analysis*. Los Angeles, CA: University of California.

Kobae, Y. (2019). Dynamic phosphate uptake in arbuscular mycorrhizal roots under field conditions. *Front. Environ. Sci.* 6:159. doi: 10.3389/fenvs.2018.00159

Lambers, H., Martinoia, E., and Renton, M. (2015). Plant adaptations to severely phosphorus-impoverished soils. *Curr. Opin. Plant Biol.* 25, 23–31. doi: 10.1016/j.pbi.2015.04.002

Li, H., Zhang, D., and Wang, X. (2019). Competition between Zea mays genotypes with different root morphological and physiological traits is dependent on phosphorus forms and supply patterns. *Plant Soil* 434, 125–137. doi: 10.1007/s11104-018-3616-7

Liu, H., Tang, C., and Li, C. (2016). The effects of nitrogen form on root morphological and physiological adaptations of maize, white lupin and faba bean under phosphorus deficiency. *AoB Plants* 8:plab006. doi: 10.1093/aobpla/plw058

López-Bucio, J., Cruz-Ramírez, A., and Herrera-Estrella, L. (2003). The role of nutrient availability in regulating root architecture. *Curr. Opin. Plant Biol.* 6, 280–287. doi: 10.1016/S1369-5266(03)00035-9

Lugli, L. F., Andersen, K. M., Aragão, L. E. O. C., Cordeiro, A. L., Cunha, H. F. V., Fuchslueger, L., et al. (2020). Multiple phosphorus acquisition strategies adopted by fine roots in low-fertility soils in Central Amazonia. *Plant Soil* 450, 49–63. doi: 10.1007/s11104-019-03963-9

Lynch, J. P. (2011). Root phenes for enhanced soil exploration and phosphorus acquisition: tools for future crops. *Plant Physiol.* 156, 1041–1049. doi: 10.1104/pp.111.175414

Lynch, J. P. (2013). Steep, cheap and deep: an ideotype to optimize water and N acquisition by maize root systems. *Ann. Bot.* 112, 347–357. doi: 10.1093/aob/mcs293

Lyu, Y., Tang, H., Li, H., Zhang, F., Rengel, Z., Whalley, W. R., et al. (2016). Major crop species show differential balance between root morphological and physiological responses to variable phosphorus supply. *Front. Plant Sci.* 7:1939. doi: 10.3389/fpls.2016.01939

Ma, Q., Chen, L., Du, M., Zhang, Y., and Zhang, Y. (2020). Localized and moderate phosphorus application improves plant growth and phosphorus accumulation in Rosa multiflora thunb. ex murr. via efficient root system development. *Forests* 11:570. doi: 10.3390/f11050570

Ma, Q., Zhang, F., Rengel, Z., and Shen, J. (2013). Localized application of NH4+-N plus P at the seedling and later growth stages enhances nutrient uptake and maize yield by inducing lateral root proliferation. *Plant Soil* 372, 65–80. doi: 10.1007/s11104-013-1735-8

McNickle, G. G. (2020). Interpreting plant root responses to nutrients, neighbours and pot volume depends on researchers' assumptions. *Funct. Ecol.* 34, 2199–2209. doi: 10.1111/1365-2435.13517

Mi, G., Chen, F., Yuan, L., and Zhang, F. (2016). Ideotype root system architecture for maize to achieve high yield and resource use efficiency in intensive cropping systems. *Adv. Agron.* 139, 73–97. doi: 10.1016/bs.agron.2016.05.002

Ni, Z., Wang, S., Chu, Z., and Jin, X. (2015). Historical accumulation of N and P and sources of organic matter and N in sediment in an agricultural reservoir in Northern China. *Environ. Sci. Pollut. Res.* 22, 9951–9964. doi: 10.1007/s11356-015-4169-4

Niu, L., Yan, Y., Hou, P., Bai, W., Zhao, R., Wang, Y., et al. (2020). Influence of plastic film mulching and planting density on yield, leaf anatomy, and root characteristics of maize on the Loess Plateau. *Crop J.* 8, 548–564. doi: 10.1016/j.cj.2019.12.002

Olsen, S., Cole, C., Watanabe, F., and Dean, L. (1954). *Estimation of Available Phosphorus in Soils by Extraction With Sodium Bicarbonate. USDA Circular No.*939. Washington, DC: United States Department of Agriculture.

Peng, Q., Wu, M., Zhang, Z., Su, R., He, H., and Zhang, X. (2020). The interaction of arbuscular mycorrhizal fungi and phosphorus inputs on selenium uptake by alfalfa (*Medicago sativa L.*) and selenium fraction transformation in soil. *Front. Plant Sci.* 11:966. doi: 10.3389/fpls.2020.00966

Pongrac, P., Castillo-Michel, H., Reyes-Herrera, J., Hancock, R. D., Fischer, S., Kelemen, M., et al. (2020). Effect of phosphorus supply on root traits of two Brassica oleracea L. *genotypes. BMC Plant Biol.* 20, 1–17. doi: 10.1186/s12870-020-02558-2

Poorter, H., Bühler, J., Van Dusschoten, D., Climent, J., and Postma, J. A. (2012). Pot size matters: a meta-analysis of the effects of rooting volume on plant growth. *Funct. Plant Biol.* 39, 839–850. doi: 10.1071/FP12049

Poorter, H., Fiorani, F., Pieruschka, R., Wojciechowski, T., van der Putten, W. H., Kleyer, M., et al. (2016). Pampered inside, pestered outside? Differences and similarities between plants growing in controlled conditions and in the field. *New Phytol.* 212, 838–855. doi: 10.1111/nph.14243

Postma, J. A., Dathe, A., and Lynch, J. P. (2014). The optimal lateral root branching density for maize depends on nitrogen and phosphorus availability. *Plant Physiol.* 166, 590–602. doi: 10.1104/pp.113.233916

Postma, J. A., and Lynch, J. P. (2011). Root cortical aerenchyma enhances the growth of maize on soils with suboptimal availability of nitrogen, phosphorus, and potassium. *Plant Physiol.* 156, 1190–1201. doi: 10.1104/pp.111.175489

Ramireddy, E., Hosseini, S. A., Eggert, K., Gillandt, S., Gnad, H., von Wirén, N., et al. (2018). Root engineering in barley: increasing cytokinin degradation produces a larger root system, mineral enrichment in the shoot and improved drought tolerance. *Plant Physiol.* 177, 1078–1095. doi: 10.1104/pp.18.00199

Santner, J., Smolders, E., Wenzel, W. W., and Degryse, F. (2012). First observation of diffusion-limited plant root phosphorus uptake from nutrient solution. *Plant, Cell Environ.* 35, 1558–1566. doi: 10.1111/j.1365-3040.2012.02509.x

Schroeder, M. S., and Janos, D. P. (2004). Phosphorus and intraspecific density alter plant responses to arbuscular mycorrhizas. *Plant Soil* 264, 335–348. doi: 10.1023/B:PLSO.0000047765.28663.49

Shah, A. N., Yang, G., Tanveer, M., and Iqbal, J. (2017). Leaf gas exchange, source–sink relationship, and growth response of cotton to the interactive effects of nitrogen rate and planting density. *Acta Physiol. Plant.* 39:119. doi: 10.1007/s11738-017-2402-0

Shao, H., Shi, D., Shi, W., Ban, X., and Chen, Y. (2019). Genotypic difference in the plasticity of root system architecture of field-grown maize in response to plant density. *Plant Soil* 439, 201–217. doi: 10.1007/s11104-019-03964-8

Shao, H., Xia, T., Wu, D., Chen, F., and Mi, G. (2018). Root growth and root system architecture of field-grown maize in response to high planting density. *Plant Soil* 430, 395–411. doi: 10.1007/s11104-018-3720-8

Shen, J., Li, C., Mi, G., Li, L., Yuan, L., Jiang, R., et al. (2013). Maximizing root/rhizosphere efficiency to improve crop productivity and nutrient use efficiency in intensive agriculture of China. *J. Exp. Bot.* 64, 1181–1192. doi: 10.1093/jxb/ers342

Teng, W., Deng, Y., Chen, X. P., Xu, X. F., Chen, R. Y., Lv, Y., et al. (2013). Characterization of root response to phosphorus supply from morphology to gene analysis in field-grown wheat. *J. Exp. Bot.* 64, 1403–1411. doi: 10.1093/jxb/ert023

Testa, G., Reyneri, A., and Blandino, M. (2016). Maize grain yield enhancement through high plant density cultivation with different inter-row and intra-row spacings. *Eur. J. Agron.* 72, 28–37. doi: 10.1016/j.eja.2015.09.006

Trouvelot, A., Kough, J. L., and Gianiazzi-Pearson, V. (1986). "Mesure du taux de mycorrhization VA d'un système radiculaire. Recherche de methods d'estimation ayant une signification fonctionnelle," in *Physiological and Genetical Aspects of Mycorrhizae*, eds J. Gianinazzi-Pearson and S. Gianinazzi (Paris: INRA Press), 217–221.

Wang, X. X., Li, H., Chu, Q., Feng, G., Kuyper, T. W., and Rengel, Z. (2020). Mycorrhizal impacts on root trait plasticity of six maize varieties along a phosphorus supply gradient. *Plant Soil* 448, 71–86. doi: 10.1007/s11104-019-04396-0

Watts-Williams, S. J., Jakobsen, I., Cavagnaro, T. R., and Grønlund, M. (2015). Local and distal effects of arbuscular mycorrhizal colonization on direct pathway Pi uptake and root growth in Medicago truncatula. *J. Exp. Bot.* 66, 4061–4073. doi: 10.1093/jxb/erv202

Williamson, L. C., Ribrioux, S. P. C. P., Fitter, A. H., and Ottoline Leyser, H. M. (2001). Phosphate availability regulates root system architecture in Arabidopsis. *Plant Physiol.* 126, 875–882. doi: 10.1104/pp.126.2.875

Yu, X., Zhang, Q., Gao, J., Wang, Z., Borjigin, Q., Hu, S., et al. (2019). Planting density tolerance of high-yielding maize and the mechanisms underlying yield improvement with subsoiling and increased planting density. *Agronomy* 9:370. doi: 10.3390/agronomy9070370

Zhang, Q., Sun, Q., Koide, R. T., Peng, Z., Zhou, J., Gu, X., et al. (2014). Arbuscular mycorrhizal fungal mediation of plant–plant interactions in a marshland plant community. *Sci. World J.* 2014:923610. doi: 10.1155/2014/923610

Zhang, W., Chen, X. X., Liu, Y. M., Liu, D. Y., Chen, X. P., and Zou, C. Q. (2017). Zinc uptake by roots and accumulation in maize plants as affected by phosphorus application and arbuscular mycorrhizal colonization. *Plant Soil* 413, 59–71. doi: 10.1007/s11104-0173213-1

Zhang, W., Tang, X., Feng, X., Wang, E., Li, H., Shen, J., et al. (2019). Management strategies to optimize soil phosphorus utilization and alleviate environmental risk in China. *J. Environ. Qual.* 48, 1167–1175. doi: 10.2134/jeq2019.02.0054

Conflict of Interest: The authors declare that the research was conducted in the absence of any commercial or financial relationships that could be construed as a potential conflict of interest.

Publisher's Note: All claims expressed in this article are solely those of the authors and do not necessarily represent those of their affiliated organizations, or those of the publisher, the editors and the reviewers. Any product that may be evaluated in this article, or claim that may be made by its manufacturer, is not guaranteed or endorsed by the publisher.

frontiers in Plant Science

PERSPECTIVE
published: 01 October 2021
doi: 10.3389/fpls.2021.686274

Adaptive Reprogramming During Early Seed Germination Requires Temporarily Enhanced Fermentation-A Critical Role for Alternative Oxidase Regulation That Concerns Also Microbiota Effectiveness

Revuru Bharadwaj[1,2], Carlos Noceda[2,3], Gunasekharan Mohanapriya[1,2], Sarma Rajeev Kumar[1,2], Karine Leitão Lima Thiers[2,4], José Hélio Costa[2,4], Elisete Santos Macedo[2], Aprajita Kumari[2,5], Kapuganti Jagadis Gupta[2,5], Shivani Srivastava[2,6], Alok Adholeya[2,6], Manuela Oliveira[2,7], Isabel Velada[2,8], Debabrata Sircar[2,9], Ramalingam Sathishkumar[1,2] and Birgit Arnholdt-Schmitt[2,4]**

[1] Plant Genetic Engineering Laboratory, Department of Biotechnology, Bharathiar University, Coimbatore, India, [2] Non-Institutional Competence Focus (NICFocus) 'Functional Cell Reprogramming and Organism Plasticity' (FunCROP), coordinated from Foros de Vale de Figueira, Alentejo, Portugal, [3] Cell and Molecular Biology of Plants (BIOCEMP)/Industrial Biotechnology and Bioproducts, Departamento de Ciencias de la Vida y de la Agricultura, Universidad de las Fuerzas Armadas-ESPE, Sangolquí, Ecuador, [4] Functional Genomics and Bioinformatics Group, Department of Biochemistry and Molecular Biology, Federal University of Ceará, Fortaleza, Brazil, [5] National Institute of Plant Genome Research, New Delhi, India, [6] Centre for Mycorrhizal Research, Sustainable Agriculture Division, The Energy and Resources Institute (TERI), TERI Gram, Gurugram, India, [7] Department of Mathematics and CIMA - Center for Research on Mathematics and Its Applications, Universidade de Évora, Évora, Portugal, [8] MED—Mediterranean Institute for Agriculture, Environment and Development, Instituto de Investigação e Formação Avançada, Universidade de Évora, Évora, Portugal, [9] Department of Biotechnology, Indian Institute of Technology Roorkee, Roorkee, India

Plants respond to environmental cues *via* adaptive cell reprogramming that can affect whole plant and ecosystem functionality. Microbiota constitutes part of the inner and outer environment of the plant. This *Umwelt* underlies steady dynamics, due to complex local and global biotic and abiotic changes. Hence, adaptive plant holobiont responses are crucial for continuous metabolic adjustment at the systems level. Plants require oxygen-dependent respiration for energy-dependent adaptive morphology, such as germination, root and shoot growth, and formation of adventitious, clonal, and reproductive organs, fruits, and seeds. Fermentative paths can help in acclimation and, to our view, the role of alternative oxidase (AOX) in coordinating complex metabolic and physiological adjustments is underestimated. Cellular levels of sucrose are an important sensor of environmental stress. We explored the role of exogenous sucrose and its interplay with AOX during early seed germination. We found that sucrose-dependent initiation of fermentation during the first 12 h after imbibition (HAI) was beneficial to germination. However, parallel upregulated *AOX* expression was essential to control negative effects by prolonged sucrose treatment. Early downregulated *AOX* activity until 12 HAI improved germination efficiency in the absence of sucrose but suppressed early germination in its presence. The results also suggest that seeds

OPEN ACCESS

Edited by:
Giuseppe Colla, University of Tuscia, Italy

Reviewed by:
Erica Lumini, Institute for Sustainable Plant Protection, National Research Council (CNR), Italy
Wei Wang, Chinese Academy of Tropical Agricultural Sciences, China

***Correspondence:**
Ramalingam Sathishkumar
rsathish@buc.edu.in
Birgit Arnholdt-Schmitt
biarnaflora@gmail.com

Specialty section:
This article was submitted to Plant Symbiotic Interactions, a section of the journal Frontiers in Plant Science

Received: *20 April 2021*
Accepted: *10 August 2021*
Published: *01 October 2021*

Citation:
Bharadwaj R, Noceda C, Mohanapriya G, Kumar SR, Thiers KLL, Costa JH, Macedo ES, Kumari A, Gupta KJ, Srivastava S, Adholeya A, Oliveira M, Velada I, Sircar D, Sathishkumar R and Arnholdt-Schmitt B (2021) Adaptive Reprogramming During Early Seed Germination Requires Temporarily Enhanced Fermentation-A Critical Role for Alternative Oxidase Regulation That Concerns Also Microbiota Effectiveness. Front. Plant Sci. 12:686274. doi: 10.3389/fpls.2021.686274

inoculated with arbuscular mycorrhizal fungi (AMF) can buffer sucrose stress during germination to restore normal respiration more efficiently. Following this approach, we propose a simple method to identify organic seeds and low-cost *on-farm* perspectives for early identifying disease tolerance, predicting plant holobiont behavior, and improving germination. Furthermore, the research strengthens the view that AOX can serve as a powerful functional marker source for seed hologenomes.

Keywords: seed quality, ROS, Warburg effect, bacterial endophytes and mycorrhizal fungi, organic seeds, biotic stress, *on-farm* seed selection

INTRODUCTION

Understanding the role of microbiota in adaptive plant robustness is important for crop improvement and developing innovative tools that could allow more efficient plant selection (Arnholdt-Schmitt et al., 2014; Arnholdt-Schmitt et al., 2015, 2018; Nogales et al., 2015). Research on the relevance of endophytic and associated microbiota and usage of microbes as bioinoculants are often hampered by low reproducibility, due to a lack of better understanding of fundamental principles of the plant-microbe interactions (Arnholdt-Schmitt, 2008; Vicente and Arnholdt-Schmitt, 2008; Campos et al., 2015; Mercy et al., 2015, 2017; Bedini et al., 2018; Albornoz et al., 2020) emphasized the need to study mycorrhizal benefits on a case-by-case basis which should consider more holistic and context-dependent views on mycorrhiza functioning at plant family and biome-wide levels. Also, it is widely confirmed that endophyte effects are genotype-specific (Abdelrazek et al., 2020a,b). Furthermore, Durán et al. (2018) identified bacterial endophytes as drivers for soil suppressive take-all disease. Nevertheless, they highlighted that they did not find a relevant correlation between disease suppression and reduced pathogen biomass. In our opinion, these are key observations. They encouraged us to initiate the work on the hypothesis that the competence of individual plant hosts for resilience plays the most critical role for beneficial or non-beneficial plant-microbe interactions, which can be superior to plant families and biome origins.

However, there is a lack of knowledge on traits that aid in (a) early prediction of the plant strength, (b) demonstration of its relevance for plant-microbe interactions, and (c) transformation of such knowledge toward user- and environment-friendly applications for sustainable agriculture. We earnestly aim with the perspective to understand these phenomena and to contribute to the knowledge base toward closing these three gaps.

Seed Germination/Reprogramming as a Model to Study Plant Adaptive Robustness

The capacity for efficient reprogramming as a trait *per se* is recognized as a marker for adaptive plant robustness (Cardoso and Arnholdt-Schmitt, 2013). Seed germination can serve as an experimental *in vitro* tool to study environmental stress-induced reprogramming and to identify early functional markers and tools for predicting plant performance under field conditions (Mohanapriya et al., 2019). Dry seeds are known to respond upon water imbibition and subsequent penetration of oxygen. Thus, radicle emergence can be seen as an indicator of environmental stress recovery from the dry-to-water imbibed conditions and low-to-high oxygen status.

Efficient seed germination under field conditions is especially required in organic agriculture, where the application of chemical herbicides and pesticides to suppress competitors shall be avoided to support healthy food and feed production and to improve the sustainability of bio-based socioeconomic systems. At the same time, organic agriculture impacts seed quality and the amount of microbiota in seeds (Cope-Selby et al., 2017; Wassermann et al., 2019). Recently, the use of the so-called "organic seeds" vs. conventionally produced seeds is raised as an ethical issue (European Parliament and of the Council, 2018). However, the better quality of organic seeds in terms of their contribution to agriculture sustainability, nutritional quality, and yield performance is under intensive debate (e.g., Bhaskar et al., 2019; Voss-Fels et al., 2019) and requires scientific validation (Simon et al., 2017; Abdelrazek et al., 2020a,b). Appropriate methods and tools are in absolute need to discriminate organic vs. conventional seeds by traits that should allow predicting the superior quality of organic seeds.

The Complex Role of Sucrose in Adaptive Reprogramming

Cellular reprogramming is an energy intensive phenomenon. Reactive oxygen species (ROS) are known to interact with redox-sensitive protein cysteine thiol groups relevant for energy metabolism and metabolic channeling linked to cell differentiation and cell cycle regulation (Bigarella et al., 2014; Dumont and Rivoal, 2019; Gupta et al., 2020a,b; Pengpeng et al., 2020; Qi et al., 2020). Sugars and sugar phosphates interact with hormone-mediated signal networks to modulate energy metabolism. Auxin-stimulated sugar metabolism is frequently reported (e.g., Zhao et al., 2021); however, only few examples revealed that sucrose can induce new cell programs (Grieb et al., 1994; see in Zavattieri et al., 2010) and also, vice versa, can change auxin metabolism (Lin et al., 2016; Meitzel et al., 2021). In maize, sucrose induced several cell cycle markers during germination than glucose (Lara-Núñez et al., 2017). Downstream of sugars, two important antagonistic protein kinases are involved in energy sensing and physiological adaptation (reviews in Bailey-Serres et al., 2018; Sakr et al., 2018; Schmidt et al., 2018). While sucrose non-fermenting-1-related protein kinase 1 is activated when energy is depleted (Schmidt et al., 2018; Wurzinger et al.,

2018; Wang et al., 2020), the target of rapamycin (TOR) is induced under conditions of energy excess to stimulate the cell cycle progression and the cell proliferation (Sangüesa et al., 2019). Sucrose can have various functions: besides its metabolic role, it acts as a signaling component (Baena-González and Hanson, 2017; Sakr et al., 2018), as an osmotic stressor that can disrupt communication within and between cells (Moon et al., 2015), shown to trigger aerobic alcohol fermentation in support of respiration, and biosynthesis of higher molecular weight compounds, such as lipids (Mellema et al., 2002).

Multifunctional Role of AOX as Switch Between Respiration and Fermentation During the Germination Process

Alcohol fermentation has been found to play a critical role in controlling tissue level pyruvate in plants, thereby, adjusting respiration rates to prevailing cellular energy status (Zabalza et al., 2009). Fan et al. (2020) identified hormone and alcohol degradation pathways that were mostly activated during the early stages of somatic embryogenesis (SE), which is a prominent example of *de novo* programming. Ethanol has been shown to reduce ROS levels and led to high induction of *alternative oxidase* (*AOX*) and *glutathione-S-transferase* transcripts (Nguyen et al., 2017). Transcriptome analyses at 2,4-dichlorophenoxyacetic acid (2,4-D) induced reprogramming indicated that the extent of aerobic fermentation is connected to cell proliferation and is regulated by interacting levels of sucrose and AOX (Costa et al., 2021). Transient upregulation of genes related to alcoholic and lactic acid fermentation is shown to be associated with glycolysis and modified complex stress signaling patterns with enhanced superoxide dismutase (SOD) and decreased transcript levels of nitric oxide (NO) producing *nitrate reductase* (NR). Furthermore, the data signaled activation of cell death-regulating system and arrested cell cycle by reducing alpha-tubulin gene transcription in the earliest step of reprogramming. Considering the generality of these observations, we proposed a reference transcriptome profile to identify virus traits that link to harmful reprogramming (Arnholdt-Schmitt et al., 2021). This approach helped to identify an early trait for combating SARS-CoV-2 that covers ROS/reactive nitrogen species (RNS) balancing, aerobic fermentation regulation, and cell cycle control (Costa et al., 2021).

In seeds, fermentation and alternative respiration (AR) are dominating metabolic reactions (Arnholdt-Schmitt et al., 2018; Mohanapriya et al., 2019). During seed germination, structural and functional acclimation of aerobic respiration is central and determines the temperature-dependent efficiency of germination (Bello and Bradford, 2016; Paszkiewicz et al., 2017). Nevertheless, markers for respiration and oxygen consumption were not superior to simple germination tests for predicting the vigor of single seeds (Powell, 2017). However, it is suggested that AR plays the most critical role during germination (Arnholdt-Schmitt et al., 2018; Mohanapriya et al., 2019). This role requires managing ROS/RNS increase and channeling energy and substance flow from fermentation, when carbohydrate storages are released and enzymes get into action (Saleh and Kalodimos, 2017), but the respiration chain is still structurally restricted and overloaded by massively incoming oxygen. AOX is mainly regulated by pyruvate (Millar et al., 1996; Hoefnagel et al., 1997; Hakkaart et al., 2006; Albury et al., 2009; Carré et al., 2011; Selinski et al., 2018) and strikingly, Ito et al. (2020) showed in *Arum* that energy-related metabolic regulation can be determined by temperature-dependent switching between AOX polymorphisms in the binding site for AOX-pyruvate. In this scenario, it might be of interest that AOX is essential in ethylene-induced drought tolerance and mediating autophagy *via* balancing ROS levels (Zhu et al., 2018). Also, thermoinhibition of carrot seed germination could be circumvented by seed priming, which was found to be linked to increased ethylene production at higher temperatures (Nascimento et al., 2013). Ethylene biosynthesis is found to be induced by hydrogen peroxide (H_2O_2) and acted positively on germination, independent of auxin-coordinated hormonal crosstalk linked to abscisic acid suppression and gibberellin activation (Wojtyla et al., 2016). During ethylene biosynthesis, cyanide is generated as a by-product of the pathway and probably shifts cytochrome oxidase (COX)-mediated respiration to AR (Siegień and Bogatek, 2006; Machingura et al., 2016). Eckert et al. (2014) stressed that microbiota has developed ethylene-producing pathways to profit during the invasion and to evade defense responses of the host plants. Additionally, Mercy et al. (2017) observed that treating mycorrhiza-infected seedlings with potassium cyanide promoted local arbuscular formation.

AOX Is a Key Molecule for Cellular Reprogramming: Toward a Perspective

Recently, we identified AOX as the stress level sensing coordinator for auxin inducible metabolic reprogramming by comparing induction of SE and seed germination (Arnholdt-Schmitt et al., 2018; Mohanapriya et al., 2019). Association of AOX to target cell reprogramming is also observed in other systems such as adventitious root development in olive (Santos Macedo et al., 2009; Porfirio et al., 2016) and elicitor-induced hairy roots (Sircar et al., 2012). Furthermore, our group had contributed to novel functional marker strategies by highlighting AOX as a marker across taxonomic borders that includes "shared" *AOX* genes in plant holobionts (Arnholdt-Schmitt, 2005a,b, 2008; Arnholdt-Schmitt et al., 2006; Campos et al., 2015; Mercy et al., 2017; Bedini et al., 2018). Based on the role of AOX in carbohydrate metabolism (Vanlerberghe et al., 1994), our approach has been stimulated to understand the role of fermentation and sugars during plant–mycorrhiza interactions (Mercy et al., 2017; Bedini et al., 2018) and had led to a privately explored patent (Lucic and Mercy, 2014). However, the early phase of reprogramming was not sufficiently considered in that research (Mercy et al., 2017) to drive our core functional marker approach (Arnholdt-Schmitt, 2008; Mercy et al., 2015). Recently, Mohanapriya et al. (2019) observed that arbuscular mycorrhizal fungi (AMF) inoculation in carrot seeds interacted with the AOX-inhibitor salicyl hydroxamic acid (SHAM) and palliated negative SHAM effects on early germination. Also, AMF effects in seeds seemed to be modified by non-culturable microbiota. Integrated *in silico* studies on experimental data revealed that endophytes interact with *AOX* expression in

species-, stress-, and developmental-dependent manner. Also, Costa et al. (2021) highlighted the importance of microbiota–plant genotype interaction and its impact on early carrot seed germination which can be modified by SHAM.

In our earlier work in Mohanapriya et al. (2019), we demonstrated successful prediction of oxycaloric equivalents from germinating seeds at 10 HAI. The present perspective questions the metabolic nature of AOX coordination and provides deeper phenotyping during germination of endophyte-free and microbiota-inoculated seeds focused at early times around 12 HAI. **Figure 1** demonstrates the step-by-step rationale of fundamental insights and deduced practical strategies (methodology of experiments is provided in **Supplementary File 1**).

In our findings, we observed that **(a)** during *Arabidopsis thaliana* seed germination *alcohol dehydrogenase* (ADH) transcript levels were increased at 12 h after seed stratification (SL) in water followed by a decline, and the increase in *ADH* transcript levels is in general accompanied by increased *AOX1a* transcript accumulation (**Figure 1B2**). **(b)** In agreement with **(a)**, germinating carrot seeds displayed a higher level of ADH activity at 12 HAI than 24 HAI. In the presence of 3% sucrose, this level was further enhanced (**Figures 1A3,B3**). **(c)** Two hours short pulses of sucrose before water imbibition enhanced early germination in seeds of two different species, viz., carrot and wheat (**Figures 1A2,E3** and **Supplementary Figure 2**). Additionally, in carrots, we showed that the effectiveness of such early sugar pulse was dependent on sucrose concentration. A short pulse could be substituted by a longer pulse at a lower concentration of sucrose (**Figure 1A2**). **(d)** On the contrary, SHAM treatment until 6 and 12 HAI suppressed germination in the presence of 3% sucrose. However, it favored early germination in the absence of sucrose (**Figure 1C1**).

(e) Three carrot native bacterial endophytes (EN1, EN2, and EN3) were used for carrot seed inoculations with two cultivars (cv. Kuroda, cv. Early Nantes) and showed a tendency to improve germination (**Figure 1D1**). However, a positive effect is dependent on cultivar-endophyte interaction. SHAM treatment reduced the early germination percentage of endophyte-treated seeds against the respective endophyte-treated controls. This was observed in all cases though to a different degree of inhibition (**Figure 1D2** and **Supplementary Table 2**). **(f)** Sucrose has displayed different impacts on endophyte-mediated effects on germination and is dependent on cultivar and endophytes. However, in no case did endophytes improved germination of sucrose-treated seeds when compared with endophyte-treated controls without sucrose (**Figure 1D2** and **Supplementary Table 2**). **(g)** In a good germinating carrot cultivar (cv. Kuroda), the two selected *Rhizophagus* species (*Rhizophagus irregularis* and *Rhizophagus proliferus*) acted negatively on early germination, while in a delayed germinating carrot cultivar (cv. Early Nantes), both *Rhizophagus* species acted positively (**Figure 1D1** and **Supplementary Table 2**). In both cultivars, sucrose could improve *Rhizophagus* effects on early germination to higher levels than the AMF-treated controls. However, this is dependent on cultivar-species interaction. In the presence of sucrose, *R. irregularis* (M1) improved germination of both cultivars compared to M1-treated control seeds in the absence of sucrose (**Figure 1D2**). **(h)** In addition, at lower concentrations of SHAM (5 mM), early germination could be improved to higher levels as compared to the AMF-treated controls (**Figure 1D2**), but this is observed only in the cv. Kuroda variety, which did not show positive AMF effects against non-AMF-treated controls (**Figure 1D1** and **Supplementary Table 2**).

In **Figure 2**, we present a simplified scheme that summarizes our conclusion based on wet-lab experiments, state-of-the-art knowledge, and our hypothetical inferences related to the dynamic metabolic interplay between sucrose, aerobic fermentation, COX-mediated respiration, AOX regulation/AR, and microbiota on cell reprogram functioning. In this scheme, we separated AOX as a macromolecule (gene/protein) from its functional pathway, AR, to highlight the outstanding position of AOX as the key and only enzyme of the pathway that, if present in an organism, is recognized to provide a central metabolism-coordinating function for efficient survival (Mohanapriya et al., 2019; Arnholdt-Schmitt et al., 2021; Costa et al., 2021). We consider that under development- and/or environment-induced conditions of rapid sucrose increase, the COX pathway is stimulated *via* enhanced glycolysis, pyruvate production, and increased tricarboxylic acid (TCA) cycle, in a way that the respiratory chain can get overloaded by electrons followed by enhanced ROS/RNS levels and, on the other hand, restricted due to rapidly consumed oxygen and/or yet low numbers of functional mitochondria concerning the presence of oxygen during germination. In response, aerobic alcoholic and lactic fermentation are stimulated (refer points a, b, and c; Costa et al., 2021). At the same time, AOX is activated [refer point d and in Mohanapriya et al. (2019), Costa et al. (2021)] mainly through *AOX* gene sequence-dependent pyruvate regulation and ROS/RNS.

Depending on stress level and the amount of sucrose and duration of the situation of high sugar-level, anaerobic glycolysis can reach high turnover during cell reprogramming and high levels of adenosine triphosphate production even corresponding to the Warburg effect. This latter hypothesis is supported by parallel research on auxin-induced callus growth (Costa et al., 2021), where we observed a rapid increase in *ADH1* transcripts of 1,777% and a parallel increase in *LDH* (*Lactate dehydrogenase*) transcripts of 346%. Warburg effects are increasingly recognized also in human systems (Kutschera et al., 2020; Melkonian and Schury, 2020) as being part of normal physiology. However, in plants, they are studied still more concerning photosynthesis (Kutschera et al., 2020) and anaerobic conditions are best explored under flooding conditions and are related to anaerobic tolerance in rice (Narsai et al., 2017). It is shown that AOX plays a beneficial role under low oxygen and especially during reoxygenation (Jayawardhane et al., 2020).

Under increased sucrose, fermentation can escape feedback downregulation with the help of enhanced AR, since AOX-transferred electrons enable the continuation of the TCA cycle for metabolic reorganization though with relatively less energy efficiency. Thus, fermentation and AOX are complementing each other to maintain metabolic and energetic homeostasis thereby avoiding inefficient situations when the respiration chain is overloaded with oxygen availability. As soon as oxidative stress gets sufficiently diminished at equilibrated oxygen availability in the COX pathway, AOX will be downregulated and normal

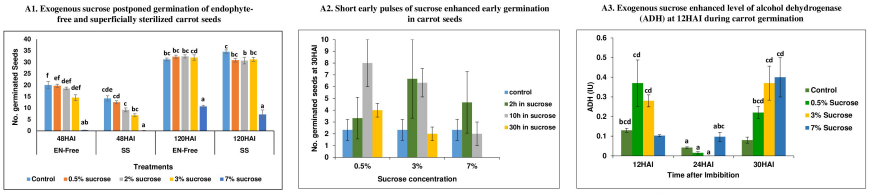

B1. SHAM affects early germination, this is linked to expression of *AtAOX1a*

Germination at 72HAI	Wild type	Anti-Sense (suppressed expression)	Overexpression
Control	ALL	ALL	ALL
0.5 mM SHAM	FEW	ALL	NONE
1.5 mM SHAM	ca. 50%	ALL	FEW
2.5 mM SHAM	NONE	NONE	NONE

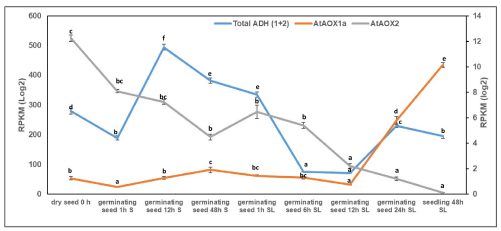

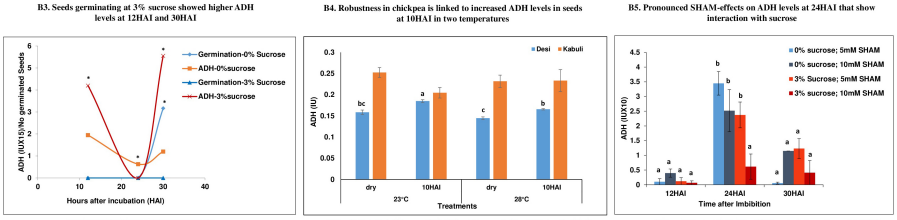

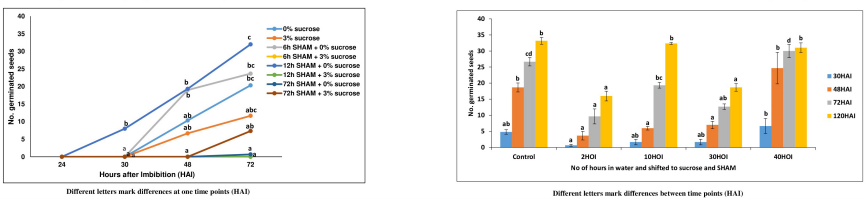

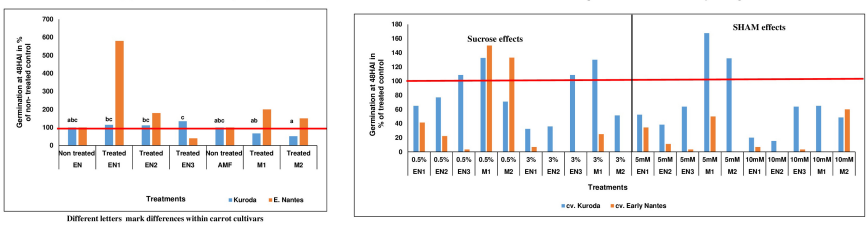

Perspectives for simple and rapid *on-farm* and *service* seed improvement – open for validation

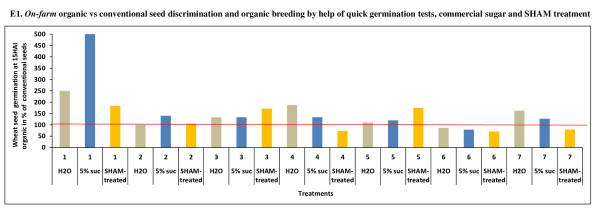

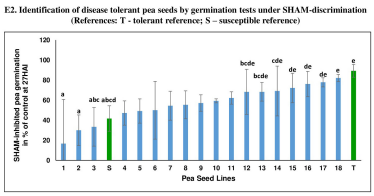

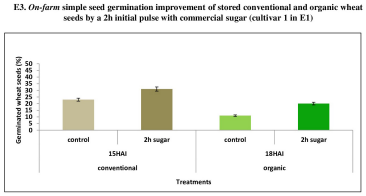

FIGURE 1 | *(Continued)*

FIGURE 1 | (Continued)
Step-by-step rationale of the perspective. **(A1)** Exogenous sucrose postponed germination of endophyte-free and superficially sterilized carrot seeds: Sucrose inhibited early germination [at 48 h after imbibition (HAI)] depending on increasing sugar concentrations. This trend is the same for endophyte-free seeds that were superficially sterilized. At 120 HAI, the effect of 0.5–3% sucrose could not be noticed anymore, while 7% sucrose inhibited germination for a prolonged time. This observation indicates a critical role of sucrose during the induction of adaptive performance. To confirm, the role of sucrose, in **Supplementary Figure 1**, the effect of sucrose is shown for auxin-dependent early induction of somatic embryogenesis (SE) as the most studied example of *de novo* programming. It demonstrates that (a) sugar is essential for cell reprogramming since SE induction was not observed at around 45 DAI (days after inoculation) in controls, but only at 2 and 3% sucrose supply and (b) that SE can be optimized with the help of increasing amounts of exogenous sucrose since SE induction efficiency is highest at 3% sucrose (**Supplementary Table 1**). Cell reprogramming competes with cell division. This is a common insight, which got here validated again through the observed delay in embryonic vs. non-embryonic callus emergence at lower sucrose concentrations. As a general tendency, at higher sucrose levels, less number of seeds showed callus growth, which was later demonstrated to be embryogenic, in comparison to the higher number of seeds with (non-embryogenic) callus growth at lower sucrose levels (**Supplementary Figure 1**). **(A2)** Short early pulses of sucrose enhanced early germination in carrot seeds: A total of 3% sucrose applied for 2 or 10 h imbibition enhanced early germination for about the same degree compared to the control and longer pulse of 30 h. A lower sucrose concentration of 0.5% had the highest effect only by a longer pulse of 10 h and, at 7% sucrose, a higher effect against the control was only indicated when given as a short pulse of 2 h. This observation was confirmed with a second carrot cultivar in a rapid *on-farm* check by using a ca. 5% solution of commercial sugar (significant) (**Supplementary Figure 2**). **(A3)** Exogenous sucrose enhanced the level of alcohol-dehydrogenase (ADH) at 12 HAI during carrot germination: At 12 HAI, treatment with 0.5 and 3% sucrose resulted in an increase in ADH activity as compared to the control, while for 7% sucrose no effect is observed. At 24 HAI, the control indicated a decline of ADH values. In the presence of 0.5 and 3% sucrose, this decline is not avoided or might even have been strengthened. However, at 30 HAI, a second phase started, where sucrose enhanced the levels of ADH in a concentration-dependent manner including a positive effect of 7% sucrose. **(B1)** Salicyl hydroxamic acid (SHAM) affects early germination and this links to expression of *AtAOX1a*: In wild-type *Arabidopsis thaliana* seeds, while monitoring germination at 72 HAI, showed that SHAM treatment led to reduced germination rates. This inhibition is dependent on its concentration of 0.5 or 1.5 mM. However, when alternative oxidase (AOX) had been silenced (antisense), SHAM did not affect germination. On the contrary, when AOX was constitutively overexpressed (OE), SHAM indicated stronger inhibition of germination than in the wild type. Nevertheless, the three genotypes germinated with similar efficiency about their respective controls. This latter observation points to the fact that AOX is critically important for germination, if present. However, in case it is not present or activated (antisense) alternative pathways can substitute the functional role of AOX during germination. **(B2)** *AtAOX1a* and *AtADH1 + 2* transcripts accumulated simultaneously: A study on ADH transcript accumulation in wild-type *A. thaliana* confirmed a biphasic activation of *ADH* during germination. A first increase was observed 12 h after stratification (significant), which includes the imbibition of water. The second enhancement occurred from 12 h SL shortly before root emergence was monitored at 24 h SL. In parallel to increased *ADH* transcript accumulation, *AOX1a* transcripts accumulated during both phases, i.e., induction and early initiation of germination. After early induction, *ADH* transcripts showed a high decline (significant) until the end of the dark stratification phase, while *AOX1a* transcript levels remained more stable. During the second phase at the initiation of exponential root length growth in light observed at 48 h SL, *AOX1a* transcript accumulation keeps on enhancing, while the increase of *ADH* transcripts stopped at that time point. This is also indicated in the first phase. *AOX2* transcript accumulation is differentially regulated in comparison to *AOX1a* and showed continuous downregulation during the whole period, which appeared to be stronger in the SL phase. **(B3)** Seeds germinating at 3% sucrose showed higher ADH levels at 12 and 30 HAI: During early germination of carrot seeds, ADH levels follow a parable, when monitored between 12 and 30 HAI. This is observed in control seeds and seeds germinating at 3% sucrose. Nevertheless, suppressed germination at 3% sucrose is linked to higher levels of ADH at 12 and 30 HAI. This means the more efficient germination in control seeds is linked at these two-time points to lower levels of ADH. Under both conditions, in the absence of exogenous sucrose and at 3% sucrose, 24 HAI displayed a turning point with the lowest ADH activity levels. However, ADH activity at 24 HAI is higher in controls (significant) than under conditions of sucrose-supplementation. **(B4)** Early chickpea plant vigor is critical for plant productivity under terminal drought conditions (Sivasakthi et al., 2017). From the two principle chickpea types, Desi and Kabuli, vast field experience has shown that Desi is superior in terms of multistress tolerance and yield performance (Purushothaman et al., 2014). In former research, we could discriminate both types at 10 HAI by a lower oxycaloric equivalent (Rq/RCO_2; calorespirometric ratio) value due to differential carbon use and, thus, predict *a posteriori* better yield stability of Desi (Mohanapriya et al., 2019). In this study, we show that Desi increased the level of ADH at 10 HAI during germination (significant at 23 and 28°C), while this is not seen in Kabuli. The reached level of ADH is higher at 23°C than at 28°C. **(B5)** Pronounced SHAM effects on ADH levels at 24 HAI that show interaction with sucrose: During the germination of carrot seeds, the most pronounced effect of SHAM treatment on ADH levels is observed at 24 HAI. At that time point, SHAM stimulated ADH levels compared to levels observed at 12 and 30 HAI. This happened independently of the presence of sucrose (3%). However, under both conditions, 5 mM SHAM showed a stronger stimulating effect on ADH levels (significant) at 24 HAI than 10 mM SHAM. But the level of SHAM-enhanced ADH is higher at both tested concentrations of SHAM when sucrose is not present. On the contrary, at time points 12 and 30 HAI, a higher ADH level in the 0% sucrose controls is associated with the higher concentration of 10 mM SHAM versus 5 mM SHAM. In the presence of 3% sucrose, ADH activity is at any time point higher at 5 mM SHAM than at 10 mM SHAM. Together, these observations point to the importance of differential AOX activity regulation for optimized germination during all three time points independently of the presence or absence of exogenous sucrose. **(C1)** SHAM pulses $\leq$12 HAI impact germination efficiency and interact with sucrose effects: In control seeds, short pulses of SHAM (10 mM) until 12 HAI enhanced germination efficiency and were more effective than pulses until 6 HAI. However, prolonged SHAM treatment of 72 HAI suppressed early germination. In contrast, at 3% exogenous sucrose, early germination efficiency is reduced against 0% sucrose controls (confirming panel **A1**) and SHAM pulses until 6 and 12 HAI led to complete suppression of early germination. However, from 48 HAI onward to 72 HAI, continuous SHAM treatment in the presence of 3% sucrose increased germination, but along with 0% sugar continuous SHAM suppressed germination also at 72 HAI. Collectively, these results show that plastic AOX regulation is critical for the timing of germination in controls and under conditions of sucrose supplementation. **(C2)** 10 and 30–40 HAI are critical times for sucrose–SHAM interaction during carrot germination: A total of 10 h of previous water imbibition reduced the strong negative effects of the combination of exogenous sucrose (3%) and SHAM (5 mM) on germination efficiency that was observed at only 2 h of previous water imbibition (significant). Also, during the phase of initiated root emergence at 30 Hours of imbibition (HOI), a transfer from water to media supplemented with sucrose and SHAM suppressed germination (significant). Water imbibition until 40 h before transfer to sucrose- and SHAM-containing media relieved and even supported germination when monitored at 30 and 48 HAI (significant). However, this increase in germination efficiency seemed to be restricted from 72 HAI onward (significant). **(D)** Sucrose and SHAM can improve the effect of arbuscular mycorrhizal fungi (AMF) on early germination: In panel **D1**, it is shown that carrot seeds treated with native endophytes (EN1—endophyte 1; EN2—endophyte 2; EN3—endophyte 3; isolated from cv. Kuroda) tend to improve early germination at 48 HAI in both the cultivars (not seen for EN3 in cv. Early Nantes). Exogenous sucrose had differential effects depending on endophyte and cultivar (Panel **D2**), but in no case does sucrose enhances early germination rates compared to the respective endophyte-treated controls (as shown also in **Supplementary Table 2**). However, SHAM treatment (Panel **D2**) reduced early germination against endophyte-treated controls in all cases (as shown also in **Supplementary Table 2**). In a separate trial, two AMF species (*R. irregularis*—M1 and *R. proliferus*—M2) were tested and acted negatively on germination in cv. Kuroda, but positively in slowly germinating seeds of cv. Early Nantes (Panel **D1**). Nevertheless, the effect of M1 on early germination could be improved in cv. Kuroda by 0.5 and 3% sucrose (Panel **D2**). However, this was not seen for M2. In the better germinating cv. Kuroda, the lower concentration of 5 mM SHAM (Panel **D2**) improved the effect of both mycorrhiza species on early germination. In later germinating seeds of cv. Early Nantes, 0.5% sucrose improved the already positive effect on germination (Panel **D1**) of *Rhizophagus* species M1 (Panel **D2**). In this cultivar, SHAM decreased
(Continued)

FIGURE 1 | (Continued)
the germination rate to the level of the untreated controls (**Supplementary Table 2**). **(E1)** *On-farm* organic vs. conventional seed discrimination and organic breeding with the help of quick germination tests, commercial sugar, and SHAM treatment: Seeds from six of seven winter wheat cultivars originated from organic agricultural management could be discriminated at 15 HAI through better germination against conventionally produced seeds when germinated in 5% sugar solution. In water, seeds of only four cultivars showed better germination than organic seeds. When conventionally produced material is compared, seeds of the first cultivar showed poor germination. This was much more pronounced when tested in a 5% sugar solution instead of water. Seeds of the second cultivar demonstrated the highest germination rates among all tested cultivars (as shown in **Supplementary Figure 4**). This was observed for seeds originating from both agricultural conditions, although higher germination in 5% sugar solution indicated the presence of microbiota (Panel **E1**). In contrast to all other cultivars, seeds of the second cultivar did not differ in germination rates for organic vs. conventional production under SHAM treatment when compared to the water control (as shown in also **Supplementary Figure 4**). This signals already low levels of AOX at 15 HAI for this cultivar no matter from which agricultural management system seeds originated. Overall, these observations indicate the interplay between plant genotype, sugar, and AOX activity that impacts differential germination capacities between organic and conventional seeds. **(E2)** Identification of disease tolerant pea seeds by germination tests under SHAM discrimination (T-tolerant reference; S-susceptible reference): Pea lines with differential degrees of root rot disease susceptibility could be ranked by employing SHAM inhibition. The most tolerant line (T) showed the lowest degree of SHAM-related inhibition of germination monitored at 27 HAI. This indicates the reasonability of germination tests under SHAM discrimination for the selection of seed vigor and plant robustness. **(E3)** *On-farm* simple seed germination improvement of stored conventional and organic wheat seeds by a 2 h initial pulse with commercial sugar (first cultivar in 1E1): This figure demonstrates the general potential of improving early germination through a short pulse of sugar its validity across species (in this study winter wheat, but also refer for carrot in Panel **A2** and **Supplementary Figure 2**), agricultural management practices and also related to the aging of seeds.

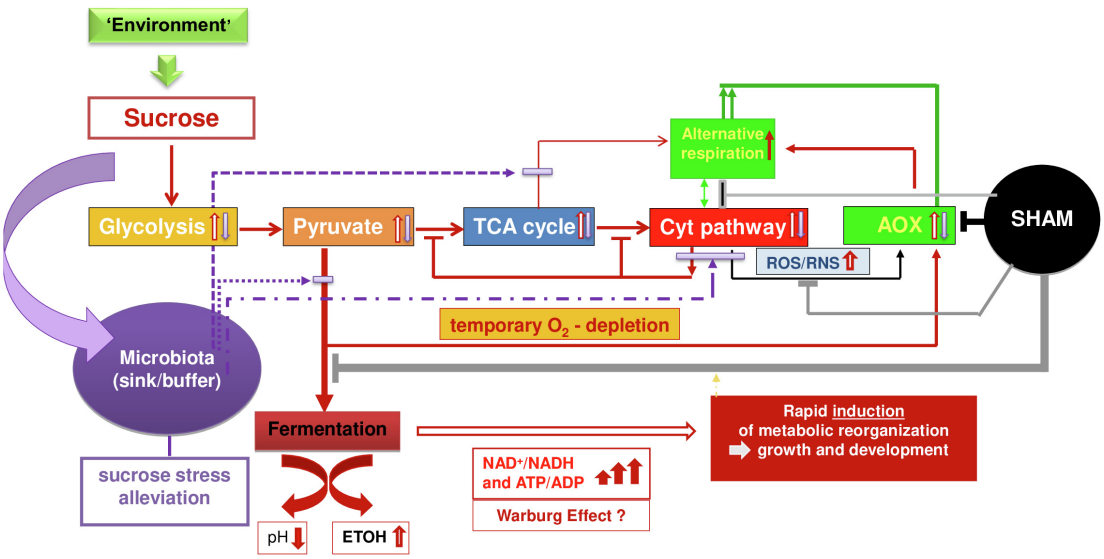

FIGURE 2 | A simplified scheme on hypothesis and conceptualization for working out metabolic principles on dynamic cell reprogram functioning (details explained in the text).

respiration will reach priority again for driving growth and development. Fermentation and AOX downregulation will again be regulated in adaptation to sucrose- and COX-mediated respiration-transmitted conditions embedded in adaptive hormonal crosstalk and overall complex cellular and apoplastic network signaling. Thus, rapid downregulation indicates efficient adaptation of COX-mediated respiration, a dynamic trait appropriate to mark seed vigor (Mohanapriya et al., 2019).

Sucrose can improve early germination of *Rhizophagus*-treated seeds (as shown in point g) while non-AMF-treated seeds respond upon sucrose typically with a delay in germination (as shown in **Figure 1A1**). This suggests that AMF and its associated bacteria (Pandit et al., under review) can alleviate or buffer the negative effects of sucrose on germination to relevant degrees by providing an additional sink. This is not indicated with the three tested endophytes (f). Also, early germination of endophyte-treated seeds is reduced at 48 HAI through the continuous presence of SHAM when compared to endophyte-treated controls (e). On the contrary, when seeds from the cv. Kuroda were inoculated with *Rhizophagus*, SHAM treatment (5 mM) could improve early germination to higher levels than observed in AMF-treated controls. This observation is in agreement with the palliating effects observed by *Scutellospora calospora* on negative SHAM effects on carrot germination by using the same cultivar (Mohanapriya et al., 2019). In an overall assessment, it is inferred that AMF treatment might improve early germination by alleviating stress-induced by rapid sucrose excess through two mechanisms: providing an additional sink for sucrose and supplying an enhanced capacity and/or engagement of AR. *Rhizophagus* spores were shown to be a rich source for polymorphic *AOX* gene sequences (Campos et al., 2015). We believe that there could be an operation of two separate mechanisms since we observed differential effects on early germination of M1-treated seeds upon SHAM treatment in the two selected cultivars (**Figure 1D**). However, M1-treated seeds of both cultivars showed improvement in

early germination when sucrose was provided (**Figure 1D**). We tend to interpret that the isolated native carrot endophytes were already well integrated into the internal host cell habitat. Thus, their reinoculation tended to influence early germination positively, but could not provide a striking new advantage or disadvantage when sucrose is enhanced or SHAM treatment reduced the level of AR. However, we reported that endophytes modulate *AOX* transcripts in species-, stress-, and development-dependent manner, and endophytes could have modified the effect of AMF inoculation on seed germination efficiency (Mohanapriya et al., 2019).

OUTLOOK

The observations offer new perspectives for low-cost prediction of plant holobiont behavior of seeds and for providing simple and rapid *on-farm* support toward sustainable agriculture. We propose three tools for validation:

(A) Seed selection with the help of short germination tests under SHAM discrimination. This tool provides modalities to identify seeds with higher seed vigor, general adaptive plant robustness, and superior internal seed quality related to the content of secondary metabolites (**Figures 1E1,E2** and **Supplementary Figures 3**, **4**).

(B) Discrimination of organic vs. conventionally produced seeds with the help of short duration germination tests in water solutions with 5% commercial sugar (**Figure 1E1**).

(C) Germination improvement by 2-h pulses of commercial sugar (**Figures 1A1,E3** and **Supplementary Figure 1**).

Furthermore, we encourage developing novel tests for AMF functionality in germinating seeds in the presence of sucrose. This approach targets compatibility between selected plants and AMF strains to support plant holobiont plasticity.

Our results suggest that polymorphic *AOX* gene sequences of symbiotic partners can impact plant–AMF compatibility. Therefore, we want to accomplish wider screening of major *AOX* polymorphisms in species-specific target cells for evaluating plant performance (Abe et al. 2002; Arnholdt-Schmitt, 2015; Nogales et al., 2016) and in AMF sources (Arnholdt-Schmitt, 2008; Vicente and Arnholdt-Schmitt, 2008; Campos et al., 2015). Such a strategy needs to also include near neighboring polymorphisms in conserved functional sites that can discriminate differentially regulated *AOX1* and *AOX2* (Costa et al., 2009). This approach would include a screening of compatible *AOX* polymorphisms from both partners in the proposed functional tests to identify the best plant–AMF combinations.

We hypothesize that the observed integration of bacterial endophytes into host plants with similar sensitivity against SHAM effects might point to synchronized AOX regulation in plant holobionts. Into this derivation would fit that we observed the same tendency of inhibiting sucrose effects on endophyte-free and superficially sterilized seeds (**Figure 1A1**), which we noticed also for SE induction (unpublished). Vicente et al. (2015) highlighted a "provocative" lack of interest in bacterial *AOX*. They anticipated that bacteria-harboring *AOX* could facilitate adaptation to extreme conditions, which could also be of interest when thinking about plant endophytes and AMF-associated bacteria (Pandit et al., under review).

This present perspective is complementing Mohanapriya et al. (2019) and Costa et al. (2021). Joining the central figures of these publications is thought of as one teaching tool that can help to explain a straightforward way from fundamental interdisciplinary research to the application that might support sustainable socioeconomies because of the diversity of emergent environmental changes.

DEDICATION

The authors want to dedicate their work to FREEDOM and ETHICS.

DATA AVAILABILITY STATEMENT

The original contributions presented in the study are included in the article/**Supplementary Material**, further inquiries can be directed to the corresponding authors.

AUTHOR CONTRIBUTIONS

RB performed lab analyses on carrot germination, endophyte isolation, and inoculation trials related to **Figures 1A1–3,B3,4,5**, **C1,2,D**. JHC coordinated transcriptome analyses supported by KT. JHC, RS, and CN discussed initially the approach of this manuscript with BA-S. GM carried out work on **Supplementary Figure 1** and **Supplementary Table 1**. SS was responsible for AMF inoculation trials under the head of AA and EM performed pea studies for **Figure 1E2** under the responsibility of BA-S. Under the supervision of KG and EM together with AK performed germination analyses of transgenic *Arabidopsis*, and AK carried out the ADH analyses on chickpea. BA-S performed *on-farm* analyses (**Figures 1E1,E3**). CN was responsible for statistics and was in part supported by MO. RB and IV helped BA-S in the literature search. DS contributed with **Supplementary Figure 3**. BA-S initiated the scientific approach, coordinated overall research, and discussion, and wrote the manuscript. All the co-authors commented on research and manuscript during its development and agreed to manuscript submission. RB organized manuscript submission.

FUNDING

RS, GM, and BA-S acknowledge support for academic cooperation and mobility of researchers by the India-Portugal Bilateral Cooperation Program (2013–2015), funded by "Fundação para a Ciência e Tecnologia" (FCT), Portugal, and the Department of Science and Technology (DST), India. RS lab is financially supported by UGC-SAP and DST-FIST. GM was grateful to UGC, India, for a doctoral grant

from the BSR fellowship. KG, MO, and BA-S acknowledge support by the India-Portugal Bilateral Cooperation Program "DST/INT/Portugal/P-03/2017." MO research was partially supported by National Funds through FCT, Fundação para a Ciência e a Tecnologia projects UIDB/04674/2020 (CIMA). BA-S wants to thank RS for enabling intensive external online supervision of RB on the presented research and excellent collaboration and communication of RB. RB and SS acknowledge the infrastructure and stay support provided by DBT-TDNBC-DEAKIN-Research Network Across continents for learning and innovation (DTD-RNA) for AMF-related work at The Energy and Resources Institute, TERI, India. JHC was grateful to CNPq for the researcher fellowship (CNPq grant 309795/2017-6). KT was grateful to CNPq for the doctoral fellowship. BA-S was grateful to SK for his support in facilitating the coordination of the Indian FunCROP team. CN acknowledges the international scientific network BIOALI-CYTED, which contributed to establish FunCROP contacts. BA-S wants to acknowledge especially the extraordinary engagement of CN for online collaboration with RB on data evaluation and presentation and overall manuscript discussion. BA-S appreciates the collaboration of LIVESEED partners with seed material and information on this material and thanks for supporting EM (European Horizon 2020 project LIVESEED Grant No. 727230).

SUPPLEMENTARY MATERIAL

The Supplementary Material for this article can be found online at: https://www.frontiersin.org/articles/10.3389/fpls.2021.686274/full#supplementary-material

Supplementary Figure 1 | Exogenous sucrose delayed callus emergence and was necessary for SE.

Supplementary Figure 2 | A total of 2-h pulse with commercial sugar improved carrot germination efficiency monitored at 40 and 50 HAI.

Supplementary Figure 3 | Effect of SHAM treatment on accumulation of soluble and wall-bound phenolics **(A)** and flavonoids and lignin **(B)** in elicitor-treated hairy roots of *Daucus carota*. Values obtained in only elicitor-treated root were considered as 100% and results were expressed in terms of percentage of maximum. The terms E and NE in the x-axis legend denote -with and -without elicitor, respectively. * Soluble phenolics. Values are mean of three independent experiments ± SD.

Supplementary Figure 4 | Rapid germination check of organic and conventional seeds from seven cultivars in water (control) or under SHAM (5 mM) treatment.

Supplementary Table 1 | Effect of exogenous sucrose concentration on carrot SE callus induction.

Supplementary Table 2 | Microbiota effect on the carrot seed germination at different sucrose and SHAM concentrations.

Supplementary File 1 | Materials and methods.

REFERENCES

Abdelrazek, S., Choudhari, S., Thimmapuram, J., Simon, P., Colley, M., Mengiste, T., et al. (2020a). Changes in the core endophytic mycobiome of carrot taproots in response to crop management and genotype. *Sci. Rep.* 10:13685. doi: 10.1038/s41598-020-70683-x

Abdelrazek, S., Simon, P., Colley, M., Mengiste, T., and Hoagland, L. (2020b). Crop management system and carrot genotype affect endophyte composition and *Alternaria dauci* suppression. *PLoS One* 15:e0233783. doi: 10.1371/journal.pone.0233783

Abe, F., Saito, K., Miura, K., and Toriyama, K. (2002). A single nucleotide polymorphism in the alternative oxidase gene among rice varieties differing in low temperature tolerance. *FEBS Lett.* 527, 181–185. doi: 10.1016/s0014-5793(02)03218-0

Albornoz, F. E., Orchard, S., Standish, R. J., Dickie, I. A., Bending, G. D., Hilton, S., et al. (2020). Evidence for niche differentiation in the environmental responses of co-occurring mucoromycotinian fine root endophytes and glomeromycotinian arbuscular mycorrhizal fungi. *Microb. Ecol.* 81, 864–873. doi: 10.1007/s00248-020-01628-0

Albury, M. S., Elliott, C., and Moore, A. L. (2009). Towards a structural elucidation of the alternative oxidase in plants. *Physiol. Plant* 137, 316–327. doi: 10.1111/j.1399-3054.2009.01270.x

Arnholdt-Schmitt, B. (2005a). Efficient cell reprogramming as a target for functional-marker strategies? Towards new perspectives in applied plant-nutrition research. *J. Plant Nutr. Soil Sci.* 168, 617–624.

Arnholdt-Schmitt, B. (2005b). Functional markers and a 'systemic strategy': convergency between plant breeding, plant nutrition and molecular biology. *Plant Physiol. Biochem.* 43, 817–820. doi: 10.1016/j.plaphy.2005.08.011

Arnholdt-Schmitt, B. (2008). "A novel gene-candidate approach of socio-economic interest?–breeding on efficient plant genotype - mycorrhiza interaction," in *Proceedings of the COST 870 Meeting from Production to Application of Arbuscular Mycorrhizal Fungi in Agricultural Systems: a Multidisciplinary Approach*, (Denmark: Department of Integrated Pest Management).

Arnholdt-Schmitt, B., Costa, J. H., and de Melo, D. F. (2006). AOX–a functional marker for efficient cell reprogramming under stress? *Trends Plant Sci.* 11, 281–287. doi: 10.1016/j.tplants.2006.05.001

Arnholdt-Schmitt, B. (2015). "From AOX diversity to functional marker development," in *Alternative Respiratory Pathways in Higher Plants*, eds K. J. Gupta, L. A. J. MuR, and B. NeelwarnE (Oxford: John Wiley and Sons), 233–243.

Arnholdt-Schmitt, B., Hansen, L. D., and Nogales, A. (2015). Calorespirometry, oxygen isotope analysis and functional-markerï£¡assisted selection ('CalOxy-FMAS') for genotype screening: a novel concept and tool kit for predicting stable plant growth performance and functional marker identification. *Brief. Funct. Genomics.* 15, 10–15. doi: 10.1093/bfgp/elv008

Arnholdt-Schmitt, B., Mohanapriya, G., Sathishkumar, R., Macedo, E. S., and Costa, J. H. (2018). "Predicting biomass production from plant robustness and germination efficiency by calorespirometry," in *Biofuels: Greenhouse Gas Mitigation and Global Warming. Next Generation Biofuels and Role of Biotechnology*, eds A. Kumar, S. Ogita, and Y. Yau (New Delhi: Springer Nature), 81–94.

Arnholdt-Schmitt, B., Valadas, V., and Doering, M. (2014). Functional marker development is challenged by the ubiquity of endophytes – a practical perspective. *Brief. Funct. Genom.* 15, 16–21. doi: 10.1093/bfgp/elu049

Arnholdt-Schmitt, B., Mohanapriya, G., Bharadwaj, R., Noceda, C., Macedo, E. S., Sathishkumar, R., et al. (2021). From plant survival under severe stress to anti-viral human defense– a perspective that calls for common efforts. *Front. Immunol.* 12:673723. doi: 10.3389/fimmu.2021.673723

Baena-González, E., and Hanson, J. (2017). Shaping plant development through the SnRK1-TOR metabolic regulators. *Curr. Opin. Plant Biol.* 35, 152–157. doi: 10.1016/j.pbi.2016.12.004

Bailey-Serres, J., Pierik, R., Ruban, A., and Wingler, A. (2018). The dynamic plant: capture, transformation, and management of energy. *Plant Physiol.* 176, 961–966. doi: 10.1104/pp.18.00041

Bedini, A., Mercy, L., Schneider, C., Franken, P., and Lucic-Mercy, E. (2018). Unraveling the initial plant hormone signaling, metabolic mechanisms and plant defense triggering the endomycorrhizal symbiosis behavior. *Front. Plant Sci.* 9:1800. doi: 10.3389/fpls.2018.01800

Bello, P., and Bradford, K. (2016). Single-seed oxygen consumption measurements and population-based threshold models link respiration and germination rates under diverse conditions. *Seed Sci. Res.* 26, 199–221. doi: 10.1017/S0960258516000179

Bhaskar, A. V. V., Baresel, J. P., Weedon, O., and Finckh, M. R. (2019). Effects of ten years organic and conventional farming on early seedling traits of evolving winter wheat composite cross populations. *Sci. Rep.* 9:9053. doi: 10.1038/s41598-019-45300-1

Bigarella, C. L., Liang, R., and Ghaffari, S. (2014). Stem cells and the impact of ROS signaling. *Development* 141, 4206–4218. doi: 10.1242/dev.107086

Boratyn, G. M., Thierry-Mieg, J., Thierry-Mieg, D., Busby, B., and Madden, T. L. (2019). Magic-BLAST, an accurate RNA-seq aligner for long and short reads. *BMC Bioinformatics* 20:405. doi: 10.1186/s12859-019-2996-x

Campos, C., Cardoso, H., Nogales, A., Svensson, J., Lopez-Ráez, J. A., Pozo, M. J., et al. (2015). Intra and inter-spore variability in rhizophagus irregularis AOX gene. *PLoS One* 10:e0142339. doi: 10.1371/journal.pone.0142339

Cardoso, H. G., and Arnholdt-Schmitt, B. (2013). "Functional marker development across species," in *Selected Traits in Diagnostics in Plant Breeding*, eds T. Lübberstedt and R. K. Varshney (Netherlands: Springer), 467–515.

Carré, J. E., Affourtit, C., and Moore, A. L. (2011). Interaction of purified alternative oxidase from thermogenic Arum maculatum with pyruvate. *FEBS Lett.* 585, 397–401. doi: 10.1016/j.febslet.2010.12.026

Cope-Selby, N., Cookson, A., Squance, M., Donnison, I., Flavell, R., and Farrar, K. (2017). Endophytic bacteria in miscanthus seed: implications for germination, vertical inheritance of endophytes, plant evolution and breeding. *GCB Bioenergy* 9, 57–77.

Costa, J. H., Cardoso, H. G., Campos, M. D., Zavattieri, A., Frederico, A. M., de Melo, D. F., et al. (2009). Daucus carota L.—an old model for cell reprogramming gains new importancethrough a novel expansion pattern of alternative oxidase (AOX) genes. *Plant Physiol. Biochem.* 47, 753–759.

Costa, J. H., Mohanapriya, G., Bharadwaj, R., Noceda, C., Thiers, K. L. L., Shahid, A., et al. (2021). ROS/RNS balancing, aerobic fermentation regulation and cell cycle control – a complex early trait ('CoV-MAC-TED') for combating SARS-CoV-2-induced cell reprogramming. *Front. Immunol.* 12:673692. doi: 10.3389/fimmu.2021.673692

Doner, L. W., and Becard, G. (1991). Solubilization of gellan gels by chelation of cations. *Biotechnol. Tech.* 5, 25–28.

Dumont, S., and Rivoal, J. (2019). Consequences of oxidative stress on plant glycolytic and respiratory metabolism. *Front. Plant Sci.* 10:166. doi: 10.3389/fpls.2019.00166

Durán, P., Tortella, G., Viscardi, S., Barra, P. J., Carrión, V. J., Mora, M. L., et al. (2018). Microbial community composition in take-all suppressive soils. *Front. Microbiol.* 9:2198. doi: 10.3389/fmicb.2018.02198

Eckert, C., Xu, W., Xiong, W., Lynch, S., Ungerer, J., Tao, L., et al. (2014). Ethylene-forming enzyme and bioethylene production. *Biotechnol. Biofuels* 7:33. doi: 10.1186/1754-6834-7-33

Fan, Y., Yu, X., Guo, H., Wei, J., Guo, H., Zhang, L., et al. (2020). Dynamic transcriptome analysis reveals uncharacterized complex regulatory pathway underlying dose iba induced embryogenic redifferentiation in cotton. *Int J. Mol. Sci.* 21:426. doi: 10.3390/ijms21020426

Grieb, B., Groß, U., Pleschka, E., Arnholdt-Schmitt, B., and Neumann, K. H. (1994). Embryogenesis of photoautotrophic cell cultures of Daucus carota L. *Plant Cell Tissue Organ. Cult.* 38, 115–122.

Gupta, K. J., Hancock, J. T., Petrivalsky, M., Kolbert, Z., Lindermayr, C., Durner, J., et al. (2020a). Recommendations on terminology and experimental best practice associated with plant nitric oxide research. *New Phytol.* 225, 1828–1834. doi: 10.1111/nph.16157

Gupta, K. J., Kolbert, Z., Durner, J., Lindermayr, C., Corpas, F. J., Brouquisse, R., et al. (2020b). Regulating the regulator: nitric oxide control of post-translational modifications. *New Phytol.* 227, 1319–1325.

Hakkaart, G. A., Dassa, E. P., Jacobs, H. T., and Rustin, P. (2006). Allotopic expression of a mitochondrial alternative oxidase confers cyanide resistance to human cell respiration. *EMBO Rep.* 7, 341–345. doi: 10.1038/sj.embor.7400601

Hirschauer, N., and Becker, C. (2020). Paradigmenwechsel Warum statistische Signifikanztests abgeschafft werden sollten. *Signifikanztests Forschung Lehre* 6:20.

Hoefnagel, M., Rich, P. R., Zhang, Q., and Wiskich, J. T. (1997). Substrate kinetics of the plant mitochondrial alternative oxidase and the effects of pyruvate. *Plant Physiol.* 115, 1145–1153. doi: 10.1104/pp.115.3.1145

Ito, K., Ogata, T., Seito, T., Umekawa, Y., Kakizaki, Y., Osada, H., et al. (2020). Degradation of mitochondrial alternative oxidase in the appendices of Arum maculatum. *Biochem. J.* 477, 3417–3431. doi: 10.1042/BCJ20200515

Jayawardhane, J., Cochrane, D. W., Vyas, P., Bykova, N. V., Vanlerberghe, G. C., and Igamberdiev, A. U. (2020). Roles for plant mitochondrial alternative oxidase under normoxia, hypoxia, and reoxygenation conditions. *Front. Plant Sci.* 11:566. doi: 10.3389/fpls.2020.00566

Kagi, J. H., and Vallee, B. L. (1960). The role of zinc in alcohol dehydrogenase. V. The effect of metal-binding agents on thestructure of the yeast alcohol dehydrogenase molecule. *J. Biol. Chem.* 235, 3188–3192.

Kutschera, U., Pieruschka, R., Farmer, S., and Berry, J. A. (2020). The Warburg-effects: basic metabolic processes with reference to cancer development and global photosynthesis. *Plant Signal Behav.* 15:1776477. doi: 10.1080/15592324.2020.1776477

Lara-Núñez, A., García-Ayala, B. B., Garza-Aguilar, S. M., Flores-Sánchez, J., Sánchez-Camargo, V. A., Bravo-Alberto, C. E., et al. (2017). Glucose and sucrose differentially modify cell proliferation in maize during germination. *Plant Physiol. Biochem.* 113, 20–31. doi: 10.1016/j.plaphy.2017.01.018

Lin, X. Y., Ye, Y. Q., Fan, S. K., Jin, C. W., and Zheng, S. J. (2016). Increased sucrose accumulation regulates iron-deficiency responses by promoting auxin signaling in arabidopsis plants. *Plant Physiol.* 170, 907–920. doi: 10.1104/pp.15.01598

Lucic, E, and Mercy, L. (2014). A method of mycorrhization of plants and use of saccharides in mycorrhization. *Eurpean Patent EP2982241A1*.

Machingura, M., Salomon, E., Jez, J. M., and Ebbs, S. D. (2016). The β-cyanoalanine synthase pathway: beyond cyanide detoxification. *Plant Cell Environ.* 39, 2329–2341. doi: 10.1111/pce.12755

Meitzel, T., Radchuk, R., McAdam, E. L., Thormählen, I., Feil, R., Munz, E., et al. (2021). Trehalose 6-phosphate promotes seed filling by activating auxin biosynthesis. *New Phytol.* 229, 1553–1565. doi: 10.1111/nph.16956

Melkonian, E. A., and Schury, M. P. (2020). *Biochemistry, Anaerobic Glycolysis*. Available online at: https://www.ncbi.nlm.nih.gov/books/NBK546695/ (accessed Jan 2021).

Mellema, S., Eichenberger, W., Rawyler, A., Suter, M., Tadege, M., and Kuhlemeier, C. (2002). The ethanolic fermentation pathway supports respiration and lipid biosynthesis in tobacco pollen. *Plant J.* 30, 329–336. doi: 10.1046/j.1365-313x.2002.01293.x

Mercy, L., Lucic-Mercy, E., Nogales, A., Poghosyan, A., Schneider, C., and Arnholdt-Schmitt, B. (2017). A functional approach towards understanding the role of the mitochondrial respiratory chain in an endomycorrhizal symbiosis. *Front. Plant Sci.* 8:417. doi: 10.3389/fpls.2017.00417

Mercy, L., Svensson, J. T., Lucic, E., Cardoso, H. G., Nogales, A., Döring, M., et al. (2015). "AOX gene diversity in arbuscular mycorrhizal fungi (AMF) products – a special challenge," in *Alternative Respiratory Pathways in Higher Plants*, eds K. J. Gupta, L. Mur, and B. Neelwarne (Oxford: John Wiley and Sons Inc), 305–310.

Millar, A. H., Hoefnagel, M., Day, D. A., and Wiskich, J. T. (1996). Specificity of the organic acid activation of alternative oxidase in plant mitochondria. *Plant Physiol.* 111, 613–618. doi: 10.1104/pp.111.2.613

Mohanapriya, G., Bharadwaj, R., Noceda, C., Costa, J. H., Kumar, S. R., Sathishkumar, R., et al. (2019). Alternative Oxidase (AOX) senses stress levels to coordinate auxin-induced reprogramming from seed germination to somatic embryogenesis—a role relevant for seed vigor prediction and plant robustness. *Front. Plant Sci.* 10:1134. doi: 10.3389/fpls.2019.01134

Moon, H., Lee, H., Paek, K., and Park, S. (2015). Osmotic stress and strong 2,4-D shock stimulate somatic-to-embryogenic transition in *Kalopanax septemlobus* (Thunb.) Koidz. *Acta Physiol. Plant* 37:1710. doi: 10.1007/s11738-014-1710-x

Mortazavi, A., Williams, B. A., Mccue, K., Schaeffer, L., and Wold, B. (2008). Mapping and quantifying mammalian transcriptomes by RNA-Seq. *Nat Methods* 5, 621–628.

Narsai, R., Secco, D., Schultz, M. D., Ecker, J. R., Lister, R., and Whelan, J. (2017). Dynamic and rapid changes in the transcriptome and epigenome during germination and in developing rice (Oryza sativa) coleoptiles under anoxia and re-oxygenation. *Plant J.* 89, f805–f824. doi: 10.1111/tpj.13418

Nascimento, W. M., Huber, D. J., and Cantliffe, D. J. (2013). Carrot seed germination and respiration at high temperature in response to seed maturity and priming. *Seed Sci. Technol.* 41, 164–169.

Nguyen, H. M., Sako, K., Matsui, A., Suzuki, Y., Mostofa, M. G., Ha, C. V., et al. (2017). Ethanol enhances high-salinity stress tolerance by detoxifying reactive

oxygen species in arabidopsis thaliana and rice. *Front. Plant Sci.* 8:1001. doi: 10.3389/fpls.2017.01001

Nogales, A., Muñoz-Sanhueza, L., Hansen, L. D., and Arnholdt-Schmitt, B. (2015). Phenotyping carrot (*Daucus carota* L.) for yield-determining temperature response by calorespirometry. *Planta* 241, 525–538. doi: 10.1007/s00425-014-2195-y

Nogales, A., Nobre, T., Cardoso, H. G., Muñoz-Sanhueza, L., Valadas, V., Campos, M. D., et al. (2016). Allelic variation on DcAOX1 gene in carrot (*Daucus carota* L.): an interesting simple sequence repeat in a highly variable intron. *Plant Gene* 5, 49–55. doi: 10.1016/j.plgene.2015.11.001

Paszkiewicz, G., Gualberto, J. M., Benamar, A., Macherel, D., and Logan, D. C. (2017). Arabidopsis seed mitochondria are bioenergetically active immediately upon imbibition and specialize via biogenesis in preparation for autotrophic growth. *Plant Cell* 29, 109–128. doi: 10.1105/tpc.16.00700

Pengpeng, J., Chenyu, D., Penghu, C., Dong, S., Ruizhuo, O., and Yuqing, M. (2020). The role of reactive oxygen species in tumor treatment. *RSC Adv.* 10, 7740–7750.

Porfirio, S., Calado, M. L., Noceda, C., Cabrita, M. J., da Silva, M. G., Azadi, P., et al. (2016). Tracking biochemical changes during adventitious root formation in olive (Olea europaea L.). *Sci. Hort.* 204, 41–53. doi: 10.1016/j.scienta.2016.03.029

Powell, A. A. (2017). *A review of the Principles and Use of the Q2 Seed Analyser*. Aberdeen: International Seed Testing Association.

Purushothaman, R., Upadhyaya, H. D., Gaur, P. M., Gowda, C. L. L., and Krishnamurthy, L. (2014). Kabuli and desi chickpeas differ in their requirement for reproductive duration. *Field Crops Res.* 163, 24–31. doi: 10.1016/j.fcr.2014.04.006

Qi, W., Ma, L., Wang, F., Wang, P., Wu, J., Jin, J., et al. (2020). Reactive oxygen species as important regulators of cell division. *Biorxiv*. [Preprint] doi: 10.1101/2020.03.06.980474

European Parliament and of the Council. (2018). *Regulation (EU) 2018/848 of the European Parliament and of the Council of 30 May 2018 on organic production and labelling of organic products and repealing Council Regulation (EC) No 834/2007*. Brussels: European Parliament and of the Council.

Sakr, S., Wang, M., Dédaldéchamp, F., Perez-Garcia, M. D., Ogé, L., Hamama, L., et al. (2018). The Sugar-Signaling Hub: Overview of Regulators and Interaction with the Hormonal and Metabolic Network. *Int. J. Mol. Sci.* 19:2506. doi: 10.3390/ijms19092506

Saleh, T., and Kalodimos, C. G. (2017). Enzymes at work are enzymes in motion. *Science* 355, 247–248. doi: 10.1126/science.aal4632

Sangüesa, G., Roglans, N., Baena, M., Velázquez, A. M., Laguna, J. C., and Alegret, M. (2019). mTOR is a Key Protein Involved in the Metabolic Effects of Simple Sugars. *Int. J. Mol. Sci.* 20:1117. doi: 10.3390/ijms20051117

Santos Macedo, E., Cardoso, H. G., Hernández, A., Peixe, A. A., Polidoros, A., Ferreira, A., et al. (2009). Physiologic responses and gene diversity indicate olive alternative oxidase as a potential source for markers involved in efficient adventitious root induction. *Physiol. Plant* 137, 532–552. doi: 10.1111/j.1399-3054.2009.01302.x

Saraiva, K. D., Oliveira, A. E., Santos, C. P., Lima, K. T., Sousa, J. M., Melo, D. F., et al. (2016). Phylogenetic analysis and differential expression of EF1α genes in soybean during development, stress and phytohormone treatments. *Mol. Genet. Genom.* 291, 1505–1522. doi: 10.1007/s00438-016-1198-8

Schmidt, R. R., Weits, D. A., Feulner, C. F. J., and van Dongen, J. T. (2018). Oxygen sensing and integrative stress signaling in plants. *Plant Physiol.* 176, 1131–1142. doi: 10.1104/pp.17.01394

Selinski, J., Hartmann, A., Deckers-Hebestreit, G., Day, D. A., Whelan, J., and Scheibe, R. (2018). Alternative oxidase isoforms are differentially activated by tricarboxylic acid cycle intermediates. *Plant Physiol.* 176, 1423–1432. doi: 10.1104/pp.17.01331

Siegień, I., and Bogatek, R. (2006). Cyanide action in plants — from toxic to regulatory. *Acta Physiol. Plant.* 28, 483–497.

Simon, P. W., Navazio, J. P., Colley, M., McCluskey, C., Zystro, J., Hoagland, L., et al. (2017). The CIOA (carrot improvement for organic agriculture) project: location, cropping system and genetic background influence carrot performance including top height and flavour. *Acta Horticulturae* 1153, 1–8. doi: 10.17660/ActaHortic.2017.1153.1

Sircar, D., Cardoso, H. G., Mukherjee, C., Mitra, A., and Arnholdt-Schmitt, B. (2012). Alternative oxidase (AOX) and phenolic metabolism in methyl jasmonate-treated hairy root cultures of Daucus carota L. *J Plant Physiol.* 169, 657–663. doi: 10.1016/j.jplph.2011.11.019

Sivasakthi, K., Tharanya, M., Kholová, J, Wangari Muriuki, R., Thirunalasundari, T., and Vadez, V. (2017). Chickpea genotypes contrasting for vigor and canopy conductance also differ in their dependence on different water transport pathways. *Front Plant Sci.* 8:1663. doi: 10.3389/fpls.2017.01663

Srivastava, S., Conlan, X. A., Cahill, D. M., and Adholeya, A. (2016). Rhizophagus irregularis as an elicitor of rosmarinic acid and antioxidant production by transformed roots of Ocimum basilicum in an in vitro co-culture system. *Mycorrhiza* 26, 919-930.

Vanlerberghe, G. C., Vanlerberghe, A. E., and McIntosh, L. (1994). Molecular genetic alteration of plant respiration (silencing and overexpression of alternative oxidase in transgenic tobacco). *Plant Physiol.* 106, f1503–f1510. doi: 10.1104/pp.106.4.1503

Vicente, C., Costa, J. H., and Arnholdt-Schmitt, B. (2015). "Bacterial AOX: a provocative lack of interest!," in *Alternative Respiratory Pathways in Higher Plants*, eds K. J. Gupta, L. A. Mur, and B. Neelwarne (Hoboken, NJ: Wiley Publishing group), 319–322.

Vicente, S. L. C., and Arnholdt-Schmitt, B. (2008). "Characterization of mediterranean AMs: initiation of a novel functional marker approach," in *Proceedings of the COST 870 Meeting*, Greece.

Voss-Fels, K. P., Cooper, M., and Hayes, B. J. (2019). Accelerating crop genetic gains with genomic selection. *Theor. Appl. Genet.* 132, 669–686. doi: 10.1007/s00122-018-3270-8

Wang, W. R., Liang, J. H., Wang, G. F., Sun, M. X., Peng, F. T., and Xiao, Y. S. (2020). Overexpression of PpSnRK1α in tomato enhanced salt tolerance by regulating ABA signaling pathway and reactive oxygen metabolism. *BMC Plant Biol.* 20:128. doi: 10.1186/s12870-020-02342-2

Wassermann, B., Cernava, T., Müller, H., Berg, C., and Berg, G. (2019). Seeds of native alpine plants host unique microbial communities embedded in cross-kingdom networks. *Microbiome* 7:108. doi: 10.1186/s40168-019-0723-5

Wojtyla, Ł, Lechowska, K., Kubala, S., and Garnczarska, M. (2016). Different modes of hydrogen peroxide action during seed germination. *Front. Plant Sci.* 7:66. doi: 10.3389/fpls.2016.00066

Wurzinger, B., Nukarinen, E., Nägele, T., Weckwerth, W., and Teige, M. (2018). The SnRK1 kinase as central mediator of energy signaling between different organelles. *Plant Physiol.* 176, 1085–1094. doi: 10.1104/pp.17.01404

Zabalza, A., van Dongen, J. T., Froehlich, A., Oliver, S. N., Faix, B., Gupta, K. J., et al. (2009). Regulation of respiration and fermentation to control the plant internal oxygen concentration. *Plant Physiol.* 149, 1087–1098. doi: 10.1104/pp.108.129288

Zavattieri, M. A., Frederico, A. M., Lima, M., Sabino, R., and Arnholdt-Schmitt, B. (2010). Induction of somatic embryogenesis as an example of stress-related plant reactions. *J. Biotechnol.* 13:1. doi: 10.2225/vol13-issue1-fulltext-4

Zhao, J., Li, W., Sun, S., Peng, L., Huang, Z., He, Y., et al. (2021). The rice small auxin-up rna gene ossaur33 regulates seed vigor via sugar pathway during early seed germination. *Int. J. Mol. Sci.* 22:1562. doi: 10.3390/ijms22041562

Zhu, T., Zou, L., Li, Y., Yao, X., Xu, F., Deng, X., et al. (2018). Mitochondrial alternative oxidase-dependent autophagy involved in ethylene-mediated drought tolerance in *Solanum lycopersicum*. *Plant Biotechnol. J.* 16, 2063–2076. doi: 10.1111/pbi.12939

Conflict of Interest: The authors declare that the research was conducted in the absence of any commercial or financial relationships that could be construed as a potential conflict of interest.

Publisher's Note: All claims expressed in this article are solely those of the authors and do not necessarily represent those of their affiliated organizations, or those of the publisher, the editors and the reviewers. Any product that may be evaluated in this article, or claim that may be made by its manufacturer, is not guaranteed or endorsed by the publisher.

frontiers in Plant Science

ORIGINAL RESEARCH
published: 11 October 2021
doi: 10.3389/fpls.2021.736613

Dose-Dependent Application of Straw-Derived Fulvic Acid on Yield and Quality of Tomato Plants Grown in a Greenhouse

Peijia Zhang[1,2], Hongjia Zhang[3], Guoqing Wu[3], Xiaoyuan Chen[3], Nazim Gruda[4], Xun Li[1], Jinlong Dong[1] and Zengqiang Duan[1]**

[1] State Key Laboratory of Soil and Sustainable Agriculture, Institute of Soil Science, Chinese Academy of Sciences, Nanjing, China, [2] University of Chinese Academy of Sciences, Beijing, China, [3] Nutrition and Health Research Institute, COFCO, Beijing, China, [4] Institute of Crop Science and Resource Conservation, Division of Horticultural Sciences, University of Bonn, Bonn, Germany

OPEN ACCESS

Edited by:
Youssef Rouphael,
University of Naples Federico II, Italy

Reviewed by:
Hadi Pirasteh-Anosheh,
National Salinity Research Center, Agricultural Research, Education and Extension Organization, Iran
Athanasios Koukounaras,
Aristotle University of Thessaloniki, Greece
Michela Schiavon,
University of Padova, Italy

***Correspondence:**
Jinlong Dong
jldong@issas.ac.cn
orcid.org/0000-0002-7766-4409
Zengqiang Duan
zqduan@issas.ac.cn

Specialty section:
This article was submitted to Crop and Product Physiology, a section of the journal Frontiers in Plant Science

Received: 05 July 2021
Accepted: 30 August 2021
Published: 11 October 2021

Citation:
Zhang P, Zhang H, Wu G, Chen X, Gruda N, Li X, Dong J and Duan Z (2021) Dose-Dependent Application of Straw-Derived Fulvic Acid on Yield and Quality of Tomato Plants Grown in a Greenhouse. Front. Plant Sci. 12:736613. doi: 10.3389/fpls.2021.736613

Fulvic acids are organic compounds widely distributed in soils, and the application of fulvic acids is thought to increase crop yield and quality. However, the effects vary among various sources and doses of fulvic acids and environmental and growth conditions of crops. Here, we investigated the effects of bioresource-derived (corn straw) fulvic acids on plant production and quality of tomato plants and soil chemical properties in soil cultures while experiments on seed germination and hydroponics were conducted to explore the underlying mechanism. Base dressing with 2.7 g kg^{-1} increased the yield of tomato by 35.0% at most as increased fruit number. Fulvic acids increased the concentrations of minerals, such as Ca, Fe, and Zn and the concentrations of citric, malic, and some amino acids in berries of tomato but did not affect the concentrations of soluble sugars and aromatic substances in tomato fruits. Similarly, fulvic acids at 80–160 mg L^{-1} increased germination rate, growth vigor, and radicle elongation of tomato seeds while it increased plant biomass, concentrations of nutrients, and root length of tomato plants in hydroponics to the greatest extent in general. The increases in yield and quality can be attributed to the improvement in root growth and, thus, increased nutrient uptake. In addition, the base application of fulvic acids improved soil cation exchange capacity and soil organic matter to an extent. In conclusion, base dressing and the addition into solution of fulvic acids at moderate doses facilitate root growth and nutrient uptake and, thus, vegetable production and quality; therefore, fulvic acids can be an effective component for designing new biofertilizers for sustainable agricultural production.

Keywords: humic substances, nutritional quality, plant biomass, seed germination, soil organic matter

INTRODUCTION

Fulvic acids are one portion of soil humic substances based on the solubility in strong acid and base solutions; the other two main portions are humic acids and humins (Hayes, 2006; Ahmad et al., 2018). Fulvic acids consist of a group of soluble organic compounds widely distributed in nature and are one of the critical components of soil organic substances (Piccolo, 2002;

Qin et al., 2016; Shah et al., 2018). These organic compounds contain many active functional groups, such as carbonyl, carboxyl, hydroxyl, phenolic hydroxyl, and quinone, and these are capable of chelating and exchanging anions or ions (Calvo et al., 2014; de Melo et al., 2016; Zhang et al., 2020). The mechanisms by which humic-like substances improve plant growth can be attributed to the increased ability of regulating membrane permeability and intracellular signaling, thus increasing root growth (Blomster et al., 2011), increasing concentrations of chlorophyll and photosynthetic activity (Haghighi et al., 2012), and activating carbon and nitrogen metabolism (Jannin et al., 2012). In addition, the biochemical fulvic acids encompass amino acids, vitamins, trace elements, and hormones, and all those compounds can stimulate cell division, root growth, and nutrient uptake and improve the antistress ability of plants and, thus, promote the growth and, thus, yield of crops (De Pascale et al., 2018; Shah et al., 2018; Qin and Leskovar, 2020). For example, fulvic acids are demonstrated to relieve Pb toxicity to plants by reducing its uptake, thus alleviating various morphological, physiological, and biochemical functions of plants (Shahid et al., 2012).

In recent decades, numerous studies confirm the effectiveness of fulvic acids in agriculture. Fulvic acids are demonstrated to increase the yield and quality of cotton plants, soil fertility, fertilizer-use efficiency, and net profit (Geng et al., 2020). The application of fulvic acids alleviates the damage on wheat plants under salinity stress by improving antioxidant-defense systems, thus increasing growth and production (Elrys et al., 2020). With respect to vegetable production, fulvic acids increase the size and number of tomatoes while decreasing the incidence of cracking and blossom-end rotting (Suh et al., 2014). As a result of increased plant growth, fulvic acids are recommended as an essential constituent to achieve the goal of high yield and quality and sustainable agriculture in horticulture particularly (Olk et al., 2018).

However, due to the complex composition of fulvic acids, in-depth trials have not been not comprehensively investigated, especially the effects of bioresource fulvic acids on the yield and quality of vegetables and the underlying mechanisms. Bioresource fulvic acids are renewable and recyclable, and thus, the popular agricultural fulvic acids in recent decades are considerable for sustainable agriculture (Quilty and Cattle, 2011; Rose et al., 2014).

This study investigates the effects of straw-derived fulvic acids on vegetable plants. We carried out soil experiments, seed germination, and hydroponic cultures to explore the effects of various doses and application patterns on the production, yield, and quality of tomato plants and the underlying mechanisms that potentially facilitate the design of new biofertilizers by using fulvic acids.

MATERIALS AND METHODS

Bioresource-derived fulvic acids, abbreviated as Zhongliang or ZL in the study, were produced by the national company COFCO Nutrition and Health Research Institute, Beijing, China (**Table 1**). ZL fulvic acids are derived from corn straw. The lignocellulosic corn straws were pretreated by continuous steam explosion and then hydrolyzed by a series of enzymes (cellulase, hemicellulase, and β-glucosidase) to get a sugar solution. The sugar solution was fermented by using a pentose/hexose co-fermentation strain (C5 strains, Green Tech America, United States) to get the mature fermented mash. Then, the mash was rectified to obtain biofuel ethanol from the top of the rectification tower while the residual mash was obtained from the bottom of the rectification tower. The residual mash was separated from the supernatant and then evaporated, concentrated, and tube-bundle-dried to get the final fulvic acids.

Experiment 1: Soil Culture of Tomato Plants

Experiment 1 was a soil culture to explore the effects of fulvic acids on the yield and quality of a fruit vegetable and soil fertility (**Supplementary Figure 1**). A randomized complete block design with 11 treatments consisted of various methods of fulvic acid application, i.e., top dressing, foliar, and base dressing (**Table 2**). Another commercial fulvic acid produced by QuanlinJiayou Co., Ltd. (Jiayou or JY) that was the most effective and popular product in China was used to compare with our product and to demonstrate the effectiveness of our Zhongling (ZL) fulvic acids. Five replicates were set for each treatment.

The soil was collected from the top 0–20 cm in a high tunnel vegetable farm managed for 18 years in Shanghai, China (**Table 3**). In this area of the Yangtze River Delta, rice was

TABLE 1 | The chemical properties of fulvic acids of Zhongliang used in this study.

Items	Value	Items	Value	Items	Value
Fulvic acids	69.5%	Ca (g kg^{-1})	9.25	As (μg g^{-1})	2.36
pH	3.94	Mg (g kg^{-1})	5.22	Cd (μg g^{-1})	0.23
Water content	6.11%	Fe (μg g^{-1})	1123	Cr (μg g^{-1})	18.9
Ach content	19.1%	Mn (μg g^{-1})	135	Hg (μg g^{-1})	0
Total C	30.3%	Cu (μg g^{-1})	2.54	Pb (μg g^{-1})	2.00
Total N	5.63%	Zn (μg g^{-1})	52.3		
Total P (P_2O_5)	0.26%				
Total K (K_2O)	3.09%				

TABLE 2 | The treatments of soil culture for tomato growth (Experiment 1).

Fertilization	Chemicals	Rates	Abbreviation
Control	Water	Local practice	Control
Top dressing	ZL fulvic	0.3 g kg^{-1}	ZL Top
Foliar application	acids	100 mg L^{-1}	ZL Foliar
Top dressing + Foliar		0.3 g kg^{-1} + 100 mg L^{-1}	ZL T + F
Top dressing	JY fulvic	0.3 g kg^{-1}	JY Top
Foliar application	acids	100 mg L^{-1}	JY Foliar
Top dressing + Foliar		0.3 g kg^{-1} + 100 mg L^{-1}	JY T + F
Base dressing	ZL fulvic	0.3 g kg^{-1}	Base 0.3
Base dressing	acids	0.9 g kg^{-1}	Base 0.9
Base dressing		2.7 g kg^{-1}	Base 2.7
Base dressing		8.1 g kg^{-1}	Base 8.1

TABLE 3 | The chemical properties of the experimental soil for Experiment 1.

pH	EC(dS m^{-1})	SOM%	Available N(μg g^{-1})	Available P(μg g^{-1})	Available K(μg g^{-1})	CEC(cmol kg^{-1})
7.5	0.47	1.9	342	169	303	19.4

produced for several hundred years before, and then the fields were used for vegetable production in the recent two decades. The base dressing followed the local practice, 5 kg mixed soils were loaded into a pot, watered to 100% field capacity, and stabilized for 1 week before being transplanted. The seeds of the tomato cultivar *Hezuo906* is an anti-mosaic-virus cultivar, which was sterilized, germinated, and nurtured. Tomato seeds were soaked in 0.5% NaClO solution for 20 min, then washed by deionized water twice, and placed in Petri dishes to be germinated in a dark incubation chamber (CWI800, Sheyan, Shanghai, China) at 25°C. The 3-day-germinated seeds were sown into a peat-pearlite mixture (2:1, v/v) in a naturally lit greenhouse and watered with a mixture of 1% urea and 1% potassium phosphate. Twenty-day-old seedlings with four true leaves were transplanted into pots. Soils in pots were watered to 80% field capacity at a frequency of 1 or 2 days. Foliar spray and top dressing were conducted every 10 days six times commencing from the initial fruiting stage. The soils were covered by plastic films when the foliar application was conducted to avoid fulvic acids dropping into the soils. The temperature and light intensity were recorded every 10 min by loggers L95-82 and L99-LX (Hangzhou Loggertech Co., China), respectively. The entire growth period was 126 days from August 31 to January 03 in the same naturally lit greenhouse with an average temperature of 18.7°C ± 3.6°C, a light intensity of 253 ± 212 μmol m^{-2} s^{-1}, and daily light integral of 12.6 ± 4.3 μmol m^{-2} day^{-1}.

Experiment 2: Germination of Tomato Seeds

Experiments 2 and 3 were conducted to explore the mechanisms of fulvic acids increasing the production and quality of vegetables. We conducted Experiment 2 to explore the stimulation of fulvic acids on seed germination rate and radicle elongation (**Supplementary Figure 2**). It was a randomized complete block design with eight concentrations of fulvic acids in solution: 0, 10, 20, 40, 80, 160, 320, and 640 mg L^{-1} with three replicates for each treatment. Two Chinese cultivars, i.e., *Huangmenren* (Jinfa Seed Company, Cangzhou, China) and *Zizhenzhu* (Huashu Seed Company, Qingxian, China) were used, and seeds were sterilized and germinated as in Experiment 1. The temperature and humidity in the incubation chamber were 28°C and 70%, respectively. The seed germination experiment lasted for 7 days. The fulvic acid solution was supplied daily to avoid water deficiency.

Experiment 3: Hydroponic Experiment With Tomato Plants

We conducted a hydroponic experiment with tomato plants to explore the effects of fulvic acids on root elongation and plant production (**Supplementary Figure 3**). The experiment was a randomized complete block design with eight concentrations of fulvic acids and four replicates for each treatment. Eight concentrations of fulvic acids in hydroponic nutrient solution were 0, 10, 20, 40, 80, 160, 320, and 640 mg L^{-1}.

Tomato seeds of cultivar cv. *Zizhenzhu* were sterilized, germinated, and grown till transplanting as in Experiment 1. Seedlings with four true leaves in similar sizes were selected and then transplanted into containers with 5 L 1/2 Hoagland nutrient solution, and the solutions were shifted to a full-strength nutrient solution at the second week. The macronutrients of Hoagland solution consisted of 4 mM $Ca(NO_3)_2{\cdot}4H_2O$, 6 mM KNO_3, 1 mM $NH_4H_2PO_4$, and 2 mM $MgSO_4{\cdot}7\ H_2O$, and the micronutrients were the universal formula (mg L^{-1}): 2.86, H_3BO_3; 13.9, $FeSO_4{\cdot}7H_2O$; 1.81, $MnCl_2{\cdot}4H_2O$; 0.22, $ZnSO_4{\cdot}7H_2O$; 0.08, $CuSO_4{\cdot}5H_2O$; and 0.02, $(NH_4)_6Mo_7O_4{\cdot}4H_2O$. The nutrient solution's pH was maintained at about 6.5 by daily adjusting using 0.25 M H_2SO_4 or 0.5 M NaOH. All the plants were harvested after growth for 21 days from June 24 to July 15.

Sampling Methods

The tomato fruits were harvested twice a week once matured and stored in a −20°C fridge. All the fruits were cut finely and homogenized thoroughly after final harvest, using a fruit blender. The homogenates were centrifuged at 3,000 *g* for 10 min and filtered by a syringe filter (0.45 μM) for biological analysis. At the final harvest, the leaves, stems, and roots of tomatoes were separated and collected. Separated tissues were cleaned and green-killed, then dried at 65°C to a constant weight to record the dry mass. Fresh portions were stored in a −20°C fridge till analysis. After plant sampling, the soils in pots were sieved at 1 mm after mixing and air-drying to determine soil chemical properties.

Measurements of Seed Germination and Radicle Length

We took daily photos of each Petri dish in Experiment 2 with a digital camera (5D Mark IV, Cannon, Germany). The germination rates were achieved by counting the number of germinated seeds in the photos. The radicle length of each seed was measured by ImageJ (Version 1.51a, National Institute of Health, United States). The germination rate and vigor index are calculated using Equations (1) and (2), respectively.

$$Germination\ rate = \frac{Number\ of\ germinated\ seeds}{Total\ number\ of\ seeds\ sown} \times 100\% \quad (1)$$

$$Vigor\ index = (mean\ radicle\ length) \times \sum \frac{G_n}{D_n} \quad (2)$$

where G_n is the number of germinated seeds at the nth day and D_n is the number of the nth day.

Determinations of Root Morphology

The fresh roots in Experiment 3 were washed by deionized water three times and scanned (V700, Epson, Japan) to obtain root images. The images were then analyzed by WinRhizo Pro (Version 2013, Regent, Canada) to determine root length and the number of root tips.

Determinations of Soil Property

Soil organic matter (SOM) was determined by dichromate titration. Soil pH was extracted by deionized water at a soil–water ratio of 1:2.5 and determined by a pH meter. Soil available N was determined by the alkali-hydrolyzed reduction diffusing method using 1 M NaOH. Available P was extracted by 0.5 M $NaHCO_3$ and determined by the molybdenum-antimony anti-spectrophotometric method. Available K was extracted by 1 M CH_3COONH_4 and determined by ammonium acetate extraction-flame photometry (Bao, 2000).

Determination of Tomato Quality

The total soluble solids in the juice of tomato fruits were analyzed by a portable digital sugar meter (PAL-1, Atago, Japan). The fruit juice was used for the determination of various compounds. The concentrations of C and N in the ground plant tissues were measured by a CNS analyzer (Vario MAX CNS, Elementar, Germany). The concentrations of P, K, Ca, Mg, S, Fe, Mn, Cu, and Zn were determined by an ICP-OES (Optima 8000, PerkinElmer, Germany), using the HNO_3-H_2O_2-digested solutions or the fruit juice of the tomato. The concentrations of heavy metals Cd, Cr, and Pb were measured by an ICP-MS (X Series II, Thermo Fisher, United States). The concentrations of metalloids As and Hg were measured by an X-ray Fluorescence Spectrometer (Axios-Advanced, PANalytical, Netherlands). The quantity and composition of metabolites in tomato fruits were determined by LC-MS (Thermo Vanquish UHPLC, Company Thermo Fisher, United States), coupled with an Orbitrap Q Exactive series mass spectrometer (Orbitrap Q Exactive, Company Thermo Fisher, United States). The fresh tomato fruits (100 mg) were individually ground using a blender and centrifuged and then the homogenate was passed through a 0.45-μM membrane. The supernatant was injected onto an Hyperil Gold column (100 mm × 2.1 mm, 1.9 μm), using a 16-min linear gradient at a flow rate of 0.2 mL min^{-1} for analysis. The Orbitrap Q Exactive series mass spectrometer was operated in positive/negative polarity mode with spray voltage of 3.2 kV, capillary temperature of 320°C, sheath gas flow rate of 35 arb, and aux gas flow rate of 10 arb.

Statistical Analysis

All the data were analyzed according to the experimental design, using SPSS 22 software (SPSS Statistics 22.0, IBM, United States). Pictures were drawn by Origin 2016 (Origin 2016, OriginLab, United States) and ImageJ (ImageJ 1.8.0, National Institutes of Health, United States). The means of these parameters were compared using Duncan's multiple range test at $P < 0.05$.

RESULTS

Effects of Fulvic Acids on Soil-Culture Tomatoes

Moderate doses of fulvic acids applied by base and top dressing improved the yield and nutrient quality of tomato fruits in general. More specifically, base dressing of ZL fulvic acids of 2.7 g kg^{-1} increased the yield and fruit number of tomatoes in soil cultures by 35.0 and 44.4% greater than other doses (**Figure 1**). The other commercial JY fulvic acids with top dressing increased the total biomass of tomato plants by 22.4% (**Table 4**).

The base dressing of 0.9 and 2.7 g kg^{-1} tended to increase fold changes of essential and non-essential amino acids (**Figure 2**).

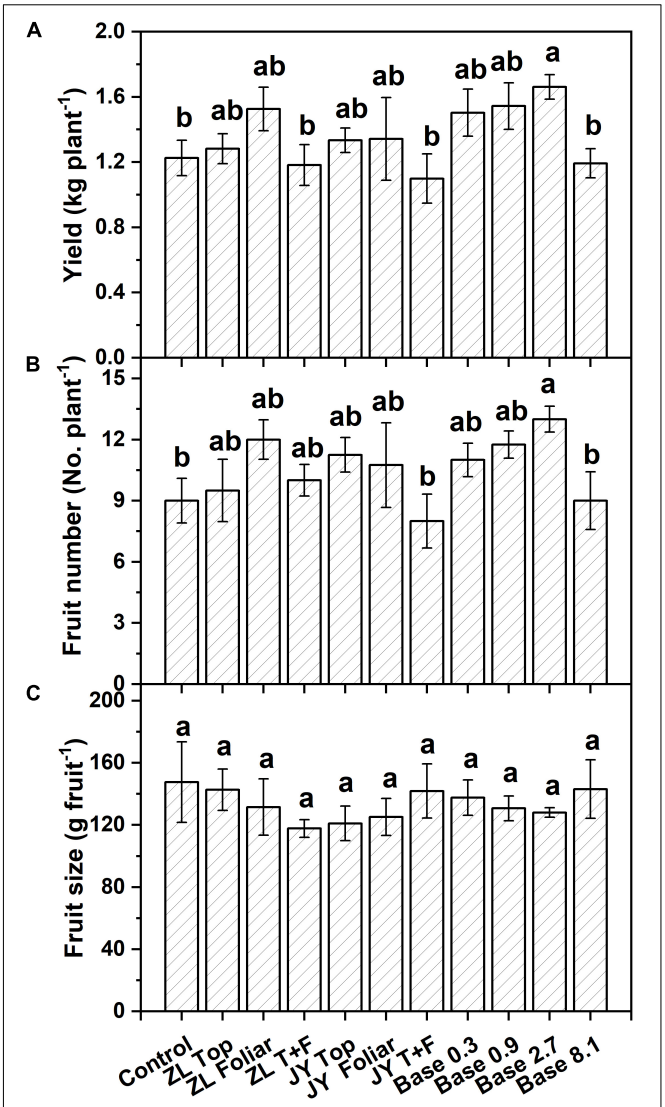

FIGURE 1 | The effect of fulvic acids on total yield **(A)**, fruit number **(B)**, and fruit size **(C)** of tomato plants cv. *Hezuo906* grown in soil culture for 126 days from transplanting at the final harvest. Data are means ± s.e ($N = 5$). The same letters denote insignificant differences ($P < 0.05$) among treatments according to Duncan's new multiple range test (Experiment 1).

TABLE 4 | The effect of fulvic acids on plant height, leaf number, and dry matter of stem, leaf, and the entire plants of tomato plants cv. *Hezuo906* grown in the soil culture for 126 days from transplanting (Experiment 1).

	Plant height (m)	Leaf number (No. plant^{-1})	Root	Stem	Leaf	Total	Root/shoot
			(g plant^{-1})				
Control	1.08 a	10.3 c	1.83 bc	20.5 ab	34.5 ab	56.8 ab	0.033 ab
ZL top	1.15 a	12.7 abc	1.85 bc	20.6 ab	30.5 ab	53.0 ab	0.036 ab
ZL foliar	1.15 a	11.3 bc	1.44 bc	15.5 b	26.6 b	43.5 b	0.034 ab
ZL T + F	1.17 a	15.7 a	1.72 bc	20.8 ab	34.6 ab	57.2 ab	0.033 ab
JY top	1.24 a	15.8 a	2.00 ab	26.6 a	40.9 a	69.5 a	0.031 b
JY foliar	1.16 a	15.8 a	1.33 c	18.3 ab	30.0 ab	49.7 b	0.028 b
JY T + F	1.11 a	13.7 abc	1.56 bc	18.2 ab	34.5 ab	54.2 ab	0.031 b
Base 0.3	1.28 a	12.0 abc	1.49 bc	19.8 ab	31.4 ab	52.7 ab	0.029 b
Base 0.9	1.09 a	13.0 abc	1.65 bc	18.7 ab	36.4 ab	56.7 ab	0.031 b
Base 2.7	1.09 a	12.8 abc	1.71 bc	19.4 ab	34.9 ab	56.0 ab	0.032 ab
Base 8.1	1.22 a	14.8 ab	2.38 a	19.9 ab	38.9 a	61.2 ab	0.041 a

Total biomass is the biomass of entire plants but without fruits. Root/shoot is the ratio of root dry biomass to shoot dry biomass. Data are means (N = 5). The same letters denote insignificant differences (P < 0.05) among treatments according to Duncan's new multiple range test.

Base dressing of 2.7 g kg^{-1} fulvic acids increased fold changes of phenylalanine, valine, and methionine by 55, 56, and 61%, respectively. Compared with the control, ZL fulvic acids by top and foliar application increased the fold changes of linolenic and linoleic acid by 209 and 275%, respectively. Fulvic acids increased fold changes of citric and malic acid with the greatest increased by 291 and 67% in JY top dressing treatment, 211 and 42% in Base 2.7 (**Figure 2**). However, fulvic acids in all treatments did not affect fold changes of soluble sugar (glucose, fructose, maltose, and sucrose) and some aromatic substances (β-lonone, citral, and eugenol) (**Figure 2**).

The base dressing of 2.7 g kg^{-1} also increased the concentrations of mineral elements in tomato juice, especially Mg by 55.9%, Ca by 31.4%, and Zn by 43.1% (**Table 5**). The concentrations of Mg, S, Ca, and Fe increased in all modes of application.

Fulvic acids by top and base dressing tended to decrease soil pH and increase the soil CEC and SOM across all treatments while foliar application did not affect these soil properties (**Table 6**). More specifically, Base 2.7 treatment decreased soil pH from 8.06 to 7.81 while it increased EC by 102.9%.

Effects of Fulvic Acids on Germination of Tomato Seeds

The seed germination rates of both tomato cultivars increased and then decreased when the concentration of fulvic acids increased after 7 days (**Figures 3A,B**). Specifically, the most effective seed germination rate was 12.9% greater than the control when fulvic acids were at a concentration of 80 mg L^{-1} on average. Fulvic acids of 80 mg L^{-1} also increased the radicle length and vigor index by 32.2 and 49.7% compared with the control, respectively (**Figure 3**). The promotion of seed germination by fulvic acids on tomato seed cv. *Huangmeiren* was greater than that of cv. *Zizhenzhu*. The average seed germination rates of *Huangmeiren* and *Zizhenzhu* across the various concentrations of fulvic acids were 62.6 and 89.9%, respectively.

Effects of Fulvic Acids on Hydroponic Tomatoes

Similar to seed germination, the effects on total biomass, foliar *C*/*N* ratio, and root growth of tomato plants in hydroponics increased at first and then decreased when the fulvic acid concentrations increased (**Table 7** and **Figure 4**). Fulvic acids increased the total biomass and foliar C/N ratio by 40.8 and 14.5% at concentrations of 160 mg L^{-1}, respectively, compared with the control. Fulvic acids increased the root length and number of lateral root tips of hydroponic tomato plants (**Figure 4**). The optimal concentration of fulvic acids on root growth was 80 mg L^{-1}, which increased root length and root tips by 44.4 and 13.8% when compared with the control, respectively (**Figure 4** and **Supplementary Figure 4**). Fulvic acids of 80 mg L^{-1} also increased the concentrations of mineral elements in the leaf, especially Fe, by 109% compared with the control (**Table 7**).

Another soil-culture experiment with pak choi was conducted to expand the application of fulvic acids on leafy vegetables with shallow roots using the soils in Experiment 1 and a series of concentrations of fulvic acids the same as Experiments 2 and 3 (**Supplementary Figure 5**). The aboveground portions of pak choi were harvested on the 21st and 30th day from seeding, respectively. The yield and mineral concentrations in the edible portion were measured (**Supplementary Table 1** and **Supplementary Figure 6**). The analysis of the cost and benefit of fulvic acid application is calculated in **Supplementary Table 2**. Results are shown in the **Supplementary Material**.

DISCUSSION

Humic substances are the end products of microbial decomposition derived from plant residuals, which play key roles in various soils and influence plant functions. Fulvic acids are components of humic substances according to their solubility and molecular weight. There are similarities between humic substances and fulvic acids, but the effects on plants depend on the source organic matter, the plant species, and the growth medium (Calvo et al., 2014). Although the effects of humic-like fertilizers differ, studies confirm their effectiveness and economic value in agricultural production. However, it lacks studies focusing on the effects of renewable sources of fulvic acids on vegetable production and yield under various growth mediums and the underlying mechanisms. Our study investigates the effects of straw-derived fulvic acids on the entire growth period of tomato from seed to fruit under either hydroponic or soil culture and give certain explanations on how fulvic acids work.

Fulvic Acids Increased the Yield and Production of Vegetables

Fulvic acids at moderate concentrations and applications of base and top dressing increased the production and yield of tomato

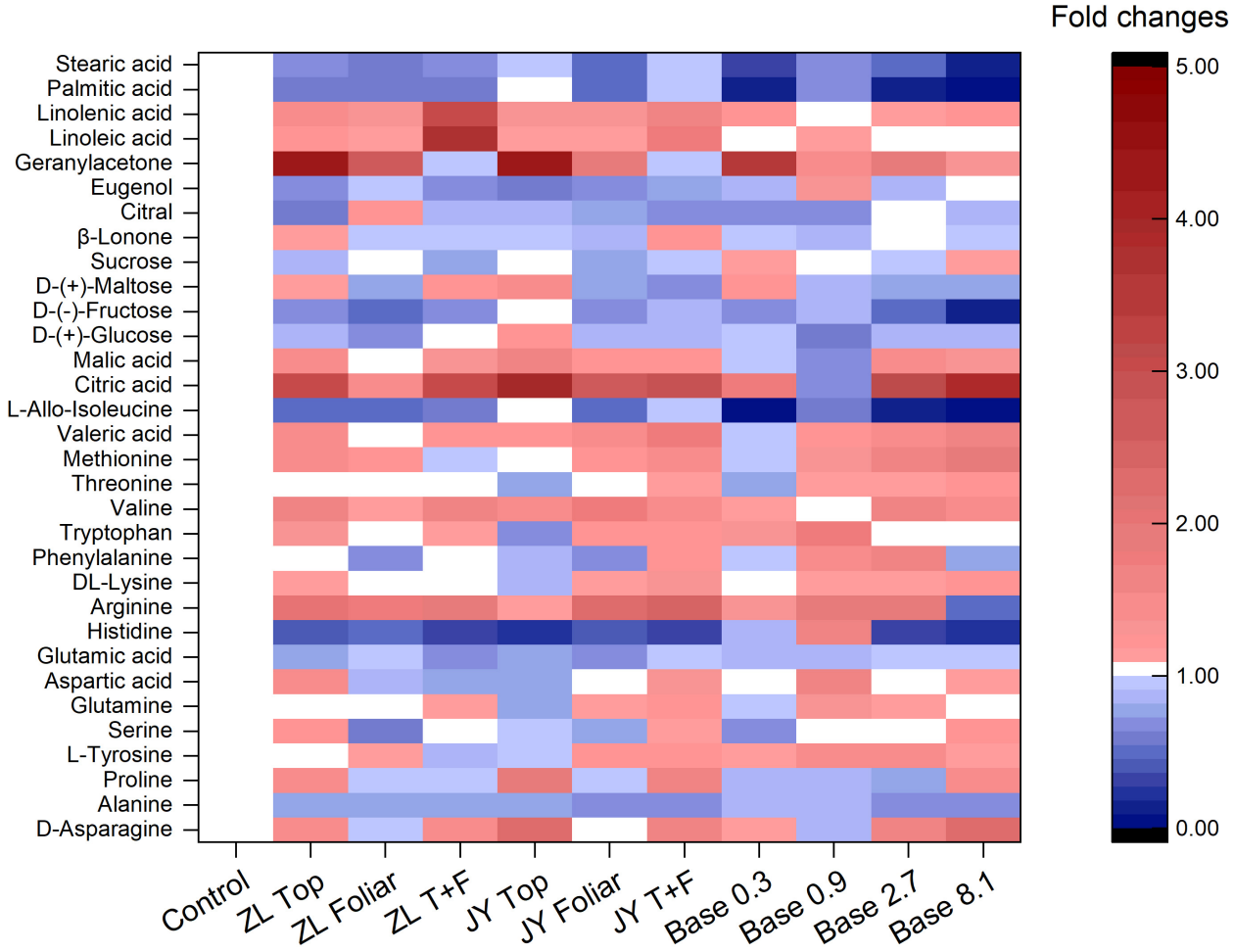

FIGURE 2 | The effect of fulvic acids on the fold changes of quality-related can carbon containing substances in fruit juices of tomato plants grown in soil cultures (Experiment 1).

TABLE 5 | The effect of fulvic acids on mineral concentration ($\mu g\ g^{-1}$) in fruit juices of tomato plants cv. *Hezuo906* grown in the soil culture for 126 days from transplanting (Experiment 1).

	K	P	Mg	S	Ca	Fe	Zn	Mn	Cu
Control	1755 bc	144.8 ab	38.3 c	37.6 a	11.8 bc	0.30 d	0.320 c	0.110 d	0.095 d
ZL top	2049 ab	152.4 ab	54.3 ab	45.9 a	13.3 bc	0.66 ab	0.480 ab	0.203 ab	0.143 abc
ZL foliar	1789 bc	135.8 ab	53.9 ab	43.7 a	15.0 abc	0.54 bcd	0.445 bc	0.175 bcd	0.136 abcd
ZL T + F	1520 c	98.4 b	63.4 a	44.7 a	16.0 abc	0.60 abc	0.540 ab	0.213 ab	0.129 cd
JY top	1889 bc	119.6 ab	54.0 ab	43.8 a	20.5 a	0.52 bcd	0.533 ab	0.178 bcd	0.123 cd
JY foliar	1597 c	104.7 b	47.7 bc	40.5 a	12.5 bc	0.44 cd	0.410 bc	0.147 cd	0.114 cd
JY T + F	2196 a	179.3 a	59.5 a	48.2 a	13.4 bc	0.67 ab	0.635 a	0.253 a	0.163 a
Base 0.3	1712 bc	117.9 ab	36.9 c	39.0 a	9.7 c	0.35 cd	0.350 c	0.128 d	0.098 d
Base 0.9	1899 bc	149.8 ab	46.8 bc	41.0 a	11.3 bc	0.40 cd	0.430 bc	0.138 d	0.125 cd
Base 2.7	2064 ab	136.0 ab	50.9 abc	40.5 a	15.5 abc	0.47 bcd	0.458 abc	0.152 cd	0.134 abc
Base 8.1	2251 a	165.7 ab	59.7 a	45.7 a	17.9 ab	0.80 a	0.623 a	0.197 abc	0.157 ab

Data are means (N = 5). The same letters denote insignificant differences ($P < 0.05$) among treatments according to Duncan's new multiple range test.

plants in our study (**Table 4**, **Figures 1**, **4** and **Supplementary Figure 6**). The yield increments of tomato and pak choi can reach 35.0 and 54% (**Figure 1** and **Supplementary Figure 6**) while fulvic acids increased the total biomass of hydroponic tomato plants by 40.8% at most (**Figure 4C**). The improved yield could contribute to the farmer's income to an extent

TABLE 6 | The effect of fulvic acids on the properties of soils where tomato plants cv. *Hezuo906* were grown for 126 days from transplanting (Experiment 1).

	pH	EC (dS m^{-1})	SOM (%)	Available N ($\mu g\ g^{-1}$)	Available P ($\mu g\ g^{-1}$)	Available K ($\mu g\ g^{-1}$)	CEC (cmol kg^{-1})
Control	8.06 ab	0.34 cd	1.87 c	106 b	151 a	110 b	18.9 b
ZL top	7.81 de	0.52 bc	1.91 bc	114 b	152 a	108 b	19.2 ab
ZL foliar	8.14 a	0.30 d	1.88 c	110 b	154 a	112 b	19.2 ab
ZL T + F	7.90 cd	0.45 cd	1.90 bc	113 b	144 a	115 ab	19.4 ab
JY top	7.75 de	0.57 bc	1.93 bc	113 b	152 a	107 b	19.4 ab
JY foliar	8.02 abc	0.36 cd	1.88 c	108 b	154 a	103 b	19.1 ab
JY T + F	7.74 e	0.50 bcd	1.91 bc	111 b	144 a	116 ab	19.4 ab
Base 0.3	8.05 abc	0.35 cd	1.92 bc	110 b	149 a	102 b	19.3 ab
Base 0.9	8.00 bc	0.41 cd	1.94 bc	107 b	151 a	108 b	19.6 ab
Base 2.7	7.81 de	0.69 b	1.96 ab	116 b	148 a	105 b	19.5 ab
Base 8.1	7.46 f	1.68 a	2.01 a	161 a	144 a	136 a	19.8 a

Data are means (N = 5). The same letters denote insignificant differences ($P < 0.05$) among treatments according to Duncan's new multiple range test. EC, electrical conductance; SOM, soil organic matter; CEC, cation exchange capacity.

(**Supplementary Table 2**). Similarly, humic-like substances were reported to increase the production of various vegetable plants. Atiyeh et al. (2002) report that humic substances extracted from vermicompost of pig manures and food waste increased the shoot and root dry masses of tomato seedlings with the optimal concentration of the humic substance being 0.2–0.5 g kg^{-1}. Karakurt et al. (2009) treated 20 ml L^{-1} humic-like substances with soil and increased the early and final yield of peppers by 38.3 and 11.8% compared with the control. The optimal doses in Karakurt et al. (2009) were lower than our current study; however, the fulvic acids in our study increased the plant yield to a greater extent. Our study demonstrates that fulvic acids have little effect on fruit size (**Figure 1C**), different from previous studies (Ferrara and Brunetti, 2010; Naidu et al., 2013; Suh et al., 2014). These differences in our study could be attributed to the variety of crops and the methods of cultivation, and the extent of increments and the specific performances also differed from the species of the plants and the sources of the humic-like substances (Morard et al., 2010). Haghighi et al. (2012) conclude that the mechanism of the increase in yield was the stimulation on N metabolism and photosynthesis activity, and Anjum et al. (2011) record that the application of fulvic acids increased the net photosynthesis, transpiration rate, and intercellular concentration of CO_2—effects that were related to plant growth promotion.

Fulvic Acids Increased the Quality of Vegetables

In our study, fulvic acids increased the concentrations of minerals and carbon-containing substances related to product quality in the edible portion of vegetables (**Table 7**, **Supplementary Table 1**, **Figure 2**, and **Supplementary Figure 6**). Several studies confirm an improvement of vegetable quality by humic-like substance application (Haghighi and Teixeira Da Silva, 2013). Fulvic acids are demonstrated to improve the produce quality, e.g., by inducing the accumulation of secondary metabolites, vitamins, antioxidants, and minerals (Calvo et al., 2014; Gruda et al., 2018), confirming our results.

More specifically, fulvic acids increase the concentrations of minerals at moderate doses, especially Mg, Fe, and Zn in either tomato or pak choi (**Table 5** and **Supplementary Table 1**). It is demonstrated that the application of humic acids enhances the accumulation of minerals such as Ca, Fe, Mg, and Zn in soil-cultured garlic (Denre et al., 2014). Similarly, humic substances increased the concentrations of P and Fe in grapes (Sánchez-Sánchez et al., 2006). With respect to carbon-containing substances, base dressing of 2.7 g kg^{-1} fulvic acids increased fold changes of phenylalanine, valine, and methionine, which possibly improved the fragrance of tomato berries (Ou et al., 2007), and the increased arginine contributed to an improvement in the quality of fruit berries (Micallef and Shelp, 1989; Nasibi et al., 2011). Consistent with our study, humic acids increased the concentrations of linolenic and linoleic acid in rapeseed (Amiri et al., 2020), the titratable acids in citrus (Hameed et al., 2018), and the amino acids in tomatoes (Yildirim, 2007). However, fulvic acids did not affect fold changes of soluble sugar and some aromatic substances (**Figure 2**), similar to a previous study (Canellas et al., 2013). That could be attributed to the application of fulvic acids that decreased the activity of enzymes involved in glucose metabolism (Canellas et al., 2015). The metabolites alternatively could be used to increase the growth of plants (Canellas et al., 2013), which confirms our results of tomato production and yield (**Table 4** and **Figures 1**, **2**). According to Trevisan et al. (2011), Jannin et al. (2012), and Canellas et al. (2015), the effects of fulvic acids on nutrients may be attributed to the regulation of enzymes and genes that are involved in the primary metabolism, and thus affect the transformation and accumulation of metabolic substances.

The increased quality indicators in tomato fruits by fulvic acids indicates an improved fruit quality and, thus, human nutrition in general. However, the quality of vegetables was not always improved by fulvic acids, such as some reduced sugars in tomato fruits (**Figure 2**) and mineral concentration in the edible portion of pak choi (**Supplementary Table 1**), so one need to be cautious when applying. These findings suggest that plant biostimulants, i.e., fulvic acids, may be used to improve product quality of vegetables in a sustainable way (Gruda et al., 2018). This will be imperative in the near future due to projected climate changes with high temperatures, water scarcity (Gruda et al., 2019a,b), and high CO_2 concentrations (Dong et al., 2018, 2020).

The Reasons for Increased Yield and Quality

The increases in production and quality might be attributed to the stimulants on plant growth, especially the promotion of root growth and, thus, the uptake of minerals. In our study, fulvic acids increased root growth of germinated seeds (**Figure 3**) and increased the root length and number of lateral root tips of hydroponic tomato plants (**Figures 4A,B**) while the uptake of mineral nutrients and the plant biomass

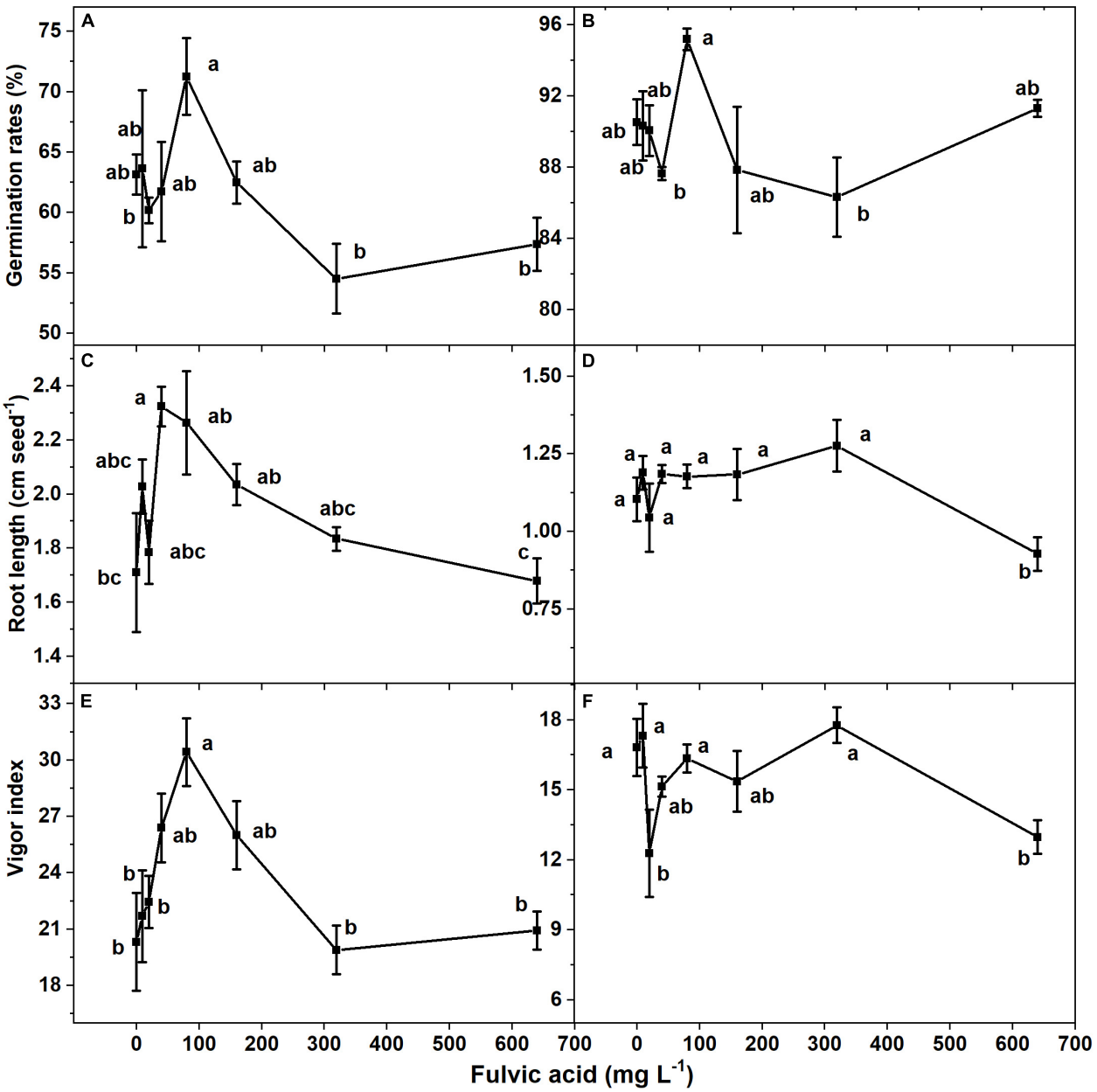

FIGURE 3 | The effect of fulvic acids on the germination rate, root length, and vigor index in of tomato seeds cv. *Huangmeiren* **(A,C,E)** and cv. *Zizhenzhu* **(B,D,F)** germinated for 7 days. Data are means ± s.e (N = 3). The same letters denote insignificant differences ($P < 0.05$) among treatments according to Duncan's new multiple range test (Experiment 2).

increased (**Table 7** and **Figure 4**). Fulvic acids are demonstrated to increase the root length of wheat seeds (Qin et al., 2016) and tomato plants (Dobbss et al., 2007, 2010) although humic extracts from hydrochar and Amazonian Dark Earth increased radicles and seminal lateral roots of maize seeds (Bento et al., 2020). The effects on root growth could be attributed to the hormone-like molecules and their auxin- and gibberellin-like effects that can promote the elongation of root cells, coleoptiles, and hypocotyls (Zhao and Zhong, 2013; Canellas et al., 2015), confirming the characteristics of our microbially fermented fulvic acids. According to Blomster et al. (2011), fulvic acids enhance the activity of auxin signaling and the involved enzymes to increase the growth of roots. However, the current study lacks specific explanation; the roles and mechanisms by which humic substances affect plant growth need further investigation.

The increased root growth was observed to increase the nutrient uptake of vegetable plants. Fulvic acids increased the concentrations of Ca, Fe, and Zn in leaves in hydroponic tomato plants, especially Fe by 109% at most (**Table 7**). Similar to the effects on Fe in our study, humic acid improved the utilization

TABLE 7 | The effect of fulvic acids (FA) on nutrient concentration in leaves of tomato plants cv. *Zizhenzhu* in hydroponics for 21 days from transplanting (Experiment 3).

FA (mg L^{-1})	P	K	Ca	Mg	S	Fe	Mn	Zn
	($\mu g\ g^{-1}$)							
0	45.5 a	339 a	143 a	33.8 a	56.2 abc	2.46 b	1.18 a	0.435 ab
10	41.8 a	287 ab	138 a	29.1 a	50.1 abc	1.51 b	0.83 a	0.411 ab
20	42.3 a	262 b	143 a	32.7 a	44.4 c	1.66 b	0.73 a	0.387 b
40	40.3 a	279 b	136 a	33.1 a	46.1 bc	1.48 b	0.88 a	0.447 ab
80	43.8 a	289 ab	151 a	32.3 a	49.7 abc	9.43 a	1.17 a	0.440 ab
160	41.3 a	287 ab	138 a	32.4 a	48.4 bc	1.85 b	1.09 a	0.561 a
320	43.7 a	296 ab	141 a	29.6 a	57.0 ab	2.69 b	1.10 a	0.499 ab
640	42.0 a	280 b	133 a	27.7 a	61.3 a	3.66 b	0.92 a	0.484 ab

Data are means (N = 4). The same letters denote insignificant differences (P < 0.05) among treatments according to Duncan's new multiple range test.

efficiency of Fe in both the whole plant and roots of tomato seedlings in hydroponics by 46 and 161%, respectively (Adani et al., 1998) while several studies report that fulvic acids can promote the absorption of Fe (Pinton et al., 1997, 1999; Halim et al., 2003; Cerozi, 2020). The effects on the concentrations of Fe could be attributed to the regulation of gene expression, which is related to reduction and transport of Fe, thus improving the iron chelation and availability and, thus, the root uptake (Bocanegra et al., 2006; Elena et al., 2009). In addition, similarly to natural chelators, fulvic acids chelate Fe and other micronutrients and move them through membranes, thus enhancing the mineral accumulation in plants (Calvo et al., 2014).

According to Calvo et al. (2014), humic substances stimulate the growth of root and chelate ions and, thus, increase plant uptake of nutrients. Humic substances upregulate the activities of genes and enzymes involved in the root-to-shoot translocation of nutrients (Mora et al., 2010). Better root growth facilitates the uptake of more nutrients due to the greater surface area. On the other hand, the effect can be attributed to the acidity of fulvic acids (**Table 1**), which decreases the pH of growth medium and, thus, improves the bioavailability of nutrients (Muscolo et al., 2007). Humic substances are reported to increase the root length and diameter of tomato seedlings and the yield of greenhouse-cultured tomato (Qin and Leskovar, 2020), and they also conclude that the increments were attributed to improvement on the structure of roots. The increase in nutrient uptake further contributed to the promotion on biomass, thus increasing the yield and quality. The *C*/*N* ratio of hydroponic plants shared the similar trends with root growth (**Figure 4**), which indicated the accumulation of carbohydrate contributing to plant yield and similar to a previous study (Aminifard et al., 2012).

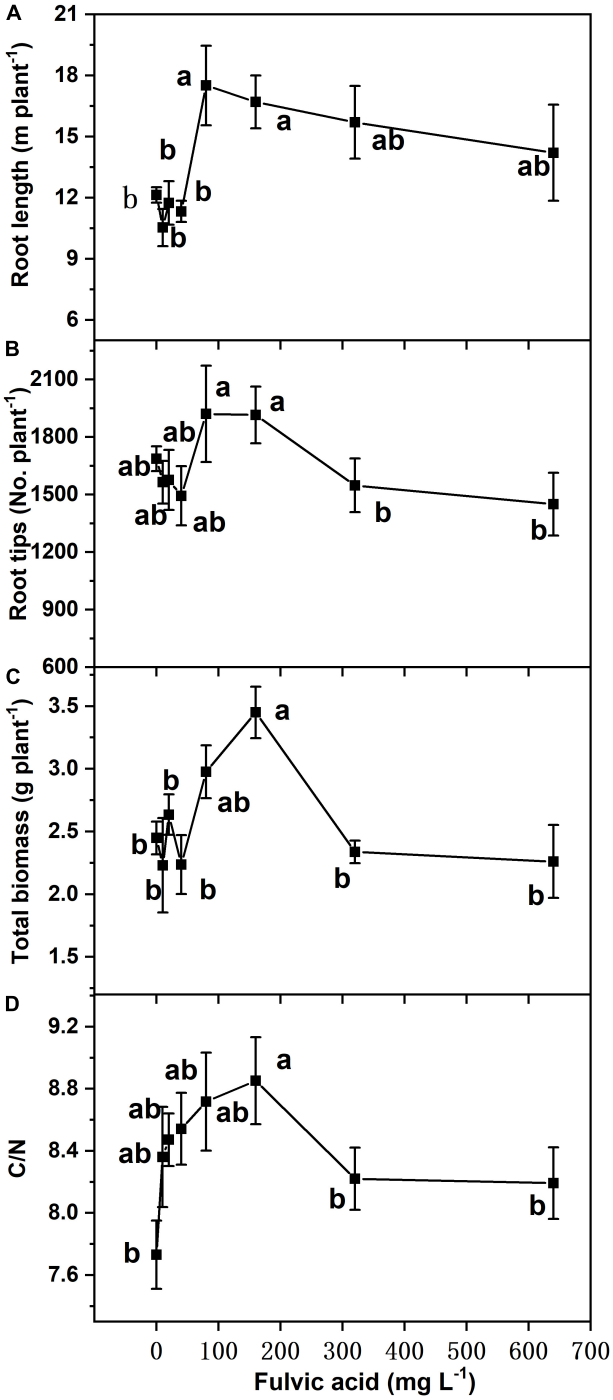

FIGURE 4 | The effect of fulvic acids on root length **(A)**, root tips **(B)**, total biomass **(C)**, and ratio of carbon to nitrogen **(D)** in leaves of tomato plants cv. *Zizhenzhu* grown in hydroponics for 21 days. Data are means ± s.e (*N* = 4). The same letters denote insignificant differences ($P < 0.05$) among treatments according to Duncan's new multiple range test (Experiment 3).

Fulvic Acids Increased the Germination of Seeds

Similar to the root growth of plants, fulvic acids at moderate concentrations increased the germination rate and vigor index of tomato seeds (**Figure 3**). Several other studies confirm our results that fulvic acids increase the germination of seeds. Soluble humates extracted from vermicomposted cattle manure in the soil substrate increased the germination rate of tomato seeds by 31.6% (Olivares et al., 2015). Humic substances

increased the germination rate and vigor index of cucumber seeds (Ahmed and Awad, 2020). Compared with our study, the humates in Olivares et al. (2015) increased the germination rate of tomato seeds to a greater extent, which might be attributed to their combined application of plant growth–promoting bacterium. The promotion on seed germination might be attributed to the auxin-like substances in humic products that can increase the activity of amylase and promote seed respiration (Zandonadi et al., 2007; Canellas et al., 2010; Canellas and Olivares, 2014). The different performances of seed germination between *Huangmeiren* and *Zizhenzhu* also indicate that fulvic acids facilitate the germination of cultivar with greater germination rates.

Fulvic Acids Affected the Chemical Properties of Soil

Fulvic acids by top and base dressing tended to decrease soil pH and increase the soil CEC and SOM across all treatments while foliar application did not affect these soil properties (**Table 6**). Base dressing of 8.1 g kg^{-1} decreased soil pH while increasing soil EC, SOM, concentrations of available N, available K, and CEC to the greatest extent. The decrease in soil pH by fulvic acid application could be attributed to the acidity from fulvic acids (Sharif et al., 2002; Tahir et al., 2011). According to Suntari et al. (2015), fulvic acids increase soil fertility indicated by the increased concentration of available N. However, fulvic acids did not affect soil available P in our study, inconsistent with other reports finding that humic substances could enhance this parameter (Cimrin and Yilmaz, 2005; Jones et al., 2007). We believe that the result of our study can be attributed to the high level of P in the experimental soils (**Table 2**).

CONCLUSION

Our study demonstrates that the moderate application of bioresource compounds, i.e., straw-extracted and microbially fermented fulvic acids, enhanced seed germination, production and yield of vegetables, and vegetable quality to an extent in both hydroponics and soil cultures. The improvement in the growth and quality of vegetables can be attributed to the promotion of root elongation and, thus, increased nutrient uptake by more likely the auxin-like substances. Also, fulvic acids can improve soil fertility indicated by the increased SOM and soil CEC. Our study confirms that optimal concentrations of fulvic acids were 2.7 g kg^{-1} as base dressing and 80–160 mg L^{-1} in solutions as seed soaking, top dressing, and hydroponic application. Future studies should aim to specify the effective components of fulvic acids and to explore the underlying mechanisms of how fulvic acids work from molecular perspectives.

DATA AVAILABILITY STATEMENT

The original contributions presented in the study are included in the article/**Supplementary Material**, further inquiries can be directed to the corresponding authors.

AUTHOR CONTRIBUTIONS

PZ: conceptualization, methodology, software, and writing—original draft. GW and ZD: resources. XC and PZ: investigation and formal analysis. HZ: investigation and resources. JD: conceptualization, data curation, and writing—review and editing. NG and XL: writing—review and editing. ZD: supervision and project administration. All authors contributed to the article and approved the submitted version.

ACKNOWLEDGMENTS

We thank the funding supports from the National Key R&D Program of China (2018YFD1100103) and the Strategic Priority Research Program of the Chinese Academy of Sciences (XDA23020401). The joint funding support and supply of fulvic acids from the Nutrition and Health Research Institute, COFCO, were much appreciated. We greatly appreciate the support of the Jiwu Shi, a local farmer, for providing the tomato seeds *Hezuo906* and technical advice.

SUPPLEMENTARY MATERIAL

The Supplementary Material for this article can be found online at: https://www.frontiersin.org/articles/10.3389/fpls.2021.736613/full#supplementary-material

REFERENCES

Adani, F., Genevini, P., Zaccheo, P., and Zocchi, G. (1998). The effect of commercial humic acid on tomato plant growth and mineral nutrition. *J. Plant Nutr.* 21, 561–575. doi: 10.1080/01904169809365424

Ahmad, T., Khan, R., and Nawaz Khattak, T. (2018). Effect of humic acid and fulvic acid based liquid and foliar fertilizers on the yield of wheat crop. *J. Plant Nutr.* 41, 2438–2445. doi: 10.1080/01904167.2018.1527932

Ahmed, H. M. H., and Awad, A. E. (2020). Influence of humic substances on cucumber seeds storability and root rot diseases incidence under salinity conditions. *J. Plant. Nutr. Soil Sci.* 32, 51–73. doi: 10.9734/ijpss/2020/v32i130235

Aminifard, M., Aroiee, H., Nemati, H., Azizi, M., and Jaafar, H. (2012). Fulvic acid affects pepper antioxidant activity and fruit quality. *Afr. J. Biotechnol.* 11, 179–185. doi: 10.5897/AJB12.1507

Amiri, M., Rad, A., Valadabadi, A., Sayfzadeh, S., and Zakerin, H. R. (2020). Response of rapeseed fatty acid composition to foliar application of humic acid under different plant densities. *Plant Soil Environ.* 65, 303–308. doi: 10.17221/220/2020-PSE

Anjum, S., Wang, L. C., Farooq, M., Xue, L., and Ali, S. (2011). Fulvic acid application improves the maize performance under well-watered and drought conditions. *J. Agron. Crop. Sci.* 197, 409–417. doi: 10.1111/j.1439-037X.2011.00483.x

Atiyeh, R. M., Lee, S., Edwards, C. A., Arancon, N. Q., and Metzger, J. D. (2002). The influence of humic acids derived from earthworm-processed organic wastes

on plant growth. *Bioresour. Technol.* 84, 7–14. doi: 10.1016/S0960-8524(02)00017-2

Bao, S. D. (2000). *Soil and Agricultural Chemistry Analysis*. Beijing: China Agriculture Press.

Bento, L., Melo, C., Ferreira, O., Moreira, A., Mounier, S., Piccolo, A., et al. (2020). Humic extracts of hydrochar and amazonian dark earth: molecular characteristics and effects on maize seed germination. *Sci. Total Environ.* 708:135000. doi: 10.1016/j.scitotenv.2019.135000

Blomster, T., Salojarvi, J., Sipari, N., Brosche, M., Ahlfors, R., Keinänen, M., et al. (2011). Apoplastic reactive oxygen species transiently decrease auxin signaling and cause stress-induced morphogenic response in arabidopsis. *Plant Physiol.* 157, 1866–1883. doi: 10.1104/pp.111.181883

Bocanegra, M. P., Lobartini, J. C., and Orioli, G. A. (2006). Plant uptake of iron chelated by humic acids of different molecular weights. *Commun. Soil Sci. Plant Anal.* 37, 239–248. doi: 10.1080/00103620500408779

Calvo, P., Nelson, L., and Kloepper, J. W. (2014). Agricultural uses of plant biostimulants. *Plant Soil* 383, 3–41. doi: 10.1007/s11104-014-2131-8

Canellas, L. P., Balmori, D. M., Médici, L. O., Aguiar, N. O., Campostrini, E., Rosa, R. C. C., et al. (2013). A combination of humic substances and *Herbaspirillum seropedicae* inoculation enhances the growth of maize (*Zea mays* L.). *Plant Soil* 366, 119–132. doi: 10.1007/s11104-012-1382-5

Canellas, L. P., and Olivares, F. L. (2014). Physiological responses to humic substances as plant growth promoter. *Chem. Biol. Technol. Agric.* 1:3. doi: 10.1186/2196-5641-1-3

Canellas, L. P., Olivares, F. L., Aguiar, N. O., Jones, D. L., Nebbioso, A., Mazzei, P., et al. (2015). Humic and fulvic acids as biostimulants in horticulture. *Sci. Hortic.* 196, 15–27. doi: 10.1016/j.scienta.2015.09.013

Canellas, L. P., Piccolo, A., Dobbss, L. B., Spaccini, R., Olivares, F. L., Zandonadi, D. B., et al. (2010). Chemical composition and bioactivity properties of size-fractions separated from a vermicompost humic acid. *Chemosphere* 78, 457–466. doi: 10.1016/j.chemosphere.2009.10.018

Cerozi, B. D. S. (2020). Fulvic acid increases iron bioavailability in aquaponic systems: theoretical designs and practical considerations to prevent iron deficiency in plants. *Aquac. Eng.* 90:102091. doi: 10.1016/j.aquaeng.2020.102091

Cimrin, K. M., and Yilmaz, I. (2005). Humic acid applications to lettuce do not improve yield but do improve phosphorus availability. *Acta Agric. Scand. B Soil Plant Sci.* 55, 58–63. doi: 10.1080/09064710510008559

de Melo, B. A., Motta, F. L., and Santana, M. H. (2016). Humic acids: structural properties and multiple functionalities for novel technological developments. *Mater. Sci. Eng. C Mater. Biol. Appl.* 62, 967–974. doi: 10.1016/j.msec.2015.12.001

De Pascale, S., Rouphael, Y., and Colla, G. (2018). Plant biostimulants: innovative tool for enhancing plant nutrition in organic farming. *Eur. J. Hortic. Sci.* 82, 277–285. doi: 10.17660/eJHS.2017/82.6.2

Denre, M., Soumya, G., and Kheyali, S. (2014). Effect of humic acid application on accumulation of mineral nutrition and pungency in garlic (*Allium sativum* L.). *Int. J. Biotechnol. Mol. Biol. Res.* 5, 7–12. doi: 10.5897/IJBMBR2014.0186

Dobbss, L., Canellas, L., Olivares, F., Aguiar, N., Peres, L., Azevedo, M., et al. (2010). Bioactivity of chemically transformed humic matter from vermicompost on plant root growth. *J. Agric. Food Chem.* 58, 3681–3688. doi: 10.1021/jf904385c

Dobbss, L. B., Medici, L. O., Peres, L. E. P., Pino-Nunes, L. E., Rumjanek, V. M., Façanha, A. R., et al. (2007). Changes in root development of Arabidopsis promoted by organic matter from oxisols. *Ann. Appl. Biol* 151, 199–211. doi: 10.1111/j.1744-7348.2007.00166.x

Dong, J., Gruda, N., Lam, S. K., Li, X., and Duan, Z. (2018). Effects of elevated CO2 on nutritional quality of vegetables: a review. *Front. Plant Sci.* 9:00924. doi: 10.3389/fpls.2018.00924

Dong, J., Gruda, N., Li, X., Tang, Y., Zhang, P., and Duan, Z. (2020). Sustainable vegetable production under changing climate: the impact of elevated CO2 on yield of vegetables and the interactions with environments-a review. *J. Clean. Prod.* 253:119920.

Elena, A., Diane, L., Eva, B., Marta, F., Roberto, B., Zamarreño, A. M., et al. (2009). The root application of a purified leonardite humic acid modifies the transcriptional regulation of the main physiological root responses to Fe deficiency in Fe-sufficient cucumber plants. *Plant Physiol. Biochem.* 47, 215–223. doi: 10.1016/j.plaphy.2008.11.013

Elrys, A. S., Abdo, A. I. E., Abdel-Hamed, E. M. W., and Desoky, E.-S. M. (2020). Integrative application of licorice root extract or lipoic acid with fulvic acid improves wheat production and defenses under salt stress conditions. *Ecotoxicol. Environ. Saf.* 190:110144. doi: 10.1016/j.ecoenv.2019.110144

Ferrara, G., and Brunetti, G. (2010). Effects of the times of application of a soil humic acid on berry quality of table grape (*Vitis vinifera* L.) cv Italia. *Span. J. Agric. Res.* 8, 817–822. doi: 10.5424/1283

Geng, J., Yang, X., Huo, X., Chen, J., Lei, S., Li, H., et al. (2020). Determination of the best controlled-release potassium chloride and fulvic acid rates for an optimum cotton yield and soil available potassium. *Front. Plant Sci.* 11:562335. doi: 10.3389/fpls.2020.562335

Gruda, N., Bisbis, M., and Tanny, J. (2019a). Impacts of protected vegetable cultivation on climate change and adaptation strategies for cleaner productiona review. *J. Clean. Prod.* 225, 324–339. doi: 10.1016/j.jclepro.2019.03.295

Gruda, N., Bisbis, M., and Tanny, J. (2019b). Influence of climate change on protected cultivation: Impacts and sustainable adaptation strategiesa review. *J. Clean. Prod.* 225, 481–495. doi: 10.1016/j.jclepro.2019.03.210

Gruda, N., Savvas, D., Colla, G., and Rouphael, Y. (2018). Impacts of genetic material and current technologies on product quality of selected greenhouse vegetablesa review. *Eur. J. Hortic. Sci.* 83, 319–328. doi: 10.17660/eJHS.2018/83.5.5

Haghighi, M., Kafi, M., and Fang, P. (2012). Photosynthetic activity and N metabolism of lettuce as affected by humic acid. *Int. J. Veg. Sci.* 18, 182–189. doi: 10.1080/19315260.2011.605826

Haghighi, M., and Teixeira Da Silva, J. A. (2013). Amendment of hydroponic nutrient solution with humic acid and glutamic acid in tomato (*Lycopersicon esculentum* Mill.) culture. *J. Soil Sci. Plant Nutr.* 59, 642–648. doi: 10.1080/00380768.2013.809599

Halim, M., Conte, P., and Piccolo, A. (2003). Potential availability of heavy metals to phytoextraction from contaminated soils induced exogenous humic substances. *Chemosphere* 52, 265–275. doi: 10.1016/S0045-6535(03)00185-1

Hameed, A., Fatma, S., Wattoo, J. I., Yaseen, M., and Ahmad, S. (2018). Accumulative effects of humic acid and multinutrient foliar fertilizers on the vegetative and reproductive attributes of citrus (*Citrus reticulata* cv. kinnow mandarin). *J. Plant Nutr.* 41, 2495–2506. doi: 10.1080/01904167.2018.1510506

Hayes, M. H. B. (2006). Solvent systems for the isolation of organic components from soils. *Soil Sci. Soc. Am. J.* 70, 986–994. doi: 10.2136/sssaj2005.0107

Jannin, L., Arkoun, M., Ourry, A., Laîné, P., Goux, D., Garnica, M., et al. (2012). Microarray analysis of humic acid effects on *Brassica napus* growth: involvement of N, C and S metabolisms. *Plant Soil* 359, 297–319. doi: 10.1007/s11104-012-1191-x

Jones, C., Jacobsen, J., and Mugaas, A. (2007). Effect of low-rate commercial humic acid on phosphorus availability, micronutrient uptake, and spring wheat yield. *Commun. Soil Sci. Plant Anal.* 38, 921–933. doi: 10.1080/00103620701277817

Karakurt, Y., Unlu, H., Unlu, H., and Padem, H. (2009). The influence of foliar and soil fertilization of humic acid on yield and quality of pepper. *Acta Agric. Scand. B Soil Plant Sci.* 59, 233–237. doi: 10.1080/09064710802022952

Micallef, B., and Shelp, B. (1989). Arginine metabolism in developing soybean cotyledons: I. relationship to nitrogen nutrition. *Plant Physiol.* 90, 624–630. doi: 10.1104/pp.90.2.624

Mora, V., Bacaicoa, E., Zamarreno, A. M., Aguirre, E., Garnica, M., Fuentes, M., et al. (2010). Action of humic acid on promotion of cucumber shoot growth involves nitrate-related changes associated with the root-to-shoot distribution of cytokinins, polyamines and mineral nutrients. *J. Plant Physiol.* 167, 633–642. doi: 10.1016/j.jplph.2009.11.018

Morard, P., Eyheraguibel, B., Morard, M., and Silvestre, J. (2010). Direct effects of humic-like substance on growth, water, and mineral nutrition of various species. *J. Plant Nutr.* 34, 46–59. doi: 10.1080/01904167.2011.531358

Muscolo, A., Sidari, M., Francioso, O., Tugnoli, V., and Nardi, S. (2007). The auxin-like activity of humic substances is related to membrane interactions in carrot cell cultures. *J. Chem. Ecol.* 33, 115–129. doi: 10.1007/s10886-006-9206-9

Naidu, Y., Meon, S., and Siddiqui, Y. (2013). Foliar application of microbial-enriched compost tea enhances growth, yield and quality of muskmelon (*Cucumis melo* L.) cultivated under fertigation system. *Sci. Hortic.* 159, 33–40. doi: 10.1016/j.scienta.2013.04.024

Nasibi, F., Yaghoobi, M. M., and Kalantari, K. M. (2011). Effect of exogenous arginine on alleviation of oxidative damage in tomato plant underwater stress. *J. Plant Interact.* 6, 291–296. doi: 10.1080/17429145.2010.539708

Olivares, F., Aguiar, N., Rosa, R., and Canellas, L. (2015). Substrate biofortification in combination with foliar sprays of plant growth promoting bacteria and humic substances boosts production of organic tomatoes. *Sci. Hortic.* 183, 100–108. doi: 10.1016/j.scienta.2014.11.012

Olk, D. C., Dinnes, D. L., Rene Scoresby, J., Callaway, C. R., and Darlington, J. W. (2018). Humic products in agriculture: potential benefits and research challengesa review. *J. Soils Sediments* 18, 2881–2891. doi: 10.1007/s11368-018-1916-4

Ou, X., Ren, X., and Zhou, Y. (2007). Comparison of amino acid contents and composistion in the stem tips of leaf-vegerable sweet potato cultivars. *J. Food. Sci. Tech.* 7, 120–125. doi: 10.16429/j.1009-7848.2007.04.021

Piccolo, A. (2002). *The Supramolecular Structure Of Humic Substances: A Novel Understanding Of Humus Chemistry And Implications In Soil Science*. Cambridge, MA: Academic Press, 57–134.

Pinton, R., Cesco, S., Nobili, M., Santi, S., and Varanini, Z. (1997). Water and pyrophosphate extractable humic substances fractions as a source of iron for Fe-deficient cucumber plants. *Biol. Fertil. Soils* 26, 23–27. doi: 10.1007/s003740050337

Pinton, R., Cesco, S., Santi, S., Agnolon, F., and Varanini, Z. (1999). Water-extractable humic substances enhance Fe deficiency responses by Fe-deficient cucumber plants. *Plant Soil* 210, 145–157. doi: 10.1023/A:1004329513498

Qin, K., and Leskovar, D. (2020). Humic substances improve vegetable seedling quality and post-transplant yield performance under stress conditions. *Agriculture* 10:10070254. doi: 10.3390/agriculture10070254

Qin, Y., Zhu, H., Zhang, M., Zhang, H., Xiang, C., and Li, B. (2016). GC-MS analysis of membrane-graded fulvic acid and its activity on promoting wheat seed germination. *Molecules* 21:21101363. doi: 10.3390/molecules21101363

Quilty, J. R., and Cattle, S. R. (2011). Use and understanding of organic amendments in Australian agriculture: a review. *Soil Res.* 49, 1–26.

Rose, M. T., Patti, A. F., Little, K. R., Brown, A. L., Jackson, W. R., and Cavagnaro, T. R. (2014). *A Meta-Analysis And Review Of Plant-Growth Response To Humic Substances: Practical Implications For Agriculture*. Cambridge, MA: Academic Press, 37–89.

Sánchez-Sánchez, A., Sánchez-Andreu, J., Juárez, M., Jordá, J., and Bermúdez, D. (2006). Improvement of iron uptake in table grape by addition of humic substances. *J. Plant Nutr.* 29, 259–272. doi: 10.1080/01904160500476087

Shah, Z. H., Rehman, H. M., Akhtar, T., Alsamadany, H., Hamooh, B. T., Mujtaba, T., et al. (2018). Humic substances: determining potential molecular regulatory processes in plants. *Front. Plant Sci.* 9:e00263. doi: 10.3389/fpls.2018.00263

Shahid, M., Dumat, C., Silvestre, J., and Pinelli, E. (2012). Effect of fulvic acids on lead-induced oxidative stress to metal sensitive *Vicia faba* L. plant. *Biol. Fertil. Soils* 48, 689–697. doi: 10.1007/s00374-012-0662-9

Sharif, M., Khattak, R. A., and Sarir, M. S. (2002). Effect of different levels of lignitic coal derived humic acid on growth of maize plants. *Commun. Soil Sci. Plant Anal.* 33, 3567–3580. doi: 10.1081/CSS-120015906

Suh, H. Y., Yoo, K. S., and Suh, S. G. (2014). Effect of foliar application of fulvic acid on plant growth and fruit quality of tomato (*Lycopersicon esculentum* L.). *Hortic. Environ. Biotechnol.* 55, 455–461. doi: 10.1007/s13580-014-0004-y

Suntari, R., Retnowati, R., Soemarno, S., and Munir, M. (2015). Determination of urea-humic acid dosage of vertisols on the growth and production of rice. *Agrivita* 37, 185–192. doi: 10.17503/Agrivita-2015-37-2-p185-192

Tahir, M. M., Khurshid, M., Khan, M. Z., Abbasi, M. K., and Kazmi, M. H. (2011). Lignite-derived humic acid effect on growth of wheat plants in different soils. *Pedosphere* 21, 124–131. doi: 10.1016/s1002-0160(10)60087-2

Trevisan, S., Botton, A., Vaccaro, S., Vezzaro, A., Quaggiotti, S., and Nardi, S. (2011). Humic substances affect Arabidopsis physiology by altering the expression of genes involved in primary metabolism, growth and development. *Environ. Exp. Bot.* 74, 45–55. doi: 10.1016/j.envexpbot.2011.04.017

Yildirim, E. (2007). Foliar and soil fertilization of humic acid affect productivity and quality of tomato. *Acta Agric. Scand. B Soil Plant Sci.* 57, 182–186. doi: 10.1080/09064710600813107

Zandonadi, D. B., Canellas, L. P., and Facanha, A. R. (2007). Indolacetic and humic acids induce lateral root development through a concerted plasmalemma and tonoplast H+ pumps activation. *Planta* 225, 1583–1595. doi: 10.1007/s00425-006-0454-2

Zhang, Z., Shi, W., Ma, H., Zhou, B., Li, H., Lü, C., et al. (2020). Binding mechanism between fulvic acid and heavy metals: Integrated interpretation of binding experiments, fraction characterizations, and models. *Water Air Soil Pollut.* 231:184. doi: 10.1007/s11270-020-04558-2

Zhao, G., and Zhong, T. (2013). Influence of exogenous IAA and GA on seed germination, vigor and their endogenous levels in *Cunninghamia lanceolata*. *Scand. J. For. Res.* 28, 511–517. doi: 10.1080/02827581.2013.783099

Conflict of Interest: The authors declare that the research was conducted in the absence of any commercial or financial relationships that could be construed as a potential conflict of interest.

frontiers in Microbiology

ORIGINAL RESEARCH
published: 25 October 2021
doi: 10.3389/fmicb.2021.763038

Isolation and Evaluation of Rhizosphere Actinomycetes With Potential Application for Biocontrolling *Fusarium* Wilt of Banana Caused by *Fusarium oxysporum* f. sp. *cubense* Tropical Race 4

Lu Zhang[1†], Huixi Zhang[2†], Yating Huang[1], Jun Peng[3], Jianghui Xie[2] and Wei Wang[2]*

[1] Ministry of Education Key Laboratory for Ecology of Tropical Islands, College of Life Sciences, Hainan Normal University, Haikou, China, [2] Key Laboratory of Biology and Genetic Resources of Tropical Crops, Ministry of Agriculture, Institute of Tropical Bioscience and Biotechnology, Chinese Academy of Tropical Agricultural Sciences, Haikou, China, [3] Institute of Environment and Plant Protection, Chinese Academy of Tropical Agricultural Sciences, Haikou, China

OPEN ACCESS

Edited by:
Maurizio Ruzzi, University of Tuscia, Italy

Reviewed by:
Anna Maria Vettraino, University of Tuscia, Italy
Chunyu Li, Institute of Fruit Tree Research, Guangdong Academy of Agricultural Sciences, China

***Correspondence:**
Wei Wang
wangweisys@ahau.edu.cn

† These authors have contributed equally to this work and share first authorship

Specialty section:
This article was submitted to Microbe and Virus Interactions with Plants, a section of the journal Frontiers in Microbiology

Received: *23 August 2021*
Accepted: *20 September 2021*
Published: *25 October 2021*

Citation:
Zhang L, Zhang H, Huang Y, Peng J, Xie J and Wang W (2021) Isolation and Evaluation of Rhizosphere Actinomycetes With Potential Application for Biocontrolling Fusarium Wilt of Banana Caused by Fusarium oxysporum f. sp. cubense Tropical Race 4. Front. Microbiol. 12:763038. doi: 10.3389/fmicb.2021.763038

Fusarium wilt of banana caused by *Fusarium oxysporum* f. sp. *cubense* tropical race 4 (TR4) is globally one of the most destructive soil-borne fungal diseases. Biological control using environmental microorganisms is considered as an alternative and sustainable strategy. Actinomycetes have the potential to explore biocontrol agents due to their production of diverse metabolites. The isolation and identification of high-efficiency and broad-spectrum antagonistic actinomycetes are the key for the application of biocontrol agents. In the present study, 60 actinomycetes were obtained from the rhizosphere soil of *Machilus pingii* in the primitive ecological natural reserve of Hainan province, China. Seventeen isolates and their extracts exhibited significant antifungal activity against *F. oxysporum* TR4. Particularly, strain BITDG-11 with the strongest inhibition ability had a broad-spectrum antifungal activity. The assay of its physiological and biochemical profiles showed that strain BITDG-11 had the ability to produce IAA and siderophores and had a positive response to gelatin liquefaction and nitrate reduction. Enzyme activities of chitinase, β-1,3-glucanase, lipase, and urease were also detected. Average nucleotide identity calculated by comparison with the standard strain genome of *Streptomyces albospinus* JCM3399 was 86.55% below the novel species threshold, suggesting that the strain could be a novel species. In addition, *Streptomyces* BITDG-11 obviously reduced the disease index of banana plantlets and promoted plant growth at 45 days post inoculation. The higher and lasting expression levels of defense genes and activities of antioxidant enzymes were induced in the roots of banana. Genome sequencing revealed that the *Streptomyces* BITDG-11 chromosome contained large numbers of conserved biosynthesis gene clusters encoding terpenes, non-ribosomal peptides, polyketides, siderophores, and ectoines.

Fifteen bioactive secondary metabolites were further identified from *Streptomyces* BITDG-11 extract by gas chromatography–mass spectrometry. Dibutyl phthalate demonstrating a strong antifungal activity was the major compound with the highest peak area. Hence, *Streptomyces* sp. BITDG-11 has a great potential to become an essential constituent of modern agricultural practice as biofertilizers and biocontrol agents.

Keywords: *Streptomyces* isolation, banana *Fusarium* wilt, antifungal activity, plant-growth promotion, biosynthetic gene clusters, GC-MS

INTRODUCTION

Banana (*Musa* spp.) is one of the world's most important staple and cash crops and widely cultivated in 135 countries in tropical and subtropical regions. Annual banana production in the world is estimated at over 145 million tons (Ploetz, 2015a). Due to the lack of effective cross-breeding techniques, commercial banana cultivars are usually multiplied by using vegetative propagation, resulting in a narrow genetic diversity and a susceptible defect to pests and diseases (Wang et al., 2012). *Fusarium* wilt of banana caused by *Fusarium oxysporum* f. sp. *cubense* is one of the most destructive soil-borne fungal diseases and seriously threatens the global banana industry. The causal agents are subdivided into four races based on the banana cultivars infected (Dita et al., 2018). *F. oxysporum* tropical race 4 (TR4) distributed in the main producing areas globally can infect almost all banana cultivars (Pegg et al., 2019). It can be spread by banana material, soil and machinery, irrigation water, etc. (Ploetz, 2015b).

Until now, there is a lack of a commercially effective method of controlling *Foc* TR4 due to the limited knowledge about its disease epidemiology (Bubici et al., 2019; Pegg et al., 2019). Selection of *F. oxysporum* TR4-resistant cultivars seems to be an optimal control strategy, but a productive alternative to the main cultivar Cavendish has not yet been found (Ploetz, 2015b). The poor fertility of Cavendish limits the improvement program through conventional breeding (Zorrilla-Fontanesi et al., 2020). Fungicides lead to chlorotic symptoms and unsatisfactory control efficiency for soil-borne pathogen due to a vascular pathogen penetrating into the plant roots or stems (Nel et al., 2010). Moreover, long-term use of fungicides causes safety concerns and enhances pathogenic resistance (Bubici et al., 2019). Crop rotation is also ineffective as *F. oxysporum* TR4 has a long survival in the soil beyond 20 years, even in the absence of host plants (Ploetz, 2015b). Therefore, before resistant cultivars are obtained, agronomic management approaches will be considered as the main strategy for controlling *Foc* TR4 with *F. oxysporum* TR4.

Recently, biological control using beneficial microorganisms has drawn the attention of scientists because of their economic and environmental advantages (Qi et al., 2019; Jing et al., 2020; Wei et al., 2020). Numerous microbial species have been identified as having the ability for biocontrol, such as *Bacillus* spp., *Burkholderia* spp., *Pseudomonas* spp., *Rhizobium* spp., and *Stenotrophomonas* spp., as well as other genera reported (Bubici et al., 2019). Particularly, *Streptomyces* can develop a symbiotic interaction with plants to promote growth of the host and produce diverse metabolites to inhibit the infection of pathogens (Chen et al., 2018; van der Heul et al., 2018; Bergeijk et al., 2020). *Streptomyces* belonging to the actinomycetes family make up 1–20% of the culturable soil microbes (Olanrewaju and Babalola, 2019). A variety of bioactive compounds are produced with different bioactivities such as antimicrobial, antiviral, and anticancer properties (Bergeijk et al., 2020). Approximately two-thirds of natural antibiotics have been isolated from actinomycetes, and 75% of them are from the *Streptomyces* genus (Franco-Correa et al., 2010). They are the primary antibiotic-producing organisms exploited by the pharmaceutical industry (Olanrewaju and Babalola, 2019). Our previous studies also evidenced that the application of *Streptomyces* sp. could increase the diversity of antagonistic microbes and reduce the disease incidence of *Fusarium* wilt of banana (Jing et al., 2020; Li et al., 2021a; Yun et al., 2021). However, environmental factors limited their stability and biocontrol efficiency against phytopathogens (Saravanan et al., 2003). Thus, the isolation and screening of high efficiency and broad-spectrum antagonistic microorganisms are still key for the application of biocontrol agents.

The extreme niches contribute to the rapid expansion of *Streptomyces* into various species clusters (Bull and Stach, 2007). This ecological diversity drives the evolution of secondary metabolic repertoires and the production of some novel metabolites (Bergeijk et al., 2020). Specialized metabolites were isolated from marine organisms such as arctic *Streptomyces nitrosporeus* (Yang et al., 2013) and desert-dwelling *Streptomyces* sp. (Sayed et al., 2019). In the present study, our aim is to screen and identify actinomycetes with excellently antagonistic *F. oxysporum* TR4 from the primitive ecological environment. We further assessed its efficacy in the management of the pathogen and antifungal mechanisms. Hence, *Streptomyces* have a great potential to become an essential constituent of modern agricultural practice as biofertilizers and biocontrol agents.

MATERIALS AND METHODS

Soil Sampling

The rhizosphere soil of *Machilus pingii* was collected from the primitive ecological nature reserve of 'Yingge' mountain (1109°43′05″E, 19°02′03″N) in Hainan province, China. The subtropical region has a hot climate in summer (23–36°C) and cold in winter (16–24°C) with an average humidity of 60–80% and annual rainfall of 1,500–2,600 mm. The samples were

transported to the laboratory in sterile polythene bags and stored in an insulated container at 4°C.

Isolation of Actinomycetes

Actinomycetes were isolated by a gradient dilution separation method (Sadeghian et al., 2016). The air-dried soil was ground to powder and passed through a 60-mesh sieve. Five grams of soil samples were dissolved in 45 ml of sterile water. After being incubated at 55°C for 20 min in a water bath, the mixture was cultured at 28°C, 180 rpm, for 1 h. The homogenate was diluted with sterile water into 10^{-1}, 10^{-2}, and 10^{-3} using a serial dilution method (Li et al., 2021a). One hundred fifty microliters of each dilution were spread on the four-separation agar media, namely, humic acid–vitamin (HV), glucose–aspartic acid (GA), starch casein agar (SCA), and Gause's No. 1. These media were supplemented with potassium dichromate (50 mg/L) and nystatin (50 mg/L) to inhibit fungal and bacterial contamination. The plates were cultured at 28°C for 5–7 days. The colonies were streaked repeatedly on the ISP2 agar medium for purification until a single colony was obtained. The purified isolates were kept on the Gause's No. 1 agar medium at 4°C and 20% (v/v) of glycerol at −80°C.

Preliminary Screening for Antagonistic Actinomycetes Against *F. oxysporum* TR4

The antagonistic activity of actinomycetes against *F. oxysporum* TR4 was initially assayed using an agar diffusion method (Wei et al., 2020). A 5-mm hyphal disk of *F. oxysporum* TR4 was manufactured using a hole puncher and placed in the middle of a potato dextrose agar (PDA, 200 g/L of potato, 20 g/L of dextrose, and 16 g/L of agar) plate. The selected isolate was inoculated in four symmetrical points of about 2.5-cm distance from the pathogen. The *F. oxysporum* TR4 plate without the inoculation of the isolate was used as a control. All plates were cultured at 28°C for 5–7 days under dark conditions. The inhibition activity was measured until the mycelia of *F. oxysporum* TR4 covered the entire surface of the plate. The inhibition percentage was calculated using the following formula:

$$\text{the inhibitory percentage of growth} = [(\text{C} - -\text{T})/\text{C}] \times 100\%$$

where C and T were growth diameters of tested pathogens in the control and treated plates, respectively.

Secondary Screening of Antagonistic Actinomycetes Against *F. oxysporum* TR4

Selected actinomycetes with antifungal activity in a preliminary screening were subjected to small-scale fermentation. Briefly, the actinomycete was cultured in a broth medium (15 g of corn flour, 3 g of beef extract, 10 g of yeast extract, 10 g of soluble starch, 10 g of glucose, 0.5 g of K_2HPO_4, 0.5 g of NaCl, 2 g of $CaCO_3$, 0.5 g of $MgSO_4$, pH 7.2–7.4) at 28°C, 180 rpm, for 7 days. The fermentation broth was centrifuged at 13,000 rpm, and the supernatant was mixed with an equal volume of ethanol (95%, v/v). The extract was concentrated using a separating funnel and evaporated with a rotary evaporator (EYELA, N-1300, Japan). The dried extract was diluted with ethanol (50%, v/v) to a final concentration of 10 mg/ml. Antifungal activity was determined by the agar diffusion method as mentioned above after the plates were cultured at 28°C for 7 days.

Growth Characteristics of the Selected Actinomycetes

To detect the growth characteristics of actinomycetes, the isolate was first cultured in six standard ISP media (yeast extract–malt agar, ISP2; oatmeal agar, ISP3; inorganic salts–starch agar, ISP4; glycerol–asparagine agar, ISP5; peptone yeast–iron agar, ISP6; tyrosine agar, ISP7), PDA, and Gause's No. 1 (Shirling and Gottlieb, 1968). These plates were incubated at 28°C for 7 days under dark conditions. Colors of substrate and aerial mycelia as well as diffusible pigments were judged by comparing them with the ISCC-NBS color charts (Qi et al., 2019). Some biochemical profiles including nitrate reduction, gelation liquefaction, hydrolysis of cellulose, starch, Tween 20, Tween 40, Tween 80, and urease activities were also measured according to the previous description of Li et al. (2016). IAA production was qualitatively assayed as the development of pink color in the plate. Liquid chrome azurol S (CAS) assay was used to assess siderophore production on ISP2 (Milagres et al., 1999). Chitinase activity was quantitated by measuring the reducing end group of *N*-acetyl glucosamine (Lee et al., 2012). The β-1,3-glucanase activity was measured using laminarin (Sigma, MA, United States) as a substrate (Lee et al., 2012). Resistance evaluation to 20 standard antibiotics was tested by a disk diffusion method (Jing et al., 2020).

Assay of Broad-Spectrum Antifungal Activity of the Selected Actinomycetes

To detect the broad-spectrum antifungal activity of actinomycete, 18 phytopathogenic fungi were selected, namely, *Fusarium graminearum* Schwabe (ATCC MYA-4620), *Botrytis cinerea* (ATCC 11542), *Cryphonectria parasitica* (ATCC 9414), *Colletotrichum acutatum* (ATCC 56815), *Curvularia fallax* (ATCC 34598), *Colletotrichum fragariae* (ATCC 58689), *Colletotrichum gloeosporioides* (ATCC MYA-456), *Colletotrichum gloeosporioides* (Penz) Saec (ATCC 36351), *Curvularia lunata* (ATCC 42011), *Colletotrichum musae* (ATCC 44422), *Fusarium oxysporum* f. sp. *cubense* race 1 (ATCC 31271), *Fusarium oxysporum* f. sp. *cubense* tropical race 4 (ATCC 76255), *Fusarium oxysporum* (Schl.) f. sp. *cucumerinum* (ATCC 204378), *Fusarium oxysporum* f. sp. *lycopersici* (ATCC MYA-1199), *Colletotrichum gloeosporioides* Penz. (ATCC MYA-4130), *Alternaria tenuissima* (ATCC 96828), *Pyricularia oryzae* (ATCC 52083), and *Colletotrichum fructicola* (ATCC 16103). These phytopathogenic fungi were kept in the National Banana Industry Research and Development Center, China Academy of Tropical Agricultural Sciences, Haikou, China. Antifungal activities of the selected actinomycetes were evaluated based on the radial growth inhibition of phytopathogenic fungi *in vitro* (Wei et al., 2020). The control plates were poured with only phytopathogenic fungi. All experiments were performed in triplicate.

Stable Characteristics and Safe Evaluation of the Isolate Extract

The extract stock was diluted to 80 μg/ml using sterile water. Seven temperature gradients, namely, 50, 60, 70, 80, 90, 100, and 121°C, were selected to treat the isolate extract for 1 h. Different pH values were prepared from 3 to 10 at an interval of one unit using 1 mol/L HCl or 1 mol/L NaOH. The extract was irradiated by an ultraviolet lamp with an illumination intensity of 100 μW cm^{-2} for 1, 3, 5, 7, 9, 11, and 13 h. Antifungal activity against *F. oxysporum* TR4 was used to evaluate extract stability after treatment of different physical factors. Hemolytic assay of human red blood cells treated with the extract was carried out to test its safety as in our previous description (Li et al., 2021b).

Genome Sequencing and Molecular Identification of the Selected Actinomycetes

The actinomycete strain with the highest antifungal activity was identified by using a molecular procedure. The isolate was cultured in the ISP2 liquid medium at 28°C for 4 days. Total genomic DNA was extracted using a Rapid Bacterial Genomic DNA Isolation Kit (Biotech Corporation, Beijing, China) according to the standard manufacturer protocol. The complete genome was sequenced using a paired-end sequencing method in the Illumina HiSeq × Ten platform (Illumina, San Diego, CA, United States) by the Shanghai Majorbio Bio-pharm Technology Co., Ltd. A multilocus sequence analysis (MLSA) was performed using 31 housekeeping genes, namely, *dnaG*, *frr*, *infC*, *nusA*, *pgk*, *pyrG*, *rplA*, *rplB*, *rplC*, *rplD*, *rplE*, *rplF*, *rplK*, *rplL*, *rplM*, *rplN*, *rplP*, *rplS*, *rplT*, *rpmA*, *rpoB*, *rpsB*, *rpsC*, *rpsE*, *rpsI*, *rpsJ*, *rpsK*, *rpsM*, *rpsS*, *smpB*, and *tsf*, from the selected actinomycete genome (Brady et al., 2008). The MLSA phylogenetic tree was constructed using the neighbor-joining method in MEGA 7.0 (Kumar et al., 2016). The confidence level was investigated using bootstrap analysis on 1,000 replicates. Average nucleotide identity (ANI) between genomes was calculated using the online OrthoANI (Yoon et al., 2017). The genome sequence of the standard strain (*Streptomyces albospinus* JCM3399) was downloaded from the public genome database of EzBioCloud[1].

Genomic Annotation of the Selected Actinomycetes

Sequencing data of the genome were analyzed on an online platform of Majorbio Cloud[2]. Clean sequences were assembled using SOAPdenovo v2.04. The open reading frames (ORFs) and genome annotation were predicted by the Rapid Annotation using Subsystem Technology (Brettin et al., 2015). These genes were annotated using the Clusters of Orthologous Groups (COGs) and Kyoto Encyclopedia of Genes and Genomes (KEGG) (Ogata et al., 1999; Tatusov et al., 2000). Identification of potential biosynthetic gene clusters (BGCs) was proposed by the bioinformatics tool website antiSMASH v4.0.2 software (Weber et al., 2015)[3]. Gene function analysis was performed through manual BLAST on NCBI[4]. The genome sequence data (accession number: SRR15506182) was deposited in the GenBank database.

Evaluation of Biocontrol and Plant Growth Promotion Under Greenhouse Conditions

The biocontrol and growth-promoting effects of the selected actinomycete were evaluated in greenhouse experiments. The genotype (cv. Brazilian, AAA group) of banana susceptible to *F. oxysporum* TR4 was multiplied by micropropagation. Plantlets with four to five leaves were transferred to soil and grew at 28°C with 70–80% of relative humidity. The selected actinomycete was cultured in a sterilized soybean liquid medium at 180 rpm for 7 days at 28°C. *F. oxysporum* TR4 was inoculated into a PDA broth at 200 rpm for 10 days at 28°C. The conidial suspension was filtered through eight layers of sterile gauze. The spore suspension of *F. oxysporum* TR4 was adjusted to 10^6 CFU ml^{-1} with sterile distilled water. Roots of banana plantlets were wounded with a scalpel and then dipped into 30 ml of fungal inoculum suspension for 30 min. The fermentation broth of the selected actinomycete (10^6 CFU g^{-1} soil) was also added to the roots of each plant. Three experimental groups were set, namely, medium treatment (T1), selected actinomycete + *F. oxysporum* TR4 treatment (T2), and *F. oxysporum* TR4 treatment (T3). The banana plantlets were kept in a greenhouse and maintained at approximately 70% of relative humidity at 28°C. The expression levels of defense genes and antioxidant enzyme activity were determined at 1, 2, 3, 4, 5, and 6 days post inoculation (dpi). Plant growth indicators including chlorophyll content, leaf area, leaf thickness, stem diameter, plant height, dry weight, and fresh weight were also measured at 45 dpi (Wei et al., 2020). The disease index was evaluated according to the description of Jing et al. (2020). Data were acquired from three independent experiments, and 36 plantlets were selected for each experiment. All experiments were carried out in triplicates.

Measurement of Antioxidant Enzyme Activity in Roots of Banana Plantlets

Five grams of frozen root samples were ground in 10 ml of precooled phosphate buffer (50 mM, pH 7.8) containing 2% of polyvinylpyrrolidone. The homogenate was transferred to a 15-ml tube and centrifuged at 15,000 rpm for 15 min at 4°C. The supernatant was used to determine the activity of superoxide dismutase (SOD), catalase (CAT), peroxidase (POD), and polyphenol oxidase (PPO) activities as described by Sun et al. (2013). H_2O_2 levels were measured according to the method of Ferguson et al. (1983). The content of malondialdehyde (MDA) was assayed using the thiobarbituric acid reaction method (Zhang et al., 2009).

Expression Analysis of Defense Genes

Total RNA of banana roots was extracted by the routine TRIzol method. The quality and quantity of RNA were measured by NanoDrop (Thermo Scientific, United States). cDNA was synthesized using the M-MLV reverse transcriptase (Takara,

[1]https://www.ezbiocloud.net/search?tn=Nocardioides

[2]www.majorbio.com

[3]http://antismash.secondarymetabolites.org/#!/start

[4]https://www.ncbi.nlm.nih.gov/

Kyoto, Japan) after treatment with the RNase-free DNase (Takara, Kyoto, Japan). Quantitative real-time polymerase chain reaction (qRT-PCR) was performed in a LightCycler® 480 System (Roche Diagnostics, Mannheim, Germany). A 10-μl reaction system contained 50 ng of first-strand cDNA, 10 μM of forward and reverse primers, and 5 μl of TB Green Advantage qPCR Premix (2×) (Takara, Kyoto, Japan). The reaction program was set as follows: 95°C for 1 min, followed by 40 cycles of denaturation at 92°C for 5 s, annealing at 60°C for 30 s, and extension at 72°C for 30 s. The representative defense marker genes such as *Maβ-1,3-Glu* (accession number: AF001523) and mitogen-activated protein kinase 1 (*MaMAPK1*, accession number: XM018826311) were selected. Results were normalized using the expression levels of 18S *rRNA* gene (accession number: U42083). The prime sequences were shown in our previous study (Zhang et al., 2019). The data obtained from different PCR runs were analyzed using the mean of CT values from three biological replicates. The expression ratios were calculated using the $2^{-\Delta\Delta Ct}$ method (Zhang et al., 2019).

Component Identification of Actinomycete Extract by Gas Chromatography–Mass Spectrometry

The chemical compounds in the extract were identified using gas chromatography–mass spectrometry (GC-MS) as in our previous description (Li et al., 2021b). The strain extract was first dissolved in the chromatographic-grade methanol and filtered through a 0.2-μm filter. The solution was injected into a gas capillary column (DB-FFAP, 30 m × 0.25 mm × 0.25 μm) of a gas chromatography (5973 Inert XL MSD, Agilent, United States). Helium was used as a carrier gas with a flow rate of 1 ml min^{-1}. The mass spectrometer (EI with replaceable horn) was operated in the electron ionization (EI) mode at 70 eV with a continuous scan from 50 to 800 *m*/*z*. The peaks were identified by matching the mass spectra with the National Institute of Standards and Technology (NIST, United States) library.

Statistical Analysis

All experiments were performed in three biological triplicates. Data were expressed as the mean ± standard deviation. The greenhouse experiments were carried out in a randomized design. All data were analyzed using analysis of variance (ANOVA) by the SPSS statistical package (version 22, SPSS Inc., Chicago, IL, United States). The *t*-test compared the mean of an outcome variable for different subjects. The LSD's multiple range test was applied to determine the significant difference at the level of $p < 0.05$.

RESULTS

Actinomycete Isolation

The primitive nature reserve of 'Yingge' mountain possessing great biodiversity was selected for the isolation of antifungal actinomycetes. A total of 60 actinomycetes were isolated from the rhizosphere soil of *M. pingii* using four culture media of HV (18), GA (12), SCA (10), and Gause's No. 1 (20). Isolated actinomycetes showed well-developed aerial and substrate mycelia in **Figure 1**. Most aerial mycelia appeared hairy, granular, or powdery. Some isolates produced colored pigments in the substrate and were hard to pick from the media. It was a representative trait of the genus *Streptomyces*. All the isolates were deposited at the National Banana Industry Research and Development Center, the Institute of Tropical Bioscience and Biotechnology, China Academy of Tropical Agricultural Sciences, Haikou, China.

Antifungal Activity Assay of the Isolated Actinomycetes

Initially, all the isolates were subjected to a primary screening test against *F. oxysporum* TR4. We assessed the inhibition ability of the mycelial growth of *F. oxysporum* TR4. By antagonistic experiments in plates, 17 out of 60 isolates showed significant antifungal activities (**Supplementary Figure 1**), accounting for 28.3% of the total actinomycetes screened. The inhibitory activity of each isolate was further determined. Eleven actinomycetes owned more than 60% of antifungal activity against *F. oxysporum* TR4. Particularly, the strain numbered BITDG-11 had the best antifungal activity. The inhibition rate reached 80.48 ± 1.49%.

A small-scale fermentation of the 17 isolates with prominent zones of inhibition from the primary screening was carried out. The antagonistic ability of their extracts was further investigated. The results demonstrated that extracts of all the selected isolates showed antifungal activity against *F. oxysporum* TR4, ranging from 27 to 60% (**Supplementary Figure 1**). The strong inhibition zone sizes were observed in extracts of four isolates (BITDG-11, BITDH-4, BITDG-7, BITDG-19, and BITDA-7). The inhibition rates were 58.44, 45.10, 43.92, 42.89, and 42.62%, respectively. Combined with primary and rescreening results, strain BITDG-11 was selected as an excellent isolate for the subsequent study.

Growth Characteristics of Strain BITDG-11

The cultural traits of strain BITDG-11 were recorded on eight media selected (**Table 1**). It had a good growth on ISP2 and a moderate growth on the rest of the media except for ISP4. The color of aerial mycelia varied from white to dark gray. Aerial hypha exhibited dark gray on ISP3, pale yellow on ISP5, and white on ISP2, ISP6, ISP7, PDA, and Gause's No. 1 media. Light yellow colors of the hyphal substrate were observed on all the media except for light gray on ISP5. Soluble pigment was produced on ISP5, ISP7, and Gause's No. 1. Production of melanin pigment on ISP7 could be taken as an identification criterion for the genus *Streptomyces* (Atta et al., 2011). Therefore, strain BITDG-11 exhibited typical morphological characteristics of *Streptomyces*.

The analysis of physiological and biochemical characteristics showed that strain BITDG-11 had the ability to hydrolyze starch and produce IAA. A positive response was observed to gelatin liquefaction and nitrate reduction. Enzyme activities of lipase and urease were also detected (**Figure 2A**). The level of chitinase was sharply increased during the exponential phase and reached the peak (3.50 U/mg protein) at 72 h (**Figure 2B**). The highest level of β-1,3-glucanase (0.49 U/mg protein) was found at 72 h

FIGURE 1 | Growth characteristics of 60 actinomycetes isolated from the rhizosphere soil of *Machilus pingii* in the primitive ecological natural reserve.

TABLE 1 | Growth characteristics of *Streptomyces* BITDG-11 on different media.

Medium	Growth	Aerial mycelium	Substrate mycelium	Soluble pigment	Colony characteristics
Yeast extract malt extract dextrose agar (ISP2)	Good	White	Lemon yellow	No	Hard and wrinkle
Oatmeal agar (ISP3)	Moderate	Dark gray	Rice yellow	No	Powder and dry
Inorganic salts starch agar (ISP4)	Normal	Creamy white	Light yellow	No	Powder and dry
Glycerol asparagine agar (ISP5)	Moderate	Pale yellow	Light gray	Light yellow	Compact and hard
Peptone yeast extract iron agar (ISP6)	Moderate	White	Pale yellow	No	Compact and wrinkle
Tyrosine agar (ISP7)	Moderate	White	Light yellow	Light purple	Powder and loose
Potato dextrose agar (PDA)	Moderate	White	Light yellow	No	Powder and dry
Gause's No. 1	Moderate	White	Light yellow	Light yellow	Powder and dry

of the incubation period (**Figure 2C**). Antibiotic susceptibility testing revealed that strain BITDG-11 manifested tolerance to 15 out of 22 kinds of antibiotics and sensitivity to erythromycin, kanamycin, gentamicin, amikacin, neomycin, midenomycin, and ofloxacin (**Supplementary Table S1**).

Identification of Strain BITDG-11

Based on the alignment of 16S *rRNA* sequence (1,523 bp, accession number: MW110901), the sequence shared 98.80% of similarity with that of *S. albospinus* NBRC 13846. It confirmed that the strain belonged to a member of the genus *Streptomyces*. However, 58% of the bootstrap value in the neighbor-joining tree indicated that strain BITDG-11 was not distinguished from closely related species using 16S *rRNA* genes.

In order to further identify the species of strain BITDG-11, its whole genome was sequenced. Sequences of 31 housekeeping genes were selected to perform the MLSA. The method was considered as an alternative strategy for defining the *Streptomyces* systematics due to the high efficiency of species resolution and reproducibility (Rong and Huang, 2010). The neighbor-joining tree based on MLSA showed that strain BITDG-11

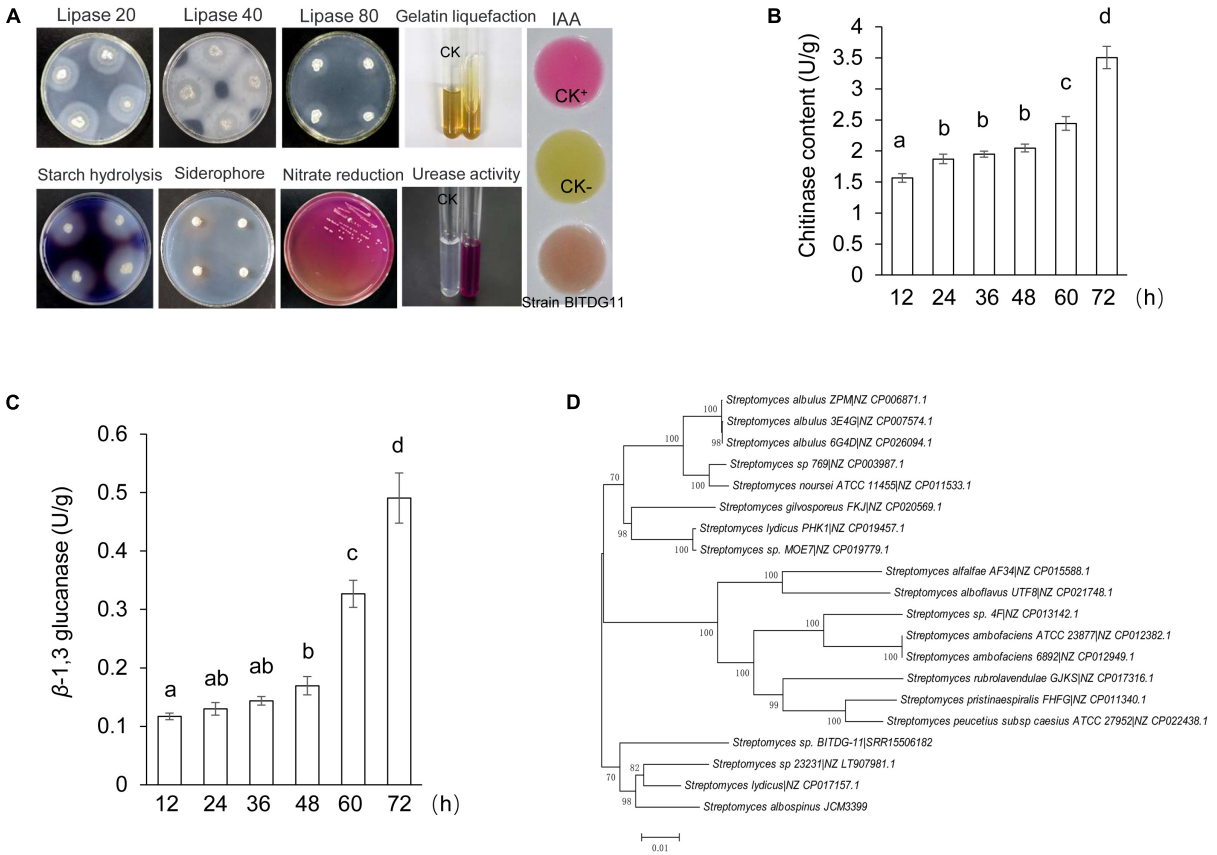

FIGURE 2 | Physicochemical property and identification of *Streptomyces* BITDG-11. **(A)** Physicochemical properties of *Streptomyces* BITDG-11. **(B)** Measurement of chitinase production during the culture process of *Streptomyces* BITDG-11. **(C)** Measurement of β-1,3-glucanase production. Data are the mean values from three biological repeats. Different lowercase letters indicate a significant difference in comparison with the initial time point of the strain growth (LSD's multiple range test, $p < 0.05$). **(D)** Construction of phylogenetic tree based on MLSA using the neighbor-joining method. The confidence level at all nodes was investigated using bootstrap analysis on 1,000 replicates.

formed a distinct clade with *S. albospinus* JCM3399 with 70% of bootstrap value (**Figure 2D**). We further compared the strain BITDG-11 genome (accession number: SRR15506182) with the standard strain genome (*S. albospinus* JCM3399) (**Supplementary Table S2**). The ANI of 86.55% was below the threshold value of 95–96% for distinguishing a novel species (Richter and Rosselló-Móra, 2009). Thus, strain BITDG-11 might be a novel species of the genus *Streptomyces* and named after *Streptomyces* sp. BITDG-11.

Assay of a Broad-Spectrum Antifungal Activity

To assess whether *Streptomyces* BITDG-11 had a broad-spectrum antifungal activity, 18 fungal pathogens were selected in our study. Compared with the growth diameters of different phytopathogenic fungi in the control plate, the strain had strong antifungal activities against all pathogens selected (**Figure 3**). The inhibition rates ranged from 65 to 90%. The maximal and minimal inhibition rates were observed against *C. parasitica* (96.78% ± 1.83) and *C. musae* (65.01% ± 1.87), respectively.

Stability Evaluation of *Streptomyces* BITDG-11 Extract

To explore and apply *Streptomyces* BITDG-11 as biopesticides in the future, the stability of the extract expressed as antifungal activity was evaluated after treatment in different temperatures, pH values, and UV doses, respectively. The results showed that different temperatures reduced antifungal activity of the extract against *F. oxysporum* TR4, but 57.05% was kept after treatments at 121°C for 1 h (**Figure 4A**). For different pH treatments, the strongest antifungal activity was detected at pH 7.0–8.0 and decreased to 52% at pH 3.0 (**Figure 4B**). Additionally, the extract stability was negatively correlated with the increase of UV dose. A slight decrease was observed in the activity change of the extract treated with UV radiation after 7 h (**Figure 4C**). Although an obvious decrease (LSD's multiple range test, $p < 0.05$) of antifungal activity was detected in *Streptomyces* BITDG-11 extract after treatment with different physical factors, more than 50% of residual antifungal activity was retained in all the groups. It suggested that the *Streptomyces* BITDG-11 extract was relatively stable to some extent. To investigate the extract toxicity on eukaryotic cells, hemolytic activity was

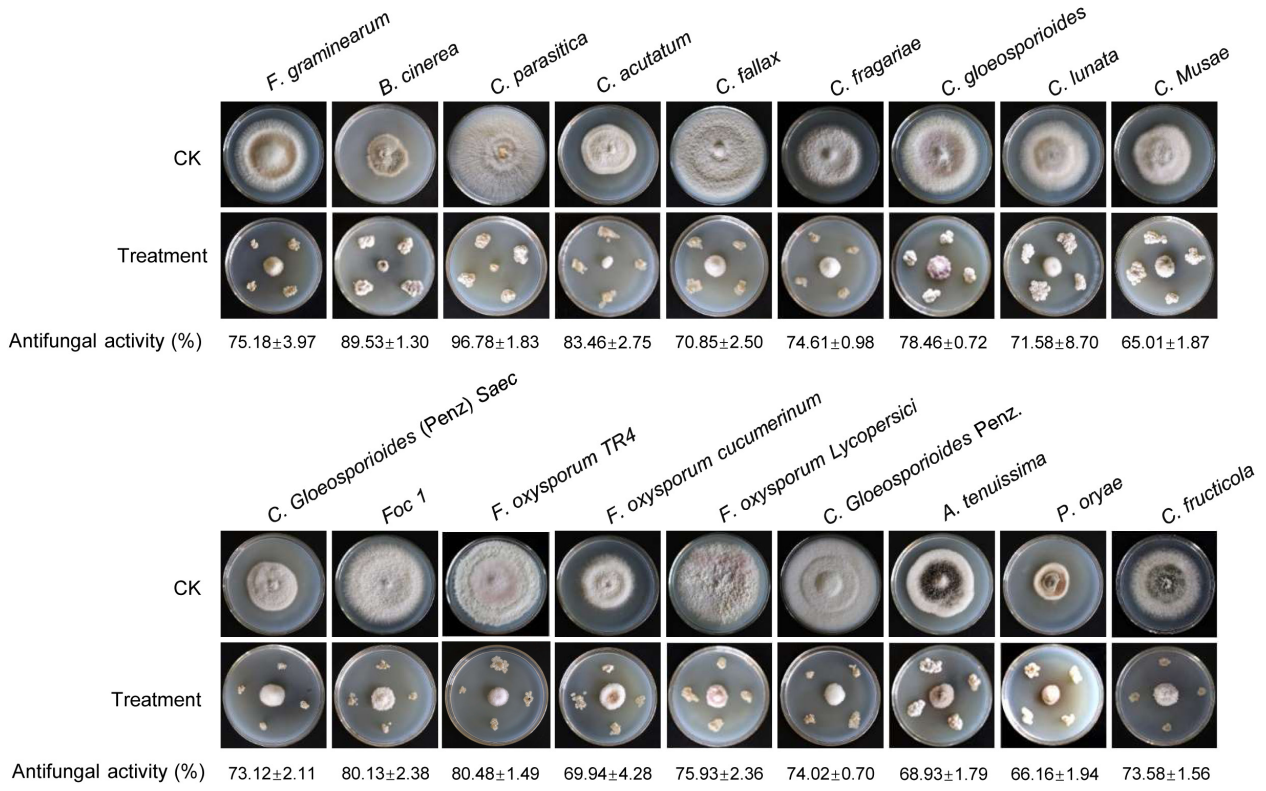

FIGURE 3 | Determination of a broad-spectrum antifungal activity of *Streptomyces* BITDG-11 against the 18 selected phytopathogenic fungi. Different data below the picture indicate antifungal activity of *Streptomyces* BITDG-11 against different phytopathogenic fungi.

analyzed. Human red blood cells were measured as the release of hemoglobin after treatment at 37°C for 1 h. Compared with the 100% hemolytic activity of Triton X-100 (0.1%, v/v), no obvious hemolytic activity was observed in the extract treatment group (**Supplementary Figure 2**).

Streptomyces BITDG-11 Improving Resistance to *F. oxysporum* TR4 and Promoting Growth of Banana Plantlets

Streptomyces BITDG-11 perfectly inhibited the growth of different phytopathogenic fungi *in vitro*, indicating that it was a promising biocontrol agent. With an objective to evaluate *in vivo* biocontrol efficiency, we analyzed the effects of *Streptomyces* BITDG-11 fermentation broth on the infection inhibition of *F. oxysporum* TR4. By contrast, the bottom leaves of banana plantlets exhibited a significant chlorotic symptom at 45 dpi in the T3 group (**Figure 5A**). No obvious disease symptom was detected in the group of *Streptomyces* BITDG-11 + *F. oxysporum* TR4. Therefore, the protective treatment with *Streptomyces* BITDG-11 effectively prevented the infection of *F. oxysporum* TR4 and reduced disease index of plants (**Figure 5B**). We also evaluated actinomycetes and fungal numbers in the rhizosphere of banana seedlings (**Supplementary Figure 3**). The colony-forming units of *F. oxysporum* TR4 were very low when compared to other treated soils. The results showed that *Streptomyces* BITDG-11 significantly increased competing bacterial and fungal counts along with the pathogen in the soil.

Moreover, various agronomic traits of plant health and condition were measured in **Figures 5C–H**. *Streptomyces* BITDG-11 significantly (LSD's multiple range test, $p < 0.05$) increased the fresh and dry weight of banana plantlets at 45 dpi (**Figure 5C**). Compared to those of control (T1, 45.5 ± 2.2 cm) or *F. oxysporum* TR4 treatment (T3, 34.0 ± 1.8 cm), the height of banana plantlets treated with *Streptomyces* BITDG-11 + *F. oxysporum* TR4 reached 50.9 ± 2.0 cm (**Figure 5D**). *F. oxysporum* TR4 significantly inhibited the increase of plant agronomic indicators (**Figures 5E–H**). Similar plant-growth-promoting effects were observed in stem diameters. Although no obvious difference of leaf thickness was detected between dual disposal and controls, a significant increase was found in leaf area and chlorophyll content of plants treated with *Streptomyces* BITDG-11.

Streptomyces BITDG-11 Enhancing the Antioxidant Abilities of Banana Plantlets

As is well-known, the stress condition could induce the production of reactive oxygen species, thereby resulting in oxidative damage of plant cells. This effect can be assayed by quantifying H_2O_2 content and CAT activity. In our study, H_2O_2 content in banana roots was increased after *F. oxysporum* TR4

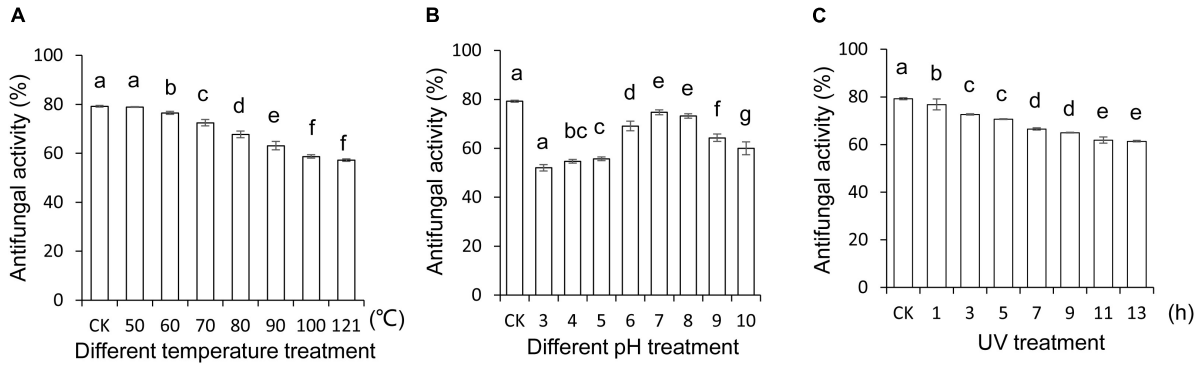

FIGURE 4 | Stability evaluation of the *Streptomyces* BITDG-11 extract after treatment at different temperatures **(A)**, pH values **(B)**, and UV doses **(C)**. Data are the mean values from three biological repeats. Different lowercase letters indicated a significant difference of antifungal activity in comparison with the control (LSD's multiple range test, $p < 0.05$).

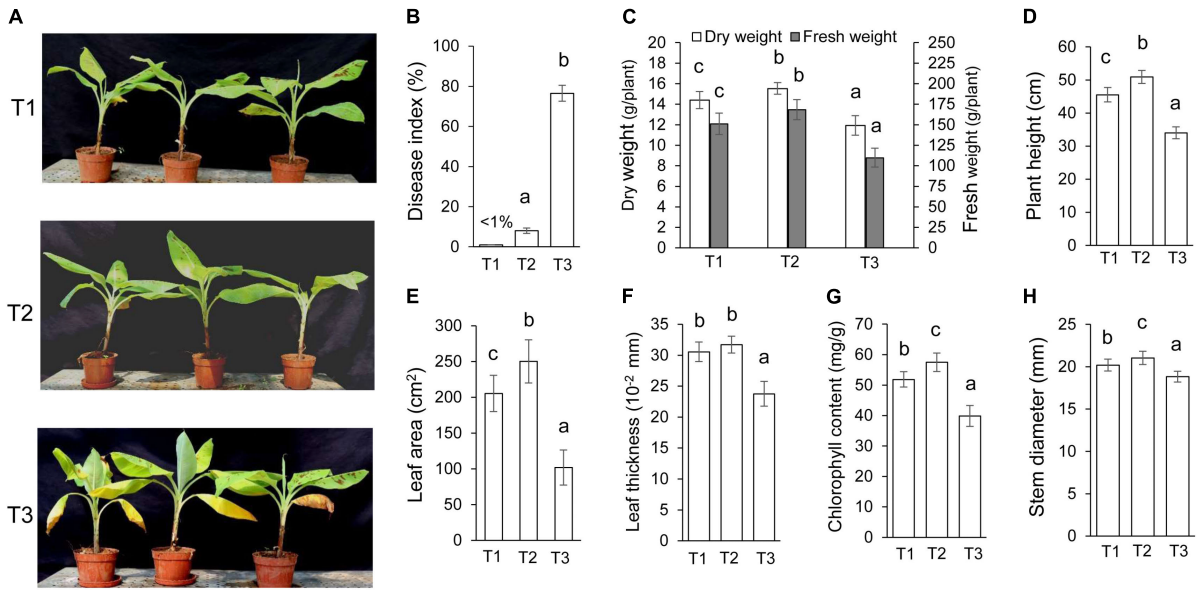

FIGURE 5 | Assay of chlorotic symptoms and plant growth promotion after treatment with *Streptomyces* BITDG-11 at 45 dpi. T1: medium treatment, T2: *Streptomyces* BITDG-11 + *F. oxysporum* TR4 treatment; T3: *F. oxysporum* TR4 treatment. **(A)** Chlorotic symptoms of banana plantlets in different treatment groups. **(B)** Quantitative analysis of disease indexes in different treatment groups. Measurement of physiological indicators including plant dry and fresh weight **(C)**, plant height **(D)**, leaf area **(E)**, leaf thickness **(F)**, chlorophyll content **(G)**, and stem diameter **(H)** in different treatment groups. Error bars indicated standard errors of the means of three repeated experiments. Different letters indicated a significant difference in comparison with the treatment group of *F. oxysporum* TR4 (LSD's multiple range test, $p < 0.05$).

treatment (**Figure 6A**). Although a similar increase was detected in banana roots treated with *F. oxysporum* TR4 + *Streptomyces* BITDG-11, H_2O_2 content was reduced significantly (LSD's multiple range test, $p < 0.05$) by inducing high CAT activity (**Figure 6B**). Hence, *Streptomyces* BITDG-11 effectively alleviated the cell membrane damage. It was supported by the fact that MDA content was lower in roots treated with *Streptomyces* BITDG-11 (**Figure 6C**). Moreover, the strain also increased the higher activities of defense-related enzymes (PPO, POD, and SOD) in comparison with *F. oxysporum* TR4 or control treatment alone (**Figures 6D–F**). The maximal values of POD, PPO, and SOD were 83.20, 70.67, and 351.31 U/g in the banana roots after inoculation with *Streptomyces* BITDG-11 combined with the challenge with *F. oxysporum* TR4 at 3, 6, and 2 dpi, respectively.

Streptomyces BITDG-11 Increasing the Expression of Defense Genes

To further determine the defense mechanism of *Streptomyces* BITDG-11-induced resistance to *Fusarium* wilt of banana, the transcription levels of *MaMAPK1* (early defense response marker gene) and *Maβ-1,3-Glu* (downstream defense marker gene) were analyzed by qRT-PCR (**Figure 7**). In comparison with control and *F. oxysporum* TR4-only treatment, the transcripts

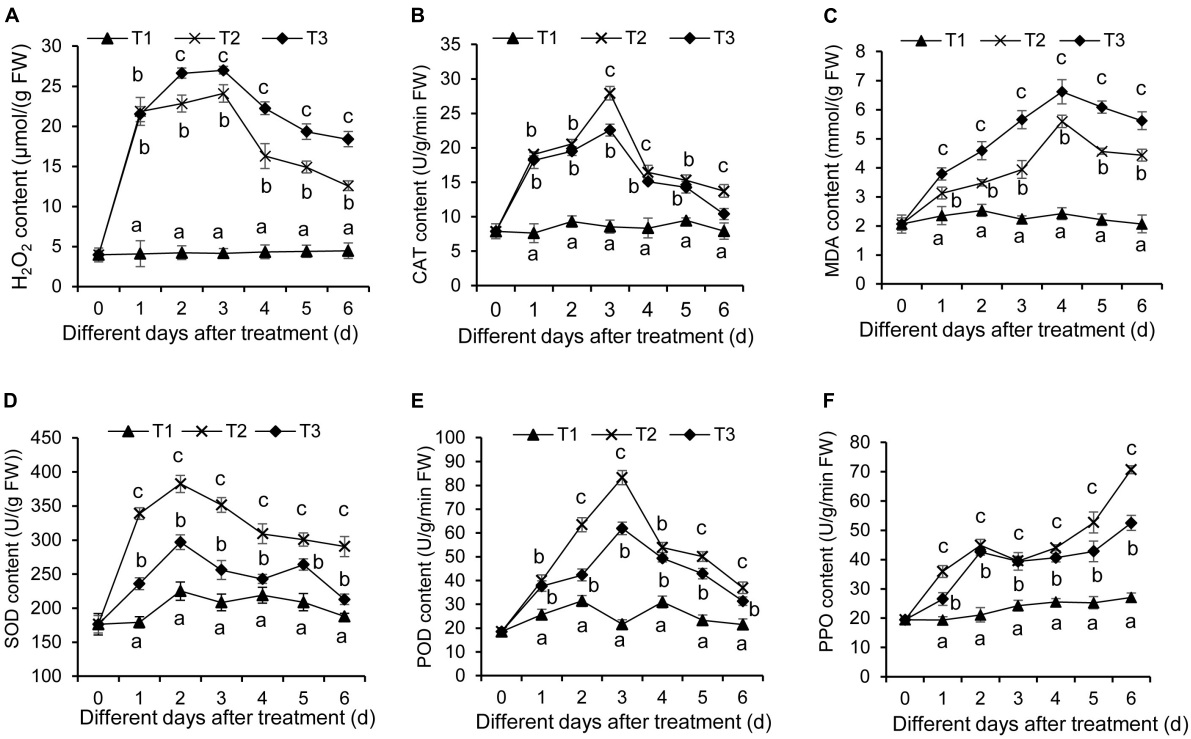

FIGURE 6 | Determination of hydrogen peroxide **(A)**, CAT **(B)**, MDA **(C)**, SOD **(D)**, POD **(E)**, and PPO **(F)** in banana roots after treatment with *Streptomyces* BITDG-11 at different time points. T1–T3 represent different treatment groups as in the description in **Figure 5**. Error bars indicate standard errors of the means of three repeated experiments. Different letters indicate a significant difference in comparison with the medium treatment group at the same time points (LSD's multiple range test, $p < 0.05$).

of two tested genes were much stronger in the banana roots treated with *Streptomyces* BITDG-11 + *F. oxysporum* TR4 and reached their maximum values at 4 and 3 dpi, respectively. In addition, high transcription levels of defense genes were kept by *Streptomyces* BITDG-11 treatment until 6 dpi. These results indicated that *Streptomyces* BITDG-11 could prime the banana plants to enhance resistance to *F. oxysporum* TR4 by simultaneously activating the *MAPK*-mediated signaling pathway of defense response.

Bioinformatics Analysis of the Genome

The *Streptomyces* BITDG-11 genome was sequenced and contained 10,590,458 bp. The genome with 71.78% of GC content included seven *rRNA* genes, 78 *tRNA* genes, and 10,366 coding sequences (CDSs) (**Figure 8A**). By annotation, 68.45, 28.51, and 57.77% of CDSs were assigned to COG, KEGG, and GO, respectively. For 7,096 genes in COG, the top five categories contained transcription (749), amino acid transport and metabolism (502), energy production and conversion (398), and carbohydrate transport and metabolism (393). Notably, 2,402 of COG genes were clustered into an unknown function category (**Figure 8B**). The GO annotation showed that these genes were classified mainly into the biological process (2063), cellular component (2113), and molecular function (5023) (**Supplementary Figure 4**). Interestingly, 78% of genes participated in the regulation of metabolism in KEGG (**Supplementary Figure 5**). By analysis of the antiSMASH software, 43 BGCs related to biosynthesis of the secondary metabolites were found in genome sequences of *Streptomyces* BITDG-11 (**Supplementary Table S3**). BGCs included one terpene-type I PKS-nucleoside-NRPS, one type III PKS, one thiopeptide-transatpks-type I PKS-NRPS, five terpene, three NRPS, four type I PKS, one type II PKS, one type I PKS-NRPS, one NRPS-lantipeptide, one lantipeptide-terpene, two lantipeptide, three bacteriocin, one ectoine, two butyrolactone, one terpene-NRPS, one type II PKS-oligosaccharide-type I PKS, one transatpks-NRPS, two siderophore, one indole, etc. Genome analysis further revealed that seven BGCs showed more than 70% of similarity with toyocamycin (100%), naringenin (100%), lantipeptide B (100%), ectoine (100%), mannopeptimycin (81%), desferrioxamine (80%), and rimocidin (72%) (**Figure 8C**).

Identification of the Chemical Composition of the *Streptomyces* BITDG-11 Extract

Gas chromatography–mass spectrometry was performed to identify the chemical composition in the *Streptomyces* BITDG-11 extract. In a comparison of their mass spectra with the NIST library, 15 compounds were identified based on their retention time and molecular weight (**Table 2**). The peak area represented the proportion of the given

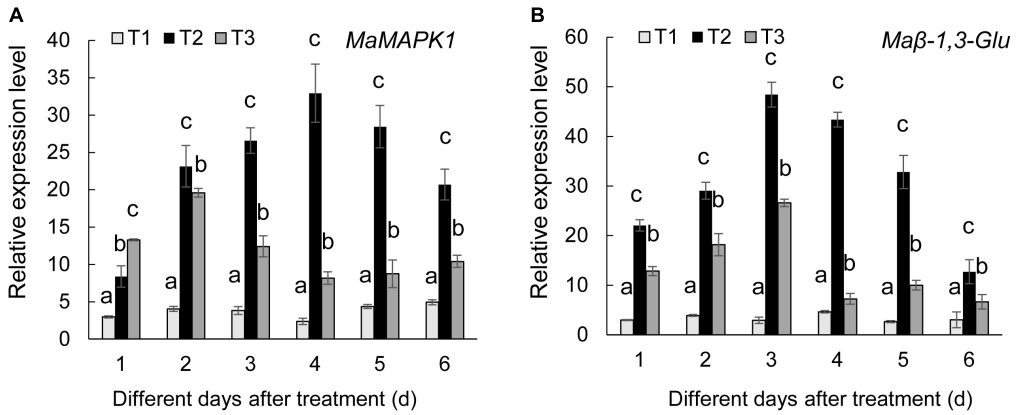

FIGURE 7 | Expression levels of the selected *MaMAPK1* **(A)** and *Maβ-1,3-Glu* **(B)** in banana roots after treatment with *Streptomyces* BITDG-11 at different time points. T1–T3 represent different treatment groups as in the description in **Figure 5**. Error bars indicate standard errors of the means of three repeated experiments. Different letters indicate significant differences in comparison with the medium treatment group at the same time points (LSD's multiple range test, $p < 0.05$).

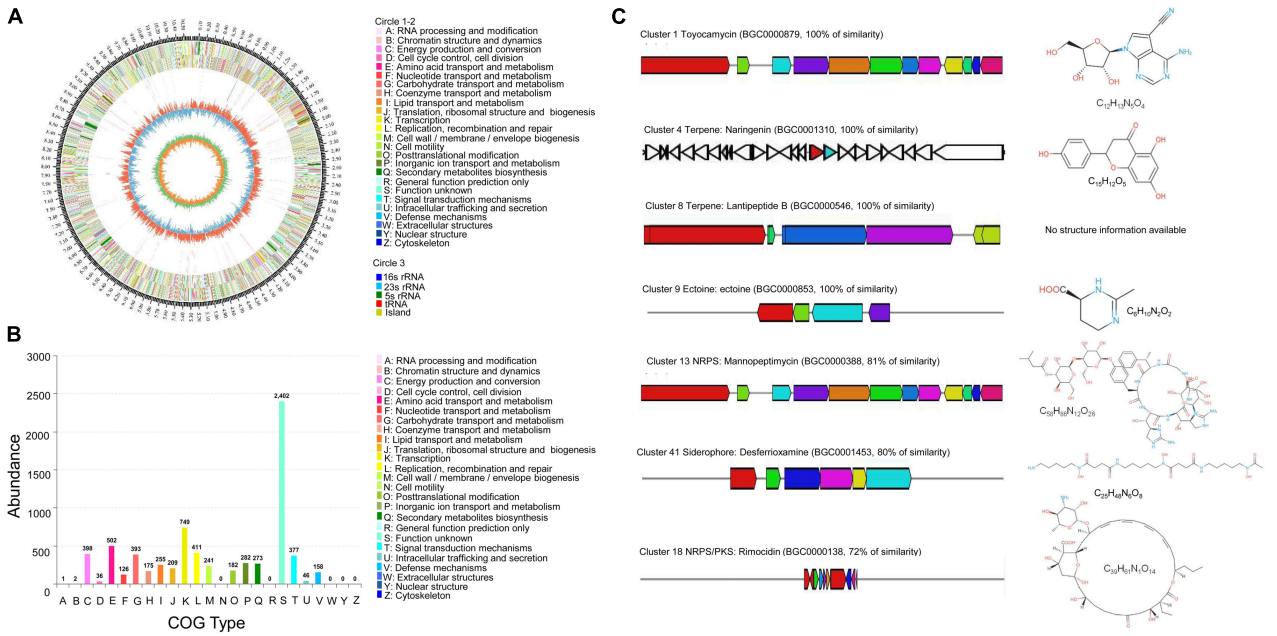

FIGURE 8 | Genome information and function annotation of *Streptomyces* BITDG-11. **(A)** Circular map of *Streptomyces* BITDG-11 genome. From outside to center, ring 1 is the mark of genome size. Rings 2 and 3 represent CDS on the forward/reverse strand. Different colors indicate the functional category of different COGs of CDS. Ring 4 is tRNA and rRNA. Ring 5 shows the G + C content. The outward red part indicates that the GC content of this region is higher than the average GC content of the whole genome. The inward blue part indicates that the GC content of this region is lower than the average GC content of the whole genome, followed by a G + C skew in ring 6. **(B)** COG annotation of *Streptomyces* BITDG-11 genome. **(C)** Biosynthesis gene clusters demonstrating more than 70% similarity with the known sequences.

compound in the total extract. According to the available library data, chemical compounds were identified as tetradecanoic acid, tricosene, *cis*-1-chloro-9-octadecene, pentadecanoic acid, *n*-hexadecanoic acid, linoleic acid ethyl ester, dibutyl phthalate, 1,2-bis(*p*-(trans-styryl)phenyl)-*cis*-ethylene, 3,3′-dihydroxy-4,4′-dinitrohexafluorobiphenyl, 1,2-bis(*p*-(*cis*-styryl)phenyl)-*trans*-ethylene, 4′-(3-(6-methyl-3-pyridyl)-1-(*p*-tolyl)-2-pyrazolin-5-yl)acetanilide, colchiceinamide, 3,3′-dihydroxy-4,4′-dinitrohexafluorobiphenyl, 2-imidazoline, 3,5-di(4-chlorophenyl)-1-(4-fluorophenyl), naphtho[2,3-c]furan-1(3H)-one, 4-(3,4-dimethoxyphenyl)-3a,4,9,9a-tetrahydro-6,7-dimethoxy, and bis(2-ethylhexyl) phthalate.

DISCUSSION

Fusarium wilt of banana is globally one of the most destructive soil-borne fungal diseases. Fungicides cause serious problems for

TABLE 2 | Identification of chemical composition of the *Streptomyces* BITDG-11 extract by GC-MS.

Compounds name	Retention time (min)	Peak area (Ab*s)	Baseline height (Ab)	Absolute height (Ab)	Peak width 50% (min)	Molecular weight (amu)
Tetradecanoic acid	31.323	4,364,641	287,197	437,164	0.369	228.209
Tricosene	33.202	1,720,859	386,105	770,438	0.168	322.36
cis-1-Chloro-9-octadecene	33.521	10,411,455	1,506,075	1,927,431	0.235	286.243
Pentadecanoic acid	33.622	12,986,919	1,792,774	2,386,203	0.411	242.225
n-Hexadecanoic acid	35.434	54,441,054	8,332,937	9,724,659	0.512	256.24
Linoleic acid ethyl ester	35.97	4,713,086	1,093,523	2,704,558	0.193	308.272
Dibutyl phthalate	37.9	176,228,995	28,511,169	29,838,598	0.277	278.152
1,2-Bis(*p*-(*trans*-styryl)phenyl)-*cis*-ethylene	40.836	556,397	218,880	1,503,957	0.218	384.188
3,3′-Dihydroxy-4,4′-dinitrohexafluorobiphenyl	42.237	242,647	76,237	1,438,498	0.117	383.982
1,2-Bis(*p*-(*cis*-styryl)phenyl)-*trans*-ethylene	42.824	549,444	96,391	1,506,214	0.193	384.188
4′-(3-(6-Methyl-3-pyridyl)-1-(*p*-tolyl)-2-pyrazolin-5-yl) acetanilide	43.067	1,251,949	273,496	1,728,673	0.168	384.195
Colchiceinamide	43.914	365,851	103,654	1,704,206	0.092	384.169
3,3′-Dihydroxy-4,4′-dinitrohexafluorobiphenyl	44.292	47,927	27,767	1,674,508	0.101	383.982
Naphtho[2,3-c]furan-1(3*H*)-one, 4-(3,4-dimethoxyphenyl)-3a,4,9,9a-tetrahydro-6,7-dimethoxy	47.119	1,012,098	226,056	1,885,888	0.151	384.157

**represents the multiplication sign.*

human health and environment pollution (Bubici et al., 2019). Biological control is considered as an alternative and sustainable strategy. In recent decades, the potential of plant-growth-promoting *Streptomyces* has been revealed for inhibiting pathogen infection and improving crop yield (Dias et al., 2017; Vurukonda et al., 2018). Although several antagonistic *Streptomyces* were investigated as biological control agents (Vurukonda et al., 2018; Jing et al., 2020; Wei et al., 2020; Li et al., 2021a), field application was limited due to the unstable and deficient antimicrobial activity. Therefore, screening highly efficient and broad-spectrum antagonistic *Streptomyces* is still the key for development of biocontrol agents. In the present study, 17 out of 60 actinomycetes obtained from the rhizosphere soil of *M. pingii* had antifungal activity against *F. oxysporum* TR4. Particularly, *Streptomyces* BITDG-11 showed the strongest growth inhibition for *F. oxysporum* TR4 and broad-spectrum antifungal activities against the 18 selected phytopathogenic fungi. In greenhouse experiments, the application of *Streptomyces* BITDG-11 could significantly alleviate the development of leaf chlorotic symptom and decrease the disease incidence of *F. oxysporum* TR4. Similar antagonistic effects of *Streptomyces* were found in controlling other phytopathogenic diseases (Chen et al., 2019; Xu et al., 2019; Sharma and Manhas, 2020; Zhang K. et al., 2020).

The antifungal mechanism of *Streptomyces* BITDG-11 might be related with its ability to produce hydrolytic enzymes including β-1,3-glucanase and chitinase (**Figures 2B,C**). These enzymes lead to the destruction of the fungal cell wall and leakage of cell contents, inhibiting the growth of phytopathogenic fungi (Hong et al., 2017). Similar reports showed that *Streptomyces cavourensis* SY224 prevented the infection of *Colletotrichum gloeosporioides* by producing hydrolytic enzymes (Lee et al., 2012). Antifungal activity of *Trichoderma harzianum* QTYC77 against *F. oxysporum* f. sp. *cucumerinum* was related to the secretion of chitinase and β-1,3-glucanase (Zhang S. et al., 2020). The cell-free culture filtrate of *Streptomyces violaceusniger* MTCC 3959 exhibited a broad range of antifungal activity against both white rot and brown rot fungi through the production of chitinase and β-1,3-glucanase (Nagpure et al., 2014). Heterologous expression of chitinase from *T. harzianum* increased inhibition activity of *B. cinerea* (Deng et al., 2019). Mycotoxin production enhanced the fungal infection on plants by repressing chitinase gene expression of the biocontrol agent *Trichoderma atroviride* (Lutz et al., 2004). Indeed, *Streptomyces* BITDG-11 had the potential to degrade starch and cellulose on plate experiments. It was supported by the identification of glucanase and amylase genes in the genome of *Streptomyces* BITDG-11. Together, these findings indicated that the hydrolytic enzymes of *Streptomyces* may be linked to their antagonistic activity against phytopathogenic fungi.

Apart from the generated hydrolytic enzymes, *Streptomyces* species were prolific producers of bioactive metabolites (van der Heul et al., 2018; Bergeijk et al., 2020). Several commercial biofungicides were developed such as rhizovit, mycostop, thatch control, and Actinovate® from different *Streptomyces* species (Sharma and Manhas, 2020). Therefore, the antifungal activity of the *Streptomyces* BITDG-11 extract was evaluated against *F. oxysporum* TR4 in the present study. The results showed that the methanol extract could effectively inhibit the mycelial growth of *F. oxysporum* TR4. Although different physical factors were selected to treat the *Streptomyces* BITDG-11 extract, more than 50% of antifungal activity was retained in all the treatment groups, suggesting that the steadily secondary metabolites with antifungal efficiency were produced in the culture filtrate. Similarly, various metabolites were identified from *Streptomyces* as biocontrol agents, and none of them had any negative effect on plants (van der Heul et al., 2018; Olanrewaju and Babalola, 2019; Bergeijk et al., 2020). It was supported by our results that no hemolytic activity was detected in human red cells treated with the *Streptomyces* BITDG-11 extract (**Supplementary Figure 2**), suggesting that the extract had non-specific cell lytic activity and toxicity to eukaryotic

cells. Furthermore, 15 bioactive secondary metabolites were further identified from the *Streptomyces* BITDG-11 extract by GC-MS. Among these compounds, alkanoic acids including tetradecanoic acid, pentadecanoic acid, and linoleic acid were a main type of antifungal production. The previous study reported that tetradecanoic acid had the potential for controlling *Culex quinquefasciatus* and *Aedes aegypti* mosquitoes (Sivakumar et al., 2011). Its isomers can be successfully applied to agriculture and pharmacy industries due to their excellent anti-elastase, anti-urease, and antioxidant activities (Sokmen et al., 2014). The addition of exogenous pentadecanoic acid promoted lipopeptide production and enhanced the antifungal activities of *Bacillus amyloliquefaciens* (Ding et al., 2019). Linoleic acid ethyl ester was critical for fungal response to salicylic acid, mycelial growth, and virulence (Zhang et al., 2017). Particularly, dibutyl phthalate was the major compound with the highest peak number and area in the *Streptomyces* BITDG-11 extract. The compounds produced by *Streptomyces* strain KX852460 had a high antifungal activity against *Rhizoctonia solani* (Ahsan et al., 2017). Other antibacterial and antifungal agents including 9-octadecene, colchiceinamide, and bis-(2-ethylhexyl) phthalate were also detected in microbial culture by the high-performance liquid chromatographic method (Hughes and Davis, 1981; Al-Bari et al., 2005; Thekkangil and Suchithra, 2019). A 9-octadecene compound identified from *Streptomyces albidoflavus* STV1572a contributed to the infection inhibition of *Trichophyton mentagrophytes* (Thekkangil and Suchithra, 2019).

In greenhouse experiments, *Streptomyces* BITDG-11 inhibited the infection of *F. oxysporum* TR4 and promoted the growth of banana seedlings. The possible mechanism might be related to the ability of *Streptomyces* BITDG-11 to produce IAA, siderophore, and antifungal compounds. Siderophore- and IAA-producing actinomycetes in rhizosphere were known to promote plant growth and stress tolerance in main crops (Dias et al., 2017; Vurukonda et al., 2018). Siderophores not only inhibited the growth of phytopathogens but also increased the iron supply to plants and microorganisms (El-Tarabily et al., 2009). This might explain our observation that *Streptomyces* BITDG-11 significantly increased plant height, fresh and dry weight, and chlorophyll content.

Additionally, the interaction of plant and antagonistic agents induces the production of specific root exudates and alters the microbial community diversity (Khamna et al., 2009). We also found that *Streptomyces* BITDG-11 improved the fungal and bacterial abundance to inhibit the growth of *F. oxysporum* TR4 in the rhizosphere soil of banana plantlets. These microbes play an important role in maintaining the stability of the soil ecosystem and reducing plant susceptibility to pathogens (Palaniyandi et al., 2011; Zhou et al., 2019; Trivedi et al., 2020). Accumulated evidences indicated that the plant immune system could be triggered after inoculation with pathogens or beneficial microbes (de Lamo and Takken, 2020). *Streptomyces* BITDG-11 induced higher and lasting expression levels of defense genes in roots of banana seedlings. Moreover, higher activities of antioxidant enzymes such as SOD, CAT, POD, and PPO were detected in the treatment group of *Streptomyces* BITDG-11 + *F. oxysporum* TR4 over pathogen only or control. POD could directly inhibit the spore germination and mycelia growth of some pathogenic fungi like *Pseudocercospora abelmoschi* (Joseph et al., 1998). Enhanced activities of antioxidant enzymes were also reported in bacterium-treated banana plantlets demonstrating tolerance to banana bunchy top disease (Kavino et al., 2007). A recent report showed that combining different *Streptomyces* strains reduced the disease incidence of *Botrytis gray* mold by improving the activity of antioxidant enzymes in chickpea (Vijayabharathi et al., 2018). The higher activity of antioxidant enzymes in banana roots could be another additional mechanism attributing to the increase of the host immune response to pathogens. These findings opened up the possibility of priming defense reactions by *Streptomyces* BITDG-11 inoculation and thus enhanced disease resistance against pathogens.

Genome sequencing further revealed that the *Streptomyces* BITDG-11 chromosome contained a large number of conserved BGC encoding terpenes, non-ribosomal peptides, polyketides, siderophores, and ectoines. These BGCs had been proven to participate in the regulation of antimicrobial activities of *Streptomyces* strains (Bergeijk et al., 2020). Some compounds such as toyocamycin, naringenin, and ectoine analogs showed a 100% similarity with known structures. Toyocamycin produced by *Streptomyces* belonged to a member of the nucleoside antibiotic family. The compound had been recognized as a promising fungicide for the control of plant diseases (Shentu et al., 2018; Ma et al., 2020). Naringenin exhibited both antimicrobial and antioxidant activities (Ng et al., 2019). As a compatible solute and chemical chaperone, ectoine widely synthesized by bacteria enhanced a cellular defense against detrimental effects (Czech et al., 2019).

A detailed survey and analysis revealed that low similarity was found in other BGCs, suggesting *Streptomyces* BITDG-11 had a great potential for producing novel secondary metabolites. It was supported that 33.9% of genes clustered into the unknown function category in COG. The predicted cluster 12 containing 43 necessary genes showed 81% similarity with the biosynthetic gene cluster of mannopeptimycin. The compound was a novel class of lipoglycopeptide antibiotics active against multidrug-resistant pathogens (Magarvey et al., 2006). Cluster 17 exhibited 72% similarity with the biosynthetic gene cluster of rimocidin, a structurally unique type polyketide belonging to a polyene macrolide (Jeon et al., 2016). Rimocidin produced by *Streptomyces rimosus* M527 demonstrated a strong broad-spectrum antifungal activity (Zhao et al., 2019). Cluster 41 had 80% similarity with the known sequence responsible for the biosynthesis of siderophore. The production of siderophores was further confirmed by the appearance of a yellow halo around the colony on CAS agar (**Figure 2A**). Catechol-siderophore such as coelichelin (cluster 26) identified from the *Streptomyces* species was previously characterized with 2,3-dihydroxybenzoate (2,3-DHB) as a key functional group (Reitz and Butler, 2019). A recent study demonstrated that 2,3-DHB was a common precursor during the biosynthesis of the catecholate siderophores in *Streptomyces* sp. MBT76 (Gubbens et al., 2017). A similar functional crosstalk was also found during the biosynthesis of enterobactin and other secondary metabolites such as benzoxazoles and caboxamycin in other *Streptomyces* species (Cano-Prieto et al., 2015; Losada et al., 2017). The antiSMASH analysis showed a large number of PKS and NRPS gene cluster

distributed in the genome of *Streptomyces* BITDG-11, whether a similar crosstalk exists in *Streptomyces* BITDG-11 merits further investigation.

CONCLUSION

In our study, 60 actinomycetes were isolated from the rhizosphere soil of *M. pingii*. Among 17 isolates with antagonistic ability against *F. oxysporum* TR4, strain BITDG-11 had high and broad-spectrum antifungal activity. The strain can produce IAA, siderophores, chitinase, β-1,3-glucanase, lipase, and urease. The molecular identification suggested that strain BITDG-11 might belong to a novel species of the genus *Streptomyces*. It obviously promoted the plant growth of banana plantlets and reduced the disease incidence by inducing the expression levels of defense genes and the activities of antioxidant enzymes. Genomic sequencing and analysis revealed that the *Streptomyces* BITDG-11 chromosome contained 43 conserved biosynthesis gene clusters encoding terpenes, non-ribosomal peptides, polyketides, siderophores, ectoines, etc. Among 15 bioactive secondary metabolites identified by GC-MS in the *Streptomyces* BITDG-11 extract, dibutyl phthalate was the major compound with the highest peak area. These results implied that *Streptomyces* BITDG-11 might be developed as a multifunctional biopesticide against a wide range of phytopathogens and as a bioinoculant to enhance plant growth.

DATA AVAILABILITY STATEMENT

The datasets presented in this study can be found in online repositories. The names of the repository/repositories and accession number(s) can be found in the article/ **Supplementary Material**.

AUTHOR CONTRIBUTIONS

LZ, HZ, and WW developed the ideas and designed the experimental plans. WW and JX supervised the research and provided the fund support. LZ, HZ, and YH performed the experiments. JP, WW, and JX provided the materials. LZ, JP and WW analyzed the data. LZ and WW prepared the manuscript. All the authors contributed to the article and approved the submitted version.

FUNDING

This work was supported by the National Natural Science Foundation of China (31770476, 32072504 and 31661143003), the Natural Science Foundation of Hainan (320CXTD441), and the China Agriculture Research System (CARS-31).

ACKNOWLEDGMENTS

We thank Zhufeng Gao for providing help with this work.

SUPPLEMENTARY MATERIAL

The Supplementary Material for this article can be found online at: https://www.frontiersin.org/articles/10.3389/fmicb.2021.763038/full#supplementary-material

Supplementary Table S1 | Antibiotic sensitivity test of *Streptomyces* BITDG-11.

Supplementary Table S2 | Calculation of ANI value.

Supplementary Table S3 | Genome-wide analysis of *Streptomyces* BITDG-11 for biosynthesis gene clusters of the biosynthesis of secondary metabolites by the online antiSMASH v4.2.0 software.

REFERENCES

Ahsan, T., Chen, J., Zhao, X., Irfan, M., and Wu, Y. (2017). Extraction and identification of bioactive compounds (eicosane and dibutyl phthalate) produced by *Streptomyces* strain KX852460 for the biological control of *Rhizoctonia solani* AG-3 strain KX852461 to control target spot disease in tobacco leaf. *AMB Exp.* 7:54. doi: 10.1186/s13568-017-0351-z

Al-Bari, M., Bhuiyan, M., Flores, M., Petrosyan, P., Garcia-Varela, M., and Islam, M. (2005). *Streptomyces bangladeshensis* sp. nov., isolated from soil, which produces bis-(2-ethylhexyl)phthalate. *Int. J. Syst. Evol. Microbiol.* 55, 1973–1977. doi: 10.1099/ijs.0.63516-0

Atta, H. M., El-Sehrawi, M. H., Awny, N. M., and El-Mesady, N. I. (2011). Microbiological studies on cultural, physiological characteristics and antimicrobial activities of *Streptomyces cyaneus*-AZ-13Zc. *Researcher* 3, 80–90.

Bergeijk, D., Terlouw, B. R., Medema, M. H., and Wezel, G. (2020). Ecology and genomics of actinobacteria: new concepts for natural product discovery. *Nat. Rev. Microbiol.* 18, 546–558. doi: 10.1038/s41579-020-0379-y

Brady, C., Cleenwerck, I., Venter, S., Vancanneyt, M., Swings, J., and Coutinho, T. (2008). Phylogeny and identification of *Pantoea* species associated with plants, humans and the natural environment based on multilocus sequence analysis (MLSA). *Syst. Appl. Microbiol.* 31, 447–460. doi: 10.1016/j.syapm.2008.09.004

Brettin, T., Davis, J. J., Disz, T., Edwards, R. A., Gerdes, S., Olsen, G. J., et al. (2015). *RASTtk*: a modular and extensible implementation of the RAST algorithm for building custom annotation pipelines and annotating batches of genomes. *Sci. Rep.* 5, 1–6. doi: 10.1038/srep08365

Bubici, G., Kaushal, M., Prigigallo, M. I., Cabanas, G. L., and Mercado-Blanco, J. (2019). Biological control agents against fusarium wilt of banana. *Front. Microbiol.* 10:1290. doi: 10.3389/fmicb.2019.01290

Bull, A. T., and Stach, J. E. M. (2007). Marine actinobacteria: new opportunities for natural product search and discovery. *Trends Microbiol.* 5, 491–499. doi: 10.1016/j.tim.2007.10.004

Cano-Prieto, C., Garcia-Salcedo, R., Sanchez-Hidalgo, M., Brana, A. F., Fiedler, H. P., Mendez, C., et al. (2015). Genome mining of Streptomyces sp. Tü 6176: characterization of the nataxazole biosynthesis pathway. *ChemBioChem* 16, 1461–1473. doi: 10.1002/cbic.201500153

Chen, X., Hu, L., Huang, X., Zhao, L., Miao, C., Chen, Y., et al. (2019). Isolation and characterization of new phenazine metabolites with antifungal activity against root-rot pathogens of *Panax notoginseng* from *Streptomyces*. *J. Agric. Food Chem.* 67, 11403–11407. doi: 10.1021/acs.jafc.9b04191

Chen, Y., Zhou, D., Qi, D., Gao, Z., Xie, J., and Luo, Y. (2018). Growth promotion and disease suppression ability of a *Streptomyces* sp. CB-75 from banana rhizosphere soil. *Front. Microbiol.* 8:2704. doi: 10.3389/fmicb.2017.02704

Czech, L., Hoppner, A., Kobus, S., Seubert, A., Riclea, R., Dickschat, J. S., et al. (2019). Illuminating the catalytic core of ectoine synthase through structural and biochemical analysis. *Sci. Rep.* 9:364. doi: 10.1038/s41598-018-36247-w

de Lamo, F. J., and Takken, F. L. (2020). Biocontrol by *Fusarium oxysporum* using endophyte-mediated resistance. *Front. Plant Sci.* 11:37. doi: 10.3389/fpls.2020.00037

Deng, J., Shi, D., Mao, H., Li, Z., Liang, S., Ke, Y., et al. (2019). Heterologous expression and characterization of an antifungal chitinase (Chit46) from

Trichoderma harzianum GIM 3.442 and its application in colloidal chitin conversion. *Int. J. Biol. Macromol.* 134, 113–121. doi: 10.1016/j.ijbiomac.2019.04.177

Dias, M. P., Bastos, M. S., Xavier, V. B., Cassel, E., Astarita, L. V., and Santarém, E. R. (2017). Plant growth and resistance promoted by *Streptomyces* spp. in tomato. *Plant Physiol. Biochem.* 118, 479–493. doi: 10.1016/j.plaphy.2017.07.017

Ding, L., Guo, W., and Chen, X. (2019). Exogenous addition of alkanoic acids enhanced production of antifungal lipopeptides in *Bacillus amyloliquefaciens* Pc3. *Appl. Microbiol. Biotechnol.* 103, 5367–5377. doi: 10.1007/s00253-019-09792-1

Dita, M., Barquero, M., Heck, D., Mizubuti, E. S., and Staver, C. P. (2018). Fusarium wilt of banana: current knowledge on epidemiology and research needs toward sustainable disease management. *Front. Plant Sci.* 9:1468. doi: 10.3389/fpls.2018.01468

El-Tarabily, K. A., Nassar, A. H., Hardy, G. E., and Sivasithamparam, K. (2009). Illuminating the catalytic core of ectoine synthase through structural and biochemical analysis. *J. Appl. Microbiol.* 106, 13–26. doi: 10.1111/j.1365-2672.2008.03926.x

Ferguson, I. B., Watkins, C. B., and Harman, J. E. (1983). Inhibition by calcium of senescence of detached cucumber cotyledons: effect on ethylene and hydroperoxide production. *Plant Physiol.* 71, 182–186. doi: 10.1104/pp.71.1.182

Franco-Correa, M., Quintana, A., Duque, C., Suarez, C., Rodríguez, M. X., and Barea, J. M. (2010). Evaluation of actinomycete strains for key traits related with plant growth promotion and mycorrhiza helping activities. *Appl. Soil Ecol.* 45, 209–217. doi: 10.1016/j.apsoil.2010.04.007

Gubbens, J., Wu, C., Zhu, H., Filippov, D., Florea, B., Rigali, S., et al. (2017). Intertwined precursor supply during biosynthesis of the catecholate-hydroxamate siderophores qinichelins in *Streptomyce*s sp. MBT76. *ACS Chem. Biol.* 12, 2756–2766. doi: 10.1021/acschembio.7b00597

Hong, S. H., Song, Y. S., Seo, D. J., Kim, K. Y., and Jung, W. J. (2017). Antifungal activity and expression patterns of extracellular chitinase and β-1,3-glucanase in *Wickerhamomyces anomalus* eg2 treated with chitin and glucan. *Microb. Pathog.* 110, 159–164. doi: 10.1016/j.micpath.2017.06.038

Hughes, J., and Davis, P. (1981). High-performance liquid chromatographic determination of N,N-dimethylcolchiceinamide and its metabolites, N-methylcolchiceinamide and colchiceinamide, in microbial culture. *J. Chromatogr.* 219, 321–324. doi: 10.1016/s0021-9673(00)87945-5

Jeon, B. J., Kim, J. D., Han, J. W., and Kim, B. S. (2016). Antifungal activity of rimocidin and a new rimocidin derivative BU 16 produced by *Streptomyces mauvecolor* BU 16 and their effects on pepper anthracnose. *J. Appl. Microbiol.* 120, 1219–1228. doi: 10.1111/jam.13071

Jing, T., Zhou, D., Zhang, M., Yun, T., Qi, D., Wei, Y., et al. (2020). Newly isolated *Streptomyces* sp. JBS5-6 as a potential biocontrol agent to control banana Fusarium wilt: genome sequencing and secondary metabolite cluster profiles. *Front. Microbiol.* 11:3036. doi: 10.3389/fmicb.2020.602591

Joseph, L. M., Koon, T. T., and Man, W. S. (1998). Antifungal effects of hydrogen peroxide and peroxidase on spore germination and mycelial growth of *Pseudocercospora* species. *Can. J. Bot.* 76, 2119–2124. doi: 10.1139/b98-166

Kavino, M., Harish, S., Kumar, N., Saravanakumar, D., Damodaran, T., Soorianathasundaram, K., et al. (2007). Rhizosphere and endophytic bacteria for induction of systemic resistance of banana plantlets against bunchy top virus. *Soil Biol. Biochem.* 39, 1087–1098. doi: 10.1016/j.soilbio.2006.11.020

Khamna, S., Yokota, A., Peberdy, J. F., and Lumyong, S. (2009). Antifungal activity of *Streptomyces* spp. isolated from rhizosphere of Thai medicinal plants. *Inter. J. Integr. Biol.* 6, 143–147.

Kumar, S., Stecher, G., and Tamura, K. (2016). MEGA7: molecular evolutionary genetics analysis version 7.0 for bigger datasets. *Mol. Biol. Evol.* 33, 1870–1874. doi: 10.1093/molbev/msw054

Lee, S. Y., Tindwa, H., Lee, Y. S., Naing, K. W., Hong, S. H., Nam, Y., et al. (2012). Biocontrol of anthracnose in pepper using chitinase, beta-1,3 glucanase, and 2-furancarboxaldehyde produced by *Streptomyces cavourensis* SY224. *J Microbiol Biotechnol.* 22, 1359–1366. doi: 10.4014/jmb.1203.02056

Li, C., Jin, P., Liu, C., Ma, Z., Zhao, J., Li, J., et al. (2016). *Streptomyces bryophytorum* sp. nov., an endophytic actinomycete isolated from moss (*Bryophyta*). *Anton. Leeuw.* 109, 1209–1215. doi: 10.1007/s10482-016-0722-5

Li, X., Jing, T., Zhou, D., Zhang, M., Qi, D., Zang, X., et al. (2021a). Biocontrol efficacy and possible mechanism of *Streptomyces* sp. H4 against postharvest anthracnose caused by *Colletotrichum fragariae* on strawberry fruit. *Postharvest Biol. Tec.* 175:111401. doi: 10.1016/j.postharvbio.2020.111401

Li, X., Li, K., Zhou, D., Zhang, M., Qi, D., Jing, T., et al. (2021b). Biological control of banana wilt disease caused by *Fusarium oxyspoum* f. sp. *cubense* using *Streptom*yces sp. H4. *Biol. Control* 155:104524. doi: 10.1016/j.biocontrol.2020.104524

Losada, A. A., CanoPrieto, C., GarciaSalcedo, R., Brana, A. F., Mendez, C., Salas, J. A., et al. (2017). Caboxamycin biosynthesis pathway and identification of novel benzoxazoles produced by cross−talk in *Streptomyces* sp. NTK 937. *Microb. Biotechnol.* 10, 873–885. doi: 10.1111/1751-7915.12716

Lutz, M., Wenger, S., Maurhofer, M., Défago, G., and Duffy, B. (2004). Signaling between bacterial and fungal biocontrol agents in a strain mixture. *FEMS Microbiol. Ecol.* 48, 447–455. doi: 10.1016/j.femsec.2004.03.002

Ma, Z., Hu, Y., Liao, Z., Xu, J., Xu, X., Bechthold, A., et al. (2020). Cloning and overexpression of the toy cluster for titer improvement of toyocamycin in *Streptomyces diastatochromogenes*. *Front. Microbiol.* 11:2074.

Magarvey, N. A., Haltili, B., He, M., Greenstein, M., and Hucul, J. (2006). Biosynthetic pathway for mannopeptimycins, lipoglycopeptide antibiotics active against drug-resistant gram-positive pathogens. *Antimicrob. Agents Ch.* 50, 2167–2177. doi: 10.1128/AAC.01545-05

Milagres, A., Machuca, A., and Napoleao, D. (1999). Detection of siderophore production from several fungi and bacteria by a modification of chrome azurol s (cas) agar plate assay. *J. Microbiol. Meth.* 37, 1–6. doi: 10.1016/S0167-7012(99)00028-7

Nagpure, A., Choudhary, B., and Gupta, R. K. (2014). Mycolytic enzymes produced by *Streptomyces violaceusniger* and their role in antagonism towards wood-rotting fungi. *J. Basic. Microbiol.* 54, 397–407. doi: 10.1002/jobm.201200474

Nel, B., Steinberg, C., Labuschagne, N., and Viljoen, A. (2010). Isolation and characterization of nonpathogenic *Fusarium oxysporum* isolates from the rhizosphere of healthy banana plants. *Plant Pathol.* 55, 207–216. doi: 10.1111/j.1365-3059.2006.01343.x

Ng, K. R., Lyu, X., Mark, R., and Chen, W. N. (2019). Antimicrobial and antioxidant activities of phenolic metabolites from flavonoid-producing yeast: Potential as natural food preservatives. *Food Chem.* 270, 123–129. doi: 10.1016/j.foodchem.2018.07.077

Ogata, H., Goto, S., Sato, K., Fujibuchi, W., Bono, H., and Kanehisa, M. (1999). KEGG: Kyoto encyclopedia of genes and genomes. *Nucleic Acids Res.* 27, 29–34. doi: 10.1093/nar/27.1.29

Olanrewaju, O. S., and Babalola, O. O. (2019). *Streptomyces*: implications and interactions in plant growth promotion. *Appl. Microbiol. Biotech.* 103, 1179–1188. doi: 10.1007/s00253-018-09577-y

Palaniyandi, S. A., Yang, S. H., Cheng, J. H., Meng, L., and Suh, J. W. (2011). Biological control of anthracnose (*Colletotrichum gloeosporioides*) in yam by *Streptomyces* sp. MJM5763. *J. Appl. Microbiol.* 111, 443–455. doi: 10.1111/j.1365-2672.2011.05048.x

Pegg, K. G., Coates, L. M., O'Neill, W. T., and Turner, D. W. (2019). The epidemiology of Fusarium wilt of banana. *Front. Plant Sci.* 10:1395. doi: 10.3389/fpls.2019.01395

Ploetz, R. C. (2015a). Fusarium wilt of banana. *Phytopathology* 105, 1512–1521. doi: 10.1094/PHYTO-04-15-0101-RVW

Ploetz, R. C. (2015b). Management of Fusarium wilt of banana: A review with special reference to tropical race 4. *Crop. Prot.* 73, 7–15. doi: 10.1016/j.cropro.2015.01.007

Qi, D., Zou, L., Zhou, D., Chen, Y., Gao, Z., Feng, R., et al. (2019). Taxonomy and broad-spectrum antifungal activity of *Streptomyces* sp. SCA3-4 isolated from rhizosphere soil of *Opuntia stricta*. *Front. Microbiol.* 10:1390. doi: 10.3389/fmicb.2019.01390

Reitz, Z., and Butler, A. (2019). Precursor-directed biosynthesis of catechol compounds in *Acinetobacter bouvetii* DSM 14964. *Chem. Commun.* 56, 12222–12225. doi: 10.1039/d0cc04171h

Richter, M., and Rosselló-Móra, R. (2009). Shifting the genomic gold standard for the prokaryotic species definition. *Proc. Natl. Acad. Sci. USA* 106, 19126–19131. doi: 10.1073/pnas.0906412106

Rong, X., and Huang, Y. (2010). Taxonomic evaluation of the Streptomyces griseus clade using multilocus sequence analysis and DNA-DNA hybridization, with

proposal to combine 29 species and three subspecies as 11 genomic species. *Int. J. Syst. Evol. Microbiol.* 60, 696–703. doi: 10.1099/ijs.0.012419-0

Sadeghian, M., Bonjar, G., and Sirchi, G. (2016). Postharvest biological control of apple bitter rot by soil-borne Actinomycetes and molecular identification of the active antagonist. *Postharvest Biol. Tec.* 112, 46–54. doi: 10.1016/j.postharvbio.2015.09.035

Saravanan, T., Muthusamy, M., and Marimuthu, T. (2003). Development of integrated approach to manage the Fusarial wilt of banana. *Crop. Prot.* 9, 1117–1123. doi: 10.1016/S0261-2194(03)00146-7

Sayed, A. M., Hassan, M. H., Alhadrami, H. A., Hassan, H. M., Goodfellow, M., and Rateb, M. E. (2019). Extreme environments: microbiology leading to specialized metabolites. *J. Appl. Microbiol.* 128, 630–657. doi: 10.1111/jam.14386

Sharma, M., and Manhas, R. K. (2020). Purification and characterization of salvianolic acid b from *Streptomyces* sp. m4 possessing antifungal activity against fungal phytopathogens. *Microbiol. Res.* 237:126478. doi: 10.1016/j.micres.2020.126478

Shentu, X., Cao, Z., Xiao, Y., Tang, G., Ochi, K., and Yu, X. (2018). Substantial improvement of toyocamycin production in *Streptomyces diastatochromogenes* by cumulative drug-resistance mutations. *PLoS One* 13:e0203006. doi: 10.1371/journal.pone.0203006

Shirling, E. B., and Gottlieb, D. (1968). Cooperative description of type cultures of *Streptomyces*. II. Species descriptions from first study. *Int. J. Syst. Bacteriol.* 18, 87–89. doi: 10.1099/00207713-18-2-69

Sivakumar, S., Jebanesan, A., Govindarajan, M., and Rajasekar, P. (2011). Larvicidal and repellent activity of tetradecanoic acid against *Aedes aegypti* (Linn.) and *Culex quinquefasciatus* (Say.) (Diptera:Culicidae). *Asian Pac. J. Trop. Med.* 4, 706–710. doi: 10.1016/S1995-7645(11)60178-8

Sokmen, B., Hasdemir, B., Yusafoglu, A., and Yanardag, R. (2014). Some monohydroxy tetradecanoic acid isomers as novel urease and elastase inhibitors and as new antioxidants. *Appl. Biochem. Biotechnol.* 172, 1358–1364. doi: 10.1007/s12010-013-0595-2

Sun, D., Lu, X., Hu, Y., Li, W., Hong, K., Mo, Y., et al. (2013). Methyl jasmonate induced defense responses increase resistance to *Fusarium oxysporum* f. sp. *cubense* race 4 in banana. *Sci. Hortic.* 164, 484–491.

Tatusov, R. L., Galperin, M. Y., Natale, D. A., and Koonin, E. V. (2000). The COG database: a tool for genome-scale analysis of protein functions and evolution. *Nucleic Acids Res.* 28, 33–36. doi: 10.1093/nar/28.1.33

Thekkangil, A., and Suchithra, T. (2019). Antidermatophytic lead compounds from *Streptomycetes albidoflavus* STV1572a against Tinea infections by *Tricophyton mentagrophytes*. *Microbl. Pathog.* 142:104037. doi: 10.1016/j.micpath.2020.104037

Trivedi, R., Leach, J. E., Tringe, S. G., Sa, T., and Singh, B. (2020). Plant-microbiome interactions: from community assembly to plant health. *Nat. Rev. Microbiol.* 18, 607–621. doi: 10.1038/s41579-020-0412-1

van der Heul, H. U., Bilyk, B. L., McDowall, K. J., Seipke, R. F., and van Wezel, G. P. (2018). Regulation of antibiotic production in Actinobacteria: new perspectives from the post-genomic era. *Nat. Prod. Rep.* 35, 575–604. doi: 10.1039/c8np00012c

Vijayabharathi, R., Gopalakrishnan, S., Sathya, A., Vasanth Kumar, M., Srinivas, V., and Mamta, S. (2018). *Streptomyces* sp. as plant growth-promoters and host-plant resistance inducers against *Botrytis cinerea* in chickpea. *Biocontrol. Sci. Techn.* 28, 1140–1163. doi: 10.1080/09583157.2018.1515890

Vurukonda, S., Giovanardi, D., and Stefani, E. (2018). Plant growth promoting and biocontrol activity of *Streptomyces* spp. as endophytes. *Int. J. Mol. Sci.* 19:952. doi: 10.3390/ijms19040952

Wang, W., Hu, Y., Sun, D., Staehelin, C., Xin, D., and Xie, J. (2012). Identification and evaluation of two diagnostic markers linked to Fusarium wilt resistance (race 4) in banana (*Musa* spp.). *Mol. Biol. Rep.* 39, 451–459. doi: 10.1007/s11033-011-0758-6

Weber, T., Blin, K., Duddela, S., Krug, D., Kin, H., Bruccoleri, R., et al. (2015). Antismash 3.0-a comprehensive resource for the genome mining of biosynthetic gene clusters. *Nucleic Acids Res.* 43, W237–W243. doi: 10.1093/nar/gkv437

Wei, Y., Zhao, Y., Zhou, D., Qi, D., Li, K., Tang, W., et al. (2020). A newly isolated *Streptomyces* sp. YYS-7 with a broad-spectrum antifungal activity improves the banana plant resistance to *Fusarium oxysporum* f. sp. *cubense* tropical race 4. *Front. Microbiol.* 11:1712. doi: 10.3389/fmicb.2020.01712

Xu, T., Cao, L., Zeng, J., Franco, C., and Zhu, Y. (2019). The antifungal action mode of the rice endophyte *Streptomyces hygroscopicus* osish-2 as a potential biocontrol agent against the rice blast pathogen. *Pestic. Biochem. Phys.* 160, 58–69. doi: 10.1016/j.pestbp.2019.06.015

Yang, A., Si, L., Shi, Z., Tian, L., Liu, D., Zhou, D., et al. (2013). Nitrosporeusines A and B, unprecedented thioester-bearing alkaloids from the Arctic *Streptomyces nitrosporeus*. *Org. Lett.* 15, 5366–5369. doi: 10.1021/ol4026809

Yoon, S. H., Ha, S. M., Kwon, S., Lim, J., and Kim, Y. (2017). Introducing EzBioCloud: a taxonomically united database of 16S rRNA gene sequences and whole-genome assemblies. *Int. J. Syst. Evol. Microbiol.* 67:1613. doi: 10.1099/ijsem.0.001755

Yun, T., Zhang, M., Zhou, D., Jing, T., Zang, X., Qi, D., et al. (2021). Anti-Foc RT4 activity of a newly isolated *Streptomyces* sp. 5-10 from a medicinal plant (*Curculigo capitulata*). *Front Microbiol.* 11:610698. doi: 10.3389/fmicb.2020.610698

Zhang, K., Gu, L., Zhang, Y., Liu, Z., and Li, X. (2020). Dinactin from a new producer, *Streptomyces badius* gz-8, and its antifungal activity against the rubber anthracnose fungus *Colletotrichum gloeosporioides*. *Microbiol. Res.* 240:126548. doi: 10.1016/j.micres.2020.126548

Zhang, L., Yuan, L., Staehelin, C., Li, Y., Ruan, J., Liang, Z., et al. (2019). The LYSIN MOTIF-CONTAINING RECEPTOR-LIKE KINASE 1 protein of banana is required for perception of pathogenic and symbiotic signals. *New Phytol.* 223, 1530–1546. doi: 10.1111/nph.15888

Zhang, S., Sun, F., Liu, L., Bao, L., Fang, W., Yin, C., et al. (2020). Dragonfly-associated *Trichoderma harzianum* QTYC77 is not only a potential biological control agent of *Fusarium oxysporum* f. sp. *cucumerinum* but also a source of new antibacterial agents. *J. Agric. Food Chem.* 2020, 14161–14167. doi: 10.1021/acs.jafc.0c05760

Zhang, W., Jiang, B., Li, W., Song, H., Yu, Y., and Chen, J. (2009). Polyamines enhance chilling tolerance of cucumber (Cucumis sativus L.) through modulating antioxidative system. *Sci. Hortic.* 122, 200–208. doi: 10.1016/j.scienta.2009.05.013

Zhang, Y., Wei, Z., Liu, C., Chen, Q., Xu, B., Guo, Z., et al. (2017). Linoleic acid isomerase gene *FgLAI12* affects sensitivity to salicylic acid, mycelial growth and virulence of *Fusarium graminearum*. *Sci. Rep.* 7:46129. doi: 10.1038/srep46129

Zhao, Y., Song, Z., Ma, Z., Bechthold, A., and Yu, X. (2019). Sequential improvement of rimocidin production in *Streptomyces rimosus* M527 by introduction of cumulative drug-resistance mutations. *J. Ind. Microbiol. Biotechnol.* 46, 697–708. doi: 10.1007/s10295-019-02146-w

Zhou, D., Jing, T., Chen, Y., Wang, F., Qi, D., Feng, R., et al. (2019). Deciphering microbial diversity associated with Fusarium wilt-diseased and disease-free banana rhizosphere soil. *BMC Microbiol.* 19:15316. doi: 10.1186/s12866-019-1531-6

Zorrilla-Fontanesi, Y., Pauwels, L., Panis, B., Signorelli, S., Vanderschuren, H., and Swennen, R. (2020). Strategies to revise agrosystems and breeding to control Fusarium wilt of banana. *Nat. Food* 1, 599–604. doi: 10.1038/s43016-020-00155-y

Conflict of Interest: The authors declare that the research was conducted in the absence of any commercial or financial relationships that could be construed as a potential conflict of interest.

Publisher's Note: All claims expressed in this article are solely those of the authors and do not necessarily represent those of their affiliated organizations, or those of the publisher, the editors and the reviewers. Any product that may be evaluated in this article, or claim that may be made by its manufacturer, is not guaranteed or endorsed by the publisher.

frontiers in Plant Science

ORIGINAL RESEARCH
published: 29 October 2021
doi: 10.3389/fpls.2021.759463

Efficiency of the Hydroponic System as an Approach to Confirm the Solubilization of $CaHPO_4$ by Microbial Strains Using *Glycine max* as a Model

Mateus Neri Oliveira Reis[1,2], *Layara Alexandre Bessa*[1,2], *Andressa Pereira de Jesus*[1], *Fabiano Guimarães Silva*[2], *Marialva Alvarenga Moreira*[3] *and Luciana Cristina Vitorino*[1]*

[1] *Laboratory of Agricultural Microbiology, Instituto Federal Goiano – Rio Verde Campus, Highway Sul Goiana, Rio Verde, Brazil,* [2] *Laboratory of Plant Mineral Nutrition and CEAGRE – Exponential Agriculture Center of Excellence, Instituto Federal Goiano, Rio Verde, Brazil,* [3] *Empresa de Pesquisa Agropecuária de Minas Gerais (EPAMIG), Santa Rita Experimental Field, Prudente de Morais, Brazil*

OPEN ACCESS

Edited by:
Maurizio Ruzzi,
University of Tuscia, Italy

Reviewed by:
Ida Romano,
University of Naples Federico II, Italy
Everlon Cid Rigobelo,
São Paulo State University, Brazil
Tofazzal Islam,
Bangabandhu Sheikh Mujibur Rahman Agricultural University, Bangladesh

***Correspondence:**
Luciana Cristina Vitorino
luciana.vitorino@ifgoiano.edu.br

Specialty section:
This article was submitted to Plant Symbiotic Interactions, a section of the journal Frontiers in Plant Science

Received: *16 August 2021*
Accepted: *27 September 2021*
Published: *29 October 2021*

Citation:
Reis MNO, Bessa LA, de Jesus AP, Guimarães Silva F, Moreira MA and Vitorino LC (2021) Efficiency of the Hydroponic System as an Approach to Confirm the Solubilization of $CaHPO_4$ by Microbial Strains Using Glycine max as a Model. Front. Plant Sci. 12:759463. doi: 10.3389/fpls.2021.759463

The sustainable development of agriculture can be stimulated by the great market availability of bio-inputs, including phosphate-solubilizing microbial strains. However, these strains are currently selected using imprecise and questionable solubilization methodologies in solid or liquid media. We hypothesized that the hydroponic system could be a more efficient methodology for selecting phosphate-solubilizing strains as plant growth promoters. This methodology was tested using the plant *Glycine max* as a model. The growth-promoting potential of the strains was compared with that of the Biomaphos® commercial microbial mixture. The obtained calcium phosphate ($CaHPO_4$) solubilization results using the hydroponic system were inconsistent with those observed in solid and liquid media. However, the tests in liquid medium demonstrated poor performances of *Codinaeopsis* sp. (328EF) and *Hamigera insecticola* (33EF) in reducing pH and solubilizing $CaHPO_4$, which corroborates with the effects of biotic stress observed in *G. max* plants inoculated with these strains. Nevertheless, the hydroponic system allowed the characterization of *Paenibacillus alvei* (PA12), which is also efficient in solubilization in a liquid medium. The bacterium *Lysinibacillus fusiformis* (PA26) was the most effective in $CaHPO_4$ solubilization owing to the higher phosphorus (P) absorption, growth promotion, and physiological performance observed in plants inoculated with this bacterium. The hydroponic method proved to be superior in selecting solubilizing strains, allowing the assessment of multiple patterns, such as nutritional level, growth, photosynthetic performance, and anatomical variation in plants, and even the detection of biotic stress responses to inoculation, obtaining strains with higher growth promotion potential than Biomaphos®. This study proposed a new approach to confirm the solubilizing activity of microorganisms previously selected *in vitro* and potentially intended for the bio-input market that are useful in P availability for important crops, such as soybeans.

Keywords: phosphate solubilizing microorganisms, PSM, bio-inputs, plant nutrition, plant growth promotion

INTRODUCTION

The world population is estimated to reach ∼9.735 billion people by 2050 (United Nations, 2019). Associated with the pressure for agriculture to meet the needs of human development, it is necessary to implement sustainable agricultural practices that increase productivity integrated with conservation measures (Taveira et al., 2019). The current productivity of important crops such as soybean is affected by phosphorus (P) deficiency in acidic soils since P plays a key role in the symbiotic capacity of nitrogen (N_2) fixation (Sulieman and Tran, 2017; Wang et al., 2020; Jaiswal et al., 2021). Current agricultural practices use fertilizers to add P to the soil, however, the use of phosphate fertilizers is expensive and unsustainable (Situmorang et al., 2015). Nonetheless, these fertilizers are easily precipitated with aluminum (Al), iron (Fe), and calcium (Ca), forming low-solubility complexes that are not used by plants (Penn and Camberato, 2019). In this context, the dissemination of more economical and ecologically appropriate technologies to improve P availability in soil has become urgent.

Currently, the use of phosphate-solubilizing microbes (PSMs) has been shown as a promising method since they play a key role in P dynamics in soil and the subsequent availability of this element to plants (Islam and Hossain, 2012; Kafle et al., 2019). PSMs fractionate insoluble P forms into soluble forms through various biological mechanisms, including the production of organic acids and extracellular enzymes, which convert insoluble forms of P into forms available for plant absorption (Hanif et al., 2015; Li et al., 2015; Baliah et al., 2016; Gurikar et al., 2016; Doilom et al., 2020; Sarr et al., 2020; Zúñiga-Silgado et al., 2020). The organic acids produced include glycolic, 2-ketogluconic, acetic, citric, propionic, succinic, tartaric, formic, fumaric, lactic, malic, butyric, gluconic, valeric, oxalic, and citric acids (Hwangbo et al., 2003; Chen et al., 2006; Patel et al., 2008; Scervino et al., 2010; Zhu et al., 2012; Jog et al., 2014; Mehta et al., 2015; Yadav et al., 2015). However, despite their importance, few PSM strains are currently available in the global market for inoculants. This is partly due to faulty strain selection mechanisms, which often present a high potential for *in vitro* systems but a reduced potential for field systems.

Phosphate-solubilizing microbes strains are usually selected through screening in solid media containing phosphate sources, such as calcium phosphate ($CaHPO_4$), $Ca_3(PO_4)_2$, aluminum phosphate ($AlPO_4$), or iron phosphate ($FePO_4$). In these media, halo measurements determine the efficiency of the isolate in solubilizing the insoluble phosphate source. However, this qualitative method is considered inefficient for selection, as many isolates that do not produce any visible halo on solid media can solubilize various types of insoluble inorganic phosphates in liquid media (e.g., Nautiyal, 1999; Bashan et al., 2013; Salcedo et al., 2014; Sousa et al., 2016). Therefore, potential strains are commonly excluded by this screening. Another selection methodology is screening in a liquid culture medium. This methodology is currently accepted as the most reliable method, but it also presents inconsistencies as a colorimetric method. The most widespread protocol for solubilizing strains in a liquid medium for determining free P is described by Murphy and Riley (1962). This protocol is based on the reaction of an ascorbic acid (vitamin C) stock solution with added molybdate, forming a blue phosphomolybdenum complex proportional to the amount of free P in the sample. Nonetheless, this method is highly susceptible to chemical interference from reducing agents present in the culture medium, such as ascorbate, which affects the formation of the blue complex and leads to under- or over-estimated free P concentrations (Jarvie et al., 2002; Kowalenko and Babuin, 2007; Kowalenko, 2008; Nagul et al., 2015; Anschutz and Deborde, 2016).

In this study, tests were performed using $CaHPO_4$ as a phosphate source, and the hydroponic method was compared with classic methodologies in solid and liquid media, for the selection of phosphate-solubilizing strains. The effects of the strains on plant growth promotion were evaluated. The methodology was tested using *Glycine max* plants as a model because their seedlings are easy to obtain and because of the current need for developing biotechnologies for the cultivation of this oilseed. In addition, the growth-promoting potential of the tested strains was compared with that of the commercial product Biomaphos®, which consisted of a mixture of *Bacillus megaterium* and *B. subtilis* bacteria. We hypothesized that the hydroponic system could be more efficient in selecting phosphate-solubilizing strains, which are plant growth promoters, independent of other nutrients. The hydroponic system requires the presence of a root system, which provides data related to the effect of the isolates on growth promotion and photochemical and photosynthetic performance. Furthermore, the effectiveness of this system was proposed based on the greater induction of plant-microorganism interactions, since in the water-plant condition, root exudates are easily adsorbed in the solution (Hoffland et al., 2006) and are freer to stimulate the tested microorganisms. This study proposed a more efficient approach for selecting strains with the potential to satisfy the current demand for bio-inputs applied to P availability in important crops, such as soybeans.

MATERIALS AND METHODS

Microbial Strains

The potential of eight rhizospheric or endophytic microbial strains was evaluated, with six previously isolated from *Hymenaea courbaril* (for further information see Rocha et al., 2020) and two from Arecaceae *Butia purpurascens* (for further information see da Silva et al., 2018) (**Table 1**). These strains currently belong to the microorganism collection of the Agricultural Microbiology Laboratory of the IFGoiano Rio Verde campus, Brazil. The potential of these strains was compared with that of the commercial product Biomaphos® (BIOMA, Brazil), which consisted of a mixture of BRM034840 and BRM033112-B strains from *B. megaterium* and *B. subtilis*. The bacterial strains were reactivated in nutrient agar medium (3 g of meat extract, 5 g of peptone, 25 g of agar, and H_2O qs 1 L) for 48 h at 35°C in an incubation chamber, and then reactivated in potato dextrose agar (PDA; infusion of 200 g of potato, 20 g of dextrose, and 15 g of agar) for 7 days at 35°C in an incubator.

TABLE 1 | Microbial strains were used to compare experimental methodologies for the evaluation of the solubilization capacity of calcium phosphate ($CaHPO_4$).

Strain	Type	Strain code
Penicillium sheari	Fungus	HSCR15-F(SC15)
Epicoccum keratinophilum	Fungus	HSCR4-F(SC4)
Hamigera insecticola	Fungus	BP33EF-F(33EF)
Codinaeopsis sp.	Fungus	BP328EF-F(328EF)
Bacillus cereus	Bacterium	HSCE5-B(SC5)
Bacillus thuringiensis	Bacterium	HSCR10-B(SC10)
Paenibacillus alvei	Bacterium	HPAR12-B(PA12)
Lysinibacillus fusiformis	Bacterium	HPAR26-B(PA26)
Bacillus megaterium and *Bacillus subtilis*	Bacteria	BRM034840 e BRM033112-B (Biomaphos®)

In the strain codes HSCR and HPAR, isolated from Hymenaea courbaril; BP, isolated from Butia purpurascens; E, endophytic; R, rhizospheric.

Qualitative Assessment of the Solubilization Capacity of $CaHPO_4$ in Solid Medium

Bacterial and fungal strains were inoculated in Petri dishes containing GELP culture medium (10 g glucose, 5 g peptone, 0.05 g yeast extract, and 15 g agar). We added 25 ml of calcium dichloride ($CaCl_2$) (10%) and 12.5 ml of dipotassium hydrogen phosphate (K_2HPO_4) (10%) to form an inorganic phosphate precipitate from $CaHPO_4$ (10%), as described by Sylvester-Bradley et al. (1982). The ability of the microorganism to solubilize $CaHPO_4$ was confirmed by observing a clear halo around the colony of the bacteria or fungus, in contrast to the opaque medium (Souchie et al., 2007). Plates containing GELP culture medium with $CaHPO_4$ added without inoculum were used as negative controls for solubilization.

The capacity of the strains to solubilize $CaHPO_4$ was compared by measuring the diameters of the solubilization zones (halos) around the colonies after 7 days of incubation. The solubilization index (SI) was calculated using the method proposed by Berraquero et al. (1976):

$$SI = \frac{(\text{total diameter including colony and halo})}{(\text{colony diameter})}$$

The SI of the strains was classified according to the methods of Silva Filho and Vidor (2000) as low ($SI < 2$), medium ($2 < SI < 3$), or high ($SI > 3$). The test was conducted in triplicate for each strain tested.

Quantitative Assessment of $CaHPO_4$ Solubilization in Liquid Medium

For this test, bacterial samples were grown under constant agitation using an orbital shaker (NT 712, NOVA TÉCNICA, Brazil) rotating at 90 rpm for 24 h at 30°C in 7 ml of liquid GL culture medium (10 g glucose, 2 g yeast extract). Then, 3 ml of the samples were aseptically removed from each culture to determine the optical density (OD) at 600 nm. All bacterial samples had their OD adjusted to 0.1 by dilution with saline solution (0.85%). Fungal samples were grown in a PDA medium for 4 days at 30°C. $CaHPO_4$ solubilization in liquid medium was quantified by inoculating 1 ml of the previously standardized bacterial culture in 10 ml of liquid GL medium, with 1.26 g L^{-1} of the $CaHPO_4$ phosphate source. For the evaluation of fungi, 5 mm diameter disks with mycelial growth were removed, which were inoculated in 10 ml of medium (one disk per glass). The cultures were agitated at 90 rpm and 30°C for 72 h. The test was performed in triplicate for each strain tested, using GL medium without inoculum as a negative control. After growth, the pH was measured, and the amount of inorganic P was determined using the vitamin C colorimetric method at 725 nm, according to the methods of Gadagi and Sa (2002).

The *in vitro* solubilization experiments were conducted in a completely randomized design, considering nine treatments with microorganisms (eight strains + Biomaphos®) and a control treatment (without inoculation). $CaHPO_4$ solubilization means and pH were subjected to a one-way ANOVA to evaluate only the treatment effect. When significant, the effects were evaluated using the Scott-Knott test at 5% significance probability.

In vivo Assessment of the Solubilizing Potential of $CaHPO_4$ Using a Hydroponic System

Inoculum Preparation

Bacterial inoculates were prepared in nutrient broth for 24 h at 30°C under constant agitation at 90 rpm. The cell concentration in each culture was estimated by CFU counting in nutrient agar and was standardized to 10^4 ml^{-1} using 0.85% saline solution. The fungal mycelia were cultivated in a PDA medium for 14 days at 30°C. Subsequently, the plates were superficially washed using 10 ml of 0.85% saline solution per plate, and the spore concentration was determined by counting them in a Neubauer chamber (hemocytometer) using an optical microscope (BA210, MOTIC, Canada) (40–100 × magnification). The spore concentration of the cultures was adjusted to 10^5 ml^{-1}.

Root Colonization and Microscopic Examination

This test was conducted to verify the colonizing potential of the strains to be tested in a hydroponic system. The test was conducted using *G. max* seeds of the Bonus 8579 RSF IPRO cultivar (BRASMAX, Brazil). The seeds were disinfected to remove epiphytes, successively washed in running water, and agitated in water and neutral detergent (Tween) for 5 min. Then, the seeds were immersed in 70% ethanol for 1 min, followed by immersion in sodium hypochlorite (2.5% active chlorine) for 1 min and 30 s, and then again in 70% ethanol for 30 s. Finally, the seeds were washed three times in autoclaved distilled water and planted in plastic trays containing autoclaved sand as substrate, where the seedlings remained for 7 days in a BOD Camera (SSBODU320, PROLAB, Brazil) at 25°C (77F) and 12/12 h photoperiod. During this period, the seedlings were aseptically watered once a day with sterilized water. The plants were then carefully removed from the sand, and the roots

were detached and washed four times with sterilized distilled water under vigorous agitation. The roots were then submerged in the previously prepared inoculum solutions and deposited in Petri dishes containing GELP medium. Plates containing roots immersed in autoclaved distilled water were used as a negative control and incubated at 28°C for 48 h. Subsequently, the roots were prefixed with glutaraldehyde, post-fixed with osmium tetraoxide, dehydrated in an ethanol series, transferred to amyl acetate, and critically dried in a dryer with carbon dioxide (CO_2), following the methodology described by Ghosh et al. (2016). Then, they were coated with gold using an ion jet to evaluate microbial colonization under a scanning electron microscope (Jeol JSM-IT300LV, JEOL USA, Inc., Peabody, MA, US).

Experiment in the Hydroponic System

The experiment was conducted in a greenhouse at the Plant Tissue Culture Laboratory of the IFGoiano Rio Verde campus (17° 48' 15.9' 'S – 50° 54' 19,5" W), from July to August 2020, under an average temperature of 26.85°C and relative humidity of 23.7%. Soybean seeds of the same cultivar were subjected to the same disinfestation and germination treatment in autoclaved sand, where the seedlings remained until they reached a mean size of 15 cm, and then transferred to 4 L pots containing the hydroponic nutrient solution proposed by Hoagland and Arnon (1950) with half ionic strength for 15 days of adaptation. After this period, the plants were subjected to a nutrient solution with full ionic strength.

The inoculation of microorganisms occurred during phase R5 of soybean development. For this, 10 ml of the previously prepared inoculate solutions were added to the nutrient solution along with 10 g L^{-1} of aseptic glucose to stimulate microbial growth in the nutrient solution. Biometric, physiological, and anatomical evaluations were conducted after 10 days of exposure to the tested strains. Plants grown in a nutrient solution without adding microorganisms and grown in a nutrient P-free solution (without the addition of $CaHPO_4$) were used as control treatments.

The *in vivo* experiment was conducted in randomized blocks, with nine treatments with microorganisms (eight strains + Biomaphos®) and two control treatments (plants grown in a nutrient solution without microorganisms and plants grown in P-free nutrient solution). All treatments were evaluated in five repetitions, with each repetition consisting of two plants per pot. The results obtained for biometric analyses, tissue P content, and physiological and anatomical analyses were subjected to ANOVA to evaluate the treatment effect. When significant, the effects were evaluated using the Scott-Knott test at 5% probability.

Subsequently, all variables were evaluated using a correlation matrix and combined in a principal component analysis (PCA). Since these variables had different measurement units, a correlation PCA was performed which was constructed using standardized data with a mean of 0 and a standard deviation of 1. The number of components was chosen as a function of the eigenvalues (>1) and explained variance (above 80%). The variables were also evaluated using Pearson's correlation coefficient, and the strength of the relationship was analyzed through R-values and the significance of the interaction at 5% probability. All statistical tests were performed in the R software version 4.0.4 (R Core Team, 2021), using the "ExpDes.pt" (Ferreira et al., 2014) and "FactoMineR" (Husson et al., 2010) packages.

Biometric and Tissue P Content Evaluations

The biometric variables plant height, stem diameter (SD), root length (RL), number of leaves (LN), and biomass were evaluated. For biomass evaluation, the plants were segmented into leaves, stems, and roots, and the material was dried in a forced-air oven at 65°C to a constant mass. Subsequently, the dry mass (DM) of each plant part was determined. The sum of the values corresponding to the biomass of each structural component of the plants (LDM + SDM + RDM) enabled the determination of the total DM (TDM).

Leaves, stems, and roots were oven-dried at 65°C until they reached a constant weight (Oven; SL-102/1152, SOLAB, Brazil) and crushed in a Willey mill with a 20 mm-mesh sieve (R-TE-680, TECNAL, Brazil). Finally, the P content was estimated according to the procedure described by Malavolta et al. (1997).

Anatomical Evaluation of the Root

The diameter of the root pot elements was evaluated as an indication of root development because it is commonly associated with P availability to plants (Rosolem and Marcello, 1998). Thus, root samples were fixed in glutaraldehyde solution (2.5%) and paraformaldehyde (4%) in sodium cacodylate buffer (pH 7.2) and added to 5 mM calcium chloride (Karnovsky, 1965). The roots were cross-sectioned into 5-μm-thick slices and stained with toluidine blue at pH 6.8 (O'Brien et al., 1964). In these sections, the diameter of the vessel elements was measured using the Anati Quanti 2 software (Aguiar et al., 2007). Each repetition was measured 15 times, and the treatments were evaluated in quintuplicate.

Gas Exchange

Gas exchange was evaluated from 7:00 AM to 10:00 AM on the third leaf counted from the apex of the plant using an infrared gas analyzer with a fluorometer (LI-6800xt, LI-COR Inc., Lincoln, USA) and photosynthetically active radiation (1,000 μmol photons m^{-2} s^{-1}) at a block temperature of 27°C and relative humidity of ∼70%. The net photosynthesis rate (*A*) (μmol CO_2 m^{-2} s^{-1}), stomatal conductance (g_{sw}) (mol of H_2O m^{-2} s^{-1}), transpiration (*E*) (H_2O m^{-2} s^{-1}), and internal carbon concentration (*Ci*) (mmol m^{-2} s^{-1}) were measured (see Hunt, 2003).

Photosynthetic Pigments

The concentration of photosynthetic pigments was evaluated using leaf disks (three fresh matter mass disks of 5 mm diameter each). These disks were covered with a DMSO solution and saturated with calcium carbonate ($CaCO_3$) (Santos et al., 2007). Subsequently, they were stored in tubes wrapped in Al foil for 24 h at 65°C. The absorbance of the obtained extract was determined by spectrophotometry at 664, 649, and 480 nm. Chlorophyll *a*, *b*, and total and carotenoid concentrations were

determined according to the methods described by Wellburn (1994).

Chlorophyll *a* Fluorescence

Chlorophyll *a* fluorescence OJIP transient was determined using a portable FluorPen FP 100 fluorometer (Photon Systems Instruments, Drasov, Czech Republic). The third leaf of all sample units was previously dark-adapted for 30 min for complete oxidation of the photosynthetic electron transport system. They were later subjected to a 3,000 μmol m^{-2} s^{-1} blue light pulse, with minimum fluorescence (F_0) and maximum fluorescence (F_M). These values were used to estimate several PSII bioenergetic indices, according to the methods described by Strasser et al. (2000). The values of the specific light absorption flow per reaction center (ABS/RC), energy flow captured per reaction center at $t = 0$ (TRo/RC), electron transport flow per reaction center (ETo/RC), specific energy dissipation flow at the level of the antenna complex chlorophylls (DIo/RC), photosynthetic performance index (Pi_Abs) that incorporates energy cascade processes from the first absorption events to PQ reduction, the maximum quantum yield of primary photochemistry (PHI_Po), the probability of an exciton moving an electron through the electron transport chain after quinone (PSI_O), and the quantum yield of electron transport (PHI_Eo) after dark adaptation of the leaves (30 min) were determined in this study.

Chlorophyll *a* fluorescence in *G. max* leaves was also evaluated using the modulated Imaging-PAM fluorometer to obtain fluorescence images. Initially, the initial fluorescence (F0) and maximum fluorescence (Fm) were determined in leaves pre-adapted to the dark for 30 min. Then, it was possible to calculate the potential quantum yield of photosystem II (PSII) (Genty et al., 1989). Sequentially, the fluorescence in the light-adapted sample before the saturation pulse (F) and Fm in a light-adapted sample (Fm') were used to obtain the effective quantum yield of photochemical energy conversion in PSII, $\Phi II = (Fm'\text{-}F)/Fm'$.

TABLE 2 | Evaluation of calcium phosphate ($CaHPO_4$) solubilization in solid medium (GELP) by rhizospheric or endophytic bacterial and fungal strains from *Hymenaea courbaril* or endophytic bacterial and fungal strains from *Butia purpurascens*.

Microorganisms	Solubility index	Solubilization capacity
SC10	1.25 a	Low
PA12	NS	NS
Biomaphos®	1.27 a	Low
SC5	1.14 a	Low
SC15	NS	NS
PA26	NS	NS
SC4	NS	NS
33EF	NS	NS
328EF	NS	NS
Control	NS	NS

Means followed by the same lowercase letter in the column do not significantly differ according to the Scott-Knott test at 5% probability. NS, did not form a solubilization halo.

TABLE 3 | Evaluation of calcium phosphate ($CaHPO_4$) solubilization in liquid medium (GL) by rhizospheric or endophytic bacterial and fungal strains from *Hymenaea courbaril* or endophytic bacterial and fungal strains from *Butia purpurascens*.

Treatments	pH	Soluble P (mg L^{-1})
SC10	4.79 c	5.53 a
PA12	4.80 c	5.62 a
Biomaphos®	4.89 c	4.61 b
SC5	4.96 b	5.13 a
SC15	5.28 b	3.15 c
PA26	5.48 b	3.69 b
SC4	5.53 b	3.18 c
33EF	6.37 a	1.82 d
328EF	6.49 a	1.48 d
Control	6.73 a	0.33 e

Means followed by the same lowercase letter in the column did not differ significantly according to the Scott-Knott test at 5% probability.

RESULTS

In vitro Experiment: Solid Culture Medium

In a solid medium, only the *B. thuringiensis* (SC10), *B. megaterium*, *B. subtilis* (Biomaphos®), and *B. cereus* (SC5) strains demonstrated potential for $CaHPO_4$ solubilization through the production of solubilization halos. The solubilizing capacity of these strains was classified as low (SI < 2) (**Table 2**).

In vitro Experiment: Liquid Culture Medium

B. thuringiensis (SC10), *Paenibacillus alvei* (PA12), and *B. cereus* (SC5) strains showed the highest solubilization efficiency in a liquid medium containing $CaHPO_4$ as a phosphate source. All microbial strains reduced the pH of the medium compared with the control without inoculation, except for fungal *Hamigera insecticola* (33EF) and *Codinaeopsis* sp. (328EF) strains, which presented the lowest solubilization means (**Table 3**).

Root Colonization

All bacteria and fungi evaluated demonstrated the ability to effectively colonize the root system, forming large superficial aggregates (**Supplementary Figures 1, 2**). Electron microscopy analyses showed the formation of protein crystals in *B. thuringiensis* (SC10) colonies and bacterial spores in *Lysinibacillus fusiformis* (PA26) root colonies (**Figures 1A–D**). They also found a large concentration of fungal spores in *Codinaeopsis* sp. (328E) colonies (**Figures 1E,F**).

In vivo Experiment: Hydroponic Cultivation

Evaluation of Growth Promotion

The exposition of *G. max* seedlings to the microorganisms tested did not affect the height of the plants; the means ranged between a minimum of 84.8 cm in plants inoculated with *Epicoccum keratinophilum* (SC4) and a maximum of 93.8 cm in plants treated with *P. alvei* (PA12). However, the development of plants

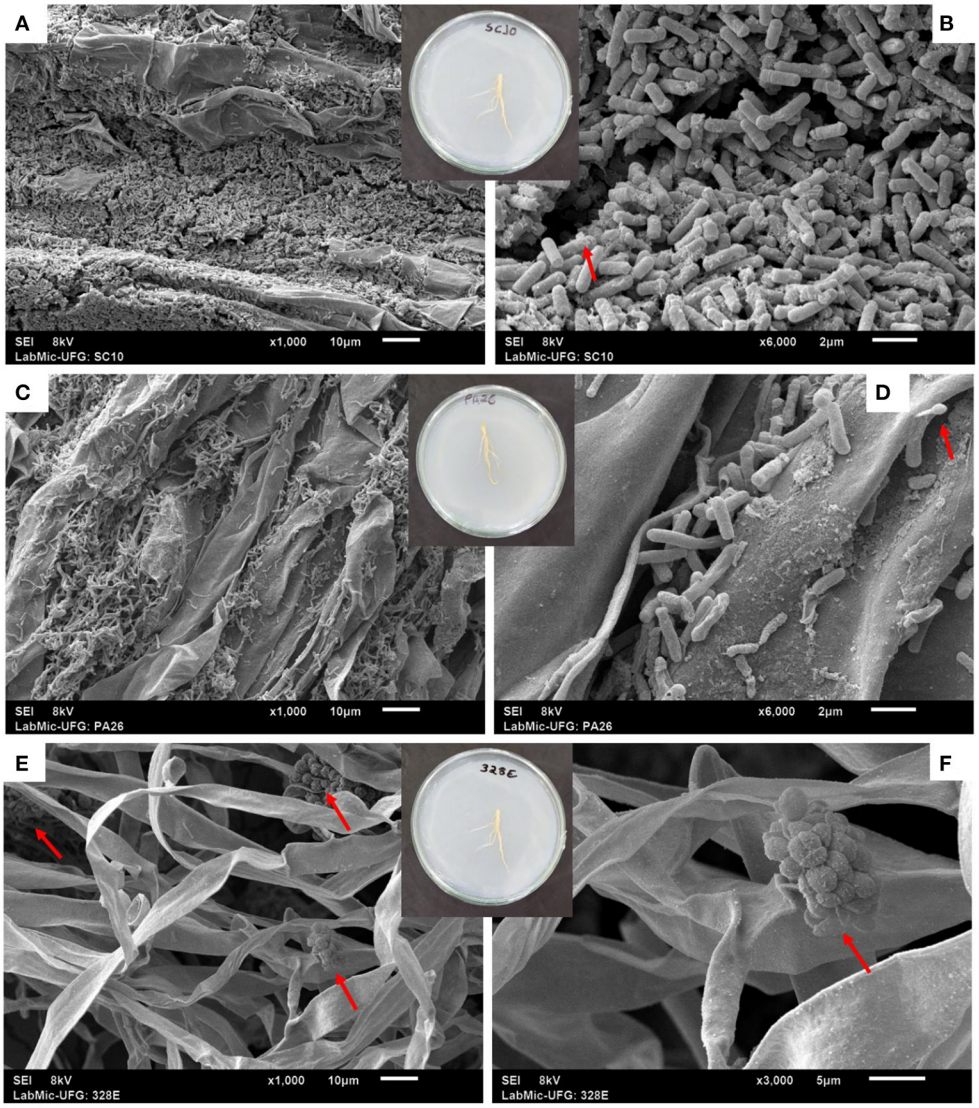

FIGURE 1 | Microscopic aspects of root colonization in soybean plants (*Glycine max)* treated with the bacterial strains SC10 = *Bacillus thuringiensis* **(A,B)** and PA26 = *Lysinibacillus fusiformis* **(C,D)**, and the fungal strain 328EF = *Codinaeopsis* sp. **(E,F)**. Red arrows indicate the presence of protein crystals **(B)** and spores **(D–F)**.

in a control solution without P was significantly affected by the unavailability of this element, with a mean height for these plants of only 64.25 cm (**Supplementary Figure 3A**). Similar results were obtained for RL, which remained statistically equal in plants inoculated with different microorganisms and in a solution without microorganisms, with the means ranging between a minimum of 46.5 cm in plants inoculated with *E. keratinophilum* (SC4) and without microorganisms and a maximum of 93.8 cm in plants treated with *P. alvei* (PA12). Plants kept in a nutrient solution without P also had their RL affected, with a mean of 34 cm (**Supplementary Figure 3B**).

Standard deviation means also followed the same pattern: not differing between plants grown in a solution without microorganisms and inoculated plants, ranging from a minimum of 0.38 mm in non-inoculated plants to a maximum of 0.46 mm in plants treated with *P. alvei* (PA12). As described for the previous variables, plants subjected to a nutrient solution without P also presented low SD development (0.16 mm) (**Supplementary Figure 3C**). However, the LN was significantly affected by the inoculation treatments, with the highest values for plants inoculated with *P. alvei* (PA12), *L. fusiformis* (PA26), and *Penicillium sheari* (SC15) (21.2, 20.2, and 19.6 leaves, respectively). The absence of P in the solution also affected the LN in the plants, with a mean of only 3.25 leaves in plants developed with this treatment (**Figure 2A**).

The dry matter mass of leaves, stems, and roots did not differ between plants inoculated with microorganisms and plants grown in a solution without microorganisms. Leaf dry matter

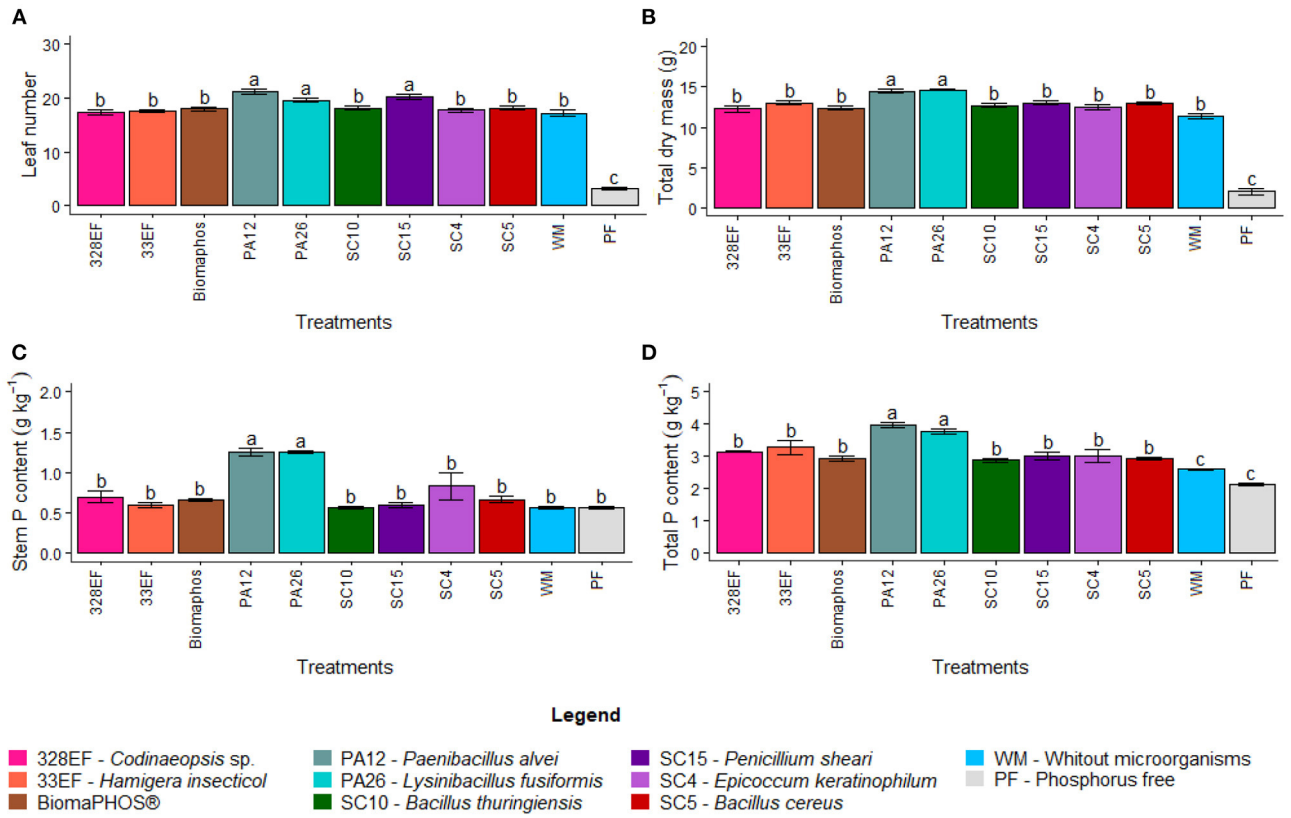

FIGURE 2 | Number of leaves **(A)**, total dry mass **(B)**, P tissue content in the stem **(C)**, and total P tissue content **(D)** in soybean plants (*Glycine max)* grown in nutrient solution providing calcium phosphate ($CaHPO_4$) as the phosphate source and inoculated with four bacterial strains and four fungal strains. Means followed by the same lowercase letter do not differ from one another according to the Scott-Knott test at 5% probability.

means varied between a minimum of 4.39 g in non-inoculated plants and a maximum of 5.2 g in plants treated with *L. fusiformis* (PA26) (**Supplementary Figure 4A**). Shoot dry matter mass followed a similar trend, ranging from a minimum of 4.05 g in non-inoculated plants and a maximum of 5.31 g in plants treated with *L. fusiformis* (PA26) (**Supplementary Figure 4B**). Root dry matter also followed the pattern described above, ranging from a minimum of 2.91 g in non-inoculated plants to a maximum of 4.12 g in plants treated with *L. fusiformis* (PA26) (**Supplementary Figure 4C**). However, plants grown in a solution without P presented the lowest values for LDM, SDM, and RDM (0.196, 1.036, and 0.847 g, respectively).

For TDM, the highest values were observed for plants inoculated with *P. alvei* (PA12) and *L. fusiformis* (PA26) (14.63 and 14.43 g, respectively). Plants grown in solution without microorganisms had a mean of 11.35 g TDM, but plants kept in solution without P had the lowest values (2.08 g) (**Figure 2B**).

P Absorption Performance Evaluation in P Tissue Content

Phosphorus content did not differ in leaves of plants subjected to the different treatments evaluated, and the means ranged between a minimum of 0.67 g in plants grown without P and a maximum of 1.30 g kg^{-1} in plants treated with *P. alvei* (PA12) (**Supplementary Figure 5A**). Stem P content was affected by the inoculation treatments, being higher in plants inoculated with *P. alvei* (PA12) and *L. fusiformis* (PA26) (1.25 and 1.25 g kg^{-1}, respectively) (**Figure 2C**). The P content in roots was higher for plants inoculated with *Codinaeopsis* sp. (328EF), *H. insecticola* (33EF), *P. alvei* (PA12), *L. fusiformis* (PA26), *B. thuringiensis* (SC10), and *P. sheari* (SC15) (1.50, 1.57, 1.40, 1.45, 1.35, and 1.35 g kg^{-1}, respectively) (**Supplementary Figure 5B**). The evaluation of total P content showed the highest means in plants inoculated with the bacteria *P. alvei* (PA12) and *L. fusiformis* (PA26) (3.95 and 3.77 g kg^{-1}), while the lowest means were verified in plants growing in a solution without microorganisms (2.58 g kg^{-1}) and P-free (2.13 g kg^{-1}) (**Figure 2D**).

Photosynthetic Performance Assessment: Gas Exchange

Microbial inoculation significantly affected gas exchange rates in *G. max*. The net CO_2 assimilation rate (*A*) was higher in plants inoculated with the strains *P. alvei* (PA12), *L. fusiformis* (PA26), *B. cereus* (SC5), and *P. sheari* (SC15) at 8.41, 7.43, 9.65, and 8.78 μmol CO_2 m^{-2} s^{-1}, respectively (**Figure 3A**). However, these plants presented low rates of internal CO_2 (*Ci*) concentration, respectively 235.56, 219.9, 230.85, and 230.24 mmol m^{-2} s^{-1}, while the highest means were verified in plants grown in a

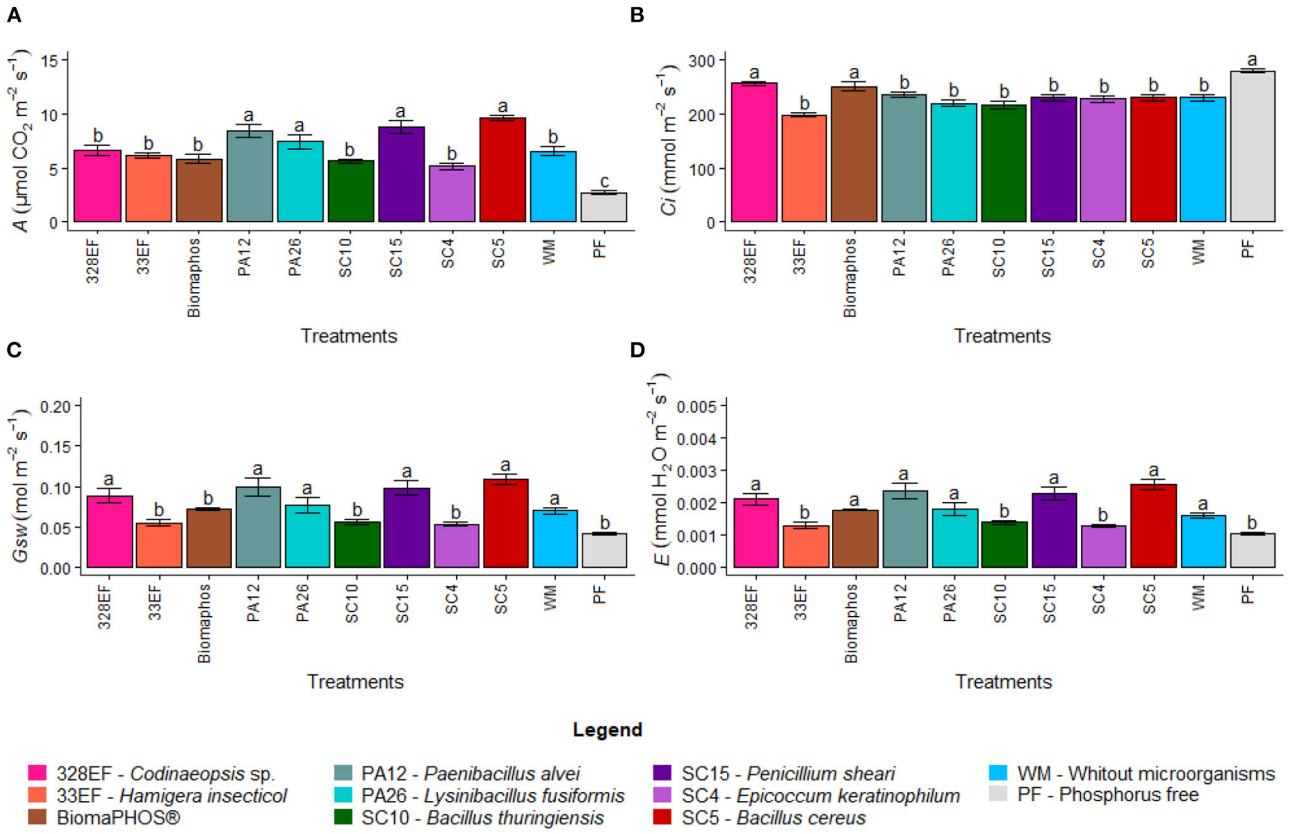

FIGURE 3 | Photosynthetic rate (*A*) **(A)**, internal CO_2 concentration (*Ci*) **(B)**, stomatal conductance (*Gsw*) **(C)**, and transpiration rate (*E*) **(D)** in soybean plants (*G. max)* grown in nutrient solution providing calcium phosphate ($CaHPO_4$) as a phosphate source and inoculated with four bacterial strains and four fungal strains. Means followed by the same letter do not differ from one another according to the Scott-Knott test at 5% probability.

solution without P (280.32 mmol m^{-2} s^{-1}) and inoculated with *Necropsied* sp. (328EF) and Biomaphos® (256.96 and 251.16 mmol m^{-2} s^{-1}) (**Figure 3B**). A behavior similar to that observed for *A* was observed for stomatal conductance (*Gsw*), with the highest means obtained for inoculation treatments with *Necropsied* sp. (328EF), *P. alvei* (PA12), *L. fusiformis* (PA26), *P. sheari* (SC15), and *B. cereus* (SC5) strains (0.072, 0.099, 0.077, 0.098, and 0.109 mol m^{-2} s^{-1}, respectively), and for plants grown in solution without microorganisms (0.07 mol m^{-2} s^{-1}) (**Figure 3C**). The transpiration rate (*E*) was higher in plants grown in a solution without microorganisms (0.0016) and inoculated with *Necropsied* sp. (328EF), Biomaphos®, *P. alvei* (PA12), *L. fusiformis* (PA26), *P. sheari* (SC15), and *B. cereus* (SC5) at 0.0021, 0.0018, 0.0024, 0.0018, 0.0023, and 0.0026 *E,* respectively (**Figure 3D**).

Photosynthetic Performance Assessment: Photosynthetic Pigments

Chlorophyll *a* content increased in plants inoculated with *H. insecticola* (33EF), *P. alvei* (PA12), *L. fusiformis* (PA26), *P. sheari* (SC15), *E. keratinophilum* (SC4), and *B. cereus* (SC5) at 42.437, 49.240, 47.717, 47.571, 41.469, and 46.052 μmol m^{-2}, respectively (**Figure 4A**). Chlorophyll *b* content also increased following a pattern similar to that observed for chlorophyll *a*, but it was higher in plants subjected to inoculation with *Necropsied* sp. (328EF), *H. insecticola* (33EF), *P. alvei* (PA12), *L. fusiformis* (PA26), *P. sheari* (SC15), *E. keratinophilum* (SC4), and *B. cereus* (SC5) strains (11.644, 13.723, 13.069, 13.726, 12.231, 12.269, and 12.704 μmol m^{-2}) (**Figure 4B**).

Microbial inoculation also affected the carotenoid content, which was higher in plants inoculated with *H. insecticola* (33EF), *P. alvei* (PA12), *L. fusiformis* (PA26), *P. sheari* (SC15), and *B. cereus* (SC5), with mean values of 10.458, 12.275, 12.084, 11.034, and 11.382 μmol m^{-2} (**Figure 4C**). Similar to other chlorophylls, the total chlorophyll content varied, with the highest means obtained in plants treated with *H. insecticola* (33EF), *P. alvei* (PA12), *L. fusiformis* (PA26), *P. sheari* (SC15), *E. keratinophilum* (SC4), and *B. cereus* (SC5) (56.161, 62.309, 61.444, 59.802, 53.738, and 58.756 μmol m^{-2}). However, much lower mean values were observed in plants grown in a solution without P (33.832 μmol m^{-2}) (**Figure 4D**).

Photosynthetic Performance Assessment: Chlorophyll a Fluorescence

As expected, the specific energy flows of the active reaction centers ABS/RC and DIo/RC were similarly affected by microbial

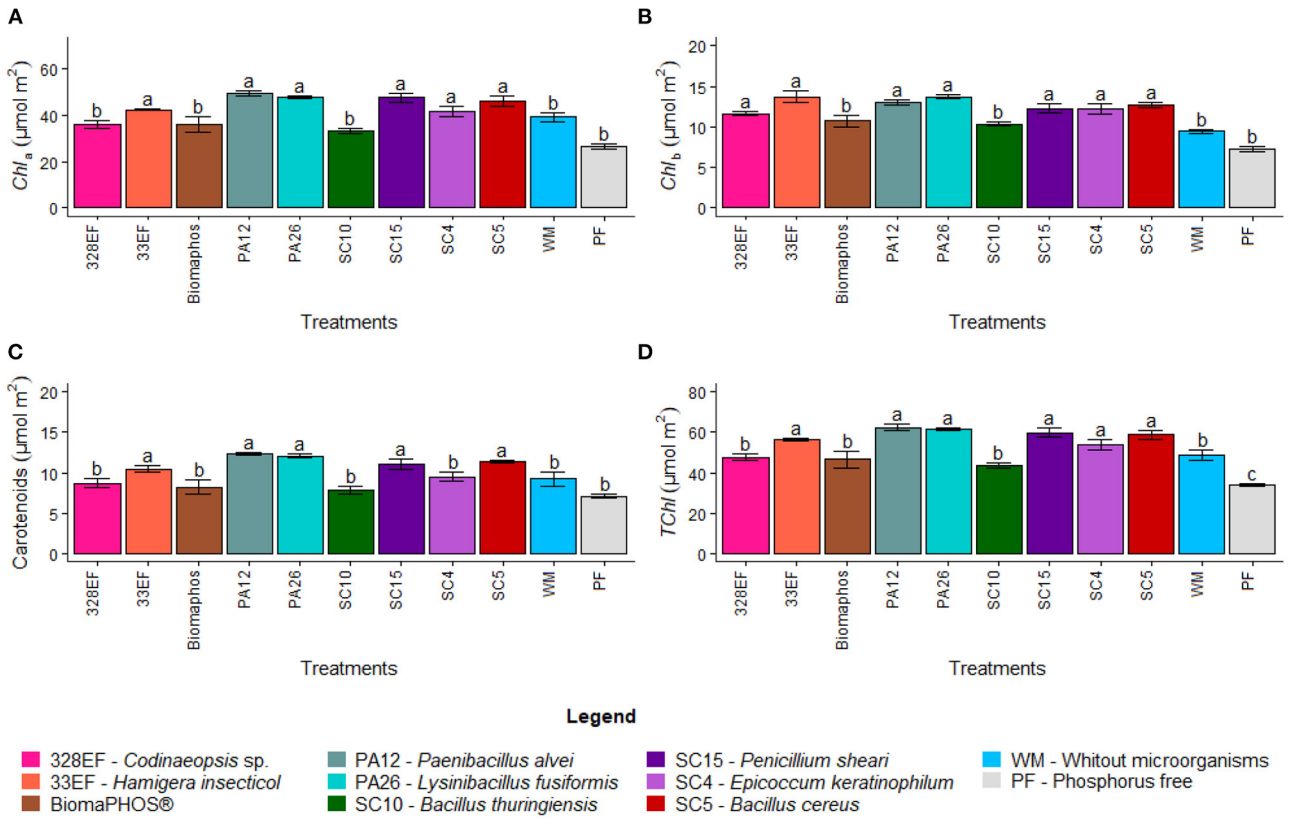

FIGURE 4 | Chlorophyll *a* content **(A)**, chlorophyll *b* content **(B)**, carotenoid content **(C)**, and total chlorophyll **(D)** in soybean plants (*G. max*) grown in nutrient solution providing calcium phosphate ($CaHPO_4$) as a phosphate source and inoculated with four bacterial strains and four fungal strains. Means followed by the same letter do not differ from one another according to the Scott-Knott test at 5% probability.

inoculation; therefore, the lowest mean ABS/RC values were observed in plants grown with the microorganisms *P. alvei* (PA12), *L. fusiformis* (PA26), *B. thuringiensis* (SC10), *P. sheari* (SC15), and *B. cereus* (SC5) (2.986, 2.962, 3.127, 2.989, and 2.859, respectively), as well as in plants grown in a solution without microorganisms (2.935) (**Figure 5A**). The lowest mean DIo/RC values were obtained in plants subjected to the same treatment sequence as above (0.714, 0.686, 0.842, 0.796, 0.660, and 0.667, respectively) (**Figure 5B**). The means observed for TRo/RC and ETo/RC were not affected by any of the evaluated treatments. TRo/RC values ranged from a minimum of 2.193 in plants inoculated with *P. sheari* (SC15) and a maximum of 2.546 in plants treated with *H. insecticola* (33EF), whereas ETo/RC means varied between a minimum of 0.985 in plants grown in nutrient P-free solution and a maximum of 1.384 in plants treated with the fungus *H. insecticola* (33EF) (**Supplementary Figures 6A,B**).

The kinetic parameters of Chl *a* fluorescence were also significantly affected by inoculation with microorganisms. The maximum quantum yield of primary photochemistry (Phi_Po) was higher for plants inoculated with *P. alvei* (PA12), *L. fusiformis* (PA26), and *B. cereus* (SC5) (0.763, 0.769, and 0.769, respectively), as well as in plants grown in a solution without microorganisms (0.752) (**Figure 5C**). The probability of an exciton moving an electron through the electron transport chain after quinone (Qa) (Psi_o) was reduced in plants inoculated with *Codinaeopsis* sp. (328EF) (0.443) and under P-free solution (0.406) (**Supplementary Figure 6C**). The means observed for the quantum yield of electron transport (Phi_Eo) followed the same pattern reported previously for Psi_o, with reduced values under *Codinaeopsis* sp. (328EF) (0.323) and P-free solution (0.277) (**Supplementary Figure 6D**). The photosynthetic performance index (Pi_ABS) was higher in plants inoculated with *P. alvei* (PA12), *L. fusiformis* (PA26), and *B. cereus* (SC5) (1.244, 1.289, and 1.255), suggesting that these plants have better performance in converting light energy into chemical energy (**Figure 5D**).

Fluorescence imaging analyses confirmed the superiority of the behavioral pattern of chlorophyll *a* fluorescence in plants inoculated with *P. alvei* (PA12), *L. fusiformis* (PA26), and *B. cereus* (SC5) and the inferiority of the pattern observed in plants grown in a P-free solution, as well as in plants inoculated with *E. keratinophilum* (SC4), *Codinaeopsis* sp. (328EF), and *H. insecticola* (33EF) (**Figure 6**).

Assessment of Anatomical Performance: Root Anatomy

The inoculation treatments affected the diameter of the root vessel elements. Therefore, the highest means were observed in plants inoculated with *P. alvei* (PA12), *L. fusiformis* (PA26),

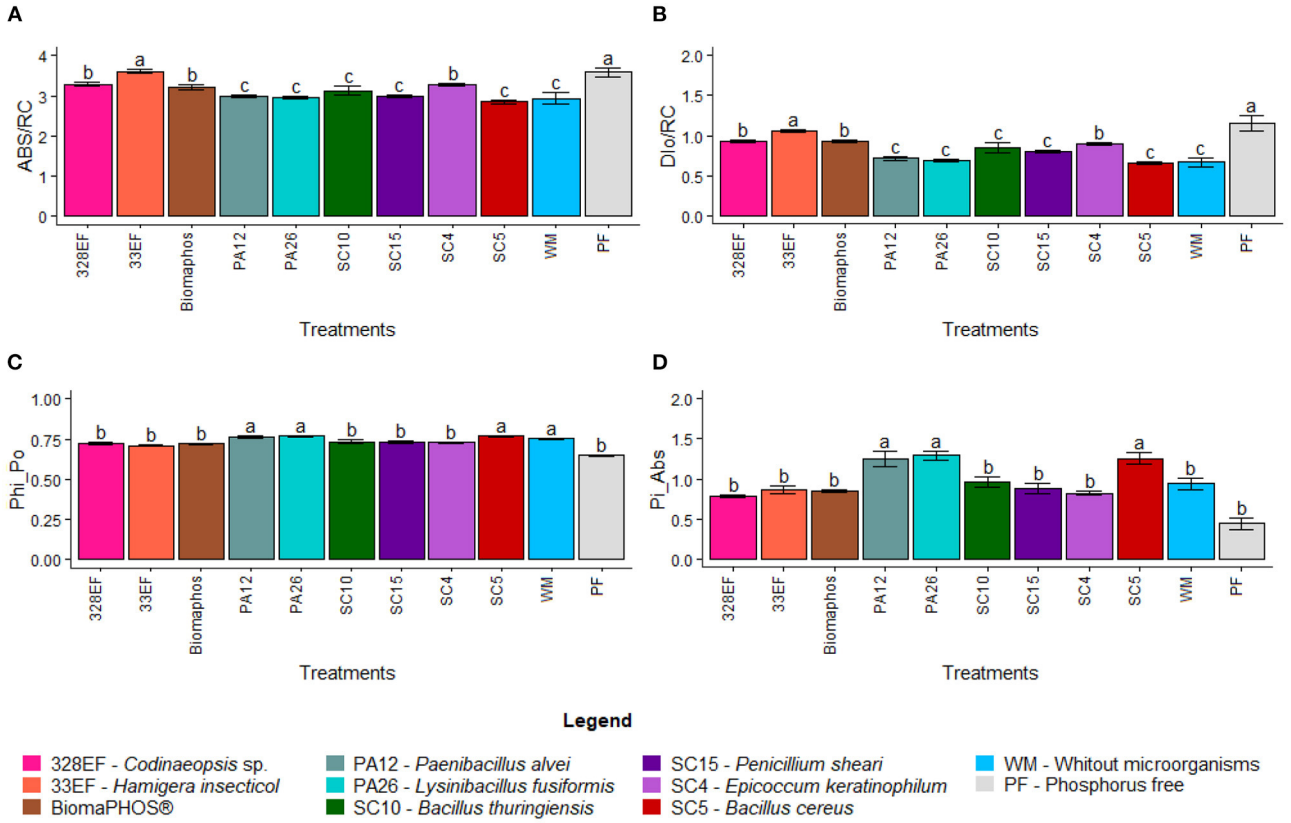

FIGURE 5 | Absorption flow by RC (ABS/RC) **(A)**, specific energy dissipation flow (DIo/RC) **(B)**, the maximum quantum yield of primary photochemistry (PHI_Po) **(C)**, and photosynthetic performance index (Pi_Abs) **(D)** in soybean plants (*G. max)* grown in nutrient solution providing calcium phosphate ($CaHPO_4$) as a phosphate source and inoculated with four bacterial strains and four fungal strains. Means followed by the same letter do not differ from one another according to the Scott-Knott test at 5% probability.

P. sheari (SC15), *E. keratinophilum* (SC4), and *B. cereus* (SC5) (55.383, 52.223, 49.943, 49.867, and 49.32 μm, respectively). In contrast, the lowest means were observed in plants grown in a P-free solution (28.787 μm), followed by a solution without microorganisms (39.91 μm) (**Figure 7**).

Anatomical analyses showed superior development of vessel elements and root caliber of plants treated with *P. alvei* (PA12) and *L. fusiformis* (PA26) strains. Root development was compromised in plants grown in a P-free solution, as well as in plants not subjected to microbial action (**Figure 8**).

PCA and Correlation Between Variables

The two-dimensional graph of principal components showed a negative correlation between the parameters DIo/RC, ABS/RC, TRo/RC, and *Ci* and the other biometric parameters: fluorescence, photosynthetic pigment content, and gas exchange, signaling the means for plants subjected to *E. keratinophilum* (SC4), *Codinaeopsis* sp. (328EF), Biomaphos®, and *H. insecticola* (33EF); plants grown in P-free solution accounted for most of the variation found in these variables. Thus, these plants were mainly associated with negative photosynthetic performance indices. On the other hand, the means verified in plants inoculated with *P. alvei* (PA12), *L. fusiformis* (PA26), and *B. cereus* (SC5) defined most of the variation in growth parameters, P content, photosynthetic performance, and photosynthetic pigments. These symbiotic microorganisms seem to improve the overall performance of the inoculated *G. max* plants (**Figure 9A**). The negative correlation between DIo/RC, ABS/RC, TRo/RC, and *Ci* means and the other biometric parameters (fluorescence, photosynthetic pigment content, and gas exchange) was more evident when the graphic pattern of the correlations between all variables was analyzed (**Figure 9B**).

DISCUSSION

Solubilization Results Obtained Using *in vitro* Methodologies Are Not Consistent With the Hydroponic System

Tests conducted in solid medium attested to the solubilizing potential of *B. thuringiensis* (SC10), *B. cereus* (SC5), and Biomaphos®, while in a liquid medium, the capacity was observed for *B. thuringiensis* (SC10), *P. alvei* (PA12), and *B. cereus* (SC5). The superposition of the two strains in these results

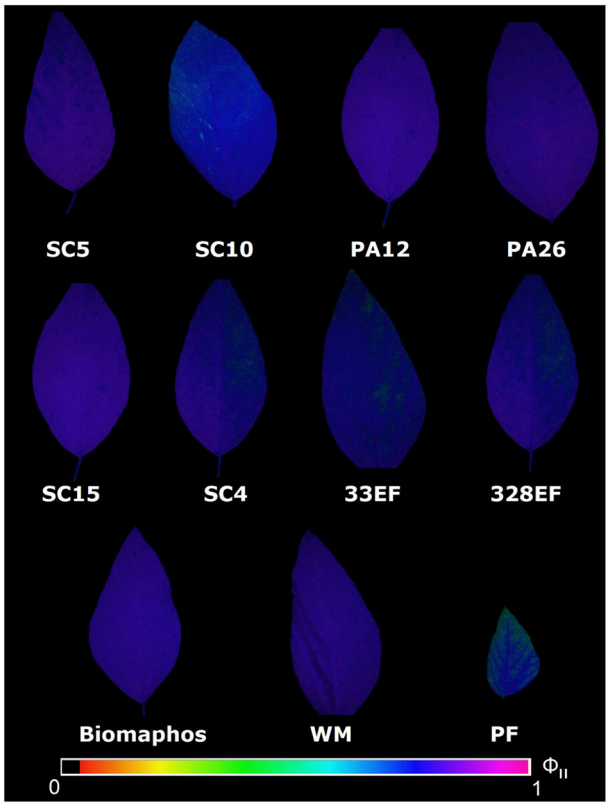

FIGURE 6 | Fluorescence images of chlorophyll-*a* obtained for the effective quantum yield of photochemical energy conversion in PSII (ΦII) in leaves of *Glycine max* grown in nutrient solution providing calcium phosphate ($CaHPO_4$) as a phosphate source and inoculated with four bacterial strains and four fungal strains. SC5, *Bacillus cereus*; SC10, *B. thuringiensis;* PA12, *Paenibacillus alvei*; PA26, *Lysinibacillus fusiformis*; SC15, *Penicillium sheari*; SC4, *Epicoccum keratinophilum*; 33EF, *Hamigera insecticola*; 328E, *Codinaeopsis* sp.; Biomaphos®, *B. megaterium* and *B. subtilis*; WM, without microorganisms; PF, phosphorus-free.

showed a low coherence between these two methodologies. However, *in vivo* analysis using the hydroponic system showed that *P. alvei* (PA12) and *L. fusiformis* (PA26), strains not shown to solubilize $CaHPO_4$ in any of the *in vitro* tests were more efficient at promoting growth and providing free P to the plant, which was demonstrated by the higher total P content in *G. max* tissues. In fact, *in vitro* solubilizing potential assessments were susceptible to the influence of many factors, as they significantly modify the living conditions of microorganisms. The growth temperature, pH, and nutritional composition of the culture medium could affect growth and metabolism (e.g., Gibson and Mitchell, 2004; Walpola et al., 2012; Tan and Ramamurthi, 2014; Yang et al., 2018), including the ability of isolates to produce organic acids or phosphatase enzymes directly associated with the potential of the microorganism to release P from forms where it is immobilized as $CaHPO_4$, $Ca_3(PO_4)_2$, $AlPO_4$, and $FePO_4$.

In general, solubilization in a liquid culture medium is considered more reliable, as it is a quantitative methodology (Sousa et al., 2016). In this methodology, free P could be quantified, and the access of organic acids and phosphatase enzymes to the phosphate source was more direct. However, the absence of a host and the impossibility of quantifying the actual P absorbed by the plant made this methodology questionable. Therefore, the use of *G. max* as a model for growth, tissue content, and photosynthetic and anatomical performance evaluations characterized *P. alvei* (PA12) and *L. fusiformis* (PA26) strains was more effective in the solubilization of $CaHPO_4$ because of its general effects on general growth promotion.

Paenibacillus is one of the Firmicutes genera predominantly found in association with plants (Yadav et al., 2017), and the potential of *P. alvei* has already been described in the literature as a disease suppressor and an inducer of crop growth and yield (Schoina et al., 2011; Kumar et al., 2012; Kalaiselvi et al., 2019). *Lysinibacillus* species have also drawn attention as effective bioremediation, biostimulant, and biocontrol agents (Ahsan and Shimizu, 2021). In the studies

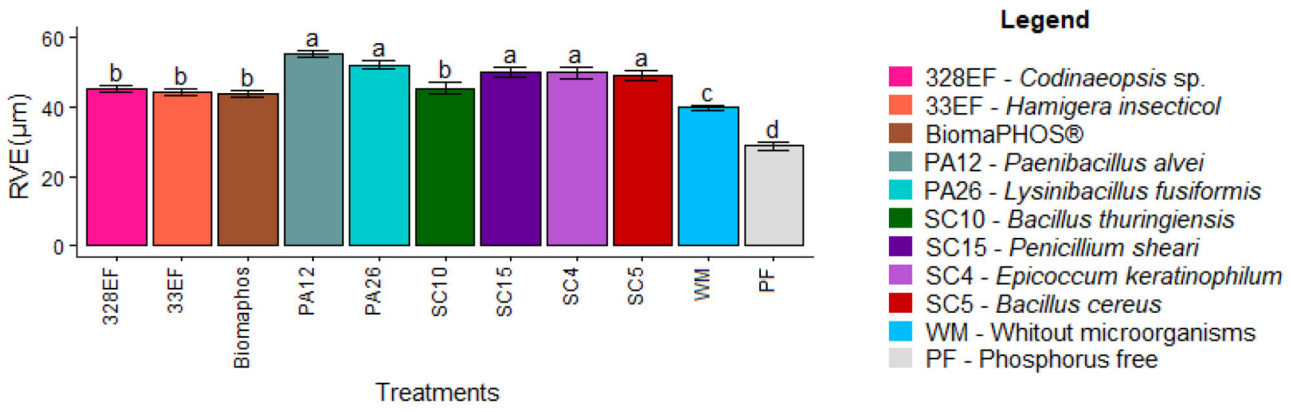

FIGURE 7 | Diameter of root vessel elements (RVE) in soybean plants (*G. max*) cultivated in nutrient solution providing calcium phosphate ($CaHPO_4$) as a phosphate source and inoculated with four bacterial strains and four fungal strains. Means followed by the same letter do not differ from one another according to the Scott-Knott test at 5% probability.

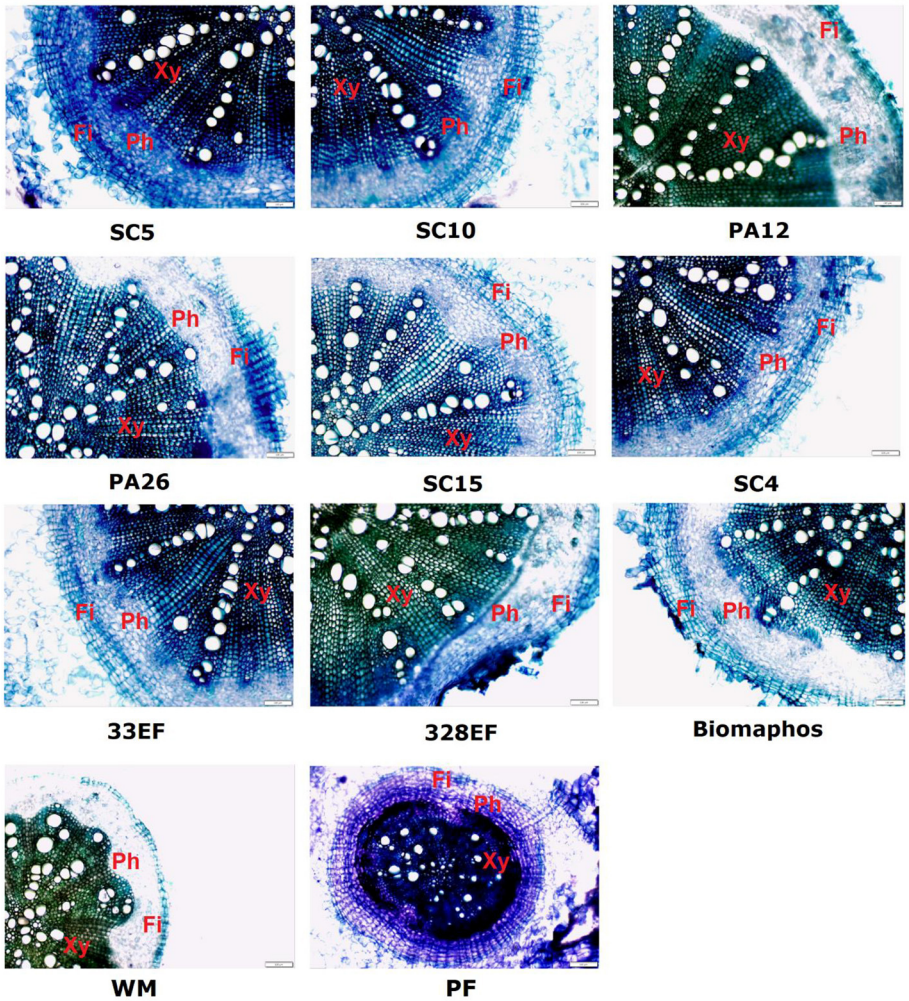

FIGURE 8 | Cross-sections showing different anatomical regions (Xy, Xylem; Ph, Phloem; Fi, Fibers) of soybean roots (*G. max*) grown in nutrient solution providing calcium phosphate ($CaHPO_4$) as a phosphate source and inoculated with four bacterial strains and four fungal strains. SC5, *B. cereus*; SC10, *B. thuringiensis*; PA12, *P. alvei*; PA26, *L. fusiformis*; SC15, *P. sheari*; SC4, *E. keratinophilum*; 33EF, *H. insecticola*; 328EF, *Codinaeopsis* sp.; Biomaphos®, *B. megaterium* and *B. subtilis*; WM, without microorganisms; PF, phosphorus-free.

by Vendan et al. (2010) and He et al. (2014), *L. fusiformis* was described as an effective phosphate solubilizer, although other functional traits have already been associated with this species, such as auxin synthesis and fungal biocontrol (Hanh and Mongkolthanaruk, 2017; Passera et al., 2021). Our work corroborated the direct association between these species and plant growth promotion.

The Hydroponic System Allows the Association of Phosphate Solubilization With Growth Promotion and Improved Photosynthetic and Anatomical Performance

The inoculation of *P. alvei* (PA12) and *L. fusiformis* (PA26) strains in the nutrient solution resulted in higher P absorption by *G. max* plants, and this better nutritional aspect improved growth, such as increased LN and TDM. Some studies have confirmed that solubilizing strains improve the nutritional status of plants, which results in increased chlorophyll concentrations and improved gas exchange parameters (Singh et al., 2018; Linu et al., 2019; Liu et al., 2020; Borowiak et al., 2021).

Plants inoculated with *P. alvei* (PA12) and *L. fusiformis* (PA26) strains also showed improved photosynthetic rates compared with plants grown in a solution without microorganisms. High *A* values are closely related to high RuBisCO activity (Bowes, 1991). Studies have suggested that an optimal P supply increases RuBisCO concentration and activity in leaves (Warren and Adams, 2002; Lin et al., 2009; e.g., Alori et al., 2017; Wang et al., 2018). Chu et al. (2018) demonstrated that decreased photosynthetic rates in *G. max* could be due

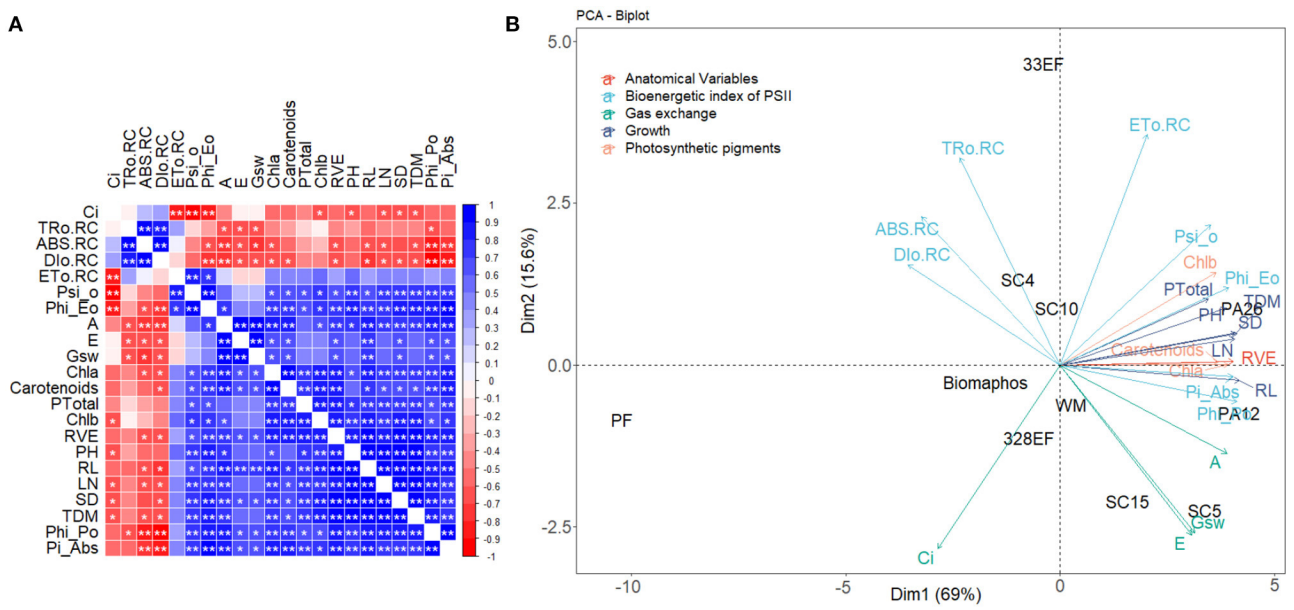

FIGURE 9 | Analysis of the main components of growth variables, photosynthetic pigments, gas exchange, chlorophyll-*a* fluorescence parameters, and anatomical development of root vessel elements **(A)** and correlations between the means observed for these variables **(B)** in soybean plants (*Glycine max*) grown in nutrient solution providing calcium phosphate ($CaHPO_4$) as a phosphate source and inoculated with four bacterial strains and four fungal strains. SC5, *B. cereus*; SC10, *B. thuringiensis*; PA1, *P. alvei*; PA26, *L. fusiformis*; SC15, *P. sheari*; SC4, *E. keratinophilum*; 33EF, *H. insecticola*; 328EF, *Codinaeopsis* sp.; Biomaphos®, *B. megaterium* and *B. subtilis*; WM, without microorganisms; PF, phosphorus-free.

to the stress caused by low P availability, as it participates in the structural regulation of the leaf, ATP synthesis, CO_2 absorption and transport, photosynthetic electron transport, and determination of the levels of enzymes related to the Calvin cycle. Thus, phosphate-solubilizing microorganisms can play an important role in photosynthetic performance by increasing P availability for plants (e.g., Wu et al., 2019; Anbi et al., 2020).

The inoculation of *G. max* with *P. alvei* (PA12) and *L. fusiformis* (PA26) bacteria also resulted in increased concentrations of photosynthetic pigments compared with plants that grew without microbial inoculation or P administration. These solubilizing strains ensured the necessary supply for pigment synthesis by increasing P release and absorption by plants. Some studies have reported that P deficiency decreases chlorophyll synthesis (Choi and Lee, 2012; Viégas et al., 2018), and that root colonization by growth-promoting microorganisms, such as phosphate solubilizers, can increase the synthesis of carotenoids (Vafadar et al., 2014; Chen et al., 2017), and plant resistance to biotic and abiotic stress factors (Vafadar et al., 2014) by protecting the photosynthetic apparatus, reducing photodamage, and photoinhibition effects (Sharma et al., 2015; Uarrota et al., 2018). Furthermore, microorganisms can affect the N_2 fixation process and the synthesis of growth-promoting substances and other compounds, such as auxins, which also have a positive effect on photosynthetic pigment production (Bashan and De-Bashan, 2010; Ahemad and Kibret, 2014; Santos et al., 2019). Phosphate-solubilizing microorganisms influence some growth-associated compounds, such as cytokinins (Abbamondi et al., 2016; Kudoyarova et al., 2017), which have a positive effect on chlorophyll biosynthesis, delaying senescence, and programmed death processes (Kunikowska et al., 2013; Zwack and Rashotte, 2013; Danilova et al., 2020; Zhang et al., 2021). Jinal et al. (2021) demonstrated that inoculation of maize seeds with *Lysinibacillus* can improve the growth and synthesis of chlorophylls-a and -b. The effects observed on the concentration of photosynthetic pigments in *G. max*, induced by *P. alvei* (PA12) and *L. fusiformis* (PA26) may be associated with the phosphate solubilizer and phytohormone producer potential (Vendan et al., 2010; Hanh and Mongkolthanaruk, 2017) of these species.

In general, plants treated with *P. alvei* (PA12) and *L. fusiformis* (PA26) absorbed more P, which is an adaptive reflection of the increased diameter of RVE. The roots were efficiently colonized by these bacteria. Microbial colonization is commonly related to increased size and density of the primary root and root hairs (Verbon and Liberman, 2016), which are important for increasing P absorption (Gahoonia et al., 2001). However, *in vitro* culture conditions seem to stress *L. fusiformis* (PA26), with evidence of spore formation in the root colonies of this strain. This occurs because when many species of the order Bacillales are subjected to abiotic stress, they tend to sporulate as a resistance mechanism (Paredes-Sabja et al., 2011; Tan and Ramamurthi, 2014). Spore inactivity may explain the inefficiency of this strain in solubilizing $CaHPO_4$ in a liquid medium.

The Hydroponic System Allows Separating Growth-Promoting Action From Biotic Stress Induction Through Photosynthetic Performance

Microbial inoculation affected ABS/RC and DIo/RC parameters. An increased ABS/RC ratio indicates that plants grown in P-free solution and plants inoculated with *Codinaeopsis* sp. (328EF), *H. insecticola* (33EF), Biomaphos®, and *E. keratinophilum* (SC4) showed a higher density of absorbed photons per reaction center than PSII, possibly because of the inactivation of some reaction centers or increased antenna size to compensate for energy loss as heat (Schöttler and Tóth, 2014; Urban et al., 2017). This observation suggests competition between the plants and the tested strains, which negatively affects performance (Pi_Abs). Some studies have shown that symbiotic microorganisms can become opportunistic pathogens under excess water conditions, such as in hydroponic systems (Aung et al., 2018). Thus, plants reduce the number of active reaction centers, which is considered a mechanism used by leaves under stress against photo-oxidative damage and excess light energy absorption (Kalaji et al., 2014, 2018). Image fluorescence showed decreased photochemical performance in plants inoculated with *E. keratinophilum* (SC4), *Codinaeopsis* sp. (328EF), and *H. insecticola* (33EF), at physiological stress conditions. Previous studies have described species of these genera as producers of secondary metabolites and antagonists to phytopathogens (e.g., Breinholt et al., 1997; Giridharan et al., 2014; Braga et al., 2018; Puri et al., 2018; Zhu et al., 2021); however, when we forced the interaction of these species with *G. max* plants, biotic stress responses were observed in the plants.

The phytopathogenic opportunism of *Codinaeopsis* sp. (328EF), when interacting with *G. max* roots, was also confirmed by the high sporulation observed *via* electron microscopy during colonization by this strain. Phytopathogenic fungi often sporulate in the presence of host tissues (Su et al., 2012), which is a mechanism used to stimulate the *in vitro* sporulation of this class of fungi (e.g., Crous et al., 2006; Li et al., 2007; Liu et al., 2010). The biotin present in plant tissues may change the synthesis of wall polysaccharides and oleic acid, triggering the selective expression of genes involved in sporulation (Su et al., 2012).

Plants inoculated with *P. alvei* (PA12) and *L. fusiformis* (PA26) presented low ABS/RC and DIo/RC values, which is compatible with non-inoculated plants and indicates the absence of biotic stress promotion by these strains since the potential of these plants to capture photons was not reduced. Plants often try to improve their adaptability under stress by adjusting energy distribution. Therefore, higher DIo/RC values indicate a shift from photochemically active centers to photochemically inactive PSII centers (Malnoë, 2018; Guidi et al., 2019). Likewise, the high Pi_Abs values observed in plants treated with *P. alvei* (PA12) and *L. fusiformis* (PA26) indicate high vitality, which, in general, is due to the significantly increased density of chlorophyll reaction centers. The Pi_Abs value reflects the functionality of both photosystems I and II and represents quantitative information about the current state of plant performance under stress conditions (Strasser et al., 2004). These high values reflected positive *P. alvei* (PA12) and *L. fusiformis* (PA26) inoculation effects on Phi_Po, indicating improved photosynthetic functionality (Ivanov et al., 2017; Dalal and Tripathy, 2018).

The Hydroponic System Proved the Positive Effect of Microbial Inoculation on P Absorption and Photosynthetic Performance in *G. max*

Plants grown without the inoculation of microorganisms presented tissue P contents compatible with those observed in plants grown in P-free solution, which negatively affected pigment synthesis, photosynthetic performance (Pi_Abs), and pigment development in RVE. Rhizobacteria or growth-promoting fungi can induce metabolic processes that improve photosynthetic and developmental yields (e.g., De Andrade et al., 2019; Bakhshandeh et al., 2020; Kartik et al., 2020; Moretti et al., 2020; Jabborova et al., 2021). Some studies have shown that inoculation can be important under stressful conditions to improve the resilience, development, and productivity of different plant species (Bruno et al., 2020; Forouzi et al., 2020; Prittesh et al., 2020; e.g., Batool et al., 2020).

Component analysis showed that non-inoculated plants were not related to negative fluorescence factors, nor positive developmental and physiological performance factors. Plants under P-free solution and inoculated with microorganisms *Codinaeopsis* sp. (328EF), *H. insecticola* (33EF), Biomaphos®, and *E. keratinophilum* (SC4) were strongly correlated with DIo/RC, ABS/RC, TRo/RC, and Ci parameters, which are negatively related to positive biometric and physiological patterns, reinforcing the hypothesis that these patterns constitute biotic stress responses in *G. max*.

CONCLUSION

Calcium phosphate solubilization results obtained using a hydroponic system were inconsistent with those observed in solid and liquid media; however, tests in liquid medium demonstrated the poor performance of *Codinaeopsis* sp. (328EF) and *H. insecticola* (33EF) in reducing the pH and levels of solubilizing phosphates, corroborating the effects of biotic stress observed in *G. max* plants inoculated with these strains. On the other hand, the hydroponic system allowed the characterization of *P. alvei* (PA12), which was also efficient in solubilizing $CaHPO_4$ in a liquid medium, and *L. fusiformis* (PA26) was the most effective in $CaHPO_4$ solubilization because of its better effects on P absorption, growth promotion, and physiological performance observed in plants inoculated with these bacteria. Therefore, the use of a hydroponic system indicated strains with higher potential than Biomaphos® for growth promotion. These results demonstrated the effectiveness of this approach in confirming the functional traits of strains previously selected as solubilizers, as it allowed the evaluation of tissue nutritional content patterns, growth patterns, photosynthetic performance, anatomical patterns, and even the detection of

biotic stress responses to inoculation, the latter making the use of strains unfeasible.

DATA AVAILABILITY STATEMENT

The original contributions presented in the study are included in the article/**Supplementary Material**, further inquiries can be directed to the corresponding author/s.

AUTHOR CONTRIBUTIONS

MR: methodology, investigation, and writing—original draft. LB: supervision, resources, and writing—review and editing. AJ: methodology and investigation. FG and MM: writing—review and editing. LV: conceptualization, investigation, resources, and writing—review and editing. All authors contributed to the article and approved the submitted version.

ACKNOWLEDGMENTS

The authors would like to thank the Coordination for the Improvement of Higher Education Personnel (CAPES) for the Master's grant for the student Mateus Neri Oliveira Reis, and the Foundation for Research Support of the State of Goiás (FAPEG) and the IFGoiano, Rio Verde campus for the infrastructure and the students involved in the study. We would also like to thank the Regional Center for Technological Development and Innovation (CRTI) for providing scanning electron microscopy (SEM) photos, and the company Vitale Corp Agroscience for their support and input.

SUPPLEMENTARY MATERIAL

The Supplementary Material for this article can be found online at: https://www.frontiersin.org/articles/10.3389/fpls.2021.759463/full#supplementary-material

REFERENCES

Abbamondi, G. R., Tommonaro, G., Weyens, N., Thijs, S., Sillen, W., Gkorezis, P., et al. (2016). Plant growth-promoting effects of rhizospheric and endophytic bacteria associated with different tomato cultivars and new tomato hybrids *Chem. Biol. Technol.* 3, 1–10. doi: 10.1186/s40538-015-0051-3

Aguiar, T. V., Sant'anna-Santos, B. F., Azevedo, A. A., and Ferreira, R. S. (2007). Anati Quanti: software de análises quantitativas para estudos em anatomia vegetal. *Planta Daninha* 25, 649–659. doi: 10.1590/S0100-83582007000400001

Ahemad, M., and Kibret, M. (2014). Mechanisms and applications of plant growth promoting rhizobacteria: current perspective. *J. King Saud Univ. Sci.* 26, 1–20. doi: 10.1016/j.jksus.2013.05.001

Ahsan, N., and Shimizu, M. (2021). *Lysinibacillus* Species: their potential as effective bioremediation, biostimulant, and biocontrol agents. *Rev. Agric. Sci.* 9, 103–116. doi: 10.7831/ras.9.0_103

Alori, E. T., Glick, B. R., and Babalola, O. O. (2017). Microbial phosphorus solubilization and its potential for use in sustainable agriculture. *Front. Microbiol.* 8:971. doi: 10.3389/fmicb.2017.00971

Anbi, A. A., Mirshekari, B., Eivazi, A., Yarnia, M., and Behrouzyar, E. K. (2020). PGPRs affected photosynthetic capacity and nutrient uptake in different Salvia species. *J. Plant Nutr.* 43, 108–121. doi: 10.1080/01904167.2019.1659342

Anschutz, P., and Deborde, J. (2016). Spectrophotometric determination of phosphate in matrices from sequential leaching of sediments. *Limnol. Oceanogr. Methods* 14, 245–256. doi: 10.1002/lom3.10085

Aung, K., Jiang, Y., and He, S. Y. (2018). The role of water in plant–microbe interactions. *Plant J.* 93, 771–780. doi: 10.1111/tpj.13795

Bakhshandeh, E., Pirdashti, H., Shahsavarpour Lendeh, K., Gilani, Z., Yaghoubi Khanghahi, M., and Crecchio, C. (2020). Effects of plant growth promoting microorganisms inoculums on mineral nutrition, growth and productivity of rice (*Oryza sativa* L.). *J. Plant Nutr.* 43, 1643–1660. doi: 10.1080/01904167.2020.1739297

Baliah, N. T., Pandiarajan, G., and Kumar, B. M. (2016). Isolation, identification and characterization of phosphate solubilizing bacteria from different crop soils of Srivilliputtur Taluk, Virudhunagar District, Tamil Nadu. *Trop. Ecol.* 57, 465–474.

Bashan, Y., and De-Bashan, L. E. (2010). How the plant growth-promoting bacterium *Azospirillum* promotes plant growth—a critical assessment. *Adv. Agron.* 108, 77–136. doi: 10.1016/S0065-2113(10)08002-8

Bashan, Y., Kamnev, A. A., and de-Bashan, L. E. (2013). A proposal for isolating and testing phosphate-solubilizing bacteria that enhance plant growth. *Biol. Fertil. Soils.* 49:1. doi: 10.1007/s00374-012-0756-4

Batool, T., Ali, S., Seleiman, M. F., Naveed, N. H., Ali, A., Ahmed, K., et al. (2020). Plant growth promoting rhizobacteria alleviates drought stress in potato in response to suppressive oxidative stress and antioxidant enzymes activities. *Sci. Rep.* 10:16975. doi: 10.1038/s41598-020-73489-z

Berraquero, F. R., Baya, A. M., and Cormenzana, A. R. (1976). Establecimiento de índices para el estudio de la solubilización de fosfatos por bacterias del suelo. *Ars Pharm.* 17, 399–406.

Borowiak, K., Wolna-Maruwka, A., Niewiadomska, A., Budka, A., Schroeter-Zakrzewska, A., and Stasik, R. (2021). The effects of various doses and types of effective microorganism applications on microbial and enzyme activity of medium and the photosynthetic activity of scarlet sage. *Agronomy* 11:603. doi: 10.3390/agronomy11030603

Bowes, G. (1991). Growth at elevated CO_2: photosynthetic responses mediated through rubisco. *Plant Cell Environ.* 14, 795–806. doi: 10.1111/j.1365-3040.1991.tb01443.x

Braga, R. M., Padilla, G., and Araújo, W. L. (2018). The biotechnological potential of *Epicoccum* spp.: diversity of secondary metabolites. *Crit. Rev. Microbiol.* 44, 759–778. doi: 10.1080/1040841X.2018.1514364

Breinholt, J., Kjoer, A., Olsen, C. E.,Rassing, B. R., and Rosendahl, C. N. (1997). Hamigerone and Dihydrohamigerone: two acetate-derived, antifungal metabolites from *Hamigera avellanea*. *Acta Chem. Scand.* 51, 1241–1244. doi: 10.3891/acta.chem.scand.51-1241

Bruno, L. B., Karthik, C., Ma, Y., Kadirvelu, K., Freitas, H., and Rajkumar, M. (2020). Amelioration of chromium and heat stresses in *Sorghum bicolor* by Cr6+ reducing-thermotolerant plant growth promoting bacteria. *Chemosphere* 244:125521. doi: 10.1016/j.chemosphere.2019.125521

Chen, S., Zhao, H., Zou, C., Li, Y., Chen, Y., Wang, Z., et al. (2017). Combined inoculation with multiple arbuscular mycorrhizal fungi improves growth, nutrient uptake and photosynthesis in cucumber seedlings. *Front. Microbiol.* 8:2516. doi: 10.3389/fmicb.2017.02516

Chen, Y. P., Rekha, P. D., Arun, A. B., Shen, F. T., Lai, W. A., and Young, C. C. (2006). Phosphate solubilizing bacteria from subtropical soil and their tricalcium phosphate solubilizing abilities. *Appl. Soil Ecol.* 34, 33–41. doi: 10.1016/j.apsoil.2005.12.002

Choi, J. M., and Lee, C. W. (2012). Influence of elevated phosphorus levels in nutrient solution on micronutrient uptake and deficiency symptom development in strawberry cultured with fertigation system. *J. Plant Nutr.* 35, 1349–1358. doi: 10.1080/01904167.2012.684127

Chu, S., Li, H., Zhang, X., Yu, K., Chao, M., Han, S., et al. (2018). Physiological and proteomics analyses reveal low-phosphorus stress affected the regulation of photosynthesis in soybean. *Int. J. Mol. Sci.* 19:1688. doi: 10.3390/ijms19061688

Crous, P. W., Slippers, B., Wingfield, M. J., Rheeder, J., Marasas, W. F., Philips, A. J., et al. (2006). Phylogenetic lineages in the Botryosphaeriaceae. *Stud. Mycol.* 55, 235–253. doi: 10.3114/sim.55.1.235

da Silva, C. F., Vitorino, L. C., Soares, M. A., and Souchie, E. L. (2018). Multifunctional potential of endophytic and rhizospheric microbial isolates associated with *Butia purpurascens* roots for promoting plant growth. *Antonie van Leeuwenhoek* 111, 2157–2174. doi: 10.1007/s10482-018-1108-7

Dalal, V. K., and Tripathy, B. C. (2018). Water-stress induced downsizing of light-harvesting antenna complex protects developing rice seedlings from photo-oxidative damage. *Sci. Rep*. 8:5955. doi: 10.1038/s41598-017-14419-4

Danilova, M. N., Doroshenko, A. S., Kudryakova, N. V., Klepikova, A. V., Shtratnikova, V. Y., and Kusnetsov, V. V. (2020). The crosstalk between cytokinin and auxin signaling pathways in the control of natural senescence of *Arabidopsis thaliana* leaves. *Russ. J. Plant Physiol*. 67, 1028–1035. doi: 10.1134/S1021443720060035

De Andrade, F. M., de Assis Pereira, T., Souza, T. P., Guimarães, P. H. S., Martins, A. D., Schwan, R. F., et al. (2019). Beneficial effects of inoculation of growth-promoting bacteria in strawberry. *Microbiol. Res*. 223, 120–128. doi: 10.1016/j.micres.2019.04.005

Doilom, M., Guo, J. W., Phookamsak, R., Mortimer, P. E., Karunarathna, S. C., Dong, W., et al. (2020). Screening of phosphate-solubilizing fungi from air and soil in Yunnan, China: four novel species in aspergillus, gongronella, penicillium, and talaromyces. *Front. Microbiol*. 11:2443. doi: 10.3389/fmicb.2020.585215

Ferreira, E., Cavalcanti, P., and Nogueira, D. (2014). ExpDes: an R package for ANOVA and experimental designs. *Appl. Math*. 5, 2952–2958. doi: 10.4236/am.2014.519280

Forouzi, A., Ghasemnezhad, A., and Nasrabad, R. G. (2020). Phytochemical response of Stevia plant to growth promoting microorganisms under salinity stress. *S. Afr. J. Bot*. 134, 109–118. doi: 10.1016/j.sajb.2020.04.001

Gadagi, R. S., and Sa, T. (2002). New isolation method for microorganisms solulbilizing iron and aluminum phosphates using dyes. *J. Soil Sci. Plant Nutr*. 48, 615–618. doi: 10.1080/00380768.2002.10409246

Gahoonia, T. S., Nielsen, N. E., Joshi, P. A., and Jahoor, A. (2001). A root hairless barley mutant for elucidating genetic of root hairs and phosphorus uptake. *Plant Soil*. 235, 211–219.

Genty, B., Briantais, J. M., and Baker, N. R. (1989). The relationship between the quantum yield of photosynthetic electron transport and quenching of chlorophyll fluorescence. *Biochim. Biophys. Acta* 990, 87–92. doi: 10.1016/S0304-4165(89)80016-9

Ghosh, R., Barman, S., Mukherjee, R., and Mandal, N. C. (2016). Role of phosphate solubilizing Burkholderia spp. for successful colonization and growth promotion of *Lycopodium cernuum L. (Lycopodiaceae)* in lateritic belt of Birbhum district of West Bengal, India. *Microbiol. Res*. 183, 80–91. doi: 10.1016/j.micres.2015.11.011

Gibson, B. R., and Mitchell, D. T. (2004). Nutritional influences on the solubilization of metal phosphate by ericoid mycorrhizal fungi. *Mycol. Res.* 108, 947–954. doi: 10.1017/s095375620400070x

Giridharan, P., Verekar, S. A., Gohil, A. R., Mishra, P. D., Khanna, A., and Deshmukh, S. K. (2014). Antiproliferative activity of hamigerone and radicinol isolated from *Bipolaris papendorfii*. *Biomed Res. Int.* 2014:890904. doi: 10.1155/2014/890904

Guidi, L., Lo Piccolo, E., and Landi, M. (2019). Chlorophyll fluorescence, photoinhibition and abiotic stress: does it make any difference the fact to be a C3 or C4 species? *Front. Plant Sci*. 10:174. doi: 10.3389/fpls.2019.00174

Gurikar, C., Naik, M. K., and Sreenivasa, M. Y. (2016). "Azotobacter: PGPR activities with special reference to effect of pesticides and biodegradation," in *Microbial Inoculants in Sustainable Agricultural Productivity*, eds D. Singh, H. Singh, and R. Prabha (New Delhi: Springer), 229–244. doi: 10.1007/978-81-322-2647-5_13

Hanh, H. T. T., and Mongkolthanaruk, W. (2017). Correlation of growth and IAA production of *Lysinibacillus fusiformis* UD 270. *J. Appl. Phys. Sci*. 3, 98–106. doi: 10.20474/japs-3.3.3

Hanif, K., Hameed, S., Imran, A., Naqqash, T., Shahid, M., and Van Elsas, J. D. (2015). Isolation and characterization of a β-propeller gene containing phosphobacterium Bacillus subtilis strain KPS-11 for growth promotion of potato (*Solanum tuberosum* L.). *Front. Microbiol*. 6:583. doi: 10.3389/fmicb.2015.00583

He, H., Qian, T. -T., Liu, W. -J., Jiang, H., and Yu, H. -Q. (2014). Biological and chemical phosphorus solubilization from pyrolytical biochar in aqueous solution. *Chemosphere* 113, 175–181. doi: 10.1016/j.chemosphere.2014.05.039

Hoagland, D. R., and Arnon, D. I. (1950). "The water-culture method for growing plants without soil," in *second ed. Circular. California Agricultural Experiment Station* (California City, CA: Agricultural Experiment Station), 347.

Hoffland, E., Wei, C., and Wissuwa, M. (2006). Organic anion exudation by lowland rice (*Oryza sativa* L.) at zinc and phosphorus deficiency. *Plant Soil* 283, 155–162. doi: 10.1007/s11104-005-3937-1

Hunt, S. (2003). Measurements of photosynthesis and respiration in plants. *Physiol. Plant*. 117, 314–325. doi: 10.1034/j.1399-3054.2003.00055.x

Husson, F., Le, S., and Pages, J. (2010). *Exploratory Multivariate Analysis by Example Using R*. London; New York, NY: Chapman and Hall. doi: 10.1201/b10345

Hwangbo, H., Park, R. D., Kim, Y. W., Rim, Y. S., Park, K. H., Kim, T. H., et al. (2003). 2-Ketogluconic acid production and phosphate solubilization by *Enterobacter* intermedium. *Curr. Microbiol*. 47, 0087–0092. doi: 10.1007/s00284-002-3951-y

Islam, M. T., and Hossain, M. M. (2012). "Plant probiotics in phosphorus nutrition in crops, with special reference to rice," in *Bacteria in Agrobiology: Plant Probiotics*, ed D. Maheshwari (Berlin, Heidelberg: Springer), 325–363. doi: 10.1007/978-3-642-27515-9_18

Ivanov, A. G., Velitchkova, M. Y., Allakhverdiev, S. I., and Huner, N. P. (2017). Heat stress-induced effects of photosystem I: an overview of structural and functional responses. *Photosynth. Res*. 133, 17–30. doi: 10.1007/s11120-017-0383-x

Jabborova, D., Enakiev, Y., Sulaymanov, K., Kadirova, D., Ali, A., and Annapurna, K. (2021). Plant growth promoting bacteria *Bacillus subtilis* promote growth and physiological parameters of *Zingiber officinale* Roscoe. *Plant Sci. Today* 8, 66–71. doi: 10.14719/pst.2021.8.1.997

Jaiswal, S. K., Mohammed, M., Ibny, F. Y., and Dakora, F. D. (2021). Rhizobia as a source of plant growth-promoting molecules: potential applications and possible operational mechanisms. *Front. Sustain. Food Syst*. 4:311. doi: 10.3389/fsufs.2020.619676

Jarvie, H. P., Withers, J. A., and Neal, C. (2002). Review of robust measurement of phosphorus in river water: sampling, storage, fractionation and sensitivity. *Hydrol. Earth Syst. Sci*. 6, 113–131. doi: 10.5194/hess-6-113-2002

Jinal, H. N., Gopi, K., Kumar, K., and Amaresan, N. (2021). Effect of zinc-resistant *Lysinibacillus* species inoculation on growth, physiological properties, and zinc uptake in maize (*Zea mays* L.). *Environ. Sci. Pollut. Res*. 28, 6540–6548. doi: 10.1007/s11356-020-10998-4

Jog, R., Pandya, M., Nareshkumar, G., and Rajkumar, S. (2014). Mechanism of phosphate solubilization and antifungal activity of Streptomyces spp. isolated from wheat roots and rhizosphere and their application in improving plant growth. *Microbiology* 160, 778–788. doi: 10.1099/mic.0.074146-0

Kafle, A., Cope, K. R., Raths, R., Krishna Yakha, J., Subramanian, S., Bücking, H., et al. (2019). Harnessing soil microbes to improve plant phosphate efficiency in cropping systems. *Agronomy* 9:127. doi: 10.3390/agronomy9030127

Kalaiselvi, P., Jayashree, R., and Poornima, R. (2019). Plant growth promoting Bacillus spp. and Paenibacillus alvei on the growth of Sesuvium portulacastrum for phytoremediation of salt affected soils. *Int. J. Curr. Microbiol. Appl. Sci*. 8, 2847–2858. doi: 10.20546/ijcmas.2019.804.332

Kalaji, H. M., Baba, W., Gediga, K., Goltsev, V., Samborska, I. A., Cetner, M. D., et al. (2018). Chlorophyll fluorescence as a tool for nutrient status identification in rapeseed plants. *Photosynth. Res*. 136, 329–343. doi: 10.1007/s11120-017-0467-7

Kalaji, H. M., Schansker, G., Ladle, R. J., Goltsev, V., Bosa, K., Allakhverdiev, S. I., et al. (2014). Frequently asked questions about in vivo chlorophyll fluorescence: practical issues. *Photosynth. Res*. 122, 121–158. doi: 10.1007/s11120-014-0024-6

Karnovsky, M. J. (1965). A formaldehyde-glutaraldehyde fixative of high osmolality for use in electron microscopy. *J. Cell Biol.* 27, 137–138.

Kartik, V. P., Jinal, H. N., and Amaresan, N. (2020). Inoculation of cucumber (*Cucumis sativus* L.) seedlings with salt-tolerant plant growth promoting bacteria improves nutrient uptake, plant attributes and physiological profiles. *J. Plant Growth Regul*. 40, 1728–1740. doi: 10.1007/s00344-020-10226-w

Kowalenko, C. G. (2008). Extraction times and analysis methods influence soil test measurements of phosphorus and sulphur. *Can. J. Soil Sci*. 88, 733–747. doi: 10.4141/CJSS08008

Kowalenko, C. G., and Babuin, D. (2007). Interference problems with phosphoantimonylmolybdenum colorimetric measurement of phosphorus in

soil and plant materials. *Commun. Soil Sci. Plant Anal.* 38, 1299–1316. doi: 10.1080/00103620701328594

Kudoyarova, G. R., Vysotskaya, L. B., Arkhipova, T. N., Kuzmina, L. Y., Galimsyanova, N. F., Sidorova, L. V., et al. (2017). Effect of auxin producing and phosphate solubilizing bacteria on mobility of soil phosphorus, growth rate, and P acquisition by wheat plants. *Acta Physiol. Plant.* 39, 1–8. doi: 10.1007/s11738-017-2556-9

Kumar, P., Khare, S., and Dubey, R. C. (2012). Diversity of bacilli from disease suppressive soil and their role in plant growth promotion and yield enhancement. *N. Y. Sci. J.* 5, 90–111.

Kunikowska, A., Byczkowska, A., Doniak, M., and Kazmierczak, A. (2013). Cytokinins résumé: their signaling and role in programmed cell death in plants. *Plant Cell Rep.* 32, 771–780. doi: 10.1007/s00299-013-1436-z

Li, W. C., Zhou, J., Guo, S. Y., and Guo, L. D. (2007). Endophytic fungi associated with lichens in Baihua mountain of Beijing, China. *Fungal Divers.* 25, 69–80.

Li, X., Luo, L., Yang, J., Li, B., and Yuan, H. (2015). Mechanisms for solubilization of various insoluble phosphates and activation of immobilized phosphates in different soils by an efficient and salinity-tolerant *Aspergillus niger* strain An2. *Appl. Biochem. Biotechnol.* 175, 2755–2768. doi: 10.1007/s12010-014-1465-2

Lin, Z. H., Chen, L. S., Chen, R. B., Zhang, F. Z., Jiang, H. X., and Tang, N. (2009). CO_2 assimilation, ribulose-1, 5-bisphosphate carboxylase/oxygenase, carbohydrates and photosynthetic electron transport probed by the JIP-test, of tea leaves in response to phosphorus supply. *BMC Plant Biol.* 9, 1–12. doi: 10.1186/1471-2229-9-43

Linu, M. S., Asok, A. K., Thampi, M., Sreekumar, J., and Jisha, M. S. (2019). Plant growth promoting traits of indigenous phosphate solubilizing *Pseudomonas aeruginosa* isolates from chilli (*Capsicum annuum* L.) rhizosphere. *Commun. Soil Sci. Plant Anal.* 50, 444–457. doi: 10.1080/00103624.2019.1566469

Liu, A. R., Chen, S. C., Wu, S. Y., Xu, T., Guo, L. D., Jeewon, R., et al. (2010). Cultural studies coupled with DNA based sequence analyses and its implication on pigmentation as a phylogenetic marker in *Pestalotiopsis* taxonomy. *Mol. Phylogenetics Evol.* 57, 528–535. doi: 10.1016/j.ympev.2010.07.017

Liu, J., Qi, W., Li, Q., Wang, S. G., Song, C., and Yuan, X. Z. (2020). Exogenous phosphorus-solubilizing bacteria changed the rhizosphere microbial community indirectly. *3 Biotech.* 10, 1–11. doi: 10.1007/s13205-020-2099-4

Malavolta, E., Vitti, G. C., and de Oliveira, S. A. (1997). *Evaluation of Plant Nutrient Status: Principles and Their Application*, 2 Ed. (Piracicaba: Brazilian Association for Potash and Phosphate Research).

Malnoë, A. (2018). Photoinhibition or photoprotection of photosynthesis? Update on the (newly termed) sustained quenching component qH. *Environ. Exp. Bot.* 154, 123–133. doi: 10.1016/j.envexpbot.2018.05.005

Mehta, P., Walia, A., and Shirkot, C. K. (2015). Functional diversity of phosphate solubilizing plant growth promoting rhizobacteria isolated from apple trees in the trans Himalayan region of Himachal Pradesh, India. *Biol. Agric. Hortic.* 31, 265–288. doi: 10.1080/01448765.2015.1014420

Moretti, L. G., Crusciol, C. A., Kuramae, E. E., Bossolani, J. W., Moreira, A., Costa, N. R., et al. (2020). Effects of growth-promoting bacteria on soybean root activity, plant development, and yield. *Agron. J.* 112, 418–428. doi: 10.1002/agj2.20010

Murphy, J. A. M. E. S., and Riley, J. P. (1962). A modified single solution method for the determination of phosphate in natural waters. *Anal. Chim. Acta* 27, 31–36. doi: 10.1016/S0003-2670(00)88444-5

Nagul, E. A., McKelvie, I. D., Worsfold, P., and Kolev, S. D. (2015). The molybdenum blue reaction for the determination of orthophosphate revisited: opening the black box. *Anal. Chim. Acta* 890, 60–82. doi: 10.1016/j.aca.2015.07.030

Nautiyal, C. S. (1999). An efficient microbiological growth medium for screening phosphate solubilizing microorganisms. *FEMS Microbiol. Lett.* 170, 265–270. doi: 10.1111/j.1574-6968.1999.tb13383.x

O'Brien, T., Feder, N., and McCully, M. E. (1964). Polychromatic staining of plant cell walls by toluidine blue O. *Protoplasma* 59, 368–373. doi: 10.1007/BF01248568

Paredes-Sabja, D., Setlow, P., and Sarker, M. R. (2011). Germination of spores of Bacillales and Clostridiales species: mechanisms and proteins involved. *Trends Microbiol.* 19, 85–94. doi: 10.1016/j.tim.2010.10.004

Passera, A., Rossato, M., Oliver, J. S., Battelli, G., Cosentino, E., Sage, J. M., et al. (2021). Characterization of *Lysinibacillus fusiformis* strain S4C11*: in vitro*, in planta, and in silico analyses reveal a plant-beneficial microbe. *Microbiol. Res.* 244:126665. doi: 10.1016/j.micres.2020.126665

Patel, D. K., Archana, G., and Kumar, G. N. (2008). Variation in the nature of organic acid secretion and mineral phosphate solubilization by *Citrobacter* sp. DHRSS in the presence of different sugars. *Curr. Microbiol.* 56, 168–174. doi: 10.1007/s00284-007-9053-0

Penn, C. J., and Camberato, J. J. (2019). A critical review on soil chemical processes that control how soil pH affects phosphorus availability to plants. *Agriculture* 9:120. doi: 10.3390/agriculture9060120

Prittesh, P., Avnika, P., Kinjal, P., Jinal, H. N., Sakthivel, K., and Amaresan, N. (2020). Amelioration effect of salt-tolerant plant growth-promoting bacteria on growth and physiological properties of rice (*Oryza sativa*) under salt-stressed conditions. *Arch. Microbiol.* 202, 2419–2428. doi: 10.1007/s00203-020-01962-4

Puri, S. K., Habbu, P. V., Kulkarni, P. V., and Kulkarni, V. H. (2018). Nitrogen containing secondary metabolites from endophytes of medicinal plants and their biological/pharmacological activities - a review. *Sys. Rev. Pharm.* 9, 22–30. doi: 10.5530/srp.2018.1.5

R Core Team (2021). *R: A Language and Environment for Statistical Computing*. Vienna: R foundation for statistical computin. Avaliable online at: https://www.R-project.org/ (accessed March 27, 2021).

Rocha, A. F. S., Vitorino, L. C., Bessa, L. A., Costa, R. R. G. F., Brasil, M. S., and Souchie, E. L. (2020). Soil parameters affect the functional diversity of the symbiotic microbiota of Hymenaea courbaril L., a Neotropical fruit tree. *Rhizosphere* 16:100237. doi: 10.1016/j.rhisph.2020.100237

Rosolem, C. A., and Marcello, C. S. (1998). Soybean root growth and nutrition as affected by liming and phosphorus application. *Sci. Agric.* 55, 448–455. doi: 10.1590/S0103-90161998000300013

Salcedo, L. D. P., Prieto, C., and Correa, M. F. (2014). Screening phosphate solubilizing actinobacteria isolated from the rhizosphere of wild plants from the Eastern Cordillera of the Colombian Andes. *Afr. J. Microbiol. Res.* 8, 734–742. doi: 10.5897/AJMR2013.5940

Santos, M. S., Nogueira, M. A., and Hungria, M. (2019). Microbial inoculants: reviewing the past, discussing the present and previewing an outstanding future for the use of beneficial bacteria in agriculture. *AMB Express* 9, 1–22. doi: 10.1186/s13568-019-0932-0

Santos, R. P., da Cruz, A. C. F., Iarema, L., Fernandes, K. R. G., Kuki, K. N., and Otoni, W. C. (2007). Avaliação da eficiência do dimetilsulfóxido na extração de pigmentos foliares de *Vitis vinifera* x *V. rotundifolia* e *V. riparia* propagadas *in vitro*. *Rev Bras Biocienc.* 5, 888–890.

Sarr, P. S., Tibiri, E. B., Fukuda, M., Zongo, A. N., and Nakamura, S. (2020). Phosphate-solubilizing fungi and alkaline phosphatase trigger the P solubilization during the co-composting of sorghum straw residues with Burkina Faso phosphate rock. *Front. Environ. Sci.* 8:174. doi: 10.3389/fenvs.2020.559195

Scervino, J. M., Mesa, M. P., Della Mónica, I., Recchi, M., Moreno, N. S., and Godeas, A. (2010). Soil fungal isolates produce different organic acid patterns involved in phosphate salts solubilization. *Biol. Fertil. Soils.* 46, 755–763. doi: 10.1007/s00374-010-0482-8

Schoina, C., Stringlis, I. A., Pantelides, I. S., Tjamos, S. E., and Paplomatas, E. J. (2011). Evaluation of application methods and biocontrol efficacy of *Paenibacillus alvei* strain K-165, against the cotton black root rot pathogen *Thielaviopsis basicola*. *Biol. Control.* 58, 68–73. doi: 10.1016/j.biocontrol.2011.04.002

Schöttler, M. A., and Tóth, S. Z. (2014). Photosynthetic complex stoichiometry dynamics in higher plants: environmental acclimation and photosynthetic flux control. *Front. Plant Sci.* 5:188. doi: 10.3389/fpls.2014.00188

Sharma, N., Yadav, K., Cheema, J., Badda, N., and Aggarwal, A. (2015). Arbuscular mycorrhizal symbiosis and water stress: a critical review. *Pertanika J. Trop. Agric. Sci.* 38, 427–453.

Silva Filho, G. N., and Vidor, C. (2000). Solubilização de fostatos por microrganismos na presença de fontes de carbono. *Rev. Bras. Ciênc. Solo* 24, 311–319. doi: 10.1590/S0100-06832000000200008

Singh, A. V., Prasad, B., and Goel, R. (2018). Plant growth promoting efficiency of phosphate solubilizing Chryseobacterium sp. PSR 10 with different doses of N and P fertilizers on lentil (*Lens culinaris* var. PL-5) growth and yield. *Int. J. Curr. Microbiol. Appl. Sci.* 7, 2280–2289. doi: 10.20546/ijcmas.2018.705.265

Situmorang, E. C., Prameswara, A., Sinthya, H. C., Toruan-Mathius, N., and Liwang, T. (2015). Indigenous phosphate solubilizing bacteria from peat soil for an eco-friendly biofertilizer in oil palm plantation. *KnE Energy*. 1, 65–72. doi: 10.18502/ken.v1i1.324

Souchie, E. L., de Souza Abboud, A. C., and Caproni, A. L. (2007). Solubilização de fosfato in vitro por microorganismos rizosféricos de guandu. *Biosci. J.* 23, 53–60.

Sousa, C. A., Junior, M. D. A. L., Fracetto, G. G. M., Freire, F. J., and Sobral, J. K. (2016). Evaluation methods used for phosphate-solubilizing bacteria. *Afr. J. Biotechnol*. 15, 1796–1805. doi: 10.5897/AJB2015.15020

Strasser, R. J., Srivastava, A., and Tsimilli-Michael, M. (2000). "The fluorescence transient as a tool to characterize and screen photosynthetic samples," in *Probing Photosynthesis: Mechanisms, Regulation and Adaptation*, eds M. Yunus, U. Pathre, and P. Mohanty (London; New York, NY: Chapman and Hall), 445–483.

Strasser, R. J., Tsimilli-Michael, M., and Srivastava, A. (2004). "Analysis of the chlorophyll a fluorescence transient," in *Chlorophyll a Fluorescence*, eds G. C. Papageorgiou, and Govindjee (Dordrecht: Springer), 321–362. doi: 10.1007/978-1-4020-3218-9_12

Su, Y. Y., Qi, Y. L., and Cai, L. (2012). Induction of sporulation in plant pathogenic fungi. *Mycology* 3, 195–200. doi: 10.1080/21501203.2012.719042

Sulieman, S., and Tran, L. S. P. (2017). *Legume Nitrogen Fixation in Soils With Low Phosphorus Availability: Adaptation and Regulatory Implication*. Cham: Springer International Publishing. doi: 10.1007/978-3-319-55729-8

Sylvester-Bradley, R., Asakawa, N., Torraca, S. L., Magalhães, F. M., Oliveira, L. A., and Pereira, R. M. (1982). Levantamento quantitativo de microrganismos solubilizadores de fosfatos na rizosfera de gramíneas e leguminosas forrageiras na Amazônia. *Acta Amazon*. 12, 15–22. doi: 10.1590/1809-439219821 21015

Tan, I. S., and Ramamurthi, K. S. (2014). Spore formation in *Bacillus subtilis*. *Environ. Microbiol. Rep*. 6, 212–225. doi: 10.1111/1758-2229.12130

Taveira, L. R. S., Carvalho, T. S. D., Teixeira, A. F. D. S., and Curi, N. (2019). Sustainable productive intensification for family farming in developing tropical countries. *Ciênc. Agrotec*. 43, 1–12. doi: 10.1590/1413-7054201943012819

Uarrota, V. G., Stefen, D. L. V., Leolato, L. S., Gindri, D. M., and Nerling, D. (2018). "Revisiting carotenoids and their role in plant stress responses: from biosynthesis to plant signaling mechanisms during stress," in *Antioxidants and Antioxidant Enzymes in Higher Plants*, eds D. Gupta, J. Palma, and F. Corpas (Cham: Springer), 207–232. doi: 10.1007/978-3-319-75088-0_10

United Nations (2019). Selected results of the 2019 UN world population projections. *Popul. Dev. Rev*. 45, 689–694. doi: 10.1111/padr.12288

Urban, L., Aarrouf, J., and Bidel, L. P. (2017). Assessing the effects of water deficit on photosynthesis using parameters derived from measurements of leaf gas exchange and of chlorophyll a fluorescence. *Front. Plant Sci*. 8:2068. doi: 10.3389/fpls.2017.02068

Vafadar, F., Amooaghaie, R., and Otroshy, M. (2014). Effects of plant-growth-promoting rhizobacteria and arbuscular mycorrhizal fungus on plant growth, stevioside, NPK, and chlorophyll content of *Stevia rebaudiana*. *J. Plant Interact*. 9, 128–136. doi: 10.1080/17429145.2013.779035

Vendan, R. T., Yu, Y. J., Lee, S. H., and Rhee, Y. H. (2010). Diversity of endophytic bacteria in ginseng and their potential for plant growth promotion. *J. Microbiol.* 48, 559–565. doi: 10.1007/s12275-010-0082-1

Verbon, E. H., and Liberman, L. M. (2016). Beneficial microbes affect endogenous mechanisms controlling root development. *Trends Plant Sci.* 21, 218–229. doi: 10.1016/j.tplants.2016.01.013

Viégas, I. D. J. M., Cordeiro, R. A. M., de Almeida, G. M., Silva, D. A. S., da Silva, B. C., Okumura, R. S., et al. (2018). Growth and visual symptoms of nutrients deficiency in mangosteens (*Garcinia mangostana* L.). *Am. J. Plant Sci.* 9, 1014–1028. doi: 10.4236/ajps.2018.95078

Walpola, B. C., Keum, M.-J., and Yoon, Y.-H. (2012). Influence of different ph conditions and phosphate sources on phosphate solubilization by Pantoea agglomerans DSM3493. *Korean J. Soil. Sci.* 45, 998–1003. doi: 10.7745/KJSSF.2012.45.6.998

Wang, J., Chen, Y., Wang, P., Li, Y. S., Wang, G., Liu, P., et al. (2018). Leaf gas exchange, phosphorus uptake, growth and yield responses of cotton cultivars to different phosphorus rates. *Photosynthetica* 56, 1414–1421. doi: 10.1007/s11099-018-0845-1

Wang, Y., Yang, Z., Kong, Y., Li, X., Li, W., Du, H., et al. (2020). GmPAP12 is required for nodule development and nitrogen fixation under phosphorus starvation in soybean. *Front. Plant Sci*. 11:450. doi: 10.3389/fpls.2020.00450

Warren, C. R., and Adams, M. A. (2002). Phosphorus affects growth and partitioning of nitrogen to rubisco in *Pinus pinaster*. *Tree Physiol*. 22, 11–19. doi: 10.1093/treephys/22.1.11

Wellburn, A. R. (1994). The spectral determination of chlorophylls a and b, as well as total carotenoids, using various solvents with spectrophotometers of different resolution. *J. Plant Physiol*. 144, 307–313. doi: 10.1016/S0176-1617(11)81192-2

Wu, F., Li, J., Chen, Y., Zhang, L., Zhang, Y., Wang, S., et al. (2019). Effects of phosphate solubilizing bacteria on the growth, photosynthesis, and nutrient uptake of *Camellia oleifera* Abel. *Forests* 10:348. doi: 10.3390/f10040348

Yadav, A. N., Verma, P., Singh, B., Chauhan, V. S., Suman, A., and Saxena, A. K. (2017). Plant growth promoting bacteria: biodiversity and multifunctional attributes for sustainable agriculture. *Adv. Biotechnol. Microbiol.* 5, 1–16. doi: 10.19080/AIBM.2017.05.555671

Yadav, H., Gothwal, R. K., Solanki, P. S., Nehra, S., Sinha-Roy, S., and Ghosh, P. (2015). Isolation and characterization of thermo-tolerant phosphate-solubilizing bacteria from a phosphate mine and their rock phosphate solubilizing abilities. *Geomicrobiol. J.* 32, 475–481. doi: 10.1080/01490451.2014.943856

Yang, E., Fan, L., Yan, J., Jiang, Y., Doucette, C., Fillmore, S., and Walker, B. (2018). Influence of culture media, pH and temperature on growth and bacteriocin production of bacteriocinogenic lactic acid bacteria. *AMB Express* 8, 1–14. doi: 10.1186/s13568-018-0536-0

Zhang, W., Peng, K., Cui, F., Wang, D., Zhao, J., Zhang, Y., et al. (2021). Cytokinin oxidase/dehydrogenase OsCKX11 coordinates source and sink relationship in rice by simultaneous regulation of leaf senescence and grain number. *Plant Biotechnol. J.* 19, 335–350. doi: 10.1111/pbi.13467

Zhu, H. J., Sun, L. F., Zhang, Y. F., Zhang, X. L., and Qiao, J. J. (2012). Conversion of spent mushroom substrate to biofertilizer using a stress-tolerant phosphate-solubilizing *Pichia farinose* FL7. *Bioresour. Technol.* 111, 410–416. doi: 10.1016/j.biortech.2012.02.042

Zhu, J., Li, Z., Lu, H., Liu, S., Ding, W., Li, J., et al. (2021). New diphenyl ethers from a fungus *Epicoccum sorghinum* L28 and their antifungal activity against phytopathogens. *Bioorg. Chem.* 115:105232. doi: 10.1016/j.bioorg.2021.105232

Zúñiga-Silgado, D., Rivera-Leyva, J. C., Coleman, J. J., Sánchez-Reyez, A., Valencia-Díaz, S., Serrano, M., et al. (2020). Soil type affects organic acid production and phosphorus solubilization efficiency mediated by several native fungal strains from Mexico. *Microorganisms* 8:1337. doi: 10.3390/microorganisms 8091337

Zwack, P. J., and Rashotte, A. M. (2013). Cytokinin inhibition of leaf senescence. *Plant Signal. Behav*. 8:e24737. doi: 10.4161/psb.24737

Conflict of Interest: The authors declare that the research was conducted in the absence of any commercial or financial relationships that could be construed as a potential conflict of interest.

Publisher's Note: All claims expressed in this article are solely those of the authors and do not necessarily represent those of their affiliated organizations, or those of the publisher, the editors and the reviewers. Any product that may be evaluated in this article, or claim that may be made by its manufacturer, is not guaranteed or endorsed by the publisher.

frontiers in Plant Science

ORIGINAL RESEARCH
published: 04 November 2021
doi: 10.3389/fpls.2021.697184

2-Keto-L-Gulonic Acid Improved the Salt Stress Resistance of Non-heading Chinese Cabbage by Increasing L-Ascorbic Acid Accumulation

Mingfu Gao[1,2], Hao Sun[1,3], Meijun Shi[1,2], Qiqi Wu[1,2], Dongxu Ji[1,2], Bing Wang[1,2], Lixin Zhang[4], Yang Liu[5], Litao Han[5], Xicheng Ruan[5], Hui Xu[1,3] and Weichao Yang[1,3*]*

[1]Key Laboratory of Pollution Ecology and Environmental Engineering, Institute of Applied Ecology, Chinese Academy of Sciences, Shenyang, China, [2]University of Chinese Academy of Sciences, Beijing, China, [3]CAS Engineering Laboratory for Green Fertilizers, Institute of Applied Ecology, Chinese Academy of Sciences, Shenyang, China, [4]State Key Laboratory of Bioreactor Engineering and School of Biotechnology, East China University of Science and Technology (ECUST), Shanghai, China, [5]Yikang Environment Biotechnology Development Co., Ltd, Shenyang, China

Salt stress has long been a prominent obstacle that restricts crop growth, and increasing the L-ascorbic acid (ASA) content of crops is an effective means of alleviating this stress. 2-Keto-L-gulonic acid (2KGA) is a precursor used in industrial ASA production as well as an ASA degradation product in plants. However, to date, no study has investigated the effects of 2KGA on ASA metabolism and salt stress. Here, we evaluated the potential of using 2KGA to improve crop resistance to salt stress (100 mM NaCl) through a cultivation experiment of non-heading Chinese cabbage (*Brassica campestris* ssp. *chinensis*). The results showed that the leaf and root biomass were significantly improved by 2KGA application. The levels of metabolites and enzymes related to stress resistance were increased, whereas the hydrogen peroxide (H_2O_2) and malondialdehyde (MDA) contents were decreased. Lipid peroxidation and cell membrane damage were alleviated following 2KGA treatment. Positive correlations were found between photosynthetic pigments and organic solutes, ASA and photosynthetic pigments, and ASA and antioxidant enzymes. In contrast, negative correlations were observed between antioxidant enzymes and H_2O_2/MDA. Moreover, the expression levels of *L-gulono-1,4-lactone oxidase*, *GDP-mannose pyrophosphorylase*, *dehydroascorbate reductase-3*, and *ascorbate peroxidase* were increased by 2KGA treatment. These results suggested that exogenous 2KGA application can relieve the inhibitory effect of salt stress on plant growth, and the promotion of ASA synthesis may represent a critical underlying mechanism. Our findings have significant implications for the future application of 2KGA or its fermentation residue in agriculture.

Keywords: 2-keto-L-gulonic acid, L-ascorbic acid, organic acid, salt stress, lipid peroxidation, non-heading Chinese cabbage

OPEN ACCESS

Edited by:
Youssef Rouphael,
University of Naples Federico II, Italy

Reviewed by:
Gholamreza Gohari,
University of Maragheh, Iran
Maria Grazia Annunziata,
University of Potsdam, Germany
Fernanda Fidalgo,
University of Porto, Portugal

***Correspondence:**
Hui Xu
xuhui@iae.ac.cn
Weichao Yang
yangweichao@iae.ac.cn

Specialty section:
This article was submitted to Plant Abiotic Stress, a section of the journal Frontiers in Plant Science

Received: *19 April 2021*
Accepted: *18 October 2021*
Published: *04 November 2021*

Citation:
Gao M, Sun H, Shi M, Wu Q, Ji D, Wang B, Zhang L, Liu Y, Han L, Ruan X, Xu H and Yang W (2021) 2-Keto-L-Gulonic Acid Improved the Salt Stress Resistance of Non-heading Chinese Cabbage by Increasing L-Ascorbic Acid Accumulation. Front. Plant Sci. 12:697184. doi: 10.3389/fpls.2021.697184

INTRODUCTION

Abiotic stress refers to specific environmental factors that are unfavorable for plant survival and development, such as high temperature, drought, and saline-alkali soils (Zandalinas et al., 2020). There are large areas of saline-alkali soils globally, and crops grown in these soils usually have a low yield and are of poor quality (Zhao et al., 2014). Moreover, hydroponic agriculture with desalinated seawater is also associated with the detrimental effects of salt stress (Santos et al., 2019). These observations highlight that saline-alkali soils or environments constitute key factors that restrict the sustainable development of agriculture.

L-ascorbic acid (ASA, vitamin C) is a non-enzymatic antioxidant commonly found in plants and plays a vital role in protecting plants from oxidative damage caused by abiotic stress. ASA is employed as an electron donor by ascorbate peroxidase (APX; EC 1.11.1.11), which catalyzes the conversion of hydrogen peroxide (H_2O_2) to water and O_2 (Tyagi et al., 2020). Simultaneously, humans must obtain ASA from the diet, especially vegetables and fruits, to maintain good health. Current evidence shows that the fluctuation of ASA metabolism in plants greatly influences the resistance of plants to salt stress. Several studies have emphasized that increasing ASA levels can strengthen the salt stress tolerance of plants. Liu et al. (2013) demonstrated that, in tobacco, the knock-in of cDNA encoding L-galactose-1,4-lactone dehydrogenase (GLDH; EC 1.3.2.3), which catalyzes the conversion of L-galactono-1,4-lactone to ASA, increased *GLDH* expression and ASA content, thereby enhancing salt stress tolerance in the plant. Similarly, the overexpression of *dehydroascorbate reductase* [encoding dehydroascorbate reductase (EC 1.8.5.1), the enzyme that catalyzes the regeneration of ASA from dehydroascorbic acid] in rice also increased ASA content, consequently enhancing the adaptability of rice to salt stress (Kim et al., 2014). Moreover, the application of exogenous ASA can also increase the ASA content and salt stress resistance of plants (Shalata and Neumann, 2001). Despite these benefits of ASA, concerns regarding the use of genetically modified crops and the inherent instability of ASA have complicated their application in agriculture. Additionally, low ASA synthesis in plants under abiotic stress can greatly inhibit their growth and development (Huang et al., 2005; Gao and Zhang, 2008). Combined, the above evidence suggests that increasing the level of ASA can enhance the ability of plants to resist salt stress.

2-Keto-L-gulonic acid (2KGA) is an intermediate metabolite of ASA metabolism in plants and is produced *via* the degradation of ASA (Jia et al., 2019). In grape tissues, 2KGA is used to synthesize tartaric acid (Jia et al., 2019). However, no study to date has investigated the effects of 2KGA on ASA metabolic activities or plant growth and development. Interestingly, 2KGA, mainly produced *via* two-step microbial fermentation using sorbitol as a substrate, is also a key precursor used in the chemical synthesis of ASA (Yang et al., 2017). Currently, the global production of 2KGA is approximately 160,000–180,000 tons per year (Xu et al., 2021), and the application of this organic acid is merely limited to the industrial production of ASA. In addition, more than 50,000 tons of fermentation residue are discarded every year from the ASA industry in China (Kong et al., 2014), with 2KGA accounting for approximately 25–30% of this residue. Unlike many industrial waste products, this fermentation residue does not contain harmful chemicals or an excess of heavy metals; nonetheless, it is now treated as a wastewater (Xu et al., 2021). One study showed that treatment with the 2KGA-containing fermentation residue can increase the biomass and ASA content of plants in saline soil (Kong et al., 2014), suggesting that it has potential for agricultural application. However, this fermentation residue is a solution comprising a mixture of organic acids, such as 2KGA, oxalic acid, formic acid, and acetic acid, among others. To assess its suitability for use in agriculture, it is necessary to investigate the effects of 2KGA in isolation.

Non-heading Chinese cabbage (*Brassica campestris* ssp. *chinensis*) is widely cultivated in China, including in hydroponic agriculture. In this study, this crop plant was used as the research material to determine whether 2KGA can enhance the resistance of crops to salt stress. In addition to ASA, organic solute [e.g., soluble carbohydrates (SC), soluble proteins (SP), and proline] and photosynthetic pigment contents and the activities of antioxidant enzymes [e.g., superoxide dismutase (EC 1.15.1.1), peroxidase (EC 1.11.1.1), APX, and catalase (EC 1.11.1.6)] are also known to be important for plant resistance to salt stress (Nounjan et al., 2012; Ahanger et al., 2019); here, these parameters were also examined to evaluate the potential of 2KGA in relieving salt stress in plants. Furthermore, we measured the expression levels of genes involved in the ASA biosynthesis and recycling pathways to reveal the effect of 2KGA treatment on plant ASA metabolism under salt stress. The aim of this study was to provide a basis for the future application of 2KGA or its fermentation residue in agriculture.

MATERIALS AND METHODS

Plant Materials and Cultivation Conditions

The experiment was conducted in a laboratory of the Institute of Applied Ecology, Chinese Academy of Sciences, Shenyang, China. 2KGA (>99.4%) was supplied by Northeast Pharmaceutical Group Co., Ltd., Shenyang, China. Non-heading Chinese cabbage seeds were soaked in 8% sodium hypochlorite solution for 10 min, washed with desalinated water at least three times, and then placed on moist germination paper. After 6 days, the cabbage seedlings at the first new leaf stage were transplanted into 1/2 Hoagland nutrient solution. When the third new leaf appeared, the seedlings were divided into the following three groups (90 seedlings per group): Group 1 (CK group), in which cabbage seedlings were transplanted into fresh 1/2 Hoagland nutrition solution as a control; group 2 (Na^+ group), in which the fresh 1/2 Hoagland nutrient solution was supplemented with NaCl (final concentration: 100 mM); and group 3 (Na^++2KGA group), in which the fresh 1/2 Hoagland nutrient solution was supplemented with NaCl (final concentration: 100 mM) and 2KGA (final concentration: 1 mM;

Figure 1). The cultivation conditions of the seedlings were as previously reported (Lacerda et al., 2003). During the experiment, the temperature was set at 26 ± 2°C, the relative humidity at 60 ± 10%, and the illumination at 8,000 lx. Plant samples were collected on days 3, 6, and 9 after the nutrient solution was replaced.

Analysis of Photosynthetic Pigments

The assay for photosynthetic pigment content was based on the method of Lichtenthaler (1987). Photosynthetic pigments were extracted from leaves with 95% ethanol. The absorbance of the extract was measured at the 470, 649, and 665 nm wavelengths. Full details are provided in **Supplementary Method 1**. Chlorophyll a (Chla), chlorophyll b (Chlb), total chlorophyll (Chlab), and carotenoid (Car) contents were calculated according to the following formulas:

$$C_{Chla} = 13.36 \times A_{665} - 5.19 \times A_{649} \ (\mu g/ml)$$
$$C_{Chlb} = 27.43 \times A_{649} - 8.12 \times A_{665} \ (\mu g/ml)$$
$$C_{Chlab} = 5.24 \times A_{665} + 22.24 \times A_{649} \ (\mu g/ml)$$
$$C_{Car} = (1{,}000 \times A_{470} - 2.13 \times C_{Chla} - 97.64 \times C_{Chlb})/209 \ (\mu g/ml)$$

Leaf and Root Sampling

Leaves and roots were collected on day 9 for the determination of the relevant parameters. The length and width of the leaves were measured. Total root length (the sum of detectable primary and lateral root lengths), root tip number, root average diameter, and surface area were measured using a Microtek ScanMaker i800 plus scanner, and the related parameters were collected *via* the instrument's supporting software. Root morphology was observed under a microscope. Fresh plant samples were directly weighed to record fresh weight and then dried to constant weight at 75°C to record dry weight. Fresh roots were soaked in desalinated water, placed at 4°C in the dark for 24 h, and then weighed to determine root turgor weight. Root relative water content was calculated according to the reported formula (Annunziata et al., 2017):

Root relative water content = (root fresh weight – root dry weight)/(root turgor weight – root dry weight) × 100%.

Determination of Soluble Carbohydrate, Soluble Protein, Proline, and ASA Content in the Leaves

Soluble carbohydrate content in the leaves was determined using the phenol-sulfuric acid method (Nielsen, 2010). Leaves (0.5 g) were chopped and placed in a centrifuge tube containing 5 ml of desalinated water. The tube was placed in a boiling water bath for 30 min and then cooled to room temperature. Next, the samples were centrifuged at 7,200 × *g* for 10 min at room temperature. The supernatant was transferred to a graduated test tube, and desalinated water was added to a total volume of 10 ml, yielding the extract solution. A 1-ml aliquot of extract, 0.5 ml of phenol solution (9% *w*/*v*), and 2.5 ml of concentrated sulfuric acid (98%) were placed in a stoppered glass test tube, mixing, and placed in a boiling water bath for 15 min. After cooling to room temperature, the absorbance was measured at 490 nm. SC content was calculated using a glucose standard curve.

Soluble proteins concentration was assessed using the Bradford assay (Bradford, 1976). Proline was extracted from the leaves using sulfosalicylic acid (3% *w*/*v*) and quantified based on a

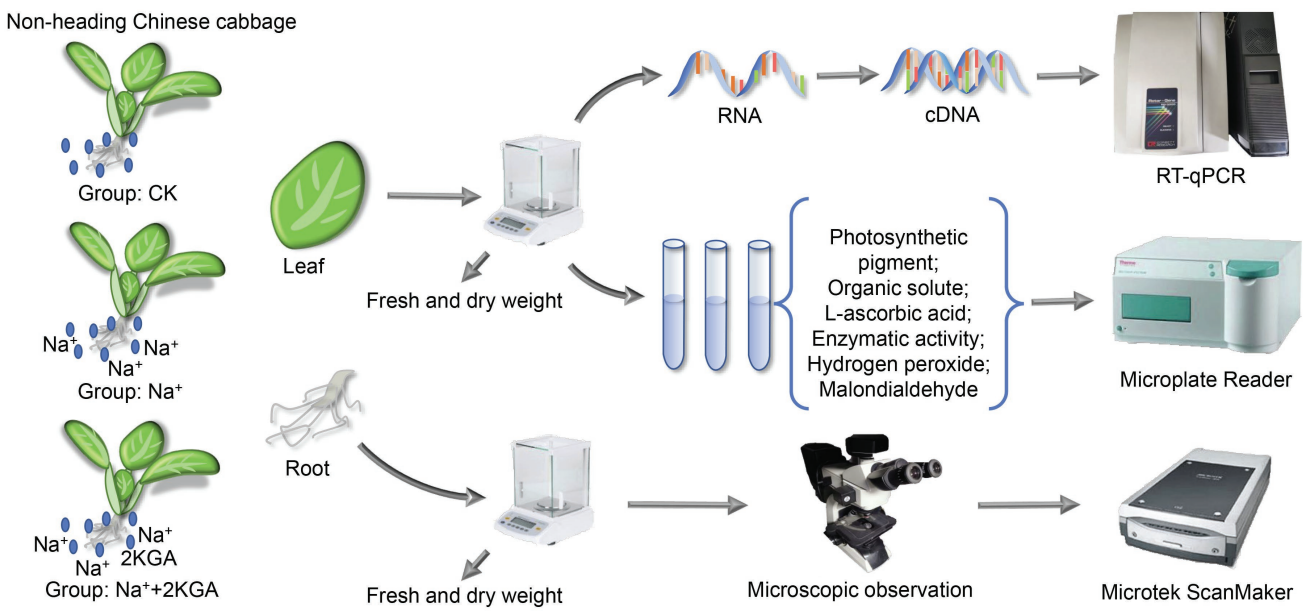

FIGURE 1 | The experimental setup of the study. 2KGA, 2-keto-L-gulonic acid. CK, seedlings were cultivated in 1/2 Hoagland nutrition solution; Na^+, the 1/2 Hoagland nutrient solution was supplemented with NaCl (100 mM); and Na^++2KGA, 1/2 Hoagland nutrient solution was supplemented with NaCl (100 mM) and 2KGA (1 mM).

previous report (Ghoulam et al., 2002). Details of the method are provided in **Supplementary Methods 2**, **3**.

Ascorbic acid content was measured using a HPLC as previously reported (Cronje et al., 2012), with some modifications. The leaves (0.3 g) were ground with liquid nitrogen and dissolved in 5 ml of 1% (*w*/*v*) metaphosphate in an ice bath. The homogenate was centrifuged at 7,200 × *g* for 10 min at 4°C, and the resulting supernatant was diluted with metaphosphate and filtered using a 0.22-μm injection filter. A 20-μl aliquot of the filtered solution was injected into an AQ-C18 column for analysis. The detection conditions were as follows: mobile phase, 95% 20 mM phosphate buffer, pH 2.8 ± 0.1, and 5% acetonitrile; flow rate, 1 ml/min; temperature, 40°C; detection wavelength, 243 nm. The ASA content of the samples was determined according to a standard curve.

Antioxidant Enzyme Activity

Leaf samples (0.2 g) in 2 ml of PBS (20 mM, pH 7.2 ± 0.1) supplemented with 0.1 mM EDTA-Na, 0.5 mM ASA, and polyvinylpyrrolidone (0.1% *w*/*v*) were evenly ground in an ice bath using a mortar and pestle. The homogenate was centrifuged at 7,200 × *g* for 10 min at 4°C, and the supernatant was collected as the crude enzyme solution. The activities of superoxide dismutase (SODa), ascorbate peroxidase (APXa), catalase (CATa), and peroxidase (PODa) were assayed as previously described (Azevedo Neto et al., 2006; Wang et al., 2014). More details of the experiment are provided in **Supplementary Method 4**.

Measurement of H_2O_2 and Malondialdehyde Levels

The H_2O_2 content was determined using potassium iodide (KI; Velikova et al., 2000). Leaf samples (0.5 g) were ground in an ice bath with 5 ml of trichloroacetic acid (TCA, 0.1% *w*/*v*). The homogenate was centrifuged at 7,200 × *g* for 10 min at 4°C, and 0.5 ml of the supernatant was mixed with 0.5 ml of 0.1 mol/l potassium phosphate buffer (pH 7.0 ± 0.1) and 1 ml of 1 mol/L KI solution and kept at room temperature in the dark for 1 h. Absorbance was then determined at 390 nm. The H_2O_2 concentration was calculated using a H_2O_2 standard curve.

Malondialdehyde (MDA) content was determined using the thiobarbituric acid (TBA) method (Li and Yi, 2012). One gram of sample was mixed with 2 ml of TCA (10% *w*/*v*) and a small amount of quartz sand and ground to obtain the homogenate. Subsequently, 8 ml of TCA (10% *w*/*v*) was added to allow the even mixing of the homogenate. The homogenate was then centrifuged at 7,200 × *g* for 10 min at 4°C, and the supernatant was used as the sample extract solution. Then, 2 ml of the extract solution was added to 2 ml of TBA (0.6% *w*/*v*) solution and the mixture were placed in a boiling water bath for 15 min to initiate the reaction. The mixture was subsequently rapidly cooled and centrifuged at 7,200 × *g* for 3 min at room temperature. The absorbance of the supernatant was measured at 450, 532, and 600 nm. The MDA concentration was calculated using the following formula:

$$C_{MDA} = 6.45 \times (A_{532} - A_{600}) - 0.56 \times A_{450} \ (\mu mol/L)$$

The Expression of Genes Related to ASA Accumulation

The expression levels of *L-gulono-1,4-lactone oxidase* (*GLO*), *GDP-mannose pyrophosphorylase* (*GMP*), *Myo-inositol oxygenase* (*MIOX*), and *GLDH* in the ASA biosynthesis pathway and *monodehydroascorbate reductase* (*MDHAR*), *dehydroascorbate reductase-1* (*DHAR1*), *dehydroascorbate reductase-3* (*DHAR3*), and *APX* in the ASA recycling pathway were examined. Total RNA was extracted from leaves according to the instructions of the SteadyPure Universal RNA Extraction Kit (Code No. AG21017; Accurate Bio, Inc., Hunan, China). cDNA was prepared using Evo M-MLV RT Premix for qPCR (Code No. AG11706; Accurate Bio, Inc., Hunan, China). qPCR was performed using the SYBR Green Premix Pro Taq HS qPCR Kit (Code No. AG11701; Accurate Bio, Inc., Hunan, China). Details of the primers used are shown in **Supplementary Table S1**. Relative gene expression levels were calculated using the $2^{-\Delta\Delta Ct}$ method (Livak and Schmittgen, 2001).

Statistical Analysis

Two-tailed Student's *t* tests were used for statistical analysis. A value of $p < 0.05$ was considered statistically significant. Each parameter was evaluated in at least three biological replicates. Spearman's method was used to analyze putative correlations among the metabolites. Cytoscape 3.7.2 was used to plot the correlation networks.

RESULTS

Leaves and Photosynthetic Pigments

We found that salt stress significantly inhibited seedling growth. Compared with the CK (control) group, seedlings in the Na^+ group were stunted and the leaves were significantly smaller (**Figure 2A**). Additionally, the fresh and dry weights of the salt-stressed leaves were reduced by 48.21 and 51.37%, respectively, compared with those of the CK group (**Figure 2B**). However, the addition of 2KGA (Na^++2KGA group) significantly increased the fresh weight and dry weight of the seedlings under stress by 45.77 and 48.44%, respectively, thereby effectively counteracting the negative impact of stress on seedling growth.

To improve the resistance of plants to salt stress, their photosynthetic efficiency must be enhanced by increasing the photosynthetic pigment content. Compared with those of the Na^+ group, leaves in the Na^++2KGA group exhibited a greater accumulation of photosynthetic pigments. The Chlab content was also significantly greater in the leaves of the Na^++2KGA group on day 6; however, no difference in the Chla/Chlb ratio was observed between the two groups. Interestingly, 2KGA treatment led to a marked increase in carotenoid content, with the highest increase (12.5%) being recorded on day 3. Correspondingly, the Chlab/Car ratio of the Na^++2KGA group was lower (**Figure 2C**).

Root Growth and Development

Compared with the CK group, Na^+-only treatment significantly reduced the root fresh weight and dry weight by 41.17 and 39.56%, respectively (**Figures 3A**,**B**), while the total root

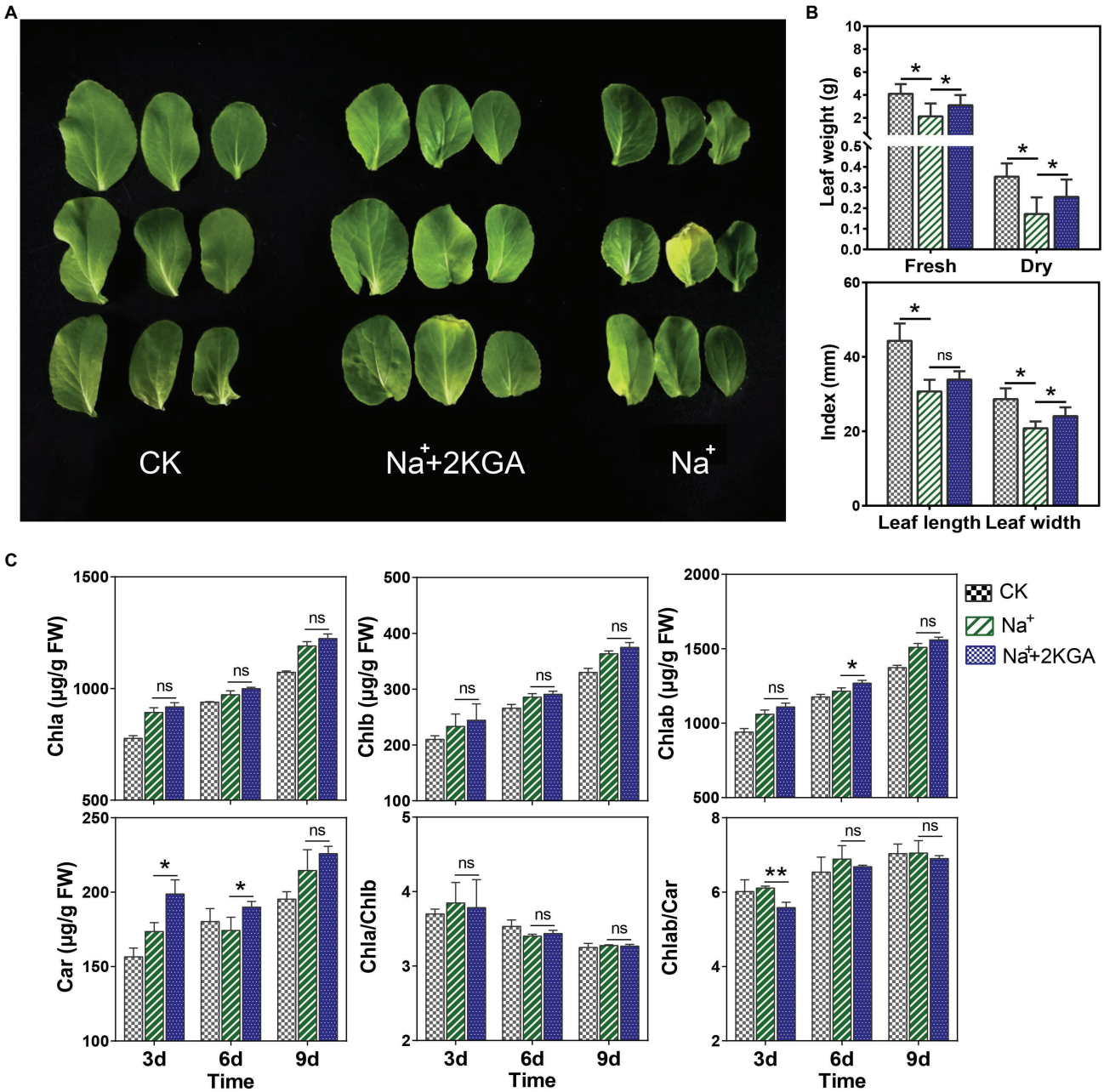

FIGURE 2 | Leaf morphology, biomass, and photosynthetic pigment content. The morphology **(A)**, biomass, length, and width **(B)**, and photosynthetic pigment content **(C)** of the leaves. Chla, chlorophyll a; Chlb, chlorophyll b; Car, carotenoids; Chlab, total chlorophyll; Chla/Chlb, the ratio of chlorophyll a content to chlorophyll b content; Chlab/Car, the ratio of total chlorophyll content to carotenoid content; FW, fresh weight; and ns, not significant; $^{*}p<0.05$, $^{**}p<0.01$.

length, root surface area, average diameter, and root tip number were reduced by 12.89, 37.73, 32.90, and 16.94%, respectively. However, 2KGA supplementation relieved the inhibitory influence of salt stress on the roots. The corresponding root indices in the Na^++2KGA group showed increases of 43.73, 37.27, 32.72, 42.56, 5.92, and 86.86% compared to the Na^+ group. Surprisingly, even under salt stress, the addition of 2KGA (Na^++2KGA group) increased the total root length and root tip number by 15.62 and 55.21%, respectively, compared with that of the CK group. Moreover, microscopic analysis showed that the roots of the Na^++2KGA group contained more and longer fine roots (**Figure 3C**). Unlike with the plant biomass, no significant changes in water content or root relative water content were recorded between the Na^+ and Na^++2KGA groups (**Supplementary Figure S1**).

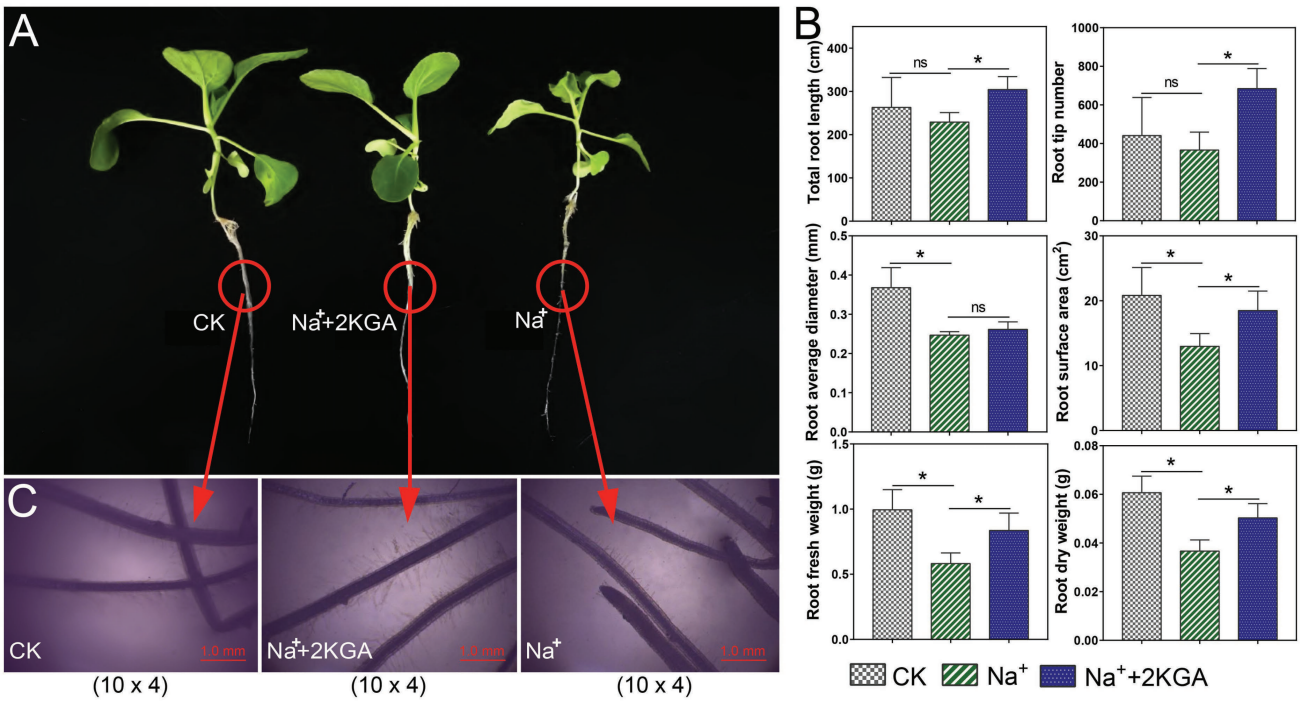

FIGURE 3 | Root morphology and indexes for each experimental group. The morphology of intact plants **(A)** and roots (10 × 4; magnification: ×40; **C**), and root-related parameters **(B)**. Five root samples of each biological replicate were scanned. Total root length was calculated as the sum of detectable primary and lateral root lengths. ns, not significant, $^{*}p < 0.05$.

Organic Solutes, ASA, Antioxidant Enzymes, H_2O_2, and MDA

Under salt stress, plants must increase their levels of anti-osmotic organic solutes (such as SC, SP, and proline) to maintain cell morphology and balance osmotic pressure. In the early stage of stress (day 3), the SC concentration of the Na^+ group increased by 30.47% compared with that of the CK group. Subsequently, however, the SC levels in the Na^+ group decreased rapidly and were lower than those of the CK group on days 6 and 9. There was no significant difference in SC content between the Na^++2KGA and Na^+ groups on day 3; however, the SC content in the Na^++2KGA group remained at a high level on days 6 and 9, showing increases of 81.68 and 98.03%, respectively, relative to those of the Na^+ group (**Figure 4**).

The SP concentration displayed a continuous increase over time. The Na^++2KGA group had a greater SP content than the Na^+ group, showing increases of 7.37, 9.53, and 4.74% on days 3, 6, and 9, respectively. From day 6, proline accumulation was significantly improved in the Na^+ group and was 6.15-fold higher compared with that of the CK group. The proline content in the Na^++2KGA group was similar, albeit slightly greater, to that of the Na^+ group. The ASA content of all the groups peaked on day 3. Compared with the Na^+ group, the ASA content in the Na^++2KGA group was significantly increased (16.24%). After day 3, the ASA content of each group began to decline and was lower in the Na^+ and Na^++2KGA groups than in the CK group on days 6 and 9; however, the ASA level was always higher in the Na^++2KGA group than in the Na^+ group (**Figure 4**).

Superoxide dismutase was 7.90% higher in the Na^++2KGA group compared with that of the Na^+ group on day 9. Meanwhile, PODa in the Na^++2KGA group was 9.63, 10.17, and 18.15% higher on days 3, 6, and 9, respectively, compared with that of the Na^+ group. Additionally, compared with the Na^+ group, APXa in the Na^++2KGA group was increased by 27.80, 11.03, and 10.29% on days 3, 6, and 9, respectively. Similarly, 2KGA caused a continuous increase in CATa of 31.85, 21.97, and 23.19% on days 3, 6, and 9 compared to that of Na^+ (**Figure 4**).

In plants, MDA is a product of cell membrane lipid oxidation and is a biochemical marker for assessing the degree of membrane lipid peroxidation (Silva et al., 2010). The results showed that H_2O_2 and MDA remained at a stable level in the seedlings under normal growth conditions but increased under salt stress. In the early stage (day 3), 2KGA did not affect H_2O_2 metabolism; from day 6, however, the H_2O_2 level in the Na^++2KGA group decreased rapidly compared with that of the Na^+ group and was reduced by 16.16% on day 9. Simultaneously, the MDA content decreased by 8.97% on day 9. These results indicated that membrane lipid peroxidation was attenuated following 2KGA treatment. The level of H_2O_2 in the Na^++2KGA group was similar to that of the control group on day 9 (**Figure 4**).

Analysis of Correlations Among Leaf Metabolites

Under salt stress, variations in the levels of organic solutes and photosynthetic pigments and activities of antioxidant enzymes in leaves were correlated with H_2O_2 and MDA contents

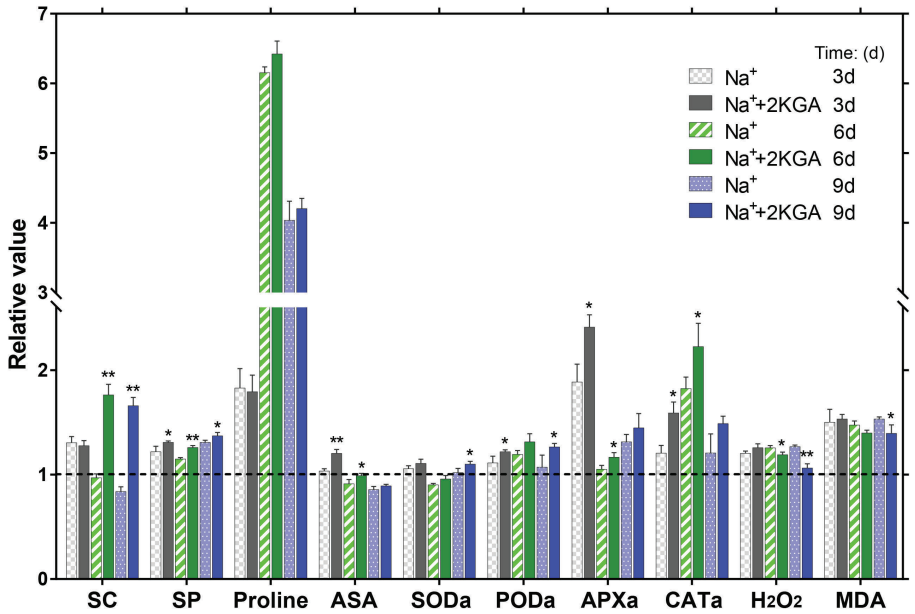

FIGURE 4 | Variations in the contents of organic solutes, ASA, antioxidant enzymes, H_2O_2, and MDA in seedling leaves at different time points. Data were normalized relative to the control (CK) group. The absolute results are shown in **Supplementary Table S2**. SC, soluble carbohydrate; SP, soluble protein; ASA, L-ascorbic acid; SODa, superoxide dismutase activity; PODa, peroxidase activity; APXa, ascorbate peroxidase activity; CATa, catalase activity; H_2O_2, hydrogen peroxide; and MDA, malondialdehyde. $^*p<0.05$, $^{**}p<0.01$.

(**Supplementary Figure S2**). Under 2KGA treatment, changes in photosynthetic pigment levels were correlated with the osmotic resistance of organic solute contents (**Figure 5A**). The Chla/Chlb ratio was negatively correlated with SP and proline levels and positively correlated with SC levels; however, Chlab/Car levels were positively correlated with SP and proline content and negatively correlated with SC content. Antioxidant enzyme activity was negatively correlated with H_2O_2 and MDA concentrations (**Figure 5B**). ASA content was positively correlated with antioxidant enzyme activity and photosynthetic pigment levels (**Figure 5C**).

ASA-Related Gene Expression

The expression levels of *GLO* and *GMP*, genes acting in the ASA biosynthesis pathway, were significantly increased in the Na^++2KGA group relative to those of the Na^+ group; in particular, the *GLO* expression level was consistently higher in the Na^++2KGA group than in the Na^+ group (**Figure 6**). *MIOX* and *GLDH* levels were not significantly different between the Na^+ and Na^++2KGA groups.

In the ASA recycling pathway, 2KGA treatment did not affect the expression of *MDHAR* or *DHAR1*. Compared to the Na^+ group, the expression level of *DHAR3* was significantly increased on day 6 in the Na^++2KGA group, but no significant difference was observed between the two groups on day 9. Furthermore, the expression of *DHAR3* was lower in both the Na^+ and Na^++2KGA groups than in the control group ($p<0.05$; **Supplementary Figure S3**). The expression of *APX* in the Na^++2KGA group was higher than that in the Na^+ group at each sampling time point (**Figure 6**). The results of nucleic acid quality assessment are provided in **Supplementary Table S3** and **Supplementary Figure S4**.

DISCUSSION

We have previously shown that a 2KGA-rich fermentation residue from the vitamin C industry could increase soil organic matter content and endogenous ASA concentrations in crops, thereby leading to increased crop yields in saline soil (Kong et al., 2014). However, this fermentation residue was a mixture, and its main effectors had not been identified. The 2KGA content in the residue varies between 25 and 30%, that of oxalic acid is approximately 1–2%, while the levels of other organic acids comprise less than 1%; much of the rest is water. This suggested that the 2KGA component of the residue might be a key to enhancing ASA production in plants. In this study, we found that 2KGA treatment increased the biomass of non-heading Chinese cabbage subjected to salt stress.

In this study, under salt stress, the levels of H_2O_2 and MDA in non-heading Chinese cabbage seedlings were significantly increased, and peroxidative damage in the cell membrane was aggravated, resulting in the inhibition of seedling leaf and root development. However, the observed increase in leaf and root biomass, especially that of roots, in the Na^++2KGA group suggested that 2KGA could effectively relieve this inhibitory effect and promote seedling growth and development. Because it has been shown that enhancing endogenous ASA levels can promote root development (Aghaei et al., 2008), we speculated that these effects were most likely related to an increase in

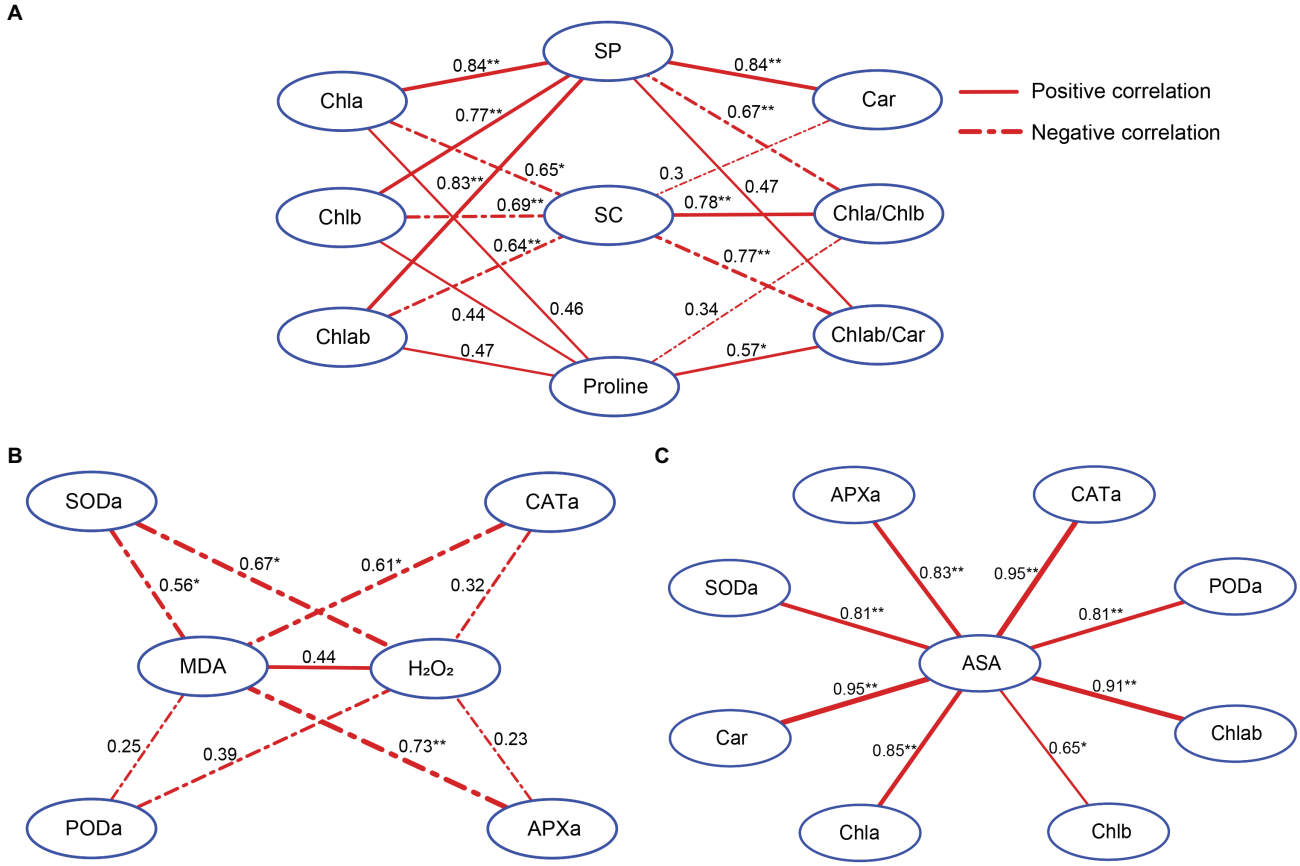

FIGURE 5 | The correlations among different metabolites in seedling leaves. **(A)** The correlation between photosynthetic pigment and organic solute contents. **(B)** The correlation between antioxidant enzyme activities and H_2O_2/MDA levels. **(C)** The correlation among ASA, antioxidant enzyme activity, and photosynthetic pigment content. Chla, chlorophyll a; Chlb, chlorophyll b; Car, carotenoids; Chlab, total chlorophyll; Chla/Chlb, the ratio of chlorophyll a content to chlorophyll b content; Chlab/Car, the ratio of total chlorophyll content to carotenoid content; SC, soluble carbohydrate; SP, soluble protein; SODa, superoxide dismutase activity; PODa, peroxidase activity; APXa, ascorbate peroxidase activity; CATa, catalase activity; H_2O_2, hydrogen peroxide; MDA, malondialdehyde; and ASA, L-ascorbic acid. The data correspond to the absolute value of the correlation coefficient. $^*p<0.05$, $^{**}p<0.01$.

ASA levels in the seedlings. In general, fluctuations in the concentrations of anti-osmotic organic solutes (including ASA), photosynthetic pigments, and antioxidant enzymes are essential for plants to resist salt stress.

Salt stress reduces the osmotic potential of plant cells by creating a high-salinity environment, which results in osmotic stress. The latter will lead to a reduction in the relative water content of plants and is not conducive to the maintenance of cell morphology (Annunziata et al., 2017). Osmotic adjustment represents an adaptive mechanism that helps cells maintain osmotic pressure and ensures normal metabolism and crop growth. In this study, we found that 2KGA treatment increased the SC, SP, and free proline contents in the leaves of non-heading Chinese cabbage under salt stress. The accumulation of SC is especially important for osmotic regulation, while SP and proline are believed to play a more important role in protecting cells from oxidative damage and enhancing defensive responses (Zhang et al., 2011; Li et al., 2019; Alfosea-Simón et al., 2020).

In the present study, the photosynthetic pigment content was found to be correlated with the SC level. When 2KGA was added under conditions of salt stress, the Chlab/Car ratio was negatively correlated with SC content. The results also showed that SC content was significantly increased on day 3 post stress induction and then rapidly decreased in the CK and Na^+ groups, while the addition of 2KGA could effectively reverse the loss of SC content. Simultaneously, the Na^++2KGA group had a lower ratio of Chab/Car. Under all treatments, the photosynthetic pigment content continuously increased along with the growth of the seedlings. Under salt stress, photosynthetic pigments accumulated at a high level, and the variations in H_2O_2 and MDA contents were positively correlated with photosynthetic pigment levels. This indicated that enhanced photosynthesis was a defense mechanism employed by seedlings to resist salt stress, and the addition of 2KGA further promoted the accumulation of photosynthetic pigments. This was in agreement with the results of previous studies, in which an increase in photosynthetic pigment levels was shown to improve photosynthetic efficiency and promote plant growth (Garg et al., 2002; Li and Yi, 2020). In contrast, in a recent study, Gautam et al. (2020) found that the photosynthetic efficiency of tobacco

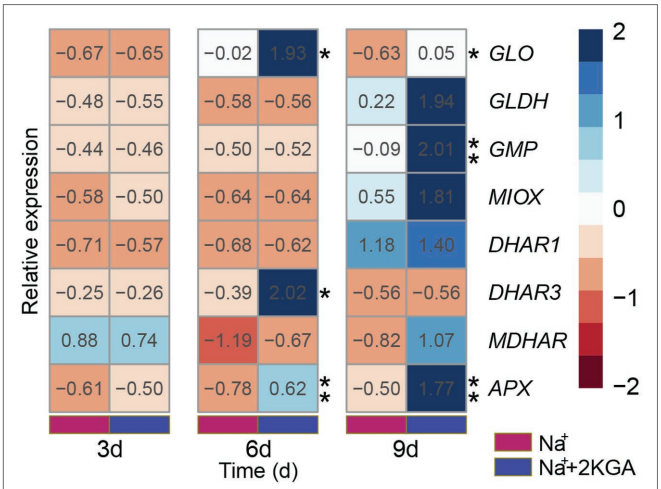

FIGURE 6 | Relative gene expression related to ASA accumulation. Data were normalized relative to that of the control (CK) group. *GLO*, *L-gulono-1,4-lactone oxidase*; *GLDH*, *L-galactose-1,4-lactone dehydrogenase*; *GMP*, *GDP-mannose pyrophosphorylase*; *MIOX*, *Myo-inositol oxygenase*; *DHAR1*, *dehydroascorbate reductase-1*; *DHAR3*, *dehydroascorbate reductase-3*; *MDHAR*, *monodehydroascorbate reductase*; *APX*, *ascorbate peroxidase*. $^{*}p < 0.05$, $^{**}p < 0.01$.

was reduced under salt stress. Differences in crop species investigated, time of action, or salt stress intensity might explain these discrepant results.

Photosynthesis is the primary means by which plants obtain carbon sources in the environment. However, in this study, the increase in photosynthetic pigment concentrations did not improve SC content in seedlings. Interestingly, photosynthetic pigment levels were positively correlated with variations in SP and proline content, indicating that seedlings could respond to salt stress by increasing photosynthetic pigment production and adjusting the Chla/Chlb and Chlab/Car ratios. Combined, these observations suggested that the addition of 2KGA enhanced the ability of the seedlings to regulate photosynthetic pigment levels, thereby resisting salt stress.

The photosynthesis system is also one of the main sites of reactive oxygen species (ROS) production in plant cells (Foyer and Noctor, 2011). Here, we found that salt stress increased the H_2O_2 content. The accumulation of ROS leads to an increase in antioxidant enzyme activity (Attia et al., 2020; Li and Yi, 2020). Accordingly, PODa, CATa, and APXa were higher in the Na^+ group than in the CK group and were positively correlated with fluctuations in H_2O_2 and MDA levels (**Supplementary Figure S2**). However, with the application of 2KGA, the activities of all four enzymes increased relative to those in the Na^+ group, and they were all negatively correlated with H_2O_2 and MDA contents. These results suggested that salt stress promoted the increase in H_2O_2 and MDA concentrations in seedlings, which subsequently led to a passive increase in antioxidant enzyme activities. Nevertheless, the addition of 2KGA enhanced antioxidant enzyme activity in the leaves, leading to faster H_2O_2 and MDA clearance.

Our findings demonstrated that the application of 2KGA could significantly increase ASA concentrations in non-heading Chinese cabbage seedlings exposed to salt stress. ASA content was positively correlated with antioxidant enzyme activities and photosynthetic pigment levels, indicating that the increase in ASA levels promoted the increase in antioxidant enzyme activities and photosynthetic pigment contents in the seedlings. Plants use ASA to remove large amounts of ROS produced by the photosynthesis system to avoid peroxidative damage (Talla et al., 2011), which is indicative of the importance of ASA in the protection of the photosynthesis system. Lim et al. (2012) reported that under salt stress, increasing endogenous ASA content in the tomato could enhance the photosynthetic pigment content. Meanwhile, exogenous ASA application can reportedly increase the levels of endogenous ASA and the activities of antioxidant enzymes in plants under heavy metal stress and salt stress (Athar et al., 2008; Chao and Kao, 2010). The above results suggested that ASA has a crucial function in plant defenses against salt stress.

To explore the mechanism underlying the 2KGA-mediated enhancement of ASA synthesis in non-heading Chinese cabbage under salt stress, we analyzed the expression levels of eight genes involved in the ASA accumulation. *DHAR3* was more highly expressed in the Na^++2KGA group relative to that in the Na^+ group, but only in the early stage of the experiment; in later stages, *DHAR3* expression was downregulated in both groups. This observation may explain why the ASA content was lower in the salt-stressed groups than in the CK group. The increase in *GMP* expression in the Na^++2KGA group reached significance only on day 9, and its contribution to ASA accumulation in the early stage was thus likely to have been limited. At present, GLO is the only confirmed enzyme involved in the synthesis of ASA in the L-gulose pathway. The expression level of *GLO* in the Na^++2KGA group was maintained at a higher level throughout the whole test period compared with that in the Na^+ group, while greater ASA accumulation was also observed in the former. An earlier study on the potato showed that an increase in *GLO* expression promoted the accumulation of ASA and enhanced abiotic stress tolerance (Lim et al., 2012). As a downstream product of ASA metabolism, the ketone group of 2KGA can be reduced to a hydroxyl group (Jia et al., 2019), which has the possibility of forming gulonic acid, a precursor in gulonolactone synthesis (catalyzed by GLO and converted to ASA) in plants (Cruz-Rus et al., 2012). This suggests strongly that exogenous 2KGA supplementation may increase the endogenous 2KGA content in non-heading Chinese cabbage. Meanwhile, the higher levels of gulonic acid and gulonolactone, both ASA precursors, finally leads to an increase in ASA content *via* GLO catalytic activity. The increase in *GMP* and *DHAR3* expression levels also exerted a positive effect on plant ASA accumulation (Lin et al., 2011; Wang et al., 2019). Moreover, in agreement with the observed increase in APX enzyme activity, *APX* gene expression was found to be upregulated with 2KGA administration, which further implied that 2KGA enhanced the resistance of non-heading Chinese cabbage seedlings to salt stress by increasing the endogenous ASA content. APX catalyzes the conversion of H_2O_2 to water and O_2, with ASA serving as the reductant

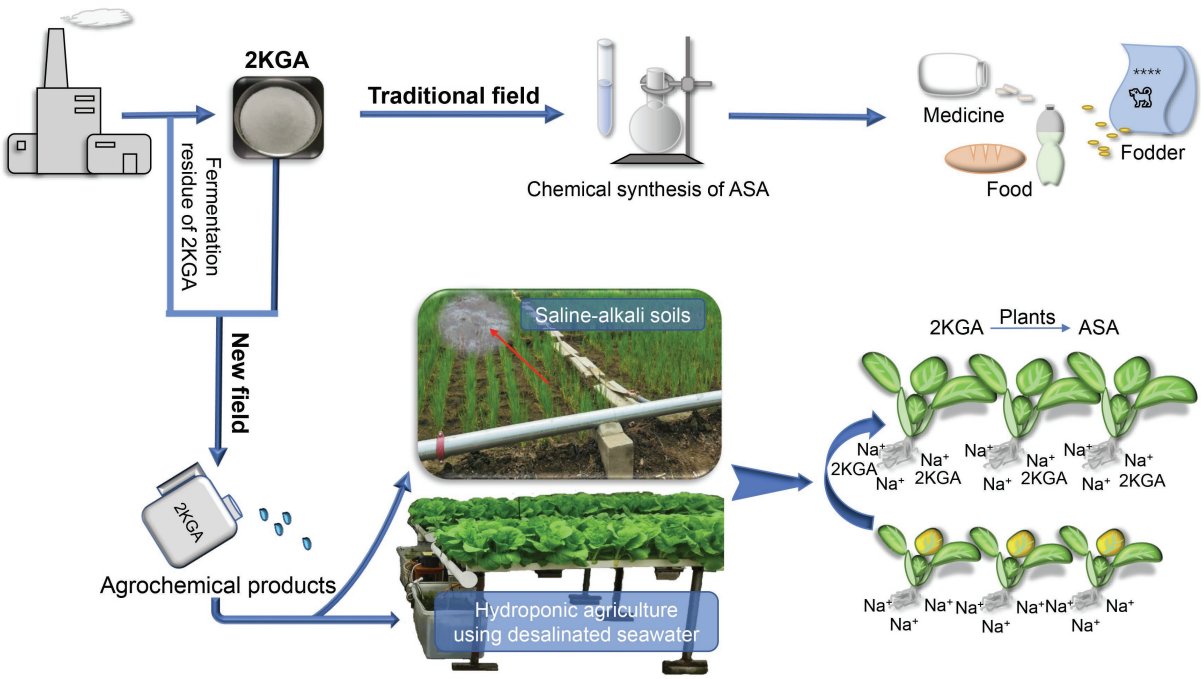

FIGURE 7 | The prospect for the application of 2KGA and its fermentation residue. 2KGA, 2-keto-L-gulonic acid; ASA, L-ascorbic acid.

(Tyagi et al., 2020). Thus, the higher ASA content and APXa in the Na^++2KGA group explains why the level of H_2O_2 was lower in this group than in the Na^+ group.

Although we demonstrated that 2KGA can relieve the inhibition of salt stress on the growth of non-heading Chinese cabbage seedlings, this is a preliminary study in this field. Many aspects remain to be explored, such as whether 2KGA has the same effect on different crops, whether 2KGA influences acetylsalicylic acid synthesis and carbon and nitrogen metabolism, and how 2KGA can efficiently be applied in agricultural practice. As a precursor of industrial ASA synthesis, 2KGA is produced on a large scale using a two-step microbial fermentation process; however, that 2KGA is only used in the chemical synthesis step of ASA production. In addition, a large amount of fermentation residue is discarded from the ASA industry. This provides a reliable industrial base for the application of 2KGA or its fermentation residue in a new field, that is, agriculture. Consequently, given the function of 2KGA against salt stress and its availability in the ASA industry, the prospect of applying 2KGA in agriculture, such as for crop cultivation in saline-alkali soils and hydroponic agriculture, merits further investigation (**Figure 7**).

CONCLUSION

In summary, to the best of our knowledge, this is the first study to report that 2KGA relieves the inhibitory effect of salt stress on non-heading Chinese cabbage, which has laid the foundation for the future application of 2KGA in agriculture. Meanwhile, a potential novel direction for the study of plant ASA metabolism was also identified. Our findings suggest that exogenous 2KGA application strengthens non-heading Chinese cabbage defenses against salt stress, for which the promotion of ASA accumulation may represent a crucial underlying mechanism.

DATA AVAILABILITY STATEMENT

The original contributions presented in the study are included in the article/**Supplementary Material**; further inquiries can be directed to the corresponding authors.

AUTHOR CONTRIBUTIONS

MG and HX: conceptualization. MG, MS, QW, and DJ: methodology. HS: software. MG and MS: validation. MG and BW: formal analysis. YL, LH, and XR: resources. MG: investigation, data curation, writing-original draft, and visualization. MG, HX, HS, and WY: writing-review and editing. WY and LZ: supervision. HX: project administration. All authors contributed to the article and approved the submitted version.

FUNDING

This work was supported by the National Key Research and Development Program of China (grant number 2020YFA0907800), the Science and Technology Plan Project of Shenyang (grant number 20-203-5-48), and the Open Research Project of Shouguang Facilities Agriculture Center in the Institute of Applied Ecology (grant number 2018SG-S-02).

ACKNOWLEDGMENTS

We thank Shuang Kong and Xiaohuan Lv for their support and Shuang Ma for her guidance during the experiments.

SUPPLEMENTARY MATERIAL

The Supplementary Material for this article can be found online at: https://www.frontiersin.org/articles/10.3389/fpls.2021.697184/full#supplementary-material

REFERENCES

Aghaei, K., Ehsanpour, A. A., and Komatsu, S. (2008). Proteome analysis of potato under salt stress. *J. Proteome Res.* 7, 4858–4868. doi: 10.1021/pr800460y

Ahanger, M. A., Aziz, U., Alsahli, A. A., Alyemeni, M. N., and Ahmad, P. (2019). Influence of exogenous salicylic acid and nitric oxide on growth, photosynthesis, and ascorbate-glutathione cycle in salt stressed *Vigna angularis*. *Biomol. Ther.* 10:42. doi: 10.3390/biom10010042

Alfosea-Simón, M., Zavala-Gonzalez, E. A., Camara-Zapata, J. M., Martínez-Nicolás, J. J., Simón, I., Simón-Grao, S., et al. (2020). Effect of foliar application of amino acids on the salinity tolerance of tomato plants cultivated under hydroponic system. *Sci. Hortic* 272:109569. doi: 10.1016/j.scienta.2020.109509

Annunziata, M. G., Ciarmiello, L. F., Woodrow, P., Maximova, E., Fuggi, A., and Carillo, P. (2017). Durum wheat roots adapt to salinity remodeling the cellular content of nitrogen metabolites and sucrose. *Front. Plant Sci.* 7:2035. doi: 10.3389/fpls.2016.02035

Athar, H. R., Khan, A., and Ashraf, M. (2008). Exogenously applied ascorbic acid alleviates salt-induced oxidative stress in wheat. *Environ. Exp. Bot.* 63, 224–231. doi: 10.1016/j.envexpbot.2007.10.018

Attia, H., Al-Yasi, H., Alamer, K., Ali, E., Hassan, F., Elshazly, S., et al. (2020). Induced anti-oxidation efficiency and others by salt stress in *Rosa damascena* miller. *Sci. Hortic* 274:109681. doi: 10.1016/j.scienta.2020.109681

Azevedo Neto, A. D., Prisco, J. T., Enéas-Filho, J., Abreu, C. E. B., and Gomes-Filho, E. (2006). Effect of salt stress on antioxidative enzymes and lipid peroxidation in leaves and roots of salt-tolerant and salt-sensitive maize genotypes. *Environ. Exp. Bot.* 56, 87–94. doi: 10.1016/j.envexpbot.2005.01.008

Bradford, M. M. (1976). A rapid and sensitive method for the quantitation of microgram quantities of protein utilizing the principle of protein-dye binding. *Anal. Biochem.* 72, 248–254. doi: 10.1016/0003-2697(76)90527-3

Chao, Y. Y., and Kao, C. H. (2010). Heat shock-induced ascorbic acid accumulation in leaves increases cadmium tolerance of rice (*Oryza sativa* L.) seedlings. *Plant Soil* 336, 39–48. doi: 10.1007/s11104-010-0438-7

Cronje, C., George, G. M., Fernie, A. R., Bekker, J., Kossmann, J., and Bauer, R. (2012). Manipulation of L-ascorbic acid biosynthesis pathways in *Solanum lycopersicum*: elevated GDP-mannose pyrophosphorylase activity enhances L-ascorbate levels in red fruit. *Planta* 235, 553–564. doi: 10.1007/s00425-011-1525-6

Cruz-Rus, E., Amaya, I., and Valpuesta, V. (2012). The challenge of increasing vitamin C content in plant foods. *Biotechnol. J.* 7, 1110–1121. doi: 10.1002/biot.201200041

Foyer, C. H., and Noctor, G. (2011). Ascorbate and glutathione: the heart of the redox hub. *Plant Physiol.* 155, 2–18. doi: 10.1104/pp.110.167569

Gao, Q., and Zhang, L. (2008). Ultraviolet-B-induced oxidative stress and antioxidant defense system responses in ascorbate-deficient *vtc1* mutants of *Arabidopsis thaliana*. *J. Plant Physiol.* 165, 138–148. doi: 10.1016/j.jplph.2007.04.002

Garg, A. K., Kim, J. K., Owens, T. G., Ranwala, A. P., Choi, Y. D., Kochian, L. V., et al. (2002). Trehalose accumulation in rice plants confers high tolerance levels to different abiotic stresses. *Proc. Natl. Acad. Sci. U. S. A.* 99, 15898–15903. doi: 10.1073/pnas.252637799

Gautam, R., Meena, R. K., Woch, N., and Kirti, P. B. (2020). Ectopic expression of *BrALDH7B2* gene encoding an antiquitin from *Brassica rapa* confers tolerance to abiotic stresses and improves photosynthetic performance under salt stress in tobacco. *Environ. Exp. Bot.* 180:104223. doi: 10.1016/j.envexpbot.2020.104223

Ghoulam, C., Foursy, A., and Fares, K. (2002). Effects of salt stress on growth, inorganic ions and proline accumulation in relation to osmotic adjustment in five sugar beet cultivars. *Environ. Exp. Bot.* 47, 39–50. doi: 10.1007/s11104-010-0438-7

Huang, C., He, W., Guo, J., Chang, X., Su, P., and Zhang, L. (2005). Increased sensitivity to salt stress in an ascorbate-deficient *Arabidopsis* mutant. *J. Exp. Bot.* 56, 3041–3049. doi: 10.1093/jxb/eri301

Jia, Y., Burbidge, C. A., Sweetman, C., Schutz, E., Soole, K., Jenkins, C., et al. (2019). An aldo-keto reductase with 2-keto-L-gulonate reductase activity functions in L-tartaric acid biosynthesis from vitamin C in *Vitis vinifera*. *J. Biol. Chem.* 294, 15932–15946. doi: 10.1074/jbc.RA119.010196

Kim, Y. S., Kim, I. S., Shin, S. Y., Park, T. H., Park, H. M., Kim, Y. H., et al. (2014). Overexpression of dehydroascorbate reductase confers enhanced tolerance to salt stress in rice plants (*Oryza sativa* L. *japonica*). *J. Agron. Crop Sci.* 200, 444–456. doi: 10.1111/jac.12078

Kong, T., Xu, H., Wang, Z., Sun, H., and Wang, L. (2014). Effect of a residue after evaporation from industrial vitamin C fermentation on chemical and microbial properties of alkali-saline soil. *Pak. J. Pharm. Sci.* 27, 1069–1074. doi: 10.1002/smll.200900562

Lacerda, C. F., Cambraia, J., Oliva, M. A., Ruiz, H. A., and Prisco, J. T. (2003). Solute accumulation and distribution during shoot and leaf development in two sorghum genotypes under salt stress. *Environ. Exp. Bot.* 49, 107–120. doi: 10.1016/S0098-8472(02)00064-3

Li, Q., Wang, G., Guan, C., Yang, D., Wang, Y., Zhang, Y., et al. (2019). Overexpression of *LcSABP*, an orthologous gene for salicylic acid binding protein 2, enhances drought stress tolerance in transgenic tobacco. *Front. Plant Sci.* 10:200. doi: 10.3389/fpls.2019.00200

Li, L., and Yi, H. (2012). Effect of sulfur dioxide on ROS production, gene expression and antioxidant enzyme activity in *Arabidopsis* plants. *Plant Physiol. Biochem.* 58, 46–53. doi: 10.1016/j.plaphy.2012.06.009

Li, L., and Yi, H. (2020). Photosynthetic responses of *Arabidopsis* to SO_2 were related to photosynthetic pigments, photosynthesis gene expression and redox regulation. *Ecotoxicol. Environ. Saf.* 203:111019. doi: 10.1016/j.ecoenv.2020.111019

Lichtenthaler, H. K. (1987). Chlorophylls and carotenoids: pigments of photosynthetic biomembranes. *Methods Enzymol.* 148, 350–382. doi: 10.1016/0076-6879(87)48036-1

Lim, M. Y., Pulla, R. K., Park, J. M., Harn, C. H., and Jeong, B. R. (2012). Over-expression of *L-gulono-γ-lactone oxidase* (*GLO*ase) gene leads to ascorbate accumulation with enhanced abiotic stress tolerance in tomato. *In Vitro Cell Dev. Biol. Plant* 48, 453–461. doi: 10.1007/s11627-012-9461-0

Lin, L., Shi, Q., Wang, H., Qin, A., and Yu, X. (2011). Over-expression of tomato GDP-mannose pyrophosphorylase (GMPase) in potato increases ascorbate content and delays plant senescence. *Agric. Sci. China* 10, 534–543. doi: 10.1016/S1671-2927(11)60034-5

Liu, W., An, H., and Yang, M. (2013). Overexpression of *Rosa roxburghii* L-galactono-1,4-lactone dehydrogenase in tobacco plant enhances ascorbate accumulation and abiotic stress tolerance. *Acta Physiol. Plant.* 35, 1617–1624. doi: 10.1007/s11738-012-1204-7

Livak, K. J., and Schmittgen, T. D. (2001). Analysis of relative gene expression data using real-time quantitative PCR and the 2(-Delta Delta C(T)) method. *Methods* 25, 402–408. doi: 10.1006/meth.2001.1262

Nielsen, S. S. (eds). (2010). "Phenol-sulfuric acid method for total carbohydrates," in *Food Analysis Laboratory Manual* (Switzerland: Springer International Publishing), 47–53.

Nounjan, N., Nghia, P. T., and Theerakulpisut, P. (2012). Exogenous proline and trehalose promote recovery of rice seedlings from salt-stress and differentially modulate antioxidant enzymes and expression of related genes. *J. Plant Physiol.* 169, 596–604. doi: 10.1016/j.jplph.2012.01.004

Santos, F. S. S. D., Viana, T. V. D. E. A., Costa, S. C., Sousa, G. G. D., and Azevedo, B. M. D. (2019). Growth andyieldofsemi-hydroponic bell pepper underdesalination waste-water and organic and mineralfertilization. *Rev. Caatinga* 32, 1005–1014. doi: 10.1590/1983-21252019v32n417rc

Shalata, A., and Neumann, P. M. (2001). Exogenous ascorbic acid (vitamin C) increase resistance to salt stress and reduces lipid peroxidation. *J. Exp. Bot.* 52, 2207–2211. doi: 10.1093/jexbot/52.364.2207

Silva, E. N., Ferreira-Silva, S. L., Viégas, R. A., and Silveira, J. A. G. (2010). The role of organic and inorganic solutes in the osmotic adjustment of drought-stressed jatropha curcas plants. *Environ. Exp. Bot.* 69, 279–285. doi: 10.1016/j.envexpbot.2010.05.001

Talla, S., Riazunnisa, K., Padmavathi, L., Sunil, B., Rajsheel, P., and Raghavendra, A. S. (2011). Ascorbic acid is a key participant during the interactions between chloroplasts and mitochondria to optimize photosynthesis and protect against photoinhibition. *J. Biosci.* 36, 163–173. doi: 10.1007/s12038-011-9000-x

Tyagi, S., Shumayla, , Verma, P. C., Singh, K., and Upadhyay, S. K. (2020). Molecular characterization of *ascorbate peroxidase* (*APX*) and *APX-related* (*APX-R*) genes in *Triticum aestivum* L. *Genomics* 112, 4208–4223. doi: 10.1016/j.ygeno.2020.07.023

Velikova, V., Yordanov, I., and Edreva, A. (2000). Oxidative stress and some antioxidant systems in acid rain-treated bean plants. *Plant Sci.* 151, 59–66. doi: 10.1016/S0168-9452(99)00197-1

Wang, W., Qiu, X., Kim, H. S., Yang, Y., Hou, D., Liang, X., et al. (2019). Molecular cloning and functional characterization of a sweetpotato chloroplast *IbDHAR3* gene in response to abiotic stress. *Plant Biotechnol. Rep.* 14, 9–19. doi: 10.1007/s11816-019-00576-7

Wang, L., Wang, Y., Wang, X., Li, Y., Peng, F., and Wang, L. (2014). Regulation of POD activity by pelargonidin during vegetative growth in radish (*Raphanus sativus* L.). *Sci. Hortic* 174, 105–111. doi: 10.1016/j.scienta.2014.05.014

Xu, H., Yang, W., and Li, J. (2021). New progress on the second step of the mixed fermentation for vitamin C. *China J. Microbiol.* 41, 1–9. doi: 10.3969/j.issn.1005-7021.2021.02.001

Yang, W., Han, L., Mandlaa, M., Zhang, H., Zhang, Z., and Xu, H. (2017). A plate method for rapid screening of *Ketogulonicigenium vulgare* mutants for enhanced 2-keto-L-gulonic acid production. *Braz. J. Microbiol.* 48, 397–402. doi: 10.1016/j.bjm.2017.02.002

Zandalinas, S. I., Fichman, Y., Devireddy, A. R., Sengupta, S., Azad, R. K., and Mittler, R. (2020). Systemic signaling during abiotic stress combination in plants. *Proc. Natl. Acad. Sci. U. S. A.* 117, 13810–13820. doi: 10.1073/pnas.2005077117

Zhang, C., Liu, J., Zhang, Y., Cai, X., Gong, P., Zhang, J., et al. (2011). Overexpression of *SlGMEs* leads to ascorbate accumulation with enhanced oxidative stress, cold, and salt tolerance in tomato. *Plant Cell Rep.* 30, 389–398. doi: 10.1007/s00299-010-0939-0

Zhao, X., Bian, X., Li, Z., Wang, X., Yang, C., Liu, G., et al. (2014). Genetic stability analysis of introduced *Betula pendula*, *Betula kirghisorum*, and *Betula pubescensfamilies* in saline-alkali soil of northeastern China. *Scand. J. Forest Res.* 29, 639–649. doi: 10.1080/02827581.2014.960892

Conflict of Interest: YL, LH, and XR were employed by the company Yikang Environment Biotechnology Development Co., Ltd., Shenyang, China.

The remaining authors declare that the research was conducted in the absence of any commercial or financial relationships that could be construed as a potential conflict of interest.

Publisher's Note: All claims expressed in this article are solely those of the authors and do not necessarily represent those of their affiliated organizations, or those of the publisher, the editors and the reviewers. Any product that may be evaluated in this article, or claim that may be made by its manufacturer, is not guaranteed or endorsed by the publisher.

frontiers in Plant Science

ORIGINAL RESEARCH
published: 18 November 2021
doi: 10.3389/fpls.2021.775785

Co-composted Biochar Enhances Growth, Physiological, and Phytostabilization Efficiency of *Brassica napus* and Reduces Associated Health Risks Under Chromium Stress

Muhammad Naveed[1], Bisma Tanvir[1], Wang Xiukang[2]*, Martin Brtnicky[3,4], Allah Ditta[5,6], Jiri Kucerik[4], Zinayyera Subhani[7], Muhammad Zubair Nazir[1], Maja Radziemska[3,8], Qudsia Saeed[1] and Adnan Mustafa[9]**

[1] Institute of Soil and Environmental Sciences, University of Agriculture, Faisalabad, Pakistan, [2] College of Life Sciences, Yan'an University, Yan'an, China, [3] Department of Agrochemistry, Soil Science, Microbiology and Plant Nutrition, Faculty of AgriSciences, Mendel University in Brno, Brno, Czechia, [4] Faculty of Chemistry, Institute of Chemistry and Technology of Environmental Protection, Brno University of Technology, Brno, Czechia, [5] Department of Environmental Sciences, Shaheed Benazir Bhutto University, Sheringal, Upper Dir, Pakistan, [6] School of Biological Sciences, The University of Western Australia, Perth, WA, Australia, [7] Faculty of Life Sciences, University of Central Punjab, Lahore, Pakistan, [8] Institute of Environmental Engineering, Warsaw University of Life Sciences, Warsaw, Poland, [9] Biology Centre, The Soil and Water Research Infrastructure (SoWa RI), Czech Academy of Sciences, Ceske Budejovice, Czechia

Among heavy metals, chromium (Cr) contamination is increasing gradually due to the use of untreated industrial effluents for irrigation purposes, thereby posing a severe threat to crop production. This study aimed to evaluate the potential of compost, biochar (BC), and co-composted BC on the growth, physiological, biochemical attributes, and health risks associated with the consumption of *Brassica* grown on Cr-contaminated soil. Results revealed that Cr stress (Cr-25) significantly reduced the growth and physiological attributes and increased antioxidant enzyme activities in *Brassica*, but the applied amendments considerably retrieved the negative effects of Cr toxicity through improving the growth and physiology of plants. The maximum increase in plant height (75.3%), root length (151.0%), shoot dry weight (139.4%), root dry weight (158.5%), and photosynthetic rate (151.0%) was noted with the application of co-composted BC under Cr stress (Cr-25) in comparison to the control. The application of co-composted BC significantly reduced antioxidant enzyme activities, such as APX (42.5%), GP (45.1%), CAT (45.4%), GST (47.8%), GR (47.1%), and RG (48.2%), as compared to the control under Cr stress. The same treatment reduced the accumulation of Cr in grain, shoot, and roots of *Brassica* by 4.12, 2.27, and 2.17 times and enhanced the accumulation in soil by 1.52 times as compared to the control. Moreover, the application of co-composted BC significantly enhanced phytostabilization efficiency and reduced associated health risks with the consumption of *Brassica*. It is concluded that

OPEN ACCESS

Edited by:
Maurizio Ruzzi, University of Tuscia, Italy

Reviewed by:
Lorenzo Rossi, University of Florida, United States
Huagang Huang, Sichuan Academy of Agricultural Sciences, China
Parvaiz Ahmad, Sri Pratap College Srinagar, India

***Correspondence:**
Muhammad Naveed
muhammad.naveed@uaf.edu.pk
Wang Xiukang
wangxiukang@yau.edu.cn
Adnan Mustafa
adnanmustafa780@gmail.com

Specialty section:
This article was submitted to Plant Abiotic Stress, a section of the journal Frontiers in Plant Science

Received: *14 September 2021*
Accepted: *19 October 2021*
Published: *18 November 2021*

Citation:
Naveed M, Tanvir B, Xiukang W, Brtnicky M, Ditta A, Kucerik J, Subhani Z, Nazir MZ, Radziemska M, Saeed Q and Mustafa A (2021) Co-composted Biochar Enhances Growth, Physiological, and Phytostabilization Efficiency of Brassica napus and Reduces Associated Health Risks Under Chromium Stress. Front. Plant Sci. 12:775785. doi: 10.3389/fpls.2021.775785

the application of co-composted BC in Cr-contaminated soil can significantly enhance the growth, physiological, and biochemical attributes of *Brassica* by reducing its uptake in plants and enhanced phytostabilization efficiency. The tested product may also help in restoring the soils contaminated with Cr.

Keywords: chromium, *Brassica*, health risks, phytostabilization, heavy metals

INTRODUCTION

The contamination of heavy metals (HMs) in soil is a serious threat to sustainable crop production and soil quality because these metals are non-degradable and persist in soil for longer durations (Kamran et al., 2019). HMs accumulation deteriorates the physicochemical and biological properties of soil, which results in poor nutrient availability and ultimately decreased crop yield (Mehmood et al., 2018b). Naturally, HMs are the constituent of sediments, adsorbed on soil organic matter, and their toxicity increased as free ions in soil solution (Abbas et al., 2020). Modern agricultural practices, especially excessive use of inorganic fertilizers and agrochemicals, have polluted soil and ultimately resulted in enhanced environmental degradation and threatened sustainability (Ditta et al., 2015; Murtaza et al., 2021b). Moreover, the application of organic waste manure, sewage sludge, and irrigation with industrial effluents contributes significant amounts of HMs into agricultural systems (Kamran et al., 2019; Bashir et al., 2020a,b).

Among HMs, chromium (Cr) is considered a major environmental pollutant due to its severe toxicity and recalcitrant nature (Ali et al., 2018). Industrial effluents from electroplating, catalytic manufacturing and wood preservation, leather tanning, and alloy preparation contain large amounts of Cr, which are the major sources of Cr contamination in the soil (Govil and Krishna, 2018). In the environment, Cr exits in various oxidation states, but Cr(III) and Cr(VI) are dominant in soil (Junaid et al., 2016; Bashir et al., 2020a). Cr(III) is an essential micronutrient for animals and involved in cell metabolism (de Oliveira et al., 2014), relatively stable, and 10–100 times less toxic as compared to Cr(VI) (Tepanosyan et al., 2020). Cr(VI) is a highly soluble, potentially mobile across membranes with strong oxidation potential, toxic, allergenic, carcinogenic, and irritant that damages the liver, kidney, and lungs (Bashir et al., 2020a,b; Tepanosyan et al., 2020).

The application of contaminated water with a higher concentration of Cr to the agricultural land not only results in detrimental effects on plant growth and loss of production, food security, and animal health but also affects the overall ecosystem (Mehmood et al., 2021). Cr phytotoxicity severely affects seed germination, decreases root growth and shoot growth, and ultimately reduces biomass production (Bashir et al., 2020a,b). Cr disrupts photosynthesis, nutrient utilization, water relation, and enzymatic activity which produces reactive oxygen species (ROS) that oxidize lipids, protein, and nucleic acid and ultimately result in plant death (de Oliveira et al., 2014; Bashir et al., 2020b; Murtaza et al., 2021b).

Various physical (e.g., soil incineration, landfill, excavation, and soil flushing), chemical (e.g., oxidation–reduction), and biological techniques (e.g., phytoremediation and biodegradation) have been used for remediation of metal-contaminated soils or conversion into less toxic form and reduced bioavailability to plants (Mustafa et al., 2020; Sabir et al., 2020; Irshad et al., 2021). Physical and chemical remediation techniques are laborious, time-consuming, and energy-consuming, and considerable toxic waste products are the main cause of limited application despite high efficiency and utility (Mustafa et al., 2020; Sabir et al., 2020). Among organic amendments, farmyard manure, animal waste, and compost are used to reduce HMs uptake for a shorter duration because these amendments improve soil physicochemical properties, nutrient uptake, soil aggregation, and maintain soil quality (Mehmood et al., 2018a; Chukwuka et al., 2020; Hu et al., 2020; Murtaza et al., 2021a). It is, therefore, a need of the hour to develop efficient *in situ* immobilization techniques that should be cost-effective, less destructive, and environment friendly for soil restoration.

In recent years, biochar (BC) is gaining popularity for the restoration of metal-contaminated sites and carbon sequestration in the soil for longer periods due to its recalcitrant nature, cost-effective, and ecofriendly approach (Mehmood et al., 2018a; Kamran et al., 2019). BC is a fine-grained black color porous material with carbonaceous nature produced from organic wastes (e.g., crop residues, sewage slug, animal wastes, and farmyard manure) at high temperatures under limited or no oxygen supply (Abbas et al., 2020; Hu et al., 2020). BC has unique physicochemical properties such as porous structure, high surface area, variety of oxygen-containing functional groups that make it an excellent material for soil fertility improvement, carbon sequestration, wastewater treatment, metal stabilization, and organic pollutant degradation in soil (Mehmood et al., 2018a,b; Chukwuka et al., 2020; Hu et al., 2020; Murtaza et al., 2021a). BC has a stable carbon pool that influences soil physicochemical and biological properties and directly increases soil organic carbon contents (Sarfraz et al., 2019; Ijaz et al., 2020; Ullah et al., 2020). The application of BC in agricultural soil improves aeration, increases nutrient availability, and increases soil organic matter, a microbial activity that ultimately increases crop production, decreases fertilizer requirement and nutrient leaching, and reduces soil erosion by controlling soil pollution (Doumer et al., 2016; Rizwan et al., 2021). BC reduces metal mobility through physical adsorption, ion exchange, surface precipitation, and metal complexation (Sarfraz et al., 2019; Irshad et al., 2021); cation exchange; and electrostatic interaction in metal-contaminated soil (Brassard et al., 2016). The adsorption property and high carbon contents of BC make it an excellent material to minimize Cr toxicity in the terrestrial ecosystem (Jia et al., 2017).

Various studies reported that combined application of compost and BC could be a better approach as BC increases compost stability and improves the productiveness of the soil, HM adsorption, and production of crop and carbon sequestration (Agegnehu et al., 2015; Coelho et al., 2018). The mixing of BC and compost adds value in increasing soil fertility by different aspects such as reducing the volatility of ammonia from manure or minimizing methane emission (Coelho et al., 2018). Compost provides high nutrients to the soil compared to BC, whereas BC could be reducing the decomposition rate of compost (Ditta et al., 2015). Many studies showed the combined application of BC and compost had a synergistic impact in improving soil structure, water-holding capacity, and nutrient contents under field conditions with reduced fertilizer use and nutrient loss from soil (Agegnehu et al., 2015). BC co-composting can reduce compost decomposition, decrease nutrient loss in the environment, improve soil structure by direct organic matter addition, and increase microbial biodiversity and activity in the soil. We hypothesized that co-composted BC could act as a better ameliorant for improving growth, physiology, and antioxidant machinery by retrieving the harmful effects of Cr in Cr-contaminated soil. The objectives of this study were to investigate the impact of compost, BC, and co-composted BC on growth, physiological, antioxidant, and biochemical attributes of *Brassica* grown under Cr-contaminated soil and the phytostabilization efficiency of compost, BC, and co-composted BC in addition to the Cr-contaminated soil and associated health risk assessment of *Brassica* grown under Cr stress.

RESULTS

Growth Attributes

Results of this study showed that the application of compost, BC, and co-composted BC significantly ($p < 0.05$) improved the growth of *Brassica* under Cr contamination (**Figure 1**). It was observed that the application of co-composted BC (Com-BC-2) resulted in the maximum increase in plant height (49.8%), root length (85.6%), shoot fresh (72.9%) and dry weight (70.0%), and root fresh (89.6%) and dry weight (74.0%) as compared to the control under normal soil, i.e., 0 mg Cr kg^{-1} (**Figure 1**). Soil spiked with Cr (25 mg Cr kg^{-1}) decreased the growth parameters of *Brassica*. However, the application of co-composted BC resulted in the maximum increase in shoot and root length, shoot fresh and dry weight, and root fresh and dry weight of *Brassica* by 75.3, 151.0, 140.0, 139.4, 193.9, and 158.5%, respectively, as compared to the control (Cr-25). It was followed by sole application of BC and compost in comparison to the controls under normal (Cr-0) and Cr stress (Cr-25).

Physiological Attributes

The application of BC and co-composted BC significantly ($p < 0.05$) enhanced the physiological attributes of *Brassica* under normal soil (Cr-0) or contaminated soil (Cr-25) when compared to the control (**Figure 2**). Under normal soil (Cr-0), the application of compost, BC, and co-composted BC significantly improved the physiological attributes of *Brassica* as compared to the control under Cr stress (Cr-25). In the case of chlorophyll contents (SPAD index), the maximum increase (2.25 times) was noticed with co-composted BC as compared to the control under normal soil (Cr-0). In soil spiked with Cr-25 concentration, the application of co-composted BC increased 2.17 times more chlorophyll contents (SPAD index) than the control under Cr stress (Cr-25). The same treatment caused an increase in 151.0, 104.3, 127.0, and 101.6% in photosynthetic rate, transpiration rate, stomatal conductance, and relative water contents, respectively, with the application of co-composted BC under Cr contamination (Cr-25). It was followed by BC and compost application under Cr contamination.

Antioxidant Enzyme Activities

Under Cr stress (Cr-25), the maximum APX (56.78 mol min^{-1} mg^{-1} protein), GP (88.43 mol min^{-1} mg^{-1} protein), CAT (16.87 nmol min^{-1} mg^{-1} protein), GST (267.13 μmol min^{-1} mg^{-1} protein), GR (30.70 mol min^{-1} mg^{-1} protein), and RG (133.27 nmol min^{-1} mg^{-1} protein) values were recorded without any treatment (**Figure 3**). The application of organic amendments (compost, BC, and co-composted BC) significantly reduced antioxidant enzyme activities as compared to the control. The maximum decrease in APX (42.5%), GP (45.1%), CAT (45.4%), GST (47.8%), GR (47.1%), and RG (48.2%) was observed with the application of co-composted BC in comparison to the control treatment.

Bean Weight and Total Soluble Sugars

Bean weight was significantly reduced under Cr stress, while a significant increase was noted with the application of compost, BC, and co-composted BC under Cr stress, i.e., Cr-25 (**Figure 4**). Under Cr stress, the minimum bean weight (3.29 g) was noted in the control treatment without any amendment, while the maximum bean weight (15.13 g) was recorded with the application of co-composted BC under normal conditions (Cr-0). The maximum bean weight (10.76) recorded with the application of co-composted BC was 3.27 times more as compared to the control (Cr-25). In the case of total sugar content (TSC), an opposite trend was recorded with the application of compost, BC, and co-composted BC (**Figure 4**). The maximum TSC (16.5) was observed under the control treatment (Cr-25), while the minimum TSC (7.83) was observed with the application of co-composted BC under normal conditions (Cr-0). The application of co-composted BC significantly reduced TSC (36.8%) in *Brassica* as compared to the control under Cr stress (Cr-25).

Chromium Accumulation

With the application of compost, BC, and co-composted BC, Cr accumulation in grain, root, and shoot samples of *Brassica* was significantly reduced in comparison to the control under Cr stress (**Figure 5**). However, Cr accumulation in soil was significantly enhanced with the application of co-composted BC in comparison to the control under Cr stress (Cr-25). With the application of co-composted BC, the minimum accumulation in grain (1.06 μg kg^{-1} DW), shoot (3.40 mg kg^{-1} DW), and root (5.33 mg kg^{-1} DW) portions of *Brassica* were 4.12, 2.27, and 2.17 times less as compared to that observed in the control

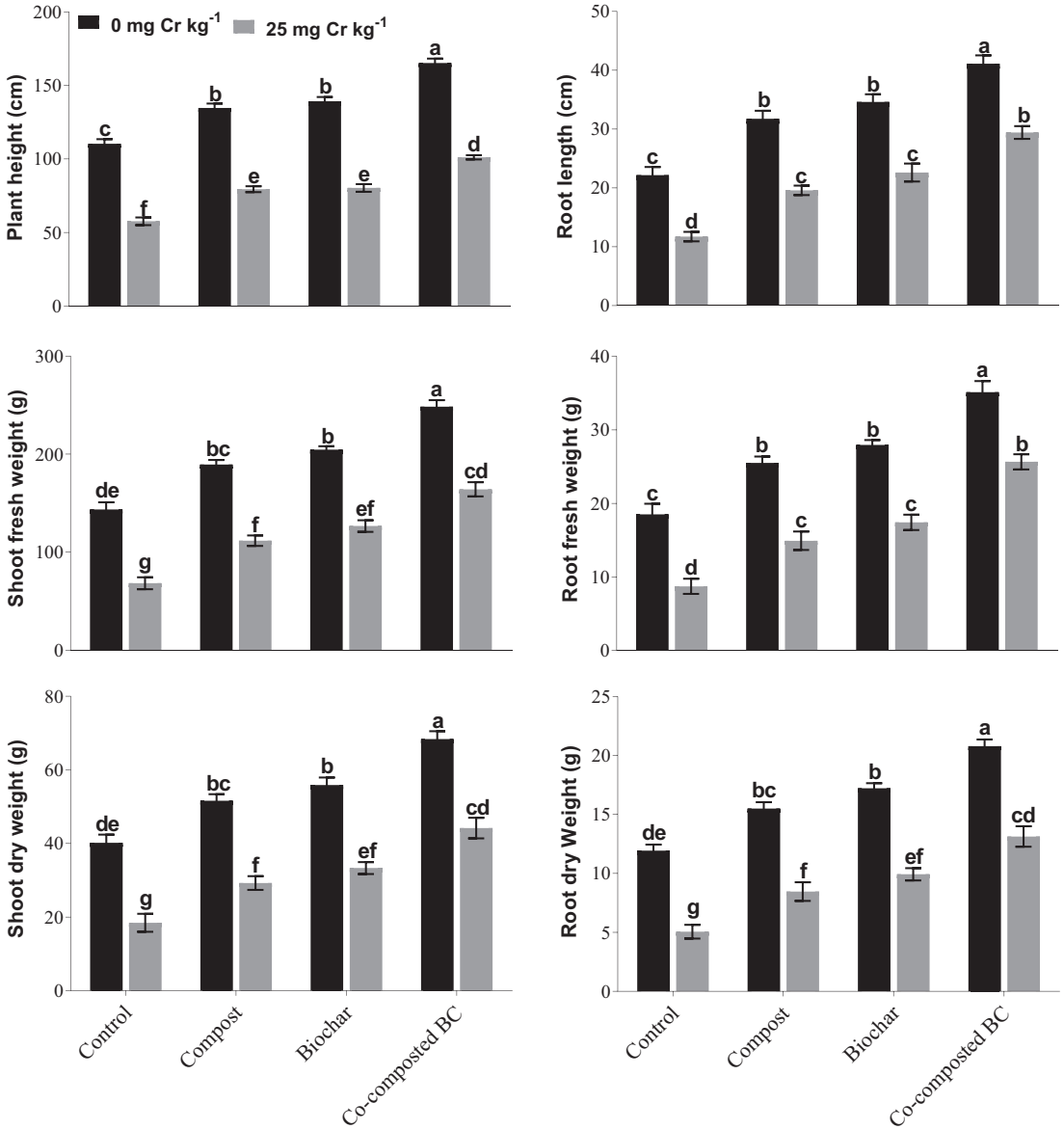

FIGURE 1 | Impact of compost, biochar, and co-composted biochar on growth and yield parameters of *Brassica*. The values are presented as mean ± standard error ($n = 3$). The values sharing the same letter(s) in bars are statistically non-significant with each other at $p < 0.05$.

treatment under Cr stress (Cr-25). The Cr accumulation in soil was maximum (20.33 mg kg^{-1} soil) with the application of co-composted BC and it was 1.52 times more as compared to that observed in the control treatment without any amendment under Cr stress (Cr-25). Moreover, significant positive and negative correlations were observed among Cr concentration in plant parts and growth and physiological attributes of *Brassica* (**Figure 6**).

Phytostabilization Efficiency and Health Risk Assessment

To estimate the phytostabilization potential of different amendments, bioconcentration factor (BCF), bioaccumulation factor (BAF), and bioaccumulation concentration (BAC) of *Brassica* were calculated (**Figure 7**). The application of compost, BC, and co-composted BC showed significant potential for the phytostabilization of Cr in the soil in comparison to the control treatment. The minimum values of BCF (0.43%), BAF (0.0000526%), and BAC (0.1667) were recorded with the application of co-composted BC as compared to the control under Cr stress (Cr-25). The health risk assessment was determined by calculating the daily intake of metal (DIM), hazard index (HI), cancer risk (CR), and total hazard quotient (THQ). The application of compost, BC, and co-composted BC significantly reduced the health risks associated with the accumulation of Cr in the edible portion of *Brassica* (**Figure 8**).

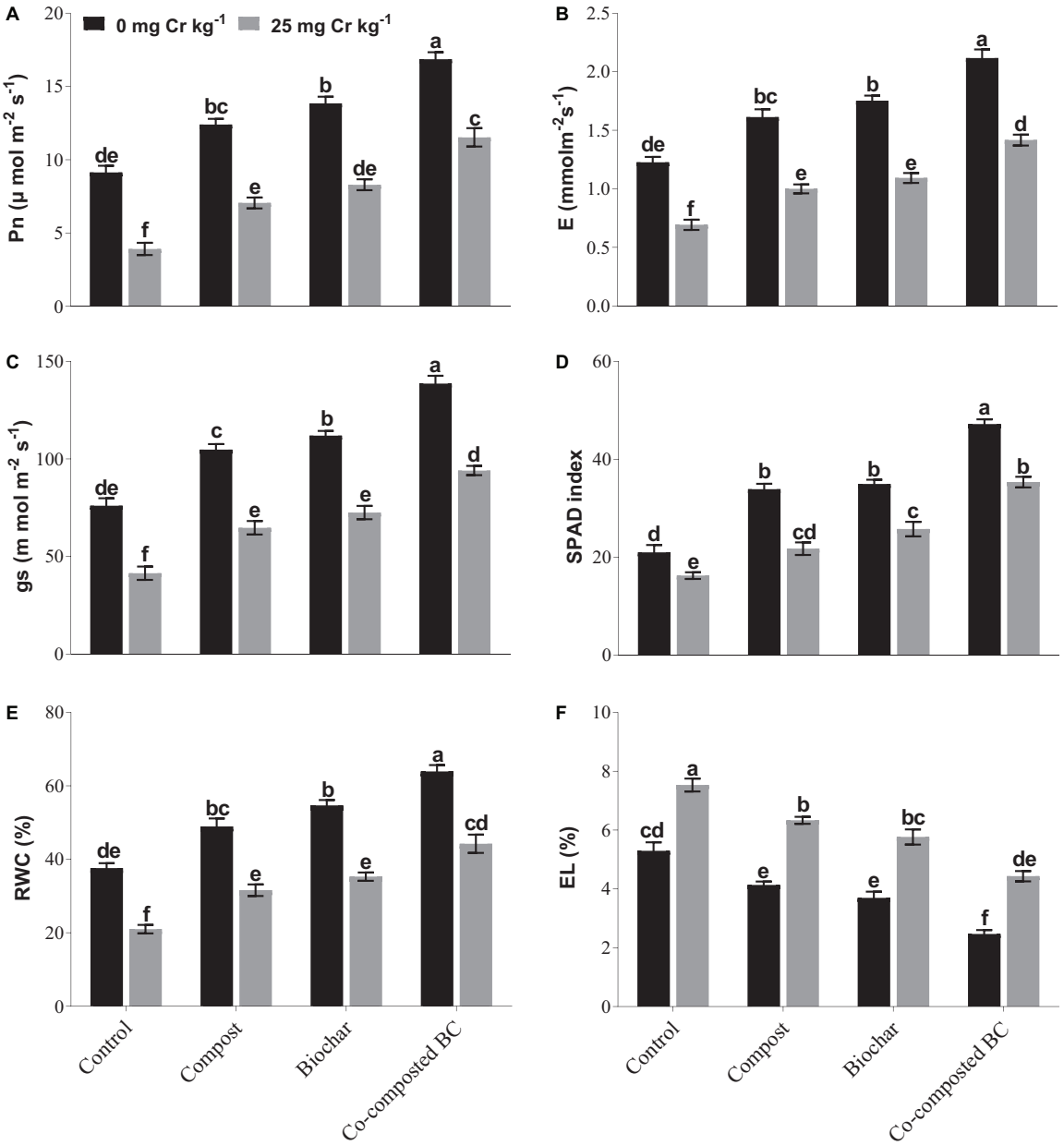

FIGURE 2 | Impact of compost, biochar, and co-composted biochar on physiological parameters of *Brassica*. **(A)** Photosynthetic rate, **(B)** transpiration rate, **(C)** stomatal conductance, **(D)** chlorophyll content, **(E)** relative water content, and **(F)** electrolyte leakage. The values are presented as mean ± standard error ($n = 3$). The values sharing the same letter(s) in bars are statistically non-significant with each other at $p < 0.05$.

With the application of co-composted BC, the minimum values of DIM (8.667×10^{-6}), HI (5.667×10^{-6}), CR (0.431), and THQ (3.2×10^{-7}) were recorded, and these were 4.21, 4.24, 4.00, and 4.00 times less as compared to the control treatment without any amendment under Cr stress (Cr-25).

DISCUSSION

Results showed that the application of compost, BC, and co-composted BC significantly ($p < 0.05$) improved the growth attributes of *Brassica* in uncontaminated and contaminated soil (Cr-25). The soil under Cr stress (Cr-25) showed reduced shoot and root length, shoot fresh and dry weight, and root fresh and dry weight of *Brassica* (**Figure 1**). Many researchers have reported reduced morphological parameters under Cr stress (Adrees et al., 2015; Maqbool et al., 2018). Cr toxicity inhibits cell division and elongation in plant root cells (Adrees et al., 2015), thus reducing root surface area for enhanced water and nutrient uptake from the soil (Medda and Mondal, 2017; Ahmad et al., 2020) and ultimately growth and biomass production. Our findings are in line with the study by Jun et al. (2009) that Cr-contaminated soil

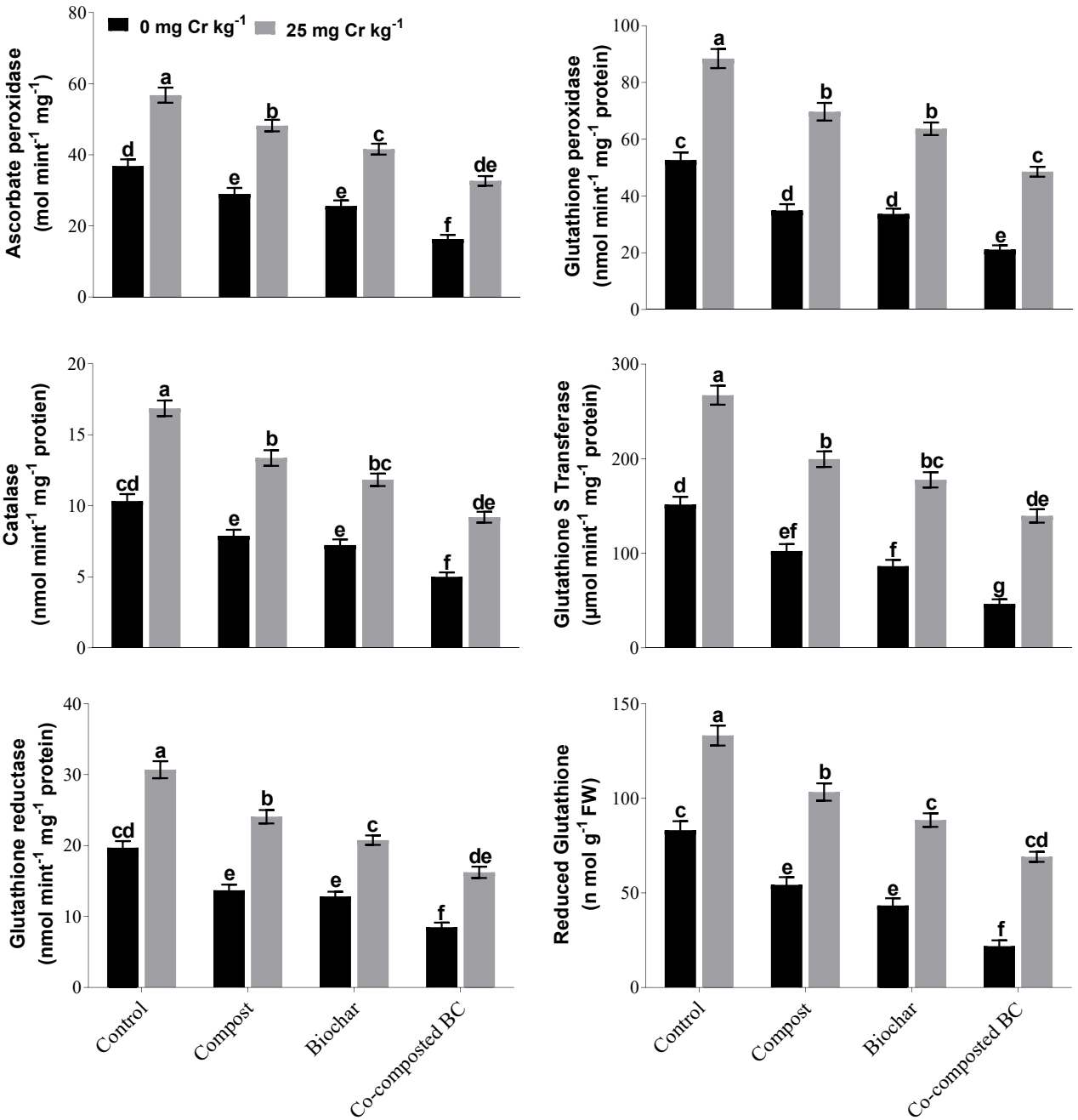

FIGURE 3 | Impact of compost, biochar, and co-composted biochar on antioxidant activities of *Brassica*. The values are presented as mean ± standard error ($n = 3$). The values sharing the same letter(s) in bars are statistically non-significant with each other at $p < 0.05$.

reduced shoot length, root growth, and biomass production in cereals, vegetables, and forages.

Our results showed that plant growth significantly improved with the application of compost, BC, and co-composted BC. Novak et al. (2019) observed growth improvement when different combinations of BC and compost were used under Cd-contaminated soil. Abbas et al. (2020) observed that a combination of BC (3%) and AMS (5%) increased shoot length (93%), root length (222%), shoot dry weight (60%), and root dry weight (164%) of maize grown in Cr-contaminated soil. Arshad et al. (2017) reported that the pine wood chip BC produced at 450°C significantly improved maize root and shoot fresh weight, root length, and root surface area. Similarly, various studies have reported that BC application improved plant growth under a Cr stress environment (Agegnehu et al., 2017; Arshad et al., 2017). BC addition improves nutrient retention

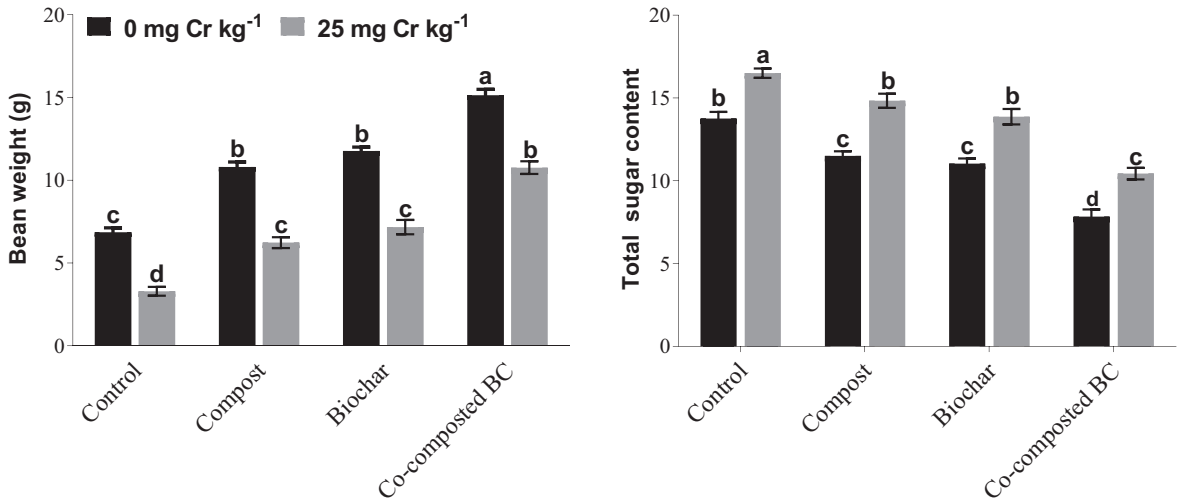

FIGURE 4 | Impact of compost, biochar, and co-composted biochar on bean weight and total sugar contents (TSCs) of *Brassica napus*. The values are presented as mean ± standard error (n = 3). The values sharing the same letter(s) in bars are statistically non-significant with each other at $p < 0.05$.

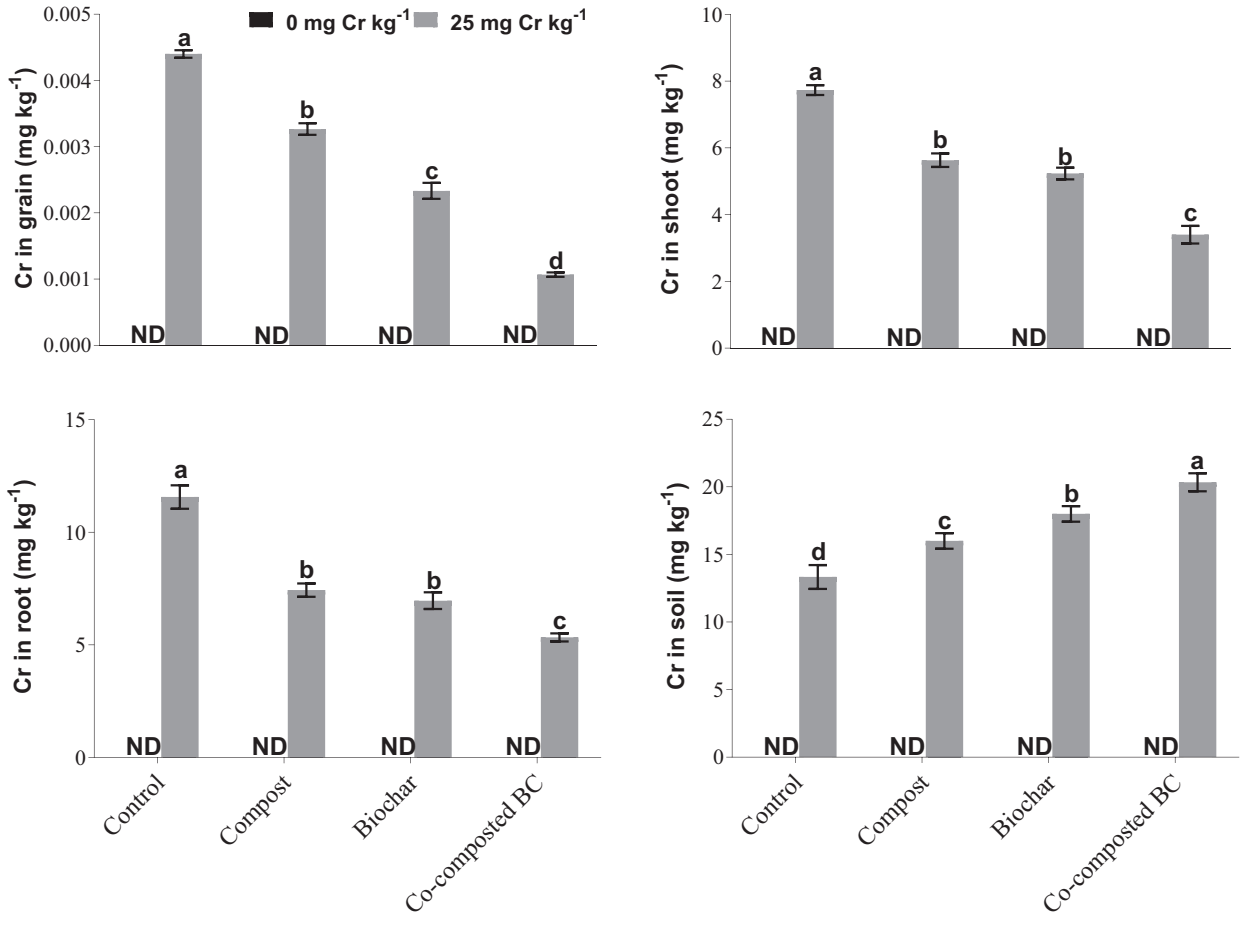

FIGURE 5 | Impact of compost, biochar, and co-composted biochar on Cr accumulation in different portions of *Brassica napus*. The values are presented as mean ± standard error (n = 3). The values sharing the same letter(s) in bars are statistically non-significant with each other at $p < 0.05$.

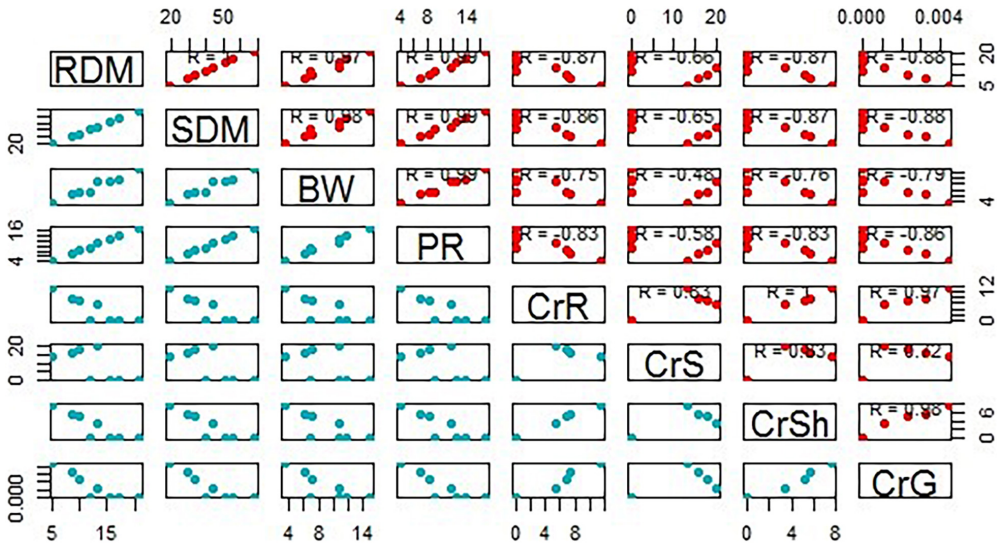

FIGURE 6 | A scatter matrix plot demonstrating pairwise scatter plots of variables in a matrix format, determining variables correlation. BW, bean weight; SDM, shoot dry mass; RDM, root dry mass; PR, photosynthetic rate; CrS, Cr in soil; CrR, Cr in the root; CRSh, Cr in the shoot; CrG, Cr in grain.

and water uptake and increases organic carbon (Rizwan et al., 2016; Cheng et al., 2020), thus enhancing soil fertility and boosting vegetative growth (Ali et al., 2018). In addition, the combined compost and BC influenced soil properties, such as pH, cation exchange capacity (CEC), soil organic matter, and nutrients availability, and ultimately increased soil fertility and plant growth (Agegnehu et al., 2017). In this study, an increase in plant growth parameters might be due to decreased Cr bioavailability with enhanced nutrient uptake under BC-amended Cr-contaminated soil. It may also be the BC -mediated conversion of Cr(VI) to Cr(III) in soil, which is relatively less mobile and less toxic (Rizwan et al., 2016).

Cr toxicity severely affects plant physiology and our results showed that the application of compost, BC, and co-composted BC significantly ($p < 0.05$) improved physiological attributes of *Brassica* in soil under Cr stress (Cr-25). Cr toxicity severely affects chlorophyll contents by disrupting chloroplast and discontinuing electron transport chain reaction, relative water contents, and electrolyte leakage in leaves. Many studies have shown that Cr toxicity damages photosynthetic machinery and produces a large amount of ROS in plants, which results in reduced growth (Ali et al., 2018; Bashir et al., 2020a).

Results of this study demonstrated that the application of compost, BC, and co-composted BC significantly reduced Cr uptake from soil under Cr contamination (Cr-25). Mustafa et al. (2020) observed that BC applied at the rate of 1 and 2% (w/w) reduced Cr uptake by 21 and 41%, respectively, under 500 μM of Cr stress. Similarly, Ali et al. (2018) observed that the application of BC efficiently removed Cr(VI) from wastewater. Cheng et al. (2020) noticed bamboo BC reduced Cu, Ni, Hg, and Cr uptake from water and soils. The reduction in Cr uptake might be due to the high surface area of BC that facilitates sorption, ion exchange, electrostatic interaction, complexation, precipitation, and co-precipitation (Rizwan et al., 2016). BC surface contains phenolic, hydroxyl, and carboxylic functional groups that facilitate metal binding (Mehmood et al., 2021; Murtaza et al., 2021a).

Under normal conditions, plants produce ROS in a controlled amount but under stress conditions; their production increases many times, which leads to oxidative stress, membrane permeability, DNA damage, and even cell death (Ahmad et al., 2010, 2019; Kohli et al., 2019). Plants have developed certain antioxidant enzymes to scavenge ROS and produce resistance against stress (Ditta and Khalid, 2016; Niamat et al., 2019). It was observed in many studies that the application of organic amendments enhanced resistance of plants against abiotic stresses (Seneviratne et al., 2017; Ali et al., 2018; Niamat et al., 2019). Our results showed that the application of co-composted BC indirectly influenced the antioxidant activity by reducing Cr bioavailability. In our findings, CAT activity was increased under Cr stress (Cr-25) in the control treatment. BC addition increased CAT activity (38.79%) in *Zea maize and Brassica rapa* (Ali et al., 2018; Bashir et al., 2020b). Similarly, Arshad et al. (2017) observed significant reductions in antioxidant enzyme activities under increasing levels of Cr stress. BC addition markedly improved antioxidant enzyme activities under Cr stress, which might be due to reduced Cr uptake (Seneviratne et al., 2017). Our results showed CAT, GSH, GR, GP, GPX, and GST activities in *Brassica* leaves increased under Cr stress (Cr-25), and the application of compost, BC, and co-composted BC reduced antioxidant activities. As discussed earlier, it was observed increased antioxidants activity in *B. napus* under Cd-spiked soil (Sabir et al., 2020).

This study results showed the co-composted BC significantly reduced Cr uptake in the *Brassica* plants. Novak et al. (2019) observed that the combined BC and compost reduced Cd uptake in plants. Seneviratne et al. (2017) also noted a significant reduction in cadmium (19.4%) and lead (22.0%) uptake when BC at the rate of 40 t ha^{-1} was applied in *Vigna radiata*.

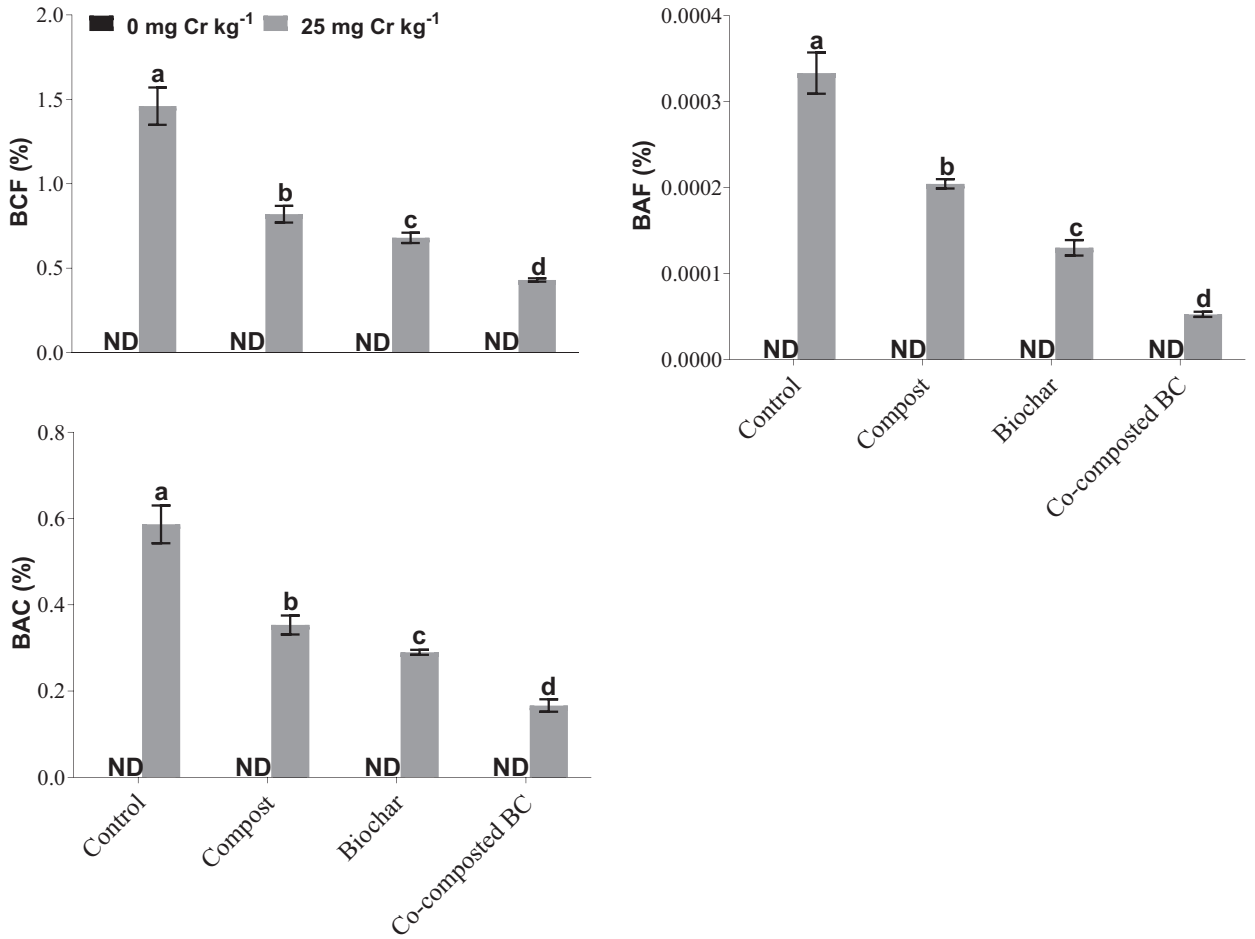

FIGURE 7 | Impact of compost, biochar, and co-composted biochar on bioconcentration factor (BCF), bioaccumulation factor (BAF), and bioaccumulation concentration (BAC) of *Brassica napus*. The values are presented as mean ± standard error (n = 3). The values sharing the same letter(s) in bars are statistically non-significant with each other at $p < 0.05$.

It was observed by many researchers that BC reduced HMs bioavailability by manipulating soil pH, precipitation, sorption, and changing HMs redox state (Ditta and Khalid, 2016; Rizwan et al., 2016; Cheng et al., 2020). BC contains a variety of oxygen-containing functional groups (such as carbonyl, carboxylic, hydroxyl, and phenol) that might be involved in complexation with HMs and cation exchange process with metals cations present on BC surface (Seneviratne et al., 2017; Niamat et al., 2019). With time, BC undergoes an oxidation process and new reactive sites are formed on BC surface that facilitates HMs immobilization (Bian et al., 2014) and ultimately results in reduced HMs uptake in plants. Such mechanisms of applied amendments might have resulted in reduced values of metal uptake in *Brassica* plants grown in this study and hence improved phytostabilization efficiency (**Figure 7**) and reduced health-associated risks (**Figure 8**). This was further evidenced by the negative correlations observed among Cr concentration in roots and shoots and growth and physiological parameters recorded for *Brassica* (**Figure 6**). The BCF and BAC values have further shown that the *Brassica* has the potential to extract Cr at higher concentrations and hence can be grown in metal-contaminated soils. Moreover, the values for DIMs and health risk index (HRI) were <1, which indicated that the consumption of *Brassica* was safe with no associated health risks.

MATERIALS AND METHODS

Soil Sampling and Analysis

The contamination-free surface soil (0–15 cm) was collected from the research area of the Institute of Soil and Environmental Sciences, University of Agriculture Faisalabad. The soil was air-dried, ground, and sieved (2 mm) to remove stones and other undesired plant materials. Composite sampling was followed for soil homogenization. For pre-sowing analysis, the soil sample was taken from the composite sample.

Standard procedures were followed for basic soil analysis regarding physicochemical properties. Soil pH was determined by making a saturated soil paste of 250 g soil and pH was measured

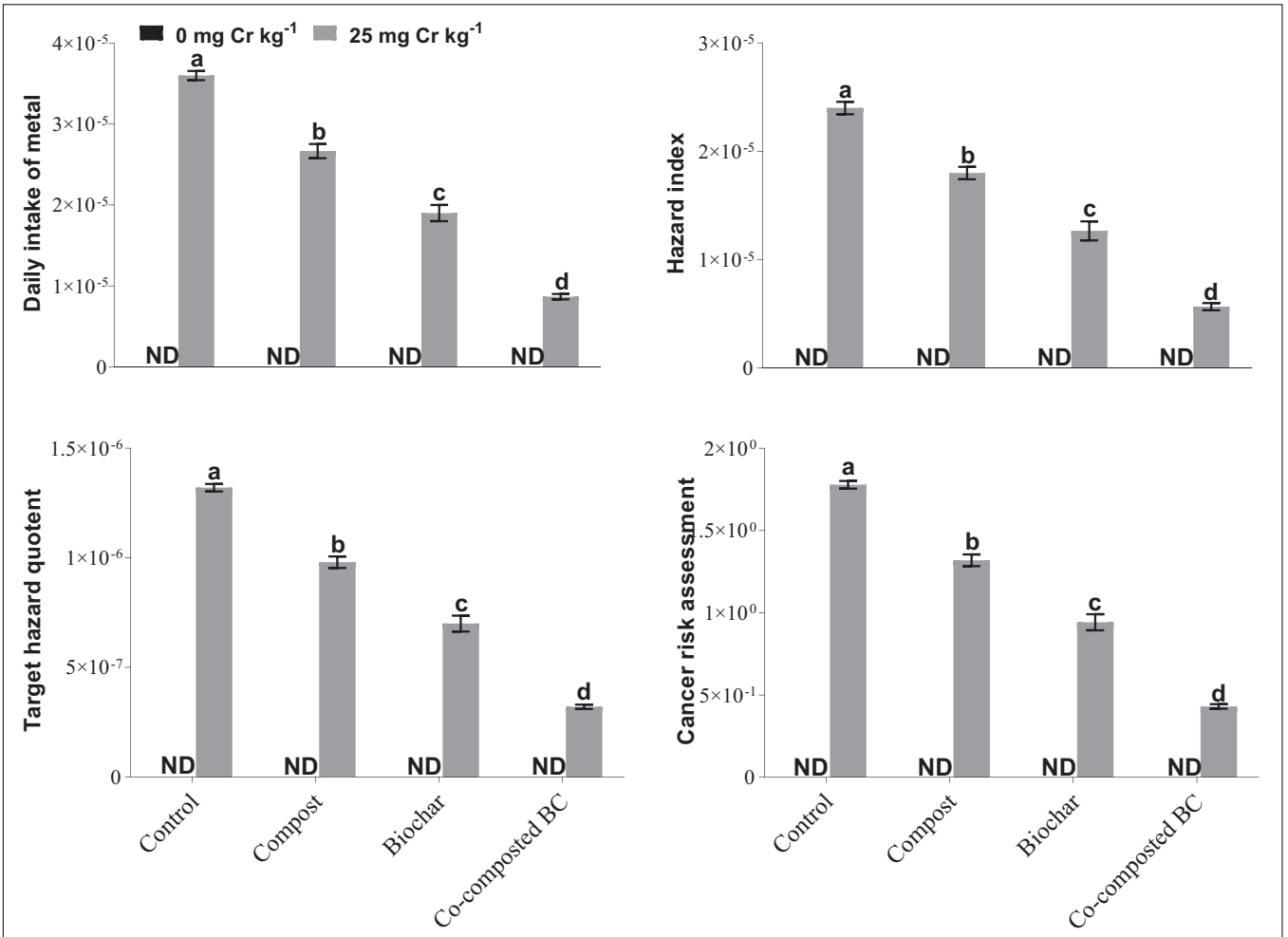

FIGURE 8 | Impact of compost, biochar, and co-composted biochar on health risk assessment for the accumulation of Cr in *Brassica napus*. The values are presented as mean ± standard error ($n = 3$). The values sharing the same letter(s) in bars are statistically non-significant with each other at $p < 0.05$.

with a pH meter (Kent Eil 7015) (US Salinity Laboratory Staff, 1954). The electrical conductivity (EC) of soil was determined by taking soil extract from saturated soil paste, and extract EC was determined using EC meter (US Salinity Laboratory Staff, 1954). Soil texture was determined with the hydrometer method, and soil organic matter was determined by the potassium dichromate method (Moodie et al., 1959). Soil CEC was determined by the ammonium acetate method (Chapman, 1965), total soil nitrogen was determined through the Kjeldahl method (Jackson, 1962), soil available P by using $NaHCO_3$ (Watanabe and Olsen, 1965), and soil K was determined through ammonium acetate (1N, pH = 7.0) method (US Salinity Laboratory Staff, 1954). Different physicochemical properties of soil are provided in **Table 1**.

For bioavailable Cr concentration, the soil sample (10 g) was extracted with AB-DTPA solution (20 ml) and shaking at 180 rpm on a reciprocal shaker for 15 min (Soltanpour and Schwab, 1977). Concentrated HNO_3 (100 ml) was added to the extract and analyzed for bioavailable Cr using atomic absorption spectrophotometer (PerkinElmer Model 700, United States). For total Cr concentration in soil, the method proposed by Soltanpour and Schwab (1977) was adopted. Briefly, soil samples (0.5 g) were digested with 15 ml of three acids mixture (HNO_3, H_2SO_4, and $HClO_4$ in a ratio of 5:1:1) and heated at 160°C in digestion chamber until a colorless solution appeared. After digestion, the samples were cooled, filtered, and diluted to a 50-ml solution using a volumetric flask with deionized water. An atomic absorption spectrophotometer (PerkinElmer Model 700) was used for the determination of total Cr concentration in the samples.

Compost, Biochar, and Co-composted Biochar Production and Characterization

For compost preparation, a locally fabricated composting unit was used involving animal manure as an easily available raw material (Ditta et al., 2015, 2018a,b). The animal manure was collected from Animal Husbandry Farm, the University of Agriculture, Faisalabad, and sun-dried to remove excess moisture and unwanted plant debris, stone, and plastic material. During

TABLE 1 | Physicochemical characteristics and nutritional composition of compost, biochar, co-composted biochar, and soil utilized in this study.

Physical/ chemical properties	Soil	Compost	Biochar	Co-composted biochar
Textural class	Sandy clay loam	–	–	–
Sand (%)	56 ± 3.21	–	–	–
Silt (%)	24 ± 1.86	–	–	–
Clay (%)	20 ± 1.57	–	–	–
pH	7.88 ± 0.35	6.85 ± 0.03	7.964 ± 0.08	7.01 ± 0.09
Electrical conductivity (dS m^{-1})	1.06 ± 0.08	1.2 ± 0.01	2.75 ± 0.07	1.58 ± 0.08
Cation exchange capacity ($cmol_c$ kg^{-1})	6.85 ± 1.62	73.01 ± 2.11	98.46 ± 2.86	92.35 ± 2.38
Moisture %	26 ± 1.26	10.57 ± 1.18	4.25 ± 0.19	7.32 ± 1.08
Organic matter (%)	0.72 ± 0.18	–	–	–
Carbon (g kg^{-1})	–	199.2 ± 3.68	633.51 ± 5.67	398.92 ± 4.33
Nitrogen (g kg^{-1})	–	21.8 ± 1.26	11.25 ± 0.86	16.42 ± 0.67
Total phosphorus (g kg^{-1})	–	0.42 ± 0.05	1.43 ± 0.54	1.18 ± 0.67
Total potassium (g kg^{-1})	–	1.67 ± 0.18	9.29 ± 0.22	7.32 ± 0.63
Zinc (mg kg^{-1})	–	47.0 ± 3.70	45.61 ± 2.91	46.27 ± 2.87
Iron (mg kg^{-1})	–	70.8 ± 4.09	85.31 ± 4.76	82.29 ± 3.67

The values are presented as mean ± SE (n = 3).

composting, 50% moisture at 65°C was maintained with 50-rpm speed and this process was completed after 40 days. Co-composted BC was prepared by mixing 30% (w/w) wheat straw BC with composted material during the last week of composting. For wheat straw BC preparation, straw feedstock was collected from the field area of the Department of Agronomy, University of Agriculture Faisalabad, washed with tap water to remove dust, sun-dried, and crushed. Sanchez et al. (2009) described a process that was followed for BC production in which feedstock was filled in a Pyrex flask having 2 L capacity. BC was prepared in a muffle furnace (Gallonhop, England) at 400°C under an oxygen-limited environment, with 20 min of retention time at heating at the rate of 10°C min^{-1} increase in temperature. Gases and water vapor produced during pyrolysis were removed by using a silicon-made bent glass rod attached to the flask outlet. After pyrolysis, the furnace remained closed until 20°C, and the prepared BC was stored in plastic bags for further analysis.

For pH and EC, each compost, BC, and co-composted BC was separately mixed with deionized water in 1:20 ratio (w/v), shaken for 1 h, and pH and EC were measured using pH meter (PHS-38W) and EC meter (4510 conductivity meter). Nutrient analysis was carried out through wet digestion of each sample using H_2SO_4 and H_2O_2 (Wolf, 1982). In 1 g of each sample, H_2SO_4 (15 ml) was added and placed in the sample overnight. On the next day, the digestion mixture was heated on a hotplate until the boiling started. In the boiling digestion mixture, H_2O_2 (10 ml) was added repeatedly until a colorless solution appeared. The volume of the digested sample was made 50 ml in a volumetric flask using deionized water and preserved until the analysis was performed. Total nitrogen was determined through the Kjeldahl method (US Salinity Laboratory Staff, 1954), P was measured by $NaHCO_3$ method using a spectrophotometer (UV-1201, Shimadzu, Tokyo, Japan), and K was determined using a flame photometer (PFP7, Jenway, Essex, United Kingdom). Different physicochemical properties of compost, BC, and co-composted BC are given in **Table 1**.

Pot Experiment

After the preparation of different organic amendments, a pot experiment was conducted in rain-protected wirehouse of Institute of Soil and Environmental Sciences (31.439052° N, 73.069335° E), University of Agriculture Faisalabad, Pakistan. In each pot, 10 kg soil was used and recommended rate of NPK (90:60:75 kg ha^{-1}) using urea, di-ammonium phosphate, and sulfate of potash fertilizer was mixed. Compost, BC, and co-composted BC were applied at the rate of 2% (w/w). For Cr contamination, the soil was spiked with potassium dichromate ($K_2Cr_2O_7$) solution at two levels (0 and 25 ppm) and applied to plants at a three-leaf stage after complete germination. In each pot, six seeds of *B. napus* (cv. AARI canola) were sown, and each treatment was applied in triplicate. The pots were placed in the wirehouse under natural conditions as day/night temperature of 25°C/15°C and relative humidity of 50%/70%, respectively. Recommended agronomic practices were followed during the course of the study. The harvesting was done after 60 days of plant growth at maturity. Data regarding growth, physiological, and biochemical parameters were measured as follows.

Growth and Physiological Parameters

After harvesting the plants, data regarding various growth and yield parameters were taken following standard procedures. For shoot and root length, measuring tape was used. For fresh biomass, the root and shoot samples were weighed on a digital balance. For dry biomass, the samples were put in a drying oven at 65°C for 48 h or until a constant weight was obtained. The shoot samples with grain pods were dried in sun. The threshing of shoot samples was done to separate grains, and the grain yield was measured by weighing the grains on a digital balance. Plant physiological attributes such as photosynthetic rate, transpiration rate, and stomatal conductance were measured by using an infrared gas analyzer (IRGA; Analytical Development Company, Hoddesdon, England) at morning time (Ben-Asher et al., 2006). Chlorophyll contents were measured in the morning time with a portable chlorophyll meter (SPAD-502, Konica-Minolta, Japan) following the method suggested by Arnon (1949), while relative water contents were measured using the method suggested by Barrs and Weatherley (1962).

To assess membrane permeability against Cr stress, electrolyte leakage was determined following the method suggested by Lutts et al. (1996). Briefly, the youngest fully expanded leaf sample (1 cm) from each replicate was taken into a vial (10 ml) and

washed three times with distilled water to remove any dust material. Each vial with leaf sample was placed in the shaker (100 rpm) at room temperature (25°C) for 24 h. On the following day, the EC of the leaf sample in the vial was measured using an EC meter and denoted as EC_1. Then, each leaf sample in the vial was autoclaved at 121°C for 20 min. After cooling the samples, again EC was measured using an EC meter and denoted as EC_2. The electrolyte leakage was determined by using the following formula:

$$\text{Electrolyte leakage (\%)} = \frac{EC_1}{EC_2} \times 100$$

Antioxidant Enzyme Activity

For different antioxidant enzyme activities, fully expanded, uppermost fresh leaf samples after 40 days of germination were used. For this purpose, 0.5 g leaves were homogenized in 3 ml Tris buffer (50 mM) having pH 7.8, centrifuged at 12,000 rpm for 20 min, and the total soluble enzyme activities were calculated by using a spectrophotometer. Leaf CAT activity was measured following the method suggested by Aebi (1983), while ascorbate peroxidase activity was measured by using a spectrophotometer at 290 nm (Nakano and Asada, 1981). The method suggested by Fryer et al. (1998) was used for the determination of glutathione reductase and that by Rahman et al. (2006) for the measurement of reduced glutathione activity, in which DTNB (5,5′-dithiobis-2-nitrobenzoic acid) reduced to TNB (2-nitro-5-thiobenzoic acid) and changed the absorbance. For glutathione peroxidase activity, the method suggested by Rahman et al. (2006) was followed. Similarly, the methodology suggested by Habig et al. (1974) was followed for glutathione-*S*-transferase activity in leaf samples.

For the determination of TSC, the method suggested by Yem and Willis (1954) was used. Briefly, 0.5 g of ground leaf samples were extracted in ethanol solution (80%). Then, 10 ml of extract solution was taken in a 25-ml test tube along with 6 ml anthrone reagent and heated in the water bath for 10 min. Anthrone reagent was freshly prepared by taking 150 mg of anthrone in 72% pure H_2SO_4. Heated samples were cooled for 10 min, and the absorbance was measured at 625 nm using a spectrophotometer (UV-1201, Shimadzu, Tokyo, Japan).

Evaluation of Phytoimmobilization Efficiency

For BAC and BCF, the following equations were used to assess the phytoimmobilization/phytostabilization potential of *B. napus* as proposed by Amin et al. (1954) and Zhuang et al. (2007).

$$\text{BAC} = \frac{\text{Ni}\left[\text{shoot}\right]}{\text{Ni}\left[\text{soil}\right]}$$

where Ni [shoot] and Ni [soil] are the concentrations of Ni in the shoots and the soil, respectively.

$$BCF = \frac{M\ (\textit{h}\text{arvested tissue})}{M\ (\text{soil water})}$$

where M (harvested tissue) is the metal concentration in the harvested plant parts (root, shoot, and grains), and M (soil water) is the total amount of applied metal for the corresponding treatment.

Intake of Heavy Metals From Vegetables and Health Risk Assessment

The DIM index was calculated by using the following equation (Latif et al., 2018):

$$DIM = \frac{M \times I \times K}{W}$$

where M is the concentration of HMs in plants (mg kg^{-1}), K is the conversion factor, I is the daily intake of vegetables, and W is the average body weight (BW). The average adult BW was considered 60 kg, while the average daily vegetable intake for adults was considered 0.345 kg^{-1} $person^{-1}$ (Latif et al., 2018).

The HRI for Ni caused by the consumption of contaminated vegetables was calculated using the following equation (Jan et al., 2010):

$$HRI = \frac{DIM}{Rfd}$$

where *DIM* is the daily intake of metals and *Rfd* is the reference oral dose. According to US-EPA IRIS, the *Rfd* value for Ni is 0.02 mg kg^{-1} BW day^{-1}.

Statistical Analysis

Data collected were evaluated using analysis of variance (ANOVA), and treatment means were compared by using Tukey's HSD test at 5% probability level using Statistix 8.1 (Analytical Software, Tallahassee, FL, United States) (Little and Hills, 1978). The figures were plotted using GraphPad Prism computer-based software (GraphPad Software, San Diego, CA, United States). The correlation matrix was computed using R software (https://www.R-project.org/).

CONCLUSION

The results showed that Cr stress (Cr-25) significantly reduced growth, physiological and biochemical parameters of *Brassica* under the control treatment without any amendment. The application of compost, BC, and co-composted BC significantly alleviated Cr stress and enhanced various growth, physiological, and biochemical parameters. With the application of co-composted BC, the maximum increase in growth, physiological, and biochemical parameters of *Brassica* was recorded in comparison to the control treatment without any amendment under Cr stress (Cr-25). Similarly, the application of co-composted BC maximized the phytostabilization efficiency as revealed through the minimum values of BCF, BAF, and BAC of *Brassica* as compared to the control treatment under Cr stress (Cr-25). Moreover, the same treatment significantly reduced the health risks associated with the consumption of *Brassica* under Cr stress (Cr-25) as clear from the lowest values of DIM, HI, CR, and THQ. In conclusion, the application of co-composted BC could serve as an effective amendment in the alleviation of Cr stress in *Brassica* via phytostabilization and reduction in associated health risks.

DATA AVAILABILITY STATEMENT

The original contributions presented in the study are included in the article/supplementary material, further inquiries can be directed to the corresponding authors.

AUTHOR CONTRIBUTIONS

AM, WX, and MN: conceptualization. BT: methodology. BT, AD, and MB: software. AM, MN, and MZN: validation. MB and JK: formal analysis. ZS and QS: resources. BT and QS: data curation. MN: writing—original draft preparation. AM, JK, and MR: writing—review and editing. AM and WX: supervision. MN and AD: project administration. WX and MB: funding acquisition. All authors have read and agreed to the published version of the manuscript.

FUNDING

This research received financial support from Higher Education (HEC) Pakistan via NRPU Project No. 6443/Punjab/NRPU/R&D/HEC/2016.

ACKNOWLEDGMENTS

We highly acknowledge the Institute of Soil and Environmental Sciences, University of Agriculture, Faisalabad, Pakistan, for providing space to conduct this experiment.

REFERENCES

Abbas, A., Azeem, M., Naveed, M., Latif, A., Bashir, S., Ali, A., et al. (2020). Synergistic use of biochar and acidified manure for improving growth of maize in chromium contaminated soil. *Int. J. Phytoremediation* 22, 52–61. doi: 10.1080/15226514.2019.1644286

Adrees, M., Ali, S., Iqbal, M., Bharwana, S. A., Siddiqi, Z., Farid, M., et al. (2015). Mannitol alleviates chromium toxicity in wheat plants in relation to growth, yield, stimulation of anti-oxidative enzymes, oxidative stress and Cr uptake in sand and soil media. *Ecotoxicol. Environ. Saf.* 122, 1–8. doi: 10.1016/j.ecoenv.2015.07.003

Aebi, H. (1983). Catalase in vitro. *Methods Enzymol.* 105, 121–126. doi: 10.1016/s0076-6879(84)05016-3

Agegnehu, G., Bass, A. M., Nelson, P. N., Muirhead, B., Wright, G., and Bird, M. I. (2015). Biochar and biochar-compost as soil amendments: effects on peanut yield, soil properties and greenhouse gas emissions in tropical North Queensland. *Austr. Agric. Ecosyst. Environ.* 213, 72–85. doi: 10.1016/j.agee.2015.07.027

Agegnehu, G., Srivastava, A. K., and Bird, M. I. (2017). The role of biochar and biochar-compost in improving soil quality and crop performance: a review. *Appl. Soil Ecol.* 119, 156–170. doi: 10.1016/j.apsoil.2017.06.008

Ahmad, I., Tahir, M., Daraz, U., Ditta, A., Hussain, M. B., and Khan, Z. U. H. (2020). "Responses and tolerance of cereal crops to metals and metalloids toxicity" in *Agronomic Crops*. ed. H. Mirza (Singapore: Springer). 235–264. doi: 10.1007/978-981-15-0025-1_14

Ahmad, P., Jaleel, C. A., Salem, M. A., Nabi, G., and Sharma, S. (2010). Roles of enzymatic and nonenzymatic antioxidants in plants during abiotic stress. *Crit. Rev. Biotechnol.* 30, 161–175. doi: 10.3109/07388550903524243

Ahmad, P., Tripathi, D. K., Deshmukh, R., Singh, V. P., and Corpas, F. J. (2019). Revisiting the role of ROS and RNS in plants under changing environment. *Environ. Exp. Bot.* 161, 1–3. doi: 10.1016/j.envexpbot.2019.02.017

Ali, S., Rizwan, M., Bano, R., Bharwana, S. A., Ur Rehman, M. Z., Hussain, M. B., et al. (2018). Effects of biochar on growth, photosynthesis, and chromium (Cr) uptake in Brassica rapa L. under Cr stress. *Arab. J. Geosci.* 11, 1–9.

Amin, H., Arain, B. A., Jahangir, T. M., Abbasi, M. S., and Amin, F. (1954). Accumulation and distribution of lead (Pb) in plant tissues of guar (Cyamopsis tetragonoloba L.) and sesame (Sesamum indicum L.): profitable phytoremediation with biofuel crops. *Geol. Ecol. Landsc.* 2, 51–60. doi: 10.1080/24749508.2018.1452464

Arnon, D. I. (1949). Copper enzymes in isolated chloroplasts, oxidase in Beta vulgaris. *Plant Physiol.* 24, 1–11. doi: 10.1104/pp.24.1.1

Arshad, M., Khan, A. H. A., Hussain, I., Anees, M., Iqbal, M., Soja, M. G., et al. (2017). The reduction of chromium (VI) phytotoxicity and phytoavailability to wheat (Triticum aestivum L.) using biochar and bacteria. *Appl. Soil Ecol.* 114, 90–98. doi: 10.1016/j.apsoil.2017.02.021

Barrs, H. D., and Weatherley, P. E. (1962). A re-examination of the relative turgidity technique for estimating water deficits in leaves. *Aust. J. Bio. Sci.* 15, 413–428.

Bashir, M. A., Naveed, M., Ahmad, Z., Gao, B., Mustafa, A., and Núñez-Delgado, A. (2020a). Combined application of biochar and sulfur regulated growth, physiological, antioxidant responses and Cr removal capacity of maize (Zea mays L.) in tannery polluted soils. *J. Environ. Manag.* 259:110051. doi: 10.1016/j.jenvman.2019.110051

Bashir, M. A., Naveed, M., Ashraf, S., Mustafa, A., Ali, Q., Rafique, M., et al. (2020b). Performance of Zea mays L. cultivars in tannery polluted soils: management of chromium phytotoxicity through the application of biochar and compost. *Physiol. Plant* 173, 129–147. doi: 10.1111/ppl.13277

Ben-Asher, J. I., Tsuyuki, B. A., and Bravdo Sagih, M. (2006). Irrigation of grapevines with saline water: i. Leaf area index, stomatal conductance, transpiration and photosynthesis. *Agric. Water Manag.* 83, 13–21.

Bian, R., Joseph, S., Cui, L., Pan, G., Li, L., Liu, X., et al. (2014). A three-year experiment confirms continuous immobilization of cadmium and lead in contaminated paddy field with biochar amendment. *J. Hazard. Mater.* 272, 121–128. doi: 10.1016/j.jhazmat.2014.03.017

Brassard, P., Godbout, S., and Raghavan, V. (2016). Soil biochar amendment as a climate change mitigation tool: key parameters and mechanisms involved. *J. Environ. Manag.* 181, 484–497. doi: 10.1016/j.jenvman.2016.06.063

Chapman, H. D. (1965). "Cation-exchange capacity" in *Methods Soil Analysis: part 2 Chemical Microbiological Properties*. in (ed) A. G. Norman. (Madison: American Society of Agronomy). 9, 891–901.

Cheng, S., Chen, T., Xu, W., Huang, J., Jiang, S., and Yan, B. (2020). Application research of biochar for the remediation of soil heavy metals contamination: a review. *Molecules* 25:3167. doi: 10.3390/molecules25143167

Chukwuka, K. S., Akanmu, A. O., Umukoro, O. B., Asemoloye, M. D., and Odebode, A. C. (2020). "Biochar: a vital source for sustainable agriculture," in *Biostimulants in Plant Science,* eds. S. M. Mirmajlessi and R. Radhakrishnan (London, UK: IntechOpen).

Coelho, M. A., Fusconi, R., Pinheiro, L., Ramos, I. C., and Ferreira, A. S. (2018). The combination of compost or biochar with urea and NBPT can improve nitrogen-use efficiency in maize. *An. Braz. Acad. Sci.* 90, 1695–1703. doi: 10.1590/0001-3765201820170416

de Oliveira, L. M., Ma, L. Q., Santos, J. A., Guilherme, L. R., and Lessl, J. T. (2014). Effects of arsenate, chromate, and sulfate on arsenic and chromium uptake and translocation by arsenic hyperaccumulator *Pteris vittata* L. *Environ. Pollut.* 184, 187–192. doi: 10.1016/j.envpol.2013.08.025

Ditta, A., and Khalid, A. (2016). "Bio-organo-phos: a sustainable approach for managing phosphorus deficiency in agricultural soils" in *Organic Fertilizers - From Basic Concepts to Applied Outcomes*. eds M. Larramendy and S. Soloneski (Croatia: In Tech), 109–136. doi: 10.5772/62473

Ditta, A., Arshad, M., Zahir, Z. A., and Jamil, A. (2015). Comparative efficacy of rock phosphate enriched organic fertilizer vs. mineral phosphatic fertilizer for nodulation, growth and yield of lentil. *Int. J. Agric. Biol.* 17, 589?595.

Ditta, A., Imtiaz, M., Mehmood, S., Rizwan, M. S., Mubeen, F., Aziz, O., et al. (2018a). Rock phosphate enriched organic fertilizer with phosphate solubilizing microorganisms improves nodulation, growth and yield of legumes. *Commun. Soil Sci. Plant Anal.* 49, 2715–2725. doi: 10.1080/00103624.2018.1538374

Ditta, A., Muhammad, J., Imtiaz, M., Mehmood, S., Qian, Z., and Tu, S. (2018b). Application of rock phosphate enriched composts increases nodulation, growth and yield of chickpea. *Int. J. Recycl. Org. Waste Agric.* 7, 33–40. doi: 10.1007/s40093-017-0187-1

Doumer, M. E., Rigol, A., Vidal, M., and Mangrich, A. S. (2016). Removal of Cd, Cu, Pb, and Zn from aqueous solutions by biochars. *Environ. Sci. Pollut. Res.* 23, 2684–2692.

Fryer, M. J., Andrews, J. R., Oxborough, K., Blowers, D. A., and Baker, N. R. (1998). Relationships between CO2 assimilation, photosynthetic electron transport and active O2 metabolism in leaves of maize in the field during periods of low temperature. *Plant Physiol.* 116, 571–580. doi: 10.1104/pp.116.2.571

Govil, P. K., and Krishna, A. K. (2018). Soil and water contamination by potentially hazardous elements: a case history from India. *Environ. Geochem.* 2018, 567–597.

Habig, W. H., Pabst, M. J., and Jacoby, W. B. (1974). Glutathione S-transferases: the first enzymatic step in mercapturic acid formation. *J. Biol. Chem.* 249, 7130–7139.

Hu, B., Ai, Y., Jin, J., Hayat, T., Alsaedi, A., Zhuang, L., et al. (2020). Efficient elimination of organic and inorganic pollutants by biochar and biochar-based materials. *Biochar* 2, 47–64. doi: 10.1016/j.wasman.2021.01.037

Ijaz, M., Rizwan, M. S., Sarfraz, M., Ul-Allah, S., Sher, A., Sattar, A., et al. (2020). Biochar reduced cadmium uptake and enhanced wheat productivity in alkaline contaminated soil. *Int. J. Agric. Biol.* 24, 1633–1640. doi: 10.17957/IJAB/15.1605

Irshad, S., Xie, Z., Mehmood, S., Nawaz, A., Ditta, A., and Mahmood, Q. (2021). Insights into conventional and recent technologies for arsenic bioremediation: a systematic review. *Environ. Sci. Pollut. Res.* 28, 18870–18892. doi: 10.1007/s11356-021-12487-8

Jackson, M. L. (1962). Interlayering of expansible layer silicates in soils by chemical weathering. *Clays Clay Miner* 11, 29–46. doi: 10.1346/ccmn.1962.0110104

Jan, F. A., Ishaq, M., Khan, S., Ihsanullah, I., Ahmad, I., and Shakirullah, M. (2010). A comparative study of human health risks via consumption of food crops grown on wastewater irrigated soil (Peshawar) and relatively clean water irrigated soil (lower Dir). *J. Hazard. Mater.* 179, 612–621. doi: 10.1016/j.jhazmat.2010.03.047

Jia, W., Wang, B., Wang, C., and Sun, H. (2017). Tourmaline and biochar for the remediation of acid soil polluted with heavy metals. *J. Environ. Chem. Eng.* 5, 2107–2114. doi: 10.1016/j.jece.2017.04.015

Jun, R., Ling, T., and Guanghua, Z. (2009). Effects of chromium on seed germination, root elongation and coleoptile growth in six pulses. *Int. J. Environ. Sci. Technol.* 6, 571–578. doi: 10.1007/bf03326097

Junaid, M., Hashmi, M. Z., Malik, R. N., and Pei, D. S. (2016). Toxicity and oxidative stress induced by chromium in workers exposed from different occupational settings around the globe: a review. *Environ. Sci. Pollut. Res.* 23, 20151–20167. doi: 10.1007/s11356-016-7463-x

Kamran, M., Malik, Z., Parveen, A., Huang, L., Riaz, M., Bashir, S., et al. (2019). Ameliorative effects of biochar on rapeseed (Brassica napus L.) growth and heavy metal immobilization in soil irrigated with untreated wastewater. *J. Plant Growth Regul.* 39, 266–281.

Kohli, S. K., Khanna, K., Bhardwaj, R., Abd Allah, E. F., Ahmad, P., and Corpas, F. J. (2019). Assessment of Subcellular ROS and NO Metabolism in Higher Plants: multifunctional Signaling Molecules. *Antioxidants* 8:641. doi: 10.3390/antiox8120641

Latif, A., Bilal, M., Asghar, W., Azeem, M., Ahmad, M. I., Abbas, A., et al. (2018). Heavy metal accumulation in vegetables and assessment of their potential health risk. *J. Environ. Ana. Chem.* 5:234.

Little, T. M., and Hills, F. J. (1978). *Agricultural Experimentation: design and analysis*. New York: John Wiley Sons. Ins.

Lutts, S., Kinet, J. M., and Bouharmont, J. (1996). NaCl-induced senescence in leaves of rice (Oryza sativa L.) cultivars differing in salinity resistance. *Ann. Bot.* 78, 389–398.

Maqbool, A., Ali, S., Rizwan, M., Ishaque, W., Rasool, N., Ur Rehman, M. Z., et al. (2018). Management of tannery wastewater for improving growth attributes and reducing chromium uptake in spinach through citric acid application. *Environ. Sci. Pollut. Res.* 25, 10848–10856. doi: 10.1007/s11356-018-1352-4

Medda, S., and Mondal, N. K. (2017). Chromium toxicity and ultrastructural deformation of Cicer arietinum with special reference of root elongation and coleoptile growth. *Ann. Agrar. Sci.* 15, 396–401. doi: 10.1016/j.aasci.2017.05.022

Mehmood, S., Rizwan, M., Bashir, S., Ditta, A., Aziz, O., Yong, L. Z., et al. (2018a). Comparative Effects of Biochar, Slag and Ferrous–Mn Ore on Lead and Cadmium Immobilization in Soil. *Bull. Environ. Contam. Toxicol.* 100, 286–292. doi: 10.1007/s00128-017-2222-3

Mehmood, S., Saeed, D. A., Rizwan, M., Khan, M. N., Aziz, O., Bashir, S., et al. (2018b). Impact of different amendments on biochemical responses of sesame (Sesamum Indicum L.) plants grown in lead-cadmium contaminated soil. *Plant Physiol. Biochem.* 132, 345–355. doi: 10.1016/j.plaphy.2018.09.019

Mehmood, S., Wang, X., Ahmed, W., Imtiaz, M., Ditta, A., Rizwan, M., et al. (2021). Removal mechanisms of slag against potentially toxic elements in soil and plants for sustainable agriculture development: a critical review. *Sustainability* 13:5255. doi: 10.3390/su13095255

Moodie, C. D., Smith, H. W., and Mcreery, R. A. (1959). *Laboratory Manual for Soil Fertility*. Washington: State college of Washington. 31–39.

Murtaza, G., Ahmed, Z., Usman, M., Tariq, W., Ullah, Z., Shareef, M., et al. (2021a). Biochar induced modifications in soil properties and its impacts on crop growth and production. *J. Plant Nutr.* 44, 1677–1691. doi: 10.1080/01904167.2021.1871746

Murtaza, G., Ditta, A., Ullah, N., Usman, M., and Ahmed, Z. (2021b). Biochar for the management of nutrient impoverished and metal contaminated soils: preparation, applications, and prospects. *J. Soil Sci. Plant Nutrit.* 21, 2191–2213.

Mustafa, A., Minggang, X., Shah, S. A. A., Abrar, M. M., Nan, S., Baoren, W., et al. (2020). Soil aggregation and soil aggregate stability regulate organic carbon and nitrogen storage in a red soil of southern China. *J. Environ. Manag.* 270:110894. doi: 10.1016/j.jenvman.2020.110894

Nakano, Y., and Asada, K. (1981). Hydrogen peroxide is scavenged by ascorbate-specific peroxidase in spinach chloroplasts. *Plant Cell Physiol.* 22, 867–880. doi: 10.1016/s0005-2728(00)00256-5

Niamat, B., Naveed, M., Ahmad, Z., Yaseen, M., Ditta, A., Mustafa, A., et al. (2019). Calcium-enriched animal manure alleviates the adverse effects of salt stress on growth, physiology and nutrients homeostasis of Zea mays L. *Plants* 8:480. doi: 10.3390/plants8110480

Novak, J. M., Ippolito, J. A., Watts, D. W., Sigua, G. C., Ducey, T. F., and Johnson, M. G. (2019). Biochar compost blends facilitate switchgrass growth in mine soils by reducing Cd and Zn bioavailability. *Biochar* 1, 97–114.

Rahman, I., Kode, A., and Biswas, S. K. (2006). Assay for quantitative determination of glutathione and glutathione disulfide levels using enzymatic recycling method. *Nat. Protoc.* 1:3159.

Rizwan, M. S., Imtiaz, M., Zhu, J., Yousaf, B., Hussain, M., Ali, L., et al. (2021). Immobilization of Pb and Cu by organic and inorganic amendments in contaminated soil. *Geoderma* 385:114803. doi: 10.1016/j.geoderma.2020.114803

Rizwan, M., Ali, S., Qayyum, M. F., Ibrahim, M., Zia-ur-Rehman, M., Abbas, T., et al. (2016). Mechanisms of biochar-mediated alleviation of toxicity of trace elements in plants: a critical review. *Environ. Sci. Pollut. Res.* 23, 2230–2248. doi: 10.1007/s11356-015-5697-7

Sabir, A., Naveed, M., Bashir, M. A., Hussain, A., Mustafa, A., Zahir, Z. A., et al. (2020). Cadmium mediated phytotoxic impacts in Brassica napus: managing growth, physiological and oxidative disturbances through combined use of biochar and *Enterobacter* sp. MN17. *J. Environ. Manag.* 265:110522. doi: 10.1016/j.jenvman.2020.110522

Sanchez, M. E., Lindao, E., Margaleff, D., Martinez, O., and Moran, A. (2009). Pyrolysis of agricultural residues from rape and sunflowers: production and characterization of bio-fuels and biochar soil management. *J. Anal. Appl. Pyrol.* 85, 142–144.

Sarfraz, R., Hussain, A., Sabir, A., Fekih, I. B., Ditta, A., and Xing, S. (2019). Role of Biochar and plant growth-promoting rhizobacteria to enhance soil carbon sequestration– a review. *Environ. Monit. Assess.* 191:251. doi: 10.1007/s10661-019-7400-9

Seneviratne, M., Weerasundara, L., Ok, Y. S., Rinklebe, J., and Vithanage, M. (2017). Phytotoxicity attenuation in Vigna radiata under heavy metal stress at the presence of biochar and N fixing bacteria. *J. Environ. Manag.* 186, 293–300. doi: 10.1016/j.jenvman.2016.07.024

Soltanpour, P. N., and Schwab, A. P. (1977). A new soil test for simultaneous extraction of macro- and micro-nutrients in alkaline soils. *Commun. Soil Sci. Plant Anal.* 8, 195–207. doi: 10.1080/00103627709366714

Tepanosyan, G., Sahakyan, L., Maghakyan, N., and Saghatelyan, A. (2020). Combination of compositional data analysis and machine learning approaches to identify sources and geochemical associations of potentially toxic elements in soil and assess the associated human health risk in a mining city. *Environ. Pollut.* 261:114210. doi: 10.1016/j.envpol.2020.114210

Ullah, N., Ditta, A., Khalid, A., Mehmood, S., Rizwan, M. S., Mubeen, F., et al. (2020). Integrated effect of algal biochar and plant growth promoting rhizobacteria on physiology and growth of maize under deficit irrigations. *J. Plant. Nutr. Soil Sci.* 20, 346–356. doi: 10.1007/s42729-019-00112-0

US Salinity Laboratory Staff. (1954). *Diagnosis and improvement of saline and alkali soils.* USDA handbook no. 60, Washington, USA: Government Printing Office. 160.

Watanabe, F. S., and Olsen, S. R. (1965). Test of an ascorbic acid method for determining phosphorus in water and NaHCO3 extracts from soil. *Soil Sci. Soc. Am.* 29, 677–678. doi: 10.2136/sssaj1965.03615995002900060025x

Wolf, B. (1982). A comprehensive system of leaf analyses and its use for diagnosing crop nutrient status. *Commun. Soil Sci. Plant Anal.* 13, 1035–1059. doi: 10.1080/00103628209367332

Yem, E. O., and Willis, A. J. (1954). The estimation of carbohydrates in plant extracts by anthrone. *Biochem. J.* 57, 508–514. doi: 10.1042/bj0570508

Zhuang, X., Chen, J., Shim, H., and Bai, Z. (2007). New advances in plant growth-promoting rhizobacteria for bioremediation. *Environ. Int.* 33, 406–413. doi: 10.1016/j.envint.2006.12.005

Conflict of Interest: The authors declare that the research was conducted in the absence of any commercial or financial relationships that could be construed as a potential conflict of interest.

Publisher's Note: All claims expressed in this article are solely those of the authors and do not necessarily represent those of their affiliated organizations, or those of the publisher, the editors and the reviewers. Any product that may be evaluated in this article, or claim that may be made by its manufacturer, is not guaranteed or endorsed by the publisher.

frontiers in Plant Science

ORIGINAL RESEARCH
published: 19 November 2021
doi: 10.3389/fpls.2021.749422

Biostimulant Capacity of an Enzymatic Extract From Rice Bran Against Ozone-Induced Damage in *Capsicum annum*

*Sandra Macias-Benitez†, Salvadora Navarro-Torre†, Pablo Caballero, Luis Martín, Elisa Revilla, Angélica Castaño and Juan Parrado**

Departamento de Bioquímica y Biología Molecular, Facultad de Farmacia, Universidad de Sevilla, Seville, Spain

OPEN ACCESS

Edited by:
Maurizio Ruzzi, University of Tuscia, Italy

Reviewed by:
George Komis, Palacký University Olomouc, Czechia
Kamrun Nahar, Sher-e-Bangla Agricultural University, Bangladesh
Kundan Kumar, Birla Institute of Technology and Science, India

***Correspondence:**
Juan Parrado
parrado@us.es

† These authors have contributed equally to this work and share first authorship

Specialty section:
This article was submitted to Plant Abiotic Stress, a section of the journal Frontiers in Plant Science

Received: *29 July 2021*
Accepted: *19 October 2021*
Published: *19 November 2021*

Citation:
Macias-Benitez S, Navarro-Torre S, CaballeroP, Martín L, Revilla E, Castaño A and Parrado J (2021) Biostimulant Capacity of an Enzymatic Extract From Rice Bran Against Ozone-Induced Damage in Capsicum annum. Front. Plant Sci. 12:749422. doi: 10.3389/fpls.2021.749422

Ozone is a destructive pollutant, damaging crops, and decreasing crop yield. Therefore, there is great interest in finding strategies to alleviate ozone-induced crop losses. In plants, ozone enters leaves through the stomata and is immediately degraded into reactive oxygen species (ROS), producing ROS stress in plants. ROS stress can be controlled by ROS-scavenging systems that include enzymatic or non-enzymatic mechanisms. Our research group has developed a product from rice bran, a by-product of rice milling which has bioactive molecules that act as an antioxidant compound. This product is a water-soluble rice bran enzymatic extract (RBEE) which preserves all the properties and improves the solubility of proteins and the antioxidant components of rice bran. In previous works, the beneficial properties of RBEE have been demonstrated in animals. However, to date, RBEE has not been used as a protective agent against oxidative damage in agricultural fields. The main goal of this study was to investigate the ability of RBEE to be used as a biostimulant by preventing oxidative damage in plants, after ozone exposure. To perform this investigation, pepper plants (*Capsicum annuum*) exposed to ozone were treated with RBEE. RBEE protected the ozone-induced damage, as revealed by net photosynthetic rate and the content of photosynthetic pigments. RBEE also decreased the induction of antioxidant enzyme activities in leaves (catalase, superoxide dismutase, and ascorbate peroxidase) due to ozone exposure. ROS generation is a common consequence of diverse cellular traumas that also activate the mitogen-activated protein kinase (MAPK) cascade. Thus, it is known that the ozone damages are triggered by the MAPK cascade. To examine the involvement of the MAPK cascade in the ozone damage *CaMPK6-1*, *CaMPK6-2*, and *CaMKK5* genes were analyzed by qRT-PCR. The results showed the involvement of the MAPK pathway in both, not only in ozone damage but especially in its protection by RBEE. Taken together, these results support that RBEE protects plants against ozone exposure and its use as a new biostimulant could be proposed.

Keywords: ozone, ROS, rice bran, enzymatic extract, MAPK

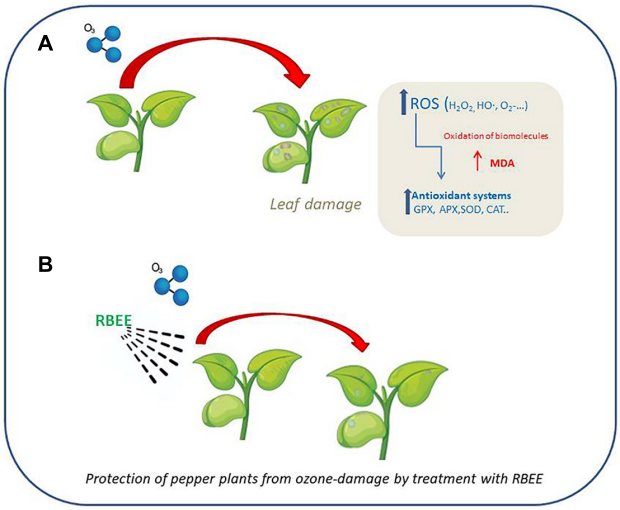

GRAPHICAL ABSTRACT | Explanatory diagram of the protective action of RBEE against the oxidizing agent ozone.

INTRODUCTION

Ozone (O_3) is a destructive pollutant with negative effects on human and ecosystem health that induces abiotic stress in plants – affecting photosynthetic carbon assimilation, stomatal conductance, and plant growth – that damages crops and decreases crop yield (Ainsworth et al., 2012).

In plants, O_3 enters through the stomata and is degraded into secondary reactive oxygen species (ROS), including H_2O_2, $O_2^{\cdot-}$, and $HO^{\cdot}$, in the apoplastic space (Vainonen and Kangasjärvi, 2015). High levels of ROS can lead to ROS stress that causes direct or indirect ROS-mediated damage on a variety of molecules including lipid peroxidation in cellular membranes, protein denaturation, carbohydrate oxidation, and pigment breakdown (Sharma et al., 2012). Even more, ROS stress can eventually lead to changes in gene expression and even cell death. However, ROS are generated in the metabolism of plant cells and therefore plants need systems that scavenge oxidizing species. Constitutive enzymatic and non-enzymatic systems in cells protect them from ROS-induced damage and are inducible under biotic and abiotic stress that triggers a rapid increase in ROS, including O_3 exposure (Sachdev et al., 2021). Enzymatic ROS-scavenging mechanisms include antioxidant enzymes such as superoxide dismutase (SOD), catalase (CAT), ascorbate peroxidase (APX), glutathione peroxidase (GP), guaiacol peroxidase (GPX) and dehydroascorbate reductase (DHAR) (Gill and Tuteja, 2010).

Specific ROS also act as "second messengers" in signal transduction pathways that lie downstream initial event in cells. The mitogen-activated protein kinase (MAPK) cascade is one of the signaling pathways sensitive to the cell's redox status. Therefore ROS generation is a common consequence of diverse cellular traumas that activate the MAPK cascade and studies in different plants have demonstrated that O_3 exposure activates some components of the MAPK cascade (Marcus et al., 2000; Liu et al., 2015; Liu and He, 2017).

Studies on the effect of O_3 on agricultural productivity showed an estimated 5–15% crop yield loss in the United States (Avnery et al., 2011) and a 5% in Europe (Mills et al., 2007). To alleviate the drop in crop productivity, the main defense strategy over the past four decades has been the application of chemicals, mainly synthetic antioxidants (fungicides, insecticides, herbicides, nematocides, growth regulators, antitranspirants, antioxidants from the rubber industry, etc.) (Didyk and Blum, 2010). These xenobiotic products have varied protection capacity with some producing ineffective or even detrimental side effects. The most effective product was found to be EDU (ethylene diurea– (*N*-[2-(2-oxo-1-imidazolidinyl) ethyl]-N0 phenylurea), developed by the duPont Chemical company (Archambault et al., 2000) whose main mechanism of action is not yet clear. Currently, more effective alternatives are being sought, such as extracts of plant origin, which do not generate environmental toxicity.

Rice Bran is a by-product of rice (*Oryza sativa*) milling that retains most of the bioactive compounds present in rice grain. These bioactives include naturally occurring antioxidants, mainly γ-oryzanol, tocopherols, tocotrienols, and polyphenols. Besides that, rice bran is also a good source of protein and fat (Goufo and Trindade, 2014). However, the low bioavailability of its biopolymers and bioactive compounds due to its high insolubility is the main drawback when considering rice bran as a biostimulant. Using enzymatic technology, our group has developed a process that enables obtaining a stable, water-soluble rice bran enzymatic extract (RBEE) from rice bran. RBEE has shown a high content in bioactive compounds, particularly phytosterols, γ–oryzanol, and tocols, and an increased content in peptides and free amino acids (Santa-María et al., 2010).

According to its content in bioactive compounds, RBEE has shown both *in vivo* and *in vitro* functional properties such as antioxidant capacity (Santa-María et al., 2010), hypocholesterolemic activity (Revilla et al., 2009), and antiproliferative and inmunoactivatory abilities (Revilla et al., 2013). Beneficial effects found in cells and animal models, especially those derived from its antioxidant capacity, lead us to consider the use of RBEE as a biostimulant in agriculture.

This work aims to evaluate the biostimulant capacity of RBEE. To this end, we propose studying the role of RBEE in plant protection against abiotic stress mediated by ROS, specifically in O_3 exposure. We chose pepper plants (*Capsicum annuum*) since pepper is a vegetable crop of great agricultural and economic importance being the second most traded spice in the world. Heavy losses in pepper production are frequently caused by abiotic stresses including O_3 exposition, in fact *Capsicum* pepper cultivation is almost entirely located in regions where O_3 concentration is increasing to phytotoxic levels (Bortolin et al., 2016). For these reasons pepper plants are an interesting research target to evaluate the negative effects of O_3.

Pepper plants exposed to O_3 were treated with RBEE and antioxidant enzyme activities and specific functional parameters were analyzed. Treatment with RBEE improved

physiological parameters, such as net photosynthetic rate and photosynthetic pigments content in plants exposed to with O_3. RBEE treatment also decreased the induction of antioxidant enzyme activities in leaves (CAT, SOD, GPX, and APX) due to O_3 exposure.

Additionally, to search whether MAPK cascade is involved in the protective role of RBEE against O_3-induced damage we analyzed the transcriptional expression of *CaMPK6-1*, *CaMPK6-2*, and *CaMKK5* genes. The high expression of genes studied strongly support that RBEE protective capacity involved the MAPK signaling cascade.

MATERIALS AND METHODS

Rice Bran Enzymatic Extract Preparation

Rice bran (*O. sativa* var. *indica*) raw material was provided by Herba Ricemills, S.L.U (Sevilla, Spain). Rice bran is obtained during the polishing/milling of raw rice grains once their husks have been stripped. Rice bran was processed by enzymatic hydrolysis using the hydrolytic agent (Biocom, Spain) subtilisin (EC 3.4.21.62), a protease from *Bacillus licheniformis* as hydrolytic agent (Biocom, Spain) in a bioreactor with controlled temperature (60°C) and pH (pH 8), using the pH-stat method (Parrado et al., 2006). The processing of this product follows different steps, including solid separation and concentration. The final product RBEE is a brown syrup that is completely water-soluble.

Rice bran enzymatic extract bran macro and micronutrient composition was characterized as previously described (Parrado et al., 2006).

Plant Treatment

Capsicum annum L. var. *grossum* (pepper) plants were raised from seeds in plastic pots containing an organic commercial substrate (Gramoflor GmbH und Co., KG.) and Osmocote® (NPK 15-9-12), and grown inside the University of Seville Glasshouse General Services on a phytoclimatic chamber, with a controlled temperature of 18–22°C, 50% relative humidity, adequate irrigation with tap water and a photoperiod of 16 h light (1200 $\mu mol.m^{-2}.\ s^{-1}$)/8 h darkness. After 8 days of transplantation, 20 pepper plants were selected and divided in 4 treatments (5 plants per treatment): control plants (C), plants treated with RBEE, control plants under O_3 exposition (C + O_3), and plants treated with RBEE under O_3 exposition (RBEE + O_3).

To evaluate the protection capacity of the treatment with RBEE, RBEE and RBEE + O_3 plants were foliar sprayed with an aqueous solution of RBEE at 0.1% a total of four times at 5-day intervals. At the same time, control plants (C and C + O_3) were sprayed with distilled water the same times. After 5 days of the last spray treatment, C + O_3 and RBEE + O_3 plants were transferred to another phytoclimatic chamber with an O_3 generator (ZONOSISTEM GM 5000 O3 Generator) attached and exposed to three consecutive fumigations with 100 ppB of O_3 for 6 h (from 10:00 a.m. to 4:00 p.m.). After O_3 fumigation, plants of all treatments were sprayed again with the corresponding solution (RBEE 0.1% or distilled water).

Finally, 24 h after the last exposure to O_3, foliar samples were taken from each plant and the analyses described below were carried out.

Physiological Status in Plants

Determination of Net Photosynthetic Rate

Twenty-four hours after the las ozone treatment, the net photosynthetic rate (A_N) was measured in plants using an IRGA (LI-6400XT, LI-COR Inc., Nev., EEUU) with a light chamber for the leaf (Li-6400-02B, Li-Cor Inc.). Measurements (n = 20) were performed between 10 a.m. and 2 p.m. hours under a photosynthetic photon flux density of 1500 $\mu mol.m^{-2}.s^{-1}$, a deficit of vapor pressure of 2–3 kPa, a temperature around 25°C, and a CO_2 concentration environment of 400 $\mu mol.mol^{-1}$ air. Each measurement was recorded after the stabilization of the exchange of gases was equilibrated (120 s).

Chlorophyll Content in Leaves

Chlorophyll content was extracted from random leaves from plants of each treatment. Fifty milligrams of leaves were homogenized in acetone 100% (v/v) and saline solution 0.9% (w/v) using a homogenizer (Hiscox and Israelstam, 1979). The total chlorophyll content was determined at 652 nm by using the absorbance coefficient of extinction 34.5 $cm^{-1} \cdot \mu g^{-1}$ (Arnon, 1949):

$$Abs_{652nm} = [\text{chlorophyll}] \cdot 34.5\ cm^{-1} \cdot \mu g^{-1}.$$

Delayed Fluorescence Measurements

Delayed fluorescence (DF) was detected using a plant imaging system (NightShade LB 985, Berthold Technologies, Germany) equipped with a deeply cooled CCD camera according to López-Jurado et al. (2020). From plants of each treatment, 2–3 intact leaves of approximately the same size were separated and placed in the plant imaging system. The leaves were illuminated for 20 s with light supplied from far red (730 nm), red (660 nm), green (565 nm), and blue (470 nm) LED panels at 2, 105, 40, and 110 $\mu mol.m^{-2}.s^{-1}$, respectively. Immediately after the LEDs were turned off, DF was measured, and the recorded intensities of light were converted to counts per second (cps). Data were then normalized to each leaf area to obtain comparable cps values across treatments.

Oxidative Stress Evaluation in Plants

Determination of Lipid Peroxidation

To quantify lipid peroxidation in leaf homogenates malondialdehyde (MDA) content was determined using the thiobarbituric acid reactive substances (TBARS) assay (Esterbauer and Cheeseman, 1990). Samples of 1 g of leaves were homogenized with 2 ml of 0.1% trichloroacetic acid (TCA). The homogenates were centrifuged at 8000 × g for 10 min at 4°C, and the supernatants were filtered through a 0.2 mm aseptic filter. Then, 0.3 ml of each sample was mixed with 0.9 ml of 20% TCA containing 0.5% TBA. The solutions were heated at 95°C for 1 h, immediately cooled, and centrifuged as above. Finally,

the absorbance at 532 and 600 nm of the supernatants was recorded, and MDA concentration was calculated by subtracting the non-specific absorption at 600 nm from the absorption at 532 nm by using the absorbance coefficient of extinction 156 mM^{-1} cm^{-1}. The results obtained were expressed in $nmol.g^{-1}$ fresh weight (FW).

Antioxidant Enzymes Analyses

To observe the stress of plants, enzymatic activities of APX, SOD, guaiacol peroxidase (GPX), and CAT were measured as described by Duarte et al. (2015). Briefly, vegetal extract was extracted in extraction buffer (50 mM sodium phosphate buffer; pH 7.6) from 500 mg of leaves. Catalase activity was determined at 240 nm in a reaction solution containing the assay buffer (50 mM sodium phosphate buffer, pH 7.0) and 100 mM H_2O_2. APX activity was assayed in the assay buffer with 12 mM H_2O_2 and 0.25 mM L-ascorbate and measured at 290 nm. SOD activity was determined by monitorization of the pyrogallol oxidation at 325 nm by the addition of 3 mM pyrogallol. Guaiacol peroxidase activity was measured at 470 nm in a reaction mixture containing the assay buffer, 2 mM H_2O_2, and 20 mM guaiacol. To determine the auto-oxidation of the substrates, control assays were performed in absence of enzymatic extract samples (Duarte et al., 2015). Finally, the total protein content in the enzymatic extracts was measured according to Bradford (1976).

Oxidative Stress Index

Oxidative stress index (OSI) is a parameter that expresses the global oxidative stress in plants (Pérez-Palacios et al., 2017). It was calculated with the formula described in Paredes-Páliz et al. (2018). Values greater than 1 indicated that the leaves were stressed, whereas values less than 1 indicated that the leaves were without oxidative stress.

Plant RNA Extraction and qRT-PCR Assay

RNA was extracted from 100 mg of leaves using RNeasy® Plant Mini Kit (Qiagen, Germany) following the manufacturer's instructions. Then, RNA samples were treated with DNA-free™ kit (ThermoFisher, United States) to remove the residual DNA. Immediately, RNA samples were retrotranscripted to cDNA using QuantiTect® Reverse Transcription kit (Qiagen, Germany) according to the manufacturer's instructions, and the expression of *CaMPK6-1*, *CaMPK6-2* (*Arabidopsis* orthologs AtMPK6, Liu et al., 2015), and *CaMKK5* (*Arabidopsis* orthologs AtMKK5, Liu et al., 2015) genes were analyzed by qPCR by triplicate. qPCR was performed using SensiFAST™ SYBR® No-ROX kit (Bioline, France) and primers described in **Table 2** following the supplier's instructions, in a LightCycler® 480 II thermo-cycler (Roche, Switzerland) under the next conditions: 95°C for 2 min and 50 cycles at 95°C for 5 s, followed by 60°C for 10 s, and finally 72°C for 15 s. The beta-tubulin housekeeping gene was used to normalize results from different samples. Primers used in these assays are described in **Table 1**. Expression signals were quantified and normalized using LightCycler® 480 Software version 1.5 (Roche). The expression fold was calculated according to Livak and Schmittgen (2001):

$$\Delta Cq = AVECq\left(TargetAssay\right) - AVECq\left(ReferenceAssay\right)$$

$$\Delta\Delta Cq = \Delta Cq\left(TestSample\right) - \Delta Cq(ReferenceSample)$$

$$RQ = 2^{-\Delta\Delta Cq}.$$

Statistical Analysis

Statistical analysis was performed using Statistica software version 6.0 (StatSoft Inc.). First, the normality was checked by the Kolmogorov–Smirnov test. The means of the different treatments were compared using two-way ANOVA and the statistic differences were carried out by Tukey test (*F*-test).

RESULTS

Rice Bran Enzymatic Extract Chemical Characterization

The enzymatic process of obtaining the new water-soluble biostimulant (RBEE) from rice bran has been previously shown (Parrado et al., 2006). The biological tool involved in the enzymatic process for obtaining the RBEE is subtilisine (EC 3.4.21.62). This protease extracts, solubilizes, and hydrolyzes the initial insoluble proteins in brans, reducing the size of original rice bran proteins to soluble peptides. This process also led to the solubilization of hydrophobic compounds as lipids and bioactive metabolites in an emulsion (w/o). The chemical composition is shown in **Table 2**.

The two major components in RBEE are the proteins and lipids in equal amounts. Protein fraction is mainly comprised of peptides <5 kDa (see **Supplementary Figure SM1**). These peptides interact with the lipid fraction that allows fatty acids and hydrophobic bioactive compounds such as polyphenols, phytosterols, tocopherols, and tocotrienols (Revilla et al., 2009) to be soluble in water, leading to a greater bioavailability.

Rice bran is rich in prominent bioactives such as phytosterols. Interestingly, our RBEE retains major phytosterols described in rice bran (Santa María et al., 2016), the most abundant phytochemical found being γ–oryzanol (**Table 2**).

Other bioactive molecules such as tocopherols and tocotrienols (vitamin E) are also present in rice bran. Seven homologs of tocols were identified in RBEE (α-, β-, γ-, and δ-tocopherols and α-, γ-, and δ-tocotrienols). Among these, γ-tocotrienols were the most abundant, followed by α-tocopherols and α-tocotrienols (**Table 2**).

Rice bran enzymatic extract components also include polyunsaturated fatty acids, so linoleic acid and linolenic acid constitute 35.76% of total fatty acid content (**Table 2**). Finally, RBEE also contains flavonoids (flavonols, 0.62 mg/g; flavanols, 2.90 mg/g) and phenolic acids (20.14 mg/g).

Accordingly, the enzymatic process increases the bioavailability of RB without losing bioactive components.

TABLE 1 | Primers for qRT-PCR amplifications.

Protein	Accession numbers	Primer	Sequence	References
Beta tubulin	EF495259.1	*BTF*	5′-GAGGGTGAGTGAGCAGTTC-3′	Guo et al., 2012
		BTR	5′-CTTCATCGTCATCTGCTGTC-3′	
CaMPK6-1	CA08g04480	*MK6-1F*	5′-AAAGCCTCTGTTTCCTGGTAG-3′	Liu et al., 2015
		MK6-1R	5′-CTCCTTCTGGGATCAAATGTC-3′	
CaMPK6-2	CA03g14570	*MK6-2F*	5′-CAGAGATCATGTACACCA-3′	
		MK6-2R	5′-TCGCACCTGTTATTCTCCTTCTG-3′	
CaMKK5	CA03g36820	*MKK5F*	5′-GATTTCATTGCCTGCTGTTTG-3′	
		MKK5R	5′-GTGCCTGATGGACCTGATTAC-3′	

TABLE 2 | Analytical composition of RBEE.

Chemical composition (%, w/w)		Tocols (mg/kg)			
		Tocopherols		Tocotrienols	
Total protein	40.6 ± 1.9	α-Tocoferol	44 ± 3	α-Tocotrienol	25 ± 2
Fat	29.7 ± 1.6	β-Tocoferol	10 ± 2	β-Tocotrienol	–
Carbohydrates	21.3 ± 2.8	γ-Tocoferol	38 ± 4	γ-Tocotrienol	62 ± 4
Ash	8.4 ± 0.6	δ-Tocoferol	7 ± 1	δ-Tocotrienol	87 ± 5
		Total	99 ± 7	Total	174 ± 10
Ca (mg/kg)	599				
Mg (mg/100 g)	787				
Fe (mg/100 g)	18				
Vitamin B1 (mg/100 g)	<0.1				
Vitamin B2 (mg/100 g)	24.1				
Sterols		**Fatty acid composition (mg/100 mg)**			
γ–Oryzanol (mg/g)	10.6 ± 0.4	$C_{14:0}$ myristic acid		0.25 ± 0.04	
Brassicasterol (μg/g)	13.2 ± 1.5	$C_{16:0}$ palmitic acid		18.40 ± 3.11	
2,4-Methylenecholesterol (μg/g)	7.5 ± 2.5	$C_{16:1}$ palmitoleic acid		0.14 ± 0.05	
Campesterol (μg/g)	648.5 ± 23	$C_{18:0}$ stearic acid		1.79 ± 0.38	
Stigmasterol (μg/g)	414.6 ± 29	$C_{18:1}$ oleic acid		41.72 ± 4.14	
δ-7-Campesterol (μg/g)	22.5 ± 1.8	$C_{18:2}$ linoleic acid		35.00 ± 0.12	
Clerosterol (μg/g)	63.5 ± 4.7	$C_{18:3}$ linolenic acid		0.76 ± 0.28	
β-Sitosterol (μg/g)	1538.9 ± 98.6	$C_{20:1}$ peanut acid		0.58 ± 0.16	
Sitostanol (μg/g)	55.7 ± 3.8	Saturated		20.44	
δ-Avenasterol (μg/g)	524.2 ± 50.8	Unsaturated		42.44	
δ-5-2,4-Stigmasterol (μg/g)	37.4 ± 2.1	Polyunsaturated		35.76	
δ-7-Stigmasterol (μg/g)	22.8 ± 2.6				
δ-7-Avenasterol (μg/g)	20.3 ± 3.5				
Cholesterol (μg/g)	27.6 ± 3.6				
Others (μg/g)	79.5 ± 6.6				
Total (μg/g)	3530.1 ± 60.0				

All data are presented as mean ± SD of three independent experiments.

Physiological Status in Plants

After the experiments, the physiological status in pepper plants was determined by assaying diverse parameters, such as net photosynthetic rate, chlorophyll content, and DF.

The net photosynthetic rate was significantly affected by O_3 exposure (**Figure 1A**). After the treatments with RBEE, plants showed similar values to the control plants indicating that the RBEE does not interfere with the photosynthesis. However, when the plants were exposed to O_3 this rate significantly decreased. This decrease was recovered by 88% in the plants exposed to O_3 and treated with RBEE.

The total chlorophyll content in plants was significantly affected by both O_3 exposure and RBEE treatment (**Figure 1B**). Leaves of control plants treated with ozone showed 4.6-folds less content of total chlorophyll than non O_3-exposed control plants. However, despite RBEE treatment did not recover the content of total chlorophyll under O_3 conditions, this treatment improved this content by 53%.

To monitor plant stress status, DF closely related to photosynthetic reactions and chlorophyll content was also measured (Zhang et al., 2019). Both RBEE treatment and O_3 exposure produced a significant decrease in DF emissions. The lowest measurements were detected in untreated, O_3-fumigated

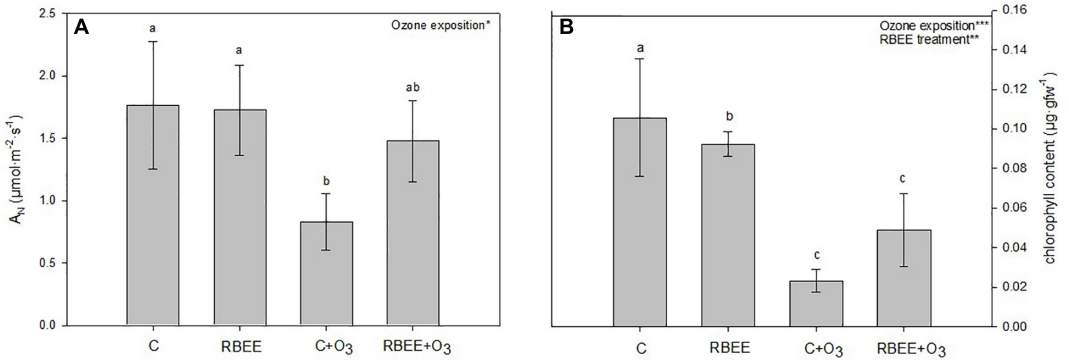

FIGURE 1 | Physiological parameters. **(A)** Net photosynthetic rate (A_N) and **(B)** total chlorophyll content in pepper plants in response to two conditions of ozone (O_3) (0 and 100 ppm) under a treatment without and with rice bran enzymatic extract (RBEE). Values represent mean ± SD, $n = 5$. Different letters indicate means that are significantly different from each other (two-way ANOVA, O_3 exposition × RBEE treatment; HSD test, $P < 0.05$). O_3 exposition and RBEE treatment in the corner of the panel indicate main or interaction significant effects (*$P < 0.05$; **$P < 0.01$; ***$P < 0.0001$).

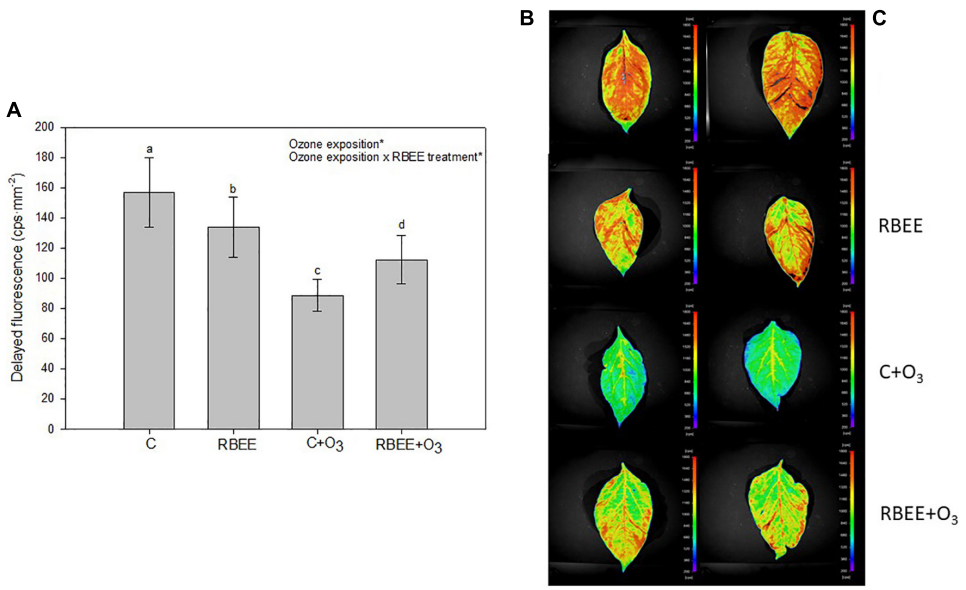

FIGURE 2 | Delayed fluorescence in leaves of pepper plants in response to two conditions of ozone (O_3) (0 and 100 ppm) under a treatment without and with rice bran enzymatic extract (RBEE). **(A)** Counts per second (cps) values for each treatment. Values represent mean ± SD, $n = 5$. Different letters indicate means that are significantly different from each other (two-way ANOVA, O_3 exposition × RBEE treatment; HSD test, $P < 0.05$). O_3 exposition and ozone exposition × RBEE treatment in the corner of the panel indicate main or interaction significant effects (*$P < 0.0001$); **(B)** photographs taken by the plant imaging system NightShade LB 985. The color scale mirrors the detected counts per second (cps) of delayed fluorescence emission in leaves.

plants, and the RBEE and RBEE + O_3 plants showed a less substantial decrease in DF emissions than the C + O_3 plants (**Figures 2A,B**). Although O_3 also produced a loss of DF signals in the RBEE-treated plants, this decrease was much less marked compared to C + O_3 plants, highlighting a lower stress state of these plants.

These results suggest that RBEE protects plants against photosynthetic damages by O_3 exposure and maintain the physiological status of plants under these conditions. With the naked eye, although with less significant differences, we could also observe the attenuation of the visible foliar symptoms caused by ozone in the plants treated with RBEE before ozonization. C + O_3 plants showed a more widespread chlorosis, as well as the appearance of small brown spots that were not present on RBEE + O_3 plants (**Supplementary Figure SM2**).

Oxidative Stress Level in Plants

To observe the oxidative stress after O_3 exposure and RBEE treatment, antioxidant enzyme activities were measured. Both variables had significant effects on these activities (**Figure 3**). As expected, O_3-exposed plants showed a significant increase in their enzymatic activities in comparison with the control to alleviate the oxidative stress caused by ozone, underline that SOD and APX showed more activity than the other enzymes.

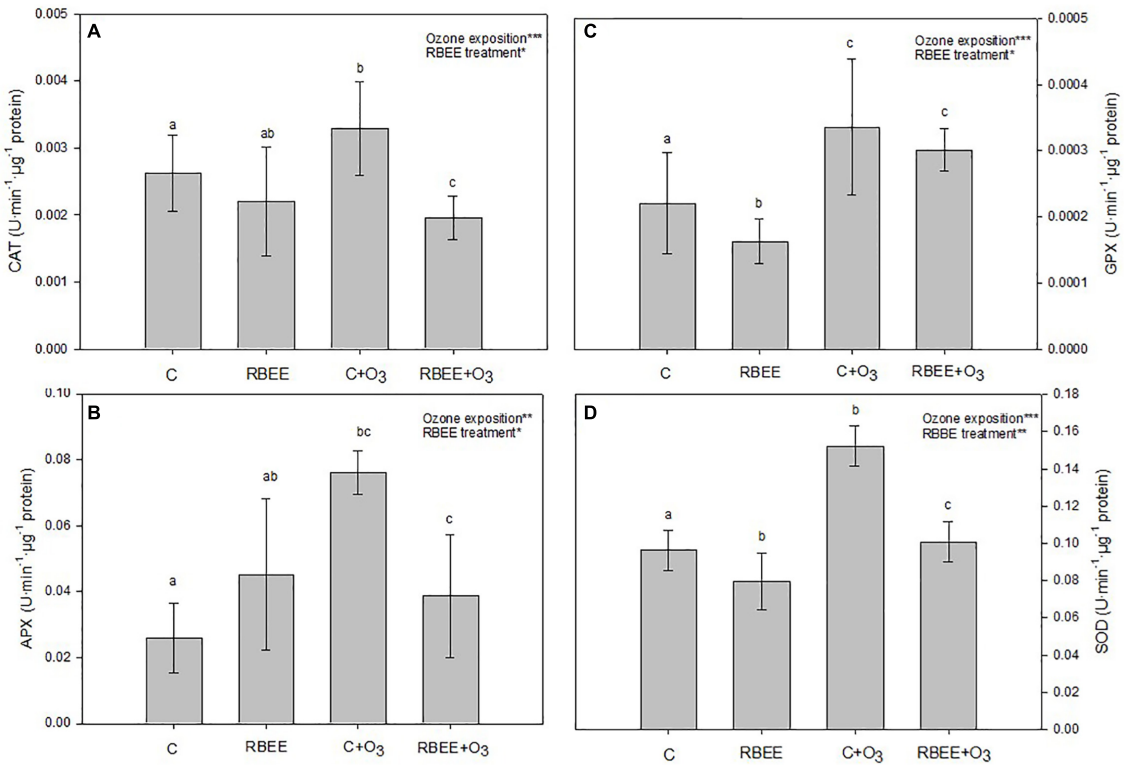

FIGURE 3 | Antioxidant enzyme activities. **(A)** Catalase (CAT), **(B)** ascorbate peroxidase (APX), **(C)** guaiacol peroxidase (GPX), and **(D)** superoxide dismutase (SOD) activities from leaves of pepper plants in response to two conditions of ozone (O_3) (0 and 100 ppm) under a treatment without and with rice bran enzymatic extract (RBEE). Values represent mean ± SD, $n = 5$. Different letters indicate means that are significantly different from each other (two-way ANOVA, O_3 exposition × RBEE treatment; HSD test, $P < 0.05$). O_3 exposition and RBEE treatment in the corner of the panels indicate main or interaction significant effects (*$P < 0.01$; **$P < 0.001$; ***$P > 0.0001$).

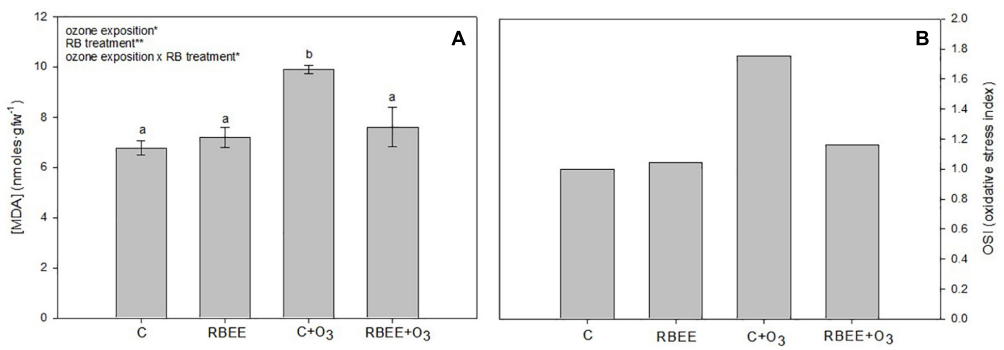

FIGURE 4 | Malondialdehyde concentration (MDA) **(A)** and oxidative stress index (OSI) **(B)** in leaves of pepper plants in response to two conditions of ozone (O_3) (0 and 100 ppm) under a treatment without and with rice bran enzymatic extract (RBEE). Values represent mean ± SD, $n = 5$. Different letters indicate means that are significantly different from each other (two-way ANOVA, O_3 exposition × RBEE treatment; HSD test, $P < 0.05$). O_3 exposition, RBEE treatment, and O_3 exposition × RBEE treatment in the corner of the panels indicate main or interaction significant effects (*$P < 0.01$; **$P < 0.001$).

Nevertheless, the activity of enzymes decreased both in an O_3 environment and when plants were treated with RBEE but no exposed to O_3, with the insignificant exception of the APX activity without ozone exposure (**Figure 3B**). In absence of O_3, the activities decrease 16, 26, and 17%, in CAT, GPX, and SOD, respectively. In O_3-exposed plants, the decreases were 41, 49, 10, and 34% in CAT, APX, GPX, and SOD, respectively, being the APX activity the most affected.

To check the lipid peroxidation of plants, the content of MDA, commonly used as a marker of oxidative stress (Oszlányi et al., 2020), was measured in our leaf samples. As shown in **Figure 4A**, higher concentrations of MDA were recorded in

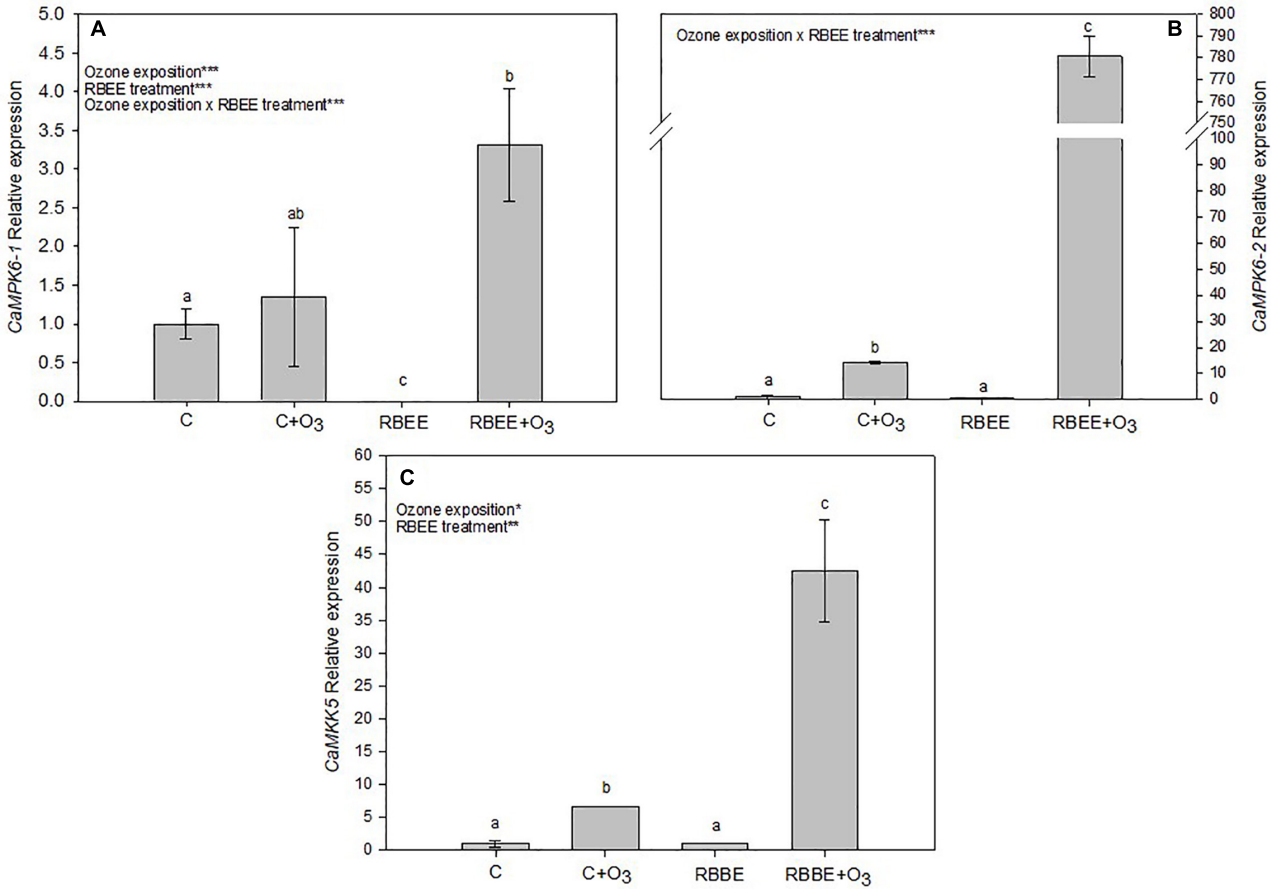

FIGURE 5 | Relative expression of **(A)** *CaMPK6-1*, **(B)** *CaMPK6-2*, and **(C)** *CaMKK5* in leaves of pepper plants in response to two conditions of ozone (O_3) (0 and 100 ppm) under a treatment without and with rice bran enzymatic extract (RBEE). For each gene, the expression level is relative to that of control plants (without RBEE treatment and without O_3 exposition) considered as 1. Values represent relative expression ± SD, $n = 3$. Different letters indicate means that are significantly different from each other (two-way ANOVA, O_3 exposition × RBEE treatment; HSD test, $P < 0.05$). O_3 exposition, RBEE treatment, and O_3 exposition × RBEE treatment in the corner of the panels indicate main or interaction significant effects (*$P < 0.05$; **$P < 0.001$; ***$P < 0.0001$).

the C + O_3 plants, which presented a significant increase in MDA content compared to all other experimental plants. On the other hand, the plants sprayed with RBEE showed similar levels of lipid peroxidation to those of the control plants, showing the protective effect of RBEE treatment against oxidative stress caused by O_3 exposure.

All these positive effects of RBEE in plants in an O_3 environment were also reflected in the OSI (**Figure 4B**). The OSI shows that O_3-exposed plants treated with RBEE contain more similar stress levels to that of the control plants. These results support the protective effects of RBEE against O_3-induced oxidative damage. Furthermore, RBEE application in leaves did not produce any oxidative stress in pepper plants.

Mitogen-Activated Protein Kinase Genes Expression

This study also checked the expression of some MAPK genes involved in oxidative stress in plants (Liu and He, 2017). As suspected, expression of *CaMPK6-1*, *CaMPK6-2*, and *CaMKK5* genes increased in leaves of O_3-exposed plants (**Figure 5**). RBEE did not give rise to the expression of these genes in plants in the absence of an O_3 environment. Surprisingly, however, after O_3 exposure, RBEE treated leaves showed a huge overexpression of these MAPK genes, these being expressions of 4.89, 55.31, and 6.39-folds higher than in the O_3-exposed control plant for *CaMPK6-1*, *CaMPK6-2*, and *CaMKK5* genes, respectively (**Figure 5**). This result could indicate that the O_3-oxidated RBEE produces the induction of gene expression by acting as a transcription inductor. However, this fact should be studied to understand the mechanism involved in this process.

DISCUSSION

Biostimulants have been defined as "a formulated product of biological origin that improves plant productivity as a consequence of the novel, or emergent properties of the complex of constituents, and not as a sole consequence of the presence of known essential plant nutrients, plant growth

regulators, or plant protective compounds" (Yakhin et al., 2017). Present results show a new product, an enzymatic extract from rice bran that protects against O_3-induced damage. O_3 treatment induces a decrease in net photosynthetic rate, chlorophyll content, and DF in pepper leaves which was partially reversed after foliar treatment with RBEE (**Figures 1A,B**, **2A**, respectively). Thus, we can propose that RBEE may exert a biostimulant effect on pepper plants mainly based on its bioactive compounds.

Rice bran enzymatic extract, the enzymatically obtained extract from rice bran, shows a notable total antioxidant capacity (Revilla et al., 2009) and has been evaluated as a protector against lipid and protein oxidation in rat brain homogenate (Parrado et al., 2003). Additionally, we tested the antioxidant capacity of RBEE in two cell models: keratinocyte monolayers and reconstructed human epidermis both irradiated with UVB, and found that RBEE decreased lipid peroxidation in both systems (Santa-María et al., 2010).

Rice bran enzymatic extract is rich in prominent bioactive molecules. Many components of the extract may contribute to its antioxidant capacity. The most abundant phytochemical is γ-oryzanol, which is a natural antioxidant composed of ferulic acid esters of sterols and triterpene alcohols with high scavenging activity of free radicals, mainly mediated by ferulic acid moiety (Lemus et al., 2014; Minatel et al., 2016; Massarolo et al., 2017; Zduńska et al., 2018). RBEE also contains tocols (both tocopherols and tocotrienols) that act as antioxidants due to their ability to donate phenolic hydrogens (electrons) to lipid radicals (Xu et al., 2001). Polyunsaturated fatty acids which act as radical scavenging agents are also present in RBEE, contributing to the antioxidant activity. So, other natural substances such as *Rosa rubiginosa* oil (Franco et al., 2007), grape seed oil (Bail et al., 2008), and soybean-germ oil (Chen et al., 2019) are used for cosmetic purposes due to their polyunsaturated fatty acid content, which acts as a radical scavenging agent.

Rice bran enzymatic extract is also rich in PHs. PHs exhibit different antioxidant and free radicals scavenging activities (Li et al., 2008), mainly conferred by some nitrogenous compounds contained therein such as glycine, betaine, and proline (du Jardin, 2015). Moreover, PHs have shown an ability to enhance antioxidant mechanisms in plants (Gurav and Jadhav, 2013). It is worth noting that PHs, mainly those resulting from the enzymatic hydrolysis of protein substrates into low molecular weight peptides and free amino acids, have shown multiple biostimulant capabilities. Protein hydrolysates are included within the biostimulant classification (du Jardin, 2015). The direct effects in plants include modulating N uptake and assimilation, acting on signaling pathways in the root, regulating enzymes involved in this process (du Jardin, 2015), possessing hormonal activity similar to auxin and gibberellin (Colla et al., 2014), and producing antioxidant activity (Li et al., 2008; Gurav and Jadhav, 2013). In addition, when applied to soils, PHs have shown indirect effects on plant growth and nutrition by increasing the availability of nutrients and their acquisition by the roots – enhancing the microbial activity and biomass of the soil, soil respiration, and their fertility in general (du Jardin, 2015; Rodríguez-Morgado et al., 2015).

It is worthing to note that mixture of these bioactive molecules, as is the case of RBEE, has been reported to greatly enhance the antioxidant activity of rice bran oil (Perez-Ternero et al., 2017).

According to the RBEE antioxidant capacity, we have selected an acute O_3 treatment as an abiotic stressor. O_3 is degraded in the apoplast into secondary ROS (Vainonen and Kangasjärvi, 2015) and high levels of ROS can lead to ROS stress that induces the enzymatic and non-enzymatic-systems that protect cells from ROS (Sachdev et al., 2021). Accordingly all the enzymatic activities assayed – CAT, GPX, APX, and SOD – were induced after O_3 treatment. Induction was significantly reversed by the foliar treatment with RBEE (**Figure 3**). The effect on enzymatic activities could be correlated with the antioxidant effect of RBEE, thus the lipid peroxidation induced by O_3 treatment was significantly alleviated by RBEE (**Figure 4A**). Consequently, the antioxidant effect is reflected in the OSI values (**Figure 4B**).

Unlike other enzymes assayed, a surprising result was the induction of APX after the application of RBEE in plants not treated with O_3 (**Figure 3B**). We can speculate that this APX induction may be due to a hormetic effect induced by RBEE, stimulating a cellular system that could be essential for plant defense under stress. At the physiological level, hormesis is an adaptive response of an organism to a low-level stress factor accompanied by over-compensation when homeostasis is interrupted (Mattson, 2008; Calabrese, 2009; Wiegant et al., 2012). Hormesis is the cellular response in plants that occurs after an initial exposure to low levels of biotic or abiotic stressors – such as herbicides, temperature, chemicals, and radiation – which predisposes them to stimulate cellular defense mechanisms at subsequent sources of stress (Agathokleous and Calabrese, 2020; Berry and López-Martínez, 2020). For example, low doses of some herbicides such as 2,4-dichlorophenoxyacetic acid, glyphosate, and paraquat have been shown to trigger auxin production and antioxidant defense. The biostimulant-induced hormesis response of beneficial organisms allows plants to tolerate stress (Ahkami et al., 2017) through activation of secondary metabolisms and gene expression to recover homeostasis (Vargas-Hernandez et al., 2017). Application of biostimulants at right time can therefore facilitate increased plant growth while combined application of multiple biostimulants can be effective in reducing environmental drastic impacts (Dong et al., 2020).

In plants, the mechanism of hormesis is still unknown. The most probable pathways for hormetic responses are the induction of ROS by mild stress which leads to the activation of antioxidant defenses, stress-signaling hormones, or adaptive growth responses (Poschenrieder et al., 2013). Thus, induction of low and sub-toxic concentrations of ROS by mild stressors, such as which occurs as a result of foliar application of RBEE, has shown the ability to develop a hormetic effect, activating antioxidative defense and adaptive responses. RBEE is rich in 18C-unsaturated fatty acids (UFAs): oleic (18:1), linoleic (18:2), and α-linolenic (18:3) acids (**Table 2**). Besides their roles as ingredients and modulators of cellular membranes, reserves of carbon and energy, stocks of extracellular barrier constituents (e.g., cutin and suberin), or precursors of various bioactive

molecules (e.g., jasmonates and nitroalkenes), recent works have pointed the role of 18C-UFAs as regulators of stress signaling (He and Ding, 2020). Oleic acid has been implicated in plant immunity against pathogens (Mandal et al., 2012). Even more, linoleic acid may regulate plant defense through ROS production (Yaeno et al., 2004). In this context, we can assume that RBEE application may induce a mild increase in ROS due to UFAs content that underly the induction of APX activity.

Ascorbate peroxidase is an H_2O_2-scavenging enzyme and is indispensable for the protection of chloroplasts and other cell constituents from damage by H_2O_2 and hydroxyl radicals (OH.). APX has been identified in most higher plants and comprises a family of isoenzymes present in different plant cell compartments, including apoplast (Sofo et al., 2015). As compared to catalase, it is more vital in stress as it has a high affinity for hydrogen peroxide (Afzal et al., 2014). Accordingly, we have found that APX activity exceeds catalase activity 10 times (**Figures 3A,B**). After O_3 enters the leaves through the stomata, it rises to the apoplast where it is immediately degraded into secondary ROS. Detoxification of ROS in the apoplast can therefore be considered as an early line of defense against O_3 (Kangasjärvi et al., 2005; Castagna and Ranieri, 2009). APX uses ascorbate as its specific electron donor to reduce H_2O_2 to water. Ascorbate is believed to be the major redox buffer and ROS scavenger in the apoplast (Foyer and Noctor, 2009). Thus, we can speculate that pretreatment with RBEE induced ROS generation that slightly stimulates APX activity, probably at the apoplast, the gate of entrance, that facilitates posterior induction and consequently protection against O_3 exposure. The APX result could be working in tandem with the decrease in chlorophyll content and DF found in the same group of plants (**Figures 1B**, **2A**). This effect could be due to linoleic acid present in RBEE as it has been shown that linoleic acid decreased the chlorophyll concentration and photosynthetic efficiency in *Cylindrospermopsis raciborskii* (Xu et al., 2016).

Protein phosphorylation mediated by protein kinase cascades is one of the most important post-translational modifications that coordinate response in cells. One relevant protein-kinase based amplification cascade is the MAPK cascade. The MAPK cascade is a complex signaling pathway hierarchically organized at least three sequentially acting serine/threonine kinases – a MAP kinase kinase kinase (MAPKKK), a MAP kinase kinase (MAPKK), and finally, the MAPK itself – with each phosphorylating, and hence activating, the next kinase. In this cascade, MAPKs phosphorylate specific substrate proteins, such as transcription factors and enzymes, and subsequently trigger cellular responses and rapidly transform upstream signals into appropriate intracellular responses (Liu et al., 2015). MAPK cascade is involved in many aspects of plant physiology, including cell division (Komis et al., 2011), plant growth and development (Xu and Zhang, 2015), plant resistance to pathogens (Bigeard et al., 2015) and insect herbivores (Hettenhausen et al., 2015), and plant response to abiotic stresses (Liu, 2012; Smékalová et al., 2014). It has been described as an interplay between MAPK cascade and ROS; so exogenous application of H_2O_2 or O_3 activates components of MAPK cascades. On the other hand, manipulating MAPK cascades results in initiation of ROS responses (Šamajová et al., 2013). In this context, the present work analyses the role of the MAPK cascade in the protective effect of RBEE against O_3 damage.

The majority of MAPK and MAPKK members are constitutively expressed in pepper plants. In leaves, the transcript level of *CaMPK1* is the highest, followed by *CaMPK6-2*, and *CaMPK19-2*. Among MAPKK genes, *CaMKK5* exhibits the highest transcript levels. Under the challenges of heat shock, salt stress, or pathogen inoculation, most of the MAPKs and MAPKKs in the pepper genome were significantly transcriptionally modified (Liu et al., 2015). Accordingly, after O_3 exposure, we found induction of the studied MAPKs. It is worth noting the relevant role that MPK3/MPK6 play in ROS response and O_3 sensitivity. AtMPK3/AtMPK6 in *A. thaliana* (Ahlfors et al., 2004) and the orthologs SIPK/WIPK in tobacco (Marcus et al., 2000), have been found to regulate for O_3 sensitivity; in fact RNAi-mediated silencing of MPK6 renders the plant more sensitive to O_3 (Miles et al., 2005). In these lines we found increased CaMAPK6-1 and CaMAPK6-2 after pepper plants exposition to O_3. Moreover, induction of CaMKK5 may be related to CaMAPK6-1 and CaMAPK6-2. It has been described in *Arabidopsis* that MKK5 was involved in MPK3/MPK6 activation in response to O_3 exposure (Vainonen and Kangasjärvi, 2015) and interestingly in pepper CaMPKK5 interacts with CaMPK3, CaMPK6-1, and CaMPK6-2 (Liu et al., 2015). But surprisingly, after O_3 exposure, RBEE treated leaves showed a huge expression of these MAPK genes, being higher than in the control plants under O_3 in *CaMPK6-1*, *CaMPK6-2*, and *CaMKK5* genes (**Figure 5**). As previously indicated, the MAPK cascade is involved in many aspects of plant physiology including the defense response against stress. The presence of multiple genes' family members in genomes of different plant species encoding for MAPKKKs, MAPKKs, and MAPKs, and the fact that one MAPK cascade may be associated with more than one upstream or downstream partner (Liu et al., 2015) made it difficult to elucidate specific mechanism mediated by MAPK modules. How ROS activates MAPK cascades still remains unclear. It is possible that plants not only use MAPK cascades to transduce ROS signaling to gene expression and sometimes cell death, but also initiate the negative feedback regulation by MAPK cascades to maintain ROS homeostasis. The different combinations of the three tiers of kinases, distribution, time point-dependent activation, strength, duration, and availability of substrates of MAPK cascades may determine the feed-forward or feed-back outcomes (Liu and He, 2017). However, our results unequivocally indicate that both the damage induced by O_3 and the activation of the protection systems against it induced by RBEE take place through the transcriptional induction of the MAPK cascade.

CONCLUSION

Rice bran enzymatic extract, an enzymatic extract of plant origin, reversed the O3-induced decrease in physiological parameters as net photosynthetic rate, chlorophyll content, and DF. Thus, the results of our study highlight the potential use of RBEE as an effective biostimulant plant protector against oxidative stress caused by O_3. Present results also point out that MAPK cascade

is involved in both, O_3-induced damage and RBEE protection. However, more studies are needed to clarify how this kinase pathway is involved.

Thus, we contribute to the general efforts done in the last decade searching new non-chemical alternative products to protect crops against damages caused by environmental oxidative stress.

DATA AVAILABILITY STATEMENT

The original contributions presented in the study are included in the article/**Supplementary Material**, further inquiries can be directed to the corresponding author.

AUTHOR CONTRIBUTIONS

SM-B, SN-T, ER, AC, and JP designed the study. SM-B, SN-T, and LM performed the research. SM-B, SN-T, PC, ER, AC, and JP analyzed the data and wrote the manuscript. All authors contributed to the article and approved the submitted version.

FUNDING

This study is part of I + D + i Project RTI2018-097425-B100 funded by MCIN/AEI/10.13039/501100011033 and by "ERDF A way of making Europe".

ACKNOWLEDGMENTS

We are particularly grateful with Emilia Sanz-Rios for help with language corrections. We thank the University of Seville Greenhouse General Service (CITIUS) for their collaboration and providing the facilities.

SUPPLEMENTARY MATERIAL

The Supplementary Material for this article can be found online at: https://www.frontiersin.org/articles/10.3389/fpls.2021.749422/full#supplementary-material

REFERENCES

Afzal, F., Khurshid, R., Ashraf, M., and Gul Kazi, A. (2014). "Reactive Oxygen Species and Antioxidants in Response to Pathogens and Wounding," in *Oxidative Damage to Plants Antioxid*, ed. P. Ahamad (Amsterdam: Elsevier), 397–424. doi: 10.1016/B978-0-12-799963-0.00013-7

Agathokleous, E., and Calabrese, E. J. (2020). A global environmental health perspective and optimisation of stress. *Sci. Total Environ.* 704:135263. doi: 10.1016/j.scitotenv.2019.135263

Ahkami, A. H., Allen White, R., Handakumbura, P. P., and Jansson, C. (2017). Rhizosphere engineering: enhancing sustainable plant ecosystem productivity. *Rhizosphere* 3, 233–243. doi: 10.1016/J.RHISPH.2017.04.012

Ahlfors, R., Macioszek, V., XRudd, J., Brosché, M., Schlichting, R., Scheel, D., et al. (2004). Stress hormone-independent activation and nuclear translocation of mitogenactivated protein kinases in *Arabidopsis thaliana* during ozone exposure. *Plant J.* 40, 512–522. doi: 10.1111/J.1365-313X.2004.02229.X

Ainsworth, E. A., Yendrek, C. R., Sitch, S. S., Collins, W. J. C., and Emberson, L. D. (2012). The effects of tropospheric ozone on net primary productivity and implications for climate change. *Annu. Rev. Plant Biol.* 63, 637–661. doi: 10.1146/ANNUREV-ARPLANT-042110-103829

Archambault, D. J., Archambault, D. J., Slaski, J. J., and Li, X. (2000). *Ozone protection in plants: the potential use of chemical protectants to measure atmospheric oxidant damage in Alberta crops*. Edmonton: Alberta Environment. doi: 10.5962/bhl.title.115607

Arnon, D. I. (1949). Copper enzymes in isolated chloroplasts. Polyphenoloxidase in Beta vulgaris. *Plant Physiol.* 24, 1–15. doi: 10.1104/PP.24.1.1

Avnery, S., Mauzerall, D. L., Liu, J., and Horowitz, L. W. (2011). Global crop yield reductions due to surface ozone exposure: 2. Year 2030 potential crop production losses and economic damage under two scenarios of O3 pollution. *Atmos. Environ.* 45, 2297–2309. doi: 10.1016/J.ATMOSENV.2011.01.002

Bail, S., Stuebiger, G., Krist, S., Unterweger, H., and Buchbauer, G. (2008). Characterisation of various grape seed oils by volatile compounds, triacylglycerol composition, total phenols and antioxidant capacity. *Food Chem.* 108, 1122–1132. doi: 10.1016/J.FOODCHEM.2007.11.063

Berry, R., and López-Martínez, G. (2020). A dose of experimental hormesis: when mild stress protects and improves animal performance. *Comp. Biochem. Physiol. A Mol. Integr. Physiol.* 242:110658. doi: 10.1016/j.cbpa.2020.110658

Bigeard, J., Colcombet, J., and Hirt, H. (2015). Signaling mechanisms in pattern-triggered immunity (PTI). *Mol. Plant* 8, 521–539. doi: 10.1016/J.MOLP.2014.12.022

Bortolin, R. C., Caregnato, F. F., Divan Junior, A. M., Zanotto-Filho, A., Moresco, K. S., de Oliveira Rios, A., et al. (2016). Chronic ozone exposure alters the secondary metabolite profile, antioxidant potential, anti-inflammatory property, and quality of red pepper fruit from Capsicum baccatum. *Ecotoxicol. Environ. Saf.* 129, 16–24. doi: 10.1016/J.ECOENV.2016.03.004

Bradford, M. M. (1976). A rapid and sensitive method for the quantitation of microgram quantities of protein utilizing the principle of protein-dye binding. *Anal. Biochem.* 72, 248–254. doi: 10.1016/0003-2697(76)90527-3

Calabrese, E. J. (2009). Hormesis: a Conversation with a Critic. *Environ. Health Perspect.* 117:1339. doi: 10.1289/EHP.0901002

Castagna, A., and Ranieri, A. (2009). Detoxification and repair process of ozone injury: from O3 uptake to gene expression adjustment. *Environ. Pollut.* 157, 1461–1469. doi: 10.1016/J.ENVPOL.2008.09.029

Chen, J., Tang, G., Zhou, J., Liu, W., and Bi, Y. (2019). The characterization of soybean germ oil and the antioxidative activity of its phytosterols. *RSC Adv.* 9, 40109–40117. doi: 10.1039/C9RA08771K

Colla, G., Rouphael, Y., Canaguier, R., Svecova, E., and Cardarelli, M. (2014). Biostimulant action of a plant-derived protein hydrolysate produced through enzymatic hydrolysis. *Front. Plant Sci.* 5:448. doi: 10.3389/fpls.2014.00448

Didyk, N. P., and Blum, O. B. (2010). Natural antioxidants of plant origin against ozone damage of sensitive crops. *Acta Physiol. Plant* 33, 25–34. doi: 10.1007/S11738-010-0527-5

Dong, C., Wang, G., Du, M., Niu, C., Zhang, P., Zhang, X., et al. (2020). Biostimulants promote plant vigor of tomato and strawberry after transplanting. *Sci. Hortic.* 267:109355. doi: 10.1016/J.SCIENTA.2020.109355

du Jardin, P. (2015). Plant biostimulants: definition, concept, main categories and regulation. *Sci. Hortic.* 196, 3–14. doi: 10.1016/J.SCIENTA.2015.09.021

Duarte, B., Goessling, J., Marques, J., and Caçador, I. (2015). Ecophysiological constraints of Aster tripolium under extreme thermal events impacts: merging biophysical, biochemical and genetic insights. *Plant Physiol. Biochem.* 97, 217–228. doi: 10.1016/J.PLAPHY.2015.10.015

Esterbauer, H., and Cheeseman, K. (1990). Determination of aldehydic lipid peroxidation products: malonaldehyde and 4-hydroxynonenal. *Methods Enzymol.* 186, 407–421. doi: 10.1016/0076-6879(90)86134-H

Foyer, C., and Noctor, G. (2009). Redox regulation in photosynthetic organisms: signaling, acclimation, and practical implications. *Antioxid. Redox Signal.* 11, 861–905. doi: 10.1089/ARS.2008.2177

Franco, D., Pinelo, M., Sineiro, J., and Núñez, M. J. (2007). Processing of Rosa rubiginosa: extraction of oil and antioxidant substances. *Bioresour. Technol.* 98, 3506–3512. doi: 10.1016/J.BIORTECH.2006.11.012

Gill, S. S., and Tuteja, N. (2010). Reactive oxygen species and antioxidant machinery in abiotic stress tolerance in crop plants. *Plant Physiol. Biochem.* 48, 909–930. doi: 10.1016/J.PLAPHY.2010.08.016

Goufo, P., and Trindade, H. (2014). Rice antioxidants: phenolic acids, flavonoids, anthocyanins, proanthocyanidins, tocopherols, tocotrienols, γ-oryzanol, and phytic acid. *Food Sci. Nutr.* 2, 75–104. doi: 10.1002/FSN3.86

Guo, W., Chen, R., Gong, Z., Yin, Y., Ahmed, S., and He, Y. (2012). Exogenous abscisic acid increases antioxidant enzymes and related gene expression in pepper (*Capsicum annuum*) leaves subjected to chilling stress. *Genet. Mol. Res.* 11, 4063–4080. doi: 10.4238/2012.SEPTEMBER.10.5

Gurav, R. G., and Jadhav, J. P. (2013). A novel source of biofertilizer from feather biomass for banana cultivation. *Environ. Sci. Pollut. Res.* 20, 4532–4539. doi: 10.1007/s11356-012-1405-z

He, M., and Ding, N.-Z. (2020). Plant Unsaturated Fatty Acids: multiple Roles in Stress Response. *Front. Plant Sci.* 11:562785. doi: 10.3389/FPLS.2020.562785

Hettenhausen, C., Schuman, M., and Wu, J. (2015). MAPK signaling: a key element in plant defense response to insects. *Insect Sci.* 22, 157–164. doi: 10.1111/1744-7917.12128

Hiscox, J. D., and Israelstam, G. F. (1979). A method for the extraction of chlorophyll from leaf tissue without maceration. *Can. J. Bot.* 57, 1332–1334. doi: 10.1139/b79-163

Kangasjärvi, J., Jaspers, P., and Kollist, H. (2005). Signalling and cell death in ozone-exposed plants. *Plant Cell Environ.* 28, 1021–1036. doi: 10.1111/J.1365-3040.2005.01325.X

Komis, G., Illés, P., Beck, P., and Šamaj, J. (2011). Microtubules and mitogen-activated protein kinase signalling. *Curr. Opin. Plant Biol.* 14, 650–657. doi: 10.1016/J.PBI.2011.07.008

Lemus, C., Angelis, A., Halabalaki, M., and Skaltsounis, A. L. (2014). 'γ-Oryzanol. An Attractive Bioactive Component from Rice Bran,' in *Wheat and Rice in Disease Prevention and Health*, eds R. R. Watson, V. R. Preedy, and S. Zibadi (London: Elsevier Inc.), 409–430. doi: 10.1016/B978-0-12-401716-0.00032-5

Li, Y., Jiang, B., Zhang, T., Mu, W., and Liu, J. (2008). Antioxidant and free radical-scavenging activities of chickpea protein hydrolysate (CPH). *Food Chem.* 106, 444–450. doi: 10.1016/j.foodchem.2007.04.067

Liu, Y. (2012). Roles of mitogen-activated protein kinase cascades in ABA signaling. *Plant Cell Rep.* 31, 1–12. doi: 10.1007/S00299-011-1130-Y

Liu, Y., and He, C. (2017). A review of redox signaling and the control of MAP kinase pathway in plants. *Redox Biol.* 11:192. doi: 10.1016/J.REDOX.2016.12.009

Liu, Z., Shi, L., Liu, Y., Tang, Q., Shen, L., Yang, S., et al. (2015). Genome-wide identification and transcriptional expression analysis of mitogen-activated protein kinase and mitogen-activated protein kinase kinase genes in Capsicum annuum. *Front. Plant Sci.* 6:780. doi: 10.3389/FPLS.2015.00780

Livak, K., and Schmittgen, T. (2001). Analysis of relative gene expression data using real-time quantitative PCR and the 2(-Delta Delta C(T)) Method. *Methods* 25, 402–408. doi: 10.1006/METH.2001.1262

López-Jurado, J., Balao, F., and Mateos-Naranjo, E. (2020). Polyploidy-mediated divergent light-harvesting and photoprotection strategies under temperature stress in a Mediterranean carnation complex. *Environ. Exp. Bot.* 171:103956. doi: 10.1016/J.ENVEXPBOT.2019.103956

Mandal, M., Chandra-Shekara, A., Jeong, R., Yu, K., Zhu, S., Chanda, B., et al. (2012). Oleic acid-dependent modulation of NITRIC OXIDE ASSOCIATED1 protein levels regulates nitric oxide-mediated defense signaling in Arabidopsis. *Plant Cell* 24, 1654–1674. doi: 10.1105/TPC.112.096768

Marcus, A. S., Godfrey, P. M., and Brian, E. E. (2000). Ozone treatment rapidly activates MAP kinase signalling in plants. *Plant J.* 22, 367–376. doi: 10.1046/J.1365-313X.2000.00741.X

Massarolo, K. C., Denardi de Souza, T., Collazzo, C. C., Badiale Furlong, E., and de Souza Soares, L. A. (2017). The impact of Rhizopus oryzae cultivation on rice bran: gamma-oryzanol recovery and its antioxidant properties. *Food Chem.* 228, 43–49. doi: 10.1016/J.FOODCHEM.2017.01.127

Mattson, M. (2008). Hormesis defined. *Ageing Res. Rev.* 7, 1–7. doi: 10.1016/J.ARR.2007.08.007

Miles, G. P., Samuel, M. A., Zhang, Y., and Ellis, B. E. (2005). RNA interference-based (RNAi) suppression of AtMPK6, an Arabidopsis mitogen-activated protein kinase, results in hypersensitivity to ozone and misregulation of AtMPK3. *Environ. Pollut.* 138, 230–237. doi: 10.1016/J.ENVPOL.2005.04.017

Mills, G., Buse, A., Gimeno, B., Bermejo, V., Holland, M., Emberson, L., et al. (2007). A synthesis of AOT40-based response functions and critical levels of ozone for agricultural and horticultural crops. *Atmos. Environ.* 41, 2630–2643. doi: 10.1016/J.ATMOSENV.2006.11.016

Minatel, I. O., Francisqueti, F. V., Corrêa, C. R., and Lima, G. P. P. (2016). Antioxidant Activity of γ-Oryzanol: a Complex Network of Interactions. *Int. J. Mol. Sci.* 17:1107. doi: 10.3390/IJMS17081107

Oszlányi, R., Mirmazloum, I., Pónya, Z., Szegő, A., Jamal, S., Bat-Erdene, O., et al. (2020). Oxidative stress level and dehydrin gene expression pattern differentiate two contrasting cucumber F1 hybrids under high fertigation treatment. *Int. J. Biol. Macromol.* 161, 864–874. doi: 10.1016/J.IJBIOMAC.2020.06.050

Paredes-Páliz, K., Rodríguez-Vázquez, R., Duarte, B., Caviedes, M. A., Mateos-Naranjo, E., Redondo-Gómez, S., et al. (2018). Investigating the mechanisms underlying phytoprotection by plant growth-promoting rhizobacteria in Spartina densiflora under metal stress. *Plant Biol.* 20, 497–506. doi: 10.1111/plb.12693

Parrado, J., Miramontes, E., Jover, M., Gutierrez, J. F., Collantes de Terán, L., and Bautista, J. (2006). Preparation of a rice bran enzymatic extract with potential use as functional food. *Food Chem.* 98, 742–748. doi: 10.1016/J.FOODCHEM.2005.07.016

Parrado, J., Miramontes, E., Jover, M., Márquez, J. C., Mejias, M. A., De Teran, L. C., et al. (2003). Prevention of brain protein and lipid oxidation elicited by a water-soluble oryzanol enzymatic extract derived from rice bran. *Eur. J. Nutr.* 42, 307–314. doi: 10.1007/S00394-003-0424-4

Pérez-Palacios, P., Agostini, E., Ibáñez, S. G., Talano, M. A., Rodríguez-Llorente, I. D., Caviedes, M. A., et al. (2017). Removal of copper from aqueous solutions by rhizofiltration using genetically modified hairy roots expressing a bacterial Cu-binding protein. *Environ. Technol.* 38, 2877–2888. doi: 10.1080/09593330.2017.1281350

Perez-Ternero, C., Alvarez de Sotomayor, M., and Herrera, M. D. (2017). Contribution of ferulic acid, γ-oryzanol and tocotrienols to the cardiometabolic protective effects of rice bran. *J. Funct. Foods* 32, 58–71. doi: 10.1016/j.jff.2017.02.014

Poschenrieder, C., Cabot, C., Martos, S., Gallego, B., and Barceló, J. (2013). Do toxic ions induce hormesis in plants?. *Plant Sci.* 212, 15–25. doi: 10.1016/j.plantsci.2013.07.012

Revilla, E., Maria, C. S., Miramontes, E., Bautista, J., García-Martínez, A., Cremades, O., et al. (2009). Nutraceutical composition, antioxidant activity and hypocholesterolemic effect of a water-soluble enzymatic extract from rice bran. *Food Res. Int.* 42, 387–393. doi: 10.1016/J.FOODRES.2009.01.010

Revilla, E., Santa-María, C., Miramontes, E., Candiracci, M., Rodríguez-Morgado, B., Carballo, M., et al. (2013). Antiproliferative and immunoactivatory ability of an enzymatic extract from rice bran. *Food Chem.* 136, 526–531. doi: 10.1016/J.FOODCHEM.2012.08.044

Rodríguez-Morgado, B., Gómez, I., Parrado, J., García-Martínez, A. M., Aragón, C., and Tejada, M. (2015). Obtaining edaphic biostimulants/biofertilizers from different sewage sludges. Effects on soil biological properties. *Environ. Technol.* 36, 2217–2226. doi: 10.1080/09593330.2015.1024760

Sachdev, S., Ansari, S. A., Ansari, M. I., Fujita, M., and Hasanuzzaman, M. (2021). Abiotic Stress and Reactive Oxygen Species: generation, Signaling, and Defense Mechanisms. *Antioxidants* 10:277. doi: 10.3390/ANTIOX10020277

Šamajová, O., Plíhal, O., Al-Yousif, M., Hirt, H., and Šamaj, J. (2013). Improvement of stress tolerance in plants by genetic manipulation of mitogen-activated protein kinases. *Biotechnol. Adv.* 31, 118–128. doi: 10.1016/J.BIOTECHADV.2011.12.002

Santa María, C., Revilla, E., Rodríguez-Morgado, B., Castaño, A., Carbonero, P., Gordillo, B., et al. (2016). Effect of rice parboiling on the functional properties

of an enzymatic extract from rice bran. *J. Cereal Sci.* 72, 54–59. doi: 10.1016/J.JCS.2016.09.010

Santa-María, C., Revilla, E., Miramontes, E., Bautista, J., García-Martínez, A., Romero, E., et al. (2010). Protection against free radicals (UVB irradiation) of a water-soluble enzymatic extract from rice bran. Study using human keratinocyte monolayer and reconstructed human epidermis. *Food Chem. Toxicol.* 48, 83–88. doi: 10.1016/J.FCT.2009.09.019

Sharma, P., Jha, A. B., Dubey, R. S., and Pessarakli, M. (2012). Reactive Oxygen Species, Oxidative Damage, and Antioxidative Defense Mechanism in Plants under Stressful Conditions. *J. Bot.* 2012:217037. doi: 10.1155/2012/217037

Smékalová, V., Doskočilová, A., Komis, G., and Šamaj, J. (2014). Crosstalk between secondary messengers, hormones and MAPK modules during abiotic stress signalling in plants. *Biotechnol. Adv.* 32, 2–11. doi: 10.1016/J.BIOTECHADV.2013.07.009

Sofo, A., Scopa, A., Nuzzaci, M., and Vitti, A. (2015). Ascorbate peroxidase and catalase activities and their genetic regulation in plants subjected to drought and salinity stresses. *Int. J. Mol. Sci.* 16, 13561–13578. doi: 10.3390/IJMS160613561

Vainonen, J. P., and Kangasjärvi, J. (2015). Plant signalling in acute ozone exposure. *Plant Cell Environ.* 38, 240–252. doi: 10.1111/PCE.12273

Vargas-Hernandez, M., Macias-Bobadilla, I., Guevara-Gonzalez, R. G., Romero-Gomez, S., de, J., Rico-Garcia, E., et al. (2017). Plant hormesis management with biostimulants of biotic origin in agriculture. *Front. Plant Sci.* 8:1762. doi: 10.3389/FPLS.2017.01762

Wiegant, F. A. C., de Poot, S. A. H., Boers-Trilles, V. E., and Schreij, A. M. (2012). Hormesis and Cellular Quality Control: a Possible Explanation for the Molecular Mechanisms that Underlie the Benefits of Mild Stress. *Dose Response* 11, 413–430. doi: 10.2203/DOSE-RESPONSE.12-030.WIEGANT

Xu, J., and Zhang, S. (2015). Mitogen-activated protein kinase cascades in signaling plant growth and development. *Trends Plant Sci.* 20, 56–64. doi: 10.1016/J.TPLANTS.2014.10.001

Xu, S., Yang, S.-Q., Yang, Y.-J., Xu, J.-Z., Shi, J.-Q., and Wu, Z.-X. (2016). Influence of linoleic acid on growth, oxidative stress and photosynthesis of the cyanobacterium Cylindrospermopsis raciborskii. *N. Z. J. Mar. Freshw. Res.* 51, 223–236. doi: 10.1080/00288330.2016.1197286

Xu, Z., Hua, N., and Godber, J. (2001). Antioxidant activity of tocopherols, tocotrienols, and gamma-oryzanol components from rice bran against cholesterol oxidation accelerated by 2,2′-azobis(2-methylpropionamidine) dihydrochloride. *J. Agric. Food Chem.* 49, 2077–2081. doi: 10.1021/JF0012852

Yaeno, T., Matsuda, O., and Iba, K. (2004). Role of chloroplast trienoic fatty acids in plant disease defense responses. *Plant J.* 40, 931–941. doi: 10.1111/J.1365-313X.2004.02260.X

Yakhin, O. I., Lubyanov, A. A., Yakhin, I. A., and Brown, P. H. (2017). Biostimulants in plant science: a global perspective. *Front. Plant Sci.* 7:2049. doi: 10.3389/fpls.2016.02049

Zduńska, K., Dana, A., Kolodziejczak, A., and Rotsztejn, H. (2018). Antioxidant Properties of Ferulic Acid and Its Possible Application. *Skin Pharmacol. Physiol.* 31, 332–336. doi: 10.1159/000491755

Zhang, Y., Fu, Y., Fan, J., Li, Q., Francis, F., and Chen, J. (2019). Comparative transcriptome and histological analyses of wheat in response to phytotoxic aphid Schizaphis graminum and non-phytotoxic aphid Sitobion avenae feeding. *BMC Plant Biol.* 19:547. doi: 10.1186/S12870-019-2148-5

Conflict of Interest: The authors declare that the research was conducted in the absence of any commercial or financial relationships that could be construed as a potential conflict of interest.

Publisher's Note: All claims expressed in this article are solely those of the authors and do not necessarily represent those of their affiliated organizations, or those of the publisher, the editors and the reviewers. Any product that may be evaluated in this article, or claim that may be made by its manufacturer, is not guaranteed or endorsed by the publisher.

frontiers in Plant Science

ORIGINAL RESEARCH
published: 29 November 2021
doi: 10.3389/fpls.2021.780099

The Use of Interactions Between Microorganisms in Strawberry Cultivation (*Fragaria x ananassa* Duch.)

Magdalena Drobek[1], Justyna Cybulska[1], Anna Gałązka[2], Beata Feledyn-Szewczyk[2], Anna Marzec-Grządziel[2], Lidia Sas-Paszt[3], Agata Gryta[1], Paweł Trzciński[3], Artur Zdunek[1] and Magdalena Frąc[1]*

[1] *Institute of Agrophysics, Polish Academy of Sciences, Lublin, Poland,* [2] *The Institute of Soil Science and Plant Cultivation (IUNG)–State Research Institute, Puławy, Poland,* [3] *National Institute of Horticultural Research, Skierniewice, Poland*

As the market indicates a growing interest in organically grown fruit, there is a need for biostimulants to counter the adverse effects of pathogenic fungi and fungal-like-pathogens. Four microbial pathogens (*Botrytis cinerea*, *Verticillium* sp., *Phytophthora* sp., and *Colletotrichum* sp.) which are the most often causes of strawberry diseases were selected. Five kinds of biostimulants (C1, C2, C3, C4, and C5) containing bacterial consortia were developed to combat the pathogens. The antagonistic effect of selected microorganisms against strawberry pathogens was observed. The effectiveness of various beneficial bacteria in combating fungal pathogens of cv. Honeoye strawberries was compared and the impact of their activity on fruit quality was assessed. The most significant effect on the strawberry firmness was found for the C2 consortium, which provided the strawberries infected with the pathogens group (MIX: *B. cinerea*, *Verticillium* sp., *Phytophthora* sp., and *Colletotrichum* sp.) with a 140% increase in maximum load in a puncture test compared to the positive control (C0). Strawberries contaminated with *Phytophthora* sp. after the application of Consortium C4 (C4) showed the largest increase (127%) in soluble solid content (SSC) when compared to the C0. Fruit contaminated with *Colletotrichum* sp. and *B. cinerea* after the application of C2 and Consortium 5 (C5), respectively, had the highest levels of anthocyanins and total phenolic content, when compared to C0. The largest increase, which reached as high as 25%, in D-galacturonic acid content was observed for the group of pathogens after Consortium 1 (C1) application. The extraction of strawberry pectin allowed for the study of the rheological properties of pectin solutions; on this basis, strawberry pectin from the control (NC) was distinguished as it showed the highest viscosity (0.137–0.415 Pas). Taking into account the individual effects of bacteria on strawberry pathogenic fungi and fungal-like-pathogens, it is possible to reduce the adverse effects of fungal disease and to improve the properties of strawberries by selecting the appropriate bacterial consortium. Interactions between microorganisms are often complex and not fully understood, which suggests the need for further research in this direction.

Keywords: antagonistic microorganisms, pectin, strawberry, organic fruit, biostimulants

OPEN ACCESS

Edited by:
Maurizio Ruzzi,
University of Tuscia, Italy

Reviewed by:
Sezai Ercisli,
Atatürk University, Turkey
Jorge Poveda,
Public University of Navarre, Spain

****Correspondence:***
Justyna Cybulska
j.cybulska@ipan.lublin.pl

Specialty section:
This article was submitted to Crop and Product Physiology, a section of the journal Frontiers in Plant Science

Received: *20 September 2021*
Accepted: *04 November 2021*
Published: *29 November 2021*

Citation:
Drobek M, Cybulska J, Gałązka A, Feledyn-Szewczyk B, Marzec-Grządziel A, Sas-Paszt L, Gryta A, Trzciński P, Zdunek A and Frąc M (2021) The Use of Interactions Between Microorganisms in Strawberry Cultivation (Fragaria x ananassa Duch.). Front. Plant Sci. 12:780099. doi: 10.3389/fpls.2021.780099

INTRODUCTION

The strawberry is one of the most frequently preferred fruit by consumers due to availability year around and suitable for both organic and conventional production (Balci, 2021; Juric et al., 2021). Excessive pesticide use in conventional crops may lead to their accumulation in the fruit. For this reason, alternative control measures, which include the biopesticides or antagonistic microorganisms (Jensen et al., 2013). The organic farming system differs from the conventional one in prohibition of synthetic plant protection products (pesticides) and mineral fertilizers. The chemical plant protection products are replaced with organic fertilizers, which contain, among others, manure, compost, green manure, beneficial microorganisms (Ponder and Hallmann, 2019). In the context of organic fertilizers, the concept of biostimulants appears. Biostimulants are defined by the European Biostimulants Industry Council as "substance (s) and/or microorganisms whose function, when applied to plants or the rhizosphere, is to stimulate natural processes to increase/benefit nutrient uptake, nutrient efficiency, tolerance to abiotic stress, and quality of the crops "(European Biostimulants Industry Council [EBIC], 2021). It has been proven that biostimulants increase plant yield and improve fruit quality. Additionally, consumers are more interested in ecological products each year, bearing in mind the safety of food and the environment (Kovačević et al., 2015).

The microbiota present on healthy strawberries is complex and includes potential plant pathogens, human pathogens, mycotoxin-producing moulds and plant disease biocontrol agents (Jensen et al., 2013). Some of these microorganisms are antagonistic to the others. Notable bacterial antagonism against pathogenic fungi occurs with considerable frequency and is the result, among other causes, of the production of antibiotics and biosurfactants, as well as competition and parasitism (Berg et al., 2000). The mechanisms of action differ depending on the bacterial strain. The most common strawberry pathogens include fungi from the genera *Botrytis*, *Verticillium*, *Phytophthora*, *Colletotrichum*, *Penicillium*, *Alternaria*, *Cladosporium*, *Rhizopus*, *Aureobasidium,* and *Cryptococcus* (Tournas and Katsoudas, 2005). Bacterial populations on strawberry plants are dominated by *Pseudomonas* spp., *Stenotrophomonas* spp., *Bacillus* spp., and *Arthrobacter* spp. (Krimm et al., 2005).

One of the main strawberry postharvest diseases is grey mould which is caused by *Botrytis cinerea*. A grey coating appears on the leaves and fruit causing the plants to die off and the fruit to dry and rot (Jin et al., 2017). Research results suggest that the following microorganisms are active in combating grey rot: *Clonostachys rosea* (Cota et al., 2009), *Rhodotorula glutinis* (Srivastava et al., 2011), *Paenibacillus polymyxa* (Santiago et al., 2016), *Bacillus* sp. (Cruz et al., 2018), *Streptomyces* sp. (Kim et al., 2015), and *Pseudomonas* sp. (Haggag and Abo El Soud, 2012). The withering of strawberry plants is mainly caused by *Verticillium dahliae*, which attacks the plant's vascular system and blocks the transport of water and nutrients (Sowik et al., 2001). Research indicates that *P. polymyxa* (Zhang et al., 2018), *Bacillus* sp. (Milijasevic-Marcic et al., 2018), and *Streptomyces* sp. (Olanrewaju and Babalola, 2019) are disease-inhibiting bacteria. Fungus-like pathogens of the genus *Phytophthora* including *Phytophthora megasperma*, *Phytophthora cryptogea*, *Phytophthora capsici*, *Phytophthora Citricola,* and *Phytophthora cactorum* can cause diseases of the root, crown and strawberry fruit. Infected plants suddenly lose healthy shoots. A relatively rare disease is red stele in strawberries (*Phytophthora fragariae*). Infected plants become stunted and the leaves turn yellow or red (Wilcox et al., 1993). *Streptomyces griseus* has shown promising results as an antifungal agent against *P. capsici*, as it produces numerous antibiotics that inhibit mycelium growth of *P. capsici*, *Pythium* spp., *Phytophthora* spp., *Rhizoctonia solani*, *Alternaria brassicicola*, and *Botrytis* sp. (Nguyen et al., 2015). The fungi belonging to the species of *Colletotrichum asianum*, *Colletotrichum fructicola*, *Colletotrichum tropicale*, *Colletotrichum dianesei*, *Colletotrichum karstii* (Lima et al., 2013), *Colletotrichum gloeosporioides* (Tang et al., 2019), and *Colletotrichum acutatum* (Moreira et al., 2014) cause anthracnose of fruit, which in the case of strawberries is manifested by the appearance of dry spots on immature fruit, and the browning and drying of flowers and shoots (Lima et al., 2013). It has been shown that the fungi *Aureobasidium pullulans*, *Diaporthe* sp., and *Nigrospora oryzae* inhibits the development of *C. acutatum* (Landum et al., 2016). Useful fungi and bacteria limit the growth and development of pathogens by activating antagonistic mechanisms such as parasitism, antibiotics, and competition (Poveda et al., 2020).

We investigated the impact of various biostimulants containing fungi and bacteria on the quality characteristics of strawberry fruit infected with microbial pathogens. The experiment included four fungal pathogens responsible for the most common strawberry diseases. Bacterial consortia with potentially antagonistic effects were applied to the infected plants infected with *B. cinerea, Verticillium* sp., *Phytophthora* sp., and *Colletotrichum* sp. The results allow for a preliminary selection of microorganisms that can be used to combat strawberry fungal diseases.

MATERIALS AND METHODS

Crop Conditions

The experiment was set up in triplicate for each of the 36 variants (**Figure 1**) and the research material consisted of strawberry cv. Honeoye. Each strawberry plant was grown in a separate pot without undercutting or root curling in a greenhouse at 23°C. Each pot contained 4 kg of soil collected from an organic experimental field of the Institute of Soil Science and Plant Cultivation - State Research Institute (Puławy, Poland) located in Grabów (Poland) and it was subjected to chemical and microbiological analysis. The soil was characterized as Cambisol with a loamy sand texture. Clover was used as a pre-crop. The soil composition was as follows: humus 1.9%, P_2O_5 10.1 mg 100 g^{-1} soil, K_2O 5.0 mg 100 g^{-1} soil, Mg 10.6 mg 100 g^{-1} soil, N-NO_3 8.92 mg kg^{-1} DM of soil, N-NH_4 2.29 mg kg^{-1} DM of soil, pH 5.9. Keramzite was placed at the bottom of each pot in a volume of 0.5 l. The soil was fertilized in autumn with manure (pH = 8.6, nutrient content: N 5.06 mg kg^{-1}, P_2O_5 2.47 mg

kg^{-1}, K_2O 6.90 mg kg^{-1}, CaO 3.04 mg kg^{-1}, MgO 2.38 mg kg^{-1}, S 0.69 mg kg^{-1}) and potassium salt (LUVENA, 100 kg ha^{-1}). Bioilsa® (NaturalCrop, Poland) fertilizer was applied in a quantity corresponding to a dose of 150 kg ha^{-1}.

Plants were treated with five consortia (C1, C2, C3, C4, and C5) and a control (C0) was prepared, in which no consortia were applied (**Figure 1**). The consortia consisted of the following bacterial strains: AF117AB (*P. polymyxa*), Sp115AD (*Bacillus subtilis*), AF75AB2, Sp115AD, AF75BC (*Bacillus* sp.), AF75AA, AF75AD (*Streptomyces* sp.), JAFGU (*Lysobacter* sp.), and AF70AC (*Pseudomonas* sp.). The bacterial strains used in the experiment originated from the SYMBIOBANK collection of the Research Institute of Horticulture in Skierniewice and were selected based on a previous study as microorganisms with potentially beneficial properties in terms of plant biostimulation and protection. The bacterial consortia, with a population size of 10^8 cfu (colony-forming units) in 1 ml, were applied to the soil in a volume of 10 ml per pot directly to the roots at planting time and twice after planting at intervals of 3–4 weeks. The objects called "Consortium C0," in which bacteria were not introduced, were the control for the ones containing bacterial consortia with their potential for plant biostimulation and protection, while NC objects constituted controls without pathogen contamination.

The next step was the infection of plants with five phytopathogenic fungi and fungus-like pathogens (BC, V, P, C, and MIX) and the submission of the control (NC) in which the plants were not treated with pathogens (**Figure 1**). Two days after plant inoculation with bacterial consortia, the plants were infected with the following pathogens: G277/18 (*Botrytis cinerea*), G296/18 (*Verticillium* sp.), G408/18 (*Phytophthora* sp.), G171/18 (*Colletotrichum* sp.). Strains of *B. cinerea*, *Phytophthora* sp., and *Verticillium* sp. were isolated from infected strawberry roots (Oszust et al., 2020), while *Colletotrichum* sp. was isolated from infected strawberry fruit (Malarczyk et al., 2020) at the Institute of Agrophysics of the Polish Academy of Sciences (Lublin, Poland). In the case of *B. cinerea* and *Colletotrichum* sp. the strawberry flowers were infected with 10 ml of pathogen suspension using an inoculum adjusted to 1,000 conidia in 1 ml. In contrast, *Phytophthora* sp. and *Verticillium* sp. were added to the soil as a pathogen inoculum suspension of 10^5 cfu ml^{-1} (10 ml was applied) and 10^4 cfu g^{-1} of soil, respectively.

At the harvest maturity stage, the strawberries (developed and grown, and the sepals easily detach from the stalk) were collected on March 23, 2019.

Firmness

Firmness is one of main parameter of texture which determine overall quality evaluation by consumers (Harker et al., 2003). For soft fruit puncture test is the most common method used for determination of firmness (Døving and Måge, 2002). Fresh fruit firmness (n) was determined by a puncture test by using a universal test machine (Lloyd LRX, Lloyd Instruments). The strawberry was placed on the platform of the device and the aluminium probe (3 mm diameter) was lowered with a constant plunger speed (20 mm min^{-1}) to a constant depth (6 mm). The maximum force required to penetrate the strawberry to a set depth was a measure of tissue firmness (Fraeye et al., 2009). The test was carried out on twenty strawberries for each replicate of the variant. Average fruit firmness was expressed in terms of *N*.

Shape

The shape of the fruit is a hormone-regulated trait and many factors can alter the final shape including environmental conditions (Rey-Serra et al., 2021). The shape was determined in accordance with the method proposed by Ishikawa et al. (2018). The length (the longer dimension was measured from the fruit's tip to the base) and width (the shorter dimension of the fruit, was measured as a transverse measurement at the thickest point) of the fruit were determined. The quotient of length and width was calculated. Fruits are classified as flattened (quotient < 1), round (quotient $= 1$), or oblong (quotient > 1). The test was carried out on fifteen strawberries for each replicate of the variant.

Fresh Weight of Fruit

Fresh weight is the weight of the fruit on the day it is harvested. It is determined by a weight method to initially determine the size of the fruit (Reyes-Yanes et al., 2020). The purpose of determining the fresh weight is to obtain information on the effectiveness of the cultivation methods. Comparison the fresh weight, dry weight and shape provides information on the hydration level of the fruit and the tissue density (Miller et al., 2000). To determine the fresh weight of fruit (FWF), each fruit was weighed to three decimal places. The results were summed and averaged. The average fresh fruit weight was expressed in g.

Dry Weight of Fruit

The dry matter allows the determination of the product residue after the removal of water from it (Ozdemir and Topuz, 2004). The drying oven method is a validated standardized method that is readily available (International Organization for Standardization, 2000). Dry weight (DW) was determined according to the procedure described in standard PN ISO 1026:2000 (International Organization for Standardization, 2000). In Brief, 0.5 g of strawberries were taken from each variant in triplicate and weighed to the nearest 0.001 g. The strawberries were then placed in an oven at 105°C, after 24 h the fruit was weighed, placed in the oven for 2 h and weighed again. The procedure was repeated until no further weight loss was noted. The average dry weight of one fruit was expressed as a percentage of fresh weight.

Soluble Sugar Content

The soluble solid content (SSC) is a measure of the total soluble solid, which includes sugars, organic acids, amino acids, and more, and it is associated with consumer preference for fruit (Crisosto et al., 2003). The refractometric method is used because of the optical properties of sugars and sugar alcohols which are majority of soluble solids of most fruit (Magwaza and Opara, 2015). SSC was determined using a refractometer (PAL-BX/RI, ATAGO, Japan) and expressed in percentage terms. A minimum of five fresh strawberries were picked and juiced. One drop of juice was applied to the refractometer glass and the measurement

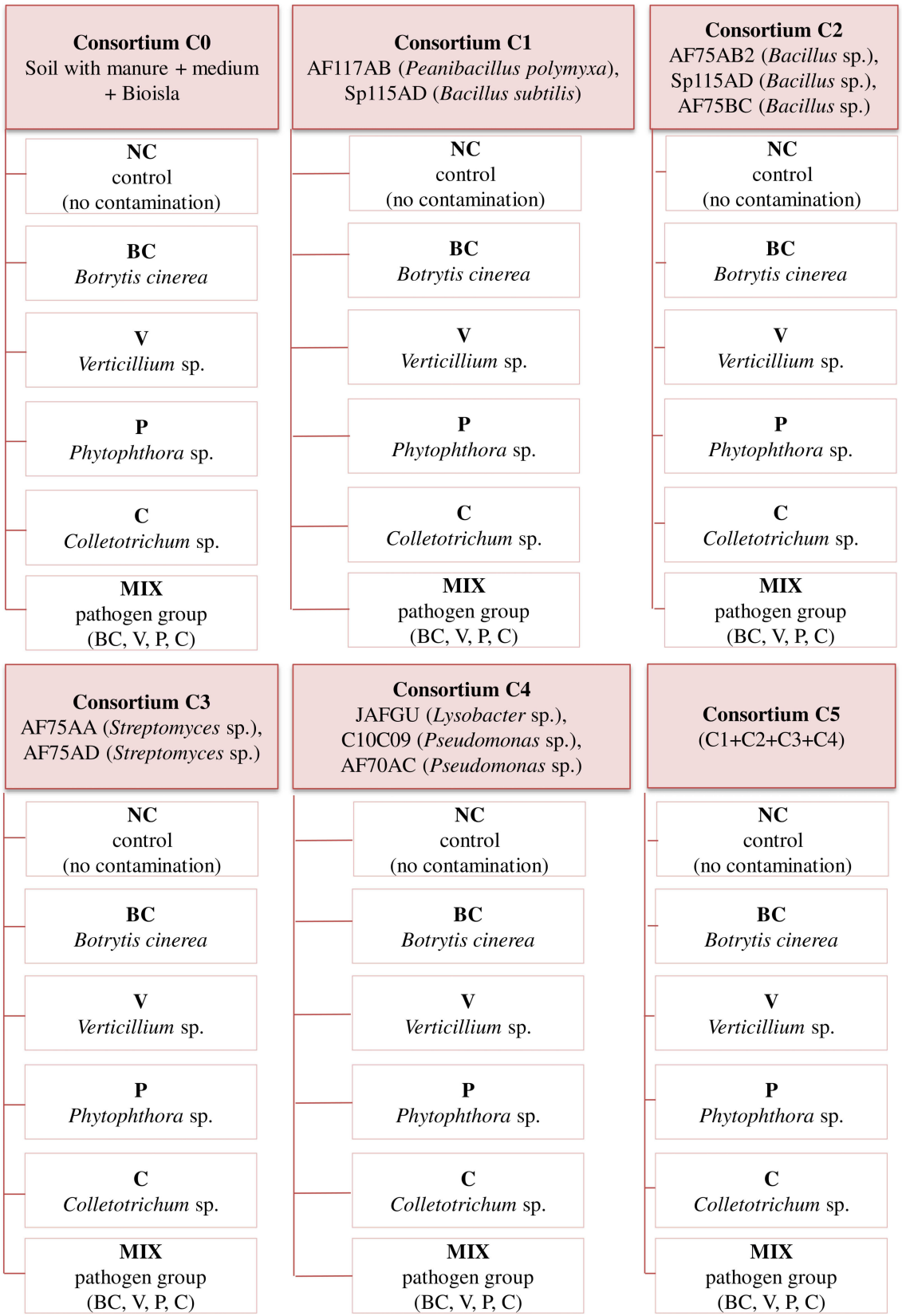

FIGURE 1 | Experimental design outlining 36 variants of the experiment.

was performed; the soluble sugar content was expressed in percentage terms. The measurement was performed in triplicate for each variant of the experiment.

Total Phenolic Content

Due to the strong antioxidant activity of most phenolic compounds in fruits, the total polyphenol content is determined for the evaluation of health-promoting properties. The Folin-Ciocalteu method has been used for many years and is still relevant today due to its high accuracy (Carmona-Hernandez et al., 2021). Phenolic compounds (PC) were determined according to the procedure proposed by Folin and Ciocalteu (1927) and Nunes et al. (2001), with some modifications. From each variant of the experiment, five fruit were taken in triplicate and then juiced. Then, 0.5 ml of the clear juice was diluted by adding 9.5 ml of deionized water. The resulting solution was spiked with 5 ml of Folin-Ciocalteu reagent (1:9 dilution) and 4 ml of sodium carbonate (0.075 g ml^{-1}). The mixture was left to stand for 30 min at 30°C, and then transferred to an ice bath (0°C) for 30 min. The absorbance of the solutions was measured at 760 nm. The content of phenolic compounds was determined using gallic acid solution as a standard, and the phenol concentration was expressed in mg 100 g^{-1} FW.

Anthocyanins Content

Anthocyanin is natural dye responsible for the color of the fruit and belongs to antioxidants which demonstrate health beneficial properties. The spectrophotometric method based on the reversible discoloration of anthocyanin depending on the pH is commonly used to measure the anthocyanin content (Johnson et al., 2020). The anthocyanins content (AC) was determined according to a previous procedure described by Nunes et al. (2001) and consisted of measuring the content of pelargonidin-3-glucoside [the main pigment in strawberries (Nunes et al., 2001)]. For each variant, 2 g of strawberry pulp was collected in triplicate. Subsequently, 18 ml of 0.5% (v/v) HCl in methanol was added to the pulp and the mixture was incubated in a refrigerator (4°C) for 1 h to extract the pigment. After incubation, the mixture was centrifuged and the supernatant was used to determine the anthocyanin content through the use of spectrophotometry at 520 nm. The anthocyanin content was calculated using the following formula: A_{520} * dilution factor * [molecular weight of pelargonidin-3-glucoside (PGN)/molar extinction coefficient (MEC)], where PGN = 433.2, MEC = 2.908 * 10^4. The result was expressed in terms of an average of three repetitions in terms of mg 100 g^{-1} FW.

Pectin Extraction

Pectin are one of the basic components of the cell wall. It has been shown that oxalate-soluble pectin play a significant role in shaping the texture of the fruit, which directly affects, among others, resistance to mechanical damage (Makarova and Shakhmatov, 2020). Strawberry pectin analysis was carried out according to the procedure proposed by Koubala et al. (2008) and Min et al. (2011) with some modifications. 1 g of pulp was taken in triplicate from each experimental variant. 35 ml of 0.25% ammonium oxalate (pH = 4.6) was added to the pulp and the mixture was transferred to a water bath (85°C) for 1 h. After incubation, the mixture was centrifuged (20,000 × *g*) for 10 min and the supernatant was collected. Three volumes of 96% ethanol were added to the supernatant and the solution was incubated in a refrigerator (4°C) for 24 h. The next step was to centrifuge (20,000 × *g*, 10 min) the solution and discard the supernatant. The remaining residue contained pectin, it was washed twice with 96% ethanol, dried and used to determine the D-galacturonic acid content.

Galacturonic Acid Content

Content of galacturonic acid as the main component of pectin determines suitability of fruit for processing (gelling, production of ascorbic acid) (Ben Abdallah et al., 2018). The content of D-galacturonic acid (GalA) in strawberries was determined using a continuous flow analyser (CFA), SanPlus (Skalar, Netherlands) according to the procedure recommended by the manufacturer. The applied automatic colorimetric method of measurement of GalA content is based on a color reaction, where the color intensity is measured at a wavelength of 520 nm (Ognyanov et al., 2021). 10 mg of dried pectin was dissolved in 12 ml of deionised water. The resulting solution was diluted 10 times and the D-galacturonic acid content was determined. The result is expressed in g kg^{-1} DW.

Rheological Properties

The rheological properties, which demonstrate the relationship between the structural, mechanical and sensory properties, are among the basic parameters of pectin (Xie et al., 2021). The rheological properties were measured using a Discovery HR-1 hybrid rheometer (TA Instruments, United States) with a cone-plate sensor. In brief, 1% aqueous solutions of strawberry pectin extracted with ammonium oxalate were prepared according to a procedure described elsewhere (Koubala et al., 2008; Min et al., 2011). For each variant of the experiment, pectin solutions were prepared in triplicate and each measurement was carried out at a temperature of 20 ± 0.5°C. Viscosity was measured at a constant shear rate of 10 s^{-1} (three repetitions), and the flow curves were determined based on measurements at variable shear rates of 10 and 600 s^{-1}. Flow curves were described using the Ostwald–de Waele model as represented by the following equation:

$$\sigma = k\gamma^{n}$$

where σ is shear stress (Pa), k is consistency index (Pas^n), γ is shear rate (s^{-1}) and n is flow behaviour index.

Antagonistic Properties of Consortia Against Fungal Pathogens

Antagonistic properties of consortia against fungal pathogens are determined in order to test the effectiveness of the tested bacterial consortia in combating fungal and fungal-like pathogens in the strawberry (Win et al., 2021). *In vitro* confrontations of four separate bacterial consortia and their mixtures (C5) against four selected phytopathogenic fungi and fungal-like-pathogens were set up using the plate culture method (Petri dish diameter 90 mm) with potato dextrose agar (PDA). Paper discs (5 mm diameter)

were surface sterilized with UV light, dipped in 30 μl of bacterial consortia suspension (10^8 cfu ml^{-1}) and placed in duplicates on Petri dishes inoculated with fungal pathogens. The pathogen inoculation included 150 μl of inoculum of a 7-day old culture of *B. cinerea* G277/18, *Phytophthora* sp. G408/18, *Verticillium* sp. G296/18, and *Colletotrichum* sp. G171/18 suspended with 10 ml of sterile water. The concentration of *B. cinerea* and *Colletotrichum* sp. was 10^3 jtk ml^{-1}, *P. cactorum* 10^5 jtk ml^{-1}, and *Verticillium* sp. 10^4 jtk g^{-1}. The pathogen-inoculated plates with discs soaked in bacterial consortia were incubated at 26°C in the dark. The observations were recorded 4 days after inoculation by measuring the fungal growth inhibition zone around the paper discs containing bacterial consortia.

Characteristics of Soil Used for Strawberry Cultivation

Characteristics of soil used for strawberry cultivation is a source of information about the processes during the growth and development of plants, which can have a direct impact on the quality of the fruit. Methods determining the content of proteins, enzymes, carbon and nitrogen in soil provide information on the level of soil degradation and allow the assessment of the importance of the biological consortia used (Wang et al., 2017). Soil samples were taken by complete randomization from a depth of 0–15 cm. The soil was dried at 23°C and sieved through a sieve with a mesh diameter of 2 mm. Total glomalin content (TG), easily extractable fractions of glomalin (EEG) (Wrigth and Upadhyaya, 1998), soil enzyme activity (dehydrogenase DHA) (Klein et al., 1964), acidic phosphatase (ACP), alkaline phosphatase (ALP) (Tabatabai and Bremner, 1969), as well as the carbon and nitrogen content in the biomass were determined in the samples.

Principal Component Analysis

Principal component analysis (PCA) is used to discover regularities between variables. It consists in determining the components which are a linear combination of the examined variables. PCA enables the identification of those initial variables that have a significant impact on the appearance of individual principal components (Yagmur and Gunes, 2021). In order to assess the relationship between the studied parameters, PCA analysis was performed using STATISTICA software (Statistica v.12, StatSoft Inc., United States).

Statistical Analysis

The obtained results were analysed with STATISTICA software (Statistica v.12, StatSoft Inc., United States) using a two-way analysis of variance (ANOVA) followed by the Tukey HSD test or Tuckey for different N, F-Welch and RIR Tuckey test for unequal numbers or ANOVA Kruskal–Wallis test; significant differences were determined at $P < 0.05$.

RESULTS AND DISCUSSION

Strawberries are in high demand because of their taste and health-promoting properties resulting from the presence of antioxidants and vitamins. The development of organic farming and the promotion of a healthy lifestyle has significantly increased the demand for organically grown fruit. The recent guidelines of the European Green Deal and Biodiversity Strategy have led to the use of sustainable practices, such as organic farming, and to a reduction in the use of chemical pesticides (European Commission, 2019). These measures have led to fruit producers ensuring the high quality of their strawberries by using natural plant protection preparations. For this purpose, plant extracts, microbial consortia that antagonize strawberry pathogens (Ornelas-Paz et al., 2013) and plant protective hormones (Poveda, 2020) are both desirable and beneficial in terms of biocontrol. For economic reasons, it is important that ecological preparations not only increase the quality of the fruit, but also guarantee a plentiful harvest, reasonable production costs and that the market price of the fruit should be taken into consideration. Therefore, bacterial strains with potentially antagonistic properties against main fungal and fungal-like pathogens were selected for this study.

Strawberry Quality

The shape of strawberries has a significant influence over visual quality and consumer interest. Based on previous findings, auxin derived from achene is responsible for cell division and expansion (Zahedipour-Sheshglani and Asghari, 2020), this changes the shape of the strawberry. Consumers prefer round strawberries (Zahedipour-Sheshglani and Asghari, 2020). The change in shape from oblong (in C0) to round after the use of the appropriate consortium was noted in strawberry P (C4 and C5) and (**Figure 2D**), which makes them the most attractive to the consumer. Strawberry V (C4), P (C3), and MIX (C2) were distinguished by their flattened shape (**Figures 2C,D,F**). The remaining fruits were characterized as oblong.

An important parameter for assessing the quality of strawberries is firmness. Ensuring the proper firmness of the fruit allows for longer storage periods and facilitates transport over greater distances (Liu et al., 2019). The highest increase in firmness was observed for MIX-infected strawberries treated with C2, the maximum load in this case was on average 2.4 times higher than in the control (C0) (**Figure 2F**). A statistically significant increase in the maximum load value as compared to the control was also observed in the NC (C1), P (C4), and C (C5) groups (**Figures 2A,D,E**). It is assumed that the reason for the increase in the firmness of strawberries infected with selected pathogens could be the activity of bacterial consortia associated with the production of metabolites limiting mycelium growth and leading to an improvement in the quality and firmness of the fruit. Strawberries soften during ripening, mainly by degrading the middle lamina of the cell wall of the cortical parenchyma cells (Qin et al., 2017). One of the reasons for this degradation may be the activity of fungal pathogens attacking the fruit during ripening and storage (Ahmadi-Afzadi et al., 2013). The treatment of strawberries with *Hanseniaspora uvarum* yeast and infection with *B. cinerea* has been shown to preserve fruit firmness as compared to the control (Qin et al., 2017). The impact of the investigated bacterial consortia and fungal and fungal-like pathogens on the firmness of strawberries has not

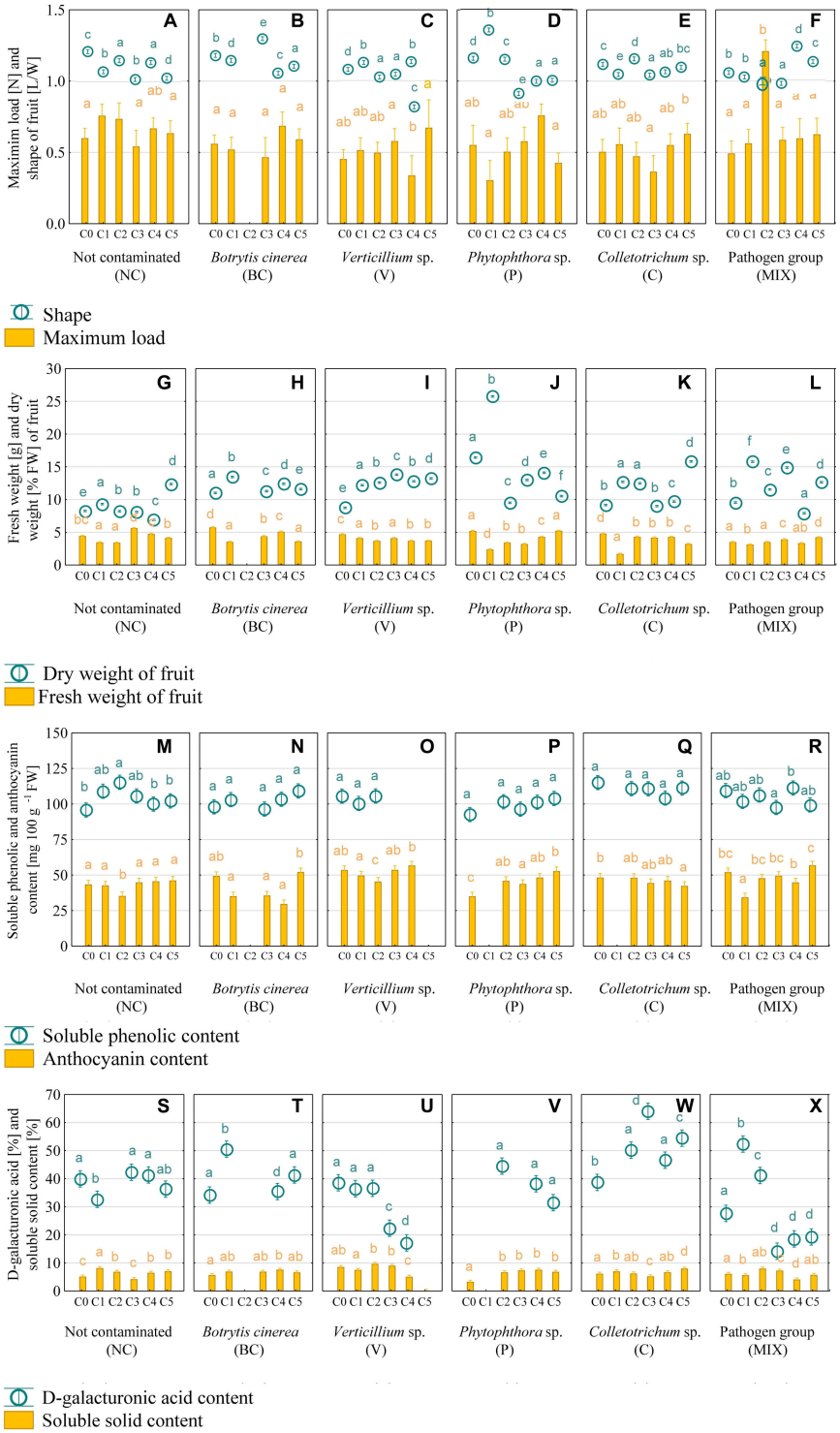

FIGURE 2 | Firmness of strawberries and shape **(A–F)**, fresh and dry weight **(G–L)**, soluble phenolic and anthocyanin content **(M–R)**, and D-galacturonic acid and soluble solid content **(S–X)** in strawberry fruit. C0, control (not contaminated); C1, Consortium 1; C2, Consortium 2; C3, Consortium 3; C4, Consortium 4; C5, Consortium 5. A statistical analysis was performed for each pathogen group of plants separately. The data are means ± SD ($n > 3$). Different letters (a–f) indicate the differences between consortia ($P < 0.05$) as determined by the following statistical test: ANOVA Tuckey test for different N for maximum load **(C–E)** and shape **(A–F)**; F-Welch test and RIR Tuckey test for unequal numbers for **(A,B,F)**, ANOVA and Tuckey test HSD for fresh weight **(G,H,L)**, dry weight **(L)**, anthocyanin **(N–Q)**, soluble phenolic **(N–Q)**, D-galacturonic acid **(W)**, soluble solid content **(W,X)**; F-Welch and *post hoc* for fresh weight **(I–K)**, dry weight **(J,K)**, anthocyanin **(M,R)**, soluble phenolic **(M,R)**, D-galacturonic acid **(S–U,X)**, soluble solid content **(S–U)**; ANOVA Kruskal–Wallis test for dry weight **(G–I)**, D-galacturonic acid **(V)**, soluble solid content **(V)**.

yet been investigated. The production of various metabolites that dissolve mycelium might play a role (Olanrewaju and Babalola, 2019). It is known that treating strawberries with beneficial microorganisms can improve the quality and properties of the stored fruit, including firmness (Fan et al., 2009). The antifungal activity of *Bacillus* sp. isolates against *C. acutatum* (Moreira et al., 2014) and *Phytophthora infestans* (Caulier et al., 2018), *Lysobacter* sp. and *Pseudomonas* sp. against *Colletotrichum* sp. (Tang et al., 2019), *S. griseus* against *P. capsici* (Nguyen et al., 2015) and *Lysobacter* sp. against *P. infestans* (Lazazzara et al., 2017) have been confirmed.

Fruit firmness is closely related to the dry matter content. Their soft texture and high water content make strawberry fruit susceptible to mechanical and physical damage which facilitates the penetration of microorganisms (Siebeneichler et al., 2020). In General, fruit with a higher tissue density exhibits a higher dry matter content and a greater degree of firmness compared to fruit with a lower tissue density (Tarantino et al., 2018). This relationship was observed for the strawberries NC (C1) and C (C5), with an increase in firmness and dry matter compared to the control (**Figures 2A,E**, **3A,E**). An inverse relationship was observed in samples P (C4) and MIX (C2), fruit with a higher degree of firmness had a lower or comparable to the control dry content (**Figures 2D,F**, **3D,F**). It is assumed that the decrease in the firmness of fruit with a high dry matter content is caused by a relatively high cell fragility, low turgor pressure or a low degree of adhesion between the adjacent strawberry tissue cells (Harker et al., 2000).Tissue hydration has a great impact not only on firmness, but also on fresh fruit weight. Studies have shown that strawberries may contain 84–92% water, depending on the variety and cultivation method (Liu et al., 2019). Only the C3 bacterial consortium increased the fresh matter content over the no contaminated (NC) strawberry by 63% (**Figure 3G**) and C3 and C5 consortia increased the fresh matter content in MIX-infected strawberry by 21% on average (**Figure 3L**). The higher fresh weight combined with the lower dry weight values indicate a higher water content in the strawberries belonging to these groups.

One of the factors determining consumer interest in strawberries is the SSC content, which is defined as the aggregate concentration of sugars (80–90% of the SSC), acids and other solutes in the cell juice (Mackenzie et al., 2011). The average content of SSC in the tested fruits was 6% (**Figures 2S–X**), which is the same as other studies which reported the content of SSC in strawberries to be within the range of 4–10% (Chen H. et al., 2018). In most cases, the SSC content was greater than or comparable to the control (C0) in strawberries treated with the bacterial consortia. A statistically significant decrease in the SSC value by 0.9–3.4% compared to the control (C0) was observed in groups V (C4), C (C3), and MIX (C1 and C4) (**Figures 2U,W,X**). The occurrence of differences in the content of SSC in the tested strawberries is natural and may result from differences in the cultivation method (Cao et al., 2015) consisting of treating the fruit with different bacterial consortia. The SSC content is influenced by various factors, such as genetics, climate, water management and cultivation practices. Positive correlations between the nutrient content, e.g., phosphorus and an increase in SSC content was noted for the strawberries (Valentinuzzi et al., 2015). This effect may occur due to the ability of bacteria to dissolve phosphates, which lowers soil pH and increases phosphorus availability through the production of organic acids. Moreover, an increase in the content of phosphorus in the fruit was shown after the treatment of strawberry seedlings with *Bacillus* sp. and *Klebsiella planticola* (Tomic et al., 2015).

Polyphenols and anthocyanins are responsible for the bright red colour of strawberries and play a key role as bioactive ingredients (de Andrade et al., 2019). The mean content of polyphenols in the tested fruit was in the range of 93–115 mg 100 g^{-1}, while the anthocyanins content was in the range of 31–57 mg 100 g^{-1}. The increase in polyphenol content was only observed in the NC group (C2) and was 20% greater than in the control (C0) (**Figure 2M**). None of the preparations used caused a statistically significant decrease in the content of polyphenols in strawberry cv. Honeoye. Unlike the case of polyphenols, a decrease in the content of anthocyanins in strawberry NC (C2), V (C2), and MIX (C1) was noted (**Figures 2M,O,R**). However, an increase in anthocyanin content at the level of 25–51% compared to the control (C0) occurred only in the group of *Phytophthora* sp. infected strawberries treated with C2, C3, C4, and C5 consortia (**Figure 2P**). It is predicted that the changes to the level of total phenolic compounds and anthocyanins may be due to the presence of pathogenic fungi, and fungal-like-pathogens, and beneficial bacteria. The bacterial synthesis of plant hormones or amino acids may enter the shikimic acid metabolic pathway, thereby acting as the precursors of phenolic acids (Cisternas-Jamet et al., 2020). The increase in anthocyanin content may be attributed to the release of anthocyanins from degraded cellular components (López-Ortiz et al., 2019), the activity of the enzymes responsible for the synthesis of anthocyanins and also the activity of microorganisms. Lingua et al. (2013) demonstrated the positive effect of bacteria of the genus *Pseudomonas* on the anthocyanin (cyanidine-3-glucoside and pelargonidine-3-glucoside) concentration in strawberries. However, the anthocyanin content shows a high degree of variability with respect to species, varieties, growth conditions and the degree of fruit ripeness (Todeschini et al., 2018).

The content of galacturonic acid (**Figure 2**), which is the main component of pectin, is important in fruit processing. Pectins have stabilizing and gelling properties, which is why they are used in the production of jam, juice, drinks, and jellies (Ben Abdallah et al., 2018). In addition, galacturonic acid is extracted from fruit for the synthesis of ascorbic acid (Agius et al., 2003). The content of galacturonic acid may vary; in a previous study, a ripe strawberry of the cultivar Chandler was found to contain about 330 mg of galacturonic acid g^{-1} DW (Paniagua et al., 2017). The use of consortia resulted in an increase in the galacturonic acid content of $\geq$400 mg g^{-1} DW (>40%) for strawberry grown in the following variants: BC (C1), C (C2, C3, C4, and C5), and MIX (C1 and C2) (**Figures 2T,W,X**), which was greater than the control (C0). Relatively large fluctuations in the content of galacturonic acid confirms the complexity of the processes caused by the activity of microorganisms, which are affected by

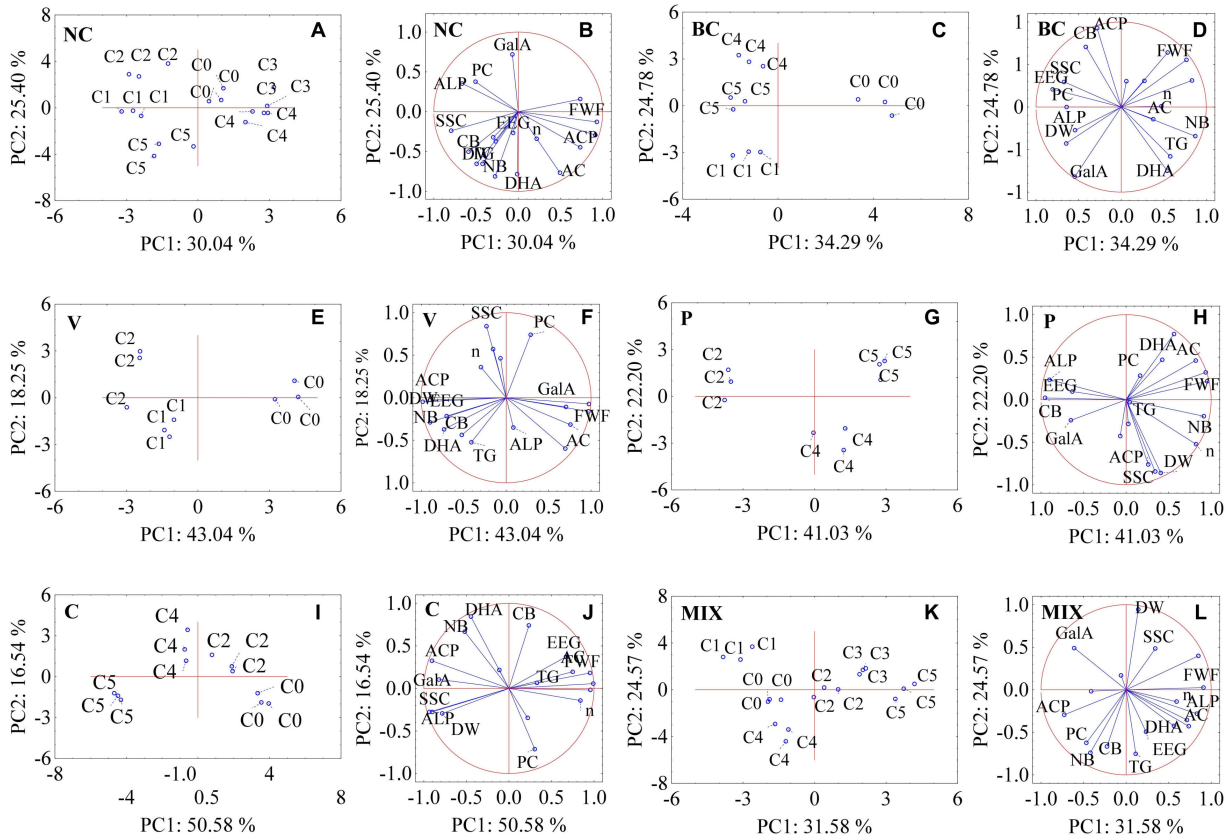

FIGURE 3 | Principal component analysis (PCA) showing interrelation of microbiological consortia used and quality parameters of strawberry fruit and soil. **(A,B)** NC (no contamination), **(C,D)** BC (*B. cinerea*), **(E,F)** V (*Verticillium* sp.), **(G,H)** P (*Phytophthora* sp.), **(I,J)** C (*Colletotrichum* sp.), **(K,L)** MIX (pathogen group: BC, V, P, C.); C0, control (no bacterial consortia); C1, Consortium 1; C2, Consortium 2; C3, Consortium 3; C4, Consortium 4; C5, Consortium 5; FWF, fresh weight of fruit; DW, dry weight of fruit; SSC, soluble solid content; PC, content of phenolic compounds; AC, content of anthocyanins; GalA, content of D-galacturonic acid; n, viscosity; TG, total glomalin; EEG, easily extractable glomalin; DHA, dehydrogenase activity; ACP, acid phosphatase activity; ALP, alkaline phosphatase activity; CB, carbon inbiomass; NB, nitrogen in biomass.

plant variety, growth conditions, pathogen infections and the consortia used.

Rheological Properties

The rheological properties of liquids determine the behaviour of the solution at all of the production stages, such as filling, mixing, packaging and removal from the package (Lee et al., 2009). Pectin solutions are used for the production of yoghurts, jelly, juices (Ke et al., 2020), paints, pastes and medicines (Jouini et al., 2018), due to their gelling, stabilizing and flavour-enhancing properties (Ke et al., 2020).

The viscosity of 1% solutions of strawberry pectin extracted with ammonium oxalate is shown in **Table 1**. The increase in viscosity as compared to the control (C0) occurred in NC (C3), BC (C1, C4, and C5), C (C2), and MIX (C2, C3, C4, and C5) strawberries. Also, contamination with pathogens (BC, V, C, and MIX) significantly lowered the viscosity of the strawberry pectin solutions in the controls (C0) as compared to the control of uninfected NC strawberries (C0). These results show that the use of appropriate consortia, dedicated to a specific pathogen, can increase the viscosity of pectin solutions. The decrease in viscosity may be attributed to the activity of microorganisms that soften the fruit cell walls though pectin degradation (Mierczyńska et al., 2014). Viscosity depends, among other factors, on the molecular weight of the pectin molecules, their degree of methylation and pH, which may be affected by fungi and bacteria associated with strawberries at all stages of growth and ripening. It has been proven that viscosity increases with increasing pectin concentration (Chan et al., 2017).

The rheological data of the 1% pectin solutions were suitably adjusted by the Ostwald–de Waele model with a high coefficient of determination of $R^2 > 0.996$. Higher values of the coefficient k correspond to the higher viscosity of the samples. Based on the *k*-factor analysis, pectin solutions were obtained with a viscosity higher than that of the control (C0) in the NC (C3) and BC (C4 and C5) groups (**Table 1**). The antagonistic interactions of the microorganisms used led to the modification of pectin, an increase in apparent viscosity and the coefficient *k*, which is associated with an increase in the molar mass of pectin (Fracasso et al., 2018). The high molar mass of pectin promotes the formation of a gel structure (O'Donoghue and Somerfield, 2008). However, for some applications a lower viscosity may be seen as

TABLE 1 | Parameters of the Ostwald–de Waele model describing the rheological properties of 1% strawberry pectin solutions.

Contamination	Consortium	Viscosity [Pas]	Upward curve			Downward curve		
			k	*n*	R^2	*k*	*n*	R^2
NC	C0	$0.34^{f} \pm 0.02$	$0.92^{d} \pm 0.10$	$0.79^{ab} \pm 0.01$	1.00	$1.06^{c} \pm 0.12$	$0.77^{ab} \pm 0.01$	1.00
	C1	$0.20^{b} \pm 0.00$	$0.54^{bcd} \pm 0.23$	$0.80^{ab} \pm 0.07$	1.00	$0.66^{a} \pm 0.10$	$0.76^{ab} \pm 0.02$	1.00
	C2	$0.14^{aa} \pm 0.00$	$0.15^{ab} \pm 0.11$	$0.95^{c} \pm 0.01$	1.00	$0.18^{b} \pm 0.02$	$0.93^{c} \pm 0.01$	1.00
	C3	$0.42^{g} \pm 0.00$	$1.40^{e} \pm 0.16$	$0.74^{a} \pm 0.01$	1.00	$1.66^{d} \pm 0.21$	$0.74^{a} \pm 0.05$	1.00
	C4	$0.14^{a} \pm 0.00$	$0.09^{a} \pm 0.01$	$0.95^{c} \pm 0.02$	1.00	$0.11^{b} \pm 0.01$	$0.93^{c} \pm 0.01$	1.00
	C5	$0.28^{d} \pm 0.00$	$0.71^{cd} \pm 0.03$	$0.80^{ab} \pm 0.00$	1.00	$0.81^{a} \pm 0.09$	$0.78^{ab} \pm 0.01$	1.00
BC	C0	$0.10^{a} \pm 0.00$	$0.13^{a} \pm 0.01$	$0.96^{b} \pm 0.00$	1.00	$0.15^{a} \pm 0.01$	$0.94^{a} \pm 0.01$	1.00
	C1	$0.12^{b} \pm 0.00$	$0.14^{a} \pm 0.00$	$0.94^{b} \pm 0.00$	1.00	$0.16^{a} \pm 0.02$	$0.93^{a} \pm 0.01$	1.00
	C2	–	–	–	–	–	–	–
	C3	–	–	–	–	–	–	–
	C4	$0.28^{c} \pm 0.00$	$0.77^{b} \pm 0.07$	$0.78^{a} \pm 0.01$	1.00	$0.92^{b} \pm 0.11$	$0.76^{c} \pm 0.01$	1.00
	C5	$0.32^{d} \pm 0.00$	$0.79^{b} \pm 0.12$	$0.78^{a} \pm 0.00$	1.00	$1.21^{c} \pm 0.04$	$0.71^{b} \pm 0.02$	1.00
V	C0	$0.20^{c} \pm 0.00$	$0.54^{a} \pm 0.18$	$0.80^{a} \pm 0.05$	1.00	$0.67^{ab} \pm 0.11$	$0.76^{a} \pm 0.02$	1.00
	C1	$0.25^{d} \pm 0.00$	$0.63^{a} \pm 0.06$	$0.80^{a} \pm 0.01$	1.00	$0.73^{b} \pm 0.08$	$0.78^{a} \pm 0.01$	1.00
	C2	$0.15^{a} \pm 0.00$	$0.41^{a} \pm 0.21$	$0.82^{a} \pm 0.08$	1.00	$0.55^{ab} \pm 0.08$	$0.76^{a} \pm 0.02$	1.00
	C3	$0.17^{b} \pm 0.00$	$0.30^{a} \pm 0.02$	$0.85^{a} \pm 0.01$	1.00	$0.38^{a} \pm 0.05$	$0.82^{a} \pm 0.03$	1.00
	C4	–	–	–	–	–	–	–
	C5	–	–	–	–	–	–	–
P	C0	–	–	–	–	–	–	–
	C1	–	–	–	–	–	–	–
	C2	$0.03^{a} \pm 0.00$	$0.03^{a} \pm 0.00$	$0.99^{a} \pm 0.01$	1.00	$0.03^{aa} \pm 0.00$	$0.97^{b} \pm 0.00$	1.00
	C3	–	–	–	–	–	–	–
	C4	$0.28^{c} \pm 0.00$	$0.75^{c} \pm 0.09$	$0.79^{b} \pm 0.01$	1.00	$0.90^{c} \pm 0.12$	$0.76^{a} \pm 0.01$	1.00
	C5	$0.21^{b} \pm 0.00$	$0.48^{b} \pm 0.03$	$0.81^{b} \pm 0.00$	1.00	$0.55^{b} \pm 0.07$	$0.79^{a} \pm 0.01$	1.00
C	C0	$0.26^{c} \pm 0.00$	$0.78^{b} \pm 0.23$	$0.77^{a} \pm 0.05$	1.00	$0.93^{c} \pm 0.01$	$0.74^{a} \pm 0.01$	1.00
	C1	–	–	–	–	–	–	–
	C2	$0.29^{d} \pm 0.00$	$0.65^{b} \pm 0.05$	$0.81^{a} \pm 0.00$	1.00	$0.71^{b} \pm 0.06$	$0.80^{b} \pm 0.00$	1.00
	C3	–	–	–	–	–	–	–
	C4	$0.07^{b} \pm 0.00$	$0.09^{a} \pm 0.01$	$0.97^{b} \pm 0.01$	1.00	$0.11^{a} \pm 0.01$	$0.94^{c} \pm 0.01$	1.00
	C5	$0.06^{a} \pm 0.00$	$0.06^{a} \pm 0.00$	$0.10^{b} \pm 0.00$	1.00	$0.07^{a} \pm 0.01$	$0.97^{d} \pm 0.01$	1.00
MIX	C0	$0.03^{b} \pm 0.00$	$0.05^{a} \pm 0.01$	$0.96^{a} \pm 0.04$	1.00	$0.06^{ab} \pm 0.01$	$0.93^{a} \pm 0.01$	1.00
	C1	$0.02^{a} \pm 0.00$	$0.02^{a} \pm 0.00$	$0.10^{a} \pm 0.01$	1.00	$0.02^{a} \pm 0.00$	$0.98^{c} \pm 0.00$	1.00
	C2	$0.17^{f} \pm 0.00$	$0.34^{b} \pm 0.05$	$0.85^{b} \pm 0.02$	1.00	$0.40^{c} \pm 0.05$	$0.82^{b} \pm 0.01$	1.00
	C3	$0.09^{d} \pm 0.00$	$0.09^{a} \pm 0.00$	$0.97^{a} \pm 0.00$	1.00	$0.10a^{b} \pm 0.02$	$0.95^{a} \pm 0.01$	1.00
	C4	$0.06^{c} \pm 0.00$	$0.08^{a} \pm 0.01$	$0.97^{a} \pm 0.01$	1.00	$0.09^{ab} \pm 0.01$	$0.95^{a} \pm 0.01$	1.00
	C5	$0.10^{e} \pm 0.00$	$0.10^{a} \pm 0.00$	$0.96^{a} \pm 0.00$	1.00	$0.11^{b} \pm 0.01$	$0.94^{a} \pm 0.01$	1.00

NC, control (no contamination); BC, B. cinerea; V, Verticillium sp.; P, Phytophthora sp.; C, Colletotrichum sp.; MIX, pathogen group (BC, V, P, and C); C0, control (no bacterial consortia); C1, Consortium 1; C2, Consortium 2; C3, Consortium 3; C4, Consortium 4; C5, Consortium 5. Different letters (a–f) indicate differences between experimental variants ($P < 0.05$) as determined by the Tukey HSD test. A statistical analysis was performed for each infected group of plants separately. Data are means ± SD ($n = 3$).

a positive property of the solutions due to pelargonidine lower energy consumption during processing (Venzon et al., 2015).

Flow curves reveal pseudoplastic, non-Newtonian behaviour due to the melt flow index values n ($n < 1$). The 1% pectin solutions tested are classified as shear thinned. Their viscosity decreases as the shear rate increases. Based on a previous study, the lower the n coefficient, the greater the degree of pseudoplasticity (Lee et al., 2009). The values of n for the tested solutions were in the range of 0.713–0.996. In comparison, the n values for 2% strawberry pectin solutions were 0.52, while for 5% strawberry pectin solutions they were 0.54 (Mierczyńska et al., 2017). Pseudoplastic fluid behaviour is important in the food industry (gelatinization of jellies and jams, thickening of juices and purees, and stabilization of liquids) (Grassino et al., 2016) and in medicine production (thickening of syrups or ointment, encapsulation of preparations) (Jouini et al., 2018).

The differences in the values of viscosity and in the flow of pectin solutions refers to the molecular properties of the samples, such as the chemical composition of neutral sugars, galacturonic acid content and the degree of pectin esterification (Fracasso et al., 2018). Microorganisms may have an indirect

effect on the chemical composition of the samples (Erturk et al., 2012). The use of beneficial microorganisms such as *Pseudomonas* sp., *Bacillus* sp., and *Azospirillum* sp. results in an increase in plant biomass and fruit yields (Erturk et al., 2012). In addition, it was found that beneficial fungi and plant growth-promoting bacteria show antagonism to the pathogens *C. acutatum*, *Macrophomina phaseolina,* and *Fusarium solani* in strawberry plants (Pastrana et al., 2016). Inoculation with beneficial bacteria in order to increase plant growth also has potential environmental benefits; it could reduce the use of agricultural chemicals and facilitate adaptation to sustainable management practices (Erturk et al., 2012).

Antagonistic Properties of Consortia Against Fungal Pathogens

In Petri dish-based assays carried out for the determination of the antifungal properties of the tested bacterial consortia, C4 and C5 did not show any clear zone of inhibition in the growth of the tested fungi, and fungal-like-pathogens or only indicated very weak inhibition (**Table 2**). The inhibitory effect was observed for C1, C2, and C3, with evident growth inhibition of all of the tested fungal pathogens in the case of C1 and C2, thereby confirming the antagonistic properties of the bacterial strains present in these consortia, which was observed in a greenhouse experiment. Other studies are consistent with the obtained results and confirm the antagonism of the tested bacterial consortia (contained *Bacillus* sp., *P. polymyxa*, and *Streptomyces* sp.) against strawberry pathogenic microorganisms (Chen P.H. et al., 2018; Li et al., 2021).

Influence of Microbial Activity on Soil Composition

The content of nutrients, proteins, and soil enzyme activity plays a key role in the functioning of the ecosystem. The cultivation of plants is accompanied by a decrease in soil productivity related to the depletion of nutrients, the release of toxic metabolites, and the development of pathogenic fungi (Gałązka, 2013). Total glomalin (TG) is one of the glycoproteins produced by arbuscular mycorrhizal fungi that live in symbiosis with plants and facilitate the uptake of water and nutrients from the environment. Easily extractable glomalin (EEG) has a more immunoreactive fraction than TG (Wrigth and Upadhyaya, 1998). For this reason, an increase in TG and EEG levels is desirable in the context of promoting plant growth. An increase in the TG content as compared to the control (C0) was only observed in the strawberry NC (C5), while an increase in EEG content may be observed in the strawberry BC (C5) (**Table 3**).

The data shows the significant influence of the type of infectious pathogen and the bacterial consortium used on enzyme activity. The increase in acid phosphatase content as compared to the control (C0) characterized the strawberry fruit in the groups NC (C3, C4, and C5), BC (C2, C3, and C4), V (C1, C2, C3, and C4), and C (C2, C3, C4, and C5), while an increase in the content of alkaline phosphatase occurred in groups BC (C1 and C3), V (C3 and C4), P (C2, C3, C4, and C5), C (C4 and C5), and MIX (C2, C3, and C5) (**Table 3**). Increased phosphatase activity is associated with a higher content of organic matter in the soil (Singh et al., 2018). In contrast to phosphatase, a statistically significant increase in dehydrogenase content was observed in strawberry V (C1 and C3), C (C1, C2, C3, C4, and C5), and MIX (C2, C4, and C5) (**Table 3**). The increase in dehydrogenase activity may be explained by the greater availability of nutrients (Kanchikerimath and Singh, 2001).

Principal Component Analysis

The relationships between the parameters studied were analysed using the PCA method (**Figure 3**). The distribution of individual samples on the plane is shown in **Figures 3A,C,E,G,I,K**. The first two factors (PC1 and PC2) explain over 50% of the total variance among the analysed samples for all of the investigated variables. For all of the tested samples, the first axis (PC1) accounted for over 30% of the total variance. The samples that explain the PC1 and PC2 axis positively have the greatest impact on the tested infection factor. On this basis, we may distinguish C0 and C3 for the NC control (**Figure 3A**), C0 for BC (**Figure 3C**), C0 for V (**Figure 3E**), C5 for P (**Figure 3G**), C2 for C (**Figure 3I**), and C3 for MIX (**Figure 3K**). An analysis of the PCA1-PCA2 observation charts (**Figures 3A,C,E,G,I,K**) confirms the results of the analyses above; the need to select an appropriate consortium which acts antagonistically against individual pathogens in order to obtain the highest quality of fruit.

An analysis of the PCA variable charts allowed for the identification of certain dependencies between the examined parameters in all of the studied groups, a positive correlation was found between DW and SSC, which was consistent with the results of other studies (Jorquera-Fontena et al., 2014). The increase in the content of anthocyanins (AC) was accompanied by an increase in the content of phenols (PC)

TABLE 2 | Antifungal properties of the bacterial consortia used in the test expressed as the inhibition zone diameter (mm).

Fungal pathogen/bacterial consortium	Inhibition zone [mm]				
	C1	C2	C3	C4	C5
Colletotrichum sp. (C) G171/18	37.3 ± 2.5^{a}	37.6 ± 2.0^{a}	15.3 ± 1.5^{b}	0.0 ± 0.0^{d}	6.3 ± 0.6^{c}
Phytophthora sp. (P) G408/18	56.0 ± 1.0^{a}	57.6 ± 2.0^{a}	48.6 ± 1.5^{b}	0.0 ± 0.0^{c}	0.0 ± 0.0^{c}
Verticillium sp. (V) G296/18	40.6 ± 6.0^{a}	6.6 ± 0.5^{c}	15.3 ± 0.6^{b}	0.0 ± 0.0^{c}	14.3 ± 1.1^{b}
Botrytis cinerea (B) G277/18	42.0 ± 6.0^{a}	39.6 ± 7.6^{a}	12.6 ± 2.1^{b}	11.7 ± 3.0^{b}	6.3 ± 0.6^{b}

Different letters (a–d) indicate differences between consortia ($P < 0.05$) as determined by the Tukey HSD test separately for each pathogen, ±standard deviation; C1, Consortium 1; C2, Consortium 2; C3, Consortium 3; C4, Consortium 4; C5, Consortium 5.

TABLE 3 | Parameters of the quality of soil from strawberry cultivation.

Contamination	Consortium	Total glomalin [mg g^{-1}]	Easily extractable glomalin [mg g^{-1}]	Dehydrogenase activity [μg TPF g^{-1} DW of soil 24 h^{-1}]	Acid phosphatase activity [μg PNP g^{-1} DW of soil h^{-1}]	Alkaline phosphatase activity [μg PNP g^{-1} DW of soil h^{-1}]	Carbon in biomass [μg g^{-1}]	Nitrogen in biomass [μg g^{-1}]
NC	C0	$4.7^{a} \pm 0.6$	$2.6^{a} \pm 0.1$	$90.9^{a} \pm 2.1$	$77.1^{a} \pm 0.6$	$77.5^{abc} \pm 0.7$	$330.0^{a} \pm 14.4$	$33.0^{ab} \pm 1.2$
	C1	$5.3^{ab} \pm 0.3$	$2.9^{a} \pm 0.2$	$90.9^{a} \pm 2.8$	$74.6^{a} \pm 1.7$	$75.5^{ab} \pm 1.9$	$376.9^{a} \pm 8.4$	$34.7^{ab} \pm 0.4$
	C2	$5.0^{ab} \pm 0.4$	$3.0^{a} \pm 0.3$	$89.8^{a} \pm 2.6$	$76.7^{a} \pm 1.5$	$84.5^{c} \pm 2.7$	$308.6^{a} \pm 50.3$	$33.7^{ab} \pm 1.4$
	C3	$5.0^{ab} \pm 0.3$	$3.0^{a} \pm 0.1$	$92.5^{a} \pm 3.2$	$92.9^{b} \pm 0.5$	$69.8^{a} \pm 3.1$	$305.5^{a} \pm 48.5$	$32.4^{a} \pm 1.4$
	C4	$4.9^{ab} \pm 0.4$	$3.0^{a} \pm 0.0$	$94.0^{a} \pm 2.2$	$93.5^{b} \pm 2.5$	$71.8^{ab} \pm 2.6$	$297.8^{a} \pm 46.8$	$36.1^{bc} \pm 0.6$
	C5	$6.0^{b} \pm 0.5$	$3.0^{a} \pm 0.2$	$102.9^{a} \pm 3.7$	$88.8^{c} \pm 0.5$	$78.2^{b} \pm 4.3$	$366.1^{a} \pm 52.4$	$39.0^{c} \pm 1.3$
BC	C0	$5.6^{b} \pm 0.2$	$2.7^{a} \pm 0.1$	$90.2^{c} \pm 2.7$	$79.7^{d} \pm 0.3$	$67.2^{ab} \pm 5.4$	$384.8^{a} \pm 18.8$	$38.8^{a} \pm 2.3$
	C1	$5.4^{ab} \pm 0.2$	$2.9^{ab} \pm 0.2$	$90.5^{c} \pm 3.6$	$75.0^{c} \pm 1.6$	$78.8^{c} \pm 1.7$	$368.7^{a} \pm 44.7$	$35.0^{b} \pm 0.7$
	C2	$4.7^{b} \pm 0.3$	$2.9^{ab} \pm 0.3$	$84.7^{bc} \pm 1.9$	$85.4^{a} \pm 2.1$	$65.0^{a} \pm 2.7$	$325.0^{a} \pm 7.2$	$23.9^{c} \pm 0.9$
	C3	$5.3^{ab} \pm 0.3$	$3.1^{ab} \pm 0.1$	$80.3^{ab} \pm 0.9$	$88.9^{ab} \pm 0.9$	$80.0^{c} \pm 2.8$	$339.7^{a} \pm 26.2$	$26.2^{c} \pm 0.6$
	C4	$4.9^{ab} \pm 0.3$	$3.0^{ab} \pm 0.1$	$76.7^{a} \pm 3.4$	$93.0^{b} \pm 2.4$	$74.5^{bc} \pm 2.0$	$462.4^{b} \pm 3.9$	$32.4^{b} \pm 0.2$
	C5	$5.3^{ab} \pm 0.2$	$3.1^{b} \pm 0.1$	$78.9^{ab} \pm 1.0$	$85.1^{a} \pm 0.6$	$68.1^{ab} \pm 3.7$	$466.0^{b} \pm 14.6$	$33.2^{b} \pm 0.8$
V	C0	$4.6^{a} \pm 0.2$	$2.9^{a} \pm 0.0$	$88.7^{ac} \pm 2.2$	$83.2^{a} \pm 1.8$	$63.1^{a} \pm 0.9$	$481.5^{a} \pm 22.5$	$33.1^{a} \pm 1.6$
	C1	$5.1^{a} \pm 0.6$	$3.1^{a} \pm 0.1$	$100.3^{b} \pm 1.6$	$94.7^{b} \pm 2.0$	$63.5^{a} \pm 0.4$	$503.6^{a} \pm 8.9$	$37.8^{b} \pm 1.0$
	C2	$4.8^{a} \pm 0.2$	$3.1^{a} \pm 0.2$	$98.1^{ab} \pm 7.9$	$94.4^{b} \pm 3.4$	$61.9^{a} \pm 5.4$	$511.6^{a} \pm 48.3$	$37.7^{b} \pm 1.6$
	C3	$5.0^{a} \pm 0.9$	$3.2^{a} \pm 0.2$	$107.7^{b} \pm 2.1$	$95.4^{b} \pm 1.9$	$81.8^{c} \pm 2.8$	$477.2^{a} \pm 10.6$	$38.4^{b} \pm 1.2$
	C4	$4.0^{a} \pm 0.2$	$2.8^{a} \pm 0.1$	$96.0^{ab} \pm 0.9$	$97.2^{b} \pm 1.8$	$72.1^{d} \pm 1.4$	$446.1^{a} \pm 55.4$	$32.0^{a} \pm 1.5$
	C5	$5.3^{a} \pm 0.8$	$2.9^{a} \pm 0.1$	$82.6^{c} \pm 2.1$	$85.9^{a} \pm 2.0$	$66.6^{ad} \pm 2.7$	$448.9^{a} \pm 18.8$	$22.5^{c} \pm 2.6$
P	C0	$5.2^{a} \pm 0.0$	$2.8^{a} \pm 0.1$	$94.4^{b} \pm 1.5$	$91.7^{a} \pm 1.2$	$69.1^{b} \pm 1.6$	$483.5^{ab} \pm 28.0$	$36.8^{a} \pm 1.7$
	C1	$5.0^{ab} \pm 0.0$	$2.8^{a} \pm 0.1$	$82.3^{a} \pm 0.8$	$89.3^{a} \pm 3.4$	$65.5^{b} \pm 1.2$	$462.3^{ab} \pm 36.7$	$34.5^{ab} \pm 1.7$
	C2	$4.6^{ab} \pm 0.1$	$3.0^{a} \pm 0.1$	$86.0^{a} \pm 2.4$	$88.1^{a} \pm 0.5$	$87.3^{c} \pm 2.9$	$522.9^{b} \pm 15.6$	$31.4^{b} \pm 1.5$
	C3	$3.9^{b} \pm 0.3$	$3.0^{a} \pm 0.1$	$86.8^{a} \pm 4.0$	$95.4^{a} \pm 5.0$	$80.2^{a} \pm 2.3$	$487.0^{ab} \pm 30.5$	$32.1^{b} \pm 0.6$
	C4	$4.9^{ab} \pm 0.8$	$2.8^{a} \pm 0.1$	$85.0^{a} \pm 4.0$	$93.1^{a} \pm 2.6$	$79.2^{a} \pm 0.4$	$394.7^{ac} \pm 46.0$	$35.8^{a} \pm 1.1$
	C5	$4.7^{ab} \pm 0.6$	$2.7^{a} \pm 0.3$	$89.6^{ab} \pm 2.5$	$88.5^{a} \pm 3.7$	$78.6^{a} \pm 0.7$	$333.0^{c} \pm 42.5$	$36.0^{a} \pm 0.4$
C	C0	$4.3^{a} \pm 0.8$	$2.6^{a} \pm 0.1$	$57.7^{c} \pm 0.5$	$71.8^{c} \pm 2.6$	$59.1^{a} \pm 0.4$	$313.0^{a} \pm 34.7$	$33.7^{a} \pm 0.7$
	C1	$3.8^{a} \pm 0.4$	$2.6^{a} \pm 0.2$	$76.0^{ab} \pm 1.8$	$79.6^{ac} \pm 1.3$	$59.1^{a} \pm 0.3$	$364.7^{ac} \pm 13.4$	$38.1^{b} \pm 0.8$
	C2	$4.1^{a} \pm 0.4$	$2.6^{a} \pm 0.1$	$80.9^{b} \pm 1.9$	$80.6^{a} \pm 3.7$	$59.1^{a} \pm 1.1$	$394.5^{c} \pm 15.3$	$35.9^{ab} \pm 1.9$
	C3	$4.8^{a} \pm 0.2$	$2.5^{a} \pm 0.2$	$73.7^{a} \pm 1.0$	$86.2^{ab} \pm 1.3$	$61.6^{ab} \pm 1.1$	$455.4^{d} \pm 26.8$	$36.7^{b} \pm 0.2$
	C4	$4.4^{a} \pm 0.4$	$2.6^{a} \pm 0.2$	$101.6^{d} \pm 3.0$	$90.1^{b} \pm 4.6$	$62.9^{b} \pm 1.7$	$362.7^{ac} \pm 10.0$	$36.5^{ab} \pm 1.2$
	C5	$3.9^{a} \pm 0.3$	$2.3^{a} \pm 0.1$	$78.1^{ab} \pm 2.9$	$93.9^{b} \pm 3.1$	$70.2^{c} \pm 0.7$	$309.7^{a} \pm 9.6$	$35.9^{ab} \pm 0.7$
MIX	C0	$4.7^{ab} \pm 0.1$	$2.8^{ab} \pm 0.0$	$74.1^{a} \pm 3.3$	$92.7^{b} \pm 5.5$	$68.3^{a} \pm 0.9$	$330.0^{ab} \pm 2.0$	$36.4^{a} \pm 1.4$
	C1	$4.0^{a} \pm 0.3$	$2.7^{a} \pm 0.0$	$78.1^{a} \pm 2.3$	$84.8^{ab} \pm 4.7$	$58.5^{e} \pm 1.5$	$323.2^{ab} \pm 12.5$	$32.3^{b} \pm 0.9$
	C2	$4.4^{ab} \pm 0.5$	$2.9^{ab} \pm 0.1$	$96.5^{bc} \pm 4.3$	$86.4^{ab} \pm 4.2$	$80.8^{d} \pm 2.7$	$333.2^{ab} \pm 13.5$	$36.0^{a} \pm 0.4$
	C3	$4.4^{ab} \pm 0.3$	$3.0^{ab} \pm 0.1$	$80.4^{a} \pm 0.8$	$82.7^{ac} \pm 0.6$	$75.2^{bc} \pm 1.0$	$303.4^{a} \pm 13.1$	$33.0^{b} \pm 1.9$
	C4	$5.0^{b} \pm 0.3$	$3.1^{b} \pm 0.3$	$95.4^{b} \pm 1.1$	$88.1^{ab} \pm 1.6$	$70.1^{ab} \pm 1.9$	$347.4^{b} \pm 24.4$	$38.0^{a} \pm 0.4$
	C5	$4.6^{ab} \pm 0.3$	$2.9^{ab} \pm 0.2$	$102.7^{c} \pm 1.7$	$73.3^{c} \pm 1.6$	$79.3^{cd} \pm 2.9$	$332.0^{ab} \pm 17.8$	$31.4^{b} \pm 0.7$

NC, control (no contamination); BC, B. cinerea; V, Verticillium sp.; P, Phytophthora sp.; C, Colletotrichum sp.; MIX, pathogen group (BC, V, P, and C); C0, control (no bacterial consortia); C1, Consortium 1; C2, Consortium 2; C3, Consortium 3; C4, Consortium 4; C5, Consortium 5. A statistical analysis was performed for each infected group of plants separately. Data are means ± SD (n = 3). Different letters (a–e) indicate differences between the experimental variants ($P < 0.05$) as determined by the following statistical tests: ANOVA Tuckey (HSD) test (total glomalin: NC, BC, V, C, MIX; easily extractable glomalin: BC, V, C, MIX; dehydrogenase: BC, P, C, MIX; acid phosphatase: BC, P, C, MIX; alkaline phosphatase: NC, BC, P, MIX; carbon: NC, P, MIX; nitrogen: NC, P), F-Welch test and RIR Tuckey test for unequal numbers (Total glomalin: P; easily extractable glomalin: NC, P; dehydrogenase: V, acid phosphatase: NC, V; alkaline phosphatase: V, C; carbon: BC, V, C; nitrogen: BC, V, C, MIX), ANOVA Kruskal–Wallis test (dehydrogenase: NC).

only in strawberries infected with *Phytophthora* sp. (**Figure 3H**). A positive correlation between the content of anthocyanins and polyphenols indicates a high antioxidant activity (Dembczyński et al., 2015). It was observed that an increase in total glomalin (TG) and easily extractable fractions of glomalin (EEG) in the soil were related to an increase in the level of nitrogen (NB) and carbon in biomass (CB) for the NC, V, and MIX groups (**Figures 1B,F,L**). Glomalin contains approximately 30% of soil carbon and is the main component of soil organic matter (Gałązka, 2013), which is associated with a positive correlation between TG and EEG and CB. The growth of glomalin-producing bacteria (TG and EEG) requires a sufficiently high nitrogen concentration thereby explaining the positive correlation between TG, EEG, and NB (Gałązka, 2013). On the other hand, it is believed that an excessively high nitrogen level in the soil leads to a significant reduction in the activity of dehydrogenases involved in the transformation of soil

carbon. High dehydrogenase activity provides favourable conditions for the development of microorganisms in the soil environment (Koper and Siwik-Ziomek, 2006). A positive correlation between dehydrogenase activity (DHA) and CB was noted for the uninfected samples and those infected by *Verticillium* sp., *Colletotrichum* sp. and a mixture of pathogens (**Figures 1B,F,J,L**), which is consistent with the results of the studies by Turski and Wyczółkowski (2008). Our research confirms that there is only a positive correlation between acid phosphatase and alkaline phosphatase for the group infected with *Colletotrichum* sp. (**Figure 3J**). For the remaining groups studied, there is either a negative or an absence of any correlation between these enzymes. This situation may be explained by the development of soil microorganisms limiting the activity of certain enzymes. It is assumed that an excess of inorganic phosphorus inhibits the synthesis of phosphatases (Nahas et al., 1982).

CONCLUSION

The interaction of beneficial bacteria and pathogenic fungi or fungal-like-pathogens makes it possible to preserve the high quality of strawberry fruit. The beneficial effects of the selected consortia were confirmed by comparing the results produced by infected strawberries with those of a positive control. On this basis, Consortium C2, which is composed of *Bacillus* sp. strains, was singled out as one of the most effective against selected pathogens in terms of maintaining the firmness of strawberries contaminated with a group of pathogens. There was an increase in strawberry firmness as compared to the positive control after the use of selected antifungal consortia. The microorganisms contained in the consortia also influenced an improvement in the biochemical properties of the strawberries, such as the soluble solids content and anthocyanins content. The application of consortia C2, C3, C4, and C5 was accompanied by an increase in the SSC in the fruit infected with *Verticillium* sp. as compared to the control, thereby improving the flavour of the strawberries. Consortium C5 significantly increased the level of anthocyanins in strawberries contaminated with *Phytophthora* sp. and *B. cinerea*, and in the control, it also increased the health-promoting properties of the strawberries. The impact of the tested consortia on the pectin content of the strawberries was noted. In comparing the fruit samples with untreated beneficial microorganisms (C0), it may be seen that the group of pathogens (MIX) reduced the content of D-galacturonic acid and thus pectin to the greatest extent. The following consortia: C2 (the control), C1 (*B. cinerea*), C2, C3, and C5 (*Colletotrichum* sp.) and C1 (the pathogens group) may be identified as causing the highest increase in the content of extracted pectin in infected fruit as compared to Consortium C0. The decrease in viscosity was related to the increase in pectin content, which is indicated by the negative correlation between these values for the aforementioned groups (*B. cinerea, Colletotrichum* sp., pathogens group). For consortia C2 (control), C3 and C5 (*Colletotrichum* sp.) and C1 (pathogens group) the viscosity decreased by more than one and a half times as compared to Consortium C0.

Based on our research results, we may conclude that the tested consortia show a high degree of antagonism toward the tested fungus and allow for high-quality fruit to be obtained. The use of bacterial consortia also has the potential for reducing environmental pollution and the amount of fungicide residues in the fruit. However, more research is still required to identify the most effective consortia for combating strawberry and other soft fruit fungal diseases.

DATA AVAILABILITY STATEMENT

The original contributions presented in the study are included in the article, further inquiries can be directed to the corresponding author.

AUTHOR CONTRIBUTIONS

MD: writing – original draft, methodology, investigation, data curation, visualization, and formal analysis. JC: writing – review and editing, conceptualization, methodology, resources, supervision, and data curation. AnG: writing – review and editing, methodology, investigation, resources, and data curation. BF-S: writing – review and editing, methodology, and resources. AM-G: methodology and investigation. LS-P: writing – review and editing, and resources. AgG: methodology, investigation, and data curation. PT: investigation. AZ: resources, supervision, and data curation. MF: writing – review and editing, conceptualization, resources, data curation, supervision, project administration, and funding acquisition. All authors contributed to the article and approved the submitted version.

FUNDING

This manuscript was financed by The National Centre for Research and Development within the framework of the BIOSTRATEG project, contract number BIOSTRATEG3/344 33/16/NCBR/ 2018.

REFERENCES

Agius, F., González-Lamothe, R., Caballero, J. L., Muñoz-Blanco, J., Botella, M. A., and Valpuesta, V. (2003). Engineering increased vitamin C levels in plants by overexpression of a D-galacturonic acid reductase. *Nat. Biotechnol.* 21, 177–181. doi: 10.1038/nbt777

Ahmadi-Afzadi, M., Tahir, I., and Nybom, H. (2013). Impact of harvesting time and fruit firmness on the tolerance to fungal storage diseases in an apple germplasm collection. *Postharvest Biol. Technol.* 82, 51–58. doi: 10.1016/j.postharvbio.2013.03.001

Balci, G. (2021). Effects of melatonin applications on certain biochemical characteristics of strawberry seedlings in lime stress conditions. *Turk. J. Agric. For.* 45, 285–289. doi: 10.3906/tar-2006-83

Ben Abdallah, D., Frikha-Gargouri, O., and Tounsi, S. (2018). Rizhospheric competence, plant growth promotion and biocontrol efficacy of *Bacillus amyloliquefaciens* subsp. plantarum strain

32a. *Biol. Control* 124, 61–67. doi: 10.1016/j.biocontrol.2018.01.013

Berg, G., Kurze, S., Buchner, A., Wellington, E. M., and Smalla, K. (2000). Successful strategy for the selection of new strawberry-associated rhizobacteria antagonistic to *Verticillium* wilt. *Can. J. Microbiol.* 46, 1128–1137. doi: 10.1139/w00-101

Cao, F., Guan, C., Dai, H., Li, X., and Zhang, Z. (2015). Soluble solids content is positively correlated with phosphorus content in ripening strawberry fruits. *Sci. Hortic.* 195, 183–187. doi: 10.1016/j.scienta.2015.09.018

Carmona-Hernandez, J. C., Taborda-Ocampo, G., and González-Correa, C. H. (2021). Folin-Ciocalteu reaction alternatives for higher polyphenol quantitation in colombian passion fruits. *Int. J. Food Sci.* 2021:8871301. doi: 10.1155/2021/8871301

Caulier, S., Gillis, A., Colau, G., Licciardi, F., Liépin, M., Desoignies, N., et al. (2018). Versatile antagonistic activities of soil-borne *Bacillus* spp. and *Pseudomonas* spp. against *Phytophthora infestans* and other potato pathogens. *Front. Microbiol.* 9, 1–15. doi: 10.3389/fmicb.2018.00143

Chan, S. Y., Choo, W. S., Young, D. J., and Loh, X. J. (2017). Pectin as a rheology modifier: Origin, structure, commercial production and rheology. *Carbohydr. Polym.* 161, 118–139. doi: 10.1016/j.carbpol.2016.12.033

Chen, H., Liu, Z., Cai, K., Xu, L., and Chen, A. (2018). Grid search parametric optimization for FT-NIR quantitative analysis of solid soluble content in strawberry samples. *Vib. Spectrosc.* 94, 7–15. doi: 10.1016/j.vibspec.2017.10.006

Chen, P. H., Chen, R. Y., and Chou, J. Y. (2018). Screening and evaluation of yeast antagonists for biological control of *B. cinerea* on strawberry fruits. *Mycobiology* 46, 33–46. doi: 10.1080/12298093.2018.1454013

Cisternas-Jamet, J., Salvatierra-Martínez, R., Vega-Gálvez, A., Stoll, A., Uribe, E., and Goñi, M. G. (2020). Biochemical composition as a function of fruit maturity stage of bell pepper (Capsicum annum) inoculated with *Bacillus amyloliquefaciens*. *Sci. Hortic.* 263:109107. doi: 10.1016/j.scienta.2019.109107

Cota, L. V., Maffia, L. A., Mizubuti, E. S. G., and Macedo, P. E. F. (2009). Biological control by *Clonostachys rosea* as a key component in the integrated management of strawberry gray mold. *Biol. Control* 50, 222–230. doi: 10.1016/j.biocontrol.2009.04.017

Crisosto, C. H., Crisosto, G. M., and Metheney, P. (2003). Consumer acceptance of 'Brooks' and 'Bing'cherries is mainly dependent on fruit SSC and visual skin color. *Postharvest Biol. Technol.* 28, 159–167. doi: 10.1016/S0925-5214(02)00173-4

Cruz, A. F., Barka, G. D., Sylla, J., and Reineke, A. (2018). Biocontrol of strawberry fruit infected by *Botrytis cinerea*: Effects on the microbial communities on fruit assessed by next-generation sequencing. *J. Phytopathol.* 166, 403–411. doi: 10.1111/jph.12700

de Andrade, F. M., de Assis Pereira, T., Souza, T. P., Guimarães, P. H. S., Martins, A. D., Schwan, R. F., et al. (2019). Beneficial effects of inoculation of growth-promoting bacteria in strawberry. *Microbiol. Res.* 223–225, 120–128. doi: 10.1016/j.micres.2019.04.005

Dembczyński, R., Białas, W., Olejnik, A., Kowalczewski, P., Drożdżyńska, A., and Jankowski, T. (2015). Acquisition of anthocyanins from chokeberry fruit, elderberry, blackcurrant and black carrot root by extraction method. *Zywn. Nauk. Technol. Jakosc/Food. Sci. Technol. Qual.* 22, 165–181. doi: 10.15193/zntj/2015/102/080

Døving, A., and Måge, F. (2002). Methods of testing strawberry fruit firmness. *Acta Agricult. Scand. Sec. B-Plant Soil Sci.* 52, 43–51. doi: 10.1080/090647102320260035

Erturk, Y., Ercisli, S., and Cakmakci, R. (2012). Yield and growth response of strawberry to plant growth-promoting *Rhizobacteria* inoculation. *J. Plant Nutr.* 35, 817–826. doi: 10.1080/01904167.2012.663437

European Biostimulants Industry Council (EBIC) (2021). https://biostimulants.eu/.

European Commission (2019). The European Green Deal, Communication from the Commission to the European Parliament, the European Council, the Council, the European Economic and Social Committee and the Committee of the Regions. Brussels: European Commission.

Fan, Y., Xu, Y., Wang, D., Zhang, L., Sun, J., Sun, L., et al. (2009). Effect of alginate coating combined with yeast antagonist on strawberry (Fragaria × ananassa) preservation quality. *Postharvest Biol. Technol.* 53, 84–90. doi: 10.1016/j.postharvbio.2009.03.002

Folin, O., and Ciocalteu, V. (1927). On tyrosine and tryptophane determinations in proteins. *J. Biol. Chem.* 73, 50–627.

Fracasso, A. F., Perussello, C. A., Carpiné, D., Petkowicz, C. L., de, O., and Haminiuk, C. W. I. (2018). Chemical modification of citrus pectin: Structural, physical and rheological implications. *Int. J. Biol. Macromol.* 109, 784–792. doi: 10.1016/j.ijbiomac.2017.11.060

Fraeye, I., Knockaert, G., Buggenhout, S., Van, Duvetter, T., Hendrickx, M., et al. (2009). Enzyme infusion and thermal processing of strawberries: Pectin conversions related to firmness evolution. *Food Chem.* 114, 1371–1379. doi: 10.1016/j.foodchem.2008.11.041

Gałązka, A. (2013). Characteristics of glomalins and the influence of different cultivation systems on their content in soil. *Polish J. Agron.* 15, 75–82.

Grassino, A. N., Brnčić, M., Vikić-Topić, D., Roca, S., Dent, M., and Brnčić, S. R. (2016). Ultrasound assisted extraction and characterization of pectin from tomato waste. *Food Chem.* 198, 93–100. doi: 10.1016/j.foodchem.2015.11.095

Haggag, W. M., and Abo El Soud, M. (2012). Production and optimization of *Pseudomonas fluorescens* biomass and metabolites for biocontrol of strawberry grey mould. *Am. J. Plant Sci.* 3, 836–845. doi: 10.4236/ajps.2012.37101

Harker, F. R., Elgar, H. J., Watkins, C. B., Jackson, P. J., and Hallett, I. C. (2000). Physical and mechanical changes in strawberry fruit after high carbon dioxide treatments. *Postharvest Biol. Technol.* 19, 139–146. doi: 10.1016/S0925-5214(00)00090-9

Harker, F. R., Gunson, F. A., and Jaeger, S. R. (2003). The case for fruit quality: an interpretive review of consumer attitudes, and preferences for apples. *Postharvest Biol. Technol.* 28, 333–347. doi: 10.1016/S0925-5214(02)00215-6

International Organization for Standardization (2000). *Fruit and vegetable products - determination of dry matter content by drying under reduced pressure and of water content by azeotropic distillation*. Geneva: International Organization for Standardization.

Ishikawa, T., Hayashi, A., Kyutoku, Y., Dan, I., Wada, T., Oku, K., et al. (2018). Classification of strawberry fruit shape by machine learning. Int. Arch. Photogramm. Remote Sens. *Spat. Inf. Sci.* XLII, 4–7. doi: 10.5194/isprs-archives-XLII-2-463-2018

Jensen, B., Knudsen, I. M. B., Andersen, B., Nielsen, K. F., Thrane, U., Jensen, D. F., et al. (2013). Characterization of microbial communities and fungal metabolites on field grown strawberries from organic and conventional production. *Int. J. Food Microbiol.* 160, 313–322. doi: 10.1016/j.ijfoodmicro.2012.11.005

Jin, P., Wang, H., Zhang, Y., Huang, Y., Wang, L., and Zheng, Y. (2017). UV-C enhances resistance against gray mold decay caused by *Botrytis cinerea* in strawberry fruit. *Sci. Hortic.* 225, 106–111. doi: 10.1016/j.scienta.2017.06.062

Johnson, J., Collins, T., Walsh, K., and Naiker, M. (2020). Solvent extractions and spectrophotometric protocols for measuring the total anthocyanin, phenols and antioxidant content in plums. *Chem. Papers* 74, 4481–4492. doi: 10.1007/s11696-020-01261-8

Jorquera-Fontena, E., Alberdi, M., and Franck, N. (2014). Pruning severity affects yield, fruit load and fruit and leaf traits of 'Brigitta' blueberry. *J. Soil Sci. Plant Nutr.* 14, 855–868. doi: 10.4067/s0718-95162014005000068

Jouini, M., Abdelhamid, A., Chaouch, M. A., Le Cerf, D., Bouraoui, A., Majdoub, H., et al. (2018). Physico-chemical characterization and pharmacological activities of polysaccharides from *Opuntia microdasys* var. rufida cladodes. *Int. J. Biol. Macromol.* 107, 1330–1338. doi: 10.1016/j.ijbiomac.2017.10.003

Juric, S., Vlahovicek-Kahlina, K., Duralija, B., Bandic, L. M., Nekic, P., and Vincekovic, M. (2021). Stimulation of plant secondary metabolites synthesis in soilless cultivated strawberries (*Fragaria x ananassa* Duchesne) using zinc-alginate microparticles. *Turk. J. Agric. For.* 45, 324–334.

Kanchikerimath, M., and Singh, D. (2001). Soil organic matter and biological properties after 26 years of maize-wheat-cowpea cropping as affected by manure and fertilization in a Cambisol in semiarid region of India. *Agric. Ecosyst. Environ.* 86, 155–162. doi: 10.1016/S0167-8809(00)00280-2

Ke, J., Jiang, G., Shen, G., Wu, H., Liu, Y., and Zhang, Z. (2020). Optimization, characterization and rheological behavior study of pectin extracted from chayote (*Sechium edule*) using ultrasound assisted method. *Int. J. Biol. Macromol.* 147, 688–698. doi: 10.1016/j.ijbiomac.2020.01.055

Kim, Y. S., Lee, I. K., and Yun, B. S. (2015). Antagonistic effect of Streptomyces sp. BS062 against *Botrytis* diseases. *Mycobiology* 43, 339–342. doi: 10.5941/MYCO.2015.43.3.339

Klein, D. A., Loh, T. C., and Goulding, R. L. (1964). Soil dehydrogenase activity. *Soil Sci.* 98, 371–376. doi: 10.1016/0038-0717(71)90049-6

Koper, J., and Siwik-Ziomek, A. (2006). Effect of long-term fertilization on the activity of dehydrogenases in soil and the content of organic carbon and total nitrogen. *Zesz. Probl. Postêpów Nauk Rol.* 1, 197–202.

Koubala, B. B., Mbome, L. I., Kansci, G., Mbiapo, F. T., and Crepeau, M. (2008). Physicochemical properties of pectins from ambarella peels (*Spondias cytherea*) obtained using different extraction conditions. *Food Chem.* 106, 1202–1207. doi: 10.1016/j.foodchem.2007.07.065

Kovačević, D. B., Putnik, P., Dragović-Uzelac, V., Vahčić, N., Babojelić, M. S., and Levaj, B. (2015). Influences of organically and conventionally grown strawberry cultivars on anthocyanins content and color in purees and low-sugar jams. *Food Chem.* 181, 94–100.

Krimm, U., Abanda-Nkpwatt, D., Schwab, W., and Schreiber, L. (2005). Epiphytic microorganisms on strawberry plants (*Fragaria ananassa* cv. Elsanta): Identification of bacterial isolates and analysis of their interaction with leaf surfaces. *FEMS Microbiol. Ecol.* 53, 483–492. doi: 10.1016/j.femsec.2005.02.004

Landum, M. C., Félix, M., do, R., Alho, J., Garcia, R., Cabrita, M. J., et al. (2016). Antagonistic activity of fungi of Olea europaea L. against *Colletotrichum acutatum*. *Microbiol. Res.* 183, 100–108. doi: 10.1016/j.micres.2015.12.001

Lazazzara, V., Perazzolli, M., Pertot, I., Biasioli, F., Puopolo, G., and Cappellin, L. (2017). Growth media affect the volatilome and antimicrobial activity against *Phytophthora infestans* in four *Lysobacter* type strains. *Microbiol. Res.* 201, 52–62. doi: 10.1016/j.micres.2017.04.015

Lee, C. H., Moturi, V., and Lee, Y. (2009). Thixotropic property in pharmaceutical formulations. *J. Control. Release* 136, 88–98. doi: 10.1016/j.jconrel.2009.02.013

Li, X., Jing, T., Zhou, D., Zhang, M., Qi, D., Zang, X., et al. (2021). Biocontrol efficacy and possible mechanism of Streptomyces sp. H4 against postharvest anthracnose caused by Colletotrichum fragariae on strawberry fruit. *Postharv. Biol. Tech.* 175:111401. doi: 10.1016/j.postharvbio.2020.111401

Lima, N. B., Marcus, M. V., De Morais, M. A., Barbosa, M. A. G., Michereff, S. J., Hyde, K. D., et al. (2013). Five *Colletotrichum* species are responsible for mango anthracnose in northeastern Brazil. *Fungal Divers* 61, 75–88. doi: 10.1007/s13225-013-0237-6

Lingua, G., Bona, E., Manassero, P., Marsano, F., Todeschini, V., Cantamessa, S., et al. (2013). Arbuscular mycorrhizal fungi and plant growth-promoting *Pseudomonads* increases anthocyanin concentration in strawberry fruits (Fragaria x ananassa var. Selva) in conditions of reduced fertilization. *Int. J. Mol. Sci.* 14, 16207–16225. doi: 10.3390/ijms140816207

Liu, B., Wang, K., Shu, X., Liang, J., Fan, X., and Sun, L. (2019). Changes in fruit firmness, quality traits and cell wall constituents of two highbush blueberries (*Vaccinium corymbosum* L.) during postharvest cold storage. *Sci. Hortic.* 246, 557–562. doi: 10.1016/j.scienta.2018.11.042

López-Ortiz, A. L. L., Méndez, L., Cornelio, D., Adriana, L., and Jorge, E. J. M. (2019). Understanding the drying kinetics of phenolic compounds in strawberries: An experimental and density functional theory study. *Innov. Food Sci. Emerg. Technol.* 60:102283. doi: 10.1016/j.ifset.2019.102

Mackenzie, S. J., Chandler, C. K., Hasing, T., and Whitaker, V. M. (2011). The role of temperature in the late-season decline in soluble solids content of strawberry fruit in a subtropical production system. *Hort Sci.* 46, 1562–1566.

Magwaza, L. S., and Opara, U. L. (2015). Analytical methods for determination of sugars and sweetness of horticultural products—A review. *Sci. Hortic.* 184, 179–192. doi: 10.1016/j.scienta.2015.01.001

Makarova, E. N., and Shakhmatov, E. G. (2020). Structural characteristics of oxalate-soluble polysaccharides from Norway spruce (*Picea abies*) foliage. *Carbohydr. Poly.* 246:116544. doi: 10.1016/j.carbpol.2020.116544

Malarczyk, D. G., Panek, J., and Frąc, M. (2020). Triplex Real Time PCR approach for the detection of crucial fungal berry pathogens-*Botrytis* spp., *Colletotrichum* spp. and *Verticillium* spp. *Int. J. Mol. Sci.* 21, 1–17. doi: 10.3390/ijms21228469

Mierczyńska, J., Cybulska, J., Pieczywek, P. M., and Zdunek, A. (2014). Effect of storage on rheology of water-soluble, chelate-soluble and diluted alkali-soluble pectin in carrot cell walls. *Food Bioprocess Technol.* 8, 171–180. doi: 10.1007/s11947-014-1392-9

Mierczyńska, J., Cybulska, J., and Zdunek, A. (2017). Rheological and chemical properties of pectin enriched fractions from different sources extracted with citric acid. *Carbohydr. Polym.* 156, 443–451. doi: 10.1016/j.carbpol.2016.09.042

Milijasevic-Marcic, S., Todorovic, V., Stanojevic, O., Beric, T., Stankovic, S., Todorovic, B., et al. (2018). Antagonistic potential of *Bacillus* spp. isolates against bacterial pathogens of tomato and fungal pathogen of pepper. *J. Pestic. Phytomedicine* 33, 9–18. doi: 10.2298/pif1801009m

Miller, W. R., McDonald, R. E., and Chaparro, J. (2000). Tolerance of selected orange and mandarin hybrid fruit to low-dose irradiation for quarantine purposes. *HortScience* 35, 1288–1291. doi: 10.21273/HORTSCI.35.7.1288

Min, B., Lim, J., Ko, S., Lee, K., Ho, S., and Lee, S. (2011). Environmentally friendly preparation of pectins from agricultural by products and their structural/rheological characterization. *Bioresour. Technol.* 102, 3855–3860. doi: 10.1016/j.biortech.2010.12.019

Moreira, R. R., Nesi, C. N., May, and De Mio, L. L. (2014). Bacillus spp. and *pseudomonas* putida as inhibitors of the *Colletotrichum acutatum* group and potential to control glomerella leaf spot. *Biol. Control* 72, 30–37. doi: 10.1016/j.biocontrol.2014.02.001

Nahas, E., Ternezi, H. F., and Rossi, A. (1982). Effect of carbon source and pH on the production and secretion of acid phosphatase and alkaline phosphatase in *Neurospora crassa*. *J. Gen. Microbiol.* 128, 2017–2021.

Nguyen, X. H., Naing, K. W., Lee, Y. S., Kim, Y. H., Moon, J. H., and Kim, K. Y. (2015). Antagonism of antifungal metabolites from *Streptomyces griseus* H7602 against *Phytophthora capsici*. *J. Basic Microbiol.* 55, 45–53. doi: 10.1002/jobm.201300820

Nunes, C. M. N., Brecht, J. K., Morais, A. M. M. B., and Sargent, S. A. (2001). Possible influences of water loss and polyphenol oxidase activity on anthocyanin content and discoloration in fresh ripe strawberry (cv . Oso Grande) during storage at 1 °C. *J. Food Sci.* 70, 79–84. doi: 10.1111/j.1365-2621.2005.tb09069.x

O'Donoghue, E. M., and Somerfield, S. D. (2008). Biochemical and rheological properties of gelling pectic isolates from buttercup squash fruit. *Food Hydrocoll.* 22, 1326–1336. doi: 10.1016/j.foodhyd.2007.07.002

Ognyanov, M., Remoroza, C. A., Schols, H. A., Petkova, N. T., and Georgiev, Y. N. (2021). Structural study of a pectic polysaccharide fraction isolated from "mountain tea"(*Sideritis scardica* Griseb.). *Carbohydr. Poly.* 260:117798. doi: 10.1016/j.carbpol.2021.117798

Olanrewaju, O. S., and Babalola, O. O. (2019). *Streptomyces*: implications and interactions in plant growth promotion. *Appl. Microbiol. Biotechnol.* 103, 1179–1188. doi: 10.1007/s00253-018-09577-y

Ornelas-Paz, J. D. J., Yahia, E. M., Ramírez-Bustamante, N., Pérez-Martínez, J. D., Escalante-Minakata, M. D. P., Ibarra-Junquera, V., et al. (2013). Physical attributes and chemical composition of organic strawberry fruit (*Fragaria x ananassa* Duch, Cv. Albion) at six stages of ripening. *Food Chem.* 138, 372–381. doi: 10.1016/j.foodchem.2012.11.006

Oszust, K., Cybulska, J., and Frąc, M. (2020). How do *Trichoderma* genus fungi win a nutritional competition battle against soft fruit pathogens? A report on niche overlap nutritional potentiates. *Int. J. Mol. Sci.* 21, 1–19. doi: 10.3390/ijms21124235

Ozdemir, F., and Topuz, A. (2004). Changes in dry matter, oil content and fatty acids composition of avocado during harvesting time and post-harvesting ripening period. *Food Chem.* 86, 79–83. doi: 10.1016/j.foodchem.2003.08.012

Paniagua, C., Santiago-Doménech, N., Kirby, A. R., Gunning, A. P., Morris, V. J., Quesada, M. A., et al. (2017). Structural changes in cell wall pectins during strawberry fruit development. *Plant Physiol. Biochem.* 118, 55–63. doi: 10.1016/j.plaphy.2017.06.001

Pastrana, A. M., Basallote-Ureba, M. J., Aguado, A., Akdi, K., and Capote, N. (2016). Biological control of strawberry soil-borne pathogens *Macrophomina phaseolina* and *Fusarium solani*, using *Trichoderma asperellum* and *Bacillus* spp. *Phytopathol. Mediterr.* 55, 109–120. doi: 10.14601/Phytopathol

Ponder, A., and Hallmann, E. (2019). The effects of organic and conventional farm management and harvest time on the polyphenol content in different raspberry cultivars. *Food Chem.* 301:125295. doi: 10.1016/j.foodchem.2019.125295

Poveda, J. (2020). Use of plant-defense hormones against pathogen-diseases of postharvest fresh produce. *Physiol. Mol. Plant Pathol.* 111:101521. doi: 10.1016/j.pmpp.2020.101521

Poveda, J., Barquero, M., and González-Andrés, F. (2020). Insight into the microbiological control strategies against B. cinerea using systemic plant resistance activation. *Agronomy* 10:1822. doi: 10.3390/agronomy10111822

Qin, X., Xiao, H., Cheng, X., Zhou, H., and Si, L. (2017). *Hanseniaspora uvarum* prolongs shelf life of strawberry via volatile production. *Food Microbiol.* 63, 205–212. doi: 10.1016/j.fm.2016.11.005

Reyes-Yanes, A., Martinez, P., and Ahmad, R. (2020). Real-time growth rate and fresh weight estimation for little gem romaine lettuce in aquaponic grow beds. *Comp. Electr. Agricult.* 179:105827. doi: 10.1016/j.compag.2020.105827

Rey-Serra, P., Mnejja, M., and Monfort, A. (2021). Shape, firmness and fruit quality QTLs shared in two non-related strawberry populations. *Plant Sci.* 11:111010. doi: 10.1016/j.plantsci.2021.111010

Santiago, R., Huiliñir, C., Cottet, L., and Castillo, A. (2016). Microbiological characterization for a new wild strain of *Paenibacillus polymyxa* with antifungal activity against *Botrytis cinerea*. *Biol. Control* 103, 251–260. doi: 10.1016/j.biocontrol.2016.10.002

Siebeneichler, T. J., Crizel, R. L., Camozatto, G. H., Paim, B. T., da Silva, Messias, R., et al. (2020). The postharvest ripening of strawberry fruits induced by abscisic acid and sucrose differs from their in vivo ripening. *Food Chem.* 317, 126–407. doi: 10.1016/j.foodchem.2020.126407

Singh, G., Bhattacharyya, R., Das, T. K., Sharma, A. R., Ghosh, A., Das, S., et al. (2018). Crop rotation and residue management effects on soil enzyme activities, glomalin and aggregate stability under zero tillage in the Indo-Gangetic Plains. *Soil. Tillage Res.* 184, 291–300. doi: 10.1016/j.still.2018.08.006

Sowik, I., Bielenin, A., and Michalczuk, L. (2001). In vitro testing of strawberry resistance to *Verticillium dahliae* and *Phytophthora cactorum*. *Sci. Hortic.* 88, 31–40. doi: 10.1016/S0304-4238(00)00195-3

Srivastava, R., Tripathi, B. M., Singh, R. K., Srivastva, P., Kumari, P., Srivastav, M., et al. (2011). Profiling of plant growth promoting bacteria associated with Jaunpuri giant radish rhizosphere. *Int. J. Agric. Biol.* 13, 9–17.

Tabatabai, M. A., and Bremner, J. M. (1969). Use of p-nitrophenyl phosphate for assay of soil phosphatase activity. *Soil Biol. Biochem.* 1, 301–307. doi: 10.1016/0038-0717(69)90012-1

Tang, B., Laborda, P., Sun, C., Xu, G., Zhao, Y., and Liu, F. (2019). Improving the production of a novel antifungal alteramide B in *Lysobacter enzymogenes* OH11 by strengthening metabolic flux and precursor supply. *Bioresour. Technol.* 273, 196–202. doi: 10.1016/j.biortech.2018.10.085

Tarantino, A., Lops, F., Disciglio, G., and Lopriore, G. (2018). Effects of plant biostimulants on fruit set, growth, yield and fruit quality attributes of 'Orange rubis®' apricot (*Prunus armeniaca* L.) cultivar in two consecutive years. *Sci. Hortic.* 239, 26–34. doi: 10.1016/j.scienta.2018.04.055

Todeschini, V., Aitlahmidi, N., Mazzucco, E., Marsano, F., Gosetti, F., Robotti, E., et al. (2018). Impact of beneficial microorganisms on strawberry growth, fruit production, nutritional quality, and volatilome. *Front. Plant Sci.* 9, 1–22. doi: 10.3389/fpls.2018.01611

Tomic, J. M., Milivojevic, J. M., and Pesakovic, M. I. (2015). The response to bacterial inoculation is cultivar-related in strawberries. *Turkish J. Agric. For.* 39, 332–341. doi: 10.3906/tar-1410-16

Tournas, V. H., and Katsoudas, E. (2005). Mould and yeast flora in fresh berries, grapes and citrus fruits. *Int. J. Food Microbiol.* 105, 11–17. doi: 10.1016/j.ijfoodmicro.2005.05.002

Turski, M., and Wyczółkowski, A. (2008). Influence of diversified use of soils from loess on respiration activity of dehydrogenases. *Acta Agrophysica* 12, 801–811.

Valentinuzzi, F., Mason, M., Scampicchio, M., Andreotti, C., Cesco, S., and Mimmo, T. (2015). Enhancement of the bioactive compound content in strawberry fruits grown under iron and phosphorus deficiency. *J. Sci. Food Agric.* 95, 2088–2094. doi: 10.1002/jsfa.6924

Venzon, S. S., Canteri, M. H. G., Granato, D., Demczuk, B., Maciel, G. M., Stafussa, A. P., et al. (2015). Physicochemical properties of modified citrus pectins extracted from orange pomace. *J. Food Sci. Technol.* 52, 4102–4112. doi: 10.1007/s13197-014-1419-2

Wang, W., Zhong, Z., Wang, Q., Wang, H., Fu, Y., and He, X. (2017). Glomalin contributed more to carbon, nutrients in deeper soils, and differently associated with climates and soil properties in vertical profiles. *Sci. Rep.* 7, 1–13. doi: 10.1038/s41598-017-12731-7

Wilcox, W. F., Scott, P. H., Hamm, P. B., Kennedy, D. M., Duncan, J. M., Brasier, C. M., et al. (1993). Identity of a *Phytophthora* species attacking raspberry in Europe and North America. *Mycol. Res.* 97, 817–831. doi: 10.1016/S0953-7562(09)81157-X

Win, T. T., Bo, B., Malec, P., and Fu, P. (2021). The effect of a consortium of *Penicillium* sp. and *Bacillus* spp. in suppressing banana fungal diseases caused by *Fusarium* sp. and *Alternaria* sp. *J. Appl. Microbiol.* 2021:15067. doi: 10.1111/jam.15067

Wrigth, S. F., and Upadhyaya, A. (1998). A survey of soils for aggregate stability and glomalin, a glycoprotein produced by hyphae of arbuscular mycorrhizal fungi. *Plant Soil* 198, 97–107.

Xie, F., Wang, Z., and Liu, J. (2021). Effects of pectins with different structural and conformational characteristics on gelatinization and retrogradation of corn starch. *Starch-Stärke* 73:2100094. doi: 10.1002/star.202100094

Yagmur, B., and Gunes, A. (2021). Evaluation of the effects of plant growth promoting rhizobacteria (pgpr) on yield and quality parameters of tomato plants in organic agriculture by principal component analysis (PCA). *Gesunde Pflanzen* 73, 219–228. doi: 10.1007/s10343-021-00543-9

Zahedipour-Sheshglani, P., and Asghari, M. (2020). Impact of foliar spray with 24-epibrassinolide on yield, quality, ripening physiology and productivity of the strawberry. *Sci. Hortic.* 268, 109–376. doi: 10.1016/j.scienta.2020.109376

Zhang, F., Li, X. L., Zhu, S. J., Ojaghian, M. R., and Zhang, J. Z. (2018). Biocontrol potential of *Paenibacillus polymyxa* against *Verticillium dahliae* infecting cotton plants. *Biol. Control* 127, 70–77. doi: 10.1016/j.biocontrol.2018.08.021

Conflict of Interest: The authors declare that the research was conducted in the absence of any commercial or financial relationships that could be construed as a potential conflict of interest.

Publisher's Note: All claims expressed in this article are solely those of the authors and do not necessarily represent those of their affiliated organizations, or those of the publisher, the editors and the reviewers. Any product that may be evaluated in this article, or claim that may be made by its manufacturer, is not guaranteed or endorsed by the publisher.

frontiers in Plant Science

REVIEW
published: 01 December 2021
doi: 10.3389/fpls.2021.746780

Sorghum-Phosphate Solubilizers Interactions: Crop Nutrition, Biotic Stress Alleviation, and Yield Optimization

Asfa Rizvi[1], Bilal Ahmed[2]*, Mohammad Saghir Khan[3], Shahid Umar[1] and Jintae Lee[2]*

[1]Department of Botany, School of Chemical and Life Sciences, Jamia Hamdard, New Delhi, India, [2]School of Chemical Engineering, Yeungnam University, Gyeongsan, South Korea, [3]Department of Agricultural Microbiology, Faculty of Agricultural Sciences, Aligarh Muslim University, Aligarh, India

Sweet sorghum [*Sorghum bicolor* (L.) Moench] is a highly productive, gluten-free cereal crop plant that can be used as an alternative energy resource, human food, and livestock feed or for biofuel-ethanol production. Phosphate fertilization is a common practice to optimize sorghum yield but because of high cost, environmental hazards, and soil fertility reduction, the use of chemical P fertilizer is discouraged. Due to this, the impetus to search for an inexpensive and eco-friendly microbiome as an alternative to chemical P biofertilizer has been increased. Microbial formulations, especially phosphate solubilizing microbiome (PSM) either alone or in synergism with other rhizobacteria, modify the soil nutrient pool and augment the growth, P nutrition, and yield of sorghum. The use of PSM in sorghum disease management reduces the dependence on pesticides employed to control the phytopathogens damage. The role of PSM in the sorghum cultivation system is, however, relatively unresearched. In this manuscript, the diversity and the strategies adopted by PSM to expedite sorghum yield are reviewed, including the nutritional importance of sorghum in human health and the mechanism of P solubilization by PSM. Also, the impact of solo or composite inoculations of biological enhancers (PSM) with nitrogen fixers or arbuscular mycorrhizal fungi is explained. The approaches employed by PSM to control sorghum phytopathogens are highlighted. The simultaneous bio-enhancing and biocontrol activity of the PS microbiome provides better options for the replacement of chemical P fertilizers and pesticide application in sustainable sorghum production practices.

Keywords: sorghum, phosphate solubilizers, microbiome, phytopathogens, antagonists, P-nutrition

OPEN ACCESS

Edited by:
Giuseppe Colla, University of Tuscia, Italy

Reviewed by:
Kanchan Vishwakarma, Swedish University of Agricultural Sciences, Sweden
Mohamed Sheteiwy, Mansoura University, Egypt

****Correspondence:***
Bilal Ahmed
bilal22000858@yu.ac.kr
Asfa Rizvi
asfarizvi09@gmail.com

Specialty section:
This article was submitted to Plant Abiotic Stress, a section of the journal Frontiers in Plant Science

Received: *24 July 2021*
Accepted: *01 November 2021*
Published: *01 December 2021*

Citation:
Rizvi A, Ahmed B, Khan MS, Umar S and Lee J (2021) Sorghum-Phosphate Solubilizers Interactions: Crop Nutrition, Biotic Stress Alleviation, and Yield Optimization. Front. Plant Sci. 12:746780. doi: 10.3389/fpls.2021.746780

INTRODUCTION

The constantly increasing human populations and regularly declining agricultural soils have placed extra pressure on sustainable agriculture systems to eliminate human food hunger worldwide (Díaz-Rodríguez et al., 2020). Globally, P fertilization is a common practice to improve sorghum production (Gemenet et al., 2016), but the intemperate application or unrelenting long-term utilization of chemical-P fertilizers cause environmental pollution and

reduce soil quality (Alori et al., 2017; Li et al., 2020). The efficiency of P solubilizer is very low (15–20%) due to its rapid fixation in acidic and alkaline soils, both of which are predominant worldwide (Aziz et al., 2014). Though the majority of global soils contain sufficient reserves of total P, most of it remains inaccessible, and soils thus become deficient in P. So, to maintain sorghum production, P fertilizers are applied regularly. The high cost of chemical-P fertilizer acts as a motivator in the quest for an alternative where naturally-occurring P sources such as rock phosphate (RP) serve as a P reservoir. Regrettably, RP is not easily available to plants in soils with a pH > 5.5–6, and farmers thus cannot use RP in sorghum fields (Gurdeep and Reddy, 2015). However, the microbial fertilizers, especially phosphate biofertilizers, augment the P use efficiency (PUE) and thereby improve plant P uptake. Collectively, the phosphate solubilizing microbiome (PSM) represents a group of soil organisms that make P available to plants from both inorganic and organic sources by solubilizing and mineralizing complex P compounds (Zaidi et al., 2009; Chawngthu et al., 2020). Among PSM inhabiting a particular environment, bacteria (Rezakhani et al., 2020), fungi (Elfiati et al., 2021), and actinomycetes (Saif et al., 2014) supply mineral nutrients especially P to various food crops including sorghum growing in different agroclimatic regions worldwide (Abawari et al., 2020; Chen et al., 2021). The PSM intervention in sorghum cultivation practices seems to be an incredibly attractive and highly promising approach to ameliorate sorghum production in P-deficient soil (dos Santos et al., 2017). Apart from supplying P, PSM plays an important role in suppressing the damaging impact of phytopathogens causing severe sorghum yield losses (Gopalakrishnan et al., 2015; Mitra et al., 2020). The PSM-mediated management of P nutrition and sorghum phytopathogens is considered an inexpensive and environmentally friendly biotechnological approach and appears to be a realistic substitute to chemical P fertilizers and hazardous pesticides (Saraf et al., 2014; Kumar et al., 2020). However, due to the competition among/between indigenous/introduced microbiome, soil environment, and other factors, the competence of PSM to survive and colonize in the rhizosphere is greatly challenged (Soumare et al., 2020). Despite this, the PSM, when applied as microbiological formulations in field/greenhouse, has been found to enhance the growth and yield of many food crops (Ahmed et al., 2017; Batool and Iqbal, 2019), including sorghum (Vijayalakshmi et al., 2020), by various direct and indirect mechanisms (Khan et al., 2014; Herrera-Quiterio et al., 2020).

Sorghum, a multipurpose cereal crop belonging to the family Poaceae, ranks fourth in terms of worldwide production after wheat, rice, and corn (Shoemaker and Bransby, 2010; Kumar et al., 2017a). It is typically cultivated in the semi-arid tropics (Almodares and Hadi, 2009) and has several economically important potential uses such as food (grain), feed (grain and biomass), biofuel (ethanol production), fiber (paper), fermentation (methane production), and fertilizer (Hasibuan and Nazir, 2017; Dar et al., 2018). Due to excessive pressure on the production of rice for human consumption, there is an urgent need to search for any nutrition-rich alternative food substitutes for rice to satisfy human food demands. Sweet sorghum in this context can serve as a potential food alternative in many countries (Marles et al., 2018). Different approaches like crop rotation, use of resistant cultivars, and agrochemicals to combat phytopathogens have been adopted to enhance the yield and quality of sweet sorghum, but due to several reasons, especially the cost, technical difficulties, emergence of resistance among pathogens against toxic chemicals, residual toxicity to non-target organisms, or environmental pollution, the implementation of such methods/chemicals is discouraged in sorghum cultivation practices. The utilization of microbiological fertilizers particularly PSM is an alternative option to plant growth and production of sweet sorghum under biotic stress conditions. However, little research has been conducted and very little information is available on the ameliorative role of PSM in relation to the growth and yield of sorghum, particularly under biotic stressed conditions. Acknowledging the importance of human food and lack of information on the role of PSM in sorghum production in high throughput agricultural practices, this review attempts to provide the latest information on the biodiversity and physiological variations of PSM and its importance in sorghum P nutrition, biotic stress alleviation and yield optimization/stability in changing agro-ecosystems worldwide. This review further explains the mechanistic basis of disease suppression and highlights the potential role of single and/or composite PSM formulations in sorghum-soil systems. The understanding of the relationship between the PSM and related rhizobacteria and arbuscular mycorrhizal fungi may help in better management of P fertilization and biotic stress alleviation in sorghum growing in different agrosystems while reducing the risk of chemical pollution.

SORGHUM: FOOD, NUTRITIONAL COMPOSITION, AND HUMAN HEALTH

Sorghum, which is naturally gluten free, is a major cereal grown as a food and feed crop (Kumar et al., 2017b; Zhao et al., 2019). Sorghum is known by different names, such as great millet and guinea corn in West Africa; kafir corn in South Africa; dura in Sudan; jowar in India, and kaoliang in China. Among sorghum-producing countries, the United States is a major sorghum producer, but only a small fraction of grain is consumed here as human food; instead, it is mainly used as animal fodder. Worldwide, sorghum is consumed in various forms, such as alcoholic and non-alcoholic beverages, baked bread, tortillas, porridges, couscous, gruel, steam-cooked products, expanded snacks, cookies, etc. (Murty and Subramanian, 1982). Sorghum can also be processed into starch, flour, grits, and flakes and is used to produce a wide range of industrial products. Due to its nutritional importance, sorghum is incorporated into the human diet more specifically for people who are intolerant to wheat (Kulamarva et al., 2009). It is consumed mostly in northern China, India, and southern Russia, where about 85% of the crops are consumed directly as human food (Dicko et al., 2006).

Nutritionally, sweet sorghum is quite high (62%) in carbohydrates (Barcelos et al., 2016) and has a higher energy output than sugarcane, sugar beet, corn, and wheat

(Dar et al., 2018). Sorghum provides important minerals, vitamins, protein, and micronutrients essential for optimal health, growth, and development (Awika and Rooney, 2004; Kulamarva et al., 2009). Recently (Tasie and Gebreyes, 2020), observed proximate composition values such as moisture, ash, crude fat, crude fiber, and crude protein, and CHO in different sorghum varieties, which varied from 9.66 to 12.94, 1.12 to 2.29, 2.48 to 4.60, 2.17 to 8.59, 8.20 to 16.48, and 67.56 to 76.42, respectively. The highest mineral content in sorghum varieties was (mg/100 g): P (368), Na (6), Mg (208), K (314), Ca (67), Fe (14), and Zn (6). The maximum tannin was recorded in Lalo (3,337 mg/100 g) and Dano (2,474 mg/100 g). Based on the high mineral value, sorghum varieties such as Miskir, Abshir, ESH-1, Meko-1, Red Swazi, and Karimtams can be considered for food product development. Sorghum also contains various phenolics like flavonoids (Shahidi and Naczk, 1995), which inhibit tumor development (Awika and Rooney, 2004), and antioxidants, which make the grain suitable for producing functional foods. It is a gluten-free cereal, which has importance in the occurrence of Celiac Disease (CD), an immunological response to gluten intolerance. The starches and sugars in sorghum are released more slowly than in other cereals (Léder, 2004) and it is thus beneficial for diabetic persons (Toomey, 1988).

WHY IS PSM SO IMPORTANT IN SORGHUM PLANT SYSTEMS?

Chemical fertilization (e.g., NPK) in agriculture is documented as a successful practice to manage soil fertility and concurrently to increase the quality and yield of cereal crops (Mojid et al., 2012; Saïdou et al., 2018), including sorghum (Sebnie et al., 2020), in different agro-ecological regions. Among plant nutrients, P is the major nutrient after N and is the second most deficient plant nutrient (Munir et al., 2004). Under a P-deficient environment, plants show altered growth and metabolism, and a reduction from 5 to 15% in crop yield has been reported (Shenoy and Kalagudi, 2005). So, to overcome the low P availability and to allow sorghum plants to grow normally, P fertilizers are used in cultivation practices (Roy and Khandaker, 2010). Sorghum requires high levels of chemical fertilizer for optimal growth, which causes a shift in the soil microbial community (Chu et al., 2007; Wang et al., 2018) and environmental degradation leading to human health problems (Adesemoye and Kloepper, 2009; Kang et al., 2011) These problems accentuate the need for new technologies in sorghum production systems to achieve sustainable production systems. The PSM of plant-growth-promoting microbes is of particular interest as it can, either alone or in combination with other related PGPR/AM-fungi, reduce the adverse impact of chemical fertilizers and simultaneously enhances plants' tolerance to environmental stress (Bhardwaj et al., 2014). Additionally, the PSM promotes root morphogenesis and gradually increases plant height, stem diameter, number of leaves per plant, leaf area, and yield along with protecting plants from phytopathogens attack (Pandey and Gupta, 2020). Also, P supplied either through solubilization or mineralization by PSM participates in cell division, growth of new tissues and nucleic acid structure, protein synthesis regulation, respiration, signal transduction, macro-molecular biosynthesis, phospholipids, carbon metabolism and a wide range of enzymes, energy transfer, and photosynthesis (Kouas et al., 2005; Hameeda et al., 2008). To fulfill P demands, the PSM has been found to be very useful (Qarni et al., 2021). The PSM-sorghum plant synergy could, therefore, be of great practical importance in the management of P nutrition, biotic stress, and yield optimization. Once developed, the PSM formulation benefits sorghum in several ways due to its ability to (i) release P nutrients slowly and as per the need of plants; (ii) complement other minerals; (iii) supply essential agroactive biological enhancers to plants; and (iv) alleviate biotic stress (Khan et al., 2014; García-Fraile et al., 2015; Yadav and Sarkar, 2019). Broadly, the utilization of microbes mediated rock phosphate solubilization has multiple advantages over conventional chemical P fertilizers in sorghum cultivation practices. These advantages are as follows: (i) the PSM-based formulations are safer than chemical fertilizers; (ii) there is no chance of deposition of either toxic materials or microbiome in the food chain; (iii) the self-replicating ability of microbes evades the requirement for repetitive application; and (iv) they reduce dependence on pesticides. Put together, the PSM along with RP could be an incredibly strong strategy to advance the biological and physicochemical fertility of the soil, which eventually enhances the sorghum production at a low cost. While the literature regarding PGPR interactions with the top three cereals (maize, wheat, and rice) is quite sizeable, a search conducted using the words "PSM" and "sorghum" as keywords revealed very few papers in the scientific literature. Also, when searching PSM and sorghum diseases, very few scientific studies are available. Collectively, the amount of information regarding the interactions between PSM (bacteria/fungi/actinomycetes) and sweet sorghum is limited.

OVERVIEW OF PSM: DEFINITION, BIODIVERSITY, AND P-SOLUBILIZATION

A group of beneficial soil microbiomes, including bacteria, fungi, and actinomycetes, capable of mineralizing/solubilizing complex P into soluble forms are termed phosphate-solubilizing microorganisms (Tian et al., 2021). The PSM has been recovered from different ecological habitats (**Table 1**) using standard microbiological methods (**Figure 1**). *Pseudomonas* and *Bacillus* among bacteria and *Aspergillus* and *Penicillium* among fungi are the most efficacious P solubilizers (Li et al., 2016; Zhu et al., 2018). P-solubilizing fungi (PSF) are better P solubilizers than other PSMs due to their ability to do the following: (i) retain a P-dissolving ability after repeated subculturing; (ii) traverse longer distances more easily in any environment; and (iii) produce more organic acids (Venkateswarlu et al., 1984). Among mineral phosphate solubilization (mps) mechanisms, the organic acid (OA) theory is the most widely accepted mechanism of solubilization and supply of P to plants (**Table 2**). The OA lowers the pH of the environment and causes discharge of P ions from the P mineral by H^+ exchange for Ca^{2+} (Goldstein et al., 1993). The variation in pH and the amount of P solubilized

TABLE 1 | Phosphate solubilizing microbiome biodiversity in different agroecological habitat.

PSM groups	Source/Origin	Media used	References
Bacterial genera			
Enterobacter	*Capsicum chinense* rhizosphere	PVK	Mendoza-Arroyo et al., 2020
Pseudomonas spp.	wheat, barley, maize, oat, faba beans, peas	NBRIP	Elhaissoufi et al., 2020
Acinetobacter, *Pseudomonas, Massilia*, *Bacillus*, *Arthrobacter, Stenotrophomonas, Ochrobactrum*, and *Cupriavidus*	Bulk soil	NBRIP	Wan et al., 2020
Burkholderia cepaciam, *B. contaminans*	Sweet corn rhizosphere	PVK	Pande et al., 2020
Endophytes			
Aneurinibacillus sp. and *Lysinibacillus* sp.	Banana tree roots	NBRIP	Matos et al., 2017
Nitrogen-fixing bacteria			
Mesorhizobium spp.	Chickpea root nodules		Muleta et al., 2021
Rhizobium, *Agrobacterium*, *Phyllobacterium*	Root nodules of *Acacia cyanophylla*	PVK	Lebrazi et al., 2020
Mesorhizobium ciceri, *M. tamadayense*	*Cicer canariense* nodules	NBRIP	Menéndez et al., 2020
Azotobacter	Maize rhizospheres	PVK and NBRIP	Nosrati et al., 2014; Bjelić et al., 2015
Azospirillum strain	Wheat rhizospheres	PVK, MPVK, and LB	Ayyaz et al., 2016
A. vinelandii	Soil	MPVK	El-Badry et al., 2016
P-solubilizing fungi (PSF)			
Aspergillus hydei, *Gongronellahydei*, *P. soli,* and *Talaromyces yunnanensis*	*Quercus rubra* rhizosphere	PVK	Doilom et al., 2020
Trichoderma koningiopsis	Rice plant	NBRIP	Tandon et al., 2020;
Penicillium guanacastense	*Pinus massoniana* rhizosphere	NBRIP	Qiao et al., 2019
Actinomycetes			
Streptomyces roseocinereus and *S. natalensis*	Moroccan oat rhizosphere	MPVK	Chouyia et al., 2020

NBRIP, national botanical research institute phosphate medium; PVK, Pikovskaya medium; MPVK, modified Pikovskaya medium; LB, luria bertani.

by PSM has also been unrelated (Asea et al., 1988), which suggests the involvement of mechanisms other than the OA in the P solubilization process which is influenced by many factors (Mohamed et al., 2018). The complex organic P compounds (phosphates, phospholipids, phytin etc.) in contrast are mineralized enzymatically by alkaline and acid phosphatases (Behera et al., 2017; Din et al., 2019), phytases (Din et al., 2019), and phospholipases (Walpola and Yoon, 2012) excreted by PSM.

Mechanisms Used by PSM to Facilitate Sorghum Plant Growth

Most of the cultivable soils in the world have insufficient elemental nutrients like P, N, K, and Zn, or these are unavailable to the plants. Also, poor agricultural practices, such as the disproportionate use of fertilizers, lead to undesirable effects such as soil fertility reduction. Indeed, a major part of chemical fertilizers applied to augment sorghum production is wasted further polluting the agroecosystem (Garnett et al., 2009). Below are some of the main mechanisms used by PSM to optimize the use of crop nutrients and help promote sorghum production.

Apart from supplying inherently P to plants, the P-dissolving microbiome benefits the plants by providing N through BNF, growth modulating enzymes, phytohormones, and antimicrobial compounds, which directly or indirectly affect the growth and development of sorghum (**Table 3**). The direct growth stimulation by PSM includes the acquisition of nutrients, such as P through solubilization/mineralization and N through N_2 fixation, phytohormone production, and facilitation of resource while indirectly they promote growth by suppression of plant pathogens and induction of resistance in host plants against pathogens (**Figure 2**).

The plant growth-promoting substances released by PSM include (i) phytohormones, such as indoleacetic acid (Lebrazi et al., 2020; Qarni et al., 2021) and gibberellin (Pandya et al., 2018; Kang et al., 2019), (ii) asymbiotic (Nosrati et al., 2014; Ayyaz et al., 2016) or symbiotic N_2 fixation (Muleta et al., 2021), (iii) biocontrol of phytopathogens through antifungal compounds and antibiotics (Olanrewaju and Babalola, 2019; Mitra et al., 2020) or lytic enzymes (Hamane et al., 2020; Naziya et al., 2020), and (iv) secretion of siderophores (Aallam et al., 2021) and HCN (Naziya et al., 2020; Boubekri et al., 2021). In addition to these biological enhancers, the phosphate dissolving bacteria (Kalam et al., 2020; Zhao et al., 2021), actinomycetes (Chukwuneme et al., 2020), and fungi (Ali et al., 2019) also release 1-aminocyclopropane-1-carboxylate (ACC) deaminase to protect plants from attack by pathogens. Phosphate solubilizing microbiota can also protect sorghum plants from biotic stress and stimulate growth indirectly by destructing the metabolism of attacking pathogens and/or stimulate the plant's immune system. Thus, the indirect mechanisms of PSM could be extremely useful and of great practical interest under field conditions because they provide a chance for growers to avoid the use of chemical biocides (Adesemoye and Kloepper, 2009; Khatoon et al., 2020) and, therefore, protect soils and crops from chemical toxicity.

PSM-SORGHUM INTERACTIONS: INOCULATION EFFECTS ON GROWTH, CROP NUTRITION, AND GRAIN YIELD

Application of microbes-based bio-fertilizers in agro-ecosystems is beneficial for plant growth and yield enhancement in both

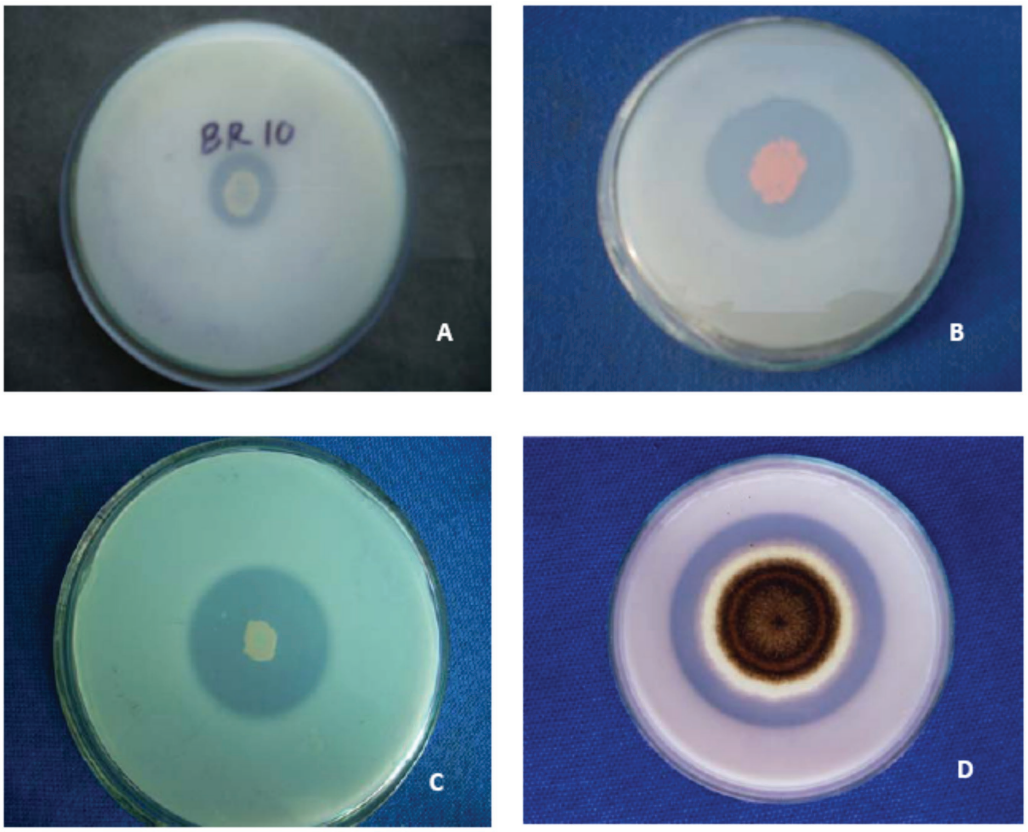

FIGURE 1 | Demonstration of solubilization of insoluble tri-calcium phosphate by species of- **(A)** *Pseudomonas* **(B)** *Serratia* **(C)** *Bacillus* and **(D)** *Aspergillus* on Pikovskaya (1948) medium.

TABLE 2 | Organic acids secreted by PSM.

PSM	Organic acids	References
Phosphate solubilizing bacteria		
Bacillus, *Burkholderia, Paenibacillus* sp.	Gluconic, oxalic, citric, tartaric, succinic, formic, and acetic acid	Chawngthu et al., 2020
Pantoea, *Pseudomonas*, *Serratia*, and *Enterobacter*	Oxalic, citric, gluconic succinic, and fumaric acids	Rfaki et al., 2020
Bacillus sp. strain AZ17	Pyruvic, succinic, fumaric, malic, tartaric, and oxalic acids	Zúñiga-Silgado et al., 2020
Pseudomonas sp. strain AZ5, *Bacillus* sp. strain AZ17	Acetic, oxalic and gluconic acids, acetic, citric, and lactic acids	Zaheer et al., 2019
Phosphate solubilizing fungi		
Rhizopus stolonifer and *R. oryzae*	Oxalic, lactic, citric, succinic, gluconic, malic, fumaric, acetic acid, and propionic acids	Mohammed, 2020
Trichoderma and *Aspergillus*	Oxalic, citric, formic, tartaric, malic, acetic, and citric acids	Li et al., 2016
Penicillium oxalicum and *A. niger*	Gluconic acid, oxalic, propionic, and malic acids	Li et al., 2016
Phosphate solubilizing actinomycetes		
Streptomyces sp. KP109810, *Streptomyces* sp. CTM396	Gluconic acid	Farhat et al., 2015

conventional (Kalayu, 2019) and extreme environments (Kamali and Mehraban, 2020; Rizvi et al., 2020). Among microbial formulations, the research on PSMs impacting growth, crop nutrition, and yield of cereal crops under greenhouse/field trials are quite large (**Table 4**). The literature regarding PSM application in sorghum cultivation systems in different agroecological regions is, however, lacking. Considering this gap, the beneficial influence of PSM including PS bacteria (PSB), fungi (PSF), and actinomycetes (PSA) used either alone or in combination with other conventional PGPR or arbuscular mycorrhizal (AM) fungi is highlighted. A model explaining the ameliorative impact of the PSM on morphological, cellular, and physiological activities of the sorghum plant is presented in **Figure 3**.

Inoculation Effects of Single PSM

The inoculation of the P-solubilizing microbiome is considered a promising and inexpensive microbiological option, not to mention the most sustainable one, in food production systems because it increases the P bioavailability without destructing the soil-plant systems. Sorghum, considered a substitute to rice, adapts well to P deficient soils employing absorption and solubilization mechanisms including interaction with PSM. The direct application of RP either alone or/and followed by the inoculation of the PSM is however, a suitable alternative to

TABLE 3 | Plant-growth-promoting active biomolecules released by PSM.

Soil microbiome	Source	PGP activities	References
Mesorhizobium spp.	Chickpea root nodules	IAA, ACC deaminase, siderophores, HCN	Muleta et al., 2021
Streptomyces alboviridis P18–*S. griseorubens* BC3–*S. griseorubens* BC10 and *Nocardiopsis alba* BC11	Desert soils of Morocco	IAA, siderophore, HCN, and ammonia	Boubekri et al., 2021
Staphylococcus sp., *Bacillus firmus*, *B. safensis*, and *B. licheniformis*	Soils of rock P mines	IAA, ACC Deaminase	Qarni et al., 2021
Penicillium sp. and *Penicillium oxalicum*	Soils of rock P mines	IAA	Qarni et al., 2021
Burkholderia ubonensis	Woodland soil of a Chinese fir plantation	IAA, ACC deaminase, nitrogenase, iron carriers	Zhao et al., 2021
Streptomyces roseocinereus MS1B15	Moroccan oat rhizosphere	IAA, Siderophores, ACC deaminase, N_2fixation, antimicrobial activity	Chouyia et al., 2020
Bacillus strains	Rhizosphere, leaf endosphere, and sap of P-efficient tropical maize genotypes	IAA	de Sousa et al., 2021
Agrobacterium tumefaciens syn. *Rhizobium radiobacter*	Nodules of *Leucaena leucocephala*	Zinc solubilization, IAA, N_2 fixation, siderophores, EPS, salt tolerance	Verma et al., 2020
S. roseocinereus, S. natalensis	Oat rhizospheres	Siderophores, IAA, ACC deaminase, antimicrobial activity against *Fusarium oxysporum*, *Botrytis cinerea*, *Phytophthora cactorum*, and *Phytophthora cryptogea*	Chouyia et al., 2020
Agrobacterium sp. NA11001, *Phyllobacterium* sp. C65, *Bacillus* sp. CS14, and *Rhizobium* sp. V3E1.	Root nodules of *Acacia cyanophylla*	IAA	Lebrazi et al., 2020
Alternaria, Aspergillus, Chaetomium, Curvularia, Fusarium, Melanaspora, Nigrospora, Penicillium and *Trichoderma*	*Chilli rhizosphere*	IAA, siderophores, HCN, chitinase	Naziya et al., 2020
Acinetobacter sp., PGP27, *Ensifer meliloti*	Faba bean and wheat rhizosphere	K solubilization, IAA, EPS	Bechtaoui et al., 2019
Bacillus sp.	*Stevia rebaudiana rhizosphere*	IAA, siderophores	Prakash and Arora, 2019
Lysinibacillus fusiformis, *Bacillus* sp., *Paenibacillus* sp.	Roots of wheat	IAA,siderophore production, protease activity, antibacterial and antifungal inhibition	Akinrinlola et al., 2018
Mesorhizobium ciceri and *M. mediterraneum*	Chickpea nodules	N_2 fixation, IAA	Zafar et al., 2017
Klebsiella sp. Br1, *K. pneumoniae* Fr1, *B. pumilus* S1r1, *Acinetobacter* sp. S3r2	Maize roots	N_2 fixation,auxin production	Kuan et al., 2016
Mucror, Penicillium	*Panax ginseng* rhizosphere	IAA	Hussein and Joo, 2015

supply P to the growing sorghum crops. Recently (Mattos et al., 2020), evaluated the effect of PSB inoculation on two sorghum genotypes (BR007-efficient and responsive and SC283-efficient and non-responsive) with different P sources (RP and triple superphosphate, TSP). The sorghum genotypes were inoculated separately with the PSB *Bacillus* strains (B116 and B70) and were cultivated in greenhouse and field soils fertilized with TSP, RP, ½TSP + ½RP. The PSB inoculation significantly increased the root biomass and P content under greenhouse and grain yield and grain P content of genotype BR007 grown in the field but had no effect on genotype SC283. The application of PSB as P-bioinoculant with RP acted as a promising alternative to reduce the use of synthetic chemical fertilizers leading to sustainable production of sorghum. The findings of this experiment, however, suggested that the impact of PSB inoculation varied according to (i) sorghum genotype, (ii) P source, and (iii) phosphobacterial strains. A field experiment by (Shete et al., 2018) conducted for three consecutive rabi seasons applying a drought-tolerant PSB strain with or without N and P sources showed a variable effect on the growth and yield of rabi sorghum. The sorghum seed inoculated with PSB strain (Acc. No.1/2012) and 100% recommended N and 75% recommended P_2O_5 demonstrated the highest plant height (199.9 cm), grain yield (18.13 q/ha), stover yield (62.96 q/ha), 1,000 grain weight (28.86 g), P uptake (14.14 kg/ha), benefit: cost ratio (3.17) and PSB counts (4.67×10^4) at flowering stage. The results firmly indicate a saving of 25% of chemical P fertilizer for rabi sorghum under dryland conditions. Seed inoculation with *Pseudomonas putida* strain 168 in other experiments resulted in the highest dried forage, maximum dry matter digestibility, and crude protein while *P. putida* strain 41 produced maximum water-soluble carbohydrates. Seed inoculation with bacterial strains alone (especially strain 168) increased nutrient uptake, plant growth and consequently enhanced the yield. Among the PSB strains, *P. putida* strain 168 was superior compared even to dual culture application suggesting the antagonism between the two PSB strains (Ehteshami et al., 2014). In a similar investigation, the PSB significantly increased the shoot growth, ear head weight, and P content in both roots and shoots, and the grain yield of sorghum rose under a greenhouse environment, compared to plants grown without bacterial cultures and treated with RP and single superphosphate (Vikram, 2007). The inoculation of PSF, *Aspergillus terreus*, and *Penicillium pinophilum* in association with the reactive phosphate rock (RPR) improved the shoot growth, P-uptake, and enhanced the dry matter yield of sorghum, when grown under greenhouse conditions. The PSF application increased the shoot dry matter yield by 30% while the plant

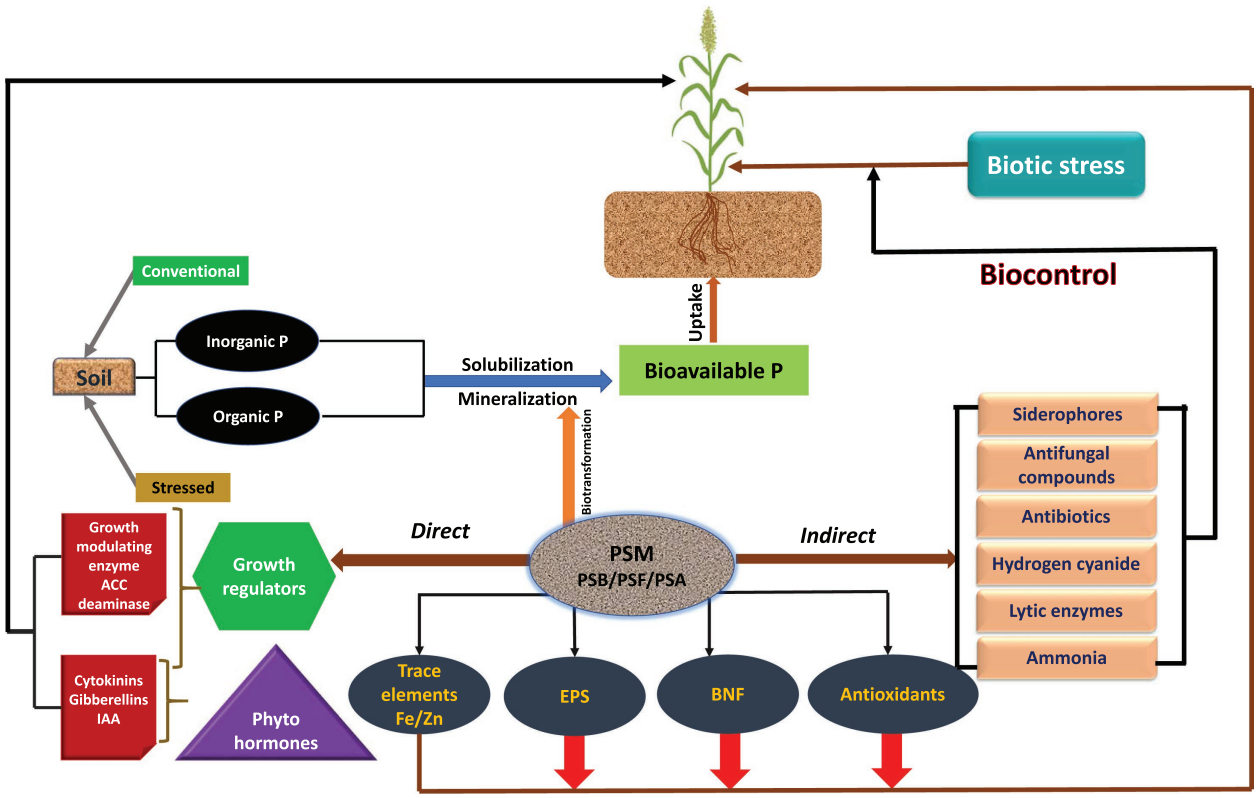

FIGURE 2 | Mechanism used by phosphate solubilizing microbiome (PSM) to facilitate sorghum plant growth.

height was enhanced by 42% compared to the uninoculated plants. The PSF inoculation, however, did not affect the root growth of sorghum plants. Moreover, the PSF substantially increased the P concentration by 61 and 71% in the absence and presence of RPR and 110 and 265% in the P accumulation of sorghum relative to the control, respectively. The PSF application, therefore, showed a more obvious beneficial impact on organ growth and sorghum P uptake (Steiner et al., 2016). A study conducted by Srinivasan et al. (2012) revealed that PSB identified using BIOLOG belonging to *Pseudomonas*, *Xanthomonas*, *Bacillus*, *Aerococcus*, *Alteromonas*, *Erwinia*, and *Enterobacter* while PSF identified as *Aspergillus* and *Penicillium* produced IAA and gibberellic acid (GA). The IAA produced by the bacterial cultures ranged between 0.74 and 9.53 μg 25 ml^{-1} while GA varied between 2.08 and 12.55 μg 25 ml^{-1}. The amount of IAA secreted by the PSF differed from 2.33 to 8.69 μg 25 ml^{-1} and GA ranged from 3.44 to 14.80 μg 25 ml^{-1}. Among the two P-solubilizers, PSF was superior to PSB in terms of P solubilization and increased maximally the stem girth, root length, root dry matter, and total dry matter of sorghum plants.

Inoculative Synergism Between PSM, N_2 Fixers, and AM-Fungi

The impact of mixed formulations of bio-enhancers belonging to two or more physiologically related/divergent groups has generally been excellent in promoting crop performance compared to single or mono culture applications (Keller-Pearson et al., 2020; Dierks et al., 2021; Nogales et al., 2021). During composite application, the synergistic or additive effect of the interacting microbe is expected on growth, crop nutrition, and yield of crops. For example, bio-fertilizer organisms can improve the growth of a plant independently through N_2 fixation or through the production of growth hormones or synergistically through both mechanisms simultaneously. Therefore, a synergistic relationship promotes the growth, crop nutrition, and yield of plants more efficiently than solo culture because the microbial pairing allows the plants to achieve greater absorption of minerals (NPK) and other elements. However, little is known about the synergistic effect of PSM and other PGPR or AM-fungi on sorghum (Cobb et al., 2016). The combined effect of two or more PSM together or PSM with N_2 fixers or AM fungi on sorghum is reviewed and highlighted.

Composite Application of Phosphate Solubilizers

Some recent data by Rezakhani et al. (2020) indicate that the single-and dual cultures of PSB, *Pseudomonas* sp. FA1, and *Bacillus simplex* UT1 and different concentrations of silicon had variable impact on the morphological, nutritional uptake of P, Si and K, and physiological activities of *Sorghum bicolor* plant fertilized with soluble or insoluble P (RP; Rezakhani et al., 2020). In this sense, the RP-fertilized sorghum had better root and shoot biomass while the PSB strains and Si levels applied independently augmented all the measured bio-chemical

TABLE 4 | Inoculation effects of PSM on the performance of cereal crops grown in different agroecological systems.

PSM inoculants	Growth parameters of cereals	Experimental conditions	References
Sorghum			
Bacillus simplex and *Pseudomonas* sp.	Growth, plant dry matter, and P use efficiency	Greenhouse	Rezakhani et al., 2020
Aspergillus terreus and *Penicillium pinophilum*	P uptake and dry matter yield	Greenhouse	Steiner et al., 2016
Streptomyces sp.	Growth and yield enhancement	Field	Alekhya and Gopalakrishnan, 2016
Maize			
Azospirillum brasilense, *B. subtilis, P. fluorescens*	Improved P uptake efficiency and greater yield	Greenhouse	Pereira et al., 2020
Achromobacter xylooxidans, Leclerciaa decarboxylata	Increased photosynthetic rate, stomatal conductance, chlorophyll, carotenoids, and grain yield	Greenhouse	Danish et al., 2020
B. subtilis	Increased productivity and shoots P	Field	Lobo et al., 2019
Aspergillus flavus	Growth and mineral contents	Greenhouse	Omomowo et al., 2020
Streptomyces sp. KP109810	Efficient promotion of maize growth and P content	Greenhouse	Mohammed, 2020
Wheat			
Streptomyces alboviridis P18– *S. griseorubens* BC3– *S. griseorubens* BC10 and *Nocardiopsis alba* BC11	Improved root length, root volume, root dry weight, shoot length, and shoot dry weight		Boubekri et al., 2021
Paenibacillus sp.	Significantly increased the plant height, biomass, root growth, and P uptake		Chen and Liu, 2019
Streptomyces	Plant height, root and shoot dry matter and p uptake	Greenhouse	El-Dsouky et al., 2019
Rice			
Pantoea sp.	Significantly increased the plant height, biomass, root growth, and P uptake	Field	Chen and Liu, 2019
Aspergillus niger	Increased grain yield	Field	Asuming-Brempong and Anipa, 2014
Streptomyces KT 6-4-1	Increased root length, plant height, and dry mass	Greenhouse	Chaiharn et al., 2018
Millet			
Bacillus strains	Enhanced biomass production and accumulation of N P K in the shoot	Greenhouse	Ribeiro et al., 2018
Bacillus sp. (C2) and *Pseudomonas* sp.	Increased height, total chlorophyll, IAA, starch, fresh and dry weight		Harinathan et al., 2016
Barley			
Streptomyces roseocinereus MS1B15	Plant growth and P uptake	Greenhouse	Chouyia et al., 2020

properties. Application of *Pseudomonas* sp. FA1 and *B. simplex* UT1 and Si with soluble P or insoluble P significantly enhanced P-use efficiency of sorghum plants. As a co-culture, both *B. simplex* and *Pseudomonas* sp. considerably increased the dry matter and P uptake of sorghum plants when raised with both forms of P fertilizer. While comparing the inoculation effects of the two PSB, *Pseudomonas* sp. was more efficacious than *B. simplex*. The composite culture of PSB with Si had the largest increase in P uptake and other growth indices. The results clearly suggest that the co-application of PSB and Si along with RP fertilization may serve as a substitute for chemical P fertilizer in sustainable sorghum cultivation practices. Studies by (Jisha and Alagawadi, 1996) revealed a variable impact of dual inoculation of PSB bacteria, *P. striata*, or *B. polymyxa* with the cellulolytic fungus, *Trichoderma harzianum*, on the nutrient uptake and yield of *Sorghum* grown in a vertisol treated with cotton stalks. Composite application of *B. polymyxa* or *P. striata* with *T. harzianum* increased the size and weight of the earhead, the number of spikelets per ear, and the straw and grain yield, and N and P uptake significantly relative to uninoculated control and single PSB application. Grain yield was increased by 6–8% due to co-inoculation over mono P-solubilizers inoculation and by 28–30% over *T. harzianum* alone.

Synergism Between PSM and N_2 Fixers

Among phytonutrients, N and P are the two major nutrients that affect many important cellular processes like root elongation, proliferation and changes of root architecture, seed development, and maturity of plants growing both under conventional and stressful conditions (Liu et al., 2020; Patel and Panchal, 2020). The combined inoculation of PSM and N_2 fixers benefit plants better than either group of organisms used alone while substantially reducing the application of chemical fertilizers under field conditions (Gheliya et al., 2018; Li et al., 2020). Considering this (Afifi et al., 2014), in a field experiment conducted at Ismailia Agricultural Research Station, Agriculture Research Centre (ARC), Egypt, evaluated the impact of an associative N_2 fixer, *Azospirillum brasilense*, PSB *B. megaterium,* and potassium solubilizing bacterium (KSB) *B. circulans*, applied either alone or in combined forms and treated individually

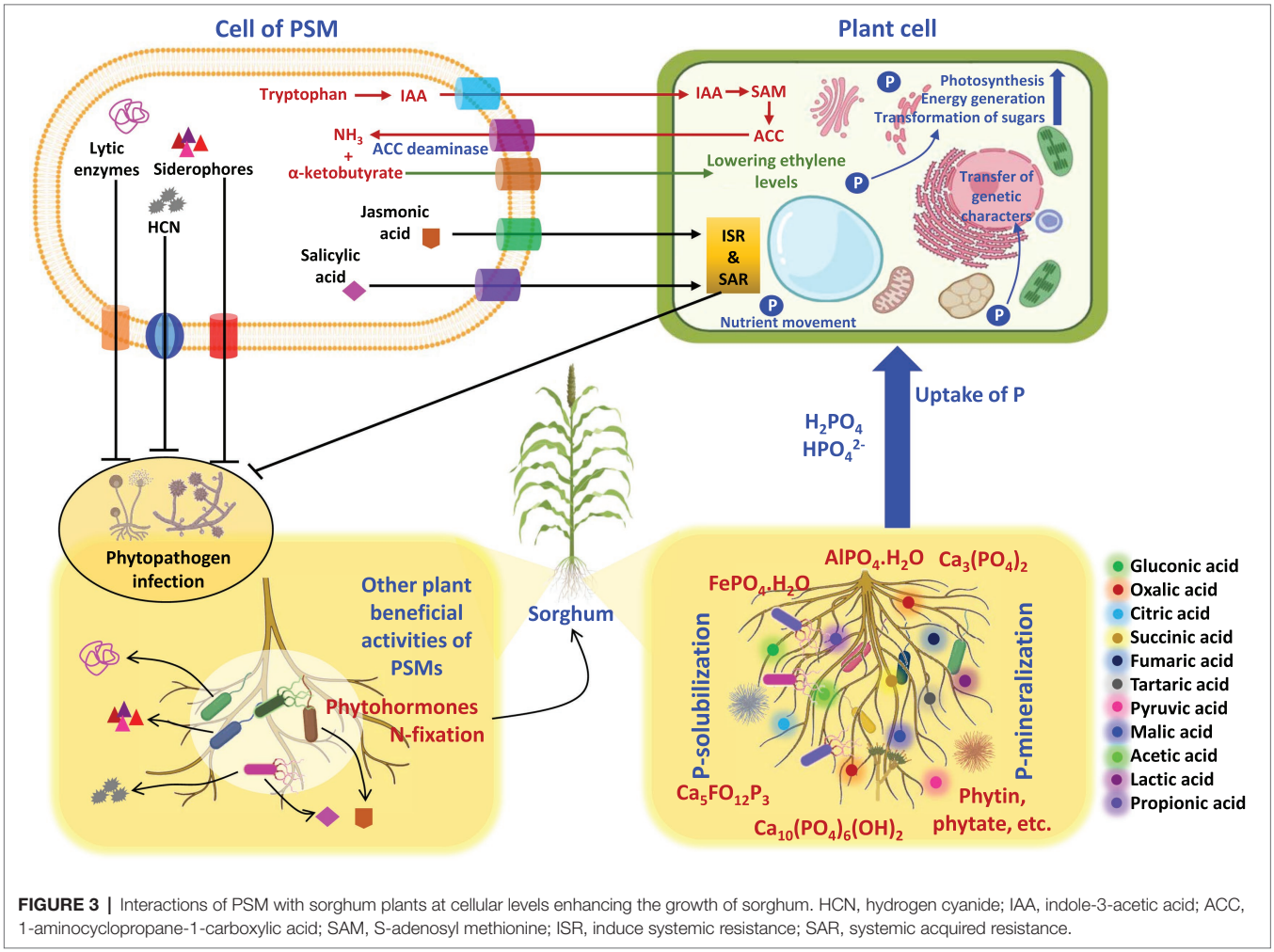

FIGURE 3 | Interactions of PSM with sorghum plants at cellular levels enhancing the growth of sorghum. HCN, hydrogen cyanide; IAA, indole-3-acetic acid; ACC, 1-aminocyclopropane-1-carboxylic acid; SAM, S-adenosyl methionine; ISR, induce systemic resistance; SAR, systemic acquired resistance.

with either humic or fulvic acids, on the availability of N, P, and K and their overall impact on morphology, physiology, and the yield attributes of *S. bicolor* (cv. Dorado) in the presence of 50% of the recommended dose of mineral NPK. Half of the recommended dose (175 kg/fed) of ammonium sulfate (20.5%) was added during sowing and 30 and 60 days after sowing with *A. brasilense* only. Half of the recommended dose of P (100 kg/fed) as super phosphate (15.5% P_2O_5) was applied during soil preparation containing *B. megaterium* only, while half of the recommended dose (25 kg/fed) of potassium sulfate (48% K_2O) was applied once only at 60 days before the earing stage inoculated with *B. circulans* only. The application of bacterial cultures either alone or as a mixture was more effective and maximally enhanced the growth and the yield of sorghum plants. Among all formulations, the mixture of bacterial cultures and humic acid demonstrated the highest populations of bacterial group in the sorghum rhizosphere. Biological features such as plant height, plant dry weight, and number of branches and biochemical attributes like nitrogenase, dehydrogenase, and phosphatase activities were significantly increased in the presence of co-culture of *A. brasilense*, *B. megaterium*, and *B. circulans* plus humic acid after 45 and 75 days of sorghum growth. Also, the NPK, crude protein, and total carbohydrates (%) were at maximum in sorghum grains. The *A. brasilense*, *B. megaterium*, and *B. circulans* when used together exhibited the highest grains yield (3.55 ton/fed) and 1,000 grains weight over control (full NPK). The findings clearly revealed that each bacterial stain could reduce the half doses of NPK through P and K solubilization and N-fixation processes. In a similar recent study, the impact of the asymbiotic nitrogen fixer (*A. chroococcum*) and P solubilizer (*B. megaterium*) on growth, yield parameters, and nutrient uptake of *Sorghum bicolor* grown under greenhouse conditions varied considerably (Vijayalakshmi et al., 2020). The formulations consisting of *A. chroococcum* and *B. megaterium* magnified the microbial populations in soil and through synergistic interaction increased the bioavailability of N and P and some other nutrients in the soil during sorghum harvest. The dual culture of N_2 fixer and P solubilizer applied with a 100% recommended dose of fertilizer (RDF) had a maximum beneficial impact on growth (plant height, length, and dry weight of root and shoot), nutrient uptake (NPK), and grain yield of sorghum compared to the uninoculated plants at harvest. The maximum number of grains (190/plant) and grain weight (5.23 g/plant) were observed with 100% RDF and combined formulations of *Azotobacter* with

PSB, which was followed by the 75% RDF with *Azotobacter* and PSB. A profound increase in the yield of sorghum was attributed as being largely due to the supply of N and P by the N_2 fixer and PSB to sorghum crops. This increase was well supported by enhancement in N (highest N 1.9%) and P (highest P uptake 0.41%) uptake by sorghum plants due to inoculation of *Azotobacter* with PSB along with 100% RDF at harvest compared to uninoculated and unfertilized control plants. In a similar greenhouse experiment (Alagawadi and Gaur, 1988, 1992), observed a significant increase in the yield of sorghum due to combined inoculation of PSB, *P. striata* or *B. polymyxa* and N_2 fixing *A. brasilense* which indicated a positive interaction between the dissimilar groups of bacteria. The yields were, however, markedly further enhanced by the application of 40 kg N as urea and 60 kg P_2O_5 (rock phosphate) per ha along with bacterial cultures over sole application of fertilizer or only bacterial inoculation. Due to this, it was suggested that 40 kg N could be saved and the whole quantity of super phosphate could be replaced by RP plus inoculation of *A. brasilense* and *P. striata* or *B. polymyxa*. The population counts of *Azospirillum* and phosphate-solubilizing bacteria in the rhizosphere of sorghum were higher in the respective inoculation treatments than in uninoculated treatments.

Synergism Between PSM and AM-Fungi

The AM-fungi during interaction receive sugars, amino acids, vitamins, and other organic substances from the host plant. In return, it absorbs minerals, especially P from the soil, and enhances the growth and yield of the host plant (Johansson et al., 2004). Agronomically, when the two dissimilar groups of beneficial organisms are applied in crop cultivation, the yield of many crops increases substantially (Saxena et al., 2013; Nacoon et al., 2020). Like other PGPR, AM- fungi and PSB interact synergistically wherein PSB solubilize sparingly available P compounds into orthophosphate that AM-fungi absorbs and transport to the host plants (Ordoñez et al., 2016). The reports on the inoculation effects of single or multiple PGPR on many cereal crops are numerous (Wahid et al., 2016; Naseri et al., 2018), but there is a scarcity of information on the synergistic effect of the PSM and AM-fungi on sorghum plants. Below, the role of composite application of PSM and AM fungi in the growth and yield promotion is highlighted.

Principally, AM-fungi provide nutrients to their host plants by producing hyphae that grow out from plant roots, effectively increasing the soil volume from which immobile nutrients can be acquired. So, mycorrhizal agricultural crops perform better and can be more productive compared with non-mycorrhizal plants. In addition, AM-fungi increase and improve the amounts of secondary compounds in plants (Mohamed et al., 2014). The synergy between AM-fungi and PSB with NPK fertilizer demonstrated variable growth and yield impact on greenhouse-grown sweet sorghum under saline conditions (Ramadhani and Widawati, 2020). The dual inoculation of AM-fungi and PSB in the presence of varying doses of NPK increased the plant height, the number of leaves, plant fresh weight, plant dry weight, and P of sweet sorghum plant. The AM-fungi and PSB applied with 25% NPK produced the highest increase in all the biological features of sorghum plants, suggesting that the colonization between AM-fungi and PSB with NPK fertilizer could be a suitable and economical option for enhancing sorghum production even under saline conditions. The results of a study conducted by (Ziaeyan et al., 2016) showed that the plants inoculated with a combination of PSB and AM-fungi expressed synergistic effect to increase the efficiency of P fertilizer and growing conditions and yield of sorghum. The combined application of 25 mg P_2O_5 per kg of soil along with the PSB and AM-fungi maximally enhanced the biological attributes and therefore, could be recommended to save the P application in sorghum cultivation systems. Nitroxin, a bio-fertilizer prepared from a mixture of asymbiotic N_2 fixers *Azospirillum* and *Azotobacter* and AM-fungus (*Glomus mosseae*), mitigated the deleterious effects of stress by increasing the amounts of photosynthetic pigments, soluble proteins and osmotic regulation and decreasing electrolyte leakage in sorghum and, hence, increased the yield significantly. Mechanistically, the interacting bacterial genera had N_2 fixation, P solubilization, and iron releasing abilities, as well as the capability to secret plant hormones such as auxin, cytokinin, and gibberellin and a growth modulating enzyme, ACC-deaminase, which together enhanced the yield substantially (Olanrewaju et al., 2017).

The interactions between PSM, N_2 fixers, and AM-fungi in terms of facilitating plant growth, nutrient uptake, and yield have been reported in numerous studies in the literature. The information regarding the inoculative effect of PSM, N_2 fixers AM fungi on sorghum is scanty. Widada et al. (2007) demonstrated that sorghum plants inoculated with PSB (*Pseudomonas* sp.), N_2 fixer (*Azospirillum lipoferum*), and AM-fungi (*Glomus manihotis* and *Entrophospora colombiana*) and grown in acid and P deficient soils improved the plant dry weight and nutrients (such as N, P, Fe, and Zn) uptake, which were enhanced further by dual inoculation of selected microbiome compared to the single inoculation. Dual inoculation of AM-fungi with PSB and AM-fungi and N_2 fixer increased plant dry weight by 112 and 64 times compared to the uninoculated plant, respectively. The selected rhizobacteria also improved plant colonization by AM-fungi. These results suggest that the tripartite interaction between PSB, N_2 fixer, and AM-fungi can be an excellent strategy for optimizing sorghum production since no antagonisms among interacting organisms were observed.

BIOTIC STRESS ALLEVIATION BY PSM

Pathogenic microorganisms are a major and continuing threat to food production and ecosystem stability worldwide. Yield, grain quality, and production stability of sorghum are constrained by various biotic (Kumar and Ram, 2014) and abiotic (Tari et al., 2013) stressors, resulting in poor marketability and utilization and causing severe economic losses. Among biotic factors, numerous fungal and bacterial diseases (**Table 5**) are of prime concern in sorghum-producing areas across the world. Attempts have been made to reduce pesticide use, develop stress-resistant varieties, enhance ecological fitness, and create

TABLE 5 | An overview of various diseases caused in sorghum following biotic stress.

Diseases	Causal organism	Major organs affected	Hotspot locations	References
Bacterial diseases				
Bacterial leaf streak	*Xanthomonas campestris* pv. Holcicola	Leaves	Wide geographical distribution	Wang et al., 2021
Bacterial leaf stripe	*Burkholderia andropogonis*	Leaves, flower buds, peduncles	Semi-arid and tropical regions	Mareya et al., 2020
Bacterial leaf spot	*Pseudomonas syringae*	Leaves	Argentina, Bulgaria, China, Hungary, India, Italy, Mexico, Africa, Rumania, Yugoslavia, Venezuela	Hernandez et al., 1992
Fungal diseases				
Anthracnose	*Colletotrichum sublineolum*	All above-ground parts	United States, India, Mexico, Nigeria	Abreha et al., 2021
Charcoal rot	*Macrophomina phaseolina* (Tassi) Goid	Root and stalk	India, Africa, Australia, United States	Mahmoud et al., 2018
Downy mildew	*Peronosclerospora sorghi*	Seedling and leaves	Africa, Asia, Mexico, America	Prom et al., 2015
Covered kernel smut	*Sporisorium sorghi*	Kernels	Ethiopia, Africa	Nigusie and Ademe, 2020
Head smut	*Sporisorium holci-sorghi*	Panicle	Africa, Europe, North and South America, Mexico, Asia, Australia, New Zealand	Wagari, 2019
Loose kernel smut	*Sporisorium cruentum*	Kernels and panicles	Egypt	Moharam, 2018
Rust	*Puccinia purpurea*	Leaves	Nigeria, India, Mexico, United States	Wang et al., 2014
Rough leaf spot	*Ascochyta sorghi*	Leaves	China	Xu et al., 2019
Leaf blight	*Helminthosporium turcicum*	Leaves	Mexico, Brazil, India, Sudan, Nigeria, Niger, Kenya, and Ethiopia	Das and Rajendrakumar, 2016
Ergot	*Claviceps sorghi*	Spikelets	Israel	Shimshoni et al., 2017
Pokkah Boeng (twisted top)	*Fusarium subglutinans*	Leaf and top	India	Das et al., 2019
Zonate leaf spot	*Gloeocercospora sorghi*	Leaves	China	Jiang et al., 2018
Sooty stripe	*Ramulispora sorghi*	Leaves	United States	Brady et al., 2011
Grain mold	*Aspergillus* sp., *Penicillium* sp.	Grains	Asia and Africa	Das et al., 2020
Target leaf spot	*Bipolaris sorghicola*	Leaves	United States, India, Japan	Kimball et al., 2019

a sustainable production system in order to enhance efficiency, grain quality, and profitability (Sharma, 1985; Kumar et al., 2014). None of these approaches have, however, been completely successful due to several reasons such as the production cost, lethal impacts of agrochemicals, emergence of resistance among pathogens toward one or multiple biocides/pesticides, and lack of genetic resistance to sorghum varieties. These factors have generated interest among sorghum growers in employing biotechnological options, including the use of inexpensive PSM in the management of sorghum phytopathogens (Khasa, 2017; Nepomuceno et al., 2019; Mitra et al., 2020). The application of PSM in the abatement of phytopathogens has certain advantages, such as (i) not causing environmental hazards; (ii) precluding residual toxicity; and (iii) blocking the emergence of resistance among pathogens attacking sorghum. PSM controls the pathogen damage by one or simultaneous mechanisms through biocide compounds and optimizes the yields (Zaidi et al., 2014; Choudhary et al., 2016). The literature on the role of PSM in the management of phytopathogens affecting sorghum is, however, without doubt, lacking.

Mechanism of Disease Suppression

The PSM controls the phytopathogens attack by synthesizing pivotal molecules like siderophores (Sarr et al., 2020), antibiotics (Raaijmakers and Mazzola, 2012), lytic enzymes (Herrera-Quiterio et al., 2020), cyanogenic compounds (Munir et al., 2019), and through induction of systemic resistance (ISR; Audenaert et al., 2002). Due to this, the soil PSM improves the growth and grain yield of sorghum by suppressing the damaging impact of biotic stresses. Below are some of the main mechanisms employed by PSM to manage phytopathogens and to boost sorghum yields.

Siderophores

Under iron-starved conditions, numerous PSMs, including bacteria, fungi, and actinomycetes, produce a wide range of siderophores (Maldonado et al., 2020; Aallam et al., 2021) with relatively low molecular weight (below ≈2 kDa) and ferric ion-specific chelating agents at neutral to alkaline pH to solubilize, capture, and transport inorganic iron to cell (Sandy and Butler, 2009). They are, therefore, exploited in the management of plant diseases (Verma et al., 2011; Jyothi et al., 2020). The siderophore positive rhizobacteria protect the plants from damages by preventing the iron acquisition (Estrella and Chet, 1998) and, hence, limiting the proliferation and root colonization by phytopathogens (O'sullivan and O'Gara, 1992).

Charcoal rot of sorghum caused by *Macrophomina phaseolina*, a soil-and seed-borne disease of sorghum, is endemic to tropical and temperate regions of the world (Kumar et al., 2016). Charcoal root causes considerable yield losses due to a lack of genetic-resistant sorghum varieties. Up to 64% yield losses are reported in India by this disease during the post-rainy season (Das et al., 2008). In order to control the attack of this phytopathogen (Gopalakrishnan et al., 2011), isolated siderophore-positive PSB, *Pseudomonas plecoglossicida*, *B. altitudinis*, *E. ludwigii*, *Acinetobacter tandoii*, and *P. monteilii* from the rhizospheres of a system of rice intensification (SRI) fields and tested their biocontrol activity against *M. phaseolina*. Interestingly, all PSB showed strong

antagonistic activity in dual culture assay, blotter paper assay, and *in vivo* greenhouse and inhibited the growth of *M. phaseolina*. No charcoal rot infection was observed in *P. plecoglossicida*-treated sorghum roots indicating the complete inhibition of pathogen whereas the roots treated with other isolates had 49–76% less charcoal rot infection compared to the control. All PSB increased root and shoot dry mass by 15–20% and 15–23% over control under greenhouse experiment. Also, all PSB adapted well to the sorghum rhizosphere as indicated by the reduction in charcoal rot disease. Similar antifungal activities (inhibition of growth, biomass, microsclerotia production, spore germination) of the secondary metabolites (antifungal volatile and siderophores) and the cell-free culture filtrates (CFCFs) of the selected fluorescent pseudomonad strains (SRB129, SRB288, and *Pseudomonas chlororaphis* SRB127) against the mycelial growth of *M. phaseolina* that varied from 30.5 to 76.5% in dual culture assay is reported (Das et al., 2008) The CFCF of the fluorescent pseudomonads @ 20% (v/v) significantly decreased the formation and germination of microsclerotia of *M. phaseolina*. Siderophore-positive bacterium *P. chlororaphis* (SRB127) controlled the charcoal rot of sorghum most efficiently under field conditions. As seed treatment, the bacterium reduced the charcoal rot incidence by >40% and crop-lodging by >20% and increased the sorghum grain mass. Under glasshouse conditions, the bacterium survived in the sorghum rhizosphere without any significant reduction in its population. Similarly, *Streptomyces* isolated from medicinal plant rhizosphere inhibited the fungal activity of phytopathogenic fungi *A. brassicicola*, *C. gloeosporioides*, *Fusarium oxysporum*, *P. digitatum*, and *S. rolfsii* through siderophores (Khamna et al., 2009). de Los Santos-Villalobos et al. (2012) reported the inhibition of *Colletotrichum* species (causing anthracnose in sorghum) due to the release of hydroxamate siderophore by *B. cepacia* in a Petri-dish bioassay test. Interestingly, even the lowest concentration ($0.64\,\mu g\,ml^{-1}$) of siderophore inhibited the pathogen by 91%. Other phytopathogenic fungi capable of inflicting damage to sorghum for example, grain mold diseases of sorghum (*Aspergillus* and *Penicillium*) has also been controlled by siderophore rich culture and free supernatant of *Alcaligenes* sp., and *P. aeruginosa* (Sayyed and Patel, 2011). The siderophore based biological control measures, therefore, be adopted in sorghum cultivation practices due to reasons, as they are (i) inexpensive and non-destructive (safer) for the environment; (ii) self-replicating and do not require repeat application; and (iii) there is no emergence of resistance among target organisms (Sayyed et al., 2004).

Growth Modulating Enzyme

Production of 1-aminocyclopropane-1-carboxylate (ACC) deaminase by PSM is considered yet another most powerful management biological weapon for plants growing under abiotic stress (Glick, 2014). After infection by phytopathogens, ethylene, a stress hormone is produced in all higher plants, which causes senescence, chlorosis, abscission, and wilting in plants, worsening the detrimental impact of pathogens (Dubois et al., 2018; Sharma et al., 2019; Etesami and Glick, 2020). The damaging impact of stress hormone can be annulled by the ACC deaminase, a multimeric enzyme, secreted by PSM bacteria (Zhao et al., 2021), fungi (Aban et al., 2017), and actinomycetes (Chukwuneme et al., 2020), which cleaves ACC (precursor of ethylene) to produce α-ketobutyrate and ammonia and thereby decreases the ethylene levels in host plants (Gupta and Pandey, 2019; Orozco-Mosqueda et al., 2021). The decrease in the levels of ACC and ethylene prevents the ethylene-mediated plant growth inhibition. PSM endowed with this capability can benefit the sorghum plants by reducing the stress and increasing plant growth (Santana et al., 2020). As an example, (Mareque et al., 2015) reported that the majority of the PSB, such as *Pantoea, Enterobacter, Serratia, Pseudomonas, Acinetobacter*, and *Stenotrophomonas* (Gammaproteobacteria phylum), *Achromobacter*, *Herbaspirillum*, and *Ralstonia* (Betaproteobacteria), *Rhizobium* (Alphaproteobacteria), *Chryseobacterium* (Bacterioidetes), *Bacillus, Staphylococcus*, *Brevibacillus,* and *Paenibacillus* (Firmicutes), and *Kocuria* (Actinobacteria), isolated from roots and stems of sweet sorghum plants exhibited ACC deaminase activity. Of these, ACC deaminase positive *Rhizobium* sp. UYSB13 and PSB bacterium *Pantoea* sp. UYSB45 showed a significant difference from the negative control in the stem height and dry weight (roots and shoots). Additionally, the ACC deaminase positive *Rhizobium* sp. UYSB12 and *Enterobacter* sp. UYSB34 significantly enhanced the root and the shoot dry weights of sweet sorghum.

Antimicrobials

The antibiotic-mediated inhibition of plant pathogens by rhizosphere-inhabiting biocontrol microorganisms is well (Babalola, 2010; Raaijmakers and Mazzola, 2012) are the most common and have been used in disease management through antibiotics, for example, the suppression of take all disease in wheat by 2,4-diacetylphloroglucinol (Weller et al., 2007). A variety of antibiotics have been identified: amphisin, 2,4-diacetylphloroglucinol (DAPG), oomycin A, phenazine, pyoluteorin, pyrrolnitrin, tensin, tropolone, and cyclic lipopeptides produced by pseudomonads (Raaijmakers and Mazzola, 2012; Saraf et al., 2014), and oligomycin A, kanosamine, zwittermicin A, and xanthobaccin produced by *Bacillus*, *Streptomyces*, and (Milner et al., 1996; Hashidoko et al., 1999; Mavrodi et al., 2012) diffusible products like 2, 4-diacetylphloroglucinol, phenazines, pyoluteorin, pyrrolnitrin, etc., or volatile compounds such as dimethyl disulfide, cyanogenic compounds, etc. (Olanrewaju and Babalola, 2019; Pandey and Gupta, 2020). One problem in depending too much on PSM-based antibiotics as biocontrol agents is, however, that with the increased use of PSM, phytopathogens may also develop resistance to microbe-mediated antibiotics in a manner similar to those exhibited for conventional antibiotics. This can though, be obviated by incorporating an HCN-positive PSM (Mahdi et al., 2020) with antibiotics producing PSM (Hamdali et al., 2008) so that the HCN-positive strain kills the pathogens while avoiding the emergence of antibiotic resistance among phytopathogens. The combination of HCN and antibiotics positive PSM looks a promising strategy that will synergistically control the phytopathogen attack.

Hydrolytic Enzymes

A number of hydrolytic enzymes, such as, cellulases, chitinase, β-1,3-glucanase, protease, lipase, and peroxidase, are released by the PSM (Liu et al., 2016; Nandimath et al., 2017). The cell wall of plant pathogenic fungi, for instance *F. oxysporum*, is mainly composed of β-1,3-glucan layers that are highly susceptible to lysis by β-1,3-glucanase. Following degradation, there occurs the leakage of inner cellular contents to the exterior environment and, finally, due to the osmotic imbalance, the pathogenic fungi collapses (Singh et al., 1999). For instance, some PSFs, such as *Acrocalymma* sp., *otryobambusa fusicoccum,* and *Phoma* sp., produce lytic enzymes such as chitinases and glucanases (Silveira et al., 2021) and catalase and cellulases (Amin et al., 2020), and many PS actinomycetes such as *S. fulvissimus*, *Streptoverticillium olivoverticillatum*, *S. nogalater*, *S. longisporoflavus,* and *S. cellulosae* produce cellulase, chitinase, pectinase, lipase, and amylase (Nandimath et al., 2017), which lyse the cell walls of pathogenic fungi attacking sorghum. Similarly, number of PSB belonging to the genera *Chrysobacterium, Bacillus, Pseudomonas, Mycobacterium, Staphylococcus, Curtobacterium, Enterobacter, Agrobacterium, Ochrobactrum, Serratia, Stenotrophomonas,* and *Acinetobacter* produced lytic enzymes, such as proteases, celluloses, lipases, esterases, and amylases, which exhibited activity against *Fusarium*, *Aspergillus*, and *Colletotrichum* (Herrera-Quiterio et al., 2020). In a similar study, phosphate solubilizing *B. subtilis* BN1 isolated from the chirpine (*Pinus roxburghii*) rhizosphere exhibited strong antagonistic activity resulting in vacuolation, hyphal squeezing, swelling, abnormal branching, and lysis of *M. phaseolina*, *F. oxysporum,* and *R. solani*. The inhibition of fungal growth by *B. subtilis* BN1 was attributed due to the secretion of lytic enzymes, chitinase, and β-1,3-glucanase, which degrades the hyphae and digest the fungal cell wall (Singh et al., 2008). The CFCF of BN1 also showed a strong but concentration-dependent antifungal activity and completely inhibited the fungal growth at 60% CFCF concentration. *Pseudomonas putida* in yet another experiment demonstrated antifungal activity against *A. alternata, F. oxysporum, and R. solani* through chitinase, β-1,3 glucanase, salicylic acid, siderophore, and HCN (Selvakumar et al., 2009). The PS bacterium *Serratia marcescens* inhibited the growth of *Sclerotium rolfsii* (Ordentlich et al., 1988) while *Paenibacillus* sp. strain 300 and actinomycetes *Streptomyces* sp. strain 385 suppressed *F. oxysporum* fsp. *Cucumerinum*. Extracellular chitinase and laminarinase synthesized by *Pseudomonas stutzeri* degraded the mycelia of *F. solani* (Lim et al., 1991). These and other related studies that are not included in this review suggests that, in the absence of high level of genetic resistance in high-yielding sorghum varieties, the PSM as bio-antagonists could safely be used to effectively manage the biotic stresses of sorghum and hence to reduce losses in yield and quality of sorghum cultivated in different regions of the world.

CONCLUSION

The unwarranted and imprudent application of agrochemicals in sorghum cultivation practices and their hazardous impact on the soil environment warrants the use of a low-cost and environmentally friendly P-solubilizing microbiome as a prospective alternative to P fertilizers and pesticides. Due to the exorbitant cost of chemical fertilizers, harmful impact of pesticides, and lack of high level of genetic resistance, the novel PSM discovered so far and discussed herein applied either alone or in synergism with compatible organisms can be a useful component in the management of P fertilization, yield optimization, and integrated sorghum disease management. The application of PSM-based (microphos) formulations in sorghum cultivation is likely to provide economic benefit to sorghum growers while reducing the risk of environmental pollution.

Future Prospects

The studies surveyed and presented herein are though directly relevant to improving food production, deciphering the detailed molecular and ecological relationships between PSM, N_2 fixers, and AM-fungi is indispensable to developing a better understanding of the synergistic relationship between three functionally divergent groups of the soil microbiome. Also, the rhizosphere competence and colonization effect of different PSM strains and their interaction with functionally unrelated plant beneficial bacteria should further be investigated under complex and variable natural conditions with the aim of producing "microphos: PSM based biofertilizer" to alleviate the biotic stresses and consequently augmenting sweet sorghum production in different agroecosystems. Continued research is, however, needed to develop novel strategies to ameliorate the yield and upgrade the efficiency of PSM to manage the attack of phytopathogens causing huge losses to sweet sorghum in variable agroclimatic conditions. To achieve this, scientists, institutions, and manufacturers need to work together to find solutions to nutrition and disease management and to optimize sorghum yield to eradicate hunger worldwide.

AUTHOR CONTRIBUTIONS

All authors listed have made substantial, direct and intellectual contributions to the work, and approved it for publication.

FUNDING

This work was supported by the Priority Research Centers Program through the National Research Foundation of Korea (NRF) funded by the Ministry of Education (2014R1A6A1031189) to JL and also supported by the NRF grant funded by the Korean government (MSIT; 2021R1G1A1094698) to BA.

ACKNOWLEDGMENTS

One of the authors, AR, is thankful to DST-SERB for National Post-doctoral Fellowship (PDF/2020/000127).

REFERENCES

Aallam, Y., Dhiba, D., Lemriss, S., Souiri, A., Karray, F., El Rasafi, T., et al. (2021). Solation and characterization of phosphate solubilizing *Streptomyces* sp. endemic from sugar beet fields of the Beni-Mellal region in Morocco. *Microorganisms* 9:914. doi: 10.3390/microorganisms9050914

Aban, J. L., Barcelo, R. C., Oda, E. E., Reyes, G. A., Balangcod, T. D., Gutierrez, R. M., et al. (2017). Auxin production, phosphate solubilisation and ACC deaminase activity of root symbiotic fungi (RSF) from *Drynaria quercifolia* L. *Bull. Environ. Pharmacol. Life Sci.* 6, 26–31.

Abawari, R. A., Tuji, F. A., and Yadete, D. M. (2020). Phosphate solubilizing bio-fertilizers and their role in bio-available P nutrient: an overview. *Int. J. Appl. Agric. Sci.* 6, 162–171. doi: 10.11648/j.ijaas.20200606.11

Abreha, K. B., Ortiz, R., Carlsson, A. S., and Geleta, M. (2021). Understanding the sorghum–*Colletotrichum sublineola* interactions for enhanced host resistance. *Front. Plant Sci.* 12:641969. doi: 10.3389/fpls.2021.641969

Adesemoye, A. O., and Kloepper, J. W. (2009). Plant–microbes interactions in enhanced fertilizer-use efficiency. *Appl. Microbiol. Biotechnol.* 85, 1–12. doi: 10.1007/s00253-009-2196-0

Afifi, M. M. I., El-Sayed, G. A. M., Manal, A., El-Gamal, H., and Massoud, O. N. (2014). Synergistic effect of biofertilizers containing N-fixer, P and K solubilizers and humic substances on Sorghum bicolor productivity. *Middle East J. Appl. Sci.* 4, 1065–1074.

Ahmed, B., Zaidi, A., Khan, M. S., Rizvi, A., Saif, S., and Shahid, M. (2017). "Perspectives of plant growth promoting rhizobacteria in growth enhancement and sustainable production of tomato," in *Microbial Strategies for Vegetable Production*. eds. A. Zaidi and M. Khan (Cham, Switzerland: Springer), 125–149.

Akinrinlola, R. J., Yuen, G. Y., Drijber, R. A., and Adesemoye, A. O. (2018). Evaluation of *bacillus* strains for plant growth promotion and predictability of efficacy by *in vitro* physiological traits. *Int. J. Microbiol.* 2018, 1–11. doi: 10.1155/2018/5686874

Alagawadi, A. R., and Gaur, A. C. (1988). Interaction between *Azospirillum brasilense* and phosphate solubilizing bacteria'and their influence on yield and nutrient uptake of sorghum (*Sorghum bicolor* L.). *Zentralbl. Mikrobiol.* 143, 637–643. doi: 10.1016/S0232-4393(88)80090-8

Alagawadi, A. R., and Gaur, A. C. (1992). Inoculation of *Azospirillum brasilense* and phosphate-solubilizing bacteria on yield of sorghum [*Sorghum bicolor* (L.) Moench] in dry land. *Trop. Agric.* 69, 347–350.

Alekhya, G., and Gopalakrishnan, S. (2016). Plant growth-promotion by *Streptomyces* spp. in sorghum (*Sorghum bicolor* L.). *Afr. J. Biotechnol.* 15, 1781–1788. doi: 10.5897/AJB2016.15423

Ali, S., Khan, S. A., Hamayun, M., Iqbal, A., Khan, A. L., Hussain, A., et al. (2019). Endophytic fungi from *Caralluma acutangula* can secrete plant growth promoting enzymes. *Fresenius Environ. Bull.* 28, 2688–2696.

Almodares, A., and Hadi, M. R. (2009). Production of bioethanol from sweet sorghum: a review. *Afr. J. Agric. Res.* 4, 772–780.

Alori, E. T., Glick, B. R., and Babalola, O. O. (2017). Microbial phosphorus solubilization and its potential for use in sustainable agriculture. *Front. Microbiol.* 8:971. doi: 10.3389/fmicb.2017.00971

Amin, B. A. Z., Farhan, H., Hina, A., Muhammad, A., Akhtar, I., Usman, I., et al. (2020). Characterization and cellulolytic enzyme potential of P solubilizers from pine forests of lower Himalaya. *Int. J. Agric. Biol.* 24, 1242–1250.

Asea, P. E. A., Kucey, R. M. N., and Stewart, J. W. B. (1988). Inorganic phosphate solubilization by two *Penicillium* species in solution culture and soil. *Soil Biol. Biochem.* 20, 459–464. doi: 10.1016/0038-0717(88)90058-2

Asuming-Brempong, S., and Anipa, B. (2014). The use of rock phosphate and phosphate solubilising fungi (*aspergillus Niger*) to improve the growth and the yield of upland rice on typic kandiudalf. *West Afr J. App. Ecol.* 22, 27–39.

Audenaert, K., Pattery, T., Cornelis, P., and Höfte, M. (2002). Induction of systemic resistance to *Botrytis cinerea* in tomato by *Pseudomonas aeruginosa* 7NSK2: role of salicylic acid, pyochelin, and pyocyanin. *Mol. Plant-Microbe Interact.* 15, 1147–1156. doi: 10.1094/MPMI.2002.15.11.1147

Awika, J. M., and Rooney, L. W. (2004). Sorghum phytochemicals and their potential impact on human health. *Phytochemistry* 65, 1199–1221. doi: 10.1016/j.phytochem.2004.04.001

Ayyaz, K., Zaheer, A., Rasul, G., and Mirza, M. S. (2016). Isolation and identification by 16S rRNA sequence analysis of plant growth-promoting azospirilla from the rhizosphere of wheat. *Braz. J. Microbiol.* 47, 542–550. doi: 10.1016/j.bjm.2015.11.035

Aziz, T., Sabir, M., Farooq, M., Maqsood, M. A., Ahmad, H. R., and Warraich, E. A. (2014). "Phosphorus deficiency in plants: responses, adaptive mechanisms, and signaling," in *Plant Signaling: Understanding the Molecular Crosstalk*. eds. K. Hakeem, R. Rehman and I. Tahir (Switzerland: Springer Nature), 133–148.

Babalola, O. O. (2010). Beneficial bacteria of agricultural importance. *Biotechnol. Lett.* 32, 1559–1570. doi: 10.1007/s10529-010-0347-0

Barcelos, C. A., Maeda, R. N., Santa Anna, L. M. M., and Pereira, N. Jr. (2016). Sweet sorghum as a whole-crop feedstock for ethanol production. *Biomass Bioenergy* 94, 46–56. doi: 10.1016/j.biombioe.2016.08.012

Batool, S., and Iqbal, A. (2019). Phosphate solubilizing rhizobacteria as alternative of chemical fertilizer for growth and yield of *Triticum aestivum* (Var. galaxy 2013). *Saudi J. Biol. Sci.* 26, 1400–1410. doi: 10.1016/j.sjbs.2018.05.024

Bechtaoui, N., Raklami, A., Tahiri, A.-I., Benidire, L., El Alaoui, A., Meddich, A., et al. (2019). Characterization of plant growth promoting rhizobacteria and their benefits on growth and phosphate nutrition of faba bean and wheat. *Biol. Open* 8:bio043968. doi: 10.1242/bio.043968

Behera, B. C., Yadav, H., Singh, S. K., Mishra, R. R., Sethi, B. K., Dutta, S. K., et al. (2017). Phosphate solubilization and acid phosphatase activity of *Serratia* sp. isolated from mangrove soil of Mahanadi river delta, Odisha, India. *J. Genet. Eng. Biotechnol.* 15, 169–178. doi: 10.1016/j.jgeb.2017.01.003

Bhardwaj, D., Ansari, M. W., Sahoo, R. K., and Tuteja, N. (2014). Biofertilizers function as key player in sustainable agriculture by improving soil fertility, plant tolerance and crop productivity. *Microb. Cell Factories* 13:66. doi: 10.1186/1475-2859-13-66

Bjelić, D., Marinković, J., Tintor, B., Tančić, S., Nastasić, A., and Mrkovački, N. (2015). Screening of Azotobacter isolates for PGP properties and antifungal activity. *Zb. Matice Srp. Prir. Nauk.* 65–72. doi: 10.2298/ZMSPN1529065B

Boubekri, K., Soumare, A., Mardad, I., Lyamlouli, K., Hafidi, M., Ouhdouch, Y., et al. (2021). The screening of potassium-and phosphate-solubilizing actinobacteria and the assessment of their ability to promote wheat growth parameters. *Microorganisms* 9:470. doi: 10.3390/microorganisms9030470

Brady, C. R., Noll, L. W., Saleh, A. A., and Little, C. R. (2011). Disease severity and microsclerotium properties of the sorghum sooty stripe pathogen, *Ramulispora sorghi*. *Plant Dis.* 95, 853–859. doi: 10.1094/PDIS-10-10-0742

Chaiharn, M., Pathom-Aree, W., Sujada, N., and Lumyong, S. (2018). Characterization of phosphate solubilizing *Streptomyces* as a biofertilizer. *Chiang Mai J. Sci.* 45, 701–716.

Chawngthu, L., Hnamte, R., and Lalfakzuala, R. (2020). Isolation and characterization of rhizospheric phosphate solubilizing bacteria from wetland paddy field of Mizoram, India. *Geomicrobiol J.* 37, 366–375. doi: 10.1080/01490451.2019.1709108

Chen, Q., and Liu, S. (2019). Identification and characterization of the phosphate-solubilizing bacterium *Pantoea* sp. S32 in reclamation soil in Shanxi, China. *Front. Microbiol.* 10:2171. doi: 10.3389/fmicb.2019.02171

Chen, J., Zhao, G., Wei, Y., Dong, Y., Hou, L., and Jiao, R. (2021). Isolation and screening of multifunctional phosphate solubilizing bacteria and its growth-promoting effect on Chinese fir seedlings. *Sci. Rep.* 11:9081. doi: 10.1038/s41598-021-88635-4

Choudhary, D. K., Kasotia, A., Jain, S., Vaishnav, A., Kumari, S., Sharma, K. P., et al. (2016). Bacterial-mediated tolerance and resistance to plants under abiotic and biotic stresses. *J. Plant Growth Regul.* 35, 276–300. doi: 10.1007/s00344-015-9521-x

Chouyia, F. E., Romano, I., Fechtali, T., Fagnano, M., Fiorentino, N., Visconti, D., et al. (2020). P-solubilizing *Streptomyces roseocinereus* MS1B15 with multiple plant growth-promoting traits enhance barley development and regulate rhizosphere microbial population. *Front. Plant Sci.* 11:1137. doi: 10.3389/fpls.2020.01137

Chu, H., Lin, X., Fujii, T., Morimoto, S., Yagi, K., Hu, J., et al. (2007). Soil microbial biomass, dehydrogenase activity, bacterial community structure in response to long-term fertilizer management. *Soil Biol. Biochem.* 39, 2971–2976. doi: 10.1016/j.soilbio.2007.05.031

Chukwuneme, C. F., Babalola, O. O., Kutu, F. R., and Ojuederie, O. B. (2020). Characterization of actinomycetes isolates for plant growth promoting traits and their effects on drought tolerance in maize. *J. Plant Interact.* 15, 93–105. doi: 10.1080/17429145.2020.1752833

Cobb, A. B., Wilson, G. W. T., Goad, C. L., Bean, S. R., Kaufman, R. C., Herald, T. J., et al. (2016). The role of arbuscular mycorrhizal fungi in grain production and nutrition of sorghum genotypes: enhancing sustainability through plant-microbial partnership. *Agric. Ecosyst. Environ.* 233, 432–440. doi: 10.1016/j.agee.2016.09.024

Danish, S., Zafar-ul-Hye, M., Mohsin, F., and Hussain, M. (2020). ACC-deaminase producing plant growth promoting rhizobacteria and biochar mitigate adverse effects of drought stress on maize growth. *PLoS One* 15:e0230615. doi: 10.1371/journal.pone.0230615

Dar, R. A., Dar, E. A., Kaur, A., and Phutela, U. G. (2018). Sweet sorghum-a promising alternative feedstock for biofuel production. *Renew. Sust. Energ. Rev.* 82, 4070–4090. doi: 10.1016/j.rser.2017.10.066

Das, I. K., Aruna, C., and Tonapi, V. A. (2020). *Sorghum Grain Mold*. Hyderabad, India: ICAR-Indian Institute of Millets Research, 1–86.

Das, I. K., Indira, S., Annapurna, A., and Seetharama, N. (2008). Biocontrol of charcoal rot in sorghum by fluorescent pseudomonads associated with the rhizosphere. *Crop Prot.* 27, 1407–1414. doi: 10.1016/j.cropro.2008.07.001

Das, I. K., Kumar, S., Kannababu, N., and Tonapi, V. A. (2019). Pokkah boeng resistance in popular rabi sorghum cultivars and effects of the disease on leaf chlorophyll. *Indian Phytopathol.* 72, 421–426. doi: 10.1007/s42360-019-00146-5

Das, I. K., and Rajendrakumar, P. (2016). "Disease resistance in sorghum," in *Biotic Stress Resistance in Millets*. eds. I. K. Das and P. G. Padmaja (Amsterdam, The Netherlands: Elsevier), 23–67.

de Los Santos-Villalobos, S., Barrera-Galicia, G. C., Miranda-Salcedo, M. A., and Peña-Cabriales, J. J. (2012). *Burkholderia cepacia* XXVI siderophore with biocontrol capacity against *Colletotrichum gloeosporioides*. *World J. Microbiol. Biotechnol.* 28, 2615–2623. doi: 10.1007/s11274-012-1071-9

de Sousa, S. M., de Oliveira, C. A., Andrade, D. L., de Carvalho, C. G., Ribeiro, V. P., Pastina, M. M., et al. (2021). Tropical *bacillus* strains inoculation enhances maize root surface area, dry weight, nutrient uptake and grain yield. *J. Plant Growth Regul.* 40, 867–877. doi: 10.1007/s00344-020-10146-9

Díaz-Rodríguez, A. M., Gastelum, L. A. S., Pablos, C. M. F., Parra-Cota, F. I., Santoyo, G., Puente, M. L., et al. (2020). The current and future role of microbial culture collections in food security worldwide. *Front. Sustain. Food Syst.* 4:614739. doi: 10.3389/fsufs.2020.614739

Dicko, M. H., Gruppen, H., Traoré, A. S., Voragen, A. G. J., and Van Berkel, W. J. H. (2006). Sorghum grain as human food in Africa: relevance of content of starch and amylase activities. *Afr. J. Biotechnol.* 5, 384–395.

Dierks, J., Blaser-Hart, W. J., Gamper, H. A., Nyoka, I. B., Barrios, E., and Six, J. (2021). Trees enhance abundance of arbuscular mycorrhizal fungi, soil structure, and nutrient retention in low-input maize cropping systems. *Agric. Ecosyst. Environ.* 318:107487. doi: 10.1016/j.agee.2021.107487

Din, M., Nelofer, R., Salman, M., Khan, F. H., Khan, A., Ahmad, M., et al. (2019). Production of nitrogen fixing Azotobacter (SR-4) and phosphorus solubilizing *aspergillus Niger* and their evaluation on *Lagenaria siceraria* and *Abelmoschus esculentus*. *Biotechnol. Rep.* 22:e00323. doi: 10.1016/j.btre.2019.e00323

Doilom, M., Guo, J.-W., Phookamsak, R., Mortimer, P. E., Karunarathna, S. C., Dong, W., et al. (2020). Screening of phosphate-solubilizing fungi from air and soil in Yunnan, China: four novel species in *Aspergillus, Gongronella, Penicillium,* and *Talaromyces*. *Front. Microbiol.* 11:585215. doi: 10.3389/fmicb.2020.585215

dos Santos, C. L. R., Alves, G. C., de Matos Macedo, A. V., Giori, F. G., Pereira, W., Urquiaga, S., et al. (2017). Contribution of a mixed inoculant containing strains of *Burkholderia* spp. and *Herbaspirillum* sp. to the growth of three sorghum genotypes under increased nitrogen fertilization levels. *Appl. Soil Ecol.* 113, 96–106. doi: 10.1016/j.apsoil.2017.02.008

Dubois, M., Van den Broeck, L., and Inzé, D. (2018). The pivotal role of ethylene in plant growth. *Trends Plant Sci.* 23, 311–323. doi: 10.1016/j.tplants.2018.01.003

Ehteshami, S. M. R., Abbasi, M. R., Khavazi, K., and And Zand, B. (2014). Effect of phosphate solubilizing bacteria strains (*Pseudomonas putida*) on forage quality and quantity of sorghum cultivars in Varamin. *J. Plant Proc. Function* 2, 1–11.

El-Badry, M. A., Elbarbary, T. A., Ibrahim, I. A., and Abdel-Fatah, Y. M. (2016). *Azotobacter vinelandii* evaluation and optimization of Abu Tartur Egyptian phosphate ore dissolution. *Saudi J. Pathol. Microbiol* 1, 80–93.

El-Dsouky, M. M., Mohamed, H. M., El-Rewainy, H. M., and Farid, A.-S. M. (2019). Effect of inoculation with phosphate solubilizing actinomycete isolates on phosphorous uptake and growth of wheat grown in calcareous sandy soil. *Assiut J. Agric. Sci.* 50, 307–315. doi: 10.21608/ajas.2019.41287

Elfiati, D., Delvian, D., Hanum, H., Susilowati, A., and Rachmat, H. H. (2021). Potential of phosphate solubilizing fungi isolated from peat soils as inoculant biofertilizer. *Biodiversitas J. Biol. Divers.* 22, 3042–3048. doi: 10.13057/biodiv/d220605

Elhaissoufi, W., Khourchi, S., Ibnyasser, A., Ghoulam, C., Rchiad, Z., Zeroual, Y., et al. (2020). Phosphate solubilizing rhizobacteria could have a stronger influence on wheat root traits and aboveground physiology than rhizosphere P solubilization. *Front. Plant Sci.* 11:979. doi: 10.3389/fpls.2020.00979

Estrella, A. H., and Chet, I. (1998). Biocontrol of bacteria and phytopathogenic fungi. *Agric. Biotechnol.* 263–282.

Etesami, H., and Glick, B. R. (2020). Halotolerant plant growth–promoting bacteria: prospects for alleviating salinity stress in plants. *Environ. Exp. Bot.* 178:104124. doi: 10.1016/j.envexpbot.2020.104124

Farhat, M. B., Boukhris, I., and Chouayekh, H. (2015). Mineral phosphate solubilization by *Streptomyces* sp. CTM396 involves the excretion of gluconic acid and is stimulated by humic acids. *FEMS Microbiol. Lett.* 362:fnv008. doi: 10.1093/femsle/fnv008

García-Fraile, P., Menéndez, E., and Rivas, R. (2015). Role of bacterial biofertilizers in agriculture and forestry. *AIMS Bioeng.* 2, 183–205. doi: 10.3934/bioeng.2015.3.183

Garnett, T., Conn, V., and Kaiser, B. N. (2009). Root based approaches to improving nitrogen use efficiency in plants. *Plant Cell Environ.* 32, 1272–1283. doi: 10.1111/j.1365-3040.2009.02011.x

Gemenet, D. C., Leiser, W. L., Beggi, F., Herrmann, L. H., Vadez, V., Rattunde, H. F. W., et al. (2016). Overcoming phosphorus deficiency in west African pearl millet and sorghum production systems: promising options for crop improvement. *Front. Plant Sci.* 7:1389. doi: 10.3389/fpls.2016.01389

Gheliya, K. P., Bhalu, V. B., Mathukia, R. K., Hadavani, J. K., and Kamani, M. D. (2018). Effect of phosphate and potash solubilizing bacteria on growth and yield of popcorn (*Zea mays* L. var. *Everta*). *Int. J. Pure Appl. Biosci.* 6, 167–174. doi: 10.18782/2320-7051.6918

Glick, B. R. (2014). Bacteria with ACC deaminase can promote plant growth and help to feed the world. *Microbiol. Res.* 169, 30–39. doi: 10.1016/j.micres.2013.09.009

Goldstein, A. H., Rogers, R. D., and Mead, G. (1993). Mining by microbe. *Bio/Technology* 11, 1250–1254.

Gopalakrishnan, S., Humayun, P., Kiran, B. K., Kannan, I. G. K., Vidya, M. S., Deepthi, K., et al. (2011). Evaluation of bacteria isolated from rice rhizosphere for biological control of charcoal rot of sorghum caused by *Macrophomina phaseolina* (Tassi) Goid. *World J. Microbiol. Biotechnol.* 27, 1313–1321. doi: 10.1007/s11274-010-0579-0

Gopalakrishnan, S., Srinivas, V., Prakash, B., Sathya, A., and Vijayabharathi, R. (2015). Plant growth-promoting traits of *Pseudomonas geniculata* isolated from chickpea nodules. *3 Biotech* 5, 653–661. doi: 10.1007/s13205-014-0263-4

Gupta, S., and Pandey, S. (2019). ACC deaminase producing bacteria with multifarious plant growth promoting traits alleviates salinity stress in French bean (*Phaseolus vulgaris*) plants. *Front. Microbiol.* 10:1506. doi: 10.3389/fmicb.2019.01506

Gurdeep, K., and Reddy, M. S. (2015). Effects of phosphate-solubilizing bacteria, rock phosphate and chemical fertilizers on maize-wheat cropping cycle and economics. *Pedosphere* 25, 428–437. doi: 10.1016/S1002-0160(15)30010-2

Hamane, S., Zerrouk, M. H., Lyemlahi, A. E., Aarab, S., Laglaoui, A., Bakkali, M., et al. (2020). "Screening and characterization of phosphate-solubilizing rhizobia," in *Phyto-Microbiome in Stress Regulation*. eds. M. Kumar, V. Kumar and R. Prasad (Switzerland: Springer Nature), 113–124.

Hamdali, H., Hafidi, M., Virolle, M. J., and Ouhdouch, Y. (2008). Growth promotion and protection against damping-off of wheat by two rock phosphate solubilizing actinomycetes in a P-deficient soil under greenhouse conditions. *Appl. Soil Ecol.* 40, 510–517. doi: 10.1016/j.apsoil.2008.08.001

Hameeda, B., Harini, G., Rupela, O. P., Wani, S. P., and Reddy, G. (2008). Growth promotion of maize by phosphate-solubilizing bacteria isolated from composts and macrofauna. *Microbiol. Res.* 163, 234–242. doi: 10.1016/j.micres.2006.05.009

Harinathan, B., Sankaralingam, S., Palpperumal, S., Kathiresan, D., Shankar, T., and Prabhu, D. (2016). Effect of phosphate solubilizing bacteria on growth

and development of pearl millet and ragi. *J. Adv. Biol. Biotechnol.* 7, 1–7. doi: 10.9734/JABB/2016/26290

Hashidoko, Y., Nakayama, T., Homma, Y., and Tahara, S. (1999). Structure elucidation of xanthobaccin A, a new antibiotic produced from *Stenotrophomonas* sp. strain SB-K88. *Tetrahedron Lett.* 40, 2957–2960. doi: 10.1016/S0040-4039(99)00336-6

Hasibuan, S., and Nazir, N. (2017). The development strategy of sustainable bioethanol industry on iconic Sumba island, eastern Indonesia. *Int. J. Adv. Sci. Eng. Inf. Technol.* 7, 276–283. doi: 10.18517/ijaseit.7.1.1796

Hernandez, J., Garrido, M. J., Lopez, O., and Trujillo, G. E. (1992). The bacterial leaf spot of sorghum caused by *pseudomonas syringae* pv. Syringae in Venezuela. *Fitopatol Venez* 5, 39–42.

Herrera-Quiterio, A., Toledo-Hernández, E., Aguirre-Noyola, J. L., Romero, Y., Ramos, J., Palemón-Alberto, F., et al. (2020). Antagonic and plant growth-promoting effects of bacteria isolated from mine tailings at El Fraile, Mexico. *Rev. Argent. Microbiol.* 52, 231–239. doi: 10.1016/j.ram.2019.08.003

Hussein, K. A., and Joo, J. H. (2015). Isolation and characterization of rhizomicrobial isolates for phosphate solubilization and indole acetic acid production. *J. Korean Soc. Appl. Biol. Chem.* 58, 847–855. doi: 10.1007/s13765-015-0114-y

Jiang, Y., Xu, J., Hu, L., Liu, K.-J., Xu, X.-D., Liu, Z., et al. (2018). First report of sorghum zonate leaf spot caused by *Gloeocercospora sorghi* in China. *Plant Dis.* 102:1033. doi: 10.1094/PDIS-08-17-1217-PDN

Jisha, M. S., and Alagawadi, A. R. (1996). Nutrient uptake and yield of sorghum (*Sorghum bicolor* L. Moench) inoculated with phosphate solubilizing bacteria and cellulolytic fungus in a cotton stalk amended vertisol. *Microbiol. Res.* 151, 213–217. doi: 10.1016/S0944-5013(96)80046-2

Johansson, J. F., Paul, L. R., and Finlay, R. D. (2004). Microbial interactions in the mycorrhizosphere and their significance for sustainable agriculture. *FEMS Microbiol. Ecol.* 48, 1–13. doi: 10.1016/j.femsec.2003.11.012

Jyothi, V., Sowmya, H. V., and Thippeswamy, B. (2020). Siderophore production by phosphate solubilizing fungi from rhizospheric soil of medicinal plants. *Int. J. Biol. Biotechnol.* 17, 599–606.

Kalam, S., Basu, A., and Podile, A. R. (2020). Functional and molecular characterization of plant growth promoting bacillus isolates from tomato rhizosphere. *Heliyon* 6:e04734. doi: 10.1016/j.heliyon.2020.e04734

Kalayu, G. (2019). Phosphate solubilizing microorganisms: promising approach as biofertilizers. *Int. J. Agron.* 2019:4917256. doi: 10.1155/2019/4917256

Kamali, S., and Mehraban, A. (2020). Effects of Nitroxin and arbuscular mycorrhizal fungi on the agro-physiological traits and grain yield of sorghum (Sorghum bicolor L.) under drought stress conditions. *PLoS One* 15:e0243824. doi: 10.1371/journal.pone.0243824

Kang, J., Amoozegar, A., Hesterberg, D., and Osmond, D. L. (2011). Phosphorus leaching in a sandy soil as affected by organic and inorganic fertilizer sources. *Geoderma* 161, 194–201. doi: 10.1016/j.geoderma.2010.12.019

Kang, S.-M., Hamayun, M., Khan, M. A., Iqbal, A., and Lee, I.-J. (2019). *Bacillus subtilis* JW1 enhances plant growth and nutrient uptake of Chinese cabbage through gibberellins secretion. *J. Appl. Bot. Food Qual.* 92, 172–178. doi: 10.5073/JABFQ.2019.092.023

Keller-Pearson, M., Liu, Y., Peterson, A., Pederson, K., Willems, L., Ane, J.-M., et al. (2020). Inoculation with arbuscular mycorrhizal fungi has a more significant positive impact on the growth of open-pollinated heirloom varieties of carrots than on hybrid cultivars under organic management conditions. *Agric. Ecosyst. Environ.* 289:106712. doi: 10.1016/j.agee.2019.106712

Khamna, S., Yokota, A., and Lumyong, S. (2009). Actinomycetes isolated from medicinal plant rhizosphere soils: diversity and screening of antifungal compounds, indole-3-acetic acid and siderophore production. *World J. Microbiol. Biotechnol.* 25, 649–655. doi: 10.1007/s11274-008-9933-x

Khan, M. S., Zaidi, A., and Ahmad, E. (2014). "Mechanism of phosphate solubilization and physiological functions of phosphate-solubilizing microorganisms," in *Phosphate Solubilizing Microorganisms*. eds. M. Khan, A. Zaidi and J. Musarrat (Switzerland: Springer International Publishing), 31–62.

Khasa, Y. P. (2017). "Microbes as biocontrol agents," in *Probiotics and Plant Health*. eds. V. Kumar, M. Kumar, S. Sharma and R. Prasad (Switzerland: Springer), 507–552.

Khatoon, Z., Huang, S., Rafique, M., Fakhar, A., Kamran, M. A., and Santoyo, G. (2020). Unlocking the potential of plant growth-promoting rhizobacteria on soil health and the sustainability of agricultural systems. *J. Environ. Manag.* 273:111118. doi: 10.1016/j.jenvman.2020.111118

Kimball, J., Cui, Y., Chen, D., Brown, P., Rooney, W. L., Stacey, G., et al. (2019). Identification of QTL for target leaf spot resistance in *Sorghum bicolor* and investigation of relationships between disease resistance and variation in the MAMP response. *Sci. Rep.* 9:18285. doi: 10.1038/s41598-019-54802-x

Kouas, S., Labidi, N., Debez, A., and Abdelly, C. (2005). Effect of P on nodule formation and N fixation in bean. *Agron. Sustain. Dev.* 25, 389–393. doi: 10.1051/agro:2005034

Kuan, K. B., Othman, R., Abdul Rahim, K., and Shamsuddin, Z. H. (2016). Plant growth-promoting rhizobacteria inoculation to enhance vegetative growth, nitrogen fixation and nitrogen remobilisation of maize under greenhouse conditions. *PLoS One* 11:e0152478. doi: 10.1371/journal.pone.0152478

Kulamarva, A. G., Sosle, V. R., and Raghavan, G. S. V. (2009). Nutritional and rheological properties of sorghum. *Int. J. Food Prop.* 12, 55–69. doi: 10.1080/10942910802252148

Kumar, P., Aeron, A., Shaw, N., Singh, A., Bajpai, V. K., Pant, S., et al. (2020). Seed bio-priming with tri-species consortia of phosphate solubilizing rhizobacteria (PSR) and its effect on plant growth promotion. *Heliyon* 6:e05701. doi: 10.1016/j.heliyon.2020.e05701

Kumar, A. A., Gorthy, S., Sharma, H. C., Huang, Y., Sharma, R., and Reddy, B. V. S. (2014). "Understanding genetic control of biotic stress resistance in sorghum for applied breeding," in *Genetics, Genomics and Breeding of Sorghum*. Florida, USA: CRC Press, 220–247.

Kumar, P., Gupta, V., Tiwari, A., and Kamle, M. (2016). "*Macrophomina phaseolina*: the most destructive soybean fungal pathogen of global concern," in *Current Trends in Plant Disease Diagnostics and Management Practices, Fungal Biology*. Switzerland: Springer Nature, 1–11.

Kumar, A. P. K., McKeown, P. C., Boualem, A., Ryder, P., Brychkova, G., Bendahmane, A., et al. (2017a). TILLING by sequencing (TbyS) for targeted genome mutagenesis in crops. *Mol. Breeding* 37:14. doi: 10.1007/s11032-017-0620-1

Kumar, G. K., and Ram, M. R. (2014). Phosphate solubilizing rhizobia isolated from *Vigna trilobata*. *Am. J. Microbiol. Res.* 2, 105–109. doi: 10.12691/ajmr-2-3-4

Kumar, S. V., Sajeevkumar, V. A., George, J., and Kumar, S. (2017b). Enhancing properties of polyvinyl alcohol film using sorghum starch nanocrystals. *Defence Life Sci. J.* 2, 169–177. doi: 10.14429/dlsj.2.11380

Lebrazi, S., Niehaus, K., Bednarz, H., Fadil, M., Chraibi, M., and Fikri-Benbrahim, K. (2020). Screening and optimization of indole-3-acetic acid production and phosphate solubilization by rhizobacterial strains isolated from *Acacia cyanophylla* root nodules and their effects on its plant growth. *J. Genet. Eng. Biotechnol.* 18:71. doi: 10.1186/s43141-020-00090-2

Léder, I. (2004). Sorghum and millets. Cultivated Plants, primarily as food sources. *EOLSS* 1, 66–84.

Li, Z., Bai, T., Dai, L., Wang, F., Tao, J., Meng, S., et al. (2016). A study of organic acid production in contrasts between two phosphate solubilizing fungi: *Penicillium oxalicum* and *aspergillus Niger*. *Sci. Rep.* 6:25313. doi: 10.1038/srep25313

Li, Y., Wang, C., Wang, T., Liu, Y., Jia, S., Gao, Y., et al. (2020). Effects of different fertilizer treatments on rhizosphere soil microbiome composition and functions. *Land* 9:329. doi: 10.3390/land9090329

Lim, H.-S., Kim, Y.-S., and Kim, S.-D. (1991). Pseudomonas stutzeri YPL-1 genetic transformation and antifungal mechanism against *Fusarium solani*, an agent of plant root rot. *Appl. Environ. Microbiol.* 57, 510–516. doi: 10.1128/aem.57.2.510-516.1991

Liu, G., Deng, L., Wu, R., Guo, S., Du, W., Yang, M., et al. (2020). Determination of nitrogen and phosphorus fertilisation rates for tobacco based on economic response and nutrient concentrations in local stream water. *Agric. Ecosyst. Environ.* 304:107136. doi: 10.1016/j.agee.2020.107136

Liu, G., Han, Y., Jiang, Y., Wang, Y., Lv, P., and Li, H. (2016). "Genomics approaches to biotic stress resistance," in *The Sorghum Genome*. eds. S. Rakshit and Y. H. Wang (Switzerland: Springer Nature), 149–167.

Lobo, L. L. B., dos Santos, R. M., and Rigobelo, E. C. (2019). Promotion of maize growth using endophytic bacteria under greenhouse and field conditions. *Aust. J. Crop. Sci.* 13, 2067–2074. doi: 10.21475/ajcs.19.13.12.p2077

Mahdi, I., Fahsi, N., Hafidi, M., Allaoui, A., and Biskri, L. (2020). Plant growth enhancement using rhizospheric halotolerant phosphate solubilizing bacterium *Bacillus licheniformis* QA1 and *Enterobacter asburiae* QF11 isolated from

Chenopodium quinoa willd. *Microorganisms* 8:948. doi: 10.3390/microorganisms8060948

Mahmoud, A. F., Abou-Elwafa, S. F., and Shehzad, T. (2018). Identification of charcoal rot resistance QTLs in sorghum using association and in silico analyses. *J. Appl. Genet.* 59, 243–251. doi: 10.1007/s13353-018-0446-5

Maldonado, S., Rodríguez, A., Ávila, B., Morales, P., González, M. P., Araya Angel, J. P. A., et al. (2020). Enhanced crop productivity and sustainability by using native phosphate solubilizing rhizobacteria in the agriculture of arid zones. *Front. Sustain. Food Syst.* 4:607355. doi: 10.3389/fsufs.2020.607355

Mareque, C., Taulé, C., Beracochea, M., and Battistoni, F. (2015). Isolation, characterization and plant growth promotion effects of putative bacterial endophytes associated with sweet sorghum (*Sorghum bicolor* (L) Moench). *Ann. Microbiol.* 65, 1057–1067. doi: 10.1007/s13213-014-0951-7

Mareya, C. R., Tugizimana, F., Di Lorenzo, F., Silipo, A., Piater, L. A., Molinaro, A., et al. (2020). Adaptive defence-related changes in the metabolome of *Sorghum bicolor* cells in response to lipopolysaccharides of the pathogen *Burkholderia andropogonis*. *Sci. Rep.* 10:7626. doi: 10.1038/s41598-020-64186-y

Marles, J., Apriyanto, E., and Harsono, P. (2018). Growth and yield response of three sorghum varieties in coastal land using organic materials and arbuscular mycorrhizal fungi. *Naturalis* 7, 29–40.

Matos, A. D. M., Gomes, I. C. P., Nietsche, S., Xavier, A. A., Gomes, W. S., Dos Santos, J. A., et al. (2017). Phosphate solubilization by endophytic bacteria isolated from banana trees. *An. Acad. Bras. Cienc.* 89, 2945–2954. doi: 10.1590/0001-3765201720160111

Mattos, B. B., Marriel, I. E., De Sousa, S. M., Lana, U. G. D. E. P., Schaffert, R. E., Gomes, E. A., et al. (2020). Sorghum genotypes response to inoculation with phosphate solubilizing bacteria. *Brazilian J. Maize Sorghum* 19:14. doi: 10.18512/rbms2020v19e1177

Mavrodi, D. V., Mavrodi, O. V., Parejko, J. A., Bonsall, R. F., Kwak, Y.-S., Paulitz, T. C., et al. (2012). Accumulation of the antibiotic phenazine-1-carboxylic acid in the rhizosphere of dryland cereals. *Appl. Environ. Microbiol.* 78, 804–812. doi: 10.1128/AEM.06784-11

Mendoza-Arroyo, G. E., Chan-Bacab, M. J., Aguila-Ramírez, R. N., Ortega-Morales, B. O., Canché Solís, R. E., Chab-Ruiz, A. O., et al. (2020). Inorganic phosphate solubilization by a novel isolated bacterial strain *Enterobacter* sp. ITCB-09 and its application potential as biofertilizer. *Agriculture* 10:383. doi: 10.3390/agriculture10090383

Menéndez, E., Pérez-Yépez, J., Hernández, M., Rodríguez-Pérez, A., Velázquez, E., and León-Barrios, M. (2020). Plant growth promotion abilities of phylogenetically diverse Mesorhizobium strains: effect in the root colonization and development of tomato seedlings. *Microorganisms* 8:412. doi: 10.3390/microorganisms8030412

Milner, J. L., Silo-Suh, L., Lee, J. C., He, H., Clardy, J., and Handelsman, J. O. (1996). Production of kanosamine by *Bacillus cereus* UW85. *Appl. Environ. Microbiol.* 62, 3061–3065. doi: 10.1128/aem.62.8.3061-3065.1996

Mitra, D., Anđelković, S., Panneerselvam, P., Senapati, A., Vasić, T., Ganeshamurthy, A. N., et al. (2020). Phosphate-solubilizing microbes and biocontrol agent for plant nutrition and protection: current perspective. *Commun. Soil Sci. Plant Anal.* 51, 645–657. doi: 10.1080/00103624.2020.1729379

Mohamed, A. A., Eweda, W. E. E., Heggo, A. M., and Hassan, E. A. (2014). Effect of dual inoculation with arbuscular mycorrhizal fungi and Sulphur-oxidising bacteria on onion (*Allium cepa* L.) and maize (*Zea mays* L.) grown in sandy soil under green house conditions. *Ann. Agric. Sci.* 59, 109–118. doi: 10.1016/j.aoas.2014.06.015

Mohamed, E. A. H., Farag, A. G., and Youssef, S. A. (2018). Phosphate solubilization by *Bacillus subtilis* and *Serratia marcescens* isolated from tomato plant rhizosphere. *J. Environ. Prot.* 9, 266–277. doi: 10.4236/jep.2018.93018

Mohammed, A. F. (2020). Influence of *Streptomyces* sp. Kp109810 on solubilization of inorganic phosphate and growth of maize (*Zea mays* L.). *J. Appl. Plant Prot.* 9, 17–24. doi: 10.21608/japp.2020.130644

Moharam, M. H. A. (2018). First report of loose kernel smut of sorghum caused by *Sporisorium cruentum* in Egypt. *New Dis. Rep.* 37:9. doi: 10.5197/j.2044-0588.2018.037.009

Mojid, M. A., Wyseure, G. C. L., and Biswas, S. K. (2012). Requirement of nitrogen, phosphorus and potassium fertilizers for wheat cultivation under irrigation by municipal wastewater. *J. Soil Sci. Plant Nutr.* 12, 655–665. doi: 10.4067/S0718-95162012005000023

Muleta, A., Tesfaye, K., Selassie, T. H. H., Cook, D. R., and Assefa, F. (2021). Phosphate solubilization and multiple plant growth promoting properties of *Mesorhizobium* species nodulating chickpea from acidic soils of Ethiopia. *Arch. Microbiol.* 203, 2129–2137. doi: 10.1007/s00203-021-02189-7

Munir, I., Bano, A., and Faisal, M. (2019). Impact of phosphate solubilizing bacteria on wheat (*Triticum aestivum*) in the presence of pesticides. *Braz. J. Biol.* 79, 29–37. doi: 10.1590/1519-6984.172213

Munir, I., Ranjha, A. M., Sarfraz, M., Obaid-ur-Rehman, Mehdiand, S. M., and Mahmood, K. (2004). Effect of residual phosphorus on sorghum fodder in two different texturedsoils. *Int. J. Agric. Biol.* 6, 967–969.

Murty, D. S., and Subramanian, V. (1982). Sorghum roti: I. Traditional methods of consumption and standard procedures for evaluation. 73–78.

Nacoon, S., Jogloy, S., Riddech, N., Mongkolthanaruk, W., Kuyper, T. W., and Boonlue, S. (2020). Interaction between phosphate solubilizing bacteria and arbuscular mycorrhizal fungi on growth promotion and tuber inulin content of *Helianthus tuberosus* L. *Sci. Rep.* 10:4916. doi: 10.1038/s41598-020-61846-x

Nandimath, A. P., Karad, D. D., Gupta, S. G., and Kharat, A. S. (2017). Consortium inoculum of five thermo-tolerant phosphate solubilizing Actinomycetes for multipurpose biofertilizer preparation. *Iran. J. Microbiol.* 9:295.

Naseri, R., Barary, M., Zarea, M. J., Khavazi, K., Tahmasebi, Z., and Yaghotipoor, A. (2018). Effect of phosphate solubilizing bacteria and mycorrhizal fungi on phenological and physiological characteristics of wheat under dryland conditions. *J. Crop Ecophysiol.* 12, 211–236.

Naziya, B., Murali, M., and Amruthesh, K. N. (2020). Plant growth-promoting fungi (PGPF) instigate plant growth and induce disease resistance in *Capsicum annuum* L. upon infection with *Colletotrichum capsici* (Syd.) Butler & Bisby. *Biomol. Ther.* 10:41. doi: 10.3390/biom10010041

Nepomuceno, R. A., Brown, C. M. B., Mojica, P. N., and Brown, M. B. (2019). Biological control potential of vesicular arbuscular mycorrhizal root inoculant (VAMRI) and associated phosphate solubilizing bacteria, *Pseudochrobactrum asaccharolyticum* against soilborne phytopathogens of onion (*Allium cepa* L. var. red creole). *Arch. Phytopathol. Plant Protect.* 52, 714–732. doi: 10.1080/03235408.2019.1644058

Nigusie, Z., and Ademe, A. (2020). Evaluation of insecticidal botanicals against sorghum covered smut (*Sphacelotheca sorghi*) at Wag-Lasta areas, Ethiopia. *Cogent Food Agric.* 6:1745132. doi: 10.1080/23311932.2020.1745132

Nogales, A., Rottier, E., Campos, C., Victorino, G., Costa, J. M., Coito, J. L., et al. (2021). The effects of field inoculation of arbuscular mycorrhizal fungi through rye donor plants on grapevine performance and soil properties. *Agric. Ecosyst. Environ.* 313:107369. doi: 10.1016/j.agee.2021.107369

Nosrati, R., Owlia, P., Saderi, H., Rasooli, I., and Malboobi, M. A. (2014). Phosphate solubilization characteristics of efficient nitrogen fixing soil *Azotobacter* strains. *Iran. J. Microbiol.* 6:285.

O'sullivan, D. J., and O'Gara, F. (1992). Traits of fluorescent *Pseudomonas* spp. involved in suppression of plant root pathogens. *Microbiol. Rev.* 56, 662–676. doi: 10.1128/mr.56.4.662-676.1992

Olanrewaju, O. S., and Babalola, O. O. (2019). Streptomyces: implications and interactions in plant growth promotion. *Appl. Microbiol. Biotechnol.* 103, 1179–1188. doi: 10.1007/s00253-018-09577-y

Olanrewaju, O. S., Glick, B. R., and Babalola, O. O. (2017). Mechanisms of action of plant growth promoting bacteria. *World J. Microbiol. Biotechnol.* 33:197. doi: 10.1007/s11274-017-2364-9

Omomowo, I. O., Shittu, O. E., Omomowo, O. I., and Majolagbe, O. N. (2020). Influence of phosphate solubilizing non-toxigenic *Aspergillus flavus* strains on maize (*Zea mays* L.) growth parameters and mineral nutrients content. *AIMS Agric. Food* 5, 408–421. doi: 10.3934/agrfood.2020.3.408

Ordentlich, A., Elad, Y., and Chet, I. (1988). The role of chitinase of *Serratia marcescens* in biocontrol of *Sclerotium rolfsii*. *Phytopathology* 78, 84–88.

Ordoñez, Y. M., Fernandez, B. R., Lara, L. S., Rodriguez, A., Uribe-Velez, D., and Sanders, I. R. (2016). Bacteria with phosphate solubilizing capacity alter mycorrhizal fungal growth both inside and outside the root and in the presence of native microbial communities. *PLoS One* 11:e0154438. doi: 10.1371/journal.pone.0154438

Orozco-Mosqueda, M., Flores, A., Rojas-Sánchez, B., Urtis-Flores, C. A., Morales-Cedeño, L. R., Valencia-Marin, M. F., et al. (2021). Plant growth-promoting bacteria as bioinoculants: attributes and challenges for sustainable crop improvement. *Agronomy* 11:1167. doi: 10.3390/agronomy11061167

Pande, A., Kaushik, S., Pandey, P., and Negi, A. (2020). Isolation, characterization, and identification of phosphate-solubilizing *Burkholderia cepacia* from the sweet corn cv. Golden bantam rhizosphere soil and effect on growth-promoting activities. *Int. J. Veg. Sci.* 26, 591–607. doi: 10.1080/19315260.2019.1692121

Pandey, S., and Gupta, S. (2020). Evaluation of *pseudomonas* sp. for its multifarious plant growth promoting potential and its ability to alleviate biotic and abiotic stress in tomato (*Solanum lycopersicum*) plants. *Sci. Rep.* 10:20951. doi: 10.1038/s41598-020-77850-0

Pandya, N. D., Desai, P. V., Jadhav, H. P., and Sayyed, R. Z. (2018). Plant growth promoting potential of *aspergillus* sp. NPF7, isolated from wheat rhizosphere in South Gujarat, India. *Environ. Sustain.* 1, 245–252. doi: 10.1007/s42398-018-0025-z

Patel, P., and Panchal, K. (2020). Effect of free-living nitrogen fixing and phosphate solubilizing bacteria on growth of *Gossypium hirsutum* L. *Asian J. Biol. Life Sci.* 9, 169–176. doi: 10.5530/ajbls.2020.9.26

Pereira, S. I. A., Abreu, D., Moreira, H., Vega, A., and Castro, P. M. L. (2020). Plant growth-promoting rhizobacteria (PGPR) improve the growth and nutrient use efficiency in maize (*Zea mays* L.) under water deficit conditions. *Heliyon* 6:e05106. doi: 10.1016/j.heliyon.2020.e05106

Pikovskaya, R. I. (1948). Mobilization of phosphorus in soil in connection with vital activity of some microbial species. *Mikrobiologiya* 17, 362–370.

Prakash, J., and Arora, N. K. (2019). Phosphate-solubilizing *Bacillus* sp. enhances growth, phosphorus uptake and oil yield of *Mentha arvensis* L. *3 Biotech* 9:126. doi: 10.1007/s13205-019-1660-5

Prom, L. K., Perumal, R., Montes-Garcia, N., Isakeit, T., Odvody, G. N., Rooney, W. L., et al. (2015). Evaluation of Gambian and Malian sorghum germplasm against downy mildew pathogen, Peronosclerospora sorghi, in Mexico and the USA. *J. Gen. Plant Pathol.* 81, 24–31. doi: 10.1007/s10327-014-0557-8

Qarni, A., Billah, M., Hussain, K., Shah, S. H., Ahmed, W., Alam, S., et al. (2021). Isolation and characterization of phosphate solubilizing microbes from rock phosphate mines and their potential effect for sustainable agriculture. *Sustainability* 13:2151. doi: 10.3390/su13042151

Qiao, H., Sun, X.-R., Wu, X.-Q., Li, G.-E., Wang, Z., and Li, D.-W. (2019). The phosphate-solubilizing ability of *Penicillium guanacastense* and its effects on the growth of *Pinus massoniana* in phosphate-limiting conditions. *Biol. Open* 8:bio046797. doi: 10.1242/bio.046797

Raaijmakers, J. M., and Mazzola, M. (2012). Diversity and natural functions of antibiotics produced by beneficial and plant pathogenic bacteria. *Annu. Rev. Phytopathol.* 50, 403–424. doi: 10.1146/annurev-phyto-081211-172908

Ramadhani, I., and Widawati, S. R. I. (2020). Synergistic interaction of arbuscular mycorrhizal fungi and phosphate-solubilizing bacteria on *Sorghum bicolor* (L.) moench growth under saline condition. *Microbiol. Indones.* 14, 73–82. doi: 10.5454/mi.14.2.4

Rezakhani, L., Motesharezadeh, B., Tehrani, M. M., Etesami, H., and Hosseini, H. M. (2020). Effect of silicon and phosphate-solubilizing bacteria on improved phosphorus (P) uptake is not specific to insoluble P-fertilized sorghum (*Sorghum bicolor* L.) plants. *J. Plant Growth Regul.* 39, 239–253. doi: 10.1007/s00344-019-09978-x

Rfaki, A., Zennouhi, O., Aliyat, F. Z., Nassiri, L., and Ibijbijen, J. (2020). Isolation, selection and characterization of root-associated rock phosphate solubilizing bacteria in moroccan wheat (*Triticum aestivum* L.). *Geomicrobiol J.* 37, 230–241. doi: 10.1080/01490451.2019.1694106

Ribeiro, V. P., Marriel, I. E., de Sousa, S. M., Lana, U. G. P., Mattos, B. B., de Oliveira, C. A., et al. (2018). Endophytic *bacillus* strains enhance pearl millet growth and nutrient uptake under low-P. *Braz. J. Microbiol.* 49, 40–46. doi: 10.1016/j.bjm.2018.06.005

Rizvi, A., Zaidi, A., Ameen, F., Ahmed, B., AlKahtani, M. D. F., and Khan, M. S. (2020). Heavy metal induced stress on wheat: phytotoxicity and microbiological management. *RSC Adv.* 10, 38379–38403. doi: 10.1039/D0RA05610C

Roy, P. R. S., and Khandaker, Z. H. (2010). Effects of phosphorus fertilizer on yield and nutritional value of sorghum (*Sorghum bicolor*) fodder at three cuttings. *Bangladesh J. Anim. Sci.* 39, 106–115. doi: 10.3329/BJAS.V39I1-2.9683

Saïdou, A., Balogoun, I., Ahoton, E. L., Igué, A. M., Youl, S., Ezui, G., et al. (2018). "Fertilizer recommendations for maize production in the South Sudan and Sudano-Guinean zones of Benin," in *Improving the Profitability, Sustainability and Efficiency of Nutrients Through Site Specific Fertilizer Recommendations in West Africa Agro-Ecosystems*. eds. A. Bationo, D. Ngaradoum, S. Youl, F. Lompo and J. O. Fening (Switzerland: Springer Nature), 215–234.

Saif, S., Khan, M. S., Zaidi, A., and Ahmad, E. (2014). "Role of phosphate-solubilizing actinomycetes in plant growth promotion: current perspective," in *Phosphate Solubilizing Microorganisms*. eds. M. Khan, A. Zaidi and J. Musarrat (Switzerland: Springer Nature), 137–156.

Sandy, M., and Butler, A. (2009). Microbial iron acquisition: marine and terrestrial siderophores. *Chem. Rev.* 109, 4580–4595. doi: 10.1021/cr9002787

Santana, S. R. A., Voltolini, T. V., dos Reis Antunes, G., da Silva, V. M., Simões, W. L., Morgante, C. V., et al. (2020). Inoculation of plant growth-promoting bacteria attenuates the negative effects of drought on sorghum. *Arch. Microbiol.* 202, 1015–1024. doi: 10.1007/s00203-020-01810-5

Saraf, M., Pandya, U., and Thakkar, A. (2014). Role of allelochemicals in plant growth promoting rhizobacteria for biocontrol of phytopathogens. *Microbiol. Res.* 169, 18–29. doi: 10.1016/j.micres.2013.08.009

Sarr, P. S., Tibiri, E. B., Fukuda, M., Zongo, A. N., and Nakamura, S. (2020). Phosphate-solubilizing fungi and alkaline phosphatase trigger the P solubilization during the co-composting of sorghum straw residues with Burkina Faso phosphate rock. *Front. Environ. Sci.* 8:559195. doi: 10.3389/fenvs.2020.559195

Saxena, J., Chandra, S., and Nain, L. (2013). Synergistic effect of phosphate solubilizing rhizobacteria and arbuscular mycorrhiza on growth and yield of wheat plants. *J. Soil Sci. Plant Nutr.* 13, 511–525. doi: 10.4067/S0718-95162013005000040

Sayyed, R. Z., Naphade, B. S., and Chincholkar, S. B. (2004). Ecologically competent rhizobacteria for plant growth promotion and disease management. *Recent Trends Biotechnol.* 1–16.

Sayyed, R. Z., and Patel, P. R. (2011). Biocontrol potential of siderophore producing heavy metal resistant *Alcaligenes* sp. and *Pseudomonas aeruginosa* RZS3 Vis-a-Vis organophosphorus fungicide. *Indian J. Microbiol.* 51, 266–272. doi: 10.1007/s12088-011-0170-x

Sebnie, W., Mengesha, M., Girmay, G., Feyisa, T., Asgedom, B., Beza, G., et al. (2020). Evaluation of micro-dosing fertilizer application on sorghum (*sorghum bicholor* L) production at wag-Lasta areas of Amhara region, Ethiopia. *Sci. Rep.* 10:6889. doi: 10.1038/s41598-020-63851-6

Selvakumar, G., Joshi, P., Nazim, S., Mishra, P. K., Bisht, J. K., and Gupta, H. S. (2009). Phosphate solubilization and growth promotion by *Pseudomonas fragi* CS11RH1 (MTCC 8984), a psychrotolerant bacterium isolated from a high altitude Himalayan rhizosphere. *Biologia* 64, 239–245. doi: 10.2478/s11756-009-0041-7

Shahidi, F., and Naczk, M. (1995). Food phenolics: sources, chemistry, effects and aplications technomic publishing. *Inc. P.* 247:260.

Sharma, H. C. (1985). Strategies for pest control in sorghum in India. *Int. J. Pest Manag.* 31, 167–185.

Sharma, A., Kumar, V., Sidhu, G. P. S., Kumar, R., Kohli, S. K., Yadav, P., et al. (2019). "Abiotic stress management in plants: role of ethylene," in *Molecular Plant Abiotic Stress: Biology and Biotechnology*. eds. A. Roychoudhury and D. K. Tripathi (New Jersey, USA: John Wiley & Sons), 185–208.

Shenoy, V. V., and Kalagudi, G. M. (2005). Enhancing plant phosphorus use efficiency for sustainable cropping. *Biotechnol. Adv.* 23, 501–513. doi: 10.1016/j.biotechadv.2005.01.004

Shete, M. H., Murumkar, D. R., Indi, D. V., and Tirmali, A. M. (2018). Effect of drought tolerant strains of phosphate solubilizing bacteria on growth and yield of *Rabi sorghum*. *Indian J. Dryl. Agric. Res. Dev.* 33, 59–63. doi: 10.5958/2231-6701.2018.00011.8

Shimshoni, J. A., Cuneah, O., Sulyok, M., Krska, R., Sionov, E., Barel, S., et al. (2017). Newly discovered ergot alkaloids in sorghum ergot *Claviceps africana* occurring for the first time in Israel. *Food Chem.* 219, 459–467. doi: 10.1016/j.foodchem.2016.09.182

Shoemaker, C. E., and Bransby, D. I. (2010). "The role of sorghum as a bioenergy feedstock," in *Sustainable Alternative Fuel Feedstock Opportunities, Challenges and Road maps for Six US Regions. Proceeedings of the Sustainable Feedstocks for Advance Biofuels Workshop, Atlanta, GA*. eds. R. Braun, D. Karlen and D. Johnson; September 28–30, 2010; Soil and Water Conserv. Soc., Ankeny, IA; 149–159.

Silveira, A. A. C., de Araújo, L. G., de Filippi, M. C. C., de Faria, F. P., and Sibov, S. T. (2021). Biochemical characterization of multifunctional endophytic fungi from *Bambusa oldhamii* Munro. *Pesqui. Agropecuária Trop.* 50, 1–8. doi: 10.1590/1983-40632020v5066370

Singh, N., Pandey, P., Dubey, R. C., and Maheshwari, D. K. (2008). Biological control of root rot fungus *Macrophomina phaseolina* and growth enhancement of *Pinus roxburghii* (Sarg.) by rhizosphere competent *Bacillus subtilis* BN1. *World J. Microbiol. Biotechnol.* 24, 1669–1679. doi: 10.1007/s11274-008-9680-z

Singh, P. P., Shin, Y. C., Park, C. S., and Chung, Y. R. (1999). Biological control of fusarium wilt of cucumber by chitinolytic bacteria. *Phytopathology* 89, 92–99. doi: 10.1094/PHYTO.1999.89.1.92

Soumare, A., Boubekri, K., Lyamlouli, K., Hafidi, M., Ouhdouch, Y., and Kouisni, L. (2020). From isolation of phosphate solubilizing microbes to their formulation and use as biofertilizers: status and needs. *Front. Bioeng. Biotechnol.* 7:425. doi: 10.3389/fbioe.2019.00425

Srinivasan, R., Alagawadi, A. R., Yandigeri, M. S., Meena, K. K., and Saxena, A. K. (2012). Characterization of phosphate-solubilizing microorganisms from salt-affected soils of India and their effect on growth of sorghum plants [Sorghum bicolor (L.) Moench]. *Ann. Microbiol.* 62, 93–105. doi: 10.1007/s13213-011-0233-6

Steiner, F., Lana, M. D. O. C., and Zoz, T. (2016). Phosphate solubilizing fungi enhance the growth and phosphorus uptake of sorghum plants. *Rev. Bras. Milho Sorgo* 15, 30–38. doi: 10.18512/1980-6477/rbms.v15n1p30-38

Tandon, A., Fatima, T., Shukla, D., Tripathi, P., Srivastava, S., and Singh, P. C. (2020). Phosphate solubilization by *Trichoderma koningiopsis* (NBRI-PR5) under abiotic stress conditions. *J. King Saud Univ.* 32, 791–798. doi: 10.1016/j.jksus.2019.02.001

Tari, I., Laskay, G., Takács, Z., and Poór, P. (2013). Response of sorghum to abiotic stresses: a review. *J. Agron. Crop Sci.* 199, 264–274. doi: 10.1111/jac.12017

Tasie, M. M., and Gebreyes, B. G. (2020). Characterization of nutritional, antinutritional, and mineral contents of thirty-five sorghum varieties grown in Ethiopia. *Int. J. Food Sci.* 2020:8243617. doi: 10.1155/2020/8243617

Tian, J., Ge, F., Zhang, D., Deng, S., and Liu, X. (2021). Roles of phosphate solubilizing microorganisms from managing soil phosphorus deficiency to mediating biogeochemical P cycle. *Biology* 10:158. doi: 10.3390/biology10020158

Toomey, G. (1988). Sorghum as substitute: food enterprises for Indian women. *IDRC Reports*, 17, no. 3.

Venkateswarlu, B., Rao, A. V., and Raina, P. (1984). Evaluation of phosphorus solubilisation by microorganisms isolated from Aridisols. *J. Indian Soc. Soil Sci.* 32, 273–277.

Verma, M., Singh, A., Dwivedi, D. H., and Arora, N. K. (2020). Zinc and phosphate solubilizing *rhizobium radiobacter* (LB2) for enhancing quality and yield of loose leaf lettuce in saline soil. *Environ. Sustain.* 3, 209–218. doi: 10.1007/s42398-020-00110-4

Verma, V. C., Singh, S. K., and Prakash, S. (2011). Bio-control and plant growth promotion potential of siderophore producing endophytic *Streptomyces* from *Azadirachta indica* A. *Juss. J. Basic Microbiol.* 51, 550–556. doi: 10.1002/jobm.201000155

Vijayalakshmi, V., Pradeep, S., Manjunatha, H., Krishna, V., and Jyothi, V. (2020). The impact of nitrogen fixers and phosphate solubilizing microbes on sorghum (*Sorghum bicolor*) yield. *Curr. Biotechnol.* 9, 198–208. doi: 10.2174/2211550109666191218125559

Vikram, A. (2007). Efficacy of phosphate solubilizing bacteria isolated from vertisols on growth and yield parameters of sorghum. *Res. J. Microbiol.* 2, 550–559. doi: 10.3923/jm.2007.550.559

Wagari, M. K. (2019). Importance and management of sorghum smuts with special reference to: the covered kernel smut (*Sphacelotheca sorghi* [Link] Clinton), Loose Kernel Smut (*Sphacelotheca cruenta* [Kuhn] Potter) and Head Smut (Sphacelotheca). *Green. J. Agri. Sci.* 9, 447–458.

Wahid, F., Sharif, M., Steinkellner, S., Khan, M. A., Marwat, K. B., and Khan, S. A. (2016). Inoculation of arbuscular mycorrhizal fungi and phosphate solubilizing bacteria in the presence of rock phosphate improves phosphorus uptake and growth of maize. *Pak. J. Bot.* 48, 739–747.

Walpola, B. C., and Yoon, M.-H. (2012). Prospectus of phosphate solubilizing microorganisms and phosphorus availability in agricultural soils: a review. *Afr. J. Microbiol. Res.* 6, 6600–6605.

Wan, W., Qin, Y., Wu, H., Zuo, W., He, H., Tan, J., et al. (2020). Isolation and characterization of phosphorus solubilizing bacteria with multiple phosphorus sources utilizing capability and their potential for lead immobilization in soil. *Front. Microbiol.* 11:752. doi: 10.3389/fmicb.2020.00752

Wang, X., Mace, E., Hunt, C., Cruickshank, A., Henzell, R., Parkes, H., et al. (2014). Two distinct classes of QTL determine rust resistance in sorghum. *BMC Plant Biol.* 14:366. doi: 10.1186/s12870-014-0366-4

Wang, Q., Shakoor, N., Boyher, A., Veley, K. M., Berry, J. C., Mockler, T. C., et al. (2021). Escalation in the host-pathogen arms race: a host resistance response corresponds to a heightened bacterial virulence response. *PLoS Pathog.* 17:e1009175. doi: 10.1371/journal.ppat.1009175

Wang, Q., Wang, C., Yu, W., Turak, A., Chen, D., Huang, Y., et al. (2018). Effects of nitrogen and phosphorus inputs on soil bacterial abundance, diversity, and community composition in Chinese fir plantations. *Front. Microbiol.* 9:3354. doi: 10.3389/fmicb.2018.03354

Weller, D. M., Landa, B. B., Mavrodi, O. V., Schroeder, K. L., De La Fuente, L., Bankhead, S. B., et al. (2007). Role of 2, 4-diacetylphloroglucinol-producing fluorescent *pseudomonas* spp. in the defense of plant roots. *Plant Biol.* 9, 4–20. doi: 10.1055/s-2006-924473

Widada, J., Damarjaya, D. I., and Kabirun, S. (2007). "The interactive effects of arbuscular mycorrhizal fungi and rhizobacteria on the growth and nutrients uptake of sorghum in acid soil," in *First International Meeting on Microbial Phosphate Solubilization*. eds. E. Velázquez and C. Rodríguez-Barrueco (Switzerland: Springer Nature), 173–177.

Xu, J., Jiang, Y., Hu, L., Liu, K.-J., Xu, X.-D., Qin, P.-W., et al. (2019). First report of rough leaf spot of sorghum caused by *Ascochyta sorghi* in China. *Plant Dis.* 103:149. doi: 10.1094/PDIS-11-17-1850-PDN

Yadav, K. K., and Sarkar, S. (2019). Biofertilizers, impact on soil fertility and crop productivity under sustainable agriculture. *Environ. Ecol.* 37, 89–93.

Zafar, M., Ahmed, N., Mustafa, G., Zahir, Z. A., and Simms, E. L. (2017). Molecular and biochemical characterization of rhizobia from chickpea (*Cicer arietinum*). *Pak. J. Agric. Sci.* 54, 373–381. doi: 10.21162/PAKJAS/17.5874

Zaheer, A., Malik, A., Sher, A., Qaisrani, M. M., Mehmood, A., Khan, S. U., et al. (2019). Isolation, characterization, and effect of phosphate-zinc-solubilizing bacterial strains on chickpea (*Cicer arietinum* L.) growth. *Saudi J. Biol. Sci.* 26, 1061–1067. doi: 10.1016/j.sjbs.2019.04.004

Zaidi, A., Ahmad, E., and Khan, M. S. (2014). "Role of phosphate-solubilizing microbes in the management of plant diseases," in *Phosphate Solubilizing Microorganisms*. eds. M. Khan, A. Zaidi and J. Musarrat (Switzerland: Springer Nature), 225–256.

Zaidi, A., Khan, M., Ahemad, M., and Oves, M. (2009). Plant growth promotion by phosphate solubilizing bacteria. *Acta Microbiol. Immunol. Hung.* 56, 263–284. doi: 10.1556/AMicr.56.2009.3.6

Zhao, Z.-Y., Che, P., Glassman, K., and Albertsen, M. (2019). "Nutritionally enhanced sorghum for the arid and semiarid tropical areas of Africa," in *Sorghum*. eds. Z. Y. Zhao and J. Dahlberg (Switzerland: Springer Nature), 197–207.

Zhao, G., Wei, Y., Chen, J., Dong, Y., Hou, L., and Jiao, R. (2021). Screening, identification and growth-promotion products of multifunctional bacteria in a Chinese fir plantation. *Forests* 12:120. doi: 10.3390/f12020120

Zhu, J., Li, M., and Whelan, M. (2018). Phosphorus activators contribute to legacy phosphorus availability in agricultural soils: a review. *Sci. Total Environ.* 612, 522–537. doi: 10.1016/j.scitotenv.2017.08.095

Ziaeyan, H., Farahbakhash, A. R., Besharati, H., and Joukar, L. (2016). Interaction effects of phosphate solubilizing bacteria and mycorrhiza on the growth and phosphorus uptake of sorghum. *J. Water Soil* 30:5.

Zúñiga-Silgado, D., Rivera-Leyva, J. C., Coleman, J. J., Sánchez-Reyez, A., Valencia-Díaz, S., Serrano, M., et al. (2020). Soil type affects organic acid production and phosphorus solubilization efficiency mediated by several native fungal strains from Mexico. *Microorganisms* 8:1337. doi: 10.3390/microorganisms8091337

Conflict of Interest: The authors declare that the research was conducted in the absence of any commercial or financial relationships that could be construed as a potential conflict of interest.

Publisher's Note: All claims expressed in this article are solely those of the authors and do not necessarily represent those of their affiliated organizations, or those of the publisher, the editors and the reviewers. Any product that may be evaluated in this article, or claim that may be made by its manufacturer, is not guaranteed or endorsed by the publisher.

frontiers in Plant Science

ORIGINAL RESEARCH
published: 13 December 2021
doi: 10.3389/fpls.2021.779382

Melatonin Enhances Drought Tolerance by Regulating Leaf Stomatal Behavior, Carbon and Nitrogen Metabolism, and Related Gene Expression in Maize Plants

*Chengfeng Zhao, Haoxue Guo, Jiarui Wang, Yifan Wang and Renhe Zhang**

College of Agronomy, Northwest A&F University, Yangling, China

It is commonly known that exogenously applied melatonin can alleviate the impact of drought stress, but the mechanism used by melatonin to regulate stomatal behavior and carbon (C) and nitrogen (N) metabolism to increase drought resistance remains elusive. Herein, our aim was to investigate the influence of exogenous melatonin on the regulation of C and N metabolism in maize plants under water deficit. In this study, we analyzed stomatal behavior, the key components of C and N metabolism, and the gene expression and activity of enzymes involved in the C and N metabolism in maize plants. The results showed that the application of melatonin (100 μM) significantly increased maize growth and sustained the opening of stomata, and secondarily increased the photosynthetic capacity in maize. Under drought stress, foliar application of melatonin induced the gene transcription and activities of sucrose phosphate synthetase, ADP-glucose pyrophosphorylase, phosphoenolpyruvate carboxylase, and citrate synthase, resulting in the enhancement of sucrose and starch synthesis and the tricarboxylic acid (TCA) cycle. This enhancement in sugar biosynthesis and the TCA cycle might lead to stronger N assimilation. As anticipated, NO_3^- reduction and NH_4^+ assimilation were also strengthened after melatonin treatment under drought stress. An increase was observed in some key enzymatic activities and transcription involved in nitrogen metabolism, such as that of nitrate reductase, nitrite reductase, glutamate synthase, and glutamine synthetase, in melatonin-treated, drought-stressed maize. Moreover, melatonin attenuated the drought-induced damage by reducing protein degradation and increasing the level of proline. Conclusively, our results indicate that exogenous melatonin enhances drought tolerance in maize *via* promoting stomatal opening and regulating C and N metabolism and related gene expression.

Keywords: maize, drought, melatonin, stomatal behavior, carbon and nitrogen metabolism

OPEN ACCESS

Edited by:
Maurizio Ruzzi,
University of Tuscia, Italy

Reviewed by:
Parvaiz Ahmad,
Sri Pratap College Srinagar, India
Hayssam M. Ali,
King Saud University, Saudi Arabia

****Correspondence:***
Renhe Zhang
zhangrenhe@nwsuaf.edu.cn

Specialty section:
This article was submitted to Plant Abiotic Stress, a section of the journal Frontiers in Plant Science

Received: *18 September 2021*
Accepted: *15 November 2021*
Published: *13 December 2021*

Citation:
Zhao C, Guo H, Wang J, Wang Y and Zhang R (2021) Melatonin Enhances Drought Tolerance by Regulating Leaf Stomatal Behavior, Carbon and Nitrogen Metabolism, and Related Gene Expression in Maize Plants. Front. Plant Sci. 12:779382. doi: 10.3389/fpls.2021.779382

INTRODUCTION

Maize (*Zea mays* L.) is one of the most important grain crops cultivated worldwide but is extremely sensitive to drought stress (Li Z. et al., 2021). Water is a crucial environmental factor for crop production, and soil water deficits limit crop growth and yield (Yang et al., 2019). Water scarcity compromises economic output and food security worldwide, and in the past decade, global losses

in crop production due to drought totaled approximately $30 billion (Riemann et al., 2015; Gupta et al., 2020).

Drought is complex abiotic stress, and a series of morphological, physiological, and biochemical changes take place during the response of plants to drought stress (Shah et al., 2020), which include plant growth (Todaka et al., 2017), leaf stomatal behavior (Indira et al., 2021), photosynthetic activity (Zhou et al., 2019), cellular redox homeostasis (Zhang et al., 2019), and metabolism homeostasis (Pinheiro and Chaves, 2011). These changes are usually interconnected. Specifically, osmotic stress caused by drought induces the accumulation of abscisic acid (ABA), which, at high levels, can promote stomata closure and decrease the internal carbon dioxide concentration (Ci) (Riemann et al., 2015; Kong et al., 2016; Zhou et al., 2019). Following stomatal closure and the decrease in Ci, the activity of the carboxylating enzyme Rubisco has been shown to decrease, which leads to electron accumulation and reactive oxygen species (ROS) overproduction, eventually resulting in oxidative damage and a series of subsequent side effects, such as leaf peroxidation, and degradation of chlorophyll, proteins, and nucleic acids (Campos et al., 2019; Sharma and Zheng, 2019; Sharma et al., 2020).

To cope with drought stress, the plants have evolved various metabolic adaptation mechanisms to defend against the adverse effects of stress, in which the coordinated regulation of carbon (C) and nitrogen (N) metabolism is one of the most important mechanisms (Ren et al., 2020). C and N metabolism are two of the most important metabolic processes in plants, and they are tightly related to each other (Yu et al., 2021). Metabolic processes involving C include reactions in photosynthesis and respiration (Cui et al., 2019). Photosynthesis and mitochondrial respiration provide C skeletons and an energy source for various biological processes, such as N assimilation and amino acid biosynthesis (Qiao et al., 2019). The growth and yield of plants are determined to a large extent by the capacity of photosynthesis (Cui et al., 2019). However, water deficit limits photosynthesis, which causes depletion of energy and sugar and diminishes plant production (Hu et al., 2020). N is a crucial structural component of nitrogenous compounds, such as amino acids, proteins, nucleic acids, chlorophyll, and enzymes (Qiao et al., 2019). Thus, N directly or indirectly affects plant photosynthesis through its effects on chlorophyll, photosynthetic rate, and the main enzymes of dark reactions and photorespiration (Zhong et al., 2019). The first step in N uptake and utilization is that nitrate reductase (NR) and nitrite reductase (NiR) convert nitrate (NO_3^-) into ammonium (NH_4^+) (Xie et al., 2019). Then, NH_4^+ is further assimilated to glutamate *via* glutamine synthetase (GS) and glutamate oxoglutarate aminotransferase (GOGAT) or glutamate dehydrogenase (GDH) (Rajasekhar and Oelmüller, 2010; Xie et al., 2019). Subsequently, glutamate acts as a donor of the amino group that distributes N to all other N-containing metabolites and macromolecules (Xie et al., 2019). The studies have shown that N assimilation plays a pivotal role in the acclimation of plant photosynthesis to drought stress (Xie et al., 2019; Zhong et al., 2019). Moreover, the C metabolism provides the energy and organic carbon skeletons for N assimilation and amino acid biosynthesis (Zhong et al., 2019). Therefore, the balance between C and N metabolism provides essential contributions to drought tolerance (Liu et al., 2014; Ren et al., 2020).

Melatonin (N-acetyl-5-methoxytryptamine) is a new plant growth regulator that is widely found in bacteria, fungi, plants, and algae (Kanwar et al., 2018; Debnath et al., 2020). Previous reports demonstrated that melatonin is involved in multiple biological processes in plants, such as seed germination (Li C. et al., 2021), root growth (Boyko et al., 2020), flowering (Kolar et al., 2003), leaf senescence (Ahmad et al., 2020), increased photosynthetic capacity (Ahmad et al., 2019), and moderation of oxidative damage (Qi et al., 2018; Kaya et al., 2019, 2020; Siddiqui et al., 2020). Furthermore, many studies have shown that the antioxidant action of melatonin can substantially enhance the tolerance of plants under biotic and abiotic stresses, such as pathogen infections (Li et al., 2019), drought (Sharma et al., 2020), cold (Wang et al., 2020), heat (Wei et al., 2015), salt, and UV stress (Yao et al., 2020; Zhang et al., 2020). In addition, melatonin may enhance plant stress resistance by regulating C or N metabolism. A previous study has suggested that metabolites, such as carbohydrates, organic acids, and amino acids accumulate after the application of melatonin to increase cold stress tolerance in Bermuda grass (Hu et al., 2016). A recent study in cotton revealed that melatonin enhances pollen fertility by balancing the carbohydrates of drought-stressed anthers (Hu et al., 2020). However, most of these studies on melatonin-enhancing stress resistance focused only on C or N metabolism, and currently, there is no report that combined C and N metabolism to study how melatonin alleviates drought stress.

Given the essential contributions of C and N metabolism and melatonin to the drought resistance of maize and the regulatory role of melatonin on primary metabolism, we hypothesize that the melatonin-induced drought resistance of maize depends to a large extent on the coordinated modulation of C and N metabolism. Therefore, we investigated the possible role of melatonin in maize response to soil drought stress by determining the photosynthetic capacity, leaf stomatal behavior, the amounts of various metabolites related to C and N metabolism, and the gene expression and activities of some key enzymes involved in C and N metabolism. The current study aimed to explore how melatonin enhances drought tolerance by regulating the coordination of C and N metabolism. The results will contribute to further understanding of the role played by melatonin in alleviating drought stress.

MATERIALS AND METHODS

Plant Materials and Treatments

A pot experiment was conducted from May to August 2020 at the rainproof shed of the Maize Experimental Station of Northwest A&F University, Shaanxi, China. Maize (*Z. mays* L. "Shaandan 609") seeds were sown in plastic pots of uniform size (diameter 26 cm and depth 38 cm), each filled with 15 kg air-dried soil and 10 g compound fertilizer containing 24% N, 6% P_2O_5, and 10% K_2O. The soil water content is expressed as a percentage maximum of pot capacity (Ogbaga et al., 2014). All plants were watered to 85% before the seven-leaf stage. Afterward, half of the

pots were exposed to drought conditions. During this period, all pots were sprayed with either melatonin (100 μM) or distilled water at 8 p.m. every day. The sprayed melatonin solution was prepared by dissolving 1.15 g melatonin powder in 25 ml ethanol as a stock solution. Subsequently, a melatonin solution of the desired concentration was obtained by further dilution with distilled water, including 0.05% (v/v) Tween-20 as a surfactant. In the present study, the maize seedlings were subjected to four treatment regimes: (1) distilled water pretreatment plus ample water (Control, CK); (2) 100 μM melatonin plus ample water (MT); (3) distilled water pretreatment plus drought (DS); (4) 100 μM melatonin plus drought (DS + MT). The melatonin concentration (100 μM) applied in this study was chosen based on a study by Guo et al. (2020a). The experiment was stopped when the soil water content decreased to 50%, i.e., after drought for 6 days. At the end of the treatments, the fully expanded third leaf from the top of the plant was gathered, rapidly frozen in liquid nitrogen, and stored at −80°C for the following measurements.

Plant Growth Attributes

The plant leaf was measured with a tape measure on the last day of the experiment to calculate the leaf area, as described by Ahmad et al. (2019): leaf area = leaf length × maximum leaf width × 0.75. The aboveground plant parts from each group were sampled, and their fresh biomass was determined. Then, the aboveground parts of the maize plant were oven-dried at 105°C for 45 min and then maintained at 80°C for 48 h to obtain a stable dry weight. The amount of chlorophyll in the fully expanded third leaf from the top was determined using a SPAD-502 Plus chlorophyll meter (Plus, Konica Minolta, Japan).

To evaluate the water stress effects, measurements of the relative water content of leaves (RWC) were performed based on the method of Li et al. (2014) with some modifications. Briefly, a total of 1 g of fresh leaves tissue was immediately excised and weighed (fresh weight, WF), and again weighed after floating leaf segments on the water for 12 h in the dark (saturated weight, WS) and after oven-drying at 85°C for 24 h to a constant weight (WD). The RWC was calculated as follows:

$$\mathrm{RWC}\,(\%) = \left[(\mathrm{WF} - \mathrm{WD}) \,/\, (\mathrm{WS} - \mathrm{WD})\right] \times 100 \quad (1)$$

Determination of Gas Exchange Parameters and Chlorophyll Fluorescence

Gas exchange parameters, such as photosynthetic rate (Pn), intercellular CO_2 concentrations (Ci), stomata conductance (Gs), and transpiration rates (Tr) were recorded between 10:00 a.m. and 12:00 a.m. on the fully expanded third leaf from the top with an LI-6400XT portable photosynthesis system (LI-COR, Biosciences, Lincoln, NE, United States). During the measurement period, the photosynthetic photon flux density (PPFD) was controlled at 1,200 μmol m^{-2} s^{-1} (light saturation), the blocking temperature was at 25°C, the CO_2 concentration in the air entering the leaf chamber was at 400 μmol mol^{-1}, and the relative humidity was at 50–70%, according to Dai et al. (2020). Each treatment was replicated three times.

The eighth leaf was selected to evaluate chlorophyll fluorescence *via* the saturation pulse technique, using the Pulse Amplitude Modulated system (Dual-PAM-100, Heinz Walz, Effeltrich, Germany). The maximum efficiency of PSII photochemistry (Fv/Fm), quantum efficiency of PSII [Y(II)], quantum yield regulated energy dissipation of PSII [Y(NPQ)], the quantum yield of non-regulated energy dissipation of PSII [Y(NO)], and photosynthetic electron flows through PSII [ETR(II)] were imaged and calculated after adaptation in the dark for 30 min (Guo et al., 2020b).

Quantification of Carbohydrates

The amounts of sucrose, glucose, and fructose were determined by using high-performance liquid chromatography (HPLC) (Xu et al., 2020). Briefly, a frozen leaf sample (1.0 g) was ground in 5 ml of extraction buffer (ethanol: chloroform: water = 12: 5: 3), and transferred to a centrifuge tube containing 25 ml of ultrapure water. Then, the mixture was heated to 80°C in a water bath for 1 h. After cooling to room temperature, the mixture was centrifuged at 10,000 × *g* for 15 min. The supernatant was filtered into a 50 ml volumetric flask, and the volume was brought to 50 ml with ultrapure water. This solution was used to quantitate the sugars, and the residue was used to quantitate the starch.

Starch was quantified in leaves with the Anthrone method as described by Hansen and Moller (1975). The starch was extracted with 20 ml of deionized water and heated in boiling water for 15 min using the residue obtained in the above extraction process. Then, the residue was extracted with 2 ml of 9.2 M perchloric acid and heated in boiling water for 15 min. After the mixture was centrifuged at 4,000 × *g* for 15 min, the supernatant was brought to a final volume of 50 ml with distilled water. Then, 2.0 ml of the supernatant was mixed with 10 ml of anthrone reagent (1.0 g of anthrone dissolved in 500 ml 72% sulfuric acid) and boiled for 10 min. After this treatment, the tube was rapidly cooled to room temperature, and the absorbance was measured at 630 nm.

NO_3^-, NO_2^-, and NH_4^+ Measurements

The foliar NO_3^-, NO_2^-, and NH_4^+ were extracted from the tissue of each freeze-dried leaf by homogenizing with deionized water. The amount of NO_3^- was spectrophotometrically determined at 410 nm by nitration of salicylic acid, as previously described by Cataldo et al. (1975). The amount of NO_2^- was assayed by measuring the absorbance changes at 620 nm obtained by known concentrations of KNO_3 (Barro et al., 1991). NH_4^+ was quantified by measuring the absorbance changes at 620 nm based on Brautigam et al. (2007), with $(NH_4)_2SO_4$ as the standard.

Quantification of Soluble Protein, Free Amino Acids, and Proline

First, 0.5 g of leaf tissues were ground in 5 ml pre-cooled 50 mM phosphate buffer (pH 7.8). The homogenate was centrifuged at 12,000 × *g* and 4°C for 20 min. The soluble protein concentration in the leaves was quantified using the Coomassie brilliant blue G-250 reagent according to Bradford (1976) with bovine serum

albumin (BSA) as a standard. The free amino acid content was determined by the ninhydrin method (Yemm et al., 1955), with glycine as the standard. Proline was determined according to the method of Ye et al. (2015). Briefly, 0.5 g of fresh leaves were homogenized in 5 ml of 3% aqueous sulfosalicylic acid. Then, the mixtures of 2 ml of supernatant, 2 ml of ninhydrin reagent, and 2 ml of glacial acetic acid were boiled for 30 min, cooled, and centrifuged at 10,000 × *g* for 10 min. The absorbance was recorded at 520 nm, and the amount of proline was calculated according to a standard curve.

Enzymatic Activity Assay

Nitrate reductase (NR) and nitrite reductase (NiR) were measured in maize leaves (0.5 g), which were homogenized with 2 ml buffer containing 0.1 M Tris–HCl (pH 7.5), 10 mM cysteine, 1 mM ethylene diamine tetraacetic acid (EDTA), and 5 μM flavin adenine dinucleotide (FAD). Then, the homogenate was centrifuged at 15,000 × *g* for 20 min at 4°C, and all the extraction steps were performed on ice. The activities of NR and NiR were measured based on the method of Barro et al. (1991).

To determine the activities of glutamine synthetase (GS), glutamate synthetase (GOGAT), and glutamate dehydrogenase (GDH), corn leaves (0.5 g) were grounded in 3 ml buffer containing 50 mM Tris–HCl (pH 8.0), 2 mM Mg^{2+}, 2 mM DTT, and 0.4 M sucrose. Extracts were centrifuged at 10,000 × *g* for 10 min at 4°C, and all operations were performed on ice. GS activity was determined according to the description of O'Neal and Joy (1973). GOGAT was measured as described by Matoh and Takahashi (1982). The activity of GDH was assessed as per Loyola-Vargas and de Jimenez (1984).

The frozen leaf samples (0.5 g) were extracted in 5 ml 100 mM Tris–HCl buffer (pH 7.0) containing 5 mM $MgCl_2$, 2 mM EDTA-Na_2, 2 mM dithiothreitol (DTT), 2% β-mercaptoethanol, 0.2% BSA, and 2% polyvinylpolypyrrolidone (PVP), and the homogenates were centrifuged at 10,000 × *g* and 4°C for 10 min. All the steps were performed on ice. After centrifugation, the supernatant was analyzed to determine if sucrose phosphate synthase (SPS), sucrose synthase (SuSy), acid invertase (AI), and alkaline invertase (NI) were present according to the method of Hu et al. (2020).

To determine ADP glucose pyrophosphorylase (AGPase) activity, 0.5 g maize leaf tissues were mixed with 50 mM HEPES-NaOH buffer, then centrifuged at 4°C for 10 min at 10,000 × *g*. The supernatant was used to determine the activity of AGPase according to Schaffer and Petreikov (1997). All extractions were carried out on the ice.

Citrate synthase (CS) activity in the frozen leaf samples (0.5 g) was extracted with 5 ml 200 mM Tris–HCl buffer (pH 8.2) containing 0.1% Triton X-100 and 10 mM erythorbic acid (Terrier et al., 2001). The samples were grounded in an ice bath, and the homogenates were centrifuged at 5,000 × *g* for 20 min at 4°C. The supernatant was used to determine the activity of CS according to Johnson et al. (1994).

The frozen leaf samples (0.5 g) were grounded with 5 ml 100 mM phosphate buffer (pH 7.2–7.4) in an ice bath, and the homogenates were centrifuged at 3,000 × *g* and 4°C for 20 min. The supernatant was then used for the enzymatic assay. The activity of phosphoenolpyruvate carboxylase (PEPC) was determined using a detection kit (Jingkang, Shanghai).

RNA Extraction and Real-Time Quantitative PCR Assay

The frozen leaf samples (approximately 100 mg) were grounded into powder under liquid nitrogen, and the total RNA of the different treatments was extracted using TRIzol reagent (Thermo Fisher, MA, United States). Then, 2 μg of total RNA was reverse transcribed according to the instructions of the reagent manufacturer (HiScript II Q-RT SuperMix for qPCR, Vazyme, China). The primer sequences for RT-PCR were designed by Primer-BLAST (GenBank, NCBI) and are shown in **Table 1**. qRT-PCR was performed using the CFX96 real-time PCR detection system (Bio-Rad, Hercules, CA, United States) with SYBR Green I (Bio-Rad). The two-step PCR method was performed, and the PCR conditions were as follows: pre-denaturation at 95°C for 30 s, 40 cycles of 95°C for 5 s, and 60°C for 30 s. The results were calculated according to the $2^{-\Delta\Delta\ CT}$ method (Mohd et al., 2011). Three biological replicates were performed, and β-actin was used as an internal reference gene.

Statistical Analysis

ANOVA was performed for the results using SPSS 25.0 software, and then Duncan's multiple range test was carried out, with $P < 0.05$ indicating a significant difference. A SigmaPlot 10.0 was used to draw the figures. All the values are presented as the mean ± SD.

RESULTS

Effects of Melatonin on Maize Growth Under Drought Stress

In the present study, we evaluated the effects of MT, drought stress, and their combination on the growth of maize to understand the role of melatonin in drought tolerance in maize plants. As shown in **Figure 1**, there were no significant effects on maize seedling growth between melatonin-treated and non-treated under the well-irrigated conditions. The water deficit caused a significant inhibition of plant growth, with the aboveground biomass accumulation and leaf area of non-treated maize seedlings decreasing by 36.0 and 42.0%, respectively, compared with control (**Figures 1A,B**). In comparison, exogenous melatonin application mitigated the drought stress, and the aboveground biomass accumulation and leaf area of melatonin-treated seedlings increased by 30.6 and 11.5%, respectively, compared with that of the non-treated seedlings (**Figures 1A,B**). Drought stress resulted in a sharp decrease in chlorophyll and the RWC, while the application of exogenous melatonin reversed these trends to some extent (**Figures 1C,D**). In relation to control, water deficit substantially reduced chlorophyll and the RWC by 30.17 and 40.19%, respectively. However, melatonin treatment caused significant recovery of chlorophyll and the RWC by

TABLE 1 | Primers used for real-time PCR (RT-PCR) amplification.

Genes	Sense primer	Anti-sense primer
*ZmSh1*_sucrose synthase	GATGCCCTGTTTGATAGTGA	ATCGTCGTGCCCTTGTAG
*Zmsps1*_sucrose phosphate synthetase	CCAGCGGCATGTGAATTTGAT	CACCAGTATAGTTAGCAGTGTCC
*ZmAgp1*_ADP-glucose pyrophosphorylase	GTTGTTTGAGGAGCATAAT	ACAGATAAGCCTGAACCC
*Zmcts1*_citrate synthase	TGCTCACAGTGGAGTTTTGC	AACACTCTTCGGCCTCTCAA
*ZmPEPC*_phosphoenolpyruvate carboxylase	GAAGACACGCTCATCCTCACC	CAGTTCGGCATTTCCATCC
*ZmRCA1*_RuBisCo activase	GCAAAGGCCAGGGAAAATCG	ATGTTCATCAGGGTGGCGTT
*ZmrbcS*_RuBisco small subunit	GCAGGAGGCCATCAAATCCT	AAGCAAGCAAAGGGTACGGT
*ZmrbcL*_RuBisCo large subunit	TGATGGGACAACCACTTCGG	GTACAGCCACCACCTACGAT
*ZmGln1-3*_cytosolic glutamine synthetase	CGAAGCGATTGCAAAGCCATTG	GTTCTGTTTTGGCACACCAC
*ZmGS2*_plastidic glutamine synthetase	TGTGAAGCAGCTGAAGGATG	CGTATCCGAATATCCGATGAA
*Zmgdh1*_glutamate dehydrogenase	GTCATAAACAAGGATAATGCTAACG	CCAGTATGTCGGGGAGGAT
*Zmfgs1*_glutamate synthase	CTGATCGTTCTGAAGCACCT	AGCAGACATACGGAGACCAT
*ZmNR*_nitrate reductase	ATGATCCAGTTCGCCATCTC	GTCCGTGGTACGTCGTAGGT
*ZmNiR*_nitrite reductase	CTTCATGGGCTGCCTCAC	CGCTTGACGAAGGTCCTACT
ZmActin	CCATCACTGCCACACAGAAAAC	AGGAACACGGAAGGACATACCAG

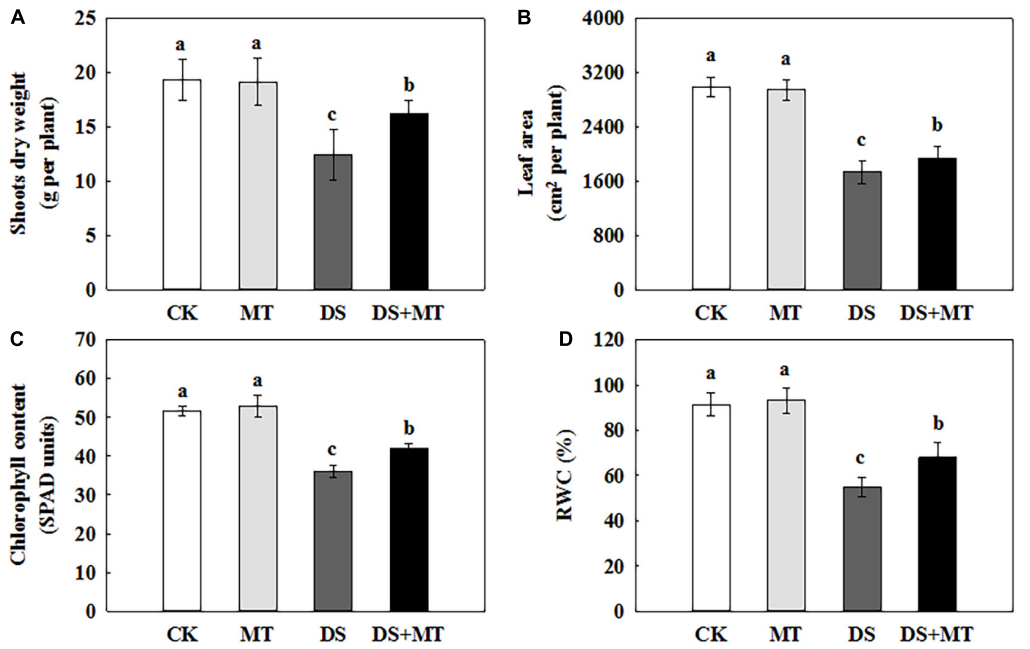

FIGURE 1 | Effects of drought and exogenous melatonin on plant growth, chlorophyll content, and relative water content (RWC) in leaves of maize. **(A)** Shoot dry weight, **(B)** whole plant leaf area, **(C)** the chlorophyll content in leaves, and **(D)** the leaf relative water content. Values are the averages of three replicates ± SD. Different letters indicate significant differences according to Duncan's multiple range tests ($P < 0.05$).

16.93 and 24.41%, respectively, compared with the drought stress treatment.

Effects of Melatonin on Stomatal Behavior Under Drought Stress

The SEM stomatal images showed that the stomata were almost completely closed by drought stress (**Figure 2B**), stomatal aperture exhibited a 72.3% decrease in comparison with control (**Figure 3C**). Moreover, drought stress also led to the stomata being shorter, narrower, and thinner. The stomatal length, width, and density in the plants that underwent drought stress alone were 82.3, 76.7, and 79.1% of that of control, respectively (**Figures 3A,B,D**). Compared with the plants that received limited water, the stomata remained partially open in the melatonin-treated maize under drought stress (**Figure 2D**). Correspondingly, the stomatal aperture of melatonin-treated plants was 1.3-fold higher than that of stressed plants (**Figure 3C**). The melatonin-treated plants had longer and wider stomata under drought stress. The stomatal length and width in maize seedlings treated with melatonin were increased by 11.9 and 12.0%, respectively, in contrast to the drought stress-treated plants (**Figures 3A,B**). In addition, the stomatal length

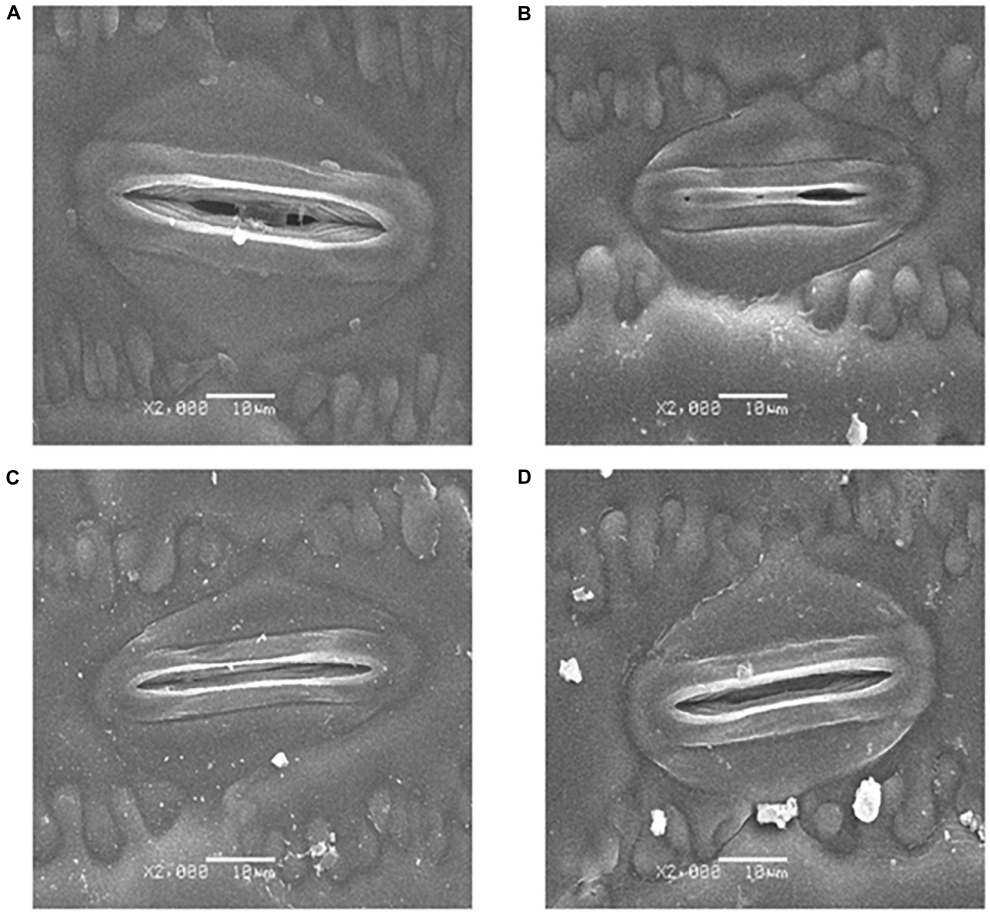

FIGURE 2 | Effects of drought and exogenous melatonin on stomata in leaves. **(A)** Stomata from well-watered plants. **(B)** Stomata from drought-treated plants. **(C)** Stomata from well-watered plants that were also treated with 100 μM melatonin. **(D)** Stomata from drought-treated plants that were also treated with 100 μM melatonin. Magnification 2000 X, scale bars = 10.0 μm.

and width were not affected by the application of melatonin compared with the well-watered plants (**Figures 3A,B**), but the stomatal density of melatonin-treated plants under soil drought stress was less than that of control (**Figure 3D**). Under well-watered conditions, the application of melatonin decreased the stomatal aperture by 36.2%, but it had no effect on other characteristics of stomata (**Figure 3**).

Effects of Melatonin on Photosynthesis of Plants Under Drought Stress

Under well-watered conditions, the application of exogenous melatonin resulted in no obvious change in the ability to photosynthesize (**Figure 4**). After 7 days of drought stress, the Pn, Ci, Gs, and Tr were decreased by 58.3, 55.3, 70.4, and 51.7%, respectively, compared with control (**Figure 4**). In contrast, the exogenous melatonin-treated plants exhibited fewer negative effects of drought stress, with a decrease of only 46.0, 31.5, 50.0, and 31.2% for Pn, Ci, Gs, and Tr, respectively, compared with control (**Figure 4**). These data suggest that there was an increased photosynthetic performance for the melatonin-treated plants compared with the non-treated plants under drought stress. In addition, the melatonin treatment increased the Rubisco activity from 25.5 to 38.31 mg g^{-1} h^{-1} FW, and the change in Rubisco activity was parallel with the expression of *ZmRCA1*, *ZmrbcL*, and *ZmrbcS* (**Table 2** and **Figure 5**). These results further support the ability of melatonin-treated plants to maintain photosynthetic C assimilation during drought stress.

To further investigate the alterations of photosynthesis in maize plants exposed to soil drought stress, multiple chlorophyll fluorescence parameters, such as Fv/Fm, Y(II), Y(NPQ), Y(NO), and ETR(II) were calculated (**Table 2**). The results of fluorescence measurement showed that the application of melatonin did not change the chlorophyll fluorescence parameters under the well-irrigated condition (**Table 2**). Compared with control, drought stress markedly reduced the Fv/Fm, Y(II), and ETR(II) by 7.0, 47.6, and 47.5%, respectively. However, melatonin application resulted in the significant reversal of the Fv/Fm, Y(II), and ETR(II) by 5.1, 50.9, and 53.7%, respectively. Moreover, the opposite effects were observed in Y(NPQ) and Y(NO), and the Y(NPQ) and Y(NO) of non-irrigated plants not treated with melatonin were 53.0 and 17.2% higher than the CK

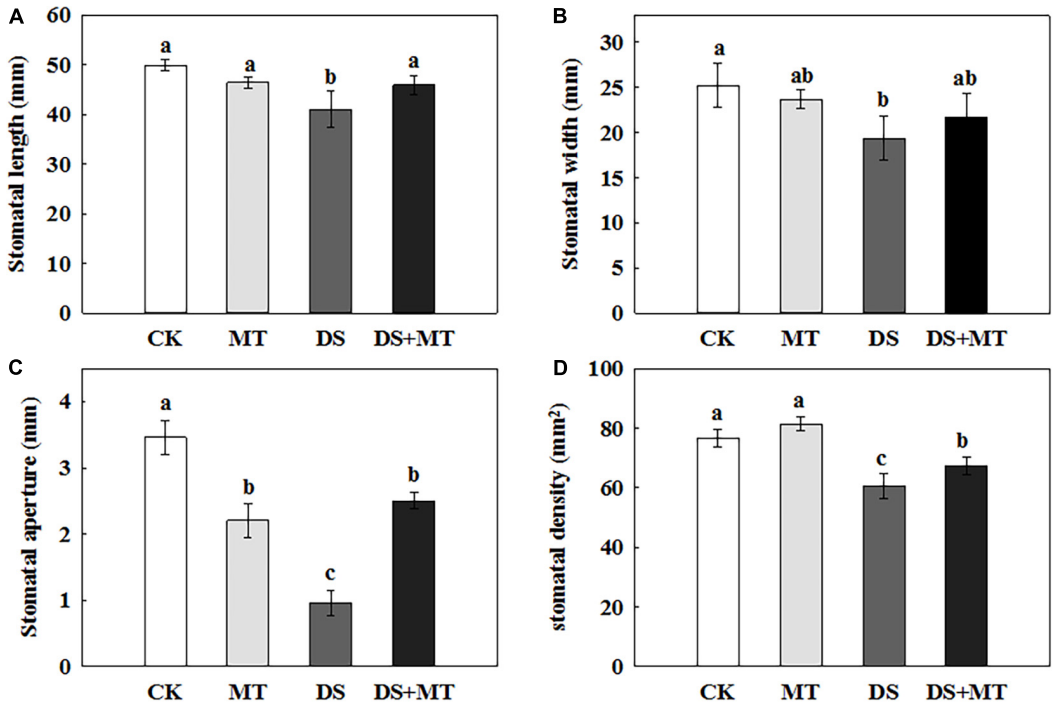

FIGURE 3 | Effects of drought and exogenous melatonin on stomatal characteristics in leaves of maize. **(A)** Stomatal length, **(B)** stomatal width, **(C)** stomatal aperture, and **(D)** stomatal density. Values are the averages of three replicates ± SD. Different letters indicate significant differences according to Duncan's multiple range tests ($P < 0.05$).

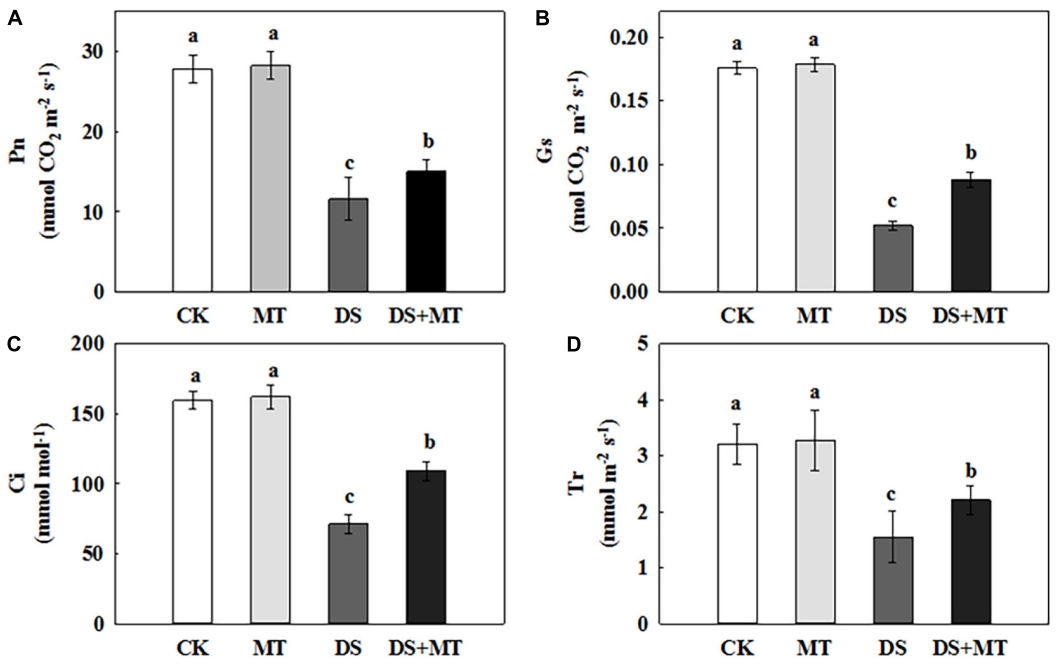

FIGURE 4 | Effects of drought and exogenous melatonin on gas exchange parameters in leaves of maize. **(A)** Net photosynthetic rate (Pn), **(B)** stomatal conductance (Gs), **(C)** intercellular CO_2 concentration (Ci), and **(D)** transpiration rate (Tr). Values are the averages of three replicates ± SD. Different letters indicate significant differences according to Duncan's multiple range tests ($P < 0.05$).

seedlings. Compared with the untreated seedlings that underwent water restriction, melatonin treatment significantly decreased the Y(NPQ) and Y(NO) levels, with Y(NO) being decreased to the normal level.

Effects of Melatonin on Carbon Metabolites Under Drought Stress

Carbon metabolism is tightly linked with photosynthesis. To elucidate how melatonin regulates C metabolic homeostasis in maize under drought stress, we further measured the amount of carbohydrate and analyzed the activities of C-metabolizing enzymes in different treatments (**Table 3** and **Figure 6**). Exogenously applied melatonin did not affect the amounts of soluble sugar, sucrose, starch, or fructose under normal conditions (**Figure 6**). In relation to control, there was a remarkable decrease in sucrose and starch in maize leaves (74.2 and 51.1% of control plants), when subjected to drought (**Figures 6B,C**). In contrast, melatonin treatment substantially increased the concentrations of sucrose and starch by 105.9 and 40.8%, respectively, compared with the drought-stressed plants (**Figures 6B,C**). Drought stress increased glucose and fructose levels by 97.9 and 66.4%, respectively, compared with control (**Figures 6A,D**). However, after 7 days of drought stress, the glucose and fructose in maize seedlings treated with melatonin were reduced by 18.7 and 20.5%, respectively, in contrast to the non-treated plants (**Figures 6A,D**).

Under normal growth conditions, all the C-metabolizing enzymatic activities that were evaluated in maize leaves were not altered by exogenous melatonin (**Table 3**). Compared with the control, soil water deficit caused considerable increases in SS and INV activity in melatonin-treated (1.3-fold and 1.7-fold of the control plants) and -untreated (1.7-fold and 2.7-fold of the control plants) maize seedlings, but the extent of increase of melatonin treatment was significantly lower than that of drought stress treatment (**Table 3**). In contrast to the control plants, water restriction resulted in a drastic decline of the activities of SPS, AGPase, PEPC, and CS by 34.9, 31.1, 22.0, and 40.5%, respectively. Compared with the drought stress treatment, the activities of SPS, AGPase, PEPC, and CS in melatonin-treated plants were increased by 60.5, 25.1, 53.6, and 33.6, respectively, with the activities of SPS and PEPC being notably higher than those of control. Furthermore, we found that the melatonin-mediated modulation of C-metabolizing enzymes was due to the induced expression of key genes encoding these enzymes, namely, *ZmSh1*, *ZmAgp1*, *Zmcts1*, *Zmsps1*, *and ZmPEPC* (**Figure 5**).

Effects of Melatonin on Nitrogen Metabolism Under Drought Stress

Nitrogen metabolism is closely associated with chlorophyll fluorescence and C assimilation. Under the well-irrigated condition, exogenous melatonin application resulted in no remarkable changes in the amounts of primary N metabolites (**Figure 7**). Water stress led to a significant reduction of soluble protein, NO_3^-, and NO_2^- by 29.8, 31.9, and 25.5%, respectively, compared with control. However, in drought-stressed plants, the melatonin treatment increased soluble protein, NO_3^-, and NO_2^- by 23.4, 18.9, and 15.1%, respectively (**Figure 7**). Under water deficit, free amino acids, NH_4^+, and proline in untreated plants were increased by 56.1, 49.5, and 61.4%, while in melatonin-treated plants, these were increased by 23.2, 28.3, and 132.9%, respectively (**Figure 7**).

The activities of the six N metabolic enzymes were hardly affected by exogenous melatonin under the well-watered condition. Due to the suppression of the expression of *ZmNR*, *ZmNiR*, *ZmGln1-3* and *ZmGS2*, and *Zmfgs1*, which are the key genes encoding NR, NiR, GS, and GOGAT in drought-stressed plants, these enzymatic activities decreased by 36.8, 37.3, 40.4, and 31.9%, respectively, compared with that in the control plants (**Table 4** and **Figure 5**). Exogenous melatonin-treated leaves exhibited higher NR, NiR, GS, and GOGAT activities than the drought-stressed leaves, and the expression of the respective genes was also higher in the melatonin-treated leaves compared with the drought-stressed plants (**Table 4** and **Figure 5**). In contrast, withholding irrigation significantly increased the foliar GDH amination and GDH deamination activities compared with the control plants, with an average increase of 2.2- and 1.5-time (**Table 4**). The qRT-PCR analyses indicated that the transcript levels of *Zmgdh1*, a key gene encoding GDH, were also dramatically induced by drought stress (**Figure 5**). However, the GDH amination and deamination activities (79.4 and 68.1% of drought stressed plants, respectively) and *Zmgdh1* expression were notably inhibited by the addition of 100 μM melatonin compared with the drought stress treatment (**Table 4** and **Figure 5**).

DISCUSSION

Exogenous Melatonin Enhanced Photosynthetic Carbon Assimilation by Promoting Stomatal Opening Under Drought Stress

Water deficit stress severely inhibits plant growth and development by affecting various aspects of plants physiology and biochemistry (Meng et al., 2014; Guo et al., 2020a; Gupta et al., 2020). Various types of research have demonstrated that exogenously applied melatonin can enhance drought tolerance in plants (Guo et al., 2020a; Hu et al., 2020; Khattak et al., 2021). Our results showed that the growth of maize was critically suppressed by water deficit because the drought-stressed plants exhibited lower values of leaf area and shoot dry weight compared with the control plants (**Figure 1**). In contrast, foliar-applied melatonin mitigates plant growth inhibition caused by drought stress, indicating that the exogenous melatonin application increased the tolerance to water deficit in plants (**Figure 1**). Moreover, we also observed that there was a reduction of the chlorophyll content and RWC after 7 days of drought stress, while melatonin treatment attenuated the decrease in chlorophyll content and RWC (**Figure 1**). Similar research results were observed in previous reports (Huang et al., 2019; Dai et al., 2020). These consequences may be due to the application of melatonin, which can facilitate photosynthesis.

TABLE 2 | Effects of drought and exogenous melatonin on PSII chlorophyll fluorescence parameters and Rubisco activity in leaves of maize.

Parameters	CK	MT	DS	DS + MT
Fv/Fm	0.815 ± 0.04^{a}	0.817 ± 0.05^{a}	0.758 ± 0.02^{c}	0.797 ± 0.03^{b}
Y(II)	0.431 ± 0.04^{a}	0.438 ± 0.02^{a}	0.226 ± 0.03^{c}	0.341 ± 0.02^{b}
Y(NPQ)	0.296 ± 0.01^{c}	0.286 ± 0.02^{c}	0.453 ± 0.03^{a}	0.369 ± 0.02^{b}
Y(NO)	0.273 ± 0.02^{b}	0.276 ± 0.01^{b}	0.320 ± 0.02^{a}	0.290 ± 0.04^{b}
ETR(II)	38.7 ± 1.46^{a}	38.6 ± 1.56^{a}	20.3 ± 1.67^{c}	31.2 ± 1.55^{b}
Rubisco activity (mg g^{-1} h^{-1} FW)	30.63 ± 1.88^{b}	31.82 ± 1.45^{b}	25.52 ± 1.48^{c}	38.31 ± 1.01^{a}

The values are the averages of three replicates ± SD. Different letters indicate significant differences according to Duncan's multiple range tests ($P < 0.05$).
Fv/Fm, quantitative values of maximum PSII yield; Y(II), effective quantum yield of PSII; Y(NPQ), quantum yield of regulatory energy dissipation; Y(NO), quantum yield of non-regulatory energy dissipation; ETR(II), electron transport rate of PSII.

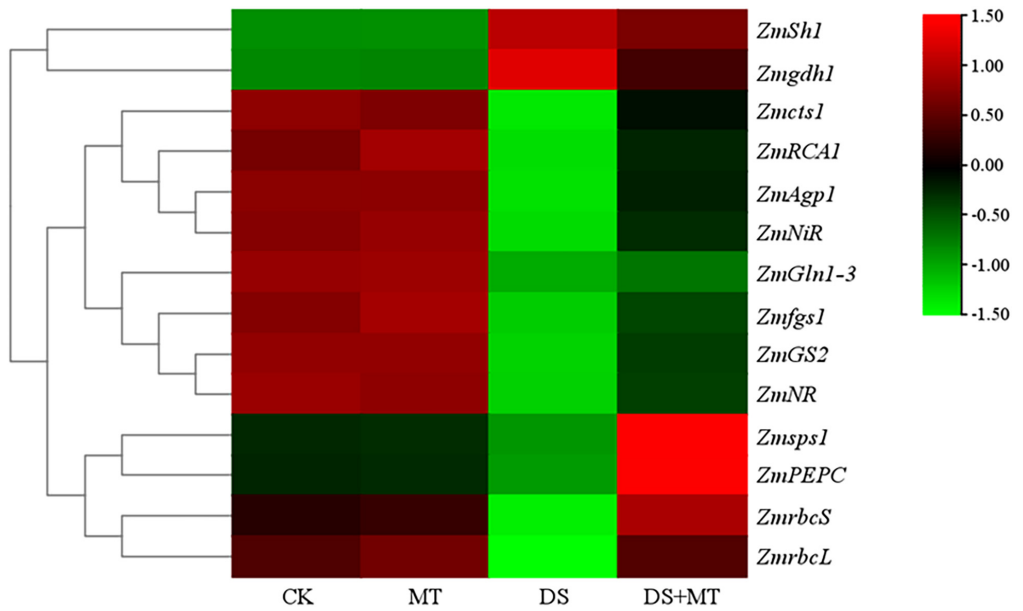

FIGURE 5 | A hierarchical clustering heat map of genes encoding enzymes involved in the processes of photosynthetic carbon assimilation, carbon metabolism, and nitrogen assimilation. Normalization of expression values was performed by log10 (FPKM). For each gene, low expression is indicated by green; high expression is indicated by red.

TABLE 3 | The effects of drought and exogenous melatonin on C-related enzymatic activities in leaves of maize.

Parameters	CK	MT	DS	DS + MT
SS activity (mg g^{-1} h^{-1}FW)	17.31 ± 1.02^{a}	16.96 ± 2.09^{a}	28.92 ± 2.10^{c}	22.29 ± 1.99^{b}
SPS activity (mg g^{-1} h^{-1}FW)	63.19 ± 4.23^{b}	64.17 ± 3.11^{b}	46.84 ± 3.11^{c}	75.19 ± 1.78^{a}
INV activity (mg g^{-1} h^{-1}FW)	5.48 ± 0.30^{a}	5.82 ± 0.86^{a}	15.00 ± 1.62^{c}	9.43 ± 1.26^{b}
AGPase activity (mg g^{-1} h^{-1}FW)	24.04 ± 1.40^{a}	25.09 ± 1.02^{a}	16.56 ± 0.93^{c}	20.71 ± 2.34^{b}
PEPC activity (μmol CO_2 mg^{-1} h^{-1})	53.27 ± 4.47^{b}	55.63 ± 3.40^{b}	41.56 ± 5.08^{c}	65.77 ± 6.15^{a}
CS activity (mg g^{-1} h^{-1}FW)	19.14 ± 1.63^{c}	19.87 ± 1.27^{c}	11.39 ± 1.26^{b}	15.22 ± 1.28^{a}

The values are the averages of three replicates ± SD. Different letters indicate significant differences according to Duncan's multiple range tests ($P < 0.05$).
SS, sucrose synthase; SPS, sucrose phosphate synthetase; INV, invertase; AGPase, ADP-glucose pyrophosphorylase; PEPC, phosphoenolpyruvate carboxylase; CS, citrate synthase.

Our results indicate that the water deficit significantly decreased photosynthetic activity in maize (**Figure 4**). Photosynthesis is the principal process of capturing light energy to synthesize carbohydrates, and it is closely related to the growth of plants. However, photosynthesis is sensitive to drought stress, and a water deficit notably inhibits photosynthesis in many plants (Velikova et al., 2018; Zhou et al., 2019; Sharma et al., 2020). In general, the decrease in photosynthetic activity is limited by the

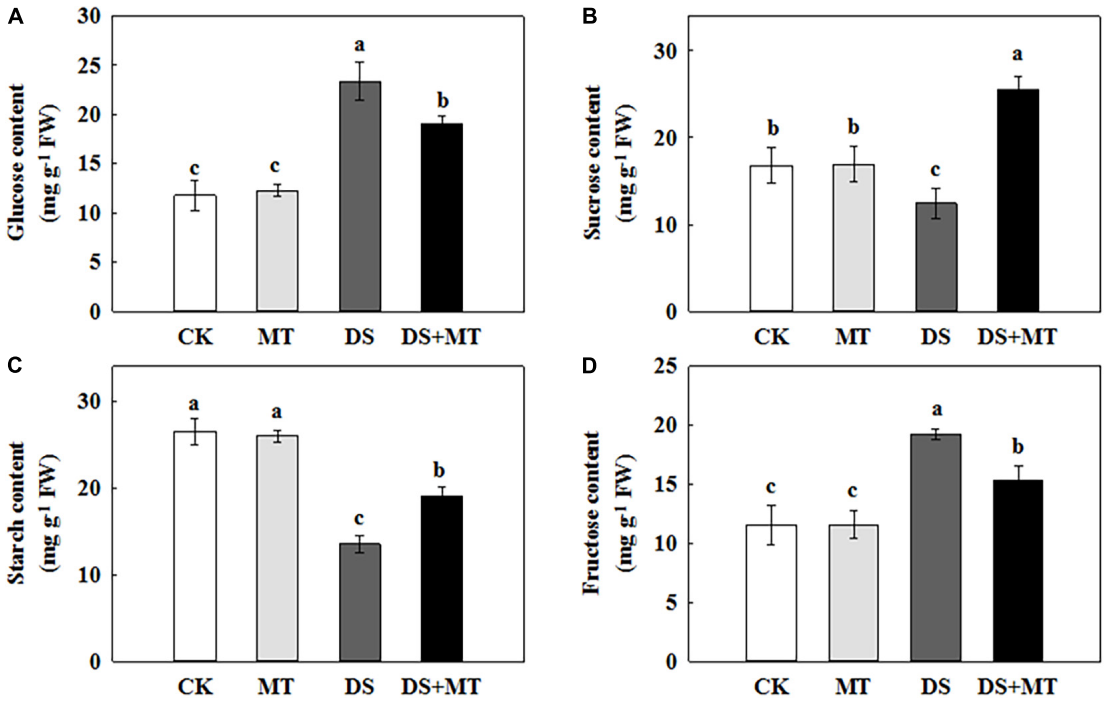

FIGURE 6 | Effects of drought and exogenous melatonin on the sugar content in leaves of maize. **(A)** Glucose content, **(B)** sucrose content, **(C)** starch content, and **(D)** fructose content. Values are the averages of three replicates ± SD. Different letters indicate significant differences according to Duncan's multiple range tests ($P < 0.05$).

reduction in CO_2 diffusion to the chloroplast, which is induced by stomatal closure (Liu et al., 2013; Ye et al., 2016). The closure of stomata restricts the mesophyll transport of CO_2, resulting in a decrease in the concentration of CO_2 in the intercellular airspaces of leaves. Low intercellular carbon dioxide (Ci) will decrease the activities of key enzymes, such as Rubisco to limit the photosynthesis rate (Flexas et al., 2006; Chaves et al., 2009; Zhong et al., 2019). As expected, our results confirmed that drought caused the stomata to close almost completely (**Figure 2**). The Ci and Pn level, and the activity of Rubisco, and the expression of several genes encoding key enzymes in Rubisco also decreased under the drought conditions (**Figures 4**, **5** and **Table 2**). These results further support the conclusion that the stomatal closure in water-stressed plants may be one of the reasons for the decrease in photosynthesis. However, the melatonin treatment increased the stomatal aperture and partially opened stomata under a water deficit (**Figure 2**). In addition, melatonin significantly increased stomatal density and stomatal length compared with water deficit stress (**Figure 3**). We speculate that in response to drought stress, an optimization strategy for stomatal structure and distribution would be beneficial. Similar research results were obtained in rape, with low stomatal width and high stomatal density observed in rape plants that experienced drought (Dai et al., 2020). Correspondingly, the higher Rubisco activity and Pn value were observed in melatonin-treated plants compared with the drought-stressed plants (**Figures 3**, **4** and **Table 2**), indicating that melatonin increased the C fixation and photosynthetic activity in maize plants under drought stress.

Chlorophyll fluorescence is an important indicator that can be used to characterize the photosynthetic capacity and energy conversion efficiency of PSII in plants (Mathur et al., 2019). Many studies have demonstrated that severe or long-term water deficit leads to photo-inhibition in the PSII reaction center (Huang et al., 2019; Zhou et al., 2019). Consistent with these findings, a large decrease in Fv/Fm, Y(II), and ETR(II) was observed in drought-stressed plants (**Table 2**). Fv/Fm, Y(II), and ETR(II) decreased, while Y(NPQ) and Y(NO) increased, indicating that drought stress-induced severe damage to the PSII complexes in maize seedlings. This was attributed to the fact that the limitation of ambient CO_2 diffusion to the site of carboxylation resulted in a relative excess of light energy and electron sinks, and led to photo-inhibition or photo-oxidation (Atkin and Macherel, 2009; Zhong et al., 2018). However, exogenous melatonin treatment can increase the photosynthetic efficiency and protect the maize plants from photo-inhibition caused by drought, because among plants exposed to drought stress, those treated with exogenous melatonin exhibited enhanced Fv/Fm, Y(II), and ETR(II), and decreased Y(NPQ) and Y(NO) levels (**Table 2**). Consistent with the current results, a previous study demonstrated that melatonin-treated tomato plants displayed significantly increased Fv/Fm and ΦPSII compared with the non-treated plants under water deficit conditions (Liu et al., 2015). Additionally, the application of melatonin produces a protective effect on chlorophyll (Campos et al., 2019; Li Z. et al., 2021). The amount of chlorophyll in melatonin-treated maize plants was higher as compared with the non-treated plants under drought

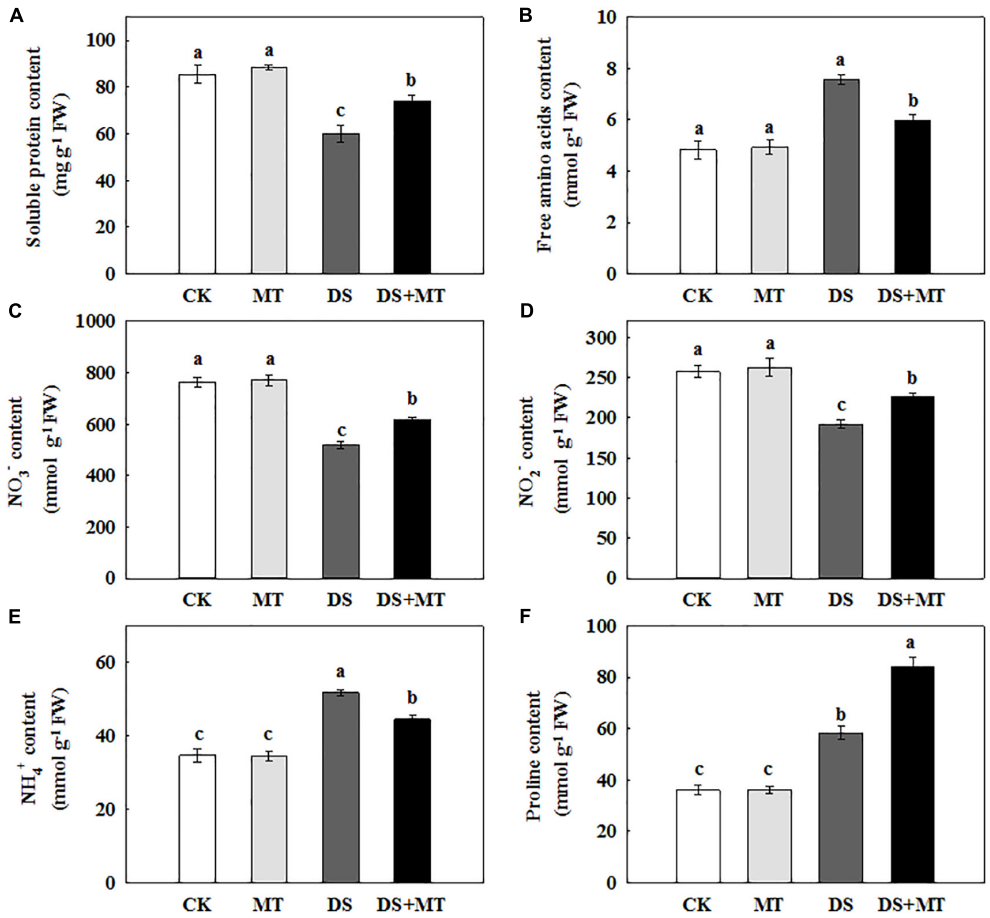

FIGURE 7 | Effects of drought and exogenous melatonin on soluble protein, free amino acid, inorganic N compounds, and proline content in the leaves of maize. **(A)** Soluble protein content, **(B)** free amino acid content, **(C)** nitrate (NO_3^-) content, **(D)** nitrite (NO_2^-) content, **(E)** ammonium (NO_4^-) content, and **(F)** proline content. Values are the averages of three replicates ± SD. Different letters indicate significant differences according to Duncan's multiple range tests ($P < 0.05$).

stress in this study (**Figure 1C**), confirming that exogenous melatonin slows damage to the photosynthetic apparatus.

Exogenous Melatonin Mitigated Drought Stress by Maintaining Carbohydrate Balance

In view of the inhibition of the photosynthetic capacity by soil water restriction, we observed that there was low carbohydrate synthesis in the drought-stressed maize plants (**Figure 6**). Plant growth and carbohydrate metabolism are closely linked because carbohydrates are the structural components and the energy source for the production and maintenance of biomass (Song et al., 2020). In higher plants, carbohydrates, such as sucrose and starch are created in photosynthetically active leaves (sources) and then exported to support sinks, which allow leaf expansion, and stem and root growth (Adams et al., 2013; Song et al., 2020). In the present study, we found that drought stress-induced a pronounced decrease in the activity and gene transcription of the main enzymes (AGPase and SPS) involved in starch and sucrose synthesis, leading to a lower starch and sucrose level in the leaves (**Figures 5**, **7** and **Table 3**). This phenomenon is attributed to the growth inhibition observed in drought-stressed plants. Similar results were reported in soybean (Du et al., 2020). Along with the enhancement of the activity and gene transcription of AGPase and SPS (**Table 3** and **Figure 5**), foliar spraying of melatonin facilitated starch and sucrose biosynthesis in maize leaves compared with the drought-stressed plants (**Figure 6**). These results demonstrated that melatonin treatment supports the growth of maize plants by the accumulation of additional photosynthates. The positive correlation between melatonin and carbohydrate synthesis was confirmed in the previous studies (Campos et al., 2019; Hu et al., 2020).

In addition, we observed that the levels of glucose and fructose were significantly enhanced in the water deficit-stressed maize plants compared with the control plants (**Figure 6**). Higher concentrations of glucose and fructose in the leaves of drought-stressed plants might be attributed to the enhancement of SS and INV activities (**Table 3**) because both enzymes can fragment sucrose into hexose sugars (Gandin et al., 2009). This phenomenon also partially explains why the sucrose content in the leaves decreased under a water deficit. Another possible

TABLE 4 | The effects of drought and exogenous melatonin on N-related enzymatic activities in leaves of maize.

Parameters	CK	MT	DS	DS + MT
NR activity (mmol NO_2^- mg^{-1} h^{-1} FW)	0.37 ± 0.01^a	0.34 ± 0.02^a	0.23 ± 0.01^c	0.27 ± 0.01^b
NiR activity (mmol NO_2^- mg^{-1} min^{-1} FW)	0.51 ± 0.03^a	0.53 ± 0.01^a	0.32 ± 0.01^c	0.43 ± 0.02^b
GS activity (mg g^{-1} h^{-1} FW)	70.46 ± 5.81^a	71.57 ± 5.86^a	42.11 ± 4.62^c	56.62 ± 4.26^b
GOGAT activity (mmol mg^{-1} Prot min^{-1})	3.98 ± 0.18^a	4.08 ± 0.15^a	2.71 ± 0.13^c	3.40 ± 0.15^b
NAD-GDH activity (nmol mg^{-1} Prot min^{-1})	4.20 ± 0.24^c	4.25 ± 0.31^c	9.38 ± 0.13^a	6.39 ± 0.21^b
NADH-GDH activity (nmol mg^{-1} Prot min^{-1})	11.09 ± 0.45^c	11.13 ± 0.37^c	16.52 ± 0.52^a	13.11 ± 0.33^b

The values are the averages of three replicates ± SD. Different letters indicate significant differences according to Duncan's multiple range tests ($P < 0.05$).
NR, nitrate reductase; NiR, nitrite reductase; GS, glutamine synthetase; GOGAT, glutamate synthetase; NAD-GDH, deaminating glutamate dehydrogenase; NADH-GDH, aminating glutamate dehydrogenase.

reason for the increase in glucose and fructose level is that drought stress inhibits the tricarboxylic acid (TCA) cycle. It has been reported that water restriction repressed the activity of the TCA cycle, which would reduce the oxidation of glucose and result in a depletion of the ATP pool (Nguyen et al., 2010; Hu et al., 2020). Our results are in agreement with this interpretation, as we found that drought stress decreased the activity and gene transcription of PEPC and CS, and increased the amounts of glucose and fructose in the leaves, compared with the control plants. However, recent research indicated that melatonin was involved in regulating the TCA cycle and could enhance energy production in water-stressed anthers (Hu et al., 2020). Our work further confirmed the protective role of melatonin on energy production in maize under drought stress. Exogenously applied melatonin increased energy production in drought-stressed plants (**Figure 6**). This increased energy can be further used for plant growth, thus promoting the growth of plants subjected to drought stress. Furthermore, the enhancements in the activities of the TCA cycle induced by melatonin under drought stress will provide more C skeletons and energy for the biosynthesis of downstream amino acids.

Exogenous Melatonin Improved Nitrogen Metabolism Under Drought Stress

Soil water deficit often causes a decrease in the activities of N assimilation enzymes and the synthesis of N-containing compounds to disrupt N metabolism (Zhong et al., 2018; Xie et al., 2019). In this regard, several previous studies have shown that drought stress can inhibit the uptake of NO_3^-, resulting in a decrease in NR activity (Miranda-Apodaca et al., 2020; Ren et al., 2020). In this study, consistent with the decrease in NO_3^- and NO_2^- (**Figure 7**), drought stress triggered a marked diminution in NR and NiR activities, which reflects the decrease in the N assimilation capacity under a water deficit. Additionally, although the NR and NiR activities decreased under drought, it was also observed that NH_4^+ accumulated in maize leaves (**Table 4** and **Figure 7**). This increment can be explained by the glycine oxidation in activated photorespiration (Zhong et al., 2018). Under drought stress, the expression levels of the *ZmNR and ZmNiR* genes, which encode the NR and NiR enzymes, were enhanced in the melatonin-treated plants (**Table 4** and **Figure 5**). Correspondingly, the melatonin-treated plants under drought stress exhibited higher NR and NiR transcription and activity than untreated plants (**Table 4** and **Figure 5**). In drought-stressed plants that were treated with melatonin, the increased NO_3^- and NO_2^- levels were in accordance with the increase in NR and NiR activities (**Figure 7**). In this context, induced NO_3^- reduction by melatonin treatment resulted in the maintenance of the osmotic pressure in photosynthetic cells (Zhong et al., 2019). Moreover, NO_3^- reduction is a process with a high energy requirement, and increased NO_3^- reduction in leaves would be facilitated due to the excessive energy derived from the photosynthetic apparatus (Sunil et al., 2013; Zhong et al., 2018).

The excessive accumulation of NH_4^+ in plant leaves due to drought stress has a toxic effect on plants because a high level of NH_4^+ triggers protein extrusion and cytosolic pH disturbances (Xie et al., 2019). In plants, NH_4^+ must be assimilated *via* the GS/GOGAT cycle and GDH pathway into glutamine and glutamate (Liu et al., 2019). However, GDH has a lower affinity for NH_4^+, and the GDH pathway is markedly activated only when the GS/GOGAT cycle is restrained (Xie et al., 2019). In this study, consistent with the transcription data of genes encoding GS and GOGAT (**Figure 5**), there were dramatically decreased GS and GOGAT activities in the plants exposed to drought (**Table 4**), and this could be another important reason for the accumulation of NH_4^+. Those results are consistent with those reported previously (Jing et al., 2021). In contrast, our results show that melatonin mitigates the toxic effect of NH_4^+, because the NH_4^+ assimilation was notably strengthened in melatonin-treated drought-stressed plants by enhancing the activity and gene transcription of GS and GOGAT, and decreasing the GDH activity and *Zmgdh1* (**Table 4** and **Figure 5**). This phenomenon can be explained by the enhancement of photosynthesis and the TCA cycle, which promotes the synthesis of the C skeleton and reduces the power and provides sufficient substrates and energy for the biosynthesis of amino acids. Thus, the GS/GOGAT cycle was enhanced in plants under drought, which subsequently promoted the synthesis of glutamate and other amino acids (Liang et al., 2018; Xie et al., 2019). These results indicate the positive impact of melatonin upon coordinated C assimilation and N metabolism in plants.

It was also observed that drought substantially increased the free amino acid and proline levels in the maize leaves compared with the control treatment (**Figures 7B,F**), and this may have occurred because N metabolism is involved in osmotic adjustment. The synthesis and accumulation of amino acids are often a strategy to enable plants to withstand

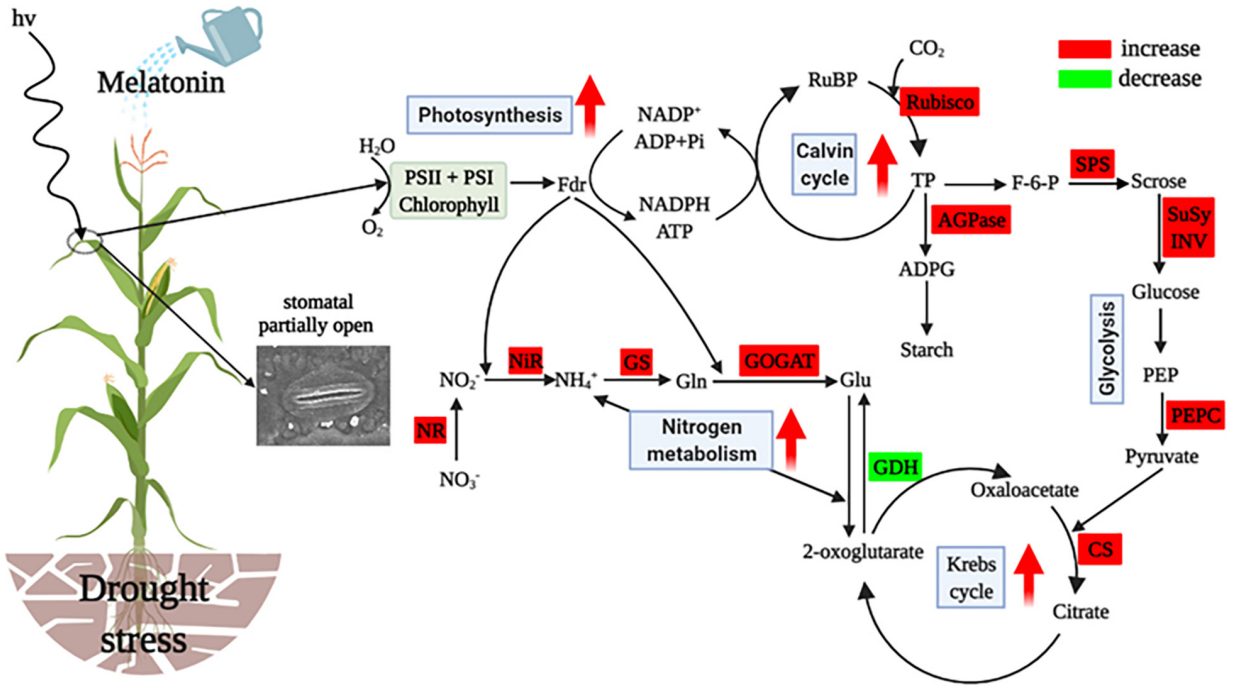

FIGURE 8 | Simplified representation of exogenous melatonin affecting C and N metabolism in leaves of drought-stressed maize. Metabolism and parameters that increased or decreased it are indicated by the red or green boxes in melatonin-treated plants when compared with drought-stressed plants. The red arrows in the figure denote increased or enhanced processes. RuBP, ribulose-l,5-disphosphate; Rubisco, ribulose bisphosphate carboxylase oxygenase; TP, triose phosphate; AGPase, ADP-glucose pyrophosphorylase; ADPG, adenosine diphosphate glucose; F-6-P, fructose-6-phosphate; SPS, sucrose phosphate synthetase; SuSy, sucrose synthase; INV, invertase; PEP, phosphoenolpyravate; PEPC, phosphoenolpyravate carboxylase; CS, citrate synthase; GDH, glutamate dehydrogenase; Glu, glutamate; GOGAT, glutamate synthetase; Gln, glutamine; GS, glutamine synthetase; NH_4^+, ammonia; NiR, nitrite reductase; NO_2^+, nitrite; NR, nitrate reductase; NO_3^+, nitrate. This figure was created using BioRender (https://biorender.com/).

adverse environmental conditions because amino acids can serve as osmotica to maintain the stability of the cellular structure and cell osmotic pressure under drought conditions (Meng et al., 2014; Zhong et al., 2018). The treatment of melatonin dramatically enhanced the levels of soluble protein and proline, and vastly decreased the free amino acid content in maize leaves under water-limiting conditions (**Figure 7**). These results indicate exogenously applied melatonin in drought-stressed plants regulated cell turgor by producing additional substances that regulated osmolarity, maintained membrane integrity. Stability in protein synthesis can increase the resistance of plants to stress (Georgiadou et al., 2018). Most soluble proteins are enzymes that are involved in various metabolic pathways in plants (Sun et al., 2020). Thus, they are an important index for measuring the protein damage in the process of plant metabolism and are usually positively correlated with soil drought stress tolerance (Xie et al., 2019). In our experiments, soil drought stress significantly diminished the soluble protein content, indicating that water deficit led to protein degradation and protein damage (**Figure 7A**). Evidence has shown that the degradation of intracellular proteins (e.g., chloroplast proteins) is an important mechanism of the N remobilization under drought stress (Ren et al., 2020). During drought stress, the abundance and activity of enzymes that control N and C metabolism are affected by the degradation of chloroplast proteins (Ishida et al., 2008). For example, drought stress-induced chloroplast proteins inactivation and degradation, resulting in an enhancement of the free amino acid content and the loss of function of plastid enzymes (e.g., GS) (Reguera et al., 2013). In our experiment, we found that the melatonin-treated plants had less proteins degradation than the non-treated plants under drought stress, along with an upregulated expression of *ZmGS2*, stabled chloroplast function, and increased capacity for N assimilation. Taken together, exogenously applied melatonin plays a positive role in the coordination of C and N metabolism under drought stress.

CONCLUSION

Based on the analysis mentioned above, the present study suggests that water deficit critically disturbs the processes of C and N metabolism, resulting in inhibited crop growth. However, exogenously applied melatonin mitigated drought stress through coordinated regulation of C and N metabolism in maize. The protective effects of exogenous melatonin on maize were mainly due to ameliorated stomatal opening and photosynthetic activity of maize, which indirectly promoted the synthesis of photosynthetic end products and energy production, and enhanced N assimilation and NH_4^+ detoxification, and thus

consequently increased maize growth under the water restriction conditions (**Figure 8**). Overall, the results of this study provide valuable information for maize drought tolerance induced by melatonin and a new theoretical basis for the application of melatonin on crops grown in arid areas. Future research should explore the molecular mechanisms of functions of melatonin and the practical use of melatonin in crop production.

DATA AVAILABILITY STATEMENT

The datasets presented in this study can be found in online repositories. The names of the repository/repositories and accession number(s) can be found in the article/supplementary material.

AUTHOR CONTRIBUTIONS

RZ and CZ conceived and designed the experiments. CZ, HG, JW, and YW conducted the experiment and collected data for preliminary analysis. CZ, RZ, and HG further analyzed the data and wrote the manuscript. All authors reviewed and commented on the manuscript and approved the submitted version.

FUNDING

This study was supported by the National Key Research and Development Program of China (2017YFD0300304) and the Key Research and Development Program of Shaanxi Province (2017ZDCXL-NY-02-02).

REFERENCES

Adams, W. W., Muller, O., Cohu, C. M., and Demmig-Adams, B. (2013). May photoinhibition be a consequence, rather than a cause, of limited plant productivity? *Photosynthesis Res.* 117, 31–44. doi: 10.1007/s11120-013-9849-7

Ahmad, S., Kamran, M., Ding, R., Meng, X., Wang, H., Ahmad, I., et al. (2019). Exogenous melatonin confers drought stress by promoting plant growth, photosynthetic capacity and antioxidant defense system of maize seedlings. *PeerJ* 7:e7793. doi: 10.7717/peerj.7793

Ahmad, S., Su, W. N., Kamran, M., Ahmad, I., Meng, X. P., Wu, X. R., et al. (2020). Foliar application of melatonin delay leaf senescence in maize by improving the antioxidant defense system and enhancing photosynthetic capacity under semi-arid regions. *Protoplasma* 257, 1079–1092. doi: 10.1007/s00709-020-01491-3

Atkin, O. K., and Macherel, D. (2009). The crucial role of plant mitochondria in orchestrating drought tolerance. *Ann. Bot.* 103, 581–597. doi: 10.1093/aob/mcn094

Barro, F., Fontes, A., and Maldonado, J. (1991). Organic nitrogen content and nitrate and nitrite reductase activities in tritordeum and wheat grown under nitrate or ammonium. *Plant Soil* 135, 251–256. doi: 10.1007/BF00010913

Boyko, E. V., Golovatskaya, I. F., Bender, O. G., and Plyusnin, I. N. (2020). Effect of short-term treatment of roots with melatonin on photosynthesis of cucumber leaves. *Russ. J. Plant Physiol.* 67, 351–359. doi: 10.1134/s102144372002003x

Bradford, M. M. (1976). A rapid and sensitive method for the quantitation of microgram quantities of protein utilizing the principle of protein-dye binding. *Anal. Biochem.* 72, 248–254. doi: 10.1006/abio.1976.9999

Brautigam, A., Gagneul, D., and Weber, A. P. M. (2007). High-throughput colorimetric method for the parallel assay of glyoxylic acid and ammonium in a single extract. *Anal. Biochem.* 362, 151–153. doi: 10.1016/j.ab.2006.12.033

Campos, C. N., Avila, R. G., de Souza, K. R. D., Azevedo, L. M., and Alves, J. D. (2019). Melatonin reduces oxidative stress and promotes drought tolerance in young *Coffea arabica* L. plants. *Agric. Water Manage.* 211, 37–47. doi: 10.1016/j.agwat.2018.09.025

Cataldo, D. A., Maroon, M., Schrader, L. E., and Youngs, V. L. (1975). Rapid colorimetric determination of nitrate in plant tissue by nitration of salicylic acid. *Commun. Soil Sci. Plant Anal.* 6, 71–80. doi: 10.1080/00103627509366547

Chaves, M. M., Flexas, J., and Pinheiro, C. (2009). Photosynthesis under drought and salt stress: regulation mechanisms from whole plant to cell. *Ann. Bot.* 103, 551–560. doi: 10.1093/aob/mcn125

Cui, G. C., Zhang, Y., Zhang, W. J., Lang, D. Y., Zhang, X. J., Li, Z. X., et al. (2019). Response of carbon and nitrogen metabolism and secondary metabolites to drought stress and salt stress in plants. *J. Plant Biol.* 62, 387–399. doi: 10.1007/s12374-019-0257-1

Dai, L., Li, J., Harmens, H., Zheng, X., and Zhang, C. (2020). Melatonin enhances drought resistance by regulating leaf stomatal behaviour, root growth and catalase activity in two contrasting rapeseed (*Brassica napus* L.) genotypes. *Plant Physiol. Biochem.* 149, 86–95. doi: 10.1016/j.plaphy.2020.01.039

Debnath, B., Li, M., Liu, S., Pan, T. F., Ma, C. L., and Qiu, D. L. (2020). Melatonin-mediate acid rain stress tolerance mechanism through alteration of transcriptional factors and secondary metabolites gene expression in tomato. *Ecotoxicol. Environ. Saf.* 200:110720. doi: 10.1016/j.ecoenv.2020.110720

Du, Y. L., Zhao, Q., Chen, L. R., Yao, X. D., Zhang, H. J., Wu, J. J., et al. (2020). Effect of drought stress during soybean R2-R6 growth stages on sucrose metabolism in leaf and seed. *Int. J. Mol. Sci.* 21:618. doi: 10.3390/ijms21020618

Flexas, J., Bota, J., Galmes, J., Medrano, H., and Ribas-Carbo, M. (2006). Keeping a positive carbon balance under adverse conditions: responses of photosynthesis and respiration to water stress. *Physiol. Plant.* 127, 343–352. doi: 10.1111/j.1399-3054.2006.00621.x

Gandin, A., Lapointe, L., and Dizengremel, P. (2009). The alternative respiratory pathway allows sink to cope with changes in carbon availability in the sink-limited plant *Erythronium americanum*. *J. Exp. Bot.* 60, 4235–4248. doi: 10.1093/jxb/erp255

Georgiadou, E. C., Kowalska, E., Patla, K., Kulbat, K., Smolinska, B., Leszczynska, J., et al. (2018). Influence of heavy metals (Ni, Cu, and Zn) on nitro-oxidative stress responses, proteome regulation and allergen production in basil (*Ocimum basilicum* L.) plants. *Front. Plant Sci.* 9:862. doi: 10.3389/fpls.2018.00862

Guo, Y. Y., Li, H. J., Liu, J., Bai, Y. W., Xue, J. Q., and Zhang, R. H. (2020a). Melatonin alleviates drought-induced damage of photosynthetic apparatus in maize seedlings. *Russ. J. Plant Physiol.* 67, 312–322. doi: 10.1134/s1021443720020053

Guo, Y. Y., Li, H. J., Zhao, C. F., Xue, J. Q., and Zhang, R. H. (2020b). Exogenous melatonin improves drought tolerance in maize seedlings by regulating photosynthesis and the ascorbate-glutathione cycle. *Russ. J. Plant Physiol.* 67, 809–821. doi: 10.1134/S1021443720050064

Gupta, A., Rico-Medina, A., and Caño-Delgado, A. I. (2020). The physiology of plant responses to drought. *Science* 368, 266–269. doi: 10.1126/science.aaz7614

Hansen, J., and Moller, I. (1975). Percolation of starch and soluble carbohydrates from plant tissue for quantitative determination with anthrone. *Anal. Biochem.* 68, 87–94. doi: 10.1016/0003-2697(75)90682-x

Hu, W., Cao, Y., Loka, D. A., Harris-Shultz, K. R., Reiter, R. J., Ali, S., et al. (2020). Exogenous melatonin improves cotton (*Gossypium hirsutum* L.) pollen fertility under drought by regulating carbohydrate metabolism in male tissues. *Plant Physiol. Biochem.* 151, 579–588. doi: 10.1016/j.plaphy.2020.04.001

Hu, Z. R., Fan, J. B., Xie, Y., Amombo, E., Liu, A., Gitau, M. M., et al. (2016). Comparative photosynthetic and metabolic analyses reveal mechanism of improved cold stress tolerance in bermudagrass by exogenous melatonin. *Plant Physiol. Biochem.* 100, 94–104. doi: 10.1016/j.plaphy.2016.01.008

Huang, B., Chen, Y. E., Zhao, Y. Q., Ding, C. B., Liao, J. Q., Hu, C., et al. (2019). Exogenous melatonin alleviates oxidative damages and protects photosystem II in maize seedlings under drought stress. *Front. Plant Sci.* 10:677. doi: 10.3389/fpls.2019.00677

Indira, P., Hadas, G., Annat, Z., Gal, S., and Tamir, K. (2021). Intraspecific plasticity in hydraulic and stomatal regulation under drought is linked to aridity at the seed source in a wild pear species. *Tree Physiol.* 41, 960–973. doi: 10.1093/TREEPHYS/TPAA159

Ishida, H., Yoshimoto, K., Masanori, I., Reisen, D., Yano, Y., Makino, A., et al. (2008). Mobilization of Rubisco and stroma-localized fluorescent proteins of chloroplasts to the vacuole by an ATG gene-dependent autophagic process. *Plant Physiol.* 148, 142–155. doi: 10.1104/pp.108.122770

Jing, T., Yue, P., and Zhong, Z. (2021). Drought, salinity, and low nitrogen differentially affect the growth and nitrogen metabolism of *Sophora japonica* (L.) in a semi-hydroponic phenotyping platform. *Front. Plant Sci.* 12:715456. doi: 10.3389/FPLS.2021.715456

Johnson, J. F., Allan, D. L., and Vance, C. P. (1994). Phosphorus stress-induced proteoid roots show altered metabolism in *Lupinus albus*. *Plant Physiol.* 104, 657–665. doi: 10.1104/pp.104.2.657

Kanwar, M. K., Yu, J., and Zhou, J. (2018). Phytomelatonin: recent advances and future prospects. *J. Pineal Res.* 65, e12526. doi: 10.1111/jpi.12526

Kaya, C., Higgs, D., Ashraf, M., Alyemeni, M. N., and Ahmad, P. (2020). Integrative roles of nitric oxide and hydrogen sulfide in melatonin-induced tolerance of pepper (*Capsicum annuum* L.) plants to iron deficiency and salt stress alone or in combination. *Physiol. Plant.* 168, 256–277. doi: 10.1111/ppl.12976

Kaya, C., Okant, M., Ugurlar, F., Alyemeni, M. N., Ashraf, M., and Ahmad, P. (2019). Melatonin-mediated nitric oxide improves tolerance to cadmium toxicity by reducing oxidative stress in wheat plants. *Chemosphere* 225, 627–638. doi: 10.1016/j.chemosphere.2019.03.026

Khattak, W. A., He, J. Q., Abdalmegeed, D., Hu, W., Wang, Y. H., and Zhou, Z. G. (2021). Foliar melatonin stimulates cotton boll distribution characteristics by modifying leaf sugar metabolism and antioxidant activities during drought conditions. *Physiol. Plant* 1–18. doi: 10.1111/ppl.13526

Kolar, J., Johnson, C. H., and Machackova, I. (2003). Exogenously applied melatonin (N-acetyl-5-methoxytryptamine) affects flowering of the short-day plant *Chenopodium rubrum*. *Physiol. Plant.* 118, 605–612. doi: 10.1034/j.1399-3054.2003.00114.x

Kong, X. Z., Zhou, S. M., Yin, S. H., Zhao, Z. X., Hanand, Y. Y., and Wang, W. (2016). Stress-inducible expression of an F-box gene TaFBA1 from wheat enhanced the drought tolerance in transgenic tobacco plants without impacting growth and development. *Front. Plant Sci.* 7:1295. doi: 10.3389/fpls.2016.01295

Li, T. T., Hu, Y. Y., Du, X. H., Tang, H., Shen, C. H., and Wu, J. S. (2014). Salicylic acid alleviates the adverseeffects of salt stress in *Torreya grandis* cv. *Merrillii* seedlings by activating photosynthesis and enhancing antioxidant systems. *PLoS One* 9:e109492. doi: 10.1371/journal.pone.0109492

Li, C., He, Q. L., Zhang, F., Yu, J. W., Li, C., Zhao, T. L., et al. (2019). Melatonin enhances cotton immunity to *Verticillium* wilt via manipulating lignin and gossypol biosynthesis. *Plant J.* 100, 784–800. doi: 10.1111/tpj.14477

Li, C., Bin, L., Liantao, L., Wenjing, D., Dan, J., Jin, L., et al. (2021). Melatonin promotes seed germination under salt stress by regulating ABA and GA3 in cotton (*Gossypium hirsutum* L.). *Plant Physiol. Biochem.* 162, 506–516. doi: 10.1016/J.PLAPHY.2021.03.029

Li, Z., Su, X. Y., Chen, Y. L., Fan, X. C., He, L. Z., Guo, J. M., et al. (2021). Melatonin improves drought resistance in maize seedlings by enhancing the antioxidant system and regulating abscisic acid metabolism to maintain stomatal opening under PEG-induced drought. *J. Plant Biol.* 64, 299–312. doi: 10.1007/s12374-021-09297-3

Liang, B., Ma, C., Zhang, Z., Wei, Z., Gao, T., Zhao, Q., et al. (2018). Long-term exogenous application of melatonin improves nutrient uptake fluxes in apple plants under moderate drought stress. *Environ. Exp. Bot.* 155, 650–661. doi: 10.1016/j.envexpbot.2018.08.016

Liu, C. G., Wang, Y. J., Pan, K. W., Zhu, T. T., Li, W., and Zhang, L. (2014). Carbon and nitrogen metabolism in leaves and roots of dwarf bamboo (*Fargesia denudata* Yi) subjected to drought for two consecutive years during sprouting period. *J. Plant Growth Regul.* 33, 243–255. doi: 10.1007/s00344-013-9367-z

Liu, D., Wu, L. T., Naeem, M. S., Liu, H. B., Deng, X. Q., Xu, L., et al. (2013). 5-Aminolevulinic acid enhances photosynthetic gas exchange, chlorophyll fluorescence and antioxidant system in oilseed rape under drought stress. *Acta Physiol. Plant.* 35, 2747–2759. doi: 10.1007/s11738-013-1307-9

Liu, J. L., Wang, W. X., Wang, L. Y., and Sun, Y. (2015). Exogenous melatonin improves seedling health index and drought tolerance in tomato. *Plant Growth Regulat.* 77, 317–326. doi: 10.1007/s10725-015-0066-6

Liu, X. M., Zhu, H., Wang, L., Bi, S. S., Zhang, Z. H., Meng, S. Y., et al. (2019). The effects of magnetic treatment on nitrogen absorption and distribution in seedlings of Populus x euramericana 'Neva' under NaCl stress. *Sci. Rep.* 9:10025. doi: 10.1038/s41598-019-45719-6

Loyola-Vargas, V. M., and de Jimenez, E. S. (1984). Differential role of glutamate dehydrogenase in nitrogen metabolism of maize tissues. *Plant Physiol.* 76, 536–540. doi: 10.1104/pp.76.2.536

Mathur, S., Tomar, R. S., and Jajoo, A. (2019). Arbuscular *Mycorrhizal fungi* (AMF) protects photosynthetic apparatus of wheat under drought stress. *Photosynth. Res.* 139, 227–238. doi: 10.1007/s11120-018-0538-4

Matoh, T., and Takahashi, E. (1982). Changes in the activities of ferredoxin- and NADH-glutamate synthase during seedling development of peas. *Planta* 154, 289–294. doi: 10.1007/BF00393905

Meng, J. F., Xu, T. F., Wang, Z. Z., Fang, Y. L., Xi, Z. M., and Zhang, Z. W. (2014). The ameliorative effects of exogenous melatonin on grape cuttings under water-deficient stress: antioxidant metabolites, leaf anatomy, and chloroplast morphology. *J. Pineal Res.* 57, 200–212. doi: 10.1111/jpi.12159

Miranda-Apodaca, J., Agirresarobe, A., Martinez-Goni, X. S., Yoldi-Achalandabaso, A., and Perez-Lopez, U. (2020). N metabolism performance in *Chenopodium quinoa* subjected to drought or salt stress conditions. *Plant Physiol. Biochem.* 155, 725–734. doi: 10.1016/j.plaphy.2020.08.007

Mohd, A., Glyn, M., and Sibte, H. (2011). Analysis of rpoS and bolA gene expression under various stress-induced environments in planktonic and biofilm phase using 2-ΔΔCT method. *Mol. Cell. Biochem.* 357, 275–282. doi: 10.1007/s11010-011-0898-y

Nguyen, G. N., Hailstones, D. L., Wilkes, M., and Sutton, B. G. (2010). DROUGHT STRESS: role of carbohydrate metabolism in drought-induced male sterility in rice anthers*. *J. Agronomy Crop Sci.* 196, 346–357. doi: 10.1111/j.1439-037X.2010.00423.x

Ogbaga, C. C., Stepien, P., and Johnson, G. N. (2014). Sorghum (*Sorghum bicolor*) varieties adopt strongly contrasting strategies in response to drought. *Physiol. Plant.* 152, 389–401. doi: 10.1111/ppl.12196

O'Neal, D., and Joy, K. (1973). Glutamine synthetase of pea leaves. I. purification, stabilization, and pH optima. *Arch Biochem. Biophys.* 159, 120–122.

Pinheiro, C., and Chaves, M. M. (2011). Photosynthesis and drought: can we make metabolic connections from available data? *J. Exp. Bot.* 62, 869–882. doi: 10.1093/jxb/erq340

Qi, Z. Y., Wang, K. X., Yan, M. Y., Kanwar, M. K., Li, D. Y., Wijaya, L., et al. (2018). Melatonin alleviates high temperature-induced pollen abortion in *Solanum lycopersicum*. *Molecules* 23:386. doi: 10.3390/molecules23020386

Qiao, Y., Yin, L., Wang, B., Ke, Q., Deng, X., and Wang, S. (2019). Melatonin promotes plant growth by increasing nitrogen uptake and assimilation under nitrogen deficient condition in winter wheat. *Plant Physiol. Biochem.* 139, 342–349. doi: 10.1016/j.plaphy.2019.03.037

Rajasekhar, V. K., and Oelmüller, R. (2010). Regulation of induction of nitrate reductase and nitrite reductase in higher plants. *Physiol. Plant.* 71, 517–521. doi: 10.1111/j.1399-3054.1987.tb02893.x

Reguera, M., Peleg, Z., Abdel-Tawab, Y. M., Tumimbang, E. B., Delatorre, C. A., and Blumwald, E. (2013). Stress-induced cytokinin synthesis increases drought tolerance through the coordinated regulation of carbon and nitrogen assimilation in rice. *Plant Physiol.* 163, 1609–1622. doi: 10.1104/pp.113.227702

Ren, J., Xie, T., Wang, Y., Li, H., Liu, T., Zhang, S., et al. (2020). Coordinated regulation of carbon and nitrogen assimilation confers drought tolerance in maize (*Zea mays* L.). *Environ. Exp. Bot.* 176:104086. doi: 10.1016/j.envexpbot.2020.104086

Riemann, M., Dhakarey, R., Hazman, M., Miro, B., Kohli, A., and Nick, P. (2015). Exploring jasmonates in the hormonal network of drought and salinity responses. *Front. Plant Sci.* 6:1077. doi: 10.3389/fpls.2015.01077

Schaffer, A. A., and Petreikov, M. (1997). Sucrose-to-starch metabolism in tomato fruit undergoing transient starch accumulation. *Plant Physiol.* 113, 739–746. doi: 10.1104/pp.113.3.739

Shah, T. M., Imran, M., Atta, B. M., Ashraf, M. Y., Hameed, A., Waqar, I., et al. (2020). Selection and screening of drought tolerant high yielding chickpea genotypes based on physio-biochemical indices and multi-environmental yield trials. *BMC Plant Biol.* 20:171. doi: 10.1186/s12870-020-02381-9

Sharma, A., and Zheng, B. (2019). Melatonin mediated regulation of drought stress: physiological and molecular aspects. *Plants (Basel)* 8:190. doi: 10.3390/plants8070190

Sharma, A., Wang, J. F., Xu, D. B., Tao, S. C., Chong, S. L., Yan, D. L., et al. (2020). Melatonin regulates the functional components of photosynthesis, antioxidant system, gene expression, and metabolic pathways to induce drought resistance

in grafted *Carya cathayensis* plants. *Sci. Total Environ.* 713:136675. doi: 10.1016/j.scitotenv.2020.136675

Siddiqui, M. H., Alamri, S., Khan, M. N., Corpas, F. J., Al-Amri, A. A., Alsubaie, Q. D., et al. (2020). Melatonin and calcium function synergistically to promote the resilience through ROS metabolism under arsenic-induced stress. *J. Hazard. Mater.* 398:122882. doi: 10.1016/j.jhazmat.2020.122882

Song, Q. B., Liu, Y. F., Pang, J. Y., Yong, J. W. H., Chen, Y. L., Bai, C. M., et al. (2020). Supplementary calcium restores peanut (*Arachis hypogaea*) growth and photosynthetic capacity under low nocturnal temperature. *Front. Plant Sci.* 10:1637. doi: 10.3389/fpls.2019.01637

Sun, J. B., Li, W. B., Li, C. Q., Chang, W. J., Zhang, S. Q., Zeng, Y. B., et al. (2020). Effect of different rates of nitrogen fertilization on crop yield, soil properties and leaf physiological attributes in banana under subtropical regions of China. *Front. Plant Sci.* 11:613760. doi: 10.3389/fpls.2020.613760

Sunil, B., Talla, S. K., Aswani, V., and Raghavendra, A. S. (2013). Optimization of photosynthesis by multiple metabolic pathways involving interorganelle interactions: resource sharing and ROS maintenance as the bases. *Photosyn. Res.* 117, 61–71. doi: 10.1007/s11120-013-9889-z

Terrier, N., Sauvage, F. X., Ageorges, A., and Romieu, C. (2001). Changes in acidity and in proton transport at the tonoplast of grape berries during development. *Planta* 213, 20–28. doi: 10.1007/s004250000472

Todaka, D., Zhao, Y., Yoshida, T., Kudo, M., Kidokoro, S., Mizoi, J., et al. (2017). Temporal and spatial changes in gene expression, metabolite accumulation and phytohormone content in rice seedlings grown under drought stress conditions. *Plant J.* 90, 61–78. doi: 10.1111/tpj.13468

Velikova, V., Tsonev, T., Tattini, M., Arena, C., Krumova, S., Koleva, D., et al. (2018). Physiological and structural adjustments of two ecotypes of *Platanus orientalis* L. from different habitats in response to drought and re-watering. *Conserv. Physiol.* 6:coy073. doi: 10.1093/conphys/coy073

Wang, M., Zhang, S., and Ding, F. (2020). Melatonin mitigates chilling-induced oxidative stress and photosynthesis inhibition in tomato plants. *Antioxidants (Basel)* 9:218. doi: 10.3390/antiox9030218

Wei, W., Li, Q. T., Chu, Y. N., Reiter, R. J., Yu, X. M., Zhu, D. H., et al. (2015). Melatonin enhances plant growth and abiotic stress tolerance in soybean plants. *J. Exp. Bot.* 66, 695–707. doi: 10.1093/jxb/eru392

Xie, T., Gu, W., Wang, M., Zhang, L., Li, C., Li, C., et al. (2019). Exogenous 2-(3,4-Dichlorophenoxy) triethylamine ameliorates the soil drought effect on nitrogen metabolism in maize during the pre-female inflorescence emergence stage. *BMC Plant Biol.* 19:107. doi: 10.1186/s12870-019-1710-5

Xu, H. F., Zou, Q., Yang, G. X., Jiang, S. H., Fang, H. C., Wang, Y. C., et al. (2020). MdMYB6 regulates anthocyanin formation in apple both through direct inhibition of the biosynthesis pathway and through substrate removal. *Horticul. Res.* 7:72. doi: 10.1038/s41438-020-0294-4

Yang, M., Geng, M., Shen, P., Chen, X., Li, Y., and Wen, X. (2019). Effect of post-silking drought stress on the expression profiles of genes involved in carbon and nitrogen metabolism during leaf senescence in maize (*Zea mays* L.). *Plant Physiol. Biochem.* 135, 304–309. doi: 10.1016/j.plaphy.2018.12.025

Yao, J. W., Ma, Z., Ma, Y. Q., Zhu, Y., Lei, M. Q., Hao, C. Y., et al. (2020). Role of melatonin in UV-B signaling pathway and UV-B stress resistance in *Arabidopsis thaliana*. *Plant Cell Environ.* 44, 114–129. doi: 10.1111/pce.13879

Ye, J., Wang, S., Deng, X., Yin, L., Xiong, B., and Wang, X. (2016). Melatonin increased maize (*Zea mays* L.) seedling drought tolerance by alleviating drought-induced photosynthetic inhibition and oxidative damage. *Acta Physiologiae Plant.* 38, 1–13. doi: 10.1007/s11738-015-2045-y

Ye, T. T., Shi, H. T., Wang, Y. P., and Chan, Z. L. (2015). Contrasting changes caused by drought and submergence stresses in bermudagrass (*Cynodon dactylon*). *Front. Plant Sci.* 6:951. doi: 10.3389/fpls.2015.00951

Yemm, E. W., Cocking, E. C., and Ricketts, R. E. (1955). The determination of amino-acids with ninhydrin. *Analyst* 80, 209–214. doi: 10.1039/AN9558000209

Yu, W., Mao, W. Y., Ting, L. Y., Li, Q. Q., Mei, F. D., Chang, W. X., et al. (2021). Influence of different nitrogen sources on carbon and nitrogen metabolism and gene expression in tea plants (*Camellia sinensis* L.). *Plant Physiol. Biochem.* 167, 561–566. doi: 10.1016/J.PLAPHY.2021.08.034

Zhang, C., Shi, S., Liu, Z., Yang, F., and Yin, G. (2019). Drought tolerance in alfalfa (*Medicago sativa* L.) varieties is associated with enhanced antioxidative protection and declined lipid peroxidation. *J. Plant Physiol.* 232, 226–240. doi: 10.1016/j.jplph.2018.10.023

Zhang, T. G., Shi, Z. F., Zhang, X. H., Zheng, S., Wang, J., and Mo, J. N. (2020). Alleviating effects of exogenous melatonin on salt stress in cucumber. *Sci. Horticul.* 262:109070. doi: 10.1016/j.scienta.2019.109070

Zhong, C., Bai, Z. G., Zhu, L. F., Zhang, J. H., Zhu, C. Q., Huang, J. L., et al. (2019). Nitrogen-mediated alleviation of photosynthetic inhibition under moderate water deficit stress in rice (*Oryza sativa* L.). *Environ. Exp. Bot.* 157, 269–282. doi: 10.1016/j.envexpbot.2018.10.021

Zhong, C., Cao, X., Bai, Z., Zhang, J., Zhu, L., Huang, J., et al. (2018). Nitrogen metabolism correlates with the acclimation of photosynthesis to short-term water stress in rice (*Oryza sativa* L.). *Plant Physiol. Biochem.* 125, 52–62. doi: 10.1016/j.plaphy.2018.01.024

Zhou, R., Kan, X., Chen, J., Hua, H., Li, Y., Ren, J., et al. (2019). Drought-induced changes in photosynthetic electron transport in maize probed by prompt fluorescence, delayed fluorescence, P700 and cyclic electron flow signals. *Environ. Exp. Bot.* 158, 51–62. doi: 10.1016/j.envexpbot.2018.11.005

Conflict of Interest: The authors declare that the research was conducted in the absence of any commercial or financial relationships that could be construed as a potential conflict of interest.

Publisher's Note: All claims expressed in this article are solely those of the authors and do not necessarily represent those of their affiliated organizations, or those of the publisher, the editors and the reviewers. Any product that may be evaluated in this article, or claim that may be made by its manufacturer, is not guaranteed or endorsed by the publisher.

frontiers in Plant Science

ORIGINAL RESEARCH
published: 16 December 2021
doi: 10.3389/fpls.2021.759929

Coated Diammonium Phosphate Combined With Humic Acid Improves Soil Phosphorus Availability and Photosynthesis and the Yield of Maize

Qi Chen[1], Zhaoming Qu[1], Zeli Li[1], Zixin Zhang[1], Guohua Ma[1], Zhiguang Liu[1], Yanfeng Wang[2], Liang Wu[2], Fuli Fang[2], Zhanbo Wei[3] and Min Zhang[1]**

[1] National Engineering Research Center for Efficient Utilization of Soil and Fertilizer Resources, College of Resources and Environment, Shandong Agricultural University, Tai'an, China, [2] Key Laboratory of Crop Specific Fertilizer, Ministry of Agriculture, Xinyangfeng Agricultural Technology Co., Ltd., Jingmen, China, [3] Institute of Applied Ecology, Chinese Academy of Sciences, Shenyang, China

OPEN ACCESS

Edited by:
Maurizio Ruzzi, University of Tuscia, Italy

Reviewed by:
Subhan Danish, Bahauddin Zakariya University, Pakistan
Shah Fahad, The University of Haripur, Pakistan

***Correspondence:**
Zhanbo Wei
huanke217@163.com
Min Zhang
minzhang-2002@163.com

Specialty section:
This article was submitted to Plant Nutrition, a section of the journal Frontiers in Plant Science

Received: *17 August 2021*
Accepted: *15 November 2021*
Published: *16 December 2021*

Citation:
Chen Q, Qu Z, Li Z, Zhang Z, Ma G, Liu Z, Wang Y, Wu L, Fang F, Wei Z and Zhang M (2021) Coated Diammonium Phosphate Combined With Humic Acid Improves Soil Phosphorus Availability and Photosynthesis and the Yield of Maize. Front. Plant Sci. 12:759929. doi: 10.3389/fpls.2021.759929

Controlled release phosphorus (P) fertilizers and humic acid (HA) applications are two effective and significant techniques or measures for preventing P loss and enhancing maize development. However, the underlying physiological mechanism of how the controlled release P fertilizers combined with HA affect the maize production and P-use efficiency (PUE) remains unknown. The effects of applying coated diammonium phosphate (CDAP) and HA together on soil nutrient supply intensity, soil phosphatase activity, photosynthesis, endogenous hormone contents, and yield of maize, as well as PUE, were examined in this study. In a pot experiment, two types of P fertilizers—CDAP and diammonium phosphate (DAP)– as well as two HA application rates (0 and 45 kg ha^{-1}) and two P levels (60 and 75 kg P_2O_5 ha^{-1}) were utilized. Results showed that the key elements that influence the growth and yield of the maize were the availability of P content in soil, plant photosynthesis, and hormone levels. The combination of CDAP and HA had a greater impact on yield and PUE over the course of 2 years than either DAP alone or DAP combined with HA. Besides, using CDAP in combination with HA increased the yield and PUE by 4.2 and 8.4%, respectively, as compared to the application of CDAP alone at 75 kg P_2O_5 ha^{-1}. From the twelve-leaf to milk stages, the available P content in the soil was increased by an average of 38.6% with the combination of CDAP and HA compared to the application of CDAP alone at 75 kg P_2O_5 ha^{-1}. In addition, the application of CDAP combined with HA boosted the activities of ATP synthase, as well as the content of cytokinin (CTK), and hence improved the maize photosynthetic rate (Pn). When compared to the application of CDAP alone or DAP combined with HA, the Pn of CDAP + HA treatments was enhanced by 17.9–35.1% at the same P rate. In conclusion, as an environmentally friendly fertilizer, the combined application of CDAP and HA improved the intensity of the soil nutrient supply, regulated photosynthetic capabilities, and increased the yield and PUE, which is important for agricultural production, P resource conservation, and environmental protection.

Keywords: phosphorus use efficiency, economic benefits, phosphate release, endogenous hormone, phosphatase

INTRODUCTION

Phosphorus (P), as a structural element, is one of the essential macronutrients for plant growth and development (Johnston and Poulton, 2019; Ding et al., 2021). The P deficiency limits virtually all major metabolic processes, in plants, such as photosynthesis and respiration (Plaxton and Tran, 2011). However, agricultural production of over 40% of the world's arable land is limited by P deficiency (Balemi and Negisho, 2012; Zhu et al., 2018). Therefore, P fertilizers are commonly applied to meet crop demand. Because of sorption, precipitation (usually by interaction with Ca^{2+} and Mg^{2+} in calcareous soils, and Fe^{3+} and Al^{3+} in acidic soils), and microbial immobilization, the P-use efficiency (PUE) of most crops is only 10–15% (Castro and Torrent, 1998; Roberts and Johnston, 2015; Zhu et al., 2018). The applied P accumulates in soils and causes soil degradation and environmental concerns, such as water eutrophication (Leslie et al., 2017). Moreover, the detrimental effects of climate change on P transport in soil and lake eutrophication, such as global warming, drought, and heavy rainfalls, have been exposed (Piao et al., 2010; Fahad et al., 2016, 2020). China is the largest producer and consumer of P fertilizers in the world, but the reserve of phosphate rock, the main source of phosphate in fertilizer, is limited (Zhang et al., 2008; Ma et al., 2011). Therefore, effective P management is of importance for PUE improvement, resource reservation, and environmental protection.

Effective P management involving appropriate P fertilizers is vital for high PUE (Zheng et al., 2016; Tian et al., 2018). Many environmentally friendly methods for increasing P availability have been proposed, including the use of P-solubilizing microorganisms (Adnan et al., 2020; Wahid et al., 2020), partial acidification of rock phosphates (Sarkar et al., 2018), combined application of biochar and P fertilizers (Fahad et al., 2016), and foliar application of P fertilizers (Rafiullah et al., 2020). The application of controlled-release fertilizers is one of these methods. Controlled-release P fertilizers show high PUE in both acidic and alkaline soils. The PUE of controlled-release P fertilizers was reported to be higher than that of water-soluble P fertilizers (Sarkar et al., 2018). Coated diammonium phosphate (CDAP), a controlled-release P fertilizer, releases P according to the demand of the plant, which not only improves PUE and crop yield but also reduces the environmental risk posed by the excessive use of fertilizers (Cruz et al., 2017; Lu et al., 2019). Chen et al. (2020) demonstrated that compared to diammonium phosphate (DAP), CDAP significantly increased maize yield and PUE by 9.65 and 7.72%, respectively.

Humic acid (HA) applied to soil as an activator is also reported to increase the availability of soil P (Zhu et al., 2018). HA consists of aromatic and aliphatic structures harboring various functional groups (mainly oxygen-containing), such as carboxyl (–COOH) and phenolic hydroxyl (–OH). Studies have shown that HA application reduced P fixation, improved the efficiency of low and high solubility P sources, increased P availability, and improved PUE (Çimrin et al., 2010; Rosa et al., 2018; Shafi et al., 2020; Xu et al., 2021). HA improved soil structure by encouraging the formation of stable aggregates, which increased the productivity of soil crops (Zhou et al., 2019). In addition, HA has been shown to improve certain aspects of growth in essential agronomic crops like soybean, wheat, rice, and maize (Calvo et al., 2014; Rosa et al., 2018). As a plant biostimulant, HA increases photosynthesis, reduces transpiration, stimulates root and shoot growth, and enhances stress resistance of plants (Canellas et al., 2013; Dantas et al., 2018; Xu et al., 2021), and is linked with changes in the hormone contents and enzyme activities and enhancement of H^+-ATPase activity (Zandonadi et al., 2010; Calvo et al., 2014). However, since HA is a weak nutritional material, it cannot supply the nutrient requirements in crop production on its own.

Many research has been conducted on the effects of HA application, the combination of water-soluble P fertilizer and HA, and HA mixed with urea or controlled-release urea on soil quality, plant development, and fertilizer use efficiency (Shafi et al., 2020; Li Z. L. et al., 2021; Xu et al., 2021). Rosa et al. (2018) found that combining HA with phosphate fertilizers (e.g., single superphosphate) boosted root dry matter, and nutrient uptake increased the shoot dry matter output, as compared to biomass produced in soil that had not been treated with HA. To our knowledge, few studies on the effects of combining HA with controlled release P fertilizer on crop production have been conducted. We hypothesized that the combined application of CDAP and HA would improve crop growth, crop yield, and PUE. This study was aimed to: (1) investigate the effects of CDAP combined with HA on soil P availability, (2) understand the roles of photosynthesis and endogenous hormones in the increase of maize production when CDAP and HA are applied together, and (3) determine the factors that influence crop yield and PUE. Findings from this study should give a technological foundation for developing an effective fertilization strategy using controlled-release P fertilizers and biostimulants.

MATERIALS AND METHODS

Soil, Coated Diammonium Phosphate, and Humic Acid Used

The soil for the pot experiment was acquired from a field at the research farm of the National Engineering Laboratory for Efficient Utilization of Soil Fertility Resources (NELEUSFR), Shandong Agricultural University (SDAU), China. It is classified as Typic Hapludalf (Soil Survey Staff, USDA, 1999) or Typic-Hapli-Udic Argosols (Chinese Soil Taxonomy, CRGCST, 2001). Physical and chemical properties of the soil were as follows: pH: 7.83 (1:2.5 soil to water ratio), organic matter content: 12.10 g kg^{-1}, total P: 0.32 g kg^{-1}, available P: 13.50 mg kg^{-1}, NO_3^--N: 71.45 mg kg^{-1}, NH_4^+-N: 9.45 mg kg^{-1}, and available K: 92.32 mg kg^{-1}.

The controlled-release P fertilizer, the CDAP (17.2% N, 44.0% P_2O_5), was prepared by NELEUSFR, SDAU, China. The coating consisted of 10% of paraffin and 90% of polyurethane. Resin-coated controlled-release urea (43.0% N; 3-month release period) was purchased from Kingenta Ecological Engineering Group Co., Ltd., Shandong, China. The other fertilizers, urea (46% N), DAP (18.0% N, 46.0% P_2O_5), and potassium chloride (60.0% K_2O), were purchased from the local market. The HA (2.0-0%-3.0%

N-P_2O_5-K_2O) was purchased from Quanlin Jiayou Fertilizer Co., Ltd., Shandong, China. It had a pH of 5.40 (1:2.5 soil to HA ratio).

Pot Experiment

The pot experiment was carried out in the research farm of NELEUSFR, SDAU, China. With an average annual temperature of 13.2°C, the experiment location has a moderate continental monsoon climate. The following nine treatments were put up, each with four replications: (1) Control (no P fertilization); (2) P, 100% (DAP at 75 kg P_2O_5 ha^{-1}); (3) P, 80% (DAP at 60 kg P_2O_5 ha^{-1}); (4) CP,100% (CDAP at 75 kg P_2O_5 ha^{-1}); 5) CP, 80% (CDAP at 60 kg P_2O_5 ha^{-1}); (6) P, 100% + HA (DAP at 75 kg P_2O_5 ha^{-1} combined with HA); (7) P, 80% + HA (DAP at 60 kg P_2O_5 ha^{-1} combined with HA); (8) CP, 100% + HA (CDAP at 75 kg P_2O_5 ha^{-1} combined with HA); and (9) CP, 80% + HA (CDAP at 60 kg P_2O_5 ha^{-1} combined with HA).

In each ceramic pot (36.0 cm in height, 30.0 cm in diameter), 1 kg sand was first placed in the bottom to improve aeration and to promote more oxygen supply to the root system (Li Z. L. et al., 2021), and then 20 kg of soil was placed on the top of the sand layer (Yu et al., 2021). Before usage, the test soil was air-dried, blended equally, and sieved. The sand (0.35–0.5 mm) used was purchased from the local market.

For the control treatment, nitrogen and potassium fertilizers were applied once as a basal fertilizer at 225 kg N ha^{-1} and 150 kg K_2O ha^{-1}, respectively, whereas for the other treatments, nitrogen, P, and potassium fertilizers were applied at 225 kg N ha^{-1}, 75 or 60 kg P_2O_5 ha^{-1}, and 150 kg K_2O ha^{-1}, respectively (Zheng et al., 2016). These fertilizer rates were calculated based on the common practices in the area. For all treatments, both coated controlled-release nitrogen and conventional nitrogen were used to provide 60 and 40% of the total applied nitrogen, respectively (Zheng et al., 2016; Qu et al., 2020). HA was applied at 45 kg ha^{-1}.

On June 20, 2017, three seeds of maize (*Zea mays* L. cv. Zhengdan 958) were sown in each container. At the three-leaf stage, the seedlings were reduced to one. Agricultural management, such as pest and weed control, was performed as needed according to local practices. In 2018, the experiment was repeated using the same pots. Maize was planted on June 12, 2018, and harvested on September 26, 2018.

Maize ears were harvested after maturity on September 29, 2017, and September 26, 2018, respectively. To deactivate enzymes, kernels and plant samples were oven-dried at 105°C for 15 min, then dried at 65°C to a constant weight (Zheng et al., 2016; Gao et al., 2021). The biomass and yield of the maize were measured.

Sampling Analyses

To learn the nutrient release pattern of CDAP, 10 g of CDAP was placed in a glass bottle containing 200 ml distilled water and incubated at 25°C. The solution in the bottle was sampled at days 1, 3, 5, 7, 10, 14, 28, 42, 56, 70, 84, 98, and 112 and analyzed for N and P concentrations according to the National Standard of the People's Republic of China—Slow-Release Fertilizers (Liu et al., 2009). The functional groups of HA were identified with an FT-IR TENSOR analyzer (Bruker Co., Germany).

In 2017, at the growth stages of seedling (V3), six-leaf (V6), twelve-leaf (V12), and milk stages (R3) of soil samples were taken from 0 to 20 cm layer of each pot, air-dried, ground, and sieved to < 2 mm; plant height was measured from the soil surface to the top of the plant stem; the diameter of the maize stem was measured at the middle of the third node from the soil surface; The readings from the Soil Plant Analysis Development (SPAD) chlorophyll meter were taken between 09:00 and 11:00 a.m. (SPAD-502, Minolta, Japan). Soil available P was extracted with 0.5 M $NaHCO_3$ (pH = 8.5) and quantified using an automatic chemical analyzer (Smartchem200, AMS, Italy). Soil NO_3^--N and NH_4^+-N were extracted with 0.01 M $CaCl_2$ (1:10 soil to water ratio) and measured with a continuous-flow injection analyzer (AA3-A001-02E, Bran-Luebbe, Germany; Houba et al., 1986; Dou et al., 2000). Soil available K was extracted with 1.0 M CH_3COONH_4 and determined using a flame photometer (Lu, 2000).

In 2018, at the V12 stage, the photosynthetic rates were determined between 09:00 and 11:00 a.m. using a LI-6400XT portable photosynthesis system (LI-Cor, Lincoln, NE, United States). Then, the fresh plant leaves, roots, and soil were sampled and frozen in liquid nitrogen for biochemical analysis. Contents of phosphoenolpyruvate carboxylase (PEPC), ADP-glucose pyrophosphorylase (AGPase), adenosine triphosphate (ATP) synthase, pyruvate phosphate dikinase (PPDK), auxin–indole-3-acetic acid (IAA), cytokinin (CTK), abscisic acid (ABA), and gibberellin (GA) of maize leaves were measured using the ELISA kit from Shanghai HengYuan Biological Technology Co., Ltd. (Shanghai, China) according to the manufacturer's instructions. Acid phosphatase (AP) and alkaline phosphatase (ALP) activities of maize root and soil were determined using the ELISA kit.

Total P content in the plant was measured using the molybdenum-antimony method after digestion with H_2SO_4-H_2O_2 (Lu, 2000). For the P fertilization treatments, PUE was calculated as follows (Devkota et al., 2013):

PUE (%) = (maize P uptake– maize P uptake in Control)/total P from fertilizer × 100%

Statistical Analyses

Data were collected and analyzed with Microsoft Excel 2010, and figures were generated using SigmaPlot software (Version 12.5, MMIV, Systat Software Inc., San Jose, CA, United States; **Figures 1**–**7**) and Origin software (Version 2021b, OriginLab Corporation, MA, United States; **Figure 8** and Spearman's correlation analysis in **Figure 9**). Analysis of variance technique (one-way ANOVA) with mean separation using Duncan's test ($P < 0.05$) was performed with IBM SPSS Statistics 22 (SPSS Inc., IL, United States).

Origin software was used to determine the determinants on the application of different fertilizations in impacting maize yield and PUE using the chord diagram, principal component analysis, and Spearman's correlation analysis (Hou et al., 2019; Li R. C. et al., 2021). With the exception of the control treatment, data were collected and divided into four categories: (1) uncoated DAP treatments (Un-P; the mean value of P 100% and P 80% treatments); (2) coated DAP treatments (CP; the mean value of

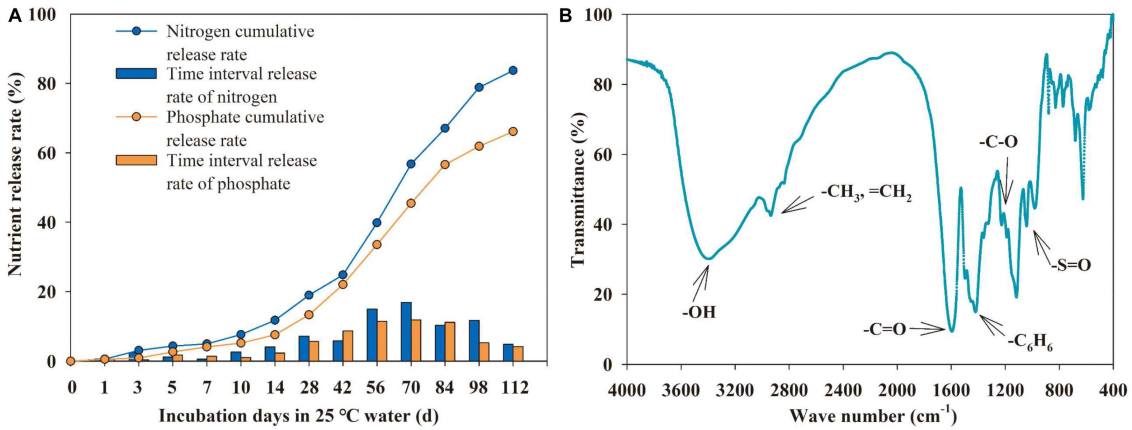

FIGURE 1 | Release rates and accumulative release rates of nutrient from coated diammonium phosphate (CDAP) in 25°C water **(A)**; infrared spectrogram of humic acid (HA) **(B)**.

CP 100% and CP 80% treatments); (3) uncoated DAP combined with HA treatments (P + HA; the mean value of P 100% + HA and P 80% + HA treatments); (4) coated DAP combined with HA treatments (CP + HA; the mean value of CP 100 % + HA and CP 80% +HA treatments).

RESULTS

Nutrient Release Pattern of Coated Diammonium Phosphate and Functional Groups of Humic Acid

Under laboratory conditions in water (25°C), nutrient release from CDAP followed a linear pattern over time (**Figure 1A**). By day 112, the cumulative release rates of P and N from CDAP reached 66.1 and 83.7%, respectively. The release of P and N was steady during the first 10 days (5.2 and 7.7% released, respectively), accelerated during the days 10–28 (8.1, 11.3% released, respectively), and slowed down afterward. However, the final cumulative release rates of P and N were different.

The FT-IR spectrum of HA displayed several characteristic peaks (**Figure 1B**). The peaks at 1,226 and 1,188 cm^{-1} are due to the existence of the C-O group. The peak at 1,117 cm^{-1} is be attributed to the C-H stretching of the benzene ring or C-O stretching. The characteristic peak at 3,396 cm^{-1} corresponds to the stretching vibration of O-H in an aromatic ring (Sarlaki et al., 2021).

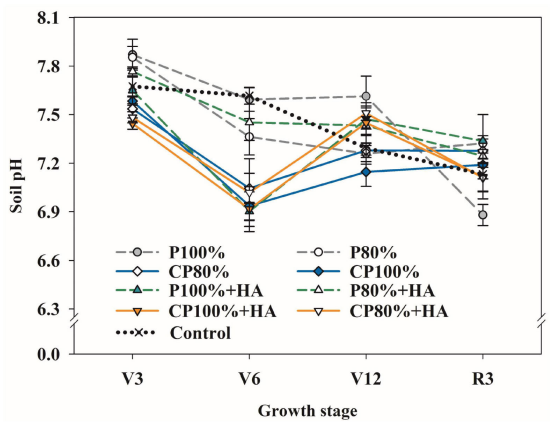

FIGURE 2 | Changes of soil pH in different fertilization treatments. Control, no P fertilizer added; P 100%, diammonium phosphate (DAP) at 75 kg P_2O_5 ha^{-1}; P80%, DAP at 60 kg P_2O_5 ha^{-1}; CP 100%, coated DAP (CDAP) at 75 kg P_2O_5 ha^{-1}; CP 80%, CDAP at 60 kg P_2O_5 ha^{-1}; P 100% + HA, DAP at 75 kg P_2O_5 ha^{-1} and humic acid (HA); P 80% + HA, DAP at 60 kg P_2O_5 ha^{-1} and HA; CP 100% + HA, CDAP at 75 kg P_2O_5 ha^{-1} and HA; CP 80% + HA, CDAP at 60 kg P_2O_5 ha^{-1} and HA. V3, seedling stage; V6, six-leaf stage; V12, twelve-leaf stage; R3, milk stage.

Soil pH and Contents of Available Nutrients

The dominant form of orthophosphate ion present in the soil is pH dependent. At the V3 stage, the soil pH in CP 100%, P 100% + HA, and CP 100% +HA was 0.29, 0.22, and 0.10 units, respectively, lower than that in P 100% (**Figure 2**). The soil pH in CP 80%, P 80% + HA, and CP 80% + HA was significantly reduced by 0.33, 0.43, and 0.39 units, respectively, while that in P 80% was only reduced by 0.02 units compared to P1 00%. The P 100% treatment resulted in the highest soil pH at the V12 stage. From the V12 to the R3 stage, the largest decrease in soil pH (0.7 units) occurred in P 100%.

Soil available P content was affected by the P fertilizers and fertilizer application rate (**Figure 3A**). The control treatment displayed the lowest soil available P content at the V3, V6, V12, and R3 growth stages. The application of CDAP significantly increased the soil available P content during the late growth stages of maize. At the V12 stage, soil available P content in CP 100%, P 100% + HA, and CP 100% + HA was 1.3, 8.0, and 16.7%, respectively, higher than that in P 100%. At the lower P application level (60 kg P_2O_5 ha^{-1}), the CP 80%, P 80% + HA, and CP 80% + HA treatments significantly increased the soil available P content by 38.8, 50.6, and 19.5%, respectively, compared to the P 100% treatment. When

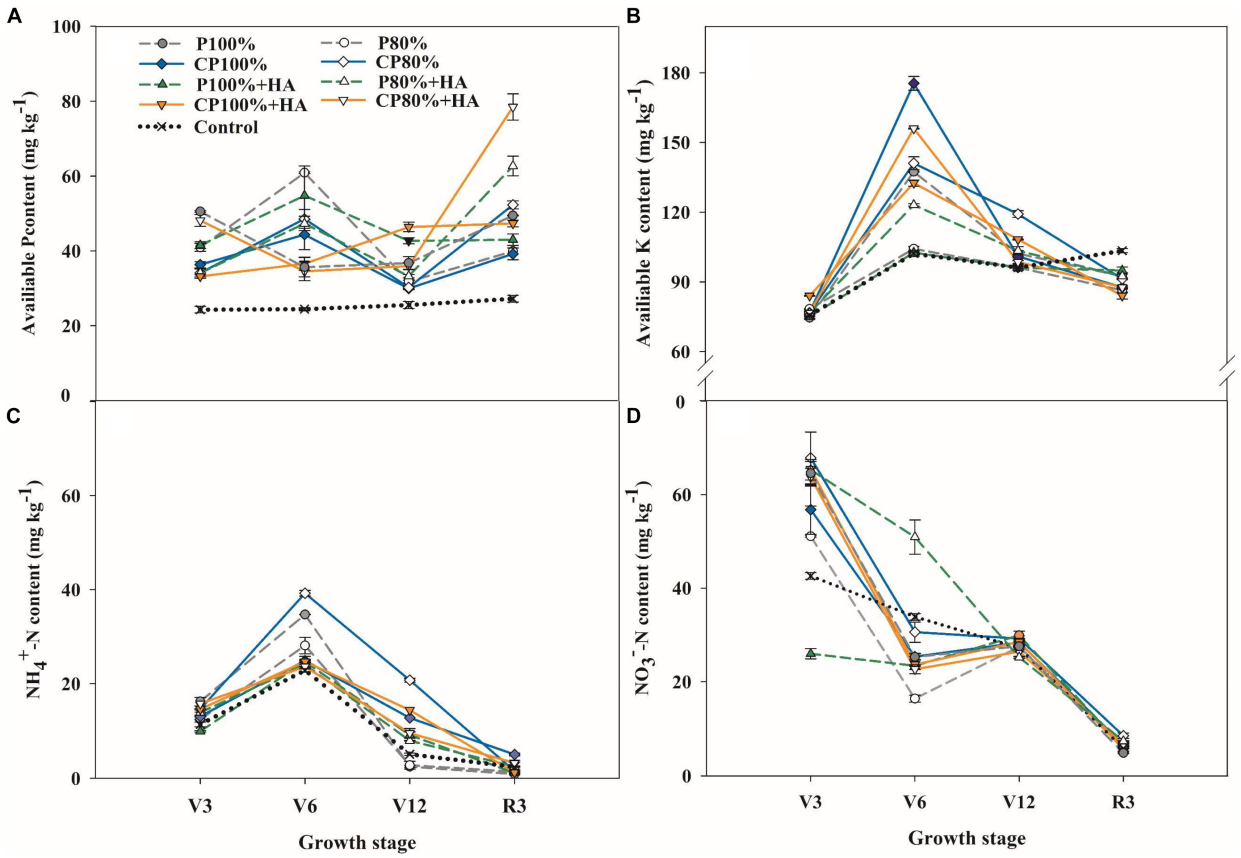

FIGURE 3 | Changes of soil available P **(A)**, available K **(B)**, NH_4^+-N **(C)**, and NO_3^--N **(D)** contents in different fertilization treatments. Control, no P fertilizer added; P 100%, diammonium phosphate (DAP) at 75 kg P_2O_5 ha^{-1}; P80%, DAP at 60 kg P_2O_5 ha^{-1}; CP 100%, coated DAP (CDAP) at 75 kg P_2O_5 ha^{-1}; C P80%, CDAP at 60 kg P_2O_5 ha^{-1}; P100%+HA, DAP at 75 kg P_2O_5 ha^{-1} and combined with humic acid (HA); P 80% + HA, DAP at 60 kg P_2O_5 ha^{-1} and combined with HA; CP 100% + HA, CDAP at 75 kg P_2O_5 ha^{-1} and combined with HA; CP 80% + HA, CDAP at 60 kg P_2O_5 ha^{-1} and combined with HA. V3, seedling stage; V6, six-leaf stage; V12, twelve-leaf stage; R3, milk stage.

coated with polyurethane or applied together with HA, the DAP increased the soil available P content at the late growth stages of maize. At the V12 and R3 stages, soil available P content in CP 100%, P 100% + HA, and CP 100% + HA was 18.1, 35.7, and 61.8%, respectively, higher than that in P100%. The average soil available P content in CP 100% + HA was 47.8 mg kg^{-1}, significantly higher than that in CP 100% by 9.5%.

Soil inorganic N (NO_3^--N and NH_4^+-N) content (**Figures 3C,D**) was high at the early growth stages and decreased at the late growth stages of maize in all treatments. At the V6, V12, and R3 stages, soil inorganic N content in the treatments with combined application of P fertilizer (CDAP or DAP) and HA was higher than that in the treatments applied with DAP only. At the V12 stage, the inorganic N content in CP 100% and P 100% + HA was higher than that in P 100%. The highest inorganic N content was found in CP 80% while the lowest was in P 100% at the V12 stage. In the treatments with P fertilization, soil available K content was low at the V3 stage, which increased rapidly to the highest value at the V6 stage and then decreased afterward (**Figure 3B**). At the V6 stage, soil available K content in CP 100% and CP 80% was 27.7 and 2.7%, respectively, higher than that in P 100%.

Acid Phosphatase and Alkaline Phosphatase Activities of Root and Soil

Phosphatase is a very important hydrolase that is ubiquitous in plants and soil. The root AP activity was increased by 11.6 and 17.2%, while the root ALP activity was increased by 24.7 and 89.5% in CP 100% and P 100% + HA, respectively, compared to P 100% (**Figures 4A,B**). The CP 100% + HA treatment increased the activities of root AP and ALP by 18.1 and 50.1%, respectively, compared to CP 100%. The root AP and ALP activities in CP 80% + HA were higher than those in CP 100%, though the P application rate was 20% lower in CP 80% + HA.

The highest soil AP activity was found in P 80% + HA, while the highest soil ALP activity was found in CP 100% (**Figures 4C,D**). There were no significant differences in soil AP activity between the treatments with 75 kg P_2O_5 ha^{-1}. There were no significant differences in soil ALP activity between P 100% + HA and P 100%. The combined application of CDAP and HA did not have a clear effect on soil AP and ALP activities.

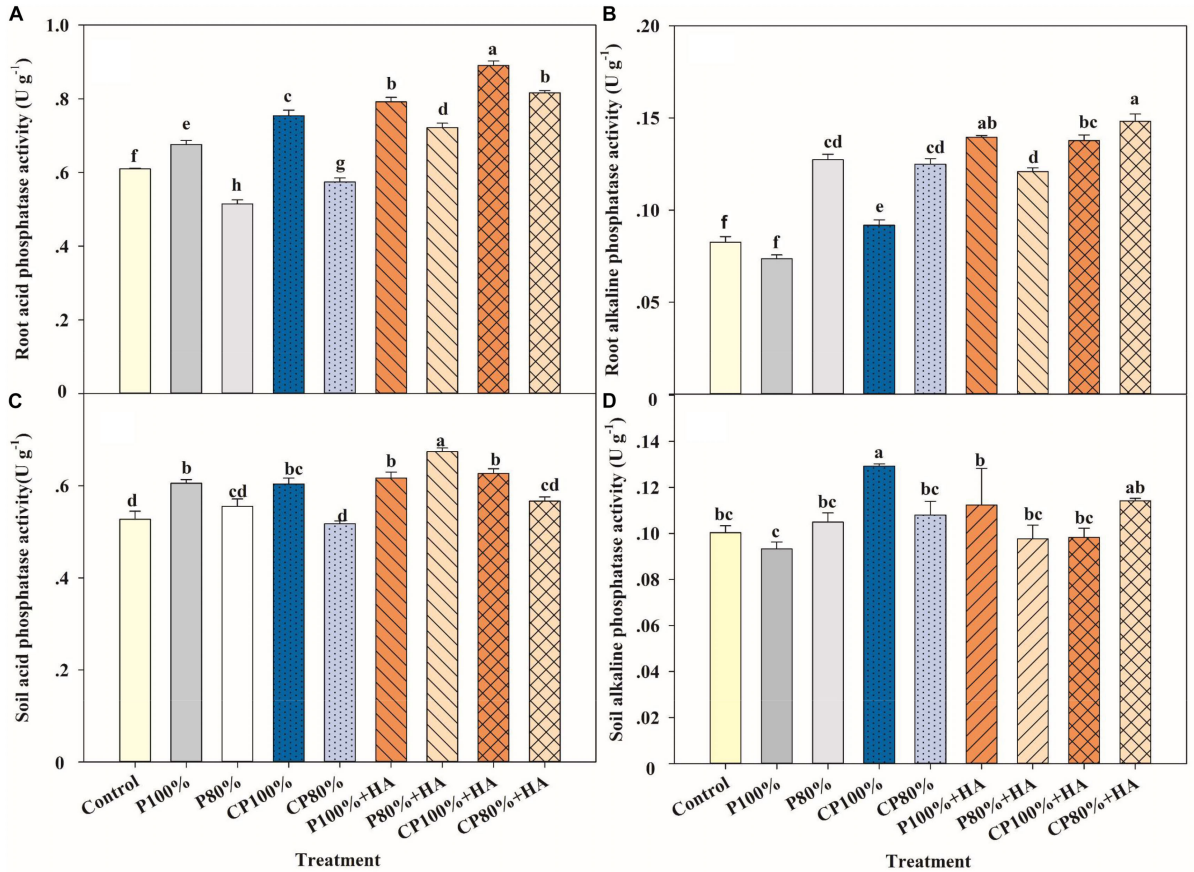

FIGURE 4 | Activities of root acid phosphatase **(A)**, root alkaline phosphatase **(B)**, soil acid phosphatase **(C)**, and soil alkaline phosphatase **(D)** in different fertilization treatments at the twelve-leaf stage of maize. Control, no P fertilizer added; P 100%, diammonium phosphate (DAP) at 75 kg P_2O_5 ha^{-1}; P80%, DAP at 60 kg P_2O_5 ha^{-1}; CP 100%, coated DAP (CDAP) at 75 kg P_2O_5 ha^{-1}; CP 80%, CDAP at 60 kg P_2O_5 ha^{-1}; P 100% + HA, DAP at 75 kg P_2O_5 ha^{-1} and combined with humic acid (HA); P 80% + HA, DAP at 60 kg P_2O_5 ha^{-1} and combined with HA; CP 100% + HA, CDAP at 75 kg P_2O_5 ha^{-1} and combined with HA; CP 80% +HA, CDAP at 60 kg P_2O_5 ha^{-1} and combined with HA. Different letters above the bars indicate significant differences at $P < 0.05$ followed by Duncan's multiple range test.

Soil Plant Analysis Development Value, Photosynthetic Rate, and Photosynthesis Enzyme Activities

The readings from the SPAD value were employed to indicate the chlorophyll content of leaves, and the SPAD-502 chlorophyll meters were used to estimate it. All treatments exhibited an increasing trend in SPAD values over time (**Figure 5**). At the V12 stage, the SPAD value in the treatments with the application of CDAP, the treatments with the combined application of DAP and HA, and the treatments with the combined application of CDAP and HA were 2.1–8.4%, 4.9–7.9%, and 8.2–12.9%, respectively, higher than that in the treatments with the application of DAP at the same P rate. In addition, the SPAD value was significantly increased in CP 80%, P 80% + HA, and CP 80% + HA by 9.5, 12.5, and 21.1%, respectively, compared to P 100%, though 20% less P was applied in these treatments. The application of HA increased the leaf SPAD value of maize.

Photosynthesis is a fundamental physiological process of maize that uses light energy to accumulate organic matter. The combined application of CDAP and HA enhanced photosynthesis at the V12 stage, a vital growth stage of maize (**Figure 6**). The photosynthetic rate in CP 100% + HA was the highest of all the treatments. For the treatments with 75 kg P_2O_5 ha^{-1}, the photosynthetic rate was in the order of CP 100% + HA > P 100% + HA > CP 100%. Of the treatments with 60 kg P_2O_5 ha^{-1}, P 80% + HA had the highest photosynthetic rate. Photosynthesis, a process that involves many enzymes, is strongly affected by the orthophosphate concentrations in cytosol and chloroplast. The different P treatments showed different effects on the activities of photosynthesis-related enzymes (**Figure 6** and **Supplementary Figure 1**). Of all the treatments, P 80% had the lowest PEPC and PPDK activities (**Supplementary Figure 1**). The addition of HA significantly increased the activities of PEPC, ATP synthase, and PPDK.

Endogenous Hormones in Maize Leaf

Endogenous hormones serve a critical role in plant growth and development, even at very low levels. **Figure 7** showed the contents of IAA, ABA, CTK, and GA in maize leaves during the V12 stage. Compared to P 100%, the CTK and GA contents

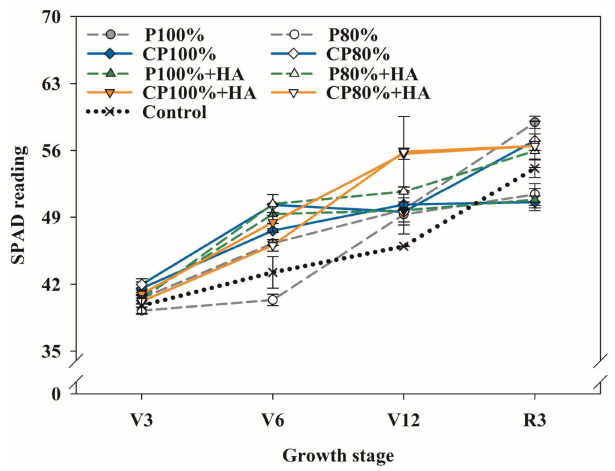

FIGURE 5 | Changes in the reading of Soil Plant Analysis Development (SPAD) chlorophyll meter with maize growth in different fertilization treatments. Control, no P fertilizer added; P 100%, diammonium phosphate (DAP) at 75 kg P_2O_5 ha^{-1}; P 80%, DAP at 60 kg P_2O_5 ha^{-1}; CP 100%, coated DAP (CDAP) at 75 kg P_2O_5 ha^{-1}; CP 80%, CDAP at 60 kg P_2O_5 ha^{-1}; P 100% + HA, DAP at 75 kg P_2O_5 ha^{-1} and combined with humic acid (HA); P 80% +H A, DAP at 60 kg P_2O_5 ha^{-1} and combined with HA; CP 100% + HA, CDAP at 75 kg P_2O_5 ha^{-1} and combined with HA; CP 80% + HA, CDAP at 60 kg P_2O_5 ha^{-1} and combined with HA. V3, seedling stage; V6, six-leaf stage; V12, twelve-leaf stage; R3, milk stage.

in CP 100% were increased by 32.4 and 21.1%, respectively. The P 100% + HA treatment increased IAA content by 34.6% and CTK content by 27.2%. The CP 100% + HA treatment increased IAA, CTK, and GA contents by 5.8, 46.4, and 21.5%, respectively. Moreover, the IAA and CTK contents were 30.5 and 10.6%, respectively, higher in CP 100% + HA and 63.3 and 9.2%, respectively, higher in CP 80% + HA than those in CP 100%.

Maize Plant Height and Stem Diameter

Changes in plant height and stem diameter at different maize growth stages are presented in **Table 1**. The maize plants in the control treatment were the shortest with the slenderest stems at the V3, V6, V12, and R3 stages. Compared to P 100%, the treatments with CP 100%, P 100% + HA, and CP 100% + HA increased the plant height by 3.7, 7.3, and 9.9%, respectively, while CP 80%, P 80% + HA, and CP 80% + HA increased the plant height by 7.8, 6.6, and 10.1%, respectively. At the V3 stage, CP 100%, P 100% + HA, and CP 100% + HA increased the diameter of the maize stem by 10.4–20.0%, 10.1–15.1%, and 7.8–12.6%, respectively, compared to P 100%.

Maize Yield, P-Use Efficiency, and Net Profit of Maize Production

In both 2017 and 2018, the maize yield of the control treatment was significantly lower than that of the other treatments (**Table 2**). Compared to P 100%, the 2-year average grain yield in CP 100% and P 100% + HA was significantly higher by 13.5 and 10.3%, respectively, while that in CP 80% and P 80% + HA, the grain yield was higher by 11.0 and 10.0%, respectively. The grain yield in CP 100% + HA was 17.2 and 16.0% higher than that in P 100% in 2017 and 2018, respectively. In 2018, the highest yield was obtained in CP 100% + HA, which was 4.2 and 4.7% higher than that in CP 100% and P 100% + HA, respectively. The PUE of CDAP or DAP combined with HA was significantly higher than that of DAP (**Table 2**). The 2-year average PUE in CP 100%, P 100% + HA, and CP 100% + HA was 24.4, 13.8, and 27.8 percentage points, respectively, higher than that in P 100%. The

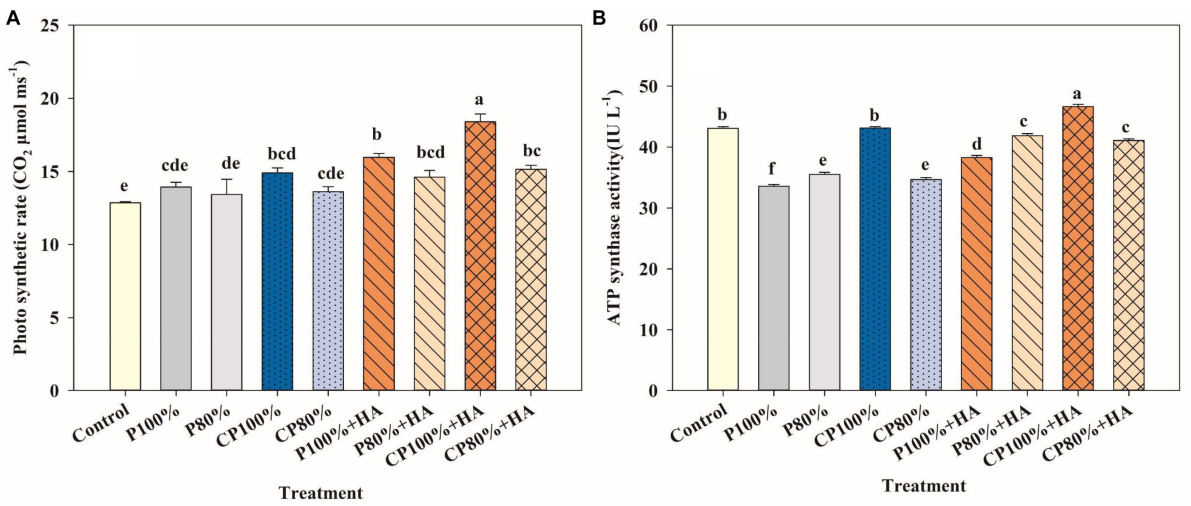

FIGURE 6 | Photosynthetic rate **(A)** and ATP synthase activity **(B)** of maize in different fertilization treatments at the twelve-leaf stage. Control, no P fertilizer added; P 100%, diammonium phosphate (DAP) at 75 kg P_2O_5 ha^{-1}; P80%, DAP at 60 kg P_2O_5 ha^{-1}; CP 100%, coated DAP (CDAP) at 75 kg P_2O_5 ha^{-1}; CP 80%, CDAP at 60 kg P_2O_5 ha^{-1}; P 100% + HA, DAP at 75 kg P_2O_5 ha^{-1} and combined with humic acid (HA); P 80% + HA, DAP at 60 kg P_2O_5 ha^{-1} and combined with HA; CP 100% + HA, CDAP at 75 kg P_2O_5 ha^{-1} and combined with HA; CP 80% + HA, CDAP at 60 kg P_2O_5 ha^{-1} and combined with HA. Different letters above the bars indicate significant differences at $P < 0.05$ followed by Duncan's multiple range test.

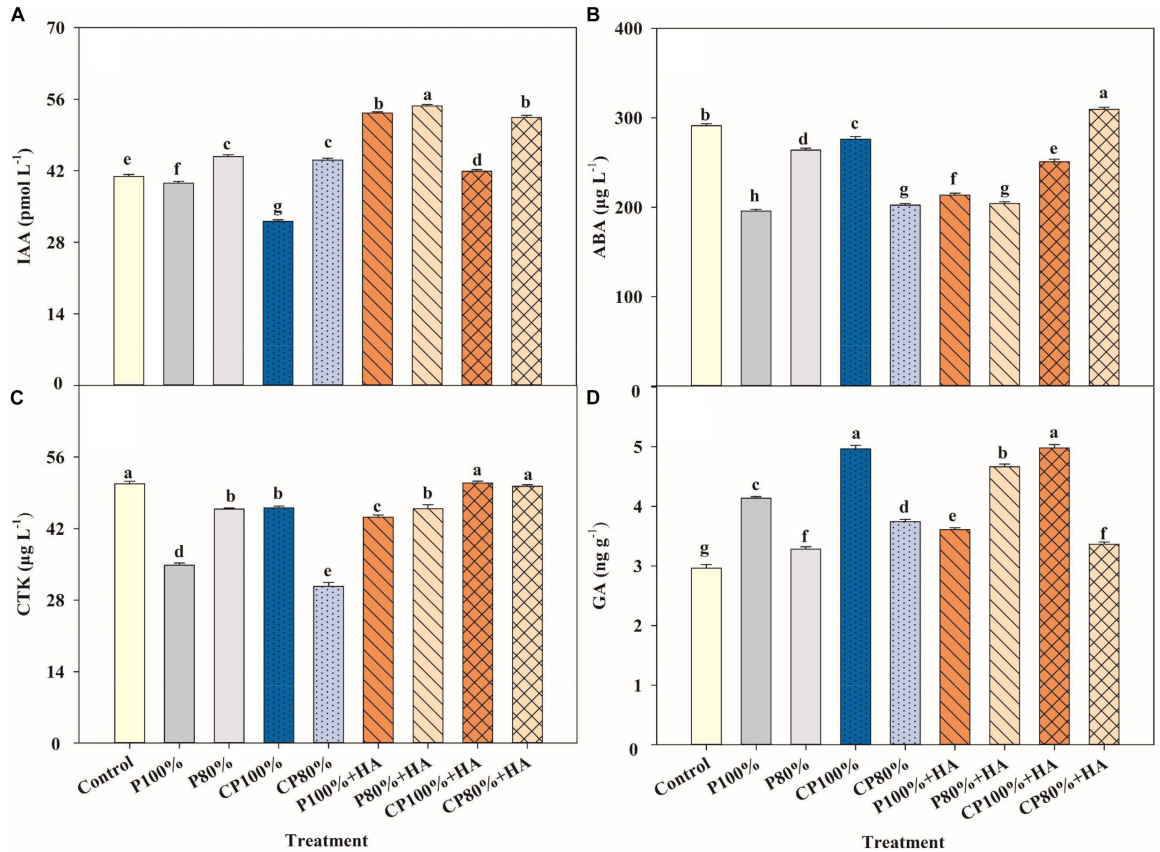

FIGURE 7 | Auxin indole-3-acetic acid (IAA) **(A)**, abscisic acid (ABA) **(B)**, cytokinin (CTK) **(C)** and gibberellin GA **(D)** contents of maize leaves in different fertilization treatments at the twelve-leaf stage. Control, no P fertilizer added; P 100%, diammonium phosphate (DAP) at 75 kg P_2O_5 ha^{-1}; P80%, DAP at 60 kg P_2O_5 ha^{-1}; CP 100%, coated DAP (CDAP) at 75 kg P_2O_5 ha^{-1}; CP8 0%, CDAP at 60 kg P_2O_5 ha^{-1}; P 100% + HA, DAP at 75 kg P_2O_5 ha^{-1} and combined with humic acid (HA); P 80% + HA, DAP at 60 kg P_2O_5 ha^{-1} and combined with HA; CP 100% + HA, CDAP at 75 kg P_2O_5 ha^{-1} and combined with HA; CP 80% + HA, CDAP at 60 kg P_2O_5 ha^{-1} and combined with HA. Different letters above the bars indicate significant differences at $P < 0.05$ followed by Duncan's multiple range test.

CP 80%, P 80% + HA, and CP 80% + HA treatments achieved a higher average of PUE than the P 100% treatment by 26.4, 20.7, and 27.4 percentage points, respectively.

When DAP was used in combination with HA, or when CDAP was applied alone or in combination with HA, the maize production cost was higher than when DAP was applied alone (**Table 3**). However, the application of CDAP, alone or together with HA, generally increased the maize grain yield. Of all treatments, CP 100% achieved the highest average net income. Compared to P 100%, the average net income of CP 100% and CP 80% was increased by 483.1 and 440.8 USD ha^{-1}, respectively, while that of P 100% + HA and P 80% + HA was increased by 287.1 and 321.5 USD ha^{-1}, respectively. The highest income was achieved by the CP 100% + HA treatment, which was 485.6 and 198.5 USD ha^{-1} greater than that by the P 100% and P 100%+HA treatments, respectively.

Correlation Analysis

Correlation analysis showed that there was a positive effect with the application of CDAP in combination with HA on yield, biomass, height, available P content, soil AP, soil ALP, root AP, root ALP, IAA, ABA, CTK, GA, PEPC, AGPase, and ATP synthase (**Figure 8A**). In addition, it was obvious that the contribution of the application of CDAP combined with HA respond to these indices than other treatments, including the combination of DAP and HA and application of CDAP and DAP, respectively. Principal component analysis revealed that the 21 parameters were divided into PC 1 (53.6%) and PC 2 (22.3%). PC 1 and PC 2 explained 53.2% of the differences among the 21 indicators (**Figure 8B**). In addition, pH and AGPase were distributed in the second quadrant, and they had a negative relationship with the other parameters mainly distributed in the first and fourth quadrants.

DISCUSSION

Effects of Coated Diammonium Phosphate on P Supply Intensity in the Soil Solution and Its Availability

It is important to balance fertilizer input and crop uptake in high-yielding maize production (Shoji et al., 2001; Geng et al., 2015).

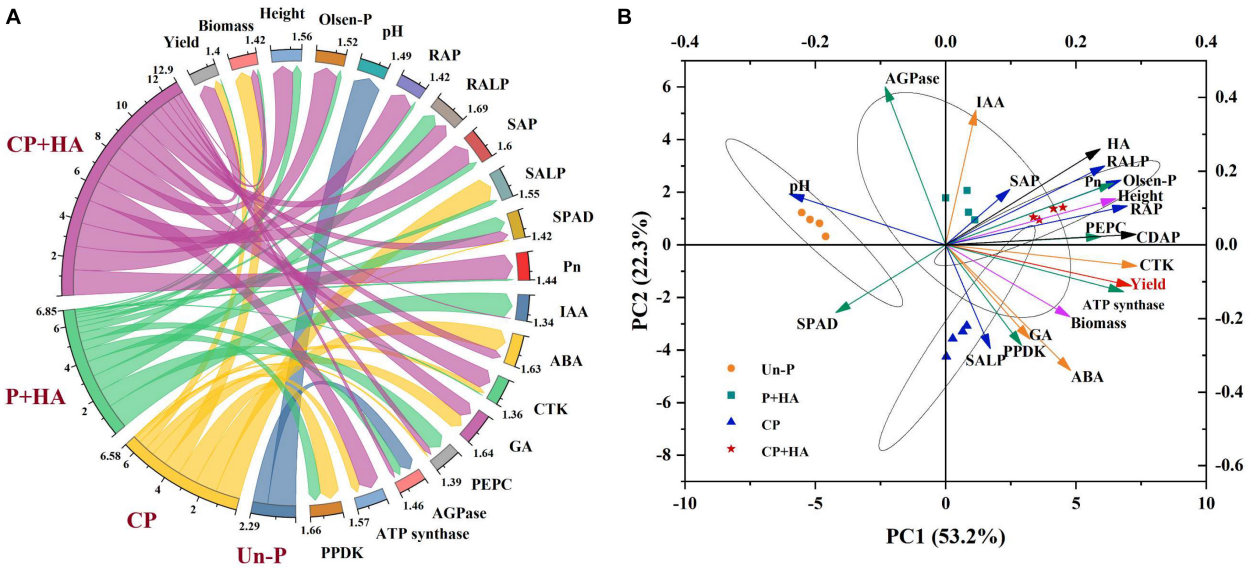

FIGURE 8 | (A) Chord diagram for showing the effects of the different treatments on these indices. This plot links these treatments *via* ribbons to their associated indexes. **(B)** Principal component analysis shows the relationship among grain yield, growth parameters, and soil nutrient. Height, plant height; SAP, soil acid phosphatase; SALP, soil alkaline phosphatase; RAP, root acid phosphatase; RALP, root alkaline phosphatase; Pn, photosynthetic rate; PEPC, Phosphoenolpyruvate carboxylase; AGPase, ADP-glucose pyrophosphorylase; PPDK, pyruvate phosphate dikinase; IAA, indole-3-acetic acid auxin; CTK, cytokinin; ABA, abscisic acid; GA, gibberellin. Un-P, uncoated DAP treatments (P 100% and P 80% treatments); CP, coated DAP treatments (CP 100% and CP 80% treatments); P + HA, uncoated DAP combined with HA treatments (P 100% + HA and P 80% +HA treatments); CP + HA, coated DAP combined with HA treatments (CP 100% + HA and CP 80% + HA treatments).

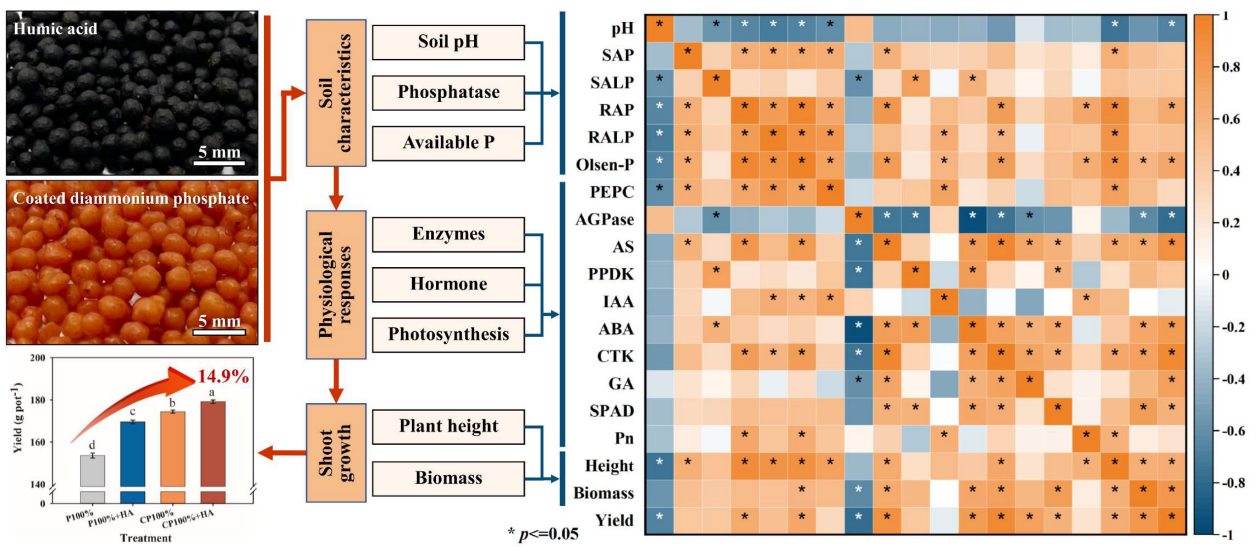

FIGURE 9 | Correlation relations between maize yield and different indices. Spearman's correlation between soil variables, growth parameters, and maize yields. Blue represents negative correlation and red represents positive correlation. The darker the color, the stronger the correlation, and vice versa (*$P \leq 0.05$). Height, plant height; SAP, soil acid phosphatase; SALP, soil alkaline phosphatase; RAP, root acid phosphatase; RALP, root alkaline phosphatase; Pn, photosynthetic rate; PEPC, Phosphoenolpyruvate carboxylase; AGPase, ADP-glucose pyrophosphorylase; PPDK, pyruvate phosphate dikinase; IAA, indole-3-acetic acid auxin; CTK, cytokinin; ABA, abscisic acid; GA, gibberellin.

The nutrient release curve of CDAP (**Figure 1A**) is similar to the sigmoidal nutrient uptake curve of maize (Bender et al., 2013). Lu et al. (2020) reported similar results pertaining to the nutrient release characteristics of CDAP that match with the nutrient uptake requirement of maize much better than the conventional P fertilizer. Based on soil available P changes during maize growth (**Figure 3A**), it is speculated that CDAP had a longer P-release period in the pot experiment than in the

TABLE 1 | Plant height and stem diameter of maize in different fertilization treatments.

Treatment[a]	Plant height (cm)				Plant stem diameter (mm)			
	V3[b]	V6	V12	R3	V3	V6	V12	R3
Control	54.3a[c]	95.3a	210.0a	223.1a	10.0d	20.3b	21.9a	25.5a
P100%	60.5a	112.6a	202.5a	224.0a	12.8abc	25.9a	25.5a	28.2a
P80%	57.9a	111.9a	234.8a	233.4a	11.2cd	22.2ab	23.2a	26.6a
CP100%	62.9a	116.0a	234.0a	232.3a	14.1a	24.7ab	24.9a	27.5a
CP80%	61.8a	117.0a	241.0a	241.5a	13.4ab	24.6ab	25.1a	27.8a
P100%+HA	63.4a	120.9a	239.8a	240.4a	14.1a	25.0ab	24.2a	27.8a
P80%+HA	62.4a	111.3a	236.3a	238.8a	12.9abc	22.1ab	22.2a	26.4a
CP100%+HA	59.3a	114.1a	245.5a	246.3a	14.4a	23.8ab	24.4a	26.4a
CP80%+HA	59.2a	114.5a	232.0a	246.6a	12.1bc	23.7ab	25.2a	26.0a

[a]*Control, no P fertilizer added; P 100%, diammonium phosphate (DAP) at 75 kg P_2O_5 ha^{-1}; P 80%, DAP at 60 kg P_2O_5 ha^{-1}; CP 100%, coated DAP (CDAP) at 75 kg P_2O_5 ha^{-1}; CP 80%, CDAP at 60 kg P_2O_5 ha^{-1}; P100%+HA, DAP at 75 kg P_2O_5 ha^{-1} and combined with humic acid (HA); P 80% + HA, DAP at 60 kg P_2O_5 ha^{-1} and combined with HA; CP 100% + HA, CDAP at 75 kg P_2O_5 ha^{-1} and combined with HA; CP 80% + HA, CDAP at 60 kg P_2O_5 ha^{-1} and combined with HA.*
[b]*Growth stages: V3, seedling stage; V6, six-leaf stage; V12, twelve-leaf stage; R3, milk stage.*
[c]*Means within each column followed by the same letters were not significantly different based on one-way ANOVA followed by Duncan's test ($P < 0.05$).*

TABLE 2 | Maize yield and phosphorus use efficiency (PUE) in different fertilization treatments.

Treatment[a]	Kernel (ear^{-1})	Plant biomass (g pot^{-1})	Yield (g pot^{-1})	Yield change vs. P100% (%)	PUE (%)	PUE change vs. P100%
2017						
Control	487b[b]	267.0d	130.3d	−9.1	–	–
P100%	543ab	301.2c	143.4c	0.0	16.7f	–
P80%	488b	304.0c	140.8c	−1.8	17.2f	0.5
CP100%	556ab	329.2a	166.2a	15.9	37.2c	20.5
CP80%	492b	318.1b	159.4b	11.1	39.3c	22.6
P100%+HA	600a	308.1c	159.1b	10.9	25.2e	8.5
P80%+HA	517b	324.2ab	158.9b	10.8	33.0d	16.3
CP100%+HA	523b	322.9ab	168.1a	17.2	40.3b	23.5
CP80%+HA	515b	319.9ab	161.2b	12.4	42.2a	25.5
2018						
Control	508c	319.5e	149.6e	−8.8	–	–
P100%	585abc	334.6d	164.0d	0.0	15.5f	–
P80%	573bc	347.4c	164.5d	0.3	16.6f	1.1
CP100%	650ab	372.8a	182.6bc	11.3	43.8c	28.3
CP80%	651ab	359.1bc	181.8c	10.9	45.7b	30.3
P100%+HA	629ab	376.0a	180.0c	9.7	34.6e	19.1
P80%+HA	603ab	351.7c	179.3c	9.3	40.6d	25.1
CP100%+HA	669a	382.9a	190.3a	16.0	47.5b	32.1
CP80%+HA	650ab	370.7ab	186.7ab	13.8	44.9a	29.4

[a]*Control, no P fertilizer added; P 100%, diammonium phosphate (DAP) at 75 kg P_2O_5 ha^{-1}; P 80%, DAP at 60 kg P_2O_5 ha^{-1}; CP 100%, coated DAP (CDAP) at 75 kg P_2O_5 ha^{-1}; CP 80%, CDAP at 60 kg P_2O_5 ha^{-1}; P 100% + HA, DAP at 75 kg P_2O_5 ha^{-1} and combined with humic acid (HA); P 80% + HA, DAP at 60 kg P_2O_5 ha^{-1} and combined with HA; CP 100% + HA, CDAP at 75 kg P_2O_5 ha^{-1} and combined with HA; CP 80% + HA, CDAP at 60 kg P_2O_5 ha^{-1} and combined with HA.*
[b]*Means within each column in each year followed by the same letters were not significantly different based on one-way ANOVA followed by Duncan's test ($P < 0.05$).*

laboratory incubation (**Figure 1A**). First, the coating of CDAP was done by a polyurethane block copolymer containing soft and hard segments, with swelling properties for gradual nutrient release (Hou et al., 2015; Lu et al., 2016). Second, the nutrient release from coated fertilizers is greatly affected by humidity and temperature (Yang et al., 2011). Although soil temperature (26.1°C on average) during maize growth in the pot experiment was closer to the incubation temperature in the laboratory, soil moisture was low compared with the moisture condition in laboratory incubation (Li et al., 2020), which might have greatly slowed down the P release. Our findings were in line with those of Zheng et al. (2016), who discovered changes in nutrient release characteristics between field soils and laboratory soils.

Sufficient nutrient supply is a requirement for high crop yield. In this study, the maize yield in CP 100% and CP 80% was increased by 13.5 and 11.0%, respectively, compared to P 100%

TABLE 3 | Cost and net profits of maize production in different fertilization treatments.

Treatment[b]	Cost[a](USD ha^{-1} year^{-1})		Total income(USD ha^{-1})		Net income(USD ha^{-1})			
	P fertilizer	Labor	2017	2018	2017	2018	Average	Change vs. P100%
Control	405.4	72.5	3403.5d[c]	3906.7e	2925.6e	3428.8d	3177.2e	−4.0
P100%	633.2	72.5	3744.8c	4282.7d	3039.1d	3577.0c	3308.0d	–
P80%	590.0	72.5	3676.2c	4295.5d	3013.7d	3633.0c	3323.3d	0.5
CP100%	690.4	72.5	4339.9a	4768.5bc	3576.8a	4005.4a	3791.1a	14.6
CP80%	633.8	72.5	4162.1b	4748.6c	3455.6b	4042.1a	3748.8ab	13.3
P100%+HA	759.4	72.5	4154.6b	4699.8c	3322.5c	3867.6b	3595.1c	8.7
P80%+HA	712.9	72.5	4149.4b	4680.9c	3363.7c	3895.3b	3629.5c	9.7
CP100%+HA	813.1	72.5	4390.0a	4969.0a	3504.2b	4083.1a	3793.6a	14.7
CP80%+HA	756.6	72.5	4209.7b	4875.5ab	3380.4c	4046.2a	3713.3b	12.3

[a]*Based on the current mean market price. Data in the table were calculated based on the current mean market price; maize, 313.4 USD t^{-1}; CDAP (coated diammonium phosphate), 557.4 USD t^{-1}; DAP (diammonium phosphate), 447.8 USD t^{-1}; Urea, 238.8 USD t^{-1}; Controlled-release urea, 348.4 USD t^{-1}; Potassium chloride, 373.1 USD t^{-1}; humic acid (HA), 302 USD t^{-1}; Labor cost for seeding, field management, and harvest, 72.5 USD ha^{-1}; and other costs including those for machinery, irrigation, pesticides, insecticides, seeds, and other materials and expenses, 1320.5 USD ha^{-1}.*

[b]*Control, no P fertilizer added; P 100%, DAP at 75 kg P_2O_5 ha^{-1}; P 80%, DAP at 60 kg P_2O_5 ha^{-1}; CP 100%, CDAP at 75 kg P_2O_5 ha^{-1}; CP 80%, CDAP at 60 kg P_2O_5 ha^{-1}; P 100% + HA, DAP at 75 kg P_2O_5 ha^{-1} and combined with HA; P 80% + HA, DAP at 60 kg P_2O_5 ha^{-1} and combined with HA; CP 100% +HA, CDAP at 75 kg P_2O_5 ha^{-1} and combined with HA; CP 80% + HA, CDAP at 60 kg P_2O_5 ha^{-1} and combined with HA.*

[c]*Means within each column followed by the same letters were not significantly different based on one-way ANOVA followed by Duncan's test ($P < 0.05$).*

(**Table 1**). The coating of CDAP not only separates DAP from direct contact with the soil, thus preventing P from fixation by the soil *via* sorption, complexation, and precipitation (Roberts and Johnston, 2015) but also stops DAP from rapid dissolution and loss of surface runoff and subsurface flow (Hively et al., 2006; Holman et al., 2008). The V12 stage is a highly P-demanding growth stage of maize, during which a large amount of P is needed for grain development in the later stages (Bender et al., 2013). The application of CDAP increased the activity of phosphatase, AP in particular, in the root by 11.5–24.7% at the V12 stage (**Figure 4**), leading to higher P availability due to more organic P being hydrolyzed.

Additionally, the application of conventional P fertilizer (i.e., DAP) resulted in a higher soil available P content at the V3 stage (**Figure 2**), which would lead to a higher P content in the maize plant (Bender et al., 2013). However, high available P would inhibit the synthesis and the activity of phosphatase and in turn, would slow down the decomposition of protein-phytic acid-mineral element complex. Consequently, the availability of mineral elements would be decreased (Sarah et al., 2018). As CDAP released P into the soil solution at a rate that matches the maize demand, maize growth was not limited by P, resulting in a high grain yield.

Effects of Humic Acid on the P Availability and Maize Growth

Humic acid, as a P activator, accelerated P transformation into bioavailable forms. On the one hand, soil pH was lower in the treatments with combined application of HA and DAP than in the treatments with an application of DAP alone at the V3 stage. The presence of HA increases the altering of the root exudate profile and it also enhances the release of oxalate and citrate from maize roots, compared to maize not treated with HA (Canellas et al., 2008; Rosa et al., 2018; Ma et al., 2021). Additionally, H^+ is produced during HA decomposition (Hue, 1991), leading to an available P increase in calcareous soils with the dissolution of insoluble P compounds. On the other hand, the adsorption of HA generates a repulsive negative electric potential on the adsorption plane and a steric hindrance on the mineral surface, further inhibiting P binding on the soil surface (Wang, 2016). Additionally, HA complexes with Ca^{2+}, Fe^{3+}, and Al^{3+}, reduce P precipitation with these cations. This was associated with the rich functional groups in HA, such as O-H in aromatic rings, C-O, and C-H in benzene rings (**Figure 1B**; Sarlaki et al., 2021). Furthermore, the application of HA increased the phosphatase (i.e., soil AP and root AP) activity (**Figure 4**) and in turn the amount of P released from the soil solid phase or from P fertilizers (Nardi et al., 2017; Zhu et al., 2018), leading to an increase in the available P content (**Figure 3A**). Therefore, HA protected P fertilizer to avoid wasting and improved the P availability in soil.

In addition to the P availability in soil, the HA use increased the growth of maize. As a biostimulant, HA possesses aliphatic and aromatic structures with various functional groups (mainly oxygen-containing). Its phenolic and quinone groups interact with enzymes in plant cell and stimulate plant metabolism, thereby promoting growth and improving crop yield (Fan et al., 2015). In this study, the photosynthetic rate of maize leaves at the key growth stage was enhanced by the application of HA (**Figure 6**). The application of HA improved photosynthesis by increasing the activities of PEPC, ATP synthase, and PPDK (**Figure 6** and **Supplementary Figure 1**) and influenced the important metabolic pathways in photosynthesis, such as photosynthetic carbon assimilation, oxidative phosphorylation, and photosynthetic phosphorylation (Gao et al., 2017; Nardi et al., 2017).

The endogenous hormone plays a key role in regulating plant growth and developmental processes as well as in regulating plant responses to the external environment (Fahad et al., 2015a,b). The P 100% + HA treatment increased the IAA, ABA, and CTK contents in maize leaves by 34.6, 9.1, and 27.2%, respectively, compared to the P 100% treatment at the V12 stage. These results are in confirmation with the reports by Nardi et al. (2017). Nardi et al. (2002) suggested that humic-like substances behave as signaling molecules in the rhizosphere, eliciting the production of phytohormones. Moreover, HA stimulates the expression of *IAA5* and *IAA19*, two early auxin-responsive genes (Nardi et al., 2002). These phytohormones can act either locally (at the site of their synthesis) or transported to some other sites within the maize plant body to mediate growth and development responses of both under ambient and stressful conditions (Peleg and Blumwald, 2011; Fahad et al., 2015a). Furthermore, IAA and HA can enhance the synthesis and activity of plasma membrane H^+-ATPase, an enzyme that converts energy for transmembrane transportation of nutrients including P, then energizes secondary ion transporters, and promotes the nutrient uptake of maize (Zandonadi et al., 2010).

Interactive Effects of Coated Diammonium Phosphate and Humic Acid

The interactive effect of CDAP and HA improved maize grain yield and PUE (**Figure 9**). The CDAP synchronized the P supply with plant demand. The HA increased the photosynthetic rate of maize to accumulate organic matter. Additionally, the functional groups of HA, such as –COOH and –OH (**Figure 1B**), adsorb to the soil surface and react with soil minerals, influencing metal speciation and solubility and reducing P fixation (Nardi et al., 2017; Sarlaki et al., 2021), which is conducive to meeting the P demand of maize in the early growth stage. Furthermore, some studies have shown that HA was capable of promoting root growth and modifying root architecture (Olaetxea et al., 2018) as well as modifying the gene expression of the main high-affinity root transporters of phosphate to increase the phosphate root uptake (Jindo et al., 2016; Olaetxea et al., 2018). Therefore, the combination of CDAP and HA was able to improve the overall P nutrition in maize plants. Besides, the contents of IAA and CTK in maize leaves were improved when treated with CDAP combined with HA. Meanwhile, the ATP synthase activity and the photosynthetic rate were improved (**Figure 9**) leading to better crop growth and grain development.

The interactive effect of CDAP and HA on maize yield was not significant in 2017. This may be because maize is a highly P-efficient crop and not very sensitive to P levels in soil (Ciarelli et al., 1998; Ci et al., 2012). However, the yield in CP 100% + HA was significantly higher than that in CP 100% in 2018. This is because the combination of CDAP and HA exerts beneficial effects on plant growth by improving the soil structure, fertility, and quality (Calvo et al., 2014; Raiesi, 2021; Xu et al., 2021), and two consecutive years of application eventually resulted in significant changes. The combination of CDAP and HA provides an HA-incorporated enhanced-efficiency P fertilizer for environmentally friendly fertilization (**Figure 9**), and future research should include P-inefficient crops (e.g., wheat).

CONCLUSION

The application of CDAP combined with HA increased the soil available P content, improved the root acid phosphatase activity, ATP synthase activity, and cytokinin content, increased the photosynthetic rate, and plant height, and eventually increased the maize grain yield and PUE. When P was applied at 75 kg P_2O_5 ha^{-1}, higher maize grain yield was obtained by CDAP-HA combination than by CDAP alone or DAP-HA combination, and in the second year of cultivation, these differences became bigger and significant. Even at 60 kg P_2O_5 ha^{-1}, the combined application of CDAP and HA presented a higher grain yield and PUE in the second year than the conventional fertilization. Overall, the combined application of CDAP and HA is of significance in improving PUE, reducing P loss to the environment, ensuring food security, realizing sustainable utilization of land and fertilizer resources, and increasing the economic return of crops. Future studies should be conducted in different regions with various soil types and crops to develop an effective strategy of fertilization with controlled-release fertilizers and biostimulants (e.g., HA).

DATA AVAILABILITY STATEMENT

The original contributions presented in the study are included in the article/**Supplementary Material**, further inquiries can be directed to the corresponding author/s.

AUTHOR CONTRIBUTIONS

QC, ZGL, ZW, and MZ contributed to the conception and design of the study. QC, ZQ, ZL, ZZ, and GM organized the database. QC, YW, LW, and FF contributed to investigating and obtaining the resources. QC, ZGL, ZW, and MZ wrote sections of the manuscript. QC wrote the first draft of the manuscript. All authors contributed to the article and approved the submitted version.

FUNDING

This study was supported by the Key Research and Development Program of Shandong (Grant No. 2019GNC106011), the National Natural Science Foundation of China (Grant No. 41977019), and the Strategic Priority Research Program of the Chinese Academy of Sciences (Grant No. XDA28090200).

SUPPLEMENTARY MATERIAL

The Supplementary Material for this article can be found online at: https://www.frontiersin.org/articles/10.3389/fpls.2021.759929/full#supplementary-material

REFERENCES

Adnan, M., Fahad, S., Zamin, M., Shah, S., Mian, I. A., and Danish, S. (2020). R coupling phosphate-solubilizing bacteria with phosphorus supplements improve maize phosphorus acquisition and growth under lime induced salinity stress. *Plants* 9:900. doi: 10.3390/plants9070900

Balemi, T., and Negisho, K. (2012). Management of soil phosphorus and plant adaptation mechanisms to phosphorus stress for sustainable crop production: a review. *J. Soil Sci. Plant Nutr.* 12, 574–562. doi: 10.4067/S0718-95162012005000015

Bender, R. R., Haegele, J. W., Ruffo, M. L., and Below, F. E. (2013). Nutrient uptake, partitioning, and remobilization in modern, transgenic insect-protected maize hybrids. *Agron J.* 105, 161–170. doi: 10.2134/agronj2012.0352

Calvo, P., Nelson, L., and Kloepper, L. K. (2014). Agricultural uses of plant biostimulants. *Plant Soil.* 383, 3–41. doi: 10.1007/s11104-014-2131-8

Canellas, L. P., Balmori, D. M., Médici, L. O., Aguiar, M. O., Campostrini, E., Rosa, R. C. C., et al. (2013). A combination of humic substances and Herbaspirillum seropedicae inoculation enhances the growth of maize (*Zea mays* L.). *Plant Soil* 366, 119–132. doi: 10.1007/s11104-012-1382-5

Canellas, L. P., Teixeira Junior, L. R. L., Dobbss, L. B., Silva, C. A., Medici, L. O., Zandonadi, D. B., et al. (2008). Humic acids crossinteractions with root and organic acids. *Ann. Appl. Biol.* 153, 157–166. doi: 10.1111/j.1744-7348.2008.00249.x

Castro, B., and Torrent, J. (1998). Phosphate sorption by calcareous vertisols and inceptisols as evaluated from extended P-sorption curves. *Eur. J. Soil Sci.* 49, 661–667. doi: 10.1046/j.1365-2389.1998.4940661.x

Chen, Q., Li, Z. L., Qu, Z. M., Zhou, H. Y., Qi, Y. J., Liu, Z. G., et al. (2020). Maize yield and root morphological characteristics affected by controlled-release diammonium phosphate and *Paecilomyces variotii* extracts. *Field Crop. Res.* 22:107862. doi: 10.1016/j.fcr.2020.107862

Ci, X. K., Li, M. S., Xu, J. S., Lu, Z. Y., Bai, P. F., Ru, G. L., et al. (2012). Trends of grain yield and plant traits in Chinese maize cultivars from the 1950s to the 2000s. *Euphytica* 185, 395–406. doi: 10.1007/s10681-011-0560-5

Ciarelli, D. M., Furlani, A. M. C., Dechen, A. R., and Lima, M. (1998). Genetic variation among maize genotypes for phosphorus-uptake and phosphorus-use efficiency in nutrient solution. *J. Plant Nutr.* 21, 2219–2229. doi: 10.1080/01904169809365556

Çimrin, K. M., Türkmen, Ö, Turan, M., and Tuncer, B. (2010). Phosphorus and humic acid application alleviate salinity stress of pepper seedling. *Afr. J. Biotechnol.* 9, 5845–5851.

CRGCST (2001). *(Cooperative Research Group on Chinese Soil Taxonomy), Chinese Soil Taxonomy*. Beijing: Science Press.

Cruz, D. F. D., Bortoletto-Santos, R., Guimarães, G. G. F., Polito, W. L., and Ribeiro, C. (2017). Role of polymeric coating on the phosphate availability as a fertilizer: insight from phosphate release by castor polyurethane coatings. *J. Agric. Food Chem.* 65, 5890–5895. doi: 10.1021/acs.jafc.7b01686

Dantas, R. S., Alberto, S. C., and Henrique, J. G. M. M. (2018). Wheat nutrition and growth as affected by humic acid-phosphate interaction. *J. Plant Nutr. Soil Sci.* 181, 870–877. doi: 10.1002/jpln.201700532

Devkota, M., Martius, C., Lamers, J. P. A., Sayre, K. D., Devkota, K. P., and Vlek, P. L. G. (2013). Tillage and nitrogen fertilization effects on yield and nitrogen use efficiency of irrigated cotton. *Soil Till Res.* 134, 72–82. doi: 10.1016/j.still.2013.07.009

Ding, W. L., Cong, W. F., and Lambers, H. (2021). Plant phosphorus-acquisition and -use strategies affect soil carbon cycling. *Trends Ecol. Evol.* 36, 899–906. doi: 10.1016/j.tree.2021.06.005

Dou, H., Alva, A. K., and Appel, T. (2000). An evaluation of plant-available soil nitrogen in selected sandy soils by electro-ultrafiltration, KCl, and CaCl2 extraction methods. *Biol. Fertil. Soils* 30, 328–332. doi: 10.1007/s003740050011

Fahad, S., Hasanuzzaman, M., Alam, M., Ullah, H., Saeed, M., Ali Khan, I., et al. (2020). *Environment, Climate, Plant and Vegetation Growth*. Switzerland: Springer Nature. doi: 10.1007/978-3-030-49732-3

Fahad, S., Hussain, S., Matloob, A., Khan, F. A., Khaliq, A., Saud, S., et al. (2015a). Phytohormones and plant responses to salinity stress: a review. *Plant Growth Regul.* 75, 391–404. doi: 10.1007/s10725-014-0013-y

Fahad, S., Nie, L., Chen, Y., Wu, C., Xiong, D., Saud, S., et al. (2015b). Crop plant hormones and environmental stress. *Sustain. Agric. Rev.* 15, 371–400. doi: 10.1007/978-3-319-09132-7_10

Fahad, S., Hussain, S., Saud, S., Hassan, S., Tanveer, M., Ihsan, M. Z., et al. (2016). A combined application of biochar and phosphorus alleviates heat-induced adversities on physiological, agronomical and quality attributes of rice. *Plant Physiol. Bioch.* 103, 191–198. doi: 10.1016/j.plaphy.2016.03.001

Fan, H. M., Li, T., Sun, X., Sun, X. Z., and Zheng, C. S. (2015). Effects of humic acid derived from sediments on the postharvest vase life extension in cut chrysanthemum flowers. *Postharvest. Biol. Tec.* 101, 82–87. doi: 10.1016/j.postharvbio.2014.09.019

Gao, J., Zhao, B., Dong, S., Liu, P., Ren, B., and Zhang, J. (2017). Response of summer maize photosynthate accumulation and distribution to shading stress assessed by using 13CO2 stable isotope tracer in the field. *Front. Plant Sci.* 8:1821. doi: 10.3389/fpls.2017.01821

Gao, Y. X., Song, X., Liu, K. X., Li, T. G., Zheng, W. K., Wang, Y., et al. (2021). Mixture of controlled-release and conventional urea fertilizer application changed soil aggregate stability, humic acid molecular composition, and maize nitrogen uptake. *Sci. Total Environ.* 789:147778. doi: 10.1016/j.scitotenv.2021.147778

Geng, J. B., Ma, Q., Zhang, M., Li, C. L., Liu, Z. G., Lyu, X. X., et al. (2015). Synchronized relationships between nitrogen release of controlled release nitrogen fertilizers and nitrogen requirements of cotton. *Field Crops Res.* 184, 9–16. doi: 10.1016/j.fcr.2015.09.001

Hively, W. D., Gerard-Marchant, P., and Steenhuis, T. S. (2006). Distributed hydrological modeling of total dissolved phosphorus transport in an agricultural landscape. II. dissolved phosphorus transport. *Hydrol. Earth Syst. Sci.* 10, 263–276. doi: 10.5194/hess-10-263-2006

Holman, I. P., Whelan, M. J., Howden, N. J. K., Bellamy, P. H., Willby, N. J., Rivas-Casado, M., et al. (2008). Phosphorus in groundwater-an overlooked contributor to eutrophication. *Hydrol. Process* 22, 5121–5127. doi: 10.1002/hyp.7198

Hou, J., Dong, Y. J., Liu, C. S., Gai, G. S., Hu, G. Y., Fan, Z. Y., et al. (2015). Nutrient release characteristics of coated fertilizers by superfine phosphate rock powder and its effects on physiological traits of Chinese Cabbage. *J. Plant Nutr.* 38, 1254–1274. doi: 10.1080/01904167.2014.983119

Hou, L. Y., Mulla, S. I., Niño-Garcia, J. P., Ning, D., Rashid, A., Hu, A., et al. (2019). Deterministic and stochastic processes driving the shift in the prokaryotic community composition in wastewater treatment plants of a coastal Chinese city. *Appl. Microbiol. Biot.* 103, 9155–9168. doi: 10.1007/s00253-019-10177-7

Houba, V. J. G., Novozansky, I., Huybregts, A. W. M., and Van der Lee, J. J. (1986). Comparison of soil extractions by 0.01 M CaCl2, by EUF and by some conventional extraction procedures. *Plant Soil* 76, 433–437. doi: 10.1007/BF02375149

Hue, N. V. (1991). Effects of organic acids/anions on P sorption and Phyto availability in soils with different mineralogies. *Soil Sci.* 152, 463–471. doi: 10.1097/00010694-199112000-00009

Jindo, K., Soares, T. S., Peres, L. E. P., Azevedo, I. G., Aguiar, N. O., Mazzei, P., et al. (2016). Phosphorus speciation and high-affinity transporters are influenced by humic substances. *J. Plant Nutr. Soil Sci.* 179, 206–214. doi: 10.1002/jpln.201500228

Johnston, A. E., and Poulton, P. R. (2019). Phosphorus in agriculture: a review of results from 175 Years of research at Rothamsted. UK. *J. Environ. Qual.* 48, 1133–1144. doi: 10.2134/jeq2019.02.0078

Leslie, J. E., Weersink, A., Yang, W., and Fox, G. (2017). Actual versus environmentally recommended fertilizer application rates: implications for water quality and policy. *Agr. Ecosyst. Environ.* 240, 109–120. doi: 10.1016/j.agee.2017.02.009

Li, R. C., Gao, Y. X., Chen, Q., Li, Z. L., Gao, F., Meng, Q. M., et al. (2021). Blended controlled-release urea with straw returning improved soil nitrogen availability, soil microbial community, and root morphology of wheat grown. *Soil Till Res.* 212:105045. doi: 10.1016/j.still.2021.105045

Li, Z. L., Liu, Z. G., Zhang, M., Chen, Q., Zheng, L., Li, Y. C., et al. (2021). The combined application of controlled-release urea and fulvic acid improved the soil nutrient supply and maize yield. *Arch. Agron. Soil Sci.* 67, 633–646. doi: 10.1080/03650340.2020.1742326

Li, Z. L., Liu, Z. G., Zhang, M., Li, C. L., Li, Y. C., Wan, Y. S., et al. (2020). Effects of controlled-release potassium chloride on soil available potassium, nutrient absorption and yield of maize plants. *Soil Till Res.* 2019:104438. doi: 10.1016/j.still.2019.104438

Liu, Z. G., Wan, L. B., Zhang, M., Cao, Y. P., Xu, Q. M., Chen, H. K., et al. (2009). *State Regular of the People's Republic of China-Slow Release Fertilizer (GB/T23348-2009)*. Beijing: China Regular Press.

Lu, H., Tian, H. Y., Liu, Z. G., Zhang, M., Zhao, C. H., Guo, Y. L., et al. (2019). Polyolefin wax modification improved characteristics of nutrient release from

biopolymer-coated phosphorus fertilizers. *ACS Omega* 4, 20402–20409. doi: 10.1021/acsomega.9b03348

Lu, H., Tian, H. Y., Zhang, M., Liu, Z. G., Chen, Q., Guan, R., et al. (2020). Water polishing improved controlled-release characteristics and fertilizer efficiency of castor oil-based polyurethane coated diammonium phosphate. *Sci. Rep.* 10:5763. doi: 10.1038/s41598-020-62611-w

Lu, P. F., Zhang, Y. F., Jia, C., Li, Y. F., Zhang, M., and Mao, Z. Q. (2016). Degradation of polyurethane coating materials from liquefied wheat straw for controlled release fertilizers. *J. App. Polym. Sci.* 133, 2–9. doi: 10.1002/app.44021

Lu, R. K. (2000). *The Analysis Method of Soil Agro-Chemistry*. Beijing: Chinese Agricultural Academic Press.

Ma, W. Q., Ma, L., Li, J. H., Wang, F. H., Sisák, I., and Zhang, F. S. (2011). Phosphorus flows and use efficiencies in production and consumption of wheat, rice, and maize in China. *Chemosphere* 84, 814–821. doi: 10.1016/j.chemosphere.2011.04.055

Ma, X. M., Liu, Y., Shen, W. J., and Kuzyakov, Y. (2021). Phosphatase activity and acidification in lupine and maize rhizosphere depend on phosphorus availability and root properties: coupling zymography with planar optodes. *Appl. Soil Ecol.* 167:104029. doi: 10.1016/j.apsoil.2021.104029

Nardi, S., Ertani, A., and Francioso, O. (2017). Soil-root cross-talking: the role of humic substances. *J. Plant Nutr. Soil Sci.* 180, 5–13. doi: 10.1002/jpln.201600348

Nardi, S., Pizzeghello, D., Muscolo, A., and Vianello, A. (2002). Physiological effects of humic substances on higher plants. *Soil Biol. Biochem.* 34, 1527–1536. doi: 10.1016/S0038-0717(02)00174-8

Olaetxea, M., de Hitaa, D., García, C. A., Fuentes, M., Baigorri, R., Mora, V., et al. (2018). Hypothetical framework integrating the main mechanisms involved in the promoting action of rhizospheric humic substances on plant root- and shoot- growth. *Appl. Soil Ecol.* 123, 521–537. doi: 10.1016/j.apsoil.2017.06.007

Peleg, Z., and Blumwald, E. (2011). Hormone balance and abiotic stress tolerance in crop plants. *Curr. Opin. Plant Biol.* 14, 290–295. doi: 10.1016/j.pbi.2011.02.001

Piao, S. L., Ciais, P., Huang, Y., Shen, Z. H., Peng, S. S., Li, J. S., et al. (2010). The impacts of climate change on water resources and agriculture in China. *Nature* 467, 43–51. doi: 10.1038/nature09364

Plaxton, W. C., and Tran, H. T. (2011). Metabolic adaptations of phosphate-starved plants. *Plant Physiol.* 156, 1006–1015. doi: 10.1104/pp.111.175281

Qu, Z. M., Qi, X. C., Shi, R. G., Zhao, Y. J., Hu, Z. P., Chen, Q., et al. (2020). Reduced N fertilizer application with optimal blend of controlled-release urea and urea improves tomato yield and quality in greenhouse production system. *J. Soil Sci. Plant Nut.* 20, 1741–1750. doi: 10.1007/s42729-020-00244-8

Rafiullah, Khan, M. J., Muhammad, D., Fahad, S., Adnan, M., Wahid, F., et al. (2020). Phosphorus nutrient management through synchronization of application methods and rates in wheat and maize crops. *Plants* 9:1389. doi: 10.3390/plants9101389

Raiesi, F. (2021). The quantity and quality of soil organic matter and humic substances following dry-farming and subsequent restoration in an upland pasture. *Catena* 202:105249. doi: 10.1016/j.catena.2021.105249

Roberts, T. L., and Johnston, A. E. (2015). Phosphorus use efficiency and management in agriculture. *Resour. Conserv. Recycl.* 105, 275–281. doi: 10.1016/j.resconrec.2015.09.013

Rosa, S. D., Silva, C. A., and Maluf, H. (2018). Wheat nutrition and growth as affected by humic acid-phosphate interaction. *J. Plant Nutr. Soil Sci.* 181, 870–877.

Sarah, K., Alizadeh, A. A., and Khodayar, H. (2018). The effect of humic acid on leaf morphophysiological and phytochemical properties of *Echinacea purpurea* L. under water deficit stress. *Sci. Hortic-amsterdam* 239, 314–323. doi: 10.1016/j.scienta.2018.03.015

Sarkar, A., Biswas, D. R., Datta, A. C., Roy, T., Moharana, P. C., Biswas, S. S., et al. (2018). Polymer coated novel controlled release rock phosphate formulations for improving phosphorus use efficiency by wheat in an Inceptisol. *Soil Till Res.* 180, 48–62. doi: 10.1016/j.still.2018.02.009

Sarlaki, E., Paghaleh, A. S., Kianmehr, M. H., and Vakilian, K. A. (2021). Valorization of lignite wastes into humic acids: process optimization, energy efficiency and structural features analysis. *Renew Energ.* 163, 105–122. doi: 10.1016/j.renene.2020.08.096

Shafi, M. I., Adnan, M., Fahad, S., Wahid, F., Khan, A., Yue, Z., et al. (2020). Application of single superphosphate with humic acid improves the growth, yield and phosphorus uptake of wheat (*Triticum aestivum* L.) in Calcareous Soil. *Agronomy* 10:1224. doi: 10.3390/agronomy10091224

Shoji, S., Delgado, J., Mosier, A., and Miura, Y. (2001). Use of controlled release fertilizers and nitrification inhibitors to increase nitrogen use eficiency and to conserve air and water quality. *Commun. Soil Sci. Plant* 32, 1051–1070. doi: 10.1081/CSS-100104103

Tian, X. F., Li, C. L., Zhang, M., Li, T., Lu, Y. Y., and Liu, L. F. (2018). Controlled release urea improved crop yields and mitigated nitrate leaching under cotton-garlic intercropping system in a 4-year field trial. *Soil Till Res.* 175, 158–167. doi: 10.1016/j.still.2017.08.015

USDA (1999). "Soil survey staff., soil taxonomy," in *A Basic System of Soil Classification for Making and Interpreting Soil Surveys*, 2nd Edn, ed. Soil Survey Staff (Washington, DC.: U.S. Gov. Print. Office).

Wahid, F., Fahad, S., Danish, S., Adnan, M., Yue, Z., Saud, S., et al. (2020). Sustainable management with mycorrhizae and phosphate solubilizing bacteria for enhanced phosphorus uptake in calcareous soils. *Agriculture* 10:334. doi: 10.3390/agriculture10080334

Wang, Y. (2016). A five-year P fertilization pot trial for wheat only in a rice-wheat rotation of Chinese paddy soil: interaction of P availability and microorganism. *Plant Soil* 399, 305–318. doi: 10.1007/s11104-015-2681-4

Xu, J. C., Mohamed, E., Li, Q., Lu, T., Yu, H. J., and Jiang, W. J. (2021). Effect of humic acid addition on buffering capacity and nutrient storage capacity of soilless substrates. *Front. Plant Sci.* 12:644229. doi: 10.3389/fpls.2021.644229

Yang, Y. C., Zhang, M., Zheng, L., Cheng, D. D., Liu, M., and Geng, Y. Q. (2011). Controlled release urea improved nitrogen use efficiency, yield, and quality of wheat. *Agron J.* 103, 479–485. doi: 10.2134/agronj2010.0343

Yu, X. J., Chen, Q., Shi, W. C., Gao, Z., Sun, X., Dong, J. J., et al. (2021). Interactions between phosphorus availability and microbes in a wheat-maize double cropping system: a reduced fertilization scheme. *J. Integr. Agr.*

Zandonadi, D. B., Santos, M. P., Dobbss, L. B., Olivares, L. F., Canellas, L. P., Binzel, M. L., et al. (2010). Nitric oxide mediates humic acids-induced root development and plasma membrane H+-ATPase activation. *Planta* 231, 1025–1036. doi: 10.1007/s00425-010-1106-0

Zhang, W. F., Ma, W. Q., Ji, Y. X., Fan, M. S., Oenema, O., and Zhang, F. S. (2008). Efficiency, economics, and environmental implications of phosphorus resource use and the fertilizer industry in China. *Nutr. Cycl. Agroecosyst.* 80, 131–144. doi: 10.1007/s10705-007-9126-2

Zheng, W. K., Zhang, M., Liu, Z. G., Zhou, H. Y., Lu, H., Zhang, W. T., et al. (2016). Combining controlled-release urea and normal urea to improve the nitrogen use efficiency and yield under wheat-maize double cropping system. *Field Crop Res.* 197, 52–62. doi: 10.1016/j.fcr.2016.08.004

Zhou, L., Monreal, C. M., Xu, S. T., McLaughlin, N. B., Zhang, H. Y., Hao, G. C., et al. (2019). Effect of bentonite-humic acid application on the improvement of soil structure and maize yield in a sandy soil of a semi-arid region. *Geoderma* 338, 269–280. doi: 10.1016/j.geoderma.2018.12.014

Zhu, J., Li, M., and Whelan, M. (2018). Phosphorus activators contribute to legacy phosphorus availability in agricultural soils: a review. *Sci. Total Environ.* 612, 522–537. doi: 10.1016/j.scitotenv.2017.08.095

Conflict of Interest: YW and LW were employed by the company Xinyangfeng Agricultural Technology Co., Ltd.

The remaining authors declare that the research was conducted in the absence of any commercial or financial relationships that could be construed as a potential conflict of interest.

Publisher's Note: All claims expressed in this article are solely those of the authors and do not necessarily represent those of their affiliated organizations, or those of the publisher, the editors and the reviewers. Any product that may be evaluated in this article, or claim that may be made by its manufacturer, is not guaranteed or endorsed by the publisher.

frontiers in Plant Science

ORIGINAL RESEARCH
published: 04 January 2022
doi: 10.3389/fpls.2021.712363

Physiological Biochemistry-Combined Transcriptomic Analysis Reveals Mechanism of *Bacillus cereus* G2 Improved Salt-Stress Tolerance of *Glycyrrhiza uralensis* Fisch. Seedlings by Balancing Carbohydrate Metabolism

*Xiang Xiao[1], Qiuli Wang[1], Xin Ma[1], Duoyong Lang[2], Zhenggang Guo[3] and Xinhui Zhang[1,4]**

[1] College of Pharmacy, Ningxia Medical University, Yinchuan, China, [2] Laboratory Animal Center, Ningxia Medical University, Yinchuan, China, [3] College of Pastoral Agriculture Science and Technology, Lanzhou University, Lanzhou, China, [4] Ningxia Engineering and Technology Research Center of Hui Medicine Modernization, Ningxia Collaborative Innovation Center of Hui Medicine, Key Laboratory of Ningxia Minority Medicine Modernization, Ministry of Education, Ningxia Medical University, Yinchuan, China

OPEN ACCESS

Edited by:
Maurizio Ruzzi, University of Tuscia, Italy

Reviewed by:
Hongxia Zhang, Ludong University, China
Fengjuan Yang, Shandong Agricultural University, China

***Correspondence:**
Xinhui Zhang
zhang2013512@163.com

Specialty section:
This article was submitted to Plant Abiotic Stress, a section of the journal Frontiers in Plant Science

Received: *20 May 2021*
Accepted: *16 November 2021*
Published: *04 January 2022*

Citation:
Xiao X, Wang Q, Ma X, Lang D, Guo Z and Zhang X (2022) Physiological Biochemistry-Combined Transcriptomic Analysis Reveals Mechanism of Bacillus cereus G2 Improved Salt-Stress Tolerance of Glycyrrhiza uralensis Fisch. Seedlings by Balancing Carbohydrate Metabolism. Front. Plant Sci. 12:712363. doi: 10.3389/fpls.2021.712363

Salt stress severely threatens the growth and productivity of *Glycyrrhiza uralensis*. Previous results found that *Bacillus cereus* G2 enhanced several carbohydrate contents in *G. uralensis* under salt stress. Here, we analyzed the changes in parameters related to growth, photosynthesis, carbohydrate transformation, and the glycolysis Embden-Meyerhof-Parnas (EMP) pathway-tricarboxylic acid (TCA) cycle by G2 in *G. uralensis* under salt stress. Results showed that G2 helped *G. uralensis*-accumulating photosynthetic pigments during photosynthesis, which could further increase starch, sucrose, and fructose contents during carbohydrate transformation. Specifically, increased soluble starch synthase (SSS) activity caused to higher starch content, which could induce α-amylase (AM) and β-amylase (BM) activities; increased sucrose content due to the increase of sucrose synthase (SS) activity through upregulating the gene-encoding SS, which decreased cell osmotic potential, and consequently, induced invertase and gene-encoding α-glucosidase that decomposed sucrose to fructose, ultimately avoided further water loss; increased fructose content-required highly hexokinase (HK) activity to phosphorylate in *G. uralensis*, thereby providing sufficient substrate for EMP. However, G2 decreased phosphofructokinase (PFK) and pyruvate kinase (PK) activities during EMP. For inducing the TCA cycle to produce more energy, G2 increased PDH activity that enhanced CA content, which further increased isocitrate dehydrogenase (ICDH) activity and provided intermediate products for the *G. uralensis* TCA cycle under salt stress. In sum, G2 could improve photosynthetic

efficiency and carbohydrate transformation to enhance carbohydrate products, thereby releasing more chemical energy stored in carbohydrates through the EMP pathway-TCA cycle, finally maintain normal life activities, and promote the growth of *G. uralensis* under salt stress.

Keywords: salt stress, *Bacillus cereus* G2, photosynthesis, carbohydrate transformation, glycolysis, tricarboxylic acid cycle

INTRODUCTION

In plants, salt stress leads to reduced water uptake, excessive accumulation of toxic elemental ions, and production of reactive oxygen species (ROS) causing oxidative stress (Salimi et al., 2016; Ahmadi et al., 2018). This combination of osmotic, ionic, and oxidative effects promotes cellular damage, declines K^+ and Ca^{2+} efficiency, reduces photosynthetic rate, impairs metabolism, and ultimately inhibits plant growth and reduces productivity (Salimi et al., 2016; Brahimova et al., 2021). In response to salt-stressed condition, carbohydrate accumulation can be an important part of radical scavenging, osmo-protection, and carbon storage in plants (Keunen et al., 2013; Zhu et al., 2016; Li et al., 2020). Carbohydrates, as the products of photosynthesis, are not only the substrates for respiration but also important substances related to the growth and energy metabolism in plants (Raessler et al., 2010). Salt stress directly reduced CO_2 availability through diffusion limitation of stomata and mesophyll or change photosynthetic metabolism, and also affected oxidative stress and thus indirectly affected leaf photosynthesis (Chaves et al., 2008). Some studies showed that salt stress typically reduced the chlorophyll (Chl) content in plants (Khoshbakht et al., 2015; Ibrahim et al., 2017), while other studies reported increased Chl concentration with increasing salinity stress in salt-tolerant plants (Borghesi et al., 2011; Huang et al., 2015; Qiu et al., 2017). Salt stress caused inhibition of carbon assimilation by affecting the activities of carbon metabolism-related enzymes and the contents of carbohydrate (Li et al., 2020). The glycolysis (EMP) pathway-tricarboxylic acid (TCA) cycle serves as the primary pathway for carbohydrate catabolism, providing sufficient energy for the plant's life activities (Jiang, 2011). Moreover, salt stress led to the disorder of EMP metabolism, which posed a threat to plant respiration metabolism (Zhong et al., 2016). Salt stress also inhibited the TCA cycle, followed by a significant decrease in adenosine triphosphate (ATP) content, resulting in insufficient energy supply and further inhibition of plants' growth (Li et al., 2015, 2020). Thus, it can be concluded that plants exposed to salt stress are unable to maintain the required carbohydrate and energy levels, and, consequently, certain measures must be adopted to regulate carbohydrate metabolism in salt-stressed plants.

Plant endophytes have great potential to enhance plant growth and alleviate salt stress without harming the environment (Fan et al., 2020; Molina-Montenegro et al., 2020). Previous studies revealed that endophytes increased salt tolerance of plants by regulating carbohydrate metabolism (Ali et al., 2014; Ghaffari et al., 2016; Win et al., 2018). Specifically, wild-type bacterial endophytes significantly increased the total Chl contents of tomato plants under salt stress (Ali et al., 2014). Endophyte (*Penicillium funiculosum* LHL06) significantly increased Chl contents and the photosynthesis rate of *Glycine max* L. under salt stress (Khan et al., 2011). Moreover, the endophytic fungus *Piriformospora indica* increased the starch concentration in barley plants under salt stress (Ghaffari et al., 2016). Therefore, carbohydrate regulation may be one of the important strategies for improving plant salt tolerance by endophytes. However, the deep mechanisms of endophytes on carbohydrate regulation in plants exposed to salt stress are largely unknown.

Glycyrrhiza uralensis Fisch., as an important windbreak and sand fixation plant in desert areas, widely grown in arid and semiarid regions of the world, especially in the harsh northwestern region of China, and suffers from salt stress year-round (Li et al., 2016; Wang C. et al., 2020). *Bacillus cereus* (G2), as an endophyte found by our laboratory, enhanced several carbohydrate contents in *G. uralensis* under salt stress, but the mechanism has not been thoroughly studied (Zhang, unpublished). During their seedling stage, plants are sensitive to adverse external factors; therefore, the seedlings stage is the optimum time to research plants' abiotic tolerance (El Atta et al., 2016). Therefore, in order to reveal the behind mechanism of G2 on carbohydrate metabolism in *G. uralensis* seedlings subjected to salt stress, this study analyzed parameters related to photosynthesis, carbohydrate transformation, and EMP pathway-TCA cycle at physiological biochemistry and transcriptome levels. This study not only provided valuable information for exploring the mechanism of G2 improving the salt tolerance of *G. uralensis*, but also laid the foundation for cultivating high-quality and high-yield *G. uralensis*.

MATERIALS AND METHODS

Plant Material

Glycyrrhiza uralensis seeds were collected from wild *G. uralensis* plants in Urad front flag, Inner Mongolia, China, in September, 2019. Healthy seeds were selected and stored in a kraft paper bag at 4°C until use.

Bacillus cereus G2 Material and Culture Suspension

Bacillus cereus (G2) was isolated from *G. uralensis* roots and identified by Sangon Biotech (Shanghai) Co., Ltd. This strain was deposited at the China General Microbiological Culture Collection Center under the accession No. CGMCC No. 16671, and under the accession No. MT803148 in NCBI.

The strain of G2 was cultured at 30°C for 2 days in a beef extract peptone AGAR medium, which contained 1-g L^{-1} tryptone, 3-g L^{-1} beef extract, 5-g L^{-1} NaCl, and 16-g L^{-1} agar, and the pH of the medium after autoclaving was 6.9–7.1. Then, G2 was grown in a sterilized LB liquid medium, which contained 2.5-g tryptone, 0.75-g beef extract, 1.25-g NaCl, and 250-ml distilled water, and the pH of the medium after autoclaving was 6.9–7.1. The bacteria culture suspension was incubated in a shaking incubator of 180 rpm at 28°C for 2 days.

Plant Growing Condition and Treatment

All of the seeds of *G. uralensis* were steeped with concentrated sulfuric acid (H_2SO_4) for 1.5 h, and then surface sterilized with 0.1% (v/v) H_2O_2 for 10 min, rinsed for three times in distilled water, and soaked in distilled water for 9 h at room temperature. Then, 75 water-absorbing, full-filled seeds were selected, blotted surface moisture, and sown evenly in each pot filled with 1,900-g high-pressure sterilized and a fully dried sand medium collected from native desert regions, which did not contain any nutrients. Then, pre-irrigated with 300 ml of distilled water as the control group (CK) or with 300 ml of distilled water containing 75-mM NaCl as the salt stress group (S). The above experiment was carried out in an indoor environment with natural light and an air temperature of 23–28°C during the day and night. After 35 days, G2 treatment was initiated when the third true leaf appeared in most of the *G. uralensis* seedling. The bacteria culture suspension with G2 was centrifuged at 8,000 rpm for 10 min, and it was washed in sterile distilled water, and the optical density (600 nm) of the bacterial strain was adjusted to 1 ($\sim 10^8$ cfu ml^{-1}) using sterile distilled water. Both CK and S groups were divided into two subgroups, and were watered either 300-ml distilled water or 300-ml of distilled water, containing 10^8-cfu ml^{-1} G2. Three replications per treatment were used, and each replication comprised two pots. All pots were randomly arranged and periodically rotated to minimize the effects of environmental heterogeneity.

At 10 days after G2 treatment, the plants were collected and used in subsequent experiments. Generally, three pots of each treatment, firstly, the numbers of plants per pot were recorded for calculation of the survival rate, and all the plants in the pot were taken out of the soil, and then growth indicators were recorded; then, the samples were oven dried at 60°C for 48 h and weighed. The rest three pots of each treatment – all seedlings were taken out of the soil between 9:00 a.m. and 10:00 a.m. and cleaned immediately with distilled water, and then parts of leaves were collected and mixed for determination of Chl contents, and the rest samples were immediately stored at −80°C to measure their physiological and biochemical characteristics.

Measurement of Photosynthetic Pigment Contents

About 0.2-g fresh leaves material of *G. uralensis* was extracted with 15 ml of a solution that contained ethanol and acetone (1:2, v/v) for 24 h at room temperature in the dark. To calculate the contents of Chl *a*, Chl *b*, and carotenoids (Car), the absorbance was measured at 663, 645, and 470 nm, respectively (Wellburn, 1994).

Measurement of Carbohydrate Contents

About 0.2-g fresh *G. uralensis* seedlings material was homogenized in 2-ml 80% (v/v) ethanol, and then 80°C water bath for 30 min and centrifuged at 1,000 rpm for 5 min, and the supernatants were analyzed for total soluble sugar (TSS), sucrose, fructose, and starch contents. The TSS content was analyzed by anthrone colorimetry (Li et al., 2020), specifically 100-μL supernatant was mixed with 5-ml anthracite reagent, and incubation was performed for 10 min at 100°C, 630-nm colorimetric analysis. The contents of sucrose and fructose were analyzed by Tang (1999), as follows: Sucrose analysis: 400-μL supernatant added to 200-μL 2-M NaOH that was boiled for 5 min, and then added 3-ml 30% (v/v) HCl, 1-mL.1% m-dihydroxybenzene, which were 80°C water bathed for 10 min, 480-nm colorimetric analysis. The mixtures for the fructose analysis contained 100-μL supernatant, 0.2-ml 80% (v/v) ethanol, 0.8-ml 0.1% m-dihy-droxybenzene, and 2.8-ml 30% (v/v) HCl, and then were 80°C water bathed for 10 min, 480-nm colorimetric analysis. The residues were extracted with 2 ml of 9.2-M perchloric acid, the volumes were adjusted to 10 ml in volumetric flasks, and the supernatants were analyzed to determine the starch contents by anthrone colorimetry (Gao, 2006).

Measurement of Carbohydrate Transformation-Related Enzyme Activities

About 0.2-g fresh *G. uralensis* seedlings material was homogenized in 2-ml water and centrifuged at 3,000 rpm for 10 min. Then, the amylase determination was carried out according to the method of Devi et al. (2007) with minor modification. α-Amylase (AM) activity was determined after destroying the β-amylase (BM) by heating the enzyme at 70°C for 20 min and estimating reducing sugars formed from 2% starch in a 50-mM sodium acetate buffer (pH 5.0) in the presence of 1-mM $CaCl_2$ at 37°C. BM was extracted with a 100-mM sodium acetate buffer (pH 3.6), containing 1-mM EDTA. The activity of BM was determined by estimating the reducing sugars formed after the enzyme action on 1% starch prepared in a 50-mM sodium acetate buffer (pH 5.0), containing 1-mM EDTA. The soluble starch synthase (SSS), granule-bound starch synthase (GBSS), and ADP-glucose pyrophosphorylase (AGP) were determined using reagent kits (Beijing Solarbio Science & Technology Co., Ltd.) according to the manufacturer's instructions. The GBSS, SSS, and AGP were determined by recording the increase of NADPH at 340 nm. The sucrose phosphate synthase (SPS) and sucrose synthase (SS) activities were measured using the m-dihydroxybenzene method (Tang, 1999) with minor modification. The mixtures for the SPS analysis contained 50-mM Tris–HCl (pH 7.0), 10-mM $MgCl_2$, 10-mM fructose-6-phosphate, 3-mM UDP-glucose, and 100 μL of crude enzyme. For the SS activity, the reaction mixtures contained 50-mM Tris–HCl (pH 7.0), 10-mM $MgCl_2$, 10-mM fructose,

3-mM UDP-glucose, and 100 μL of crude enzyme. The invertase extraction and determination were carried out according to the method of Scholes et al. (1996). About 0.2-g fresh *G. uralensis* seedlings material was homogenized on an ice bath in 3 ml of extracting solution and centrifuged at 10,000 rpm for 10 min, and enzyme activity was detected in the supernatants. The amount of the compound formed by the reaction of reducing sugar with 3,5-dini-trosalicylic acid indicates its activity, and the absorbance is measured at 510 nm.

Measurement of Intermediate Contents in the EMP and Tricarboxylic Acid Cycle Pathway

The pyruvate (PA) and citrate (CA) contents were determined using reagent kits (Beijing Solarbio Science & Technology Co., Ltd.) according to the manufacturer's instructions. PA content was determined using 2,4-dinitrophenylhydrazine as the substrate to record the absorbance at 520 nm. CA content was determined by the reduction of Cr^{6+} at 545 nm.

Measurement of Enzyme Activities in the EMP and Tricarboxylic Acid Cycle Pathway

The hexokinase (HK), phosphofructokinase (PFK), and pyruvate kinase (PK) were determined using reagent kits (Beijing Solarbio Science & Technology Co., Ltd.) according to the manufacturer's instructions. HK was determined using glucose as the substrate to record the increase in absorbance at 340 nm caused by the enzymatic reduction of $NADP^+$. PFK was determined using 6-phosphate-fructose as the substrate to record the decrease in absorbance at 340 nm caused by the enzymatic oxidation of NADH. PK was determined using phosphoenolpyruvate (PEP) as the substrate to record the decrease in absorbance at 340 nm caused by the enzymatic oxidation of NADH.

The malate dehydrogenase (MDH), pyruvate dehydrogenase (PDH), isocitrate dehydrogenase (ICDH), and succinate dehydrogenase (SDH) were determined using reagent kits (Beijing Solarbio Science & Technology Co., Ltd.) according to the manufacturer's instructions. The MDH activity was determined using oxaloacetate as the substrate to record the decrease in absorbance at 340 nm caused by the enzymatic oxidation of NADH. PDH catalyzed dehydrogenation of PA and reduced 2,6-DCPIP at the same time. The PDH activity was determined by recording a decrease in absorbance at 605 nm. The ICDH activity was determined by measuring ketoglutaric acid production at 340 nm, and the SDH activity was determined by recording the reduction rate of 2,6-DCPIP at 600 nm.

RNA Extraction, cDNA Library Construction, and RNA-Seq

Transcriptome sequencing was carried out by Beijing Baimeike Company. The experimental process followed the method provided by Oxford Nanopore Technologies (ONT), which mainly included the following steps: (i) *G. uralensis* seedlings collected of four treatments (CK, CK + G2, S, and S + G2) were grounded, grouped by weight, and biologically replicated for RNA preparation. Three biological replicates per sample were used for the RNA-Seq experiments. (ii) Total RNA was extracted from the tissue using TRIzol reagent (Takara, Kyoto, Japan) according to the manufacturer's instructions. RNA purity was tested using the Nano Photometer spectrophotometer (IMPLEN, Westlake Village, United States). (iii) Library construction: primer annealing, reverse transcription into cDNA, plus switch Oligo; synthesis of complementary chains; DNA damage repair and terminal repair and magnetic bead purification. (iv) The cDNA libraries were sequenced using the Illumina NovaSeq 6000 platform.

Transcriptome Data Assembly

Filter the low-quality (length less than 500 bp, Qscore less than 7) sequence and ribosomal RNA sequence from the original landing sequence, and obtain the full-length sequence according to the presence of primers at both ends of the sequence. Polish the full-length sequence obtained in the previous step to obtain the consistent sequence. Contig comparisons with reference genomes or constructed contig sequences were performed to remove redundancy.

Transcription Quantification

Transcriptome sequencing can be simulated as a random sampling process. In order to make the number of fragments truly reflect the expression level of transcripts, it is necessary to normalize the number of mapped reads in the sample. CPM (counts per million) (Zhou et al., 2014) was used as an indicator to measure the expression level of transcripts or genes. The calculation formula of CPM was as follows (reads mapped to a transcript means the number of reads compared to the transcript; total reads aligned in the sample represent the total number of fragments compared to the reference transcriptome):

$$\mathrm{CPM} = \frac{\text{reads } \textit{mapped to transcript}}{\textit{total reads aligned in sample}} \times 1,000,000$$

Quantification of Gene/Transcript Expression Levels and Differential Expression Analysis

Full length reads were mapped to the reference transcriptome sequence. Reads with match quality above 5 were further used to quantify. Expression levels were estimated by reads per gene/transcript per 10,000 reads mapped. For the samples with biological replicates: differential expression analysis of two conditions/groups was performed using the DESeq R package (1.18.0). DESeq provided statistical routines for determining differential expression in digital gene expression data using a model based on the negative binomial distribution. The resulting *p*-values were adjusted using the Benjamini and Hochberg's approach for controlling the false discovery rate. Genes with a *p*-value < 0.05 and fold change ≥ 1.5 found by DESeq were assigned as differentially expressed.

Reverse Transcriptase-Polymerase Chain Reaction and Quantitative Real-Time-Polymerase Chain Reaction

Reverse transcriptase-polymerase chain reaction RT-PCR and quantitative real-time-polymerase chain reaction (qRT-PCR) were performed on the same RNA pools, which were previously used in RNA-Seq for 10 key DEGs of carbohydrate metabolism in*G. uralensis*, respectively. Gene-specific primers were designed based on the sequencing data using the Primer-BLAST tool. The primer sequences used for conventional PCR and qRT-PCR analysis are listed in **Supplementary Table 1**. First-strand cDNAs were synthesized from 2 μg of DNase-treated total RNA using RevertAid RT Reverse Transcription Kit (Servicebio, China). As for RT-PCR, target genes were amplified using a polymerase chain reaction (PCR) thermal cycler (ABI 2720, United States), photographed by FR-980B gel imaging system (FuRi Science & Technology Co., Ltd.), and analyzed with pixel quantitation software Image J 2 (Rawak Software Inc.). qRT-PCR was performed by Wuhan Servicebio Technology CO., LTD. using 2 × SYBR Green qPCR Master Mix (High ROX). The reaction mixture (20 μL) contained 2 × ChamQ SYBR Green qPCR Master Mix 10 μL, 1 μL of primer, 1 μL of template cDNA,.4 μL of 50 × ROX Reference Dye 1 and 7.6 μL of ddH2O. Amplifications were performed under the following conditions: 95°C for 10 min, followed by 40 cycles of 95°*C* for 15 s and 60°*C* for 60 s. Relative expression for each sample was calculated using the $2^{-\Delta\Delta Ct}$ methods with normalization to the internal control genes.

Statistical Analyses

All treatments have three replication operations presented as the mean ± SD of each experiment. The one-way ANOVA was carried out, and physiological data were tested for significant treatment differences using Duncan's multiple range tests, and $p < 0.05$ was considered to be statistically significant. The correlation analysis of photosynthetic pigments contents, carbohydrates contents, enzymes activities, and intermediates contents of carbohydrate transformation and EMP pathway-TCA cycle in *G. uralensis* under four different conditions was determined. Principal component analysis (PCA) of the response variables photosynthetic pigments contents, carbohydrates contents, enzymes activities, and intermediates contents of carbohydrate transformation and EMP pathway-TCA cycle was performed to separate plants in different treatments. The first two principal components, which accounted for the highest variation, were then used to plot two-dimensional scatter plots. The qRT-PCR data were tested for significant treatment differences using the Student's *T*-test, and $p < 0.05$ was considered to be statistically significant. All statistical analyses were performed using SPSS Statistics 25, Origin 2018 Statistics, and GraphPad Prism 8.0.1.

RESULTS

Effect of *Bacillus cereus* G2 on the Growth Parameters of *Glycyrrhiza uralensis* Seedlings

The growth situation of *G. uralensis* seedling under all treatments (CK, CK + G2, S, and S + G2) is shown in **Figure 1A**. Salt stress significantly decreased plant height, leaf number, lateral root number, fresh weight, dry weight, and survival rate, but increased the root diameter. Interestingly, G2 significantly increased plant height, stem diameter, fresh weight, and dry weight of *G. uralensis* under salt stress (**Figure 1B**).

Effect of *Bacillus cereus* G2 on Carbohydrate Contents in *Glycyrrhiza uralensis* Seedlings

Salt stress significantly decreased the contents of TSS, starch, fructose, sucrose, and the ratio of sucrose/starch, while G2 significantly increased the contents of TSS, starch, fructose, and sucrose in *G. uralensis* under salt stress (**Figure 2**). TSS, sucrose, and fructose were very positively correlated with one another (**Figure 9** and **Supplementary Figure 1A**).

Effect of *Bacillus cereus* G2 on Photosynthesis in *Glycyrrhiza uralensis* Seedlings

Salt stress significantly increased Chl *a*, Chl *b*, and Chl *a* + *b* contents in *G. uralensis*. Interestingly, G2 significantly further increased the Chl *a* and Car contents in *G. uralensis* under salt stress (**Figure 3**).

In carbon fixation in the photosynthetic organisms pathway (**Table 1** and **Figure 4**) according to transcriptomic analysis, glyceraldehyde-3-phosphate dehydrogenase ($NADP^+$) (GPD), ribulose-bisphosphate carboxylase small chain (Rubisco), and ribose 5-phosphate isomerase (RPI) A were differentially expressed in S vs. CK comparison. Specifically, the gene (*Glyur002595s00035357*)-encoding GPD, the genes (*Glyur000604s00024572* and *Glyur001973s00030832*)-encoding Rubisco, and the gene (*Glyur004632s00040687*)-encoding RPI were upregulated in S vs. CK comparison. However, G2 had no significant effect on the genes related to carbon fixation in the photosynthetic organisms pathway.

In the relationship between carbohydrates and photosynthetic pigments (**Figure 9** and **Supplementary Figure 1A**), fructose content was negatively correlated with Chl *a* and Chl *a* + *b* contents; the ratio of sucrose/starch was very negatively correlated with Chl *a* and Chl *a* + *b* contents, and negatively correlated with Chl *b* and Car contents.

Effect of *Bacillus cereus* G2 on Enzymes Related to Carbohydrate Transformation in *Glycyrrhiza uralensis* Seedlings

Salt stress significantly increased AGP activity but decreased SSS activity, while G2 significantly increased the activities of SSS, AM, and BM in *G. uralensis* under salt stress (**Figures 5**, **8**). Salt stress significantly decreased the activities of SPS, SS, and NI, while G2 significantly increased the activities of SS, NI, and AI in *G. uralensis* under salt stress (**Figures 6**, **8**).

In the starch and sucrose metabolism pathway (**Table 1** and **Figure 4**), β-glucosidase, β-fructofuranosidase (INV),

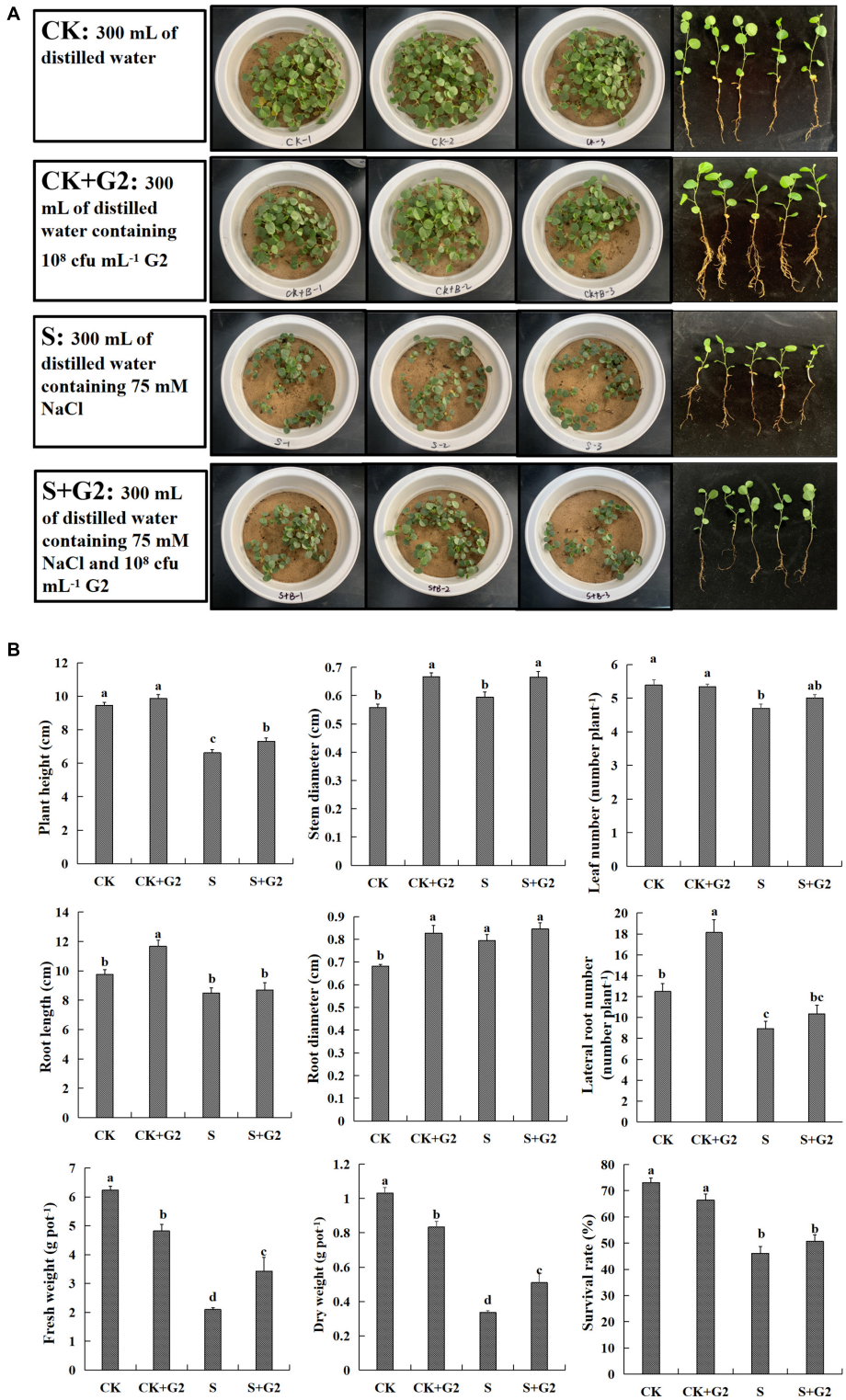

FIGURE 1 | (A) A part of the experiment layout of *Glycyrrhiza uralensis* Fisch. seedlings grown in control and salt stress conditions without or with *Bacillus cereus* G2. **(B)** Effects of *B. cereus* G2 on growth parameters of *G. uralensis* seedlings under control and salt stress conditions. CK, control group; S, salt stress group; CK + G2, control combined with the G2 group; S + G2, salt stress combined with the G2 group. The different letters within the different treatments in the same parameter indicate the significant difference at the 0.05 level. Values are means ± SE (n = 3).

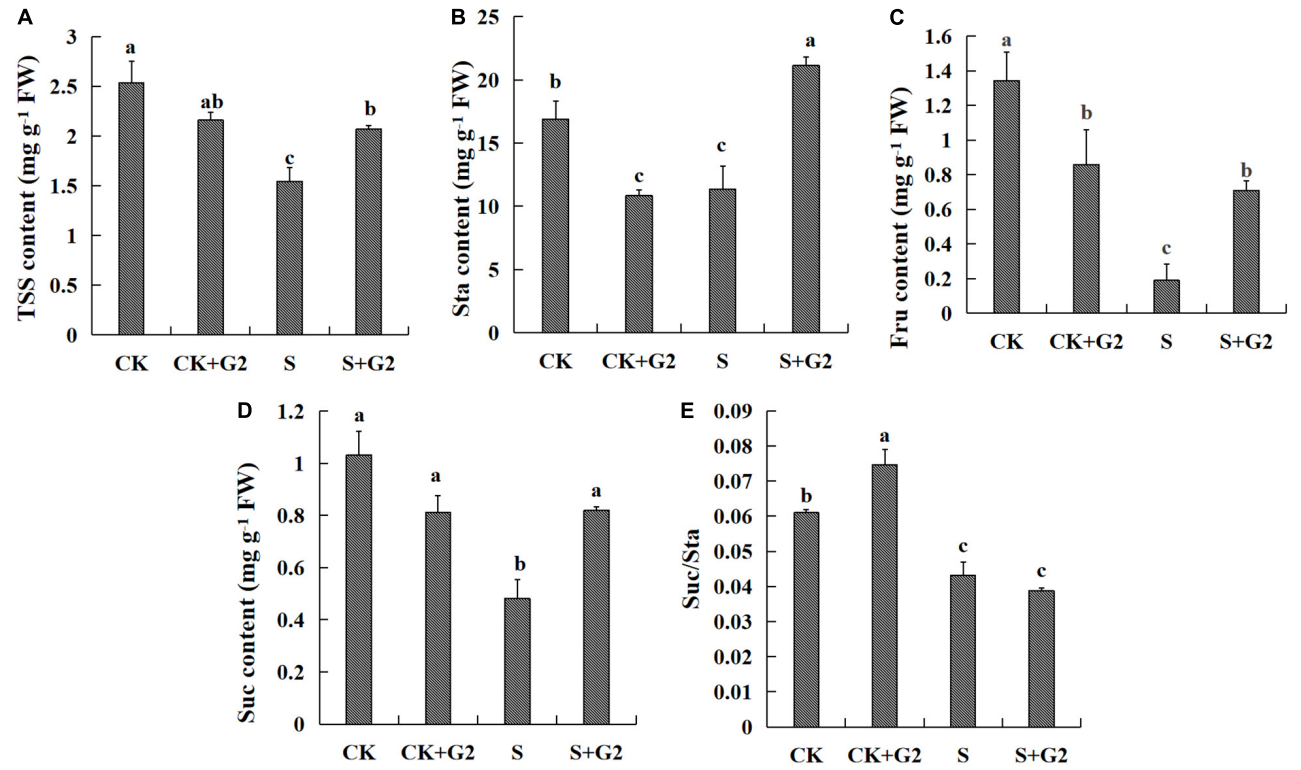

FIGURE 2 | Effects of *B. cereus* G2 on carbohydrates contents in *G. uralensis* seedlings under control and salt stress conditions. CK, control group; S, salt stress group; CK + G2, control combined with the G2 group; S + G2, salt stress combined with the G2 group. The different letters within the different treatments in the same parameter indicate the significant difference at the 0.05 level. Values are means ± SE (n = 3). **(A)** TSS: total soluble sugar. **(B)** Sta: starch. **(C)** Fru: fructose. **(D)** Suc: sucrose. **(E)** Suc/Sta: sucrose/starch.

α-glucosidase, trehalose 6-phosphate synthase/phosphatase (TPS), BM, SS, and HK were differentially expressed under different treatments. Specifically, the genes (*Glyur000779s00022830* and *Glyur000585s00027748*)-encoding β-glucosidase and the gene (*Glyur000324s00015431*)-encoding HK were upregulated, but the gene (*Glyur000214s00016036*)-encoding β-glucosidase, the gene (*Glyur000064s00005640*)-encoding INV, the genes (*Glyur000018s00003759* and *Glyur000231s00022077*)-encoding TPS and the genes (*Glyur000047s00004005* and *Glyur000067s00006388*)-encoding BM were downregulated in S vs. CK comparison. However, the gene (*Glyur000005s00001105*)-encoding α-glucosidase, the gene (*Glyur000018s00003759*)-encoding TPS, and the gene (*Glyur001957s00039090*)-encoding SS were upregulated in S + G2 vs. S comparison.

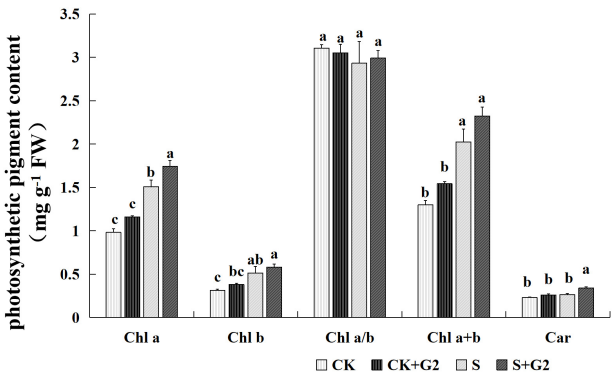

FIGURE 3 | Effects of *B. cereus* G2 inoculation on photosynthetic pigment contents in *G. uralensis* seedlings under control and salt stress conditions. CK, control group; S, salt stress group; CK + G2, control combined with the G2 group; S + G2, salt stress combined with the G2 group. The different letters within the different treatments in the same parameter indicate the significant difference at the 0.05 level. Values are means ± SE (n = 3). Chl *a*, chlorophyll *a*; Chl *b*, chlorophyll *b*; Car, carotenoids.

In the relationship between carbohydrate and carbohydrate transformation parameters (**Figure 9** and **Supplementary Figure 1B**), TSS content was very positively correlated with SS and SPS activities and positively correlated with NI activity, and very negatively correlated with AGP activity. Starch content was very positively correlated with SSS and AM and positively correlated with the activities of GBSS and BM. Sucrose and fructose contents were very positively correlated with SS activity and positively correlated with NI activity, and very negatively correlated with AGP activity. The ratio of sucrose/starch was positively correlated with SPS activity and negatively correlated with the activities of GBSS and AM.

TABLE 1 | Regulation of carbohydrate metabolism-related DEGs in *G. uralensis* by salt stress or *B. cereus* G2.

Pathway	Enzyme name	Definition (EC)	Gene ID	Regulated	
				S vs. CK comparison	S + G2 vs. S comparison
Carbon fixation in photosynthetic organisms	GPD	Glyceraldehyde-3-phosphate dehydrogenase (NADP+) (phosphorylating) (EC:1.2.1.13)	*Glyur002595s00035357*	Up	–
	Rubisco	Ribulose-bisphosphate carboxylase small chain (EC:4.1.1.39)	*Glyur000604s00024572*	Up	–
			Glyur001973s00030832	Up	–
	RPI	Ribose 5-phosphate isomerase (EC:5.3.1.6)	*Glyur004632s00040687*	Up	–
Starch and sucrose metabolism	β-Glucosidase	Beta-glucosidase (EC:3.2.1.21)	*Glyur000779s00022830*	Up	–
			Glyur000585s00027748	Up	–
			Glyur000214s00016036	Down	–
	INV, sacA	Beta-fructofuranosidase (EC:3.2.1.26)	*Glyur000064s00005640*	Down	–
	α-Glucosidase	Alpha-glucosidase (EC:3.2.1.20)	*Glyur000005s00001105*	–	Up
	TPS	Trehalose 6-phosphate synthase/phosphatase (EC:2.4.1.15 3.1.3.12)	*Glyur000018s00003759*	Down	Up
			Glyur000231s00022077	Down	–
	BM	Beta-amylase (EC:3.2.1.2)	*Glyur000047s00004005*	Down	–
			Glyur000067s00006388	Down	–
	SS	Sucrose synthase (EC:2.4.1.13)	*Glyur001957s00039090*	–	Up
	HK	Hexokinase (EC:2.7.1.1)	*Glyur000324s00015431*	Up	–
EMP-TCA cycle	HK	Hexokinase (EC:2.7.1.1)	*Glyur000324s00015431*	Up	–
	PFK, pfkA	6-Phosphofructokinase 1 (EC:2.7.1.11)	*Glyur000219s00011582*	Up	–
	PDC	Pyruvate decarboxylase (EC:4.1.1.1)	*Glyur000136s00007955*	Up	–
			Glyur003994s00042985	Up	Down
	ADH	S-(hydroxymethyl)glutathione dehydrogenase/alcohol dehydrogenase (EC:1.1.1.284 1.1.1.1)	*Glyur000038s00004477*	Up	–
	ALDH	Aldehyde dehydrogenase (NAD+) (EC:1.2.1.3)	*Glyur000698s00016570*	Up	–
	pdhB, PDHB	Pyruvate dehydrogenase E1 component beta subunit (EC:1.2.4.1)	*Glyur000278s00017282*	Up	–
	pdhD, DLD, lpd	Dihydrolipoamide dehydrogenase (EC:1.8.1.4)	*Glyur000082s00007586*	Up	–

CK, control group; S, salt stress group; S + G2, salt stress combined with G2 group.
"–" means normal.

Effect of *Bacillus cereus* G2 on the Levels of Intermediates and Enzymes in the EMP Pathway-Tricarboxylic Acid Cycle of *Glycyrrhiza uralensis* Seedlings

In the EMP pathway, salt stress significantly decreased HK activity, while increased PFK and PK activities in *G. uralensis*. Interestingly, G2 only significantly increased HK activity under salt stress but decreased PK and PFK activities in *G. uralensis* under salt stress. As for the TCA cycle, salt stress significantly decreased PDH and SDH activities and CA content, but increased MDH activity in *G. uralensis*. Interestingly, G2 significantly increased PDH and ICDH activities and CA content, but decreased SDH activity under salt stress condition (**Figures 7**, **8**).

In the EMP pathway-TCA cycle (**Table 1** and **Figure 4**), HK, PFK, pyruvate decarboxylase (PDC), S-(hydroxymethyl)glutathione dehydrogenase/alcohol dehydrogenase (ADH), aldehyde dehydrogenase (NAD^+) (ALDH), pyruvate dehydrogenase E1 component beta subunit (pdhB), and dihydrolipoamide dehydrogenase (pdhD) were differentially expressed under different treatments. Specifically, the gene (*Glyur000324s00015431*)-encoding HK, the gene (*Glyur000219s00011582*)-encoding PFK, the genes (*Glyur000136s00007955* and *Glyur003994s00042985*)-encoding PDC, the gene (*Glyur000038s00004477*)-encoding ADH, the gene (*Glyur000698s00016570*)-encoding ALDH, the gene (*Glyur000278s00017282*)-encoding pdhB, and the gene (*Glyur000082s00007586*)-encoding pdhD were upregulated in S vs. CK comparison, while only the gene (*Glyur003994s00042985*)-encoding PDC was downregulated in S + G2 vs. S comparison.

In the relationship between EMP pathway-TCA cycle parameters and carbohydrates (**Figure 9** and **Supplementary Figure 1C**), the HK activity was positively correlated with the

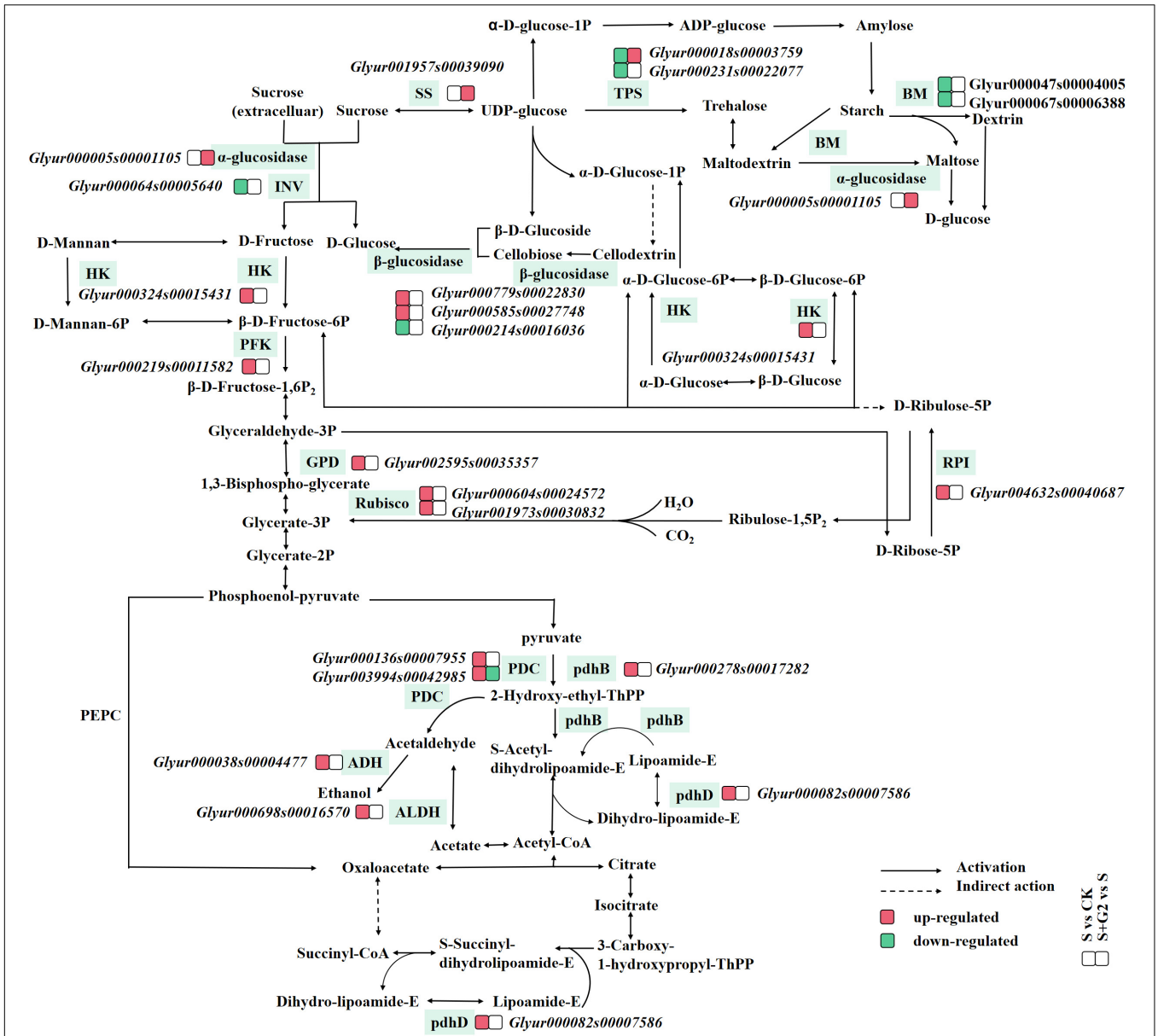

FIGURE 4 | A figure of the mechanism by which *B. cereus* G2 improves the salt tolerance of *G. uralensis* by regulating DEGs related to carbohydrate metabolism. CK, control group; S, salt stress group; S + G2, salt stress combined with the G2 group; GPD, glyceraldehyde-3-phosphate dehydrogenase (NADP+); Rubisco, ribulose-bisphosphate carboxylase small chain; RPI, ribose 5-phosphate isomerase A; INV, beta-fructofuranosidase; TPS, trehalose 6-phosphate synthase/phosphatase; BM, beta-amylase; SS, sucrose synthase; HK, hexokinase; PFK, 6-phosphofructokinase 1; pdhB, pyruvate dehydrogenase E1 component beta subunit; PDC, pyruvate decarboxylase; ADH, S-(hydroxymethyl)glutathione dehydrogenase/alcohol dehydrogenase; pdhD, dihydrolipoamide dehydrogenase; ALDH, aldehyde dehydrogenase.

ratio of sucrose/starch; the PFK activity was very negatively correlated with the contents of TSS, sucrose, and fructose; the PK activity was very negatively correlated with the contents of TSS, sucrose, fructose, and the ratio of sucrose/starch; the PDH activity was very positively correlated with the contents of TSS, sucrose, and fructose and positively correlated with the ratio of sucrose/starch; the MDH activity was very negatively correlated with the contents of TSS, sucrose, and fructose and negatively correlated with the ratio of sucrose/starch; the CA content was only very positively correlated with the starch content.

Principal Component Analysis

The results of PCA related to photosynthetic pigment contents, starch, and sucrose metabolism and EMP pathway-TCA cycle indexes that we measured revealed a closer association between biological replicates than between salinity or G2 treatments (**Supplementary Figures 2A,B**). PC1 explaining 42.9% of

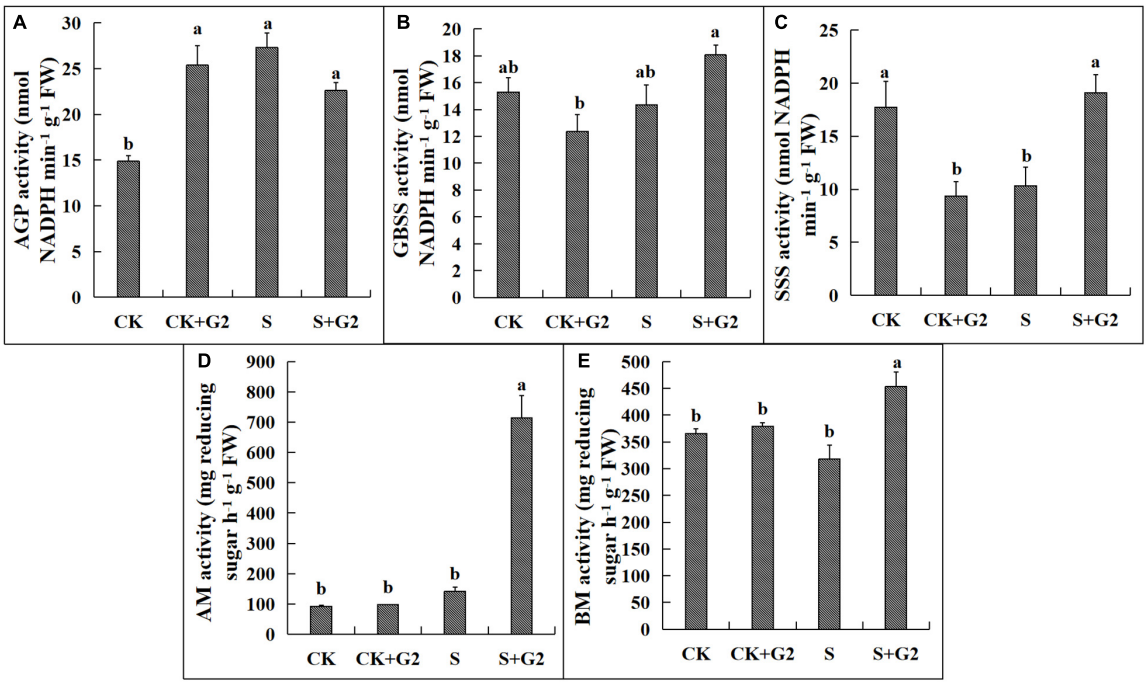

FIGURE 5 | Effects of *B. cereus* G2 on enzymes related to starch synthesis and decomposition in *G. uralensis* seedlings under control and salt stress conditions. CK, control group; S, salt stress group; CK + G2, control combined with the G2 group; S + G2, salt stress combined with the G2 group. The different letters within the different treatments in the same parameter indicate the significant difference at the 0.05 level. Values are means ± SE (n = 3). **(A)** AGP: ADP-glucose pyrophosphorylase. **(B)** GBSS: granule-bound starch synthase. **(C)** SSS: soluble starch synthase. **(D)** AM: α-amylase; **(E)** BM: β-amylase.

total variation uncovered differences between plants of CK and S treatments, while PC2, accounting for 26.5% of total variation, distinctly separated the plants provided with S and S + G2 treatments. PC1 formation covers photosynthetic pigment contents, sucrose synthesis, and EMP indices, while PC2 formation covers starch synthesis and decomposition indices. PC1 clearly separated S-treated *G. uralensis* from control *G. uralensis* because of photosynthetic pigment contents, sucrose synthesis, and EMP indices. PC2 clearly separated S + G2-treated *G. uralensis* from S-treated *G. uralensis* because of starch synthesis and decomposition indices.

The results of PCA related to gene expression in carbon fixation in photosynthetic organisms, starch, and sucrose metabolism and the EMP pathway-TCA cycle pathway also revealed a relatively closer association between biological replicates than between salinity or G2 treatments (**Supplementary Figures 2C,D**). PC1 explaining 44.2% of total variation revealed differences between plants of CK and S treatments, while PC2 accounting for 19.2% of total variation distinctly separated the plants provided with S and S + G2 treatments, which is consistent with the result of the PCA in the physiological biochemical level. PC1 formation covered the genes related to the synthesis and decomposition of sucrose and fructose, while PC2 formation covers the genes-encoding pdhD, PFK, and PDC-2. PC1 clearly separated S-treated *G. uralensis* from control *G. uralensis* because of the genes related to the synthesis and decomposition of sucrose and fructose indices. PC2 clearly separated S + G2-treated *G. uralensis* from S-treated *G. uralensis* because of the genes-encoding pdhD, PFK, and PDC-2.

The Polymerase Chain Reaction Expression Level of the Ley DEGs Related to Carbohydrate Metabolism in *Glycyrrhiza uralensis* Seedlings

To elucidate the correlation between mRNA transcript levels and gene expression levels and further analyze the carbohydrate metabolism-related genes expression level, transcriptional analysis of 10 DEGs in carbohydrate metabolism was conducted *via* RT-PCR and qRT-PCR in *G. uralensis* seedlings under four treatments (CK, CK + G2, S, and S + G2). The genes-encoding β-glucosidase, INV, α-glucosidase, BM, and SS in carbohydrate transformation and HK, PFK, pdhB, and pdhD in the EMP pathway-TCA cycle were used for this study. The RT-PCR results are shown in **Supplementary Figure 3**. The qRT-PCR results (**Figure 10**) showed that salt stress downregulated the genes-encoding INV, BM, and one of the gene-encoding β-glucosidase, while upregulated the genes-encoding HK, PFK, pdhB, pdhD, and one of the gene-encoding β-glucosidase in *G. uralensis* seedlings. G2 downregulated the genes-encoding INV, HK, PFK, pdhB, pdhD, and one of the genes encoding β-glucosidase, while G2 upregulated the genes encoding α-glucosidase under salt stress in *G. uralensis* seedlings.

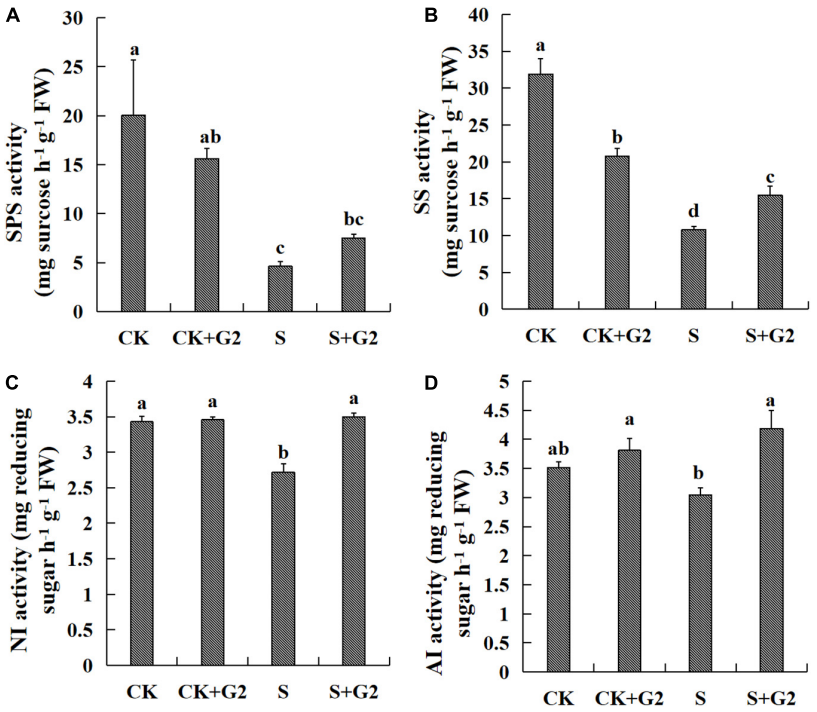

FIGURE 6 | Effects of *B. cereus* G2 on enzymes related to sucrose synthesis and decomposition in *G. uralensis* seedlings under control and salt stress conditions. CK, control group; S, salt stress group; CK + G2, control combined with the G2 group; S + G2, salt stress combined with the G2 group. The different letters within the different treatments in the same parameter indicate the significant difference at the 0.05 level. Values are means ± SE (n = 3). **(A)** SPS: sucrose-phosphate synthase. **(B)** SS: sucrose synthase. **(C)** NI: neutral invertase. **(D)** AI: acid invertase.

DISCUSSION

Effect of G2 on Growth in *Glycyrrhiza uralensis* Under Salt Stress

Growth inhibition is the most frequent and significant effect of salt stress on plants, and it is mainly manifested as a decrease in biomass (Zhang et al., 2018). Present results also showed that salt stress inhibited the growth of *G. uralensis*, and this effect was partly reversed by G2 inoculation (**Figure 2**), agreeing with previous findings on wheat (*Triticum turgidum* subsp. *durum*) (Ibarra-Villarreal et al., 2021), soybean (*G. max* L.) (El-Esawi et al., 2018), and *Artemisia ordosica* (Hou et al., 2021). Specifically, G2 significantly increased plant height, stem diameter, fresh weight, and dry weight of *G. uralensis* seedlings under salt stress (**Figure 1B**).

Effect of G2 on Photosynthesis in *Glycyrrhiza uralensis* Under Salt Stress

Carbohydrate is produced during photosynthesis and acts as a substrate for respiration, which reflects the balance between plant carbon acquisition and expenditure (Liu et al., 2016). We mainly analyzed the genes in carbon fixation in photosynthetic organisms and the contents of photosynthetic pigments.

Our transcriptomic analysis showed that salt stress upregulated the genes-encoding RPI, Rubisco, and GPD in carbon fixation in photosynthetic organisms. The pathway of carbon fixation in photosynthetic organisms is mainly divided into three stages: the carboxylation stage, the reduction stage, and the regeneration stage. In the carboxylation stage, Rubisco as the key enzyme in the first step converted ribulose-1,5-bisphosphate (RuBP) and atmospheric CO_2 into two molecules of 3-phosphoglycerate (3-PGA). Salt stress-induced stomatal closure generally causes a decline in the available CO_2; in this case, Rubisco uses O_2 that leads to the formation of 2-phosphoglycolate, which is a toxic two-carbon compound and inhibits at least two key enzymes of carbon metabolism, thus attenuates the net photosynthesis rate (Frukh et al., 2019). In our study, salt stress upregulated genes-encoding Rubisco; on the one hand, salt stress promoted the synthesis of 3-PGA, therefore promoted the energy storage process of photosynthesis at the substrate level; on the other hand, salt stress might promote the synthesis of 2-PGA, thereby weakening photosynthesis. However, the direction of Rubisco regulation depends on the partial pressure of CO_2 and O_2 in the environment, which need to be further analyzed. In the reduction stage, GPD catalyzes the reduction of 1,3-bisphosphoglycerate by NADPH to produce 3-phosphoglyceraldehyde (G3P) and $NADP^+$; then, PGA can accept electrons from NADPH to decrease ROS production, and G3P can be used to synthesize starch in the chloroplast or can be transported to the cytoplasm for sucrose biosynthesis (Chintakovid et al., 2017). In this study, salt stress upregulated the gene-encoding GPD, therefore promoted the energy storage process of photosynthesis. However, whether the upregulation

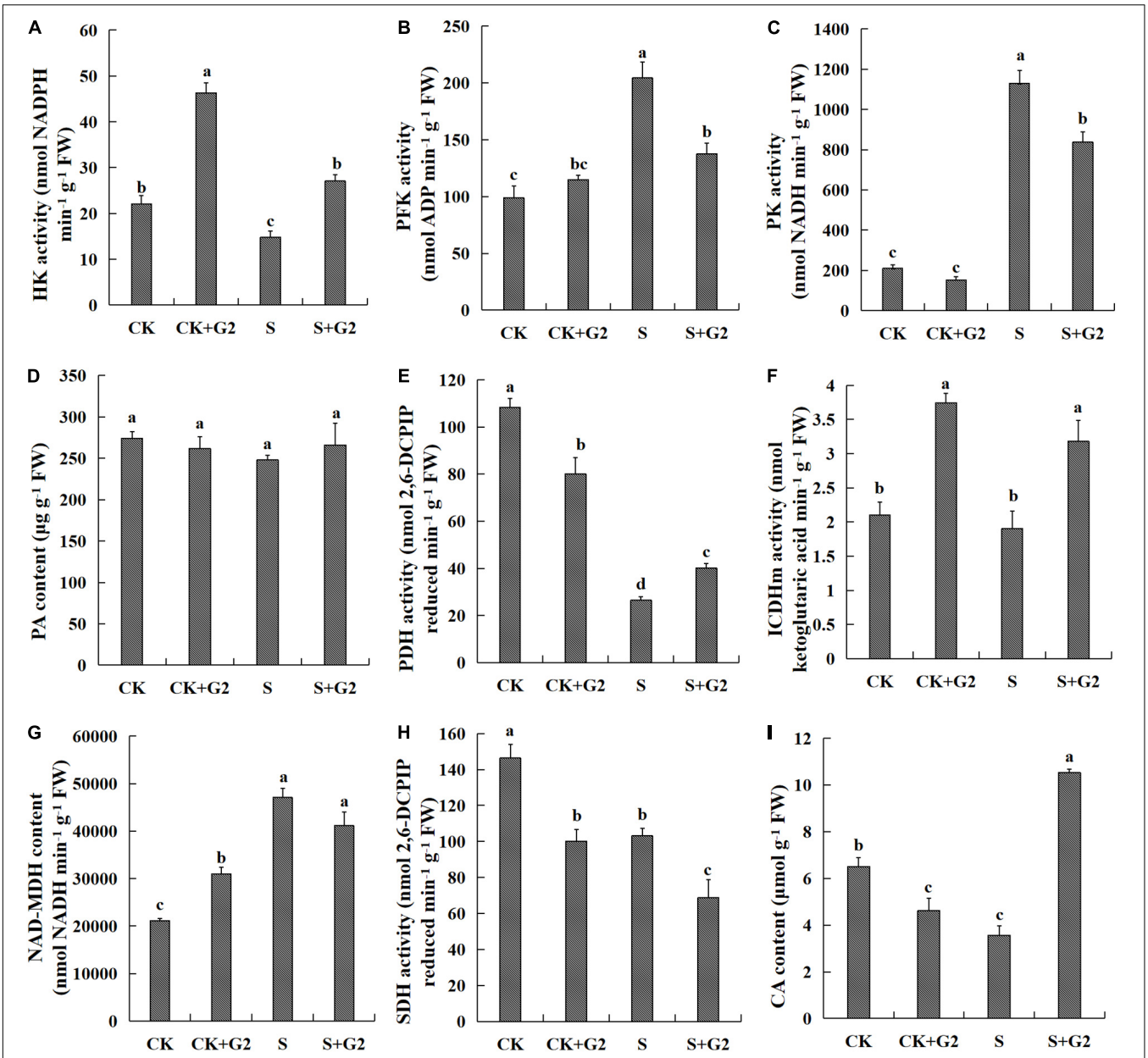

FIGURE 7 | Effects of *B. cereus* G2 on EMP-TCA-related enzyme activities and intermediate contents in *G. uralensis* seedlings under control and salt stress conditions. CK, control group; S, salt stress group; CK + G2, control combined with the G2 group; S + G2, salt stress combined with the G2 group. The different letters within the different treatments in the same parameter indicate the significant difference at the 0.05 level. Values are means ± SE (n = 3). **(A)** HK: hexokinase. **(B)** PFK: phosphofructokinase. **(C)** PK: pyruvate kinase. **(D)** PA: pyruvate. **(E)** PDH: pyruvate dehydrogenase. **(F)** ICDH: isocitrate dehydrogenase. **(G)** MDH: malate dehydrogenase. **(H)** SDH: succinate dehydrogenase. **(I)** CA: citrate.

of the GPD gene under salt stress can help *G. uralensis* reduce the production of ROS and promote the synthesis of starch and sucrose remains to be confirmed by further studies. In the regeneration stage, RPI not only isomerizes ribose-5-phosphate into ribulose-5-phosphate but also helps in the regeneration of the Rubisco substrate (Moigne et al., 2020); therefore, the upregulation of the gene-encoding RPI could contribute to providing sufficient Rubisco substrates for *G. uralensis* seedling under salt stress. However, our results found that G2 had little effect on the gene related to carbon fixation in photosynthetic organisms in *G. uralensis* under salt stress.

Salt stress generally reduced Chl content (Rabiei et al., 2020); however, some studies have reported increased Chl content with increasing salt stress in salt-tolerant plants (Borghesi et al., 2011; Huang et al., 2015; Qiu et al., 2017). In our study, salt stress also increased contents of Chl *a*, *b*, and *a* + *b* in *G. uralensis*, and then, maybe, leading to highly efficient photosynthesis in terms of light reaction, which is further supported by our

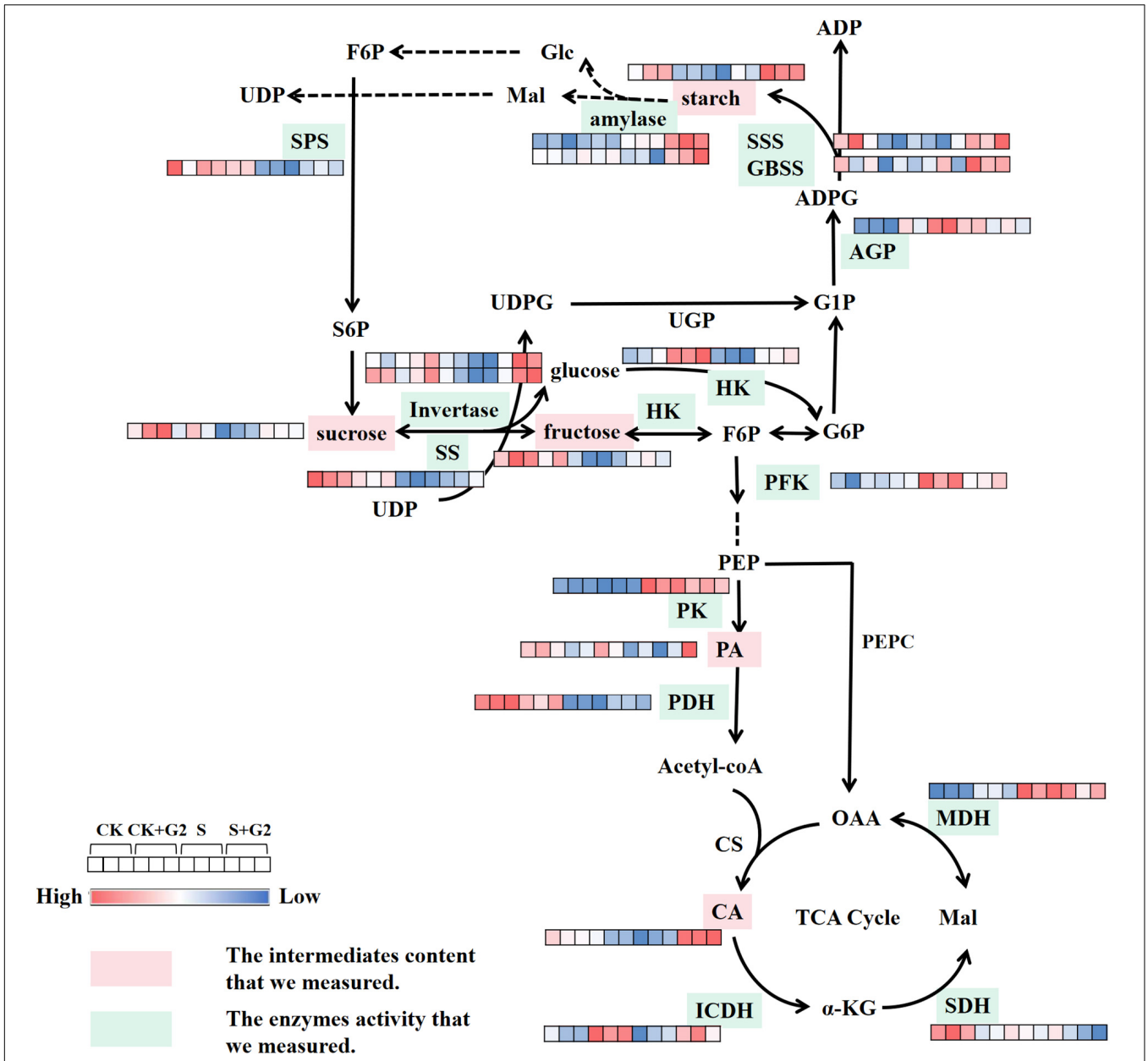

FIGURE 8 | A figure of the mechanism by which *B. cereus* G2 improves the salt tolerance of *G. uralensis* by regulating enzymes and intermediates related to carbohydrate metabolism. CK, control group; S, salt stress group; CK + G2, control combined with the G2 group; S + G2, salt stress combined with the G2 group. SPS, sucrose-phosphate synthase; SS, sucrose synthase; AGP, ADP-glucose pyrophosphorylase; GBSS, granule-bound starch synthase; HK, hexokinase; PFK, phosphofructokinase; PK, pyruvate kinase; PA, pyruvate; PDH, pyruvate dehydrogenase; CA, citrate; ICDH, isocitrate dehydrogenase; SDH, succinate dehydrogenase; MDH, malate dehydrogenase.

observation that *G. uralensis* leaves under salt stress exhibited greener compared to that under control conditions (**Figure 1A**). Interestingly, G2 further increased Chl *a* and Car contents in *G. uralensis* exposed to salt stress, which possibly helped improve the photosynthetic rate of *G. uralensis* and promote plants to resist oxidative stress caused by salt stress (Gururani et al., 2015), thus accumulating more photosynthetic products. Carbohydrates are important substrates of metabolism that helps the plants in various physiological events by regulating the import of carbon to the metabolical sink (Aliche et al., 2019). In this study, salt stress resulted in a significant decrease in starch and TSS contents, and decreased *G. uralensis* growth and yield; in this case, *G. uralensis* thus could require the enhanced photosynthetic rate to synthesize more photosynthetic products to maintain the normal metabolism under salt stress, which may be the reason for the increase of Chl content under salt stress. Moreover, G2 significantly increased the starch and TSS contents in *G. uralensis* under salt stress, which could attribute

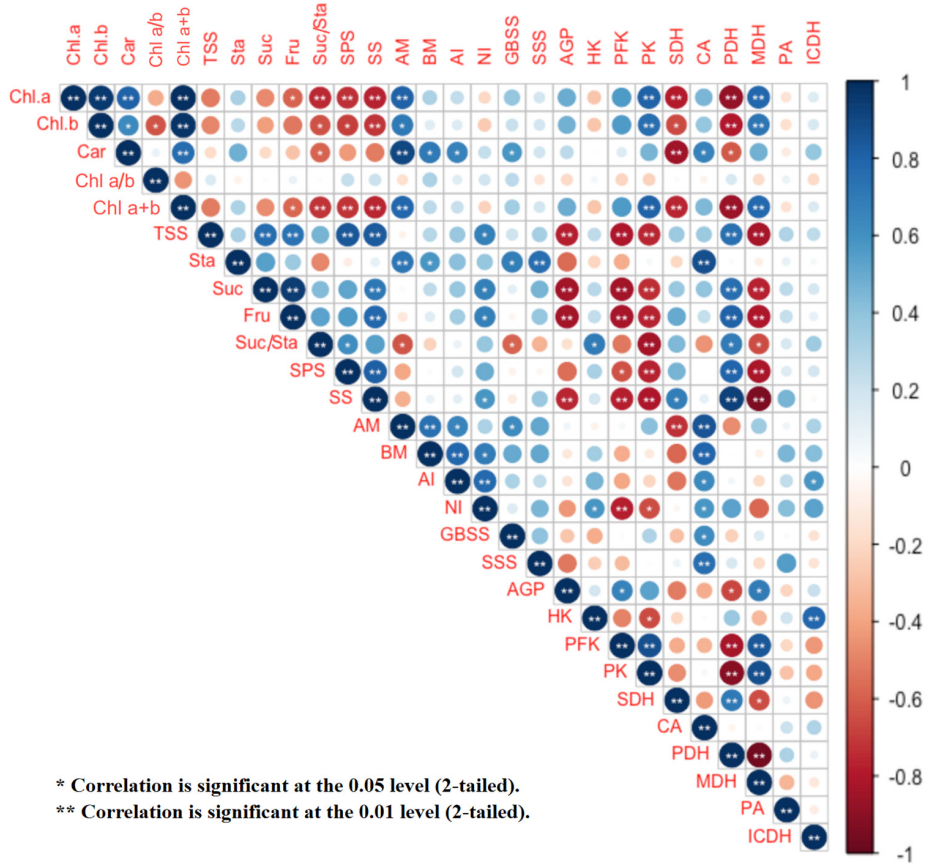

FIGURE 9 | Correlation analysis among *G. uralensis* photosynthetic pigment contents, starch and sucrose metabolism, EMP and TCA cycle indexes in the four treatments (CK, CK + G2, S, and S + G2). CK, control group; S, salt stress group; CKEE + G2, control combined with the G2 group; S + G2, salt stress combined with the G2 group. Chl *a*, chlorophyll *a*; Chl *b*, chlorophyll *b*; Car, carotenoids; AGP, ADP-glucose pyrophosphorylase; GBSS, granule-bound starch synthase; SSS, soluble starch synthase; AM, α-amylase; BM, β-amylase; SPS, sucrose-phosphate synthase; SS, sucrose synthase; AI, acid invertase; NI, neutral invertase; HK, hexokinase; PFK, phosphofructokinase; PK, pyruvate kinase; PDH, pyruvate dehydrogenase; ICDH, isocitrate dehydrogenase; SDH, succinate dehydrogenase; MDH, malate dehydrogenase; PA, pyruvate; CA, citrate; TSS, total soluble sugar; Sta, starch; Fru, fructose; Suc, sucrose.

to improve the photosynthetic rate caused by increased Chl *a* and Car contents.

It was concluded that the G2 increased carbohydrate contents mainly by increasing photosynthetic pigments rather than by regulating the gene related to carbon fixation in photosynthetic organisms in *G. uralensis* under salt stress.

Effect of G2 on Carbohydrate Transformation in *Glycyrrhiza uralensis* Under Salt Stress

Carbohydrate contents are not only related to photosynthesis but also closely related to the key enzymes in its synthesis and decomposition. Maintenance of the balance among the production, translocation, partition, and use of carbohydrate is important for plants' normal growth. Starch, sucrose, and fructose are the important components of carbohydrate.

Starch is a major storage form of carbohydrate and an energy carrier in plant storage organs. In the present study, salt stress significantly decreased starch content, while G2 significantly increased starch content in *G. uralensis* under salt stress (**Figure 2**). In starch synthesis, AGP catalyzes the conversion of glucose 1-phosphase and ATP to produce the precursor for starch biosynthesis, ADP-glucose (Sun et al., 2021), while GBSS and SSS catalyze the elongation of a-1,4-glucosidic bonds on amylose and amylopectin molecules, respectively, by the transfer of glucose from ADPG (Wu et al., 2020). Transcriptomic analysis showed that the genes related to starch synthesis had no differential expression in *G. uralensis* both in S vs. CK and S + G2 vs. S comparisons. However, different results were found when the activities of enzymes related to starch synthesis were measured. Specifically, salt stress significantly increased AGP activity but decreased SSS activity, while G2 significantly increased the activity of SSS in *G. uralensis* under salt stress (**Figure 3**), which could be the result of the combined action of all genes-encoding AGP and SSS. The results indicating that the decrease of starch under salt stress were mainly due to the inhibition of amylopectin synthesis, while the accumulation of starch by G2 under salt stress was also mainly due to the promotion of amylopectin synthesis. In starch decomposition, amylase catalyzes the hydrolysis of

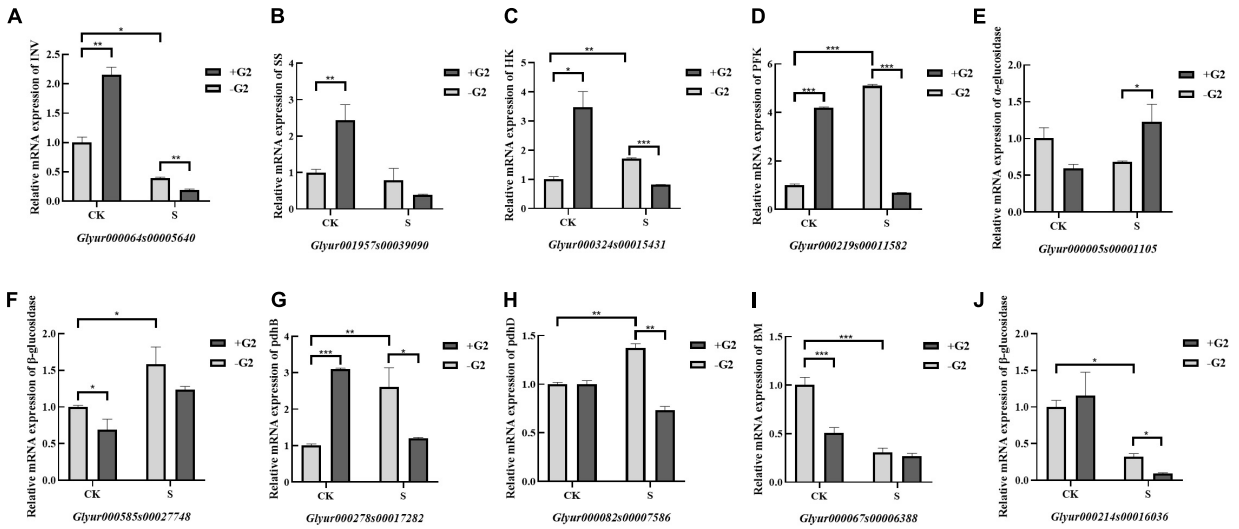

FIGURE 10 | Expression of carbohydrate metabolism-related genes (qRT-PCR) in *G. uralensis* in four treatments (CK, CK + G2, S, and S + G2). CK, control group; S, salt stress group; CK + G2, control combined with the G2 group; S + G2, salt stress combined with the G2 group (mean ± SD; $^{*}p < 0.05$; $^{**}p < 0.01$; $^{***}p < 0.001$). **(A)** INV: beta-fructofuranosidase. **(B)** SS: sucrose synthase. **(C)** HK: hexokinase. **(D)** PFK: 6-phosphofructokinase 1. **(E)** α-glucosidase: alpha-glucosidase. **(F,J)** β-glucosidase: beta-glucosidase. **(G)** pdhB: pyruvate dehydrogenase E1 component beta subunit. **(H)** pdhD: dihydrolipoamide dehydrogenase **(I)** BM: beta-amylase.

starch to a mixture of smaller oligosaccharides (Baslam et al., 2020). Specifically, starch grains are attacked by AM to release linear and branched oligosaccharides, and then BM catalyzes branched oligosaccharides to release maltose disaccharides (Lloyd and Kötting, 2016). G2 had no effect on the genes-encoding AM and BM by transcriptomic analysis and the gene *Glyur000067s00006388* by qRT-PCR, but G2 increased AM and BM activities in *G. uralensis* under salt stress that helped starch hydrolysis and provided energy for subsequent life activities of plants, which could be the result of the combined action of all genes-encoding AM and BM. Furthermore, S + G2 treatment increased AM and BM activities, and the variation activity of AM was higher than BM, which was possibly due to excessive starch content required increased AM activity to decompose and produce linear and branched oligosaccharides, thus providing sufficient substrates for subsequent carbohydrate metabolism, whereas BM only catalyzed branched oligosaccharides. Moreover, starch content was very positively correlated with SSS and AM activities and positively correlated with BM activity (**Figure 7**), which also indicated that the decrease of starch content in *G. uralensis* under salt stress was mainly attributed to the decrease of SSS activity, while the increase of starch content by G2 in *G. uralensis* under salt stress was also mainly due to the increase of SSS activity firstly, and then the elevated starch required higher activities of amylase for decomposing, which thus improved the activities of AM and BM.

Sucrose is the main product of plant photosynthesis, which not only acts as a carbon and energy source but also plays a key role as a signaling molecule to regulate the growth of source and sink tissues and the sugar-mediated feedback repression of photosynthesis (Gil et al., 2013). In the present study, salt stress markedly decreased sucrose content, while G2 significantly increased sucrose content in *G. uralensis* under salt stress. SPS is responsible for the synthesis of sucrose from glucose and fructose, and AI, NI, and α-glucosidase catalyze the sucrose to glucose and fructose (Lombardo et al., 2011; Bilska-Kos et al., 2020), while SS has a dual role in the synthesis and hydrolysis of sucrose (Yang et al., 2020). In sucrose synthesis, salt stress had no significantly effect on the genes-encoding SPS and SS by transcriptomic analysis and the gene *Glyur001957s00039090* by qRT-PCR, but salt stress significantly decreased SS and SPS activities that inhibited the synthesis of sucrose, which could be the result of the combined action of all genes-encoding SS and SPS. G2 upregulated the gene *Glyur001957s00039090*-encoding SS by transcriptomic analysis, and G2 also increased SS activity in *G. uralensis* under salt stress that promoted the synthesis of sucrose, which suggested that G2 promoted the synthesis of sucrose, mainly by regulating SS activity resulted from upregulation of the gene *Glyur001957s00039090*. The activity of SS is highly correlated with sucrose content so that changes in SS activity may largely explain the reduced sucrose content in *G. uralensis* under S condition and the increased sucrose content in *G. uralensis* under S + G2 condition. In sucrose decomposition, salt stress downregulated the gene *Glyur000064s00005640*-encoding INV by transcriptomic and qRT-PCR analysis, and salt stress also decreased NI activity that inhibited the hydrolysis of sucrose, which indicated that salt stress inhibited the hydrolysis of sucrose mainly by regulating NI activity resulted from downregulation of the gene *Glyur000064s00005640*. However, G2 downregulated the gene *Glyur000064s00005640*-encoding INV by qRT-PCR analysis, but G2 increased NI and AI activities in *G. uralensis* under salt stress that promoted the hydrolysis of sucrose, which indicated

that gene *Glyur000064s00005640* is not the key gene that controlled NI and AI activities. Moreover, G2 upregulated the gene *Glyur000005s00001105*-encoding α-glucosidase by transcriptomic and qRT-PCR analyses, which suggested that G2 promoted the hydrolysis of sucrose under salt stress. Owing to sucrose accumulation under the S + G2 condition, the cell osmotic potential decreased. In order to avoid further water loss of leaves, G2 promoted sucrose hydrolysis and increased the accumulation of reducing sugar in *G. uralensis* under salt stress not only by upregulating invertase but also by upregulating α-glucosidase, thus could help *G. uralensis* produce more energy to cope with salt stress by facilitating sucrose hydrolysis. Correlation analysis results showed that sucrose content was positively correlated with NI activity, which indicated that the overmuch sucrose required higher NI activity for decomposition, which thus improved the activity of NI.

As for fructose, salt stress resulted in a significant decrease in fructose content, while G2 resulted in a significant increase in fructose content in *G. uralensis*. In fructose synthesis, invertases and α-glucosidase mentioned above can catalyze the cleavage of sucrose to glucose and fructose; therefore, these enzymes not only participate in sucrose hydrolysis but also contribute to the production of fructose. In the present study, salt stress downregulated the gene *Glyur000064s00005640*-encoding INV by transcriptomic and qRT-PCR analyses, and salt stress also decreased NI activity that inhibited the production of fructose, which indicated that salt stress inhibited the production of fructose mainly by regulating NI activity caused by downregulation of the gene *Glyur000064s00005640*. G2 downregulated the gene *Glyur000064s00005640*-encoding INV by qRT-PCR analysis, but G2 increased NI and AI activities in *G. uralensis* under salt stress that promoted the production of fructose, which indicated that gene *Glyur000064s00005640* is not the key gene that regulated NI and AI activities under the S + G2 condition, and the potential reason needs further studies. Moreover, G2 upregulated the gene *Glyur000005s00001105*-encoding α-glucosidase by transcriptomic and qRT-PCR analyses, which further verified G2 promoted the production of fructose under salt stress not only by upregulating invertase but also by upregulating α-glucosidase. In fructose decomposition, HK, as a key enzyme in EMP, can phosphorylate glucose and fructose and induce leaf senescence (Sun et al., 2021). In the present study, salt stress upregulated gene *Glyur000324s00015431*-encoding HK by transcriptomic and qRT-PCR analyses, but salt stress decreased HK activity that inhibited the phosphorylation of fructose. However, G2 downregulated gene *Glyur000324s00015431*-encoding HK by qRT-PCR analysis, but G2 increased HK activity in *G. uralensis* under salt stress that promoted the phosphorylation of fructose and thus provided sufficient substrates for EMP. These results suggested that the gene *Glyur000324s00015431* might not be the pivotal gene that controlled HK activity, and the reason needs further studies. The activity of NI is highly correlated with fructose content so that changes in NI activity may largely explain the reduced fructose content in *G. uralensis* under the S condition and the increased fructose content in *G. uralensis* under the S + G2 condition, and then the overmuch fructose content required higher HK activity to decompose, which thus improved the HK activity.

In the starch and sucrose metabolism pathway, in addition to the genes mentioned above, the genes-encoding β-glucosidase and TPS in *G. uralensis* were affected by salt or G2. β-Glucosidase can catalyze the hydrolysis of the β-glycosidic linkage from the nonreducing end of isoflavone glucosides, disaccharides, oligosaccharides, aryl-glucosides, and alkyl-glucosides (Maitan-Alfenas et al., 2014). However, as a major component of the primary cell wall of many plant tissues, β-glucosidase may be involved in the production of signaling molecules through its specific hydrolytic activity, thus improving the plant's salt tolerance (Mostek et al., 2016). In our study, salt stress downregulated the gene *Glyur000214s00016036*-encoding β-glucosidase by transcriptomic and qRT-PCR analyses, but upregulated the gene *Glyur000585s00027748*-encoding β-glucosidase by transcriptomic and qRT-PCR analyses and the gene *Glyur000779s00022830*-encoding β-glucosidase by transcriptomic analysis in *G. uralensis*, which implied that β-glucosidase could involve in the starch and sucrose metabolism pathway through affecting hydrolytic activity. G2 downregulated the gene *Glyur000214s00016036*-encoding β-glucosidase by qRT-PCR analysis but had no significant effect on genes-encoding β-glucosidase by transcriptomic analysis in *G. uralensis* under salt stress; thus, the effect of β-glucosidase by G2 on *G. uralensis* remains to be further studied. TPS can catalyze UDP-glucose and glucose-6-phosphate to form trehalose 6-phosphate (Tre6P), and then trehalose 6-phosphate phosphatase (TPP) can catalyze trehalose from Tre6P (Wang P. et al., 2020). Overexpression of the TPS gene in plants can enhance the ability of plant cells to scavenge ROS, promote the low accumulation of O_2 and H_2O_2, thereby reducing cell death and enhancing salt tolerance and permeability of plants (Wang P. et al., 2020). In the present study, salt stress downregulated the genes (*Glyur000018s00003759* and *Glyur000231s00022077*)-encoding TPS, while G2 upregulated the gene *Glyur000018s00003759*-encoding TPS under salt stress in *G. uralensis* that may alleviate the oxidative stress caused by salt stress, thus improving the salt tolerance of *G. uralensis*.

Normal carbohydrate metabolism persists when plants grow unstressed conditions; in such a case, energy is stored in the form of starch, and the accumulation of TSS usually remains very limited. TSS concentrations are required for osmo-protection and carbon storage in plants subjected to salt stress (Neera and Amrit, 2018).

Effect of G2 on the EMP-Tricarboxylic Acid Cycle in *Glycyrrhiza uralensis* Under Salt Stress

The EMP pathway-TCA cycle plays an important role in the aerobic respiration of plants, providing ATP, reductants, and metabolites needed for plant growth and development (Jiang, 2011). Sucrose and starch are sources of the EMP substrate fructose (Li et al., 2020), and they store chemical energy that can be released in the form of ATP through the EMP pathway-TCA cycle (Bandehagh and Taylor, 2020), and our study found that G2 increased the sucrose, starch, and fructose contents, which

result in the EMP pathway being promoted from the substrate and energy level. In plants, HK, PFK, and PK are crucial for regulating the EMP pathway. HK is supposed to act as a sugar sensor and/or interact with other enzymes directly in supplying metabolic pathways (Kim et al., 2013). PFK is the rate-limiting enzyme in the EMP pathway because of its low catalytic efficiency and irreversible catalytic reaction (Wen et al., 2020). PK, a transferase involved in the final step of EMP, catalyzes PEP and adenosine diphosphate (ADP), resulting in one molecule of PA and one molecule of ATP. In our study, salt stress upregulated the gene *Glyur000324s00015431*-encoding HK by transcriptomic and qRT-PCR analyses, but decreased HK activity that inhibited the EMP process at the substrate level. However, G2 downregulated gene *Glyur000324s00015431*-encoding HK by qRT-PCR analysis, but increased HK activity in *G. uralensis* under salt stress. These results implied that the gene *Glyur000324s00015431* might not be the pivotal gene that regulates HK activity. The increase of HK activity by G2 could not only promote the EMP process at the substrate level but also help to alleviate the oxidative stress caused by the decrease of HK activity in *G. uralensis* under salt stress (Poór et al., 2019). Salt stress upregulated the gene *Glyur000219s00011582*-encoding PFK in transcriptomic and qRT-PCR results and also increased PFK and PK activity in *G. uralensis*, resulting in increased respiration in response to elevated energy requirements of *G. uralensis* from exposure to salt (Jacoby et al., 2011), which suggested that salt stress produced more energy by regulating PK and PFK resulted from upregulation of the gene *Glyur000219s00011582*. The increased PFK and PK activities may contribute to the acceleration of glucose catabolism, further produce more energy to remedy the inadequacy of energy caused by insufficient carbon sources, and, finally, maintain the *G. uralensis*'s normal life activities under salt stress, which is supported by the previous studies in tomato (Poór et al., 2019) and mangrove tree (Suzuki et al., 2005). However, G2 downregulated the gene *Glyur000219s00011582*-encoding PFK by qRT-PCR analysis and also decreased PFK and PK activities in *G. uralensis* under salt stress, which suggested that the EMP process was slowed down by regulating PK and PFK resulted from downregulation of the gene *Glyur000219s00011582*. In which case, the decrease of PFK and PK activities may be due to *G. uralensis*-elevated energy requirements from exposure to salt had been alleviated by G2. Additionally, an induced CA content can enhance the inhibitory effect of ATP and thus inhibit PFK activity (Sadka et al., 2019), which may help to explain why the process of EMP was slowed down.

In addition to the genes-encoding HK and PFK mentioned above, PDC, ADH, and ALDH-related genes in the EMP pathway were affected by salt or G2 in *G. uralensis*. There are three enzymes in the anaerobic metabolic pathway, PDC, ADH, and lactate dehydrogenase (LDH), in which PDC converted PA to acetaldehyde that was transformed to ethanol by ADH. Acetaldehyde and acetaldehyde are harmful to plant cells (Pan et al., 2019). ALDH further oxidizes acetaldehyde into carboxylic acids that can help cope with salt stress (Tagnon and Simeon, 2017). In our study, all of the DEGs-encoding PDC, ADH, and ALDH were upregulated in S vs. CK comparison, indicating that salt stress could firstly cause to produce more acetaldehyde and ethanol in *G. uralensis* by upregulating genes-encoding PDC and ADH and thus injure plant cells; in such a case, ALDH was upregulated timely for oxidizing excessive acetaldehyde into carboxylic acids that help *G. uralensis* cope with salt stress. However, only the gene-encoding PDC was downregulated in S + G2 vs. S comparison in *G. uralensis,* suggesting that G2 could protect plant cells from the impairment caused by toxic acetaldehyde and ethanol in *G. uralensis* under salt stress.

Pyruvate as the final product of the EMP pathway not only plays an important role in improving the salt tolerance of plants (Wu et al., 2013) but also links the EMP pathway with the TCA cycle. In our study, salt stress caused the PA production enzyme (PK) activity to increase and the PA decomposition enzyme (PDH) activity to decrease, but salt stress had no significant effect on PA content. This phenomenon may be due to the anaplerotic function of phosphoenolpyruvate carboxylase (PEPC) that replenished the TCA cycle with intermediates by catalyzing PA to produce oxaloacetate (**Figures 4**, **8**), which finally ensured the normal progress of the TCA in *G. uralensis* under salt stress, which is supported by the results in peanut (*Arachis hypogaea* L.) (Pan et al., 2017). However, G2 caused the PA production enzyme (PK) activity to decrease and the PA decomposition enzyme (PDH) activity to increase, but had no significant effect on PA content in *G. uralensis* under salt stress, which may be due to G2 alleviated the inhibition to the TCA cycle from exposure to salt, and the TCA cycle can proceed normally, and the replenishment mechanism of PEPC was weakened, thereby reducing the consumption of PA in *G. uralensis* under salt stress.

The TCA cycle as the most effective way for an organism to obtain energy from the oxidation of sugar and other substances (Yu et al., 2021) can produce the largest amount of energy to plant and provide ATP and reductants for adaptive processes, such as ion exclusion, compatible solute synthesis, and ROS detoxification under salt stress (Che-Othman et al., 2019). Firstly, PDH as a bridge linking the EMP pathway to the TCA cycle can catalyze the oxidative decarboxylation of PA into acetyl CoA, which is the main input of energy in several steps of the TCA cycle (Saha et al., 2012). PDH complex is a complex consisting of three components: pdhB, dihydrolipoyl acetyltransferase (pdhC), and pdhD. In our study, salt stress upregulated the genes *Glyur000278s00017282* and *Glyur000082s00007586*-encoding pdhD and pdhB by transcriptomic and qRT-PCR analyses, but decreased PDH activity in *G. uralensis* that possibly inhibits energy production. However, G2 downregulated the genes *Glyur000278s00017282* and *Glyur000082s00007586*-encoding pdhD and pdhB by qRT-PCR analysis, but increased PDH activity in *G. uralensis* under salt stress that could provide energy for subsequent life activities of *G. uralensis*. These results indicated that the process of oxidative decarboxylation of pyruvate to acetyl-coA is complex, and the key genes regulating PDH need to be further identified. CA is the first organic acid generated in the TCA cycle, and the increase of CA content could help to resist the ionic stress in the plant (Torre-González et al., 2017). In our study, salt stress significantly decreased the CA content, while G2 significantly increased the CA content under salt stress, which potentially indicates an increased capacity for

acetyl-CoA-dependent synthesis of organic acid resulted from the increase of PDH activity in *G. uralensis* by G2. These results are supported by Che-Othman et al. (2019) for wheat. Moreover, CA can inhibit PFK activity by enhancing the inhibitory effect of ATP under S + G2 treatment, thus slowing down the EMP process in *G. uralensis*, which is strongly supported by the results from Sadka et al. (2019). The next three important steps in the TCA cycle are conversion of isocitrate to α-ketoglutarate catalyzed by ICDH, succinate to fumarate catalyzed by SDH with the generation of energy in the form of $FADH_2$, and malate to oxaloacetate catalyzed by MDH (Saha et al., 2012). Specifically, ICDH regulates nitrogen assimilation by maintaining the 2-oxoglutarate level (Bustamante et al., 2019), thereby linking C and N metabolism, and relates to plant antioxidants (Liu et al., 2010). In our study, G2 increased ICDH activity in *G. uralensis* under salt stress, which could affect C and N metabolism and antioxidant system. The accumulated CA under the S + G2 condition resulted from the increase of PDH activity needs higher ICDH to catalyze, thereby the ICDH activity was increased under the S + G2 condition. SDH plays a key role in mitochondrial metabolism both as a member of the electron transport chain and the TCA cycle (Araújo et al., 2011). Salt stress decreased SDH activity in *G. uralensis*, which could attribute to chloride that has a strong inhibitory effect on SDH activity, which is supported by Nunes-Nesi et al. (2013). However, G2 decreased SDH activity in *G. uralensis* under salt stress, which may attribute to the mitigation of chlorine toxicity. The TCA cycle is completed by MDH, which, as a salt-sensitive enzyme, is thought to play a protective role by counteracting the damaging effect of salt by increasing the malate through conformational change (Saha et al., 2012). Salt stress enhanced MDH activity in *G. uralensis*, and the more active MDH could offset the damaging effect of salinity by conformational changes, thus protecting *G. uralensis* from salt stress.

It was concluded that the G2 slowed-down EMP pathway may be attributed to the following reasons. Firstly, G2 alleviated the elevated energy requirements from exposure to salt, thereby decreased PFK and PK activities in *G. uralensis* under salt stress. Secondly, increased CA content inhibited PFK activity by enhancing the inhibitory effect of ATP under the S + G2 condition. Moreover, G2 increased HK activity, which may inhibit the production of ROS and increased ICDH activity, which may affect the production of plant antioxidants, thus possibly improving salt tolerance of *G. uralensis* by affecting the antioxidant system. PDH, as a key enzyme for major energy regulation in the TCA cycle, was promoted by G2 under salt stress in *G. uralensis*, which activated the TCA cycle, resulting in the production of large amounts of intermediates and energy to support *G. uralensis* growth under salt stress.

CONCLUSION

G2 improved Chl content in *G. uralensis* under salt stress, which may lead to highly efficient photosynthesis in terms of light reaction. Second, it increased carbohydrate contents in *G. uralensis* due to balanced regulation of related enzymes, thus increased *G. uralensis* growth and yield under salt stress, and the increase of TSS content induced by G2 plays a protective role in osmoregulation in *G. uralensis* seedlings under salt stress. Third, it alleviated the elevated energy requirements from exposure to salt, thereby slowing down the EMP process in *G. uralensis* under salt stress. Fourth, it provided energy for the subsequent life activities of *G. uralensis* under salt stress through regulating the TCA cycle. Therefore, G2 can effectively regulate and accumulate carbohydrate, improve salt tolerance, and thereby promote the growth of *G. uralensis* seedlings under salt stress.

DATA AVAILABILITY STATEMENT

The data presented in the study are deposited in the GEO repository, accession number GSE187003 (https://www.ncbi.nlm.nih.gov/geo/query/acc.cgi?acc=GSE187003).

AUTHOR CONTRIBUTIONS

XX performed the experiment and wrote the manuscript. QW made the tables. XM modified the language. DL modified the details and made the figures. XZ provided the ideas and revised the manuscript. ZG revised the manuscript. All authors contributed to the article and approved the submitted version.

FUNDING

This work was supported by the project of the National Natural Science Foundation of China (31860343 and 82160724) and the Ningxia Science and Technology Innovation Leader Program (2020GKLRLX12).

SUPPLEMENTARY MATERIAL

The Supplementary Material for this article can be found online at: https://www.frontiersin.org/articles/10.3389/fpls.2021.712363/full#supplementary-material

Supplementary Figure 1 | A correlation line graph between carbohydrates and photosynthetic pigment contents, carbohydrates transformation, and EMP pathway-TCA cycle indexes in *G. uralensis* seedlings. **(A)** The causal relationship between photosynthetic pigment contents and carbohydrates in *G. uralensis* seedlings. **(B)** The causal relationship between starch and sucrose-related enzymes and carbohydrates in *G. uralensis* seedlings. **(C)** The causal relationship between EMP pathway-TCA cycle-related enzymes and intermediates and carbohydrates in *G. uralensis* seedlings. The solid and dotted lines indicate the positive and negative effects, respectively. CK, control group; S, salt stress group; CK + G2, control combined with the G2 group; S + G2, salt stress combined with the G2 group. The different letters within the different treatments in the same parameter indicate the significant difference at the 0.05 level. Values are means ± SE (n = 3). Chl *a*, chlorophyll *a*; Chl *b*, chlorophyll *b*; Car, carotenoids; AGP, ADP-glucose pyrophosphorylase; GBSS, granule-bound starch synthase; SSS, soluble starch synthase; AM, α-amylase; BM, β-amylase; SPS, sucrose-phosphate synthase; SS, sucrose synthase; AI, acid invertase; NI, neutral invertase; HK, hexokinase; PFK, phosphofructokinase; PK, pyruvate kinase; PDH, pyruvate dehydrogenase; ICDH, isocitrate dehydrogenase; SDH, succinate dehydrogenase; MDH, malate dehydrogenase; Sta, starch; Fru, fructose; Suc, sucrose.

Supplementary Figure 2 | Principal component analysis of enzyme activity and gene expression in photosynthesis, starch and sucrose metabolism, and EMP and TCA cycle indexes of *G. uralensis* seedlings under four treatments (CK, CK + G2, S, and S + G2). **(A)** Ordering distribution and interpretation of the 12 principal components related to enzyme activity. **(B)** The contribution of the variables related to photosynthetic pigments content, starch and sucrose metabolism, and EMP and TCA cycle indexes to the principal components. **(C)** Ordering distribution and interpretation of the 12 principal components related to gene expression. **(D)** The contribution of the variables related to carbon fixation in the photosynthetic organisms pathway, starch and sucrose metabolism, and EMP and TCA cycle indexes to the principal components. The depth of the color of the arrow line represents the degree of contribution. The angle of the arrow line represents correlations. CK, control group; S, salt stress group; CK + G2, control combined with the G2 group; S + G2, salt stress combined with the G2 group.

Supplementary Figure 3 | Expression of carbohydrate metabolism-related genes (RT-PCR) in *G. uralensis* in four treatments (CK, CK + G2, S, and S + G2). CK, control group; S, salt stress group; CK + G2, control combined with the G2 group; S + G2, salt stress combined with the G2 group.

REFERENCES

Ahmadi, F. I., Karimi, K., and Struik, P. C. (2018). Effect of exogenous application of methyl jasmonate on physiological and biochemical characteristics of *Brassica napus* L. cv. Talaye under salinity stress. *South Afr. J. Bot.* 115, 5–11. doi: 10.1016/j.sajb.2017.11.018

Ali, S., Charles, T. C., and Glick, B. R. (2014). Amelioration of high salinity stress damage by plant growth-promoting bacterial endophytes that contain ACC deaminase. *Plant Physiol. Biochem.* 80, 160–167.

Aliche, E. B., Theeuwen, T. P. J. M., Oortwijn, M., Visser, R. G. F., and van der Linden, C. G. (2019). Carbon partitioning mechanisms in POTATO under drought stress. *Plant Physiol. Biochem.* 146, 211–219. doi: 10.1016/j.plaphy.2019.11.019

Araújo, W. L., Nunes-Nesi, A., Osorio, S., Usadel, B., Fuentes, D., Nagy, R., et al. (2011). Antisense inhibition of the iron-sulphur subunit of succinate dehydrogenase enhances photosynthesis and growth in tomato via an organic acid-mediated effect on stomatal aperture. *Plant Cell* 23, 600–627. doi: 10.1105/tpc.110.081224

Bandehagh, A., and Taylor, N. L. (2020). Can alternative metabolic pathways and shunts overcome salinity induced inhibition of central carbon metabolism in crops? *Front. Plant Sci.* 11:1072. doi: 10.3389/fpls.2020.01072

Baslam, M., Mitsui, T., Sueyoshi, K., and Ohyama, T. (2020). Recent advances in carbon and nitrogen metabolism in C3 plants. *Int. J. Mol. Sci.* 22:318. doi: 10.3390/ijms22010318

Bilska-Kos, A., Mytych, J., Suski, S., Magoń, J., and Zebrowski, J. (2020). Sucrose phosphate synthase (SPS), sucrose synthase (SUS) and their products in the leaves of Miscanthus × giganteus and *Zea mays* at low temperature. *Planta* 252:23. doi: 10.1007/s00425-020-03421-2

Borghesi, E., González-Miret, M. L., Escudero-Gilete, M. L., Malorgio, F., Heredia, F. J., and Meléndez-Martínez, A. J. (2011). Effects of salinity stress on carotenoids, anthocyanins, and color of diverse tomato genotypes. *J. Agric. Food Chem.* 59, 11676–11682. doi: 10.1021/jf2021623

Brahimova, U., Kumari, P., Yadav, S., Rastogi, A., and Brestic, M. (2021). Progress in understanding salt stress response in plants using biotechnological tools. *J. Biotechnol.* 329, 180–191. doi: 10.1016/j.jbiotec.2021.02.007

Bustamante, M. A., Nogués, I., Jones, S., and Allison, G. G. (2019). The effect of anaerobic digestate derived composts on the metabolite composition and thermal behaviour of rosemary. *Sci. Rep.* 9:6489.

Chaves, M. M., Flexas, J., and Pinheiro, C. (2008). Photosynthesis under drought and salt stress: regulation mechanisms from whole plant to cell. *Ann. Bot.* 103, 551–560. doi: 10.1093/aob/mcn125

Che-Othman, M. H., Jacoby, R. P., Millar, A. H., and Taylor, N. L. (2019). Wheat mitochondrial respiration shifts from the TCA cycle to the GABA shunt under salt stress. *New Phytol.* 225, 1166–1180. doi: 10.1111/nph.15713

Chintakovid, N., Maipoka, M., Phaonakrop, N., Mickelbart, M. V., Roytrakul, S., and Chadchawan, S. (2017). Proteomic analysis of drought-responsive proteins in rice reveals photosynthesis-related adaptations to drought stress. *Acta Physiol. Plant.* 39:240. doi: 10.1007/s11738-017-25

Devi, R., Munjral, N., Gupta, A. K., and Kaur, N. (2007). Cadmium induced changes in carbohydrate status and enzymes of carbohydrate metabolism, glycolysis and pentose phosphate pathway in pea. *Environ. Exp. Bot.* 61, 167–174. doi: 10.1016/j.envexpbot.2007.05.006

El Atta, H. A., Aref, I. M., and Ahmed, A. I. (2016). Seed size effects on the response of seedlings of *Acacia asak* (Forssk.) Willd. to water stress. *Pakistan J. Bot.* 48, 439–446.

El-Esawi, M. A., Alaraidh, I. A., Alsahli, A. A., Alamri, S. A., Ali, H. M., and Alayafi, A. A. (2018). Bacillus firmus (SW5) augments salt tolerance in soybean (*Glycine max* L.) by modulating root system architecture, antioxidant defense systems and stress-responsive genes expression. *Plant Physiol. Biochem.* 132, 375–384. doi: 10.1016/j.plaphy.2018.09.026

Fan, D., Subramanian, S., and Smith, D. L. (2020). Plant endophytes promote growth and alleviate salt stress in Arabidopsis thaliana. *Sci. Rep.* 10, 12740. doi: 10.1038/s41598-020-69713-5

Frukh, A., Siddiqi, T. O., Iqbal, M., Khan, R., and Ahmad, A. (2019). Modulation in growth, biochemical attributes and proteome profile of rice cultivars under salt stress. *Plant Physiol. Biochem.* 146, 55–70. doi: 10.1016/j.plaphy.2019.11.011

Gao, J. F. (2006). *Experimental Guide For Plant Physiology*. Beijing: Higher Education Press.

Ghaffari, M. R., Ghabooli, M., Khatabi, B., Hajirezaei, M. R., Schweizer, P., and Salekdeh, G. H. (2016). Metabolic and transcriptional response of central metabolism affected by root endophytic fungus piriformospora indica under salinity in barley. *Plant Mol. Biol.* 90, 699–717. doi: 10.1007/s11103-016-0461-z

Gil, R., Boscaiu, M., Lull, C., Bautista, I., Lidón, A., and Vicente, O. (2013). Are soluble carbohydrates ecologically relevant for salt tolerance in halophytes? *Funct. Plant Biol.* 40, 805–818. doi: 10.1071/fp12359

Gururani, M. A., Venkatesh, J., and Tran, L. P. (2015). Regulation of photosynthesis during abiotic stress-induced photoinhibition. *Mol. Plant* 8, 1304–1320. doi: 10.1016/j.molp.2015.05.005

Hou, L., Li, X., He, X., Zuo, Y., Zhang, D., and Zhao, L. (2021). Effect of dark septate endophytes on plant performance of *Artemisia ordosica* and associated soil microbial functional group abundance under salt stress. *Appl. Soil Ecol.* 165:103998. doi: 10.1016/j.apsoil.2021.103998

Huang, C. J., Wei, G., Jie, Y. C., Xu, J. J., and Zhao, S. Y. (2015). Responses of gas exchange, chlorophyll synthesis and ROS-scavenging systems to salinity stress in two ramie (*Boehmeria nivea* L.) cultivars. *Photosynthetica* 53, 455–463. doi: 10.1007/s11099-015-0127-0

Ibarra-Villarreal, A., Gándara-Ledezma, A., Godoy-Flores, A. D., Herrera-Sepúlveda, A., Díaz-Rodríguez, A. M., Parra-Cota, F. I, et al. (2021). Salt-tolerant Bacillus species as a promising strategy to mitigate the salinity stress in wheat (*Triticum turgidum* subsp. durum). *J. Arid Environ.* 186:104399. doi: 10.1016/j.jaridenv.2020.104399

Ibrahim, W., Ahmed, I. M., Chen, X., and Wu, F. (2017). Genotype-dependent alleviation effects of exogenous GSH on salinity stress in cotton is related to improvement in chlorophyll content, photosynthetic performance, and leaf/root ultrastructure. *Environ. Sci. Pollut. Res.* 24, 9417–9427. doi: 10.1007/s11356-017-8611-7

Jacoby, R. P., Taylor, N. L., and Millar, A. H. (2011). The role of mitochondrial respiration in salinity tolerance. *Trends Plant Sci.* 16, 614–623. doi: 10.1016/j.tplants.2011.08.002

Jiang, D. A. (2011). *Plant Physiology*. Beijing: Higher Education Press.

Keunen, E., Peshev, D., Vangronsveld, J., Wim, V., and Cuypers, A. (2013). Plant sugars are crucial players in the oxidative challenge during abiotic stress: extending the traditional concept. *Plant Cell Environ.* 36, 1242–1255. doi: 10.1111/pce.12061

Khan, A. L., Hamayun, M., Kim, Y. H., Kang, S. M., and Lee, I. J. (2011). Ameliorative symbiosis of endophyte (*Penicillium funiculosum* LHL06) under salt stress elevated plant growth of *Glycine max* L. *Plant Physiol. Bioch.* 49, 852–861. doi: 10.1016/j.plaphy.2011.03.005

Khoshbakht, D., Ramin, A. A., and Baninasab, B. (2015). Effects of sodium chloride stress on gas exchange, chlorophyll content and nutrient concentrations of nine citrus rootstocks. *Photosynthetica* 53, 241–249.

Kim, Y. M., Heinzel, N., Giese, J. O., Koeber, J., and Hajirezaei, M. R. (2013). A dual role of tobacco hexokinase 1 in primary metabolism and sugar sensing. *Plant Cell Environ.* 36, 1311–1327. doi: 10.1111/pce.12060

Li, L., Xing, W. W., Shao, Q. S., Shu, S., Sun, J., and Guo, S. R. (2015). The effects of grafting on glycolysis and the tricarboxylic acid cycle in Ca(NO3)2-stressed cucumber seedlings with pumpkin as rootstock. *Acta Physiol. Plant.* 37, 259. doi: 10.1007/s11738-015-1978-5

Li, S., Li, Y., Gao, Y., He, X., and Li, Q. (2020). Effects of CO2 enrichment on non-structural carbohydrate metabolism in leaves of cucumber seedlings under salt stress. *Sci. Hortic.* 265:109275. doi: 10.1016/j.scienta.2020.109275

Li, Y. P., Yu, C. X., Qiao, J., Zang, Y. M., Xiang, Y., Ren, G. X., et al. (2016). Effect of exogenous phytohormones treatment on glycyrrhizic acid accumulation and preliminary exploration of the chemical control network based on glycyrrhizic acid in root of *Glycyrrhiza uralensis*. *Rev. Bras. Farmacogn.*26, 490–496. doi: 10.1016/j.bjp.2016.02.009

Liu, J., Wu, N., Wang, H., Sun, J., Peng, B., Jiang, P., et al. (2016). Nitrogen addition affects chemical compositions of plant tissues, litter and soil organic matter. *Ecology* 97, 1796–1806. doi: 10.1890/15-1683.1

Liu, Y., Shi, Y., Song, Y., Wang, T., and Yu, L. (2010). Characterization of a stress-induced NADP-isocitrate dehydrogenase gene in maize confers salt tolerance in *Arabidopsis*. *J. Plant Biol.* 53, 107–112. doi: 10.1007/s12374-009-9091-1

Lloyd, J. R., and Kötting, O. (2016). *Starch Biosynthesis And Degradation In Plants*. Hoboken, NJ: John Wiley & Sons, Ltd, doi: 10.1002/9780470015902.a0020124.pub2

Lombardo, V. A., Osorio, S., Borsani, J., Lauxmann, M. A., Bustamante, C. A., Budde, C. O., et al. (2011). Metabolic profiling during peach fruit development and ripening reveals the metabolic networks that underpin each developmental stage. *Plant Physiol.* 157, 1696–1710. doi: 10.1104/pp.111.186064

Maitan-Alfenas, G. P., Lage, L., Almeida, M. N. D., Visser, E. M., Rezende, S. T. D., and Guimaraes, V. M. (2014). Hydrolysis of soybean isoflavones by *Debaryomyces hansenii* UFV-1 immobilised cells and free β-glucosidase. *Food Chem.* 146, 429–436. doi: 10.1016/j.foodchem.2013.09.099

Moigne, T. L., Crozet, P., Lemaire, S. D., and Henri, J. (2020). High-resolution crystal structure of chloroplastic ribose-5-phosphate isomerase from *Chlamydomonas reinhardtii*-an enzyme involved in the photosynthetic calvin-benson cycle. *Int. J. Mol. Sci.* 21:7787. doi: 10.3390/ijms21207787

Molina-Montenegro, M. A., Acuña-Rodríguez, I. S., Torres-Díaz, C., Gundel, P. E., and Dreyer, I. (2020). Antarctic root endophytes improve physiological performance and yield in crops under salt stress by enhanced energy production and Na+sequestration. *Sci. Rep.* 10:5819. doi: 10.1038/s41598-020-62544-4

Mostek, A., Brner, A., and Weidner, S. (2016). Comparative proteomic analysis of β-aminobutyric acid-mediated alleviation of salt stress in barley. *Plant Physiol. Biochem.* 99, 150–161. doi: 10.1016/j.plaphy.2015.12.007

Neera, G., and Amrit, B. (2018). Salicylic acid improves arbuscular mycorrhizal symbiosis, and chickpea growth and yield by modulating carbohydrate metabolism under salt stress. *Mycorrhiza.* 28, 727–746. doi: 10.1007/s00572-018-0856-6

Nunes-Nesi, A., Araújo, W. L., Obata, T., and Fernie, A. R. (2013). Regulation of the mitochondrial tricarboxylic acid cycle. *Curr. Opin. Plant Biol.* 16, 335–343. doi: 10.1016/j.pbi.2013.01.004

Pan, D. L., Wang, G., Wang, T., Jia, Z. H., Guo, Z. R., and Zhang, J. Y. (2019). AdRAP2.3, a Novel Ethylene Response Factor VII from Actinidia deliciosa, enhances waterlogging resistance in transgenic tobacco through improving expression levels of PDC and ADHgenes. *Int. J. Mol. Sci.* 20:1189. doi: 10.3390/ijms20051189

Pan, L., Zhang, J., Chen, N., Chen, M., Wang, M., and Wan, T. (2017). Molecular characterization and expression profiling of the phosphoenolpyruvate carboxylase genes in peanut (*Arachis hypogaea* L.). *Russian J. Plant Physiol.* 64, 576–587. doi: 10.1134/S1021443717040100

Poór, P., Patyi, G., Takács, Z., Szekeres, A., and Tari, I. (2019). Salicylic acid-induced ROS production by mitochondrial electron transport chain depends on the activity of mitochondrial hexokinases in tomato (*Solanum lycopersicum* L.). *J. Plant Res.* 132, 273–283. doi: 10.1007/s10265-019-01085-y

Qiu, T., Jiang, L. L., Li, S. Z., and Yang, Y. F. (2017). Small-scale habitat-specific variation and adaptive divergence of photosynthetic pigments in different alkali soils in reed identified by common garden and genetic tests. *Front. Plant Sci.* 7:2016. doi: 10.3389/fpls.2016.02016

Rabiei, Z., Hosseini, S. J., Pirdashti, H., and Hazrati, S. (2020). Physiological and biochemical traits in coriander affected by plant growth-promoting rhizobacteria under salt stress. *Heliyon* 6:e05321. doi: 10.1016/j.heliyon.2020.e05321

Raessler, M., Wissuwa, B., Breul, A., Unger, W., and Grimm, T. (2010). Chromatographic analysis of major non-structural carbohydrates in several wood species – an analytical approach for higher accuracy of data. *Anal. Methods* 2:532. doi: 10.1039/b9ay00193j

Sadka, A., Shlizerman, L., Kamara, I., and Blumwald, E. (2019). Primary metabolism in citrus fruit as affected by its unique structure. *Front. Plant Sci.* 10:1167. doi: 10.3389/fpls.2019.01167

Saha, P., Kunda, P., and Biswas, A. K. (2012). Influence of sodium chloride on the regulation of krebs cycle intermediates and enzymes of respiratory chain in mungbean (*Vigna radiata* L. wilczek) seedlings – sciencedirect. *Plant Physiol. Biochem.* 60, 214–222. doi: 10.1016/j.plaphy.2012.08.008

Salimi, F., Shekari, F., and Hamzei, J. (2016). Methyl jasmonate improves salinity resistance in *German chamomile* (*Matricaria chamomilla* L.) by increasing activity of antioxidant enzymes. *Acta Physiol. Plant.* 38:1. doi: 10.1007/s11738-015-2023-4

Scholes, J., Bundock, N., Wilde, R., and Rolfe, S. (1996). The impact of reduced vacuolar invertase activity on the photosynthetic and carbohydrate metabolism of tomato. *Planta* 200, 265–272. doi: 10.1007/BF00208317

Sun, L., Song, F., Zhu, X., Liu, S., Liu, F., Wang, Y., et al. (2021). Nano-zno alleviates drought stress via modulating the plant water use and carbohydrate metabolism in maize. *Arch. Agron. Soil Sci.* 67, 245–259. doi: 10.1080/03650340.2020.1723003

Suzuki, M., Hashioka, A., Mimura, T., and Ashihara, H. (2005). Salt stress and glycolytic regulation in suspension-cultured cells of the mangrove tree *Bruguiera sexangula*. *Physiol. Plant.* 123, 246–253. doi: 10.1111/j.1399-3054.2005.00456.x

Tagnon, M. D., and Simeon, K. O. (2017). Aldehyde dehydrogenases may modulate signaling by lipid peroxidation-derived bioactive aldehydes. *Plant Signal. Behav.* 12:e1387707. doi: 10.1080/15592324.2017.1387707

Tang, Z. C. (1999). *Experimental Guide of Modern Plant Physiology*. Beijing: Science Press.

Torre-González, A. D. L., Albacete, A., Sánchez, E., Blasco, B., and Ruiz, J. M. (2017). Comparative study of the toxic effect of salinity in different genotypes of tomato plants: carboxylates metabolism. *Sci. Hortic.* 217, 173–178. doi: 10.1016/j.scienta.2017.01.045

Wang, C., Chen, L., Cai, Z., Chen, C., and Mei, Y. (2020). Comparative proteomic analysis reveals the molecular mechanisms underlying the accumulation difference of bioactive constituents in *Glycyrrhiza uralensis* Fisch under salt stress. *J. Agric. Food Chem.* 68, 1480–1493. doi: 10.1021/acs.jafc.9b04887

Wang, P., Lei, X., Lü, J., and Gao, C. (2020). Overexpression of the thtps gene enhanced salt and osmotic stress tolerance in *Tamarix hispida*. *J. For. Res.* doi: 10.1007/s11676-020-01224-5

Wellburn, A. R. (1994). The spectral determination of chlorophyll a and chlorophyll b, as well as total carotenoids, using various solvents with spectrophotometers of different resolution. *J. Plant Physiol.* 144, 307–313. doi: 10.1016/S0176-1617(11)81192-2

Wen, J., Wang, W., Xu, K., Ji, D., Xu, Y., Chen, C., et al. (2020). Comparative analysis of proteins involved in energy metabolism and protein processing in Pyropia haitanensis at different salinity levels. *Front. Mar. Sci.* 7:415. doi: 10.3389/fmars.2020.00415

Win, K. T., Tanaka, F., Okazaki, K., and Ohwaki, Y. (2018). The ACC deaminase expressing endophyte *Pseudomonas* spp. Enhances NaCl stress tolerance by reducing stress-related ethylene production, resulting in improved growth, photosynthetic performance, and ionic balance in tomato plants. *Plant Physiol. Biochem.* 127, 599–607. doi: 10.1016/j.plaphy.2018.04.038

Wu, D., Cai, S., Chen, M., Ye, L., Chen, Z., Zhang, H., et al. (2013). Tissue metabolic responses to salt stress in wild and cultivated barley. *PLoS One* 8:e55431. doi: 10.1371/journal.pone.0055431

Wu, P., Li, X., Liu, X., Xu, X., and Li, L. (2020). Comparison of transcriptomic and proteomic analyses to construct a model for the promotion of starch synthesis by ABA in *Euryale ferox* Salisb. seeds. *Res. Square* [Preprint]. doi: 10.21203/rs.3.rs-18154/v1

Yang, Z., Li, J. L., Liu, L. N., Xie, Q., and Sui, N. (2020). Photosynthetic regulation under salt stress and salt-tolerance mechanism of sweet sorghum. *Front. Plant Sci.* 10:1722.

Yu, H., Yuan, Y., Wang, S., Wu, G., Xu, H., Wei, J., et al. (2021). Interspecies evolution and networks investigation of the auxin response protein (AUX/IAA) family reveals the adaptation mechanisms of halophytes crops in nitrogen starvation agroecological environments. *Agriculture* 11:780. doi: 10.3390/agriculture11080780

Zhang, W., Yu, X., Li, M., Lang, D., Zhang, X., and Xie, Z. (2018). Silicon promotes growth and root yield of Glycyrrhiza uralensis under salt and drought stresses through enhancing osmotic adjustment and regulating antioxidant metabolism. *Crop Prot.* 107, 1–11. doi: 10.1016/j.cropro.2018.01.005

Zhong, M., Yuan, Y., Shu, S., Sun, J., Guo, S., Yuan, R., et al. (2016). Effects of exogenous putrescine on glycolysis and Krebs cycle metabolism in cucumber leaves subjected to salt stress. *Plant Growth Regul.* 79, 319–330.

Zhou, X., Lindsay, H., and Robinson, M. D. (2014). Robustly detecting differential expression in RNA sequencing data using observation weights. *Nucleic Acids Res.* 42:e91. doi: 10.1093/nar/gku310

Zhu, Y., Guo, J., Feng, R., Jia, J., Han, W., and Gong, H. (2016). The regulatory role of silicon on carbohydrate metabolism in *Cucumis sativus* L. under salt stress. *Plant Soil* 406, 231–249. doi: 10.1007/s11104-016-2877-2

Conflict of Interest: The authors declare that the research was conducted in the absence of any commercial or financial relationships that could be construed as a potential conflict of interest.

frontiers in Plant Science

ORIGINAL RESEARCH
published: 07 January 2022
doi: 10.3389/fpls.2021.767335

Effects of Preharvest Methyl Jasmonate and Salicylic Acid Treatments on Growth, Quality, Volatile Components, and Antioxidant Systems of Chinese Chives

Cheng Wang†, Jing Zhang†, Jianming Xie, Jihua Yu, Jing Li, Jian Lv, Yanqiang Gao, Tianhang Niu and Bakpa Emily Patience*

College of Horticulture, Gansu Agricultural University, Lanzhou, China

OPEN ACCESS

Edited by:
Youssef Rouphael, University of Naples Federico II, Italy

Reviewed by:
Ebrahim Hadavi, Islamic Azad University of Karaj, Iran
Asgar Ali, University of Nottingham Malaysia, Malaysia
Anna Spinardi, University of Milan, Italy

***Correspondence:**
Jianming Xie
xiejianming@gsau.edu.cn

† These authors have contributed equally to this work and share first authorship

Specialty section:
This article was submitted to Crop and Product Physiology, a section of the journal Frontiers in Plant Science

Received: *30 August 2021*
Accepted: *26 November 2021*
Published: *07 January 2022*

Citation:
Wang C, Zhang J, Xie J, Yu J, Li J, Lv J, Gao Y, Niu T and Patience BE (2022) Effects of Preharvest Methyl Jasmonate and Salicylic Acid Treatments on Growth, Quality, Volatile Components, and Antioxidant Systems of Chinese Chives. Front. Plant Sci. 12:767335. doi: 10.3389/fpls.2021.767335

Methyl jasmonate (MeJA) and salicylic acid (SA) regulate the production of biologically active compounds in plants and stimulate the accumulation of plant aromatic substances. However, the underlying mechanisms of how MeJA and SA influence characteristic flavor compounds and the antioxidant activity of vegetables are poorly understood. Five MeJA and SA concentrations were used to investigate the dose-dependent effects of these phytohormones on the dry and fresh weight; chlorophyll abundance; the contents of vitamin C, soluble protein, and sugar, nitrate, total phenols, flavonoids, volatile components, and enzymatically produced pyruvic acid; and antioxidant activity in Chinese chive. We found that MeJA and SA at concentrations of 500 and 150 μM, respectively, significantly increased the levels of total chlorophyll, phenols and flavonoids, vitamin C, and volatile components and significantly reduced the accumulation of nitrate. In addition, compared with the control, 500 μM of MeJA significantly increased the soluble sugar and protein content, and 150 μM SA significantly increased the dry and fresh weight of Chinese chive. Furthermore, these concentrations of MeJA and SA significantly increased the enzymatic pyruvate content and the amount of sulfide and aromatic volatile compounds and improved the characteristic flavor compounds. The 2,2-diphenyl-1-picrylhydrazyl radical scavenging capacity, Trolox-equivalent antioxidant capacity, and ferric-reducing antioxidant capacity were significantly improved after a preharvest treatment with 500 μM MeJA and 150 μM SA, which could improve the antioxidant activity, thus improving the postharvest quality and preservation characteristics of Chinese chives. Taken together, a preharvest treatment with 500 μM MeJA and 150 μM SA is optimal to improve the growth, quality, antioxidant activity, and flavor of Chinese chive, thereby enhancing its commercial value.

Keywords: methyl jasmonate, salicylic acid, antioxidant activity, quality, volatile compositions

INTRODUCTION

Fruits and vegetables contain a large amount of nutrients required by the human body, and their minerals, vitamins, and antioxidants are important for maintaining human health. As such, plants play a key role in maintaining a balanced diet and in well-being (Gbska et al., 2020). Phenols, carotenoids, alkaloids, and organosulfur compounds are the main phytochemical categories (Liu, 2004). Organosulfur compounds are the main flavor precursors of Allium plants, and they endow Allium vegetables with great nutritional and medicinal value (Jones, 2004; Yabuki et al., 2010). Flavonoids have antifungal activity in plants and are therefore involved in pathogen defense (Napal et al., 2009). Phenolics and flavonoids play an important role as antioxidants in raw food materials (Nayak et al., 2013; Ahmed and Eun, 2017). The nutritional value of vegetables is also greatly improved (Soppelsa et al., 2018).

Chinese chive (*Allium tuberosum* Rottler ex Spreng.) is a popular vegetable in China. As a commercial crop, Chinese chives are cultivated all over China (Mau et al., 2001). Similar to that of garlic (*Allium sativum* L.), Chinese chive has a distinctive odor due to volatile compounds and is rich in nutrients, such as vitamins, proteins, carbohydrates, and cellulose (Rose et al., 2005; Gao et al., 2018). Studies have shown that it is also rich in saponins, alkaloids, phenylpropanoid glucoside, polysaccharides, phenols, flavonoids, and sulfur compounds (Zhang et al., 2016; Tang et al., 2017). This is because Chinese chive can produce sulfur-containing metabolites-S-alk(alkene) cysteine sulfoxides (CSOs), which have an extremely high nutritional and medicinal value (Rabinowitch and Currah, 2002). CSOs are the main flavor precursors of Allium vegetables (Liu et al., 2021). The flavor of Allium plants is produced by the hydrolysis of CSOs by alliinase when the cells are ruptured, and the amount of pyruvate produced in the hydrolysis reaction is equivalent to that of CSOs, which can be used to evaluate the flavor of Chinese chive (Wall and Corgan, 1992). Chinese chive is a vegetable that has been used for both food and in medicine (Leelarungrayub et al., 2006; Bernaert et al., 2012). It has anti-inflammatory, anticancer, antibacterial, and antioxidant activities, which are mainly related to its sulfur-containing compounds (Rattanachaikunsopon and Phumkhachorn, 2009; Hong et al., 2014; Zeng et al., 2017). Additionally, Chinese chives are considered as a health food that can improve the kidney function (Masuda and Mihara, 1988; Block et al., 1992), and they are used for sexual enhancement, nocturnal emission, abdominal pain, and diarrhea in traditional Chinese medicine (Jiangsu, 1979). Therefore, increasing the nutritional quality, antioxidant activity, and organosulfur compounds could be a good strategy to enhance the potential health benefits of Allium vegetables, including Chinese chives.

Jasmonic acid (JA) and methyl jasmonate (MeJA) and their derivatives are ubiquitous lipid-based plant hormones (Sheard et al., 2010). MeJA is a natural plant growth regulator, which has a wide range of physiological effects on plant growth, development, and abiotic tolerance, such as postharvest preservation, quality improvement, secondary metabolite synthesis, and stress response (Meir et al., 1996; Delker et al., 2006; Donati et al., 2018). Based on these reports, MeJA treatment can regulate the antioxidant system, including phenolic substances and antioxidant-related enzymes, to regulate postharvest fruit quality and stress responses (Marjorie et al., 2016; Serna-Escolano et al., 2019; Min et al., 2021). Studies have also shown that MeJA can affect the biosynthesis of fruit components, such as carotene, chlorophyll, and vitamins (Saniewski and Czapski, 1983; Pérez et al., 1993; Wolucka et al., 2005). In addition, Shi et al. (2021) showed that MeJA induced the accumulation of tea (*Camellia sinensis* L.) aroma precursors and improved the quality of fresh leaves. Moreover, it has been observed that the application of MeJA significantly enhanced the flavor quality of fruits and vegetables, such as peaches (*Prunus persica* L. Batsch), strawberries (*Fragaria* × *ananassa* Duch.), sweet basil (*Ocimum basilicum*), and tomatoes (*Solanum lycopersicum* L. cv. Messina) (Ziosi et al., 2008; Fernando et al., 2010; Zhang et al., 2012; Misra et al., 2014). Salicylic acid (SA) can maintain plant growth and development and respond to abiotic stress (Miura and Tada, 2014). Studies have reported that the application of MeJA and SA increased the amounts of bioactive substances in oil palm seedlings (*Elaeis guineensis* Jacq.) and mangosteen (*Garcinia mangostana* L.) during cold storage, thereby enhancing their antioxidant activity (Arthy et al., 2018; Mustafa et al., 2018a). The exogenous application of SA increased the stomatal conductance of barley (*Hordeum vulgare* L.) leaves under drought stress, thereby increasing dry matter content (Habibi, 2012). Huang et al. (2010) showed that SA treatment induces the accumulation of flavonoids and carotenoids, thereby enhancing the antioxidant activity of preharvest navel oranges (*Citrus sinensis* Osb.). Li et al. (2019) found that SA treatment increased the flavonoid content in tea. Martínez-Esplá et al. (2018) showed that preharvest SA treatment increases the antioxidant compounds of plums (*Prunus salicina* Lindl.).

Previous studies on MeJA and SA have mostly focused on stress tolerance, postharvest quality, and the preservation of fruits (Kim et al., 2009; Ibrahim et al., 2018; Se et al., 2020). Despite being a Chinese characteristic flavor vegetable, few studies have been conducted on the flavor quality and antioxidant activity of Chinese chive compared with those on that of tomatoes, onions, and garlic. As such, there are no data on the effects of exogenous hormones on the volatile components of Chinese chives, and there are few reports on the effects of the exogenous application of MeJA and SA on the growth physiology, quality, and antioxidant activity of Chinese chives. We hypothesized that the preharvest application of MeJA and SA promotes the growth of Chinese chive, improves the quality, volatile content, and antioxidant activity, thus improving the characteristic flavor, postharvest quality, preservation characteristics, and its commercial value. The objective of this study was to determine the effects of preharvest MeJA and SA treatments on the growth physiology, quality, volatile content, and antioxidant activity of Chinese chive and to identify suitable spraying concentrations of these compounds for this crop for better Chinese chive cultivation.

MATERIALS AND METHODS

Plant Materials and Experimental Sites

The seeds of the Chinese chive cultivar "Chive God F1," cultivated by the Fugou County Seed and the Seedling Research Institute of Henan Province, were used as the experimental material for this study. Seedlings were cultivated in Wushan (N 34°25′–34°57′, E 104°34′–105°08′), China, in the core demonstration area for Chinese chives, in May 2020. Wushan has a temperate continental semi-humid monsoon climate, with an annual average temperature of 10°C and a precipitation of 500 mm. The soil type at the test site was sandy loam, and the soil fertility was medium and uniform.

Methods and Treatments

The experiment was set up in a completely randomized design with 11 treatments and three replicates. The plot size for each planting area was 2.7 m × 3.3 m (plant, 460 holes). On May 21, 2021, Chinese chive seedlings were transplanted into a plastic greenhouse (10 m × 30 m) with a row spacing of 20 cm, a hole spacing of 10 cm, and three seedlings per hole. Each plot was treated with exogenous hormones: an aqueous solution of MeJA (containing 0.1% ethanol and 0.1% Tween-20) at five concentrations: 50, 150, 300, 500, or 800 μM; an aqueous solution of SA (containing 0.1% ethanol and 0.1% Tween-20) at five concentrations: 50, 150, 300, 500, or 800 μM; and a control solution (0 μM; containing 0.1% ethanol and 0.1% Tween-20). Three liters of the aqueous solution of each treatment was sprayed on the leaves of the Chinese chive between 7:00 and 8:00 every morning. All treatments were applied for 3 days in a row (June 16, 2021 to June 18, 2021). After 35 days (June 25, 2021), the Chinese chive had attained the commercial standard, and plants from all plots were collected. Fifteen holes (three plants per hole) were randomly selected from each plot, with five holes for each of the three biological replicates. All samples were immediately frozen in liquid nitrogen and stored at −80°C prior to analysis.

Growth and Photosynthetic Pigments Analysis

During harvest, 15 holes of Chinese chives (roots and shoots) were randomly selected from each plot within each treatment to record the fresh weight, and the dry weight was recorded after drying the plants at 105°C for 30 min, followed by 75°C for 72 h to a constant weight per a previously published method (Noreen et al., 2020).

The Chinese chive samples were taken using the same sampling method described above to determine the chlorophyll content. The photosynthetic pigments in the leaves were determined according to the method described by Arnon (1949) using the 80% acetone extraction technique. Briefly, a sample was obtained using a r puncher (0.5 cm diameter), 0.1 g of leaves was placed in a 25 ml test tube with a stopper, and 10 ml of 80% acetone was added, mixed well, sealed with a parafilm, and then chlorophyll was extracted in the dark for 48 h until the leaves turned white. The optical density of each extract was measured at 663 and 645 nm using a UV-1780 spectrophotometer [Shimadzu Instruments (Suzhou) Co., Ltd., Suzhou, China]. The Chl.a, Chl.b, and total Chls (Chl.T) were calculated with the following formulas:

$$\begin{aligned}\text{Chl.a (mg g}^{-1}\text{ FW)} &= [12.71 \times D663 - 2.59 \times D645] \\ &\times (V/1000W) \\ \text{Chl.b (mg g}^{-1}\text{ FW)} &= [22.88 \times D645 - 4.67 \times D643] \\ &\times (V/1000W) \\ \text{Chl.T (mg g}^{-1}\text{ FW)} &= [20.29 \times D645 + 8.04 \times D663] \\ &\times (V/1000W)\end{aligned}$$

Where V and W represent the total volume of extract (ml) and fresh weight of the sample (g), respectively.

Nutritional Parameters Analysis

The vitamin C content was determined using the 2,6-dichloroindophenol stain method (Arya et al., 2000). The soluble protein content was determined using the Coomassie Brilliant Blue method (Bradford, 1976). The soluble sugar content was determined using the anthrone–sulfuric acid assay method (Wen et al., 2005). The nitrate content was determined according to Cataldo et al. (1975) with slight modifications.

Total Phenol and Flavonoid Analysis

The total phenol content was determined using the Folin-Ciocalteu method with a slight modification (Hand et al., 2017). Briefly, a crude extract of phenols (0.2 ml) was obtained by extraction with 50% methanol (0.2 ml), which was mixed with distilled water (4.8 ml), followed by Folin-Ciocalteu's phenol reagent (0.5 ml) and 20% sodium carbonate solution (2.5 ml). After incubating in water bath at 50°C for 30 min in the dark, the absorbance of the extract was measured at 760 nm using a UV-1780 spectrophotometer (Shimadzu Instruments, Suzhou, China). The results were compared with the calibration curve of gallic acid and expressed in milligrams of gallic acid equivalent (GAE) per gram of sample (mg GAE g^{-1}).

The flavonoid content was determined following the method of sodium nitrite-aluminum nitrate (Chang et al., 2002) with a slight modification. A crude extract of phenol (1 ml) was obtained by extraction with 50% methanol, which was evenly mixed with 50% methanol (1 ml) and 5% ammonium nitrite (0.5 ml). After incubating for 5 min, 10% aluminum nitrate (0.5 ml) was added. After incubation for 6 min, 4% sodium hydroxide (2 ml) was added. After incubating for 10 min, the absorbance of the extract was measured at 510 nm using a UV-1780 spectrophotometer [Shimadzu Instruments (Suzhou) Co., Ltd., Suzhou, China]. The results were compared with the rutin calibration curve and expressed as rutin equivalent (RE) mg (mg RE g^{-1}) per gram of sample.

Electronic Nose Analysis of Volatile Content

A portable electronic nose (PEN3) electronic nose (Airsense Analytics GmbH, Schwerin, Germany) was used to analyze the

volatile components of the samples. The PEN3 E-nose was equipped with a sensor array composed of 10 chemical sensing elements. The signal response of the sensor is expressed as (G/G0), which is defined as the ratio of the electrical conductivity of volatile matter to that of pure air (Cai et al., 2020). There were some differences in the types of sensitive substances, which could be detected by each sensor. **Table 1** lists the substance types and performance descriptions of the 10 sensors. The electronic nose analysis of the volatile components of Chinese chive was performed according to Jia et al. (2020), with a slight modification. Chinese chives were fully ground (1.5 g) in a headspace bottle using 0.75 g anhydrous sodium sulfate and distilled water (2 ml). The bottle was then heated in a magnetic mixer at 70°C for 15 min to equilibrate the internal headspace gas, and then the injection needle was inserted into the headspace bottle for measurement of volatile compounds. The detection conditions were as follows: flush time of 60 s, sensor zero-time of 5 s, presample time of 5 s, injection flow rate of 400 ml min^{-1}, and a measurement time of 120 s. Based on the data obtained at each time point, the average value of the stable maximum response of each sensor of three parallel samples was obtained, and a characteristic radar map was established.

Enzymatically Produced Pyruvic Acid in Chinese Chive

The content of enzymatically produced pyruvic acid in Chinese chive leaves was determined according to the method of Liu et al. (2021) with a slight modification. Briefly, the sample was divided into two portions. One part was extracted by grinding with ultrapure water and quartz sand. Then, 1 ml of the extract was added to 2 ml 8% trichloroacetic acid and 1 ml 0.1% 2,4-dinitrophenylhydrazine and mixed well. The mixture was incubated in a water bath at 37°C for 10 min, and then 5 ml of 1.5 M NaOH was added. The other part of the sample was placed in a boiling water bath for 10 min to inactivate alliinase, followed by the same method as described for the other section to determine the background pyruvate levels. Absorbance was measured at 520 nm using a spectrophotometer. The enzymatically produced pyruvic acid was the pyruvic acid content in leaves minus the background pyruvic acid content. Pyruvate was determined using a standard sodium pyruvate curve.

TABLE 1 | Substance type and performance description represented by 10 sensors of electronic nose.

Array serial number	Sensor name	Substance types	Sensor performance description
1	W1C	Aromatic	Aromatic components, benzenes
2	W5S	Broadrange	High sensitivity, sensitive to nitrogen oxides
3	W3C	Aromatic	Sensitive aromatic components, ammonia
4	W6S	Hydrogen	Mainly selective to hydride
5	W5C	Arom-aliph	Aromatic components of short-chain alkanes
6	W1S	Broad-methane	Sensitive to methyl groups
7	W1W	Sulfur-organic	Sensitive to sulfides
8	W2S	Broad-alcohol	Sensitive to alcohols, aldehydes and ketones
9	W2W	Sulph-chlor	Aromatic components, sensitive to organic sulfides
10	W3S	Methane-aliph	Sensitive to long-chain alkanes

Antioxidant Parameters Analysis

The total antioxidant capacity of Chinese chive was determined according to the kit instructions (Suzhou Keming, Suzhou, China), including 2,2-diphenyl-1-picrylhydrazyl (DPPH) radical scavenging activity, ferric-reducing antioxidant power (FRAP), and 2,2'-azino-bis(3-ethylbenzothiazoline-6-sulfonic acid (ABTS) radical scavenging activity. Briefly, using a precooled mortar, the leaf tissue was ground (0.1 g) in 1 ml of precooled extract. The homogenate was centrifuged at 4°C at 10,000 × *g* for 10 min, and the supernatant was collected for testing. According to the instructions of the DPPH radical scavenging activity and FRAP kits, the respective solutions were mixed and allowed to react at room temperature in the dark for 20 min and at room temperature for 20 min. A microplate reader (SpectraMax i3, Molecular Devices, Sunnyvale, CA, United States) was used to measure absorbance at 515 and 593 nm. The same extraction method was used to extract the supernatant from the sample to determine ABTS radical scavenging activity. When the tested substance was added to the ABTS+ solution, antioxidants reacted with ABTS+ and faded the reaction system. The change in absorbance was measured at 734 nm. The antioxidant capacity of the Chinese chive was quantified by the change in absorbance and Trolox was used as the control system.

Statistical Analysis

All experimental data were analyzed using IBM Statistical Product and Service Solutions (SPSS) Statistics version 21.0, and the statistical significance of treatment means was evaluated using Duncan's multiple range test ($p < 0.05$). All data were presented as mean ± SE. Data figures, correlation analysis, and principal component analysis (PCA) were generated using Origin Pro (2019b).

RESULTS

Effect of Methyl Jasmonate and Salicylic Acid Treatments on Dry and Fresh Weight of Chinese Chive

The application of SA treatment had a significant effect on the dry weight and fresh weight of the shoots and roots of Chinese chives (**Figures 1B,D**). The fresh weight of roots, shoots, and plants treated with 150 μM SA increased significantly by 69, 55, and 58%, respectively, and the dry weight increased by 85, 33, and 50%, respectively, compared with that of the control (0 μM). With the increase in the SA concentration, the dry and fresh weight of Chinese chives exhibited a decreasing trend. However, the application of MeJA had no significant effect on the dry and fresh weights of Chinese chives (**Figures 1A,C**).

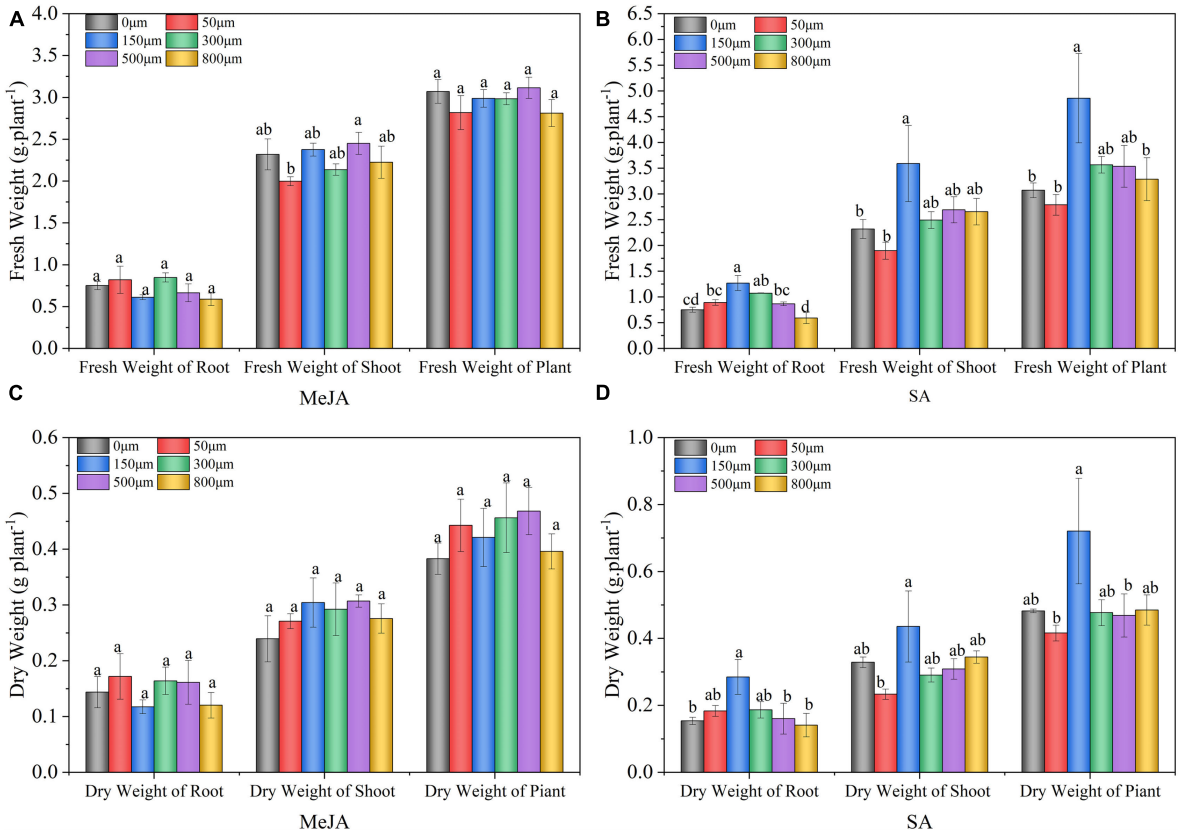

FIGURE 1 | Fresh **(A,B)** and dry weight **(C,D)** of Chinese chives affected by methyl jasmonate (MeJA) and salicylic acid (SA) treatments. Data represent the mean ± SE (n = 3). Different lowercase letters indicate statistical significance by Duncan's multiple range test ($p < 0.05$).

Effect of Methyl Jasmonate and Salicylic Acid Treatments on Photosynthetic Pigment Contents of Chinese Chive

Compared with the control (0 μM) treatment, 500 μM MeJA significantly increased Chl.a and Chl.T by 5 and 8%, respectively, in Chinese chives (**Figure 2A**); however, 800 μM MeJA significantly decreased Chl.a and Chl.T content. Treatment with 150 μM SA significantly increased Chl.b and Chl.T content by 23 and 8%, respectively, compared with the control (0 μM) (**Figure 2B**). When treated with 300–800 μM SA, the content of Chl.a, Chl.b, and Chl.T in Chinese chives decreased significantly compared with the control (0 μM).

Effect of Methyl Jasmonate and Salicylic Acid Treatments on Vitamin C, Soluble Sugar, Soluble Protein, and Nitrate Content of Chinese Chive

The contents of vitamin C, soluble sugar, and soluble protein in Chinese chives treated with MeJA were significantly higher than those in the control (0 μM) (**Figures 3A–C**). The vitamin C, soluble sugars, and protein contents in Chinese chives treated with 500 μM MeJA significantly increased by 44, 10, and 72%, respectively, compared with those in the control (0 μM). However, 50–500 μM SA treatment had no significant effect on the soluble sugar content. SA at 800 μM significantly decreased the vitamin C and soluble sugar content of Chinese chives (**Figures 3A,B**); however, there was no significant effect on the soluble protein content (**Figure 3C**). Compared with the control (0 μM), treatment with SA (150–800 μM) and MeJA significantly reduced the nitrate content of Chinese chive (**Figure 3D**).

Effect of Methyl Jasmonate and Salicylic Acid Treatments on Total Phenol and Flavonoid Content of Chinese Chive

The methyl jasmonate and salicylic acid treatments had significant effects on the total phenol and flavonoid contents of Chinese chive (**Figure 4**). Treatment with different concentrations of SA significantly increased the total phenol content (**Figure 4A**). After 150 μM SA treatment, the total phenol content significantly increased by 29% compared with the control (0 μM). However, treatment with different concentrations of MeJA significantly increased the total phenol content of Chinese chive (18.2%) at a concentration of 500 μM. Treatment with different concentrations of MeJA and SA significantly increased the flavonoid content of Chinese chive compared with the control (0 μM) (**Figure 4B**). The flavonoid

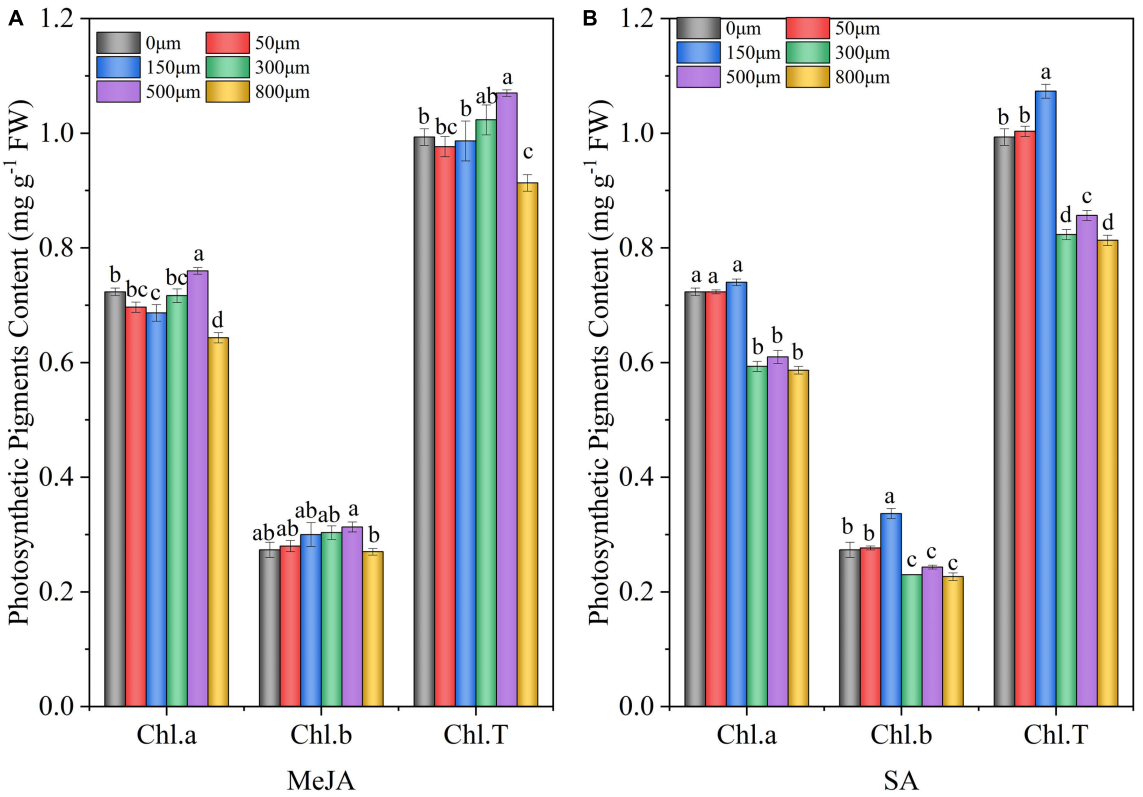

FIGURE 2 | Chlorophyll (Chl) Chl.a, Chl.b, and Chl.T contents of Chinese chives, as affected by MeJA **(A)** and SA **(B)** treatments. Data represent the mean ± SE (n = 3). Different lowercase letters indicate statistical significance by Duncan's multiple range test ($p < 0.05$).

content in Chinese chive was significantly increased by 133% and 70 after treatment with 500 μM MeJA and 150 μM SA.

Effect of Methyl Jasmonate and Salicylic Acid Treatments on Volatile Composition and Flavor Intensity of Chinese Chive

The 10 sensors of the electronic nose all responded to the volatile compounds of Chinese chive treated with different concentrations of MeJA and SA, and the responses of different sensors were differed (**Figures 5A,B**). The signal responses to the sensors were expressed by G/G0, which was defined as the ratio of the electrical conductivity of volatiles to that of pure air. The radar chart shows the response of the different sensors of the electronic nose to volatile substances in Chinese chive. In **Figure 5**, the relative resistivity (G/G0) values of the W5S and W2W sensors were higher than those of the other sensors, indicating that the volatile components of Chinese chive, such as nitrogen oxides, aromatics, and organic sulfides, were more sensitive to the sensor. As can be seen from the radar map, the contours of 500 μM MeJA and 50 μM SA were the largest. After treatment with different concentrations of MeJA and SA, the outline of the radar map gradually changed, indicating that the composition of volatile compounds in Chinese chives changed. In addition, the heat map showed an increase or decrease in volatile content after MeJA and SA treatments compared with the control (0 μM) treatment (**Figures 5C,D**). With the exception of W1C and W5S, the relative resistivity of the other eight sensors treated with 500 μM MeJA was increased compared with that of the control (0 μM) sensors, which indicated that treatment with 500 μM MeJA increased the amounts of most of the volatile components, such as sulfides, aromatics, and organic sulfides. Moreover, treatment with 50 and 150 μM SA increased the amounts of characteristic aromatic substances, such as aromatics and sulfides, compared with the control (0 μM).

The methyl jasmonate and salicylic acid treatments had a significant effect on the total flavor intensity (sulfur compounds) of Chinese chive, characterized by the pyruvate produced by alliinase (**Table 2**). Treatment with 500 μM MeJA and 50 and 150 μM SA significantly increased the enzymatic pyruvate content compared with the control (0 μM).

Classification Model of Volatile Composition of Chinese Chive Using Principal Component Analysis

The principal component analysis was used to study the volatile components of Chinese chives treated with MeJA and SA (**Figure 6**). The first and second principal components captured most of the variation within the different MeJA and SA concentrations. The sum of the first two principal components treated by MeJA reached 95.2%, of which PC1 and PC2 explained

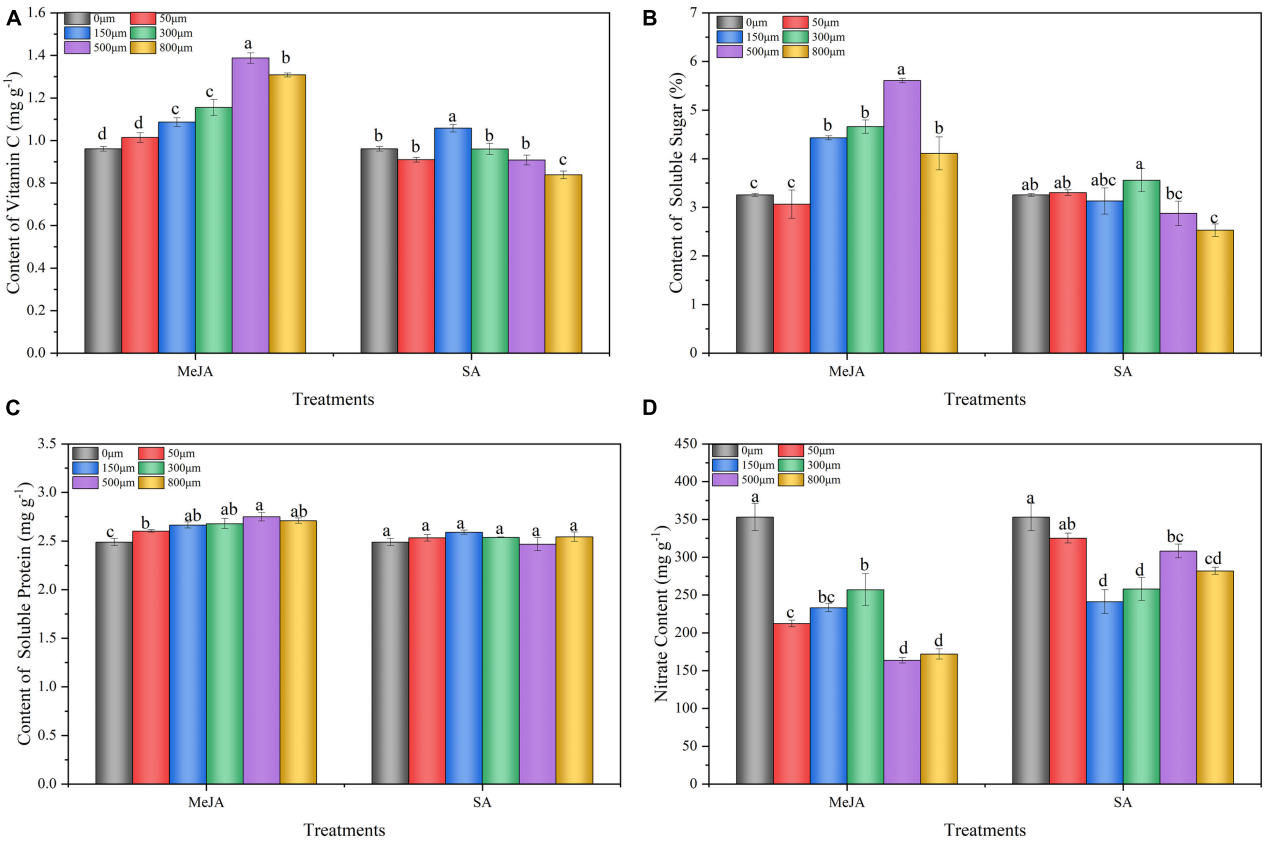

FIGURE 3 | Vitamin C **(A)**, soluble sugar **(B)**, soluble protein **(C)**, and nitrate **(D)** contents of Chinese chives as affected by MeJA and SA treatments. Data represent the mean ± SE (n = 3). Different lowercase letters indicate statistical significance by Duncan's multiple range test ($p < 0.05$).

56.7 and 38.5% of the total variance, respectively (**Figure 6A**). The sum of the first two principal components treated by SA reached 96.3%, of which PC1 and PC2 explained 83.5 and 12.8% of the total variance, respectively (**Figure 6B**). In addition, it can be seen from the loading plot that W1W and W5C had strong loadings with the first and second principal component and W3C and W2W had strong loadings with the first and second principal component and thus were used as representative factors reflecting the volatile components of Chinese chives treated with different concentrations of MeJA and SA, indicating these treatments have considerable effects on the sulfide, organic sulfides, and aromatic volatile components of Chinese chive.

Effect of Methyl Jasmonate and Salicylic Acid Treatments on the Antioxidant Activities of Chinese Chive

The methyl jasmonate and salicylic acid treatments had a significant effect on the antioxidant activity of Chinese chives (**Figure 7**). All antioxidant activity determination methods, such as DPPH radical scavenging activity (**Figure 7A**), FRAP (**Figure 7B**), and ABTS radical scavenging activity (**Figure 7C**), indicated significantly higher antioxidant activity in MeJA (150–500 μM) and SA (150 μM)-treated Chinese chives than in the control (0 μM). The highest scavenging capacity was recorded in Chinese chives treated with 500 μM MeJA and 150 μM SA. The scavenging ability of samples treated with 800 μM MeJA and 300–800 μM SA showed a downward trend.

Correlation Analysis and Principal Component Analysis

The correlation analysis of the parameters observed in this study showed that Chl.a had a significantly correlated with the Chl.T at $p < 0.01$ after MeJA and SA treatment, and Chl.b had a significantly correlated with soluble sugar and Chl.T at $p < 0.5$ (**Figures 8A,B**). DPPH had a significantly correlated with vitamin C and W1W after MeJA treatment ($p < 0.5$), and it had a significantly correlated with soluble sugar ($p < 0.01$); ABTS had a significantly correlated with FRAP and flavonoids ($p < 0.5$); soluble protein had a significantly correlated with flavonoids ($p < 0.01$); total phenols had a significantly correlated with flavonoids ($p < 0.5$) (**Figure 8A**); however, nitrate had a significantly negatively correlated with flavonoids and soluble proteins ($p < 0.5$). After SA treatment, the DPPH had a significantly correlated with vitamin C at $p < 0.5$; FRAP had a significantly correlated with soluble sugar and protein at $p < 0.5$; soluble protein had a significantly correlated with sugar and flavonoids at $p < 0.5$ (**Figure 8B**); however, nitrate had a

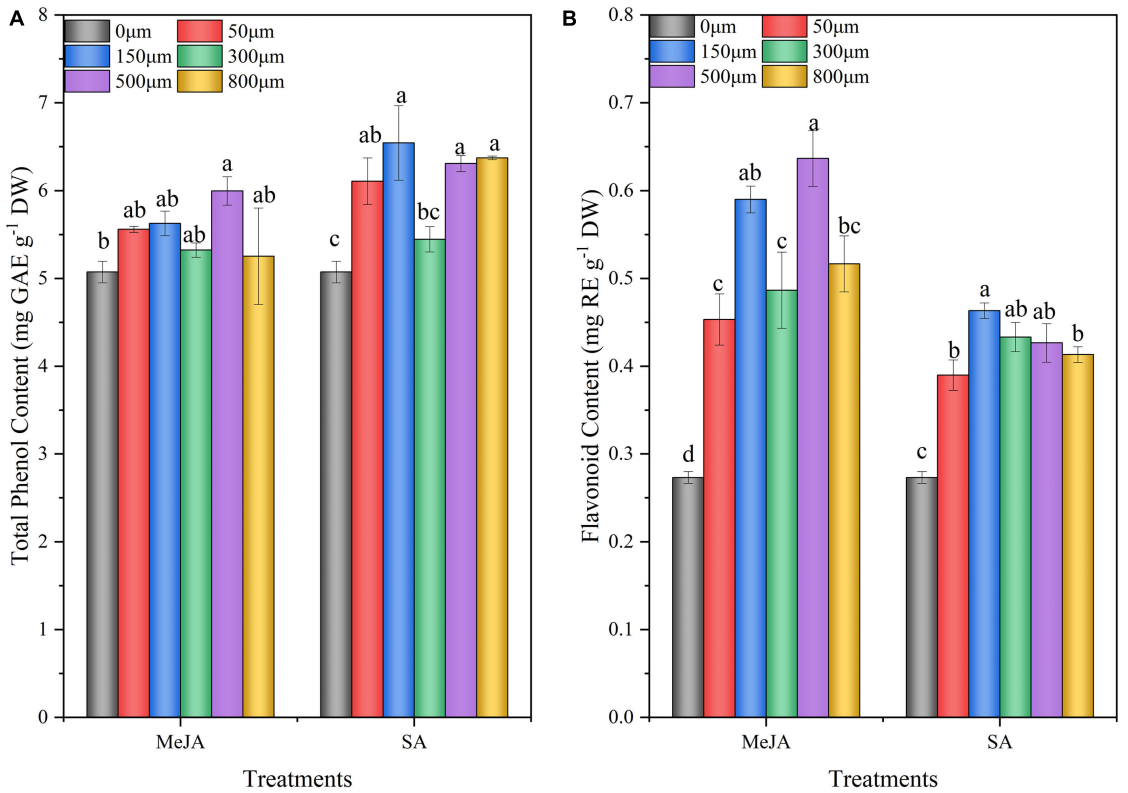

FIGURE 4 | Total phenol **(A)** and flavonoid **(B)** content of Chinese chives as affected by MeJA and SA treatments. Data represent the mean ± SE (n = 3). Different lowercase letters indicate statistical significance by Duncan's multiple range test ($p < 0.05$).

negatively correlated with flavonoids ($p < 0.5$), and negatively correlated with ABTS ($p < 0.01$).

The PCA of the parameters observed in this study is shown in **Figures 8C,D**. The different concentrations of MeJA and SA treatments and various parameters constituted the corresponding groups. The sum of the first two principal components treated with MeJA reached 68.3% (**Figure 8C**). PC1 accounted for 50.5% of the total variance. PC2 accounted for 17.8% of the total variance. The sum of the first two principal components treated by SA was 61.3% (**Figure 8D**). PC1 accounted for 38.6% of the total variance. PC2 accounted for 23% of the total variance. In addition, it can be seen from the loading plot that flavonoids and Chl.a showed strong loadings with the first and second principal component, soluble sugar and Chl.a showed strong loadings with the first and second principal component and thus can be used as representative factors to reflect the effects of different concentrations of MeJA and SA on the growth physiology, quality, volatile content, and antioxidant potential of Chinese chive (**Figures 8C,D**).

DISCUSSION

Exogenous application of MeJA and SA can induce different biochemical, morphological, and physiological responses of plants (Huang et al., 2017). In our study, we found that MeJA had no significant effect on the fresh and dry weights of Chinese chives (**Figures 1A,C**). Our results contradict the findings of Baek et al. (2021), who reported that MeJA treatment increased biomass in tomatoes. However, Kurowska et al. (2020) showed that the application of MeJA significantly reduced the first leaf sheath and dry leaf weight of barley seedlings. This suggests that different plants, tissue types, and developmental stages respond differently to MeJA. SA promoted plant growth by improving plant photosynthesis and significantly promoted the fresh and dry weight of shoot and root (Gururani et al., 2013). Our results showed that SA (150 μM) treatment significantly increased the fresh and dry weights of root, shoot, and plants (**Figures 1B,D**). Since the treatments were applied during the peak growth period of Chinese chive, the increase in fresh and dry weight could be attributed to the effect of SA on alleviating biotic and abiotic stresses in the plant, thus increasing net photosynthetic rate and productivity (Hasanuzzaman et al., 2017). In addition, we observed that both 800 μM MeJA and SA inhibited the growth of Chinese chive. This may be due to the effects of high concentrations of MeJA and SA on plants similar to abiotic stress, reducing plant photosynthesis and thus inhibits plant growth (Kang et al., 2012; Kurowska et al., 2020).

Among studies on the effects of JA on plant photosynthesis, the most controversial research is the effect on photosynthetic plant pigments (Shu et al., 2016). *Exogenous JA significantly inhibited photosynthesis in broccoli (*Brassica oleracea L.)

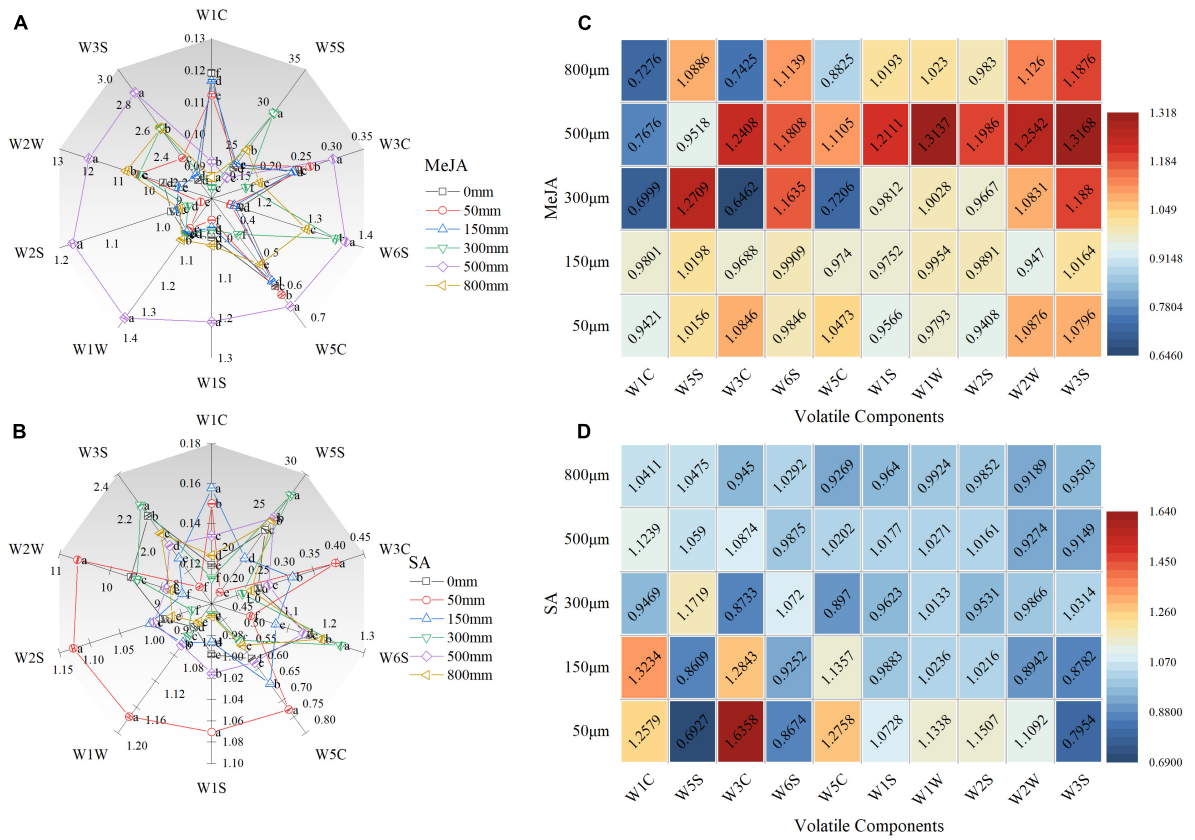

FIGURE 5 | Radar map of volatile components of Chinese chives as affected by MeJA **(A)** and SA **(B)**. The radar map is represented by the signal response value (G/G0) of the electronic nose sensor, and G/G0 is defined as the ratio of the electrical conductivity of volatile matter to that of pure air. The data were normalized to 0 mm concentration. The increase or decrease in the amounts of volatile components after each treatment is compared with that in the control (0 μM). The color code shows that different numbers of volatile components were detected, and the proportion changes are related to the control (0 μM) level **(C,D)**. Data represent the mean ± SE (n = 3). Different lowercase letters indicate statistical significance by Duncan's multiple range test ($p < 0.05$).

and *tomato*, but promoted *photosynthesis and chlorophyll accumulation in rapeseed (*Brassica napus L.*)* (Rahnamaie-Tajadod et al., 2017; Ding et al., 2018*)*. In the present study, we found that the total chlorophyll content after 500 μM MeJA treatment was significantly higher than that in the control (**Figure 2A**), *which was similar to that* reported by Ji et al. (2018) *on maize seedlings (*Zea mays *L.). In addition, exogenous application of JAs increased photosynthetic pigments in a dose-dependent manner, thereby increasing photosynthetic efficiency (*Sirhindi et al., 2020*). The same results were shown in our study, where chlorophyll increased with increasing MeJA concentration (50–500 μM).* Previous studies have shown that *SA application increased the chlorophyll content of wheat (*Triticum aestivum *L.)* (Singh and Usha, 2003*). Our results showed that treatment with 150 μM SA significantly increased Chl.b and Chl.*T content (**Figure 2B**), *which was similar to that* reported by Zhang et al. (2021). *However, the high concentrations of MeJA (800 μM) and SA (300–800 μM) significantly reduced the total chlorophyll content. This may be due to the* fact that the *high concentrations of MeJA and SA can activate genes related to chlorophyll catabolism, which is related to the degradation of chlorophyll* (Zhu et al., 2015). *In addition, chlorophyll is the most prominent natural pigment in green vegetables and has significant antioxidant activity* (Lanfer-Marquez et al., 2005*). The chlorophyll can also reflect the senescence of plants and the maturity, color, quality, and freshness of fruits and vegetables through changes in its structure* (Wang et al., 2005).

The nutritional properties of vegetables are not only protective compounds that maintain their quality, but also guarantee nutritional value (Mustafa et al., 2018b). The preharvest treatment of exogenous MeJA and SA simulated biological stress and increased phytochemical compounds in different crops (Ku and Juvik, 2013; Sariñana-Aldaco et al., 2020). Our results showed that the contents of vitamin C, soluble sugar, soluble protein, total phenol, and flavonoid in Chinese chives treated with MeJA (500 μM) preharvest were significantly higher than those in the control (**Figures 3A–C**, **4**), which was similar to the results of Min et al. (2021). The increase of total phenols and flavonoids in MeJA treatment may be due to the regulation of various physiological and metabolic processes, thus affecting the nutritional quality of crops. However, our results contradict the findings of Yamamoto et al. (2020), who reported that MeJA treatment significantly reduced flavonoids in citrus, indicating that MeJA has different regulation of bioactive substances in different crops, which is

TABLE 2 | Characteristic flavor of Chinese chives as affected by methyl jasmonate (MeJA) and salicylic acid (SA) treatments.

EPY (μg ml^{-1})	0 mm	50 mm	150 mm	300 mm	500 mm	800 mm
MeJA	16.5 ± 0.3d	29.9 ± 0.8a	23.3 ± 0.5b	24.3 ± 0.7b	32.0 ± 0.9a	20.5 ± 0.6c
SA	16.5 ± 0.3d	66.9 ± 0.4a	67.6 ± 0.5a	50.1 ± 1.7b	23.0 ± 0.5c	8.2 ± 0.3e

Data represent the mean ± SE (n = 3). Different lowercase letters indicate statistical significance by Duncan's multiple range test ($p < 0.05$).

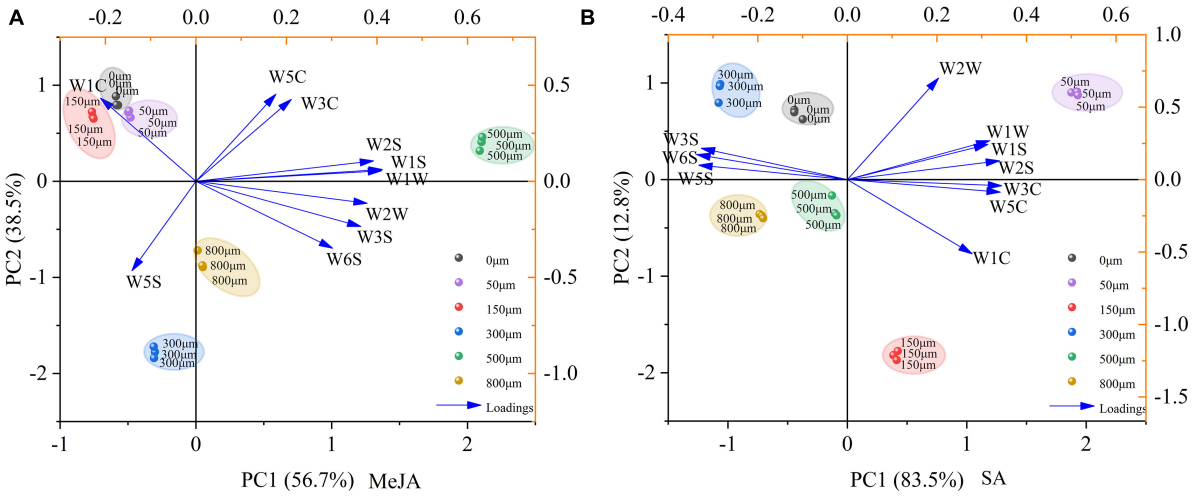

FIGURE 6 | Principal component analysis (PCA) of volatile composition of Chinese chives after MeJA **(A)** and SA **(B)** treatments for a score scatterplot and a loading plot. PCA was based on the ratio of the electrical conductivity of volatiles to that of pure air (G/G0) in response to 10 sensors as variables. PCA aims to solve multicollinearity among multiple covariables, represents the differences between samples, and provides information from electronic nose pattern recognition files.

worthy of further study. SA affects the phenylpropanoid pathway by inducing its key enzymes phenylalanine ammonia lyase and chalcone synthase, resulting in the accumulation of phenolic compounds (Ghasemzadeh et al., 2012). In the present study, we found that SA (150 μM) treatment significantly increased the content of vitamin C, total phenols, and flavonoids in Chinese chive (**Figures 3A**, **4**). Flavonoids are widely found in plants and play important roles in antioxidant, anticancer, antibacterial, and antimutagenic effects, and they are also one of the antioxidants produced by plants for their own survival (Treutter, 2006; Ghasemzadeh et al., 2010; Sharma et al., 2014). The MeJA and SA treatments increased the contents of total phenols and flavonoids in Chinese chives, thus improving the antioxidant activity of Chinese chives. In addition, we observed that both MeJA and SA treatments reduced the nitrate content of Chinese chives (**Figure 3D**). This may be because the reduction in nitrogen (N) uptake as an immediate consequence after MeJA treatment and the concomitant reactivation of endogenous N from leaves to roots, thereby reducing nitrate accumulation in leaves (Rossato et al., 2002). In general, preharvest MeJA (500 μM) and SA (150 μM) treatments improved the nutritional quality and safety quality of Chinese chives.

The MeJA treatment can trigger biosynthesis of volatile secondary metabolites and non-volatile secondary metabolites (Cheong and Choi, 2003). A sensor equipped with an electronic nose can simulate human olfactory factors and specific fingerprints of volatile tissues (Schaller et al., 1998; Benedetti et al., 2008). We detected volatile components of Chinese chives by electronic nose mainly nitrogen oxides (W5S), aromatics, and organic sulfides (W2W) (**Figures 5A,B**), which are more sensitive to the sensors of electronic nose and are characteristic aromatic substances of Chinese chives (Abbey et al., 2001). The volatile components of Chinese chives were dominated by methionine produced methyl sulfide, followed by Alliin produced allyl sulfide (Yabuki et al., 2010). The treatment with MeJA (500 μM) and SA (50 and 150 μM) increased the volatile composition of sulfur-containing compounds and enhanced the characteristic aromatic substances of Chinese chives. Meanwhile, we found that in addition to W1C and W5S, the relative resistivity of the other eight sensors treated with 500 μM MeJA was increased compared with that of the control sensors (**Figure 5C**), which indicated that treatment with this concentration of MeJA increased the content of most of the volatile components in Chinese chives, such as ammonia-based aromatic components (W3C), organic sulfides (W2W), hydrides (W6S), methyl groups (W1S), sulfides (W1W), alcohols, aldehydes, and ketones (W2S), short-chain alkane aromatic components (W5C), and long-chain alkanes (W3S). This may be because JA, as a lipid-based plant hormone, forms hydroperoxide through lipoxygenase pathway, and then oxidizes into short-chain aldehydes and ketones, increasing the hydride and aldehydes and ketones volatile components of Chinese chive (Li et al., 2010). Alcohols, aldehydes, and ketones have obvious odors (Tian et al., 2017), which may contribute greatly to the aroma of Chinese chive except aromatic hydrocarbons and sulfides. The aroma intensity of most long-chain alkanes is weak and contributes little to the aroma of food (Peng et al., 2014).

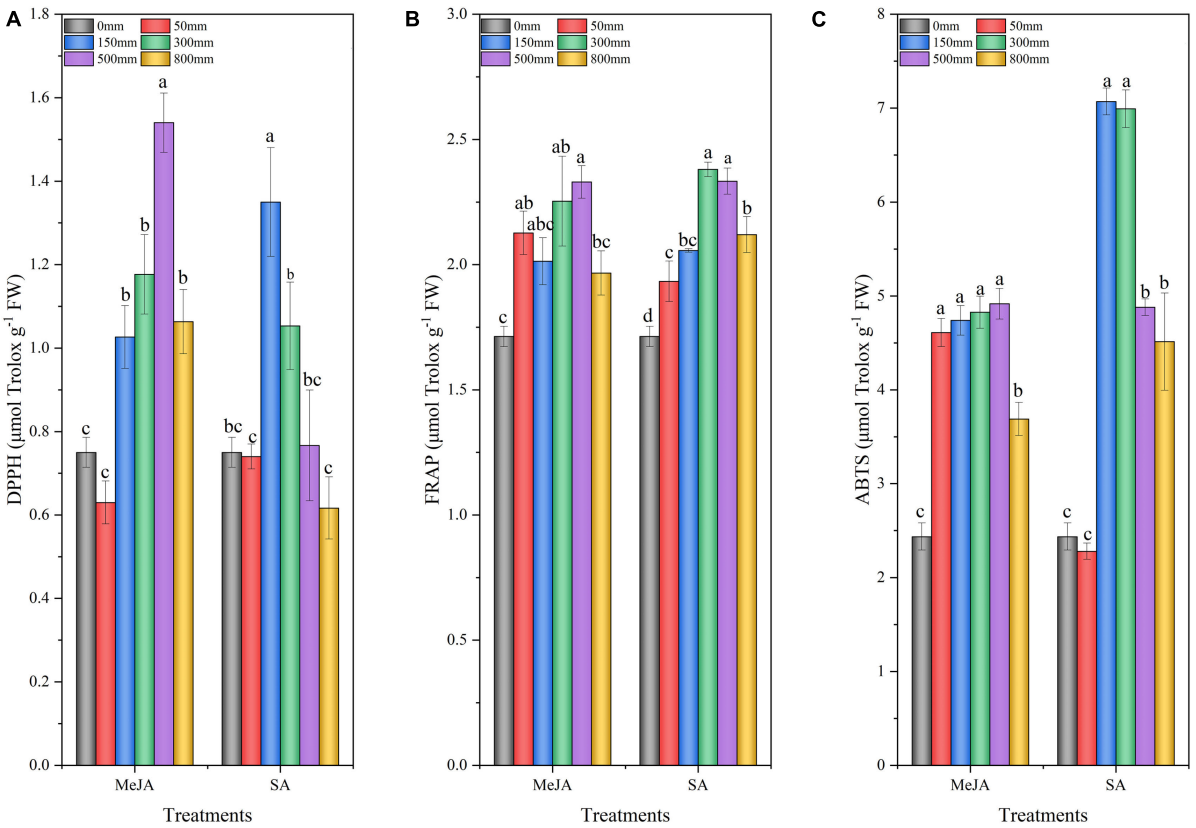

FIGURE 7 | The 2,2-diphenyl-1-picrylhydrazyl (DPPH) radical scavenging capacity **(A)**, ferric-reducing antioxidant power (FRAP) **(B)**, and Trolox-equivalent antioxidant capacity (ABTS) **(C)** of Chinese chives as affected by MeJA and SA treatments. Data represent the mean ± SE (n = 3). Different lowercase letters indicate statistical significance by Duncan's multiple range test ($p < 0.05$).

However, compared with the control, 500 μM MeJA treatment increased the content of long-chain alkanes, which requires further study to determine the contribution of long-chain alkanes to aroma. The loading plots further indicated that different concentrations of MeJA and SA treatment had considerable effects on the volatile components compared with the control, such as sulfide, aromatic components (ammonia), short-chain alkane aromatic components, methyls, alcohols, aldehydes and ketones, organic sulfides (**Figure 6**). In addition, we found that 500 μM MeJA and 150 μM SA significantly increased the enzymatic pyruvate content (**Table 2**), which was consistent with the results of electronic nose testing that increased the content of organic sulfur compounds, thereby improving the flavor intensity of Chinese chives.

Previous studies have shown an increase in plant antioxidant activity after application of MeJA (Wang et al., 2008; Szymanowska et al., 2015), and this was similarly observed for DPPH, FRAP, and ABTS activity of the Chinese chive with MeJA application in this study (**Figure 7**). The improvement of antioxidant capacity of plants is related to the increase of phenols and other bioactive substances (Flores et al., 2015). In this study, the increase in the content of bioactive substances such as total phenols and flavonoids may be responsible for the improved scavenging and reducing abilities of Chinese chives after MeJA (500 μM) and SA (150 μM) treatments. However, this contradicts the study that Mustafa et al. (2016) reduced the content of antioxidants by applying MeJA in carambola (*Averrhoa carambola*). This result indicates that the JA signal is involved in the balance of the redox reaction (Dong et al., 2010), which is worthy of further study. The antioxidant activities (DPPH, ABTS, and FRAP) after MeJA treatment had a significant correlation with organic sulfur compounds, vitamin C, flavonoids, and soluble sugars (**Figures 8A,B**). SA processing showed similar results. This further indicated that the improvement of antioxidant capacity of Chinese chive could be closely related to the increase in the content of bioactive substances. JA, MeJA, and SA are the most widely used elicitors that promote the production of more bioactive compounds in plants, which in turn improve the nutritional quality and antioxidant activity of plants (Baenas et al., 2014). PCA analysis showed that MeJA (500 μM) and SA (150 μM) positively regulate Chl.a, Chl.T, Chl.b, sulfides, total phenols, FRAP, DPPH, soluble sugar, ABTS, flavonoids, vitamin C, and soluble protein. In general, MeJA and SA enhance the bioactive substances content and antioxidant activity, thereby improving the medicinal value, postharvest quality, and preservation characteristics, thus increasing the commercial value of Chinese chives.

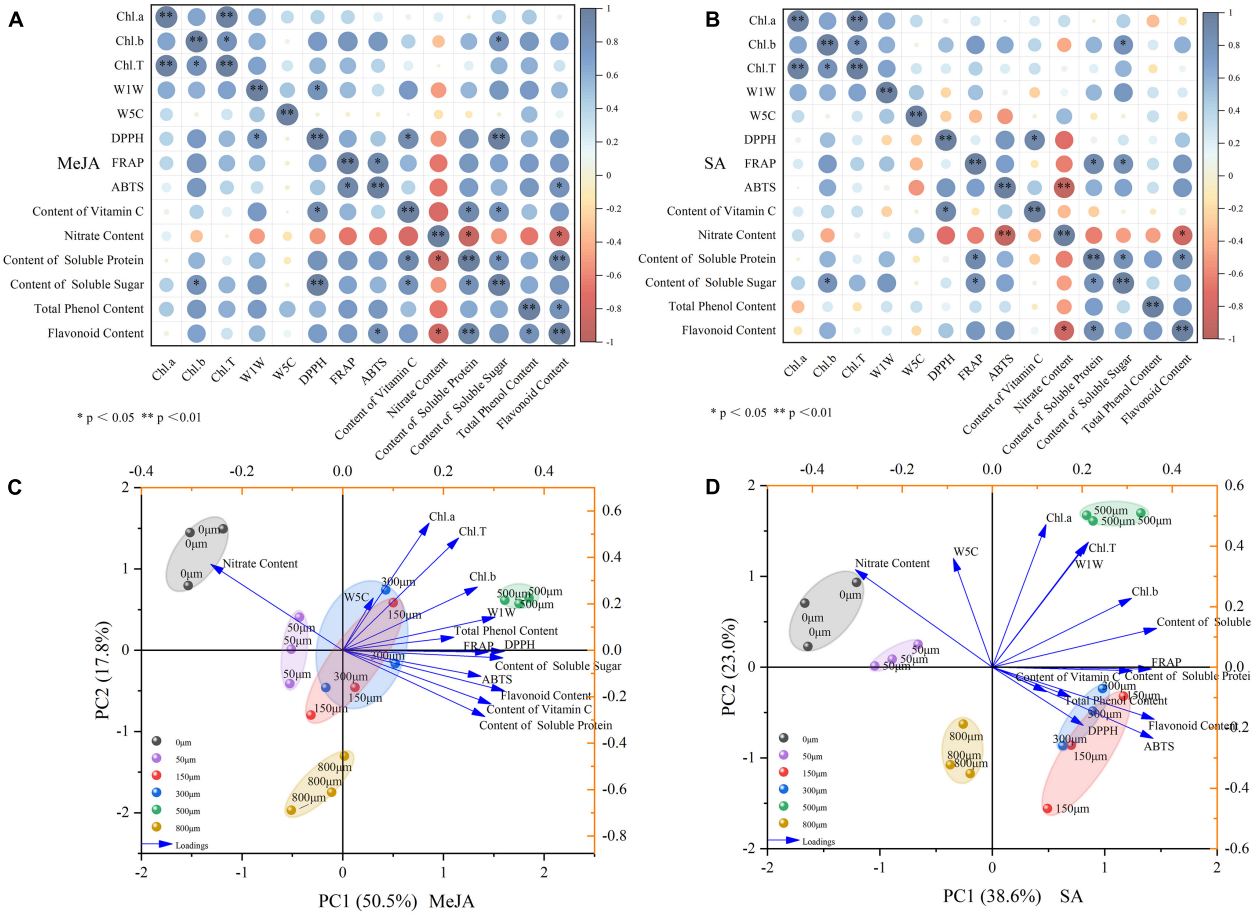

FIGURE 8 | The heat map shows the correlation analysis between the observed parameters processed by MeJA **(A)** and SA **(B)**. The score plot and loading plot show the PCA analysis of the observation parameters processed by MeJA **(C)** and SA **(D)**. Pearson correlation analysis and PCA was carried out with chlorophyll, soluble protein, soluble sugar, total phenols, flavonoids, antioxidant activity, and volatile components as variables. ** and ** denote correlation coefficients that are significant at $p < 0.05$ and 0.01 level, respectively.

CONCLUSION

Our results suggest that preharvest treatments with 500 μM MeJA and 150 μM SA significantly increased the content of total chlorophyll, soluble sugar, total phenols and flavonoids, volatile components, and antioxidant activity of Chinese chive. In addition, 500 μM MeJA and 150 μM SA significantly increased the soluble protein content, and the dry and fresh weight, respectively. Simultaneously, 500 μM MeJA and 150 μM SA significantly increased the enzymatic pyruvate content, effectively increased the amounts of sulfide and aromatic volatile components, and improved the characteristic flavor compounds of Chinese chive. In addition, the antioxidant activity was improved after preharvest treatment with 500 μM MeJA and 150 μM SA, which could improve the postharvest quality and preservation characteristics, and therefore enhance the commercial value. In conclusion, preharvest treatment with 500 μM MeJA and 150 μM SA could be the best option for improving the growth physiology, quality, antioxidant activity, and the flavor of Chinese chive.

DATA AVAILABILITY STATEMENT

The original contributions presented in the study are included in the article/supplementary material, further inquiries can be directed to the corresponding author/s.

AUTHOR CONTRIBUTIONS

CW, JZ, JX, and JY conceived and designed the experiments. CW, JZ, and YG analyzed the data. CW wrote the manuscript. CW, JZ, JLi, TN, and JLv were involved in the related discussion. JX, JZ, and BP helped to improve the quality of the manuscript. All authors have read and agreed to the published version of the manuscript.

FUNDING

This research was funded by the National Key Research and Development Program of China (2016YFD0201005), Special Fund for Technical System of Melon and Vegetable Industry of Gansu Province (GARS-GC-1), and Special Fund for Guiding Scientific and Technological Innovation and Development of Gansu Province (2018ZX-02), China.

REFERENCES

Abbey, L., Aked, J., and Joyce, D. C. (2001). Discrimination amongst Alliums using an electronic nose. *Ann. Appl. Biol.* 139, 337–342. doi: 10.1111/j.1744-7348.2001.tb00147.x

Ahmed, M., and Eun, J. B. (2017). Flavonoids in fruits and vegetables after thermal and nonthermal processing: A review. *Crit. Rev. Food Sci. Nutr.* 2017, 1–30. doi: 10.1080/10408398.2017.1353480

Arnon, D. I. (1949). Copper enzymes in isolated chloroplasts. Polyphenoloxidase in Beta vulgaris. *Plant Physiol.* 24:1. doi: 10.1104/pp.24.1.1

Arthy, S., Yasmeen, S., Sivakumar, M., and Asgar, A. (2018). Role of benzoic and salicylic acids in the immunization of oil palm seedlings-challenged by Ganoderma boninense. *Indust. Crops Prod.* 122, 358–365. doi: 10.1016/j.indcrop.2018.06.005

Arya, S. P., Mahajan, M., and Jain, P. (2000). Non-spectrophotometric methods for the determination of Vitamin C. *Anal. Chim. Acta* 2000:909. doi: 10.1016/s0003-2670 (00) 00909-0

Baek, M. W., Choi, H. R., Yun Jae, L., Kang, H.-M., Lee, O.-H., Jeong, C. S., et al. (2021). Preharvest Treatment of Methyl Jasmonate and Salicylic Acid Increase the Yield, Antioxidant Activity and GABA Content of Tomato. *Agronomy* 11:2293. doi: 10.3390/agronomy11112293

Baenas, N., Garcia-Viguera, C., and Moreno, D. A. (2014). Biotic Elicitors Effectively Increase the Glucosinolates Content in Brassicaceae Sprouts. *J. Agr. Food Chem.* 62, 1881–1889. doi: 10.1021/jf404876z

Benedetti, S., Buratti, S., Spinardi, A., Mannino, S., and Mignani, I. (2008). Electronic nose as a non-destructive tool to characterise peach cultivars and to monitor their ripening stage during shelf-life. *Postharvest Biol. Techno.* 47, 181–188. doi: 10.1016/j.postharvbio.2007.06.012

Bernaert, N., De Paepe, D., Bouten, C., De Clercq, H., Stewart, D., Van Bockstaele, E., et al. (2012). Antioxidant capacity, total phenolic and ascorbate content as a function of the genetic diversity of leek (Allium ampeloprasum var. porrum). *Food Chem.* 134, 669–677. doi: 10.1016/j.foodchem.2012.02.159

Block, E., Naganathan, S., Putman, D., and Zhao, S. H. (1992). Allium chemistry: HPLC analysis of thiosulfinates from onion, garlic, wild garlic (ramsoms), leek, scallion, shallot, elephant (great-headed) garlic, chive, and Chinese chive. Uniquely high allyl to methyl ratios in some garlic samples. *J. Agricult. Food Chem.* 40, 2418–2430. doi: 10.1021/jf00024a017

Bradford, M. M. (1976). A rapid and sensitive method for the quantitation of microgram quantities of protein utilizing the principle of protein-dye binding. *Anal. Biochem.* 72, 248–254. doi: 10.1016/0003-2697(76)90527-3

Cai, J. S., Zhu, Y. Y., Ma, R., Thakur, K., and Wei, Z. J. (2020). Effects of roasting level on physicochemical, sensory, and volatile profiles of soybeans using electronic nose and HS-SPME-GC-MS. *Food Chem.* 340:127880. doi: 10.1016/j.foodchem.2020.127880

Cataldo, D., Maroon, M., Schrader, L., and Youngs, V. (1975). Rapid colorimetric determination of nitrate in plant tissue by nitration of salicylic acid. *Comm. Soil Sci. Plant Anal.* 6, 71–80. doi: 10.1080/00103627509366547

Chang, C. C., Yang, M. H., Wen, H. M., and Chern, J. C. (2002). Estimation of Total Flavonoid Content in Propolis by Two Complementary Colorimetric Methods. *J. Food Drug Anal.* 10, 178–182. doi: 10.3168/jds.S0022-0302(02)74323-3

Cheong, J. J., and Choi, Y. D. (2003). Methyl jasmonate as a vital substance in plants. *Trends Genet.* 19, 409–413. doi: 10.1016/S0168-9525(03)00138-0

Delker, C., Stenzel, I., Hause, B., Miersch, O., and Wasternack, C. (2006). Jasmonate Biosynthesis in Arabidopsis thaliana - Enzymes, Products, Regulation. *Plant Biol.* 8, 297–306. doi: 10.1055/s-2006-923935

Ding, F., Wang, M., and Zhang, S. (2018). Sedoheptulose-1,7-Bisphosphatase is Involved in Methyl Jasmonate- and Dark-Induced Leaf Senescence in Tomato Plants. *Internat. J. Mole. Sci.* 2018:19. doi: 10.3390/ijms19113673

Donati, L., Ferretti, L., Fralliciardi, J., Rosciani, R., Valletta, A., Pasqua, G., et al. (2018). Stilbene biosynthesis and gene expression in response to methyl jasmonate and continuous light treatment in Vitis vinifera cv. Malvasia del Lazio and V. rupestris Du Lot cell cultures. *Physiol. Plant.* 2018:12813. doi: 10.1111/ppl.12813

Dong, J., Wan, G., and Liang, Z. (2010). Accumulation of salicylic acid-induced phenolic compounds and raised activities of secondary metabolic and antioxidative enzymes in Salvia miltiorrhiza cell cultures. *J. Biotechnol.* 148, 99–104. doi: 10.1016/j.jbiotec.2010.05.009

Fernando, D., La, P., and Moreno, G (2010). Effect of (-)and (+)-methyl jasmonate on the bioformation of aroma-active esters in strawberry fruits. *Eur. Food Res. Tech.* 231, 829–834. doi: 10.1007/s00217-010-1339-y

Flores, G., Blanch, G. P., and Luisa, R. (2015). Postharvest treatment with (-) and (+)-methyl jasmonate stimulates anthocyanin accumulation in grapes. *LWT - Food Sci. Tech.* 62, 807–812. doi: 10.1016/j.lwt.2014.12.033

Gao, Q., Li, X. B., Sun, J., Xia, E. D., Tang, F., Cao, H. Q., et al. (2018). Isolation and identification of new chemical constituents from Chinese chive (Allium tuberosum) and toxicological evaluation of raw and cooked Chinese chive. *Food Chem. Toxicol.* 112, 400–411. doi: 10.1016/j.fct.2017.02.011

Gbska, D., Guzek, D., Groele, B., and Gutkowska, K. (2020). Fruit and Vegetable Intake and Mental Health in Adults: A Systematic Review. *Nutrients* 12:12010115. doi: 10.3390/nu12010115

Ghasemzadeh, A., Jaafar, H., and Rahmat, A. (2010). Antioxidant Activities, Total Phenolics and Flavonoids Content in Two Varieties of Malaysia Young Ginger (Zingiber officinale Roscoe). *Molecules* 15:15064324. doi: 10.3390/molecules15064324

Ghasemzadeh, A., Jaafar, H. Z., and Karimi, E. (2012). Involvement of salicylic acid on antioxidant and anticancer properties, anthocyanin production and chalcone synthase activity in ginger (Zingiber officinale Roscoe) varieties. *Int. J. Mol. Sci.* 13, 14828–14844. doi: 10.3390/ijms131114828

Gururani, M. A., Upadhyaya, C. P., Baskar, V., Venkatesh, J., Nookaraju, A., and Park, S. W. (2013). Plant Growth-Promoting Rhizobacteria Enhance Abiotic Stress Tolerance in Solanum tuberosum Through Inducing Changes in the Expression of ROS-Scavenging Enzymes and Improved Photosynthetic Performance. *Journal of Plant Growth Regulation* 32, 245–258. doi: 10.1007/s00344-012-9292-6

Habibi, G. (2012). Exogenous salicylic acid alleviates oxidative damage of barley plants under drought stress. *Acta Biolog. Szegediensis* 56, 57–63.

Hand, M. J., Taffouo, V. D., Nouck, A. E., Nyemene, K., Brice, T., Meguekam, T. L., et al. (2017). Effects of Salt Stress on Plant Growth, Nutrient Partitioning, Chlorophyll Content, Leaf Relative Water Content, Accumulation of Osmolytes and Antioxidant Compounds in Pepper (Capsicum annuum L.) Cultivars. *Notul. Bot. Horti Agrobot. Cluj-Nap.* 45, 481–490. doi: 10.15835/nbha45210928

Hasanuzzaman, M., Nahar, K., Bhuiyan, T. F., Anee, T. I., and Fujita, M. (2017). *Salicylic Acid: An All-Rounder in Regulating Abiotic Stress Responses in Plants. Phytohormones - Signaling Mechanisms and Crosstalk in Plant Development and Stress Responses*. London: Intechopen, doi: 10.5772/intechopen.68213

Hong, J., Chen, T. T., Hu, P., Yang, J., and Wang, S. Y. (2014). Purification and characterization of an antioxidant peptide (GSQ) from Chinese leek (Allium tuberosum Rottler) seeds. *J. Funct. Foods* 10, 144–153. doi: 10.1016/j.jff.2014.05.014

Huang, H., Bei, L., Liangyu, L., and Susheng, S. (2017). Jasmonate action in plant growth and development. *J. Exp. Bot.* 2017, 1349–1359. doi: 10.1093/jxb/erw495

Huang, R., Xia, R., Lu, Y., Hu, L., and Xu, Y. (2010). Effect of pre-harvest salicylic acid spray treatment on post-harvest antioxidant in the pulp and peel of 'Cara cara' navel orange (Citrus sinenisis L. Osbeck). *J. Sci. Food Agricult.* 88, 229–236. doi: 10.1002/jsfa.3076

Ibrahim, D. S., Eissa, A. M., and Khalil, H. (2018). Alleviation of salinity stress by exogenous plant growth regulators in three citrus rootstocks. *Middle East J.* 2018:2018.

Ji, B., Li, Z., Gu, W., Li, J., and Wei, S. (2018). Methyl jasmonate pretreatment promotes the growth and photosynthesis of maize seedlings under saline

conditions by enhancing the antioxidant defense system. *Internat. J. Agricult. Biol.* 20, 1454–1462. doi: 10.17957/IJAB/15.0701

Jia, L. e., Ma, Y., Wang, D., Ji, Y., Xie, L., and Zhao, X. (2020). *Study on the Quality Change of Fresh-Cut Chinese Chive Chopped Pieces Northern Horticulture*, 468, 95–102. doi: 10.11973/bfyy.20200099

Jiangsu (1979). *New Medicinal College. The dictionary of Chinese herbal medicines*. Shanghai: Shanghai People's Publishing Press.

Jones, M. G. (2004). Biosynthesis of the flavour precursors of onion and garlic. *Journal of Exp. Bot.* 2004:1961. doi: 10.2337/diacare.22.12.1961

Kang, G., Li, G., Xu, W., Peng, X., Han, Q., Zhu, Y., et al. (2012). Proteomics Reveals the Effects of Salicylic Acid on Growth and Tolerance to Subsequent Drought Stress in Wheat. *J. Prot. Res.* 11:6066. doi: 10.1021/pr300728y

Kim, E. H., Kim, Y. S., Park, S. H., Koo, Y. J., Yang, D. C., Chung, Y. Y., et al. (2009). Methyl Jasmonate Reduces Grain Yield by Mediating Stress Signals to Alter Spikelet Development in Rice. *Plant Physiol.* 149, 1751–1760. doi: 10.1104/pp.108.134684

Ku, K. M., and Juvik, J. A. (2013). Environmental Stress and Methyl Jasmonate-mediated Changes in Flavonoid Concentrations and Antioxidant Activity in Broccoli Florets and Kale Leaf Tissues. *Hortscience* 48, 996–1002. doi: 10.21273/HORTSCI.48.8.996

Kurowska, M. M., Daszkowskagolec, A., Gajecka, M., Koscielniak, P., Bierza, W., and Szarejko, I. (2020). Methyl Jasmonate Affects Photosynthesis Efficiency, Expression of HvTIP Genes and Nitrogen Homeostasis in Barley. *Internat. J. Mole. Sci.* 21:4335. doi: 10.3390/ijms21124335

Lanfer-Marquez, U. M., Barros, R., and Sinnecker, P. (2005). Antioxidant activity of chlorophylls and their derivatives. *Food Res. Internat.* 38, 885–891. doi: 10.1016/j.foodres.2005.02.012

Leelarungrayub, N., Rattanapanone, V., Chanarat, N., and Gebicki, J. M. (2006). Quantitative evaluation of the antioxidant properties of garlic and shallot preparations. *Nutrition* 22, 266–274. doi: 10.1016/j.nut.2005.05.010

Li, Q., Li, D., and Li, D. (2010). The biosynthesis and regulation mechanism of jasmonic acid and methyl jasmonate. *Bull. Biotechnol.* 2010, 53–57.

Li, X., Zhang, L. P., Zhang, L., Yan, P., Ahammed, G., and Han, W. Y. (2019). Methyl Salicylate Enhances Flavonoid Biosynthesis in Tea Leaves by Stimulating the Phenylpropanoid Pathway. *Molecules* 24:24020362. doi: 10.3390/molecules24020362

Liu, N., Tong, J., Hu, M., Ji, Y., and Wu, Z. (2021). Transcriptome landscapes of multiple tissues highlight the genes involved in the flavor metabolic pathway in Chinese chive (Allium tuberosum). *Genomics* 113:5. doi: 10.1016/j.ygeno.2021.05.005

Liu, R. H. (2004). Potential synergy of phytochemicals in cancer prevention: mechanism of action. *J. Nutr.* 134, 3479S–3485S. doi: 10.1093/jn/134.12.3479S

Marjorie, R. D., Tomas, L., Liliana, C., Adriano, N. N., Jorge, R., Laura, J., et al. (2016). Methyl Jasmonate: An Alternative for Improving the Quality and Health Properties of Fresh Fruits. *Molecules* 21:21060567. doi: 10.3390/molecules21060567

Martínez-Esplá, A., Zapata, P. J., Valero, D., Martínez-Romero, D., Díaz-Mula, H. M., Serrano, M., et al. (2018). Preharvest treatments with salicylates enhance nutrient and antioxidant compounds in plum at harvest and after storage. *J. Sci. Food Agricult.* 2018:8770. doi: 10.1002/jsfa.8770

Masuda, H., and Mihara, S. (1988). Olfactive properties of alkylpyrazines and 3-substituted 2-alkylpyrazines. *J. Agricult. Food Chem.* 36, 584–587. doi: 10.1021/jf00081a044

Mau, J., Chen, C., and Hsieh, P. (2001). Antimicrobial effect of extracts from Chinese chive, cinnamon, and corni fructus. *J. Agric. Food Chem.* 49, 183–188. doi: 10.1021/jf000263c

Meir, S., Philosoph-Hadas, S., Lurie, S., Droby, S., Akerman, M., Zauberman, G., et al. (1996). Reduction of chilling injury in stored avocado, grapefruit, and bell pepper by methyl jasmonate. *Can. J. Bot.* 74, 870–874. doi: 10.1139/b96-108

Min, W. B., Han, R. C., Solomon, T., Jeong, C. S., and Tilahun, S. (2021). Preharvest Methyl Jasmonate Treatment Increased the Antioxidant Activity and Glucosinolate Contents of Hydroponically Grown Pak Choi. *Antioxidants* 10:131. doi: 10.3390/antiox10010131

Misra, R. C., Maiti, P., Chanotiya, C. S., Shanker, K., and Ghosh, S. (2014). Methyl jasmonate-elicited transcriptional responses and pentacyclic triterpene biosynthesis in sweet basil. *Plant Physiol.* 164:232884. doi: 10.1104/pp.113.232884

Miura, K., and Tada, Y. (2014). Regulation of water, salinity, and cold stress responses by salicylic acid. *Front. Plant Sci.* 5:4. doi: 10.3389/fpls.2014.00004

Mustafa, M. A., Ali, A., Seymour, G., and Tucker, G. (2016). Enhancing the antioxidant content of carambola (Averrhoa carambola) during cold storage and methyl jasmonate treatments. *Postharv. Biol. Tech.* 118, 79–86. doi: 10.1016/j.postharvbio.2016.03.021

Mustafa, M. A., Ali, A., Seymour, G., and Tucker, G. (2018a). Delayed pericarp hardening of cold stored mangosteen (Garcinia mangostana L.) upon pre-treatment with the stress hormones methyl jasmonate and salicylic acid. *Sci. Horticult.* 230, 107–116. doi: 10.1016/j.scienta.2017.11.017

Mustafa, M. A., Ali, A., Seymour, G., and Tucker, G. (2018b). Treatment of dragonfruit (Hylocereus polyrhizus) with salicylic acid and methyl jasmonate improves postharvest physico-chemical properties and antioxidant activity during cold storage. *Sci. Horticult.* 231, 89–96. doi: 10.1016/j.scienta.2017.09.041

Napal, G., Carpinella, M. C., and Palacios, S. M. (2009). Antifeedant activity of ethanolic extract from Flourensia oolepis and isolation of pinocembrin as its active principle compound. *Bioresour. Tech.* 99, 3669–3673. doi: 10.1016/j.biortech.2009.02.050

Nayak, B., Rui, H. L., and Tang, J. (2013). Effect of Processing on Phenolic Antioxidants of Fruits, Vegetables, and Grains—A Review. *Crit. Rev. Food Sci. Nut.* 55:654142. doi: 10.1080/10408398.2011.654142

Noreen, S., Sultan, M., Akhter, M. S., Shah, K. H., Ummara, U., Manzoor, H., et al. (2020). Foliar Fertigation of Ascorbic Acid and Zinc Improves Growth, Antioxidant Enzyme Activity and Harvest Index in Barley (Hordeum vulgare L.) Grown under Salt Stress - ScienceDirect. *Plant Physiol. Biochem.* 2020:7. doi: 10.1016/j.plaphy.2020.11.007

Peng, Z., Li, Y., Lian, S., Xie, Z., and Ye, H. (2014). Study on the aroma components of rice and glutinous rice. *Winemak. Sci. Tech.* 2014, 42–46. doi: 10.13746/j.njkj.2014.0291

Pérez, A., Sanz, C., Richardson, D. G., and Olías, J. (1993). Methyl jasmonate vapor promotes β-carotene synthesis and chlorophyll degradation in Golden Delicious apple peel. *J. Plant Growth Regulat.* 12, 163–167. doi: 10.1007/BF00189648

Rabinowitch, H., and Currah, L. (2002). Allium crop science: recent advances. *Cabi. Bookshop* 2, 159–220. doi: 10.1079/9780851995106.0000

Rahnamaie-Tajadod, R., Loke, K. K., Goh, H. H., and Noor, N. M. (2017). Differential Gene Expression Analysis in Polygonum minus Leaf upon 24 h of Methyl Jasmonate Elicitation. *Front. Plant Sci.* 1:109. doi: 10.3389/fpls.2017.00109

Rattanachaikunsopon, P., and Phumkhachorn, P. (2009). Shallot (Allium ascalonicum L.) oil: Diallyl sulfide content and antimicrobial activity against food-borne pathogenic bacteria. *Afr. J. Microbiol. Res.* 3:80482. doi: 10.1271/bbb.80482

Rose, P., Whiteman, M., Moore, P. K., and Zhu, Y. Z. (2005). Bioactive S-alk(en)yl cysteine sulfoxide metabolites in the genus Allium: the chemistry of potential therapeutic agents. *Nat. Prod. Rep.* 22, 351–368. doi: 10.1039/b417639c

Rossato, L., Macduff, J. H., Laine, P., Le Deunff, E., and Ourry, A. (2002). Nitrogen storage and remobilization in Brassica napus L. during the growth cycle: effects of methyl jasmonate on nitrate uptake, senescence, growth, and VSP accumulation. *J. Exp. Bot.* 53, 1131–1141. doi: 10.1093/jexbot/53.371.1131

Saniewski, M., and Czapski, J. (1983). The effect of methyl jasmonate on lycopene and β-carotene accumulation in ripening red tomatoes. *Experientia* 39, 1373–1374. doi: 10.1007/BF01990110

Sariñana-Aldaco, O., Sánchez-Chávez, E., Troyo-Diéguez, E., Tapia-Vargas, L. M., Díaz-Pérez, J. C., and Preciado-Rangel, P. (2020). Foliar Aspersion of Salicylic Acid Improves Nutraceutical Quality and Fruit Yield in Tomato. *Agriculture* 10:482. doi: 10.3390/agriculture10100482

Schaller, E., Bosset, J. O., and Escher, F. (1998). 'Electronic Noses' and Their Application to Food. *LWT - Food Sci. Tech.* 31, 305–316. doi: 10.1006/fstl.1998.0376

Se, A., Mr, A., Mjg, A., Ms, B., Gm, B., Dv, A., et al. (2020). Enhancing antioxidant systems by preharvest treatments with methyl jasmonate and salicylic acid leads to maintain lemon quality during cold storage. *Food Chem.* 338:128044. doi: 10.1016/j.foodchem.2020.128044

Serna-Escolano, V., Valverde, J. M., García-Pastor, M., Valero, D., Castillo, S., Guillén, F., et al. (2019). Pre-harvest methyl jasmonate treatments increase

antioxidant systems in lemon fruit without affecting yield or other fruit quality parameters. *J. Sci. Food Agricult.* 2019:9746. doi: 10.1002/jsfa.9746

Sharma, K., Assefa, A. D., Kim, S., Ko, E. Y., Lee, E. T., and Park, S. W. (2014). Evaluation of total phenolics, flavonoids and antioxidant activity of 18 Korean onion cultivars: a comparative study. *J. Sci. Food Agricult.* 94, 1521–1529. doi: 10.1002/jsfa.6450

Sheard, L. B., Xu, T., Mao, H., Withers, J., Ben-Nissan, G., Hinds, T. R., et al. (2010). Jasmonate perception by inositol-phosphate-potentiated COI1–JAZ co-receptor. *Nature* 2010:9430. doi: 10.1038/nature09430

Shi, J., Wang, J., Lv, H., Peng, Q., Schreiner, M., Baldermann, S., et al. (2021). Integrated proteomic and metabolomic analyses reveal the importance of aroma precursor accumulation and storage in methyl jasmonate-primed tea leaves. *Hortic Res.* 8:95. doi: 10.1038/s41438-021-00528-9

Shu, S., Tang, Y., Yuan, Y., Sun, J., Zhong, M., and Guo, S. (2016). The role of 24-epibrassinolide in the regulation of photosynthetic characteristics and nitrogen metabolism of tomato seedlings under a combined low temperature and weak light stress. *Plant Physiol. Biochem.* 107, 344–353. doi: 10.1016/j.plaphy.2016.06.021

Singh, B., and Usha, K. (2003). Salicylic acid induced physiological and biochemical changes in wheat seedlings under water stress. *Plant Growth Regulat.* 39, 137–141. doi: 10.1023/A:1022556103536

Sirhindi, G., Mushtaq, R., Gill, S. S., Sharma, P., Abd Allah, E. F., and Ahmad, P. (2020). Jasmonic acid and methyl jasmonate modulate growth, photosynthetic activity and expression of photosystem II subunit genes in Brassica oleracea L. *Scient. Rep.* 10:14. doi: 10.1038/s41598-020-65309-1

Soppelsa, S., Kelderer, M., Casera, C., Bassi, M., and Andreotti, C. (2018). Use of Biostimulants for Organic Apple Production: Effects on Tree Growth, Yield, and Fruit Quality at Harvest and During Storage. *Frontiers in Plant Science* 9:1342. doi: 10.3389/fpls.2018.01342

Szymanowska, U., Zotek, U., Kara, M., and Baraniak, B. (2015). Anti-inflammatory and antioxidative activity of anthocyanins from purple basil leaves induced by selected abiotic elicitors. *Food Chem.* 172, 71–77. doi: 10.1016/j.foodchem.2014.09.043

Tang, X., Olatunji, O. J., Zhou, Y., and Hou, X. (2017). In vitro and in vivo aphrodisiac properties of the seed extract from Allium tuberosum on corpus cavernosum smooth muscle relaxation and sexual behavior parameters in male Wistar rats. *BMC Compl. Altern Med.* 17:510. doi: 10.1186/s12906-017-2008-5

Tian, H., Zhang, Y., Wu, Y., Qin, L., Chen, C., Xiao, L., et al. (2017). Using Gas Chromatography-Mass Spectrometry and Electronic Nose to Identify the Aroma Components of Chicken Essence Seasoning. *Food Sci.* 2017, 191–197. doi: 10.7506/spkx1002-6630-201702031

Treutter, D. (2006). Significance of flavonoids in plant resistance: a review. Environmental Chemistry Letters. *Environ. Chem. Lett.* 4, 147–157. doi: 10.1007/s10311-006-0068-8

Wall, M. M., and Corgan, J. N. (1992). Relationship between pyruvate analysis and flavor perception for onion pungency determination. *Hortsci. Publ. Am. Soc. Sci.* 27:223846. doi: 10.1007/BF00223846

Wang, Q., Chen, J., Stamps, R. H., and Li, Y. (2005). Correlation of Visual Quality Grading and SPAD Reading of Green-Leaved Foliage Plants. *J. Plant Nutr.* 28, 1215–1225. doi: 10.1081/PLN-200063255

Wang, S. Y., Bowman, L., and Min, D. (2008). Methyl jasmonate enhances antioxidant activity and flavonoid content in blackberries (Rubus sp.) and promotes antiproliferation of human cancer cells. *Food Chem.* 107, 1261–1269. doi: 10.1016/j.foodchem.2007.09.065

Wen, C. F., Dong, A. W., Li, G. Z., Shu, L., and Yong, L. (2005). Determination of Total Sugar and Reducing Sugar in Viola Philippicassp Munda W. Becker by Anthrone Colorimetry. *Guangzh. Food Sci. Tech.* 2005:44. doi: 10.3969/j.issn.1673-9078.2005.03.044

Wolucka, B. A., Goossens, A., and Inzé, D. (2005). Methyl jasmonate stimulates the de novo biosynthesis of vitamin C in plant cell suspensions. *J. Exp. Bot.* 56, 2527–2538. doi: 10.1093/jxb/eri246

Yabuki, Y., Mukaida, Y., Saito, Y., Oshima, K., Takahashi, T., Muroi, E., et al. (2010). Characterisation of volatile sulphur-containing compounds generated in crushed leaves of Chinese chive (Allium tuberosum Rottler). *Food Chem.* 120, 343–348. doi: 10.1016/j.foodchem.2009.11.028

Yamamoto, R., Ma, G., Zhang, L., Hirai, M., and Kato, M. (2020). Effects of Salicylic Acid and Methyl Jasmonate Treatments on Flavonoid and Carotenoid Accumulation in the Juice Sacs of Satsuma Mandarin In Vitro. *Appl. Sci.* 10:8916. doi: 10.3390/app10248916

Zeng, Y., Li, Y., Yang, J., Pu, X., Du, J., Yang, X., et al. (2017). Therapeutic Role of Functional Components in Alliums for Preventive Chronic Disease in Human Being. *Evid. Based Compl. Altern. Med.* 2017:9402849. doi: 10.1155/2017/9402849

Zhang, Q., Li, D., Wang, Q., Song, X., Wang, Y., Yang, X., et al. (2021). Exogenous Salicylic Acid Improves Chilling Tolerance in Maize Seedlings by Improving Plant Growth and Physiological Characteristics. *Agronomy* 11:1341. doi: 10.3390/agronomy11071341

Zhang, W. N., Zhang, H. L., Lu, C. Q., Luo, J. P., and Zha, X. Q. (2016). A new kinetic model of ultrasound-assisted extraction of polysaccharides from Chinese chive. *Food Chem.* 212, 274–281. doi: 10.1016/j.foodchem.2016.05.144

Zhang, X., Sheng, J., Li, F., Meng, D., and Lin, S. (2012). Methyl jasmonate alters arginine catabolism and improves postharvest chilling tolerance in cherry tomato fruit. *Postharv. Biol. Tech.* 64, 160–167. doi: 10.1016/j.postharvbio.2011.07.006

Zhu, X., Chen, J., Xie, Z., Gao, J., Ren, G., Gao, S., et al. (2015). Jasmonic acid promotes degreening via MYC2/3/4- and ANAC019/055/072-mediated regulation of major chlorophyll catabolic genes. *Plant* J. 2015:13030. doi: 10.1111/tpj.13030

Ziosi, V., Bonghi, C., Bregoli, A. M., Trainotti, L., Biondi, S., Sutthiwal, S., et al. (2008). Jasmonate-induced transcriptional changes suggest a negative interference with the ripening syndrome in peach fruit. *J. Exp. Bot.* 59, 563–573. doi: 10.1093/jxb/erm331

Conflict of Interest: The authors declare that the research was conducted in the absence of any commercial or financial relationships that could be construed as a potential conflict of interest.

Publisher's Note: All claims expressed in this article are solely those of the authors and do not necessarily represent those of their affiliated organizations, or those of the publisher, the editors and the reviewers. Any product that may be evaluated in this article, or claim that may be made by its manufacturer, is not guaranteed or endorsed by the publisher.

frontiers in Plant Science

ORIGINAL RESEARCH
published: 03 February 2022
doi: 10.3389/fpls.2021.808711

Integration of Phenomics and Metabolomics Datasets Reveals Different Mode of Action of Biostimulants Based on Protein Hydrolysates in *Lactuca sativa* L. and *Solanum lycopersicum* L. Under Salinity

Mirella Sorrentino[1,2], Klára Panzarová[1], Ioannis Spyroglou[3], Lukáš Spíchal[4], Valentina Buffagni[5], Paola Ganugi[5], Youssef Rouphael[2], Giuseppe Colla[6], Luigi Lucini[5] and Nuria De Diego[4]**

[1] Photon Systems Instruments (PSI), spol. S.r.o., Drásov, Czechia, [2] Department of Agricultural Sciences, University of Naples Federico II, Portici, Italy, [3] Plant Sciences Core Facility, Central European Institute of Technology, Masaryk University, Brno, Czechia, [4] Centre of the Region Haná for Biotechnological and Agricultural Research, Czech Advanced Technology and Research Institute, Palacký University, Olomouc, Czechia, [5] Department for Sustainable Food Process, DiSTAS, Università Cattolica del Sacro Cuore, Piacenza, Italy, [6] Department of Agriculture and Forest Sciences, University of Tuscia, Viterbo, Italy

OPEN ACCESS

Edited by:
Marco Landi,
University of Pisa, Italy

Reviewed by:
Antonio Ferrante,
University of Milan, Italy
Anket Sharma,
University of Maryland, United States

***Correspondence:**
Luigi Lucini
luigi.lucini@unicatt.it
Nuria De Diego
nuria.de@upol.cz

Specialty section:
This article was submitted to Crop and Product Physiology, a section of the journal Frontiers in Plant Science

Received: 03 November 2021
Accepted: 21 December 2021
Published: 03 February 2022

Citation:
Sorrentino M, Panzarová K, Spyroglou I, Spíchal L, Buffagni V, Ganugi P, Rouphael Y, Colla G, Lucini L and De Diego N (2022) Integration of Phenomics and Metabolomics Datasets Reveals Different Mode of Action of Biostimulants Based on Protein Hydrolysates in Lactuca sativa L. and Solanum lycopersicum L. Under Salinity. Front. Plant Sci. 12:808711. doi: 10.3389/fpls.2021.808711

Plant phenomics is becoming a common tool employed to characterize the mode of action of biostimulants. A combination of this technique with other omics such as metabolomics can offer a deeper understanding of a biostimulant effect *in planta*. However, the most challenging part then is the data analysis and the interpretation of the omics datasets. In this work, we present an example of how different tools, based on multivariate statistical analysis, can help to simplify the omics data and extract the relevant information. We demonstrate this by studying the effect of protein hydrolysate (PH)-based biostimulants derived from different natural sources in lettuce and tomato plants grown in controlled conditions and under salinity. The biostimulants induced different phenotypic and metabolomic responses in both crops. In general, they improved growth and photosynthesis performance under control and salt stress conditions, with better performance in lettuce. To identify the most significant traits for each treatment, a random forest classifier was used. Using this approach, we found out that, in lettuce, biomass-related parameters were the most relevant traits to evaluate the biostimulant mode of action, with a better response mainly connected to plant hormone regulation. However, in tomatoes, the relevant traits were related to chlorophyll fluorescence parameters in combination with certain antistress metabolites that benefit

the electron transport chain, such as 4-hydroxycoumarin and vitamin K1 (phylloquinone). Altogether, we show that to go further in the understanding of the use of biostimulants as plant growth promotors and/or stress alleviators, it is highly beneficial to integrate more advanced statistical tools to deal with the huge datasets obtained from the -omics to extract the relevant information.

Keywords: vegetal-based protein hydrolysates, multivariate statistical analysis, metabolomics, secondary metabolism, salt stress, *Lactuca sativa* L., *Solanum lycopersicum* L., high-throughput phenotyping

INTRODUCTION

Changes in climate patterns are dramatically influencing some agricultural areas with special impact in arid, semi-arid, and coastal agricultural areas (Corwin, 2020). Soil salinity already covers 20% of total cultivated and 33% of the irrigated agricultural lands worldwide, and is expected to increase at a faster rate than now by the year 2050 (Mukhopadhyay et al., 2021). The high salt concentration in the soil reduces plant growth and, hence, yield in two ways: increasing the osmotic potential of the soil solution, making it harder for the plant to extract water, and accumulating into the root and shoot tissue at a concentration that can be toxic for the plant (Munns and Tester, 2008). The extent of salinity damage to the fitness and final yield of the crop can change according to the species. For example, lettuce (*Lactuca sativa* L.) reduces plant growth and yield under salt stress conditions (Moncada et al., 2020). However, tomatoes (*Solanum lycopersicum* L.) can maintain the fruit yield and increase their quality under moderate stress (Meza et al., 2020), whereas severe salt stress reduced tomato growth and provoked severe damages, especially in young seedlings (Ali et al., 2021).

To reduce the yield loss connected to salinity, scientists are moving toward the selection of more tolerant genotypes through breeding, genetic engineering, and marker-assisted selection (MAS) (Munns and James, 2000; Yamaguchi and Blumwald, 2005). However, these methods are expensive, time-consuming, and, in the case of genetic engineering, received with suspicion by the general public (Yamaguchi and Blumwald, 2005; Halford and Shewry, 2000). A more sustainable alternative is represented by the use of protein hydrolysates (PHs), a class of non-microbial plant biostimulants obtained from the partial hydrolysis of protein sources of plant or animal origin (Colla and Rouphael, 2015). Many works from the last years have enlightened the effects of PHs as stress alleviators on different crops growing in saline conditions (Van Oosten et al., 2017; Dell'Aversana et al., 2020; Di Mola et al., 2021). Nonetheless, it is important to remember that the effects of the PHs on crops can vary with the plant species or varieties, the time of the application, and the dose (Lisiecka et al., 2011).

Before a new potential PH-based biostimulant is put on the market, it is essential to test its effects in multiple conditions and on different crops. High-throughput automated platforms for plant phenotyping have proven to improve and speed up the biostimulant testing process (Rouphael et al., 2018). Different sensors can be implemented in high-throughput phenotyping platforms, allowing the user to monitor the effects of the PH applications on many morpho-physiological traits throughout the entire crop life cycle (Paul et al., 2019a,b). As a result, we can define in which crop, developmental stage, and dosage the application is recommended. Besides, a deeper physiological study allows the characterisation of their mode of action. This information can be used for further possible applications.

The use of other -omic approaches, such as metabolomics, allows studying the biostimulant effect in a more complex manner, supporting, and integrating the phenomics data to better understand the biochemical processes activated in the plants by the biostimulants application. However, the data analysis and interpretation of the complex omics datasets can become another challenging bottleneck. Here, we investigated the mechanism of action of a set of 7 PHs in lettuce and tomato subjected to early and late salinity stress. We hypothesise that salinity will reduce plant growth and change the physiology of the plant in tomato and lettuce. However, the PH application will ameliorate the salt negative effect in both plant species. Besides, a deep data analysis using advanced statistical tools will allow us (i) to understand better the effect of the PHs on two species, lettuce and tomato, selected for their economic importance, their distinct architecture, and purpose, and their different sensitivity to salinity stress, (ii) to evaluate the biological translation from the results obtained in PH-primed Arabidopsis grown under salt stress (Sorrentino et al., 2021) to other crops under similar growing conditions, and (iii) to demonstrate the necessity of the use of statistical approaches to simplify complex omic datasets allowing identification of the traits relevant for the understanding of a biostimulant mechanism of action.

MATERIALS AND METHODS

Plant Material and Growing Conditions

Seeds of *Lactuca sativa* L. var. capitata (Salanova cv Aquino) and *Solanum lycopersicum* L. cv MicroTom were sown in 250 ml pots filled with 235 g of a mixture of sieved peat (Substrate 2, Klasmann-Deilmann GmbH, Geeste, Germany) and river sand in 1:1 proportion. All the pots were watered up to 55% of the soil relative water content (SRWC). The water holding capacity of the substrate was calculated as described by Junker et al. (2015). The covered pots were stratified at 4°C in the dark for two days. After that, the pots were moved to a climate-controlled growth chamber (FS-WI, Photon Systems Instruments, Czechia) under long-day conditions (16 h light/8 h dark). The climate conditions in the growth chamber were set at 21/19°C for day/night temperature with 60% relative humidity (RH) and

120 μmol m^{-2} s^{-1} cool-white LED (6,500 K) and 5.5 μmol m^{-2} s^{-1} far-red LED (735 nm) lighting. These conditions were kept constant throughout the entire experiment. The pots were kept covered with a plastic lid for the first 24 h to maintain the soil moisture before it was removed.

Selection of the Plants

Eight days after lettuce stratification and ten days after tomato stratification, when most of the germinated seedlings had reached the 2-true-leaf stage, a top view RGB picture of all plantlets was taken using the top view RGB2 camera in the PlantScreen^{TM} Compact system (Photon Systems Instruments, Brno, Czechia). The plants with areas between the 1st and the 4th quartile of the normal distribution of the population were used for the experiment. In the tomato experiment, each variant counted 6 plantlets as biological replicates, with a total of 96 plants. For the lettuce experiment, each variant counted 8 plantlets as biological replicates, with a total of 128 plants.

High-Throughput Phenotyping

To investigate the effects of PHs application on the morpho-physiological parameters of lettuce and tomato grown under salt stress conditions, trays containing two pots with one plantlet each were automatically transported within PlantScreen^{TM} Compact System on conveyor belts between the light-isolated imaging cabinets, weighing and watering station, and the dark/light acclimation chamber. The trays were measured thrice a week, ending with 10 phenotyping rounds distributed in 21 days for lettuce and 24 days for tomato (**Figure 1**), with the starting point before the first salt application (Day of Phenotyping 1, henceforth defined as DoP 1). The phenotyping protocol used was the same for both crops. Physiological measurements [Chlorophyll Fluorescence (ChlF) and Thermal Imaging (IR)], being sensitive to circadian rhythm regulation mechanisms (Cano-Ramirez and Dodd, 2018), were always performed in the morning. A single round measuring protocol consisted of an initial 15 min light-adaptation period inside the acclimation chamber, followed by IR, and red-green-blue (RGB) top view imaging (RGB2). Next, 15 min dark-adaptation was applied, followed by chlorophyll fluorescence kinetic imaging, RGB side view imaging (RGB1), and weighing and watering (**Figure 1A**). Due to the limited capacity of the phenotyping system for the lettuce experiment, the trays were divided into 3 blocks with 16 trays each. The measuring round for one block lasted for 2 h and 45 min. The PlantScreen^{TM} Analyser software (PSI, Czechia) was used to automatically process, re-analyse, and export the data.

Biostimulants Selection and Application

Seven PHs obtained by enzymatic hydrolysis of vegetal-derived proteins were selected from a batch of eleven PHs that were previously screened for their mode of action (Sorrentino et al., 2021) and used for the experiment. They included PHs from different plant sources belonging to the botanical families of Fabaceae (O), Malvaceae (C), Brassicaceae (F), Solanaceae (B), and Graminaceae (P), and two commercial products [Trainer® (D) and Vegamin® (H)], commercialised by Hello Nature Inc. (former Italpollina) (Anderson, IN, United States) and used as positive controls. The PH was obtained through enzymatic hydrolysis of the dry biomass and was then analysed for their total nitrogen and carbon content. For a detailed description of the procedure, see Sorrentino et al. (2021) and Ceccarelli et al. (2021).

Biostimulants were applied to leaves through spraying once a week, using only distilled water for the controls or the given PH in a concentration of 3 mL/L for the treated plants. A total of 4 foliar applications of PHs were done throughout the experiment (**Figure 1B**). The first spraying (priming) was performed one day before the first salt application. Two hours before and after the spraying of the plants, the relative humidity in the growing chamber (FS-WI) was increased up to 80% to promote the stomata opening.

Due to the limited capacity of the phenotyping platform, the lettuce experiment was divided into two rounds, each consisting of 64 plants. The substances B, C, and F were tested in the first round, while D, H, O, and P in the second round.

Watering and Salt Treatment

All the pots were watered after each phenotyping round at up to 55% SRWC with a modified Hoagland solution [0.36 g/L Ca $(NO_3)_2$, 0.1 g/L KH_2PO_4, 0.80 g/L KNO_3, 0.04 g/L NH_4NO_3, 0.13 g/L $MgSO_4$, and 0.01 mg/L of MIKROM fertilizer (Cifo Srl, S.Giorgio di Piano (BO), Italy)] using the Weighing and Watering station in the PlantScreen^{TM} Compact. The solution was freshly prepared before each watering round and the pH was adjusted to a value of 5.7.

Starting from 2 weeks after stratification, the plants belonging to the stress group were subjected twice a week to salt application, ending with 6 applications for both crops (**Figure 1B**). In the lettuce assay, our objective was to reach a concentration of 40 mM NaCl in the soil, corresponding to moderate stress (Freitas et al., 2019). To avoid osmotic shock to the plants and NaCl accumulation in the soil, all the pots were first watered up to 55% of SRWC with plain nutrient solution. The plants belonging to the stress group were then given 40 ml each of an 80 mM NaCl solution (8.7 mS/cm). In the end, after a couple of hours from the salt application, all the plants were watered again of up to 100% of their SRWC to create drainage of the solution from the pot. The same setup was used with tomato, but in this case, the salt solution increased to 120 mM NaCl (14 mS/cm) to reach a concentration of around 60 mM NaCl in the pot, corresponding to moderate salt stress (Meza et al., 2020; **Figure 1B**). The two NaCl concentrations used in the experiments were the result of several preliminary tests conducted on both crops (data not shown).

Imaging Protocol and Data Analysis

Red-Green-Blue Imaging

Red green blue imaging using high-resolution top-view and side-view RGB cameras and an optimised image segmentation algorithm for automated analysis were used to calculate the number of plant-specific pixels throughout the whole experiment. The RGB images were processed as described by Awlia et al. (2016) and Paul et al. (2019a,b).

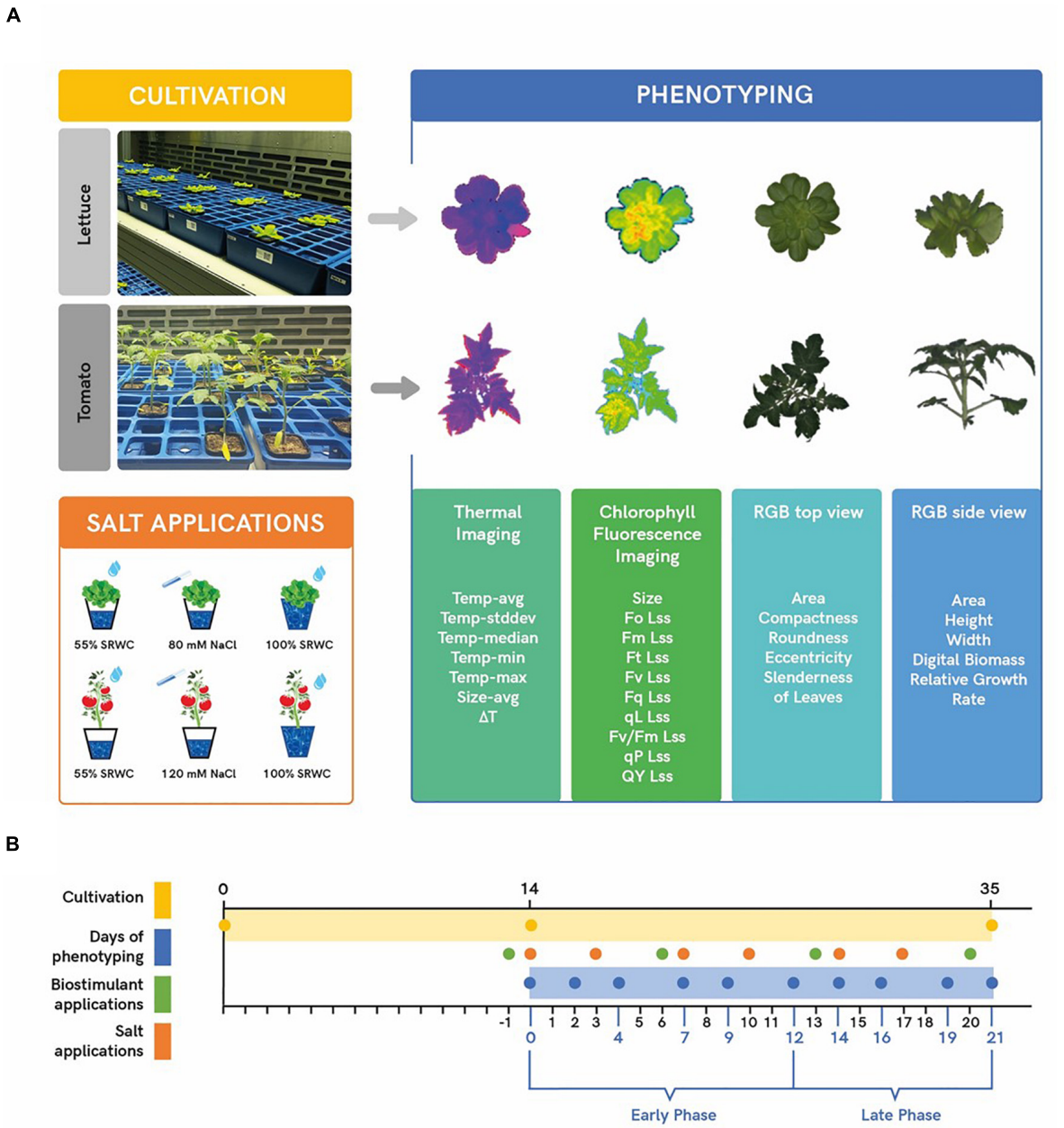

FIGURE 1 | Scheme of plant cultivation and phenotyping protocol. Plants were manually transferred from the cultivation chamber to PlantScreen^{TM} Compact System for imaging using four different sensors (thermal camera, chlorophyll fluorescence, and top and side RGB). The resulting false-color, segmented images, and list of extracted parameters obtained from the sensors are shown **(A)**. Timeline of plant cultivation (yellow bar) and phenotyping protocol (blue bar). Green dots show four-time points of the foliar application for the selected biostimulants and the orange dots show six timepoints for the salt treatment **(B)**.

Projected shoot area (PSA) from the top (PSA_{top}) and the side view (PSA_{side}) was used to calculate the Digital Biomass (DM) of each plant (Rahaman et al., 2017):

$$\sqrt{PSA_{side}^2 \times PSA_{top}}$$

Digital Biomass, corresponding to the approximate volume, was then used to calculate the Relative Growth Rate (RGR), where T_1 and T_2 indicate the time interval (days), while DM_1 and DM_2 indicate the corresponding digital biomass:

$$(\ln\ DM_2 - \ln DM_1)/(T_2 - T_1)$$

Relative growth rate (RGR) was calculated twice during the experiment: from DoP 0 to DoP 12 (**Early Phase**) for both crops, and from DoP 12 to DoP 21 for lettuce plants, or to DoP 24 for tomato plants (**Late Phase**).

Chlorophyll Fluorescence Imaging

To assess the effects of salt stress and biostimulants application on the photosynthetic performance of the plants, ChlF measurements were acquired using an enhanced version of the FluorCam FC-800MF pulse amplitude modulated (PAM) chlorophyll fluorometer incorporated into the PlantScreen^{TM} Compact System (for more details, see Henley, 1993). After 15 min of dark adaptation, the light curve protocol, as described in Awlia et al. (2016), was used to quantify the rate of photosynthesis at different photon irradiances (Rascher et al., 2000). Four actinic light irradiances [Lss (Light steady-state) 1: 180 μmol m^{-2} s^{-1}; Lss2: 480 μmol m^{-2} s^{-1}; Lss3; 780 μmol m^{-2} s^{-1} and Lss4: 1,080 μmol m^{-2} s^{-1}] with a duration of 60 s were used to quantify the rate of photosynthesis. The raw data were automatically processed using the PlantScreen^{TM} Analyser software (PSI, Brno, Czechia). From the measured fluorescence transient states, the basic ChlF parameters were derived (i.e., F0, Fm, Ft, and Fv), which were used to calculate a range of parameters characterizing the plant photosynthetic performance (i.e., Fv/Fm, Fv′/Fm′, NPQ, and ΦPSII). We chose to evaluate the parameters obtained after the exposure of the plants to the light of intensity 480 μmol m^{-2} s^{-1} (Lss2) since they provide the highest discriminative power between control and stress plants.

Thermal Imaging

To determine the leaf temperature of the plants, we used the thermal imaging unit implemented into the PlantScreen^{TM} Compact system, which allows assessing the canopy temperature from the top view. The thermal imaging unit incorporated in the PlantScreen^{TM} Compact System consists of a light-isolated box with one top view camera mounted on a static frame and a temperature sensor to increase contrast for the image-processing step. The imaged area is 440 mm × 340 mm (height × width). To assess the Spatio-temporal variations in temperature over plant surface, we used an FLIR A615 thermal camera with 45o lenses and a resolution of 640 × 480 pixels and high-speed infrared windowing option and <50 mK thermal sensitivity (FLIR Systems Inc., Boston, MA, United States). The canopy temperature of each plant was automatically extracted with PlantScreen^{TM} Analyser software (PSI, Brno, Czechia) by mask application, background subtraction, and pixel-by-pixel integration of values across the entire plant surface area.

To minimize the influence of the differences in environmental conditions and image acquisition timing among individual plants, the average canopy temperature of each plant (T_{avg}) was normalised with the actual temperature inside the Thermal Imaging box and expressed as canopy temperature depression or δT (°C) (Hou et al., 2019).

Untargeted Metabolomic Analysis

At the end of the experiment, at DoP 21 and 24 in lettuce and tomato, respectively, the third true leaf of each plant was harvested and freeze-dried. The material from control plants and plants treated with the 7 PHs was used for the metabolomic analysis. Lyophilised plant material (50 mg for lettuce and 250 mg for tomato) was extracted in twenty volumes (w/v) of methanol/water solution (70:30, v/v), acidified with 0.1% formic acid by Ultra-Turrax (Polytron PT, City, Switzerland), centrifuged, and then filtered through a 0.22 μm membrane as previously reported (Paul et al., 2019a,b). Untargeted metabolomics was performed using a 6,550 iFunnel quadrupole-time-of-flight mass spectrometer and a 1,200 series ultra-high-pressure liquid chromatographic system (UHPLC-ESI/QTOF-MS) from Agilent Technologies (Santa Clara, CA, United States) as previously described (Miras-Moreno et al., 2021). Briefly, 6 μL were injected and a reverse-phase chromatography was applied under a water-acetonitrile gradient elution (6 to 94% acetonitrile in 33 min). The mass spectrometer worked in positive ionisation (ESI+) and in SCAN mode for the acquisition of accurate masses ranging from 100 to 1,200 m/z. Four replicates were analysed for each treatment and samples were randomly sequenced. Quality Controls (QCs) were prepared by pooling all the extracts and were analysed throughout the chromatographic sequence using the same chromatographic conditions as samples but were acquired in data-dependent MS/MS mode (1Hz, 50–1,200m/z, 12 precursors per cycle) at different collision energies (10, 20, and 40eV).

Agilent Profinder B.07 (Agilent Technologies) software was used for mass (5-ppm tolerance), retention time (0.05min maximum shift) alignment, and for processing all the mass features from UHPLC-ESI/QTOF-MS raw data. The combination of monoisotopic mass, isotopes accurate spacing, and isotope ratio was used for annotation using the PlantCyc 12.6 database (Plant Metabolic Network)[1], as previously reported (Pretali et al., 2016; Schläpfer et al., 2017). Only those compounds identified in 75% of the replications within at least one treatment were retained. Thereafter, MS/MS confirmations from QCs were carried out using the software MS-DIAL 4.24 (Tsugawa et al., 2015), formerly using MS/MS experimental spectra available in the software (Mass Bank of North America), and then using MS-Finder *in silico* fragmentation (Tsugawa et al., 2016). The annotation process corresponded to level 2 of confidence as set out in the COSMOS Metabolomics Standards Initiative (Salek et al., 2015).

Statistical Analysis

For the phenotyping data, statistical differences between treatments and time points were determined by Mixed model analysis (McCulloch and Searle, 2000; Boisgontier and Cheval, 2016) and multiple pairwise comparisons using *post hoc* Tukey's test (*P*-value <0.05). The statistical analysis was implemented in R studio (R GUI 4.0.3) using the "lmer" and "emmeans" packages (R Core Team, 2014; Bates et al., 2015; Russell, 2020). Then, to define the specificities of each crop and their response to the foliar application with PHs, and to go further in the mode of action, hierarchical clustering was applied with the use of "Ward's" linkage method to find similarities between crops, growth conditions, and the best and worse performed biostimulant and to identify clusters (Saxena et al., 2017). Finally, random forest classification was also applied to identify the significant variables for the treatment classification (Qi, 2012).

[1]http://www.plantcyc.org

Concerning metabolomics, the software Agilent Mass Profiler Professional B.12.06 (from Agilent Technologies, Santa Clara, CA, United States) was used for data normalisation and baselining (Mimmo et al., 2017). Then, unsupervised hierarchical cluster analysis (HCA) based on fold-change heatmaps (Squared Euclidean distance) was used to naively describe patterns across treatments. Thereafter, supervised multivariate statistics were performed in SIMCA 13 (Umetrics, Malmo, Sweden), where orthogonal projection to latent structures discriminant analysis (OPLS-DA) was carried out. Each supervised model (separate models for tomato and lettuce, and then a comprehensive model for salt-stressed versus control plants), was validated by CV-ANOVA, checked for overfitting by permutation testing (N = 200), and then inspected for goodness-of-fit (R2Y) and prediction ability (Q2Y). After that, variable importance in projection (VIP) ranking was used to identify the most discriminant compounds in each OPLS-DA model. Finally, ANOVA (P-value <0.01, Bonferroni multiple testing correction) and fold-change (FC) analysis (FC $\geq$ 1.3) were combined into Volcano Plots, and differential compounds were imported into the Omic Viewer Pathway Tool of PlantCyc (Stanford, CA, United States) software (Caspi et al., 2013) for biochemical interpretations.

RESULTS

Development of the Experimental Protocol for Salt and Biostimulants Applications

To effectively characterise the outcome of biostimulants applications on lettuce and tomato performance in the early vegetative growth phase, we first optimised the experimental protocol for plant cultivation, mild-salt stress application, and the stress response quantification. The crops were analysed in independent experiments as they are very diverse in their tolerance to salinity, and two different concentrations of NaCl in the nutrient solution were used to water the plants as described in Materials and Methods (**Figure 1**). Lettuce and tomato plants were grown for 35 and 39 days, respectively, and this period corresponded to the complete head maturation in lettuce and the beginning of the flowering stage in tomatoes.

The PHs were applied *via* foliar spraying with solutions of 3 mL/L each (**Figure 1**; Di Mola et al., 2019a,b). The morpho-physiological traits of the plants were quantified dynamically throughout the trial to monitor their growth performance and physiological status. As a result, we could clearly distinguish two periods in the experiment, an early and late phase, in which the response of the plants to the salt stress and to the interaction with the biostimulants applications were diverse. It is well-known that plants respond to salt stress in two phases (Ugena et al., 2018): a rapid and osmotic phase, described here as the early phase (DoP 0-12), and a slower ionic phase due to the ion toxicity, referred to as the late phase (DoP 12-21 in lettuce or DoP 12-24 in tomato) (**Figure 2**).

Lettuce and Tomato Plants Have Different Physiological Responses to Mild Salinity

In lettuce, salt stress reduced plant growth in the later phase of the experiment after 4 salt applications (after DoP 14) (**Figures 2A1,A2**), and the reduction was similar in the lettuce plants from the first and second trials with 35 and 29% lower digital biomass (DB) than their correspondent controls, respectively (**Supplementary Figures 1A1,B1**). We further assessed other morphological parameters, such as roundness,

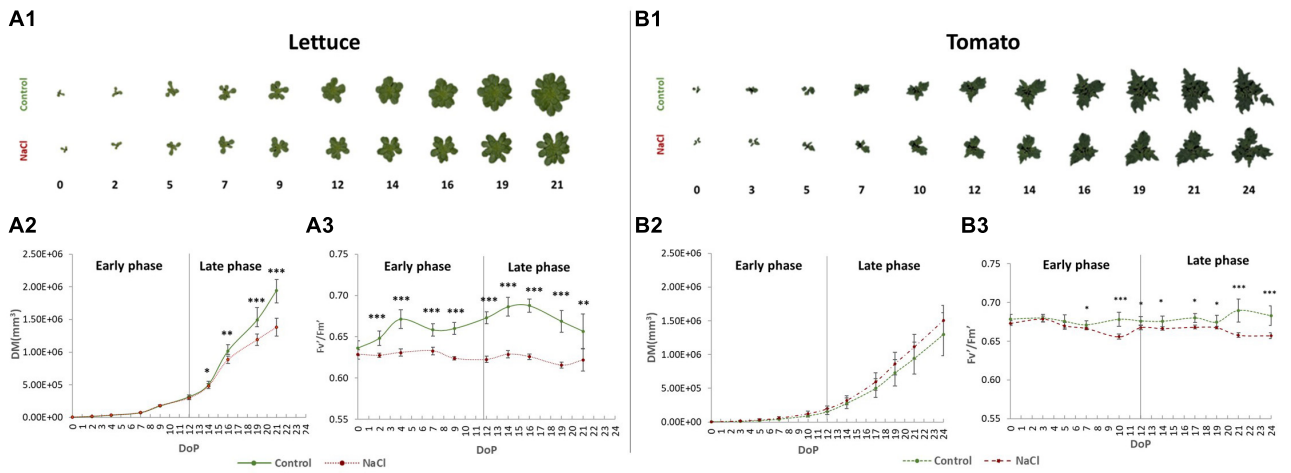

FIGURE 2 | Salinity response in tomato and lettuce plants. The RGB top view colour-segmented images of lettuce **(A1)** and tomato **(B1)** control and salinity-stressed plants over the time-course of the experiment. Digital biomass (DB) of the lettuce **(A2)** and tomato **(B2)** plants. The maximum quantum efficiency of photosystem II in the light-adapted state (Fl′/Fm′) for lettuce [full line, **(A3)**] and tomato [dashed line, **(B3)**] plants. Values represent the average of 8 (lettuce) and 6 (tomato) biological replicates per treatment, error bars represent standard deviation. The significant differences between control and salt treatment are indicated with *, **, and *** for p-values below 0.05, 0.01, and 0.001, respectively. Data and images shown are from the 1st round of the lettuce experiment.

compactness, and slenderness of the leaves (SOL), showing that they did not differ between the rounds, but differed between the controls and salt-stressed plants in the late phase, with the less compact, round, and more SOL in the stressed lettuce (**Figure 2A1** and **Supplementary Figures 1A,B**).

The photosynthetic performance of the plants during the development and with the progression of the salt stress was also affected (**Figure 2A3** and **Supplementary Figures 1C,D**). In the two rounds that were analysed, the most significant differences were observed in the late phase between the controls and the NaCl-treated lettuce plants. We showed that the maximum quantum yield of PSII photochemistry for the light-adapted (Fv′/Fm′) state and PSII operating efficiency (ΦPSII) were significantly reduced in the stressed plants, whereas the non-photochemical quenching (NPQ) was increased compared to the controls (**Figure 2A3** and **Supplementary Figures 1C,D**). Altogether, our data demonstrate that in lettuce, only the late phase of salt stress imposition (after DoP12) was important to detect the differences in growth and in fluorescence-related parameters between treatments.

In tomato plants, the growth of the plant was not affected by the mild salt stress (**Figures 2B1,B2**). The remaining morphological parameters did not show differences between control and salt stress, except for the higher slenderness of the leaves (SOL) in salt-stressed plants during the transition from the early to late phase (**Supplementary Figures 2A1–A4**). Regarding the physiology, however, there were significant differences in several fluorescence-related parameters at the end of the early phase and late phase of the salt stress (**Figure 2B3** and **Supplementary Figure 2B**). In salt-stressed tomatoes, we observed a significant reduction in Fv′/Fm′ and ΦPSII, and increased NPQ values compared to the controls.

Protein Hydrolysates Specifically Improve Growth Performance of Lettuce Plants

In the following step, we analysed how the foliar application of selected PHs could modify the responses observed in salt-stressed and non-stressed plants. In lettuce plants, the substance P increased the DB at the late phase of stress after 3 foliar applications under both growth conditions (DoP13) (**Figures 3A1,A2**, **Supplementary Figure 3B1**, and **Supplementary Tables 1A,B**). The substances D and H also improved the DB, but only when plants were grown under salt stress conditions. Other morphological traits, such as roundness, compactness, or SOL, did not change (**Supplementary Figures 3A2–A4,B1–B4** and **Supplementary Tables 1A,B**). Similarly, the foliar application with substance P increased the RGR of the plants in the early phase under control conditions (**Figures 3A1,A2** and **Supplementary Figures 6A1,A2**). Other PHs did not modify the RGR of the plants compared to their respective controls (salt or control) in both the early and late phases. Interestingly, application of the PHs increased the final biomass (**Supplementary Figures 6B,C**), especially the dry weight of the aerial part of the plants when the substances B, C, F, and P were applied to plants grown under control and salt stress conditions, or when the substance O was applied under control conditions.

The application of biostimulants had a mild impact on the photosynthetic performance of the lettuce plants both under control and salt stress conditions. We showed that the plants treated with the substances P and H increased Fv′/Fm′ and ΦPSII values both under control and stress conditions, while we observed reduced NPQ levels along with the experiment (**Figures 3A1,A2**, **Supplementary Figures 3C,D, 4C,D**, and **Supplementary Table 2A**).

In tomato plants, the application of PHs did not have any effect on the morphological traits; the differences in DB, RGR, and fresh and dry weight were only due to the growth conditions. Digital biomass (DB), along with the fresh weights of the plants, were similar in PH-treated plants and control plants during both phases of the experiment (**Figures 3B1,B2**, **Supplementary Figures 5A,B, 7**, and **Supplementary Table 1C**). Similarly, no significant improvement of the photosynthetic efficiency of the plants was observed in tomato plants sprayed with PHs in any growth conditions (**Figures 3B1,B2**, **Supplementary Figures 5C,D**, and **Supplementary Table 2C**).

We have further analysed the impact of PHs applications on the leaf surface temperature profile of both crops using thermal image analysis. The salt stress significantly increased the temperature of the leaf surface in lettuce but not in tomato plants (**Supplementary Figure 8**). Similarly, the changes of the temperature by the application with biostimulants were more visible in lettuce than in tomato plants. We showed that the lettuce plants treated with the substances C and F had a significantly reduced surface temperature when grown both under control and stress conditions (**Figures 3A1,A2**, **Supplementary Figures 8A,B**, and **Supplementary Table 3A**). In tomatoes, the biostimulants reduced the temperature of the leaf surface after the first application in plants that were under control and salt stress conditions. However, in the late phase, they increased the temperature over the respective control in almost all the cases (**Supplementary Figure 8C** and **Supplementary Table 3A**).

Investigating the Mode of Action of the Protein Hydrolysates Through the Plant Biostimulant Characterisation Index

To simplify the results and to identify the specific mode of action of the 7 PHs, we used the Plant Biostimulant Characterisation (PBC) index as described previously (Ugena et al., 2018; Sorrentino et al., 2021). For the calculation of the PBC indexes, we selected the five traits (DB, RGR, Fv′/Fm′, ΦPSII, and ΔT) that provided the highest discriminative power between the different treatments (**Supplementary Tables 1–3**). The PBC indexes for the Early Phase (from DoP 0 to 12) and the Late Phase (from DoP 12 to 21 in lettuce or from DoP 12 to 24 in tomato) were calculated independently since we could observe different responses of the plants treated with the 7 PHs in the two phases. To determine the index value, the log2 of the ratio between the biostimulant treated plants and untreated ones was determined for each crop and growth conditions, and then represented

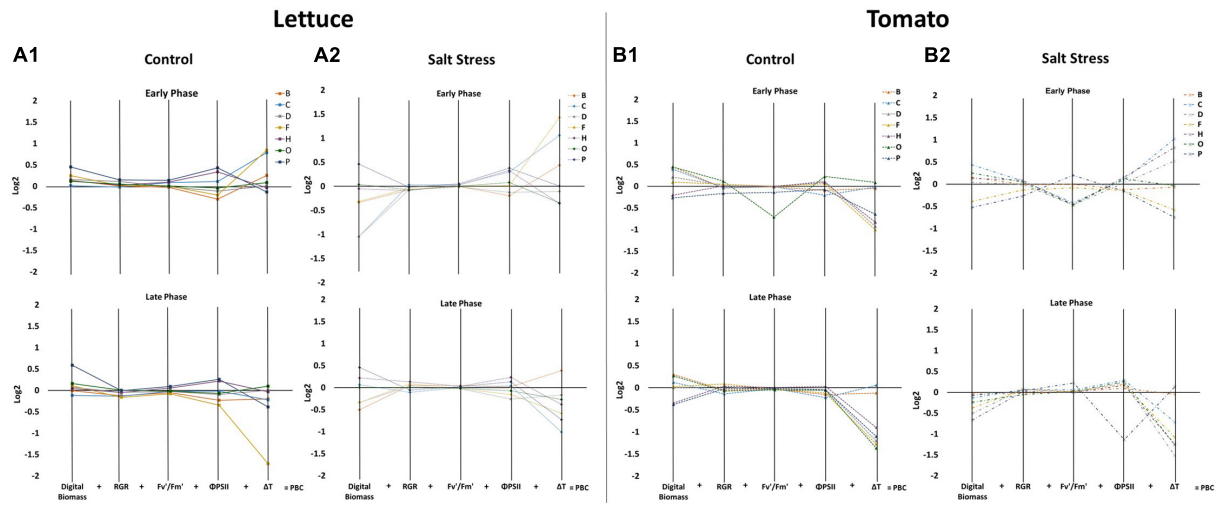

FIGURE 3 | Characterisation of the effect of biostimulants on the performance of tomato and lettuce plants grown under control and salinity conditions. Parallel coordinate plots of the 5 main morpho-physiological parameters (Digital Biomass, RGR, Fv′/Fm′, ΦPSII and △T) are shown for lettuce plants grown in control [full lines, **(A1)**] and salt stress conditions [dotted lines, **(A2)**], for tomato plants grown in control [dashed lines, **(B1)**], and salt stress conditions [dotted and dashed lines, **(B2)**]. The values represent the log2 of the ratio between the plants treated with the 7 protein hydrolysates (PHs) and their respective controls, the sum of the resulting 5 values corresponds to the Plant Biostimulant Characterisation (PBC) index, used for the characterisation of the PHs. Data are shown for the early (0–12 Days of Phenotyping) and the late phase (12–21 Days of Phenotyping) of the plant growth.

in parallel plots (**Figure 3**). Then, the five obtained values represented in each parallel plot were summed to end with a unique number that represents the PBC index (for further detail see Sorrentino et al., 2021) which was included in **Table 1**. The calculated PBC index for each compound, growing condition, and phase of the trial could be negative (red) or positive (blue), providing information about the mode of action of that specific combination (**Table 1**). More in detail, the substances with positive PBC indexes (darker blue) in control conditions are characterised as plant growth promoters, whereas the negative (darker red) are plant growth inhibitors. Overall, our data clearly showed that in lettuce plants, the substance P was both the best growth promotor and stress alleviator, improving the fitness of the plants in all growing conditions and both stages of the trial. The second best was H, while the absolute worst was B (**Table 1A**). Some of the other PHs proved to be beneficial to the crop only in a specific growing condition and/or phase of the trial. For example, F showed an effect as a growth promotor, but only in the late phase of the experiment, while O acted as a stress alleviator in the early phase, but its effect fainted in the Later Phase (**Table 1A**).

For tomato, the absolute best performer was the substance O, followed by D, F, and H, all acting as growth promotors and stress alleviators. Contrarily, the plants treated with the substance B showed the worst performances, especially in salt stress conditions (**Table 1B**).

The results obtained from the PBC index were also corroborated by a cluster analysis performed with the complete phenotyping data set (**Figure 4**). In lettuce, the plants treated with H and P were located in an independent cluster that was divided into two subclusters due to the growth conditions (control or salt) but independent of the stress and unstressed control plants (**Figure 4A**). Contrarily, the rest of the substances were located with their respective controls that were only separated by the stress effect (**Figures 4A,B**). In tomato plants, except for the substances B and C, all PHs were beneficial for the plant fitness, especially when they were grown under salt stress conditions (**Figure 4C**). Altogether, we could conclude that H and P were the best growth promotors and stress alleviators, whereas B was a plant growth inhibitor.

The Applications of Protein Hydrolysates Activate Different Metabolic Pathways in Lettuce and Tomato Plants

An untargeted metabolomic analysis (UHPLC/QTOF-MS) was performed to understand the molecular mechanisms triggered by PH treatments in tomato and lettuce plants grown under either control or salinity conditions. The untargeted profiling allowed to putatively annotate more than 2,000 compounds; the whole list of metabolites, together with the composite mass spectra and individual abundances are provided as **Supplementary Material** (**Supplementary Table 5A** for lettuce, **Supplementary Table 5B** for tomato). The metabolomics dataset included a broad biochemical diversity, including metabolites from a large range of metabolic processes of primary and secondary metabolism. Multivariate statistics were applied to the metabolomic dataset highlighting the similarities or dissimilarities among the metabolomic profiles across treatments. At first, the unsupervised and supervised statistics were carried out separately, while considering the metabolomics datasets from lettuce and tomato. These statistics served as the first step of interpretation to point out the similarities or dissimilarities among all treatments.

TABLE 1 | Classification of 7 protein hydrolysates (PHs) using Plant Biostimulant Characterisation (PBC) index.

	(A) Lettuce				(B) Tomato			
	Control		*NaCl*		*Control*		*NaCl*	
	Early phase	Late phase	Early phase	Late phase	Early phase	Late phase	Early phase	Late phase
B	−0.38	−0.21	−1.04	−0.78	0.35	0.18	0.09	0.10
C	−0.54	−0.07	−1.73	1.01	0.17	−0.32	0.84	1.00
D	0.12	−0.10	−1.18	−0.42	1.27	1.14	1.14	1.33
F	−0.73	1.23	−1.77	0.15	1.21	1.24	0.92	1.00
H	0.63	0.30	0.53	1.00	0.73	0.63	1.36	0.77
O	0.15	−0.02	0.38	0.19	1.96	1.45	1.49	1.23
P	1.37	1.32	0.84	1.29	0.60	0.64	0.34	0.36

The PBC index values for each substance, in Early (0-12 Days of Phenotyping for both crops) and in Late Phase of the experiment (21-21 or 12-24 Days of Phenotyping for lettuce or tomato, respectively). The PBC index of the 7 studied PHs in lettuce (A) and tomato (B) plants under control and salinity conditions. White corresponds to 0, positive values are highlighted in blue and negative values are highlighted in red, the farther the value from 0, the darker is the corresponding hue.

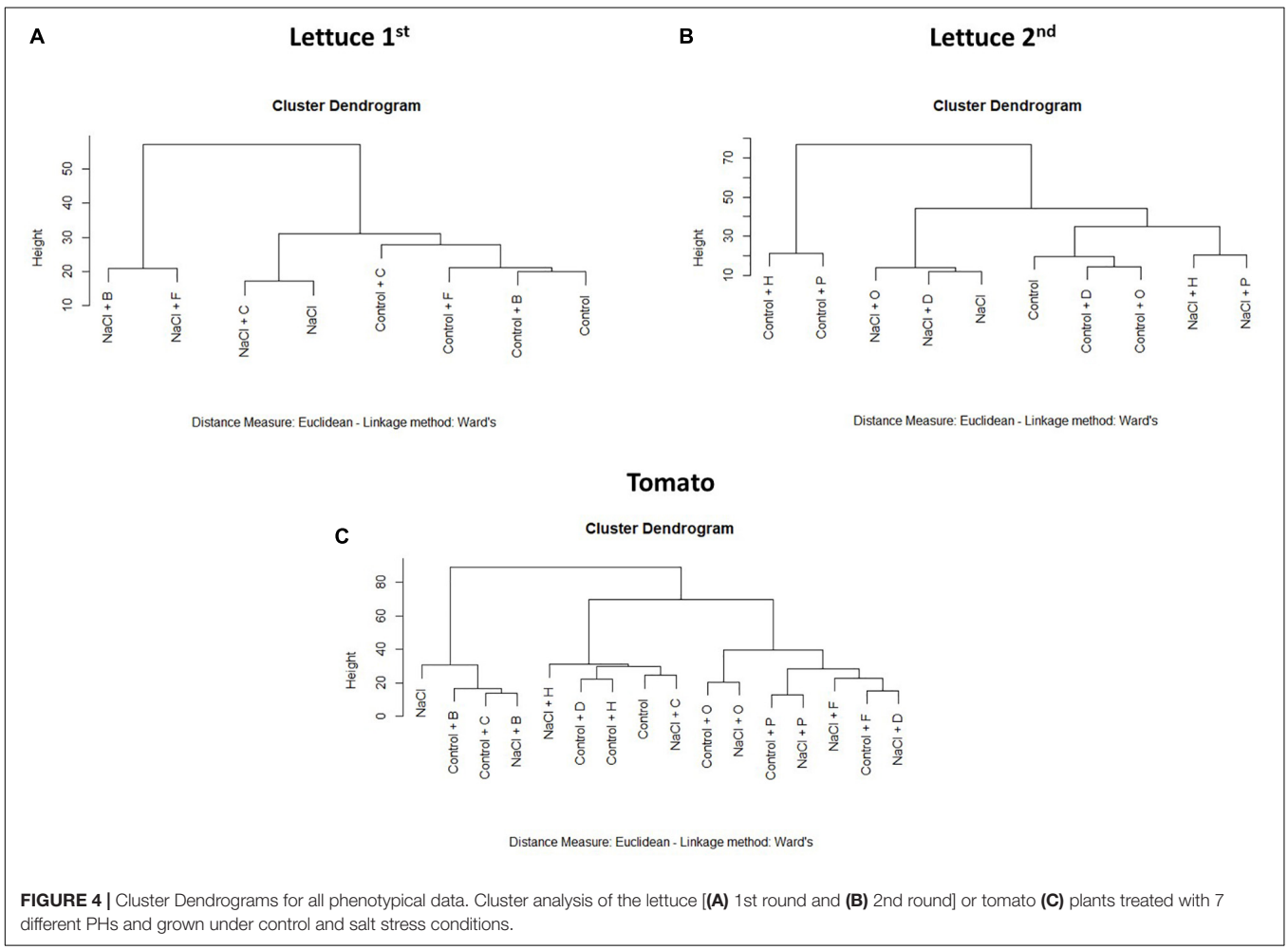

FIGURE 4 | Cluster Dendrograms for all phenotypical data. Cluster analysis of the lettuce [**(A)** 1st round and **(B)** 2nd round] or tomato **(C)** plants treated with 7 different PHs and grown under control and salt stress conditions.

When the lettuce plants were analysed, the unsupervised fold-change-based hierarchical clustering output (**Figure 5A**) naively evidenced that within each trial (first for PHs B, C, F, and second for D, H, O, P), the salinity application was the main clustering factor. Nevertheless, the score plot from the supervised OPLS-DA multivariate modelling (**Figure 5B**) allowed to efficiently discriminate among the different groups of treatments, whereas control samples from the two different trials merged into the score-plot. The model was validated (P-value < 0.001), parameters of the OPLS-DA were excellent (R2Y = 0.983, Q2Y = 0.935), and overfitting was avoided through permutation testing. Therefore, discriminant compounds (VIP

score > 1.2 – **Supplementary Table 6A**) were exported and were considered. Overall, primary and secondary metabolites were equally represented among the VIP discriminants. In more detail, the most represented primary metabolites included carbohydrates, membrane lipids, hormones (mainly brassinosteroids, a cytokinin, and two gibberellins), and electron-carriers (quinol and quinones). Among secondary metabolites, the most represented compounds were phenylpropanoids, alkaloids, and isoprenoids. Exploring the OPLS-DA score plot (**Figure 5B**), the variants showed a clear distribution through all score spaces with a clear separation between stressed and non-stressed plants treated with the same PHs. Under non-saline conditions, the plants treated with B, C, and F presented metabolomic signatures similar to the untreated control, depicting a separated group of responses. However, a second group formed by the plants treated with H, O, and P, corresponding to the best performing biostimulants according to the phenotyping data, formed an independent group under control and salt stress conditions (**Figure 5B**).

Different results were obtained in tomato plants. As a preliminary approach, unsupervised HCA (**Figure 6A**) suggests that salinity did not have a primary effect on metabolic signatures. Tomato samples clustered in two main groups, distinguishing PH treatments, with a cluster including O, P, F, and H, and a second group containing those plants treated with the substance B and C, more similar to untreated controls. These results were further confirmed by the OPLS-DA supervised statistics which allowed separating better the samples in the score space according to the combined treatments (**Figure 6B**). The model parameters of the OPLS-DA were excellent (R2Y = 0.981, Q2Y = 0.941), validation was adequate (*P*-value <0.001), and overfitting could be excluded by permutation testing. Discriminant compounds (VIP score > 1.1 – **Supplementary Table 6B**) are mainly related to secondary metabolism (phenylpropanoids and to a lesser extent terpenoids and alkaloids), cofactors/electron carriers, and phytohormones (gibberellins, brassinosteroids, jasmonate, and IAA-conjugates). Primary metabolites range from carbohydrates, lipids, organic acids, and nucleic acid components. OPLS-DA evidenced that some PHs (O, P, H, D) were better able to minimize the differences between stressed and non-stressed plants, so the plants were grouped independently of the plant growth conditions. This feature might imply a hierarchically stronger effect of the biostimulant above salt stress, and thus, the ability of these PHs to well-play as stress alleviator on plant metabolism (**Figure 6B**).

Biochemical Insights on the Metabolomic Reprogramming Triggered by the Best and the Worst Performers Protein Hydrolysates

To further understand the differences between the mode of action of good and bad performing biostimulants, we analysed the plants treated with the best substance, H, as plant growth promotor and stress alleviator and with the worst, B, as growth inhibitor [according to the PBC indexes and the cluster analysis (**Figures 3**, **4** and **Table 1**)]. The two corresponding sub-datasets were then considered, including 669 compounds for lettuce and 1,090 for tomato. The HCA confirmed the strongest effect of salinity above the PH-treatments in lettuce, whereas PHs had a hierarchically stronger effect on tomatoes (**Supplementary Figures 9A,B**). Indeed, for lettuce, the two main clusters divided stressed from non-stressed plants, even though the metabolic profiles of control plants were more similar to B-treated plants. On the other hand, the metabolic signatures of tomato samples merged in two main clusters, one including H-treated plants and a second cluster grouped controls and B-treated. Consistent results were obtained by OPLS-DA where the separation of treatments could be observed in the score plot hyperspace (**Supplementary Figures 9A,B**). The OPLS-DA model was robust, being R2Y = 0.996 and Q2Y = 0.987 in lettuce (*P*-value < 0.001) and R2Y = 0.996 and Q2Y = 0.977 in tomato (*P*-value < 0.001). Thereafter, the Volcano plot analysis (*P*-value < 0.01, FC ≥ 1.3) was applied to identify differential compounds. Overall, we evidenced that 414 (in lettuce, **Supplementary Table 7A**) and 261 compounds (in tomato, **Supplementary Table 7B**) were significantly modulated by treatments compared to control. The Pathway Tool analysis from PlantCyc was applied to simplify the interpretation in terms of plant metabolism. **Figures 7A**, **8A** show the biosynthetic processes modulated by treatments, along with cumulate FC values. Overall, biosynthesis processes related to secondary metabolism were generally decreased in both crops (**Figures 7B**, **8B**), except for tomato plants treated with PH B under non-stress conditions. In both species, N-containing compounds (mostly alkaloids), phenylpropanoids, and terpenes underwent the most evident modulation. In lettuce, several membrane lipids were impaired, such as long-chain fatty acid (also in the epoxy form) and sterols. Phytohormones were broadly affected by the treatments in lettuce, whereas in tomato, we evidenced a weaker impact (**Figures 7C**, **8C**). The main modulations concerned gibberellins, which decreased in both crops. In treated lettuce, a reduction of brassinosteroids, auxin-conjugates (IAA-Ile, IAA-Leu, IAA-Asp), and N-glycosylated cytokinins were observed. The ethylene precursor (1-aminocyclopropane-1-carboxylate, ACC) down-accumulated only in control plants of lettuce treated with H-substance. In tomatoes, changes in cytokinin content with the main accumulation of trans-zeatin-O-glucoside-7-*N*-glucoside in response to PH B (either under control conditions or salt stress and to H in control conditions).

Similar results were obtained when the effect of the two PHs (B and H) was investigated with respect of their ability as growth improvers and stress alleviators by independently exploring non-stressed and salt-stressed plants. Two different OPLS-DA models were validated regardless of the plant species, one considering metabolomics data from salt-stressed plants and the other including non-stressed plants (**Supplementary Figures 10A,B**). Validation parameters were excellent in both models, showing a R2Y = 0.992 and Q2Y = 0.964 (*P*-value = 1.57 e-17) for non-stressed samples and R2Y = 0.996 and Q2Y = 0.949 (*P*-value = 6.41 e-15) for samples grown under salt stress. The strongest discriminant compounds were selected from each model through the VIP method

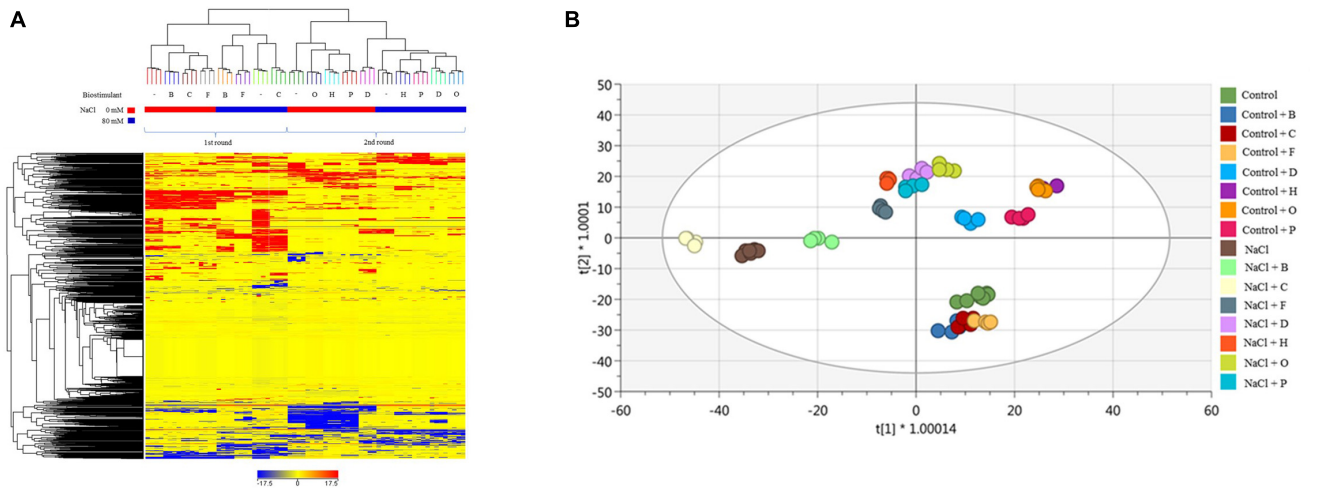

FIGURE 5 | Metabolomic analysis of lettuce plants. Unsupervised hierarchical cluster analysis carried out from ultra-high-pressure liquid chromatographic system (UHPLC-ESI/QTOF-MS) metabolomics analysis of lettuce plants treated with 7 PHs under control and salt stress (NaCl) conditions. The fold-change-based heat map was used to build hierarchical clusters (linkage rule: Ward, distance: Euclidean) **(A)**. Score plot of orthogonal projection to latent structures discriminant analysis (OPLS-DA) supervised modelling carried out on untargeted metabolomics profiles of lettuce plants after 7 PHs application, under control and salt stress (NaCl) conditions (R2Y = 0.98, Q2Y = 0.93) **(B)**.

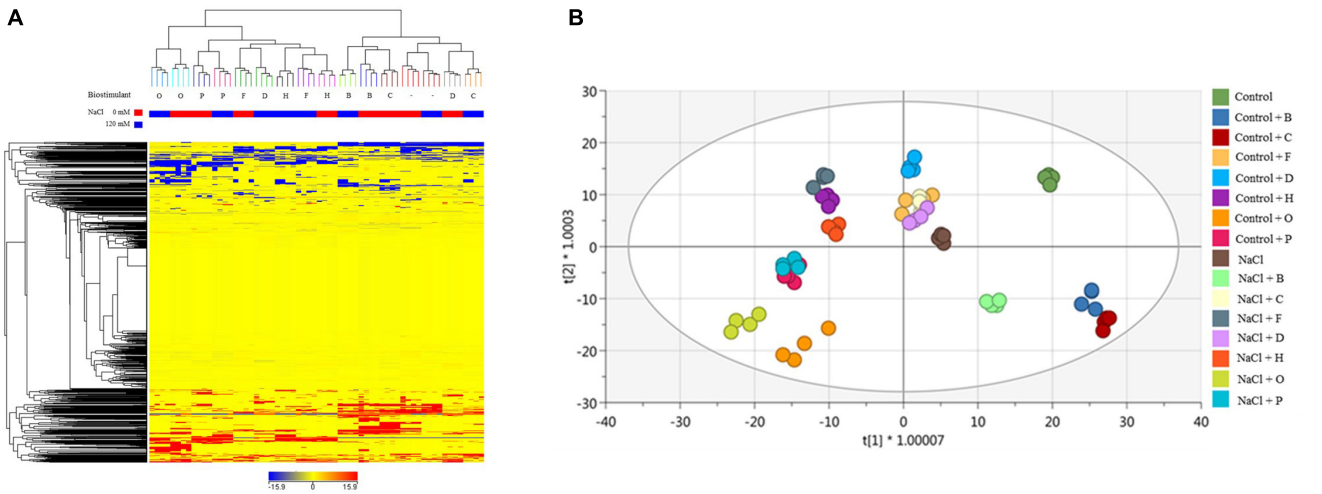

FIGURE 6 | Metabolomic analysis of tomato plants. Unsupervised hierarchical cluster analysis carried out from UHPLC-ESI/QTOF-MS metabolomics analysis of tomatoes treated with 7 PHs under control and salt stress (NaCl) conditions. The fold-change-based heat map was used to build hierarchical clusters (linkage rule: Ward, distance: Euclidean) **(A)**. Score plot of orthogonal projection to latent structures discriminant analysis (OPLS-DA) supervised modelling carried out on untargeted metabolomics profiles of lettuce plants after 7 PHs application, under control and salt stress (NaCl) conditions (R2Y = 0.98, Q2Y = 0.94) **(B)**.

(VIP score > 1.20). A total of 310 (salinity, **Supplementary Table 8A**) and 333 (control, **Supplementary Table 8B**) metabolites were considered and exported along with their FC values into the Omic Viewer Pathway Tool of PlantCyc for interpretations (**Supplementary Figures 11A–C, 12A–C**). Half of the total discriminant compounds were classified as secondary metabolites. However, whereas B substance downregulated the accumulation of secondary metabolites (phenylpropanoids, terpenes, and N-containing compounds), H increased them along with the levels of others such as fatty acid/lipids, cofactors, and electron carriers.

Regarding phytohormones, several discriminant compounds were differentially modulated by the two PHs. Under non-stress conditions, brassinosteroids [3-dehydroteasterone and (22S,24R)-22-hydroxy-5α-ergostan-3-one] strongly down-accumulated in response to PH B but not to PH H, which, on the other hand, remarkably induced a strong accumulation of methyl (indol-3-yl) acetate (MeIAA), a storage form of IAA. Among cytokinins, two glycosylated forms of trans-zeatin accumulated by H applications, whereas only one (*trans*-zeatin-7-*N*-glucoside) in response to B. The PH-treated plants caused a depletion in the ethylene precursor [1-aminocyclipropane-1-carboxylate (ACC)],

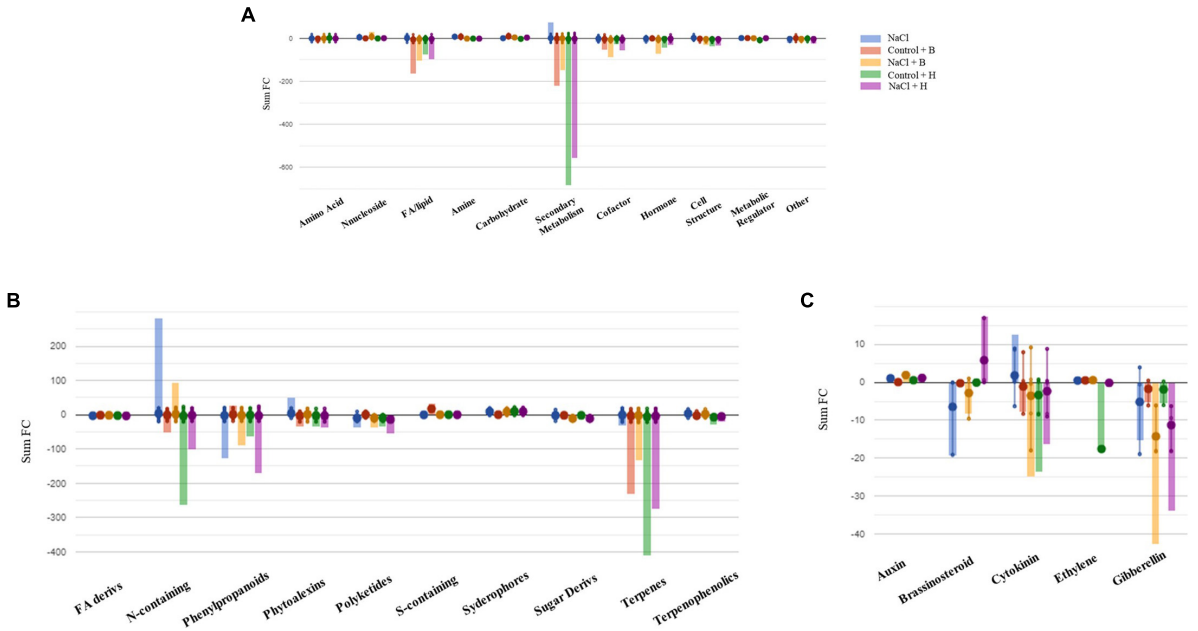

FIGURE 7 | Metabolic changes in lettuce plants. Metabolic processes **(A)**, secondary metabolism **(B)**, and **(C)** hormone biosynthesis were impaired by treatments in lettuce plants compared to control samples. Differential metabolites from the Volcano analysis (*P*-value <0.01, FC ≥ 1.3) were elaborated using the Omics Viewer Dashboard of the Plant Cyc pathway Tool software (www.pmn.plantcyc.com). The large dots represent the average (mean) of all log Fold-change (FC) for metabolites, and the small dots represent the individual log FC for each metabolite. The *x*-axis represents each set of subcategories, while the *y*-axis corresponds to the cumulative log FC. FA/Lipid: fatty acids and lipids, Amine: amines and polyamines, Cofactor: cofactors, prosthetic groups, electron carriers, and vitamins, FA Derives: fatty acid derivatives, N-containing: Nitrogen-containing secondary metabolites, S-containing: Sulfur-containing secondary metabolites, Sugar Derives: sugar derivatives.

but PH H had the strongest effect. Under salinity conditions, MeIAA showed the same modulations recorded in control plants. The only cytokinin found as discriminant (cis-zeatin) accumulated in response to the substance H.

Integrative Analysis of Phenomic and Metabolomics Datasets

The multivariate generalisation of the squared Pearson correlation coefficient was investigated through co-inertia (CIA) in terms of global similarity between the integrated phenotyping and metabolomic datasets (**Supplementary Figure 13**). The overall correlation between the two datasets was expressed as the RV coefficient. This is a measure of global similarity between the datasets and assumes values between 0 and 1. The closer to 1, the higher the similarity between the datasets (Robert and Escoufier, 1976). The overall similarity in structure between phenotyping and metabolomics data was higher in lettuce than in tomato with an RV coefficient equal to 0.37 and 0.29, respectively. However, the obtained RV for both crops reflected the lack of joint structure in these two datasets (phenomics and metabolomics). Altogether, we could say that according to the low synchrony obtained between the phenotypical and metabolomics data after CIA analysis, the changes in the metabolic content do not define the phenotype of the plants.

To deal with this low concordance between the two datasets, we decided to work with the phenotypical and metabolomic data obtained from the plants treated with the substance H as plant growth promotor and stress alleviator, and with the substance B that worked as a growth inhibitor in both lettuce and tomato plants. As the first step, we used the random forest classification method to identify the most important phenotyping traits for each species. As a result, in lettuce, the importance was mainly focused on morphological traits, whereas in tomato the physiology was most relevant (**Supplementary Tables 4A,B**). Concretely, the volume represented as DB was the parameter with the highest discriminative power between treatments, followed by the physiological parameter, water use efficiency (WUE), related to water balance. However, in tomatoes, the most important parameters were related to the photosynthetic performance of the plant, with QY_max and QY_Lss4 as the main ones. The two crops respond in a different way to the changes in the growth conditions, where not only the growth conditions but also whatever treatment applied is included. Once defined, the main phenotypical traits, the correlated metabolites ($p < 0.05$) were identified performing a correlation matrix (**Supplementary Tables 9A,B**). For lettuce, many secondary metabolites, including alkaloids, terpenoids, and phenols or certain metabolites involved in amino acid metabolism (mainly degradation compounds) were negatively correlated with the volume of lettuce plants. However, this phenotyping trait was positively correlated with IAA, IAA-Asp, and L-arginine-succinate, among others. In tomato, however, QY_max was positively correlated to certain secondary metabolites, such as the phenol 4-hydroxycoumarin,

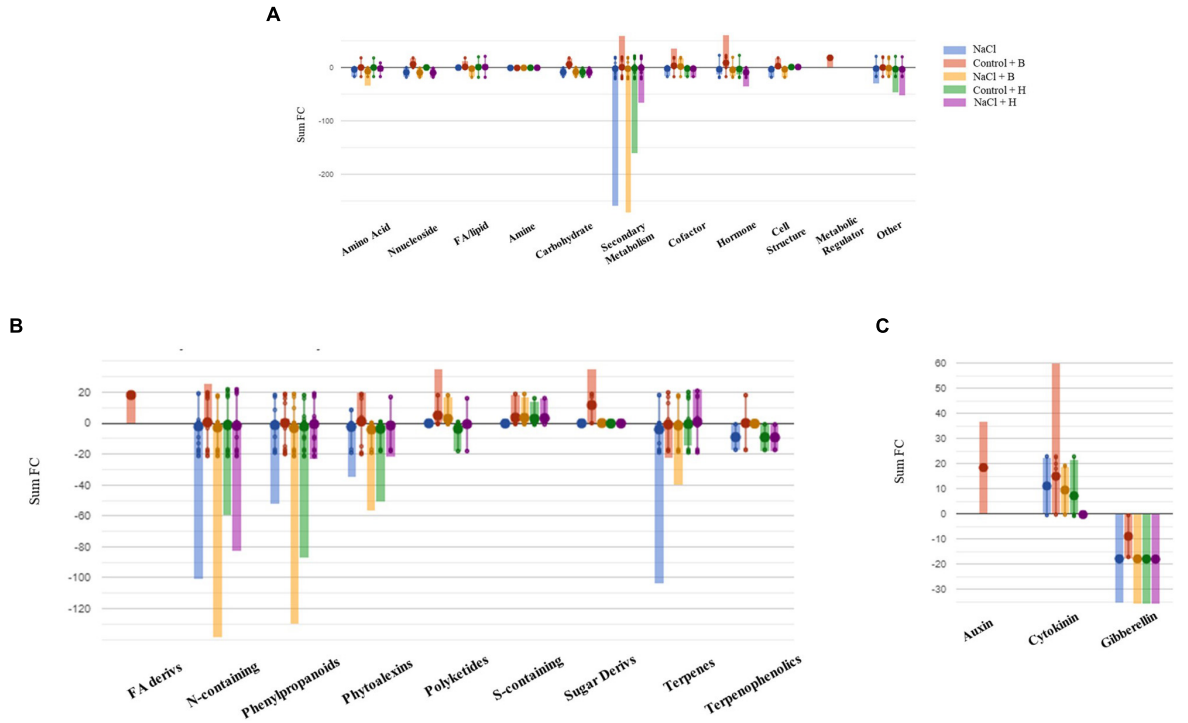

FIGURE 8 | Metabolic changes in tomato plants. Metabolic processes **(A)**, secondary metabolism **(B)**, and **(C)** hormone biosynthesis were impaired by treatments in tomato plants compared to control samples. Differential metabolites from the Volcano analysis (*P*-value <0.01, FC ≥ 1.3) were elaborated using the Omics Viewer Dashboard of the Plant Cyc pathway Tool software (www.pmn.plantcyc.com). The large dots represent the average (mean) of all log Fold-change (FC) for metabolites, and the small dots represent the individual log FC for each metabolite. The *x*-axis represents each set of subcategories, while the *y*-axis corresponds to the cumulative log FC. FA/Lipid: fatty acids and lipids, Amine: amines and polyamines, Cofactor: cofactors, prosthetic groups, electron carriers, and vitamins, FA Derives: fatty acid derivatives, N-containing: Nitrogen-containing secondary metabolites, S-containing: Sulfur-containing secondary metabolites, and Sugar Derives: sugar derivatives.

and the vitamin K1 (phylloquinone), among others, and the carbohydrate D-erythrose 4-phosphate.

DISCUSSION

In the last years, the use of plant phenotyping approaches is becoming an efficient tool for characterizing the mode of action of biostimulants obtained from many different sources and in many plant species (Briglia et al., 2019; Danzi et al., 2019; Akhtar et al., 2020; Mutale-joan et al., 2020). Non-invasive approaches allow the simultaneous study of the crops grown under different growth conditions treated with biostimulant substances for a better understanding of their mode of action. To this end, our study could be another example of this type of study. We show that two distance crops, such as lettuce and tomato, differ in the response to salt stress alone or the interaction between the stress and the application of PHs based biostimulants. The PH application modified the kinetics of the curves for the different phenotyping traits, including plant growth, fluorescence-related parameters, and thermal imaging. This separated the plant response in the early and late phases, with it being more evident for lettuce than for tomato plants (**Supplementary Figures 1–8**). However, the effect was different for both crops and from the one obtained in previous studies performed in Arabidopsis (Sorrentino et al., 2021). Whereas in lettuce, the biostimulant application induced changes during the early phase and after a low number of applications, in the case of tomato the changes were mainly visible at the late phase.

To go further in the understanding of the biostimulant mode of action, we probed the combination of phenotyping experiments with other omics, especially metabolomics, which can give additional information. In this context, the most difficult part is the data management, as both –omics approaches are ending with a huge amount of data to process and interpret. Thanks to the fast evolution of the data analysis based on multivariate statistical analysis, this is possible, and this aims to be a good example of such approaches. For that, the first step done was the clustering of the variants analysed independently for both lettuce and tomato using phenomic data (**Figure 4**). The high dimensionality of the data is a characteristic that creates many challenges in clustering and data analysis in general. The clustering tree is defined by the analysis of the L_K norm distances that depend on the value of K (Euclidean, Manhattan, Minkowski, etc.). The most often L_k norm used is Euclidean distance. In this regard, Aggarwal et al. (2001) showed some interesting results comparing different L_K norm distances. More specifically, they stress that the meaningfulness of L_K norm

(K = 1 for Manhattan, K = 2 for Euclidean, etc.) is worse on high dimensions. This means that the Manhattan distance is preferred in situations where the number of traits (metabolomics or phenomics) is considerably large. That is the reason why Euclidean and Manhattan distances were both examined in this study. However, in this case, the results were not significantly different for both lettuce and tomato. One of the reasons for this result could be that there was a clear different response of the plant when the H or B substance was applied.

As the second step, after the performance of the metabolic analysis and data processing, the concordance between both datasets (phenomics + metabolomics) was performed using CIA analysis. This tool is becoming a particularly attractive method for the identification of relationships between large datasets, but it is mainly used in ecology or genetics (Bady et al., 2004; Genitsaris et al., 2016; Devarajan et al., 2021). However, there are not any case studies using this tool for integrating phenotyping data with other omics. In our study, we observed low values of the RV coefficient between both datasets (phenomics + metabolomics) (**Supplementary Figure 13**). This would mean that the metabolic profiling cannot explain the phenotypes of the plants, making the integration of both data more difficult. One of the reasons for this could be that the most of modulated metabolites were secondary metabolites, including alkaloids, phenylpropanoids, and terpenes (**Figures 7**, **8** and **Supplementary Table 7**). On the contrary, relevant molecules, such as plant growth regulators, are not so abundant and mainly appeared in lettuce. For example, in lettuce plants, there was a clear reduction of the conjugated forms of IAA, most probably to maintain the pool of IAA and thus allow the plant growth (reviewed by Ludwig-Müller, 2011). Besides, the precursor of ethylene, ACC, was also reduced in lettuce plants treated with the H substance when plants were grown under control conditions. It could mean that the H application can reduce the ethylene synthesis and with that, its negative effects (i.e., growth inhibition). However, recent studies also showed that ACC itself is enough to reduce the plant growth (Vanderstraeten et al., 2019).

To solve the low concordance between the phenotyping and metabolomic data, we decided to identify the most significant traits for each treatment (or treatment + biostimulant) among the phenotyping traits identified. For that, we used a random forest classifier. Such a tool is mainly used in plant science for machine learning approaches applied in image analysis (Barradas et al., 2021; Singh et al., 2016), but it has never been used for characterizing the biostimulant mode of action. Apart from a powerful classification method, the random forest has the advantage of revealing the significance of the traits used for identifying (classifying) treatments. This is done using the decrease in classification accuracy if a specific variable – trait is removed. The random forest classifiers applied for lettuce and tomato have high accuracy percentages (>95%), which makes them valid for the interpretation of the significant traits. The significant traits found for lettuce were the volume (based on the DB) and WUE. The most relevant result was the volume that positively correlated with the IAA levels (**Supplementary Table 9**). Higher IAA levels in leaves can improve cell extensibility and consequently induce leaf growth (Veselov et al., 2002). Additionally, under stress conditions, the IAA accumulation can be a stress tolerance mechanism that permits the plant to keep growing (De Diego et al., 2012). Besides, this result could also explain the aforementioned reduction of the conjugation of IAA with certain amino acids observed in the plants treated with the H substance, and hence, their better growth under both control and stress conditions. The amide-linked IAA-amino acid conjugates are considered reversible storage forms with no or low biological activity (Mellor et al., 2016), with the Gretchen Hagen3 (GH3) family of auxin-inducible acyl amido synthetases as the enzymes converting IAA to IAA-amino acids. Thus, we could think that the application of the substance H in lettuce has downregulated the activity of GH3 to reduce auxin-conjugates and maintain the IAA levels as a stress response strategy.

In tomato, the most important trait was the QY_max, which was positively correlated to D-erythrose 4-phosphate (**Supplementary Table 9**), an intermediate in the pentose phosphate pathway, and the Calvin cycle that serves as a precursor in the shikimate pathway (Billakurthi and Schreier, 2020). This result could also explain the positive correlation with other metabolites product of this pathway, such as 4-hydroxycoumarin and vitamin K1 (phylloquinone). The hydroxycoumarins have been described as efficient antibacterial compounds that can improve plant stress resistance (Yang et al., 2018). Vitamin K1 has been detected inside thylakoid membranes as an electron carrier and is a key element within the photosystem I redox chain (reviewed by Lüthje et al., 2013). Thus, it serves as a mobile carrier transferring the electrons across the plasma membrane and contributes to the maintenance of a suitable redox state of some important proteins embedded in the plasma membrane with protective functions against stress. The better performance in tomato plants can, thus, be related to the use of D-erythrose 4-phosphate as a precursor for the synthesis of antistress compounds from the shikimate pathway.

CONCLUSION

We assume that PH-based biostimulants improve the plant growth and salt stress response in crops, such as lettuce and tomato, through different mechanisms. For a better understanding of the mechanism of action, it was necessary to use powerful statistical tools which helped to simplify the results and, hence, their interpretation. Thus, we observed that for lettuce, the most interesting traits to study the PHs based biostimulants are those representing the aerial biomass (i.e., volume). These were correlated with altered levels of certain phytohormones, such as auxin and ethylene, and consequently with plant growth. However, in tomatoes, the chlorophyll fluorescence-related parameters were the most relevant defining the plant growth capacity and salt stress tolerance affecting also the stress-related metabolites from the shikimate pathway. We believe that these results corroborated the relevant role of the multivariate statistical analysis as a further step to uncover key traits and metabolites for a deeper understanding of the biostimulant mode of action.

DATA AVAILABILITY STATEMENT

The original contributions presented in the study are included in the article/**Supplementary Material**, further inquiries can be directed to the corresponding authors.

AUTHOR CONTRIBUTIONS

YR, LL, and GC prepared and selected the protein hydrolysates. MS and KP designed the phenotyping experiments. MS performed the experiments, the image processing, and image-based data analysis. LL, VB, and PG carried out the untargeted metabolomics and performed the analysis of the metabolomic data. IS and ND performed the multivariate statistical analysis. All authors discussed the results and contributed to writing the manuscript.

FUNDING

This work was supported by European Union's Horizon 2020 Research and Innovation Program under the Marie Skłodowska- Curie grant agreement no. 675006, by Italian Ministry of Education, University and Research (MiUR) under the PRIN 'PHOBOS' (no. 2017FYBLPP), by European Regional Development Fund-Project "SINGING PLANT" (No. CZ.02.1.01/0.0/0.0/16_026/0008446) with financial contribution from the Ministry of Education, Youths and Sports of the Czech Republic through the National Programme for Sustainability II funds and by the ERDF project "Plants as a tool for sustainable global development" (No. CZ.02.1.01/0.0/0.0/16_019/0000827) from the Ministry of Education, Youth and Sports of the Czech Republic.

ACKNOWLEDGMENTS

We thank Hello Nature Inc. (former Italpollina) (Anderson, IN, United States) for helping in the development of tested protein hydrolysates and providing them. Plant Sciences Core Facility of CEITEC Masaryk University and Phenotyping and Cultivation facility of PSI Research Center is acknowledged for the technical support.

SUPPLEMENTARY MATERIAL

The Supplementary Material for this article can be found online at: https://www.frontiersin.org/articles/10.3389/fpls.2021.808711/full#supplementary-material

Supplementary Figure 1 | Morphological and physiological parameters of lettuce plants under control and stress conditions. Digital biomass [DM, **(A1–B1)**], roundness **(A2–B2)**, compactness **(A3–B3)**, and slenderness of leaves [SOL, **(A4–B4)**] in lettuce plants grown under control or salt stress conditions for 21 days of phenotyping (DoP). Variations of maximum quantum yield of PSII photochemistry for the light-adapted state [Fv′/Fm′, **(C1–D1)**], PSII operating efficiency [ΦPSII, **(C2–C3)**] and non-photochemical quenching [NPQ, **(C3–D3)**]. The values were obtained after the exposure of the plants to a light intensity of 480 μmol m^{-2} s^{-1} (Lss2). Morphological and physiological values shown represent the average of 8 biological replicates per variant. Error bars represent standard deviation. The significant differences between control and salt treatment are indicated with *, **, and *** for *p*-values below 0.05, 0.01, and 0.001, respectively.

Supplementary Figure 2 | Morphological and physiological parameters of tomato plants under control and stress conditions. Digital biomass [DB, **(A1)**], roundness **(A2)**, compactness **(A3)**, and slenderness of leaves [SOL, **(A4)**] in tomato plants grown under control or salt stress conditions for 24 days of phenotyping (DoP). The maximum quantum yield of PSII photochemistry for the light-adapted state [Fv′/Fm′, **(C1)**], PSII operating efficiency [ΦPSII, **(C2)**], and non-photochemical quenching [NPQ, **(C3)**]. The values were obtained after the exposure of the plants to a light intensity of 480 μmol m^{-2} s^{-1} (Lss2). Morphological and physiological values shown represent the average of 6 biological replicates per variant. Error bars represent standard deviation. The significant differences between control and salt treatment are indicated with *, **, and *** for *p*-values below 0.05, 0.01, and 0.001, respectively.

Supplementary Figure 3 | Morphological and physiological parameters of lettuce plants treated with 7 different under control conditions. Digital biomass [DB, **(A1–B1)**], roundness **(A2–B2)**, compactness **(A3–B3)**, and slenderness of leaves [SOL, **(A4–B4)**] of lettuce plants treated with 7 PHs and grown under control conditions for 21 days of phenotyping (DoP). The maximum quantum yield of PSII photochemistry for the light-adapted state [Fv′/Fm′, **(C1–D1)**], PSII operating efficiency [ΦPSII, **(C2–C3)**] and non-photochemical quenching [NPQ, **(C3–D3)**]. The values were obtained after the exposure of the plants to a light intensity of 480 μmol m^{-2} s^{-1} (Lss2). Morphological and physiological values shown represent the average of 8 biological replicates per variant. Error bars represent standard deviation.

Supplementary Figure 4 | Morphological and physiological parameters of lettuce plants treated with 7 different under salt stress conditions. Digital biomass [DM, **(A1–B1)**], roundness **(A2–B2)**, compactness **(A3–B3)**, and slenderness of leaves [SOL, **(A4–B4)**] of lettuce plants treated with 7 PHs and grown under salt stress conditions for 21 days of phenotyping (DoP). The maximum quantum yield of PSII photochemistry for the light-adapted state [Fv′/Fm′, **(C1–D1)**], PSII operating efficiency [ΦPSII, **(C2–C3)**] and non-photochemical quenching [NPQ, **(C3–D3)**]. The values were obtained after the exposure of the plants to a light intensity of 480 μmol m^{-2} s^{-1} (Lss2). Morphological and physiological values shown represent the average of 8 biological replicates per variant. Error bars represent standard deviation.

Supplementary Figure 5 | Morphological and physiological parameters of tomato plants grown in control and salt stress conditions: PHs treated and untreated lettuce plants. Digital biomass [DM, **(A1–B1)**], roundness **(A2–B2)**, compactness **(A3–B3)**, and slenderness of leaves [SOL, **(A4–B4)**] of tomato plants treated with 7 PHs and grown under control and salt stress conditions for 24 days of phenotyping (DoP). The maximum quantum yield of PSII photochemistry for the light-adapted state [Fv′/Fm′, **(C1–D1)**], PSII operating efficiency [ΦPSII, **(C2–C3)**] and non-photochemical quenching [NPQ, **(C3–D3)**]. Values were obtained after the exposure of the plants to the light of intensity 480 μmol m^{-2} s^{-1} (Lss2). Morphological and physiological values shown represent the average of 6 biological replicates per variant. Error bars represent standard deviation. The significant differences between control and salt treatment are indicated with *, **, and *** for *p*-values below 0.05, 0.01, and 0.001, respectively.

Supplementary Figure 6 | Relative Growth Rate and final biomass of lettuce plants treated with PHs. Relative Growth Rate [RGR, **(A1–A2)**] of the different treatments over time, calculated for the early phase (from DoP 0 to DoP 12) and for the late Phase (from DoP 12 to DoP 21) in lettuce plants treated with 7 PHs grown under control or salt stress conditions. Total fresh **(B1–B2)** and dry **(C1–C2)** weight of the final aboveground biomass per variant. Values represent the average of the 8 biological replicates per variant. Error bars represent standard deviation. Different letters indicate significant differences according to the one-way ANOVA post hoc Tukey's test ($p < 0.05$).

Supplementary Figure 7 | Relative Growth Rate and final biomass of tomato plants treated with PHs. Relative Growth Rate [RGR, **(A1–A2)**] of the different treatments over time, calculated for the early phase (from DoP 0 to DoP 12) and for the late Phase (from DoP 12 to DoP 24) in tomato plants sprayed with 7 PHs,

grown under control conditions or salt stress. Total fresh **(B1–B2)** and dry **(C1–C2)** weight of the final aboveground biomass per variant. Values represent the average of the 6 biological replicates per variant. Error bars represent standard deviation. Different letters indicate significant differences according to the one-way ANOVA post hoc Tukey's test ($p < 0.05$).

Supplementary Figure 8 | Temperature of the leaves for lettuce and tomato plants under control and salt stress conditions. Canopy temperature depression measured on lettuce [**(A1–A3, B1–B3)**, full and dotted lines] and tomato [**(C1–C3)**, dashed and dotted + dashed lines] plants, untreated or treated with the biostimulant substances, grown under control or salt stress conditions. Values represent the average of the 8 biological replicates per treatment in lettuce and 6 biological replicates in tomato, error bars represent standard deviation. The significant differences between control and salt treatment are indicated with *, **, and *** for *p*-values below 0.05, 0.01, and 0.001, respectively.

Supplementary Figure 9 | Metabolomic analysis for the best (H) and worst (B) performing biostimulants. Unsupervised hierarchical cluster analysis carried out from UHPLC-ESI/QTOF-MS metabolomics analysis of lettuce **(A)** and tomato **(B)** plants treated with PH B or H, grown under control or salt stress conditions. The fold-change-based heat map was used to build hierarchical clusters (linkage rule: Ward, distance: Euclidean). Score plot of orthogonal projection to latent structures discriminant analysis (OPLS-DA) supervised modelling carried out on untargeted metabolomics profiles of lettuce **(C)** and tomato **(D)** plants after B and H application grown under control and salt stress (NaCl) condition.

Supplementary Figure 10 | Score plot of metabolomics profiles. Score plot orthogonal projection to latent structures discriminant analysis (OPLS-DA) supervised modelling carried out on untargeted metabolomics profiles of tomato and lettuce plants after B and H application grown under control **(A)** or salt stress **(B)** conditions.

Supplementary Figure 11 | Identified metabolites in control conditions. Metabolic processes **(A)**, secondary metabolism **(B)**, and hormone biosynthesis **(C)** were impaired by treatments in lettuce and tomato plants grown under control conditions. Differential metabolites (VIP score > 1.20) along with their fold-change (FC) values were elaborated using the Omic Viewer Dashboard of the PlantCyc pathway Tool software (www.pmn.plantcyc.com). The large dots represent the average (mean) of all log FC for metabolites, and the small dots represent the individual log FC for each metabolite. The *x*-axis represents each set of subcategories, while the *y*-axis corresponds to the cumulative log FC. FA/Lipid: fatty acids and lipids, Amine: amines and polyamines, Cofactor: cofactors, prosthetic groups, electron carriers, and vitamins, N-containing: Nitrogen-containing secondary metabolites, S-containing: Sulphur-containing secondary metabolites, Sugar Derives: sugar derivatives.

Supplementary Figure 12 | Identified metabolites in plant under salt stress conditions. Metabolic processes **(A)**, secondary metabolism **(B)**, and hormone biosynthesis **(C)** were impaired by treatments in lettuce and tomato plants grown under salt stress conditions. Differential metabolites (VIP score > 1.20) along with their fold-change (FC) values were elaborated using the Omic Viewer Dashboard of the PlantCyc pathway Tool software (https://plantcyc.org/). The large dots represent the average (mean) of all log FC for metabolites, and the small dots represent the individual log FC for each metabolite. The *x*-axis represents each set of subcategories, while the *y*-axis corresponds to the cumulative log FC. FA/Lipid: fatty acids and lipids, Amine: amines and polyamines, Cofactor: cofactors, prosthetic groups, electron carriers, and vitamins, N-containing: Nitrogen-containing secondary metabolites, S-containing: Sulphur-containing secondary metabolites, and Sugar Derivs: sugar derivatives.

Supplementary Figure 13 | Graphical output of co-Inertia analysis (CIA). Scatter plot of tomato **(A)** and lettuce **(B)** samples. Each sample is represented by an arrow whose length is proportional to the divergence between the phenomic and the metabolomic datasets. Eigenvalues of the co-inertia analysis for tomato **(C)** and lettuce **(D)**. Correlation circles **(E,F)** showing the projections of the PCA axes (from the phenomic datasets) onto the axes of the co-inertia analysis (*x* axes) and projections of the PCA axes (from the metabolomic datasets) onto the axes of the co-inertia analysis (*y* axes). These four circles represent a view of the rotations needed to associate the two datasets for tomato **(E)** and the two datasets for lettuce **(F)**.

Supplementary Table 1 | Pairwise comparisons test using mixed models for determining the significant differences between the means of the morphological parameters in lettuce (1st round, A, 2nd round, B) and tomato (C) plants treated with 7 PHs grown under control or salt stress conditions at different time points. The *p*-values below 0.05 are highlighted in green.

Supplementary Table 2 | Pairwise comparisons test using mixed models for determining the significant differences between the means of the photosynthetic parameters in lettuce (1st round, A, 2nd round, B) and tomato (C) plants treated with 7 PHs grown under control or salt stress conditions at different time points. The *p*-values below 0.05 are highlighted in green.

Supplementary Table 3 | Pairwise comparisons test using mixed models for determining the significant differences between the means of the difference between the canopy and air temperature in lettuce (1st round, A, 2nd round, B) and tomato (C) plants treated with 7 PHs grown under control or salt stress conditions at different time points. The *p*-values below 0.05 are highlighted in green.

Supplementary Table 4 | Importance of variables for lettuce (A) and tomato (B) plants based on the random forest classifier used for treatment classification based on a mean decrease in classification accuracy measure.

Supplementary Table 5 | Whole dataset produced from untargeted metabolomics carried out in lettuce (A) and tomato (B) plants treated with 7 PHs grown under control or salt stress conditions. Compounds are presented with individual intensities and composite mass spectra.

Supplementary Table 6 | Discriminant metabolites identified by the variable importance in projection (VIP) analysis following OPLS-DA modelling of the metabolome in lettuce (A) and tomato (B) plants treated with 7 PHs grown under control or salt stress condition. Compounds were selected as discriminant by possessing a VIP score > 1.20.

Supplementary Table 7 | Differential metabolites derived from Volcano analysis ($p < 0.01$, FC ≥ 1.3) in lettuce (A) and tomato (B) plants treated with PH B, and PH H grown under control or salt stress conditions.

Supplementary Table 8 | Discriminant metabolites identified by the variable importance in projection (VIP) analysis following OPLS-DA modelling of the metabolome of lettuce and tomato plants treated with PH H and PH B grown under control (A) or salt stress (B) conditions along with their LogFC values in comparison to control samples. Compounds were selected as discriminant by possessing a VIP score > 1.20.

Supplementary Table 9 | Correlation matrix between the most important phenotyping traits (according to the random forest analysis) and the metabolites for lettuce (A) and tomato plants (B).

REFERENCES

Aggarwal, C. C., Hinneburg, A., and Keim, D. A. (2001). "On the Surprising Behavior of Distance Metrics in High Dimensional Space," in *Database Theory — ICDT 2001. ICDT 2001. Lecture Notes in Computer Science*, eds J. Van den Bussche and V. Vianu (Berlin: Springer), doi: 10.1007/3-540-44503-X_27

Akhtar, S. S., Amby, D. B., Hegelund, J. N., Fimognari, L., Großkinsky, D. K., Westergaard, J. C., et al. (2020). *Bacillus licheniformis* FMCH001 increases water use efficiency via growth stimulation in both normal and drought conditions. *Front. Plant Sci.* 11:297. doi: 10.3389/fpls.2020.00297

Ali, M., Kamran, M., Abbasi, G. H., Saleem, M. H., Ahmad, S., Parveen, A., et al. (2021). Melatonin-induced salinity tolerance by ameliorating osmotic and oxidative stress in the seedlings of two tomato (*Solanum lycopersicum* L.) cultivars. *J. Plant Growth Regul.* 40, 2236–2248. doi: 10.1007/s00344-020-10273-3

Awlia, M., Nigro, A., Fajkus, J., Schmoeckel, S. M., Negrão, S., Santelia, D., et al. (2016). High-throughput non-destructive phenotyping of traits that contribute

to salinity tolerance in *Arabidopsis thaliana*. *Front. Plant Sci.* 7:1414. doi: 10.3389/fpls.2016.01414

Bady, P., Dolédec, S., Dumont, B., and Fruget, J.-F. (2004). Multiple co-inertia analysis: a tool for assessing synchrony in the temporal variability of aquatic communities. *C. R. Biol.* 327, 29–36. doi: 10.1016/j.crvi.2003.10.007

Barradas, A., Correia, P. M. P., Silva, S., Mariano, P., Pires, M. C., Matos, A. R., et al. (2021). Comparing machine learning methods for classifying plant drought stress from leaf reflectance spectra in *Arabidopsis thaliana*. *Appl. Sci.* 11:6392. doi: 10.3390/app11146392

Bates, D., Mächler, M., Bolker, B., and Walker, S. (2015). Fitting linear mixed-effects models using lme4. *J. Stat. Softw.* 67, 1–48. doi: 10.18637/jss.v067.i01

Billakurthi, K., and Schreier, T. B. (2020). Insights into the control of metabolism and biomass accumulation in a staple C4 grass. *J. Exp. Bot.* 71, 5298–5301. doi: 10.1093/jxb/eraa307

Boisgontier, M. P., and Cheval, B. (2016). The anova to mixed model transition. *Neurosci. Biobehav. Rev.* 68, 1004–1005. doi: 10.1016/j.neubiorev.2016.05.034

Briglia, N., Petrozza, A., Hoeberichts, F. A., Verhoef, N., and Povero, G. (2019). Investigating the impact of biostimulants on the row crops corn and soybean using high-efficiency phenotyping and next generation sequencing. *Agronomy* 9:761. doi: 10.3390/agronomy9110761

Cano-Ramirez, D. L., and Dodd, A. N. (2018). New connections between circadian rhythms, photosynthesis, and environmental adaptation. *Plant Cell Environ.* 41, 2515–2517. doi: 10.1111/pce.13346

Caspi, R., Dreher, K., and Karp, P. D. (2013). The challenge of constructing, classifying, and representing metabolic pathways. *FEMS Microbiol. Lett.* 345, 85–93. doi: 10.1111/1574-6968.12194

Ceccarelli, A. V., Miras-Moreno, B., Buffagni, V., Senizza, B., Pii, Y., Cardarelli, M., et al. (2021). Foliar application of different vegetal-derived protein hydrolysates distinctively modulates tomato root development and metabolism. *Plants* 10:326. doi: 10.3390/plants10020326

Colla, G., and Rouphael, Y. (2015). Biostimulants in horticulture. *Sci. Hortic.* 196, 1–2. doi: 10.1016/j.scienta.2015.10.044

Corwin, D. L. (2020). Climate change impacts on soil salinity in agricultural areas. *Eur. J. Soil Sci.* 72, 842–862. doi: 10.1111/ejss.13010

Danzi, D., Briglia, N., Petrozza, A., Summerer, S., Povero, G., Stivaletta, A., et al. (2019). Can high throughput phenotyping help food security in the Mediterranean area?. *Front. Plant Sci.* 10:15. doi: 10.3389/fpls.2019.00015

De Diego, N., Perez-Alfocea, F., Cantero, E., Lacuesta, M., and Moncalean, P. (2012). Physiological response to drought in radiata pine: phytohormone implication at leaf level. *Tree Physiol.* 32, 435–449. doi: 10.1093/treephys/tps029

Dell'Aversana, E., D'Amelia, L., De Pascale, S., and Carillo, P. (2020). "Use of biostimulants to improve salinity tolerance in agronomic crops," in *Agronomic Crops*, ed. M. Hasanuzzaman (Springer: Singapore), doi: 10.1007/978-981-15-0025-1_2

Devarajan, A. K., Muthukrishanan, G., Truu, J., Truu, M., Ostonen, I., Kizhaeral, S., et al. (2021). The foliar application of rice phyllosphere bacteria induces drought-stress tolerance in *Oryza sativa* (L.). *Plants* 10:387. doi: 10.3390/plants10020387

Di Mola, I., Conti, S., Cozzolino, E., Melchionna, G., Ottaiano, L., Testa, A., et al. (2021). Plant-based protein hydrolysate improves salinity tolerance in hemp: agronomical and physiological aspects. *Agronomy* 11:342. doi: 10.3390/agronomy11020342

Di Mola, I., Cozzolino, E., Ottaiano, L., Giordano, M., Rouphael, Y., Colla, G., et al. (2019a). Effect of vegetal- and seaweed extract-based biostimulants on agronomical and leaf quality traits of plastic tunnel-grown baby lettuce under four regimes of nitrogen fertilization. *Agronomy* 9:571. doi: 10.3390/agronomy9100571

Di Mola, I., Ottaiano, L., Cozzolino, E., Senatore, M., Giordano, M., El-Nakhel, C., et al. (2019b). Plant-based biostimulants influence the agronomical, physiological, and qualitative responses of baby rocket leaves under diverse nitrogen conditions. *Plants* 8:522. doi: 10.3390/plants8110522

Freitas, W. E., de, S., Oliveira, A. B., de Mesquita, R. O., Carvalho, H. H., de, et al. (2019). Sulfur-induced salinity tolerance in lettuce is due to a better P and K uptake, lower Na/K ratio and an efficient antioxidative defense system. *Sci. Hortic.* 257:108764. doi: 10.1016/j.scienta.2019.108764

Genitsaris, S., Monchy, S., Breton, E., Lecuyer, E., and Christaki, U. (2016). Small-scale variability of protistan planktonic communities relative to environmental pressures and biotic interactions at two adjacent coastal stations. *Mar. Ecol. Prog. Ser.* 548, 61–75. doi: 10.3354/meps11647

Halford, N. G., and Shewry, P. R. (2000). Genetically modified crops: methodology, benefits, regulation and public concerns. *Br. Med. Bull.* 56, 62–73. doi: 10.1258/0007142001902978

Henley, W. J. (1993). Measurement and interpretation of photosynthetic light-response curves in algae in the context of photoinhibition and diel changes. *J. Phycol.* 29, 729–739.

Hou, M., Tian, F., Zhang, T., and Huang, M. (2019). Evaluation of canopy temperature depression, transpiration, and canopy greenness in relation to yield of soybean at reproductive stage based on remote sensing imagery. *Agric. Water Manag.* 222, 182–192. doi: 10.1016/j.agwat.2019.06.005

Junker, A., Muraya, M. M., Weigelt-Fischer, K., Arana-Ceballos, F., Klukas, C., Melchinger, A. E., et al. (2015). Optimizing experimental procedures for quantitative evaluation of crop plant performance in high throughput phenotyping systems. *Front. Plant Sci.* 5:770. doi: 10.3389/fpls.2014.00770

Lisiecka, J., Knaflewski, M., Spiżewski, T., Frąszczak, B., Kałużewicz, A., and Krzesinski, W. (2011). The effect of animal protein hydrolysate on quantity and quality of strawberry daughter plants cv. 'Elsanta'. *Acta Sci. Pol. Hortorum Cultus* 10, 31–40. doi: 10.5586/aa.2014.012

Ludwig-Müller, J. (2011). Auxin conjugates: their role for plant development and in the evolution of land plants. *J. Exp. Bot.* 62, 1757–1773. doi: 10.1093/jxb/erq412

Lüthje, S., Möller, B., Perrineau, F. C., and Wöltje, K. (2013). Plasma membrane electron pathways and oxidative stress. *Antioxid. Redox Signal.* 18, 2163–2183. doi: 10.1089/ars.2012.5130

McCulloch, C. E., and Searle, S. R. (2000). "Generalized, linear, and mixed models," in *Wiley Series in Probability and Statistics*, eds W. A. Shewhart and S. S. Wilks (New York: Wiley), doi: 10.1002/0471722073

Mellor, N., Band, L. R., Pìnèík, A., Novák, O., Rashed, A., and Holman, T. (2016). Dynamic regulation of auxin oxidase and conjugating enzymes AtDAO1 and GH3 modulates auxin homeostasis. *Proc. Natl. Acad. Sci. U. S. A.* 113, 11022–11027. doi: 10.1073/pnas.1604458113

Meza, S. L. R., Egea, I., Massaretto, I. L., Morales, B., Purgatto, E., Egea-Fernández, J. M., et al. (2020). Traditional tomato varieties improve fruit quality without affecting fruit yield under moderate salt stress. *Front. Plant Sci.* 11:587754. doi: 10.3389/fpls.2020.587754

Mimmo, T., Tiziani, R., Valentinuzzi, F., Lucini, L., Nicoletto, C., Sambo, P., et al. (2017). Selenium biofortification in *Fragaria* × *ananassa*: implications on strawberry fruits quality, content of bioactive health beneficial compounds and metabolomic profile. *Front. Plant Sci.* 8:1887. doi: 10.3389/fpls.2017.01887

Miras-Moreno, B., Zhang, L., Senizza, B., and Lucini, L. (2021). A metabolomics insight into the Cyclic Nucleotide Monophosphate signaling cascade in tomato under non-stress and salinity conditions. *Plant Sci.* 309:110955. doi: 10.1101/2021.03.22.436432

Moncada, A., Vetrano, F., and Miceli, A. (2020). Alleviation of salt stress by plant growth-promoting bacteria in hydroponic leaf lettuce. *Agronomy* 10:1523. doi: 10.3390/agronomy10101523

Mukhopadhyay, R., Sarkar, B., Jat, H. S., Sharma, P. C., and Bolan, N. S. (2021). Soil salinity under climate change: challenges for sustainable agriculture and food security. *J. Environ. Manage.* 280:111736. doi: 10.1016/j.jenvman.2020.111736

Munns, R., and James, R. A. (2000). Screening methods for salinity tolerance: a case study with tetraploid wheat. *Plant Soil* 253, 201–218. doi: 10.1023/a:1024553303144

Munns, R., and Tester, M. (2008). Mechanisms of Salinity Tolerance. *Annu. Rev. Plant Biol.* 59, 651–681. doi: 10.1146/annurev.arplant.59.032607.092911

Mutale-joan, C., Redouane, B., Najib, E., Yassine, K., Lyamlouli, K., Sbabou, L., et al. (2020). Screening of microalgae liquid extracts for their biostimulant properties on plant growth, nutrient uptake and metabolite profile of *Solanum lycopersicum* L. *Sci. Rep.* 10:2820. doi: 10.1038/s41598-020-59840-4

Paul, K., Sorrentino, M., Lucini, L., Rouphael, Y., Cardarelli, M., Bonini, P., et al. (2019a). A combined phenotypic and metabolomic approach for elucidating the biostimulant action of a plant-derived protein hydrolysate on tomato grown under limited water availability. *Front. Plant Sci.* 10:493. doi: 10.3389/fpls.2019.00493

Paul, K., Sorrentino, M., Lucini, L., Rouphael, Y., Cardarelli, M., Bonini, P., et al. (2019b). Understanding the biostimulant action of vegetal-derived protein hydrolysates by high-throughput plant phenotyping and metabolomics: a case study on tomato. *Front. Plant Sci.* 10:47. doi: 10.3389/fpls.2019.00047

Pretali, L., Bernardo, L., Butterfield, T. S., Trevisan, M., and Lucini, L. (2016). Botanical and biological pesticides elicit a similar Induced Systemic Response in tomato (*Solanum lycopersicum*) secondary metabolism. *Phytochemistry* 130, 56–63. doi: 10.1016/j.phytochem.2016.04.002

Qi, Y. (2012). "Random forest for bioinformatics," in *Ensemble machine learning*, eds C. Zhang and Y. Q. Ma (Springer: Boston), 307–323.

R Core Team (2014). *R: A Language and Environment for Statistical Computing*. Vienna: R Foundation for Statistical Computing.

Rahaman, M. M., Ahsan, M. A., Gillani, Z., and Chen, M. (2017). Digital biomass accumulation using high-throughput plant phenotype data analysis. *J. Integr. Bioinform.* 14:20170028. doi: 10.1515/jib-2017-0028

Rascher, U., Liebig, M., and Lüttge, U. (2000). Evaluation of instant light-response curves of chlorophyll fluorescence parameters obtained with a portable chlorophyll fluorometer on site in the field. *Plant Cell Environ.* 23, 1397–1405.

Robert, P., and Escoufier, Y. (1976). A unifying tool for linear multivariate statistical methods: the RV- coefficient. *Appl. Stat.* 25:257. doi: 10.2307/2347233

Rouphael, Y., Spíchal, L., Panzarová, K., Casa, R., and Colla, G. (2018). High-throughput plant phenotyping for developing novel biostimulants: from lab to field or from field to lab?. *Front. Plant Sci.* 9:1197. doi: 10.3389/fpls.2018.01197

Russell, L. (2020). *Emmeans: Estimated Marginal Means, Aka Least-Squares Means, R package version 1.4.5*. Available online at: https://cran.r-project.org/web/packages/emmeans/index.html (Accessed December 22, 2020).

Salek, R. M., Neumann, S., Schober, D., Hummel, J., Billiau, K., Kopka, J., et al. (2015). COordination of Standards in MetabOlomicS (COSMOS): facilitating integrated metabolomics data access. *Metabolomics* 11, 1598–1599. doi: 10.1007/s11306-015-0822-7

Saxena, A., Prasad, M., Gupta, A., Bharill, N., Patel, O. P., Tiwari, A., et al. (2017). A review of clustering techniques and developments. *Neurocomputing* 267, 664–681. doi: 10.1016/j.neucom.2017.06.053

Schläpfer, P., Zhang, P., Wang, C., Kim, T., Banf, M., Chae, L., et al. (2017). Genome-wide prediction of metabolic enzymes, pathways, and gene clusters in plants. *Plant Physiol.* 173, 2041–2059. doi: 10.1104/pp.16.01942

Singh, A., Ganapathysubramanian, B., Singh, A. K., and Sarkar, S. (2016). Machine learning for high-throughput stress phenotyping in plants. *Trends Plant Sci.* 21, 110–124. doi: 10.1016/j.tplants.2015.10.015

Sorrentino, M., De Diego, N., Ugena, L., Spíchal, L., Lucini, L., Miras-Moreno, B., et al. (2021). Seed priming with protein hydrolysates improves arabidopsis growth and stress tolerance to abiotic stresses. *Front. Plant Sci.* 12:626301. doi: 10.3389/fpls.2021.626301

Tsugawa, H., Cajka, T., Kind, T., Ma, Y., Higgins, B., Ikeda, K., et al. (2015). MS-DIAL: data-independent MS/MS deconvolution for comprehensive metabolome analysis. *Nat. Methods* 12, 523–526. doi: 10.1038/nmeth.3393

Tsugawa, H., Kind, T., Nakabayashi, R., Yukihira, D., Tanaka, W., Cajka, T., et al. (2016). Hydrogen Rearrangement Rules: computational MS/MS Fragmentation and Structure Elucidation Using MS-FINDER Software. *Anal. Chem.* 88, 7946–7958. doi: 10.1021/acs.analchem.6b00770

Ugena, L., Hılová, A., Podlešáková, K., Humplík, J. F., Doležal, K., De Diego, N., et al. (2018). Characterization of biostimulant mode of action using novel Multi-Trait High-Throughput Screening of Arabidopsis germination and rosette growth. *Front. Plant Sci.* 9:1327. doi: 10.3389/fpls.2018.01327

Van Oosten, M. J., Pepe, O., De Pascale, S., Silletti, S., and Maggio, A. (2017). The role of biostimulants and bioeffectors as alleviators of abiotic stress in crop plants. *Chem. Biol. Technol. Agric.* 4:5. doi: 10.1186/s40538-017-0089-5

Vanderstraeten, L., Depaepe, T., Bertrand, S., and Van Der Straeten, D. (2019). The ethylene precursor ACC affects early vegetative development independently of ethylene signaling. *Front. Plant Sci.* 10:1591. doi: 10.3389/fpls.2019.01591

Veselov, D., Mustafina, A., Sabirjanova, I., Akhiyarova, G. R., Dedov, A. V., Veselov, S. U., et al. (2002). Effect of PEG-treatment on the leaf growth response and auxin content in shoots of wheat seedlings. *Plant Growth Regul.* 38, 191–194. doi: 10.1023/A:1021254702134

Yamaguchi, T., and Blumwald, E. (2005). Developing salt-tolerant crop plants: challenges and opportunities. *Trends Plant Sci.* 10, 615–620. doi: 10.1016/j.tplants.2005.10.002

Yang, L., Wu, L., Yao, X., Zhao, S., Wang, J., Li, S., et al. (2018). Hydroxycoumarins: new, effective plant-derived compounds reduce *Ralstonia pseudosolanacearum* populations and control tobacco bacterial wilt. *Microbiol. Res.* 215, 15–21. doi: 10.1016/j.micres.2018.05.011

Conflict of Interest: MS and KP were employed by company Photon Systems Instruments (PSI).

The remaining authors declare that the research was conducted in the absence of any commercial or financial relationships that could be construed as a potential conflict of interest.

Publisher's Note: All claims expressed in this article are solely those of the authors and do not necessarily represent those of their affiliated organizations, or those of the publisher, the editors and the reviewers. Any product that may be evaluated in this article, or claim that may be made by its manufacturer, is not guaranteed or endorsed by the publisher.

frontiers in Plant Science

ORIGINAL RESEARCH
published: 14 February 2022
doi: 10.3389/fpls.2022.814401

Multiple Arbuscular Mycorrhizal Fungal Consortia Enhance Yield and Fatty Acids of *Medicago sativa*: A Two-Year Field Study on Agronomic Traits and Tracing of Fungal Persistence

Elisa Pellegrino[1]*, *Marco Nuti*[1,2] *and Laura Ercoli*[1]

[1] Institute of Life Sciences, Scuola Superiore Sant'Anna, Pisa, Italy, [2] University of Pisa, Pisa, Italy

Arbuscular mycorrhizal fungi are promoted as biofertilizers due to potential benefits in crop productivity, and macro- and microelement uptake. However, crop response to arbuscular mycorrhizal fungi (AMF) inoculation is context-dependent, and AMF diversity and field establishment and persistence of inoculants can greatly contribute to variation in outcomes. This study was designed to test the hypotheses that multiple and local AMF inoculants could enhance alfalfa yield and fatty acids (FA) compared to exotic isolates either single or in the mixture. We aimed also to verify the persistence of inoculated AMF, and which component of the AMF communities was the major driver of plant traits. Therefore, a field experiment of AMF inoculation of alfalfa (*Medicago sativa* L.) with three single foreign isolates, a mixture of the foreign isolates (FMix), and a highly diverse mixture of local AMF (LMix) was set up. We showed that AMF improved alfalfa yield (+ 68%), nutrient (+ 147% N content and + 182% P content in forage), and FA content (+ 105%). These positive effects persisted for at least 2 years post-inoculation and were associated with enhanced AMF abundance in roots. Consortia of AMF strains acted in synergy, and the mixture of foreign AMF isolates provided greater benefits compared to local consortia (+ 20% forage yield, + 36% forage N content, + 18% forage P content, + 20% total FA in forage). Foreign strains of *Funneliformis mosseae* and *Rhizophagus irregularis* persisted in the roots of alfalfa 2 years following inoculation, either as single inoculum or as a component of the mixture. Among inoculants, *F. mosseae* BEG12 and AZ225C and the FMix exerted a higher impact on the local AMF community compared with LMix and *R. irregularis* BEG141. Finally, the stimulation of the proliferation of a single-taxa (*R. irregularis* cluster1) induced by all inoculants was the main determinant of the host benefits. Crop productivity and quality as well as field persistence of inoculated AMF support the use of mixtures of foreign AMF. On the other hand, local mixtures showed a lower impact on native AMF. These results pave the way for extending the study on the effect of AMF mixtures for the production of high-quality forage for the animal diet.

Keywords: biofertilization, *Funneliformis mosseae*, *Rhizophagus irregularis*, microbial consortia, crop yield and quality, local and foreign AM fungal inocula, fatty acids (FAs)

OPEN ACCESS

Edited by:
Maurizio Ruzzi,
University of Tuscia, Italy

Reviewed by:
Sidney Luiz Stürmer,
Regional University of Blumenau, Brazil
Teresa Dias,
Universidade de Lisboa, Portugal

***Correspondence:**
Elisa Pellegrino
elisa.pellegrino@santannapisa.it

Specialty section:
This article was submitted to Plant Nutrition, a section of the journal Frontiers in Plant Science

Received: *13 November 2021*
Accepted: *12 January 2022*
Published: *14 February 2022*

Citation:
Pellegrino E, Nuti M and Ercoli L (2022) Multiple Arbuscular Mycorrhizal Fungal Consortia Enhance Yield and Fatty Acids of Medicago sativa: A Two-Year Field Study on Agronomic Traits and Tracing of Fungal Persistence. Front. Plant Sci. 13:814401. doi: 10.3389/fpls.2022.814401

INTRODUCTION

The management of soil biota is considered a key strategy to maintain and improve ecological services in agro-ecosystems (De Vries et al., 2013; Toju et al., 2018). The plant symbiotic arbuscular mycorrhizal fungi (AMF) support plant growth, productivity, and soil fertility (e.g., Smith and Read, 2008; Gianinazzi et al., 2010). However, the evidence of crop benefits following field application of fungal inoculum suggests that intensive agricultural practices, such as frequent and deep tillage, high P or N fertilizer rate, long fallow, and continuous cropping, have a negative impact on AMF abundance in soil (e.g., Jasper et al., 1989; Lekberg and Koide, 2005; Roldan et al., 2007; Duan et al., 2010; Higo et al., 2013; Sheng et al., 2013; van der Heyde et al., 2017). In the European Union (EU), AMF are cataloged as plant biostimulants according to the new Regulation (EU) 2019/1009, based on the functions of stimulating plant nutrition processes and tolerance to abiotic stresses and improving the quality of the agricultural product (EU, 2019). AMF represent an important segment of the global biostimulant market, estimated in 2018 at about $ 2.0 billion (Rouphael and Colla, 2018). Despite the huge commercial interest in microbial and non-microbial plant biostimulants, associated with a growing body of research, the detailed molecular, cellular, and physiological mechanisms underlying plant-biostimulant interactions under different environments and management strategies remain largely unknown. Therefore, there is an urgent need to better elucidate the causal/functional mechanisms of biostimulants and their potential side-effects on the environment (e.g., invasiveness and threat to soil and plant biodiversity and ecosystem functioning, Hart et al., 2017).

In addition to the enhanced crop productivity (Lekberg and Koide, 2005; Pellegrino et al., 2011, 2015a; Pellegrino and Bedini, 2014), arbuscular mycorrhizal (AM) fungal addition through field inoculation can increase macro- and microelement content (Karandashov and Bucher, 2005; Veresoglou et al., 2012; Lehmann et al., 2014; Lehmann and Rillig, 2015; Ercoli et al., 2017a; Coccina et al., 2019; Pellegrino et al., 2020a) and nutraceuticals (Baslam et al., 2013; Saleh et al., 2020). Lekberg and Koide (2005), applying a meta-analysis approach on experimental results from field and glasshouse trials, demonstrated a large increase of mycorrhizal colonization in inoculation trials, suggesting that low inoculum potential can limit mycorrhizal colonization. Furthermore, they also showed that yield or biomass positive response to increased mycorrhizal colonization is non-linear, as management practices, site and climate, inherent inoculum potential, available soil P concentrations, and interactions between plant and fungal species modulate the plant response to increased mycorrhizal colonization.

In addition to abundance, AM fungal diversity can also limit AM fungal-derived benefits if different AM fungal species or isolates provide complementary benefits to the host plant (van der Heijden et al., 1998a,b; Verbruggen et al., 2010, 2013). Some pot studies with sterilized soil inoculated by a common bacterial community and AMF inocula have shown that plant growth and nutrient uptake were more promoted by diverse inocula, composed of a mixture of AM fungal taxa belonging to different species of the same family (Edathil et al., 1996; van der Heijden et al., 1998a,b) or to different families (Thonar et al., 2014; Crossay et al., 2019; Parvin et al., 2020), than single-species inocula. These results are supported by a meta-analysis of Hoeksema et al. (2010) in which AM fungal inoculum complexity (multispecies and whole soil inocula vs. single species inocula) was positively related to plant benefits. Conversely, other studies showed that pot inoculation with multiple AM fungal species could not outweigh single inoculants in terms of plant biomass response, while plant diversity and nutrient uptake [e.g., phosphorus (P) and nitrogen (N)] were even decreased (van der Heijden et al., 2003; Jansa et al., 2008). However, due to the different functional traits among AMF (Munkvold et al., 2004; Thonar et al., 2011; Treseder et al., 2018), and because the interactions among AMF are not always synergistic (Koide, 2000; Jansa et al., 2008), the effectiveness of AM fungal mixed inocula have to be evaluated in the field, where a local microbial community (including AMF and many other microbial groups) is present. However, when a crude inoculum is applied (composed of AM fungal spores, roots, and soil), the method utilized for the production of different isolates may include their associated microbial communities and metabolites that are likely to have an effect on the inoculation outcomes, thus representing a confounding effect (Bianciotto and Bonfante, 2002).

However, the effectiveness of AM fungal inocula should be confirmed by pieces of evidence of their establishment and persistence in the field. Attempts to directly track inoculants in the field are few due to the fact that morphological methods (i.e., staining and counting at the microscope) cannot be applied because many AM fungal species colonizing the same root are morphologically indistinguishable, while current molecular markers can hardly distinguish among closely related taxa and the detection of specific fungal species isolates remains challenging in the field (Hart et al., 2015). An earlier study, based on the amplification of ca. 2,200-bp-long central stretch of the nuclear rDNA cistron and the barcoding of SSU-ITS2-LSU sequences (550, 200, and 580 bp, respectively), successfully tracked the establishment and persistence of two isolates of *F. mosseae* (IMA1 = BEG12 and AZ22C) in alfalfa up to 2 years (Pellegrino et al., 2012). Similarly, other studies using different molecular targets and approaches [e.g., the LSU of ribosomal RNA gene or the mitochondrial LSU DNA (mtLSU) and cloning and sequencing; a fragment of the RNA polymerase II gene (RPB1) and qPCR; mt cox3-rnl intergenic mtDNA region, and droplet digital PCR] could detect root establishment and persistence of some AM fungal isolates in field-inoculated crops up to 3 years (Farmer et al., 2007; Sýkorová et al., 2012; Thioye et al., 2019).

Alfalfa (*Medicago sativa* L.) is a perennial herbaceous legume and one of the most important forage crops in the world due to its high feeding value and yield potential (Radović et al., 2009). Moreover, alfalfa supports important functions in sustaining agricultural systems, such as diversification of crop rotations, conserving soil water, improving soil structure by the development of a large root system, and increasing soil fertility through biological N fixation (Carlsson and Huss-Danell, 2003; Hakl et al., 2017; Sun and Li, 2019). Alfalfa's global cultivation area exceeds 35 million ha (Radović et al., 2009) with an

estimated world production of around 436 million tons in 2006 (FAO, 2006). Alfalfa contains a high quantity of macro- and microelements, and a high amount of fatty acids (FA), such as linoleic acid (C18:2) and the α-linolenic acid (C18:3) (Boufaïed et al., 2003) that are fundamental for animal health (Radović et al., 2009). The composition of fats from food animals is a major human health concern, and particularly important is the content of total polyunsaturated FA (ΣPUFA), α-linolenic acid (ALA, 18:3), and linoleic acid (LA, 18:2), ALA, and LA belonging to the n-3 (omega-3) and n-6 (omega-6) fatty acid family, respectively (Calviello and Serini, 2010). An increase of PUFAs and conjugated linoleic acids (CLA), such as ALA and LA in the human diet, has been shown to reduce the risk of cardiovascular disease, diabetes, cancers, and obesity (Pariza et al., 2001). Since animals cannot synthesize ALA or LA *de novo*, their content in forage plants, among which alfalfa is one of the main sources, is of primary importance in producing beef and milk with high levels of omega-3 FA and CLA (Dhiman et al., 1999; French et al., 2000; Scollan et al., 2001; Pintus et al., 2013).

To our knowledge, no information is available about the role played by AMF in plant FA synthesis, despite the fact that C in the mycorrhizal roots, received by the host plant in the form of monosaccharides, is stored primarily as lipids and many of the genes induced in mycorrhizal roots are predicted to function in lipid metabolism (Rich et al., 2017; Roth and Paszkowski, 2017). This study was designed to test the following multiple hypotheses: (i) alfalfa yield and quality is limited by AM fungal diversity and multiple AM fungal inoculants could act in synergy to promote crop growth and FA concentration; (ii) environmental pressure could select for highly efficient AM fungi and therefore a mixture of native AM fungal isolates could provide greater benefits compared to an exotic mixture. Finally, we aimed to verify the persistence of inoculated AMF in the field, and which component of the AM fungal communities found in the plots was the major driver of plant traits. To these aims, a field experiment of AM fungal inoculation of alfalfa with single foreign isolates, a mixture of the foreign isolates, and a highly diverse mixture of local AMF was set up and plants and fungal traits were assessed for 2 years, together with the molecular assessment of inoculum persistence and native AM fungal communities.

MATERIALS AND METHODS

Fungal Material

The experiment compared five AM fungal inoculum treatments: (1) *Funneliformis mosseae* BEG 12, (2) *Funneliformis mosseae* AZ225C, (3) *Rhizophagus irregularis* BEG141, (4) a mixture of the above foreign isolates (Fmix) and (5) a mixture of local strains of AMF (Lmix). The Lmix was isolated from an alfalfa soil located in Manciano and was composed by *Funneliformis coronatum*, *Funneliformis geosporum*, *Funneliformis mosseae*, *Rhizophagus clarus*, *Rhizophagus irregularis*, *Glomus* sp., *septoglomus viscosum*, *Claroideoglomus etunicatum*, *Diversispora spurca*, *Acaulospora rugosa*, *Acaulospora cavernata*, *Acaulospora spinosa*, *Scutellospora auriglobа* and *Scutellospora calospora* (14 AM fungal species belonging to five families) (Pellegrino et al., 2020b). The foreign AMF isolates were obtained from the collection of the Scuola Superiore Sant'Anna, Italy. Details about the geographical origin, collector, and original inoculum supplier are given in **Supplementary Table 1**.

The inocula of single foreign AM fungal isolates (BEG12, AZ225C, BEG141) were produced in 15 L pots (four pots for treatment). Each pot was filled with sandy soil and Terragreen (1:1 by volume) and 1.5 L of starting crude inoculum. The substrate was previously steam-sterilized (121°C for 25 min, on two consecutive days) to kill native AMF. The Fmix was obtained at the end of inoculum production, by mixing equal quantities of the foreign AMF isolates. The Lmix was produced in 15 L pots (four pots), by adding 1.5 L soil of the experimental site to 13.5 L of the substrate. Additional four 15 L-pots were set up for the inoculation of control plots, by mixing equal quantities of sterilized single foreign AM fungal inocula and soil from the experimental site (a total of 1.5 L) to 13.5 L of the substrate (mock inoculum). Sudan grass (*Sorghum sudanense* L.) was used as a host plant (10 plants per pot). All pots received 1.5 L of a deionized water filtrate from the single foreign AM fungal inocula, and from the soil of the experimental site. Although the amount of microbial filtrate used at the start of the propagation was very large to minimize the differences among AM fungal inoculants, we cannot exclude that the differences in socialization among AM fungal isolates and microbes could lead to the end of the production phase to distinct microbial communities in the inoculants. Pots were irrigated with tap water and supplied with half-strength Hoagland's solution every month (1.5 L per pot). After the 3-month growth, Sudan grass was harvested, and soil and roots were removed from the pots and air-dried. Then, the roots were cut, mixed with the soil, and stored in polyethylene bags at 4°C, until field inoculation. The AM fungal treatments were thus composed of AMF, microbes, soil, and roots, while the control was only composed of microbes, soil, and roots.

Experimental Site and Climatic Data

The experiment was carried out at Manciano (Grosseto), Italy (47° 16′ 36.5″ N–70° 14′ 53″ E; 447 m above sea level). Main soil physical and chemical properties were: 322.9 g kg^{-1} sand, 308.5 g kg^{-1} silt, 368.6 g kg^{-1} clay (hydrometric method, Gee and Bauder, 1986); 7.1 pH (deionized H_2O 1:2.5 w/v); 28.7 g kg^{-1} organic matter (Walkley–Black wet combustion method; Nelson and Sommers, 1982); 1.47 g kg^{-1} total N (Kjeldahl digestion; Bremner and Mulvaney, 1982);0.84 g kg^{-1} total P (colorimetry using perchloric acid digestion; Olsen and Sommers, 1982); 8.3 mg kg^{-1} available P (colorimetry using a solution of sodium bicarbonate; Olsen and Sommers, 1982); 163.2 mg kg^{-1} exchangeable K (Thomas, 1982); 30.1 meq 100 g^{-1} Cation Exchange Capacity (displacement with 0.1 M $BaCl_2$ triethanolamine, Hendershot and Duquette, 1986). The soil of the area is a *Haplic Calcisol*, according to the FAO classification system (IUSS, 2015), and an Inceptisol, according to the USDA classification (Soil Survey Staff, 1999). The climate of the site is cold, humid Mediterranean (Csa) according to the Köppen-Geiger climate classification (Kottek et al., 2006). Mean annual maximum and minimum air temperatures averaged over 1996–2015 are 20.2 and 9.3°C, respectively, and

annual precipitation was 769 mm (Vallebona et al., 2015). During the field experiment (November 2011–August 2013), maximum and minimum temperatures were 19.3 and 9°C, respectively, while total precipitation was 1,730 mm and had a peak of 207 mm during the 3rd decade of November 2012 (**Supplementary Figure 1**).

Field Experiment Setup

A 2-year field AMF inoculation experiment was set up with alfalfa (*Medicago sativa* L., var. Giulia) as the host crop. Conventional tillage was performed at the beginning of September 2011 and consisted of moldboard plowing (30 cm depth), disking twice (15 cm depth), and harrowing (20 cm depth) (Ercoli et al., 2017b). Plots of 25 m^2 size (5 m × 5 m) were designed within the field and hand inoculated with 0.4 kg m^{-2} of inoculum, incorporated into the soil by hand hoeing at ca. 10 cm depth (19 October 2011). The mean number of spores/sporocarps per g of inoculum ranged from 10 to 25, corresponding to 4,000–10,000 spores/sporocarps per m^2. The plots were hand-seeded on 20 October 2011 with 5 g m^{-2} of alfalfa seeds. The preceding crop was barley. Neither chemical fertilization nor chemical nor mechanical weed control was applied. Alfalfa was cut when regrowth at the crown was initiated, on June 20 and August 6, 2012 and on 17 June and 18 August 2013. The experiment design was a nested split-plot with three replicates. The main plot factor was the age of cultivation (first and second year), the sub-plot factor was the AMF inoculation (BEG12, AZ225C, BEG141, Fmix, Lmix, and mock inoculum as control), and the cut was a nested factor within the year of cultivation.

Sampling and Measurements

One month after crop emergence (December 2011), and at the beginning of spring growth in the two following years (2012 and 2013), six alfalfa plants from each replicated plot were sampled and AMF root colonization was assessed under a stereomicroscope (Olympus SZX 9, Olympus Optics, Tokyo, Japan), after clearing and staining with lactic acid instead of phenol (Phillips and Hayman, 1970), following the gridline intersect method (McGonigle et al., 1990). In both years and for both cuts, alfalfa shoots were harvested from one square meter for each replicated plot. A subsample of shoots was partitioned into stems and leaves, and dry weight was determined after oven drying at 75°C. Shoot N and P concentrations were determined by the Kjeldahl method and by the ammonium-molybdophosphoric blue color method, respectively (Jones et al., 1991). Protein concentration was calculated by multiplying the shoot N concentration × 6.25 (Lynch and Barbano, 1999). At the first cut of each year of cultivation, a root sample was extracted from the soil (about 100 g fresh weight) and assessed for AMF colonization applying the previously described procedure.

Fatty acids of alfalfa shoots from both cuts in the 2 years were extracted and methylated by a one-step procedure using toluene as solvent (Sukhija and Palmquist, 1988). Methyl nonadecanoate was used as an internal standard. Fatty acid methyl esters were quantified by gas chromatography using an HP 5890 chromatography (Hewlett Packard Co., Palo Alto, CA, United States), under the following conditions: 60-m × 0.32-mm DB-23 capillary column, 0.25 μm film thickness, H_2 as a carrier gas, 2.8 cm^3 min^{-1} volumetric flow rate, injector split 1/100 at 240°C, septum purge vent at 2 ml min^{-1}, flame ionization detector at 250°C, and 15 kPa of heat pressure. The initial temperature was 150°C, which was increased by 5°C min^{-1} up to 200°C. Fatty acid methyl esters in toluene were directly injected through the split injection port. The peak area of Fas was measured using a Turbochrom 3 analytical system (version 3.3; PE Nelson, Cupertino, CA, United States). Each peak was identified and quantified using pure methyl ester standards (Alltech, Deerfield, IL, United States). Total volatile fatty acids were calculated.

Extraction of Genomic DNA, PCR Amplification, Cloning, and Sequencing of Arbuscular Mycorrhizal Fungi Inoculants

In a further experiment, DNA was extracted from 50 spores of the foreign *F. mosseae* isolates BEG12 and AZ225C, from 20 spore clusters (ca. 25 spores each) of the foreign *R. irregularis* isolate BEG141 and from the roots of Sudan grass host plants grown in pots for the production of Lmix inoculum. Spores were crushed in microtubes on ice and the DNA was extracted using 50 μl of extraction buffer (100 mM Tris–HCl, 100 mM NaCl, 2 mM MgCl2, and 2% Triton-X100, pH 8). Genomic DNA was extracted from a subsample of 100-mg fresh weight of roots collected from the Sudan grass pots (four replicates), using the Dneasy®Plant Mini Kit (Qiagen, Germantown, MD, United States). PCR amplification was performed using the primer pair NS31 and LSUGlom1, targeting a portion of the small subunit ribosomal RNA (SSU rRNA 18S) gene, the internal transcribed spacer (ITS1), the 5.8S, the ITS2, and a portion of the LSU rRNA gene (Pellegrino et al., 2012). The NS31/LSUGlom1 PCR amplicons were generated in volumes of 20 μl with 0.5 U of HotStarTaq DNA Polymerase (Qiagen, Germantown, MD, United States), 10 μM of each primer (NS31 /LSUGlom1), 0.2 mM of each dNTP, 1 mM of $MgCl_2$, and 1 × reaction buffer, using a touchdown thermal cycling on an S1000 Thermal CyclerTM (BIORAD, Hercules, CA, United States). The temperature profile was as follows: denaturation and enzyme activation at 95°C for 15 min, 20 cycles with denaturation at 95°C for 30 s, primer annealing for 1 min starting at 62°C and decreasing by 0.5°C per cycle to 52°C, extension at 72°C for 135 s and 20 cycles with denaturation at 95°C for 30 s, primer annealing at 52°C for 1 min, extension at 72°C for 135 s, and a final extension at 72°C for 10 min. The QIAquick (Qiagen, Germantown, MD, United States) purified PCR amplicons of DNA from the spore samples and the Wizard®SV (Promega Corporation, Madison, WA, United States) gel-purified amplicons of DNA from the root samples were ligated into the pGem®-T Easy vector (Promega, Corporation, Madison, WA, United States) to transform XL10-Gold®Ultracompetent *Escherichia coli* cells (Agilent Technologies, Milano, Italy). On average, sixty-five recombinant clones per amplicon library were screened for the ca. 2,200-bp-long NS31-Glom1 fragment on agarose gels [2% ultrapure agarose (VWR) stained with 0.5 μg ml^{-1} ethidium

bromide]. The variable SSU, ITS2, and LSU fragments of the vector inserts (2.2 kb long) were sequenced from plasmids, using the GenElute^{TM} Plasmid Miniprep Kit (Sigma-Aldrich, St Louis, MO, United States). Sequencing reactions were set up with the vector primers SP6 and T7 using the 3730XL Genetic Analyser automated sequencer (Life Technologies, Carlsbad, CA, United States) at the DNA Services of the University of Illinois in Chicago, United States.

Molecular Tracing of Arbuscular Mycorrhizal Fungi Inoculants in Roots of *M. sativa* Plants

At the onset of spring growth in 2013 (on the 2-year crop), 100 mg of fresh roots were collected from each replicate plot, and genomic DNA was extracted and amplified using NS31/LSUGlom1 primers, as described above. After screening on agarose, on average seventy recombinant clones were sequenced as described above. Plasmids (1184) were sequenced and phylogenetically identified targeting *F. mosseae* and *R. irregularis*, and other Glomeromycota taxa.

Statistical Analysis

All results except for AM fungal root colonization were analyzed by a three-way ANOVA using a general mixed model including crop age (Age), AM fungal inoculant (Inoc), and cut (Cut) as fixed factors. Given our experimental design, the effect of the year of growth is completely confounded with the crop age and thus it was not possible to discriminate the effect of climatic conditions from the effect of crop age. Plots-within-replicates were included as a random factor to account for grouping factors and repeated measures in the same plots (Onofri et al., 2016). AM fungal root colonization was analyzed by a two-way ANOVA using a general mixed model and including Inoc and crop stage (1 month, 1st year, and 2nd year) as fixed factors and plots-within-replicates as a random factor. The relative abundances of AM fungal phylotypes (native *F. mosseae* and *R. irregularis*, and other Glomeromycota) in roots were analyzed by a one-way ANOVA to test the effect of Inoc. Data were ln or arcsine-transformed when needed to fulfill the assumptions of the ANOVA. *Post hoc* Tukey-B significant difference test was used for comparison among treatments. Finally, one-way ANOVA was performed to test the effect of inoculants on plant growth, N and P content of forage, and on single and total fatty acid content accumulated over cuts and years (data were transformed, when necessary, as described above). Differences between means were determined using orthogonal contrasts: inoculated (+ Myc) vs. control, single AM fungal isolates vs. mixture inoculants (Single vs. Mixture), and foreign vs. local AM fungal mixtures (Fmix vs. Lmix). The means given in tables and figures are for untransformed data. Analyses were performed using the SPSS software package version 21 (SPSS Inc., Chicago, IL, United States).

To understand the functional relationship between AM fungal community within the roots of alfalfa and plant performance, and which were the phylotypes mainly responsible for the measured plant traits, a two-step approach was utilized: (i) a multivariate descriptive analysis of the AM fungal community within the roots of the 2-year crop, and a multivariate descriptive analysis of the corresponding plant traits; (2) a test of the relationships between the biological community (AMF) and plant traits matrices. Thus, firstly, a non-metric multidimensional scaling analysis (nMDS) was done on the Bray-Curtis similarity matrix calculated on the fourth-root AM fungal relative abundances of phylotypes retrieved within the roots of inoculated and not-inoculated 2-year alfalfa (Kruskal, 1964). Moreover, the principal component analysis (PCA) was performed on the Euclidian distance matrix calculated on the square root of the plant traits (plant growth, N and P concentration of forage, and fatty acid composition) (Abdi and Williams, 2010). Then, a RELATE analysis, based on Spearman rank and 999 permutations, allowed to test the significance of the relationship between the two matrices ($\rho = 1$ perfect relationship) (Clarke and Warwick, 2001), while the BEST analysis, based on BioEnv methods (all combinations), Spearman rank and 999 permutations. Allowed to find the best descriptor of such relationship (Clarke et al., 2008). Finally, the Distance-based linear method (DistLM) analysis using a stepwise selection and the Akaike's information criterion (AICc) was applied to measure the significance and the variance explained by the best descriptor/s (Knorr et al., 2000), and the Distance-based redundancy analysis was used to plot the first and second axes of the DistLM (Legendre and Anderson, 1999). Analyses were performed using PRIMER 7 and PERMANOVA + software (Primer-e, Auckland, New Zealand) (Anderson et al., 2008; Clarke and Gorley, 2015).

Phylogenetic Analysis

The Glomeromycota affiliation of the sequences was verified in similarity searches using the Basic Local Alignment Search Tool (BLAST) in the National Center for Biotechnology Information (NCBI) database. No chimeric sequences were detected among the newly generated AM fungal SSU and ITS2-LSU sequences (1,324 sequences for each fragment). Here, 20 and 24 newly generated partial SSU (ca. 550 bp), ITS2 (ca. 165 bp) and LSU (ca. 400 bp) sequences of the isolates *F. mosseae* BEG12 and AZ225C, and 39 sequences of the native *F. mosseae* were aligned together with 17 public sequences of isolate BEG12 of *F. mosseae*, one sequence of the isolate *Funneliformis caledonium* BEG20, and one sequence of the isolate *Funneliformis geosporum* BEG11 using MAFFT online service (MAFFT version 7[1]; Kuraku et al., 2013; Katoh et al., 2019). Moreover, 17 newly generated partial SSU (ca. 720 bp), 5.8S and ITS2 (ca. 430 bp), and LSU (ca. 365 bp) sequences of the isolate *R. irregularis* BEG141, and 40 sequences of the native *R. irregularis* were aligned together with five sequences of the isolate *R. irregularis* DAOM181602, three sequences of the isolate *R. irregularis* MUCL43194/DAOM197198, four sequences of the isolate *R. irregularis* DAOM229456, and two sequences of the isolate *R. irregularis* MUCL41833, and one sequence of the isolate *R. intraradices* FL208. The multiple alignments were separately computed for the SSU and ITS2-LSU fragments and then concatenated using SEAVIEW[2] (Gouy et al., 2010). Two

[1]https://mafft.cbrc.jp/alignment/server/large.html

[2]http://doua.prabi.fr/software/seaview

phylogenetic trees (*F. mosseae* and *R. irregularis* trees) were built by neighbor-joining (NJ) analysis using built-in MEGA11[3] (Tamura et al., 2021) and the Kimura 2-parameter model (Kimura, 1980). Branch support values correspond to 1,000 bootstrap replicates. The phylograms were drawn by MEGA 11 and edited by Adobe Illustrator 2021. Then, after having validated the DNA marker for the molecular discrimination among the foreign isolates of *F. mosseae* (12 and AZ225C) and *R. irregularis* (BEG141) and the native phylotypes of *F. mosseae* and *R. irregularis,* two further multiple sequence alignments were derived, including 478 and 332 newly generated sequences of *F. mosseae* and *R. irregularis*, respectively, derived from the roots sampled in the 2-year crop. Phylogenetic discrimination of non-native AM fungal strains relied on branch support of ≥ 70%. This approach of sequence analysis enabled to discriminate native from inoculated non-native strains through molecular barcoding and the phylogenetic divergence. The relative abundances of AM fungal intraradical communities (*F. mosseae* BEG12, AZ225C, BE141, native *F. mosseae*, native *R. irregularis,* and other Glomeromycota taxa) were calculated based on the ratio between the number of sequences affiliated to each phylotype and the total number of sequences of the clone library of each sample, and one-way ANOVA was performed to test the effect of inoculants and the *Post hoc* Tukey-B test was used for comparison among treatments. Cluster/Similarity Profile (SIMPROF) analyses were used to group the different samples into clusters based on their similarity/homogeneity of AM fungal intraradical communities (relative abundances of phylotypes) and to group the different phylotypes based on their similarity of occurrence. Relative abundance data were initially log(X + 1) transformed (Clarke and Warwick, 2001) and the Bray-Curtis similarity was calculated. The SIMPROF cluster analysis was performed to objectively define the groups within the dendrogram. Moreover, the relative abundances of the AM fungal phylotypes were represented by a shaded plot. The analyses were performed using PRIMER 7 and PERMANOVA + software (Primer-e, Auckland, New Zealand) (Anderson et al., 2008; Clarke and Gorley, 2015). All new sequences were uploaded in NCBI[4] and are available under the submission numbers SUB10633042 (OL412293-OL412393) and SUB10648656 (OL441688-OL441757) for the SSU of *F. mosseae* and *R. irregularis*, respectively; SUB10638254 (OL435161-OL435261) for the ITS2 of *F. mosseae*; SUB10649136 (OL449343-OL449412) for the 5.8S-ITS2 of *R. irregularis*; SUB10638603 (OL422707-OL422807) and SUB10649570 (OL442685-OL442754) for the LSU of F. *mosseae* and *R. irregularis*, respectively.

RESULTS

Arbuscular Mycorrhizal Fungal Root Colonization

Arbuscular mycorrhizal (AM) fungal root colonization was influenced by the interaction of AM fungal inoculant and crop stage (**Supplementary Table 2**). Over time and with crop aging, root colonization increased with all treatments, but the rate of increase differed among control and inoculants (**Figure 1**). One month after seeding, AM fungal root colonization was higher with all inoculants compared with uninoculated control, ranging from 22% for BEG141 to 34% for Fmix. However, differences among inoculants were statistically not significant. Functional root nodules were observed in all plant samples without differences among treatments (data not shown). Similarly, at the beginning of the spring growth of the first year, root colonization was higher with all inoculants compared with the uninoculated control, and the range of variation among inoculants was small (from 37% for BEG141 to 41% for Fmix). At the onset of the spring growth of the second year, root colonization increased in the uninoculated control compared with the previous year, although the difference was statistically not significant. AM fungal root colonization in the 2-year plants did not further increase with all inoculants. At this crop stage, differences in root colonization among inoculation treatments were small (36–41%) and statistically not significant. Averaged over inoculants, root colonization was 30, 39, and 39% 1 month after seeding, at the onset of the spring growth of the first year and of the second year, respectively.

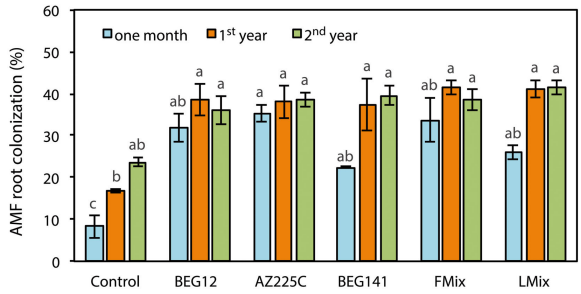

FIGURE 1 | Arbuscular mycorrhizal (AM) fungal root colonization of alfalfa (*Medicago sativa* L.) as influenced by the interaction AM fungal inoculant [*Funneliformis mosseae* BEG12, *F. mosseae* AZ225C, *Rhizophagus irregularis* BEG141, foreign mixture (FMix) (BEG12, AZ225C, and BEG141), local mixture (LMix) of 14 AM fungal species belonging to five families, and mock-inoculated control] and crop stage (1 month, 1-year and 2-year). Data are mean ± SE (n = 3). Different letters indicate significant differences at $P \leq 0.001$ (**Supplementary Table 2**).

Plant Growth, Forage Yield, and N and P Content

Leaf DW accumulated over years and cuts was increased by 64% by inoculation and was 99% higher with inoculum mixture (Fmix and Lmix) compared with single inoculants (BEG12, AZ225C, BEG141), and 19% higher with Fmix than Lmix (**Figure 2A**). Calculating the quantity of stem DW accumulated over years and cuts, it is evident that it was increased by 75% by inoculation, and it was 15% higher with inoculum mixture compared with single inoculants, and 21% higher with Fmix than Lmix (**Figure 2B**). Forage DW accumulated over years and cuts was increased by 68% by inoculation, it was 12% higher with inoculum mixtures compared with single inoculants and was 20% higher with

[3]https://www.megasoftware.net
[4]https://submit.ncbi.nlm.nih.gov

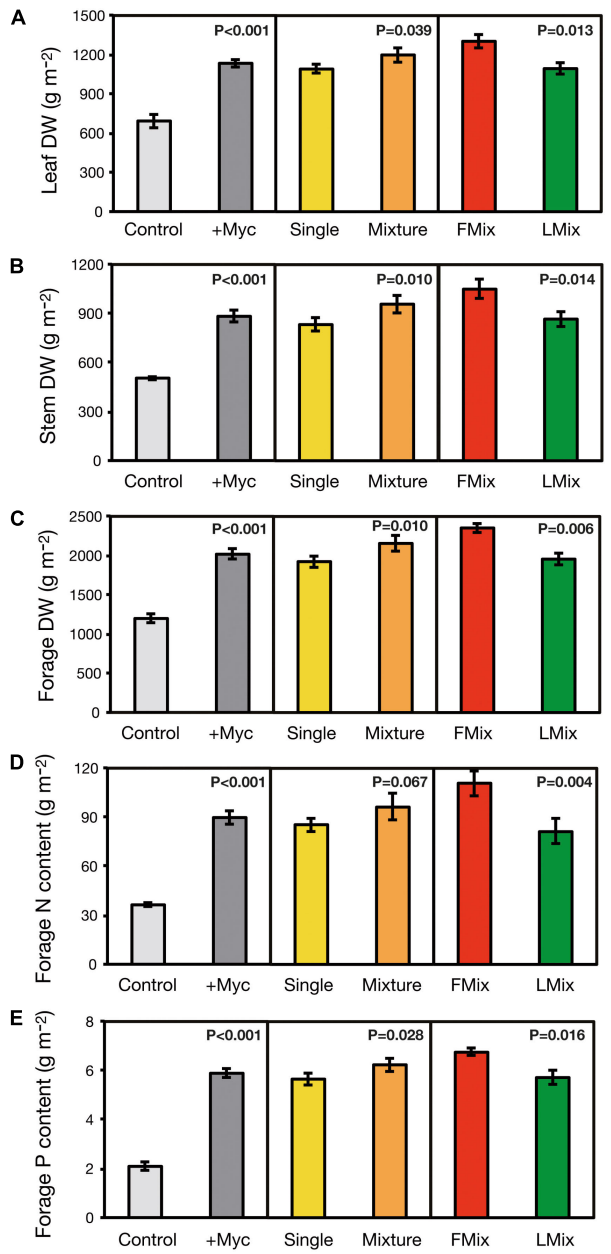

FIGURE 2 | Leaf, stem, and forage dry weight **(A–C)** of alfalfa (*M. sativa*), and forage nitrogen (N) and phosphorus (P) content **(D,E)** accumulated over years and cuts as affected by AM fungal inoculation. Results of orthogonal contrasts used for discriminating the differences between means: inoculated (+ Myc) vs. control, single fungal isolates vs. mixture inoculants (Single vs. Mixture), and foreign vs. local AM fungal mixtures (FMix vs. LMix) [Inoculants: *F. mosseae* BEG12, *F. mosseae* AZ225C, *R. irregularis* BEG141, foreign mixture-FMix (BEG12, AZ225C, and BEG141), local mixture-LMix of 14 AM fungal species belonging to five families, and mock-inoculated control]. Data are mean ± SE (three plot replicates per inoculum treatment).

Fmix than Lmix (**Figure 2C**). Forage N content accumulated over years and cuts was increased by 147% by inoculation, was unchanged when treated with inoculum mixture compared with single inoculants, and was 36% higher with Fmix than with Lmix (**Figure 2D**). Forage P content accumulated over years and cuts was increased by 182% by inoculation, was 10% higher with inoculum mixture compared with single inoculants, and 18% higher with Fmix than with Lmix (**Figure 2E**). Details about plant growth, forage yield, and N and P content across years and cuts are given in **Supplementary Results** and **Supplementary Figures 2–4**.

Fatty Acid Profile

Arbuscular mycorrhizal (AM) fungal inoculation significantly influenced the forage FA profile of alfalfa (**Supplementary Table 4**). While nearly all FA examined had significant interactions between inoculation and age and between inoculation and cut, these interactions tended to be small compared with the sources of variation of inoculation. Therefore, these interactions are only reported in **Supplementary Tables 5**, **6**, while the effect of inoculation, being of primary interest, is here illustrated. Fatty acids 18:3 (α-linolenic acid, omega-3) and 18:2 (linoleic acid, omega-6) were the predominant ones, comprising from 44 to 47% and 29 to 31%, respectively, of the total FA concentration in all treatment combinations (**Supplementary Table 5**). Fatty acids 16:0 and 18:1 were similar to each other in concentration, i.e., comprising from 11 to 15% and from 7 to 12% of the total FA, respectively, in all treatment combinations. Finally, FA18:0 had the smallest fraction, accounting for 2–3% of the total FA analyzed.

Arbuscular mycorrhizal (AM) fungal inoculation increased the concentration of all FA in forage compared with control, except for 18:0, and the increases were fairly similar across crop ages and cuts (**Supplementary Table 5**). Moreover, TFA, averaged over crop age and cut, were increased by 24% compared with uninoculated control. When significant differences occurred among inoculants, Fmix was the most effective in increasing FA concentration in alfalfa forage.

Fatty acids content in forage of all FA accumulated over years and cuts was increased by AM fungal inoculation, and increases ranged from 74 to 189% in 16:0 and 18:1, respectively (**Figure 3**). Moreover, the content of all FA, except 18:0, was higher with inoculum mixture compared with single inoculants, and the increase ranged from 10 to 19% in 18:0 and 18:2, respectively. Finally, the content of all FA was higher when plants were inoculated with Fmix than with Lmix, and the increase ranged from 18 to 28% in 18:3 and 18:0, respectively. Similarly, TFA content was increased by 105% following inoculation and was 17% greater when inoculation was performed with an inoculum mixture than with a single inoculant and 20% greater when a mixture of foreign inoculants was applied, compared with a local one.

Molecular Discrimination Among Non-native and Native *F. mosseae* and *R. irregularis*

The c. 2,200-bp-long central stretch of the nuclear rDNA cistron, obtained using the PCR primers NS31 and LSUGlom1, provided sufficient phylogenetic resolution to discriminate the inoculated isolates from native strains of *F. mosseae* and *R. irregularis*.

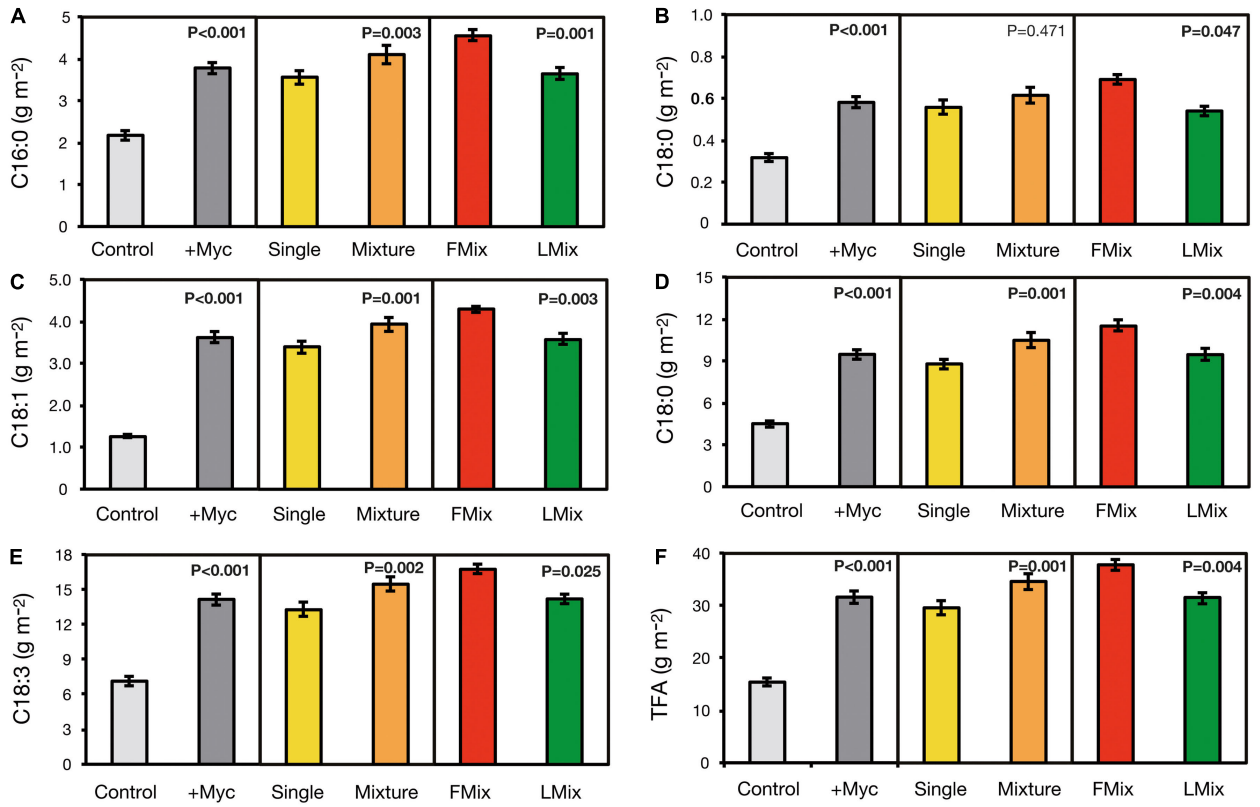

FIGURE 3 | The single **(A–E)** and total fatty acid **(F)** content of alfalfa (*Medicago sativa* L.) accumulated over cuts and years as affected by AM fungal inoculation. Results of orthogonal contrasts used for discriminating the differences between means: inoculated (+ Myc) vs. control, single arbuscular mycorrhizal (AM) fungal isolates vs. mixture inoculants (Single vs. Mixture), and foreign vs. local AM fungal mixtures (FMix vs. LMix) [Inoculants: *F. mosseae* BEG12, *F. mosseae* AZ225C, *R. irregularis* BEG141, foreign mixture-FMix (BEG12, AZ225C, and BEG141), local mixture-LMix of 14 AM fungal species belonging to five families, and mock-inoculated control]. Data are mean ± SE (three plot replicates per inoculum treatment).

However, similarly to Pellegrino et al. (2012), in the case of *F. mosseae* BEG12 and AZ225C, the discrimination was possible using the concatenated sequences of the variable 3′ end of the SSU rRNA gene (ca. 550 bp), ITS2 (ca. 165 bp), and the variable 5′ end of the LSU (400) rRNA gene (**Figure 4A** and **Supplementary Figure 5**). In the case of *R. irregularis* BEG141, the discrimination was possible using longer concatenated sequences of the variable 3′ end of the SSU rRNA gene (ca. 720), the 5.8S and ITS2 (ca. 430 bp), and LSU (ca. 365 bp) (**Figure 4B** and **Supplementary Figure 6**). The sequences (obtained from spores) of the inoculated *F. mosseae* BEG12 and AZ225C, and *R. irregularis* BEG141 clustered distinctly from those of the native strains of both AM fungal species, amplified from the roots of Sudan grass grown in pots for the production of the Lmix inoculum (**Figure 4** and **Supplementary Figures 5**, **6**). The partial sequences of the nuclear rDNA cistron of the *F. mosseae* BEG12 isolate clustered into two phylogenetic subclusters, whereas those of *F. mosseae* AZ225C and *R. irregularis* BEG141 both grouped into only one cluster.

Reference sequences of *F. mosseae* BEG12 from NCBI clustered together with the sequences two phylogenetic subclusters of the inoculated *F. mosseae* BEG12 maintained in cultivation since 2010 at the AM fungal bank of the Institute of Life Science (Scuola Superiore Sant'Anna, Pisa, Italy) (**Figure 4A** and **Supplementary Figure 5**). Since no reference sequences of SSU and ITS2 were available for *R. irregularis,* BEG141 and only three sequences available for LSU were included in the alignment as input for the tree building of four different isolates of *R. irregularis* and one of *R. intraradices* (**Figure 4B** and **Supplementary Figure 6**). The sequences of *R. irregularis* MUCL43194/DAOM197198 grouped into a unique, well-supported cluster, as well as the sequences of *R. irregularis* MUCL41833. Conversely, the sequences of *R. irregularis* DAOM181602 were grouped into two distinct clusters, as well as those of DAOM229456. The sequences of the local strain of *F. mosseae* were grouped into one cluster, whereas those of *R. irregularis* were more divergent and grouped into nine distinct clusters (**Figure 4** and **Supplementary Figures 5**, **6**).

Tracing Non-native and Native Strains of *F. mosseae* and *R. irregularis* in the Field

Using the validated molecular markers, foreign and local strains of *F. mosseae* and *R. irregularis* were successfully traced within the roots of the polyannual forage crop alfalfa 2 years following inoculation. However, AZ225C was the most persistent both as

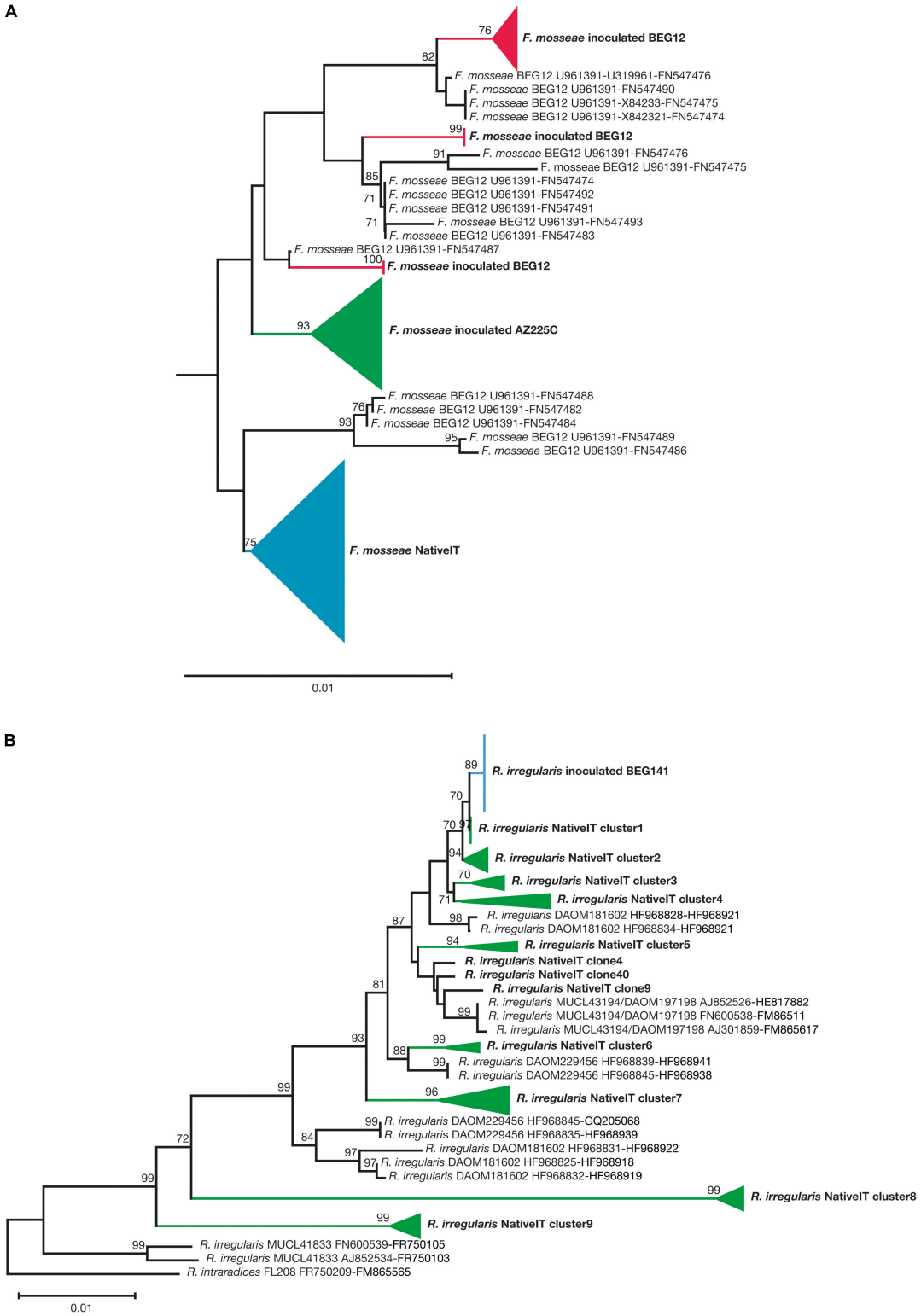

FIGURE 4 | Neighbor-joining (NJ) collapsed tree of the nuclear ribosomal rDNA sequences of *F. mosseae,* originating from local strains and the non-native inoculated isolates BEG12and AZ225C **(A)**. The tree is composed of 20 and 24 newly generated sequences of BEG12 and AZ225C, respectively, 39 native *F. mosseae* sequences, plus 17 sequences of BEG12 as reference. NJ collapsed tree of the nuclear ribosomal rDNA sequences of *R. irregularis,* originating from local strains and the non-native inoculated isolates BEG141 **(B)**. The tree is composed of 17 newly generated sequences of BEG141 and 40 native *R. irregularis* sequences, plus 14 sequences of *R. irregularis* isolates as reference (DAOM181602, MUCL43194/DAOM197198, DAOM229456, and MUCL41833) The NJ *F. mosseae* tree is based

(Continued)

FIGURE 4 | on concatenated sequences of the small subunit ribosomal RNA gene (SSU; ca. 550 bp), the internal transcribed spacer 2 (ITS2; ca. 165 bp) and the large subunit ribosomal RNA gene (LSU; ca. 400 bp). The NJ *R. irregularis* tree is based on concatenated sequences of the small subunit ribosomal RNA gene SSU (ca. 720 bp), 5.8S, and ITS2 (ca. 430 bp), and LSU (ca. 365 bp). Bootstrap values (based on 1,000 replicates) are shown at the nodes. The scale bar indicates substitutions per site. Clades formed by sequences of native and inoculated *F. mosseae* and *R. irregularis* strains are shown by colored branches and triangles. The concatenated sequences AJ245637-AJ239122-AJ5110241 of the isolate BEG11 of *Funneliformis geosporum* were used as an outgroup to root the *F. mosseae* tree, while the concatenated sequences FR750209-FM865565 of the isolate of *R. intraradices* FL208 were used as an outgroup to root the *R. irregularis* tree. The *F. mosseae* tree is outgroup-truncated. The newly generated sequences are highlighted in boldface, and their accession numbers are indicated in **Supplementary Figure 3**.

single inoculum or mixture, followed by BEG12 and BEG141 (**Supplementary Table 7**). This is also evidenced by the cluster analysis and the associated shade plot based on the AM fungal community found in the inoculated and control plots (**Figure 5**). Control replicates clustered together and separately from the inoculated plots, which were separated according to inoculation treatment, except for BEG141. Overall, local *F. mosseae* were similarly abundant to the other Glomeromycota taxa, but they were differently retrieved in the treated plots. In the BEG12 and AZ225C plots over 60% of the retrieved sequences were assigned to *F. mosseae* either inoculated or local, whereas in the BEG141 plots local *F. mosseae* accounted only for 7.4% (**Supplementary Table 7**). Comparing control and Lmix, local *F. mosseae* and other Glomeromycota taxa accounted for 44 and 37% of the total retrieved taxa in the control plots, while they accounted for 39 and 45%, respectively, in the Lmix plots. Finally, clusters 1–9 of local *R. irregularis* formed a unique group across the treated replicates, although clusters 5 and 6 were more abundant in the control, BEG12, and BEG141 plots.

These results are also supported by the NJ trees built focusing on *F. mosseae* and *R. irregularis* and by the relative abundance pie charts based on inoculum treatments (**Supplementary Figures 7**, **8**). In detail, the NJ tree of *F. mosseae* clearly showed that the sequences retrieved in the alfalfa roots collected from the plots inoculated by BEG12, AZ225C, and Fmix clustered into three groups, phylogenetically affiliated to BEG12, AZ225C, and the local sequences of *F. mosseae*. Among these, 86% of the sequences affiliated to BEG12 were retrieved in the plots originally inoculated with this isolate, while the remaining were retrieved in the Fmix plots (14%) and no sequences were found in the other treatments. Similarly, 81% of the sequences affiliated to AZ225C were retrieved in the plots inoculated with AZ225C and 19% in the Fmix plots. Finally, the sequences phylogenetically affiliated to the native *F. mosseae* were retrieved in all the inoculated plots but were more abundant in the control plots, and their occurrence decreased progressively from Lmix (30%) to BEG141 (7%) (**Supplementary Figure 7**). As regard *R. irregularis*, the NJ tree showed that the sequences retrieved in the alfalfa roots collected from the treated plots were grouped into 10 clusters (**Supplementary Figure 8**), one cluster composed of sequences phylogenetically affiliated to BEG141 and the others composed by the sequences affiliated to the nine clusters of local *R. irregularis* strains initially found (**Figure 4B**). About 88% of the sequences affiliated to BEG141 were retrieved in the plots originally inoculated with this isolate, while the remaining were retrieved in the Fmix plots (12%) and no sequences were found in the other treatments. Regarding local *R. irregularis* clusters, the relative abundance of clusters 1, 4, and 6 differed among treatments, while the abundances of the others did not change (**Supplementary Figure 8**).

Exploring the Relationship Between the Components of Arbuscular Mycorrhizal Fungal Communities in Alfalfa Roots and Plant Traits

In the nMDS plot, representing the AM fungal communities within the roots of the 2-year alfalfa, the inoculum treatments were well separated along a first and second axis (**Figure 6A**), and the nMDS stress (0.09) supported this representation of the dissimilarity among samples. Moreover, the PCA, based on the corresponding plant traits, well separated the non-inoculated plots from the inoculated ones along the first axis, as well as the different inoculants along the second axis (**Figure 6B**). Overall, local *R. irregularis* clusters 1–4, and 7–9, and *F. mosseae* AZ225C and BEG12 were positively and strongly correlated with all plant traits. The relationship of the two matrices was also shown to be significant by the RELATE analysis, for which the ρ was equal to 0.46 and the significance level of sample statistic after 999 permutations were equal to 0.4% (**Figure 6C**). Nevertheless, the BEST analysis allowed us to highlight that together local *R. irregularis* cluster1 and cluster6 were the best predictors of the plant traits (correlation:0.656). Finally, although the marginal test of the DistLM analysis highlighted that many phylotypes were significantly correlated with the plant traits and explained a relevant part of the total variation (**Supplementary Table 8**), the local *R. irregularis* cluster1 alone was sufficient to describe the majority of the diversity inside the plant traits (49.2% of the total variance explained; $P = 0.003$). This is also detectable from the plot of the dbRDA of the DistLM axes (**Figure 6D**) showing that the increase in the abundance of the local *R. irregularis* cluster1 well explains the distribution of the samples in the multivariate space based on plant traits (**Figure 6B**).

DISCUSSION

Arbuscular Mycorrhizal Fungal Inoculation Enhances Alfalfa Yield and Fatty Acid Concentration in Forage

Overall, AM fungal field inoculation enhanced crop yield and FA concentration in both years of cultivation. AM fungal root colonization was greatly increased by inoculation and the effect was the highest at the beginning of crop growth. Indeed, already 1 month following inoculation, all inoculants reached the saturation (ca. 40%) within the roots of alfalfa, compared with

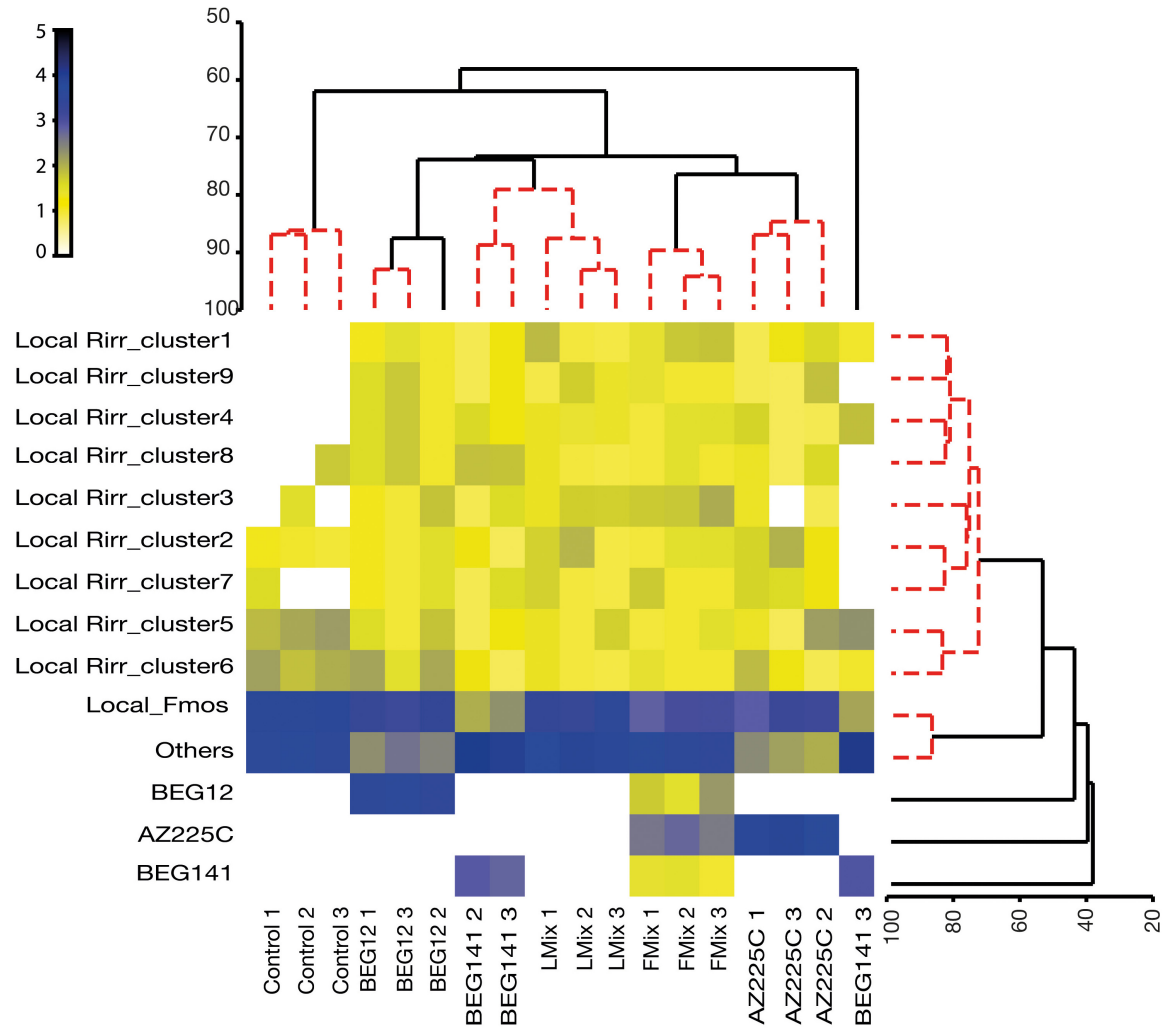

FIGURE 5 | Dendrogram of Similarity Profile (SIMPROF) cluster analysis (horizontal dendrogram) grouping the different samples collected at the beginning of spring growth (roots of 2-year alfalfa, *M. sativa*) [three fields replicate plots treated by mock-inoculated control (Control), *F. mosseae* isolates BEG12 and AZ225C, *R. irregularis* isolate BEG141, foreign mixture-FMix (BEG12, AZ225C, and BEG141), local mixture-LMix of 14 AM fungal species belonging to five families] into clusters based on their similarity/homogeneity of AM fungal intraradical communities [relative abundances of phylotypes of non-native/inoculated *F. mosseae* BEG12 and AZ225C, non-native/inoculated *R. irregularis* BEG141, native *F. mosseae* (Local Fmos) and native *R. irregularis* (Local Rirr_cluster1-9) and other Glomeromycota taxa (others)]. Vertical dendrogram groups the different phylotypes based on their similarity of occurrence. Red clusters are supported by the SIMPROF analysis. Relative abundance input data were log(X + 1) transformed and Bray-Curtis similarity was calculated and shown as a shaded plot.

control having less than 10% of colonization. This suggests a high infectivity of the AM fungal inoculants under field conditions. This is in agreement with the root colonization pattern reported in a previous study on alfalfa field-inoculated with two single isolates of *F. mosseae* (IMA1 = BEG12 and AZ225C) (Pellegrino et al., 2012). In the study of Pellegrino et al. (2012), already 3 months after crop emergence, AM fungal colonization in the inoculated plants reached 30%, while in the control plots were low (3%), and the rate of colonization did not change with crop aging, supporting the high infectivity of the inoculants on alfalfa and a saturation level similar to the one in our research. Our data evidenced that native AMF occurring into control plots were less infective, because up to 2 years from crop seeding their presence in plant roots was still lower compared with inoculated plots. Thus, these results support the high infectivity (54%–80%) found in a pot experiment with a 4-month-old alfalfa inoculated by *F. mosseae* IMA1 and AZ225C, and by *R. irregularis* IMA6 (= BEG141) (Avio et al., 2006). Other studies carried in pots with isolates of *F. mosseae* and *Rhizophagus intraradices*, reported in 8-month-old alfalfa plants root colonization up to 60% (Wang et al., 2020; Li et al., 2021). Thus, our results confirm the high mycotrophic behavior of this important forage crop previously described in controlled conditions.

In the first year of growth, the higher AM fungal root colonization detected in inoculated alfalfa compared with uninoculated controls was associated with a general improvement of plant growth, due to an increase of the growth of stems and leaves and consequently of forage. However, this

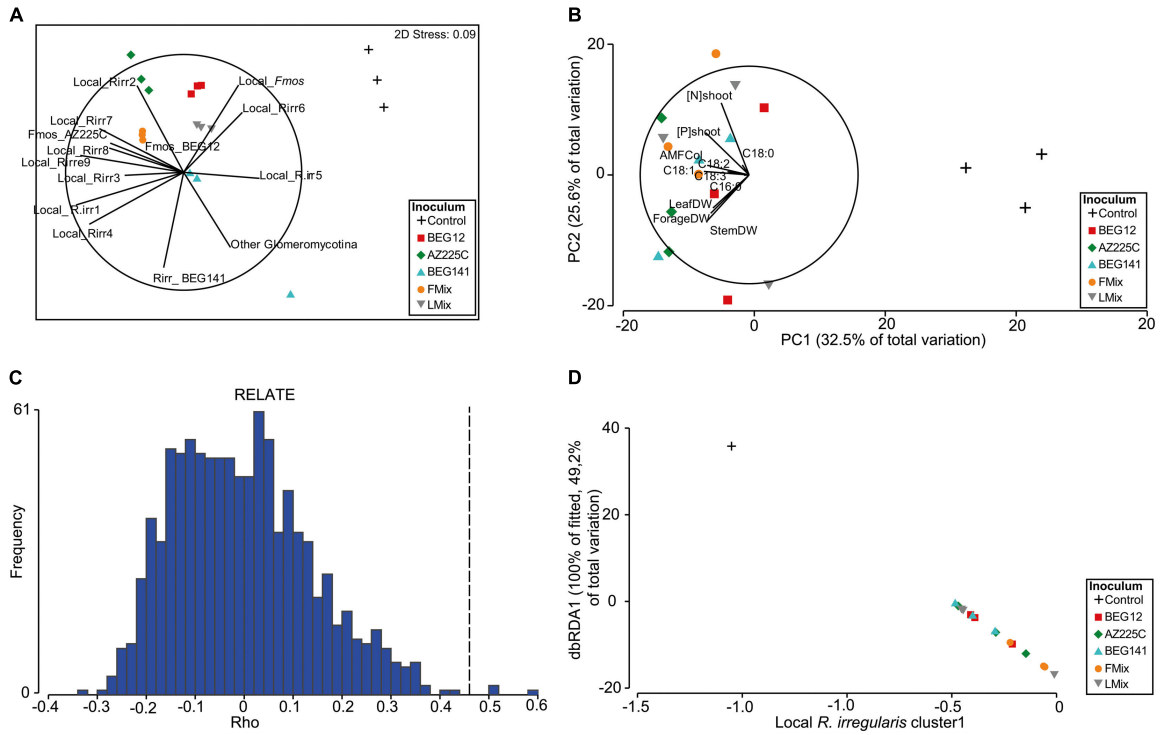

FIGURE 6 | Non-metric multidimensional scaling analysis (nMDS) plot based on the Bray-Curtis similarity matrix calculated on the fourth-root AM fungal relative abundances of phylotypes retrieved within the roots of inoculated and not-inoculated 2-year alfalfa **(A)**. A principal component analysis (PCA) plot was performed on the Euclidian distance matrix calculated on the square root of the plant traits (plant growth, N and P concentration of forage, and fatty acid composition) **(B)**. RELATE analysis based on Spearman rank and 999 permutations for testing the significance of the relationship between the two matrices **(C)**. Distance-based redundancy analysis plot used to visualize the first and second axes of the Distance-based linear method (DistLM) analysis applied to measure the significance and the variance explained by the best descriptor **(D)**.

fungal trait could not fully explain the variability in plant growth, since inoculants colonizing the roots of alfalfa at a similar rate differently influenced plant growth. In this regard, Lekberg and Koide (2005) found a significant but weak relationship between a change in mycorrhizal colonization and a change in yield. Therefore, while an increase in mycorrhizal colonization appears to be associated with an increase in yield, the mycorrhizal colonization cannot be the sole predictor of an increase in yield, and the characterization of the AM fungal components of the root community assemblages became essential for dissecting functionality (Vályi et al., 2016). Indeed, AMF taxa can greatly differ in the spread of external mycelium or hyphae architecture, thus affecting yield and nutrient uptake (Munkvold et al., 2004; Avio et al., 2006).

The positive effect of field AM fungal inoculation on N and P concentration in forage irrespective of inoculants is consistent with the results on Egyptian clover (*Trifolium alexandrinum* L.) and alfalfa (Pellegrino et al., 2011, 2012). A generalized positive effect of AM fungal inoculation on plant P concentration was reported by Lekberg and Koide (2005) taking into consideration 25 field trials. About the effect of AM fungal inoculation on plant N concentration, while a generalized increase was reported by Delavaux et al. (2017) looking only to greenhouse trials, the effect in the field is less clear and poorly studied (Pellegrino et al., 2015a). However, in Pellegrino et al. (2011) a strong variability among AM fungal inoculants was reported on forage nutrient concentrations in pots where no other AMF occur. This suggests that the interactions of AM fungal inoculants with the native AM fungal community are likely to be responsible for the lack of differences in fungal physiological traits (van der Heijden and Scheublin, 2007). In addition, in the field, the outcome of the inoculation is influenced also by the disturbance history (i.e., reduced disturbance and shorter fallow) (Lekberg and Koide, 2005), and/or by soil nutrient availability (i.e., N and P) and soil pH (Han et al., 2020).

So far, a unique study in a field-grown crop analyzed the effect of AMF on fatty acid content and composition (Igiehon et al., 2021). In contrast with our results highlighting an increase in the amount of fatty acids, Igiehon et al. (2021) found a lower amount of fatty acids in seeds of soybean when plants were inoculated with AMF and no changes of fatty acids when soybean was inoculated with AMF plus strain of *Rhizobium* sp. However, similar to our results, the composition of polyunsaturated FA (PUFA), monounsaturated FA (MUFA), and saturated FA (SFA) was greatly modified by AMF and *Rhizobium* in comparison with the uninoculated control. Moreover, drought stress was shown to enhance the fatty acid contents in seeds of some inoculated soybean plants through upregulation and downregulation of

specific fatty acids (Hou et al., 2006; Igiehon et al., 2021). Under water-deficit conditions, plants colonized by mycorrhizal fungi have better growth than those that are not, and the response is more evident in perennial plants (Jayne and Quigley, 2014). Therefore, our results largely confirm the hypothesis that AM fungal inoculation supports plant growth and total fatty acid content in drought conditions, likely to occur in the area where our trial was run. A higher concentration of oleic acid (C18:1), linoleic acids (C18:2), and α-linolenic acid (C18:3), we found in all inoculated alfalfa plots, is a desirable quality in forage for animal nutrition, since these components are associated with several health and nutritional benefits (Radović et al., 2009; González-Fernández et al., 2020). The fatty acid auxotrophy of AMF is supported by recent studies showing that lipids synthesized by the host plants (e.g., palmitic, oleic, and myristic acids) are transferred to the fungi, lacking genes encoding fatty acid synthases (Stumpe et al., 2005; Trépanier et al., 2005; Sugiura et al., 2020). However, our results suggested that AMF, in addition to using fatty acids as C and energy source, can stimulate their synthesis in the aboveground part of the plant. This is in line with recent results reporting that AMF is involved in the stimulation of the synthesis of secondary metabolites plant (Baslam and Goicoechea, 2012; Zouari et al., 2014; Kaur and Suseela, 2020). Moreover, the use of AM fungi in pasture management could provide benefits for animals, derived products, and humans. In this regard, cows grazing in AM fungal inoculated pasture produced high-quality milk (Masoero et al., 2021).

Multiple Arbuscular Mycorrhizal Fungal Inoculants Act in Synergy to Promote Alfalfa Yield and Fatty Acids Concentration in Forage

In this study, mixed AM fungal inocula performed better than single inocula both in terms of plant growth, P uptake, and FA content and composition. However, no difference in AM fungal root colonization was reported. Several studies carried out in pot conditions with sterilized substrate showed that AM fungal mixed inocula promoted markedly plant performance (e.g., Edathil et al., 1996; Maherali and Klironomos, 2007; Thonar et al., 2014; Martignoni et al., 2021), whereas the few studies performed in the field do not allow to reach conclusive assessments (e.g., Powell, 1977, 1979; Clarke and Mosse, 1981; Pellegrino et al., 2011; Pellegrino and Bedini, 2014). Recently, some meta-analyses synthesized the literature on this topic, but merging the data obtained from lab experiments with the few obtained from the field (e.g., Rúa et al., 2016; Yang et al., 2017; Zhang et al., 2019). Significant differences were found in cereal yield (i.e., wheat, rice, and corn) if mixed inocula were compared with single inocula and substrate sterilization was not applied, whereas no differences were found if the substrate sterilization was applied with or without application of a microbial supplement (Zhang et al., 2019). These results may derive from complementarity among AM fungal species, which can provide a greater crop benefit (Koide, 2000; Thonar et al., 2014). A mixed and more complex inoculum can be more efficient across a range of soil parameters, climatic conditions, and host plants (species or even varieties/genotypes) increasing plant nutrient uptake, decreasing nutrient losses, and improving soil aggregation. The greater efficiency of mixed inocula can be the result of a large variability among AM fungal taxa in foraging strategies and extraradical mycelium development (spread of the mycelium, hyphal architecture, or anastomosis frequency). This variability may enhance the ability of the inoculum to adapt and thus be more efficient and/or more persistent in many environments. Indeed, the structure of the AM fungal extraradical mycelium (ERM) that is largely variable among AM fungal species or even isolates among species was linked to specific functions (Munkvold et al., 2004; Avio et al., 2006; Thonar et al., 2011; Treseder et al., 2018). For example, a high positive correlation was highlighted between ERM interconnectedness (anastomosis frequency and number) and plant growth variables (total shoot biomass), or between anastomosis frequency and root P content (Avio et al., 2006). Moreover, a crop genotype inoculated with an AM fungal mixture may have a great probability to find among the AMF components the taxa with a higher host preference and a life history strategy adapted to local agricultural soil. In this regard, Wagg et al. (2015) using a model plant-mycorrhizal system, suggested that the fungal composition rather than the diversity of species may be more important in determining how plant species function within a community.

Multiple Arbuscular Mycorrhizal Fungal Inoculants Composed of Foreign Arbuscular Mycorrhizal Fungi Provide Greater Benefits to Alfalfa Compared to a Mixture of Local Arbuscular Mycorrhizal Fungi

Foreign isolates combined in the mixture performed better than the local-isolate mixture composed of 14 AM fungal species belonging to seven genera and five families. This is in agreement with the results recorded in the field by Pellegrino et al. (2011) On the contrary, Pellegrino and Bedini (2014) reported that the locally sourced AM fungal mixed inoculum was more effective than a foreign mixture inoculum. The greater effectiveness of foreign mixtures is in accordance with the results of the meta-analysis of Rúa et al. (2016) concluding that the geographic origin of plants relative to the origin of AMF and soil is important for describing the effect of inoculation on plant biomass. Indeed, if plants and soil are sympatric (i.e., locally sourced), but allopatric to the fungus (i.e., foreign origin), the positive effect of inoculation is greater than when all three components are allopatric. In agreement, Klironomos (2003) reported positive responses using local plants and fungi, and parasitic or no responses using foreign plant or fungal genotypes. Kiers et al. (2011) explained this concept by the bidirectionality of mutualism and the reward for individuals showing the best rate of exchange. Indeed, plants and fungi are able to detect variation in the resources supplied by their partners, allowing them to adjust their own resource allocation accordingly. In addition to this concept, the taxonomic resolution of the AM fungal diversity in the inocula is the main factor of plant functionality, as the

functional benefit was found at AM fungal family level, and not at species scale (Yang et al., 2017). Thus, an inoculum composed of many AM fungal families would allow maintaining a full complement of ecosystem functions, rather than an inoculum composed of many species belonging to the same o few families. Therefore, our hypothesis of greater host benefits from local AM fungal isolates than foreign isolates has to be rejected, probably due to the legacy of the agricultural practices (tillage, fertilization, pesticides, etc.) potentially selecting for less advantageous AM fungal strains. Finally, we would like to highlight, as previously mentioned, that in this study inoculants were composed of spores, roots, and soil (crude inoculum). Thus, during the process of production of the different AM fungal isolates and mixtures, AMF may have had socialized differently with the microbial community. This means that, although a significant microbial filtrate was applied at the start of the process of production to minimize microbial differences, at the end of the production phase the variabilities in crop response might be due not only to the AM fungal species identity but also to differences in microbial associated groups. Indeed, from the mycorrhizosphere and the spores of different AM fungal isolates many different bacterial taxa were detected (Bharadwaj et al., 2008). The multiple services provided by AMF were shown to be the result of the synergistic activity of the diverse bacterial communities living in the mycorrhizosphere, strictly associated with the spores and with the extraradical mycelium, which played many plant growth-promoting roles (e.g., nitrogen fixation, P solubilization, production of indole acetic acid, siderophores, and antibiotics) (Frey-Klett et al., 2007).

Molecular Discrimination of Foreign Inoculants and Native *F. mosseae* and *R. irregularis*

In this work, consistently with Pellegrino et al. (2012), the phylogenetic information contained in the polymorphic 3′ end of the nuclear SSU rRNA gene, ITS2, and the 5′ end of the LSU rRNA gene were sufficient for discriminating among foreign inoculants and local strains of *F. mosseae*. Moreover, the phylogenetic information contained in the 5.8S in addition to that contained in the partial SSU, complete ITS2, and partial LSU, allowed also to discriminate foreign inoculants and local isolates of *R. irregularis*. Thus, in our field site, these regions gave sufficient variation to reach a good resolution among closely related AM fungal isolates for both AM fungal species. Molecular discrimination of foreign inoculants might have been facilitated by the fact that both *F. mosseae* isolates BEG12 and AZ225C, and *R. irregularis* BEG141 have a distant origin. Indeed, *F. mosseae* isolates BEG12 and AZ225C are originated from United Kingdom and Arizona (United States), and *R. irregularis* BEG141 from France. Despite the fact that a high rDNA sequence polymorphism was proved within individuals (e.g., Hijri et al., 1999; Lanfranco et al., 1999; Jansa et al., 2002; Thiéry et al., 2012), other researchers (Krüger et al., 2009, 2012; Stockinger et al., 2010), similarly to our findings, proved that the combination of the highly polymorphic ITS region with variable SSU and LSU regions can be used to achieve phylogenetic species- and strain-level resolution in AMF. In this regard, Farmer et al. (2007) could discriminate isolates of *R. irregularis* BEG141 and *C. etunicatum* BEG168, using only the variable domains of the LSU of ribosomal RNA gene, whereas more recent studies proved that other molecular markers (i.e., mtLSU, RPB1, and mt cox3-rnl intergenic mtDNA region) are even more efficient in the discrimination of foreign AM fungal isolates in the field (Sýkorová et al., 2012; Buysens et al., 2017; Kokkoris et al., 2019; Thioye et al., 2019). Very recently, to overcome the difficulties of the lack of consensus barcoding region for the determination of AM fungal taxa, Kolaříková et al. (2021) developed a fine and promising approach to sequence an AM fungal marker within the ribosome-encoding operon (rDNA) which covers all the three widely applied variable molecular markers (SSU, ITS, and LSU). In detail, they amplified a ca. 2.5 kb of the rDNA, spanning the majority of the SSU gene, the complete ITS region, and a part of LSU rRNA gene, and sequenced the PCR products using a PacBio platform and the Single-Molecule Real-Time sequencing. This approach proved to be able to obtain a robust phylogenetic assignment of several Glomeromycota lineages occurring in complex AM fungal assemblages, could overcome the site- and inoculation-specificity of the molecular approach we proposed.

Persistence of Inoculated Arbuscular Mycorrhizal Fungi in the Field and Effects on Native Arbuscular Mycorrhizal Fungi

Using the validated molecular approach, foreign strains of *F. mosseae* and *R. irregularis* were found to persist in the roots of the poliannual forage crop alfalfa 2 years following inoculation with single-foreign isolate inoculum or the mixture of those isolates. Similarly, in potatoes, the inoculated *R. irregularis* BEG141 and *R. etunicatum* BEG168 were found to persist in roots 6 weeks following inoculation (Farmer et al., 2007). In this study, a nested PCR using taxon-specific primers, targeting the variables domains of the LSU of ribosomal RNA gene, and a cloning-sequencing approach was applied. Moreover, using other molecular markers, such as the mtLSU (cloning and sequencing approach) and a fragment of RPB1 (qPCR approach), Sýkorová et al. (2012) and Thioye et al. (2019) successfully traced two haplotypes of *R. irregularis* BEG140 in roots of field-inoculated *Phalaris arundinacea* and *R. irregularis* IR27 in roots of jujube (*Ziziphus mauritiana*), respectively. *Rhizophagus irregularis* BEG140 was reported to survive and proliferate up to 3 years in the field and was found more often in the inoculated than in control plots (Sýkorová et al., 2012), while *R. irregularis* IR27 was reported to persist in jujube tree roots up to 18 months. More recently, Buysens et al. (2017), using a qPCR approach and amplifying the mtLSU RNA gene, performed for the first time the absolute quantification in the field of the isolate *R. irregularis* MUCL 41833, and found a significant correlation between mtLSU_MUCL41833 and total, arbuscular and vesicular colonization of roots of three varieties of potatoes at three growing stages (i.e., flowering, before defoliation and harvest). Finally, Kokkoris et al. (2019) successfully traced the *R. irregularis* DAOM 197198 using specific primers, targeting the mt cox3-rnl intergenic mtDNA region, and a probe in a droplet

digital PCR. The inoculated isolate was found in all the plots (inoculated and non-inoculated) and its abundance increased over time, supporting the hypothesis of the spreading of the isolate beyond inoculated plots. Conversely, Berruti et al. (2017), using a next-generation sequencing-based on the amplification of only ca. 420 bp of the 18S V3-V4 hypervariable domains (SSU), found a lack of field persistence of the AM fungal components of microbial mixed inoculum in maize at the V8-9 stage. Therefore, long-term inoculation trials are needed for monitoring the evolution of the AM fungal native community and to track the persistence of the inoculated AMF.

In our study, among the foreign-inoculated AM fungal isolates, *F. mosseae* AZ225C was the most persistent both as single inoculum or mixture, followed by BEG12 and BEG141. This is in agreement with a previous study (Pellegrino et al., 2012), where at 2 years post-inoculation, the isolate AZ225C was more persistent in roots of *M. sativa* with respect to IMA1, although it declines from the establishment (i.e., 3 months following plant emergence; from 100 to 16%). In the previous study (Pellegrino et al., 2012), IMA1, despite still stimulating crop performance, did not persist after 2 years. This inconsistency proves the high site-specificity of the outcome of the inoculation related to climate, texture, and chemical properties of soil (Ciccolini et al., 2015; Pellegrino et al., 2015a,b, 2020a), or the genetic variability in AM fungal compatibility with different genotypes of the same plant species (*M. sativa* L. var. Giulia vs. cv. Messe) (Pellegrino et al., 2012). In this regard, a large variability in compatibility was proved for AMF in *Triticum turgidum* (Singh et al., 2012), and in *Triticum aestivum* L. (Pellegrino et al., 2020a).

Comparing mock-inoculated control and LMix, while the abundance of the local *F. mosseae* cluster was reduced, the abundance of the native *R. irregularis* clusters and other Glomeromycota taxa was promoted. The change of assemblages with LMix in comparison with those observed with single foreign inoculants of *F. mosseae* BEG12 and AZ225 (i.e., a strong decrease in the abundance of other Glomeromycota), supports the fact that inoculation with local AM fungal mixture or with the less persistent *R. irregularis* BEG141 determines a less environmentally impacting shift of the local fungal community. This is also associated with similarities in the outcome of the symbiosis in terms of plant performance (i.e., plant growth and nutrient and FA content).

The fact that sequences phylogenetically affiliated to the local *F. mosseae* were retrieved in all the inoculated plots, but were more abundant in the control plots, support the high ubiquity of this species (generalist) across a wide range of agro-climatic conditions and geographically areas (Öpik et al., 2006). Finally, no sequences similar to those of BEG12, AZ225C, and BEG141 were found in the roots of mock-inoculated alfalfa (controls) or the roots of alfalfa inoculated with LMix. This could support the absence of spreading of the inoculated AM fungal isolates, at least up to 2 years following inoculation and in such specific management, and in such a no-tilled polyannual forage. However, we cannot exclude a low fungal abundance as well as an insufficient sampling effort due to the used cloning and Sanger sequencing approach. Finally, since we inoculated crude inocula and the method of propagation cannot fully eliminate differences in microbial communities, we could not exclude that the outcome of field persistence can be due not only to the identities of inoculated AMF but also to the associated microbes that might affect the establishment/persistence, with consequences in the soil/rhizospheric microbial communities.

Components of Arbuscular Mycorrhizal Fungal Communities in Alfalfa Roots Best Explain Plant Traits

Unexpectedly, although a high diversity in the composition of AM fungal assemblages was found among inoculated treatments, small differences were found in plant traits, such as growth and nutrient uptake, with the exception of FA. Total fatty acids (TFA) were increased with inoculum mixtures compared with single inoculants, while the content of the majority of FA was higher when plants were inoculated with FMix than with LMix. However, by relating the AM fungal assemblages within the roots of the 2-year alfalfa with the corresponding plant traits, the only change in abundance of the local *R. irregularis* cluster1 induced by all inoculation treatments was sufficient to describe the majority of the diversity inside the overall studied plant traits. Thus, we can speculate that the main determinant of the improved host benefit across the inoculation treatments is related to the stimulation of the proliferation of a single-taxa rather than to the increase in abundance of the inoculated isolates. Overall, these results suggest an environmental-driven selection for highly efficient AMF and support the use of native mixture inoculants having a lower risk of including invasive isolates (Hart et al., 2017).

CONCLUSION

The data presented in this study demonstrated that: (i) field application of AM fungal inocula improved alfalfa yield, nutrient and fatty acid concentration up to 2 years post-inoculation and enhanced AM fungal abundance in roots; (ii) multiple AM fungal inoculants can act in synergy to achieve the effects on crop yield and quality; (iii) a mixture of foreign AM fungal isolates provided greater benefits compared to local consortia; (iv) foreign strains of *F. mosseae* and *R. irregularis* persisted in the roots of the polyannual crop 2 years following inoculation either as single inoculum or as component of the mixture; (v) among inoculants, *F. mosseae* BEG12 and AZ225C and the foreign mixture exerted an higher environmental impact on the local AM fungal community compared with the local AM fungal mixture and *R. irregularis* BEG141; (vi) the stimulation of the proliferation of a single-taxa, such as the local *R. irregularis* cluster1, induced by all inoculation treatments was the main determinant of the improved host benefits, suggesting an environmental-driven selection for a highly efficient AM fungal strain. The results on crop productivity and quality as well as on-field persistence of inoculated AMF support the use of mixtures of foreign AM fungal isolates. On the other hand, taking into consideration the effects on the native AMF, the local AM fungal mixture shows a lower impact. These results pave the way for extending the study on the effect of exotic and native mixtures for the production of

high-quality forage for the animal diet, allowing to assess the fatty acid profile in milk or meat, and derived products, and finally to evaluate AM fungal benefits on human health.

DATA AVAILABILITY STATEMENT

The datasets presented in this study can be found in online repositories. The names of the repository/repositories and accession number(s) can be found in the article/**Supplementary Material**.

AUTHOR CONTRIBUTIONS

EP conceived and designed the study and collected and analyzed the samples. EP and LE analyzed the data. EP, LE, and MN discussed the results. EP and LE wrote the manuscript. All authors reviewed and approved the manuscript before its submission.

FUNDING

This study was funded by the European Agricultural Fund for Rural Development 2007–2013 in Tuscany (Italy), measure 124 (FORMANOVA; project leader: Enrico Bonari). EP was supported by European Agricultural Fund for Rural Development 2014–2020 in Tuscany (Italy), measure 16.2—EIP-AGRI Agriculture and Innovation (title: Development of the production process of biological fertilizers and their application for food and feed crops in Tuscan agriculture—FERTIBIO project; ARTEA Code CUP ARTEA 828090; project leader: Laura Ercoli).

SUPPLEMENTARY MATERIAL

The Supplementary Material for this article can be found online at: https://www.frontiersin.org/articles/10.3389/fpls.2022.814401/full#supplementary-material

REFERENCES

Abdi, H., and Williams, L. J. (2010). Principal component analysis. *WIRES Comput. Stat.* 2, 433–459. doi: 10.1002/wics.101

Anderson, M. J., Gorley, R. N., and Clarke, R. K. (2008). *Permanova+ for Primer: guide to Software and Statistical Methods*. Plymouth: PRIMER-E.

Avio, L., Pellegrino, E., Bonari, E., and Giovannetti, M. (2006). Functional diversity of arbuscular mycorrhizal fungal isolates in relation to extraradical mycelial networks. *New Phytol.* 172, 347–357. doi: 10.1111/j.1469-8137.2006.01839.x

Baslam, M., and Goicoechea, N. (2012). Water deficit improved the capacity of arbuscular mycorrhizal fungi (AMF) for inducing the accumulation of antioxidant compounds in lettuce leaves. *Mycorrhiza* 22, 347–359. doi: 10.1007/s00572-011-0408-9

Baslam, M., Garmendia, I., and Goicoechea, N. (2013). Enhanced accumulation of vitamins, nutraceuticals and minerals in lettuces associated with arbuscular mycorrhizal fungi (AMF): a question of interest for both vegetables and humans. *Agriculture* 3, 188–209. doi: 10.3390/agriculture3010188

Berruti, A., Lumini, E., and Bianciotto, V. (2017). AMF components from a microbial inoculum fail to colonize roots and lack soil persistence in an arable maize field. *Symbiosis* 72, 73–80. doi: 10.1007/s13199-016-0442-7

Bharadwaj, D. P., Lundquist, P. O., Persson, P., and Alström, S. (2008). Evidence for specificity of cultivable bacteria associated with arbuscular mycorrhizal fungal spores. *FEMS Microbiol. Ecol.* 65, 310–322. doi: 10.1111/j.1574-6941.2008.00515.x

Bianciotto, V., and Bonfante, P. (2002). Arbuscular mycorrhizal fungi: a specialised niche for rhizospheric and endocellular bacteria. *Anton. van Lee.* 81, 365–371. doi: 10.1023/A:1020544919072

Boufaïed, H., Chouinard, P. Y., Tremblay, G. F., Petit, H. V., Michaud, R., and Bélanger, G. (2003). Fatty acids in forages. I. Factors affecting concentrations. *Can. J. Anim. Sci.* 83, 501–511. doi: 10.4141/A02-098

Bremner, J. M., and Mulvaney, C. S. (1982). "Nitrogen-total" in *Methods of Soil Analysis. Part 2. Chemical and Microbiological Properties*. eds A. L. Page, R. H. Miller, and D. R. Keeney (Madison: American Society of Agronomy). 595–624.

Buysens, C., Alaux, P. L., César, V., Huret, S., Declerck, S., and Cranenbrouck, S. (2017). Tracing native and inoculated Rhizophagus irregularis in three potato cultivars (Charlotte, Nicola and Bintje) grown under field conditions. *Appl. Soil Ecol.* 115, 1–9. doi: 10.1016/j.apsoil.2017.03.007

Calviello, G., and Serini, S. (2010). *Dietary Omega-3 Polyunsaturated Fatty Acids and Cancer*. New York: Springer.

Carlsson, G., and Huss-Danell, K. (2003). Nitrogen fixation in perennial forage legumes in the field. *Plant Soil* 253, 353–372. doi: 10.1023/A:1024847017371

Ciccolini, V., Bonari, E., and Pellegrino, E. (2015). Land-use intensity and soil properties shape the composition of fungal communities in Mediterranean peaty soils drained for agricultural purposes. *Biol. Fert. Soils* 51, 719–731. doi: 10.1007/s00374-015-1013-4

Clarke, C., and Mosse, B. (1981). Plant growth responses to vesicular-arbuscular mycorrhiza XII. Field inoculation responses of barley at two soil P levels. *New Phytol.* 87, 695–703. doi: 10.1111/j.1469-8137.1981.tb01704.x

Clarke, K. R., and Gorley, R. N. (2015). *Getting Started with PRIMER v7*. Plymouth: PRIMER-E.

Clarke, K. R., and Warwick, R. (2001). *Change in marine communities: an approach to statistical analysis and interpretation*. Plymouth: PRIMER-E.

Clarke, K. R., Somerfield, P. J., and Gorley, R. N. (2008). Testing of null hypotheses in exploratory community analyses: similarity profiles and biota-environment linkage. *J. Exp. Mar. Biol. Ecol.* 366, 56–69. doi: 10.1016/j.jembe.2008.07.009

Coccina, A., Cavagnaro, T. R., Pellegrino, E., Ercoli, L., McLaughlin, M. J., and Watts-Williams, S. J. (2019). The mycorrhizal pathway of zinc uptake contributes to zinc accumulation in barley and wheat grain. *BMC Plant Biol.* 19:133. doi: 10.1186/s12870-019-1741-y

Crossay, T., Majorel, C., Redecker, D., Gensous, S., Medevielle, V., Durrieu, G., et al. (2019). Is a mixture of arbuscular mycorrhizal fungi better for plant growth than single-species inoculants? *Mycorrhiza* 29, 325–339. doi: 10.1007/s00572-019-00898-y

De Vries, F. T., Thébault, E., Liiri, M., Birkhofer, K., Tsiafouli, M. A., Bjørnlund, L., et al. (2013). Soil food web properties explain ecosystem services across European land use systems. *P. Natl. Acad. Sci.* 110, 14296–14301. doi: 10.1073/pnas.1305198110

Delavaux, C. S., Smith-Ramesh, L. M., and Kuebbing, S. E. (2017). Beyond nutrients: a meta-analysis of the diverse effects of arbuscular mycorrhizal fungi on plants and soils. *Ecology* 98, 2111–2119. doi: 10.1002/ecy.1892

Dhiman, T. R., Anand, G. R., Satter, L. D., and Pariza, M. W. (1999). Conjugated linoleic acid content of milk from cows fed different diets. *J. Dairy Sci.* 82, 2146–2156. doi: 10.3168/jds.S0022-0302(99)75458-5

Duan, T., Shen, Y., Facelli, E., Smith, S. E., and Nan, Z. (2010). New agricultural practices in the Loess Plateau of China do not reduce colonizatioion by arbuscular mycorrhizal or root invading fungi and do not carry a yield penalty. *Plant Soil* 331, 265–275. doi: 10.1007/s11104-009-0251-3

Edathil, T. T., Manian, S., and Udaiyan, K. (1996). Interaction of multiple VAM fungal species on root colonization, plant growth and nutrient status of tomato seedlings (Lycopersicon esculentum Mill.). *Agr. Ecosyst. Environ.* 59, 63–68. doi: 10.1016/0167-8809(96)01040-7

Ercoli, L., Masoni, A., Mariotti, M., Pampana, S., Pellegrino, E., and Arduini, I. (2017b). Effect of preceding crop on the agronomic and economic performance of durum wheat in the transition from conventional to reduced tillage. *Eur. J. Agron.* 82, 125–133. doi: 10.1016/j.eja.2016.10.010

Ercoli, L., Schüßler, A., Arduini, I., and Pellegrino, E. (2017a). Strong increase of durum wheat iron and zinc content by field-inoculation with arbuscular mycorrhizal fungi at different soil nitrogen availabilities. *Plant Soil* 419, 153–167. doi: 10.1007/s11104-017-3319-5

EU (2019). *E.U. Regulation of the European Parliament and of the Council Laying Down Rules on the Making Available on the Market of EU Fertilising Products and Amending Regulations (EC) No 1069/2009 and (EC) No 1107/2009 and Repealing Regulation (EC) No 2003/2003. 2019*. Available online at: https://eur-lex.europa.eu/legal-content/EN/TXT/?uri=OJ:L:2019:170:TOC (accessed on 1 March 2021).

FAO (2006). *FAOSTAT*. Italy: Food and Agriculture Organization of the United Nations.

Farmer, M. J., Li, X., Feng, G., Zhao, B., Chatagnier, O., Gianinazzi, S., et al. (2007). Molecular monitoring of field-inoculated AMF to evaluate persistence in sweet potato crops in China. *Appl. Soil Ecol.* 35, 599–609. doi: 10.1016/j.apsoil.2006.09.012

French, P., Stanton, C., Lawless, F., O'Riordan, E. G., Monahan, F. J., Caffrey, P. J., et al. (2000). Fatty acid composition, including conjugated linoleic acid, of intramuscular fat from steers offered grazed grass, grass silage, or concentrate-based diets. *J. Anim. Sci.* 78, 2849–2855. doi: 10.2527/2000.78112849x

Frey-Klett, P., Garbaye, J. A., and Tarkka, M. (2007). The mycorrhiza helper bacteria revisited. *New Phytol.* 176, 22–36. doi: 10.1111/j.1469-8137.2007.02191.x

Gee, G. W., and Bauder, J. W. (1986). "Particle-size analysis" in *Methods of Soil Analysis, Part–1 - Physical Mineral Methods*, 2nd Edn, ed. A. Klute (Madison: American Society of Agronomy Book Series). 383–411.

Gianinazzi, S., Gollotte, A., Binet, M. N., van Tuinen, D., Redecker, D., and Wipf, D. (2010). Agroecology: the key role of arbuscular mycorrhizas in ecosystem services. *Mycorrhiza* 20, 519–530. doi: 10.1007/s00572-010-0333-3

González-Fernández, M. J., Ortea, I., and Guil-Guerrero, J. L. (2020). α-Linolenic and γ-linolenic acids exercise differential antitumor effects on HT-29 human colorectal cancer cells. *Toxicol. Res.* 9, 474–483. doi: 10.1093/toxres/tfaa046

Gouy, M., Guindon, S., and Gascuel, O. (2010). SeaView version 4: a multiplatform graphical user interface for sequence alignment and phylogenetic tree building. *Mol. Biol. Evol.* 27, 221–224. doi: 10.1093/molbev/msp259

Hakl, J., Pisarčik, M., Hrevušová, Z., and Šantrůček, J. (2017). In-field lucerne root morphology traits over time in relation to forage yield, plant density, and root disease under two cutting managements. *Field Crop. Res.* 213, 109–117. doi: 10.1016/j.fcr.2017.07.017

Han, Y., Feng, J., Han, M., and Zhu, B. (2020). Responses of arbuscular mycorrhizal fungi to nitrogen addition: a meta-analysis. *Glob. Change Biol.* 26, 7229–7241. doi: 10.1111/gcb.15369

Hart, M. M., Aleklett, K., Chagnon, P. L., Egan, C., Ghignone, S., and Helgason, T. (2015). Navigating the labyrinth: a guide to sequence-based, community ecology of arbuscular mycorrhizal fungi. *New Phytol.* 207, 235–247. doi: 10.1111/nph.13340

Hart, M. M., Antunes, P. M., Chaudhary, V. B., and Abbott, L. K. (2017). Fungal inoculants in the field: is the reward greater than the risk? *Funct. Ecol.* 32, 126–135. doi: 10.1111/1365-2435.12976

Hendershot, W. H., and Duquette, M. (1986). A simple barium chloride method for determining cation exchange capacity and exchangeable cations. *Soil Sci. Soc. Am. J.* 50, 605–608. doi: 10.2136/sssaj1986.03615995005000030013x

Higo, M., Isobe, K., Yamaguchi, M., Drijber, R. A., Jeske, E. S., and Ishii, R. (2013). Diversity and vertical distribution of indigenous arbuscular mycorrhizal fungi under two soybean rotational systems. *Biol. Fert. Soils* 49, 1085–1096. doi: 10.1007/s00374-013-0807-5

Hijri, M., Hosny, M., van Tuinen, D., and Dulieu, H. (1999). Intraspecific ITS polymorphism in Scutellospora castanea (Glomales, Zygomycota) is structured within multinucleate spores. *Fungal Genet. Biol.* 26, 141–151. doi: 10.1006/fgbi.1998.1112

Hoeksema, J. D., Chaudhary, V. B., Gehring, C. A., Johnson, N. C., Karst, J., Koide, R. T., et al. (2010). A meta-analysis of context-dependency in plant response to inoculation with mycorrhizal fungi. *Ecol. Lett.* 13, 394–407. doi: 10.1111/j.1461-0248.2009.01430.x

Hou, G., Ablett, G. R., Pauls, K. P., and Rajcan, I. (2006). Environmental effects on fatty acid levels in soybean seed oil. *J. Amer. Oil Chem. Soc.* 83, 759–763.

Igiehon, N. O., Babalola, O. O., Cheseto, X., and Torto, B. (2021). Effects of rhizobia and arbuscular mycorrhizal fungi on yield, size distribution and fatty acid of soybean seeds grown under drought stress. *Microbiol. Res.* 242:126640. doi: 10.1016/j.micres.2020.126640

IUSS (2015). *FAO Soils Portal, World reference base for soil resources 2014: international Soil Classification System for Naming Soils and Creating Legends for Soil Maps, Update 2015, World Soil Resources Reports 106*. Rome: Food and Agriculture Organization of the United Nations.

Jansa, J., Mozafar, A., Banke, S., McDonald, B. A., and Frossard, E. (2002). Intra-and intersporal diversity of ITS rDNA sequences in Glomus intraradices assessed by cloning and sequencing, and by SSCP analysis. *Mycol. Res.* 106, 670–681. doi: 10.1017/S0953756202006032

Jansa, J., Smith, F. A., and Smith, S. E. (2008). Are there benefits of simultaneous root colonization by different arbuscular mycorrhizal fungi? *New Phytol.* 177, 779–789. doi: 10.1111/j.1469-8137.2007.02294.x

Jasper, D. A., Abbott, L. K., and Robson, A. D. (1989). Hyphae of a vesicular—arbuscular mycorrhizal fungus maintain infectivity in dry soil, except when the soil is disturbed. *New Phytol.* 112, 101–107. doi: 10.1111/j.1469-8137.1989.tb00314.x

Jayne, B., and Quigley, M. (2014). Influence of arbuscular mycorrhiza on growth and reproductive response of plants under water deficit: a meta-analysis. *Mycorrhiza* 24, 109–119. doi: 10.1007/s00572-013-0515-x

Jones, J. B. Jr., Wolf, B., and Mills, H. A. (1991). *Plant Analysis Handbook II: a Practical Sampling, Preparation, Analysis, and Interpretation Guide*. Athens: Micro-Macro Publishing Inc.

Karandashov, V., and Bucher, M. (2005). Symbiotic phosphate transport in arbuscular mycorrhizas. *Trends Plant Sci.* 10, 22–29. doi: 10.1016/j.tplants.2004.12.003

Katoh, K., Rozewicki, J., and Yamada, K. D. (2019). MAFFT online service: multiple sequence alignment, interactive sequence choice and visualization. *Brief. Bioinform.* 20, 1160–1166. doi: 10.1093/bib/bbx108

Kaur, S., and Suseela, V. (2020). Unraveling arbuscular mycorrhiza-induced changes in plant primary and secondary metabolome. *Metabolites* 10:335. doi: 10.3390/metabo10080335

Kiers, E. T., Duhamel, M., Beesetty, Y., Mensah, J. A., Franken, O., Verbruggen, E., et al. (2011). Reciprocal rewards stabilize cooperation in the mycorrhizal symbiosis. *Science* 333:880. doi: 10.1126/science.1208473

Kimura, M. (1980). A simple method for estimating evolutionary rates of base substitutions through comparative studies of nucleotide sequences. *J. Mol. Evol.* 16, 111–120.

Klironomos, J. N. (2003). Variation in plant response to native and exotic arbuscular mycorrhizal fungi. *Ecology* 84, 2292–2301. doi: 10.1890/02-0413

Knorr, E. M., Ng, R. T., and Tucakov, V. (2000). Distance-based outliers: algorithms and applications. *VLDB J.* 8, 237–253. doi: 10.1007/s007780050006

Koide, R. T. (2000). Functional complementarity in the arbuscular mycorrhizal symbiosis. *New Phytol.* 147, 233–235. doi: 10.1046/j.1469-8137.2000.00710.x

Kokkoris, V., Li, Y., Hamel, C., Hanson, K., and Hart, M. (2019). Site specificity in establishment of a commercial arbuscular mycorrhizal fungal inoculant. *Sci. Total Environ.* 660, 1135–1143. doi: 10.1016/j.scitotenv.2019.01.100

Kolaříková, Z., Slavíková, R., Krüger, C., Krüger, M., and Kohout, P. (2021). PacBio sequencing of Glomeromycota rDNA: a novel amplicon covering all widely used ribosomal barcoding regions and its applicability in taxonomy and ecology of arbuscular mycorrhizal fungi. *New Phytol.* 231, 490–499. doi: 10.1111/nph.17372

Kottek, M., Grieser, J., Beck, C., Rudolf, B., and Rubel, F. (2006). World map of the Köppen-Geiger climate classification updated. *Meteorol. Z.* 15, 259–263. doi: 10.1127/0941-2948/2006/0130

Krüger, M., Krüger, C., Walker, C., Stockinger, H., and Schüßler, A. (2012). Phylogenetic reference data for systematics and phylotaxonomy of arbuscular mycorrhizal fungi from phylum to species level. *New Phytol.* 193, 970–984. doi: 10.1111/j.1469-8137.2011.03962.x

Krüger, M., Stockinger, H., Krüger, C., and Schüßler, A. (2009). DNA-based species level detection of Glomeromycota: one PCR primer set for all arbuscular

mycorrhizal fungi. *New Phytol.* 183, 212–223. doi: 10.1111/j.1469-8137.2009.02835.x

Kruskal, J. B. (1964). Nonmetric multidimensional scaling: a numerical method. *Psychometrika* 29, 115–131. doi: 10.1007/BF02289694

Kuraku, S., Zmasek, C. M., Nishimura, O., and Katoh, K. (2013). aLeaves facilitates on-demand exploration of metazoan gene family trees on MAFFT sequence alignment server with enhanced interactivity. *Nucleic Acids Res.* 41, W22–W28. doi: 10.1093/nar/gkt389

Lanfranco, L., Delpero, M., and Bonfante, P. (1999). Intrasporal variability of ribosomal sequences in the endomycorrhizal fungus Gigaspora margarita. *Mol. Ecol.* 8, 37–45. doi: 10.1046/j.1365-294X.1999.00535.x

Legendre, P., and Anderson, M. J. (1999). Distance-based redundancy analysis: testing multispecies responses in multifactorial ecological experiments. *Ecol. Monogr.* 69, 1–24.

Lehmann, A., and Rillig, M. C. (2015). Arbuscular mycorrhizal contribution to copper, manganese and iron nutrient concentrations in crops–a meta-analysis. *Soil Biol. Biochem.* 81, 147–158. doi: 10.1016/j.soilbio.2014.11.013

Lehmann, A., Veresoglou, S. D., Leifheit, E. F., and Rillig, M. C. (2014). Arbuscular mycorrhizal influence on zinc nutrition in crop plants–a meta-analysis. *Soil Biol. Biochem.* 69, 123–131. doi: 10.1016/j.soilbio.2013.11.001

Lekberg, Y., and Koide, R. T. (2005). Is plant performance limited by abundance of arbuscular mycorrhizal fungi? A meta-analysis of studies published between 1988 and 2003. *New Phytol.* 168, 189–204. doi: 10.1111/j.1469-8137.2005.01490.x

Li, Y., Duan, T., Nan, Z., and Li, Y. (2021). Arbuscular mycorrhizal fungus alleviates alfalfa leaf spots caused by Phoma medicaginis revealed by RNA-seq analysis. *J. Appl. Microbiol.* 130, 547–560.

Lynch, J. M., and Barbano, D. M. (1999). Kjeldahl nitrogen analysis as a reference method for protein determination in dairy products. *J. AOAC Int.* 82, 389–1398. doi: 10.1093/jaoac/82.6.1389

Maherali, H., and Klironomos, J. N. (2007). Influence of phylogeny on fungal community assembly and ecosystem functioning. *Science* 316, 1746–1748. doi: 10.1126/science.1143082

Martignoni, M. M., Garnier, J., Zhang, X., Rosa, D., Kokkoris, V., Tyson, R. C., et al. (2021). Co-inoculation with arbuscular mycorrhizal fungi differing in carbon sink strength induces a synergistic effect in plant growth. *J. Theor. Biol.* 531:110859. doi: 10.1016/j.jtbi.2021.110859

Masoero, G., Ariotti, R., Giovannetti, G., Ercole, E., Cugnetto, A., and Nuti, M. (2021). Connecting the use of biofertilizers on maize silage or meadows with progress in milk quality and economy. *J. Agron. Res.* 3, 26–45. doi: 10.14302/issn.2639-3166.jar-21-3817

McGonigle, T. P., Miller, M. H., Evans, D. G., Fairchild, G. L., and Swan, J. A. (1990). A new method which gives an objective measure of colonization of roots by vesicular—arbuscular mycorrhizal fungi. *New Phytol.* 115, 495–501. doi: 10.1111/j.1469-8137.1990.tb00476.x

Munkvold, L., Kjøller, R., Vestberg, M., Rosendahl, S., and Jakobsen, I. (2004). High functional diversity within species of arbuscular mycorrhizal fungi. *New Phytol.* 164, 357–364. doi: 10.1111/j.1469-8137.2004.01169.x

Nelson, D. W., and Sommers, L. (1982). "Total carbon, organic carbon, and organic matter" in *Methods of Soil Analysis. Part 2 Chemical and Microbiological Properties*. eds A. L. Page, R. H. Miller, and D. R. Keeney (Madison: American Society of Agronomy). 539–579.

Olsen, S. R., and Sommers, L. E. (1982). "Phosphorus" in *Methods of Soil Analysis Part 2, Chemical and Microbiological Properties*. 2nd Edn. ed. A. L. Page (Madison: American Society of Agronomy). 403–430.

Onofri, A., Seddaiu, G., and Piepho, H. P. (2016). Long-term experiments with cropping systems: Case studies on data analysis. *Eur. J. Agron.* 77, 223–235. doi: 10.1016/j.eja.2016.02.005

Öpik, M., Moora, M., Liira, J., and Zobel, M. (2006). Composition of root-colonizing arbuscular mycorrhizal fungal communities in different ecosystems around the globe. *J. Ecol.* 94, 778–790. doi: 10.1111/j.1365-2745.2006.01136.x

Pariza, M. W., Park, Y., and Cook, M. E. (2001). The biologically active isomers of conjugated linoleic acid. *Prog. Lipid Res.* 40, 283–298. doi: 10.1016/S0163-7827(01)00008-X

Parvin, S., Van Geel, M., Yeasmin, T., Verbruggen, E., and Honnay, O. (2020). Effects of single and multiple species inocula of arbuscular mycorrhizal fungi on the salinity tolerance of a Bangladeshi rice (Oryza sativa L.) cultivar. *Mycorrhiza* 30, 431–444. doi: 10.1007/s00572-020-00957-9

Pellegrino, E., and Bedini, S. (2014). Enhancing ecosystem services in sustainable agriculture: biofertilization and biofortification of chickpea (Cicer arietinum L.) by arbuscular mycorrhizal fungi. *Soil Biol. Biochem.* 68, 429–439. doi: 10.1016/j.soilbio.2013.09.030

Pellegrino, E., Bedini, S., Avio, L., Bonari, E., and Giovannetti, M. (2011). Field inoculation effectiveness of native and exotic arbuscular mycorrhizal fungi in a Mediterranean agricultural soil. *Soil Biol. Biochem.* 43, 367–376. doi: 10.1016/j.soilbio.2010.11.002

Pellegrino, E., Bosco, S., Ciccolini, V., Pistocchi, C., Sabbatini, T., Silvestri, N., et al. (2015b). Agricultural abandonment in Mediterranean reclaimed peaty soils: long-term effects on soil chemical properties, arbuscular mycorrhizas and CO2 flux. *Agr. Ecosyst. Environ.* 199, 164–175. doi: 10.1016/j.agee.2014.09.004

Pellegrino, E., Gamper, H. A., Ciccolini, V., and Ercoli, L. (2020b). Forage rotations conserve diversity of arbuscular mycorrhizal fungi and soil fertility. *Front. Microbiol.* 10:2969. doi: 10.3389/fmicb.2019.02969

Pellegrino, E., Öpik, M., Bonari, E., and Ercoli, L. (2015a). Responses of wheat to arbuscular mycorrhizal fungi: a meta-analysis of field studies from 1975 to 2013. *Soil Biol. Biochem.* 84, 210–217. doi: 10.1016/j.soilbio.2015.02.020

Pellegrino, E., Piazza, G., Arduini, I., and Ercoli, L. (2020a). Field inoculation of bread wheat with Rhizophagus irregularis under organic farming: variability in growth response and nutritional uptake of eleven old genotypes and a modern variety. *Agronomy* 10:333. doi: 10.3390/agronomy10030333

Pellegrino, E., Turrini, A., Gamper, H. A., Cafà, G., Bonari, E., Young, J. P. W., et al. (2012). Establishment, persistence and effectiveness of arbuscular mycorrhizal fungal inoculants in the field revealed using molecular genetic tracing and measurement of yield components. *New Phytol.* 194, 810–822. doi: 10.1111/j.1469-8137.2012.04090.x

Phillips, J. M., and Hayman, D. S. (1970). Improved procedures for clearing roots and staining parasitic and vesicular-arbuscular mycorrhizal fungi for rapid assessment of infection. *Trans. Br. Mycol. Soc.* 55, 158–161. doi: 10.1016/S0007-1536(70)80110-3

Pintus, S., Murru, E., Carta, G., Cordeddu, L., Batetta, B., Accossu, S., et al. (2013). Sheep cheese naturally enriched in α-linolenic, conjugated linoleic and vaccenic acids improves the lipid profile and reduces anandamide in the plasma of hypercholesterolaemic subjects. *Brit. J. Nutr.* 109, 1453–1462. doi: 10.1017/S0007114512003224

Powell, C. L. (1977). Mycorrhizas in hill country soils: III. Effect of inoculation on clover growth in unsterile soils. *New Zeal. J. Agr. Res.* 20, 343–348. doi: 10.1080/00288233.1977.10427345

Powell, C. L. (1979). Spread of mycorrhizal fungi through soil. *New Zeal. J. Agr. Res.* 22, 335–339. doi: 10.1080/00288233.1979.10430756

Radović, J., Sokolović, D., and Marković, J. J. B. A. H. (2009). Alfalfa-most important perennial forage legume in animal husbandry. *Biotechnol. An. Husb.* 25, 465–475.

Rich, M. K., Nouri, E., Courty, P. E., and Reinhardt, D. (2017). Diet of arbuscular mycorrhizal fungi: bread and butter? *Trends Plant Sci.* 22, 652–660. doi: 10.1016/j.tplants.2017.05.008

Roldan, A., Salinas-Garcia, J. R., Alguacil, M. M., and Caravaca, F. (2007). Soil sustainability indicators following conservation tillage practices under subtropical maize and bean crops. *Soil Till. Res.* 93, 273–282. doi: 10.1016/j.still.2006.05.001

Roth, R., and Paszkowski, U. (2017). Plant carbon nourishment of arbuscular mycorrhizal fungi. *Curr. Opin. Plant Biol.* 39, 50–56. doi: 10.1016/j.pbi.2017.05.008

Rouphael, Y., and Colla, G. (2018). Synergistic biostimulatory action: designing the next generation of plant biostimulants for sustainable agriculture. *Front. Plant Sci.* 9:1655. doi: 10.3389/fpls.2018.01655

Rúa, M. A., Antoninka, A., Antunes, P. M., Chaudhary, V. B., Gehring, C., Lamit, L. J., et al. (2016). Home-field advantage? Evidence of local adaptation among plants, soil, and arbuscular mycorrhizal fungi through meta-analysis. *BMC Evol. Biol.* 16:122. doi: 10.1186/s12862-016-0698-9

Saleh, A. M., Abdel-Mawgoud, M., Hassan, A. R., Habeeb, T. H., Yehia, R. S., and AbdElgawad, H. (2020). Global metabolic changes induced by arbuscular mycorrhizal fungi in oregano plants grown under ambient and elevated levels of atmospheric CO2. *Plant Physiol. Biochem.* 151, 255–263. doi: 10.1016/j.plaphy.2020.03.026

Scollan, N. D., Choi, N. J., Kurt, E., Fisher, A. V., Enser, M., and Wood, J. D. (2001). Manipulating the fatty acid composition of muscle and adipose tissue in beef cattle. *Brit. J. Nutr.* 85, 115–124. doi: 10.1079/BJN2000223

Sheng, M., Lalande, R., Hamel, C., and Ziadi, N. (2013). Effect of long-term tillage and mineral phosphorus fertilization on arbuscular mycorrhizal fungi in a humid continental zone of Eastern Canada. *Plant Soil* 369, 599–613. doi: 10.1007/s11104-013-1585-4

Singh, A. K., Hamel, C., DePauw, R. M., and Knox, R. E. (2012). Genetic variability in arbuscular mycorrhizal fungi compatibility supports the selection of durum wheat genotypes for enhancing soil ecological services and cropping systems in Canada. *Can. J. Microbiol.* 58, 293–302. doi: 10.1139/w11-140

Smith, S. E., and Read, D. J. (2008). *Mycorrhizal Symbiosis*. Amsterdam: Academic Press.

Soil Survey Staff. (1999). *Soil Taxonomy. A Basic System of Soil Classification for Making and Interpreting Soil Surveys. USDA. Agricultural Handbook 436*. Washington: United States Department of Agriculture.

Stockinger, H., Krüger, M., and Schüßler, A. (2010). DNA barcoding of arbuscular mycorrhizal fungi. *New Phytol.* 187, 461–474.

Stumpe, M., Carsjens, J. G., Stenzel, I., Göbel, C., Lang, I., Pawlowski, K., et al. (2005). Lipid metabolism in arbuscular mycorrhizal roots of Medicago truncatula. *Phytochemistry* 66, 781–791. doi: 10.1016/j.phytochem.2005.01.020

Sugiura, Y., Akiyama, R., Tanaka, S., Yano, K., Kameoka, H., Marui, S., et al. (2020). Myristate can be used as a carbon and energy source for the asymbiotic growth of arbuscular mycorrhizal fungi. *P. Natl. Acad. Sci. U. S. A.* 117, 25779–25788.

Sukhija, P. S., and Palmquist, D. L. (1988). Rapid method for determination of total fatty acid content and composition of feedstuffs and feces. *J. Agr. Food Chem.* 36, 1202–1206. doi: 10.1021/jf00084a019

Sun, T., and Li, Z. (2019). Alfalfa-corn rotation and row placement affects yield, water use, and economic returns in Northeast China. *Field Crop. Res.* 241:107558. doi: 10.1016/j.fcr.2019.107558

Sýkorová, Z., Börstler, B., Zvolenská, S., Fehrer, J., Gryndler, M., Vosátka, M., et al. (2012). Long-term tracing of Rhizophagus irregularis isolate BEG140 inoculated on *Phalaris arundinacea* in a coal mine spoil bank, using mitochondrial large subunit rDNA markers. *Mycorrhiza* 22, 69–80. doi: 10.1007/s00572-011-0375-1

Tamura, K., Stecher, G., and Kumar, S. (2021). MEGA11: molecular evolutionary genetics analysis version 11. *Mol. Biol. Evol.* 38, 3022–3027. doi: 10.1093/molbev/msab120

Thiéry, O., Moora, M., Vasar, M., Zobel, M., and Öpik, M. (2012). Inter-and intrasporal nuclear ribosomal gene sequence variation within one isolate of arbuscular mycorrhizal fungus, Diversispora sp. *Symbiosis* 58, 135–147. doi: 10.1007/s13199-012-0212-0

Thioye, B., van Tuinen, D., Kane, A., de Faria, S. M., Ndiaye, C., Duponnois, R., et al. (2019). Tracing Rhizophagus irregularis isolate IR27 in Ziziphus mauritiana roots under field conditions. *Mycorrhiza* 29, 77–83.

Thomas, G. W. (1982). "Exchangeable cations" in *Methods of Soil Analysis, Part 2, Chemical and Microbiological Properties*. eds A. L. Page, R. H. Miller, and D. R. Keeney (Madison: American Society of Agronomy). 159–165.

Thonar, C., Frossard, E., Šmilauer, P., and Jansa, J. (2014). Competition and facilitation in synthetic communities of arbuscular mycorrhizal fungi. *Mol. Ecol.* 23, 733–746. doi: 10.1111/mec.12625

Thonar, C., Schnepf, A., Frossard, E., Roose, T., and Jansa, J. (2011). Traits related to differences in function among three arbuscular mycorrhizal fungi. *Plant Soil* 339, 231–245. doi: 10.1007/s11104-010-0571-3

Toju, H., Peay, K. G., Yamamichi, M., Narisawa, K., Hiruma, K., Naito, K., et al. (2018). Core microbiomes for sustainable agroecosystems. *Nat. Plants* 4, 247–257. doi: 10.1038/s41477-018-0139-4

Trépanier, M., Bécard, G., Moutoglis, P., Willemot, C., Gagné, S., Avis, T. J., et al. (2005). Dependence of arbuscular-mycorrhizal fungi on their plant host for palmitic acid synthesis. *Appl. Environ. Microb.* 71, 5341–5347. doi: 10.1128/AEM.71.9.5341-5347.2005

Treseder, K. K., Allen, E. B., Egerton-Warburton, L. M., Hart, M. M., Klironomos, J. N., Maherali, H., et al. (2018). Arbuscular mycorrhizal fungi as mediators of ecosystem responses to nitrogen deposition: a trait-based predictive framework. *J. Ecol.* 106, 480–489. doi: 10.1111/1365-2745.12919

Vallebona, C., Pellegrino, E., Frumento, P., and Bonari, E. (2015). Temporal trends in extreme rainfall intensity and erosivity in the Mediterranean region: a case study in southern Tuscany, Italy. *Clim. Change* 128, 139–151. doi: 10.1007/s10584-014-1287-9

Vályi, K., Mardhiah, U., Rillig, M. C., and Hempel, S. (2016). Community assembly and coexistence in communities of arbuscular mycorrhizal fungi. *ISME J.* 10, 2341–2351. doi: 10.1038/ismej.2016.46

van der Heijden, M. G., and Scheublin, T. R. (2007). Functional traits in mycorrhizal ecology: their use for predicting the impact of arbuscular mycorrhizal fungal communities on plant growth and ecosystem functioning. *New Phytol.* 174, 244–250. doi: 10.1111/j.1469-8137.2007.02041.x

van der Heijden, M. G., Boller, T., Wiemken, A., and Sanders, I. R. (1998a). Different arbuscular mycorrhizal fungal species are potential determinants of plant community structure. *Ecology* 79, 2082–2091. doi: 10.2307/176711

van der Heijden, M. G., Klironomos, J. N., Ursic, M., Moutoglis, P., Streitwolf-Engel, R., Boller, T., et al. (1998b). Mycorrhizal fungal diversity determines plant biodiversity, ecosystem variability and productivity. *Nature* 396, 69–72. doi: 10.1038/23932

van der Heijden, M. G., Wiemken, A., and Sanders, I. R. (2003). Different arbuscular mycorrhizal fungi alter coexistence and resource distribution between co-occurring plant. *New Phytol.* 157, 569–578. doi: 10.1046/j.1469-8137.2003.00688.x

van der Heyde, M., Ohsowski, B., Abbott, L. K., and Hart, M. (2017). Arbuscular mycorrhizal fungus responses to disturbance are context-dependent. *Mycorrhiza* 27, 431–440. doi: 10.1007/s00572-016-0759-3

Verbruggen, E., Röling, W. F., Gamper, H. A., Kowalchuk, G. A., Verhoef, H. A., and van der Heijden, M. G. (2010). Positive effects of organic farming on below-ground mutualists: large-scale comparison of mycorrhizal fungal communities in agricultural soils. *New Phytol.* 186, 968–979. doi: 10.1111/j.1469-8137.2010.03230.x

Verbruggen, E., van der Heijden, M. G., Rillig, M. C., and Kiers, E. T. (2013). Mycorrhizal fungal establishment in agricultural soils: factors determining inoculation success. *New Phytol.* 197, 1104–1109. doi: 10.1111/j.1469-8137.2012.04348.x

Veresoglou, S. D., Chen, B., and Rillig, M. C. (2012). Arbuscular mycorrhiza and soil nitrogen cycling. *Soil Biol. Biochem.* 46, 53–62. doi: 10.1016/j.soilbio.2011.11.018

Wagg, C., Barendregt, C., Jansa, J., and van der Heijden, M. G. (2015). Complementarity in both plant and mycorrhizal fungal communities are not necessarily increased by diversity in the other. *J. Ecol.* 103, 1233–1244. doi: 10.1111/1365-2745.12452

Wang, X., Ding, T., Li, Y., Guo, Y., Li, Y., and Duan, T. (2020). Dual inoculation of alfalfa (Medicago sativa L.) with Funnelliformis mosseae and Sinorhizobium medicae can reduce Fusarium wilt. *J. Appl. Microbiol.* 129, 665–679. doi: 10.1111/jam.14645

Yang, H., Zhang, Q., Koide, R. T., Hoeksema, J. D., Tang, J., Bian, X., et al. (2017). Taxonomic resolution is a determinant of biodiversity effects in arbuscular mycorrhizal fungal communities. *J. Ecol.* 105, 219–228. doi: 10.1111/1365-2745.12655

Zhang, S., Lehmann, A., Zheng, W., You, Z., and Rillig, M. C. (2019). Arbuscular mycorrhizal fungi increase grain yields: a meta-analysis. *New Phytol.* 222, 543–555. doi: 10.1111/nph.15570

Zouari, I., Salvioli, A., Chialva, M., Novero, M., Miozzi, L., Tenore, G. C., et al. (2014). From root to fruit: rNA-Seq analysis shows that arbuscular mycorrhizal symbiosis may affect tomato fruit metabolism. *BMC Genomics* 15:221. doi: 10.1186/1471-2164-15-221

Conflict of Interest: The authors declare that the research was conducted in the absence of any commercial or financial relationships that could be construed as a potential conflict of interest.

frontiers in Plant Science

ORIGINAL RESEARCH
published: 17 February 2022
doi: 10.3389/fpls.2022.790504

Myco-Synergism Boosts Herbivory-Induced Maize Defense by Triggering Antioxidants and Phytohormone Signaling

Raufa Batool[1], Muhammad Jawad Umer[2], Yangzhou Wang[3], Kanglai He[1], Muhammad Zeeshan Shabbir[4], Tiantao Zhang[1], Shuxiong Bai[1], Jie Chen[5] and Zhenying Wang[1]**

[1] State Key Laboratory for Biology of Plant Diseases and Insect Pests, Institute of Plant Protection, Chinese Academy of Agricultural Sciences, Beijing, China, [2] State Key Laboratory of Cotton Biology, Institute of Cotton Research, Chinese Academy of Agricultural Sciences (ICR, CAAS), Anyang, China, [3] Insect Ecology, Institute of Plant Protection, Jilin Academy of Agricultural Sciences, Changchun, China, [4] Institute of Plant Protection, Guangdong Academy of Agricultural Sciences, Guangzhou, China, [5] School of Agriculture and Biology, Shanghai Jiao Tong University, Shanghai, China

OPEN ACCESS

Edited by:
Maurizio Ruzzi, University of Tuscia, Italy

Reviewed by:
Enrique Quesada Moraga, University of Córdoba, Colombia
Yong Liu, Hunan Academy of Agricultural Sciences, Chinese Academy of Agricultural Sciences (CAAS), China

***Correspondence:**
Jie Chen
jiechen59@sjtu.edu.cn
Zhenying Wang
wangzy61@163.com;
zywang@ippcaas.cn

Specialty section:
This article was submitted to Crop and Product Physiology, a section of the journal Frontiers in Plant Science

Received: *06 October 2021*
Accepted: *17 January 2022*
Published: *17 February 2022*

Citation:
Batool R, Umer MJ, Wang Y, He K, Shabbir MZ, Zhang T, Bai S, Chen J and Wang Z (2022) Myco-Synergism Boosts Herbivory-Induced Maize Defense by Triggering Antioxidants and Phytohormone Signaling. Front. Plant Sci. 13:790504. doi: 10.3389/fpls.2022.790504

Background: Biocontrol strategies are the best possible and eco-friendly solution to develop resistance against *O furnacalis* and improve the maize yield. However, the knowledge about underlying molecular mechanisms, metabolic shifts, and hormonal signaling is limited.

Methods: Here, we used an axenic and a consortium of entomopathogenic *Beauveria bassiana* OFDH1-5 and a pathogen-antagonistic *Trichoderma asperellum* GDFS1009 in maize and observed that consortium applications resulted in higher chlorophyll contents and antioxidants activities [superoxide dismutase (SOD), peroxidase (POD), proline, protease, and polyphenol oxidase (PPO)] with a decrease in *O. furnacalis* survival. We performed a comprehensive transcriptome and an untargeted metabolome profiling for the first time at a vegetative stage in fungal inoculated maize leaves at 0-, 12-, 24-, 48-, and 72-h post insect infestation.

Results: The consortium of *B. bassiana* and *T. asperellum* leads to 80–95% of *O. furnacalis* mortality. A total of 13,156 differentially expressed genes were used for weighted gene coexpression network analysis. We identified the six significant modules containing thirteen candidate genes [protein kinase (GRMZM2G025459), acyl-CoA dehydrogenase (GRMZM5G864319), thioredoxin gene (GRMZM2G091481), glutathione *S*-transferase (GRMZM2G116273), patatin-like phospholipase gene (GRMZM2G154523), cytochrome P450 (GRMZM2G139874), protease inhibitor (GRMZM2G004466), (AC233926.1_FG002), chitinase (GRMZM2G453805), defensin (GRMZM2G392863), peroxidase (GRMZM2G144153), GDSL- like lipase (AC212068.4_FG005), and Beta-glucosidase (GRMZM2G031660)], which are not previously reported that are highly correlated with Jasmonic acid - Ethylene (JA-ET) signaling pathway and antioxidants. We detected a total of 130 negative and 491

positive metabolomic features using a ultrahigh-performance liquid chromatography ion trap time-of-flight mass spectrometry (UHPLC-QTOF-MS). Intramodular significance and real time-quantitative polymerase chain reaction (RT-qPCR) expressions showed that these genes are the true candidate genes. Consortium treated maize had higher jasmonic acid (JA), salicylic acid (SA), and ethylene (ET) levels.

Conclusion: Our results provide insights into the genetics, biochemicals, and metabolic diversity and are useful for future biocontrol strategies against ACB attacks.

Keywords: myco-synergism, *Ostrinia furnacalis*, *Beauveria bassiana*, *Trichoderma asperellum*, antioxidants myco-synergism triggers herbivory-induced defense

INTRODUCTION

Maize plants undergo several challenges during their growth, including pathogenic infections, environmental stresses, and insect attacks (Batool et al., 2020). Asian corn borer, *Ostrinia furnacalis* (Guenée), is among the most destructive insect pests of maize in Southeast and East Asia, especially China, causing an estimated yield loss of 6–9 million tons annually (He et al., 2003). Based on the importance of sustainable and eco-friendly agricultural practices (Guo et al., 2019), *O. furnacalis* control strategies have been shifted toward the application of biological control agents rather than harmful chemical pesticides (Mitchell et al., 2016; Batool et al., 2020). The *Trichoderma* spp. is traditionally viewed as a kind of biocontrol fungi against a range of plant pathogens (Dou et al., 2020), however, *Trichoderma* spp. has also been found with some functions against plant insects in different ways. More interestingly, in our previous study, we proved that *T. asperellum* and *Beauveria bassiana* are great entomopathogenic against *O. furnacalis* in maize (Batool et al., 2020). The plant herbivory response is a dynamic process that temporally and spatially regulates proteins, metabolic profiles, and transcript patterns (Ehlting et al., 2008; Barah and Bones, 2015). This suggests that it is essential to study the plant herbivory defense mechanisms at transcriptional and metabolic levels in response to insect-feeding and pre-inoculated entomopathogenic fungal strains (Li et al., 2016).

To combat herbivory, plants have evolved a broad range of defense mechanisms (Abebe, 2021). The morphological structures such as trichomes, waxy leaf surface, and numerous secondary metabolites act as the first barrier or the constitutive defense against herbivore attack. Plants have also developed an induced defense response, which affects the herbivore's survival, growth, and development directly through the production of defensive proteins and secondary metabolites, and indirectly through the secretion of volatile compounds to attract the pests (Guo et al., 2019). Plant-induced defense is initiated by the perception of insect-feeding-derived elicitor, and it is a sophisticated mechanism to balance the growth and defense. When plants are exposed to a herbivore attack, different receptors and transporters could be activated and pass the signals through different signal molecules to activate the genes involved in the biosynthesis of phytohormones such as jasmonic acid (JA), ethylene (ET), and salicylic acid (SA), secondary metabolites, and defensive enzymes, which are toxic, repellent, interfere in the digestive system, survival, and nutrient absorption of insects (Qi et al., 2018). JA and SA accumulate and exhibit a major role in regulating the plant defense mechanisms against herbivory (Tzin et al., 2015; Guo et al., 2019). JA-induced signaling is primarily regulated upon insect feeding, whereas salicylic acid regulates the response to phloem-feeding insects (Tzin et al., 2015; Heidel-Fischer et al., 2018). Herbivory-induced defensive enzymes, including enzymatic [superoxide dismutase (SOD), peroxidase (POD), polyphenol oxidase (PPO), and protease] and non-enzymatic (proline) antioxidants in maize plants, help to develop resistance against a corn borer and are responsible for the regulation of plant defense mechanism through the production of secondary metabolites and reactive oxygen species (ROS) scavenging (Batool et al., 2020). *Trichoderma* is also capable of stimulating an induced systemic resistance (ISR) plant defense response against aphids, caterpillars, and nematodes, modulated by crosstalk between SA and JA (Di Lelio et al., 2021).

Entomopathogenic fungi have traditionally been assumed to help regulate insect populations. So far, they have aroused a limited interest as plant growth promoters, alongside of protecting plant form herbivores (González-Guzmán et al., 2020, 2021). However, some hypocrealean ascomycetes, such as *B. bassiana*, play other poorly understood ecological roles that might be useful in developing novel strategies for both increased crop production and crop protection (Sánchez-Rodríguez et al., 2018). Sánchez-Rodríguez et al. (2018) concluded in their study that *B. bassiana* successfully colonized the plant and boosted the spike production in wheat inoculated with seed-dressing and soil drenching methods and caused a 30–75% larval mortality after consuming the endophytically-colonized leaves. In their work, González-Guzmán et al. (2020) also examined the performance of two wheat varieties inoculated with entomopathogenic fungi including *B. bassiana* and *Metarhizium brunneum* by soil drenching and seed coating method and found an increased yield with no significant difference in plant heights. Their results support the seed-dressing method of inoculating with entomopathogenic fungi as a promising green technology for crop protection and enhancement with no negative effect on plant performance. Landa et al. (2013) identified the endophytic colonization of the Opium poppy plant by *B. bassiana* and concluded that it can protect the plant from stem gall wasp. The *B. bassiana, M, brunneum,* and *Isaria farinosa*

were also found to increase the iron (Fe) availability in soil differently depending on particle size, increased plant height, and inflorescences the production of sunflower grown (Raya-Díaz et al., 2017).

Advances in omics and quantitative biology offer several ways to identify gene networks and their regulatory mechanisms in living systems. One such promising approach is the RNA-Sequence-based weighted gene co-expression network analysis (WGCNA) (Langfelder and Horvath, 2008). The WGCNA is a useful method to identify modules/networks of coexpressed genes. Furthermore, the correlation of these modules with phenotypic traits was useful to detect the key genes within the networks (Umer et al., 2020). However, no such large-scale study regarding the synergistic interaction of *B. bassiana* OFDH1-5 and *T. asperellum* GDFS1009 in triggering the omics-based regulatory mechanisms of defense genes, biochemical enzymes, and phytohormones induced by the *O. furnacalis* herbivory, are available.

Here, we hypothesized that the consortium of entomopathogenic *B. bassiana* OFDH1-5 and pathogenic antagonistic *T. asperellum* GDFS1009 fungal inoculants can trigger the enhanced defense response in maize, then the normal herbivory-induced response by an enhanced expression of defense-related genes, antioxidants production, phytohormone synthesis, digestive enzyme inhibitors, etc. So, we performed the physiological, biochemical, transcriptome, metabolome, and phytohormonal level analysis in field-grown vegetative stage maize inoculated with *B. bassiana* OFDH1-5 and *T. asperellum* GDFS1009, singly and in the consortium at 0-, 12-, 24-, 48-, and 72-h under *O. furnacalis* feeding. By integrating differentially expressed genes (DEGs) and biochemical antioxidants through weighted gene coexpression network analysis (WGCNA), we revealed gene networks and key candidate genes linked to JA, SA, and ethylene biosynthesis pathway and production of antioxidants and insect cuticle and digestive enzyme inhibiters. Our results highlight the positive impact of *B. bassiana* OFDH1-5 and *T. asperellum* GDFS1009 on increasing the herbivory-induced defenses and restricting the survival and growth of *O. furnacalis*.

MATERIALS AND METHODS

Plant Growth and Treatments

Maize variety "Jingke 968" was planted in an open field located at the Gongzhuling Experimental Station of the Institute of Plant Protection, CAAS, Gongzhuling, China (43°30′ N, 124°47′ E; 224.9 m above sea level) on May 11, 2018, and May 06, 2019. The treatments include: (CK) untreated control, (BB-1) seed treatment with *B. bassiana* OFDH1-5, (BB-2) soil drenching with *B. bassiana* OFDH1-5, (TH-1) seed treatment with *T. asperellum* GDFS1009, (TH-2) soil drenching with *T. asperellum* GDFS1009, (BT-1) seed treatment with consortium of *B. bassiana* OFDH1-5 and *T. asperellum* GDFS1009, (BT-2) soil drenching with a consortium of *B. bassiana* OFDH1-5 + *T. asperellum* GDFS1009, and (IC) no inoculation. All treatments except CK were infested with *O. furnacalis* larvae. Each treatment was replicated three times.

The *B. bassiana* OFDH1-5 (ACCC32726) sourced through Jilin Academy of Agricultural Sciences, Gongzhuling, China and the *T. asperellum* GDFS1009 (CGMCC NO. 9512) obtained from the School of Agriculture and Biology, Shanghai Jiao Tong University, Shanghai, China, were selected for this study based on the previous results (Batool et al., 2020). Fungal strains were grown and conidial suspensions of *B. bassiana* OFDH1-5 (1×10^9), *T. asperellum* GDFS1009 (1×10^9), and combined suspension of *B. bassiana* OFDH1-5 + *T. asperellum* GDFS1009 ($5.9 \times 10^5 + 8.4 \times 10^8$) in 1:1 were prepared as described by Batool et al. (2020). An interaction analysis to check the synergistic effect of two strains was performed based on laboratory pathogenicity analysis data (**Supplementary Table 1**). Surface-sterilized maize seeds were soaked in respective conidial suspension and placed in a shaker incubator (HZP-250) at 25 ± 2°C and 200 rpm for 12 h (Motholo, 2019), and then dried under a laminar air flow hood before planting (Cherry et al., 2004). For insect control-IC, control-CK, and soil drenching treatments BB-2, TH-2, and BT-2, seeds were soaked in a sterilized.1% (v/v) tween 80. For soil drenching treatments, 30 ml/plant fungal suspension was applied around the root zone after 1 week of germination.

Fifty plants per treatment were planted and replicated three times with 5 m spacing between rows. Plants of each treatment were planted 2.5 m apart from each other to hinder communication. The field conditions and management were consistent with the common local farming agricultural practices and covered with nylon netting to prevent insect immigration. All the plants selected for this experiment were healthy and developmentally similar.

Confirmation of Endophytic Colonization of Plants

To confirm the endophytic colonization of plants by fungal stains, a re-isolation method was used. Leaves were surface-sterilized in 1% sodium hypochlorite for 3 min, 70% ethanol for 1 min followed by washing with sterilized distilled water three times. Leaves were then cut into small segments by using sterilized scissors and placed on potato dextrose agar (PDA) plates. After incubation of 3–7 days at 25 ± 2°C, the presence or absence of fungal growth from leaves was recorded and the colonization % was calculated (Quesada-Moraga et al., 2006).

Insect Infestation and Plant Sampling

The *O. furnacalis* neonates were obtained from the Institute of Plant Protection, CAAS, and reared on an artificial diet. Insect infestation for larval survival and maize damage rating was carried out at the vegetative and silking stage, representing 1st and 2nd generation infestation, respectively. Healthy plants were infested artificially with 60 neonates (<24 h old) on June 30 and June 25 for 1st generation infestation, and on August 10 and 6 for the 2nd generation infestation in 2018 and 2019, respectively. The infestation was done during the

evening to avoid exposure of neonate to direct sunlight and high temperature.

For antioxidants, chlorophyll, and molecular assays, 3rd instar larvae of *O. furnacalis* were placed on each leaf of healthy vegetative stage plants covered with small net cages to restrict their movement. Damaged leaves around the larval feeding site were collected in three replicates at 0-, 12-, 24-, 48-, and 72-h post infestation and immediately frozen in liquid nitrogen. Samples were stored at −80°C until further analysis (Guo et al., 2019).

Maize Damage Rating and Larval Mortality

When fifth instar *O. furnacalis* larvae were observed around the maize field of 1st generation on July 28 and 23 and of 2nd generation on September 9 and 4 (ready to harvest), maize plants were dissected to record the larval mortality rate (%), plant height, tunnel number, tunnel length, kernel number kernel weight, and fungal outgrowth on larval cadavers (Xie et al., 2015).

Measurement of Plant Antioxidants and Chlorophyll Content

Enzymatic antioxidants including POD, SOD, protease, polyphenol oxidase, proline content, and chlorophyll content were estimated in maize leaves at 0-, 12-, 24-, 48-, and 72-h post infestation. Detailed protocols are described in our previous article Batool et al. (2020).

Transcriptome Profiling and Bioinformatics Analysis

The RNA was isolated using the TIANGEN kit (Beijing, China), following the manufacturer's instructions. Sequencing libraries were generated using NEBNext Ultra^{TM} RNA Library Prep Kit for Illumina (New England Biolabs, Ipswich, MA, United States) according to the manufacturer's instructions, and index codes were added to attribute sequences of each sample. Library quality was assessed on the Agilent Bioanalyzer 2100 system. Clean reads were then mapped with the reference genome sequence by Hisat2 tools soft (Kim et al., 2015). Gene function was annotated based on database information. DEGs were identified using the DESeq2 with P-value < 0.05 (Wang et al., 2010). We used KOBAS software to test the statistical enrichment of DEGs in kyoto encyclopedia of genes and genomes (KEGG) pathways.

Weighted Gene Co-expression Network Analysis for Identification of Key Candidate Genes Involved in Maize Defense

Weighted gene coexpression network analysis (WGCNA) was performed in R (version 4.1.2) using default parameters to simplify genes into expressed modules to identify the defense-related hub genes (Langfelder and Horvath, 2008). The fragments per kilobase of transcript per million mapped reads (FPKM) values were normalized, and an adjacency matrix was constructed. The plant antioxidant and the chlorophyll analysis data, used as phenotypic data, were imported into the WGCNA package, and correlation between antioxidants and chlorophyll data and gene modules were calculated using the default settings. The WGCNA package was used to convert the adjacency matrix into a topological overlap matrix (TOM). After constructing a network, the transcripts with identical expression patterns were grouped into one module, and eigengenes were also calculated for these modules. The genes from each module were exported using the default parameters for cytoscape export.

Validation of Intramodular Candidates Through Real Time-Quantitative Polymerase Chain Reaction

Validation of gene expression by RT-qPCR was carried out in three biological replicates on Applied Biosystems 7500 Fast Real-Time PCR System (Applied Biosystems, Foster City, CA, United States) using an SYBR Green (TAKARA Bio Inc., Japan) following the manufacturer's guide. The RNA was isolated using a TIANGEN kit (Beijing, China) and the complementary DNAs (cDNAs) were synthesized using the One-Step gDNA Removal and cDNA Synthesis SuperMix (TransGen Biotech Co., Ltd., Beijing, China) by using the user's manual. The amplification program followed was 95°C (15 s), followed by 40 cycles at 60°C (60 s), and 95°C (30 s). Actin (accession number-EU585777.1) was used as a reference gene. Fold changes of gene expression level were calculated using the $2^{-\Delta\Delta CT}$ method (Guo et al., 2019). Primers used are given in **Supplementary Table 4**.

Metabolome Profiling and Quantification of Phytohormones

Metabolite extraction and analysis were performed by using ultra-high-performance liquid chromatography-mass spectroscopy (UHPLC-MS, ExionLC, AB SCIEX; Waters, Manchester, United Kingdom) by following the protocol described by Yu et al. (2020). Quantification of SA, JA, and ET was done by following Guo et al. (2021). All the samples were collected as three biological replicates.

Data Analysis

Data collected from the maize physiological and biochemical experiments were analyzed using Statistix 8.1 software and the significance of $p < 0.05$ was applied. Alignment of RNA-seq data was done with HISAT2 software. Assembling of transcripts with mapped reads was done by using String Tie. To quantify the expression levels of transcripts for each sample, we used Asprofile software. The WGCNA was performed in R packages (version 4.1.2). Statistical comparisons of metabolite concentration were made using a SAS statistics package version 9.2 (SAS Institute Inc, 2015) and a significance level of $P < 0.05$ was applied.

RESULTS

Confirmation of Endophytic Colonization of Plants

By a re-isolation method, the mycelia growth of *B. bassiana* OFDH1-5 and *T. asperellum* GDSF1009 were observed growing

from leaf segments placed in PDA plates after 3 days, whereas, in the control treatment, no fungal growth was observed. In comparison with the soil drenching treatments, 19.6 and 15.9%, 42.2 and 39.44%, and 55 and 43.17% higher growth was recorded in seed coated treatment BB-1, TH-1, and BT-1 in 2018 and 2019, respectively (**Table 1** and **Figure 1**).

Larval Survival Rate

The *B. bassiana* OFDH1-5 and *T. asperellum* GDFS1009 significantly affected the mortality rate of *O. furnacalis* larvae in both generations. In both generations, 89.38 and 92.28% of larval mortality was observed in BT-1 treatment (a consortium of both fungi) of 2018 and 2019, respectively, followed by 73.03 and 69.68% mortality was observed in BB-1, which was higher than IC. Plants inoculated with soil drenching method (BB-2, TH-2, and BT-2) showed relatively low mortality (60–65%, 40–50%, and 70–80%) in comparison with plants inoculated with seed treatment method (BB-1, TH-1, and BT-1) in 2018 and 2019, respectively (**Table 2**).

Maize Growth and Damage Rating

The consortium of *B. bassiana* OFDH1-5 + *T. asperellum* GDFS1009 has a positive effect on plant growth and damage rating. In Generation 1, the highest number of tunnels and tunnel lengths were recorded in the insect control treatment (IC), whereas this damage was reduced up to 86.3 and 94.6% in BT-1 in 2018, and 92.2 and 96.7% in 2019, respectively. The second lowest damage was recorded in BB-1 with 77.7 and 81.8% reduction in the number of tunnels and 91.3 and 93.8% reduction in tunnel lengths in 2018 and 2019, respectively. Similar results were recorded in generation 2 with the highest number of tunnels and tunnel lengths in IC and lowest (82.9 and 93% in 2018, and 84.9 and 95.6% in 2019) in BT-1 (**Table 2**).

Over the 2-year average, plant heights were reduced up to 25.65% in the insect control treatment (IC) compared to the untreated control, while application of *B. bassiana* OFDH1-5 and *T. asperellum* GDFS1009 reduced the negative effect of *O. furnacalis* feeding and increased the plant heights up to 30.65, 29.1, and 34.5% in BB-1, TH-1, and BT-1, respectively. Less effect on plant height was seen in plants inoculated with the soil drenching method (**Table 3**). Additionally, the application of entomopathogenic fungi significantly increased the grain yield. The maximum increase in the average number of kernels per ear was recorded as 55.2 and 70.9% in BT-1, followed by 53.4 and 69.1% in BB-1, and 47.9 and 56.6% in TH-1 in 2018 and 2019, respectively. Similar patterns of increase in weight per 100 kernels were observed with 53.3 and 79.8% in BT-1, 46.2 and 65.7% in BB-1, and 36.1 and 43.4% in TH-1 in 2018 and 2019, respectively. In contrast, the maximum reduction in grain yield was recorded in insect control (IC) treatment with 20.6 and 29.1% in the number of kernels per ear, and 21.1 and 32.1% in weight per 100 kernels in the year 2018 and 2019, respectively, compared to untreated control (CK) (**Table 3**).

Larval cadavers were collected from the field to determine the percentage (%) of cadavers showing a fungal outgrowth collected from the field. The highest number of cadavers (%) with fungal outgrowth was observed as 87.33 and 91.83% in seed treated consortium treatment (BT-1) in 2018 and 2019, respectively, at Generation 1 infestation. Similarly, in Generation 2 infestation, 89.68 and 84.07% cadavers were detected in BT-1 with fungal outgrowth in 2018 and 2019, respectively, followed by 71–74% in seed treated with *B. bassiana* treatment (BB-1) (**Table 4** and **Figure 2**). Based on agronomic field data, samples from BB-1, TH-1, BT-1 (inoculated through seed treatment method), and IC were used for further analysis.

TABLE 1 | Percentage (%) endophytic colonization of plants by fungal isolates among different treatments in 2018 and 2019.

Treatments	Endophytic colonization (%)	
	2018	2019
CK	0 ± 0^{f}	0 ± 0^{f}
BB-1	85.02 ± 1.67^{a}	82.40 ± 0.73^{b}
BB-2	68.33 ± 2.55^{c}	69.28 ± 1.50^{c}
TH-1	86.67 ± 0.96^{a}	89.70 ± 2.01^{a}
TH-2	50.01 ± 1.67^{d}	54.32 ± 0.35^{d}
BT-1	83.33 ± 0.96^{b}	89.87 ± 1.20^{a}
BT-2	46.67 ± 2.55^{e}	51.07 ± 0.65^{e}
IC	0 ± 0^{f}	0 ± 0^{f}

Mean ± SD followed by different lowercase letters indicate significant differences among the treatments ($p < 0.05$). Treatments include: (CK) untreated control, (BB-1) seed treatment with B. bassiana OFDH1-5, (BB-2) soil drenching with B. bassiana OFDH1-5, (TH-1) seed treatment with T. asperellum GDFS1009, (TH-2) soil drenching with T. asperellum GDFS1009, (BT-1) seed treatment with consortium of B. bassiana OFDH1-5 and T. asperellum GDFS1009, (BT-2) soil drenching with a consortium of B. bassiana OFDH1-5 + T. asperellum GDFS1009, (IC) no inoculation.

Transcriptome Responses Triggered by *B. bassiana* OFDH1-5 and *T. asperellum* GDFS1009

For transcriptome profiling, four treatments (BB-1, TH-1, BT-1, and IC) in three replicates at 0-, 12-, 24-, 48-, and 72-h post *O. furnacalis* infestation were used to construct 60 cDNA libraries. A total of 458.04 Gb clean data was obtained and the clean data of each sample reached 5.71 Gb, and the Q30 base percentage was 93.24% and above. Clean reads were aligned with a designated reference genome (ZmB73_RefGen_v4) and the comparison efficiency ranged from 79.13 to 89.36% (**Supplementary Table 2**). Based on the comparison results, the gene expression level analysis was performed and the differentially expressed genes were identified according to their expression levels | log2 (fold-change)| > 1 and an adjusted *P*-value < 0.05 in each pairwise comparison. The abundance of upregulated genes was higher than downregulated genes compared to all-time points (**Supplementary Table 3**). Identified genes in all samples were hierarchically clustered relative to control. The difference in color indicates high (red) and low (green) expressions (**Figure 3A**). The principal component analysis revealed the variability among transcriptome data of different samples. Clustering of samples away from each other and control group (IC) indicates a fungal inoculation and *O. furnacalis*-induced changes in gene expression specially

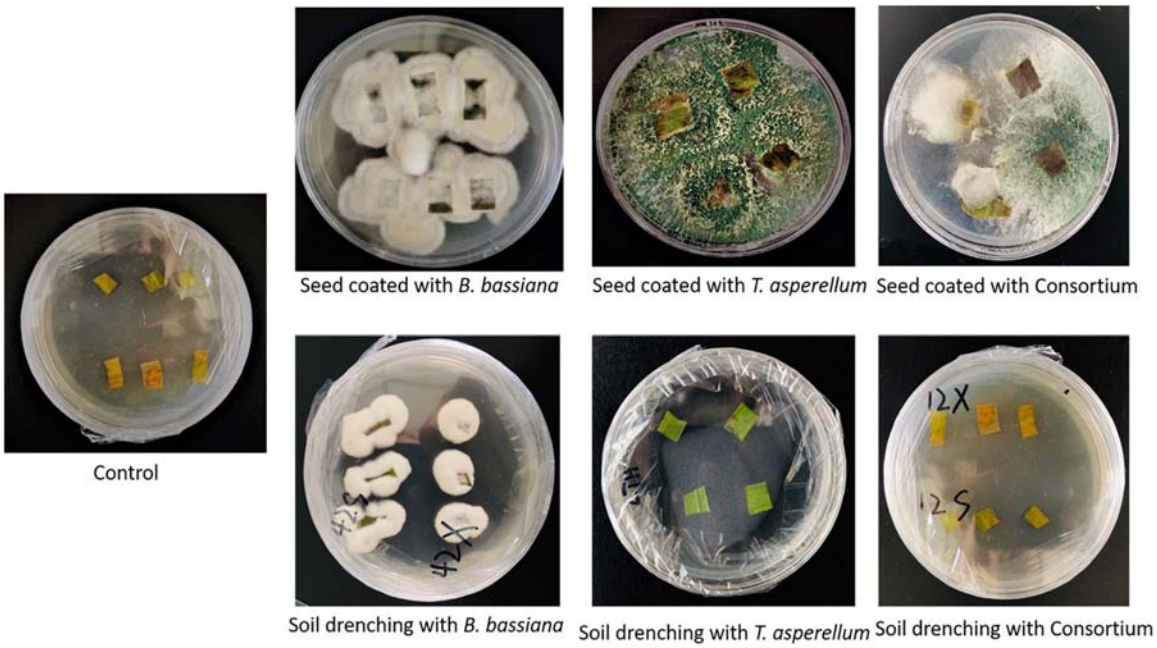

FIGURE 1 | Confirmation of endophytic colonization of plants by fungal isolates through the re-isolation method.

TABLE 2 | Differential effect of single and consortium of *B. bassiana* OFDH1-5 and *T. asperellum* GDFS1009 inoculation on larval survival rate, number, and length of tunnels under *O. furnacalis* attack for two generations in 2018 and 2019.

Treatments	Mortality (%)		Number of tunnels/plant		Length of tunnels (cm)	
	2018	2019	2018	2019	2018	2019
Generation 1 (vegetative stage)						
CK	0 ± 0^{h}	0 ± 0^{g}	0 ± 0^{f}	0 ± 0^{g}	0 ± 0^{f}	0 ± 0^{g}
BB-1	73.03 ± 0.02^{c}	69.68 ± 0.075^{c}	1.033 ± 0.19^{d}	1.073 ± 0.15^{e}	0.652 ± 0.05^{ef}	0.576 ± 0.08^{e}
BB-2	61.11 ± 0.05^{e}	62.43 ± 0.12^{d}	1.533 ± 0.1^{c}	1.66 ± 0.09^{d}	1.687 ± 0.045^{d}	1.319 ± 0.02^{d}
TH-1	67.51 ± 0.08^{d}	61.16 ± 0.14^{d}	2.05 ± 0.05^{b}	2.083 ± 0.1^{c}	2.43 ± 0.12^{c}	2.087 ± 0.09^{c}
TH-2	52.33 ± 0.07^{f}	42.57 ± 0.12^{e}	2.233 ± 0.12^{b}	2.56 ± 0.03^{b}	4.147 ± 0.15^{b}	4.125 ± 0.2^{b}
BT-1	89.38 ± 0.1^{a}	92.28 ± 0.03^{a}	0.633 ± 0.07^{e}	0.46 ± 0.06^{f}	0.405 ± 0.06^{f}	0.309 ± 0.03^{f}
BT-2	81.47 ± 0.08^{b}	71.43 ± 0.08^{b}	1.383 ± 0.08^{c}	1.49 ± 0.22^{de}	1.185 ± 0.14^{de}	1.27 ± 0.06^{d}
IC	24.08 ± 0.08^{g}	15.52 ± 0.46^{f}	4.633 ± 0.06^{a}	5.9 ± 0.3^{a}	7.486 ± 0.6^{a}	9.337 ± 0.8^{a}
Generation 2 (silking stage)						
CK	0 ± 0^{h}	0 ± 0^{h}	0 ± 0^{g}	0 ± 0^{g}	0 ± 0^{g}	0 ± 0^{h}
BB-1	71.08 ± 0.06^{c}	74.03 ± 0.014^{c}	1.683 ± 0.12^{ef}	1.676 ± 0.05^{e}	3.037 ± 0.13^{e}	2.547 ± 0.03^{f}
BB-2	59.17 ± 0.06^{e}	61.07 ± 0.05^{e}	2.317 ± 0.11^{d}	2.527 ± 0.02^{d}	5.333 ± 0.06^{d}	5.69 ± 0.1^{d}
TH-1	62.45 ± 0.05^{d}	65.57 ± 0.08^{d}	3.3 ± 0.28^{c}	3.411 ± 0.1^{c}	13.993 ± 0.08^{c}	11.33 ± 1.7^{c}
TH-2	43.17 ± 0.1^{f}	48.54 ± 0.06^{f}	4.3 ± 0.22^{b}	5.01 ± 0.08^{b}	17.894 ± 0.8^{b}	20.573 ± 0.7^{b}
BT-1	86.05 ± 0.09^{a}	89.67 ± 0.09^{a}	1.117 ± 0.1^{f}	1.25 ± 0.1^{f}	1.403 ± 0.06^{f}	1.103 ± 0.1^{g}
BT-2	81.47 ± 0.03^{b}	83.53 ± 0.05^{b}	2.1 ± 0.1^{de}	2.347 ± 0.09^{de}	5.425 ± 0.16^{d}	4.573 ± 0.67^{de}
IC	16.15 ± 0.1^{g}	17.07 ± 0.05^{g}	6.567 ± 0.4^{a}	8.267 ± 0.5^{a}	20.055 ± 0.83^{a}	25.097 ± 0.9^{a}

Mean ± SD followed by different lowercase letters indicate significant differences among the treatments ($p < 0.05$). Treatments include: (CK) untreated control, (BB-1) seed treatment with B. bassiana OFDH1-5, (BB-2) soil drenching with B. bassiana OFDH1-5, (TH-1) seed treatment with T. asperellum GDFS1009, (TH-2) soil drenching with T. asperellum GDFS1009, (BT-1) seed treatment with consortium of B. bassiana OFDH1-5 and T. asperellum GDFS1009, (BT-2) soil drenching with a consortium of B. bassiana OFDH1-5 + T. asperellum GDFS1009, (IC) no inoculation.

in consortium treatment (BT) (**Figure 3B**). In total, 13,156 common DEG's were identified in all the combinations at different time points.

To explore the response of different processes in combined *B. bassiana* OFDH1-5 and *T. asperellum* GDFS1009 treatments, we analyzed the KEGG enrichment analysis of common DEG's. The sets of DEG's were assigned to significant KEGG Pathways ($P > 0.05$) (**Supplementary Figure 1**), and the top enriched resistance related pathways in IC vs. BB, IC vs. TH, and IC vs. BT at 12-, 24-, 48-, and 72-h were listed in **Figure 3C**, which show

TABLE 3 | Differential effect of single and consortium of *B. bassiana* OFDH1-5 and *T. asperellum* GDFS1009 inoculation on maize yield under *O. furnacalis* attack in 2018 and 2019.

Treatments	Kernel number/ear		100 kernel weight		Height (cm)	
	2018	2019	2018	2019	2018	2019
CK	692.78 ± 0.5^{g}	706.03 ± 0.7^{g}	20.56 ± 0.5^{c}	21.27 ± 0.8^{c}	316.62 ± 0.5^{a}	311.34 ± 1.38^{b}
BB-1	843.3 ± 0.8^{a}	846.27 ± 0.29^{b}	23.92 ± 0.6^{a}	23.95 ± 0.56^{b}	298.43 ± 1.13^{e}	304.27 ± 0.27^{c}
BB-2	793.63 ± 0.6^{e}	789.15 ± 0.5^{e}	21.03 ± 0.19^{bc}	21.65 ± 0.50^{c}	279.61 ± 1.2^{f}	296.05 ± 1.23^{e}
TH-1	813.68 ± 1.25^{c}	793.93 ± 1.0^{d}	22.27 ± 0.45^{b}	20.72 ± 0.65^{cd}	307.07 ± 0.4^{c}	298.43 ± 1.13^{e}
TH-2	780.23 ± 0.4^{f}	740.81 ± 0.7^{f}	20.44 ± 0.5^{c}	17.83 ± 0.5^{e}	301.46 ± 1.2^{d}	279.50 ± 0.6^{f}
BT-1	853.23 ± 0.9^{b}	855.3 ± 0.7^{a}	25.06 ± 0.11^{a}	25.98 ± 0.52^{a}	311.34 ± 1.4^{b}	316.62 ± 0.5^{a}
BT-2	797.92 ± 0.61^{d}	801.63 ± 0.5^{c}	21.82 ± 0.7^{bc}	23.21 ± 0.2^{b}	300.23 ± 0.8^{d}	300.25 ± 0.8^{d}
IC	549.8 ± 1.03^{h}	500.41 ± 1.01^{h}	16.36 ± 0.3^{d}	14.45 ± 0.50^{f}	238.74 ± 1.2^{g}	228.38 ± 1.01^{g}

Mean ± SD followed by different lowercase letters indicate significant differences among the treatments ($p < 0.05$). Treatments include (CK) untreated control, (BB-1) seed treatment with B. bassiana OFDH1-5, (BB-2) soil drenching with B. bassiana OFDH1-5, (TH-1) seed treatment with T. asperellum GDFS1009, (TH-2) soil drenching with T. asperellum GDFS1009, (BT-1) seed treatment with consortium of B. bassiana OFDH1-5 and T. asperellum GDFS1009, (BT-2) soil drenching with a consortium of B. bassiana OFDH1-5 + T. asperellum GDFS1009, (IC) no inoculation.

TABLE 4 | Percentage (%) of cadavers showing fungal outgrowth collected from the field.

Treatments	Cadavers with fungal outgrowth (%)	
	2018	2019
Generation 1 (vegetative stage)		
CK	0 ± 0^{f}	0 ± 0^{e}
BB-1	74.00 ± 0.67^{b}	71.68 ± 0.75^{b}
BB-2	54.11 ± 2.05^{d}	62.93 ± 0.23^{c}
TH-1	54.67 ± 0.78^{d}	59.36 ± 0.34^{c}
TH-2	20.08 ± 0.477^{e}	32.37 ± 1.12^{d}
BT-1	87.33 ± 1.13^{a}	91.83 ± 2.01^{a}
BT-2	58.67 ± 1.08^{c}	61.39 ± 1.08^{c}
IC	0 ± 0^{f}	0 ± 0^{e}
Generation 2 (silking stage)		
CK	0 ± 0^{g}	0 ± 0^{g}
BB-1	71.58 ± 0.35^{b}	74.32 ± 0.24^{b}
BB-2	56.67 ± 0.76^{cd}	61.75 ± 1.15^{c}
TH-1	49.45 ± 1.35^{e}	47.57 ± 0.48^{e}
TH-2	24.17 ± 1.71^{f}	28.50 ± 1.06^{f}
BT-1	89.65 ± 1.09^{a}	84.07 ± 0.19^{a}
BT-2	59.97 ± 0.53^{c}	57.09 ± 0.35^{d}
IC	0 ± 0^{g}	0 ± 0^{g}

Mean ± SD followed by different lowercase letters indicate significant differences among the treatments ($p < 0.05$). Treatments include (CK) untreated control, (BB-1) seed treatment with B. bassiana OFDH1-5, (BB-2) soil drenching with B. bassiana OFDH1-5, (TH-1) seed treatment with T. asperellum GDFS1009, (TH-2) soil drenching with T. asperellum GDFS1009, (BT-1) seed treatment with consortium of B. bassiana OFDH1-5 and T. asperellum GDFS1009, (BT-2) soil drenching with a consortium of B. bassiana OFDH1-5 + T. asperellum GDFS1009, (IC) no inoculation.

FIGURE 2 | Field collected dead larvae showing the existence of fungal outgrowth from the larval cadavers.

uniquely induced genes enriched in a higher number of metabolic processes in consortium treatment (BT).

B. bassiana OFDH1-5 and *T. asperellum* GDFS1009 Triggered Antioxidants and Chlorophyll Content in *O. furnacalis*-Induced Defense

The antioxidant enzyme activities started to increase at 12-h in all the infested treatments and reached a maximum point at 24-h of insect feeding and gradually decreased until 48-h, while polyphenol oxidase (PPO) reached the maximum at 48-h. The production of antioxidant enzymes was further triggered by entomopathogenic fungal treatments and the highest productions were observed in consortium treatment (BT-1). An increase of 132. 5-, 385. 3-, 100. 6-, and 277.7-folds were recorded in SOD, POD, proline, and protease activities at 24-h of *O. furnacalis* feeding. In the case of PPO, a 522.7-fold increase was recorded at 48-h and the lowest enzyme activities were observed in IC treatment (**Figures 4A–E**).

Chlorophyll content was observed to be gradually decreased from 0-h to 72-h due to *O. furnacalis* feeding, but fungal inoculation increased the chlorophyll content. The maximum content of chlorophyll-a and chlorophyll-b were recorded in BT-1, followed by TH-1, and BB-1 compared to insect control (IC). Chlorophyll-a, chlorophyll-b, and carotenoid were reduced up to 80-, 86-, and 86.3-folds, respectively, in the insect control (IC) (**Figures 4F–I**).

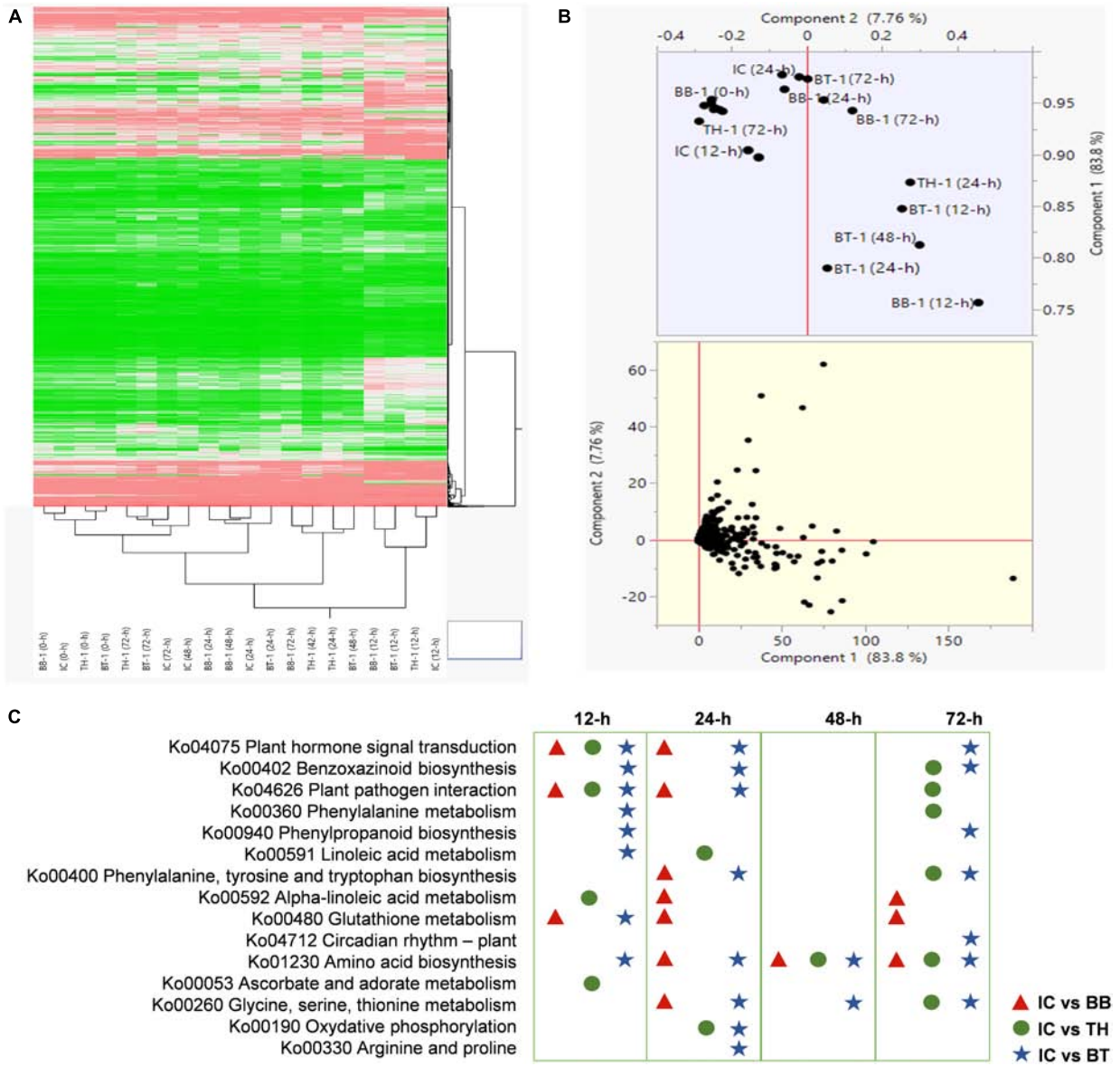

FIGURE 3 | Transcriptome response of maize inoculated with single and consortium of *Beauveria bassiana* OFDH1-5 and *Trichoderma asperellum* GDFS1009 to *Ostrinia furnacalis*. **(A)** Hierarchical Cluster dendrogram of differentially expressed genes, the difference in color indicate high (red) and low (green) expression. **(B)** PCA plot showing variability of transcriptome data; **(C)** top enriched resistance related pathways in IC vs. BB, IC vs. TH, IC vs. BT at 12-, 24-, 48-, and 72-h.

Co-expression Network Analysis for the Identification of Hub Genes Involved in Maize Defense

The FPKM values of 13,156 common DEGs and plant biochemical parameters (SOD, POD, proline, protease, PPO, Chl-a, chl-b, carotenoids, and chl-a + b) at different time points were used for the weighted gene coexpression network analysis and the module trait correlations were calculated. Thirty-three gene modules were identified based on coexpression patterns. Each module is represented by a different color and presented as a cluster dendrogram and network heatmap (**Figures 5A–D**).

Among the 33 identified modules, only six showed significant correlations with the phenotypic data. The blue module with 326 genes showed significant correlations with SOD, proline, protease, and PPO with correlation coefficients (r^2) of 0.93, 0.82, 0.7, and 0.75, respectively. The darkgrey module possessing 149 genes showed positive correlations with POD (r^2 = 0.84), PPO (r^2 = 0.73), and protease (r^2 = 0.95). The green-yellow module, having 223 genes, showed significant positive correlations with POD (r^2 = 0.71), SOD (r^2 = 0.81), proline (r^2 = 0.73), protease (r^2 = 0.71), and PPO (r^2 = 0.9). Grey60 module consists of 57 genes, and it showed a positive correlation with carotenoids (r^2 = 0.73). Magenta module with 98 genes showed positive

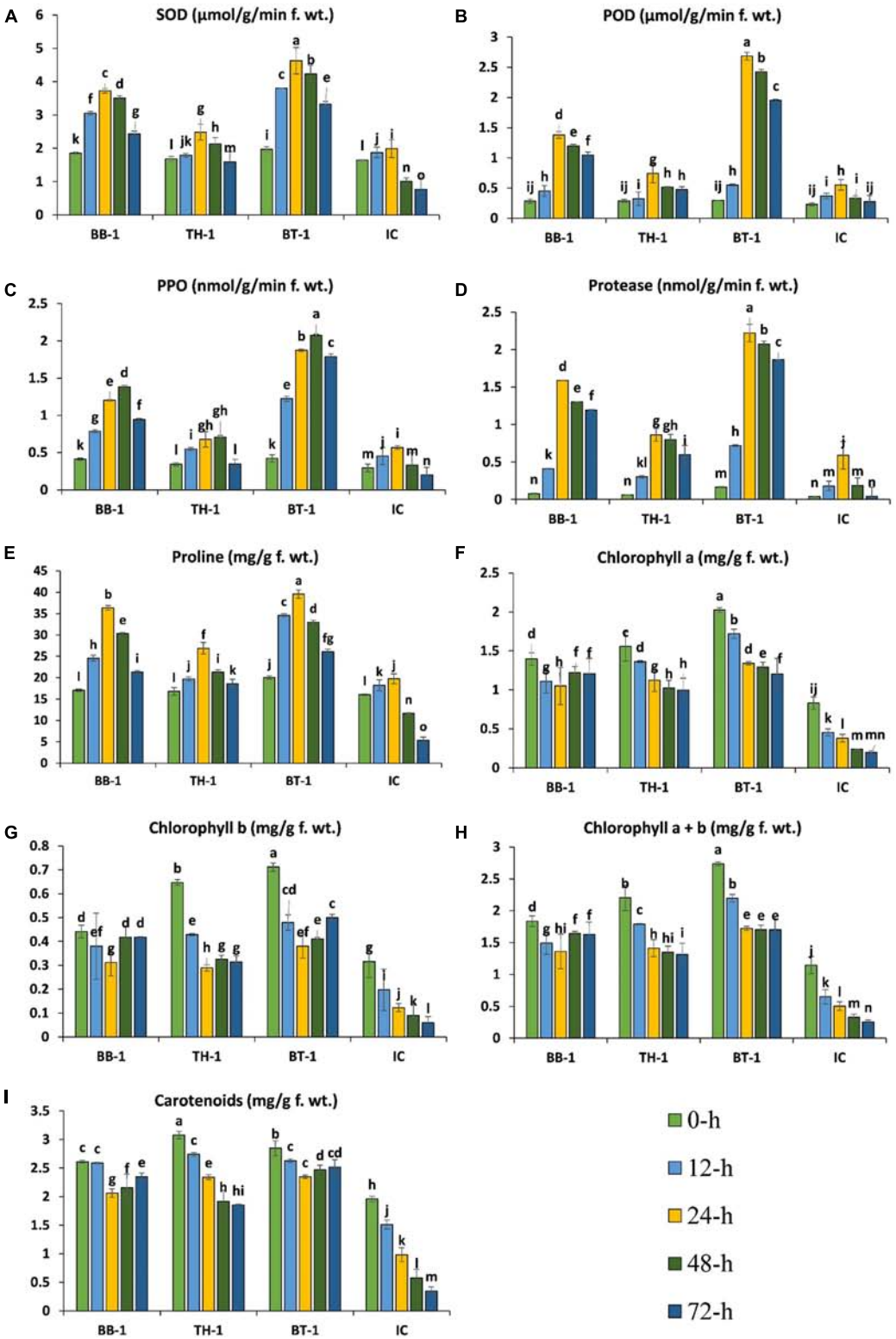

FIGURE 4 | *Beauveria bassiana* OFDH1-5 and *T. asperellum* GDFS1009 induced response of maize antioxidants and chlorophyll content under *O. furnacalis* attack. **(A)** Superoxide dismutase (SOD); **(B)** peroxidase (POD); **(C)** polyphenol oxidase (PPO); **(D)** protease; **(E)** proline; **(F)** chlorophyll a; **(G)** chlorophyll b; **(H)** chlorophyll a + b; **(I)** carotenoids. Different lowercase letters above each bar indicate significant differences among treatments ($p < 0.05$). Treatments include (BB-1) seed treatment with *B. bassiana* OFDH1-5, (TH-1) seed treatment with *T. asperellum* GDFS1009, (BT-1) seed treatment with a consortium of *B. bassiana* OFDH1-5 and *T. asperellum* GDFS1009, (IC) no inoculation.

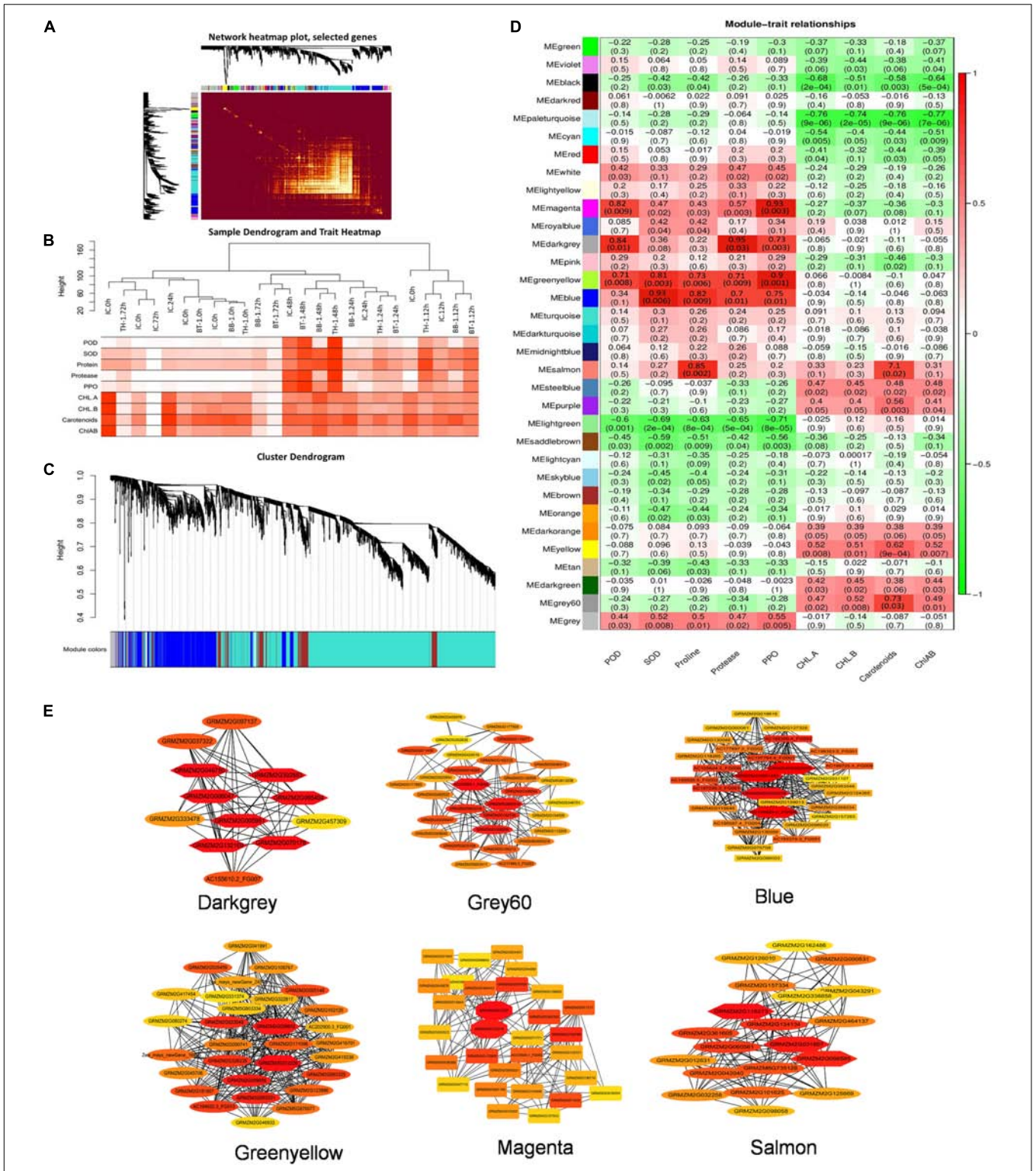

FIGURE 5 | Weighted gene coexpression network analysis (WGCNA) analysis to identify key candidate genes involved in maize defense. **(A)** Cluster dendrogram and network heatmap of genes subjected to coexpression module calculation. **(B)** Sample dendrogram and module trait heatmap of each time point. **(C)** Hierarchical clustering presenting eleven modules having coexpressed genes. Each leaflet in the tree corresponds to an individual gene. **(D)** Module-trait associations based on Pearson correlations. The color key from green to red represents r^2 values ranging from –1 to 1. **(E)** Gene networks of six highly correlated modules with phenotypic traits. Genes in different red shape due to the highest weight within the module represents hub genes (key candidate genes) and are coded for gene descriptors based on annotation. Treatments include (BB-1) seed treatment with *B. bassiana* OFDH1-5, (TH-1) seed treatment with *T. asperellum* GDFS1009, (BT-1) seed treatment with a consortium of *B. bassiana* OFDH1-5 and *T. asperellum* GDFS1009, (IC) no inoculation.

correlations with POD (r^2 = 0.82) and with PPO (r^2 = 0.93). Salmon module with 145 genes showed a correlation with proline (r^2 = 0.85) (**Figure 5D**). The hub genes from these modules were selected by the cytoscape built-in extension, namely "CytoHubba," visualizing the gene networks (**Figure 5E**). Furthermore, to find out the genes involved in maize defense within these gene networks, gene annotation information was extracted from maize reference genome (ZmB73_Ref-Gen_v4).

Real Time-Quantitative Polymerase Chain Reaction Validation of Intramodular Hub Genes

Selected hub genes were further validated by performing RT-qPCR at different time points, thus, narrowing down the number of selected genes. Finally, from 28 hub genes, we selected 13 key candidate genes with stable and consistent expressions responsible for maize defense against *O. furnacalis* (**Figure 6**). The RT-qPCR results were consistent with the RNA-seq data (**Supplementary Figure 2**). All the key candidate genes, along with other hub genes, are shown in **Table 5**.

B. bassiana OFDH1-5 and *T. asperellum* GDFS1009-Enhanced Expression of *Key Candidate Genes in Maize Defense Response* Against *O. furnacalis* Herbivory

Three key genes in the blue module were identified as protein kinase gene (GRMZM2G025459), which participates in the phytohormone signaling pathway to initiate a defense response and to regulate the expression of genes involved in ion homeostasis and oxidative stress responses, acyl-CoA dehydrogenase (GRMZM5G864319), which is involved in an alpha-linolenic acid metabolism of jasmonic acid pathway and thioredoxin gene (GRMZM2G091481), which acted as an important component of the signaling pathway in plant antioxidant networks. Similarly, in the salmon module, the Glutathione *S*-transferase was identified as a key gene (GRMZM2G116273), which plays a crucial role in plant oxidative stress response against high ROS (reactive oxygen species) levels generated by the insect attack.

Four genes, (GRMZM2G144153, AC212068.4_FG005, GRMZM2G392863, and GRMZM2G004466) were identified as key genes in darkgrey module. These genes were identified as glutathione peroxidase, GDSL- like lipase, defensin, and protease inhibitor. Glutathione peroxidase gene (GRMZM2G144153) is known to be activated upon a cell wall damage by insect feeding. In addition, it is also involved in the ROS scavenging, lignification of the cell wall, and synthesis of phenolic compounds. The GDSL- like lipase (AC212068.4_FG005) acts as an elicitor of systemic resistance linked with ET pathways. Upon insect feeding, its expression depending upon the ethylene signaling generates the systemic signals which translocate to other healthy parts of plants and propagate a systemic resistance throughout the plant. The defensin gene (GRMZM2G392863) has a great insecticidal property of inhibiting insect digestive enzymes; α-amylase play a crucial role in breaking down plant starch and hydrolyze proteins. Protease inhibitor genes (GRMZM2G004466) were characterized as key genes. One more protease inhibitor gene (AC233926.1_FG002) was identified in the grey60 module as a key gene. They were found to participate in the reduction of insect growth, and, thereby, suppress the infection process by inhibiting extracellular proteases released by insects.

Patatin-like phospholipase gene (GRMZM2G154523) is responsible for the synthesis of linolenic acid, as a precursor of jasmonic acid biosynthesis pathway and chitinase gene (GRMZM2G453805), expressed by plants and acted as a self-defense mechanism against insect attack, were found as defense-related hub genes in the green-yellow module.

Beta-glucosidase 18 and cytochrome p450 (GRMZM2G031660 and GRMZM2G139874), which participate in various detoxification and biosynthetic pathways to protect the plant, were found as key genes in the magenta module. All genes showed differential expression patterns among all fungal-inoculated treatments, with the highest expression levels at 24- and 48-h post larval infestation specially in BT-1. The role and expression patterns of all key genes in maize defense response are shown in **Table 5**, **Figure 6**, and **Supplementary Figure 2**.

Metabolomic Adjustments Triggered by *B. bassiana* OFDH1-5 and *T. asperellum* GDFS1009

To obtain complete insights of *B. bassiana* OFDH1-5 and *T. asperellum* GDFS1009 inoculated maize under the *O. furnacalis* attack, we performed a comprehensive untargeted metabolomic analysis of all BB-1, TH-1, BT-1, and IC at 0-, 12-, 24-, 48-, and 72-h by UHPLC-QTOF-MS for the first time. The principal component analysis (PCA) analysis clearly showed the diversity among samples. Interestingly 0-h samples grouped indicating less diversity and other samples clustering away from control showed diversity in metabolomic data (**Figure 7A**). Through electrospray ionization (ESI) total of 7,367 NEG (negative) and 13,183 POS (positive) mass/retention time features were detected (**Supplementary Data 4**), and further 130 NEG and 491 POS differentially annotated and abundant metabolomic features were filtered based on different classes (**Supplementary Data 5** and **Figure 7B**). Within the POS metabolic features, 9 fall in alkaloids and derivatives class, 26 in benzenoids, 3 in hydrocarbons, 194 in lipids and lipid-like molecule, 17 in nucleosides, nucleotides, and analogs, 47 in organic acids and derivatives, 11 in organic nitrogen compounds, 37 in organic oxygen compounds, 78 in organoheterocyclic compounds, 8 in organooxygen compounds, 57 in phenylpropanoids and polyketides and 1 each in hydrocarbon derivatives, organic compounds, organonitrogen compounds and lignans, neolignans, and related compounds. In the case of NEG metabolic features, 10 fall in benzenoids class, 15 each in nucleosides, nucleotide and analogs class and organic acid and derivative class, 1 in organic compounds, 16 in organic oxygen compounds, 13 in organoheterocyclic compounds, 6 in organooxygen compounds, 13 in phenylpropanoids and polyketides, and 41 in lipids and lipid-like molecules class

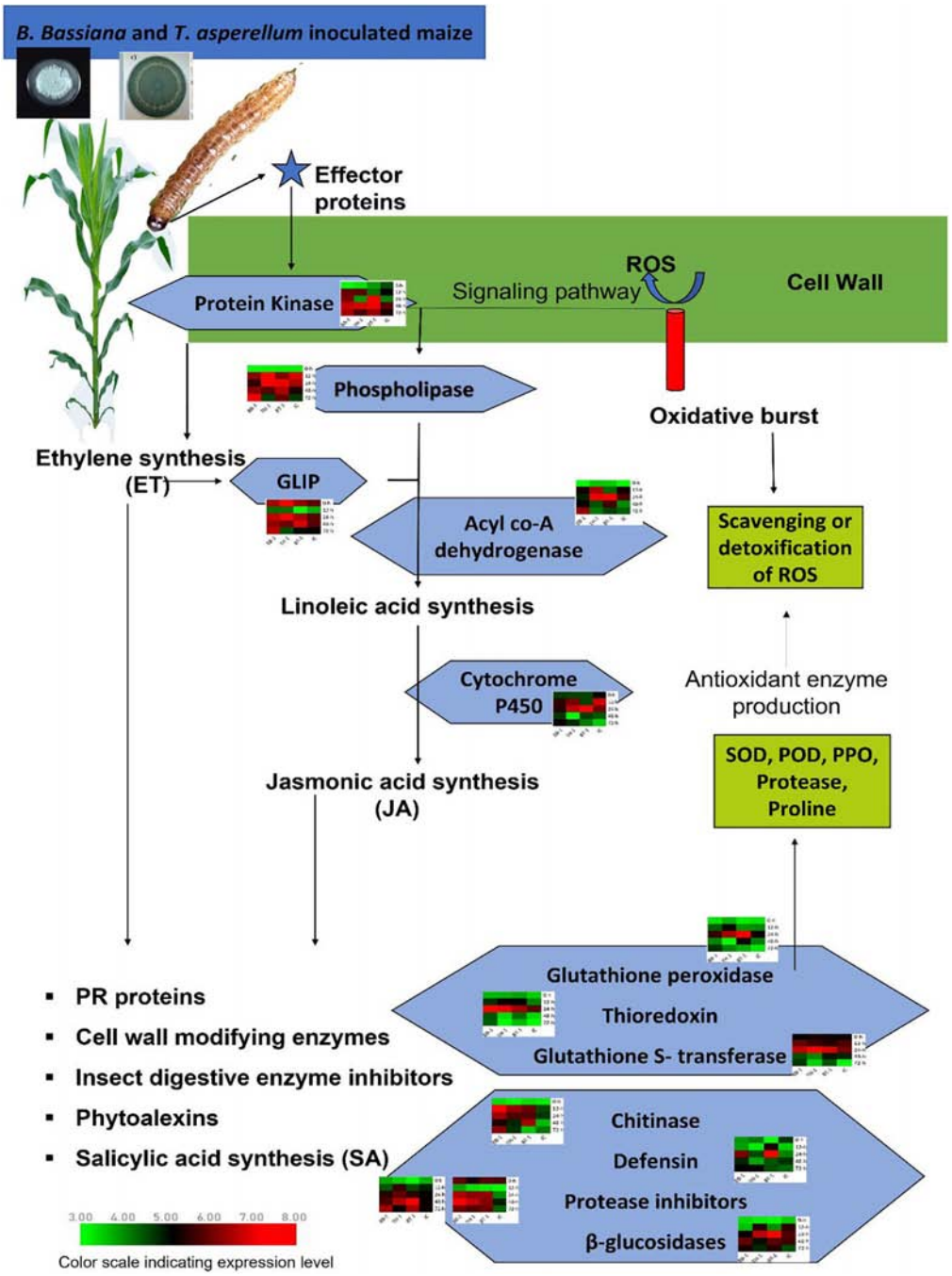

FIGURE 6 | Schematic representation of transcriptional strategies employed by maize inoculated with a consortium of *B. bassiana* OFDH1-5 and *T. asperellum* GDFS1009 compared with single inoculation to induce enhanced expression of key genes to involve in initiating signaling pathway to activate phytohormone biosynthesis pathways which regulate the production and expression of defense genes to induce maize resistance against *O. furnacalis*. Treatments include (BB-1) seed treatment with *B. bassiana* OFDH1-5, (TH-1) seed treatment with *T. asperellum* GDFS1009, (BT-1) seed treatment with a consortium of *B. bassiana* OFDH1-5 and *T. asperellum* GDFS1009, (IC) no inoculation.

(**Figure 7B**). Through hierarchical clustering, metabolites were divided into five clusters. Obvious changes were seen in the abundance of all metabolites belonging to different classes with a higher abundance of malonic acid, succinic acid, threonic acid, and gluconolactone in cluster 1, silicristin and mulberrin in cluster 2, etrogol and jasmonic acid in cluster 3, and betaine, L-threonine, L-carnitine, and thermophilin in cluster 5 were observed in a consortium treatment (BT-1). In cluster 4, all inoculated treatments have shown higher abundance as compared to control (IC) (**Figure 7C**).

TABLE 5 | Selected hub genes from all coexpressed modules with functional annotation.

Gene ID	Module	Annotation	Identified as key candidate gene
GRMZM2G144153	Darkgrey	Glutathione peroxidase	✓
AC212068.4_FG005	Darkgrey	GDSL-like lipase	✓
GRMZM2G046750	Darkgrey	Protease inhibitor	×
GRMZM2G392863	Darkgrey	Defensin like protein	✓
GRMZM2G004466	Darkgrey	Protease inhibitor	✓
GRMZM2G005991	Darkgrey	Protease inhibitor	×
GRMZM2G132169	Darkgrey	Laccase (L-ascorbate oxidase precursor)	×
GRMZM5G865319	Grey60	Serpin	×
AC233926.1_FG002	Grey60	Protease inhibitor	✓
GRMZM2G171444	Yellow	Ribosomal protein L19	×
AC200099.4_FG006	Blue	Cytochrome P450	×
GRMZM2G025459	Blue	Protein kinase	✓
GRMZM2G091481	Blue	Thioredoxin	✓
GRMZM5G864319	Blue	Acyl-CoA dehydrogenase	✓
GRMZM2G035708	Darkgreen	Photosynthetic NDH subunit	×
GRMZM2G453805	Green yellow	Chitinase	✓
GRMZM2G154523	Green yellow	Patatin-like phospholipase	✓
GRMZM2G031660	Magenta	Beta-glucosidase 18	✓
GRMZM2G139874	Magenta	Cytochrome P450	✓
GRMZM2G023152	Purple	*O*-methyltransferase ZRP4	×
AC225718.2_FG009	Purple	Wound-induced protein	×
GRMZM2G116273	Salmon	Glutathione *S*-transferase	✓
GRMZM2G031607	Salmon	SGS domain-containing protein	×
GRMZM2G096585	Salmon	peptidyl-prolyl isomerase	×
GRMZM2G310368	Steel blue	Ethylene-responsive transcription factor	×
Zea_mays_newGene_38529	Steel blue	Plant transposase	×
Zea_mays_newGene_15021	Steel blue	Plant transposase	×
Zea_mays_newGene_17096	White	Ribosomal protein S19e	×

B.bassiana OFDH1-5 and *T. asperellum* GDFS1009-Enhanced Phytohormone Concentration Induced by *O. furnacalis* Herbivory

To determine changes in stress-related phytohormones, we quantified JA, ET, and SA. A significant increase in the contents of phytohormones was recorded in all fungal inoculated treatments, but highest in consortium treatment (BT-1) at 24-h post infestation with an increase of 32.2, 37.4, and 77.5% in JA, SA, and ET, respectively (**Figure 7D**).

DISCUSSION

Ostrinia furnacalis is one of the most destructive insect pests of maize and it is responsible for major yield losses. It causes major damage at whorl stage plants by feeding in leaves and boring in maize stalk. Besides other pest control strategies, the biological control approach is of the highest interest because of its eco-friendly nature. The latest research proved that a consortium of biological control agents was effective against maize pests (Sarma et al., 2015; Batool et al., 2020). In our previous study (Batool et al., 2020), we have investigated and concluded that the entomopathogenic strain, *B. bassiana,* and plant pathogen antagonistic strain, *T. asperellum,* have both strong synergistic potential and can be used in the consortium to enhance their biological control activity. They inhibit the insect survival and damage on maize plants by inhibiting the immune response of *O. furnacalis* at the transcriptome level. Based on our previous findings, in the present investigation, we further investigated the effect of *B. bassiana*, *T. asperellum,* and their consortium on insect survival, maize damage, and growth, at field level under natural environmental conditions. Furthermore, WGCNA was used for the first time in an entomopathogenically inoculated maize to integrate transcriptome and biochemical data and an untargeted metabolite profiling at the vegetative stage of maize to identify the candidate genes and metabolites associated with the regulation of defensive biochemical enzymes, and induction of maize resistance and maize defense pathways against *O. furnacalis*.

Both entomopathogenic/antagonistic fungi can colonize the plant endophytically and can induce a defensive response upon insect feeding as a challenge, thereby killing or arresting the growth of insects (Batool et al., 2020). Plants can provide a suitable environment for entomopathogenic fungi and their insecticidal activity can suppress the infection and facilitate plants by increasing insect resistance and plant growth (Gupta et al., 2016). Plant colonization largely depends upon the method of

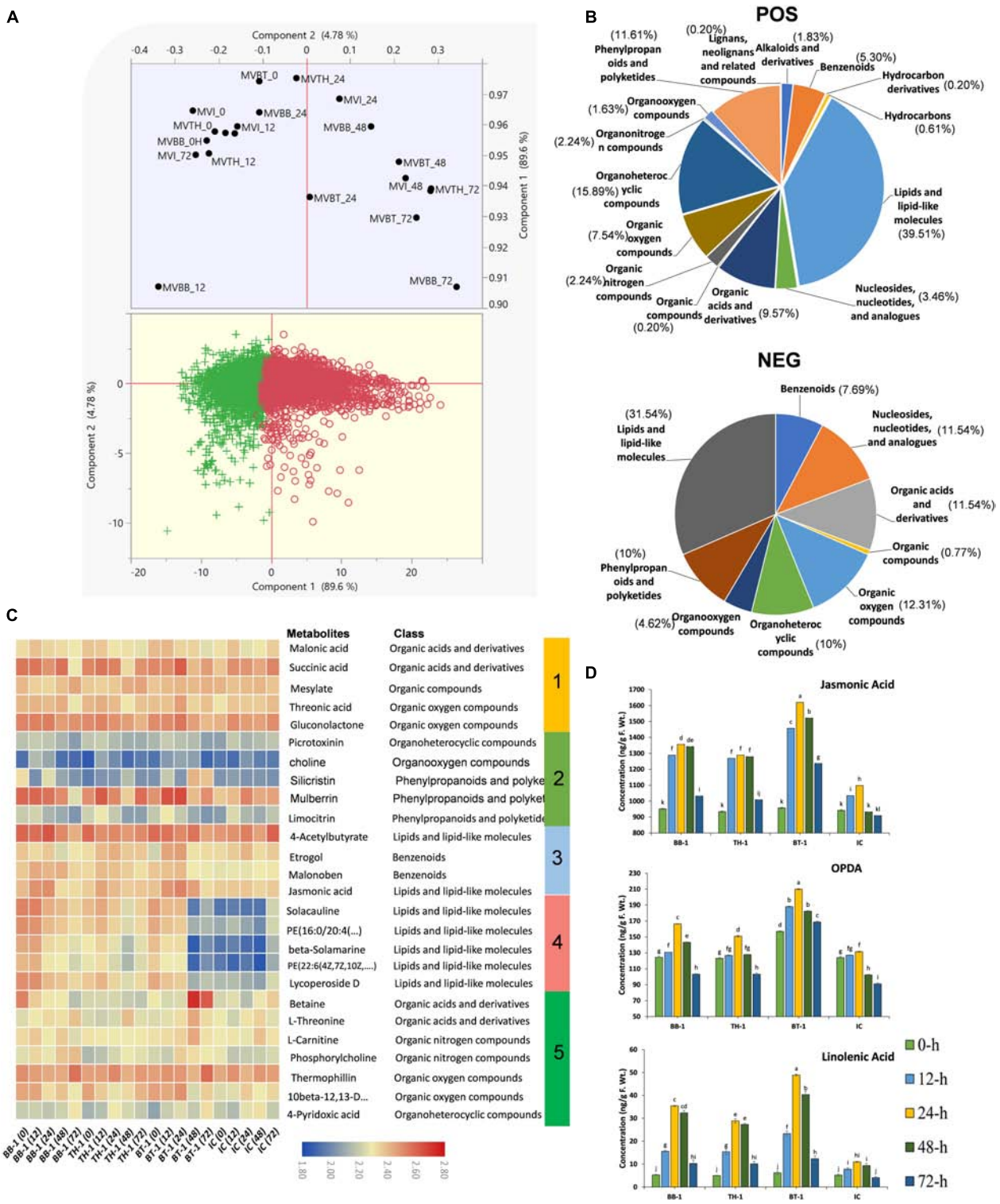

FIGURE 7 | Metabolome profiling of maize inoculated with single and consortium of *B. bassiana* OFDH1-5 and *T. asperellum* GDFS1009 and subjected to *O. furnacalis* attack. **(A)** PCA plot show divergence in metabolome data among treatments (MVBB, MVTH, MVBT, and MVI stands for BB-1, TH-1, BT-1, and IC, respectively). **(B)** Pie chart showing the percentage distribution of differentially annotated metabolites in different classes. **(C)** Hierarchical clustering of identified abundant metabolites. **(D)** Concentration of phytohormones in maize plants. Data is mean of three replicates and different lower-case letters above each bar indicate significant differences among treatments ($p < 0.05$). Treatments include (BB-1) seed treatment with *B. bassiana* OFDH1-5, (TH-1) seed treatment with *T. asperellum* GDFS1009, (BT-1) seed treatment with a consortium of *B. bassiana* OFDH1-5 and *T. asperellum* GDFS1009, (IC) no inoculation.

application and the seed treatment method was proven to be more effective (Batool et al., 2020). The seed treatment has the advantage of colonizing radical and plumule at the same time, as they are close to seed and can colonize the whole plant during its growth (Muvea et al., 2014). Our results were also in accordance with the findings of pathogenicity against *O. furnacalis* and reducing its survival, tunnel number and length, and increasing grain yield and plant growth in the consortium-treated Plants (BT-1). Some previous research also showed that the growth of entomopathogenic fungi in plants can prevent plant herbivory, and the *B. bassiana* have insecticidal activity against several insects including corn borers (Wagner and Lewis, 2000). *Trichoderma* is generally known for the function to induce the ISR of the whole maize plant against plant diseases and pest insects through colonization of maize roots (Rivas-Franco et al., 2020). The activity of *T. asperellum* was relatively low as compared to others, but its pathogenic activity was enhanced by the co-cultivation with *B. bassiana*. Shakeri and Foster (2007) also stated that the *Trichoderma* pathogenicity against borer larvae was lower and it can be increased by modifying them at the genetic level. Trichoderma could generate synergistic action with other biocontrol organisms, including the entomopathogenic fungi (Netzker et al., 2015), describing the use of consortium technique to enhance the activity through intercommunication.

In response to an insect attack, plants produce several defensive antioxidants including, SOD, POD, protease, PPO, and proline to scavenge ROS. These enzymes were considered the most important plant defense-related enzymes against herbivores (Guo et al., 2017; Batool et al., 2020). We also observed that antioxidant activities such as SOD, POD, PPO, protease, and proline were increased in all insect-infested plants, with a maximum increase at 24-h post infestation, while these enzyme activities were relatively higher in entomopathogenic fungal inoculated plants. The results revealed that these biocontrol agents enhanced the defense mechanism in plants by enhancing the production of defensive enzymes. Consortium treatment showed a maximum increase among all treatments. Some previous studies also reported the induction of SOD, POD, proline, protease, and PPO by biological control agents (Bano and Muqarab, 2017). PPO and protease play a defensive role against insect attack and induce resistance in plants (Joe and Muthukumaran, 2008). The chlorophyll content is one of the important components for plant growth and we observed that the chlorophyll content was increased in plants treated with entomopathogenic fungi compared to the insect control (IC). The same trend was recorded in previous studies (Bano and Muqarab, 2017; Batool et al., 2020). SOD is considered as the first enzyme in the scavenging process of ROS and its augmented scavenging action and detoxified by POD and act as a signaling agent to activate defensive genes in plants (Bano and Muqarab, 2017). Proline is best known as hydroxyl radical scavenger also serves as an energy source in plants. PPO is an important enzyme, which induces insect resistance in plants by participating in cell lignification and oxidation of polyphenols. Protease also has a defensive role against insect attacks (Batool et al., 2020).

With rapid development in bioinformatics, the weighted gene co-expression analysis (WGCNA) approach has been developed to explore the functionality of transcriptome. WGCNA was used to detect the genes which co-express (Lin et al., 2019). The relationship between trait and module identifies the most vital hub genes, which supports an efficacious way to explore the in-depth mechanism of complex traits (Lv et al., 2020). Considering the importance of fungal inoculants against the control of *O. furnacalis*, plant yield, and maize defense through augmented production of enzymatic and non-enzymatic antioxidants. We also integrated these biochemical enzymes and compounds with plant transcriptome at 0-, 12-, 24-, 48-, and 72-h. We performed a transcriptome-based analysis to identify DEGs in different combinations. The DEGs were then analyzed by WGCNA along with biochemical parameters and 33 gene modules represented by different colors were identified. Among them, 6 were significantly correlated with SOD, POD, PPO, protease, proline, and chlorophyll content. All genes contained in modules were functionally annotated to identify hub genes and 28 hub genes were identified and validated through RT-qPCR. Finally, 13 genes were characterized as the key candidates that are involved in maize defense mechanism against *O. furnacalis* based on significant correlation of hub genes from the module with biochemical enzymes and chlorophyll content, and expression pattern of selected genes. Gamboa-Tuz et al. (2018) also identified stress related hub genes from papaya leaves and roots. Pan et al. (2020) correlated transcriptome through WGCNA to identify key genes in maize against herbivore.

Activity of Identified Candidate Genes in Phytohormone Signaling and Biosynthesis Pathways

Insect herbivores induce the expressions of genes associated with the phytohormone signaling pathway (Li et al., 2016). Plant recognizes herbivore damage as a primary signal and triggers the expression of defense related genes. Initially, when an insect starts feeding, the plant reacts to it by producing ROS and effector proteins to activate the expression of signaling molecules and initiate signaling pathways of systemic resistance (Almagro et al., 2009). We identified four such signaling related genes; protein kinase (GRMZM2G025459), GDSL-like Lipase (AC212068.4_FG005), Patatin-like phospholipase (GRMZM2G154523), and Cytochrome P450 (GRMZM2G139874), which showed a high response against *O. furnacalis* feeding in fungal inoculated treatments. The activity of GDSL- like lipase (GLIP) is highly dependent on the Ethylene ET- the pathway to generate systemic signals to produce GLIP in the uninfected part of the plants to protect it from the insect (Kwon et al., 2009). They also reported the reduction in the growth of *Pseudomonas syringae* by the accumulation of GLIP 1 in all parts of the plant. Patatin like phospholipase is a signaling molecule responsible for the release of linolenic acid from phospholipids to biosynthesize jasmonic acid (JA) (Ryu, 2004). Meijer and Munnik (2003) observed the presence of phospholipases in wounded tomatoes and many other plants. Dhondt et al. (2002) also found three lipase genes in response to external elicitor or infection before the accumulation of JA. Acyle co-A dehydrogenase gene (GRMZM5G864319) was also

identified as a candidate gene that participates in the linolenic acid metabolism of the JA biosynthesis pathway (Tang et al., 2015). Cytochrome P450 (CYP) participates in plant growth promotion and protection from biotic and abiotic stresses through detoxification and biosynthesis pathways. To date, the involvement of cytochrome p450 in different metabolic pathways including allene oxide synthesis in the jasmonic acid pathway, hormone metabolism, and biosynthesis of phytoalexin has been confirmed (Jun et al., 2015). *CYP74A* (allene oxide synthase, AOS) catalyzes the dehydration of hydroperoxide to an instable allene oxide in the JA biosynthetic pathway and plays an important role in wound-induced defense against biotic attacks (Park et al., 2002).

Gene Expression Regulating Antioxidant Enzyme Production

Biosynthesis of JA- and ET- activate the production of PR-proteins, cell wall modifying enzymes, salicylic acid synthesis, and phytoalexins as a defense response to induce systemic resistance. In the present investigation, the genes encoding defensive enzymes and proteins such as Thioredoxin (GRMZM2G091481), Glutathione Peroxidase (GRMZM2G144153), Glutathione *S*-transferase (GRMZM2G116273), Defensin like protein (GRMZM2G392863), protease inhibitor (GRMZM2G004466), protease inhibitor (AC233926.1_FG002), Chitinase (GRMZM2G453805), Beta-glucosidase 18 (GRMZM2G031660) were upregulated with higher expressions in consortium treatment (BT-1). The expression patterns of these genes coincide with the levels of biochemical enzymes produced in all treatments, which indicates that the over expressions of these genes may regulate higher production of enzymatic (SOD, POD, PPO, and Protease) and non-enzymatic (proline) antioxidants to initiate maize defense responses, such as lignification, suberization, insect growth inhibition, and scavenging of ROS.

Genes Mediating Redox Signaling

Enzymatic and non-enzymatic antioxidants reduce the level of ROS and SOD is considered as the first and most important enzyme in the scavenging process as it catalyzes O_2^- into H_2O_2. The accumulation of the highest H_2O_2 is toxic for plants and POD detoxifies them (Bano and Muqarab, 2017; Batool et al., 2020). Peroxidases are the most important enzyme and they participate in different physiological processes of the plant (Almagro et al., 2009). Besides ROS scavenging, peroxidase encoding genes are also involved in lignin and suberin production to link the cell wall components. POD belongs to the PR-protein9 subfamily. The highest expression of POD increases the structure barrier and stops the infection. The expression of peroxidase genes in plants was induced by biotic and abiotic stresses (Sasaki et al., 2007). Thioredoxin genes were found to be associated with ROS scavenging enzymes such as ascorbate, POD, SOD, and catalase through disulfite bridge (Dos Santos and Rey, 2006), Moreover, Glutathione *S*-transferase detoxify electrophilic compounds in the scavenging process, also interact with plant thioredoxin (Yamazaki et al., 2004). Several stress conditions accumulate high ROS levels and resulted in the increased expression of the thioredoxin gene to participate in oxidative stress-linked signaling to induce high levels of antioxidant enzymes in potato plants (Dos Santos and Rey, 2006).

Genes Inhibiting Insect Digestive Enzyme

Polyphenol oxidase is a plant antioxidant enzyme important for regulating insect feeding, growth, development and defense response against herbivory and its production can be associated with the expression of different proteins and enzymes that can restrict the nutrient uptake of insects and attack their digestive track, e.g., chitinase, protease inhibitors and α-amylase inhibitors (Abebe). The chitinase enzyme is very important and it inhibits insect chewing and killing by degrading the insect skeleton (Zhong et al., 2021). The highest expression of chitinase reduces the insect induced damage and survival rate. Bordoloi et al. (2021) also identified two chitinase genes *viz*. TEA028279 and TEA019397 in tea plants with high expression under stress conditions with jasmonate and salicylic acid in their promoter upstream region to degrade chitin, of insect's exoskeleton. Similarly, defensin gene also prevents the insect chewing by inhibiting insect's digestive enzyme such as α-amylase and protease and makes it difficult to breakdown plant starch. Defensin express continuously in leaves stomatal cells, cell wall, peripheral layer of root, seed, and flowers, which indicate that they play an important role in protecting all entry points of plants from pest and pathogens. Khairutdinov et al. (2017) reported the inhibition of α-amylase activity by *PsDef1* defensin gene in pine pest *Panolis flammea.* The inhibitory action of α-amylase by the defensin gene in *Sorghum bicolor, Vigna unguiculata,* and *Tephrosia villosa* have also been studied (Kovaleva et al., 2020). Similar to defensin, protease inhibitors and β-glucosidase are also important for inhibiting insect gut digestive enzymes like proteases to prevent its feeding. Guedes and Cutler (2014) reported the role of insecticidal protease inhibitors in tobacco, rice, oilseed rape, sugarcane, and brassica. Expressions of protease inhibitors have been detected in wounds and induce defense against plant herbivory and pathogen attack (Clemente et al., 2019). Maize, almond, and white mustard defensive β-glucosidases were shown to restrict the digestion of lepidopteran larvae (Vassão et al., 2018).

High accumulation of metabolites contributes to acclimation of maize pre-inoculated with entomopathogenic fungi in response to *O. furnacalis* stress. In our study, significant accumulation of organic acids, benzoxazinoids, phenylpropanoids and polyketides, and lipid-like molecules were observed with higher levels in consortium treatment. Benzoxazinoid is an important defensive secondary metabolite in maize defense against *O. furnacalis* (Guo et al., 2019). However, this untargeted metabolome profiling was performed for the first time in maize plants inoculated with a consortium of *B. bassiana* and *T. asperellum* in response to *O. furnacalis* attack. We found that the contents of benzoxazinoids were changed after insect attack but higher contents were seen in inoculated treatments as compared to control. Accumulation of organic compounds plays a key role in defense against biotic and abiotic stresses (Zhang et al., 2020). We found that the accumulation of metabolites belonging to benzoxazinoids,

lipid-like molecules, organic compounds and phenylpropanoids can be a common mechanism in plant adaptation to different stresses. JA contents, expression levels of genes involved in JA biosynthetic pathway and JA-dependent metabolite adjustment in lipid-like molecules, which plays a defensive role, increased during *O. furnacalis* feeding in consortium inoculated plants, indicating its enhanced protective mechanism in JA-dependent maize resistance to *O. furnacalis*. Similar findings were reported by Guo et al. (2019) in *O. furnacalis* induced direct and in direct defenses. Jasmonates are responsible for regulating nearly all biosynthetic pathways that lead to metabolites (Martínez-Medina et al., 2021). According to the significant impact of *B. bassiana* and *T. asperellum* on JA, significant changes in secondary metabolites were triggered. Similarly, previous research also reported a strong impact on plant metabolites, primary metabolism, and changes in defensive compounds (Martínez-Medina et al., 2021).

Among consortium of biocontrol agents used against pest attack, one acts as a stress inducer and the other acts as a control agent. The combined application of BCAs by different mechanisms effectively controlled the incidence of *Duponchelia fovealis* in strawberry plants (Araujo et al., 2020).

CONCLUSION

By comprehensive physiological, biochemical, transcriptomic, metabolomic, and phytohormone analysis in maize inoculated with *B. bassiana* and *T. asperellum,* applied singly and in the consortium, we revealed enhanced maize defenses against *O. furnacalis herbivory*. Our study indicates that consortium of *B. bassiana* and *T. asperellum* can synergistically suppress *O. furnacalis* immune response and enhance maize immune response in the field by directly inducing enhanced expression of defense genes and indirectly activating antioxidants and phytohormone production as compared to normal herbivory-induced defenses. They can regulate the coordinated gene network expression related to defense signaling and antioxidants response and within these networks, certain genes make a key contribution to trait variation. Higher phytohormone content diverse metabolome abundance in consortium treatments was also highlighted in our results indicating the importance of JA, SA, and ethylene in plant defense. The correlation between the expression of these genes and enzymatic (SOD, POD, PPO, and protease) and non-enzymatic (proline) antioxidants, phytohormone synthesis, and metabolite adjustments were identified the first time in *B. bassiana* OFDH1-5, *T. asperellum* GDFS1009 consortium inoculated maize against *O. furnacalis* attack. The advantages of fungal BCAs are economic mass production, easy-to-use, sustainable control efficacy, and environmental safety suggest a bright future of mycoinsecticides in the world. Moreover, this study opens up new insight for future studies to focus on how certain changes in the gene networks and metabolites through biocontrol agents can affect above and below ground maize defense and other pathways. On the basis of current results, we believe that defense against ACB attack in maize is not a single gene-controlled process. Multiple genes are involved at the same time. Future research must focus on metabolic-gene clusters.

DATA AVAILABILITY STATEMENT

The datasets presented in this study is submitted in (https://www.ncbi.nlm.nih.gov/bioproject) repository, BioProject: PRJNA797234.

AUTHOR CONTRIBUTIONS

ZW and JC contributed to conceptualization and supervision. RB contributed to methodology, formal analysis, data curation, visualization, investigation, preparation, and writing of the original draft. MU contributed to software, formal analysis, review, and editing. YW provided resources. KH, MS, TZ, and SB were involved in the review and editing. All authors contributed to the article and approved the submitted version.

FUNDING

This study was supported by Agricultural Science and Technology Innovation Program (CAAS-ZDRW202004) and China Agriculture Research System of MOF and MARA.

ACKNOWLEDGMENTS

We acknowledge the lab members of State Key Laboratory for Biology of Plant Diseases and Insect Pest, Institute of Plant Protection, Chinese Academy of Agricultural Sciences, Beijing, China and biomarker company for helping us during this study.

SUPPLEMENTARY MATERIAL

The Supplementary Material for this article can be found online at: https://www.frontiersin.org/articles/10.3389/fpls.2022.790504/full#supplementary-material

REFERENCES

Abebe, W. (2021). Review on plant defense mechanisms against insect pests. *Int. J. Novel Res. Interdiscip. Stud.* 8, 15–39.

Almagro, L., Gomez Ros, L. V., Belchi-Navarro, S., Bru, R., Ros Barcelo, A., and Pedreno, M. A. (2009). Class III peroxidases in plant defence reactions. *J. Exp. Bot.* 60, 377–390. doi: 10.1093/jxb/ern277

Araujo, E. S., Benatto, A., Rizzato, F. B., Poltronieri, A. S., Poitevin, C. G., Zawadneak, M. A., et al. (2020). Combining biocontrol agents with different mechanisms of action to control *Duponchelia fovealis*, an invasive pest in South America. *J. Crop Prot.* 134:105184. doi: 10.1016/j.cropro.2020.105184

Bano, A., and Muqarab, R. (2017). Plant defence induced by PGPR against *Spodoptera litura* in tomato (*Solanum lycopersicum* L.). *Plant Biol.* 19, 406–412. doi: 10.1111/plb.12535

Barah, P., and Bones, A. M. (2015). Multidimensional approaches for studying plant defence against insects: from ecology to omics and synthetic biology. *J. Exp. Bot.* 66, 479–493. doi: 10.1093/jxb/eru489

Batool, R., Umer, M. J., Wang, Y., He, K., Zhang, T., Bai, S., et al. (2020). Synergistic effect of *Beauveria bassiana* and *Trichoderma asperellum* to induce maize (*Zea mays* L.) defense against the Asian corn borer, *Ostrinia furnacalis* (Lepidoptera, Crambidae) and larval immune response. *Int. J. Mol. Sci.* 21:8215. doi: 10.3390/ijms21218215

Bordoloi, K., Dihingia, P., Krishnatreya, D., and Agarwala, N. (2021). Genome-wide identification, characterization and expression analysis of the expansin gene family under drought stress in tea (*Camellia sinensis* L.). *J. Plant Sci. Today* 8, 32–44.

Cherry, A. J., Banito, A., Djegui, D., and Lomer, C. (2004). Suppression of the stem-borer *Sesamia calamistis* (Lepidoptera; Noctuidae) in maize following seed dressing, topical application and stem injection with African isolates of *Beauveria bassiana*. *Int. J. Pest Manag.* 50, 67–73.

Clemente, M., Corigliano, M. G., Pariani, S. A., Sanchez-Lopez, E. F., Sander, V. A., and Ramos-Duarte, V. A. (2019). Plant serine protease inhibitors: biotechnology application in agriculture and molecular farming. *Int. J. Mol. Sci.* 20:1345. doi: 10.3390/ijms20061345

Dhondt, S., Gouzerh, G., Müller, A., Legrand, M., and Heitz, T. (2002). Spatio-temporal expression of patatin-like lipid acyl hydrolases and accumulation of jasmonates in elicitor-treated tobacco leaves are not affected by endogenous levels of salicylic acid. *Plant J.* 32, 749–762. doi: 10.1046/j.1365-313x.2002.01465.x

Di Lelio, I., Coppola, M., Comite, E., Molisso, D., Lorito, M., Woo, S. L., et al. (2021). Temperature differentially influences the capacity of *Trichoderma* species to induce plant defense responses in tomato against insect pests. *Front. Plant Sci.* 12:678830. doi: 10.3389/fpls.2021.678830

Dos Santos, C. V., and Rey, P. (2006). Plant thioredoxins are key actors in the oxidative stress response. *Trends Plant Sci.* 11, 329–334. doi: 10.1016/j.tplants.2006.05.005

Dou, K., Lu, Z., Wu, Q., Ni, M., Yu, C., Wang, M., et al. (2020). MIST: a multilocus identification system for *Trichoderma*. *Appl. Environ. Microbiol.* 86:e01532-20. doi: 10.1128/AEM.01532-20

Ehlting, J., Chowrira, S. G., Mattheus, N., Aeschliman, D. S., Arimura, G., and Bohlmann, J. (2008). Comparative transcriptome analysis of *Arabidopsis thaliana* infested by diamond back moth (*Plutella xylostella*) larvae reveals signatures of stress response, secondary metabolism, and signalling. *BMC Genomics* 9:154. doi: 10.1186/1471-2164-9-154

Gamboa-Tuz, S. D., Pereira-Santana, A., Zamora-Briseno, J. A., Castano, E., Espadas-Gil, F., Ayala-Sumuano, J. T., et al. (2018). Transcriptomics and co-expression networks reveal tissue-specific responses and regulatory hubs under mild and severe drought in papaya (*Carica papaya* L.). *Sci Rep.* 8:14539. doi: 10.1038/s41598-018-32904-2

González-Guzmán, A., Raya-Diaz, S., Sacristán, D., Yousef, M., Sánchez-Rodríguez, A. R., Barrón, V., et al. (2021). Effects of entomopathogenic fungi on durum wheat nutrition and growth in the field. *Eur. J. Agron.* 128:126282.

González-Guzmán, A., Sacristán, D., Quesada-Moraga, E., Torrent, J., del Campillo, M. C., and Sánchez-Rodríguez, A. R. (2020). Effects of entomopathogenic fungi on growth and nutrition in wheat grown on two calcareous soils: influence of the fungus application method. *Ann. Appl. Biol.* 177, 26–40. doi: 10.1111/aab.12596

Guedes, R. N., and Cutler, G. C. (2014). Insecticide-induced hormesis and arthropod pest management. *Pest Manage. Sci.* 70, 690–697. doi: 10.1002/ps.3669

Guo, J., Guo, J., He, K., Bai, S., Zhang, T., Zhao, J., et al. (2017). Physiological responses induced by *Ostrinia furnacalis* (Lepidoptera: Crambidae) feeding in maize and their effects on *O. furnacalis* performance. *J. Econ. Entomol.* 110, 739–747. doi: 10.1093/jee/tox060

Guo, J., Qi, J., He, K., Wu, J., Bai, S., Zhang, T., et al. (2019). The Asian corn borer *Ostrinia furnacalis* feeding increases the direct and indirect defence of mid-whorl stage commercial maize in the field. *Plant Biotechnol. J.* 17, 88–102. doi: 10.1111/pbi.12949

Guo, Q., Li, X., Niu, L., Jameson, P. E., and Zhou, W. (2021). Transcription-associated metabolomic adjustments in maize occur during combined drought and cold stress. *Plant Physiol.* 186, 677–695. doi: 10.1093/plphys/kiab050

Gupta, H., Saini, R., Pagadala, V., Kumar, N., Sharma, D., and Saini, A. J. (2016). Analysis of plant growth promoting potential of endophytes isolated from *Echinacea purpurea* and *Lonicera japonica*. *J. Soil Sci. Plant Nutr.* 16, 558–577.

He, K., Wang, Z., Zhou, D., Wen, L., Song, Y., and Yao, Z. (2003). Evaluation of transgenic Bt corn for resistance to the Asian corn borer (Lepidoptera: Pyralidae). *J. Econ. Entomol.* 96, 935–940. doi: 10.1093/jee/96.3.935

Heidel-Fischer, H. M., Musser, R. O., and Vogel, H. (2018). "Plant transcriptomic responses to herbivory," in *Annual Plant Reviews Online*, Vol. 47, eds C. Voelckel and G. Jander, New York, NY: Wiley. 155–196. doi: 10.1002/9781118829783.ch5

Joe, M. M., and Muthukumaran, N. (2008). Role of certain elicitors on the chemical induction of resistance in tomato against the leaf caterpillar *Spodoptera litura* Fab. *Not. Bot. Horti Agrobot. Cluj Napoca* 36, 71–75.

Jun, X., Wang, X.-Y., and Guo, W.-Z. (2015). The cytochrome P450 superfamily: key players in plant development and defense. *J. Integr. Agric.* 14, 1673–1686. doi: 10.1016/s2095-3119(14)60980-1

Khairutdinov, B. I., Ermakova, E. A., Yusypovych, Y. M., Bessolicina, E. K., Tarasova, N. B., Toporkova, Y. Y., et al. (2017). NMR structure, conformational dynamics, and biological activity of PsDef1 defensin from *Pinus sylvestris*. *Biochim. Biophys. Acta Proteins Proteom.* 1865, 1085–1094. doi: 10.1016/j.bbapap.2017.05.012

Kim, D., Langmead, B., and Salzberg, S. L. (2015). HISAT: a fast spliced aligner with low memory requirements. *Nat. Methods* 12, 357–360. doi: 10.1038/nmeth.3317

Kovaleva, V., Bukhteeva, I., Kit, O. Y., and Nesmelova, I. V. (2020). Plant defensins from a structural perspective. *Int. J. Mol. Sci.* 21:5307. doi: 10.3390/ijms21155307

Kwon, S. J., Jin, H. C., Lee, S., Nam, M. H., Chung, J. H., Kwon, S. I., et al. (2009). GDSL lipase-like 1 regulates systemic resistance associated with ethylene signaling in *Arabidopsis*. *Plant J.* 58, 235–245. doi: 10.1111/j.1365-313X.2008.03772.x

Landa, B. B., López-Díaz, C., Jiménez-Fernández, D., Montes-Borrego, M., Muñoz-Ledesma, F. J., Ortiz-Urquiza, A., et al. (2013). In-planta detection and monitorization of endophytic colonization by a *Beauveria bassiana* strain using a new-developed nested and quantitative PCR-based assay and confocal laser scanning microscopy. *J. Inverteb. Pathol.* 114, 128–138. doi: 10.1016/j.jip.2013.06.007

Langfelder, P., and Horvath, S. (2008). WGCNA: an R package for weighted correlation network analysis. *BMC Bioinformatics* 9:559. doi: 10.1186/1471-2105-9-559

Li, J., Zhu, L., Hull, J. J., Liang, S., Daniell, H., Jin, S., et al. (2016). Transcriptome analysis reveals a comprehensive insect resistance response mechanism in cotton to infestation by the phloem feeding insect *Bemisia tabaci* (whitefly). *Plant Biotechnol. J.* 14, 1956–1975. doi: 10.1111/pbi.12554

Lin, C. T., Xu, T., Xing, S. L., Zhao, L., Sun, R. Z., Liu, Y., et al. (2019). Weighted gene co-expression network analysis (WGCNA) reveals the hub role of protein ubiquitination in the acquisition of desiccation tolerance in *Boea hygrometrica*. *Plant Cell Physiol.* 60, 2707–2719. doi: 10.1093/pcp/pcz160

Lv, L., Zhang, W., Sun, L., Zhao, A., Zhang, Y., Wang, L., et al. (2020). Gene co-expression network analysis to identify critical modules and candidate genes of drought-resistance in wheat. *PLoS One* 15:e0236186. doi: 10.1371/journal.pone.0236186

Martínez-Medina, A., Mbaluto, C. M., Maedicke, A., Weinhold, A., Vergara, F., and Van Dam, N. M. (2021). Leaf herbivory counteracts nematode-triggered repression of jasmonate-related defences in tomato roots. *Plant Physiol.* 187, 1762–1778. doi: 10.1093/plphys/kiab368

Meijer, H. J., and Munnik, T. (2003). Phospholipid-based signaling in plants. *Annu. Rev. Plant Biol.* 54, 265–306. doi: 10.1146/annurev.arplant.54.031902.134748

Mitchell, C., Brennan, R. M., Graham, J., and Karley, A. J. (2016). Plant defense against herbivorous pests: exploiting resistance and tolerance traits for sustainable crop protection. *Front. Plant. Sci.* 7:1132. doi: 10.3389/fpls.2016.01132

Motholo, L. F. (2019). *Endophytic Establishment of Beauveria bassiana in Wheat (Triticum aestivum) and Its Impact on Diuraphis noxia*. Potchefstroom: North-West University- Potchefstroom Campus.

Muvea, A. M., Meyhöfer, R., Subramanian, S., Poehling, H.-M., Ekesi, S., and Maniania, N. K. (2014). Colonization of onions by endophytic fungi and their

impacts on the biology of *Thrips tabaci*. *PLoS One* 9:e108242. doi: 10.1371/journal.pone.0108242

Netzker, T., Fischer, J., Weber, J., Mattern, D. J., Konig, C. C., Valiante, V., et al. (2015). Microbial communication leading to the activation of silent fungal secondary metabolite gene clusters. *Front. Microbiol.* 6:299. doi: 10.3389/fmicb.2015.00299

Pan, Y., Zhao, S. W., Tang, X. L., Wang, S., Wang, X., Zhang, X. X., et al. (2020). Transcriptome analysis of maize reveals potential key genes involved in the response to belowground herbivore *Holotrichia parallela* larvae feeding. *Genome* 63, 1–12. doi: 10.1139/gen-2019-0043

Park, J. H., Halitschke, R., Kim, H. B., Baldwin, I. T., Feldmann, K. A., and Feyereisen, R. (2002). A knock-out mutation in allene oxide synthase results in male sterility and defective wound signal transduction in *Arabidopsis* due to a block in jasmonic acid biosynthesis. *Plant J.* 31, 1–12. doi: 10.1046/j.1365-313x.2002.01328.x

Qi, J., Malook, S. U., Shen, G., Gao, L., Zhang, C., Li, J., et al. (2018). Current understanding of maize and rice defense against insect herbivores. *Plant Divers.* 40, 189–195. doi: 10.1016/j.pld.2018.06.006

Quesada-Moraga, E., Landa, B. B., Muñoz-Ledesma, J., Jiménez-Díaz, R. M., and Santiago-Alvarez, C. (2006). Endophytic colonization of opium poppy, *Papaver somniferum*, by an entomopathogenic *Beauveria bassiana* strain. *Mycopathologia* 161, 323–329. doi: 10.1007/s11046-006-0014-0

Raya-Díaz, S., Quesada-Moraga, E., Barrón, V., Del Campillo, M. C., and Sánchez-Rodríguez, A. R. (2017). Redefining the dose of the entomopathogenic fungus *Metarhizium brunneum* (Ascomycota, Hypocreales) to increase Fe bioavailability and promote plant growth in calcareous and sandy soils. *Plant Soil* 418, 387–404. doi: 10.1007/s11104-017-3303-0

Rivas-Franco, F., Hampton, J. G., Narciso, J., Rostás, M., Wessman, P., Saville, D. J., et al. (2020). Effects of a maize root pest and fungal pathogen on entomopathogenic fungal rhizosphere colonization, endophytism and induction of plant hormones. *Biol. Control* 150:104347. doi: 10.1016/j.biocontrol.2020.104347

Ryu, S. B. (2004). Phospholipid-derived signaling mediated by phospholipase A in plants. *Trends Plant Sci.* 9, 229–235. doi: 10.1016/j.tplants.2004.03.004

Sánchez-Rodríguez, A. R., Raya-Díaz, S., Zamarreño, ÁM., García-Mina, J. M., del Campillo, M. C., and Quesada-Moraga, E. (2018). An endophytic *Beauveria bassiana* strain increases spike production in bread and durum wheat plants and effectively controls cotton leafworm (*Spodoptera littoralis*) larvae. *Biol. Control* 116, 90–102. doi: 10.1016/j.biocontrol.2017.01.012

Sarma, B. K., Yadav, S. K., Singh, S., and Singh, H. B. (2015). Microbial consortium-mediated plant defense against phytopathogens: readdressing for enhancing efficacy. *Soil Biol. Biochem.* 87, 25–33. doi: 10.1016/j.soilbio.2015.04.001

SAS Institute Inc (2015). *Base SAS 9.2 Procedures Guide Pdf.* Cary, NC: SAS Institute Inc.

Sasaki, K., Yuichi, O., Hiraga, S., Gotoh, Y., Seo, S., Mitsuhara, I., et al. (2007). Characterization of two rice peroxidase promoters that respond to blast fungus-infection. *Mol. Genet. Genomics* 278, 709–722. doi: 10.1007/s00438-007-0286-1

Shakeri, J., and Foster, H. A. (2007). Proteolytic activity and antibiotic production by *Trichoderma harzianum* in relation to pathogenicity to insects. *Enzyme Microb. Technol.* 40, 961–968.

Tang, J. D., Perkins, A., Williams, W. P., and Warburton, M. L. (2015). Using genome-wide associations to identify metabolic pathways involved in maize aflatoxin accumulation resistance. *BMC Genomics* 16:673. doi: 10.1186/s12864-015-1874-9

Tzin, V., Fernandez-Pozo, N., Richter, A., Schmelz, E. A., Schoettner, M., Schafer, M., et al. (2015). Dynamic maize responses to aphid feeding are revealed by a time series of transcriptomic and metabolomic assays. *Plant Physiol.* 169, 1727–1743. doi: 10.1104/pp.15.01039

Umer, M. J., Bin Safdar, L., Gebremeskel, H., Zhao, S., Yuan, P., Zhu, H., et al. (2020). Identification of key gene networks controlling organic acid and sugar metabolism during watermelon fruit development by integrating metabolic phenotypes and gene expression profiles. *Hortic. Res.* 7:193. doi: 10.1038/s41438-020-00416-8

Vassão, D. G., Wielsch, N., Gomes, A. M. D. M. M., Gebauer-Jung, S., Hupfer, Y., Svatoš, A., et al. (2018). Plant defensive β-glucosidases resist digestion and sustain activity in the gut of a lepidopteran herbivore. *Front. Plant Sci.* 9:1389. doi: 10.3389/fpls.2018.01389

Wagner, B. L., and Lewis, L. C. (2000). Colonization of corn, *Zea mays*, by the entomopathogenic fungus *Beauveria bassiana*. *Appl. Environ. Microbiol.* 66, 3468–3473. doi: 10.1128/aem.66.8.3468-3473.2000

Wang, L., Feng, Z., Wang, X., Wang, X., and Zhang, X. (2010). DEGseq: an R package for identifying differentially expressed genes from RNA-seq data. *Bioinformatics* 26, 136–138. doi: 10.1093/bioinformatics/btp612

Xie, H., Liu, K., Sun, D., Wang, Z., Lu, X., and He, K. (2015). A field experiment with elevated atmospheric CO_2-mediated changes to C_4 crop-herbivore interactions. *Sci. Rep.* 5:13923 . doi: 10.1038/srep13923

Yamazaki, D., Motohashi, K., Kasama, T., Hara, Y., and Hisabori, T. (2004). Target proteins of the cytosolic thioredoxins in *Arabidopsis thaliana*. *Plant Cell Physiol.* 45, 18–27. doi: 10.1093/pcp/pch019

Yu, X., Xiao, J., Chen, S., Yu, Y., Ma, J., Lin, Y., et al. (2020). Metabolite signatures of diverse *Camellia sinensis* tea populations. *Nat. Commun.* 11:5586.

Zhang, Y., Bouwmeester, H. J., and Kappers, I. F. (2020). Combined transcriptome and metabolome analysis identifies defence responses in spider mite-infested pepper (*Capsicum annuum*). *J. Exp. Bot.* 71, 330–343. doi: 10.1093/jxb/erz422

Zhong, X., Feng, P., Ma, Q., Zhang, Y., Yang, Y., and Zhang, J. (2021). Cotton chitinase gene GhChi6 improves the *Arabidopsis* defense response to aphid attack. *Plant. Mol. Biol. Rep.* 39, 251–261. doi: 10.1007/s11105-020-01248-5

Conflict of Interest: The authors declare that the research was conducted in the absence of any commercial or financial relationships that could be construed as a potential conflict of interest.

Publisher's Note: All claims expressed in this article are solely those of the authors and do not necessarily represent those of their affiliated organizations, or those of the publisher, the editors and the reviewers. Any product that may be evaluated in this article, or claim that may be made by its manufacturer, is not guaranteed or endorsed by the publisher.

frontiers in Plant Science

SYSTEMATIC REVIEW
published: 01 March 2022
doi: 10.3389/fpls.2022.816438

A Global Network Meta-Analysis of the Promotion of Crop Growth, Yield, and Quality by Bioeffectors

Michelle Natalie Herrmann[1,2], Yuan Wang[1,3], Jens Hartung[2], Tobias Hartmann[2,4], Wei Zhang[1,3], Peteh Mehdi Nkebiwe[2], Xinping Chen[1,3], Torsten Müller[2] and Huaiyu Yang[1,3]**

[1] College of Resources and Environment, Academy of Agricultural Sciences, Southwest University, Chongqing, China, [2] Institute of Crop Science, University of Hohenheim, Stuttgart, Germany, [3] Interdisciplinary Research Center for Agriculture Green Development in Yangtze River Basin, Southwest University, Chongqing, China, [4] Crop Production, Landwirtschaftskammer des Saarlandes, Bexbach, Germany

Bioeffector (BE) application is emerging as a strategy for achieving sustainable agricultural practices worldwide. However, the effect of BE on crop growth and quality is still controversial and there is still no adequate impact assessment that determines factors on the efficiency of BE application. Therefore, we carried out a network metaanalysis on the effect of BEs using 1,791 global observations from 186 studies to summarize influencing factors and the impact of BEs on crop growth, quality, and nutrient contents. The results show that BEs did not only improve plant growth by around 25% and yield by 30%, but also enhanced crop quality, e.g., protein (55% increase) and soluble solids content (75% increase) as well as aboveground nitrogen (N) and phosphate (P) content by 28 and 40%, respectively. The comparisons among BE types demonstrated that especially non-microbial products, such as extracts and humic/amino acids, have the potential to increase biomass growth by 40–60% and aboveground P content by 54–110%. The soil pH strongly influenced the efficiency of the applied BE with the highest effects in acidic soils. Our results showed that BEs are most suitable for promoting the quality of legumes and increasing the yield of fruits, herbs, and legumes. We illustrate that it is crucial to optimize the application of BEs with respect to the right application time and technique (e.g., placement, foliar). Our results provide an important basis for future research on the mechanisms underlying crop improvement by the application of BEs and on the development of new BE products.

Keywords: biostimulants, biofertilizers, sustainable agriculture, nutrient use efficiency, pH, PGPR

OPEN ACCESS

Edited by:
Youssef Rouphael, University of Naples Federico II, Italy

Reviewed by:
Vijay S. Meena, The International Maize and Wheat Improvement Center (CIMMYT), India
Cinzia Margherita Bertea, University of Turin, Italy

****Correspondence:***
Michelle Natalie Herrmann
m.herrmann@uni-hohenheim.de
Huaiyu Yang
yanghuaiyu@swu.edu.cn

Specialty section:
This article was submitted to Plant Nutrition, a section of the journal Frontiers in Plant Science

Received: *16 November 2021*
Accepted: *31 January 2022*
Published: *01 March 2022*

Citation:
Herrmann MN, Wang Y, Hartung J, Hartmann T, Zhang W, Nkebiwe PM, Chen X, Müller T and Yang H (2022) A Global Network Meta-Analysis of the Promotion of Crop Growth, Yield, and Quality by Bioeffectors. Front. Plant Sci. 13:816438. doi: 10.3389/fpls.2022.816438

INTRODUCTION

The use of bioeffectors (BEs) has been proposed as a promising solution for the challenges of sustainable agriculture (Povero et al., 2016). A BE is defined as organic material and/or microorganisms applied to living plants or soil to enhance nutrient uptake, stimulate growth, improve stress tolerance and crop-quality traits, regardless of its nutrient contents (Van Oosten et al., 2017; Rouphael and Colla, 2018; Schütz et al., 2018; Ricci et al., 2019). Typical BEs include amino acids and other organic compounds, seaweed extracts, and botanicals as well

as microorganisms including fungi and bacteria. Numerous studies have demonstrated that the application of BEs is beneficial to plants in all developmental stages (Qiu et al., 2020; Rouphael and Colla, 2020b) and may increase yield (Schütz et al., 2018).

Microbial products can directly influence nutrient availability in soil or nutrient uptake by plants. For example, N-fixing bacteria are able to sequester nitrogen (N_2) from the air, thereby increasing the pool of reactive N in the soil. Phosphate (P)-solubilizing bacteria (PSB) can transform phosphate from insoluble compounds to bioavailable ones by releasing protons, exudates, such as chelates, and other substances. Previous studies have determined that symbiotic arbuscular mycorrhiza fungi (AMF) promoted phosphate, nitrogen, and micronutrient acquisition through spatial enlargement of the influence of the rhizosphere (Watts-Williams and Cavagnaro, 2014). The stimulation of plant nutrient acquisition by BEs is beneficial, especially under nutrient-poor conditions and it reduces the dependency of agriculture on the application of inorganic fertilizers (Oldroyd and Leyser, 2020). Further, in high-input agricultural systems, the application of BEs can facilitate fertilizer and pesticide use without risking yield decline. Some plant growth-promoting microbes can alter the hormone balance in plants and improve plant performance. Meents et al. (2019), for instance, reported that the beneficial fungi *Piriformospora indica* increased auxin levels in plants thereby promoting root growth.

Besides selected microbial organisms, BEs also comprise a variety of processed substances from soil and plants, such as humic acids, amino acids, and extracts, from seaweeds and other plants. These products are diverse in terms of their potential influence on plants and the microbial community in the soil. Extracts can directly influence plant growth by bioactive compounds or indirectly by ameliorating soil characteristics (Shukla et al., 2018). By altering soil water holding capacity, they indirectly improve soil growing conditions and nutrient availability for plants (Khan et al., 2009). Extracts also interact with the soil microbial community and promote the function of beneficial fungi (e.g., AMF) by increasing infectivity, spore production, colonization, and hyphae growth (Khan et al., 2009). Humic and amino acids can stimulate the proton pump of the plant (Jindo et al., 2012), thereby supporting the plant's own nutrient solubilizing pathway and increasing nutrient availability in the rhizosphere. Additionally, the complexation of micronutrients by organic acids, reduction of Fe(III) to Fe(II), and the presence of organic radicals and phenolic compounds are further possible explanations for an increased nutrient availability in soil after the application of organic acids (Adani et al., 1998).

BEs have further been shown to improve plant tolerance to abiotic and biotic stress. Two main pathways are described: Firstly, beneficial microbes can adapt themselves to extreme conditions, such as salinity and cold temperatures (Selvakumar et al., 2008; Upadhyay et al., 2009). Microbes can then increase the tolerance of plants to abiotic stress by ameliorating plant performance under these conditions (Van Oosten et al., 2017). Secondly, microbes and natural compounds can produce substances that promote stress adaptation by the plant (Van Oosten et al., 2017).

Considering the recent public awareness on environmental degradation and pollution by agricultural production, the topic of BE-use in sustainable agriculture is becoming increasingly important. However, BEs as living organisms or natural extracts are influenced by edaphic and environmental factors after application. This leads to unreliable outcomes for farmers, thereby limiting their practical use and adoption. Despite decades of research on this topic, the efficiency of BEs varies widely among published studies (Schmidt and Gaudin, 2018). In particular, the pivotal factors determining the effects of BEs, such as crop specificity and mode of action, are still unclear. Moreover, most data from Chinese BE studies are not included in previously published metaanalyses.

The goal of this study was to systematically quantify the improvement of plant performance and other important indicators (e.g., quality, nutrient acquisition) *via* BE application in general, but also under given local agricultural conditions (e.g., pH, crop type). Another aim was to specify practical and efficient application strategies of BEs. To achieve these goals, a network metaanalysis was conducted to primarily determine whether BEs show a global positive effect on plant biomass, yield, aboveground nutrient content, nutrient use efficiencies, and quality indicators (protein- and soluble-solids content). Secondly, crucial factors that influence the efficiency of BEs were determined. Therefore, we analyzed variables, such as crop type, edaphic pH, and other aspects, in crop production on a global scale.

MATERIALS AND METHODS

Data Collection

In this metaanalysis, we compiled a global dataset by retrieving peer-reviewed studies published until December 2021 using Scopus by Elsevier, ISI-Web of Science, the search engines of Microsoft Academic, and Hohsearch (search engine of the University of Hohenheim, Stuttgart, Germany). Studies in Chinese were extracted from the China Knowledge Resource Integrated Database (CNKI). "Biofertilizer," "biostimulant," or "bioeffector" together with "nutrient" or "quality" were selected as keywords. This resulted in more than 2,000 possibly fitting studies. Studies were sorted by relevance prior to checking them. Literature searches were terminated if 20 studies in succession did not fit into the inclusion criteria defined below. We filtered the studies by the following inclusion criteria: (i) the standard errors and the number of replicates that were reported. These values were needed to calculate the effect sizes. (ii) The experiment had to be laid out in the soil. (iii) The only difference between the control and the treatment group was the BE application. (iv) Germination trials were excluded. (v) The study stated at minimum two predefined response variables. (vi) The agricultural crops were used for food, fodder, or biomass production. A PRISMA flowchart is included in the **Supplementary Materials** (**Supplementary Figure 1**).

Preprocessing of Data

When data were available in graphs only, the program GetData Graph Digitizer (Ver. 2.22) was used to extract means and

standard errors. To convert the concentration of available N and P in soil from g kg^{-1} to kg ha^{-1}, the bulk density was estimated according to the United States Department of Agriculture – Natural Resources Conservation Service (2019). The effective root zone was determined as 0.5 m. If only the total N of the soil was analyzed, then the available N was estimated based on the calculation by Sponagel et al. (2005). When organic fertilizers were used and in case their nutrient composition was not analyzed, estimated nutrient contents were used from Herbert et al. (2019). If it could not be estimated, the study was not considered in the investigations of nutrient-use efficiency. Additionally, the shoot biomass for the calculation of nutrient use efficiencies was transformed into kg ha^{-1} by considering plant densities indicated in the papers or estimated based on a common agricultural practice (**Supplementary Table 1**). pH values were adapted in case it was measured in $CaCl_2$ or KCl, according to Reuter et al. (2008), to convert values to measurements in water. If the method was not given, it was assumed to be measured in water. For all the other measurements, methods were considered similar, and no transformation of the values was implemented.

The potential influencing variables BE, geographic region, application strategy, and application time were categorized. The BEs including microorganisms were categorized according to Schütz et al. (2018). Botanicals, as well as sea-weed extracts, were summarized as the group of "extracts." Humic/amino acids formed another category. Substances not fitting into these categories were pooled in the group "others." The combination treatment was subdivided into a dual combination, which included two different microorganism categories, a combination of more than two microorganism categories, and a mixture of microorganisms and non-microbes.

In the case of BE application, it is very likely that different effects must be expected for different management regimes. As nutrient balances vary largely across the world and locally adapted strategies are needed (Haygarth and Rufino, 2021), the World Bank (2019) classification of regions was applied to account for this variation. This categorization of the countries was chosen as a broad indicator for the agricultural practice in the countries. According to the set of the experiment, we divided the data into pot and field trials. The grouping into perennial or annual did not happen according to the biological capability of growing several seasons, but according to the layout of the experiments. If the plants in the experiment had been growing for several seasons or the BE application was conducted for more than 1 year on the same plant, the study was identified as perennial.

Furthermore, the data were subdivided according to the application strategy. We identified four different modes of application. The BEs were applied either (1) to the seed, (2) in the soil, (3) to the seedling, or (4) by foliar application. Additionally, a combination of two or more above-mentioned modes of application was also considered. Concerning application time, we distinguished between a single application, before/at sowing or after sowing, or a multiple application. The pH range was divided into five subgroups, namely, $\leq$ 5.5 "strongly acidic," 5.5 $<$ pH $\leq$ 6.5 "slightly acidic," 6.5 $<$ pH $\leq$ 7.5 "neutral," 7.5 $<$ pH $\leq$ 8.5 "slightly alkaline," pH $>$ 8.5 "strongly alkaline."

Statistical Approach

Determination of effect sizes is one option in metaanalyses to handle the variation of units and measurements and to enable the calculation of overall effects, thereby enabling the comparison of effects between studies (Sánchez-Meca and Marín-Martínez, 1998). For calculating the effect size, the treatment means were standardized by dividing them by their standard error. Additionally, the correction of bias according to Hedges (1981), which includes the repetition number, was added to the calculation. A logarithmic transformation was then applied to further stabilize the variance and counteract the right-skewness of the effect sizes. Effect sizes in the current study were calculated for the following traits: yield, shoot biomass, root biomass, aboveground nutrient content of N and P, nutrient

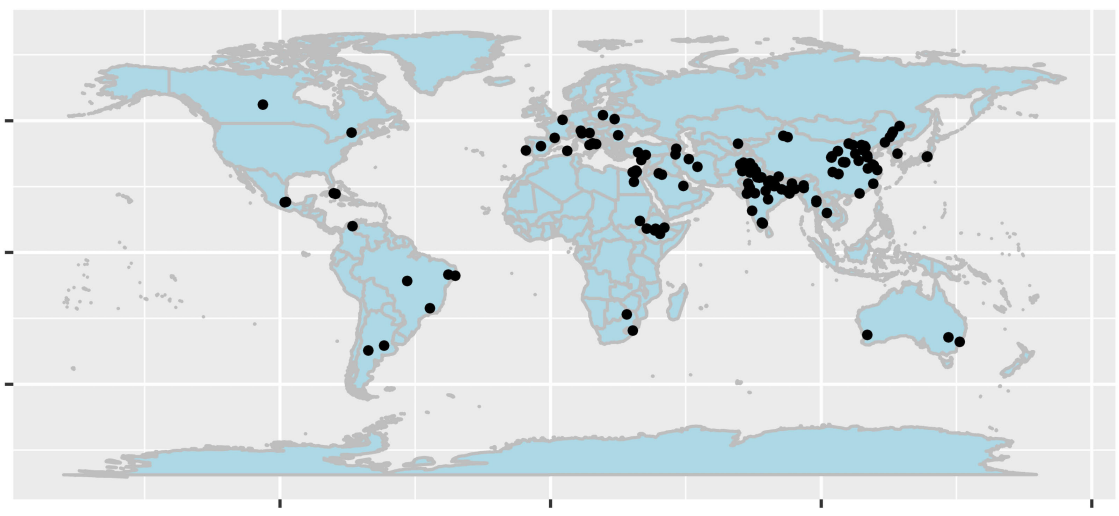

FIGURE 1 | Location of studies included in the data set. The figure was created by the R package ggmap (Kahle and Wickham, 2013).

use efficiency of N and P, as well as the quality parameters of protein and soluble solids content. We defined shoot biomass as the total aboveground plant material and yield as the main marketable product. Nutrient use efficiency was defined as the biomass divided through the total amount of available N and P in soil, respectively (available nutrient in soil + input through fertilizers).

Publication bias can strongly affect the results of metaanalyses, thereby altering or overestimating the outcomes (Levine et al., 2009). It was assumed that articles will be more likely to be published if they prove positive effects, similar to medical studies (Joober et al., 2012). In our study, when a strong right skewness was observed, the statistical approach by Carrijo et al. (2017) was followed. Therefore, independently for every group of effect size, when the effect sizes of studies exceeded the mean plus three times the standard error, they were excluded from the analysis. After the exclusion, 186 out of 197 studies were used for the final analysis including a total amount of 1,791 observations. For the first time, 64 studies conducted in China (423 observations) were included. The locations of those studies when identifiable are shown in **Figure 1**. The 186 studies, which were finally included in the metaanalysis, are listed in the references.

It is important to consider the methodological quality of the studies as it could strongly influence the outcome of a metaanalysis (Moher et al., 1998). Therefore, we included the impact-factor of the journal, where the study was published as a covariate in our model. In later steps, the covariate was again removed from the model, as it was not significant in any case.

In the collected data structure, several treatments correspond to the same control. Therefore, to quantify the impact of each BE type of one study and still avoid correlation of effect sizes, a network metaanalysis was necessary using a linear mixed model described by Madden et al. (2016). This approach has the advantage that it enables us to compare treatments indirectly even if they never occurred together in the same study. A random study effect was included in the model as just a sample of available studies was chosen, and the aim of the analysis was to generalize our result for future studies to be published. The model can be described as follows:

$$y_{ijklmnopqr} = \mu + b_j + \tau_i + (\alpha\tau)_{ik} + \beta_{li} + \gamma_{mi} + (\delta\tau)_{in} + \theta_{oi} + (\vartheta\tau)_{iq} + (\phi\tau)_{iq} + (\kappa\tau)_{ir} + e_{ijklmnopqr},$$

where μ is the intercept, b_j is the random effect of the jth study, τ_i is the main effect for the ith treatment (with levels control and treatment). β_{li}, γ_{mi} , and θ_{oi} are the effect of the lth application time, the mth BE, and the oth mode of application, respectively. These factors are nested within treatment, as in the control BEs were not applied at all. $(\alpha\tau)_{ik}$, $(\delta\tau)_{in}$,$(\vartheta\tau)_{iq}$, $(\phi\tau)_{iq}$, and $(\kappa\tau)_{ir}$ are the interaction effects of the ith treatment and kth testing system, the nth crop, pth perennial or annual, qth geographical region, and the rth pH-effect, respectively. We did not fit the main effects for these latter terms as we were only interested in the differences of control and treatment depending on these factors. The value $e_{ijklmnopqr}$ is the error of mean effect size $y_{ijklmnopqr}$ with a homogeneous error variance.

For all factors in the model above, our main focus was on the differences between control and treatment, and differences between these differences across treatments. Contrasts were used to calculate the difference of the differences between control and treatment. As the data were logarithmically transformed prior to analysis, differences correspond to ratios on the original scale. The back-transformed value from a difference of differences corresponds to an odds ratio.

To avoid overfitting, which means that additional non-significant factors in the model mask the effects of other factors, we performed a model selection. To implement this, we switched the method for variance component estimation to maximum likelihood. We then used the Akaike Information Criterion (AIC, Wolfinger, 1993) selection criterion to find the best model for our data. Since the AIC can only be used for comparisons of models which have identical data sets, an auxiliary dataset was created by omitting all observations for which data for at least one of the parameters of the full model was lacking. Afterward, the model selection was carried out using this auxiliary dataset. It was assumed that the best-selected model through the model selection is transmissible to the entire dataset later since studies were considered as random samples.

In none of the final models from the model selection, BE types were included as factors. Since one of our initial focuses was to investigate the differences between BE types, selected models of shoot and root biomass, yield, aboveground P as well as N content, and nutrient use efficiencies were expanded by the BE type. This resulted in slightly higher AIC and changed mean effects (**Supplementary Table 2**). Further analyses for all other factors were conducted with the non-expanded model and only BE types were investigated using the expanded model.

After finding the best model *via* AIC, the restricted maximum likelihood estimation was applied (Patterson and Thompson, 1971). Confidence limits were calculated for each difference between treatment and control and the contrasts of the differences among treatments. We considered estimates to be significantly different from zero when their p-Values were below or equal to 0.05, and in tendency when their p-Values were below or equal to 0.1. Afterward, differences and contrasts [as well as their lower and upper bounds of the confidence limit ($\alpha = 0.05$)] were backtransformed to the original scale for presentation purposes only. Standard errors were backtransformed using the approximate delta method (Xu and Long, 2005). Normal distribution and homogeneous variances of residuals (on the transformed scale) were checked graphically.

The illustration of the graphs was implemented in R with the package ggplot2 (Wickham, 2016). The figures depict the median and confidence limits of the subgroup analysis, as well as the overall effects, which we defined as the difference of the main effects τ_i, namely the difference of treatment and control factors.

RESULTS

The results of the model selection are shown in the **Supplementary Materials** (**Supplementary Table 3**). In the root biomass investigation, no data was available for perennial

crops and field trials. Those parameters were therefore not considered in the analysis. The country grouping was also not relevant for the model of root biomass as experiments were exclusively laid out under controlled greenhouse conditions. A summary of the significant parameters in each model and the most important influencing factors for each indicator are provided (**Supplementary Table 4**).

Assessment of Bioeffector Effects on Crop Growth and Yield

As shown in **Figure 2A**, shoot biomass was significantly enhanced due to BE application by 26%. The variable soil pH influenced the outcome clearly (**Figure 2B**). A significant increase of biomass by BE application was observed in slightly acidic and strongly acidic soils, with strongly acidic soils showing the highest median of 58% increase. Regarding the mode of application, BE input *via* soil (38% increase) and foliar application (34% increase) as well as a combination of several different modes (48% increase) was more beneficial for plant biomass production than seed inoculation or application during early plant developmental stages (12% and 0.6% increase) (**Figure 2C**). **Figure 2D** illustrates that a significant increase of shoot biomass occurred in pot trials (33% increase). The efficiency of BE application differed among countries (**Figure 2E**), with middle-income economies obtaining the highest efficiencies (46% increase for lower-middle-income economies and 35% increase for upper-middle-income economies).

When adding the BE types to the model, non-microbial products attained the highest responses with a shoot biomass increase of 57%, 41%, and 42% for extracts, humic and amino acids, and the combination of microbes and non-microbial substances, respectively (**Figure 3A**).

The yield was significantly augmented by 30% (**Figure 4A**). Almost all crop types responded significantly to BE application, except the group "others." Herbs and fruits increased in yield the most with 47% and 40% (**Figure 4B**). Pot-trials obtained a significantly higher yield increase than field trials with a 45% and 16% increase, respectively (**Figure 4C**). When investigating the expanded model, all BE types induced significant yield increases (**Figure 3B**), and the combination of microbes and non-microbial products stood out with an increase of 55% (**Figure 3B**).

Root biomass responded positively to BE application with an increase of 69% (**Figure 5A**). As shown in **Figure 5B**, in strongly acidic soils with pH levels < 5.5, root growth was extremely enhanced by 161%, whereas in other pH levels the effect was below the overall median. For strongly alkaline soils, data was limited in the dataset. Therefore, no definite statement can be given. The comparison of the mode of application resulted in significant increases for nearly every application mode, except the inoculation of the seedling (**Figure 5C**). The combination of several modes of application resulted in exceptionally high root growth with a 173% increase. The analysis of the model extended with the variable BE type led to no clear differentiation among the BE types except for AMF as well as the combination of

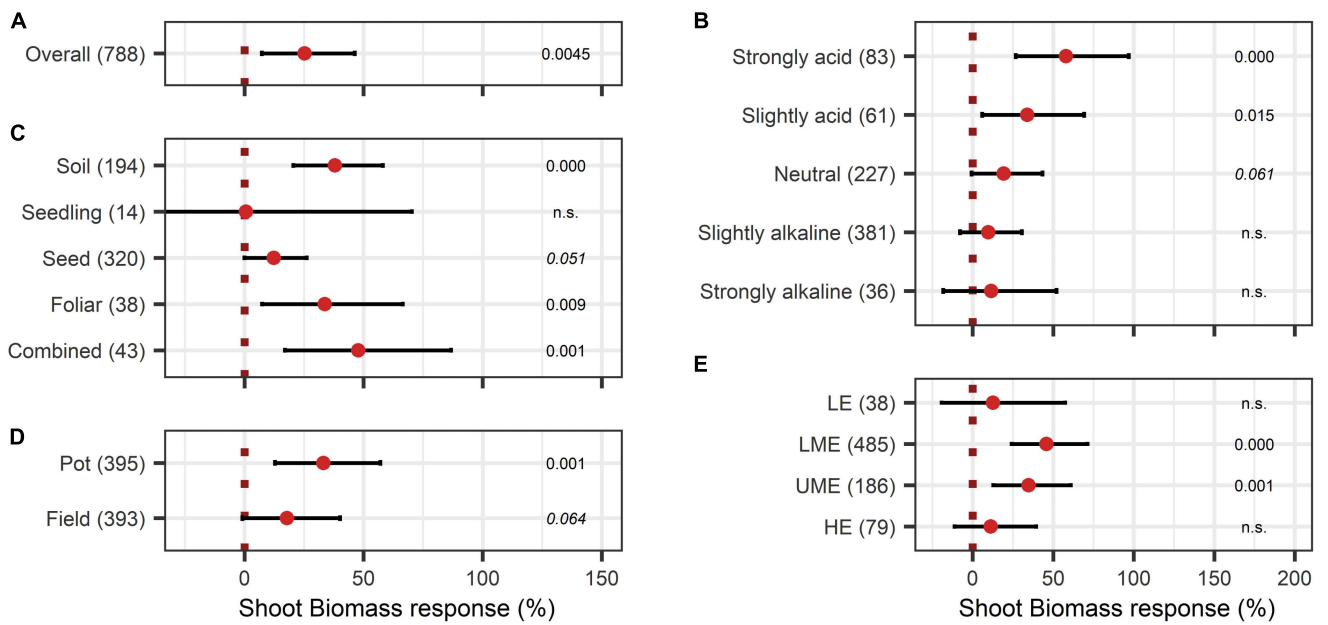

FIGURE 2 | Response of shoot biomass. **(A)** Overall biomass effect of all observations (median). **(B–E)** are subgroup analyses on biomass response: **(B)** pH categories, **(C)** mode of application, **(D)** test system, **(E)** country grouping (LE: low income economies, LME: lower middle income economies, UME: upper middle income economies, HE: high income economies). Dots mark the median, lines mark the 95% confidence interval. If the line crosses the vertical dotted line, the impact of bioeffectors is not significant ($\alpha = 0.05$). Numbers beside are the *p*-Values. *p*-Values > 0.1 were denoted as non-significant (n.s.), *p*-Values between 0.1 and 0.05 were shown in italics to indicate tendencies and *p*-Values ≤ 0.05 indicating significance were shown in regular font. The number of observations per treatment is indicated by the number in brackets.

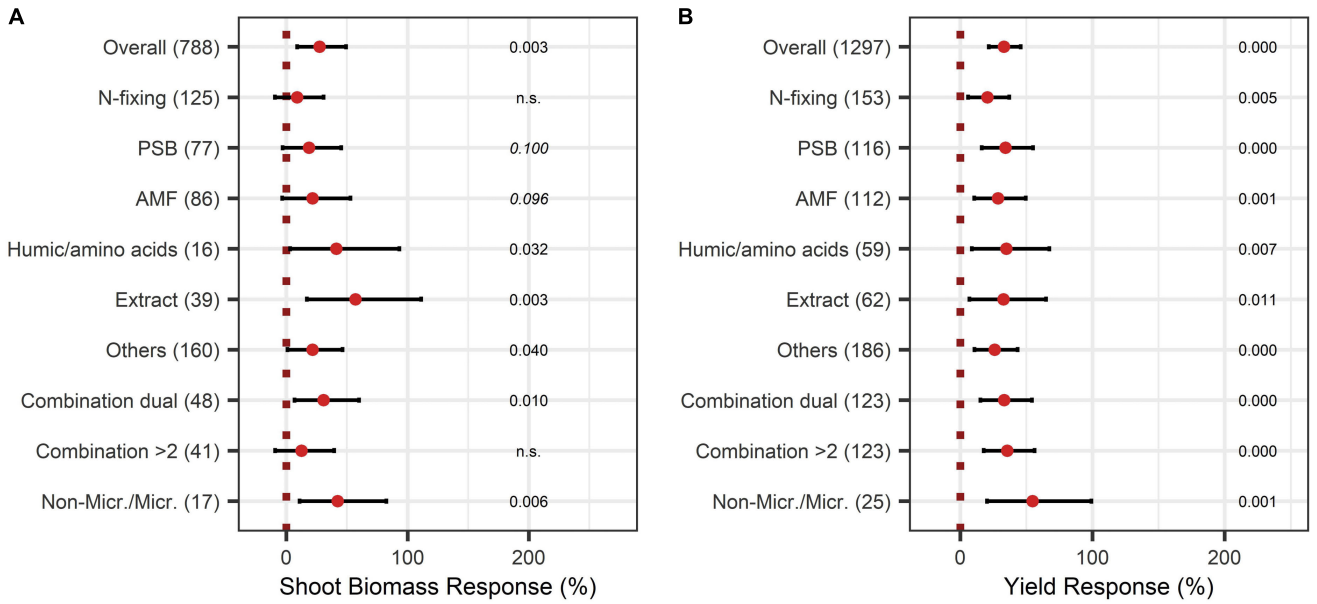

FIGURE 3 | Response of shoot **(A)** and yield **(B)** for different BE types according to the expanded model. Dots mark the median and lines mark the 95% confidence interval. If the line crosses the dotted line, the impact of bioeffectors is not significant ($\alpha = 0.05$). Numbers beside are the *p*-Values. *p*-Values > 0.1 were denoted as non-significant (n.s.), *p*-Values between 0.1 and 0.05 are shown in italics to indicate tendencies, and *p*-Values $\leq$ 0.05 indicating significance were shown in regular font. The number of observations per treatment is indicated by the number in brackets.

microbes and non-microbial substances, which led to the highest root biomass improvements (**Figure 5D**).

Assessment of Bioeffector Effects on Crop Quality Indicators

Concerning the crop quality improving aspects after BEs application, soluble solids content and protein content were investigated. Soluble solids showed a positive increase with an overall BE effect of 55% (**Figure 6A**) and also, with BE application protein content strongly increased by 75% (**Figure 7A**). The content of soluble solids depended on the test system, crop type, and pH (**Figure 6**), whereas protein content was additionally affected by the mode of BE application, the geographic region, and if the plant was perennial or annual (**Figure 7**). Here, foliar application resulted in a strong increase in protein content by 157%, whereas seed and soil application led to increases of 45% and 105%, respectively (**Figure 7F**). Crop types, such as fruits and vegetables, for which quality aspects are important for selling, showed no significant increase in soluble solids content as well as in protein content by BE application (**Figures 6C**, **7C**). In legumes, soluble solids content was significantly enhanced by 181% and protein content by 99% (**Figures 6C**, **7C**). Protein content was more increased in perennial crops (138%) than in annual crops (29%) (**Figure 7D**). From slightly acidic to slightly alkaline environments, the median responses of soluble solids content were the most pronounced with increases from 53% to 73%, but significant responses could be obtained only in slightly alkaline conditions (**Figure 6B**). Additionally, protein contents were significantly increased in neutral environments by 180%, whereas increases were clearly lower in other soil pH ranges (**Figure 7B**). The median increase of soluble solids content in the field (76%) compared to pot trials (37%) due to BE application was higher and more significant (**Figure 6D**), whereas for protein content, results were similar (74% for field and 77% for pot trials) (**Figure 7G**).

Assessment of Bioeffector Effects on Crop Nutrient Content and Nutrient Use Efficiency

The BE application showed significant improvements in aboveground nutrient content and nutrient use efficiency. The response of aboveground P content (40%) was slightly larger than the improvement of aboveground N content (28%) (**Figures 8A**, **9A**). Crop types differed in their response to BE application regarding aboveground N and P content. Aboveground N content was especially enhanced in legumes (81%) (**Figure 8B**). Also, cereals and oilseed crops have the tendency to attain positive outcomes with an increase of 37%. For aboveground P content, differences were marginal among cereals, legumes, and fruits (61% to 87%) (**Figure 9B**). The application time after sowing led to the highest increase with regard to aboveground N and P content (64% and 73%) (**Figures 8C**, **9C**). Both aboveground nutrient content responses did not differ in the test systems (**Figures 8D**, **9D**). Soil (79%), foliar (49%), and a combination of different methods of application (90%) improved aboveground P content significantly (**Figure 9E**). In the case of aboveground N content, only soil application (104%) led to significant increases while seed application (29%) showed a tendency to increase N content (**Figure 8E**).

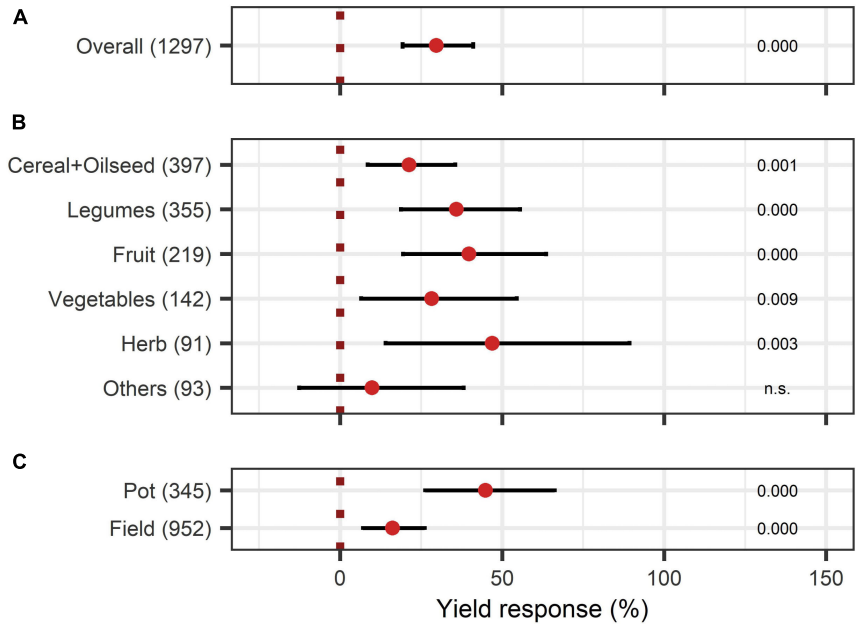

FIGURE 4 | Response of yield. **(A)** Overall yield effect of all observations (median), **(B,C)** are subgroup analyses on yield response: **(B)** crop types, **(C)** test system. Dots mark the median and lines mark the 95% confidence interval. If the line crosses the dotted line, the impact of bioeffectors is not significant ($\alpha = 0.05$). Numbers beside are the *p*-Values. *p*-Values > 0.1 were denoted as non-significant (n.s.), *p*-Values between 0.1 and 0.05 are shown in italics to indicate tendencies, and *p*-Values ≤ 0.05 indicating significance were shown in regular font. The number of observations per treatment is indicated by the number in brackets.

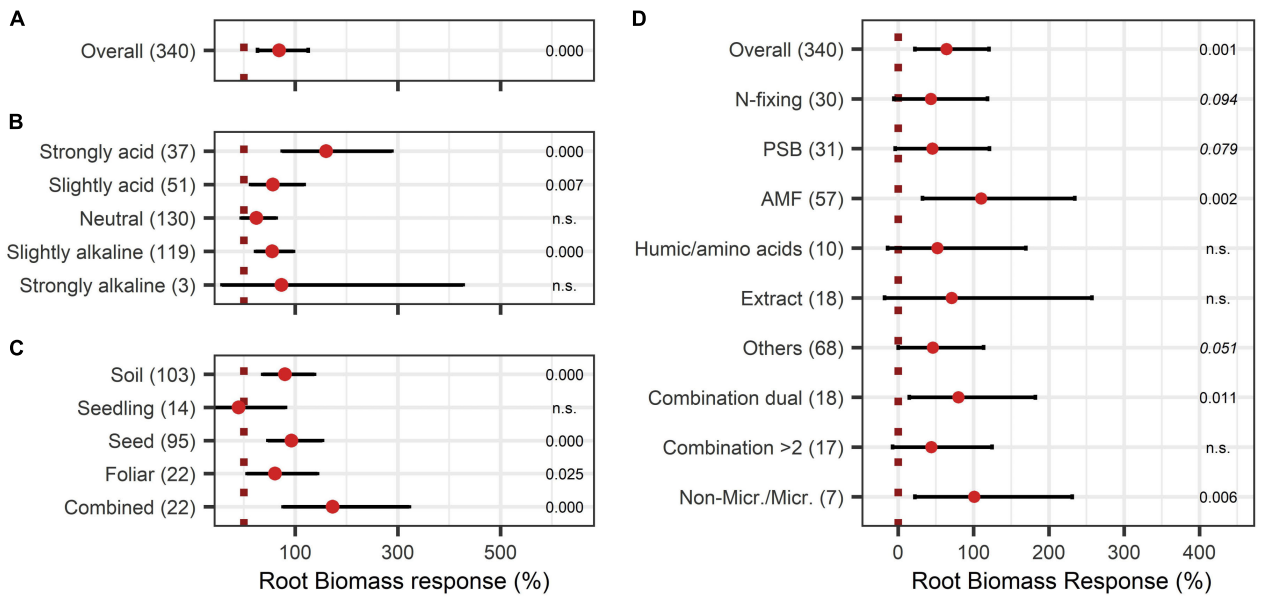

FIGURE 5 | Response of Root biomass. **(A)** Overall root biomass effect of all observations (median), **(B,C)** are subgroup analyses on root biomass response: **(B)** pH categories, **(C)** mode of application. **(D)** BE types and overall median according to the expanded model. Dots mark the median and lines mark the 95% confidence interval. If the line crosses the dotted line, the impact of bioeffectors is not significant ($\alpha = 0.05$). Numbers beside are the *p*-values. *p*-Values > 0.1 were denoted as non-significant (n.s.), *p*-Values between 0.1 and 0.05 are shown in italics to indicate tendencies, and *p*-Values ≤ 0.05 indicating significance were shown in regular font. The number of observations per treatment is indicated by the number in brackets.

Aboveground N content was significantly enhanced in strongly acidic environments by BE application (116%) (**Figure 8F**). For aboveground P content, a tendency toward higher efficiencies in lower pH levels was indicated; however, aboveground P content was again lower in strongly acidic soils (27% increase) compared to slightly acidic soils (72% increase) (**Figure 9F**).

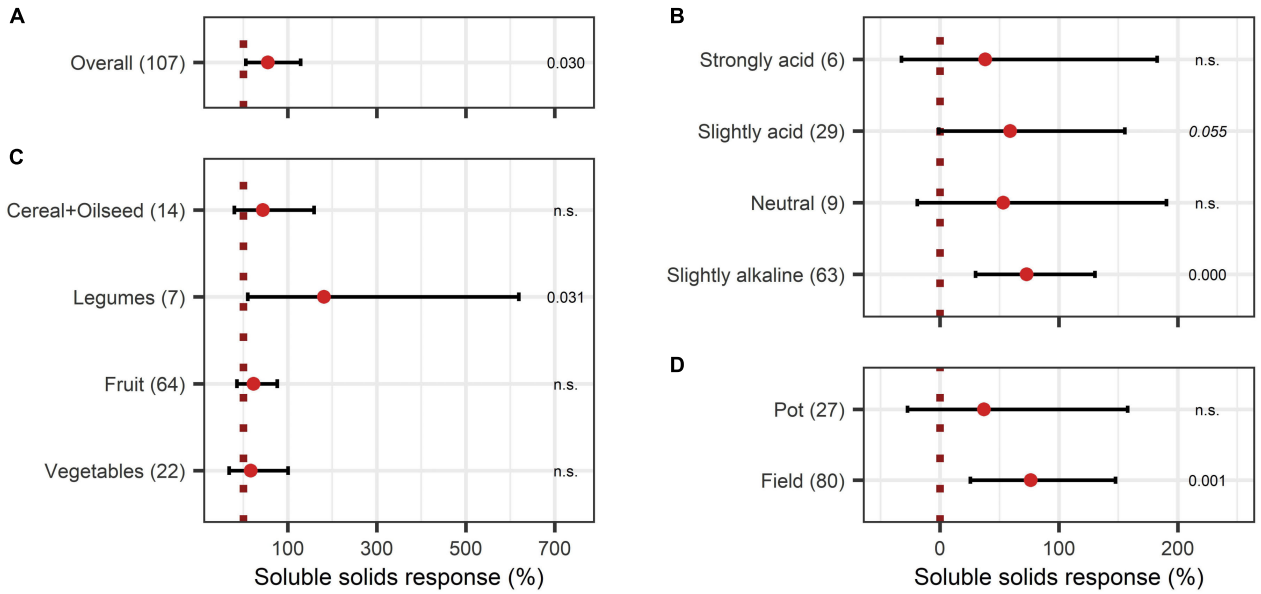

FIGURE 6 | Response of soluble solids. **(A)** Overall soluble solids increase of all observations (median), **(B–D)** are subgroup analyses on soluble solids response: **(B)** pH categories, **(C)** crop type, **(D)** test system. Dots mark the median, lines mark the 95% confidence interval. If the line crosses the dotted line, the impact of bioeffectors is not significant ($\alpha = 0.05$). Numbers beside are the *p*-Values. *p*-Values > 0.1 were denoted as non-significant (n.s.), *p*-Values between 0.1 and 0.05 are shown in italics to indicate tendencies, and *p*-Values ≤ 0.05 indicating significance were shown in regular font. The number of observations per treatment is indicated by the number in brackets.

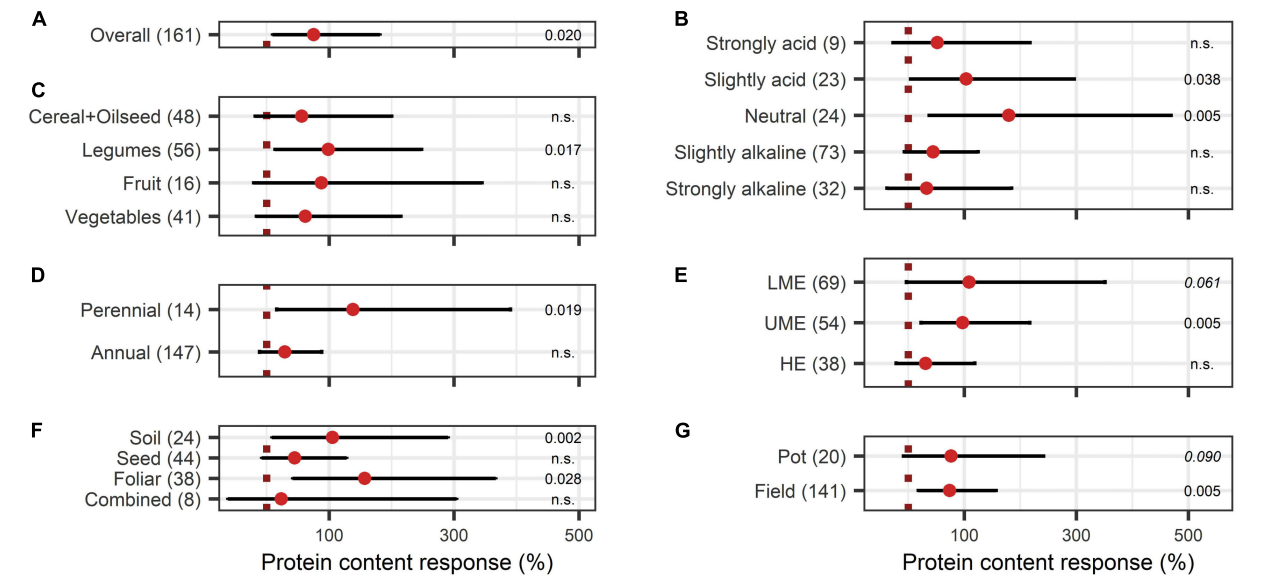

FIGURE 7 | Response of protein content. **(A)** Overall protein increase of all observations (median), **(B–G)** are subgroup analyses on protein response: **(B)** pH categories, **(C)** crop types, **(D)** perennial or annual **(E)** country grouping (LME: lower-middle-income economies, UME: upper-middle-income economies, HE: high income economies), **(F)** mode of application, **(G)** test system. Dots mark the median and lines mark the 95% confidence interval. If the line crosses the dotted line, the impact of bioeffectors is not significant ($\alpha = 0.05$). Numbers beside are the *P*-values. *P*-values > 0.1 were denoted as non-significant (n.s.), *p*-Values between 0.1 and 0.05 are shown in italics to indicate tendencies, and *p*-Values ≤ 0.05 indicating significance were shown in regular font. The number of observations per treatment is indicated by the number in brackets.

For both nutrients, the highest improvements of aboveground content were achieved in lower-middle-income economies with 71% increases for N and 76% increases for P (**Figures 8G**, **9G**). In accordance with the increase of biomass, extracts improved aboveground P content by 110% when examining it with the extended model (**Figures 10A,B**). In the case of aboveground

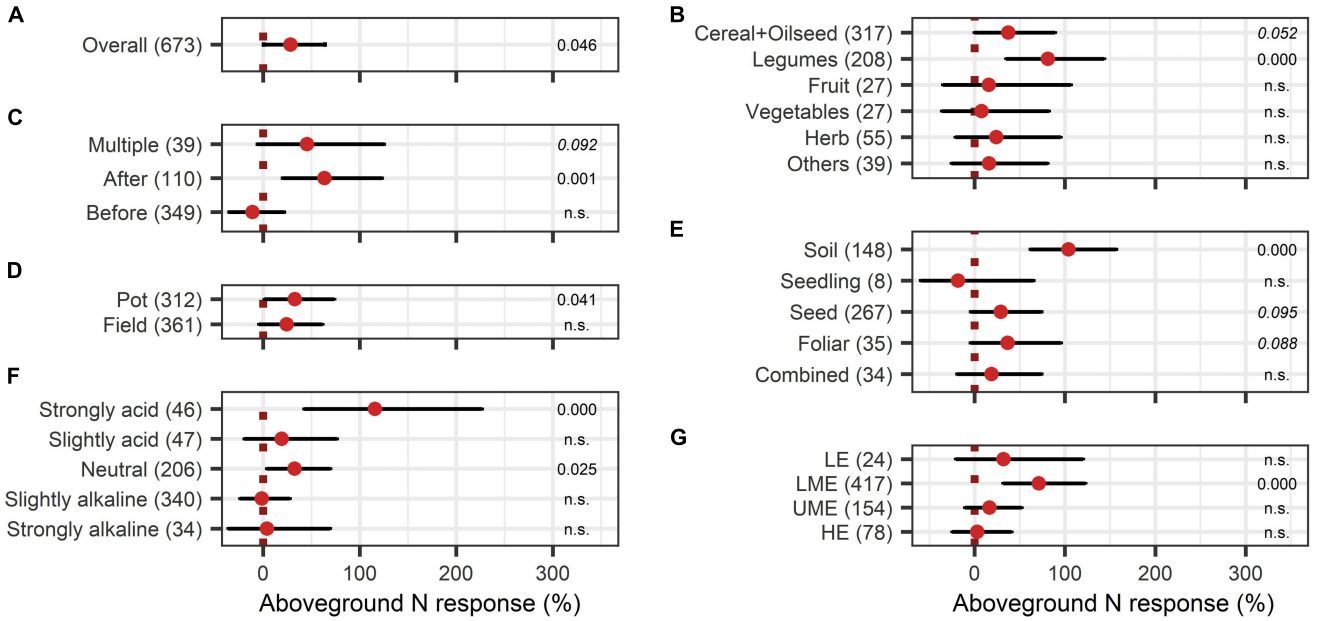

FIGURE 8 | Response of aboveground N content. **(A)** Overall aboveground N increase of all observations (median), **(B–G)** are subgroup analyses on aboveground N response: **(B)** crop type, **(C)** time of application relative to sowing, **(D)** test system, **(E)** mode of application, **(F)** pH categories, **(G)** country grouping (LE: low-income economies, LME: lower-middle-income economies, UME: upper-middle-income economies, HE: high-income economies). Dots mark the median, lines mark the 95% confidence interval. If the line crosses the dotted line, the impact of bioeffectors is not significant ($\alpha = 0.05$). Numbers beside are the *p*-Values. *p*-Values > 0.1 were denoted as non-significant (n.s.), *p*-Values between 0.1 and 0.05 are shown in italics to indicate tendencies and *p*-Values ≤ 0.05 indicating significance were shown in regular font. The number of observations per treatment is indicated by the number in brackets.

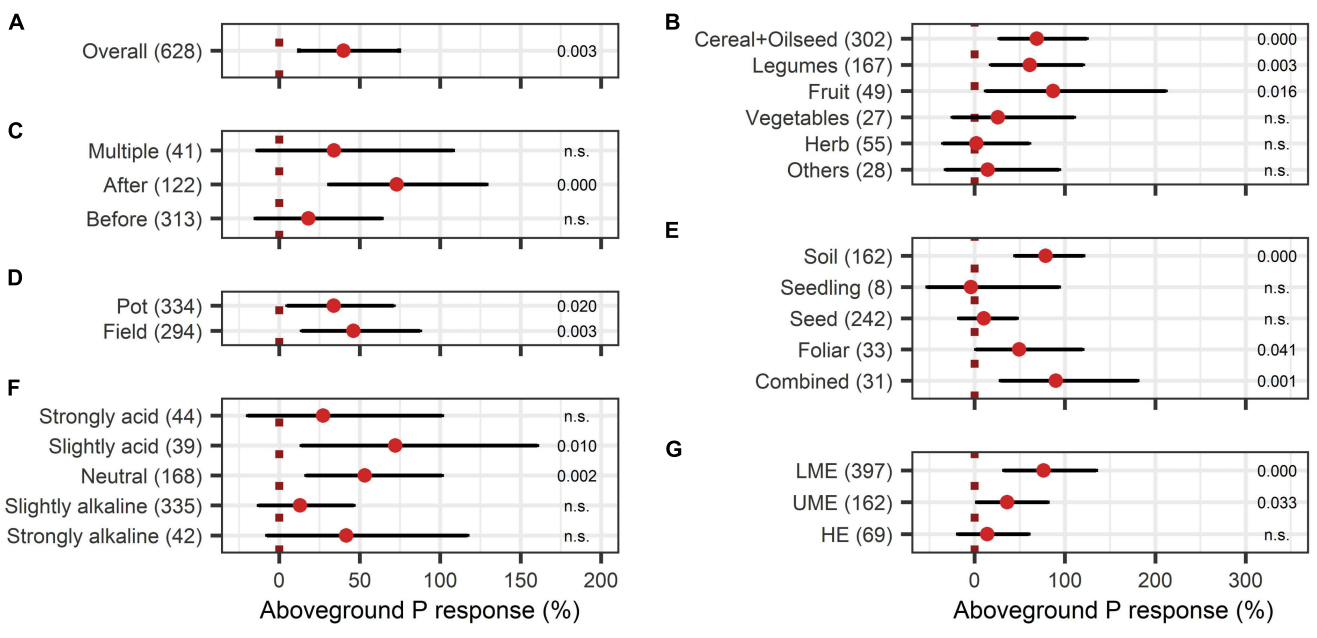

FIGURE 9 | Response of aboveground P content. **(A)** Overall aboveground P increase of all observations (median), **(B–G)** are subgroup analyses on aboveground P response: **(B)** crop type, **(C)** time of application relative to sowing, **(D)** test system, **(E)** mode of application, **(F)** pH categories, **(G)** country grouping (LE: low-income economies, LME: lower-middle-income economies, UME: upper-middle-income economies, HE: high-income economies). Dots mark the median and lines mark the 95% confidence interval. If the line crosses the dotted line, the impact of bioeffectors is not significant ($\alpha = 0.05$). Numbers beside are the *P*-values. *P*-values > 0.1 were denoted as non-significant (n.s.), *p*-Values between 0.1 and 0.05 are shown in italics to indicate tendencies, and *p*-Values ≤ 0.05 indicating significance were shown in regular font. The number of observations per treatment is indicated by the number in brackets.

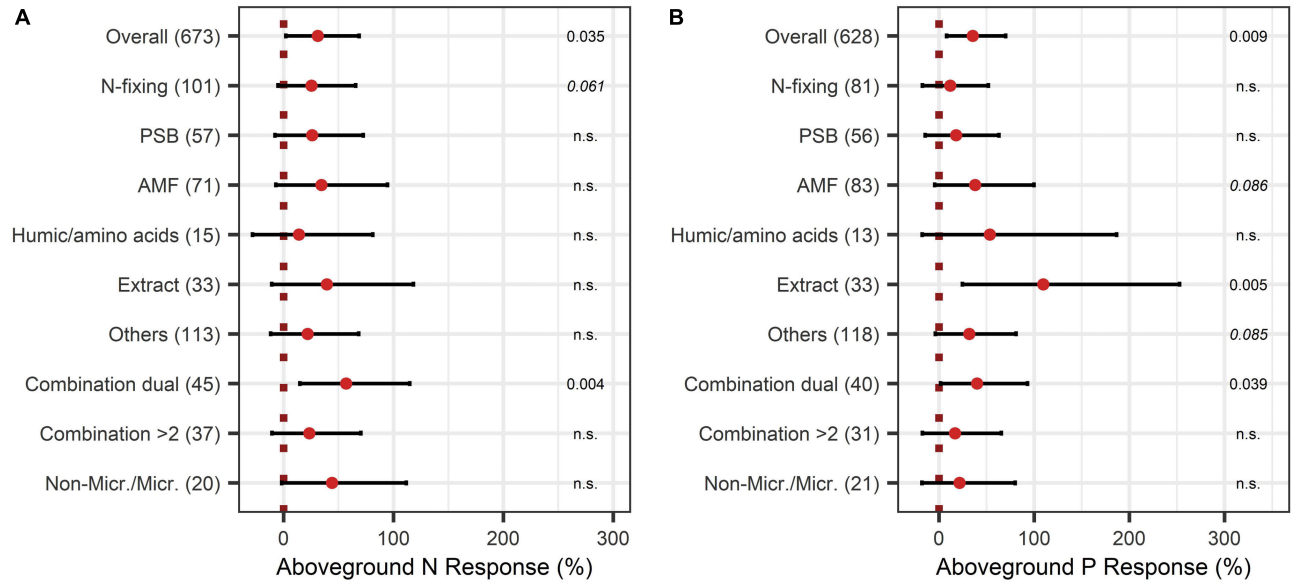

FIGURE 10 | Response of aboveground N **(A)** and P **(B)** content by different BE types. Dots mark the median, lines mark the 95% confidence interval. If the line crosses the dotted line, the impact of bioeffectors is not significant ($\alpha = 0.05$). Numbers beside are the *P*-values. *P*-values > 0.1 were denoted as non-significant (n.s.), *p*-Values between 0.1 and 0.05 are shown in italics to indicate tendencies, and *p*-Values ≤ 0.05 indicating significance were shown in regular font. The number of observations per treatment is indicated by the number in brackets.

P content, extracts and a dual combination treatment achieved significant positive results and AMF and others enhanced aboveground P content in tendency, whereas N was significantly increased by dual combinations and in tendency improved by N-fixing bacteria.

The overall effect of N-use efficiency was significantly enhanced by BE application with an increase of 36% (**Figure 11A**). Also, P-use efficiency was significantly improved by 22% (**Figure 12A**). To achieve enhanced nutrient-use efficiency, the application time needs to be considered for N, whereas the mode of application was the decisive factor for P. To increase N-use efficiency the most, an application time point after sowing should be preferred, which resulted in the highest improvements of 53% compared to 41% for multiple treatments and 17% for an application time before or at sowing (**Figure 11B**). For P-use efficiency, foliar application (40%) as well as soil application (39%) were the most suitable methods (**Figure 12C**). Moreover, N-use efficiency and P-use efficiency were dependent on soil pH. In both cases, the trend of higher efficiencies in lower pH levels was approximately visible (**Figures 11C**, **12B**). While the test system (field or pot) did not alter the results for N-use efficiency (**Figure 11D**), pot trials (26%) showed a higher median than field trials (18%) for P-use efficiency (**Figure 12D**). In the models of N- and P-use efficiency, country grouping was included as a factor. The median response of BE application on N- and P-use efficiency was especially high in lower-middle-income (50% and 34%, respectively) and upper-middle-income countries (52% and 23%, respectively), whereas it was slightly reduced in low- (21% and 15%, respectively) and high-income economies (24% and 17%, respectively) (**Figures 11E**, **12E**).

When the models of N-use efficiency were expanded by BE types, N-use efficiency was shown to be significantly improved by all BE types (**Figure 13A**). In particular, extracts and also humic and amino acids, and the dual combination treatment attained high responses for both nutrients, with 64%, 46%, and 45% for N-use efficiency (**Figure 13A**) and 109%, 54%, and 40% for P-use efficiency, respectively (**Figure 13B**). For the application of microbes, a combination of two different inoculants appeared to be more beneficial to improve N- and P-use efficiency than the application of only one BE type (**Figures 13A,B**).

DISCUSSION

The General Impact of Bioeffectors

In this metaanalysis, BE application had a positive impact on the shoot and root biomass, yield, and analyzed quality indicators as well as on aboveground nutrient uptake.

Since the outcome of a metaanalysis strongly depends on the input data, it can be assumed that the current results could be slightly biased due to a higher chance of publication success for studies with positive BE effects and missing unpublished study data. But given the number of studies published on the positive impact of BEs, it is likely that the results indicate an existing effect but may overestimate the magnitude. The higher biomass translated directly into higher yields underlining the economic opportunity going along with BE application.

The benefit of BEs on nutrient uptake and nutrient use efficiency was already summarized by previous reviews (Kumar and Aloke, 2020; Rouphael and Colla, 2020a,b). In the current study, the strong increase of plant macronutrient uptake by BE

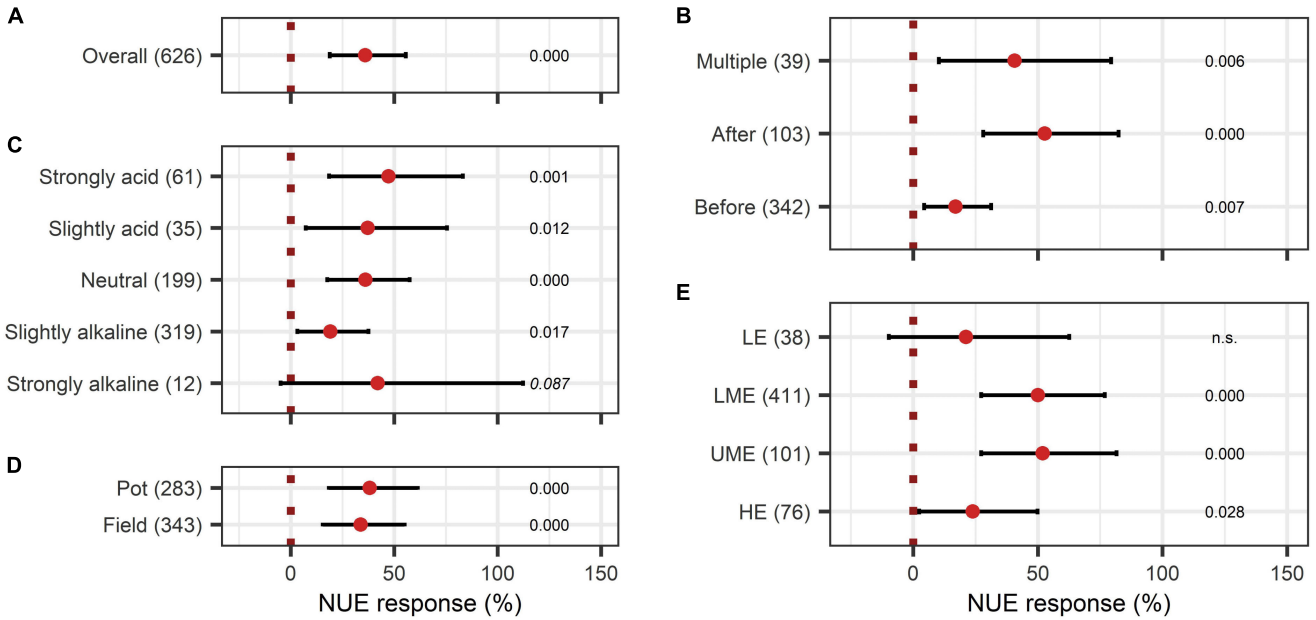

FIGURE 11 | Response of Nitrogen use efficiency (NUE). **(A)** Overall NUE increase of all observations (median), **(B–E)** are subgroup analyses on NUE: **(B)** time of application relative to sowing, **(C)** pH categories, **(D)** test system, **(E)** country grouping (LE: low-income economies, LME: lower-middle-income economies, UME: upper-middle-income economies, HE: high-income economies). Dots mark the median, lines mark the 95% confidence interval. If the line crosses the dotted line, the impact of bioeffectors is not significant ($\alpha = 0.05$). Numbers beside are the *P*-values. *P*-values > 0.1 were denoted as non-significant (n.s.), *p*-Values between 0.1 and 0.05 are shown in italics to indicate tendencies, and *p*-Values ≤ 0.05 indicating significance are shown in regular font. The number of observations per treatment is indicated by the number in brackets.

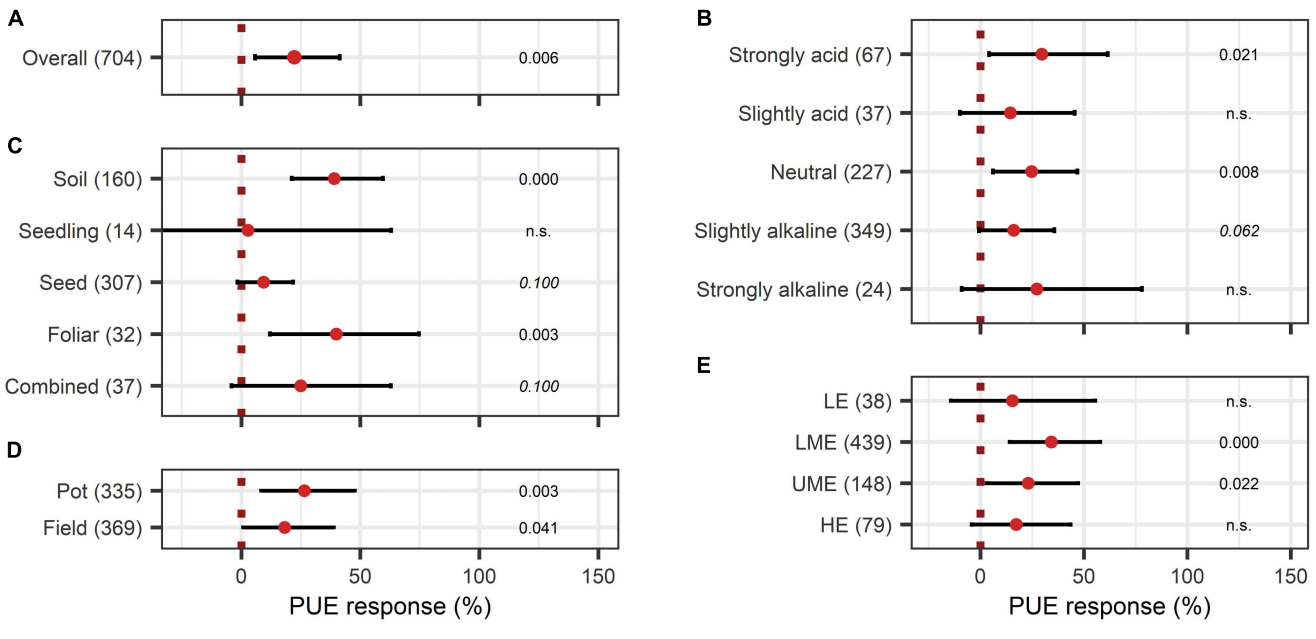

FIGURE 12 | Response of Phosphate use efficiency (PUE). **(A)** Overall PUE increase of all observations (median), **(B–E)** are subgroup analyses on PUE: **(B)** pH levels, **(C)** mode of application, **(D)** test system, **(E)** country grouping (LE: low-income economies, LME: lower-middle-income economies, UME: upper-middle income economies, HE: high-income economies). Dots mark the median and lines mark the 95% confidence interval. If the line crosses the dotted line, the impact of bioeffectors is not significant ($\alpha = 0.05$). Numbers beside are the *p*-Values. *p*-Values > 0.1 were denoted as non-significant (n.s.), *p*-Values between 0.1 and 0.05 were shown in italics to indicate tendencies, and *p*-Values ≤ 0.05 indicating significance were shown in regular font. The number of observations per treatment is indicated by the number in brackets.

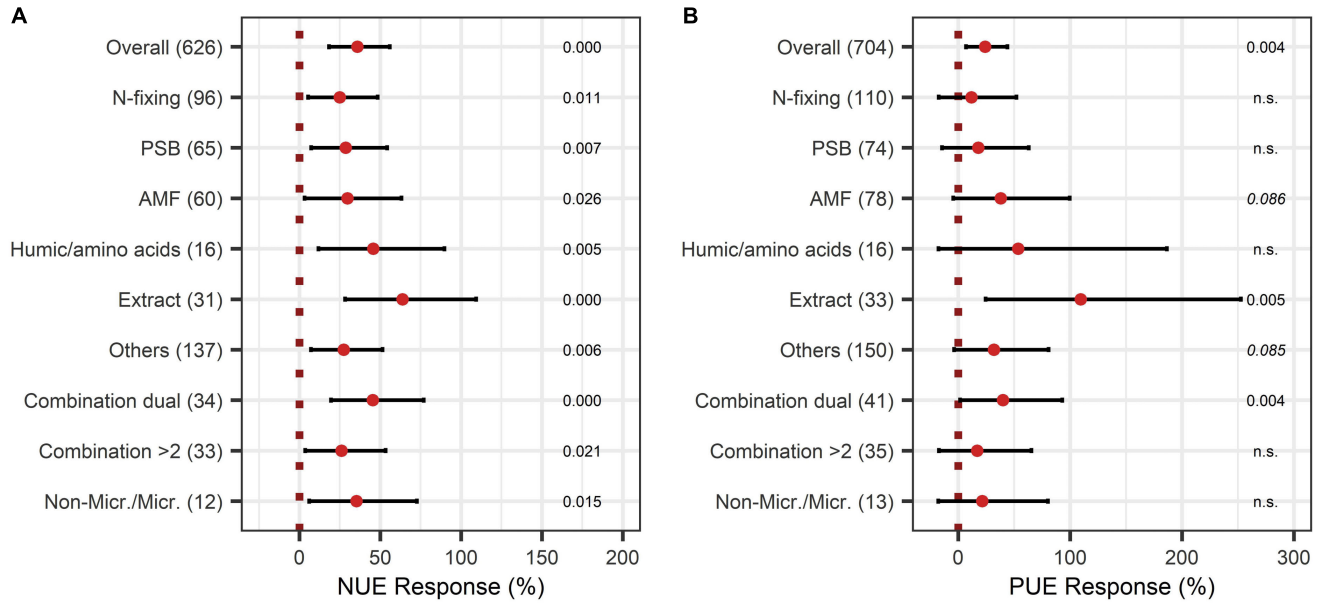

FIGURE 13 | Response of Nitrogen use efficiency (NUE) **(A)** and Phosphate use efficiency (PUE) **(B)** by different BE types according to the expanded model. Dots mark the median, lines mark the 95% confidence interval. If the line crosses the dotted line, the impact of bioeffectors is not significant ($\alpha = 0.05$). Numbers beside are the *p*-Values. *p*-Values > 0.1 were denoted as non-significant (n.s.), *p*-Values between 0.1 and 0.05 were shown in italics to indicate tendencies, and *p*-Values ≤ 0.05 indicating significance were shown in regular font. The number of observations per treatment is indicated by the number in brackets.

application, in general, could be confirmed. Moreover, BEs can contribute to the production of high-quality food and fodder. In this study, they enhanced protein content and soluble solids content, which are some of the most important indicators for taste and nutritional value. These results agree with findings from previous studies, which investigated other quality indicators (Paradikovic et al., 2011; Maach et al., 2021).

The comparison of different BE types according to the categorization above was not included in any model for the analysis of plant growth or quality traits. One could hypothesize that the type of BE is not crucial for the success of the usage, which is consistent with recent findings from the metaanalysis by Lekfeldt et al. (2021). However, BEs are selected for studies based on the experimental setting and research question, and only a few studies directly compared BE types. Thus, the results of this analysis could be biased due to non-random selection of the BE types. The expansion of the selected models with BE types resulted in only slight increases of the AIC value. Significant deviations from the main effect of extracts and humic/ amino acids on shoot biomass, as well as the effect of a combination of microbial and non-microbial products on shoot biomass and yield, could be detected with the expanded model. Additionally, a combination of two different microbial strains could exploit synergies and increased biomass as well as aboveground N content, which was also highlighted by a recent review (Santoyo et al., 2021). The increase in aboveground P content and P-use efficiency by PSB was not outstanding. Raymond et al. (2020) suggested that P solubilizing capabilities of bacteria suffice to cover the demands of the bacteria, but not to support plant P acquisition. Therefore, the improvement of aboveground P content might be caused by an improved spatial acquisition rather than an enhanced mobilization of bound phosphate in soil. Nevertheless, the P in the microbial biomass pool enters the nutrient cycle and becomes available to plants in the long term. The improvement of P nutrition through extracts, humic, and amino acids, however, did not go along with a proportional root growth increase. Thus, it cannot be related exclusively to enhanced spatial P acquisition. Other mechanisms and interactions related to the application of humic and amino acids and extracts need to be considered, such as humic–metal complexes, influence on soil biota, and increase of nutrient translocation (Anitha, 2020; Shukla and Prithiviraj, 2021). However, these mechanisms need to be clarified in future experimental studies.

In accordance with previous metaanalyses (Rubin et al., 2017; Schmidt and Gaudin, 2018), stronger positive effects on shoot biomass in pot trials than in field trials could be confirmed. This could also explain higher overall responses of root biomass compared to shoot biomass as root biomass was only investigated in pot experiments. Weinmann and Neumann (2020) suggested that BEs efficiency is higher in pot trials due to the limited soil volume, which leads to an artificially high concentration of the BE inoculant around the densely growing root. In contrast to pot trials, the root is not restricted in its growth direction in the field. This could hinder the establishment of symbiosis with BEs, as they are outcompeted by native microbial communities, which are spatially closer to the root (Weinmann and Neumann, 2020). However, in the results of aboveground N and P content, the higher efficiency of BEs in pot trials could not be identified. To clarify this contradiction, it would be helpful to reveal underlying

mechanisms to avoid results that are influenced by experimental approaches (e.g., higher application rates in pot trials, controlled conditions in the greenhouse) rather than by the test system.

Crop Types and Soil pH Determined the Effect Size of Bioeffectors

It was shown that the potential in achieving certain inoculation aims depends on the crop type as yield, aboveground nutrient contents, as well as quality traits response differed with the crop type. This may be the result of specialized symbiosis of plants and microbes to acquire nutrients in the soil, such as N-fixing bacteria and legumes, while other crop types lack this intense mutualistic interaction. In this study, the increase of aboveground N content in cereals and legumes indicates the development of more effective symbiosis with soil microorganisms, which is known to exist in these crop types (Rosenblueth et al., 2018). However, the potential amount of nitrogen fixation is lower in cereals than in legumes (Cooper and Scherer, 2012), which is also reflected by the results of this study.

Soil physicochemical characteristics can impact the success of BE application (Weinmann and Neumann, 2020). In this study, it was highlighted that the pH level of the soil strongly influences the outcome of a BE application. As mentioned above, most of the BEs can mobilize insoluble nutrients, such as P, in several ways. BEs act as a counterpart against nutrient fixation in soil by acidification, which is regarded as the most crucial impact of soil microbes (Raymond et al., 2020). However, the results imply that this mechanism is restricted to slight pH decreases as the efficacy of BEs decreased in almost any case in strongly alkaline soils. Additionally, the results from this analysis suggest that the highest benefit of BE application occurs in strongly acidic environments with the highest increase in shoot and root biomass. It also shows that the effectiveness of BE application to improve plant growth traits tends to increase with decreasing soil pH, especially for shoot biomass. In these soils, nutrients, such as P, become insoluble due to reaction with Al and Fe (Margenot et al., 2018). By an enhanced root growth, as demonstrated in this study, the acquisition of scarce soluble nutrients can be improved. BEs could support root growth in acidic environments by chelating detrimental Fe and Al-cations and forming metal–humic complexes (Khan et al., 2009; Anitha, 2020).

The Right Time and Right Way to Use Bioeffectors

It remains an open research question whether better-adapted application methods could improve the effectiveness of BE application. Application methods should be highly effective and easily adoptable in common agricultural schemes (Weinmann and Neumann, 2020). In the present metaanalysis, it was shown that investigated methods of application had a significant impact on growth parameters, quality traits, and aboveground nutrient content. Foliar and soil application seem to be the most promising application methods to achieve reliable growth gains, improve nutritional quality, and increase nutrient uptake. The application time influenced aboveground N and P content and N-use efficiency. Consistently, an application time after sowing obtained highest efficiencies in all cases, in which application time was included in the model.

The country grouping provided a broad indicator for agronomical production regimes. Most of the investigated effects showed a dependency on management; however, in almost none of the cases the impact was negative, and for yield, country grouping was not included in the model. It could therefore be argued that the benefits from BE application are realizable in any region. Yet, differences in efficiency across countries could be detected regarding shoot biomass, aboveground N and P content, as well as N- and P-use efficiency. This may be due to different baselines of N- and P-use efficiency in the regions and therefore, varying improvement opportunities for growth and nutrient uptake. In the study of Omara et al. (2019), low-income economies and high-income economies obtained N-use efficiencies above the global average, while China and India, which contributed to a great extent to the data for this study, showed N-use efficiencies below the global average (Omara et al., 2019). One could hypothesize that BEs can especially support these countries with a low nutrient use efficiency, while in countries that already have a high efficacy, BEs cannot contribute much to ameliorate nutrient use efficiency even more.

CONCLUSION AND OUTLOOK

Reducing mineral fertilizer input while maintaining high yield levels is crucially important in sustainable agricultural production. As demonstrated in this study, BEs can contribute to achieve this goal by improving plant growth by 26%, yield by 30%, and P and N uptake by 40% and 28%, respectively. In contrast to studies focusing on single microbial BEs, we could show that non-microbial BEs and composite products with combinations of different microbial and non-microbial BEs are most promising as they increased biomass by 40%–60%. However, the results are not consistent. The application time, the application mode (e.g., foliar, placement, and combinations), and soil characteristics, especially the pH level, need to be considered to guarantee effective action of BEs. In summary, the effects of BEs on crop growth traits were strongest for the following: application after sowing; foliar application, a combination of several different application methods, and a soil application; as well as under acidic soil conditions especially regarding biomass response and nutrient uptake. Harmonizing BE types, application mode, crop type, and soil characteristics should be the focus of future studies. Further research is needed to clarify the mechanisms of non-microbial products, especially their influence on plant P uptake.

DATA AVAILABILITY STATEMENT

The data analyzed in this study is subject to the following licenses/restrictions: The datasets, SAS scripts and R scripts of the current study are available from the corresponding author on reasonable request. Requests to access these datasets should be directed to MH, m.herrmann@uni-hohenheim.de.

AUTHOR CONTRIBUTIONS

HY and MH conceptualized the study. MH and YW collected the data. JH and MH implemented the statistical analysis. MH drafted and wrote the manuscript. HY and TM complemented the work. HY, TM, and XC supervised the work. All authors read and revised the manuscript and approved the final version.

FUNDING

This study was financially supported by the Scientific Research Startup Foundation of Southwest University to HY (SWU019012) and the Deutsche Forschungsgemeinschaft (DFG, German Research Foundation) – 328017493/GRK 2366 (Sino-German International Research Training Group AMAIZE-P). MH also would like to thank the Studienstiftung des Deutschen Volkes for the financial support of her educational stay at the South West University in Chongqing (China).

ACKNOWLEDGMENTS

The authors would like to thank Drs. Xiaozhong Wang and Wushuai Zhang for the advice and Ms. Yue Wu for her support in the early stage of the project.

SUPPLEMENTARY MATERIAL

The Supplementary Material for this article can be found online at: https://www.frontiersin.org/articles/10.3389/fpls.2022.816438/full#supplementary-material

REFERENCES

Adani, F., Genevini, P., Zaccheo, P., and Zocchi, G. (1998). The effect of commercial humic acid on tomato plant growth and mineral nutrition. *J. Plant Nutr.* 21, 561–575. doi: 10.1080/01904169809365424

Anitha, K. V. (2020). Role of biostimulants in uptake of nutrients by plants. *J. Pharmacogn. Phytochem.* 9, 563–567. doi: 10.22271/phyto.2020.v9.i3v.11492

Carrijo, D. R., Lundy, M. E., and Linquist, B. A. (2017). Rice yields and water use under alternate wetting and drying irrigation: a meta-analysis. *Field Crops Res.* 203, 273–280. doi: 10.1016/j.fcr.2016.12.002

Cooper, J. E., and Scherer, H. W. (2012). "Nitrogen Fixation," in *Marschner's Mineral Nutrition of Higher Plants*, ed. P. Marschner (London: Academic Press), 389–408. doi: 10.1016/B978-0-12-384905-2.00016-9

Haygarth, P. M., and Rufino, M. C. (2021). Local solutions to global phosphorus imbalances. *Nat. Food* 2, 459–460. doi: 10.1016/j.wasman.2018.11.020

Hedges, L. V. (1981). Distribution theory for Glass's estimator od effect size and related estimators. *J. Educ. Stat.* 6, 107–128. doi: 10.3102/10769986006002107

Herbert, S., Hashemi, M., Chickering-Sears, C., and Weis, S. (2019). *Plant nutrients from manure*. Available online at: https://ag.umass.edu/sites/ag.umass.edu/files/fact-sheets/pdf/PlantNutrientsfromManure09-52.pdf. [Accessed 21 June 2019].

Jindo, K., Martim, S. A., Navarro, E. C., Pérez-Alfocea, F., Hernandez, T., Garcia, C., et al. (2012). Root growth promotion by humic acids from composted and non-composted urban organic wastes. *Plant Soil* 353, 209–220. doi: 10.1007/s11104-011-1024-3

Joober, R., Schmitz, N., Annable, L., and Boksa, P. (2012). Publication bias: What are the challenges and can they be overcome? *J. Psychiatry Neurosci.* 37, 149–152. doi: 10.1503/jpn.120065

Kahle, D., and Wickham, H. (2013). ggmap: Spatial Visualization with ggplot2. *R J.* 5, 144–161. doi: 10.32614/RJ-2013-014

Khan, A., Jilani, G., Akhtar, M. S., Naqvi, S. M. S., and Rasheed, M. (2009). Phosphorus solubilizing bacteria: occurrence, mechanisms and their role in crop production. *J. Agric. Biol. Sci.* 1, 48–58.

Kumar, H. D., and Aloke, P. (2020). Role of Biostimulant Formulations in Crop Production: An Overview International. *IJASVM* 8, 38–46.

Lekfeldt, J. D. S., Nkebiwe, P. M., Symanczik, S., Mäder, M., Bar-Tal, A., Biró, B., et al. (2021). To BE, or not to BE . a meta-analysis on the effectiveness of bio-effectors (BEs) on maize, wheat and tomato performance from greenhouse to field scales across Europe and Israel. *Manuscript Preparation*.

Levine, T. J., Asada, K. J., and Carpenter, C. (2009). Sample Sizes and Effect Sizes are Negatively Correlated in Meta-Analyses: Evidence and Implications of a Publication Bias Against NonSignificant Findings. *Comm. Monogr.* 76, 286–302. doi: 10.1080/03637750903074685

Maach, M., Boudouasar, K., Akodad, M., Skalli, A., Moumen, A., and Baghour, M. (2021). Application of biostimulants improves yield and fruit quality in tomato. *Internat. J. Veg. Sci.* 27, 288–293. doi: 10.1080/19315260.2020.1780536

Madden, L. V., Piepho, H. P., and Paul, P. A. (2016). Statistical models and methods for network meta-analysis. *Phytopathology* 106, 792–806. doi: 10.1094/PHYTO-12-15-0342-RVW

Margenot, A. J., Sommer, R., and Parikh, S. J. (2018). Soil phosphatase activities across a liming gradient under long-term managements in Kenya. *Soil Sci. Soc. Am. J.* 82, 850–861. doi: 10.2136/sssaj2017.12.0420

Meents, A. K., Furch, A. C. U., Almeida-Trapp, M., Özyürek, S., Scholz, S. S., Kirbis, A., et al. (2019). Beneficial and Pathogenic Arabidopsis Root-Interacting Fungi Differently Affect Auxin Levels and Responsive Genes During Early Infection. *Front. Plant Sci.* 2019:380. doi: 10.3389/fmicb.2019.00380

Moher, D., Pham, B., Jones, A., Cook, D. J., Jadad, A. R., Moher, M., et al. (1998). Does quality of reports of randomized trials affect estimates of intervention efficacy reported in meta-analysis? *Lancet* 352, 609–613. doi: 10.1016/s0140-6736(98)01085-x

Oldroyd, G., and Leyser, O. (2020). A plant's diet, surviving in a variable nutrient environment. *Science* 368:eaba0196. doi: 10.1126/science.aba0196

Omara, P., Aula, L., Oyebiyi, F., and Raun, W. R. (2019). World Cereal Nitrogen Use Efficiency Trends: Review and Current Knowledge. *Agrosyst. Geosci. Environ.* 2:180045. doi: 10.2134/age2018.10.0045

Paradikovic, N., Vinkovic, T., Vinkovic, V. I., Zuntar, I., Bojic, M., and Medic-Saric, M. (2011). Effect of natural biostimulants on yield and nutritional quality: an example of sweet yellow pepper (Capsicum annuum L.) plants. *J. Sci. Food Agric.* 91, 2146–2152. doi: 10.1002/jsfa.4431

Patterson, H. D., and Thompson, R. (1971). Recovery of interblock information when block sizes are unequal. *Biometrika* 58, 545–554. doi: 10.1093/biomet/58.3.545

Povero, G., Mejia, J. F., Di Tommaso, D., Piaggesi, A., and Warrior, P. (2016). A Systematic Approach to Discover and Characterize Natural Plant Biostimulants Front. *Plant Sci.* 7:435. doi: 10.3389/fpls.2016.00435

Qiu, Y., Amirkhani, M., Mayton, H., Chen, Z., and Taylor, A. G. (2020). Biostimulant Seed Coating Treatments to Improve Cover Crop Germination and Seedling Growth. *Agronomy* 10:154. doi: 10.3390/agronomy10020154

Raymond, N. S., Gómez-Muñoz, B., van der Bom, F. J. T., Nybroe, O., Jensen, L. S., Müller-Stöver, D. S., et al. (2020). Phosphate-solubilising microorganisms for improved crop productivity: a critical assessment. *New Phytol.* 229, 1268–1277. doi: 10.1111/nph.16924

Reuter, H. I., Lado, L. R., Hengl, T., and Monranarella, L. (2008). Continental-scale digital soil mapping using European soil profile data: soil pH. *Hamburger Beiträge zur Physischen Geographie und Landschaftsökologie* 19, 91–102.

Ricci, M., Tilbury, L., Daridon, B., and Sukalac, K. (2019). General principles to justify plant biostimulant claims. *Front. Plant Sci.* 10:494. doi: 10.3389/fpls.2019.00494

Rosenblueth, M., Ormeño-Orrilo, E., López-López, A., Rogel, M. A., Reyes-Hernández, B. J., Martínez-Romero, J. C., et al. (2018). Nitrogen Fixation in Cereals. *Front. Microbiol.* 9:1794. doi: 10.3389/fmicb.2018.01794

Rouphael, Y., and Colla, G. (2018). Synergistic Biostimulatory Action: Designing the next generation of plant biostimulants for sustainable agriculture. *Front. Plant Sci.* 9, 1655. doi: 10.3389/fpls.2018.01655

Rouphael, Y., and Colla, G. (2020a). Toward a Sustainable Agriculture Through Plant Biostimulants: From Experimental Data to Practical Applications. *Agronomy* 10:1461. doi: 10.3390/agronomy10101461

Rouphael, Y., and Colla, G. (2020b). Editorial: Biostimulants in Agriculture. *Front. Plant Sci.* 11:40. doi: 10.3389/fpls.2020.00040

Rubin, R. L., van Groenigen, K. J., and Hungate, B. A. (2017). Plant growth promoting rhizobacteria are more effective under drought: a meta-analysis. *Plant Soil* 416, 309–323. doi: 10.1007/s11104-017-3199-8

Sánchez-Meca, J., and Marín-Martínez, F. (1998). Weighting by inverse variance or by sample size in Meta-analysis: A simulation study. *Educ. Psychol. Meas.* 58, 211–220. doi: 10.1177/0013164498058002005

Santoyo, G., Guzmán-Guzmán, P., Parra-Cota, F. I, de los Santos-Villalobos, S., Orozco-Mosqueda, M. D. C., and Glick, B. R. (2021). Plant Growth Stimulation by Microbial Consortia. *Agronomy* 11:219. doi: 10.3390/agronomy11020219

Schmidt, J. E., and Gaudin, A. (2018). What is the agronomic potential of biofertilizers for maize? A meta-analysis. *FEMS Microbiol. Ecol.* 94:7. doi: 10.1093/femsec/fiy094

Schütz, L., Gattinger, A., Meier, M., Müller, A., Boller, T., Mäder, P., et al. (2018). Improving Crop Yield and Nutrient Use Efficiency *via* Biofertilization – A Global Meta-analysis. *Front. Plant Sci.* 2018:2204. doi: 10.3389/fpls.2017.02204

Selvakumar, G., Kundu, S., Joshi, P., Nazim, S., Gupta, A. D., Mishra, P. K., et al. (2008). Characterization of a cold-tolerant plant growth-promoting bacterium *Pantoea dispersa* 1A isolated from a sub-alpine soil in the North Western Indian Himalayas. *World J. Microb. Biotechnol.* 24, 955–960. doi: 10.1007/s11274-007-9558-5

Shukla, P. S., Borza, T., Critchley, A. T., Hiltz, D., Norrie, J., and Prithiviray, B. (2018). *Ascophyllum nodosum* extract mitigates salinity stress in *Arabidopsis thaliana* by modulating the expression of miRNA involved in stress tolerance and nutrient acquisition. *PLoS One* 2018:206221. doi: 10.1371/journal.pone.0206221

Shukla, P. S., and Prithiviraj, B. (2021). Ascophyllum nodosum Biostimulant Improves the Growth of Zea mays Grown Under Phosphorus Impoverished Conditions. *Front. Plant Sci.* 2021:601843. doi: 10.3389/fpls.2020.601843

Sponagel, H., Grottenthaler, W., Hartmann, K. J., Hartwich, R., Janetzko, P., Joisten, H., et al. (2005). *Bodenkundliche Kartieranleitung*. Hannover: Bundesanstalt für Geowissenschaften und Rohstoffe.

United States Department of Agriculture – Natural Resources Conservation Service (2019). *Estimating Moist Bulk Density by Texture*. Available online at: https://www.nrcs.usda.gov/wps/portal/nrcs/detail/soils/survey/office/ssr10/tr/?cid=nrcs144p2_074844. [Accessed 21 June 2019]

Upadhyay, S. K., Singh, D. P., and Saikia, R. (2009). Genetic Diversity of Plant Growth Promoting Rhizobacteria Isolated from Rhizospheric Soil of Wheat Under Saline Condition. *Curr. Microbiol.* 59, 489–496. doi: 10.1007/s00284-009-9464-1

Van Oosten, M. J., Pepe, O., de Pascale, S., Silletti, S., and Maggio, A. (2017). The role of biostimulants and bioeffectors as alleviators of abiotic stress in crop plants. *Chem. Biol. Technol. Agric.* 4:5. doi: 10.1186/s40538-017-0089-5

Watts-Williams, S. J., and Cavagnaro, T. R. (2014). Nutrient interactions and arbuscular mycorrhizas: a meta-analysis of a mycorrhiza-defective mutant and wild-type tomato genotype pair. *Plant Soil* 384, 79–92. doi: 10.1007/s11104-014-2140-7

Weinmann, M., and Neumann, G. (2020). *Bio-effectors to optimize the mineral nutrition of crop plants", in Achieving sustainable crop nutrition*. Cambridge: Burleigh Dodds Series in Agricultural Science, doi: 10.19103/AS.2019.0062.27

Wickham, H. (2016). *ggplot2: Elegant Graphics for Data Analysis*. New York, NY: Springer-Verlag. doi: 10.1007/978-3-319-24277-4

Wolfinger, R. (1993). Covariance structure selection in general mixed models. *Commun. Stat. Simul. Comput.* 22, 1079–1106. doi: 10.1080/03610919308813143

World Bank (2019). *Countries and Economies*. Available online at: https://data.worldbank.org/country. [Accessed on 7 Jan 2021].

Xu, J., and Long, J. S. (2005). *Using the Delta Method to Construct Confidence Intervals for Predicted Probabilities, Rates, and Discrete Changes*. Available online at: https://jslsoc.sitehost.iu.edu/stata/ci_computations/spost_deltaci.pdf [Accessed on 13 Mar 2021].

Conflict of Interest: The authors declare that the research was conducted in the absence of any commercial or financial relationships that could be construed as a potential conflict of interest.

Publisher's Note: All claims expressed in this article are solely those of the authors and do not necessarily represent those of their affiliated organizations, or those of the publisher, the editors and the reviewers. Any product that may be evaluated in this article, or claim that may be made by its manufacturer, is not guaranteed or endorsed by the publisher.

frontiers in Microbiology

ORIGINAL RESEARCH
published: 02 March 2022
doi: 10.3389/fmicb.2022.826827

Identification and Characterization of *Bacillus tequilensis* GYUN-300: An Antagonistic Bacterium Against Red Pepper Anthracnose Caused by *Colletotrichum acutatum* in Korea

Hyeok-Tae Kwon[1†], Younmi Lee[1,2†], Jungyeon Kim[1], Kotnala Balaraju[1,2], Heung Tae Kim[3] and Yongho Jeon[1]*

[1] Department of Plant Medicals, Andong National University, Andong, South Korea, [2] Agricultural Science and Technology Research Institute, Andong National University, Andong, South Korea, [3] Department of Plant Medicine, Chungbuk National University, Cheongju, South Korea

OPEN ACCESS

Edited by:
Maurizio Ruzzi,
University of Tuscia, Italy

Reviewed by:
Asgar Ali,
University of Nottingham Malaysia Campus, Malaysia
Yameen Siddiqui,
Putra Malaysia University, Malaysia

***Correspondence:**
Yongho Jeon
yongbac@andong.ac.kr

[†]*These authors share first authorship*

Specialty section:
This article was submitted to Microbe and Virus Interactions with Plants, a section of the journal Frontiers in Microbiology

Received: *01 December 2021*
Accepted: *11 February 2022*
Published: *02 March 2022*

Citation:
Kwon H-T, Lee Y, Kim J, Balaraju K, Kim HT and Jeon Y (2022) Identification and Characterization of Bacillus tequilensis GYUN-300: An Antagonistic Bacterium Against Red Pepper Anthracnose Caused by Colletotrichum acutatum in Korea. Front. Microbiol. 13:826827. doi: 10.3389/fmicb.2022.826827

Anthracnose is a fungal disease caused by *Colletotrichum* species and has detrimental effects on many crops, including red pepper. This study used *Bacillus tequilensis* GYUN-300 (GYUN-300), which exhibit antagonistic activity against the fungal pathogen, *Colletotrichum acutatum*. This pathogen causes anthracnose that manifests primarily as a fruit rot in red pepper. There have been little efforts to identify antagonistic bacteria from mushrooms; this strain of bacteria was identified as *B. tequilensis* using BIOLOG and 16S rDNA sequencing analysis. The genetic mechanism underpinning the biocontrol traits of GYUN-300 was characterized using the complete genome sequence of GYUN-300, which was closely compared to related strains. GYUN-300 inhibited mycelial growth and spore germination of *C. acutatum* under *in vitro* conditions. Important antagonistic traits, such as siderophore production, solubilization of insoluble phosphate, and production of lytic enzymes (cellulase, protease, and amylase), were observed in GYUN-300, These trains promoted growth in terms of seed germination and vigorous seedling growth compared to the non-treated control. When red pepper fruits were treated with GYUN-300, the preventive and curative effects were 66.6 and 38.3% effective, respectively, in wounded red pepper fruits; there was no difference between the preventive and curative effects in non-wounded red pepper fruits. Furthermore, GYUN-300 was resistant to several commercial fungicides, indicating that GYUN-300 bacterial cells may also be used synergistically with chemical fungicides to increase biocontrol efficiency. Based on *in vitro* results, GYUN-300 played a role to control anthracnose disease effectively in field conditions when compared to other treatments and non-treated controls. The results from this study provide a better understanding of the GYUN-300 strain as an effective biocontrol agent against red pepper anthracnose; this form of biocontrol provides an environment-friendly alternative to chemical fungicides.

Keywords: *Bacillus tequilensis*, anthracnose, fungicide resistance, fungal pathogen, genome sequence, microbial pesticide

INTRODUCTION

Red pepper (*Capsicum annuum* L.) is a vegetable crop belonging to the Solanaceae family, with the cultivation area of 33,373 hectares. The total production of chili pepper recorded as 92,756 tons in the year 2021 in Korea[1] (Kim et al., 2014). To meet the demands of a growing population, an increased production of red pepper along with other vegetables are required in Korea. Therefore, a large quantity of chemical pesticides is utilized annually to control various bacterial, fungal, and viral diseases on red pepper crops in Korea (Hong et al., 2015). Among all pathogens that cause diseases in red peppers, anthracnose caused by a wide range of *Colletotrichum* species results in serious losses of fruits during the pre- and post-harvest stages (Ali et al., 2016), while occasionally damaging the stem and foliage (Mishra et al., 2018; Mongkolporn and Taylor, 2018). To date, 24 *Colletotrichum* species infecting red peppers have been identified; the most common species are *Colletotrichum acutatum* and *Colletotrichum gloeosporioides*, which inflict serious damage to red pepper (Kim et al., 2008; Parisi et al., 2020). The fungal species of *Colletotrichum* cause anthracnose in several plants, including red peppers (Siddiqui and Ali, 2014). Anthracnose was responsible for a 10% annual reduction in pepper productivity in South Korea (Kim et al., 2008). Anthracnose in red pepper is associated with several *Colletotrichum* species, including *C. acutatum* (Harp et al., 2014), this may also infect other fruit and vegetable crops (Han et al., 2015). Red pepper anthracnose is typically characterized by dark brown to black, circular water-soaked spots with concentric rings of black acervuli developing beneath the skin of the fruit (Parisi et al., 2020); the spots are often numerous and coalesce, causing softening and fruit rot (Montri et al., 2009).

Anthracnose is usually controlled by the application of chemical fungicides in field conditions. The increased use of chemical fungicides has led to the development of resistance in fungal strains (Onyeka et al., 2006). In particular, *C. acutatum* is resistant to specific chemical fungicides, including carbendazim, benomyl, and copper oxide (Peres et al., 2002; Jayasinghe and Fernando, 2009). The continuous use of chemical pesticides increases public concern regarding the risks associated with hazardous residues on agricultural products and its adverse effects on biodiversity in ecosystems (Meena et al., 2020). In addition, disease control by chemical pesticides is cost-effective for farmers in developing countries (Wesseling et al., 1997; Bordoh et al., 2020). For these reasons, biological control using antagonistic microorganisms has emerged as environment-friendly alternative to control plant diseases (Köhl et al., 2019; De la Lastra et al., 2021). Antagonistic microorganisms produce a variety of secondary metabolites to combat plant pathogens (Hossain et al., 2015; Köhl et al., 2019; Cellini et al., 2021). They induce resistance against pathogen infections in plant tissues without direct antagonistic interactions with the pathogen itself (Sharma et al., 2019). Similarly, a previous study by Ali et al. (2015) reported that the red pepper anthracnose was suppressed by an antimicrobial organic compound, propolis under post-harvest conditions. Additional indirect interaction with pathogens occurs during competition for nutrients and space, antibiotic production, colonization, induced systemic resistance (ISR), and parasitism against target plant pathogens (Kloepper et al., 2004; Kim et al., 2012); however, antagonistic microorganisms often do not exhibit consistent disease suppression compared to the commercial fungicides (Sang et al., 2013). Plant growth-promoting rhizobacteria (PGPR) are antagonistic to plant pathogens as they produce secondary metabolites, including siderophores, lytic enzymes, and antibiotics (Conn et al., 2008); they also produce plant growth regulators, such as indole-3-acetic acid (IAA), and solubilization of insoluble phosphates (Goswami et al., 2016).

There are several studies on antibiotic production by antagonistic microbes, such as *Bacillus* sp., *Pseudomonas* sp., and *Streptomyces* sp. (Beneduzi et al., 2012; Ngalimat et al., 2021; Yang et al., 2021). *Bacillus* spp., produce spores, which may be used to develop an effective microbial biopesticide formulation in the form of a biocontrol agent (BCA). Previously, many studies have demonstrated that several secondary metabolites produced by antagonistic bacteria play key roles in controlling various phytopathogens (Han et al., 2015). To date, there have been no reports on the isolation of these bacteria from the edible mushroom, locally known as "Sanghwang." It is a popular medicinal mushroom wildly cultivated in China, Japan, and Korea (Chen et al., 2016). This is grown on different trees, such as Oak and mulberry (Sliva, 2010), and being used as a traditional medicine to treat various health disorders, such as inflammation, gastroenteric, lymphatic diseases, and cancers (Jang et al., 2015). This further may exhibits biocontrol potential against anthracnose caused by *C. acutatum* in red pepper. This study sought to meet two key objectives: (i) evaluate the potential efficacy of the selected PGPR strain, *Bacillus tequilensis* GYUN-300, as a BCA against red pepper anthracnose under *in vitro* and field conditions; and (ii) evaluate its complete genome sequence for determining divergent genomic characteristics among other *Bacillus* strains.

MATERIALS AND METHODS

Isolation of Antagonistic Bacteria From Mushroom

Fresh sanghwang mushrooms were purchased from the local traditional market and thoroughly washed with water in the laboratory. Thereafter, 5 g of mushroom was ground in 10 mL sterilized distilled water (SDW) and diluted to 10^{-8}. Next, 100 μL of the diluted samples were plated onto nutrient agar plates; single colonies were selected 48 h after incubation at 28°C. Of the 20 total isolates obtained, only one isolate (i.e., GYUN-300) was selected for further study based on primary screening on *in vitro* antagonistic activity.

[1] https://kostat.go.kr

Source of Fungal Pathogens Used

The pathogen *C. acutatum* KACC42403 as obtained from Korean Agricultural Culture Collection (KACC), Agricultural Microbiology Division, RDA, South Korea. Other two pathogens, *C. acutatum* ANBPC, and *C. acutatum* ANYPC, were isolated from the infected fruits. After cutting the small sections of the lesion from the infected fruit, they were surfaces sterilized in 70% ethanol for 30 s and were rinsed twice in SDW. Thus, surface sterilized tissues were placed onto potato dextrose agar (PDA) medium. The fungal colonies were obtained after incubating the plates at 25°C for 7 days. The isolates ANBPC and ANYPC were recovered from these colonies. The cultures were stored on PDA plates at 10°C for further use.

In vitro Antagonistic Activity of GYUN-300

Bacteria isolated from sanghwang mushrooms were diluted to 10^{-6} and 10^{-5} in SDW and placed onto tryptic soy agar (TSA) plates. Out of several bacterial isolates, only GYUN-300 was selected based on its *in vitro* antagonistic activity against *C. acutatum* isolates. The isolate GYUN-300 was maintained at −80°C in tryptic soy broth (TSB) with glycerol (20%) for long-term storage. To prepare bacterial suspensions, a culture from the −80°C stock was grown on TSA plates for 3 days at 28°C; single colonies were transferred to TSB and incubated for 48 h at 28°C under shaking conditions (150 rpm). Bacteria were pelleted after centrifugation for 5 min at 8,000 × *g* and suspended in SDW to obtain a final concentration of 1×10^6 colony-forming units (CFU)/mL prior to application. The *in vitro* antifungal activity of bacterial cell suspensions of GYUN-300 was tested against *C. acutatum* isolates using a dual culture plate assay. Briefly, the fungal pathogenic isolates, *C. acutatum* KACC42403, *C. acutatum* ANBPC, and *C. acutatum* ANYPC were cultured on potato dextrose agar (PDA) medium for 7 days at 25°C to obtain mycelial plugs for the *in vitro* antagonism tests. The mycelial plugs (6 mm in diameter) of *C. acutatum* were placed onto the center of the PDA plates, and 10 μl of antagonistic bacterial GYUN-300 cell suspensions (1×10^6 CFU/mL) impregnated on sterile paper discs (6 mm in diameter) were placed on the top, bottom, right, and left sides of the plate 30 mm away from the center of the plate; plates treated with SDW served as the non-treated control. The growth inhibition distance between the bacterial suspension and pathogen was measured 7 days after incubation at 25°C in comparison with the non-treated control. Each treatment consisted of five replicates (Petri dishes), and the experiment was carried out at least twice.

Preparation of Fungal Pathogen Inocula

Conidial suspensions (100 μL) were spread onto PDA plates and incubated at 25°C for 7 days. The conidia were harvested by pouring SDW onto a PDA plate containing pathogenic fungi, and scraped. The suspensions were filtered through a double-layered cheesecloth. The concentration of spore suspensions was adjusted to 10^5 conidia/mL using a hemocytometer prior to its application.

Inhibition of Spore Germination of *Colletotrichum acutatum* Through Treatment With GYUN-300 Bacterial Cell Suspensions

Conidial germination and appressorium formation from *C. acutatum* were tested on a cover glass surface treated with GYUN-300 bacterial suspensions and its culture filtrate (CF) using a method described by Kim et al. (1998). Briefly, conidia from the cultures grown on PDA plates for 7 days were harvested and washed twice with ice-cold SDW. Conidial suspensions (10^6 CFU/mL) of 100 μL were mixed into Eppendorf tubes containing bacterial cell suspensions of GYUN-300 or its CF, and incubated for 48 h at 25°C. Conidial germination and the formation of appressorium and primary hyphae in the GYUN-300 or its CF treatment were assessed at different durations (i.e., 8, 16, 24, 32, 40, and 48 h) in Petri dishes containing moist paper. At minimum, 50 measurements were carried out per structure with a ProgRes SpeedXT ^{core} 3 Imager microscope using a differential interference contrast illumination.

Inhibition of Fungal Mycelial Growth by Volatile Compounds From GYUN-300

An I-plate assay (Sharifi and Ryu, 2016) and dual culture plate assays (Chaurasia et al., 2004) were carried out to evaluate the ability of the GYUN-300 stain to inhibit fungal growth through the production of volatile compounds. For the I-plate assay, one compartment of the I-plate contained TSA medium to inoculate GYUN-300, while the other side contained PDA to culture the fungal pathogen, *C. acutatum* KACC42403; the plate treated with SDW served as the non-treated control. Mycelial growth inhibition was observed 7 days after incubation at 25°C. For the dual culture plate assay, a Petri dish containing PDA medium was inoculated with a pathogenic mycelial plug on one side just 10 mm from the edge of the plate, and cell suspensions of GYUN-300 were used to inoculate the other side just 10 mm from the edge of the plate, by streaking on the same Petri dish without contacting the fungal pathogen. The inhibitory effect of GYUN-300 on fungal mycelia was measured 7 days after incubation at 25°C. Each test was conducted in triplicate, and three independent measurements were taken for each plate.

Identification of Antagonistic Bacteria Using MicroLog System

The putative *Bacillus* isolate was tested for the utilization of 95 carbon sources using the BIOLOG program (Jeon et al., 2003). Briefly, bacterial cells cultured on TSA medium for 24 h at 28°C were suspended in an inoculating fluid (i.e., 0.4% NaCl, 0.03% Pluronic F-68, and 0.01% gellan gum). They were inoculated onto GENIII MicroPlates (BIOLOG Inc., BiOLOG GP MicroPlateTM, Hayward, CA, United States), and incubated at 28°C. After 24 h of incubation, turbidity in the wells was measured using a MicroLogTM 3-Automated Microstation system (BIOLOG, Hayward, CA, United States). Bacteria were identified using the MicroLog Gram-positive database (ver. 4.0; BIOLOG).

Molecular Identification of GYUN-300

The selective isolate, GYUN-300, was subjected to molecular identification based on the sequence homology of its 16S rDNA gene (Weisburg et al., 1991). The genomic DNA (gDNA) of GYUN-300 was isolated using a kit (BioFact Genomic DNA Extraction Kit, Biofact Co., Seoul, South Korea) as per the manufacturer's instructions. The 16S rDNA gene was amplified using polymerase chain reaction (PCR) with Taq DNA polymerase, and primers 27F (5'-AGA GTT TGA TCM TGG CTC AG-3') and 1492R (5'-GGY TAC CTT GTT ACG ACT T-3') were used for amplification. The thermal cycling conditions were: denaturation at 94°C for 5 min followed by 35 cycles at 94°C for 30 s, annealing at 55°C for 30 s, and extension at 72°C for 1 min. At the end of the cycle, the reaction mixture was held at 72°C for 10 min, and then cooled to 4°C. The PCR product was purified using a PCR gel purification kit (BIOFACT Co., Seoul, South Korea), according to the manufacturer's instructions. The purified PCR product was sequenced using an automated sequencer (Genetic Analyzer 3130; Applied Biosystems, Carlsbad, CA, United States), in which the same primers were used utilized. The sequence was compared with the reference bacterial species contained in a genomic database using the Basic Local Alignment Search Tool (BLAST) from the National Center for Biotechnology Information (NCBI). Sequence alignment and phylogenetic tree construction were carried out using the MEGA 4.0 program (Biodesign Institute, Tempe, AZ, United States).

GYUN-300 Whole-Genome Sequence Analysis and Annotation

Bacterial gDNA was extracted using a FastDNA^{TM} SPIN Kit for Soil (MP Biomedicals, Santa Anna, CA, United States), according to the manufacturer's instructions. The concentration of extracted DNA was determined using a Qubit 2.0 fluorometer (Invitrogen, Carlsbad, CA, United States). The contamination of DNA or the cultured strain was tested by sequencing the 16S rRNA gene using an ABI 3730 DNA sequencing machine (Applied Biosystems, Foster City, CA, United States). The integrity of the gDNA was verified using agarose gel electrophoresis, and quantified using a Qubit 2.0 fluorometer (Invitrogen, Carlsbad, CA, United States). Then, sequencing libraries were prepared according to the manufacturer's instructions for 20 kb template preparation using the BluePippin Size-Selection System using PacBio DNA Template Prep Kit 1.0. Briefly, 10 μg of the gDNA was sheared to 20 kb using g-tubes (Covaris); they were then purified, end-repaired, and the blunt-end SMARTbell adapters were ligated. The libraries were quantified using a Qubit 2.0 fluorometer (Invitrogen, Carlsbad, CA, United States) and qualified using the DNA 12000 chip (Agilent Technologies, Waldbronn, Germany). Subsequently, the libraries were sequenced using PacBio P6C4 chemistry in the 8-well SMART Cell v3 in PacBio RSII.

The genome of the GYUN-300 strain was constructed *de novo* using PacBio sequencing data; sequencing analysis was carried out at Chunlab, Inc., PacBio sequencing data were assembled with PacBio SMRT Analysis 2.3.0, using the HGAP2 protocol (Pacific Biosciences, Menlo Park, CA, Inc., United States); the resultant contigs of the PacBio sequencing data were prototyped using Circlator 1.4.0 (Sanger Institute). Gene-finding and functional annotation pipeline of the whole-genome assembly used in the EzBioCloud genome database, and the protein-coding sequences (CDSs) were predicted using Prodigal 2.6.2 (Hyatt et al., 2010). The gene encoding tRNA was identified using the tRNAscan-SE 1.3.1 (Schattner et al., 2005), while the rRNA and other non-coding RNAs were analyzed using the Rfam 12.0 database (Nawrocki and Eddy, 2013). The CRISPRs were detected by PilerCR 1.06 (Edgar, 2007) and CRT 1.2 (Bland et al., 2007). The CDSs were classified into groups based on their roles, referencing the orthologous groups[2] (EggNOG 4.5) (Powell et al., 2014). For more functional annotation, the predicted CDSs were compared with the Swissprot (UniProt Consortium, 2015), KEGG (Kanehisa et al., 2014), and SEED (Overbeek et al., 2005) databases using the UBLAST program (Edgar, 2007).

In vitro Enzyme Activity by Antagonistic Bacteria

The ability of bacteria to produce various enzymes, such as cellulase, protease, and amylase was tested under *in vitro* conditions. Cellulase production was assessed by inoculation of GYUN-300 cell suspensions on TSA media supplemented with 5 g/L carboxymethyl cellulose (CMC). Sterilized filter paper discs (6 mm diameter) impregnated with 10 μL bacterial cell suspensions were placed on Petri dishes at four sides 15–20 mm away from the edge of plates, then incubated at 28°C for 5 days. After pouring 0.1% Congo Red solution onto the surface of Petri dishes, and retained for 5–10 min; Plates were then de-stained using a 1 M NaCl solution. The development of a clear halo around the colonies indicated a positive reaction and the production of cellulase by bacteria. For protease activity, bacterial isolates were inoculated on gelatin media (i.e., gelatin 5 g, beef extract 3 g, protease peptone 5 g, agar 15 g, distilled water 1,000 mL); plates were then incubated at 28°C for 2–3 days. After dispensing plates with 1% tannic solution for 5 min for staining, they were washed with SDW; Protease activity was recorded through the development of a clear zone (halo) around the colonies, indicating that proteins were hydrolyzed by the bacteria. Amylase production was assessed through the inoculation of the GYUN-300 isolate on TSA media supplemented with 0.5% soluble starch. Sterile paper discs (6 mm) impregnated with bacterial cell suspensions were plated on solid media, and Petri dishes were incubated at 28°C for 2–3 days. After pouring iodine solution (0.3 g iodine and 0.6 g KI/L) on the surface of Petri plates, any clear halo development around colonies was indicative of a positive reaction and the production of amylase and degradation of starch by bacteria.

Determination of Siderophore Production and Phosphate Solubilization

The procedure developed by Schwyn and Neilands (1987) using Chrome Azurol S (CAS) media was used to evaluate

[2]http://eggnogdb.embl.de

the ability of bacteria to produce siderophores. Briefly, 10 μL GYUN-300 bacterial suspensions were inoculated on iron-free King B solid media and incubated at 28°C for 2–3 days. Then, CAS agar (15 mL) was poured onto the GYUN-300 bacterial cultures, and after a few hours the plates were checked for the appearance of a halo around bacterial colonies, with a color change from blue to orange. The halo diameter was calculated by subtracting the diameter of the colony from the total diameter of the halo and the colony, a procedure developed by Gaur (1990) was used to determine the ability of bacteria to degrade the inorganic phosphates from the soil. Briefly, sterile paper discs (6 mm diameter) impregnated with 10 μL of GYUN-300 bacterial suspensions were placed onto the surface of tricalcium phosphate medium (i.e., glucose 10 g, tricalcium phosphate 5 g, $MgCl_2$ $6H_2O$ 5 g, $MgSO_4$ $7H_2$ 0.025 g, $(NH_4)_2SO_4$ 0.1 g, agar 20 g, distilled water 1,000 mL). After 15 days of incubation at 28°C, the appearance of a halo around the colony indicated phosphate solubilization. The phosphate solubilization ability was directly reflected by the halo diameter size; all experiments were carried out in triplicate.

Disease Control of Red Pepper Anthracnose by GYUN-300 Bacterial Suspensions

An indoor experiment was conducted to examine the preventive and curative effects of GYUN-300 bacterial suspensions on anthracnose in wounded and non-wounded red pepper fruits (cv. Geochanghan). Fully ripened red pepper fruits, procured from the field were selected for the experiment. Fruits were surface sterilized in 70% ethanol for 3 min, immersed in 1% NaOCl for 1 min, and rinsed 2–3 times in SDW; the surface-sterilized red pepper fruits were air-dried at room temperature. Nearly five wounds were inflicted on the surface of fruits using a sterile needle, and one set of non-wounded red pepper fruits were also used in this experiment. To test for preventive effects, wounded or non-wounded fruits were treated with antagonistic bacterial suspensions of GYUN-300 (10^7 CFU/mL) using a spray method (50 μL per fruit). Fruits treated with chemical pyraclostrobin and SDW served as positive and negative controls, respectively. After sufficient drying at room temperature, 10 μL of *C. acutatum* spore suspensions (10^5 conidia/mL) were inoculated on wounded or non-wounded sites, dried at room temperature, then placed in plastic square plates (40 cm × 40 cm) containing filter paper under moist conditions. The disease index (DI), using the formula (DI = sum of disease ratings in fruits/total number of fruits assessed) was recorded 10 days after incubation at 25°C in comparison with a non-treated control, from which the control value (%) was calculated. To test for curative effects, wounded or non-wounded red pepper fruits were inoculated with 10 μL of *C. acutatum* spore suspensions (10^5 conidia/ml), dried at room temperature, and placed in plastic square plates (40 cm × 40 cm) containing wet paper to maintain the humidity. Plates were incubated at 25°C for 10 days, treated with antagonistic bacterial suspensions, and incubated at 25°C for another 4 days; then the disease index, from which the control value (%) was recorded. Fruits treated with pyraclostrobin and SDW served as positive and negative controls, respectively.

Effect of Antagonistic Bacteria on Growth in Red Pepper Seed Germination

Red pepper seeds (cv. Geochanghan) used for growth promotion were purchased from the local market. Seeds were washed with tap water to remove the coated chemical fungicides and then surface-disinfected with 1% NaOCl for 10 min; they were then rinsed in SDW and dried completely on filter paper. The bacterial inoculum was prepared by culturing on TSA plates for 3 days at 28°C, and cell suspensions were prepared at 10^6 CFU/mL prior to inoculation. *Bacillus velezensis* AK-0 and *Serratia plymuthica* GYUN-8 were used as positive controls. They are commercially available in the market as biocontrol agents (BCAs), with names, Tangeokil and Serratan for AK-0 and GYUN-8, respectively in Korea. These BCAs are produced by Koreabio, Co. Ltd., South Korea; while seeds treated with SDW served as negative controls. Dried seeds were coated with bacterial cell suspensions (10^6 CFU/mL) by immersing for 30 min, placed between double-layered wet papers, and incubated in a growth chamber at 25°C for 6 days. Then, seed germination (root length in mm) was measured and compared to that of the non-treated control; this experiment was repeated at least once.

Growth Promotion Effect on Red Pepper Seedlings

To investigate the ability of GYUN-300 to promote growth, surface-sterilized red pepper seeds were sown in plastic trays (36 pots per tray) containing garden soil. After germination, 3-week-old red pepper seedlings were soil drenched with 25 mL of 3-days-old cultured bacterial suspensions (10^6 CFU/mL) of GYUN-300, GYUN-8, or AK-0. Observations of growth promotion were recorded once every 7 days up to 40 days of the growing period; Seedlings were watered once every 3 days. The average length (cm) of seedlings was measured; this measurement was constrained to the length of the aboveground biomass. Four replications were used per treatment; each replication consisted of 20 seedlings under greenhouse conditions.

Fungicidal Resistance Test to GYUN-300 Bacterial Suspensions

To investigate the fungicidal resistance to GYUN-300, 11 types of chemical fungicides currently used to control red pepper anthracnose in Korea were used (**Supplementary Table 1**). A single colony of GYUN-300 was inoculated into TSB and incubated under shaking conditions (180 rpm) at 28°C for 3 days. From this, 100 μL of the suspensions were spread onto freshly prepared TSA plates. Sterile paper discs (6 mm in diameter) impregnated with 10 μL of chemical fungicides at different concentrations (i.e., 0.5×, 1.0×, and 2.0×) were placed onto the TSA plates. Results were observed after 3 days of incubation at 28°C; the experiment was carried out in triplicate. Bacterial resistance to fungicides was determined based on the inhibition zone.

Field Evaluation of the Application of GYUN-300 on Disease Suppression of Red Pepper Anthracnose

A field experiment was conducted to investigate the biological control of red pepper anthracnose using GYUN-300 antagonistic bacteria in Korea. At first, the seedlings were raised in plastic trays (36 pots per tray) by placing a single seed per pot. Three-week-old red pepper seedlings were transplanted to a field belongs to Andong National University, located at Andong, Gyeongbuk Province, South Korea. Seedlings were planted at a distance of 100 cm between rows and 40 cm between plants. After preparing the field, the soil was fertilized with NPK before starting the transplantation. The planting row was covered with non-woven fabric material for weed control. Antagonistic microorganism treatments were grouped into three: soil drenching, foliar spray, and foliar spray + soil drench. The GYUN-8 and AK-0 bacteria were used as positive controls, Pyraclostrobin was used as chemical control, and water treatment was served as non-treated control. Bacterial cell suspensions prepared at a concentration of 10^7 CFU/mL were used for all treatments. The field was irrigated 10 days intervals. The first dose was administered on June 17, 2020, and a total of nine treatments were administered at 10 days intervals until August 31, 2020. The pyraclostrobin emulsion was used as chemical control, and tap water was used as negative control. The disease incidence (%) was calculated from the disease index ratings (**Supplementary Table 2**). Four replications were used per treatment; each replication consisted of 20 plants under field conditions.

Statistical Analysis

The data were subjected to analysis of variance (ANOVA) using SAS JMP software ver. 3. (SAS Institute Inc, 1995). The experiments were set up as completely randomized block designs under field conditions. Significant differences between treatment means were determined using the least significant difference (LSD) at $p < 0.05$. All experiments were carried out at least twice; data were analyzed separately for each experiment. The results of one representative experiment are shown.

RESULTS

In vitro Antagonistic Activity of GYUN-300

The GYUN-300 bacterium was tested for *in vitro* antagonistic activity against three fungal pathogenic isolates; *C. acutatum* KACC42403, ACPP014, and ACPP015, all of which cause anthracnose disease in red pepper fruits (**Figure 1**). The mycelial growth of all three pathogenic fungal isolates was inhibited at a greater level than the non-treated control. Among the three fungal isolates, the mycelial growth of isolate *C. acutatum* KACC42403 was greatly inhibited by GYUN-300 7 days after incubation at 25°C, when compared the growth inhibition of the other two pathogens. GYUN-300 was most effective with an average inhibition zone of 28, 25.3, and 25.5 mm against *C. acutatum* KACC42403, ACPP014, and ACPP015, respectively (**Supplementary Table 3**). The dual culture plate assay on the PDA medium exhibited greater inhibition of mycelial growth of *C. acutatum* KACC42403 on PDA plates 5 days after incubation at 25°C, while growth inhibition was not observed in the non-treated control (**Figure 2**).

Effect of GYUN-300 Cell Suspensions or Culture Filtrate Treatment on Conidial Germination of *Colletotrichum acutatum* Under *in vitro* Conditions

When conidial spores of *C. acutatum* KACC42403 were treated with GYUN-300 bacterial cell suspensions (10^6 CFU/mL) or their CF under *in vitro* conditions, there were different levels of damages in the conidia germination and germ tube lengths; these were compared to the non-treated control. Conidial spore germination analysis using a hemocytometer showed greater inhibition percentage of spores after 16 h incubation in GYUN-300 cell suspensions-treated conidia compared to CF-treated conidia. After 48 h of incubation, the conidial germination rate was 40 and 43% in the GYUN-300 cell suspension and its CF treatments, respectively (**Figure 3A**); while the spore germination increased drastically in the non-treated control. GYUN-300-treated conidia resting on the hard glass surface did not germinate, while from 16 h onward, water-treated conidia germinated and formed appressoria through germ tubes (**Figure 3B**). At 48 h, all conidia had germinated and appressoria were formed through germ tubes in the water-treated control; this did not occur with the GYUN-300-treated conidia. At 16 h itself, there was a suppression of conidial germination, resulting in gall-like formation on the hyphal wall without further leading to germination during 48 h of incubation. This result suggests that GYUN-300 cell suspensions played a role effectively in suppressing conidial germination of *C. acutatum* KACC42403 (**Figure 3B**).

Inhibitory Effects of Volatile Organic Compounds Produced by GYUN-300 on *in vitro* Fungal Growth of *Colletotrichum acutatum*

We tested the effect of bacterial volatile organic compounds (VOCs) released by GYUN-300 cells on the inhibition of mycelial growth of *C. acutatum* KACC42403 under *in vitro* conditions using the I-plate or dual culture plate assays. Exposing *C. acutatum* KACC42403 to VOCs released by GYUN-300 bacterial suspensions significantly inhibited fungal mycelial growth 7 days after incubation at 25°C (**Figure 4**). When bacterial cells colonized the entire Petri dish, fungal growth had been drastically reduced by 20% greater in I-plate assay in comparison with the growth reduction of the same fungal pathogen in the dual culture plate assay. This was because the spread of the bacterial inoculum was relatively lower than that observed in the I-plate assay; the specific VOCs involved are yet to be determined.

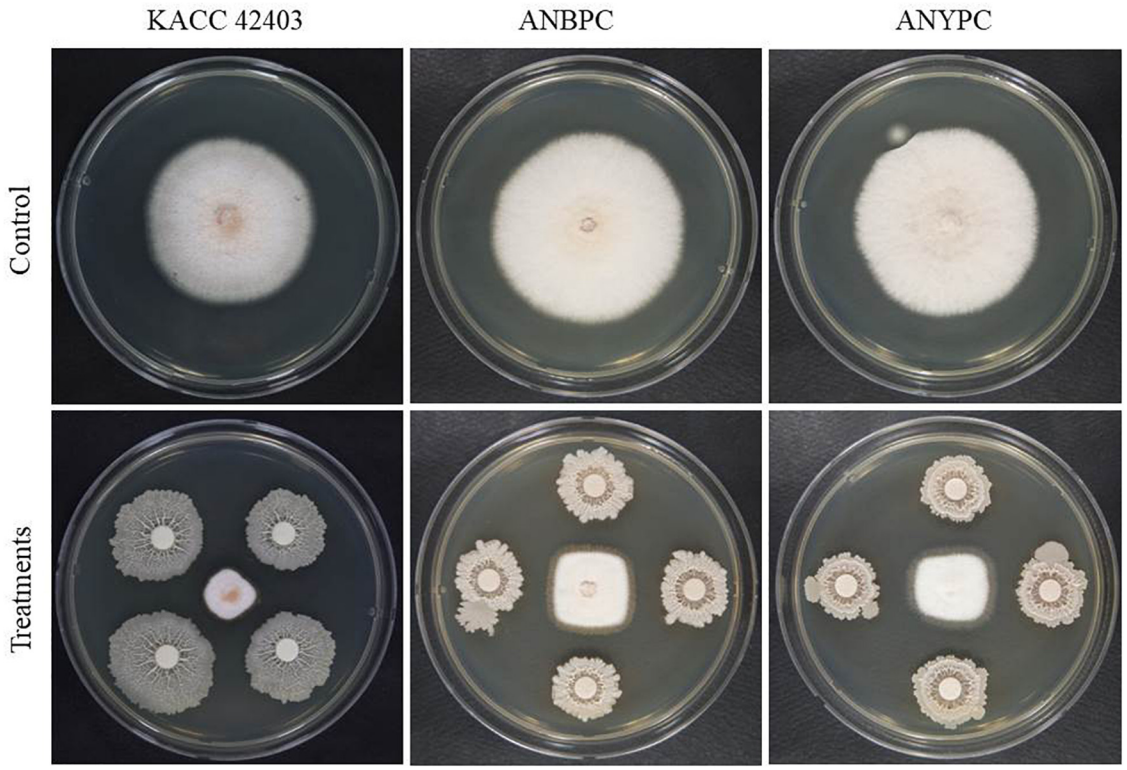

FIGURE 1 | *In vitro* antagonistic activity of *Bacillus tequilensis* GYUN-300 on the inhibition of Colletotrichum *acutatum* fungal stains in comparison with the non-treated control. Mycelial growth of fungal pathogens on potatoes dextrose agar plates was recorded 7 days after incubation at 25°C. The experiment was repeated at least once, with each treatment carried out in replicate.

Morphological Analysis of *Colletotrichum acutatum* in the Presence or Absence of GYUN-300 Cell Suspensions

Distinct morphological characterization of the mycelial growth of *C. acutatum* in the presence or absence of GYUN-300 cell suspensions were carried out *in vitro* using a dual culture plate assay (**Supplementary Figure 1**). The mycelium grown in the presence of GYUN-300 was elongated, where hyphae were formed producing gall-like formations on the mycelia. This was considered deformed mycelia, and mycelial growth was healthy without any signs of deformation when it was grown without the presence of the GYUN-300 cell suspensions.

Identification of Antagonistic Bacteria Using MicroLog System

The characteristics of GYUN-300 based on carbon source utilization and various chemical reagents assessed by the MicroLog system revealed that GYUN-300 was sensitive to various carbon sources, such as glycol-L-Proline, maltose, and D-fructose (**Supplementary Table 4**). By contrast, antibiotics, such as rifamycin SV, vancomycin, and minocycline, showed a negative reaction to the chemical substances (**Supplementary Table 5**). These traits were compared with *Bacillus subtilis*, where they were found to have a 57% probability of occurring compared with the existing database. The bacteria was identified as *Bacillus* sp., based on carbohydrate and chemical utilization, as this method identifies specific bacteria by matching with carbon utilization in the database.

Molecular Identification of GYUN-300

The isolate GYUN-300 was characterized using 16S rDNA gene sequencing. Comparison of the specific sequence of the ribosomal gene with sequences deposited in GenBank (accession no. OK001770) suggest that the GYUN-300 isolate belonged to the *Bacillus* genus, and shared the highest homology with *B. tequilensis* (99.93%). In the phylogenetic tree, GYUN-300 was clustered with other *Bacillus* spp. and was closely related to *B. tequilensis* (**Supplementary Figure 2**); thus, molecular characteristics confirmed this species as *B. tequilensis*. In the phylogenetic tree, the isolate was clustered with other *Bacillus* species that was closely related to *B. tequilensis*.

GYUN-300 Whole-Genome Sequence Analysis and Annotation

PacBio RSII NGS equipment was used at a sequencing depth of 179.34× to obtain complete sequence data for GYUN-300. The generated raw data were assembled using the HGAP2 protocol to obtain a FASTA file consisting of one contig. In

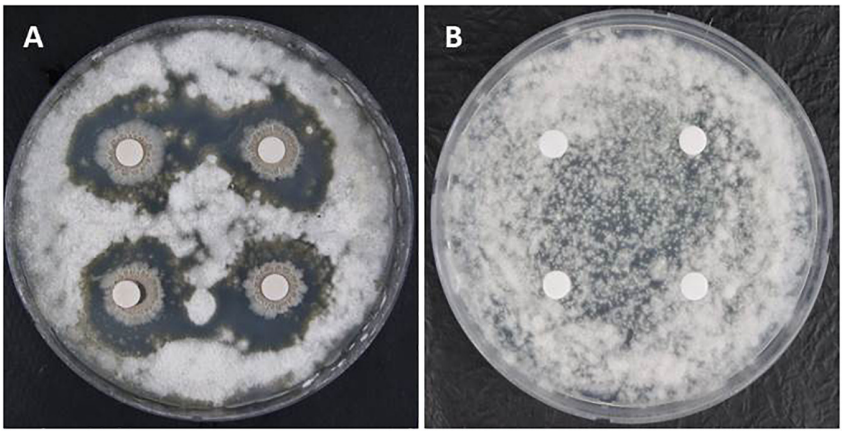

FIGURE 2 | Dual culture plate assay for the *in vitro* inhibition of *Colletotrichum acutatum* mycelial growth using an antagonistic bacterium GYUN-300: **(A)** sterile paper discs loaded with bacterial suspensions (10^8 CFU/mL) placed onto the potato dextrose agar (PDA) plates containing pathogenic fungal spores; and **(B)** sterile paper discs (6 mm in diameter) loaded with sterilized distilled water (SDW) served as the non-treated control. The inhibition zone was measured 7 days after incubation at 25°C. The experiment was repeated at least once, with each treatment carried out in triplicates (Petri dishes).

genome analysis, GYUN-300 was identified as *B. tequilensis*, where its core genome coverage was 96.7%. The genome of the *B. tequilensis* GYUN-300 (GYUN-300) strain consisted of a circular chromosome of 4,220,345 bp, with 4,789 predicted protein-coding sequences (CDSs), 38 rRNA genes, 86 rRNA genes, and an average G + C content of 43.6% based on the NCBI Prokaryotic Genomes Automatic Annotation Pipeline (PGAAP) analysis (**Figure 5A** and **Table 1**); the full genome sequence was deposited in NCBI under the GenBank accession number OK001770. Comparative analysis between the genome sequences of GYUN-300 and four other *Bacillus* strains showed a similar genome (**Table 1**). The genome of the GYUN-300 strain was compared with the four closest known evolutionary relatives: *B. subtilis* subsp. *subtilis* NCIB 3610, *B. subtilis* subsp. *spizizenii* TU-B-10, and *B. subtilis* subsp. *inaquosorum* KCTC 13429. Most genes in GYUN-300 were associated with secondary metabolite biosynthesis, transport, amino acid metabolism, carbohydrate metabolism, and catabolism. The first outer circle in the gray of the genome map represents one contig, the second circle represents the forward, the third circle represents the CDSs on the reverse strand, and the fourth circle indicates the tRNA and rRNA positions (**Figure 5A**). In addition to the gDNA, it was determined that the genome was likely to have an additional plasmid form. The fifth circle represents the GC skew, used as a reference point; values higher than this are indicated in green, while lower values are indicated in red. The sixth circle is GC ratio metric, where values greater than the average GC ratio, were expressed in blue, and lower values were represented in yellow; the GC skew and GC ratio were expressed at 10 kb intervals.

Venn diagrams (**Figure 5B**) compare the common CDSs among *B. tequilensis* GYUN-300, *B. subtilis* subsp. *subtilis* NCIB 3610, and *B. subtilis* subsp. *spizizenii* TU-B-10. This section summarizes the unique protein-encoding genes from the total genes of GYUN-300 is presented here. There were 3637 common high-expression gene families shared among GYUN-300, NCIB 3610, and TU-B-10 (**Figure 5B**), while 391, 113, and 389 genes were determined to be unique for GYUN-300, NCIB 3610, and TU-B-10, respectively. All predicted CDSs of GYUN-300 were compared in the clusters of orthologous genes (COG) database to identify homologous amino acid sequences. Each functionally annotated protein was assigned a COG number, representing a class of proteins; then, proteins were subjected to functional clustering analysis according to the COG function (**Figure 5C**). The detection of secondary metabolites from GYUN-300 was analyzed using antiSMASH (**Figure 5D**). A total of 12 biosynthetic gene clusters were detected in GYUN-300. Clusters 1, 3, 5, 7, and 12 showed 100% similarity to fengycin, sublancin 168 A, bacillibactin, subtilosinA, and bacillaene, respectively; cluster 10 showed 78% similarity to surfactin.

Production of Lytic Enzymes, Siderophore Production, and Phosphate Solubilization by Antagonistic Bacteria

The antagonistic bacterium, GYUN-300, was considered for the production of hydrolyzing enzymes, such as cellulase, protease, and amylase, under *in vitro* conditions (**Supplementary Figure 3A**). GYUN-300 was found to produce protease at a greater level with an average inhibition zone of 25 mm. By contrast, other enzymatic activities, such as cellulase and amylase, had inhibition zones of 18 and 23 mm, respectively. GYUN-300 displayed strong inhibitory activity against fungal pathogens and showed strong amylase activity (**Supplementary Figure 3A**). There was greater production of all three enzymes (i.e., cellulase, protease, and amylase) by GYUN-300 compared with the non-treated control (SDW); this was in terms of inhibition zones around inoculation sites on the solid media in Petri dishes through the degradation of various substrates, such as CMC, proteins, and soluble starch, respectively.

The capacity of GYUN-300 to produce siderophores was qualitatively observed using a CAS assay. The positive reaction

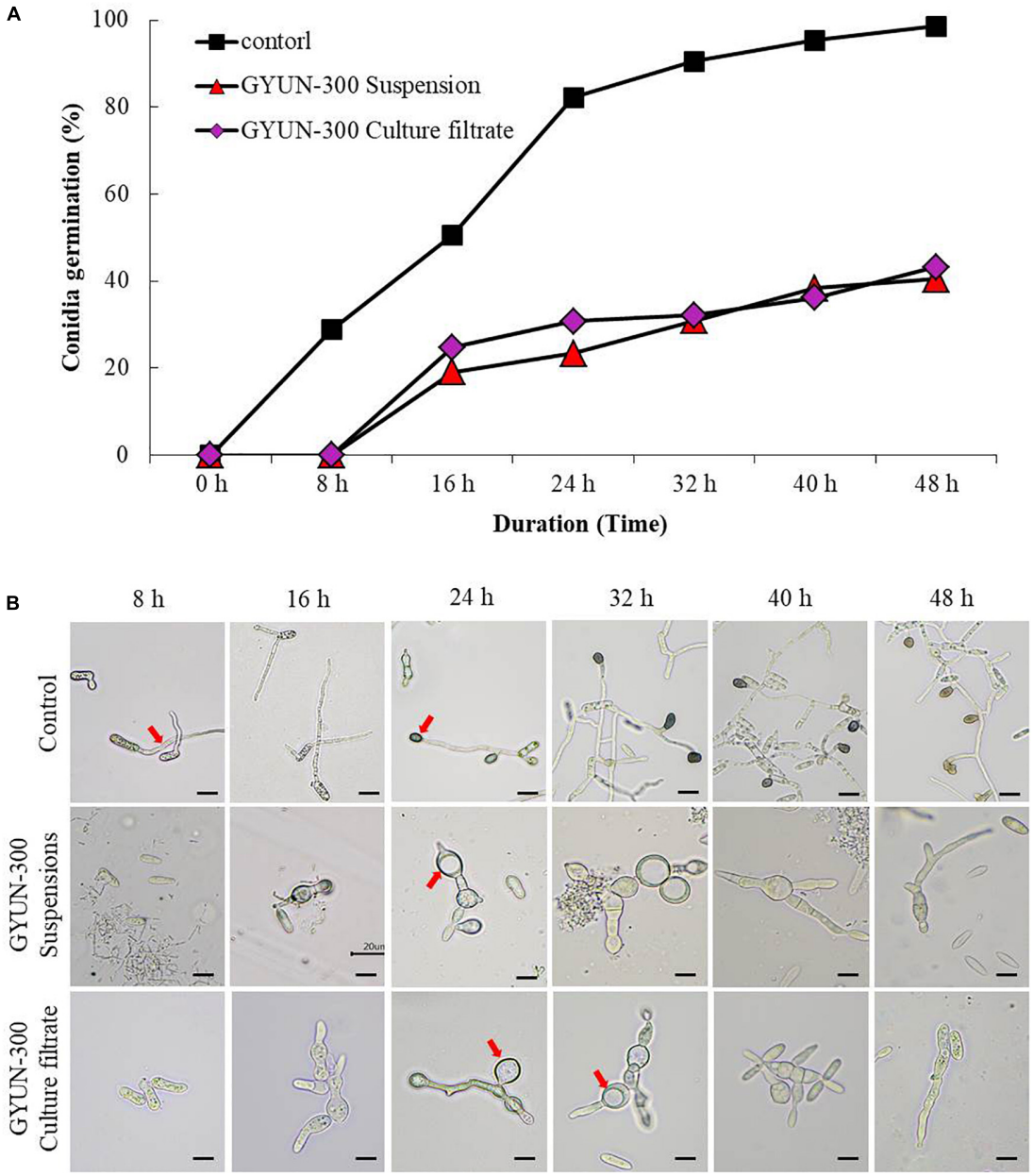

FIGURE 3 | Effect of bacterial cell suspensions and culture filtrate (CF) of *Bacillus tequilensis* GYUN-300 treatment on conidia germination rate (%) of *Colletotrichum acutatum* and microscopic observation: **(A)** Conidial germination rate (%) was suppressed by CF and bacterial cell suspensions, while the germination rate (%) was increased in the non-treated control; and **(B)** microscopic observations of *C. acutatum* fungal spore germination after GYUN-300 treatment during the incubation period from 8 to 48 h. The germination counting was carried out using a hemocytometer. Bar = 10 μm. The experiment was repeated at least once, with treatments repeated in triplicate producing similar results.

of the qualitative assay results in a color change in the CAS agar medium from blue to orange around the inoculation site (**Supplementary Figure 3B**). The color changed from blue to light orange 4 days after incubating the plates at 28°C, while there was no color development around the non-treated control (SDW). This result suggests that siderophores produced by this bacterium helped to obtain dissolved iron by binding to Fe^{3+}; this enables competition with pathogens for available iron, which is essential for survival. The phosphate solubilization ability of the bacterium GYUN-300 was determined on tricalcium phosphate medium, where GYUN-300 solubilized the inorganic phosphate at a moderate level. This converted phosphorous into an available form, which is important as it is one of the major essential macronutrients for plant growth and development (**Supplementary Figure 3B**); there was no growth inhibition in the water-treated control.

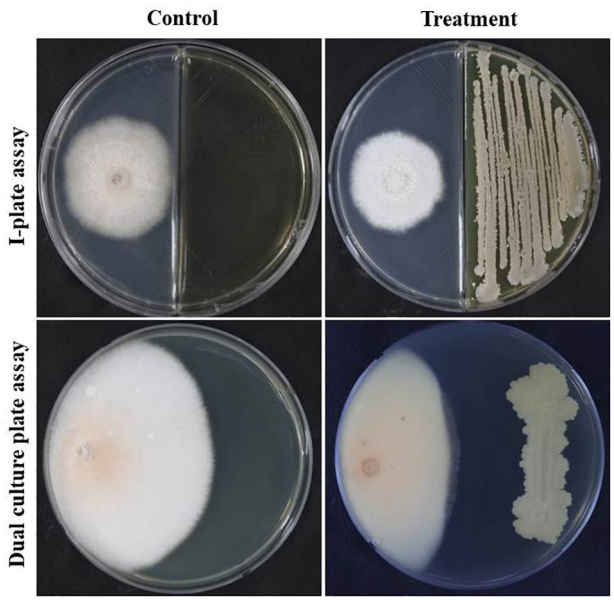

FIGURE 4 | Inhibition of *Colletotrichum acutatum* mycelial growth by bacterial volatiles produced by GYUN-300 under *in vitro* conditions using the I-plate and dual culture plate assays. Growth inhibition was observed in the I-plate and dual culture plate assays by volatiles in comparison with the non-treated control.

Control of Red Pepper Anthracnose by GYUN-300 Bacterial Suspensions

For anthracnose disease control by GYUN-300 bacterial suspensions, the red pepper fruits were treated with conidia suspensions on wounded or non-wounded fruits. In terms of preventive effects, where fruits were inoculated with pathogens after treatment with bacterial suspensions, the GYUN-300 bacterial treatment significantly ($P < 0.05$) controlled the anthracnose by 66.6%. This was higher than the chemical, GYUN-8, and AK-0 treatments, where they controlled the anthracnose by 56.6, 40, and 62.5%, respectively (**Figure 6A**). By contrast, in terms of the curative effect of wounded red pepper fruits, the GYUN-300 treatment controlled the anthracnose by 38.3%; this level of control was lower than the other treatments (**Figure 6B**). GYUN-300 treatment by the preventive method was better than the curative effect in wounded red pepper fruits. When GYUN-300 treatment was tested on non-wounded red pepper fruits, there was no significant difference in the control value among the three treatments. However, GYUN-8 treatment exhibited a greater control value (95.8%) than the other three treatments in terms of its protective effect (**Figure 7A**). In terms of the curative effects, the disease control using the chemical, GYUN-300, and AK-0 treatments was the same as that for the protective effects of non-wounded red pepper fruits; however, the GYUN-8 treatment exhibited less control than its protective effect (**Figure 7B**). The level of disease control with the non-treated control was zero in all treatments. These results suggest that the GYUN-300 strain is more effective as a preventive method compared to its curative effect.

Effect of GYUN-300 Treatment on Seed Germination and Growth Promotion in Red Pepper

A double-layered wet paper method was used to evaluate the growth promoting effect of GYUN-300 on red pepper seed germination under *in vitro* conditions. The average length of seedlings was higher in the AK-0 treated seedlings than other treatments (**Supplementary Figure 4A**). However, seedling length in GYUN-300 treated seedlings was higher than the non-treated control and GYUN-8-treated seedlings. The average seedling lengths were 31.7, 29.2, 39.6, and 25.3 mm, in the GYUN-300, GYUN-8, AK-0 treatments, and control, respectively. Similarly, the plant growth-promoting ability of GYUN-300 on red pepper seedlings was greater in terms of plant height compared to that in the non-treated control and other treatments, such as GYUN-8 and AK-0 (**Supplementary Figure 4B**); this indicates that GYUN-300 may be used for growth promotion.

Fungicidal Resistance to the Bacterium GYUN-300

The GYUN-300 strain was tested for resistance against various chemical fungicides under *in vitro* conditions. The bacterium GYUN-300 showed resistance against nine of the ten chemical fungicides tested in this study; while the bacterium showed sensitive to the fungicide Acibenzolar-S-methyl/Chlorothalonil, which inhibited bacterial growth on the TSA plates (**Supplementary Table 6**). This result suggests that most chemical fungicides used to control red pepper anthracnose do not affect GYUN-300 cell growth. These results suggest that GYUN-300 cells may be used synergistically with the chemical fungicides to control plant disease.

Effect of GYUN-300 on Disease Control of Red Pepper Anthracnose Under Field Conditions

Based on the *in vitro* results of disease suppression by GYUN-300, we tested the ability of GYUN-300 bacterial cells to suppress red pepper anthracnose caused by *C. acutatum* under field conditions. There was greater reduction in disease incidence (%) in the GYUN-300 treatment by foliar spray in comparison with the soil drench or combined application of soil drench + foliar spray (**Figure 8**). The disease incidence (%) was recorded as only 14% at both concentrations (500× and 100×) of GYUN-300 cell suspensions using a foliar spray method, while the disease incidence was 24.5% by combined method of spray + soil drench. On the other hand, the disease incidence was found at a greater level (56%) in both positive controls GYUN-8 and AK-0 by foliar spray method. Whereas, the disease incidence in chemical control (Pyraclostrobin) was observed as 46.1%, this is better than positive controls and non-treated control. Overall, all treatments with GYUN-300 showed better performance in controlling disease incidence (%) compared with the chemical treatments and non-treated control. These results suggest that

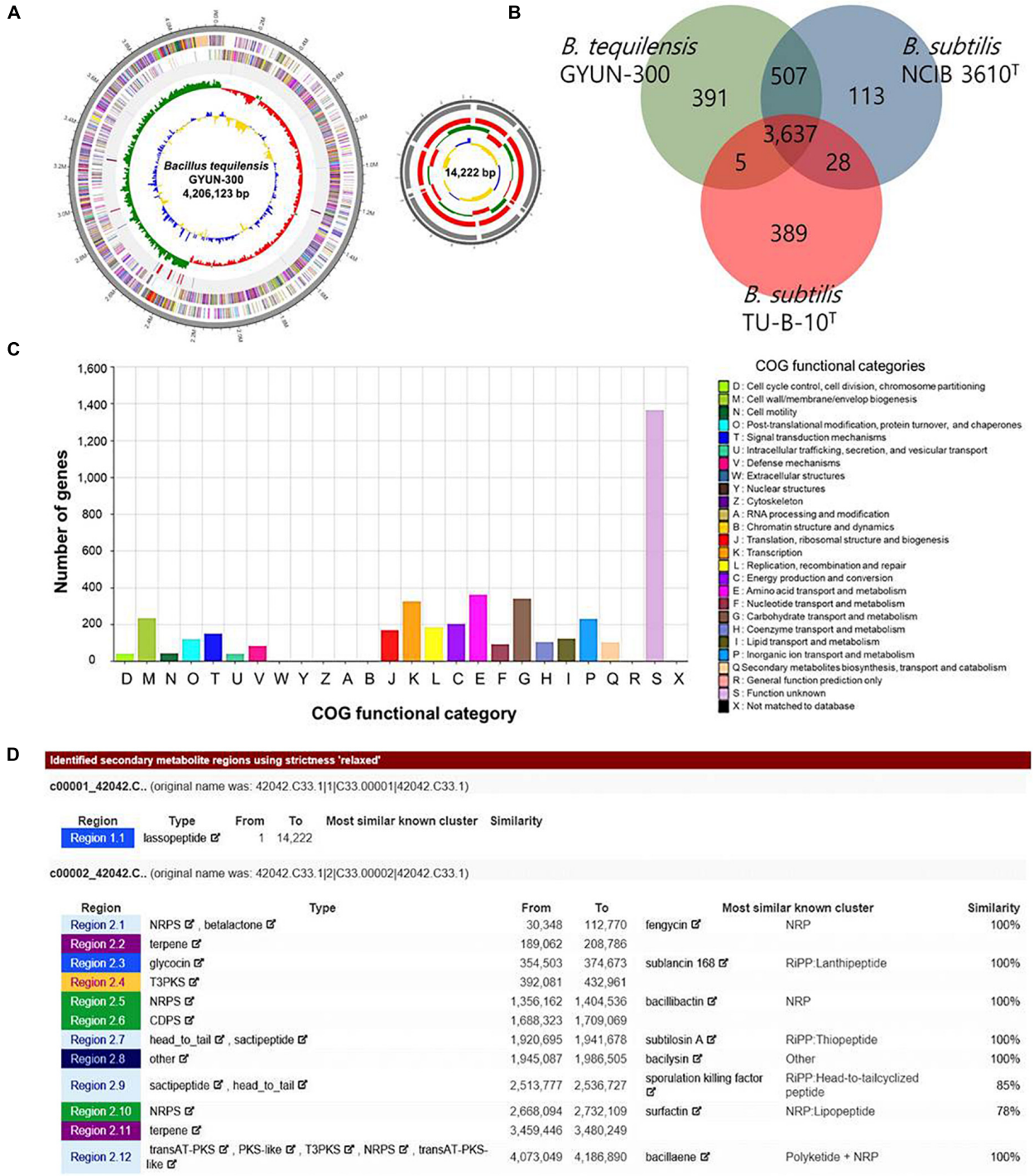

Region	Type	From	To	Most similar known cluster		Similarity
Region 1.1	lassopeptide	1	14,222			
Region 2.1	NRPS, betalactone	30,348	112,770	fengycin	NRP	100%
Region 2.2	terpene	189,062	208,786			
Region 2.3	glycocin	354,503	374,673	sublancin 168	RiPP:Lanthipeptide	100%
Region 2.4	T3PKS	392,081	432,961			
Region 2.5	NRPS	1,356,162	1,404,536	bacillibactin	NRP	100%
Region 2.6	CDPS	1,688,323	1,709,069			
Region 2.7	head_to_tail, sactipeptide	1,920,695	1,941,678	subtilosin A	RiPP:Thiopeptide	100%
Region 2.8	other	1,945,087	1,986,505	bacilysin	Other	100%
Region 2.9	sactipeptide, head_to_tail	2,513,777	2,536,727	sporulation killing factor	RiPP:Head-to-tailcyclized peptide	85%
Region 2.10	NRPS	2,668,094	2,732,109	surfactin	NRP:Lipopeptide	78%
Region 2.11	terpene	3,459,446	3,480,249			
Region 2.12	transAT-PKS, PKS-like, T3PKS, NRPS, transAT-PKS-like	4,073,049	4,186,890	bacillaene	Polyketide + NRP	100%

FIGURE 5 | Whole-genome map of *Bacillus tequilensis* GYUN-300 and annotation. **(A)** Marked characteristics shown from the outside to the center; coding sequence (CDS) on forward strand, CDS on reverse strand, tRNA, rRNA, guanine-cytosine (GC)-content, and GC skew. CDS genome consists of a single circular chromosome that is 4.2 mb in size, and represents one contig from the outer part of the circle; the second circle represents forward, the third represents reverse strain, and the fourth circle represents tRNA and rRNA positions; **(B)** distribution of orthologous genes in the *Bacillus tequilensis* GYUN-300, *B. subtilis* subsp. *subtilis* NCIB 3610^T, and *B. subtilis* subsp. *spizizenii* TU-B-10^T genomes. The Venn diagram shows the summary of unique SNPs from total genes of the *B. tequilensis* GYUN-300 strain. This analysis exploits all CDS of the genomes and is not restricted to the core genome; **(C)** the clusters of orthologous genes (COG) function annotation of *B. tequilensis* GYUN-300, and distribution of genes in different COG function categories; and **(D)** analysis of secondary metabolites of GYUN-300 using the antiSAMASH program.

TABLE 1 | Genomic features of the *Bacillus tequilensis* GYUN-300 genome and comparison with genomes of other *Bacillus* subsp. belonging to the *Bacillus subtilis* group.

Taxon name	Strain name	No. of contigs	Genome size	DNA G + C content (%)	No. of CDSs	No. of rRNA genes	No. of tRNA genes
B. tequilensis	GYUN-300	2	4 220 345	43.6	4,789	38	86
B. subtilis subsp. *subtilis*	NCIB 3610^T	2	4 299 822	43.3	4,329	30	88
B. subtilis subsp. *spizizenii*	TU-B-10^T	1	4 207 222	43.8	4,144	30	92
B. subtilis subsp. *inaquosorum*	KCTC 13429^T	1	4 350 498	43.8	4,280	27	86

GYUN-300 is a potential candidate for the biological control of red pepper anthracnose in Korea.

DISCUSSION

Bacillus species are widespread in and produce numerous antibiotic compounds that are active against several phytopathogens as an alternative to chemical fertilizers and synthetic pesticides (Shahid et al., 2021). In this study, we isolated the *B. tequilensis* GYUN-300 strain from fresh sanghwang mushroom, as it exhibits potent antagonistic activity against red pepper anthracnose caused by *C. acutatum* under *in vitro* and field conditions. Previously, several *Bacillus* species have demonstrated antagonistic activity against several *Colletotrichum* species, including *C. acutatum* (Han et al., 2015; Caulier et al., 2019).

This study describes the isolation, identification, and characterization of an antagonistic *Bacillus* sp. isolated from an edible mushroom. GYUN-300 was confirmed as *B. tequilensis* based on its morphology and the BIOLOG program results. Furthermore, the GYUN-300 strain was characterized by molecular analysis using 16S rDNA sequencing; this strain was identified as *B. tequilensis* GYUN-300. The GYUN-300 strain showed 99.9% homology with the reported database strains of other *B. tequilensis*. Anthracnose from *Colletotrichum* may cause considerable damage to various crops, including red pepper (Than et al., 2008; Kim et al., 2010); *Colletotrichum* spp. are frequently associated with several pepper diseases worldwide (Liu et al., 2016). There are limited reports on microbial-based control of anthracnose disease, and to the best of our knowledge, this is the first report on the use of the GYUN-300 as a potential BCA for red pepper anthracnose; this is also the first analysis of the whole-genome sequencing of GYUN-300. The results provide an understanding of the biocontrol mechanism of the GYUN-300 strain, providing a possible alternative BCA to control red pepper anthracnose in Korea.

It was found that treatment with GYUN-300 CF was equally effective as the cell suspensions in inhibiting the conidial germination of *C. acutatum* under *in vitro* conditions. Similarly, a recent study by Choub et al. (2021b) reported that the CF from *B. velezensis* CE100 exhibited antifungal activity against *Colletotrichum gloeosporioides* through the production of cyclic tetrapeptides from the CF. Another study reported that the CF from *B. subtilis* inhibited the growth and spore germination of *C. gloeosporioides* through mycolytic enzyme-mediated antagonism (Ashwini and Srividya, 2014). Recently, Sarwar et al. (2018) reported that the growth of various phytopathogens, such as *Fusarium moniliforme*, *Fusarium oxysporum*, *Fusarium solani*, and *Trichoderma atroviride*, was suppressed by *Bacillus* spp. through the production of a broad spectrum of lipopeptide biosurfactants. This is supported by recent reports (Jayapala et al., 2019; Wu et al., 2019), which have demonstrated that *Bacillus* spp. played a role in producing antibiotic compounds to protect red pepper from anthracnose and wilt diseases caused by *Colletotrichum capsici* and *Rhizoctonia solani*, respectively. Zalila-Kolsi et al. (2016) reported that a few *Bacillus* species isolated from wheat rhizosphere soil exhibited *in vitro* antagonistic activity against several phytopathogenic fungi, including *F. graminearum*, which causes durum wheat disease.

The microscopic observations in this study indicate that the suppressive effects of bacterial suspensions of GYUN-300 and its CF may be due to antibiosis mechanisms. The GYUN-300 strain affected the conidial germ tube and mycelial morphology of *C. acutatum* KACC42403, causing severe damage to the fungal hyphae. Numerous studies have demonstrated the antifungal mechanisms of soluble non-volatile bioactive compounds, such as lipopeptides and proteins, produced by various *Bacillus* species against several soil-borne diseases (Zhang et al., 2020). Conversely, the suppression of mycelial growth of fungal phytopathogens caused by bacterial antagonists has been attributed to VOCs, involved in biocontrol interactions by *Bacillus species* against fungal pathogens, such as *Botrytis cinerea* (Sharifi and Ryu, 2016), *Penicillium expansum*, *Alternaria alternata* (Gao et al., 2018), and *C. gloeosporioides* (Chowdhury et al., 2015).

The whole-genome sequence of GYUN-300 was characterized; this consisted of a 4.22 Mb chromosome, and this genome was compared to other *Bacillus* species (**Table 1**). In particular, biocontrol-related genes and gene clusters involved in the antibiotic may produce differences in biocontrol targets and efficacy between GYUN-300 and other *Bacillus subtilis* strains. These results suggest that all other strains may prevent the host plant from the disease by genes involved in the synthesis of secondary metabolites and exhibit strong antifungal activities against various fungal phytopathogens (Pusztahelyi et al., 2015; Costa et al., 2019). *Bacillus* species produce cyclic lipopeptides (CLPs), known for their broad-spectrum antagonistic activity mediated by secondary metabolites (Kim et al., 2021). This may have contributed to antagonistic activity against *C. acutatum*. Whole-genome comparisons revealed that the GYUN-300 strain showed high similarity to *B. subtilis* subsp. *subtilis* NCIB 3610^T, *B. subtilis* TU-B-10^T, and *B. subtilis* subsp. *inaquosorm* KCTC

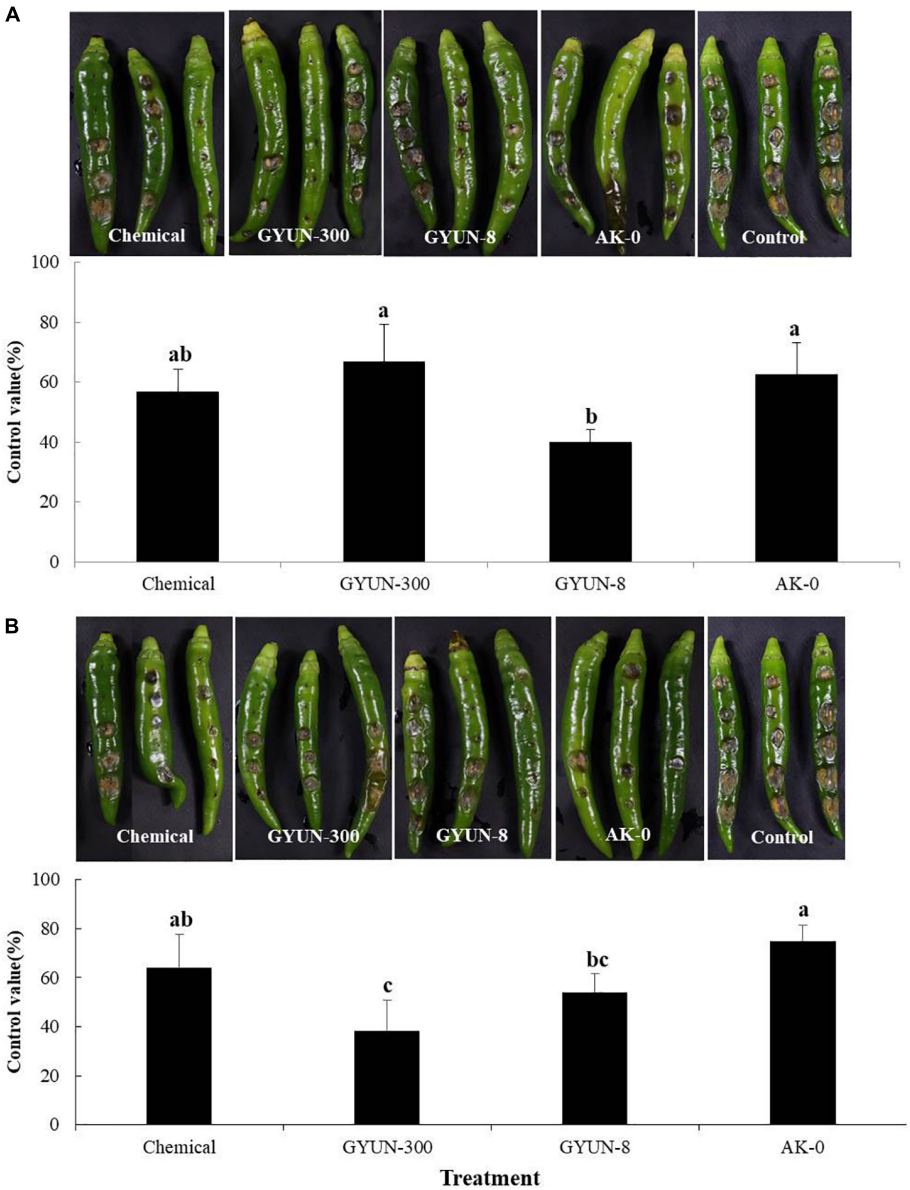

FIGURE 6 | Protective and curative effects of GYUN-300 on disease suppression of red pepper anthracnose in wounded fruits. **(A)** For protective effects, bacterial suspensions (10^7 CFU/mL) were sprayed on the detached green pepper fruits, followed by inoculation with *Colletotrichum acutatum* conidia suspensions (10^5 conidia/mL) on the same day. The disease severity (%) was recorded 10 days after incubation at 25°C. **(B)** For curative effects, symptom development was observed 10 days after pathogen inoculation with *C. acutatum* conidia suspensions (10^5 conidia/mL) on detached green pepper fruits, followed by treatment with bacterial suspensions (10^7 CFU/mL) using a spray method. Disease severity (%) was recorded 10 days after incubation at 25°C. The experiment was carried out two times with six replicates (fruits) per treatment, showing similar results. Bars with the same letters do not differ significantly between each other according to the least significant difference (LSD; $p < 0.05$).

13429^T strains currently used as BCAs in field conditions (Zhang et al., 2016; Gu et al., 2021). The COG database was used to functionally categorize predicted proteins from the distribution of genes (Galperin et al., 2015), and the COG categories were compared among the four strains, including GYUN-300. The COGs of the four strains showed highly similar distributions, suggesting that these strains have comparable biological characteristics. A total of 12 putative biosynthetic gene clusters for secondary metabolites were detected in the GYUN-300 genome. Some are involved in the metabolism of amino acids, carbohydrates, lipid transport and metabolism, and catabolism of secondary metabolite biosynthesis (Zhang et al., 2016). These functions are important for antagonistic agents against various phytopathogens, including *C. acutatum*, which causes red pepper anthracnose. The genome of GYUN-300 was investigated for the presence of gene clusters involved in the biosynthesis of CLPs that

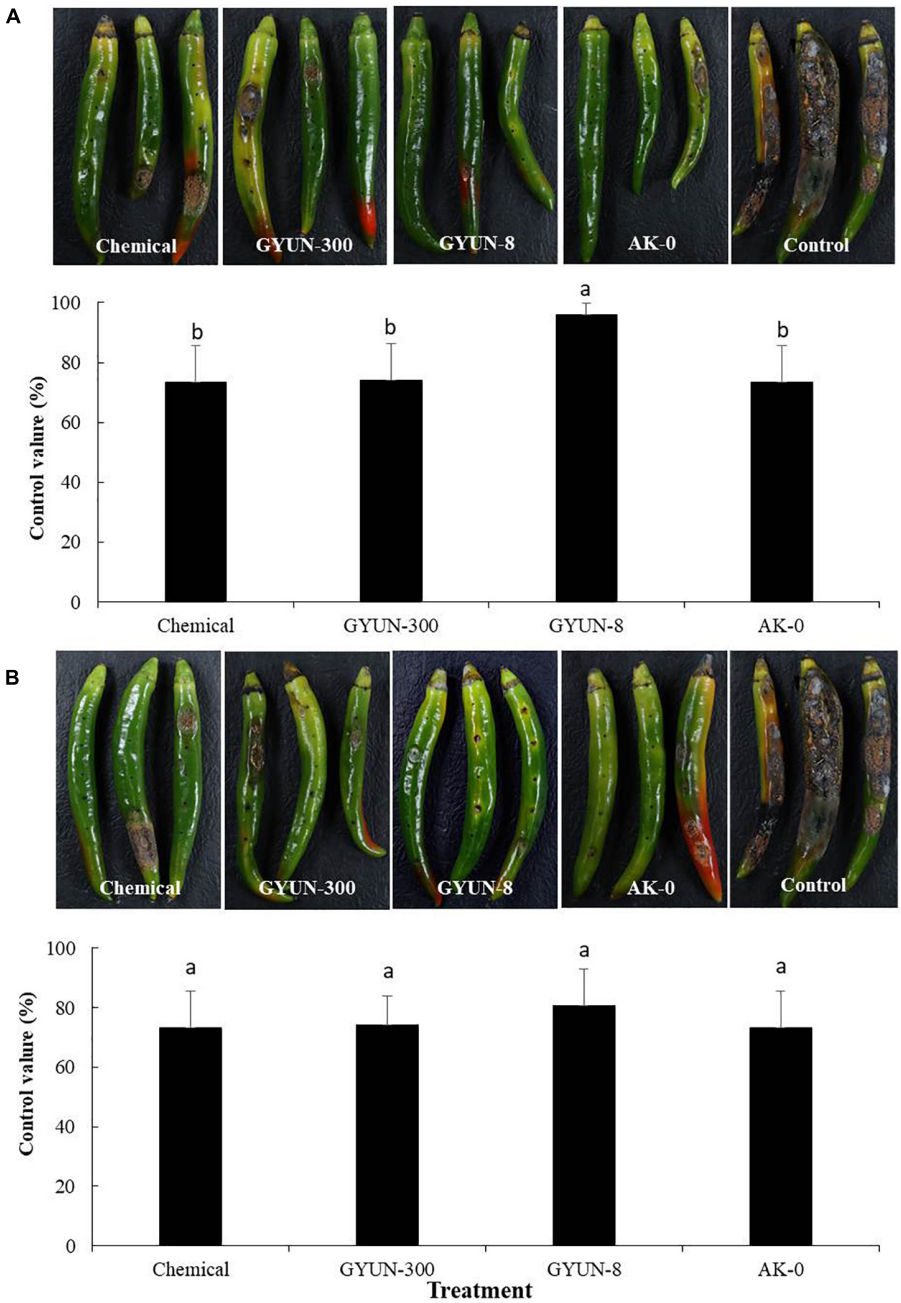

FIGURE 7 | Protective and curative effects of GYUN-300 on disease suppression of red pepper anthracnose in non-wounded fruits. **(A)** For protective effects, bacterial suspensions (10^7 CFU/mL) were sprayed on the detached green pepper fruits without wounding, followed by inoculation with *Colletotrichum acutatum* conidia suspensions (10^5 conidia/ml) on the same day. Disease severity (%) was recorded 14 days after incubation at 25°C. **(B)** For curative effects, symptoms were observed 14 days after pathogen inoculation with *C. acutatum* conidia suspensions (10^5 conidia/mL) on detached green pepper fruits without wounding, followed by treatment with bacterial suspensions (10^7 CFU/mL) using a spray method. Disease severity (%) was recorded 10 days after incubation at 25°C. The experiment was carried out two times with six replicates (fruits) per treatment, showing similar results. Bars with the same letters do not differ significantly between each other according to the least significant difference (LSD; $p < 0.05$).

were predicted by antiSMASH analysis; this is a web server and stand-alone tool for the automatic genomic identification and analysis of biosynthetic gene clusters.[3]

[3]http://antismash.secondarymetabolites.org

Furthermore, the GYUN-300 strain produced hydrolytic enzymes, such as cellulase, protease, amylase, and siderophores, as well as phosphate solubilization, which are common features of antagonistic bacterial isolates (Belbahri et al., 2017). Siderophores are powerful ferric iron-chelating

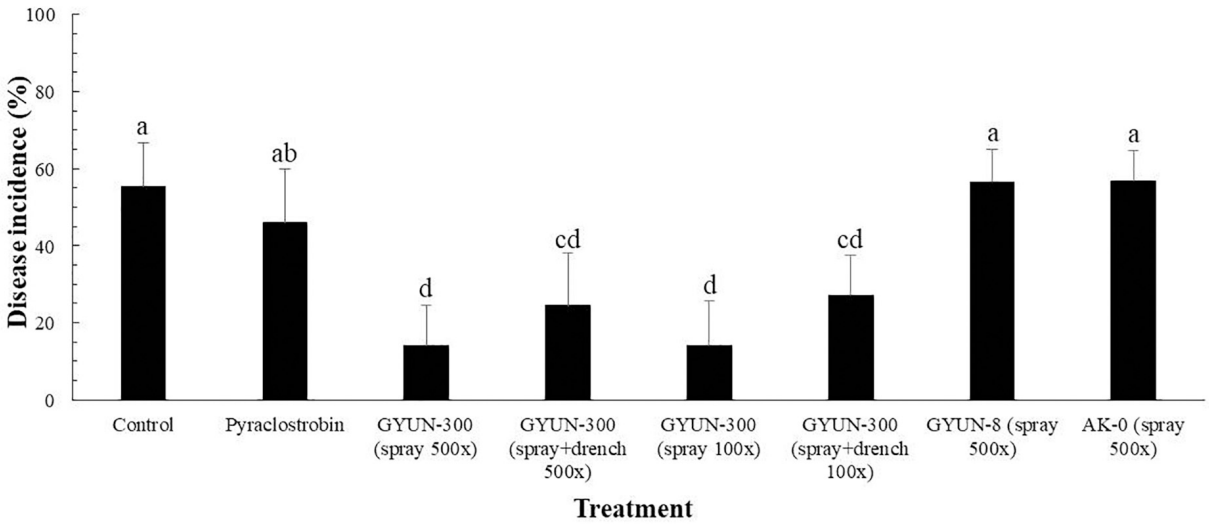

FIGURE 8 | Effect of GYUN-300 treatment on disease suppression of anthracnose caused by *Colletotrichum acutatum* under field conditions. Various treatments of GYUN-300 were compared with the chemical controls and non-treated control. Bars with the same letters do not differ significantly between each other according to the least significant difference (LSD; $p < 0.05$).

molecules produced by microorganisms that acquire iron, which is essential for crop growth. Siderophores differ from one another in their chemical structure and properties (Ahmed and Holmström, 2014), and have been suggested as environment-friendly alternatives to hazardous pesticides (Schenk et al., 2012). Siderophore-producing bacteria improve iron nutrition and slow down pathogen growth by limiting iron availability for pathogens (Nabila and Kasiamdari, 2021). However, the development of fungicide resistance in antagonistic bacteria is an increasing threat in plant disease management (Alizadeh et al., 2020). At times, the antagonistic bacteria in combination with agrochemicals are effective in suppressing pathogen growth at a greater level when compared with individual treatments under field conditions (Ons et al., 2020). This is in agreement with the results from this study, suggesting that GYUN-300 cell suspensions may be used in synergy with chemical fungicides.

The red pepper anthracnose disease was suppressed by GYUN-300 at a greater level in comparison with other positive controls, such as GYUN-8 and AK-0, and chemical control under field conditions. Similarly, a recent study by Choub et al. (2021a) reported that the field application of *B. velezensis* CE 100 culture broth resulted in a 1.3-fold and 6.9-fold decrease in anthracnose disease severity on walnut trees compared to the conventional and control groups, respectively. Previously, Park et al. (2001) reported to suppress the anthracnose disease in cucumber by the application of *Bacillus amyloliquefaciens* EXTN-1, and another strain *Bacillus vallismortis* BS07 suppressed the disease incidence (%) of anthracnose caused by *C. acutatum* on red pepper fruits at a greater level in comparison with the chemical control under field conditions (Park et al., 2013), which is in agreement with our results. Additionally, our results are supported by a recent study (Prihatiningsih et al., 2019), which displayed the control of red pepper anthracnose using microencapsulated *B. subtilis* B298 by spray method under field conditions. On the other hand, recently our team (Kim et al., 2021) reported to show the disease control of anthracnose caused by *C. gloeosporioides* on fresh apples using a biocontrol agent *B. velezensis* AK-0.

In conclusion, the GYUN-300 strain isolated from the edible sanghwang mushroom exhibited significant antagonistic activity against red pepper anthracnose caused by *C. acutatum*. The strain was identified as *B. tequilensis* GYUN-300 based on whole-genome sequence analysis. The strain exhibits *in vitro* antagonistic activity and suppression of conidial germination and *in planta* disease control of anthracnose. GYUN-300 suspension treatment has also demonstrated to control red pepper anthracnose in field conditions in Andong, Gyeongbuk Province, South Korea. Whole-genome sequencing revealed that the core genome of GYUN-300 was very similar to various *B. subtilis* strains. The differences between the various *B. tequilensis* strains in terms of control targets and efficacies may be attributed to variations in genes or gene clusters responsible for the biocontrol mechanism. Several CLP products of this strain were determined by analyzing secondary metabolite BGCs using antiSMASH software. GYUN-300 possessed several biosynthetic compounds, which may play an important role in controlling red pepper anthracnose through a mechanism of antibiosis. Overall, the results of this study indicate that GYUN-300 shows as an eco-friendly BCA against phytopathogens. Future research should investigate the signaling pathways involved in the antagonistic effects of secondary metabolites against pathogenic fungi.

DATA AVAILABILITY STATEMENT

The datasets presented in this study can be found in online repositories. The names of the repository/repositories and accession number(s) can be found in the article/ **Supplementary Material**.

AUTHOR CONTRIBUTIONS

H-TK and YL designed the experimental setup and performed laboratory experiments. JK involved in the field experiment. KB and HK analyzed the data and wrote the manuscript. YJ supervised the project. All authors have reviewed and approved the manuscript.

FUNDING

This work was supported by the Korean Institute of Planning and Evaluation for Technology in Food, Agriculture, Forestry (IPET) through the Crop Viruses and Pests Response Industry Technology Development Program, funded by the Ministry of Agriculture, Food, and Rural Affairs (MAFRA; Grant No. 320042-5).

SUPPLEMENTARY MATERIAL

The Supplementary Material for this article can be found online at: https://www.frontiersin.org/articles/10.3389/fmicb.2022.826827/full#supplementary-material

REFERENCES

Ahmed, E., and Holmström, S. J. M. (2014). Siderophores in environmental research: roles and applications. *Microb. Biotechnol.* 7, 196–208. doi: 10.1111/1751-7915.12117

Ali, A., Bordoh, P. K., Singh, A., Siddiqui, Y., and Droby, S. (2016). Post-harvest development of anthracnose in pepper (*Capsicum* spp): etiology and management strategies. *Crop Prot.* 90, 132–141.

Ali, A., Wei, Y. Z., and Mustafa, M. A. (2015). Exploiting propolis as an antimicrobial edible coating to control post-harvest anthracnose of bell pepper. *Pack. Tech. Sci*. 28, 173–179.

Alizadeh, M., Vasebi, Y., and Safaie, N. (2020). Microbial antagonists against plant pathogens in Iran: a review. *Open Agric.* 5, 404–440.

Ashwini, N. and Srividya, S. (2014). Potentiality of Bacillus subtilis as biocontrol agent for management of anthracnose disease of chilli caused by Colletotrichum gloeosporioides OGC1. *3 Biotech* 4, 127–136. doi: 10.1007/s13205-013-0134-4

Belbahri, L., Chenari Bouket, A., Rekik, I., Alenezi, F. N., Vallat, A., Luptakova, L., et al. (2017). Comparative genomics of *Bacillus amyloliquefaciens* strains reveals a core genome with traits for habitat adaptation and a secondary metabolites rich accessory genome. *Front. Microbiol.* 8:1438. doi: 10.3389/fmicb.2017.01438

Beneduzi, A., Ambrosini, A., and Passaglia, L. M. P. (2012). Plant growth-promoting *rhizobacteria* (PGPR): their potential as antagonists and biocontrol agents. *Genet. Mol. Biol.* 35, 1044–1051. doi: 10.1590/s1415-47572012000600020

Bland, C., Ramsey, T. L., Sabree, F., Lowe, M., Brown, K., Kyrpides, N. C., et al. (2007). CRISPR Recognition Tool (CRT): a tool for automatic detection of clustered regularly interspaced palindromic repeats. *BMC Bioinformatics* 8:209. doi: 10.1186/1471-2105-8-209

Bordoh, P. K., Ali, A., Dickinson, M., Siddiqui, Y., and Romanazzi, G. (2020). A review on the management of postharvest anthracnose in dragon fruits caused by *Colletotrichum* spp. *Crop Prot*. 130:105067.

Caulier, S., Nannan, C., Gillis, A., Licciardi, F., Bragard, C., and Mahillon, J. (2019). Overview of the antimicrobial compounds produced by members of the *Bacillus subtilis* group. *Front. Microbiol.* 10:302. doi: 10.3389/fmicb.2019.00302

Cellini, A., Spinelli, F., Donati, I., Ryu, C. M., and Kloepper, J. W. (2021). Bacterial volatile compound-based tools for crop management and quality. *Trends Plant Sci*. 26, 968–983. doi: 10.1016/j.tplants.2021.05.006

Chaurasia, B., Pandey, A., Palni, L. M. S., Trivedi, P., Kumar, B., and Colvin, N. (2004). Diffusible and volatile compounds produced by an antagonistic *Bacillus subtilis* strain cause structural deformations in pathogenic fungi in vitro. *Microbiol. Res.* 160, 75–80. doi: 10.1016/j.micres.2004.09.013

Chen, H., Tian, T., Miao, H., and Zhao, Y. Y. (2016). Traditional uses, fermentation, phytochemistry and pharmacology of *Phellinus linteus*: a review. *Fitoterapia* 113, 6–26. doi: 10.1016/j.fitote.2016.06.009

Choub, V., Maung, C. E. H., Won, S. J., Moon, J. H., Kim, K. Y., Han, Y. S., et al. (2021b). Antifungal Activity of Cyclic Tetrapeptide from *Bacillus velezensis* CE 100 against plant pathogen *Colletotrichum gloeosporioides*. *Pathogens* 10:209. doi: 10.3390/pathogens10020209

Choub, V., Ajuna, H. B., Won, S. J., Moon, J. H., Choi, S. I., Maung, C. E. H., et al. (2021a). Antifungal activity of *Bacillus velezensis* CE 100 against anthracnose disease (*Colletotrichum gloeosporioides*) and growth promotion of walnut (*Juglans regia* L.) trees. *Int. J. Mol. Sci*. 22:10438. doi: 10.3390/ijms221910438

Chowdhury, S. P., Hartmann, A., Gao, X., and Borriss, R. (2015). Biocontrol mechanism by root-associated *Bacillus amyloliquefaciens* FZB42–a review. *Front. Microbiol*. 6:780. doi: 10.3389/fmicb.2015.00780

Conn, V. M., Walker, A. R., and Franco, C. M. M. (2008). Endophytic actinobacteria induce defense pathways in *Arabidopsis thaliana*. *Mol. Plant Microbe Interact*. 21, 208–218. doi: 10.1094/MPMI-21-2-0208

Costa, J. H., Wassano, C. I., Angolini, C. F. F., Scherlach, K., Hertweck, C., and Fill, T. P. (2019). Antifungal potential of secondary metabolites involved in the interaction between citrus pathogens. *Sci. Rep*. 9:18647. doi: 10.1038/s41598-019-55204-9

De la Lastra, E., Camacho, M., and Capote, N. (2021). Soil bacteria as potential biological control agents of *Fusarium* species associated with asparagus decline syndrome. *Appl. Sci.* 11:8356.

Edgar, R. C. (2007). Piler-CR: fast and accurate identification of CRISPR repeats. *BMC Bioinformatics* 8:18. doi: 10.1186/1471-2105-8-18

Galperin, M. Y., Makarova, K. S., Wolf, Y. I., and Koonin, E. V. (2015). Expanded microbial genome coverage and improved protein family annotation in the COG database. *Nucleic Acids Res*. 43, D261–D269. doi: 10.1093/nar/gku1223

Gao, H., Li, P., Xu, X., Zeng, Q., and Guan, W. (2018). Research on Volatile Organic Compounds From *Bacillus subtilis* CF-3: biocontrol Effects on Fruit Fungal Pathogens and Dynamic Changes During Fermentation. *Front. Microbiol*. 9:456. doi: 10.3389/fmicb.2018.00456

Gaur, A. C. (1990). "Physiological functions of phosphate solubilizing microorganisms," in *Phosphate Solubilizing Micro-Organisms as Biofertilizers*, ed. A. C. Gaur (New Delhi: Omega Scientific Publisher), 16–72.

Goswami, D., Thakker, J. N., and Dhandhukia, P. C. (2016). Portraying mechanics of plant growth promoting *rhizobacteria* (PGPR): a review. *Cogent Food Agric.* 2:1127500.

Gu, X., Zeng, Q., Wang, Y., Li, J., Zhao, Y., Li, Y., et al. (2021). Comprehensive genomic analysis of *Bacillus subtilis* 9407 reveals its biocontrol potential against bacterial fruit blotch. *Phytopathol. Res.* 3:34.

Han, J. H., Shim, H., Shin, J. H., and Kim, K. S. (2015). Antagonistic activities of *Bacillus* spp. strains isolated from tidal flat sediment towards anthracnose pathogens *Colletotrichum acutatum* and *C. gloeosporioides* in South Korea. *Plant Pathol. J.* 31, 165–175. doi: 10.5423/PPJ.OA.03.2015.0036

Harp, T., Kuhn, P., Roberts, P. D., and Pernezny, K. L. (2014). Management and cross-infectivity potential of *Colletotrichum acutatum* causing anthracnose on bell pepper in Florida. *Phytoparasitica* 42, 31–39.

Hong, S. J., Kim, Y. K., Jee, H. J., Shin, C. K., Kim, M. J., Park, J. H., et al. (2015). Control of Pepper Anthracnose Caused by *Colletotrichum acutatum* using alternate application of agricultural organic materials and iminoctadine tris + thiram. *Korean J. Pestic. Sci*. 19, 428–439.

Hossain, M. J., Ran, C., Liu, K., Ryu, C. M., Rasmussen-Ivey, C. R., Williams, M. A., et al. (2015). Deciphering the conserved genetic loci implicated in plant disease control through comparative genomics of *Bacillus amyloliquefaciens* subsp. *plantarum*. *Front. Plant Sci*. 6:631. doi: 10.3389/fpls.2015.00631

Hyatt, D., Chen, G. L., LoCascio, P. F., Land, M. L., Larimer, F. W., and Hauser, L. J. (2010). Prodigal: prokaryotic gene recognition and translation initiation site identification. *BMC Bioinformatics* 11:119. doi: 10.1186/1471-2105-11-119

Jang, E. H., Jang, S. Y., Cho, I. H., Hong, D., Jung, B., Park, M. J., et al. (2015). Hispolon inhibits the growth of estrogen receptor positive human breast cancer cells through modulation of estrogen receptor alpha. *Biochem. Biophys. Res. Commun*. 463, 917–922. doi: 10.1016/j.bbrc.2015.06.035

Jayapala, N., Mallikarjunaiah, N. H., Puttaswamy, H., Gavirangappa, H., and Ramachandrappa, N. S. (2019). *Rhizobacteria Bacillus* spp. induce resistance against anthracnose disease in chili (*Capsicum annuum* L.) through activating host defense response. *Egypt. J. Biol. Pest Control* 29:45.

Jayasinghe, C., and Fernando, T. (2009). First Report of *Colletotrichum acutatum* on *Mangifera indica* in Sri Lanka. *Ceylon J. Sci*. 38:31034.

Jeon, Y. H., Chang, S. P., Hwang, I., and Kim, Y. H. (2003). Involvement of growth-promoting rhizobacterium Paenibacillus polymyxa in root rot of stored Korean ginseng. *J. Microbiol. Biotechnol*. 13, 881–891.

Kanehisa, M., Goto, S., Sato, Y., Kawashima, M., Furumichi, M., and Tanabe, M. (2014). Data, information, knowledge and principle: back to metabolism in KEGG. *Nucleic Acids Res*. 42, D199–D205. doi: 10.1093/nar/gkt1076

Kim, H. S., Sang, M. K., Jung, H. W., Jeun, Y. C., Myung, I. S., and Kim, K. D. (2012). Identification and characterization of *Chryseobacterium wanjuense* strain KJ9C8 as a biocontrol agent against Phytophthora blight of pepper. *Crop Prot*. 32, 129–137.

Kim, J. S., Jee, H. J., Gwag, J. G., Kim, C. K., and Shim, C. K. (2010). Evaluation on red pepper germplasm lines (*Capsicum* spp.) for resistance to anthracnose caused by *Colletotrichum acutatum*. *Plant Pathol. J*. 26, 273–279.

Kim, J. T., Park, S. Y., Choi, W. B., Lee, Y. H., and Kim, H. T. (2008). Characterization of *Collectotrichum* isolates causing anthracnose of pepper in Korea. *Plant Pathol. J*. 24, 17–23.

Kim, S., Park, M., Yeom, S. I., Kim, Y. M., Lee, J. M., Lee, H. A., et al. (2014). Genome sequence of the hot pepper provides insights into the evolution of pungency in *Capsicum* species. *Nat. Genet*. 46, 270–278. doi: 10.1038/ng.2877

Kim, Y. K., Li, D., and Kolattukudy, P. E. (1998). Induction of Ca^{2+}-calmodulin signaling by hard-surface contact primes *Colletotrichum gloeosporioides* conidia to germinate and form appressoria. *J. Bacteriol*. 180, 5144–5150. doi: 10.1128/JB.180.19.5144-5150.1998

Kim, Y. S., Lee, Y. M., Cheon, W. S., Park, J. W., Kwon, H. T., Balaraju, K., et al. (2021). Characterization of *Bacillus velezensis* AK-0 as a biocontrol agent against apple bitter rot caused by *Colletotrichum gloeosporioides*. *Sci. Rep*. 11:626. doi: 10.1038/s41598-020-80231-2

Kloepper, J. W., Ryu, C. M., and Zhang, S. (2004). Induced systemic resistance and promotion of plant growth by *Bacillus* spp. *Phytopathology* 94, 1259–1266. doi: 10.1094/PHYTO.2004.94.11.1259

Köhl, J., Kolnaar, R., and Ravensberg, W. J. (2019). Mode of action of microbial biological control agents against plant diseases: relevance Beyond Efficacy. *Front. Plant Sci*. 10:845. doi: 10.3389/fpls.2019.00845

Liu, F., Tang, G., Zheng, X., Li, Y., Sun, X., Qi, X., et al. (2016). Molecular and phenotypic characterization of *Colletotrichum* species associated with anthracnose disease in peppers from Sichuan Province, China. *Sci. Rep*. 6:32761. doi: 10.1038/srep32761

Meena, R. S., Kumar, S., Datta, R., Lal, R., Vijayakumar, V., Brtnicky, M., et al. (2020). Impact of Agrochemicals on soil microbiota and management: a review. *Land* 9:34. doi: 10.1016/j.wasman.2016.11.028

Mishra, R., Rout, E., and Joshi, R. K. (2018). Identification of resistant sources against anthracnose disease caused by *Colletotrichum truncatum* and *Colletotrichum gloeosporioides* in *Capsicum annuum* L. *Proc. Natl. Acad. Sci. India Sect. B Biol. Sci*. 89, 517–524.

Mongkolporn, O., and Taylor, P. W. J. (2018). Chili anthracnose: *colletotrichum* taxonomy and pathogenicity. *Plant Pathol*. 67, 1255–1263.

Montri, P., Taylor, P. W. J., and Mongkolporn, O. (2009). Pathotypes of *Colletotrichum capsici*, the causal agent of chili anthracnose, in Thailand. *Plant Dis*. 93, 17–20. doi: 10.1094/PDIS-93-1-0017

Nabila, N., and Kasiamdari, R. S. (2021). Antagonistic activity of siderophore-producing bacteria from black rice rhizosphere against rice blast fungus *Pyricularia oryzae*. *Microbiol. Biotechnol. Lett*. 49, 217–224. doi: 10.48022/mbl.2011.11009

Nawrocki, E. P., and Eddy, S. R. (2013). Infernal 1.1: 100-fold faster RNA homology searches. *Bioinformatics* 29, 2933–2935. doi: 10.1093/bioinformatics/btt509

Ngalimat, M. S., Mohd Hata, E., Zulperi, D., Ismail, S. I., Ismail, M. R., Mohd Zainudin, N. A. I., et al. (2021). Plant Growth-Promoting Bacteria as an Emerging Tool to Manage Bacterial Rice Pathogens. *Microorganisms* 9:682. doi: 10.3390/microorganisms9040682

Ons, L., Bylemans, D., Thevissen, K., and Cammue, B. P. A. (2020). Combining biocontrol agents with chemical fungicides for integrated plant fungal disease control. *Microorganisms* 8:1930. doi: 10.3390/microorganisms8121930

Onyeka, T. J., Petro, D., Etienne, S., Jacqua, G., and Ano, G. (2006). Optimizing controlled environment assessment of levels of resistance to anthracnose disease of yam using tissue culture-derived whole plants. *J. Phytopathol*. 154, 286–292.

Overbeek, R., Begley, T., Butler, R. M., Choudhuri, J. V., Chuang, H., Cohoon, M., et al. (2005). The subsystems approach to genome annotation and its use in the project to annotate 1000 genomes. *Nucleic Acids Res.* 33, 5691–5702. doi: 10.1093/nar/gki866

Parisi, M., Alioto, D., and Tripodi, P. (2020). Overview of biotic stresses in pepper (*Capsicum* spp.): sources of genetic resistance, Molecular Breeding and Genomics. *Int. J. Mol. Sci*. 21:2587. doi: 10.3390/ijms21072587

Park, J. W., Balaraju, K., Kim, J. W., Lee, S. W., and Park, K. S. (2013). Systemic resistance and growth promotion of chili pepper induced by an antibiotic producing *Bacillus vallismortis* strain BS07. *Biol. Control* 65, 246–257. doi: 10.1016/j.biocontrol.2013.02.002

Park, K. S., Ahn, I. P., and Kim, C. H. (2001). Systemic resistance and expression of the pathogenesis-related genes mediated by the plant growth-promoting rhizobacterium *Bacillus amyloliquefaciens* EXTN-1 against anthracnose disease in cucumber. *Mycology* 29, 48–53.

Peres, N. A. R., Souza, N. L., Zitko, S. E., and Timmer, L. W. (2002). Activity of Benomyl for Control of Postbloom Fruit Drop of Citrus Caused by *Colletotrichum acutatum*. *Plant Dis*. 86, 620–624. doi: 10.1094/PDIS.2002.86.6.620

Powell, S., Forslund, K., Szklarczyk, D., Trachana, K., Roth, A., Huerta-Cepas, J., et al. (2014). eggNOG v4.0: nested orthology inference across 3686 organisms. *Nucleic Acids Res*. 42, D231–D239. doi: 10.1093/nar/gkt1253

Prihatiningsih, N., Djatmiko, H. A., and Erminawati, W. (2019). Bio-management of anthracnose disease in chilli with microencapsulates containing *Bacillus subtilis* B298. *Earth Environ. Sci*. 250:012041. doi: 10.1088/1755-1315/250/1/012041

Pusztahelyi, T., Holb, I. J., and Pócsi, I. (2015). Secondary metabolites in fungus-plant interactions. *Front. Plant Sci*. 6:573. doi: 10.3389/fpls.2015.00573

Sang, M. K., Shrestha, A., Kim, D. Y., Park, K. S., Park, C. H., and Kim, K. D. (2013). Biocontrol of phytophthora blight and anthracnose in pepper by sequentially selected antagonistic *rhizobacteria* against *Phytophthora capsici*. *Plant Pathol. J*. 29, 154–167. doi: 10.5423/PPJ.OA.07.2012.0104

Sarwar, A., Brader, G., Corretto, E., Aleti, G., Abaidullah, M., Sessitsch, A., et al. (2018). Qualitative analysis of biosurfactants from *Bacillus* species exhibiting antifungal activity. *PLoS One* 13:e0198107. doi: 10.1371/journal.pone.0198107

SAS Institute Inc (1995). *JMP statistics and graphics guide, version 3*. Cary, NC. USA: SAS Institute Inc.

Schattner, P., Brooks, A. N., and Lowe, T. M. (2005). The tRNAscan-SE, snoscan and snoGPS web servers for the detection of tRNAs and snoRNAs. *Nucleic Acids Res*. 33, 686–689.

Schenk, P. M., Carvalhais, L. C., and Kazan, K. (2012). Unraveling plantmicrobe interactions: can multi-species transcriptomics help? *Trends Biotechnol*. 30, 177–184. doi: 10.1016/j.tibtech.2011.11.002

Schwyn, B., and Neilands, J. B. (1987). Universal chemical assay for the detection and determination of siderophores. *Anal. Biochem*. 160, 47–56. doi: 10.1016/0003-2697(87)90612-9

Shahid, I., Han, J., Hanooq, S., Malik, K. A., Borchers, C. H., and Mehnaz, S. (2021). Profiling of Metabolites of *Bacillus* spp. and Their Application in Sustainable Plant Growth Promotion and Biocontrol. *Front. Sustain. Food Syst*. 5:605195. doi: 10.3389/fsufs.2021.605195

Sharifi, R., and Ryu, C. M. (2016). Are bacterial volatile compounds poisonous odors to a fungal pathogen *Botrytis cinerea*, alarm signals to *Arabidopsis*

seedlings for eliciting induced resistance, or both? *Front. Microbiol.* 7:196. doi: 10.3389/fmicb.2016.00196

Sharma, S., Chen, C., Navathe, S., Chand, R., and Pandey, S. P. (2019). A halotolerant growth promoting *rhizobacteria* triggers induced systemic resistance in plants and defends against fungal infection. *Sci. Rep*. 9:4054. doi: 10.1038/s41598-019-40930-x

Siddiqui, Y., and Ali, A. (2014). "*Colletotrichum gloeosporioides* (Anthracnose)," in *Postharvest Decay: control Strategies*, ed. S. Bautista-Banos (London, UK: Elsevier), 337–371.

Sliva, D. (2010). Medicinal mushroom *Phellinus linteus* as an alternative cancer therapy. *Exp. Ther. Med*. 1, 407–411.

Than, P. P., Prihastuti, H., Phoulivong, S., Taylor, P. W. J., and Hyde, K. D. (2008). Chilli anthracnose disease caused by *Colletotrichum* species. *J. Zhejiang Univ. Sci. B* 9, 764–778. doi: 10.1631/jzus.B0860007

UniProt Consortium (2015). UniProt: a hub for protein information. *Nucleic Acids Res.* 43, D204–D212. doi: 10.1093/nar/gku989

Weisburg, W. G., Barns, S. M., Pelletier, D. A., and Lane, D. J. (1991). 16S ribosomal DNA amplification for phylogenetic study. *J. Bacteriol.* 173, 697–703. doi: 10.1128/jb.173.2.697-703.1991

Wesseling, C., McConnell, R., Partanen, T., and Hogstedt, C. (1997). Agricultural pesticide use in developing countries: health effects and research needs. *Int. J. Health Serv*. 27, 273–308. doi: 10.2190/E259-N3AH-TA1Y-H591

Wu, Z., Huang, Y., Li, Y., Dong, J., Liu, X., and Li, C. (2019). Biocontrol of *Rhizoctonia solani* via Induction of the Defense Mechanism and Antimicrobial Compounds Produced by *Bacillus subtilis* SL-44 on Pepper (*Capsicum annuum* L.). *Front. Microbiol*. 10:2676. doi: 10.3389/fmicb.2019.02676

Yang, D., Wang, L., Wang, T., Zhang, Y., Zhang, S., and Luo, Y. (2021). Plant Growth-Promoting *Rhizobacteria* HN6 Induced the Change and Reorganization of *Fusarium* Microflora in the Rhizosphere of Banana Seedlings to Construct a Healthy Banana Microflora. *Front. Microbiol*. 12:685408. doi: 10.3389/fmicb.2021.685408

Zalila-Kolsi, I., Mahmoud, A. B., Ali, H., Sellami, S., Nasfi, Z., Tounsi, S., et al. (2016). Antagonist effects of Bacillus spp. strains against *Fusarium graminearum* for protection of durum wheat (*Triticum turgidum* L. subsp. *durum*). *Microbiol. Res*. 192, 148–158. doi: 10.1016/j.micres.2016.06.012

Zhang, D., Yu, S., Yang, Y., Zhang, J., Zhao, D., Pan, Y., et al. (2020). Antifungal effects of volatiles produced by *Bacillus subtilis* against *Alternaria solani* in potato. *Front. Microbiol*. 11:1196. doi: 10.3389/fmicb.2020.01196

Zhang, N., Yang, D., Kendall, J. R. A., Borriss, R., Druzhinina, I. S., Kubicek, C. P., et al. (2016). Comparative Genomic Analysis of *Bacillus amyloliquefaciens* and *Bacillus subtilis* Reveals Evolutional Traits for Adaptation to Plant-Associated Habitats. *Front. Microbiol*. 7:2039. doi: 10.3389/fmicb.2016.02039

Conflict of Interest: The authors declare that the research was conducted in the absence of any commercial or financial relationships that could be construed as a potential conflict of interest.

Publisher's Note: All claims expressed in this article are solely those of the authors and do not necessarily represent those of their affiliated organizations, or those of the publisher, the editors and the reviewers. Any product that may be evaluated in this article, or claim that may be made by its manufacturer, is not guaranteed or endorsed by the publisher.

frontiers in Plant Science

ORIGINAL RESEARCH
published: 02 March 2022
doi: 10.3389/fpls.2022.828267

Application of a Biostimulant (Pepton) Based in Enzymatic Hydrolyzed Animal Protein Combined With Low Nitrogen Priming Boosts Fruit Production Without Negatively Affecting Quality in Greenhouse-Grown Tomatoes

Tania Mesa[1], Javier Polo[2], Andrea Casadesús[1], Íñigo Gómez[1] and Sergi Munné-Bosch[1,3]*

[1]Department of Evolutionary Biology, Ecology and Environmental Sciences, Faculty of Biology, University of Barcelona, Barcelona, Spain, [2]R&D Department, APC Europe S.L., Granollers, Spain, [3]Research Institute of Nutrition and Food Safety, Faculty of Biology, University of Barcelona, Barcelona, Spain

OPEN ACCESS

Edited by:
Maurizio Ruzzi, University of Tuscia, Italy

Reviewed by:
Vasileios Fotopoulos, Cyprus University of Technology, Cyprus
Athanasios Koukounaras, Aristotle University of Thessaloniki, Greece

***Correspondence:**
Javier Polo
javier.polo@apc-europe.com

Specialty section:
This article was submitted to Crop and Product Physiology, a section of the journal Frontiers in Plant Science

Received: *03 December 2021*
Accepted: *21 January 2022*
Published: *02 March 2022*

Citation:
Mesa T, Polo J, Casadesús A, Gómez Í and Munné-Bosch S (2022) Application of a Biostimulant (Pepton) Based in Enzymatic Hydrolyzed Animal Protein Combined With Low Nitrogen Priming Boosts Fruit Production Without Negatively Affecting Quality in Greenhouse-Grown Tomatoes. Front. Plant Sci. 13:828267. doi: 10.3389/fpls.2022.828267

Improved nutrient use efficiency together with the use of biostimulants have been little explored thus far to improve fruit yield and quality in economically relevant crops. The aim of this study was to determine the additive or synergistic effects, if any, of the application of an enzyme hydrolyzed animal protein biostimulant (Pepton) combined with priming with low nitrogen (N) in the production and quality of greenhouse tomatoes. Biostimulant treatment (Pepton at a dose equivalent of 4 kg/ha) was applied by ferti-irrigation for 2 months during the vegetative phase both in controls (watered with nutrient solution) and nutrient efficient crop (NEC), in which plants were primed with low N by exposing them to a 30% N deficiency for 2 months, and then recovered for 1 month before fruit production. Foliar water and N contents, pigments, maximum PSII efficiency (Fv/Fm ratio), and phytohormones [including abscisic acid (ABA), salicylic acid (SA), jasmonic acid (JA), and cytokinins] were measured prior and at 4 and 8 weeks after the first application. Fruit production and quality [as indicated by total soluble sugars (TSS) and acidity (TA), and the contents of lycopene, vitamin E, and vitamin C] were measured 1 month later at harvest. Priming with low N availability (NEC plants) doubled ($p < 0.001$) fruit production (due to an increase in the number of fruits), tended to increase ($p = 0.057$) by 20% the amount of TSS and increased ($p < 0.05$) the contents of lycopene (by 90%) and vitamin E (by 40%). Pepton displayed a tendency, almost significant, to improve ($p = 0.054$) total fruit production both in control and NEC plants, thus showing an additive effect to low N priming in boosting fruit production. Pepton maintained fruit quality in terms of sugar

accumulation, total acidity and the contents of carotenoids, vitamins C and E. Pepton-related improvement in fruit production seemed to be related, at least partially, to an increased accumulation of cytokinins and photosynthetic pigments in leaves, which might favor vegetative vigor and ultimately fruit yield. In conclusion, Pepton application was effective in improving the yield of greenhouse tomatoes showing additive effect with low N priming, without negatively affecting fruit quality.

Keywords: biostimulant, cytokinins, nitrogen efficient crops, production, tomato

INTRODUCTION

Rising productivity to feed the escalating global population and increasing the use efficiency of the resources without harming the ecosystems are two of the greatest challenges that the agricultural sector is facing these days. Moreover, current agriculture has to face more frequent and long-lasting unfavorable environmental and soil conditions, which have a direct negative impact on crop productivity. A technological innovation proposed to solve these problems is the application of natural biostimulants that can enhance flowering, plant growth, fruit set, crop productivity, and nutrient use efficiency, while also improving abiotic stress tolerance (Rouphael and Colla, 2020). One of the main important nutrients for plant growth and development is nitrogen (N), which at the same time is one of the major limiting nutrients in most economically relevant crops (Flores et al., 2004; Padilla et al., 2018). Because of this, and to ensure high crop yield, it is very common among farmers to conduct excessive N applications that end up leaching into groundwater, threatening both the environment and human health (Padilla et al., 2018; Burri et al., 2019). Hence, it is of great importance to develop new techniques that help farmers optimize crop production, while using the minimum N input to reduce its harmful effects on the environment and human health.

Enzymatically hydrolyzed protein-based biostimulants may be an adequate approach to both raise productivity and increase the use efficiency of some nutrients such as N (Colla et al., 2014, 2017). Pepton 85/16® (Pepton) is a natural biostimulant obtained by the enzymatical hydrolysis of animal proteins that is available in a micro-granular form and highly soluble in water (APC Europe S.L., Spain). Pepton has been proved to have beneficial effects on crops under stress conditions such as intense cold or heat episodes, mild stress ambient field conditions, and water and nutrient stress. It has also been observed that it exerts a positive effect on the hormonal profile enhancing abiotic stress defenses (Polo et al., 2006; Marfà et al., 2009; Polo and Mata, 2018; Casadesús et al., 2019, 2020). However, little is still known about the possible effects of this biostimulant on plants under low nutrient availability conditions and the improvement of nutrient use efficiency. Priming with low N has been previously shown as a useful technique with a great potential to increase productivity since it can ameliorate nutrient use efficiency in wheat (Gao et al., 2019). However, to our knowledge, its potential beneficial effects on improving the yield and quality of tomatoes, and most particularly in combination with biostimulant application, has not been explored thus far.

Tomato (*Solanum lycopersicum* L.) is one of the most cultivated crops with a cultivation area of 5.03 million hectares (FAOSTAT, 2019). Its fruits are highly valued by consumers due to their organoleptic characteristics and nutritional value, as they constitute an important source of vitamins C and E and lycopene, among other nutrients and antioxidants (Asensio et al., 2019). It is of great interest to increase the nutrient use efficiency of tomato plants, without affecting their production, since large amounts of fertilizer are usually applied to obtain their maximum yield (Abenavoli et al., 2016). Therefore, this work aimed to assess to what extent an enzymatically hydrolyzed protein-based biostimulant (Pepton) can improve fruit production and quality both in control and in low N primed conditions, and establish a mechanism of action, with an emphasis on the possible role of endogenous phytohormone contents.

MATERIALS AND METHODS

Experimental Design

Seeds of tomato plants (*Solanum lycopersicum* cv. Ailsa Craig) were obtained from the Experimental Field Facilities of the University of Barcelona (Barcelona, NE, Spain). Seeds were sown on 7th March 2019, in 1 L pots in a climate-controlled growth chamber (16 h day/8 h night, at 22°C), using a substrate based on 50% peat, 25% perlite, 25% vermiculite, $CaCO_3$ at 1 g/L and essential micronutrients at 0.05 g/L. On 8th April, seedlings were transferred to 3 L pots and placed in a glass greenhouse (25.6°C mean temperature, 33.8°C highest temperature average with an absolute maximum of 41.0°C, and 60.1% mean relative humidity) with 20 cm between pots. Then, on 10th June, four treatments were established including: Control plants without Pepton, Control plants with Pepton, Nitrogen Efficient Crop (NEC) without Pepton, and NEC with Pepton. Control plants were irrigated with 50% Hoagland nutrient solution (Hoagland and Arnon, 1950) throughout the experiment. In contrast, NEC plants were primed with low N by irrigating plants for 8 weeks with a nutrient solution deficient by 30% N relative to controls and then recovered with the same nutrient solution as used for controls (50% Hoagland solution). Pepton was applied by ferti-irrigation once every 2 weeks during the first 2 months at a dose equivalent of 4 kg/ha (0.2 g of Pepton dissolved in 0.5 L of

irrigation water), corresponding with the supplier recommendation for this crop. All applications were performed 1 h before sunset. All plants were subject to "topping" at week seven of starting treatments due to excessive growth in the greenhouse, so that this pruning caused the plants to stop flowering and setting new fruits.

Leaf samples were collected on 16th June (week 0), 16th July (week 4), and 13th August (week 8) at predawn (1 h before sunrise). In each sampling, one young, fully developed leaf from eight randomly selected plants per treatment was sampled. The apical leaflet was used to determine the chlorophyll fluorescence and the adjacent leaflet was used to determine the water, carbon (C), and N status, and the leaflet mass per area ratio (LMA). The other adjacent leaflet was immediately frozen in liquid N_2 and stored at −80°C for subsequent biochemical analyses. Fruit samplings from the same plants were performed between 4th September and 7th September. All fruits (from breaker to red ripe stages) of each plant were harvested for the estimation of yield. In addition, four ripe tomatoes on the red ripe stage were chosen for fruit quality analysis: one was frozen in liquid N_2 and stored at −80°C for subsequent biochemical analyses (total carotenoids, lycopene, and vitamins C and E) and three were used to analyze total soluble sugars (TSS) and titratable acidity (TA).

Pepton Composition

Pepton is an enzymatically hydrolyzed protein product that contains L-α amino acids (84.8%), free amino acids (16.5%), organic-nitrogen (12.0%), iron (3,000 ppm), and potassium (4.0%). The complete chemical composition of this biostimulant can be found in Polo and Mata (2018).

Total Production, TSS, and TA

Total production was estimated as the total amount of fruits produced per plant, the total biomass of fruits produced per plant and the fresh mass per fruit unit. The fresh mass of fruits was measured by weighing freshly harvested fruits. For estimating fruit quality, 1 ml of juice from a pool of three tomatoes was used to determine TSS using a digital refractometer HI 96801 (Hannah Instruments, Italy). Then, 10 ml of juice were diluted in 100 ml of MiliQ water and used for TA determination with 0.1 M NaOH and 1% phenolphthalein as an indicator to estimate citric acid content. The TSS/TA ratio was then calculated.

Fruit Total Carotenoids, Lycopene, and Vitamins C and E

For the quantification of total carotenoids, 100 mg of ground frozen fruit were extracted with acetone 80% (v/v) using ultrasonication (Branson 2510 ultrasonic cleaner, Bransonic, Danbury, CT, United States). The extract was then centrifuged for 10 min at 4°C and 13,000 rpm, and the supernatant was collected. The pellet was re-extracted until it was colorless, pooling at the end all the supernatants. Total carotenoids were analyzed using UV/Visible spectrophotometry of double beam using a CE Aquarius UCE7400 (Cecil Instruments Ltd., Cambridge, United Kingdom). The absorbance of the supernatants was read at 470, 646, 663, and 750 nm, respectively. Carotenoid content was calculated following the equations developed by Lichtenthaler and Wellburn (1983).

Quantification of lycopene content was performed as described by Fish et al. (2002). Around 500 mg of ground frozen fruit were extracted with 800 µl MiliQ water, 1.5 ml acetone, 1.5 ml ethanol, and 3 ml hexane. The pellet was re-extracted with hexane until it was colorless. The absorbance of the supernatants was read at 503 and 800 nm.

The analysis of vitamin C was adapted from Takahama and Oniki (1992) and Queval and Noctor (2007). Around 100 mg of ground frozen fruit were extracted with 6% meta-phosphoric acid (w/v) and 0.2 mM DTPA using ultrasonication and centrifugation for 10 min at 4°C and 13,000 rpm. The contents of ascorbic acid (AA) and dehydroascorbic acid (DHA) were determined spectrophotometrically (xMark Microplate Spectrophotometer, Bio-Rad, Hercules, CA, United States) with quartz microplates reading the absorbance at 265 nm. Total ascorbate was calculated as the sum of AA + DHA.

For vitamin E analyses, 100 mg of ground frozen fruit were extracted with methanol and 5 ppm (w/v) of tocol as an internal standard. Extractions were performed as above. The extracts were then filtered with a hydrophobic PTFE filter of 0.22 µm (Phenomenex, Torrance, CA, United States) and injected into the HPLC system (consisting of a Waters 600 controller pump, a Waters 717 plus auto-sampler, and a Jasco FP-1520 fluorescence detector). Fluorescence detection was at an excitation wavelength of 295 nm and emission at 330 nm. The mobile phase was a mixture of *n*-hexane and 1,4-dioxane (95.5:4.5, v/v) at a flow rate of 0.7 ml/min. Tocochromanols were separated using an Inertsil 100A column (5 µm, 30 × 250 mm, GL Sciences Inc., Tokyo, Japan). A calibration curve was established with each of the tocochromanols analyzed using authentic standards from Sigma-Aldrich (Steinheim, Germany).

Leaf Water Status, C and N Contents, and LMA

Relative water content (RWC) was calculated using the formula $RWC = 100 \times (FW - DW) / (TW - DW)$, where FW is the fresh mass measured on the sampling date, TW is the turgid mass measured after rehydrating the leaves for 24 h in the dark at 4°C, and DW is the dry mass measured after oven-drying the leaves at 80°C until constant weight. Leaflet area was measured with a flatbed scanner and processed with ImageJ (1.52p, National Institutes of Health, Bethesda, MD, United States). The LMA was calculated as DW/Leaflet area.

For C and N analyses, 3 mg of dry leaflets were ground, weighed, placed in tin capsules, sealed and analyzed using an organic elemental analyzer (Thermo EA 1108, Thermo Scientific, Milan, Italy). Standard conditions recommended by the supplier were applied (Combustion reactor at 1,000°C, reactor chromatographic column at 60°C, helium flow 120 ml/min and 10 ml oxygen circuit at 100 kPa).

Photosynthetic Pigments and Chlorophyll Fluorescence

For total chlorophyll and carotenoid content measurements, methanolic extracts were prepared using 100 mg of frozen ground leaves and diluted 1:10 (v/v) with methanol. The absorbance of the supernatants was read at 470, 653, 666, and 750 nm using a UV/Visible spectrophotometer of double beam (CE Aquarius UCE7400, Cecil Instruments Ltd., Cambridge, United Kingdom). Chlorophyll a, chlorophyll b, and carotenoid contents were calculated following the equations developed by Lichtenthaler (1987).

The maximum efficiency of PSII photochemistry (or F_v/F_m ratio), an indicator of photoinhibition (Takahashi and Badger, 2011), was determined by measuring chlorophyll fluorescence from leaves by using a portable fluorimeter Mini-PAM II (Photosynthesis Yield Analyser, Walz, Germany) in dark-adapted leaves for 1 h, as described by van Kooten and Snel (1990).

Stress-Related Phytohormones and Cytokinins

Phytohormones, including the stress-related phytohormones, abscisic acid (ABA), salicylic acid (SA), jasmonic acid (JA), and the cytokinins, *trans*-zeatin (*t*-Z), and its riboside *trans*-zeatin riboside (*t*-ZR), were analyzed by the extraction of 100 mg of frozen ground leaves with methanol containing deuterium-labeled hormones, which were used as internal standards. The extracts were subject to ultrasonication and vortexing for 30 min. After centrifugation for 10 min at 4°C and 13,000 rpm, the supernatant was collected, and the pellet was re-extracted. The supernatants were then filtered with a hydrophobic PTFE filter of 0.22 µm (Phenomenex, Torrance, CA, United States) prior to analysis. Hormone levels were analyzed by UHPLC-ESI-MS/MS as described by Müller and Munné-Bosch (2011). Quantification was made considering the recovery rates for each sample by using the deuterium-labeled internal standards.

Statistical Analyses

Statistical analyses were performed by a three-way ANOVA for foliar analyses and a two-way ANOVA for fruit analyses. The Tuckey test was used as a *post hoc* method. In all cases, differences were considered significant at a probability level of $p < 0.05$ and a trending toward statistical significance at a probability level of p between 0.1 and 0.05 (Fisher, 1950; These et al., 2016). All statistical tests were performed with RStudio (Boston, MA, United States).

RESULTS AND DISCUSSION

Low N Priming and Pepton Application Improve Fruit Production

Biostimulants have been considered innovative tools that are able to improve plant growth and productivity and help alleviate the effects of abiotic stresses. Furthermore, some biostimulants, such as Pepton, that are enzymatically hydrolyzed animal protein-based biostimulants can promote circular economy helping recycle animal waste products and reduce the use of limited resources of nature (Casadesús et al., 2020). Previous studies have shown that Pepton can improve crop performance against different abiotic stresses including water and temperature stress conditions. In the present study, fruit production was stimulated by the NEC treatment as compared to controls, whereas fruit size remained unaffected (**Figure 1**). NEC treatment increased the production of greenhouse-grown tomato fruits, estimated as total fresh matter of fruits per plant, by 1.7-fold, which was associated with an increase in the number of fruits per plant by 1.8-fold. However, no significant differences were observed for fruit size. A trend toward statistical significant effect ($p = 0.054$) was observed for fruit production in Pepton-treated plants, with an increase in fruit production by 32% relative to controls both in N-fed (Controls) and low N-primed plants (NEC; **Figure 1**). This increase in yield in both groups of plants supplemented with Pepton has an important economic relevance for producers with very positive return on investment. In a previous study, Polo and Mata (2018) found similar results, with a yield increased by 27% when Pepton was applied at similar doses (4 Kg/Ha) in gold cherry tomatoes growing under low stress ambient field conditions. N is a crucial nutrient for plant growth and development, so one might expect that plants with higher N availability (control, N-fed plants) would show increased fruit production, as previously observed in several economically important crops, including tomatoes (Warner et al., 2004). It is also true, however, that low N priming can be used in crops to improve nutrient efficiency, showing a great potential to increase yields (Gao et al., 2019). In the present study, we observed that plants have acclimated to a deprived nutrient availability during the vegetative growth for 2 months allowing them to become more efficient in their N use and, therefore, increase their total fruit production considerably. It is noteworthy, however, that aside from low N priming, the pruning of plants performed after 7 weeks of treatment may play a role in the observed effects. Topping might have caused a severe loss of aboveground biomass favoring fruit set and ripening, but at the same time reduced a significant amount of biomass previously consuming root N. Therefore, as pruning was performed just before the end of N deprivation, it may have had an impact on the recovery phase in the NEC treatment helping boost production relative to controls. In other words, NEC treatment may would not have had such a positive effect compared to controls if all plants had not been pruned.

The Positive Effects of Combined Low N Priming and Pepton Application on Fruit Production Did Not Negatively Affect Fruit Quality

Total soluble sugars and TA are important components of flavor exerting their effect not only through their content but also through their ratio (Xu et al., 2018; Navarro and Munné-Bosch, 2022). However, the effects of some nutrients' availability, such as a decrease in the N dose, on tomato quality are still controversial as it has been seen to both increase (Aziz, 1968; Bénard et al., 2009; Truffault et al.,

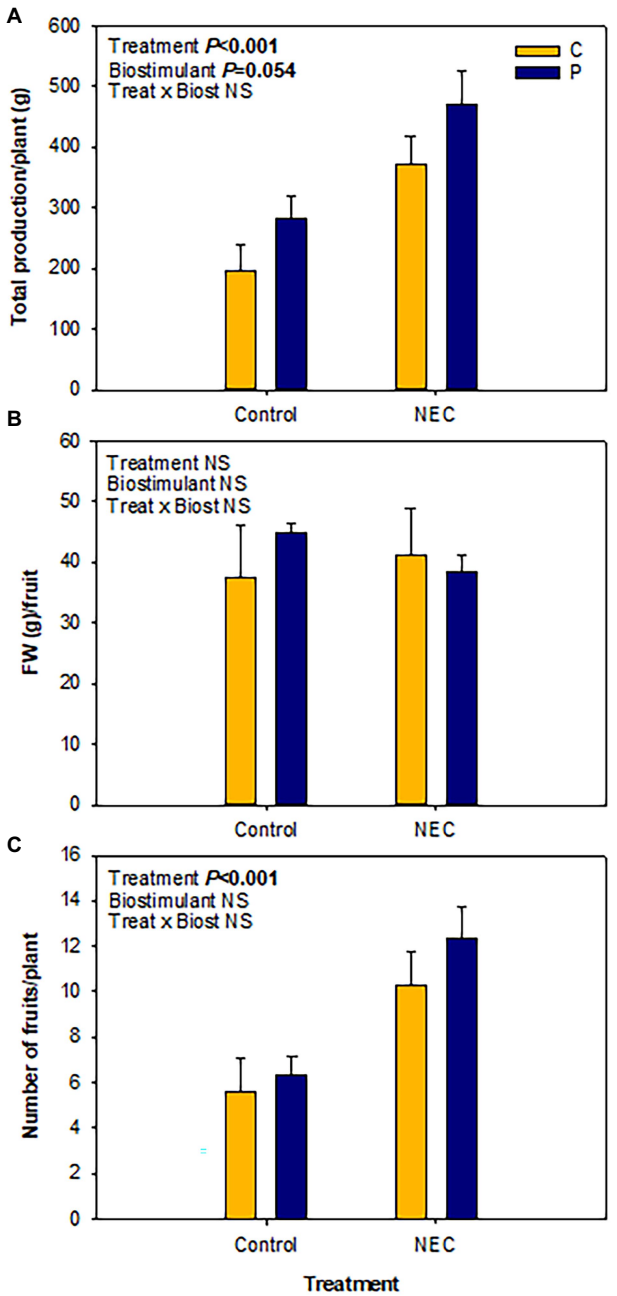

FIGURE 1 | Effects of low nitrogen (N) priming and Pepton application on fruit production in greenhouse-grown tomato plants. **(A)** Total fruit production per plant, **(B)** average fresh weight of ripen fruits, and **(C)** number of ripen fruits per plant, in Pepton-treated plants (P) or untreated controls (C) either fed with nitrogen in a 50% Hoagland solution (Control) or exposed to low nitrogen priming (NEC). NEC stands for Nitrogen Efficient Crop (these plants were exposed to a 30% N deficiency relative to controls for 2 months and then recovered for 1 month with the same nutrient solution used for controls before estimation of fruit production, see section Materials and Methods for details). Data are mean of $n = 8 \pm$ SE. p values of two-way ANOVA are shown in the inlets and values of $p > 0.10$ were considered as not significant (NS).

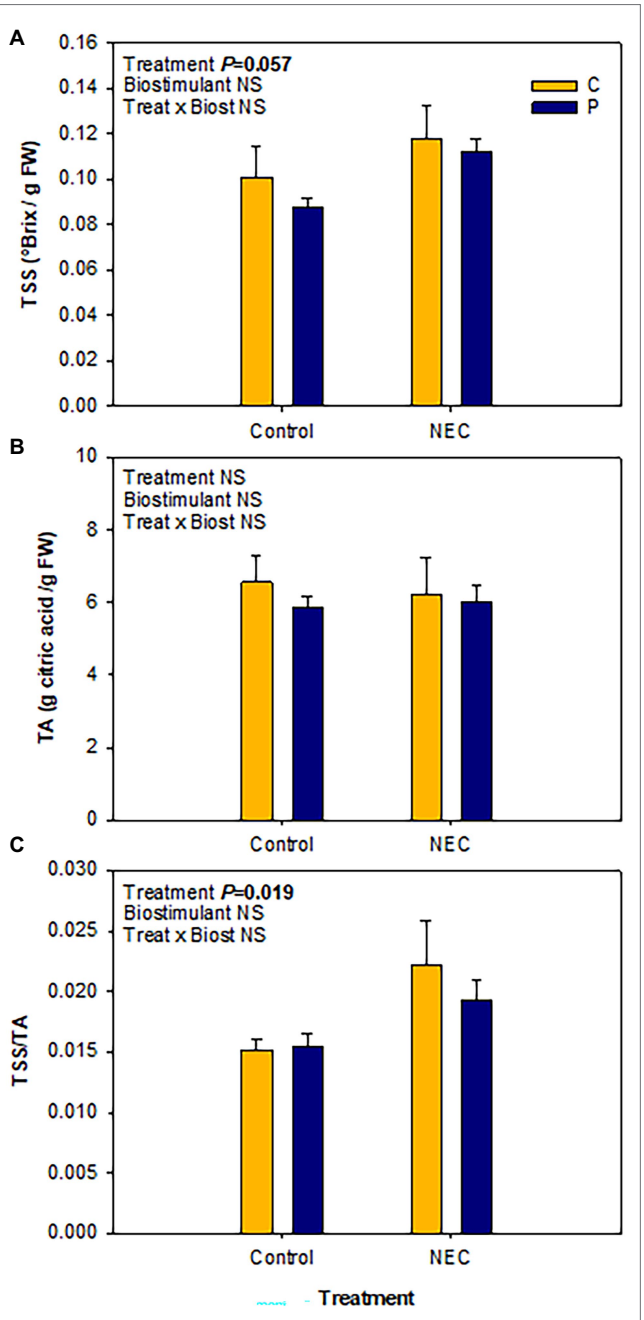

FIGURE 2 | Effects of low nitrogen priming and Pepton application on fruit quality, in terms of soluble sugar accumulation and acidity, in greenhouse-grown tomato plants. **(A)** Total soluble sugars (TSS), **(B)** total acidity (TA), and **(C)** TSS/TA ratio in mature fruits of Pepton-treated plants (P) or untreated controls (C) either fed with nitrogen in a 50% Hoagland solution (Control) or exposed to low nitrogen priming (NEC). NEC stands for Nitrogen Efficient Crop (see **Figure 1** legend and section Materials and Methods for details). Data are mean of $n = 8 \pm$ SE. p values of two-way ANOVA are shown in the inlets and values of $p > 0.10$ were considered as NS.

2019) and decrease (Hernández et al., 2020; Navarro and Munné-Bosch, 2022) the TSS/TA ratio. In the present study, fruit quality was improved by the NEC treatment, particularly, a significant increase in the TSS/TA ratio was observed together with a trend toward statistical significant increase of TSS (**Figure 2**). Moreover, the quality of the tomato

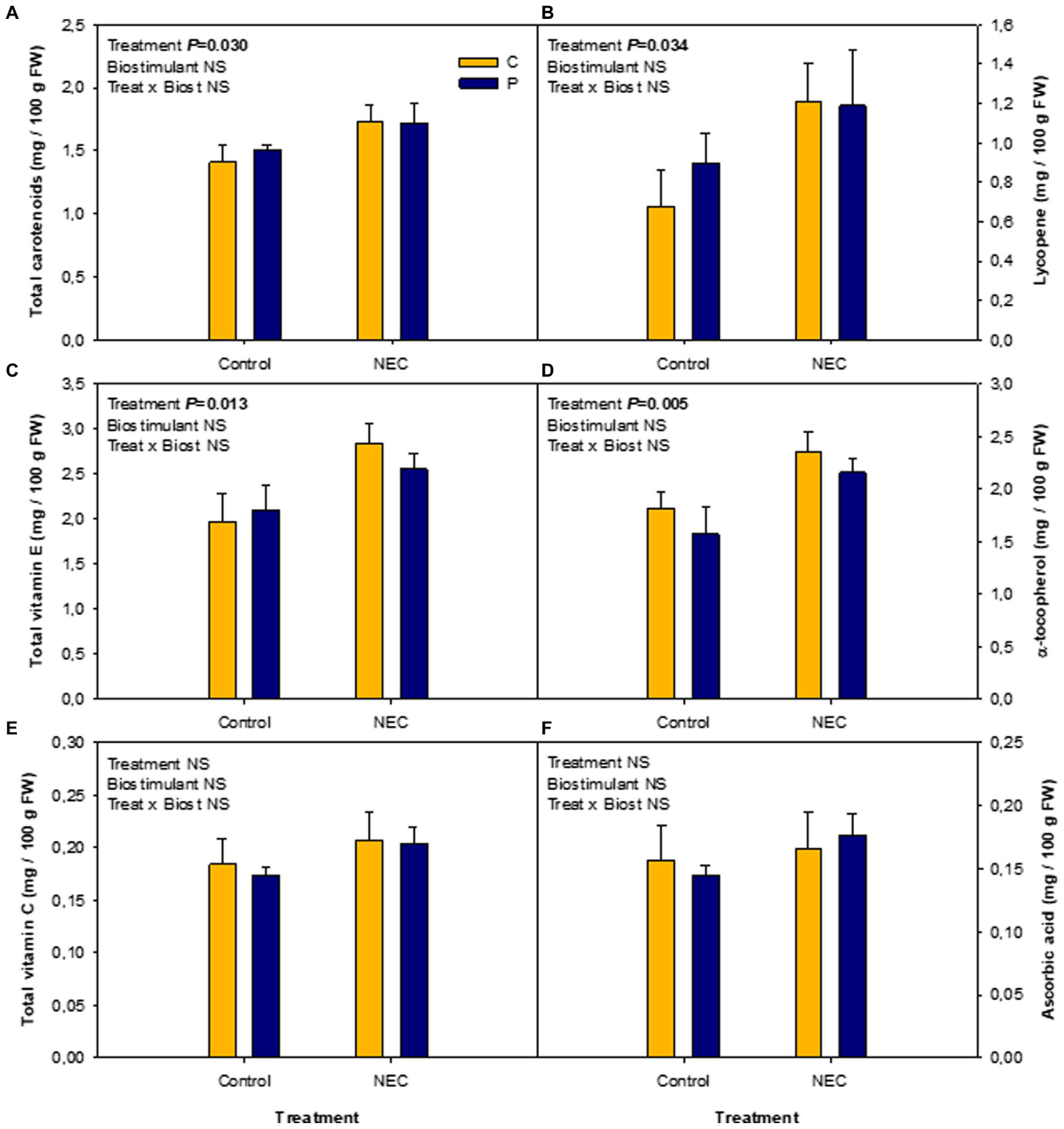

FIGURE 3 | Effects of low nitrogen priming and Pepton application on fruit quality, in terms of carotenoid, vitamin E, and vitamin C accumulation, in greenhouse-grown tomato plants. **(A)** Total carotenoids, **(B)** lycopene, **(C)** total vitamin E, **(D)** α-tocopherol, **(E)** total vitamin C, and **(F)** ascorbic acid contents in mature fruits of Pepton-treated plants (P) or untreated controls (C) either fed with nitrogen in a 50% Hoagland solution (Control) or exposed to low nitrogen priming (NEC). NEC stands for Nitrogen Efficient Crop (see **Figure 1** legend and section Materials and Methods for details). Data are mean of $n = 8 \pm$ SE. p values of two-way ANOVA are shown in the inlets and values of $p > 0.10$ were considered as NS.

fruits was not affected by the application of Pepton, thus showing that this biostimulant can increase fruit yield without a negative impact on the TSS/TA ratio. Other quality parameters related to the antioxidant composition of the fruits, were also unaffected by the biostimulant, again indicating that it would be a great option to increase the production without negative implications on the fruit quality (**Figure 3**). Furthermore, NEC treatment did improve the total carotenoids and vitamin E contents by increasing their major components, lycopene, and α-tocopherol, respectively. Total carotenoids and lycopene contents increased by NEC treatment by 18 and 52%, respectively, relative to controls.

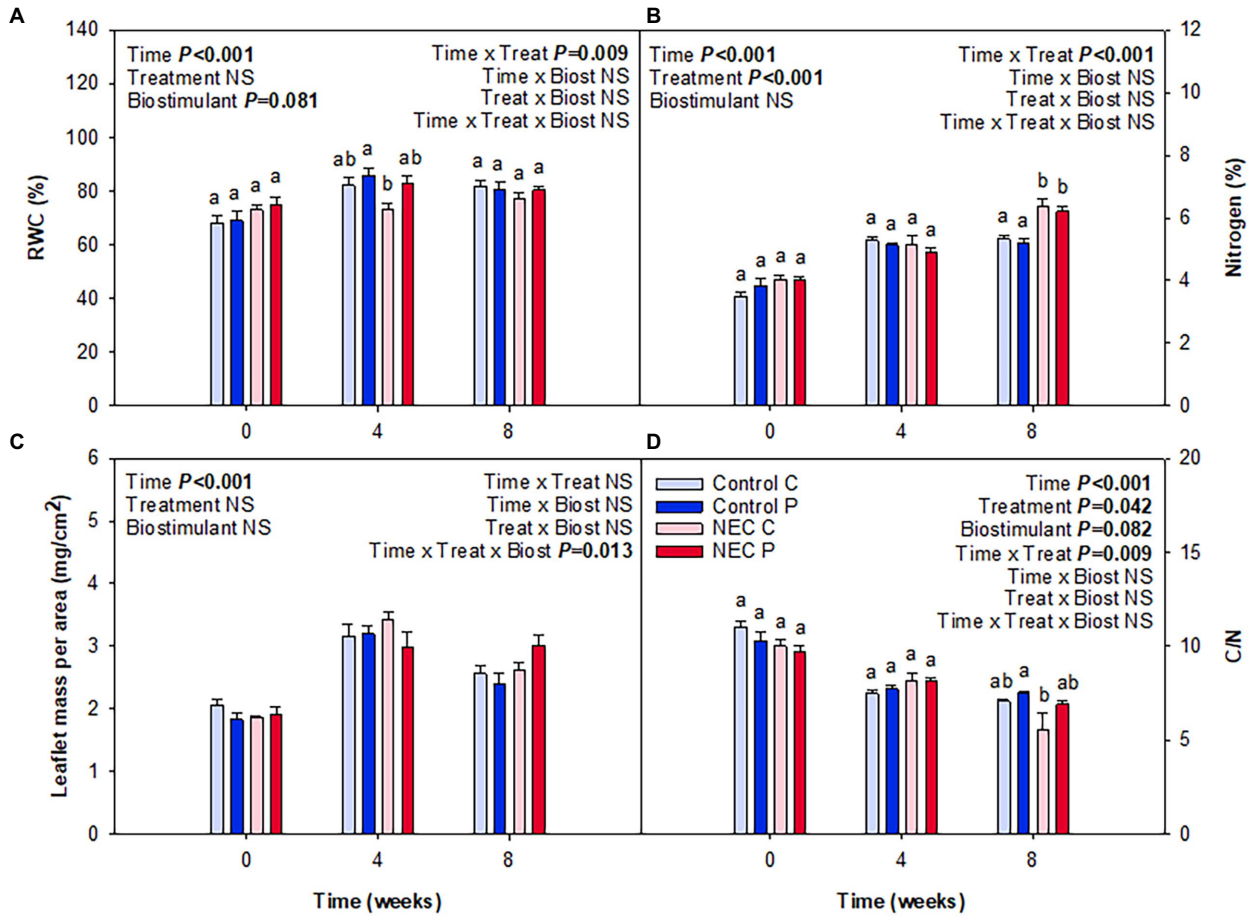

FIGURE 4 | Effects of low nitrogen priming and Pepton application on leaf water and nitrogen contents in greenhouse-grown tomato plants. **(A)** Relative leaf water content (RWC), **(B)** nitrogen content (expressed as a percentage of dry mass), **(C)** leaflet mass per area ratio (LMA), and **(D)** carbon to nitrogen (C/N) ratio. NEC stands for Nitrogen Efficient Crop (see **Figure 1** legend and section Materials and Methods for details). Measurements on leaves were performed before treatments (week 0), and in the middle (week 4) and end (week 8) of treatments. Data are mean of $n = 8 \pm$ SE. p values of three-way ANOVA are shown in the inlets and values of $p > 0.10$ were considered as NS. Different letters indicate differences in Tukey's HSD multiple comparison test.

Vitamin E in fruits also increased in response to the NEC treatment by 33% relative to the controls, mainly associated with an increase of α-tocopherol (**Figure 3**). In contrast, total vitamin C and ascorbic acid contents remained unaffected by treatments.

Effects of Low N Priming and Pepton Application on Fruit Production Differ on a Mechanistic Level

When analyzing water and N contents in leaves, it was observable that a significant increase of N content occurred due to the NEC treatment, especially at week 8 of treatment. This increase was reflected in the percentage of total N and the C/N ratio (**Figure 4**). Pruning during week 7 may have caused this effect. Despite plants suffering 30% N deficiency, the removal of a significant part of the aerial biomass may have largely alleviated stress and have led to an improvement of N use in all treatments, but most particularly in those already suffering a N deficiency. Differences between NEC and control treatments were small but significant, with an increase in foliar N by 15% in the former compared to the latter. In contrast, Pepton treatment did not additionally increase foliar N contents, but showed a trend to improve the RWC ($p = 0.081$), an effect that appeared to be more apparent before than after pruning (week 4 relative to week 8; **Figure 4**). The contents of photosynthetic pigments were also positively affected by either the NEC treatment, the biostimulant or both, depending on the parameter (**Figure 5**). The most striking effects were observed for the biostimulant combined with the NEC treatment. Pepton application significantly helped to maintain the contents of chlorophyll a + b and total carotenoids higher than in controls, an effect that was particularly observed at week 8 in NEC plants treated with Pepton (**Figure 5**). On the other side, NEC treatment alone

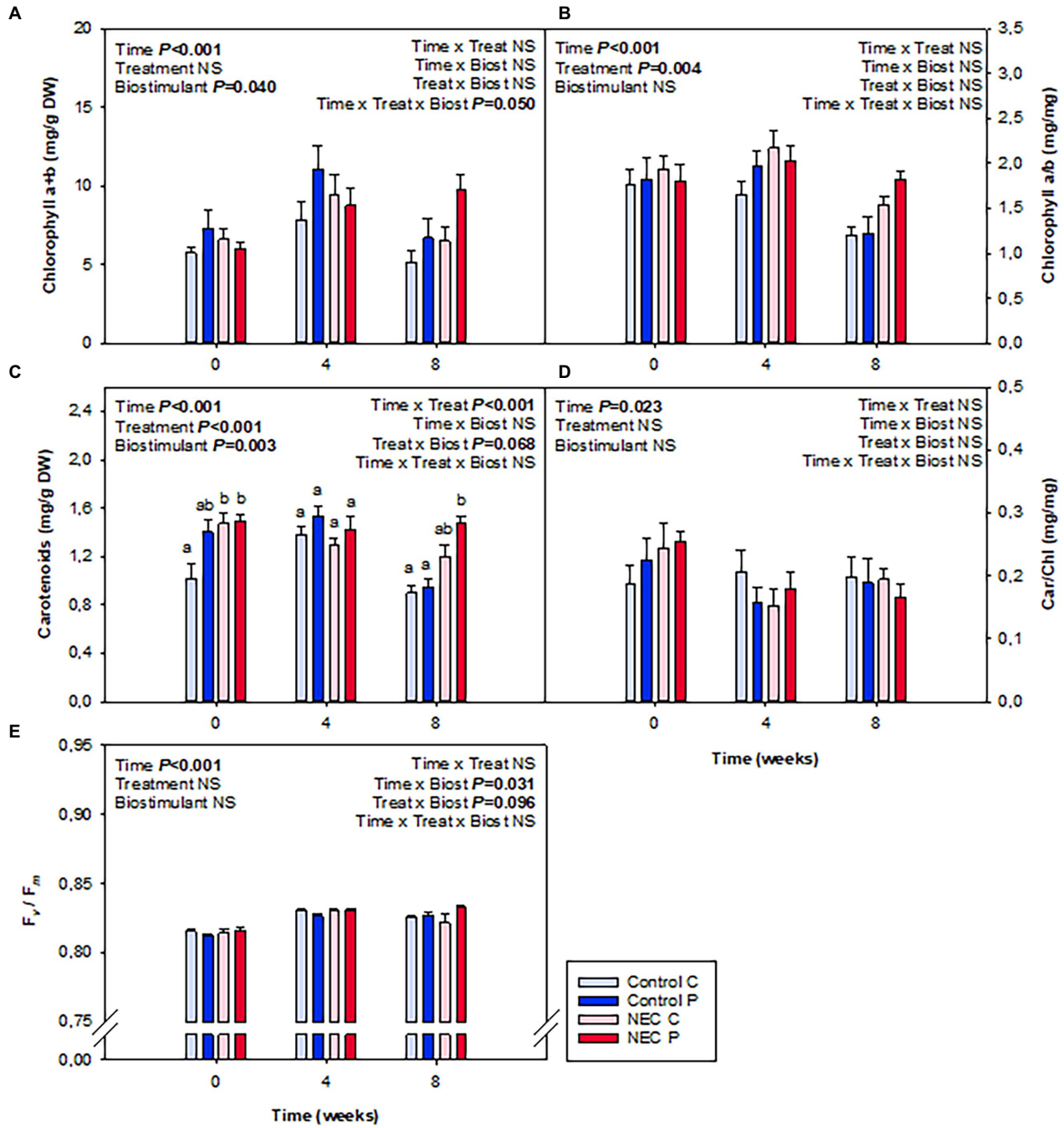

FIGURE 5 | Effects of low nitrogen priming and Pepton application on photosynthetic pigment contents and photoinhibition in leaves of greenhouse-grown tomato plants. **(A)** Chlorophyll a + b, **(B)** chlorophyll a/b ratio (Chl a/b), **(C)** carotenoids, **(D)** carotenoids/chlorophylls ratio (Car/Chl), and **(E)** maximum efficiency of photosystem II photochemistry (F_v/F_m), an indicator of photoinhibition. NEC stands for Nitrogen Efficient Crop (see **Figure 1** legend and section Materials and Methods for details). Measurements on leaves were performed before treatments (week 0), and in the middle (week 4) and end (week 8) of treatments. Data are mean of $n = 8 \pm$ SE. p values of three-way ANOVA are shown in the inlets and values of $p > 0.10$ were considered as NS. Different letters indicate differences in Tukey's HSD multiple comparison test.

helped maintain carotenoids content and the chlorophyll a/b ratio high at week 8, but not as high as when combined with Pepton (**Figure 5**). This Pepton-related differential behavior in NEC plants may be attributed to an increased endogenous concentration of cytokinins, and most particularly of the active form *t*-Z, but not of any of the stress-related phytohormones, ABA, SA, or JA (**Figures 6, 7**). NEC treatment had an impact on the endogenous content

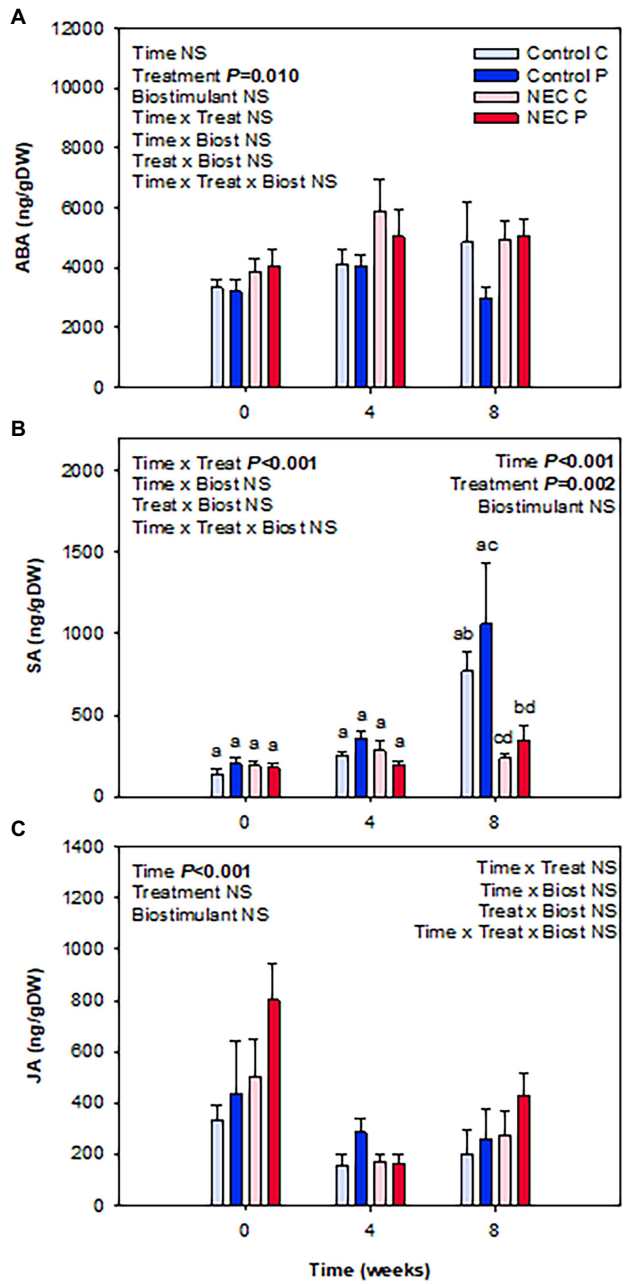

FIGURE 6 | Effects of low nitrogen priming and Pepton application on the endogenous contents of stress-related phytohormones in leaves of greenhouse-grown tomato plants. **(A)** Abscisic acid (ABA), **(B)** salicylic acid (SA), and **(C)** jasmonic acid (JA). NEC stands for Nitrogen Efficient Crop (see **Figure 1** legend and section Materials and Methods for details). Measurements on leaves were performed before treatments (week 0), and in the middle (week 4) and end (week 8) of treatments. Data are mean of $n = 8 \pm$ SE. p values of three-way ANOVA are shown in the inlets and values of $p > 0.10$ were considered as NS. Different letters indicate differences in Tukey's HSD multiple comparison test.

of ABA, which was most evident at week 4, but most particularly in the endogenous content of SA at week 8 (**Figure 6**). As SA is a well-known growth inhibitor (Abreu and Munné-Bosch, 2009), reduced contents of SA in leaves of NEC may contribute to enhanced yields in low N-primed plants, an effect that occurred both with and without Pepton application. In contrast, Pepton doubled the endogenous contents of *t*-Z in combination with the NEC treatment (**Figure 7**), thus showing a possible link with the maintenance of chlorophyll contents (**Figure 5**). It is well-known that high cytokinins contents may have an anti-senescing effect and help maintain the photosynthetic apparatus active for longer (Müller and Munné-Bosch, 2021), which in this case might contribute to increase fruit yield in greenhouse-grown tomatoes subject to a combination of Pepton application and low N priming. It is interesting to note that this cytokinin-mediated effect was not observed for NEC only, thus indicating differential mechanisms of action upon the application of Pepton. It was only the combination of low N priming together with Pepton application that caused additive effects on yield, enhanced cytokinin contents and a maintenance of chlorophyll contents. It is tempting to speculate that the composition of peptides in Pepton may cause such an effect, since previous studies have shown a crosstalk between peptide and cytokinin signaling in plants (Leibfried et al., 2005; Fukuda and Higashiyama, 2011; Sakakibara, 2021), an aspect that warrants further investigations.

Another important point that needs consideration is the application and interpretation of statistical evaluation of results in the study of the application of biostimulants to improve crop yields and produce quality, either in the field or in controlled trials, as that performed in the present study. Statistical analyses generally rely on p values to demonstrate relationships and the traditional level of significance ($p < 0.05$) can indeed be negatively impacted by small sample size, bias, and random error, so that in psychology and biochemical research has sometimes evolved to include interpretation of statistical trends, correction factors for multiple analyses, and acceptance of statistical significance for $p > 0.05$ for complex relationships such as effect modification (These et al., 2016). We suggest that in very particular cases, where biostimulants may have relatively effects by themselves but they can indeed modify the effect of another treatment, as it occurred in our study with low N priming, it is suggested to consider p values close to 0.05 as showing a trend to significant effect and must not be disregarded. As shown in the present study, these effects may be out of the classical p value but at the same time represent important increases in yield that if confirmed under field conditions will lead to important economical revenues. It is therefore of value to include results with a trend to statistically significant results, so that these positive effects can be scalable and therefore adequately tested in the field in future studies. Furthermore, we strongly encourage research that relies on various yield and quality parameters, instead of using only one parameter, since any small unavoidable bias due to the intrinsic methodology used on the latter case can lead to equivocal interpretation of results.

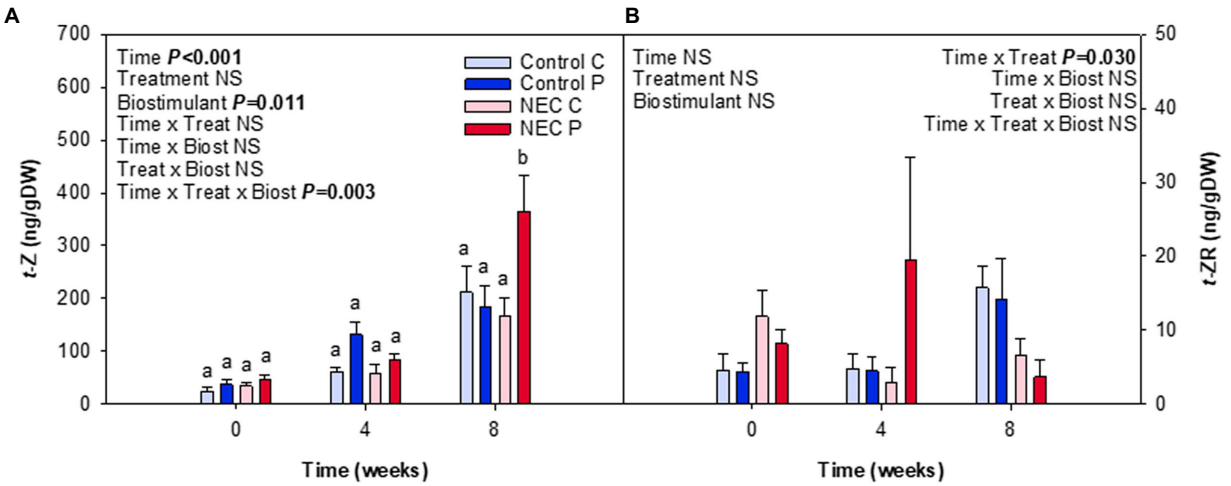

FIGURE 7 | Effects of low nitrogen priming and Pepton application on the endogenous contents of cytokinins in leaves of greenhouse-grown tomato plants. **(A)** *trans*-zeatin (*t*-Z) and **(B)** *trans*-zeatin (*t*-ZR). NEC stands for Nitrogen Efficient Crop (see **Figure 1** legend and section Materials and Methods for details). Measurements on leaves were performed before treatments (week 0), and in the middle (week 4) and end (week 8) of treatments. Data are mean of $n = 8 \pm$ SE. *p* values of three-way ANOVA are shown in the inlets and values of $p > 0.10$ were considered as NS. Different letters indicate differences in Tukey's HSD multiple comparison test.

CONCLUSION

It is concluded that priming with low N availability (NEC plants) doubled fruit production (due to an increase in the number of fruits), increased by 20% the amount of total soluble sugars and increased the contents of lycopene (by 90%) and vitamin E (by 40%). Furthermore, it is also stated that pruning the plants may have helped NEC treatment boost the production since there was a reduction of the root N-consuming biomass. Pepton treatment showed a trend to improve total fruit production both in control and NEC plants, thus indicating an additive effect to low N priming in boosting fruit production. Pepton maintained fruit quality in terms of sugar accumulation, total acidity, and the contents of carotenoids, vitamins C and E. Pepton-related improvement in fruit production seemed to be related, at least in part, to an increased accumulation of cytokinin and photosynthetic pigments in leaves, which might favor vegetative vigor and ultimately fruit yield. It should be noted that the observed effects may at least be partially attributed to the pruning that was carried out 7 weeks after treatment, thus it imperative to carry out future research to unravel the mechanisms underlying the interactive effects of low N priming with biostimulant application and pruning.

DATA AVAILABILITY STATEMENT

The original contributions presented in the study are included in the article/supplementary material, further inquiries can be directed to the corresponding author.

AUTHOR CONTRIBUTIONS

JP and SM-B conceived and designed the experiments with the help of AC. AC, IG, and TM performed the experiments. AC and TM prepared the figures and performed the statistical analyses. SM-B wrote the first draft of the manuscript with the help of TM and JP. All authors contributed to the article and approved the submitted version.

FUNDING

This study was partially funded by the European Union Regional Development Fund within the framework of the ERDF Operational Program of Catalonia 2014–2020 with the reference RD17-1-0096 (Generalitat de Catalunya, Spain) and by APC Europe S.L. The funders were not involved in the study design, collection, analysis, interpretation of data, the writing of this article, or the decision to submit it for publication.

ACKNOWLEDGMENTS

The authors are deeply indebted to *Serveis de Camps Experimentals* and *Serveis Científico-tècnics* from the University of Barcelona for their help in growing the plants. We are also very grateful to David H. Fresno for his help with some samplings and biochemical analyses.

REFERENCES

Abenavoli, M., Longo, C., Lupini, A., Miller, A., Araniti, F., Mercati, F., et al. (2016). Phenotyping two tomato genotypes with different nitrogen use efficiency. *Plant Physiol. Biochem.* 107, 21–32. doi: 10.1016/j.plaphy.2016.04.021

Abreu, M. E., and Munné-Bosch, S. (2009). Salicylic acid deficiency in *NahG* transgenic lines and *sid2* mutants increases seed yield in the annual plant *Arabidopsis thaliana*. *J. Exp. Bot.* 60, 1261–1271. doi: 10.1093/jxb/ern363

Asensio, E., Sanvicente, I., Mallor, C., and Menal-Puey, S. (2019). Spanish traditional tomato. Effects of genotype, location and agronomic conditions

on the nutritional quality and evaluation of consumer preferences. *Food Chem.* 270, 452–458. doi: 10.1016/j.foodchem.2018.07.131

Aziz, A. B. (1968). Seasonal Changes in the Physical and Chemical Composition of Tomato Fruits as Affected by Nitrogen Levels. Mededelingen Landbouwhogeschool, Wageningen, Netherlands, 68, 1–6.

Bénard, C., Gautier, H., Bourgaud, F., Grasselly, D., Navez, B., Caris-Veyrat, C., et al. (2009). Effects of low nitrogen supply on tomato (*Solanum lycopersicum*) fruit yield and quality with special emphasis on sugars, acids, ascorbate, carotenoids, and phenolic compounds. *J. Agric. Food Chem.* 57, 4112–4123. doi: 10.1021/jf8036374

Burri, N., Weatherl, R., Moeck, C., and Schirmer, M. (2019). A review of threats to groundwater quality in the anthropocene. *Sci. Total Environ.* 684, 136–154. doi: 10.1016/j.scitotenv.2019.05.236

Casadesús, A., Pérez-Llorca, M., Munné-Bosch, S., and Polo, J. (2020). An enzymatically hydrolyzed animal protein-based biostimulant (Pepton) increases salicylic acid and promotes growth of tomato roots under temperature and nutrient stress. *Front. Plant Sci.* 11:953. doi: 10.3389/fpls.2020.00953

Casadesús, A., Polo, J., and Munné-Bosch, S. (2019). Hormonal effects of an enzymatically hydrolyzed animal protein-based biostimulant (Pepton) in water-stressed tomato plants. *Front. Plant Sci.* 10:758. doi: 10.3389/fpls.2019.00758

Colla, G., Hoagland, L., Ruzzi, M., Cardarelli, M., Bonini, P., Canaguier, R., et al. (2017). Biostimulant action of protein hydrolysates: unravelling their effects on plant physiology and microbiome. *Front. Plant Sci.* 8:2202. doi: 10.3389/fpls.2017.02202

Colla, G., Rouphael, Y., Canaguier, R., Svecova, E., and Cardarelli, M. (2014). Biostimulant action of a plant-derived protein hydrolysate produced through enzymatic hydrolysis. *Front. Plant Sci.* 5:448. doi: 10.3389/fpls.2014.00448

FAOSTAT (2019). Food and Agriculture Organization of the United Nations. Available at: http://www.fao.org/faostat/en/ (Accessed October 28, 2021).

Fish, W., Perkins-Veazie, P., and Collins, J. (2002). A quantitative assay for lycopene that utilizes reduced volumes of organic solvents. *J. Food Compos. Anal.* 15, 309–317. doi: 10.1006/jfca.2002.1069

Fisher, R. A. (1950). *Statistical Methods for Research Workers. 11th Edn. Biological Monographs and Manuals*. Edinburgh, UK: Oliver and Boyd.

Flores, P., Botella, M., Cerdá, A., and Martínez, V. (2004). Influence of nitrate level on nitrate assimilation in tomato (*Lycopersicon esculentum*) plants under saline stress. *Can. J. Bot.* 82, 207–213. doi: 10.1139/b03-152

Fukuda, H., and Higashiyama, T. (2011). Diverse functions of plant peptides: entering a new phase. *Plant Cell Physiol.* 52, 1–4. doi: 10.1093/pcp/pcq193

Gao, J., Luo, Q., Sun, C., Hu, H., Wang, F., Tian, Z., et al. (2019). Low nitrogen priming enhances photosynthesis adaptation to water-deficit stress in winter wheat (*Triticum aestivum* L.) seedlings. *Front. Plant Sci.* 10:818. doi: 10.3389/fpls.2019.00818

Hernández, V., Hellín, P., Fenoll, J., and Flores, P. (2020). Impact of nitrogen supply limitation on tomato fruit composition. *Sci. Hortic.* 264:109173. doi: 10.1016/j.scienta.2020.109173

Hoagland, D. R., and Arnon, D. I. (1950). The Water-Culture Methods for Growing Plants Without Soil. California Agricultural Experiment Station Circular 347, College of Agriculture, University of California, USA.

Leibfried, A., To, J. P., Busch, W., Stehling, S., Kehle, A., Demar, M., et al. (2005). WUSCHEL controls meristem function by direct regulation of cytokinin-inducible response regulators. *Nature* 438, 1172–1175. doi: 10.1038/nature04270

Lichtenthaler, H. K. (1987). Chlorophylls and carotenoids: pigments of photosynthetic biomembranes. *Methods Enzymol.* 148, 350–382. doi: 10.1016/0076-6879(87)48036-1

Lichtenthaler, H., and Wellburn, A. (1983). Determinations of total carotenoids and chlorophylls a and b of leaf extracts in different solvents. *Biochem. Soc. Trans.* 11, 591–592. doi: 10.1042/bst0110591

Marfà, O., Cáceres, R., Polo, J., and Ródenas, J. (2009). Animal protein hydrolysate as a biostimulant for transplanted strawberry plants subjected to cold stress. *Acta Hortic.* 842, 315–318. doi: 10.17660/actahortic.2009.842.57

Müller, M., and Munné-Bosch, S. (2011). Rapid and sensitive hormonal profiling of complex plant samples by liquid chromatography coupled to electrospray ionization tandem mass spectrometry. *Plant Methods* 7:37. doi: 10.1186/1746-4811-7-37

Müller, M., and Munné-Bosch, S. (2021). Hormonal impact on photosynthesis and photoprotection in plants. *Plant Physiol.* 185, 1500–1522. doi: 10.1093/plphys/kiaa119

Navarro, M., and Munné-Bosch, S. (2022). Reduced phosphate availability improves tomato quality through hormonal modulation in developing fruits. *J. Plant Growth Regul.* 41, 153–162. doi: 10.1007/s00344-020-10290-2

Padilla, F., Gallardo, M., and Manzano-Agugliaro, F. (2018). Global trends in nitrate leaching research in the 1960–2017 period. *Sci. Total Environ.* 643, 400–413. doi: 10.1016/j.scitotenv.2018.06.215

Polo, J., Barroso, R., Ródenas, J., Azcón-Bieto, J., Cácerres, R., and Marfá, O. (2006). Porcine hemoglobin hydrolysate as a biostimulant for lettuce plants subjected to conditions of thermal stress. *HortTechnology* 16, 483–487. doi: 10.21273/HORTTECH.16.3.0483

Polo, J., and Mata, P. (2018). Evaluation of a biostimulant (Pepton) based in enzymatic hydrolyzed animal protein in comparison to seaweed extracts on root development, vegetative growth, flowering, and yield of gold cherry tomatoes grown under low stress ambient field conditions. *Front. Plant Sci.* 8:2261. doi: 10.3389/fpls.2017.02261

Queval, G., and Noctor, G. (2007). A plate reader method for the measurement of NAD, NADP, glutathione, and ascorbate in tissue extracts: application to redox profiling during *Arabidopsis* rosette development. *Anal. Biochem.* 363, 58–69. doi: 10.1016/j.ab.2007.01.005

Rouphael, Y., and Colla, G. (2020). Editorial: biostimulants in agriculture. *Front. Plant Sci.* 11:40. doi: 10.3389/fpls.2020.00040

Sakakibara, H. (2021). Cytokinin biosynthesis and transport for systemic nitrogen signaling. *Plant J.* 105, 421–430. doi: 10.1111/tpj.15011

Takahama, U., and Oniki, T. (1992). Regulation of peroxidase-dependent oxidation of phenolics in the apoplast of spinach leaves by ascorbate. *Plant Cell Physiol.* 33, 379–387.

Takahashi, S., and Badger, M. R. (2011). Photoprotection in plants: a new light on photosystem II damage. *Trends Plant Sci.* 16, 53–60. doi: 10.1016/j.tplants.2010.10.001

These, M. S., Ronna, B., and Ott, U. (2016). P value interpretations and considerations. *J. Thorac. Dis.* 8, E928–E931. doi: 10.21037/jtd.2016.08.16

Truffault, V., Marlene, R., Brajeul, E., Vercambre, G., and Gautier, H. (2019). To stop nitrogen overdose in soilless tomato crop: a way to promote fruit quality without affecting fruit yield. *Agronomy* 9:80. doi: 10.3390/agronomy9020080

van Kooten, O., and Snel, J. F. H. (1990). The use of chlorophyll fluorescence nomenclature in plant stress physiology. *Photosynth. Res.* 25, 147–150. doi: 10.1007/BF00033156

Warner, J., Zhang, T. Q., and Hao, X. (2004). Effects of nitrogen fertilization on fruit yield and quality of processing tomatoes. *Can. J. Plant Sci.* 84, 865–871. doi: 10.4141/P03-099

Xu, S., Sun, X., Lu, H., Yang, H., Ruan, Q., Huang, H., et al. (2018). Detecting and monitoring the flavor of tomato (*Solanum lycopersicum*) under the impact of postharvest handlings by physicochemical parameters and electronic nose. *Sensors* 18:1847. doi: 10.3390/s18061847

Conflict of Interest: JP is employed by APC Europe S.L.

The remaining authors declare that the research was conducted in the absence of any commercial or financial relationships that could be construed as a potential conflict of interest.

Publisher's Note: All claims expressed in this article are solely those of the authors and do not necessarily represent those of their affiliated organizations, or those of the publisher, the editors and the reviewers. Any product that may be evaluated in this article, or claim that may be made by its manufacturer, is not guaranteed or endorsed by the publisher.

frontiers in Plant Science

ORIGINAL RESEARCH
published: 18 March 2022
doi: 10.3389/fpls.2022.860484

Root Reinforcement Improved Performance, Productivity, and Grain Bioactive Quality of Field-Droughted Quinoa (*Chenopodium quinoa*)

Salma Toubali[1,2,3], Mohamed Ait-El-Mokhtar[1,2], Abderrahim Boutasknit[1,2,3], Mohamed Anli[1,2,3], Youssef Ait-Rahou[1,2], Wissal Benaffari[1,2,3], Hela Ben-Ahmed[3], Toshiaki Mitsui[4], Marouane Baslam[4] and Abdelilah Meddich[1,2,3]**

[1]Center of Agrobiotechnology and Bioengineering, Research Unit Labelled CNRST (Centre AgroBiotech-URL-CNRST-05), Physiology of Abiotic Stresses Team, Cadi Ayyad University, Marrakesh, Morocco, [2]Laboratory of Agro-Food, Biotechnologies and Valorization of Plant Bioresources (AGROBIOVAL), Faculty of Science Semlalia, Cadi Ayyad University, Marrakesh, Morocco, [3]Laboratoire Mixte Tuniso-Marocain (LMTM) de Physiologie et Biotechnologie Végétales et Changements Climatiques LPBV2C, Tunis, Tunisia, [4]Laboratory of Biochemistry, Faculty of Agriculture, Niigata University, Niigata, Japan

OPEN ACCESS

Edited by:
Youssef Rouphael,
University of Naples Federico II, Italy

Reviewed by:
Yousef Sohrabi,
University of Kurdistan, Iran
Arafat Abdel Hamed Abdel Latef,
South Valley University, Egypt

***Correspondence:**
Marouane Baslam
mbaslam@gs.niigata-u.ac.jp
Abdelilah Meddich
a.meddich@uca.ma

Specialty section:
This article was submitted to Plant Abiotic Stress, a section of the journal Frontiers in Plant Science

Received: 23 January 2022
Accepted: 28 February 2022
Published: 18 March 2022

Citation:
Toubali S, Ait-El-Mokhtar M, Boutasknit A, Anli M, Ait-Rahou Y, Benaffari W, Ben-Ahmed H, Mitsui T, Baslam M and Meddich A (2022) Root Reinforcement Improved Performance, Productivity, and Grain Bioactive Quality of Field-Droughted Quinoa (Chenopodium quinoa). Front. Plant Sci. 13:860484. doi: 10.3389/fpls.2022.860484

Modern agriculture is facing multiple and complex challenges and has to produce more food and fiber to feed a growing population. Increasingly volatile weather and more extreme events such as droughts can reduce crop productivity. This implies the need for significant increases in production and the adoption of more efficient and sustainable production methods and adaptation to climate change. A new technological and environment-friendly management technique to improve the tolerance of quinoa grown to maturity is proposed using native microbial biostimulants (arbuscular mycorrhizal fungi; AMF) alone, in the consortium, or in combination with compost (Comp) as an organic matter source under two water treatments (normal irrigation and drought stress (DS)). Compared with controls, growth, grain yield, and all physiological traits under DS were significantly decreased while hydrogen peroxide, malondialdehyde, and antioxidative enzymatic functions were significantly increased. Under DS, biofertilizer application reverted physiological activities to normal levels and potentially strengthened quinoa's adaptability to water shortage as compared to untreated plants. The dual combination yielded a 97% improvement in grain dry weight. Moreover, the effectiveness of microbial and compost biostimulants as a biological tool improves grain quality and limits soil degradation under DS. Elemental concentrations, particularly macronutrients, antioxidant potential (1,1-diphenyl-2-picrylhydrazyl radical scavenging activity), and bioactive compounds (phenol and flavonoid content), were accumulated at higher levels in biofertilizer-treated quinoa grain than in untreated controls. The effects of AMF + Comp on post-harvest soil fertility traits were the most positive, with significant increases in total phosphorus (47%) and organic matter (200%) content under drought conditions. Taken together, our data demonstrate that drought stress strongly influences the physiological traits, yield, and quality of quinoa.

Microbial and compost biostimulation could be an effective alternative to ensure greater recovery capability, thereby maintaining relatively high levels of grain production. Our study shows that aboveground stress responses in quinoa can be modulated by signals from the microbial/compost-treated root. Further, quinoa grains are generally of higher nutritive quality when amended and inoculated with AMF as compared to non-inoculated and compost-free plants.

Keywords: biostimulants, root-shoot-grain circuit, seed quality, drought tolerance, antioxidants, pseudocereal, soil health, endogenous mycorrhiza

INTRODUCTION

By 2050, the world's population is expected to reach 9.7 billion, 34% higher than current levels. This will require raising overall food production by about 70% (FAO, 2017). Nearly all of this population increase will occur in many developing economies. This implies the need for significant increases in the production of several key commodities. Demand for (pseudo)cereals, for both food and animal feeds, will need to rise to some 3 billion tons, *vs* 2.1 billion today, by 2050. Major cereal crops, including wheat, rice, barley, and corn, are progressively failing to withstand the growing salinity and water scarcity present in marginal environments that are highly vulnerable to climate variability, such as shifts in growing season conditions (IPCC, 2014). Therefore, there is an urgent need to identify alternative ways to sustain and, possibly, increase agricultural production in areas where the cultivation of traditional crops has become greatly complicated and even sometimes uneconomic. Quinoa (*Chenopodium quinoa* Wild.) is an annual herbaceous pseudocereal crop originating from the Andean Mountains, where it has developed tolerance to several abiotic stresses (Di Fabio and Parraga, 2017). Quinoa grains—known as the "mother grain" of the Incan Empire—are a gluten-free alternative to starchy grains and have a low glycaemic index (Gordillo-Bastidas et al., 2016). Deemed the "Queen of Superfoods," this plant was prized for its nutritional qualities as it contains all nine essential amino acids, carbohydrates, poly-unsaturated fatty acids, fiber, vitamins, and minerals (Ruiz-Lozano et al., 2016; Vilcacundo and Hernández-Ledesma, 2017). The grains also contain a large amount of phenolics, flavonols, and betalains (Abderrahim et al., 2015; Escribano et al., 2017). Such is the value of the plant that the UN marked 2013 as the International Year of Quinoa owing to its biodiversity and nutritional value and its role in providing food security and nutrition and poverty eradication, as well as its adaptability to thrive in a wide range of agroecosystems, as it grows at an exceptional range of altitudes, temperatures, humidities, and under different soil conditions (Bazile et al., 2013; Hussain et al., 2018).[1] Due to its superior nutritional profile and stress tolerance, interest in quinoa is increasing worldwide, although it is still an underutilized crop with few breeding programs (Massawe et al., 2016).

More frequent and severe droughts are expected across many regions in the 21st century (Schwalm et al., 2017). Drought has a negative effect on growth, physiology, and yield (Fischer et al., 2017; Miranda-Apodaca et al., 2018). With climate change, growing alterations in the frequency, duration, and intensity of droughts and impending water disputes, the potential gains in welfare from selecting/cultivating effective drought-tolerant (DT) crops and using smart agronomical techniques, are enormous. In the past decade, total investment in drought-resistance research has clearly exceeded US$1 billion (Lybbert and Bell, 2010b). Yet, (marginal) farmers—who are typically faced with poor soils, erratic weather and limited or no access to irrigation, and other inputs—may lack the control to perceive subtle differences in the value of competing varieties and their views of the relative yield benefit of DT varieties are conditioned by (1) drought pressure: if increased cost is not associated with benefit or if the yield is comparatively lower in DT varieties than in conventional varieties when water is plentiful and (2) if the relative benefits of DT varieties fade as drought severity increases (Lybbert and Bell, 2010a). Recently, Jarvis et al. sequenced the approximately 1.5-gigabase-long genome of *C. quinoa* (Jarvis et al., 2017). Using the information gained from the genome to improve quinoa production will require robust breeding efforts and fundamental research to identify the defenses mechanism used by quinoa.

To date, manipulating a plant's genetic makeup is a time-consuming option to enrich the new genetic variant. It is a tedious process and has several significant challenges under natural field conditions. Therefore, the demand for sustainable cropping systems has encouraged the search for technologies—from treated seeds and crop protection products to data analysis apps and precision spraying—and alternatives to increase crop production and quality/functionality with improved defense mechanisms, especially under stressful conditions. While farmer stakeholders may be able to afford to invest, small/marginal farmers have little or no access to affordable institutional credit. Further, farmers must learn how to best use these technologies to improve their farming business. To address these issues, there has been an upsurge in agricultural technologies and products. Different soil management practices that can enhance soil fertility, water availability, and the root zone could be efficient drought mitigation tools in irrigated and non-irrigated regions (Phillips et al., 2020).

In recent years, the use of plant biostimulants, either non-microbial or microbial, has become a popular option to enhance water and crop productivity and adapt crops to rapidly changing environmental conditions. The biofertilizer industry has witnessed a relatively stable market growth following the COVID-19

[1]http://www.fao.org/quinoa-2013/en/

pandemic, with a similar trend of high demand existing in 2020. The global biofertilizer market is estimated to be worth US$ 2.6 billion in 2021 and is expected to reach a value of US$ 4.5 billion by 2026, at a compound annual growth rate (CAGR) of 12%. The need to increase food production combined with the imperative need to preserve natural resources has led to an upsurge in materials with low environmental impact but high efficiency, with natural-based substances being prioritized over synthetic inputs. The FAO recently recognized the potential of microbiomes in food production/safety, health enhancement, and environmental sustainability (FAO, 2019). Arbuscular mycorrhizal fungi (AMF) have been identified as microorganism targets that increase abiotic stress tolerance (Abdel Latef and Chaoxing, 2011). More than two-thirds of terrestrial plants acquire mineral nutrients from the soil by the root pathway *via* root epidermal cells and root hairs, and the mycorrhizal pathway (Smith and Smith, 2011). AMF recruit distinct microbes into their hyphosphere to shape the "second genome of AMF," which significantly contributes to soil organic nutrient mobilization and turnover (Zhang et al., 2021). By colonizing the rhizosphere/endo-rhizosphere of plants, these beneficial microorganisms promote growth through various direct and indirect mechanisms (Harrison, 2005; Maillet et al., 2011). In addition, AMF application induces antioxidant enzyme activity and osmolyte accumulation under various stressful conditions, including water shortage (Meddich et al., 2018; Ben-Laouane et al., 2019, 2020; Anli et al., 2020a; Boutasknit et al., 2020b). While plants are known to establish symbiotic relationships and the role of microorganisms in managing (a)biotic stresses is gaining importance, our understanding of those relationships under a stressful environment is rudimentary. Recent research has suggested that AMF should be combined with organic amendments to increase soil fertility (Anli et al., 2020a; Ben-Laouane et al., 2020; Boutasknit et al., 2020a, 2021a; Renaut et al., 2020). Organic compost is increasingly (re)used in (modern) agriculture as a mulch to provide surface protection and it also seems to be beneficial for field crops as an alternative to chemical fertilizer overuse (Raklami et al., 2019b). It is applied to increase plant and soil health, reduce nutrient losses by volatilization or leaching, prevent soil erosion, and improve soil water retention, soil carbon content, and the long-term fertility of agricultural soils. Many stormwater manuals continue to recommend compost as an organic matter source in bioretention soils (PGC, 2014; VTSM, 2017). Quality green composts can provide nutrients and improve physical soil conditions for plant growth (Cogger, 2005). Such composts contain important concentrations of nitrogen (N), phosphorus (P), and potassium (K^+) as well as a wide range of micronutrients, including magnesium, copper, and iron (Meddich et al., 2015).

Our growing understanding of the interconnectedness of microbiomes and organic amendment in environmental and food systems suggests that soil biofertilizer innovations have the potential to improve sustainable food, feed, and biofuel production while embracing the principles of circularity. The role of organic compounds and microorganisms in plant growth, nutrient management, and biocontrol activity is very well established. Despite the promise of biofertilizer applications, the rush to develop them should be tempered by the need to fully understand the systems in which they function and to characterize the biochemical pathways or interactions in crop systems. To the best of our knowledge, this is the first study to investigate the role of the dual application of AMF combined with compost on quinoa plants subjected to drought stress under field conditions. Moreover, quinoa seeds have potential health benefits and recent food trends and high demand have led to the adaptation and commercial production of quinoa seeds. Thus, the main objective of this research was to assess root reinforcement through a synergistic application of multiple soil biofertilizers (integrating organic amendments and native AMF) to mitigate the adverse effects of drought stress on the physiology, growth, yield, grain quality (antioxidant potential) of quinoa, and post-harvest agricultural soil fertility by regulating soil nutrient status and plant physiological processes. We hypothesized that "manipulating"/shaping the below-ground conditions in which plants grow could ultimately be beneficial. This study provides evidence toward selecting assemblages adapted to abiotic stress, improving resistance against stressors to promote the health and drought tolerance of plants.

MATERIALS AND METHODS

Growth Conditions of Plants in the Field, Biofertilizer Material, and Collection of Vegetal Samples

Quinoa (*Chenopodium quinoa* Willd.) cv. Titicaca has been used in this study based on its high nutritional value, early-maturity standard, top performance, and extensive cultivation (high potential of adaptation in the poor organic/mineral matters) in the Andean states, Sahel, the Middle East, and North African regions (Alvar-Beltrán et al., 2020; Miller et al., 2021; Fghire et al., 2022). Quinoa seeds were surface sterilized with sodium hypochlorite solution containing 0.02% Tween 20 for 10 min. After successive washings in sterile water, the seeds were placed on 1% agar plates containing 1/2 Murashige and Skoog (1/2 MS) medium and incubated in dark conditions at 30°C for 3 days. The uniform looking seedlings were transplanted in the field at a spacing of 20 cm (same row) × 80 cm (between rows) at Saada fields, Marrakesh, Morocco (31°37′39.9″ N and 08°07′46.7″ W), during February–June 2020. The climate of this location is semi-arid, with an average annual temperature of 19.6°C and an average annual rainfall of 250 mm (from September to June). Meteorological data (minimum and maximum temperature, minimum and maximum relative humidity, wind speed, solar radiation, and rainfall) were measured by iMETOS® ag weather stations installed in the field and presented in **Supplementary Figure S1**.

The fields have never been treated before with chemical fertilizers or other organic fertilizers. The physicochemical characteristics of the agricultural soil are reported in **Table 1**. All agronomic practices were performed uniformly for the quinoa plants, following the local cultural practices. We number the weeks according to the plants growing dates. Week 0 coincides with seedling emergence. Plants were subjected to two water regimes: 100% field capacity (FC; WW; well-watered regularly at 8 l/h) and 50% FC (DS; drought stress *ca*. 4 l/h) conditions

TABLE 1 | Physicochemical parameters of agricultural soil and compost used.

	Soil	Compost
Sand (%)	52	
Clay (%)	24	
Loam (%)	24	
pH	7.90 ± 0.07	7.74 ± 0.01
EC (mS cm^{-2})	1.70 ± 0.60	5.46 ± 0.20
TKN (%)	0.15 ± 0.01	1.32 ± 0.01
NH_4^+ (%)	–	0.09 ± 0.01
NO_3^- (%)	–	0.31 ± 0.01
TOC (%)	1.30 ± 0.30	5.72 ± 0.45
OM (%)	2.24 ± 0.50	9.86 ± 0.78
C/N	–	7.49 ± 0.00
NH_4^+ / NO_3^-	–	0.29 ± 0.00
Polsen (ppm)	31.00 ± 2.00	489.95 ± 20.3
Na^+ (mg g^{-1})	1.24 ± 0.08	2.11 ± 0.05
K^+ (mg g^{-1})	1.43 ± 0.01	5.59 ± 0.15
Ca^{2+} (mg g^{-1})	17.77 ± 2.03	37.38 ± 1.84

EC, electrical conductivity; TKN, total Kjeldahl nitrogen; TOC, total organic carbon; OM, organic matter; C/N, carbon-to-nitrogen ratio; and P, phosphorus. Values represent the mean ± standard deviation (SD).

applied from week 1 until harvest. The field plots were irrigated at five-day intervals using drip irrigation system lines, with appropriate internal drippers, placed on the soil surface of each furrow. The WW plots received 100% FC of the weekly calculated crop evapotranspiration for the 5 days before each irrigation. Crop evapotranspiration was determined according to Xu et al. (2018) using potential evapotranspiration multiplied by the crop coefficient, which was adjusted according to crop growth stage.

We extracted and isolated an indigenous consortium of AMF isolated from the Tafilalet palm grove located 500 km southeast of Marrakesh (Morocco) and containing a mixture of 15 species: *Acaulospora delicata*, *A. leavis*, *Acaulospora* sp., *Claroideoglomus claroideum*, *Glomus aggregatum*, *G. claroides*, *G. clarum*, *G. deserticola*, *G. heterosporum*, *G. macrocarpum*, *G. microcarpum*, *G. versiforme*, *Glomus* sp., *Rhizophagus intraradices*, and *Pacispora boliviana* (Meddich et al., 2015). These species belong to five genera: *Glomus* (60% of the total community), *Acaulospora* (20%), *Claroideoglomus*, *Rhizophagus*, and *Pacispora* (all these three 6.7%). The number of AMF spores detected in this inoculum was 47 spores/100 g of the soil sample. The inoculum was enriched in propagules by co-cultivation with *Zea mays* L. as the host plant under controlled greenhouse conditions. Corn roots containing hyphae, vesicles, and spores were harvested, cut into small pieces and used as the inoculum. Inoculation of quinoa plants was performed by adding 2 g (/plant) of the inoculum (roots and substrate containing spores) to the quinoa root system. Non-mycorrhizal (NM) treatments received an equal quantity of both non-inoculated (and non-mycorrhizal) *Z. mays* roots to match "organic matter" in the pots and filtered inoculum in an attempt to restore other soil free-living microorganisms accompanying the AMF. The filtrate for each pot was obtained by passing the mycorrhizal inoculum in 20 ml of distilled water through a layer of 15- to 20-mm filter papers (Whatman, GE Healthcare, Buckinghamshire, United Kingdom).

The compost used in this study was prepared from green waste (quack grass) as described by Meddich et al. (2016). The physicochemical properties of the compost are presented in **Table 1**. The compost was applied to the corresponding plot at a rate of 1.2 Kg/plot (10 t/ha).

Each water regime (WW or DS) comprised four treatments: (1) Control: non-inoculated and non-amended, (2) AMF: seedlings inoculated with the indigenous AMF consortium, (3) Comp: seedlings amended with compost, and (4) AMF + Comp: joint application of AMF and Comp. The experimental design was carried out as a split-plot based on a randomized complete block design with three replications. The fields were divided into 24 plots, 0.8 m wide separated from each other by 0.5 m; of six rows each (∼ 60 plants per plot). Each plot was randomly assigned a watering regime (WW or DS) comprising biofertilizers (or not) treatments, with three replicates, for a total of 24 (2×4×3).

Harvesting, Plant Growth, and Yield Parameters

After 4 months of cultivation, at the harvest time and within each plot, individual plant samples were manually collected at the same time of the day (10 am to 1 pm). Ten representative plant samples from each plot were collected. Roots were collected using a shovel from 30 cm depth of each plant's system, avoiding brace roots, cutting using garden shears, and kept into an aluminum foil bag and then pooled. Roots were vortexed for 2 min in epiphyte removal buffer to remove rhizosphere soil, rinsed twice in root washing buffer, gently wiped, and placed in aluminum foil bags for the subsequent analyses.

The growth performance of quinoa plants was assessed by measuring the seed yield, shoot height (SH), root elongation (RE), biomass production (PDM; plant dry matter), and seeds dry matter (SDM). DM was obtained after drying samples at 80°C until the weight remained constant. Seed samples were cleaned and stored (4°C) for subsequent analyses. The tolerance index (TI) was calculated using the DMs according to the methods described by Parvez et al. (2020) using the following formula:

$$\text{Tolerance index (TI)}(\%) = \left(\frac{\text{DM}_{\text{stressed plants}}}{\text{DM}_{\text{well-watered}}}\right) \times 100$$

Mycorrhization Assessement

The harvested roots were washed with distilled water and cleared with 10% KOH at 90°C for 30 min. Then, they were rewashed and acidified with 2% HCl for 10 min and stained with Trypan blue at 90°C for 20 min, according to Phillips and Hayman (1970). Root fragments of 1 cm long were observed in the glycerol droplet. The microscopic assessment of mycorrhizal root colonization rates (F %: frequency and I %: intensity) was performed according to the method of Derkowska et al. (2008) using 20 randomly selected root fragments repeated five times for each sample.

$$\text{Mycorrhizal frequency (F)}(\%) = \left(\frac{\text{Infected root segments}}{\text{Total roots segments}}\right) \times 100$$

$$\text{Mycorrhizal intensity}\,(\text{I})(\%) = \frac{(95n5 + 70n4 + 30n3 + 5n2 + n1)}{\text{Total roots segments}}$$

Where n represents fragments with an index of 0, 1, 2, 3, 4, or 5 with the following infection rates: $100 > n5 > 90$; $90 > n4 > 50$; $50 > n3 > 10$; $10 > n2 > 1$; and $1 > n1 > 0$.

Grain Mineral Composition Analysis

Mineral concentrations (K, Ca, and Na) in grain were determined after digestion using ICP/OES Ultima Expert (inductively coupled plasma/optical emission spectrometry, iCAP 6500 Duo, Horiba Inc., Burlington, ON, Canada). The total phosphorus in grains was determined according to the method described by Olsen and Sommers (1982).

Measurement of Chlorophyll and Carotenoids Concentration

The concentration of chlorophyll *a*, *b*, total chlorophyll, and carotenoids was determined using the method of Lichtenthaler (1987). Leaf tissue (100 mg) was homogenized in 80% pre-chilled acetone. After centrifugation at 10,000 $\times g$ for 10 min, the supernatants were pooled and the absorbance of the extract was read at 480, 645, and 663 nm using a UV/visible spectrophotometer (UV-3100 PC spectrophotometer).

Total Soluble Sugars and Protein Quantification

The quantity of total soluble sugars (TSS) content was determined according to Kochert (1978) in 0.25 ml of the supernatant mixed with 0.25 ml of phenol and 1.25 ml of sulfuric acid. After 15 min, TSS content was determined by measuring the absorbance at 485 nm and calculated using the standard glucose curve.

Total soluble proteins were determined according to the technique described by Bradford (1976). Samples (1 g) were homogenized with 4 ml of 1 M phosphate buffer (pH 7.2) and then centrifuged at 18,000 *x g* for 15 min at 4°C. The absorbance was read at 595 nm.

Stress Indicators (Malondialdehyde and Hydrogen Peroxide) Determination

Hydrogen peroxide (H_2O_2) concentration in seeds and leaves was determined by the method described by Velikova et al. (2000). Briefly, samples were homogenized with 5 ml 10% (w/v). Trichloroacetic acid (TCA) in an ice bath and then centrifuged at 12,000 × *g* for 10 min at 4°C. The supernatant (0.5 ml) was recovered to determine the content of H_2O_2 and 0.5 ml of potassium phosphate buffer (10 mM, pH 7) and 1 ml of iodic potassium (1 M) was added. After 1 h of incubation, the absorbance at 390 nm was recorded and plotted against a standard H_2O_2 curve. The blank was made by replacing the sample extract with 10% TCA.

Lipid peroxidation as malondialdehyde (MDA) equivalent was evaluated in seeds and leaves tissues. MDA content was estimated by seed samples (0.1 g) in 3 ml of 0.1% (w/v) TCA and centrifuged at 18,000 × *g* for 10 min as described by Rao and Sresty (2000). Supernatant was mixed with 3 ml of 0.1% TCA containing 0.5% (w/v) thiobarbituric acid (TBA). The mixture was then heated in a water bath at 100°C for 30 min and immediately cooled in an ice bath. The absorbance was read at 440, 532, and 600 nm. The concentration of MDA (nmol g^{-1} DW) was calculated by using the extinction coefficient of 155 mM cm^{-1}, and the results were expressed as nmol MDA equivalents per grams.

Preparation of Methanolic Extracts

Two grams of ground quinoa seeds was mixed with 50 ml of 80% (v/v) methanol at room temperature with frequent agitation. The mixtures were then left in a shaking incubator prior to filtration (Buckner funnel and Whatman No. 1) for 24 h and were then centrifuged at 3,500 × *g* for 10 min at 5°C. The clarified extract was collected and then evaporated to dryness using a rotary evaporator at 40°C. Finally, the extract was reconstituted in sterile distilled water, freeze-dried, and stored at 4°C in an airtight container until further use.

Determination of Total Phenols and Flavonoids Content and 1,1-Diphenyl-2-Picrylhydrazyl Radical Scavenging Assay in Quinoa Grain

The total phenolic content (TPC) was measured using the Singleton et al. (1999) assay with slight modifications. To determine the total flavonoids, gallic acid standard was used to prepare the calibration curve. Briefly, a 250 µl aliquot of appropriately diluted methanolic extract solution (with distilled water) was placed in a test tube, to which 2.5 ml of 1 N Folin–Ciocalteu reagent solution was added. The mixture was incubated at room temperature for 3 min. Then, 250 µl of 10% sodium carbonate (Na_2CO_3) solution was added and kept in a dark place for 90 min. The absorbance of the extract solution and different concentrations of quercetin standard was measured at 760 nm. The TPC was calculated using an established formula and was expressed as milligrams of gallic acid equivalents (GAE) per g of quinoa sample DM (mg GAE/g DM).

The total flavonoids content (TFC) was determined using the colorimetric method described by Li et al. (2006). A quercetin standard was used to prepare the calibration standard curve to determine the TFC. A 0.5 ml aliquot of appropriately diluted methanol extract solution was taken in a test tube, to which 0.3 ml of 5% sodium nitrate solution was added. The mixture was kept at room temperature for 5 min. Then, 0.3 ml of 10% aluminum nitrate was added to each test tube, kept in a dark place for 6 min, and the reaction was stopped by adding 2 ml of 1 M sodium hydroxide. The absorbance of the extract solution and different concentrations of quercetin standard were measured at 510 nm. The standard calibration curve was prepared by plotting the concentration *vs* quercetin absorbance. Finally, The TFC was calculated using an established formula and was expressed as mg of quercetin equivalents.

The free radical scavenging activity of the quinoa seeds was assessed using the modified 1,1-diphenyl-2-picrylhydrazyl (DPPH)

radical scavenging assays of Athamena et al. (2010). A 50 µl aliquot of appropriately diluted methanol extract solution was placed in a test tube, to which 2 ml of freshly prepared 0.1 mM DPPH methanol solution was added. An equal amount of methanol was used as a control. After vigorously shaken incubation for 20 min in a dark place at room temperature, the absorbance of the extract solution and different concentrations of ascorbic acid standard were measured at 517 nm. The scavenging activity was calculated using the following formula:

$$\text{DPPH radical scavenging}(\%) = \left(\frac{A_{control} - A_{sample}}{A_{control}}\right) \times 100$$

The IC50 (half-maximal inhibitory concentration) value was also calculated for the dose inhibition curve in linear range by plotting the extract concentration vs. the corresponding scavenging effect.

Antioxidant Enzymes Activities of Quinoa

Ground samples (100 mg) were mixed with 4 ml of 0.1 M sodium phosphate buffer (pH 7) containing 5% insoluble polyvinylpyrrolidone (PVPP) and 0.1 mM ethylene diamine tetraacetic acid (EDTA). The homogenate was centrifuged at 18,000 × *g* for 10 min at 4°C, and the supernatant was collected and used to measure antioxidant enzymes activities. Total soluble proteins were determined according to the technique described by Bradford (1976).

Superoxide dismutase (*SOD, EC1.15.1.1*) activity was assayed using the method of Beyer and Fridovich (1987). One unit of SOD activity was defined as the amount of enzyme leading to 50% inhibition of nitro blue tetrazolium (NBT) reduction at 25°C. The SOD activity was expressed at unit mg protein^{-1} min^{-1}.

Ascorbate peroxidase (*APX, EC1.11.1.11*) activity was measured according to the method of Amako et al. (1994). APX was assayed as a decrease in absorbance at 290 nm for 1 min. The assay mixture contained 100 µl of extract sample, 50 mM potassium phosphate buffer (pH 7.6) including 0.2 mM EDTA, 100 µM H_2O_2, and 0.5 mM ascorbate. The reaction was initiated by adding the enzyme extract, and the decrease in absorbance was recorded. One enzyme unit was defined as µmol mg^{-1} protein oxidized ascorbate per min.

Peroxidase (*POX, EC 1.11.1.7*) activity was measured using the guaiacol test by monitoring the change of absorbance at 470 nm. The activity was assayed for 3 min in a reaction solution containing 3 ml of 1 M potassium phosphate buffer (pH 7.0), 20 mM guaiacol, 40 mM H_2O_2, and 0.1 ml enzyme extract in a 3 ml volume (Polle et al., 1994). POX activity was determined by its ability to convert guaiacol to tetraguaiacol ($\varepsilon = 26.6\ mM^{-1}\ cm^{-1}$). One unit of POX activity was defined as an absorbance change of 0.01 unit min^{-1}.

Polyphenol oxidase (*PPO, EC 1.14.18.1*) activity was estimated by the method of Hori et al. (1997). The assay solution contained 20 mM catechol in 0.1 M phosphate buffer (pH 7). The reaction was started by adding 100 ml of the enzymatic extract. PPO activity was expressed in enzyme unit mg^{-1} protein. One unit of PPO activity was defined as the amount of enzyme causing an increase in the absorbance of 0.001/min at 420 nm.

Soil Analyses

The physicochemical properties of agricultural field soil were analyzed at plant harvest on samples taken near the roots to assess the effect of compost and/or AMF applied alone or in combination with soil fertility. Five homogeneous rhizospheric soil samples at a 0–20 cm depth were collected for each treatment. The samples were dried and sieved to measure the pH, electrical conductivity (EC), total organic carbon (TOC), organic matter (OM), and assimilable phosphorus (AP). The pH and EC were measured in a diluted soil suspension 1/5 (v/v) using a pH meter HI 9025 and a conductivity meter HI-9033 (Hanna Instruments, Padua, Italy), respectively. Total TOC and OM were measured according to the method described by Aubert (1978), which consists of the oxidation of organic matter by potassium dichromate in the presence of sulfuric acid. The AP concentration was determined according to Olsen and Sommers (1982).

Statistical Analysis

Statistical analysis was carried out with the software package CoStat version 6.400 (CoHort Software). Data were analyzed by employing a three-way multivariate analysis of variance (MANOVA) followed by the Student–Newman–Keuls test using a significance level of 5% ($p \leq 0.05$). The normality of residuals was tested using the Shapiro–Wilk test. Mycorrhizal root colonization rates were arcsin-square root transformed to fit the assumption of normal distribution. Different lower cases indicate significant differences among treatments at $p \leq 0.05$. In order to integrate all the data, a complete dataset comprising all growth, physiological, and biochemical data was subjected to Principal Components Analysis (PCA). The PCA was performed using XLSTAT v. 2016 (Addinsoft, NY, United States). Initially, index values for each treatment were calculated by assessing the response of drought stress compared to its control value. The responses of all the traits under each treatment were combined and used as index values for PCA analysis. These index values were used to identify the correlation of response variable vectors and treatments across the ordination space. Percentage contributions of principal component (PC) variables are shown in **Supplementary Table S2**. The heatmap was performed using the software GraphPad® Prism v9.0 GraphPad (San Diego, CA, United States). Data are presented as mean ± standard error (SE) of three independent biological replicates.

RESULTS AND DISCUSSION

Drought remains one of the most damaging environmental stresses limiting crop production worldwide. Increasing food supply significantly in an unstable environment in the required timeframe is time-consuming. Hence, it is essential to find eco-friendly strategies that allow plants to withstand drought, focus on biomass and functionality, ensure food security, and mitigate the damage occurring in drought-prone areas. To our knowledge, this is the first study to summarize the extent to which the effect of single and multiple combinations of endogenous AMF and/or compost-based amendments are crucial to improve the fitness and health of quinoa—an immense industrial crop—under field drought conditions. Therefore, this

method could be used for designing a functionally reliable system which could be termed "plant probiotics."

Effect of Drought Stress and Biofertilizers on the Root, Plant Growth, and Yield

The AMF infection frequency and intensity were estimated in the root system of quinoa plants (**Figure 1**). Under field conditions, the non-inoculated plants exhibited mycorrhizal infections with or without stress. The addition of AMF alone successfully infected quinoa roots and showed the highest root mycorrhizal frequency (57%) and intensity (44%) regardless of the water regime. The application of drought stress significantly ($p < 0.001$, **Supplementary Table S1**) reduced mycorrhizal frequency and intensity in all the treatments. The negative effect of drought on the AMF colonization of quinoa plants is in line with several studies showing that mycorrhizal infection decreased in drought-treated host plants (Baslam and Goicoechea, 2012; Meddich et al., 2015; Anli et al., 2020a). Drought induces inhibition of AMF spore germination and hyphal growth, thereby decreasing mycorrhizal colonization (Rydlová and Püschel, 2020). In addition, soil moisture plays a vital role in spore germination and/or development (Püschel et al., 2021). The supply of compost significantly ($p < 0.001$, **Supplementary Table S1**) decreased mycorrhizal frequency by *ca*. 40 and 30% and intensity by *ca*. 50 and 30% in AMF-inoculated plants under non-stressed and stressed conditions, respectively. The application of organic amendments including compost and mineral nutrients may reduce AMF root colonization and activity owing to the release of mineralized P in the soil and/or diffusion of decomposition products, which reduces the establishment and maintenance of the symbioses (Gryndler et al., 2008; Baslam et al., 2011). Other studies, in contrast, have revealed that compost application could have a positive effect on AMF growth and sporulation (Cavagnaro et al., 2015; Anli et al., 2020a,b). There may be several reasons for this favorable effect of compost on AMF; N- and humic acid-rich compost (Gryndler et al., 2009), moderate level of soil assimilable P (Yang et al., 2017), and/or compost with no AM fungal spores that could outcompete the native microbial community once the compost is applied to the soil (Yang et al., 2018).

Several studies have been conducted which demonstrate the beneficial effects of AMF and/or compost on plant performance.

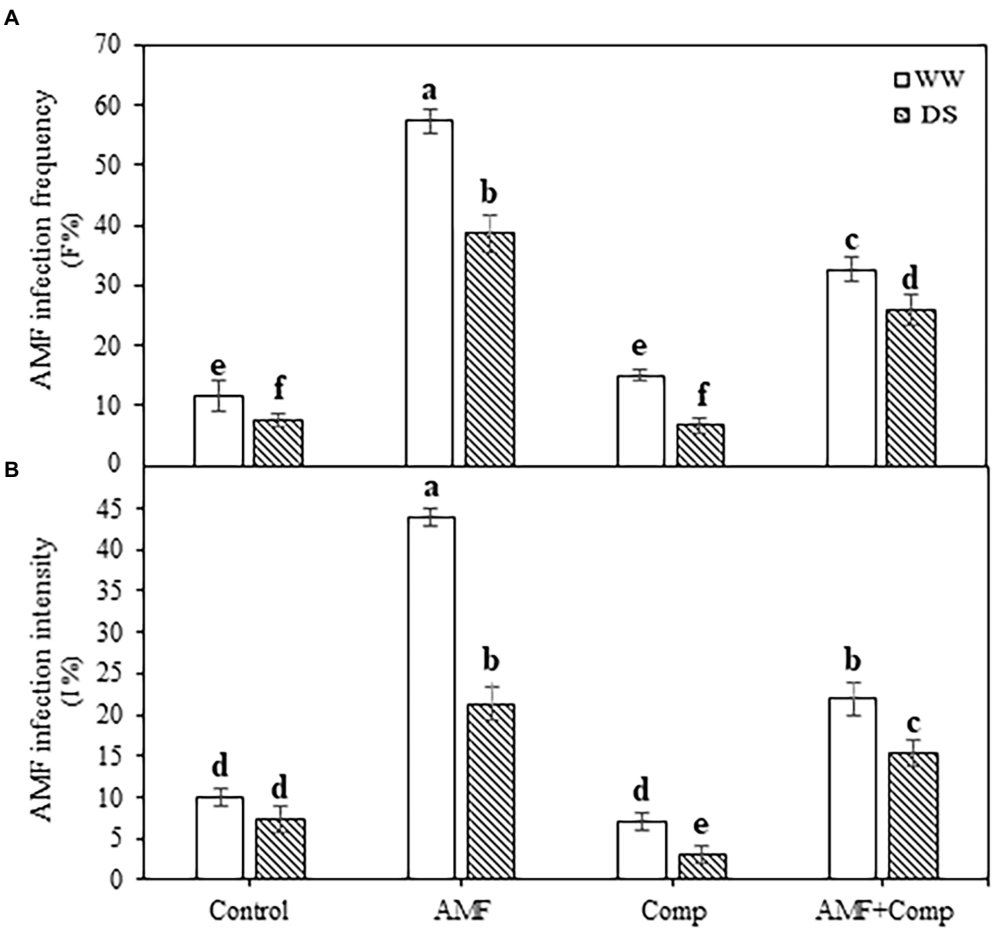

FIGURE 1 | Effects of water regimes (WW; well-watered or DS: drought stress) on AMF infection **(A)** frequency and **(B)** intensity of non-amended and non-inoculated quinoa (control) and quinoa inoculated with arbuscular mycorrhizal fungi (AMF) and/or amended with compost (Comp). Data are mean ± SD. Means followed by the same letters are not significantly different at $p < 0.05$.

Here, we also showed that mycorrhizal symbiosis in the presence or absence of compost improved quinoa biomass and grain quality. In addition to the lower AMF colonization levels under drought stress, we observed higher growth traits in the treated plants relative to those in the control non-amended and non-inoculated plants. These results indicate that compost supply and AMF colonization improved the growth of treated plants. Drought stress jeopardizes plant growth and causes a series of physiological, biochemical, and molecular changes. A large number of studies have reported that biofertilizers enhance the ability of plants to tolerate drought stress through multiple mechanisms in leaves and below-ground, including soil structure improvement, increased formation of soil aggregates, and increases in soil nutrient and moisture retention. Plant nutrient and water absorption have been found to be accelerated due to the vast networks of extraradical mycelium, plant photosynthetic, and defense mechanisms which alleviate harmful reactive oxygen species (ROS) effects have been found to be improved and increases in the expression of drought-resistance genes have been observed (Mo et al., 2016). Here, we were interested in determining whether biofertilizer application would improve quinoa grain traits under drought stress.

The deleterious effect of water stress was observed on all growth parameters (shoot height, root elongation, and plant and grain dry weights) and quinoa yield cultivated under field conditions (**Table 2**). The results revealed that the growth traits and yield of plants were significantly ($p < 0.001$, **Supplementary Table S1**) reduced under water scarcity. However, biofertilizer application mitigated the negative effect of water deficit and improved the growth of quinoa as compared to the controls. The application of compost and AMF, separately or in combination, significantly increased plant biomass under stressed and non-stressed conditions compared to non-inoculated and non-amended plants. In fact, the highest plant growth values were obtained when the compost was combined with AMF (AMF + Comp). Under DS conditions, the AMF + Comp treatment increased plant dry weight (*ca.* 200%), grain dry weight (*ca.* 100%), shoot height (*ca.* 70%), root elongation (32%), and yield (*ca.* 100%) in comparison with stressed control plants.

The tolerance index data revealed that the quinoa variety used (Titicaca) was highly tolerant of water deficit (76%; **Table 2**). Our results are in agreement with previous reports (Finlay, 2008; Anli et al., 2020a), showing that AMF inoculation combined with compost application yielded the highest values of plant growth parameters. The beneficial effect of mycorrhizal symbiosis and compost application on the growth of quinoa under drought could be explained by the greater uptake of low mobility nutrients, such as P and N contained in the substrate. Several studies have indicated that compost, AMF, and PGPR improve plant growth through the assimilation of immobile soil nutrients such as N and P (Tanwar et al., 2013; Baslam et al., 2014; Abdel Latef et al., 2016; Al-Karaki, 2016; Barje et al., 2016; Frosi et al., 2016; Yang et al., 2018; Raklami et al., 2019a; Anli et al., 2021). Previous reports have demonstrated that crops inoculated with AMF accumulated more N and P in leaves than non-mycorrhizal plants when subjected to drought stress (Meddich et al., 2015). Nadeem et al. (2014) showed that AMF could regulate mineral nutrition by solubilizing soil nutrients and producing plant growth regulators (i.e., hormones). This improvement in growth traits could also be due to the growth-promoting mechanisms employed by AMF through the production of phytohormones and the solubilization of minerals (Finlay, 2008). In addition, compost is used as a soil amendment in agriculture to improve organic C supply and increase the storage capacity of water and nutrients in the soil, resulting in a higher photosynthesis rate, growth, and plant stress tolerance (Anli et al., 2020a; Boutasknit et al., 2021b). In this study, growth improvement was accompanied by better quantitative productivity. The significant boost in yield was observed in plants inoculated with AMF and amended with compost.

Biofertilizers Enhanced Nutrient Uptake and the Concentration of Nutrients in Quinoa Grains

Cereal crops such as quinoa provide key nutritional elements to the human diet. However, abiotic stresses can negatively impact the concentration and distribution of nutrients in cereal grains. Indeed, P, K^+, and Ca^{2+} contents were significantly ($p < 0.001$, **Supplementary Table S1**) decreased under water-deficit conditions. In contrast, Na^+ uptake was significantly ($p < 0.001$, **Supplementary Table S1**) higher in stressed plants). Elemental

TABLE 2 | Growth performance, yield, and tolerance index of non-amended and non-inoculated quinoa (control), and quinoa inoculated with arbuscular mycorrhizal fungi (AMF) and/or amended with compost (Comp) subjected to different water regimes (WW; well-watered or DS: drought stress).

		Shoot height (cm)	Root elongation (cm)	Plant dry weight (g/plant)	Grain dry weight (g/plant)	Yield (tons/ha)
WW	Control	97.3 ± 2.5^{c}	44.2 ± 0.7^{de}	5.7 ± 0.2^{e}	15.6 ± 0.7^{d}	3.9 ± 0.2^{d}
	AMF	116.7 ± 2.9^{b}	53.7 ± 1.5^{b}	18.0 ± 1.3^{b}	24.0 ± 1.0^{b}	6.0 ± 0.3^{b}
	Comp	110.3 ± 0.6^{b}	43.3 ± 1.4^{e}	14.9 ± 0.6^{c}	21.5 ± 0.5^{c}	5.4 ± 0.1
	AMF + Comp	123.3 ± 3.0^{a}	57.3 ± 1.4^{a}	21.6 ± 0.5^{a}	32.0 ± 2.6^{a}	8.0 ± 0.7^{a}
DS	Control	77.3 ± 2.9^{d}	35.5 ± 0.9^{g}	4.4 ± 0.4^{f}	7.9 ± 1.4^{f}	1.9 ± 0.3^{f}
	AMF	112.0 ± 1.7^{b}	45.9 ± 1.9^{cd}	9.5 ± 0.5^{d}	15.0 ± 1.0^{d}	3.8 ± 0.2^{d}
	Comp	108.0 ± 7.2^{b}	39.2 ± 0.8^{f}	7.1 ± 0.3^{e}	12.0 ± 1.0^{e}	3.0 ± 0.2^{e}
	AMF + Comp	110.0 ± 4.6^{b}	47.2 ± 0.7^{c}	9.7 ± 0.8^{d}	15.6 ± 0.5^{d}	3.9 ± 0.1^{d}
				Tolerance index (%)		
				76.72 ± 5.1		

Values represent the mean ± standard deviation (SD; n = 3). Means followed by the same letters are not significantly different ($p \leq 0.05$).

concentrations, particularly macronutrients, were greater in biofertilizer-treated quinoa grain than in untreated plants (**Table 3**). Under water-deficiency conditions, the dual application of AMF and compost showed the most significant increase in P, K^+, and Ca^{2+} nutrients and a maximum decrease in Na^+ (74%) content as compared to control plants under the same condition. This was followed by the application of AMF alone, which registered a significant increase in P and Ca^{2+} uptake. Cakmak reported that biofortification of cereals by using breeding or fertilizer techniques is considered a viable way to increase the concentrations of essential nutrients in the grain (Cakmak, 2008). Several studies showed that AMF inoculation affects the yield and nutrition of crops (i.e., bread and durum wheat, barley, sorghum, legume, and other food crops; Lehmann et al., 2014; Watts-Williams and Cavagnaro, 2014; Lehmann and Rillig, 2015), which has led to AMF being proposed as one part of the solution to food security (Thirkell et al., 2017), but there has been little focus on the effects on the grain. In our study, the highest elemental macronutrients in quinoa grain in decreasing order were P, K, and Ca. Phosphorus element plays critical roles in plant function, as it is a building block of nucleic acids and phospholipids. Our data showed that AMF-colonizing quinoa root systems supplemented with compost increased the P concentration by *ca*. 10× compared to untreated plants under both WW and DS conditions. Mycorrhizae are beneficial particularly for P nutrition since the influx of P in mycorrhizal roots can be 3–5× higher than the P influx in non-mycorrhizal roots (Smith and Read, 2008). This nutrient uptake is generally improved in AMF-treated plants (Smith and Smith, 2011) and is more important when different fungi colonize plant roots. Tian et al. (2013) reported that different AMF species act differently in terms of growth, P uptake, and P transporter gene expression in maize and that simultaneous root colonization with these species induces the greatest expression of P transporters. Watts-Williams and Gilbert (2021) showed higher macronutrient P, Mg, K, and S, and micronutrient Zn concentrations in mycorrhizal barley grain than in the mock-inoculated plants.

Furthermore, several studies have indicated that compost and AMF improve plant growth by absorbing immobile soil nutrients such as N and P (Baslam et al., 2014; Al-Karaki, 2016; Barje et al., 2016; Frosi et al., 2016; Raklami et al., 2019b). Colonization by AMF results in the establishment of extensive hyphal networks and the secretion of glomalin, supplying plants with water and nutrients (P, N, K^+, Ca^{2+}, and Zn), which improves soil structure and hence productivity (Ben-Laouane et al., 2020). AMF extraradical hyphae can spread ~12 cm further beyond the root system, thus providing a greatly enhanced absorption area over roots, allowing plants to absorb root-inaccessible mineral nutrients (Bonfante and Anca, 2009; Kiers et al., 2011). Li et al. (1991) revealed that >75% of P acquired by mycorrhizal plants could be attributed to these extraradical hyphae. In addition, AMF modify root system elements, including morphology and diameter, and promote the development of a dense root system which improves plant functioning (Elsen et al., 2003). Under water-deficit conditions, plants improve in root fineness, root-shoot ratio, root number, and root hair length to mitigate the deleterious effects. Our data may suggest a modification in AMF-induced root morphology resulting in improved uptake, as observed, of mineral elements, including P, K, and *Ca*. The addition of compost to low OM soil can provide essential nutrients for plant growth and development and promote the plant's biological activity, which can further sustain the slow release of nutrients from the organic amendment (Scotti et al., 2015). The societal implications of these results are that from a human nutrition perspective (bioavailability), quinoa plants treated with AMF provide a more nutrient-rich grain, thus contributing to greater nutrition for consumers.

Biofertilizers Restore Abnormalities in Photosynthetic Machinery and Metabolite Content in Quinoa Grown Under Droughted-Field Conditions

The grain yield of cereals is determined by the synergistic interaction between source activity and sink (developing grains) capacity. A strong source with sufficient reserves is necessary for grain filling, and a high sink capability promotes reserve remobilization from the source to the sink (Camargo et al., 2016). We evaluated the protective role of compost-derived and rhizosphere-enriched AMF isolates application on chlorophylls as the major pigment used in photosynthesis under normal and drought conditions. Our results showed that concentration of Chl *a*, *b*, and total Chl significantly ($p < 0.001$; **Supplementary Table S1**) decreased under DS conditions

TABLE 3 | Seeds mineral composition of non-amended and non-inoculated quinoa (control) and quinoa inoculated with arbuscular mycorrhizal fungi (AMF) and/or amended with compost (Comp) subjected to different water regimes (WW; well-watered or DS: drought stress) after 4 months of cultivation.

		Na^+ (mg/g DM)	Ca^{2+} (mg/g DM)	K^+ (mg/g DM)	P (mg/g DM)
WW	Control	0.46 ± 0.001^{e}	7.59 ± 0.03^{c}	3.90 ± 0.50^{g}	0.02 ± 0.002^{e}
	AMF	0.46 ± 0.001^{f}	9.65 ± 0.07^{a}	11.47 ± 0.42^{c}	0.32 ± 0.007^{a}
	Comp	0.39 ± 0.001^{g}	9.01 ± 0.02^{b}	11.54 ± 0.24^{b}	0.03 ± 0.005^{de}
	AMF + Comp	0.28 ± 0.001^{h}	9.45 ± 0.05^{a}	13.60 ± 0.45^{a}	0.22 ± 0.012^{b}
DS	Control	1.61 ± 0.010^{a}	6.35 ± 0.09^{f}	2.31 ± 0.74^{h}	0.01 ± 0.001^{f}
	AMF	1.09 ± 0.001^{c}	6.71 ± 0.01^{d}	6.67 ± 0.01^{f}	0.04 ± 0.003^{d}
	Comp	1.14 ± 0.001^{b}	6.46 ± 0.02^{e}	6.71 ± 0.24^{e}	0.02 ± 0.001^{de}
	AMF + Comp	0.92 ± 0.001^{d}	7.61 ± 0.01^{c}	7.17 ± 0.18^{d}	0.10 ± 0.001^{c}

Na^+, sodium; Ca^{2+}, calcium: K^+, potassium; and P, phosphorus; Values represent the mean ± standard deviation (SD; n = 3). Means followed by the same letters are not significantly different ($p \leq 0.05$).

(**Table 4**). One of the most important responses of plants to drought stress is the decline in concentrations of photosynthetic pigments, which may be due to a decrease in the protein, N, and Mg concentrations observed in the present study. A reduction in the chlorophyll content under water deficit suggests a breakdown of the chlorophyll structure and mechanisms of chloroplast dismantling (Rangani et al., 2016). Both Chl biosynthesis and degradation are linked with photosystem (PS) assembly and disassembly because Chl molecules are intimately integrated within PS subunits. The PS II light collection system in plants consists of several chlorophyll-binding proteins that perform essential functions, including the efficient collection of light energy for photosynthesis (Rangani et al., 2016). Concentrations of chlorophylls decreased in untreated and treated plants when subjected to drought. Concentrations of all pigments were significantly higher in treated plants than untreated plants. Applying biofertilizers induced a significant increase in the photosynthetic pigments as compared with non-inoculated with AMF and non-amended with compost. Indeed, the AMF and compost bicombination showed the highest values of these parameters under WW conditions. When water deficit was applied, all the biofertilizer treatments could maintain higher chlorophyll content than non-amended and non-inoculated control plants. A higher photosynthetic pigment under drought stress conditions suggests a better performance of the photosynthetic apparatus (Anli et al., 2020a; Ben-Laouane et al., 2020). Similar results were found in maize (Quiroga et al., 2017), quinoa (Ramzani et al., 2017), and date palm (Anli et al., 2020a). Hashem et al. (2019) showed that organic amendment and AMF mitigated the abiotic stress-induced decline in photosynthesis by improving chlorophyll biosynthesis. Several molecular and biochemical mechanisms have been proposed to explain the enhanced performance upon drought mediated by AM symbiosis and/or compost in the host plant (Fileccia et al., 2017; Balestrini et al., 2020).

Since pseudocereals, including quinoa, are broadleaf plants with seeds characterized by excellent nutrient profiles that can be ground into flour, providing a gluten-free alternative to regular cereal-based flour; we next sought to analyze the carotenoids—can be not only provitamin A but also strong antioxidants with various health-promoting properties—soluble sugars, and proteins in the leaves (source) and seeds (sink). Water deficit resulted in a significant decrease in carotenoid (32 and 15%), sugar (52 and 33%), and protein (33 and 32%) concentrations ($p < 0.001$; **Supplementary Table S1**) in quinoa grains and leaves, respectively, as compared to non-stressed untreated plants (**Figure 2**). The supply of biofertilizers induced a significant increase in these parameters compared to untreated plants regardless of the water regime. Under drought stress, the most significant increases (220 and 111%) were recorded for TSS content in grains and leaves, respectively, in plants treated with dual AMF and compost application. Quiroga et al. found similar results regarding carotenoid content in maize (Quiroga et al., 2017). The synergistic effect of AMF and compost in improving the total content of carotenoids might be due, at least partially, to nutrient availability (Fileccia et al., 2017). Tang et al. (2015, 2016) suggested that quinoa seeds consumption over other cereals is a way to increase the intake of carotenoids. Copetta et al. (2011) observed that the use of AMF and compost improved the quality of plants by improving their organic (sugar and protein) osmolyte composition through increasing the photosynthetic machinery. The increase in protein and sugar concentration could be related to the increased mineral release from the compost and the improvement of its uptake by AMF, resulting in high phytohormone levels, thereby boosting the photosynthetic apparatus and source-sink dynamics. Previous studies showed that sugar metabolism genes tend to be upregulated in plants treated with beneficial microbes under abiotic stresses (Ahanger et al., 2014; Bárzana et al., 2015). Studies have revealed that enhancement of the accumulation of osmolytes, including proteins and sugars, is regulated through modulations in their assimilatory pathways with up- and downregulation of their synthesis and catabolism (Wu et al., 2017). Begum et al. (2019) suggested that the AMF inoculation of drought-stressed plants may have improved synthesis and downregulated the catabolism of osmolytes, resulting in significant increases in their accumulation. Ahanger et al. (2018) reported that crops exhibiting higher accumulation of osmolytes show improved tolerance and growth performance under stress through tissue water content and protein structure maintenance and functioning. Osmolyte accumulation is considered a ubiquitous response for accelerating water uptake under drought conditions, and the biofertilizer-mediated enhancement in their accumulation shown *herein* justifies the beneficial role of AMF and compost in improving the grain performance of quinoa under water-deficit conditions. Keunen et al. (2013) showed that sugars are key ROS scavengers and are assumed to regulate the interplay between ROS signaling and stress tolerance.

TABLE 4 | Leaf chlorophyll content of non-amended and non-inoculated quinoa (control) and quinoa inoculated with arbuscular mycorrhizal fungi (AMF) and/or amended with compost (Comp) subjected to different water regimes (WW; well-watered or DS: drought stress) after 4 months of cultivation.

		Chlorophyll *a* (mg/g DM)	Chlorophyll *b* (mg/g DM)	Total chlorophyll (mg/g DM)
WW	Control	5.75 ± 0.09^{e}	0.69 ± 0.05^{d}	6.45 ± 0.03^{e}
	AMF	9.03 ± 0.01^{b}	1.61 ± 0.00^{b}	10.65 ± 0.01^{b}
	Comp	8.48 ± 0.41^{c}	1.68 ± 0.14^{a}	10.17 ± 0.55^{c}
	AMF + Comp	10.84 ± 0.10^{a}	1.83 ± 0.19^{a}	12.68 ± 0.29^{a}
DS	Control	3.87 ± 0.17^{f}	0.54 ± 0.04^{e}	4.41 ± 0.22^{f}
	AMF	6.23 ± 0.05^{d}	1.13 ± 0.06^{c}	7.36 ± 0.12^{d}
	Comp	6.46 ± 0.10^{d}	1.23 ± 0.12^{c}	7.69 ± 0.02^{d}
	AMF + Comp	6.40 ± 0.15^{d}	1.30 ± 0.18^{c}	7.70 ± 0.03^{c}

Values represent the mean ± standard deviation (SD; n = 3). Means followed by the same letters are not significantly different ($p \leq 0.05$).

Biofertilizer Application Rescues Oxidative Stress Levels and Antioxidative Enzyme Activity in Quinoa Grains and Leaves

Drought stress and biofertilizers significantly ($p < 0.001$, **Supplementary Table S1**) affected MDA and H_2O_2 concentrations

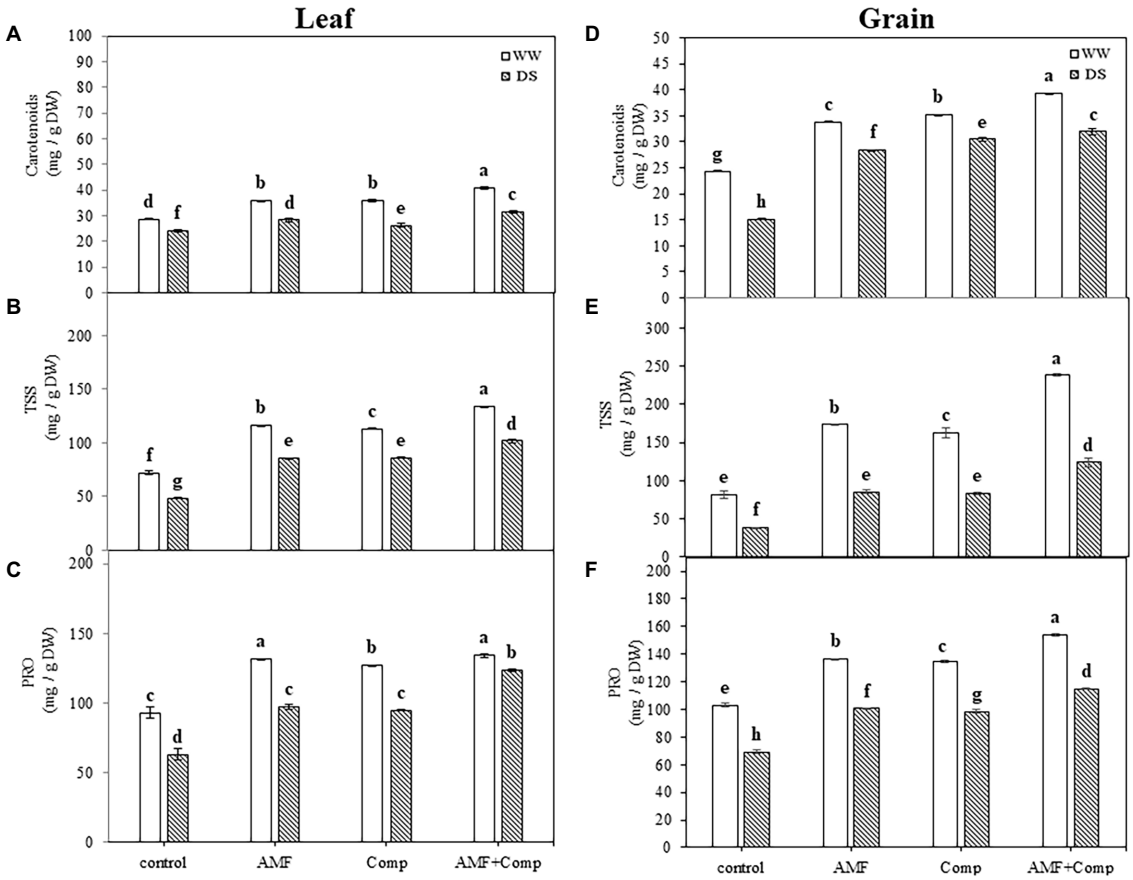

FIGURE 2 | Effects of water regimes (WW; well-watered or DS: drought stress) on leaves and seeds **(A,D)** carotenoids, **(B,E)** total soluble sugar content, and **(C,F)** protein content of non-amended and non-inoculated quinoa (control), and quinoa inoculated with arbuscular mycorrhizal fungi (AMF) and/or amended with compost (Comp). Data are mean ± SD. Means followed by the same letters are not significantly different at $p < 0.05$.

in quinoa leaves and grains (**Figure 3**). MDA and H_2O_2 concentrations were markedly increased in leaves and grains in non-treated plants, especially under DS conditions. Drought-induced oxidative damage resulting from increased ROS, including H_2O_2, leads to lipid peroxidation and membrane dysfunction, thus affecting normal cellular functioning. The H_2O_2 generated at various sites in different plant organelles may diffuse through membranes, causing damage over long distances. Increased membrane damage, lipid peroxidation, in crops due to excessive generation of ROS has been well documented. Drought influences plant growth transitions by causing a surge in H_2O_2 accumulation and impeding membrane integrity (Singh et al., 2016). Stresses upregulate lipoxygenase activity and alter the poly-unsaturated fatty acid composition, leading to disruption in membranes' structural and functional integrity (Nahar et al., 2016). Lipid peroxidation levels in leaves and grains in the droughted cultures were decreased in the presence of AMF and/or compost. Similarly to MDA concentrations, H_2O_2 levels were significantly lower in the cultures inoculated with AMF and/or amended with compost than in non-AMF and compost-free plants. Quinoa inoculated with mixed AMF species and amended with compost, the dual combination, showed the lowest oxidative stress values in leaves by 72 and 52% and grains by 70 and 50% in MDA and H_2O_2, respectively. These could be attributed to reducing the ROS concentrations to minimal possible levels, thus protecting the major metabolic processes. A reduction in oxidative stress subsequently decreases the level of lipid peroxidation (Schützendübel and Polle, 2002), which is a process in which ROS obtain electrons from the lipid bilayer (cell membrane), leading to deleterious oxidation of most cell components. Maintaining low concentrations of ROS benefits tissues in regulating and integrating key developmental events, including cell proliferation, signaling, and programmed cell death (Neill et al., 2002; Miller et al., 2010).

Furthermore, the application of AMF and/or compost decreased the activity of the antioxidant enzymes in quinoa grains and leaves compared to untreated plants, regardless of the water regime applied. This decrease was more noticeable in the combined treatment for CAT (50 and 62%) and SOD (both 30%) activities in grains and leaves, respectively, under drought stress than in untreated plants (**Figure 4**). In contrast, in untreated quinoa plants, SOD, CAT, POX, and PPO activities were significantly increased ($p < 0.001$, **Supplementary Table S1**) under water shortage (**Figure 4**). The high antioxidant levels in quinoa grains and leaves grown in soil non-inoculated with AMF and non-amended

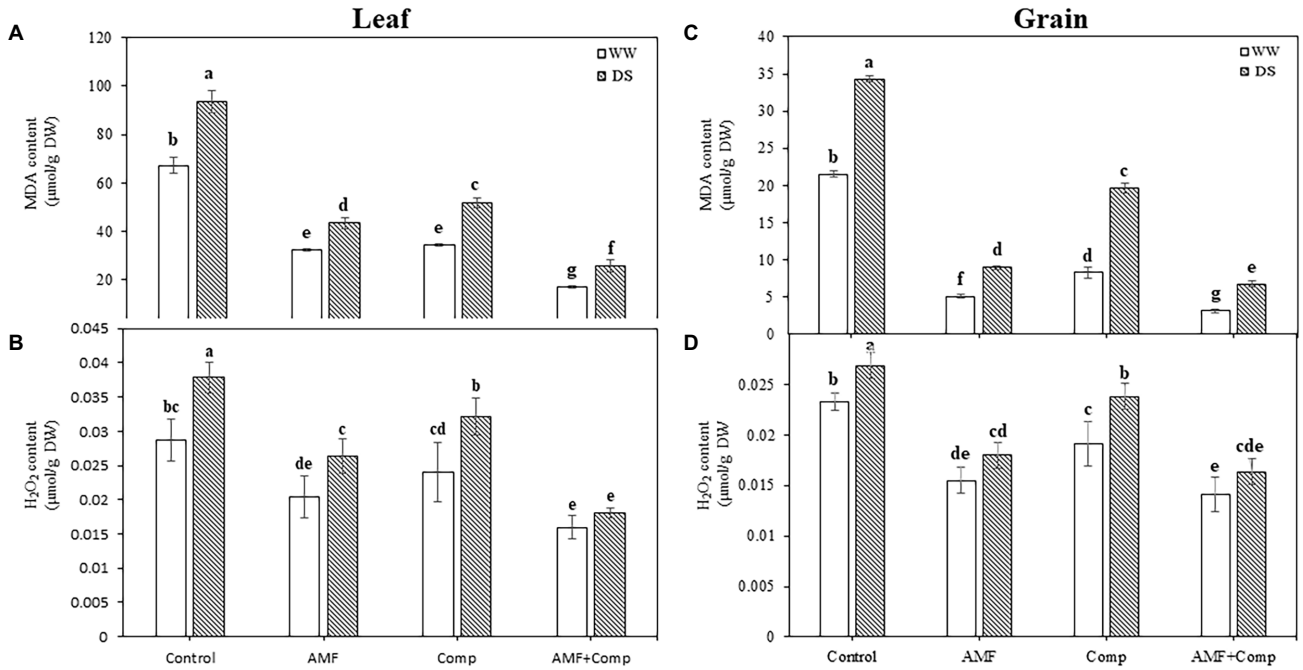

FIGURE 3 | Effects of water regimes (WW; well-watered or DS: drought stress) on leaves and seeds **(A,C)** lipid peroxidation (MDA) and **(B,D)** hydrogen peroxide (H_2O_2) content in seeds of non-amended and non-inoculated quinoa (control), and quinoa inoculated with arbuscular mycorrhizal fungi (AMF) and/or amended with compost (Comp). Data are mean ± SD. Means followed by the same letters are not significantly different at $p < 0.05$.

by compost, independently of the water regime, may be linked to the damaging effect of the high level of H_2O_2 and MDA content. Several studies have shown increased antioxidant activity in drought-stressed plants, which detoxifies ROS damage and alleviates oxidative stress (Gill and Tuteja, 2010; Shahid et al., 2014; Meddich et al., 2018). The significant increase in these enzymes limits cell damage and improves the antioxidant capacity of plants to defend themselves against stress, suggesting that AMF symbiosis and/or compost could help quinoa plants reduce the oxidative damage in response to water deficiency. Increased SOD activity prevents the generation of toxic hydroxyl radicals through the Haber-Weiss reaction, which can otherwise induce severe damage to the membrane and organelle functioning. CAT and peroxidases neutralize cytosolic H_2O_2 excess, while other enzymes, i.e., APX, AsA, and GSH act on the AsA-GSH pathway to neutralize plastidial and mitochondrial H_2O_2. In drought-stressed quinoa plants, biofertilizers mediated the upregulation of antioxidant functioning and redox homeostasis maintenance more than biofertilizer-treated plants under well-watered conditions and were thus able to prevent the harmful effects of drought stress to a considerable extent.

AMF and Compost Enhance the Bioactive Compounds of Quinoa Grains Under Droughted-Field Conditions

TPC, TFC, and DPPH were progressively influenced by drought stress and biofertilizer application. In this investigation, a significant decrease in the TPC (76%) and TFC (70%) under drought stress *vs* WW was observed in quinoa grains. However, the antioxidant activity determined by the DPPH radical scavenging activity showed a significant increase (42%) in the untreated treatment (**Figure 5**). The application of AMF and compost, separately or in combination, increased these parameters significantly more than in stressed controls. Indeed, AMF-inoculated quinoa yielded the highest TPC improvement (525%) in grains under drought stress. It has been reported that AMF symbiosis under drought improves non-enzymatic antioxidant activities, which counteracts water-deficit effects in other cereals (Bahraminia et al., 2020). Previous studies demonstrated increased phenol and flavonoid content as drought severity increased (Gharibi et al., 2016; Siracusa et al., 2017). In plant tissues under control conditions, Robbins showed that phenylalanine produced widely dispersed phenolic acids, i.e., hydroxycinnamic acids (Robbins, 2003). The most common forms of flavonoids are glycoside derivatives, even though these compounds occasionally occur as a glycone in plants (Sarker and Oba, 2018). Flavonoids represent 60% of total dietary phenolic compounds, with the most predominant flavonoids being flavonols and the most prevalent naturally occurring flavonols being the glycosides of quercetin (Harborne and Williams, 2000). Moreover, our observation provides supportive evidence for a similar result for cereal grains (Adom and Liu, 2002; Ma et al., 2016; Kiani et al., 2021). As observed in this study, the induction of the synthesis of phenolic compounds by mycorrhization has also been shown by Hazzoumi et al. (2015), thus providing evidence of an active secondary metabolism. The increase in phenolic metabolism in response to mycorrhization would be responsible for the resistance of mycorrhizal plants to drought. The plants would respond more quickly and produce large quantities of phenolic compounds that can intervene in the defense reactions. Furthermore, phenols and flavonoids may be involved as signal

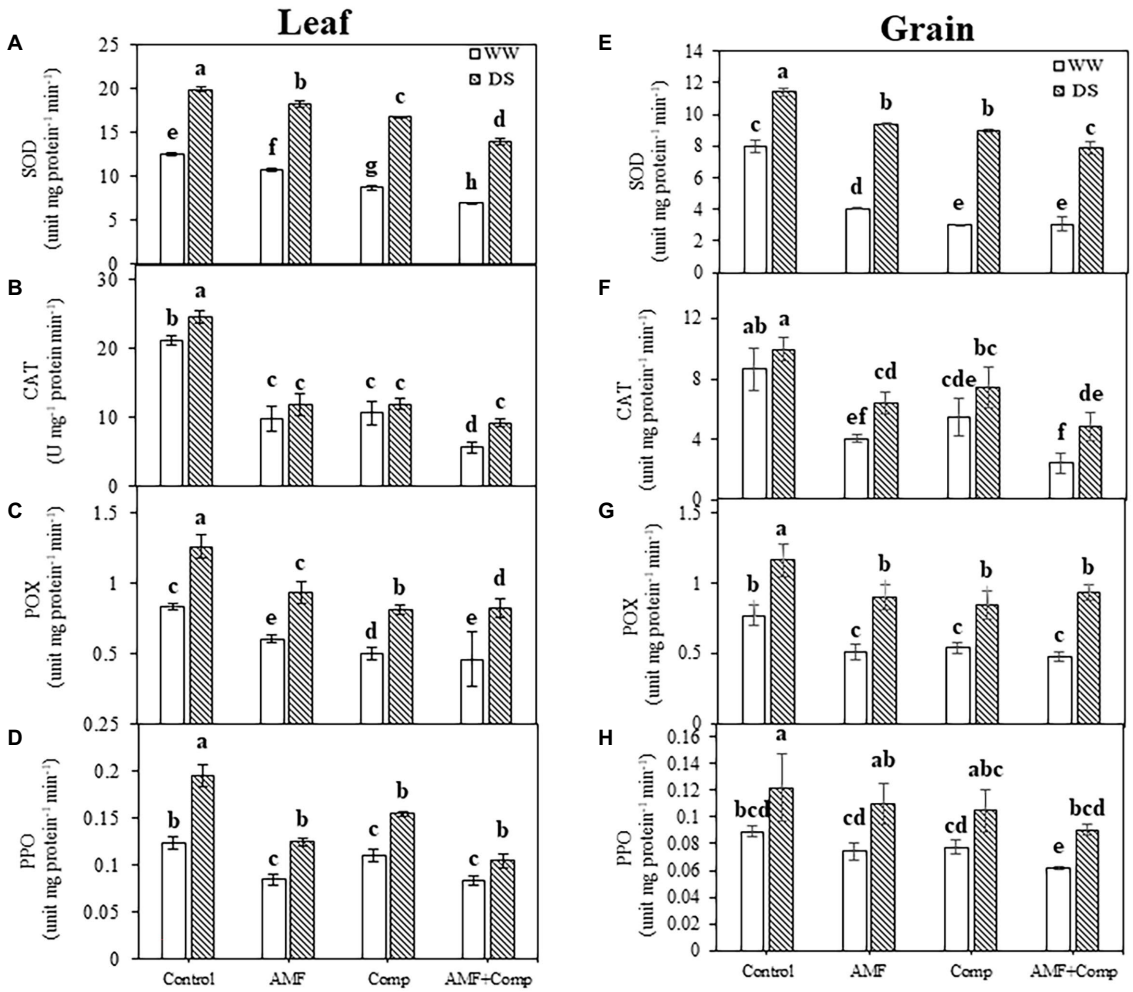

FIGURE 4 | Effects of water regimes (WW; well-watered or DS: drought stress) on leaves and seeds antioxidant enzyme activity **(A,E)** superoxide dismutase (SOD), **(B,F)** catalase (CAT), **(C,G)** peroxidase (POX), and **(D,H)** polyphenol oxidase (PPO) of non-amended and non-inoculated quinoa (control), and quinoa inoculated with arbuscular mycorrhizal fungi (AMF) and/or amended with compost (Comp). Data are mean ± SD. Means followed by the same letters are not significantly different at $p < 0.05$.

molecules in plant-AMF interactions (Morandi et al., 1984), where some new phenolic molecules are produced during the establishment of AMF colonization (Charitha Devi and Reddy, 2002). Interestingly, Fiasconaro et al. reported that compost-treated soil increased TPC in peppers grown under drought conditions (Fiasconaro et al., 2019).

The high antioxidant activity induced by DPPH activity suggested the accumulation of phenolic compounds, which play an essential role in scavenging ROS under stressful conditions (Gengmao et al., 2015). Furthermore, high levels of phenols in plants can markedly improve their resilience during exposure to water stress and lead to better adaptation and survival (Liu et al., 2011). This accumulation of the essential non-enzymatic antioxidants, TPC and TFC, provides further evidence that phenol and flavonoid compounds play vital physiological and biochemical roles in cells, particularly in ROS scavenging and in helping overcome stresses (Tohidi et al., 2017; Sharma et al., 2019), and in particular, those evoked by oxidative stress during drought stress (Hura et al., 2007). From a societal and human nutrition perspective, the increase of these bioactive compounds in biofertilizer-treated quinoa grains could be very useful in preventing various diseases, including cancer and cardiovascular disease. Thus, the "empowerment of these compounds in plants, especially in grains, can limit human diseases (Uttara et al., 2009) and take the food industry to another level of quality/functionality."

Biofertilizers Improved Soil Fertility Traits in Post-harvest Agricultural Soil

The results of soil analyses after the cultivation of quinoa and the application of the different treatments are shown in **Table 5**. Compared to the initial properties (**Table 1**), the soil TOC, OM, and P were significantly improved after biofertilizer application ($p < 0.01$, **Supplementary Table S1**). pH values decreased after the experiment in quinoa plants treated with AMF + Comp reaching a pH value of 7.7 under stressed conditions. The dual application

of biofertilizers significantly improved the concentrations of OM and TOC by *ca*. 200% and AP by ~50% under droughted-field conditions. The improved soil physicochemical properties after harvest under water deficit and biofertilizer application, especially compost, could be due to the adequate and balanced quantity of nutrients and OM provided by this amendment and the processes launched by chemical and biological activity. Montiel-Rozas et al. showed that the application of organic amendments soil microbial activity, increasing OM degradation and mineralization processes (Montiel-Rozas et al., 2016). Similarly, Gaiotti et al. have highlighted that the inoculation with microorganisms and application of compost effectively improved soil quality, especially OM and mineral nutrition (Gaiotti et al., 2017). Moreover, AMF could promote soil quality *via* multiple mechanisms such as P solubilization, soil structure and aggregates *via* glomalin production (Ben-Laouane et al., 2020, 2021). Biofertilizers are not fertilizers in themselves but potentially enhance the release of naturally reserved nutrients in the soil (Schütz et al., 2018). Pii et al. (2015) showed that microbial inoculants enhance the decomposition process fostering the release of essential plant nutrients produced from the natural process of OM decomposition and which induce overall crop productivity. Thus, the application of nutrient-rich biofertilizers made from organic amendments and microorganisms that can induce such phenomena as P solubilization and mineral absorption is essential in the recovery of soil nutrients under water deficit and to enhance plant life growth and yield. Therefore, in this study, scaling up the biofertilizer formulation and application in field trial provided optimum growth conditions for maintaining the viability of the microorganisms, under unfavorable conditions, and added to the compost carrier to ensure that the nutrients are made available to the plant. Thus, the need to use a cheap and readily available organic matter coupled with indigenous microorganism strains should be an integral component of agricultural practice and industrial methods to enhance soil quality and essential nutrient content, due to the direct and indirect effects, and hence to increase yield performance and stimulate the concentration and distribution of nutrients in quinoa.

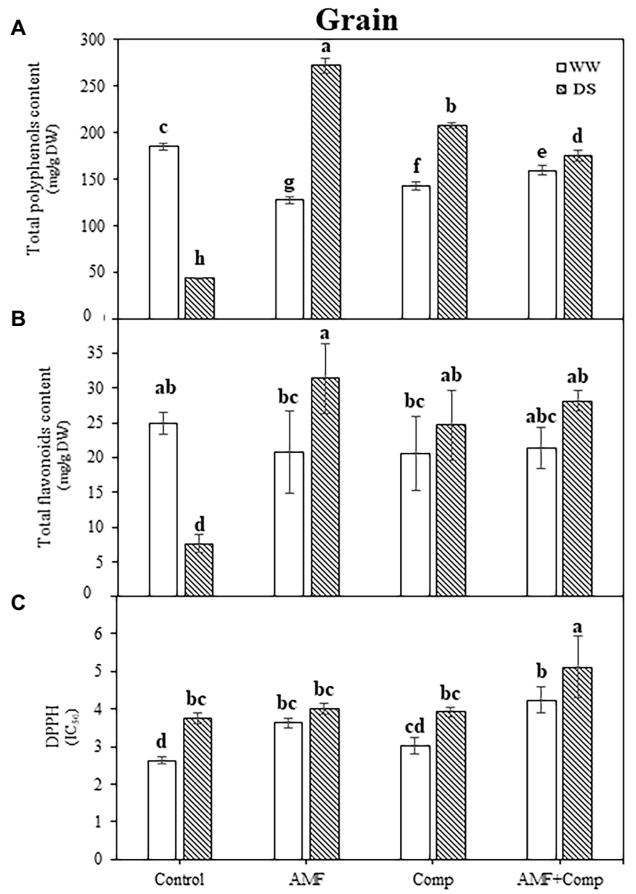

FIGURE 5 | Effects of water regimes (WW; well-watered or DS: drought stress) on seed antioxidant properties **(A)** total phenolics, **(B)** total flavonoids, and **(C)** DPPH (2,2-diphenyl-1-picrylhydrazyl) of non-amended and non-inoculated quinoa (control), and quinoa inoculated with arbuscular mycorrhizal fungi (AMF) and/or amended with compost (Comp). Data are mean ± SD. Means followed by the same letters are not significantly different at $p < 0.05$.

Principal Component Analysis and Heat Map Revealed the Potential of Biofertilizer Applications to Mitigate Drought and Support Better Quinoa Grains

The principle component analysis (PCA; **Figure 6A**) and heat map (**Figure 6B**) were performed to elaborate on the interactions

TABLE 5 | Main characteristics of different treatments on agricultural soil physicochemical parameters after harvest.

		pH	EC (mS/cm²)	TOC (%)	OM (%)	P (ppm)
WW	Control	7.99 ± 0.08^{a}	0.74 ± 0.01^{d}	1.14 ± 0.05^{d}	1.97 ± 0.09^{d}	29.98 ± 1.65^{c}
	AMF	7.91 ± 0.07^{ab}	0.89 ± 0.01^{bc}	2.14 ± 0.02^{c}	3.70 ± 0.04^{c}	33.70 ± 3.67^{c}
	Comp	7.88 ± 0.11^{ab}	0.80 ± 0.00^{cd}	2.67 ± 0.07^{b}	4.60 ± 0.21^{b}	36.62 ± 2.10^{b}
	AMF + Comp	7.81 ± 0.00^{ab}	0.76 ± 1.35^{d}	2.94 ± 0.02^{a}	5.07 ± 0.04^{a}	44.32 ± 3.59^{a}
DS	Control	8.02 ± 0.07^{a}	0.74 ± 0.01^{d}	1.00 ± 0.08^{e}	1.74 ± 0.14^{e}	29.72 ± 4.86^{c}
	AMF	7.93 ± 0.04^{ab}	0.93 ± 0.04^{b}	2.11 ± 0.11^{c}	3.64 ± 0.20^{c}	30.52 ± 4.66^{c}
	Comp	7.95 ± 0.06^{ab}	0.96 ± 0.01^{b}	2.65 ± 0.10^{b}	4.57 ± 0.17^{b}	35.29 ± 3.59^{b}
	AMF + Comp	7.71 ± 0.16^{ab}	1.16 ± 0.15^{a}	3.02 ± 0.06^{a}	5.22 ± 0.11^{a}	43.78 ± 3.64^{a}

EC, electric conductivity; TOC, total organic content; OM, organic matter; and P, available phosphorus. Values represent the mean ± standard deviation (SD; n = 3). Means followed by the same letters are not significantly different ($p \leq 0.05$).

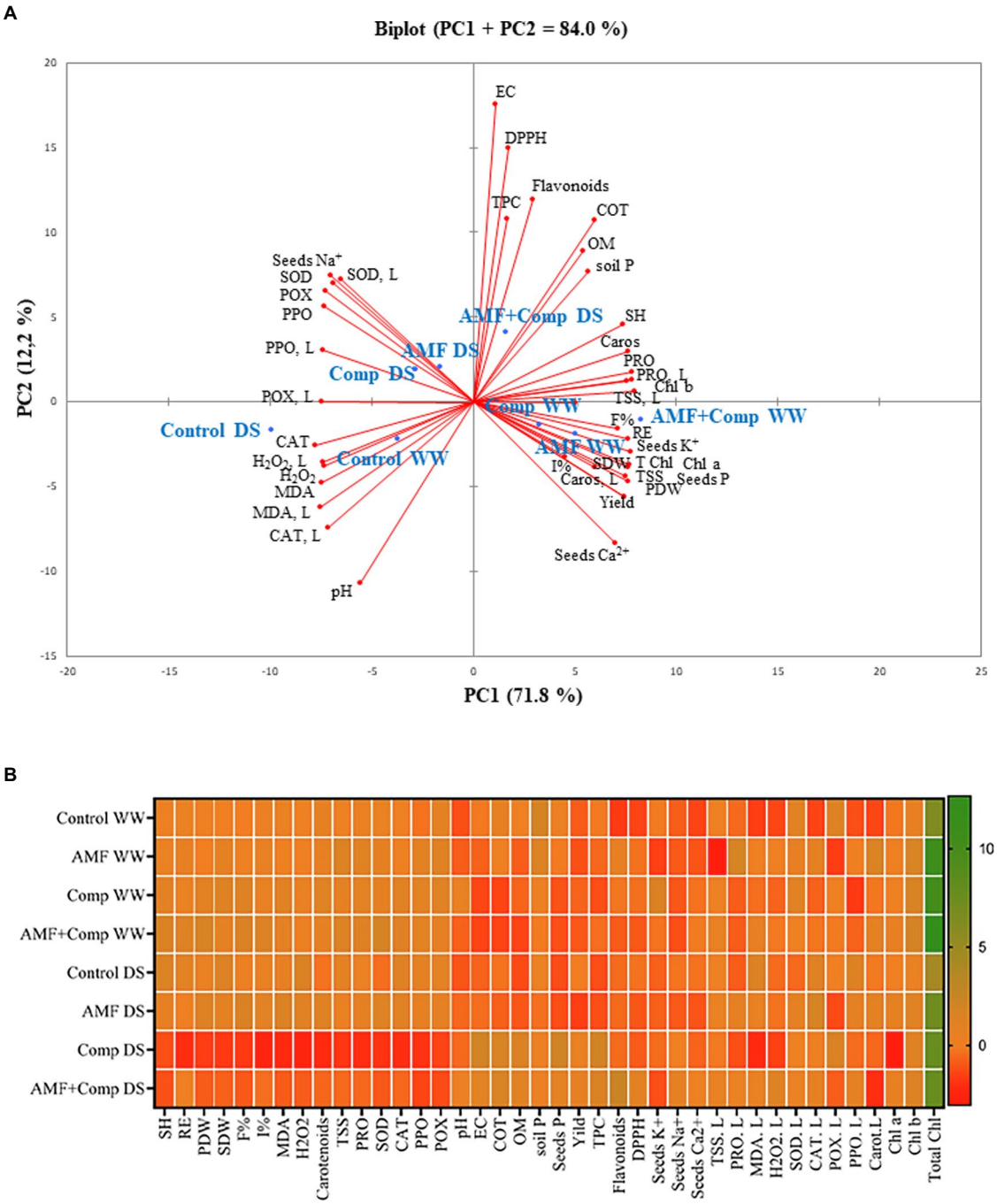

FIGURE 6 | The principal component analysis (PCA) **(A)** and heat map **(B)** measured variables and applied treatments. AMF, arbuscular mycorrhizal fungi consortium; AP, soil available phosphorous; Ca^{2+}, seed calcium; Caros, seed corotenoid; Caros, L; leaf carotenoid; CAT, seed catalase activity; CAT, L, leaf catalase activity; Chl, leaf chorophyll; Comp, compost; DS, drought stress; EC, electrical conductivity; F%, AMF colonization frequency; I%, AMF colonization intensity; K^+, seed potassium; Na^+, seed sodium; OM, organic matter; P, seed phosphorus; PDW, plant dry weight; PPO, seed polyphenol oxidase activity; PPO, L, leaf PPO; POX, seed peroxidase activity; POX, L, leaf POX; Prot, seed protein; Prot, L, leaf protein; RE, root elongation; SDW, seed dry weight; SH, shoot height; SOD, seed superoxide dismutase activity; SOD, L, leaf SOD; TFC, seed total flavonoid; TOC, total organic carbon; TPC, seeds total phenol; TSS, seed total soluble sugar; TSS, L, leaf total soluble sugar; and WW, well-watered.

across the different treatments applied and traits. The PCA shows that treatments and variables were associated (83%) with the first (PC1) and the second (PC2) components, of which PC1 was the major component (71%; **Figure 6A** and **Supplementary Table S2**). The heat map analysis indicates that the highest values of soil fertility (TOC, OM, and AP), plant growth (PH, RE, PDW, and SDW), yield, and grain traits (K, TSS, protein, and carotenoids) were found in

AMF + Comp-treated quinoa. DPPH radical scavenging activity and EC registered the highest values in the dual inoculation and compost under DS conditions. The single application of AMF was correlated with F%, I%, and grain P and Ca, under WW conditions, and with grain TPC and TFC under stressful conditions. Regarding irrigation, the drought stress conditions were associated mainly with low nutrient and bioactive compound content in grains, oxidative damage, and low soil fertility, leading to reduced grain quality and yield. In fact, the lowest values for these parameters were recorded in the controls under drought conditions, which showed the highest accumulation of Na^+, oxidative stress markers (H_2O_2 and MDA), and detoxifying enzymes (SOD, CAT, PPO, and POX).

In general, our study demonstrates that the combination of AMF + Comp was the most efficient treatment to improve the yield and performance parameters of quinoa grains, principally regarding the concentration of the non-enzymatic antioxidants of phenolic and flavonoid compounds, under drought stress. Moreover, under the same condition, the dual combination improved plant growth, yields, and grain quality seemed to be influenced by the increase in grain nutrient status (P, K, and Ca^{2+}).

CONCLUSION

Drought is the most important environmental stress factor that significantly reduces plant growth, biochemical processes, and crop production and nutritive quality worldwide. Taken together, our data suggest that drought stress limited quinoa growth, yield, and grain nutritional status/bioactive compounds and increased grain stress indicators. The overall conclusion of this study is that reinforcing the root system and altering the microbial population around the plant's rhizosphere, thereby disturbing the biological activities of the soils' ecosystem, increase the soil's traits, and in turn, quinoa yield/productivity and grain quality under normal and droughted-field conditions. AMF and the provision of green compost have an influential role in improving and preserving quinoa grain yield and functionality under water shortage conditions by boosting their bioactive compounds, including flavonoid and phenolic compound concentrations, ultimately improving the beneficial health effects for the final consumer. The potential of such native AMF + compost-based fertilizer applications could help plant growth, performance, and grain biofortification and mitigate global drought—a global mitigation strategy that farmers could implement as it is eco-friendly, cost-effective, easy to apply, and precludes the need for further subsidies.

Altogether, our results suggest that using a locally produced compost and water stress-adapted endogenous AMF can benefit the vegetative growth of crops and the quality of the grain. This is an important finding since grain biofortification under water limitation is one of the main effects of climate change in agricultural areas worldwide, where the use of efficient biotechnological tools can partially counter the deleterious effects of drought. In the application of industrial biotechnology, it is more attractive and more promising to reveal the powerful features of natural consortia and organic amendments and combine to execute new functions. This knowledge is crucial to boost grain quality and bioactive compounds at the industrial and pharmaceutical levels and has the potential for extensive application with all the subsequent benefits for humanity.

DATA AVAILABILITY STATEMENT

The original contributions presented in the study are included in the article/**Supplementary Material**, further inquiries can be directed to the corresponding authors.

AUTHOR CONTRIBUTIONS

AM and MB designed and supervised the research. ST performed the experiments and carried out the analysis. MA-E-M, AB, MA, YA-R, and WB contributed to the analytic tools. ST, MA-E-M, and MB performed the data analysis and interpretation. HB-A and TM contributed to the conception and design of the work. MB and ST wrote the manuscript. MB and MA-E-M revised and finalized the manuscript. All authors read, commented on, and approved the manuscript.

FUNDING

The present study was supported by the Tuniso-Moroccan Mixed Laboratories (LMTM) of Plant Physiology and Biotechnology and Climate Change LPBV2C and FOSC project (Sus-Agri-CC) from the European Union's Horizon 2020 research and innovation program under grant agreement N862555. This work was also funded by Grant-in-Aid for Early-Career Scientists to MB (JSPS KAKENHI grant number 20K15425) and Grant for Promotion of KAAB Projects (Niigata University).

SUPPLEMENTARY MATERIAL

The Supplementaryfor this article can be found online at: https://www.frontiersin.org/articles/10.3389/fpls.2022.860484/full#supplementary-material

REFERENCES

Abdel Latef, A. A. H., and Chaoxing, H. (2011). Effect of arbuscular mycorrhizal fungi on growth, mineral nutrition, antioxidant enzymes activity and fruit yield of tomato grown under salinity stress. *Sci. Hortic.* 127, 228–233. doi: 10.1016/j.scienta.2010.09.020

Abdel Latef, A. A. H., Hashem, A., Rasool, S., Abd-Allah, E. F., Alqarawi, A. A., Egamberdieva, D., et al. (2016). Arbuscular mycorrhizal symbiosis and abiotic stress in plants: a review. *J. Plant Biol.* 59, 407–426. doi: 10.1007/s12374-016-0237-7

Abderrahim, F., Huanatico, E., Segura, R., Arribas, S., Gonzalez, M. C., and Condezo-Hoyos, L. (2015). Physical features, phenolic compounds, betalains

and total antioxidant capacity of coloured quinoa seeds (*Chenopodium quinoa* Willd.) from Peruvian Altiplano. *Food Chem.* 183, 83–90. doi: 10.1016/j.foodchem.2015.03.029

Adom, K. K., and Liu, R. H. (2002). Antioxidant activity of grains. *J. Agric. Food Chem.* 50, 6182–6187. doi: 10.1021/jf0205099

Ahanger, M. A., Alyemeni, M. N., Wijaya, L., Alamri, S. A., Alam, P., Ashraf, M., et al. (2018). Potential of exogenously sourced kinetin in protecting *Solanum lycopersicum* from NaCl-induced oxidative stress through up-regulation of the antioxidant system, ascorbate-glutathione cycle and glyoxalase system. *PLoS One* 13:e0202175. doi: 10.1371/journal.pone.0202175

Ahanger, M. A., Tyagi, S. R., Wani, M. R., and Ahmad, P. (2014). Drought tolerance: role of organic osmolytes, growth regulators, and mineral nutrients. *Physiol. Mechanisms Adapt. Strategies Plants Under Changing Environ.* 1, 1–376. doi: 10.1007/978-1-4614-8591-9

Al-Karaki, G. N. (2016). Application of mycorrhizal fungi in landscape turfgrass establishment under arid and semiarid environments. *AGROFOR Int. J.* 1, 154–161. doi: 10.7251/agreng1602154a

Alvar-Beltrán, J., Verdi, L., Marta, A. D., Dao, A., Vivoli, R., Sanou, J., et al. (2020). The effect of heat stress on quinoa (cv. Titicaca) under controlled climatic conditions. *J. Agric. Sci.* 158, 255–261. doi: 10.1017/S0021859620000556

Amako, K., Chen, G. X., and Asada, K. (1994). Separate assays specific for ascorbate peroxidase and guaiacol peroxidase and for the chloroplastic and cytosolic isozymes of ascorbate peroxidase in plants. *Plant Cell Physiol.* 35, 497–504. doi: 10.1093/oxfordjournals.pcp.a078621

Anli, M., Baslam, M., Tahiri, A., Raklami, A., Symanczik, S., Boutasknit, A., et al. (2020a). Biofertilizers as strategies to improve photosynthetic apparatus, growth, and drought stress tolerance in the date palm. *Front. Plant Sci.* 11:516818. doi: 10.3389/fpls.2020.516818

Anli, M., El Kaoua, M., Ait-El-Mokhtar, M., Boutasknit, A., Ben-Laouane, R., Toubali, S., et al. (2020b). Seaweed extract application and arbuscular mycorrhizal fungal inoculation: a tool for promoting growth and development of date palm (*Phoenix dactylifera* L.) cv «Boufgous». *S. Afr. J. Bot.* 132, 15–21. doi: 10.1016/j.sajb.2020.04.004

Anli, M., Symanczik, S., El Abbassi, A., Ait-El-Mokhtar, M., Boutasknit, A., Ben-Laouane, R., et al. (2021). Use of arbuscular mycorrhizal fungus *Rhizoglomus irregulare* and compost to improve growth and physiological responses of *Phoenix dactylifera* 'Boufgouss'. *Plant Biosyst.* 155, 763–771. doi: 10.1080/11263504.2020.1779848

Athamena, S., Chalghem, I., Kassah-Laouar, A., Laroui, S., and Khebri, S. (2010). Activite anti-oxydante et antimicrobienne d'extraits de *Cuminum cyminum* L. *Leban. Sci. J.* 11, 69–81.

Aubert, G. (1978). *Méthodes d'analyses des sols*. Centre national de documentation pédagogique, Centre régional de documentation pédagogique, Marseille.

Bahraminia, M., Zarei, M., Ronaghi, A., Sepehri, M., and Etesami, H. (2020). Ionomic and biochemical responses of maize plant (*Zea mays* L.) inoculated with *Funneliformis mosseae* to water-deficit stress. *Rhizosphere* 16:100269. doi: 10.1016/j.rhisph.2020.100269

Balestrini, R., Brunetti, C., Chitarra, W., and Nerva, L. (2020). Photosynthetic traits and nitrogen uptake in crops: which is the role of arbuscular mycorrhizal fungi? *Plants.* 9, 1105 doi: 10.3390/plants9091105

Barje, F., Meddich, A., El Hajjouji, H., El Asli, A., Ait Baddi, G., El Faiz, A., et al. (2016). Growth of date palm (*Phoenix dactylifera* L.) in composts of olive oil mill waste with organic household refuse. *Compost Sci. Util.* 24, 273–280. doi: 10.1080/1065657X.2016.1171738

Bárzana, G., Aroca, R., and Ruiz-Lozano, J. M. (2015). Localized and non-localized effects of arbuscular mycorrhizal symbiosis on accumulation of osmolytes and aquaporins and on antioxidant systems in maize plants subjected to total or partial root drying. *Plant Cell Environ.* 38, 1613–1627. doi: 10.1111/pce.12507

Baslam, M., and Goicoechea, N. (2012). Water deficit improved the capacity of arbuscular mycorrhizal fungi (AMF) for inducing the accumulation of antioxidant compounds in lettuce leaves. *Mycorrhiza* 22, 347–359. doi: 10.1007/s00572-011-0408-9

Baslam, M., Pascual, I., Sánchez-Díaz, M., Erro, J., García-Mina, J. M., and Goicoechea, N. (2011). Improvement of nutritional quality of greenhouse-grown lettuce by arbuscular mycorrhizal fungi is conditioned by the source of phosphorus nutrition. *J. Agric. Food Chem.* 59, 11129–11140. doi: 10.1021/jf202445y

Baslam, M., Qaddoury, A., and Goicoechea, N. (2014). Role of native and exotic mycorrhizal symbiosis to develop morphological, physiological and biochemical responses coping with water drought of date palm, *Phoenix dactylifera*. *Trees* 28, 161–172. doi: 10.1007/s00468-013-0939-0

Bazile, D., Fuentes, F., Mujica, A., Bhargava, A., and Srivastava, S. (2013). *Quinoa: Botany, Production and Uses*. Wallingford: CABI.

Begum, N., Ahanger, M. A., Su, Y., Lei, Y., Mustafa, N. S. A., Ahmad, P., et al. (2019). Improved drought tolerance by AMF inoculation in maize (*Zea mays*) involves physiological and biochemical implications. *Plan. Theory* 8:579. doi: 10.3390/plants8120579

Ben-Laouane, R., Ait-El-Mokhtar, M., Anli, M., Boutasknit, A., Ait Rahou, Y., Raklami, A., et al. (2021). Green compost combined with mycorrhizae and rhizobia: a strategy for improving alfalfa growth and yield under field conditions. *Gesunde Pflanz.* 73, 193–207. doi: 10.1007/s10343-020-00537-z

Ben-Laouane, R., Baslam, M., Ait-El-Mokhtar, M., Anli, M., Boutasknit, A., Ait-Rahou, Y., et al. (2020). Potential of native arbuscular mycorrhizal fungi, rhizobia, and/or green compost as alfalfa (*Medicago sativa*) enhancers under salinity. *Microorganisms* 8:1695. doi: 10.3390/microorganisms8111695

Ben-Laouane, R., Meddich, A., Bechtaoui, N., Oufdou, K., Wahbi, S., Ben Laouane, R., et al. (2019). Effects of arbuscular mycorrhizal fungi and rhizobia symbiosis on the tolerance of *Medicago Sativa* to salt stress. *Gesunde Pflanz* 71, 135–146. doi: 10.1007/s10343-019-00461-x

Beyer, W. F., and Fridovich, I. (1987). Assaying for superoxide dismutase activity: Some large consequences of minor changes in conditions. *Anal. Biochem.* 161, 559–566. doi: 10.1016/0003-2697(87)90489-1

Bonfante, P., and Anca, I. (2009). Plants, mycorrhizal fungi, and bacteria: a network of interactions. *Annu. Rev. Microbiol.* 63, 363–383. doi: 10.1146/annurev.micro.091208.073504

Boutasknit, A., Ait-Rahou, Y., Anli, M., Ait-El-Mokhtar, M., Ben-Laouane, R., and Meddich, A. (2021a). Improvement of garlic growth, physiology, biochemical traits, and soil fertility by *Rhizophagus irregularis* and compost. *Gesunde Pflanz* 73, 149–160. doi: 10.1007/s10343-020-00533-3

Boutasknit, A., Anli, M., Tahiri, A., Raklami, A., Ait-El-Mokhtar, M., Ben-Laouane, R., et al. (2020a). Potential effect of horse manure-green waste and olive pomace-green waste composts on physiology and yield of garlic (*Allium sativum* L.) and soil fertility. *Gesunde Pflanz* 72, 285–295. doi: 10.1007/s10343-020-00511-9

Boutasknit, A., Baslam, M., Ait-El-Mokhtar, M., Anli, M., Ben-Laouane, R., Douira, A., et al. (2020b). Arbuscular mycorrhizal fungi mediate drought tolerance and recovery in two contrasting carob (*Ceratonia siliqua* L.) ecotypes by regulating stomatal, water relations, and (In)organic adjustments. *Plants* 9:80. doi: 10.3390/plants9010080

Boutasknit, A., Baslam, M., Anli, M., Ait-El-Mokhtar, M., Ben-Laouane, R., Ait-Rahou, Y., et al. (2021b). Impact of arbuscular mycorrhizal fungi and compost on the growth, water status, and photosynthesis of carob (*Ceratonia siliqua*) under drought stress and recovery. *Plant Biosyst.* 1–17. doi: 10.1080/11263504.2021.1985006

Bradford, M. M. (1976). A rapid and sensitive method for the quantitation of microgram quantities of protein utilizing the principle of protein-dye binding. *Anal. Biochem.* 72, 248–254. doi: 10.1016/0003-2697(76)90527-3

Cakmak, I. (2008). Enrichment of cereal grains with zinc: agronomic or genetic biofortification? *Plant Soil* 302, 1–17. doi: 10.1007/s11104-007-9466-3

Camargo, A. V., Mott, R., Gardner, K. A., Mackay, I. J., Corke, F., Doonan, J. H., et al. (2016). Determining phenological patterns associated with the onset of senescence in a wheat MAGIC mapping population. *Front. Plant Sci.* 7:1540. doi: 10.3389/fpls.2016.01540

Cavagnaro, T. R., Bender, S. F., Asghari, H. R., and van der Heijden, M. G. A. (2015). The role of arbuscular mycorrhizas in reducing soil nutrient loss. *Trends Plant Sci.* 20, 283–290. doi: 10.1016/j.tplants.2015.03.004

Charitha Devi, M., and Reddy, M. N. (2002). Phenolic acid metabolism of groundnut (*Arachis hypogaea* L.) plants inoculated with VAM fungus and rhizobium. *Plant Growth Regul.* 37, 151–156. doi: 10.1023/A:1020569525965

Cogger, C. G. (2005). Potential compost benefits for restoration of soils disturbed by urban development. *Compost Sci. Util.* 13, 243–251. doi: 10.1080/1065657X.2005.10702248

Copetta, A., Bardi, L., Bertolone, E., and Berta, G. (2011). Fruit production and quality of tomato plants (*Solanum lycopersicum* L.) are affected by green compost and arbuscular mycorrhizal fungi. *Plant Biosyst.* 145, 106–115. doi: 10.1080/11263504.2010.539781

Derkowska, E., Sas-Paszt, L., Sumorok, B., Szwonek, E., and Gluszek, S. (2008). The influence of mycorrhization and organic mulches on mycorrhizal frequency in apple and strawberry roots. *J. Fruit Ornam. Plant Res.* 16, 227–242.

Di Fabio, A., and Parraga, G. (2017). "Origin, production and utilization of pseudocereals," in *Pseudocereals Chemistry Technology*. eds. C. Y. Haros and R. Schönlechner, 1st Edn. (Willey, Chichester: Pseudocereals: Chemistry and Technology) 1–27.

Elsen, A., Beeterens, R., Swennen, R., and De Waele, D. (2003). Effects of an arbuscular mycorrhizal fungus and two plant-parasitic nematodes on Musa genotypes differing in root morphology. *Biol. Fertil. Soils* 38, 367–376. doi: 10.1007/s00374-003-0669-3

Escribano, J., Cabanes, J., Jiménez-Atiénzar, M., Ibañez-Tremolada, M., Gómez-Pando, L. R., García-Carmona, F., et al. (2017). Characterization of betalains, saponins and antioxidant power in differently colored quinoa (*Chenopodium quinoa*) varieties. *Food Chem.* 234, 285–294. doi: 10.1016/j.foodchem.2017.04.187

FAO (2017). *FAO*, The Future of Food and Agriculture: Trends and Challenges. Available at: http://www.fao.org/3/a-i6583e.pdf (Accessed January 8, 2021).

FAO (2019). *FAO*, Proactive Approaches to Drought Preparedness—where are we now and where do we go from here? Food and Agriculture Organization of the United Nations, Rome, Italy.

Fghire, R., Anaya, F., Issa Ali, O., Lamnai, K., Foughali, B., Faghire, M., et al. (2022). Effects of deficit irrigation and fertilization on quinoa (*Chenopodium quinoa* Willd.) water status and yield productions. *Gesunde Pflanzen* 74, 97–110. doi: 10.1007/s10343-021-00591-1

Fiasconaro, M. L., Lovato, M. E., Antolín, M. C., Clementi, L. A., Torres, N., Gervasio, S., et al. (2019). Role of proline accumulation on fruit quality of pepper (*Capsicum annuum* L.) grown with a K-rich compost under drought conditions. *Sci. Hortic.* 249, 280–288. doi: 10.1016/j.scienta.2019.02.002

Fileccia, V., Ruisi, P., Ingraffia, R., Giambalvo, D., Frenda, A. S., and Martinelli, F. (2017). Arbuscular mycorrhizal symbiosis mitigates the negative effects of salinity on durum wheat. *PLoS One* 12:e0184158. doi: 10.1371/journal.pone.0184158

Finlay, R. D. (2008). Ecological aspects of mycorrhizal symbiosis: With special emphasis on the functional diversity of interactions involving the extraradical mycelium. *J. Exp. Bot.* 59, 1115–1126. doi: 10.1016/B978-0-12-410397-9.00004-4

Fischer, S., Wilckens, R., Jara, J., Aranda, M., Valdivia, W., Bustamante, L., et al. (2017). Protein and antioxidant composition of quinoa (*Chenopodium quinoa* Willd.) sprout from seeds submitted to water stress, salinity and light conditions. *Ind. Crop. Prod.* 107, 558–564. doi: 10.1016/j.indcrop.2017.04.035

Frosi, G., Barros, V. A., Oliveira, M. T., Cavalcante, U. M. T., Maia, L. C., and Santos, M. G. (2016). Increase in biomass of two woody species from a seasonal dry tropical forest in association with AMF with different phosphorus levels. *Appl. Soil Ecol.* 102, 46–52. doi: 10.1016/j.apsoil.2016.02.009

Gaiotti, F., Marcuzzo, P., Belfiore, N., Lovat, L., Fornasier, F., Tomasi, D., et al. (2017). Influence of compost addition on soil properties, root growth and vine performances of *Vitis vinifera* cv cabernet sauvignon. *Sci. Hortic.* 225, 88–95. doi: 10.1016/j.scienta.2017.06.052

Gengmao, Z., Yu, H., Xing, S., Shihui, L., Quanmei, S., and Changhai, W. (2015). Salinity stress increases secondary metabolites and enzyme activity in safflower. *Ind. Crop. Prod.* 64, 175–181. doi: 10.1016/j.indcrop.2014.10.058

Gharibi, S., Tabatabaei, B. E. S., Saeidi, G., and Goli, S. A. H. (2016). Effect of drought stress on total phenolic, lipid peroxidation, and antioxidant activity of *Achillea* species. *Appl. Biochem. Biotechnol.* 178, 796–809. doi: 10.1007/s12010-015-1909-3

Gill, S. S., and Tuteja, N. (2010). Reactive oxygen species and antioxidant machinery in abiotic stress tolerance in crop plants. *Plant Physiol. Biochem.* 48, 909–930. doi: 10.1016/j.plaphy.2010.08.016

Gordillo-Bastidas, E., Roura, R., Rizzolo, D., Massanés, T., and Gomis, R., et al. (2016). Quinoa (Chenopodium quinoa Willd), from nutritional value to potential health benefits: an integrative review.. *J. Nutr. Food Sci.* 6: 255. doi: 10.4172/2155-9600.1000497

Gryndler, M., Hršelová, H., Cajthaml, T., Havránková, M., Řezáčová, V., Gryndlerová, H., et al. (2009). Influence of soil organic matter decomposition on arbuscular mycorrhizal fungi in terms of asymbiotic hyphal growth and root colonization. *Mycorrhiza* 19, 255–266. doi: 10.1007/s00572-008-0217-y

Gryndler, M., Sudová, R., Püschel, D., Rydlová, J., Janoušková, M., and Vosátka, M. (2008). Cultivation of high-biomass crops on coal mine spoil banks: can microbial inoculation compensate for high doses of organic matter? *Bioresour. Technol.* 99, 6391–6399. doi: 10.1016/j.biortech.2007.11.059

Harborne, J. B., and Williams, C. A. (2000). Advances in flavonoid research since 1992. *Phytochemistry* 55, 481–504. doi: 10.1016/S0031-9422(00)00235-1

Harrison, M. J. (2005). Signaling in the arbuscular mycorrhizal symbiosis. *Annu. Rev. Microbiol.* 59, 19–42. doi: 10.1146/annurev.micro.58.030603.123749

Hashem, A., Kumar, A., Al-Dbass, A. M., Alqarawi, A. A., Al-Arjani, A. B. F., , Singh, G., , Farooq, M., , and Abd_Allah, E. F., (2019). Arbuscular mycorrhizal fungi and biochar improves drought tolerance in chickpea. *Saudi J. Biol. Sci.* 26, 614–624. doi: 10.1016/j.sjbs.2018.11.005

Hazzoumi, Z., Moustakime, Y., Hassan Elharchli, E., and Joutei, K. A. (2015). Effect of arbuscular mycorrhizal fungi (AMF) and water stress on growth, phenolic compounds, glandular hairs, and yield of essential oil in basil (*Ocimum gratissimum* L.). *Chem. Biol. Technol. Agric.* 2:10. doi: 10.1186/s40538-015-0035-3

Hori, K., Wada, A., and Shibuta, T. (1997). Changes in phenoloxidase activities of galls on leaves of *Ulmus davidana* formed by *Tetraneura fusiformis* (Homoptera: Eriosomatidae). *Appl. Entomol. Zool.* 32, 365–371. doi: 10.1303/aez.32.365

Hura, T., Grzesiak, S., Hura, K., Thiemt, E., Tokarz, K., and Wędzony, M. (2007). Physiological and biochemical tools useful in drought-tolerance detection in genotypes of winter triticale: accumulation of ferulic acid correlates with drought tolerance. *Ann. Bot.* 100, 767–775. doi: 10.1093/aob/mcm162

Hussain, M., Farooq, S., Hasan, W., Ul-Allah, S., Tanveer, M., Farooq, M., et al. (2018). Drought stress in sunflower: physiological effects and its management through breeding and agronomic alternatives. *Agric. Water Manag.* 201, 152–166. doi: 10.1016/j.agwat.2018.01.028

IPCC (2014). *IPCC Fifth Assessment Synthesis Report-Climate Change 2014 Synthesis Report*. Contribution of Working Groups I, II and III to the Fifth Assessment Report of the Intergovernmental Panel on Climate Change eds. R. K. Pachauri and L. A. Meyer (Switzerland: IPCC Geneva), 151.

Jarvis, D. E., Ho, Y. S., Lightfoot, D. J., Schmöckel, S. M., Li, B., Borm, T. J. A., et al. (2017). The genome of *Chenopodium quinoa*. *Nature* 542, 307–312. doi: 10.1038/nature21370

Keunen, E., Peshev, D., Vangronsveld, J., Van Den Ende, W., and Cuypers, A. (2013). Plant sugars are crucial players in the oxidative challenge during abiotic stress: extending the traditional concept. *Plant Cell Environ.* 36, 1242–1255. doi: 10.1111/pce.12061

Kiani, R., Arzani, A., and Mirmohammady Maibody, S. A. M. (2021). Polyphenols, flavonoids, and antioxidant activity involved in salt tolerance in wheat, *Aegilops cylindrica* and their amphidiploids. *Front. Plant Sci.* 12:646221. doi: 10.3389/fpls.2021.646221

Kiers, E. T., Duhamel, M., Beesetty, Y., Mensah, J. A., Franken, O., Verbruggen, E., et al. (2011). Reciprocal rewards stabilize cooperation in the mycorrhizal symbiosis. *Science* 333, 880–882. doi: 10.1126/science.1208473

Kochert, G. (1978). Carbohydrate determination by the phenol-sulfuric acid method. In: Handbook of Physiological Methods. *Handb. Phycol. methods, Phycol. Biochem. Methods*. eds. J. A. Helebust and J. S. Craig Cambridge: Cambridge University Press. 95–97.

Lehmann, A., and Rillig, M. C. (2015). Arbuscular mycorrhizal contribution to copper, manganese and iron nutrient concentrations in crops – a meta-analysis. *Soil Biol. Biochem.* 81, 147–158. doi: 10.1016/j.soilbio.2014.11.013

Lehmann, A., Veresoglou, S. D., Leifheit, E. F., and Rillig, M. C. (2014). Arbuscular mycorrhizal influence on zinc nutrition in crop plants – a meta-analysis. *Soil Biol. Biochem.* 69, 123–131. doi: 10.1016/j.soilbio.2013.11.001

Li, X. L., George, E., and Marschner, H. (1991). Extension of the phosphorus depletion zone in VA-mycorrhizal white clover in a calcareous soil. *Plant Soil* 136, 41–48. doi: 10.1007/BF02465218

Li, Y., Guo, C., Yang, J., Wei, J., Xu, J., and Cheng, S. (2006). Evaluation of antioxidant properties of pomegranate peel extract in comparison with

pomegranate pulp extract. *Food Chem.* 96, 254–260. doi: 10.1016/j.foodchem.2005.02.033

Lichtenthaler, H. K. (1987). Chlorophylls and carotenoids: pigments of photosynthetic biomembranes. *Methods Enzymol.* 148, 350–382. doi: 10.1016/0076-6879(87)48036-1

Liu, H., Wang, X., Wang, D., Zou, Z., and Liang, Z. (2011). Effect of drought stress on growth and accumulation of active constituents in salvia miltiorrhiza Bunge. *Ind. Crop. Prod.* 33, 84–88. doi: 10.1016/j.indcrop.2010.09.006

Lybbert, T. J., and Bell, A. (2010a). Stochastic benefit streams, learning, and technology diffusion: why drought tolerance is not the new Bt. *AgBioforum* 13, 13–24. http://hdl.handle.net/10355/7074

Lybbert, T. J., and Bell, A. (2010b). Why drought tolerance is not the new Bt. *Nat. Biotechnol.* 28, 553–554. doi: 10.1038/nbt0610-553

Ma, D., Li, Y., Zhang, J., Wang, C., Qin, H., Ding, H., et al. (2016). Accumulation of phenolic compounds and expression profiles of phenolic acid biosynthesis-related genes in developing grains of white, purple, and red wheat. *Front. Plant Sci.* 7:528. doi: 10.3389/fpls.2016.00528

Maillet, F., Poinsot, V., André, O., Puech-Pagés, V., Haouy, A., Gueunier, M., et al. (2011). Fungal lipochitooligosaccharide symbiotic signals in arbuscular mycorrhiza. *Nature* 469, 58–63. doi: 10.1038/nature09622

Massawe, F., Mayes, S., and Cheng, A. (2016). Crop diversity: an unexploited treasure trove for food security. *Trends Plant Sci.* 21, 365–368. doi: 10.1016/j.tplants.2016.02.006

Meddich, A., Ait El Mokhtar, M., Bourzik, W., Mitsui, T., Baslam, M., and Hafi, M. (2018). "Optimizing growth and tolerance of date palm (*Phoenix dactylifera* L.) to drought, salinity, and vascular fusarium-induced wilt (*Fusarium oxysporum*) by application of arbuscular mycorrhizal fungi (AMF)," in *Root Biology*. eds. B. Giri, R. Prasad and A. Varma, 52, 239–258. doi: 10.3166/rcma.26.451-469

Meddich, A., Elouaqoudi, F., Khadra, A., and Bourzik, W. (2016). Valorization of green and industrial waste by composting process. *J. Rev. Compos. Adv. Mater.* 26, 451–469.

Meddich, A., Jaiti, F., Bourzik, W., Asli, A.El, and Hafidi, M. (2015). Use of mycorrhizal fungi as a strategy for improving the drought tolerance in date palm (*Phoenix dactylifera*). *Sci. Hortic.* 192, 468–474. doi:10.1016/j.scienta.2015.06.024.

Miller, M. J., Kendall, I. P., Capriles, J. M., Bruno, M. C., Evershed, R. P., and Hastorf, C. A. (2021). Quinoa, potatoes, and llamas fueled emergent social complexity in the Lake Titicaca Basin of the Andes. *Proc. Natl. Acad. Sci. U. S. A.* 118:e2113395118. doi: 10.1073/pnas.2113395118

Miller, G., Suzuki, N., Ciftci-Yilmaz, S., and Mittler, R. (2010). Reactive oxygen species homeostasis and signalling during drought and salinity stresses. *Plant Cell Environ.* 33, 453–467. doi: 10.1111/j.1365-3040.2009.02041.x

Miranda-Apodaca, J., Yoldi-achalandabaso, A., Aguirresarobe, A., del Canto, A., and Pérez-López, U. (2018). Similarities and differences between the responses to osmotic and ionic stress in quinoa from a water use perspective. *Agric. Water Manag.* 203, 344–352. doi: 10.1016/j.agwat.2018.03.026

Mo, Y., Wang, Y., Yang, R., Zheng, J., Liu, C., Li, H., et al. (2016). Regulation of plant growth, photosynthesis, antioxidation and osmosis by an arbuscular mycorrhizal fungus in watermelon seedlings under well-watered and drought conditions. *Front. Plant Sci.* 7:644. doi: 10.3389/fpls.2016.00644

Montiel-Rozas, M. D. M., López-García, Á., Kjøller, R., Madejón, E., and Rosendahl, S. (2016). Organic amendments increase phylogenetic diversity of arbuscular mycorrhizal fungi in acid soil contaminated by trace elements. *Mycorrhiza* 26, 575–585. doi: 10.1007/s00572-016-0694-3

Morandi, D., Bailey, J. A., and Gianinazzi-Pearson, V. (1984). Isoflavonoid accumulation in soybean roots infected with vesicular-arbuscular mycorrhizal fungi. *Physiol. Plant Pathol.* 24, 357–364. doi: 10.1016/0048-4059(84)90009-2

Nadeem, S. M., Ahmad, M., Zahir, Z. A., Javaid, A., and Ashraf, M. (2014). The role of mycorrhizae and plant growth promoting rhizobacteria (PGPR) in improving crop productivity under stressful environments. *Biotechnol. Adv.* 32, 429–448. doi: 10.1016/j.biotechadv.2013.12.005

Nahar, K., Hasanuzzaman, M., Alam, M. M., Rahman, A., Suzuki, T., and Fujita, M. (2016). Polyamine and nitric oxide crosstalk: antagonistic effects on cadmium toxicity in mung bean plants through upregulating the metal detoxification, antioxidant defense and methylglyoxal detoxification systems. *Ecotoxicol. Environ. Saf.* 126, 245–255. doi: 10.1016/j.ecoenv.2015.12.026

Neill, S., Desikan, R., and Hancock, J. (2002). Hydrogen peroxide signalling. *Curr. Opin. Plant Biol.* 5, 388–395. doi: 10.1016/S1369-5266(02)00282-0

Olsen, S., and Sommers, L. (1982). Methods of soil analysis. Part 2. Chemical and microbiological properties of phosphorus. *ASA Monograp* 9, 403–430.

Parvez, S., Abbas, G., Shahid, M., Amjad, M., Hussain, M., Ahmad, S., et al. (2020). Effect of salinity on physiological, biochemical and photostabilizing attributes of two genotypes of quinoa (*Chenopodium quinoa* Willd.) exposed to arsenic stress. *Ecotoxicol. Environ. Saf.* 187:109814. doi: 10.1016/j.ecoenv.2019.109814

PGC (2014). (Prince George's County). Stormwater Management Design Manual. Available at: https://www.princegeorgescountymd.gov/DocumentCenter/View/4782/Stormwater-Management-Design-Manual-PDF (accessed April 25, 2021).

Phillips, J. M., and Hayman, D. S. (1970). Improved procedures for clearing roots and staining parasitic and vesicular-arbuscular mycorrhizal fungi for rapid assessment of infection. *Trans. Br. Mycol. Soc.* 55, 158–IN18. doi: 10.1016/S0007-1536(70)80110-3

Phillips, C. L., Light, S. E., Gollany, H. T., Chiu, S., Wanzek, T., Meyer, K., et al. (2020). Can biochar conserve water in Oregon agricultural soils? *Soil Tillage Res.* 198:104525. doi: 10.1016/j.still.2019.104525

Pii, Y., Mimmo, T., Tomasi, N., Terzano, R., Cesco, S., and Crecchio, C. (2015). Microbial interactions in the rhizosphere: beneficial influences of plant growth-promoting rhizobacteria on nutrient acquisition process. A review. *Biol. Fertil. Soils* 51, 403–415. doi: 10.1007/s00374-015-0996-1

Polle, A., Otter, T., and Seifert, F. (1994). Apoplastic peroxidases and lignification in needles of Norway spruce (*Picea abies* L.). *Plant Physiol.* 106, 53–60. doi: 10.1104/pp.106.1.53

Püschel, D., Bitterlich, M., Rydlová, J., and Jansa, J. (2021). Drought accentuates the role of mycorrhiza in phosphorus uptake. *Soil Biol. Biochem.* 157:108243. doi: 10.1016/j.soilbio.2021.108243

Quiroga, G., Erice, G., Aroca, R., Chaumont, F., and Ruiz-Lozano, J. M. (2017). Enhanced drought stress tolerance by the arbuscular mycorrhizal symbiosis in a drought-sensitive maize cultivar is related to a broader and differential regulation of host plant aquaporins than in a drought-tolerant cultivar. *Front. Plant Sci.* 8:1056. doi: 10.3389/fpls.2017.01056

Raklami, A., Bechtaoui, N., Tahiri, A.-I., Anli, M., Meddich, A., and Oufdou, K. (2019a). Use of rhizobacteria and mycorrhizae consortium in the open field as a strategy for improving crop nutrition, productivity and soil fertility. *Front. Microbiol.* 10:1106. doi: 10.3389/fmicb.2019.01106

Raklami, A., Oufdou, K., Tahiri, A.-I., Mateos-Naranjo, E., Navarro-Torre, S., Rodríguez-Llorente, I. D., et al. (2019b). Safe cultivation of *Medicago sativa* in metal-polluted soils from semi-arid regions assisted by heat- and metallo-resistant PGPR. *Microorganisms* 7:212. doi: 10.3390/microorganisms7070212

Ramzani, P. M. A., Shan, L., Anjum, S., Khan, W., Ronggui, H., Iqbal, M., et al. (2017). Improved quinoa growth, physiological response, and seed nutritional quality in three soils having different stresses by the application of acidified biochar and compost. *Plant Physiol. Biochem.* 116, 127–138. doi: 10.1016/j.plaphy.2017.05.003

Rangani, J., Parida, A. K., Panda, A., and Kumari, A. (2016). Coordinated changes in antioxidative enzymes protect the photosynthetic machinery from salinity induced oxidative damage and confer salt tolerance in an extreme halophyte Salvadora persica L. *Front. Plant Sci.* 7:50. doi: 10.3389/fpls.2016.00050

Rao, K. V. M., and Sresty, T. V. S. (2000). Antioxidative parameters in the seedlings of pigeonpea (*Cajanus cajan* (L.) Millspaugh) in response to Zn and Ni stresses. *Plant Sci.* 157, 113–128. doi: 10.1016/S0168-9452(00)00273-9

Renaut, S., Daoud, R., Masse, J., Vialle, A., and Hijri, M. (2020). Inoculation with *Rhizophagus irregularis* does not alter arbuscular mycorrhizal fungal community structure within the roots of corn, wheat, and soybean crops. *Microorganisms* 8:83. doi: 10.3390/microorganisms8010083

Robbins, R. J. (2003). Phenolic acids in foods: an overview of analytical methodology. *J. Agric. Food Chem.* 51, 2866–2887. doi: 10.1021/jf026182t

Ruiz-Lozano, J. M., Aroca, R., Zamarreño, Á. M., Molina, S., Andreo-Jiménez, B., Porcel, R., et al. (2016). Arbuscular mycorrhizal symbiosis induces strigolactone biosynthesis under drought and improves drought tolerance in lettuce and tomato. *Plant Cell Environ.* 39, 441–452. doi: 10.1111/pce.12631

Rydlová, J., and Püschel, D. (2020). Arbuscular mycorrhiza, but not hydrogel, alleviates drought stress of ornamental plants in peat-based substrate. *Appl. Soil Ecol.* 146:103394. doi: 10.1016/j.apsoil.2019.103394

Sarker, U., and Oba, S. (2018). Drought stress enhances nutritional and bioactive compounds, phenolic acids and antioxidant capacity of *Amaranthus* leafy vegetable. *BMC Plant Biol.* 18:258. doi: 10.1186/s12870-018-1484-1

Schütz, L., Gattinger, A., Meier, M., Müller, A., Boller, T., Mäder, P., et al. (2018). Improving crop yield and nutrient use efficiency via biofertilization—A global meta-analysis. *Front. Plant Sci.* 8:2204. doi: 10.3389/fpls.2017.02204

Schützendübel, A., and Polle, A. (2002). Plant responses to abiotic stresses: heavy metal-induced oxidative stress and protection by mycorrhization. *J. Exp. Bot.* 53, 1351–1365. doi: 10.1093/jexbot/53.372.1351

Schwalm, C. R., Anderegg, W. R. L., Michalak, A. M., Fisher, J. B., Biondi, F., Koch, G., et al. (2017). Global patterns of drought recovery. *Nature* 548, 202–205. doi: 10.1038/nature23021

Scotti, R., Bonanomi, G., Scelza, R., Zoina, A., and Rao, M. A. (2015). Organic amendments as sustainable tool to recovery fertility in intensive agricultural systems. *J. Soil Sci. Plant Nutr.* 15, 333–352. doi: 10.4067/S0718-95162015005000031

Shahid, M., Pourrut, B., Dumat, C., Nadeem, M., Aslam, M., and Pinelli, E. (2014). Heavy-metal-induced reactive oxygen species: phytotoxicity and physicochemical changes in plants. *Rev. Environ. Contam. Toxicol.* 232, 1–44. doi: 10.1007/978-3-319-06746-9_1

Sharma, A., Shahzad, B., Rehman, A., Bhardwaj, R., Landi, M., and Zheng, B. (2019). Response of phenylpropanoid pathway and the role of polyphenols in plants under abiotic stress. *Molecules* 24:2452. doi: 10.3390/molecules24132452

Singh, R., Singh, S., Parihar, P., Mishra, R. K., Tripathi, D. K., Singh, V. P., et al. (2016). Reactive oxygen species (ROS): beneficial companions of plants' developmental processes. *Front. Plant Sci.* 7:1299. doi: 10.3389/fpls.2016.01299

Singleton, V. L., Orthofer, R., and Lamuela-Raventós, R. M. (1999). Analysis of total phenols and other oxidation substrates and antioxidants by means of folin-ciocalteu reagent. *Methods Enzymol.* 299, 152–178. doi: 10.1016/S0076-6879(99)99017-1

Siracusa, L., Gresta, F., Sperlinga, E., and Ruberto, G. (2017). Effect of sowing time and soil water content on grain yield and phenolic profile of four buckwheat (*Fagopyrum esculentum* Moench.) varieties in a Mediterranean environment. *J. Food Compos. Anal.* 62, 1–7. doi: 10.1016/j.jfca.2017.04.005

Smith, S. E., and Read, D. J. (2008). *Mycorrhizal Symbiosis. 3rd Edn*. New York: Academic Press.

Smith, S. E., and Smith, F. A. (2011). Roles of arbuscular mycorrhizas in plant nutrition and growth: new paradigms from cellular to ecosystem scales. *Annu. Rev. Plant Biol.* 62, 227–250. doi: 10.1146/annurev-arplant-042110-103846

Tang, Y., Li, X., Chen, P. X., Zhang, B., Hernandez, M., Zhang, H., et al. (2015). Characterization of fatty acid, carotenoid, tocophenol/tocotrienol compositions and antioxidant activities in seeds of three *Chenopodium quinoa* Willd. Genotypes. *Food Chem.* 174, 502–508. doi: 10.1016/j.foodchem.2014.11.040

Tang, Y., Li, X., Chen, P. X., Zhang, B., Liu, R., Hernandez, M., et al. (2016). Assessing the fatty acid, carotenoid, and tocopherol compositions of amaranth and quinoa seeds grown in Ontario and their overall contribution to nutritional quality. *J. Agric. Food Chem.* 64, 1103–1110. doi: 10.1021/acs.jafc.5b05414

Tanwar, A., Aggarwal, A., Yadav, A., and Parkash, V. (2013). Screening and selection of efficient host and sugarcane bagasse as substrate for mass multiplication of *Funneliformis mosseae*. *Biol. Agric. Hortic.* 29, 107–117. doi: 10.1080/01448765.2013.771955

Thirkell, T. J., Charters, M. D., Elliott, A. J., Sait, S. M., and Field, K. J. (2017). Are mycorrhizal fungi our sustainable saviours? Considerations for achieving food security. *J. Ecol.* 105, 921–929. doi: 10.1111/1365-2745.12788

Tian, Y., Lei, Y., Zheng, Y., and Ca, Z. (2013). Synergistic effect of colonization with arbuscular mycorrhizal fungi improves growth and drought tolerance of *Plukenetia volubilis* seedlings. *Acta Physiol. Plant.* 35, 687–696. doi: 10.1007/s11738-012-1109-5

Tohidi, B., Rahimmalek, M., and Arzani, A. (2017). Essential oil composition, total phenolic, flavonoid contents, and antioxidant activity of thymus species collected from different regions of Iran. *Food Chem.* 220, 153–161. doi: 10.1016/j.foodchem.2016.09.203

Uttara, B., Singh, A. V., Zamboni, P., and Mahajan, R. T. (2009). Oxidative stress and neurodegenerative diseases: a review of upstream and downstream antioxidant therapeutic options. *Curr. Neuropharmacol.* 7, 65–74. doi: 10.2174/157015909787602823

Velikova, V., Yordanov, I., and Edreva, A. (2000). Oxidative stress and some antioxidant systems in acid rain-treated bean plants. *Plant Sci.* 151, 59–66. doi: 10.1016/S0168-9452(99)00197-1

Vilcacundo, R., and Hernández-Ledesma, B. (2017). Nutritional and biological value of quinoa (*Chenopodium quinoa* Willd.). *Curr. Opin. Food Sci.* 14, 1–6. doi: 10.1016/j.cofs.2016.11.007

VTSM (2017). Vermont Agency of Natural Resources. Vermont Stormwater Management Manual (VTSM). Rule and Design Guidance. Available at: https://dec.vermont.gov/sites/dec/files/wsm/stormwater/docs/Permitinformation/2017%20VSMM_Rule_and_Design_Guidance_04172017.pdf (accessed April 25, 2021).

Watts-Williams, S. J., and Cavagnaro, T. R. (2014). Nutrient interactions and arbuscular mycorrhizas: a meta-analysis of a mycorrhiza-defective mutant and wild-type tomato genotype pair. *Plant Soil* 384, 79–92. doi: 10.1007/s11104-014-2140-7

Watts-Williams, S. J., and Gilbert, S. E. (2021). Arbuscular mycorrhizal fungi affect the concentration and distribution of nutrients in the grain differently in barley compared with wheat. *Plants People Planet* 3, 567–577. doi: 10.1002/ppp3.10090

Wu, H. H., Zou, Y. N., Rahman, M. M., Ni, Q. D., and Wu, Q. S. (2017). Mycorrhizas alter sucrose and proline metabolism in trifoliate orange exposed to drought stress. *Sci. Rep.* 7, 1–10. doi: 10.1038/srep42389

Xu, T., Guo, Z., Liu, S., He, X., Meng, Y., Xu, Z., et al. (2018). Evaluating different machine learning methods for upscaling evapotranspiration from flux towers to the regional scale. *J. Geophys. Res. Atmos.* 123, 8674–8690. doi: 10.1029/2018JD028447

Yang, W., Gu, S., Xin, Y., Bello, A., Sun, W., and Xu, X. (2018). Compost addition enhanced hyphal growth and sporulation of arbuscular mycorrhizal fungi without affecting their community composition in the soil. *Front. Microbiol.* 9:169. doi: 10.3389/fmicb.2018.00169

Yang, W., Guo, Y., Wang, X., Chen, C., Hu, Y., Cheng, L., et al. (2017). Temporal variations of soil microbial community under compost addition in black soil of Northeast China. *Appl. Soil Ecol.* 121, 214–222. doi: 10.1016/j.apsoil.2017.10.005

Zhang, L., Zhou, J., George, T. S., Limpens, E., and Feng, G. (2021). Arbuscular mycorrhizal fungi conducting the hyphosphere bacterial orchestra. *Trends Plant Sci.* 12, 1–10. doi: 10.1016/j.tplants.2021.10.008

Conflict of Interest: The authors declare that the research was conducted in the absence of any commercial or financial relationships that could be construed as a potential conflict of interest.

Publisher's Note: All claims expressed in this article are solely those of the authors and do not necessarily represent those of their affiliated organizations, or those of the publisher, the editors and the reviewers. Any product that may be evaluated in this article, or claim that may be made by its manufacturer, is not guaranteed or endorsed by the publisher.

frontiers in Plant Science

ORIGINAL RESEARCH
published: 21 March 2022
doi: 10.3389/fpls.2022.806781

Iron Oxide and Silicon Nanoparticles Modulate Mineral Nutrient Homeostasis and Metabolism in Cadmium-Stressed *Phaseolus vulgaris*

Lyubka Koleva[1], Aisha Umar[2], Nasim Ahmad Yasin[3], Anis Ali Shah[4], Manzer H. Siddiqui[5]*, Saud Alamri[5], Luqman Riaz[6], Ali Raza[7], Talha Javed[7,8] and Zunera Shabbir[9]*

[1] Department of Plant Physiology and Biochemistry, Agricultural University, Plovdiv, Bulgaria, [2] Institute of Botany, University of Punjab, Lahore, Pakistan, [3] Senior Superintendent Garden, RO-II Office, University of Punjab, Lahore, Pakistan, [4] Department of Botany, Division of Science and Technology, University of Education, Lahore, Pakistan, [5] Department of Botany and Microbiology, King Saud University, Riyadh, Saudi Arabia, [6] Department of Environmental Sciences, University of Narowal, Punjab, Pakistan, [7] Key Laboratory of Ministry of Education for Genetics, Breeding and Multiple Utilization of Crops, Centre of Legume Crop Genetics and Systems Biology/College of Agriculture, Oil Crop Research Institute, Fujian Agriculture and Forestry University (FAFU), Fuzhou, China, [8] College of Agriculture, Fujian Agriculture and Forestry University, Fuzhou, China, [9] Agronomy, Horticulture, and Plant Science Department, South Dakota State University, Brookings, SD, United States

OPEN ACCESS

Edited by:
Maurizio Ruzzi, University of Tuscia, Italy

Reviewed by:
Parvaiz Ahmad, Government Degree College, Pulwama, India
Basharat Ali, University of Agriculture, Faisalabad, Pakistan

***Correspondence:**
Anis Ali Shah
anisalibot@gmail.com
Manzer H. Siddiqui
mhsiddiqui@ksu.edu.sa

Specialty section:
This article was submitted to Plant Abiotic Stress, a section of the journal Frontiers in Plant Science

Received: *01 November 2021*
Accepted: *21 January 2022*
Published: *21 March 2022*

Citation:
Koleva L, Umar A, Yasin NA, Shah AA, Siddiqui MH, Alamri S, Riaz L, Raza A, Javed T and Shabbir Z (2022) Iron Oxide and Silicon Nanoparticles Modulate Mineral Nutrient Homeostasis and Metabolism in Cadmium-Stressed Phaseolus vulgaris. Front. Plant Sci. 13:806781. doi: 10.3389/fpls.2022.806781

The application of nanoparticles (NPs) has been proved as an efficient and promising technique for mitigating a wide range of stressors in plants. The present study elucidates the synergistic effect of iron oxide nanoparticles (IONPs) and silicon nanoparticles (SiNPs) in the attenuation of Cd toxicity in *Phaseolus vulgaris*. Seeds of *P. vulgaris* were treated with IONPs (10 mg/L) and SiNPs (20 mg/L). Seedlings of uniform size were transplanted to pots for 40 days. The results demonstrated that nanoparticles (NPs) enhanced growth, net photosynthetic rate, and gas exchange attributes in *P. vulgaris* plants grown in Cd-contaminated soil. Synergistic application of IONPs and SiNPs raised not only K^+ content, but also biosynthesis of polyamines (PAs), which alleviated Cd stress in *P. vulgaris* seedlings. Additionally, NPs decreased malondialdehyde (MDA) content and electrolyte leakage (EL) in *P. vulgaris* plants exposed to Cd stress. These findings suggest that stress alleviation was mainly attributed to the enhanced accumulation of K^+ content, improved antioxidant defense system, and higher spermidine (Spd) and putrescine (Put) levels. It is suggested that various forms of NPs can be applied synergistically to minimize heavy metal stress, thus increasing crop production under stressed conditions.

Keywords: growth, potassium, polyamines, antioxidant, stress, cadmium

INTRODUCTION

Mining operation, industrial waste, and pollutants emitted during agricultural and industrial operations (Palansooriya et al., 2020; Raghib et al., 2020) release substantial quantities of toxic heavy metals (As, Cd, Hg, Pb) into the environment. The quantity of harmful heavy metals in the soil environment has steadily increased over time, which produces negative effects on plant growth and their developmental process, which is a great challenge for the sustainability of agriculture (Afzal et al., 2019). Among the numerous heavy metals, Cd content in the environment has risen owing to excessive use of chemical fertilizers and pesticides besides mining sources (Seshadri et al., 2016; Manzoor et al., 2019). Although the concentration of Cd reported in the environment is low, it is considered extremely toxic due to its higher mobility in media and living cells (Rahman and Singh, 2019; Kaya et al., 2020a), which is raising concerns for agriculture. It was reported that Cd exposure reduces seed sprouting, root elongation, shoot development, and the number of leaves per plant (Kaya et al., 2020b; Seifikalhor et al., 2020). In addition, it also results in the overproduction of reactive oxygen species (ROS) (Moradi-Marjaneh et al., 2019), which influence plant physiological, biochemical, and molecular characteristics (Raza et al., 2020). Plants can avoid, tolerate, and immobilize heavy metals in soil (Kumar and Prasad, 2018; Mei et al., 2020) by activating signaling molecules that regulate ROS production, phytohormone synthesis, and calcium calmodulin pathways (Bali et al., 2019). The activated pathways include the production of nitric oxide (NO), glutathione, phytohormones, and antioxidant enzymes (Dias et al., 2019; Rady et al., 2019), which lead to Cd chelation and reduced oxidative damage.

Nanoparticles (NPs) with a size of 100 nm exhibit unique properties such as increased reaction site, high surface activity, better catalytic efficiency, and unique magnetic characteristics (Yang et al., 2017, 2018; Wang et al., 2019), which have assisted in agriculture promotion by alleviating abiotic stress in plants (Adeel et al., 2019). Many researchers have reported that NPs improve seed germination, rhizome development, and quality of crops cultivated in stressed conditions (Ghafariyan et al., 2013; Palchoudhury et al., 2018; Kah et al., 2019). Nanotechnology research offers a new pathway for soil pollution remediation (Liu et al., 2021), since it has the potential to enhance plants' antioxidative defense systems, thus reducing the bioaccumulation of ROS in plants (Usman et al., 2020; Wang et al., 2020). As documented, NPs when applied in soil (Li et al., 2021) or sprayed *via* foliar (Toumey, 2020), results in a reduction of Cd and Pd toxicity in rice seedlings (Hussain et al., 2020). It was observed that the Si improved hydraulic conductivity in applied plants through enhancing K^+ concentration in xylem sap resulting in improved xylem hydraulic conductivity and osmotic gradient (Chen et al., 2016). Similarly, exogenously applied Fe modulates K^+ uptake and translocation in crop plants (Okturen Asri and Sonmez, 2014).

Potassium is a crucial phytonutrient required by plants for the maintenance of growth (Jaiswal et al., 2016), stomatal conductance, gaseous exchange (Hasanuzzaman et al., 2018), photosynthate production, and antioxidative defense system (Xu et al., 2020). Approximately 10% of plant biomass is composed of K, which not only acts as a co-factor for various enzymes involved in photosynthesis and protein stabilization, but it also hinders Cd-translocation and escalates the production of crucial amino acids, carbohydrates, and nitrogenous compounds. Potassium improves plant stress tolerance by regulating the biosynthesis of polyamines (Karimi, 2017). Polyamines regulate physiochemical procedures of plants under normal conditions and also induce modification in the expression level of stress-responsive genes besides detoxifying metals by vacuolar compartmentalization (Spormann et al., 2021).

Considering the background information, we hypothesized that the synergistic effect of NPs can mitigate Cd stress; and regulate polyamine synthesis, K^+ metabolism, and antioxidant enzymes. Therefore, the objective of the present study was to explore the individual and combined role of IONPs and SiNPs application in mitigation of Cd toxicity through regulation of K^+ metabolism and antioxidant enzymes in *P. vulgaris* exposed to Cd-contaminated conditions.

MATERIALS AND METHODS

A total of 85 soil samples were collected (0–30 cm) from an agricultural field (2-ha area) in the vicinity of the campus site. The soil was sieved through a 4 mm mesh to remove plant parts, debris, then thoroughly mixed and conditioned for 1 week at 35% of water holding capacity (WHC) before the experiment. The physicochemical properties of the soil such as pH, electrical conductivity (EC), organic matter, and metal content (Cd, Zn, Fe, Ni, Pb) were measured using standard protocols (Bouyoucos, 1962; Page et al., 1982). The physicochemical properties of the soil were as follows; pH (7.13), EC (1.87), and organic content (0.45%). The total concentration of Cd, Zn, Fe, Ni, and Pb in soil was quantified as 5.87, 34.98, 37.91, 13.28, and 35.18 mg/kg, respectively. The soil was contaminated by mixing $CdCl_2$. Cadmium concentrations in the soil were kept as 0 mM $CdCl_2$, 1 mM $CdCl_2$, 1.5 mM $CdCl_2$, and 2 mM $CdCl_2$. Both IONPs and SiNPs were purchased from Alfa Aesar. A pilot project was carried out to find out the toxic concentration of Cd that affects the growth of *P. vulgaris*. A 10 mg/L IONPs and 20 mg/L SiNPs were found to be effective against selected Cd toxic levels. Iron oxide nanoparticles (IONPs) obtained from Alfa Aesar were having 99% purity, size 15–25 nm, and 4.67 density. Silicon nanoparticles obtained from Alfa Aesar were having 98% purity, size 40–100 nm, and 4.7 density. The solution used during the experiment was prepared using deionized H_2O.

Seed Priming With Iron Oxide Nanoparticles and Silicon Nanoparticles

Seeds of *P. vulgaris* were surface sterilized using 2.5% sodium hypochlorite solution for 2 min and then washed with deionized H_2O to remove chlorophyll (Chl) contents. IONPs and SiNPs were weighed and added in deionized H_2O followed by ultra-sonication for half-hour and their desired concentrations (IONPs = 10 mg/L) and (SiNPs = 20 mg/L) were achieved. After that sterilized seeds of *P. vulgaris* were soaked in an NP solution.

In the case of the control treatment, seeds were treated with deionized H_2O. In the next step, soaked seeds were dried and stored at 4°C for further experiments.

Seed Sowing and Greenhouse Conditions

The current study was executed at the university site (32°′N, 74°′E, 236m altitude). Ten seeds were sown in plastic pots of 40 × 45 cm containing 20kg treated soil. These pots were kept in the greenhouse condition with an average temperature of 20/15°C (day/night), average humidity of 50/70% late afternoon/morning, and a natural photoperiod. After germination, thinning was done and 8 plants were retained per pot. Regular weeding was done and plants were watered daily to uphold 70% of the field maximum moisture capacity throughout the growth period.

Determination of Growth and Leaf Relative Water Content

Plants were uprooted after 40 days and growth characteristics (root and shoot fresh weight, root and shoot dry weight) were estimated. Leaf relative water content (LRWC) values from *P. vulgaris* leaf samples were estimated using the following equation as given by Smart and Bingham (1974);

$$\text{LRWC}(\%) = \text{LFW} - \text{LDW}/\text{LTW} - \text{LDW} \times 100$$

Where LRWC = Leaf relative water content
LFW = Leaf fresh weight
LDW = Leaf dry weight
LTW = Leaf turgid weight

Estimation of Photosynthetic Pigments

Arnon method (1949) was used for the estimation of photosynthetic pigments. Approximately 100 mg leaf extract was mixed with 80% acetone and centrifuged for 5 min at 10,000 rpm. The optical density (OD) of filtrates was then measured using a spectrophotometer (Hitachi U-2001, Tokyo, Japan).

Determination of Malondialdehyde Content and Electrolyte Leakage

Malondialdehyde (MDA) content was determined according to the method of Cavalcanti et al. (2004). Briefly, 0.5 g samples were homogenized using mortar and pestle in 4 mL of trichloroacetic acid (TCA) (1% w/v) at 4°C. The homogenous mixture was then centrifuged for 20 min at 12,000 rpm to collect the supernatant. One milliliter of this supernatant was added to 3 mL of reaction mixture containing TCA (20% w/v) and thiobarbituric acid (0.5% w/v). The reaction mixture was incubated at 95°C for half-hour and the reaction was stopped by placing it in an ice bath. The absorbance value of the fraction was measured at 440, 532, and 600 nm.

The method of Blum and Ebercon (1981) was used for the determination of electrolyte leakage. A dry leaf sample (0.2 g) was floated in deionized H_2O (50 mL) for 24 h at room temperature with shaking. The electrolyte content in the solution was quantified and recorded as CO. After 20 min of boiling the sample, the electrolyte content in the solution was recorded as C1. Electrolyte leakage was measured in percentage as per the following formula:

$$\text{Relative electrolyte leakage} = \text{CO}/\text{C1} \times 100$$

Determination of Antioxidant Enzymes

About 1 g leaf samples were homogenized in a solution of potassium phosphate buffer solution (100 mM), polyvinyl pyrrolidone (1% w/v), ethylenediamine tetraacetic acid (0.1 mM) and triton X-100 (0.5%). The homogenate was filtered through cheesecloth and centrifuged at 18,000 rpm for 20 min at 4°C. The resultant supernatant was used for the estimation of antioxidative enzymes and was stored at −80°C for analysis. The method of Aebi (1974) was used for the determination of catalase (CAT) activity. Briefly, potassium phosphate buffer (50 mM) and plant extract were used in the reaction (3 mL). To start the reaction, 10 mM H_2O_2 was added. 1 unit of CAT is defined as the number of enzymes, which release 1/2 of peroxide oxygen from 10 mM H_2O_2 solution in 100 s at 25°C. Superoxide dismutase (SOD) activity was measured according to the method of Beyer and Fridovich (1987). The reaction mixture (30 mL) for the determination of SOD was composed of potassium phosphate buffer (50 mM), methionine (9.9 mM), nitroblue tetrazolium (57 mM), and plant extract. The reaction mixture was started by light illumination. One unit of SOD is defined as the enzyme which causes a 50% decrease of SOD inhabitable reduction.

Determination of Proline Content

To determine proline content, dry leaf samples (0.5 g) were extracted in sulfosalicylic acid (3%) and then filtered (Bates et al., 1973). Afterward, 2 mL of leaf extract was mixed in ninhydrin solution (2 mL) and glacial acetic acid (2 mL). Plant samples were incubated at 100°C for 1 h and cooled in an ice bath. Four milliliters of toluene was vigorously added to the mixture. The absorbance value was calibrated at 520 nm using a spectrophotometer. Proline content was estimated using a standard curve.

Determination of Cadmium Content

Following Cd treatment, *P. vulgaris* seedlings were rinsed with deionized H_2O. Seedlings were dried at 80°C for 24 h. The plant material was digested in HNO_3:$HCLO_4$. About 1 g plant sample was homogenized in 50 mM Tris (hydroxymethyl) aminomethane (Tris–HCl), 250 mM sucrose, and 1 mM DL-dithiothreitol. The homogenous mixture obtained was centrifuged at 3,000 rpm for 5 min for the isolation of the cell wall. The supernatant obtained was centrifuged at 20,000 rpm for 45 min. Cd was determined using ICP (ICP-AES, Thermo Elemental, United States) (Wang et al., 2009).

Determination of Nutritional Content

A flame photometer (Jenway PFP-7) was used for the determination of nutritional content (Mo^+, Ca^+, K^+, Mn^+) from

the digested plant samples. K^+ content was quantified with the help of a standard solution.

Determination of Gaseous Exchange

Assessments of gaseous exchange attributes, net CO_2 uptake, net photosynthesis (Pn), stomatal conductance (Gs), and transpiration rate (E), were performed at 10:00 a.m. at 27°C during the daytime on completely expanded leaves using a portable gas exchange system (Holá et al., 2010).

Determination of Polyamine Activity

The concentration of hydrogen peroxide produced during polyamine oxidation assisted in the estimation of polyamine oxidase (PAO) activity. The foliage plant sample was mixed with potassium phosphate buffer (0.1 mM at pH 6.5 in an pre-chilled mortar and pestle. The resultant supernatant (0.5 mL) was obtained by centrifugation of this mixture at 10,000 g at 4°C for 20 min followed by mixing with 4-aminoantipyrine/*N*,*N*-dimethylaniline solutions (0.4 mL), 0.2 mL horseradish POD (250 U/mL), and 5 mL of K_3PO_4 buffer (100 mM at pH 6.5). For the determination of polyamine oxidase, putrescine (30 mL of 20 mM) was homogenized in enzyme extract to initiate reaction according to Zhao et al. (2004).

Determination of Nitric Oxide Content

Nitric oxide activity was quantified using the nitric oxide detection kit (Solarbio Life Science, Beijing, China) following the manufacturer's instructions.

Estimation of Soluble Protein Content

Leaf samples (1 g) were extracted using KH_2PO_4 (4 mL at pH 6.8) following centrifugation at 3,600 rpm for 30 min. The resultant supernatant was collected and a 20 μL aliquot of the extract was collected and homogenized with the Bradford color reagent (1 mL). The spectrophotometer calibration was carried out at 595 nm as per the procedure described by Bradford (1976).

Statistical Analysis

Data reported in the experiment was mean of 5 replicates. Statistical package XL-STAT was carried out for analysis of variance (ANOVA). Subsequently, Tukey's test was conducted to determine the significant differences among the values.

RESULTS

Effect of Iron Oxide Nanoparticles and Silicon Nanoparticles on Growth Attributes of *Phaseolus vulgaris*

Table 1 shows the role of IONPs and SiNPs, alone or in combination, on the growth of *P. vulgaris* seedlings grown in normal and Cd-contaminated soil. Synergistic application of NPs improved shoot fresh weight and root fresh weight by 39 and 40%, respectively, as compared to IONPs-only treated *P. vulgaris* seedlings grown in non-contaminated soil. When *P. vulgaris* seedlings were exposed to 2 mM $CdCl_2$, combined treatment of IONPs and SiNPs increased shoot fresh weight and root fresh weight by 45 and 19%, respectively, as compared to SiNP-treated *P. vulgaris* seedlings grown in Cd-contaminated media. Likewise, combined and synergistic treatments involving NPs enhanced root dry weight and shoot dry weight in *P. vulgaris* seedlings grown in normal and Cd-contaminated conditions (**Table 1**).

Effect of Iron Oxide Nanoparticles and Silicon Nanoparticles on Leaf Relative Water Content and Net Photosynthetic Rate of *Phaseolus vulgaris*

When *P. vulgaris* seedlings were grown in non-contaminated media, combined treatment of IONPs and SiNPs enhanced LRWC content by 9 and 4% in comparison with IONPs-only and SiNPs-only treatment, respectively. A similar trend of net

TABLE 1 | Effect of IONPs and SiNPs on root fresh weight, shoot fresh weight, root dry weight, shoot dry weight, leaf relative water content, and net photosynthetic rate of *Phaseolus vulgaris* grown in different concentrations of Cd.

Treatments	Root FW (g plant^{-1})	Shoot FW (g plant^{-1})	Root DW (g plant^{-1})	Shoot DW (g plant^{-1})	LRWC (%)	Net Photosynthetic rate (μmol m^{-2} s^{-1})
Cd0 + IONPs	4.21 ± 0.45ab	25.12 ± 1.89b	0.33 ± 0.0021b	2.76 ± 0.54bc	82 ± 6.76	1.98 ± 0.35cd
Cd0 + SiNPs	3.76 ± 0.37cd	23.18 ± 1.46bc	0.28 ± 0.0031bc	2.34 ± 0.38bc	86 ± 5.27	2.19 ± 0.76c
Cd0 + IONPs + SiNPs	5.89 ± 0.89a	34.98 ± 2.87a	0.56 ± 0.0039a	3.54 ± 0.39a	90 ± 5.87	3.17 ± 0.38a
Cd1 + IONPs	3.78 ± 0.37c	21.12 ± 1.78c	0.21 ± 0.0035cd	2.09 ± 0.54cd	78 ± 3.98	2.19 ± 0.57bc
Cd1 + SiNPs	2.56 ± 0.87de	18.98 ± 1.67d	0.28 ± 0.0076bc	2.56 ± 0.43c	80 ± 4.18	2.67 ± 0.18bc
Cd1 + IONPs + SiNPs	4.18 ± 0.48b	24.78 ± 1.09bc	0.39 ± 0.0072ab	2.98 ± 0.15ab	90 ± 5.28	3.08 ± 0.24ab
Cd2 + IONPs	2.76 ± 0.27d	18.23 ± 1.04de	0.17 ± 0.0043d	1.89 ± 0.76 d	72 ± 3.67	1.09 ± 0.12d
Cd2 + SiNPs	2.23 ± 0.45de	20.89 ± 1.09cd	0.26 ± 0.0021c	2.08 ± 0.45cd	80 ± 4.27	1.89 ± 0.38cd
Cd2 + IONPs + SiNPs	3.89 ± 0.48bc	23.89 ± 1.34bc	0.32 ± 0.0028b	2.65 ± 0.16c	92 ± 4.87	2.76 ± 0.17b
Cd3 + IONPs	1.89 ± 0.56e	13.76 ± 1.09f	0.17 ± 0.0021d	1.09 ± 0.78e	63 ± 3.87	0.98 ± 0.002d
Cd3 + SiNPs	2.67 ± 0.72de	15.27 ± 1.38e	0.13 ± 0.0065de	1.56 ± 0.37de	76 ± 4.76	1.67 ± 0.21cd
Cd3 + IONPs + SiNPs	3.89 ± 0.51bc	18.28 ± 1.02de	0.28 ± 0.0078bc	2.78 ± 0.28b	84 ± 5.98	2.09 ± 0.54bc

Here IONPs, SiNPs, Cd0, Cd1, Cd2, Cd3 indicates iron oxide nanoparticles, silicon nanoparticles, 0 mM $CdCl_2$, 1 mM $CdCl_2$, 1.5 mM $CdCl_2$, 2 mM $CdCl_2$. Different letters indicate significant difference among the treatments ($P \leq 0.05$).

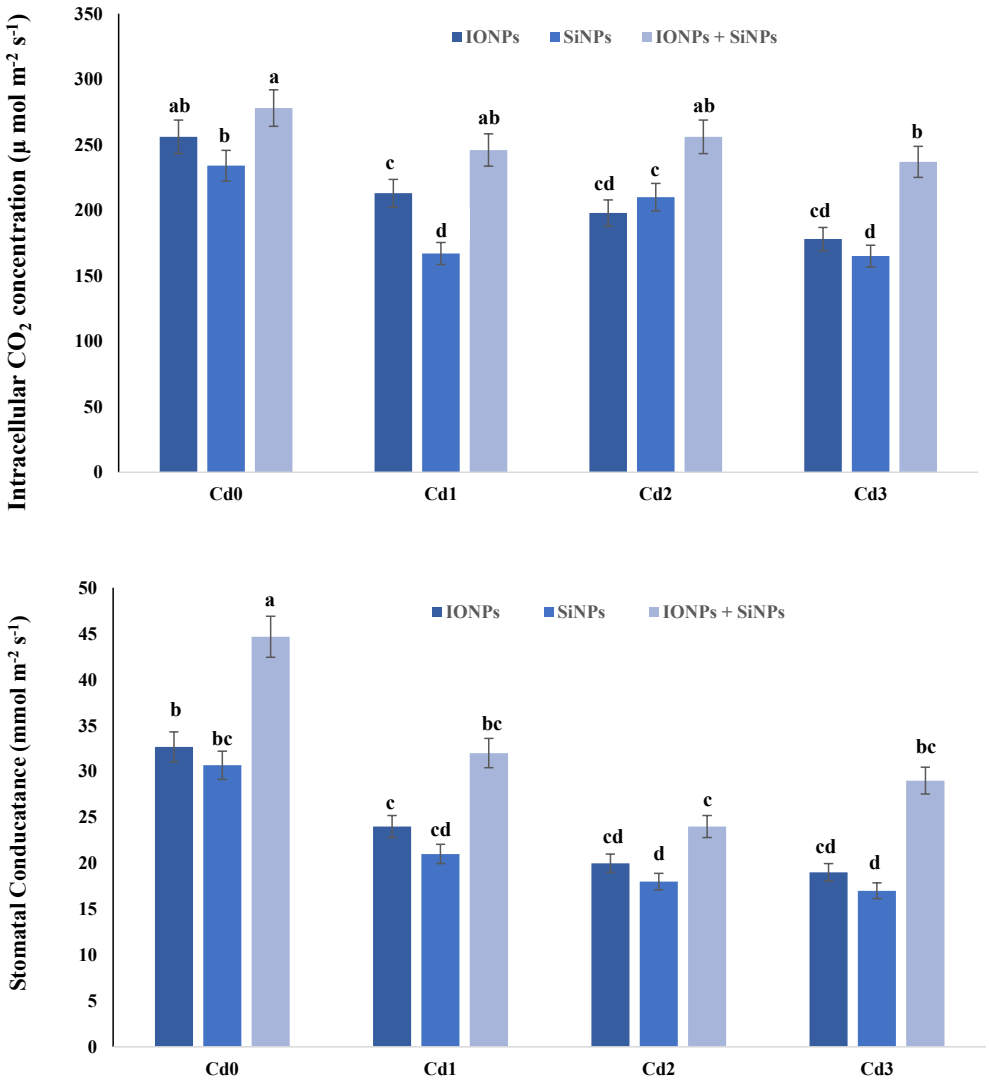

FIGURE 1 | Effect of IONPs and SiNPs on intercellular CO_2 concentration and stomatal conductance of *Phaseolus vulgaris* grown in different concentrations of Cd. Here IONPs, SiNPs, Cd0, Cd1, Cd2, and Cd3 indicate iron oxide nanoparticles, silicon nanoparticles, 0 mM $CdCl_2$, 1 mM $CdCl_2$, 1.5 mM $CdCl_2$, and 2 mM $CdCl_2$. Different letters indicate significant difference among the treatments ($P \leq 0.05$).

photosynthetic rate was observed in *P. vulgaris* seedlings exposed to different concentrations of $CdCl_2$ (**Table 1**).

Effect of Iron Oxide Nanoparticles and Silicon Nanoparticles on Gas Exchange Parameters of *Phaseolus vulgaris*

In the case of *P. vulgaris* seedlings grown in non-contaminated soil, synergistic application of IONPs and SiNPs increased intercellular CO_2 concentration and stomatal conductance by 8 and 18%, respectively, in comparison with alone application of IONP and SiNP treatment. When *P. vulgaris* seedlings were treated with 1 mM $CdCl_2$, 1.5 mM $CdCl_2$, and 2 mM $CdCl_2$, intercellular CO_2 concentration decreased by 20, 29, and 43%, respectively, as compared to Cd0 treatment. Synergistic application of IONP and SiNP increased intercellular CO_2 concentration in *P. vulgaris* seedlings grown in 1.5 mM $CdCl_2$ by 22 and 7%, respectively, in comparison with alone treatments of IONPs and SiNPs. Likewise, synergistic application of IONP and SiNP enhanced stomatal conductivity in *P. vulgaris* seedlings grown in Cd0-treatment and Cd-contaminated soil (**Figure 1**).

Effect of Iron Oxide Nanoparticles and Silicon Nanoparticles on Malondialdehyde Content and Electrolyte Leakage in *Phaseolus vulgaris*

Figure 2 shows that the application of IONPs and SiNPs reduced MDA content and EL leakage in *P. vulgaris* seedlings grown in non-contaminated and Cd-polluted soil. Synergistic application

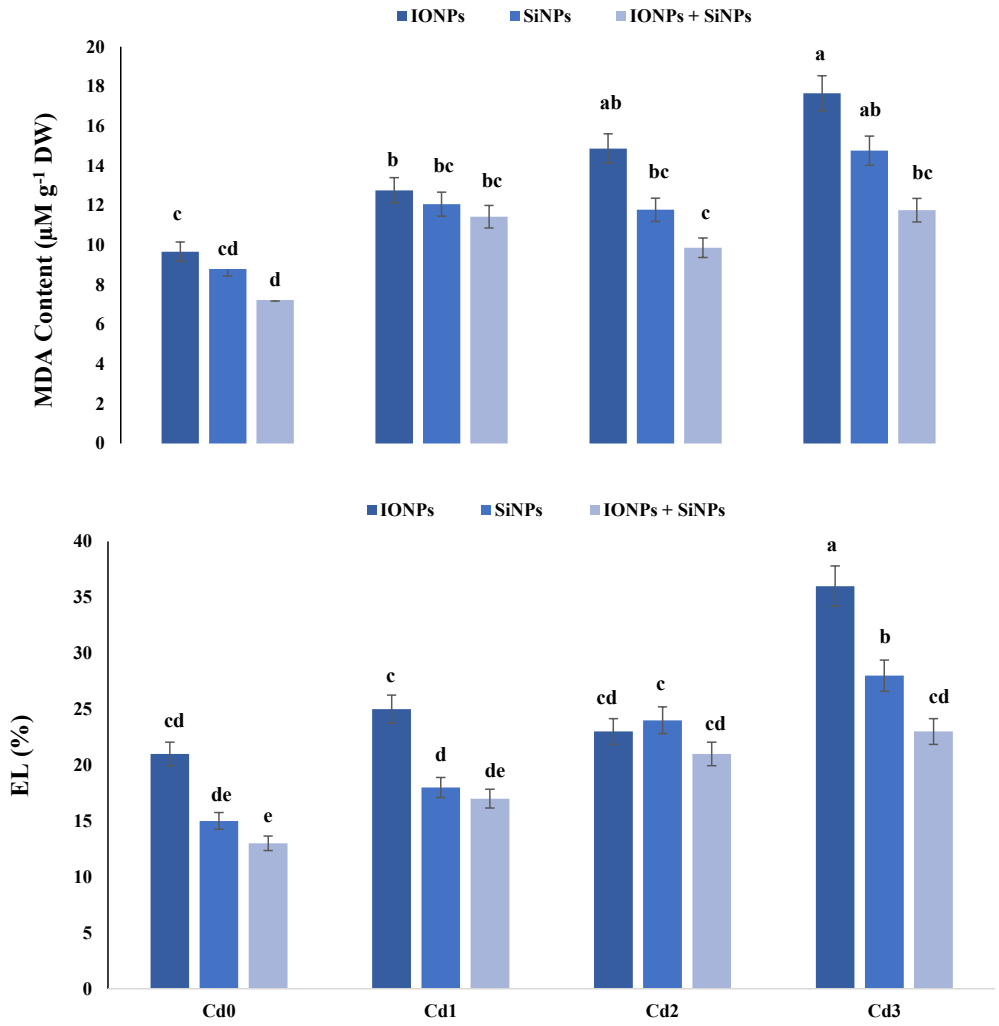

FIGURE 2 | Effect of IONPs and SiNPs on MDA content and EL of *Phaseolus vulgaris* grown in different concentrations of Cd. Here IONPs, SiNPs, Cd0, Cd1, Cd2, and Cd3 indicate iron oxide nanoparticles, silicon nanoparticles, 0 mM $CdCl_2$, 1 mM $CdCl_2$, 1.5 mM $CdCl_2$, and 2 mM $CdCl_2$. Different letters indicate significant difference among the treatments ($P \leq 0.05$).

of IONPs and SiNPs reduced MDA content by 50 and 20% as compared to individual application of IONPs and SiNPs, respectively, in *P. vulgaris* seedlings grown in 1.5 mM $CdCl_2$-contaminated soil.

Electrolyte leakage was also reduced in *P. vulgaris* seedlings treated with combined application of IONPs and SiNPs, in comparison with individual treatments. In the case of *P. vulgaris* seedlings grown in 2 mM $CdCl_2$, combined application of IONPs and SiNPs reduced EL by 56 and 21%, respectively, in comparison with individual treatments of IONPs and SiNPs (**Figure 2**).

Effect of Iron Oxide Nanoparticles and Silicon Nanoparticles on Polyamine Content in *Phaseolus vulgaris* Seedlings

Figure 3 shows the effect of IONPs and SiNPs on spermidine (Spd) and putrescine (Put) content of *P. vulgaris* seedlings grown in normal and Cd-contaminated soil. Application of IONPs and SiNPs, alone or in combination, escalated Spd and Put content in *P. vulgaris*. Combined treatment of IONPs and SiNPs enhanced Spd content by 91% as compared to individual application of SiNPs in *P. vulgaris* seedlings grown in 1 mM $CdCl_2$. Likewise, Put content also increased when *P. vulgaris* seedlings were treated with IONPs and SiNPs in combination. The combined application of IONPs and SiNPs enhanced Put content by more than onefold in comparison with SiNPs-only treatment in *P. vulgaris* seedlings grown in 2 mM $CdCl_2$.

Effect of Iron Oxide Nanoparticles and Silicon Nanoparticles on Nitric Oxide and Proline Content of *Phaseolus vulgaris*

Nitric oxide and proline (Pro) content are considered as stress markers in plants. During the current study, IONPs and SiNPs enhanced nitric oxide and proline

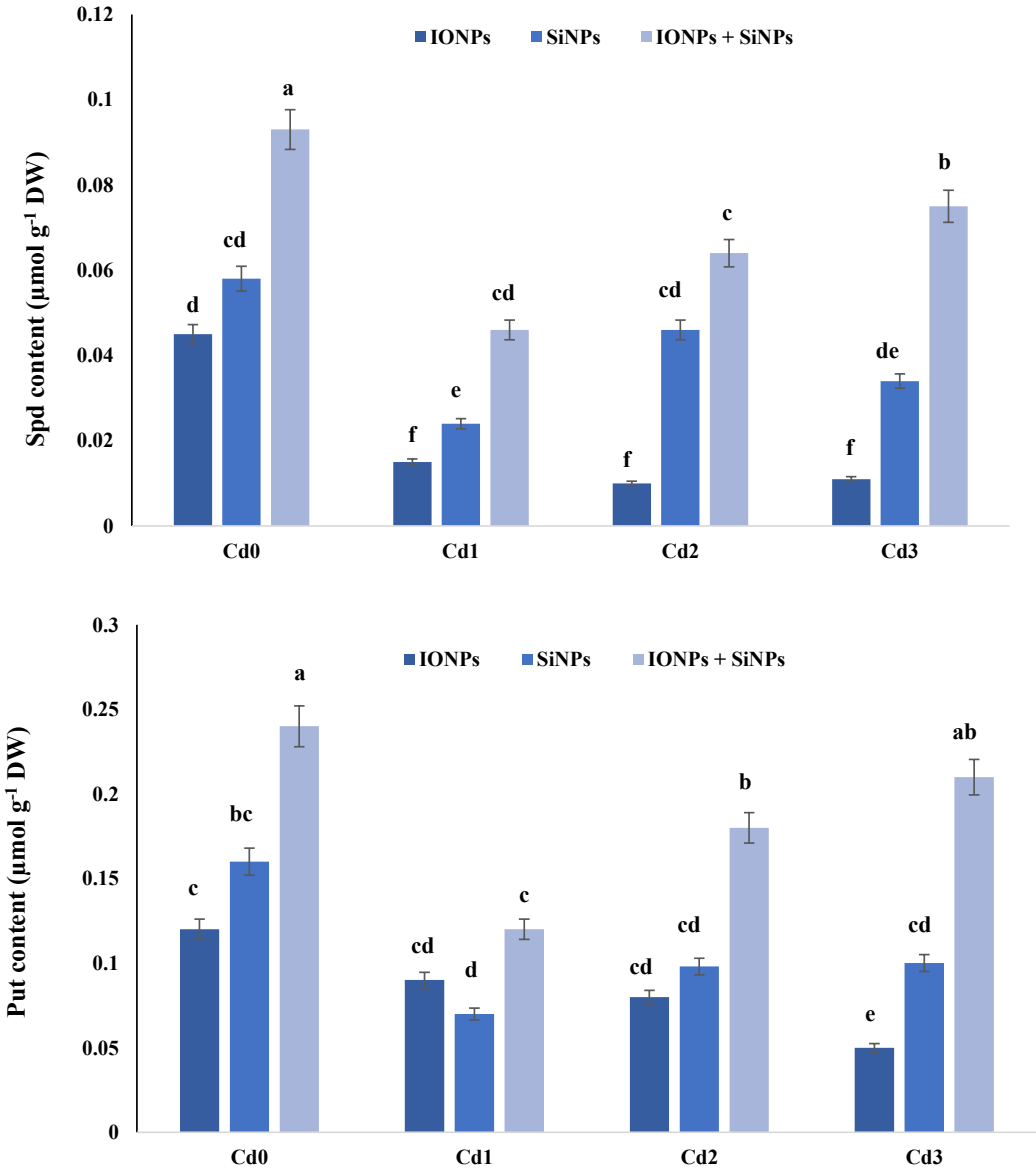

FIGURE 3 | Effect of IONPs and SiNPs on PAs content of *Phaseolus vulgaris* grown in different concentrations of Cd. Here IONPs, SiNPs, Cd0, Cd1, Cd2, and Cd3 indicate iron oxide nanoparticles, silicon nanoparticles, 0 mM $CdCl_2$, 1 mM $CdCl_2$, 1.5 mM $CdCl_2$, and 2 mM $CdCl_2$. Different letters indicate significant difference among the treatments ($P \leq 0.05$).

content in *P. vulgaris* seedlings grown in normal and Cd-contaminated soil. In the case of *P. vulgaris* seedlings grown in control conditions, synergistic application of IONPs and SiNPs enhanced NO content by 44 and 50%, respectively, in comparison with individual application of IONPs and SiNPs. When *P. vulgaris* seedlings were exposed to 2 mM $CdCl_2$, combined application of IONPs and SiNPs enhanced NO content by more than onefold and 60% as compared to IONPs-only and SiNPs-only treatment. Similarly, IONPs and SiNPs also enhanced proline content in *P. vulgaris* seedlings grown in normal and Cd-contaminated conditions (**Figure 4**).

Effect of Iron Oxide Nanoparticles and Silicon Nanoparticles on the Activity of Antioxidant Enzymes in *Phaseolus vulgaris*

Figure 5 explains the role of IONPs and SiNPs on the activity of SOD and CAT in *P. vulgaris* seedlings grown in control and Cd-contaminated conditions. In the case of *P. vulgaris* seedlings grown in Cd0 treatment, combined application of IONPs and SiNPs improved the activity of SOD by 41 and 71%, respectively, in comparison with IONPs-only and SiNPs-only treatment. Synergistic treatment of IONPs and SiNPs enhanced

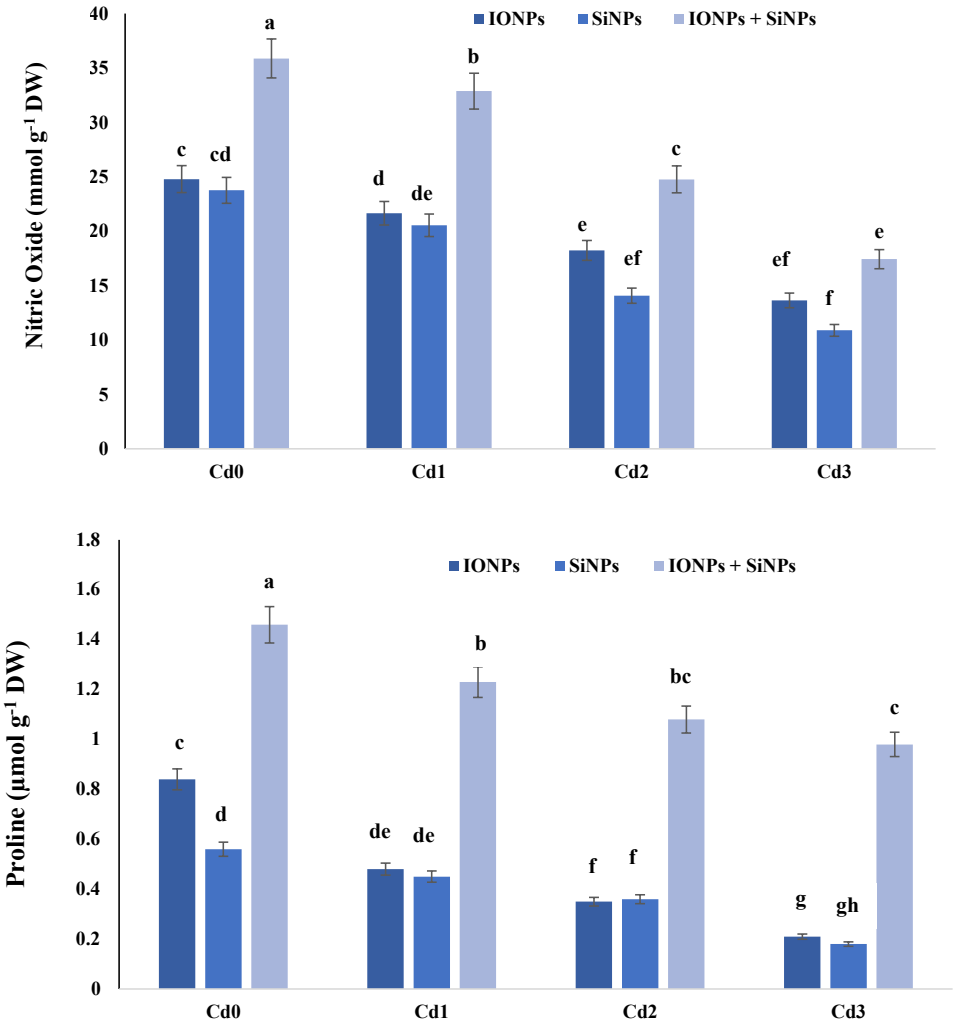

FIGURE 4 | Effect of IONPs and SiNPs on nitric oxide and proline content of *Phaseolus vulgaris* grown in different concentrations of Cd. Here IONPs, SiNPs, Cd0, Cd1, Cd2, and Cd3 indicate iron oxide nanoparticles, silicon nanoparticles, 0 mM $CdCl_2$, 1 mM $CdCl_2$, 1.5 mM $CdCl_2$, and 2 mM $CdCl_2$. Different letters indicate significant difference among the treatments ($P \leq 0.05$).

SOD content by 72 and 90% as compared to individual treatments of IONPs and SiNPs, respectively, in *P. vulgaris* seedlings grown in 2 mM $CdCl_2$. Likewise, combined treatment of IONPs and SiNPs enhanced CAT activity in *P. vulgaris* seedlings grown in normal and $CdCl_2$-contaminated conditions. The combined application of IONPs and SiNPs escalated CAT activity by 71 and 50%, as compared to IONPs-only and SiNPs-only treatment, respectively, in *P. vulgaris* seedling exposed to 2 mM $CdCl_2$.

Effect of Iron Oxide Nanoparticles and Silicon Nanoparticles on Cadmium Uptake of *Phaseolus vulgaris*

Table 2 shows that NP treatment reduced Cd uptake in *P. vulgaris* seedlings grown in $CdCl_2$-contaminated soil. Synergistic application of IONPs and SiNPs reduced Cd uptake by 68% in *P. vulgaris* seedling grown in 2 mM $CdCl_2$.

Effect of Iron Oxide Nanoparticles and Silicon Nanoparticles on Photosynthetic Pigmentation of *Phaseolus vulgaris*

Table 3 shows the role of IONPs and SiNPs on photosynthetic pigmentation of *P. vulgaris* grown in normal and Cd toxic conditions. IONPs and SiNPs orchestered carotenoids content, Chl *a*, Chl *b*, and total Chl content in *P. vulgaris* seedlings.

Effect of Iron Oxide Nanoparticles and Silicon Nanoparticles on the Nutritional Content of *Phaseolus vulgaris*

Table 4 describes the role of IONPs and SiNPs on the nutritional content of *P. vulgaris* seedlings grown in normal and different concentrations of $CdCl_2$. A combined application of IONPs and SiNPs increased K^+ content by 31 and 24%, respectively, as

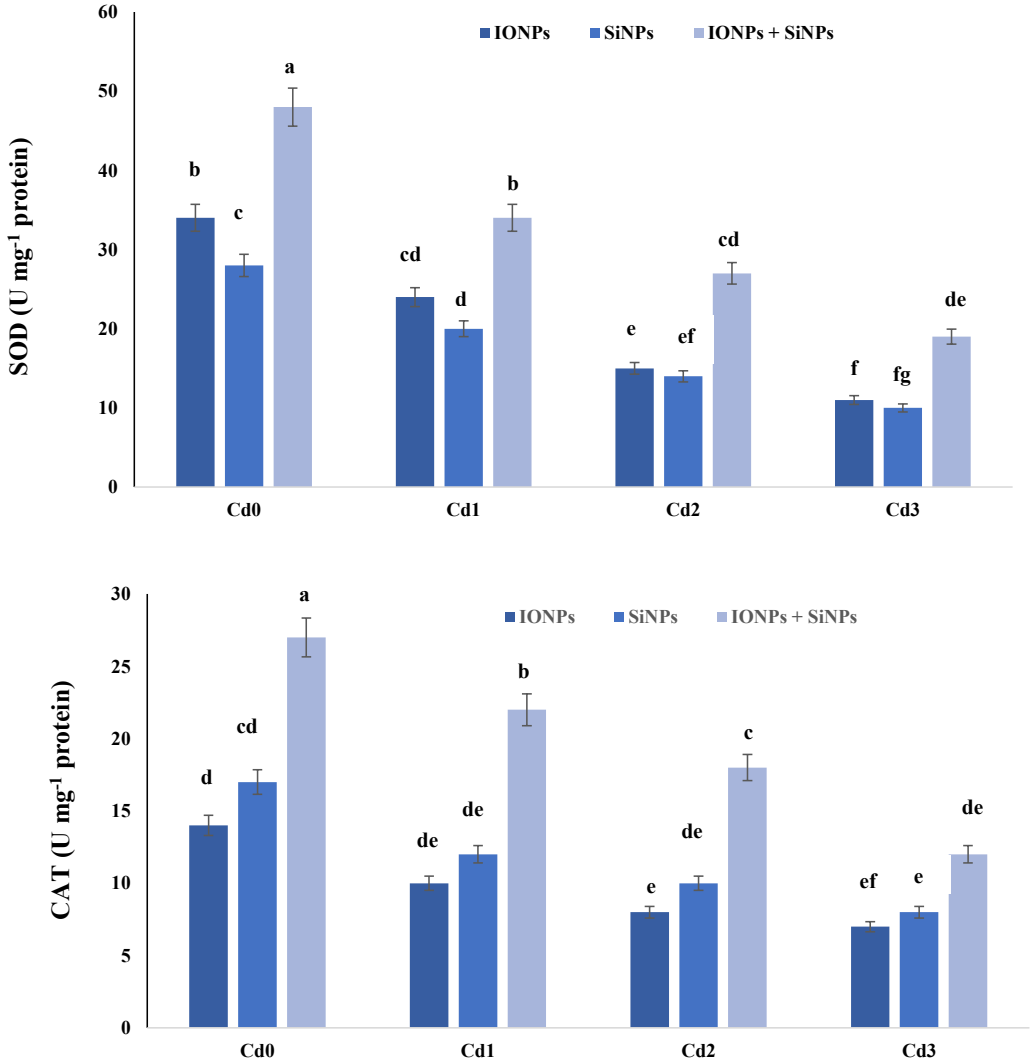

FIGURE 5 | Effect of IONPs and SiNPs on SOD and CAT activity of *P. vulgaris* grown in different concentrations of Cd. Here IONPs, SiNPs, Cd0, Cd1, Cd2, and Cd3 indicate iron oxide nanoparticles, silicon nanoparticles, 0 mM $CdCl_2$, 1 mM $CdCl_2$, 1.5 mM $CdCl_2$, and 2 mM $CdCl_2$. Different letters indicate significant difference among the treatments ($P \leq 0.05$).

compared to IONPs-only and SiNPs-only treated *P. vulgaris* seedlings grown in non-contaminated potted soil.

DISCUSSION

Cadmium toxicity reduces the ability of plants to absorb key nutrients (Mg, Ca, P, K) and water content from soil (Yang et al., 2020). Potassium is considered as crucial for plant growth, development, and metabolomics (Hasanuzzaman et al., 2018) because it alleviates abiotic stresses (Raza et al., 2021) by restricting transportation and accumulation of heavy metals in plants (Kerchev et al., 2020). Additionally, potassium not only immobilizes heavy metal content (Liu et al., 2018) but also behaves antagonistically to Cd and detoxifies Cd within plants (Shamsi et al., 2008). Cadmium is a non-essential metal and is involved in the hindrance of plant growth (Shah et al., 2020a) by causing a reduction in water content, biomass, fresh and dry weight of plants, as well as disruption in redox reaction (Raza et al., 2020). Potassium application stabilizes chlorophyll architecture, which leads to the regulation of photosynthate production (Hasanuzzaman et al., 2018). It was also documented that K^+ application enhanced growth and yield in apple dwarf rootstock seedlings (Xu et al., 2020) *via* Cd assimilation by increased accumulation of K^+ in plants (Norvell et al., 2000). In addition, the increase in K^+ enhanced the activity of antioxidant enzymes and reduced MDA content in plants exposed to Cd toxicity. The results of the present study also indicated that synergistic application of IONPs and SiNPs enhanced K^+ content in *P. vulgaris* seedlings grown in normal and Cd-contaminated soil. In the present study, IONPs and SiNPs treatment increased LRWC in *P. vulgaris* seedling

TABLE 2 | Effect of IONPs and SiNPs on root Cd content, shoot Cd content, translocation factor, and metal tolerance index of *Phaseolus vulgaris* grown in different concentrations of Cd.

Treatments	Root (μg g^{-1} DW)	Shoot (μg g^{-1} DW)
Cd0 + IONPs	ND	ND
Cd0 + SiNPs	ND	ND
Cd0 + IONPs + SiNPs	ND	ND
Cd1 + IONPs	0.013 ± 0.002	0.05 ± 0.0002
Cd1 + SiNPs	0.014 ± 0.003	0.04 ± 0.0001
Cd1 + IONPs + SiNPs	0.005 ± 0.004	0.002 ± 0.0003
Cd2 + IONPs	0.017 ± 0.001	0.009 ± 0.0001
Cd2 + SiNPs	0.015 ± 0.003	0.007 ± 0.0004
Cd2 + IONPs + SiNPs	0.019 ± 0.008	0.005 ± 0.0002
Cd3 + IONPs	0.021 ± 0.005	0.003 ± 0.0005
Cd3 + SiNPs	0.041 ± 0.0003	0.006 ± 0.0007
Cd3 + IONPs + SiNPs	0.049 ± 0.002	0.029 ± 0.0006

Here IONPs, SiNPs, Cd0, Cd1, Cd2, Cd3 indicates iron oxide nanoparticles, silicon nanoparticles, 0 mM $CdCl_2$, 1 mM $CdCl_2$, 1.5 mM $CdCl_2$, 2 mM $CdCl_2$.

(**Table 1**). Before, it was also reported that SiNP treatment enhanced gas exchange characteristics in plants exposed to Cd-contaminated media (Ur Rahman et al., 2021). Cadmium stress destabilized photosynthetic apparatus, yet IONPs and SiNPs application reduced injury to photosynthetic machinery. Iron oxide nanoparticles increased root and shoot length in *Arachis hypogaea* plants (Rizwan et al., 2019). In the present research, it was noted also that that synergistic application of IONPs and SiNPs increased photosynthesis and gas exchange characteristics in *P. vulgaris* seedlings.

Proline is crucial for the sustenance of metabolomics in plants (Ahmad et al., 2019). It was noted in the present investigation that *P. vulgaris* seedlings treated with IONPs and SiNPs showed an increased level of proline under Cd stress. The increased level of proline in NP-treated plants might lead to activation of proline synthesizing genes involved in the regulation of water content in plants.

Membrane stability is an essential characteristic required for the effective survival of plants under abiotic stress since damage to it will lead to cellular death. MDA is an indicator of cellular damage and membrane stability (Shah et al., 2020b). Under stress conditions, the generation of MDA and peroxidation of lipids increased causing damage to plants. In this study, Cd stress amplified MDA and EL in *P. vulgaris* plants grown in Cd-contaminated soil. Cadmium decreases the stability of membranous molecules due to the enhanced accumulation of ROS. Previous researchers revealed the role of IONPs and SiNPs in alleviating abiotic stresses in plants.

TABLE 3 | Effect of IONPs and SiNPs on carotenoids, total chlorophyll content, Chlb, and Chla of *Phaseolus vulgaris* grown in different concentrations of Cd.

Treatments	Carotenoids	Total Chlorophyll	Chlb	Chla
Cd0 + IONPs	4.87 ± 0.89ab	1.42 ± 0.071a	0.55 ± 0.032ab	0.87 ± 0.043
Cd0 + SiNPs	3.78 ± 0.76b	1.10 ± 0.032bc	0.34 ± 0.026c	0.76 ± 0.031
Cd0 + IONPs + SiNPs	4.93 ± 0.51a	1.19 ± 0.024bc	0.65 ± 0.016a	0.54 ± 0.017
Cd1 + IONPs	3.23 ± 0.47bc	0.81 ± 0.027c	0.35 ± 0.034bc	0.46 ± 0.026
Cd1 + SiNPs	3.02 ± 0.39c	0.66 ± 0.046	0.28 ± 0.026cd	0.38 ± 0.027
Cd1 + IONPs + SiNPs	3.16 ± 0.23bc	1.3 ± 0.037b	0.41 ± 0.017b	0.89 ± 0.031
Cd2 + IONPs	3.09 ± 0.42bc	0.78 ± 0.045c	0.31 ± 0.015cd	0.47 ± 0.025
Cd2 + SiNPs	2.89 ± 0.25cd	0.65 ± 0.067cd	0.23 ± 0.019cd	0.42 ± 0.027
Cd2 + IONPs + SiNPs	3.87 ± 0.31ab	0.96 ± 0.047bc	0.37 ± 0.023bc	0.59 ± 0.015
Cd3 + IONPs	2.78 ± 0.18cd	0.79 ± 0.067cd	0.24 ± 0.021cd	0.55 ± 0.036
Cd3 + SiNPs	2.67 ± 0.24d	0.65 ± 0.078cd	0.21 ± 0.054d	0.44 ± 0.045
Cd3 + IONPs + SiNPs	3.54 ± 0.26bc	1.13 ± 0.037ab	0.38 ± 0.018bc	0.75 ± 0.029

Here IONPs, SiNPs, Cd0, Cd1, Cd2, Cd3 indicates iron oxide nanoparticles, silicon nanoparticles, 0 mM $CdCl_2$, 1 mM $CdCl_2$, 1.5 mM $CdCl_2$, 2 mM $CdCl_2$. Different letters indicate significant difference among the treatments ($P \leq 0.05$).

TABLE 4 | Effect of IONPs and SiNPs on Mo^+, Ca^+, K^+, and Mn^+ of *Phaseolus vulgaris* grown in different concentrations of Cd.

Treatments	Mo^+ content (meq. g^{-1} DW)	Ca^{+2} content (meq. g^{-1} DW)	K^+ content (meq. g^{-1} DW)	Mn^{+2} content (meq. g^{-1} DW)
Cd0 + IONPs	21.78 ± 1.87ab	13.56 ± 1.03b	14.87 ± 1.02bc	30.89 ± 2.56b
Cd0 + SiNPs	17.56 ± 1.08cd	15.78 ± 1.09ab	15.76 ± 1.13b	25.78 ± 1.47c
Cd0 + IONPs + SiNPs	27.98 ± 1.56a	19.87 ± 1.27a	19.56 ± 1.07a	45.98 ± 2.58a
Cd1 + IONPs	17.98 ± 1.08c	10.89 ± 1.07cd	12.56 ± 1.23cd	22.65 ± 1.45cd
Cd1 + SiNPs	15.82 ± 1.23d	11.25 ± 1.12bc	13.76 ± 1.09c	18.65 ± 1.38de
Cd1 + IONPs + SiNPs	20.56 ± 1.34b	15.89 ± 1.06ab	16.78 ± 1.56ab	24.98 ± 2.45cd
Cd2 + IONPs	13.98 ± 1.07d	10.46 ± 1.18c	09.87 ± 0.97d	14.76 ± 1.43e
Cd2 + SiNPs	14.89 ± 1.04de	11.34 ± 1.14bc	11.57 ± 1.09cd	16.34 ± 1.28de
Cd2 + IONPs + SiNPs	19.78 ± 1.37bc	12.45 ± 1.09bc	14.27 ± 1.06bc	21.59 ± 1.92d
Cd3 + IONPs	10.34 ± 1.08f	9.56 ± 1.07de	7.65 ± 0.67ef	12.98 ± 1.03ef
Cd3 + SiNPs	12.87 ± 1.17e	11.67 ± 1.56d	10.78 ± 1.08e	14. 45 ± 1.78e
Cd3 + IONPs + SiNPs	13.89 ± 1.67de	14.87 ± 1.45cd	14.87 ± 1.09de	25.89 ± 2.67c

Here IONPs, SiNPs, Cd0, Cd1, Cd2, Cd3 indicates iron oxide nanoparticles, silicon nanoparticles, 0 mM $CdCl_2$, 1 mM $CdCl_2$, 1.5 mM $CdCl_2$, 2 mM $CdCl_2$. Different letters indicate significant difference among the treatments ($P \leq 0.05$).

The total antioxidant activity of a plant is a good indicator of how well the plant's antioxidant system is functioning in the presence of oxidative stress. Plants have a variety of antioxidative defense systems to deal with oxidative stress, particularly those produced by the generation of excess ROS as a result of abiotic stress. Superoxide peroxidase (SOD) is the first line of defense that is involved in the conversion of superoxide anion to peroxide. Catalase (CAT) is also a crucial antioxidant that plays an important role in plants' defensive approach to abiotic stresses. This enzyme is involved in the conversion of H_2O_2 to O_2 and H_2O. Current research reported that IONPs and SiNPs enhanced the activity of CAT in *P. vulgaris* seedlings exposed to Cd stress.

Nanoparticles reduced MDA levels, while they increased peroxidase (POD) and SOD activity in metal-stressed wheat plants (Sardar et al., 2022). Additionally, osmoregulators control the structure of organelles and macromolecules in plants by adjusting osmosis and aid in the reduction of Cd-induced toxicity in plants (Thind et al., 2021). In the present study, we also noticed that Cd inhibited the production of total soluble proteins and proline concentration in *P. vulgaris* seedlings. The findings of the present study were in line with the findings of Azizi et al. (2021). Application of NPs in the present study enhanced proline accumulation in Cd treated *P. vulgaris* seedlings. Enhanced accumulation of proline and soluble sugar may be due to augmented proline playing some vital roles in scavenging ROS, adjusting osmotic equilibrium and determining the membrane attributes in plants exposed to stress (Aswani et al., 2019). Many authors investigated the positive effect of NPs on the enhancement of proline accumulation under stress conditions in broad bean plants in addition to adjusted antioxidant enzyme activities, soluble sugars, and amino acids (Sadak and Bakry, 2020). Furthermore, Azimi et al. (2021) claimed that NP supply can decline salt stress in tomatoes by improving photosynthetic machinery, phenolics, and antioxidant enzyme activities and yield as well.

Cadmium phytotoxicity increased the formation of ROS and produced oxidative burst by interfering with the antioxidant defense system (Kamran et al., 2021), which promotes the MDA content due to the high accumulation of lipid peroxidation of the membrane. During the normal metabolism, the plants have established well-organized antioxidant enzyme defense mechanisms to eliminate the ROS (Fan et al., 2020). This is because SOD acts as the first line of defense in plants against ROS. Superoxide dismutase converts the O_2^- to less toxic H_2O_2, and it forms the first line of defense in the antioxidant system of plants; to this end, CAT scavenges the H_2O_2 to water and oxygen molecules (Orabi and Abou-Hussein, 2019). The ameliorative influence of the NPs on Cd stress was also assessed by Hussain et al. (2018) in the wheat plant. This apparently will promote antioxidant impairments by decreasing H_2O_2 and MDA content and enhancing the activities of SOD, CAT, and increased tolerance against abiotic toxicity (Sharma et al., 2019).

CONCLUSION

Cadmium toxicity enhanced oxidative stress in *P. vulgaris* seedlings. Application of IONPs and SiNPs escalated the activity of antioxidant enzymes besides incrementation in K^+ content. Additionally, synergistic application of IONPs and SiNPs increase NO content and Pro content in *P. vulgaris* seedlings grown in normal and $CdCl_2$-polluted soil. Cd-stress alleviation is credited to increased activity of antioxidant enzymes and maintenance of PAs and K^+ metabolism. It is further added that mechanisms and molecules involved in the interaction of different NPs can be exploited for the mitigation of numerous stresses in plants.

DATA AVAILABILITY STATEMENT

The original contributions presented in the study are included in the article/supplementary material, further inquiries can be directed to the corresponding author/s.

AUTHOR CONTRIBUTIONS

LK contributed toward designing the research and conceptualization. AU and AAS performed the experiments. AAS performed the statistical analysis. NAY and ZS contributed to the review and drafting. LR contributed to writing the manuscript. AR and TJ drafted the manuscript. MHS and SA were involved in funding acquisition and writing. All authors contributed to the article and approved the submitted version.

ACKNOWLEDGMENTS

The authors would like to extend their sincere appreciation to the Researchers Supporting Project Number (RSP-2021/194), King Saud University, Riyadh, Saudi Arabia.

REFERENCES

Adeel, M., Ma, C., Ullah, S., Rizwan, M., Hao, Y., Chen, C., et al. (2019). Exposure to nickel oxide nanoparticles insinuates physiological, ultrastructural and oxidative damage: a life cycle study on *Eisenia fetida*. *Environ. Pollut.* 254:113032. doi: 10.1016/j.envpol.2019.113032

Aebi, H. (1974). "Catalalse," in *Methods of Enzymatic Analysis*, ed. H. U. Bergmeyer (NewYork, NY: Academic press), 673–684.

Afzal, I., Shinwari, Z. K., Sikandar, S., and Shahzad, S. (2019). Plant beneficial endophytic bacteria: mechanisms, diversity, host range and genetic determinants. *Microbiol. Res.* 221, 36–49. doi: 10.1016/j.micres.2019.02.001

Ahmad, L., Siddiqui, Z. A., and Abd Allah, E. F. (2019). Effects of interaction of Meloidogyne incognita, Alternaria dauci and Rhizoctonia solani on the growth, chlorophyll, carotenoid and proline contents of carrot in three types of soil. *Acta Agric. Scand. Sect. B Soil Plant Sci.* 69, 324–331. doi: 10.1080/09064710.2019.1568541

Aswani, V., Rajsheel, P., Bapatla, R. B., Sunil, B., and Raghavendra, A. S. (2019). Oxidative stress induced in chloroplasts or mitochondria promotes proline accumulation in leaves of pea (*Pisum sativum*): another example of

chloroplastmitochondria interactions. *Protoplasma* 256, 449–457. doi: 10.1007/s00709-018-1306-1

Azimi, F., Oraei, M., Gohari, G., Panahirad, S., and Farmarzi, A. (2021). Chitosan-selenium nanoparticles (Cs–Se NPs) modulate the photosynthesis parameters, antioxidant enzymes activities and essential oils in *Dracocephalum moldavica* L. under cadmium toxicity stress. *Plant Physiol. Biochem.* 167, 257–268.

Azizi, M., Fard, E. M., and Ghabooli, M. (2021). Piriformospora indica affect drought tolerance by regulation of genes expression and some morphophysiological parameters in tomato (*Solanum lycopersicum* L.). *Sci. Hortic.* 287:110260. doi: 10.1016/j.scienta.2021.110260

Bali, A. S., Sidhu, G. P. S., Kumar, V., and Bhardwaj, R. (2019). "Mitigating cadmium toxicity in plants by phytohormones," in *Cadmium Toxicity and Tolerance in Plants,* eds M. Hasanuzzaman, M. N. V. Prasad, and M. Fujita (London: Academic Press), 375–396.

Bates, L. S., Waldren, R. P., and Teare, I. D. (1973). Rapid determination of free proline for water-stress studies. *Plant Soil* 39, 205–207. doi: 10.1007/BF00018060

Beyer, W. F. Jr., and Fridovich, I. (1987). Assaying for superoxide dismutase activity: some large consequences of minor changes in conditions. *Anal. Biochem.* 161, 559–566. doi: 10.1016/0003-2697(87)90489-1

Blum, A., and Ebercon, A. (1981). Cell membrane stability as a measure of drought and heat tolerance in wheat 1. *Crop Sci.* 21, 43–47. doi: 10.2135/cropsci1981.0011183X002100010013x

Bouyoucos, G. J. (1962). Hydrometer method improved for making particle size analyses of soils 1. *Agron. J.* 54, 464–465. doi: 10.2134/agronj1962.00021962005400050028x

Bradford, M. M. (1976). A rapid and sensitive method for the quantitation of microgram quantities of protein utilizing the principle of protein-dye binding. *Anal. Biochem.* 72, 248–254. doi: 10.1006/abio.1976.9999

Cavalcanti, F. R., Oliveira, J. T. A., Martins-Miranda, A. S., Viégas, R. A., and Silveira, J. A. G. (2004). Superoxide dismutase, catalase and peroxidase activities do not confer protection against oxidative damage in salt-stressed cowpea leaves. *New Phytol.* 163, 563–571. doi: 10.1111/j.1469-8137.2004.01139.x

Chen, D., Cao, B., Wang, S., Liu, P., Deng, X., Yin, L., et al. (2016). Silicon moderated the K deficiency by improving the plant-water status in sorghum. *Sci. Rep.* 6:22882. doi: 10.1038/srep22882

Dias, M. C., Mariz-Ponte, N., and Santos, C. (2019). Lead induces oxidative stress in *Pisum sativum* plants and changes the levels of phytohormones with antioxidant role. *Plant Physiol. Biochem.* 137, 121–129. doi: 10.1016/j.plaphy.2019.02.005

Fan, W. J., Feng, Y. X., Li, Y. H., Lin, Y. J., and Yu, X. Z. (2020). Unraveling genes promoting ROS metabolism in subcellular organelles of *Oryza sativa* in response to trivalent and hexavalent chromium. *Sci. Total Environ.* 744:140951. doi: 10.1016/j.scitotenv.2020.140951

Ghafariyan, M. H., Malakouti, M. J., Dadpour, M. R., Stroeve, P., and Mahmoudi, M. (2013). Effects of magnetite nanoparticles on soybean chlorophyll. *Environ. Sci. Technol.* 47, 10645–10652. doi: 10.1021/es402249b

Hasanuzzaman, M., Bhuyan, M. H. M., Nahar, K., Hossain, M., Mahmud, J. A., Hossen, M., et al. (2018). Potassium: a vital regulator of plant responses and tolerance to abiotic stresses. *Agronomy* 8:31.

Holá, D., Benešová, M., Honnerová, J., Hnilička, F., Rothová, O., Kočová, M., et al. (2010). The evaluation of photosynthetic parameters in maize inbred lines subjected to water deficiency: can these parameters be used for the prediction of performance of hybrid progeny? *Photosynthetica* 48, 545–558. doi: 10.1007/s11099-010-0072-x

Hussain, A., Ali, S., Rizwan, M., ur Rehman, M. Z., Javed, M. R., Imran, M., et al. (2018). Zinc oxide nanoparticles alter the wheat physiological response and reduce the cadmium uptake by plants. *Environ. Pollut.* 242, 1518–1526. doi: 10.1016/j.envpol.2018.08.036

Hussain, B., Lin, Q., Hamid, Y., Sanaullah, M., Di, L., Khan, M. B., et al. (2020). Foliage application of selenium and silicon nanoparticles alleviates Cd and Pb toxicity in rice (*Oryza sativa* L.). *Sci. Total Environ.* 712:136497. doi: 10.1016/j.scitotenv.2020.136497

Jaiswal, D. K., Verma, J. P., Prakash, S., Meena, V. S., and Meena, R. S. (eds). (2016). "Potassium as an important plant nutrient in sustainable agriculture: a state of the art," in *Potassium Solubilizing Microorganisms for Sustainable Agriculture*, (Berlin: Springer), 21–29.

Kah, M., Tufenkji, N., and White, J. C. (2019). Nano-enabled strategies to enhance crop nutrition and protection. *Nat. Nanotechnol.* 14, 532–540. doi: 10.1038/s41565-019-0439-5

Karimi, R. (2017). Potassium-induced freezing tolerance is associated with endogenous abscisic acid, polyamines and soluble sugars changes in grapevine. *Sci. Hortic.* 215, 184–194.

Kamran, M., Wang, D., Alhaithloul, H. A. S., Alghanem, S. M., Aftab, T., Xie, K., et al. (2021). Jasmonic acid-mediated enhanced regulation of oxidative, glyoxalase defense system and reduced chromium uptake contributes to alleviation of chromium (VI) toxicity in choysum (*Brassica parachinensis* L.). *Ecotoxicol. Environ. Saf.* 208:111758. doi: 10.1016/j.ecoenv.2020.111758

Kaya, C., Akram, N. A., Ashraf, M., Alyemeni, M. N., and Ahmad, P. (2020a). Exogenously supplied silicon (Si) improves cadmium tolerance in pepper (*Capsicum annuum* L.) by up-regulating the synthesis of nitric oxide and hydrogen sulfide. *J. Biotechnol.* 316, 35–45. doi: 10.1016/j.jbiotec.2020.04.008

Kaya, C., Ashraf, M., Alyemeni, M. N., and Ahmad, P. (2020b). The role of nitrate reductase in brassinosteroid-induced endogenous nitric oxide generation to improve cadmium stress tolerance of pepper plants by upregulating the ascorbate-glutathione cycle. *Ecotoxicol. Environ. Saf.* 196:110483. doi: 10.1016/j.ecoenv.2020.110483

Kerchev, P., van der Meer, T., Sujeeth, N., Verlee, A., Stevens, C. V., Van Breusegem, F., et al. (2020). Molecular priming as an approach to induce tolerance against abiotic and oxidative stresses in crop plants. *Biotechnol. Adv.* 40:107503. doi: 10.1016/j.biotechadv.2019.107503

Kumar, A., and Prasad, M. N. V. (2018). Plant-lead interactions: transport, toxicity, tolerance, and detoxification mechanisms. *Ecotoxicol. Environ. Saf.* 166, 401–418. doi: 10.1016/j.ecoenv.2018.09.113

Li, M., Zhang, P., Adeel, M., Guo, Z., Chetwynd, A. J., Ma, C., et al. (2021). Physiological impacts of zero valent iron, Fe3O4 and Fe2O3 nanoparticles in rice plants and their potential as Fe fertilizers. *Environ. Pollut.* 269:116134. doi: 10.1016/j.envpol.2020.116134

Liu, G., Lin, S., Pile, L. S., Fang, Z., and Wang, G. G. (2018). Effect of potassium permanganate and pyrolysis temperature on the biochar produced from rice straw and suitability of biochars for heavy metal (Cd & Pb) immobilization in paper sludge. *Fresenius Environ. Bull.* 27, 9008–9018.

Liu, Y., Wu, T., White, J. C., and Lin, D. (2021). A new strategy using nanoscale zero-valent iron to simultaneously promote remediation and safe crop production in contaminated soil. *Nat. Nanotechnol.* 16, 197–205. doi: 10.1038/s41565-020-00803-1

Manzoor, A., Ahmad, T., Bashir, M. A., Hafiz, I. A., and Silvestri, C. (2019). Studies on colchicine induced chromosome doubling for enhancement of quality traits in ornamental plants. *Plants* 8:194. doi: 10.3390/plants8070194

Mei, X., Li, Q., Wang, H., Fang, H., Chen, H., Chen, X., et al. (2020). Effects of cultivars, water regimes, and growth stages on cadmium accumulation in rice with different radial oxygen loss. *Plant Soil* 453, 529–543. doi: 10.1007/s11104-020-04634-w

Moradi-Marjaneh, R., Hassanian, S. M., Mehramiz, M., Rezayi, M., Ferns, G. A., Khazaei, M., et al. (2019). Reactive oxygen species in colorectal cancer: the therapeutic impact and its potential roles in tumor progression via perturbation of cellular and physiological dysregulated pathways. *J. Cell. Physiol.* 234, 10072–10079. doi: 10.1002/jcp.27881

Norvell, W. A., Wu, J., Hopkins, D. G., and Welch, R. M. (2000). Association of cadmium in durum wheat grain with soil chloride and chelate-extractable soil cadmium. *Soil Sci. Soc. Am. J.* 64, 2162–2168. doi: 10.2136/sssaj2000.6462162x

Okturen Asri, F., and Sonmez, S. (2014). "Effects of potassium and iron applications on nutrient concentrations of tomato plants grown in soilless culture," in *Proceedings of the VI Balkan Symposium on Vegetables and Potatoes*, Vol. 1142, Zagreb, 329–334.

Orabi, S. A., and Abou-Hussein, S. D. (2019). Antioxidant defense mechanisms enhance oxidative stress tolerance in plants. A review. *Curr. Sci. Int.* 8, 565–576.

Page, A. L., Miller, R. H., Keeney, D. R., and Baker, D. E. (1982). *Methods of Soil Analysis. II. Chemical and Microbiogical Properties,* 2nd Edn. Madison, WI: American Society of Agronomy.

Palansooriya, K. N., Shaheen, S. M., Chen, S. S., Tsang, D. C., Hashimoto, Y., Hou, D., et al. (2020). Soil amendments for immobilization of potentially toxic elements in contaminated soils: a critical review. *Environ. Int.* 134:105046. doi: 10.1016/j.envint.2019.105046

Palchoudhury, S., Jungjohann, K. L., Weerasena, L., Arabshahi, A., Gharge, U., Albattah, A., et al. (2018). Enhanced legume root growth with pre-soaking in α-Fe 2 O 3 nanoparticle fertilizer. *RSC Adv.* 8, 24075–24083.

Rady, M. M., Elrys, A. S., El-Maati, M. F. A., and Desoky, E. S. M. (2019). Interplaying roles of silicon and proline effectively improve salt and cadmium stress tolerance in Phaseolus vulgaris plant. *Plant Physiol. Biochem.* 139, 558–568. doi: 10.1016/j.plaphy.2019.04.025

Raghib, F., Naikoo, M. I., Khan, F. A., Alyemeni, M. N., and Ahmad, P. (2020). Interaction of ZnO nanoparticle and AM fungi mitigates Pb toxicity in wheat by upregulating antioxidants and restricted uptake of Pb. *J. Biotechnol.* 323, 254–263. doi: 10.1016/j.jbiotec.2020.09.003

Rahman, Z., and Singh, V. P. (2019). The relative impact of toxic heavy metals (THMs)(arsenic (As), cadmium (Cd), chromium (Cr)(VI), mercury (Hg), and lead (Pb)) on the total environment: an overview. *Environ. Monit. Assess.* 191:419. doi: 10.1007/s10661-019-7528-7

Raza, A., Charagh, S., Zahid, Z., Mubarik, M. S., Javed, R., Siddiqui, M. H., et al. (2021). Jasmonic acid: a key frontier in conferring abiotic stress tolerance in plants. *Plant Cell Rep.* 40, 1513–1541. doi: 10.1007/s00299-020-02614-z

Raza, A., Habib, M., Kakavand, S. N., Zahid, Z., Zahra, N., Sharif, R., et al. (2020). Phytoremediation of cadmium: physiological, biochemical, and molecular mechanisms. *Biology* 9:177. doi: 10.3390/biology9070177

Rizwan, M., Ali, S., Ali, B., Adrees, M., Arshad, M., Hussain, A., et al. (2019). Zinc and iron oxide nanoparticles improved the plant growth and reduced the oxidative stress and cadmium concentration in wheat. *Chemosphere* 214, 269–277. doi: 10.1016/j.chemosphere.2018.09.120

Sadak, M. S., and Bakry, B. A. (2020). Zinc-oxide and nano ZnO oxide effects on growth, some biochemical aspects, yield quantity, and quality of flax (*Linum uitatissimum* L.) in absence and presence of compost under sandy soil. *Bull. Natl. Res. Centre* 44, 1–12.

Sardar, R., Ahmed, S., and Yasin, N. A. (2022). Titanium dioxide nanoparticles mitigate cadmium toxicity in *Coriandrum sativum* L. through modulating antioxidant system, stress markers and reducing cadmium uptake. *Environ. Pollut.* 292:118373. doi: 10.1016/j.envpol.2021.118373

Seifikalhor, M., Hassani, S. B., and Aliniaeifard, S. (2020). Seed priming by cyanobacteria (*Spirulina platensis*) and salep gum enhances tolerance of maize plant against cadmium toxicity. *J. Plant Growth Regul.* 39, 1009–1021. doi: 10.1007/s00344-019-10038-7

Seshadri, B., Bolan, N. S., Wijesekara, H., Kunhikrishnan, A., Thangarajan, R., Qi, F., et al. (2016). Phosphorus-cadmium interactions in paddy soils. *Geoderma* 270, 43–59. doi: 10.1016/j.geoderma.2015.11.029

Shah, A. A., Ahmed, S., Ali, A., and Yasin, N. A. (2020a). 2-Hydroxymelatonin mitigates cadmium stress in *Cucumis sativus* seedlings: modulation of antioxidant enzymes and polyamines. *Chemosphere* 243:125308. doi: 10.1016/j.chemosphere.2019.125308

Shah, A. A., Khan, W. U., Yasin, N. A., Akram, W., Ahmad, A., Abbas, M., et al. (2020b). Butanolide alleviated cadmium stress by improving plant growth, photosynthetic parameters and antioxidant defense system of *Brassica oleracea*. *Chemosphere* 261:127728. doi: 10.1016/j.chemosphere.2020.127728

Shamsi, I. H., Jilani, G., Guo-Ping, Z., and Kang, W. (2008). Cadmium stress tolerance through potassium nutrition in soybean. *Asian J. Chem.* 20:1099.

Sharma, P., Jha, A. B., and Dubey, R. S. (2019). "Oxidative stress and antioxidative defense system in plants growing under abiotic stresses," in *Handbook of Plant and Crop Stress*, 4th Edn, ed. M. Pessarakli (Boca Raton, FL: CRC Press), 93–136.

Smart, R. E., and Bingham, G. E. (1974). Rapid estimates of relative water content. *Plant Physiol.* 53, 258–260. doi: 10.1104/pp.53.2.258

Spormann, S., Soares, C., Teixeira, J., and Fidalgo, F. (2021). Polyamines as key regulatory players in plants under metal stress—A way for an enhanced tolerance. *Ann. Appl. Biol.* 178, 209–226.

Thind, S., Hussain, I., Ali, S., Rasheed, R., and Ashraf, M. A. (2021). Silicon application modulates growth, physio-chemicals, and antioxidants in wheat (*Triticum aestivum* L.) exposed to different cadmium regimes. *Dose Response* 19:15593258211014646. doi: 10.1177/15593258211014646

Toumey, C. (2020). *Notes on Environmental Nanoscience*. Doctoral dissertation. Berlin: Nature Portfolio.

Ur Rahman, S., Xuebin, Q., Zhao, Z., Du, Z., Imtiaz, M., Mehmood, F., et al. (2021). Alleviatory effects of Silicon on the morphology, physiology, and antioxidative mechanisms of wheat (*Triticum aestivum* L.) roots under cadmium stress in acidic nutrient solutions. *Sci. Rep.* 11:1958. doi: 10.1038/s41598-020-80808-x

Usman, M., Farooq, M., Wakeel, A., Nawaz, A., Cheema, S. A., Ur Rehman, H., et al. (2020). Nanotechnology in agriculture: current status, challenges and future opportunities. *Sci. Total Environ.* 721:137778. doi: 10.1016/j.scitotenv.2020.137778

Wang, B., He, J., Bianchi, V., and Shamsi, S. A. (2009). Combined use of chiral ionic liquid and CD for MEKC: part II. Determination of binding constants. *Electrophoresis* 30, 2820–2828. doi: 10.1002/elps.200800852

Wang, Y., Jiang, F., Ma, C., Rui, Y., Tsang, D. C., and Xing, B. (2019). Effect of metal oxide nanoparticles on amino acids in wheat grains (*Triticum aestivum*) in a life cycle study. *J. Environ. Manag.* 241, 319–327. doi: 10.1016/j.jenvman.2019.04.041

Wang, Z., Yue, L., Dhankher, O. P., and Xing, B. (2020). Nano-enabled improvements of growth and nutritional quality in food plants driven by rhizosphere processes. *Environ. Int.* 142:105831. doi: 10.1016/j.envint.2020.105831

Xu, X., Du, X., Wang, F., Sha, J., Chen, Q., Tian, G., et al. (2020). Effects of potassium levels on plant growth, accumulation and distribution of carbon, and nitrate metabolism in apple dwarf rootstock seedlings. *Front. Plant Sci.* 11:904. doi: 10.3389/fpls.2020.00904

Yang, J., Cao, W., and Rui, Y. (2017). Interactions between nanoparticles and plants: phytotoxicity and defense mechanisms. *J. Plant Interact.* 12, 158–169. doi: 10.1080/17429145.2017.1310944

Yang, J., Jiang, F., Ma, C., Rui, Y., Rui, M., Adeel, M., et al. (2018). Alteration of crop yield and quality of wheat upon exposure to silver nanoparticles in a life cycle study. *J. Agric. Food Chem.* 66, 2589–2597. doi: 10.1021/acs.jafc.7b04904

Yang, Y., Xiong, J., Tao, L., Cao, Z., Tang, W., Zhang, J., et al. (2020). Regulatory mechanisms of nitrogen (N) on cadmium (Cd) uptake and accumulation in plants: a review. *Sci. Total Environ.* 708:135186. doi: 10.1016/j.scitotenv.2019.135186

Zhao, W., Sun, G., and Li, S. (2004). Polyamines and plant stress resistance. *J. South. Agric.* 35, 443–447.

Conflict of Interest: The authors declare that the research was conducted in the absence of any commercial or financial relationships that could be construed as a potential conflict of interest.

Publisher's Note: All claims expressed in this article are solely those of the authors and do not necessarily represent those of their affiliated organizations, or those of the publisher, the editors and the reviewers. Any product that may be evaluated in this article, or claim that may be made by its manufacturer, is not guaranteed or endorsed by the publisher.

frontiers | Frontiers in Plant Science

ORIGINAL RESEARCH
published: 06 April 2022
doi: 10.3389/fpls.2022.837695

Foliar Application of an Inositol-Based Plant Biostimulant Boosts Zinc Accumulation in Wheat Grains: A μ-X-Ray Fluorescence Case Study

Douglas C. Amaral[1] *and Patrick H. Brown*[2]*

[1] Division of Agriculture and Natural Resources, University of California, Davis, Davis, CA, United States, [2] Department of Plant Sciences, University of California, Davis, Davis, CA, United States

There has been much interest in the incorporation of organic molecules or biostimulants into foliar fertilizers with the rationalization that these compounds will enhance the uptake, or subsequent mobility of the applied nutrient. The objective of this research was to investigate the effects of an inositol-based plant stimulant on the mobility and accumulation of foliar-applied zinc (Zn) in wheat plants (*Triticum aestivum* L.). High-resolution elemental imaging with micro-X-ray fluorescence (μ-XRF) was utilized to examine Zn distribution within the vascular bundle of the leaf and whole grains. The inclusion of *myo*-inositol with Zinc sulfate, significantly increased Zn concentration in shoots in contrast to untreated controls and Zn sulfate applied alone. Foliar Zn treated plants increased Zn in grains by 5–25% with *myo*-inositol plus Zn treated plants significantly increasing grain Zn concentration compared to both Zn treated and non-treated controls. XRF imaging revealed Zn enrichment in the bran layer and germ, with a very low Zn concentration present in the endosperm. Plants treated with Zn plus *myo*-inositol showed an enhanced and uniform distribution of Zn throughout the bran layer and germ with an increased concentration in the endosperm. While our data suggest that foliar application of *myo*-inositol in combination with Zn may be a promising strategy to increase the absorption and mobility of Zn in the plant tissue and subsequently to enhance Zn accumulation in grains, further research is needed to clarify the mechanisms by which *myo*-inositol affects plant metabolism and nutrient mobility.

Keywords: biofortification, foliar fertilizer, biostimulant, wheat, zinc, μ-XRF

OPEN ACCESS

Edited by:
Maurizio Ruzzi,
University of Tuscia, Italy

Reviewed by:
Fahim Nawaz,
Muhammad Nawaz Shareef University of Agriculture, Pakistan
Nacer Bellaloui,
Crop Genetics Research Unit (USDA-ARS), United States

***Correspondence:**
Patrick H. Brown
phbrown@ucdavis.edu

Specialty section:
This article was submitted to Plant Nutrition, a section of the journal Frontiers in Plant Science

Received: *16 December 2021*
Accepted: *31 January 2022*
Published: *06 April 2022*

Citation:
Amaral DC and Brown PH (2022) Foliar Application of an Inositol-Based Plant Biostimulant Boosts Zinc Accumulation in Wheat Grains: A μ-X-Ray Fluorescence Case Study. Front. Plant Sci. 13:837695. doi: 10.3389/fpls.2022.837695

INTRODUCTION

Wheat (*Triticum aestivum* L.) is a cereal grass widely cultivated for their edible grains. Among widely cultivated food crops, wheat plays a particularly important role in daily energy intake, especially in the developing world. Modern wheat cultivars are however a poor source of micronutrients (e.g., Zn and Fe) and when used as a dominant part of daily calorie intake, a wheat based diet often fails to meet human Zn and Fe requirements (Cakmak et al., 2010). To meet human dietary needs in wheat dominant diets, it is estimated that grain Zn concentrations should

be increased from the current average of 20–35 mg kg^{-1} to greater than 50 mg kg^{-1} (Cakmak et al., 2010). Foliar fertilization can be used to effectively enrich Zn grain though the efficiency of transport of foliar applied Zn to grain is generally low (Erenoglu et al., 2011).

Foliar application of nutrients in crop plants is an important agricultural practice world-wide (Fernández et al., 2013). Foliar fertilization is essential where soil conditions such as high pH, limit the availability of soil applied fertilizers and where there is a need to ensure nutrient adequacy at critical stages of plant growth (Tian et al., 2015). Many factors may influence the efficacy of foliar fertilizers such as the physiological status and phenological stage of the plant, the mobility of the nutrient within the plant, or the presence of abiotic stresses (Fernández and Brown, 2013; Fernández et al., 2013). For example, Zn fertilizers, when applied *via* foliar fertilization, must readily penetrate the leaf and remain soluble to promote the translocation from leaves to phloem-fed tissues (White and Broadley, 2011; Saa et al., 2018). However, it has been reported that foliar application of common sources of Zn such as Zinc sulfate ($ZnSO_4$) and Zn-EDTA may not improve the mobility of Zn in plant tissues (Doolette et al., 2018). Thus, enhancing the efficiency of the foliar applied nutrients by adopting new strategies is of great importance not only from an economic, agronomic and environmental point of view, but also as a means to correct human nutrient deficiencies.

The use of plant biostimulants, such as inositol compounds, is emerging as a central feature in plant biochemistry and physiology (Yakhin et al., 2017). Inositol which is well known for acting as a stress-ameliorator in plants (Hu et al., 2018; Mukherjee et al., 2019) may also control multiple aspects of plant signaling and physiology (Jia et al., 2019). Previous reports suggest that exogenous application of inositol could not only alleviate stress but also alter gene expression involved in cell wall biosynthesis, regulation of phytohormones, redox reactions, and chromosome modifications (Chatterjee and Majumder, 2010; Donahue et al., 2010; Ye et al., 2016). In addition, some inositol isoforms (e.g., *myo*-inositol) may act as a strong chelator of metal cations possibly facilitating absorption and transport of nutrients. Given the important role of inositol in cellular functioning, especially its protective functions under biotic and abiotic stresses, surprisingly little is known about exogenous application of inositol in plants such as responses to nutrient availability and effects on mobility.

The development of new techniques that will help improve the efficacy of foliar applied nutrients by enhancing the absorption, translocation, and its utilization by plants with the ultimate goal of improving the quality and yields of crops is mandatory. Due to its capacity to potentially facilitate ion transmembrane transport, we hypothesize that *myo*-inositol applied in combination with Zn may increase its absorption, transport, and accumulation in plant tissues. Here, our goal was to provide comprehensive information on the mobility and distribution of foliar applied zinc, with or without *myo*-inositol, in wheat leaves and its accumulation and localization in grains using X-ray fluorescence (XRF) synchrotron-based techniques which represents a powerful tool for characterizing *in vivo* nutrient mobility and distribution in plants.

MATERIALS AND METHODS

Plant Culture

Sterilized wheat seeds (*Triticum aestivum* L., cv. Patwin 515) were soaked in deionized water for 24 h and then germinated in containers filled with a soil mixture containing (% of volume) 40% peat, 35% silica clay, 20% perlite, and 5% gravel. 10-day-old seedlings of uniform height were transplanted into each 5L pot, one plant per pot, and the pots were transferred to a controlled environment greenhouse with day/night temperature of 25/20°C and day/night humidity of 70/85%. Lighting was provided by LED grow lights with 16-h day length. Plants were watered as needed with a nutrient solution [1.2 mM KNO_3, 0.8 mM $Ca(NO_3)_2$, 0.8 mM NH_4NO_3, 0.3 mM KH_2PO_4, and 0.2 mM $MgSO_4$, 12 μM Fe-EDTA, 0.25 μM $Na_2B_8O_{13}{\cdot}4H_2O$, 1.5 μM $MnSO_4$, 0.25 μM $ZnSO_4$, 0.5 μM $CuSO_4$, and 0.04 μM Na_2MoO_4]. Each treatment and analyses were conducted in four biological replicates.

Foliar Treatments

During stem elongation (flag leaf ligule and collar visible) plants were treated with the following treatments: water sprayed control (no added Zn, "*-Zn-CK*"), zinc sulfate control (added Zn, "*+Zn-CK*"), *myo*-inositol (no added Zn, "*-Zn+Ino*"), and *myo*-inositol plus zinc sulfate (added Zn, "*+Zn +Ino*"). $ZnSO^{-4}$ was applied at the final concentration of 250 mg L^{-1}, and *myo*-inositol was applied at the concentration of 0.25% v/v. The selected concentration was based on previous experiments (data not shown). *Myo*-inositol was selected due to its capacity to potentially facilitate ion transmembrane transport. The treatments were applied to the leaves of wheat 8 h before darkness (10 a.m.). The soil was covered to prevent inadvertent spray drift. Foliar application was repeated 15 days after initial application. To avoid the possibility that the effect of the foliar spray was a consequence of alleviation of secondary nutrient deficiency, all plants were grown with continuous and abundant soil nutrient.

Elemental Analysis

At plant maturity, shoot and grains were collected and prepared for elemental analysis. The wheat grains were removed from panicles and dehusked, and several dehusked grains were set aside for X-ray fluorescence (XRF) imaging. Leaves and grains were oven-dried at 65°C for 72 h and ground using a stainless-steel mill (0.2-mm screen). Ground, dry plant samples (0.1 g) were digested with concentrated trace-metal grade (TMG) HNO_3. Total concentrations of elements (i.e., Zn, Fe, Cu, and Mn) in the filtrates were analyzed using inductively coupled plasma mass spectroscopy (ICP-MS; Agilent 7500a, United States). Standard Reference Material (SRM) Tomato Leaves (NIST 1573a) were used to verify the results and gave excellent recoveries for all the elements of interest (≥94%).

Elemental Mapping

μ-X-Ray Fluorescence Sample Preparation

Mid-sections of leaves were obtained from plants treated with different foliar treatments. Leaf cross-sections (30 μm) were sectioned with a cryotome (LEICA, CM1850) at a temperature of −20°C. Single sections of each treatment were selected under light microscopy for their ultrastructural integrity and then freeze-dried under −20°C for 3 days prior to XRF analysis. The dehusked grains were set in epoxy (EPO-TEK 301-2FL) resin, cured, and cut into thin sections.

μ-X-Ray Fluorescence Analyses

X-ray fluorescence imaging of the grain and leaf thin sections was conducted at the Stanford Synchrotron Radiation Laboratory (SSRL) at beam lines 10–2 and 2–3. Experiments at Beam Line 10–2 were recorded at 10500 eV, using a 20 μm (H) × 20 μm (V) beam spot size, a 20 μm × 20 μm pixel size, and 200 ms dwell time per pixel. The incident X-ray beam of 2 μm at beam line 2–3 was focused using a pair of Kirkpatrick–Baez mirrors, and the incident beam was monochromatized using a Si(111) double-crystal monochromator. Micro-XRF maps were obtained by rastering the beam at 5 μm steps, with a count time of 100 ms per step. Fluorescence intensities of P, S, Cl, K, Ca, Mn, Fe, Ni, Cu, and Zn were monitored. Fluorescence signal intensities for Zn and any other elements were calculated with SMAK (Sam's Microprobe Analysis Kit, Version 1.5).

Experimental Design and Statistical Analysis

The experimental design was a randomized complete design with a full factorial structure. Each treatment and analyses were conducted in four biological replicates. Analysis of variance (ANOVA) was performed with SigmaPlot (Systat Software, Inc., Version 14.0). If significant differences ($P < 0.05$) were identified, a Tukey test was used to distinguish differences between the groups.

RESULTS

Grain Yield and Plant Biomass

Plant biomass and yield were determined at full plant maturity (**Figure 1**). Treatments did not significantly affect plant biomass (i.e., straw) or yield (i.e., whole grain mass) however the use of *myo*-inositol increased grain yield on average by up to 15% compared to -Zn-CK.

Total Zn Concentration in Shoots and Grains

All treatments affected shoot zinc concentrations (**Figure 2**). Shoot Zn concentrations ranged from 15.2 to 53.1 mg kg^{-1} and were significantly affected by both Zn treatments, with +Zn+Ino treated plants having significantly more zinc than the non-treated control (-Zn-CK) by nearly fourfold and significantly increasing shoot Zn by 13 mg kg^{-1} approximately 40% in contrast to +Zn-Ino treatments. Total zinc concentrations in shoots were lowest for the control and *myo*-inositol treated plants, while shoot zinc in plants treated with zinc alone or applied with *myo*-inositol was significantly higher ($p = 0.001$).

Similar, though smaller trends were observed in the grains where Zn-treated plants both with and without *myo*-inositol had increased zinc concentration compared with non-treated control (**Figure 2**). In the absence of added zinc, *myo*-inositol had no effect on grain zinc levels, with the addition of both *myo*-inositol and Zn grain zinc levels increased by 20 ppm ($p < 0.05$). Zinc values in unpolished grains ranged from 55.5 to 75.6 mg kg^{-1} for -Zn-CK and +Zn+Ino treatments, respectively. On average, Zn treated plants increased zinc in grains by 5–25% with +Zn+Ino significantly increasing grain zinc concentration compared to both Zn-treated ($p = 0.018$) and non-treated controls ($p = 0.003$).

Distribution Patterns of Zinc in Leaf and Grain of Wheat Plants

Micro-XRF mapping was performed to investigate the effects of different foliar applied Zn and *myo*-inositol treatments on the distribution and localization of zinc in leaves of wheat at full plant maturity. The cross sections of wheat leaves are composed of upper and lower epidermis, parenchyma, and vascular tissue (xylem and phloem). Spatial imaging of zinc was also performed on cross-sections of unpolished wheat grains collected during plant harvest. The cross sections of unpolished wheat grains are composed of bran layer, endosperm, and germ. The normalized XRF intensities of each map indicates the relative distribution for each individual element.

X-ray fluorescence images showed that wheat leaves exhibited differential zinc distribution on plant tissue with a higher degree of distribution to the mesophyll and vascular tissues (**Figure 3**). When adjusted to the same relative scale, the zinc distribution on the +Zn-CK and +Zn+Ino treated plants was much more extensive and higher in fluorescence intensity than on the −Zn-CK and −Zn+Ino treated plants with +Zn+Ino treated plants showing a higher intensity when compared to +Zn-CK treated plants. This finding corroborates with the ICP-MS data (**Figure 2**), suggesting that *myo*-inositol applied *via* foliar spray in combination with Zn may facilitate solute movement into plant cells.

Images obtained from a longitudinal cross-section of wheat grains show the distribution of zinc (**Figure 4**). In −Zn-CK and −Zn+Ino treatments, zinc was distributed in highest concentration in the bran layer and germ, with a very small concentration present in the endosperm. For +Zn-CK and +Zn+Ino treated plants, zinc was also present in highest concentration in the bran layer and germ, but exhibited an increased concentration in the endosperm, with +Zn+Ino showing an enhanced and uniform distribution of zinc throughout the grain. Furthermore, intensity analysis across a single scan line through the grain confirmed that the peak of Zn intensities in the bran layer, endosperm, and germ was noticeably increased in the +Zn+Ino treatment.

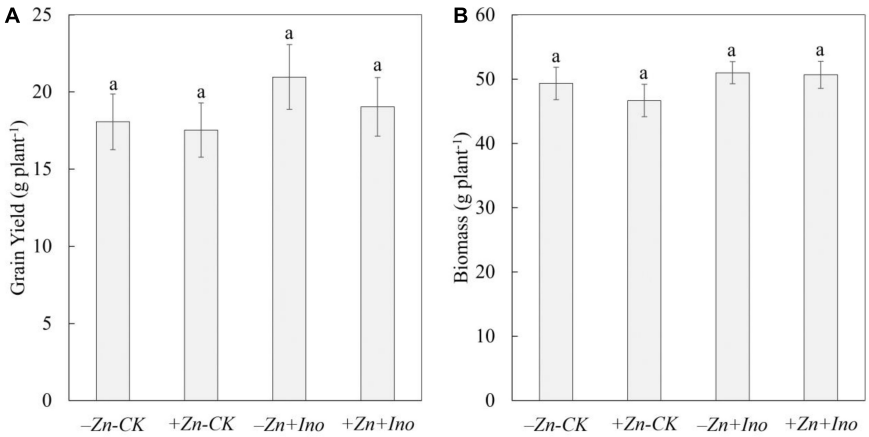

FIGURE 1 | Grain yield **(A)** and plant biomass **(B)** of wheat treated with different foliar fertilizers. Data points and error bars represent means and SE of four replicates. Different letters denote significant differences ($p < 0.05$, $n = 4$).

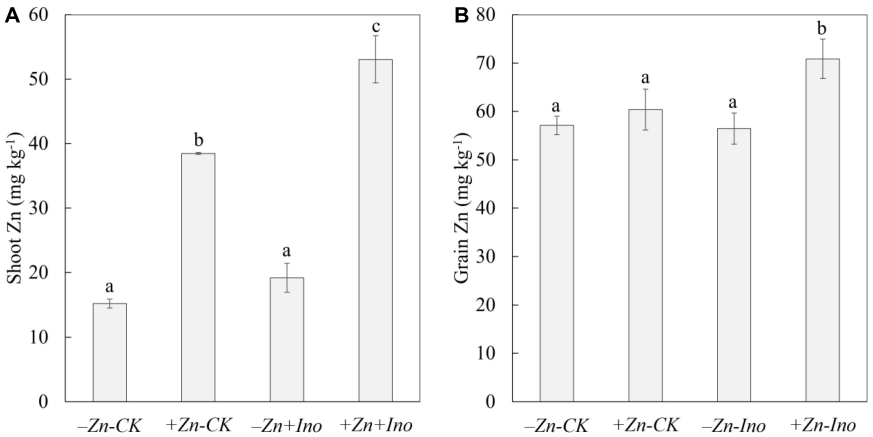

FIGURE 2 | Zinc (Zn) concentrations in shoots **(A)** and grains **(B)** of wheat plants treated with different foliar fertilizers. Data points and error bars represent means and SE of four replicates. Different letters denote significant differences ($p < 0.05$, $n = 4$).

All treatments showed the same pattern of distribution for other plant nutrients (data not shown). Iron, manganese, and copper follow a similar allocation pattern as zinc. Calcium was distributed throughout the grain with highest levels in the germ and bran layer, and lowest in the endosperm. Potassium and phosphorus follow a similar distribution pattern as calcium, with potassium being more abundant in the endosperm.

Plant Nutrients

Of the other plant nutrients analyzed (i.e., Fe, Mn, and Cu), none were significantly affected by the treatments compared to the −Zn-CK suggesting that foliar application of Zn and *myo*-inositol, alone or in combination, may increase total grain zinc in wheat without negatively affecting grain Fe, Mn, or Cu (**Figure 5**).

In the shoots, +Zn-CK treatment increased the concentration of Mn (155.9 mg kg^{-1}) and Cu (4.5 mg kg^{-1}), and slightly decreased Fe (21.7 mg kg^{-1}) concentration compared to the −Zn-CK (Mn: 148.8 mg kg^{-1}; Cu: 3.8 mg kg^{-1}, and Fe: 24.6 mg kg^{-1}). −Zn+Ino also enhanced Mn (151.9 mg kg^{-1}) and Cu (3.9 mg kg^{-1}), and reduced Fe concentration (18.3 mg kg^{-1}). +Zn+Ino increased Mn concentration by 13% (168.5 mg kg^{-1}) and Cu by 15% (4.4 mg kg^{-1}) but did not affect Fe concentration (23.7 mg kg^{-1}).

In grains, +Zn-CK, −Zn+Ino, and +Zn+Ino decreased Mn concentration by 5% (71.2 mg kg^{-1}), 10% (68.0 mg kg^{-1}), and 4% (72.4 mg kg^{-1}), respectively, compared to the −Zn-CK (75.4 mg kg^{-1}). Fe and Cu concentration in −Zn-CK, +Zn-CK, −Zn+Ino, and +Zn+Ino treatments were consistent showing concentrations of 57.7 and 10.1 mg kg^{-1}, 56.1 and 9.3 mg kg^{-1}, 50.8 and 9.4 mg kg^{-1}, and 61.4 and 10.0 mg kg^{-1}, respectively.

DISCUSSION

Zinc sulfate ($ZnSO_4$) and Zn-EDTA are two common forms of foliar-applied Zn fertilizers (White and Broadley, 2009, 2011). However, low or limited mobility of zinc in leaves when applied

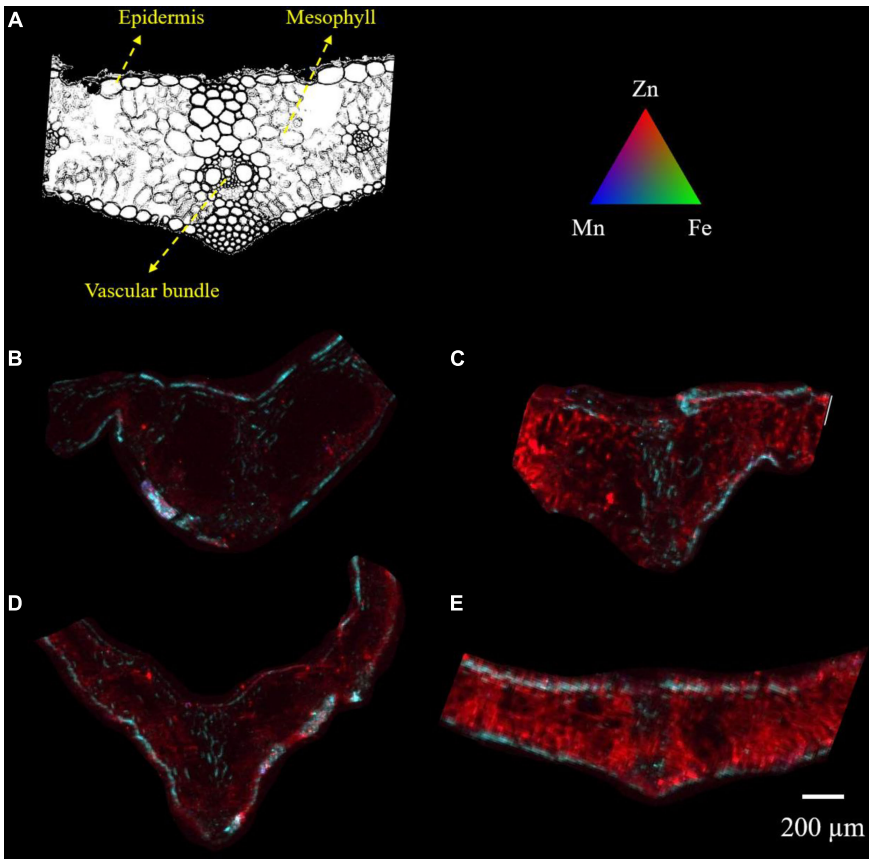

FIGURE 3 | Microscope cross section **(A)** and µ-XRF elemental maps **(B–E)** for Zn (red), Fe (green), and Mn (blue) of wheat leaf treated with different foliar fertilizers: −Zn-CK **(B)**, +Zn-CK **(C)**, −Zn+Ino **(D)**, and +Zn+Ino **(E)**. Pixel brightness for µ-XRF map **(B–E)** is displayed in RGB, with the brightest spots corresponding to the highest elemental fluorescence. Scale bar: 200 µm. *n* = 4, representative images shown.

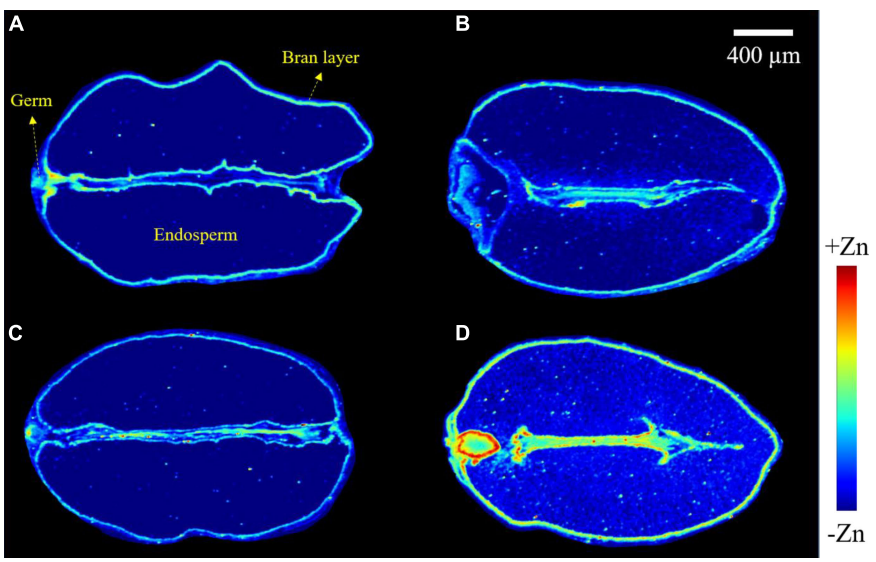

FIGURE 4 | Micro X-ray fluorescence (µ-XRF) elemental maps for Zn of grains collected from wheat plants subject to different foliar fertilizers: −Zn-CK **(A)**, +Zn-CK **(B)**, −Zn+Ino **(C)**, and +Zn+Ino **(D)**. Pixel brightness for µ-XRF maps **(A–D)** is displayed in RGB, with the brightest spots corresponding to the highest elemental fluorescence. Scale bar: 400 µm. *n* = 4, representative images shown.

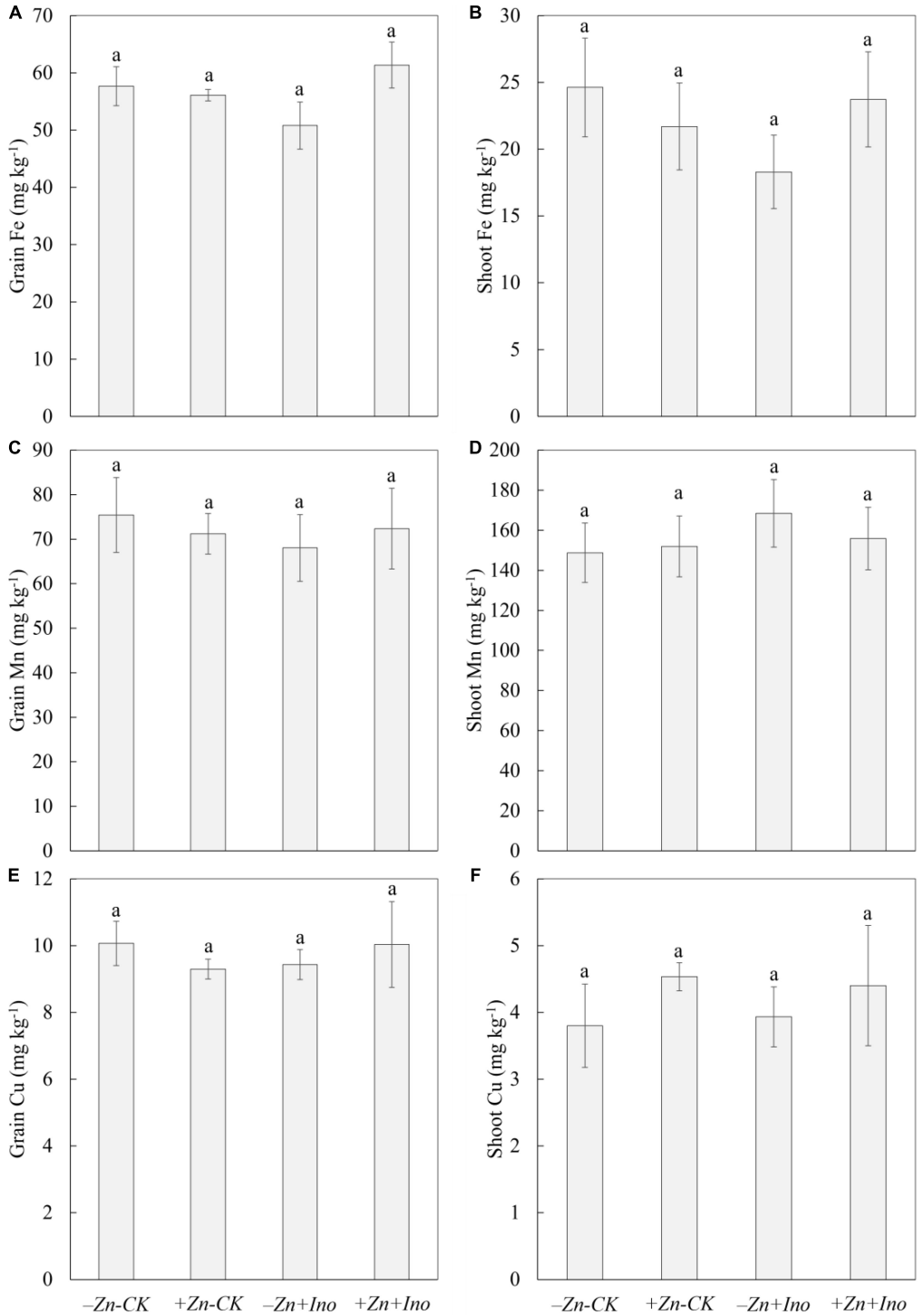

FIGURE 5 | Concentrations of Fe **(A,B)**, Mn **(C,D)**, and Cu **(E,F)** in leaves and grains of wheat plants treated with different foliar fertilizers. Data points and error bars represent means and SE of four replicates ($p < 0.05$, $n = 4$).

in the form of SO_4 (Tian et al., 2015) or chelated with EDTA (Doolette et al., 2018) has been reported. To improve the efficacy of foliar applied Zn, we focused on developing new strategies aiming to increase Zn transport from leaf surface to phloem-fed tissues and subsequently improving its transport and accumulation in grains.

Results from the present study showed clearly increased accumulation of Zn in both leaf and grains of wheat after

the application of $ZnSO_4$ in combination with *myo*-inositol, while $ZnSO_4$ applied alone increased shoot Zn significantly but had only slightly increased Zn distribution and accumulation in grains (**Figures 2–4**). *Myo*-inositol applied alone slightly increased shoot Zn concentrations (**Figure 2A**) suggesting this product may also influence root Zn uptake or Zn transport of previously acquired Zn, this effect is being examined in separate experiments. The significant positive effect of +Zn+Ino on shoot (**Figure 2A**) and grain (**Figure 2B**) Zn concentrations and changes within organ Zn distribution suggests *myo*-inositol may alter both Zn penetration into the shoot tissue and the subsequent intercellular mobility of acquired Zn. While Zn has been reported as having a poor leaf penetration and low mobility in the phloem (White and Broadley, 2011), this study showed evidence that *myo*-inositol may improve Zn mobility in the plant tissue (**Figure 3**) resulting in greater phloem Zn transport, and higher grain Zn concentrations (**Figure 4**) than $ZnSO_4$ alone.

The role of inositol in plant metabolism is uncertain. Inositol may function in various plant signaling pathways, such as energy homeostasis, phosphate sensing, and immune responses (Williams et al., 2015). However, its existence and function in plants is newly emerging and little is known about its use as a plant stimulant. Inositol has been proposed to be an important component for stomatal regulation in plants as it is implicated in abscisic acid-mediated signaling (Perera et al., 2008). Recently, (Hu et al., 2018) showed that exogenous application of *myo*-inositol not only improved the photosynthetic activity and plant growth in *Malus hupehensis* plants, but also up-regulated stomatal apertures allowing those plants to modulate transpirational water losses and the uptake of CO_2. While the mechanisms of absorption of solutes through the stomata are not very well understood (Fernández and Brown, 2013), it can be highly significant as the number of stomata contributing to uptake proved to be highly variable in the leaf surface (Eichert et al., 2008). For example, in *Vicia faba*, exogenously administered phosphatidyl-inositol induced stomatal opening and swelling in guard cell protoplasts (Lee et al., 2007). Thus, by up-regulating stomatal apertures, *myo*-inositol application may result in an improved distribution of permeability on the leaf surface possibly enhancing the diffusion of solutes into the stomatal pores. Li et al. (2019) studying the pathways in which foliar-applied $ZnSO_4$ moves through the sunflower leaf surface, considering the potential importance of the cuticle, stomata and trichomes, demonstrated that there is no indication that the stomata played a major role in the foliar absorption of $ZnSO_4$. This corroborates our hypothesis where $ZnSO_4$ applied alone increased Zn in plant tissue only by twofold, while *myo*-inositol applied in combination with $ZnSO_4$ in the same concentration (250 mg L^{-1}) enhanced plant Zn by nearly fourfold compared to the control, possibly by modulating stomatal opening and increasing Zn absorption by the leaf.

An oxidized form of inositol is also the most common and important sugar implicated in polysaccharide synthesis for cell walls (Loewus and Murthy, 2000; Cui et al., 2013). In addition to cell wall biosynthesis, inositol and its derivatives provide components for other vital pathways such as, but not limited to, biotic and abiotic stress response, plant growth and development, signaling transduction, and substrate transportation (Ye et al., 2016). Some recent studies have reported the benefits of non-foliar applied *myo*-inositol in plants under different conditions (Liu et al., 2006; Lee et al., 2007; Perera et al., 2008; Zhai et al., 2016; Belgaroui et al., 2018; Mukherjee et al., 2019). For example, in apple rootstock *Malus hupehensis*, root-applied *myo*-inositol alleviates salt-induced inhibition of growth not only acting in antioxidant defenses, but also mediating Na^+ and K^+ homeostasis and the osmotic balance (Hu et al., 2018). In contrast, very little is known regarding foliar application of *myo*-inositol and its possible benefits in plants. It has been reported that Zn is coordinated to P as Zn-Phytic acid (inositol-6-phosphate), which is composed of six Pi molecules linked to a *myo*-inositol, in roots and in leaves of *Arabidopsis lyrata* (Sarret et al., 2003; Bouain et al., 2014). According to Bouain et al. (2014), the occurrence of co-regulation of Pi–Zn nutrition in cells of intact plants may impact both P and Zn uptake and transport within a plant body. When exposed to a combination of $ZnSO_4$ and *myo*-inositol, wheat plants showed an increased accumulation of Zn in both shoots and grains. We speculated that the increased Zn concentration in response to *myo*-inositol application might be a gene-mediated response strategy related to ion transmembrane transport, leading to absorption of Zn as it has recently been shown that exogenous *myo*-inositol could alter gene expression and signaling transduction in plant cells (Ye et al., 2016). Furthermore, several genes related to substance transport in response to *myo*-inositol *application* were identified suggesting that *myo*-inositol might act as a regulator mediating the transportation of carbohydrates and other substances. However, no further evidence on its implication in the regulation of Zn transport and/or signaling has been discovered. Therefore, further research should focus on the role of *myo*-inositol in co-regulating Zn transport and signaling crosstalk.

On the basis of existing knowledge of inositol function in plants we propose two main mechanisms to explain the increased plant Zn accumulation and transport due to *myo*-inositol application (1) *myo*-inositol may have changed plant stomatal regulation and increased Zn absorption by wheat leaves; and (2) *myo*-inositol may have changed cell permeability by gene-mediated response strategy related to ion transmembrane transport, facilitating Zn absorption by the leaf. To our understanding, this is the first study utilizing μ-XRF to show visual evidence for the *in situ* investigation of Zn in wheat leaves and grains after foliar application of *myo*-inositol. We found that *myo*-inositol significantly affected Zn transport and distribution in leaf and grains of wheat. Additionally, *myo*-inositol treated plants increased plant yield by 5–15% compared to the controls. The results suggested that *myo*-inositol could affect the physiological status of plant cells and might also influence the mobility of Zn in the plant tissue. The observations above introduce many important points considering the form in which foliar applied Zn penetrates the leaf and how Zn is redistributed in leaf tissue when applied in combination with *myo*-inositol. While further research is required to better understand the specific absorption or uptake pathway of different foliar Zn fertilizers and/or plant stimulants, the results show

evidence that *myo*-inositol may improve the efficiency of foliar-applied $ZnSO_4$.

CONCLUSION

The diet of much of the world's population is based on cereals such as wheat that contain insufficient amounts of numerous nutrients (e.g., Zn, Fe, Cu, and Mn) to meet daily needs. Our results showed that foliar application of *myo*-inositol in combination with Zn may be a promising strategy to increase the absorption and mobility of Zn in the plant tissue and subsequently to enhance Zn accumulation in grains without affecting other essential metals such as Fe, Mn and Cu or decreasing grain yield. Further research is needed to clarify the mechanisms by which *myo*-inositol affects plant metabolism and to identify stimulant properties that can considerably increase grain micronutrients under a wide range of field conditions to maximize plant response to foliar applications.

DATA AVAILABILITY STATEMENT

The original contributions presented in the study are included in the article/supplementary material, further inquiries can be directed to the corresponding author.

AUTHOR CONTRIBUTIONS

DA and PB designed the study. DA performed the experiments, analytical determinations, carried out the data analyses, and wrote the first draft of the manuscript. PB was responsible for the revision of the final manuscript. Both authors have given final approval for this version of the manuscript.

FUNDING

This research was supported by the CH Biotech R&D Co., and Loveland Products.

ACKNOWLEDGMENTS

We thank Leah Hartman and Andrea Tinajero for analytical assistance, and Miguel Guillen and Luis Sanchez for sampling assistance. We also thank Davith Hin and Jianguo Chen for greenhouse assistance. DA thank all the staff of BL 10-2, and BL 2–3 at the SSRL for their kind support. Use of the Synchrotron Radiation Lightsource, SLAC National Accelerator Laboratory, is supported by the United States Department of Energy, Office of Science, Office of Basic Energy Sciences, under Contract No. DE-AC02-76SF00515.

REFERENCES

Belgaroui, N., Lacombe, B., Rouached, H., and Hanin, M. (2018). Phytase overexpression in *Arabidopsis* improves plant growth under osmotic stress and in combination with phosphate deficiency. *Sci. Rep.* 8:1137. doi: 10.1038/s41598-018-19493-w

Bouain, N., Shahzad, Z., Rouached, A., Khan, G. A., Berthomieu, P., Abdelly, C., et al. (2014). Phosphate and zinc transport and signalling in plants: toward a better understanding of their homeostasis interaction. *J. Exp. Bot.* 65, 5725–5741. doi: 10.1093/jxb/eru314

Cakmak, I., Pfeiffer, W. H., and McClafferty, B. (2010). Biofortification of durum wheat with zinc and iron. *Cereal Chem.* 87, 10–20. doi: 10.1094/cchem-87-1-0010

Chatterjee, J., and Majumder, A. L. (2010). Salt-induced abnormalities on root tip mitotic cells of *Allium cepa*: prevention by inositol pretreatment. *Protoplasma* 245, 165–172. doi: 10.1007/s00709-010-0170-4

Cui, M., Liang, D., Wu, S., Ma, F. W., and Lei, Y. S. (2013). Isolation and developmental expression analysis of L-myo-inositol-1-phosphate synthase in four Actinidia species. *Plant Physiol. Biochem.* 73, 351–358. doi: 10.1016/j.plaphy.2013.10.015

Donahue, J. L., Alford, S. R., Torabinejad, J., Kerwin, R. E., Nourbakhsh, A., Ray, W. K., et al. (2010). The *Arabidopsis thaliana* myo-inositol 1-Phosphate Synthase1 gene is required for myo-inositol synthesis and suppression of cell death. *Plant Cell* 22, 888–903. doi: 10.1105/tpc.109.071779

Doolette, C. L., Read, T. L., Li, C., Scheckel, K. G., Donner, E., Kopittke, P. M., et al. (2018). Foliar application of zinc sulphate and zinc EDTA to wheat leaves: differences in mobility, distribution, and speciation. *J. Exp. Bot.* 69, 4469–4481. doi: 10.1093/jxb/ery236

Eichert, T., Kurtz, A., Steiner, U., and Goldbach, H. E. (2008). Size exclusion limits and lateral heterogeneity of the stomatal foliar uptake pathway for aqueous solutes and water-suspended nanoparticles. *Physiol. Plant* 134, 151–160. doi: 10.1111/j.1399-3054.2008.01135.x

Erenoglu, E. B., Kutman, U. B., Ceylan, Y., Yildiz, B., and Cakmak, I. (2011). Improved nitrogen nutrition enhances root uptake, root-to-shoot translocation and remobilization of zinc (65Zn) in wheat. *New Phytol.* 189, 438–448. doi: 10.1111/j.1469-8137.2010.03488.x

Fernández, V., and Brown, P. H. (2013). From plant surface to plant metabolism: the uncertain fate of foliar-applied nutrients. *Front. Plant Sci.* 4:289. doi: 10.3389/fpls.2013.00289

Fernández, V., Sotiropoulos, T., and Brown, P. H. (2013). *Foliar Fertilization: Scientific Principles and Field Pratices*. Paris: International fertilizer industry association (IFA), 144.

Hu, L. Y., Zhou, K., Li, Y. T. S., Chen, X. F., Liu, B. B., Li, C. Y., et al. (2018). Exogenous myo-inositol alleviates salinity-induced stress in *Malus hupehensis* Rehd. *Plant Physiol. Biochem.* 133, 116–126. doi: 10.1016/j.plaphy.2018.10.037

Jia, Q., Kong, D. F., Li, Q. H., Sun, S., Song, J. L., Zhu, Y. B., et al. (2019). The function of inositol phosphatases in plant tolerance to abiotic stress. *Int. J. Mol. Sci.* 20:15. doi: 10.3390/ijms20163999

Lee, Y., Kim, Y. W., Jeon, B. W., Park, K. Y., Suh, S. J., Seo, J., et al. (2007). Phosphatidylinositol 4,5-bisphosphate is important for stomatal opening. *Plant J.* 52, 803–816. doi: 10.1111/j.1365-313X.2007.03277.x

Li, C., Wang, P., van der Ent, A., Cheng, M. M., Jiang, H. B., Read, T. L., et al. (2019). Absorption of foliar-applied Zn in sunflower (*Helianthus annuus*): importance of the cuticle, stomata and trichomes. *Ann. Bot.* 123, 57–68. doi: 10.1093/aob/mcy135

Liu, H. T., Gao, F., Cui, S. J., Han, J. L., Sun, D. Y., and Zhou, R. G. (2006). Primary evidence for involvementof IP3 in heat-shock signal transduction in *Arabidopsis*. *Cell Res.* 16, 394–400. doi: 10.1038/sj.cr.7310051

Loewus, F. A., and Murthy, P. P. N. (2000). myo-Inositol metabolism in plants. *Plant Sci.* 150, 1–19. doi: 10.1016/s0168-9452(99)00150-8

Mukherjee, R., Mukherjee, A., Bandyopadhyay, S., Mukherjee, S., Sengupta, S., Ray, S., et al. (2019). Selective manipulation of the inositol metabolic pathway for induction of salt-tolerance in indica rice variety. *Sci. Rep.* 9:5358. doi: 10.1038/s41598-019-41809-7

Perera, I. Y., Hung, C. Y., Moore, C. D., Stevenson-Paulik, J., and Boss, W. F. (2008). Transgenic *Arabidopsis* plants expressing the type 1 inositol 5-phosphatase exhibit increased drought tolerance and altered abscisic acid signaling. *Plant Cell* 20, 2876–2893. doi: 10.1105/tpc.108.061374

Saa, S., Negron, C., and Brown, P. (2018). Foliar zinc applications in Prunus: from lab experience to orchard management. *Sci. Hortic.* 233, 233–237. doi: 10.1016/j.scienta.2018.01.040

Sarret, G., Saumitou-Laprade, P., Bert, V., Proux, O., Hazemann, J. L., Traverse, A., et al. (2003). Forms of zinc accumulated in the hyperaccumulator *Arabidopsis halleri*. *Plant Physiol.* 130, 1815–1826. doi: 10.1104/pp.007799

Tian, S., Lu, L., Xie, R., Zhang, M., Jernstedt, J. A., Hou, D., et al. (2015). Supplemental macronutrients and microbial fermentation products improve the uptake and transport of foliar applied zinc in sunflower (*Helianthus annuus* L.) plants. Studies utilizing micro X-ray florescence. *Front. Plant Sci.* 5:808. doi: 10.3389/fpls.2014.00808

White, P. J., and Broadley, M. R. (2009). Biofortification of crops with seven mineral elements often lacking in human diets - iron, zinc, copper, calcium, magnesium, selenium and iodine. *New Phytol.* 182, 49–84. doi: 10.1111/j.1469-8137.2008.02738.x

White, P. J., and Broadley, M. R. (2011). Physiological limits to zinc biofortification of edible crops. *Front. Plant Sci.* 2:80. doi: 10.3389/fpls.2011.00080

Williams, S. P., Gillaspy, G. E., and Perera, I. Y. (2015). Biosynthesis and possible functions of inositol pyrophosphates in plants. *Front. Plant Sci.* 6:67. doi: 10.3389/fpls.2015.00067

Yakhin, O. I., Lubyanov, A. A., Yakhin, I. A., and Brown, P. H. (2017). Biostimulants in plant science: a global perspective. *Front. Plant Sci.* 7:2049.

Ye, W. X., Ren, W. B., Kong, L. Q., Zhang, W. J., and Wang, T. (2016). Transcriptomic profiling analysis of *Arabidopsis thaliana* treated with exogenous myo-inositol. *PLoS One* 11:e0161949. doi: 10.1371/journal.pone.0161949

Zhai, H., Wang, F. B., Si, Z. Z., Huo, J. X., Xing, L., An, Y. Y., et al. (2016). A myo-inositol-1-phosphate synthase gene, IbMIPS1, enhances salt and drought tolerance and stem nematode resistance in transgenic sweet potato. *Plant Biotechnol. J.* 14, 592–602. doi: 10.1111/pbi.12402

Conflict of Interest: The authors declare that the research was conducted in the absence of any commercial or financial relationships that could be construed as a potential conflict of interest.

frontiers | Frontiers in Plant Science

SYSTEMATIC REVIEW
published: 14 April 2022
doi: 10.3389/fpls.2022.836702

A Meta-Analysis of Biostimulant Yield Effectiveness in Field Trials

*Jing Li, Thijs Van Gerrewey and Danny Geelen**

HortiCell, Department of Plants and Crops, Faculty of Bioscience Engineering, Ghent University, Ghent, Belgium

Today's agriculture faces many concerns in maintaining crop yield while adapting to climate change and transitioning to more sustainable cultivation practices. The application of plant biostimulants (PBs) is one of the methods that step forward to address these challenges. The advantages of PBs have been reported numerous times. Yet, there is a general lack of quantitative assessment of the overall impact of PBs on crop production. Here we report a comprehensive meta-analysis on biostimulants (focus on non-microbial PBs) of over one thousand pairs of open-field data in a total of 180 qualified studies worldwide. Yield gains in open-field cultivation upon biostimulant application were compared across different parameters: biostimulant category, application method, crop species, climate condition, and soil property. The overall results showed that (1) the add-on yield benefit among all biostimulant categories is on average 17.9% and reached the highest potential via soil treatment; (2) biostimulant applied in arid climates and vegetable cultivation had the highest impact on crop yield; and (3) biostimulants were more efficient in low soil organic matter content, non-neutral, saline, nutrient-insufficient, and sandy soils. This systematic review provides general biostimulant application guidelines and gives consultants and growers insights into achieving an optimal benefit from biostimulant application.

Keywords: meta-analysis, biostimulant, crop yield, sustainable agriculture, open-field trial, climate, soil quality

OPEN ACCESS

Edited by:
Giuseppe Colla,
University of Tuscia, Italy

Reviewed by:
Renato De Mello Prado,
São Paulo State University, Brazil
Paolo Bonini,
Ngalab, Spain

****Correspondence:***
Danny Geelen
Danny.Geelen@UGent.be

Specialty section:
This article was submitted to Crop and Product Physiology, a section of the journal Frontiers in Plant Science

Received: *15 December 2021*
Accepted: *25 March 2022*
Published: *14 April 2022*

Citation:
Li J, Van Gerrewey T and Geelen D (2022) A Meta-Analysis of Biostimulant Yield Effectiveness in Field Trials. Front. Plant Sci. 13:836702. doi: 10.3389/fpls.2022.836702

INTRODUCTION

By 2050, the risk of hunger is predicted to rise by 30% due to climate change and the expected population increase (Van Dijk et al., 2021). To meet future food production requirements, the impact of climate change on crop production needs to be addressed. How we will achieve this ambitious goal is currently debated. Various conventional (e.g., fertilization) and novel bioengineering strategies (e.g., genetically modified crops) are extensively developed to boost crop production and ensure food security and safety (Bailey-Serres et al., 2019). As a general consensus is emerging synthetic fertilizers that cause environmental threats to the local and global ecosystems (Koli et al., 2019), plant biostimulants (PBs) are potentially a tool to mitigate climate change-induced stress and reduce the dependency on chemical fertilizers (Hunter et al., 2017). The European Commission aims to replace 30% of chemical fertilizers with bio-based alternatives by 2050 (Hansen, 2018). The application of PBs, is a more sustainable agricultural practice to preserve crop yield under reduced fertilizer conditions (Gupta et al., 2020). The global market value of PBs is expected to reach USD 3 billion in 2021, with a cumulative annual growth rate (CAGR) of about 13% until 2025 (EBIC, 2021). Nevertheless, there is no clear view of how efficient PBs really are.

The European Commission has categorized PBs under the framework of fertilizing products [Regulation (Eu) 2019/1009, 2019]. Briefly, it states that PBs are products that stimulate plant growth and improve one or more additional functions: nutrient use efficiency, abiotic stress tolerance, crop quality traits, and availability of confined nutrients in the soil or plant rhizosphere. Furthermore, Regulation (EU) 2019/1009 cataloged two distinct categories based on whether the stimulatory bioactivity is of microbial or non-microbial origin, and this may require an even more refined classification (Rouphael and Colla, 2020). Within the most accepted subcategories, microbial PBs consist of arbuscular mycorrhizal fungi (AMF) and plant growth-promoting rhizobacteria (PGPR) (Rouphael and Colla, 2020). Commonly, 6 subcategories of non-microbial PBs are distinguished: chitosan (Chi), humic and fulvic acids (HFA), animal and vegetal protein hydrolysates (PHs), phosphites (Phi), seaweed extracts (SWE), and silicon (Si). More recently, an additional group of PBs that have received much attention are the plant extract-based PBs (PE) (excluding SWE) and are included as a separate class of PBs (Du Jardin, 2015; Bio4Safe, 2021). Aside from these complex mixtures of PBs, products with a single active compound are not included in this review because we consider that the majority of PBs are complex mixtures (Du Jardin, 2015; García-García et al., 2020). The European Biostimulant Industry Council (EBIC) proposed several general principles to regulate and justify the claims made by manufacturers with regards to PBs efficiency (Ricci et al., 2019). A European legal framework for PBs regarding standardization of sampling, denominations, marking, and test methods are currently under development and will be fully released in 2024 (CEN Technical Committees, 2021). Therefore, sufficient high-quality and credible experimental data is required from PBs producers to support the claims of PBs products and provide valuable practical advice for the users. Recently, a biostimulant database was launched for growers, gathering PBs product information, plant trails, and scientific data on crop quality, water nutrient use efficiency, and stress tolerance (Bio4Safe, 2021). However, an overall in-depth evaluation of PBs performance is still missing.

Crop yield enhancement is a popular claim listed in the product description of many PBs (Ricci et al., 2019). As various environmental factors and management practices influence yield performance (Liliane and Charles, 2020), empirical knowledge that depends on different experimental conditions is of critical value for the farmer. Because of the variability in agronomic management and environmental conditions, studies with similar or identical PBs have resulted in different effectiveness data (Schütz et al., 2018). As crop yield is a multi-trait property, meta-analysis has been conducted to gain insight into the impact of soil property (Oldfield et al., 2019), climate change (Challinor et al., 2014), and microbial PBs application (Schütz et al., 2018). Hence, effectiveness remains poorly understood to what extent these variables affect non-microbial PBs (designated as biostimulants in later text).

In this study, we performed a meta-analysis to (1) estimate crop yield improvement by biostimulants, (2) understand the relationship between crop yield and biostimulant application method, and (3) assess the impact of environmental variables on the performance of biostimulants in open-field cultivation.

MATERIALS AND METHODS

Literature Review

Thomson Reuters' Web of Science, Elsevier's Scopus, and Google Scholar were queried until July 2021 for peer-reviewed publications identified using the keywords "biostimulant AND crop AND (yield OR biomass)". Additional studies were also selected based on citations occurring in the selected papers and relevant reviews. Studies were selected for the analyses using five criteria: (1) crop yield data were obtained from open-field trials or walk-in tunnels (open on both sides), excluding pot and greenhouse experiments; (2) marketable crop yield was reported as it represents traceable agro-economic value; (3) the studies contained pairwise comparisons between single biostimulant-treated and corresponding non-treated control plants, using the same application method under the same geo-climatic and crop management; (4) the yield means, their standard deviation (SD), and the number of replications were provided separately; (5) the studies were written in English and available in full text. A total of 1,108 paired observations from 181 empirical studies (**Supplementary Data 1**) were identified after two rounds of screening of titles, abstracts, and full texts analyzed in this study following the PRISMA-P statement (**Supplementary Figure 1**) (Page et al., 2021).

Data Collection

Experimental crop yield data were collected from the original tables or extracted from the attached figures using WebPlotDigitizer (Rohatgi, 2020). The methodology section obtained other information, including the field site location, crop species, soil properties, biostimulant product information, application method, dose, frequency, and whether interannual studies were performed. All data were compiled in one dataset (**Supplementary Data 2**) after conversion to uniform metrics for each variable.

Moderator Variables

Four main groups of moderator variables were considered to investigate further potential crop yield effectors, including experimental-, plant-, climate-, and soil-related parameters. **Table 1** shows the classifications of all categorical moderators.

Biostimulant Categories and Methods of Application

The classification of biostimulants was based on the main bioactive substances: Chi, HFA, PHs, Phi, SWE, Si, and PE (Du Jardin, 2015; Rouphael and Colla, 2020). Detailed information about the available natural resources and the major bioactive compounds of these biostimulants are shown in **Supplementary Table 1**. Moringa leaf extract (MLE) was separated as a subgroup of interest, and the rest were other PE under the PE group.

The application methods are specified as foliar, soil, and seed treatment. Direct biostimulant application in the soil and introduction *via* irrigation water were considered soil treatments.

TABLE 1 | The description of classifications involved in categorical moderators.

Categorical moderators	Classifications involved
Climate categories[a]	A (Af, Am, As, Aw); B (BWk, BWh, BSk, BSh); C (Cfa, Cfb, Csa, Csb, Cwa); D (Dfa, Dfb, Dfc, Dsa).
Crop species in categories	Cereals (wheat, maize, oat, barley, rice, quinoa); Fruits (including nuts) (grape, mango, apricot, cherry, plum, mandarin, blueberry, apple, strawberry, pear, pistachio nut, papaya, citrus, sugarcane); Legumes (soybean, faba bean, black gram, common bean, pea, cowpea, mung bean, snap bean); Others (fennel, berseem clover, cardoon, dragonhead, geranium, sesame, lemon, hyssop, grass mixture, ryegrass, timothy, alfalfa, cotton, basil, honeysuckle, rape, vetch, chamomile, olive, zinnia, sugar beet, niger, milk thistle, meadow, mint, red clover); Root/tuber crops (potato); Vegetables (eggplant, rocket, tomato, okra, sweet pepper, onion, pepper, lettuce, garlic, broccoli, carrot, endive, cabbage, spinach, cucumber, celery).
Degree of soil pH	Strongly acid (5.1–5.5); Moderately acid (5.6–6.0); Slightly acid (6.1–6.5); Neutral (6.6–7.3); Moderately alkaline (7.9–8.4); Strongly alkaline (8.5–9.0).
Degree of soil salinity by ECe (dS/m)	Nonsaline (0–2.0); Slightly saline (2.1–4.0); Moderately saline (4.1–8.0); Strongly saline (>8.1).
Soil P Levels (ppm)	Very low (<16); Low (16–25); Medium (26–35); Optimal (>36).
Soil K levels (ppm)	Very low (<61); Low (61–60); Medium (91–130); Optimal (>131).

[a]*According to Köppen-Geiger climate classification (Peel et al., 2007) on main climates, A, equatorial; B, arid; C, warm temperate; D, snow; on precipitation: W, desert; S, steppe; f, fully humid; s, summer dry; w, winter dry; m, monsoonal; on temperature: h, hot arid; k, cold arid; a, hot summer; b, warm summer; c, cool summer.*

Biostimulant application frequency indicates the total number of foliar applications, where "0" indicates continuous treatment with a specific time interval. The biostimulant application dose was only defined within dose-response studies, where "1" was used for the highest biostimulant concentration, "0" for non-treated conditions, and the other doses were expressed as corresponding relative concentrations. For interannual studies, annual crop cultivation was labeled as "0" while the rest of continuous crop production was marked as the order of successive years.

Crop Categories and Environmental Parameters

Cultivated crop species were grouped into 6 main crop categories (cereals, vegetables, fruits, legumes, root/tuber crops, and other crops) following the Food and Agriculture Organization of the United Nations (FAO) classification of agricultural crops (FAO, 2005). In addition, sugar crops (sugar cane and sugar beet), medicinal plants (e.g., cardoon, zinnia, and basil), oilseed crops (rapeseed and olive), grasses (e.g., alfalfa, ryegrass, and timothy), spice crops (cinnamon and fennel), and fiber crops (cotton) were added to the "other crops" class due to the limited number of relevant studies.

The locations, including city and country names, were converted to latitude and longitude with decimal degree coordinates. Next, the climate zone was categorized according to the Köppen-Geiger climate classification (Peel et al., 2007) using R software version 4.0.2 (R Core Team, 2020) equipped with package "kgc" version 1.0.0.2 (Bryant et al., 2017). Finally, the geographical map of the identified studies was visualized using ArcMap (Esri, 2020). Four main climates (equatorial, arid, warm temperate, and boreal) and six subclasses (desert, steppe, monsoonal, summer dry, winter dry, and fully humid) are determined by vegetation and temperature and precipitation, were covered in this study. As regular irrigation was commonly applied during cultivation, studies with artificial drought stress experiments were excluded.

For soil physicochemical properties, soil texture was assigned to 12 classes according to the fractions of clay, silt, and sand particles in the topsoil (0–30 cm), as described by the soil texture triangle (Soil Science Division Staff, 1993). Soil acidity and alkalinity, a measure for soil reaction, were expressed as soil pH measured in water or converted in CaCl2 or KCl (Land Resources Management Unit Commission, 2010). The soil pH levels ranged from 3.5 to 8.4 and were split into six groups (strongly acid, moderately acid, slightly acid, neutral, moderately alkaline, and strongly alkaline) triangle (Soil Science Division Staff, 1993). Electrical conductivity (EC) of soil standard saturated paste extract (ECe), a measure for soil salinity, was represented as the standard EC, and EC measured in soil-water extracts were converted (Kargas et al., 2018). The degree of soil salinity was allocated into five levels (non-saline, slightly saline, moderately saline, and strongly saline) for all soils (Smith and Doran, 1997). The soil organic matter (SOM) was considered a critical indicator of soil health (Soil Health Institute, 2018). SOM was transposed from available soil organic carbon (SOC), which assumedly contributed to 58% of the mass of SOM (Edwards, 2021). Soil total nitrogen (N) indicates the percentage of organic and inorganic N forms (Marx et al., 1996). Furthermore, soil available nutrients for plant uptake are associated with three macronutrients, N, phosphorus (P), and potassium (K) content (ppm concentrations), where soil available N content (ppm) only includes plant-available nitrate- and ammonium-N (Horneck et al., 2011). For easier understanding in agronomy guide, soil fertility was interpreted to four levels (very low, low, medium, and optimal) based on available P and K concentrations and the expected yield potential without fertilization for most agronomic crops (Snyder et al., 1993).

Missing Values

If the studies only provided the dry biomass, the fresh weight was computed according to the calculated water contents (Spungen, 2005). When outcome errors were unavailable in the original text, the SD was estimated in percentage based on the mean SD of the existing studies per crop category (Schütz et al., 2018). The estimated SD for cereals was 4.25%, legumes 13.4%, root/tuber crops 9.51%, vegetables 9.67%, fruits 16.5%, and for

other crops (grasses and medical plants 8.84%, sugar crops 1.55%, oilseed crops 8.92%). Thus, more importantly, the availability of complete raw datasets combined with other descriptive records of trail-related conditions is critical for proper statistical analysis and justifying biostimulant claims of manufacturers (Ricci et al., 2019).

Data Analysis

The primary outcome of crop yield was defined as the fresh weight ($kg{\cdot}m^{-2}$) of marketable product, in the case of cereals, the seed or grain yield, shoot biomass for most vegetables or other crops, fruit yield for fruits, and tuber yield for root/tuber crops. The yield response (%) to biostimulant application was calculated using the Equation (1),

$$\textit{Yield response}\ (\%) = \frac{\textit{Yield}_{\textit{with biostimulant}}}{\textit{Yield}_{\textit{without biostimulant}}} \times 100\% \qquad (1)$$

where "$Yield_{with\ biostimulant}$" is the crop yield after treatment with a single biostimulant product and "$Yield_{without\ biostimulant}$" is the crop yield under non-treated control conditions. A meta-analysis was conducted in R with package "metafor" version 3.0-2 (Viechtbauer, 2010). First, the effect size was calculated with log-transformed ratios of the means and confidence intervals (CI) of each means, with yield response as the main outcome. The variables were assigned according to the major influencing factors of crop production. Next, random-effect models (RE) were fitted with categorical moderators using the restricted maximum-likelihood (REML) estimator method. For categorical moderators, forest plots were applied to visualize the meta-analyses. On the other hand, linear meta-regression analysis on continuous variables was conducted by fitting mixed-effect models (ME). The ME performance was evaluated by R^2 for variance explained (Nakagawa and Schielzeth, 2013). We also investigated the between-study heterogeneity by determining I^2 of each model (Inthout et al., 2016). To further explore the causes of heterogeneity, influence diagnostics was applied to remove outlier cases with large DFBETAS (indicating the change of SDs after study exclusion from model fitting). As a result, twenty-one of the 1,108 studies were removed. Additionally, to eliminate the systematic publication bias in meta-analysis, we evaluated the comprehensiveness of collected data by assessing the asymmetry of the funnel plot with the "regtest" function. Since the asymmetry test was not significant ($p > 0.05$) (**Supplementary Figure 2**), we thus addressed no issues on publication bias in our dataset and included all the data for this study.

RESULTS

Following a literature survey and selection using the quality criteria described previously, 1,087 paired observations in 180 studies were retained for data extraction and comparison. Most of these studies were performed in the Eurasian and Mediterranean regions under arid and warm temperate climates. The smaller subsection of studies was from the Americas and Southeast Asia, and a single study was conducted in Southern Africa and one in Australia (**Figure 1**).

PE Is the Most Efficient Biostimulant

The average yield increases induced by reported biostimulant applications in open-field varied between 8.5 and 30.8% between the category (**Figure 2**). The overall average in crop yield response was 17.9% (CI 16.7–19.0%). The best performing category was PE, with a yield increase of 26.6% (CI 23.1–30.1%). Amongst MLE showed the highest improvement (+30.8%; CI 26.1–35.6%) while other PE (+22.3%; CI 17.2–27.3%). The biostimulant group with the lowest yield enhancement was Phi (+8.6%; CI 4.6–12.5%), and it was derived from the smallest dataset with 18 comparisons from three studies. The other four biostimulant categories, Chi, HFA, PHs, and SWE, showed an intermediate increase of 14.8–17.1%. Regarding the impact of the commercial status of biostimulants, non-marketed biostimulants tended to represent a stronger yield enhancement effect (+21.8%; CI 20.0–23.5%) than commercially purchased products (+14.4%; CI 12.7–16.0%). For SWE, commercial or non-commercial sources resulted in a similar yield increase of about 16.5–18.0%. The variation in results was the largest for Si, while SWE showed the most consistent yield increase.

Yield Effectiveness Affected by Biostimulant Application Method

Since the application methodology is an important efficacy determinant, the yield increase across different application methods (foliar, seed, and soil) and associated variables (frequency, dose, and interannual application) were compared (**Figure 3**). An unexpected result was that soil treatment, an indirect application method, resulted in the most substantial yield increase (+28.8%; CI 24.0–33.6%). Foliar treatments, representing over 85% of the studies, and seed application were similar in an average yield increase of about 17.0% (**Figure 3A**). In several studies, different dilutions of the biostimulant were tested. Here, we set the highest dose to "1" and calculated the effectiveness of dose responses (**Figure 3B**). The positive yield effect increased with higher doses, as was expected. However, the regression slope was very shallow, indicating that the doses applied were, in general, close to the saturation level. Single spray applications resulted in a comparably stronger yield increment (+14.9%; CI 12.3–17.6%) with subsequent sprayings of up to four times, resulting in only a slight further increase in yield reaching 16.6–18.6% (**Figure 3C**). More frequent spraying was counterproductive, with lower yield benefits between 11.3 and 14.3%. When comparing the use of biostimulant within annual or continuous crop production studies, a slightly higher yield improvement in the first 2 years of interannual cultivation was observed (∼18.3–20.4%) rather than the single growth season (+16.7%; CI 15.0–18.4%) (**Figure 3D**). However, the efficiency of biostimulant application decreased in the third year (+12.9%; CI 10.6–15.3%) in interannual studies.

Vegetables Respond the Most to Yield Improvement

The effectiveness of biostimulant application was compared across different crop types: cereals, fruits, legumes, root/tubers, vegetables, and other crops (**Figure 4**). A sound comparison was

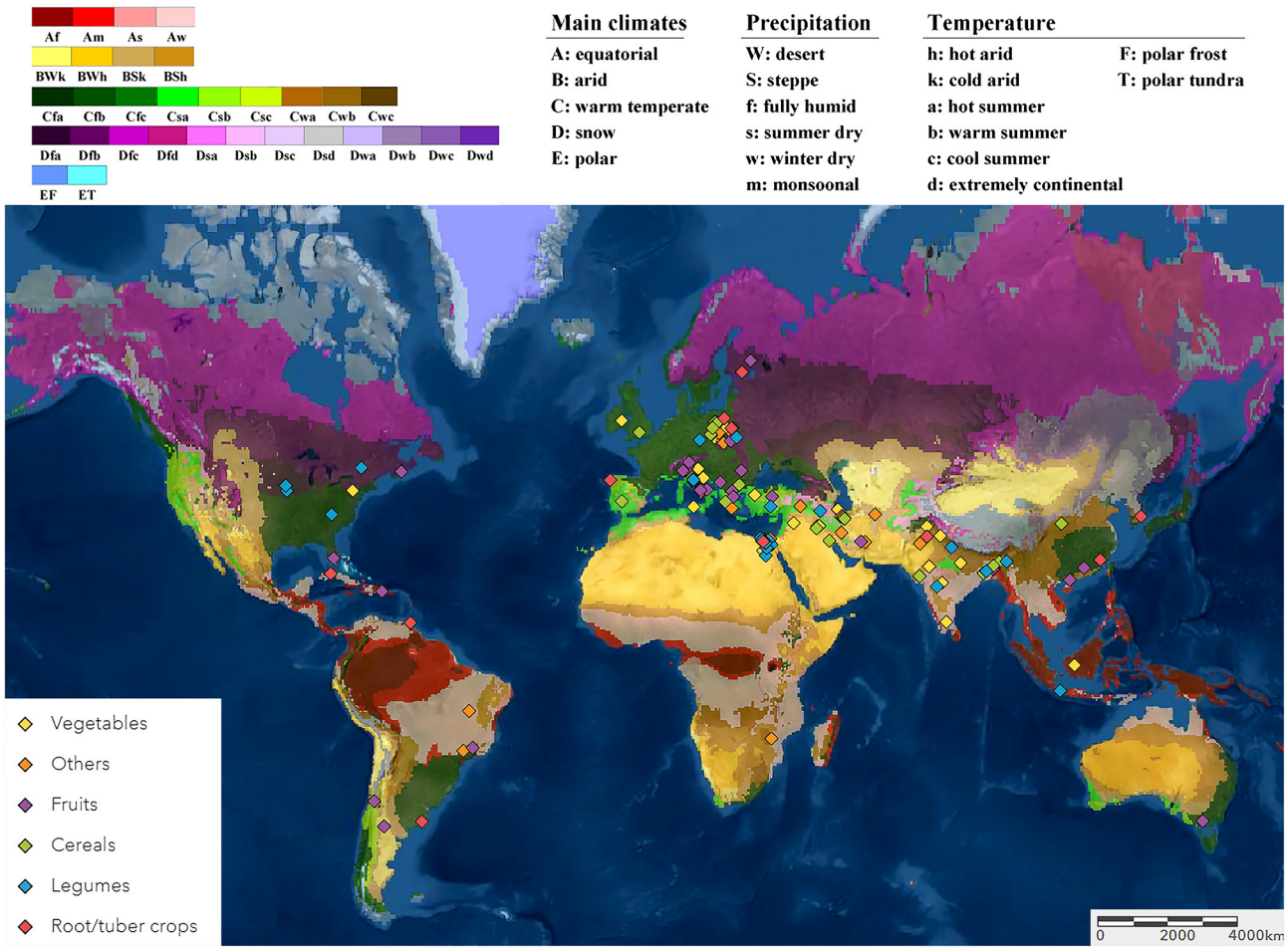

FIGURE 1 | The locations of the open-field studies included in the meta-analysis as displayed on the Köppen-Geiger climate classification (Peel et al., 2007) on the world map (Esri, 2009). The studies were grouped based on the six crop categories of cultivation (cereals, legumes, vegetables, fruits, root/tuber crops, and other crops).

possible because the number of studies was similar across the different crop types. Vegetable crops showed the highest and roots/tubers the lowest yield benefit, differing by more than two-fold (+22.8% compared to +10.6%). Legumes were significantly better at responding to biostimulant applications than fruits, cereals, and other crops.

Yield Effectiveness Varied in Climate and Soil Properties

The impact of climate conditions on biostimulant performance was analyzed by comparing the yield increase across four main climate categories (equatorial, arid, warm temperate, and boreal) and six precipitation types (desert, steppe, monsoonal, summer dry, winter dry, and fully humid) (**Figure 5**). The effect of biostimulant was most positive in climates with seriously limited water availability (arid and desert). Moreover, yield gain showed a clear negative trend with increased precipitation, with fully humid climate conditions as the least favorable for biostimulant efficiency. Overall, water availability was revealed as a critical factor, positively correlating with the effect of biostimulants. At the same time, temperature negatively impacted the more extreme side of the spectrum. Next, we compared soil physical and chemical parameters: textures, pH, salinity, and SOM (**Figure 6**). For most soil types, the average effect of biostimulant was within the same interval range. However, pure clay had a clear lower impact (+13.5%), even though soils with a high clay component were among the best scoring soils (e.g., silty clay loam; +26.3%) (**Figure 6A**). In general, regarding the soil pH levels, mild soil acidity or alkalinity were better than soils with a neutral or more extreme low or high pH (**Figure 6B**). Moderate alkaline soil reveals the highest potential response to biostimulant application. Soil salinity strongly positively correlated with biostimulant effectiveness (**Figure 6C**), in line with the water availability correlation shown in **Figure 5**. Finally, we compared biostimulant effectiveness across soils with different SOM content. Here, we found a robust negative trend between SOM and yield response after biostimulant application (**Figure 6D**). A negative correlation was also observed with

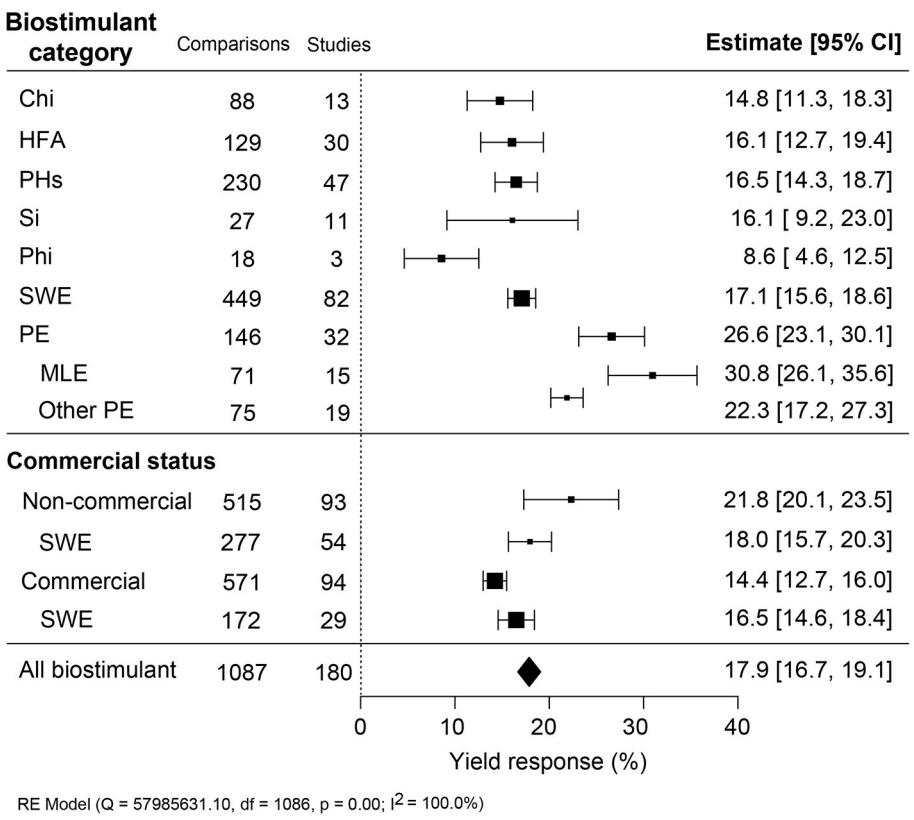

FIGURE 2 | Percentage yield response to biostimulant application affected by the biostimulant category and the commercial status of biostimulant products. The point size correlates to the estimate's precision, and the error bars represent 95% confidence intervals (CI) of mean estimated effect sizes. The number of comparisons and studies is indicated in each line. The combined effect estimates and the heterogeneity test on the random-effect model (RE) are summarized at the bottom, where the heterogeneity test is significant ($p < 0.001$) and $I^2 \geq 75\%$ implies substantial heterogeneity. Chi, Chitosan; HFA, humic and fulvic acids; PHs, protein hydrolysates; Si, silicons; Phi, phosphite; SWE, seaweed extracts; PE, plant extracts; MLE, moringa leaf extract.

increasing soil total N (%) and soil available N content (ppm) (**Figures 7A,B**). Concerning soil P and K levels, the analysis revealed that biostimulants function better in poor soils deficient in P and K nutrients (**Figures 7C,D**).

DISCUSSION

Biostimulant Effectiveness

A large body of published data demonstrates the positive impact of numerous types of biostimulants on a wide range of crops using different application methods under various conditions. However, for biostimulants to become standard practice, these products will require consistency and reproducibility in the beneficial effects they are claimed to have on crop production. A standardization for measuring the effectiveness of biostimulants is required to distinguish the good from the bad (Ricci et al., 2019). Variation in biostimulant effectiveness is expected as different crops respond differently to biostimulants, and the environmental conditions are likely also influencing the effects. Therefore, a one-to-one comparison of biostimulant effectiveness based on published data is not likely to be very reliable. In this study, we looked at the bigger picture and queried the literature for data published on the effectiveness of biostimulants. To allow for sound comparisons, the study focused on biostimulants derived from natural resources categorized according to their origin and chemical properties (Geelen and Xu, 2020) and restricted to crop yield experiments in open fields that are closer to an application and commercialization target. The main result from the meta-analysis was that it revealed correlations between biostimulant effectiveness and impactors that have, insofar as we are aware, not previously been completely recognized.

Since most authors wish to report successful biostimulants, it is fair to assume that publications are biased toward the positive. This does, however, not prevent the identification of correlations between the effects and the materials and application conditions used. With the high yield gain found, one would expect widespread use of biostimulants in many crop production systems. This is currently not the case, and we, therefore, assume that the average yield increase reported here is an overestimation of what can be expected in a commercial context. Noteworthy here is that the efficiency of non-commercial products was 7% higher than commercial ones (**Figure 2**). Indeed, a more conservative estimation of the yield increase is warranted, and there is a need for a more systematic collection of yield data

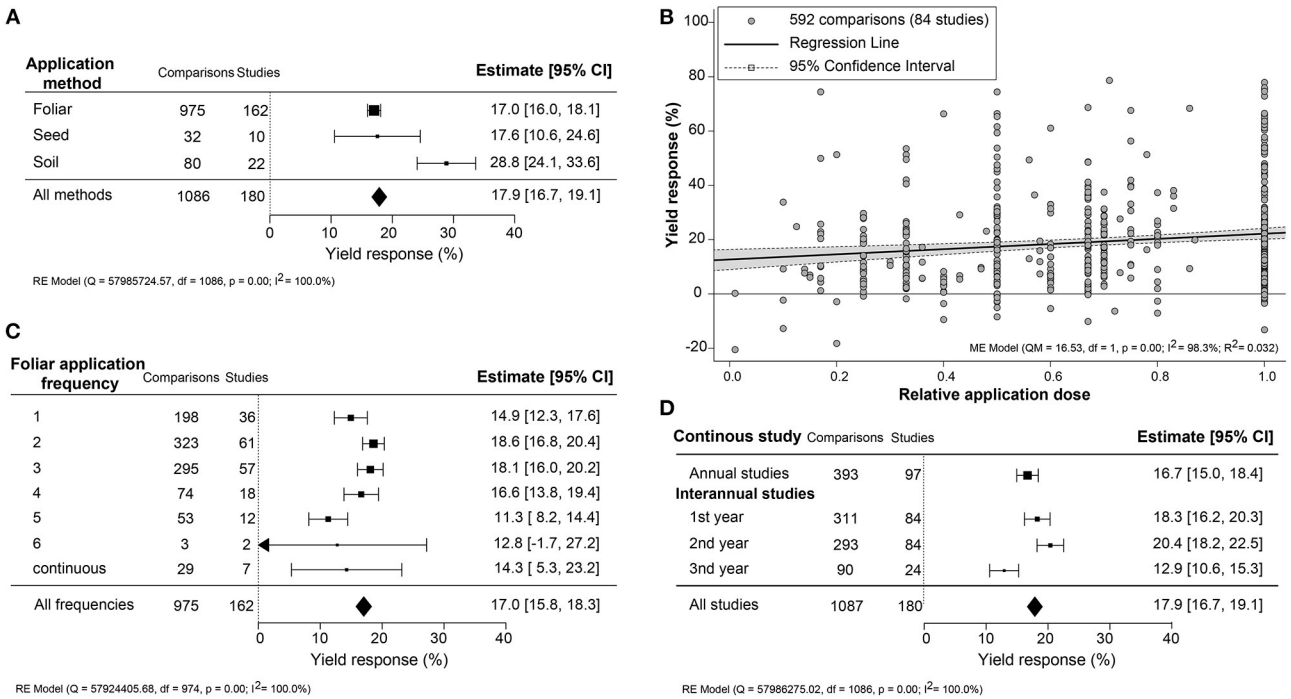

FIGURE 3 | Percentage yield response to biostimulant application affected by the different application management practices, including **(A)** application method, **(B)** frequency, **(C)** concentration, and **(D)** interannual studies. The point size correlates to the estimate's precision, and the error bars represent 95% confidence intervals (CI) of mean estimated effect sizes. The number of comparisons and studies is indicated in each line or legend. The combined effect estimates and the test of heterogeneity on the models [random-effect models (RE) in **(A,B,D)**, and mixed-effect model (ME) in **(C)**] were summarized at the bottom, where the heterogeneity test is significant ($p < 0.001$) and $I^2 \geq 75\%$ implies substantial heterogeneity.

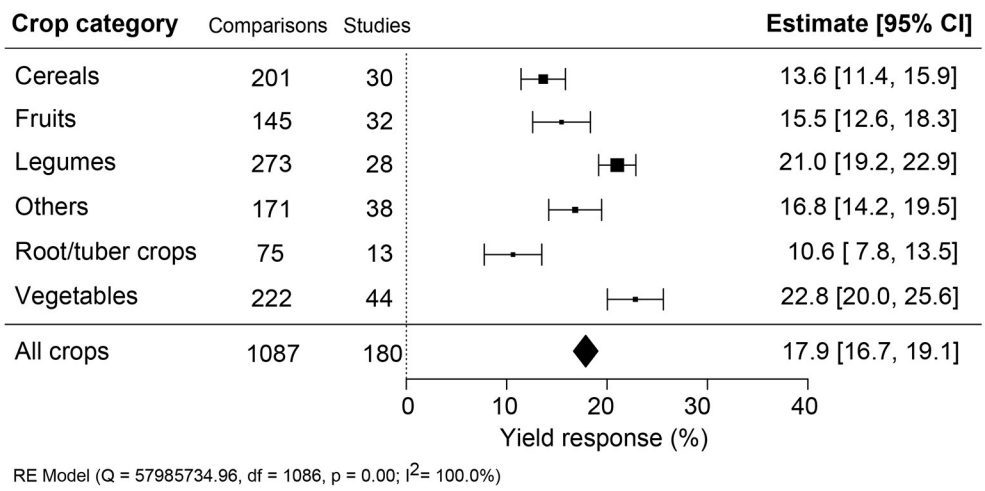

FIGURE 4 | Percentage yield response to biostimulant application affected by the crop categories. The point size correlates to the estimate's precision, and the error bars represent 95% confidence intervals (CI) of mean estimated effect sizes. The number of comparisons and studies is indicated in each line. The combined effect estimates and the heterogeneity test on the random-effect model (RE) were summarized at the bottom, where the heterogeneity test is significant ($p < 0.001$) and $I^2 \geq 75\%$ implies substantial heterogeneity.

to conclude the effectiveness of commercial crop production systems (Geelen and Xu, 2020). Previously, a meta-analysis focusing on humic substances under controlled environment and field studies reported an estimated just above 20% of the increase in dry weight of shoot and root (Rose et al., 2014), which is close to the yield gain we found (+17.9%) (**Figure 2**). In the case of microbial PBs, Schütz et al. (2018) found that the yield benefit in field trials was between +8.5 and +20.0%. Taken together, the

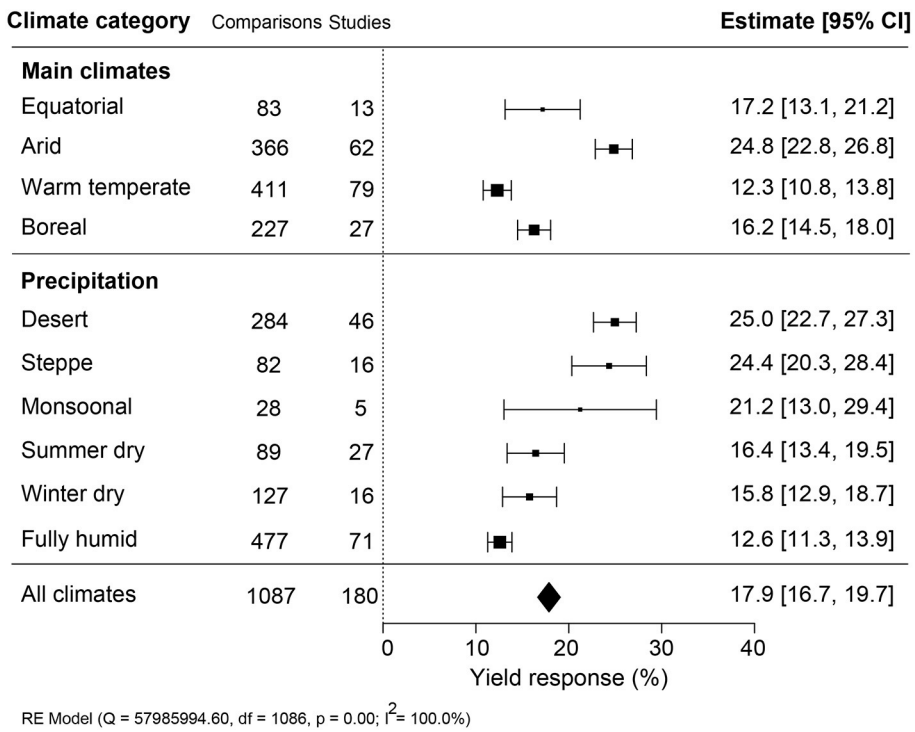

FIGURE 5 | Percentage yield response to biostimulant application affected by the climate categories that were subgrouped into main climates and precipitation types. The point size correlates to the estimate's precision, and the error bars represent 95% confidence intervals (CI) of mean estimated effect sizes. The number of comparisons and studies is indicated in each line. The combined effect estimates and the heterogeneity test on the random-effect model (RE) were summarized at the bottom, where the heterogeneity test is significant ($p < 0.001$) and $I^2 \geq 75\%$ implies substantial heterogeneity.

published data show some level of consistency across the different biostimulants analyzed. Chemical fertilizers also contribute to a yield gain, and here the average contribution was estimated to be around 40–60% (Stewart et al., 2005). Considering that biostimulants are commonly applied as supplements under conventional fertilization schemes and in many cases usually contain NPK fertilizers, the net positive effect of the bioactive ingredients is expected to be a considerable fraction of the total yield gain. Nevertheless, biostimulants sustainably improve the yield and provide a solution to reducing the dependency on synthetic fertilizer.

The extent of yield improvement varied across categories, with PE and MLE as the best performing biostimulants (**Figure 2**). MLE has been historically tested on many different crops displaying beneficial effects on seed germination, plant growth and yield, nutrient use efficiency, quality traits, and tolerance to abiotic stresses (Zulfiqar et al., 2020). The significant profitability and variability in MLE and other PE efficacy might be due to their complex composition of plant metabolites, containing many macro and mineral nutrients, osmoprotectants, and antioxidants (Soares et al., 2021). PE also likely contains plant hormones, which, in small quantities, are known to harbor the capacity to stimulate crop production (Harms and Oplinger, 1988). None of the MLE products used are, insofar we know, commercialized. This contrasts with SWE, for which more than 60% of the products analyzed are commercialized. Moreover, from over 40% of the total dataset, we estimated the effect of SWE products with more confidence compared to the other biostimulant categories. The consistency in yield benefits linked with SWE application is likely a result of the standardization of SWE extraction and formulation methods. The use of SWE as a plant growth regulator can be traced back as far as the Roman Empire (Henderson, 2004), with the first commercial product marketed in 1952 (Milton, 1952). The technology of SWE production has developed into a mainstream hot-alkaline extraction method involving specific manufacturing conditions, allowing strong consistency in production and quality (Craigie, 2011). However, the more recently discovered biostimulants like PE show batch variations, and their processing methodology is not well-established (García-García et al., 2020).

While many biostimulants are typically complex mixtures, Phi and Si are simple inorganic salts. Despite their less complex chemical composition, the average effectiveness of Phi was the lowest, and that of Si showed the greatest variability. Compared to these products, PBs consisting of complex mixtures were more effective, and it will be a challenge to determine their mechanism of action. It also remains to be demonstrated whether the complex biostimulants exert stronger bioactivity because of synergistic interactions between bioactive ingredients (García-García et al., 2020). Therefore, further standardization in biostimulant production procedures is forecasted to improve

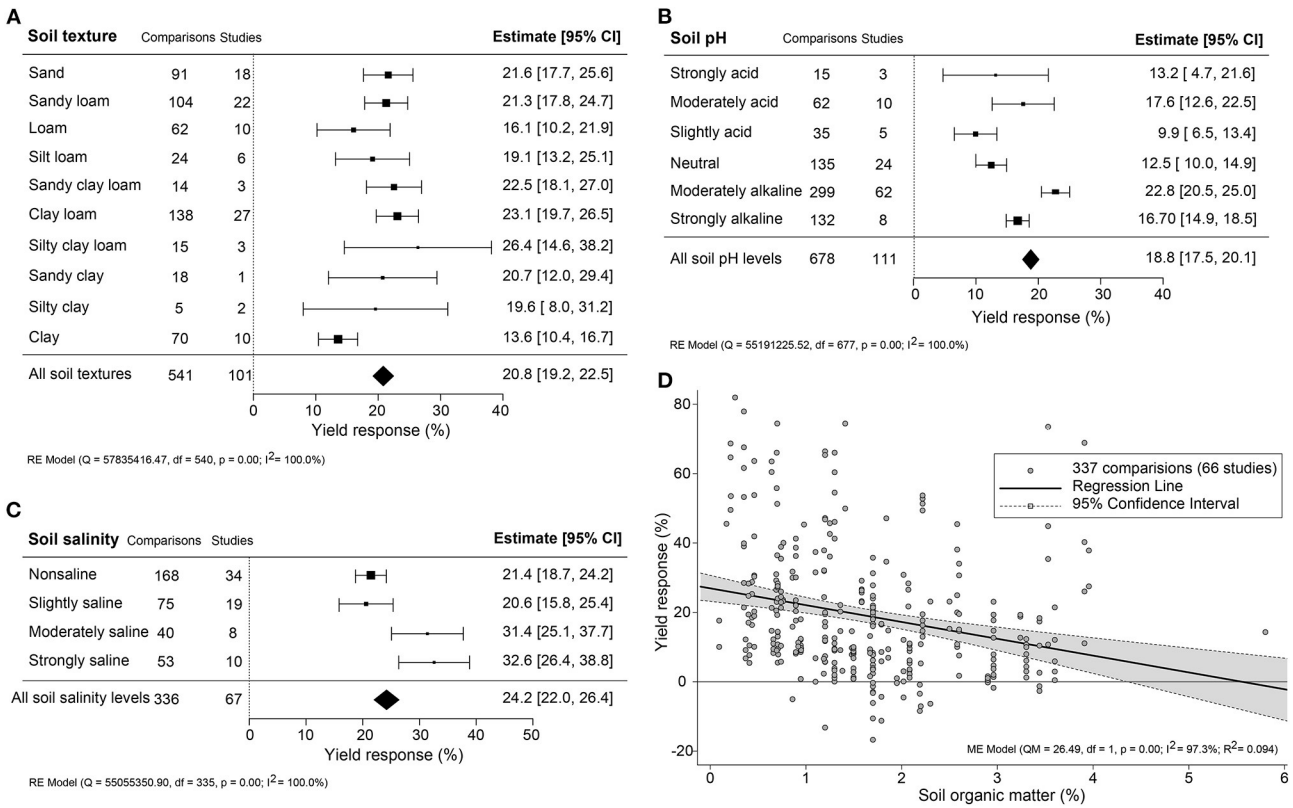

FIGURE 6 | Percentage yield response to biostimulant application affected by the soil properties, including soil **(A)** texture, **(B)** pH, **(C)** salinity, and **(D)** organic matter (%). The point size correlates to the estimate's precision, and the error bars represent 95% confidence intervals (CI) of mean estimated effect sizes. The number of comparisons and studies is indicated in each line or each legend. The combined effect estimates and the heterogeneity test on the models [random-effect models (RE) in **(A–C)**, and mixed-effect model (ME) in **(D)**] were summarized at the bottom, where the heterogeneity test is significant ($p < 0.001$) and $I^2 \geq 75\%$ implies substantial heterogeneity.

the consistency in effectiveness and reproducibility on yield gaining benefits.

Impact of Biostimulant Application Methodology

Biostimulants applied via soil resulted in about 10% higher yield benefits than foliar and seed applications (**Figure 3A**). This outcome is surprising as foliar and seed applications deliver the biostimulants directly to the plant, allowing faster uptake of the bioactive ingredients (Niu et al., 2021). For instance, surface spraying acts more directly and results in rapid responses to ripen fruits (Fernández and Eichert, 2009). Soil application of biostimulants likely has a different mode of action related to nutrient uptake efficiency or enhancing microbial activity on and around the crop. Nutrient availability is a major yield factor that can be improved by either providing higher levels of mineral or organic nutrients or by altering the microbial community interacting with the root system (Schütz et al., 2018; Kour et al., 2019; Oldroyd and Leyser, 2020). HFA, PHs, SWE, and PGPR have been shown to stimulate micro and macronutrient uptake efficiency, either by direct activation of ion transporters, mineral utilization, or improving soil quality and mineral recycling (for an extensive review, see Halpern et al., 2015).

Foliar application is the favored method because it can be merged with conventional spraying practices. Remarkably, single biostimulant sprays were nearly as effective as multiple applications (**Figure 3C**). This suggests that the yield benefit is likely due to nutrient supply and other rapid-growth stimulation induced upon spraying the crop once or twice. Also noteworthy is that applications above 4 times resulted in a negative trend with lower efficiency. The diminishing returns of higher biostimulant application frequencies may be caused by changes in the uptake and assimilation rate of effective agents throughout the germination, vegetative, and reproductive plant developmental stages (Bulgari et al., 2019). Colla et al. (2015) recommended lowering the dosage when frequently applying biostimulant to avoid growth inhibition caused by overdose. In general, the efficiency of biostimulants depends on the plant's nutrient uptake rate, which is highest prior to maximum growth rates depending on the crop type (Jones et al., 2011; Nguyen et al., 2019). For example, SWE application was best during the tilling stage (Stamatiadis et al., 2021) and best during the seedling stage of sugarcane (Chen et al., 2021). Moreover, the sensitivity of plants

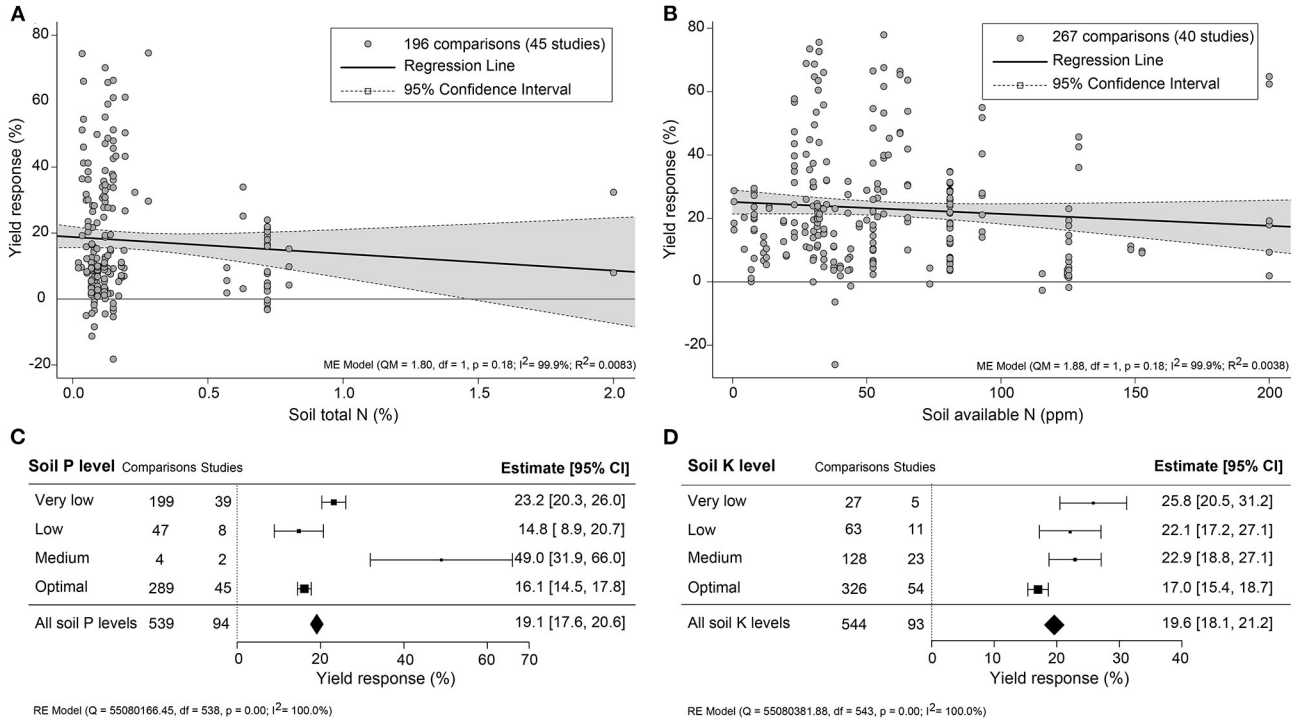

FIGURE 7 | Percentage yield response to biostimulant application as affected by the macronutrient levels, including **(A)** soil total N (%), **(B)** soil available N (ppm), soil **(C)** P, and **(D)** K levels. The point size correlates to the estimate's precision, and the error bars represent 95% confidence intervals (CI) of mean estimated effect sizes. The number of comparisons and studies is indicated in each line or each legend. The combined effect estimates and the heterogeneity test on the models [mixed-effect models (ME) in **(A,B)**, and random-effect models (RE) in **(C,D)**] were summarized at the bottom, where the heterogeneity test is significant ($p < 0.001$) and $I^2 \geq 75\%$ implies substantial heterogeneity.

is regulated by their daily circadian clock that also may influence the effectiveness of the biostimulant (Belbin et al., 2019). It is thus suggested to spray biostimulants in the early morning or late afternoon because of the open stomata (Specialty Fertilizers, 2015). Summarily, we strongly advise following the optimized biostimulant application in crop management.

Comparison Between Crop Categories

Vegetable and legume crops showed the highest gain in yield upon biostimulant application (**Figure 4**). A previous meta-analysis study on the crop yield improvement via biofertilization with microbial PBs argued that vegetables require higher fertilizer concentrations for optimal growth, and legumes engage in symbiotic nitrogen fixation, which is stimulated upon the addition of microbial PBs (Schütz et al., 2018). As our analysis included only non-microbial PBs, the stronger legume response is not likely attributed to the stimulation of symbiotic interactions with nitrogen-fixing bacteria. It is currently unclear why vegetable and legume crops are more responsive to biostimulant application.

Biostimulants Are More Efficient Under Suboptimal Growing Conditions

Overall, biostimulants showed the strongest crop yield effects in soils of low quality (acid and alkaline soils, saline soils, barren soils with low SOM, and P- or K-deficient soils) (**Figures 6B–D**, **7C,D**). In these soils, the cation exchange capacity (CEC) is inherently nutrient-poor (Brown and Lemon, 2021). Soil rich in clay component or SOM, for instance, has a higher CEC value and typically retains higher levels of nutrients, and therefore supporting sustained crop growth and higher yield (Bayu, 2020). The yield gap of cultivation in poor soils is thus much larger than in fertile soils (Evans and Fischer, 1999). Therefore, we suggest combining biostimulant applications with "Integrated Fertility Management" to maximize yield potential and reduce crop loss risk under climate change scenarios.

Open-field production systems are exposed to variations in climate conditions and, therefore, at risk of abiotic and biotic stresses and degradation of the soil conditions (drought, salinity, nutrient deficiency) (Challinor et al., 2014; Mickelbart et al., 2015). Biostimulants are propagated as a solution to safeguard crop yield under suboptimal growth conditions (Yakhin et al., 2017). In agreement with this view, the effectiveness of biostimulant application was the highest under suboptimal growing conditions of arid climates with low precipitation conditions (**Figure 5**). A similar conclusion was made from a meta-analysis on the yield improvement using microbial PBs (Schütz et al., 2018). In arid climate conditions, crops are exposed to more extreme temperature

conditions, which strongly impacts crop fertility (Thakur et al., 2010; Deryng et al., 2014; De Storme and Geelen, 2014). How PBs can mitigate environmental stresses is not well understood. Exogenously applied compounds may elicit a stress response that prepares the plant for subsequent stresses caused by limitations in water, soil fertility, or unfavorable temperature conditions (Ahmad et al., 2019). Molecules that can elicit a stress response are present in biostimulants and have been shown to induce stress-related genes (Geelen and Xu, 2020; González-Morales et al., 2021). Phytohormones are also commonly present in biostimulants, and their interactions with plants are known to enhance osmolyte accumulation and tolerance to stress (Sharma et al., 2019). In addition, plant-derived biostimulants contain antioxidants and improve the adaptation to unfavorable growing conditions by eliminating reactive oxygen species (ROS) (Drobek et al., 2019). Therefore, the bioactive compounds in biostimulants may evoke either stress alleviation (e.g., suppression of ROS) or induce stress response factors that trigger the immunity against abiotic stresses (Brown and Saa, 2015), validating the hypothesis that biostimulants are more effective under suboptimal growth conditions.

CONCLUSIONS

This review underscores the importance of evaluating the biostimulant application methodology and the crop cultivation conditions. The study indicates that the impact of biostimulant application on crop yield depends on the type of products and application management. Our results also provide various environment-specific assessments of biostimulant performance in open-field conditions, which can be used to set up more effective farming practices for future biostimulant application strategies. In conclusion, biostimulants improve crop yield by reducing yield reductions under stress conditions. This approach can help improve food security for the growing world population under increasing climate change threats.

DATA AVAILABILITY STATEMENT

The original contributions presented in the study are included in the article/**Supplementary Material**, further inquiries can be directed to the corresponding author/s.

AUTHOR CONTRIBUTIONS

JL: conceptualization, investigation, formal analysis, data curation, visualization, and writing—original draft. TV: writing—review and editing and supervision. DG: conceptualization, funding acquisition, writing—review and editing, and supervision. All authors contributed to the article and approved the submitted version.

FUNDING

This research was supported by Fonds Wetenschappelijk Onderzoek – Vlaanderen (FWO) under project Bio2Bio (S006017N) and under project BioSUNmulant by European Union's Horizon 2020 research and innovation program under grant agreement of sustainable and resilient agriculture for food and non-food systems (FACCE SURPLUS, No. 652615) and with Flanders Innovation & Entrepreneurship (VLAIO) (HBC.2019.2244). JL was supported by the China Scholarship Council (CSC) Grant No. 201706350259.

ACKNOWLEDGMENTS

We thank Ms. Halimat Ogunsanya, Ms. Brechtje de Haas, Dr. Hoang Khai Trinh (HortiCell Lab, Ghent University) for their critical comments and suggestions.

SUPPLEMENTARY MATERIAL

The Supplementary Material for this article can be found online at: https://www.frontiersin.org/articles/10.3389/fpls.2022.836702/full#supplementary-material

REFERENCES

Ahmad, B., Zaid, A., Sadiq, Y., Bashir, S., and Wani, S.H. (2019). Role of selective exogenous elicitors in plant responses to abiotic stress tolerance. *Plant Abiotic Stress Tolerance* 273–290. doi: 10.1007/978-3-030-06118-0_12

Bailey-Serres, J., Parker, J.E., Ainsworth, E.A., Oldroyd, G.E., and Schroeder, J.I. (2019). Genetic strategies for improving crop yields. *Nature* 575, 109–118. doi: 10.1038/s41586-019-1679-0

Bayu, T. (2020). Review on contribution of integrated soil fertility management for climate change mitigation and agricultural sustainability. *Cogent Environ. Sci.* 6, 1823631. doi: 10.1080/23311843.2020.1823631

Belbin, F.E., Hall, G.J., Jackson, A.B., Schanschieff, F.E., Archibald, G., Formstone, C., et al. (2019). Plant circadian rhythms regulate the effectiveness of a glyphosate-based herbicide. *Nat. Commun.* 10, 3704. doi: 10.1038/s41467-019-11709-5

Bio4Safe, I.S.P. (2021). *Biostimulant Database*. Available online at: https://bio4safe.eu/ (accessed March 10, 2022).

Brown, K., and Lemon, J. (2021). *Cations and Cation Exchange Capacity*. Available online at: https://www.soilquality.org.au/factsheets/cation-exchange-capacity (accessed October 25, 2021).

Brown, P., and Saa, S. (2015). Biostimulants in agriculture. *Front. Plant Sci.* 6:671. doi: 10.3389/fpls.2015.00671

Bryant, C., Wheeler, N.R., Rubel, F., and French, R.H. (2017). kgc: Koeppen-Geiger Climatic Zones. Austria: The R Project for Statistical Computing

Bulgari, R., Franzoni, G., and Ferrante, A. (2019). Biostimulants application in horticultural crops under abiotic stress conditions. *Agronomy* 9, 306. doi: 10.3390/agronomy9060306

CEN Technical Committees (2021). *CEN/TC 455 - Plant Biostimulants and Agricultural Micro-Organisms* (Brussels).

Challinor, A.J., Watson, J., Lobell, D.B., Howden, S.M., Smith, D.R., and Chhetri, N. (2014). A meta-analysis of crop yield under climate change and adaptation. *Nat. Clim. Chang.* 4, 287–291. doi: 10.1038/nclimate2153

Chen, D., Zhou, W., Yang, J., Ao, J., Huang, Y., Shen, D., et al. (2021). Effects of seaweed extracts on the growth, physiological activity, cane yield and sucrose content of sugarcane in China. *Front. Plant Sci.* 12, 659130. doi: 10.3389/fpls.2021.659130

Colla, G., Nardi, S., Cardarelli, M., Ertani, A., Lucini, L., Canaguier, R., et al. (2015). Protein hydrolysates as biostimulants in horticulture. *Sci. Hortic.* 196, 28–38. doi: 10.1016/j.scienta.2015.08.037

Craigie, J.S. (2011). Seaweed extract stimuli in plant science and agriculture. *J. Appl. Phycol.* 23, 371–393. doi: 10.1007/s10811-010-9560-4

De Storme, N., and Geelen, D. (2014). The impact of environmental stress on male reproductive development in plants: biological processes and molecular mechanisms. *Plant Cell Environ.* 37, 1–18. doi: 10.1111/pce.12142

Deryng, D., Conway, D., Ramankutty, N., Price, J., and Warren, R. (2014). Global crop yield response to extreme heat stress under multiple climate change futures. *Environ. Res. Lett.* 9, 034011. doi: 10.1088/1748-9326/9/3/034011

Drobek, M., Frac, M., and Cybulska, J. (2019). Plant biostimulants: importance of the quality and yield of horticultural crops and the improvement of plant tolerance to abiotic stress-a review. *Agronomy* 9, 335. doi: 10.3390/agronomy9060335

Du Jardin, P. (2015). Plant biostimulants: definition, concept, main categories and regulation. *Sci. Hortic.* 196, 3–14. doi: 10.1016/j.scienta.2015.09.021

EBIC. (2021). *Economic Overview of the European Biostimulants Market*. Available online at: https://biostimulants.eu/highlights/economic-overview-of-the-european-biostimulants-market/ (accessed March 10, 2022).

Edwards, T. (2021). *What Is Soil Organic Carbon?* Available online at: https://www.agric.wa.gov.au/measuring-and-assessing-soils/what-soil-organic-carbon (accessed October 21, 2021).

Esri (2009). *"World Imagery" [basemap]*. Available online at: https://www.arcgis.com/home/item.html?id=10df2279f9684e4a9f6a7f08febac2a9 (accessed October 21, 2021).

Esri (2020). *"Koeppen-Geiger_Observed_and_Predicted_Climate_Shifts"[basemap]*. ArcGIS REST Services Directory. Available online at: https://www.arcgis.com/home/item.html?id=3205557fc36445a38fe961cb3d030089 (accessed July 19, 2021).

Evans, L., and Fischer, R. (1999). Yield potential: its definition, measurement, and significance. *Crop Sci.* 39, 1544–1551. doi: 10.2135/cropsci1999.3961544x

FAO (2005). *A System of Integrated Agricultural Censuses and Surveys: World programme for the census of agriculture 2010*. Rome: Food and Agriculture Organization of the United Nations.

Fernández, V., and Eichert, T. (2009). Uptake of hydrophilic solutes through plant leaves: current state of knowledge and perspectives of foliar fertilization. *CRC Crit. Rev. Plant Sci.* 28, 36–68. doi: 10.1080/07352680902743069

García-García, A.L., García-Machado, F.J., Borges, A.A., Morales-Sierra, S., Boto, A., and Jiménez-Arias, D. (2020). Pure organic active compounds against abiotic stress: a biostimulant overview. *Front. Plant Sci.* 11, 575829. doi: 10.3389/fpls.2020.575829

Geelen, D., and Xu, L. (2020). *The Chemical Biology of Plant Biostimulants*. Hoboken, NJ: John Wiley & Sons, Incorporated.

González-Morales, S., Solís-Gaona, S., Valdés-Caballero, M.V., Juárez-Maldonado, A., Loredo-Treviño, A., and Benavides-Mendoza, A. (2021). Transcriptomics of biostimulation of plants under abiotic stress. *Front. Genet.* 12, 583888. doi: 10.3389/fgene.2021.583888

Gupta, A., Rico-Medina, A., and Cano-Delgado, A.I. (2020). The physiology of plant responses to drought. *Science* 368, 266–269. doi: 10.1126/science.aaz7614

Halpern, M., Bar-Tal, A., Ofek, M., Minz, D., Muller, T., and Yermiyahu, U. (2015). The use of biostimulants for enhancing nutrient uptake. *Adv. Agron.* 130, 141–174. doi: 10.1016/bs.agron.2014.10.001

Hansen, J. (2018). *EU Must Get Serious About Promoting the Circular Economy [WWW Document]*. Available online at: https://www.theparliamentmagazine.eu/articles/partner_article/fertilizers-europe/eu-must-get-serious-about-promoting-circular-economy (accessed October 21, 2021).

Harms, C.L., and Oplinger, E.S. (1988). *Plant Growth Regulators: Their Use in Crop Production*. Ames, IA: North Central Region Extension Publication.

Henderson, J. (2004). *The Roman Book of Gardening*. London: Routledge.

Horneck, D.A., Sullivan, D.M., Owen, J.S., and Hart, J.M. (2011). *Soil Test Interpretation Guide*. Corvallis, OR: Oregon State University Extension Service.

Hunter, M.C., Smith, R.G., Schipanski, M.E., Atwood, L.W., and Mortensen, D.A. (2017). Agriculture in 2050: recalibrating targets for sustainable intensification. *Bioscience* 67, 386–391. doi: 10.1093/biosci/bix010

Inthout, J., Ioannidis, J.P., Rovers, M.M., and Goeman, J.J. (2016). Plea for routinely presenting prediction intervals in meta-analysis. *BMJ Open* 6, e010247. doi: 10.1136/bmjopen-2015-010247

Jones, C., Olson-Rutz, K., and Dinkins, C. (2011). *Nutrient Uptake Timing by Crops*. Montana: Montana State University.

Kargas, G., Chatzigiakoumis, I., Kollias, A., Spiliotis, D., Massas, I., and Kerkides, P. (2018). Soil Salinity assessment using saturated paste and mass soil:water 1:1 and 1:5 ratios extracts. *Water* 10, 1589. doi: 10.3390/w10111589

Koli, P., Bhardwaj, N.R., and Mahawer, S.K. (2019). "Agrochemicals: harmful and beneficial effects of climate changing scenarios," in *Climate Change and Agricultural Ecosystems*. eds K. K. Choudhary, A. Kumar, and A. K. Singh (Duxford: Elsevier), 65–94.

Kour, D., Rana, K., Yadav, A., Yadav, N., Kumar, M., Kumar, V., et al. (2019). Microbial biofertilizers: bioresources and eco-friendly technologies for agricultural and environmental sustainability. *Biocatal. Agric. Biotechnol.* 23, 101487. doi: 10.1016/j.bcab.2019.101487

Land Resources Management Unit and Commission (2010). *Map of Soil pH in Europe* (Brussels).

Liliane, T.N., and Charles, M.S. (2020). Factors affecting yield of crops. *Agron. Clim. Change Food Secur.* 9, 1–16. doi: 10.5772/intechopen.90672

Marx, E.S., Hart, J.M., and Stevens, R.G. (1996). *Soil Test Interpretation Guide*. Corvallis, OR: Oregon State University Extension Service.

Mickelbart, M.V., Hasegawa, P.M., and Bailey-Serres, J. (2015). Genetic mechanisms of abiotic stress tolerance that translate to crop yield stability. *Nat. Rev. Genet.* 16, 237–251. doi: 10.1038/nrg3901

Milton, R. (1952). Improvements in or relating to horticultural and agricultural fertilizers. *British Patent* 664989, 9.

Nakagawa, S., and Schielzeth, H. (2013). A general and simple method for obtaining R2 from generalized linear mixed-effects models. *Methods Ecol. Evol.* 4, 133–142. doi: 10.1111/j.2041-210x.2012.00261.x

Nguyen, M.L., Spaepen, S., Du Jardin, P., and Delaplace, P. (2019). Biostimulant effects of rhizobacteria on wheat growth and nutrient uptake depend on nitrogen application and plant development. *Arch. Agron. Soil Sci.* 65, 58–73. doi: 10.1080/03650340.2018.1485074

Niu, J., Liu, C., Huang, M., Liu, K., and Yan, D. (2021). Effects of Foliar fertilization: a review of current status and future perspectives. *J. Soil Sci. Plant Nutr.* 21, 104–118. doi: 10.1007/s42729-020-00346-3

Oldfield, E.E., Bradford, M.A., and Wood, S.A. (2019). Global meta-analysis of the relationship between soil organic matter and crop yields. *Soil* 5, 15–32. doi: 10.5194/soil-5-15-2019

Oldroyd, G.E., and Leyser, O. (2020). A plant's diet, surviving in a variable nutrient environment. *Science* 368, eaba0196. doi: 10.1126/science.aba0196

Page, M.J., Mckenzie, J.E., Bossuyt, P.M., Boutron, I., Hoffmann, T.C., Mulrow, C.D., et al. (2021). The PRISMA 2020 statement: an updated guideline for reporting systematic reviews. *Int. J. Surg.* 88, 105906. doi: 10.1016/j.ijsu.2021.105906

Peel, M.C., Finlayson, B.L., and Mcmahon, T.A. (2007). Updated world map of the Köppen-Geiger climate classification. *Hydrol. Earth Syst. Sci.* 11, 1633–1644. doi: 10.5194/hess-11-1633-2007

R Core Team (2020). *R: A Language and Environment for Statistical Computing*. Available online at: https://www.r-project.org/ (accessed March 10, 2022).

Regulation (Eu) 2019/1009 (2019). *Regulation (EU) 2019/1009 of the European Parliament and of the Council of 5 June 2019 Laying Down Rules on the Making Available on the Market of EU Fertilising Products and Amending Regulations (EC) No 1069/2009 and (EC) No 1107/2009 and Repealing Regula*.

Ricci, M., Tilbury, L., Daridon, B., and Sukalac, K. (2019). General principles to justify plant biostimulant claims. *Front. Plant Sci.* 10, 494. doi: 10.3389/fpls.2019.00494

Rohatgi, A. (2020). *Webplotdigitizer: Web Based Tool to Extract Data From Plots, Images, and Maps*. Available online at: https://automeris.io/WebPlotDigitizer

Rose, M.T., Patti, A.F., Little, K.R., Brown, A.L., Jackson, W.R., and Cavagnaro, T.R. (2014). A meta-analysis and review of plant-growth response to humic substances: practical implications for agriculture. *Adv. Agron.* 124, 37–89. doi: 10.1016/B978-0-12-800138-7.00002-4

Rouphael, Y., and Colla, G. (2020). Editorial: biostimulants in agriculture. *Front. Plant Sci.* 11, 40. doi: 10.3389/fpls.2020.00040

Schütz, L., Gattinger, A., Meier, M., Müller, A., Boller, T., Mäder, P., et al. (2018). Improving crop yield and nutrient use efficiency via biofertilization—A global meta-analysis. *Front. Plant Sci.* 8, 2204. doi: 10.3389/fpls.2017.02204

Sharma, A., Shahzad, B., Kumar, V., Kohli, S.K., Sidhu, G.P.S., Bali, A.S., et al. (2019). Phytohormones regulate accumulation of osmolytes under abiotic stress. *Biomolecules* 9, 285. doi: 10.3390/biom9070285

Smith, J.L., and Doran, J.W. (1997). Measurement and use of pH and electrical conductivity for soil quality analysis. *Methods Assess. Soil Qual.* 49, 169–185.

Snyder, C., Chapman, S., Sabbe, W., and Baker, W. (1993). *Understanding the Numbers on Your Soil Test Report*. St Paul, MN: FSA (USA).

Soares, T.F.S.N., Silva, A.V.C.D., and Muniz, E.N. (2021). Moringa leaf extract: A cost-effective and sustainable product to improve plant growth. *South Afr. J. Bot.* 141, 171–176. doi: 10.1016/j.sajb.2021.04.007

Soil Health Institute (2018). *North American Project to Evaluate Soil Health Measurements*. Available online at: https://soilhealthinstitute.org/ (accessed October 21, 2021).

Soil Science Division Staff (1993). *Examination and Description of Soil Profiles*. U.S. Department of Agriculture Handbook 18. Available online at: https://www.nrcs.usda.gov/wps/portal/nrcs/detail/soils/ref/?cid=nrcs142p2_054253 (accessed March 25, 2021).

Specialty Fertilizers, I. (2015). Recommendations for efficient foliar application. Available online at: https://icl-sf.com/global-en/article/recommendations-for-efficient-foliar-application/ (accessed August, 9, 2021).

Spungen, J. (2005). *Bowes & Church's Food Values of Portions Commonly Used*. Philadelphia, PA: Lippincott Williams & Wilkins.

Stamatiadis, S., Evangelou, E., Jamois, F., and Yvin, J.-C. (2021). Targeting Ascophyllum nodosum (L.) Le Jol. extract application at five growth stages of winter wheat. *J. Appl. Phycol.* 33, 1–10. doi: 10.1007/s10811-021-02417-z

Stewart, W., Dibb, D., Johnston, A., and Smyth, T. (2005). The contribution of commercial fertilizer nutrients to food production. *Agron. J.* 97, 1–6. doi: 10.2134/agronj2005.0001

Thakur, P., Kumar, S., Malik, J.A., Berger, J.D., and Nayyar, H. (2010). Cold stress effects on reproductive development in grain crops: an overview. *Environ. Exp. Bot.* 67, 429–443. doi: 10.1016/j.envexpbot.2009.09.004

Van Dijk, M., Morley, T., Rau, M.L., and Saghai, Y. (2021). A meta-analysis of projected global food demand and population at risk of hunger for the period 2010–2050. *Nat. Food* 2, 494–501. doi: 10.1038/s43016-021-00322-9

Viechtbauer, W. (2010). Conducting meta-analyses in R with the metafor. *J. Stat. Softw.* 36, 1–48. doi: 10.18637/jss.v036.i03

Yakhin, O.I., Lubyanov, A.A., Yakhin, I.A., and Brown, P.H. (2017). Biostimulants in plant science: a global perspective. *Front. Plant Sci.* 7, 2049. doi: 10.3389/fpls.2016.02049

Zulfiqar, F., Casadesús, A., Brockman, H., and Munné-Bosch, S. (2020). An overview of plant-based natural biostimulants for sustainable horticulture with a particular focus on moringa leaf extracts. *Plant Sci.* 295, 110194. doi: 10.1016/j.plantsci.2019.110194

Conflict of Interest: The authors declare that the research was conducted in the absence of any commercial or financial relationships that could be construed as a potential conflict of interest.

Publisher's Note: All claims expressed in this article are solely those of the authors and do not necessarily represent those of their affiliated organizations, or those of the publisher, the editors and the reviewers. Any product that may be evaluated in this article, or claim that may be made by its manufacturer, is not guaranteed or endorsed by the publisher.

frontiers | Frontiers in Microbiology

ORIGINAL RESEARCH
published: 03 May 2022
doi: 10.3389/fmicb.2022.889073

Designing Synergistic Biostimulants Formulation Containing Autochthonous Phosphate-Solubilizing Bacteria for Sustainable Wheat Production

Mahreen Yahya[1], Maria Rasul[1,2], Yasra Sarwar[3], Muhammad Suleman[1,4], Mohsin Tariq[5], Syed Zajif Hussain[6], Zahid Iqbal Sajid[1], Asma Imran[1], Imran Amin[7], Thomas Reitz[8,9], Mika Tapio Tarkka[8,9] and Sumera Yasmin[1]**

[1] Soil and Environmental Biotechnology Division, National Institute for Biotechnology and Genetic Engineering College, Pakistan Institute of Engineering and Applied Sciences (NIBGE-C, PIEAS), Faisalabad, Pakistan, [2] Department of Environment and Energy, Sejong University, Seoul, South Korea, [3] Health Biotechnology Division, National Institute for Biotechnology and Genetic Engineering College, Pakistan Institute of Engineering and Applied Sciences (NIBGE-C, PIEAS), Faisalabad, Pakistan, [4] School of Life Sciences, Institute of Microbiology, Lanzhou University, Lanzhou, China, [5] Department of Bioinformatics and Biotechnology, Government College University Faisalabad (GCUF), Faisalabad, Pakistan, [6] Department of Chemistry and Chemical Engineering, SBA School of Science and Engineering (SBA-SSE), Lahore University of Management Sciences (LUMS), Lahore, Pakistan, [7] Agricultural Biotechnology Division, National Institute for Biotechnology and Genetic Engineering College, Pakistan Institute of Engineering and Applied Sciences (NIBGE-C, PIEAS), Faisalabad, Pakistan, [8] Soil Ecology Department, UFZ-Helmholtz-Centre for Environmental Research, Halle, Germany, [9] German Centre for Integrative Biodiversity Research (iDiv) Halle-Jena-Leipzig, Leipzig, Germany

OPEN ACCESS

Edited by:
Maurizio Ruzzi,
University of Tuscia, Italy

Reviewed by:
Hassan Javed Chaudhary,
Quaid-i-Azam University, Pakistan
Tania Taurian,
Universidad Nacional de Río Cuarto, Argentina

***Correspondence:**
Mika Tapio Tarkka
mika.tarkka@ufz.de
Sumera Yasmin
sumeraimran2012@gmail.com

Specialty section:
This article was submitted to Microbe and Virus Interactions with Plants, a section of the journal Frontiers in Microbiology

Received: *03 March 2022*
Accepted: *04 April 2022*
Published: *03 May 2022*

Citation:
Yahya M, Rasul M, Sarwar Y, Suleman M, Tariq M, Hussain SZ, Sajid ZI, Imran A, Amin I, Reitz T, Tarkka MT and Yasmin S (2022) Designing Synergistic Biostimulants Formulation Containing Autochthonous Phosphate-Solubilizing Bacteria for Sustainable Wheat Production. Front. Microbiol. 13:889073. doi: 10.3389/fmicb.2022.889073

Applying phosphate-solubilizing bacteria (PSB) as biofertilizers has enormous potential for sustainable agriculture. Despite this, there is still a lack of information regarding the expression of key genes related to phosphate-solubilization (PS) and efficient formulation strategies. In this study, we investigated rock PS by *Ochrobactrum* sp. SSR (DSM 109610) by relating it to bacterial gene expression and searching for an efficient formulation. The quantitative PCR (qPCR) primers were designed for PS marker genes glucose dehydrogenase (*gcd*), pyrroloquinoline quinone biosynthesis protein C (*pqqC*), and phosphatase (*pho*). The SSR-inoculated soil supplemented with rock phosphate (RP) showed a 6-fold higher expression of *pqqC* and *pho* compared to inoculated soil without RP. Additionally, an increase in plant phosphorous (P) (2%), available soil P (4.7%), and alkaline phosphatase (6%) activity was observed in PSB-inoculated plants supplemented with RP. The root architecture improved by SSR, with higher root length, diameter, and volume. *Ochrobactrum* sp. SSR was further used to design bioformulations with two well-characterized PS, *Enterobacter* spp. DSM 109592 and DSM 109593, using the four organic amendments, biochar, compost, filter mud (FM), and humic acid. All four carrier materials maintained adequate survival and inoculum shelf life of the bacterium, as indicated by the field emission scanning electron microscopy analysis. The FM-based bioformulation was most efficacious and enhanced not only wheat grain yield (4–9%) but also seed P (9%). Moreover, FM-based bioformulation enhanced soil available P (8.5–11%) and phosphatase activity (4–5%). Positive correlations were observed between the

PSB solubilization in the presence of different insoluble P sources, and soil available P, soil phosphatase activity, seed P content, and grain yield of the field grown inoculated wheat variety Faisalabad-2008, when di-ammonium phosphate fertilizer application was reduced by 20%. This study reports for the first time the marker gene expression of an inoculated PSB strain and provides a valuable groundwork to design field scale formulations that can maintain inoculum dynamics and increase its shelf life. This may constitute a step-change in the sustainable cultivation of wheat under the P-deficient soil conditions.

Keywords: marker genes, *gcd*, *pqqC*, *pho*, *Ochrobactrum*, FESEM, bioformulations, FISH

INTRODUCTION

Phosphorus (P) is an essential key macro-nutrient for the optimal plant growth (Brito et al., 2020; Chandran et al., 2021) and a crucial element for various physiological and biochemical functions at plant cellular level (Bechtaoui et al., 2021). The complex dynamics of P in soil makes it a limited resource for plant uptake (Bindraban et al., 2020). To satisfy the rising P nutrition requirements of crops and to boost agricultural production, the conventional agriculture relies on agrochemicals, a practice that compromises the human and environmental health (Akanmu et al., 2021). Further, the global P input into croplands is expected to increase by up to 86% by 2050 (Mogollón et al., 2018), and thus sustainable means for P fertilization are urgently needed.

The application of bacteria that are beneficial for crop production, commonly termed as plant growth-promoting bacteria, has been adopted as a potent, biological alternative for the mineral fertilization. The bacterial inoculants can be used as biofertilizers and biostimulants to improve the soil nutrient availability, plant nutrient uptake and assimilation, and root growth, since their biological activities include, e.g., mineral and organic phosphate solubilization (PS), nitrogen fixation, siderophore, and indole-3-acetic acid production (Castiglione et al., 2021). Among the plant beneficial bacteria, the biofertilizer group phosphate-solubilizing bacteria (PSB) are promising candidates to satisfy the P requirements of the plants by converting unavailable soil inorganic (P_i) and organic (P_o) forms of phosphate into plant-available orthophosphates through dissolution and absorption (Chen and Liu, 2019). The P_i-solubilizing microorganisms secrete organic acids to dissolve phosphate minerals, whereas the organic phosphates are hydrolyzed by acid and alkaline phosphatases as well as phytases (Liu et al., 2020). In general, the application of PSB in soil decreases the pH locally and consequently makes the P bound in minerals available to the plant and strengthens the activity of other beneficial microorganisms (Etesami et al., 2021).

At present, the research on the genes of PSB related to P_i solubilization is mainly focused on *pyrroloquinoline quinone–glucose dehydrogenase (gcd)* and six redox–coenzyme *pyrroloquinoline quinone* genes *pqq A*, *B*, *C*, *D*, *E*, *F*, and *G* (Bhanja et al., 2021). By contrast, the organic phosphates are hydrolyzed by acid phosphatases, alkaline phosphatases, and phytases (inositol phosphate phosphatases) that are encoded by *phosphatase* (*pho*) genes (Sarr et al., 2020). The knowledge on the genetic potential of PSB is still scanty, and the molecular studies to understand how PSB brings out the P solubilization are inconclusive (Liu et al., 2018).

In spite to the wide varieties of PSB, i.e., *Acinetobacter*, *Bacillus*, *Enterobacter Ochrobactrum*, and *Pseudomonas*, there are still relatively limited studies on P-solubilizing pathways and expression patterns of genes related to phosphate-solubilizing that need to be further studied. For this reason, the first aim of this work was to construct primers and to provide expression analysis of key PS related genes, i.e., *gcd*, *pqqC*, and *pho* of selected PSB.

Although an elite strain with a high and consistent PS activity is an essential prerequisite for the development of successful inoculant, the non-biological components for bioformulations are still key bottlenecks in commercial development of the inoculants (Mendoza-Suárez et al., 2021). The choice of carrier material is fundamental, because carrier is the sole delivery vehicle of live microorganism from the production unit to the plants in the field (Vassilev et al., 2020). The main roles of a good carrier material are as follows: (i) To provide an optimal microenvironment for microorganisms to maintain microbial viability and longer shelf life without any need for special storage and (ii) to support the strain(s) competitive abilities with the usually much better adapted, native soil microflora (Soumare et al., 2020). Besides, the carrier material must be readily available, easily pulverized and sterilized, cost-effective, compatible with the environment, acquiescent to nutrient supplement, and un-harmful to the user (Koskey et al., 2021). The carrier materials can be organic [e.g., compost (CM), biochar (BC), peat, biogas, humic acid (HA), slurry, etc.] or inorganic (e.g., talc, perlite, lignin, zeolite, etc.) origin, or even synthesized from specific compounds (Mitter et al., 2021). The by-products from the food and agricultural industries are also important sources for the development of biostimulants. The PSB-based carrier materials can include extracts from food waste, manures, vermicomposting, aquaculture waste streams or even sewage treatments (Madende and Hayes, 2020).

Despite the great potential and long-term expedient effects, the biostimulants/biofertilizers still face major challenges that limit their use in agriculture. These challenges are often associated with limited shelf life and survival of inoculated strain in the field, in variable environments and with different host plants (Mitter et al., 2021). For this reason,

the various commercial bioinoculants did not function under field conditions with a similar efficacy as in greenhouse or laboratory conditions (Stamenkovi et al., 2018; Santos et al., 2019; Vassilev et al., 2020). Mostly, the reasons for that were inadequate formulations with carriers that did not support the survival and growth of the microorganisms and/or were not stable under field conditions (Fasusi et al., 2021). Furthermore, the simultaneous application of two or more plant growth promoting rhizobacteria (PGPR) as consortium can improve the plant growth and can cause substantial increment in the crop yield (Shahzad et al., 2017; Backer, 2018; Mpanga et al., 2019). Bacteria in the consortium can efficiently colonize in rhizosphere than single bacterium (Molina-Romero et al., 2021) and they not only reduce the application chemical fertilizers but also allow the plants to utilize P already present in the soil (Lobo et al., 2019). Hence, the second aim of this study was to design a successful bioformulation based on PSB consortium with optimal shelf life and agro-industrial by-products as sole carbon source/organic amendments. We expected that this approach is expedient for developing a robust and effective alternative for mineral P fertilization.

We hypothesized that (H1) the autochthonous PSB that can solubilize different unavailable forms of phosphate, may have the genetic potential to express key genes responsible for PS and improve root architecture concomitantly under P-deficient conditions. We assumed (H2) that designing biostimulants based on a PSB consortium and using different agro-industrial by-products as organic amendments could result in a product with a long shelf life and survival in the wheat rhizosphere. We also expected (H3) correlations between P solubilization from the different insoluble phosphate sources by PSB and increased soil available P, consequently also resulting in improved wheat root growth, and grain yield.

MATERIALS AND METHODS

The PSB and Evaluation of Their P-Solubilization Potential in Different Insoluble P Sources

The PSB *Enterobacter* spp. ZW9, ZW32 (GenBank accession numbers MK422617 and MK817561) and *Ochrobactrum* sp. SSR (GenBank accession number MK422612) used in this study were isolated from the wheat rhizosphere and characterized in our previous study (Yahya et al., 2021). These PSB are non-pathogenic, compatible with each other and were also submitted to DSMZ (https://www.dsmz.de/) culture collection under the accession numbers DSM 109610 and DSM 109592, DSM 109593 for *Ochrobactrum* sp. SSR, *Enterobacter* sp. ZW9 and *Enterobacter* sp. ZW32, respectively.

In the current study, an *in vitro* assay was carried out to assess the P-solubilization potential of P-solubilizing bacteria SSR, ZW32 and ZW9 in the presence of different insoluble P sources. The three PSB strains were cultured in rock phosphate (RP) broth medium (Nguyen et al., 1992) and phytate broth medium (Howson and Davis, 1983) supplemented with insoluble P sources, i.e., RP and phytate, respectively. The flasks were kept at 28 ± 2°C and 180 rpm. An un-inoculated medium was used as a control. The P-solubilizing abilities of PSB were quantitatively estimated at 3, 5, 7, 10, and 15 days post-inoculation (DPI). To get the cell-free supernatant, the cultures were centrifuged at 4,000 rpm for 10 min at 4°C. The supernatant obtained was used for available P quantification as described by Murphy and Riley (1962) using the molybdenum blue method.

Expression Analysis of Genes Responsible for P-Solubilization in Soil Amended With RP Using Quantitative Real-Time PCR (qRT-PCR)

Based on the *in vitro* P-solubilizing efficacy and genetic potential (**Table 1**), *Ochrobactrum* sp. SSR was selected for expression analysis of PS-related genes as compared to the other two potential PSB (*Enterobacter* spp. ZW32 and ZW9). Therefore, a pot experiment was carried out in the soil amended with RP to evaluate the effect of SSR inoculation on wheat growth and root architecture concomitantly with expression of key PS related genes.

Effects of *Ochrobactrum* sp. SSR Inoculation on Wheat Plants and Soil Amended With RP

The PSB *Ochrobactrum* sp. SSR was evaluated for phosphate-solubilizing potential in soil amended with insoluble RP under the greenhouse conditions at National Institute for Biotechnology and Genetic Engineering (NIBGE), Faisalabad (31°25′0″N 73°5′28″E). Seeds of the wheat variety Faisalabad-2008 were surface sterilized with sodium hypochlorite (1.5%) and sequentially washed with sterile water. For the inoculum preparation, a single colony of SSR was grown in Luria–Bertani (LB) broth medium at 28 ± 2°C for 24–48 h. Sterilized seeds were inoculated with SSR (1×10^9 CFU ml^{-1}) for 30 min. Un-inoculated seeds dipped in LB medium were used as control. Two seeds per treatment were sown in cylindrical pots (10-cm diameter) filled with 300-g soil (loam texture, 0.57 % organic matter, pH 8, and 2 mg kg^{-1} available P) per pot.

The four biological treatments, i.e., T_1: SSR-inoculated seeds and soil amended with 45-mg P in the form of RP; T_2: Un-inoculated seeds and soil supplemented with 45-mg P in the form of RP; T_3: SSR-inoculated seeds and soil without RP; T_4: Un-inoculated seeds and soil without RP, each with six biological replicates, were arranged in a completely randomized design. All pots were provided with basic nutrient solution (Hoagland and Arnon, 1950) before sowing. Then T1 and T2 were provided with Hoagland without any P source while, T3 and T4 received Hoagland solution with complete nutrients. After germination, two plants per pot were grown and pots were watered as per requirement.

The plants were uprooted 30 days after sowing (DAS) and the plant growth parameters, i.e., root length, shoot length, plant dry, and fresh weight were determined. The root morphological parameters, i.e., root length (cm), root surface area (cm^2), root volume (cm^3), root length per volume (cm m^{-3}), root diameter (cm), number of crossings, number of forks, and tips were

TABLE 1 | The qPCR primers for quantification of genes encoding for proteins involved in PS, i.e., *gcd, pqqC*, and *pho*.

Bacterial strain	Primer name	Primer sequence	Product length (bp)	Gene length (bp)	Reference
Ochrobactrum sp. SSR	F26_pqqC_F	GGGCTTGACCCCGACTATGT	360	783	This study
	R26_pqqC_R	CGACGGCATCCTGCTTTTCC			
	F_pqqE_F	TTYTAYACCAACCTGATCACSTC	725	-	Perez et al., 2007
	R_pqqE_F	TBAGCATRAASGCCTGRCG			
	F12_gcd_F	TCACGACCTCTGGGACTACG	847	2439	Rasul et al., 2021
	R12_gcd_R	CTTCCACAATTCCCGACCCG			
	P12_gcd_F	ATGTCACGGGCGTCGATCTG	131	265	This study
	P12_gcd_R	CGTGATCATCGGTCCGCCTA			
	P26_pqqC_F	GCTTTGCGGTGGGTGCTT	78	222	This study
	P26_pqqC_R	GTTCTGTCAGCGACGATGCG			
	P30_phosphatase_F	ATGCGCGACCGAAAGACC	19	191	Rasul et al., 2021
	P30_phosphatase_R	TGCTGGCGACGAGACGAA			

measured by using a rhizoscanner (Epson photo scanner V-700, USA) accompanied with WinRHIZO software (Regent Int. Co., Ltd. Canada).

Plant P was analyzed by the tri-acid digestion method according to Tandon (1993). Rhizosphere soil was analyzed for available P by the Olsen method (Olsen, 1954) and alkaline phosphatase activity by following the *p*-nitrophenyl method (Tabatabai and Bremner, 1969).

Quantitative Real Time PCR (qRT-PCR)

To validate the persistence of inoculated PSB, wheat rhizosphere soil was collected from inoculated treatments of the pot experiment at 30 DAS and qRT-PCR was performed for expression analysis of PSB genes. Strain-specific (*Ochrobactrum* sp. SSR) primers for genes, i.e., glucose dehydrogenase (*gcd*), pyrroloquinoline quinone biosynthesis protein C gene *pqqC* and phosphatase (*pho*) responsible for P solubilization were used for expression analysis.

Primers Designing and Phylogenetic Analysis of PS-Related Genes

The primers for the amplification of *pqqC* genes of *Ochrobactrum* sp. SSR, encoding proteins involved in inorganic P solubilization were designed according to Rasul et al. (2021). The primers for *gcd* and *pho* gene of *Ochrobactrum* sp. SSR have been designed and reported in our preceding study (Rasul et al., 2021). The primers used in PCR amplification to evaluate the functionality and to authenticate the predicted sizes of amplicons (**Table 1**). The PCR conditions were 98°C for 3 min, followed by 35 cycles of 95°C for 60 s followed by 54°C for 60 s, 72°C for 60 s and final elongation at 72°C for 10 min. The amplified PCR-products were run on agarose gel (1%) at 80 V for 45 min. The PCR products were purified using PCR purification kit (QIAGEN Science, USA) and sequenced by Macrogen (Seoul, Korea). The obtained sequences were aligned and compared to sequences available at NCBI (https://www.ncbi.nlm.nih.gov/) and deposited to GenBank. Phylogenetic analysis was carried out by using MEGA6 software by using maximum likelihood method (Kumar et al., 2016).

Primer Design for qRT-PCR

Gcd and *pqqC* primers for qRT-PCR were designed for *Ochrobactrum* sp. SSR and were used in PCR amplifications to verify the amplification of the predicted amplicon sizes (**Table 1**). The primers for *pho* gene were designed and reported in the previous study (Rasul et al., 2021). The *Gcd* gene was selected as reference gene to normalize and validate qRT-PCR experiment by screening relative expression (based on fold change values) of candidate genes, i.e., *pqqC* and *pho* genes.

The RNA Extraction and cDNA Synthesis

The RNA was extracted from the soil with FastRNA spin Kit (MP, Biomedical, USA) by following the manufacturer's instructions. The cDNA was synthesized using First-Strand cDNA Synthesis Kit (Invitrogen, California, USA). The quality and quantity of cDNA were analyzed using Nanodrop 2000 (Thermo 262 Scientific, United States).

Expression Analysis by qRT-PCR

Bio-Rad RT-PCR (Bio-Rad, Hercules, USA) with SYBR Premix ExTaq kit (Takara Bio, USA) were used for expression analysis. A 25-μL reaction mixture contained 12.5-μL SYBR Green Master, 0.2-μL forward primer (10 μM), 0.2-μL reverse primer (10 μM), 2-μL cDNA, and 10.1 μL deionized water. The amplification conditions were as follows: The initial denaturation at 95°C for 5 min, 35 cycles of 95°C for 30 s followed by 54°C for 30 s, and 72°C for 30 s. The melting curve was analyzed from 54°C to determine the primer specificity.

The data were calculated as described by Javaid et al. (2016) and the expression level of target gene *pqqC* and *pho* were normalized with the C_t-value of reference gene (*gcd*). All samples were analyzed in three replicates.

Designing of Bioformulations Based on PSB-Consortium and Organic Amendments

Four different carrier materials, i.e., BC, CM, filter mud (FM), and HA were used to design bioformulations with PSB consortium comprising of well characterized strains (*Ochrobactrum sp.* SSR, *Enterobacter* spp. ZW32, and ZW9). The BC was obtained from wheat straw by pyrolysis in an automated furnace at 350°C with a resident time of 1 h and at a constant heat rate, i.e., 10°C min^{-1} (Abbas et al., 2020). The CM was derived from cow dung together with nitrogen-rich plant material and was obtained from Microbial Ecology Lab (NIBGE, Pakistan). The FM was obtained from decantation and filtration of sugarcane waste product (Suleman et al., 2018). The HA was extracted by alkali treatment of lignite as described by Ghani et al. (2021).

The standard procedures were followed for the characterization of carrier materials. The pH of the carrier materials was estimated by using pH meter (Phs-3c, Rex, China) according to Thomas (1996). The electric conductivity of soil was determined by using electric conductivity meter (DDS307A, Rex, Shanghai; Rhoades, 1993). The soil organic matter was estimated by Walkley black wet digestion method (Nelson and Sommers, 1996). Kjeldal method was used to measure total nitrogen (Bremner and Mulvaney, 1982). Elemental analysis of N and C was further validated by using CHNS analyzer (Perkin Elmer, Massachusetts, United States). The total P was determined by vanadate-molybdate method (Olsen, 1954).

The carrier materials were ground, sieved through 2-mm sieve and autoclaved. For the development of consortium, PSB strains, i.e., *Ochrobactrum* sp. SSR, *Enterobacter* spp. ZW32, and ZW9 were grown in LB broth medium separately at 28 ± 2°C for 24–48 h. The consortium (1×10^9 CFU ml^{-1}) was developed by mixing equal volume of each of the bacterium that are grown in LB. The bacterial suspension was mixed uniformly and aseptically with the carrier material to allow an adequate evenness to the final mix. Each carrier was prepared aseptically by adding 300 ml of bacterial suspension to 700 g of carrier and mixed well. The negative controls were also prepared by aseptically adding 300 ml of un-inoculated LB broth to 700 g of carrier. Each bioformulation and negative controls were prepared in triplicates, stored in polythene bags and were incubated at 28°C until the sampling time (Pastor-Bueis et al., 2019).

Shelf Life Study of Bioformulations

The survival of the inoculated PSB was assessed in all tested formulation at different time intervals, i.e., after 15, 30, 60, 90, 180, and 270 days. Three samples from each formulation were collected at each sampling date and analyzed for survival of the PSB inoculum. The bacterial viability was estimated for each sample by four-fold serial dilutions on LB agar and NBRIP (National Botanical Research Institute's Phosphate) (Nautiyal, 1999) agar supplemented with tri-calcium phosphate as source of P. The mean values of PSB viable count per gram of carrier material was calculated at each time interval and plotted on logarithmic scale (Pastor-Bueis et al., 2019).

Morphological and Elemental Analysis of Bioformulations by Scanning Electron Microscopy With Energy Disruptive X-Ray Spectroscopy Microanalysis (SEM/EDS)

Morphology or surface features of PSB inoculated and un-inoculated bioformulations were observed using field emission scanning electron microscopy (FESEM). The predominant chemical elements were determined by element microanalysis through EDS with a JEOL SEM microscope JSM 6490-LV model at a voltage range 10–20 kV and 1,000–10,000 magnification (Shahzad et al., 2019).

In-vivo Evaluation of Bioformulations in Earthen Pots Under Net House Conditions

The bioformulations were evaluated for their impact on wheat grain yield and plant P content under net house conditions at NIBGE, Faisalabad (31°23'45.1 "N, 73°01'3.4"E) in earthen pots through wheat-growing season November 2018 to April 2019. The seeds of wheat variety Faisalabad-2008 were surface sterilized as illustrated in preceding section. After sterilization, the seeds were pelleted with each bioformulation (@ 50-kg seeds kg^{-1}carrier material), separately and kept for 30 min. Un-inoculated pelleted seeds (with carrier materials) were used as control.

The sowing was done in the earthen pots (30-cm diameter) filled with 12-kg soil (loamy texture, pH 8.2, soil available P 1.9 mg kg^{-1} and organic matter 0.6%) and watered prior to sowing. The soil was supplemented with 80% recommended di-ammonium phosphate (DAP) dose (i.e., 20% reduced DAP). Eight treatments, six biological replicates, and four plants per pot were arranged in two factorial completely randomized design (**Supplementary Table S2**). Fertilizers were applied as per the recommendations, where DAP (150-mg kg^{-1} soil) and urea (75-mg kg^{-1} soil) in split doses were supplemented at the time of sowing and with first and second watering.

After 35 days of sowing plants were uprooted and multiple plant growth parameters (root length, shoot length, and plant dry weight) were evaluated. At maturity, plants were harvested and wheat yield parameters, i.e., number of tillers, grain yield, plant biomass, and plant height were recoded. Plant P content (Tandon, 1993), available P (Olsen, 1954), and alkaline phosphatase activity of soil (Tabatabai and Bremner, 1969) were analyzed by standard protocols.

In planta Evaluation of Bioformulation for Wheat Yield Parameters Under Field Conditions

Microplot Experiment

Based on the improved wheat yield and higher P-solubilizing potential in the net house experiment, the FM-based bioformulation was selected and evaluated in microplots at NIBGE. Each microplot was of the size of 1.5 × 1.5 m.

Three biological replicates for three treatments including seeds primed with bioformulation and soil supplemented with 80% of the recommended dose of DAP, i.e., 20% reduced dose and un-inoculated controls supplemented with 80 and 100% DAP

doses, respectively, were arranged in randomized complete block design. Seed pelleting of the wheat variety, Faisalabad-2008, was carried out as described in the previous section. The seeds were sown with the help of a dibbler in microplots. Fertilizers were applied as per recommendations (N: P, 15:100-kg ha^{-1}). The DAP and urea in split doses were applied at the time of sowing and subsequently with first and second irrigations.

Field Trial

A field trial was conducted to evaluate the selected bioformulation during winter season of November 2019–April 2020 at NIBGE, Faisalabad (31°23'45.1 "N, 73°01'3.4"E).Three biological replicates for three treatments, i.e., seeds primed with selected bioformulation provided with 80% recommended dose of DAP and un-inoculated controls supplemented with 80 and 100% doses of DAP, respectively were arranged in randomized complete block design. The seeds were sown by drill method in a plots size of 6 m × 6 m. Doses of fertilizers, treatments, and controls were similar to that applied in microplot experiment. While, standard agronomic practices were maintained throughout the experiment.

Estimation of Wheat Yield Parameters, Seed P, Available Soil P, and Phosphatase Activity

At maturity, the plants from both microplots and field trial were harvested and wheat yield parameters, i.e., number of tillers, grain yield, plant biomass, and plant height were recoded. Plant P content (Tandon, 1993), available P (Olsen, 1954), and alkaline phosphatase activity of soil (Tabatabai and Bremner, 1969) were analyzed by standard protocols.

Detection of Inoculated PSB

The survival of inoculated PSB was evaluated through the viable count method (Somasegaran and Hoben, 2012). The persistence of inoculated PSB was confirmed by fluorescent *in situ* hybridization (FISH) equipped with confocal laser-scanning microscopy (CLSM) (Amann et al., 1995). Inoculated *Ochrobactrum* sp. SSR was detected by hybridizing the Cy3-labeled ALF1b probe. While FLUOS-labeled probe "EUB338" was used for the total bacterial population (Manz et al., 1996). An Argon–Ion laser was used for excitation of FLOUS at 488 nm and Cy3 at 514 nm. FV10-ASW 1.7 software was used for imaging (Schneider et al., 2012).

The morphological characteristics and multiple plant growth promoting traits, i.e., phosphate solubilization, production of gluconic acid, and zinc solubilization of re-isolated PSB were compared to that of inoculated PSB (Yasmin et al., 2016).

Statistical Analysis

The data derived from *in vitro* experiments, pot experiment and field trials were statistically analyzed by ANOVA. The least significant difference (LSD) compared the variations between the treatments at 1 and 5% confidence level for lab assessments and field trials respectively, by using software STATISTIX-10 (Tallahassee, FL, USA). For the principal component analysis SPSS 23.0 software (SPSS Inc., USA) was used. Box plots were generated for analysis of wheat yield parameters and soil parameters in an earthen pot experiment by using Origin Software 2020b (Origin Lab Corporation Northampton, MA, USA).

RESULTS

The PSB and Evaluation of Their P-Solubilization Potential in Different Insoluble P Sources

All tested PSB strains, i.e., *Ochrobactrum* sp. SSR, *Enterobacter* spp. ZW32, and ZW9 exhibited P-solubilizing activity in RP medium and phytate medium (**Supplementary Table S1**). The highest level of solubilized P from RP (112 μg ml^{-1}) was detected with SSR 15 DPI. The maximum P solubilization from phytate occurred 10 DPI for ZW32 and 3 DPI for ZW9 and SSR (**Supplementary Table S1**). The P released from phytate by SSR at 15 DPI (22 μg ml^{-1}) was considerably lower than from RP (112 μg ml^{-1}) (**Supplementary Table S1**).

Phylogenetic Analysis of Genes Responsible for P-Solubilization

The PQQ biosynthesis protein C related gene *pqqC* (GenBank under accession number OL342768) was amplified from genomic DNA of SSR. It showed 98% identity to *pqqC* nucleotide sequence of *Ochrobactrum* sp. (**Figure 1**).

Expression Analysis of *gcd*, *PqqC*, and *pho* Genes by qRT-PCR

The persistence of *Ochrobactrum* sp. SSR in wheat rhizosphere was estimated by gene expression analysis of the *gcd, pqqC*, and *pho* genes gene. Among the tested treatments, the highest abundance of SSR was observed in RP amended soil. The supplementation of the soil with RP led to increased *gcd*, *pqqC*, and *pho* expression level (**Figure 2D**).

The relative expression level of *pqqC* and *pho* gene was 23-fold and 29-fold higher than reference gene *gcd* in SSR inoculated treatment supplemented with RP, while the expression level of *pho* gene was 3-fold higher than *pqqC* gene. On the other hand, the relative expression level of *pqqC* and *pho* gene was 17-fold and 23-fold higher, respectively, than the reference gene *gcd* in SSR inoculated treatment without RP (**Figure 2D**), while the expression level of *pho* gene was 6-fold higher than that of *pqqC* gene. Collectively, the SSR-inoculated treatment supplemented with RP showed high expression levels for *pqqC* and *pho* gene, i.e., 6-fold higher compared to inoculated treatment without RP (**Figure 2D**).

Effects of PSB Inoculation on Wheat Plants and Soil Amended With Rock Phosphate

The effect of *Ochrobactrum* sp. SSR on wheat variety Faisalabad-2008 was evaluated in soil either amended or not with RP under controlled conditions. Increases in shoot length, root length, plant fresh weight and dry weight were recorded in plants with SSR and soil amended with RP as compared to the un-inoculated control. These changes were significant in the presence and

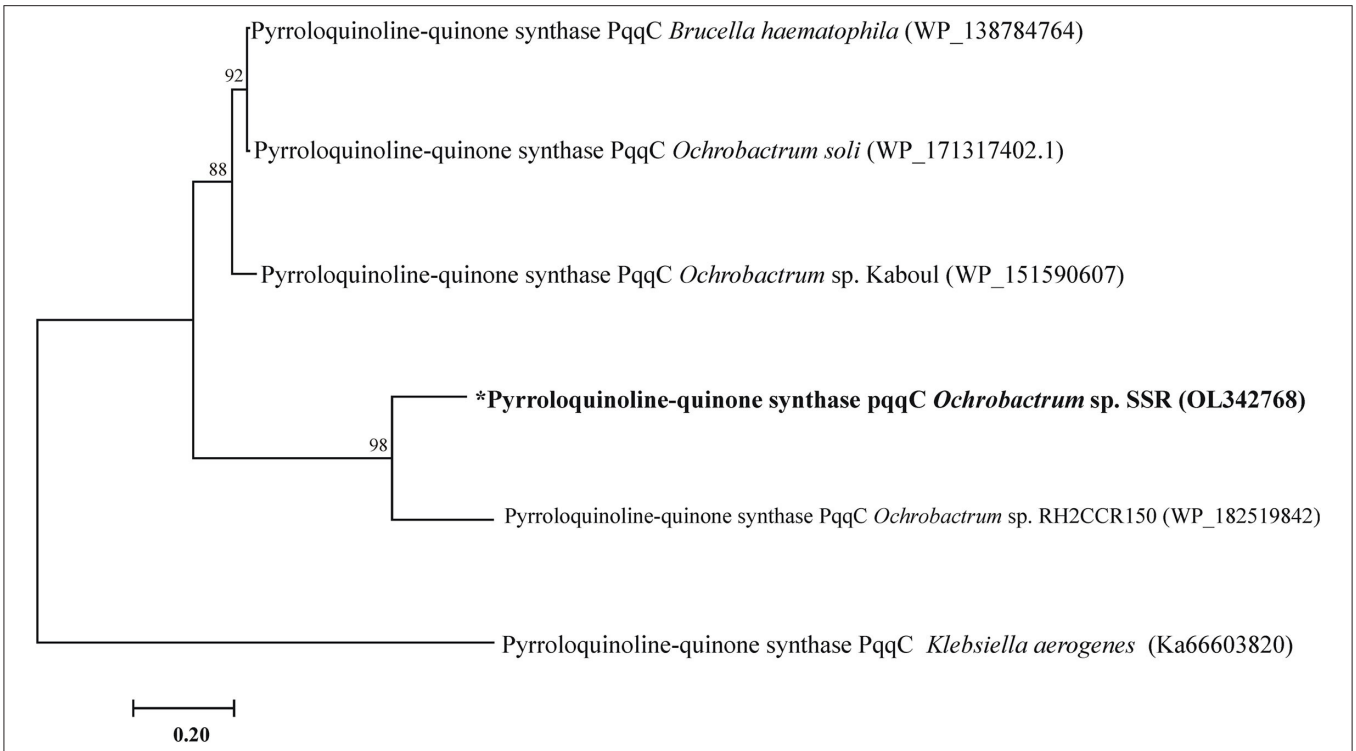

FIGURE 1 | Phylogenetic tree of pqqC gene of *Ochrobactrum* sp. SSR. Phylogenetic trees was constructed by maximum likelihood method.

absence of RP (**Figures 2A,B**; **Table 2**). The root morphological traits, i.e., root length, root volume, root surface area, root projection area, root tips and number of forks were also enhanced in inoculated plants (**Figure 2C**; **Supplementary Table S3**). Furthermore, we also observed increases in plant P (1.2–2.2%), available soil P (3.8–4.7 $\mu g\, g^{-1}$) and alkaline phosphatase activity (5.6–6.2 μmoles g^{-1} of soil h^{-1}) upon the treatment with the PSB (**Table 2**).

Shelf Life Study of Bioformulations

The survival of the three PSB, *Ochrobactrum* sp. SSR, *Enterobacter* spp. ZW32, and ZW9, was evaluated in bioformulations that were based on four carrier materials. These included BC, CM, FM, and HA. The PSB were less abundant in CM than other carrier materials at 15 DPI (**Figure 3**). All carriers maintained the inoculated PSB up to 180 DPI. However, after the course of 270 days, the FM showed significantly higher levels of the PSB than other carrier materials.

The inoculated PSB bacteria and the morphology of the bioformulations were investigated by FESEM. The PSB were detected in all four inoculated carrier materials (**Figures 4A,D,G,J**). Energy-dispersive X-ray spectroscopy was used to analyze the elemental composition of the surfaces of the bioformulations (**Figures 4C,F,I,L**). The data of SEM/EDS, CNHS, and biochemical analysis validates the presence of essential elements, i.e., N, K, C, and O in all tested carrier materials (**Figure 4**; **Supplementary Table S4**). However, it is also indicated that FM has more P than HA and CM. Only very low amounts of heavy metals Cu, Fe, and Cd were detected in the tested carrier materials (**Figure 5**).

In-vivo Evaluation of Bio-Formulations in Earthen Pots Under Net House Conditions

All bioformulations enhanced the wheat plant growth in the pot experiment under net-house conditions up to variable extent (**Figure 5**). However, FM-based bioformulation showed significant increase in grain yield as compared to respective control, i.e., un-inoculated carrier material (**Figure 5B**). Seed P increased significantly in FM-based bioformulated plants compared to un-inoculated FM (**Figure 5D**; **Supplementary Table S5**), with concomitantly increased soil available P (6.23 $\mu g\ g^{-1}$ soil) and alkaline phosphatase activity (24 μmoles g^{-1} of soil h^{-1}) (**Figures 5E,F**; **Supplementary Table S6**).

The Performance of the Filter Mud Bioformulation in the Field

Based on the persistence of inoculum in FM, and the highly promising plant growth promoting effects of the PSB with FM in the earthen pot experiment, FM-based bioformulation was tested under field conditions. The FM-based PSB bioformulation enhanced not only wheat grain yield and plant biomass, but also seed P, soil available P, and soil alkaline phosphatase activity (**Table 3**).

A positive correlation was found between P-solubilization by SSR, ZW32, and ZW9 in presence of different insoluble P sources,

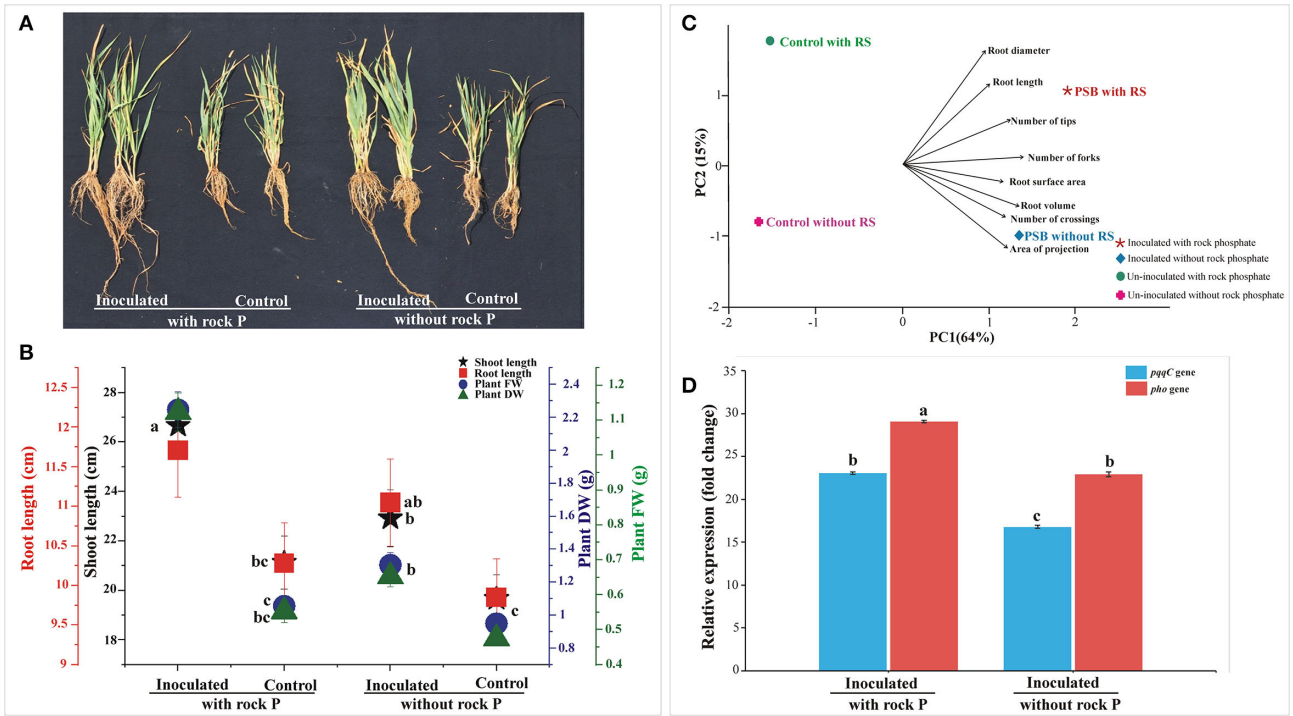

FIGURE 2 | *In vivo* Screening of PSB inoculation in soil amended with RP and analysis of bacterial gene expression. The data was recorded at 30 days of cultivation. Plants were used to evaluate different plant growth parameters **(A,B)** and root parameters **(C)**. Principal component analysis linking SSR inoculation to wheat root architecture **(C)**. The components elucidate a total variance of 79%. The loadings showed strength and direction of root parameters in dataset. The relative expression profile of *pqqC* and *pho* encoding gene of *Ochrobactrum* sp. SSR, expressed in the soil of the different treatments **(D)**. The data represents the relative fold changes in the expression values of the *pqqC* and phosphatase gene of *Ochrobactrum* sp. SSR in the soil with respect to *gcd* gene. Bars with distinct alphabetical letters are significantly different at $p \leq 0.05$.

TABLE 2 | Evaluation of PSB on wheat grown in soil amended with unavailable form of P under controlled conditions.

Treatments	Fresh weight (g plant^{-1})	Dry weight (g plant^{-1})	Shoot length (cm)	Root Length (cm)	Plant P(%)[a]	Soil available P[b]	Phosphatase activity[c]
Inoculated with RP	2.25 ± 0.11 A	1.12 ± 0.06 A	26.67 ± 1.33 A	11.71 ± 0.59 A	2.25 ± 0.16 A	4.70 ± 0.23 A	6.24 ± 0.31 A
Control with RP	1.06 ± 0.05 C	0.55 ± 0.03 BC	21.13 ± 1.06 BC	10.28 ± 0.51 BC	0.94 ± 0.07 C	3.12 ± 0.16 C	3.03 ± 0.15 C
Inoculated without RP	1.31 ± 0.07 B	0.65 ± 0.03 B	22.92 ± 1.15 B	11.05 ± 0.55 AB	1.19 ± 0.06 B	3.81 ± 0.19 B	5.65 ± 0.26 B
Control without RP	0.95 ± 0.05 C	0.48 ± 0.02 C	19.66 ± 0.98 C	9.85 ± 0.49 C	0.58 ± 0.03 D	2.33 ± 0.15 D	2.66 ± 0.15 D

Evaluation of PSB on wheat growth, in soil amended with unavailable form of P under controlled conditions. The data were collected 30 DAS and shown as averages ± standard deviation of six replicates.

[a]Plant P Content is given in % of the total plant weight, [b]Soil available P is represented by μg/gram of soil weight. [c]Soil phosphatase activity is presented in μmoles/g of soil/h. The mean values followed by different letters are significantly different at $p > 0.05$ according to LSD.

and soil available P, soil phosphatase activity, seed P content, and grain yield of field grown inoculated wheat variety Faisalabad-2008 with 20% reduced DAP fertilization application (**Figure 6**). The PCA plot revealed correlation between different parameters, where the two principal components contributed up to 87% toward variance on *x*-axis (PC1 = 68%) and *y*-axis (PC2 = 19%). The plants inoculated with *Ochrobactrum* sp. SSR had significant (positive) impact on the grain yield, plant tillers, soil available P, soil phosphatase activity, seed P content of the wheat plants. No parameter was found to have negative effects by inoculation with the potential PSB.

Detection of Inoculated PSB

The presence of inoculated PSB in wheat rhizosphere soil from earthen pot experiment was confirmed by plating and counting the bacteria and FISH at 35 days after seeding (**Figure 7**). The root colonization was studied by FISH–CLSM of inoculated wheat roots. The FLUOS-labeled green probe EUB338 showed the total bacterial population (**Figure 7**). The Cy3-labeled ALF1b probe predominantly detects the presence of *Ochrobactrum* sp. SSR population in the PSB inoculated treatments as indicated by red cells (**Figures 7B–E**). Of note, the highest density of the red cells was observed in FM carrier material (**Figure 7D**).

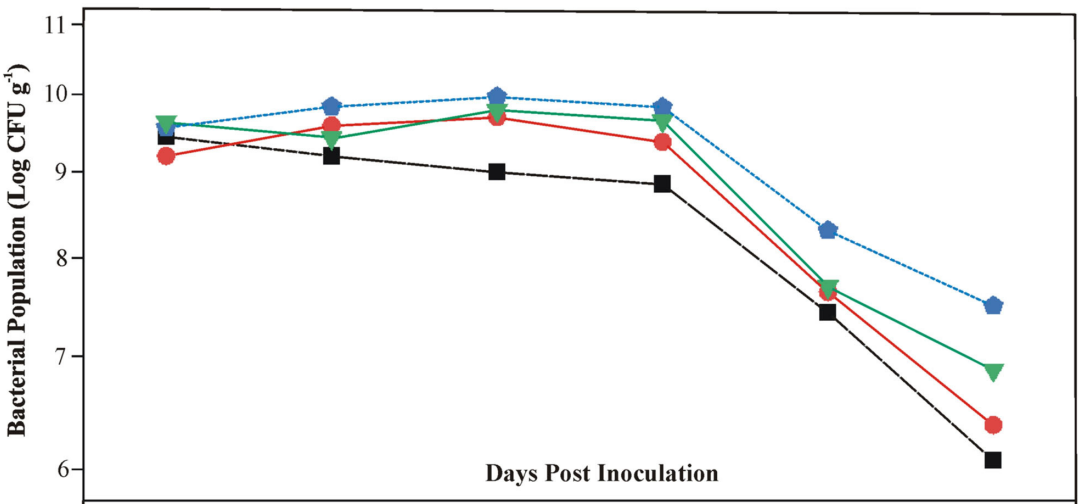

	15	30	60	90	180	270
Biochar	9.52 A	9.20 B	9.00 B	8.85 C	7.43 A	6.08 C
Compost	9.20 B	9.59 AB	9.70 A	9.38 B	7.64 A	6.38 BC
Filter Mud	9.57 A	9.84 A	9.97 A	9.83 A	8.31 A	7.50 A
Humic acid	9.64 A	9.43 AB	9.79 A	9.65 A	7.70 A	6.87 B
F value	9.40***	2.63 ns	9.74***	28.8***	1.22 ns	11.2***

FIGURE 3 | The shelf life of bioformulations to assess the survival of inoculated PSB in different carrier materials. Each point represents decimal logarithmic of viable cells g^{-1} carrier material and it is the mean value of three replicas. The ANOVA has been performed within each sampling date, thus within each column in data table, and the F and significance values (***$p \leq 0.001$, ns not significant) are provided; the values followed by the same letter, within each column, are not significantly different at $p < 0.05$ in the LSD test.

The re-isolated colonies of PSB, i.e., *Ochrobactrum* sp. SSR, *Enterobacter* spp. ZW32, and ZW9 were identified based on their morphological characteristics and plant growth promoting attributes, i.e., phosphate solubilization (279–359 μg ml^{-1}), gluconic acid production (113–129 μg ml^{-1}), and indole acetic acid production (30–45 μg ml^{-1}).

DISCUSSION

The development and use of the microbial inoculants has elicited great interest in the recent years since it presents a sustainable alternative for the application of chemicals fertilizes (Romano et al., 2020). However, the biofertilizer products still face major challenges, associated with the limited shelf life and the persistence of inoculant in different environments, and this limits their use in agriculture (Basu et al., 2021). To tackle this problem, we constructed a bioformulation that entails three plant growth promoting bacteria carried by FM. Our results suggest that the designed bioformulation has a long shelf life, is persistent in soil, and effective for both greenhouse and field applications.

The applied bacterial strains solubilized RP and phytate. Previously these bacteria were reported to solubilize P from tricalcium phosphate (Yahya et al., 2021). Our data supports the view that the utilization of multiple P sources by bacteria assures that they release P in different substrates and environments, and exhibit a strong potential for applications (Wan et al., 2020). We suggest that the successive analysis of TCP, RP and phytate solubilization by potentially novel plant beneficial bacteria provides a useful approach to obtain PSB that release P effectively in different soils.

To determine the genetic features of SSR that may contribute to the higher P solubilization, *pqqC* gene related to PQQ biosynthesis was amplified and analyzed phylogenetically. To this end new primers were designed that specifically amplify *pqqC* gene of *Ochrobactrum* genus. The *pqqC* encodes pyrroloquinoline quinone biosynthesis protein C, a well characterized enzyme that catalyze the final step of PQQ biosynthesis pathway. It is involved in oxidation and cyclization of 3*a*-(2-amino-2-carboxy-ethyl)-4 and 5-dioxo hexahydoquinoline dicarboxylic acid in the final step of PQQ biosynthesis (Meyer et al., 2011). In our previous studies, we revealed *gcd* (accession numbers MK883706), *pho* (accession

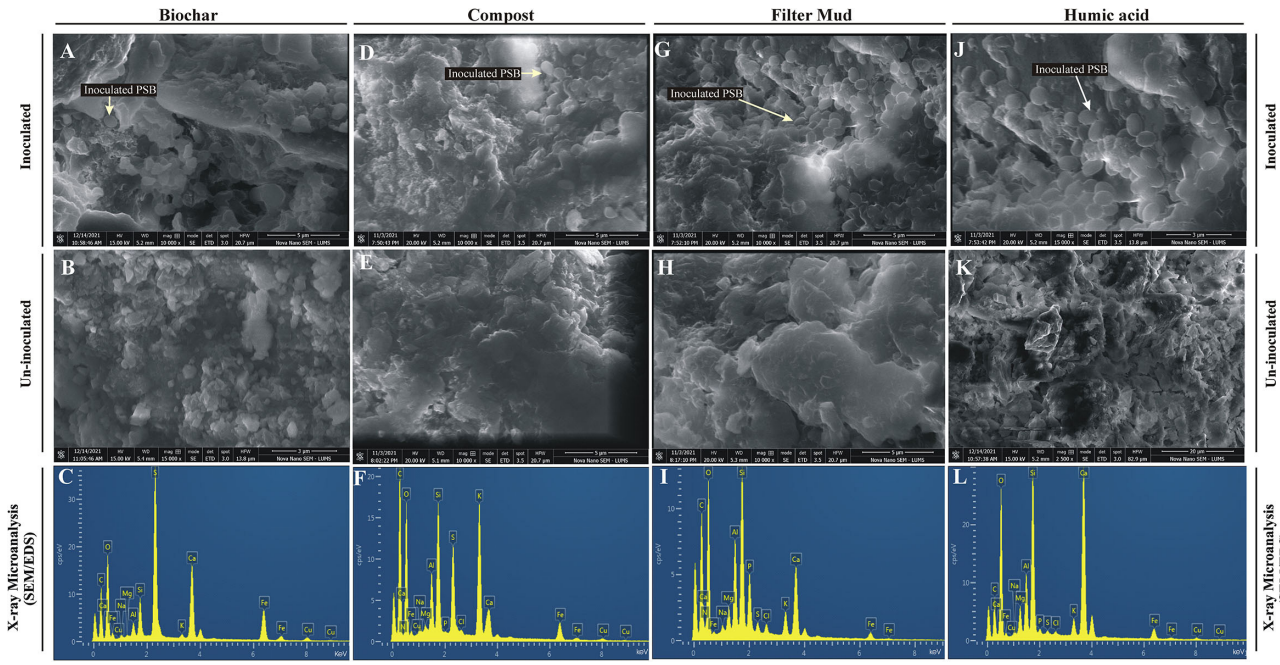

FIGURE 4 | Field emission scanning electron microscopic analysis and energy dispersive X-ray spectroscopy of bioformulations. FESEM analysis of inoculated Biochar **(A)**, compost **(D)**, filter mud **(G)** and Humic acid **(J)** to visualize PSB and composition/ structure of carrier materials compared to non-inoculated filter mud **(B)**, compost **(E)**, Biochar **(H)** and Humic acid **(K)**. The chemical elements microanalysis of the filter mud **(C)**, compost **(F)**, Biochar **(I)** and Humic acid **(L)** is analyzed through EDS.

numbers MK883704; Rasul et al., 2021), and *pqqE* genes (accession numbers MT897167; Yahya et al., 2021) containing *Ochrobactrum* sp. SSR is multifaceted PSB. The *pqqC* and *pqqE* genes of strain SSR were amplified and known as most essential genes of PQQ operon. The biosynthesis of PQQ is only accomplished when the complex of gene products, i.e., pqq A, B, D, and F gets attached to pqqC at the C-terminal and with pqqE at the N-terminal (Bhanja et al., 2021). The amplification of these essential genes is the significant contribution and can provide novel insights into understanding the PQQ biosynthesis pathway in *Ochrobactrum* sp.

New primers for qPCR were designed and reported for the first time as marker genes to directly link the gene expression with phosphate-solubilizing activity. These primers were successfully applied for real time quantitative analysis of functional genes, i.e., *pqqC, pho* and *gcd* in inoculated soils of a pot experiment. We observed higher soil available P and soil phosphatase activities with concomitant increased expression of *pqqC* and *pho* genes related to SSR in RP amended soil as compared to inoculated soil with available P. This significant increase in soil available P corresponds to high rock P-solubilizing potential of *Ochrobactrum* sp. SSR *in vitro*. The SSR performed profoundly even in the absence of un-available P source but more efficiently in the presence of un-available P rock-phosphate as validated by higher expression level of marker genes, i.e., *pqqC* and *pho* relative to the *gcd* expression level. The developed qPCR primers are useful molecular tools to quantitatively trace functional gene expression and abundance of SSR that can be linked to its P-solubilizing activity in the wheat rhizosphere. Our results are in line with globally coordinated nutrient addition experiments carried out in the UK, the USA, and South Africa by Widdig et al. (2019), which described that the P-solubilizing microbes can work more effectively in nutrient deprived soils. This leads to an increase in relative-abundance of PSB in plant rhizosphere. Similarly, a case study of rhizosphere soil from temperate beech forest revealed P-solubilizing efficacy of PSB get lowered in nutrient rich soils than soils with low nutrient availability (Nicolitch et al., 2016). Moreover, another study demonstrated that application of PSB in the soil significantly increased the soil available P and soil phosphatase activity in semi-arid soils with concomitant increased expression of *gdh* and *pqqC* genes in a microcosmic experiment (Saadouli et al., 2021).

The effects of PSB inoculation were not limited to phosphate solubilization only, but also extended to multiple root morphological traits, thus improving acquisition of P (**Table 2**). Inoculated wheat plants showed significant improvement in both above ground plant traits (i.e., plant P and shoot length) and belowground plant traits (i.e., root length, soil available P, and phosphates activity). This finding is consistent with the recent study by Elhaissoufi et al. (2020), reported improved above and below ground parameters of PSB-inoculated wheat plants. The root morphological traits indicated root proliferation that significantly correlated with root/shoot P contents. This roots foraging and proliferation could lead to a greater P uptake.

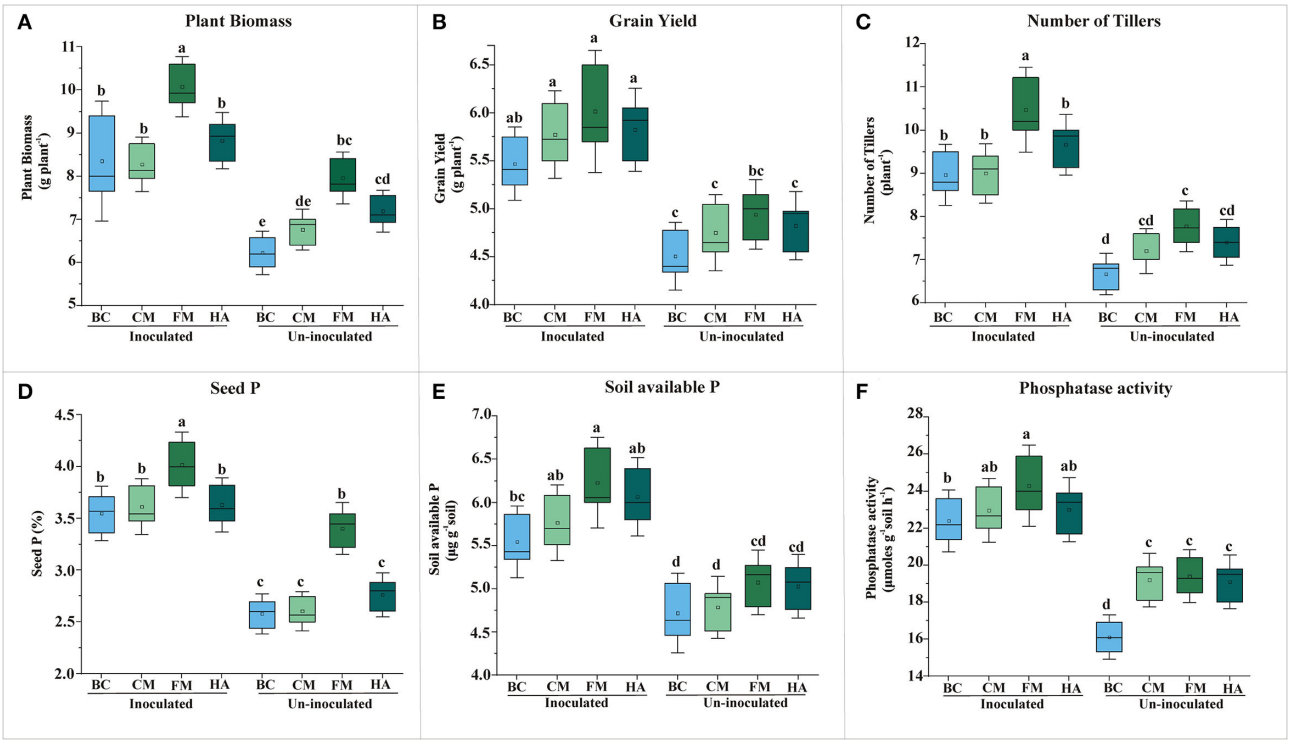

FIGURE 5 | Evaluation of PSB bioformulations for plant yield and soil P contents of wheat grown soil compared to un-inoculated controls. The effect of bioformulation on plant biomass **(A)**, grain yield **(B)**, number of tillers **(C)**, seed P **(D)**, available P of soil **(E)**, and phosphatase activity **(F)**. The mean values are an average of six biological replicates organized in completely randomized design. The mean values followed by different letters are significantly different at $p = 0.05$. BC, Biochar; CM, Compost; FM, Filter mud; HA, Humic acid.

TABLE 3 | Effect of Filter mud bioformulation and PSB consortium on plant growth and yield of wheat in microplots and field conditions.

Microplot trial	Treatments	No. of tillers (tillers plant^{-1})	Plant height (cm)	Plant biomass (kg plot^{-1})	Grain yield (kg plot^{-1})	Seed P content (%)	Soil available P (µg g^{-1} soil)	Phosphatase activity(µmoles g^{-1} soil h^{-1})
	Inoculated (80%)	13.33 ± 0.76 A	106.67 ± 5.03 A	2.36 ± 0.18 A	0.93 ± 0.04 A	4.15 ± 0.30 A	6.06 ± 0.28 A	26.63 ± 1.19 A
	Un-inoculated (80%)	8.53 ± 0.43 C	98.33 ± 5.03 A	1.93 ± 0.11 B	0.83 ± 0.04 B	3.36 ± 0.14 B	3.73 ± 0.27 C	19.33 ± 0.85 B
	Un-inoculated (100%)	10.07 ± 0.60 B	104.33 ± 5.51 A	2.11 ± 0.17 AB	0.87 ± 0.03 AB	3.68 ± 0.16 B	5.73 ± 0.31 B	24.73 ± 1.04 A
Field trial	**Treatments**	**No. of tillers (tillers m^{-2})**	**Plant height (cm)**	**Plant biomass (kg ha^{-1})**	**Grain yield (kg ha^{-1})**	**Seed P content (%)**	**Soil available P (µg g^{-1} soil)**	**Phosphatase activity (µmoles g^{-1} soil h^{-1})**
	Inoculated (80%)	468 ± 27 A	106 ± 5.31 A	14,667 ± 733 A	4,805 ± 224 A	4.60 ± 0.32 A	7.34 ± 0.34 A	26.67 ± 1.61 A
	Un-inoculated (80%)	369 ± 20 B	104 ± 5.03 A	12,317 ± 615 B	4,127 ± 220 B	3.30 ± 0.20 B	4.67 ± 0.20 C	19.67 ± 0.97 B
	Un-inoculated (100%)	389 ± 17 B	105 ± 5.22 A	13,167 ± 658AB	4,556 ± 210 AB	4.23 ± 0.23 A	5.91 ± 0.29 B	21.33 ± 1.12 B

Wheat grown in microplots under net house and field conditions during winter wheat season 2018–2019. The FM bioformulation Inoculated and respective un-inoculated control were supplemented with 20% reduced application of DAP. Seeds were pelleted with FM bioformulation containing PSB consortium (1 × 10^9 CFU ml^{-1}). The mean values are an average of three biological replicates arranged in completely randomized design. The mean values followed by different letters are significantly different at $p > 0.05$ according to LSD. Area of each microplot was 2.25 m^2 with a total number of 54 plants grown in each microplot. Each treatment of field trial has plot size of 6 m × 6 m and seed rate was @123.5 kg ha^{-1}.

After the confirmation of genetic potential of SSR to solubilize recalcitrant-P, the present work is focused on designing the optimal inoculant formulation based on this elite strain SSR along with two other well-characterized and compatible PSB strains *Enterobacter* spp. ZW32 and ZW9 to develop consortium for wheat to be applied under field conditions. Application of consortium can improve plant growth and increase the crop yield as compared to application of single bacterium (Backer, 2018; Mpanga et al., 2019). Although an elite PSB strains with consistent performance under field conditions

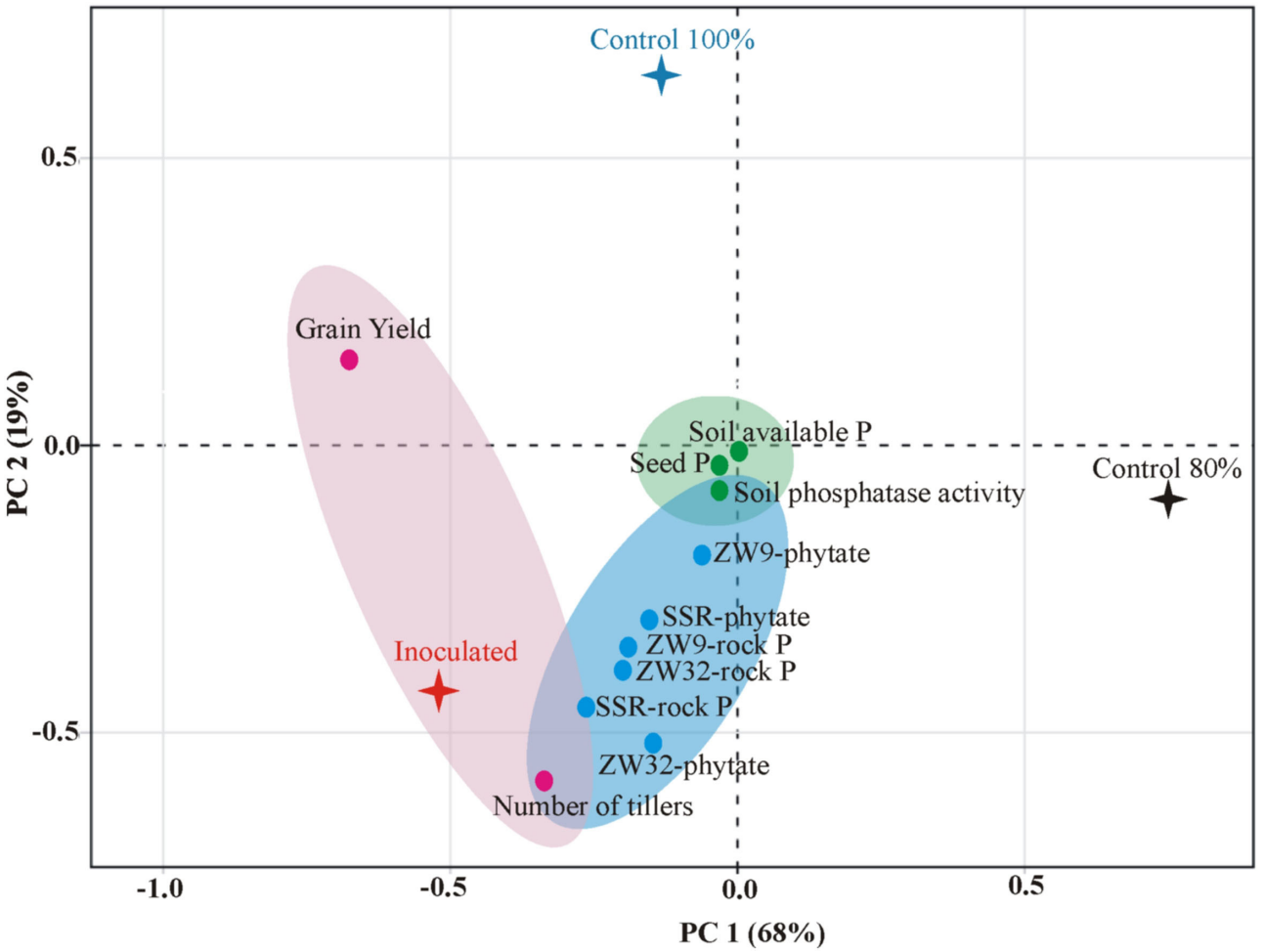

FIGURE 6 | Principal component analysis depicting the response of PSB inoculation to wheat yield parameters, plant, and soil P content. The components elucidate a total variance of 87%. The points represent mean values of each combination of seed P, wheat yield parameters (grain yield and number of tillers), soil P contents (available P and phosphatase activity), and the treatments (PSB inoculation and un-inoculated controls).

is essential for successful inoculant development, the non-biological components are still the key bottlenecks in commercial development of the inoculants (Pastor-Bueis et al., 2019; Mendoza-Suárez et al., 2021). Four different carrier materials, i.e., BC; CM; FM, and HA were used to design bioformulations with PSB-consortium based on autochthonous strain *Ochrobactrum* sp. SSR. Two other PSB strains used in consortium were well characterized *Enterobacter* spp. DSM 109592 and DSM 109593.

The elemental analysis of all carrier materials was performed with SEM accompanied with EDS. The data of SEM/EDS (**Figure 4**), CNHS, and biochemical analysis validates the presence of essential elements, i.e., N, K, C, and O in the tested carrier materials (**Supplementary Table S4**). However, P content of FM was higher than HA and CM. Non-significant amount of heavy metals Cu, Fe, and Cd were detected in all tested carrier materials. The essential heavy metals such as Cu, Fe, Mn, and Zn are required for various biochemical and physiological processes of plant (Yan et al., 2020), but they may become toxic when present in excess. Therefore, the carrier materials with low amount of essential heavy metals are the potential candidates for the development of successful bioformulation.

The shelf-life assessment of well-characterized biostimulants revealed that all carriers maintained adequate survival of PSB to a variable extent up to 180 days period. The FM showed significantly higher bacterial load as compared to rest of the tested carrier materials predominantly up to 270 DPI (**Figure 3**). The persistence of inoculated PSB in carrier materials was further validated by FESEM. This indicates that FM-based carrier material provided more suitable microenvironment for inoculated PSB and maintained longer shelf life. This is an essential attribute of carrier materials for maintenance of microbial-viability without any special need of storage facility (Soumare et al., 2020). Besides, very few studies have focused on selection and development of

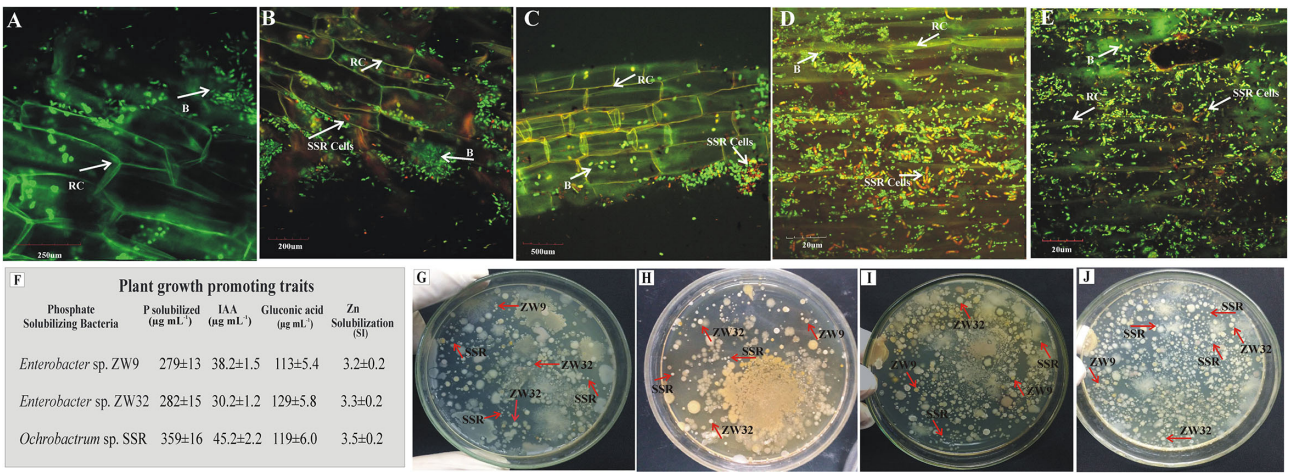

FIGURE 7 | Re-isolation and detection of inoculated P-solubilizing bacteria. The CLSM of wheat roots at 35 days post inoculation of P-solubilizing bacteria in the pot experiment under net house conditions. The FLUOS-labeled oligonucleotide probes showed green fluorescent signals for total bacterial population and Cy3-labeled oligonucleotide probes showed red fluorescent signals for inoculated *Ochrobactrum* sp. SSR. **(A)** Control treatments without inoculation and from the PSB inoculated pots with carrier materials **(B)** Biochar, **(C)** CM, **(D)** FM, and **(E)** HA after hybridizing with fluorescently labeled probes. The plant growth promoting traits of re-isolated PSB strains for their confirmation in comparison to pure PSB **(F)**. The plates depicting the re-isolated colonies of SSR, ZW32, and ZW9 from BC **(G)**, CM **(H)**, FM **(I)** and HA **(J)** in inoculated treatments. *Enterobacter* spp. ZW9, ZW32, *Ochrobactrum* sp. SSR. B, bacteria; RC, root cells.

carrier materials and their effect on bioinoculum as most of studies emphasized on the performance of microbial inoculants (Koskey et al., 2021).

After designing of potential biostimulants with adequate shelf life, the next step was to evaluate the inoculants under field conditions. The FM-based bioformulation showed a pronounced effect on wheat growth as indicated by significant improved grain yield (16%) and seed P content (15%) with concomitant inceresed in soil available P (18%) under net house conditions (**Figure 5**). Under the field conditions, significant increase in grain yield (5%), plant biomass (10%), soil available P (7%), and soil phosphatase activity (27 μmol g^{-1} soil h^{-1}) were observed in FM-based bioformulation compared to un-inoculated 80 and 100% controls (**Table 3**). The results are in line with some previous studies that shows the enhanced rice growth (Tahir et al., 2013) and wheat grain yield (Suleman et al., 2018) under agro–ecological conditions when seed pelleted with FM and PSB. Therefore, the FM can be adopted as a potent carrier material for the PSB aimed at improved soil nutrient availability, enhanced wheat grain yield, and decipher a key role as green alternative for imminent agricultural sustainability. Multiple traits of the PSB are directly involved in the bioavailability and P uptake by the plants. The PSB-enhanced nutrient-sensing capacity of the plants, which has already been made available by the secretion of bacterial organic acids (Chungopast et al., 2021; Yahya et al., 2021). The PSB modulates the morphology of root architecture and alleviates the P-stress by making P available in the soil and stimulating the plants to uptake P. This tripartite system could lead to improved crop vigor and yield.

The principal component analysis indicates a positive correlation between P solubilization by SSR, ZW32, and ZW9 in presence of different insoluble phosphate sources, and soil available-P, soil phosphatase activity, seed P content and grain yield of field grown inoculated wheat variety Faisalabad-2008 with 20% reduced application of DAP fertilizer (**Figure 6**). The agronomic performance of the potential inoculant tested under field trial, appraise the superiority of the inoculant. The various studies demonstrate that P-solubilizing microbes showed best effect with reduced application of DAP fertilizers (Suleman et al., 2018; Rosa et al., 2020; Rasul et al., 2021; Yahya et al., 2021).

The survival of inoculated PSB strains in wheat-rhizosphere was validated by viable count and FISH-CLSM, this shows that the inoculated PSB were rhizosphere-competent phosphobacteria. Furthermore, the plant growth promoting attributes of re-isolated PSB were compared to their pure cultures, indicates the persistence of inoculated PSB (**Figure 7**). The persistent colonization of PGPR in the rhizosphere is an indication that bacteria can carry out their functions (Hakim et al., 2021; Lopes et al., 2021) and form an association with local microbial community (Santoyo et al., 2021).

The ecological approach developed in the present study enabled us the development of biostimulators that can act as a soil conditioner in agriculture. These potential formulations can be a substitute to chemical fertilizers to optimize the use of natural phosphate in the world and improve resilience and yield of wheat crop. The deployment of such biostimulants containing multifaceted autochthonous *Ochrobactrum* sp. SSR and *Enterobacter* spp. ZW32 and ZW9 can offer a potential approach to mitigate P-induced stress in wheat plants. *Ochrobactrum*

sp. SSR exhibit pronounced potential in terms of modification of root morphology/architecture and increased real-time PS related genes expression to aid in transformation of insoluble P compounds into available forms for plant uptake, stimulate plant growth, and increase the crop yield.

CONCLUSIONS

This study provides a solid foundation to design well-characterized biostimulant formulation that deployed the multifaceted PSB and organic amendments based on agro-industrial by-products to improve the wheat growth and yield under P-deficient conditions. This is the first comprehensive research work that reports amplification of PS-related genes, i.e., *gcd*, *pqqC*, *pqqE*, and *pho* and real time expression of these genes by autochthonous *Ochrobactrum* sp. SSR, to release P from recalcitrant P forms. The successful biostimulant developed in this study is not only well-characterized but also extended the shelf life of highly efficient rhizosphere-competent P-solubilizers that ultimately led to sustainable wheat production for global food security.

DATA AVAILABILITY STATEMENT

The datasets presented in this study can be found in online repositories. The names of the repository/repositories and accession number(s) can be found in the article.

AUTHOR CONTRIBUTIONS

MY analyzed the data, wrote the manuscript, and executed statistical analysis. SY and MT performed data analysis and review the manuscript. MTT, TR, MR, and MY designed the primers. YS, IA, and MY performed the expression analysis. ZS, MT, and MS performed elemental analysis of carrier materials. AI helped in FISH analysis and in biochemical analysis of soils. SY conceived and supervised the whole study and edited the manuscript. All authors contributed to the article and approved the submitted version.

ACKNOWLEDGMENTS

We are highly grateful to Dr. Kalsoom Akhtar (DCS, NIBGE) from Industrial Biotechnology Division and Dr. Muhammad Afzal from Soil and Environmental Biotechnology Division for providing HA and guidance. Thanks is due to Mr. M. Sarwar (Technical Assistant, NIBGE) for his help in net house and field experiments.

SUPPLEMENTARY MATERIAL

The Supplementary Material for this article can be found online at: https://www.frontiersin.org/articles/10.3389/fmicb.2022.889073/full#supplementary-material

REFERENCES

Abbas, A., Naveed, M., Azeem, M., Yaseen, M., Ullah, R., and Alamri, S., et al. (2020). Efficiency of wheat straw biochar in combination with compost and biogas slurry for enhancing nutritional status and productivity of soil and plant. *Plants*. 9:1516. doi: 10.3390/plants9111516

Akanmu, A. O., Babalola, O. O., Venturi, V., Ayilara, M. S., Adeleke, B. S., Amoo, A. E., et al. (2021). Plant disease management: leveraging on the plant-microbe-soil interface in the biorational use of organic amendments. *Front. Plant Sci.* 12, 700507. doi: 10.3389/fpls.2021.700507

Amann, R. I., Ludwig, W., and Schleifer, K. H. (1995). Phylogenetic identification and in situ detection of individual microbial cells without cultivation. *Microbiol rev.* 59, 143–169. doi: 10.1128/mr.59.1.143-169.1995

Backer, R., Rokem, J. S., Ilangumaran, G., Lamont, J., Praslickova, D., Ricci, E., et al. (2018). Plant growth-promoting rhizobacteria: context, mechanisms of action, and roadmap to commercialization of biostimulants for sustainable agriculture, *Front. Plant Sci*. 1473. doi: 10.3389/fpls.2018.01473

Basu, A., Prasad, P., Das, S. N., Kalam, S., Sayyed, R., Reddy, M., et al. (2021). Plant growth promoting rhizobacteria (PGPR) as green bioinoculants: recent developments, constraints, and prospects. *Sustainability* 13, 1140. doi: 10.3390/su13031140

Bechtaoui, N., Rabiu, M. K., Raklami, A., Oufdou, K., Hafidi, M., and Jemo, M. (2021). Phosphate-dependent regulation of growth and stresses management in plants. *Front. Plant Sci.* 12, 679916. doi: 10.3389/fpls.2021.679916

Bhanja, E., Das, R., Begum, Y., and Mondal, S. K. (2021). Study of pyrroloquinoline quinine from phosphate-solubilizing microbes responsible for plant growth: in silico approach. *Front. Agron.* 3, 667339. doi: 10.3389/fagro.2021.667339

Bindraban, P. S., Dimkpa, C. O., and Pandey, R. (2020). Exploring phosphorus fertilizers and fertilization strategies for improved human and environmental health. *Biol. Fertil.* 56, 299–317. doi: 10.1007/s00374-019-01430-2

Bremner, J., and Mulvaney, C. (1982). "Nitrogen-total," in *Methods of Soil Analysis. Part 2. Chemical and Microbial Properties. No. 9*. Page, A. L., Miller, R. H., and Keeney, D. R. Madison, WI: American Society of Agronomy and Soil Science Society of America. Inc.

Brito, L. F., López, M. G., Straube, L., Passaglia, L. M., and Wendisch, V. F. (2020). Inorganic phosphate solubilization by rhizosphere bacterium Paenibacillus sonchi: gene expression and physiological functions. *Front. Microbiol.* 11, 588605. doi: 10.3389/fmicb.2020.588605

Castiglione, A., Brick, C., Holden, S., Miles-urdan, E., and Aron, A. (2021). Discovering the psychological building blocks underlying climate action-a longitudinal study of real-world activism. 1–34. doi: 10.31234/osf.io/jqz29

Chandran, H., Meena, M., and Swapnil, P. (2021). Plant growth-promoting rhizobacteria as a green alternative for sustainable agriculture. *Sustainability.* 13: 10986. doi: 10.3390/su131910986

Chen, Q., and Liu, S. (2019). Identification and characterization of the phosphate-solubilizing bacterium Pantoea sp. S32 in reclamation soil in Shanxi, China. *Front. Microbiol.* 10, 2171. doi: 10.3389/fmicb.2019.02171

Chungopast, S., Thongjoo, C., Islam, A. M., and Yeasmin, S. (2021). Efficiency of phosphate-solubilizing bacteria to address phosphorus fixation in Takhli soil series: a case of sugarcane cultivation, Thailand. *Plant Soil.* 460, 347–357. doi: 10.1007/s11104-020-04812-w

Elhaissoufi, W., Khourchi, S., Ibnyasser, A., Ghoulam, C., Rchiad, Z., Zeroual, Y., et al. (2020). Phosphate solubilizing rhizobacteria could have a stronger influence on wheat root traits and aboveground physiology than rhizosphere P solubilization. *Front. Plant Sci.* 11, 979. doi: 10.3389/fpls.2020.00979

Etesami, H., Jeong, B. R., and Glick, B. R. (2021). Contribution of arbuscular mycorrhizal fungi, phosphate–solubilizing bacteria, and silicon to p uptake by plant. *Front. Plant Sci.* 12, 699618. doi: 10.3389/fpls.2021.699618

Fasusi, O. A., cruz, C., and Babalola, O. O. (2021). Agricultural sustainability: microbial biofertilizers in rhizosphere management. *Agriculture.* 11, 163. doi: 10.3390/agriculture11020163

Ghani, M. J., Akhtar, K., Khaliq, S., Akhtar, N., and Ghauri, M. A. (2021). Characterization of humic acids produced from fungal liquefaction of low-grade Thar coal. *Process Biochem.* 107, 1–12. doi: 10.1016/j.procbio.2021.05.003

Hakim, S., Naqqash, T., Nawaz, M. S., Laraib, I., Siddique, M. J., Zia, R., et al. (2021). Rhizosphere engineering with plant growth-promoting microorganisms for agriculture and ecological sustainability. *Front. Sustain. Food Systs.* 5, 617157. doi: 10.3389/fsufs.2021.617157

Hoagland, D. R., and Arnon, D. I. (1950). The water-culture method for growing plants without soil, Circular. *Calif. Agri. Exper. Stat.* 347, 32. Available online at: http://hdl.handle.net/2027/uc2.ark:/13960/t51g1sb8j

Howson, S., and Davis, R. (1983). Production of phytate-hydrolysing enzyme by some fungi. *Enzyme Microbial Technol.* 5, 377–382. doi: 10.1016/0141-0229(83)90012-1

Javaid, S., Amin, I., Jander, G., Mukhtar, Z., Saeed, N. A., and Mansoor, S. (2016). A transgenic approach to control hemipteran insects by expressing insecticidal genes under phloem-specific promoters. *Sci. Rep.* 6, 1–11. doi: 10.1038/srep34706

Koskey, G., Mburu, S. W., Awino, R., Njeru, E. M., and Maingi, J. M. (2021). Potential use of beneficial microorganisms for soil amelioration, phytopathogen biocontrol, and sustainable crop production in smallholder agroecosystems. *Front. Sustain. Food Syst.* 5, 606308. doi: 10.3389/fsufs.2021.606308

Kumar, S., Stecher, G., and Tamura, K. (2016). MEGA7: molecular evolutionary genetics analysis version 7.0 for bigger datasets. *Mol. Biol. Evol.* 33, 1870–1874. doi: 10.1093/molbev/msw054

Liu, J., Cade-Menun, B. J., Yang, J., Hu, Y., Liu, C. W., Tremblay, J., et al. (2018). Long-term land use affects phosphorus speciation and the composition of phosphorus cycling genes in agricultural soils. *Front. Microbiol.* 9, 1643. doi: 10.3389/fmicb.2018.01643

Liu, X., Yuan, Z., Liu, X., Zhang, Y., Hua, H., and Jiang, S. (2020). Historic trends and future prospects of waste generation and recycling in China's phosphorus cycle. *Environ. Sci. Technol.* 54, 5131–5139. doi: 10.1021/acs.est.9b05120

Lobo, C. B., Juarez Tomas, M. S., Viruel, E., Ferrero, M. A., and Lucca, M. E. (2019). Development of low-cost formulations of plant growth-promoting bacteria to be used as inoculants in beneficial agricultural technologies. *Microbiol. Res.* 219, 12–25. doi: 10.1016/j.micres.2018.10.012

Lopes, M. J. D. S., Dias-Filho, M. B., and Gurgel, E. S. C. (2021). Successful plant growth-promoting microbes: Inoculation methods and abiotic factors. *Front. Sustain. Food Syst.* 5, 606454. doi: 10.3389/fsufs.2021.606454

Madende, M., and Hayes, M. (2020). Fish by-product use as biostimulants: An overview of the current state of the art, including relevant legislation and regulations within the EU and USA. *Molecules.* 25, 1122. doi: 10.3390/molecules25051122

Manz, W., Amann, R., Ludwig, W., Vancanneyt, M., and Schleifer, K. H. (1996). Application of a suite of 16S rRNA-specific oligonucleotide probes designed to investigate bacteria of the phylum cytophaga-flavobacter-bacteroides in the natural environment. *Microbiol.* 142, 1097–1106. doi: 10.1099/13500872-142-5-1097

Mendoza-Suárez, M., Andersen, S. U., Poole, P. S., and Sánchez-Cañizares, C. (2021). Competition, nodule occupancy, and persistence of inoculant strains: key factors in the rhizobium-legume symbioses. *Front. Plant Sci.* 12, 690567. doi: 10.3389/fpls.2021.690567

Meyer, J. B., Frapolli, M., Keel, C., and Maurhofer, M. (2011). Pyrroloquinoline quinone biosynthesis gene pqqC, a novel molecular marker for studying the phylogeny and diversity of phosphate-solubilizing pseudomonads. *Appl. Environ. Microbiol.* 77, 7345–7354. doi: 10.1128/AEM.05434-11

Mitter, E. K., Tosi, M., Obregón, D., Dunfield, K. E., and Germida, J. J. (2021). Rethinking crop nutrition in times of modern microbiology: innovative biofertilizer technologies. *Front. Sustain. Food Syst.* 5, 606815. doi: 10.3389/fsufs.2021.606815

Mogollón, J., Beusen, A., Van Grinsven, H., Westhoek, H., and Bouwman, A. (2018). Future agricultural phosphorus demand according to the shared socioeconomic pathways. *Glob. Environ. Chang.* 50, 149–163. doi: 10.1016/j.gloenvcha.2018.03.007

Molina-Romero, D., Juárez-Sánchez, S., Venegas, B., Ortíz-González, C. S., Baez, A., Morales-García, Y. E., et al. (2021). A bacterial consortium interacts with different varieties of maize, promotes the plant growth, and reduces the application of chemical fertilizer under field conditions. *Front. Sustain. Food Syst.* 4, 616757. doi: 10.3389/fsufs.2020.616757

Mpanga, I. K., Nkebiwe, P. M., Kuhlmann, M., Cozzolino, V., Piccolo, A., Geistlinger, J., et al. (2019). The form of N supply determines plant growth promotion by P-solubilizing microorganisms in maize. *Microorganisms.* 7, 111. doi: 10.3390/microorganisms7020038

Murphy, J., and Riley, J. P. (1962). A modified single solution method for the determination of phosphate in natural waters. *Anal. Chim. Acta.* 27, 31–36. doi: 10.1016/S0003-2670(00)88444-5

Nautiyal, C. S. (1999). An efficient microbiological growth medium for screening phosphate solubilizing microorganisms. *FEMS Microbiol. Lett.* 170, 265–270. doi: 10.1111/j.1574-6968.1999.tb13383.x

Nelson, D., and Sommers, L. E. (1996). "Total carbon, organic carbon, and organic matter," in *Methods of Soil Analysis: Part 2 Chemical and Microbiological Properties*, *Vol. 9*. Page, A. L., Miller, R. H., and Keeny, D. R. Madison, WI: ASA and SSSA. p. 539–579. doi: 10.2134/agronmonogr9.2.2ed.c29

Nguyen, C., Yan, W., Le tacon, F., and Lapeyrie, F. (1992). Genetic variability of phosphate solubilizing activity by monocaryotic and dicaryotic mycelia of the ectomycorrhizal fungus Laccaria bicolor (Maire) PD Orton. *Plant Soil.* 143, 193–199. doi: 10.1007/BF00007873

Nicolitch, O., Colin, Y., Turpault, M.-P., and Uroz, S. (2016). Soil type determines the distribution of nutrient mobilizing bacterial communities in the rhizosphere of beech trees. *Soil Biol.Biochem.* 103, 429–445. doi: 10.1016/j.soilbio.2016.09.018

Olsen, S. R. (1954). *Estimation of available phosphorus in soils by extraction with sodium bicarbonate*. Washington, DC: US Department of Agriculture.

Pastor-Bueis, R., Sánchez-Cañizares, C., James, E. K., and González-Andrés, F. (2019). Formulation of a highly effective inoculant for common bean based on an autochthonous elite strain of Rhizobium leguminosarum bv. phaseoli, and genomic-based insights into its agronomic performance. *Front. Microbio.* 10, 2724. doi: 10.3389/fmicb.2019.02724

Perez, E., Sulbaran, M., Ball, M. M., and Yarzabal, L. A. (2007). Isolation and characterization of mineral phosphate-solubilizing bacteria naturally colonizing a limonitic crust in the south-eastern Venezuelan region. *Soil Biol. Biochem.* 39, 2905–2914. doi: 10.1016/j.soilbio.2007.06.017

Rasul, M., Yasmin, S., Yahya, M., Breitkreuz, C., Tarkka, M., and Reitz, T. (2021). The wheat growth-promoting traits of *Ochrobactrum* and *Pantoea* species, responsible for solubilization of different P sources, are ensured by genes encoding enzymes of multiple P-releasing pathways. *Microbiol. Res.* 246, 126703. doi: 10.1016/j.micres.2021.126703

Rhoades, J. D. (1993). Electrical conductivity methods for measuring and mapping soil salinity. *ADV AGRON.* 49, 201–251. doi: 10.1016/S0065-2113(08)60795-6

Romano, I., Ventorino, V., and Pepe, O. (2020). Effectiveness of plant beneficial microbes: overview of the methodological approaches for the assessment of root colonization and persistence. *Front. Plant Sci.* 11, 6. doi: 10.3389/fpls.2020.00006

Rosa, P. A. L., Mortinho, E. S., Jalal, A., Galindo, F. S., Buzetti, S., Fernandes, G. C., et al. (2020). Inoculation with growth-promoting bacteria associated with the reduction of phosphate fertilization in sugarcane. *Front. Environ. Sci.* 8, 32. doi: 10.3389/fenvs.2020.00032

Saadouli, I., Mosbah, A., Ferjani, R., Stathopoulou, P., Galiatsatos, I., Asimakis, E., et al. (2021). The impact of the inoculation of phosphate-solubilizing bacteria pantoea agglomerans on phosphorus availability and bacterial community dynamics of a semi-arid soil. *Microorganisms.* 9, 1661. doi: 10.3390/microorganisms9081661

Santos, M. S., Nogueira, M. A., and Hungria, M. (2019). Microbial inoculants: reviewing the past, discussing the present and previewing an outstanding future for the use of beneficial bacteria in agriculture. *AMB Express.* 9, 1–22. doi: 10.1186/s13568-019-0932-0

Santoyo, G., Urtis-Flores, C. A., Loeza-Lara, P. D., Orozco-Mosqueda, M., and Glick, B. R. (2021). Rhizosphere colonization determinants by plant growth-promoting rhizobacteria (PGPR). *Biology.* 10, 475. doi: 10.3390/biology10060475

Sarr, P. S., Tibiri, E. B., Fukuda, M., Zongo, A. N., Compaore, E., and Nakamura, S. (2020). Phosphate-solubilizing fungi and alkaline phosphatase

trigger the P solubilization during the co-composting of sorghum straw residues with Burkina Faso phosphate rock. *Front. Environ. Sci.* 8, 559195. doi: 10.3389/fenvs.2020.559195

Schneider, C. A., R, W. S., and Eliceiri, K. W. (2012). NIH Image to ImageJ: 25 years of image analysis. *Nat. Methods.* 9, 671–675. doi: 10.1038/nmeth.2089

Shahzad, A., Saeed, H., Iqtedar, M., Hussain, S. Z., et al. (2019). Size-controlled production of silver nanoparticles by Aspergillus fumigatus BTCB10: likely antibacterial and cytotoxic effects. *J. Nanomater.* 2019, 1–14. doi: 10.1155/2019/5168698

Shahzad, S., Khan, M. Y., Zahir, Z. A., Asghar, H. N., and Chaudhry, U. K. (2017). Comparative effectiveness of different carriers to improve the efficacy of bacterial consortium for enhancing wheat production under salt affected field conditions. *Pak. J. Bot* 49, 1523–1530.

Somasegaran, P., and Hoben, H. J. (2012). *Handbook for rhizobia: methods in legume-Rhizobium technology*. New York, NY: Springer-Verlag.

Soumare, A., Boubekri, K., Lyamlouli, K., Hafidi, M., Ouhdouch, Y., and Kouisni, L. (2020). From isolation of phosphate solubilizing microbes to their formulation and use as biofertilizers: status and needs. *Front. Bioeng. Biotechnol.* 7, 425. doi: 10.3389/fbioe.2019.00425

Stamenkovi,ć, S., Beškoski, V., Karabegovi,ć, I., Lazi,ć, M., and Nikoli,ć, N. (2018). Microbial fertilizers: A comprehensive review of current findings and future perspectives. *Span. J. Agric. Res.* 16, 2171–9292. doi: 10.5424/sjar/2018161-12117

Suleman, M., Yasmin, S., Rasul, M., Yahya, M., Atta, B. M., and Mirza, M. S. (2018). Phosphate solubilizing bacteria with glucose dehydrogenase gene for phosphorus uptake and beneficial effects on wheat. *PLoS ONE.* 13, e0204408. doi: 10.1371/journal.pone.0204408

Tabatabai, M., and Bremner, J. (1969). Use of p-nitrophenyl phosphate for assay of soil phosphatase activity. *Soil Biol. Biochem.* 1, 301–307. doi: 10.1016/0038-0717(69)90012-1

Tahir, M., Mirza, M. S., Zaheer, A., Dimitrov, M. R., Smidt, H., and Hameed, S. (2013). Isolation and identification of phosphate solubilizer Azospirillum, Bacillus and Enterobacter strains by 16SrRNA sequence analysis and their effect on growth of wheat (Triticum aestivum L.). *Aust. J. Crop Sci.* 7, 1284–1292.

Tandon, H. L. S. (1993). *Methods of Analysis of Soils, Plants, Waters, and Fertilizers*. New Delhi: Fertiliser Development and Consultation Organization.

Thomas, G. W. (1996). Soil pH and soil acidity. *Methods of soil analysis: part 3 chemical methods*. 5, 475–490. doi: 10.2136/sssabookser5.3.c16

Vassilev, N., Vassileva, M., Martos, V., Garcia Del Moral, L. F., Kowalska, J., Tylkowski, B., et al. (2020). Formulation of microbial inoculants by encapsulation in natural polysaccharides: focus on beneficial properties of carrier additives and derivatives. *Front. Plant Sci.* 11, 270. doi: 10.3389/fpls.2020.00270

Wan, W., Qin, Y., Wu, H., Zuo, W., He, H., Tan, J., et al. (2020). Isolation and characterization of phosphorus solubilizing bacteria with multiple phosphorus sources utilizing capability and their potential for lead immobilization in soil. *Front. Microbiol.* 11, 752. doi: 10.3389/fmicb.2020.00752

Widdig, M., Schleuss, P.-M., Weig, A. R., Guhr, A., Biederman, L. A., Borer, E. T., et al. (2019). Nitrogen and phosphorus additions alter the abundance of phosphorus-solubilizing bacteria and phosphatase activity in grassland soils. *Front. Environ. Sci.* 7, 185. doi: 10.3389/fenvs.2019.00185

Yahya, M., Islam, E.u, Rasul, M., Farooq, I., Mahreen, N., Tawab, A., Irfan, M., et al. (2021). Differential root exudation and architecture for improved growth of wheat mediated by phosphate solubilizing bacteria. *Front. Microbiol.* 12, 744094. doi: 10.3389/fmicb.2021.744094

Yan, A., Wang, Y., Tan, S. N., Mohd Yusof, M. L., Ghosh, S., and Chen, Z. (2020). Phytoremediation: a promising approach for revegetation of heavy metal-polluted land. *Front. Plant Sci.* 11, 359. doi: 10.3389/fpls.2020.00359

Yasmin, S., Zaka, A., Imran, A., Zahid, M. A., Yousaf, S., Rasul, G., et al. (2016). Plant growth promotion and suppression of bacterial leaf blight in rice by inoculated bacteria. *PLoS ONE.* 11, e0160688. doi: 10.1371/journal.pone.0160688

Conflict of Interest: The authors declare that the research was conducted in the absence of any commercial or financial relationships that could be construed as a potential conflict of interest.

Publisher's Note: All claims expressed in this article are solely those of the authors and do not necessarily represent those of their affiliated organizations, or those of the publisher, the editors and the reviewers. Any product that may be evaluated in this article, or claim that may be made by its manufacturer, is not guaranteed or endorsed by the publisher.

frontiers | Frontiers in Plant Science

ORIGINAL RESEARCH
published: 18 May 2022
doi: 10.3389/fpls.2022.879545

Photosynthetic Pigments and Biochemical Response of Zucchini (*Cucurbita pepo* L.) to Plant-Derived Extracts, Microbial, and Potassium Silicate as Biostimulants Under Greenhouse Conditions

Doaa Y. Abd-Elkader[1], Abeer A. Mohamed[2], Mostafa N. Feleafel[1], Asma A. Al-Huqail[3], Mohamed Z. M. Salem[4]*, Hayssam M. Ali[3] and Hanaa S. Hassan[1]*

[1] Department of Vegetable, Faculty of Agriculture (EL-Shatby), Alexandria University, Alexandria, Egypt, [2] Plant Pathology Institute, Agriculture Research Center (ARC), Alexandria, Egypt, [3] Chair of Climate Change, Environmental Development and Vegetation Cover, Department of Botany and Microbiology, College of Science, King Saud University, Riyadh, Saudi Arabia, [4] Forestry and Wood Technology Department, Faculty of Agriculture (El-Shatby), Alexandria University, Alexandria, Egypt

OPEN ACCESS

Edited by:
Youssef Rouphael, University of Naples Federico II, Italy

Reviewed by:
Antonio Ferrante, University of Milan, Italy
Alexios A. Alexopoulos, University of Peloponnese, Greece

***Correspondence:**
Mohamed Z. M. Salem
zidan_forest@yahoo.com
Asma A. Al-Huqail
aalhuquail@ksu.edu.sa

Specialty section:
This article was submitted to Crop and Product Physiology, a section of the journal Frontiers in Plant Science

Received: *01 March 2022*
Accepted: *19 April 2022*
Published: *18 May 2022*

Citation:
Abd-Elkader DY, Mohamed AA, Feleafel MN, Al-Huqail AA, Salem MZM, Ali HM and Hassan HS (2022) Photosynthetic Pigments and Biochemical Response of Zucchini (Cucurbita pepo L.) to Plant-Derived Extracts, Microbial, and Potassium Silicate as Biostimulants Under Greenhouse Conditions. Front. Plant Sci. 13:879545. doi: 10.3389/fpls.2022.879545

There are many technological innovations in the field of agriculture to improve the sustainability of farmed products by reducing the chemicals used. Uses of biostimulants such as plant extracts or microorganisms are a promising process that increases plant growth and the efficient use of available soil resources. To determine the effects of some biostimulants' treatments on the photosynthetic pigments and biochemicals composition of zucchini plants, two experiments were conducted in 2019 and 2020 under greenhouse conditions. In this work, the effects of beneficial microbes (*Trichoderma viride* and *Pseudomonas fluorescens*), as well as three extracts from *Eucalyptus camaldulensis* leaf extract (LE), *Citrus sinensis* LE, and *Ficus benghalensis* fruit extract (FE) with potassium silicate (K_2SiO_3) on productivity and biochemical composition of zucchini fruits, were assessed as biostimulants. The results showed that *E. camaldulensis* LE (4,000 mg/L) + K_2SiO_3 (500 mg/L) and *T. viride* (10^6 spore/ml) + K_2SiO_3 (500 mg/L) gave the highest significance yield of zucchini fruits. Furthermore, the total reading response of chlorophylls and carotenoids was significantly affected by biostimulants' treatments. The combination of K_2SiO_3 with *E. camaldulensis* LE increased the DPPH scavenging activity and the total phenolic content of zucchini fruits, in both experiments. However, the spraying with K_2SiO_3 did not observe any effects on the total flavonoid content of zucchini fruits. Several phenolic compounds were identified *via* high-performance liquid chromatography (HPLC) from the methanol extracts of zucchini fruits such as syringic acid, eugenol, caffeic acid, pyrogallol, gallic acid, ascorbic acid, ferulic acid, α-tocopherol, and ellagic acid. The main elemental content (C and O) analyzed *via* energy-dispersive X-ray spectroscopy (EDX) of leaves was affected by the application of biostimulants. The success of this work could lead to the development of cheap and easily available safe biostimulants for enhancing the productivity and biochemical of zucchini plants.

Keywords: zucchini plants, beneficial microbes, plant-derived biostimulants, potassium silicate, phenolic compounds

INTRODUCTION

In agricultural performance, plant biostimulants are including different bioactive natural substances such as plant extracts, beneficial microorganisms, macroalgae seaweeds extracts, humic acid, fulvic acid, silicon, animal protein hydrolysate, vegetal protein hydrolysate, and bacteria belonging to the genera *Azotobacter*, *Rhizobium*, and *Azospirillum* (Chiaiese et al., 2018; Ricci et al., 2019).

In the recent years, the use of external preparations capable of stimulating plant growth by working on plant metabolism has become suitable for enhancing the efficiency of chemical fertilizers (Baroccio et al., 2017). Increasing yield is often associated with better-quality vegetables or fruits. According to the previous studies, biostimulants have a positive effect on the production of vegetables and fruits (Kocira et al., 2017; Goñi et al., 2018; Milić et al., 2018; Tarantino et al., 2018). In modern agriculture, biostimulants are the important strategies in the production of horticultural crops and consist of highly heterogeneous classes of compounds with a wide range of actions to improve quantitative and qualitative crops (Drobek et al., 2019).

Zucchini or squash (*Cucurbita pepo* L.), a highly polymorphic vegetable crop, is growing during the summer season in Egypt and all over the world (Ezzo et al., 2012; Mahmoud, 2016; Contreras et al., 2020), as a result of its economic importance and nutritional value. However, the increasing demand of consumers, in the local and international markets for fresh fruits of zucchini all year round, led to an increase in planting zucchini in the greenhouse (Formisano et al., 2020a,b). Zucchini is one of the most significant vegetable cash crops, especially, in newly reclaimed areas of Egypt, due to its high-yielding potential per unit area in the short-growing season. Therefore, improving the agricultural practices of zucchini production is of great economic interest. This may be achieved by applying simple applicable modern and low-cost strategies such as the use of silica compounds, *Trichoderma*, or plant-growth-promoting-rhizobacteria (PGPR) and plant extracts that stimulate the growth and development of this plant and then increase the productivity, which is safe for humans and environments (Savvas et al., 2009; Formisano et al., 2021; Novello et al., 2021).

Silicon (Si) is a biostimulant in the group of inorganic products. Foliar application of Si, as potassium silicates, is a relatively new technique of feeding vegetable plants, with several roles in plant physiology, regulation of ions uptake and increased tolerance of plants to various biotic and abiotic stresses (Artyszak, 2018). Moreover, Si stimulates the growth, development, and yield components of many vegetable species by correcting the levels of endogenous growth hormones (Artyszak, 2018).

Inoculating vegetable plants with *Trichoderma* or PGPR may be an effective strategy to stimulate the growth and development of plants as well as to minimize the use of synthetic fertilizers and agrochemicals. This strategy can improve plant tolerance for the abiotic stresses through induction of resistance by the production of phytohormones, enhancing soil productivity and volatile compounds that affect the plant signaling pathways (Kumar et al., 2020; Mannino et al., 2020). *Trichoderma* spp. are free-living filamentous fungi in the soil, and some of them are the most potent agents for the biocontrol of soil-borne plant pathogens (Castiglione et al., 2021). *Trichoderma* can improve soil nutrient availability and promote plant growth and biostimulant (Velmourougane et al., 2019; Chen et al., 2021).

Plant extracts contain many bioactive compounds such as sugars, amino acids, proteins, nucleic acids, polysaccharides (Fernie and Pichersky, 2015), phenolic acids, and flavonoids (Sarker and Oba, 2018; Salem et al., 2021b). Foliar application of plant extracts leads to stimulating the root growth, photosynthetic capacity, and increasing the nutrient use efficiency, which ultimately leads to the growth promotion of vegetable crops (Bulgari et al., 2015). In addition, phenolic acids and flavonoids often play the important roles in the plant's defense against disease (Sarker and Oba, 2018). However, the plant extracts can be considered a good source of natural antioxidants and antimicrobial in both *in vitro* and *in vivo* (Di Mola et al., 2019; Souri and Bakhtiarizade, 2019; Godlewska et al., 2021). The raw materials resulting from the pruning processes of *Eucalyptus camaldulensis*, *Citrus sinensis*, and *Ficus benghalensis* trees are readily available in high quantities in Egypt. The growth of these trees under Egyptian conditions is very suitable and therefore economical in use. Further, the extracts from these trees were shown potential activities against the growth of bacteria and fungi (Nair and Chanda, 2007; Ekwenye and Edeha, 2010; El-Hefny et al., 2017; Bhawana et al., 2018; Salem et al., 2019; Abdelkhalek et al., 2020; Abo-Elgat et al., 2020; Afzal et al., 2020; Fatima et al., 2020).

The present research was carried out as an attempt to apply simple applicable modern, low-cost, and safe strategies through studying the effect of the use of some natural biostimulant with silicon on the productivity and bioactive component responses of zucchini plants, grown in clay soil, under drip irrigation in the greenhouse.

MATERIALS AND METHODS

A total of two consecutive experiments were carried out in the years 2019 and 2020 under a drip irrigation system in the greenhouse, at the Experimental Station Farm of the Faculty of Agriculture, Alexandria University, Abies, Alexandria, situated in Egypt, 31° 13′ N latitude, 29° 59′ E longitude.

Soil Analysis

Prior to the initial of the first experiment, soil samples of the experimental site up to 30 cm depth were collected and analyzed for some chemical and physical properties according to the standard procedures (Sparks et al., 2020). The main physical and chemical soil characteristics at the experimental site with clay soil were 46% sand, 24% silt, and 30% clay, electrical conductivity (EC): 2.60 dS m^{-1}, pH: 8, total nitrogen (N): 0.16%, phosphorus and potassium were 0.30 ppm and 0.33 m eq l^{-1}, respectively.

Experimental Work and Treatments

The current experiments were performed to study the effect of plant extracts, K_2SiO_3, and microbial inoculation with *Trichoderma viride* (10^6 spore/ml) and *Pseudomonas fluorescens*

TABLE 1 | Treatments used in this study.

Treatment	Combination of biostimulants
Control	Without any microbial, plant extract, and potassium silicate
T. viride	*Trichoderma viride* (10^6 spore/ml)
T. viride + K_2SiO_3	*T. viride* (10^6 spore/ml) + potassium silicate (500 mg/L)
P. fluorescens	*Pseudomonas fluorescens* (10^8 CFU/ml)
P. fluorescens + K_2SiO_3	*P. fluorescens* (10^8 CFU/ml) + potassium silicate (500 mg/L)
T. viride + *P. fluorescens*	*T. viride* + *P. fluorescens*, individually (10^6 spore/ml +10^8 CFU/ml)
T.viride + *P. fluorescens* + K_2SiO_3	*T. viride* + *P. fluorescens*, individually (10^6 spore /ml +10^8 CFU/ml) + potassium silicate (500 mg/L)
E. camaldulensis LE	*Eucalyptus camaldulensis* leaf extract (4,000 mg/L)
E.camaldulensis LE + K_2SiO_3	*E. camaldulensis* leaf extract (4,000 mg/L) + potassium silicate (500 mg/L)
C. sinensis LE	*Citrus sinensis* leaf extract (4,000 mg/L)
C. sinensis LE + K_2SiO_3	*C. sinensis* leaf extract (4,000 mg/L) + potassium silicate (500 mg/L)
F. benghalensis FE	*Ficus benghalensis* fruit extract (4,000 mg/L)
F.benghalensis FE + K_2SiO_3	*F. benghalensis* fruit extract (4,000 mg/L) + potassium silicate (500 mg/L)

(10^8 CFU/ml) as biostimulants on the growth, productivity, and bioactive of zucchini fruit that is grown in greenhouse conditions. Extracts were prepared from *Eucalyptus camaldulensis* leaves, *Citrus sinensis* leaves, and *Ficus benghalensis* fruits at the concentration of 4,000 mg/L as recommended in our previous work (Hassan et al., 2021).

AZIAD F1 cultivar was used in this study, and this cultivar was imported from the Sakata Tacky Company Japan vegetable seed. It is a desirable variety in the Egyptian market and bears low temperatures and high production (Abd Elmohsen et al., 2021). Zucchini seeds were sown in late September and in late December, in the first and second experiments, respectively. Within the same plantation row, the spacing between each plant and the other was set to be 30 cm, whereas the spacing between each line and the other was 1 m (3 plants/m^2). The experimental layout was a randomized complete block design (RCBD), with three replicates. RCBD is used to control the variation in the experiment by accounting for spatial effects in the field or greenhouse, e.g., the variation in soil fertility or drainage differences in the field (Lauren, 2014). Each trial consisted of 13 treatments as shown in **Table 1**.

Each treatment was replicated three times, and each replicate consisted of 35 plants. Water irrigation was applied through the drip irrigation system. The drip irrigation system consisted of laterals GR of 16 mm in diameter with emitters at a 0.3-m distance. The emitters had a discharge rate of 4 L/h. The actual evapotranspiration of the zucchini crop (ETc), under greenhouse at "Abies, Alexandria" area conditions, was calculated and adjusted at the start of each growth stage (Feleafel and Mirdad, 2014). It was calculated by multiplying reference evapotranspiration (ET_0) for different growth stages through both two experiments (from late September 2019 up to mid-December, 2019, in the first experiment and from late December and ended in late February 2020, in the second experiment) by a crop coefficient (K_C); $ET_c = ET_0 \times K_C$ (Allen, 1998; Razmi and Ghaemi, 2011) as shown in **Supplementary Table S1**. Irrigation frequency was every 5 days, to maintain soil water above 50% soil water depletion (Qassim and Ashcroft, 2002), which is the optimum level for zucchini plants.

The treatments of inoculation with *T. viride* were used as a drench to the plants' root area, were done through the addition of 50 ml suspension, which was mixed thoroughly with the soil, and then watered and left to ensure establishment and distribution in the soil. However, inoculation with *P. fluorescens*, *T. viride* + *P. fluorescens* and application of K_2SiO_3 and three extracts from *E. camaldulensis* LE, *C. sinensis* LE, and *F. benghalensis* FE were sprayed separately on zucchini plants. All treatments were added to the plants four times during the entire growing season of zucchini plants. The first addition was after 2 weeks from the sowing date, and then, the addition was done weekly. The spraying was done for each biostimulant separately, and *P. fluorescens* was sprayed before the spraying with K_2SiO_3 at an interval of 3 days. Ammonium sulfate $(NH_4)_2SO_4$, (20.5% N), phosphoric acid (58%), and potassium sulfate (48% K_2O) were the sources of N, P_2O_5, and K_2O, respectively. Nitrogen, phosphorus, and potassium fertilizers were fertigated at rates of 143, 167, and 238 kg N, P_2O_5, and K_2O/ha, respectively, which were injected directly into the irrigation water (fertigation) using a venture injector at one time weekly through a drip irrigation system in equal doses, starting from 2 weeks after planting. Climatic data, such as maximum and minimum air temperature ($T_{maximum}$ and $T_{minimum}$ °C) and relative humidity (RH%), were collected using Testo 175-H1 as shown in **Figure 1**.

Evaluation of Productivity

Zucchini fruits were harvested after 50 days from sowing, at a rate of two times a week. For each harvest, the number of fruits was counted and weighed for each treatment and then attributed to the hectare. The number and weight of fruits were recorded after each harvesting accumulatively. The number of fruits/hectare and the total productivity/hectare for each treatment were calculated.

Photosynthetic Pigments

Extraction of chlorophylls (a and b) and carotenoids from zucchini leaves was performed in ethanol 96% (v/v) in a proportion of 1:10 (w/v). The absorbance was read at 664 and 649 nm for chlorophylls a and b, respectively, as well as at 470 nm for carotenoids (Lichtenthaler, 1987; Campobenedetto et al., 2021).

Energy-Dispersive X-Ray Spectroscopy (EDX) Analysis

Energy-dispersive X-ray spectroscopy analysis was performed to measure the changes in the elemental chemical composition of zucchini leaves (nine leaves for each treatment) due to different treatments with treated with 500 mg/L K_2SiO_3 and

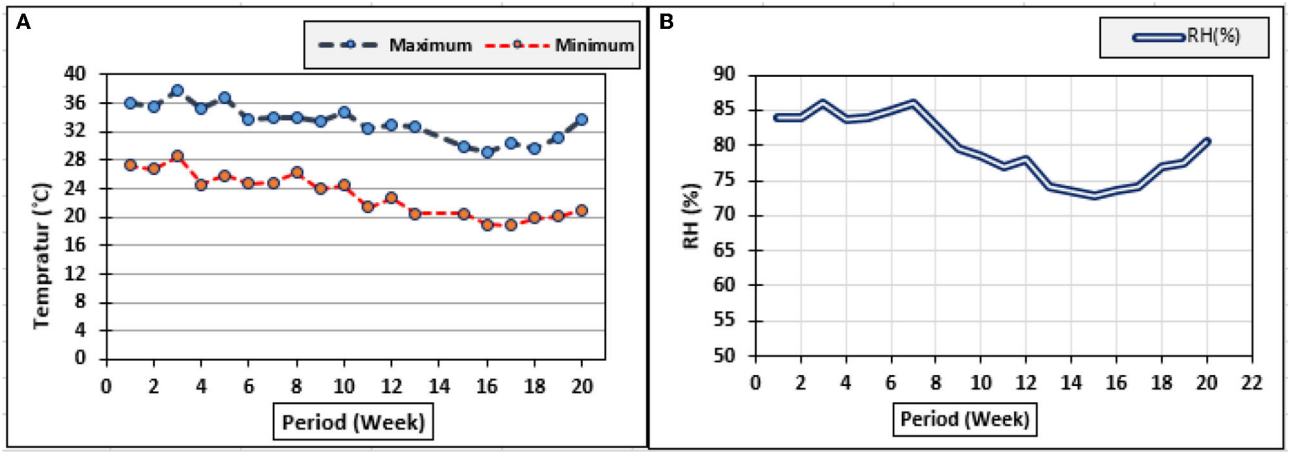

FIGURE 1 | The measured climatic conditions in the greenhouse during 2019 and 2020. **(A)** Minimum and maximum temperature (°C); **(B)** RH (%).

control treatment. Energy-dispersive spectrometry (EDX), JFC-1100E ion sputtering device (model JEOL/MP, JSMIT200 Series, Tokyo, Japan) with acceleration voltage of 20.00 kV to show the elemental compotation at three point was used (Salem et al., 2021a).

2,2-Diphenyl-1-Picrylhydrazyl (DPPH) Radical Scavenging Activity

At 1 ml of 0.1 mM 2,2-diphenyl-1-picrylhydrazyl (DPPH), we added different concentrations of the prepared zucchini fruits' methanolic extracts. After vigorous shaking, the mixture was incubated for 30 min in the dark and at 25°C. The reduction of the radical DPPH resulting from the incubation with the different dilutions of zucchini methanolic extracts was monitored by reading the color decrease at 517 nm (Mannino et al., 2020). The percentage DPPH radical scavenging activity was calculated using the formula: Inhibition (%) = $[(A_{control} - A_{sample})/A_{control}] \times 100$, where $A_{control}$ and A_{sample} are the absorbance of the control and treatments (Abd-Elkader et al., 2021).

Total Phenolic and Flavonoid Contents

Total phenolic content (TPC) was determined *via* Folin–Ciocalteu assay, as previously reported (Mannino et al., 2020). Quantification was performed using an external calibration curve with gallic acid (GA). Analyses were performed in triplicate, and data were expressed as millimole GA equivalents (GAE) per 100 g of FW., while the aluminum chloride colorimetric assay was used for total flavonoid content (TFC) determination and read at 510 nm using UV–Visible spectrophotometer Model UV 1601 version 2.40 (Shimadzu) (Marinova et al., 2005). Total flavonoids' content was expressed as mg catechin equivalents.

Fruit Extraction and HPLC Analysis of Phenolic Compounds

The extraction process was carried out on zucchini fruit samples treated with plant extracts and microbial with 500 mg/L K_2SiO_3 and control treatment. A sample was taken for each treatment from the three replicates, about 15 fruits, then, all the fruits were grated and mixed well, and 30 g was taken then extracted by 60 ml methanol by the soaking method for 1 week (Ashmawy et al., 2020; Abd-Elkader et al., 2021). The extracts were then filtered through filter paper (Whatman no. 1) and then with a cotton plug. The extracts were concentrated and stored in brown vials in the refrigerator prior HPLC analysis. The phenolic compounds from the methanol extracts of each previous treatments were identified by the Agilent ChemStation [HPLC-(Agilent, Santa Clara, CA, USA)], which is composed of a quaternary pump and UV/Vis detector and C18 column (125 mm × 4.60 mm, 5 μm particle size). Chromatograms were obtained and analyzed using HPLC. Phenolic compounds were separated by employing a mobile gradient phase of water/acetonitrile/glacial acetic acid (980/20/5, v/v/v, pH 2.68) and acetonitrile/glacial acetic acid (1,000/5, v/v) with a flow rate of 1 ml/min and detected at 325 nm. All chemical standards (HPLC grade) were purchased from Sigma-Aldrich (St. Louis, MO, USA) (Hassan et al., 2021).

Statistical Analysis

All data were analyzed by implementing the CoStat software version 6.303 (CoHort Software 798 Lighthouse Ave. PMB 320, Monterrey, CA, 93940, USA) package through a two-way analysis of variance (ANOVA). A Tukey's honestly significant difference (HSD) test ($p < 0.05$) was used to separate the means (Steel and Torrie, 1980).

RESULTS

Productivity Parameters of Zucchini

Figure 2A shows that spraying of plants with K_2SiO_3 and biostimulants led to a significant increase in fruits number (ha) compared to control. The fruits number/ha was significantly increased as zucchini plants were treated with *E. camaldulensis* LE and *E. camaldulensis* LE + K_2SiO_3 in the two consecutive experiments. In addition, plants sprayed with microbial and plant extracts were significantly increased the fruits number/ha

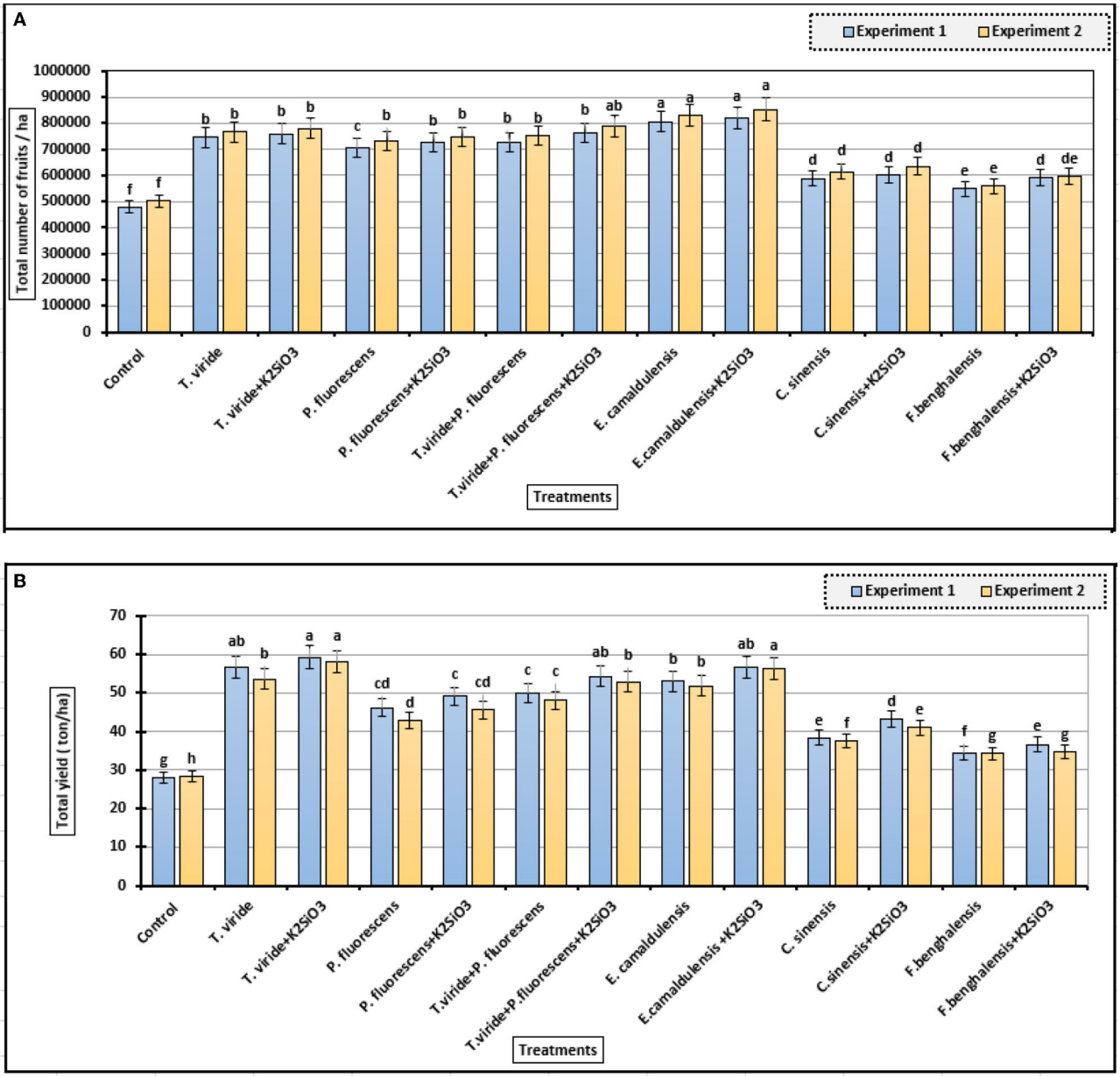

FIGURE 2 | Fruits number and total yield of zucchini as affected by biostimulant treatments. **(A)** Total number of fruits/ha and **(B)** The total yield (ton/ha) (means ± S.E) of zucchini as affected by the extracts, microbial inoculations, and K_2SiO_3. Letters in the figure indicated that the means ± S.E of treatments with the same letter/s were not significantly different according to Tukey's HSD level of probability.

as compared to the control treatment. Moreover, spraying plants with K_2SiO_3 at 500 mg/L with microbial or plant extracts were maximized the increase in fruits number/ha compared to biostimulant treatments without K_2SiO_3 in the two experiments.

The total yield/ha of zucchini fruits (**Figure 2B**) showed a significant difference among treatments with the highest values of 59.25 and 58 ton/ha, with the treatment of *T. viride* + K_2SiO_3, in the first and second experiments, respectively. *E. camaldulensis* LE + K_2SiO_3 treatment, also, gave a higher mean value in both experiments (56.67 and 56.34 ton/ha). It is noted that the use of K_2SiO_3 with microbial and plant extracts as biostimulants led to an increase in total productivity/ha of zucchini in both experiments.

Photosynthetic Pigments

Table 2 presents the effect of K_2SiO_3 and plant extract or beneficial microbes as biostimulants on the content of photosynthetic pigments (total chlorophylls, chlorophylls a, b, and total carotenoids) of zucchini leaves. The results indicated a significant increase in the content of pigments as affected by

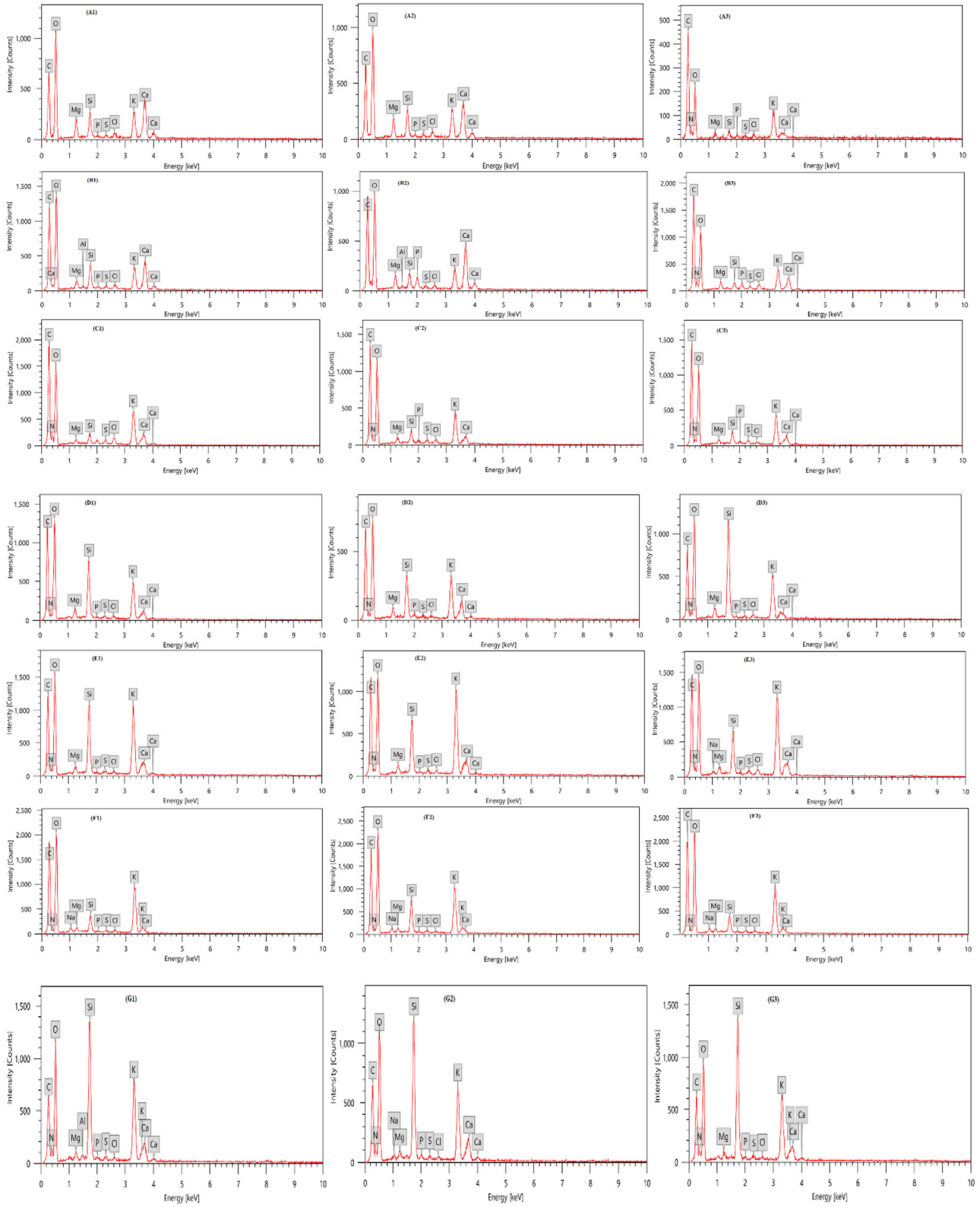

FIGURE 3 | Elemental compositions of zucchini leaves with EDX analysis as affected by plant extracts, microbial inoculations, and potassium silicates biostimulants. Analysis was taken from three points for each treatment. **(A1–A3)** Control; **(B1–B3)** *T. viride* + K_2SiO_3; **(C1–C3)** *P. fluorescens* + K_2SiO_3; **(D1–D3)** *T. viride* + *P. fluorescens* + K_2SiO_3; **(E1–E3)** *E. camaldulensis* LE + K_2SiO_3; **(F1–F3)** *C. sinensis* LE + K_2SiO_3; **(G1–G3)** *F. benghalensis* FE + K_2SiO_3.

TABLE 2 | Effect of plant extracts, microbial inoculations, and potassium silicates biostimulants, on photosynthetic pigments content of leaves in the second experiment.

Treatment	Experiment 1				Experiment 2			
	Chlorophyll a	Chlorophyll b	Total chlorophylls	Total carotenoids	Chlorophyll a	Chlorophyll b	Total chlorophylls	Total carotenoids
	(mg/100 g fw)	(mg/100 g fw)	(mg/100 g fw)	(mg/100 g fw)	(mg/100 g fw)	(mg/100 g fw)	(mg/100 g fw)	(mg/100 g fw)
Control	14.8 ± 0.21e	10.3 ± 0.13e	25.1 ± 0.51f	2.83 ± 0.32e	15.7 ± 0.33e	11.4 ± 0.55e	27.1 ± 0.13e	2.92 ± 0.13d
T. viride	24.6 ± 0.11ab	18.3 ± 0.25ab	42.9 ± 0.32ab	3.62 ± 0.42b	24.9 ± 0.24ab	18.8 ± 0.31ab	43.7 ± 0.21ab	3.72 ± 0.32ab
T. viride + K_2SiO_3	25.3 ± 0.12a	19.0 ± 0.14a	44.3 ± 0.43a	3.81 ± 0.11ab	25.6 ± 0.42a	19.7 ± 0.44a	45.3 ± 0.21a	3.97 ± 0.14a
P. fluorescens	20.1 ± 0.12bc	16.3 ± 0.52bc	36.4 ± 0.22cd	3.32 ± 0.14c	21.1 ± 0.11bc	16.9 ± 0.23b	38.0 ± 0.10c	3.48 ± 0.33ab
P. fluorescens + K_2SiO_3	21.2 ± 0.31b	17.0 ± 0.32b	38.2 ± 0.31c	3.49 ± 0.15b	22.0 ± 0.14bc	17.8 ± 0.21ab	39.8 ± 0.42bc	3.56 ± 0.42ab
T. viride + *P. fluorescens*	22.1 ± 0.13b	18.0 ± 0.22ab	40.1 ± 0.11b	3.45 ± 0.21ab	22.9 ± 0.51bc	17.9 ± 0.24ab	40.8 ± 0.14bc	3.50 ± 0.16b
T. viride + *P. fluorescens* + K_2SiO_3	23.4 ± 0.11ab	19.1 ± 0.11a	42.5 ± 0.10ab	3.59 ± 0.23b	24.0 ± 0.33ab	20.1 ± 0.25a	4.1 ± 0.23ab	3.64 ± 0.17ab
E. camaldulensis	24.4 ± 0.23ab	18.9 ± 0.21ab	43.3 ± 0.10ab	3.90 ± 0.22a	25.0 ± 0.22a	19.3 ± 0.51a	44.3 ± 0.31ab	4.02 ± 0.23a
E. camaldulensis + K_2SiO_3	25.6 ± 0.11a	20.2 ± 0.33a	45.8 ± 0.22a	4.01 ± 0.24a	26.0 ± 0.14a	20.8 ± 0.34a	46.8 ± 0.26a	4.13 ± 0.52a
C. sinensis	17.7 ± 0.14c	12.4 ± 0.51cd	30.1 ± 0.32e	3.01 ± 0.11b	17.9 ± 0.21cd	12.9 ± 0.42d	30.8 ± 0.31d	3.12 ± 0.22c
C. sinensis + K_2SiO_3	18.1 ± 0.21c	13.9 ± 0.22c	32.0 ± 0.12d	3.15 ± 0.32c	19.2 ± 0.41c	15.2 ± 0.32c	34.4 ± 0.42cd	3.21 ± 0.13bc
F. benghalensis	15.6 ± 0.05d	11.3 ± 0.11d	26.9 ± 0.33f	2.93 ± 0.36d	16.1 ± 0.44d	11.9 ± 0.52e	28.0 ± 0.34e	2.98 ± 0.16d
F. benghalensis + K_2SiO_3	17.3 ± 0.11c	14.9 ± 0.22c	32.2 ± 0.41d	3.10 ± 0.51c	18.2 ± 0.51c	14.2 ± 0.32c	32.4 ± 0.15cd	3.17 ± 0.05b

Letters in the figure indicated that the means ± S.E of treatments with the same letter/within the same column were not significantly different according to Tukey's HSD at a 0.05 level of probability.

the biostimulant treatments. It is clear from the results that the values obtained from the different photosynthetic pigments were affected by the different treatments of the biostimulant used. *T. viride* + K_2SiO_3, and *E camaldulensis* + K_2SiO_3 treatments increased all the photosynthetic pigment contents, but the effect was most significant by the treatment *E. camaldulensis* LE+ K_2SiO_3, in both experiments. In addition, **Table 2** shows the application of the treatments *T. viride* and *E. camaldulensis* LE improved the chlorophyll pigment of leaves compared to the other treatments, in both experiments.

Elemental Compositions of Leaves by EDX Analysis

Table 3 and **Figure 3** presents an EDX analysis to measure the changes in the elements' compositions of the leaves due to different treatments of biostimulants, which are six treatments in addition to the control. There was a significant effect of treatments on the elemental percentages with the highest values obtained with treatments *P. fluorescens* + K_2SiO_3, *T. viride* + *P. fluorescens* + K_2SiO_3, and *E. camaldulensis* LE + K_2SiO_3 on C, Mg, and Si elements. Also, there was a significant effect of treatments on elements N, P, and Ca percentages whereas the highest value was obtained by the plants treated with *T. viride* + K_2SiO_3. Moreover, the highest value of element K was obtained by treatment *E. camaldulensis* LE + K_2SiO_3.

DPPH Scavenging Activity

In **Figure 4**, all DPPH scavenging activity data of the zucchini fruits parameter were significantly influenced by the biostimulant applications. Our data indicated that the *E. camaldulensis* LE + K_2SiO_3 treatment increased the DPPH scavenging activity mean value of zucchini fruits (75.93 and 76.21%) followed by *E. camaldulensis* LE (72.24 and 73.45%) in the first and second experiments, respectively (**Figure 4**). In addition, the combination of K_2SiO_3 with plant extract and microbial stimulants had no effect on improving DPPH in zucchini fruits, in both experiments.

Total Phenolic and Flavonoid Contents

Significant differences were found among the total phenolic contents of zucchini fruit samples in (**Figure 5A**), in both experiments. The values varied in a wide range with an average value of 150 to 300 mg GAE/100 g FW. In our two experimental conditions, the highest value was found with the treatment *E. camaldulensis* LE + K_2SiO_3 (300 mg GAE/100 g FW), followed by *E. camaldulensis* LE (289 mg GAE/100 g FW) and *T. viride* + *P. fluorescens* + K_2SiO_3 (287 mg GAE/100 g FW), whereas the lowest content was found in the control treatment.

The higher values of flavonoid content were recorded in biostimulant-treated zucchini plants with *T. viride* + *P. fluorescens* (104 mg QE/100 g sample), *T. viride* + *P. fluorescens* + K_2SiO_3 (110 mg QE/100 g sample), *E. camaldulensis* LE (116 mg QE/100 g sample), and *E. camaldulensis* LE + K_2SiO_3 (115 mg QE/100 g FW sample) treatments, with no significant difference among other treatments (**Figure 5B**). On the other hand, the spraying with K_2SiO_3 did not show any effects on the total flavonoids' content of zucchini fruits in both experiments.

HPLC Analysis of Phenolic Compounds in Zucchini Fruits

Table 4 presents the phytochemicals in terms of the phenolic compounds identified in the methanol extracts (MEs) of zucchini

TABLE 3 | Effect of plant extracts, microbial inoculations, and potassium silicates biostimulants, on elemental composition (Atom%) of zucchini leaves in the second experiment.

Treatment	Elements									
	C	N	O	Mg	Si	P	S	Cl	K	Ca
Control	37.60 ± 0.33c	10.90 ± 0.88b	35.74 ± 0.93d	0.40 ± 0.05b	0.36 ± 0.04d	0.23 ± 0.03b	0.11 ± 0.01c	0.09 ± 0.01c	1.21 ± 0.04c	0.27 ± 0.04b
T. viride + K_2SiO_3	46.17 ± 0.22ab	25.19 ± 0.57a	40.21 ± 0.64c	0.16 ± 0.02d	0.77 ± 0.03c	0.64 ± 0.03a	0.12 ± 0.01b	0.15 ± 0.01ab	1.97 ± 0.08c	3.01 ± 0.06a
P. fluorescens + K_2SiO_3	47.88 ± 0.20a	4.28 ± 0.34c	43.65 ± 0.50b	0.39 ± 0.03c	0.63 ± 0.03c	0.13 ± 0.01c	0.20 ± 0.01a	0.20 ± 0.01a	2.13 ± 0.04b	0.50 ± 0.20b
T. viride + *P. fluorescens* + K_2SiO_3	48.86 ± 0.34a	5.55 ± 0.32c	44.02 ± 0.49b	0.62 ± 0.03a	4.64 ± 0.07a	0.06 ± 0.01d	0.13 ± 0.0b	0.18 ± 0.01ab	2.66 ± 0.06b	0.26 ± 0.01b
E. camaldulensis LE + K_2SiO_3	49.79 ± 0.54a	4.32 ± 0.33c	43.80 ± 0.48b	0.51 ± 0.03a	2.23 ± 0.05b	0.05 ± 0.01d	0.14 ± 0.01b	0.20 ± 0.03a	4.55 ± 0.06 a	0.69 ± 0.03 b
C. sinensis LE + K_2SiO_3	43.54 ± 0.28b	1.10 ± 0.20d	47.47 ± 0.39a	0.24 ± 0.02c	0.87 ± 0.03c	0.10 ± 0.01c	0.12 ± 0.01b	0.16 ± 0.01ab	3.15 ± 0.04ab	0.14 ± 0.01b
F. benghalensis FE + K_2SiO_3	41.90 ± 0.33b	9.89 ± 0.41b	41.99 ± 0.52c	0.40 ± 0.03b	5.64 ± 0.08a	0.12 ± 0.02c	0.14 ± 0.01b	0.11 ± 0.01 b	3.44 ± 0.06ab	0.72 ± 0.031b

Letters in figure indicated that means ± S.E of treatments with the same letter/s were not significantly different according to Tukey's HSD at 0.05 level of probability.

fruits treated with plant extracts and microbial with K_2SiO_3 added only, which are six treatments in addition to the control treatment. The HPLC separation chromatograms are shown in **Supplementary Figure S1**. Ferulic (21.12 μg/ml), caffeic (19.63 μg/ml), and ellagic (18.33 μg/ml) acids were the most abundant compounds in zucchini fruit ME as affected by control. Zucchini fruit ME from plants treated with *T. viride* + K_2SiO_3 showed the presence of eugenol (35.16 μg/ml) and ellagic acid (17.36 μg/ml) as the main compounds. Eugenol (18.05 μg/ml) and caffeic acid (16.26 μg/ml) were the abundant compounds in ME from zucchini fruit treated with *P. fluorescens* + K_2SiO_3. Interestingly, α-tocopherol (22.01 μg/ml) with syringic acid (13.30 μg/ml) were the most abundant compounds in ME from fruits treated with *T. viride* + *P. fluorescens* + K_2SiO_3. The ME from fruits of the plants treated with *E. camaldulensis* LE + K_2SiO_3 identified *p*-coumaric acid (25.51 μg/ml), ferulic acid (20.11 μg/ml), and caffeic acid (18.87 μg/ml) as the abundant compounds. The ME of fruits from plants treated with *C. sinensis* LE + K_2SiO_3 identified pyrogallol (28.5 μg/ml), ferulic acid (18.09 μg/ml), and gallic acid (12.66 μg/ml) as the abundant compounds. Syringic (18.69 μg/ml) and caffeic (15.26 μg/ml) acids were the most abundant compounds in ME from fruits of zucchini collected from plants treated with *F. benghalensis* FE + K_2SiO_3.

DISCUSSION

The development of eco-friendly products to improve the growth and yield of horticulture has spurred a massive interest in commercial, especially in poor countries. The use of biostimulants has become increasingly common in modern agriculture and in the global market for the sale of agricultural products (Xu and Geelen, 2018). The biostimulants used may be a substance of natural origin or microorganisms that work or a mixture of them that improve the condition of crops and resist some pathogens and stress conditions to which plants are exposed without causing harmful side effects to the environment or humans (Du Jardin, 2015). The advantage of using biomass contained in plant extracts is its low cost (Tembo et al., 2018). Conversion of plant biomass in plant extracts, showing the action of biostimulants or plant growth, can be supportive to farmers in developing countries that cannot afford synthetic biostimulants, because of their high costs (Fite et al., 2020).

In this study, photosynthetic pigments and productivity were affected by the application of different biostimulants used. The results illustrated generally that *E camaldulensis* LE or *Trichoderma viride* with K_2SiO_3 increased the previous characters. *Eucalyptus* leaf extract increased photosynthetic pigments and the production of zucchini plants. These results might be due to many species of eucalyptus have high rich in carotenoids, carbohydrates, phenols, flavonoids, and antioxidants. Due to these compounds detected in *E camaldulensis* LE, it can be considered a biostimulant to enhance growth and productivity. Also, allelopathic activity and this activity can be the important catalysts in reducing diseases and increasing total yield (El-Rokiek et al., 2019). The

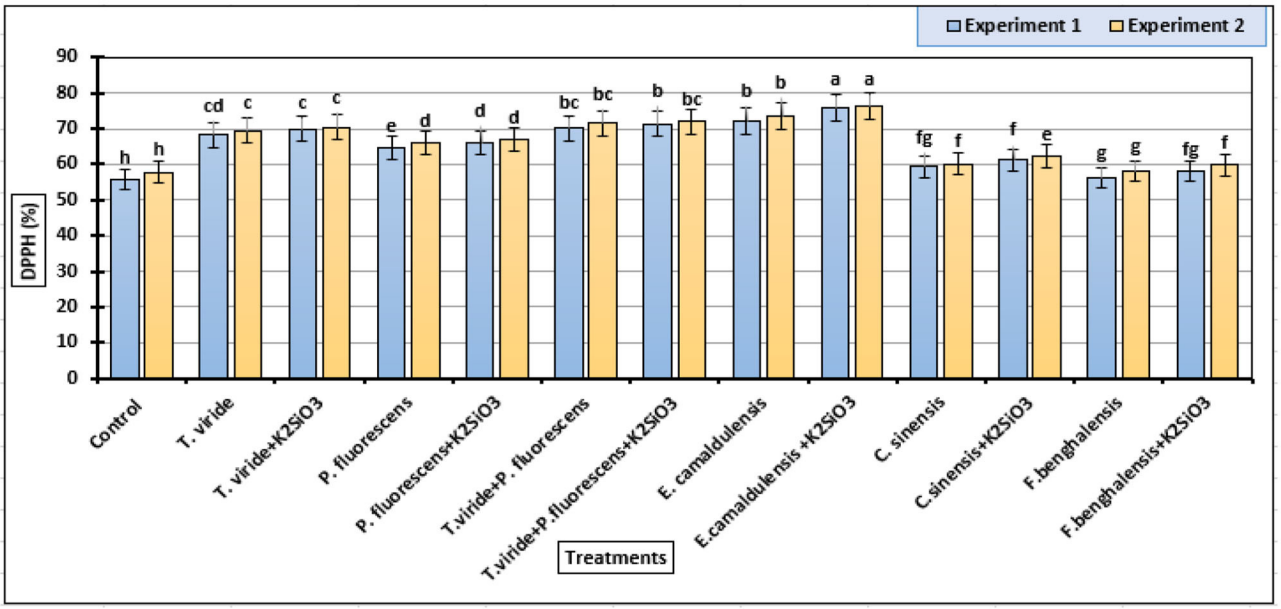

FIGURE 4 | DPPH (2,2-diphenyl-1-picrylhydrazyl) inhibition percentages (means ± S.E) of methanol extracts from zucchini fruits as affected by the plant extracts, microbial inoculations, and potassium silicate biostimulants. Letters in the figure indicated that means ± S.E of treatments with the same letter/s were not significantly different according to Tukey's HSD at a 0.05 level of probability.

induced metabolism of the photosynthetic pigments signified the increased growth parameters of the used leaf extract. In this response, the photosynthetic pigments of seedling broccoli significantly increased by *Eucalyptus* leaf extract (Mohsen et al., 2018). Furthermore, the application of *T. viride* seems to have affected photosynthetic pigments and the total yield characteristics of *Brassica* leafy crops similar to what has been shown for the control. *Trichoderma* is a genus of filamentous fungi that include several species described as biostimulants and/or biological control agents in agriculture (Velasco et al., 2021). Almost, microbial is widely used as a biofertilizer almost for all crops with or without amendments (Vinale et al., 2008; Schuster and Schmoll, 2010; Reynolds, 2016). Similarly, the PGPR increases both the growth parameters and yield attributes of onions and zucchini with the triple inoculation treatments (Tinna et al., 2020; Novello et al., 2021).

The role of microbial or *Trichoderma* in increased crop yield and quality was achieved mainly by the ability to degrade complex organic compounds present in the soil. Complex organic compounds were made available to plants in a simpler form, so that they could be absorbed (Khan et al., 2017; Thapa et al., 2020).

It is clear from previous studies that treating plants with silicon benefits their leaf structure by improving plant leaf erection, which leads to increased light interception and reduced self-shading, which leads to improved photosynthesis (Galindo et al., 2021). In this regard, silicon has a positive effect on chlorophyll pigments, which leads to an improvement in growth, which in turn affects the production of plants (Thorne et al., 2020; Salim et al., 2021). It is noted that there is an effect of the use of biostimulants on the metabolism of plants and the final quality (Colla et al., 2015). Plant growth, quality, tolerance to abiotic and biotic stresses, photosynthesis, and using nutrients, fertilizers, and water are able to be enhanced by plant-derived biostimulants (PDBs) by modulating plant biochemical, molecular, and physiological processes (Rouphael and Colla, 2020b; Godlewska et al., 2021; Mosa et al., 2021b). Our previous work (Hassan et al., 2021) showed that the most abundant phenolic compounds in *Eucalyptus camaldulensis* LE were pyrogallol, caffeic acid, and *p*-coumaric acid, in *Citrus sinensis* LE were syringic and ferulic acids, and in *Ficus benghalensis* were gallic, p-coumaric, and syringic acids.

In addition, the application of biostimulants increased the biochemical compounds with potential effect on the nutrient content of plants. The shorter growing cycle of plants may result in biostimulation if the beneficial microbe has higher performance (i.e., *Trichoderma viride*), in improving the N uptake efficiency (Fiorentino et al., 2018). Moreover, the increase in the root system caused by the application of *Trichoderma* to the roots may have contributed to the increased N uptake of zucchini plants. This has also been observed when correlating the use of *Trichoderma* with the N content of leaves from several vegetable crops such as lettuce and tomato (Fiorentino et al., 2016; Sani et al., 2020).

Similar observations to our results were found after the use of microbial based on the enhanced yield by microbial inoculants has been linked in some cases to increased nutrient uptake and improved nutrient status of the cucumber and lettuce (Abdelaziz and Pokluda, 2009; El-Saady and Omar, 2017). Furthermore, some reports showed that *Pseudomonas* spp. was significantly

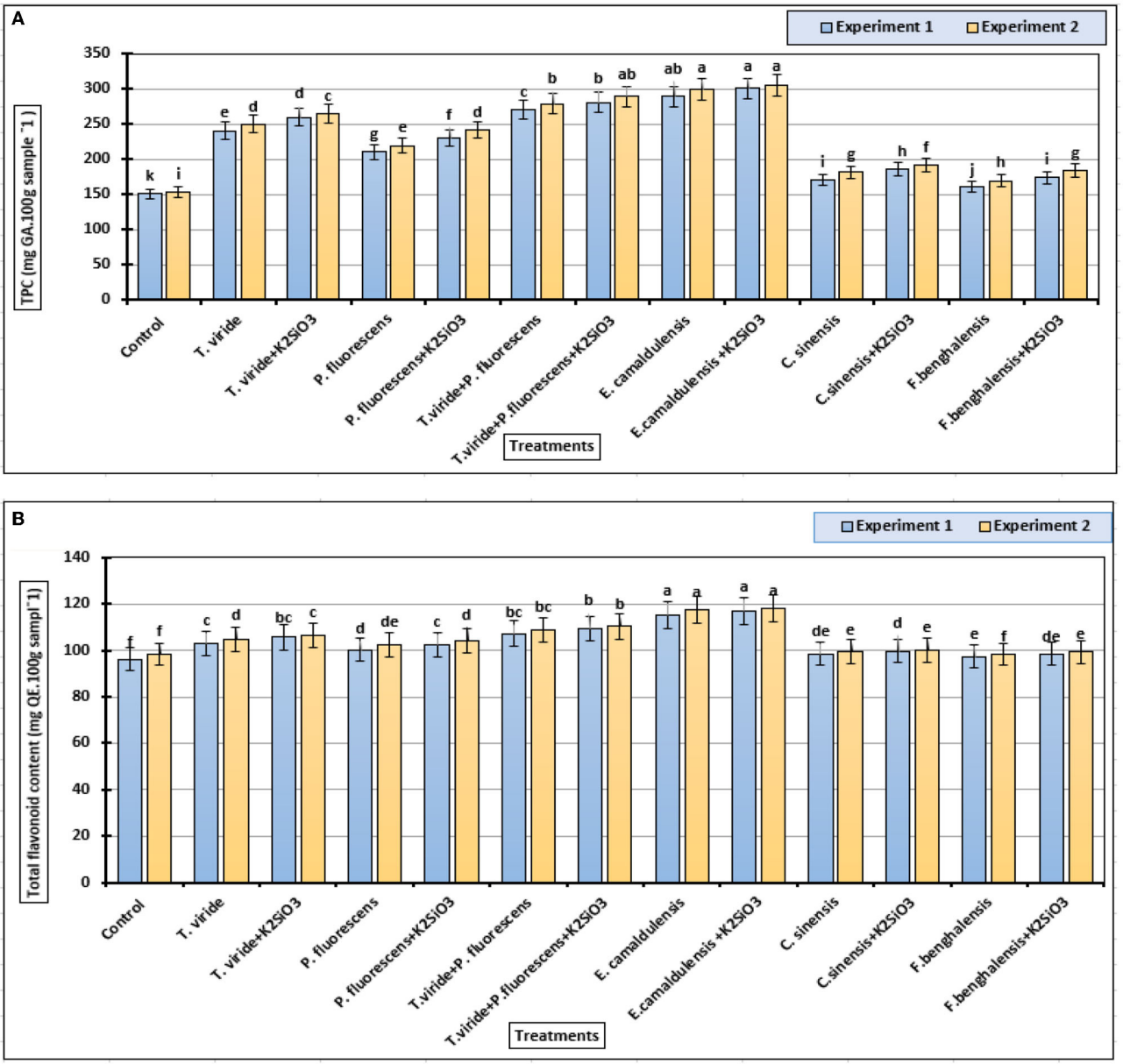

FIGURE 5 | Phenolic and flavonoid contents (means ± S.E) of zucchini fruits as affected by the plant extracts, microbial inoculations, and potassium silicate biostimulants. **(A)** Total phenolic content and **(B)** total flavonoid content. Letters in the figure indicated that the means ± S.E of treatments with the same letter/s were not significantly different according to Tukey's HSD at a 0.05 level of probability.

increased the uptake of P, Fe, Ca, and manganese (Mn) in some vegetables, e.g., eggplant and tomato (Calvo et al., 2014; Chrysargyris et al., 2020).

Some studies that are similar to our results were found after the use of PDBs in agriculture leads to an improvement in the crop's quality with an increase in bioactive components (Di Mola et al., 2019). It can be said that biological stimulants have a positive effect on a number of chemical properties of fruits and vegetables. It is evident that the use of several types of PDBs has potential effects on the development and quality of several plant species, for example, tomato (Souri and Bakhtiarizade, 2019), rocket (Di Mola et al., 2019), and zucchini (Hassan et al., 2021).

Consistence with the present findings, PDBs as the foliar application were enhanced the total phenolic contents, antioxidant activity, and nutrient contents of tomato plants compared to the control (Chiaiese et al., 2018). Furthermore, these findings, generally, agreed with those previously reported on spinach and broccoli (Fan et al., 2011; Kałuzewicz et al., 2017), where they concluded that the use of biostimulants enhanced the phenolic content.

TABLE 4 | Effect of plant extracts, microbial inoculations, and potassium silicate biostimulants on phenolic compounds identified in zucchini fruits methanol extract in the second experiment.

Compound	Phenolic compounds (μg/ml) in zucchini fruits ME as plants treated with						
	Control	*T.viride* + K_2SiO_3	*P. fluorescens* + K_2SiO_3	*T. viride* + *P. fluorescens* + K_2SiO_3	*E. camaldulensis* LE + K_2SiO_3	*C. sinensis* LE + K_2SiO_3	*F. benghalensis* FE + K_2SiO_3
Myricetin	nd	10.33	nd	nd	nd	nd	nd
Syringic acid	9.22	9.14	8.12	13.30	nd	nd	18.69
p-Coumaric acid	9.68	nd	nd	8.09	25.51	8.23	nd
Eugenol	nd	35.16	18.05	nd	nd	nd	4.36
Vanillin	nd	nd	nd	nd	5.42	7.55	nd
Caffeic acid	19.63	6.47	16.26	5.36	18.87	6.98	15.26
4-Hydroxybenzoic acid	nd	nd	nd	nd	nd	7.12	nd
Pyrogallol	14.51	nd	nd	nd	nd	28.5	3.75
Gallic acid	nd	8.16	7.14	nd	5.12	12.66	12.44
Ascorbic acid	nd	nd	nd	nd	10.61	8.23	nd
Ferulic acid	21.12	nd	nd	6.12	20.11	18.09	nd
α-Tocopherol	7.45	nd	nd	22.01	nd	nd	nd
Salicylic acid	nd	9.12	9.56	nd	nd	nd	nd
Catechol	5.18	nd	nd	6.23	nd	nd	nd
Ellagic acid	18.33	17.36	8.49	5.14	nd	nd	nd
Protocatechuic acid	nd	10.68	2.21	nd	nd	nd	nd

nd, not detected; ME, methanol extract.

Foliar application of Si has biostimulation effects, and also, it can be used by plants to augment their defenses against the entrance of toxic ions *via* the root apoplast (Verma et al., 2021b).

The phenolic contents were ranged between 96.2 and 117.3 mg GAE/100 g of FW, as affected by different biostimulant treatments. Other studies showed that the average phenolic content of zucchini fruits of was 8.67 mg GAE/g FW (Hamissou et al., 2013).

Zucchini plants treated with the following treatments *T. viride* + K_2SiO_3, *P. fluorescens* + K_2SiO_3, *T. viride* + *P. fluorescens* + K_2SiO_3, *E. camaldulensis* LE + K_2SiO_3, *C. sinensis* LE+K_2SiO_3, and *F. benghalensis* FE + K_2SiO_3 showed several phenolic compounds (myricetin, syringic acid, *p*-coumaric acid, eugenol, vanillin, caffeic acid, 4-hydroxybenzoic acid, pyrogallol, gallic acid, ascorbic acid, ferulic acid, α-tocopherol, salicylic acid, catechol, ellagic acid, and protocatechuic acid) in the methanol extract with different concentrations compared with the control treatment. These phenolic compounds or PDBs are playing the important roles in regulating plant metabolic processes (Boudet, 2007; Lin et al., 2016; Mosa et al., 2021a). Simple phenolic acids such as hydroxybenzoic and hydroxycinnamic acids are derived from phenylpropanoid pathway (Mandal et al., 2010).

This study clarified the importance of the role played by Si element as a biostimulant in spraying on zucchini plants and increasing the efficiency of plant extract or microbial biostimulant. Si improves the growth of the plant by role defending the plant by increasing some different biochemical mechanisms in plants such as antimicrobial enzymes, flavonoids, and pathogen-related proteins (Verma et al., 2021a), chlorophyll pigments, and antioxidants (Thorne et al., 2020; Salim et al., 2021). Studies have also shown that one of the beneficial properties of Si is its positive effects on abiotic stress tolerance and resistance to pathogens and diseases and thus has an effective role in improving overall productivity (Savvas and Ntatsi, 2015; Abd-Alkarim et al., 2017; Shwethakumari et al., 2021).

Plant-derived biostimulants have a positive effect on crop and vegetable plants; however, to improve their efficacy and optimize their inclusion in the industrial processes, the understanding of their action mechanism should be amended (Brown and Saa, 2015; Backer et al., 2018; Rouphael and Colla, 2020a).

CONCLUSION

The results of this study highlight the importance of biostimulant application to mitigate the effects of yield and biochemical. The potential use of some leaf extracts or microbial with K_2SiO_3 as a biostimulant was tested in zucchini plants on plant photosynthetic pigments, productivity, bioactive componence, and elements content parameters that were evaluated after its use. The productivity of zucchini plants was increased by the foliar application of the treatments *T. viride* + K_2SiO_3 or *E. camaldulensis* LE + K_2SiO_3 as well as the content of the leaves of photosynthesis pigments. HPLC analysis of phenolic compounds in zucchini fruits and elements content of leaves was affected by biostimulants (microbial and plant extract with silicon). Total phenolic contents and DPPH scavenging activity were increased significantly in plants treated with *E. camaldulensis* LE + K_2SiO_3.

DATA AVAILABILITY STATEMENT

The original contributions presented in the study are included in the article/**Supplementary Materials**, further inquiries can be directed to the corresponding author/s.

AUTHOR CONTRIBUTIONS

HH, AM, MS, and DA-E: conceptualization, formal analysis, and data curation. HH, AM, MS, AA-H, and DA-E: methodology. HH, AM, MF, MS, HA, and DA-E: software, investigation, and visualization. HH, AM, MF, AA-H, and DA-E: validation. HH, AM, MF, MS, AA-H, HA, and DA-E: resources and writing—original draft preparation. HH, AM, MF, MS, HA, AA-H, and DA-E: writing, reviewing, and editing. MF and MS: supervision. DA-E: project administration. HA and AA-H: funding acquisition. All authors have read and agreed to the published version of the manuscript.

FUNDING

This research was funded by the Deanship of Scientific Research, King Saud University, through the Vice Deanship of Scientific Research Chairs.

ACKNOWLEDGMENTS

The authors are grateful to the Deanship of Scientific Research, King Saud University, for funding through the Vice Deanship of Scientific Research Chairs.

SUPPLEMENTARY MATERIAL

The Supplementary Material for this article can be found online at: https://www.frontiersin.org/articles/10.3389/fpls.2022.879545/full#supplementary-material

REFERENCES

Abd Elmohsen, Y., Salman, S. R., Helmy, Y. I., El-Shinawy, M. Z., and Abou-Hadid, A. F. (2021). The effect of grafting on squash plants grown under low plastic tunnel in winter season. *Egy. J. Hort.* 48, 181–192. doi: 10.21608/ejoh.2021.60786.1164

Abd-Alkarim, E., Bayoumi, Y., Metwally, E., and Rakha, M. (2017). Silicon supplements affect yield and fruit quality of cucumber (*Cucumis sativus* L.) grown in net houses. *Afr. J. Agri. Res.* 12, 2518–2523. doi: 10.5897/AJAR2017.12484

Abdelaziz, M., and Pokluda, R. (2009). Response of cucumbers grown on two substrates in an open soilless system to inoculation with microorganisms. *Acta Hort* 819, 157–164. doi: 10.17660/ActaHortic.2009.819.14

Abd-Elkader, D. Y., Salem, M. Z. M., Komeil, D. A., Al-Huqail, A. A., Ali, H. M., Salah, A. H., et al. (2021). Post-harvest enhancing and *Botrytis cinerea* control of strawberry fruits using low cost and eco-friendly natural oils. *Agronomy* 11, 1246. doi: 10.3390/agronomy11061246

Abdelkhalek, A., Salem, M. Z. M., Kordy, A. M., Salem, A. Z. M., and Behiry, S. I. (2020). Antiviral, antifungal, and insecticidal activities of Eucalyptus bark extract: HPLC analysis of polyphenolic compounds. *Microb. Pathogen* 147, 104383. doi: 10.1016/j.micpath.2020.104383

Abo-Elgat, W. A. A., Kordy, A. M., Böhm, M., Cerný, R., Abdel-Megeed, A., and Salem, M. Z. M. (2020). *Eucalyptus camaldulensis*, *Citrus aurantium*, and *Citrus sinensis* essential oils as Antifungal Activity against *Aspergillus flavus*, *Aspergillus niger*, *Aspergillus terreus*, and *Fusarium culmorum*. *Processes* 8, 1003. doi: 10.3390/pr8081003

Afzal, T., Ali, Q., and Malik, A. (2020). Phenolic compounds proliferation by HPLC: To find out antibacterial activities in *Ficus benghalensis* plant extract. *Int. J. Bot. Stud.* 5, 140–144.

Allen, R. G. (1998). Crop evapotranspiration-Guideline for computing crop water requirements. *Irrig. Drain* 56, 300.

Artyszak, A. (2018). Effect of silicon fertilization on crop yield quantity and quality—a literature review in Europe. *Plants* 7, 54. doi: 10.3390/plants7030054

Ashmawy, N. A., Behiry, S. I., Al-Huqail, A. A., Ali, H. M., and Salem, M. Z. M. (2020). Bioactivity of selected phenolic acids and hexane extracts from *Bougainvilla spectabilis* and *Citharexylum spinosum* on the growth of *Pectobacterium carotovorum* and *Dickeya solani* bacteria: an opportunity to save the environment. *Processes* 8, 482. doi: 10.3390/pr8040482

Backer, R., Rokem, J. S., Ilangumaran, G., Lamont, J., Praslickova, D., Ricci, E., et al. (2018). Plant growth-promoting rhizobacteria: context, mechanisms of action, and roadmap to commercialization of biostimulants for sustainable agriculture. *Front. Plant Sci.* 9, 1473. doi: 10.3389/fpls.2018.01473

Baroccio, F., Barilaro, N., Tolomei, P., and Mascini, M. (2017). Classification of biostimulants origin using amino acids composition of hydrolyzed proteins. *J. Hortic. Sci. Res.* 1, 30–35. doi: 10.36959/745/395

Bhawana, R., Kaur, J., Vig, A. P., Arora, S., and Kaur, R. (2018). Evaluation of antibacterial potential of Ficus species. *J. Pharma. Sci. Res.* 10, 1251–1255.

Boudet, A.-M. (2007). Evolution and current status of research in phenolic compounds. *Phytochemistry* 68, 2722–2735. doi: 10.1016/j.phytochem.2007.06.012

Brown, P., and Saa, S. (2015). Biostimulants in agriculture. *Front. Plant Sci.* 6, 671. doi: 10.3389/fpls.2015.00671

Bulgari, R., Cocetta, G., Trivellini, A., Vernieri, P., and Ferrante, A. (2015). Biostimulants and crop responses: a review. *Biol. Agri. Horticul.* 31, 1–17. doi: 10.1080/01448765.2014.964649

Calvo, P., Nelson, L., and Kloepper, J. W. (2014). Agricultural uses of plant biostimulants. *Plant Soil* 383, 3–41. doi: 10.1007/s11104-014-2131-8

Campobenedetto, C., Agliassa, C., Mannino, G., Vigliante, I., Contartese, V., Secchi, F., et al. (2021). A biostimulant based on seaweed (*Ascophyllum nodosum* and *Laminaria digitata*) and yeast extracts mitigates water stress effects on tomato (*Solanum lycopersicum* L.). *Agriculture* 11, 557. doi: 10.3390/agriculture11060557

Castiglione, A. M., Mannino, G., Contartese, V., Bertea, C. M., and Ertani, A. (2021). Microbial biostimulants as response to modern agriculture needs: composition, role and application of these innovative products. *Plants* 10, 1533. doi: 10.3390/plants10081533

Chen, D., Hou, Q., Jia, L., and Sun, K. (2021). Combined use of two *Trichoderma* strains to promote growth of pakchoi (*Brassica chinensis* L.). *Agronomy* 11, 726. doi: 10.3390/agronomy11040726

Chiaiese, P., Corrado, G., Colla, G., Kyriacou, M. C., and Rouphael, Y. (2018). Renewable sources of plant biostimulation: microalgae as a sustainable means to improve crop performance. *Front. Plant Sci.* 9, 1782. doi: 10.3389/fpls.2018.01782

Chrysargyris, A., Charalambous, S., Xylia, P., Litskas, V., Stavrinides, M., and Tzortzakis, N. (2020). Assessing the biostimulant effects of a novel plant-based formulation on tomato crop. *Sustainability* 12, 8432. doi: 10.3390/su12208432

Colla, G., Nardi, S., Cardarelli, M., Ertani, A., Lucini, L., Canaguier, R., et al. (2015). Protein hydrolysates as biostimulants in horticulture. *Sci. Horticul.* 196, 28–38. doi: 10.1016/j.scienta.2015.08.037

Contreras, J. I., Baeza, R., Alonso, F., Cánovas, G., Gavilán, P., and Lozano, D. (2020). Effect of distribution uniformity and fertigation volume on the bio-productivity of the greenhouse zucchini crop. *Water* 12, 2183. doi: 10.3390/w12082183

Di Mola, I., Ottaiano, L., Cozzolino, E., Senatore, M., Giordano, M., El-Nakhel, C., et al. (2019). Plant-based biostimulants influence the agronomical,

physiological, and qualitative responses of baby rocket leaves under diverse nitrogen conditions. *Plants* 8, 522. doi: 10.3390/plants8110522

Drobek, M., Frac, M., and Cybulska, J. (2019). Plant biostimulants: importance of the quality and yield of horticultural crops and the improvement of plant tolerance to abiotic stress—a review. *Agronomy* 9, 335. doi: 10.3390/agronomy9060335

Du Jardin, P. (2015). Plant biostimulants: definition, concept, main categories and regulation. *Sci. Horticul.* 196, 3–14. doi: 10.1016/j.scienta.2015.09.021

Ekwenye, U. N., and Edeha, O. V. (2010). The antibacterial activity of crude leaf extract of *Citrus sinensis* (sweet orange). *Inter. J. Pharma Bio Sci.* 1, 743–750.

El-Hefny, M., Ashmawy, N. A., Salem, M. Z. M., and Salem, A. Z. M. (2017). Antibacterial activities of the phytochemicals-characterized extracts of *Callistemon viminalis*, E*ucalyptus camaldulensis* and *Conyza dioscoridis* against the growth of some phytopathogenic bacteria. *Microb. Pathogen* 113, 348–356. doi: 10.1016/j.micpath.2017.11.004

El-Rokiek, K. G., Dawood, M. G., Sadak, M. S., and El-Awadi, M. E.-S. (2019). The effect of the natural extracts of garlic or Eucalyptus on the growth, yield and some chemical constituents in quinoa plants. *Bull. Nat. Res. Cent.* 43, 119. doi: 10.1186/s42269-019-0161-3

El-Saady, W. A., and Omar, G. F. (2017). Impact of some bio-stimulants on growth, yield and quality of head lettuce (cv. Big bell). *Int. J. Environ.* 6, 178–187.

Ezzo, M., Glala, A., Saleh, S., and Omar, N. M. (2012). Improving squash plant growth and yielding ability under organic fertilization condition. *Austr. J. Basic Appl. Sci.* 6, 572–578.

Fan, D., Hodges, D. M., Zhang, J., Kirby, C. W., Ji, X., Locke, S. J., et al. (2011). Commercial extract of the brown seaweed *Ascophyllum nodosum* enhances phenolic antioxidant content of spinach (*Spinacia oleracea* L.) which protects *Caenorhabditis elegans* against oxidative and thermal stress. *Food Chem.* 124, 195–202. doi: 10.1016/j.foodchem.2010.06.008

Fatima, T., Mian, A. H., Khan, Z., Khan, A. M., Anwar, F., Tariq, A., et al. (2020). *Citrus sinensis* a potential solution against superbugs. *Appl. Nanosci.* 10, 5077–5083. doi: 10.1007/s13204-020-01408-9

Feleafel, M., and Mirdad, Z. (2014). Alleviating the deleterious effects of water salinity on greenhouse grown tomato. *Inter. J. Agri. Biol.* 16, 49–56.

Fernie, A. R., and Pichersky, E. (2015). focus issue on metabolism: metabolites, metabolites everywhere. *Plant Physiol.* 169, 1421–1423. doi: 10.1104/pp.15.01499

Fiorentino, N., De Rosa, A., Gioia, L., Senatore, M., Visconti, D., Ottaiano, L., et al. (2016). Effects of Trichoderma on growth and nitrogen uptake of lettuce (*Lactuca sativa* L.). *Atti del XLV Convegno della Società Italiana di Agronomia Sassari* 20, 22.

Fiorentino, N., Ventorino, V., Woo, S. L., Pepe, O., De Rosa, A., Gioia, L., et al. (2018). Trichoderma-based biostimulants modulate rhizosphere microbial populations and improve N uptake efficiency, yield, and nutritional quality of leafy vegetables. *Front. Plant Sci.* 9, 743. doi: 10.3389/fpls.2018.00743

Fite, T., Tefera, T., Negeri, M., and Damte, T. (2020). Effect of *Azadirachta indica* and *Milletia ferruginea* extracts against H*elicoverpa armigera* (Hubner) (Lepidoptera: Noctuidae) infestation management in chickpea. *Cog. Food Agri.* 6, 1712145. doi: 10.1080/23311932.2020.1712145

Formisano, L., El-Nakhel, C., Corrado, G., De Pascale, S., and Rouphael, Y. (2020a). Biochemical, physiological, and productive response of greenhouse vegetables to suboptimal growth environment induced by insect nets. *Biology* 9, 432. doi: 10.3390/biology9120432

Formisano, L., Miras-Moreno, B., Ciriello, M., El-Nakhel, C., Corrado, G., Lucini, L., et al. (2021). Trichoderma and phosphite elicited distinctive secondary metabolite signatures in zucchini squash plants. *Agronomy* 11, 1205. doi: 10.3390/agronomy11061205

Formisano, L., Pannico, A., El-Nakhel, C., Starace, G., Poledica, M., Pascale, S. D., et al. (2020b). Improved porosity of insect proof screens enhances quality aspects of zucchini squash without compromising the yield. *Plants* 9, 1264. doi: 10.3390/plants9101264

Galindo, F. S., Pagliari, P. H., Rodrigues, W. L., Fernandes, G. C., Boleta, E. H., Santini, J. M., et al. (2021). Silicon amendment enhances agronomic efficiency of nitrogen fertilization in maize and wheat crops under tropical conditions. *Plants* 10, 1329. doi: 10.3390/plants10071329

Godlewska, K., Ronga, D., and Michalak, I. (2021). Plant extracts - importance in sustainable agriculture. *Ital. J. Agronm.* 16, 1851. doi: 10.4081/ija.2021.1851

Goñi, O., Quille, P., and O'connell, S. (2018). *Ascophyllum nodosum* extract biostimulants and their role in enhancing tolerance to drought stress in tomato plants. *Plant Physiol. Biochem.* 126, 63–73. doi: 10.1016/j.plaphy.2018.02.024

Hamissou, M., Smith, A. C., Carter Jr, R. E., and Triplett Ii, J. K. (2013). Antioxidative properties of bitter gourd (*Momordica charantia*) and zucchini (*Cucurbita pepo*). *Emirat. J. Food Agri.* 25, 641–647. doi: 10.9755/ejfa.v25i9.15978

Hassan, H. S., Mohamed, A. A., Feleafel, M. N., Salem, M. Z. M., Ali, H. M., Akrami, M., et al. (2021). Natural plant extracts and microbial antagonists to control fungal pathogens and improve the productivity of zucchini (*Cucurbita pepo* L.) *in vitro* and in greenhouse. *Horticulture* 7, 470. doi: 10.3390/horticulturae7110470

Kałuzewicz, A., Gasecka, M., and Spizewski, T. (2017). Influence of biostimulants on phenolic content in broccoli heads directly after harvest and after storage. *Folia Horticul.* 29, 221–230. doi: 10.1515/fhort-2017-0020

Khan, M. Y., Haque, M. M., Molla, A. H., Rahman, M. M., and Alam, M. Z. (2017). Antioxidant compounds and minerals in tomatoes by Trichoderma-enriched biofertilizer and their relationship with the soil environments. *J. Integr. Agri.* 16, 691–703. doi: 10.1016/S2095-3119(16)61350-3

Kocira, A., Kocira, S., Swieca, M., Złotek, U., Jakubczyk, A., and Kapela, K. (2017). Effect of foliar application of a nitrophenolate–based biostimulant on the yield and quality of two bean cultivars. *Sci. Horticul.* 214, 76–82. doi: 10.1016/j.scienta.2016.11.021

Kumar, P., Sharma, N., Sharma, S., and Gupta, R. (2020). Rhizosphere stochiometry, fruit yield, quality attributes and growth response to PGPR transplant amendments in strawberry (*Fragaria* × *ananassa* Duch.) growing on solarized soils. *Sci. Horticul.* 265, 109215. doi: 10.1016/j.scienta.2020.109215

Lauren, P. (2014). *Statistics 2. RCBD Review Agriculture Innovation Program*, 1–14. Available online at: https://epakag.ucdavis.edu/media/vocational/man-stats-rcbd.pdf. (accessed October 01, 2014).

Lichtenthaler, H. K. (1987). Chlorophyll fluorescence signatures of leaves during the autumnal chlorophyll breakdown. *J. Plant Physiol.* 131, 101–110. doi: 10.1016/S0176-1617(87)80271-7

Lin, D., Xiao, M., Zhao, J., Li, Z., Xing, B., Li, X., et al. (2016). An overview of plant phenolic compounds and their importance in human nutrition and management of type 2 diabetes. *Molecules* 21, 1374. doi: 10.3390/molecules21101374

Mahmoud, A. (2016). Occurrence of Fusarium wilt on summer squash caused by *Fusarium oxysporum* in Assiut, Egypt. *J. Phytopathol. Pest Manag.* 3, 34–45.

Mandal, S. M., Chakraborty, D., and Dey, S. (2010). Phenolic acids act as signaling molecules in plant-microbe symbioses. *Plant Signa. Behav.* 5, 359–368. doi: 10.4161/psb.5.4.10871

Mannino, G., Campobenedetto, C., Vigliante, I., Contartese, V., Gentile, C., and Bertea, C. M. (2020). The application of a plant biostimulant based on seaweed and yeast extract improved tomato fruit development and quality. *Biomolecules* 10, 1662. doi: 10.3390/biom10121662

Marinova, D., Ribarova, F., and Atanassova, M. (2005). Total phenolics and total flavonoids in Bulgarian fruits and vegetables. *J. Univ. Chem. Technol. Metall.* 40, 255–260.

Milić, B., Tarlanović, J., Keserović, Z., Magazin, N., Miodragović, M., and Popara, G. (2018). Bioregulators can improve fruit size, yield and plant growth of northern highbush blueberry (*Vaccinium corymbosum* L.). *Sci. Horticul.* 235, 214–220. doi: 10.1016/j.scienta.2018.03.004

Mohsen, A., Abdelhaak, M., Abdalla, M., and El Tanbashawy, H. (2018). Response of broccoli seedling to some plant extracts. *Egy. J. Bot.* 58, 195–204. doi: 10.21608/ejbo.2017.563.1024

Mosa, W. F. A., Salem, M. Z. M., Al-Huqail, A. A., and Ali, H. M. (2021a). Application of glycine, folic acid, and moringa extract as bio-stimulants for enhancing the production of 'flame seedless' grape cultivar. *Bioresources* 16, 3391–3410. doi: 10.15376/biores.16.2.3391-3410

Mosa, W. F. A., Sas-Paszt, L., Górnik, K., Ali, H. M., and Salem, M. Z. M. (2021b). Vegetative growth, yield, and fruit quality of guava (*Psidium guajava* L.) cv. maamoura as affected by some biostimulants. *Bioresources* 16, 7379–7399. doi: 10.15376/biores.16.4.7379-7399

Nair, R., and Chanda, S. (2007). Antibacterial activities of some medicinal plants of the western region of India. *Turk. J. Biol.* 31, 231–236.

Novello, G., Cesaro, P., Bona, E., Massa, N., Gosetti, F., Scarafoni, A., et al. (2021). The effects of plant growth-promoting bacteria with biostimulant features

on the growth of a local onion cultivar and a commercial zucchini variety. *Agronomy* 11, 888. doi: 10.3390/agronomy11050888

Qassim, A., and Ashcroft, B. (2002). *Estimating Vegetable Crop Water Use With Moisture-Accounting Method# AG1192, DPI Victoria*. Available online at: http://www.dpi.vic.gov.au/agriculture/horticulture/vegetables/vegetable-growing-and-management/estim-ating-vegetable-crop-water-use (accessed October 2001).

Razmi, Z., and Ghaemi, A. A. (2011). Crop and soil-water stress coefficients of tomato in the glass-greenhouse conditions. *J. Soil Plant Inter.* 2, 75–87.

Reynolds, M. (2016). Go green for environmental sustainability: an interdisciplinary. *Biol. Chem.* 271, 4609–4612.

Ricci, M., Tilbury, L., Daridon, B., and Sukalac, K. (2019). General principles to justify plant biostimulant claims. *Front. Plant Sci.* 10, 494. doi: 10.3389/fpls.2019.00494

Rouphael, Y., and Colla, G. (2020a). Editorial: biostimulants in agriculture. *Front. Plant Sci.* 11, 40. doi: 10.3389/fpls.2020.00040

Rouphael, Y., and Colla, G. (2020b). Toward a sustainable agriculture through plant biostimulants: from experimental data to practical applications. *Agronomy* 10, 1461. doi: 10.3390/agronomy10101461

Salem, M. Z. M., Ali, H. M., and Akrami, M. (2021a). *Moringa oleifera* seeds-removed ripened pods as alternative for papersheet production: antimicrobial activity and their phytoconstituents profile using HPLC. *Sci. Rep.* 11, 19027. doi: 10.1038/s41598-021-98415-9

Salem, M. Z. M., Behiry, S. I., and El-Hefny, M. (2019). Inhibition of *Fusarium culmorum*, *Penicillium chrysogenum* and *Rhizoctonia solani* by n-hexane extracts of three plant species as a wood-treated oil fungicide. *J. Appl. Microbiol.* 126, 1683–1699. doi: 10.1111/jam.14256

Salem, M. Z. M., El-Hefny, M., Ali, H. M., Abdel-Megeed, A., El-Settawy, A., a,.A., et al. (2021b). Plants-derived bioactives: novel utilization as antimicrobial, antioxidant and phytoreducing agents for the biosynthesis of metallic nanoparticles. *Microb. Pathogen.* 158, 105107. doi: 10.1016/j.micpath.2021.105107

Salim, B. B. M., Abou El-Yazied, A., Salama, Y. A. M., Raza, A., and Osman, H.S. (2021). Impact of silicon foliar application in enhancing antioxidants, growth, flowering and yield of squash plants under deficit irrigation condition. *Ann. Agri. Sci.* 66, 176–183. doi: 10.1016/j.aoas.2021.12.003

Sani, M. N. H., Hasan, M., Uddain, J., and Subramaniam, S. (2020). Impact of application of *Trichoderma* and biochar on growth, productivity and nutritional quality of tomato under reduced N-P-K fertilization. *Ann. Agri. Sci.* 65, 107–115. doi: 10.1016/j.aoas.2020.06.003

Sarker, U., and Oba, S. (2018). Drought stress enhances nutritional and bioactive compounds, phenolic acids and antioxidant capacity of Amaranthus leafy vegetable. *BMC Plant Biol.* 18, 258. doi: 10.1186/s12870-018-1484-1

Savvas, D., Giotis, D., Chatzieustratiou, E., Bakea, M., and Patakioutas, G. (2009). Silicon supply in soilless cultivations of zucchini alleviates stress induced by salinity and powdery mildew infections. *Environ. Exper. Bot.* 65, 11–17. doi: 10.1016/j.envexpbot.2008.07.004

Savvas, D., and Ntatsi, G. (2015). Biostimulant activity of silicon in horticulture. *Sci. Horticul.* 196, 66–81. doi: 10.1016/j.scienta.2015.09.010

Schuster, A., and Schmoll, M. (2010). Biology and biotechnology of *Trichoderma*. *App. Microbiol. Biotechnol.* 87, 787–799. doi: 10.1007/s00253-010-2632-1

Shwethakumari, U., Pallavi, T., and Prakash, N. B. (2021). Influence of foliar silicic acid application on soybean (*Glycine max* L.) varieties grown across two distinct rainfall years. *Plants* 10, 1162. doi: 10.3390/plants10061162

Souri, M. K., and Bakhtiarizade, M. (2019). Biostimulation effects of rosemary essential oil on growth and nutrient uptake of tomato seedlings. *Sci. Horticul.* 243, 472–476. doi: 10.1016/j.scienta.2018.08.056

Sparks, D. L., Page, A. L., Helmke, P. A., and Loeppert, R. H. (2020). *Methods of Soil Analysis, Part 3: Chemical Methods.* Hoboken, New Jersey, U.S.: John Wiley and Sons.

Steel, R., and Torrie, J. (1980). *Principles and Procedures of Statistics, 2nd Edn*. New York, NY: McGraw-Hill.

Tarantino, A., Lops, F., Disciglio, G., and Lopriore, G. (2018). Effects of plant biostimulants on fruit set, growth, yield and fruit quality attributes of 'Orange rubis®' apricot (*Prunus armeniaca* L.) cultivar in two consecutive years. *Sci. Horticul.* 239, 26–34. doi: 10.1016/j.scienta.2018.04.055

Tembo, Y., Mkindi, A. G., Mkenda, P. A., Mpumi, N., Mwanauta, R., Stevenson, P. C., et al. (2018). Pesticidal plant extracts improve yield and reduce insect pests on legume crops without harming beneficial arthropods. *Front. Plant Sci.* 9, 1425. doi: 10.3389/fpls.2018.01425

Thapa, S., Rai, N., Limbu, A., and Joshi, A. (2020). Impact of *Trichoderma* sp. in agriculture: a mini-review. *J. Biol. Today's World* 9, 227.

Thorne, S. J., Hartley, S. E., and Maathuis, F. J. M. (2020). Is silicon a panacea for alleviating drought and salt stress in crops? *Front. Plant Sci.* 11, 1221. doi: 10.3389/fpls.2020.01221

Tinna, D., Garg, N., Sharma, S., Pandove, G., and Chawla, N. (2020). Utilization of plant growth promoting rhizobacteria as root dipping of seedlings for improving bulb yield and curtailing mineral fertilizer use in onion under field conditions. *Sci. Horticul.* 270, 109432. doi: 10.1016/j.scienta.2020.109432

Velasco, P., Rodríguez, V. M., Soengas, P., and Poveda, J. (2021). Trichoderma hamatum increases productivity, glucosinolate content and antioxidant potential of different leafy brassica vegetables. *Plants* 10, 2449. doi: 10.3390/plants10112449

Velmourougane, K., Prasanna, R., Chawla, G., Nain, L., Kumar, A., and Saxena, A. K. (2019). Trichoderma–Azotobacter biofilm inoculation improves soil nutrient availability and plant growth in wheat and cotton. *J. Basic Microbiol.* 59, 632–644. doi: 10.1002/jobm.201900009

Verma, K. K., Song, X.-P., Tian, D.-D., Guo, D.-J., Chen, Z.-L., Zhong, C.-S., et al. (2021a). Influence of silicon on biocontrol strategies to manage biotic stress for crop protection, performance, and improvement. *Plants* 10, 2163. doi: 10.3390/plants10102163

Verma, K. K., Song, X.-P., Zeng, Y., Guo, D.-J., Singh, M., Rajput, V. D., et al. (2021b). Foliar application of silicon boosts growth, photosynthetic leaf gas exchange, antioxidative response and resistance to limited water irrigation in sugarcane (*Saccharum officinarum* L.). *Plant Physiol. Biochem.* 166, 582–592. doi: 10.1016/j.plaphy.2021.06.032

Vinale, F., Sivasithamparam, K., Ghisalberti, E. L., Marra, R., Woo, S. L., and Lorito, M. (2008). Trichoderma–plant–pathogen interactions. *Soil Biol. Biochem.* 40, 1–10. doi: 10.1016/j.soilbio.2007.07.002

Xu, L., and Geelen, D. (2018). Developing biostimulants from agro-food and industrial by-products. *Front. Plant Sci.* 9, 1567. doi: 10.3389/fpls.2018.01567

Conflict of Interest: The authors declare that the research was conducted in the absence of any commercial or financial relationships that could be construed as a potential conflict of interest.

Publisher's Note: All claims expressed in this article are solely those of the authors and do not necessarily represent those of their affiliated organizations, or those of the publisher, the editors and the reviewers. Any product that may be evaluated in this article, or claim that may be made by its manufacturer, is not guaranteed or endorsed by the publisher.

frontiers | Frontiers in Plant Science

ORIGINAL RESEARCH
published: 19 May 2022
doi: 10.3389/fpls.2022.885156

Humic Acid Modified by Being Incorporated Into Phosphate Fertilizer Increases Its Potency in Stimulating Maize Growth and Nutrient Absorption

Jianyuan Jing[1†], Shuiqin Zhang[1†], Liang Yuan[1], Yanting Li[1], Chengrong Chen[2] and Bingqiang Zhao[1]*

[1] Key Laboratory of Plant Nutrition and Fertilizer, Ministry of Agriculture and Rural Affairs, Institute of Agricultural Resources and Regional Planning, Chinese Academy of Agricultural Sciences, Beijing, China, [2] School of Environment and Science, Australian Rivers Institute, Griffith University, Nathan, QLD, Australia

OPEN ACCESS

Edited by:
Nicola Tomasi,
University of Udine, Italy

Reviewed by:
Hassan Etesami,
University of Tehran, Iran
Jose M. Garcia-Mina,
University of Navarra, Spain

***Correspondence:**
Bingqiang Zhao
zhaobingqiang@caas.cn

[†] These authors have contributed equally to this work and share first authorship

Specialty section:
This article was submitted to Plant Nutrition, a section of the journal Frontiers in Plant Science

Received: 27 February 2022
Accepted: 22 April 2022
Published: 19 May 2022

Citation:
Jing J, Zhang S, Yuan L, Li Y, Chen C and Zhao B (2022) Humic Acid Modified by Being Incorporated Into Phosphate Fertilizer Increases Its Potency in Stimulating Maize Growth and Nutrient Absorption. Front. Plant Sci. 13:885156. doi: 10.3389/fpls.2022.885156

Humic acid-enhanced phosphate fertilizer (HAP) is widely applied in Chinese agriculture due to its high efficiency. Although the structural composition and physicochemical properties of humic acid (HA) are significantly altered during HAP production, a clear understanding of the mechanisms underlying the biological effects of HA extracted from HAP fertilizer (PHA) on plant growth is still lacking. In the current study, we extracted PHA from HAP and assessed its effects on the dry biomass, phosphorus (P) and nitrogen (N) uptake, and P absorption rate of maize seedlings when supplied at different concentrations (2.5, 5, 10, and 25 mg C L^{-1}) in the hydroponic culture. The root vigor, root plasma membrane H^+-ATPase activity, and root nitrate reductase activity were also determined as the representative indicators of the root capacity for nutrient absorption, and used to clarify the mechanism by which PHA affects the maize growth and nutrient absorption. The results showed that the dry biomass, phosphorus uptake, nitrogen uptake, and average phosphorus absorption rates were significantly higher by 14.7–27.9%, 9.6–35.1%, 17.9–22.4%, and 22.1–31.0%, respectively, in plants treated with 2.5–5 mg C L^{-1} PHA compared to untreated controls. Application of 10–25 mg C L^{-1} raw HA resulted in similar stimulatory effects on plant growth and nutrient absorption. However, higher levels of PHA (10–25 mg C L^{-1}) negatively impacted these indicators of plant growth. Furthermore, low PHA or high raw HA concentrations similarly improved root vigor and root plasma membrane H^+-ATPase and nitrate reductase (NR) activities. These results indicate that lower concentrations of PHA can stimulate maize seedling growth and nutrient absorption to an extent that is comparable to the effect of higher concentrations of raw HA. Thus, the proportion of HA incorporated into HAP could be lower than the theoretical amount estimated through assays evaluating the biological effects of raw HA.

Keywords: humic acid-enhanced phosphate fertilizer, humic acid, biological activity, maize, concentration

INTRODUCTION

Field application of humic acid-enhanced phosphate fertilizer (HAP) has been shown to increase crop yields and phosphorus (P) use efficiency when compared to conventional phosphate fertilizers (Li et al., 2017; Ma et al., 2019). Its higher performance is due to the effects of humic acid (HA) on P bioavailability, stimulation of plant growth, and nutrient absorption (Eyheraguibel et al., 2008; Yang et al., 2019; De Hita et al., 2020). However, only trace amounts of HA are present in HAP (i.e., typically lower than 0.5% *w*/*w*) (Zhao et al., 2020), suggesting that HA provides a greater contribution toward stimulating root growth and nutrient absorption than toward modulating P bioavailability (Eyheraguibel et al., 2008; Rose et al., 2014). Thus, the in-depth study of the bioactive effects of HA in HAP (PHA) on the production of plants cultivated in hydroponics is beneficial to clarify the mechanism that HA enhances the efficiency of phosphate fertilizer, and provides an important reference for HAP production (Urrutia et al., 2013).

Many studies have suggested that HA shows strong biological activity in promoting plant growth and the absorption of macronutrients, such as nitrogen (N) and P (Canellas et al., 2010; Jannin et al., 2012; Shah et al., 2018; De Hita et al., 2020; Jindo et al., 2020), and that these effects can be modulated by variations in the structural composition, molecular weight, and concentrations of different compounds in heterogenous HA. For example, HA that is structurally enriched in carboxyl groups and hydrophobic structures has been reported to increase the root surface area, whereas HA with a greater proportion of aromatic and carbonyl groups have been linked to the increase of root number and diameter (García et al., 2016). Alternatively, HA composed of more smaller molecular components is reportedly most effective for inducing the absorption, transport, and assimilation of NO_3^- (Albuzio et al., 1986; Nardi et al., 2000; Zanin et al., 2018; Pizzeghello et al., 2020), while HA containing a higher proportion of high molecular components has been described as a potent positive regulator of root growth in other studies (Zandonadi et al., 2007; Canellas et al., 2009). Thus, the chemical structure of HA affects its function as a plant growth stimulator, while it is uncertain which chemical structure is predominantly available.

It is well-established that high temperature can substantially alter the structural composition of HA (Zhou et al., 2019), while a lot of heat is generated by exothermic neutralization reactions between phosphoric acid and alkaline compounds during the production of phosphate fertilizers (Peng and Xiang, 2017). Hence, the incorporation of HA into the phosphate fertilizer can change its structure, which has been verified by our previous study (Jing et al., 2020). The change likely leads to differences in the effects and potency of PHA on plant growth compared to carbon equivalent concentrations of HA. Whether PHA also maintained the bioactive effects on plant growth as HA was of great significance for revealing the enhancement mechanism of PHA on the efficiency of phosphate fertilizers.

Additionally, HA concentration can also serve as an important factor that determines its effect on the stimulation of plant growth. Pizzeghello et al. (2020) identified a positive, linear, and concentration-dependent relationship between biomass production and HA concentration (ranging from 0 to 1 mg C L^{-1}) in garlic. However, work by Rose et al. (2014) indicated that plant biomass production followed a bell-shaped distribution with increasing HA concentration. Likewise, Garcia et al. (2016) observed adverse effects on the root of *Brachiaria* following the application of high concentrations of HA, which can be attributed to redox imbalance. Most of the previous studies focused on the influence of individual factors while overlooking the comprehensive contributions of structural properties, the molecular weight of constituent compounds, and concentration in the mechanistic analyses of the HA effects on plant growth.

The objective of this study is to determine the biological activity of PHA, identify the possible mechanisms by which HAP enhances plant growth and nutrient absorption, and provide a reference for the amount of HA incorporated into phosphate fertilizer. To this end, we extracted PHA from HAP and conducted a series of hydroponic experiments to assess the effects of 2.5–25 mg C L^{-1} of HA or PHA on biomass production, P and N uptake, and P absorption rate in maize. We also examine representative indicators of the root capacity for nutrient absorption, including root vigor and root plasma membrane H^+-ATPase activity, as well as root nitrate reductase activity as an indicator of nitrogen metabolism for biomass production.

MATERIALS AND METHODS

Preparation of HA and PHA

Humic acid was extracted from weathered coal (45°23′ N, 119°15′ E; Huolinhe, Tongliao, Inner Mongolia Autonomous Region, Northeast China) according to the method conducted by Zhang et al. (2017). Subsequently, HAP incorporated with 0.5% HA was manufactured, and PHA was extracted from HAP and purified as described by Jing et al. (2020). In brief, 56.03 g of potassium hydroxide was added to the mixture containing 0.50 g of HA and 46.47 g of phosphoric acid (85% in *v*/*v*) under continuous stirring, and the reaction product was immediately pulverized and grounded through a 0.85 mm sieve to obtain the HAP fertilizer. Ten samples were prepared to achieve enough amounts of HAP for the extraction of PHA. HAP was dissolved in deionized water at a solid–liquid ratio of 1:10, and the pH of the mixture was adjusted to 1.0 using 6 M HCl. After standing for 24 h, the solution was centrifuged. The insoluble portions were collected and thoroughly washed four times with deionized water at a solid–liquid ratio of 1:10 and then oven-dried at 50°C to obtain PHA.

The phosphorus content of HA and PHA was determined using inductively coupled plasma emission spectrometer (5110 ICP-OES, Agilent Technologies Inc., USA) after wet digestion with H_2SO_4-H_2O_2 (Kalra, 1998). The contents of carbon, hydrogen, oxygen, nitrogen, and sulfur in HA and PHA were determined using an element analyzer (Vario Micro Cube, Elementar Analysensysteme GmbH, Germany). The relative proportions of C-containing functional groups and the molecular weight distributions of HA and PHA were determined using solid-state ^{13}C nuclear magnetic resonance spectrometer (Bruker

TABLE 1 | Elemental composition, relative proportions of C-containing functional groups, hydrophobicity index, and the percentage of the fractions with molecular weight <3,500 Da in all the detected molecular weights of HA and PHA.

Sample	Elemental composition (%)						Relative proportions of C-containing functional groups (%)						HI	The percentage of molecular weight ≤3,500 Da (%)
	P	C	H	O	N	S	Carbonyl (220–190)	Carboxylic acid (190–160)	O-Aryl (160–140)	C-Aryl (140–110)	O-Alkyl (110–60)	O-CH_3 (60–45)	Alkyl (45–0)	
HA	0.9	59.5	2.7	31.1	2.5	0.8	0.0	9.4	5.0	81.2	4.0	0.3	0.2	6.4	56.9
PHA	1.1	48.2	3.0	26.1	1.4	0.4	0.1	7.0	6.1	82.1	4.2	0.4	0.2	7.6	75.7

Hydrophobicity index (HI) = Σ[(0–45 ppm) + (110–160 ppm)]/ Σ[(45–60 ppm) + (60–110 ppm) + (160–190 ppm) + (190–220 ppm)], calculated as Bento et al. (2020).

AVANCE III HD 400 MHz, Switzerland) and gel permeation chromatography (GPC, Shimazu LC-20A, Japan) as described by Jing et al. (2020). The data of the above parameters are presented in **Table 1** and **Supplementary Figure S1**.

Hydroponic Maize and Experimental Design

Maize hybrid ZD958, a dominant high-yield hybrid in North China, was used in this study. Hydroponic experiments on maize seedling growth were conducted in an artificial climate chamber (28°C day/21°C night, 16 h/8 h light/dark period, 300 μmol m^{-2} s^{-1} light intensity, and 70% relative humidity) at the Dezhou experimental station, Chinese Academy of Agricultural Sciences. Before hydroponic culture, maize seeds were presoaked and pregerminated as described by Jing et al. (2020), and then the endosperm of seedlings was removed, and each plant was transplanted to containers filled with Hoagland nutrient solution (pH = 6.1) (Mao and Shen, 2011) containing HA or PHA at different concentrations. According to the previous studies by our group and others (Jing et al., 2020; Rosa et al., 2021), the concentration gradient of HA or PHA was set as 2.5, 5, 10, and 25 mg C L^{-1}. The nutrient solution with 0 mg C L^{-1} of HA or PHA was set as a control. Six replicates were arranged for each treatment. During the incubation period, the nutrient solution was renewed every 72 h.

Sampling and Laboratory Analyses

During the incubation, the volume of initial and replaced nutrient solution was accurately measured, and meanwhile, the sampling of nutrient solution was conducted for the further P concentration analysis. The P concentration in the sampled nutrient solution was determined by the vanadium molybdate yellow colorimetric method (Haslemore and Roughan, 1976). Then, the P absorption rate of the plant was calculated according to formula (1).

On the 30th day after seed germination, the plant was harvested and divided into roots and shoots. All replicates for each treatment were split into two halves. One-half was stored in liquid nitrogen to retain freshness, and the remaining half was oven-dried at 105°C for 30 min and then at 75°C for 48 h to determine the dry biomass of the plants.

The fresh samples were used to measure the physiological traits as follows. The root vigor was evaluated by TTC (2, 3, 5-triphenyltetrazolium chloride) reduction method (Chen et al., 2006). The root plasma membrane (PM) H^+-ATPase activity was determined by using Plant H^+-ATP ELISA Kit (Jianglai Biological, Shanghai, China). The root nitrate reductase (NR) activity was assayed by monitoring the nitrite formation by the colorimetric method, as indicated by Jaworski (1971). The oven-dried samples were ground using a ball mill (MM400, RETSCH, Germany), and the P and N content was determined after wet digestion with H_2SO_4-H_2O_2 (Kalra, 1998). The P content was determined using the vanadium molybdate yellow colorimetric method (Johnson and Ulrich, 1959), and the N content was determined using the Kjeldahl method (Bremner, 1960).

Calculations and Statistical Analysis

Based on the decrease in the amount of P in the nutrient solution per unit time, the P absorption rates (mg day^{-1}) of a plant can be calculated as:

$$P\ absorption\ rate = \frac{C_1 \times V_1 - C_2 \times V_2}{D} \quad (1)$$

where C_1 and C_2 are the concentrations of P (mg/ml) in the initial and replacement of nutrient solution, respectively; V_1 and V_2 are the volumes of initial and replacement of nutrient solution (ml), respectively; and *D* is the number of days that the nutrient solution was used, and D was 3 days in this study.

All values are shown as the mean of all replicates. The variance among different treatments was analyzed by using SAS 9.1 (SAS Institute Inc., NC, USA). The differences in maize traits between HA and PHA treatments at the same concentration were compared with two independent sample *t*-tests, while the differences between different HA or PHA concentrations were evaluated by performing an analysis of variance (ANOVA) with the least significant difference (LSD) ($\alpha = 0.05$). LSD was also used to assess the interaction between the type and concentration of HA and PHA. We conducted a structural equation model (SEM) to explore the direct and total effects of root vigor, and root PM H^+-ATPase and root NR activities on the nutrient absorption, and Pearson correlation analysis was used to explore the relationship between nutrient absorption and root vigor or root PM H^+-ATPase activity. Graphs were compiled by using Origin 2021 (Origin Lab Corporation, MA, USA).

RESULTS

PHA Shows Stronger Stimulatory Effects on Maize Biomass Production Than HA at Low Concentrations

To better understand the effects of PHA on the growth of maize plants, we first compared biomass production between maize plants treated with different concentrations of HA or PHA. The results showed that humic acid type, the concentration, and the interaction between type and concentration significantly impacted the accumulation of maize dry biomass ($P < 0.01$) (**Supplementary Table S1**). HA led to 16.6% and 30.7% higher total dry biomass than control plants at 10 and 25 mg C L^{-1} ($P < 0.05$), respectively, although it had no significant impact on total dry biomass at the concentrations of 2.5 or 5 mg C L^{-1} (**Figure 1A**). In contrast, application of 2.5 or 5 mg C L^{-1} PHA significantly increased total dry biomass by 14.7 and 27.9%, respectively, compared to the untreated controls ($P < 0.05$), but resulted in a significant decrease in biomass of 14.5 and 24.6% at 10 and 25 mg C L^{-1} concentrations, respectively ($P < 0.05$). A comparison of HA and PHA at the equivalent carbon concentration showed that biomass production was significantly higher under PHA treatment at low concentrations (i.e., 2.5–5 mg C L^{-1}) ($P < 0.05$), whereas HA application provided significantly stronger effects than PHA at higher concentrations (i.e., 10-25 mg C L^{-1}) (**Figure 1A**). In addition, quantification of root biomass and shoot biomass under HA or PHA treatments recapitulated the effects of different concentrations on total dry biomass (**Figures 1B,C**). Taken together, these results indicated that PHA provided stronger stimulatory effects on biomass production in maize at lower concentrations than HA.

PHA Provides Its Maximal Effects on Nutrient Uptake at Lower Concentrations Than HA

Given that PHA application led to increased biomass accumulation in both above- and below-ground plant organs, we next measured P and N uptake under exposure to different concentrations of PHA or HA (**Figures 2A,B**). The results indicated that humic acid type, concentration, and the interaction between type and concentration significantly impacted P or N uptake ($P < 0.01$) (**Supplementary Table S1**). Although HA had no significant impact on P or N uptake at low concentrations (i.e., 2.5–5 mg C L^{-1}) ($P > 0.05$), at high concentrations of HA (i.e., 10–25 mg C L^{-1}), the uptake of both macronutrients was significantly greater than that observed in the untreated control plants ($P < 0.05$) (**Figures 2A,B**). Conversely, PHA treatments significantly enhanced nutrient uptake at lower concentrations (i.e., 2.5–5 mg C L^{-1}) ($P < 0.05$), but significantly reduced P and N uptake at higher concentrations ($P < 0.05$) relative to that observed in controls (**Figures 2A,B**). Maximum nutrient uptake for each treatment was observed at 25 mg C L^{-1} HA and 5 mg C L^{-1} PHA, with 58.5 and 35.1% higher P uptake corresponding to these respective treatments (**Figure 2A**), and 32.9 and 17.5% higher N uptake, respectively, compared to that of controls (**Figure 2B**).

At equivalent carbon concentrations, nutrient uptake was significantly higher under PHA treatments than that under HA treatment at low concentrations ($P < 0.05$), although no significant differences were identified between HA and PHA treatments in P uptake at 2.5 mg C L^{-1} ($P > 0.05$). At high concentrations (10–25 mg C L^{-1}), nutrient uptake was significantly higher in plants treated with HA compared to those subjected to PHA treatment ($P < 0.05$) (**Figures 2A,B**). Moreover, nutrient uptake by roots and shoots under different concentrations of HA or PHA was generally consistent with total P or N uptake (**Supplementary Figures S2A–D**).

We then compared the rates of P absorption by maize under different concentrations of HA or PHA over 30 days of cultivation (**Figure 3A**). During the cultivation, the average rates of P absorption increased along with HA concentration by 4.9, 10.5, 26.7, and 27.2% at 2.5, 5, 10, and 25 mg C L^{-1}, respectively, compared to that in the untreated controls (**Figure 3B**). In contrast, average P absorption rates increased by 21.9 and 30.6% over that in controls under treatment with 2.5 and 5 mg C L^{-1} PHA, respectively. However, average P absorption rates were lower than the rates observed in control plants, by 5.8 and 40.5% on average, under 10 and 25 mg C L^{-1} PHA, respectively (**Figure 3B**). Comparison of treatments at equivalent carbon concentrations indicated that average P absorption rates by maize were significantly higher in PHA than HA at 2.5 or 5 mg C L^{-1}, but significantly higher in HA compared to PHA at 10 or 25 mg C

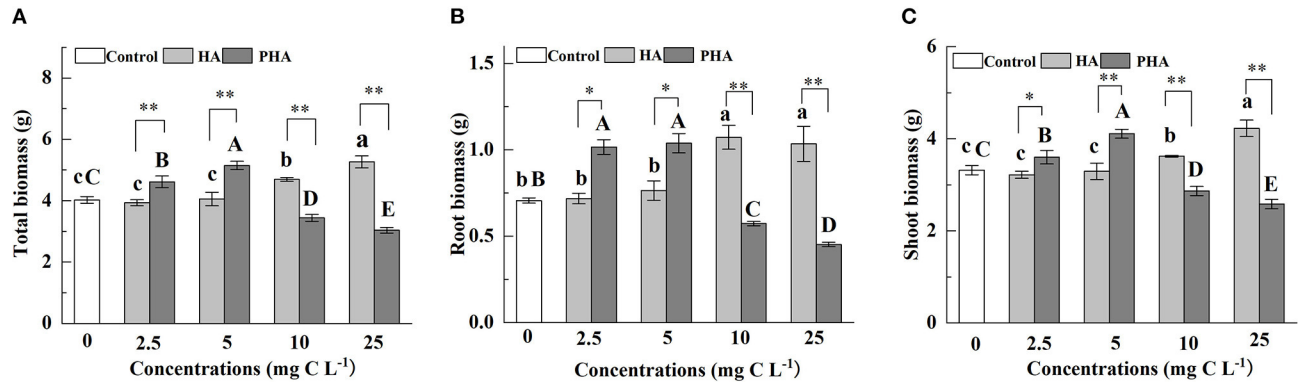

FIGURE 1 | Effects of 2.5–25 mg C L^{-1} of HA or PHA on the **(A)** total dry biomass, **(B)** root biomass, and **(C)** shoot biomass. Error bars represent standard deviations ($n = 3$). Different lowercase letters above columns indicate significant differences between HA and control treatments, while different capital letters above columns indicate significant differences between PHA and control treatments at $P < 0.05$, as determined by the LSD test. Significant differences between HA and PHA treatments at equivalent carbon concentrations were compared with two independent sample *t*-tests, $^{*}P < 0.05$; $^{**}P < 0.01$.

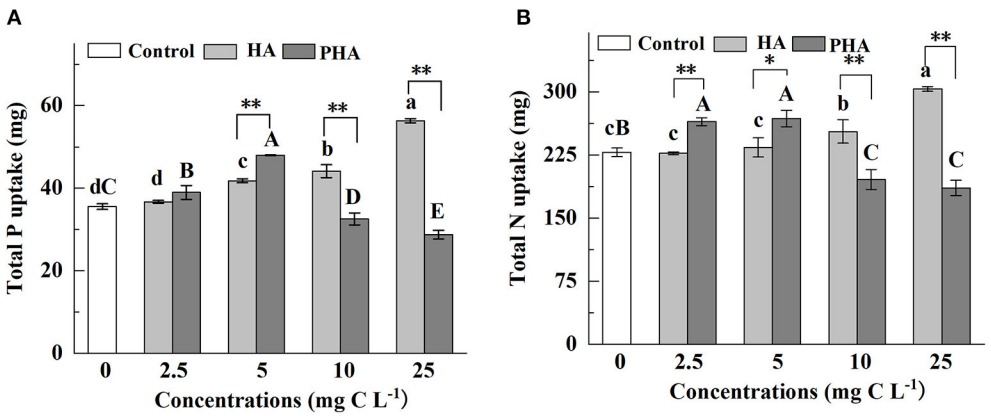

FIGURE 2 | Effects of 2.5–25 mg C L^{-1} of HA and PHA on the **(A)** total P uptake and **(B)** N uptake. Error bars represent standard deviations ($n = 3$). Different lowercase letters above the column indicate significant differences between HA and control treatments, while different capital letters above the column indicate significant differences between PHA and control treatments at $P < 0.05$, as determined by the LSD test. Significant differences between HA and PHA treatments at equivalent carbon concentrations were compared with two independent sample *t*-tests, $^{*}P < 0.05$; $^{**}P < 0.01$.

L^{-1} ($P < 0.05$). These results suggested that the positive effects of PHA on nutrient uptake were strongest at lower concentrations than those conferred by HA treatment.

PHA Provides Maximal Stimulatory Effects on Root Nutrient Absorption Capacity at Lower Concentrations Than HA

Since root vigor and root plasma membrane (PM) H^+-ATPase activity are known as representative indicators related to nutrient absorption by roots (Azevedo et al., 2019; Huang et al., 2021), we measured these traits in order to assess the effects of PHA on the capacity of root to absorb nutrients. The results showed that HA treatments resulted in significantly increased root vigor and root PM H^+-ATPase activity at concentrations of 10 or 25 mg C L^{-1} compared to the control treatments, but had no significant impact on these indicators at 2.5 or 5 mg C L^{-1} ($P > 0.05$) (**Figures 4A,B**). In agreement with our experimental results, both indicators were significantly higher at 2.5–5 mg C L^{-1} of PHA than that in controls ($P < 0.05$) (**Figures 4A,B**). However, at 10–25 mg C L^{-1} of PHA, root vigor was significantly lower than that of control plants ($P < 0.05$) (**Figure 4A**), and root PM H^+-ATPase activity was not significantly different from controls (**Figure 4B**). Notably, at 2.5 or 5 mg C L^{-1}, root vigor and root PM H^+-ATPase activity were significantly higher in PHA treatments than in HA treatments, but significantly higher in HA than PHA at 10 or 25 mg C L^{-1} ($P < 0.05$). These results suggested that both PHA and HA application could lead to higher root vigor and root PM H^+-ATPase activity than that observed in the absence of either treatment, but with maximal effects conferred at lower concentrations of PHA compared to HA.

Concentration of PHA With Largest Stimulation on Root Nitrate Reductase Is Lower Than That of HA

Since nitrate reductase (NR) activity in roots is an important indicator to assess nitrogen metabolism, we investigated whether

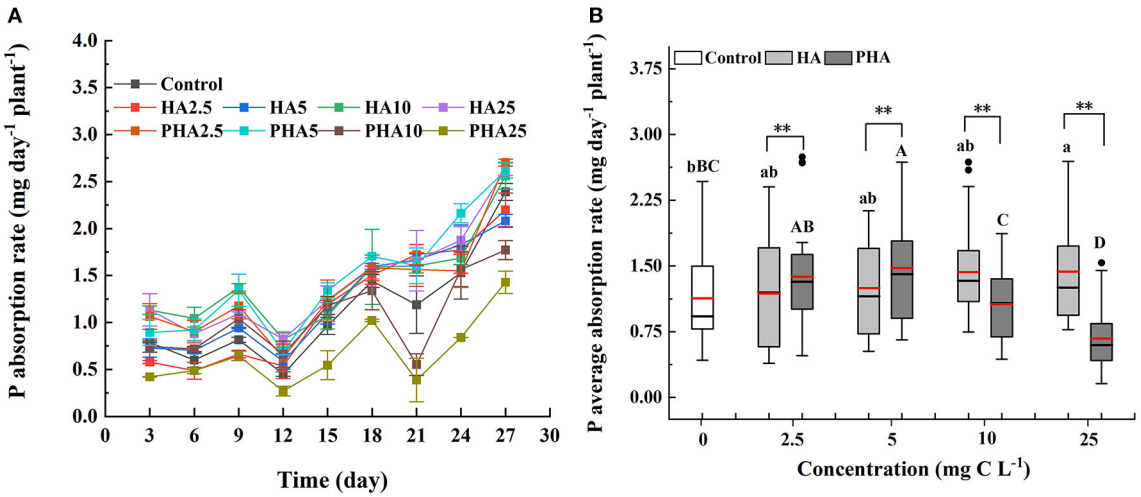

FIGURE 3 | Effects of 2.5–25 mg C L^{-1} of HA and PHA on **(A)** P absorption rate over time ($n = 3$) and **(B)** average P absorption rate ($n = 27$). **(B)** Black lines, median value; red lines, mean value; lower and upper edges of the boxes, 25th and 75th percentiles of all data; bars, 5th and 95th percentiles of all data; dots in outside the boxes, <5th and >95th percentiles of all data. Different lowercase letters above the column indicate significant differences between HA and control treatments, while different capital letters above the column indicate significant differences between PHA and control treatments at $P < 0.05$, as determined by the LSD test. Significant differences between HA and PHA treatments at equivalent carbon concentrations were compared with two independent sample *t*-tests, $^{**}P < 0.01$.

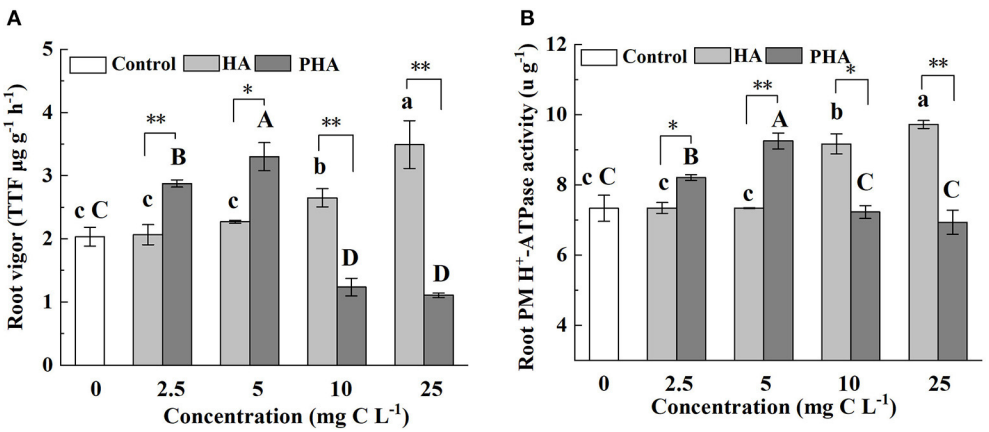

FIGURE 4 | Effects of 2.5–25 mg C L^{-1} of HA and PHA on **(A)** root vigor and **(B)** root plasma membrane (PM) H^+-ATPase activity. Different lowercase letters above the column indicate significant differences between HA and control treatments, while different capital letters above the column indicate significant differences between PHA and control treatments at $P < 0.05$, as determined by the LSD test. Significant differences between HA and PHA treatments at equivalent carbon concentrations were compared with two independent sample *t*-tests, $^{*}P < 0.05$; $^{**}P < 0.01$.

and how different concentrations of HA or PHA affected this activity. The results showed that root NR activity was significantly higher than that in control plants at high concentrations of HA (i.e., 10–25 mg C L^{-1}) ($P < 0.05$), but not significantly different from controls at 2.5 mg C L^{-1} ($P > 0.05$) (**Figure 5**). However, compared to the NR activity detected in the untreated control plants, the application of 2.5–5 mg C L^{-1} of PHA resulted in significantly elevated root NR activity, while higher concentrations (10–25 mg C L^{-1}) of HA significantly decreased root NR activity ($P < 0.05$) (**Figure 5**). As evident in the above-mentioned comparisons between equivalent treatments, root NR activity was significantly higher in PHA treatments than in HA treatments at low concentrations, but higher in HA treatments than PHA at high concentrations ($P < 0.05$). These results indicated that both PHA and HA could increase root NR activity at different concentrations.

DISCUSSION

Modification of Humic Acid *via* Its Incorporation Into Phosphate Fertilizer Lowers the Concentration Required to Stimulate Maize Growth

In this study, we show that the stimulatory effects on plant growth and nutrient absorption by HA or PHA are affected

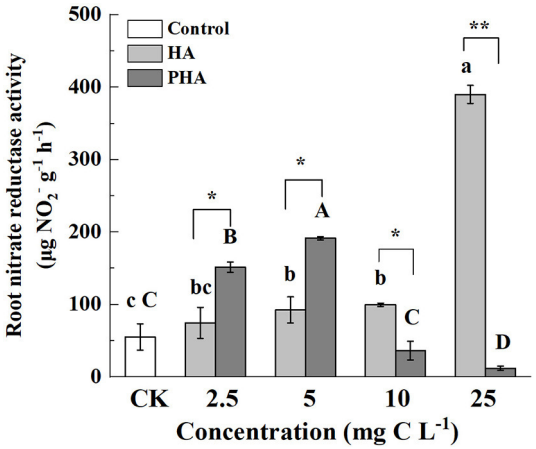

FIGURE 5 | Effects of 2.5–25 mg C L^{-1} of HA and PHA on root nitrate reductase activity. Different lowercase letters above the column indicate significant differences between HA and control treatments, while different capital letters above the column indicate significant differences between PHA and control treatments at $P < 0.05$, as determined by the LSD test. Significant differences between HA and PHA treatments at equivalent carbon concentrations were compared with two independent sample *t*-tests, $^{*}P < 0.05$; $^{**}P < 0.01$.

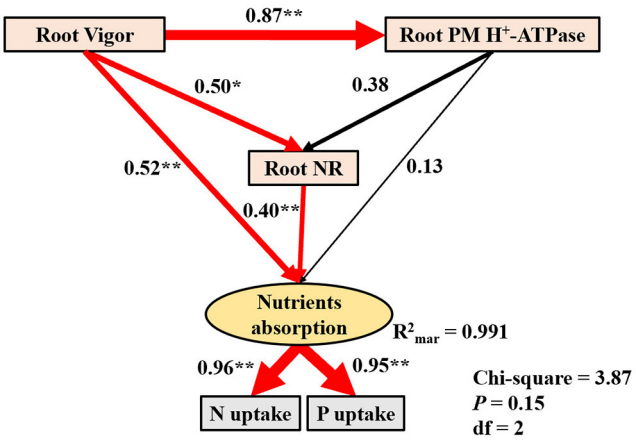

FIGURE 6 | A structural equation model to test the effects of root vigor, root PM H^{+}-ATPase, and root nitrate reductase (NR) on nitrogen and phosphorus absorption. The width of the connections represents estimates of the standardized path coefficients, with solid lines representing a positive relationship and dashed lines a negative relationship. Significant connections are shown in red and non-significant connections in black. Significance was determined at: $^{*}P < 0.05$, $^{**}P < 0.01$.

by their concentration (**Supplementary Table S1**), and the concentration of PHA required to significantly increase dry biomass and nutrient absorption is lower than that of HA, which could be explained by differences in the structural characteristics of HA and PHA. Compared with HA, PHA was characterized by the presence of more low-molecular-weight compounds and a higher hydrophobicity index, and less number of carboxylic groups (**Table 1**). Previous reports showed that HA with a larger proportion of low-molecular-weight compounds exhibits higher potency in promoting the growth of garlic (*Allium sativum* L.) plantlets than HA containing a larger proportion of high-molecular-weight compounds at concentrations ranging from 0 to 5 mg C L^{-1} (Pizzeghello et al., 2020). Similarly, HA with strong hydrophobicity and more carboxylic groups shows greater beneficial effects on root growth, root area, root mitotic site, and root PM H^{+}-ATPase activity (Jindo et al., 2012) at lower concentrations than HA with low hydrophobicity, which requires higher application rates to achieve the same results on plant productivity (Monda et al., 2018). These findings are supported by our results that show lower concentrations of PHA can provide similar stimulatory effects on plant growth as higher concentrations of HA (**Figures 1A**, **2A,B**), which can be attributed to PHA containing a greater percentage of low-molecular-weight components than HA (**Table 1**, **Supplementary Figures S1C,D**), while incongruity with the fact that PHA has less carboxyl groups than HA. The result is also inconsistent with the view that HA-mediated promotion of root growth seems to be more closely related to HA mobility, molecular conformation, and functional group distribution than to molecular weight (Olaetxea et al., 2018). The above incongruity might be attributed to the fact that there was a greater variation of the molecular weight distribution between PHA and HA than that of the carboxyl group content (**Table 1**). Additionally, the result of this research also suggests that the actual quantity of HA, added during the preparation of HAP, that is required to obtain optimal effects on plant growth could be less than that determined by theoretical calculations based on the biological effects of raw HA.

PHA Can Improve Root Vigor and Root Nitrate Reductase Activity to Enhance Absorption of Macronutrients

The increase in nutrient uptake is usually attributed to the enhancement of root physiological indexes, such as root vigor, root PM H^{+}-ATPase activity, and root nitrate reductase (NR) activity (Olaetxea et al., 2018; Azevedo et al., 2019; Zhou et al., 2022), while the primary factor varied for different environmental conditions. Therefore, we constructed a structural equation model to analyze inherent relationships between nutrient uptake and root physiological traits affected by HA or PHA. Our model showed that nutrient absorption (P or N) is directly positively influenced by root vigor (**Figure 6**), which indicated that PHA application enhances nutrient absorption through improved root vigor when compared to HA.

The higher absorption of P or N in PHA is also directly stimulated by root NR activity (**Figure 6**), since root NR catalyzes the first step in the reduction of nitrate N to organic forms in plants, and increasing NR activity promotes N accumulation (Cordeiro et al., 2011). This is consistent with previous results that higher root NR activity and more nutrient uptake were observed in maize treated with low-molecular-weight HA (Vaccaro et al., 2015; Zanin et al., 2018). Moreover, root NR activity also has positive effects on P absorption (**Figure 6**), implying that enzymes associated with N metabolism also

contribute to P uptake. This co-regulatory effect on N and P uptake could be explained by the requirement of both essential macronutrients in plant biomass production, for example, nucleic acid and nucleoprotein synthesis (Marschner, 2012). Overall, PHA can improve P or N uptake by enhancing root vigor and stimulating root NR activity.

In addition, previous studies have also reported that the positive effect of HA on root PM H^+-ATPase activity is the main factor affecting nutrient absorption (Xu et al., 2012; Olaetxea et al., 2018; Azevedo et al., 2019). However, in this study, root PM H^+-ATPase activity had no significant impact on nutrient absorption ($P > 0.05$) (**Figure 6**). Further correlation analysis revealed that P or N uptake shares a generally positive correlation with root vigor and root PM H^+-ATPase activity ($P < 0.001$, $n = 27$), although the correlation coefficients for uptake and root vigor (P uptake, $R^2 = 0.90$; N uptake, $R^2 = 0.94$) are higher than those observed for uptake and root PM H^+-ATPase activity (P uptake, $R^2 = 0.88$; N uptake, $R^2 = 0.85$), implying that nutrient uptake is more strongly affected by root vigor than PM H^+-ATPase activity. This result is supported by the lack of significant effects on nutrient absorption by root PM H^+-ATPase activity in our structural equation model.

CONCLUSION

This study has clearly demonstrated that PHA retains the bioactive effects of raw HA in stimulating maize seedling growth and P or N absorption. HA or PHA appears to increase nutrient absorption by enhancing root vigor and stimulating root NR activity. However, lower concentrations of PHA can provide similar stimulatory effects on plant growth and nutrient absorption as higher concentrations of HA. These results have indicated that the actual proportion of HA being incorporated into HAP for optimal effects on maize growth and macronutrient uptake could be lower than that determined through the assays that evaluated the biological effects of raw HA.

DATA AVAILABILITY STATEMENT

The raw data supporting the conclusions of this article will be made available by the authors, without undue reservation.

AUTHOR CONTRIBUTIONS

BZ conceived and designed the study. JJ and SZ conducted the experiments and wrote the main manuscript. LY, YL, and CC contributed to data interpretation. All authors were involved in revising the manuscript.

FUNDING

This work was financially supported by the National Key Technologies R&D Program of China during the 13th Five-Year Plan period (2016YFD0200402).

SUPPLEMENTARY MATERIAL

The Supplementary Material for this article can be found online at: https://www.frontiersin.org/articles/10.3389/fpls.2022.885156/full#supplementary-material

REFERENCES

Albuzio, A., Ferrari, G., and Nardi, S. (1986). Effects of humic substances on nitrate uptake and assimilation in barley seedlings. *Can. J. Soil Sci.* 66, 731–736. doi: 10.4141/cjss86-072

Azevedo, I. G. D., Olivares, F. L., Ramos, A. C., Bertolazi, A. A., and Canellas, L. P. (2019). Humic acids and Herbaspirillum seropedicae change the extracellular H^+ flux and gene expression in maize roots seedlings. *Chem. Biol. Technol. Agric.* 6, 8. doi: 10.1186/s40538-019-0149-0

Bento, L. R., Melo, C. A., Ferreira, O. P., Moreira, A. B., Mounier, S., Piccolo, A., et al. (2020). Humic extracts of hydrochar and Amazonian Dark Earth: molecular characteristics and effects on maize seed germination. *Sci. Total Environ.* 708, 135000. doi: 10.1016/j.scitotenv.2019.135000

Bremner, J. M. (1960). Determination of nitrogen in soil by the Kjeldahl method. *J. Agr. Sci.* 55, 11–33. doi: 10.1017/S0021859600021572

Canellas, L. P., Piccolo, A., Dobbss, L. B., Spaccini, R., Olivares, F. L., and Zandonadi, D. B., et al. (2010). Chemical composition and bioactivity properties of size-fractions separated from a vermicompost humic acid. *Chemosphere* 78, 457–466. doi: 10.1016/j.chemosphere.2009.10.018

Canellas, L. P., Spaccini, R., Piccolo, A., Dobbss, L. B., Okorokova-Facanha, A. L., and Santos, G. D. A., et al. (2009). Relationships between chemical characteristics and root growth promotion of humic acids isolated from Brazilian oxisols. *J. Soil Sci.* 174, 611–620. doi: 10.1097/SS.0b013e3181bf1e03

Chen, C. W., Yang, Y. W., Lur, H. S., Tsai, Y. G., and Chang, M. C. (2006). A novel function of abscisic acid in the regulation of rice (*Oryza sativa* L.) root growth and development. *Plant Cell Physiol.* 47, 1–13. doi: 10.1093/pcp/pci216

Cordeiro, F. C., Santa-Catarina, C., Silveira, V., and De Souza, S. R. (2011). Humic acid effect on catalase activity and the generation of reactive oxygen species in corn (*Zea mays*). *Biosci. Biotech. Bioch.* 75, 70–74. doi: 10.1271/bbb.100553

De Hita, D., Fuentes, M., Fernandez, V., Zamarreno, A. M., Olaetxea, M., and Garcia-Mina, J. M. (2020). Discriminating the short-term action of root and foliar application of humic acids on plant growth: emerging role of jasmonic acid. *Front. Plant Sci.* 11, 493. doi: 10.3389/fpls.2020.00493

Eyheraguibel, B., Silvestre, J., and Morard, P. (2008). Effects of humic substances derived from organic waste enhancement on the growth and mineral nutrition of maize. *Bioresour. Technol.* 99, 4206–4212. doi: 10.1016/j.biortech.2007.08.082

García, A. C., De Souza, L. G. A., Pereira, M. G., Castro, R. N., García-Mina, J. M., and Zonta, E., et al. (2016). Structure-property-function relationship in humic substances to explain the biological activity in plants. *Sci. Rep.* 6, 20798. doi: 10.1038/srep20798

Garcia, A. C., Olaetxea, M., Santos, L. A., Mora, V., Baigorri, R., and Fuentes, M., et al. (2016). Involvement of hormone- and ROS-signaling pathways in the beneficial action of humic substances on plants growing under normal and stressing conditions. *Biomed Res. Int.* 2016, 3747501. doi: 10.1155/2016/3747501

Haslemore, R. M., and Roughan, P. G. (1976). Rapid chemical analysis of some plant constituents. *J. Sci. Food Agr.* 27, 1171–1178. doi: 10.1002/jsfa.2740271214

Huang, C. C., Song, X., Huang, S. M., Zhang, K. K., and Yue, K. (2021). Analysis of differences in root morphology, phosphorus transport and yield of wheat with different phosphorus efficiency (in Chinese). *Acta. Agric. Boreal Sin.* 36, 169175. doi: 10.7668/hbnxb.20191728

Jannin, L., Arkoun, M., Ourry, A., Laine, P., Goux, D., and Garnica, M., et al. (2012). Microarray analysis of humic acid effects on Brassica napus growth: Involvement of N, C and S metabolisms. *Plant Soil* 359, 297–319. doi: 10.1007/s11104-012-1191-x

Jaworski, E. G. (1971). Nitrate reductase assay in intact plant tissues. *Biochem. Biophys. Res. Co.* 43, 1274–1279. doi: 10.1016/S0006-291X(71)80010-4

Jindo, K., Martim, S. A., Navarro, E. C., Perez-Alfocea, F., Hernandez, T., and Garcia, C., et al. (2012). Root growth promotion by humic acids from composted and non-composted urban organic wastes. *Plant Soil* 353, 209–220. doi: 10.1007/s11104-011-1024-3

Jindo, K., Olivares, F. L., Malcher, D. J. D. P., Sánchez-Monedero, M. A., Kempenaar, C., and Canellas, L. P. (2020). From lab to field: role of humic substances under open-field and greenhouse conditions as biostimulant and biocontrol agent. *Front. Plant Sci.* 11, 426. doi: 10.3389/fpls.2020.00426

Jing, J. Y., Zhang, S. Q., Yuan, L., Li, Y. T., Lin, Z. A., and Xiong, Q. Z., et al. (2020). Combining humic acid with phosphate fertilizer affects humic acid structure and its stimulating efficacy on the growth and nutrient uptake of maize seedlings. *Sci. Rep.* 10, 17502. doi: 10.1038/s41598-020-74349-6

Johnson, C. M., and Ulrich, A. (1959). *Analytical Methods for Use in Plant Analysis.* Berkeley: University of California, Agricultural Experiment Station.

Kalra, Y. P. (1998). Handbook of reference methods for plant analysis. *Crop Sci.* 38, 1710–1711. doi: 10.2135/cropsci1998.0011183X003800060050x

Li, J., Yuan, L., Zhao, B. Q., Li, Y. T., Wen, Y. C., and Li, W. (2017). Effect of adding humic acid to phosphorous fertilizer on maize yield and phosphorus uptake and soil available phosphorus content. *J. Plant Nutr. Fert. Sci.* 23, 641–648 (in Chinese). doi: 10.11674/zwyf.16319

Ma, M. K., Yuan, L., Li, Y. T., Gao, Q., and Zhao, B. Q. (2019). The effect of sulfonated humus acid phosphate fertilizer on enhancing grain yield and phosphorus uptake and utilization in winter wheat. *J. Plant Nutr. Fert. Sci.* 25, 362–369 (in Chinese). doi: 10.11674/zwyf.18461

Mao, D. R., and Shen, J. B. (2011). *Research Methods of Plant Nutrition.* Beijing: China Agricultural University Press.

Marschner, P. (2012). *Mineral Nutrition of Higher Plants.* Netherlands: Academic Press.

Monda, H., Cozzolino, V., Vinci, G., Drosos, M., Savy, D., and Piccolo, A. (2018). Molecular composition of the Humeome extracted from different green composts and their biostimulation on early growth of maize. *Plant Soil* 429, 407–424. doi: 10.1007/s11104-018-3642-5

Nardi, S., Pizzeghello, D., Gessa, C., Ferrarese, L., and Casadoro, G. (2000). A low molecular weight humic fraction on nitrate uptake and protein synthesis in maize seedlings. *Soil Bio. Biochem.* 32, 415–419. doi: 10.1016/S0038-0717(99)00168-6

Olaetxea, M., De Hita, D., Garcia, C. A., Fuentes, M., Baigorri, R., and Mora, V., et al. (2018). Hypothetical framework integrating the main mechanisms involved in the promoting action of rhizospheric humic substances on plant root- and shoot- growth. *Agric,. Ecosyst. Environ,. Appl. Soil Ecol.* 123, 521–537. doi: 10.1016/j.apsoil.2017.06.007

Peng, B. L., and Xiang, S. L. (2017). Study on industrial technology of fertilizer grade wet-process phosphoric acid to produce industrial MAP. *Mod. Chem. Ind.* 37, 152–155 (in Chinese). doi: 10.16606/j.cnki.issn0253-4320.2017.07.036

Pizzeghello, D., Schiavon, M., Francioso, O., Dalla Vecchia, F., Ertani, A., and Nardi, S. (2020). Bioactivity of size-fractionated and unfractionated humic substances from two forest soils and comparative effects on N and S metabolism, nutrition, and root anatomy of allium sativum L. *Front. Plant Sci.* 11, 1203. doi: 10.3389/fpls.2020.01203

Rosa, S. D., Silva, C. A., Carletti, P., and Helena Frankland Sawaya, A. C. (2021). Maize growth and root organic acid exudation in response to water extract of compost application. *J. Soil Sci. Plant Nut.* 21, 2770–2780. doi: 10.1007/s42729-021-00564-3

Rose, M. T., Patti, A. F., Little, K. R., Brown, A. L., Jackson, W. R., and Cavagnaro, T. R. (2014). Chapter two - a meta-analysis and review of plant-growth response to humic substances: practical implications for agriculture. *Adv. Agron.* 124, 37–89. doi: 10.1016/B978-0-12-800138-7.00002-4

Shah, Z. H., Rehman, H. M., Akhtar, T., Alsamadany, H., Hamooh, B. T., and Mujtaba, T., et al. (2018). Humic substances: determining potential molecular regulatory processes in plants. *Front. Plant Sci.* 9, 263. doi: 10.3389/fpls.2018.00263

Urrutia, O., Guardado, I., Erro, J., Mandado, M., and García-Mina, J. M. (2013). Theoretical chemical characterization of phosphate-metal–humic complexes and relationships with their effects on both phosphorus soil fixation and phosphorus availability for plants. *J. Sci. Food Agr.* 93, 293–303. doi: 10.1002/jsfa.5756

Vaccaro, S., Ertani, A., Nebbioso, A., Muscolo, A., Quaggiotti, S., and Piccolo, A., et al. (2015). Humic substances stimulate maize nitrogen assimilation and amino acid metabolism at physiological and molecular level. *Chem. Biol. Technol. Agr.* 2, 5. doi: 10.1186/s40538-015-0033-5

Xu, W., Shi, W., Jia, L., Liang, J., and Zhang, J. (2012). TFT6 and TFT7, two different members of tomato 14-3-3 gene family, play distinct roles in plant adaption to low phosphorus stress. *Plant Cell Environ.* 35, 1393–1406. doi: 10.1111/j.1365-3040.2012.02497.x

Yang, F., Zhang, S. S., Song, J. P., Du, Q., Li, G. X., and Tarakina, N. V., et al. (2019). Synthetic humic acids solubilize otherwise insoluble phosphates to improve soil fertility. *Angew. Chem. Int. Edit.* 58, 18883–18886. doi: 10.1002/anie.201911060

Zandonadi, D. B., Canellas, L. P., and Façanha, A. R. (2007). Indolacetic and humic acids induce lateral root development through a concerted plasmalemma and tonoplast H^+ pumps activation. *Planta* 225, 1583–1595. doi: 10.1007/s00425-006-0454-2

Zanin, L., Tomasi, N., Zamboni, A., Sega, D., Varanini, Z., and Pinton, R. (2018). Water-extractable humic substances speed up transcriptional response of maize roots to nitrate. *Environ. Exp. Bot.* 147, 167–178. doi: 10.1016/j.envexpbot.2017.12.014

Zhang, S. Q., Yuan, L., Li, W., Lin, Z. A., Li, Y. T., Hu, S. W., et al. (2017). Characterization of pH-fractionated humic acids derived from Chinese weathered coal. *Chemosphere* 166, 334–342. doi: 10.1016/j.chemosphere.2016.09.095

Zhao, B. Q., Yuan, L., Li, Y. T., and Zhang, S. Q. (2020). *Overview of Value-Added Fertilizer.* Beijing: China Agricultural Science and Technology Press.

Zhou, L. P., Yuan, L., Zhao, B. Q., Li, Y. T., and Lin, Z. A. (2019). Response of maize roots to different additive amounts of weathered coal humic acids. *Sci. Agric. Sin.* 52, 285–292 (in Chinese). doi: 10.3864/j.issn.0578-1752.2019.02.008

Zhou, L. P., Yuan, L., Zhao, B. Q., Li, Y. T., and Zhang, S. Q. (2022). Advances in humic acid structures and their regulatory role in maize roots. *J. Plant Nutr. Fert. Sci.* 28, 334–343 (in Chinese). doi: 10.11674/zwyf.2021006

Conflict of Interest: The authors declare that the research was conducted in the absence of any commercial or financial relationships that could be construed as a potential conflict of interest.

Publisher's Note: All claims expressed in this article are solely those of the authors and do not necessarily represent those of their affiliated organizations, or those of the publisher, the editors and the reviewers. Any product that may be evaluated in this article, or claim that may be made by its manufacturer, is not guaranteed or endorsed by the publisher.

frontiers | Frontiers in Plant Science

ORIGINAL RESEARCH
published: 23 May 2022
doi: 10.3389/fpls.2022.906686

Biostimulatory Action of Vegetal Protein Hydrolysate Compensates for Reduced Strength Nutrient Supply in a Floating Raft System by Enhancing Performance and Qualitative Features of "Genovese" Basil

*Michele Ciriello[1], Luigi Formisano[1], Marios C. Kyriacou[2], Giuseppe Colla[3], Giulia Graziani[4], Alberto Ritieni[4], Stefania De Pascale[1] and Youssef Rouphael[1]**

[1]Department of Agricultural Sciences, University of Naples Federico II, Naples, Italy, [2]Department of Vegetable Crops, Agricultural Research Institute, Aglantzia, Cyprus, [3]Department of Agriculture and Forest Sciences, University of Tuscia, Viterbo, Italy, [4]Department of Pharmacy, University of Naples Federico II, Naples, Italy

OPEN ACCESS

Edited by:
Rosario Paolo Mauro,
University of Catania, Italy

Reviewed by:
Dragana Jakovljević,
University of Kragujevac, Serbia
Giulia Franzoni,
University of Milan, Italy

***Correspondence:**
Youssef Rouphael
youssef.rouphael@unina.it

Specialty section:
This article was submitted to Crop and Product Physiology, a section of the journal Frontiers in Plant Science

Received: 28 March 2022
Accepted: 02 May 2022
Published: 23 May 2022

Citation:
Ciriello M, Formisano L, Kyriacou MC, Colla G, Graziani G, Ritieni A, De Pascale S and Rouphael Y (2022) Biostimulatory Action of Vegetal Protein Hydrolysate Compensates for Reduced Strength Nutrient Supply in a Floating Raft System by Enhancing Performance and Qualitative Features of "Genovese" Basil. Front. Plant Sci. 13:906686. doi: 10.3389/fpls.2022.906686

The floating raft constitutes a valuable system for growing herbs as it effectuates high yield and prime functional quality. However, the pressing need for advancing sustainability in food production dictates the reduction of chemical fertilizer inputs in such intensive production schemes through innovative cultivation practices. In this perspective, our work appraised the productive and qualitative responses of two "Genovese" basil genotypes (Eleonora and Italiano Classico) grown in a floating raft system with nutrient solutions of varied electrical conductivity (EC; 2 and 1 dS m^{-1}) combined with root application of protein hydrolysate biostimulant at two dosages (0.15 and 0.3 0 ml L^{-1} of Trainer®). The phenolic composition, aromatic profile, and antioxidant activities (ABTS, DPPH, and FRAP) of basil were determined by UHPLC/HRMS, GC/MS, and spectrophotometry, respectively. "Eleonora" demonstrated higher number of leaves (37.04 leaves per plant), higher fresh yield (6576.81 g m^{-2}), but lower polyphenol concentration (1440.81 μg g^{-1} dry weight) compared to "Italiano Classico." The lower EC solution (1 dS m^{-1}) increased total phenols (+32.5%), ABTS, DPPH, and FRAP antioxidant activities by 33.2, 17.1, and 15.8%, respectively, and decreased linalool relative abundance by 5.5%. Biostimulant application improved crop performance and increased total phenolic concentration in both genotypes, with the highest phenolic concentration (1767.96 μg g^{-1} dry weight) registered at the lowest dose. Significant response in terms of aromatic profile was detected only in "Eleonora." Our results demonstrate that the application of protein hydrolysate may compensate for reduced strength nutrient solution by enhancing yield and functional quality attributes of "Genovese" basil for pesto.

Keywords: ***Ocimum basilicum*** **L., biostimulants, hydroponic, nutrient solution concentration, volatiles, phenolics, antioxidant activities, UHPLC/HRMS**

INTRODUCTION

The ongoing quest for a healthy lifestyle and modern-day awareness exemplified in "*we are what we eat*" usher consumers to dietary schemes characterized by regular consumption of fruits and vegetables. The association between high consumption of healthy foods and low incidence of chronic disorders is attributed to the beneficial effects of the phytochemical antioxidants typical of plants (Teklić et al., 2021). Phytochemicals are classified into three groups according to their metabolic pathway: phenylpropanoids, alkaloids, and terpenoids (El-Nakhel et al., 2019). Better known as secondary metabolites, these biomolecules, crucial in defense and functional environment-plant interaction (Verma and Shukla, 2015), have always been a natural and indispensable resource for cosmetic, pharmaceutical, and agri-food industries (Mahajan et al., 2020; Ciriello et al., 2021b). Minor plant species, such as herbs, due to a heterogeneous and not fully explored reservoir of secondary metabolites, have rekindled the interest of both consumers and academics (Kwon et al., 2020; Alexopoulos et al., 2021). Basil (*Ocimum basilicum* L., *Lamiaceae*) is an irreplaceable ingredient for traditional Italian dishes ("pesto" and pizza "Margherita") and the pharma-cosmetic sector (Barátová et al., 2015; Ciriello et al., 2021a,b) due to the biosynthesis of low molecular weight organic compounds (i.e., monoterpenes and phenylpropanoids), responsible for its distinctive aroma (Dias et al., 2016). On the other hand, the outstanding nutraceutical value of basil is mainly attributable to a heterogeneous phenolic profile (rosmarinic acid, chicoric acid, caffeic acid, and p-coumaric acid) that, like aroma, is strongly affected by the interaction between genotype and environment (Jakovljević et al., 2019; Ciriello et al., 2021b). To date, phenolic compounds have become among the most investigated natural molecules (Dias et al., 2016). In addition to having a considerable impact on quality attributes (flavor and color), they possess antioxidant, antifungal, and antimicrobial properties, such as being considered multitarget drugs with potential applications in the agri-food sector as surrogates for artificial preservatives (Filip, 2017). Increasingly extreme environmental conditions combined with the demand for high-quality agricultural production have led the growers to alternative cropping systems (Alexopoulos et al., 2021; Ciriello et al., 2021a; Teklić et al., 2021). In this context, the soilless growing system is a viable strategy for the conversion and redevelopment of abandoned urban and peri-urban areas to full-scale green farms (Wortman, 2015). Among hydroponic systems, the floating system is undoubtedly the one that best lends itself to the production of aromatic herbs such as basil (Ciriello et al., 2020, 2021a). This growing system, in addition to being more economically sustainable (lower production and set-up costs), would guarantee, in line with today's market demands, a higher production all year round with standardized characteristics (Bonasia et al., 2017; Prinsi et al., 2020; Aktsoglou et al., 2021; Žlabur et al., 2021). In addition, the potential to control and manipulate the composition of the nutrient solution (NS) would positively change secondary metabolism by enhancing the phytochemical properties of grown horticultural products (Scuderi et al., 2011; Maggini et al., 2014; El-Nakhel et al., 2019; Prinsi et al., 2020; Aktsoglou et al., 2021). The unclear effects of dilute NS (nutrient stresses) on leafy vegetable yield parameters (Fallovo et al., 2009; El-Nakhel et al., 2019; Ciriello et al., 2020; Hosseini et al., 2021) have prompted growers to use concentrated NS that exceed crop needs (Yang and Kim, 2020). Consistent with the guidelines of the European Commission, the need to reduce chemical input while improving yield and quality in intensive production environments has prompted the agricultural sector to become increasingly interested in biostimulants (Carillo et al., 2019; Kerchev et al., 2020; Teklić et al., 2021). The combination of hydroponic and biostimulants appears to be a promising ecological strategy for controlled environment production of high-quality vegetables. Colla et al. (2015) reported that plant protein hydrolysates (PH's) are innovative strategies to address the above challenges. Recent work by Rouphael et al. (2021) pointed out that the use of PH's by foliar application improved the production performance of "Genovese" basil in protected cultures. The effectiveness of these natural products (derived from agricultural by-products) is also confirmed in the work of Caruso et al. (2019) and Cristofano et al. (2021) on arugula (*Eruca sativa* Mill.) and lettuce (*Lactuca sativa* L.), respectively. These results are attributable to bioactive molecules (amino acids and signaling peptides) that exert a plethora of physiological and growth effects on plants while inducing up-regulation of increasingly sought-after secondary metabolites (Colla et al., 2017; Ertani et al., 2017; Caruso et al., 2019). The possibility of sustainably increasing resource use efficiency (Rouphael et al., 2021) by partially ameliorating environmental drawbacks associated with overfertilization makes the application of PH's in floating raft systems (FRS) even more attractive. The complete absence of interactions between the roots and the agricultural soil makes the FRS suitable for studying *in vivo* the real plant responses to biostimulant integration (Tsouvaltzis et al., 2020). To date, there is a lack of information in the literature on the application mode recommended for this cropping system. However, considering that PH's improve the uptake, assimilation, and translocation of nutrients through modifications of the root system, the possibility of applying the biostimulant directly in contact with the root system (in NS) could further enhance its potential. The benefits of biostimulus on production and quality in a soilless superintensive system could be an effective tool to reduce chemical fertilizer inputs, and to improve economic and environmental sustainability. Our work aimed to evaluate the use of a PH in a NS at two different doses to assess the effects on the production performance and quality of two Genovese basil genotypes (Eleonora and Italiano Classico) grown in a FRS with two different nutrient concentrations (1 and 2 dS m^{-1}).

MATERIALS AND METHODS

Plant Material, Experimental Design, and Growth Conditions

The experimental trial was carried out in a passive ventilation greenhouse at the experimental site of the Federico II University

of Naples - Department of Agriculture (DIA) located in Portici (Naples, Italy; lat. 40°51'N, long. 14°34'E; 60 m above sea level), during the summer growing season in 2020. The experimental design was trifactorial in which two "Genovese" basil (*Ocimum basilicum* L.) genotypes [(1) Eleonora, Enza Zaden, Enkhuizen, Noord-Holland, The Netherlands: erect stem, large green, slightly serrated leaves; suitable for open field cultivation; intermediate resistance to *Peronospora belbahrii* and (2) Italiano Classico, La Semiorto Sementi, Sarno, SA, Italy; erect stem, medium height with bright green, slightly blistered "spoon" leaves] were grown in a FRS with two different concentrations of NS (1 dS m^{-1}-Half Strength and 2 dS m^{-1}-Full Strength) and two doses of biostimulants (0.15 and 0.30 ml L^{-1}) plus an untreated control (hereafter $B_{0.15}$, $B_{0.30}$, and Control, respectively). The treatments were performed in triplicate and arranged in a completely randomized block design. On 9 June (18 days after sowing), at the phenological stage of 2–3 true leaves, basil seedlings were transplanted into 54-hole polystyrene trays (52 × 32 × 6 cm; upper hole diameter: 4.5 cm; bottom hole diameter 3 cm; volume: 0.06 l) at a density of 317 plants m^{-2}. The experimental design comprised 36 experimental units, each consisting of a 54-hole tray floating in a 40-liter tank filled with 35 l of NS. The oxygenation of the NS was provided by a submersible pump (Aquaball 60, Eheim, Stuttgart, Germany).

Nutrient Solutions Management, Biostimulant Application, and Harvest

The NS (half strength and full strength) were prepared from osmosis water. The half strength NS was obtained by halving the macronutrient concentration of the full strength stock NS (14.0 mM nitrate, 1.5 mM phosphorus, 3.0 mM potassium, 1.75 mM sulfur, 4.5 mM calcium, 1.5 mM magnesium, and 1.0 mM ammonium). Micronutrient concentrations were for both solutions 15 μM iron, 9 μM manganese, 0.3 μM copper, 1.6 μM zinc, 20 μM boron, and 0.3 μM molybdenum. During the trial, the pH was continuously monitored and maintained at values of 5.8 ± 0.2. At transplanting, a legume PH (Trainer- Hello Nature USA Inc., Anderson, IN 46016) was applied to the NS at two different doses (0.15 ml L^{-1} and 0.30 ml L^{-1}). The biostimulant used, which was free of plant hormones (Rouphael et al., 2018; Paul et al., 2019), contained soluble peptides and amino acids such as Ala, Arg, Asp., Cys, Glu, Gly, His, Ile, Leu, Lys, Met, Phe, Pro, Ser, Thr, Trp, Tyr, and Val, which comprised 5% of the total nitrogen content along with soluble sugars and phenols. At the end of the experiment, 25 plants per experimental unit were sampled to determine biometric parameters such as the number of leaves per plant and fresh yield. The harvested plant material was then placed in a ventilated oven at 60°C until a constant weight was reached to determine the dry yield and the percentage of dry matter (DM = 100 × dry weight/fresh weight). Instead, a homogeneous pool of 20 plants per experimental unit was sampled and placed immediately at −80°C for future qualitative analysis. A plant material sample was freeze-dried (Alpha 1–4, Martin Christ Gefriertrocknungsanlagen GmbH, Osterode am Harz, Germany) and finely ground with a KM13 rotating blade grinder (Bosch, Gerlingen, Germany).

CIELab Color Space Determination

At harvest, color coordinates were recorded on the adaxial surface of ten healthy and fully expanded leaves per experimental unit using a Minolta Chromameter CR-400 portable colorimeter (Minolta Camera Co. Ltd., Osaka, Japan). As described by the International Commission on Illumination (CIE), the color was expressed by L, a*, and b* coordinates by which the Chroma and Hue angle were determined as follows:

$$\text{Chroma} = \left[\left(a^*\right)^2 + \left(b^*\right)^2\right]^{0.5}$$

$$\text{Hue angle} = \tan^{-1} b^* / a^*$$

Determination of ABTS, DPPH, and FRAP Antioxidant Activities

The antioxidants activities were determined following the protocols described by Graziani et al. (2021). For the determination of ABTS antioxidant activity a stock solution was prepared by mixing 44 ml of potassium persulfate (2.45 mM) with 2.50 ml of aqueous solution (7 mM) of 2,2′-azinobis-(3-ethylbenzothiazoline-6-sulfonate) radical ($ABTS^+$) and placed at 20°C (room temperature) for 12 h. The ABTS solution was diluted (1:88) with ethanol until it reached an absorbance of 0.700 ± 0.005 at 734 nm. After that, a 1 ml aliquot of ABTS solution was added to 100 ml of the filtered sample and incubated at room temperature for 2.5 min. For the antioxidant 2,2-diphenyl-1-picryl-hydrazyl (DPPH) activity, 1 ml of methanolic solution of DPPH 100 μM (absorbance of 0.90 ± 0.02 at 517 nm) was added to 0.2 ml of diluted leaf extract and incubated at room temperature for 10 min. For ferric reduction/antioxidant power (FRAP) antioxidant activity determination a FRAP reagent was prepared by mixing 1.25 ml of 2,4,6-triridyl-striazine (TPTZ; 10 mM) in 40 mM Hydrochloric acid, 1.25 ml of 20 mmol ferric chloride in water, and 12.5 ml of 0.3 M sodium acetate (pH 3.6). An aliquot of 2.850 ml of FRAP reagent was added to 0.015 ml of leaf extract and incubated at room temperature for 4 min. The absorbances of the ABTS, DPPH, and FRAP assays were measured with a UV–VIS spectrophotometer (Shimadzu, Japan) at 734, 517, and 593 nm, respectively. Results were expressed as mmol Trolox equivalents kg^{-1} dry weight (dw) of the sample. All determinations were made in triplicate.

Determination of the Polyphenol Profile by Ultra-High Performance Liquid Chromatography and Orbitrap High-Resolution Mass Spectrometry Analysis

Extraction of Polyphenolic Compounds

Polyphenolic compounds were extracted as described by Corrado et al. (2021). Briefly, 0.1 g of finely ground and freeze-dried leaves was extracted in 5 ml of an aqueous methanol solution (60:40, *v/v*). Then, the obtained solution was sonicated and centrifuged at 4,000 rpm for 15 min, and 0.05 ml of supernatant was collected, filtered, and analyzed.

Quantification of Phenolic Compounds

Quantification and separation of phenolic compounds were performed by UltraHigh-Pressure Liquid Chromatography (Dionex UltiMate 3,000 UHPLC, Thermo Fisher Scientific, Waltham, MA, United States) coupled to the Q Exactive Orbitrap LC–MS/MS Mass Spectrometer (Thermo Fisher Scientific, Waltham, MA, United States) as described by El-Nakhel et al. (2021). The polyphenols were separated by using a Luna Omega PS (1.6 m, 50 × 2.1 mm, Phenomenex, Torrance, CA, United States) at 25 ° C. The mobile phase was a two-phase solution containing water (phase A) and acetonitrile (phase B). Both mobile phases contained 0.1% formic acid (*v/v*). Polyphenolic compounds were eluted using the following gradient schedule: 0–1.3 min 5% B, 1.3–9.3 min 5–100% B, 9.3–11.3 min 100% B, 11.3–13.3 min 100–5% B, 13.3–20 min 5% B. The flow rate was 0.2 ml min^{-1}. For all compounds of interest, an ESI source (Thermo Fisher Scientific, Waltham, MA, United States) was used in negative ion mode, with full ion (MS) and all ion fragmentation (AIF) scanning events. Data acquisition and processing were performed with Quan/Qual Browser Xcalibur software, v. 3.1.66.10 Xcalibur, Thermo Fisher Scientific, (Thermo Fisher Scientific, Waltham, MA, United States). Polyphenols were expressed as μg g^{-1} dw.

Determination of Volatile Compounds

The extraction and quantification of volatile compounds (VOCs) were performed by gas chromatography combined with the mass spectrometer technique (GC/MS) after solid phase microextraction (SPME), as described in detail by Ciriello et al. (2021b).

Extraction of Volatile Compounds by the SPME Technique

An aliquot of 0.5 g of frozen sample was placed in glass vials with a screw cap and placed on a heated stirrer (30°C for 10 min) to facilitate the migration of volatile compounds into the headspace. The adsorption of VOCs was performed by introducing a divinylbenzene/carboxane/polydimethylsiloxane fiber 1 cm long and 50/30 μm thick; Supelco® (Bellefonte, PA, United States) into the headspace for 10 min.

Quantification of Volatile Compounds

SPME fiber containing the adsorbed analytes was introduced into the split–splitless injector of the gas chromatograph (GC 6890 N; Agilent, Santa Clara, CA, United States) coupled to the mass spectrometer (MS 5973 N; Agilent, Santa Clara, California, United States). The thermal desorption of the analytes occurred at 250 ° C for 10 min. The oven temperature was maintained at 50°C for 2 min and increased from 50°C to 150°C at 10°C/min and from 150°C to 280°C at 15°C/min. The injection and ion source temperatures were 250°C and 230°C, respectively, and helium (99.999%) was used as a carrier gas with a flow rate of 1 ml min^{-1}. The gas chromatograph was equipped with a capillary column (30 m × 0.250 mm) coated with a 0.25 μm 5% diphenyl/95% dimethylpolysiloxane film (Supelco®, Bellefonte, PA, United States). The mass spectrometer was set at 70 eV. Identification of VOCs identification was performed using the National Institute of Standards and Technology (NIST) Atomic Spectra Database version 1.6 (U.S. Department of Commerce, Gaithersburg, Maryland, United States).

Statistics

The experiment consisted of a randomized block design with three factors: Cultivar-CV, Biostimulant-B, and Nutrient Solution Concentration-NSC. Analysis of variance (ANOVA) was conducted for the main effects and their interactions. In the absence of significant interactions, significant main effects for factors applied at only two levels (CV and NSC) also denote significant differences between the two means. In the case of significant two-way interactions (CV × B, B × NSC, and CV × NSC), interaction means were compared using the Tukey–Kramer HSD test with statistical significance determined at the $p < 0.05$ level. All data are presented as mean ± standard error. Statistical analysis was performed using IBM SPSS 20 (Armonk, NY, United States) package for Microsoft Windows 10. Statistical processing was performed using IBM SPSS 20 (Armonk, NY, United States) package for Microsoft Windows 10.

RESULTS

Yield and Yield Parameters

Regarding the main yield parameters, the cultivar factor significantly influenced all the parameters reported in **Table 1**, except the dry yield. Although "Eleonora" had the highest number of leaves and the highest fresh yield, "Italiano Classico" was characterized by a higher percentage of dry matter. Biostimulant treatment significantly influenced all yield parameters compared to the Nutrient Solution Concentration that affected dry yield and dry matter (**Table 1**).

Biostimulant treatment showed a linear increase in leaf number, fresh yield, and dry yield as a function of the dose used (Control > $B_{0.15}$ > $B_{0.30}$), in contrast to dry matter, which showed the highest value at $B_{0.15}$. Regarding the CV × B interaction for both "Eleonora" and "Italiano Classico," the $B_{0.30}$ dose determined, compared to the Control, an average increase of 13.65 and 21.38% in the number of leaves and dry yield, respectively. The dry matter did not show the same trend since, in "Eleonora," the highest value was obtained at $B_{0.15}$, while in "Italiano Classico," the highest values were obtained at $B_{0.15}$ and $B_{0.30}$. The CV × B interaction did not influence fresh yield that was significantly influenced by the B × NSC interaction (**Figure 1**). Regardless of the NSC, the use of the biostimulant increase fresh yield (**Figure 1**) and dry yield (**Table 1**). However, for the full strength solution (FS; 2 dS m^{-1}), a linear increase of the above two parameters was observed as the concentration of the biostimulant increased. The highest dry matter values were obtained at $B_{0.15}$ for both half strength [HS;1 dS m^{-1}; (7.67%)] and FS (7.88%) nutrient solutions. On the contrary, the highest values were already observed at $B_{0.15}$ for the HS nutrient solution, which did not show significant differences compared to the $B_{0.30}$ dose. The CV × NSC interaction showed significant differences only for dry yield and dry matter. In "Italiano Classico," the use of the FS increases by 4.82 and

TABLE 1 | Analysis of variance and mean comparisons for leaf number, fresh yield, dry yield, and dry matter of Eleonora and Italiano Classico genotypes grown hydroponically under two nutrient solution and dose of biostimulant.

Treatment	Leaf number	Fresh Yield	Dry Yield	Dry matter
	No. plant^{-1}	(g m^{-2})	(g m^{-2})	(%)
Cultivar (CV)				
Eleonora	37.04 ± 0.35	6576.81 ± 126.42	486.40 ± 10.47	7.40 ± 0.06
Italiano Classico	31.34 ± 0.64	6232.70 ± 124.58	481.99 ± 11.89	7.76 ± 0.05
Biostimulant (B)				
Control	31.86 ± 1.15c	5863.99 ± 69.31c	434.65 ± 5.43c	7.40 ± 0.06c
$B_{0.15}$	34.49 ± 0.88b	6365.64 ± 99.00b	490.34 ± 6.12b	7.78 ± 0.05a
$B_{0.30}$	36.21 ± 0.71a	6984.64 ± 95.94a	527.60 ± 10.88a	7.57 ± 0.10b
Nutrient Solution Concentration (NSC)				
Half Strength (HS)	34.33 ± 0.82	6406.93 ± 97.33	479.18 ± 7.47	7.48 ± 0.05
Full Strength (FS)	34.05 ± 0.91	6402.59 ± 159.72	489.21 ± 13.88	7.68 ± 0.08
CV × B				
Eleonora × Control	35.46 ± 0.44bc	6016.81 ± 102.01	435.60 ± 9.8d	7.22 ± 0.03d
Eleonora × $B_{0.15}$	37.23 ± 0.28ab	6601.58 ± 120.67	503.25 ± 6.46bc	7.66 ± 0.08bc
Eleonora × $B_{0.30}$	38.43 ± 0.32a	7112.04 ± 133.79	520.34 ± 13.32ab	7.32 ± 0.06d
Italiano Classico × Control	28.27 ± 0.68f	5711.17 ± 37.28	433.70 ± 5.77d	7.58 ± 0.05c
Italiano Classico × $B_{0.15}$	31.74 ± 0.55d	6129.71 ± 79.32	477.42 ± 7.49c	7.89 ± 0.04a
Italiano Classico × $B_{0.30}$	34.00 ± 0.35c	6857.24 ± 126.91	534.86 ± 17.95a	7.81 ± 0.11ab
B × NSC				
Control × HS	32.40 ± 1.82	5979.71 ± 119.42 cd	442.53 ± 7.57c	7.38 ± 0.06c
$B_{0.15}$ × HS	34.58 ± 0.99	6525.28 ± 136.88b	500.34 ± 8.59b	7.67 ± 0.07b
$B_{0.30}$ × HS	36.01 ± 1.11	6715.79 ± 72.40b	494.67 ± 5.69b	7.40 ± 0.09c
Control × FS	31.33 ± 1.55	5748.27 ± 38.99d	426.76 ± 6.88c	7.42 ± 0.12c
$B_{0.15}$ × FS	34.39 ± 1.56	6206.01 ± 119.12c	480.33 ± 7.13b	7.88 ± 0.06a
$B_{0.30}$ × FS	36.42 ± 0.96	7253.49 ± 79.66a	560.53 ± 7.39a	7.74 ± 0.14ab
CV × NSC				
Eleonora × HS	37.15 ± 0.36	6624.76 ± 102.91	487.73 ± 9.05ab	7.34 ± 0.05d
Eleonora × FS	36.92 ± 0.63	6528.87 ± 238.23	485.06 ± 19.59ab	7.46 ± 0.10c
Italiano Classico × HS	31.50 ± 0.85	6189.10 ± 133.44	470.63 ± 11.72b	7.63 ± 0.05b
Italiano Classico × FS	31.17 ± 1.01	6276.31 ± 218.37	493.35 ± 20.76a	7.89 ± 0.06a
Significance				
CV	***	***	ns	***
B	***	***	***	***
NSC	ns	ns	*	***
CV× B	**	ns	**	**
B × NSC	ns	***	***	**
CV × NSC	ns	ns	*	*

Nutrient solution concentration treatments: HS, half strength; FS, full strength; Biostimulant treatments: Control; $B_{0.15}$ = 0.15 ml L^{-1} of Trainer®; $B_{0.30}$ = ml L^{-1} of Trainer®. ns, non-significant effect. Data represent means ± standard error of 3 replicates (n = 3). Treatment means within each column followed by different letters denote significant differences (p < 0.05) according to Tukey–Kramer HSD test.

**Significant effect at the 0.05 level.*

***Significant effect at the 0.01 level.*

****Significant effect at the 0.001 level.*

3.40% dry yield and dry matter, respectively. The same trend was observed in "Eleonora" only for dry matter (+1.60%).

CIELab Colorimetric Parameters

Except for the Hue angle, significant differences were observed between genotypes for leaf colorimetric characteristics (**Table 2**). "Italiano Classico" showed the highest values of L, a*, b*, and Chroma. Greenness (a*) was the only parameter influenced by the biostimulant, with the highest value obtained at $B_{0.30}$. The different NSC influenced the colorimetric parameters L, a*, and Hue angle, as opposed to b* and Chroma. The latter were significantly affected by the CV × B and CV × NSC interactions (**Table 2**). The CV × NSC interaction also influenced the a* and Hue angle parameters. The biostimulants in the HS solutions did not affect a* and Hue angle, compared to the FS nutrient solution, where the $B_{0.15}$ and $B_{0.30}$ doses increased these parameters, compared to the Control. The CV × NSC interaction showed significant differences only for the parameters L and b*. In both "Eleonora" and "Italiano Classico," the use of HS increased L; the opposite trend was observed for the b* in Eleonora, while no significant differences were registered in "Italiano Classico."

Phenolic Acids

The total phenols were influenced by the factors under investigation and their mutual interactions (**Table 3**). Chicoric acid was the

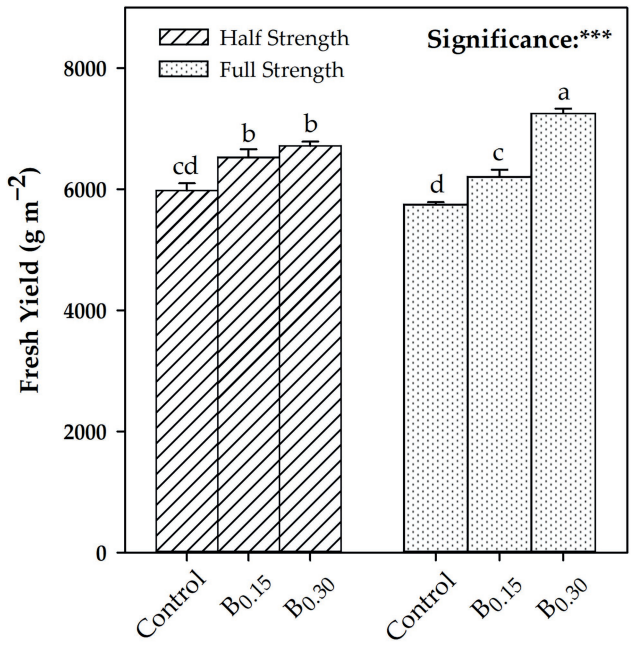

FIGURE 1 | Effects of Biostimulant × Nutrient Solution Concentration interaction for fresh yield [Nutrient solution concentration treatments: Half strength and Full Strength; biostimulant treatments: Control; B0.15 = 0.15 ml L^{-1} of Trainer®; B0.30 = ml L^{-1} of Trainer®]. Different letters denote significant differences ($p < 0.05$) according to Tukey–Kramer HSD test. ***Significant effect at the 0.001 level.

predominant compound, followed by feruloyl tartaric acid, salvianolic acid K, rosmarinic acid, caftaric acid, salvianolic acid L, and chlorogenic acid. "Italiano Classico" showed the highest content of chicoric acid, salvianolic acid K, rosmarinic acid, salvianolic acid L, and chlorogenic acid, while "Eleonora" showed the highest concentration of feruloyl tartaric acid. B and NSC treatments significantly affected the entire phenolic profile (**Table 3**). Specifically, the biostimulant at $B_{0.15}$ dose increased the total phenols by 35.63% compared to the Control. Similarly, the HS increased the total phenol by 32.50%, compared to the HS one. CV × B interaction affected all the parameters reported in **Table 3**. The $B_{0.15}$ dose increased caftaric acid, feruloyl tartaric acid, salvianolic acid K, salvianolic acid L, and total phenols for both genotypes, compared to the Control. On the other hand, the highest chicoric acid values were obtained from the Italiano Classico × $B_{0.15}$ combination (1290.32 μg g^{-1} dw) and Italiano Classico × $B_{0.30}$ (1309.98 μg g^{-1} dw). In comparison, the lowest value was obtained from the combination Eleonora × $B_{0.30}$ (11.68 μg g^{-1} dw). Except for the most and least representative phenolic acids (chicoric and chlorogenic acids, respectively), all phenolic acids were affected by the B × NSC interaction. The $B_{0.15}$ × HS combination provided the highest total phenol concentration (2045.94 μg g^{-1} dw) and feruloyl tartaric acid, salvianolic acid L, salvianolic acid K, and caftaric acid, while the highest concentration of rosmarinic acid was obtained from the Control × HS combination. Compared to the CV × NSC interaction, for both "Eleonora" and "Italiano Classico," the HS, compared to the FS, increased total phenols by 53.99 and 15.95%, respectively. Except for caftaric acid, the highest concentration of all phenolic acids was recorded for both genotypes in the HS.

Antioxidant Activities

The results of the ABTS, DPPH, and FRAP assay are presented in **Table 4** and are expressed as Trolox equivalents mmol kg^{-1} dw. The CV factor did not result in any significant differences for all antioxidant activities, in contrast to what was observed for the B and NSC factors. Specifically, application of Biostimulant at $B_{0.15}$ dose increased ABTS, DPPH, and FRAP by 32.37, 31.37, and 19.80%, respectively, compared to $B_{0.30}$ dose. Relative to the effect of nutrient solution concentrations, HS resulted in a significant increase in all antioxidant activities compared to FS. The CV × B and B × NSC interactions did not result in significant differences for all parameters reported in **Table 4**, compared to the CV × NSC interaction where differences were observed only for DPPH antioxidant activity. In "Italiano Classico," the different nutrient solution concentration did not lead to significant differences for this parameter (DPPH). In contrast, in "Eleonora," the FS reduced DPPH by 27.32%, compared to the HS.

Volatile Compounds

The percentages of the main volatile compounds are shown in **Table 5**. Linalool was the predominant compound, followed by eucalyptol, α-Bergamotene, eugenol, 1-Octen-3-ol, and β-cis-Ocimene. Except for eugenol, all volatile compounds detected were significantly affected by CV. "Eleonora" recorded the highest content of eucalyptol, α-Bergamotene, 1-Octen-3-ol, and β-cis-Ocimene, while "Italiano Classico" showed the highest value of linalool (**Table 5**). The biostimulant influenced the whole aroma profile with the highest content of linalool and eucalyptol obtained at $B_{0.30}$ and $B_{0.15}$ doses, respectively. The same compounds increased with increasing NSC (HF > HS) while the highest values of α-Bergamotene, eugenol, and β-cis-Ocimene were obtained using the HS solution. The CV × B interaction affected the entire profile of volatile compounds (**Table 5**). For "Eleonora," the $B_{0.30}$ dose increase linalool by 27.33%, compared to the control, in contrast to "Italiano Classico," where the application of the biostimulant did not result in significant differences. Furthermore, for "Eleonora," the $B_{0.15}$ dose increased eucalyptol and 1-Octen-3-ol. The highest values of α-Bergamotene, eugenol, and β-cis-Ocimene were obtained from the Eleonora × Control combination. Relative to the B × NSC interaction, at both nutrient solution concentrations, the $B_{0.30}$ dose increase linalool (+11.81%, on avg.) compared with Control. Regardless of dose, the biostimulant in the HS reduced eugenol and α-Bergamotene. The highest values of 1-Octen-3-ol (2.95%) were obtained from the combination of $B_{0.15}$ × HS combination. Except for eucalyptol, all volatile compounds were affected by the CV × NSC interaction (**Table 5**). For "Eleonora," the FS increased linalool and 1-Octen-3-ol, compared to the HS. The opposite trend was observed for α-Bergamotene, eugenol, and β-cis-Ocimene. For "Italiano Classico," only linalool was affected by the different nutrient concentrations, with the highest values recorded by the Italiano Classico × FS combination.

TABLE 2 | Analysis of variance and mean comparisons for CIELab colorimetric parameters of Eleonora and Italiano Classico genotypes grown hydroponically under two nutrient solution and dose of biostimulant.

Treatment	L*	a*	b*	Chroma	Hue angle
Cultivar (CV)					
Eleonora	44.99 ± 0.15	−6.92 ± 0.14	15.97 ± 0.17	17.04 ± 0.16	112.69 ± 0.11
Italiano Classico	45.36 ± 0.10	−7.17 ± 0.12	16.54 ± 0.12	18.09 ± 0.18	112.52 ± 0.18
Biostimulant (B)					
Control	45.15 ± 0.17	−6.82 ± 0.06b	16.38 ± 0.19	17.83 ± 0.26	112.51 ± 0.14
$B_{0.15}$	45.32 ± 0.14	−7.04 ± 0.21ab	16.35 ± 0.23	17.40 ± 0.17	112.61 ± 0.21
$B_{0.30}$	45.06 ± 0.18	−7.28 ± 0.15a	16.04 ± 0.16	17.47 ± 0.33	112.70 ± 0.19
Nutrient Solution Concentration (NSC)					
Half Strength (HS)	45.57 ± 0.06	−6.73 ± 0.08	16.17 ± 0.16	17.45 ± 0.18	112.41 ± 0.15
Full Strength (FS)	44.78 ± 0.11	−7.36 ± 0.13	16.34 ± 0.16	17.68 ± 0.24	112.80 ± 0.13
CV × B					
Eleonora × Control	44.93 ± 0.28	−6.72 ± 0.08	15.90 ± 0.16bc	17.39 ± 0.18c	112.53 ± 0.14
Eleonora × $B_{0.15}$	45.18 ± 0.26	−6.92 ± 0.33	16.33 ± 0.45ab	17.21 ± 0.31 cd	112.57 ± 0.24
Eleonora × $B_{0.30}$	44.86 ± 0.25	−7.13 ± 0.25	15.67 ± 0.14c	16.51 ± 0.24d	112.96 ± 0.11
Italiano Classico × Control	45.37 ± 0.16	−6.91 ± 0.07	16.85 ± 0.22a	18.27 ± 0.44ab	112.49 ± 0.26
Italiano Classico × $B_{0.15}$	45.46 ± 0.09	−7.16 ± 0.29	16.37 ± 0.18ab	17.58 ± 0.10bc	112.65 ± 0.36
Italiano Classico × $B_{0.30}$	45.27 ± 0.24	−7.43 ± 0.17	16.41 ± 0.19ab	18.43 ± 0.22a	112.43 ± 0.35
B × NSC					
Control × HS	45.56 ± 0.14	−6.88 ± 0.08b	16.61 ± 0.23ab	17.61 ± 0.19ab	112.84 ± 0.14ab
$B_{0.15}$ × HS	45.59 ± 0.09	−6.41 ± 0.08b	15.74 ± 0.18c	16.99 ± 0.18b	112.05 ± 0.19c
$B_{0.30}$ × HS	45.57 ± 0.12	−6.91 ± 0.15b	16.17 ± 0.31bc	17.76 ± 0.46ab	112.32 ± 0.31bc
Control × FS	44.73 ± 0.19	−6.75 ± 0.08b	16.14 ± 0.30bc	18.04 ± 0.50a	112.18 ± 0.16c
$B_{0.15}$ × FS	45.06 ± 0.21	−7.67 ± 0.18a	16.96 ± 0.23a	17.81 ± 0.14ab	113.16 ± 0.16a
$B_{0.30}$ × FS	44.56 ± 0.15	−7.65 ± 0.15a	15.91 ± 0.10c	17.18 ± 0.48ab	113.07 ± 0.09a
CV × NSC					
Eleonora × HS	45.53 ± 0.10a	−6.54 ± 0.09	15.71 ± 0.15b	17.06 ± 0.21	112.61 ± 0.17
Eleonora × FS	44.46 ± 0.10c	−7.30 ± 0.19	16.23 ± 0.28a	17.01 ± 0.27	112.76 ± 0.13
Italiano Classico × HS	45.62 ± 0.08a	−6.92 ± 0.11	16.64 ± 0.17a	17.85 ± 0.25	112.21 ± 0.23
Italiano Classico × FS	45.11 ± 0.13b	−7.41 ± 0.19	16.45 ± 0.17a	18.34 ± 0.25	112.84 ± 0.24
Significance					
CV	***	*	***	***	ns
B	ns	**	ns	ns	ns
NSC	***	***	ns	ns	**
CV× B	ns	ns	*	***	ns
B × NSC	ns	***	***	**	***
CV × NSC	**	ns	**	ns	ns

Nutrient solution concentration treatments: HS, half strength; FS, full strength; Biostimulant treatments: Control; $B_{0.15}$ = 0.15 ml L^{-1} of Trainer®; $B_{0.30}$ = ml L^{-1} of Trainer®. ns = non-significant effect. Data represent means ± standard error of 3 replicates (n = 3). Treatment means within each column followed by different letters denote significant differences ($p < 0.05$) according to Tukey–Kramer HSD test.

**Significant effect at the 0.05 level.*

***Significant effect at the 0.01 level.*

****Significant effect at the 0.001 level.*

Principal Component Analysis

A principal component analysis (PCA) for yield, visual and quality attributes was conducted to further explore differences between the two "Genovese" basil genotypes (Eleonora and Italiano Classico), grown in a FRS with two different concentrations of NS (1 dS m^{-1}-Half Strength [HS] and 2 dS m^{-1}-Full Strength [FS]) and two doses of biostimulants (0.15 and 0.30 ml L^{-1}, compared to an untreated control). The first two principal components (PCs) explained 60.7% of the cumulative variance, with PC1 and PC2 accounting for 36.1 and 24.6%, respectively (**Figure 2**). PC1 was positively correlated with all target polyphenols, volatile compounds as well as the antioxidant assays. Also, PC1 correlated negatively with the visual attributes (L, a*, b*). Furthermore, PC2 correlated positively with the three antioxidant activities and target polyphenols (**Figure 2**). Based on the angle between vectors of the examined variables, cichoric acid, chlorogenic acid, total phenols, DPPH and FRAP were found to be positively and significantly correlated among them (angle <90°) and negatively correlated with eucalyptol (angle >90°; **Figure 2**). The PC1 and PC2 score plot discriminated tested treatments into different cluster groups. On the positive side of PC1, "Italiano Classico" fertigated with HS and treated with 0.15 ml L^{-1} of PH delivered basil leaves of premium quality with high concentration of target polyphenols and antioxidant activities. At the lower right quadrant, "Eleonora" supplied with HS solution, showed the highest aroma profile, while the "Eleonora" cultivar fertigated with FS (irrespective of the biostimulant treatment) was positioned in the lower left quadrant distinguished by the poorest nutritional value (**Figure 2**).

TABLE 3 | Analysis of variance and mean comparisons for phenolic acids in Eleonora and Italiano Classico genotypes grown hydroponically under two nutrient solution and dose of biostimulant.

Treatment	Caftaric acid	Chlorogenic acid	Feruloyl tartaric acid	Salvianolic acid K	Salvianolic acid L	Rosmarinic acid	Cichoric acid	Total Phenols
Cultivar (CV)								
Eleonora	48.41 ± 4.78	40.29 ± 1.36	243.49 ± 9.56	42.27 ± 8.03	39.52 ± 9.65	36.28 ± 6.21	990.57 ± 59.63	1440.81 ± 92.40
Italiano Classico	49.30 ± 5.66	42.84 ± 2.01	166.68 ± 13.6	71.62 ± 5.66	50.96 ± 7.56	61.45 ± 3.08	1147.18 ± 59.55	1590.04 ± 86.65
Biostimulant (B)								
Control	32.74 ± 6.48c	35.38 ± 1.39c	166.50 ± 18.61c	45.01 ± 8.31c	28.99 ± 4.75b	57.78 ± 5.52a	937.10 ± 49.81c	1303.50 ± 80.99c
$B_{0.15}$	63.45 ± 5.05a	46.04 ± 1.85a	250.84 ± 13.19a	74.86 ± 10.64a	77.73 ± 13.62a	49.12 ± 5.80b	1205.92 ± 71.14a	1767.96 ± 111.20a
$B_{0.30}$	50.38 ± 4.10b	43.27 ± 1.77b	197.92 ± 13.86b	50.97 ± 7.43b	29.00 ± 2.32b	39.69 ± 8.69c	1063.60 ± 85.47b	1474.83 ± 98.81b
Nutrient Solution Concentration (NSC)								
Half Strength (HS)	58.34 ± 4.32	45.45 ± 1.33	232.89 ± 15.13	78.49 ± 6.65	65.08 ± 9.21	60.38 ± 5.75	1186.69 ± 39.37	1727.32 ± 65.05
Full Strength (FS)	39.37 ± 5.07	37.68 ± 1.59	177.28 ± 11.40	35.40 ± 4.82	25.40 ± 4.81	37.35 ± 4.24	951.05 ± 68.12	1303.54 ± 84.79
CV × B								
Eleonora × Control	47.08 ± 9.54c	38.36 ± 1.61d	223.51 ± 12.48c	28.72 ± 4.59d	27.56 ± 9.44c	62.87 ± 10.17b	1032.96 ± 38.36b	1461.07 ± 83.74d
Eleonora × $B_{0.15}$	56.88 ± 9.52b	42.28 ± 3.02c	269.12 ± 20.79a	66.02 ± 20.85bc	65.8 ± 25.4b	34.28 ± 4.61d	1121.53 ± 133.94b	1655.90 ± 216.47c
Eleonora × $B_{0.30}$	41.27 ± 5.16d	40.22 ± 2.38cd	237.85 ± 11.21b	32.06 ± 5.65d	25.19 ± 2.90c	11.68 ± 2.24e	817.21 ± 84.00c	1205.47 ± 113.17e
Italiano Classico × Control	18.40 ± 3.35e	32.41 ± 1.55e	109.49 ± 8.22e	61.30 ± 13.28c	30.41 ± 3.09c	52.68 ± 4.47c	841.24 ± 75.96c	1145.93 ± 109.18e
Italiano Classico × $B_{0.15}$	70.02 ± 2.06a	49.80 ± 0.57a	232.56 ± 14.12bc	83.69 ± 5.65a	89.67 ± 10.67a	63.96 ± 6.24ab	1290.32 ± 38.46a	1880.01 ± 50.23a
Italiano Classico × $B_{0.30}$	59.49 ± 3.76b	46.33 ± 2.1b	158.00 ± 9.03d	69.88 ± 8.24b	32.81 ± 3.09c	67.70 ± 3.67a	1309.98 ± 28.34a	1744.19 ± 33.61b
B × NSC								
Control × HS	47.03 ± 9.56c	38.72 ± 1.44	189.49 ± 27.69c	64.88 ± 11.67b	42.57 ± 3.27b	73.92 ± 5.34a	1061.13 ± 26.38	1517.73 ± 58.58c
$B_{0.15}$ × HS	76.00 ± 1.56a	49.57 ± 0.61	289.62 ± 11.66a	104.13 ± 4.63a	117.13 ± 5.68a	61.03 ± 7.53b	1348.48 ± 38.73	2045.94 ± 47.29a
$B_{0.30}$ × HS	51.98 ± 0.47b	48.07 ± 1.35	219.56 ± 19.39b	66.46 ± 9.76b	35.54 ± 1.92bc	46.19 ± 13.22c	1150.48 ± 70.42	1618.28 ± 77.63b
Control × FS	18.45 ± 3.38d	32.04 ± 1.42	143.50 ± 23.35e	25.15 ± 3.07e	15.40 ± 3.86c	41.64 ± 1.09cd	813.07 ± 63.78	1089.26 ± 84.11e
$B_{0.15}$ × FS	50.89 ± 6.83bc	42.52 ± 3.13	212.06 ± 5.27b	45.59 ± 11.57c	38.34 ± 12.76bc	37.21 ± 5.89de	1063.37 ± 112.42	1489.97 ± 145.81c
$B_{0.30}$ × FS	48.77 ± 8.53bc	38.48 ± 1.67	176.29 ± 16.78d	35.47 ± 7.19d	22.46 ± 1.73bc	33.20 ± 11.86e	976.72 ± 155.44	1331.38 ± 169.42d
CV × NSC								
Eleonora × HS	66.37 ± 3.78a	45.35 ± 1.07a	276.41 ± 10.05a	65.26 ± 11.9b	67.16 ± 14.2a	48.77 ± 10.03b	1177.81 ± 63.18ab	1747.12 ± 102.13a
Eleonora × FS	30.45 ± 1.51c	35.22 ± 0.58c	210.57 ± 4.01b	19.27 ± 0.61d	11.88 ± 1.86c	23.79 ± 4.92c	803.33 ± 48.52c	1134.50 ± 49.01c
Italiano Classico × HS	50.30 ± 6.99b	45.55 ± 2.53a	189.37 ± 19.95c	91.71 ± 1.51a	63.00 ± 12.55a	71.99 ± 2.49a	1195.58 ± 50.74a	1707.51 ± 86.35a
Italiano Classico × FS	48.3 ± 9.34b	40.14 ± 2.98b	143.99 ± 16.09d	51.54 ± 5.76c	38.92 ± 7.01b	50.91 ± 2.53b	1098.78 ± 109.14b	1472.58 ± 144.94b
Significance								
CV	ns	***	***	***	***	***	***	***
B	***	***	***	***	***	***	***	***
NSC	***	***	***	***	***	***	***	***
CV× B	***	***	***	***	**	***	***	***
B × NSC	***	ns	***	***	***	***	ns	***
CV × NSC	***	***	***	*	***	*	***	***

Nutrient solution concentration treatments: HS, half strength; FS, full strength; Biostimulant treatments: Control; $B_{0.15}$ = 0.15 ml L^{-1} of Trainer®; $B_{0.30}$ = ml L^{-1} of Trainer®. All data are expressed as μg g^{-1} dw. ns = non-significant effect. Data represent means ± standard error of 3 replicates (n = 3). Treatment means within each column followed by different letters denote significant differences (p < 0.05) according to Tukey–Kramer HSD.

**Significant effect at the 0.05 level.*

***Significant effect at the 0.01 level.*

****Significant effect at the 0.001 level.*

DISCUSSION

The PH's in Nutrient Solution Boosted Basil Yield

Soilless systems are increasingly used to maximize the yields of premium quality vegetables. Among these, the FRS is characterized by ease of use, low management costs and high functionality, allowing early production with standard characteristics even on a large scale. The surprising yield obtained in the present study confirms the high efficiency of the FRS for basil cultivation compared to soil cultivation. Compared to the results obtained by Zheljazkov et al. (2008) on 38 basil

TABLE 4 | Analysis of variance and mean comparisons for ABTS, DPPH, and FRAP antioxidant activities of Eleonora and Italiano Classico genotypes grown hydroponically under two nutrient solution and dose of biostimulant.

Treatment	ABTS	DPPH	FRAP
	(mmol Trolox eq. kg^{-1} dw)	(mmol Trolox eq. kg^{-1} dw)	(mmol Trolox eq. kg^{-1} dw)
Cultivar (CV)			
Eleonora	39.84 ± 2.87	28.63 ± 1.79	49.59 ± 2.24
Italiano Classico	39.02 ± 2.23	31.15 ± 1.62	51.86 ± 2.11
Biostimulant (B)			
Control	40.49 ± 2.69ab	30.30 ± 1.58ab	50.60 ± 2.34ab
$B_{0.15}$	44.32 ± 3.50a	33.71 ± 2.47a	55.36 ± 3.04a
$B_{0.30}$	33.48 ± 2.41b	25.66 ± 1.56b	46.21 ± 1.95b
Nutrient Solution Concentration (NSC)			
Half Strength (HS)	45.05 ± 2.42	32.25 ± 1.47	54.44 ± 1.95
Full Strength (FS)	33.81 ± 1.93	27.53 ± 1.80	47.01 ± 2.05
CV × B			
Eleonora × Control	42.18 ± 3.95	30.42 ± 1.61	52.34 ± 3.79
Eleonora × $B_{0.15}$	44.65 ± 6.03	31.81 ± 3.98	51.16 ± 4.34
Eleonora × $B_{0.30}$	32.71 ± 4.06	23.66 ± 2.59	45.28 ± 3.50
Italiano Classico × Control	38.81 ± 3.88	30.18 ± 2.89	48.87 ± 2.92
Italiano Classico × $B_{0.15}$	44.00 ± 4.18	35.61 ± 3.09	59.57 ± 3.83
Italiano Classico × $B_{0.30}$	34.24 ± 2.98	27.66 ± 1.54	47.14 ± 2.05
B × NSC			
Control × HS	46.84 ± 1.75	31.87 ± 1.37	55.34 ± 2.68
$B_{0.15}$ × HS	52.19 ± 4.23	36.88 ± 2.99	59.04 ± 3.57
$B_{0.30}$ × HS	36.13 ± 3.45	28.01 ± 1.78	48.93 ± 2.91
Control × FS	34.14 ± 3.54	28.72 ± 2.84	45.86 ± 2.81
$B_{0.15}$ × FS	36.46 ± 3.36	30.54 ± 3.73	51.68 ± 4.74
$B_{0.30}$ × FS	30.83 ± 3.29	23.31 ± 2.30	43.49 ± 2.31
CV × NSC			
Eleonora × HS	47.85 ± 3.69	33.16 ± 2.34a	55.36 ± 3.22
Eleonora × FS	31.84 ± 2.33	24.10 ± 1.75b	43.82 ± 1.62
Italiano Classico × HS	42.25 ± 3.04	31.34 ± 1.86ab	53.51 ± 2.37
Italiano Classico × FS	35.78 ± 3.06	30.95 ± 2.78ab	50.20 ± 3.55
Significance			
CV	ns	ns	ns
B	**	**	*
NSC	***	*	**
CV× B	ns	ns	ns
B × NSC	ns	ns	ns
CV × NSC	ns	*	ns

Nutrient solution concentration treatments: HS, half strength; FS, full strength; Biostimulant treatments: Control; $B_{0.15}$ = 0.15 $ml L^{-1}$ of Trainer®; $B_{0.30}$ = $ml L^{-1}$ of Trainer® ns, non-significant effect. Data represent means ± standard error of 3 replicates (n = 3). Treatment means within each column followed by different letters denote significant differences ($p < 0.05$) according to Tukey–Kramer HSD test.

**Significant effect at the 0.05 level.*

***Significant effect at the 0.01 level.*

****Significant effect at the 0.001 level.*

cultivars grown in the open field, we recorded average yields approximately 15 times higher. This result is attributable to a better allocation of water and nutritional resources and the high density adopted (317 m^{-2}; Ciriello et al., 2020). Regardless of the growing system, genetic material plays a crucial role in the productive response of basil (Žlabur et al., 2021). It should be noted that "Eleonora" showed better adaptability to the selected cropping system, producing more leaves per plant, and thus providing a higher fresh yield than "Italiano Classico," which, in contrast, had a higher dry matter percentage (**Table 1**). In hydroponic systems, yield is primarily determined by the formulation of the NS, and to this end, numerous studies have focused on seeking optimal mineral levels to achieve *ad hoc* crop-specific "recipes" (Hosseini et al., 2021). For example, some studies have shown reduced yields in spinach (*Spinacia oleracea* L.; Cocetta et al., 2014) and lettuce (Hosseini et al., 2021) when grown in nutrient solutions with suboptimal mineral concentrations. Moreover, in our study, we did not observe any significant change in fresh yield in basil grown in HS (1 dS m^{-1}) and FS (2 dS m^{-1}) nutrient solutions. Our result is in line with the observations of Hosseini et al. (2021), who reported reductions in fresh yield in basil and lettuce grown on nutrient solutions with lower EC of 0.9 dS m^{-1} and corroborated the studies of Walters and Currey (2018) on "Sweet," "Lemon," and "Holy" basil, which did not observe yield increase with EC between 1 and 4 dS m^{-1}. This shows that excess nutrients in the solution provide no benefit in terms of basil yield and negatively affect resource efficiency,

TABLE 5 | Analysis of variance and mean comparisons for volatile compounds in Eleonora and Italiano Classico genotypes grown hydroponically under two nutrient solution and dose of biostimulant.

Treatment	1-Octen-3-ol	Eucaliptol	β-cis-Ocimene	Linalool	Eugenol	α-Bergamotene
Cultivar (CV)						
Eleonora	2.73 ± 0.07	25.42 ± 0.63	2.24 ± 0.14	43.08 ± 1.23	3.86 ± 0.27	7.72 ± 0.55
Italiano Classico	2.38 ± 0.05	17.44 ± 0.30	1.67 ± 0.03	60.77 ± 0.30	3.72 ± 0.20	5.48 ± 0.15
Biostimulant (B)						
Control	2.48 ± 0.06b	20.78 ± 0.90b	2.11 ± 0.18a	49.33 ± 3.40c	4.35 ± 0.35a	7.39 ± 0.97a
$B_{0.15}$	2.81 ± 0.10a	22.64 ± 1.83a	1.9 ± 0.16ab	51.3 ± 2.86b	3.28 ± 0.23b	6.27 ± 0.25b
$B_{0.30}$	2.37 ± 0.05c	20.86 ± 1.06b	1.85 ± 0.10b	55.16 ± 1.93a	3.74 ± 0.17b	6.14 ± 0.15b
Nutrient Solution Concentration (NSC)						
Half Strength (HS)	2.53 ± 0.08	20.83 ± 1.06	2.13 ± 0.13	50.46 ± 2.49	4.09 ± 0.27	7.24 ± 0.63
Full Strength (FS)	2.57 ± 0.07	22.03 ± 1.09	1.78 ± 0.10	53.40 ± 2.09	3.49 ± 0.17	5.95 ± 0.18
CV × B						
Eleonora × Control	2.57 ± 0.1b	23.3 ± 0.74b	2.63 ± 0.16a	38.38 ± 1.6d	5.06 ± 0.46a	9.81 ± 1.31a
Eleonora × $B_{0.15}$	3.10 ± 0.04a	28.59 ± 0.61a	2.06 ± 0.32b	42.00 ± 1.09c	3.010 ± 0.2c	6.91 ± 0.21b
Eleonora × $B_{0.30}$	2.50 ± 0.02bc	24.37 ± 0.20b	2.03 ± 0.18b	48.87 ± 0.62b	3.50 ± 0.14bc	6.43 ± 0.21bc
Italiano Classico × Control	2.38 ± 0.03cd	18.26 ± 0.68c	1.60 ± 0.06c	60.27 ± 0.63a	3.64 ± 0.36bc	4.97 ± 0.22d
Italiano Classico × $B_{0.15}$	2.52 ± 0.11bc	16.69 ± 0.40c	1.74 ± 0.05bc	60.61 ± 0.47a	3.56 ± 0.41bc	5.62 ± 0.24cd
Italiano Classico × $B_{0.30}$	2.23 ± 0.07d	17.36 ± 0.18c	1.67 ± 0.05bc	61.45 ± 0.36a	3.97 ± 0.29b	5.84 ± 0.16cd
B × NSC						
Control × HS	2.33 ± 0.02c	19.74 ± 0.98	2.18 ± 0.28	47.14 ± 5.43e	5.21 ± 0.40a	8.91 ± 1.71a
$B_{0.15}$ × HS	2.95 ± 0.09a	22.14 ± 2.74	2.19 ± 0.26	49.82 ± 4.44d	3.04 ± 0.19c	6.30 ± 0.49b
$B_{0.30}$ × HS	2.33 ± 0.06c	20.61 ± 1.58	2.01 ± 0.17	54.40 ± 2.95ab	4.03 ± 0.28b	6.51 ± 0.17b
Control × FS	2.62 ± 0.08b	21.83 ± 1.46	2.04 ± 0.24	51.51 ± 4.41cd	3.5 ± 0.30bc	5.87 ± 0.50b
$B_{0.15}$ × FS	2.68 ± 0.18b	23.14 ± 2.66	1.61 ± 0.11	52.78 ± 3.93bc	3.53 ± 0.43bc	6.23 ± 0.18b
$B_{0.30}$ × FS	2.41 ± 0.09c	21.12 ± 1.57	1.68 ± 0.07	55.91 ± 2.73a	3.44 ± 0.13bc	5.76 ± 0.15b
CV × NSC						
Eleonora × HS	2.65 ± 0.12b	24.66 ± 1.00	2.62 ± 0.11a	40.94 ± 1.90d	4.34 ± 0.44a	8.95 ± 0.95a
Eleonora × FS	2.81 ± 0.08a	26.18 ± 0.74	1.86 ± 0.19b	45.23 ± 1.30c	3.38 ± 0.23b	6.48 ± 0.15b
Italiano Classico × HS	2.42 ± 0.09c	17.00 ± 0.35	1.64 ± 0.04b	59.98 ± 0.33b	3.85 ± 0.32ab	5.53 ± 0.22c
Italiano Classico × FS	2.34 ± 0.05c	17.88 ± 0.45	1.70 ± 0.05b	61.57 ± 0.32a	3.60 ± 0.25b	5.42 ± 0.21c
Significance						
CV	***	***	***	***	ns	***
B	***	***	*	***	***	***
NSC	ns	**	***	***	***	***
CV× B	***	***	**	***	***	***
B × NSC	***	ns	ns	*	***	***
CV × NSC	***	ns	***	**	*	***

Nutrient solution concentration treatments: HS, half strength; FS, full strength; Biostimulant treatments: Control; $B_{0.15}$ = 0.15 ml L^{-1} of Trainer®; $B_{0.30}$ = ml L^{-1} of Trainer®. All data are expressed as percentage relative abundance (%). ns, non-significant effect. Data represent means ± standard error of 3 replicates (n = 3). Treatment means within each column followed by different letters denote significant differences (p < 0.05) according to Tukey–Kramer HSD.

**Significant effect at the 0.05 level.*

***Significant effect at the 0.01 level.*

****Significant effect at the 0.001 level.*

economic viability, and environmental sustainability of hydroponic systems. The pressing need to ensure high yields of high-quality vegetables by adopting efficient and environmentally friendly cultivation methods makes the application of biostimulants in NS a promising ecological strategy. In our study, the application of PH's (Trainer®) in the NS increased the fresh yield, the dry yield, and the number of leaves proportional to the dose used (**Table 1**). These results highlight that applying the biostimulant directly to the NS is a beneficial strategy to increase yield in hydroponic systems, as also shown by Cristofano et al. (2021) in lettuce. The beneficial effects of PH's on yield parameters, also obtained in arugula (Caruso et al., 2019; Giordano et al., 2020), celery (*Apium graveolens* L.; Consentino et al., 2020) and basil (Rouphael et al., 2021), can be attributed to the peptides and bioactive amino acids characteristic of commercial formulations (Rouphael et al., 2021). Peptides, involved in cell differentiation and division, due to recognized hormone-like activity, modify root architecture and growth, improving uptake and crop yield (Li et al., 2016; Colla et al., 2017; Kim et al., 2019). The above effects are also attributable to amino acids

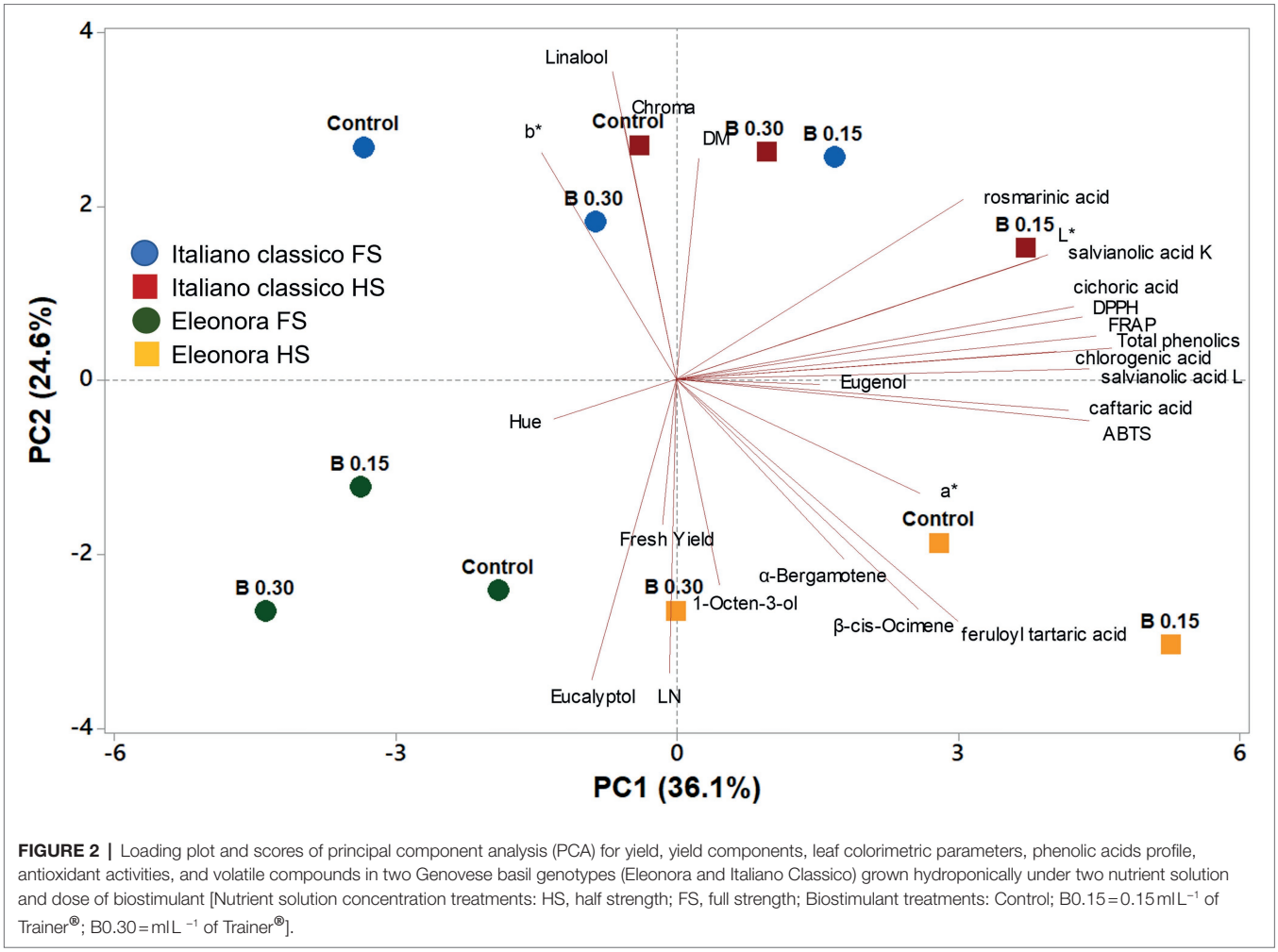

FIGURE 2 | Loading plot and scores of principal component analysis (PCA) for yield, yield components, leaf colorimetric parameters, phenolic acids profile, antioxidant activities, and volatile compounds in two Genovese basil genotypes (Eleonora and Italiano Classico) grown hydroponically under two nutrient solution and dose of biostimulant [Nutrient solution concentration treatments: HS, half strength; FS, full strength; Biostimulant treatments: Control; B0.15 = 0.15 ml L^{-1} of Trainer®; B0.30 = ml L^{-1} of Trainer®].

(easily absorbed by roots) that are involved in essential signaling processes in addition to performing physiological functions (Tsouvaltzis et al., 2020). These molecules found in Trainer® could have promoted nitrogen uptake in the rhizosphere and regulated key transcription factors and photosynthesis (Alfosea-Simón et al., 2021). In contrast to what was observed for the yield, the higher accumulation of dry matter in plants treated with the biostimulant (**Table 1**) is not widely supported in the literature. As an example, Caruso et al. (2019) recorded results comparable to ours in arugula, while Consentino et al. (2020) obtained opposite results in celery. In spinach, Rouphael et al. (2020) observed no significant difference for this parameter. The contrasting results highlight how the effects of biostimulants depend on factors such as time and mode of application, growth conditions, and genotype (Teklić et al., 2021). In line with the above, although the biostimulant, on average, increased the fresh and dry yield, integration of the PH's into the FS and HS solutions showed dose-dependent responses. While, for the FS, increasing the dose led to linear increases in fresh and dry yields, there was no apparent dose-dependent effect for the HS. Under these operating conditions, the above points out that the impact of the biostimulant could also be influenced by the mutual interaction between the application dose and the concentration of the NS.

Different Genotypes Impacted Visual Attributes of Basil Leaves

Color is a characteristic of light measurable in terms of wavelength and intensity, related to the observer's perception and to the light conditions under which it is observed, able of influencing consumer choice about food quality (Pathare et al., 2013). In basil, the bright green color of the leaves and the attraction of consumer interest is a critical industrial requirement for the preparation of a "pesto" sauce, as it reduces the use of artificial colorants (Ciriello et al., 2021b). Although the basil genotypes tested all belonged to the "Genovese" cultivar., CIELab colorimetric parameters (L, a*, b*) showed cultivar-dependent variations, with "Italiano Classico" recording the highest values of all above parameters, confirming the results of Ciriello et al. (2020) on the same basil genotypes grown in FRS. The higher values of L (brightness) and a* (greenness) in "Italiano Classico" are consistent with Chroma values, indicating a higher color intensity perceived by the consumer. The latter parameters (L and a*) were also influenced by the

NSC. In particular, the FS increased leaf brightness (higher L) and greenness (higher a*) compared to the HS, although it did not show any productive differences (**Table 2**). As argued by Fallovo et al. (2009), the more intense green leaf color could be attributed to a higher chlorophyll content (data not shown) related to the higher nitrogen levels of the FS (2 dS m^{-1}). Our color results showed that applying the biostimulant at the highest dose ($B_{0.30}$) in the NS increased only the parameter a *, compared to the Control, in agreement with Consentino et al. (2020). This result could be related again to the increase induced by biostimulants in chlorophyll content, as observed by Vernieri et al. (2006) and Aktsoglou et al. (2021) in arugula and peppermint (*Mentha* × *piperita*), respectively. However, Caruso et al. (2019) and Giordano et al. (2020), despite observing an increase in SPAD (an indirect index of chlorophyll content), did not record a change in color in arugula after the application of PH's. These results confirm once again how the effects of biostimulants differ primarily by species, but also by dose, mode of application, and different growth and development conditions.

Impact of Interactions Between Investigated Factors on Basil Quality Attributes

The inability to "escape" from possible environmental threats has "bound" plants to passive defense mechanisms based on the production of specialized metabolites that have allowed their survival over time (Trivellini et al., 2016). In medicinal plants, specialized metabolites are characterized by significant structural and chemical diversity that uniquely confers the desired technological and nutritional attributes (Dias et al., 2016; Filip, 2017). Although we had used "Genovese" genotypes characterized by a similar phenolic profile in our study, the concentration of total phenolic acids differed considerably (**Table 3**). The higher total phenolic concentration in "Italiano Classico" (**Table 3**), also obtained in other works conducted under different growth conditions, again demonstrates how the accumulation of these compounds is strongly influenced by genetics (Žlabur et al., 2021). Despite this, the antioxidant activities reported in **Table 4** were not affected by the effect of the cultivar. The explanation for this could lie in the fact that between the two genotypes tested there was only a 9.4% difference in the concentration of total phenols, but it could also be due to the synergistic effects between polyphenols and other chemical constituents, such as ascorbic acid and carotenoids that contribute to overall antioxidant activity (Graziani et al., 2021). The data in **Table 3** clearly show the influence of genetics on the diversity of the phenolic profile of the basil genotypes. Although rosmarinic acid is referred to as the most represented phenolic acid in basil (Kiferle et al., 2013; Filip, 2017; Ciriello et al., 2020), in our study, both "Eleonora" and "Italiano Classico" were characterized by a predominant concentration of chicoric acid. The influence of genotype on the predominant biosynthesis of chicoric acid was also confirmed by Kwee and Niemeyer (2011) in basil. The authors showed that 9 basil varieties out of 15 tested had the highest absolute concentration of chicoric acid. Furthermore, it is important to note that the discrepancy with the results reported in the literature is attributable not only to the genetic material but also to the different extraction methods and solvents used to determine the phenolic acids and the different growth conditions adopted (Filip, 2017). Regardless of the cultivar., the present work confirms that basil leaves contain, in addition to high levels of chicoric acid, significant amounts of salviolanic acids K and L. The important and recognized pharmacological properties of salviolanic acid could further increase the nutraceutical value of basil (Prinsi et al., 2020). The change in the entire phenolic profile in response to changing concentrations of NS (**Table 3**) confirms that nutritional stress can affect the biosynthesis and accumulation of specialized metabolites (Mahajan et al., 2020). The use of a HS increased the levels of the entire phenolic profile in both genotypes compared to what was observed in the FS, similar to what was observed in basil (Jakovljević et al., 2019), lettuce (El-Nakhel et al., 2019), artichoke (*Cynara cardunculus* subsp. *scolymus* L.), and cardoon (*Cynara cardunculus* L.; Rouphael et al., 2012). The increase in the phenolic profile showed the same trend as the ABTS, DPPH, and FRAP assays (**Table 4**), indicating how the limitation of nutrition induced an improvement in antioxidant activity. This result and the increase in the phenolic profile are probably related to the halving of nitrate in the HS, which as observed by Chishaki and Horiguchi (1997) has a more significant influence on the accumulation of phenolic acids than potassium and phosphorus deficiency. Low nitrogen levels would stimulate phenylpropanoid metabolism, inducing the accumulation of phenylalanine ammonia-lyase (PAL) and other critical enzymes involved in the biosynthesis of phenolic compounds (Fritz et al., 2006; Wada et al., 2014; Mahajan et al., 2020). This would suggest that low nitrogen levels, by decreasing growth requirements, would promote the accumulation of specialized metabolites (Prinsi et al., 2020). However, in our study, we did not observe a reduction in fresh yield at HS (**Table 1**), which justifies the high phenolic concentration as a result of ex novo synthesis rather than a deceleration of primary metabolism by increased activity of PAL or its substrate (phenylalanine; Gershenzon, 1984). Similarly to the yield parameters (**Table 1**), the application of the biostimulant in the NS significantly increase the phenolic concentration in basil. A probable reason for elucidating this interesting result could be related to the increase in production due to a better photosynthetic activity mediated by the biostimulant, which would have promoted secondary metabolism (Colla et al., 2017). However, the bioactive signal molecules characteristic of PH's, in addition to providing the plethora of physiological effects mentioned above, may have triggered the induction of the production of specialized metabolites. Based on a recent work (Kisa et al., 2021), in which a positive influence was observed on basil secondary metabolism after applying amino acids, our results could be traced to the composition of Trainer®, which is characterized by the presence of these organic molecules. One of the crucial functions of amino acids and molecules derived from them is their ability to serve as precursors for specialized plant metabolites, acting both as substrates and as activators of key enzymes such as chorismate mutase, creating points of interconnection in the biosynthesis of phenolic compounds (Feduraev et al., 2020; Kisa et al., 2021). Interestingly,

regardless of the cultivar and concentration of the nutrient solution, among the biostimulant doses tested ($B_{0.15}$ and $B_{0.30}$), the highest accumulation of total phenolics was obtained after application in the nutrient solution of the lowest dose ($B_{0.15}$) of the biostimulant, confirming that this result was not dose dependent. The justification behind the above could stem from the fact that at dose $B_{0.30}$, the biostimulant prioritized production over secondary metabolism. The variability in the composition of essential oils among basil types gives this aromatic herb a multitude of uses. The non-unique aroma of basil is determined by the various compounds that constitute its essential oils, mainly terpenoids (synthesized through the mevalonate pathway and the 2-methylitritol 4-phosphate pathway) and phenylpropanoids (synthesized through the shikimate pathway; Dudai et al., 2020; Mahajan et al., 2020). The distinctive aroma of "Genovese" basil and its derivative products (such as pesto sauce) is attributable to the dominant presence of critical aromatic molecules such as linalool and the complete absence of mint (menthol) and anise (estragole; Ciriello et al., 2021b). Not surprisingly, in the basil genotypes tested, linalool was the predominant, a compound that, in addition to uniquely characterizing the flavor of the "Genovese" genotypes, also has documented therapeutic properties (Mughal, 2019). However, the differences found in "Eleonora" (higher content of 1-Octen-3-ol, eucalyptol, β-cis-Ocimene, and α-Bergamotene) and "Italiano Classico" (higher content of linalool) in the full aroma profile reported in **Table 5** underscore the significant impact of genotype. These differences could be due to the different leaf morphology, the density of oil glands, vegetative growth, and biosynthesis of volatile odorous compounds (Khammar et al., 2021). Compared to the latter, the higher content of linalool but lower contents of eucalyptol and β-cis-ocimene contents, recorded in "Italiano Classico," compared to "Eleonora," highlights a clear genotypic effect on gene expression that regulates the conversion of its sole precursor (geranyl pyrophosphate) from the enzymes linalool synthase, 1,8-cineole synthase and β-cis-ocimene synthase (Chang et al., 2007). The basil genotypes tested showed a different response to the biostimulant (**Table 5**). As seen in peppermint and spearmint (*Mentha romana* L.; Aktsoglou et al., 2021), biostimulant in the NS did not result in any significant difference in the composition of the aroma profile of Italiano Classico. On the one hand, this result could indicate a low sensitivity of the cultivar to the biostimulant and, on the other hand, it could result from the use of insufficient doses to induce alterations in the overall composition of volatile oils. On the contrary, in "Eleonora," there was a significant effect on the whole aromatic profile caused by the application of the biostimulant. We observed a direct correlation between increasing the dose of biostimulant and the linalool content, contrary to what was observed for eugenol, β-cis-Ocimene and α-Bergamotene, which instead decreased regardless of the dose used. Since plant nutrition is known to influence the content of volatile oils (Aktsoglou et al., 2021), it is not surprising that the use of NS at different concentrations resulted in significant differences in basil flavor profile (**Table 5**). As with the biostimulant, different responses were observed for the NSC between the two basil genotypes used in the present study. In "Italiano Classico," the different NSC changed only the content of the most represented compound (linalool), while in "Eleonora," all compounds, except eucalyptol, were significantly affected by the different availability of nutrients in the nutrient solution. In any case, in both genotypes, the more concentrated nutrient solution (FS) increased the linalool content. As also seen on *Salvia sclarea* L. (Sharma and Kumar, 2012), the higher availability of nutrients, especially nitrogen, led to an increase in the linalool content, as nitrogen, involved in the biosynthesis of primary and secondary metabolites, could positively interact in its metabolic pathway, confirming our results (Khammar et al., 2021).

CONCLUSION

The challenge imposed on the agricultural sector to provide nourishment to a growing population has led to alternative production techniques such as hydroponics. However, the urgent need to reduce chemical inputs in alternative cropping systems has paved the way for biostimulants, which currently represent an environmentally sustainable strategy for horticultural production. Under the experimental conditions of our study, the varietal comparison showed that "Eleonora" provided the highest fresh yield (6576.81 $g\,m^{-2}$). At the same time, "Italiano Classico" had the highest total phenol concentration (1590.04 $\mu g\,g^{-1}$ dw). The use of NS with different concentrations did not result in significant differences in fresh yield, regardless of the cultivar., but positively impacted the aroma and phenolic profile. Specifically, the HS increased total phenols by 32.5%, compared to the FS that ensured the highest content of eucalyptol (22.0%) and linalool (53.4%). The application of biostimulants in the NS increased all biometric parameters (such as the number of leaves, fresh and dry yield) and the linalool content proportionally to the dose used, while the highest total phenol concentration was obtained from the lowest dose ($B_{0.15}$). Based on the excellent results achieved, the application of biostimulants in NS turned out to be a valid strategy to reduce chemical input. For this reason, it should also be investigated on other leafy crops to define a new production technique that can improve both yield and quality.

DATA AVAILABILITY STATEMENT

The raw data supporting the conclusions of this article will be made available by the authors, without undue reservation.

AUTHOR CONTRIBUTIONS

MC, SP, and YR: conceptualization and project administration. MC, LF, MK, GC, GG, and AR: methodology, validation, formal analysis, investigation, and writing—original draft preparation. MC and LF: software, resources, and data curation. MC, LF, and YR: writing—review and editing. SP and YR: visualization, supervision, and funding acquisition. All authors contributed to the article and approved the submitted version.

FUNDING

This research was conducted in the framework of a PhD project sponsored by the Italian Ministry of Education (PON research and innovation).

ACKNOWLEDGMENTS

We are grateful to Raffaele Romano and Fabiana Pizzolongo for providing the access to GC/MS facilities and analysis.

REFERENCES

Aktsoglou, D. C., Kasampalis, D. S., Sarrou, E., Tsouvaltzis, P., Chatzopoulou, P., Martens, S., et al. (2021). Protein hydrolysates supplement in the nutrient solution of soilless grown fresh peppermint and spearmint as a tool for improving product quality. *Agronomy* 11:317. doi: 10.3390/agronomy11020317

Alexopoulos, A. A., Marandos, E., Assimakopoulou, A., Vidalis, N., Petropoulos, S. A., and Karapanos, I. C. (2021). Effect of nutrient solution ph on the growth, yield and quality of taraxacum officinale and reichardia picroides in a floating hydroponic system. *Agronomy* 11:1118. doi: 10.3390/agronomy11061118

Alfosea-Simón, M., Simón-Grao, S., Zavala-Gonzalez, E. A., Cámara-Zapata, J. M., Simón, I., Martínez-Nicolás, J. J., et al. (2021). Physiological, nutritional and metabolomic responses of tomato plants after the foliar application of amino acids aspartic acid, glutamic acid and alanine. *Front. Plant Sci.* 11:581234. doi: 10.3389/fpls.2020.581234

Barátová, S., Mezeyova, I., Hegedusová, A., and Andrejiová, A. (2015). Impact of biofortification, variety and cutting on chosen qualitative characteristic of basil (*Ocimum basilicum* L.). *Acta Fytotech. Zootech.* 18, 71–75. doi: 10.15414/afz.2015.18.03.71-75

Bonasia, A., Lazzizera, C., Elia, A., and Conversa, G. (2017). Nutritional, biophysical and physiological characteristics of wild rocket genotypes as affected by soilless cultivation system, salinity level of nutrient solution and growing period. *Front. Plant Sci.* 8:300. doi: 10.3389/fpls.2017.00300

Carillo, P., Colla, G., El-Nakhel, C., Bonini, P., D'Amelia, L., Dell'Aversana, E., et al. (2019). Biostimulant application with a tropical plant extract enhances corchorus olitorius adaptation to sub-optimal nutrient regimens by improving physiological parameters. *Agronomy* 9:249. doi: 10.3390/agronomy9050249

Caruso, G., De Pascale, S., Cozzolino, E., Giordano, M., El-Nakhel, C., Cuciniello, A., et al. (2019). Protein hydrolysate or plant extract-based biostimulants enhanced yield and quality performances of greenhouse perennial wall rocket grown in different seasons. *Plan. Theory* 8:208. doi: 10.3390/plants8070208

Chang, X., Alderson, P. G., Hollowood, T. A., Hewson, L., and Wright, C. J. (2007). Flavour and aroma of fresh basil are affected by temperature. *J. Sci. Food Agric.* 87, 1381–1385. doi: 10.1002/jsfa.2869

Chishaki, N., and Horiguchi, T. (1997). Responses of secondary metabolism in plants to nutrient deficiency. *Soil Sci. Plant Nut.* 43, 987–991. doi: 10.1080/00380768.1997.11863704

Ciriello, M., Formisano, L., El-Nakhel, C., Corrado, G., Pannico, A., De Pascale, S., et al. (2021a). Morpho-physiological responses and secondary metabolites modulation by Preharvest factors of three hydroponically grown Genovese basil cultivars. *Front. Plant Sci.* 12:671026. doi: 10.3389/fpls.2021.671026

Ciriello, M., Formisano, L., El-Nakhel, C., Kyriacou, M. C., Soteriou, G. A., Pizzolongo, F., et al. (2021b). Genotype and successive harvests interaction affects phenolic acids and aroma profile of genovese basil for pesto sauce production. *Foods* 10:278. doi: 10.3390/foods10020278

Ciriello, M., Pannico, A., El-Nakhel, C., Formisano, L., Cristofano, F., Duri, L. G., et al. (2020). Sweet basil functional quality as shaped by genotype and macronutrient concentration reciprocal action. *Plan. Theory* 9:1786. doi: 10.3390/plants9121786

Cocetta, G., Baldassarre, V., Spinardi, A., and Ferrante, A. (2014). Effect of cutting on ascorbic acid oxidation and recycling in fresh-cut baby spinach (*Spinacia oleracea* L.) leaves. *Postharvest Biol. Technol.* 88, 8–16. doi: 10.1016/j.postharvbio.2013.09.001

Colla, G., Hoagland, L., Ruzzi, M., Cardarelli, M., Bonini, P., Canaguier, R., et al. (2017). Biostimulant action of protein hydrolysates: Unraveling their effects on plant physiology and microbiome. *Front. Plant Sci.* 8:2202. doi: 10.3389/fpls.2017.02202

Colla, G., Nardi, S., Cardarelli, M., Ertani, A., Lucini, L., Canaguier, R., et al. (2015). Protein hydrolysates as biostimulants in horticulture. *Sci. Hortic.* 196, 28–38. doi: 10.1016/j.scienta.2015.08.037

Consentino, B. B., Virga, G., la Placa, G. G., Sabatino, L., Rouphael, Y., Ntatsi, G., et al. (2020). Celery (*Apium graveolens* L.) performances as subjected to different sources of protein hydrolysates. *Plan. Theory* 9, 1–13. doi: 10.3390/plants9121633

Corrado, G., El-Nakhel, C., Graziani, G., Pannico, A., Zarrelli, A., Giannini, P., et al. (2021). Productive and morphometric traits, mineral composition and secondary Metabolome components of borage and Purslane as underutilized species for microgreens production. *Horticulturae* 7:211. doi: 10.3390/horticulturae7080211

Cristofano, F., El-Nakhel, C., Pannico, A., Giordano, M., Colla, G., and Rouphael, Y. (2021). Foliar and root applications of vegetal-derived protein Hydrolysates differentially enhance the yield and qualitative attributes of two lettuce cultivars grown in floating system. *Agronomy* 11:1194. doi: 10.3390/agronomy11061194

Dias, M. I., Sousa, M. J., Alves, R. C., and Ferreira, I. C. F. R. (2016). Exploring plant tissue culture to improve the production of phenolic compounds: A review. *Ind. Crop. Prod.* 82, 9–22. doi: 10.1016/j.indcrop.2015.12.016

Dudai, N., Nitzan, N., and Gonda, I. (2020). *Ocimum basilicum L., in Medicinal, Aromatic and Stimulant Plants*. Germany: Springer, 377–405.

El-Nakhel, C., Pannico, A., Graziani, G., Kyriacou, M. C., Gaspari, A., Ritieni, A., et al. (2021). Nutrient supplementation configures the bioactive profile and production characteristics of three brassica L. microgreens species grown in peat-based media. *Agronomy* 11:346. doi: 10.3390/agronomy11020346

El-Nakhel, C., Pannico, A., Kyriacou, M. C., Giordano, M., De Pascale, S., and Rouphael, Y. (2019). Macronutrient deprivation eustress elicits differential secondary metabolites in red and green-pigmented butterhead lettuce grown in a closed soilless system. *J. Sci. Food Agric.* 99, 6962–6972. doi: 10.1002/jsfa.9985

Ertani, A., Schiavon, M., and Nardi, S. (2017). Transcriptome-wide identification of differentially expressed genes in *Solanum lycopersicon* L. In response to an alfalfa-protein hydrolysate using microarrays. *Front. Plant Sci.* 8:1159. doi: 10.3389/fpls.2017.01159

Fallovo, C., Rouphael, Y., Rea, E., Battistelli, A., and Colla, G. (2009). Nutrient solution concentration and growing season affect yield and quality of *Lactuca sativa* L. var. acephala in floating raft culture. *J. Sci. Food Agric.* 89, 1682–1689. doi: 10.1002/jsfa.3641

Feduraev, P., Skrypnik, L., Riabova, A., Pungin, A., Tokupova, E., Maslennikov, P., et al. (2020). Phenylalanine and tyrosine as exogenous precursors of wheat (*Triticum aestivum* L.) secondary metabolism through PAL-associated pathways. *Plan. Theory* 9:476. doi: 10.3390/plants9040476

Filip, S. (2017). Basil (*Ocimum basilicum* L.) a source of valuable phytonutrients. *Int. J. Clin. Nutr. Diet.* 3, 1–5. doi: 10.15344/2456-8171/2017/118

Fritz, C., Palacios-Rojas, N., Feil, R., and Stitt, M. (2006). Regulation of secondary metabolism by the carbon-nitrogen status in tobacco: nitrate inhibits large sectors of phenylpropanoid metabolism. *Plant J.* 46, 533–548. doi: 10.1111/j.1365-313X.2006.02715.x

Gershenzon, J. (1984). Changes in the levels of plant secondary metabolites Under water and nutrient stress. *Phytochem. Adap. Stress* 18, 273–320. doi: 10.1007/978-1-4684-1206-2_10

Giordano, M., El-Nakhel, C., Caruso, G., Cozzolino, E., De Pascale, S., Kyriacou, M. C., et al. (2020). Stand-alone and combinatorial effects of plant-based biostimulants on the production and leaf quality of perennial wall rocket. *Plan. Theory* 9, 1–15. doi: 10.3390/plants9070922

Graziani, G., Gaspari, A., Di Vaio, C., Cirillo, A., Ronca, C. L., Grosso, M., et al. (2021). Assessment of in vitro bioaccessibility of polyphenols from annurca, limoncella, red delicious, and golden delicious apples using a sequential enzymatic digestion model. *Antioxidants* 10:541. doi: 10.3390/antiox10040541

Hosseini, H., Mozafari, V., Roosta, H. R., Shirani, H., Van de Vlasakker, P. C. H., and Farhangi, M. (2021). Nutrient use in vertical farming: optimal electrical conductivity of nutrient solution for growth of lettuce and basil in hydroponic cultivation. *Horticulturae* 7:283. doi: 10.3390/horticulturae7090283

Jakovljević, D., Topuzović, M., and Stanković, M. (2019). Nutrient limitation as a tool for the induction of secondary metabolites with antioxidant activity in basil cultivars. *Ind. Crop. Prod.* 138:111462. doi: 10.1016/j.indcrop.2019.06.025

Kerchev, P., Van der Meer, T., Sujeeth, N., Verlee, A., Stevens, C. V., van Breusegem, F., et al. (2020). Molecular priming as an approach to induce tolerance against abiotic and oxidative stresses in crop plants. *Biotechnol. Adv.* 40:107503. doi: 10.1016/j.biotechadv.2019.107503

Khammar, A. A., Moghaddam, M., Asgharzade, A., and Sourestani, M. M. (2021). Nutritive composition, growth, biochemical traits, essential oil content and compositions of Salvia officinalis L. grown in different nitrogen levels in soilless culture. *J. Soil Sci. Plant Nutr.* 21, 3320–3332. doi: 10.1007/s42729-021-00608-8

Kiferle, C., Maggini, R., and Pardossi, A. (2013). Influence of nitrogen nutrition on growth and accumulation of rosmarinic acid in sweet basil (*Ocimum basilicum* L.) grown in hydroponic culture. *Aust. J. Crop Sci.* 7, 321–327.

Kim, H. J., Ku, K. M., Choi, S., and Cardarelli, M. (2019). Vegetal-derived biostimulant enhances adventitious rooting in cuttings of basil, tomato, and chrysanthemum via brassinosteroid-mediated processes. *Agronomy* 9:74. doi: 10.3390/agronomy9020074

Kisa, D., İmamoğlu, R., Genç, N., Şahin, S., Qayyum, M. A., and Elmastaş, M. (2021). The interactive effect of aromatic amino acid composition on the accumulation of phenolic compounds and the expression of biosynthesis-related genes in *Ocimum basilicum*. *Physiol. Mol. Biol. Plants* 27, 2057–2069. doi: 10.1007/s12298-021-01068-1

Kwee, E. M., and Niemeyer, E. D. (2011). Variations in phenolic composition and antioxidant properties among 15 basil (*Ocimum basilicum* L.) cultivars. *Food Chem.* 128, 1044–1050. doi: 10.1016/j.foodchem. 2011.04.011

Kwon, D. Y., Kim, Y. B., Kim, J. K., and Park, S. U. (2020). Production of rosmarinic acid and correlated gene expression in hairy root cultures of green and purple basil (*Ocimum basilicum* L.). *Prep. Biochem. Biotechnol.* 51, 35–43. doi: 10.1080/10826068.2020.1789990

Li, X., Zeng, R., and Liao, H. (2016). Improving crop nutrient efficiency through root architecture modifications. *J. Integr. Plant Biol.* 58, 193–202. doi: 10.1111/jipb.12434

Maggini, R., Kiferle, C., and Pardossi, A. (2014). "Hydroponic production of medicinal plants," in *Medicinal Plants: Antioxidant Properties, Traditional Uses and Conservation Strategies.* (Hauppauge, NY: Nova Science Publishers, Inc.), 91–116.

Mahajan, M., Kuiry, R., and Pal, P. K. (2020). Understanding the consequence of environmental stress for accumulation of secondary metabolites in medicinal and aromatic plants. *J. Appl. Res. Med. Aromat. Plants* 18:100255. doi: 10.1016/j.jarmap.2020.100255

Mughal, M. H. (2019). Spices; a mechanistic anticancer treatise. *J. Nutr. Food Res. Technol.* 2, 14–19. doi: 10.30881/jnfrt.00016

Pathare, P. B., Opara, U. L., and Al-Said, F. A. J. (2013). Colour measurement and analysis in fresh and processed foods: A review. *Food Bioprocess Technol.* 6, 36–60. doi: 10.1007/s11947-012-0867-9

Paul, K., Sorrentino, M., Lucini, L., Rouphael, Y., Cardarelli, M., Bonini, P., et al. (2019). A combined phenotypic and metabolomic approach for elucidating the biostimulant action of a plant-derived protein hydrolysate on tomato grown under limited water availability. *Front. Plant Sci.* 10:493. doi: 10.3389/fpls.2019.00493

Prinsi, B., Negrini, N., Morgutti, S., and Espen, L. (2020). Nitrogen starvation and nitrate or ammonium availability differently affect phenolic composition in green and purple basil. *Agronomy* 10:498. doi: 10.3390/agronomy10040498

Rouphael, Y., Cardarelli, M., Lucini, L., Rea, E., and Colla, G. (2012). Nutrient solution concentration affects growth, mineral composition, phenolic acids, and flavonoids in leaves of artichoke and cardoon. *HortScience* 47, 1424–1429. doi: 10.21273/hortsci.47.10.1424

Rouphael, Y., Carillo, P., Colla, G., Fiorentino, N., Sabatino, L., El-Nakhel, C., et al. (2020). Appraisal of combined applications of trichoderma virens and a biopolymer-based biostimulant on lettuce agronomical, physiological, and qualitative properties under variable and regimes. *Agronomy* 10:196. doi: 10.3390/agronomy10020196

Rouphael, Y., Carillo, P., Cristofano, F., Cardarelli, M., and Colla, G. (2021). Effects of vegetal- versus animal-derived protein hydrolysate on sweet basil morpho-physiological and metabolic traits. *Sci. Hortic.* 284:110123. doi: 10.1016/j.scienta.2021.110123

Rouphael, Y., Giordano, M., Cardarelli, M., Cozzolino, E., Mori, M., Kyriacou, M. C., et al. (2018). Plant-and seaweed-based extracts increase yield but differentially modulate nutritional quality of greenhouse spinach through biostimulant action. *Agronomy* 8:126. doi: 10.3390/agronomy8070126

Scuderi, D., Restuccia, C., Chisari, M., Barbagallo, R. N., Caggia, C., and Giuffrida, F. (2011). Salinity of nutrient solution influences the shelf-life of fresh-cut lettuce grown in floating system. *Postharvest Biol. Technol.* 59, 132–137. doi: 10.1016/j.postharvbio.2010.08.016

Sharma, S., and Kumar, R. (2012). Effect of nitrogen on growth, biomass and oil composition of clary sage (*Salvia sclarea* Linn.) under mid hills of north western Himalayas. *Indian J. Nat. Prod. Resour.* 3, 79–83.

Teklić, T., Parađiković, N., Špoljarević, M., Zeljković, S., Lončarić, Z., and Lisjak, M. (2021). Linking abiotic stress, plant metabolites, biostimulants and functional food. *Ann. Appl. Biol.* 178, 169–191. doi: 10.1111/aab.12651

Trivellini, A., Lucchesini, M., Maggini, R., Mosadegh, H., Villamarin, T. S. S., Vernieri, P., et al. (2016). Lamiaceae phenols as multifaceted compounds: bioactivity, industrial prospects and role of "positive-stress". *Ind. Crop. Prod.* 83, 241–254. doi: 10.1016/j.indcrop.2015.12.039

Tsouvaltzis, P., Kasampali, D. S., Aktsoglou, D. C., Barbayiannis, N., and Siomos, A. S. (2020). Effect of reduced nitrogen and supplemented amino acids nutrient solution on the nutritional quality of baby green and red lettuce grown in a floating system. *Agronomy* 10:922. doi: 10.3390/agronomy10070922

Verma, N., and Shukla, S. (2015). Impact of various factors responsible for fluctuation in plant secondary metabolites. *J. Appl. Res. Med. Aromat. Plants* 2, 105–113. doi: 10.1016/j.jarmap.2015.09.002

Vernieri, P., Borghesi, E., Tognoni, F., Serra, G., Ferrante, A., and Piaggesi, A. (2006). Use of biostimulants for reducing nutrient solution concentration in floating system. *Acta Hortic.* 718, 477–484. doi: 10.17660/ActaHortic.2006.718.55

Wada, K. C., Mizuuchi, K., Koshio, A., Kaneko, K., Mitsui, T., and Takeno, K. (2014). Stress enhances the gene expression and enzyme activity of phenylalanine ammonia-lyase and the endogenous content of salicylic acid to induce flowering in pharbitis. *J. Plant Physiol.* 171, 895–902. doi: 10.1016/j.jplph.2014.03.008

Walters, K. J., and Currey, C. J. (2018). Effects of nutrient solution concentration and daily light integral on growth and nutrient concentration of several basil species in hydroponic production. *HortScience* 53, 1319–1325. doi: 10.21273/HORTSCI13126-18

Wortman, S. E. (2015). Crop physiological response to nutrient solution electrical conductivity and pH in an ebb-and-flow hydroponic system. *Sci. Hortic.* 194, 34–42. doi: 10.1016/j.scienta.2015.07.045

Yang, T., and Kim, H. J. (2020). Characterizing nutrient composition and concentration in tomato-, basil-, and lettuce-based aquaponic and hydroponic systems. *Water* 12:1259. doi: 10.3390/W12051259

Zheljazkov, V. D., Callahan, A., and Cantrell, C. L. (2008). Yield and oil composition of 38 basil (*Ocimum basilicum* L.) accessions grown in Mississippi. *J. Agric. Food Chem.* 56, 241–245. doi: 10.1021/jf072447y

Žlabur, J. Š., Opačić, N., Žutić, I., Voća, S., Poštek, M., Radman, S., et al. (2021). Valorization of nutritional potential and specialized metabolites of basil cultivars depending on cultivation method. *Agronomy* 11:1048. doi: 10.3390/agronomy11061048

Conflict of Interest: The authors declare that the research was conducted in the absence of any commercial or financial relationships that could be construed as a potential conflict of interest.

Publisher's Note: All claims expressed in this article are solely those of the authors and do not necessarily represent those of their affiliated organizations, or those of the publisher, the editors and the reviewers. Any product that may be evaluated in this article, or claim that may be made by its manufacturer, is not guaranteed or endorsed by the publisher.

frontiers | Frontiers in Microbiology

ORIGINAL RESEARCH
published: 09 June 2022
doi: 10.3389/fmicb.2022.885430

Evaluation and Genome Analysis of *Bacillus subtilis* YB-04 as a Potential Biocontrol Agent Against *Fusarium* Wilt and Growth Promotion Agent of Cucumber

Wen Xu[1†], Qian Yang[1,2†], Fan Yang[3†], Xia Xie[1], Paul H. Goodwin[4], Xiaoxu Deng[1], Baoming Tian[2] and Lirong Yang[1*]*

[1] Henan International Joint Laboratory of Crop Protection, Henan Biopesticide Engineering Research Center, Institute of Plant Protection Research, Graduate T&R Base of Zhengzhou University, Henan Academy of Agricultural Sciences, Zhengzhou, China, [2] School of Agricultural Sciences, Zhengzhou University, Zhengzhou, China, [3] Institute of Horticulture, Henan Academy of Agricultural Sciences, Zhengzhou, China, [4] School of Environmental Sciences, University of Guelph, Guelph, ON, Canada

OPEN ACCESS

Edited by:
Maurizio Ruzzi,
University of Tuscia, Italy

Reviewed by:
Orlando Borras-Hidalgo,
Qilu University of Technology, China
Divjot Kour,
Eternal University, India
Hesham Ali El Enshasy,
University of Technology Malaysia, Malaysia

***Correspondence:**
Baoming Tian
15071246556@163.com
Lirong Yang
luck_ylr@126.com

[†] These authors have contributed equally to this work

Specialty section:
This article was submitted to Microbe and Virus Interactions with Plants, a section of the journal Frontiers in Microbiology

Received: 28 February 2022
Accepted: 06 May 2022
Published: 09 June 2022

Citation:
Xu W, Yang Q, Yang F, Xie X, Goodwin PH, Deng X, Tian B and Yang L (2022) Evaluation and Genome Analysis of Bacillus subtilis YB-04 as a Potential Biocontrol Agent Against Fusarium Wilt and Growth Promotion Agent of Cucumber. Front. Microbiol. 13:885430. doi: 10.3389/fmicb.2022.885430

Cucumber wilt caused by *Fusarium oxysporum* f.sp. *cucumerinum* (*Foc*) is a highly destructive disease that leads to reduced yield in cucumbers. In this study, strain YB-04 was isolated from wheat straw and identified as *Bacillus subtilis.* It displayed strong antagonistic activity against *F. oxysporum* f.sp. *cucumerinum* in dual culture and exhibited significant biocontrol of cucumber *Fusarium* wilt with a higher control effect than those of previously reported *Bacillus* strains and displayed pronounced growth promotion of cucumber seedlings. *B. subtilis* YB-04 could secrete extracellular protease, amylase, cellulose, and β-1,3-glucanase and be able to produce siderophores and indole acetic acid. Inoculation with *B. subtilis* YB-04 or *Foc* increased cucumber defense-related enzyme activities for PPO, SOD, CAT, PAL, and LOX. However, the greatest increase was with the combination of *B. subtilis* YB-04 and *Foc*. Sequencing the genome of *B. subtilis* YB-04 showed that it had genes for the biosynthesis of various secondary metabolites, carbohydrate-active enzymes, and assimilation of nitrogen, phosphorous, and potassium. *B. subtilis* YB-04 appears to be a promising biological control agent against the *Fusarium* wilt of cucumber and promotes cucumber growth by genomic, physiological, and phenotypic analysis.

Keywords: ***Fusarium oxysporum* f.sp. *cucumerinum*, biocontrol agent, genome sequencing and assembly, *Bacillus subitilis*, growth promotion**

INTRODUCTION

Cucumber (*Cucumis sativus* L.) is an important vegetable crop worldwide. Cucumber wilt caused by *Fusarium oxysporum* f.sp. *cucumerinum* (*Foc*) is one of the most destructive diseases of cucumber that can lead to severe losses in yield and quality (Zhou et al., 2017). *Foc* enters root tissues by direct penetration or wounds causing visible symptoms, including necrotic lesions, vascular and root wilt, and ultimately death (Ahn et al., 1998). It can survive up to 20 years in soil (Zhao et al., 2017). Furthermore, there are no commercially available cucumber cultivars with resistance

against *Fusarium* wilt. Therefore, biological control of cucumber *Fusariu*m wilt using antagonistic microorganisms has been considered to be a promising alternative.

Beneficial microorganisms can be used as biological control agents (BCAs) against different plant diseases. Many of these are species of *Bacillus,* which are also plant growth-promoting bacteria (PGPB) that can improve plant growth by producing secondary metabolites, such as fengycin, surfactin, bacillaene, and macrolactin, siderophores, and indole acetic acid (IAA) and secreting hydrolases to suppress plant pathogens and promote plant growth (Blake et al., 2021). More importantly, *Bacillus* species have several advantages, such as rapid growth, spore production, safe, non-pathogenic nature, and adaptation to broader environmental conditions (Nayak, 2021). However, there are several problems in the field application of microbial agents, including lack of high-efficiency biocontrol, relatively short shelf life, and variable control effectiveness. Therefore, understanding the growth-promotion and biocontrol mechanisms of beneficial microorganisms can significantly contribute to improved application efficacy of BCAs.

One way to better understand these organisms is through whole genome sequencing allowing for the discovery of genes for the production of bioactive compounds responsible for biocontrol and growth promotion (Bauman et al., 2021). For instance, sequencing the complete genome of the BCA *Bacillus velezensis* 9912D revealed gene clusters for secondary metabolite synthesis, including several potentially new lantibiotics (Pan et al., 2017). Similarly, the complete genome of *Bacillus subtilis* 7PJ-16 revealed genes for biosynthesis of antimicrobial metabolites and promoting plant growth traits, indicating its ability to act as a BCA and PGPB (Xu et al., 2019). The genome of *B. subtilis* 9407 showed that it had genes for the biocontrol mechanism against bacterial fruit blotch, including genes for a newly identified subtilosin A, bacilysin, and bacillaene (Gu et al., 2021).

In this study, strain YB-04 was isolated from wheat straw. A number of BCA and PGPB traits were screened for YB-04 in culture. The genome of strain YB-04 was sequenced to identify a number of genes associated with BCA and PGPB traits. Plant growth promotion of cucumber seedlings by soil inoculation of YB-04 was assessed based on chlorophyll content and growth of shoots, roots, stems, and leaves. Biocontrol activity by YB-04 against *Fusarium* wilt of cucumber was assessed based on disease severity and disease index. Furthermore, the activities of cucumber defense-related enzymes activities, both by YB-04 alone and in combination with *Foc* inoculation, were examined. The discovery and characterization of *B. subtilis* YB-04 indicate that it is a promising BCA and PGPB of cucumber.

MATERIALS AND METHODS

Isolation of Strain YB-04 and *in vitro* Antagonism Test

Strain YB-04 was isolated from wheat straw and cultured in LB broth by a dilution plate method at 37°C, collected from a field (E113°97', N35°05') at the Henan Academy of Agricultural Sciences in Xinxiang, Henan, China in June. *Foc* was obtained from the College of Plant Protection, Henan Agricultural University. Antagonistic activity against *Foc* was performed by a dual culture where *Foc* was grown on PDA at 28°C for 5 days, and then 5 mm agar plugs were excised and transferred to the center of another PDA plate. Strain YB-04 was placed 3 cm away from the edge of the Petri dish, and the growth rate of *Foc* was measured relative to the control, which was *Foc* without strain on a plate (Xu et al., 2020).

Biocontrol Efficiency of Strain YB-04 Against Cucumber *Fusarium* Wilt and Growth Promotion on Cucumber Seedlings

Strain YB-04 was cultured in LB broth for 24 h at 37°C with shaking at 180 rpm and harvested by centrifugation (4,000 × *g* for 5 min), washed once with LB broth, and adjusted to 10^8 CFU/ml based on OD at 595 nm. *Foc* was grown on PDA at 28°C for 5 days, and then ten 5 mm agar plugs were excised and transferred to 100 ml PDB. The broths were incubated at 28°C in a shaker at 180 rpm for 3 days. The *Foc* cultures were filtered through 4 layers of sterile gauze, and the filtered spores were adjusted to 10^5 spores/ml using a hemacytometer (XB-K-25, Qiujing, Shanghai, China).

Cucumber seeds of cultivar Chuancui No. 3 were surface-sterilized in 75% ethanol (v/v) for 30 s and then rinsed with sterile water three times. The seeds were air-dried and each seed was planted in a separate pot (10 cm high, 10 cm diameter) filled with a 400 g sterilized mixture of soil. The plants were grown in the greenhouse at 25°C with a 16 h light/8 h dark photoperiod. After 10 days, each pot of cucumber seedlings was treated as follows: (1) drenching with 15 ml of YB-04 suspension; (2) first drenching with 15 ml l of YB-04 suspension and 24 h of later drenching with 15 ml *Foc* spore suspension; (3) first drenching with 15 ml of 0.1% hymexazol and 24 h later drenching with 15 ml *Foc* spore suspension; (4) drenching with 15 ml of sterile distilled water; or (5) drenching with 15 ml of sterile distilled water and 24 h later drenching with 15 ml of *Foc* spore suspension. Each treatment was performed using 12 plants with 3 replicates. At 20 and 45 days post inoculation (dpi) with YB-04, chlorophyll content, shoot height and fresh weight, root length and fresh weight, stem thickness, and leaf area were measured, and disease severity and disease index were recorded for plants inoculated with *Foc* at 45 days post YB-04 inoculation (Chen et al., 2010). In brief, disease severity was assessed using a 0–4 disease scale; 0 = leaf asymptomatic; 1 = leaf wilting below 1/4 of cucumber seedling; 2 = leaf wilting in 1/4 to 1/2 of cucumber seedling; 3 = leaf wilting above 1/2 of cucumber seedling; 4 = the whole plant was wilted and died. The disease index was calculated using $DI = [[(0 \times N0) + (1 \times N1) + (2 \times N2) + (3 \times N3) + (4 \times N4)]/T \times 4] \times 100$, where N is the number of cucumber seedlings for each disease score and T is the total number of cucumber seedlings. Disease incidence = $[N1 + N2 + N3 + N4]/T \times 100\%$. Control efficacy = (DI of control - DI of treatment)/DI of control × 100%. The chlorophyll content of leaves was measured by using a SPAD-502 Plus chlorophyll content meter (Konica

Minolta, Tokyo, JP). Root length and shoot height were measured with a ruler. The fresh weight of root and shoot was recorded with an analytical balance (ME203E, Mettler Toledo, Shanghai, China). Stem thickness was measured at 2 cm from the crown with a vernier caliper (MNT-200, Shanghai Meinaite Metals Instruments Co., Shanghai, China).

Determination of Defense Enzyme Activities in the Cucumber Leaves

After 20 days post YB-04 inoculation, leaves were harvested and stored at –80°C. In brief, 0.5 g leaves were ground in liquid nitrogen, and 1 ml of extraction buffer was added. After centrifugation at 8,000 × *g* for 10 min, the supernatant was removed for enzyme assays. Enzyme activities were measured using assay kits for PPO (Cat. No. BC0195), SOD (Cat. No. BC0175), CAT (Cat. No. BC0205), PAL (Cat. No. BC0215), and LOX (Cat. No. BC0325) following the procedures of the manufacturer (Solarbio, Beijing, China). Absorbance was determined by using a plate reader (Tecan Spark, Tecan, Switzerland).

Detection of Plant Growth-Promoting Bacteria and Biological Control Agents Traits

Protease activity was detected with single colonies of YB-04 grown at 30°C for 5 days on skim milk agar (0.1 g $CaCl_2$, 5.0 g NaCl, 10.0 g skim milk, 10.0 g peptone, and 18.0 g of agar per liter, pH 7.2). Protease activity was observed as clear zones around the colonies (Kazanas, 1968). Amylase activity was detected with single colonies grown at 30°C for 48 h on starch agar (10.0 g soluble starch, 10.0 g tryptone, 5.0 g glucose, 5.0 g NaCl, 5.0 g beef extract, and 18.0 g of agar per liter, pH 7.2). Lugol's iodine solution (1% iodine in 2% potassium iodide w/v) was added to the starch agar plate, and amylase activity was observed as a colorless halo (Al-Naamani et al., 2015). Cellulose activity was assayed with single colonies grown for 7 days at 30°C on carboxymethylcellulose agar (5.0 g CMC-Na, 0.1 g $MgSO_4{\cdot}7H_2O$, 0.25 g $(NH_4)_2SO_4$, 0.25 g K_2HPO_4, and 18.0 g of agar per liter, pH 5.5). The plates were flooded with 1% (m/v) Congo Red, and then washed with sterilized distilled water, and cellulose activity was detected as a clear zone (Teather and Wood, 1982). The β-Glucanase activity was assayed with single colonies grown at 30°C for 2 days on β-glucan agar (0.05 g glucose, 0.5 g yeast extract, 1 g peptone, 0.5 g NaCl, 0.01 g Congo Red, and 18.0 g of agar per liter, pH 7.0). The β-Glucanase activity was indicated by a clear zone around the colonies (Teather and Wood, 1982). Siderophore production was determined with single colonies grown at 30°C for 2 days in the dark on Chrome Azurol S blue agar (10 ml 20% sucrose solution, 30 ml 10% acid hydrolyzed casein, 1 ml 1 mmol/L $CaCl_2$, 5 ml 0.1 mol/L phosphate-buffered saline (pH 6.8), 50 ml CAS dyeing solution, and 18 g of agar per liter, pH 7.2). Siderophore production was indicated by a change from blue to orange around the colonies (Schwyn and Neilands, 1987). IAA production was measured with single colonies grown at 30°C for 2 days on L-tryptophan nutrient broth (3 g beef extract, 10 g peptone, 5 g NaCl,0.5 g L-tryptophan per liter, pH 7.2). After centrifugation at 14,000 × *g* for 10 min,1 ml of supernatant was mixed with 2 ml of Salkowski stain, and then kept at room temperature in the dark for 30 min (Glickmann and Dessaux, 1995). All of the above reagents were of analytical grade and produced by China National Pharmaceutical Group Corp., Shanghai, China.

Genome Sequencing and Assembly of Strain YB-04

Strain YB-04 was grown in LB broth for 16 h at 37°C by shaking at 180 rpm. Genomic DNA was extracted with a Mini-BEST Bacterial Genomic DNA Extraction Kit Ver. 3.0 following the manufacturer's instructions (Takara, Beijing, China). An approximately 10 kb insert sequencing library was constructed and sequencing was performed using the PacBio Sequel II system (Pacific Biosciences, Menlo Park, CA, United States) by Frasergen (Wuhan, Hubei, China). Sequencing reads were *de novo* assembled by using HGAP4 (Chin et al., 2013) and the Canu (v.1.6) (Koren et al., 2017) software. The depth of genome coverage was analyzed by using the align tool (BLASR, v0.4.1) (Chaisson and Tesler, 2012). The assembled complete genome sequence was deposited in NCBI GenBank (Accession number CP072525). A circular map of the genome was constructed by using Circos (v0.64) (Krzywinski et al., 2009).

Genome Annotation of Strain YB-04

The genome of strain YB-04 was annotated using Glimmer (v3.02) (Delcher et al., 2007). The tRNA and rRNA genes were identified by tRNAscan-SE (v2.0) (Lowe and Eddy, 1997) and RNAmmer (v1.2) (Lagesen et al., 2007), respectively. Functional descriptions of putative protein encoding genes were done by BLASTx with an *E*-value threshold of 1e-5 using the NCBI Non-Redundant protein database (NR), Swiss-Prot, Clusters of Orthologous Groups (COG), Kyoto Encyclopedia of Genes and Genomes (KEGG), and Gene Ontology (GO).

Phylogenetic Relationship of Strain YB-04

The 16S rRNA gene sequences of strain YB-04 and *B. velezensis FZB42*, *B. velezensis* YB-130, *B. subtilis* H1, *B. subtilis* 168, *B. licheniformis* SRCM103583, *B. licheniformis* ATCC 14580, *B. altitudinis* CHB19, *B. altitudinis* GQYP101, *B. pumilus* SF-4, and *B. pumilus* ZB201701 were obtained from the genomes (GenBank IDs: CP000560.2, CP054562.1, CP026662.1, NC_000964.3, CP035404.1, CP034569.1, CP043559.1, CP040514.1, CP047089.1, and CP029464.1, respectively). A tree of the 16S rRNA gene sequences was constructed with MEGA 7.0 using the Neighbor Joining method (Kumar et al., 2016). Average Nucleotide Identity (ANI) was calculated using an ANI calculator (Yoon et al., 2017).

Analysis of Genes Encoding CAZymes and Gene Clusters Responsible for the Biosynthesis of Secondary Metabolites

Protein-coding genes in the genome of strain YB-04 were aligned with the carbohydrate active enZYme (CAZy) database

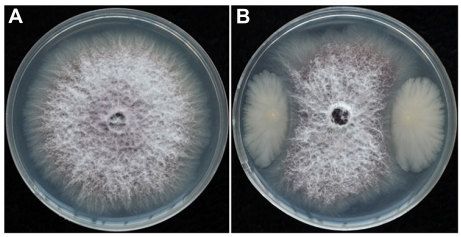

FIGURE 1 | Colony morphology of *Foc* co-cultivated with or without strain YB-04. **(A)** Colony morphology of *Foc* in PDA; **(B)** inhibition of strain YB-04 on *Foc* growth.

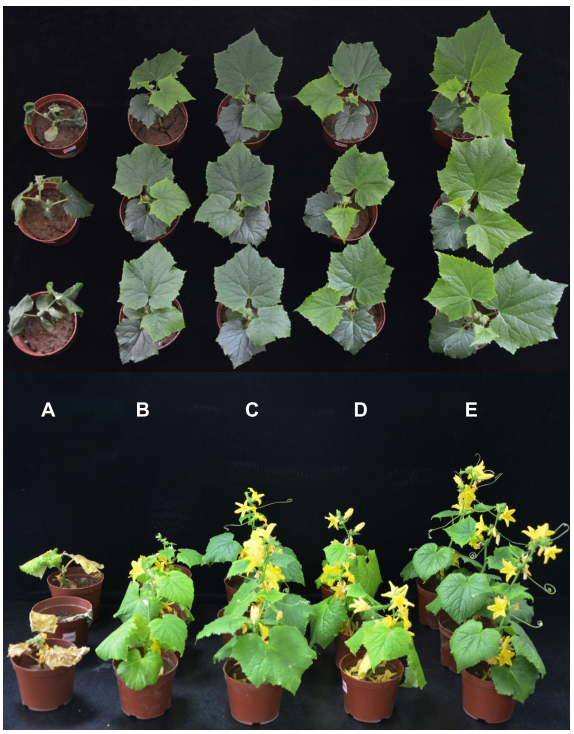

FIGURE 2 | Effect of strain YB-04 against *Fusarium* wilt and on growth-promotion of Cucumber Seedlings. **(A)** Only *Foc* inoculation; **(B)** *Foc* inoculation and hymexazol treatment; **(C)** inoculation of strain YB-04 and *Foc*; **(D)** sterile distilled water; **(E)** only strain YB-04 inoculation.

TABLE 1 | Disease incidence, disease index, and control efficacy of *B. subtilis YB-04* against cucumber *Fusarium* wilt.

Treatment	Disease incidence (%)	Disease index	Control efficacy (%)
FOC	95.07 ± 0.41a	107.51 ± 0.4a	
FOC + 0.1% Hymexazol	3.48 ± 0.15b	13.24 ± 0.14b	87.68 ± 0.08a
FOC + YB-04	2.42 ± 0.21c	8.69 ± 0.09c	91.92 ± 0.12a

Data are the mean ± standard deviation (SD); different letters (a–c) in the same column indicate significant difference at p-values < 0.05 level.

(Lombard et al., 2014) using dbCAN2 (Zhang et al., 2018) and HMMER (v3.1b2) (Finn et al., 2011) with an *E*-value threshold of 1e-15. Identification of gene clusters for the synthesis of secondary metabolites was analyzed by using antiSMASH5.0 (Blin et al., 2019).

Statistical Analysis

Statistical analysis was performed using SPSS v21.0 by one-way analysis of variance (ANOVA). Means were compared with Duncan's multiple range tests at a probability of $p \leq 0.05$.

RESULTS

Isolation of YB-04 and Wilt Disease Biocontrol Activity *in vitro* and *in vivo*

Dilution plating from surface-sterilized wheat straw yielded numerous colonies with different colony appearances. Twenty strains were purified and screened for antagonistic activity against *Foc* in dual culture and reduced wilt severity of cucumber inoculated with *Foc* in the greenhouse (data not shown). Strain YB-04 was selected based on having the greatest antagonistic activity against *Foc* in culture (**Figure 1**) and reduced wilt severity of cucumber seedlings at 20 days after *Foc* inoculation (**Figure 2**). Disease incidence, disease index, and control efficacy at 45 dpi revealed that YB-04 significantly reduced wilt symptoms caused by *Foc* to levels slightly less than the chemical fungicide hymexazol (**Table 1**).

Growth-Promotion Activity of Strain YB-04

At 20 and 45 dpi with strain YB-04, there was a significant increase in chlorophyll content, height and fresh weight of shoot, root length and fresh weight, stem thickness, and leaf area compared to non-treated cucumber seedlings (**Figure 2** and **Table 2**). At 20 dpi, the greatest increases were observed for the fresh weight of shoots and roots at 115.91 and 334.88%, respectively. At 45 dpi, the greatest increases were observed for shoot height and leaf area at 79.03 and 49.07%, respectively.

At 20 and 45 dpi with strain YB-04 and *Foc* inoculation, there was also a significant increase in chlorophyll content, height, and fresh weight of shoot, root length and fresh weight, stem thickness, and leaf area compared to that of the *Foc* inoculated cucumber seedlings (**Figure 2** and **Table 2**). This was also observed with the *Foc* inoculated seedlings treated with hymexazol. However, strain YB-04 treatment of the *Foc*-inoculated seedlings resulted in significantly higher chlorophyll content, shoot height and fresh weight, root length and fresh weight, and leaf area than *Foc*-inoculated seedlings with hymexazol. However, there was no significant difference in the stem thickness of *Foc*-inoculated seedlings with strain YB-04 or hymexazol at 45 dpi.

Effect of Strain YB-04 on Activities of Defense-Related Enzymes in Cucumber Seedlings

At 20 dpi with strain YB-04, cucumber seedlings showed significantly higher activities of SOD, CAT, PAL, and LOX,

TABLE 2 | Effects of *B. subtilis* YB-04 on growth parameters of cucumber seedlings.

		FOC	FOC + 0.1% Hymexazol	FOC + YB-04	CK	YB-04
20 days after inoculation	Chlorophyll content (SPAD)	36.20 ± 0.52d	42.13 ± 0.23c	50.97 ± 0.30a	41.87 ± 0.39c	44.17 ± 0.41b
	Shoot height (cm)	6.47 ± 0.20c	12.27 ± 0.27b	16.27 ± 0.23a	11.80 ± 0.17b	16.63 ± 0.09a
	Stem thickness (mm)	3.47 ± 0.03e	4.33 ± 0.03c	4.47 ± 0.01b	3.74 ± 0.03d	4.60 ± 0.05a
	Shoot fresh weight (g)	2.11 ± 0.02e	7.17 ± 0.04c	9.66 ± 0.08b	4.84 ± 0.06d	10.45 ± 0.07a
	Root length (cm)	7.81 ± 0.06e	19.50 ± 0.42c	21.30 ± 0.32 b	18.50 ± 0.35d	35.27 ± 0.27a
	Root fresh weight (g)	0.16 ± 0.02e	1.34 ± 0.05c	1.72 ± 0.05 b	0.43 ± 0.02d	1.87 ± 0.03a
	Leaf area (cm^2)	53.54 ± 0.70 e	74.37 ± 0.51c	84.53 ± 1.28b	71.30 ± 0.66d	103.12 ± 0.91a
45 days after inoculation	Chlorophyll content (SPAD)	10.73 ± 10.73d	30.90 ± 30.90c	41.27 ± 0.64a	34.30 ± 0.61b	42.17 ± 0.64a
	Shoot height (cm)	9.03 ± 0.24d	16.21 ± 0.52c	26.27 ± 0.69b	17.50 ± 0.69c	31.33 ± 0.66a
	Stem thickness (mm)	4.11 ± 0.06c	4.43 ± 0.02b	4.52 ± 0.02b	4.20 ± 0.04c	4.94 ± 0.03a
	Shoot fresh weight (g)	5.06 ± 0.02e	8.57 ± 0.76d	14.14 ± 0.58b	12.42 ± 0.30c	15.91 ± 0.24a
	Root length (cm)	13.02 ± 0.26d	14.77 ± 0.38c	18.97 ± 0.35b	15.02 ± 0.34c	20.40 ± 0.57a
	Root fresh weight (g)	1.88 ± 0.04d	4.74 ± 0.06c	6.21 ± 0.06a	5.58 ± 0.07b	6.35 ± 0.07a
	Leaf Area (cm^2)	44.41 ± 1.16e	78.01 ± 0.90d	106.28 ± 1.12b	91.38 ± 1.13c	136.22 ± 0.78a

Data are the mean ± standard deviation (SD); different letters (a–e) in the same line indicate significant difference at p-values < 0.05 level.

TABLE 3 | Five defense enzyme activities of cucumber leaves under different treatments.

	LOX (U/g)	PAL (U/g)	CAT (U/g)	PPO (U/g)	SOD (U/g)
FOC	1450.70 ± 28.01b	18.76 ± 0.65c	149.34 ± 7.58c	76.82 ± 1.14b	160.15 ± 0.83b
FOC + 0.1% Hymexazol	618.12 ± 9.48c	26.54 ± 0.57b	180.74 ± 4.61b	43.30 ± 0.75c	141.44 ± 1.19d
FOC + YB-04	3620.26 ± 27.82a	29.90 ± 0.92a	221.38 ± 3.38a	187.93 ± 3.85a	188.54 ± 1.05a
CK	460.10 ± 11.12d	12.64 ± 0.70e	104.99 ± 2.89e	21.72 ± 1.06d	102.22 ± 0.99e
YB-04	650.55 ± 12.38c	15.45 ± 0.63d	119.77 ± 2.48d	77.61 ± 0.62b	155.95 ± 0.97c

Data are the mean ± standard deviation (SD); different letters (a–e) in the same column indicate significant difference at p-values < 0.05 level.

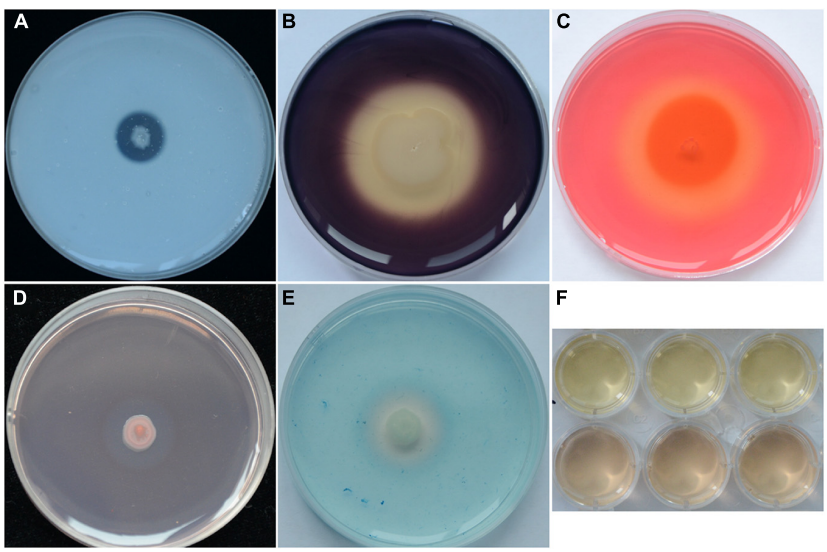

FIGURE 3 | Antifungal and PGP traits of strain YB-04. **(A)** Protease production; **(B)** amylase production; **(C)** cellulose production; **(D)** β-1,3-glucanase production; **(E)** siderophore production; **(F)** IAA production.

but not PPO, compared to non-treated seedlings (**Table 3**). Inoculation with *Foc* also significantly increased those enzyme activities, except PPO, compared to seedlings without *Foc* inoculation. The highest activities were observed with *Foc* inoculation and strain YB-04 treatment, which was significantly higher for all the enzymes compared to *Foc* inoculation. However, the activities of PAL and CAT significantly increased but LOX, PPO, and SOD significantly decreased with *Foc* inoculation and hymexazol treatment compared to *Foc* inoculation.

Detection of *in vitro* Antifungal and Growth-Promoting Traits

Strain YB-04 could secrete protease (**Figure 3A**), amylase (**Figure 3B**), cellulose (**Figure 3C**), and β-1, 3-glucanase

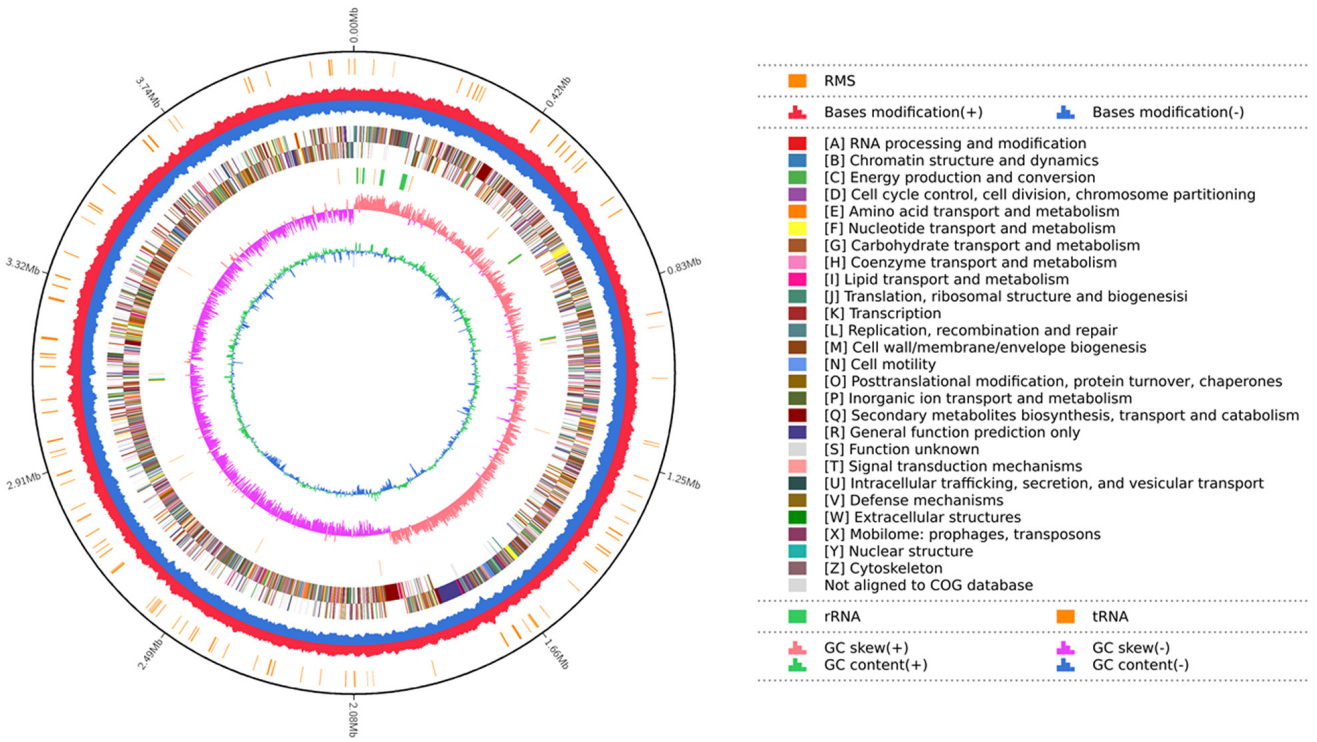

FIGURE 4 | Map of the strain YB-04 genome. The distributions of circles from outwards to inwards are as follows: ring 1 for genome size (black line); ring 2 for the restriction modification system, for forward strand (red) and reverse strand (blue); ring 3 for COG classifications of protein-coding genes on the forward strand and reverse strand; ring 4 for the distribution of tRNAs (brown) and rRNAs (green); ring 5 for GC skew; ring 6 for GC content.

(**Figure 3D**). In addition, it could produce siderophores (**Figure 3E**) and indole acetic acid (**Figure 3F**).

Genome Sequencing, Assembly, and Identification of Strain YB-04

A total of 387,797 high-quality sequencing long reads with a mean length of 10,962 bp and an N50 of 13,374 bp were generated from the genomic DNA of strain YB-04 by the Pacbio sequencing platform. Total base pairs were 4,251,215,058 bp with an 882.47X genome coverage. The YB-04 genome consisted of a single circular chromosome of 4,156,177 bp with a GC content of 43.83% (**Figure 4**). There were 4,325 protein-coding genes covering 88.62% of the genome with an average gene length of 851.6 bp, which included 87 tRNAs, 30 rRNAs (5S, 16S, 23S), and 22 sRNAs. Four gene islands, three CRISPRs, and four prophages were detected (**Supplementary Tables 1–3**). For the predicted protein encoding genes, 99.70, 90.73, 75.45, 64.30, and 53.87% could be annotated with the NR, Swiss-Prot, COG, GO, and KEGG databases, respectively (**Supplementary Table 4**).

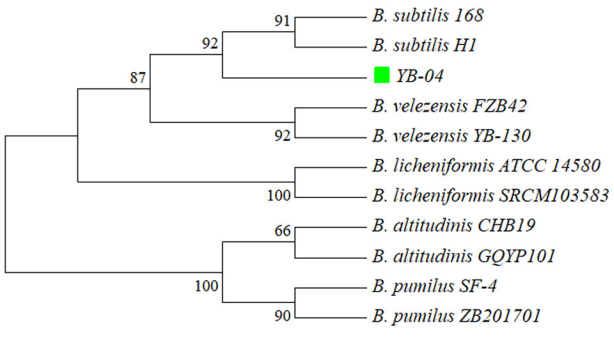

FIGURE 5 | Phylogenetic tree of *B. subtilis* YB-04 and 10 other *Bacillus* species based on 16S rRNA sequences.

A phylogenetic tree based on 16S rRNA gene sequences of strain YB-04 and 10 other *Bacillus* isolates showed that strain YB-04, *B. subtilis* 168, and *B. subtilis* H1 clustered (**Figure 5**). Strain YB-04 and *B. subtilis* 168 had the maximum ANI value of 98.74%, followed by B. *subtilis* H1with 98.65%, which is higher than the cutoff of 95–96% for bacterial species identity. ANI values between strain YB-04 and the 8 other *Bacillus* species ranged from 71.05 to 77.22% (**Figure 6**). Therefore, strain YB-04 was identified as *B. subtilis*.

Genome Analysis of Selected Genes of *Bacillus subtilis* YB-04

The genome of *B. subtilis* YB-04 had 111 genes identified as putative CAZymes, namely, 2 auxiliary activities (AAs), 7 polysaccharide lyases (PLs), 15 carbohydrate-binding modules (CBMs), 19 carbohydrate esterases (CEs) 24 glycosyltransferases (GTs), and 51 glycoside hydrolases (GHs) (**Figure 7** and

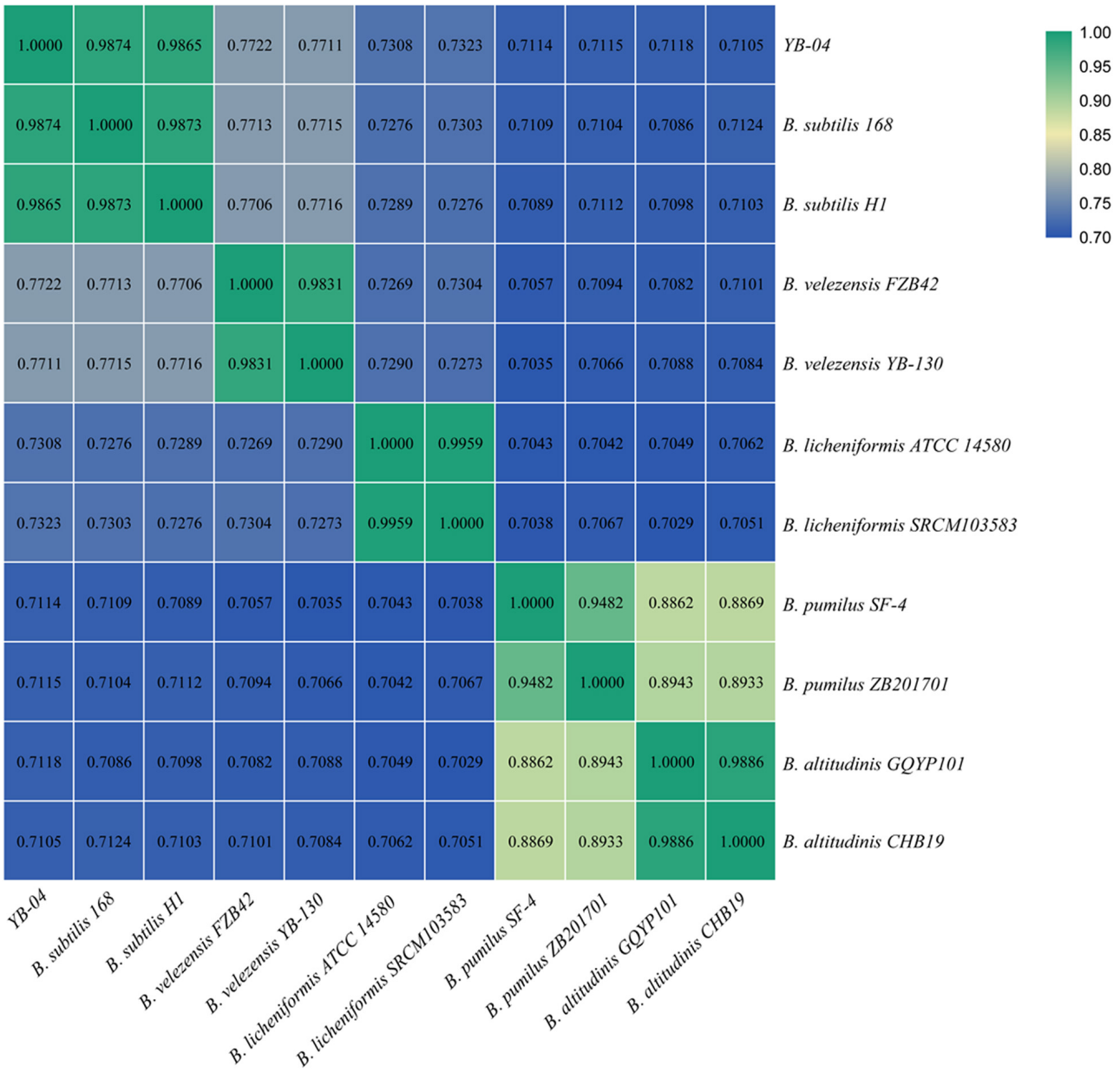

FIGURE 6 | ANI analysis of *B. subtilis* YB-04 and 10 other *Bacillus* species.

Supplementary Table 5). Six of those were classified as both GHs and CBMs.

There were 13 gene clusters predicted to be responsible for the biosynthesis of secondary metabolites. At 100% similarity, there was each matching gene clusters for bacillaene, fengycin, bacillibactin, subtilin, subtilosin A, and bacilysin synthesis. There was also one gene cluster with 82% similarity to that for surfactin synthesis. There were 6 biosynthetic gene clusters with no similarity in the antiSMASH database that appeared to be novel biosynthetic gene clusters of secondary metabolites. Based on their matches to the antiSMASH database, these were one gene cluster each for types of lanthipeptide-class-i, Type III PKS, tRNA-dependent cyclodipeptide synthases, other unspecified ribosomally synthesized, post-translationally modified peptide products, and two gene clusters, each encoding for terpenes (**Table 4**).

The genome of *B. subtilis* YB-04 contained predicted genes for an ATP-dependent phosphate uptake system *PstABCS*, phoPR operon for regulating Pho regulon in response to phosphate limitation, and alkaline phosphatase genes of *phoA* and *phoD* for phosphorus acquisition (**Table 5**). It also contained the *nasABCDEF* gene cluster for nitrite transport and reduction. Additionally, there were the potassium uptake system *ktrABCD*,

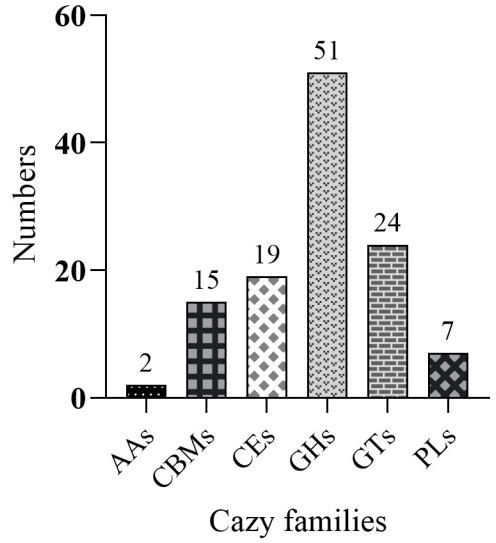

FIGURE 7 | Distribution of CAZy families in the genome of *B. subtilis* YB-04.

a putative gamma-glutamylcyclotransferase *YkqA* for potassium assimilation, and a putative potassium efflux channel *yugO*.

DISCUSSION

Fusarium wilt disease caused by *Foc* is one of the most devastating soil-borne diseases of cucumber, resulting in severe yield losses throughout the world (Zhou et al., 2018). While the use of BCAs to control plant diseases and PGPBs to improve plant growth is considered to be promising (Radhakrishnan et al., 2017; Koskey et al., 2021), new strains are needed to screen for greater efficiency, shelf life, and consistency. As part of that, an in-depth analysis of growth promotion and biocontrol traits will help in developing them into successful microbial products.

In this study, *B. subtilis* YB-04 was found to be a BCA with antagonistic activity against *Foc* in dual culture and significantly reduced *Fusarium* wilt caused by *Foc* at levels comparable to hymexazol, which is used to control the disease in China. It was also a PGPB with pronounced growth promotion on cucumber seedlings. Previously, *B. subtilis* B579, *B. subtilis* MBI600, and *B. subtilis* B068150 were also shown to significantly reduce cucumber *Fusarium* wilt and promote cucumber growth (Chen et al., 2010; Li et al., 2012; Samaras et al., 2020). Compared to those bacteria, the percentage reduction in the *Fusarium* wilt of cucumber by *B. subtilis* YB-04 was greater than those achieved by *B. subtilis* B068150, *B. subtilis* B579, or *B. subtilis* MBI600. The percentage of increased growth-promotion based on the shoot and root fresh weight and plant height by *B. subtilis* YB-04 was greater than those achieved by *B. subtilis* B579 or *B. subtilis* MBI600. Thus, *B. subtilis* YB-04 appears to be more effective as a BCA and PGPB than some of the previously described *B. subtilis* tested on cucumber.

To act as a BCA against plant pathogenic fungi, bacteria possess a number of mechanisms including synthesis of hydrolytic enzymes, production of antibiotics, and induction of systemic resistance (Morales-Cedeño et al., 2021; Saeed et al., 2021; Xu et al., 2021). In this study, *B. subtilis* YB-04 had all of those mechanisms. Hydrolytic enzyme activities including protease, amylase, cellulose, and β-1, 3-glucanase were present in pure cultures, and they can break down chitin, glucans, and other polymers in fungal cell walls, thus inhibiting the growth of fungal pathogens (Naglot et al., 2015; Li et al., 2019). Other *B. subtilis* BCAs with similar enzymes include *B. subtilis* BCC6327, *B. subtilis* ZIM3, and *B. subtilis* LR1 (Thakaew and Niamsup, 2013; Banerjee et al., 2017; Dai et al., 2020). Furthermore, a large number of CAZyme genes were found in the genome of *B. subtilis* YB-04, also suggesting that it has a strong capability to be antagonistic against fungal plant pathogens based on the potential degradation and use of fungal polymers as nutrient sources (Banani et al., 2015; Chen et al., 2018; Sui et al., 2020). In addition, gene clusters were found to be responsible for the biosynthesis of known secondary metabolites, including bacillaene, fengycin, bacillibactin, subtilin, subtilosin A, bacilysin, and surfactin, indicating antibiotic production by *B. subtilis* YB-04, which is common in *Bacillus* species (Xu et al., 2019; Su et al., 2020). Other *B. subtilis* BCAs found to produce antibiotics or have genes for antibiotic production included *B. subtilis* BSD-2 for lanthipeptide (Liu et al., 2016). Surfactin and fengycin can also be elicitors of induced systemic resistance in plants (Romero et al., 2007; Ongena et al., 2010). Many studies have reported that plant defense enzymes play important roles in disease resistance (Prasannath, 2017; Ji et al., 2020; Xu et al., 2021). Induction of the activities of defense-related enzymes in leaves following soil inoculation with *B. subtilis* YB-04 and *Foc* indicates a form of systemic resistance. Defense-related enzymes activities for PPO, SOD, CAT, PAL, and LOX could be induced by inoculation with *B. subtilis* YB-04 or *Foc* alone and the greatest increase was with the combination of *B. subtilis* YB-04 and *Foc*. Other *B. subtilis* BCAs causing host induction of defense-related enzyme activities include *B. subtilis* B579, *B. subtilis* SL-44, and *B. subtilis* CBR05 (Chen et al., 2010; Chandrasekaran and Chun, 2016; Wu et al., 2019).

All the growth parameters of cucumber seedlings measured in this study were increased with *B. subtilis* YB-04 treatment. Importantly, growth parameters were all increased much more in infected seedlings with *Foc* treated with *B. subtilis* YB-04 than those infected with *Foc* and treated with hymexazol. This indicates that *B. subtilis* YB-04 can improve plant growth while providing disease control, which would be an advantage over using hymexazol that did not promote growth. This was similar to *Pseudomonas aeruginosa* CQ-40 that controlled tomato gray mold caused by *Botrytis cinerea* and promoted the growth of tomato seedlings, whereas pyrimethanil only controlled the disease with a prevention effect of up to 64.71% (Wang et al., 2020).

To act as a PGPB, bacteria have a variety of mechanisms including the production of enzymes and siderophores for nutrient acquisition and phytohormones to promote growth, and enzymes to reduce the negative effects of various abiotic stresses

TABLE 4 | List of the putative gene clusters encoding for secondary metabolites by antiSMASH in the *B. subtilis* YB-04 genome.

Clusters	Types	Genomic locations	Most similar known clusters	Similarity
Cluster 1	NRPS	349,833–413,272	Surfactin	82%
Cluster 2	Terpene	1,124,835–1,145,348		
Cluster 3	Lanthipeptide-class-i	1,699,549–1,725,648		
Cluster 4	transAT-PKS,PKS-like,T3PKS,transAT-PKS-like,NRPS	1,747,915–1,862,664	Bacillaene	100%
Cluster 5	NRPS, betalactone	1,920,534–2,002,654	Fengycin	100%
Cluster 6	Terpene	2,073,306–2,095,204		
Cluster 7	T3PKS	2,142,940–2,184,037		
Cluster 8	NRPS	3,179,833–3,229,574	Bacillibactin	100%
Cluster 9	lanthipeptide-class-i	3,377,840–3,404,065	Subtilin	100%
Cluster 10	CDPS	3,523,308–3,544,054		
Cluster 11	Sactipeptide	3,768,784–3,790,395	Subtilosin A	100%
Cluster 12	Other	3,797,486–3,838,904	Bacilysin	100%
Cluster 13	RiPP-like	4,040,385–4,053,116		

TABLE 5 | Genes responsible for nitrogen, phosphorous, and potassium assimilation identified in the strain YB-04 genome.

Function	Gene	UniProt accession No.	Description	Best hit in YB-04	Identity
Phosphate assimilation	*phoA*	P19406	Alkaline phosphatase 4	orf00986	99.35%
	phoR	P23545	Alkaline phosphatase synthesis sensor protein PhoR	orf03027	99.48%
	phoP	P13792	Alkaline phosphatase synthesis transcriptional regulatory protein PhoP	orf03028	99.58%
	phoD	P42251	Alkaline phosphatase D	orf00275	99.49%
Phosphate transport	*pstS*	P46338	Phosphate-binding protein	orf02500	99.67%
	pstC	A0A6M4JLF7	Phosphate transport system permease protein	orf02499	99.35%
	pstB1	P46342	Phosphate import ATP-binding protein PstB 1	orf02496	99.62%
	pstB2	P46341	Phosphate import ATP-binding protein PstB 2	orf02497	99.63%
	pstA	A0A6M3ZE53	Phosphate transport system permease protein	orf02498	100.00%
Nitrate/nitrite assimilation	*nasD*	P42435	Nitrite reductase	orf00344	99.26%
	nasE	P42436	Assimilatory nitrite reductase [NAD(P)H] small subunit	orf00343	100.00%
	nasA	P42432	Nitrate transporter	orf00347	99.50%
	nasC	P42434	Assimilatory nitrate reductase catalytic subunit	orf00345	98.03%
	nasB	P42433	Assimilatory nitrate reductase electron transfer subunit	orf00346	97.54%
	nasF	P42437	Uroporphyrinogen-III C-methyltransferase	orf00342	97.30%
Potassium assimilation	*ktrC*	P39760	Ktr system potassium uptake protein C	orf01561	100.00%
	ykqA	P39759	Putative gamma-glutamylcyclotransferase YkqA	orf01560	96.75%
	ktrD	O31658	Ktr system potassium uptake protein D	orf01445	100.00%
	yugO	Q795M8	Putative potassium channel protein YugO	orf03270	100.00%
	ktrB	O32081	Ktr system potassium uptake protein B	orf03241	99.10%
	ktrA	O32080	Ktr system potassium uptake protein A	orf03240	99.10%

(Glick, 2012; Saeed et al., 2021). *B. subtilis* YB-04 produced siderophores that can improve iron uptake and alleviate harmful effects of iron on plants that have been associated with enhanced plant growth (Haas, 2003; Dimkpa et al., 2009). The genome of *B. subtilis* YB-04 also contained genes responsible for nitrogen, phosphorous, and potassium assimilation. Plant growth and development depend on macronutrients, such as nitrogen, phosphorous, and potassium, that are mostly obtained from the soil and can be made more available to plants by soil microbes that have the ability to solubilize nutrients and transfer them to plants (Glick, 2012; Rana et al., 2020). Finally, *B. subtilis* YB-04 produced IAA, which may be taken up by the cucumber seedlings stimulating the transcriptional expression of IAA responsive genes and enhancing biomass (Spaepen et al., 2014; Jiang et al., 2020).

In summary, *B. subtilis* YB-04 appears to be an effective BCA against cucumber *Fusarium* wilt and an effective PGPB of cucumber seedlings. The BCA mechanisms could include induced systemic host resistance as indicated by greater host defense-related enzyme activities, and direct pathogen inhibition through secretion of extracellular enzymes and antibiotics. The PGPB mechanisms could include nutrient acquisition *via* siderophores and enzymes for fixing nitrogen and solubilizing potassium and phosphorus, and direct plant growth enhancement through increased amounts of indole acetic acid. Compared to other *B. subtilis* strains used as cucumber

Fusarium wilt BCAs and PGPBs in cucumber, *B. subtilis* YB-04 is a more effective BCA than all those reported thus far and is a more effective PGPB than most reported so far. Thus, it appears to be a very promising novel beneficial *B. subtilis* strain for cucumber production.

DATA AVAILABILITY STATEMENT

The datasets presented in this study can be found in online repositories. The names of the repository/repositories and accession number(s) can be found in the article/ **Supplementary Material**.

AUTHOR CONTRIBUTIONS

LY and WX conceived the research and designed the experiments. QY, XX, FY, XD, and WX performed the experiments and analyzed the data. WX prepared the manuscript draft. PG, BT, and LY critically revised the manuscript. All authors approved the final version of the manuscript.

FUNDING

This research was funded by the Central Government Guiding Local Projects (2020[44]), the Special Project for Science and Technology Innovation Team of Henan Academy of Agricultural Sciences (2022TD25), and the Outstanding Youth Science and Technology Fund of Henan Academy of Agricultural Sciences (2022YQ06).

SUPPLEMENTARY MATERIAL

The Supplementary Material for this article can be found online at: https://www.frontiersin.org/articles/10.3389/fmicb.2022.885430/full#supplementary-material

REFERENCES

Ahn, P., Chung, H. S., and Lee, Y. H. (1998). Vegetative Compatibility Groups and Pathogenicity Among Isolates of *Fusarium oxysporum* f. sp. *cucumerinum*. *Plant Dis.* 82, 244–246. doi: 10.1094/PDIS.1998.82.2.244

Al-Naamani, L. S. H., Dobretsov, S., Al-Sabahi, J., and Soussi, B. (2015). Identification and characterization of two amylase producing bacteria *Cellulosimicrobium* sp. and *Demequina* sp. isolated from marine organisms. *J. Agricult. Mar. Sci.* 20, 8–15. doi: 10.24200/jams.vol20iss0pp8-15

Banani, H., Spadaro, D., Zhang, D., Matic, S., Garibaldi, A., and Gullino, M. L. (2015). Postharvest application of a novel chitinase cloned from *Metschnikowia fructicola* and overexpressed in *Pichia pastoris* to control brown rot of peaches. *Int. J. Food Microbiol.* 199, 54–61. doi: 10.1016/j.ijfoodmicro.2015.01.002

Banerjee, G., Nandi, A., and Ray, A. K. (2017). Assessment of hemolytic activity, enzyme production and bacteriocin characterization of *Bacillus subtilis* LR1 isolated from the gastrointestinal tract of fish. *Archiv. Microbiol.* 199, 115–124. doi: 10.1007/s00203-016-1283-8

Bauman, K. D., Butler, K. S., Moore, B. S., and Chekan, J. R. (2021). Genome mining methods to discover bioactive natural products. *Nat. Prod. Rep.* 38, 2100–2129. doi: 10.1039/d1np00032b

Blake, C., Christensen, M. N., and Kovacs, A. T. (2021). Molecular Aspects of Plant Growth Promotion and Protection by *Bacillus subtilis*. *Mol. Plant Microbe Interact.* 34, 15–25. doi: 10.1094/MPMI-08-20-0225-CR

Blin, K., Shaw, S., Steinke, K., Villebro, R., Ziemert, N., Lee, S. Y., et al. (2019). antiSMASH 5.0: updates to the secondary metabolite genome mining pipeline. *Nucleic Acids Res.* 47, W81–W87. doi: 10.1093/nar/gkz310

Chaisson, M. J., and Tesler, G. (2012). Mapping single molecule sequencing reads using basic local alignment with successive refinement (BLASR): application and theory. *BMC Bioinform.* 13:238. doi: 10.1186/1471-2105-13-238

Chandrasekaran, M., and Chun, S. C. (2016). Expression of PR-protein genes and induction of defense-related enzymes by *Bacillus subtilis* CBR05 in tomato (*Solanum lycopersicum*) plants challenged with *Erwinia carotovora* subsp. *carotovora*. *Biosci. Biotechnol. Biochem.* 80, 2277–2283. doi: 10.1080/09168451.2016.1206811

Chen, F., Wang, M., Zheng, Y., Luo, J., Yang, X., and Wang, X. (2010). Quantitative changes of plant defense enzymes and phytohormone in biocontrol of cucumber *Fusarium* wilt by *Bacillus subtilis* B579. *World J. Microbiol. Biotechnol.* 26, 675–684. doi: 10.1007/s11274-009-0222-0

Chen, P. H., Chen, R. Y., and Chou, J. Y. (2018). Screening and Evaluation of Yeast Antagonists for Biological Control of *Botrytis cinerea* on Strawberry Fruits. *Mycobiology* 46, 33–46. doi: 10.1080/12298093.2018.1454013

Chin, C. S., Alexander, D. H., Marks, P., Klammer, A. A., Drake, J., Heiner, C., et al. (2013). Nonhybrid, finished microbial genome assemblies from long-read SMRT sequencing data. *Nat. Methods* 10, 563–569. doi: 10.1038/nmeth.2474

Dai, J., Dong, A., Xiong, G., Liu, Y., Hossain, M. S., Liu, S., et al. (2020). Production of Highly Active Extracellular Amylase and Cellulase From *Bacillus subtilis* ZIM3 and a Recombinant Strain With a Potential Application in Tobacco Fermentation. *Front. Microbiol.* 11:1539. doi: 10.3389/fmicb.2020.01539

Delcher, A. L., Bratke, K. A., Powers, E. C., and Salzberg, S. L. (2007). Identifying bacterial genes and endosymbiont DNA with Glimmer. *Bioinformatics* 23, 673–679. doi: 10.1093/bioinformatics/btm009

Dimkpa, C. O., Merten, D., Svatoš, A., Büchel, G., and Kothe, E. (2009). Metal-induced oxidative stress impacting plant growth in contaminated soil is alleviated by microbial siderophores. *Soil Biol. Biochem.* 41, 154–162. doi: 10.1016/j.soilbio.2008.10.010

Finn, R. D., Clements, J., and Eddy, S. R. (2011). HMMER web server: interactive sequence similarity searching. *Nucleic Acids Res.* 39, W29–W37. doi: 10.1093/nar/gkr367

Glick, B. R. (2012). Plant growth-promoting bacteria: mechanisms and applications. *Scientifica* 2012:963401. doi: 10.6064/2012/963401

Glickmann, E., and Dessaux, Y. (1995). A critical examination of the specificity of the Salkowski reagent for indolic compounds produced by phytopathogenic bacteria. *Appl. Env. Microbiol.* 61, 793–796. doi: 10.1128/aem.61.2.793-796

Gu, X., Zeng, Q., Wang, Y., Li, J., Zhao, Y., Li, Y., et al. (2021). Comprehensive genomic analysis of *Bacillus subtilis* 9407 reveals its biocontrol potential against bacterial fruit blotch. *Phytopathol. Res.* 3:4. doi: 10.1186/s42483-021-00081-2

Haas, H. (2003). Molecular genetics of fungal siderophore biosynthesis and uptake: the role of siderophores in iron uptake and storage. *Appl. Microbiol. Biotechnol.* 62, 316–330. doi: 10.1007/s00253-003-1335-2

Ji, Z. L., Peng, S., Zhu, W., Dong, J. P., and Zhu, F. (2020). Induced resistance in nectarine fruit by *Bacillus licheniformis* W10 for the control of brown rot caused by *Monilinia fructicola*. *Food. Microbiol.* 92:103558. doi: 10.1016/j.fm.2020.103558

Jiang, Y., Wu, Y., Hu, N., Li, H., and Jiao, J. (2020). Interactions of bacterial-feeding nematodes and indole-3-acetic acid (IAA)-producing bacteria promotes growth of *Arabidopsis thaliana* by regulating soil auxin status. *Appl. Soil Ecol.* 147:103447. doi: 10.1016/j.apsoil.2019.103447

Kazanas, N. (1968). Proteolytic activity of microorganisms isolated from freshwater fish. *Appl. Microb.* 16, 128–132. doi: 10.1128/am.16.1.128-132

Koren, S., Walenz, B. P., Berlin, K., Miller, J. R., Bergman, N. H., and Phillippy, A. M. (2017). Canu: scalable and accurate long-read assembly via adaptive

k-mer weighting and repeat separation. *Genome Res.* 27, 722–736. doi: 10.1101/gr.215087.116

Koskey, G., Mburu, S. W., Awino, R., Njeru, E. M., and Maingi, J. M. (2021). Potential Use of Beneficial Microorganisms for Soil Amelioration, Phytopathogen Biocontrol, and Sustainable Crop Production in Smallholder Agroecosystems. *Front. Sustainab. Food Syst.* 5:606308. doi: 10.3389/fsufs.2021.606308

Krzywinski, M., Schein, J., Birol, I., Connors, J., Gascoyne, R., Horsman, D., et al. (2009). Circos: an information aesthetic for comparative genomics. *Genome Res.* 19, 1639–1645. doi: 10.1101/gr.092759.109

Kumar, S., Stecher, G., and Tamura, K. (2016). MEGA7: Molecular Evolutionary Genetics Analysis Version 7.0 for Bigger Datasets. *Mol. Biol. Evol.* 33, 1870–1874. doi: 10.1093/molbev/msw054

Lagesen, K., Hallin, P., Rodland, E. A., Staerfeldt, H. H., Rognes, T., and Ussery, D. W. (2007). RNAmmer: consistent and rapid annotation of ribosomal RNA genes. *Nucleic Acids Res.* 35, 3100–3108. doi: 10.1093/nar/gkm160

Li, L., Ma, J., Li, Y., Wang, Z., Gao, T., and Wang, Q. (2012). Screening and partial characterization of Bacillus with potential applications in biocontrol of cucumber *Fusarium* wilt. *Crop. Prot.* 35, 29–35. doi: 10.1016/j.cropro.2011.12.004

Li, Z., Ye, X., Liu, M., Xia, C., Zhang, L., Luo, X., et al. (2019). A novel outer membrane β-1,6-glucanase is deployed in the predation of fungi by myxobacteria. *ISME J.* 13, 2223–2235. doi: 10.1038/s41396-019-0424-x

Liu, H., Yin, S., An, L., Zhang, G., Cheng, H., Xi, Y., et al. (2016). Complete genome sequence of *Bacillus subtilis* BSD-2, a microbial germicide isolated from cultivated cotton. *J. Biotechnol.* 230, 26–27. doi: 10.1016/j.jbiotec.2016.05.019

Lombard, V., Golaconda Ramulu, H., Drula, E., Coutinho, P. M., and Henrissat, B. (2014). The carbohydrate-active enzymes database (CAZy) in 2013. *Nucleic Acids Res.* 42, D490–D495. doi: 10.1093/nar/gkt1178

Lowe, T. M., and Eddy, S. R. (1997). tRNAscan-SE: a program for improved detection of transfer RNA genes in genomic sequence. *Nucleic Acids Res.* 25, 955–964. doi: 10.1093/nar/25.5.955

Morales-Cedeño, L. R., Orozco-Mosqueda, M. D. C., Loeza-Lara, P. D., Parra-Cota, F. I, de los Santos-Villalobos, S., and Santoyo, G. (2021). Plant growth-promoting bacterial endophytes as biocontrol agents of pre- and post-harvest diseases:fundamentals, methods of application and future perspectives. *Microbiolog. Res.* 242:126612. doi: 10.1016/j.micres.2020.126612

Naglot, A., Goswami, S., Rahman, I., Shrimali, D. D., Yadav, K. K., Gupta, V. K., et al. (2015). Antagonistic Potential of Native Trichoderma viride Strain against Potent Tea Fungal Pathogens in North East India. *Plant Pathol. J.* 31, 278–289. doi: 10.5423/PPJ.OA.01.2015.0004

Nayak, S. K. (2021). Multifaceted applications of probiotic *Bacillus* species in aquaculture with special reference to *Bacillus subtilis*. *Rev. Aquacult.* 13, 862–906. doi: 10.1111/raq.12503

Ongena, M., Jourdan, E., Adam, A., Paquot, M., Brans, A., Joris, B., et al. (2010). Surfactin and fengycin lipopeptides of *Bacillus subtilis* as elicitors of induced systemic resistance in plants. *Environ. Microb.* 9, 1084–1090. doi: 10.1111/j.1462-2920.2006.01202.x

Pan, H. Q., Li, Q. L., and Hu, J. C. (2017). The complete genome sequence of *Bacillus velezensis* 9912D reveals its biocontrol mechanism as a novel commercial biological fungicide agent. *J. Biotechnol.* 247, 25–28. doi: 10.1016/j.jbiotec.2017.02.022

Prasannath, K. (2017). Plant defense-related enzymes against pathogens: a review. *AGRIEAST: J. Agricult. Sci.* 11, 38–48. doi: 10.4038/agrieast.v11i1.33

Radhakrishnan, R., Hashem, A., and Abd Allah, E. F. (2017). *Bacillus*: a Biological Tool for Crop Improvement through Bio-Molecular Changes in Adverse Environments. *Front. Physiol.* 8:667–667. doi: 10.3389/fphys.2017.00667

Rana, K. L., Kour, D., Kaur, T., Devi, R., Yadav, A. N., Yadav, N., et al. (2020). Endophytic microbes: biodiversity, plant growth-promoting mechanisms and potential applications for agricultural sustainability. *Antonie Van Leeuwenhoek* 113, 1075–1107. doi: 10.1007/s10482-020-01429-y

Romero, D., de Vicente, A., Rakotoaly, R. H., Dufour, S. E., Veening, J. W., Arrebola, E., et al. (2007). The iturin and fengycin families of lipopeptides are key factors in antagonism of *Bacillus subtilis* toward *Podosphaera fusca*. *Mol. Plant Microbe Interact.* 20, 430–440. doi: 10.1094/MPMI-20-4-0430

Saeed, Q., Xiukang, W., Haider, F. U., Kucerik, J., Mumtaz, M. Z., Holatko, J., et al. (2021). Rhizosphere Bacteria in Plant Growth Promotion, Biocontrol, and Bioremediation of Contaminated Sites: A Comprehensive Review of Effects and Mechanisms. *Int. J. Mol. Sci.* 22:19. doi: 10.3390/ijms221910529

Samaras, A., Nikolaidis, M., Antequera-Gomez, M. L., Camara-Almiron, J., Romero, D., Moschakis, T., et al. (2020). Whole Genome Sequencing and Root Colonization Studies Reveal Novel Insights in the Biocontrol Potential and Growth Promotion by *Bacillus subtilis* MBI 600 on Cucumber. *Front Microbiol* 11:600393. doi: 10.3389/fmicb.2020.600393

Schwyn, B., and Neilands, J. B. (1987). Universal chemical assay for the detection and determination of siderophores. *Analyt. Biochem.* 160, 47–56. doi: 10.1016/0003-2697(87)90612-9

Spaepen, S., Bossuyt, S., Engelen, K., Marchal, K., and Vanderleyden, J. (2014). Phenotypical and molecular responses of *Arabidopsis thaliana* roots as a result of inoculation with the auxin-producing bacterium *Azospirillum brasilense*. *New Phytol.* 201, 850–861. doi: 10.1111/nph.12590

Su, Z., Chen, X., Liu, X., Guo, Q., Li, S., Lu, X., et al. (2020). Genome mining and UHPLC-QTOF-MS/MS to identify the potential antimicrobial compounds and determine the specificity of biosynthetic gene clusters in *Bacillus subtilis* NCD-2. *BMC Gen.* 21:767. doi: 10.1186/s12864-020-07160-2

Sui, Y., Wisniewski, M., Droby, S., Piombo, E., Wu, X., and Yue, J. (2020). Genome Sequence, Assembly, and Characterization of the Antagonistic Yeast *Candida oleophila* Used as a Biocontrol Agent Against Post-harvest Diseases. *Front Microbiol.* 11:295. doi: 10.3389/fmicb.2020.00295

Teather, R. M., and Wood, P. J. (1982). Use of Congo red-polysaccharide interactions in enumeration and characterization of cellulolytic bacteria from the *bovine rumen*. *Appl. Env. Microbiol.* 43, 777–780. doi: 10.1128/aem.43.4.777-780

Thakaew, R., and Niamsup, H. (2013). Inhibitory Activity of *Bacillus subtilis* BCC 6327 Metabolites against Growth of Aflatoxigenic Fungi Isolated from Bird Chili Powder. *Internat. J. Biosci. Biochem. Bioinform.* 3, 27–32. doi: 10.7763/IJBBB.2013.V3.157

Wang, X., Zhou, X., Cai, Z., Guo, L., Chen, X., Chen, X., et al. (2020). A Biocontrol Strain of *Pseudomonas aeruginosa* CQ-40 Promote Growth and Control *Botrytis cinerea* in Tomato. *Pathogens* 10:1. doi: 10.3390/pathogens10010022

Wu, Z., Huang, Y., Li, Y., Dong, J., Liu, X., and Li, C. (2019). Biocontrol of *Rhizoctonia solani* via Induction of the Defense Mechanism and Antimicrobial Compounds Produced by *Bacillus subtilis* SL-44 on Pepper (*Capsicum annuum* L.). *Front. Microbiol.* 10:2676. doi: 10.3389/fmicb.2019.02676

Xu, W., Xu, L., Deng, X., Goodwin, P. H., Xia, M., Zhang, J., et al. (2021). Biological Control of Take-All and Growth Promotion in Wheat by *Pseudomonas chlororaphis* YB-10. *Pathogens* 10:7. doi: 10.3390/pathogens10070903

Xu, W., Zhang, L., Goodwin, P. H., Xia, M., Zhang, J., Wang, Q., et al. (2020). Isolation, Identification, and Complete Genome Assembly of an Endophytic *Bacillus velezensis* YB-130, Potential Biocontrol Agent Against *Fusarium graminearum*. *Front. Microbiol.* 11:598285. doi: 10.3389/fmicb.2020.598285

Xu, W.-F., Ren, H.-S., Ou, T., Lei, T., Wei, J.-H., Huang, C.-S., et al. (2019). Genomic and Functional Characterization of the Endophytic *Bacillus subtilis* 7PJ-16 Strain, a Potential Biocontrol Agent of Mulberry Fruit Sclerotiniose. *Microb. Ecol.* 77, 651–663. doi: 10.1007/s00248-018-1247-4

Yoon, S. H., Ha, S. M., Lim, J., Kwon, S., and Chun, J. (2017). A large-scale evaluation of algorithms to calculate average nucleotide identity. *Antonie Van Leeuwenhoek* 110, 1281–1286. doi: 10.1007/s10482-017-0844-4

Zhang, H., Yohe, T., Huang, L., Entwistle, S., Wu, P., Yang, Z., et al. (2018). dbCAN2: a meta server for automated carbohydrate-active enzyme annotation. *Nucleic Acids Res.* 46, W95–W101. doi: 10.1093/nar/gky418

Zhao, J., Mei, Z., Zhang, X., Xue, C., Zhang, C., Ma, T., et al. (2017). Suppression of *Fusarium* wilt of cucumber by ammonia gas fumigation via reduction

of *Fusarium* population in the field. *Sci. Rep.* 7:43103. doi: 10.1038/srep43103

Zhou, J., Wang, M., Sun, Y., Gu, Z., Wang, R., Saydin, A., et al. (2017). Nitrate Increased Cucumber Tolerance to *Fusarium* Wilt by Regulating Fungal Toxin Production and Distribution. *Toxins* 9:3. doi: 10.3390/toxins9030100

Zhou, X., Shen, Y., Fu, X., and Wu, F. (2018). Application of Sodium Silicate Enhances Cucumber Resistance to *Fusarium* Wilt and Alters Soil Microbial Communities. *Front. Plant Sci.* 9:624. doi: 10.3389/fpls.2018.00624

Conflict of Interest: The authors declare that the research was conducted in the absence of any commercial or financial relationships that could be construed as a potential conflict of interest.

Publisher's Note: All claims expressed in this article are solely those of the authors and do not necessarily represent those of their affiliated organizations, or those of the publisher, the editors and the reviewers. Any product that may be evaluated in this article, or claim that may be made by its manufacturer, is not guaranteed or endorsed by the publisher.

frontiers | Frontiers in Microbiology

ORIGINAL RESEARCH
published: 21 June 2022
doi: 10.3389/fmicb.2022.813415

A Combined Use of Rhizobacteria and Moringa Leaf Extract Mitigates the Adverse Effects of Drought Stress in Wheat (*Triticum aestivum* L.)

Irfana Lalarukh[1], Sami A. Al-Dhumri[2], Laith Khalil Tawfeeq Al-Ani[3,4], Rashid Hussain[5], Khalid Awadh Al Mutairi[6], Nida Mansoora[7], Syeda Fasiha Amjad[7]*, Mohamed H. H. Abbas[8], Ahmed A. Abdelhafez[9,10]*, Peter Poczai[11]*, Khem Raj Meena[12] and Tarek M. Galal[13,14]*

[1] Department of Botany, Government College Women University, Faisalabad, Pakistan, [2] Department of Biology, Al Khumra University College, Taif University, Taif, Saudi Arabia, [3] Department of Plant Protection, College of Agriculture Engineering Science, University of Baghdad, Baghdad, Iraq, [4] School of Biology Science, Universiti Sains Malaysia, George Town, Malaysia, [5] Department of Horticultural Sciences, Faculty of Agriculture and Environment, The Islamia University of Bahawalpur, Bahawalpur, Pakistan, [6] Department of Biology, Faculty of Science, University of Tabuk, Tabuk, Saudi Arabia, [7] Department of Botany, University of Agriculture Faisalabad, Faisalabad, Pakistan, [8] Department of Soils and Water, Faculty of Agriculture, Benha University, Benha, Egypt, [9] Department of Soils and Water, Faculty of Agriculture, New Valley University, Kharga, Egypt, [10] National Committee of Soils Science, Academy of Scientific Research and Technology, Cairo, Egypt, [11] Botany Unit, Finnish Museum of Natural History, University of Helsinki, Helsinki, Finland, [12] Department of Microbiology, College of Basic Sciences and Humanities, Dr. Rajendra Prasad Central Agricultural University, Pusa, India, [13] Department of Botany and Microbiology, Faculty of Science, Helwan University, Cairo, Egypt, [14] Department of Biology, College of Sciences, Taif University, Taif, Saudi Arabia

Less nutrient availability and drought stress are some serious concerns of agriculture. Both biotic and abiotic stress factors have the potential to limit crop productivity. However, several organic extracts obtained from moringa leaves may induce immunity in plants under nutritional and drought stress for increasing their survival. Additionally, some rhizobacterial strains have the ability to enhance root growth for better nutrient and water uptake in stress conditions. To cover the knowledge gap on the interactive effects of beneficial rhizobacteria and moringa leaf extracts (MLEs), this study was conducted. The aim of this experimental study was to investigate the effectiveness of sole and combined use of rhizobacteria and MLEs against nutritional and drought stress in wheat. Nitrogen-fixing bacteria *Pseudomonas aeruginosa* (Pa) (10^8 CFU ml^{-1}) was inoculated to wheat plants with and without foliar-applied MLEs at two different concentrations (MLE 1 = 1:15 v/v and MLE 2 = 1:30 v/v) twice at 25 and 35 days after seed sowing (50 ml per plant) after the establishment of drought stress. Results revealed that Pa + MLE 2 significantly increased fresh weight (FW), dry weight (DW), lengths of roots and shoot and photosynthetic contents of wheat. A significant enhancement in total soluble sugars, total soluble proteins, calcium, potassium, phosphate, and nitrate contents validated the efficacious effect of Pa + MLE 2 over control-treated plants. Significant decrease in sodium, proline, glycine betaine, electrolyte leakage, malondialdehyde, hydrogen peroxide, superoxide dismutase (SOD), and peroxide (POD)

OPEN ACCESS

Edited by:
Giuseppe Colla, University of Tuscia, Italy

Reviewed by:
Kamlesh Kumar Meena, National Institute of Abiotic Stress Management (ICAR), India
Faisal Zulfiqar, Islamia University of Bahawalpur, Pakistan
Olubukola Oluranti Babalola, North-West University, South Africa

***Correspondence:**
Syeda Fasiha Amjad
fasihamushadi75@gmail.com
Laith Khalil Tawfeeq Al-Ani
cmv_virus2002@yahoo.com; laith.kt77@gmail.com
Ahmed A. Abdelhafez
ahmed.aziz@agr.nvu.edu.eg
Peter Poczai
peter.poczai@helsinki.fi

Specialty section:
This article was submitted to Microbe and Virus Interactions with Plants, a section of the journal Frontiers in Microbiology

Received: *11 November 2021*
Accepted: *11 March 2022*
Published: *21 June 2022*

Citation:
Lalarukh I, Al-Dhumri SA, Al-Ani LKT, Hussain R, Al Mutairi KA, Mansoora N, Amjad SF, Abbas MHH, Abdelhafez AA, Poczai P, Meena KR and Galal TM (2022) A Combined Use of Rhizobacteria and Moringa Leaf Extract Mitigates the Adverse Effects of Drought Stress in Wheat (Triticum aestivum L.). Front. Microbiol. 13:813415. doi: 10.3389/fmicb.2022.813415

concentrations in wheat cultivated under drought stress conditions also represents the imperative role of Pa + MLE 2 over control. In conclusion, Pa + MLE 2 can alleviate nutritional stress and drought effects in wheat. More research in this field is required to proclaim Pa + MLE 2 as the most effective amendment against drought stress in distinct agroecological zones, different soil types, and contrasting wheat cultivars worldwide.

Keywords: PGPR, agroecological zones, drought stress, *Pseudomonas*, nitrogen-fixing bacteria, biofertilizers, bioinnoculants

INTRODUCTION

Crop production is always under pressure to increase and sustain the food demands, considering the estimated increase in global population that might increase from the current 7.7 billion to approximately 9.6 billion in the year 2050 (Zulfiqar et al., 2020). Moreover, constantly changing climatic conditions are the other major challenge for sustainable crop production (Wheeler and Von Braun, 2013). Several abiotic and biotic stress factors such as temperature, water-logging, salinity, drought, weed, and pest infestations critically limit crop production (Parajuli et al., 2019). Climate change leads to widely drought-affected areas, such as tropics (Grover et al., 2011).

Water constitutes approximately 80–90% of the total biomass of herbaceous plants and is crucial in almost all plant physiological processes, a principal means of nutrients and metabolite transport (Lisar et al., 2012). Water scarcity is one of the leading plant stress factors. A drought effect reduces cell turgor and water potential causing adversities in carrying out plant's normal physiological functions (Lisar et al., 2012). In fact, water is the key determining factor for crop growth and productivity, thus playing an essential role in species distribution and evolution (Ngumbi and Kloepper, 2016).

The induction of drought stress tolerance has been described by several physiological and biochemical changes (Shukla et al., 2012). In spite of these tolerance strategies including elaborated antioxidative activities, losses to crop production are increasing rapidly. Chemical fertilizers are largely being used to increase agricultural production, which is a matter of concern due to their improper use and potential adverse effects on human health and environment (Ruzzi and Aroca, 2015; Jiménez-Gómez et al., 2018). Expensive agrochemicals and synthetic fertilizers are commercially undesirable (Colla et al., 2015). Hence, to maintain and increase the yield, it is crucial to devise some efficient, low-cost, less time taking, and environment-friendly techniques to cope with drought conditions and achieve a sustainable agricultural system (Venkateswarlu and Shanker, 2009; Zulfiqar et al., 2019).

Several microorganisms, mainly bacteria, colonize the plant root zone (Kaushal and Wani, 2016; Barnawal et al., 2019). The beneficial associations between microbes and roots are an important determinant of soil texture, water conservation, and plant health. Plant growth-promoting rhizobacteria (PGPR) improve nutrient uptake by roots, growth, and consequently crop yield by causing biochemical changes in the plant body, meanwhile protecting from a variety of other plant diseases (Khan et al., 2020; Singh et al., 2021; Soumare et al., 2021). Furthermore, improvement in soil texture and fertility enhances crop production (Nardi et al., 2009).

Moringa leaf extract (MLE), as a plant biostimulant in the foliar application, enhances the growth of plants that are grown even under abiotic stress conditions (Semida and Rady, 2014). *Moringa oleifera* Lam belongs to the Moringaceae family and native to the subcontinent (Shahzad et al., 2013). Moringa leaves are rich in both micronutrients and macronutrients, i.e., N, P, Ca, K, Na, Zn, Mg, B, Cu, Mn, and Fe (Yasmeen et al., 2014). These mineral nutrients can supplement the nutritional demands of stressed grown crops and help in decreasing the use of agrochemicals and synthetic fertilizers (Zulfiqar et al., 2020). Spraying MLE diluted solution on plant leaves seems to have a considerable positive impact, i.e., delay in senescence, higher sugar contents, increased plant height, and bigger fruits and seeds (Yasmeen et al., 2013a; Nasir et al., 2014). This validates the potential effects of MLE to be used to improve plant vigor specifically in suboptimal environmental situations like drought stress as a foliar application. MLE foliar spray increased approximately 20–35% yield of several plants (Yasmeen et al., 2012).

Wheat (*Triticum aestivum* L.) is one of the most important cereal crops worldwide, considering its production and human consumption. Wheat supplements almost one-third of the total global population. Harvesting more yields to meet the future food demands of the increasing population is a major agricultural concern at all times. Different environmental factors contribute to crop yields (Yasmeen et al., 2012; Fasiha Amjad et al., 2021). Wheat in Pakistan experiences severe abiotic constraints during all developmental stages (Rashid et al., 2018), and drought stress is the main limiting factor among abiotic stresses for wheat yield (Budak et al., 2013; Mutumba et al., 2018).

Previously, the effects of exogenous applied MLE and treating plants with nitrogen-fixing bacteria (NFB) were studied solely on wheat grown at high temperatures. This study covers the knowledge gap in the combined use of NFB and MLE under normal and heat stress situations. In earlier studies, treating plants with rhizobacteria and the effects of foliar sprayed MLE were assessed solely on wheat grown under drought stress conditions by considering their ameliorative implications on various physiological and biochemical attributes but their combined implications are still not confirmed.

Therefore, this study aimed to investigate the best treatment combination for alleviation of heat stress in wheat. Anaj 17 genotype was selected because it is one of the latest genotypes developed in the past 5 years in Pakistan and it performed well under abiotic stress conditions so we wanted to check

its response to the application of MLE and rhizobacteria. It is hypothesized that the combined use of MLE and NFB might be a better approach than the sole application to improve wheat growth attributes under heat stress. This study was conducted to analyze the ameliorative and best co-application of applied amendments in alleviating the drought stress effects on wheat plants. It is hypothesized that MLE and rhizobacterial combined application might be an effective approach to improve wheat attributes than their sole applications in drought effects. In earlier studies, treating plants with rhizobacteria and the effects of foliar sprayed MLE were assessed solely on wheat grown under drought stress conditions by considering their ameliorative implications on various physiological and biochemical attributes but their combined implications are still not confirmed. Therefore, this study is conducted to analyze the ameliorative and best co-application of applied amendments in alleviating the drought stress effects on wheat plants. It is hypothesized that MLE and rhizobacterial combined application might be an effective approach to improve wheat attributes than their sole applications in drought effects.

MATERIALS AND METHODS

Experimental Site and Design

The wheat crop was sown at the experimental site of the Government College University Faisalabad (30°–31.5° N and 73°–74° E, 184.4 m above sea level). A greenhouse pot experiment was carried out from November to January. The experimental layout was a randomized complete block design (RCBD) that was replicated three times.

Soil Characteristics

The clay loam soil (8–12 inches in depth) collected from the experimental site of the Government College University Faisalabad was air-dried and sieved through a 2-mm sieve. The collected soils were sterilized through solarization, by covering the soil with a thin layer of plastic sheet. The heat from the sun builds up the temperature of the soil to kill most of the bacteria, weeds, and pests (Stapleton et al., 2008). Some soil chemical characteristics that were analyzed before the experiment include EC 7.78 (d Sm^{-1}), pH (water) 7.3; organic matter contents 1.38%; available N 0.032 ppm, available P 5.93 ppm, and available K 32.3 ppm.

Seed Collection and Sterilization

A well-adapted wheat genotype Anaj 17, which performs well under abiotic stress conditions, was selected. Seeds were disinfected using 95% ethanol and washed using 70% sodium hypochlorite solution followed by rinsing with distilled water three times.

Treatments

The treatments (two sets of pots) were as follows: (i) control (untreated with foliar spray, no bacterial inoculation], (ii) *Pseudomonas aeruginosa* (Pa) (strain) [inoculation with Pa], (iii) MLE 1 [foliar sprayed MLE at 1:15], (iv) MLE 2 [foliar sprayed MLE at 1:30], (v) Pa + MLE 1 [inoculation with Pa bacteria + foliar sprayed MLE at 1:15], and (vi) Pa + MLE 2 [inoculation with Pa bacteria + foliar sprayed MLE at 1:30].

Fertilizer and Seed Sowing

At the start of the experiment, the soil was fertilized with a basal dose of N–P–K fertilizer (0.51–0.45–0.38 N–P–K g) using urea (46% N), sulfate of potash (50% K_2O), and diammonium phosphate (46% P_2O_5, 18% N) [24]. Initially, ten seeds were sown in each pot containing 12 kg clay loamy soil (25 cm diameter × 30 cm height), and after complete emergence, they were thinned to six plants per pot.

Moringa Leaf Extract, Pa (Strain), and Establishment of Drought Stress

An aerobic PGPR strain of free-living soil nitrogen-fixing bacteria; Pa (Pa strain) isolated from the rhizosphere of wheat roots growing in local field areas by serial dilution method was used in this study. The serial dilutions up to 10^{-7} were spread on Luria-Bertani (LB) agar plates at 37°C temperature and inoculated overnight. Bacterial growth was determined by measuring optical density at 600 nm using a spectrophotometer (Gontia-Mishra et al., 2016). Before inoculation, the seeds were coated with 20% gum Arabic as an adhesive and immersed in a bacterial suspension of 10^8 CFU ml^{-1} strength just before 15 min of sowing. After 20 days of seed sowing, one set of pots (half number) was shifted to canopies for the imposition of drought stress. Well-watered conditions were maintained at 70 FC (70% field capacity), while drought stress was maintained at 45 FC (45% field capacity). The plants that remained were kept at different water regimes until harvesting.

Fresh and disease-free moringa leaves were collected and rinsed with water. Notably, a 100-g leaf sample was extracted in 1 L distilled water (1:10 w/v) for 15 min (Yasmeen et al., 2013b). Later, MLE was filtered and diluted with distilled water at two concentrations: MLE 1 = 1:20 v/v and MLE 2 = 1:30 v/v. Some chemical properties of moringa leaves are total chlorophyll = 3.79 mg g^{-1} FW, carotenoids = 1.58 mg g^{-1} FW, total phenolics = 1.68 μmol g^{-1} FW, mg g^{-1} FW, nitrogen = 14.13 mg g^{-1} DW, phosphorous = 2.98 mg g^{-1} DW, potassium = 11.97 mg g^{-1} DW, and calcium = 16.8 mg g^{-1} DW. The extracts were freshly prepared before their application. Distilled water was sprayed on control plants in both applications. MLE was sprayed to a pot-grown wheat twice after 25 and 35 days of sowing date (50 ml per plant) after the establishment of drought stress. Tween-20 surfactant was used in a foliar spray (0.1% v/v).

Harvesting and Measurement of Growth Attributes

Harvest was done after 45 days of planting. Root and shoot fresh weights (FWs) and lengths were measured immediately after harvest at the experimental site. Fresh samples were stored at -30°C in a biomedical refrigerator for fresh analysis. Three samples per treatment were oven-dried (65°C) for 3 days to

determine their dry weights (DWs) and ionic content analysis using the acid digestion method.

Photosynthetic Pigments

The chlorophyll contents of wheat leaves were determined as described by Dere et al. (1998). Notably, 0.2 g of leaves (randomly collected) were extracted in 10 ml methanol (96%) using a homogenizer at 1,000 rpm for 1 min, then filtered, and centrifuged for 10 min at 2,500 rpm. The supernatant was separated and used to determine chlorophyll contents at 666 (chlorophyll a), 653 (chlorophyll b), and 470 nm (total carotenoids) wavelengths using a spectrophotometer (Model SM1200; Randolph, NJ, United States).

Measurements of Stomatal Conductance (gs)

Stomatal conductance (gs) of fully developed leaves (three plants per treatment) was measured by putting them in a portable infrared gas analyzer chamber (Analytical Development Company, Hoddeson, United Kingdom). The measurements were made 6 days after the first MLE foliar spray.

Leaf Biochemical Analysis

Fully expanded leaves from each replicate were taken, wrapped in aluminum foils, immersed in liquid nitrogen, and transferred into plastic zipper bags. These samples were stored at –80°C for further analysis. Following, biochemical analysis was performed using a spectrophotometer (Model SM1200; Randolph, NJ, United States).

To determine osmolytes as sugars and non-enzymatic antioxidants, 50 mg of dried leaves were homogenized in 10 ml of 80% ethanol and filtered followed by the re-extraction in 10 ml ethanol, and a 20 ml of the final volume was maintained. This obtained solution was used to evaluate flavonoids (Lewis et al., 1999), soluble sugars (Dubois et al., 1956), proteins (Bradford, 1976), and proline (Bates et al., 1973) contents. Glycine betaine (GB) was assessed by following the method of Holmström et al. (2000).

Mineral Content

For the determination of P contents in wheat molybdate/ascorbic acid, the blue technique was used, and nitrate contents were assessed by Kowalenko and Lowe (1973) method using a spectrophotometer (Model SM1200; Randolph, NJ, United States). K concentration was determined using a flame photometer. Ca and Na ions were evaluated by Atomic Absorption Spectrum (AAS; Shimadzu instruments, Inc., Spectra AA-220, Kyoto, Japan).

Statistical Analysis

Statistical analysis of data was performed using a *post-hoc* test, which was performed to measure specific differences between treatments using the Duncan's Multiple Range Test (DMRT) in a completely randomized block design. The significant diffidences between treatment means were determined using analysis of variance and mean separation at a 5% significance level ($p \leq 0.05$). In addition, the Pearson correlation of different wheat attributes under drought stress and well-watered conditions was performed. Logarithmic data transformation to obtain near-normal distribution was implemented before analysis, where required.

RESULTS

Length, Fresh Weight, and Dry Weight of Roots and Shoot

All applied treatments had a significant positive effect on root and shoot FWs, DWs, and lengths under control and drought stress conditions (**Figure 1**). In this regard, Pa + MLE 1 and Pa + MLE 2 were proved significantly efficient amendments in increasing root FW and shoot FW of wheat plants during drought conditions. Furthermore, MLE 2 enhanced root DW and shoot DW at 45 FC compared with control (70 FC). The treatments MLE 2, Pa + MLE 1, and Pa + MLE 2 had a more significant effect on root length and shoot length as compared with the control under drought stress. A significant difference was observed between the given amendments and control plants which signify their effectiveness in drought stress environments.

Photosynthetic Pigments

All photosynthetic pigments such as chlorophyll a, chlorophyll b, total chlorophyll, and carotenoids were significantly affected when subjected to drought stress conditions (45 FC) as compared with well-irrigated conditions (70 FC) (**Figure 2**). All applied amendments significantly improved plant photosynthetic pigments over the control. Pa + MLE 1 and Pa + MLE 2 treatments were remained efficient in increasing chlorophyll a and chlorophyll b at 45 FC over control-treated wheat plants (70 FC). Furthermore, MLE 2 differed significantly better for the enhancement of total chlorophyll contents at 45 FC than 70 FC. Treatments MLE 2, Pa + MLE 1, and Pa + MLE 2 were significantly different for wheat carotenoid contents under drought stress as compared with the control. A significant difference was observed in MLE at both concentrations and Pa for all studied parameters in all treatment levels. The above results signify the value of given amendments in enhancing the efficiency of water uptake and use by the grown plants.

Flavonoids, Phenolics, Total Soluble Sugars, Total Soluble Proteins, and Stomatal Conductance

Flavonoids, phenolics, total soluble sugars, total soluble proteins, and stomatal conductance of wheat plants were significantly affected in drought stress (45 FC) compared with well-watered plants (70 FC) (**Figure 3**). Both sole and combined applications of Pa and MLE significantly increased plant total soluble sugars, total soluble proteins, and stomatal conductance over the control. Pa + MLE 1 and Pa + MLE 2 treatments were remained efficient in decreasing flavonoids and phenolics at 45 FC over 70 FC. Moreover, MLE 2 differed significantly better than MLE 1 and

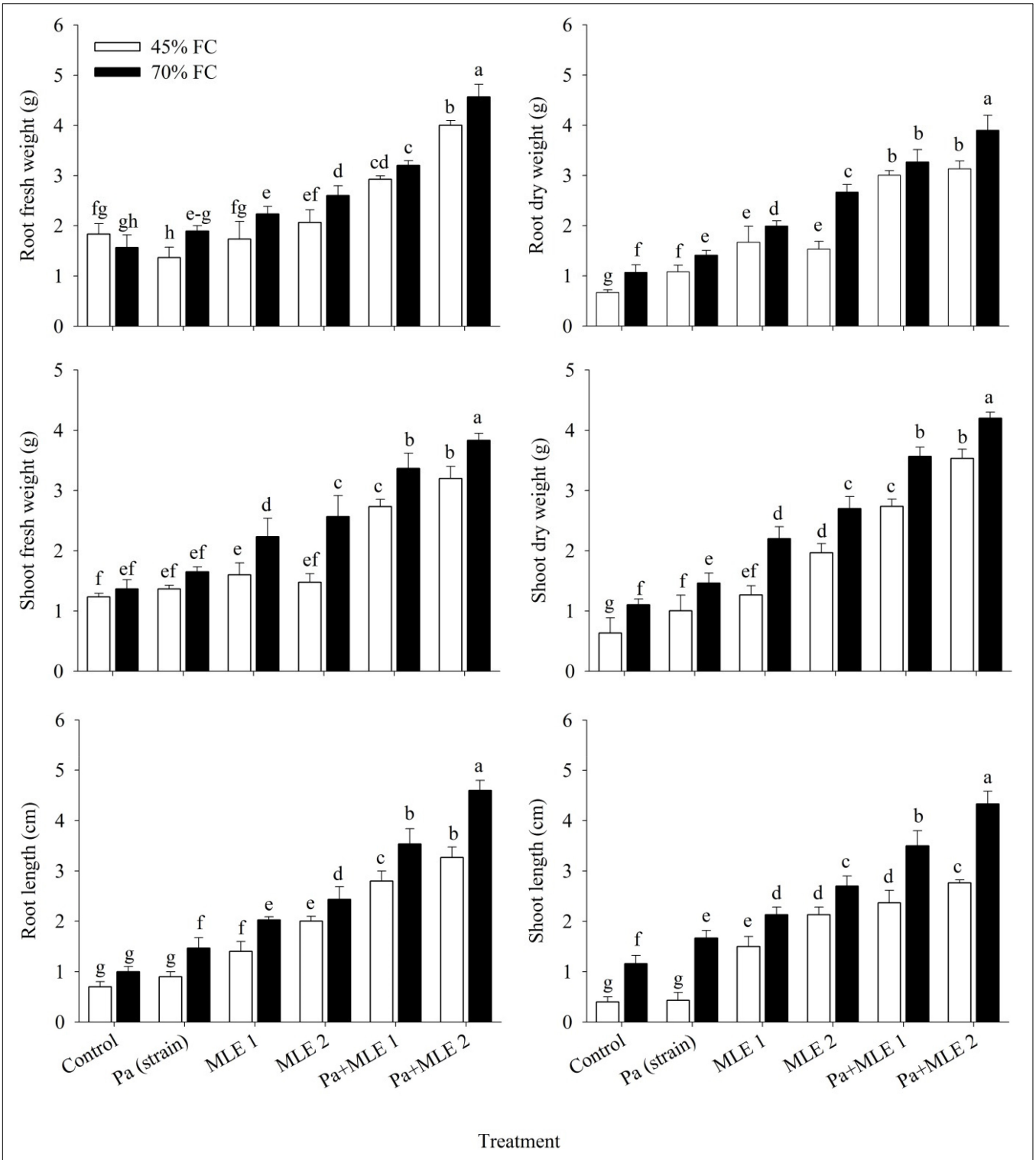

FIGURE 1 | Impact of sole and combined applications of Pa and moringa leaf extract (MLE) on different growth attributes of wheat plants under 45 FC and 70 FC irrigation levels. Different bars represent the mean values of three replicates. Error bars represent standard error (SE). Different letters on bars indicate significant difference at $p \leq 0.05$ [70 FC = well-irrigated, 45 FC = drought stress condition; C = control, Pa (strain) = *Pseudomonas aeruginosa* inoculated plants, MLE 1 = foliar-applied MLE at 1:15, and MLE 2 = foliar-applied MLE at 1:30]. Means with the same letters within the column are not significantly different.

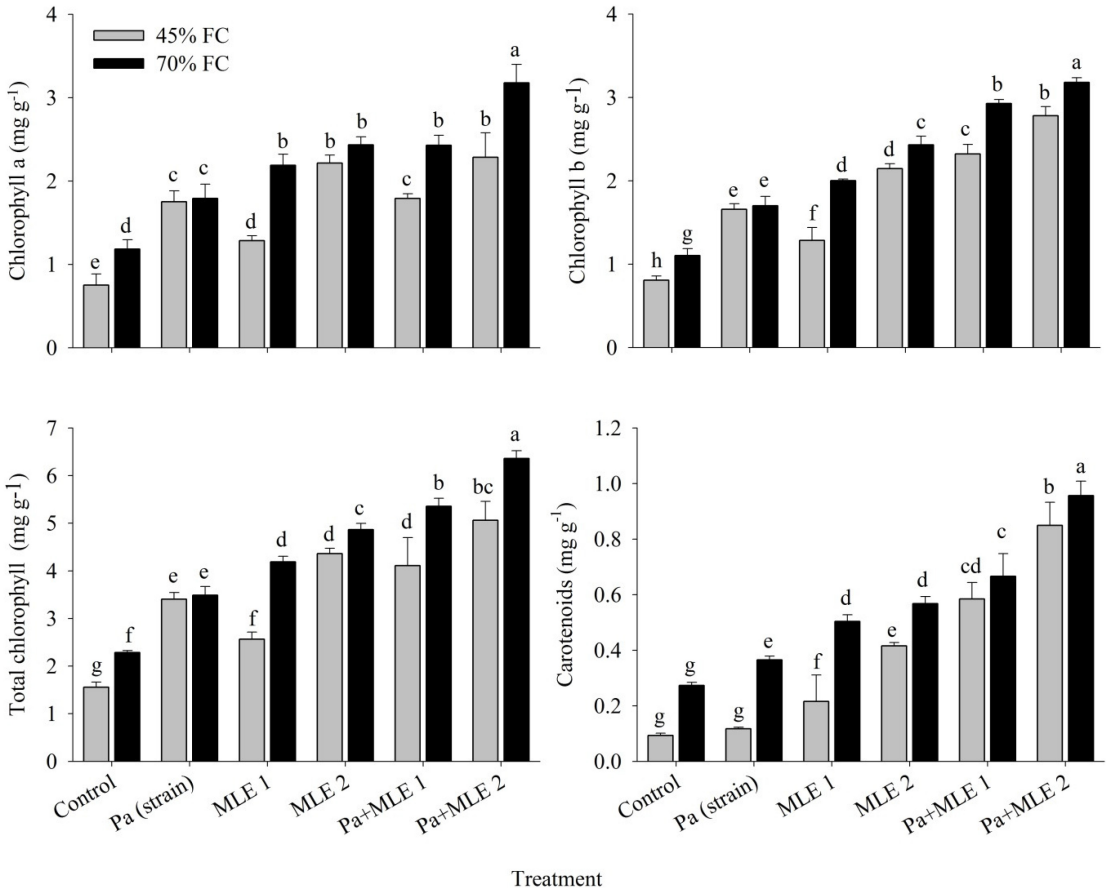

FIGURE 2 | Impact of sole and combined applications of Pa and MLE on different photosynthetic pigments of wheat plants under 45 FC and 70 FC irrigation levels. Different bars represent the mean values of three replicates. Error bars represent SE. Different letters on bars indicate significant difference at $p \leq 0.05$ [70 FC = well-irrigated, 45 FC = drought stress condition; C = control, Pa (strain) = *P. aeruginosa* inoculated plants, MLE 1 = foliar-applied MLE at 1:15, and MLE 2 = foliar-applied MLE at 1:30]. Means with the same letters within the column are not significantly different.

Pa either in sole or combined applications at 45 FC than 70 FC, while, MLE 2, Pa + MLE 1, and Pa + MLE 2 were significantly efficient in decreasing flavonoids and phenolics of wheat plants under drought stress as compared with the control. These results prove the effectiveness of these amendments in increasing the water uptake efficiency of wheat plants.

Oxidative Stress Indicators, Enzymatic Antioxidants, and Ionic Contents

Ionic nutrient contents increased significantly in plants that were irrigated at 70 FC compared with plants irrigated with water to reach only 45 FC (**Table 1**). However, in contrast, different oxidative stress indicators such as sodium, proline, GB, electrolyte leakage (EL), malondialdehyde (MDA), and hydrogen peroxide (H_2O_2) increased significantly in plants subjected to 45 FC water conditions. Furthermore, antioxidant enzyme [superoxide dismutase (SOD) and peroxide (POD)] activities were increased in drought stress.

All additives had significant positive improvements in ameliorating drought effects in wheat. These amendments were more detectable when the dose of MLE foliar application was increased. Pa and MLE decreased sodium, proline, GB, EL, MDA, H_2O_2, and SOD and POD contents significantly. Also, they increased calcium, potassium, phosphate, and nitrate concentrations in plant tissues. It is worth mentioning in this study that sole and combined applications of either MLE or Pa were better in decreasing the oxidative stress indicators and increasing nutrient contents of wheat, and this signifies the success of these ameliorating treatments for drought stress. Pa + MLE 1 and Pa + MLE 2 recorded the least oxidative stress indicators and enzymatic antioxidant activities during more nutrient assimilation in plants.

All values are the means of three replicates ± SD. Different labels represent significant different alphabets using the least significant difference (LSD) test. [70 FC = well-irrigated conditions, 45 FC = drought stress conditions; C = control, Pa (strain) = *P. aeruginosa* inoculated plants, MLE 1 = foliar applied MLE at 1:15, and MLE 2 = foliar applied MLE at 1:30] [GB = glycine betaine, EL = electrolyte leakage, MDA = malondialdehyde, H_2O_2 = hydrogen peroxide, SOD = superoxide dismutase, and POD = peroxide].

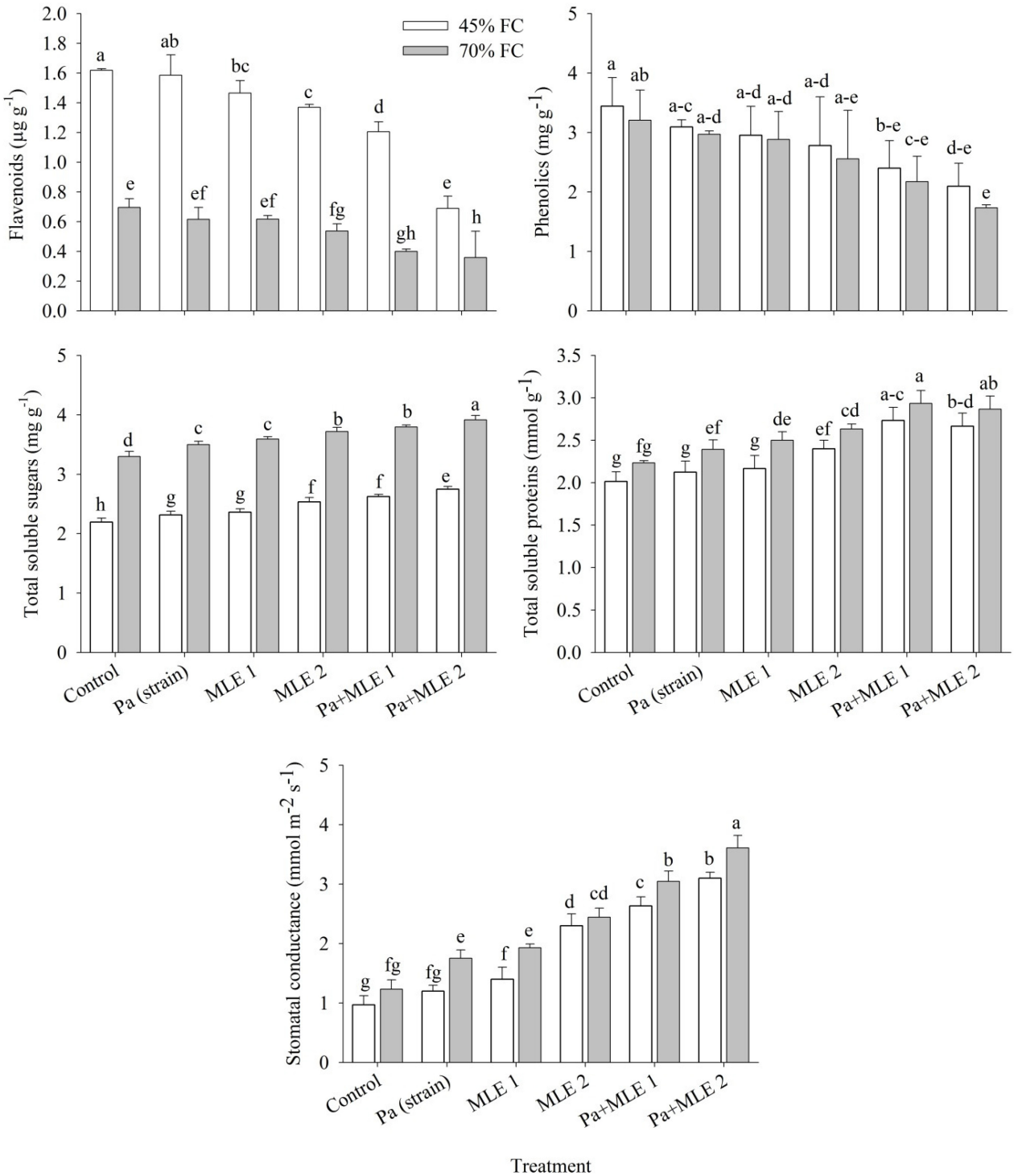

FIGURE 3 | Impact of sole and combined applications of Pa and MLE on flavonoids, phenolics, total soluble sugars, total soluble proteins, and stomatal conductance of wheat plants under 45 FC and 70 FC irrigation levels. Different bars represent the mean values of three replicates. Error bars represent SE. Different letters on bars indicate significant difference at $p \leq 0.05$ [70 FC = well-irrigated, 45 FC = drought stress condition; C = control, Pa (strain) = *P. aeruginosa* inoculated plants, MLE 1 = foliar-applied MLE at 1:15, MLE 2 = foliar-applied MLE at 1:30, and S.C. = stomatal conductance]. Means with the same letters within the column are not significantly different.

TABLE 1 | Oxidative stress indicators, enzymatic antioxidants, and ionic contents of wheat grown in well-watered and drought stress conditions.

Treatment	Proline (µg g^{-1} FW)	GB (µmol g^{-1})	EL (%)	MDA (µmol g^{-1} FW)	H_2O_2 (µmol g^{-1} FW)	SOD (U g^{-1} FW)	POD (U g^{-1} FW)	Sodium (mg g^{-1} DW)	Calcium (mg g^{-1} DW)	Potassium (mg g^{-1} DW)	Phosphate (mg g^{-1} DW)	Nitrate (mg g^{-1} DW)
45% FC												
Control	3.40 ± 0.09a	2.03 ± 0.29a	30.33 ± 2.52a	1.85 ± 0.07a	3.26 ± 0.53a	1.92 ± 0.35a	6.15 ± 1.06a	22.67 ± 1.53a	8.33 ± 0.76i	3.17 ± 0.29ef	0.02 ± 0.0h	3.18 ± 0.02e
Pa (strain)	3.27 ± 0.08b	1.83 ± 1.54ab	27.67 ± 2.08ab	1.13 ± 0.24bc	2.96 ± 0.48a-c	1.76 ± 0.13ab	4.06 ± 0.33b-d	21.67 ± 0.58ab	10.17 ± 0.76hi	4.33 ± 0.58e	0.02 ± 0.0f-h	3.27 ± 0.02e
MLE 1	3.13 ± 0.04c	1.78 ± 0.05ab	25.67 ± 1.53b	1.22 ± 0.64b	3.09 ± 0.29ab	1.77 ± 0.15ab	4.23 ± 1.03bc	20.00 ± 2.65b	12.83 ± 0.76fg	4.33 ± 0.76e	0.02 ± 0.0gh	3.25 ± 0.05e
MLE 2	2.89 ± 0.06d	1.50 ± 0.28ab	26.33 ± 0.58b	1.11 ± 0.13bc	2.68 ± 0.59a-d	1.62 ± 0.39a-c	3.79 ± 0.41b-d	16.33 ± 0.58cd	13.67 ± 1.76f	3.17 ± 0.76ef	0.03 ± 0.01e-g	3.43 ± 0.06d
Pa + MLE 1	2.77 ± 0.05de	1.22 ± 0.43a-c	20.67 ± 2.52cd	1.09 ± 0.02bc	2.53 ± 0.27a-d	1.28 ± 0.32a-d	3.05 ± 0.57de	14.67 ± 0.58de	17.67 ± 1.61cd	2.50 ± 1.0f	0.04 ± 0.01c-e	3.63 ± 0.06c
Pa + MLE 2	2.63 ± 0.09fg	1.10 ± 0.01a-c	17.67 ± 1.53de	0.78 ± 0.14b-d	2.27 ± 0.09cd	0.73 ± 0.10c-e	2.47 ± 0.56ef	13.33 ± 1.15ef	21.17 ± 0.76b	1.97 ± 0.06f	0.04 ± 0.0bc	3.87 ± 0.06b
70% FC												
Control	2.88 ± 0.09d	1.20 ± 0.04a-c	21.67 ± 2.08c	0.85 ± 0.23b-d	2.47 ± 0.27b-d	1.16 ± 1.37a-d	4.62 ± 0.55b	21.17 ± 1.26ab	11.00 ± 1.0gh	4.33 ± 1.04e	0.03 ± 0.0fg	3.23 ± 0.03e
Pa (strain)	2.75 ± 0.08ef	0.99 ± 0.28bc	19.67 ± 1.53cd	0.70 ± 0.54b-d	2.23 ± 0.22cd	0.83 ± 0.07c-e	3.08 ± 0.51de	20.00 ± 0.50b	11.67 ± 1.53gh	4.67 ± 1.53e	0.03 ± 0.0d-f	3.40 ± 0.02d
MLE 1	2.59 ± 0.07gh	1.12 ± 0.33a-c	17.00 ± 1.0d-f	0.79 ± 0.12b-d	2.32 ± 0.16cd	0.96 ± 0.27b-e	3.54 ± 0.11c-e	17.00 ± 1.0c	14.33 ± 0.58ef	6.83 ± 0.76d	0.04 ± 0.0c-e	3.48 ± 0.03d
MLE 2	2.48 ± 0.05hi	0.93 ± 0.28bc	18.00 ± 2.65c-e	0.61 ± 0.07cd	2.19 ± 0.13d	0.71 ± 0.46c-e	2.67 ± 0.09ef	14.33 ± 0.58de	16.17 ± 1.04de	8.50 ± 0.5c	0.04 ± 0.0b-d	3.63 ± 0.06c
Pa + MLE 1	2.37 ± 0.05ij	0.35 ± 0.2c	15.33 ± 1.53ef	0.55 ± 0.15d	2.14 ± 0.14d	0.43 ± 0.44de	2.48 ± 0.29ef	12.67 ± 0.58ef	19.50 ± 1.32bc	10.00 ± 0.5b	0.05 ± 0.01b	3.87 ± 0.0b
Pa + MLE 2	2.26 ± 0.07j	0.26 ± 0.06c	13.67 ± 3.21f	0.36 ± 0.22d	2.01 ± 0.83d	0.15 ± 0.06e	1.97 ± 0.48f	11.33 ± 1.1f	23.33 ± 0.76a	12.67 ± 1.2a	0.07 ± 0.01a	4.21 ± 0.1b

Means with the same letters within the column are not significantly different.

Pearson Correlation

A significant positive correlation exists between plant morphological attributes and photosynthetic pigments (**Figure 4**). This might, in turn, improve plant vigor and consequently improved plant growth. Also, the total soluble sugars, total soluble proteins, stomatal conductance, and ionic contents were increased with the given amendments. However, oxidative stress indicators, enzymatic antioxidants, flavonoids, and phenolics increased under drought stress conditions recorded significant negative correlations with plant growth parameters.

DISCUSSION

This study evaluates the effect of MLE (MLE 1 = 1:20 v/v and MLE 2 = 1:30 v/v) and PGPR strain (Pa) on drought stress tolerance ability of wheat (Anaj 17 genotype) under two irrigation regimes (45 FC and 70 FC). The use of organic or biofertilizers as a global initiative instead of costly chemical fertilizers is addressed by several researchers (Talaei et al., 2014; El-Naggar et al., 2015; El-Serafy, 2018; Rahimi et al., 2019). Plant-derived biostimulants that trigger abiotic stress tolerance to ameliorate stress-induced yield reduction involve many different mechanisms, and most of these involve phytohormones and upregulated antioxidant defense systems (Bulgari et al., 2017; Sadasivam et al., 2017).

The highest dry matter contents in both root and shoot were obtained with the combined application of Pa + MLE 2 mixture that agrees with previous findings describing that soil beneficial bacteria can promote plant growth in abiotic stress conditions. Durán et al. (2016) had similar results on lettuce inoculated with *Bacillus* sp. and *Klebsiella* sp. and concluded that inoculated plants have more DW than non-inoculated ones. In this sense, Glick et al. (2007) said that this increase in the dry matter might be the enzyme 1-aminocyclopropane-1-carboxylate (ACC) deaminase enzyme activity of bacteria to lower the stress-induced ethylene levels, leaving α-ketobutyrate and $NH4^+$ available to the plants. Moreover, according to the study by Sánchez López (2011), auxins, i.e., indole-3-acetic acid (IAA), have a stimulatory effect on secondary root development that contributes to the total biomass of the plant by increasing nutrient and water absorption in moisture deficit conditions. The results from this study are in accordance with those claimed by Mishra et al. (2012) that an increase in auxin concentration stimulates adventitious root formation and thus increases root surface area and total plant biomass, proclaiming a morphological strategy of plants to tolerate drought with the help of bacterial strains.

Photosynthetic pigment contents are considered a valuable physiological indicator for evaluating the damage caused by stress intensity. The wheat genotype in this study had more chlorophyll contents when supplemented with Pa and MLE with the highest value recorded in their combined treatment at both water regimes. This alteration is directly related to plant macronutrient contents such as nitrogen. The reactive oxygen species (ROS) produced during abiotic stress cause the reduction of chlorophyll contents by damaging photosynthetic machinery (Manivannan et al., 2007). Similar to our results, Ahmadi et al. (2013)

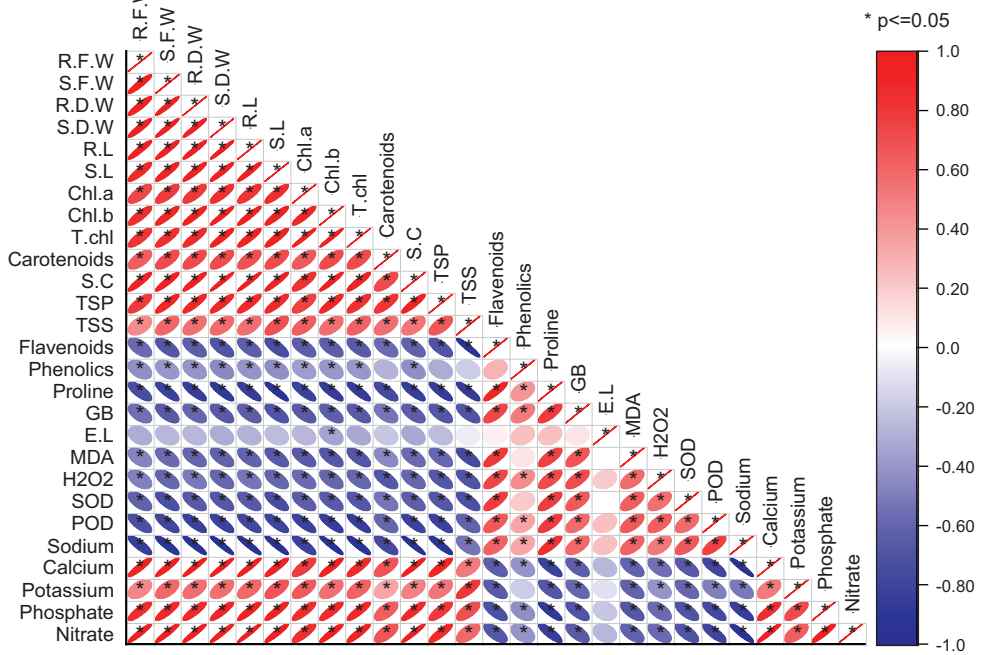

FIGURE 4 | Pearson correlation of different wheat attributes under drought stress and well-watered conditions.

also found a significant increase in chlorophyll contents by inoculating wheat with different bacterial strains (*Pseudomonas* sp. *and Azospirillum* sp.).

This study indicates that the increase in mineral nutrient contents of wheat is due to the use of biostimulants that enhanced drought stress tolerance. The inoculation with *P. aeruginosa* and MLE applied separately and in combination increased levels of sodium, calcium, potassium, phosphate, and nitrate in wheat submitted to drought. This might be due to the nutrient solubilization by added microorganisms due to the production of ACC deaminase (Mutumba et al., 2018). In addition, Römheld and Kirkby (2010) considered potassium as a key element in reducing water stress by adjusting osmoregulation in cells as a compatible solute. Zulfiqar et al. (2020) reported enhancement in soil nutrient availability and improvement in fruit quality induced by plant-derived biostimulants in stress conditions. The increase in plant nutritional status and vigor is due to improved soil microbial activity (Colla et al., 2015) and the presence of some chelating agents that enhance nutrient solubility in soil (Abou Chehade et al., 2018).

Induced tolerance by plant growth regulators is triggered by external stress factors and enhancement in plant sterols by reducing EL and regulating membrane stability (Lucini et al., 2015), thus providing an antioxidant defense system. Results of this experimental study indicate that Pa and MLE significantly improve growth, biochemical, antioxidant, and ionic attributes of wheat. Rhizobacteria potentially increase plant vigor by increasing atmospheric nitrogen fixation ability of roots and mineral absorption.

In accordance with our findings, previous studies also validate drought stress effects that consequently increase ROS that activate plant enzymatic and non-enzymatic antioxidant systems in order to balance the cellular redox state (Zulfiqar et al., 2020). Kumar et al. (2019) reported seed priming that involves plant growth regulators inducing sugar-triggered plant immunity (called "sweet immunity"—immunity by sugar compounds) having a positive priming effect on antioxidant systems. Results of our study validate that the antioxidant contents were improved using MLEs as a bioactive compound. Furthermore, a study by Rashid et al. (2018) confirmed the presence of a primary growth regulator, zeatin (a cytokinin derivative) that provided abiotic stress tolerance. Moringa extract constitutes considerable quantities of secondary metabolites, antioxidants, and osmoprotectants (Rehman et al., 2015). MLE's growth-promoting and abiotic stress tolerance inducing effects justify its use as a potential alternative to synthetic chemical fertilizers for improving wheat productivity (Nasir et al., 2016; Brockman and Brennan, 2017; Merwad, 2018; Younis et al., 2018). MLE aqueous solutions are very easy to make, cost-effective, and environment-friendly and can be used by the farmers effectively for increasing their crop yields. This study clearly reveals that all studied growth, biochemical, ionic, and antioxidant constituents of wheat plants were improved by using either of the two given amendments. Pa and MLE reduced all investigated oxidants and oxidative stress indicators. It is worth mentioning in this study that these supplementary amendments might antagonize each other's effects to some extent in their combined applications, as their sole applications had lowered physiological, biochemical, and ionic attributes. Thus, constitutive effects, i.e., Pa and MLE,

at both concentration levels were more elaborated, thus inducing drought tolerance in wheat.

CONCLUSION

The application of both nitrogen-fixing bacteria (Pa strain) and foliar sprayed MLE either in sole or combined treatments can alleviate nutrient and drought stress effects. Nevertheless, the combined application of Pa and MLE 2 (Pa + MLE 2) can efficiently improve wheat growth attributes, photosynthetic pigment contents, and nutrient uptake under drought stress. The combined supplementation of Pa and MLE had more significant positive effects compared with their sole applications. Pa + MLE 2 was also efficient in decreasing oxidative stress indicators and enzymatic antioxidants of wheat under drought stress. There is a need for more investigations at field levels by considering the effect of other environmental constraints to effectively validate these findings.

DATA AVAILABILITY STATEMENT

The original contributions presented in the study are included in the article/supplementary material, further inquiries can be directed to the corresponding author/s.

AUTHOR CONTRIBUTIONS

IL, SA-D, LA-A, RH, KAM, NM, SA, MA, AA, PP, KM, and TG: researching and writing. AA, SA, and LA-A: writing. All authors contributed to the article and approved the submitted version.

FUNDING

The research team and authors are thankful to Taif University Research Supporting project number TURSP-2020/315, Taif University, Taif, Saudi Arabia, for providing the research and lab facilities and financial support throughout the research experiment.

ACKNOWLEDGMENTS

We are thankful to the Taif University Research Supporting project number (TURSP-2020/315) Taif University, Taif, Saudi Arabia for providing the research and lab facilities and financial support throughout the research experiment. We also thank the support of the iASK Research Grant and Eötvös Research Grant (MAEÖ-00074-002/2021) for their help in publishing this research.

REFERENCES

Abou Chehade, L., Al Chami, Z., De Pascali, S. A., Cavoski, I., and Fanizzi, F. P. (2018). Biostimulants from food processing by-products: agronomic, quality and metabolic impacts on organic tomato (*Solanum lycopersicum* L.). *J. Sci. Food Agric.* 98, 1426–1436. doi: 10.1002/jsfa.8610

Ahmadi, J., Asgharzadeh, A., and Bakhtiari, S. (2013). The effect of microbial inoculants on physiological responses of two wheat cultivars under salt stress. *Int. J. Adv. Biol.* 4, 364–371.

Barnawal, D., Singh, R., and Singh, R. P. (2019). "Role of plant growth promoting rhizobacteria in drought tolerance: regulating growth hormones and osmolytes," in *PGPR Amelioration in Sustainable Agriculture*, eds A. K. Singh, A. Kumar, and P. K. Singh (Amsterdam: Elsevier), 107–128. doi: 10.1016/b978-0-12-815879-1.00006-9

Bates, L. S., Waldren, R. P., and Teare, I. D. (1973). Rapid determination of free proline for water-stress studies. *Plant Soil* 39, 205–207. doi: 10.1007/BF00018060

Bradford, M. M. (1976). A rapid and sensitive method for the quantitation of microgram quantities of protein utilizing the principle of protein-dye binding. *Anal. Biochem.* 72, 248–254. doi: 10.1016/0003-2697(76)90527-3

Brockman, H. G., and Brennan, R. F. (2017). The effect of foliar application of Moringa leaf extract on biomass, grain yield of wheat and applied nutrient efficiency. *J. Plant Nutr.* 40, 2728–2736. doi: 10.1080/01904167.2017.1381723

Budak, H., Kantar, M., and Yucebilgili Kurtoglu, K. (2013). Drought tolerance in modern and wild wheat. *Sci. World J.* 2013:548246. doi: 10.1155/2013/548246

Bulgari, R., Morgutti, S., Cocetta, G., Negrini, N., Farris, S., Calcante, A., et al. (2017). Evaluation of borage extracts as potential biostimulant using a phenomic, agronomic, physiological, and biochemical approach. *Front. Plant Sci.* 8:935. doi: 10.3389/fpls.2017.00935

Colla, G., Nardi, S., Cardarelli, M., Ertani, A., Lucini, L., Canaguier, R., et al. (2015). Protein hydrolysates as biostimulants in horticulture. *Sci. Hortic.* 196, 28–38. doi: 10.1016/j.scienta.2015.08.037

Dere, S., Güneş, T., and Sivaci, R. (1998). Spectrophotometric determination of chlorophyll-A, B and total carotenoid contents of some algae species using different solvents. *Turk. J. Bot.* 22, 13–18.

Dubois, M., Gilles, K., Hamilton, J., Rebers, P. A., and Smith, F. (1956). Colorimetric method for determination of sugars and related substances. *Anal. Chem.* 28, 350–356. doi: 10.1021/ac60111a017

Durán, P., Acuña, J. J., Armada, E., López-Castillo, O. M., Cornejo, P., Mora, M. L., et al. (2016). Inoculation with selenobacteria and arbuscular mycorrhizal fungi to enhance selenium content in lettuce plants and improve tolerance against drought stress. *J. Plant. Nutr. Soil Sci.* 16, 211–225.

El-Naggar, A. H. M., Hassan, M. R. A., Shaban, E. H., and Mohamed, M. E. A. (2015). Effect of organic and biofertilizers on growth, oil yield and chemical composition of the essential oil of *Ocimum basillicum* L. plants. *Alex. J. Agric. Res.* 60, 1–16.

El-Serafy, R. S. (2018). Growth and productivity of roselle (*Hibiscus sabdariffa* L.) as affected by yeast and humic acid. *Sci. J. Flowers Ornam. Plants* 5, 195–203. doi: 10.21608/sjfop.2018.18129

Fasiha Amjad, S., Mansoora, N., Yaseen, S., Kamal, A., Butt, B., Matloob, H., et al. (2021). Combined use of endophytic bacteria and pre-sowing treatment of thiamine mitigates the adverse effects of drought stress in wheat (*Triticum aestivum* L.) cultivars. *Sustainability* 13:6582. doi: 10.3390/su13126582

Glick, B. R., Cheng, Z., Czarny, J., and Duan, J. (2007). "Promotion of plant growth by ACC deaminase-producing soil bacteria," in *New Perspectives and Approaches in Plant Growth-Promoting Rhizobacteria Research*, eds P. A. H. M. Bakker, J. M. Raaijmakers, G. Bloemberg, M. Höfte, P. Lemanceau, and B. M. Cooke (Dordrecht: Springer), 329–339. doi: 10.1007/978-1-4020-6776-1_8

Gontia-Mishra, I., Sapre, S., Sharma, A., and Tiwari, S. (2016). Amelioration of drought tolerance in wheat by the interaction of plant growth-promoting rhizobacteria. *Plant Biol.* 18, 992–1000. doi: 10.1111/plb.12505

Grover, M., Ali, S. Z., Sandhya, V., Rasul, A., and Venkateswarlu, B. (2011). Role of microorganisms in adaptation of agriculture crops to abiotic stresses. *World J. Microbiol. Biotechnol.* 27, 1231–1240. doi: 10.1007/s11274-010-0572-7

Holmström, K.-O., Somersalo, S., Mandal, A., Palva, T. E., and Welin, B. (2000). Improved tolerance to salinity and low temperature in transgenic tobacco producing glycine betaine. *J. Exp. Bot.* 2000, 177–185. doi: 10.1093/jexbot/51.343.177

Jiménez-Gómez, A., Flores-Félix, J. D., Garcia-Fraile, P., Mateos, P. F., Menéndez, E., and Velázquez, E. (2018). Probiotic activities of Rhizobium laguerreae on

growth and quality of spinach. *Sci. Rep.* 8:295. doi: 10.1038/s41598-017-18632-z

Kaushal, M., and Wani, S. P. (2016). Plant-growth-promoting rhizobacteria: drought stress alleviators to ameliorate crop production in drylands. *Ann. Microbiol.* 66, 35–42. doi: 10.1007/s13213-015-1112-3

Khan, N., Ali, S., Tariq, H., Latif, S., Yasmin, H., and Mehmood, A. (2020). Water conservation and plant survival strategies of rhizobacteria under drought stress. *Agronomy* 10:1683. doi: 10.1002/jobm.201800309

Kowalenko, C. G., and Lowe, L. E. (1973). Determination of nitrates in soil extracts. *Soil Sci. Soc. Am. J.* 37:660. doi: 10.2136/sssaj1973.03615995003700040051x

Kumar, S., Chinnannan, K., Thamilarasan, S. K., Seralathan, M., Shanmuganathan, R., and Padikasan, I. A. (2019). Enzymatically hydrolysed sago bagasse improves physiological, biochemical and molecular attributes of *Solanum lycopersicum*. *Biocatal. Agric. Biotechnol.* 17, 499–506. doi: 10.1016/j.bcab.2019.01.005

Lewis, C. E., Walker, J. R. L., Lancaster, J. E., and Sutton, K. H. (1999). Determination of anthocyanins, flavonoids and determination phenolic acids in coloured potatoes. i: cultivars of *Solanum tuberosum* L. *J. Sci. Food Agricult.* 77, 45–57. doi: 10.1002/(sici)1097-0010(199805)77:1<45::aid-jsfa1>3.0.co;2-s

Lisar, S. Y. S., Motafakkerazad, R., Hossain, M. M., and Rahman, I. M. M. (2012). "Water stress in plants: causes, effects and responses," in *Water Stress*, eds I. M. M. Rahman and H. Hasegawa (Rijeka: InTech), 1–14. doi: 10.1007/978-1-4614-4747-4_1

Lucini, L., Rouphael, Y., Cardarelli, M., Canaguier, R., Kumar, P., and Colla, G. (2015). The effect of a plant-derived biostimulant on metabolic profiling and crop performance of lettuce grown under saline conditions. *Sci. Hortic.* 182, 124–133. doi: 10.1016/j.scienta.2014.11.022

Manivannan, P., Jaleel, C. A., Sankar, B., Kishorekumar, A., Somasundaram, R., Lakshmanan, G. A., et al. (2007). Growth, biochemical modifications and proline metabolism in *Helianthus annuus* L. as induced by drought stress. *Colloids Surf. B.* 59, 141–149. doi: 10.1016/j.colsurfb.2007.05.002

Merwad, A.-R. M. A. (2018). Using *Moringa oleifera* extract as biostimulant enhancing the growth, yield and nutrients accumulation of pea plants. *J. Plant Nutr.* 41, 425–431. doi: 10.1080/01904167.2017.1384012

Mishra, P. K., Bisht, S. C., Bisht, J. K., and Bhatt, J. C. (2012). "Cold-tolerant PGPRs as bioinoculants for stress management," in *Bacteria in Agrobiology: Stress Management*, ed. D. Maheshwari (Berlin: Springer), 95–118. doi: 10.1007/978-3-662-45795-5_6

Mutumba, F. A., Zagal, E., Gerding, M., Castillo-Rosales, D., and Paulino, L., Schoebitz, M. (2018). Plant growth promoting rhizobacteria for improved water stress tolerance in wheat genotypes. *J. Soil Sci. Plant Nutr.* 18, 1080–1096.

Nardi, S., Carletti, P., Pizzeghello, D., and Muscolo, A. (2009). "Biological activities of humic substances," in *Biophysico-chemical Processes Involving Natural Nonliving Organic Matter in Environmental Systems. Vol 2, Part 1: Fundamentals and Impact of Mineral-organic Biota Interactions on the Formation, Transformation, Turnover, and Storage of Natural Nonliving Organic Matter (NOM)*, eds N. Senesi, B. Xing, and P. M. Huang (Hoboken: Wiley), 305–340. doi: 10.1002/9780470494950.ch8

Nasir, M., Khan, A. S., Basra, S. M. A., and Malik, A. U. (2014). Foliar application of moringa leaf extract, potassium and zinc influence yield and fruit quality of Kinnow mandarin. *Sci. Hortic.* 210, 227–235. doi: 10.1016/j.scienta.2016.07.032

Nasir, M., Khan, A. S., Ahmad Basra, S. M., Malik, A. U. (2016). Foliar application of moringa leaf extract, potassium and zinc influence yield and fruit quality of 'Kinnow' mandarin. *Scientia Horticulturae* 210, 227–235. doi: 10.1016/j.scienta.2016.07.032

Ngumbi, E., and Kloepper, J. (2016). Bacterial-mediated drought tolerance: current and future prospects. *Appl. Soil Ecol.* 105, 109–125. doi: 10.1016/j.apsoil.2016.04.009

Parajuli, R., Thoma, G., and Matlock, M. D. (2019). Environmental sustainability of fruit and vegetable production supply chains in the face of climate change: a review. *Sci. Total Environ.* 650, 2863–2879. doi: 10.1016/j.scitotenv.2018.10.019

Rahimi, A., Siavash Moghaddam, S., Ghiyasi, M., Heydarzadeh, S., Ghazizadeh, K., and Popović-Djordjević, J. (2019). The influence of chemical, organic and biological fertilizers on agrobiological and antioxidant properties of Syrian Cephalaria (*Cephalaria syriaca* L.). *Agriculture* 9:122. doi: 10.3390/agriculture9060122

Rashid, N., Basra, S. M. A., Shahbaz, M., Iqbal, S., and Hafeez, M. B. (2018). Foliar applied moringa leaf extract induces terminal heat tolerance in quinoa. *Int. J. Agric. Biol.* 20, 157–164.

Rehman, H., Kamran, M., Basra, S. M. A., Afzal, I., and Farooq, M. (2015). Influence of seed priming on performance and water productivity of direct seeded rice in alternating wetting and drying. *Rice Sci.* 22, 189–196. doi: 10.1016/j.rsci.2015.03.001

Römheld, V., and Kirkby, E. A. (2010). Research on potassium in agriculture: needs and prospects. *Plant Soil* 335, 155–180. doi: 10.1007/s11104-010-0520-1

Ruzzi, M., and Aroca, R. (2015). Plant growth-promoting rhizobacteria act as biostimulants in horticulture. *Sci. Hortic.* 196, 124–134. doi: 10.1016/j.scienta.2015.08.042

Sánchez López, D. B. (2011). *Efecto de la Inoculación con Bacterias Promotoras de Crecimiento Vegetal Sobre el Cultivo de Tomate (Solanum Lycopersicum var. Sofía) bajo Invernadero. Master's thesis*. Pontificia Universidad Javeriana, Bogotá.

Sadasivam, V., Packiaraj, G., Subiramani, S., Govindarajan, S., Kumar, G. P., Kalamani, V., et al. (2017). Evaluation of seagrass liquid extract on salt stress alleviation in tomato plants. *Asian J. Plant Sci.* 16, 172–183. doi: 10.3923/ajps.2017.172.183

Semida, W. M., and Rady, M. M. (2014). Pre-soaking in 24-epibrassinolide or salicylic acid improves seed germination, seedling growth, and anti-oxidant capacity in *Phaseolus vulgaris* L. grown under NaCl stress. *J. Hortic. Sci. Biotechnol.* 89, 338–344. doi: 10.1080/14620316.2014.11513088

Shahzad, U., Khan, M. A., Jaskani, M. J., Khan, I. A., and Korban, S. S. (2013). Genetic diversity and population structure of *Moringa oleifera*. *Conserv. Genet.* 14, 1161–1172. doi: 10.1007/s10592-013-0503-x

Shukla, N., Awasthi, R. P., Rawat, L., and Kumar, J. (2012). Biochemical and physiological responses of rice (*Oryza sativa* L.) as influenced by *Trichoderma harzianum* under drought stress. *Plant Physiol. Biochem.* 54, 78–88. doi: 10.1016/j.plaphy.2012.02.001

Singh, S., Kumar, V., Dhanjal, D. S., Sonali, Dhaka, V., Thotapalli, S., et al. (2021). "Rhizosphere biology: a key to agricultural sustainability," in *Current Trends in Microbial Biotechnology for Sustainable Agriculture*, eds A. N. Yadav, J. Singh, C. Singh, and N. Yadav (Singapore: Springer Nature), 161–182. doi: 10.1007/978-981-15-6949-4_7

Soumare, A., Diédhiou, A. G., Arora, N. K., Al-Ani, L. K. T., Ngom, M., Fall, S., et al. (2021). Potential role and utilization of plant growth promoting microbes in plant tissue culture. *Front. Microbiol.* 12:649878. doi: 10.3389/fmicb.2021.649878

Stapleton, J. J., Wilen, C. A., and Molinar, R. H. (2008). *Soil Solarization for Gardens and Landscapes. Pest Note Publication, 74145*. Davis, CA: University of California Agriculture and Natural Resources.

Talaei, G. H., Vazirimehr, M. R., Shahgholi, H., Shirmohammadi, E., Sabbagh, E., and Rigi, K. (2014). Influence of biological and chemical nitrogen fertilizers on grain yield and yield components of Fennel (*Foeniculum vulgare* Mill.). *Int. J. Biosci.* 4, 206–211. doi: 10.12692/ijb/4.9.206-211

Venkateswarlu, B., and Shanker, A. K. (2009). Climate change and agriculture: adaptation and mitigation stategies. *Indian J. Agron* 54, 226–230.

Wheeler, T., and Von Braun, J. (2013). Climate change impacts on global food security. *Science* 341, 508–513.

Yasmeen, A., Basra, S. M. A., Ahmad, R., and Wahid, A. (2012). Performance of late sown wheat in response to foliar application of *Moringa oleifera* Lam. leaf extract. *Chil. J. Agric. Res.* 72:92. doi: 10.4067/s0718-58392012000100015

Yasmeen, A., Basra, S. M. A., Farooq, M., ur Rehman, H., Hussain, N., and Athar, H. R. (2013a). Exogenous application of moringa leaf extract modulates the antioxidant enzyme system to improve wheat performance under saline conditions. *Plant Growth Regul.* 69, 225–233. doi: 10.1007/s10725-012-9764-5

Yasmeen, A., Basra, S. M. A., Wahid, A., Nouman, W., and Rehman, H. U. R. (2013b). Exploring the potential of *Moringa oleifera* leaf extract (MLE) as a seed priming agent in improving wheat performance. *Turk. J. Bot.* 37, 512–520.

Yasmeen, A., Nouman, W., Basra, S. M. A., Wahid, A., and Hussain, N. (2014). Morphological and physiological response of tomato (*Solanum lycopersicum* L.) to natural and synthetic cytokinin sources: a comparative study. *Acta Physiol. Plant.* 36, 3147–3155. doi: 10.1007/s11738-014-1662-1

Younis, A., Akhtar, M. S., Riaz, A., Zulfiqar, F., Qasim, M., Farooq, A., et al. (2018). Improved cut flower and corm production by exogenous moringa leaf extract application on gladiolus cultivars. *Acta Sci. Pol. Hortorum Cultus* 17, 25–38. doi: 10.24326/asphc.2018.4.3

Zulfiqar, F., Allaire, S. E., Akram, N. A., Méndez, A., Younis, A., Peerzada, A. M., et al. (2019). Challenges in organic component selection and biochar as an

opportunity in potting substrates: a review. *J. Plant Nutr.* 42, 1386–1401. doi: 10.1080/01904167.2019.1617310

Zulfiqar, F., Casadesús, A., Brockman, H., and Munné-Bosch, S. (2020). An overview of plant-based natural biostimulants for sustainable horticulture with a particular focus on moringa leaf extracts. *Plant Sci.* 295:110194. doi: 10.1016/j.plantsci.2019.110194

Conflict of Interest: The authors declare that the research was conducted in the absence of any commercial or financial relationships that could be construed as a potential conflict of interest.

The reviewer FZ declared a shared affiliation with one of the author, RH, to the handling editor at the time of the review.

Publisher's Note: All claims expressed in this article are solely those of the authors and do not necessarily represent those of their affiliated organizations, or those of the publisher, the editors and the reviewers. Any product that may be evaluated in this article, or claim that may be made by its manufacturer, is not guaranteed or endorsed by the publisher.

frontiers | Frontiers in Plant Science

ORIGINAL RESEARCH
published: 01 July 2022
doi: 10.3389/fpls.2022.837441

Sunflower Bark Extract as a Biostimulant Suppresses Reactive Oxygen Species in Salt-Stressed Arabidopsis

*Jing Li[1], Philippe Evon[2], Stéphane Ballas[3], Hoang Khai Trinh[1,4], Lin Xu[1†], Christof Van Poucke[5], Bart Van Droogenbroeck[5], Pierfrancesco Motti[6], Sven Mangelinckx[6], Aldana Ramirez[1], Thijs Van Gerrewey[1] and Danny Geelen[1]**

[1] HortiCell, Department of Plants and Crops, Faculty of Bioscience Engineering, Ghent University, Ghent, Belgium, [2] Laboratoire de Chimie Agro-Industrielle, Université de Toulouse, Institut National de Recherche pour l'Agriculture, l'Alimentation et l'Environnement (INRAE), École Nationale Supérieure des Ingénieurs en Arts Chimiques et Technologiques (ENSIACET), Toulouse, France, [3] Ovalie Innovation, Auch, France, [4] Biotechnology Research and Development Institute (BiRDI), Can Tho University, Can Tho, Vietnam, [5] Flanders Research Institute for Agriculture, Fisheries and Food (ILVO), Melle, Belgium, [6] SynBioC, Department of Green Chemistry and Technology, Faculty of Bioscience Engineering, Ghent University, Ghent, Belgium

OPEN ACCESS

Edited by:
Youssef Rouphael,
University of Naples Federico II, Italy

Reviewed by:
Anket Sharma,
University of Maryland, College Park, United States
Miroslava Konstantinova Zhiponova,
Sofia University, Bulgaria

***Correspondence:**
Danny Geelen
Danny.Geelen@UGent.be

†Present address:
Lin Xu,
Department of Food Technology, Safety and Health, Faculty of Bioscience Engineering, Ghent University, Kortrijk, Belgium

Specialty section:
This article was submitted to Plant Abiotic Stress, a section of the journal Frontiers in Plant Science

Received: 16 December 2021
Accepted: 30 May 2022
Published: 01 July 2022

Citation:
Li J, Evon P, Ballas S, Trinh HK, Xu L, Van Poucke C, Van Droogenbroeck B, Motti P, Mangelinckx S, Ramirez A, Van Gerrewey T and Geelen D (2022) Sunflower Bark Extract as a Biostimulant Suppresses Reactive Oxygen Species in Salt-Stressed Arabidopsis. Front. Plant Sci. 13:837441. doi: 10.3389/fpls.2022.837441

A survey of plant-based wastes identified sunflower (*Helianthus annuus*) bark extract (SBE), produced via twin-screw extrusion, as a potential biostimulant. The addition of SBE to Arabidopsis (*Arabidopsis thaliana*) seedlings cultured *in vitro* showed a dose-dependent response, with high concentrations causing severe growth inhibition. However, when priming seeds with SBE, a small but significant increase in leaf area was observed at a dose of 0.5 g of lyophilized powder per liter. This optimal concentration of SBE in the culturing medium alleviated the growth inhibition caused by 100 mM NaCl. The recovery in shoot growth was accompanied by a pronounced increase in photosynthetic pigment levels and a stabilization of osmotic homeostasis. SBE-primed leaf discs also showed a similar protective effect. SBE mitigated salt stress by reducing the production of reactive oxygen species (ROS) (e.g., hydrogen peroxide) by about 30% and developing more expanded true leaves. This reduction in ROS levels was due to the presence of antioxidative agents in SBE and by activating ROS-eliminating enzymes. Polyphenols, carbohydrates, proteins, and other bioactive compounds detected in SBE may have contributed to the cellular redox homeostasis in salt-stressed plants, thus promoting early leaf development by relieving shoot apical meristem arrest. Sunflower stalks from which SBE is prepared can therefore potentially be valorized as a source to produce biostimulants for improving salt stress tolerance in crops.

Keywords: *Helianthus annuus*, plant extract, biostimulant, *in vitro* assay, salt stress, antioxidant

INTRODUCTION

Substantial losses in biomass accompany crop production and downstream processing because of inadequate harvesting methods and a lack of valorization of by-products (Parfitt et al., 2010). To reduce the ecological footprint of agricultural practices, the Food and Agriculture Organization of the United Nations (FAO) identified two primary targets: "agricultural sustainability" and "global

food losses" (FAO, 2021). In view of these targets, we urgently need to transform agricultural waste into value-added products. Crop waste is a natural resource for refining and recovering bioactive ingredients (Van Tang, 2017). Indeed, various molecules are abundant in unused biomass, some of which can be developed as plant biostimulants (PBs) (Xu and Geelen, 2018; Huang et al., 2021). The development and commercialization of PBs is a rapidly growing business, estimated at USD 3.2 billion in 2021 with a projected compound annual growth rate (CAGR) of 12.1% (Markets and Markets, 2021). Strikingly, plant extract-based PBs exhibited the highest effectiveness in yield enhancement of field crops (Li et al., 2022). Compared with synthetic chemical additives for crop improvement, PBs derived from natural resources like plant byproducts are poised to encompass a lower environmental risk and impact (Kumar et al., 2019). PBs are more likely to pass the regulatory restriction of fertilizers from natural origins imposed by legislation (Regulation [EU], 2019).

The main methods of PBs application are foliar spraying, seed priming, and soil drenching (Vertified Market Research, 2021). Hence, most primary screening assays are designed to screen putative biostimulant activity starting from seed germination and the growth responses of seedlings (García-García et al., 2020). The monitoring of seedling growth allows for *in vitro* assays under controlled conditions, short evaluation periods, and assessment of a broad spectrum of responses (Colegate and Molyneux, 2007). Subsequent bioassays are dedicated to monitoring specific plant responses. For example, seed priming tests report the effect of chemical reagents on seed germination and early seedling development (Lutts et al., 2016). Arabidopsis (*Arabidopsis thaliana*) seedlings grown *in vitro* are widely used to study the effects of exogenous chemicals on root and shoot growth (Trinh et al., 2018). An alternative to growth assays is measuring the longevity of mature leaf discs punched from mature leaves that normally senescence in a matter of days (Chiu et al., 2021). *In vitro* bioassays also allow for the quantitative impact of stress responses, and the combining of the results from multiple assays provides a reasonable indication for possible biostimulant activity under field conditions.

Plant-based raw materials are typically rich in diverse metabolites (Zulfiqar et al., 2020). Various plant extracts have also improved stress tolerance, often attributed to antioxidants (De Diego and Spíchal, 2020). Polyphenols, abundant in many plant extracts, are a class of bioactive antioxidants that scavenge *in vitro* and *in vivo* reactive oxygen species (ROS) (Stagos, 2020). For instance, many polyphenols are found in various bark by-products from woody species such as oak and willow (Dróżdż and Pyrzynska, 2017; Dou et al., 2018; Tanase et al., 2019). Sunflower (*Helianthus annuus*) seeds and florets are also rich in polyphenols with antioxidant activity (Karamać et al., 2012; Ye et al., 2015). The trichomes isolated from the surface of sunflower stems contain many flavonoids, which are typically showing antioxidant activity (Brentan Silva et al., 2017).

Sunflower is an annual crop produced for its seed and is the fourth most important oilseed crop responsible for 10% of the world's edible plant-derived oil (Dantas et al., 2017). The leaves and stems are usually not harvested and left on the field as organic compost. The worldwide production of sunflower foliage and stems is an estimated 15.2 megatons per year (United Nations Industrial Development, 2007). Because of this substantial amount of biomass, stem material is considered a source of fiber used in biocomposite panels and other fiber-rich materials. The stalks are separated into the bark (external "woody" part, 90% w/w), which is rich in lignocellulose, and the pith (internal part, 10% w/w) (Evon et al., 2018; Verdier et al., 2020). In addition to fiber, the stalks can potentially be refined through the advanced twin-screw extrusion technology and used for various added-value applications in the agrochemical industry.

This study shows that (1) sunflower bark extract (SBE) can be produced as a side stream during twin-screw extrusion of fiber from stems; (2) SBE is a complex mixture of water-soluble molecules, several of which have bioactivity on plant growth; (3) exogenous application of SBE mitigates salt stress-induced growth inhibition of *in vitro* grown Arabidopsis.

MATERIALS AND METHODS

Sunflower Stalk Collection and Bark Extraction

Sunflower stalks were collected with a forage harvester with the assistance of Ovalie Innovation in Autumn 2018 (Samaran, Gers department, southwest France). The stalks were stored in a ventilated box and dried with ventilated air at 40°C for 24 h. The bark was mechanically separated from the pith using a three-step procedure: (1) grinding of stalks using a hammer mill (Electra Goulu N, France) fitted with a 32 mm sieve; (2) de-dusting of the ground material using a vibrating sieve shaker (Ritec 600, France) equipped with a 1 mm screen; (3) aspiration of pith particles. Pith and bark particles were separated based on their differential density (i.e., 30 and 140 kg/m^3, respectively).

Here, the twin-screw extrusion technology was used as an innovative technique for the thermo-mechanical and organic solvent-free extraction of biomolecules (Evon et al., 2018; Vandenbossche et al., 2019). The bark was then fractionated into a pulp and a liquid extract made of water-soluble compounds using a co-rotating and co-penetrating twin-screw extruder (Clextral Evolum HT 53, France). The extruder barrel (1.9 m in length) consisted of eight modules, each 4D in length (D is the screw diameter, i.e., 53 mm), except for module 1, which had an 8D length. A filter section consisting of six hemispherical dishes with 1 mm diameter perforations outfitted on module 7 enabled filtrate collection. During the liquid/solid fractionation process, bark with 10.0 $\pm$ 0.1% moisture content was fed at the level of module 1 using a gravimetric feeder. Water was injected at the end of module 2 using a piston pump at a liquid/solid ratio of 2.9 (i.e., 10.2 and 29.6 kg/h for the inlet flow rates of bark and water, respectively). For optimal operation, a specific screw configuration was applied. Bilobe paddles (BL22) were positioned in module 5 to favor strong mixing between the liquid and the solid. In addition, reversed pitch screws (CF2C) were positioned in module 8, immediately downstream from the filtering sieves to separate the liquid (i.e., the filtrate)

and solid (i.e., the pulp) phases continuously by compression action. The temperature was set at 80°C in module 2, at 100°C along the extracting zone (modules 3–6), and 110°C in the pressing part (module 8). The rotation speed of the screws was set at 250 rpm.

The filtrate collected at the bottom of the filtration module (module 7) was centrifuged to remove the small solid particles and driven through the filter. Then, the clarified filtrate was concentrated by partial water evaporation and freeze-dried, producing SBE as a powder product stored in the dark at 4°C until use.

Chemical Characterization of Starting Sunflower Bark and Sunflower Bark Extract

The moisture and dry matter contents of solids in the starting sunflower bark were determined according to ISO 665:2000 (ISO, 2000). The mineral content of starting bark was quantified according to ISO 749:1977 (ISO, 1977), and lipids were assessed according to ISO 659:2009 (ISO, 2009). Cell wall polymers, including cellulose, hemicellulose, and lignin, were quantified using the ADF–NDF method (ADF for acid detergent fiber, and NDF for neutral detergent fiber) of Van Soest and Wine (1967, 1968). After 1 h of boiling in water, water-soluble compounds were calculated from biomass losses.

Inside the SBE, the soluble protein and digestible carbohydrate contents were analyzed by colorimetric methods (Deans et al., 2018). Total phenolics content (TPC) was estimated by the Folin–Ciocalteu method (Sánchez-Rangel et al., 2013). The total flavonoid content (TFC) was measured following two aluminum complexation methods using quercetin and rutin as reference flavonoids (Pękal and Pyrzynska, 2014). The total *in vitro* antioxidant capacity (TAC) of SBE was determined using the 2,2-diphenyl-1-picrylhydrazyl (DPPH) and the 2,2′-azino-bis (3-ethylbenzothiazoline-6-sulfonic acid) (ABTS) assay (Xiao et al., 2020). Trolox (TE) was used as a standard antioxidant to calculate the equivalent antioxidant capacity of samples. The DPPH assay was slightly modified (Xiao et al., 2020). A total of 20 μl sample was added with 100 μl 200 mM DPPH and 80 μl 50 mM Tris–HCl buffer (pH 7.4).

Chemical Profiling of Sunflower Bark Extract Using UHPLC-PDA-High-Resolution Mass Spectrometer Analysis

Sunflower bark extract was dissolved in water at 1 mg/mL and pushed through a 0.22 μm filter (Millix-GV, Millipore). Samples were subjected to ultra-high-performance liquid chromatography (Acquity UPLC) coupled to a PDA detector (UPLC eLambda 800 nm) and a SYNAPT G2-S High-Resolution Mass Spectrometer (HRMS) (Waters, Milford, MA, United States). Prepared samples were chromatographically separated on an ACQUITY UPLC BEH C18 column (1.7 μm, 2.1 mm × 150 mm) protected by an ACQUITY UPLC BEH C18 VanGuard Precolumn (1.7 μm, 2.1 mm × 5 mm) (Waters). The mobile phase A was 0.1% formic acid in water (solvent A) and the mobile phase B was 0.1% formic acid in acetonitrile (solvent B) at a flow rate of 0.35 mL/min with following gradient: 95% A–5% B (0–18 min), 100% B (18–25 min), 95% A–5% B (25.1–30 min). PDA data was recorded between 220 and 550 nm. Ions were detected in the positive electrospray ionization (ESI+) and negative electrospray ionization (ESI−) modes. The ESI conditions were set as follows: capillary voltage of 3.0 kV (ESI+)/2.0 kV (ESI−), source temperature of 120°C, cone voltage of 30 V (ESI+)/40 V (ESI−), and desolvation temperature of 500°C with a desolvation gas flow of 800 L/h. The collision-induced dissociation (CID) was set at 4 eV for precursor ion, and MS/MS fragment ion information was obtained with a collision energy ramp from 8 to 40 eV. The HRMS was calibrated between 50 and 1200 Da with a sodium formate solution prior to analysis. The injection volume was set at 5 μl, and each sample was analyzed in duplicate. All data were recorded at resolution mode (20,000 FWHM) in centroid full scan MS^e mode (data-independent acquisition, DIA). A 200 pg/μl leucine enkephalin solution was continuously infused during analysis to perform lockmass correction (m/z 556.2771 in positive ion mode and m/z 554.2615 in negative ion mode) during analysis. Blanks containing only the mobile phase without any sample were injected between each batch of samples.

To determine the chemical composition of SBE, the raw MS/MS data were processed for feature detection and alignment with MS-DIAL software version 4.48 (Blaženović et al., 2017). The detailed settings are listed in **Supplementary Table 1**, and are adapted from Lee et al. (2019). To gain a high confidence in the peak identification, only the features present in both runs from the same sample were considered for alignment correction. Next, aligned features meeting the criteria were selected with a total weighted similarity score of over 60 (overall library-matching score based on retention time, accurate mass, isotope ratio, and MS^E spectra) (Tsugawa et al., 2015). Then, we searched these chosen features for further compound prediction in MS-FINDER software version 3.50 (Tsugawa et al., 2016) among online metabolites databases, including PlantCyc (plant), KNApSAcK (natural product), FoodDB (Food), ChEBI (Biomolecules), and PubChem (Biomolecules), with the agreement of identification confidence levels (level 3) (Schymanski et al., 2014). In each feature, the predicted formula and structure with the top total score were reported as the final candidate compound (Tsugawa et al., 2019). Finally, the identified compounds were assigned taxonomy based on their chemical characterization represented as InChIKey (International Chemical Identifier) in ChemOnt ontology via ClassyFire (Djoumbou Feunang et al., 2016).

Pesticide Residue Detection in Sunflower Bark Extract

Lyophilized powder of SBE was analyzed for the presence of over 500 pesticide residues (Regulation [EC], 2005, 2009) (Primoris, Belgium). Briefly, the pesticide(s) were extracted from the crude sunflower bark material with acidified acetonitrile (QuEChERS extraction) or acetonitrile with 0.5% acetic acid. Pesticides were quantitatively determined using LC–MS/MS and GC–MS/MS, respectively. No chemicals above the maximum residue levels were reported (data not shown).

Plant-Based Bioassays Using Arabidopsis as the Model Plant

Root Development

Arabidopsis (Col-0) seeds were chlorine gas-sterilized for 3 h (Lindsey et al., 2017), sown on full strength Murashige and Skoog medium, and vernalized for 3 days at 4°C (Trinh et al., 2018). Next, the plates were exposed 8 h to light (room temperature 21.4°C, 40–60% humidity, light intensity 140 μmol m^{-2} s^{-1}, 14/10 h day/night photoperiod) and transferred to the dark for another 3 days to induce etiolation. Then, uniform-size of 3 DAG (days after germination) seedlings were transplanted onto the growth medium and incubated vertically for 10 days. For the dose-response experiment, the medium was supplemented with 0.1, 0.5, 1, 2, 3, 3.67, 4, and 5 g/L SBE. For the time-course analysis of primary root development, the medium was supplemented with 1 g/L or 3 g/L SBE and incubated for 6, 12, and 24 h after etiolation. Seedlings were scored for the numbers of adventitious roots (ARs), junction roots (JRs), and lateral roots (LRs) under a binocular microscope (Olympus, SZX9, Tokyo, Japan). The primary root length (PRL) was measured by image analysis using ImageJ software version 1.53n (Schindelin et al., 2012) coupled with the "NeuronJ" plugin (Meijering et al., 2004). Each treatment consisted of three plates, and each plate contained 10 seedlings.

Shoot Growth

Arabidopsis shoot growth in response to SBE application was evaluated using a shoot assay adapted from De Diego et al. (2017). Briefly, seedlings were grown as described in the root assay and, at 3 DAG, transferred to 24-well tissue culture plates (VWR, CA, United States) containing Murashige and Skoog medium (4 mL per well) supplemented with 0.5 g/L SBE and 100 mM NaCl. Since at 100 mM NaCl, Arabidopsis rosettes are more compact (Claeys et al., 2014), we assessed the shoot growth at 13 DAG by measuring the green surface area using ImageJ. Each data point corresponds to 16 seedlings per treatment. The electrolyte leakage (also called conductivity) from seedlings was measured with a conductivity meter (inoLab Cond level 1) (Jiang et al., 2017).

Floating Leaf Disc

The senescence leaf disc assay was modified from Ghosh et al. (2015) and Chiu et al. (2021). Arabidopsis was cultivated in Jiffy-7® peat pellets (Jiffy Products International AS, Norway) in a growth room (room temperature 18°C, less than 70% relative humidity, light intensity 100 μmol m^{-2} s^{-1}, 16/8 h day/night photoperiod). The chlorophyll content in fully expanded rosette leaves of the same developmental stage was determined by the SPAD-502 chlorophyll meter (Konica Minolta, Tokyo, Japan). Leaves with SPAD values from 25 to 35 were harvested from healthy plants at 30 DAG. Around 20 leaf discs were punched with a 7 mm cork borer and floated on a 5 mL solution in each petri dish (55 mm diameter). Each treatment consisted of six individual plates. Distilled water (dH_2O) was considered the blank, while 200 mM NaCl was considered the salt treatment. For exogenous SBE treatment, leaf discs were pretreated with 5 mL of dH_2O or 0.5 g/L SBE for 1 day before incubating in the blank or salt solution for another 2 days. The plates were sealed with 3M Micropore tape (3M, St. Paul, MN, United States) and placed in the growth room (room temperature 25°C, 40–60% humidity, light intensity 200 μmol m^{-2} s^{-1}, 24 h light photoperiod). After incubation, the leaf disc samples were first wrapped in dust-free tissue paper, then homogenized into powder with liquid nitrogen, and stored at −80°C for further analysis. Photosynthetic pigments of chlorophyll *a* (Chl *a*), chlorophyll *b* (Chl *b*), and carotenoids (Car) were assessed from frozen samples using a microplate reader (Tecan Infinite M200), according to Chiu et al. (2021). Malondialdehyde (MDA), as a biomarker of lipid peroxidation, was analyzed via the thiobarbituric acid (TBA)-reactive substances assay following (Hodges et al., 1999).

True Leaf Development

The true leaf assay was adapted from Rosa and Scheid (2014). Arabidopsis seeds were sown directly on the treated medium and vernalized as mentioned before (Trinh et al., 2018). Since the addition of NaCl (100 mM) in the medium induced moderate salt stress (Claeys et al., 2014), medium supplemented with 0.5 g/L SBE was prepared with or without 100 mM NaCl for the exogenous SBE application. The plates were positioned horizontally for germination in the light without etiolation and early leaf development monitoring for 10 days. The germination rate and the early development phenotypes were recorded daily at the same time each day. At 2 DAG, seed germination was evaluated by checking if the radicle was visible after testa rupture. Later, at 10 DAG, the successful emergence and expansion of the first pair of true leaves were determined by a binocular microscope at 20× zoom. If the side-view width of the true leaf had expanded larger than the hypocotyl diameter, it was then scored as a plant with expanded true leaves (**Supplementary Figure 1**). The percentage (%) of seedlings with true leaves was calculated following Equation 1:

$$\%\ \text{plants with true leaves} = \frac{\text{Number of seedlings developed with true leaves}}{\text{Number of germinated seedlings}} \quad (1)$$

This assay was performed as nine replicates for each treatment, and each plate contained 25 seeds. The harvested samples at 10 DAG were pooled into four biological replications and stored at −80°C for further analysis. The fresh weight of whole seedlings was measured and subsequently dried at 65°C for 48 h in an oven for dry biomass determination. In addition, the conductivity and MDA content in seedlings were measured as mentioned above to evaluate plasma membrane damage.

Hydrogen peroxide (H_2O_2), as one of the main ROS products, was quantified based on potassium iodide (KI) oxidation (Junglee et al., 2014). To detect *in situ* H_2O_2, histological staining with 3,3′-diaminobenzidine (DAB) on whole seedlings was performed as previously described (Daudi and O'Brien, 2012). The seedlings were imaged via an Olympus BX51 microscope (Olympus, Tokyo, Japan) equipped with differential interference contrast (DIC) optics at 10× zoom. The relative DAB staining intensity was calibrated in pseudo color and quantified in

TABLE 1 | Contents of soluble protein, digestible carbohydrate, polyphenols, and *in vitro* antioxidant capacity in SBE.

Parameters		SBE
Soluble protein content (mg g DW^{-1} BSA equivalent)		14.91 ± 0.41
Digestible carbohydrate content (mg g DW^{-1} D-glucose equivalent)		6.91 ± 0.53
Total phenolic content (TPC) (mg g DW^{-1})	AsA equivalent	6.46 ± 0.79
	CHA equivalent	29.68 ± 0.81
Total flavonoid content (TFC) (μg g DW^{-1})	QE equivalent	9.70 ± 0.29
	Rutin equivalent	15.93 ± 2.01
Total antioxidant capacity (TAC) (mg g DW^{-1} TEAC)	IC_{50} DPPH assay	20.66 ± 0.67
	IC_{50} ABTS assay	117.34 ± 3.34

Values are represented as mean ± SD (n = 3). SBE, sunflower bark extract; DW, dry weight; BSA, bovine serum albumin; AsA, ascorbic acid; CHA, chlorogenic acid; QE, quercetin; TEAC, trolox equivalent antioxidant capacity; DPPH, 2,2-diphenyl-1-picrylhydrazyl; ABTS, 2,2′-azino-bis (3-ethylbenzothiazoline-6-sulfonic acid).

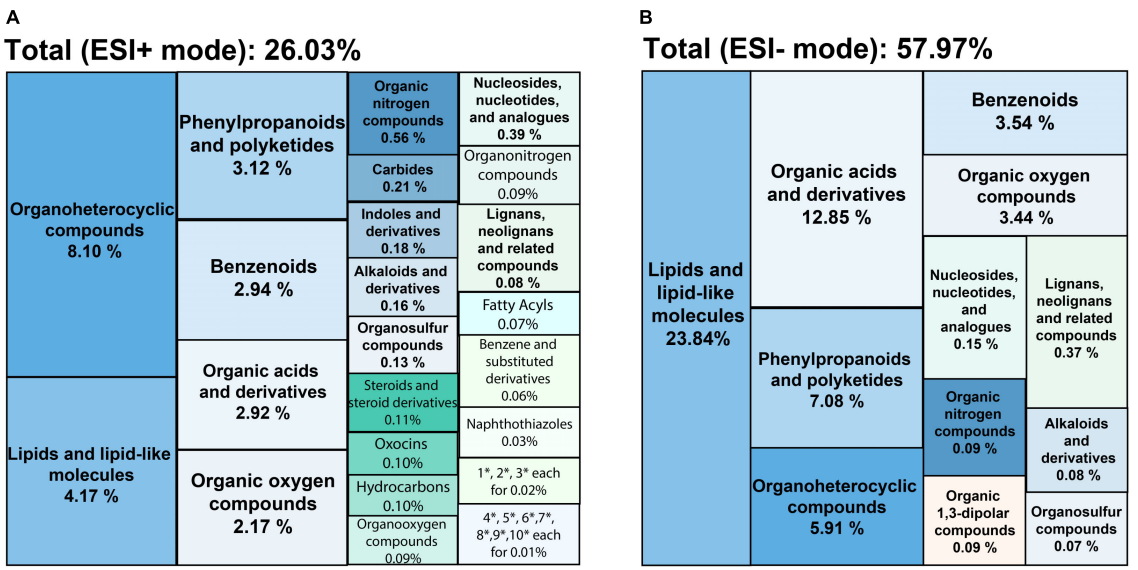

FIGURE 1 | Treemaps of chemical classifications of SBE compounds detected by UHPLC-PDA-HRMS in **(A)** ESI+ and **(B)** ESI– modes. Each color shows the chemical taxonomy at the superclass level from ChemOnt ontology. Each value indicates the relative distribution of each superclass by total peak areas. SBE, sunflower bark extract; ESI+ (–), positive (negative) electrospray ionization. Where * is short for the superclasses following, 1: cinnamic acids and derivatives; 2: quinolines and derivatives; 3: imidazopyrimidines; 4: organic phosphoric acids and derivatives; 5: pyrroloazepines; 6: coumarins and derivatives; 7: pumiliotoxins, homopumiliotoxins, and allopumiliotoxins; 8: benzothiazoles; 9: azoles; 10: lupin alkaloids.

four tissues, inclusive of cotyledons, hypocotyls, shoot apical meristems (SAMs), and root, using ImageJ coped with the "Colour Deconvolution 2" plugin (Ruifrok and Johnston, 2001; Landini et al., 2021).

The antioxidant enzyme activity was then determined following a semi high-throughput protocol (Fimognari et al., 2020) with the adapted extraction method (Noctor et al., 2016). About 300 mg grounded sample was extracted with 2 mL extraction buffer (0.1 M phosphate buffer plus 1 M EDTA; pH 7.5) and 50 mg polyvinylpyrrolidone (PVP). The mixture was centrifuged for 10 min at 4°C. Next, the total protein content was quantified in the desalted supernatant by Wizard® SV minicolumns using a spectrophotometer (DeNovix Inc., United States). Finally, the enzyme kinetic assays were performed for the activity measurement of ascorbate peroxidase (APX, EC:1.11.1.11), catalase (CAT, EC:1.11.1.6), glutathione reductase (GR, EC:1.8.1.7), glutathione *S*-transferase (GST, EC:2.5.1.18), monodehydroascorbate reductase (MR, EC:1.6.5.4), (cytoplasmic) peroxidase (POX, EC:1.11.1.5), and superoxide dismutase (SOD, EC:1.15.1.1). The antioxidative enzyme capacity, indicating the rate of catalyzed reaction by the enzyme, was calculated as a unit per mg of protein (Vanhoudt, 2014).

Statistical Analysis

The treemap was generated indicating the chemical classification of compounds identified in SBE by R software version 4.1.1 (R Core Team, 2021) coupled with "treemap" package version 2.4-3 (Tennekes and Ellis, 2021). Non-parametric Kruskal–Wallis test was used with *post hoc* Dunn's analysis ($\alpha = 0.05$) for variances in root numbers of different types. PRL was normalized and fitted in a 5-parameter logistic model of dose-response analysis using "nplr" package version 0.1-7 (Commo and Bot, 2016). The half-maximal-effect concentration (EC_{50}) was calculated on

TABLE 2 | Polyphenolic compounds of interest in SBE.

Class[1]	Subclass[1]	Parent level 1[1]	Predicted formula	Adduct	RT (min)	Precursor m/z	Area (×10^5)	Total score[2]
2-Arylbenzofuran flavonoids	NA	2-Arylbenzofuran flavonoids	$C_{25}H_{28}O_{10}$	$[M + H]^+$	7.97	489.1735	0.14	5.90
Cinnamic acids and derivatives	Cinnamic acid esters	Cinnamic acid esters	$C_{11}H_{12}O_2$	$[M + H]^+$	7.75	177.0916	0.65	5.51
	Cinnamic acids	Cinnamic acids	$C_9H_8O_2$	$[M + H]^+$	23.46	149.0597	0.53	6.33
	Hydroxycinnamic acids and derivatives	Coumaric acids and derivatives	$C_{17}H_{16}O_4$	$[M + H]^+$	9.79	285.1128	0.12	5.78
		Hydroxycinnamic acids	$C_9H_8O_3$	$[M + H]^+$	4.96	165.0547	0.39	6.14
Coumarins and derivatives	Hydroxycoumarins	6,7-Dihydroxycoumarins	$C_9H_6O_4$	$[M + H]^+$	4.20	179.0345	0.35	5.78
		7-Hydroxycoumarins	$C_{10}H_8O_4$	$[M + H]^+$	4.80	193.0505	1.43	5.98
	Furanocoumarins	Angular furanocoumarins	$C_{17}H_{12}O_6$	$[M + H - H_2O]^+$	6.04	295.0606	0.23	6.09
	Pyranocoumarins	Angular pyranocoumarins	$C_{21}H_{22}O_7$	$[M + H]^+$	7.89	387.1450	0.22	5.98
	Coumarin glycosides	Coumarin glycosides	$C_{15}H_{16}O_9$	$[M + H]^+$	4.20	341.0872	0.24	5.84
	NA	Coumarins and derivatives	$C_9H_6O_2$	$[M + H]^+$	6.44	147.0443	0.36	5.99
	Furanocoumarins	Linear furanocoumarins	$C_{13}H_{10}O_5$	$[M + H - H_2O]^+$	7.34	229.0500	0.23	5.55
Flavonoids	Flavones	3′-Prenylated flavones	$C_{20}H_{18}O_7$	$[M + H - H_2O]^+$	8.22	353.1040	0.15	5.75
	Flavans	8-Prenylated flavans	$C_{20}H_{20}O_5$	$[M + H]^+$	9.13	341.1380	0.22	6.32
	Flavonoid glycosides	Flavonoid *O*-glycosides	$C_{21}H_{20}O_{11}$	$[M + H]^+$	6.30	449.1083	0.11	6.43
	O-Methylated flavonoids	3-O-methylated flavonoids	$C_{17}H_{12}O_8$	$[M + H]^+$	7.20	345.0626	0.29	5.74
		8-O-methylated flavonoids	$C_{21}H_{22}O_8$	$[M + H]^+$	7.81	403.1376	1.58	6.04
Isoflavonoids	O-Methylated isoflavonoids	4′-O-methylated isoflavonoids	$C_{22}H_{22}O_6$	$[M + H]^+$	7.78	383.1476	0.17	5.97
	Isoflavans	Isoflavanols	$C_{15}H_{14}O_3$	$[M + H]^+$	6.90	243.1024	0.24	5.74
	Isoflavans	Isoflavanones	$C_{20}H_{20}O_6$	$[M + H]^+$	8.07	357.1351	0.93	6.28
	Isoflav-2-enes	Isoflavones	$C_{15}H_{10}O_5$	$[M + H]^+$	5.38	271.0605	0.18	6.30
	Isoflavonoid *O*-glycosides	Isoflavonoid *O*-glycosides	$C_{21}H_{20}O_9$	$[M + H]^+$	8.36	417.1198	0.33	6.52
	Furanoisoflavonoids	Pterocarpans	$C_{20}H_{18}O_5$	$[M + H - H_2O]^+$	6.93	321.1141	0.19	6.37
Stilbenes	Stilbene glycosides	Stilbene glycosides	$C_{21}H_{24}O_8$	$[M + H]^+$	6.24	405.1557	0.21	6.07
Tannins	Hydrolyzable tannins	Hydrolyzable tannins	$C_{33}H_{32}O_{11}$	$[M + H]^+$	8.79	605.2021	0.21	5.38
2-Arylbenzofuran flavonoids	NA	2-Arylbenzofuran flavonoids	$C_{26}H_{34}O_{11}$	$[M - H]^-$	6.81	521.2031	0.38	5.63
Coumarins and derivatives	Furanocoumarins	Angular furanocoumarins	$C_{17}H_{12}O_6$	$[M - H]^-$	6.60	311.0547	0.56	5.95
	Coumarin glycosides	Coumarin glycosides	$C_{16}H_{18}O_9$	$[M - H]^-$	3.84	353.0870	2.45	6.00
	NA	Coumarins and derivatives	$C_{10}H_8O_6S$	$[M - H]^-$	7.06	254.9952	0.50	4.94
Cinnamic acids and derivatives	Hydroxycinnamic acids and derivatives	Coumaric acids and derivatives	$C_{13}H_{16}O_5$	$[M - H]^-$	8.12	251.0909	0.19	5.46
		Hydroxycinnamic acids	$C_9H_8O_4$	$[M - H]^-$	6.19	179.0340	25.60	6.24
Diarylheptanoids	Linear diarylheptanoids	Linear diarylheptanoids	$C_{20}H_{24}O_3$	$[M - H]^-$	13.86	311.1670	6.64	5.30
Flavonoids	Flavones	3-Prenylated flavones	$C_{25}H_{24}O_7$	$[M - H]^-$	7.81	435.1488	0.18	5.15
	O-Methylated flavonoids	3′-O-methylated flavonoids	$C_{16}H_{12}O_6$	$[M - H]^-$	6.48	299.0578	7.24	6.38
		4′-O-methylated flavonoids	$C_{16}H_{12}O_5$	$[M - H]^-$	8.45	283.0631	0.81	6.44
		6-O-methylated flavonoids	$C_{18}H_{18}O_8$	$[M - H]^-$	4.77	361.0936	0.23	5.52

(Continued)

TABLE 2 | (Continued)

Class[1]	Subclass[1]	Parent level 1[1]	Predicted formula	Adduct	RT (min)	Precursor m/z	Area (×10^5)	Total score[2]
		7-O-methylated flavonoids	$C_{20}H_{20}O_8$	$[M-H]^-$	8.22	387.1066	0.53	6.84
		8-O-methylated flavonoids	$C_{19}H_{18}O_7$	$[M-H]^-$	8.36	357.0961	0.37	5.92
	Flavonoid glycosides	Flavonoid *O*-glycosides	$C_{26}H_{28}O_{12}$	$[M-H]^-$	7.45	531.1503	0.53	6.47
	Flavones	Flavonols	$C_{16}H_{12}O_7$	$[M-H]^-$	7.39	315.0530	1.17	6.20
Isoflavonoids	Isoflavonoid *O*-glycosides	Isoflavonoid *O*-glycosides	$C_{24}H_{24}O_{11}$	$[M-H]^-$	5.86	487.1252	0.20	5.94
Isocoumarins and derivatives	NA	Isocoumarins and derivatives	$C_{13}H_{14}O_7$	$[M-H]^-$	8.11	281.0659	0.17	5.05
Linear 1,3-diarylpropanoids	Chalcones and dihydrochalcones	2′-Hydroxy-dihydrochalcones	$C_{21}H_{24}O_5$	$[M-H]^-$	18.83	355.1559	0.75	5.06
Phenylpropanoic acids	NA	Phenylpropanoic acids	$C_9H_{10}O_5$	$[M-H]^-$	3.33	197.0450	1.16	5.67
Tannins	Hydrolyzable tannins	Hydrolyzable tannins	$C_{14}H_{18}O_9$	$[M-H]^-$	6.91	329.0877	0.20	5.64

The compounds were detected and tentatively identified via UHPLC-PDA-HRMS under ESI+ and ESI− modes.
SBE, sunflower bark extract; ESI+ (−), positive (negative) electrospray ionization; RT, retention time; NA, not available.
[1]The ontology information of identified features (class, subclass, and parent level 1) was retrieved by InChIKey according to ChemOnt chemical taxonomy (Djoumbou Feunang et al., 2016).
[2]The top-ranking score of the candidate compound was selected in the MS-FINDER program (Tsugawa et al., 2016).

the PRL inhibition effect by getEstimates function (Venturelli et al., 2016). Dynamic growth models of plant leaf area were fitted in exponential growth curves illustrating the early development patterns. One-way ANOVA analysis was applied with *post hoc* Tukey HSD test ($\alpha = 0.05$) to compare the treatment difference for other plant traits. Besides, two-way ANOVA analysis was used for two independent variables: the addition of growth media and timepoints. The statistical analysis of the remaining parameters and data visualization were performed with GraphPad Prism software version 8.0.2 (GraphPad, San Diego, CA, United States).

RESULTS

Preparation of Sunflower Bark Extract and Chemical Analysis

Aqueous extraction of sunflower bark was obtained using a twin-screw extruder as described in the materials and methods. **Supplementary Table 2** shows the chemical composition of the starting bark materials, with the insoluble fraction constituting 88% of the bark containing 50% cellulose and 15% lignin. The high content in lignocellulose promoted the separation into fiber (pulp) and a liquid filtrate, which contained the water-soluble compounds. The chemical composition and antioxidant activity of the freeze-dried liquid filtrate (SBE) contained 1.5% (w/w) soluble protein and 0.7% (w/w) carbohydrate (**Table 1**). The polyphenol content (TPC and TFC) per gram dry biomass of SBE was 6.46 mg AsA equivalents and 29.68 mg CHA equivalents with phenolic acids, and 9.70 μg QE equivalents and 15.93 μg rutin equivalents with flavonoids. TAC of SBE was represented as IC_{50} from *in vitro* antioxidant assays, which were 20.66 and 117.34 TE equivalents in the DPPH and ABTS assay, respectively.

The low molecular weight primary and secondary metabolites were characterized by untargeted metabolic profiling using UHPLC-PDA-HRMS. It resulted in 2369 LC–MS features in the ESI+ mode and 814 under the ESI− mode (the chromatograms are shown in **Supplementary Figure 2**, all the identified compounds are listed in **Supplementary Data 1**). A total of 26.03% of the ESI+ and 57.97% of the ESI− detected peaks were tentatively identified. These compounds were classified according to 35 distinct categories of plant metabolites (**Figure 1**). The lipids and lipid-like molecules, organic acids, phenylpropanoids and polyketides, benzenoids, and organoheterocyclic compounds formed the five most extensive groups representing half of the classified metabolites. SBE was particularly rich in compounds across chemical superclasses of phenylpropanoids and polyketides, organic acids and derivatives, and benzenoids, of which polyphenols are well-known antioxidants with cytoprotective activity (Kiokias et al., 2020; Šamec et al., 2021). Thereby, we further focused on the diverse proportions of non-flavonoid and flavonoid compounds of interest under the phenylpropanoids and polyketides superclass in SBE. Eleven polyphenol classes involved 20 subclasses, and 45 tentatively identified compounds were illustrated in **Table 2**.

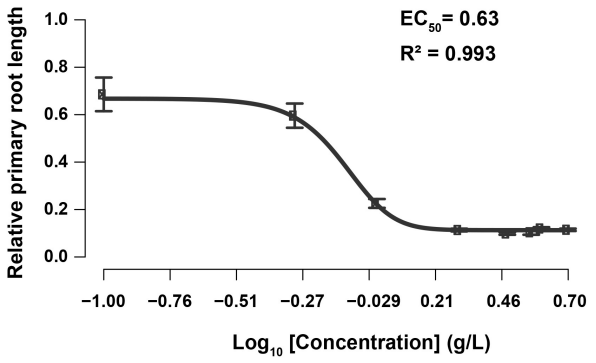

FIGURE 2 | Dose-response curve of relative primary root length to the increase of SBE concentration in the Arabidopsis root assay. Each data point indicates the mean ± SD ($n > 15$). The black line represents the 5-parameter logistic regression. SBE, sunflower bark extract; EC_{50}, half-maximal-effect concentration.

Sunflower Bark Extract Inhibited the Primary Root Growth of Non-stressed Arabidopsis Seedlings in a Dose-Response Manner

The root tip is a sensory organ that evaluates the presence of mineral nutrients and physical obstructions, adapting its growth in response to the conditions by altering the growth rate and orientation of cell division and expansion (Svolacchia et al., 2020). Hence, the primary root is very susceptible to environmental conditions, and its plasticity facilitates the detection of slight changes in the composition of the growing medium (Malamy, 2005). To test the impact of SBE application on root growth, root length (PRL) and branching (AR, LR, and JR) of *in vitro* grown Arabidopsis seedlings were determined (**Supplementary Figure 3**). Significantly less AR was formed when treated with SBE at higher doses. A strong reduction in LR number was observed at SBE levels from 1 g/L, while the effect on JR formation was more complex with a promotion up to 1 g/L SBE but a reduction from a higher concentration above 1 g/L. Furthermore, the EC_{50} of SBE inhibition of PRL was 0.63 g/L (**Figure 2**). Since root growth often shows an adaptive behavior to exogenous stimuli, the inhibition of PRL was examined at different time intervals after transfer to the medium containing SBE. Growth inhibition was observed 24 h after treatment with 1 g/L SBE, while at 3 g/L SBE inhibition occurred 6 h after treatment (**Supplementary Figure 4**). To avoid secondary effects following primary root growth inhibition, SBE was applied at 0.5 g/L in the subsequent assays (**Supplementary Figure 3**).

Priming With Sunflower Bark Extract Did Not Alter Germination Rate but Stimulated Shoot Growth

We did not observe a notable change in shoot growth after transferring 3 DAG Arabidopsis seedlings to SBE containing medium (**Figure 3B**). In addition to the seed priming experiment, there was no impairment of seed germination rate after 2 days in any of the treatments (**Supplementary Figure 5**). After 4 days, however, we observed a slight, statistically significant increase in the leaf area of seedlings grown on SBE containing medium (**Figure 4A**).

Sunflower Bark Extract Alleviated Shoot Growth Inhibition Under Salt Stress

Biostimulants typically show a more pronounced effect in plants grown under stress (Rouphael and Colla, 2020). The impact of SBE was therefore assessed under conditions of salt stress. As the suppression of shoot growth by NaCl was very notable (Claeys et al., 2014), the projected leaf area was used as a proxy for determining the effect of SBE. In the shoot assay, the shoot growth was severely inhibited in the presence of 100 mM NaCl, showing a reduced petiole length, smaller cotyledons, and delayed or even arrested emergence of the first true leaves (**Figure 3A**). In the presence of SBE, the NaCl-stressed seedlings generated a significantly larger green surface area than in control salt-stressed plants (**Figure 3B**). NaCl causes osmotic stress and ionic imbalances, affecting the integrity of the plasma membrane (Dubois and Inzé, 2020). Therefore, the seedlings were collected after 13 DAG to determine the electrolyte leakage (**Figure 3C**). Salt stressed plants grown on SBE containing medium showed much lower conductivity than the control plants, suggesting that SBE treatment protected the plants from cell membrane damage.

We then put more attention to early true leaf development in seed priming treatment. SBE did not influence the germination rate of Arabidopsis under salt stress conditions (**Supplementary Figure 5**). Since we noticed that shoot growth was enhanced in SBE containing medium, a time-course analysis was performed to determine this response in more detail (**Figure 4**). On 100 mM NaCl-containing medium, shoot development was significantly reduced, while this growth inhibition was strongly alleviated when SBE was included in the medium (**Figure 4A**). Under normal conditions, all plants expanded their first true leaves at 10 DAG, while in the presence of NaCl, only 20% of the plants produced expanded true leaves. However, the number of salt-stressed plants with expanded true leaves increased to around 80% when treated with SBE (**Figure 4B**). The addition of SBE advanced true leaf development by about 2 days, and the effects were already noticeable from 3 DAG when NaCl-induced anthocyanin accumulation as a red discoloring of the cotyledons and at the upper hypocotyl margin was observed. While less intense red coloring was shown in the presence of SBE (**Figure 4C**).

Sunflower Bark Extract Preserved Photosynthesis Pigments and Stabilized the Cell Membrane Under Salt Stress

The Arabidopsis response to salt stress includes a reduction in growth, reflected in lower fresh weight and dry weight (**Figures 5A,B**), and a bleaching effect that entails a decline of pigments, the photosynthetic chlorophyll, and carotenoids (Leschevin et al., 2021). These pigments were quantified, and chl_{a+b} was reduced twofold, whereas carotenoids were down by about threefold in 10 DAG salt-stressed seedlings (**Figures 5C,D**).

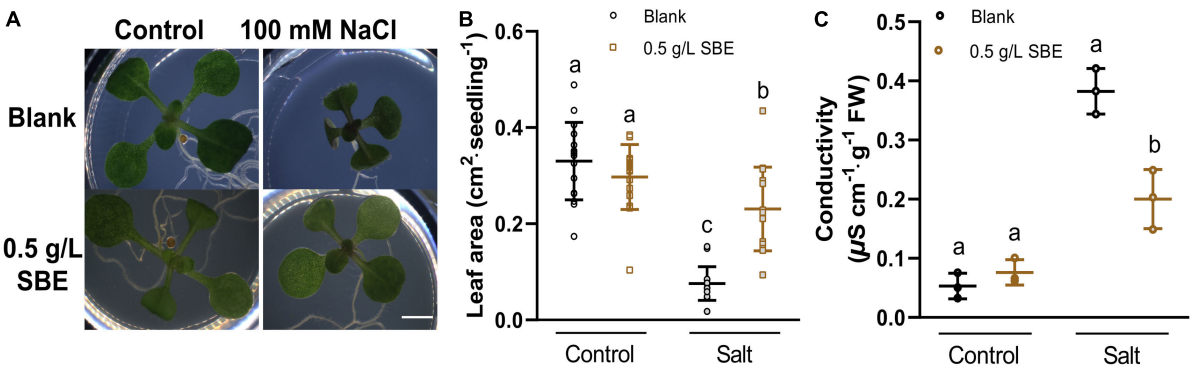

FIGURE 3 | Salt stress alleviation of SBE treatment in the Arabidopsis shoot assay. **(A)** Phenotypes of representative seedlings at 13 DAG grown on multiwell plates. Bar = 2 mm. The changes of **(B)** leaf area (n = 16) and **(C)** conductivity (n = 4) of 13 DAG seedlings. Error bars indicate SDs of the means. Different letters represent significant differences between treatments using Tukey's HSD test ($p < 0.05$). SBE, sunflower bark extract; DAG, days after germination.

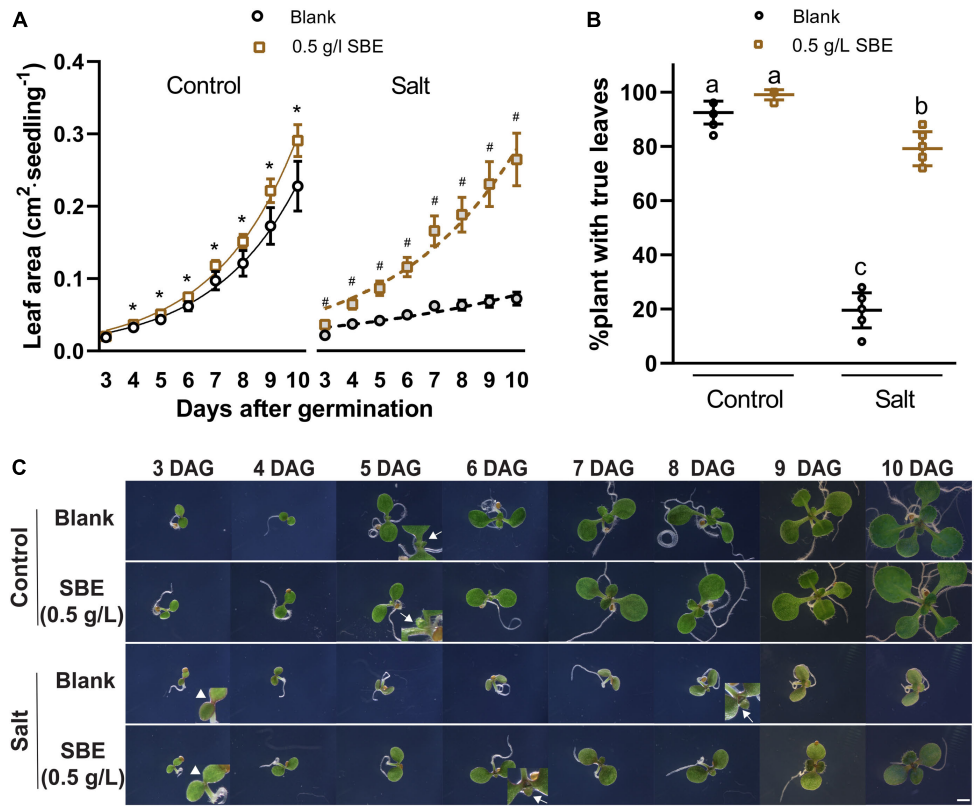

FIGURE 4 | Salt stress alleviation of SBE treatment in the Arabidopsis true leaf assay. **(A)** The dynamic growth of leaf area from 3 DAG to 10 DAG. Error bars indicate SDs of the means (n = 9). Different letters represent significant differences between treatments using Tukey's HSD test ($p < 0.05$). Fitted lines were exponential curves of dynamic leaf area growth. The symbols * and # represent significant differences between treatment with or without SBE addition under control or salt stress conditions at the same time point, respectively ($p < 0.05$). Both salt treatments were significantly different from the two non-stress treatments at every time point (label not shown). **(B)** The percentages of plants successfully developed with true leaves at 10 DAG. **(C)** Phenotype changes of representative seedlings from 3 DAG to 10 DAG focusing on the center of two cotyledons under binocular 6.3× zoom. Bar = 2 mm. Arrows without tails indicate salt stress alleviation by SBE addition on anthocyanin accumulation at the cotyledon edges of 3 DAG seedlings. Arrows with tails showed the earliest starting time point of visible true leaves. SBE, sunflower bark extract; DAG, days after germination.

This protective effect of SBE was accompanied by diminished salt stress-induced electrolyte leakage (**Figure 5E**) and MDA overaccumulation (**Figure 5F**).

To investigate whether SBE exerts a priming protective effect on mature leaves, punched leaf discs from fully developed leaves were pretreated for 1 day with SBE or water as a control

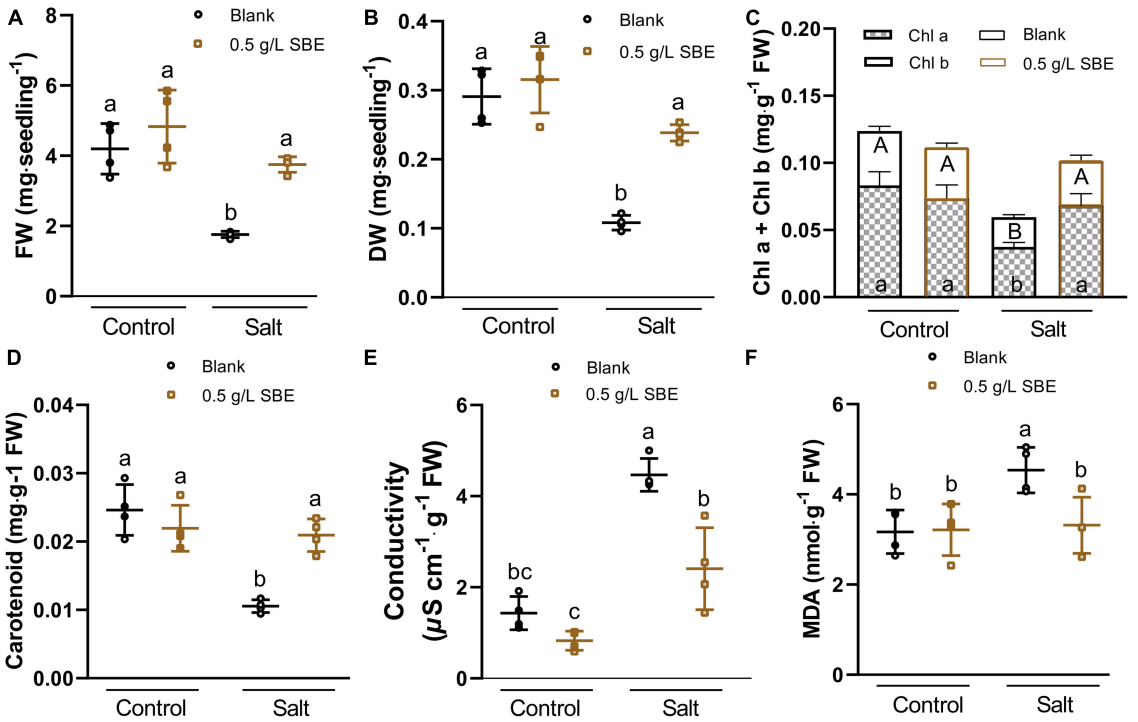

FIGURE 5 | Salt stress alleviation of SBE treatment on the physiological traits of 10 DAG Arabidopsis in the true leaf assay. **(A)** Fresh weight, and **(B)** dry weight of the whole seedlings at 10 DAG. The changes of photosynthetic pigments containing **(C)** chlorophyll a and b, **(D)** carotenoid content, **(E)** conductivity, and **(F)** MDA content. Error bars indicate SDs of the means (n = 4). Different letters represent significant differences between treatments using Tukey's HSD test ($p < 0.05$). SBE, sunflower bark extract; DAG, days after germination; FW, fresh weight; DW, dry weight; Chl a, chlorophyll a; Chl b, chlorophyll b; MDA, malondialdehyde.

(**Figure 6A**). Next, the leaves were floated for 2 days on a solution with or without 200 mM NaCl. The SBE pretreated leaves maintained a higher level of chl_{a+b} and carotenoid content under salt stress conditions (**Figures 6B,C**). Similar to the salt-stressed seedlings, SBE pretreatment dampened the accumulation of MDA production induced by salt (**Figure 6D**).

Sunflower Bark Extract Mitigates NaCl Toxicity by Suppressing Hydrogen Peroxide Overaccumulation

Salinity-induced osmotic and ionic stress affects cellular redox homeostasis by H_2O_2 overproduction causing oxidative damage to proteins and lipids (Munns and Tester, 2008; Huang et al., 2019). We, therefore, asked if SBE scavenges ROS in salt-stressed plants. The H_2O_2 levels more than doubled in salt stress seedlings at 10 DAG (**Figure 7A**). The salt-induced increase in H_2O_2 was reduced to about 60% by SBE application (**Figure 7A**). ROS reduction was already apparent after 3 DAG upon ROS staining with DAB (**Supplementary Figure 6** and **Figure 7B**), which coincides with the earliest time point when SBE started showing a significant improvement in shoot growth on NaCl containing medium (**Figure 4C**). The relative DAB staining intensity in plants grown in the presence of SBE was lower than in plants without SBE (**Figure 7B**). The quantification of DAB intensity in the cotyledons, hypocotyl, root, and SAM showed that the dampening effect of SBE occurred in all seedling organs (**Figure 7C**). H_2O_2 levels were relatively higher in the root and SAM than in cotyledons and hypocotyl. The SBE mediated reduction of ROS was most pronounced in the SAM in line with the protective effect of SBE on true leaf development under salt stress conditions.

Next, we asked whether SBE neutralizes ROS formation via the overactivation of antioxidant enzymes that are part of the plant defense system (Apel and Hirt, 2004; Bobrovskikh et al., 2020). To this end, the activity of the antioxidant enzymes was measured in control and salt-stressed seedlings grown with or without SBE supplement (**Figure 8**). In control conditions, no difference in antioxidant enzymes activity was investigated. SBE treatment of salt-stressed plants significantly increased the activity of CAT, APX, and POX (**Figures 8B–D**), which directly participate in eliminating ROS pathway by catalyzing the conversion from H_2O_2 to H_2O (Dumanović et al., 2021). In contrast, SOD, GR, GST, and MR were not significantly altered by SBE treatment (**Figure 8A** and **Supplementary Figure 7**).

DISCUSSION

This study on the analysis of potential biostimulant activity is a major step in valorizing sunflower stalks. Here, we report that SBE, a side stream obtained during fiber isolation by twin-screw extrusion, contains polyphenols and other bioactive molecules that activate ROS scavenging enzymes, thereby suppressing the

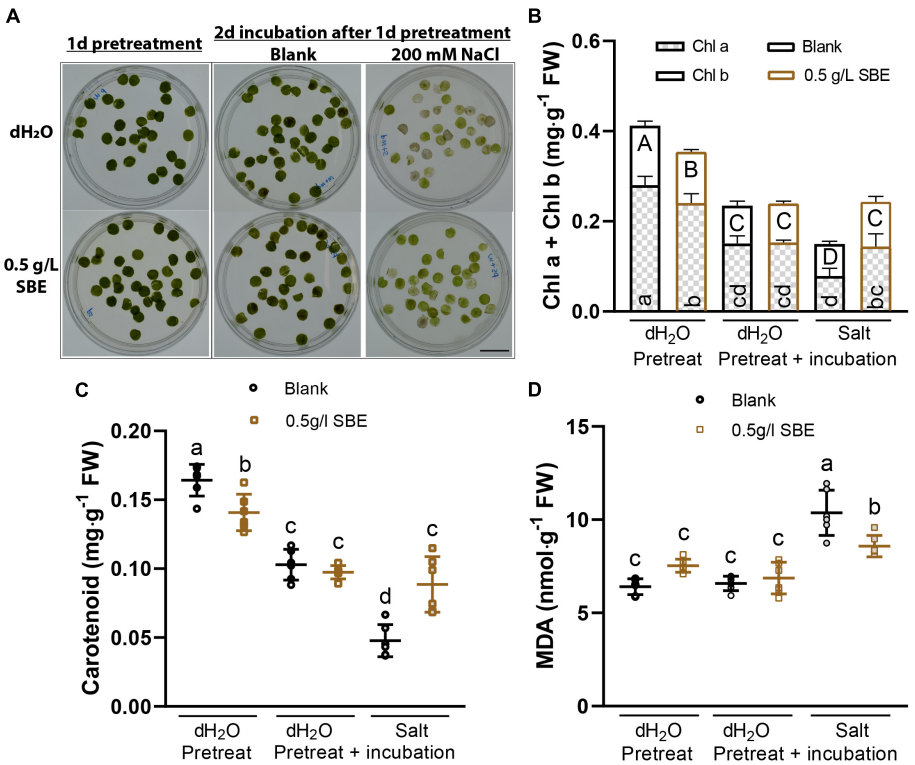

FIGURE 6 | Salt stress alleviation of SBE pretreatment on expanded Arabidopsis leaves in the leaf disc assay. **(A)** The representative image of treated leaf discs was taken before sampling. Bar = 2 cm. Photosynthetic pigments contain **(B)** chlorophyll *a* and *b*, and **(C)** carotenoid content. **(D)** MDA content. Error bars indicate SDs of the means (n = 6). Different letters represent significant differences between treatments using Tukey's HSD test ($p < 0.05$). SBE, sunflower bark extract; DAG, days after germination; FW, fresh weight; Chl a, chlorophyll a; Chl b, chlorophyll b; MDA, malondialdehyde.

oxidative damage to Arabidopsis seedlings grown on the NaCl-containing medium. Together, the results suggest that SBE is a potential source of biostimulant.

The twin-screw extrusion method is an extraction technique for separating insoluble parts (e.g., fibers) from solvent-soluble molecules in a single step. The solvent, thermal and mechanical actions are customized to extract fiber-rich plant biomass from crop waste such as sunflower stems (Evon et al., 2018; Vandenbossche et al., 2019). The extrusion method is an ecofriendly biorefinery process that meets the criteria of "green chemistry" extraction of natural products (Chemat et al., 2012). Yet, the bark extract is not economically valorized from the sunflower fiber part. SBE is an aqueous extract adhering to the guidelines of the European directive for certification of natural substances without pesticide residue and, as such, can be used to produce a novel biostimulant.

The outer bark constitutes about 90% dry weight of the whole stalk, indicating that it is much denser than the pith (Xu et al., 2020). The stems contain a considerable amount of polyphenols (Kamal, 2013). The chemical composition of an aqueous extract from sunflower bark has not yet been reported. An estimation of phenolics content (TPC) in SBE (**Table 1**) was obtained by applying a modified Folin–Ciocalteu assay to quantify TPC values against CHA (Sánchez-Rangel et al., 2013). However, the TFC values for evaluating "total" flavonoid content are not adequate based on aluminum complex reaction as the two procedures we performed are specific for different flavonoid structures (Pękal and Pyrzynska, 2014). In this situation, it is not possible to compare the accurate polyphenol content across the studies using different protocols. Therefore, to improve the coverage of present plant metabolites in SBE besides polyphenols, UHPLC-PDA-HRMS was performed for more precise detection and identification (Lai et al., 2018). Thanks to the validated algorithm increasing the accuracy of compound identification (Tsugawa et al., 2016), MS-DIAL combined with MS-FINDER is recommended to match MS^e spectra *in silico* for untargeted metabolomics (Blaženović et al., 2017; Vaniya et al., 2017). Our study thus provides the chemical composition of SBE, to some degree, revealing the plant metabolomics with both colorimetric and UHPLC-PDA-HRMS analysis.

Sunflower bark extract shows conspicuously *in vitro* activity, completely inhibiting primary root growth at doses above 1 g/L (**Supplementary Figure 3**). This strong growth inhibition contrasts with the growth-promoting effects observed in salt-stressed plants treated with more diluted SBE. Sunflowers produce a diverse set of allelochemicals that either positively or negatively affect the growth of other plant species (Macías et al., 2002). Some of these allelochemicals were already identified in sunflower stalks (Maheswari et al., 2019). Allelopathic activity in sunflower was closely linked with the presence of polyphenols

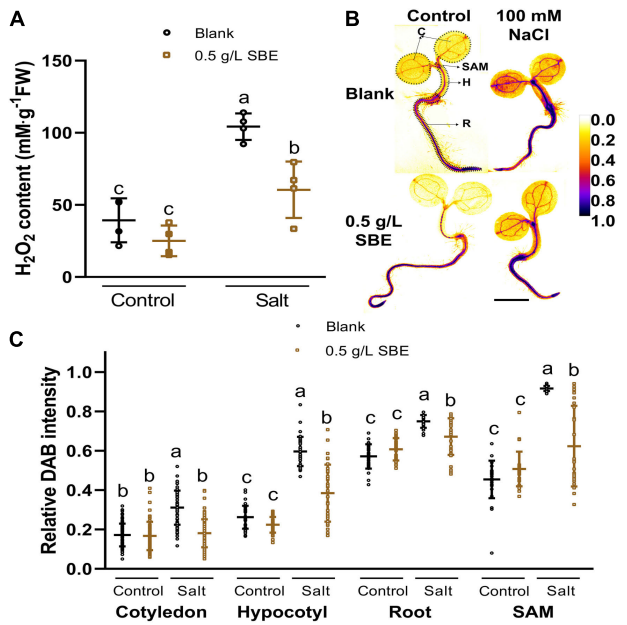

FIGURE 7 | Hydrogen peroxide accumulation of 3 DAG and 10 DAG Arabidopsis seedlings under salt stress in the true leaf assay. **(A)** H_2O_2 content in 10 DAG seedlings. **(B)** Representative images of 3 DAG seedlings after histological staining of H_2O_2 by DAB are shown in pseudo-colors of relative DAB intensity as shown in the color bar. Regions of interested organs are shown in circles with black dotted lines. Bar = 1 mm. **(C)** Relative DAB staining intensity of four organs in 3 DAG seedlings. Error bars indicate SDs of the means [$n = 4$ **(A)** and >25 **(B)**]. Different letters represent significant differences between treatments ($p < 0.05$). SBE, sunflower bark extract; DAG, days after germination; H_2O_2, hydrogen peroxide; DAB, 3′,3-diaminobenzidine; C, cotyledon; H, hypocotyl; R, root; SAM, shoot apical meristem.

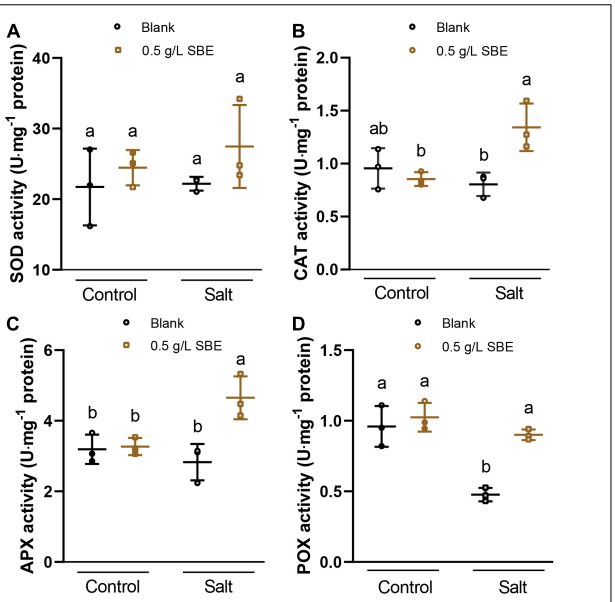

FIGURE 8 | The antioxidant activities of Arabidopsis seedlings under salt stress at 10 DAG in the true leaf assay. **(A)** SOD activity, **(B)** CAT activity, **(C)** APX activity, **(D)** POX activity. Error bars indicate SDs of the means. Different letters represent significant differences between treatments using Tukey's HSD test ($p < 0.05$). SBE, sunflower bark extract; DAG, days after germination; U, enzyme activity unit (μmol/min); SOD, superoxide dismutase; CAT, catalase; APX, ascorbate peroxidase; POX, peroxidases.

and terpenes (Rawat et al., 2017). Sunflower aqueous shoot extract partially inhibited rapeseed and *Cephalaria* seedling growth (Hamad, 2017). Natural polyphenols were extensively reported to induce cytotoxicity in plant normal cells as well as cancer cell in dose-dependent manners (Rasouli et al., 2016; Perveen, 2017). These or other allelopathic compounds are likely also present in SBE and could be responsible for the primary root growth inhibition at high doses and may also prime to trigger a plant defense response, a property of many biostimulants (Kerchev et al., 2020).

However, at 0.5 g/L, SBE protected Arabidopsis from oxidative damage induced by a moderate concentration of NaCl in the medium (**Figure 4**). Also, allelopathic extracts from *Levisticum officinale* Koch were recently identified to have a positive performance on soybean yield (Szparaga et al., 2021). One of the reasons is that some polyphenols have antioxidant activity and play a role in controlling oxidative stress in plants (reviewed in Ferdinando et al., 2012; Šamec et al., 2021). For example, quercetin suppressed the ROS toxicity of paraquat in seedlings of Arabidopsis, tobacco, and duckweed (Kurepa et al., 2016) and heavy-metal stress in Arabidopsis (Zhang et al., 2017). Recent evidence shows that flavonoids are active as cytoprotective antioxidants preventing mitochondrial signaling that regulates autophagy and apoptosis (Kicinska and Jarmuszkiewicz, 2020). Phenolic acids are also stress-relieving molecules due to their high antioxidative properties (Šamec et al., 2021), namely, caffeic and sinapic acids enhance salt tolerance in wheat seedlings when exogenously applied (Kaur et al., 2017). The reduction in ROS levels mediated by SBE is likely due to the antioxidant activity of polyphenols and possibly other molecules within a non-toxic concentration range.

Next to polyphenols, SBE contained digestible carbohydrates and soluble protein. Sugars released from carbohydrates function as energy metabolites, osmoprotectants, and signaling molecules and mitigate stress responses in plants (Rook et al., 2006; Krasensky and Jonak, 2012). Likewise, several amino acids derived from proteins have been proved to be precursors of secondary metabolites and signaling molecules tightly related to plant responses under stress (Batista-Silva et al., 2019). These water-soluble primary compounds may support plant stress adaptation and complement the ROS suppressing activity of the above-mentioned bioactive agents.

The true leaf development assay in Arabidopsis is a sensitive method for evaluating DNA damaging agents (Rosa et al., 2013). High concentrations of NaCl induce ROS formation in germinating eggplant leading to DNA damage (Kiran et al., 2020). In particular stem cells in germinating seeds and in shoot meristems are highly susceptible to DNA damage causing an arrest in leaf development (Fulcher and Sablowski, 2009). We speculate that the accumulation of H_2O_2 in SAM causes oxidative damage, including DNA damage and that this prevents

the development of the first true leaves in our experiments (**Figure 7C**). Polyphenols suppress ROS overaccumulation by neutralizing free radicals with donated electrons or hydrogen atoms with concomitant formation of stabilized phenolic radicals (Dumanović et al., 2021). In addition, polyphenols activate ROS scavenging enzymes (Kerchev et al., 2020). These enzymes function in plant defense and regulate cell growth and cell death (Mhamdi and Van Breusegem, 2018). Therefore, SBE will likely affect shoot growth under salt stress by activating ROS scavenging enzymes.

In future experiments, fractionation of SBE into less complex mixtures will be necessary to define the extent of synergism between the different bioactive molecules. Plant extract-based biostimulants are typically mixtures of bioactive compounds (García-García et al., 2020), which may explain why certain extracts are active despite the applied low dilutions. Given that the large biomass of sunflower stalks is currently underused, we anticipate that it is a suitable resource for biostimulant development and will contribute to valorization of the stems. Further studies will also focus on the consistency and reproducibility of bioactivity across separate harvested materials.

CONCLUSION

Taken together, we demonstrated that SBE can be refined from sunflower bark using water as an extraction solvent in a twin-screw extruder and that it contains bioactive molecules that act as protectants against salt stress by maintaining cellular redox homeostasis. The results highlight the potential of SBE as a source for biostimulant production that can be used for seed biopriming, soil, and foliar application. Future studies are underway to test the effectiveness of SBE biostimulant under field conditions on various crops. The characterization of the bioactive ingredients is a critical target to unravel the chemical structure and underlying mode of action.

DATA AVAILABILITY STATEMENT

The raw data supporting the conclusions of this article will be made available by the authors, without undue reservation.

AUTHOR CONTRIBUTIONS

JL, AR, and DG: conceptualization. JL: methodology and investigation and writing – original draft preparation. HKT: initial screening. SB and PE: resources. PE and JL: chemical characterization. CVP, PM, SM, and JL: chemical profiling. PE, SB, CVP, SM, TVG, and DG: writing – review and editing. DG: supervision. TVG, AR, LX, and DG: project administration. BVD, SB, PE, SM, and DG: funding acquisition. All authors contributed to the article and approved the submitted version.

FUNDING

This research was supported by Fonds Wetenschappelijk Onderzoek – Vlaanderen (FWO) under project Bio2Bio (no. S006017N), under project BioSUNmulant by European Union's Horizon 2020 Research and Innovation Program under grant agreement of sustainable and resilient agriculture for food and non-food systems (FACCE SURPLUS, no. 652615) and with Flanders Innovation and Entrepreneurship (VLAIO) (no. HBC.2019.2244). JL was supported by the China Scholarship Council (CSC) grant no. 201706350259.

ACKNOWLEDGMENTS

We thank Dr. Maaike Perneel (CropFit, Ghent University), Ms. Patricia Delaere, Mr. Christophe Petit, and Ms. Ellen van Gysegem (HortiCell Lab, Ghent University) for their technical and administrative support and Ms. Halimat Ogunsanya and Ms. Brechtje de Haas (HortiCell Lab, Ghent University) for the critical comments and suggestions.

SUPPLEMENTARY MATERIAL

The Supplementary Material for this article can be found online at: https://www.frontiersin.org/articles/10.3389/fpls.2022.837441/full#supplementary-material

REFERENCES

Apel, K., and Hirt, H. (2004). Reactive oxygen species: metabolism, oxidative stress, and signal transduction. *Annu. Rev. Plant Biol.* 55, 373–399. doi: 10.1146/ANNUREV.ARPLANT.55.031903.141701

Batista-Silva, W., Heinemann, B., Rugen, N., Nunes-Nesi, A., Araújo, W. L., Braun, H. P., et al. (2019). The role of amino acid metabolism during abiotic stress release. *Plant Cell Environ.* 42, 1630–1644. doi: 10.1111/PCE.13518

Blaženović, I., Kind, T., Torbašinović, H., Obrenović, S., Mehta, S. S., Tsugawa, H., et al. (2017). Comprehensive comparison of *in silico* MS/MS fragmentation tools of the CASMI contest: database boosting is needed to achieve 93% accuracy. *J. Cheminform.* 9:32. doi: 10.1186/s13321-017-0219-x

Bobrovskikh, A., Zubairova, U., Kolodkin, A., and Doroshkov, A. (2020). Subcellular compartmentalization of the plant antioxidant system: an integrated overview. *PeerJ.* 8:e9451. doi: 10.7717/PEERJ.9451

Brentan Silva, D., Aschenbrenner, A.-K., Lopes, N. P., and Spring, O. (2017). Direct Analyses of Secondary Metabolites by Mass Spectrometry Imaging (MSI) from Sunflower (Helianthus annuus L.) Trichomes. *Molecules* 22:774. doi: 10.3390/molecules22050774

Chemat, F., Vian, M. A., and Cravotto, G. (2012). Green Extraction of Natural Products: concept and Principles. *Int. J. Mol. Sci.* 13, 8615–8627. doi: 10.3390/IJMS13078615

Chiu, Y.-C., Chen, B.-J., Su, Y.-S., Huang, W.-D., and Chen, C.-C. (2021). A Leaf Disc Assay for Evaluating the Response of Tea (Camellia sinensis) to PEG-Induced Osmotic Stress and Protective Effects of Azoxystrobin against Drought. *Plants* 10:546. doi: 10.3390/plants10030546

Claeys, H., Landeghem, S., Van, Dubois, M., Maleux, K., Inzé, D., et al. (2014). What Is Stress? *Dose-response effects in commonly used in vitro stress assays*. *Plant Physiol.* 165, 519–527. doi: 10.1104/pp.113.234641

Colegate, S., and Molyneux, R. (2007). *Bioactive Natural Products: Detection, Isolation, and Structural Determination*. Florida: CRC Press.

Commo, F., and Bot, B. M. (2016). *R Package nplr n-Parameter Logistic Regressions. V. 0.1–7*. Seattle, Washington: Fred Hutchinson Cancer Research Center.

Dantas, M. S. M., Rolim, M. M., Duarte, A., de, S., Lima, L. E., (2017). Production and morphological components of sunflower on soil fertilized with cassava wastewater. *Rev. Ceres.* 64, 77–82. doi: 10.1590/0034-737X201764010011

Daudi, A., and O'Brien, J. A. (2012). Detection of Hydrogen Peroxide by DAB Staining in Arabidopsis Leaves. *Bio. Protoc.* 2:e263. doi: 10.21769/bioprotoc.263

De Diego, N., Fürst, T., Humplík, J. F., Ugena, L., Podlešáková, K., and Spíchal, L. (2017). An Automated Method for High-Throughput Screening of Arabidopsis Rosette Growth in Multi-Well Plates and Its Validation in Stress Conditions. *Front. Plant Sci.* 8:1702. doi: 10.3389/FPLS.2017.01702

De Diego, N., and Spíchal, L. (2020). "Use of plant metabolites to mitigate stress effects in crops," in *The Chemical Biology of Plant Biostimulants*, eds D. Geelen and L. Xu (Hoboken: Wiley Online Library), 261–300. doi: 10.1002/9781119357254.ch11

Deans, C. A., Sword, G. A., Lenhart, P. A., Burkness, E., Hutchison, W. D., and Behmer, S. T. (2018). Quantifying Plant Soluble Protein and Digestible Carbohydrate Content, Using Corn (Zea mays) As an Exemplar. *J. Vis. Exp.* 138:e58164. doi: 10.3791/58164

Djoumbou Feunang, Y., Eisner, R., Knox, C., Chepelev, L., Hastings, J., Owen, G., et al. (2016). ClassyFire: automated chemical classification with a comprehensive, computable taxonomy. *J. Cheminform.* 8:61 . doi: 10.1186/s13321-016-0174-y

Dou, J., Xu, W., Koivisto, J. J., Mobley, J. K., Padmakshan, D., Kögler, M., et al. (2018). Characteristics of Hot Water Extracts from the Bark of Cultivated Willow (Salix sp.). *ACS Sustain. Chem. Eng.* 6, 5566–5573. doi: 10.1021/ACSSUSCHEMENG.8B00498

Dróżdż, P., and Pyrzynska, K. (2017). Assessment of polyphenol content and antioxidant activity of oak bark extracts. *Eur. J. Wood Wood Prod.* 76, 793–795. doi: 10.1007/S00107-017-1280-X

Dubois, M., and Inzé, D. (2020). Plant growth under suboptimal water conditions: early responses and methods to study them. *J. Exp. Bot.* 71, 1706–1722. doi: 10.1093/jxb/eraa037

Dumanović, J., Nepovimova, E., Natić, M., Kuča, K., and Jaćević, V. (2021). The significance of reactive oxygen species and antioxidant defense system in plants: a concise overview. *Front. Plant Sci.* 11:2106. doi: 10.3389/fpls.2020.552969

Evon, P., Vandenbossche, V., Candy, L., Pontalier, P.-Y., and Rouilly, A. (2018). "Twin-screw extrusion: A key technology for the biorefinery,"," in *Biomass Extrusion and Reaction Technologies: Principles to Practices and Future Potential*, (ACS Publications), 25–44. doi: 10.1021/bk-2018-1304.ch002

FAO (2021). *Sustainable Development Goals*. Available online at: http://www.fao.org/sustainable-development-goals/indicators/en/ (accessed Jul 30, 2021)

Ferdinando, M., Di, Brunetti, C., Fini, A., Tattini, M., Di Ferdinando, M., et al. (2012). Flavonoids as Antioxidants in Plants Under Abiotic Stresses. In: Ahmad, P., Prasad, M. (eds) Abiotic Stress Responses in Plants. Springer, New York, NY. doi: 10.1007/978-1-4614-0634-1_9

Fimognari, L., Dölker, R., Kaselyte, G., Jensen, C. N. G., Akhtar, S. S., Großkinsky, D. K., et al. (2020). Simple semi-high throughput determination of activity signatures of key antioxidant enzymes for physiological phenotyping. *Plant Methods* 16, 1–19. doi: 10.1186/S13007-020-00583-8

Fulcher, N., and Sablowski, R. (2009). Hypersensitivity to DNA damage in plant stem cell niches. *Proc. Natl. Acad. Sci.* 106, 20984–20988. doi: 10.1073/PNAS.0909218106

García-García, A. L., García-Machado, F. J., Borges, A. A., Morales-Sierra, S., Boto, A., and Jiménez-Arias, D. (2020). Pure Organic Active Compounds Against Abiotic Stress: a Biostimulant Overview. *Front. Plant Sci.* 0:1839. doi: 10.3389/FPLS.2020.575829

Ghosh, A., Pareek, A., and Singla-Pareek, S. (2015). Leaf Disc Stress Tolerance Assay for Tobacco. *Bio-Protocol* 5, e1440. doi: 10.21769/bioprotoc.1440

Hamad, S. W. (2017). *Bioherbicidal Properties of Sunflower (Helianthus annuus L.) and its Activities in Weed Management*. Available online at: http://theses.ncl.ac.uk/jspui/handle/10443/3755 (accessed Sep 9, 2021)

Hodges, D. M., DeLong, J. M., Forney, C. F., and Prange, R. K. (1999). Improving the thiobarbituric acid-reactive-substances assay for estimating lipid peroxidation in plant tissues containing anthocyanin and other interfering compounds. 207, 604–611. *Planta* 245:1067. doi: 10.1007/s00425-017-2699-3

Huang, H., Ullah, F., Zhou, D.-X., Yi, M., and Zhao, Y. (2019). Mechanisms of ROS regulation of plant development and stress responses. *Front. Plant Sci.* 10:800. doi: 10.3389/fpls.2019.00800

Huang, S., Zheng, X., Luo, L., Ni, Y., Yao, L., and Ni, W. (2021). Biostimulants in bioconversion compost of organic waste: a novel booster in sustainable agriculture. *J. Clean. Prod.* 319:128704.

ISO (1977). *ISO 749:1977, Oilseed Residues — Determination of total Ash*. Geneva: ISO.

ISO (2000). *ISO 665:2000, Oilseeds—Determination of Moisture and Volatile Matter Content*. Geneva: ISO.

ISO (2009). *ISO 659:2009, Oilseeds—Determination OF Oil Content*. Geneva: ISO.

Jiang, B., Shi, Y., Zhang, X., Xin, X., Qi, L., Guo, H., et al. (2017). PIF3 is a negative regulator of the CBF pathway and freezing tolerance in Arabidopsis. *Proc. Natl. Acad. Sci.* 114, E6695–E6702. doi: 10.1073/pnas.1706226114

Junglee, S., Urban, L., Sallanon, H., and Lopez-Lauri, F. (2014). Optimized Assay for Hydrogen Peroxide Determination in Plant Tissue Using Potassium Iodide. *Am. J. Anal. Chem.* 05, 730–736. doi: 10.4236/ajac.2014.511081

Kamal, J. (2013). Quantification of alkaloids, phenols and flavonoids in sunflower (Helianthus annuus L.). *African J. Biotechnol.* 10, 3149–3151. doi: 10.4314/ajb.v10i16

Karamać, M., Kosińska, A., Estrella, I., Hernández, T., and Duenas, M. (2012). Antioxidant activity of phenolic compounds identified in sunflower seeds. *Eur. Food Res. Technol.* 235, 221–230. doi: 10.1007/s00217-012-1751-6

Kaur, H., Bhardwaj, R. D., and Grewal, S. K. (2017). Mitigation of salinity-induced oxidative damage in wheat (Triticum aestivum L.) seedlings by exogenous application of phenolic acids. *Acta Physiol. Plant.* 39:221. doi: 10.1007/s11738-017-2521-7

Kerchev, P., van der Meer, T., Sujeeth, N., Verlee, A., Stevens, C. V., Van Breusegem, F., et al. (2020). Molecular priming as an approach to induce tolerance against abiotic and oxidative stresses in crop plants. *Biotechnol. Adv.* 40:107503. doi: 10.1016/j.biotechadv.2019.107503

Kicinska, A., and Jarmuszkiewicz, W. (2020). Flavonoids and Mitochondria: activation of Cytoprotective Pathways? *Mol* 25:3060. doi: 10.3390/molecules25133060

Kiokias, S., Proestos, C., and Oreopoulou, V. (2020). Phenolic acids of plant origin—A review on their antioxidant activity *in vitro* (o/w emulsion systems) along with their in vivo health biochemical properties. *Foods* 9:534. doi: 10.3390/foods9040534

Kiran, K. R., Deepika, V. B., Swathy, P. S., Prasad, K., Kabekkodu, S. P., Murali, T. S., et al. (2020). ROS-dependent DNA damage and repair during germination of NaCl primed seeds. *J. Photochem. Photobiol. B Biol.* 213:112050. doi: 10.1016/J.JPHOTOBIOL.2020.112050

Krasensky, J., and Jonak, C. (2012). Drought, salt, and temperature stress-induced metabolic rearrangements and regulatory networks. *J. Exp. Bot.* 63, 1593–1608. doi: 10.1093/jxb/err460

Kumar, R., Kumar, R., and Prakash, O. (2019). "Chapter-5 The Impact of Chemical Fertilizers on Our Environment and Ecosystem," in *Research Trends in Environmental Sciences*, ed. P. Sharma (Delhi: Akinik Publications).

Kurepa, J., Shull, T. E., and Smalle, J. A. (2016). Quercetin feeding protects plants against oxidative stress. *F1000Research* 5:2430. doi: 10.12688/f1000research.9659.1

Lai, Z., Tsugawa, H., Wohlgemuth, G., Mehta, S., Mueller, M., Zheng, Y., et al. (2018). Identifying metabolites by integrating metabolome databases with mass spectrometry cheminformatics. *Nat. Methods* 15, 53–56. doi: 10.1038/nmeth.4512

Landini, G., Martinelli, G., and Piccinini, F. (2021). Colour deconvolution: stain unmixing in histological imaging. *Bioinformatics* 37, 1485–1487. doi: 10.1093/BIOINFORMATICS/BTAA847

Lee, J., da Silva, R. R., Jang, H. S., Kim, H. W., Kwon, Y. S., Kim, J.-H. H., et al. (2019). In silico annotation of discriminative markers of three Zanthoxylum species using molecular network derived annotation propagation. *Food Chem.* 295, 368–376. doi: 10.1016/j.foodchem.2019.05.099

Leschevin, M., Ismael, M., Quero, A., San Clemente, H., Roulard, R., Bassard, S., et al. (2021). Physiological and biochemical traits of two major Arabidopsis accessions, Col-0 and Ws, under salinity. *Front. Plant Sci* 12:639154. doi: 10.3389/fpls.2021.639154

Li, J., Van Gerrewey, T., and Geelen, D. (2022). A meta-analysis of biostimulant yield effectiveness in field trials. *Front. Plant Sci* 13:836702. doi: 10.3389/fpls.2022.836702

Lindsey, B. E., Rivero, L., Calhoun, C. S., Grotewold, E., and Brkljacic, J. (2017). Standardized method for high-throughput sterilization of Arabidopsis seeds. *J. Vis. Exp.* 2017:56587. doi: 10.3791/56587

Lutts, S., Benincasa, P., Wojtyla, L., Kubala S, S., Pace, R., Lechowska, K., et al. (2016). "Seed priming: new comprehensive approaches for an old empirical technique," in *New Challenges in Seed Biology*, eds S. Araujo and A. Balestrazzi (London: IntechOpen), 1–46. doi: 10.5772/64420

Macías, F. A., Varela, R. M., Torres, A., Galindo, J. L. G., and Molinillo, J. M. G. (2002). Allelochemicals from sunflowers: chemistry, bioactivity and applications. In: Mallik, A.U., ed Chemical Ecology of Plants: allelopathy in Aquatic and Terrestrial Ecosystems. Birkhäuser, Basel. doi: 10.1007/978-3-0348-8109-8_5

Maheswari, U. M., Murali Arthanari, P., and Uma Maheswari, C. M. (2019). Sunflower dried stalk extract: a natural Preemergence herbicide: effect on crops and weeds seed germination. *J. Pharmacogn. Phytochem.* 8, 135–137.

Malamy, J. E. (2005). Intrinsic and environmental response pathways that regulate root system architecture. *Plant Cell Environ.* 28, 67–77. doi: 10.1111/J.1365-3040.2005.01306.X

Markets and Markets (2021). *Biostimulants research global trends in 2021. MarketsandMarkets*. Available online at:https://www.biostimulant.com/blog-29-biostimulants-research-global-trends-in-2021/ (accessed on Mar 24, 2022)

Meijering, E., Jacob, M., Sarria, J. C. F., Steiner, P., Hirling, H., and Unser, M. (2004). Design and Validation of a Tool for Neurite Tracing and Analysis in Fluorescence Microscopy Images. *Cytom. Part A* 58, 167–176. doi: 10.1002/CYTO.A.20022

Mhamdi, A., and Van Breusegem, F. (2018). Reactive oxygen species in plant development. *Development* 145:dev164376. doi: 10.1242/dev.164376

Munns, R., and Tester, M. (2008). Mechanisms of salinity tolerance. *Annu. Rev. Plant Biol.* 59, 651–681. doi: 10.1146/annurev.arplant.59.032607.092911

Noctor, G., Mhamdi, A., and Foyer, C. H. (2016). Oxidative stress and antioxidative systems: recipes for successful data collection and interpretation. *Plant Cell Environ.* 39, 1140–1160. doi: 10.1111/PCE.12726

Parfitt, J., Barthel, M., and Macnaughton, S. (2010). Food waste within food supply chains: quantification and potential for change to 2050. *Philos. Trans. R. Soc. B Biol. Sci.* 365, 3065–3081. doi: 10.1098/RSTB.2010.0126

Pękal, A., and Pyrzynska, K. (2014). Evaluation of Aluminium Complexation Reaction for Flavonoid Content Assay. *Food Anal. Methods* 7, 1776–1782. doi: 10.1007/S12161-014-9814-X

Perveen, S. (2017). ""Phenolic Compounds from the Natural Sources and Their Cytotoxicity,"," in *Natural Sources, Importance and Applications*, eds M. Soto-Hernandez, M. Palma-Tenango, and M. D. R. Garcia-Mateos (London: IntechOpen), doi: 10.5772/66898

R Core Team (2021). *R: A Language and Environment for Statistical Computing*. Vienna, Austria: R Version 4. 1. 1, R Foundation for Statistical Computing.

Rasouli, H., Farzaei, M. H., Mansouri, K., Mohammadzadeh, S., and Khodarahmi, R. (2016). Plant Cell Cancer: may Natural Phenolic Compounds Prevent Onset and Development of Plant Cell Malignancy? A Literature Review. *Moecules* 21, 1104. doi: 10.3390/molecules21091104

Rawat, L. S., Maikhuri, R. K., Bahuguna, Y. M., Jha, N. K., and Phondani, P. C. (2017). Sunflower allelopathy for weed control in agriculture systems. *J. Crop Sci. Biotechnol.* 20, 45–60. doi: 10.1007/S12892-016-0093-0

Regulation [EC] (2005). *Regulation (EC) No 396/2005 of the European Parliament and of the Council of 23 February 2005 on maximum residue levels of pesticides in or on food and feed of plant and animal origin and amending Council Directive 91/414/EEC*. Available online at:https://eur-lex.europa.eu/legal-content/EN/ALL/?uri=celex%3A32005R0396 (accessed on Nov 10, 2021].

Regulation [EC] (2009). *Regulation (EC) No 1107/2009 of the European Parliament and of the Council of 21 October 2009 concerning the placing of plant protection products on the market and repealing Council Directives 79/117/EEC and 91/414/EEC*. Available online at:https://eur-lex.europa.eu/legal-content/EN/TXT/?uri=celex%3A32009R1107 (Accessed on Nov 10, 2021).

Regulation [EU] (2019). *Regulation (EU) 2019/1009 of the European Parliament and of the Council of 5 June 2019 laying down rules on the making available on the market of EU fertilising products and amending Regulations (EC) No 1069/2009 and (EC) No 1107/2009 and repealing Regula*. Available online at:https://eur-lex.europa.eu/legal-content/EN/TXT/PDF/?uri=CELEX:32019R1009&from=EN (accessed on Jul 30, 2021).

Rook, F., Hadingham, S. A., Li, Y., and Bevan, M. W. (2006). Sugar and ABA response pathways and the control of gene expression. *Plant Cell Environ.* 29, 426–434. doi: 10.1111/j.1365-3040.2005.01477.x

Rosa, M., Harder, M., Von, Cigliano, R. A., Schlögelhofer, P., and Scheid, O. M. (2013). The Arabidopsis SWR1 Chromatin-Remodeling Complex Is Important for DNA Repair. *Somatic Recombination, and Meiosis. Plant Cell* 25, 1990-2001. doi: 10.1105/TPC.112.104067

Rosa, M., and Scheid, O. (2014). DNA Damage Sensitivity Assays with Arabidopsis Seedlings. *Bio-Protocol* 4:e1093. doi: 10.21769/bioprotoc.1093

Rouphael, Y., and Colla, G. (2020). Biostimulants in agriculture. *Front. Plant Sci.* 11:40. doi: 10.3389/FPLS.2020.00040

Ruifrok, A. C., and Johnston, D. A. (2001). Quantification of histochemical staining by color deconvolution. *Anal. Quant. Cytol. Histol.* 23, 291–299.

Šamec, D., Karalija, E., Šola, I., Vujčić Bok, V., Salopek-Sondi, B., Bok, V. V., et al. (2021). The Role of polyphenols in abiotic stress response: the influence of molecular structure. *Plants* 10:118. doi: 10.3390/PLANTS10010118

Sánchez-Rangel, J. C., Benavides, J., Heredia, J. B., Cisneros-Zevallos, L., and Jacobo-Velázquez, D. A. (2013). The Folin–Ciocalteu assay revisited: improvement of its specificity for total phenolic content determination. *Anal. Methods* 5, 5990–5999. doi: 10.1039/C3AY41125G

Schindelin, J., Arganda-Carreras, I., Frise, E., Kaynig, V., Longair, M., Pietzsch, T., et al. (2012). Fiji: an open-source platform for biological-image analysis. *Nat. Methods* 9, 676–682. doi: 10.1038/nmeth.2019

Schymanski, E. L., Jeon, J., Gulde, R., Fenner, K., Ruff, M., Singer, H. P., et al. (2014). Identifying small molecules via high resolution mass spectrometry: communicating confidence. *Environ. Sci. Technol.* 48, 2097–2098. doi: 10.1021/es5002105

Van Soest, P. J., and Wine, R. H. (1967). Use of Detergents in the Analysis of Fibrous Feeds. IV. Determination of Plant Cell-Wall Constituents. *J. AOAC Int.* 50, 50–55. doi: 10.1093/JAOAC/50.1.50

Stagos, D. (2020). Antioxidant Activity of Polyphenolic Plant Extracts. *Antioxidants* 9:19. doi: 10.3390/ANTIOX9010019

Svolacchia, N., Salvi, E., and Sabatini, S. (2020). Arabidopsis primary root growth: let it grow, can't hold it back anymore! Curr. *Opin. Plant Biol.* 57, 133–141. doi: 10.1016/J.PBI.2020.08.005

Szparaga, A., Kocira, S., Findura, P., Kapusta, I., Zaguła, G., and Świeca, M. (2021). Uncovering the Multi-level Response of Glycine Max L. To the Application of Allelopathic Biostimulant From Levisticum Officinale Koch. *Sci. Rep.* 11:15360. doi: 10.1038/s41598-021-94774-5

Tanase, C., Coşarcă, S., and Muntean, D. L. (2019). A critical review of phenolic compounds extracted from the bark of woody vascular plants and their potential biological activity. *Molecules* 24:1182. doi: 10.3390/MOLECULES24061182

Tennekes, M., and Ellis, P. (2021). *treemap: Treemap visualization. R Packag. version, 2–4*. Available online at:https://cran.r-project.org/package=treemap. (accessed March 24, 2022).

Trinh, H. K., Verstraeten, I., and Geelen, D. (2018). In Vitro Assay for Induction of Adventitious Rooting on Intact Arabidopsis Hypocotyls,". *Methods Mol. Biol.* 1761, 95–102. doi: 10.1007/978-1-4939-7747-5_7

Tsugawa, H., Cajka, T., Kind, T., Ma, Y., Higgins, B., Ikeda, K., et al. (2015). MS-DIAL: data-independent MS/MS deconvolution for comprehensive metabolome analysis. *Nat. Methods* 12, 523–526. doi: 10.1038/nmeth.3393

Tsugawa, H., Kind, T., Nakabayashi, R., Yukihira, D., Tanaka, W., Cajka, T., et al. (2016). Hydrogen Rearrangement Rules: computational MS/MS Fragmentation and Structure Elucidation Using MS-FINDER Software. *Anal. Chem.* 88, 7946–7958. doi: 10.1021/acs.analchem.6b00770

Tsugawa, H., Nakabayashi, R., Mori, T., Yamada, Y., Takahashi, M., Rai, A., et al. (2019). A cheminformatics approach to characterize metabolomes in stable-isotope-labeled organisms. *Nat. Methods* 16, 295–298. doi: 10.1038/s41592-019-0358-2

United Nations Industrial Development (2007). *Industrial Biotechnology and Biomass Utilisation.Prospects and Challenges for the Developing World*. Vienna: United Nations Industrail Development

Van Soest, P. J., and Wine, R. H. (1968). Determination of Lignin and Cellulose in Acid-Detergent Fiber with Permanganate. *J. AOAC Int.* 51, 780–785. doi: 10.1093/JAOAC/51.4.780

Van Tang, N. (2017). *Recovering Bioactive Compounds from Agricultural Wastes*. Hoboken: John Wiley & Sons, Ltd, doi: 10.1002/9781119168850

Vandenbossche, V., Candy, L., Evon, P., Rouilly, A., and Pontalier, P.-Y. (2019). "0 - Extrusion," in *1*, eds F. Chemat and E. Vorobiev (Cambridge: Academic Press), 289–314. doi: 10.1016/B978-0-12-815353-6.00010-0

Vanhoudt, N. (2014). *Enzyme Analysis by Spectrophotometry - Plate Reader method*. Available online at: https://radioecology-exchange.org/sites/default/files/Enzyme%20Analysis%20by%20Spectrophotometry%20-%20Plate%20Reader%20method.pdf (accessed March 24, 2022).

Vaniya, A., Samra, S. N., Palazoglu, M., Tsugawa, H., and Fiehn, O. (2017). Using MS-FINDER for identifying 19 natural products in the CASMI 2016 contest. *Phytochem. Lett.* 21, 306–312. doi: 10.1016/j.phytol.2016.12.008

Venturelli, S., Petersen, S., Langenecker, T., Weigel, D., Lauer, U. M., and Becker, C. (2016). Allelochemicals of the phenoxazinone class act at physiologically relevant concentrations. *Plant Signal. Behav.* 11:e1176818. doi: 10.1080/15592324.2016.1176818

Verdier, T., Balthazard, L., Montibus, M., Magniont, C., Evon, P., and Bertron, A. (2020). Using glycerol esters to prevent microbial growth on sunflower-based insulation panels. *Proc. ICE - Constr. Mater.* 174, 140–149. doi: 10.1680/JCOMA.20.00002

Vertified Market Research (2021). *Global Biostimulants Market Size By Active Ingredient(Humic Substances, Microbial Amendments, Seaweed Extracts), By Application Method(Seed Treatment, Soil Treatment, Foliar Treatment), By Crop Type(Turfs and Ornamentals, Fruits and Vegetables, Row Crops)*. Available online at:https://www.verifiedmarketresearch.com/product/biostimulants-market/ (accessed on Jul 30, 2021)

Xiao, F., Xu, T., Lu, B., and Liu, R. (2020). Guidelines for antioxidant assays for food components. *Food Front.* 1, 60–69. doi: 10.1002/fft2.10

Xu, L., and Geelen, D. (2018). Developing biostimulants from agro-food and industrial by-products. *Front. Plant Sci.* 9:1567. doi: 10.3389/fpls.2018.01567

Xu, M., Qi, M., Goff, H. D., and Cui, S. W. (2020). Polysaccharides from sunflower stalk pith: chemical, structural and functional characterization. *Food Hydrocoll.* 100:105082. doi: 10.1016/J.FOODHYD.2019.04.053

Ye, F., Liang, Q., Li, H., and Zhao, G. (2015). Solvent effects on phenolic content, composition, and antioxidant activity of extracts from florets of sunflower (Helianthus annuus L.). *Ind. Crops Prod.* 76, 574–581. doi: 10.1016/J.INDCROP.2015.07.063

Zhang, X., Yang, H., and Cui, Z. (2017). Alleviating Effect and Mechanism of Flavonols in Arabidopsis Resistance under Pb-HBCD Stress. *ACS Sustain. Chem. Eng.* 5, 11034–11041. doi: 10.1021/acssuschemeng.7b02971

Zulfiqar, F., Casadesús, A., Brockman, H., and Munné-Bosch, S. (2020). An overview of plant-based natural biostimulants for sustainable horticulture with a particular focus on moringa leaf extracts. *Plant Sci.* 295:110194. doi: 10.1016/j.plantsci.2019.110194

Conflict of Interest: The authors declare that the research was conducted in the absence of any commercial or financial relationships that could be construed as a potential conflict of interest.

Publisher's Note: All claims expressed in this article are solely those of the authors and do not necessarily represent those of their affiliated organizations, or those of the publisher, the editors and the reviewers. Any product that may be evaluated in this article, or claim that may be made by its manufacturer, is not guaranteed or endorsed by the publisher.

frontiers | Frontiers in Plant Science

TYPE Original Research
PUBLISHED 28 July 2022
DOI 10.3389/fpls.2022.894985

OPEN ACCESS

EDITED BY
Maurizio Ruzzi,
University of Tuscia, Italy

REVIEWED BY
Mahmoud Yaish,
Sultan Qaboos University, Oman
Asma Imran,
National Institute for Biotechnology and Genetic Engineering, Pakistan

*CORRESPONDENCE
Marisa Díaz
mdiaz@rizobacter.com.ar
Claudio Valverde
cvalver@unq.edu.ar

†PRESENT ADDRESSES
Teresa Bach,
Independent Professional, Pergamino, Argentina
Fabián Noguera,
Independent Professional, Pergamino, Argentina

SPECIALTY SECTION
This article was submitted to Plant Symbiotic Interactions, a section of the journal Frontiers in Plant Science

RECEIVED 12 March 2022
ACCEPTED 29 June 2022
PUBLISHED 28 July 2022

CITATION
Díaz M, Bach T, González Anta G, Agaras B, Wibberg D, Noguera F, Canciani W and Valverde C (2022) Agronomic efficiency and genome mining analysis of the wheat-biostimulant rhizospheric bacterium *Pseudomonas pergaminensis* sp. nov. strain 1008^T. *Front. Plant Sci.* 13:894985. doi: 10.3389/fpls.2022.894985

Agronomic efficiency and genome mining analysis of the wheat-biostimulant rhizospheric bacterium *Pseudomonas pergaminensis* sp. nov. strain 1008^T

Marisa Díaz[1]*, Teresa Bach[1†], Gustavo González Anta[2,3,4], Betina Agaras[5], Daniel Wibberg[6], Fabián Noguera[1†], Wilter Canciani[1] and Claudio Valverde[5]*

[1]Rizobacter Argentina S.A., Buenos Aires, Argentina, [2]Escuela de Ciencias Agrarias, Exactas y Naturales, Universidad Nacional del Noroeste de la Provincia de Buenos Aires (UNNOBA), Buenos Aires, Argentina, [3]Departamento de Ciencias Naturales y Exactas, Universidad Nacional de San Antonio de Areco (UNSAdA), Buenos Aires, Argentina, [4]Indrasa Biotecnología S.A., Córdoba, Argentina, [5]Laboratorio de Fisiología y Genética de Bacterias Beneficiosas para Plantas, Centro de Bioquímica y Microbiología del Suelo, Universidad Nacional de Quilmes-CONICET, Buenos Aires, Argentina, [6]Center for Biotechnology (CeBiTec), Bielefeld University, Bielefeld, Germany

Pseudomonas sp. strain 1008 was isolated from the rhizosphere of field grown wheat plants at the tillering stage in an agricultural plot near Pergamino city, Argentina. Based on its *in vitro* phosphate solubilizing capacity and the production of IAA, strain 1008 was formulated as an inoculant for bacterization of wheat seeds and subjected to multiple field assays within the period 2010–2017. *Pseudomonas* sp. strain 1008 showed a robust positive impact on the grain yield (+8% on average) across a number of campaigns, soil properties, seed genotypes, and with no significant influence of the simultaneous seed treatment with a fungicide, strongly supporting the use of this biostimulant bacterium as an agricultural input for promoting the yield of wheat. Full genome sequencing revealed that strain 1008 has the capacity to access a number of sources of inorganic and organic phosphorus, to compete for iron scavenging, to produce auxin, 2,3-butanediol and acetoin, and to metabolize GABA. Additionally, the genome of strain 1008 harbors several loci related to rhizosphere competitiveness, but it is devoid of biosynthetic gene clusters for production of typical secondary metabolites of biocontrol representatives of the *Pseudomonas* genus. Finally, the phylogenomic, phenotypic, and chemotaxonomic comparative analysis of strain 1008 with related taxa strongly suggests that this wheat rhizospheric biostimulant isolate is a representative of a novel species within the genus *Pseudomonas*, for which the name *Pseudomonas pergaminensis* sp. nov. (type strain 1008^T = DSM 113453^T = ATCC TSD-287^T) is proposed.

KEYWORDS

PGPR, *Pseudomonas pergaminensis* sp. nov., wheat, biostimulant, agronomic efficiency, genome mining, phylogenomics

Introduction

The rhizosphere of terrestrial plants harbors complex assemblages of bacteria that are fundamental for the nutrition, health, and tolerance to biotic and abiotic stresses of the plant host (Mendes et al., 2013), being this interkingdom association a consequence of a long co-evolutionary history that shaped the current plant holobionts (Rosenberg and Zilber-Rosenberg, 2016; Lyu et al., 2021). Those plant-beneficial bacteria are collectively referred to as plant growth-promoting rhizobacteria (PGPR), a concept introduced in the late 70's (Kloepper et al., 1980). Although the taxonomic composition of the rhizosphere microbiome is certainly influenced by the plant genotype, soil features, agronomical practices, and environmental factors (Philippot et al., 2013), there are ubiquitous bacterial groups that are hallmark components of the rhizosphere niche, such as members of the *Streptomyces, Flavobacterium, Bacillus, Burkholderia,* and *Pseudomonas* genera (Mendes et al., 2011; Rey and Dumas, 2017; Imade and Babalola, 2021; Kavamura et al., 2021).

In particular, *Pseudomonas* spp. strains display a strong preference for the rhizosphere habitat in comparison to bulk soil, a feature that has been revealed by both culture-dependent and culture-independent approaches (Molina et al., 2000; Agaras et al., 2012; Tao et al., 2020; Chiniquy et al., 2021). The relative ease to isolate and culture *Pseudomonas* strains in the lab, together with the identification and characterization of a number of genetic and biochemical traits that may significantly contribute to the growth and health of the host plant, has fostered the exploitation of a number of *Pseudomonas* isolates for the development of agricultural inputs to increase the yield of different crops. The latter represents a promising conceptual solution to the worldwide demand of eco-friendly alternatives to the questioned utilization of chemical inputs in agriculture (Backer et al., 2018; Höfte, 2021; Müller and Behrendt, 2021).

A group of isolates of the genus *Pseudomonas* that have become plant biocontrol models, like *Pseudomonas protegens* CHA0, *Pseudomonas synxantha* 2–79. *Pseudomonas chlororaphis* PA23, or *Pseudomonas simiae* WCS417, have the ability to protect the roots of colonized plants from diverse phytopathogens, either through the production of antimicrobial compounds and/or by inducing systemic resistance in the plant (Ramette et al., 2011; Duke et al., 2017; Zhang et al., 2020; Höfte, 2021; Pieterse et al., 2021). On the other hand, rhizospheric isolates like *P. fluorescens* SS101 or *P. fluorescens* SBW25, do not show biocontrol capacity at all, but display plant growth-promoting traits like strong root competitiveness, stimulation of root growth and/or modulation of hormone homeostasis (Park et al., 2015; Shinde et al., 2019), and fall within the definition of plant biostimulants (Du Jardin, 2015). Usually, the *in vitro* characterization of such indirect (biocontrol) or direct (biostimulant) traits has been further mined at the genetic and/or genomic level, to unravel the underlying molecular determinants (Paterson et al., 2017; Agaras et al., 2018; Biessy et al., 2019; Pieterse et al., 2021), which may ultimately lead to biotechnological improvements of the identified plant-beneficial traits (Haskett et al., 2021).

Nevertheless, only a few thoroughly characterized *Pseudomonas* isolates with plant-beneficial traits have been registered worldwide as active ingredients for the production of commercial agricultural inputs (Basu et al., 2021; Höfte, 2021), a fact that most likely reflects the hurdles existing in the transition from the lab to the field (Backer et al., 2018). Here, we report the isolation of the *Pseudomonas* sp. isolate 1008 from the rhizosphere of field-grown wheat, which proved to be a highly efficient biostimulant of wheat crops in field assays under agronomical conditions. Further, we have determined its full genome sequence, explored its plant-beneficial genetic traits, and carried out phylogenomic, phenotypic and chemotaxonomic comparative analyses with related taxa, which strongly support that strain 1008 is a plant-biostimulant representative of a novel *Pseudomonas* species.

Materials and methods

Strain isolation and characterization

Root systems of wheat plants (stage Z.20; tillering) with their surrounding soil were sampled in a productive plot in the vicinity of Pergamino city, Province of Buenos Aires, Argentina (33° 56′ 41″ S, 60° 34′ 04″ W) (**Figure 1a**). Care was taken to avoid damaging the root systems. The plants were placed in clean plastic bags, leaving them open to avoid anoxic conditions, and were transported to the laboratory for processing without delay (**Figure 1b**). The aerial parts were cut, and the root systems were gently brushed to remove loosely adhered soil (**Figure 1c**). Each root system with its tightly associated rhizospheric soil was placed in an Erlenmeyer flask containing sterile demineralized water (pH 6.8–7) and agitated for 30 min at 200 rpm. Thereafter, aliquots of the suspensions were serially diluted with sterilized water, plated on *Pseudomonas* agar F (Merck Millipore) and incubated at 28°C for 48 h. The colonies that showed fluorescence upon exposure of plates to UV light (**Figure 1d**) were re-streaked for ensuring purity and preserved for subsequent characterization and preliminary identification. Colonies of interest were first screened on the basis of the conventional physiological tests according to Bergey's Manual of Determinative Bacteriology (Palleroni, 2015) to select candidate isolates of the species *Pseudomonas fluorescens* or closely related species (i.e., Gram-negative rods that grow in cetrimide agar: positive; oxidase test: positive; glucose fermentation: negative; motility: positive; fluorescent pigments in *Pseudomonas* F medium: positive; fluorescent pigments in *Pseudomonas* P medium: negative; growth at 41°C: negative; gelatin hydrolysis: positive). Phosphate solubilization, a feature

sought for the selection of candidates for the formulation of biofertilizer inoculants, was applied as the second screening criterion in agarized Pikovskaya's medium (Pikovskaya, 1948). The phosphate solubilizing isolates preliminary identified as *P. fluorescens* were further tested with the bioMérieux API 20 NE Gallery System. The isolate 1008, which is the subject of this study and that was originally designated as a *P. fluorescens* representative on the basis of the aforementioned biochemical and physiological tests, was selected for further characterization and development of a commercial formulation for agronomical purposes.

Phenotypic assays

Strain 1008 was routinely grown on *Pseudomonas* agar F (Merck Millipore) or nutrient agar (NA; 4% w/v blood agar base, 0.5% w/v yeast extract; Biokar). Liquid cultures were grown in tryptone soybean broth (TSB; Laboratorios Britania) or nutrient yeast broth (NYB; 2.5% w/v nutrient broth, 0.5% w/v yeast extract; Biokar), with shaking (200 rpm). In all cases, incubation temperature was 28°C. The strain was stored at −80°C as a suspension of an overnight NYB culture containing 20% w/v of glycerol. Solubilization of mineral phosphate was qualitatively assessed in agarized medium containing inorganic phosphate (Pikovskaya, 1948). The presence of a clear halo around the bacterial colonies was determined after 5 days of growth. Phosphate solubilization was quantified in liquid Pikovskaya medium with 5 g/L of $Ca_3(PO_4)_2$ (Pikovskaya, 1948) modified by buffering with 100 mM Tris and adjusting the pH to 8.0 with HCl. Samples from triplicate cultures were withdrawn to assess soluble phosphate concentration. In total, 1 mL of the cell suspension was centrifuged at 12,000 × *g* for 20 min at 4°C, and the P content in the supernatant was determined by the molybdenum blue method (Murphy and Riley, 1962). Zinc solubilization was qualitatively assessed in agarized Pikovskaya's base medium containing 1% w/v ZnO (Tagele et al., 2019). The presence of a clear halo around the bacterial colonies was determined after 48 h of growth. Extracellular protease and phospholipase C (lecithinase) activity were qualitatively assessed in skimmed milk agar or in egg yolk agar, respectively, as reported previously (Sacherer et al., 1994). Intracellular and extracellular phosphatase activities were determined enzymatically by following the hydrolysis of *p*-nitrophenyl phosphate in reactions buffered at pH 5.5 or pH 9.0 (for acid and alkaline phosphatase, respectively), as reported (Tabatabai and Bremner, 1969). Cellular siderophore production was qualitatively studied in CAS agar plates (Schwyn and Neilands, 1987). Hydrogen cyanide production was detected using the picrate filter paper method (Egan et al., 1998). Indoleacetic acid (IAA) production was analyzed in the supernatant of cultures grown for 24 h in tryptophan-amended medium (20 mg/100 ml) by colorimetry with the Salkowski reagent, as described elsewhere (Bric et al., 1991). The capacity of strain 1008 to inhibit the growth of phytopathogenic fungi was assessed with the dual culture assay on PDA plates (Muller et al., 2018). Analysis of cellular fatty acids and metabolic profiling in Biolog GenIII plates were carried out by DSMZ Services, Leibniz-Institut DSMZ - Deustsche Sammlung von Mikroorganismen und Zellkulturen GmbH, Brunswick, Germany.

Transmission electron microscopy

Cells of strain 1008 from early stationary-phase cultures in NYB were negatively stained with a solution of 2% w/v uranyl acetate for 5 min and directly observed at a magnification of 15,000–40,000× with a JEOL/JEM 1200 EX II transmission electron microscope at the Microscopy Service of the School of Veterinary Sciences (National University of La Plata, La Plata, Argentina). The dimensions of cells were analyzed in digitalized images with ImageJ[1].

Field assays

Field assays were carried out in three different locations in the Argentine Pampas, close to the cities of Pergamino, Junín, and Ferré (**Figure 1a**). The properties of the soil in each location are: typic Argiudoll – silt loam, for Pergamino; typic Hapludoll – loam/silt loam, for Junín and Ferré (Agaras et al., 2020). In the period 2010–2016, the annual average temperature ranged between 15.7 and 19°C, with an average monthly temperature range of 10 to 23 °C; the annual average rainfall ranged between 656 and 1,681 mm, with an average monthly rainfall range of 26 to 182 mm (**Supplementary Table 1**). The chemical analyses of soil samples (contents of organic carbon, nitrate, organic nitrogen, total nitrogen, and extractable phosphorus, and pH) were determined by Laboratorio SueloFértil (Pergamino, Buenos Aires[2]) using standardized agronomical protocols.

For evaluating the impact of seed inoculation with a commercial formulation based on strain 1008, seeds of different cultivars of wheat (*Triticum aestivum*) (**Supplementary Table 2**) were treated with the formulated inoculant Rizofos® following the instructions of the manufacturer (Rizobacter Argentina S.A.). Briefly, seeds were treated at a ratio of 0.8 ml of inoculant plus 0.2 ml of Premax R® bacterial protectant per 100 g of seeds in a rotary mixer at room temperature during 2 min. Seeds were immediately sown or stored at temperatures below 25°C in the dark for a period of up to 15 days before sowing. Non-treated seeds served as control. When indicated (**Supplementary Table 2**),

1 https://imagej.nih.gov/ij/

2 http://www.suelo-fertil.com.ar

10.3389/fpls.2022.894985

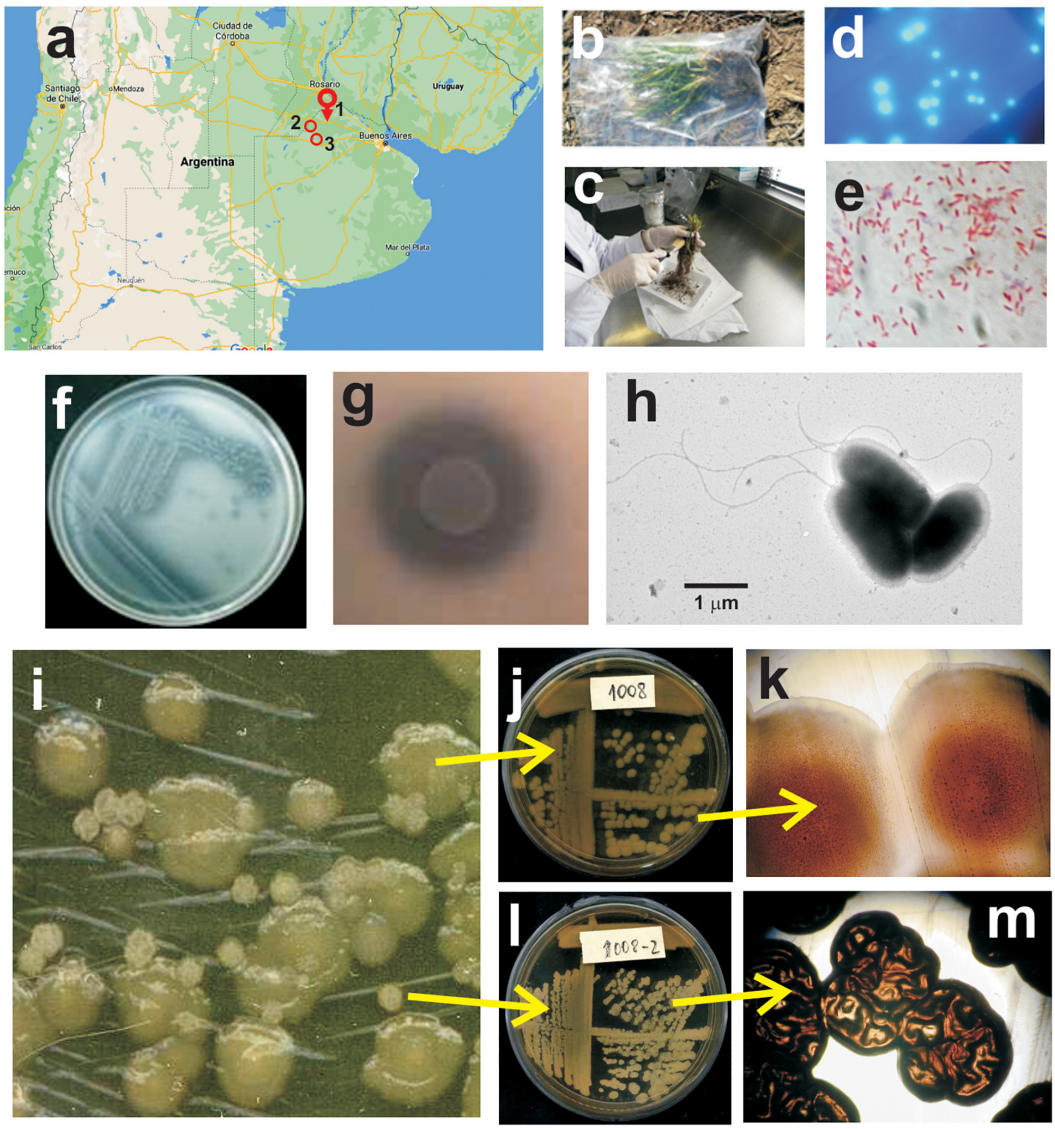

FIGURE 1
Isolation and microbiological characterization of *Pseudomonas* sp. strain 1008. **(a)** Geographic location of the wheat field plot sampled for isolation of *Pseudomonas* strain 1008 (1, Pergamino), and of the experimental field assays for evaluation of the performance of the inoculant based on strain 1008 (1, Pergamino; 2, Ferré; 3, Junín). **(b)** Wheat plants sampled at tillering stage. **(c)** Loosely adhered soil was gently brushed away from the root system. **(d)** Fluorescent colonies developed on *Pseudomonas* agar F upon plating of dilutions of rhizospheric suspensions. **(e)** Gram staining of cells from a pure culture of strain 1008. **(f)** Streaks of strain 1008 on Pikovskaya agar with calcium triphosphate as P source. **(g)** Close up of a macrocolony of strain 1008 and the surrounding calcium triphosphate solubilization halo on Pikovskaya agar. **(h)** Transmission electron micrograph showing cells of strain 1008 grown for 24 h in nutrient yeast broth at 28°C and 200 rpm. Note the flagella with a typical polar location. **(i)** Colony phase variants of strain 1008 on nutrient agar plates. The larger colonies correspond to phase variant 1 **(j,k)** whereas the smaller colonies correspond to phase variant 2 **(l,m)**. The colony morphotype of each variant is clearly distinct under magnifying lens **(k,m)**.

seeds had been previously treated with the commercial fungicide Compinche® (Rizobacter Argentina S.A.), containing difenoconazole and metalaxyl-M as active principles. Genotypes, seed treatments and fertilizer applications were those recommended by regional agronomical advisers (**Supplementary Table 2**).

Each treatment had three replicates per location in a completely randomized block design, with a plot size of 9 m^2 (6 m × 1.5 m, with 7 furrows). Sowing dates, plant densities and fungicide seed treatments were adjusted to the selected genotypes and the regional recommendations [**Supplementary Table 2**; (Agaras et al., 2020)]. At harvest, the number of plants and of spikes per m^2, and grain yield (kg/ha) were recorded. When indicated (**Supplementary Table 2**), the number of tillers per m^2, the tiller and spike dry weight, and the NDVI (Normalized Difference Vegetation Index, shown as the average

value per m^2, during tillering), were determined during early crop stages (Benedetti and Rossini, 1993).

Statistical analysis of field assays

The data set comprises twenty-five field assays under no-till management across seven campaigns, heterogeneously distributed in three geographical locations. In addition to the main effect of seed bacterization with the Rizofos® formulation containing live cells of strain 1008, the experimental plots included: the effect of seed pre-treatment with (or without) the fungicide Compinche®; five wheat genotypes (Baguette 601, Klein Tigre, Klein Rayo, Klein Yarará, and Buck SY 300); and two different forecrops (soybean or cereal/soybean). Thus, we considered that there were five additional effects that could be influencing the impact of wheat seed bacterization. First, we applied ANOVA to evaluate if those effects interacted with seed bacterization. Upon confirming that the interactions between bacterization and every additional effect were not significant, we applied Generalized Linear Mixed Models (GLMM; Di Rienzo et al., 2011) to evaluate the global effect of seed bacterization with strain 1008 on crop yield using Infostat v. 2020 software (Di Rienzo et al., 2020). GLMM were fitted to analyze the data (with n = 150 for grain yield, plant number and spike number per m^2; n = 114 for tiller number; n = 34 for tiller dry weight; n = 102 for tiller fresh weight; n = 48 for spike fresh weight), considering locations, seasons, crop genotypes, forecrops and seed pre-treatment with fungicide as random effects, and amending the variance structure to achieve homoscedasticity when corresponded (Casanoves et al., 2007; Harrison et al., 2018). The fitted models were evaluated with Akaike's (AIC) and Schwarz's (BIC) Information Criteria, looking for the lowest values for selecting the best model. Likelihood ratio between models was applied when AIC ad BIC criteria were not sufficient to select the best model (Di Rienzo et al., 2011). Finally, ANOVA tests were performed on each of the 25 field trials to specifically evaluate the impact of seed bacterization (Di Rienzo et al., 2020). If appropriate, Fisher's LSD multiple comparison method was applied to evaluate significant differences among average values. In all cases, statistics were done at $p < 0.05$. Multivariate analyses were conducted using Principal Component Analysis (PCA) of grain yield, plant number and tiller number per m^2 (n = 150, Infostat v. 2020).

DNA isolation and genome sequencing

Genomic DNA of strain 1008 was extracted with the Zymo ZR Soil Microbe DNA MiniPrep kit (Zymo Research), according to the manufacturer's guidelines. gDNA concentration and quality were assessed by UV spectrophotometry with Nanodrop ND-1000. A sample of 15 µg of gDNA in 10 mM Tris.HCl (pH 8.0) was submitted to Macrogen Inc. (Korea) for whole genome *de novo* sequencing with the PacBio RS System. Upon quality control analysis (fluorescence-based quantification, agarose gel and microfluidic electrophoresis), the gDNA was processed according to a guide for preparing SMRTbell template for sequencing on the PacBio RS System. The templates were sequenced using SMRT® sequencing. Sequencing resulted in a total of 134.530 subreads, with an average length of 9,422 bp, totalizing around 1,27 Gb, which represents 192× coverage of the genome.

Genome assembly and annotation

The raw data generated from PacBio RS II sequencing was utilized for whole-genome sequence assembly. The assembly and annotation approach was performed as described recently with smaller modifications (Wibberg et al., 2020, 2021). In brief, the assembly was performed using canu v1.6 (Koren et al., 2017) resulting in a single, circular contig. This contig was then polished based on PacBio reads using quiver 2.1 (Chin et al., 2013) and adjusted to *dnaA* as the first gene. The finished genome sequence was annotated with Prokka (Seemann, 2014) and imported into the annotation platform GenDB (Meyer et al., 2003). The annotated circular and gapless chromosome of 6,609,162 bp and a GC content of 60.7% was deposited into the NCBI database under the accession number CP078013.

Phylogenomic analysis

The phylogenetic position of strain 1008 within the genus *Pseudomonas* was inferred by a set of complementary studies based on comparative sequence analysis of single or multiple genes, and of genome properties: comparative analysis of whole genome average nucleotide identity (ANI) and tetranucleotide usage pattern (Tetra) in the JSpeciesWS server (Richter et al., 2015); average amino acid identity (AAI) at the EDGAR server (Dieckmann et al., 2021); 16S rRNA based gene tree, genome-based phylogenetic tree, and digital DDH at the Type (Strain) Genome Server (TYGS) (Meier-Kolthoff and Göker, 2019).

Genome mining

The presence of sequences related to integrated plasmids and prophages was studied with NCBI VecScreen[3], PlasmidFinder 2.1 and PHAST tools (Zhou et al., 2011; Carattoli et al., 2014). MGEfinder and ICEfinder were used to identify mobile genetic elements (Liu et al., 2018; Durrant et al., 2020). oriTfinder was used to identify DNA transfer-related

3 https://www.ncbi.nlm.nih.gov/tools/vecscreen/

modules (Li et al., 2018). Genomic islands were searched with IslandViewer 4 (Bertelli et al., 2017). Acquired genes and/or chromosomal mutations mediating antimicrobial resistance were inspected using the Resistance Gene Identifier tool[4] at the Comprehensive Antibiotic Resistance Database (Alcock et al., 2020). The presence of CRISPR/Cas elements was studied with CRISPRCasFinder and CRISPRMiner2 (Couvin et al., 2018; Zhang et al., 2018). antiSMASH v6.0 was used for predicting secondary metabolite biosynthetic gene clusters (Blin et al., 2021). Bacteriocin gene clusters were mined with BaGel4 (Van Heel et al., 2018). A list of genes related to direct and indirect plant growth promotion mechanisms, as well as for rhizosphere competence and interactions with plant cells and other microbial species, was compiled from recent works (Berendsen et al., 2015; Biessy et al., 2019; Anderson and Kim, 2020; De Vrieze et al., 2020; Keswani et al., 2020; Singh et al., 2021) and surveyed in the genome of strain 1008 by using BlastN and BlastP webservices at the NCBI webpage[5]. Type IV secretion system components were identified with OriTfinder (Li et al., 2018). Type VI secretion system components were identified with SecRet6 (Li et al., 2015).

Availability of biological material

The type strain, originally designated as 1008, was deposited in the Leibniz Institute DSMZ - German Collection of Microorganisms and Cell Cultures GmbH (DSMZ, Braunschweig, Germany) and in the American Type Culture Collection (ATCC, Manassas, VA, United States), under the accession numbers DSM 113453 and ATCC TSD-287, respectively.

Results

Isolation and characterization of a phosphate-solubilizing *Pseudomonas* isolate with plant growth-promoting features from field-grown wheat roots

Field-grown wheat plants at the tillering stage were sampled in an agricultural plot nearby the city of Pergamino (Buenos Aires province, Argentina; **Figure 1a**) to generate a collection of rhizobacterial isolates with potential to be formulated as an agricultural input. Rhizospheric suspensions were plated on *Pseudomonas* agar F, and fluorescent colonies with different morphological features were subjected to an initial set of phenotypical tests to retain those *P. fluorescens* candidates on the basis of Bergey's determinative manual. Upon further screening for phosphate-solubilizing potential, one isolate designated as 1008 was retained for further characterization of plant-growth promoting features (**Figure 1** and **Table 1**). The results of the bioMérieux API 20 NE Gallery System for strain 1008 were consistent with an isolate representative of the *P. fluorescens* lineage (**Supplementary Table 3**), which was also supported by the sequence of its 16S rDNA gene (**Supplementary Figure 1**).

Strain 1008 was selected by its phosphate-solubilizing activity in a first screening on agar plates (**Figures 1f,g** and **Table 1**). In liquid Pikovskaya medium after 24 h of growth at 28°C and 200 rpm, strain 1008 was able to solubilize an average of 22% of the insoluble calcium triphosphate (final soluble P content of 45 mg per 100 ml). It was also able to mineralize P from two types of phosphate rocks (of Chinese and Chilean origin) achieving a final soluble content of 46 mg P per 100 ml. In addition to insoluble sources of P, strain 1008 solubilized zinc in a modified Pikovskaya medium containing ZnO (**Table 1** and **Supplementary Figure 2A**).

The production of indole acetic acid (IAA)-like compounds was first detected qualitatively as a positive reaction to the Salkowski reagent in cells grown in agarized medium supplemented with 5 mM tryptophan (**Table 1**). The production of IAA was confirmed by HPLC-MS/MS analysis of liquid cultures. Strain 1008 produced IAA in a tryptophan-dependent manner reaching up to 46,7 mg/100 ml after 48 h of growth (**Supplementary Figure 2E**). The production of extracellular proteolytic and lecithinase activities were revealed in qualitative plate assays (**Table 1** and **Supplementary Figures 2B,C**). Spectrophotometric enzymatic assays revealed the production of both acid and alkaline phosphatases, with a major fraction of the activity detected in acid conditions (586 μg *p*-nitrophenol/mg bacteria.h) of which 83% was located intracellularly. By contrast, 82% of the total alkaline phosphatase activity (10 μg *p*-nitrophenol/mg bacteria.h) was detected in the culture supernatant.

TABLE 1 *In vitro* plant growth-promoting traits of *Pseudomonas* sp. strain 1008.

PGP trait	Detected (+)/Not detected (−)
Phosphate solubilization	+
Zinc solubilization	+
Alkaline phosphatase activity	+
Acid phosphatase activity	+
Tryptophan-induced IAA production	+
Lecithinase activity	+
Exoprotease activity	+
Iron sequestration in the presence of CAS	+
ACC deaminase activity	−
Hydrogen cyanide production	−
Antagonism of phytopathogenic fungi	−

4 https://card.mcmaster.ca/analyze/rgi

5 https://blast.ncbi.nlm.nih.gov/Blast.cgi

10.3389/fpls.2022.894985

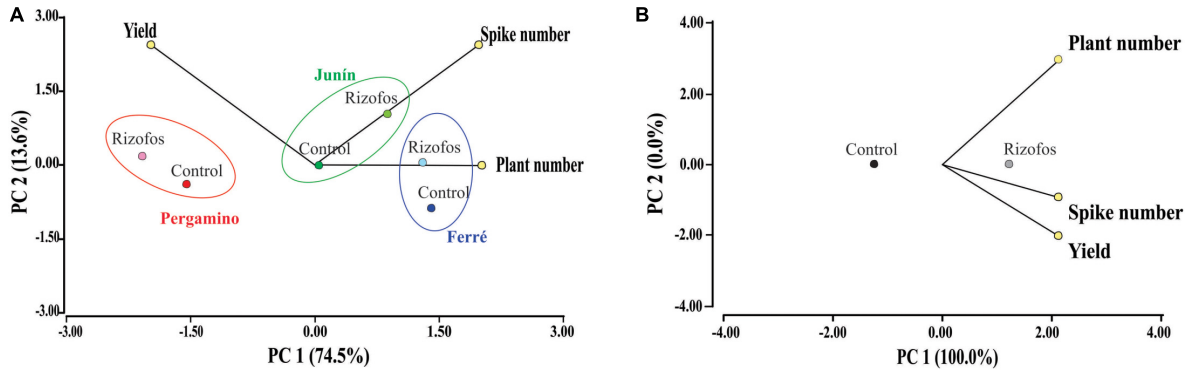

FIGURE 2
Agronomic efficiency of *Pseudomonas* sp. strain 1008. Principal component analyses of wheat parameters measured for 25 field assays (for details, see **Supplementary Table 2**). Data were partitioned by seed bacterization treatment with *Pseudomonas* sp. strain 1008, and by location **(A)**; or, only by seed bacterization treatment **(B)**. **(A)** In each location, wheat grain yield and the number of spikes per m^2 mainly explain the seed bacterization effect. Together, PC1 and PC2 explain >85% of the total variance. PC1 explains the geographical effect, whereas PC2 explains the bacterization effect for each geographical site. **(B)** Seed bacterization clearly influenced the three measured variables, explaining the whole variance. In both plots, "Rizofos" refers to the seed bacterization treatment.

Strain 1008 produced soluble and diffusible iron-chelating compounds detected in CAS plates (**Table 1** and **Supplementary Figure 2D**) and it was not able to grow on ACC as the sole C source in defined medium, thus disclosing the lack of ACC deaminase activity under the tested conditions (**Table 1**). Finally, strain 1008 did not produce hydrogen cyanide and did not inhibit the growth of a variety of phytopathogenic fungi or an oomycete in dual culture plates (**Table 1** and **Supplementary Figure 2F**).

Pure cultures of strain 1008 in NYB medium revealed polarly flagellated cells typical for the *Pseudomonas* genus, with average dimensions of 1.9 ± 0.4 μm long and 0.9 ± 0.1 μm wide (**Figure 1h**). Cells showed on average 1 or 2 polar flagella of up to 10 μm long (**Figure 1h**). Interestingly, strain 1008 showed evidence of colony phase variation in solid medium (**Figures 1i–m**). The identity of both phase variants was confirmed by 16S rDNA sequencing (**Supplementary Figure 3**). Whereas the colony morphotypes were clearly distinct (**Figures 1i–m**), both colony phase variants were undistinguishable at the cellular level (**Supplementary Figure 3**).

To summarize, strain 1008 was isolated from the rhizosphere of field grown wheat plants at the tillering stage and preliminary typed as a member of the *P. fluorescens* subgroup on the basis of phenotypical tests and its 16S rDNA sequence (**Supplementary Figure 1**; see below). *In vitro* assessment of plant growth-promoting traits revealed that strain 1008 had features that may directly impact on plant growth (such as an improvement of P availability to plant roots and production of IAA). For this reason, strain 1008 was formulated as an inoculant for wheat seed treatment and subjected to multiple field assays to evaluate its performance as a plant biostimulant.

Agronomic efficiency of *Pseudomonas* sp. strain 1008

The impact of treating wheat seeds with Rizofos®, a commercial formulation based on *Pseudomonas* strain 1008, was evaluated in a series of 25 field assays carried out in the period 2010–2017 (**Supplementary Table 2**). This dataset involved seven campaigns in two or three locations (**Figure 1a**), a total of five wheat genotypes, two different forecrops, two treatments with antifungals (Compinche®, or none), and two treatments with strain 1008 (Rizofos®, or none), under no-till management. The variables that were measured in all 25 assays were grain yield, number of plants and number of spikes per m^2 (**Supplementary Table 2**). These were used to carry out multivariate analyses.

By considering all classifiers (location, campaign, genotype, seed treatment with antifungals, forecrop, and treatment with Rizofos®), we did not find a general impact of any of the factors (**Supplementary Data 1**). If location and treatment with Rizofos® were only considered for data classification, the effect of inoculation was clear-cut, specifically based on the contribution of grain yield and spike number (**Figure 2A**). The impact of location was more evident in the plant number per m^2 (**Figure 2A**). If we only consider the impact of seed inoculation with Rizofos® in a principal component analysis, the PC1 explained 100% of the variability, with those plots in which seeds were treated with Rizofos® showing the highest values for the three variables (number of plants and of spikes per m^2, and grain yield) (**Figure 2B**). This global analysis of the field assay dataset thus indicated that all factors other than seed treatment with Rizofos® did not strongly influence the data behavior. Thus, we next proceeded to apply a generalized linear mixed model, in which all factors (except for seed treatment with

TABLE 2 Agronomic efficiency of *Pseudomonas* sp. strain 1008.

Variable	*n*	Control	+Rizofos®	SE	*P*-value
Grain yield (kg/ha)	150	4,084.4[a]	4,423.8[b]	289.0	<0.0001
Number of plants per m^2	150	n.s.	n.s.	n.s.	0.1874
Number of spikes per m^2	150	371.4[a]	388.3[b]	37.3	0.0274
Tiller number per m^2	114	n.s.	n.s.	n.s.	0.6314
NDVI at tillering	*	*	*	*	*
Tiller dry weight (g)	34	100.3[a]	101.9[b]	10.4	<0.0001
Tiller fresh weight (g)	102	452.6[a]	489.9[b]	43.9	0.0007
Spike dry weight (g)	*	*	*	*	*
Spike fresh weight (g)	48	1,815.0[a]	1,719.3[b]	86.0	0.0019

Output of GLMM applied to analyze the impact of wheat seed bacterization with *Pseudomonas* sp. strain 1008 (Rizofos®) in field assays. Adjusted average values for non-bacterized (Control) and bacterized (+Rizofos®) treatments and associated standard error (SE) are shown. Fisher's LSD test ($\alpha = 0.05$) was applied for multiple comparisons. *p*-value correction was not applied. See Supplementary Data 1 for more details of the GLMM analysis. *The model could not be built. Different superscript lowercase letters (a, b) denote statistical meaningful differences between treatment average values. n.s., there was not significant statistical difference among control and treatment with Rizofos.

Rizofos®) were considered as random effects. This allowed us to evaluate the impact that treatment of seeds with the inoculant based on strain 1008 had on the different variables recorded in the field trials (Table 2 and Supplementary Data 1).

Overall, the variables that responded better and with statistical support to the seed treatment with Rizofos® were grain yield (+8%), number of spikes (+5%), and tiller fresh weight (+8%) (Table 2). It is worth mentioning that we did not detect an interaction between the application of fungicide (Compinche®) and seed treatment with Rizofos® for any of the variables recorded in the field trials (Supplementary Data 1). In other words, the positive effects of seed inoculation with Rizofos® were not influenced by the application of the fungicide Compinche. With regards to the location of the field trials, the highest yields were registered nearby Pergamino, although there was no interaction between the location and seed inoculation with Rizofos® (Supplementary Data 1).

When the effect of Rizofos® was analyzed for each of the individual field assays by means of a simple ANOVA, we found that in 18 out of 26 cases (70%), the bacterization of seeds significantly increased the yield of wheat with $p < 0.05$ (Supplementary Table 4). If the statistical significance is relaxed at $p < 0.1$, the application of Rizofos® showed a positive yield response in 100% of the 26 field trials (Supplementary Table 4).

In summary, the application to wheat seeds of an inoculant formulated with live *Pseudomonas* sp. strain 1008 showed a robust positive impact on the grain yield in the field across a number of campaigns, soil properties, seed genotypes, and with no significant impact of the simultaneous treatment of the seeds with a fungicide.

Genomic properties of *Pseudomonas* sp. strain 1008

Prompted by the possibility to uncover the genetic basis for the biostimulant behavior of strain 1008 on the one hand, and to permit a more confident taxonomic positioning of the strain, we determined its genome sequence. The 6.6 Mb genome of this plasmid-free strain is composed by a circular chromosome with a GC content of 60.72% and is predicted to contain 6,000 protein-coding genes, five ribosomal operons and 67 tRNA genes (Table 3 and Figure 3). The size and informational content of strain 1008' genome is slightly above the average for the genus (6.3 Mb and 5,775 CDS[6], as of July 2021).

One integrative and conjugative element (ICE) of 115 kb is present in the chromosomal region 3,036,538–3,151,403 (Figure 3 and Supplementary Figure 4). It has a GC content

6 www.pseudomonas.com

TABLE 3 Description of the sequenced, assembled, and annotated whole genome of *Pseudomonas* sp. strain 1008.

Sequencing technology	PacBio RS chemistry sequencing
Polymerase subread bases	1,267,610,607 bp
Total subreads	134,530
Average subread length	9,422 bp
Average reference coverage	192×
Bio-project number	PRJNA741525
NCBI Accession number	CP078013
Genome size	6,609,162 bp
G + C content	60.72%
Chromosome	1
CDS	6,000
Coding density	89%
rRNA operons	5
tRNAs	67
Max. CDS length	14,115 bp
Mean CDS length	980 bp
Genes with COG identified	3,951
Hypothetical proteins (COGs R or S)	34%

of 56.12% (−4.6% with respect to the chromosome average; Table 3 and Supplementary Figure 4) and is flanked by perfect direct repeats of 16 bp at positions 3,036,538 – 3,036,553 (*attL*) and 3,151,388 – 3,151,403 (*attR*). This ICE encodes 91 proteins comprising a likely functional T4SS apparatus with its own relaxase and T4-coupling protein (Supplementary Figure 4). No integrated plasmids were detected, and no *oriT* or relaxase sequences were found outside the ICE region. A search at the Comprehensive Antibiotic Resistance Database using the Resistance Gene Identifier tool revealed four ORFs related to efflux pumps of the RND and MFS families (Supplementary Table 5), typical of pseudomonads (Pasqua et al., 2019). One intact 38 kb-prophage of the *Pseudomonas* phiCTX family (Hayashi et al., 1990) flanked by *attL-attR* sites was identified in between positions 1,778,760 – 1,816,567 (Figure 3). The prophage has a GC content of 57.4% and encodes 41 ORFs (Supplementary Figure 5A). Importantly, the *ctx* gene encoding a eukaryotic cell pore-forming toxin, originally described for the phiCTX phage of *P. aeruginosa* hosts (Hayashi et al., 1990), is not present in the prophage region of strain 1008 (Supplementary Figure 5A). A second but incomplete prophage region is present in positions 3,466,884 – 3,483,655 (16.7 kb; Supplementary Figure 5B), and it most likely represents a phage remnant. Importantly, according to the PathogenFinder tool of the Center for Genomic Epidemiology (Cosentino et al., 2013), the genome of *Pseudomonas* sp. strain 1008 corresponds to a microorganism not pathogenic for humans (Supplementary Figure 6). In support of the latter conclusion, strain 1008 did not show evidence of toxicity toward the nematode *Caenorhabditis elegans* and the springtail *Folsomia candida*, when applied into soil following standardized protocols (Supplementary Data 2, 3). Strain 1008 was neither pathogenic in a murine model following intranasal and oral inoculation of 1×10^8 cells (Supplementary Data 4).

The chromosome of strain 1008 contains minimal orphan CRISPR arrays, three of which seem to be derived from foreign genetic material and two appear to be a self-targeting spacer originated from the own chromosome (Supplementary Table 6). However, no CRISPR-associated (Cas) proteins were detected, so disregarding the functionality of these CRISPR loci.

Finally, a number of transposable elements were identified (Figure 3 and Supplementary Table 7), including single copies of IS66-, IS21-, and IS1182-like elements within the ICE, and one composite transposon bracketed by two IS3 elements located just downstream the ICE. In addition, three copies of IS3 were detected in the rest of the chromosome (Figure 3 and Supplementary Table 7).

The bacterial genome available in public databases with the highest similarity at the DNA sequence level to that of *Pseudomonas* sp. strain 1008 is by large that of *Pseudomonas azotoformans* F77 (GenBank accession CP019856), with an ANIm = 99.08% along a 94.4% of chromosomes alignment. We will deepen on the taxonomical implications of this finding in the next section. As expected, there is a substantial degree of synteny along both chromosomes, except for the fact that strain F77 lacks a large region of about 200 kb in the middle of the replicon, mapping to positions 3,100,000 – 3,300,000 in the chromosome of strain 1008 (Figure 3 and Supplementary Figure 7). This gap in the F77 genome may be partially explained by the insertion of the mobile genetic elements detected in the chromosome of strain 1008 (specifically, the ICE and the composite transposon; Figure 3 and Supplementary Figure 7).

Genome mining of plant growth-promoting, rhizosphere colonization and competitiveness traits of *Pseudomonas* sp. strain 1008

The complete genome of *Pseudomonas* sp. strain 1008 was annotated with state-of-the-art tools and mined to search for genetic determinants of direct and indirect plant growth-promotion, rhizosphere colonization, and competitiveness (see section "Materials and Methods"). An exhaustive list of the identified genes and operons of interest for this work is presented in Supplementary Table 8, and the physical location of a number of relevant genes/operons is shown in Figure 3.

Pseudomonas sp. strain 1008 does not have the genetic capacity to carry out biological nitrogen fixation (Supplementary Table 8), a feature that, within the genus, is only restricted to the species *Pseudomonas stutzeri* (Silby et al., 2011) and to a few number of uncharacterized isolates (Li et al., 2017). Neither it has the genetic determinants for a complete denitrification pathway, only bearing one copy of *napA* encoding the periplasmic nitrate reductase, and the *nirBD* operon encoding subunits of the periplasmic nitrite reductase (Supplementary Table 8). However, the genome of strain 1008 is equipped with a number of genes encoding enzymes that may substantially contribute to the acquisition of phosphorus from extracellular inorganic and organic sources (Figure 3 and Supplementary Table 8). For instance, we identified homologs of *acpA* (acid phosphatase), *alkP* (alkaline phosphatase), *ygiF* (inorganic triphosphatase), *phoD1* and *phoD2* (phosphatases), *phoX* (phosphatase), *ppx* (exopolyphosphatase), the *phn* operon (C-P lyase for organophosphonate utilization), and *phyPf* (phytase of the β-propeller type) (Figure 3 and Supplementary Table 8). Of these, the polypeptides encoded by *phyPf*, *acpA*, *phoD1*, *phoD2,* and *phoX*, contain signal peptides for their export across the plasma membrane (of the Sec/SPI type for the phytase, and of the TAT system for the rest). Additionally, there is one full *pqq* operon encoding enzymes for the biosynthesis of pyrroloquinoline quinone (PQQ). This redox coenzyme is required for the activity of glucose dehydrogenase, an enzyme whose critical role in the solubilization of inorganic phosphates has been demonstrated (De Werra et al., 2009).

FIGURE 3
Characteristics and features of the genome of *Pseudomonas* sp. strain 1008. The circular map of the 6.6 Mb chromosome was performed with the GCview server (http://cgview.ca/). The circles represent, from outside to inside: rings 1–6, protein coding genes in the three different reading frames, oriented in the forward (rings 1–3) and reverse (rings 4–6) orientations, respectively. Ring 7 shows GC skews, with positive and negative values being indicated with green and purple colors, respectively. Ring 8 shows G + C% content plot (black). The innermost ring indicates absolute chromosome coordinates. Positions of mobile genetic elements are indicated with arrowheads in the outermost ring. The location of an intact prophage and of an integrative and conjugative element (ICE) are indicated with boxes. Finally, the position of a number of genetic loci related to plant growth promotion and rhizosphere competitiveness are indicated with colored lines, following the reference colors of the legend positioned at the lower left corner.

The corresponding glucose dehydrogenase gene *gcd* was also identified (Figure 3 and Supplementary Table 8).

In pure cultures, strain 1008 produces IAA and this is stimulated by the addition of tryptophan (Supplementary Figure 2). Of the known pathways for the biosynthesis of auxin (Spaepen et al., 2007), we could only detect two genes probably constituting an operon encoding the enzymes for the IAM pathway: namely, the tryptophan-2-monooxygenase IaaM and the indole-3-acetamide hydrolase IaaH (Figure 3 and Supplementary Table 8). On the other hand, we did not find the cluster of genes for IAA catabolism (*iacHABICDEFG*). In addition to IAA, the genome of strain 1008 revealed its genetic potential to produce the volatile compounds acetoin and 2,3-butanediol (Figure 3 and Supplementary Table 8), which have been reported as plant biostimulants and inducers of systemic resistance (Chung et al., 2016). Under stress conditions plants produce and accumulate GABA, but its production has to be controlled because high levels of GABA can impair cell

TABLE 4 Overall genome relatedness indices derived from pairwise genomic comparison between *Pseudomonas* sp. strain 1008 and type species with the highest similarity of 16S rDNA sequences.

Type strain	16S[1]	ANIb (%)[2]	ANIm (%)[3]	dDDH[4]
P. lurida LMG 21995	99.02	90.30 (79.9)	91.73 (79.8)	67.6 (64.2 – 70.8)
P. marginalis pv. *marginalis* ICMP 3553	98.79	90.02 (76.7)	91.41 (77.8)	61.6 (58.3 - 64.8)
P. extremorientalis LMG 19695	98.57	89.92 (79.5)	91.22 (80.0)	66.9 (63.5 – 70.1)
P. azotoformans LMG 21611	99.85	89.88 (81.3)	91.22 (91.9)	66.6 (63.2 – 69.8)
*P. simiae*_CCUG_50988	98.91	89.51 (77.2)	90.96 (77.2)	62.5 (59.2 – 65.7)
P. veronii DSM 11331	98.42	86.49 (69.7)	88.87 (66.5)	n.d.
P. salomonii LMG 22120	99.09	86.34 (74.4)	88.59 (71.1)	n.d.
P. fluorescens ATCC 13525	98.79	86.11 (72.9)	88.45 (69.0)	n.d.
*P. trivialis*_LMG_21464	98.87	85.45 (62.8)	88.33 (58.8)	n.d.

[1]% identity along a 1,325 bp amplicon sequence from *Pseudomonas* sp. strain 1008, based on BlastN. [2]Pairwise average nucleotide identity calculation based on Blast (ANIb) with the % of aligned genome sequence in between parentheses. [3]Pairwise average nucleotide identity calculation based on MUMmer (ANIm) with the % of aligned genome sequence in between parentheses. [4]Digital DNA–DNA hybridization (dDDH) estimate values (%) based on *in silico* DDH according to formula d_6 [a.k.a. GGDC formula 3, TYGS server; (Meier-Kolthoff et al., 2013; Meier-Kolthoff and Göker, 2019)]; model-based confidence intervals are specified in between parentheses. Shaded cells indicate the highest scores for every genomic feature. n.d., not determined.

elongation and plant stress resistance (Li et al., 2021). The identification of *gabT* and *gabD* homologs, encoding GABA aminotransferase and succinate-semialdehyde dehydrogenase involved in GABA degradation, and the *gabP* gene, encoding the GABA permease (**Figure 3** and **Supplementary Table 8**), suggests that strain 1008 can acquire and metabolize GABA in the rhizosphere, thus indirectly modulating root GABA levels.

The type three secretion system (T3SS) is a complex protein structure evolutionary derived from the flagellar apparatus that spans the cytoplasmic and outer membranes of bacteria and the cell envelope of the eukaryotic host to deliver effectors directly into its cytosol (Galan et al., 2014). Thus, T3SSs play an important role in plant cell-bacterial interactions, with an outcome of virulent or mutualistic association, essentially depending on the nature of the transported effectors (Zamioudis and Pieterse, 2012). We have detected one T3SS locus of the Hrp-1 type in the genome of strain 1008 (**Figure 3** and **Supplementary Table 8**). The T3SS cluster is highly similar and syntenic to those of the plant-beneficial strains *P. simiae* WCS417 and *P. fluorescens* SBW25 (**Supplementary Figure 8**). Based on the lack of plant virulence of strain 1008, this T3SS gene cluster -if functional- may be instrumental for induction of systemic resistance and/or modulation of other physiological responses in root cells (Stringlis et al., 2019).

Notably, the genome of strain 1008 lacks biosynthetic gene clusters (BGCs) responsible for the production of antimicrobial compounds that are hallmarks of biocontrol strains of the species *P. protegens*, *P. chlororaphis*, *Pseudomonas donghuensis*, or *P. putida* (namely, 2,4-diacetylphloroglucinol, pyrrolnitrin, pyoluteorin, polyynes, phenazines, hydrogen cyanide, and 7-hydroxytropolone, among others; **Supplementary Table 8** and **Figure 3**). The sole exceptions are the presence of the *undA* gene, encoding an enzyme for the production of the antifungal volatile 1-undecene (Rui et al., 2014), and of a homolog of the *ycaO* gene involved in posttranslational modification of ribosomally synthesized peptides (Burkhart et al., 2017) (**Figure 3** and **Supplementary Table 8**). The number of identified BGCs of the NRPS and PKS type is also remarkably low, just two orphan NRPS clusters and none PKS clusters (**Supplementary Table 8**). Homologs of the broadly distributed genes in *Pseudomonas* species encoding the extracellular metalloprotease A (*aprA*), the extracellular phospholipase C (*plcN*), and two extracellular lipases (*lipA*, *lipB*) were identified. By contrast, no chitinase gene was detected. Strain 1008 neither possesses genes for characterized insecticidal proteins (Kupferschmied et al., 2013).

In terms of iron scavenging, we identified the *pvd* gene cluster for the biosynthesis of pyoverdine. In fact, spectroscopic signals in the UV-visible range typical of pyoverdine were detected in supernatants from cultures of strain 1008 in iron-deficient medium (**Supplementary Figure 2G**). Besides the pyoverdine gene cluster, we found genes encoding the hemophore protein HasA and the corresponding hemophore receptor. Interestingly, we did not detect the genes for biosynthesis of the siderophore achromobactin, but we identified one gene encoding a putative achromobactin receptor (**Supplementary Table 8**). No other genetic determinants for the production of additional siderophores were found. With regards to the transport of iron complexes, the genome of strain 1008 bears five genes encoding putative ferric-pyoverdine receptors and 13 genes for TonB-dependent receptors (six of which are located adjacent to iron-metabolism genes; **Supplementary Table 8**).

Effective colonization of the rhizosphere is key to execute direct and indirect mechanisms of plant growth-promotion (Lugtenberg and Kamilova, 2009). Our current studies on the root colonizing ability of strain 1008 point to a strong competitiveness to access the rhizoplane of wheat in natural soil in the presence of indigenous microorganisms and irrespective

of its initial location (bulk soil or seeds), although the survival of strain 1008 in bulk soil is severely limited in the absence of plant roots (unpublished data). The abilities to adhere to surfaces and establish biofilms, as well as to compete with other rhizobacteria, are critical factors to colonize the rhizoplane. In this sense, the genome of strain 1008 is endowed with the genetic capacity to produce polysaccharides commonly found in the extracellular matrix of biofilms (e.g., alginate, Psl, and Pel), as well as for the biosynthesis of a set of macromolecules mediating surface adhesion (cellulose, PGA adhesin, Fap amyloid fimbriae, and two large adhesins of the ShlA/HecA/FhaA family) (**Figure 3** and **Supplementary Table 8**). The rhizosphere niche colonization by strain 1008 may be facilitated by its swimming motility driven by the flagellar apparatus (**Figure 1**) encoded by the flagellar operons, as well as by twitching motility associated with pili (**Supplementary Table 8**).

Strain 1008 lacks canonical *luxIR* genes for AHL production and global coordination of gene expression according to cell density, but it possesses one AHL synthase gene of the *hdtS* type, one LuxR-solo gene, and one AHL-lactonase encoded within the ICE region (**Figure 3** and **Supplementary Table 8**). This implies that strain 1008 would be able to respond to its own and/or to foreign AHLs, and/or to interfere with cell–cell communication of other rhizobacteria. Finally, we identified genes for production of metabolites that confer protection to cells against different types of stress, namely osmotic stress [*betAB*, *ngg-asnO,* and *treY*/*treZ*, for betaine, NAGGN and trehalose biosynthesis, respectively; (Kurz et al., 2010)], oxidative stress [*ape* cluster for aryl polyene production; (Schoner et al., 2016)], and general stress [*pha* genes for polyhydroxyalkanoates; (Lopez et al., 2015)] (**Figure 3** and **Supplementary Table 8**). Collectively, the expression of these genes may confer increased fitness in the rhizosphere to strain 1008.

An interesting bacterial strategy to compete with non-kin cells is the type VI secretion system (T6SS), a contractile nanoweapon to inject toxins directly into the cell membranes, periplasm, or cytoplasm, leading to killing of competitor cells if they do not have the matching immunity protein (Ryu, 2015). The injected T6SS effectors have different biochemical activities, but the nanomachine and their injected toxins are not harmful for plant cells (Lucke et al., 2020). The genome of strain 1008 contains two complete T6SS loci, and a number of potential effector toxins of the *tse5* (four copies) and *vrgG* (three copies) types (**Figure 3** and **Supplementary Figure 9** and **Supplementary Table 8**). Besides the genetic determinants of the T6SS nanomachines, strain 1008 contains genes encoding bacteriocins (Ghequire and De Mot, 2014; Jackson et al., 2018): we identified functional homologs of S-pyocins of the *pys1* (for a colicin-like rRNAse) and PA3865 (for a tRNAse) types, as well as two copies of putative CDI toxins related to PA0041 and PA2462 proteins from *P. aeruginosa*, and three copies of a gene encoding a putative bacteriocin of the DUF692 family. It would be interesting to evaluate the functionality of the two detected T6SS loci in standard bioassays for antibacterial activity.

The broadly conserved global regulatory cascade of *Pseudomonas* species known as Gac-Rsm is fundamental to coordinate different traits for colonization of plant tissues, production of secondary metabolites and the interaction with eukaryotic organisms sharing the niche with pseudomonads (Ferreiro et al., 2018; Sobrero and Valverde, 2020). The genome of strain 1008 contains all the essential and accessory genetic elements delineating a functional Gac-Rsm cascade, including the GacS-GacA two-component system, the GacS-modulating histidine kinases RetS, LadS, and PA1611-like, three ortholog RNA binding proteins of the Rsm family (RsmA, RsmE, and RsmI), and the two cognate non-coding regulatory RNAs RsmY and RsmZ (**Supplementary Table 8**).

Phylogenomic, phenotypic and chemotaxonomic comparative analysis of *Pseudomonas* strain 1008 and related taxa

The first attempt to assign a taxonomic position to *Pseudomonas* sp. strain 1008 by comparative analysis of a 1,325 bp partial sequence of the PCR amplified 16S rDNA gene indicated that the isolate had >98.4% of sequence identity with several species belonging to the *P. fluorescens* subgroup within the *P. fluorescens* lineage (**Table 4** and **Supplementary Figure 1**). For a more detailed analysis of its phylogenetic positioning, we drew on the complete genome sequence of strain 1008. A pairwise genome comparison with a set of type species having highly similar 16S rDNA sequences revealed that the closest taxonomic species was *Pseudomonas lurida* (**Table 4**). However, the calculated ANIb and ANIm values for strain 1008 were far below the current accepted threshold of 95% for species definition (Jain et al., 2018). In addition, the dDDH values calculated for each close relative species with respect to strain 1008, were all below 70% (**Table 4**), the cutoff for delimiting species (Meier-Kolthoff et al., 2013). These findings firmly suggested that strain 1008 may be a representative of a novel *Pseudomonas* species within the *P. fluorescens* subgroup.

To get further support for this hypothesis we profited on the genome-based taxonomy service provided by the DSMZ Type (Strain) Genome Server (TYGS; Meier-Kolthoff and Göker, 2019). In agreement with the ANI similarity and dDDH data (**Table 4**), the TYGS analysis reinforced the finding that strain 1008 is a representative of a novel species of *Pseudomonas* (**Figure 4** and **Supplementary Figure 8**).

When the relatedness of the genome of strain 1008 was analyzed by comparison to all *Pseudomonas* genomes available in public databases, we found that the highest similarity indexes corresponded to the genome of *P. azotoformans* strain F77 (NCBI accession CP019856), with ANIb and AAI

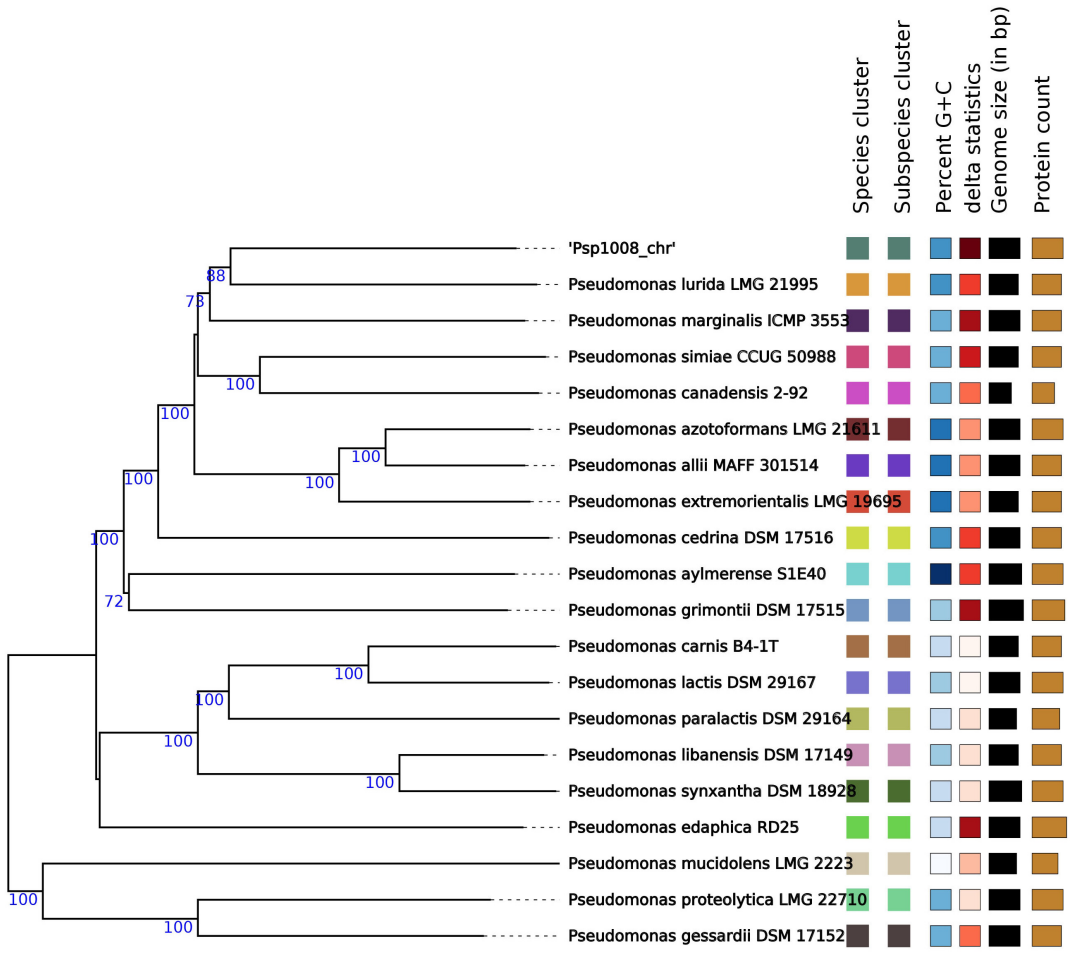

FIGURE 4
Genome BLAST Distance Phylogeny (GBDP) tree of *Pseudomonas* sp. strain 1008. The phylogenetic tree was constructed with the type (Strain) Genome Server (Meier-Kolthoff and Göker, 2019), which produces a GBDP tree by approximating intergenomic relatedness using the MASH algorithm among all type strain genomes in the TYGS database and by extracting and comparing 16S rRNA gene sequences with >14.990 type strains using BLAST as a proxy to identify the 50 closest type strains to calculate precise distances. The tree itself was constructed using FastME version 2.1.4 to infer a balanced minimum evolution tree with branch support. The tree represents only the *Pseudomonas* spp. most closely related to strain 1008. Bootstrap support values are shown at the nodes. The leaf label "Species cluster" assigns a different color to denote genomes from different type species.

(average amino acid identity) values of 99.02 and 99.64, respectively (Figure 5). However, the genomic similarity between the type strain of the *P. azotoformans* species (LMG 21611) and strain 1008 (Table 4 and Figures 4, 5) is not consistent with this finding, thus raising doubts about the taxonomical positioning of *P. azotoformans* F77. In fact, the ANIm and AAI analyses of all available genomes of isolates designated as members of the *P. azotoformans* species (including that of the species type strain), clearly support the fact that both strains 1008 and F77 are representatives of a novel species distinct from *P. azotoformans* and from closely related type species (Figures 4, 5). In addition to the evidence provided by genomic metrics, the comparison of the composition of whole-cell fatty acids and of key biochemical activities between strain 1008 and closely related taxa (Tables 5, 6), also provide phenotypic support for the separate species status that was shown by the phylogenomic analysis.

Based on the evidence described above demonstrating that strain 1008 represents a newly derived branch in the phylogenomic tree of the *P. fluorescens* lineage (Figures 4, 5), we propose a new taxonomic entity with the name "*Pseudomonas pergaminensis*" sp. nov.

Description of *Pseudomonas pergaminensis* sp. nov.

Pseudomonas pergaminensis (per ɣa mi ˈnen sis), N.L. masc./fem. adj. pergaminensis, belonging to Pergamino county

10.3389/fpls.2022.894985

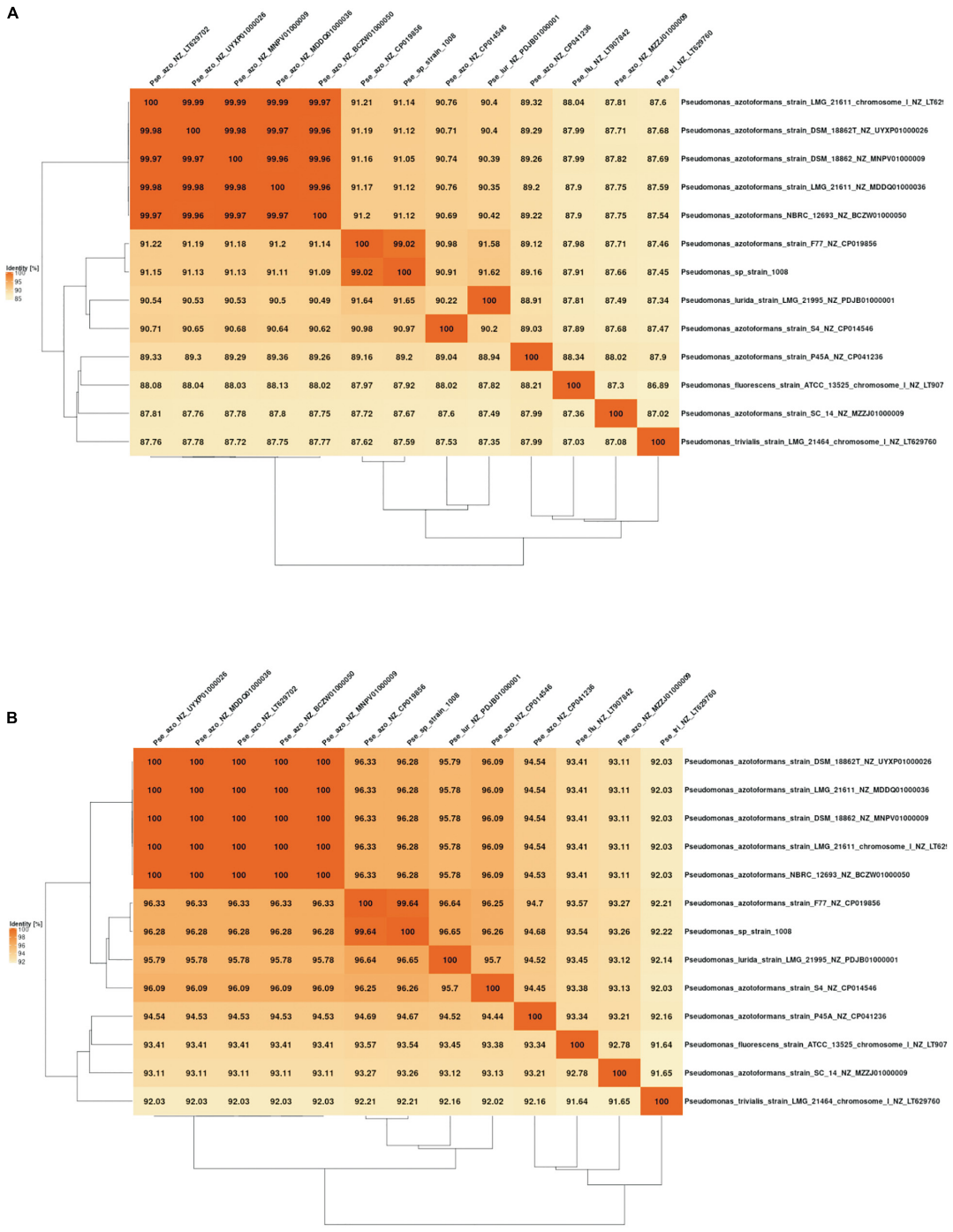

FIGURE 5
Overall genome relatedness derived from pairwise genomic comparison between *Pseudomonas* sp. strain 1008 and type species and isolates with the highest similarity of 16S rDNA sequences. **(A)** Average nucleotide identity matrix generated with the fastANI matrix tool of the EDGAR platform (https://edgar.computational.bio.uni-giessen.de/cgi-bin/edgar_login.cgi). **(B)** Average amino acid identity matrix generated with the AAI matrix tool of the EDGAR platform (https://edgar3.computational.bio.uni-giessen.de/cgi-bin/edgar.cgi).

(Province of Buenos Aires, Argentina), from where the type strain was isolated.

Cells of strain 1008^T are Gram-reaction negative, aerobic, oxidase positive, rod-shaped bacteria ranging between 0.6–1.1 mm wide × 1.2–3.2 μm long, non-endospore-forming rods. Grows on *Pseudomonas* agar F at 28°C forming circular colonies <2 mm, with smooth borders, opaque, of light beige color, and creamy texture. It may give rise to

phase-variant colonies. Growth occurs at 4–35°C but not at 37°C. Strain 1008^T grows in a pH range from 6–9, and with a NaCl concentration of up to 1% w/v. Results from tests using API 20 NE Gallery System show that the following substrates are utilized: D-glucose, D-arabinose, D-mannose, D-mannitol, *N*-acetyl-D-glucosamine, D-gluconate, capric acid, adipic acid, malic acid, and citrate. Using the Biolog GenIII system, tests positive for the utilization of the following additional substrates: dextrin, D-fructose, D-fructose-6-phosphate, D-galactose, D-fucose, L-fucose, L-rhamnose, L-galactonic acid lactone, D-galacturonic acid, D-glucuronic acid, glucuronamide, acetic acid, quinic acid, γ-amino butyric acid, formic acid, and Tween-40 (**Supplementary Data 5** and **Supplementary Figure 10**). The major cellular fatty acids are $C_{16:0}$ (30.4%), $C_{16:1w7c}$ (29.5%), $C_{18:1w7c}$ (15.3%), $C_{17:0cyclow7c}$ (9.1%), $C_{12:0\ 2OH}$ (4.3%), $C_{12:0\ 3OH}$ (3.7%), $C_{10:0\ 3OH}$ (3.0%), and $C_{12:0}$ (2.3%) (**Supplementary Data 6**). It is able to solubilize mineral phosphates and zinc oxide, to produce IAA and siderophores, to secrete proteases and phospholipases, but not chitinases. The strain 1008^T was isolated form the rhizosphere of field grown *Triticum aestivum*, in Pergamino, Buenos Aires province, Argentina, in 2003. The genomic DNA G + C content of the type strain is 60.72%. The full genome sequence of the strain 1008^T has been deposited at the NCBI GenBank under accession number CP078013. The type strain is 1008^T (= DSM 113453 = ATCC TSD-287).

Discussion

The urgent need of sustainable and eco-friendly strategies to mitigate the impact of agrochemical industry and its massive application has boosted research on plant-biostimulant microorganisms, whereas at the same time, it has exposed frequent inconsistencies between the plant-beneficial potential of isolated microorganisms studied under lab conditions and their efficiency in the field (Timmusk et al., 2017; Backer et al., 2018; Basu et al., 2021). Such hurdles may be partially reduced if the microorganisms are isolated from plant tissues of the target crop and are applied in the geographical area of origin (Armada et al., 2018; Müller and Behrendt, 2021). *Pseudomonas* sp. strain 1008 was isolated from the rhizosphere of healthy field-grown wheat plants, as a bacterium able to increase the availability of phosphate to plant roots and to produce auxin (**Figure 1** and **Supplementary Figure 2**). Based on these traits, strain 1008 was formulated as an inoculant for its application on wheat seeds before sowing and tested in a series of field trials at three different locations around the isolation site, across several campaigns involving different wheat varieties (**Figure 1a** and **Supplementary Tables 1**, **2**, **4**). Collectively, the results of the whole set of field trials strongly support the use of this biostimulant bacterium (Du Jardin, 2015) as an efficient agricultural input for promoting the yield of wheat (**Table 2** and **Supplementary Table 4**). The fact that a single seed bacterizing shot with live *Pseudomonas* sp. strain 1008 resulted in an average increase of wheat yield of 8% (median = +9.7%; **Table 2** and **Supplementary Table 4**), suggests that seedling establishment and its early development are critical stages that are strongly responsive to the presence of the bacterium and its physiological activities, and whose beneficial effects are largely transduced all along the growth cycle of the plant. Recently, it has been proposed that domestication and breeding strategies have worked against the maintenance of plant genes promoting interactions with plant-beneficial bacteria (Valente et al., 2020). In this regard, bacterization of commercial wheat seeds with strain 1008 may represent a way to by reinstate key microbial functions in the rhizosphere of seedlings by compensating the reduced ability of modern wheat varieties to interact with PGPR (Perez-Jaramillo et al., 2016; Valente et al., 2020).

Physiological and genomic plant-beneficial traits of *Pseudomonas* sp. strain 1008

In vitro, strain 1008 was capable of solubilizing phosphate from pure calcium triphosphate and from mineral phosphate rocks, mineralizing phosphate from organic esters, solubilizing zinc from ZnO, producing siderophores and extracellular lytic enzymes of the phospholipase and protease types (**Table 1** and **Supplementary Figure 2**). All these features may cooperatively contribute to enhancing nutrient availability in the rhizosphere of wheat plants.

The closest related strain to *Pseudomonas* sp. 1008 described in the literature is the isolate F77 (**Supplementary Figures 7**, **8**). Strain F77 was originally assigned to the *P. azotoformans* species, but on the basis of our phylogenomic analysis this species ascription should be revised (**Figure 5**). Strain F77 was reported as a strong biomineralizer of aluminum and iron from biotite minerals, being this feature fully dependent on the activity of the product of the *gcd* gene, encoding the periplasmic glucose dehydrogenase enzyme (Wang et al., 2020). In pseudomonads, glucose dehydrogenase drives the oxidation of glucose into gluconic acid in a reaction that requires the PQQ cofactor (Miller et al., 2010). Gluconic acid may be further oxidized in the periplasm to 2-ketogluconic acid by the activity of the product of the *gad* gene (gluconic acid dehydrogenase) (Miller et al., 2010). This pathway of glucose uptake leads to acidification of the cell environment, which indirectly facilitates solubilization of mineral phosphates. In fact, genetic data confirmed the absolute requirement of *gcd*, *gad* and *pqq* genes for solubilization of calcium triphosphate by the biocontrol rhizospheric strains *P. fluorescens* F113 and *P. protegens* CHA0 (De Werra et al., 2009; Miller et al., 2010). Gcd can also oxidize xylose (Dvorak and De Lorenzo, 2018), another abundant sugar present in plant root exudates. The genome of strain 1008 encodes *gcd*, *gad,* and *pqq* homologs (**Figure 3** and **Supplementary Table 8**), thus providing genomic support for the observed

capacity to solubilize mineral phosphates. Acidification of the extracellular environment in the rhizosphere has been found to contribute to local suppression of root immunity upon recognition of bacterial inducers of ISR, an effect that for certain rhizospheric *Pseudomonas* species required PQQ biosynthesis and gluconic acid production (Yu et al., 2019). Thus, root colonization by strain 1008 may also be promoted through this mechanism of ISR modulation associated with the control of extracellular pH driven by PQQ-dependent acidification (Yu et al., 2019), which in parallel contributes to solubilization of mineral phosphates.

Additionally, several genes of strain 1008 encode phosphatases acting on organic phosphate esters, some of which are predicted to be secreted (i.e., a β-propeller-phytase, the acid phosphatase AcpA, and the phosphatases PhoD1, PhoD2, and PhoX). Notably, strain 1008 has an *alkP* homolog, encoding an alkaline phosphatase, that is also present in only two out of the 613 complete genomes available in the PseudoDB database: the phylogenetically closest isolate "*P. azotoformans*" strain F77 and *Pseudomonas extremorientalis* BS2774, the latter being a member of a subgroup whose type species is also closely related to strain 1008 (**Table 4** and **Figure 4**). Altogether, the repertoire of genes related to the metabolism of inorganic and organic sources of phosphates present in the genome of strain 1008 (**Figure 3** and **Supplementary Table 8**) suggests its potential as a phosphorus biofertilizer in the rhizosphere of wheat.

Pseudomonas sp. strain 1008 produces auxin in a tryptophan-dependent manner (**Table 1** and **Supplementary Figure 2**). In bacteria, five different tryptophan-dependent pathways for IAA biosynthesis have been reported (Spaepen et al., 2007). By contrast, the genetic basis for the tryptophan-independent production of IAA is unknown (Spaepen et al., 2007). We could not identify the *ipdC* (IPA pathway), *oxd* and *nha1* (IAOc/IAN pathway), and *tdc* (TPM pathway) genes in the genome of strain 1008. We detected, however, a putative operon highly resembling the *iaaMH* tandem of the IAM pathway (**Figure 3** and **Supplementary Table 8**). Given that the gene responsible for the fifth biosynthetic pathway involving a tryptophan side-chain oxidase (TSO) is yet unknown (Spaepen et al., 2007), we cannot rule out the presence of a *tso* homolog in the genome of strain 1008. Besides auxin, the genome of strain 1008 has the potential to produce other phytostimulators, such as the volatiles 2,3-butanediol and acetoin [two compounds known to be involved in plant growth stimulation (Ryu et al., 2004; Chung et al., 2016)], and the cofactor PQQ, which in addition to its role in phosphate solubilization, it has been reported to act a phytostimulator with antioxidant properties in tomato and cucumber (Choi et al., 2008). With regards to modulation of plant hormone homeostasis during abiotic stress responses, the genome of strain 1008 does not encode a *bona fide* ACC deaminase gene *acdS*, but it encodes the GABA permease GabP and the GABA catabolic enzymes GabD-GabT (**Figure 3** and **Supplementary Table 8**). Thus, strain 1008 may

TABLE 5 Comparison of the relative abundance (%) of major cellular fatty acids of *Pseudomonas* sp. strain 1008 and its closest phylogenetic relatives (see **Table 4** and **Figure 4**).

Fatty acid	16:0	16:1 w7c	18:1 w7c	17:0 cyclo w7c	12:0 2OH	12:0 3OH
Pseudomonas sp. 1008	30.4	29.5	15.3	9.1	4.3	3.7
P. lurida LMG 21995	n.r.	n.r.	n.r.	n.r.	n.r.	n.r.
*P. marginalis*_ICMP_3553	32.4	26.6	14.8	7.5	n.r.	n.r.
P. extremorientalis LMG 19695	37.0	8.7	14.0	31.3	n.r.	n.r.
P. azotoformans LMG 21611	31.1	32.0	17.2	3.6	3.7	4.0
P. simiae OLi^T	30.3	27.0	12.3	11.7	n.r.	n.r.

Values were obtained from Campos et al. (2010) for *P. marginalis* ICMP 3553T, (Ivanova et al., 2002) for *P. extremorientalis* LMG 19695, (Sawada et al., 2021) for *P. azotoformans* LMG 21611, and (Vela et al., 2006) for *P. simiae* OLi^T. Values for *P. lurida* LMG 21995 could not be found in the literature. Cellular fatty acids analysis of strain 1008 was carried out by DSMZ Services, at the Leibniz-Institut DSMZ (Germany). n.r., not reported in the literature.

TABLE 6 Biochemical features differentiating *Pseudomonas* sp. strain 1008 from the type strains of closely related species (see **Table 4** and **Figure 4**).

	Strain 1008	*P. lurida*	*P. orientalis*	*P. extremorientalis*	*P. azotoformans*	*P. simiae*
Nitrate reduction	+w	−	−	−	+	+
Gelatinase	−	+	+	+	+	+
Urease	−	n.r.	+	−	−	−
Arginine dehydrolase	−	+	+	+	+	+
L-rhamnose assimilation	+w	+	+	−	−	−
N-acetyl-D-glucosamine assimilation	+	+	+	+	+	−

Data were retrieved from BacDive (https://bacdive.dsmz.de/) and from the literature (Dabboussi et al., 1999; Behrendt et al., 2007; Von Neubeck et al., 2017; Lick et al., 2020). +, positive reaction; +w, weak positive reaction; −, negative. n.r., not reported.

contribute to attenuate the GABA-mediated response to abiotic and biotic stress (Li et al., 2021) in the rhizosphere of colonized plants, in a way comparable with bacterial ACC deaminase to limit ethylene production by plant tissues (Gamalero and Glick, 2015). All these genetic traits directly related to phytoregulation suggest that cells of *Pseudomonas* sp. strain 1008 colonizing the rhizosphere of wheat may have a key role in promoting root system development locally and contributing systemically to modulation of plant responses to stresses.

With regards to indirect mechanisms of plant growth promotion, strain 1008 was unable to produce HCN [a volatile compound responsible for the inhibition of diverse phytopathogens (Blumer and Haas, 2000)] and to antagonize several phytopathogenic fungi and one oomycete *in vitro* (**Table 1** and **Supplementary Figure 2**). These findings provide stronger support toward a direct plant biostimulatory effect, rather than to an indirect biocontrol-based mechanism, as the main contribution of strain 1008 to the promotion of wheat growth and yield in the field. In this regard, mining of the full genome sequence of strain 1008 clearly indicated that this isolate was not evolved to fight pathogens with secondary metabolites typical of biocontrol PGPR, like antibiotics, antimetabolites, and lipopeptides of NRPS origin (**Figure 3** and **Supplementary Table 8**) (Keswani et al., 2020). However, the capacity to induce systemic resistance cannot be discarded for strain 1008, as typical general elicitors of ISR like LPS, flagella and siderophores of the pyoverdine type (Pieterse et al., 2014) are structural and functional components of strain 1008 (**Figure 1**, **Supplementary Figure 2**, and **Supplementary Table 8**). Furthermore, the genome of strain 1008 encodes genes for the production of the volatile compounds 2,3-butanediol and acetoin (**Figure 3** and **Supplementary Table 8**), which are also elicitors of ISR (Pieterse et al., 2014; Silva Dias et al., 2021). In addition, it has been recently proposed that certain plant-beneficial rhizobacteria may engage into a feedback loop. The recognition of key MAMPs by the plant immune system triggers a defense reaction that stimulates bacterial production of IAA, thus reinforcing development of lateral roots and ISR itself on the plant side, but also promoting root colonization by the rhizobacterium (Tzipilevich et al., 2021). It would be interesting to explore if the IAA-producer strain 1008 can also enter into such a virtuous loop with plant roots.

The compendium of genes and operons detected in the genome of *Pseudomonas* sp. strain 1008 that are potentially involved in biofertilization and phytostimulation as the main underlying mechanisms for promotion of wheat yield in the field, as well as those genetic determinants potentially relevant for rhizosphere colonization and competitiveness (**Figure 3** and **Supplementary Table 8**), set the basis for designing functional genetics screens and gene expression profiling of strain 1008, in order to provide experimental support linking the functional relevance of the cataloged genetic repertoire of plant-beneficial traits in the rhizosphere. An important issue that has to be considered when aiming to link gene functions to PGPR mechanisms and, by transition, to agronomic efficiency in the field, is that plant-beneficial rhizospheric microbes may display a set of concurring mechanisms that contribute to the overall robust performance in the field, as it has been addressed for the agronomic response of different crops to the inoculation with *Azospirillum brasilense* [i.e., the "multiple mechanisms hypothesis" (Bashan and De-Bashan, 2010; Cassán et al., 2020)]. This hypothesis may explain the overall positive impact of strain 1008 on the yield of wheat across a number of field assays carried out in different locations, with different seed genotypes and across different campaigns (**Figure 2** and **Supplementary Table 2**). Under this scenario, we have preliminary data indicating that strain 1008 promotes early root development of wheat in natural soil, and that induces root branching and expression of auxin-responsive reporter fusions in *Arabidopsis thaliana* (unpublished data). These effects would be consistent with the observed production of auxin by strain 1008 (**Supplementary Figure 2**) and with the identification of an operon encoding the auxin biosynthetic proteins IaaM-IaaH of the IAM pathway (**Figure 3** and **Supplementary Table 8**); together, these clues would point to auxin production in the rhizosphere as one of the possible mechanisms of strain 1008 contributing to the promotion of root development in the field. However, and importantly, such hypothesis needs to be challenged with targeted mutation of the *iaaMH* genes; the same reasoning applies to all other genetic traits with potential relevance in the field that were identified in the genome of strain 1008 (**Figure 3** and **Supplementary Table 8**).

Strain 1008 is a representative of the proposed novel species *Pseudomonas pergaminensis*

The initial taxonomic assignment of strain 1008 indicated that the isolate belonged to the *P. fluorescens* lineage, with its 16S rDNA sequence being 98.4–99.1% similar to those of different type species within this large and complex cluster of the *Pseudomonas* genus (**Table 4** and **Supplementary Figure 1**). On the basis of the full genome sequence, we concluded that isolate 1008 represents a novel species of the genus *Pseudomonas* (**Figure 4** and **Supplementary Figure 8**). Moreover, our genomic comparative analysis led us to conclude that this novel proposed species for strain 1008, must also include the aluminum- and iron-weathering isolate F77, which had been originally typed as a *P. azotoformans* isolate (Wang et al., 2020), and that shares an overall genomic relatedness with strain 1008 of 99.08% at the nucleotide level, and of 99.64% at the amino acid level (**Figure 5**). The phenotypic and chemotaxonomic features of strain 1008 confirmed its

differentiation from related taxa (**Tables 5**, **6**, **Supplementary Datas 5, 6**, and **Supplementary Figure 10**). The results from this polyphasic approach support the classification of 1008^T as a novel species of *Pseudomonas*, and the name of *Pseudomonas pergaminensis* is thus proposed for this strain.

Conclusion

We report the isolation, physiological characterization, and genomic analysis of a wheat rhizospheric strain representative of a novel species of the genus *Pseudomonas*, that showed a robust positive effect on the yield of field-grown wheat upon its application as a formulated inoculant on seeds. *In vitro* and genomic traits strongly suggest that *Pseudomonas pergaminensis* 1008^T acts as a plant biostimulant, rather than as a biocontrol bacterium. Full genome information will be useful for functional characterization of the mechanisms underlying the robust performance of strain 1008 in the field.

Data availability statement

The datasets presented in this study can be found in online repositories. The names of the repository/repositories and accession number(s) can be found in the article/**Supplementary Material**.

Author contributions

MD and TB isolated, characterized, and developed the commercial formulation of strain 1008. FN designed, implemented, and monitored field trials. GGA and WC supervised research and the agronomical evaluation of the commercial formulation. BA performed the statistical analysis of agronomical data and prepared DNA for genome sequencing. DW carried out genome assembly, annotation, and a set of comparative genomic tests. CV carried out genome mining, phylogenomic analysis, organized datasets, elaborated article structure, and wrote the manuscript. All authors contributed to manuscript revision, read, and approved the submitted version.

Funding

This work was supported by Rizobacter Argentina S.A. and by research grants from Universidad Nacional de Quilmes (PUNQ 1306/19, Argentina) and CONICET (11220150100388CO and 11220200101442CO, Argentina). Bioinformatics support by the BMBF-funded project "Bielefeld-Gießen Center for Microbial Bioinformatics—BiGi (Grant Number: 031A533)" within the German Network for Bioinformatics Infrastructure (de.NBI) is gratefully acknowledged. BA and CV are members of CONICET.

Conflict of interest

MD, TB, FN, and WC, were employed by Rizobacter Argentina S.A. GGA was employed by Indrasa Biotecnología S.A.

The remaining authors declare that the research was conducted in the absence of any commercial or financial relationships that could be construed as a potential conflict of interest.

The authors declare that this study received funding from Rizobacter Argentina S.A. The funder had the following involvement in the study: isolation and characterization of the bacterial strain; development of the commercial formulation tested in field assays; design, implementation, and monitoring of the agronomical evaluation of the formulation in field trials.

Publisher's note

Supplementary material

The Supplementary Material for this article can be found online at: https://www.frontiersin.org/articles/10.3389/fpls.2022.894985/full#supplementary-material

References

Agaras, B. C., Iriarte, A., and Valverde, C. F. (2018). Genomic insights into the broad antifungal activity, plant-probiotic properties, and their regulation, in *Pseudomonas donghuensis* strain SVBP6. *PLoS One* 13:e0194088. doi: 10.1371/journal.pone.0194088

Agaras, B., Noguera, F., Gonzalez Anta, G., Wall, L. G., and Valverde, C. (2020). Biocontrol potential of pseudomonads, but not their direct plant growth promoting features, is a predictor of crop productivity under field conditions. *Biol. Cont.* 413:104209. doi: 10.1016/j.biocontrol.2020.104209

Agaras, B., Wall, L. G., and Valverde, C. (2012). Specific enumeration and analysis of the community structure of culturable pseudomonads in agricultural soils under no-till management in Argentina. *Appl. Soil Ecol.* 61, 305–319. doi: 10.1016/j.apsoil.2011.11.016

Alcock, B. P., Raphenya, A. R., Lau, T. T. Y., Tsang, K. K., Bouchard, M., and Edalatmand, A. (2020). CARD 2020: antibiotic resistome surveillance with the comprehensive antibiotic resistance database. *Nucleic Acids Res.* 48, D517–D525. doi: 10.1093/nar/gkz935

Anderson, A. J., and Kim, Y. C. (2020). Insights into plant-beneficial traits of probiotic *Pseudomonas* chlororaphis isolates. *J. Med. Microbiol.* 69, 361–371. doi: 10.1099/jmm.0.001157

Armada, E., Leite, M. F. A., Medina, A., Azcón, R., and Kuramae, E. E. (2018). Native bacteria promote plant growth under drought stress condition without impacting the rhizomicrobiome. *FEMS Microbiol. Ecol.* 94:fiy092. doi: 10.1093/femsec/fiy092

Backer, R., Rokem, J. S., Ilangumaran, G., Lamont, J., Praslickova, D., Ricci, E., et al. (2018). Plant Growth-Promoting Rhizobacteria: context, Mechanisms of Action, and Roadmap to Commercialization of Biostimulants for Sustainable Agriculture. *Front. Plant Sci.* 9:1473. doi: 10.3389/fpls.2018.01473

Bashan, Y., and De-Bashan, L. E. (2010). "Chapter Two - How the Plant Growth-Promoting Bacterium Azospirillum Promotes Plant Growth—A Critical Assessment," in *Advances in Agronomy*, ed. D. L. Sparks (Cambridge, MA: Academic Press), 77–136.

Basu, A., Prasad, P., Das, S. N., Kalam, S., Sayyed, R. Z., Reddy, M. S., et al. (2021). Plant Growth Promoting Rhizobacteria (PGPR) as Green Bioinoculants: recent Developments. Constraints, and Prospects. *Sustainability* 13:1140. doi: 10.3390/su13031140

Behrendt, U., Ulrich, A., Schumann, P., Meyer, J. M., and Sproer, C. (2007). *Pseudomonas* lurida sp. nov., a fluorescent species associated with the phyllosphere of grasses. *Int. J. Syst. Evol. Microbiol.* 57, 979–985. doi: 10.1099/ijs.0.64793-0

Benedetti, R., and Rossini, P. (1993). On the use of NDVI profiles as a tool for agricultural statistics: the case study of wheat yield estimate and forecast in Emilia Romagna. *Remote Sensing Environ.* 45, 311–326. doi: 10.1016/0034-4257(93)90113-C

Berendsen, R. L., Van Verk, M. C., Stringlis, I. A., Zamioudis, C., Tommassen, J., Pieterse, C. M., et al. (2015). Unearthing the genomes of plant-beneficial *Pseudomonas* model strains WCS358, WCS374 and WCS417. *BMC Genomics* 16:539. doi: 10.1186/s12864-015-1632-z

Bertelli, C., Laird, M. R., Williams, K. P., Simon fraser university research computing group, Lau, B. Y., Hoad, G., et al. (2017). IslandViewer 4: expanded prediction of genomic islands for larger-scale datasets. *Nucleic Acids Res.* 45, W30–W35. doi: 10.1093/nar/gkx343

Biessy, A., Novinscak, A., Blom, J., Leger, G., Thomashow, L. S., Cazorla, F. M., et al. (2019). Diversity of phytobeneficial traits revealed by whole-genome analysis of worldwide-isolated phenazine-producing *Pseudomonas* spp. *Environ. Microbiol.* 21, 437–455. doi: 10.1111/1462-2920.14476

Blin, K., Shaw, S., Kloosterman, A. M., Charlop-Powers, Z., Van wezel, G. P., Medema, M. H., et al. (2021). antiSMASH 6.0: improving cluster detection and comparison capabilities. *Nucleic Acids Res.* 49, W29–W35. doi: 10.1093/nar/gkab335

Blumer, C., and Haas, D. (2000). Mechanism, regulation, and ecological role of bacterial cyanide biosynthesis. *Arch. Microbiol.* 173, 170–177. doi: 10.1007/s002039900127

Bric, J. M., Bostock, R. M., and Silverstone, S. E. (1991). Rapid in situ assay for indoleacetic Acid production by bacteria immobilized on a nitrocellulose membrane. *Appl. Environ. Microbiol.* 57, 535–538. doi: 10.1128/aem.57.2.535-538.1991

Burkhart, B. J., Schwalen, C. J., Mann, G., Naismith, J. H., and Mitchell, D. A. (2017). YcaO-Dependent Posttranslational Amide Activation: biosynthesis, Structure, and Function. *Chem. Rev.* 117, 5389–5456. doi: 10.1021/acs.chemrev.6b00623

Campos, V. L., Valenzuela, C., Yarza, P., Kampfer, P., Vidal, R., Zaror, C., et al. (2010). *Pseudomonas arsenicoxydans* sp nov., an arsenite-oxidizing strain isolated from the Atacama desert. *Syst. Appl. Microbiol.* 33, 193–197. doi: 10.1016/j.syapm.2010.02.007

Carattoli, A., Zankari, E., García-Fernández, A., Larsen, M. V., Lund, O., Villa, L., et al. (2014). *In Silico* Detection and Typing of Plasmids using PlasmidFinder and Plasmid Multilocus Sequence Typing. *Antimicrobial Agents Chemother.* 58, 3895–3903. doi: 10.1128/AAC.02412-14

Casanoves, F., Macchiavelli, R., and Balzarini, M. (2007). Models for multi-environment yield trials with fixed and random block effects and homogeneous and heterogeneous residual variances. *J. Agric. Univ. Puerto Rico* 91, 117–131. doi: 10.46429/jaupr.v91i3-4.3280

Cassán, F., Coniglio, A., López, G., Molina, R., Nievas, S., De Carlan, C. L. N., et al. (2020). Everything you must know about Azospirillum and its impact on agriculture and beyond. *Biol. Fertility Soils* 56, 461–479. doi: 10.1007/s00374-020-01463-y

Chin, C. S., Alexander, D. H., Marks, P., Klammer, A. A., Drake, J., Heiner, C., et al. (2013). Nonhybrid, finished microbial genome assemblies from long-read SMRT sequencing data. *Nat. Methods* 10, 563–569. doi: 10.1038/nmeth.2474

Chiniquy, D., Barnes, E. M., Zhou, J., Hartman, K., Li, X., Sheflin, A., et al. (2021). Microbial Community Field Surveys Reveal Abundant *Pseudomonas* Population in Sorghum Rhizosphere Composed of Many Closely Related Phylotypes. *Front. Microbiol.* 12:598180. doi: 10.3389/fmicb.2021.598180

Choi, O., Kim, J., Kim, J. G., Jeong, Y., Moon, J. S., Park, C. S., et al. (2008). Pyrroloquinoline quinone is a plant growth promotion factor produced by *Pseudomonas* fluorescens B16. *Plant Physiol.* 146, 657–668. doi: 10.1104/pp.107.112748

Chung, J.-H., Song, G. C., and Ryu, C.-M. (2016). Sweet scents from good bacteria: case studies on bacterial volatile compounds for plant growth and immunity. *Plant Mol. Biol.* 90, 677–687. doi: 10.1007/s11103-015-0344-8

Cosentino, S., Voldby Larsen, M., Moller Aarestrup, F., and Lund, O. (2013). PathogenFinder–distinguishing friend from foe using bacterial whole genome sequence data. *PLoS One* 8:e77302. doi: 10.1371/journal.pone.0077302

Couvin, D., Bernheim, A., Toffano-Nioche, C., Touchon, M., Michalik, J., Néron, B., et al. (2018). CRISPRCasFinder, an update of CRISRFinder, includes a portable version, enhanced performance and integrates search for Cas proteins. *Nucleic Acids Res.* 46, W246–W251. doi: 10.1093/nar/gky425

Dabboussi, F., Hamze, M., Elomari, M., Verhille, S., Baida, N., Izard, D., et al. (1999). Taxonomic study of bacteria isolated from Lebanese spring waters: proposal for *Pseudomonas* cedrella sp. nov. and P. orientalis sp. nov. *Res. Microbiol.* 150, 303–316. doi: 10.1016/s0923-2508(99)80056-4

De Vrieze, M., Varadarajan, A. R., Schneeberger, K., Bailly, A., Rohr, R. P., Ahrens, C. H., et al. (2020). Linking Comparative Genomics of Nine Potato-Associated *Pseudomonas* Isolates With Their Differing Biocontrol Potential Against Late Blight. *Front. Microbiol.* 11:857. doi: 10.3389/fmicb.2020.00857

De Werra, P., Péchy-Tarr, M., Keel, C., and Maurhofer, M. (2009). Role of gluconic acid production in the regulation of biocontrol traits of *Pseudomonas fluorescens* CHA0. *Appl. Environ. Microbiol.* 75, 4162–4174. doi: 10.1128/AEM.00295-09

Di Rienzo, J. A., Casanoves, F., Balzarini, M. G., Gonzalez, L., Tablada, M., and Robledo, C. W. (2020). *InfoStat versión 2020*. http://www.infostat.com.ar (accessed April 2020.)

Di Rienzo, J. A., Macciavelli, R. E., and Casanoves, F. (eds) (2011). *Modelos Lineales Mixtos: aplicaciones en InfoStat*. Córdoba: Infostat Group.

Dieckmann, M., Beyvers, S., Nkouamedjo-Fankep, R. C., Hanel, P. H. G., Jelonek, L., Blom, J., et al. (2021). EDGAR3.0: comparative genomics and phylogenomics on a scalable infrastructure. *Nucleic Acids Res.* 49, W185–W192. doi: 10.1093/nar/gkab341

Du Jardin, P. (2015). Plant biostimulants: definition, concept, main categories and regulation. *Sci. Horticult.* 196, 3–14. doi: 10.1016/j.scienta.2015.09.021

Duke, K. A., Becker, M. G., Girard, I. J., Millar, J. L., Dilantha Fernando, W. G., Belmonte, M. F., et al. (2017). The biocontrol agent *Pseudomonas* chlororaphis PA23 primes Brassica napus defenses through distinct gene networks. *BMC Genomics* 18:467. doi: 10.1186/s12864-017-3848-6

Durrant, M. G., Li, M. M., Siranosian, B. A., Montgomery, S. B., and Bhatt, A. S. (2020). A Bioinformatic Analysis of Integrative Mobile Genetic Elements

Highlights Their Role in Bacterial Adaptation. *Cell Host Microbe* 27, 140–153.e9. doi: 10.1016/j.chom.2019.10.022

Dvorak, P., and De Lorenzo, V. (2018). Refactoring the upper sugar metabolism of *Pseudomonas* putida for co-utilization of cellobiose, xylose, and glucose. *Metab. Eng.* 48, 94–108. doi: 10.1016/j.ymben.2018.05.019

Egan, S. V., Yeoh, H. H., and Bradbury, J. H. (1998). Simple picrate paper kit for determination of the cyanogenic potential of cassava flour. *J. Sci. Food Agricult.* 76, 39–48. doi: 10.3109/09637489809089388

Ferreiro, M. D., Nogales, J., Farias, G. A., Olmedilla, A., Sanjuan, J., and Gallegos, M. T. (2018). Multiple CsrA Proteins Control Key Virulence Traits in *Pseudomonas* syringae pv. tomato DC3000. *Mol. Plant Microbe Interact.* 31, 525–536. doi: 10.1094/MPMI-09-17-0232-R

Galan, J. E., Lara-Tejero, M., Marlovits, T. C., and Wagner, S. (2014). Bacterial type III secretion systems: specialized nanomachines for protein delivery into target cells. *Annu. Rev. Microbiol.* 68, 415–438. doi: 10.1146/annurev-micro-092412-155725

Gamalero, E., and Glick, B. R. (2015). Bacterial Modulation of Plant Ethylene Levels. *Plant Physiol.* 169, 13–22. doi: 10.1104/pp.15.00284

Ghequire, M. G., and De Mot, R. (2014). Ribosomally encoded antibacterial proteins and peptides from *Pseudomonas*. *FEMS Microbiol. Rev.* 38, 523–568.

Harrison, X. A., Donaldson, L., Correa-Cano, M. E., Evans, J., Fisher, D. N., Goodwin, C. E. D., et al. (2018). A brief introduction to mixed effects modelling and multi-model inference in ecology. *PeerJ* 6:e4794. doi: 10.7717/peerj.4794

Haskett, T. L., Tkacz, A., and Poole, P. S. (2021). Engineering rhizobacteria for sustainable agriculture. *ISME J.* 15, 949–964. doi: 10.1038/s41396-020-00835-4

Hayashi, T., Baba, T., Matsumoto, H., and Terawaki, Y. (1990). Phage-conversion of cytotoxin production in *Pseudomonas aeruginosa*. *Mol. Microbiol.* 4, 1703–1709. doi: 10.1111/j.1365-2958.1990.tb00547.x

Höfte, M. (2021). "The use of *Pseudomonas* spp. as bacterial biocontrol agents to control plant disease," in *Microbial Bioprotectants for Plant Disease Management*, eds J. Köhl and W. J. Ravensberg (Cambridge: Burleigh Dodds Science Publishing Limited), 1–74.

Imade, E. E., and Babalola, O. O. (2021). Biotechnological utilization: the role of Zea mays rhizospheric bacteria in ecosystem sustainability. *Appl. Microbiol. Biotechnol.* 105, 4487–4500. doi: 10.1007/s00253-021-11351-6

Ivanova, E. P., Gorshkova, N. M., Sawabe, T., Hayashi, K., Kalinovskaya, N. I., Lysenko, A. M., et al. (2002). *Pseudomonas extremorientalis* sp. nov., isolated from a drinking water reservoir. *Int. J. Syst. Evol. Microbiol.* 52, 2113–2120. doi: 10.1099/00207713-52-6-2113

Jackson, S. A., Crossman, L., Almeida, E. L., Margassery, L. M., Kennedy, J., and Dobson, A. D. W. (2018). Diverse and Abundant Secondary Metabolism Biosynthetic Gene Clusters in the Genomes of Marine Sponge Derived Streptomyces spp. Isolates. *Mar. Drugs* 16:67. doi: 10.3390/md16020067

Jain, C., Rodriguez-R, L. M., Phillippy, A. M., Konstantinidis, K. T., and Aluru, S. (2018). High throughput ANI analysis of 90K prokaryotic genomes reveals clear species boundaries. *Nat. Commun.* 9:5114. doi: 10.1038/s41467-018-07641-9

Kavamura, V. N., Mendes, R., Bargaz, A., and Mauchline, T. H. (2021). Defining the wheat microbiome: towards microbiome-facilitated crop production. *Comput. Struct. Biotechnol. J.* 19, 1200–1213. doi: 10.1016/j.csbj.2021.01.045

Keswani, C., Singh, H. B., Garcia-Estrada, C., Caradus, J., He, Y. W., Mezaache-Aichour, S., et al. (2020). Antimicrobial secondary metabolites from agriculturally important bacteria as next-generation pesticides. *Appl. Microbiol. Biotechnol.* 104, 1013–1034. doi: 10.1007/s00253-019-10300-8

Kloepper, J. W., Leong, J., Teintze, M., and Schroth, M. N. (1980). Enhanced plant growth by siderophores produced by plant growth-promoting rhizobacteria. *Nature* 286, 885–886.

Koren, S., Walenz, B. P., Berlin, K., Miller, J. R., Bergman, N. H., and Phillippy, A. M. (2017). Canu: scalable and accurate long-read assembly via adaptive k-mer weighting and repeat separation. *Genome Res.* 27, 722–736. doi: 10.1101/gr.215087.116

Kupferschmied, P., Maurhofer, M., and Keel, C. (2013). Promise for plant pest control: root-associated pseudomonads with insecticidal activities. *Front. Plant Sci.* 4:287. doi: 10.3389/fpls.2013.00287

Kurz, M., Burch, A. Y., Seip, B., Lindow, S. E., and Gross, H. (2010). Genome-driven investigation of compatible solute biosynthesis pathways of *Pseudomonas* syringae pv. syringae and their contribution to water stress tolerance. *Appl. Environ. Microbiol.* 76, 5452–5462. doi: 10.1128/AEM.00686-10

Li, H.-B., Singh, R. K., Singh, P., Song, Q.-Q., Xing, Y.-X., Yang, L.-T., et al. (2017). Genetic Diversity of Nitrogen-Fixing and Plant Growth Promoting *Pseudomonas* Species Isolated from Sugarcane Rhizosphere. *Front. Microbiol.* 8:1268. doi: 10.3389/fmicb.2017.01268

Li, J., Yao, Y., Xu, H. H., Hao, L., Deng, Z., Rajakumar, K., et al. (2015). SecReT6: a web-based resource for type VI secretion systems found in bacteria. *Environ. Microbiol.* 17, 2196–2202. doi: 10.1111/1462-2920.12794

Li, L., Dou, N., Zhang, H., and Wu, C. (2021). The versatile GABA in plants. *Plant Signal. Behav.* 16:1862565. doi: 10.1080/15592324.2020.1862565

Li, X., Xie, Y., Liu, M., Tai, C., Sun, J., Deng, Z., et al. (2018). oriTfinder: a web-based tool for the identification of origin of transfers in DNA sequences of bacterial mobile genetic elements. *Nucleic Acids Res.* 46, W229–W234. doi: 10.1093/nar/gky352

Lick, S., Krockel, L., Wibberg, D., Winkler, A., Blom, J., Bantleon, A., et al. (2020). *Pseudomonas* carnis sp. nov., isolated from meat. *Int. J. Syst. Evol. Microbiol.* 70, 1528–1540. doi: 10.1099/ijsem.0.003928

Liu, M., Li, X., Xie, Y., Bi, D., Sun, J., Li, J., et al. (2018). ICEberg 2.0: an updated database of bacterial integrative and conjugative elements. *Nucleic Acids Res.* 47, D660–D665. doi: 10.1093/nar/gky1123

Lopez, N. I., Pettinari, M. J., Nikel, P. I., and Mendez, B. S. (2015). Polyhydroxyalkanoates: much More than Biodegradable Plastics. *Adv. Appl. Microbiol.* 93, 73–106. doi: 10.1016/bs.aambs.2015.06.001

Lucke, M., Correa, M. G., and Levy, A. (2020). The Role of Secretion Systems, Effectors, and Secondary Metabolites of Beneficial Rhizobacteria in Interactions With Plants and Microbes. *Front. Plant Sci.* 11:589416. doi: 10.3389/fpls.2020.589416

Lugtenberg, B., and Kamilova, F. (2009). Plant-growth-promoting rhizobacteria. *Annu. Rev. Microbiol.* 63, 541–556.

Lyu, D., Zajonc, J., Page, A., Tanney, C. 'A. S., Shah, A., Monjezi, N., et al. (2021). Plant Holobiont Theory: the Phytomicrobiome Plays a Central Role in Evolution and Success. *Microorganisms* 9:675. doi: 10.3390/microorganisms9040675

Meier-Kolthoff, J. P., and Göker, M. (2019). TYGS is an automated high-throughput platform for state-of-the-art genome-based taxonomy. *Nat. Commun.* 10:2182. doi: 10.1038/s41467-019-10210-3

Meier-Kolthoff, J. P., Auch, A. F., Klenk, H. P., and Goker, M. (2013). Genome sequence-based species delimitation with confidence intervals and improved distance functions. *BMC Bioinformatics* 14:60. doi: 10.1186/1471-2105-14-60

Mendes, R., Garbeva, P., and Raaijmakers, J. M. (2013). The rhizosphere microbiome: significance of plant beneficial, plant pathogenic, and human pathogenic microorganisms. *FEMS Microbiol. Rev.* 37, 634–663. doi: 10.1111/1574-6976.12028

Mendes, R., Kruijt, M., De Bruijn, I., Dekkers, E., Van Der Voort, M., Schneider, J. H., et al. (2011). Deciphering the rhizosphere microbiome for disease-suppressive bacteria. *Science* 332, 1097–1100. doi: 10.1126/science.1203980

Meyer, F., Goesmann, A., Mchardy, A. C., Bartels, D., Bekel, T., Clausen, J., et al. (2003). GenDB–an open source genome annotation system for prokaryote genomes. *Nucleic Acids Res.* 31, 2187–2195. doi: 10.1093/nar/gkg312

Miller, S. H., Browne, P., Prigent-Combaret, C., Combes-Meynet, E., Morrissey, J. P., and O'gara, F. (2010). Biochemical and genomic comparison of inorganic phosphate solubilization in *Pseudomonas* species. *Environ. Microbiol. Rep.* 2, 403–411. doi: 10.1111/j.1758-2229.2009.00105.x

Molina, L., Ramos, C., Duque, E., Ronchel, M. C., GarcıìA, J. M., Wyke, L., et al. (2000). Survival of *Pseudomonas* putida KT2440 in soil and in the rhizosphere of plants under greenhouse and environmental conditions. *Soil Biol. Biochem.* 32, 315–321. doi: 10.1016/S0038-0717(99)00156-X

Müller, T., and Behrendt, U. (2021). Exploiting the biocontrol potential of plant-associated pseudomonads – A step towards pesticide-free agriculture? *Biol. Control* 155:104538. doi: 10.1016/j.biocontrol.2021.104538

Muller, T., Ruppel, S., Behrendt, U., Lentzsch, P., and Muller, M. E. H. (2018). Antagonistic Potential of Fluorescent Pseudomonads Colonizing Wheat Heads Against Mycotoxin Producing Alternaria and Fusaria. *Front. Microbiol.* 9:2124. doi: 10.3389/fmicb.2018.02124

Murphy, J., and Riley, J. P. (1962). A modified single solution method for determination of phosphate. *Anal. Chim. Acta* 27, 31–36. doi: 10.1016/S0003-2670(00)88444-5

Palleroni, N. J. (2015). "Pseudomonas," in *Bergey's Manual of Sytematics of Archaea and Bacteria*, ed. W. B. Whitman (Hoboken, NJ: John Wiley & Sons, Inc.), 9781118960608.

Park, Y.-S., Dutta, S., Ann, M., Raaijmakers, J. M., and Park, K. (2015). Promotion of plant growth by *Pseudomonas* fluorescens strain SS101 via novel volatile organic compounds. *Biochem. Biophys. Res. Commun.* 461, 361–365. doi: 10.1016/j.bbrc.2015.04.039

Pasqua, M., Grossi, M., Zennaro, A., Fanelli, G., Micheli, G., Barras, F., et al. (2019). The Varied Role of Efflux Pumps of the MFS Family in the Interplay of Bacteria with Animal and Plant Cells. *Microorganisms* 7:285. doi: 10.3390/microorganisms7090285

Paterson, J., Jahanshah, G., Li, Y., Wang, Q., Mehnaz, S., and Gross, H. (2017). The contribution of genome mining strategies to the understanding of active principles of PGPR strains. *FEMS Microbiol. Ecol.* 93:fiw249. doi: 10.1093/femsec/fiw249

Perez-Jaramillo, J. E., Mendes, R., and Raaijmakers, J. M. (2016). Impact of plant domestication on rhizosphere microbiome assembly and functions. *Plant Mol. Biol.* 90, 635–644. doi: 10.1007/s11103-015-0337-7

Philippot, L., Raaijmakers, J. M., Lemanceau, P., and Van Der Putten, W. H. (2013). Going back to the roots: the microbial ecology of the rhizosphere. *Nat. Rev. Microbiol.* 11, 789–799. doi: 10.1038/nrmicro3109

Pieterse, C. M. J., Berendsen, R. L., De Jonge, R., Stringlis, I. A., Van Dijken, A. J. H., Van Pelt, J. A., et al. (2021). *Pseudomonas simiae* WCS417: star track of a model beneficial rhizobacterium. *Plant Soil* 461, 245–263. doi: 10.1007/s11104-020-04786-9

Pieterse, C. M., Zamioudis, C., Berendsen, R. L., Weller, D. M., Van Wees, S. C., and Bakker, P. A. (2014). Induced systemic resistance by beneficial microbes. *Annu. Rev. Phytopathol.* 52, 347–375. doi: 10.1146/annurev-phyto-082712-102340

Pikovskaya, R. I. (1948). Mobilization of phosphorus in soil in connection with the vital activity of some microbial species. *Mikrobiologiva* 17, 362–370.

Ramette, A., Frapolli, M., Saux, M. F., Gruffaz, C., Meyer, J. M., Defago, G., et al. (2011). *Pseudomonas* protegens sp. nov., widespread plant-protecting bacteria producing the biocontrol compounds 2,4-diacetylphloroglucinol and pyoluteorin. *Syst. Appl. Microbiol.* 34, 180–188. doi: 10.1016/j.syapm.2010.10.005

Rey, T., and Dumas, B. (2017). Plenty Is No Plague: streptomyces Symbiosis with Crops. *Trends Plant Sci.* 22, 30–37. doi: 10.1016/j.tplants.2016.10.008

Richter, M., Rosselló-Móra, R., Oliver Glöckner, F., and Peplies, J. (2015). JSpeciesWS: a web server for prokaryotic species circumscription based on pairwise genome comparison. *Bioinformatics* 32, 929–931. doi: 10.1093/bioinformatics/btv681

Rosenberg, E., and Zilber-Rosenberg, I. (2016). Microbes Drive Evolution of Animals and Plants: the Hologenome Concept. *mBio* 7:e01395. doi: 10.1128/mBio.01395-15

Rui, Z., Li, X., Zhu, X., Liu, J., Domigan, B., Barr, I., et al. (2014). Microbial biosynthesis of medium-chain 1-alkenes by a nonheme iron oxidase. *Proc. Natl. Acad. Sci. U.S.A.* 111, 18237–18242. doi: 10.1073/pnas.1419701112

Ryu, C. M. (2015). Against friend and foe: type 6 effectors in plant-associated bacteria. *J. Microbiol.* 53, 201–208. doi: 10.1007/s12275-015-5055-y

Ryu, C. M., Farag, M. A., Hu, C. H., Reddy, M. S., Kloepper, J. W., and Pare, P. W. (2004). Bacterial volatiles induce systemic resistance in Arabidopsis. *Plant Physiol.* 134, 1017–1026. doi: 10.1104/pp.103.026583

Sacherer, P., Defago, G., and Haas, D. (1994). Extracellular protease and phospholipase C are controlled by the global regulatory gene gacA in the biocontrol strain *Pseudomonas* fluorescens CHA0. *FEMS Microbiol. Lett.* 116, 155–160. doi: 10.1111/j.1574-6968.1994.tb06694.x

Sawada, H., Fujikawa, T., Tsuji, M., and Satou, M. (2021). *Pseudomonas allii* sp. nov., a pathogen causing soft rot of onion in Japan. *Int. J. Syst. Evol. Microbiol.* [Epub ahead of print]. doi: 10.1099/ijsem.0.004582

Schoner, T. A., Gassel, S., Osawa, A., Tobias, N. J., Okuno, Y., Sakakibara, Y., et al. (2016). Aryl Polyenes, a Highly Abundant Class of Bacterial Natural Products, Are Functionally Related to Antioxidative Carotenoids. *Chembiochem* 17, 247–253. doi: 10.1002/cbic.201500474

Schwyn, B., and Neilands, J. B. (1987). Universal chemical assay for the detection and determination of siderophores. *Anal. Biochem.* 160, 47–56. doi: 10.1016/0003-2697(87)90612-9

Seemann, T. (2014). Prokka: rapid prokaryotic genome annotation. *Bioinformatics* 30, 2068–2069. doi: 10.1093/bioinformatics/btu153

Shinde, S., Zerbs, S., Collart, F. R., Cumming, J. R., Noirot, P., and Larsen, P. E. (2019). *Pseudomonas* fluorescens increases mycorrhization and modulates expression of antifungal defense response genes in roots of aspen seedlings. *BMC Plant Biol.* 19:4. doi: 10.1186/s12870-018-1610-0

Silby, M. W., Winstanley, C., Godfrey, S. A., Levy, S. B., and Jackson, R. W. (2011). *Pseudomonas* genomes: diverse and adaptable. *FEMS Microbiol. Rev* 35, 652–680. doi: 10.1111/j.1574-6976.2011.00269.x

Silva Dias, B. H., Jung, S.-H., Castro Oliveira, J. V. D., and Ryu, C.-M. (2021). C4 Bacterial Volatiles Improve Plant Health. *Pathogens* 10:682. doi: 10.3390/pathogens10060682

Singh, P., Singh, R. K., Guo, D. J., Sharma, A., Singh, R. N., Li, D. P., et al. (2021). Whole Genome Analysis of Sugarcane Root-Associated Endophyte *Pseudomonas aeruginosa* B18-A Plant Growth-Promoting Bacterium With Antagonistic Potential Against Sporisorium scitamineum. *Front. Microbiol.* 12:628376. doi: 10.3389/fmicb.2021.628376

Sobrero, P. M., and Valverde, C. (2020). Comparative Genomics and Evolutionary Analysis of RNA-Binding Proteins of the CsrA Family in the Genus *Pseudomonas*. *Front. Mol. Biosci.* 7:127. doi: 10.3389/fmolb.2020.00127

Spaepen, S., Vanderleyden, J., and Remans, R. (2007). Indole-3-acetic acid in microbial and microorganism-plant signaling. *FEMS Microbiol. Rev.* 31, 425–448. doi: 10.1111/j.1574-6976.2007.00072.x

Stringlis, I. A., Zamioudis, C., Berendsen, R. L., Bakker, P., and Pieterse, C. M. J. (2019). Type III Secretion System of beneficial rhizobacteria *Pseudomonas simiae* WCS417 and *Pseudomonas defensor* WCS374. *Front. Microbiol.* 10:1631. doi: 10.3389/fmicb.2019.01631

Tabatabai, M. A., and Bremner, J. M. (1969). Use of p-nitrophenylphosphate for assay of soil phosphatase activity. *Soil Biol. Biochem.* 1, 301–307. doi: 10.1016/0038-0717(69)90012-1

Tagele, S. B., Kim, S. W., Lee, H. G., and Lee, Y. S. (2019). Potential of Novel Sequence Type of Burkholderia cenocepacia for Biological Control of Root Rot of Maize (Zea mays L.) Caused by Fusarium temperatum. *Int. J. Mol. Sci.* 20:1005. doi: 10.3390/ijms20051005

Tao, C., Li, R., Xiong, W., Shen, Z., Liu, S., Wang, B., et al. (2020). Bio-organic fertilizers stimulate indigenous soil *Pseudomonas* populations to enhance plant disease suppression. *Microbiome* 8, 137–137. doi: 10.1186/s40168-020-00892-z

Timmusk, S., Behers, L., Muthoni, J., Muraya, A., and Aronsson, A. C. (2017). Perspectives and Challenges of Microbial Application for Crop Improvement. *Front. Plant Sci.* 8:49. doi: 10.3389/fpls.2017.00049

Tzipilevich, E., Russ, D., Dangl, J. L., and Benfey, P. N. (2021). Plant immune system activation is necessary for efficient root colonization by auxin-secreting beneficial bacteria. *Cell Host Microbe* 29, 1507–1520.e4.. doi: 10.1016/j.chom.2021.09.005

Valente, J., Gerin, F., Le Gouis, J., Moënne-Loccoz, Y., and Prigent–Combaret, C. (2020). Ancient wheat varieties have a higher ability to interact with plant growth-promoting rhizobacteria. *Plant Cell Environ.* 43, 246–260. doi: 10.1111/pce.13652

Van Heel, A. J., De Jong, A., Song, C., Viel, J. H., Kok, J., and Kuipers, O. P. (2018). BAGEL4: a user-friendly web server to thoroughly mine RiPPs and bacteriocins. *Nucleic Acids Res.* 46, W278–W281. doi: 10.1093/nar/gky383

Vela, A. I., Gutierrez, M. C., Falsen, E., Rollan, E., Simarro, I., Garcia, P., et al. (2006). *Pseudomonas simiae* sp. nov., isolated from clinical specimens from monkeys (Callithrix geoffroyi). *Int. J. Syst. Evol. Microbiol.* 56, 2671–2676. doi: 10.1099/ijs.0.64378-0

Von Neubeck, M., Huptas, C., Gluck, C., Krewinkel, M., Stoeckel, M., Stressler, T., et al. (2017). *Pseudomonas* lactis sp. nov. and *Pseudomonas* paralactis sp. nov., isolated from bovine raw milk. *Int. J. Syst. Evol. Microbiol.* 67, 1656–1664. doi: 10.1099/ijsem.0.001836

Wang, Y. L., Sun, L. J., Xian, C. M., Kou, F. L., Zhu, Y., He, L. Y., et al. (2020). Interactions between Biotite and the Mineral-Weathering Bacterium *Pseudomonas* azotoformans F77. *Appl. Environ. Microbiol.* 86:e2568–e2519. doi: 10.1128/AEM.02568-19

Wibberg, D., Price-Carter, M., Ruckert, C., Blom, J., and Mobius, P. (2020). Complete Genome Sequence of Ovine Mycobacterium avium subsp. paratuberculosis Strain JIII-386 (MAP-S/type III) and Its Comparison to MAP-S/type I, MAP-C, and M. avium Complex Genomes. *Microorganisms* 9:70. doi: 10.3390/microorganisms9010070

Wibberg, D., Stadler, M., Lambert, C., Bunk, B., Spröer, C., Rückert, C., et al. (2021). High quality genome sequences of thirteen Hypoxylaceae (Ascomycota) strengthen the phylogenetic family backbone and enable the discovery of new taxa. *Fungal Divers.* 106, 7–28. doi: 10.1007/s13225-020-00447-5

Yu, K., Liu, Y., Tichelaar, R., Savant, N., Lagendijk, E., Van Kuijk, S. J. L., et al. (2019). Rhizosphere-Associated *Pseudomonas* Suppress Local Root Immune Responses by Gluconic Acid-Mediated Lowering of Environmental pH. *Curr. Biol.* 29, 3913–3920.e4. doi: 10.1016/j.cub.2019.09.015

Zamioudis, C., and Pieterse, C. M. J. (2012). Modulation of Host Immunity by Beneficial Microbes. *Mol. Plant Microbe Interact.* 25, 139–150. doi: 10.1094/mpmi-06-11-0179

Zhang, F., Zhao, S., Ren, C., Zhu, Y., Zhou, H., Lai, Y., et al. (2018). CRISPRminer is a knowledge base for exploring CRISPR-Cas systems in microbe and phage interactions. *Commun. Biol.* 1:180. doi: 10.1038/s42003-018-0184-6

Zhang, J., Mavrodi, D. V., Yang, M., Thomashow, L. S., Mavrodi, O. V., Kelton, J., et al. (2020). *Pseudomonas synxantha* 2-79 Transformed with Pyrrolnitrin Biosynthesis Genes Has Improved Biocontrol Activity Against Soilborne Pathogens of Wheat and Canola. *Phytopathology* 110, 1010–1017. doi: 10.1094/phyto-09-19-0367-r

Zhou, Y., Liang, Y., Lynch, K. H., Dennis, J. J., and Wishart, D. S. (2011). PHAST: a fast phage search tool. *Nucleic Acids Res.* 39, W347–W352. doi: 10.1093/nar/gkr485

frontiers | Frontiers in Plant Science

TYPE Original Research
PUBLISHED 08 August 2022
DOI 10.3389/fpls.2022.920881

OPEN ACCESS

EDITED BY
Maurizio Ruzzi,
University of Tuscia, Italy

REVIEWED BY
Mukul Joshi,
Birla Institute of Technology and Science, India
Cristiano Fortuna Soares,
University of Porto, Portugal

*CORRESPONDENCE
Héctor Ocampo-Alvarez
hector.ocampo@academicos.udg.mx

†These authors have contributed equally to this work and share first authorship

SPECIALTY SECTION
This article was submitted to Crop and Product Physiology, a section of the journal Frontiers in Plant Science

RECEIVED 15 April 2022
ACCEPTED 20 July 2022
PUBLISHED 08 August 2022

CITATION
Becerril-Espinosa A, Hernández-Herrera RM, Meza-Canales ID, Perez-Ramirez R, Rodríguez-Zaragoza FA, Méndez-Morán L, Sánchez-Hernández CV, Palmeros-Suárez PA, Palacios OA, Choix FJ, Juárez-Carrillo E, Lara-González MA, Hurtado-Oliva MA and Ocampo-Alvarez H (2022) Habitat-adapted heterologous symbiont *Salinispora arenicola* promotes growth and alleviates salt stress in tomato crop plants. *Front. Plant Sci.* 13:920881. doi: 10.3389/fpls.2022.920881

Habitat-adapted heterologous symbiont *Salinispora arenicola* promotes growth and alleviates salt stress in tomato crop plants

Amayaly Becerril-Espinosa[1,2†], Rosalba M. Hernández-Herrera[3†], Ivan D. Meza-Canales[1,4], Rodrigo Perez-Ramirez[1], Fabián A. Rodríguez-Zaragoza[1], Lucila Méndez-Morán[1], Carla V. Sánchez-Hernández[5], Paola A. Palmeros-Suárez[5], Oskar A. Palacios[6], Francisco J. Choix[2,6], Eduardo Juárez-Carrillo[1], Martha A. Lara-González[1], Miguel Ángel Hurtado-Oliva[7] and Héctor Ocampo-Alvarez[1*]

[1]Departamento de Ecología, Centro Universitario de Ciencias Biológicas y Agropecuarias, Universidad de Guadalajara, Guadalajara, Mexico, [2]Consejo Nacional de Ciencia y Tecnología, Mexico City, Mexico, [3]Departamento de Botánica y Zoología, Centro Universitario de Ciencias Biológicas y Agropecuarias, Universidad de Guadalajara, Guadalajara, Mexico, [4]Instituto Transdisciplinar de Investigación y Servicios, Centro Universitario de Ciencias Exactas e Ingenierías, Universidad de Guadalajara, Guadalajara, Mexico, [5]Departamento de Producción Agrícola, Centro Universitario de Ciencias Biológicas y Agropecuarias, Universidad de Guadalajara, Guadalajara, Mexico, [6]Facultad de Ciencias Químicas, Universidad Autónoma de Chihuahua, Chihuahua, Mexico, [7]Facultad de Ciencias del Mar, Universidad Autónoma de Sinaloa, Mazatlán, Mexico

To ensure food security given the current scenario of climate change and the accompanying ecological repercussions, it is essential to search for new technologies and tools for agricultural production. Microorganism-based biostimulants are recognized as sustainable alternatives to traditional agrochemicals to enhance and protect agricultural production. Marine actinobacteria are a well-known source of novel compounds for biotechnological uses. In addition, former studies have suggested that coral symbiont actinobacteria may support co-symbiotic photosynthetic growth and tolerance and increase the probability of corals surviving abiotic stress. We have previously shown that this activity may also hold in terrestrial plants, at least for the actinobacteria *Salinispora arenicola* during induced heterologous symbiosis with a wild Solanaceae plant *Nicotiana attenuata* under *in vitro* conditions. Here, we further explore the heterologous symbiotic association, germination, growth promotion, and stress relieving activity of *S. arenicola* in tomato plants under agricultural conditions and dig into the possible associated mechanisms. Tomato plants were grown under normal and saline conditions, and germination, bacteria-root system interactions, plant growth, photosynthetic performance, and the expression of salt stress response genes were analyzed. We found an endophytic interaction between *S. arenicola* and tomato plants, which promotes germination and

shoot and root growth under saline or non-saline conditions. Accordingly, photosynthetic and respective photoprotective performance was enhanced in line with the induced increase in photosynthetic pigments. This was further supported by the overexpression of thermal energy dissipation, which fine-tunes energy use efficiency and may prevent the formation of reactive oxygen species in the chloroplast. Furthermore, gene expression analyses suggested that a selective transport channel gene, *SlHKT1,2*, induced by *S. arenicola* may assist in relieving salt stress in tomato plants. The fine regulation of photosynthetic and photoprotective responses, as well as the inhibition of the formation of ROS molecules, seems to be related to the induced down-regulation of other salt stress response genes, such as *SlDR1A*-related genes or *SlAOX1b*. Our results demonstrate that the marine microbial symbiont *S. arenicola* establishes heterologous symbiosis in crop plants, promotes growth, and confers saline stress tolerance. Thus, these results open opportunities to further explore the vast array of marine microbes to enhance crop tolerance and food production under the current climate change scenario.

KEYWORDS

***Salinispora* heterologous symbiont, marine actinobacteria, coral actinobacteria, plant salt stress, plant biostimulant, photoprotective response**

Introduction

Plant biostimulants (PBs) based on microorganisms have emerged as sustainable alternatives to traditional agrochemicals by enhancing plant stress tolerance and increasing crop yields and quality under suboptimal conditions. Nowadays, PBs are becoming essential components of strategies to mitigate the effects of climate change. In their native environments, plants live and grow with many symbiotic microorganisms. However, intensive cultivation practices and the indiscriminate use of fertilizers and agrochemicals, which at one point increased the ecological success of plants, have modified the natural microbiota of crop soils. Microorganism-based PBs take advantage of the symbiotic microorganisms that typically occur in nature and reintroduce them into empty crop soil, which enables plants to withstand environmental changes that threaten the global crop industry (Shameer and Prasad, 2018).

Currently, one of the principal problems that affects crop productivity is soil salinization. Soil salinization has increased due to the over-irrigation and over-fertilization of high-yield cropping systems, which have affected 931.67 million hectares worldwide as of 2018 (Mukhopadhyay et al., 2021). The resulting high salt concentrations in soils produce osmotic stress and cause imbalances in water and nutrient uptake by plants (Arif et al., 2020). Moreover, a high influx of Na^+ ions into the plant cells results in the displacement of K^+ ions from many enzymes and cofactors, which affects plant metabolism (Abdelaziz et al., 2019). Both ionic and osmotic stressors promote the accumulation of reactive oxygen species (ROS) and cause oxidative stress, which can damage DNA, proteins, and lipids (Shahid et al., 2020). These plant stressors affect germination, photosynthesis, growth, flowering, and many other physiological processes responsible for the low crop yields associated with saline soils (Parihar et al., 2015).

Plants have evolved complex survival responses to cope with salinity that involve coordination among many physiological and genetic processes, such as controlling water loss through stomata pore regulation, ion sequestration, metabolic and osmotic adjustments, and the activation of enzymatic and non-enzymatic mechanisms of the antioxidant system to maintain cellular redox homeostasis (Orsini et al., 2011; Abo-Ogiala et al., 2014; Adem et al., 2014; Geilfus et al., 2015; Soares et al., 2019). However, natural plant responses are not always sufficiently able to cope with stress. To our knowledge, no reliable process is available to fully restore saline soils (Shankar and Evelin, 2019). However, the inoculation of plants with certain microorganisms can increase their salt tolerance and enable them to be cultivated under saline stress conditions. Rodriguez et al. (2008) elegantly demonstrated a process, which they defined as habitat-adapted symbiosis (HAS), in which endophytic symbionts of native halophytes enable saline-sensitive plants to grow in saline soils. Since then, HAS strategies employing various halophytes from different saline habitats have been explored to relieve salt stress in salt-sensitive plant species. Some examples of HAS species that confer resistance to salt stress in plants

are the halophilic bacteria *Stenotrophomonas rhizophila*, which inhabits the halophyte *Lygeum spartum* that is native to the desert environments of Algeria; *Bacillus atrophaeus*, which is an endophyte of the halophytes *Suaeda mollis* and S*alsola tetrandra* that are native to Algeria Salt Lakes; *Jejubacter calystegiae*, which is found in the halophyte *Calystegia soldanella* that is found on sandy beaches in South Korea; and many fungus-like microorganisms like *Neocamarosporium chichastianum*, *N. goegapense*, and *Periconia macropinosa*, which has been isolated from the desert halophyte *Seidlitzia osmarinus* collected at Hoz-e Soltan Salt Lake in Iran (Jiang et al., 2021; Kerbab et al., 2021; Moghaddam et al., 2021; Dif et al., 2022). Some of these HAS species have been successfully employed in PB formulations.

Recently, it was shown that the marine actinobacteria *Salinispora arenicola* could establish a symbiotic relationship with seedlings of the wild-tobacco *Nicotiana attenuata* under *in vitro* conditions (Ocampo-Alvarez et al., 2020) and relieve saline stress during germination and early growth. As *S. arenicola* is a saline habitat symbiont that relieves saline stress in the saline-sensitive *N. attenuata*, it partially fulfills the HAS definition. However, the native habitat of *S. arenicola* is marine, and it is found within *Porites* corals where it establishes what seems to be three symbiotic trophic interactions between the coral and *Symbiodinium* sp., a phototrophic alga. Therefore, *S. arenicola* is better defined as a habitat-adapted heterologous symbiont (HAHS). Nevertheless, the potential of this HAHS species to relieve salt stress and any associated mechanisms remain unexplored in terrestrial plants of agricultural interest.

All HAS possess specific mechanisms to ameliorate saline stress in plants. A common HAS mechanism is the production of osmolytes, such as proline, trehalose, glycine betaine, or exopolysaccharides, which directly ameliorate osmotic stress by decreasing the internal osmotic potential of plants cells (Bano and Fatima, 2009; Upadhyay et al., 2012; Timmusk et al., 2014; Upadhyay and Singh, 2015). Other HAS mechanisms involve activating antioxidant systems, such as enzymes, biochemical compounds, and secondary metabolites that counteract the induced oxidative stress (Hashem et al., 2016). Moreover, several HAS also regulate phytohormone activity or biosynthesis. For example, ACC (1-aminocyclopropane-1-carboxylate) deaminase activity lowers the level of the stress-related phytohormone ethylene, thus avoiding the down-regulation of genes involved in plant growth (Glick et al., 2007). Another mechanism to cope with salinity in plants is the overexpression of specific ionic channels that counterbalance the K^+/Na^+ proportion, such as high-affinity Na^+ and K^+ transporters (i.e., High-affinity K^+, *HKT*; Na^+/K^+ antiporters, *NHX*; or inward-rectifier K^+ channel/transporters, *AKTs*; Arif et al., 2020). Different mechanisms produce different levels of protection, which may lead to improved germination, photosynthesis, growth, flowering, or yield under saline conditions.

Tomato (*Solanum lycopersicum*) is an agriculturally important crop, and its responses to salt stress have been abundantly reported. Some of the most recognizable effects of salinity in tomato plants are reduced growth; decreased dry weights (DW) of roots, stems, and leaves; and leaf senescence (Munns, 2002; Zribi et al., 2009). Growth reduction is a consequence of Na^+ accumulation due to a decline in the water potential, which affects photosynthetic activity (Iyengar and Reddy, 1996; Hanachi et al., 2014). Stomatal closure is probably the first plant protection response against desiccation and a direct factor that immediately controls carbon fixation in the case of C3 plants. Long-term exposure to saline treatments in tomatoes has been shown to result in a notable and progressive decline in photochemical processes and a notable increase in non-photochemical quenching (NPQ) that protects the plant from an overreduction of the quinone electron acceptor (QA; Zribi et al., 2009).

In this study, the properties of the marine actinobacteria *S. arenicola* as a PB and bio-protector under normal and saline conditions were evaluated in tomato plants. First, the nature of the interaction between the tomato plants and *S. arenicola* was established. Then, the potential of this actinobacteria to relieve induced salt stress during germination and plant growth was explored based on the assumption that the HAHS *S. arenicola* may possess specific activities that could alleviate salt stress in tomato plants. Finally, the photosynthetic performance, pigment composition, osmolyte content, and changes in the antioxidant properties of tomato plants were explored while scouting for changes in the expression of genes potentially involved in different mechanisms induced by salt stress conditions. Overall, our results support the potential of this marine actinobacterium to be used as a crop PB and protective agent against salt stress.

Materials and methods

Biological samples

Salinispora arenicola strain X29 (GenBank accession number MT002753[1]) was isolated from *Porites lobata* obtained from the Tropical Central Pacific coral reef system (19° 5′ 55.21″ N, 104° 23′ 24.47″ W and 19° 3′ 28.87″ N, 104° 15′ 40.25″ W) and cryopreserved at −70°C in 15% glycerol (Ocampo-Alvarez et al., 2020) until use.

The bacterial suspension used to treat Tomato plants was prepared as follows: *S. arenicola* X29 was cultivated on A1 medium (Mincer et al., 2002) under agitation at 210 rpm and 28°C for 5 days and then centrifuged at 10,000 × *g* for 5 min. The supernatant was discarded, and the pellet

1 http://www.ncb.nlm.nih.gov/genbank/index.html

was weighed and resuspended with distilled water to a final concentration of 1 mg/mL.

All experiments were conducted using tomato plants (*S. lycopersicum* L. cv. Rio Fuego; Kristen Seed, San Diego, CA, United States). Tomato seeds were cleaned by immersion on a 10% v/v household soapy solution for 1 min and washed thrice with sterile distilled water. They were then disinfected with 3% sodium hypochlorite for 10 min and washed thrice with sterile distilled water. Subsequently, the seeds were either treated with *S. arenicola* X29 or not and then sown in phytagel-agar media for the germination and fluorescence *in situ* hybridization (FISH) experiments or with peat moss in germination trays and later treated at the seedling stage with *S. arenicola* X29 for subsequent plant response analyses (**Figure 1**). The plants were grown at all times in an artificial climate growth chamber (Thermo Fisher Scientific, Waltham, MA, United States) at 28/17°C and with a 16:8 h day/night photoperiod (155–300 μm s^{-1} m^{-2}).

Root *Salinispora* colonization

Tomato seeds were cleaned as previously described and incubated for 2 h in 3 mL of *S. arenicola* X29 culture or water (i.e., control) right after cleaning (**Figure 1**). Then, the seeds were sown in sterile plates with solid plant growth media [6 g L^{-1} phytagel (Sigma-Aldrich, St. Louis, MO, United States) and 3.2 g L^{-1} Gamborg's B-5 Basal Medium with Minimal Organics (Sigma-Aldrich)], with or without 100 mM NaCl (SIGMA, Merck KGaA, Darmstadt, Germany). Seeds were then incubated at 28/17°C with a 16:8 light/dark photoperiod (155–300 μm s^{-1} m^{-2}) in a growth chamber. After 30 days, the roots were harvested, fixed with formaldehyde, and stored at −20°C until needed for Giemsa staining and FISH hybridization.

Giemsa-stained roots were then observed under a light microscope (Olympus BX41; Olympus, Tokyo, Japan; Muresu et al., 2010). FISH was performed according to the methods of de-Bashan et al. (2011) and Palacios et al. (2019). Three probes labeled with FAM dye, which have been previously reported, were used to target eubacteria: EUB-338-I (5′GCT GCC TCC CGT AGG AGT-3′), EUB-338-II (5′-GCA GCC ACC CGT AGG TGT-3′), and EUB-338-III (5′ GCT GCC ACC CGT AGG TGT-3′; Amann et al., 1990; Daims et al., 1999). The samples were visualized with a BX41 epifluorescence microscope (Olympus) using a FITC filter at 550/570 nm (excitation/emission; Olympus America, Melville, NY, United States).

Germination assays

The tomato seed germination assay was conducted according to the standard protocol of the international society for seed bioassays (ISTA), which was modified by adding the actinobacteria or A1 medium (i.e., controls) as previously described. Approximately 800 surface-sterilized seeds were mixed with 3 mL of *S. arenicola* X29 suspension culture or A1 medium (control) for 2 h (**Figure 1**). Under sterile conditions, the seeds were transferred into Petri dishes containing wet Whatman no. 5 filter paper (Whatman International Limited, Maidstone, United Kingdom).

The salt stress experiment was run with 8 mL of 100 mM NaCl or sterile distilled water (control). Four groups, each containing 100 seeds, were included in each experiment. The seeds were incubated in a growth chamber at 28°C with a 16:8 light/dark photoperiod (155–300 μm/s/m^2). Seed germination was measured every day for 8 days and only when the radicle was at least 2 mm long. The germination percentage was determined using the following formula:

$$\%\ Germination = \frac{number\ of\ germinated\ seeds}{total\ number\ of\ seeds} \times 100$$

Germination was followed daily for 8 days after sowing. The seed germination data were fitted to the Gompertz equation: $f = a\left(exp^{-exp\left[-\left(\frac{d-d_0}{b}\right)\right]}\right)$, where a represents the maximum germination percentage and d_0 represents the half time of maximum germination. Germinated seeds were grown for five additional days (13 days after sowing), and the morphological properties of the seedlings were analyzed. Specifically, the plumule and radicle lengths (cm) of the seedlings were measured, and the dry weight of the seedlings was determined after oven drying at 50°C to a constant weight. Nitrogen, carbon, and polyphenol content were determined in seedlings to evaluate any nutritional or antioxidant benefits induced by the actinobacteria.

Nitrogen and organic carbon percentages were determined according to the methodology established by the Association of Analytical Chemists (955.04; Association of Official Analytical Chemist, 1990). Total polyphenol content was evaluated with the Folin-Ciocalteu colorimetric method with a gallic acid standard (Singleton and Rossi, 1965).

Treatment of plants with *Salinispora arenicola* for growth, photosynthesis, metabolite, antioxidant capacity, and gene expression analysis

Tomato seeds were germinated in peat moss as previously described without further treatment. Fifteen-day-old seedlings were washed with distilled water to remove peat moss. The roots were incubated for 3 min in the *S. arenicola* X29 suspension at a bacteria concentration of 1 mg/mL or water (control). The treated seedlings were transplanted into pots with 500 g of soil mixture composed of vermiculite, peat moss, and soil (1v:1v:1v; **Figure 1**).

10.3389/fpls.2022.920881

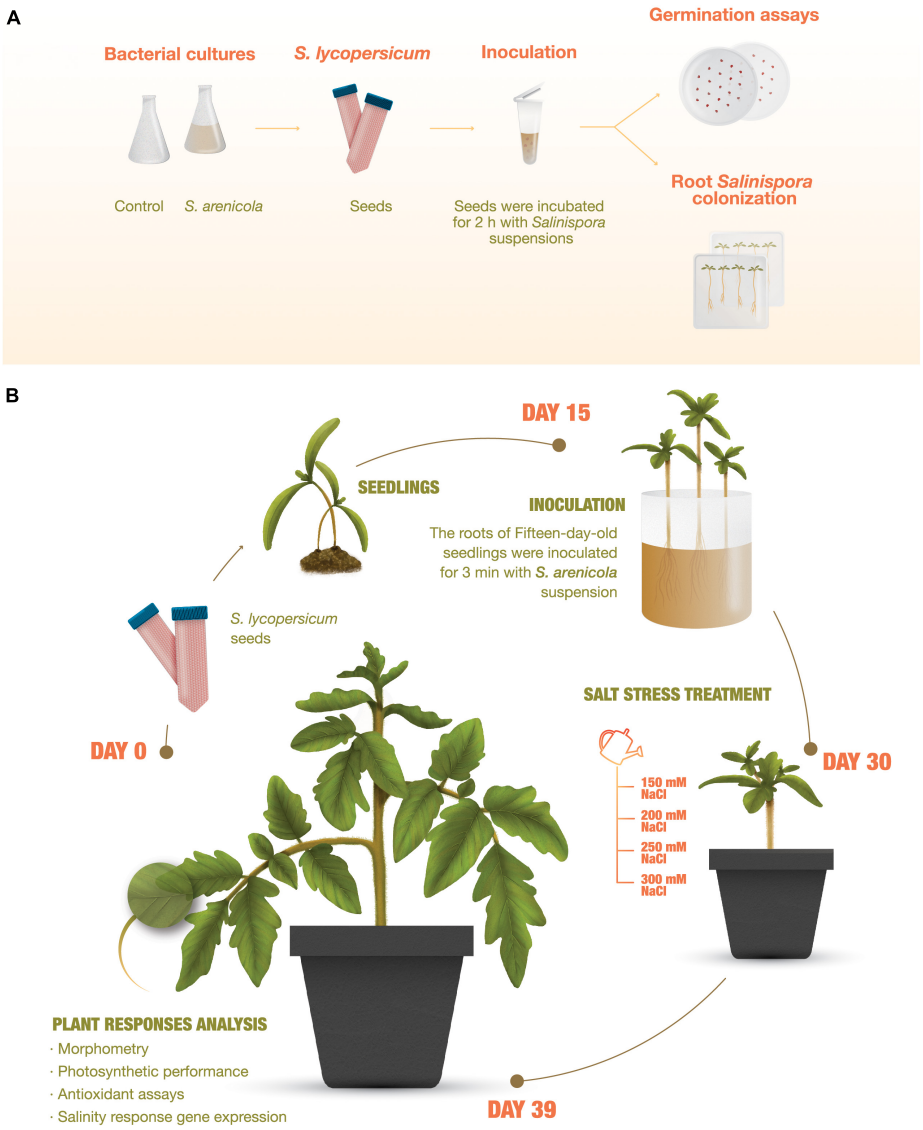

FIGURE 1
Experiment outline. **(A)** Root *Salinispora* colonization and germination assays of tomato (*Solanum lycopersicum*) plants. Seeds were sterilized, directly inoculated with *S. arenicola* X29, and sown and cultured in phytagel-agar plates. Growth and plant response analyses. **(B)** Tomato seedling roots were inoculated on day 15. On day 30, the plants were treated for 8 days with increasing NaCl concentrations and analyzed on day 39.

Salt stress treatment

Fifteen days after treatment with the *S. arenicola* suspension, a set of tomato plants was irrigated with increasing concentrations of saline water (150, 200, 250, and 300 mM NaCl) every second day. Photosynthetic performance and morphological parameters were analyzed for all treatments 9 days after inducing salt stress with saline water irrigation (Day 39, **Figure 1**). Whole leaf samples were collected, flash-frozen with liquid nitrogen, and stored at −70°C for metabolite, pigment, enzyme, or gene expression analyses.

Photosynthetic performance analysis

Chlorophyll-*a* fluorescence was measured with a non-intrusive pulse-amplitude modulated (PAM) chlorophyll-fluorometer (Junior-PAM, Heinz Walz GmbH, Effeltrich, Germany). All photosynthetic parameters from the fluorescence measurements were obtained as described by Schreiber (2004) (**Supplementary Table 1**). Two standard protocols (i.e., induction curves and rapid light response curves) were used to obtain all photosynthetic parameters for our experiments. Both protocols were performed on the second youngest,

attached, fully expanded, and healthy leaves of at least six plants per treatment. The light guide of the Junior-PAM was positioned at the midpoint of the adaxial side of the leaf for both fluorescence protocols. The protocols were initiated after 30 min of dark adaption.

The NPQ induction curves began with a saturating pulse of 10,000 μmol photons m^{-2} s^{-1} (800 ms) to measure maximum fluorescence when all PSII reaction centers were closed. This pulse was followed by 40 s of darkness to reestablish a basal F_0 measurement, after which the leaf was subjected to 20 min of high actinic light (1,500 μmol photon m^{-2} s^{-1}). Saturating light pulses (SP) were emitted during this lighting period every 30 s. The rapid light curves (RLCs) were set with 12 light levels (each turned on for 30 s): 25, 45, 65, 90, 125, 190, 285, 420, 625, 820, 1,150, and 1,500 μmol photon m^{-2} s^{-1}. As in the induction curve experiments, the RLCs began with a saturating light pulse of 10,000 μmol photons m^{-2} s^{-1} (800 ms) to measure maximum fluorescence when all PSII reaction centers were closed. All experiments began early in the morning and were completed before noon. The induction curve and RLC parameters were obtained from the automatic data output of the Junior PAM software.

Photosynthetic pigments

Photosynthetic pigments were extracted and measured using the method described by Zapata et al. (2000) following the recommendations of Osuna-Ruíz et al. (2019). Pigments were extracted from 300 mg of fresh frozen leaves in 90% acetone for 24 h at 4°C and then centrifuged at 3,220 × *g* for 10 min. The supernatants were recovered and stored at −20°C until use. Pigment quantification was performed with a 1200 Infinity HPLC system (Agilent Technologies, Santa Clara, CA, United States) coupled to a diode array detector (DAD) with a C-8 column (ZORBAX 4.6 mm × 100 mm, 3.5 μm particles). The mobile phases consisted of eluent A (methanol:acetonitrile:pyridine 0.25 M, 50:25:25, v:v:v) and eluent B (acetonitrile:acetone, 80:20, v:v) delivered with the following gradient scheme (A%/B%, min): 100/0, 0; 60/40, 22; 5/95, 28; 5/95, 38; and 0/100, 40. The flow rate was fixed at 1 mL per min. All solvents were HPLC grade (Tedia, OH, United States). Pigments were identified by comparing their retention times with standards (DHI, Hørsholm, Denmark). Pigment coefficients were calculated to evaluate the photosynthetic and photoprotective status of whole-treated plants. Total chlorophyll was obtained by the sum of Chl *a* + Chl *b* and was used as a proxy for photosynthetic capacity. The chlorophyll ratio was obtained by dividing Chl *a* by Chl *b* and was used as an estimator of LHCII antenna size and the light acclimation state. The pool size of the xanthophyll cycle pigments ($\sum XC$) was obtained by the sum content of the three xanthophyll pigments [i.e., violaxanthin (Vx), antheraxanthin (Ax), and zeaxanthin (Zx)] and was used to estimate the photoprotective capacity to dissipate thermal energy. The percentage of xanthophyll cycle pigments in deepoxidated state DEPS was obtained by the formula $\left(\frac{[Z_x]+0.5[A_x]}{\sum XC}\right) \times 100$ and was used to assess the actual photoprotective state of the $\sum XC$ pool. The β-carotene:total chlorophyll ratio, $\frac{\beta-car}{Chl\ a+b}$, was used as a proxy of the antioxidant capacity.

Total phenol, flavonoid, proline, and reducing sugar content

Phenol, flavonoid, and reducing sugar content were determined from acidified ethanol extractions conducted with fresh frozen leaves (six plants per treatment) that were pulverized and lyophilized (ILSHIN BIOBASE Table Top Freeze Dryer). A total of 25 mg of lyophilized leaves was extracted in 70% ethanol (acidified with 0.1% HCl) for 24 h at 4°C in the dark. The mixture was centrifuged at 4°C for 20 min at 10,000 × *g*, and the supernatant was collected for metabolite analysis.

Total polyphenol content was determined using the Folin-Ciocalteu (F-C) colorimetric method adjusted for micro-determination (Cao et al., 2020) with some modifications. A 100-μL aliquot of the sample extract and 500 μL of F-C reagent were mixed and incubated at room temperature for 5 min. Afterward, 400 μL of Na_2CO_3 (15%) was added to the solution. The mixture was incubated at 45°C for 10 min. A total of 200 μL of the reaction mixture was placed into a 96-well plate. The absorbance was measured at 730 nm in a microplate reader (Multiskan^{TM} GO Microplate Spectrophotometer, Thermo Fisher Scientific, Waltham, MA, United States) after mixing and an 80-min incubation in the dark. A standard curve using gallic acid was recorded (10–200 μg/mL). Phenol content was expressed as gallic acid equivalents (GAE, mg) per gram of DW (mg GAE/g DW).

The reducing sugar assay was conducted according to the methodology of Negrulescu et al. (2012) with some modifications. A 100-μL aliquot of the sample extract was added to 1,000 μL of DNS reagent (3,5-dinitro salicylic acid, Sigma Aldrich) and mixed. The samples were incubated for 10 min at 100°C. Subsequently, the mixture was allowed to cool to room temperature for 4 min, and 200 μL was placed in a microplate. The absorbance was read at 540 nm with the Multiskan^{TM} GO microplate reader (Thermo Fisher Scientific). A glucose calibration curve ranging from 1–10 mg/mL was used.

The proline assay was conducted as described by Palmeros-Suárez et al. (2015). Briefly, leaves were harvested, flash-frozen in liquid nitrogen, pulverized, and lyophilized. A total of 25 mg of powdered tissue from each sample was mixed with 100 μL of the proline extraction buffer [80% ethanol, 100 mM HEPES *N*-(2-Hydroxyethyl)piperazine-N′-(2-ethane sulfonic acid) buffer at pH 7.4, and 5 mM $MgCl_2$]. The mixture was incubated at

4°C for 10 min with shaking and then centrifuged at 10,000 × *g* at 4°C for 10 min. The supernatant was transferred to a new tube and concentrated by vacuum centrifugation using a Maxi Dry Lyo (Heto-Holten, Allerød, Denmark). The precipitate was dissolved in 100 μL of HEPES buffer (100 mM, pH 7.4) with $MgCl_2$ (5 mM). A 100-μL aliquot of the former solution was added to 200 μL of a solution containing glacial acetic acid 60% (v/v), ethanol 20% (v/v), and ninhydrin 1% (w/v). The mixture was boiled at 95°C for 20 min, cooled to room temperature, and the optical density was recorded at 520 nm in the Multiskan™ GO microplate reader (Thermo Fisher Scientific).

Antioxidant capacity

Antioxidant capacity was measured according to the methodology of Brand-Williams et al. (1995) following the recommendations of Rubio-Ochoa et al. (2019). A total of 100 μL of each sample extract and 900 μL of 0.1 M of the stable radical 2,2-diphenyl-1-picrylhydrazyl (DPPH• in 70% ethanol) were mixed for 30 min at room temperature in the dark. Subsequently, a 250-μL aliquot of each sample was placed in the 96-well Multiskan™ GO microplate (Thermo Fisher Scientific) and read at 515 nm. The result was expressed in micromol equivalents of Trolox per gram of tissue (DW) using a calibration curve ranging from 1–1,000 μM/mL.

Salinity responsive gene expression assay

Total RNA was extracted from leaves obtained from a pool of three plants using TRIzol Reagent (Invitrogen, Carlsbad, CA, United States) following manufacturer recommendations. The cDNA was obtained from 2 μg of RNA using GoScript reverse transcriptase (Promega, Madison, NJ, United States) and oligo-dT (15) primers. qPCR amplifications were performed using SYBR® Green detection in 96-well plates in a StepOnePlus System (Applied Biosystems, Foster City, CA, United States). Reactions were prepared in a total volume of 15 μL with 1.5 μL of cDNA template (1:10), 7.5 μL SYBR® Select Master Mix (Applied Biosystems), and forward and reverse gene-specific primers (300 nM). The cycling conditions were set as follows: initial denaturation step at 95°C for 5 min, followed by 40 cycles of denaturation at 95°C for 10 s, and annealing at 60°C for 30 s. A melting curve analysis was used to evaluate reaction specificity. The RT-qPCR system software automatically determined the baseline and cycle threshold (Ct). Relative expression was calculated using a comparative cycle threshold method (Livak and Schmittgen, 2001) and *SlGADPH* and *SlEF1α* as endogenous reference genes. Primers for *SlGADPH* and salinity responsive genes were reported by Devkar et al. (2020) and *SlEF1α* by Wang et al. (2020) (**Supplementary Table 2**).

Statistical analysis

The data sets were analyzed by a one-way ANOVA and *post hoc* Tukey HSD tests after both normality and homogeneity of variance were tested with Shapiro–Wilk and Bartlett tests, respectively. When these assumptions were not met, a permutational ANOVA (PERMANOVA) was used. All statistical analyses were conducted in Sigma Plot v. 12 (Systat Software, Inc., Chicago, IL, United States) and PRIMER + PERMANOVA software (Version 7.0.13; PRIMER-e, Plymouth, United Kingdom).

Results

Tomato root colonization by *Salinispora arenicola*

In a previous study (Ocampo-Alvarez et al., 2020), a close interaction between *S. arenicola* and *Nicotiana attenuata* roots was observed *in vitro*. To confirm the presence of such interactions in tomato plants in this study, tomato seeds inoculated with *S. arenicola* and controls (bacteria-free) were grown under either saline or salt-free conditions and analyzed by Giemsa staining and FISH (**Figure 2**). Colonization of *S. arenicola* was observed in the central zone of the seedling roots. Under salt-free conditions, we found the bacteria interacting with the epidermal cells of roots (**Figures 2E,F**). Interestingly, bacterial colonization was more markedly observed under saline conditions on root hairs (**Figures 2G,H**). The control seedlings showed no presence of any bacteria (**Figures 2A–D**), which confirms that *S. arenicola* interaction occurs in tomato plants and that the site of this interaction changes from epidermal cells to root hairs based on salinity conditions. As *S. arenicola* is a bacteria found in saline habitats with the capacity to sustain a heterologous symbiotic relationship with plant roots, hereinafter it is referred to as a HAHS.

Salinispora arenicola increases the germination percentage of tomato seeds under salt stress conditions

Once the interaction between *S. arenicola* and the tomato plants was confirmed, the effects of this HAHS on germination competence were evaluated (**Figure 3**). With salt-free irrigation, no differences were observed in germination kinetics between the HAHS-treated and control seeds with

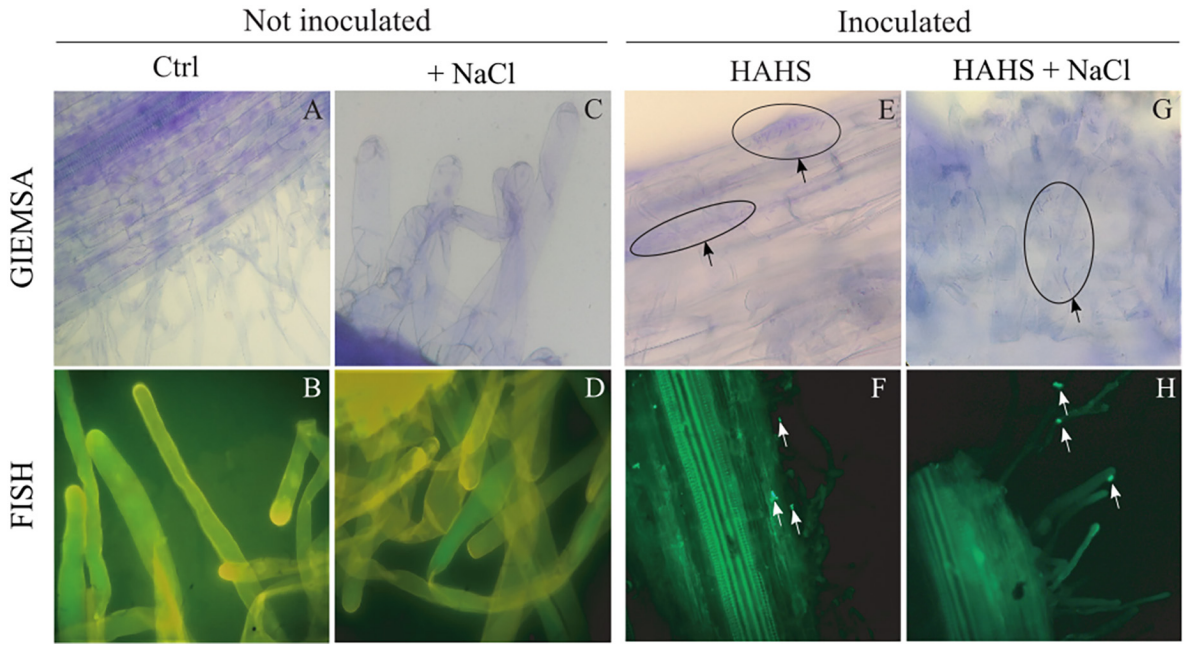

FIGURE 2
Colonization of *Salinispora arenicola* on tomato root hairs. Samples underwent Giemsa staining **(A,C,E,G)** and Fluorescence *in situ* Hybridization (FISH; **B**,**D**,**F**,**H**). Arrows indicate the presence of habitat-adapted heterologous symbiont (HAHS) bacterial cells in samples of plants inoculated under control (Ctrl; without NaCl) and NaCl conditions (100 mM).

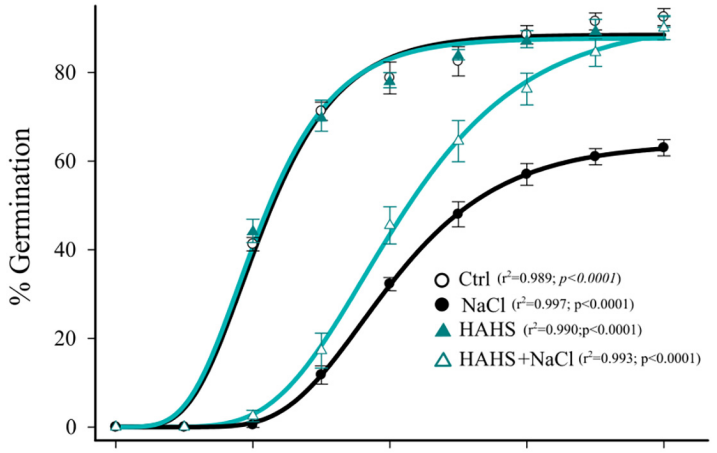

Parameter	Ctrl	HAHS	NaCl	HAHS+NaCl	ANOVA F	ANOVA P
Maximum germination percentage	88.50 ± 1.00^a	87.70 ± 0.94^a	64.03 ± 0.76^b	91.59 ± 1.73^a	119.060	<0.001
Half time of maximum germination	1.85 ± 0.04^a	1.80 ± 0.04^a	3.59 ± 0.03^b	3.62 ± 0.05^b	606.515	<0.001

FIGURE 3
Germination kinetics of HAHS-treated and control tomato seeds under saline conditions. Symbols represent the daily average germination percentage of four replicates with 100 seeds. Seed germination data were fitted to the Gompertz equation: $f = ae^{\left(-e^{-\left(\frac{d-d0}{b}\right)}\right)}$. Seeds inoculated under control (Ctrl) or habitat-adapted heterologous symbiont (HAHS) conditions with water free of NaCl or with 100 mmol NaCl (+NaCl) irrigation. Statistical significance was analyzed by a univariate analysis of variance. Lowercase letters denote statistical differences (pairwise test) among treatments for each parameter.

TABLE 1 Growth and biochemical characteristics of habitat-adapted heterologous symbiont (HAHS)-treated (B) and control (C) tomato seedlings under salt stress conditions.

	Ctrl	HAHS	NaCl	HAHS + NaCl
Plumule (cm)	6.61 ± 0.24^{b}	9.29 ± 1.18^{c}	3.84 ± 0.46^{a}	4.51 ± 0.40^{a}
Radicle (cm)	6.00 ± 0.40^{b}	7.35 ± 0.24^{c}	3.40 ± 0.21^{a}	3.96 ± 0.64^{a}
% N	5.09 ± 0.01^{b}	5.19 ± 0.01^{b}	3.74 ± 0.03^{a}	4.72 ± 0.09^{c}
% C	43.42 ± 0.09^{b}	38.72 ± 0.14^{d}	31.20 ± 0.30^{a}	41.02 ± 0.19^{c}
Polyphenols (mg/kg)	901.81 ± 6.37^{b}	600.01 ± 1.71^{d}	356.97 ± 5.52^{a}	$1{,}582.53 \pm 14.17^{c}$

Ctrl, control; HAHS-free; HAHS = *S. arenicola*; NaCl = HAHS-free and NaCl condition (100 mM); and HAHS + NaCl = *S. arenicola* and NaCl condition (100 mM).

∼90% seed germination. Salinity delayed the germination kinetics in both HAHS-treated (HAHS+NaCl) or HAHS-free seeds (NaCl). However, although NaCl treatment caused a delay in seed germination, HAHS-treated seeds reached the maximum germination percentage (∼90%) at the end of the germination assay as did the control seeds. In comparison, HAHS-free seeds with NaCl treatment only reached ∼60% germination. Salt stress affected tomato seed germination, but treatment with *S. arenicola* alleviated this stress by the end of the experiment.

Additionally, in the germinated seedlings, we measured %N, %C, and polyphenol (mg/Kg) content and the radicle and plumule heights on day 13 (Table 1). Salinity decreased the plumule and radicle lengths of both HAHS-treated and HAHS-free seedlings. Interestingly, treatment with *S. arenicola* significantly increased both length measurements under conditions of no salt stress. Seedling plumule and radicle lengths correlated nicely with nitrogen content (Pearson $r \approx 0.8$), although the relationships with polyphenols and carbon showed different patterns. Polyphenol content decreased in the control tomato seedlings under salt stress conditions but increased in the plants treated with *S. arenicola* under salt stress. The high polyphenol content in HAHS-treated tomato seedlings could be related to the enhanced antioxidant activity that protected tomato seeds during germination. This is supported by the high correlation between the germination percentage and polyphenol content (Pearson correlation: $r = 0.95$). Furthermore, high correlations were found between %N and %C content and germination (Pearson correlation: $r = 0.97$, 0.94, respectively).

Growth promoting activity of *Salinispora arenicola* with saline and salt-free irrigation

Tomato plant seedlings (15 days after germination; DAG) were submerged in either an *S. arenicola* suspension (HAHS-treatment) or water (control) before being transplanted into pots with soil and allowed to grow for 15 more days (Figure 1B). Afterward, groups of plants of each treatment were irrigated for 8 days with increasing NaCl concentrations up to 300 mM, which resulted in another two treatments: HAHS+NaCl and NaCl. Plant response parameters (i.e., plant length from the bottom to the main apex and the number of leaflets) were recorded 1 day after the last irrigation treatment (day 9 after the first irrigation). Results showed a clear and significant effect of *S. arenicola* in promoting tomato plant growth (Figure 4). With simple irrigation (salt-free), we found increases in growth of 27.2% in the shoots and 42.3% in the roots of plants treated with *S. arenicola* compared to those of the controls. In addition, leaflets and compound leaves increased in number by 20.9% and 36.3%, respectively (Figure 4).

Saline irrigation showed a slight decrease in all analyzed phenotypes for both control and HAHS-treated plants (Figure 4). Interestingly, HAHS-treated plants under salt stress conditions grew higher than control plants grown without saline stress, with a slight difference in shoot length (5.7%) and a notable difference in root length (21.1%; $P = 0.001$). Moreover, we still observed that HAHS-NaCl plants substantially outgrew bacteria free-plants under saline conditions (NaCl), with 26.8% and 42.2% differences in shoot and root lengths, respectively, and differences of 17.1% and 24.6% in the number of leaflets and compound leaves, respectively (Figure 4). Overall, although growth was affected by salinity in both control and HAHS-treated plants, *S. arenicola*-treated plants outperformed the control plants, which further suggests induced salt-tolerance activity by the actinobacteria.

Salinispora arenicola enhances photosynthetic performance and photoprotection

In line with the growth results obtained with simple water irrigation, HAHS-treated plants exhibited enhanced photosynthetic performance compared to HAHS-free plants in the form of an ∼25% larger electron transport rate (ETR_{MAX}), a marginally but statistically significant increase in the maximum photochemical quantum yield of PSII (F_V/F_M; c. 2%), and ∼15% higher dissipation of absorbed energy in the PSII antenna through a thermal dissipation pathway (NPQ; Figure 5A).

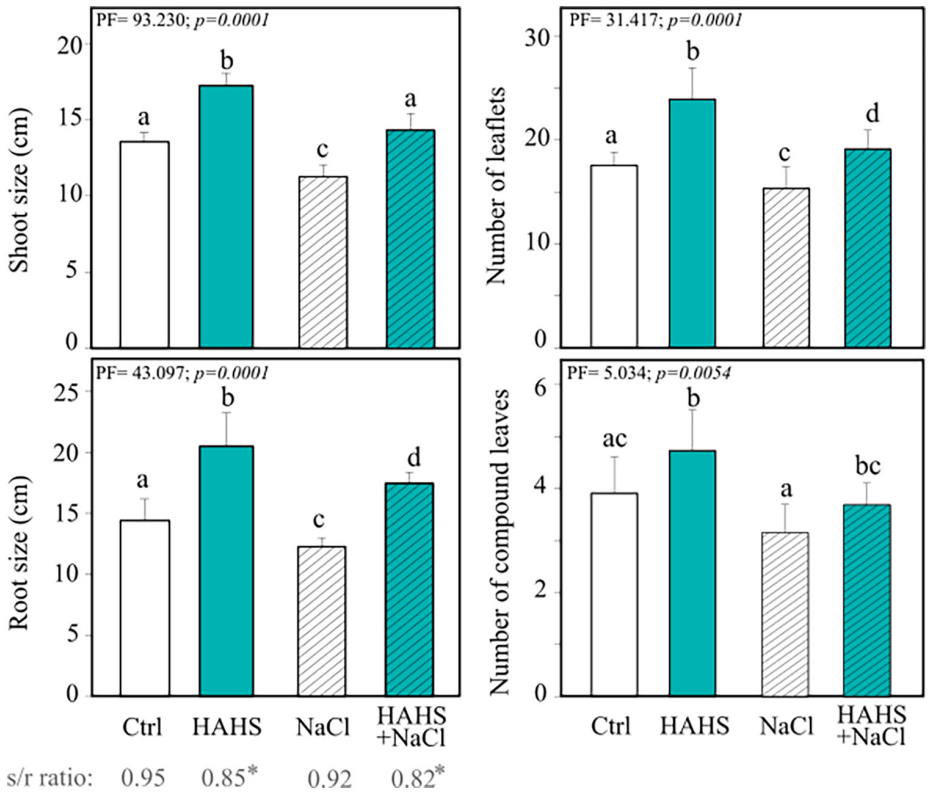

FIGURE 4
Salinispora arenicola enhances the growth of tomato plants under normal and salt stress conditions. Phenotype measurements of 39 DAG plants grown with either NaCl-free irrigation or saline irrigation that were either inoculated with a habitat-adapted heterologous symbiont (HAHS) bacterium or not (control; Ctrl). Statistical significance was determined using a permutational ANOVA (PERMANOVA; $p = 0.001$). Lowercase letters denote statistical differences (pairwise test) among conditions.

The yield coefficients of the absorbed energy distribution [effective photochemical quantum yield, Y(II); the non-regulated quantum yield of fluorescence emission from PSII, Y(NO); and light-regulated quantum yield of non-photochemical fluorescence quenching, Y(NPQ)] confirmed the bacterial benefits to photosynthetic performance. HAHS treatment induced a 40% increase of Y(II) compared to that of the control plants and a drop in the non-regulated Y(NO) and regulated Y(NPQ) energy distribution pathways in HAHS-treated compared to those of HAHS-free plants. This points to an increased capacity of HAHS-treated plants to allocate light-derived energy into the carbon assimilation pathway induced by the actinobacteria (**Figure 5B**).

Interestingly, when plants were irrigated with a saline solution, the photosynthetic parameters followed an interesting pattern of change with respect to those observed under non-stressed conditions in HAHS-free and HAHS-treated plants (**Figure 5A**). For HAHS-free plants, salt-stress induced no effect on F_V/F_M, although a reduction of ∼9% in NPQ and an increase of ∼20% in ETR_{MAX} were observed. On the other hand, HAHS-treated plants showed no increase in F_V/F_M, but in contrast, a significant increase in NPQ (∼74%) and a decrease in ETR_{MAX} (∼7%) under saline stress was observed when compared to those of the control plants. This agrees with the observed changes induced by saline stress in yield coefficients, which showed a decrease in the proportion of Y(NO) of ∼17%, a marginal reduction in Y(II) of ∼7%, and a high increase in Y(NPQ) of ∼42% in HAHS-treated plants (**Figure 5B**).

Photosynthetically related pigments and metabolites

The photosynthetic changes suggested the activity of photosynthetic and photoprotective-related pigments and metabolites. Pigment composition (**Figure 6**) and metabolite content (**Table 2**) were assessed in plant leaves collected 1 day after the last saline irrigation treatment. An increase in light collector molecules (Chl *a* by 11% and Chl *b* by 6 %) was observed in HAHS-treated plants under salt-free irrigation (**Figure 6** and **Supplementary Table 3**), which provides evidence of extended photosynthetic performance induced by the actinobacterium. The increase was higher in Chl *a* than Chl *b*, which was reflected in the Chl *a*/*b* ratio. Moreover, the

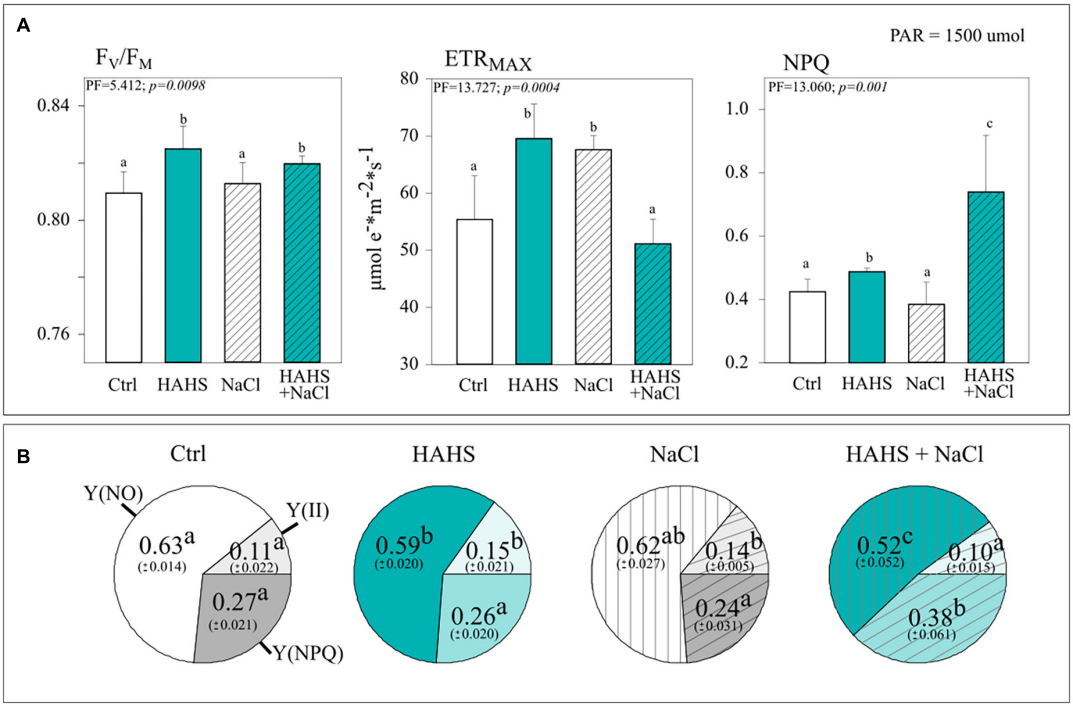

FIGURE 5
Salinispora arenicola enhances quantum yield and photoprotection under saline stress. **(A)** Photosynthethic performance parameters and **(B)** Yield coefficients of the absorbed energy distribution. Parameters were measured with a non-intrusive pulse-amplitude modulated (PAM) device (n = 6) 39 days after germination (DAG) in plants grown with either NaCl-free or saline irrigation and inoculated with a habitat-adapted heterologous symbiont (HAHS) bacteria (turquoise bars) or not (control; C, white bars). F_V/F_M, Maximum photochemical quantum yield of PSII; ETR_{MAX}, Maximum electron transfer rate; NPQ, Stern-Volmer type non-photochemical fluorescence quenching; Y(NO), Quantum yield of non-regulated heat dissipation and fluorescence emission; Y(II), Effective photochemical quantum yield of PSII; Y(NPQ), Quantum yield of light-induced non-photochemical fluorescence quenching. Statistical significance was determined separately for each irrigation scheme using a univariate analysis of variance (ANOVA; p = 0.001). Lowercase letters denote statistical differences (pairwise test) among conditions.

Xanthophyll cycle pool size $\left[\sum\left(\frac{XC}{Chl\ a+b}\right)\right]$ was reduced by 8% in HAHS-treated plants compared to that of the control plants, which was also likely due to the higher content of chlorophyll molecules. The photoprotective pigment zeaxanthin, which his related to the light-regulated energy dissipation mechanism, was not affected, although the antioxidant molecule beta-carotene increased ∼60% in HAHS-treated plants.

In HAHS-free plants, salt stress caused a significant reduction in all analyzed pigments [chl *a* (∼21%), chl *b* (∼22%), Zeaxanthin (∼11%), and Beta-carotene (∼19%)] and on the xanthophyll cycle pool size (∼16%). In contrast, treatment with HAHS prior to saline stress partially lessened the reduction in light collector molecules (chl *a* down to 12% and chl *b* to 17%) and the xanthophyll cycle pool (down to 6%) with respect to those of the control conditions. Furthermore, the content of Zeaxanthin and Beta-carotene was enriched up to 2 and 40%, respectively, which suggests induced zeaxanthin-related photoprotective and beta-carotene-related antioxidant activity by the actinobacterium *S. arenicola*.

Antioxidant metabolites, such as proline and phenol, and DPPH antioxidant activity tended to increase in plants under salinity as a strategy to mitigate stress by reducing the cellular osmotic potential and free radical scavenging. We found an increase in all of these parameters after saline irrigation. However, the increase was onefold lower in HAHS-treated plants than in untreated plants for both proline and DPPH (**Table 2**). This result implies that the symbiotic bacteria may reduce oxidative and osmotic stress and thus alleviate responses upstream, perhaps by inducing cation-transporters or reducing ROS formation.

Studies have also reported changes in sugar accumulation after saline stress (Yin et al., 2010), which are likely a consequence of a metabolic reconfiguration and redistribution of resources or an effect of photosynthetic changes. We observed a significant reduction in the content of reducing sugars (∼50%) when HAHS-free plants were treated with saline water (**Table 2**). This reduction was not observed in HAHS-treated plants. Sugar content reduction in untreated plants may be due to the observed decrease in photosynthesis (El-Beltagi et al., 2017). Overall, metabolic changes suggest that the symbiotic bacteria may lessen oxidative and osmotic stress and thereby protect plant metabolism.

10.3389/fpls.2022.920881

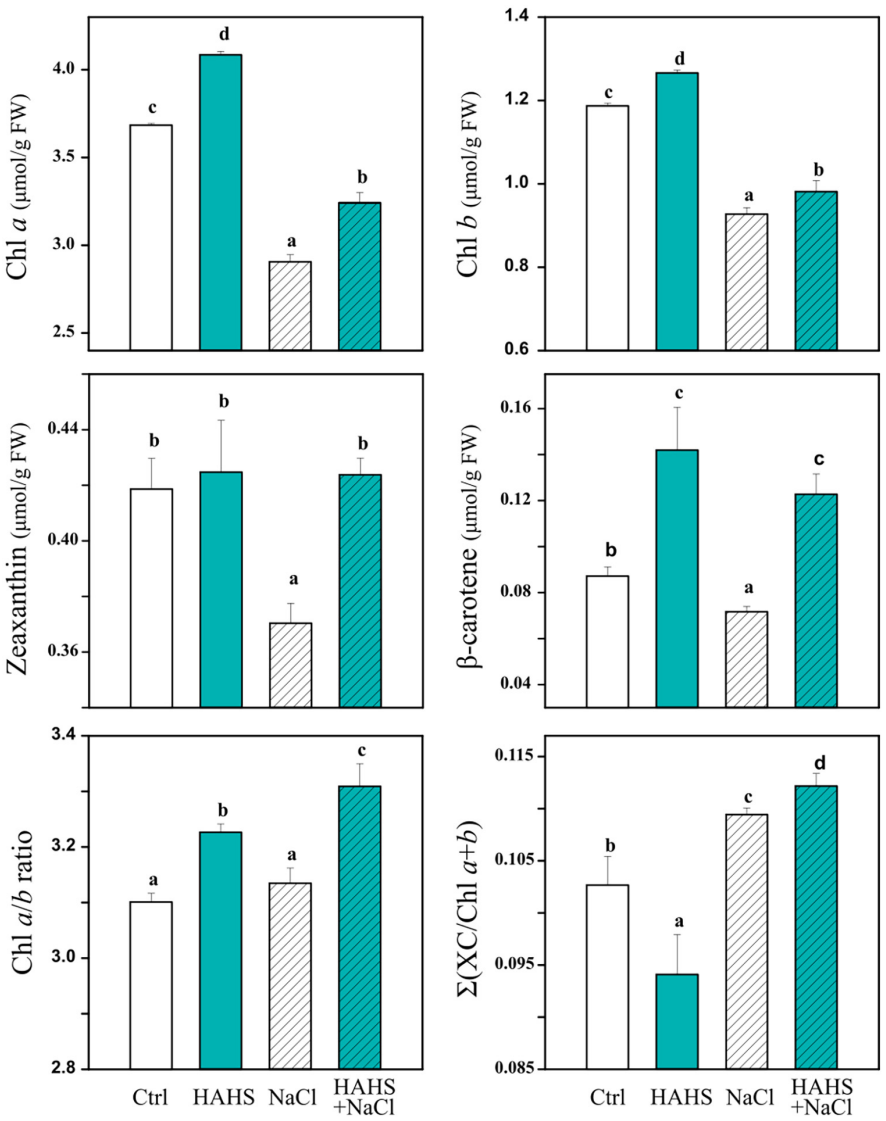

FIGURE 6
Salinispora arenicola induces changes in photosynthetically related pigments under normal and saline conditions. Plants (n = 4) 39 days after germination (DAG) were grown with either normal irrigation (white boxes) or saline irrigation (NaCl; gray boxes) and inoculated with a habitat-adapted heterologous symbiont (HAHS; B, turquoise) or not (control; C, black). Statistical significance was determined separately for each irrigation scheme using a univariate analysis of variance (ANOVA; p = 0.001). Lowercase letters denote statistical differences (pairwise test) among conditions.

TABLE 2 Proline, phenolics, antioxidant activity, and reducing sugars in tomato plant leaves.

	Ctrl	HAHS	NaCl	HAHS + NaCl
Proline	37.39 ± 1.53^{a}	35.68 ± 1.14^{a}	133.55 ± 3.23^{b}	93.08 ± 1.46^{c}
Total phenolics	5.03 ± 0.22^{a}	4.75 ± 0.28^{a}	5.47 ± 0.332^{b}	5.30 ± 0.16^{b}
DPPH antioxidant activity	3.64 ± 0.48^{a}	3.17 ± 0.45^{a}	6.50 ± 0.303^{c}	5.94 ± 0.34^{b}
Reducing sugars	41.67 ± 1.34^{c}	35.34 ± 0.92^{b}	27.33 ± 0.70^{a}	33.27 ± 2.29^{b}

DPPH is a water soluble, stable radical 2,2-diphenyl-1-picrylhydrazyl; DPPH Antioxidant activity (µg Trolox/g FW), proline (µg/mg FW), reducing sugars (mg/g FW), total phenolics (mg GAE/g FW), and flavonoids (mg/g FW) in six-week-old tomato plant leaves. Ctrl = control, habitat-adapted heterologous symbiont (HAHS)-free; HAHS = *S. arenicola*; NaCl = HAHS-free and NaCl (100 mM); and HAHS+NaCl = *S. arenicola* and NaCl (100 mM). Values are mean ± standard deviation (n = 6). Different letters indicate significant differences according to Tukey tests ($P < 0.05$).

Salinispora arenicola modulates salinity responsive gene expression

To obtain insights into the possible mechanism responsible for alleviating saline stress, the expression of the following five genes was assessed: *SlHBF7*, a transcription factor regulator of salt tolerance; *SlRD29B*, a gene involved in early responses to desiccation; *SlSDR1A*, a responsive gene involved in ABA biosynthesis; *SlHKT1,2*, a cation transmembrane transporter involved in Na^+/K^+ homeostasis; and *SlAOX1b*, a gene related with oxidative stress-related genes and ROS scavenging (**Figure 7**). Most of the genes were upregulated under salt stress conditions, with or without bacteria, except *SlRD29B*, which did not show any changes in expression. Interestingly, the expression of *SlHKT1,2* increased in HAHS-treated plants regardless of whether or not they were subjected to salt stress. *SlHKT1,2* encodes a Na^+/K^+ transporter and plays a crucial role in salinity tolerance mechanisms by alleviating osmotic stress. On the other hand, *SlAOX1b* and *SlHBF7* decreased their expression by half under salt stress conditions in HAHS-treated plants when compared to that of control plants under the same stress conditions. Therefore, HAHS treatment may induce changes that prime plants to better respond to salt-induced osmotic stress to avoid oxidative stress.

Discussion

The indiscriminate use of agrochemicals coupled with the projected increases in population growth and soil salinity are expected to negatively impact the native microbiota of soils, and thus sustainable alternatives must be explored for plant agriculture. In this study, we show a growth-promoting and induced saline resilience effect in tomato plants by the marine actinobacteria *S. arenicola*. This actinobacterium established an endophytic symbiosis with tomato plant roots (**Figure 2**). The presence of this actinobacteria on tomato seeds relieved the inhibitory effect of salt on tomato germination and enhanced tomato plant growth under normal irrigation conditions (**Figures 3**, **4**). Although salt-induced growth inhibition was still observed with HAHS-treated tomato plants, we observed enhanced quantum yield and photoprotective mechanisms (**Figure 5**). These changes appeared with increased quantities of photosynthetic pigments like Chl *a*, Chl *b*, β-carotene, and zeaxanthin along with increased amounts of reducing-sugars compared to those present in HAHS-free plants, which suggests improved photoprotection and a specific NPQ mechanism at play. Interestingly, we observed reductions in proline osmolyte and antioxidant activity in plant leaf tissues compared to that of the control plants under saline conditions (**Figure 6** and **Table 2**), which implies that the bacterial treatment might ameliorate the underlying causes that induce these responses. Furthermore, after scouting for the possible mechanisms involved in these responses based on gene expression, only two genes with significant differences in expression between HAHS-treated and HAHS-free plants were identified (**Figure 7**). The expression of *SlHKT1,2*, which is involved in ion-transporter encoding, was found to be significantly higher in HAHS-treated plants than in HAHS-free plants under both normal and saline conditions. *SlHKT1,2* expression may explain the ameliorated responses in HAHS-treated plants to salt stress by restoring the K^+/Na^+ balance and relieving osmotic stress.

Microscopic analysis showed that *S. arenicola* established a stable symbiotic interaction with tomato plants (**Figure 2**). Interestingly, this interaction was observed to change with the salinity conditions of the substrate. Under salt-free conditions, *S. arenicola* was found on epithermal roots cells, while we observed them mainly distributed on root hairs under saline conditions. Both epidermal root cells and root hairs have been recognized as active interaction sites for microbes. The roles of root hairs in plant exudation in part determine the growth of symbiotic bacteria (Mercado-Blanco and Prieto, 2012). Furthermore, an evaluation of the effect of saline stress conditions on root exudation patterns in barley plants by Knipfer et al. (2021) revealed higher water exchange by exudation in the root hair region compared to the mature region (epidermal and endodermal cells) under saline stress, whereas higher water exchange occurs in mature regions in the absence of saline stress. Similar phenomena could occur in tomato roots under saline stress, with an increase in exudation in the root hair region that produces chemotaxis of *S. arenicola* and improves colonization in this region. Moreover, *Salinispora* is an obligate halophile (Mincer et al., 2002). Therefore, it is also possible that *S. arenicola* could migrate out of the plants or to more superficial cells, such as root hairs, in salty soil. In non-salty soil, the bacteria would likely prefer deeper cells to escape low-salinity soil. However, it would be interesting to further explore and define the specific reasons behind this behavior.

Tomato seeds exposed to salt stress showed delayed germination and a reduction in the percentage of germinated seeds. Salt stress disrupts germination by decreasing water uptake due to changes in the hydraulic potential or the activity of phytohormones, such as gibberellins (GAs) and abscisic acid (ABA; Liu et al., 2018). However, HAHS-treated seeds under saline conditions showed the same overall germination percentage as that of control plants, although with a slight delay. GAs activate amylase enzymes that make endosperm energy available in the embryo for germination; however, salinity is known to affect amylase activity (Liu et al., 2018). The recovery of the germination percentage in HAHS-treated seeds may be explained by the high production of saline-stable glycosyl hydrolases by *S. areniola*, including α-amylase, endoglucanases, and endomanases, which are seen in the *S. arenicola* genome (CNS-205, T00613; Penn and Jensen, 2012) and published in the Kyoto Encyclopedia of Genes and Genomes

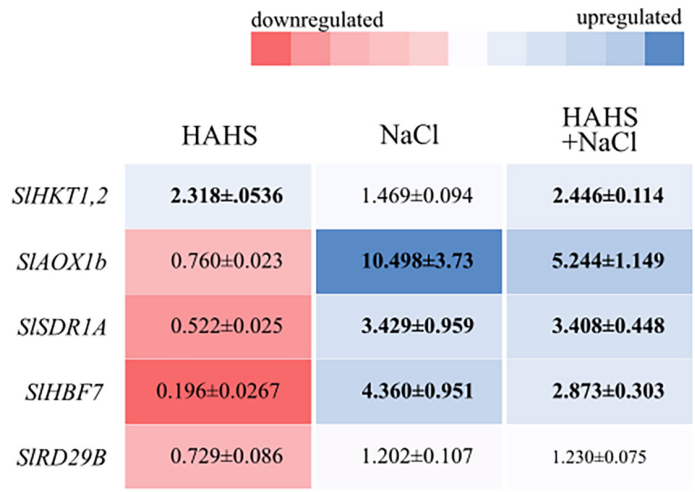

FIGURE 7
Salinispora arenicola modulates the expression of saline response genes in tomato plant leaves. Shade plot showing up- (blue) or downregulated (red) saline responsive genes in plants in the habitat-adapted heterologous symbiont (HAHS), HAHS + NaCl, and NaCl treatments. Gene expression was normalized to control expression. Black numbers inside the colored blocks indicate changes in expression at least 50% lower or higher than that of the control.

database[2]. Therefore, even if GAs are not produced in sufficient concentrations due to low water uptake during imbibition under saline conditions, the enzymes necessary for germination could be provided by the HAHS *S. arenicola*.

Salt exposure also affected the growth of tomato plants, independent of the bacterial treatment. However, HAHS-treated plants were healthier, with thicker stems, greener leaves, and fewer senescent leaves than those of HAHS-free plants. It is possible that the initial effect on growth and perhaps nutrition by HAHS treatment prior to saline irrigation may have prepared the plant to better cope with salt stress conditions. This is consistent with the onset of arrested growth. However, we observed increased photoprotection parameters, such as NPQ, and a reduction in Y(NO) and ETR_{MAX} in HAHS-treated plants under salt stress conditions. ETR_{MAX} increased in HAHS-free plants under salt stress conditions, although this does not seem to be consistent with the observed arrested growth. It could be argued that the electron flow in these plants was directed toward an alternative electron sink pathway, such as photorespiration (**Figure 8**). Photorespiration is considered to be a significant electron sink pathway for C3 plants under saline stress (Di Martino et al., 1999; Hossain and Dietz, 2016). Absicic acid-mediated stomata closure is one of the first responses to salt stress (Zhao et al., 2021). Stomata closure decreases the availability of CO_2 in leaves and increases the probability of RuBP oxygenation by Rubisco, which leads to photorespiration (Kalaji et al., 2011). Photorespiration is an energy-expensive process that affects plant growth (Walker et al., 2016). Therefore, although an increase in ETR_{MAX} was observed in NaCl-treated plants, it does not necessarily translate to increased photosynthesis and growth. HAHS-treated plants seem to prevent this scenario by redirecting quantum energy to dissipation mechanisms, as evidenced by the increase in NPQ, which is consistent with the increase in zeaxanthin pigment. The onset of this NPQ mechanism (**Figure 8**) allows the plant to reduce PSII pressure and prevent oxidative damage through the reduction of the un-regulated dissipation of energy [Y(NO)], which may result in ROS production at the photosynthetic antenna.

To avoid damage caused by the overproduction of ROS, plants employ an arsenal of antioxidant defense mechanisms, one of which involves the synthesis of molecules with antioxidant properties, such as polyphenols (Salem et al., 2014; Zhao et al., 2015). Antioxidant production is often observed as a plant tolerance mechanism to cope with salt stress (Soares et al., 2019; Akyol et al., 2020). Salt stress affects the electron transport chain, which may favor the formation of potentially harmful ROS that are then scavenged by antioxidants (Ahanger et al., 2017; Numan et al., 2018). Inoculation with several plant growth-promoting rhizobacteria (PGPR), such as *Sphingobacterium* BHU-AV3 in tomato plants, increases phenols and antioxidative enzymes and directly alleviates the induced oxidative stress (Kohler et al., 2009; Hashem et al., 2016; Vaishnav et al., 2020). As expected, phenols and the overall antioxidant activity in plant leaf tissues increased with salt stress in tomato plants. However, no significant changes were observed in phenols or antioxidant activity between HAHS-treated and HAHS-free plants (**Table 2**) that would improve the performance of the HAHS-treated plants in our experiment.

2 https://www.genome.jp/kegg/kegg2.html

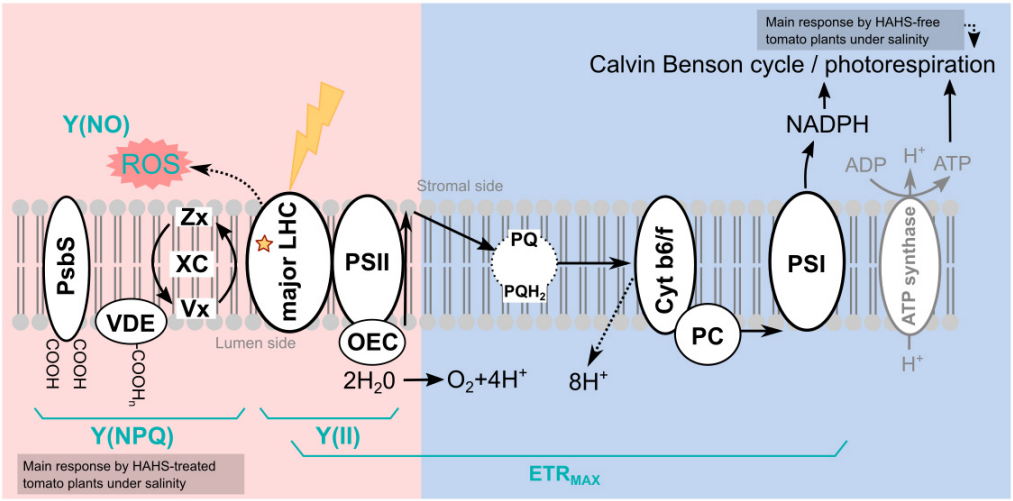

FIGURE 8
Model of habitat-adapted heterologous symbiont (HAHS)-induced changes in the light reactions of photosynthesis and associated alternative electron transfer pathways. The light energy distribution (pink side) and electron transport (blue side) of the light reactions of photosynthesis are shown. In the control plants, the photochemical energy flows to NADPH, mainly *via* the linear electron flow (LEF) pathway. Reduced Y(NO) and increased Y(II) indicate a lower probability of non-regulated dissipation but a higher probability of energy conduction to photochemistry as observed for HAHS-treated plants. As a result, plants exhibited higher F_V/F_M values and high plant growth. An increase in Chl content, the Chl *a*/*b* ratio, and beta-carotene but a reduction of XC/Chl *a*+*b* suggests a reduction of antenna size and an increase of PSII reaction centers in agreement with the increase in photosynthetic performance. High ETR_{MAX} with a small antenna and no PSII damage indicates highly efficient energy consumption in the Calvin cycle induced by HAHS interaction. Plants under salt stress without HAHS did not exhibit differences in Y(NO) or Y(NPQ) dissipation, indicating that no induced protective mechanism was present in the antenna. However, a significant increase in Y(II) linked to lower plant size was found, suggesting that a salt-induced mechanism in tomato plants without HAHS is related to the activation of alternative sinks such as photorespiration. Induced stomatal closure due to saline stress reduces CO_2/O_2 ratio increases the photorespiration probability. Photorespiration reduces the energy destined for photosynthetic Calvin Benson cycle, thereby affecting plant growth. In plants treated with HAHS under saline conditions, the HAHS protects plant photosynthesis by increasing the regulated thermal energy dissipation Y(NPQ) pathway, which decreases the potential for ROS formation in the LHCII antenna. This is also reflected in high F_V/F_M values compared to those of the control and control + NaCl plants. PsBS, pigment-binding protein associated with photosystem II (PSII); VDE, Violaxanthin De-Epoxidase; XC, Xanthophyll cycle pigments (Zx+Ax+Vx); Zx, Zeaxanthin; Ax; Antheraxanthin, Vx, Violaxanthin; LHC, Light-Harvesting Complex; PSII, Photosystem II; OEC, oxygen-evolving complex; PQ, Plastoquinone; PQH, Plastoquinol; AOX, Alternative Oxidase; Cyt b6/f, Cytochrome b6/f; PC, Plastocyanin; PSI, Photosystem I; ROS, Reactive oxygen species; ETR_{MAX}, Maximum electron transfer rate; Y(NO), Quantum yield of non-regulated heat dissipation and fluorescence emission; Y(II), Effective photochemical quantum yield of PSII; Y(NPQ), Quantum yield of light-induced non-photochemical fluorescence quenching.

It is likely that the higher NPQ levels observed in HAHS-treated plants under salt stress may contribute to avoiding ROS formation and thus reducing oxidative stress beforehand. Therefore, although antioxidant activity and metabolites were equivalent in plants with or without HAHS treatment, oxidative stress may have been reduced in HAHS-treated plants. Further experiments that analyze ROS production, ROS half-life times, and other antioxidant metabolites are needed to answer this question.

The presence of bacteria alone induced a drop in reducing sugars even though ETR_{MAX} was enhanced. An increase in ETR_{MAX} suggests an increase in sugar production. However, it is likely that the rate of sugar consumption also increased in HAHS-treated plants, with sugars being redirected to growth and development (as suggested by the high shoot and root lengths and the number of branches) to sustain the symbiotic relationship with the bacteria. The symbiotic consumption of photosynthetically produced sugars has been demonstrated for other root symbiotic interactions, such as mycorrhizal interactions (Schweiger et al., 2014). On the other hand, salt-stress conditions lowered the sugar levels in HAHS-free plants. This was also observed in ETR_{MAX} levels, which were increased by salt stress in HAHS-free plants. However, considering that growth was inhibited, the flow of the electrons at ETR_{MAX} may follow alternative electron sink pathways. Moreover, the rapid secretion of photosynthetically produced molecules other than sugars, such as osmolytes, can lead to high ETR_{MAX} but low growth rates (Demmig-Adams et al., 2017). Interestingly, salt stress conditions had no significant effect on reducing sugars in HAHS-treated plants. This may be due to a reduction in ETR_{MAX} by redirecting quantum energy to dissipative NPQ mechanisms and a decrease in the sugar used, as suggested by the reduced growth. This coordinated response may favor the plant by avoiding energy waste and oxidative stress.

Proline accumulation in the leaves and roots is considered to be a salt-sensitive trait in tomato plants that may be used to select varieties with different degrees of tolerance (Gharsallah et al., 2016). Many reports have shown that the

proline concentration increases in the shoots of plants grown under saline conditions (Vicente et al., 2004; Amini and Ehsanpour, 2005; Roy et al., 2014). Plants accumulate proline as a non-toxic and protective compatible solute, which participates in cytosolic osmotic adjustments and balances osmotic pressure differences between the cytosol and vacuoles (Parida and Das, 2005; Munns and Tester, 2008; Kamanga et al., 2020). Additionally, proline acts as an energy supplier and a signaling/regulatory molecule that can activate responses involved in the adaptation process, which helps to improve salinity tolerance (Maggio et al., 2002). In agreement with this, our experiments showed increased proline levels when plants were exposed to salt stress conditions, although this increase was lower in HAHS-treated plants (**Table 2**). As with any stimuli response mechanism, a quantitative level of damage or impact must induce a protective response of a similar scale. In this case, a lower response in HAHS-treated tomatoes does not necessarily mean a lower capacity to protect against the damaging effects of salt, as suggested by the observed growth and photosynthetic performance (**Figures 4**, **5**). Instead, this could be due to lower adverse effects produced by Na^+ ions. A potential hypothesis is that the activation of ion transporters ameliorates some of the adverse effects of Na^+. Which is line with many other studies that have shown that the activation of HKT1 transporters under saline stress conditions increases salinity tolerance in plants (Rodríguez-Navarro and Rubio, 2006). This aligns well with the observed overexpression of *SlHKT1,2* in HAHS-treated plants with regular or saline irrigation (**Figure 7**). The increased expression of *SlHKT1,2* in HAHS-treated plants, even in the absence of salt stress, could serve as a mechanism that prepares the plants to withstand stress by ameliorating other stress responses. In agreement with this, HKT1 induction has been proposed as a protective mechanism to salinity stress conditions in halophytes (Rodríguez-Navarro and Rubio, 2006) or in salt sensitive plants, where growth promoting bacteria (Zhang et al., 2008) and synthetic bacterial community (Schmitz et al., 2022) induced HKT1 expression. However, *SlHKT1,2* gene behavior in response to HAHS even in salty or regular conditions, needs further investigation. Additionally, the decreased expression of *SlAOX1b* and *SlHBF7* under saline conditions in HAHS-treated plants compared with those of the control plants indicates lower damage caused by free radicals and other salt-related effects. *Salinispora* is endemic to marine ecosystems, and *Salinispora* strains offer a vast array of potential benefits to their ubiquitous hosts. These strains are recognized for their antimicrobial activity (Cardoso-Martínez et al., 2015; Chase et al., 2021), ability to modify microbiotas (Tuttle et al., 2019), and ability to degrade recalcitrant materials. The particular strain used in this study was isolated from corals. However, many other strains have been obtained from other marine sources, including ascidians (Steinert et al., 2015), seaweeds (Jensen et al., 2005), soft corals (Louka et al., 2022), and sponges (Kim et al., 2005), which suggests that *Salinispora* is a ubiquitous symbiont. However, we were surprised to find that this actinobacterium was able to sustain a stable interaction with a terrestrial plant, although *S. arenicola* is closely related to several terrestrial actinobacteria (Trujillo et al., 2014). Thus, the ability to sustain this interaction may be due to a conserved mechanism present among terrestrial or marine actinobacteria or an evolutionary memory in *S. arenicola* metabolism that allows it to interact with terrestrial plants. A better understanding of the interactions between *S. arenicola* and terrestrial plants may allow us to identify the fundamental mechanisms necessary for sustaining symbiotic relationships, promoting growth, and alleviating saline stress. We define this interaction as a habitat-adapted heterologous symbiosis following the guidelines of Rodriguez et al. (2008). However, ecological interactions are not always positive. For example, Chhun et al. (2021) demonstrated that *S. arenicola* could inhibit the growth of some marine phototrophs. Therefore, it is essential to further study actinobacteria interactions to mitigate any potential side effects in terrestrial plants.

Data availability statement

The original contributions presented in this study are included in the article/**Supplementary material**, further inquiries can be directed to the corresponding author.

Author contributions

HO-A, AB-E, and RH-H designed and formulated the concept of the study. AB-E, RH-H, RP-R, CS-H, PP-S, EJ-C, OP, FC, ML-G, MH-O, LM-M, and HO-A performed part of the measurements in laboratory and interpreted part of the results. AB-E, IM-C, FR-Z, and HO-A carried out the analysis of the data. AB-E, RH-H, IM-C, and HO-A draft the manuscript with contributions of CS-H and PP-S. All authors approved the final manuscript.

Funding

This work was partially financed by a PRODEP project (UDG-PTC-1460) provided to HO-A, the Universidad de Guadalajara (P3E-2021; awarded to HO-A); the FORDECYT-PRONACES CONACYT Project (1576/2019) awarded to HO-A, AB-E, OP, and FC; and a CONACyT grant (INFR-2012-01188065). AB-E acknowledge CONACYT for its support through the program *Investigadoras e Investigadores por México* (No. 2196).

Acknowledgments

We thank the volunteer biology students Olmedo Valadez Leonardo and Sánchez González Ian Cristian for their help in the lab. We also thank Asdrúbal Burgos for the discussions and valuable comments on the draft. We are grateful to Andrea Liévana MacTavish for her English language review and Carolina Mateos-Salmón for the illustration in **Figure 1**.

Conflict of interest

The authors declare that the research was conducted in the absence of any commercial or financial relationships that could be construed as a potential conflict of interest.

Publisher's note

All claims expressed in this article are solely those of the authors and do not necessarily represent those of their affiliated organizations, or those of the publisher, the editors and the reviewers. Any product that may be evaluated in this article, or claim that may be made by its manufacturer, is not guaranteed or endorsed by the publisher.

Supplementary material

The Supplementary Material for this article can be found online at: https://www.frontiersin.org/articles/10.3389/fpls.2022.920881/full#supplementary-material

References

Abdelaziz, M. E., Abdelsattar, M., Abdeldaym, E. A., Atia, M. A., Mahmoud, A. W. M., Saad, M. M., et al. (2019). Piriformospora indica alters Na+/K+ homeostasis, antioxidant enzymes and LeNHX1 expression of greenhouse tomato grown under salt stress. *Sci. Hortic.* 256:108532. doi: 10.1016/j.scienta.2019.05.059

Abo-Ogiala, A., Carsjens, C., Diekmann, H., Fayyaz, P., Herrfurth, C., Feussner, I., et al. (2014). Temperature-induced lipocalin (TIL) is translocated under salt stress and protects chloroplasts from ion toxicity. *J. Plant Physiol.* 171, 250–259. doi: 10.1016/j.jplph.2013.08.003

Adem, G. D., Roy, S. J., Zhou, M., Bowman, J. P., and Shabala, S. (2014). Evaluating contribution of ionic, osmotic and oxidative stress components towards salinity tolerance in barley. *BMC Plant Biol.* 14:113. doi: 10.1186/1471-2229-14-113

Ahanger, M. A., Tomar, N. S., Tittal, M., Argal, S., and Agarwal, R. M. (2017). Plant growth under water/salt stress: ROS production; antioxidants and significance of added potassium under such conditions. *Physiol. Mol. Biol. Plants* 23, 731–744. doi: 10.1007/s12298-017-0462-7

Akyol, T. Y., Yilmaz, O., Uzilday, B., Uzilday, R. Ö, and Türkan, Ý (2020). Plant response to salinity: an analysis of ROS formation, signaling, and antioxidant defense. *Turk. J. Bot.* 44, 1–13. doi: 10.3906/bot-1911-15

Amann, R., Binder, B. J., Olson, R. J., Chisholm, S. W., Devereux, R., and Stahl, D. A. (1990). Combination of 16S rRNA-Targeted oligonucleotide probes with flow cytometry for analyzing mixed microbial populations. *Appl. Environ. Microbiol.* 57, 1919–1925. doi: 10.1128/aem.56.6.1919-1925.1990

Amini, F., and Ehsanpour, A. A. (2005). Soluble proteins, proline, carbohydrates and Na+/K+ changes in two tomato (Lycopersicon esculentum Mill.) cultivars under in vitro salt stress. *Am. J. Biochem. Biotechnol.* 1, 204–208. doi: 10.3844/ajbbsp.2005.204.208

Arif, Y., Singh, P., Siddiqui, H., Bajguz, A., and Hayat, S. (2020). Salinity induced physiological and biochemical changes in plants: an omic approach towards salt stress tolerance. *Plant Physiol. Biochem.* 156, 64–77. doi: 10.1016/j.plaphy.2020.08.042

Association of Official Analytical Chemist (1990). *Official Methods of Analysis*, 15th Edn. Washington, DC: Association of Official Analytical Chemist.

Bano, A., and Fatima, M. (2009). Salt tolerance in Zea mays (L). following inoculation with Rhizobium and *Pseudomonas*. *Biol. Fertil. Soils* 45, 405–413. doi: 10.1007/s00374-008-0344-9

Brand-Williams, W., Cuvelier, M. E., and Berset, C. L. W. T. (1995). Use a free radical method to evaluate antioxidant activity. *LWT Food Sci. Technol.* 28, 25–30. doi: 10.1016/S0023-6438(95)80008-5

Cao, W., Zhang, J. J., Liu, C. Y., Bai, W. S., and Cheng, N. (2020). A modified folin-ciocalteu method for the microdetermination of total phenolic content in honey. *Int. Food Res. J.* 27, 576–586.

Cardoso-Martínez, F., Becerril-Espinosa, A., Barrila-Ortíz, C., Torres-Beltrán, M., Ocampo-Alvarez, H., Iñiguez-Martínez, A. M., et al. (2015). Antibacterial and cytotoxic bioactivity of marine actinobacteria from Loreto bay national park, México. *Hidrobiológica* 25, 223–229.

Chase, A. B., Sweeney, D., Muskat, M. N., Guillén-Matus, D. G., and Jensen, P. R. (2021). Vertical inheritance facilitates interspecies diversification in biosynthetic gene cluster and specialized metabolites. *mBio* 12:e02700-21. doi: 10.1128/mBio.02700-21

Chhun, A., Sousoni, D., Aguiló-Ferretjans, M. D. M., Song, L., Corre, C., Christie-Oleza, J. A. A., et al. (2021). Phytoplankton trigger the production of cryptic metabolites in the marine actinobacterium *Salinispora tropica*. *Microb. Biotechnol.* 14, 291–306. doi: 10.1111/1751-7915.13722

Daims, H., Brühl, A., Amann, R., Schleifer, K. H., and Wagner, M. (1999). The domain-specific probe EUB338 is insufficient for the detection of all bacteria: development and evaluation of a more comprehensive probe set. *Syst. Appl. Microbiol.* 22, 434–444. doi: 10.1016/S0723-2020(99)80053-8

de-Bashan, L. E., Schmid, M., Rothballer, M., Hartmann, A., and Bashan, Y. (2011). Cell-cell interaction in the eukaryote-prokaryote model of the microalgae *Chlorella vulgaris* and the bacterium *Azospirillum brasilense* immobilized in polymer beads. *J. Phycol.* 47, 1350–1359. doi: 10.1111/j.1529-8817.2011.01062.x

Demmig-Adams, B., Stewart, J., and Adams, W. III (2017). Environmental regulation of intrinsic photosynthetic capacity: an integrated view. *Curr. Opin. Plant Biol.* 37, 34–41. doi: 10.1016/j.pbi.2017.03.008

Devkar, V., Thirumalaikumar, V. P., Xue, G. P., Vallarino, J. G., Tureèková, V., Strnad, M., et al. (2020). Multifaceted regulatory function of tomato SlTAF1 in the response to salinity stress. *New Phytol.* 225, 1681–1698. doi: 10.1111/nph.16247

Di Martino, C., Delene, S., Alvino, A., and Loreto, F. (1999). Photorespiration rate in spinach leaves under moderate NaCl stress. *Photosynthetica* 36, 233–242. doi: 10.1023/A:1007099627285

Dif, G., Belaouni, H. A., Yekkour, A., Goudjal, Y., Djemouai, N., Peòázová, E., et al. (2022). Performance of halotolerant bacteria associated with Sahara-inhabiting halophytes *Atriplex halimus* L. and *Lygeum spartum* L. ameliorate tomato plant growth and tolerance to saline stress: from selective isolation to genomic analysis of potential determinants. *World J. Microbiol. Biotechnol.* 38, 1–26. doi: 10.1007/s11274-021-03203-2

El-Beltagi, H. S., Ahmed, S. H., Namich, A. A. M., and Abdel-Sattar, R. R. (2017). Effect of salicylic acid and potassium citrate on cotton plant under salt stress. *Fresen. Environ. Bull.* 26, 1091–1100.

Geilfus, C. M., Mithöfer, A., Ludwig-Müller, J., Zörb, C., and Muehling, K. H. (2015). Chloride- inducible transient apoplastic alkalinizations induce stomata closure by controlling abscisic acid distribution between leaf apoplast and guard cells in salt-stressed *Vicia faba*. *New Phytol.* 208, 803–816. doi: 10.1111/nph.13507

Gharsallah, C., Fakhfakh, H., Grubb, D., and Gorsane, F. (2016). Effect of salt stress on ion concentration, proline content, antioxidant enzyme activities and gene expression in tomato cultivars. *AoB Plants* 8;lw055. doi: 10.1093/aobpla/plw055

Glick, B. R., Todorovic, B., Czarny, J., Cheng, Z., Duan, J., and McConkey, B. (2007). Promotion of plant growth by bacterial ACC deaminase. *Crit. Rev. Plant. Sci.* 26, 227–242. doi: 10.1080/07352680701572966

Hanachi, S., Van Labeke, M. C., and Mehouachi, T. (2014). Application of chlorophyll fluorescence to screen eggplant (*Solanum melongena* L.) cultivars for salt tolerance. *Photosynthetica* 52, 57–62. doi: 10.1007/s11099-014-0007-z

Hashem, A., AbdAllah, E. F., Alqarawi, A. A., Al-Huqail, A. A., Wirth, S., and Egamberdieva, D. (2016). The interaction between arbuscular mycorrhizal fungi and endophytic bacteria enhances plant growth of *Acacia gerrardii* under salt stress. *Front. Microbial.* 7:1089. doi: 10.3389/fmicb.2016.01089

Hossain, M. S., and Dietz, K. J. (2016). Tuning of redox regulatory mechanisms, reactive oxygen species and redox homeostasis under salinity stress. *Front. Plant Sci.* 7:548. doi: 10.3389/fpls.2016.00548

Iyengar, E. R. R., and Reddy, M. P. (1996). "Photosynthesis in highly salt-tolerant plants," in *Handbook of Photosynthesis*, eds M. Pesserkali, M. Dekar, and B. Rose (Abingdon: Taylor & Francis), 897–909.

Jensen, P. R., Gontang, E., Mafnas, C., Mincer, T. J., and Fenical, W. (2005). Culturable marine actinomycete diversity from tropical Pacific Ocean sediments. *Environ. Microbiol.* 7, 1039–1048. doi: 10.1111/j.1462-2920.2005.00785.x

Jiang, L. M., Lee, Y. J., Han, H. L., Lee, M. H., Jeong, J. C., Kim, C. Y., et al. (2021). Genome insights into the novel species Jejubacter calystegiae, a plant growth-promoting bacterium in saline conditions. *Diversity* 13:24. doi: 10.3390/d13010024

Kalaji, H. M., Bosa, K., Kościelniak, J., and Żuk-Gołaszewska, K. (2011). Effects of salt stress on photosystem II efficiency and CO2 assimilation of two Syrian barley landraces. *Environ. Exp. Bot.* 73, 64–72. doi: 10.1016/j.envexpbot.2010.10.009

Kamanga, R. M., Echigo, K., Yodoya, K., Mekawy, A. M. M., and Ueda, A. (2020). Salinity acclimation ameliorates salt stress in tomato (*Solanum lycopersicum* L.) seedlings by triggering a cascade of physiological processes in the leaves. *Sci. Hortic.* 270:109434. doi: 10.1016/j.scienta.2020.109434

Kerbab, S., Silini, A., Chenari Bouket, A., Cherif-Silini, H., Eshelli, M., El Houda Rabhi, N., et al. (2021). Mitigation of NaCl stress in wheat by rhizosphere engineering using salt habitat adapted PGPR halotolerant bacteria. *Appl. Sci.* 11:1034. doi: 10.3390/app11031034

Kim, T. K., Garson, M. J., and Fuerst, J. A. (2005). Marine actinomycetes related to the "Salinispora" group from the great barrier reef sponge *Pseudoceratina clavata*. *Environ. Microbiol.* 7, 509–519. doi: 10.1111/j.1462-2920.2004.00716.x

Knipfer, T., Danjou, M., Vionne, C., and Fricke, W. (2021). Salt stress reduces root water uptake in barley (*Hordeum vulgare* L.) through modification of the transcellular transport path. *Plant Cell Environ.* 44, 458–475. doi: 10.1111/pce.13936

Kohler, J., Hernández, J. A., Caravaca, F., and Roldán, A. (2009). Induction of antioxidant enzymes is involved in the greater effectiveness of a PGPR versus AM fungi with respect to increasing the tolerance of lettuce to severe salt stress. *Environ. Exp. Bot.* 65, 245–252. doi: 10.1016/j.envexpbot.2008.09.008

Liu, L., Xia, W., Li, H., Zeng, H., Wei, B., Han, S., et al. (2018). Salinity inhibits rice seed germination by reducing α-amylase activity via decreased bioactive gibberellin content. *Front. Plant Sci.* 9:275. doi: 10.3389/fpls.2018.00275

Livak, K. J., and Schmittgen, T. D. (2001). Analysis of relative gene expression data using real-time quantitative PCR and the 2_DDCT method. *Methods* 25, 402–408. doi: 10.1006/meth.2001.1262

Louka, X. P., Sklirou, A. D., Le Goff, G., Lopes, P., Papanagnou, E. D., Manola, M. S., et al. (2022). Isolation of an extract from the soft coral symbiotic microorganism Salinispora arenicola exerting cytoprotective and anti-aging effects. *Curr. Issue Mol. Biol.* 44, 14–30. doi: 10.3390/cimb44010002

Maggio, A., Miyazaki, S., Veronese, P., Fujita, T., Ibeas, J. I., Damsz, B., et al. (2002). Does proline accumulation play an active role in stress-induced growth reduction? *Plant J.* 31, 699–712. doi: 10.1046/j.1365-313X.2002.01389.x

Mercado-Blanco, J., and Prieto, P. (2012). Bacterial endophytes and root hairs. *Plant Soil* 361, 301–306. doi: 10.1007/s11104-012-1212-9

Mincer, T. J., Jensen, P. R., Kauffman, C. A., and Fenical, W. (2002). Widespread and persistent populations of a major new marine actinomycete taxon in ocean sediments. *Appl. Environ. Microbiol.* 68, 5005–5011. doi: 10.1128/AEM.68.10.5005-5011.2002

Moghaddam, M. S. H., Safaie, N., Soltani, J., and Hagh-Doust, N. (2021). Desert-adapted fungal endophytes induce salinity and drought stress resistance in model crops. *Plant Physiol. Biochem.* 160, 225–238. doi: 10.1016/j.plaphy.2021.01.022

Mukhopadhyay, R., Sarkar, B., Jat, H. S., Sharma, P. C., and Bolan, N. S. (2021). Soil salinity under climate change: challenges for sustainable agriculture and food security. *J. Environ. Manage.* 280:111736. doi: 10.1016/j.jenvman.2020.111736

Munns, R. (2002). Comparative physiology of salt and water stress. *Plant Cell Environ.* 25, 239–250. doi: 10.1046/j.0016-8025.2001.00808.x

Munns, R., and Tester, M. (2008). Mechanisms of salinity tolerance. *Annu. Rev. Plant Biol.* 59, 651–681. doi: 10.1146/annurev.arplant.59.032607.092911

Muresu, R., Maddau, G., Delogu, G., Cappuccinelli, P., and Squartini, A. (2010). Bacteria colonizing root nodules of wild legumes exhibit virulence-associated properties of mammalian pathogens. *Antoine van Leeuwenhoek* 97, 143–153. doi: 10.1007/s10482-009-9396-6

Negrulescu, A., Patrulea, V., Mincea, M. M., Ionascu, C., Vlad-Oros, B. A., and Ostafe, V. (2012). Adapting the reducing sugars method with dinitrosalicylic acid to microtiter plates and microwave heating. *J. Braz. Chem. Soc.* 23, 2176–2182. doi: 10.1590/S0103-50532013005000003

Numan, M., Bashir, S., Khan, Y., Mumtaz, R., Shinwari, Z. K., Khan, A. L., et al. (2018). Plant growth promoting bacteria as an alternative strategy for salt tolerance in plants: a review. *Microbiol. Res.* 209, 21–32. doi: 10.1016/j.micres.2018.02.003

Ocampo-Alvarez, H., Meza-Canales, I. D., Mateos-Salmón, C., Rios-Jara, E., Rodríguez-Zaragoza, F. A., Robles-Murguía, C., et al. (2020). Diving into reef ecosystems for land-agriculture solutions: coral microbiota can alleviate salt stress during germination and photosynthesis in terrestrial plants. *Front. Plant Sci.* 11:648. doi: 10.3389/fpls.2020.00648

Orsini, F., Accorsi, M., Gianquinto, G., Dinelli, G., Antognoni, F., Carrasco, K. B. R., et al. (2011). Beyond the ionic and osmotic response to salinity in *Chenopodium quinoa*: functional elements of successful halophytism. *Funct. Plant Biol.* 38, 818–831. doi: 10.1071/FP11088

Osuna-Ruíz, I., Nieves-Soto, M., Manzano-Sarabia, M., Hernández-Garibay, E., Lizardi-Mendoza, J., Burgos-Hernández, A., et al. (2019). Gross chemical composition, fatty acids, sterols and pigments in tropical seaweed species off Sinaloa, México. *Cien. Mar.* 45, 101–120. doi: 10.7773/cm.v45i3.2974

Palacios, O. A., Lopez, B. R., Bashan, Y., and de-Bashan, L. E. (2019). Early changes in nutritional conditions affect formation of synthetic mutualism between *Chlorella sorokiniana* and the bacterium *Azospirillum brasilense*. *Microb. Ecol.* 77, 980–992. doi: 10.1007/s00248-018-1282-1

Palmeros-Suárez, P. A., Massange-Sánchez, J. A., Martínez-Gallardo, N. A., Montero-Vargas, J. M., Gómez-Leyva, J. F., and Délano-Frier, J. P. (2015). The overexpression of an *Amaranthus hypochondriacus* NF-YC gene modifies growth and confers water deficit stress resistance in *Arabidopsis*. *Plant Sci.* 240, 25–40. doi: 10.1016/j.plantsci.2015.08.010

Parida, A., and Das, A. B. (2005). Salt tolerance and salinity effects on plants: a review. *Ecotoxicol. Environ. Saf.* 60, 324–349. doi: 10.1016/j.ecoenv.2004.06.010

Parihar, P., Singh, S., Singh, R., Singh, V. P., and Prasad, S. M. (2015). Effect of salinity stress on plants and its tolerance strategies: a review. *Environ. Sci. Pollut. Res.* 22, 4056–4075. doi: 10.1007/s11356-014-3739-1

Penn, K., and Jensen, P. R. (2012). Comparative genomics reveals evidence of marine adaptation in *Salinispora* species. *BMC Genomics* 13:86. doi: 10.1186/1471-2164-13-86

Rodriguez, R. J., Henson, J., Van Volkenburgh, E., Hoy, M., Wright, L., Beckwith, F., et al. (2008). Stress tolerance in plants via habitat-adapted symbiosis. *ISME J.* 2, 404–416. doi: 10.1038/ismej.2007.106

Rodríguez-Navarro, A., and Rubio, F. (2006). High-affinity potassium and sodium transport systems in plants. *J. Exp. Bot.* 57, 1149–1160. doi: 10.1093/jxb/erj068

Roy, S. J., Negrão, S., and Tester, M. (2014). Salt resistant crop plants. *Curr. Opin. Biotechnol.* 26, 115–124. doi: 10.1016/j.copbio.2013.12.004

Rubio-Ochoa, E., Pérez-Sánchez, R. E., Ávila-Val, T. C., Gómez-Leyva, J. F., and García-Saucedo, P. A. (2019). Propiedades fisicoquímicas de frutos silvestres de Rubus con potencial nutracéutico y alimenticio. *Rev. Mexicana Cienc. Agríc.* 23, 291–301. doi: 10.29312/remexca.v0i23.2028

Salem, N., Msaada, K., Dhifi, W., Limam, F., and Marzouk, B. (2014). Effect of salinity on plant growth and biological activities of *Carthamus tinctorius* L. extracts at two flowering stages. *Acta Physiol. Plant* 36, 433–445. doi: 10.1007/s11738-013-1424-5

Schmitz, L., Yan, Z., Schneijderberg, M., de Roij, M., Pijnenburg, R., Zheng, Q., et al. (2022). Synthetic bacterial community derived from a desert rhizosphere confers salt stress resilience to tomato in the presence of a soil microbiome. *ISME J.* 16, 1–14. doi: 10.1038/s41396-022-01238-3

Schreiber, U. (2004). "Pulse-amplitude-modulation (PAM) fluorometry and saturation pulse method: an overview," in *Chlorophyll a Fluorescence. Advances in Photosynthesis and Respiration*, Vol. 19, eds G. C. Papageorgiou and T. Govindjee (Dordrecht: Springer).

Schweiger, R., Baier, M., and Müller, C. (2014). Arbuscular mycorrhiza-induced shifts in foliar metabolism and photosynthesis mirror the developmental stage of the symbiosis and are only partly driven by improved phosphate uptake. *Mol. Plant Microbe Interact.* 27, 1403–1412. doi: 10.1094/MPMI-05-14-0126-R

Shahid, M. A., Sarkhosh, A., Khan, N., Balal, R. M., Ali, S., Rossi, L., et al. (2020). Insights into the physiological and biochemical impacts of salt stress on plant growth and development. *Agronomy* 10:938. doi: 10.3390/agronomy10070938

Shameer, S., and Prasad, T. N. V. K. V. (2018). Plant growth promoting rhizobacteria for sustainable agricultural practices with special reference to biotic and abiotic stresses. *Plant Growth Regul.* 84, 603–615. doi: 10.1007/s10725-017-0365-1

Shankar, V., and Evelin, H. (2019). "Strategies for reclamation of saline soils," in *Microorganisms in Saline Environments: Strategies and Functions*, eds B. Giri and A. Varma (Cham: Springer).

Singleton, V., and Rossi, J. (1965). Colorimetry of total phenolic compounds with phosphomolybdic-phosphotungstic acid reagents. *Am. J. Enol. Viticult.* 16, 144–158.

Soares, C., Carvalho, M. E., Azevedo, R. A., and Fidalgo, F. (2019). Plants facing oxidative challenges-A little help from the antioxidant networks. *Environ. Exp. Bot.* 161, 4–25. doi: 10.1016/j.envexpbot.2018.12.009

Steinert, G., Taylor, M. W., and Schupp, P. J. (2015). Diversity of Actinobacteria associated with the marine ascidian *Eudistoma toealensis*. *Mar. Biotechnol.* 17, 377–385. doi: 10.1007/s10126-015-9622-3

Timmusk, S., El-Daim, I. A. A., Copolovici, L., Tanilas, T., Kännaste, A., Behers, L., et al. (2014). Drought-tolerance of wheat improved by rhizosphere bacteria from harsh environments: enhanced biomass production and reduced emissions of stress volatiles. *PLoS One* 9:e96086. doi: 10.1371/journal.pone.0096086

Trujillo, M. E., Bacigalupe, R., Pujic, P., Igarashi, Y., Benito, P., Riesco, R., et al. (2014). Genome features of the endophytic actinobacterium *Micromonospora lupini* strain Lupac 08: on the process of adaptation to an endophytic life style? *PLoS One* 9:e108522. doi: 10.1371/journal.pone.0108522

Tuttle, R. N., Demko, A. M., Patin, N. V., Kapono, C. A., Donia, M. S., Dorrestein, P., et al. (2019). Detection of natural products and their producers in ocean sediments. *Appl. Environ. Microbiol.* 85:e02830-18. doi: 10.1128/AEM.02830-18

Upadhyay, S. K., and Singh, D. P. (2015). Effect of salt-tolerant plant growth-promoting rhizobacteria on wheat plants and soil health in a saline environment. *Plant Biol.* 17, 288–293. doi: 10.1111/plb.12173

Upadhyay, S. K., Singh, J. S., Saxena, A. K., and Singh, D. P. (2012). Impact of PGPR inoculation on growth and antioxidant status of wheat under saline conditions. *Plant Biol.* 14, 605–611. doi: 10.1111/j.1438-8677.2011.00533.x

Vaishnav, A., Singh, J., Singh, P., Rajput, R. S., Singh, H. B., and Sarma, B. K. (2020). *Sphingobacterium* sp. BHU-AV3 induces salt tolerance in tomato by enhancing antioxidant activities and energy metabolism. *Front. Microbiol.* 11:443. doi: 10.3389/fmicb.2020.00443

Vicente, O., Boscaiu, M., Naranjo, M. A., Estrelles, E., Bellés, J. M., and Soriano, P. (2004). Responses to salt stress in the halophyte *Plantago crassifolia* (Plantaginaceae). *J. Arid Environ.* 58, 463–481. doi: 10.1016/j.jaridenv.2003.12.003

Walker, B., VanLoocke, A., Bernacchi, C., and Ort, D. R. (2016). The costs of photorespiration to food production now and in the future. *Annu. Rev. Plant Biol.* 67, 107–129. doi: 10.1146/annurev-arplant-043015-111709

Wang, W. R., Liang, J. H., Wang, G. F., Sun, M. X., Peng, F. T., and Xiao, Y. S. (2020). Overexpression of PpSnRK1α in tomato enhanced salt tolerance by regulating ABA signaling pathway and reactive oxygen metabolism. *BMC Plant Biol.* 20:128. doi: 10.1186/s12870-020-02342-2

Yin, Y. G., Kobayashi, Y., Sanuki, A., Kondo, S., Fukuda, N., Ezura, H., et al. (2010). Salinity induces carbohydrate accumulation and sugar-regulated starch biosynthetic genes in tomato (*Solanum lycopersicum* L. cv.'Micro-Tom') fruits in an ABA-and osmotic stress-independent manner. *J. Exp. Bot.* 61, 563–574. doi: 10.1093/jxb/erp333

Zapata, M., Rodríguez, F., and Garrido, J. L. (2000). Separation of chlorophylls and carotenoids from marine phytoplankton: a new HPLC method using a reversed phase C8 column and pyridine-containing mobile phases. *Mar. Ecol. Prog. Ser.* 195, 29–45. doi: 10.3354/meps195029

Zhang, H., Kim, M. S., Sun, Y., Dowd, S. E., Shi, H., and Paré, P. W. (2008). Soil bacteria confer plant salt tolerance by tissue-specific regulation of the sodium transporter HKT1. *Mol. Plant Microbe Interact.* 21, 737–744. doi: 10.1094/MPMI-21-6-0737

Zhao, G. M., Han, Y., Sun, X., Li, S. H., Shi, Q. M., and Wang, C. H. (2015). Salinity stress increases secondary metabolites and enzyme activity in safflower. *Ind. Crop. Prod.* 64, 175–181. doi: 10.1016/j.indcrop.2014.10.058

Zhao, S., Zhang, Q., Liu, M., Zhou, H., Ma, C., and Wang, P. (2021). Regulation of plant responses to salt stress. *Int. J. Mol. Sci.* 22:4609. doi: 10.3390/ijms22094609

Zribi, L., Fatma, G., Fatma, R., Salwa, R., Hassan, N., and Néjib, R. M. (2009). Application of chlorophyll fluorescence for the diagnosis of salt stress in tomato "*Solanum lycopersicum* (variety Rio Grande)". *Sci. Hortic.* 120, 367–372. doi: 10.1016/j.scienta.2008.11.025

frontiers | Frontiers in Plant Science

TYPE Original Research
PUBLISHED 08 August 2022
DOI 10.3389/fpls.2022.950393

OPEN ACCESS

EDITED BY
Maurizio Ruzzi,
University of Tuscia, Italy

REVIEWED BY
Maria Giordano,
University of Naples Federico II, Italy
El-Sayed Mohamed Desoky,
Zagazig University, Egypt

*CORRESPONDENCE
Abdur Rehim
abdur.rehim@bzu.edu.pk
Yucong Geng
tiger86gyc@gmail.com

†These authors have contributed equally to this work and share first authorship

SPECIALTY SECTION
This article was submitted to Plant Nutrition, a section of the journal Frontiers in Plant Science

RECEIVED 22 May 2022
ACCEPTED 24 June 2022
PUBLISHED 08 August 2022

CITATION
Raza Q-U-A, Bashir MA, Rehim A, Ejaz R, Raza HMA, Shahzad U, Ahmed F and Geng Y (2022) Biostimulants induce positive changes in the radish morpho-physiology and yield. *Front. Plant Sci.* 13:950393. doi: 10.3389/fpls.2022.950393

Biostimulants induce positive changes in the radish morpho-physiology and yield

Qurat-Ul-Ain Raza[1†], Muhammad Amjad Bashir[2†], Abdur Rehim[1*], Rafia Ejaz[2], Hafiz Muhammad Ali Raza[1,2], Umbreen Shahzad[2], Faraz Ahmed[3] and Yucong Geng[4*]

[1]Department of Soil Science, Faculty of Agricultural Sciences and Technology, Bahauddin Zakariya University, Multan, Pakistan, [2]College of Agriculture, Bahauddin Zakariya University Multan, Bahadur Sub-Campus Layyah, Layyah, Pakistan, [3]Soil and Water Testing Laboratory, Sargodha, Pakistan, [4]KOYO Star Agriculture Technology Co., LTD., Beijing, China

An ever-increasing population has issued an open challenge to the agricultural sector to provide enough food in a sustainable manner. The upsurge in chemical fertilizers to enhance food production had resulted in environmental problems. The objective of the current study is to assess the utilization of biostimulants for sustainable agricultural production as an alternative to chemical fertilization. For this purpose, two pot experiments were conducted to examine the response of radish against individual and combined applications of biostimulants. In the first experiment, the effects of chemical fertilizer (CK), glycine (G), lysine (L), aspartic acid (A), and vitamin B complex (V) were studied. The results demonstrated that V significantly improved the transpiration rate (81.79%), stomatal conductance (179.17%), fresh weight (478.31%), and moisture content (2.50%). In the second experiment, tested treatments included chemical fertilizer (CK), Isabion® (I), glycine + lysine + aspartic acid (GLA), moringa leaf extract + GLA (M1), 25% NPK + M1 (M2). The doses of biostimulants were 5g L^{-1} glycine, 1g L^{-1} lysine, 2g L^{-1} aspartic acid, and 10 ml L^{-1} moringa leaf extract. The photosynthetic rate improved significantly with GLA (327.01%), M1 (219.60%), and M2 (22.16%), while the transpiration rate was enhanced with GLA (53.14%) and M2 (17.86%) compared to the Ck. In addition, M1 increased the stomatal conductance (54.84%), internal CO_2 concentration (0.83%), plant fresh weight (201.81%), and dry weight (101.46%) as compared to CK. This study concludes that biostimulants can effectively contribute to the sustainable cultivation of radish with better growth and yield.

KEYWORDS

biostimulants, fertilization, glycine, radish, vegetable production

Introduction

The main challenge the world is facing today is to feed its increasing population using less and highly efficient inputs (Bashir et al., 2021). It is estimated that by 2050 the population will increase to 9.7 billion; this demands a 70% increase in food production to feed such a huge population (Del Buono, 2021).

On the other hand, the key factors influencing crop productivity are limited available land, climate change, the genetic potential of crops, and depletion of natural resources (Maja and Ayano, 2021). The Green Revolution was a promising approach to food security, but in the long run, its adverse impact on agriculture, human health, and the environment were observed worldwide (John and Babu, 2021).

There is rampant overuse of chemical fertilizers and about 1.9×10^{11} tons of them are used globally (Wan et al., 2021). Conventional agricultural patterns that include excessive use of fertilizers and pesticides have increased crop production but have negatively impacted food quality and environmental sustainability (Chouhan et al., 2021). The excessive use of chemical fertilizers contributes to groundwater and atmospheric pollution, poor food quality, increased input cost with lower outputs, deterioration of the soil quality and fertility status, reduced nutrient efficiency, susceptibility to pathogens, nutrient leaching, greenhouse gases emission, and other abiotic stresses (Rahman and Zhang, 2018; Godlewska et al., 2021; Wan et al., 2021).

To improve crop yield, quality, and environmental sustainability, various breeding programs have been attempted. The need for sustainable and modernized agriculture makes it imperative to improve plant growth and development functions, stimulate plant metabolism, and improve environmental safety (Bashir et al., 2021). Biostimulants are organic/ inorganic substances gaining popularity due to their incredible benefits for better plant growth and development. They are involved in the stimulation of plant physiological processes and improved plant shoot/ root growth. They minimize chemical fertilizer use, are cost-effective, enhance plant's tolerance to biotic and abiotic stresses, boost yield, and, more importantly, offer an environmentally friendly approach (Bashir et al., 2021; Rehim et al., 2021; Bell et al., 2022; Samuels et al., 2022). European Biostimulant Industry Council (EBIC) reported that biostimulants improve the nutrient use efficiency and uptake in plants, counteract the influence of biotic and abiotic stresses, and improve crop quality (Bashir et al., 2021). Based on their origin, biostimulants are generally classified as humic, amino-acid/nitrogen-containing, inorganic, chitosan/ biopolymers, beneficial microbes, seaweed, and botanical extracts (Samuels et al., 2022).

One of the beneficial effects of biostimulants to be identified recently is crop yield enhancement. Moringa leaf extract is a potent bio-stimulator that improves plant growth and yield. It contains essential nutrients, sugars, amino acids, phytohormones, vitamins, and antioxidants. It benefits the plants by improving seed germination, nutrient status, growth and yield processes, fruit quality, chlorophyll content, and biometric attributes (Abd El-Mageed et al., 2017; Arif et al., 2022). Moreover, using biostimulants also promotes nutrient uptake, enzymatic activity, crop physiology, green leaf pigment, plant metabolism, and molecular processes (Rehim et al., 2021).

The use of amino acid-based biostimulants positively impacts the plants' metabolic processes and favors sustainable agriculture (Alfosea-Simón et al., 2020). In addition, animal-based protein hydrolysates significantly increase the gaseous exchange and chlorophyll fluorescence (Cristiano and De Lucia, 2021). Without chemical fertilizers, the foliar application of biostimulants, vitamins, and coenzyme Q10 significantly improves the radish root-shoot biomass under green-house conditions (Rehim et al., 2021). Radish is of various cultivars, including shapes (oval, round, spindle, icicle, cylindrical, long, conical, half long), color (white, red, pink, black, purple), and flavor. The crop is cultivated worldwide on a large scale; its extensive cultivation is better due to its taste, high nutritional content, low calories, and myriad health benefits (Godlewska et al., 2021). In Asia, it is one of the most economically important crops; it is cultivated for its soft leaves and root, which is consumed raw, dried, pickled, or simmered (Lee and Park, 2020). Radish has also been reported to reduce health risks associated with cancer, stone formation, constipation, jaundice, and anxiety (Godlewska et al., 2021). As per published data, biostimulants play a vital role in the yield enhancement of various vegetables along with controlled chemical fertilization. Still, there is a considerable gap in identifying the potential benefits of biostimulants for morpho-physiological parameters of radish. This makes the current study timely and important to identify the influence of biostimulants on sustainable agriculture.

Considering the positive effects of biostimulants on plant growth, development, and yield, the present study was undertaken with the following objectives: (i) identify the physiological response of radish against individual and combined use of biostimulants, (ii) estimate the efficacy of biostimulants on crop morphology, and (iii) find an alternative to minimize the use of chemical fertilizers. We hypothesized that the use of biostimulants will not just only improve the radish production but will also enhance the photosynthetic rate and other related physiological indices.

Materials and methods

Two pot experiments were conducted to assess the role of biostimulants on radish yield, morphology, and physiology. A brief description of each experiment is given below.

Experiment 1

The experiment was conducted from September to December 2021 at the research area of the Department of Soil Science (30.258° E, 71.515° N), Bahauddin Zakariya University, Multan, Pakistan. The climate of the Multan region is semi-arid to arid. The pots were lined with plastic sheets and filled with

15 kg soil having the following physicochemical properties: pH 7.7, EC 0.5 $dS{\cdot}m^{-1}$, organic matter 0.4%, saturation percentage 34%, texture loam, nitrogen (N) 221 mg kg^{-1}, phosphorus (P) 8.2 mg kg^{-1}, and potassium (K) 30.1 mg kg^{-1}.

The experiment consisted of five treatments with three replications in a completely randomized design (CRD). The tested treatments were: recommended chemical fertilizer (CK; N 61.8 kg ha^{-1}, P 49.4 kg ha^{-1}, K 61.7 kg ha^{-1}), glycine (G; $C_2H_5NO_2$), lysine (L; $C_6H_{14}N_2O_2$), aspartic acid (A; $C_4H_7NO_4$), and vitamin B complex (V; vitamin B1, B6, B12). The doses of biostimulants were maintained the same according to the crop's N requirements (61.8 kg ha−1). G, L, and A were purchased from Sigma Aldrich, while V was purchased from Martin Dow Market Ltd.

Six radish seeds (cultivar "Mino early long white," Nongwoo Bio) were sown in each pot on 24 September 2021. Smaller seedlings were later eradicated, and only two plants per pot were maintained. The foliar application was performed four times in the morning on sunny and windless days (15 October, 25 October, 5 November, and 15 November). Plants were harvested on 9 December 2021. Regular manual weed eradiation and irrigation practices were maintained during the growth period. Plant samples (rosette and root) were collected after harvesting for further analysis.

Experiment 2

The experiment was conducted between October 2021 and January 2022 at the research area of the College of Agriculture (30.97° E, 70.96° N), Bahauddin Zakariya University, Bahadur Sub-campus Layyah, Pakistan. The region has a desert climate with usually no rainfall, and similar to experiment one, the pots were lined with plastics sheets and filled with 8 kg soil (pH 7.8, EC 0.1 $dS{\cdot}m^{-1}$, organic matter 0.7%, saturation percentage 28%, texture sandy loam, N 450 mg kg^{-1}, P 7.1 mg kg^{-1}, and K 62.34 mg kg^{-1}).

The experiment comprised five treatments with three replications in a completely randomized design (CRD). The treatments included: recommended chemical fertilizer (CK; N 61.8 kg ha^{-1}, P 49.4 kg ha^{-1}, K 61.7 kg ha^{-1}), Isabion® (I), glycine + lysine + aspartic acid (GLA), moringa leaf extract + GLA (M1), 25% NPK + M1 (M2). The doses of biostimulants were 5 g L^{-1} glycine, 1 g L^{-1} lysine, 2 g L^{-1} aspartic acid, and 10 ml L^{-1} moringa leaf extract. Whereas, Isabion® was used as recommended by the manufacturer. G, L, and A were purchased from Sigma Aldrich, while I was purchased from Syngenta, Pakistan. Moringa leaf extract was prepared at the laboratory. Fresh moringa (50 g) leaves were weighed and soaked in 200 ml distilled water for 12 h, then sonicated, centrifuged, and stored supernatant for further use.

Similar to experiment one, six seeds were sown in each pot on 21 October 2021, and two healthy plants were maintained. Four foliar applications of biostimulants were applied on 16 November, 26 November, 6 December, and 16 December 2021. The crop was harvested on 13 January 2022, and plant rosette and root samples were collected for further analysis.

Gaseous exchange parameters

Gaseous exchange parameters (photosynthetic rate, transpiration rate, internal CO_2, and stomatal conductance) were measured at vegetative maturity (ten days before harvesting) using an infrared gas analyzer (IRGA; Analytical Development Company, Hoddesdon, UK). Readings were taken between 8:00 and 9:00 a.m. The IRGA chamber was attached to a fresh expanded radish leaf and logged for ten seconds (Scafaro et al., 2018; Zaheer et al., 2020).

Photosynthetic pigments

To determine the chlorophyll a + b content, fresh leaf samples (0.5 g) were collected and cut into fine pieces (<0.25 mm^2). The samples were dipped in ethanol (96% v/v) for chlorophyll extraction and placed in darkness for 24 h. Afterward, the spectrophotometer was used to determine the chlorophyll a + b contents by measuring absorbance at 665 and 649 nm. The following equation was used to calculate the chlorophyll a + b contents (mg g^{-1}).

$$\text{Chlorophyll a} + \text{b} = \frac{(5.1 \times \text{A665} + 20.24 \times \text{A649}) \times \text{V}}{\text{m}}$$

Where A665 and A649 is the absorbance value, V is the volume of solution (liters), and m is the weight (g) of the sample used (Yuan et al., 2016).

Leaf greenness index

The leaf greenness index was measured using SPAD 502 Plus Chlorophyll Meter (Konica Minolta, Osaka, Japan). Three fully expanded fresh leaves from each pot were selected, and the readings were measured three times. The average was calculated to estimate leaf greenness.

Fresh and dry weight

Plant samples (rosette and roots) were collected and washed at harvest, and fresh plant weight was measured. Later on, the samples (root and rosette) were oven-dried at 65°C until a constant weight was achieved. The plant dry weight was measured using a weighing balance and recorded in grams.

Moisture content

The moisture content in samples was determined using the following formula.

$$Moisture\ content\ (\%) = \frac{(\text{Fresh weight} - \text{Oven dry weight})}{\text{Fresh weight}} \times 100$$

Where fresh weight is the weight of plant samples at the time of harvest, and oven-dry weight was obtained after drying the samples at 65°C until a constant weight was achieved. A weighing balance was used for weighing, and readings were taken.

Biometric analysis

The biometric analysis of radish included root diameter and length. After harvest, the radish was washed, and its length was measured using a measuring tape. Whereas, the diameter of radish was determined using Vernier calipers.

Statistical analysis

Data sets were represented as means ± standard deviation (SD), and CRD was the basis of the analysis of variance (ANOVA). The least significant difference (LSD) test was used for comparison at a 5% probability level. Statistical softwares R-studio® and Statistix 9® were used for statistical analysis. Microsoft Excel 2016 was used for data processing and visualization. Pearson correlation analysis was performed using R-studio.

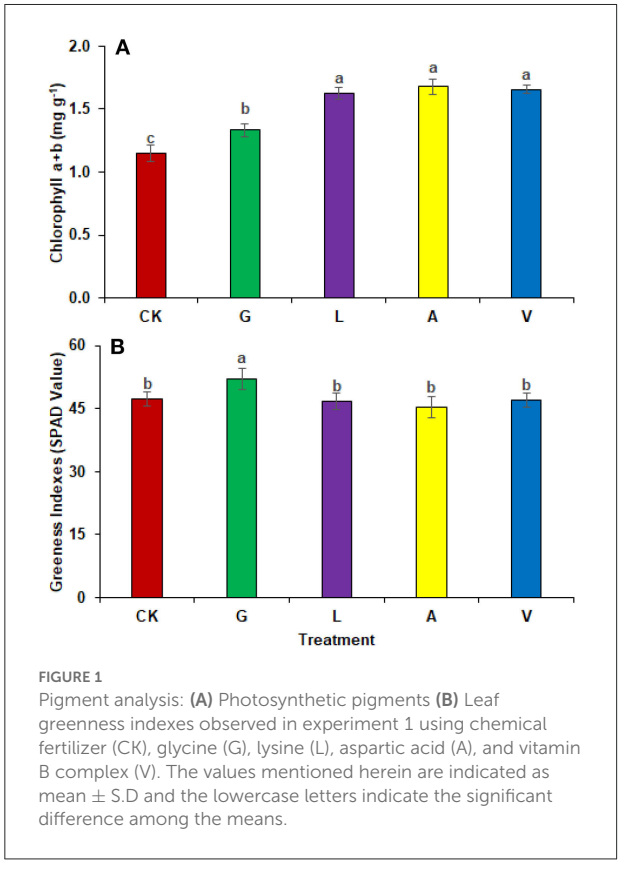

FIGURE 1
Pigment analysis: **(A)** Photosynthetic pigments **(B)** Leaf greenness indexes observed in experiment 1 using chemical fertilizer (CK), glycine (G), lysine (L), aspartic acid (A), and vitamin B complex (V). The values mentioned herein are indicated as mean ± S.D and the lowercase letters indicate the significant difference among the means.

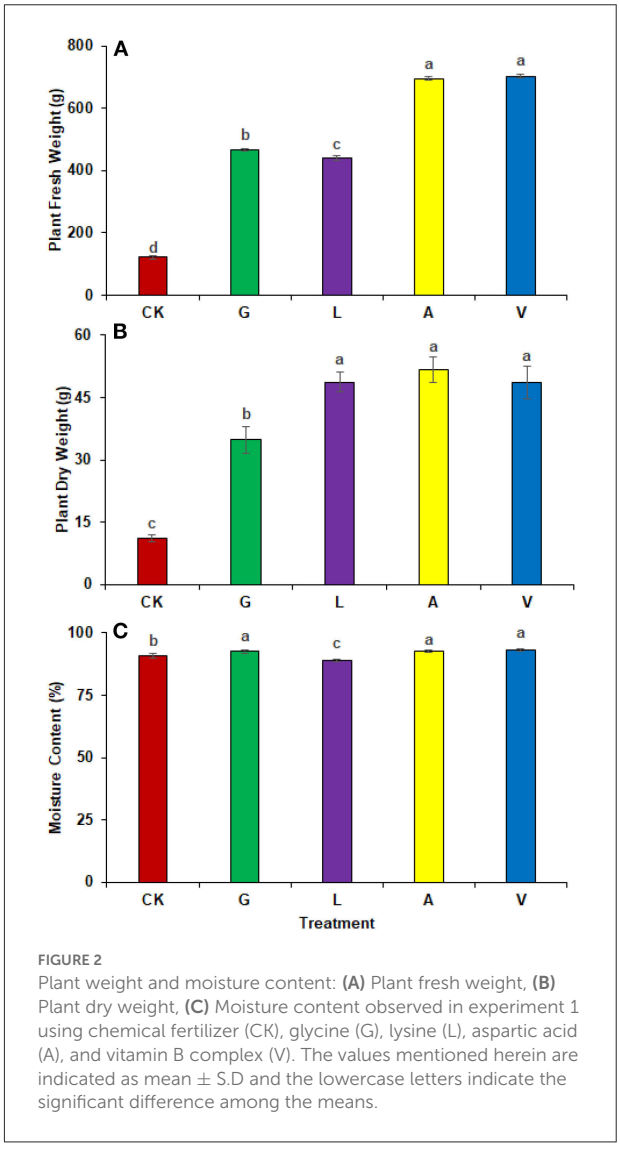

FIGURE 2
Plant weight and moisture content: **(A)** Plant fresh weight, **(B)** Plant dry weight, **(C)** Moisture content observed in experiment 1 using chemical fertilizer (CK), glycine (G), lysine (L), aspartic acid (A), and vitamin B complex (V). The values mentioned herein are indicated as mean ± S.D and the lowercase letters indicate the significant difference among the means.

Results

The radish growth performance improved significantly with the use of biostimulants. In our experiments, the control group contained plants sprayed with the recommended dose of chemical fertilizers (CK). All the treatments are compared with CK.

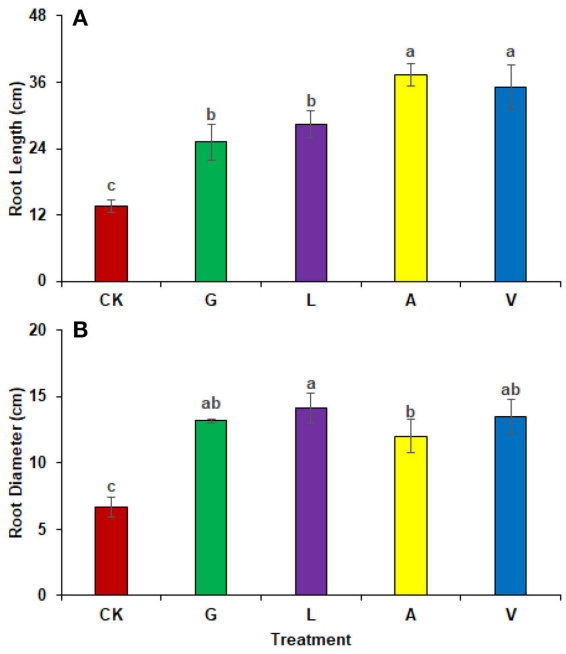

FIGURE 3
Biometric attributes of radish: **(A)** Root length **(B)** Root diameter observed in experiment 1 using chemical fertilizer (CK), glycine (G), lysine (L), aspartic acid (A), and vitamin B complex (V). The values mentioned herein are indicated as mean ± S.D and the lowercase letters indicate the significant difference among the means.

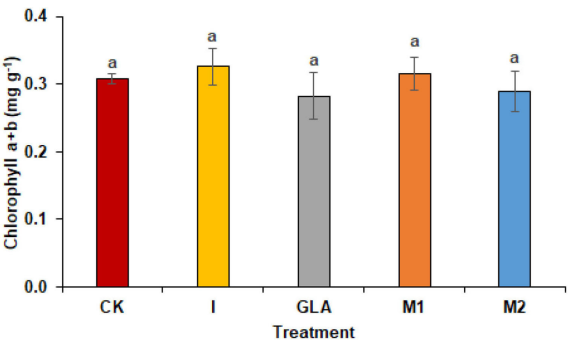

FIGURE 4
Photosynthetic pigments observed in experiment 2 using chemical fertilizer (CK), Isabion® (I), glycine + lysine + aspartic acid (GLA), moringa leaf extract + GLA (M1), 25% NPK + M1 (M2). The values mentioned herein are indicated as mean ± S.D and the lowercase letters indicate the significant difference among the means.

Experiment 1

Gaseous exchange parameters

Photosynthetic rates showed insignificant changes with the identified values as 4.03 μmol m^{-2} s^{-1} in CK, 4.23 μmol m^{-2} s^{-1} in G, 4.00 μmol m^{-2} s^{-1} in L, 4.61 μmol m^{-2} s^{-1} in A, and 3.78 μmol m^{-2} s^{-1} in V respectively. Transpiration rate was significantly increased with the application of V (81.79%), followed by A (47.77%), L (36.77%), and G (1.17%), respectively, compared with CK. The identified values were 0.97 mmol m^{-2} s^{-1} in CK, 1.17 mmol m^{-2} s^{-1} in G, 1.33 mmol m^{-2} s^{-1} in L, 1.43 mmol m^{-2} s^{-1} in A, and 1.76 mmol m^{-2} s^{-1} in V

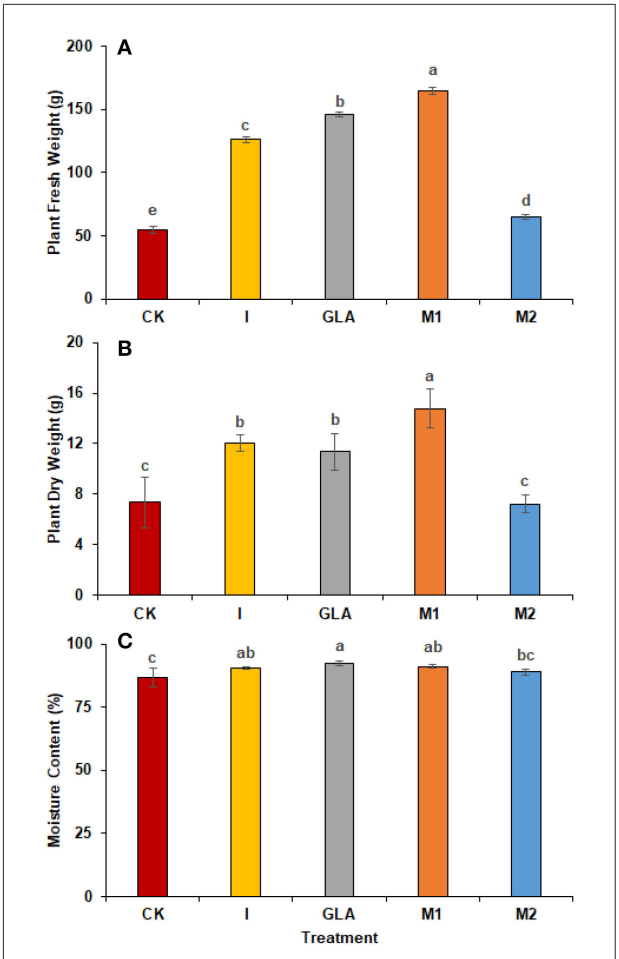

FIGURE 5
Plant weight and moisture content: **(A)** Plant fresh weight, **(B)** Plant dry weight, **(C)** Moisture content observed in experiment 2 using chemical fertilizer (CK), Isabion® (I), glycine + lysine + aspartic acid (GLA), moringa leaf extract + GLA (M1), 25% NPK + M1 (M2). The values mentioned herein are indicated as mean ± S.D and the lowercase letters indicate the significant difference among the means.

respectively. Stomatal conductance was also increased with a similar trend where V showed the highest increase (179.17%), followed by A (141.67%), L (87.50%), and G (47.92%). The values observed were 0.16 mmol m^{-2} s^{-1} in CK, 0.24 mmol m^{-2} s^{-1} in G, 0.30 mmol m^{-2} s^{-1} in L, 0.39 in A, and 0.45 mmol m^{-2} s^{-1} in V. Internal CO_2 concentration was significantly improved with the application of biostimulants. The highest increase was observed with G (15.04%), L (14.69%), V (13.81%), and A (11.70%), respectively, compared with CK. The values reported were 379.00 μmol mol^{-1} in CK, 436.00 μmol mol^{-1} in G, 434.67 μmol mol^{-1} in L, 423.33 μmol mol^{-1} in A, and 431.33 in V.

Photosynthetic pigments

The foliar application of biostimulants on radish increased the photosynthetic pigments in leaves. Chlorophyll contents were improved significantly with the application of A (45.81%), followed by V (43.89%), L (41.28%), and G (16.01%) as compared to CK (Figure 1A). The identified values were 1.15 mg g^{-1} in CK, 1.33 mg g^{-1} in G, 1.62 mg g^{-1} in L, 1.68 mg g^{-1} in A, and 1.65 mg g^{-1} in V, respectively. The SPAD measurements demonstrated that G enhanced (9.91%) the greenness index of the leaves, while the values observed were 47.31 in CK, 52.00 in G, 46.70 in L, 45.37 in A, and 46.99 in V (Figure 1B).

Fresh and dry weight

A significant improvement in plant total fresh and dry weights were observed with the application of biostimulants. The identified values were 121.33 g in CK, 466.67 g in G, 441.67 g in L, 695.00 g in A, and 701.67 g in V, respectively. The most significant change in fresh plant weight was observed in radish plants receiving V (478.31%), followed by A (472.82%), G (284.63%), and L (264.02%) (Figure 2A). In addition, plant dry weight improved significantly in A, followed by L, V, and G (364.73, 337.90, 364.73, and 212.50%) compared to the CK (Figure 2B). The identified values were 11.33 g in CK, 34.78 g in G, 48.74 g in L, 51.72 g in A, and 48.61 g in V.

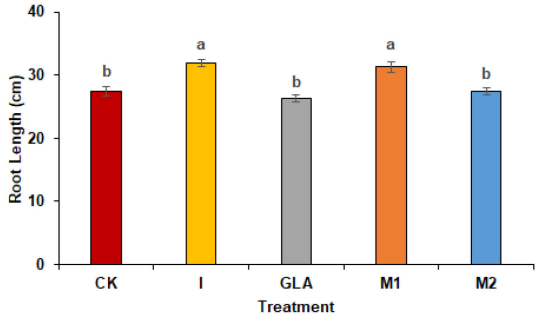

FIGURE 6
Root length of radish observed in experiment 2 using chemical fertilizer (CK), Isabion® (I), glycine + lysine + aspartic acid (GLA), moringa leaf extract + GLA (M1), 25% NPK + M1 (M2). The values mentioned herein are indicated as mean ± S.D and the lowercase letters indicate the significant difference among the means.

Moisture content

The use of biostimulants influenced radish moisture contents. The moisture contents were higher in V (2.50%), followed by A (1.94%), and G (1.92%) as compared to CK. Whereas, the identified values were 90.80% in CK, 92.55% in G, 88.97% in L, 92.56% in A, and 93.07% in V respectively (Figure 2C).

Morphological analysis

The biostimulants influenced the root length and diameter significantly. Root length was increased significantly with A (172.86%), followed by V (157.50%), L (107.27%), and G (84.10%) in comparison with CK. The identified values were 13.67 cm in CK, 25.17 cm in G, 28.33 cm in L, 37.30 cm in A, and 35.20 cm in V, respectively (Figure 3A). Similarly, root diameter was increased with L (111.89%), V (102.40%), G (97.40%), and A (79.91%) as compared to CK. The values observed were 6.67 cm in CK, 13.17 cm in G, 14.13 cm in L, 12.0 cm in A, and 13.50 cm in V, respectively (Figure 3B).

Experiment 2

Gaseous exchange parameters

Similar to experiment one, biostimulants significantly improved the plants' physiology in experiment two (Figure 4). Photosynthetic rates were significantly enhanced with GLA (327.01%), M1 (219.60%), and M2 (22.16%), respectively. The identified values were 3.64 μmol m^{-2} s^{-1} in CK, 3.42 μmol m^{-2} s^{-1} in I, 15.54 μmol m^{-2} s^{-1} in GLA, 11.63 μmol m^{-2} s^{-1} in M1, and 4.45 μmol m^{-2} s^{-1} in M2 respectively. The transpiration rate was significantly improved with GLA (53.14%) and M2 (17.86%) compared to the CK. The identified values were 4.46 mmol m^{-2} s^{-1} in CK, 4.31 mmol m^{-2} s^{-1} in I, 6.83 mmol m^{-2} s^{-1} in GLA, 4.03 mmol m^{-2} s^{-1} in M1, and 5.26 mmol m^{-2} s^{-1} in M2 respectively. In addition, the stomatal conductance was enhanced significantly with M1 (54.84%) followed by GLA (43.01%), and internal CO_2 concentration was improved with M1 and M2 (0.83 and 1.93%, respectively) compared to CK. Whereas, the values of stomatal conductance were 0.31 mmol m^{-2} s^{-1} in CK, 0.30 mmol m^{-2} s^{-1} in I, 0.44 mmol m^{-2} s^{-1} in GLA, 0.48 mmol m^{-2} s^{-1} in M1, and 0.28 mmol m^{-2} s^{-1} in M2 respectively. Moreover, the values of internal CO_2 concentration were 363.33 μmol mol^{-1} in CK,

344.67 μmol mol^{-1} in I, 338.67 μmol mol^{-1} in GLA, 366.33 μmol mol^{-1} in M1, and 370.33 in M2.

Photosynthetic pigments

The photosynthetic pigments of radish leaves showed non-significant results with the spraying of biostimulants. Chlorophyll a + b was highest in I (5.11%) and M1 (1.47%) as compared to CK. The identified values were 0.31 mg g^{-1} in CK, 0.33 mg g^{-1} in I, 0.28 mg g^{-1} in GLA, 0.31 mg g^{-1} in M1, and 0.29 mg g^{-1} in M2 respectively (Figure 4).

Fresh and dry weight

A significant increase in plant total fresh and dry weights were observed with the application of biostimulants. The highest plant fresh weight was achieved in plants receiving M1 (201.81%), followed by GLA (167.06%), I (130.47%), and M2 (18.29%). The identified values were 54.67 g in CK, 126.00 g in I, 146.00 g in GLA, 164.00 g in M1, and 64.67 g in M2, respectively (Figures 5A,B). In addition, plant dry weight was significantly improved in M1, followed by I and GLA (101.46%, 63.84%, and 54.93% higher than CK). The observed values were 7.33 g in CK, 12.01 g in I, 11.36 g in GLA, 14.77 g in M1, and 7.22 g in M2 (Figure 5C).

Moisture content

Moisture contents were also influenced by the use of biostimulants and were significantly improved with GLA (6.51%) followed by M1 (5.16%) and I (4.48%) as compared to CK. The identified values were 86.59% in CK, 90.47% in I, 92.23% in GLA, 91.06% in M1, and 88.82% in M2 respectively (Figure 6).

Morphological analysis

Radish length was influenced significantly by the use of biostimulants and was shown by I (16.52%) followed by M1 (14.09%) and M2 (0.35%) as compared to CK. The values observed were 27.42 cm in CK, 31.91 cm in I, 26.33 cm in GLA, 31.28 cm in M1, and 27.52 cm in M2, respectively (Figure 7).

Pearson correlation

Photosynthesis is strongly positively correlated with transpiration rate and moderately associated with stomatal conductance. It has a weak negative correlation with internal CO_2 assimilation and chlorophyll content. Transpiration showed a strong negative association with internal CO_2 assimilation, chlorophyll content, fresh weight, and dry weight. Moreover, a weak positive correlation was observed between stomatal conductance and root diameter. Stomatal conductance showed a strong positive association with root length and a weak positive relationship with root diameter. Internal CO_2 concentration strongly correlates with chlorophyll content, fresh weight, and dry weight. In addition, a moderate positive relation with root diameter was observed. Chlorophyll content showed a strong positive correlation with fresh and dry weight, moderate relation with root diameter, and a weak association with moisture content. Plant fresh weight had a strong positive relation with dry weight and moderate association with moisture content, root length, and diameter. Moreover, dry weight had a strong positive correlation with root diameter, moderate correlation with root length, and a weak association with moisture content. Root length and diameter were also positively correlated with each other (Figure 7).

Discussion

An increasing population along with climate change has threatened agricultural production. Today's need is to develop new sustainable products to increase production and yield and support organic farming (Godlewska et al., 2021). In this scenario, biostimulants can play an environment-friendly role to increase crop productivity, which is associated with the minimal use of chemical fertilizers. In the current study, individual and the combined application of biostimulants showed a potential to improve radish morphology, growth, and yield.

Our results demonstrated an increase in leaf gas exchange attributes. The use of biostimulants improved the transpiration rate, stomatal conductance, and internal CO_2 in plants (Figures 8, 9). Biostimulants can potentially improve water-use efficiency in plants (Jiménez-Arias et al., 2022), which also increases turgor pressure in radish leaf guard cells and increases gaseous exchange attributes. Leaf greenness and chlorophyll are essential in transmitting and absorbing solar energy (Ahmad et al., 2021). The results showed that amino acid-based biostimulants significantly improved the chlorophyll content (Figures 1, 4). The increased pigments with biostimulants can be associated with water and ion use efficiency, better stomatal conductance, photosynthetic capacity, and bioactive compounds, i.e., vitamins (Ali et al., 2020), amino acids, and mineral nutrients (Bahmani Jafarlou et al., 2022). In addition, moringa leaf extract also improves chlorophyll content with its induced sink capability through the supply and translocation of photo-assimilates from leaves to other parts of a plant that improve fruit quality (Arif et al., 2022).

In addition, the use of biostimulants showed a positive response to radish yield and growth. The results determined that the use of A, V, and M1 significantly improved the radish yield and production (Figures 2, 5). Whereas a low yield was observed with the combined use of biostimulants and mineral fertilizers. The amino acid-based biostimulants positively impact plant physiology and metabolism, while the interaction of

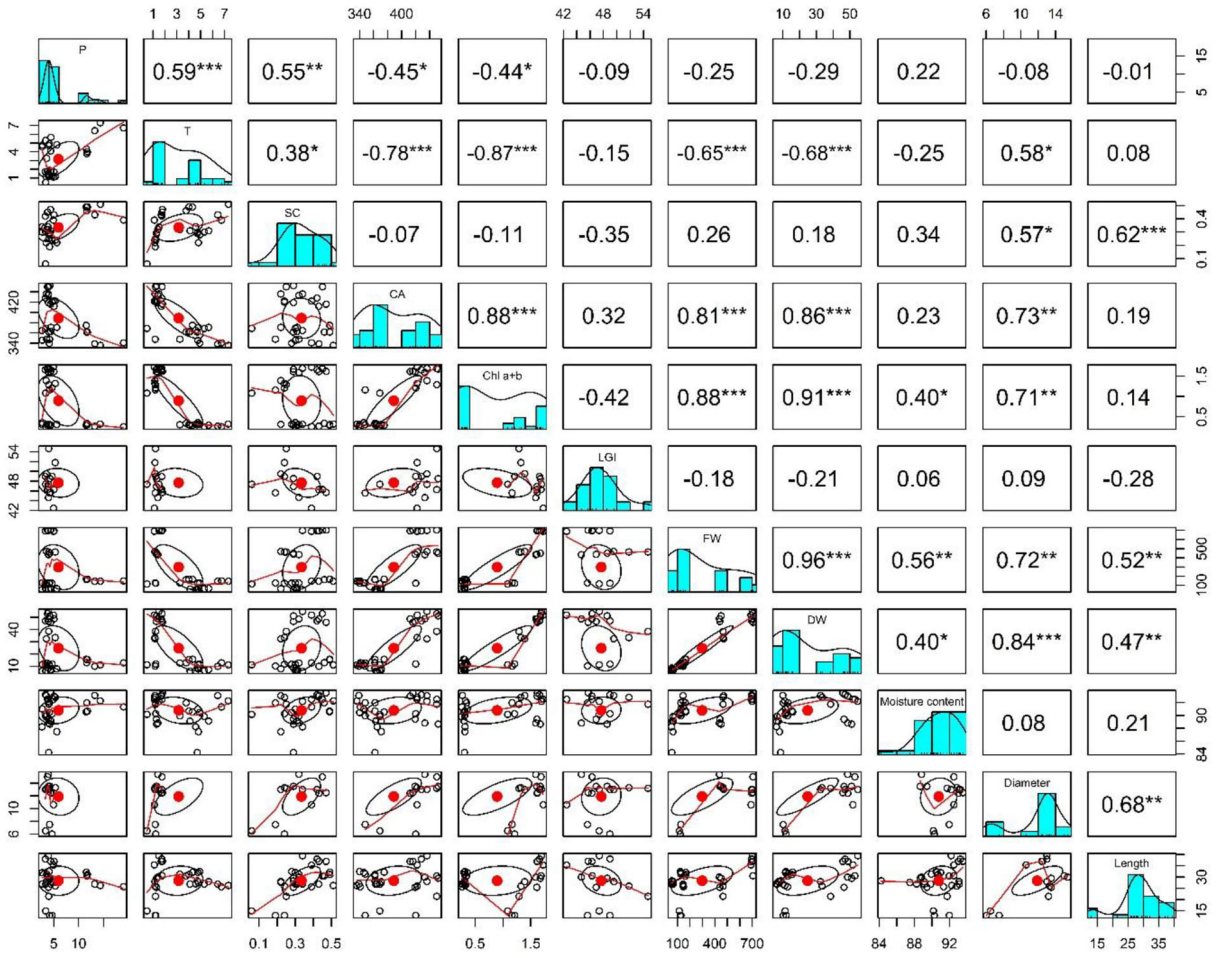

FIGURE 7
Pearson correlation indicating the relation between assessment parameters: P is Photosynthetic rate, T is Transpiration rate, SC is Stomatal conductance, CA Internal CO_2 concentration, Chl a+b is Photosynthetic pigments, LGI is Leaf greenness indexes, FW is Plant fresh weight, DW is Plant dry weight, Moisture content is Moisture content, Diameter is Root diameter, and Length is Root length. The * indicates week relationship, ** shows strong, and *** shows very strong relationship.

biostimulants when applied in combination is still unknown (Alfosea-Simón et al., 2021). Plants can produce amino acids and vitamins, but it requires considerable energy; therefore, if applied exogenously, they can save energy and improve their development at different growth stages (Popko et al., 2018). In addition, improved yield can also be related to the potential of Vitamins B_1 and B_6 to develop resistance in plants against oxidative stress (Asensi-Fabado and Munné-Bosch, 2010). Biostimulants also act as signal-transducing molecules and benefit plant physiological processes that contribute to higher yield and biomass (Khan et al., 2019).

The results of both experiments also suggest that foliar application of amino acids and vitamins improves the radish root morphology (Figures 3, 6). Previous literature reported that root growth is also stimulated with the application of biostimulants having vitamin B-complex (Rehim et al., 2021). Vitamins B_1 is a cofactor that contributes significantly to improve primary metabolic processes in plants (glycolysis, tricarboxylic acid cycle, and pentose phosphate pathway) that ultimately increases plant growth performances (Soppelsa et al., 2019). In addition, free amino acids are small molecules easily absorbed by plant leaves and roots and promote endogenous biosynthesis of plant hormones that ultimately regulate plant phenological processes (Caruso et al., 2019). Foliar application of amino acids improves plant growth, yield, and morphology in beans and radish (Kocira et al., 2020; Rehim et al., 2021). Amino acids are involved in synthesizing organic compounds and phytohormones (auxin and gibberellin) and enhancing macro and micronutrient uptake, contributing to better crop productivity (Kocira et al., 2020). Moreover, glycine has a better potential to release N molecules than urea (McCoy et al., 2020).

Although the use of chemical fertilizers contributes a lot to improving crop productivity and yield, it has adverse

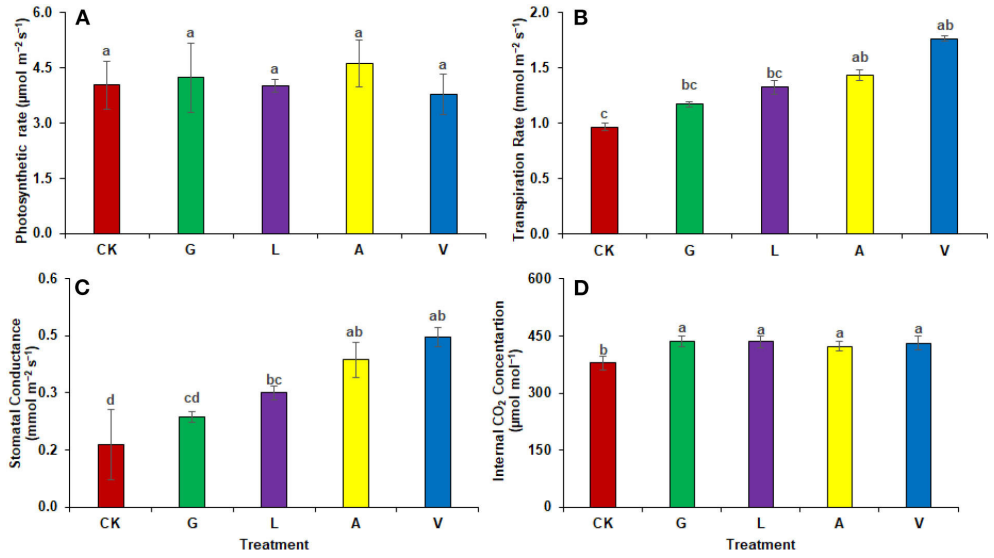

FIGURE 8
Gaseous exchange parameters: **(A)** Photosynthetic rate, **(B)** Transpiration rate, **(C)** Stomatal conductance **(D)** Internal CO_2 concentration observed in experiment 1 using chemical fertilizer (CK), glycine (G), lysine (L), aspartic acid (A), and vitamin B complex (V). The values mentioned herein are indicated as mean ± S.D and the lowercase letters indicate the significant difference among the means.

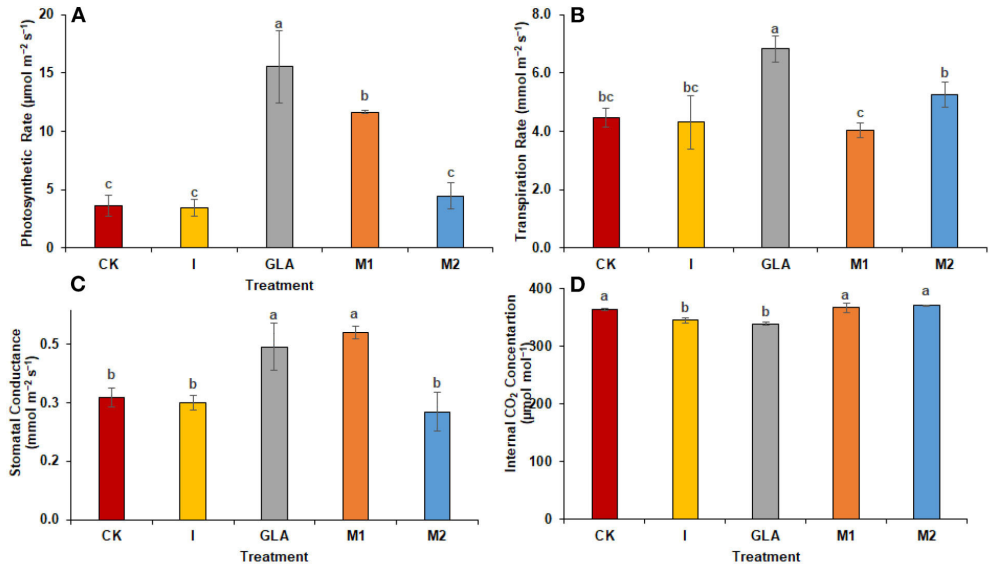

FIGURE 9
Gaseous exchange parameters: **(A)** Photosynthetic rate, **(B)** Transpiration rate, **(C)** Stomatal conductance **(D)** Internal CO_2 concentration observed in experiment 2 using chemical fertilizer (CK), Isabion® (I), glycine + lysine + aspartic acid (GLA), moringa leaf extract + GLA (M1), 25% NPK + M1 (M2). The values mentioned herein are indicated as mean ± S.D and the lowercase letters indicate the significant difference among the means.

effects on the soil, water, and environment. The results of our study demonstrated that the foliar application of biostimulants has a promising role in improving crop yield, physiology, and morphology. Moreover, it is an innovative method for the sustainable cultivation of radish. However, the long-term impact and effects of biostimulants on soil properties and field conditions need to be explored.

Conclusion

The demand for food and a safe environment is gaining attention from the scientific community, and sustainable agriculture needs effective chemical fertilizers, genetically improved plants, and growth-promoting biostimulants. Biostimulants are a rich source of biologically active compounds and can potentially improve plant metabolic processes to achieve better crop quality, yield, and productivity. The study concludes that the foliar application of biostimulants increases gaseous exchange activities and chlorophyll content in radish as well as the plant's morphology, and its fresh and dry biomass, which can be conclusive evidence to reduce chemical fertilizers. However, further studies regarding field conditions, long-term uses and impacts, effects on soil mineral status, nutrient use efficiency, and plant biochemical properties are the identified research gaps. In addition, the mechanistic approaches behind the improved results with the combined use of biostimulants need attention.

Data availability statement

The original contributions presented in the study are included in the article/supplementary material, further inquiries can be directed to the corresponding authors.

Author contributions

All authors listed have made a substantial, direct, and intellectual contribution to the work and approved it for publication.

Funding

This study acknowledges the financial aid provided by Higher Education Commission Pakistan under the indigenous Ph.D. 5000 fellowship program 520(PH-II) 2AV6-075/HEC/IS/2020 for Q-U-AR to pursue her Ph.D. at BZU Multan.

Conflict of interest

Author YG was employed by KOYO Star Agriculture Technology Co., LTD.

The remaining authors declare that the research was conducted in the absence of any commercial or financial relationships that could be construed as a potential conflict of interest.

Publisher's note

All claims expressed in this article are solely those of the authors and do not necessarily represent those of their affiliated organizations, or those of the publisher, the editors and the reviewers. Any product that may be evaluated in this article, or claim that may be made by its manufacturer, is not guaranteed or endorsed by the publisher.

References

Abd El-Mageed, T. A., Semida, W. M., and Rady, M. M. (2017). Moringa leaf extract as biostimulant improves water use efficiency, physio-biochemical attributes of squash plants under deficit irrigation. *Agric. Water Manag.* 193, 46–54. doi: 10.1016/j.agwat.2017.08.004

Ahmad, S., Cui, W., Kamran, M., Ahmad, I., Meng, X., Wu, X., et al. (2021). Exogenous application of melatonin induces tolerance to salt stress by improving the photosynthetic efficiency and antioxidant defense system of maize seedling. *J. Plant Growth Regul.* 40, 1270–1283. doi: 10.1007/s00344-020-10187-0

Alfosea-Simón, M., Simón-Grao, S., Zavala-Gonzalez, E. A., Cámara-Zapata, J. M., Simón, I., Martínez-Nicolás, J. J., et al. (2020). Application of biostimulants containing amino acids to tomatoes could favor sustainable cultivation: implications for tyrosine, lysine, and methionine. *Sustainability* 12, 1–19. doi: 10.3390/su12229729

Alfosea-Simón, M., Simón-Grao, S., Zavala-Gonzalez, E. A., Cámara-Zapata, J. M., Simón, I., Martínez-Nicolás, J. J., et al. (2021). Physiological, nutritional and metabolomic responses of tomato plants after the foliar application of amino acids aspartic acid, glutamic acid and alanine. *Front. Plant Sci.* 11, 581234. doi: 10.3389/fpls.2020.581234

Ali, Q., Perveen, R., El-Esawi, M. A., Ali, S., Hussain, S. M., Amber, M., et al. (2020). Low doses of cuscuta reflexa extract act as natural biostimulants to improve the germination vigor, growth, and grain yield of wheat grown under water stress: Photosynthetic pigments, antioxidative defense mechanisms, and nutrient acquisition. *Biomolecules* 10, 1–30. doi: 10.3390/biom10091212

Arif, Y., Bajguz, A., and Hayat, S. (2022). *Moringa oleifera Extract as a Natural Plant Biostimulant*. *J. Plant Growth Regul.* 1–16. doi: 10.1007/s00344-022-10630-4

Asensi-Fabado, M. A., and Munné-Bosch, S. (2010). Vitamins in plants: occurrence, biosynthesis and antioxidant function. *Trends Plant Sci.* 15, 582–592. doi: 10.1016/j.tplants.2010.07.003

Bahmani Jafarlou, M., Pilehvar, B., Modaresi, M., and Mohammadi, M. (2022). Seaweed Liquid Extract as an Alternative Biostimulant for the Amelioration of Salt-stress Effects in Calotropis procera (Aiton) W.T. *J. Plant Growth Regul.* 1–16. doi: 10.1007/s00344-021-10566-1

Bashir, M. A., Rehim, A., Raza, Q. U. A., Muhammad Ali Raza, H., Zhai, L., Liu, H., et al. (2021). "Biostimulants as plant growth stimulators in modernized agriculture and environmental sustainability," in *Technology in Agriculture* [Working Title] (London: IntechOpen).

Bell, J. C., Bound, S. A., and Buntain, M. (2022). "Biostimulants in agricultural and horticultural production," in *Horticultural Reviews* (Hoboken, NJ: John Wiley and Sons. Ltd), 35–95.

Caruso, G., De Pascale, S., Cozzolino, E., Cuciniello, A., Cenvinzo, V., Bonini, P., et al. (2019). Yield and nutritional quality of Vesuvian piennolo tomato PDO

as affected by farming system and biostimulant application. *Agronomy* 9, 1–14. doi: 10.3390/agronomy9090505

Chouhan, G. K., Verma, J. P., Jaiswal, D. K., Mukherjee, A., Singh, S., de Araujo Pereira, A. P., et al. (2021). Phytomicrobiome for promoting sustainable agriculture and food security: Opportunities, challenges, and solutions. *Microbiol. Res.* 248, 126763. doi: 10.1016/j.micres.2021.126763

Cristiano, G., and De Lucia, B. (2021). Petunia performance under application of animal-based protein hydrolysates: effects on visual quality, biomass, nutrient content, root morphology, and gas exchange. *Front. Plant Sci.* 12, 890. doi: 10.3389/fpls.2021.640608

Del Buono, D. (2021). Can biostimulants be used to mitigate the effect of anthropogenic climate change on agriculture? It is time to respond. *Sci. Total Environ.* 751, 141763. doi: 10.1016/j.scitotenv.2020.141763

Godlewska, K., Pacyga, P., Michalak, I., Biesiada, A., Szumny, A., Pachura, N., et al. (2021). Systematic investigation of the effects of seven plant extracts on the physiological parameters, yield, and nutritional quality of radish (Raphanus sativus var. sativus). *Front. Plant Sci.* 12, 651152. doi: 10.3389/fpls.2021.651152

Jiménez-Arias, D., Hernándiz, A. E., Morales-Sierra, S., García-García, A. L., García-Machado, F. J., Luis, J. C., et al. (2022). Applying biostimulants to combat water deficit in crop plants: research and debate. *Agronomy* 12, 571. doi: 10.3390/agronomy12030571

John, D. A., and Babu, G. R. (2021). Lessons from the aftermaths of green revolution on food system and health. *Front. Sustain. Food Syst.* 5, 21. doi: 10.3389/fsufs.2021.644559

Khan, S., Yu, H., Li, Q., Gao, Y., Sallam, B. N., Wang, H., et al. (2019). Exogenous application of amino acids improves the growth and yield of lettuce by enhancing photosynthetic assimilation and nutrient availability. *Agronomy* 9, 266. doi: 10.3390/agronomy9050266

Kocira, A., Lamorska, J., Kornas, R., Nowosad, N., Tomaszewska, M., Leszczyńska, D., et al. (2020). Changes in biochemistry and yield in response to biostimulants applied in bean (Phaseolus vulgaris L.). *Agronomy* 10, 189. doi: 10.3390/agronomy10020189

Lee, O. N., and Park, H. Y. (2020). Effects of different colored film mulches on the growth and bolting time of radish (Raphanus sativus L.). *Sci. Hortic. (Amsterdam).* 266, 109271. doi: 10.1016/j.scienta.2020.109271

Maja, M. M., and Ayano, S. F. (2021). The Impact of Population Growth on Natural Resources and Farmers' Capacity to Adapt to Climate Change in Low-Income Countries. *Earth Syst. Environ.* 5, 271–283. doi: 10.1007/s41748-021-00209-6

McCoy, R. M., Meyer, G. W., Rhodes, D., Murray, G. C., Sors, T. G., and Widhalm, J. R. (2020). Exploratory study on the foliar incorporation and stability of isotopically labeled amino acids applied to turfgrass. *Agronomy* 10, 358. doi: 10.3390/agronomy10030358

Popko, M., Michalak, I., Wilk, R., Gramza, M., Chojnacka, K., and Górecki, H. (2018). Effect of the new plant growth biostimulants based on amino acids on yield and grain quality of winter wheat. *Molecules* 23, 470. doi: 10.3390/molecules23020470

Rahman, K. M. A., and Zhang, D. (2018). Effects of fertilizer broadcasting on the excessive use of inorganic fertilizers and environmental sustainability. *Sustain.* 10, 759. doi: 10.3390/su10030759

Rehim, A., Amjad Bashir, M., Raza, Q.-U.-A., Gallagher, K., and Berlyn, G. P. (2021). Yield Enhancement of Biostimulants, Vitamin B12, and CoQ10 Compared to Inorganic Fertilizer in Radish. *Agronomy* 11, 697. doi: 10.3390/agronomy11040697

Samuels, L. J., Setati, M. E., and Blancquaert, E. H. (2022). Towards a better understanding of the potential benefits of seaweed based biostimulants in vitis vinifera L. Cultivars. *Plants* 11, 348. doi: 10.3390/plants11030348

Scafaro, A. P., Atwell, B. J., Muylaert, S., Reusel, B., Van, R.uiz, G. A., Rie, J., et al. (2018). A thermotolerant variant of rubisco activase from a wild relative improves growth and seed yield in rice under heat stress. *Front. Plant Sci.* 871, 1663. doi: 10.3389/fpls.2018.01663

Soppelsa, S., Kelderer, M., Casera, C., Bassi, M., Robatscher, P., Matteazzi, A., et al. (2019). Foliar applications of biostimulants promote growth, yield and fruit quality of strawberry plants grown under nutrient limitation. *Agronomy* 9, 483. doi: 10.3390/agronomy9090483

Wan, L. J., Tian, Y., He, M., Zheng, Y. Q., Lyu, Q., Xie, R. J., et al. (2021). Effects of chemical fertilizer combined with organic fertilizer application on soil properties, citrus growth physiology, and yield. *Agriculture* 11, 1207. doi: 10.3390/agriculture11121207

Yuan, Z., Cao, Q., Zhang, K., Ata-Ul-Karim, S. T., Tan, Y., Zhu, Y., et al. (2016). Optimal leaf positions for SPAD meter measurement in rice. *Front. Plant Sci.* 7, 719. doi: 10.3389/fpls.2016.00719

Zaheer, I. E., Ali, S., Saleem, M. H., Imran, M., Alnusairi, G. S. H., Alharbi, B. M., et al. (2020). Role of iron–lysine on morpho-physiological traits and combating chromium toxicity in rapeseed (Brassica napus L.) plants irrigated with different levels of tannery wastewater. *Plant Physiol. Biochem.* 155, 70–84. doi: 10.1016/j.plaphy.2020.07.034

frontiers | Frontiers in Plant Science

TYPE Original Research
PUBLISHED 11 August 2022
DOI 10.3389/fpls.2022.956391

OPEN ACCESS

EDITED BY
Maurizio Ruzzi,
University of Tuscia, Italy

REVIEWED BY
Philipp Franken,
Friedrich Schiller University Jena, Germany
Cristina Cruz,
University of Lisbon, Portugal

*CORRESPONDENCE
Andrea Fiorini
andrea.fiorini@unicatt.it

SPECIALTY SECTION
This article was submitted to Crop and Product Physiology, a section of the journal Frontiers in Plant Science

RECEIVED 30 May 2022
ACCEPTED 11 July 2022
PUBLISHED 11 August 2022

CITATION
Ganugi P, Fiorini A, Rocchetti G, Bonini P, Tabaglio V and Lucini L (2022) A response surface methodology approach to improve nitrogen use efficiency in maize by an optimal mycorrhiza-to-*Bacillus* co-inoculation rate.
Front. Plant Sci. 13:956391.
doi: 10.3389/fpls.2022.956391

A response surface methodology approach to improve nitrogen use efficiency in maize by an optimal mycorrhiza-to-*Bacillus* co-inoculation rate

Paola Ganugi[1], Andrea Fiorini[2]*, Gabriele Rocchetti[3], Paolo Bonini[4], Vincenzo Tabaglio[2] and Luigi Lucini[1]

[1]Department for Sustainable Food Process, Università Cattolica del Sacro Cuore, Piacenza, Italy, [2]Department of Sustainable Crop Production, Università Cattolica del Sacro Cuore, Piacenza, Italy, [3]Department of Animal Science, Food and Nutrition, Università Cattolica del Sacro Cuore, Piacenza, Italy, [4]oloBion-OMICS LIFE LAB, Barcelona, Spain

Co-inoculation of arbuscular mycorrhizal fungi (AMF) and bacteria can synergically and potentially increase nitrogen use efficiency (NUE) in plants, thus, reducing nitrogen (N) fertilizers use and their environmental impact. However, limited research is available on AMF-bacteria interaction, and the definition of synergisms or antagonistic effects is unexplored. In this study, we adopted a response surface methodology (RSM) to assess the optimal combination of AMF (*Rhizoglomus irregulare and Funneliformis mosseae*) and *Bacillus megaterium* (a PGPR—plant growth promoting rhizobacteria) formulations to maximize agronomical and chemical parameters linked to N utilization in maize (*Zea mays* L.). The fitted mathematical models, and also 3D response surface and contour plots, allowed us to determine the optimal AMF and bacterial doses, which are approximately accorded to 2.1 kg ha^{-1} of both formulations. These levels provided the maximum values of SPAD, aspartate, and glutamate. On the contrary, agronomic parameters were not affected, except for the nitrogen harvest index (NHI), which was slightly affected (p-value of < 0.10) and indicated a higher N accumulation in grain following inoculation with 4.1 and 0.1 kg ha^{-1} of AMF and *B. megaterium*, respectively. Nonetheless, the identification of the saddle points for asparagine and the tendency to differently allocate N when AMF or PGPR were used alone, pointed out the complexity of microorganism interaction and suggests the need for further investigations aimed at unraveling the mechanisms underlying this symbiosis.

KEYWORDS

biostimulants, *Bacillus megaterium*, *Rhizoglomus irregulare*, *Funneliformis mosseae*, nutrients uptake, plant growth promoting rhizobacteria

Introduction

Nitrogen (N) represents a major nutrient for plants, being an essential component of proteins, nucleotides, chlorophyll, and a broad range of secondary metabolites. Cereals grains, providing 60% of the food necessary to feed the world's population, require significant inputs of N to achieve optimum yields. Nevertheless, N availability can represent a limiting condition since nitrate (NO_3^-) and ammonium (NH_4^+), representing the readily available N pool, account for only 2% of total soil N content (Moreau et al., 2019).

At the same time, the increasing use of synthetic N fertilizers over the last decades has posed concerns about the contamination of surface and groundwater bodies by nitrate, the impairment of biodiversity, and the emission of greenhouse gases (Ahmed et al., 2017). In line with the EU "Farm to fork" strategy, which aims at increasing the agricultural land managed under organic farming by 25%, scientific efforts are being done to maintain (or even increase) crop productivity by efficiently using organic fertilizers, which have been recognized to increase N losses very often, especially if applied inappropriately (Maris et al., 2021). Such an increase in N use efficiency can significantly minimize N losses and the consequent adverse impacts on ecosystems while decreasing costs for organic fertilizers (Galloway et al., 2014).

All the pathways of N cycling in soils mainly depend on the edaphic conditions, agronomic management, climate, crop genetics, and finally determines N availability, transfer, transformation, and losses (Congreves et al., 2021). Many scientific contributions have reported best agronomic practices and breeding solutions to enhance NUE, commonly defined as the plant biomass accumulation per unit of soil N available (Peng et al., 2006; van Bueren and Struik, 2017; Anas et al., 2020). N assimilation by plants involves the GS–GOGAT pathway, for which glutamine, asparagine, glutamate, and aspartate are upstream key intermediates; once incorporated into organic compounds, N is then distributed to a broad range of different N-containing compounds. Over the last two decades, biotechnological engineering of the amino acid metabolism has led to promising results for the improvement of NUE, especially the content of glutamine, asparagine, glutamate, and aspartate has been adopted as an interesting target to carry out these studies, being involved in plant N utilization and storage after assimilation (Dellero, 2020; The et al., 2021). Recently, especially in a framework of sustainable crop production, the inoculation with beneficial microorganisms has gained importance in such plant NUE increase (Di Benedetto et al., 2017; Verzeaux et al., 2017; Dalla Costa et al., 2021).

Arbuscular mycorrhizal fungi (AMF) have been reported to increase NUE by developing the symbiotic association with most terrestrial plants, favoring access to N uptake in a larger soil volume (Verzeaux et al., 2017). Interestingly, the specific up-regulation of NO_3^- and NH_4^+ transporters has been observed in AMF colonized roots compared with the non-colonized plants (Courty et al., 2015; Garcia et al., 2016). In cereals such as sorghum, maize, and rice, AMT3.1 plant NH_4^+ transporter transcripts were specifically up-regulated following the mycorrhizal colonization (Koegel et al., 2017). Similarly, higher NUE has been observed following beneficial associations with N2-fixing bacteria such as Rhizobia, *Frankia* sp., and Cyanobacteria, and some other diazotrophs like *Azospirillum* spp., *Herbaspirillum* spp., and *Paenibacillus* spp. Interestingly, a community of mycorrhizosphere bacteria living strictly associated with AMF has been suggested to encompass improved crop performances, acting synergistically with AMF (Oldroyd et al., 2011; Santi et al., 2013; Udvardi and Poole, 2013; Agnolucci et al., 2015; Kollah et al., 2016; Mus et al., 2016; Rosenblueth et al., 2018). In this regard, a high degree of specificity between bacteria and AMF has been proposed, and this tripartite association can potentially increase NUE in plants (Tajini et al., 2012; Giovannini et al., 2020; Paul et al., 2020).

The dynamic assembly of the rhizosphere microbial community depends on a large set of factors and is driven by an intricate set of belowground chemical communications (van Dam and Bouwmeester, 2016; Qu et al., 2020). However, very little information is available in the literature regarding optimizing AMF-bacteria co-inoculation to manipulate rhizomicrobiome and improve plant performance.

The present study aimed at optimizing the co-inoculation between mycorrhiza and *Bacillus megaterium* using the response surface methodology (RSM), with reference to enhanced N utilization in maize (*Zea mays* L.). The RSM approach has been chosen to account for the interaction(s) between the fungal and bacterial inoculum in the framework of the complex rhizosphere community. Similarly, different plant-based indices of NUE (i.e., NHI and NUtE; López-Bellido and López-Bellido, 2001) and yield of maize have been considered to account for the different assimilation, metabolization, mobilization processes, as well as the translocation to reproductive portions, to overcome the temporal and spatial edges of NUE indices (Congreves et al., 2021).

Materials and methods

Experimental site and microorganism inoculation

The field experiment was conducted over one maize cropping season—between May 2021 and September 2021—at the CERZOO experimental research station in Piacenza (45°00′21.6″N, 9°42′27.1″E; altitude 68 m a.s.l.), Northern Italy. At the experimental site, the climate is temperate (Cfa following Köppen classification), with an average annual temperature of

13.2°C and cumulative annual precipitation of 837 mm (20-yr data). The soil is a fine, mixed, mesic Udertic Haplustalf based on the Keys to Soil Taxonomy (Soil Survey Staff 2014). The physicochemical properties of soil (0–30 cm soil layer) measured before starting the experiment were: organic matter content 27 g kg^{-1}; pH H_2O 7.8; bulk density 1.36 g cm^{-3}; sand 127 g kg^{-1}; silt 445 g kg^{-1}; clay 428 g kg^{-1}; soil total N 1.3 g kg^{-1}; available P (Olsen) 32 mg kg^{-1}; exchangeable K (NH_4^+ Ac) 294 mg kg^{-1}, and cation exchange capacity 30 $cmol^+$ kg^{-1}. Biostimulant treatments consisted of a seed dressing with the powder AMF-based product Aegis Sym irriga® (*Rhizoglomus irregulare* BEG72 and *Funneliformis mosseae* BEG234, 700 sp g^{-1} each species) formulation, or the PGPR Bactrium® (*Bacillus megaterium* BM77 e BM06, 5×10^9 CFU/g each species) liquid formulation, all from Athens, Agrotecnologia Naturales SL (Tarragona, Spain). The seed dressing was homogenized with maize seeds using an automated mixer.

To assess the effect of different doses of AMF and bacteria on yield and NUE in maize, nine different types of seed dressing were prepared as all the possible combinations of the three doses of AMF (low: 0.1 kg ha^{-1}; medium: 2.1 kg ha^{-1}; and high: 4.1 kg ha^{-1}) and three doses of *B. megaterium* (low: 0.1 kg ha^{-1}; medium: 2.1 kg ha^{-1}; and high: 4.1 kg ha^{-1}). As a result, the present field experiment was set up as a randomized complete block (RCB) design with 9 treatments and 4 replicates (blocks). Each plot was 28 m^2: 10 m long and 2.8 m wide (4 maize rows at a 0.7 m inter-row distance). Before planting maize, the seed dressing was carried out in the Lab separately for each treatment. In brief, each level of the 3 × 3 AMF-*B. megaterium* doses were manually mixed with maize seeds (at around 82,000 seeds ha^{-1}). Then, maize was planted with a common two-row plot seeder on 7 May 2021. Maize cropping management followed principles reported by the regulation (EU) 2018/848 on the organic farming production methods. To represent local practice under organic farming, a 170 kg N ha^{-1} slurry distribution was applied to all the plots before soil tillage (autumn 2020), and no fertilizer was applied during the cropping cycle of maize. To prevent water stress, maize was sprinkler-irrigated three times at doses of 30, 40, and 45 mm. Harvesting took place on 20 September 2021 with a plot-scale combination.

SPAD measurement

On 13 August, relative chlorophyll concentrations, defined as SPAD value, were estimated between 02:00 p.m. and 03:00 p.m. using a SPAD-502 chlorophyll meter (Minolta, Tokyo, Japan). The average value of five measurements of three leaves was taken as the maize SPAD value per plot.

Asparagine, glutamine, aspartate, and glutamate content in leaves

On 13 August, the ninth leaf of five plants per plot was sampled and stored at −20°C. The frozen samples were used to determine the content of four amino acids, namely, asparagine, glutamine, aspartate, and glutamate.

Initially, the five leaves per plot were ground together with liquid nitrogen using a pestle and mortar to obtain a homogeneous and representative final sample. Two aliquots (2 × 1 g) per plot were extracted in 10 ml of 50% methanol, 50% deionized water, and 0.01% formic acid using an Ultra-Turrax (Ika T-25, Staufen, Germany) and successively centrifuged (12,000 × g).

The different extracts were diluted 1,000-fold with deionized water and then filtered in the HPAEC vials using 0.20 μm syringe filters until instrumental analysis. The amino acid content of the hydroalcoholic leaf extracts was then investigated through High-Performance Anion Exchange Chromatography with Pulsed Amperometric Detection (HPAEC–PAD). The analyses were carried out on a Dionex ICS-5000 + instrument (Thermo Fisher Scientific, Waltham, the United States) provided with an electrochemical cell consisting of a gold-working electrode and a pH–Ag/AgCl reference electrode. The separation was performed using a Thermo Scientific™ Dionex™ AMINOPAC™ PA10 Analytical column (2 × 250 mm). The chromatographic runs were executed in a total time of 80 min, with multi-gradient elution consisting of a mobile phase of deionized water (eluent A), 250 mM aqueous sodium hydroxide (eluent B), and 1 M sodium acetate solution (eluent C). The flow rate was 0.25 ml/min, and the injection volume was 25 μl, with a column and detector compartment temperature at 30°C. Gradient elution consisted of 0–12 min with 80% of eluent A and 20% of eluent B; 12–16 min with 68% of eluent A and 32% of eluent B; 16–40 min of 36% of eluent A, 24% of eluent B, and 40% of eluent C. Also, a 40 min of equilibration phase was considered, sing 80% of eluent A and 20% of eluent B. The amino acids were detected by an ICS-5000 + electrochemical detector in integrated pulsed amperometric detection mode applying the following waveform potentials and durations: E1 = 0.13 V (t1 = 0.40 s), E2 = 0.33 V (t2 = 0.210 s), E3 = 0.55 V (t3 = 0.460 s), E4 = 0.33 V (t4 = 0.560 s), E5 = −1.67 V (t5 = 0.580 s), E6 = 0.93 V (t6 = 0.590 s), and E7 = 0.13 V (t7 = 0.600 s). For the quantification step, a calibration curve ($R2 > 0.98$) of the four amino acids was prepared by appropriately diluting an amino acid standard mix (2.5 μmol/ml in 0.1M HCl solution, provided by Merck, Darmstadt, Germany), considering the following concentration range: 25-10-5-2.5-1 μM (**Supplementary Figure 2**). The chromatographic system was controlled through the Thermo Scientific™ Dionex™ Chromeleon™ software

version 7.0 for the instrumentation command, chromatograms acquisition, and processing.

Maize yield and agronomic nitrogen use efficiency indices

At the BBCH 89, maize yield was measured by manually harvesting 8 m^2 per single plot. Plants were weighed and separated into grain and biomass (stalks). A 100-g sub-sample of each grain and biomass sample was oven-dried at 65°C until constant weight to measure dry matter content. Grain and biomass N-uptake were calculated by multiplying grain and biomass yield by their N-concentrations, determined by the Dumas combustion method with an elemental analyzer varioMax C:N (VarioMax C:NS, Elementar, Germany).

The two following N-efficiency parameters were calculated for each treatment according to López-Bellido and López-Bellido (2001): (i) N harvest index (NHI;%) as the ratio of N in grain to N in total plant biomass; and (ii) N-utilization efficiency (NUtE; kg kg^{-1}) as the ratio of grain yield to total plant N-uptake.

Statistical analysis

Data analysis was performed with Rstudio 3.6.1 software (R Core Team, 2013). On each NUE parameter, two different two-way ANOVA ($p < 0.05$) were carried out. The first ANOVA was focused on the differences between treatments, thus, the combination of AMF and bacterial doses, as well as the block, were considered as factors, respectively, represented by 9 and 3 levels. The response profiles not impacted by the microbial inoculations were plotted as box plots using the *ggplot* package to represent the data distribution according to treatments (Wickham and Chang, 2007). Successively, the second ANOVA was performed to study the effects and the interactions of the AMF and bacteria factors.

After that, response-surface analysis was performed with the *rsm* package (Lenth, 2009). According to Kumar et al. (2020), the face-centered composite design (FCDD) was used and two independent variables with three levels were selected: AMF (x1: 0.1 kg ha^{-1}; 2.1 kg ha^{-1}; 4.1 kg ha^{-1}) and B. megaterium (x2: 0.1 kg ha^{-1}; 2.1 kg ha^{-1}; 4.1 kg ha^{-1}). A full factorial design of 27 experimental runs with 12 cube points, 12 axial points, and 3 center points was chosen (**Table 1**), while SPAD values, amino acid concentrations, and other NUE parameters were considered response profiles for modeling. The experimental runs were randomized to minimize the effect of unexpected variability on the observed responses. The following second-order quadratic model was used to develop the optimization and predictive model:

$$Y = \beta_0 + (\beta_i^* x_1) + (\beta_j^* x_2) + (B_{ij}^* x_1^* x_2) + (\beta_i^* {x_1}^2) + (\beta j^* {x_2}^2); \quad (1)$$

where Y is the predicted response profile, β_0, β_i, β_j, and β_{ij} are the interactive regression coefficients, and x_1 and x_2 are the AMF and *B. megaterium* doses, respectively.

Results

Analysis of variance revealed a significant effect of the treatments on maize in terms of SPAD value and amino acid concentrations (**Table 2**). Interestingly, the highest value of SPAD (62.95 ± 1.41) was found with the intermediate dose of AMF and *B. megaterium*, corresponding to 2.1 kg ha^{-1} of each inoculum. Similarly, the same result was obtained for aspartate, whose highest concentration (0.81 ± 0.38 μM) was registered at the same treatment level, showing a content 4.7- and 3.5-folds higher than those, respectively, registered with the lowest (0.1 kg ha^{-1}) and the highest (4.1 kg ha^{-1}) doses of both inocula. Surprisingly, asparagine and glutamine concentrations reached the maximum concentration (respectively, 2.95 ± 0.52 and 0.86 ± 0.13 μM) at 2.1 + 2.1 kg ha^{-1} AMF-*B. Megaterium* combination, then decreased with the increasing dosage of AMF and raised again at the highest levels of mycorrhizal and bacterial inocula. At final, the inoculum with 2.1 + 4.1 kg ha^{-1} of AMF and *B. megaterium* combined reflected a higher glutamate content (0.82 ± 0.14 μM).

However, the ANOVA did not reveal a significant effect of the treatments for the considered agronomic parameters, except for NHI, which seemed to be slightly affected (*p*-value of < 0.10) and indicated a higher N accumulation in grain following 4.1 and 0.1 kg ha^{-1} of AMF and *B. megaterium* inoculation (**Table 2**). Box plots (**Figure 1**) provided high-level information regarding data symmetry, variance, and outliers, allowing comparisons between different treatments.

Overall, biomass and biomass N-uptake values showed a similar trend, with 2.1 + 2.1 kg ha^{-1}, 2.1 + 4.1 kg ha^{-1}, and 4.1 + 4.1 kg ha^{-1} doses of mycorrhizal and bacterial inocula that tended to increase maize performances. Biomass N-concentration tended to be the highest under 0.1 + 2.1 kg ha^{-1}, 2.1 + 0.1 kg ha^{-1}, and 4.1 + 4.1 kg ha^{-1} doses of mycorrhizal and bacterial inocula.

Grain yield values showed a tendency to be increased under 0.1 + 2.1/4.1 kg ha^{-1}, 2.1 + 2.1 kg ha^{-1}, and 4.1 + 0.1 kg ha^{-1} doses. Moreover, grain N-concentration tended to be higher (1.51 ± 0.16%) in the absence of mycorrhizal inoculation (0.1 + 4.1 kg ha^{-1} of AMF and *B. megaterium*). At last, the

10.3389/fpls.2022.956391

TABLE 1 RSM–CCD matrix for response surface analysis on the maize experiment.

Run	Coded label		Actual label	
	Factor x_1 AMF dose (ka ha^{-1})	Factor x_2 *B. megaterium* dose (ka ha^{-1})	Factor x_1 AMF dose (ka ha^{-1})	Factor x_2 *B. megaterium* dose (ka ha^{-1})
1	−1	−1	0.1	0.1
2	+1	0	4.1	2.1
3	−1	0	0.1	2.1
4	+1	+1	4.1	4.1
5	0	+1	2.1	4.1
6	0	0	2.1	2.1
7	0	−1	2.1	0.1
8	+1	−1	4.1	0.1
9	+1	−1	4.1	0.1
10	+1	0	4.1	2.1
11	+1	+1	4.1	4.1
12	−1	0	0.1	2.1
13	0	0	2.1	2.1
14	−1	+1	0.1	4.1
15	0	+1	2.1	4.1
16	+1	−1	4.1	0.1
17	−1	−1	0.1	0.1
18	+1	0	4.1	2.1
19	−1	+1	0.1	4.1
20	0	−1	2.1	0.1
21	−1	0	0.1	2.1
22	−1	−1	0.1	0.1
23	0	+1	2.1	4.1
24	0	−1	2.1	0.1
25	−1	+1	0.1	4.1
26	0	0	2.1	2.1
27	+1	+1	4.1	4.1

highest NUtE value was obtained with 4.1 kg ha^{-1} and 2.1 kg ha^{-1}, respectively, of AMF and *B. megaterium* dose.

A prediction model was developed for those indices being significantly affected (p-value of < 0.05) by AMF and *B. megaterium* treatment. The quadratic equations of the final models are given below Eqs. 1–5:

$$Y_{\text{SPAD}} = 62.57 + 0.81x_1 + 0.89x_2 - -0.39x_1x_2 - 4.39{x_1}^2 - 3.42{x_2}^2 \quad (2)$$

$$Y_{\text{ASPARTATE}} = 0.69 + 0.05x_1 + 0.02x_2 - 0.09x_1x_2 - 0.33{x_1}^2 - 0.09{x_2}^2 \quad (3)$$

$$Y_{\text{GLUTAMATE}} = 0.69 + 0.09x_1 + 0.08x_2 - 0.03x_1x_2 - 0.22{x_1}^2 - 0.07{x_2}^2 \quad (4)$$

$$Y_{\text{ASPARAGINE}} = 2.89 + 0.28x_1 - 0.02x_2 - 0.16x_1x_2 - 0.87{x_1}^2 + 0.17{x_2}^2 \quad (5)$$

$$Y_{\text{GLUTAMINE}} = 0.80 + 0.23x_1 + 0.09x_2 - 0.19x_1x_2 - 0.27{x_1}^2 + 0.14{x_2}^2 \quad (6)$$

Regarding the SPAD value, the model showed a high coefficient of determination ($R^2 = 0.9$) and a high F-value (224.9), while the p-value was < 0.05 and no significant lack of fit values (> 0.05) were found. Similarly, a high-predictive model was found for glutamine concentration, exhibiting $R^2 = 0.8$, F-value = 8.75, and a p-value of < 0.05. Glutamate, asparagine, and aspartate models showed lower R^2, being 0.5, 0.6, and 0.4, respectively, corresponding to 4.3, 6.4, and 3.9 F-values.

TABLE 2 Two−way ANOVA on SPAD value, amino acid concentrations, and agronomic parameters observed in the maize crop following AMF and *B. megaterium* treatment.

Treatment x1 + x2 (kg ha^{-1})	SPAD value	Aspartate (μ M)	Glutamate (μ M)	Asparagine (μ M)	Glutamine (μ M)	Biomass (Mg ha^{-1})	Biomass N conc. (%)	Biomass N uptake (kg ha^{-1})	Grain N conc. (%)	Grain N uptake (kg ha^{-1})	Grain yield (Mg ha^{-1})	NHI	NUtE
0.1 + 0.1	52.89 ± 0.61	0.17 ± 0.14	0.25 ± 0.07	1.57 ± 0.20	0.20 ± 0.11	8.09 ± 0.89	0.72 ± 0.07	58.8 ± 13.64	1.39 ± 0.11	132.23 ± 21.88	9.46 ± 0.85	69.36 ± 1.76	50.14 ± 4.73
0.1 + 2.1	57.01 ± 0.58	0.25 ± 0.11	0.37 ± 0.18	1.90 ± 0.47	0.35 ± 0.07	10.62 ± 0.44	0.79 ± 0.03	84.16 ± 7.21	1.49 ± 0.14	177.59 ± 23.46	11.85 ± 0.64	67.76 ± 1.08	45.56 ± 3.57
0.1 + 4.1	55.38 ± 1.01	0.32 ± 0.04	0.42 ± 0.05	2.08 ± 0.37	0.61 ± 0.04	9.16 ± 1.29	0.76 ± 0.10	69.52 ± 14.89	1.51 ± 0.16	179.71 ± 36.71	11.83 ± 1.51	72.13 ± 1.84	48.04 ± 4.49
2.1 + 0.1	58.01 ± 0.59	0.44 ± 0.35	0.54 ± 0.11	3.27 ± 0.16	0.66 ± 0.15	9.25 ± 1.14	0.8 ± 0.11	73.54 ± 8.87	1.5 ± 0.09	158.79 ± 14.48	10.58 ± 0.93	68.33 ± 3.29	45.49 ± 0.82
2.1 + 2.1	62.95 ± 1.41	0.81 ± 0.38	0.60 ± 0.22	2.95 ± 0.52	0.86 ± 0.13	11.73 ± 2.92	0.75 ± 0.10	87.02 ± 23.38	1.43 ± 0.10	170.09 ± 5.76	11.94 ± 1.27	66.55 ± 5.46	46.45 ± 1.14
2.1 + 4.1	59.93 ± 1.31	0.64 ± 0.17	0.82 ± 0.14	2.79 ± 0.33	1.18 ± 0.17	12.13 ± 3.12	0.71 ± 0.07	87.16 ± 34.15	1.44 ± 0.06	168.86 ± 26.49	11.68 ± 1.80	66.74 ± 5.24	46.22 ± 3.92
4.1 + 0.1	55.12 ± 0.55	0.46 ± 0.18	0.41 ± 0.24	2.66 ± 0.08	1.14 ± 0.15	9.39 ± 0.76	0.69 ± 0.09	64.36 ± 6.56	1.46 ± 0.15	178.73 ± 27.49	12.25 ± 1.09	73.43 ± 1.23	50.73 ± 4.99
4.1 + 2.1	58.98 ± 1.14	0.34 ± 0.16	0.68 ± 0.14	2.07 ± 0.79	0.66 ± 0.05	9.21 ± 1.63	0.72 ± 0.12	67.53 ± 23.61	1.34 ± 0.14	151.67 ± 32.63	11.25 ± 1.63	69.62 ± 4.64	52.49 ± 9.27
4.1 + 4.1	56.03 ± 0.95	0.23 ± 0.01	0.47 ± 0.16	2.52 ± 0.50	0.78 ± 0.14	11.79 ± 0.68	0.8 ± 0.17	95.04 ± 24.55	1.42 ± 0.15	150.32 ± 15.80	10.78 ± 2.23	61.48 ± 8.64	44.23 ± 10.97
Significance(*p*-value)													
Two-wayANOVA													
Treatment	**<2E−16**	**0.03**	**0.01**	**2.00E−03**	**3.11E−07**	0.27	0.86	0.37	0.83	0.33	0.38	0.07	0.71
Block	0.98	0.33	0.31	0.18	0.45	0.56	0.57	0.43	0.85	0.54	0.42	0.06	0.58
Two way ANOVA													
AMF dose	**7.74E−03**	**2.52E−03**	**2.52E−03**	**1.10E−04**	**6.37E−08**	0.41	0.66	0.60	0.28	0.79	0.55	0.43	0.64
Bacterial dose	**3.55E−03**	0.53	0.06	0.61	**1.68E−03**	**0.045**	0.71	**0.05**	0.86	0.38	0.29	8.2E−02	0.34
AMF dose * Bacterial dose	0.28	0.25	0.29	0.24	**4.40E−05**	0.58	0.53	0.38	0.26	9.07E−03	**0.02**	**5.79E−03**	0.51

Values are presented as mean ± standard error (SE). Bold values denote statistical significance at the $p < 0.05$ level. The "*" symbolizes the interaction of the two factors (AMF and bacteria) within ANOVA.

10.3389/fpls.2022.956391

10.3389/fpls.2022.956391

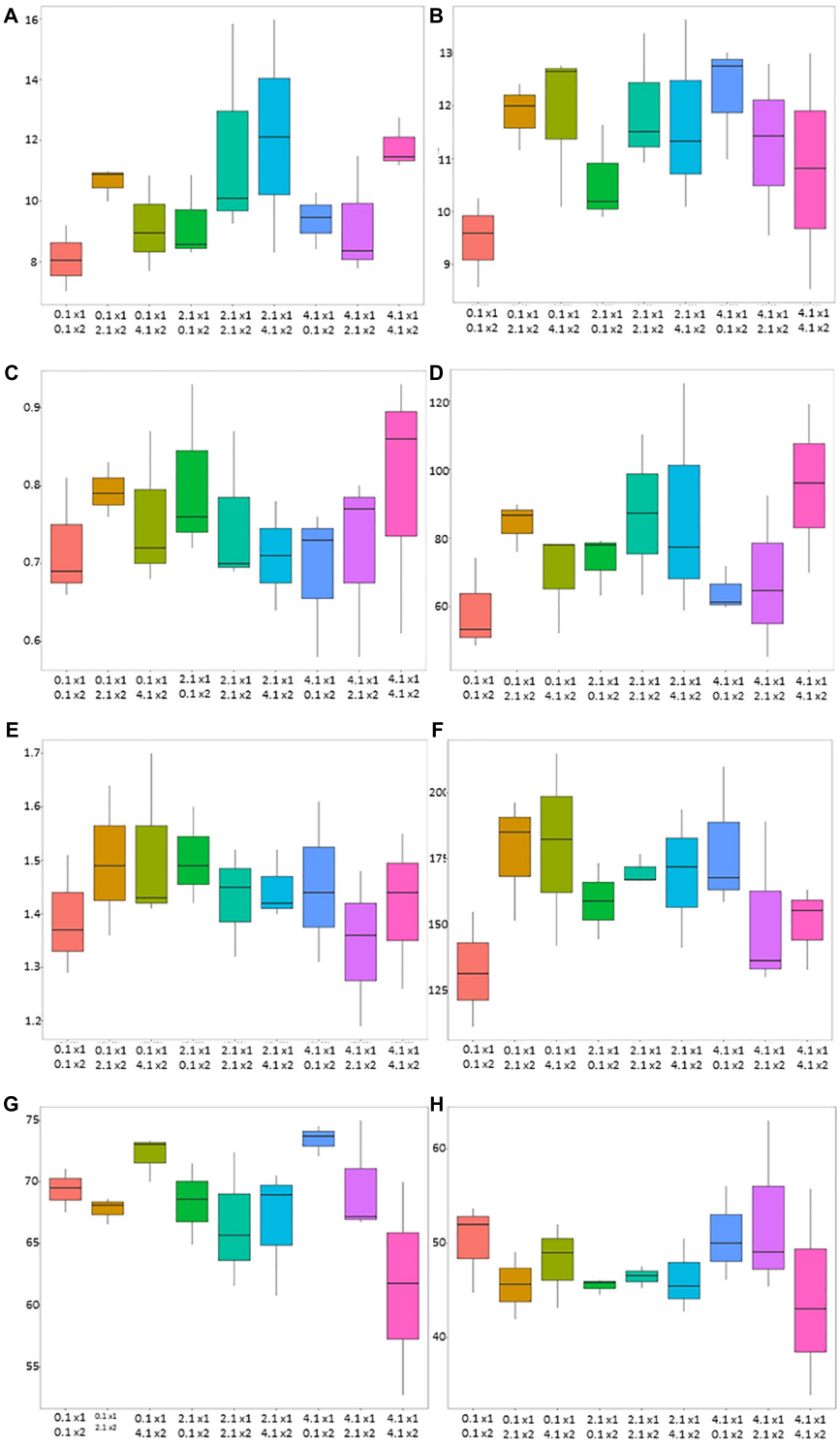

FIGURE 1
Box plot diagrams of agronomic parameters for AMF and *Bacillus megaterium* treatments on maize (*Zea mays* L.). The *X*-axis describes the combination of AMF and *B. megaterium* doses (0.1 kg ha^{-1}, 2.1 kg ha^{-1}, and 4.1 kg ha^{-1}) while the *Y*-axis represents the values for maize biomass (mg ha^{-1}) **(A)**, grain yield (mg ha^{-1}) **(B)**, biomass nitrogen concentration (%) **(C)**, biomass nitrogen-uptake (kg ha^{-1}) **(D)**, grain nitrogen concentration (%) **(E)**, grain nitrogen-uptake (kg ha^{-1}) **(F)**, NHI **(G)**, and NutE **(H)**. Each box line corresponds to the median of the data while the ends of the box show the upper (Q3) and lower quartiles.

However, in all the three cases, the *p*-value was < 0.05, and a significant lack of fit was not provided (> 0.05).

The final regression analysis equations were used for plotting 3D response surface and contour plots which represented the interaction of the input factors—AMF and *B. megaterium*—to trace the stationary point of each variable for the desired response (**Figure 2** and **Supplementary Figure 1**). This stationary point was a maximum for SPAD value, aspartate, and glutamate, indicating a maximum response of these profiles obtained with mycorrhizal and bacterial-specific doses (**Figure 2**). The RSM optimized values for maximum SPAD value (62.66) were 2.27 ka ha^{-1} for AMF and 2.35 ka ha^{-1} for *B. megaterium*. Moreover, 2.22 and 2.24 ka ha^{-1} indicated the optimized doses of mycorrhizal and bacterial inocula to reach the highest aspartate content (0.69), while 2.41 ka ha^{-1} and 3.31 ka ha^{-1} obtained the maximum glutamate concentration. Concerning asparagine and glutamine, the stationary point was represented by a saddle point (2.91 and 0.85), which consisted of an inflection point of the response surface and was, respectively, achieved with 2.40 ka ha^{-1} and 2.36 ka ha^{-1}, and with 2.99 ka ha^{-1} and 2.03 ka ha^{-1} of AMF and *B. megaterium* inocula. The contour plots of the fitted response surfaces allowed us to visualize the behavior of the fitted surface around the stationary point (**Supplementary Figure 2**). Each plot displayed a color image overlaid by the contour lines of constant responses in a two-dimensional space.

Discussion

The choice of the best AMF-bacteria combination to improve NUE and thus ensure efficient and sustainable food production has become a burning question in the perspective of developing new strategies for the ecological transition of agriculture (Agnolucci et al., 2019). *B. megaterium* and AMF are both supposed to be potential bio-fertilizer agents able to play a key role in plant growth promotion. Their single and dual inoculation has revealed beneficial emerging properties in plant symbiosis, mostly translated into enhanced plant growth, yield, and abiotic stress tolerance (Ortiz et al., 2015; Khalid et al., 2017). RSM allows testing of multiple factors with complex interactions, modeling the system mathematically and using a limited number of experimental trials. However, despite the presence of studies based on the application of RSM models to improve plant growth, yield, and NUE, the statistical optimization of the best performing inoculum which can boost plant N acquisition is still limited in literature (Peng et al., 2014; Gundi et al., 2018; Naili et al., 2018; Mazumdar et al., 2021).

Several studies have shed light on the ability of AMF or PGPR to increase plant NUE, reporting higher grain and biomass values, as well as higher levels of NUtE, in different crops. In maize, clear evidence of improved NUE have been observed following inoculation with bacterial strains of *P. fluorescens* S3X and *C. necator* 1C2 (Pereira et al., 2020), *Bacillus megaterium* (Ganugi et al., 2022), and other. Concerning AMF, positive results were reported by single inoculation with *R. irregulare* BEG72 and *F. mosseae* BEG234, and coupled application of *Rhizophagus irregularis* and *Bacillus* spp. (Adesemoye et al., 2008).

Nevertheless, understanding the specific mycorrhizal and bacterial synergic action requires considerable study since PGPR–AMF affinity and colonization efficiency seem to be strongly related to the fungus species and origin. Marulanda-Aguirre et al. (2008) found different results for *B. megaterium* when inoculated on lettuce (*Lactuca sativa* L.) coupled with *Glomus constrictum* autochthonous, *G.constrictum* from a collection or commercial *G.intraradices*. In addition, this study highlights how an optimized mycorrhizal-to-bacterial inoculation rate on maize seeds at planting might be a success factor for the establishment and effectiveness of an AMF–PGPR symbiosis. Interestingly, our optimization aimed at enhancing maize NUE revealed similar RSM values for maximum SPAD, aspartate, and glutamate concentrations, which correspond to the intermediate doses of AMF and *B. megaterium*. Together with indicating a treatment effect on these NUE indices, this point confirmed the tripartite synergy between plants, mycorrhizae, and microbial communities for plant nutrition. Such synergy can be translated into a significant increase in N acquisition compared with the single inoculation of AMF or *B. megaterium* (Hestrin et al., 2019). However, the identification of saddle points for asparagine and glutamine pointed to the complexity of microorganisms' interactions. The presence of such intricate microbial interactions indicates the need for further deep analyses, focused on experimental runs at points along this path, using the observed response values for guidance on where to locate the next factorial experiment (Lenth, 2009; Jan et al., 2021).

Despite the lack of significant treatment effect on most of the agronomic parameters, our data revealed interesting trends which is worth exploring in the future. On the one hand, it seems that maize plant biomass and biomass N-uptake could be increased by the concomitant action of AMF and *B. megaterium* at > 2.1. On the other hand, grain yield, grain N-uptake, and NHI showed a tendency to be increased preferentially by the single action of either AMF or *B. megaterium*, while lower values were registered under co-inoculation conditions. This latter statement was further corroborated by the fact that NHI (which was close to being significantly affected by the treatments) had the highest values with 4.1 kg ha^{-1} of AMF or *B. megaterium*, alternatively. These results suggest that (i) combining AMF and *B. megaterium* at a significant dose (> 2 kg ha^{-1}) may have the potential to enhance plant tissues growth toward vegetative biomass, and (ii) if AMF and

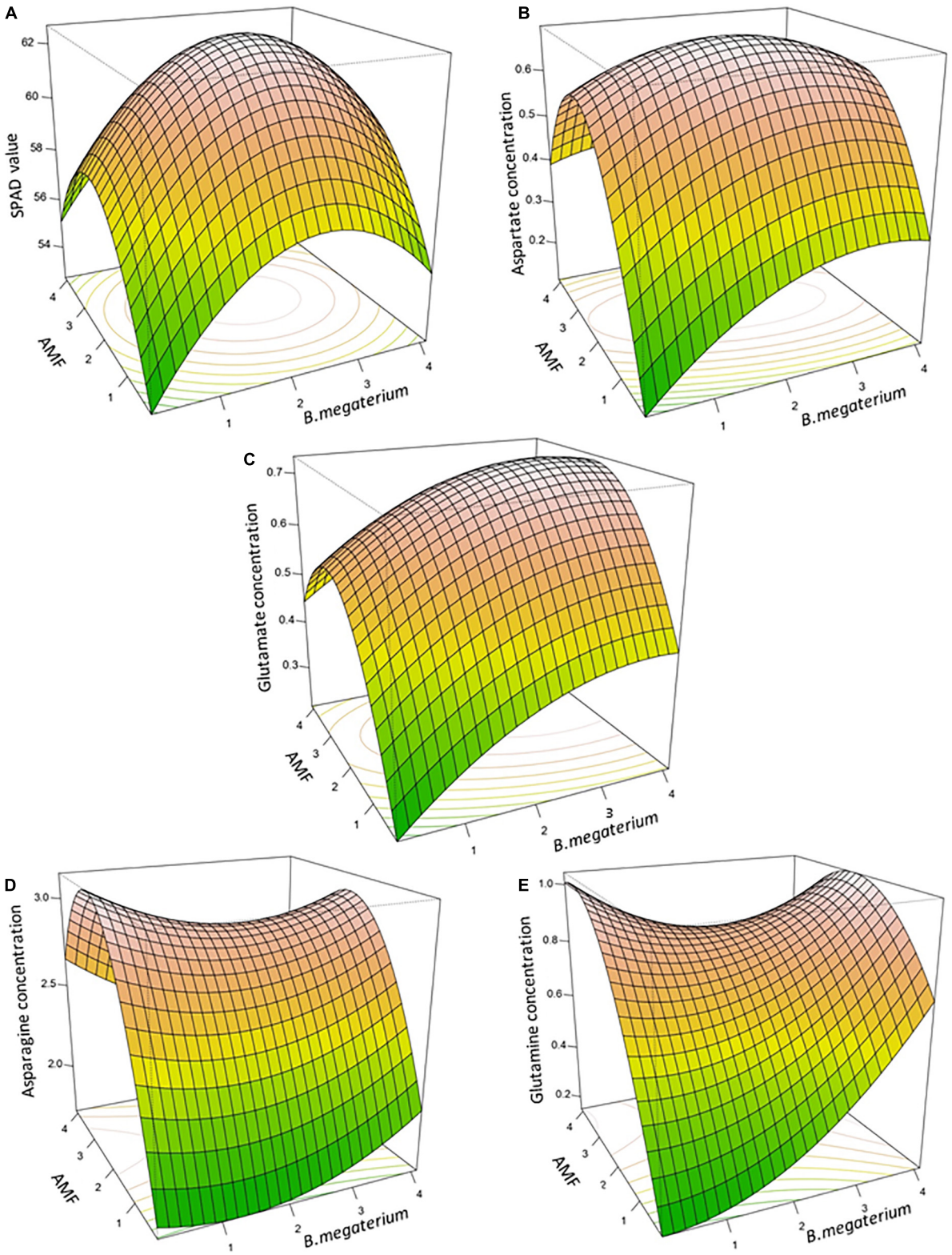

FIGURE 2
The three-dimensional response surface plots for interactive effects of *B. megaterium* and AMF co-inoculation on SPAD value **(A)**, aspartate concentration **(B)**, glutamate concentration **(C)**, asparagine concentration **(D)**, and glutamine concentration **(E)** in maize.

B. megaterium are inoculated alone, it is likely that grain-related agronomic parameters could benefit more than biomass-related ones. In fact, distinct effects provided by AMF, PGPR, and their co-inoculation in terms of drought resistance and essential oil yield have been previously reported in myrtle (Azizi et al., 2021). Similarly, it was reported that symbiotic efficiency may be hindered by interaction(s) with other biofertilizers together with being impacted by agro-practices (Kuila and Ghosh, 2022). In another work, Pacheco et al., evaluated the effect of AMF and *Pseudomonas putida* (PSB) single and co-inoculation on P uptake, productivity, and P concentration in maize (Pacheco et al., 2021). Interestingly, these authors reported that the microbial inoculants enhanced plant P uptake, that the presence of PSB increased biomass per unit of P taken up, and that the microbial inoculants altered P allocation within the plant, reducing grain P concentration (Pacheco et al., 2021). This distinct effect of the microbial inoculants on biomass production and nutrients allocation agrees with the results from Lozano Olivério Salvador and co-workers, who observed specific effects in terms of dry weight, symbiotic efficiency, chlorophyll content, and nitrogen accumulation when AMF or rhizobacteria were applied with compost to soybean (Salvador et al., 2022).

Despite the fact that mechanisms underlying the effect of single and combined inoculum are still unknown, amino acid metabolism represents an interesting target for crop NUE improvement, being actively involved in plant NUtE (Dellero, 2020). In particular, the glutamine synthetase/glutamate:2-oxoglutarate aminotransferase (GS/GOGAT) cycle represents the major route for plant ammonia assimilation, followed by asparagine synthetase (ASN) and glutamate dehydrogenase (GDH) (Harrison et al., 2000). Accordingly, experimental studies on maize have pointed out the increased concentration of aspartate and glutamate following *R. irregularis* and *Gigaspora margarita* inoculation (Matsumura et al., 2013; Hu and Chen, 2020), while the enhanced activity of ammonium assimilating enzymes (GS and GDH) have been detected with *Azospirillum* bacterial treatment (Ribaudo et al., 2001).

Here, for the first time, we reported how different rates of mycorrhiza-to-*Bacillus* co-inoculation may be considered—to some extent—as a driver of differential *N* partitioning between grain and vegetative biomass in the maize plant. This should be considered to address future studies to shed light on how such biotic interactions may steer plant physiology toward grain rather than vegetative tissues *N* accumulation.

Nevertheless, it should be stated some important aspects of the experiment. At first, it must be pointed out that the *Aegis Sym irriga*® product is predominantly but not totally made by AMF, being associated—as the most commercial inocula—to other bacteria. For this reason, the effect of this inoculum on plant-based indices of NUE, as well as that obtained following its interaction with the PGPR product, is not necessarily ascribable to the exclusive presence of mycorrhiza. Second, to further complicate matters, plant responses should be studied under a wide range of soil-climate conditions, including different soil types and soil fertility, and temperate to dry climates. Particularly, physico-chemical soil properties, such as nutrient availability, pH, structure, organic matter content, and texture, can affect the release of plant root exudates and, consequently, the availability and the interactions with soil microbial communities (Neumann et al., 2014). It is likely that plant-microbe symbiosis is profoundly influenced by external environmental conditions, namely, temperature and moisture (Cheng et al., 2019). As consequence, it should be clarified that our results are strictly related to a specific pedoclimatic experimental context and, for this reason, maximum and saddle points for each NUE index cannot be certainly considered as absolute values exactly reproducible under different plant growth conditions.

Equally, the lack of significant effects in some agronomic indices may be reasonable because of the peculiar temperate and fertile conditions underlying the study, which is why it would be unreasonable to draw a conclusion about a lack of general effect of microbial inocula on the plant NUE. Notwithstanding, the application of prediction models may considerably contribute to advancements in the agricultural sector, particularly, under challenging factors interaction conditions.

Data availability statement

The original contributions presented in this study are included in the article/**Supplementary material**, further inquiries can be directed to the corresponding author.

Author contributions

PG, AF, VT, and LL conceived the ideas and designed the methodology. PG, AF, GR, and PB collected the data. PG, GR, and PB analyzed the data. PG, AF, PB, VT, and LL wrote the original draft. AF and LL critically revised the original draft. All the authors gave final approval for the publication.

Funding

This project was funded by the Emilia-Romagna region, Italy, in the framework of the Regional Development Program PSR 2014-2020, Measure 16.1.01–Focus Area 4B (project 5150325 – INBIOS: Sviluppo di un approccio INtegrato a base di BIOStimolanti per la sostenibilità delle produzioni agrarie).

Acknowledgments

We thank the "Romeo ed Enrica Invernizzi" Foundation (Milan, Italy) for the kind support to the metabolomic facility at the Università Cattolica del Sacro Cuore.

Conflict of interest

PB was employed by company oloBion-OMICS LIFE LAB.

The remaining authors declare that the research was conducted in the absence of any commercial or financial relationships that could be construed as a potential conflict of interest.

Publisher's note

Supplementary material

The Supplementary Material for this article can be found online at: https://www.frontiersin.org/articles/10.3389/fpls.2022.956391/full#supplementary-material

References

Anas, M., Liao, F., Verma, K. K., Sarwar, M. A., Mahmood, A., Chen, Z. L., et al. (2020). Fate of nitrogen in agriculture and environment: agronomic, ecophysiological and molecular approaches to improve nitrogen use efficiency. *Biol. Res.* 53, 1–20. doi: 10.1186/s40659-020-00312-4

Adesemoye, A. O., Torbert, H. A., and Kloepper, J. W. (2008). Enhanced plant nutrient use efficiency with PGPR and AMF in an integrated nutrient management system. *Can. J. Microbiol.* 54, 876–886. doi: 10.1139/W08-081

Agnolucci, M., Avio, L., Pepe, A., Turrini, A., Cristani, C., Bonini, P., et al. (2019). Bacteria associated with a commercial mycorrhizal inoculum: Community composition and multifunctional activity as assessed by illumina sequencing and culture-dependent tools. *Front. Plant Sci.* 9:1956. doi: 10.3389/fpls.2018.01956

Agnolucci, M., Battini, F., Cristani, C., and Giovannetti, M. (2015). Diverse bacterial communities are recruited on spores of different arbuscular mycorrhizal fungal isolates. *Biol. Fertil. Soils* 51, 379–389. doi: 10.1007/s00374-014-0989-5

Ahmed, M., Rauf, M., Mukhtar, Z., and Saeed, N. A. (2017). Excessive use of nitrogenous fertilizers: An unawareness causing serious threats to environment and human health. *Environ. Sci. Pollut. Res.* 24, 26983–26987. doi: 10.1007/s11356-017-0589-7

Azizi, S., Tabari Kouchaksaraei, M., Hadian, J., Fallah Nosrat Abad, A. R., Modarres Sanavi, S. A. M., Ammer, C., et al. (2021). Dual inoculations of arbuscular mycorrhizal fungi and plant growth-promoting rhizobacteria boost drought resistance and essential oil yield of common myrtle. *For. Ecol. Manage.* 497:119478. doi: 10.1016/j.foreco.2021.119478

Cheng, Y. T., Zhang, L., and He, S. Y. (2019). Plant-microbe interactions facing environmental challenge. *Cell Host Microbe* 26, 183–192. doi: 10.1016/j.chom.2019.07.009

Congreves, K. A., Otchere, O., Ferland, D., Farzadfar, S., Williams, S., and Arcand, M. M. (2021). Nitrogen use efficiency definitions of today and tomorrow. *Front. Plant Sci.* 12:637108. doi: 10.3389/fpls.2021.637108

Courty, P. E., Smith, P., Koegel, S., Redecker, D., and Wipf, D. (2015). Inorganic nitrogen uptake and transport in beneficial plant root-microbe interactions. *CRC. Crit. Rev. Plant Sci.* 34, 4–16. doi: 10.1080/07352689.2014.897897

Dalla Costa, M., Rech, T. D., Primieri, S., Pigozzi, B. G., Werner, S. S., and Stürmer, S. L. (2021). Inoculation with isolates of arbuscular mycorrhizal fungi influences growth, nutrient use efficiency and gas exchange traits in micropropagated apple rootstock 'Marubakaido.' *Plant Cell. Tissue Organ Cult.* 145, 89–99. doi: 10.1007/s11240-020-01994-0

Dellero, Y. (2020). Manipulating amino acid metabolism to improve crop nitrogen use efficiency for a sustainable agriculture. *Front. Plant Sci.* 11:602548. doi: 10.3389/fpls.2020.602548

Di Benedetto, N. A., Corbo, M. R., Campaniello, D., Cataldi, M. P., Bevilacqua, A., Sinigaglia, M., et al. (2017). The role of plant growth promoting bacteria in improving nitrogen use efficiency for sustainable crop production: A focus on wheat. *AIMS Microbiol.* 3, 413–434. doi: 10.3934/microbiol.2017.3.413

Galloway, J. N., Winiwarter, W., Leip, A., Leach, A. M., Bleeker, A., and Erisman, J. W. (2014). Nitrogen footprints: Past, present and future. *Environ. Res. Lett.* 9:115003. doi: 10.1088/1748-9326/9/11/115003

Ganugi, P., Fiorini, A., Ardenti, F., Caffi, T., Bonini, P., Taskin, E., et al. (2022). Nitrogen use efficiency, rhizosphere bacterial community, and root metabolome reprogramming due to maize seed treatment with microbial biostimulants. *Physiol. Plant.* 174, 1–15. doi: 10.1111/ppl.13679

Garcia, K., Doidy, J., Zimmermann, S. D., Wipf, D., and Courty, P. E. (2016). Take a trip through the plant and fungal transportome of mycorrhiza. *Trends Plant Sci.* 21, 937–950. doi: 10.1016/j.tplants.2016.07.010

Giovannini, L., Palla, M., Agnolucci, M., Avio, L., Sbrana, C., Turrini, A., et al. (2020). Arbuscular mycorrhizal fungi and associated microbiota as plant biostimulants: Research strategies for the selection of the best performing inocula. *Agronomy* 10:106. doi: 10.3390/agronomy10010108

Gundi, J. S., Santos, M. S., Oliveira, A. L. M., Nogueira, M. A., Hungria, M. (2018). Development of liquid inoculants for strains of Rhizobium tropici group using response surface methodology. *Afr J Biotechnol* 17, 411–421. doi: 10.5897/AJB2018.16389

Harrison, J., Brugière, N., Phillipson, B., Ferrario-Mery, S., Becker, T., Limami, A., et al. (2000). Manipulating the pathway of ammonia assimilation through genetic 399 engineering and breeding: Consequences to plant physiology and plant development. *Plant Soil* 221, 81–93. doi: 10.1023/A:1004715720043

Hestrin, R., Hammer, E. C., Mueller, C. W., and Lehmann, J. (2019). Synergies between mycorrhizal fungi and soil microbial communities increase plant nitrogen acquisition. *Commun. Biol.* 2:233. doi: 10.1038/s42003-019-0481-8

Hu, Y., and Chen, B. (2020). Arbuscular mycorrhiza induced putrescine degradation into γ-aminobutyric acid, malic acid accumulation, and improvement of nitrogen assimilation in roots of water-stressed maize plants. *Mycorrhiza* 30, 329–339. doi: 10.1007/s00572-020-00952-0

Jan, R., Asaf, S., Numan, M., Lubna, and Kim, K. M. (2021). Plant secondary metabolite biosynthesis and transcriptional regulation in response to biotic and abiotic stress conditions. *Agronomy* 11:968. doi: 10.3390/agronomy11050968

Khalid, M., Hassani, D., Bilal, M., Asad, F., and Huang, D. (2017). Influence of bio-fertilizer containing beneficial fungi and rhizospheric bacteria on health promoting compounds and antioxidant activity of *Spinacia oleracea* L. *Bot. Stud.* 58:35. doi: 10.1186/s40529-017-0189-3

Koegel, S., Mieulet, D., Baday, S., Chatagnier, O., Lehmann, M. F., Wiemken, A., et al. (2017). Phylogenetic, structural, and functional characterization of AMT3; an ammonium transporter induced by mycorrhization among model grasses. *Mycorrhiza* 27, 695–708. doi: 10.1007/s00572-017-0786-8

Kollah, B., Patra, A. K., and Mohanty, S. R. (2016). Aquatic microphylla Azolla: A perspective paradigm for sustainable agriculture, environment and global climate change. *Environ. Sci. Pollut. Res.* 23, 4358–4369. doi: 10.1007/s11356-015-5857-9

Kuila, D., and Ghosh, S. (2022). Aspects, problems and utilization of Arbuscular Mycorrhizal (AM) application as bio-fertilizer in sustainable agriculture. *Curr. Res. Microb. Sci.* 3:100107. doi: 10.1016/j.crmicr.2022.100107

Kumar, V., Kumar, P., and Khan, A. (2020). Optimization of PGPR and silicon fertilization using response surface methodology for enhanced growth, yield and biochemical parameters of French bean (*Phaseolus vulgaris* L.) under saline stress. *Biocatal. Agric. Biotechnol.* 23:101463. doi: 10.1016/j.bcab.2019.101463

Lenth, R. V. (2009). Response-surface methods in R, using RSM. *J. Stat. Softw.* 32, 1–17. doi: 10.18637/jss.v032.i07

López-Bellido, R. J., and López-Bellido, L. (2001). Efficiency of nitrogen in wheat under Mediterranean conditions: Effect of tillage, crop rotation and N fertilization. *F. Crop. Res.* 71, 31–46. doi: 10.1016/S0378-4290(01)00146-0

Maris, S. C., Abalos, D., Capra, F., Moscatelli, G., Scaglia, F., Reyes, G. E. C., et al. (2021). Strong potential of slurry application timing and method to reduce N losses in a permanent grassland. *Agricult. Ecosyst. Environ.* 311:107329. doi: 10.1016/j.agee.2021.107329

Marulanda-Aguirre, A., Azcón, R., Ruiz-Lozano, J. M., and Aroca, R. (2008). Differential effects of a *Bacillus megaterium* strain on *Lactuca sativa* plant growth depending on the origin of the arbuscular mycorrhizal fungus coinoculated: Physiologic and biochemical traits. *J. Plant Growth Regul.* 27, 10–18. doi: 10.1007/s00344-007-9024-5

Matsumura, A., Taniguchi, S., Yamawaki, K., Hattori, R., Tarui, A., Yano, K., et al. (2013). Nitrogen uptake from amino acids in maize through arbuscular mycorrhizal symbiosis. *Am. J. Plant Sci.* 4, 2290–2294. doi: 10.4236/ajps.2013.412283

Mazumdar, D., Saha, S., and Ghoshet, S. (2021). RSM based optimization of plant growth promoting rhizobacteria and nitrogen dosage for enhanced growth and yield of mustard (*Brassica campestris* L.). *J. Plant Nutr.* 44, 2228–2244. doi: 10.1080/01904167.2021.1889585

Moreau, D., Bardgett, R. D., Finlay, R. D., Jones, D. L., and Philippot, L. (2019). A plant perspective on nitrogen cycling in the rhizosphere. *Funct. Ecol.* 33, 540–552. doi: 10.1111/1365-2435.13303

Mus, F., Crook, M. B., Garcia, K., Garcia Costas, A., Geddes, B. A., Kouri, E. D., et al. (2016). Symbiotic nitrogen fixation and the challenges to its extension to nonlegumes. *Appl. Environ. Microbiol.* 82, 3698–3710. doi: 10.1128/AEM.01055-16

Naili, F., Neifar, M., Elhidri, D., Cherif, H., Bejaoui, B., and Aroua, M. (2018). Optimization of the effect of PGPR-based biofertlizer on wheat growth and yield. *Biometric. Biostat. Int. J.* 7, 226–232. doi: 10.15406/bbij.2018.07.00213

Neumann, G., Bott, S., Ohler, M. A., Mock, H. P., Lippmann, R., Grosch, R., et al. (2014). Root exudation and root development of lettuce (*Lactuca sativa* l. Cv. Tizian) as affected by different soils. *Front. Microbiol.* 5:2. doi: 10.3389/fmicb.2014.00002

Oldroyd, G. E. D., Murray, J. D., Poole, P. S., and Downie, J. A. (2011). The rules of engagement in the legume-rhizobial symbiosis. *Annu. Rev. Genet.* 45, 119–144. doi: 10.1146/annurev-genet-110410-132549

Ortiz, N., Armada, E., Duque, E., Roldán, A., and Azcón, R. (2015). Contribution of arbuscular mycorrhizal fungi and/or bacteria to enhancing plant drought tolerance under natural soil conditions: Effectiveness of autochthonous or allochthonous strains. *J. Plant Physiol.* 174, 87–96. doi: 10.1016/j.jplph.2014.08.019

Pacheco, I., Ferreira, R., Correia, P., Carvalho, L., Dias, T., and Cruza, C. (2021). Microbial consortium increases maize productivity and reduces grain phosphorus concentration under field conditions. *Saudi J. Biol. Sci.* 28, 232–237. doi: 10.1016/j.sjbs.2020.09.053

Paul, K., Saha, C., Nag, M., Mandal, D., Naiya, H., Sen, D., et al. (2020). A tripartite interaction among the basidiomycete rhodotorula mucilaginosa, N2-fixing endobacteria, and rice improves plant nitrogen nutrition. *Plant Cell* 32, 486–507. doi: 10.1105/tpc.19.00385

Peng, S., Buresh, R. J., Huang, J., Yang, J., Zou, Y., Zhong, X., et al. (2006). Strategies for overcoming low agronomic nitrogen use efficiency in irrigated rice systems in China. *F. Crop. Res.* 96, 37–47. doi: 10.1016/j.fcr.2005.05.004

Peng, Y., He, Y., Wu, Z., Lu, J., and Li, C. S. (2014). Screening and optimization of low-cost medium for *Pseudomonas putida* Rs-198 culture using RSM. *Braz. J. Microbiol.* 45, 1229–1237. doi: 10.1590/s1517-83822014000400013

Pereira, S. I. A., Abreu, D., Moreira, H., Vega, A., and Castro, P. M. L. (2020). Plant growth-promoting rhizobacteria (PGPR) improve the growth and nutrient use efficiency in maize (*Zea mays* L.) under water deficit conditions. *Heliyon* 6:e05106. doi: 10.1016/j.heliyon.2020.e05106

Qu, Q., Zhang, Z., Peijnenburg, W. J. G. M., Liu, W., Lu, T., Hu, B., et al. (2020). Rhizosphere microbiome assembly and its impact on plant growth. *J. Agric. Food Chem.* 68, 5024–5038.

R Core Team (2013). *R: A Language and Environment for Statistical Computing*.

Ribaudo, C., Rondanini, D. P., Curá, J. A., and Fraschina, A. A. (2001). Response of *Zea mays* to the inoculation with *Azospirillum* on nitrogen metabolism under greenhouse conditions. *Biol. Plant.* 44, 631–634. doi: 10.1023/A:1013779712106

Rosenblueth, M., Ormeño-Orrillo, E., López-López, A., Rogel, M. A., Reyes-Hernández, B. J., Martínez-Romero, J. C., et al. (2018). Nitrogen fixation in cereals. *Front. Microbiol.* 9:1794. doi: 10.3389/fmicb.2018.01794

Salvador, G. L. O., Araújo, F. F., de Araujo Pereira, A. P., Bonifácio, A., and Ferreira Araujo, A. S. (2022). Rhizobacteria and arbuscular mycorrhizal fungus presented distinct and specific effects on soybean growth when inoculated with organic compost. *Rhizosphere* 22:100513. doi: 10.1016/j.rhisph.2022.100513

Santi, C., Bogusz, D., and Franche, C. (2013). Biological nitrogen fixation in non-legume plants. *Ann. Bot.* 111, 743–767. doi: 10.1093/aob/mct048

Tajini, F., Trabelsi, M., and Drevon, J. J. (2012). Combined inoculation with *Glomus intraradices* and *Rhizobium tropici* CIAT899 increases phosphorus use efficiency for symbiotic nitrogen fixation in common bean (*Phaseolus vulgaris* L.). *Saudi J. Biol. Sci.* 19, 157–163. doi: 10.1016/j.sjbs.2011.11.003

The, S. V., Snyder, R., and Tegeder, M. (2021). Targeting nitrogen metabolism and transport processes to improve plant nitrogen use efficiency. *Front. Plant Sci.* 11:628366. doi: 10.3389/fpls.2020.628366

Udvardi, M., and Poole, P. S. (2013). Transport and metabolism in legume-rhizobia symbioses. *Annu. Rev. Plant Biol.* 64, 781–805. doi: 10.1146/annurev-arplant-050312-120235

van Bueren, L. E. T., and Struik, P. C. (2017). Diverse concepts of breeding for nitrogen use efficiency. A review. *Agron. Sustain. Dev.* 37:50. doi: 10.1007/s13593-017-0457-3

van Dam, N. M., and Bouwmeester, H. J. (2016). Metabolomics in the rhizosphere: Tapping into belowground chemical communication. *Trends Plant Sci.* 21, 256–265. doi: 10.1016/j.tplants.2016.01.008

Verzeaux, J., Hirel, B., Dubois, F., Lea, P. J., and Tétu, T. (2017). Agricultural practices to improve nitrogen use efficiency through the use of arbuscular mycorrhizae: Basic and agronomic aspects. *Plant Sci.* 264, 48–56. doi: 10.1016/j.plantsci.2017.08.004

Wickham, H., and Chang, W. (2007). *ggplot2: An implementation of the grammar of graphics. GNU general public license*. Available online at: https://cran.r-project.org/web/packages/ggplot2 (accessed May 03, 2022).

frontiers | Frontiers in Plant Science

TYPE Original Research
PUBLISHED 31 August 2022
DOI 10.3389/fpls.2022.944066

OPEN ACCESS

EDITED BY
Youssef Rouphael,
University of Naples Federico II, Italy

REVIEWED BY
Sławomir Kocira,
University of Life Sciences of Lublin, Poland
Andrea Copetta,
Council for Agricultural and Economics Research (CREA), Italy

*CORRESPONDENCE
Nuria De Diego
nuria.de@upol.cz

SPECIALTY SECTION
This article was submitted to Plant Abiotic Stress, a section of the journal Frontiers in Plant Science

RECEIVED 14 May 2022
ACCEPTED 11 July 2022
PUBLISHED 31 August 2022

CITATION
Hernandiz AE, Jiménez-Arias D, Morales-Sierra S, Borges AA and De Diego N (2022) Addressing the contribution of small molecule-based biostimulants to the biofortification of maize in a water restriction scenario. *Front. Plant Sci.* 13:944066. doi: 10.3389/fpls.2022.944066

Addressing the contribution of small molecule-based biostimulants to the biofortification of maize in a water restriction scenario

Alba E. Hernandiz[1,2], David Jiménez-Arias[3,4], Sarai Morales-Sierra[5], Andres A. Borges[4] and Nuria De Diego[2]*

[1]Laboratory of Plant Growth Regulators, Faculty of Science, Palacký University, Olomouc, Czechia, [2]Centre of Region Haná for Biotechnological and Agricultural Research, Czech Advanced Technology and Research Institute, Palacký University, Olomouc, Czechia, [3]ISOPlexis, Centro de Agricultura Sustentável e Tecnologia Alimentar, Campus Universitário da Penteada, Universidade da Madeira, Funchal, Portugal, [4]Chemical Plant Defence Activators Group, Department of Life and Earth Science, IPNA-CSIC, Campus de Anchieta, San Cristóbal de La Laguna, Spain, [5]Grupo de Biología Vegetal Aplicada, Departamento de Botánica, Ecología y Fisiología Vegetal-Facultad de Farmacia, Universidad de La Laguna, San Cristóbal de La Laguna, Spain

Biostimulants have become an asset for agriculture since they are a greener alternative to traditionally used plant protection products. Also, they have gained the farmers' acceptance due to their effect on enhancing the plant's natural defense system against abiotic stresses. Besides commercially available complex products, small molecule-based biostimulants are useful for industry and research. Among them, polyamines (PAs) are well-studied natural compounds that can elicit numerous positive responses in drought-stressed plants. However, the studies are merely focused on the vegetative development of the plant. Therefore, we aimed to evaluate how drenching with putrescine (Put) and spermidine (Spd) modified the maize production and the yield quality parameters. First, a dosage optimization was performed, and then the best PA concentrations were applied by drenching the maize plants grown under well-watered (WW) conditions or water deficit (WD). Different mechanisms of action were observed for Put and Spd regarding maize production, including when both PAs similarly improved the water balance of the plants. The application of Put enhanced the quality and quantity of the yield under WW and Spd under WD. Regarding the nutritional quality of the grains, both PAs increased the carbohydrates content, whereas the contribution to the protein content changed by the interaction between compound and growth conditions. The mineral content of the grains was also greatly affected by the water condition and the PA application, with the most relevant results observed when Spd was applied, ending with flour richer in

Zn, Cu, and Ca minerals that are considered important for human health. We showed that the exogenous PA application could be a highly efficient biofortification approach. Our findings open a new exciting use to be studied deep in the biostimulant research.

KEYWORDS

drenching, mineral nutrition, polyamines, yield, *Zea mays*

Introduction

Plants are sessile organisms exposed to a rapidly changing environment. They respond to external stimuli, which might result in plant acclimation to specific growing conditions. When this is impossible, growth becomes inhibited and, later, may die. Abiotic stresses are the principal cause of severe yield losses of 50–80%, depending on the crop and geographical location (Zhang et al., 2018). The global climate change projections forecast an increase in extreme weather events' occurrence, frequency, and severity (FAO, 2018). The incidence of abiotic stresses such as drought will raise and compromise the yield of the crops, especially in arid and semiarid areas. Drought is multidimensional stress affecting plants at various developmental stages, including the plant's production (Blum, 1996). One of the most promising methods to cope with the inevitable abiotic stresses is the application of biostimulants to enhance plant resilience to environmental perturbations (Van Oosten et al., 2017). Their action relies on the "preparation" effect (priming or hardening) that their application exerts on the plants (Gebremedhn and Berhanu, 2013; Maiti and Pramanik, 2013; Savvides et al., 2016). Biostimulants have been proved to improve plant growth and photosynthesis efficiency by modifying the plant metabolism under abiotic stress conditions (Paul et al., 2019; Sorrentino et al., 2021). Moreover, the recent recognition of biostimulants as an independent group of agricultural inputs by the European Union and their contribution to more sustainable agricultural practices forecasts a growing interest in these substances (Ben Mrid et al., 2021).

Typically, biostimulants are a mixture of several substances, such as protein hydrolysates or seaweed extracts; this has been seen as a great opportunity by some companies to join the circular economy trend since they can give a second life to waste and by-products (Xu and Geelen, 2018). However, these products present the disadvantage of lack of uniformity between the batches and the problematic identification of the active substances (Yakhin et al., 2017). Studying pure organic active compounds as biostimulants will lead to a better standardization, the quality control of formulation, and an understanding of their mode and mechanism of action (García-García et al., 2020). While the effectiveness of biostimulants has been widely researched and summarized in extensive reviews (Battacharyya et al., 2015; Bulgari et al., 2015, 2019), there is a limited information available on how their application might affect the final yield and quality.

Maize (*Zea mays* L.) is one of the most important cereal crops for human nutrition in large parts of the world (Huma et al., 2019) and an essential grain used as livestock feed in the world (Loy and Lundy, 2018). Drought negatively affects the plant growth, the dry biomass content, and the yield (Anjum et al., 2017; Kim et al., 2019). The water deficit during maturation might cause problems in the grain filling stage (Zhang et al., 2019) and reduce the quality parameters such as starch, proteins (Barutcular et al., 2016), or mineral content (Aqaei et al., 2020). Maize kernel mainly comprises carbohydrates, protein, and oil (Chaudhary et al., 2014). Starch accounts for approximately 70% of the kernel weight (Orhun et al., 2013). According to the release and absorption of glucose in the intestines, starch is divided into the following three categories: Rapidly and slowly digestible starch and resistant starch; the last category has particular importance for human nutrition since its consumption has been linked to a decrease in the risk of developing type 2 diabetes and colon cancer (Hoebler et al., 1999). Protein content varies from 8 to 11% of the kernel weight on common varieties of maize (Landry and Moureaux, 1980). However, the nutritional value is poor for monogastric and human consumption due to the low content of essential amino acids such as lysine, tryptophan, and threonine (Li and Vasal, 2015). The discovery of the opaque-2 gene and its link with higher lysine and tryptophan was the beginning of the Quality Protein Maize (QPM) research, which produced hybrids whose kernels had a significant increment on the mentioned amino acids. Nevertheless, the yield was reduced in these hybrids, and their agronomical performance was deficient (Chaudhary et al., 2014). The kernel mineral composition is strongly affected by the environmental factors, soil moisture, and fertility, but it is mainly genotype dependent, with the vast variety of differences as the most significant contributor to the reported variance (Feil et al., 2005; Menkir, 2008).

The development of nutritionally enhanced food crops using traditional breeding practices and modern biotechnology approaches is known as "biofortification" (Chaudhary et al., 2014; Garg et al., 2018). The first main achievements in this field were the lysine and tryptophan enriched maizes or

vitamin A-rich orange sweet potato; much effort is put into transgenic research, although traditional breeding practices are best accepted (Garg et al., 2018). Given the exposed facts, we decided to test biostimulants as an alternative approach for maize biofortification due to their effect on plant metabolism and stress tolerance. With this aim, we applied two polyamines (PAs) with proven efficiency as stress alleviators, putrescine (Put), and spermidine (Spd) (Li et al., 2015, 2018; Marcińska et al., 2020; Islam et al., 2022), although the dose was optimized to the specific cultivar of maize used. The maize plants were treated with the two PAs *via* drenching, which has been proven to have positive results toward drought stress (Jiménez-Arias et al., 2019) because drenching provides a more extended period of continuous uptake of the supplemented substance than the foliar application (Parkunan et al., 2011). Some reports also revealed that the drench application improves soil fertility by increasing the availability of minerals, soil aeration, and water holding capacity and promotes the development of essential microbes (Battacharyya et al., 2015; du Jardin, 2015). We expect that applying PAs by drenching will improve maize's biofortification and stress tolerance.

Materials and methods

Plant material, growth conditions, and dose optimization

A local plant nursery provided a local forage variety of maize from Gran Canaria Island (*Zea mays* L. c.v. Lechucilla) in a 150-socket nursery tray. One week after sowing, the plants were placed in a growth chamber under controlled conditions with a temperature of 22°C, a photoperiod of 16-h light and 8-h dark, with a light intensity of 300–400 μmol m^{-2} s^{-1}, and a relative humidity around 60–70%. Plants in stage V1 were used for the dose optimization experiments when the lowermost leaf had a visible leaf collar (Zhao et al., 2012).

Putrescine and spermidine were purchased from Sigma–Aldrich (Put CAS number 333-93-7; Spd CAS number 124-20-9). In the direct application-optimized doses of both chemicals under two water regimes in the nursery tray, 20 plants were used as biological replicates per variant (treatment × growth condition), as described in Jiménez-Arias et al. (2022). The nursery experiment ensured the suitability of the plant for the root treatment. The treatments were applied directly to the roots of stage V1 plants, consisting of 5 ml of a half-strength Hoagland solution (Hoagland and Arnon, 1938) for the controls or containing the tested substances at the following five concentrations: 0.01, 0.1, 0.5, 1, and 2 mM for the treated plants. Twenty plants per variant were grown under a water limitation of 50% of the field capacity for a week. The two harvesting times were performed; at the dry period's beginning and end. The whole plant, including the aerial part and roots, was harvested. The dried weight (DW, mg) of the 20 plants was recorded after being oven-dried at 85°C for 48 h to calculate the relative growth ratio (RGR) (Hoffmann and Poorter, 2002),

$$\mathrm{RGR} = \left(\ln \mathrm{DW}_2 - \ln \mathrm{DW}_1\right)/(t_2 - t_1), \quad (1)$$

where DW_1 and DW_2 corresponded to the dry weights of maize seedlings at times t_1 and t_2 (beginning and end of the water deficit).

The plant water use efficiency (WUE, mg ml^{-1}) was calculated considering all the amount of water provided during the experiment timespan (Kuglitsch et al., 2008).

$$\mathrm{WUE} = \text{Plant biomass}/\text{Total irrigation} \quad (2)$$

Greenhouse experiment

Once the data was evaluated for the dosage optimization, an additional study with maize variety was conducted at a greenhouse property of the Escuela de Capacitación Agraria de Tacoronte (Tenerife), Canary Islands (28°29′47.0″N 16°25′12.0″ W) from June 2021 to August 2021. The ambient conditions were recorded daily (**Supplementary Table 1**). The average maximum and minimum temperatures were 30 and 22°C, respectively, with an average relative humidity of 80% (**Supplementary Table 1**). The soil is classified as clay–loam (35% clay, 27% silt, and 38% sand), and the experiment was organized in randomly distributed blocks of 20 m^2 blocks with three replicates, each block containing 80 plants. The seeds were sown in nursery trays and transplanted to the field after 15 days of the sowing. The irrigation was calculated according to the FAO (Rao et al., 2016), taking into account the evapotranspiration rate (ETo) provided by a nearby meteorological station, property of the island council, Cabildo de Tenerife (**Supplementary Table 1**). The soil humidity was monitored within the wet-bulb with the TEROS 12 FDR sensor (METER Group, Pullman, WA, United States). The treatments consisted of 20 ml of water for the controls or of 0.1-mM Put (CAS No.: 333-93-7) or 0.5-mM Spd (CAS No.: 124-20-9) for the treated plants; both compounds purchased from Aldrich Chemical Co. (St. Louis, MO, United States). The treatment was applied manually using a backpack sprayer with a dispenser. The solutions were applied directly to the wet soil, between the irrigation emitter and the plants, to ensure the direct availability of the root system. The treatments were applied twice, 2 and 4 weeks after the transplanting. After the second application, the water restriction for the drought variant started, and these conditions were maintained until the harvest of the maize cobs. The plants did not receive additional fertilization or protective treatment during the experiment. The weeds were manually removed every 7–10 days to avoid competition for the water.

Biomass, yield, and water status measurement

In 15 and 30 days after the onset of the water restriction, the relative water content (RWC, %) was calculated (Barrs and Weatherley, 1962). A total of 20 disks of 1-cm diameter per variant were excised from the last fully expanded leaf and immediately weighted to register the fresh weight (FW, mg). After that, the disks were submerged in distilled water for 24 h to determine the turgid weight (TW, mg). Finally, the disks were oven-dried at 85°C for 48 h to register the dry weight (DW, mg). The RWC for each disk was calculated as

$$\mathrm{RWC} = (\mathrm{FW} - \mathrm{DW})/(\mathrm{TW} - \mathrm{DW}) \quad (3)$$

The yield-related parameters were evaluated at the harvest, 45 days after the onset of the stress. The number of adequately developed maize cobs per plant and variant was counted. Ten random plants per variant were selected to determine morphometric parameters such as plant length (from insertion to the soil until the base of the flower) and width (at the middle of the stem length), and the length and width of the last fully developed leaf. The cobs to evaluate production were also obtained from the selected plants. The cobs were weighed to record the fresh weight and then oven-dried at 65°C for 1 week to reduce the possible bias due to the different moisture levels. The dry cob weight, the number and total weight of all kernels per cob, and the weight of 100 kernels (in triplicate from each cob) were registered. The total yield considering 40,000 plants ha^{-1} for the used plantation frame was also calculated using the following equation with the following formula:

$$\mathrm{Yield\ ha^{-1}} = \mathrm{Average\ kernel\ weight/Cob} \times \mathrm{Average\ cob\ number/Plant} \times \mathrm{Estimated\ plants\ ha^{-1}} \quad (4)$$

The Harvest index (HI) was also calculated from the total kernel weight (total KW) per cob and the average cob fresh weight (average cob FW) as follows:

$$\mathrm{HI} = \mathrm{Total\ KW/Average\ Cob\ FW} \quad (5)$$

The production water use efficiency (WUEp) in maize was also estimated (Kiziloglu et al., 2009). The accumulated effective crop evapotranspiration (ETc, mm) was calculated through the experiment (**Supplementary Table 1**). This term corrects the deficiencies of the ETo values by a Kc factor that depends on the moisture soil level, crop characteristics, and the stage of the crop vegetative cycle (6). For maize, the Kc values are estimated at 1.2 in the initial phases to 0.6 at the final stages (FAO).

$$\mathrm{ETc} = \mathrm{ETo\ X\ Kc} \quad (6)$$

The WUEp (kg mm^{-1}) was then calculated as the ratio between the accumulated ETc and the final yield (kg ha^{-1}).

Protein, carbohydrates, and mineral composition of the maize flour

All kernels from the selected cobs were ground to a fine powder to evaluate quality parameters. A 50 mg of the powder per sample was used for the total protein content calculated using the Kjeldahl Method (Kirk, 1950), multiplying the total nitrogen content by 6.25. An additional 100 mg of the powder was used to determine total carbohydrates using the phenol sulfuric acid method modified in multi-well plates (Jiménez-Arias et al., 2019). Finally, 1 g of the flour powder per sample was used to analyze the mineral content (Ca, Mg, K, P, Na, Cu, Zn, and Fe). Each sample was converted to ash in a muffle stove at 480°C and mineralized by the dry method with 6 N HCl. The mineral levels were determined by ICP OES Avio 500 (Perkin Elmer, Waltham, MA, United States).

Data analysis

All plant growth and production parameters were used to calculate the Plant Biostimulant Characterization Index (PBCI), a visual and helpful tool to reduce all considered variants into a single number a for better biostimulant characterization (Ugena et al., 2018; Sorrentino et al., 2021). The PBCI was used to select the best-performed concentrations in the first experiment (dose optimization) and evaluate the PA application impact on maize production.

The data were evaluated using different statistical approaches. First, using Infostat software, the normality of the variables was assessed with the Shapiro–Wilks test. After that, a two-way ANOVA ($p \leq 0.05$) followed by multiple comparisons with LSD posthoc test was used for parametric data and Kruskal–Wallis test ($\alpha = 0.05$) for nonparametric data. The multivariate statistical analyses with the yield-related parameters were also carried out for better visualization. One principal component (PC-Dim) analysis and matrix correlation were constructed in RStudio v.2021.09.1+372 using the packages *factoextra*, *ggplot2*, and *corrplot*.

Results

Nursery tray dose optimization

The dose optimization was performed in nursery trays following the protocol established by Jiménez-Arias et al. (2022). The parameters considered to evaluate the efficiency of the dose were the plant weight (shoot and root), the RGR (%), and WUE (**Supplementary Table 2**). **Table 1** displays the heatmap from the computed parameters, transformed with the log2 and relativized to the untreated maize seedlings. The drenching with Put at 0.5 and especially 0.1 mM enhanced the plant biomass (weight), RGR (%), and WUE compared to untreated seedlings

10.3389/fpls.2022.944066

TABLE 1 Heatmap summarizes the parameters estimated in maize seedlings treated with Put or Spd at five concentrations (0.01, 0.1, 0.5, and 1 or 2 mM) grown under water limitation (50% field capacity).

Compound	Concentration	Biomass	RGR	WUE	PCBI
Put	0.01	−0.003	−0.001	−0.003	**−0.008**
	0.1	0.050	0.026	0.059	**0.135**
	0.5	0.014	0.008	0.017	**0.039**
	1	−0.033	−0.018	−0.039	**−0.091**
	2	−0.021	−0.011	−0.025	**−0.057**
Spd	0.01	−0.089	−0.049	−0.106	**−0.244**
	0.1	−0.085	−0.046	−0.101	**−0.232**
	0.5	−0.044	−0.024	−0.052	**−0.120**
	2	−0.078	−0.042	−0.092	**−0.212**
	1	−0.119	−0.066	−0.143	**−0.328**

The studied parameters were plant dried weight (Plant W, mg), relative growth ratio (RGR, %), and water use efficiency (WUE, mg mL^{-1}). The table represents the ratio (log2) between the original values of each variant and the untreated plants (Control). The right panel shows the obtained PBCI values. Blue indicates a stress alleviator; orange indicates a stress inductor.

when grown under a water limitation of 50% field capacity, ending with a positive PBCI value (Table 1). Contrarily, the application of Spd did not improve the seedlings performance under the same growth conditions (Table 1 and Supplementary Table 2). The plants treated with 0.5-mM Spm presented less negative PBCI (Table 1). Thus, we selected 0.1-mM Put and 0.5-mM Spd to evaluate their impact on maize production under optimal and water deficit conditions.

The application of polyamines enhanced the RWC in maize plants

The changes in soil water content were recorded through the experiment and represented in Figure 1A. The plants under well-watered conditions were irrigated according to their water requirements estimated by FAO's reference evapotranspiration (ETo) (Supplementary Table 1). The water supply was reduced by 20% of the crops water requirements for the water stress variants. As a result, we observed that the volumetric water content in the well-watered plants was maintained between 1.7 and 1.6 m^3 m^{-3} (Figure 1A). However, in the stress variant, the water was drastically reduced to a volumetric water content of 1.4 m^3 m^{-3} for the first four days and maintained for additional 15 days. After that, it fluctuated between 1.3 and 1.1 m^3 m^{-3}.

The water status of the plants was estimated twice by the RWC, at 15 (t_1) and 30 (t_2) days after the water restriction onset (Figures 1B,C). According to ANOVA, there was a significant interaction between growth conditions and treatment for $RWCt_2$ but not for $RWCt_1$. The water restriction reduced the $RWCt_1$ in all plants compared to well-watered ones. However, the application of Put and Spd increased the $RWCt_1$ values compared to their respective controls. The Put and Spd applications kept the same trend, with an $RWCt_1$ of 4 and 2.6% for WW and 9 and 4% for WD conditions, respectively, compared to the corresponding untreated plants (Supplementary Table 3). Interestingly, no differences in $RWCt_2$ were observed among variants; only the untreated plants significantly reduced the $RWCt_2$ to 80% (Figure 1C and Supplementary Table 3). Thus, Put and Spd applications increased significantly $RWCt_2$ to 14.9 and 15.8% in the maize plants, respectively, compared to the untreated plants under WD (Supplementary Tables 1, 3).

The application of Spd by drenching reduced the biomass-related parameters under water limitation

The biomass production was evaluated by monitoring several parameters such as stem diameter, the plant length (measured from the transition to the roots, up to the emission of the anthers), length and width of the flag leaf, and the ratio length/width (L/W) for the flag leaf (Figure 2 and Supplementary Table 4). The parameters were then represented in a parallel coordinate plot, and the values were used for the PBCI calculation. None of the treatments enhanced plant biomass production in any water regime, so all presented negative PBCI values (Figure 2). The parallel coordinate plot illustrated that only Put slightly enhanced the biomass production under WW conditions; the rest of the treatments and growth conditions presented a negative effect. The thicker stem was reported for the WW control plants, with Put plants having the thinnest stem for both irrigation conditions. Interestingly, the Spd-treated plants were the only ones keeping the stem thickness irrespectively of the growth conditions (Figure 2 and Supplementary Table 4). The water limitation slightly reduced the plant height, flag leaf length, and width without significant differences (Supplementary Table 4). Overall, the highest plant length and leaves were found in the Put treated maizes under WW conditions, while the shortest plants were reported for the WD with Spd application. Regarding the leaf L/W ratio, the highest values were reported for Put and Spd in WW conditions, followed closely by the Control treatment and Put under WD (Figure 2 and Supplementary Table 4). The lowest L/W ratio was observed in the maize plants treated with Spd under WD, confirming that this treatment modified the plant stress response and hence, the growth profile.

Put enhanced yield and WUEp under optimal conditions, and Spd under water limitations

As a first step in evaluating maize's yield, the total number of cobs produced per variant was counted and represented in Figure 3A. The Put application was the most effective treatment

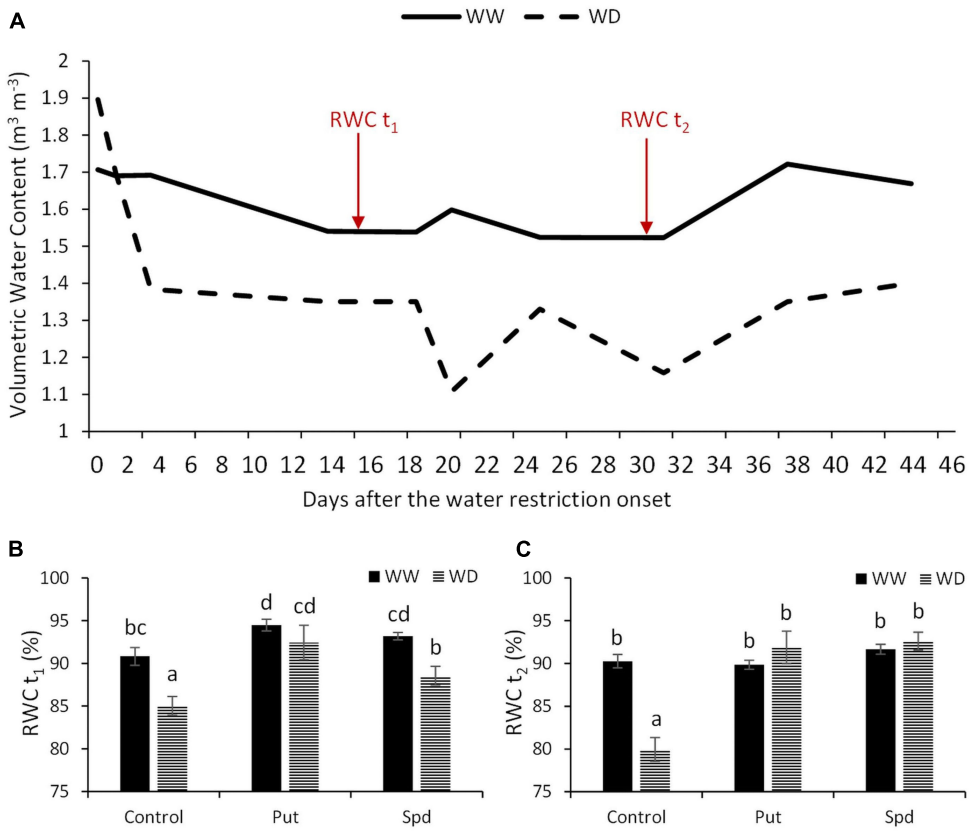

FIGURE 1
Water-related parameters in maize plants under optimal conditions and water limitation. **(A)** Volumetric water content of the soil (m^3 m^{-3}) measured with the FDR soil moisture sensor from the onset of the water restriction. Red arrows indicate the two dates (t_1, t_2), when the relative water content (RWC, %) was measured in the maize plants untreated (Control) and treated with 0.1-mM Put or 0.5-mM Spd under optimal conditions (WW) or water deficit (WD). **(B)** RWCt_1 of the plants, t_1 corresponds to15 days after the onset of the stress). **(C)** RWCt_2 (%) of the plants, t_2 corresponds to 30 days after the onset of the stress. Mean ± SE; $N = 24$. Different letters for the RWC values indicate the significant differences according to the LSD test after two-way ANOVA ($p \leq 0.05$).

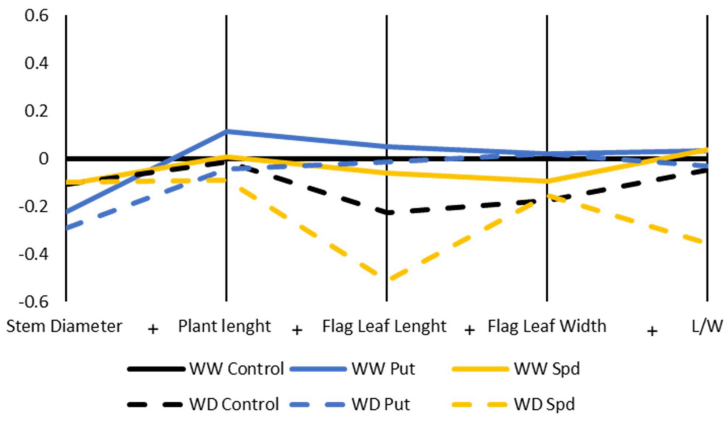

		PBCI
WW	C	0
	Put	-0.01
	Spd	-0.22
WD	C	-0.57
	Put	-0.37
	Spd	-1.21

FIGURE 2
Parallel coordinate plot and PBCI regarding the biomass-related parameters. Stem diameter (mm), plant length (cm), flag leaf length and width (cm), and length/width ratio (L/W) of maize plants treated with 0.1-mM Put or 0.5-mM Spd under optimal conditions (WW) or water deficit (WD). The plot represents the ratio (log2) between the original values of each variant and the untreated plants under WW conditions. The right panel shows the obtained PBCI values. Orange color indicates stress inductor.

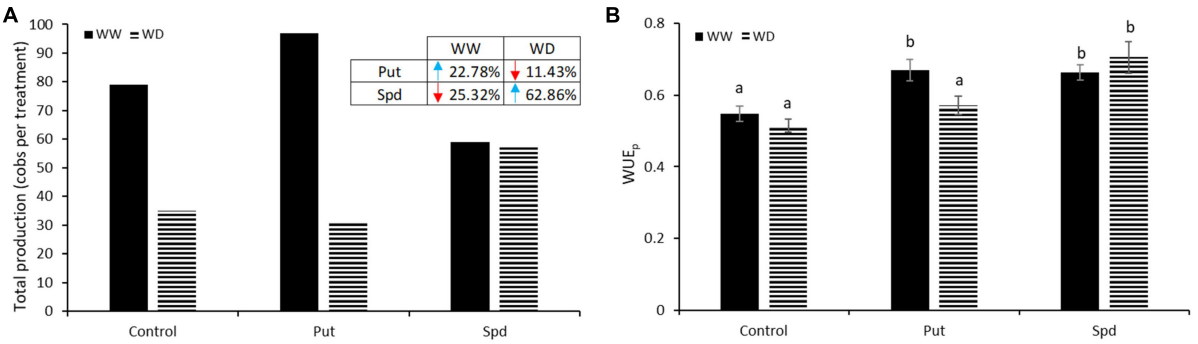

FIGURE 3
Total production and WUEp in PA treated maize plants. **(A)** Total production expressed as the sum of all cobs produced per variant in maize plants untreated (Control) and treated with 0.1-mM Put or 0.5-mM Spd grown under well water (WW) or water deficit (WD). Enclosed in the left upper table, the percentage of increment (blue, upside arrow) or reduction (orange, downside arrow) of Put and Spd treatment relative to the respective control in WW and WD conditions. **(B)** Water use efficiency calculated as the ratio between the fresh biomass production and the ETo adapted to maize crop with the FAO Kc. Different letters indicate the significant differences between the treatments and the growth conditions according to the LSD test after two-way ANOVA; $p < 0.05$.

under WW, so its plants increased the total production by 22.78%, with 97 cobs compared to 79 obtained in the controls. On the other hand, Spd reduced the production to only 59 cobs. Water limitation reduced the final yield in all treatments, except in Spd treated plants that maintained similar production as observed under WW conditions (Figure 3A) and enhanced the production by 62.78% compared to control plants under WD. However, the Put application reduced plant production by 11.43% (Figure 3A).

Crop physiologists initially considered WUE as the amount of carbon assimilated and crop yield per unit of transpiration (Viets, 1962), although the definition evolved to biomass or marketable yield produced per unit of transpiration. In this sense, this parameter is essential to better characterize the productivity of crops, especially in a water scarcity scenario. In this work, the production WUE was calculated to understand better the relationship between plant production and the water used (Figure 3B). A significant interaction between treatment and growth condition was obtained according to ANOVA ($p = 0.002$). In control plants, no differences in WUEp were observed among growth conditions. However, the PA treatments enhanced the WUEp of the treated plants under WW conditions, but only Spd application improved this parameter under WD (Figure 3B). These results pointed to WUEp increase induced by PAs as one of the primary factors conditioning maize yield under optimal and water limitation conditions.

Other parameters related to the cobs and kernel production were also determined (Supplementary Table 5). Among them, the fresh weight and length of the cobs and the final yield per hectare considering the kernel were the production-related parameters that showed a significant interactive effect on the treatment and growth conditions according to ANOVA ($p \leq 0.05$). The treatment with Put and Spd improved the fresh cob weight but reduced the length compared to the controls under WW, but not under WD (Figure 4 and Supplementary Table 5). Contrarily, the PA treatments reduced the cob length in both growth conditions except for Spd under WD. Polyamines significantly increased the yield per hectare (1.5×10^6 g ha^{-1} for Put and 1.6×10^6 g ha^{-1} for Spd) compared to untreated plants (1×10^6 g ha^{-1}) under WD conditions, reaching the level of the WW plants (Figure 4 and Supplementary Table 5). Regarding the harvest index (HI), Put-treated plants under WD overcame the levels of controls under WW conditions.

To integrate the production data, two additional PBCIs were estimated (right panel, Figure 4). As a final result, we observed that Put improved maize yield (positive values for PBCI) under WW and WD conditions. However, Spd only enhanced maize production under WD conditions and negatively affected the plants under WW (right panel, Figure 4). Altogether, the PA application by drenching enhances the quality of maize production, especially under water restrictions.

Polyamines application modifies the quality of the maize flour

As the final step, we evaluated the percentage of carbohydrates (CH) content and protein in the kernel powder obtained from each treatment and growth conditions (Figure 5 and Supplementary Table 6). According to ANOVA, both parameters were affected by the interaction between the treatment and growth conditions. Under WW conditions, the PA application did not change the carbohydrate content (Figure 5A). The reduced water availability significantly decreased the CH content for the control treatment; curiously, both PA treatments resulted in significantly higher CH content than the WD control, leveling it up to the control treatment under WW conditions (Supplementary Table 6). The water

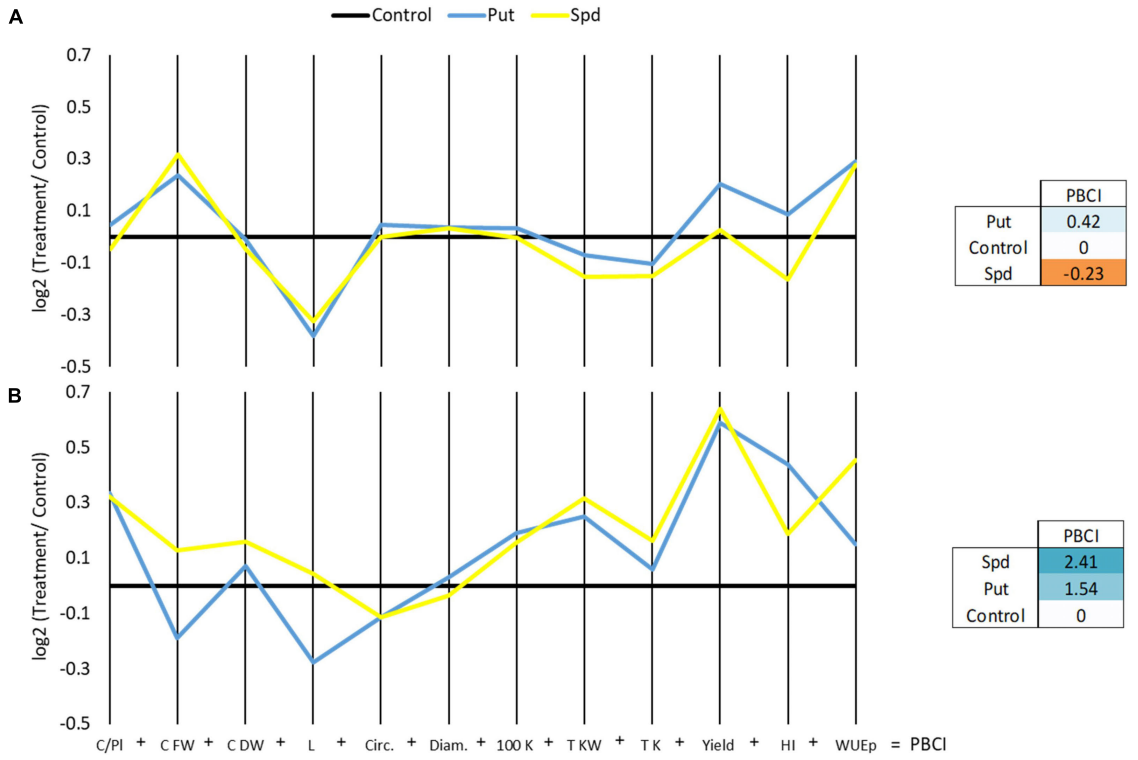

FIGURE 4
Parallel coordinates plot representing log2 of the production parameters relativized with the control of each growth condition; cobs per plant (Cobs/Pl), cobs fresh (Cob FW), and dry weight (Cob DW) (g), length [L(K)] (kernels in a line), circumference [circ. (K)] (kernel circumference) and diameter (diam.) (mm), the weight of 100 kernels (100 K DW) (g) and the total kernel weight (Total KW) (g), the total number of kernels (Total K), the yield per hectare, considering the dry kernel production [Yield(K) ha^{-1}], harvest index (HI) (Total dry kernels weight/Average cob fresh weight), and the WUE in maize plants untreated (Control) and treated with 0.1-mM Put or 0.5-mM Spd grown under well water (WW) **(A)** or water deficit (WD) **(B)**. The right panel represents the PBCI, which summarizes the plot in a single number positive (Blue color) for growth promotor or negative (orange) for stressor.

availability significantly affected the protein content (%), with higher values for the kernels from the controls under WD than under WW conditions (Figure 5B). The PA application presented a different pattern (Supplementary Table 6). Also, Put significantly increased the protein content under WW conditions but reduced them under WD compared to the respective controls. Contrarily, Spd did not affect the protein content under WD but significantly reduced it under the protein content compared to the controls under WW conditions (Figure 5B).

The mineralogical profile of the flour obtained from the dry grains was also analyzed (Table 2 and Supplementary Table 7). Significant changes were observed in the flour mineral compositions due to the treatment, growth conditions, and their interaction. As Na, P, and Cu were the most sensitive parameters because their changes were due to the interaction between the treatment and the growth conditions ($p \leq 0.006$, $p \leq 0.001$, and $p \leq 0.047$, respectively). The treated plants presented the biggest changes in Cu, mainly due to a significant increment in those treated with Spd (Table 2 and Supplementary Table 7). The WD conditions significantly reduced the Na levels of the non-treated plant, but the application with Put and Spd kept them at the same levels as the WW-variants. The water restriction significantly induced the P, K, and Mg accumulation in the plants under WD, except the Spd treated ones that kept the lower values observed in the flour from the WW plants. The opposite situation was observed for Ca, where only the Spd-treated plants from WD kept the levels of the WW ones (Table 2 and Supplementary Table 7). Altogether, the PA application modifies maize flour's chemical and mineral composition. However, the changes are also highly influenced by the growth conditions.

The multivariate statistical analysis uncovers the different effects of Put and Spd in maize

To better visualize and integrate the biomass, productivity, hydric status of the plants, and the kernel nutritional profile, we performed a principal component analysis (PCA) and correlation matrix (Figure 6). The two first PCs explained 67.3%

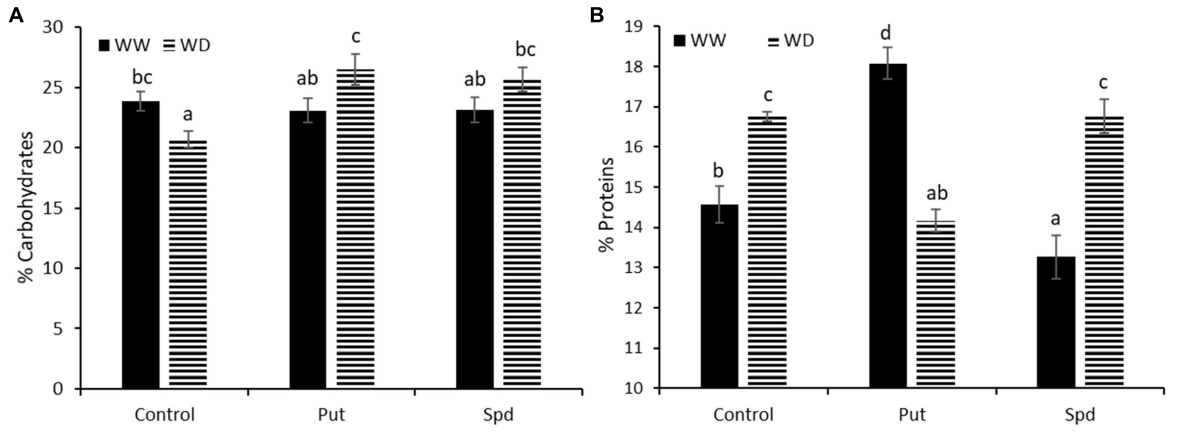

FIGURE 5
Content of carbohydrates **(A)** and protein **(B)** expressed as % of the weight of the sample WUE in maize plants untreated (Control) and treated with 0.1-mM Put or 0.5-mM Spd grown under well water (WW) or water deficit (WD). Different letters indicate the significant differences between the treatments and growth conditions according to the LSD test after two-way ANOVA, $p < 0.05$.

TABLE 2 Heatmap containing the log2 values of the different mineral elements content (ppm) in maize plants untreated (Control) and treated with 0.1-mM Put or 0.5-mM Spd grown under optimal conditions (WW) or water deficit (WD).

Growth conditions	Treatment	Ca	Fe	K	Mg	Na	P	Zn	Cu
WW	Control	0 ab	0 a	0 ab	0 ab	0 b	0 ab	0 a	0 a
	Put	0.58 ab	−2.00 a	−0.42 a	−0.24 a	0.00 b	−0.15 a	−1.77 a	0.77 a
	Spd	0.20 ab	0.38 a	−0.27 ab	−0.11 a	−0.07 b	0.14 bc	1.45 b	0.31 a
WD	Control	−0.42 a	−0.70 a	0.33 c	0.25 c	−0.22 a	0.24 c	−0.41 a	1.23 a
	Put	−0.14 ab	0.17 a	0.14 bc	0.22 bc	0.03 b	0.23 bc	−0.48 a	0.19 a
	Spd	0.72 b	−1.86 a	−0.17 ab	−0.15 a	−0.03 b	−0.08 a	−1.53 a	2.46 b

The values are relative to the control treatment under WW. The different letters indicate significant differences according to the LSD test after two-way ANOVA, $p = 0.05$. Blue indicates accumulation and red reduction.

(Dim1 = 42%; Dim2 = 25.3%) of the total model variation. As the first result, Dim1 separated the non-treated plants due to the irrigation regime (Figure 6A). However, whereas stressed Put treated plants were located close to the irrigated plants, Spd was located opposite to these plants, pointing to a different mechanism of action between these two PAs. Put treated plants under WD strongly correlated with the leaf biomass expressed as flag leaf length/width ratio and the Zn and Fe levels. This result was also evident in the negative correlation between Fe, p, K, and Mg with many production-related parameters, the plant RWC and Ca in the flour, observed in the correlation matrix (Figure 6A). Contrarily, Spd-treated plants under WD presented longer (Cob_L) and heavier (Cobs_FW) cobs, with higher content of Cu in the flour (Figure 6A). It is worth mentioning that the growth condition affected CH and protein content, presenting a higher correlation with the RWC, the kernel-related parameters, and the final yield. The PA-activated strategy conditioned the biomass production (vegetative or reproductive biomass) and the composition of the final product; in this case, the quality of the flour.

Discussion

Nowadays, the research topics need to focus on understanding how the principal abiotic stresses such as drought affect crop yield. Besides, due to the promising biostimulant efficiency to mitigate the plants' stress effect, new evidence is needed to know if they provide any quantitative or qualitative benefit in the final yield. This study aimed to evaluate using the major PAs as small molecules-based biostimulants to improve maize production under optimal and water restriction conditions. Their impact on maize biofortification is also investigated. A recent review has reported the relevance of these compounds in regulating plant tolerance/resistance to stress abiotic/biotic (Ramazan et al., 2022). When used PAs as a foliar application, the concentration range of 0.1–1 mM elicited positive responses in stressed plants (De Diego and Spíchal, 2020). In this work, we investigated their application *via* fertirrigation because it is considered an efficient agricultural method to enable plants to cope with the consequences of the water limitation during the growth and fruit production

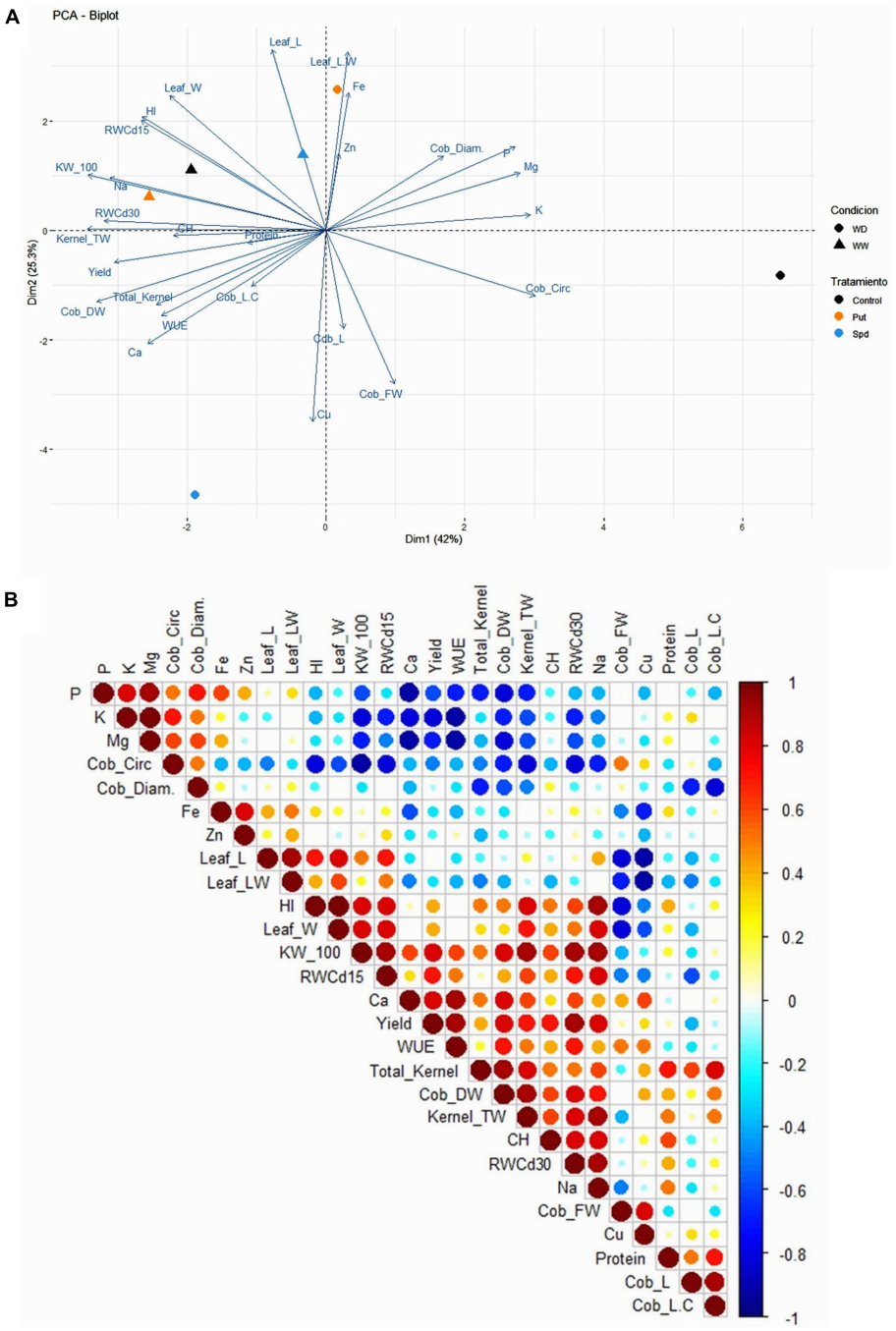

FIGURE 6
Principal component analysis **(A)** and correlation matrix **(B)** of the studied biomass parameters [flag leaf length (Leaf_L), flag leaf width (Leaf_W), and flag leaf length/width ratio (leaf_LW)], relative water content at 15 and 30 days after the stress onset (RWC 15d and RWC30d), productivity parameters [cob length (Cob_L), cob circumference (Cob_circ.), cob diameter (Cob_diam.), cob fresh weight (Cob_FW), cob dry weight (Cob_DW), weight of 100 kernels (KW_100), total number of kernels per cob (Total_Kernel); total weight of the kernels per cob (Kernel_TW), harvest index (HI), yield, water use efficiency (WUE), protein content (Protein), carbohydrates content (CH), and mineralogical profile of the kernels (P, K, Mg, Fe, Zn, Ca, Na, and Cu) in maize plants untreated (Control) and treated with 0.1-mM Put or 0.5-mM Spd grown under well water (WW) or water deficit (WD).

(Agliassa et al., 2021). The main reason is that the fertirrigation provides the plant with a longer nutrient uptake window than foliar application (Parkunan et al., 2011). However, it must be considered that different application methods can trigger different responses in the plants (Paul et al., 2019), so optimizing the dose for the root treatment was an essential step,

ending with 0.1-mM Put and 0.5-mM Spd the most effective concentrations (**Table 1**).

The application of PAs reduced the RWC losses when plants are subjected to water limitations (**Figure 2**) compared to untreated plants. Many studies have also obtained similar results and reported that the PA-induced better water balance is due to decreasing the stomatal conductance and increasing proline, anthocyanins, and soluble phenolics levels, improving membrane properties and enhancing the activity of catalase and superoxide dismutase (Farooq et al., 2009; Hassan et al., 2018). Their application has also been described as improving plant osmotic adjustment mechanisms (Choudhary et al., 2022). However, the improvement in the water balance did not influence the plant biomass but instead reduced it in the PA-treated plants (**Figure 3**). Similar results were also observed in other maize species (Li et al., 2018) and crops (Ullah et al., 2012; Liu et al., 2018). One possible explanation is that this type of treatment simulates moderate stress in the plants, so-called hardening, to be ready for fighting future adverse conditions (Duarte-Sierra et al., 2020).

The "no improvement" of the plant growth might also be an energy-saving mechanism to redirect the PA-induced/accumulated resources to the enhancement of the production of the crop. This concept has already been proposed for fruit tree management, where the application of plant growth retardants has been explored to reduce vegetative growth and obtain higher production (Köhne, 1989). According to this assumption, we expected that both PA treatments improved maize production under WW and WD. However, different responses were observed; Put enhanced the total maize yield under WW but reduced it under WD (**Figure 3**). Despite the reduced total maize yield, drenching with 0.1-mM Put ended with a positive PBCI under WD due to a higher number of cobs per plant, higher kernel weight, or yield per ha (**Figures 4**, **7A** and **Supplementary Table 5**). The exogenous application of PAs, including Put, has improved flowering and yield in many plant species (Reviewed by González-Hernández et al., 2022) and wheat production (Mostafa et al., 2010). These results could partially explain the higher number of cobs per plant. Besides, the exogenous application of 0.1-mM Put enhanced yield in winter wheat under WD and the plant biomass (Gupta and Gupta, 2011; Gupta et al., 2012). Besides, the long-term application of Put on salt-stressed rice stimulated the morphogenesis of reproductive structures, enhancing the yield compared to the unstressed plants (Ndayiragije and Lutts, 2007). This positive effect of Put was also observed in the vegetative development and yield of barley salt-stressed plants (Seleem et al., 2021). Pál et al. (2018) also suggested that Put pretreatment induces acclimation processes under controlled conditions. These results agree with ours, so the Put-treated plants presented the best growth and yield under control conditions, and they had higher biomass production and some productive parameters under WD (**Figures 4**, **6A**, **7A**).

Overall, the PA addition enhanced the production, in agreement with the findings of Liang and Lur (2002), who demonstrated that aborted maize kernels had lower endogenous PA levels. However, a much higher yield was obtained with Spd than with Put under WD (**Figures 3**, **4** and **Supplementary Table 5**). This could be because the vital biological processes, such as embryogenesis and seed settings, have been related more to the levels of Spd than Put (Feng et al., 2011; Chen et al., 2019a). The benefit of Put could be only due to its condition as a precursor of Spd synthesis (Feng et al., 2011). Furthermore, a recent study showed that high endogenous levels of Put but not of Spd could condition grain filling of wheat, and hence, yield, under drought because it induced the accumulation of endogenous ethylene and ABA in the grains, which worsened the adverse stress effects (Liu et al., 2016). Controversial results were also obtained in wheat where the exogenous Spd and Put applications had an opposite effect on florets; while Spd inhibited the floret degeneration, Put enhanced it, resulting in a reduction of fertile floret number (XiaoKang et al., 2016). Another study demonstrated that pretreatment with Spd improved the grain yield of salt-stressed rice plants (Saleethong et al., 2013). However, this response must be concentration-dependent and conditioned by the endogenous levels of the different PA forms and their crosstalk with other phytohormones. For example, the crosstalk between ethylene and PAs has also been reported to condition the seed setting in maize (Feng et al., 2011). These authors also demonstrated that high levels of PAs are needed to avoid aborted kernels. It is well known that ethylene and PAs compete for the same precursor S-adenosyl-methionine (SAM), the methionine-activated form (Podlešáková et al., 2019). This could explain that high PAs and low ethylene levels promote plant flowering and embryogenesis (reviewed by Chen et al., 2019a), where Spd is the leading PA form regulating these processes.

From our knowledge of yield quality in maize, no study focused on the impact of PAs as small molecule-based biostimulants exist in the research literature. Our work demonstrated that PA application improved both yield quantity and quality. The first two parameters analyzed were the CH and protein content (%) in the flour powder obtained from the seeds (**Figure 5** and **Supplementary Table 6**). Regarding CH, it was shown that the crosstalk between PAs and the ethylene pathway could condition plant yield and determine the grain filling and carbohydrate translocation in cereals (Yang et al., 2017). Therefore, we expected PA supplementation to induce a good CH transport, enhancing the kernel set and the final yield. As a result, WD reduced the CH content compared to the WW conditions in untreated plants, as previously observed by Hussain et al. (2020) and Abbas et al. (2021). However, opposite results were also published. For example, it has been reported that drought during the vegetative stage of maize plants induced an increment in glucose and amino acids on the grains (Harrigan et al., 2007) or did not affect

the CH content (Barutcular et al., 2016). Interestingly, the PA application increased the flour CH content in the plants under WD conditions over the levels of the WW plants (**Figure 5A** and **Supplementary Table 6**). Besides, clear evidence was found about a positive correlation between CH, the leaf RWC, and the Na content, which also positively correlates with the weight of 100 kernels and the total kernels weight (**Figure 6B**). It can be because the application of PAs under stress has been reported to protect the photosynthetic apparatus (ensuring the synthesis of photosynthates) and increase the osmotic adjustment of the plants under stress conditions (Chen et al., 2019b; Jing et al., 2019). Moreover, Xu et al. (2016) suggested that PA might be involved in the starch biosynthesis in kernels during post-anthesis when the soil is drying. Therefore, it is not surprising that those treatments reported the same yield as the proper irrigated plants and were higher than the WD control plants.

Low water availability increased the protein content in the flour, as described by Lu et al. (2015), Barutcular et al. (2016), and Abbas et al. (2021). However, other studies showed no alterations in the protein content by the water restriction (Hussain et al., 2020). Our work showed that the PA levels could be a relevant factor in determining the protein content in the flour. However, the opposite responses were obtained by the Put or Spd applications under both WW and WD conditions (**Figure 5B**). There is a direct link between the source–sink ratio during the filling stage and the final protein content in the kernels (Borrás et al., 2002). As mentioned above, Spd is considered essential for a good grain filling. Its exogenous application reduced the production and the flour protein content under WW conditions, whereas it improved the yield but not the protein level under WD (**Figures 4**, **5B**). Contrarily, the Put application enhanced the production and protein content under WW but reduced both under WD. In wheat, the Spd application may affect grain filling by regulating protein synthesis and posttranslational modification, together with a better antioxidative response under drought conditions (Li et al., 2020). This way, the maize–Spd treated plants could deal better with the water limitations, ensuring better production under this adverse condition.

On the other hand, Put exogenous application induced the increment of N content in cotton plants (*Gossypium barbadense* L.) under control conditions and salt stress (Darwish et al., 2013). Our results partially agree since we only reported a protein increment under control conditions. The different behavior observed for Put and Spd applications in the plant growth and yield quantity and quality could be because they regulated the PA synthesis, the conversion, and the terminal catabolism differently. In this regard, it has been proved that at least the synthesis of Spd and Spm *via* the activity of the spermine synthase (SPMS, E.C.2.5.1.22) and spermidine synthase (SPDS, E.C. 2.5.1.16) could condition the flowering (reviewed by Chen et al., 2019b). In addition to the SPDS, the activity of other enzymes related to the PA synthesis, such as ornithine decarboxylase (ODC, E.C. 4.1.1.17) and S-adenosyl-L-methionine decarboxylase (SAMDC, E.C. 4.1.1.50) have also been positively correlated with the grain filling rate (Yang et al., 2020). The PA oxidation *via* polyamine oxidases has been reported to regulate the plant reproductive phases (reviewed by Yu et al., 2019). In this last case, the back conversion from thermospermine or spermine to Spd was the most often identified step conditioning fertility and floral development. Cao et al. (2010) suggested that Spd, among Put and Spm, might be more closely involved in the physiological changes of the maize kernel development. Altogether, it is clear that the effect of the PA application in maize production is due to the endogenous levels and the interconversion between the different PA forms. The further studies are needed focusing on the enzymatic changes to clarify the mode of action of these compounds.

As the last step, we analyzed the mineral content of the flour. Only the limitation of water availability has induced controversial results regarding the flour mineral composition. For example, some studies did not see any effect (Feil et al., 2005), whereas others observed a reduction in K, P, and Fe (Abbas et al., 2021). Contrarily, Avila et al. (2017) reported the increment of P and Mg on grains of maize plants subjected to water limitations. These contrasting results point to a complex response of the plants that affect the metabolism in the grains and condition their mineral composition, which is regulated by the interaction of variety, genotype, and stress intensity. Our study showed that the application with PAs modified the composition under WW and WD (**Table 2**, **Supplementary Table 7**, and **Figure 7B**). Only the Spd treatment increased the Zn content in WW plants, whereas all applications enhanced the Cu under WW and WD. These two minerals have been reported to accumulate under drought stress (da Ge et al., 2010; Avila et al., 2017). Zn deficiency reduces plant growth and nutritional quality (Liu et al., 2019). In a previous experiment with wheat, it was proposed that the increment of N supply also contributed to an enhancement of the Zn concentration in the grains (Kutman et al., 2010).

Copper is also needed for the growth and development of maize and is an essential cofactor for many metalloproteins and various enzymes involved in different physiological and cellular processes such as oxidation and reduction reactions (Rajput et al., 2018). Besides, both minerals are considered essential for human health (White and Broadley, 2009; Garg et al., 2018). It is worth mentioning that the deficiencies in Cu also play a vital role in COVID-19, altering the disease outcomes and prognosis (Altooq et al., 2022). In this context, crop biofortification by applying compounds or fertilizers increases attention to assure plant and human health. Our results showed that a simple PA application could improve the content of these two minerals in the flour, especially when the plants are treated with Spd (five times more Cu under WD or three times more Zn under WW). Additionally, the Spd application also induced a significant

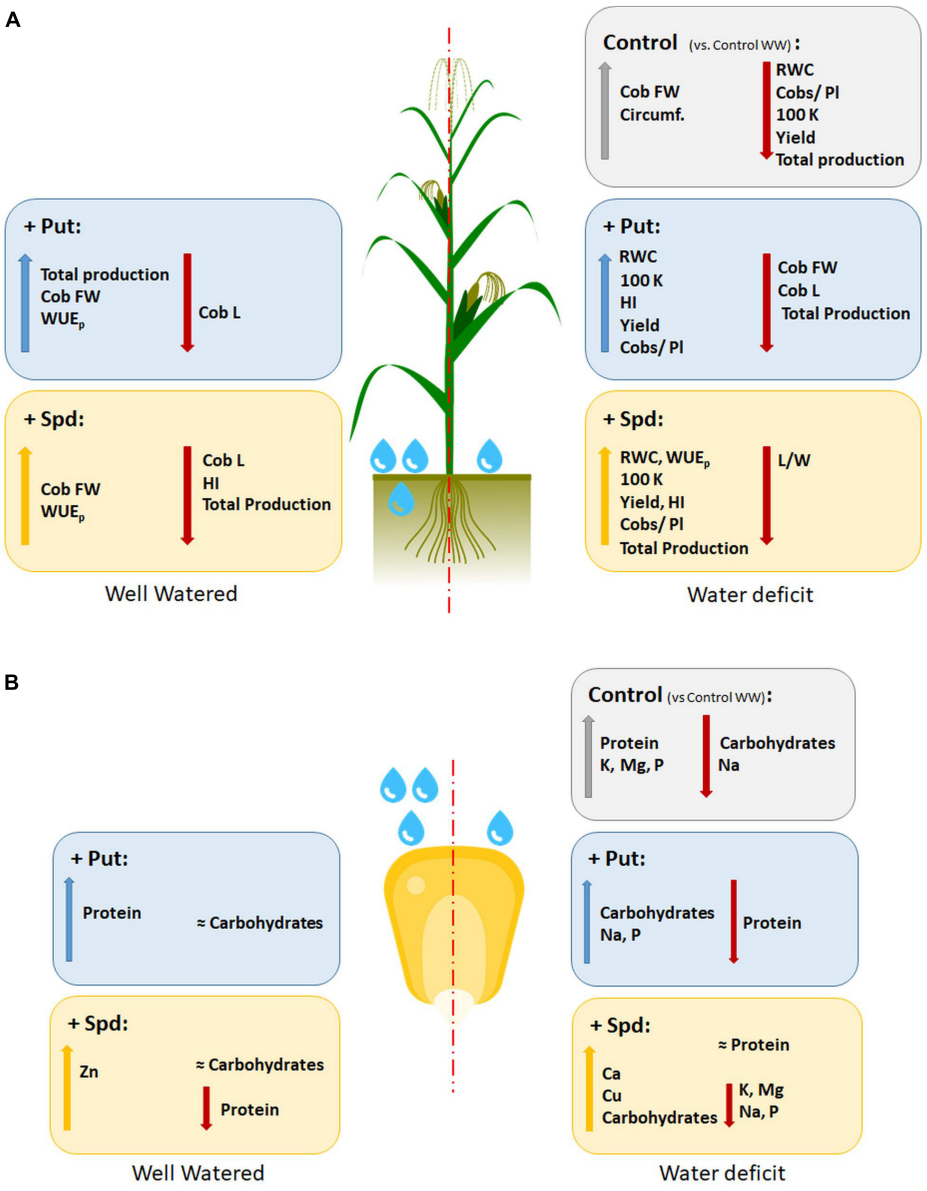

FIGURE 7
Summary of the variation of the observed parameters in maize plants untreated (Control) and treated with 0.1-mM Put or 0.5-mM Spd grown under well-water (WW) or water deficit (WD). Bold formatting of the font means the statistical effect on the increment or reduction; the total production is expressed as the sum of every cob produced per treatment and condition. The parameters displayed are the water use efficiency (WUE); leaf relative water content (RWC); flag leave length/width ration (L/W); cob fresh weight (g) (Cob FW); cob length, as kernels in the longitudinal line (Cob L); cob circumference, as the kernels in the perimeter at the center of the cob (circumf.); average cobs produced in a plant (Cobs/pl); the weight of 100 kernels (g) (100 K); harvest index (HI); yield (10^6g ha^{-1}) (Yield); % of carbohydrates; % of protein; and minerals (ppm) such as Ca, Zn, K, Mg, Na, P, and Cu.

accumulation of Ca. However, it is evident that product and crop specificities exist, so it is expected to respond differently to the treatments according to the genotype (Shahrajabian et al., 2021). From the human nutritional point of view, higher Ca content is an advantage because a recent study associates a dietary low calcium intake with a higher risk of all-cause mortality (Yoo et al., 2022). Altogether, we demonstrate that the exogenous application of PAs improves plant performance under stress conditions and can also be an efficient biofortification approach (Figure 7), especially in the case of Spd.

Conclusion

The polyamine application by drenching can improve maize production under optimal and stress conditions. However,

different polyamines induced different responses, conditioned by the growth conditions. Putrescine was the most effective treatment under well-watered conditions because it enhanced the fruit production, the WUE, and the content of Ca and Cu. The spermidine application showed better results under water deficit, with better water balance, water use efficiency, higher production, and better nutritional composition of the flour by increasing carbohydrates content, Cu and Ca. These results point to polyamine supplementation as an exciting approach for crop biofortification. Nevertheless, due to the different effects of genotype and product specificities, a higher effort should be put into elucidating and characterizing the use of these substances for crop and site-specific locations.

Data availability statement

The original contributions presented in this study are included in the article/**Supplementary material**, further inquiries can be directed to the corresponding author.

Author contributions

AH, DJ-A, AB, and NDD designed the idea of the project. AH, DJ-A, and SM-S performed the experiments. AH and NDD analyzed the data and wrote the manuscript. All authors agreed with the last version of the manuscript.

Funding

This work was funded by the project "Plants as a tool for sustainable global development" (Registration No: CZ.02.1.01/0.0/0.0/16_019/0000827) within the program Research, Development, and Education (OP RDE), and by the project AHIDAGRO 450 (MAC2/1.1b/279), Cooperation Programme INTERREG-MAC 2014-2020, with European Funds for Regional Development- 452 FEDER.

Acknowledgments

We thank Natalia Usenco for her technical support during field sample processing.

Conflict of interest

The authors declare that the research was conducted in the absence of any commercial or financial relationships that could be construed as a potential conflict of interest.

Publisher's note

All claims expressed in this article are solely those of the authors and do not necessarily represent those of their affiliated organizations, or those of the publisher, the editors and the reviewers. Any product that may be evaluated in this article, or claim that may be made by its manufacturer, is not guaranteed or endorsed by the publisher.

Supplementary material

The Supplementary Material for this article can be found online at: https://www.frontiersin.org/articles/10.3389/fpls.2022.944066/full#supplementary-material

References

Abbas, M., Abdel-Lattif, H., and Shahba, M. (2021). Ameliorative effects of calcium sprays on yield and grain nutritional composition of maize (*Zea mays* l.) cultivars under drought stress. *Agriculture* 11:285. doi: 10.3390/agriculture11040285

Agliassa, C., Mannino, G., Molino, D., Cavalletto, S., Contartese, V., Bertea, C. M., et al. (2021). A new protein hydrolysate-based biostimulant applied by fertigation promotes relief from drought stress *in Capsicum annuum* L. *Plant Physiol. Biochem.* 166, 1076–1086. doi: 10.1016/j.plaphy.2021.07.015

Altooq, N., Humood, A., Alajaimi, A., Alenezi, A. F., Janahi, M., AlHaj, O., et al. (2022). The role of micronutrients in the management of COIVD-19 and optimizing vaccine efficacy. *Hum. Nutr. Metabol.* 27:200141. doi: 10.1016/j.hnm.2022.200141

Anjum, S. A., Ashraf, U., Tanveer, M., Khan, I., Hussain, S., Shahzad, B., et al. (2017). Drought induced changes in growth, osmolyte accumulation and antioxidant metabolism of three maize hybrids. *Front. Plant Sci.* 8:69. doi: 10.3389/fpls.2017.00069

Aqaei, P., Weisany, W., Diyanat, M., Razmi, J., and Struik, P. C. (2020). Response of maize (*Zea mays* L.) to potassium nano-silica application under drought stress. *J. Plant Nutr.* 43, 1205–1216. doi: 10.1080/01904167.2020.1727508

Avila, R. G., Silva, E. M., Magalhães, P. C., Alvarenga, A. A., and Lavinsky, A. O. (2017). Drought changes yield and organic and mineral composition of grains of four maize genotypes. *Acad. J. Agri. Res.* 5, 243–250.

Barrs, H., and Weatherley, P. (1962). A Re-Examination of the relative turgidity technique for estimating water deficits in leaves. *Aust. J. Biol. Sci.* 15, 413–428. doi: 10.1071/bi9620413

Barutcular, C., Dizlek, H., El-Sabagh, A., Sahin, T., Elsabagh, M., and Islam, S. (2016). Nutritional quality of maize in response to drought stress during grain-filling stages in mediterranean climate condition. *J. Exp. Biol. Agri. Sci.* 4, 644–652. doi: 10.18006/2016.4(issue6).644.652

Battacharyya, D., Babgohari, M. Z., Rathor, P., and Prithiviraj, B. (2015). Seaweed extracts as biostimulants in horticulture. *Sci. Horticu.* 196, 39–48. doi: 10.1016/j.scienta.2015.09.012

Ben Mrid, R., Benmrid, B., Hafsa, J., Boukcim, H., Sobeh, M., and Yasri, A. (2021). Secondary metabolites as biostimulant and bioprotectant agents: a review. *Sci. Total Environ.* 777:146204. doi: 10.1016/j.scitotenv.2021.146204

Blum, A. (1996). "Crop responses to drought and the interpretation of adaptation," in *Drought Tolerance in Higher Plants: Genetical, Physiological and*

Molecular Biological Analysis, (Netherlands: Springer), 57–70. doi: 10.1007/978-94-017-1299-6_8

Borrás, L., Curá, J. A., and Otegui, M. E. (2002). Maize kernel composition and post-flowering source-sink ratio. *Crop Sci.* 42, 781–790. doi: 10.2135/cropsci2002.7810

Bulgari, R., Cocetta, G., Trivellini, A., Vernieri, P., and Ferrante, A. (2015). Biostimulants and crop responses: a review. *Biol. Agri. Hort.* 31, 1–17. doi: 10.1080/01448765.2014.964649

Bulgari, R., Franzoni, G., and Ferrante, A. (2019). Biostimulants application in horticultural crops under abiotic stress conditions. *Agronomy* 9, 306. doi: 10.3390/agronomy9060306

Cao, D. D., Hu, J., Zhu, S. J., Hu, W. M., and Knapp, A. (2010). Relationship between changes in endogenous polyamines and seed quality during development of sh2 sweet corn (*Zea mays* L.) seed. *Sci. Hort.* 123, 301–307. doi: 10.1016/j.scienta.2009.10.006

Chaudhary, D. P., Kumar, S., and Yadav, O. P. (2014). "Nutritive value of maize: Improvements, applications and constraints," in *Maize: Nutrition Dynamics and Novel Uses*, (Berlin: Springer India), 3–17. doi: 10.1007/978-81-322-1623-0_1

Chen, D., Shao, Q., Yin, L., Younis, A., and Zheng, B. (2019a). Polyamine function in plants: metabolism, regulation on development, and roles in abiotic stress responses. *Front. Plant Sci.* 9:1945. doi: 10.3389/fpls.2018.01945

Chen, D., Shao, Q., Yin, L., Younis, A., and Zheng, B. (2019b). Polyamine function in plants: metabolism, regulation on development, and roles in abiotic stress responses. *Front. Plant Sci.* 9:1945.

Choudhary, S., Wani, K. I., Naeem, M., Khan, M. M. A., and Aftab, T. (2022). Cellular responses, osmotic adjustments, and role of osmolytes in providing salt stress resilience in higher plants: polyamines and nitric oxide crosstalk. *J. Plant Growth Regul.* doi: 10.1007/s00344-022-10584-7 [Epub ahead of print].

Darwish, E., Hanafy Ahmed, A., Hamoda, S., and Alobaidy, M. (2013). Effect of putrescine and humic acid on growth, yield and chemical composition of cotton plants grown under saline soil conditions. *Environ. Sci.* 13, 479–497. doi: 10.5829/idosi.aejaes.2013.13.04.1965

De Diego, N., and Spíchal, L. (2020). "Use of plant metabolites to mitigate stress effects in crops," in *The Chemical Biology of Plant Biostimulants*, (Hoboken, NJ: John Wiley & Sons, Ltd), 261–300. doi: 10.1002/9781119357254.ch11

du Jardin, P. (2015). Plant biostimulants: definition, concept, main categories and regulation. *Sci. Hort.* 196, 3–14. doi: 10.1016/j.scienta.2015.09.021

Duarte-Sierra, A., Tiznado-Hernández, M. E., Jha, D. K., Janmeja, N., and Arul, J. (2020). Abiotic stress hormesis: an approach to maintain quality, extend storability, and enhance phytochemicals on fresh produce during postharvest. *Compr. Rev. Food Sci. Food Saf.* 19, 3659–3682. doi: 10.1111/1541-4337.12628

FAO (2018). *Climate Change and Food Security: Risks and Reponses. Watch Letter*. Rome, IT: Food and Agriculture Organization.

Farooq, M., Wahid, A., and Lee, D. J. (2009). Exogenously applied polyamines increase drought tolerance of rice by improving leaf water status, photosynthesis and membrane properties. *Acta Phys. Plant.* 31, 937–945. doi: 10.1007/s11738-009-0307-2

Feil, B., Moser, S. B., Jampatong, S., and Stamp, P. (2005). Mineral composition of the grains of tropical maize varieties as affected by pre-anthesis drought and rate of nitrogen fertilization. *Crop Sci.* 45, 516–523. doi: 10.2135/cropsci2005.0516

Feng, H. Y., Wang, Z. M., Kong, F. N., Zhang, M. J., and Zhou, S. L. (2011). Roles of carbohydrate supply and ethylene, polyamines in maize kernel set. *J. Integr. Plant Biol.* 53, 388–398. doi: 10.1111/j.1744-7909.2011.01039.x

García-García, A. L., García-Machado, F. J., Borges, A. A., Morales-Sierra, S., Boto, A., and Jiménez-Arias, D. (2020). Pure organic active compounds against abiotic stress: a biostimulant overview. *Front. Plant Sci.* 11:575829. doi: 10.3389/fpls.2020.575829

Garg, M., Sharma, N., Sharma, S., Kapoor, P., Kumar, A., Chunduri, V., et al. (2018). Biofortified crops generated by breeding, agronomy, and transgenic approaches are improving lives of millions of people around the world. *Front. Nutr.* 5:12. doi: 10.3389/fnut.2018.00012

da Ge, T., Sui, F. G., Nie, S., Sun, N. B., Xiao, H., and Tong, C. L. (2010). Differential responses of yield and selected nutritional compositions to drought stress in summer maize grains. *J. Plant Nutr.* 33, 1811–1818. doi: 10.1080/01904167.2010.503829

Gebremedhn, Y., and Berhanu, A. (2013). The role of seed priming in improving seed germination and seedling growth of maize (*Zea mays* L.) under salt stress at laboratory conditions. *Afr. J. Biotechnol.* 12, 6484–6490. doi: 10.5897/ajb2013.13102

González-Hernández, A. I., Scalschi, L., Vicedo, B., Marcos-Barbero, E. L., Morcuende, R., and Camañes, G. (2022). Putrescine: a key metabolite involved in plant development, tolerance and resistance responses to stress. *Intl. J. Mol. Sci.* 23:2971. doi: 10.3390/ijms23062971

Gupta, S., Agarwal, V. P., and Gupta, N. K. (2012). Efficacy of putrescine and benzyladenine on photosynthesis and productivity in relation to drought tolerance in wheat (*Triticum aestivum* L.). *Physiol. Mol. Biol. Plants* 18, 331–336. doi: 10.1007/s12298-012-0123-9

Gupta, S., and Gupta, N. (2011). Field efficacy of exogenously applied putrescine in wheat (*Triticum aestivum*) under water-stress conditions. *Indian J. Agri. Sci.* 81, 516–519.

Harrigan, G. G., Stork, L. A. G., Riordan, S. G., Ridley, W. P., MacIsaac, S., Halls, S. C., et al. (2007). Metabolite analyses of grain from maize hybrids grown in the United States under drought and watered conditions during the 2002 field season. *J. Agri. Food Chem.* 55, 6169–6176. doi: 10.1021/jf070493s

Hassan, F. A. S., Ali, E. F., and Alamer, K. H. (2018). Exogenous application of polyamines alleviates water stress-induced oxidative stress of *Rosa damascena* Miller var. trigintipetala Dieck. *South Afr. J. Bot.* 116, 96–102. doi: 10.1016/j.sajb.2018.02.399

Hoagland, D. R., and Arnon, D. I. (1938). *The Water-Culture Method for Growing Plants Without Soil*. California: University of California.

Hoebler, C., Karinthi, A., Chiron, H., Champ, M., and Barry, J. L. (1999). Bioavailability of starch in bread rich in amylose: metabolic responses in healthy subjects and starch structure. *Eur. J. Clin. Nutr.* 53, 360–366. doi: 10.1038/sj.ejcn.1600718

Hoffmann, W. A., and Poorter, H. (2002). Avoiding bias in calculations of relative growth rate. *Ann. Bot.* 90, 37–42. doi: 10.1093/aob/mcf140

Huma, B., Hussain, M., Ning, C., and Yuesuo, Y. (2019). Human benefits from maize. *Sch. J. Appl. Sci. Res.* 2, 4–7.

Hussain, S., Maqsood, M., Ijaz, M., Ul-Allah, S., Sattar, A., Sher, A., et al. (2020). Combined application of potassium and zinc improves water relations, stay green, irrigation water use efficiency, and grain quality of maize under drought stress. *J. Plant Nutr.* 43, 2214–2225. doi: 10.1080/01904167.2020.1765181

Islam, M. J., Uddin, M. J., Hossain, M. A., Henry, R., Begum, K., Sohel, A. T., et al. (2022). Exogenous putrescine attenuates the negative impact of drought stress by modulating physio-biochemical traits and gene expression in sugar beet (*Beta vulgaris* L.). *PLoS One* 17:e0262099. doi: 10.1371/journal.pone.0262099

Jiménez-Arias, D., García-Machado, F. J., Morales-Sierra, S., Luis, J. C., Suarez, E., Hernández, M., et al. (2019). Lettuce plants treated with L-pyroglutamic acid increase yield under water deficit stress. *Environ. Exp. Bot.* 158, 215–222. doi: 10.1016/j.envexpbot.2018.10.034

Jiménez-Arias, D., Morales-Sierra, S., Borges, A. A., Herrera, A. J., and Luis, J. C. (2022). New biostimulants screening method for crop seedlings under water deficit stress. *Agronomy* 12:728. doi: 10.3390/agronomy12030728

Jing, J. G., Guo, S. Y., Li, Y. F., and Li, W. H. (2019). Effects of polyamines on agronomic traits and photosynthetic physiology of wheat under high temperature stress. *Photosynthetica* 57, 912–920. doi: 10.32615/ps.2019.104

Kim, S. G., Lee, J. S., Bae, H. H., Kim, J. T., Son, B. Y., Kim, S. L., et al. (2019). Physiological and proteomic analyses of Korean F1 maize (*Zea mays* L.) hybrids under water-deficit stress during flowering. *Appl. Biol. Chem.* 62, 1–9. doi: 10.1186/s13765-019-0438-0

Kirk, P. L. (1950). Kjeldahl method for total nitrogen. *Anal. Chem.* 22, 354–358. doi: 10.1021/ac60038a038

Kiziloglu, F. M., Sahin, U., Kuslu, Y., and Tunc, T. (2009). Determining water-yield relationship, water use efficiency, crop and pan coefficients for silage maize in a semiarid region. *Irrig. Sci.* 27, 129–137. doi: 10.1007/s00271-008-0127-y

Köhne, J. S. (1989). Comparison of growth regulators paclobutrazol and uniconazole on avocado. South African Avocado Growers". *Assoc. Yearb.* 1989, 38–39.

Kuglitsch, F. G., Reichstein, M., Beer, C., Carrara, A., and Ceulemans, R. (2008). Characterisation of ecosystem water-use efficiency of european forests from eddy covariance measurements. *Biogeosci. Dis.* 5, 4481–4519. doi: 10.5194/bgd-5-4481-2008

Kutman, U. B., Yildiz, B., Ozturk, L., and Cakmak, I. (2010). Biofortification of durum wheat with zinc through soil and foliar applications of nitrogen. *Cereal Chem.* 87, 1–9. doi: 10.1094/CCHEM-87-1-0001

Landry, J., and Moureaux, T. (1980). Distribution and amino acid composition of protein groups located in different histological parts of maize grain. *J. Agri. Food Chem.* 28, 1186–1191. doi: 10.1021/jf60232a042

Li, G., Liang, Z., Li, Y., Liao, Y., and Liu, Y. (2020). Exogenous spermidine regulates starch synthesis and the antioxidant system to promote wheat grain filling under drought stress. *Acta Phys. Plant.* 42, 1–14. doi: 10.1007/s11738-020-03100-5

Li, J. S., and Vasal, S. K. (2015). Maize: quality Protein Maize. *Encycl. Food Grains* 4, 420–424. doi: 10.1016/B978-0-12-394437-5.00223-0

Li, L., Gu, W., Li, C., Li, W., Li, C., Li, J., et al. (2018). Exogenous spermidine improves drought tolerance in maize by enhancing the antioxidant defence system and regulating endogenous polyamine metabolism. *Crop Pasture Sci.* 69, 1076–1091. doi: 10.1071/CP18271

Li, Z., Zhou, H., Peng, Y., Zhang, X., Ma, X., Huang, L., et al. (2015). Exogenously applied spermidine improves drought tolerance in creeping bentgrass associated with changes in antioxidant defense, endogenous polyamines and phytohormones. *Plant Growth Regul.* 76, 71–82. doi: 10.1007/s10725-014-9978-9

Liang, Y.-L., and Lur, H.-S. (2002). Conjugated and free polyamine levels in normal and aborting maize kernels. *Crop Sci.* 42, 1217–1224. doi: 10.2135/cropsci2002.1217

Liu, C. J., Wang, H. R., Wang, L., Han, Y. Y., Hao, J. H., and Fan, S. X. (2018). "Effects of different types of polyamine on growth, physiological and biochemical nature of lettuce under drought stress," in *Proceedings of IOP Conference Series: Earth and Environmental Science*, (Bristol, EN: IOP Publishing), 012010. doi: 10.1088/1755-1315/185/1/012010

Liu, D. Y., Liu, Y. M., Zhang, W., Chen, X. P., and Zou, C. Q. (2019). Zinc uptake, translocation, and remobilization in winter wheat as affected by soil application of zn fertilizer. *Front. Plant Sci.* 10:426. doi: 10.3389/fpls.2019.00426

Liu, Y., Liang, H., Lv, X., Liu, D., Wen, X., and Liao, Y. (2016). Effect of polyamines on the grain filling of wheat under drought stress. *Plant Phys. Biochem.* 100, 113–129. doi: 10.1016/j.plaphy.2016.01.003

Loy, D. D., and Lundy, E. L. (2018). "Nutritional properties and feeding value of corn and its coproducts," in *Corn: Chemistry and Technology*, 3rd Edn, (Saint Paul, MA: AACC International Press), 633–659. doi: 10.1016/B978-0-12-811971-6.00023-1

Lu, D., Cai, X., Zhao, J., Shen, X., and Lu, W. (2015). Effects of drought after pollination on grain yield and quality of fresh waxy maize. *J.Sci. Food Agri.* 95, 210–215. doi: 10.1002/jsfa.6709

Maiti, R., and Pramanik, K. (2013). Vegetable seed priming?: a low cost, simple and powerful techniques for farmers' livelihood. *Intl. J. Bio Res. Stress Manag.* 4, 475–481.

Marcińska, I., Dziurka, K., Waligórski, P., Janowiak, F., Skrzypek, E., Warchoł, M., et al. (2020). Exogenous polyamines only indirectly induce stress tolerance in wheat growing in hydroponic culture under polyethylene glycol-induced osmotic stress. *Life* 10, 1–20. doi: 10.3390/life10080151

Menkir, A. (2008). Genetic variation for grain mineral content in tropical-adapted maize inbred lines. *Food Chem.* 110, 454–464. doi: 10.1016/j.foodchem.2008.02.025

Mostafa, H. A. M., Hassanein, R. A., Khalil, S. I., El-Khawas, S. A., El-Bassiouny, H. M. S., and Abd El-Monem, A. A. (2010). Effect of arginine or putrescine on growth, yield and yield components of late sowing wheat. *J. Appl. Sci. Res.* 6, 177–183.

Ndayiragije, A., and Lutts, S. (2007). Long term exogenous putrescine application improves grain yield of a salt-sensitive rice cultivar exposed to NaCl. *Plant Soil* 291, 225–238. doi: 10.1007/s11104-006-9188-y

Orhun, G. E., Onsekiz, Ç, Üniversitesi, M., and Orhun, G. E. (2013). Maize for Life. *Intl. J. Food Sci. Nutr. Eng.* 3, 13–16. doi: 10.5923/j.food.20130302.01

Pál, M., Majláth, I., Németh, E., Hamow, K. Á, Szalai, G., Rudnóy, S., et al. (2018). The effects of putrescine are partly overlapping with osmotic stress processes in wheat. *Plant Sci.* 268, 67–76. doi: 10.1016/j.plantsci.2017.12.011

Parkunan, V., Johnson, C. S., and Eisenback, J. D. (2011). Influence of acibenzolar- S-Methyl and mixture of *Bacillus* species on grwoth and vigor of cultivated tobacco. *Tob. Sci.* 48, 7–14. doi: 10.3381/10-010.1

Paul, K., Sorrentino, M., Lucini, L., Rouphael, Y., Cardarelli, M., Bonini, P., et al. (2019). A combined phenotypic and metabolomic approach for elucidating the biostimulant action of a plant-derived protein hydrolysate on tomato grown under limited water availability. *Front. Plant Sci.* 10:493. doi: 10.3389/fpls.2019.00493

Podlešáková, K., Ugena, L., Spíchal, L., Doležal, K., and De Diego, N. (2019). Phytohormones and polyamines regulate plant stress responses by altering GABA pathway. *New Biotechnol.* 48, 53–65. doi: 10.1016/j.nbt.2018.07.003

Rajput, V. D., Minkina, T., Suskova, S., Mandzhieva, S., Tsitsuashvili, V., Chapligin, V., et al. (2018). Effects of Copper Nanoparticles (CuO NPs) on Crop Plants: a Mini Review. *BioNanoSci.* 8, 36–42. doi: 10.1007/s12668-017-0466-3

Ramazan, S., Nazir, I., Yousuf, W., and John, R. (2022). Environmental stress tolerance in maize (*Zea mays*): role of polyamine metabolism. *Funct. Plant Biol.* doi: 10.1071/FP21324 [Epub ahead of print].

Rao, N. K. S., Laxman, R. H., and Shivashankara, K. S. (2016). "Physiological and morphological responses of horticultural crops to abiotic stresses," in *Abiotic Stress Physiology of Horticultural Crops*, (Berlin: Springer), 3–18. doi: 10.1007/978-81-322-2725-0_1

Saleethong, P., Sanitchon, J., Kong, -Ngern, K., and Theerakulpisut, P. (2013). Effects of exogenous spermidine (Spd) on yield, yield-related parameters and mineral composition of rice (*Oryza sativa* L. ssp.' indica') grains under salt stress. *Aust. J. Crop Sci.* 7, 1293–1301. doi: 10.3316/informit.619809711947641

Savvides, A., Ali, S., Tester, M., and Fotopoulos, V. (2016). Chemical priming of plants against multiple abiotic stresses: mission possible? *Trends Plant Sci.* 21, 329–340. doi: 10.1016/j.tplants.2015.11.003

Seleem, E. A., Ibrahim, H. M. S., and Taha, Z. K. (2021). Exogenous application of ascorbic acid and putrescine: a natural eco-friendly potential for alleviating NaCl stress in barley (*Hordeum vulgare*). *Emirates J. Food Agri.* 33, 657–670. doi: 10.9755/ejfa.2021.v33.i8.2742

Shahrajabian, M. H., Chaski, C., Polyzos, N., and Petropoulos, S. A. (2021). Biostimulants application: a low input cropping management tool for sustainable farming of vegetables. *Biomolecules* 11:698. doi: 10.3390/biom11050698

Sorrentino, M., De Diego, N., Ugena, L., Spíchal, L., Lucini, L., Miras-Moreno, B., et al. (2021). Seed priming with protein hydrolysates improves Arabidopsis growth and stress tolerance to abiotic stresses. *Front. Plant Sci.* 12:626301. doi: 10.3389/fpls.2021.626301

Ugena, L., Hýlová, A., Podlešáková, K., Humplík, J. F., Doležal, K., Diego, N., et al. (2018). Characterization of biostimulant mode of action using novel multi-trait high-throughput screening of arabidopsis germination and rosette growth. *Front. Plant Sci.* 9:1327. doi: 10.3389/fpls.2018.01327

Ullah, F., Bano, A., and Nosheen, A. (2012). Effects of plant growth regulators on growth and oil quality of canola (*Brassica napus* L.) under drought stress. *Pakistan J. Bot.* 44, 1873–1880.

Van Oosten, M. J., Pepe, O., De Pascale, S., Silletti, S., and Maggio, A. (2017). The role of biostimulants and bioeffectors as alleviators of abiotic stress in crop plants. *Chem. Biol. Technol. Agri.* 4, 1–12. doi: 10.1186/s40538-017-0089-5

Viets, F. G. (1962). Fertilizers and the efficient use of water. *Adv. Agron.* 14, 223–264. doi: 10.1016/S0065-2113(08)60439-3

White, P. J., and Broadley, M. R. (2009). Biofortification of crops with seven mineral elements often lacking in human diets - Iron, zinc, copper, calcium, magnesium, selenium and iodine. *New Phytol.* 182, 49–84. doi: 10.1111/j.1469-8137.2008.02738.x

XiaoKang, L., XiaoXia, W., YunCheng, L., and Yang, L. (2016). Effect of exogenous polyamines on mechanism of floret degeneration in wheat. *Acta Agron. Sinica* 42, 1391–1401.

Xu, L., and Geelen, D. (2018). Developing biostimulants from agro-food and industrial by-products. *Front. Plant Sci.* 871:1567. doi: 10.3389/fpls.2018.01567

Xu, Y., Qiu, M., Li, Y., Qian, X., Gu, J., and Yang, J. (2016). Polyamines mediate the effect of post-anthesis soil drying on starch granule size distribution in wheat kernels. *Crop J.* 4, 444–458. doi: 10.1016/j.cj.2016.05.004

Yakhin, O. I., Lubyanov, A. A., Yakhin, I. A., and Brown, P. H. (2017). Biostimulants in plant science: a global perspective. *Front. Plant Sci.* 7:2049. doi: 10.3389/fpls.2016.02049

Yang, W., Li, Y., Yin, Y., Qin, Z., Zheng, M., Chen, J., et al. (2017). Involvement of ethylene and polyamines biosynthesis and abdominal phloem tissues characters of wheat caryopsis during grain filling under stress conditions. *Sci. Rep.* 7:46020. doi: 10.1038/srep46020

Yang, W., Qin, Z., Sun, H., Liao, X., Gao, J., Wang, Y., et al. (2020). Yield-related agronomic traits evaluation for hybrid wheat and relations of ethylene and polyamines biosynthesis to filling at the mid-grain filling stage. *J. Integr. Agri.* 19, 2407–2418. doi: 10.1016/S2095-3119(19)62873-X

Yoo, J. Y., Cho, H. J., and Lee, J. E. (2022). Lower dietary calcium intake is associated with a higher risk of mortality in Korean adults. *J. Acad. Nutr. Diet.* S2212–S2672. doi: 10.1016/j.jand.2022.02.012

Yu, Z., Jia, D., and Liu, T. (2019). Polyamine oxidases play various roles in plant development and abiotic stress tolerance. *Plants* 8:184. doi: 10.3390/plants8060184

Zhang, H., Han, M., Comas, L. H., Dejonge, K. C., Gleason, S. M., Trout, T. J., et al. (2019). Response of maize yield components to growth stage-based deficit irrigation. *Agron. J.* 111, 3244–3252. doi: 10.2134/agronj2019.03.0214

Zhang, H., Li, Y., and Zhu, J. K. (2018). Developing naturally stress-resistant crops for a sustainable agriculture. *Nat. Plants* 4, 989–996. doi: 10.1038/s41477-018-0309-4

Zhao, X., Tong, C., Pang, X., Wang, Z., Guo, Y., Du, F., et al. (2012). Functional mapping of ontogeny in flowering plants. *Brief Bioinform.* 13, 317–328. doi: 10.1093/bib/bbr054

frontiers | Frontiers in Plant Science

TYPE Original Research
PUBLISHED 15 September 2022
DOI 10.3389/fpls.2022.960750

OPEN ACCESS

EDITED BY
Maurizio Ruzzi,
University of Tuscia,
Italy

REVIEWED BY
Jiahong Ren,
Changzhi University,
China
Guan-Xi Li,
Qufu Normal University, China

*CORRESPONDENCE
Xiao-Qin Wu
xqwu@njfu.edu.cn

SPECIALTY SECTION
This article was submitted to Plant Nutrition, a section of the journal Frontiers in Plant Science

RECEIVED 03 June 2022
ACCEPTED 19 August 2022
PUBLISHED 15 September 2022

CITATION
Kong W-L, Wang Y-H, Lu L-X, Li P-S, Zhang Y and Wu X-Q (2022) *Rahnella aquatilis* JZ-GX1 alleviates iron deficiency chlorosis in *Cinnamomum camphora* by secreting desferrioxamine and reshaping the soil fungal community. *Front. Plant Sci.* 13:960750. doi: 10.3389/fpls.2022.960750

Rahnella aquatilis JZ-GX1 alleviates iron deficiency chlorosis in *Cinnamomum camphora* by secreting desferrioxamine and reshaping the soil fungal community

Wei-Liang Kong[1,2], Ya-Hui Wang[1,2], Lan-Xiang Lu[1,2], Pu-Sheng Li[1,2], Yu Zhang[1,2] and Xiao-Qin Wu[1,2]*

[1]Co-Innovation Center for Sustainable Forestry in Southern China, College of Forestry, Nanjing Forestry University, Nanjing, Jiangsu, China, [2]Jiangsu Key Laboratory for Prevention and Management of Invasive Species, Nanjing Forestry University, Nanjing, Jiangsu, China

Plant growth-promoting rhizobacteria are important for improving plant iron nutrition, but the interactions among inoculants, host plants and soil microorganisms have not been greatly explored. *Rahnella aquatilis* JZ-GX1 was applied to treat the increasingly serious iron deficiency chlorosis in *Cinnamomum camphora*, and the resulting improvement in chlorosis was determined by assessing the contents of chlorophyll, active iron, Fe^{2+} and antioxidant enzymes in leaves, the effects on the soil microbial community and the metabolism in the rhizosphere by high-throughput sequencing techniques and liquid chromatography–mass spectrometry (LC–MS). The results showed that inoculation with JZ-GX1 significantly increased the chlorophyll content of *C. camphora*, which promoted the redistribution of active iron in roots and leaves, increased the activities of superoxide dismutase (SOD), peroxidase (POD), catalase (CAT) and ascorbate peroxidase (APX), and thus reduced membrane damage in iron-deficient *C. camphora* caused by reactive oxygen species. According to genome prediction and ultra-performance liquid chromatography–mass spectrometry (UPLC–MS) analysis, the JZ-GX1 strain could secrete desferrioxamine (DFO), and the concentration of DFO in *C. camphora* rhizosphere was 21-fold higher than that in uninoculated soil. The exogenous application of DFO increased the SPAD and Fe^{2+} contents in leaves. In addition, the inoculant affected the fungal community structure and composition in the *C. camphora* rhizosphere soil and increased the abundances of specific taxa, such as *Glomus*, *Mortierella*, *Trichoderma,* and *Penicillium*. Therefore, *R. aquatilis* JZ-GX1 application promoted iron absorption in *C. camphora* trees by secreting DFO and alleviated iron deficiency chlorosis through interactions with the local fungal community.

KEYWORDS

***Cinnamomum camphora*, iron deficiency chlorosis, *Rahnella aquatilis*, microbial community, desferrioxamine**

Introduction

Iron is one of the most important trace elements in many living organisms and mainly exists as Fe^{2+} and Fe^{3+} in nature (Liu et al., 2017). The transformation between these forms is an important redox process in living cells, and the availability and content of iron play important roles in the growth and development of plants (Ferreira et al., 2019). Although iron is abundant in the Earth's crust, ranking fourth among all elements on the Earth's surface, the solubility of iron in soil is very low due to oxidation by oxygen in the atmosphere, drought and the alkalinity of semidry calcareous soil; thus, the absorption of iron by plants is difficult (Zhou et al., 2016). The concentration of free soluble iron in soil is $<10^{-17}$ M, which is markedly lower than the optimal value for plant growth (Arikan et al., 2018). Plants growing in these soils often show iron deficiency chlorosis, which seriously affects the yield of crops (Aras et al., 2018). Therefore, iron deficiency stress has become a global problem. Over the years, researchers have also introduced many control measures to solve this problem, including soil application, trunk injection, and foliar spraying of various inorganic, organic and chelated iron fertilizers (Farshchi et al., 2021). However, these methods have many problems, such as causing slight damage to trees and environmental pollution and high cost; thus, no economic and effective method for the prevention and control of iron deficiency chlorosis in plants has been developed (Li M. et al., 2021).

A large number of microorganisms are found in plant rhizosphere soil, and among these, the bacteria beneficial to plants are called plant growth-promoting rhizobacteria (PGPR). Many studies have shown that PGPR can secrete a series of substances, including siderophores, organic acids, and volatiles, to help plants cope with iron deficiency stress (Radzki et al., 2013; Martinez-Medina et al., 2017). For example, Liu et al. (2017) effectively controlled the yellowing associated with iron deficiency in peanuts and peaches through the use of siderophore-producing bacteria. Aras et al. (2018) studied the effect of PGPR on the uptake of iron by peach trees in calcareous soil and found that the absorption and transport of malic acid released by bacteria in the rhizosphere effectively reduced the pH of leaves and that the organic acid secreted by *Azospirillum brasilense* significantly reduced the pH of cucumber hydroponic nutrient solution and increased the activity of Fe^{3+} reductase in cucumber roots. However, the mechanisms through which microorganisms promote plant iron absorption are currently mostly limited to the phenotypic and physiological responses of host plants, and few studies have investigated the changes in indigenous soil microbial communities after inoculation with exogenous bacterial agents. The effects of most microorganisms on plants in nature are accomplished through interactions (Niu et al., 2021). Due to the influence of biological and environmental factors, the effects of inocula are often not ideal. The interaction between the plant rhizosphere and microorganisms is very complex. Whether a single exogenous bacterial agent can adapt to the indigenous microbial community and exert its plant growth-promoting characteristics is currently unclear. Therefore, understanding the interactions among plants, inocula and local microorganisms is of great significance.

In recent years, with the rise and development of genomics technology, an increasing number of studies have used genomic, transcriptome, metabolome and microbiome sequencing techniques to comprehensively and deeply study the interaction mechanisms between PGPR and plants or the soil microbial community (Gamez et al., 2019; Luo et al., 2020; Yang et al., 2020; Ye et al., 2020; Priya et al., 2021). For example, Li F. et al. (2020) combined transcriptome and microbiome analyses and revealed that the rare fungus *Mortierella capitata* can promote crop growth directly by altering root gene expression levels and indirectly *via* interaction with indigenous rhizosphere bacteria. Tao et al. (2020) combined high-throughput sequencing, culturable microbiome, key microbial return and community interaction experiments and found that *Bacillus amyloliquefaciens* W19 enhanced multispecies root colonization in coordination with specific probiotic *Pseudomonas* populations in the tomato rhizosphere in the treatment of tomato bacterial wilt to ultimately result in the formation of a probiotic community that effectively helps plants resist pathogen infection. Tsai and Schmidt (2017) showed that coumarin secreted by plants is favorable for the interactions between plants and microbial communities under iron restriction. These special metabolites change the composition of root microorganisms and are necessary for plant iron uptake and immune regulation mediated by microbial communities.

Cinnamomum camphora, which belongs to Lauraceae, is the main component of subtropical evergreen broad-leaved forests and a famous tree species in landscapes (Zhong et al., 2019). Due to its good appreciation, pruning resistance, strong sprouting ability and excellent cultural value, *C. camphora* has become one of the dominant tree species in landscaping, has been widely used in parks, green spaces, street trees and courtyard greening (Chen et al., 2020) and has played an important role in improving the ecological environment of cities. *Cinnamomum camphora* contains unique chemicals and is affected by few diseases and insect pests, but due to heavy planting, lack of management and the area not suitable for the growth of the species, *C. camphora* etiolation is becoming increasingly serious in many places (Zhou H. et al., 2017; Duan et al., 2020). *Cinnamomum camphora* iron deficiency etiolation is generally characterized by varying degrees of leaf yellowing, poor tree potential, white and thin leaves in severe cases, scorched and withered spots on the tip and edge of leaves, and vulnerability to frost injury; the yellowed leaves are initially locally distributed only on the crown, and the number then increases gradually, resulting in yellowing of the whole crown, withering of shoots, sparseness of branches and leaves, shrinking of the crown, gradual exhaustion and death, which seriously affects the economic and ecological benefits of the species (Kong et al., 2020a).

The etiolation of *C. camphora* is pervasive and widespread. Researchers usually explore the cause of the disease from the perspective of the soil pH and element content, whereas the

microbial community in the underground part of *C. camphora* has rarely been investigated. In this study, nontargeted metabolic technology based on LC–MS was used to characterize the secretion and metabolism of *Rahnella aquatilis* JZ-GX1 in the rhizosphere of *C. camphora* and to identify the key substances that may affect the uptake of iron by *C. camphora*. From the point of view of soil microecology, we aimed to clarify the mechanism through which *R. aquatilis* JZ-GX1 alleviates the etiolation of *C. camphora*. A microbial amplification technique was also used to explore the effect of the JZ-GX1 strain on the community structure and composition of bacteria and fungi in the rhizosphere of *C. camphora* and to explore the soil microbial inducement that may lead to the etiolation of *C. camphora* with the aim of providing a scientific solution for the management of the disease.

Materials and methods

Plant materials, growth conditions and pot experimental design

Rahnella aquatilis JZ-GX1 (CCTCC M2012439) was isolated from the rhizosphere soils of *Pinus massoniana* in Guangxi, China, and identified by 16S rRNA sequencing (GenBank No. KC351183.1). This bacterial strain was inoculated into Luria-Bertani (LB) liquid medium and incubated in an orbital shaker (200 rpm) at 28°C for 18 h. Bacteria were collected by centrifugation at 8,000 rpm and 4°C for 15 min. The centrifuge tubes were washed with 0.1 M phosphate-buffered saline (PBS, pH 7.2), and the bacteria were then diluted to obtain 1×10^7 CFUs/ml for microbial inoculation (Kong et al., 2020b).

Three-year-old *C. camphora* seedlings were purchased from a nursery and planted in plastic pots (Φ15 × 20 cm) containing 2 kg of saline-alkali soil. The soil properties were as follows: pH 8.2; organic matter, 7.89 g/kg; available N, 37.61 mg/kg; available P, 16.07 mg/kg; available K, 153.01 mg/kg and effective Fe, 6.14 mg/kg. All the plants were cultured at 25°C under a 12-h light/12-h dark cycle until the seedlings started to exhibit yellowing. Subsequently, 60 *C. camphora* seedlings were selected, divided into three groups (20 plants per group) and administered one of the following treatments: (1) 0.1 M PBS, (2) 1.2% iron sulfate ($FeSO_4$), and (3) 10^7 CFUs/mL *R. aquatilis* JZ-GX1 suspended in PBS. The plant roots in each pot were inoculated with 50 ml of the treatment solution, and the plants were then watered daily until harvesting of the plant tissues. The harvested samples were used for various physiological and biochemical analyses.

Determination of the Chl and Fe concentrations in *Cinnamomum camphora* plants

After 30 days, the concentrations of Chl in the leaves were determined according to the method described by Zhang et al. (2009). Fresh leaf tissue (0.5 g) was extracted with 2 ml of 95% (v/v) ethanol for 24 h in the dark. The concentrations of Chl a, Chl b, and carotenoids in the extract were determined by reading the absorbances at 665, 649, and 470 nm, respectively, with a spectrophotometer (UNICOWFUV-2000, Unico, United States).

After harvest, the plants were separated into leaves, shoots and roots. Approximately 0.2 g of plant material was individually digested in 1 mol/L HCl at a 1:10 ratio (v/v) for the extraction of active Fe (Koseoglu and Acikgoz, 1995). Improved NH_4F masking method was used for the extraction of Fe^{2+} from the fresh samples. The concentrations of active Fe and Fe^{2+} in the digested solution were then determined with O-phenanthroline spectrophotometry (Ni et al., 2015).

Determination of the MDA, EL, O_2^-, and H_2O_2 levels in leaves

To analyse the mitigation of microbe-mediated iron deficiency stress in planted soil, the stress-related levels of malonaldehyde (MDA) and reactive oxygen species (ROS) in leaves were investigated (Chen et al., 2015). Young leaves on the top of the *C. camphora* trees were collected after 3, 5, 10, and 20 days of the different treatments. Malonaldehyde was extracted from leaves with 10% trichloroacetic acid, and its concentration was determined based on the absorbances at 450, 532, and 600 nm (Xu et al., 2008). The formation rate of O_2^- (Elstner and Heupel, 1976) and the level of H_2O_2 (Mukherjee and Choudhuri, 1983) in leaves were determined based on the absorbances at 530 and 436 nm, respectively. The values of electrolyte leakage (EL) were determined according to the method reported by Jiang and Zhang (2001).

Determination of antioxidant enzyme activity in leaves

To verify the levels of O_2^- and H_2O_2, ROS-scavenging antioxidant enzymes were extracted from leaves according to methods described by Liu et al. (2010). The activities of superoxide dismutase (SOD), catalase (CAT), peroxidase (POD) and ascorbate peroxidase (APX) were determined based on the absorbances at 560, 240, 470, and 340 nm, respectively (Beauchamp and Fridovich, 1971; Aebi, 1984; Zhu et al., 2004; Li J. et al., 2020). To calculate the activities of antioxidant enzymes, the protein content in each of the enzyme extracts was determined based on the absorbance at 595 nm (Bradford, 1976).

Prediction of secondary metabolites of *Rahnella aquatilis* JZ-GX1

The complete genome sequence of *R. aquatilis* JZ-GX1 has been deposited in the NCBI under GenBank accession number

SAMN18652319, and the secondary metabolites of the JZ-GX1 strain were predicted using antiSMASH online prediction software.[1] The complete gene cluster information for siderophore synthesis in the JZ-GX1 genome was determined and mapped. The secondary metabolites of JZ-GX1 and other bacteria were compared and analyzed (Blin et al., 2019).

Gene expression related to siderophore biosynthesis of JZ-GX1 under Fe deficiency

Strain JZ-GX1 was inoculated into 20 ml of MSA medium (per liter: 20 g of sucrose, 2 g of L-asparagine, 1 g of K_2HPO_4, 0.5 g of $MgSO_4{\cdot}7H_2O$) with or without 20 μM $FeCl_3{\cdot}6H_2O$ for 24 h and centrifuged at 12,000 rpm for 5 min. The bacterial cells were collected, rinsed with sterile water, frozen in liquid nitrogen, and stored at −80°C for RNA isolation. Total RNA of JZ-GX1 was extracted using a bacterial RNA extraction kit (Jiancheng Bioengineering Institute, Nanjing, China). After the detection of RNA quality and concentration, cDNA samples were prepared using HiScript II Q Select RT SuperMix for RT–qPCR (CAT: 11202ES08; Yeasen, Shanghai, China). The expression levels of related genes were calculated using ABI 7500 software (Applied Biosystems, United States), and *atpD* was used as an internal control (Li P. et al., 2021). These gene primers are shown in Supplementary Table S1.

Ultra-performance liquid chromatography–mass spectrometry spectrometric analysis

The crude siderophore extract of *R. aquatilis* JZ-GX1 was syringe-filtered using a 0.22-μm nylon filter. Filtrates were injected into a UHPLC instrument (U3000, Thermo Scientific, Germany) with a Wates BEH C18 Column (150 × 2.1 mm, 1.7 μm, United States) at 35°C, and the instrument was connected to a mass spectrometer (TripleTOF® 5600+, AB Sciex, United States). The mobile phase consisted of acetonitrile:0.1% formic acid-H_2O at a ratio of 5%:95% with a 0.3 ml/min flow rate.

The positive and negative ion modes of electrospray ionization (ESI) were detected. The source conditions of ESI were as follows: Ion Source Gas 1 (Gas1): 50 charge; Ion Source Gas 2 (Gas2): 50 magical; Curtain Gas (CUR): 25; Source Temperature: 500°C (positive ion) and 450°C (negative ion); Ion Sapary Voltage Floating (ISVF): 5,500 V (positive ion) and 4,500 V (negative ion); TOF MS scan range: 100–1,200 Dajia; ion scan range product ion scan range: 50–1,000 Da; MaOF 0.2 s; MS scan accumulation time: 0.01 s; secondary mass spectrometry was performed by information-dependent acquisition (IDA). Using high sensitivity mode, declustering potential (DP): ±60 V, collision energy: 35 ± 15 eV.

Identification of metabolites in the rhizosphere soil of *Cinnamomum camphora*

Rhizosphere soil of *C. camphora* with and without inoculation with the JZ-GX1 strain was extracted in prechilled methanol (3 ml), sonicated for 30 min and centrifuged for 20 min at 4,000×*g*. The supernatant was passed through a 0.22-μm filter for liquid chromatography combined with mass spectrometry (LC–MS) analysis at Wenxin Biotechnology Co., Ltd. (Nanjing, China; Wan et al., 2018). In brief, the extracts were separated using an ultra-performance liquid chromatography (UPLC) system (Waters Corporation, Japan). The UPLC column was an ACQUITY UPLC BEH C18 column (100 mm × 2.1 mm, 1.7 μm), which was maintained at 35°C and treated with a multistep gradient for product elution over the course of 30 min at 0.4 ml/min. The gradient was composed of A (formic acid-water, containing 0.1% formic acid) and B (formic acid-acetonitrile, containing 0.1% formic acid) as follows: 0–5 min, 5% B; 5–50 min, linear gradient from 5% to 100% B; 50–60 min, 100% B. The time-of-flight mass spectrometry (TOF-MS) parameters were as follows: positive and negative ionization modes; the ion source temperature and solvent removal temperature were 120°C and 450°C, respectively; the He carrier gas was 800 L/h; the MS scanning range was 50–1,000 MHz/z; and the resolution was 30,000 (Yang et al., 2020).

Before the identification of metabolites, the original data were analyzed by peak identification, alignment, deconvolution and normalization. Following data evaluation, including quality control and principal component analysis (PCA) analysis, OPLS-DA, a supervised multivariate method, was used to maximize metabolome differences between sample pairs. Differentially accumulated metabolites (DAMs) were set at fold change (FC) > 2 or FC < 0.5 and OPLS-DA VIP ≥ 1. Volcano map construction and unsupervised PCA clustering of the identified metabolites were performed using Ezinfo 3.0. The MetaboAnalyst 4.0 software was employed to build heatmap diagrams. Subsequently, the KEGG[2] were used to construct the metabolic pathway.

High-throughput sequencing and analysis of 16S rRNA and internal transcribed spacer regions

To investigate the effects of strain JZ-GX1 on the rhizosphere microbial community, six samples were randomly selected on the 30th day from three replicates of the inoculated and uninoculated

1 https://antismash.secondarymetabolites.org/

2 http://www.genome.jp/kegg/

treatments, and two soils from the same replicate were mixed to obtain one composite sample. After removing 0–5 cm of topsoil, the soil around the root system was gently shaken off. The soil attached to the root surface was then evaluated as rhizosphere soil. The fresh soil samples were stored at −80°C before DNA extraction and microbial community analysis. Soil DNA was extracted from 0.60 g of fresh soil using a Fast DNA® Spin Kit for Soil (MP Biomedicals, CA, United States). Two universal primer sets (515F/909R and ITS1F/ITS2) were used: the former was used to amplify the prokaryotic 16S rRNA V4 region, and the latter was used to amplify the fungal internal transcribed spacer (ITS) region (Blaalid et al., 2013). The data were analyzed with the free online platform of the Majorbio Cloud Platform,[3] and the obtained prokaryotic and fungal sequences were deposited in the Sequence Read Archive (SRA) with the accession number PRJNA733870.

Estimation of root fungal colonization frequency

The 1-cm long root segments were cleared with 10% KOH solution for 100 min at 95°C, bleached with 10% hydrogen peroxide for 15 min, acidified with 0.2 mol/L hydrochloric acid for 1 h, and finally stained with 0.05% (w/v) trypan blue in lactophenol for 3 min. After microscopic observation (Zeiss Microscope System Standard 16; Carl Zeiss Ltd.; Germany), the AMF colonization rate was expressed as the percentage of the number of fungal colonized root segments over the total number of observed root segments (Yang et al., 2021).

Data analysis and processing

The data were subjected to analysis of variance (ANOVA) followed by Duncan's multiple comparison test with SPSS 21.0 software (IBM Inc., Armonk, NY, United States), or independent samples t-test to determine significant differences ($p < 0.05$). Graphs were generated using GraphPad Prism 8.0 (GraphPad Software, Inc., United States).

Results

Rahnella aquatilis JZ-GX1 alleviated iron deficiency chlorosis in *Cinnamomum camphora*

Chlorophyll is one of the most important pigments related to photosynthesis and is widely used to evaluate the status of iron stress in plants. The application of JZ-GX1 strain significantly improved the etiolation of *C. camphora* resulting from iron deficiency (Figure 1A). Compared with CK, $FeSO_4$ and inoculation treatments significantly increased the chlorophyll b, total chlorophyll and carotenoid contents of iron-deficient *C. camphora*. Among these treatments, the inoculation treatment exerted the best effect, as observed by 154.03%, 186.64%, and 80.07% increases in these contents, respectively, but had little effect on the content of chlorophyll a (Figure 1B).

Active iron is a form of iron directly absorbed and utilized by plants that can more effectively affect the iron nutritional status of plants. The iron content of *C. camphora* seedlings grown in alkaline soil was significantly lower. The $FeSO_4$ treatment significantly increased the content of active iron in roots, whereas the JZ-GX1 treatment significantly increased the content of active iron in leaves, but the two treatments exerted no significant effect on active iron in stems (Figure 1C). The supply of exogenous inorganic iron sources and microbial inoculant not only increased the content of active iron in *C. camphora* but also affected the content of Fe^{2+}. In contrast to the active iron, the JZ-GX1 treatment did not increase the content of Fe^{2+} in roots but significantly increased the content of Fe^{2+} in stems and leaves of *C. camphora* (Figure 1D), which indicated that the JZ-GX1 strain promoted the transfer of Fe^{2+} from roots to leaves.

Rahnella aquatilis JZ-GX1 reduced oxidative damage in *Cinnamomum camphora* leaves

Under normal circumstances, the production and scavenging of ROS in plants are in a dynamic equilibrium, but iron deficiency inhibits the antioxidant system and increases the production of ROS, and these effects damage electron transport in chloroplasts and mitochondria and consequently cause oxidative stress in plants. The level of ROS in *C. camphora* leaves increased gradually, peaked on the 10th day, and then decreased, and the JZ-GX1 treatment decreased the contents of O_2^- and H_2O_2 (Figures 2A,B). Electrolyte leakage analysis showed that the CK group exhibited relatively stable EL during the detection period, whereas the JZ-GX1 treatment showed some fluctuations, but the value obtained with the JZ-GX1 treatment was generally lower than that of CK (Figure 2C). Malonaldehyde is the final product of membrane lipid peroxidation in plant cells. Compared with CK, the addition of JZ-GX1 strain significantly decreased the MDA content in leaves at all tested time points with the exception of 20 days (Figure 2D).

Rahnella aquatilis JZ-GX1 enhanced the activities of antioxidant enzymes in *Cinnamomum camphora* leaves

The exposure of plants to external environmental stress leads to the production of ROS and subsequent oxidative damage. The scavenging of ROS in plants is mainly performed by some enzyme systems and antioxidants, and SOD, POD, CAT, and APX are

3 www.majorbio.com

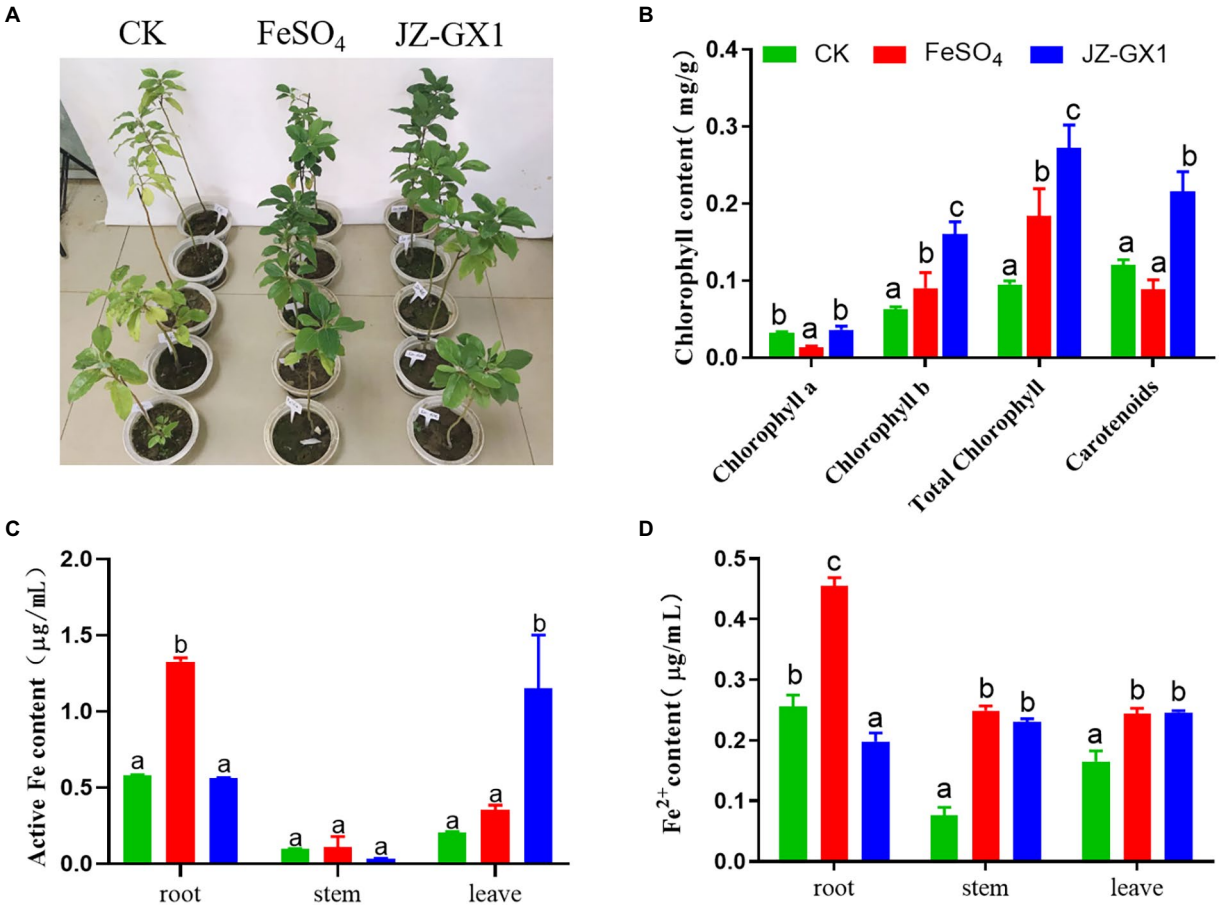

FIGURE 1
Effects of *Rahnella aquatilis* JZ-GX1 on the phenotype **(A)**, chlorophyll content **(B)**, active iron content **(C)** and Fe^{2+} content **(D)** of *Cinnamomum camphora*. The data were analyzed by one-way ANOVA followed by Duncan's post-hoc test. Different letters indicate statistically significant differences ($p<0.05$) among treatments.

important ROS-scavenging enzymes in plants. In this study, the effect of inoculation of JZ-GX1 strain on SOD enzyme activity was not obvious, only higher than that of CK on the 5th day, but lower than that of CK at other time points (Figure 3A). After the application of JZ-GX1, the activities of POD, CAT, and APX increased during culture, reached maximal levels on the 5th day, were 40.57%, 42.75%, and 21.63% higher than those obtained with the CK, respectively, and then decreased gradually but remained higher than those in the CK (Figures 3B–D).

Rahnella aquatilis JZ-GX1 secreted desferrioxamine

To explore the potential key substances of JZ-GX1 that promote iron uptake by *C. camphora*, we predicted its secondary metabolites according to its whole genome. The results showed that JZ-GX1 strain could synthesize and secrete siderophores. The comparison found that the siderophore synthesis gene cluster of JZ-GX1 strain exhibited high homology (100%) with the known DFO E synthesis gene cluster dfoJACS of *Pantoea agglomerans* (Figure 4A). In addition, at transcription level, Fe deficiency induced the upregulation of *dfoJ*, *dfoA*, *dfoC*, and *dfoS* genes in JZ-GX1 (Supplementary Figure S1).

Moreover, the supernatant organic extracts of strain JZ-GX1 were analyzed by UPLC–MS in the positive ion mode, and the mass spectrum showed a molecular ion peak at m/z 561.3599 ($[M+H]^+$), with a retention time of 4.19 min (Figure 4B), which was similar to that of the standard DFO (m/z 561.3000 ($[M+H]^+$), retention time of 4.34 min; Figure 4C). Based on the mass spectra, the compound was also identified as DFO (Supplementary Figure S2).

Application of *Rahnella aquatilis* JZ-GX1 changed the metabolite profiles in the rhizosphere soil of *Cinnamomum camphora*

To evaluate the metabolic changes in the secretions from *C. camphora* roots induced by the JZ-GX1 strain, a nontargeted

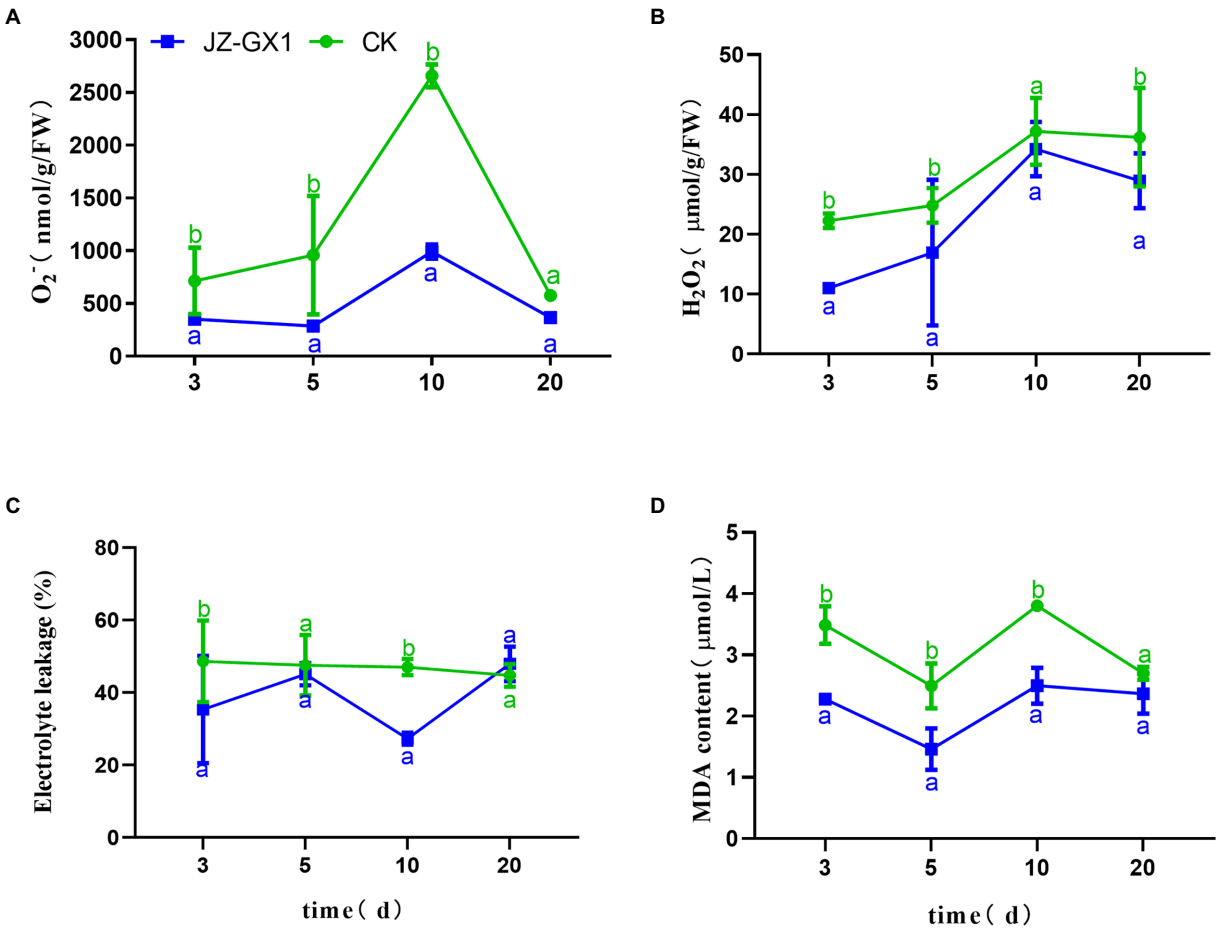

FIGURE 2
Effects of *Rahnella aquatilis* JZ-GX1 on the O_2^- **(A)**, H_2O_2 **(B)**, EL **(C)** and MDA levels **(D)** in *Cinnamomum camphora* leaves. Data are the means ± SE. Different letters indicate statistically significant differences ($p<0.05$) among treatments (*t*-test).

metabolomics detection of rhizosphere soils from etiolated and green *C. camphora* was performed based on UPLC–MS. A PCA analysis explained the metabolites of the two treatments were obviously separated on PC1, and the contribution rate of PC1 was 46.6%, the contribution rate of PC2 was 28.1%. The results from the same group of samples were concentrated, which indicated good repeatability between groups (Figure 5A). As seen in the volcano plot, a total of 381 metabolites were changed by the JZ-GX1 treatment, including 271 with increased expression and 110 with decreased expression (Figure 5B).

The main differential metabolites included phenolic acids, such as 3-O-cis-coumaroylmaslinic acid and 3-trans-caffeoyltormentic acid; amino acids, such as Arg, Cys, and His; glutinosone; tacrolimus; and other substances, such as lipoyllysine, arginyl and DFO (Figure 5C). Among the representative compounds showing significant differences, DFO exhibited 21.53-fold higher abundance in the JZ-GX1-inoculated group than in the uninoculated group (Figure 5D). According to the relatively large changes in metabolites, pathway enrichment analysis showed that the affected KEGG metabolic pathways mainly included glycolysis/gluconeogenesis, biosynthesis of isoflavonoids and phenylpropanoids, porphyrin and chlorophyll metabolism, tryptophan metabolism and biosynthesis of antibiotics (Figure 5E).

Desferrioxamine promoted iron absorption by *Cinnamomum camphora*

To explore the effects of DFO on iron absorption by *C. camphora* trees, three different concentrations of DFO were applied. The results revealed that compared with the treatment without DFO, different concentrations of DFO alleviated the iron deficiency-induced yellowing of *C. camphora* (Figure 6A). Desferrioxamine concentrations of 10, 100, and 500 μM significantly increased the SPAD value in leaves (Figure 6B). The Fe^{2+} content treated with a low concentration of DFO (10 μM) was significantly higher than that obtained with the two other concentrations (Figure 6C).

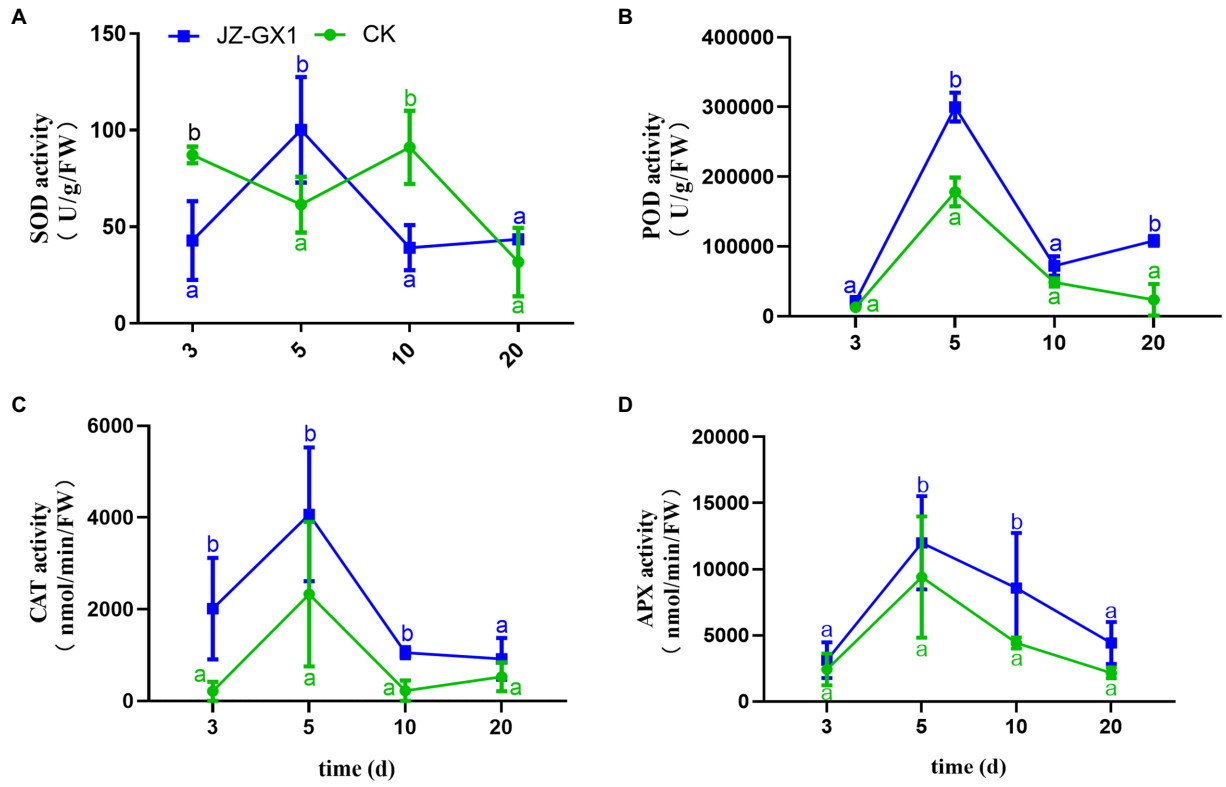

FIGURE 3
Effects of *Rahnella aquatilis* JZ-GX1 on SOD **(A)**, POD **(B)**, CAT **(C)** and APX enzyme activities **(D)** in *Cinnamomum camphora* leaves. Data are the means ± SE. Different letters indicate statistically significant differences ($p<0.05$) among treatments (*t*-test).

Effects of *Rahnella aquatilis* JZ-GX1 on microbial community composition and structure in rhizosphere of *Cinnamomum camphora*

The operational taxonomic unit (OTU) number analysis revealed a decrease in rhizosphere bacterial and fungal diversity on inoculation treatment, and the α-diversity was not affected by JZ-GX1 strain inoculation (Table 1). Regarding microbial community composition, the application increased the relative abundances of *Acidobacteriota* and *Verrucomicrobia*, slightly decreased the abundances of *Chloroflexi* and *Cyanobacteria*, and did not affect other phyla (Figure 7A). The analysis of fungal flora showed that application of the inoculum increased the relative abundances of *Basidiomycota*, *Mortierellomycota* and *Glomeromycota*, decreased the relative abundances of *Ascomycota* and *Rozellomycota*, and greatly increased the number of unclassified fungi in the rhizosphere soil of iron-deficient *C. camphora* (Figure 7B). According to the fungi functional guild (FUNGuild) prediction, the JZ-GX1 treatment also decreased the relative abundances of saprotrophic fungi, plant pathogens and animal pathogens and increased the proportions of arbuscular mycorrhizal fungi and orchid mycorrhizal (Figure 7C). The root system of *C. camphora* inoculated with JZ-GX1 formed a typical mycorrhizal structure, and a large number of arbuscules and vesicles were observed (Figures 8B–E), while the roots of most uninoculated plants were not infected by mycorrhiza (Figure 8A). The hypha colonization rate increased by 270.37% compared to CK (Figure 8F). These results indicated that the application of the JZ-GX1 strain greatly disturbed the community structure of the rhizosphere fungi of *C. camphora*.

Identification of specific fungal genera

The histogram presented in Figure 9A showed the composition of the fungal community in the rhizosphere soils of etiolated and green *C. camphora* at the genus level. Compared with those of untreated plants, the application of the JZ-GX1 strain decreased the relative abundances of *Rozellomycota*, *Nectriaceae*, *Agaricomycetes*, *Neocosmospora*, *Paraphoma*, and *Plectosphaerella* and significantly increased those of *Mortierella*, *Saitozyma*, *Penicillium*, and *Trichoderma* (Figure 9B). These microbes may be an important feature of

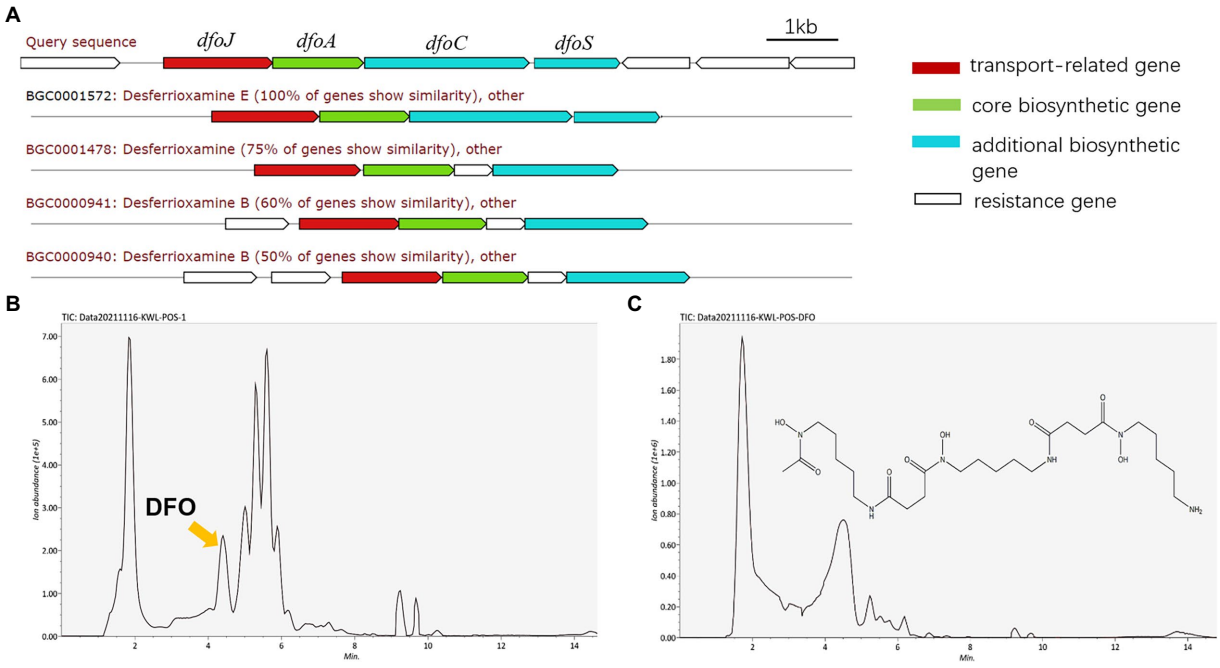

FIGURE 4
DFO, one of the predicted secondary metabolites of *Rahnella aquatilis* JZ-GX1. Biosynthetic gene cluster for DFO **(A)**, HPLC chromatogram of siderophores from JZ-GX1 culture **(B)** and DFO standard in the positive ion mode **(C)**.

the ability of the JZ-GX1 strain to alleviate *C. camphora* etiolation.

Discussion

Rahnella aquatilis JZ-GX1 reduces oxidative damage in *Cinnamomum camphora* under alkali stress by activating the antioxidant system

Under normal physiological conditions, ROS in plants are in a dynamic balance of being continuously produced and scavenged, but the exposure of plants to biotic or abiotic stress destroys this balance and increases the level of ROS (Pflugmacher et al., 2010; Wan et al., 2015; Wu et al., 2021). These increases in ROS (including H_2O_2 and O_2^-) can lead to cell membrane damage and EL and subsequently to membrane lipid peroxidation, and the degree of membrane lipid peroxidation can be reflected by the MDA content (Guo et al., 2019). In this experiment, we found that iron deficiency led to increases in the H_2O_2 and O_2^- contents in *C. camphora* leaves, which was consistent with the results obtained by Zhou C. et al. (2017) and Song et al. (2018) for peanut and chrysanthemum.

Superoxide dismutase, POD, and CAT are important active oxygen-scavenging enzymes in plants that can reduce the damage caused by membrane lipid peroxidation (Qin et al., 2018). Superoxide dismutase can catalyse the disproportionation of the superoxide anion to H_2O_2, and H_2O_2 is then decomposed into H_2O by CAT and APX (Wang et al., 2012). Peroxidase, an enzyme that is widely found in plants, contains iron in a porphyrin ring and has limited specificity. This enzyme can catalyse the decomposition of intracellular peroxidation products and plays an important role in maintaining the normal physiological function of leaves (Nounjan et al., 2021). Iron is an important cofactor in the synthesis of many enzymes. Once iron deficiency leads to decreased POD and CAT activities, plant cells accumulate more H_2O_2 (Hassan et al., 2020). In this study, the application of JZ-GX1 increased the activities of four antioxidant enzymes, reduced the production of ROS (H_2O_2 and O_2^-) and the accumulation of MDA, and effectively alleviated the oxidative stress caused by iron deficiency. In addition, due to the redox characteristics of iron ions, bioavailable Fe^{2+} is easily oxidized, and the application of JZ-GX1 improved the antioxidant capacity of trees and stabilized the transport of Fe^{2+} in plants to promote the transfer of Fe^{2+} from roots to stems and leaves compared with that observed in the CK treatment.

Desferrioxamine secreted by *Rahnella aquatilis* JZ-GX1 promotes iron absorption by *Cinnamomum camphora*

Plant growth-promoting rhizobacteria play important roles in plant growth and development and disease control and help plants cope with various abiotic stresses (such as salt, heavy metal, and drought stresses; Qin et al., 2018;

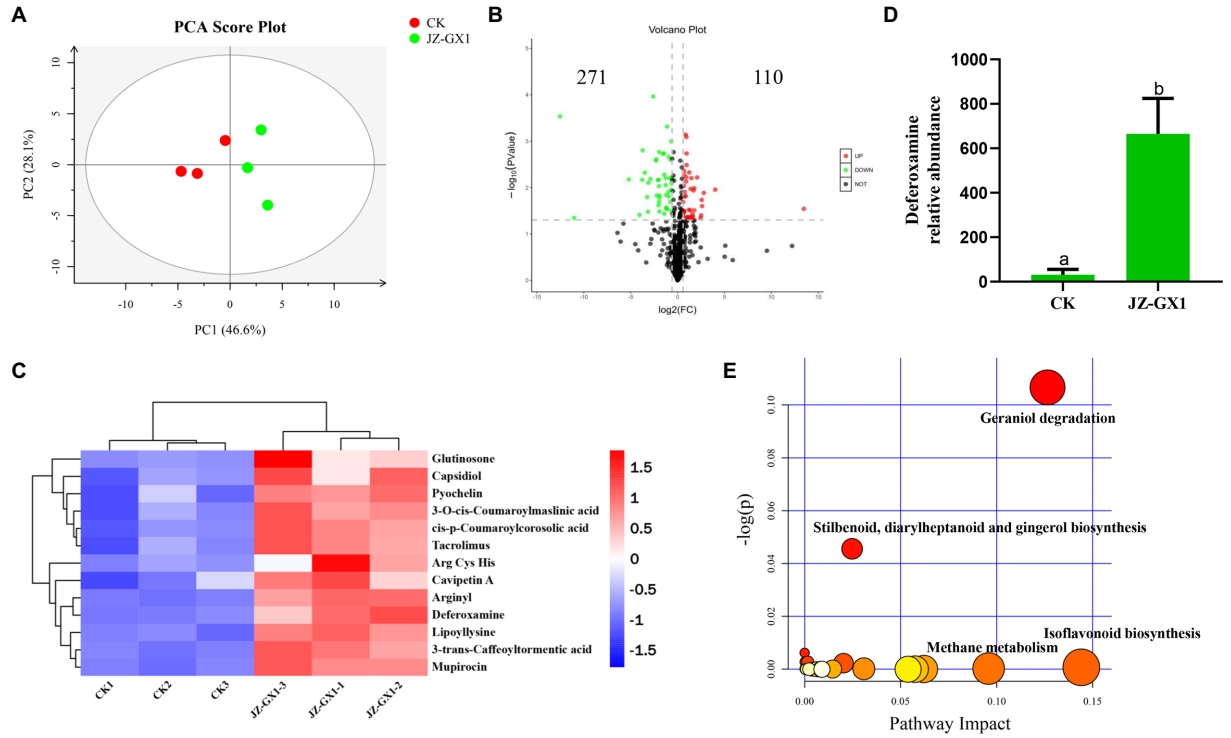

FIGURE 5
PCA analysis of the metabolites for positive mode. PC1 and PC2 are the first two principal components **(A)**, volcano plot **(B)**, heatmap analysis for the identified metabolites with significant difference being selected by PLS-DA (VIP >1, $p<0.05$) **(C)**, DFO relative abundance **(D)** and KEGG pathway analysis of the rhizosphere soil in etiolated and green *Cinnamomum camphora*. The size and color of each point represents the number of metabolites enriched in a particular pathway and the -$\log_{10}$ p-values, respectively. A larger pathway impact and –$\log_{10}$ p-values shows a greater degree of enrichment **(E)**.

Guo et al., 2020; Hassan et al., 2020). To date, most studies have focused on the secretion of active substances *in vitro* and the host responses of microorganisms, but no in-depth study has investigated how microorganisms function in complex soil environments. In this study, based on whole genome prediction and UPLC-MS spectrometric analysis, it was shown that JZ-GX1 strain could secrete DFO, and the abundance of DFO in inoculated soil was 21-fold higher than that in uninoculated soil. Desferrioxamine was the first siderophore isolated from *Streptomyces*, is the most effective iron fertilizer known thus far (Pierwola et al., 2004; Liu et al., 2019) and has been widely used as the iron source of peanut, cucumber, tobacco, wheat and other plants (Yehuda et al., 2003, 2012; Fernandez et al., 2004). Desferrioxamine secreted by JZ-GX1 strain may contribute to the iron absorption of *C. camphora*.

Iron deficiency chlorosis of *Cinnamomum camphora* may be related to the relative abundance of soil pathogenic fungi

For a long time, the physiological etiolation of *C. camphora* was considered to be related to high pH and low available iron content in soil, but the microbial flora of etiolating plant soil was ignored. The plant root microbiome is considered the second genome of plants and plays an important role in plant growth and development (Wozniak and Galazka, 2019; Cao et al., 2020). We hypothesize that the physiological etiolation of *C. camphora* may be related to the relative abundance of pathogenic fungi in its rhizosphere soil, and this hypothesis was proven by FUNGuild function prediction analysis. Iron is the core of many metabolic processes, particularly in alkaline environments, and is thus the focus of severe competition among organisms (Aznar et al., 2014). To survive, a pathogen competes for insoluble Fe^{3+} in soil; thus, the plant has less soluble iron, which results in iron deficiency chlorosis in leaves (McCully et al., 2019). In addition, a KEGG metabolic pathway analysis of soil metabolism revealed that some macrolides were highly enriched in the treatment group. JZ-GX1 promoted the secretion of antibiotics by other microorganisms, this effect could be a consequence of the change in the microbial abundance of specific taxa. Meanwhile, it cannot be excluded that DFO could also be produced by some of the microorganisms whose growth was stimulated by JZ-GX1. Therefore, exogenous beneficial microorganisms can adjust the community and structure of indigenous

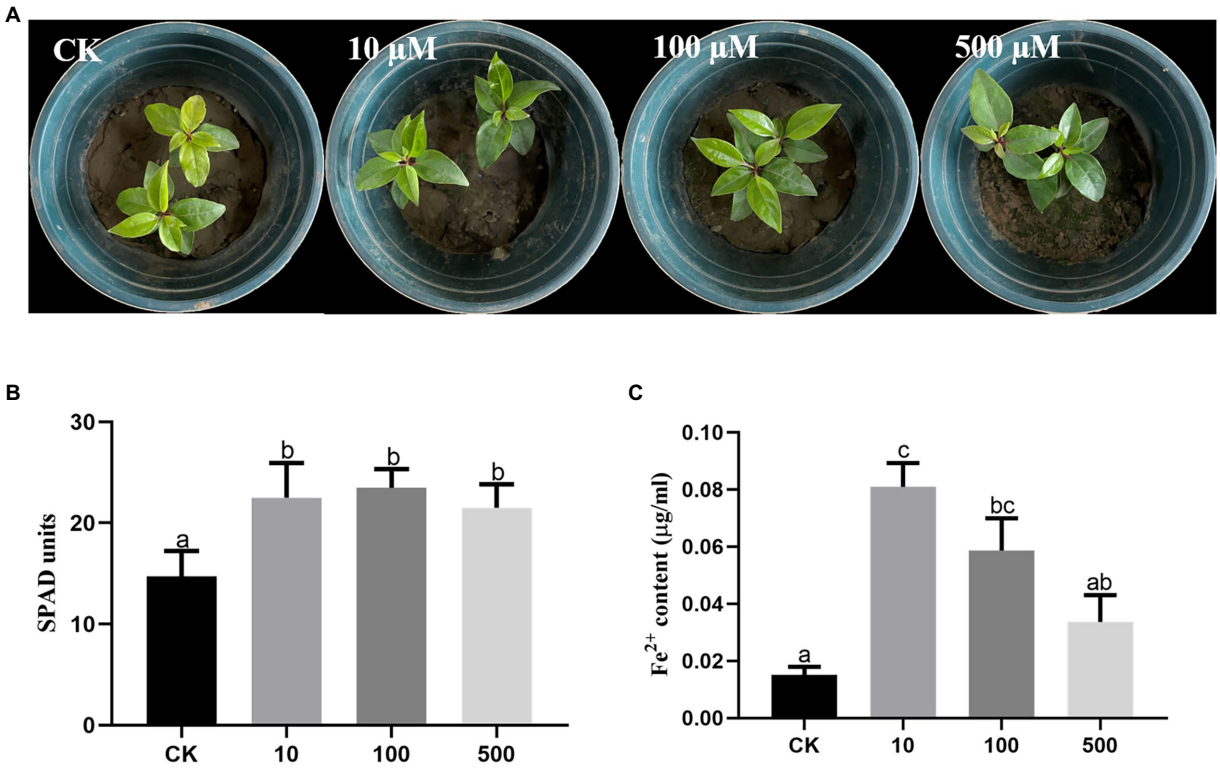

FIGURE 6
Effects of different concentrations of DFO on the growth of *Cinnamomum camphora* under iron deficiency. Plant phenotype **(A)**, SPAD **(B)** and **(C)** Fe^{2+} content. The data were analyzed by one-way ANOVA followed by Duncan's post-hoc test. Different letters indicate statistically significant differences ($p<0.05$) among treatments.

TABLE 1 Microbial α-diversity in *Rahnella aquatilis* JZ-GX1 inoculation and control treatments.

		OTU number	Shannon	Simpson	Ace	Chao1
Bacteria	Control	888[1]	6.7180 ± 0.12a	0.0046 ± 0.001a	3703.05 ± 172.72a	3692.35 ± 132.57a
	Inoculation	804[1]	6.5103 ± 0.25a	0.0058 ± 0.002a	3651.81 ± 276.79a	3632.12 ± 278.82a
Fungal	Control	190[1]	3.9162 ± 0.24a	0.0746 ± 0.02a	450.14 ± 96.34a	450.68 ± 97.19a
	Inoculation	84[1]	3.4807 ± 0.74a	0.1209 ± 0.11a	308.18 ± 72.26a	308.69 ± 72.30a

Means ± standard deviations. Same letters indicated no significant difference between control and inoculation treatments based on Student's *t*-test ($p < 0.05$). [1]Represents the OUT number.

microorganisms; this results in a decline in pathogen abundance, plants no longer lack iron, and the physiological etiolation can be alleviated.

Rahnella aquatilis JZ-GX1 regulates specific soil fungal communities by secreting DFO

Studies conducted in recent years have found that siderophores can promote the growth of some unculturable microorganisms and change the microbial community (Xavier, 2011). In view of the high abundance of DFO obtained with the JZ-GX1 treatment in this study, we speculated that the rapid and stable secretion of DFO by JZ-GX1 into the environment provides not only abundant absorbable iron but also excessive siderophores, resulting in relatively high iron concentration niches, which are beneficial to the growth of other microorganisms using homologous siderophores. Studies have shown that some fungi of *Mortierella* and *Trichoderma* can secrete hydroxamic acid siderophores, and DFO belongs to this type of siderophore (Zhao et al., 2014). Therefore, we hypothesize that the observed increases in the *Mortierella* and *Trichoderma* populations may depend on the increase in DFO abundance found in the group inoculated with the JZ-GX1 strain. In addition, the excessive secretion of DFO-bound Fe^{3+} by the JZ-GX1 strain will bring excessive redox pressure to the environment. This type of siderophore

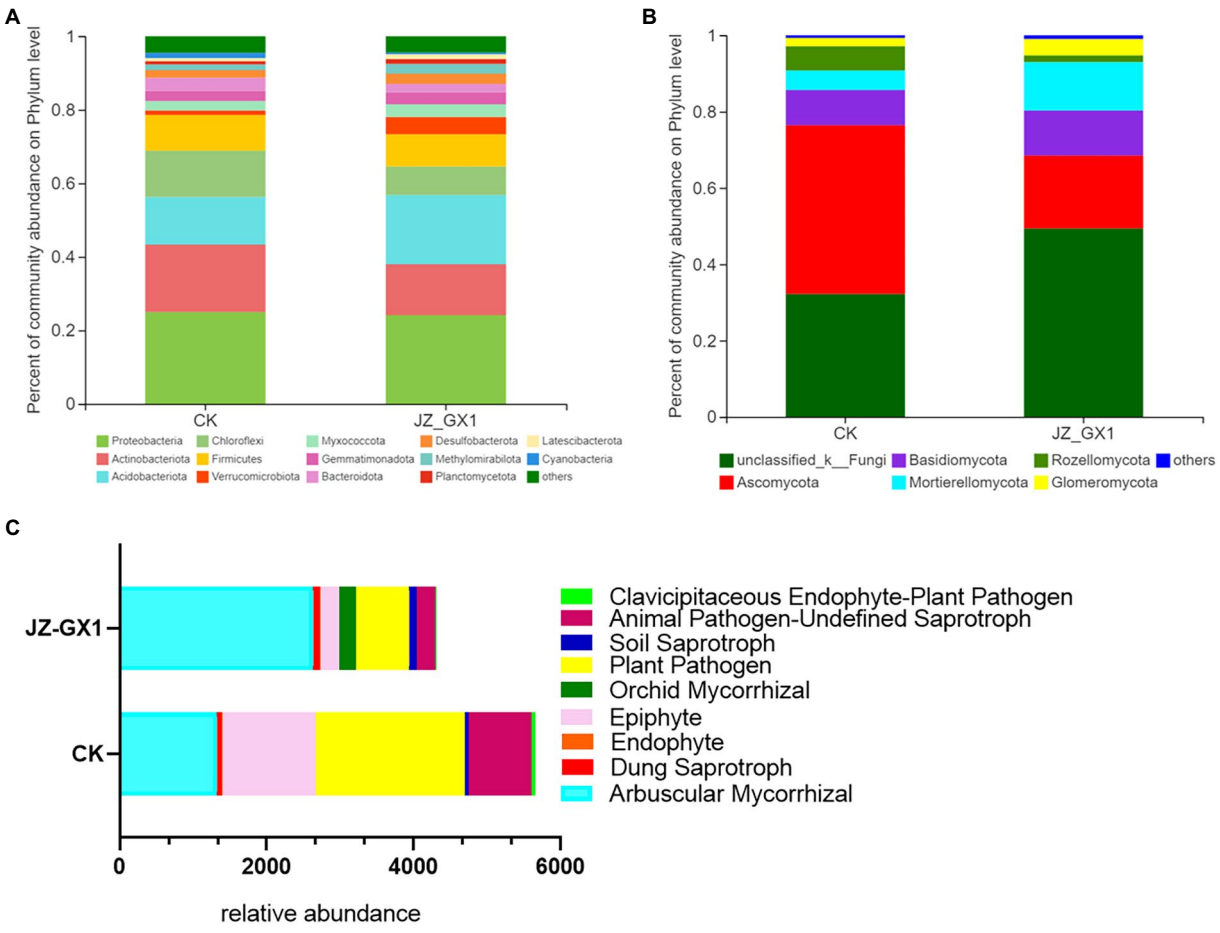

FIGURE 7
Composition and relative abundances of microorganisms in etiolated and green *Cinnamomum camphora* rhizosphere soils at the phylum level. Bacterial community structure **(A)**, fungal community structure **(B)** and FUNGuild functional prediction **(C)**.

can be recognized, absorbed and utilized by only the producer's own specific receptors on the cell membrane and not by other microorganisms, thus inhibiting the growth of some microorganisms that cannot use it (Maindad et al., 2014; Yu et al., 2017). This mechanism may explain how the JZ-GX1 strain promotes plant development as a provider of iron in the rhizosphere. Therefore, in the future, the composition of fungi and bacteria in soil can be changed by adding biological fertilizer to the plant rhizosphere, and this strategy might provide a feasible biological method for the treatment of *C. camphora* etiolation from a microbial community perspective.

Conclusion

Plant growth-promoting rhizobacteria have been widely shown to promote plant growth and stress resistance. In this study, the exogenous application of JZ-GX1 increased the contents of chlorophyll, active iron and the activities of antioxidant enzymes in leaves. After a comprehensive analysis of the microbial community structure and metabolic response of *C. camphora* rhizosphere soil after inoculation, this study proposed the possible mechanism of interactions among *R. aquatilis* JZ-GX1, native microflora and plants (Figure 10). After entering the low-iron rhizosphere soil, the JZ-GX1 strain first secretes DFO to chelate insoluble Fe^{3+} for its own needs. The Fe^{3+}-DFO complex directly provides an iron source for iron-deficient *C. camphora*. On the other hand, the removal of Fe^{3+} may limit the growth of pathogens and increase the abundances of some specific microorganisms (such as *Glomeromycota* and *Mortierella*). The mycorrhizae formed by these microorganisms indirectly promote the ability of plants to absorb iron and ultimately alleviate the etiolation of *C. camphora* caused by iron deficiency.

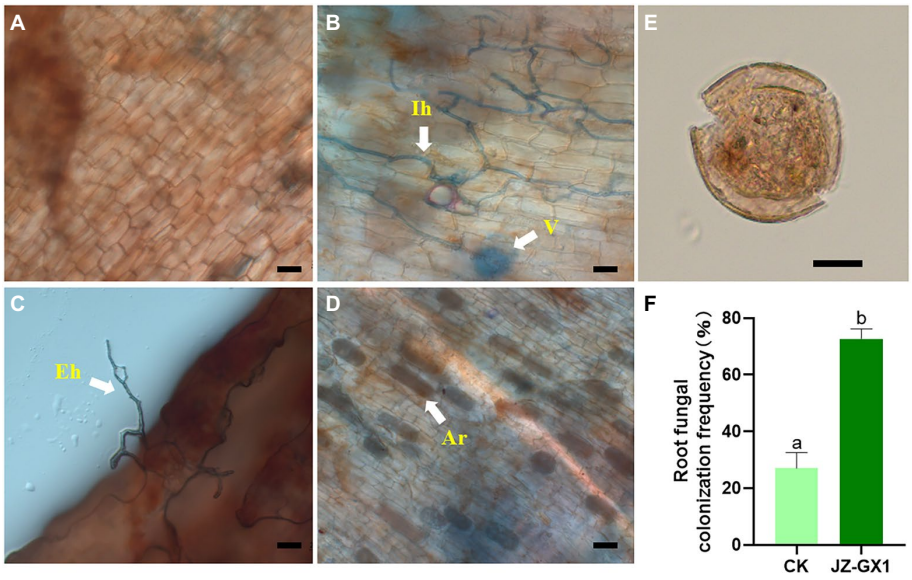

FIGURE 8
Typical structure of arbuscular mycorrhizal fungi (AMF) in the root system of *Cinnamomum camphora*. Uninfected **(A)** and infected **(B–D)** plant roots, spore morphotypes detected in the rhizosphere **(E)** and changes in root fungal colonization frequency **(F)**. Ar, arbuscule; V, vesicle; Eh, extraradical hypha; Ih, intraradical hypha. Scale bar=20μm.

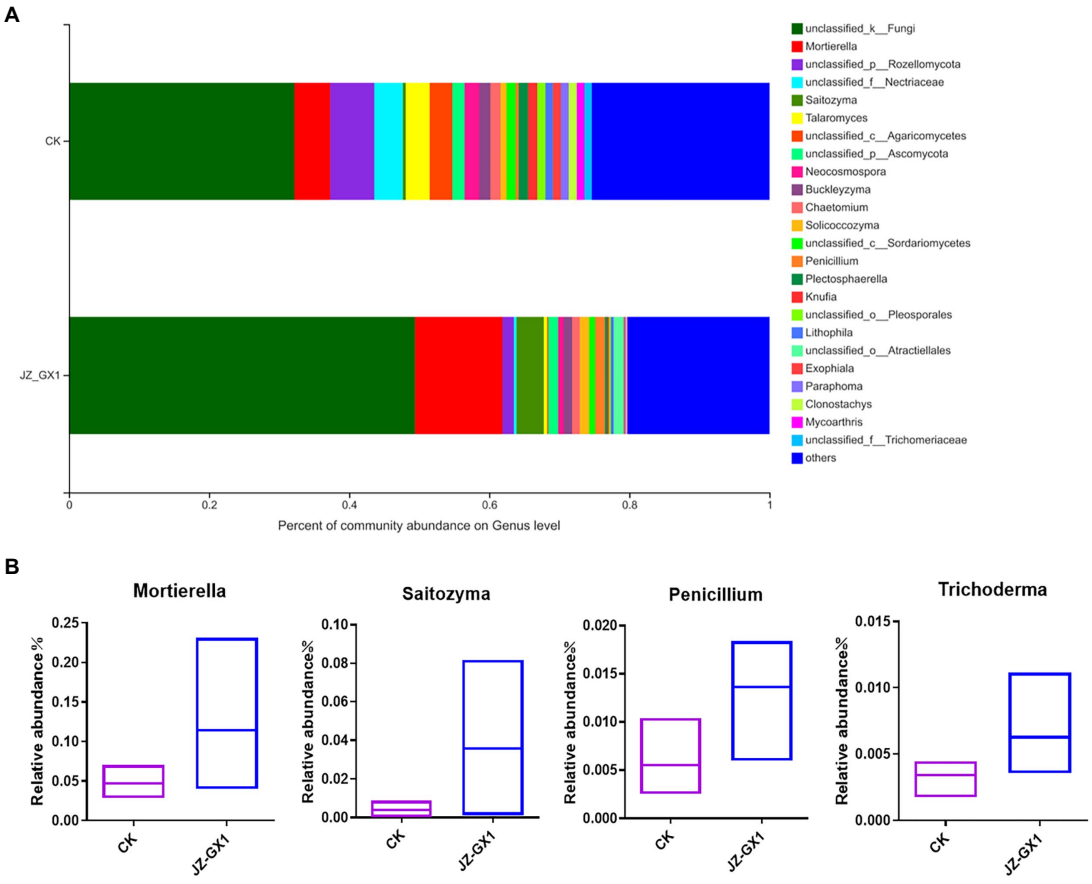

FIGURE 9
Composition of fungal communities in etiolated and green *Cinnamomum camphora* rhizosphere soils at the genus level. Proportion of fungi in each genus **(A)** and specific microorganisms **(B)**.

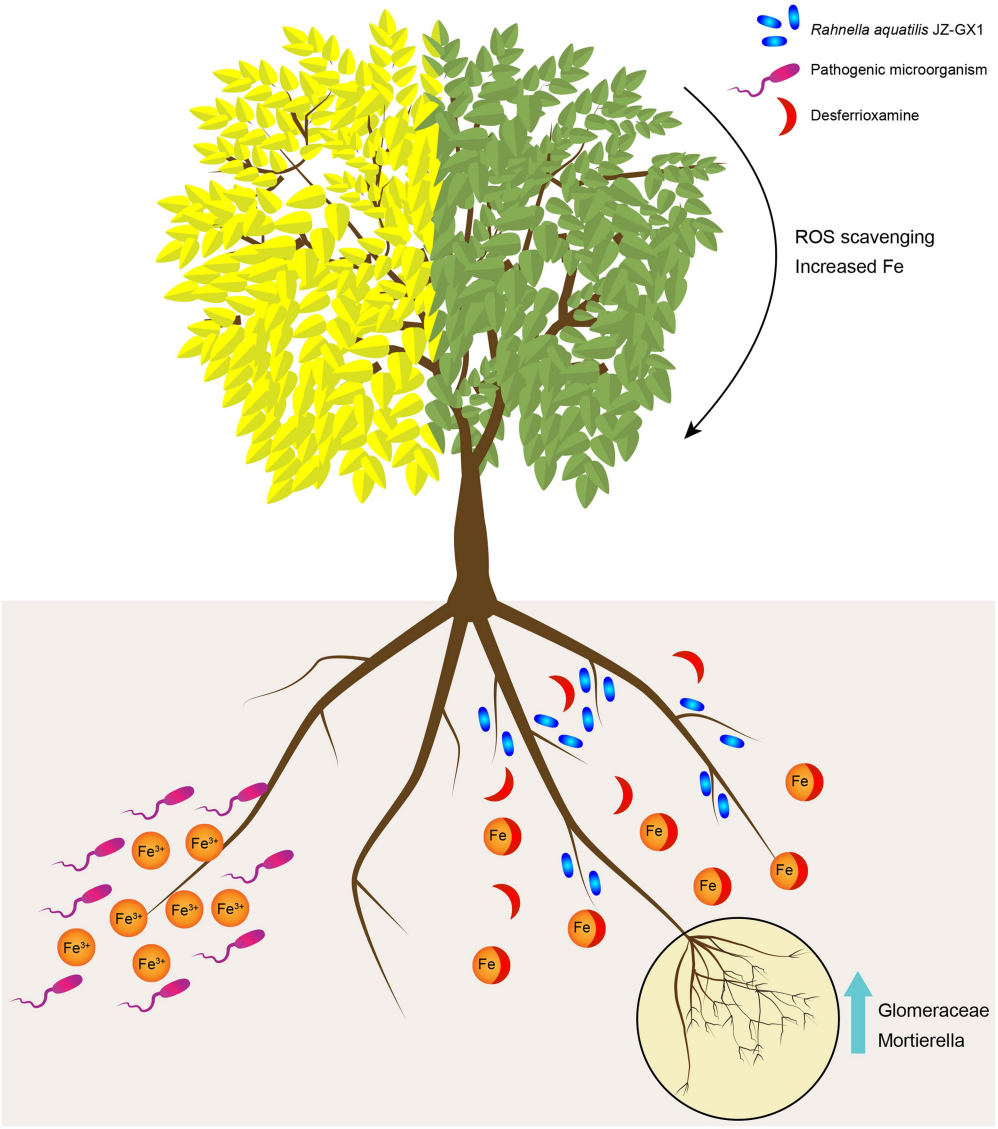

FIGURE 10
Putative model of the mechanism through which *Rahnella aquatilis* JZ-GX1 alleviates the iron deficiency-induced etiolation of *Cinnamomum camphora* by reprogramming the rhizosphere microbial community and increasing the content of DFO in soil. The JZ-GX1 strain secrete DFO to chelate insoluble Fe^{3+}, then the Fe^{3+}-DFO complex directly provides an iron source for iron-deficient *C. camphora*. At the same time, the removal of Fe^{3+} may limit the growth of pathogens and increase the population of *Glomeromycota* and *Mortierella*. The mycorrhizae formed by these microorganisms alleviate the etiolation of *C. camphora* caused by iron deficiency.

Data availability statement

The datasets presented in this study can be found in online repositories. The names of the repository/repositories and accession number(s) can be found at: https://www.ncbi.nlm.nih.gov/, PRJNA733870.

Author contributions

W-LK completed the data analysis and the first draft of the paper. W-LK, P-SL, and YZ were the finishers of the experimental research. Y-HW and L-XL participated in the experimental result analysis. X-QW directed experimental design, data analysis, and paper writing and revision. All authors contributed to the article and approved the submitted version.

Funding

This work was supported by the National Key Research and Development Program of China (2017YFD0600104), the Priority Academic Program Development of the Jiangsu Higher Education Institutions (PAPD), and the Postgraduate Research & Practice Innovation Program of Jiangsu Province (KYCX20_0872).

Conflict of interest

The authors declare that the research was conducted in the absence of any commercial or financial relationships that could be construed as a potential conflict of interest.

Publisher's note

All claims expressed in this article are solely those of the authors and do not necessarily represent those of their affiliated organizations, or those of the publisher, the editors and the reviewers. Any product that may be evaluated in this article, or claim that may be made by its manufacturer, is not guaranteed or endorsed by the publisher.

Supplementary material

The Supplementary material for this article can be found online at: https://www.frontiersin.org/articles/10.3389/fpls.2022.960750/full#supplementary-material

References

Aebi, H. (1984). "Catalase in vitro," in *Methods in Enzymology*. ed. L. Packer (Orlando: Academic Press), 121–126.

Aras, S., Arikan, S., Ipek, M., Esitken, A., Pirlak, L., Donmez, M. F., et al. (2018). Plant growth promoting rhizobacteria enhanced leaf organic acids, FC-R activity and Fe nutrition of apple under lime soil conditions. *Acta Physiol. Plant.* 40:120. doi: 10.1007/s11738-018-2693-9

Arikan, S., Esitken, A., Ipek, M., Aras, S., Sahin, M., Pirlak, L., et al. (2018). Effect of plant growth promoting rhizobacteria on Fe acquisition in peach (*Prunus Persica* L) under calcareous soil conditions. *J. Plant Nutr.* 41, 2141–2150. doi: 10.1080/01904167.2018.1482910

Aznar, A., Chen, N. W. G., Rigault, M., Riache, N., Joseph, D., Desmaele, D., et al. (2014). Scavenging iron: a novel mechanism of plant immunity activation by microbial siderophores. *Plant Physiol.* 164, 2167–2183. doi: 10.1104/pp.113.233585

Beauchamp, C., and Fridovich, I. (1971). Superoxide dismutase: improved assays and assay applicable to acrylamide gels. *Anal. Biochem.* 44, 276–287. doi: 10.1016/0003-2697(71)90370-8

Blaalid, R., Kumar, S., Nilsson, R. H., Abarenkov, K., Kirk, P. M., and Kauserud, H. (2013). ITS1 versus ITS2 as DNA metabarcodes for fungi. *Mol. Ecol. Resour.* 13, 218–224. doi: 10.1111/1755-0998.12065

Blin, K., Shaw, S., Steinke, K., Villebro, R., Ziemert, N., Lee, S. Y., et al. (2019). antiSMASH 5.0: updates to the secondary metabolite genome mining pipeline. *Nucleic Acids Res.* 47, W81–W87. doi: 10.1093/nar/gkz310

Bradford, M. M. (1976). A rapid and sensitive method for the quantitation of microgram quantities of protein utilizing the principle of protein-dye binding. *Anal. Biochem.* 72, 248–254. doi: 10.1016/0003-2697(76)90527-3

Cao, P., Li, C., Wang, H., Yu, Z., Xu, X., Wang, X., et al. (2020). Community structures and antifungal activity of root-associated endophytic actinobacteria in healthy and diseased cucumber plants and *Streptomyces* sp. HAAG3-15 as a promising biocontrol agent. *Microorganisms* 8:236. doi: 10.3390/microorganisms8020236

Chen, S., Guo, L., Bai, J., Zhang, Y., Zhang, L., Wang, Z., et al. (2015). Biodegradation of p-hydroxybenzoic acid in soil by *pseudomonas putida* CSY-P1 isolated from cucumber rhizosphere soil. *Plant Soil* 389, 197–210. doi: 10.1007/s11104-014-2360-x

Chen, J., Tang, C., Zhang, R., Ye, S., Zhao, Z., Huang, Y., et al. (2020). Metabolomics analysis to evaluate the antibacterial activity of the essential oil from the leaves of *Cinnamomum camphora* (Linn.) Presl. *J. Ethopharmacol.* 253:112652. doi: 10.1016/j.jep.2020.112652

Duan, H., Wang, D., Wei, X., Huang, G., Fan, H., Zhou, S., et al. (2020). The decoupling between gas exchange and water potential of *Cinnamomum camphora* seedlings during drought recovery and its relation to ABA accumulation in leaves. *J. Plant Ecol.* 13, 683–692. doi: 10.1093/jpe/rtaa056

Elstner, E. F., and Heupel, A. (1976). Inhibition of nitrite formation from hydroxylammoniumchloride: a simple assay for superoxide dismutase. *Anal. Biochem.* 70, 616–620. doi: 10.1016/0003-2697(76)90488-7

Farshchi, H. K., Azizi, M., Teymouri, M., Nikpoor, A. R., and Jaafari, M. R. (2021). Synthesis and characterization of nanoliposome containing Fe^{2+} element: a superior nano-fertilizer for ferrous iron delivery to sweet basil. *Sci. Hortic.* 283:110110. doi: 10.1016/j.scienta.2021.110110

Fernandez, V., Winkelmann, G., and Ebert, G. (2004). Iron supply to tobacco plants through foliar application of iron citrate and ferric dimerum acid. *Physiol. Plant.* 122, 380–385. doi: 10.1111/j.1399-3054.2004.00405.x

Ferreira, M. J., Silva, H., and Cunha, A. (2019). Siderophore-producing rhizobacteria as a promising tool for empowering plants to cope with iron limitation in saline soils: a review. *Pedosphere* 29, 409–420. doi: 10.1016/S1002-0160(19)60810-6

Gamez, R. M., Rodriguez, F., Vidal, N. M., Ramirez, S., Alvarez, R. V., Landsman, D., et al. (2019). Banana (*Musa acuminata*) transcriptome profiling in response to rhizobacteria: *bacillus amyloliquefaciens* Bs006 and *Pseudomonas fluorescens* Ps006. *BMC Genomics* 20:378. doi: 10.1186/s12864-019-5763-5

Guo, Y., Jiang, J., Pan, Y., Yang, X., Li, H., Li, H., et al. (2019). Effect of high O-2 treatments on physiochemical, lycopene and microstructural characteristics of cherry tomatoes during storage. *J. Food Process. Preserv.* 43:e14216. doi: 10.1111/jfpp.14216

Guo, J., Muhammad, H., Lv, X., Wei, T., Ren, X., Jia, H., et al. (2020). Prospects and applications of plant growth promoting rhizobacteria to mitigate soil metal contamination: a review. *Chemosphere* 246:125823. doi: 10.1016/j.chemosphere.2020.125823

Hassan, N., Ebeed, H., and Aljaarany, A. (2020). Exogenous application of spermine and putrescine mitigate adversities of drought stress in wheat by protecting membranes and chloroplast ultra-structure. *Physiol. Mol. Biol. Plants* 26, 233–245. doi: 10.1007/s12298-019-00744-7

Jiang, M. Y., and Zhang, J. H. (2001). Effect of abscisic acid on active oxygen species, antioxidative defence system and oxidative damage in leaves of maize seedlings. *Plant Cell Physiol.* 42, 1265–1273. doi: 10.1093/pcp/pce162

Kong, W., Rui, L., Ni, H., and Wu, X. (2020b). Antifungal effects of volatile organic compounds produced by *Rahnella aquatilis* JZ-GX1 against *Colletotrichum gloeosporioides* in *Liriodendron chinense* x *tulipifera*. *Front. Microbiol.* 11:1114. doi: 10.3389/fmicb.2020.01114

Kong, W., Wu, X., and Zhao, Y. (2020a). Effects of *Rahnella aquatilis* JZ-GX1 on treat chlorosis induced by iron deficiency in *Cinnamomum camphora*. *J. Plant Growth Regul.* 39, 877–887. doi: 10.1007/s00344-019-10029-8

Koseoglu, A. T., and Acikgoz, V. (1995). Determination of iron chlorosis with extractable iron analysis in peach leaves. *J. Plant Nutr.* 18, 153–161. doi: 10.1080/01904169509364892

Li, P. S., Kong, W. L., and Wu, X. Q. (2021). Salt tolerance mechanism of the Rhizosphere bacterium JZ-GX1 and its effects on tomato seed germination and seedling growth. *Front. Microbiol.* 12:657238. doi: 10.3389/FMICB.2021.657238

Li, J., Shi, C., Wang, X., Liu, C., Ding, X., Ma, P., et al. (2020). Hydrogen sulfide regulates the activity of antioxidant enzymes through persulfidation and improves the resistance of tomato seedling to copper oxide nanoparticles (CuO NPs)-induced oxidative stress. *Plant Physiol. Biochem.* 156, 257–266. doi: 10.1016/j.plaphy.2020.09.020

Li, M., Zhang, P., Adeel, M., Guo, Z., Chetwynd, A. J., Ma, C., et al. (2021). Physiological impacts of zero valent iron, Fe_3O_4 and Fe_2O_3 nanoparticles in rice plants and their potential as Fe fertilizers. *Environ. Pollut.* 269:116134. doi: 10.1016/j.envpol.2020.116134

Li, F., Zhang, S., Wang, Y., Li, Y., Li, P., Chen, L., et al. (2020). Rare fungus, *Mortierella capitata*, promotes crop growth by stimulating primary metabolisms related genes and reshaping rhizosphere bacterial community. *Soil Biol. Biochem.* 151:108017. doi: 10.1016/j.soilbio.2020.108017

Liu, Z., Guo, Y., and Bai, J. (2010). Exogenous hydrogen peroxide changes antioxidant enzyme activity and protects ultrastructure in leaves of two cucumber ecotypes under osmotic stress. *J. Plant Growth Regul.* 29, 171–183. doi: 10.1007/s00344-009-9121-8

Liu, D., Yan, R., Fu, Y., Wang, X., Zhang, J., and Xiang, W. (2019). Antifungal, plant growth-promoting, and genomic properties of an endophytic actinobacterium *Streptomyces* sp. NEAU-S7GS2. *Front. Microbiol.* 10:2077. doi: 10.3389/fmicb.2019.02077

Liu, D., Yang, Q., Ge, K., Hu, X., Qi, G., Du, B., et al. (2017). Promotion of iron nutrition and growth on peanut by *Paenibacillus illinoisensis* and *bacillus* sp strains in calcareous soil. *Braz. J. Micrology* 48, 656–670. doi: 10.1016/j.bjm.2017.02.006

Luo, Y., Zhou, M., Zhao, Q., Wang, F., Gao, J., Sheng, H., et al. (2020). Complete genome sequence of *Sphingomonas* sp. Cra20, a drought resistant and plant growth promoting rhizobacteria. *Genomics* 112, 3648–3657. doi: 10.1016/j.ygeno.2020.04.013

Maindad, D. V., Kasture, V. M., Chaudhari, H., Dhavale, D. D., Chopade, B. A., and Sachdev, D. P. (2014). Characterization and fungal inhibition activity of siderophore from wheat rhizosphere associated acinetobacter calcoaceticus strain HIRFA32. *Indian J. Microbiol.* 54, 315–322. doi: 10.1007/s12088-014-0446-z

Martinez-Medina, A., Van Wees, S. C. M., and Pieterse, C. M. J. (2017). Airborne signals from *Trichoderma* fungi stimulate iron uptake responses in roots resulting in priming of jasmonic acid-dependent defences in shoots of *Arabidopsis thaliana* and *Solanum lycopersicum*. *Plant Cell Environ.* 40, 2691–2705. doi: 10.1111/pce.13016

McCully, L. M., Bitzer, A. S., Seaton, S. C., Smith, L. M., and Silby, M. W. (2019). Interspecies social spreading: interaction between two sessile soil bacteria leads to emergence of surface motility. *Msphere* 4, e00696–e00618. doi: 10.1128/mSphere.00696-18

Mukherjee, S. P., and Choudhuri, M. A. (1983). Implications of water stress-induced changes in the levels of endogenous ascorbic acid and hydrogen peroxide in Vigna seedlings. *Physiol. Plant.* 58, 166–170. doi: 10.1111/j.1399-3054.1983.tb04162.x

Ni, L. L., Hou, S. Q., Feng, S. D., Wu, C. Y., Lu, X. L., and Wei, J. (2015). Application of improved NH4F masking method in determination of ferrous iron in plant tissues. *Plant Physiol. J.* 51, 1347–1349. doi: 10.13592/j.cnki.ppj.2015.0236

Niu, H., Leng, Y., Li, X., Yu, Q., Wu, H., Gong, J., et al. (2021). Behaviors of cadmium in rhizosphere soils and its interaction with microbiome communities in phytoremediation. *Chemosphere* 269:128765. doi: 10.1016/j.chemosphere

Nounjan, N., Kumon-Sa, N., and Theerakulpisut, P. (2021). Spermidine priming promotes germination of deteriorated seeds and reduced salt stressed damage in rice seedlings. *Notulae Botanicae Horti Agrobotanici Cluj-Napoca* 49:12130. doi: 10.15835/NBHA49112130

Pflugmacher, S., Olin, M., and Kankaanpaa, H. (2010). Oxidative stress response in the red alga *Furcellaria lumbricalis* (Huds.) Lamour. Due to exposure and uptake of the cyanobacterial toxin nodularin from *Nodularia spumigena*. *Harmful Algae* 10, 49–55. doi: 10.1016/j.hal.2010.06.004

Pierwola, A., Krupinski, T., Zalupski, P., Chiarelli, M., and Castignetti, D. (2004). Degradation pathway and generation of monohydroxamic acids from the trihydroxamate siderophore deferrioxamine B. *Appl. Environ. Microbiol.* 70, 831–836. doi: 10.1128/AEM.70.2.831-836.2004

Priya, P., Aneesh, B., and Harikrishnan, K. (2021). Genomics as a potential tool to unravel the rhizosphere microbiome interactions on plant health. *J. Microbiol. Methods* 185:106215. doi: 10.1016/J.MIMET.2021.106215

Qin, S., Feng, W. W., Zhang, Y. J., Wang, T. T., Xiong, Y. W., and Xing, K. (2018). Diversity of bacterial microbiota of coastal halophyte Limonium sinense and amelioration of salinity stress damage by symbiotic plant growth-promoting actinobacterium Glutamicibacter halophytocola KLBMP 5180. *Appl. Environ. Microbiol.* 84:e01533-18. doi: 10.1128/AEM.01533-18

Radzki, W., Gutierrez Manero, F. J., Algar, E., Lucas Garcia, J. A., Garcia-Villaraco, A., and Ramos Solano, B. (2013). Bacterial siderophores efficiently provide iron to iron-starved tomato plants in hydroponics culture. *Anton. Leeuw. Int. J. Gen. Mol. Microbiol.* 104, 321–330. doi: 10.1007/s10482-013-9954-9

Song, Y., Dong, Y., Tian, X., Wang, W., and He, Z. (2018). Mechanisms of exogenous nitric oxide and 24-Epibrassinolide alleviating chlorosis of peanut plants under iron deficiency. *Pedosphere* 28, 926–942. doi: 10.1016/S1002-0160(17)60446-6

Tao, C., Li, R., Xiong, W., Shen, Z., Liu, S., Wang, B., et al. (2020). Bio-organic fertilizers stimulate indigenous soil *pseudomonas* populations to enhance plant disease suppression. *Microbiome* 8:137. doi: 10.1186/s40168-020-00892-z

Tsai, H. H., and Schmidt, W. (2017). Mobilization of iron by plant-borne coumarins. *Trends Plant Sci.* 22, 538–548. doi: 10.1016/j.tplants.2017.03.008

Wan, Y., Zhang, Y., Zhang, L., Zhou, Z., Li, X., Shi, Q., et al. (2015). Caffeic acid protects cucumber against chilling stress by regulating antioxidant enzyme activity and proline and soluble sugar contents. *Acta Physiol. Plant.* 37, 1–10. doi: 10.1007/s11738-014-1706-6

Wan, Y., Zhang, Y., Zhang, L., Zhou, Z., Li, X., Shi, Q., et al. (2018). Diversity of bacterial microbiota of coastal halophyte limonium sinense and amelioration of salinity stress damage by symbiotic plant growth-promoting actinobacterium *Glutamicibacter halophytocola* KLBMP 5180. *Appl. Environ. Microbiol.* 84, e01533–e01518. doi: 10.1128/AEM.01533-18

Wang, C., Yang, W., Wang, C., Gu, C., Niu, D., Liu, H., et al. (2012). Induction of drought tolerance in cucumber plants by a consortium of three plant growth-promoting rhizobacterium strains. *PLoS One* 7:e52565. doi: 10.1371/journal.pone.0052565

Wozniak, M., and Galazka, A. (2019). The rhizosphere microbiome and its beneficial effects on plants – current knowledge and perspectives. *Advancements Microbiol.* 58, 59–69. doi: 10.21307/PM-2019.58.1.059

Wu, F., Ding, Y., Nie, Y., Wang, X., An, Y., Roessner, U., et al. (2021). Plant metabolomics integrated with transcriptomics and rhizospheric bacterial community indicates the mitigation effects of *Klebsiella oxytoca* P620 on p-hydroxybenzoic acid stress in cucumber. *J. Hazard. Mater.* 415:125756. doi: 10.1016/J.JHAZMAT.2021.125756

Xavier, J. B. (2011). Social interaction in synthetic and natural microbial communities. *Mol. Syst. Biol.* 7:483. doi: 10.1038/msb.2011.16

Xu, P., Guo, Y., Bai, J., Shang, L., and Wang, X. (2008). Effects of long-term chilling on ultrastructure and antioxidant activity in leaves of two cucumber cultivars under low light. *Physiol. Plant.* 132, 467–478. doi: 10.1111/j.1399-3054.2007.01036.x

Yang, C., Zhao, W., Wang, Y., Zhang, L., Huang, S., and Lin, J. (2020). Metabolomics analysis reveals the alkali tolerance mechanism in *Puccinellia tenuiflora* plants inoculated with Arbuscular Mycorrhizal fungi. *Microorganisms* 8:327. doi: 10.3390/microorganisms8030327

Yang, L., Zou, Y. N., Tian, Z. H., Wu, Q. S., and Kuča, K. (2021). Effects of beneficial endophytic fungal inoculants on plant growth and nutrient absorption of trifoliate orange seedlings. *Sci. Hortic.* 277:109815. doi: 10.1016/j.scienta.2020.109815

Ye, X., Li, Z., Luo, X., Wang, W., Li, Y., Li, R., et al. (2020). A predatory myxobacterium controls cucumber *Fusarium* wilt by regulating the soil microbial community. *Microbiome* 8:49. doi: 10.1186/s40168-020-00824-x

Yehuda, Z., Hadar, Y., and Chen, Y. (2003). Immobilized EDDHA and DFOB as iron carriers to cucumber plants. *J. Plant Nutr.* 26, 2043–2056. doi: 10.1081/PLN-120024263

Yehuda, Z., Hadar, Y., and Chen, Y. (2012). FeDFOB and FeEDDHA immobilized on Sepharose gels as an Fe sources to plants. *Plant Soil* 350, 379–391. doi: 10.1007/s11104-011-0923-7

Yu, S., Teng, C., Liang, J., Song, T., Dong, L., Bai, X., et al. (2017). Characterization of siderophore produced by *pseudomonas syringae* BAF.1 and its inhibitory effects on spore germination and mycelium morphology of *Fusarium oxysporum*. *J. Microbiol.* 55, 877–884. doi: 10.1007/s12275-017-7191-z

Zhang, H., Sun, Y., Xie, X., Kim, M., Dowd, S. E., and Paré, P. W. (2009). A soil bacterium regulates plant acquisition of iron via deficiency-inducible mechanisms. *Plant J.* 58, 568–577. doi: 10.1111/j.1365-313X.2009.03803.x

Zhao, L., Wang, F., Zhang, Y., and Zhang, J. (2014). Involvement of *Trichoderma asperellum* strain T6 in regulating iron acquisition in plants. *J. Basic Microbiol.* 54, S115–S124. doi: 10.1002/jobm.201400148

Zhong, Y., Yang, A., Li, Z., Zhang, H., Liu, L., Wu, Z., et al. (2019). Genetic diversity and population genetic structure of *Cinnamomum camphora* in South China revealed by EST-SSR markers. *Forests* 10:1019. doi: 10.3390/f10111019

Zhou, C., Guo, J., Zhu, L., Xiao, X., Xie, Y., Zhu, J., et al. (2016). *Paenibacillus polymyxa* BFKC01 enhances plant iron absorption via improved root systems and activated iron acquisition mechanisms. *Plant Physiol. Biochem.* 105, 162–173. doi: 10.1016/j.plaphy.2016.04.025

Zhou, H., Ren, J., and Li, Z. (2017). Antibacterial activity and mechanism of pinoresinol from *Cinnamomum Camphora* leaves against food-related bacteria. *Food Control* 79, 192–199. doi: 10.1016/j.foodcont.2017.03.041

Zhou, C., Zhu, L., Xie, Y., Li, F., Xiao, X., Ma, Z., et al. (2017). *Bacillus licheniformis* SA03 confers increased saline-alkaline tolerance in chrysanthemum plants by induction of abscisic acid accumulation. *Front. Plant Sci.* 8:1143. doi: 10.3389/fpls.2017.01143

Zhu, Z. J., Wei, G. Q., Li, J., Qian, Q. Q., and Yu, J. Q. (2004). Silicon alleviates salt stress and increases antioxidant enzymes activity in leaves of salt-stressed cucumber (*Cucumis sativus* L.). *Plant Sci.* 167, 527–533. doi: 10.1016/j.plantsci.2004.04.020

frontiers | Frontiers in Plant Science

TYPE Original Research
PUBLISHED 26 September 2022
DOI 10.3389/fpls.2022.983788

OPEN ACCESS

EDITED BY
Youssef Rouphael,
University of Naples Federico II, Italy

REVIEWED BY
Zhiguang Liu,
Shandong Agricultural University, China
Jianlin Shen,
Chinese Academy of Sciences (CAS), China

*CORRESPONDENCE
Xiaoqiang Jiao
xqjiao526@cau.edu.cn

SPECIALTY SECTION
This article was submitted to Plant Nutrition, a section of the journal Frontiers in Plant Science

RECEIVED 01 July 2022
ACCEPTED 08 September 2022
PUBLISHED 26 September 2022

CITATION
Gong H, Xiang Y, Wako BK and Jiao X (2022) Complementary effects of phosphorus supply and planting density on maize growth and phosphorus use efficiency. *Front. Plant Sci.* 13:983788. doi: 10.3389/fpls.2022.983788

Complementary effects of phosphorus supply and planting density on maize growth and phosphorus use efficiency

Haiqing Gong, Yue Xiang, Bilisuma Kabeto Wako and Xiaoqiang Jiao*

National Academy of Agriculture Green Development, Department of Plant Nutrition, Key Laboratory of Plant-Soil Interactions, Ministry of Education, China Agricultural University, Beijing, China

Phosphorus (P) supply and planting density regulate plant growth by altering root morphological traits and soil P dynamics. However, the compensatory effects of P supply and planting density on maize (*Zea mays* L.) growth and P use efficiency remain unknown. In this study, we conducted pot experiments of approximately 60 days to determine the effect of P supply, i.e., no P (CK), single superphosphate (SSP), and monoammonium phosphate (MAP), and different planting densities (low: two plants per pot; and high: four plants per pot) on maize growth. A similar shoot biomass accumulation was observed at high planting density under CK treatment (91.5 g plot^{-1}) and low planting density under SSP treatment (94.3 g plot^{-1}), with similar trends in P uptake, root morphological traits, and arbuscular mycorrhizal colonization. There was no significant difference in shoot biomass between high planting density under SSP (107.3 g plot^{-1}) and low planting density under MAP (105.2 g plot^{-1}); the corresponding P uptake, root growth, and P fraction in the soil showed the same trend. These results suggest that improved P supply could compensate for the limitations of low planting density by regulating the interaction between root morphological traits and soil P dynamics. Furthermore, under the same P supply, the limitations of low planting density could be compensated for by substituting MAP for SSP. Our results indicate that maize growth and P use efficiency could be improved by harnessing the compensatory effects of P supply and planting density to alter root plasticity and soil P dynamics.

KEYWORDS

maize, phosphorus supply, planting density, phosphorus use efficiency, root morphological traits, soil P dynamics

Introduction

Phosphorus (P) is an essential nutrient for plant growth and development, as well as an important factor limiting sustainable maize production (Bindraban et al., 2020; Muhaba and Dakora, 2020). Mineral P fertilizers are critical in ensuring food security (Nedelciu et al., 2020); however, P use efficiency is extremely low owing to poor P mobility (Heuer et al., 2017). Although increasing planting density is a common agronomic measure for increasing P use efficiency (Jia et al., 2018; Zhang et al., 2021), it results in reduced space for root growth. The primary mechanism for P acquisition in maize production is the morphological expansion of root systems (Zhou et al., 2019a). The low mobility of P and the compression of root space have made efficient P use under high planting density conditions difficult (Shao et al., 2018). Allowing root systems to fully develop their biological potential and increase soil P uptake will be critical to improving P use efficiency in intensive maize production.

The spatial expansion of maize roots becomes severely compressed and the competition among plant roots growing closely at high planting densities is severe due to the extent of overlap among rhizospheres, which may result in nutrient deficiencies (Thorup-Kristensen and Kirkegaard, 2016; Li et al., 2019). High planting densities decrease the number of nodal roots, lateral root density, and root biomass per unit volume of soil (Shao et al., 2018; Niu et al., 2020). In addition, root system size can be reduced at high planting density due to plant competition. The root crown angle can become more vertical to adapt to a small growing space at high planting densities (Shao et al., 2018; Tomasi et al., 2020). Furthermore, maize roots adapt to obtain P in small spaces by becoming thinner and longer, extending into soil spaces with limited carbohydrates. The root-soil contact area also increases to enhance P acquisition (Lynch et al., 2022). Root foraging for P is determined by changes in root morphology in response to soil environmental conditions, and plant productivity and P uptake may be affected by planting density due to differential competitiveness.

The plastic response of the root system is not only limited by growth area but also largely affected by P supply at high planting densities (Wang et al., 2020; Postma et al., 2021). According to Semchenko (2020), resource capture is the primary driver of root changes. Maintaining an adequate P supply in the root zone can help the root system and mycorrhizal infection expand into the soil space and acquire soil P (Deng et al., 2017). Planting density and P supply interactions can maximize the efficiency of maize roots in mobilizing and acquiring P (Schneider et al., 2019). Indeed, P supply has the potential to considerably improve P use efficiency in crop production by activating soil P (Soltangheisi et al., 2018). Initial and residual P effects are influenced by the solubility of P fertilizer, which varies widely (Gong et al., 2022). However, it is unclear whether maize dry-matter accumulation loss caused by low planting density may be compensated for by regulating root plasticity and soil P dynamics through altered P supply.

This study aims to determine the compensatory mechanisms of P supply and planting density on maize root morphology, soil P dynamics, and P uptake. The specific goals of the study were to (1) evaluate the growth and P uptake of maize under different P supplies and planting densities, and (2) to examine whether maize growth limitation due to low planting density may be compensated for by altering P supply.

Materials and methods

Experimental design

A greenhouse pot experiment was conducted from May to July 2021 at the Quzhou Experimental Station of the China Agricultural University (36°51′57″N, 150°0′37″E), in Quzhou County, Heibei Province, China. Calcareous loam soil was collected from the Quzhou Long-Term Fertilizer Station (36° 52′21″N, 115°03′15″E) of the China Agricultural University. The soil was air-dried and then sieved to pass through a 2-mm mesh. The soil type is calcareous fluvo-aquic soil from the North China Plain. The basic physical and chemical properties of the soil are as follows: pH value, 8.0; soil organic carbon content, 12.5 g kg^{-1}; total nitrogen content, 1.3 g kg^{-1}; soil Olsen-P content, 4.3 mg kg^{-1}; and soil available potassium content, 194 mg kg^{-1}. The soil properties were measured using the methods specified by Bao (2001).

The experiment was laid out in a 3×2 complete factorial design. Three P supply treatments were used: no P (CK), single superphosphate (SSP), and monoammonium phosphate (MAP). Two planting densities were tested: low (two plants per pot) and high (four plants per pot). Each of the six treatment combinations were replicated four times for a total of 24 pots. Each pot was 30 cm in diameter and 40 cm in height. A treatment rate of 150 kg P ha^{-1} was applied using the different P supplies, SSP and MAP. In the fertigation treatments, urea and muriate of potash were used as sources of nitrogen and potassium, respectively. Both nitrogen and potassium were applied at a rate of 150 kg ha^{-1}. All fertilizers were incorporated and completely mixed with soil at planting.

Maize Zhengdan 958 seeds was used in this study; they were surface sterilized in 10% (v/v) H_2O_2 for 0.5 h, washed with deionized water, a supersaturated solution of calcium sulfate ($CaSO_4$) was soaked for 1 day, and germinated in a dish with an aerated cover with wet filter paper for 3 days at 25 °C. Pots were watered daily to field capacity (18%, w/w) by watering every day. Temperatures ranged from a minimum of 20 °C at night to a maximum of 30 °C during the day.

Plant harvest and sample analysis

The plants were harvested 60 days after planting. Shoots and roots were separated and shoots were first oven-dried at 105 °C for 0.5 h and then dried at 75 °C for 4 days to constant weight. The dry samples were weighed, crushed, and homogenized. Shoot P concentration was determined according to the standard vanadomolybdate method (Murphy and Riley 1962).

The root samples were carefully and thoroughly washed in a large volume of deionized water and then scanned using the EPSON root scanning software (Epson Expression 1600 pro, Model EU-35; Epson, Tokyo, Japan) at 400 points per inch. The WinRHIZO software (Pro2004b, version 5.0; Regent Instruments Inc., QC, Canada) was used to measure total root length. Lateral root density was calculated by dividing the number of lateral roots per 5 cm of the primary root by the 5-cm length of the primary root (Wu et al., 2019). Arbuscular mycorrhizal colonization analysis was performed according to the method of Trouvelot et al. (1986). Fine roots were cut into 1-cm-long segments and thoroughly mixed. Root samples were cleared with 10% (w/v) potassium hydroxide (KOH) at 90 °C for 2 h, and mycorrhizal colonization was stained using trypan blue. All roots were dried at 75 °C for 3 days and then weighed to calculate root dry biomass. The root/shoot ratio was defined as the ratio of root dry mass to that of the shoots (Marziliano et al., 2015).

Rhizosphere soil was taken from a 0–2-mm distance around the roots and collected by clearing the roots of debris; the rhizosphere soil was the loosely attached soil particles that were removed from around the roots (Cui et al., 2020; Zhou et al., 2022). Soil samples were then air-dried and passed through a 2-mm mesh sieve. Soil P fractions were analyzed sequentially and extracted using the Hedley method (Hedley et al., 1982). Soluble P is extractable with water and $NaHCO_3$ (water-extractable P and $NaHCO_3$-extractable P), which is considered labile P, and are immediately available to plants. Moderately labile P is extractable with NaOH (NaOH-extractable P), which is available to plants. Recalcitrant forms, such as HCl-extractable P and residual P, are considered non-labile P and are only available to plants over long time periods (Cross and Schlessinger, 1995).

Statistical analysis

A two-way analysis of variance (ANOVA) test was used to examine the effects of P supply, planting density and their interacting effects on variables. All statistical analyses were performed using the SPSS statistical software (SPSS 20.0; SPSS Inc., Chicago, IL, USA). Significant differences among means were separated by the least significant difference test at the $P \leq 0.05$ probability level. The graphs were constructed using Sigmaplot (version 10.0; Systat Software Inc., San Jose, CA, USA).

Results

Shoot biomass and P content

Shoot biomass was significantly influenced by P supply and planting density ($P < 0.01$, Table 1; Figure 1A), and was higher for MAP-treated plants than for SSP or CK-treated plants at both planting densities. The high planting density concurrently improved shoot biomass: high shoot biomass was obtained under the high planting density condition, regardless of the P source. However, soil P supply intensity and planting density had complementary effects on shoot biomass. P supply intensity compensated for the reduction in shoot biomass due to the low planting density. Similar root biomass levels were recorded at the low planting density under the SSP treatment (91.5 g $plot^{-1}$) and at the high planting density under the CK treatment (94.3 g

TABLE 1 Two-way analysis of variance of phosphorus (P) supply, planting density, and their interaction.

Parameters	P supply		Planting density		P supply × Planting density	
	F-value	*P*-value	*F*-value	*P*-value	*F*-value	*P*-value
Shoot biomass	254.0	$P < 0.0001$	175.3	$P < 0.0001$	13.9	$P = 0.0008$
Shoot P uptake	61.1	$P < 0.0001$	23.2	$P = 0.0004$	1.5	$P = 0.2655$
Root biomass	71.5	$P < 0.0001$	72.7	$P < 0.0001$	2.5	$P = 0.1213$
Root length	25.7	$P = 0.0003$	46.4	$P < 0.0001$	0.5	$P = 0.4785$
Root/shoot ratio	12.3	$P = 0.0044$	6.9	$P = 0.0097$	3.0	$P = 0.0875$
Lateral root density	30.0	$P < 0.0001$	238.2	$P < 0.0001$	5.8	$P = 0.0116$
Labile P	5.3	$P = 0.0407$	2232.0	$P < 0.0001$	30.1	$P < 0.0001$
Moderately labile P	10.8	$P = 0.0064$	144.8	$P < 0.0001$	2.9	$P = 0.0969$
Non-labile P	2.1	$P = 0.1738$	9.2	P = 0.0039	2.2	$P = 0.1555$
AM colonization	21.7	$P = 0.0002$	278.2	$P < 0.0001$	0.4	$P = 0.6815$

AM, arbuscular mycorrhizal.

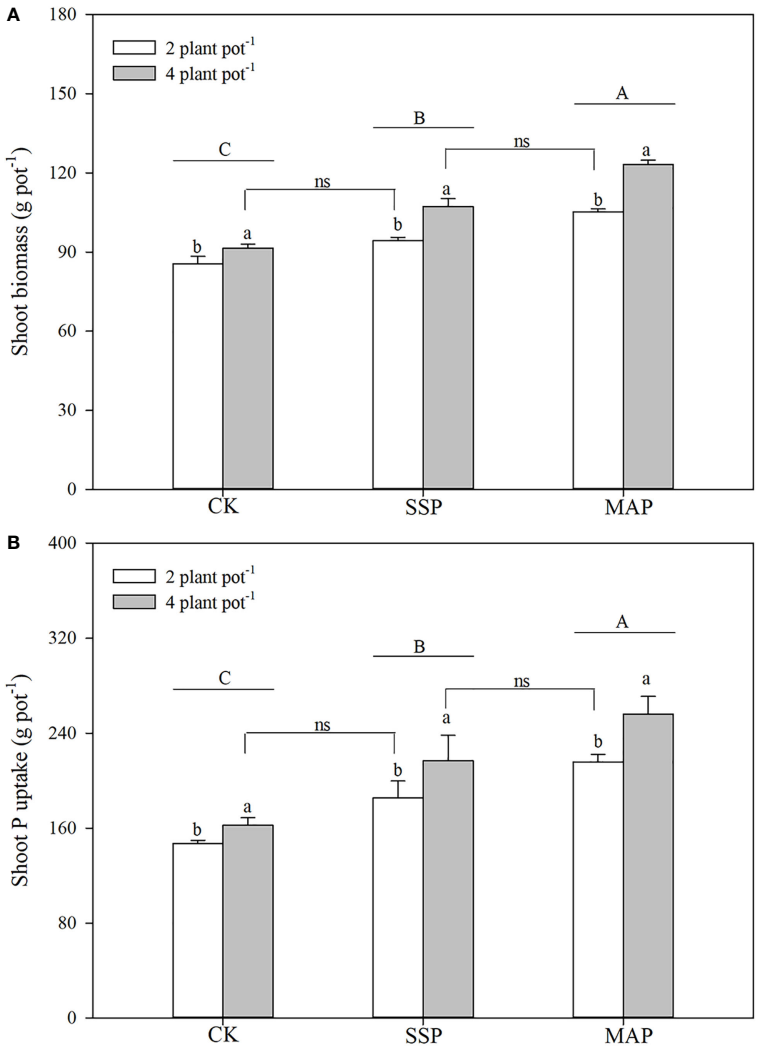

FIGURE 1
Shoot biomass **(A)**, shoot phosphorus (P) content **(B)** under two planting densities and three P fertilizer sources, no P (CK), superphosphate (SSP), and monoammonium phosphate (MAP). Different lowercase letters represent a significant difference among different planting densities at the $P < 0.05$ level, and different uppercase letters represent significant differences among different P fertilizer sources at the $P < 0.05$ level; ns indicates no significant difference at the 95% confidence interval between the two treatments.

plot^{-1}). A strong complementary effect was also found between P source and planting density. A reduction in shoot biomass due to low planting density was compensated for by substituting the MAP for the SSP treatment under the same P supply. Higher shoot biomass was recorded for the high planting density under the SSP treatment (107.3 g plot^{-1}), which was equivalent to the shoot biomass recorded for the low planting density under the MAP treatment (105.2 g plot^{-1}).

Shoot P content was strongly influenced by both P supply ($P < 0.01$) and planting density ($P < 0.01$), increasing in tandem with planting density (Table 1; Figure 1B). Shoot P content was higher in high planting densities than in low planting densities. The shoot P content observed in the low planting density under the SSP treatment was equivalent to the shoot P content observed in the high plant density under the CK treatment. This finding indicated that, although the shoot P content was limited by the low planting density, it was compensated for by P supply intensity. The shoot P content differed significantly by P source; regardless of planting density, the shoot P content was significantly higher when the MAP treatment was applied than when SSP was applied. Similar complementary effects of P sources and planting density on the shoot P content were observed. There were no significant differences in the shoot P content between the high planting density under the SSP treatment and the low planting density under the MAP treatment.

Root morphological traits

P supply and planting density significantly influenced maize root biomass ($P < 0.01$, Table 1; Figure 2A). P supply had a greater influence on root biomass in the MAP treatment than in the CK or SSP treatments, and root biomass increased as planting density increased. No significant differences were observed between the low planting density under the SSP treatment and the high planting density under the CK treatment. There was a strong complementary effect between P source and planting density on root biomass. A similar root biomass accumulation was observed at the high planting density in SSP-treated pots and the low planting density in MAP-treated pots.

Maize root length was also affected by P supply and planting density ($P < 0.01$, Table 1; Figure 2B); specifically, it was higher in the MAP-treated pots than in both the SSP- or CK-treated pots, regardless of the planting density. Furthermore, maize root length increased with planting density for both of these P sources. However, there was no significant difference in the root length between the low planting density under the SSP treatment and the high planting density under the CK treatment. Root length in SSP-treated pots at the high planting density was equivalent to that in MAP-treated pots at the low planting density.

The root/shoot ratio and lateral root density were significantly altered by P supply and planting density ($P < 0.01$, Table 1; Figures 2C, D). Thus, the root/shoot ratio and lateral root density of plants grown in SSP- and MAP-treated pots were significantly greater than those grown in CK-treated pots. However, there was no significant difference in the root/shoot ratio or lateral root density between the SSP and MAP treatments at either planting density. The effect of planting density on the root/shoot ratio and lateral root density under MAP supply was negligible. Similar to root length, there was no significant difference in the root/shoot ratio or lateral root density between the low planting density under SSP and the high planting density under the CK treatment. Similar root/shoot ratio values and lateral root densities were observed at the

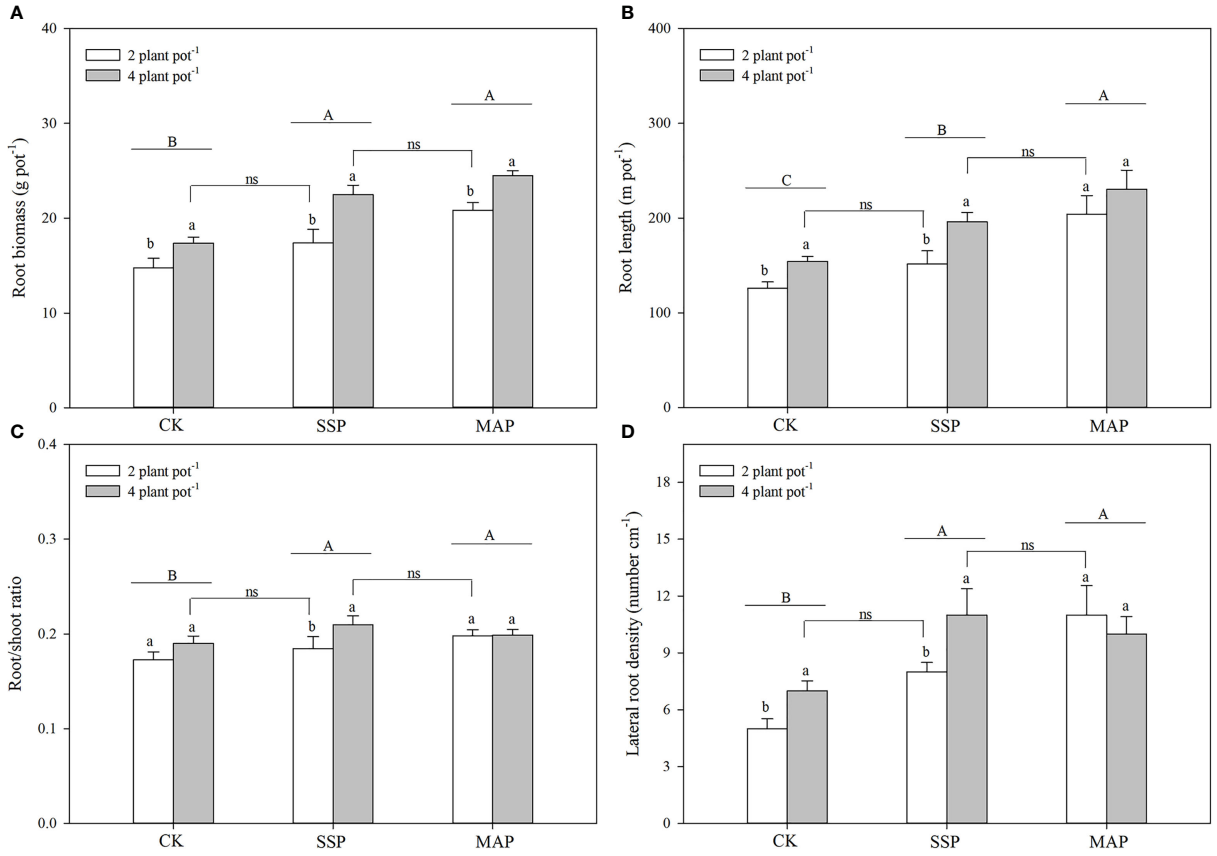

FIGURE 2
Maize root biomass **(A)**, root length **(B)**, root/shoot ratio **(C)**, and lateral root density **(D)** under two planting densities and three P fertilizer sources, no P (CK), superphosphate (SSP), and monoammonium phosphate (MAP). Different lowercase letters represent a significant difference among different planting densities at the $P < 0.05$ level, and different uppercase letters represent significant differences among different P fertilizer sources at the $P < 0.05$ level; ns indicates no significant difference at the 95% confidence interval between the two treatments.

high planting density under SSP and the low planting density under the MAP treatment.

Phosphorus fractions in the rhizosphere soil of maize

The labile P fractions accounted for only 2–8% of total P (Figure 3A). Labile P in the rhizosphere soil of maize was significantly altered by P supply and planting density ($P < 0.01$, Table 1; Figure 3B). The amount of labile P in maize plants grown with SSP or MAP was significantly greater than that of maize plants grown without P, while there was no significant difference in labile P between the SSP and MAP treatments, regardless of planting density. However, labile P in the rhizosphere soil of maize, in the high planting density under MAP was significantly greater than that of the low planting density treatment. There was no significant difference between the high planting density under the SSP treatment and the low planting density under the MAP treatment.

The moderately labile P fractions accounted for only 0.4–4% of total P (Figure 3A). Changes in the moderately labile P content of maize rhizosphere soil were mostly consistent with those for the labile P content among the treatments (Figure 3C). Moderately labile P in the maize rhizosphere soil significantly increased when P was supplied, compared with the CK treatment. A higher moderately labile P content in the maize rhizosphere soil was observed at the high planting density under the MAP treatment, whereas no significant difference was detected in moderately labile P between the high planting density under the SSP treatment and the low planting density under the MAP treatment.

The non-labile P fractions accounted for 88–98% of total P (Figure 3A). P supply and planting density had little effect on the non-labile P content in maize rhizosphere soil (Table 1; Figure 3D). However, the non-labile P content at the low planting density under the CK treatment was equivalent to

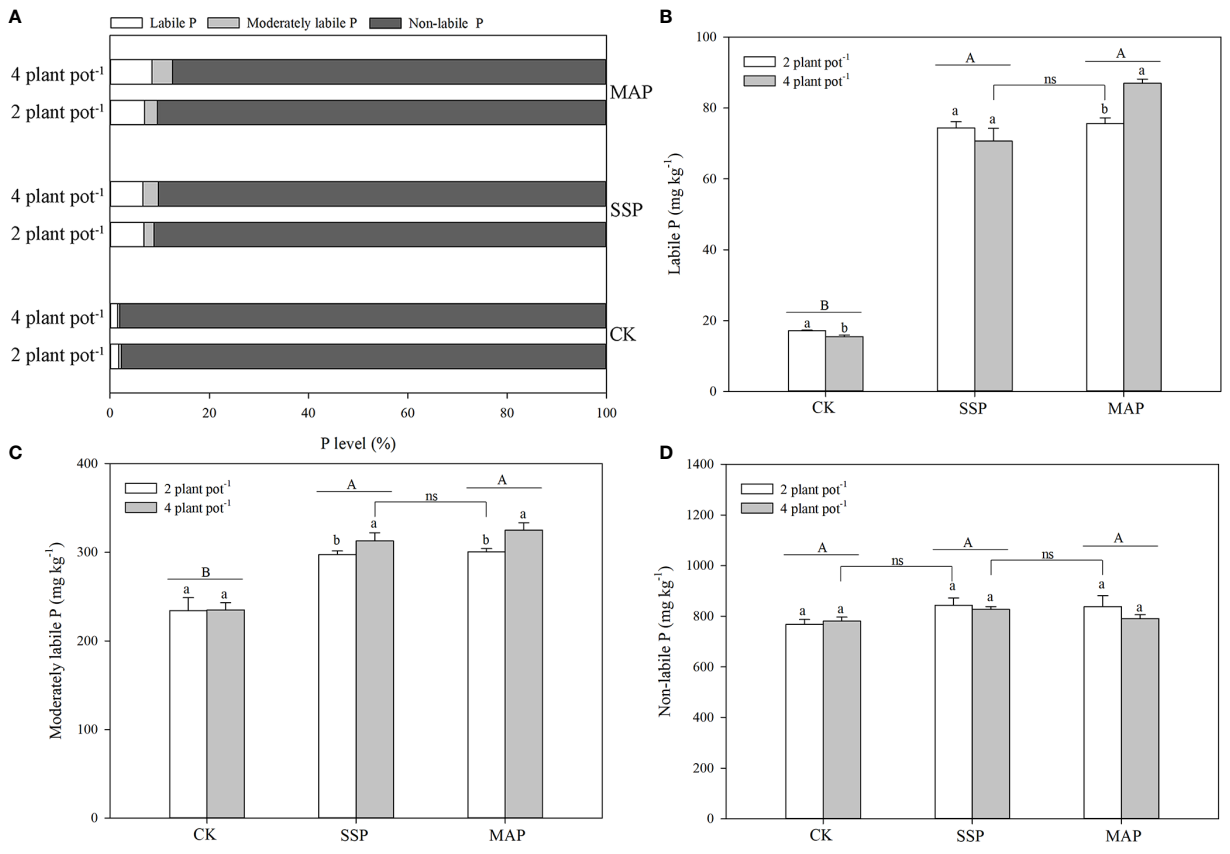

FIGURE 3
Proportions of labile, moderately labile, and non-labile P fractions under phosphate sources and cover crops under two planting densities and three P fertilizer sources **(A)**. Labile P **(B)**, moderately labile P **(C)**, and non-labile P **(D)** under two planting densities and three different P fertilizer sources, no P (CK), superphosphate (SSP), and monoammonium phosphate (MAP). Different lowercase letters represent a significant difference among different planting densities at the $P < 0.05$ level, and different uppercase letters represent significant differences among different P fertilizer sources at the $P < 0.05$ level; ns indicates no significant difference at the 95% confidence interval between the two treatments.

that at the high planting density under the SSP treatment. Similarly, the non-labile P content was higher at the high planting density under the SSP treatment than at the low planting density under the MAP treatment.

Arbuscular mycorrhizal colonization

The arbuscular mycorrhizal (AM) colonization was significantly altered by the P supply and planting densities (Table 1; Figure 4). Specifically, AM colonization decreased with P supply regardless of the planting density. The effect of AM colonization at the high planting density was greater than that at the low planting density in both SSP and MAP treatments. However, there was no significant difference in AM colonization between the high planting density under the SSP treatment and the low planting density under the CK treatment.

Discussion

Several studies have investigated the effects of P supply or planting density on maize growth (Zhang et al., 2019; Gong et al., 2021). This study confirmed prior findings by demonstrating strong interaction effects between P supply and planting density. However, little is known about whether the negative effects of low planting density on shoot biomass accumulation and P uptake can be offset by increasing P supply. P plays an important role, and aboveground biomass accumulations are a response to P availability (Cheng et al., 2020; Nkrumah et al., 2021). Shoot biomass accumulation and P uptake can be increased by intensifying the P supply or changing the P source at low planting density. Similar levels of root biomass accumulation were observed at a low planting density under SSP conditions and at a high planting density under the CK treatment. These findings suggest that limited aboveground dry-matter accumulations in maize caused by low planting density are compensated for by increasing P supply intensity. It is unclear whether substituting MAP for SSP can compensate for a low shoot biomass accumulation and P uptake caused by a low planting density. The SSP treatment resulted in a high shoot biomass accumulation and P uptake at a high planting density, which were equivalent to those at the low density under MAP treatment. These findings indicate that limited aboveground dry-matter accumulations in maize at low planting densities could be compensated for by substituting MAP for SSP.

Low planting density reduces the leaf area index and the interception of photosynthetically active radiation by the canopy, resulting in a decrease in the accumulation of aboveground dry-matter (Zhang et al., 2021). Consistently, we found that at low planting densities, shoot biomass accumulation and P uptake were lower than at high planting densities. This finding in the present study was similar to those in previous studies (Du et al., 2021; Gong et al., 2021). P supply may affect root architecture and morphology, and could facilitate the establishment of a better root system (Williamson et al.,

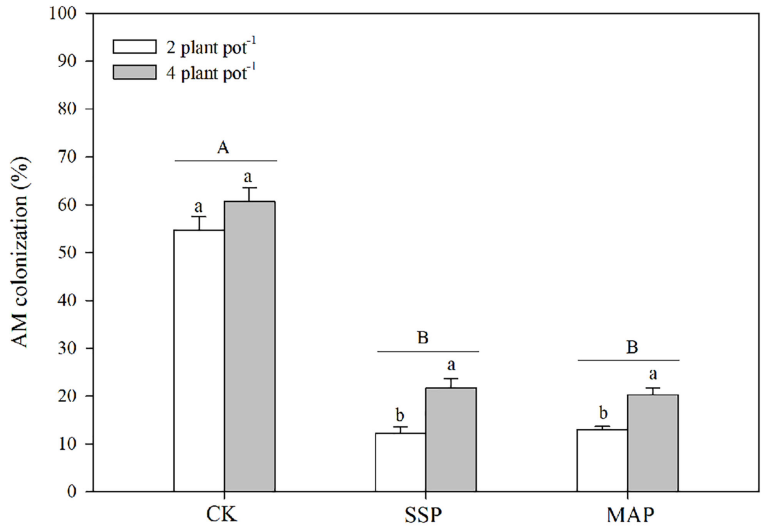

FIGURE 4
Arbuscular mycorrhizal (AM) colonization under two planting densities and three P fertilizer sources, no P (CK), superphosphate (SSP), and monoammonium phosphate (MAP). Different lowercase letters represent a significant difference among different planting densities at the $P < 0.05$ level, and different uppercase letters represent significant differences among different P fertilizer sources at the $P < 0.05$ level; ns indicates no significant difference at the 95% confidence interval between the two treatments.

2001). It may also affect P uptake by maize plants (Hopkins and Hansen, 2019; Pongrac et al., 2020). In this study on maize, root architecture, root biomass, root length, root/shoot ratio, and lateral root density were all significantly higher under P supply than under the CK treatment. Consistent with a previous study (Zhang et al., 2017), AM colonization decreased when P supply intensity increased. A high P supply intensity may have contributed to the selection of less beneficial AM species (Saia et al., 2015). These changes in maize roots effectively increased the amount of P accessible to maize plants, supporting previous findings (Gong et al., 2021). Root growth may explain the complementary effects of P supply and planting density on shoot biomass and P uptake (Zhang et al., 2014; Gong et al., 2021). The proportion of labile P and the moderately labile P content in the SSP treatment was higher than that in the CK treatment in both planting densities tested. Labile P and moderately labile P contents were transformed into other more available forms of P for plant uptake under the SSP treatment at low planting densities, compared with that under the CK treatment at high planting densities. Our study provides substantial evidence for the complementary effects of P supply intensity and planting density on shoot biomass and P uptake.

Increasing planting density is an effective method for improving output yield in agricultural systems (Li et al., 2021; Zhou et al., 2019b). A similar shoot biomass accumulation and P uptake were observed for the same P supply intensity at a high planting density under the SSP treatment and at a low planting density under the MAP treatment. Furthermore, the values of maize root-architecture components, such as root biomass, root length, root/shoot ratio, and lateral root density, were equivalent under the MAP treatment combined with a low planting density to those observed under the SSP treatment combined with a high planting density. MAP could provide readily available P to plants, and contribute indirectly to improved root growth and development because of the beneficial starter effects of MAP (Chien et al., 2011; Gong et al., 2022) because MAP is produced from ammonia and phosphoric acid, and phosphate (PO_4^{3-}) and ammonium (NH_4^+) are released upon dissolution. NH_4^+ and PO_4^{3-} ions are macronutrients that enhance root elongation (Weligama et al., 2008; Lu et al., 2019). When MAP was applied, shoot biomass and P uptake were higher than when SSP was applied at the same planting density. Low shoot biomass accumulation and P uptake due to low planting density may be compensated for by substituting MAP for SSP through exploiting the biological potential for enhancing P use efficiency. This implies a compensatory effect between P source and planting density.

Conclusions

In this study, P supply and planting density significantly modified root morphology and soil P dynamics, thereby influencing shoot biomass accumulation and P uptake. A similar shoot biomass accumulation was observed at a low planting density under SSP treatment and at a high planting density under CK treatment, with similar trends in P uptake, root morphological traits, and AM colonization. The reduction in aboveground dry-matter accumulation was fully compensated for by P supply at a low planting density. Additionally, at the same P supply level, shoot biomass accumulation and P uptake at a high planting density under SSP were equivalent to those observed at a low planting density under the MAP treatment, indicating that the reduction of aboveground dry-matter accumulation in the low planting density was fully compensated for by substituting MAP for SSP. These results contribute to our understanding of the biological potentials that can be exploited to enhance P use efficiency by optimizing the types and intensities of P fertilizer. Furthermore, our study provides new insights into the compensatory effects of P supply and planting density on maize production.

Data availability statement

The original contributions presented in the study are included in the article/Supplementary Material. Further inquiries can be directed to the corresponding author.

Author contributions

XJ conceived and designed the experiments. YX, BK, and HG performed the experiments. HG analyzed the data and wrote the manuscript. All authors reviewed and approved the manuscript for publication.

Funding

This work was supported by the National Natural Science Foundation of China (NSFC) (32172675) and by the Deutsche Forschungsgemeinschaft (DFG, German Research Foundation)-328017493/GRK 2366 (Sino-German International Research Training Group AMAIZE-P).

Conflict of interest

The authors declare that the research was conducted in the absence of any commercial or financial relationships that could be construed as a potential conflict of interest.

Publisher's note

All claims expressed in this article are solely those of the authors and do not necessarily represent those of their affiliated organizations, or those of the publisher, the editors and the reviewers. Any product that may be evaluated in this article, or claim that may be made by its manufacturer, is not guaranteed or endorsed by the publisher.

Supplementary material

The Supplementary Material for this article can be found online at: https://www.frontiersin.org/articles/10.3389/fpls.2022.983788/full#supplementary-material

References

Bao, S. (2001). *Analysis of soil agro-chemistry* (Beijing: Agricultural Press Chinese).

Bindraban, P., Dimkpa, C., and Pandey, R. (2020). Exploring phosphorus fertilizers and fertilization strategies for improved human and environmental health. *Biol. Fert. Soils.* 56 (3), 299–317. doi: 10.1007/s00374-019-01430-2

Cheng, Y., Zhang, H., Zang, R., Wang, X., Long, W., Wang, X., et al. (2020). The effects of soil phosphorus on aboveground biomass are mediated by functional diversity in a tropical cloud forest. *Plant Soil* 449 (1), 51–63. doi: 10.1007/s11104-020-04421-7

Chien, S., Prochnow, L., Prochnow, L., Tu, S., Tu, S., Snyder, C., et al. (2011). Agronomic and environmental aspects of phosphate fertilizers varying in source and solubility: an update review. *Nutr. Cycl. Agroecosys.* 89, 229–255. doi: 10.1007/s10705-010-9390-4

Cross, A., and Schlessinger, W. (1995). A literature review and evaluation of the hedley fractionation: application to the biogeochemical cycle of soil phosphorous in natural ecosystems. *Geoderma* 64, 197–214. doi: 10.1016/0016-7061(94)00023-4

Cui, J. L., Zhao, Y., Chan, T., Zhang, L., Tsang, D., and Li, X. (2020). Spatial distribution and molecular speciation of copper in indigenous plants from contaminated mine sites: Implication for phytostabilization. *J. Hazard. Mater.* 381, 121208. doi: 10.1016/j.jhazmat.2019.121208

Deng, Y., Feng, G., Chen, X., and Zou, C. (2017). Arbuscular mycorrhizal fungal colonization is considerable at optimal Olsen-p levels for maximized yields in an intensive wheat-maize cropping system. *F. Crop Res.* 209, 1–9. doi: 10.1016/j.fcr.2017.04.004

Du, X., Wang, Z., Lei, W., and Kong, L. (2021). Increased planting density combined with reduced nitrogen rate to achieve high yield in maize. *Sci. Rep.* 11, 358. doi: 10.1038/s41598-020-79633-z

Gong, H., Meng, F., Wang, G., Hartmann, T., Feng, G., Wu, J., et al. (2022). Toward the sustainable use of mineral phosphorus fertilizers for crop production in China: From primary resource demand to final agricultural use. *Sci. Total Environ.* 804, 150183. doi: 10.1016/j.scitotenv.2021.150183

Gong, H., Wako, K., Xiang, Y., and Jiao, X. (2021). Phosphorus-use efficiency modified by complementary effects of p supply intensity with limited root growth space. *Front. Plant Sci.* 12. doi: 10.3389/fpls.2021.728527

Hedley, M., Stewart, J., and Chauhan, B. (1982). Changes in inorganic and organic soil phosphorus fractions induced by cultivation practices and by laboratory incubations. *Soil Sci. Soc Am. J.* 46 (5), 970–976. doi: 10.2136/sssaj1982.03615995004600050017x

Heuer, S., Gaxiola, R., Schilling, R., Herrera-Estrella, L., López-Arredondo, D., Wissuwa, M., et al. (2017). Improving phosphorus use efficiency: a complex trait with emerging opportunities. *Plant J.* 90 (5), 868–885. doi: 10.1111/tpj.13423

Hopkins, B., and Hansen, N. (2019). Phosphorus management in high-yield systems. *J. Environ. Qual.* 48 (5), 1265–1280. doi: 10.2134/jeq2019.03.0130

Jia, Q., Sun, L., Ali, S., Zhang, Y., Liu, D., Kamran, M., et al. (2018). Effect of planting density and pattern on maize yield and rainwater use efficiency in the loess plateau in China. *Agricult. Water Manage.* 202, 19–32. doi: 10.1016/j.agwat.2018.02.011

Li, G., Cheng, Q., Li, L., Lu, D., and Lu, W. (2021). N, p and K use efficiency and maize yield responses to fertilization modes and densities. *J. Integr. Agr.* 20, 78–86. doi: 10.1016/S2095-3119(20)63214-2

Li, H., Wang, X., Brooker, R. W., Rengel, Z., Zhang, F., Davies, W., et al. (2019). Root competition resulting from spatial variation in nutrient distribution elicits decreasing maize yield at high planting density. *Plant Soil* 439, 219–232. doi: 10.1007/s11104-018-3812-5

Lu, D., Song, H., Jiang, S., Chen, X., Wang, H., and Zhou, J. (2019). Managing fertiliser placement locations and source types to improve rice yield and the use efficiency of nitrogen and phosphorus. *F. Crop Res.* 231, 10–17. doi: 10.1016/j.fcr.2018.11.004

Lynch, J., Mooney, S., Strock, C., and Schneider, H. (2022). Future roots for future soils. *Plant Cell Environ.* 45 (3), 620–636. doi: 10.1111/pce.14213

Marziliano, P., Lafortezza, R., Medicamento, U., Lorusso, L., Giannico, V., Colangelo, G., et al. (2015). Estimating belowground biomass and root/shoot ratio of phillyrea latifolia l. in the Mediterranean forest landscapes. *Ann. For. Sci.* 72 (5), 585–593. doi: 10.1007/s13595-015-0486-5

Murphy, J., and Riley, J. (1962). A modified single solution method for the determination of phosphate in natural waters. *Anal. Chim. Acta* 27, 31–36. doi: 10.1016/S0003-2670(00)88444-5

Muhaba, S., and Dakora, F. (2020). Symbiotic performance, shoot biomass and water-use efficiency of three groundnut (Arachis hypogaea l.) genotypes in response to phosphorus supply under field conditions in Ethiopia. *Front. Agr. Sci. Eng.* 7 (4), 455–466. doi: 10.15302/J-FASE-2020354

Nedelciu, C., Ragnarsdottir, K., Schlyter, P., and Stjernquist, I. (2020). Global phosphorus supply chain dynamics: Assessing regional impact to 2050. *Glob. Food secur* 26, 100426. doi: 10.1016/j.gfs.2020.100426

Niu, L., Yan, Y., Hou, P., Bai, W., Zhao, R., Wang, Y., et al. (2020). Influence of plastic film mulching and planting density on yield, leaf anatomy, and root characteristics of maize on the loess plateau. *Crop J.* 8 (4), 548–564. doi: 10.1016/j.cj.2019.12.002

Nkrumah, P., Echevarria, G., Erskine, P., Chaney, R., Sumail, S., and van der Ent, A. (2021). Contrasting phosphorus (P) accumulation in response to soil p availability in 'metal crops' from p-impoverished soils. *Plant Soil* 467 (1), 155–164. doi: 10.1007/s11104-020-04444-0

Pongrac, P., Castillo-Michel, H., Reyes-Herrera, J., Hancock, R., Fischer, S., Kelemen, M., et al. (2020). Effect of phosphorus supply on root traits of two *Brassica oleracea* l. genotypes. *BMC Plant Biol.* 20, 1–17. doi: 10.1186/s12870-020-02558-2

Postma, J., Hecht, V., Hikosaka, K., Nord, E., Pons, T., and Poorter, H. (2021). Dividing the pie: A quantitative review on plant density responses. *Plant Cell Environ.* 44, 13968. doi: 10.1111/pce.13968

Saia, S., Rappa, V., Ruisi, P., Abenavoli, M., Sunseri, F., Giambalvo, D., et al. (2015). Soil inoculation with symbiotic microorganisms promotes plant growth and nutrient transporter genes expression in durum wheat. *Front. Plant Sci.* 6. doi: 10.3389/fpls.2015.00815

Schneider, K., Thiessen Martens, J., Zvomuya, F., Reid, D., Fraser, T., Lynch, D., et al. (2019). Options for improved phosphorus cycling and use in agriculture at the field and regional scales. *J. Environ. Qual.* 48, 1247–1264. doi: 10.2134/jeq2019.02.0070

Semchenko, M. (2020). Constraints on selfish behavior in plants. *Science* 370, 1167–1168. doi: 10.1126/science.abf2785

Shao, H., Xia, T., Wu, D., Chen, F., and Mi, G. (2018). Root growth and root system architecture of field-grown maize in response to high planting density. *Plant Soil* 430, 395–411. doi: 10.1007/s11104-018-3720-8

Soltangheisi, A., Rodrigues, M., Coelho, M., Gasperini, A., Sartor, L., and Pavinato, P. (2018). Changes in soil phosphorus lability promoted by phosphate sources and cover crops. *Soil Till. Res.* 179, 20–28. doi: 10.1016/j.still.2018.01.006

Thorup-Kristensen, K., and Kirkegaard, J. (2016). Root system-based limits to agricultural productivity and efficiency: the farming systems context. *Ann. Bot.* 118, 573–592. doi: 10.1093/aob/mcw122

Tomasi, D., Gaiotti, F., Petoumenou, D., Lovat, L., Belfiore, N., Boscaro, D., et al. (2020). Winter pruning: Effect on root density, root distribution and root/canopy ratio in vitis vinifera cv. pinot gris. *Agronomy* 10 (10), 1509. doi: 10.3390/agronomy10101509

Trouvelot, A., Kough, J., and Gianiazzi-Pearson, V. (1986). "Mesure dutauxde mycorrhization VA d'un système radiculaire. recherche de methods d'estimation ayant une signifification fonctionnelle," in *Physiological and genetical aspects of mycorrhizae*. Eds. J. Gianinazzi-Pearson and S. Gianinazzi (Paris: INRA Press), 217–221.

Wang, X., Li, H., Chu, Q., Feng, G., Kuyper, T. W., and Rengel, Z. (2020). Mycorrhizal impacts on root trait plasticity of six maize varieties along a phosphorus supply gradient. *Plant Soil* 448, 71–86. doi: 10.1007/s00468-019-01858-x

Weligama, C., Tang, C., Sale, P., Conyers, K., and Liu, D. (2008). Localised nitrate and phosphate application enhances root proliferation by wheat and maximises rhizosphere alkalisation in acid subsoil. *Plant Soil* 312, 101–115. doi: 10.1007/s11104-008-9581-9

Williamson, L., Ribrioux, S., Fitter, A., and Ottoline Leyser, H. (2001). Phosphate availability regulates root system architecture in arabidopsis. *Plant Physiol.* 126, 875–882. doi: 10.1104/pp.126.2.875

Wu, Q., Du, M., Wu, J., Wang, N., Wang, B., Li, F., et al. (2019). Mepiquat chloride promotes cotton lateral root formation by modulating plant hormone homeostasis. *BMC Plant Biol.* 19, 573. doi: 10.1186/s12870-019-2176-1

Zhang, W., Chen, X., Liu, Y. M., Liu, D. Y., Chen, X., and Zou, C. (2017). Zinc uptake by roots and accumulation in maize plants as affected by phosphorus application and arbuscular mycorrhizal colonization. *Plant Soil* 413 (1), 59–71. doi: 10.1007/s11104-017-3213-1

Zhang, D., Li, H., Fu, Z., Cai, S., Xu, S., Zhu, H., et al. (2019). Increased planting density of Chinese milk vetch (Astragalus sinicus) weakens phosphorus uptake advantage by rapeseed (Brassica napus) in a mixed cropping system. *AoB Plants* 11, plz033. doi: 10.1093/aobpla/plz033

Zhang, C., Postma, J., York, L., and Lynch, J. (2014). Root foraging elicits niche complementarity-dependent yield advantage in the ancient "three sisters" (maize/bean/squash) polyculture. *Ann. Bot.* 114, 1719–1733. doi: 10.1093/aob/mcu191

Zhang, Y., Xu, Z. G., Li, J., and Wang, R. (2021). Optimum planting density improves resource use efficiency and yield stability of rainfed maize in semiarid climate. *Front. Plant Sci.* 12. doi: 10.3389/fpls.2021.752606

Zhou, B., Sun, X., Wang, D., Ding, Z., Li, C., Ma, W., et al. (2019b). Integrated agronomic practice increases maize grain yield and nitrogen use efficiency under various soil fertility conditions. *Crop J.* 7, 527–538. doi: 10.1016/j.cj.2018.12.005

Zhou, T., Wang, L., Li, S., Gao, Y., Du, Y., Zhao, L., et al. (2019a). Interactions between light intensity and phosphorus nutrition affect the p uptake capacity of maize and soybean seedling in a low light intensity area. *Front. Plant Sci.* 10. doi: 10.3389/fpls.2019.00183

Zhou, J., Zhang, L., Feng, G., and George, T. (2022). Arbuscular mycorrhizal fungi have a greater role than root hairs of maize for priming the rhizosphere microbial community and enhancing rhizosphere organic p mineralization. *Soil Biol. Biochem.* 171, 108713. doi: 10.1016/j.soilbio.2022.108713

frontiers | Frontiers in Plant Science

TYPE Review
PUBLISHED 29 September 2022
DOI 10.3389/fpls.2022.985429

OPEN ACCESS

EDITED BY
Maurizio Ruzzi,
University of Tuscia, Italy

REVIEWED BY
Satish Kumar Verma,
Banaras Hindu University, India
Antonio Ferrante,
University of Milan, Italy

*CORRESPONDENCE
Arpita Tripathi
arpitatripathi0391@gmail.com

†These authors have contributed equally to this work and share first authorship

SPECIALTY SECTION
This article was submitted to Plant Symbiotic Interactions, a section of the journal Frontiers in Plant Science

RECEIVED 03 July 2022
ACCEPTED 07 September 2022
PUBLISHED 29 September 2022

CITATION
Tripathi A, Pandey P, Tripathi SN and Kalra A (2022) Perspectives and potential applications of endophytic microorganisms in cultivation of medicinal and aromatic plants. *Front. Plant Sci.* 13:985429. doi: 10.3389/fpls.2022.985429

Perspectives and potential applications of endophytic microorganisms in cultivation of medicinal and aromatic plants

Arpita Tripathi[1,2,3*†], Praveen Pandey[1,4†], Shakti Nath Tripathi[5] and Alok Kalra[1]

[1]Microbial Technology Department, CSIR-Central Institute of Medicinal and Aromatic Plants, Lucknow, India, [2]Academy of Scientific and Innovative Research (AcSIR), Ghaziabad, India, [3]Faculty of Education, Teerthanker Mahaveer University, Moradabad, India, [4]Division of Plant Breeding and Genetic Resource Conservation, CSIR-Central Institute of Medicinal and Aromatic Plants, Lucknow, India, [5]Department of Botany, Nehru Gram Bharati Deemed to be University, Prayagraj, India

Ensuring food and nutritional security, it is crucial to use chemicals in agriculture to boost yields and protect the crops against biotic and abiotic perturbations. Conversely, excessive use of chemicals has led to many deleterious effects on the environment like pollution of soil, water, and air; loss of soil fertility; and development of pest resistance, and is now posing serious threats to biodiversity. Therefore, farming systems need to be upgraded towards the use of biological agents to retain agricultural and environmental sustainability. Plants exhibit a huge and varied niche for endophytic microorganisms inside the *planta*, resulting in a closer association between them. Endophytic microorganisms play pivotal roles in plant physiological and morphological characteristics, including growth promotion, survival, and fitness. Their mechanism of action includes both direct and indirect, such as mineral phosphate solubilization, fixating nitrogen, synthesis of auxins, production of siderophore, and various phytohormones. Medicinal and aromatic plants (MAPs) hold a crucial position worldwide for their valued essential oils and several phytopharmaceutically important bioactive compounds since ancient times; conversely, owing to the high demand for natural products, commercial cultivation of MAPs is on the upswing. Furthermore, the vulnerability to various pests and diseases enforces noteworthy production restraints that affect both crop yield and quality. Efforts have been made towards enhancing yields of plant crude drugs by improving crop varieties, cell cultures, transgenic plants, etc., but these are highly cost-demanding and time-consuming measures. Thus, it is essential to evolve efficient, eco-friendly, cost-effective simpler approaches for improvement in the yield and health of the plants. Harnessing endophytic microorganisms as biostimulants can be an effective and alternative step. This review summarizes the concept of endophytes, their multidimensional interaction inside the host plant, and the salient benefits associated with endophytic microorganisms in MAPs.

KEYWORDS

plant-microbe interaction, plant growth promotion, secondary metabolites, stress tolerance, medicinal plants, endophytic microorganisms

Introduction

Plants perform a range of fundamental functions in helping all distinct forms of living beings and release chemical signals to communicate with them. The roots give anchorage to the plant in soil and assist in the acquisition of water and nutrients, as well as produce chemical compounds that induce various types of interactions. This constitutes mutualism with the microorganisms that include fungi in mycorrhizal associations, endophytes, and plant growth-promoting rhizobacteria (PGPRs) as well as parasitism with pathogenic microorganisms, other plants, and herbivores (Badri et al., 2009). The plant roots discharge tremendous quantities of chemical compounds to fight pathogens and attract advantageous microorganisms (Badri and Vivanco, 2009). Such plant–microbe interactions occur at different trophic levels within a sophisticated arrangement of communities (Yan et al., 2019). Approximately 470 million years ago, the evolution of aquatic plants into terrestrial organisms was made possible by cooperating with soil microbes, and many of those microbe–plant interactions still persist (Bhattacharya and Medlin, 1998; Palmer et al., 2004; Ni et al., 2012; Williams et al., 2013). Some plant–microbe interactions are commensalism, where no harm is done to the plant, but the microbe gains some advantage. Several distinct interactions are advantageous to both partners (e.g., they are called mutualistic). Lastly, another group of microorganisms are pathogens and parasites to their host plants. In all the incidents, the microbe and the plant have established the ability to communicate. The microorganism recognizes and responds to the chemical signaling molecules produced by the plants. This usually results in the discharge of microbial compounds that are in turn identified by the plant, thereby generating a two-way "communication" that uses a molecular lexicon. Once a plant–microbe relationship begins, microbes and plants continue to observe their partner's physiology and coordinate their activities accordingly.

Medicinal and aromatic plants (MAPs) hold a crucial position within people's healthcare systems throughout the world. Until the arrival of advanced medicines, an oversized population in emerging nations has traditionally relied upon the products obtained from plants, particularly from forests. Numerous medicinal and aromatic crops are being exploited for economic uses. Approximately 12.5% of the more than 422,000 plant species have been universally documented for medicinal properties; however, only a couple of hundreds are known to be in cultivation (Schippmann et al., 2002). There is a need to grow MAPs to maintain their steady supply and conservation amidst decreasing stocks from natural sources and rising global interest. Apart from increasing farmers' income, MAPs cultivation also acts as insurance crops against the climate extremes. Its cultivation for essential oils and several phytopharmaceutically important compounds is an age-old aspect of agriculture; conversely, owing to the high demand for natural products, commercial cultivation of MAPs is on the upswing. Furthermore, the vulnerability to various biotic and abiotic perturbations (phytopathogens, drought, water-logging, salinity, temperature, etc.) enforces noteworthy production constraints to diminish both yield and overall quality of the crops. Until the arrival of today's medicine, a large part of the population in developing nations traditionally depended on the products obtained from plants, particularly from forests, for administering human and livestock ailments. Some efforts have been made towards enhancing yields of plant crude drugs by improving crop varieties, cell cultures, transgenic plants, etc., but these are highly cost-demanding and time-consuming measures. Thus, it is vital to evolve efficient, eco-friendly, cost-effective simpler approaches for improvement in yield and health of the plants.

Plant growth-promoting endophytic microorganisms inhabit and proliferate inside the plants without any distinct symptoms of any diseases *in-planta* (Bacon et al., 2002), and their mechanism includes both direct and indirect actions such as mineral phosphate solubilization (Verma et al., 2001), fixating nitrogen (Alishahi et al., 2020), synthesis of auxins (Patten and Glick, 2002), production of siderophore (Lodewyckx et al., 2002), and various phytohormones (Costacurta and Vanderleyden, 1995). As many abiotic stresses induce multiple physiological disturbances, which include stomatal closure and stunted plant growth, this ultimately results in lesser crop yield. It has been well reported that ACC (1-aminocyclopropane-1-carboxylic acid) deaminase-containing microbes lower the effect of stress induced by higher ethylene levels of the host plant (Penrose et al., 2001; Sessitsch et al., 2005; Glick, 2005; Sun et al., 2009; Rashid et al., 2012). Therefore, microbial treatments can protect plants from the damaging effects of environmental perturbations (Ali et al., 2014). Changes in climatic conditions such as rainfall, ambient CO_2, and varying temperatures affect

agriculture through countless constraints resulting in either low yields or sometimes death of the plants. This review reveals the role of endophytes in improving agricultural sustainability, which can serve as a valuable approach toward green cultivation of MAPs and cost-effective drug production.

Endophytes: Microbial entities for plant fitness

Endophytes, the Greek word having "endon" (within) and "phyton" (plant), was coined by De Bary (1879) for "any organism occurring within plant tissues". Bacon and White (2000) have defined endophyte in the broadest and widely accepted manner that states that endophytes include those microbes colonizing living plant internal tissues and not causing any instant, obvious ill effects. Thus, most precisely, endophytes refer to microorganisms (fungi, bacteria, actinomycetes, etc.) that spend at least a part of their life cycle establishing a relationship with a plant that remains asymptomatic (Vanessa and Christopher, 2004). Microorganisms that require living cells to grow and complete their life cycle are known as "obligate" while the others that mainly thrive on the outside of the plant tissues are termed as "epiphytes" and sometimes may enter the plant endosphere, called "opportunistic" (Hardoim et al., 2008). In this interaction, both plant and endophytic microbes live together, providing profound benefits to each other (Ting et al., 2009). These endophytes are often rhizospheric in nature, and preferable sites for their attachment and subsequent entry into the host plant could be apical root zone with thin-walled surface root layers and basal root zones with small cracks (Gagné, 1987). They proliferate in the entire host plant (Hallmann et al., 1997a), and reside within the cells, vascular tissues, or intercellular spaces (Patriquin and Dobereiner, 1978; Jacobs et al., 1985; Bell et al., 1995). Endophytic microbes could also enter through the stomata and vertically transmit from parent to offspring *via* seeds while roots have maximum colonization through epidermis formed by lateral root emergence (Roos and Hattingh, 1983; Agrawal and Shende, 1987). Which community of microbes are friends and which are foes? It is decided by the immune system of the plant itself (Zeilinger et al., 2016). The "balanced antagonism" with asymptomatic colonization between the host plant and endophytic microbes clearly shows that endophytes can live within the plant without activating any host defense mechanism and improves its self-sustenance through the production of the plant-like substances (Schulz et al., 1999; Schulz and Boyle, 2005).

The study of plant–microbe interactions helps us acknowledge natural events that influence our daily lives and could benefit befalling in sustainable resources, a smaller influence on the atmosphere and surroundings, and control of environmental pollution. The benefits of using these interactions for biotechnological applications are huge. The utilization of the pre-existing plant–microbe interactions for the promotion of growth of the plant and biocontrol diminishes the use of unnatural synthetic pesticides and fertilizers, resulting in lowering input costs and, more importantly, reducing the influence of chemical nutrients and pesticides on existing useful fiora and fauna (Boddey et al., 2003; Elmer and Reglinski, 2006; Whipps and Gerhardson, 2007). The production of beneficial compounds of industrial and pharmaceutical importance through plant–microbe symbiosis reduces the requirement to supply expensive catalysts and precursors and is energy-saving (Wu et al., 2007; Del Giudice et al., 2008). Remediation by traditional methods is costly and laborious; however, plant–microbe remediation approaches are incredibly efficient and less interfering (Anderson et al., 1993). The carbon sequestration by the plant–rhizosphere methods is probably a sustainable approach for reducing atmospheric carbon (Wu et al., 2009).

As the name implies, endophytic microorganisms live within a plant in the intercellular spaces of various plant parts such as stems, roots, petioles, leaves, etc., without imposing any apparent symptoms of disease or ill health. The symbiotic relationship of the host and its endophytes has been studied in detail and is explained as the plant partner protecting and feeding the endophytes, which, "in return", produce certain substances with bioactive capabilities (antiviral, plant growth promotion, antibacterial, antifungal, insecticidal, etc.) to augment the growth and competitiveness of the former under natural conditions. These endophytic entities defend their host plants from pathogens by secreting bioactive secondary metabolites under unfavorable environments (Azevedo et al., 2000; Strobel, 2003). The endophytic organisms are now recognized as a vital part of biodiversity, the allocation of endophytic microfiora varies with the difference according to its host. Zhang et al. (2006a) suggested that almost all of the vascular plants are known to harbor endophytic entities, especially those with medicinal values that are thought to be related to the formation of therapeutic products. Endophytic microbes are not entirely explored yet, but several investigations present them as an enormous therapeutic compound source. Worldwide, about 300,000 plants grown in an unexplored region are a host of at least one or more endophytic microbes (Araújo et al., 2001). Therefore, functionally diverse endophytes' occurrence offers a key role in ecosystems at the most plentiful biodiversity (Strobel, 2003). Survival of the endophytic microbes inside the host cell can be for a long duration. The ability of these microbes to produce bioactive secondary metabolites makes them interesting candidates to be studied and exploited in biotechnological aspects (Casella et al., 2013) to add on to the existing wealth of secondary metabolites. Such interest has been reflected in a number of recent reviews showcasing the secondary metabolite-producing abilities of these wonder

microbes (Müller, 2015). The growth and yield of several medicinal plants have been reported to be enhanced by many endophytes (Barnawal et al., 2012; Barnawal et al., 2014), especially by gene expression modulation regulated in important secondary metabolites' biosynthesis. They have also been reported to impart tolerance to the plants against a range of biotic and abiotic stresses (Pandey et al., 2016a; Pandey et al., 2016b; Lata et al., 2018).

Chemical fertilizers' indiscriminate use for boosting the productivity of crops is drastically destroying soil and environmental health (Tilman, 1998). Even then, the use of fertilizers is likely to increase further in agriculture to feed the ever-growing huge population (Vitousek et al., 1997; Frink et al., 1999). In the current scenario of global climate change, sustainable agriculture production proves to be a significant challenge. Some approaches such as the integration of microbes associated with plants in agriculture enhance the growth of the plant through different modes and alleviate several biotic and abiotic perturbations (Tanaka et al., 2005; Vega et al., 2008; Lata et al., 2018), and may serve as rescue practices under such situations.

Colonization of the endophytic microorganisms in plants

Plants exhibit a huge and varied niche for microorganisms inside the *planta* resulting in a closer association between them. Endophytes inhabit the internal plant tissue comprising different bacterial and fungal species that collectively form the "plant endomicrobiome" and can trigger various physiological responses in the plant. Colonization and benefits associated with endophytic microorganisms in plants are presented in Figure 1.

Colonization of the bacterial endophytes

Bacterial endophytes, sometimes considered a part of the population of rhizospheric microbes (Marquez-Santacruz et al., 2010), are present in various tissues such as the stem, root, leaf, tuber, and fruit, of different agricultural, horticultural, and forest species. As the endophytic bacteria are directly in contact with the plant tissues, they have the benefit of greater advantage than rhizospheric bacteria from the plants and offer more benefits to the plant other than bacteria in the rhizospheric region and outside the plants (Araujo et al., 2002). The wide-ranging and recurrent occurrence of such endophytic bacterial populations indicates that healthy plants recruit more endophytic populations (Hardoim et al., 2015) and provide these organisms with a huge and somewhat uncharted ecological niche.

The colonization of host-associated microbes occurs horizontally from the surroundings and might be vertical *via* parent to the progenies (Santoyo et al., 2016). Endophytic bacteria have several ways to enter inside the host plant tissues. Except for those microbes that are already established

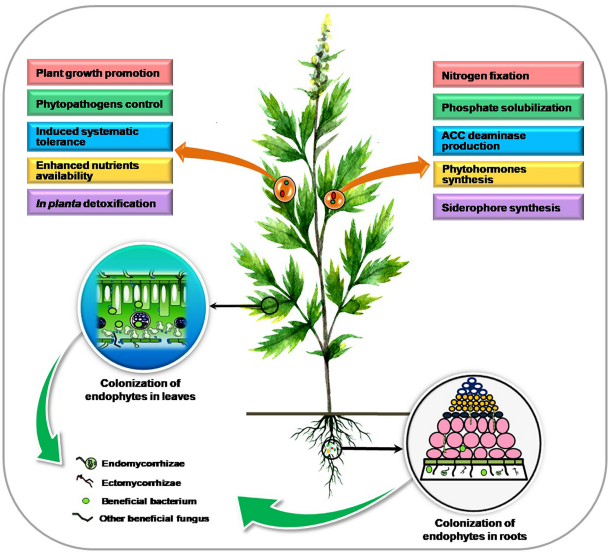

FIGURE 1
Colonization and benefits of endophytic microorganisms in plants.

inside the seeds of the plant (Truyens et al., 2014), the most frequent point of entry of endophytic bacterial endophytes inside the host plant is *via* the cracks on the roots and wounded root tissues formed as a result of growth and development of the plant (Sprent and De Faria, 1989; Sørensen and Sessitsch, 2006). This allows leakage of plant metabolites, which attract more bacteria towards it (Hallmann et al., 1997a). Other points of entry of endophytes could be lenticels present in root and shoot periderm (Scott et al., 1996), radicles of germinating seeds, or lateral root hair cells. For example, Hallmann et al. (1997b) showed that *Enterobacter asburiae* JM22, an endophytic bacterium in cotton plants, produces enzymes capable of hydrolyzing cellulose in the cell wall, assisting the entry of the bacterium inside the host plant.

Autofluorescent proteins (AFP) could be an important method as well as a tool for the visualization of the biofilm to study plant–microbe interaction. These visualization techniques also include gene expression studies using GFP (green fluorescent proteins) in which the GFP gene is integrated into the chromosome of bacteria and a plasmid containing GFP cloned cells which are visualized by confocal or epifluorescence or laser scanning microscopy (Villacieros et al., 2003; Germaine et al., 2004). In the β-glucuronidase (GUS) reporter system, staining helps in the visualization of bacterial movement and gene expression in the rhizosphere and phyllosphere, and entrance and site of pathogens can be studied by IVET (*in vivo* expression technology) (Preston et al., 2001; Leveau and Lindow, 2001; Zhang et al., 2006a).

Colonization of the fungal endophytes

For the recruitment of the endophytes, the host plant establishes symbiosis with large soil microbial diversity. Initially, attachment of the endophytic fungi might occur on the surface of roots and form structures called appressorium (Yedidia et al., 1999). After that, these attachments penetrate the outer root system and internally colonize the plant tissues (Viterbo and Chet, 2006; Nogueira-Lopez et al., 2018). Endophytic fungi mostly use two types of diffusion patterns; in the primary mechanism, fungi are vertically transmitted into progeny seed from maternal plants by which the offspring gets infected (Gagic et al., 2018). The endophytic fungi transmission among the host plants and the offspring is brought about under appropriate environmental conditions when infected seeds germinate and the endophytic fungi present inside the seed enter the seedlings after the germination of seeds (Hodgson et al., 2014).

Generally, endophytic fungi initiate from the nutrient-rich atmosphere of the rhizosphere, which also has insects and animal feeding processes, and air floating fungal spores (Rodriguez et al., 2009; Sasse et al., 2018). Many of the endophytic fungal microbes are transmitted through spores or hyphal fragments horizontally in aboveground tissues, by insects or herbivores (biotic) or rain or wind (abiotic dispersion agents) from plant to plant, thus establishing communication of fungal endophytes between several plant hosts (Wiewiora et al., 2015).

Microscopic observations of tomato roots on early colonization by the endophytic fungus *Trichoderma* illustrated no disturbance in cell integrity during this process (Chacón et al., 2007). However, in cucumber roots colonized by endophytes, various phenomena such as enhanced chitinase activity, necrosis of the penetration peg, and fluorescent products' formation in the intercellular spaces were observed. This phenomenon might be due to copious extracellular enzyme production by endophytic fungi (Suryanarayanan et al., 2012).

How endophytic microorganisms benefit the plants

Not much information exists about the mechanisms of endophyte-mediated plant growth enhancement. Endophytes can mediate plant growth improvement both directly and indirectly (Figure 2). As rhizospheric bacterium initiates its development into endophytes, it is supposed that endophytes can maintain their characteristics inside the host plant.

Direct beneficial mechanisms

Endophytic microbes help host plants directly in many ways to promote the plant's growth by improving the uptake of essential nutrients, which ultimately increases overall crop yield (Muthukumarasamy et al., 2002). A typical example is nitrogen fixation by particular endophytes in leguminous crops (Stacey et al., 2006). Additionally, several researchers have stated that endophytic bacteria effectively associate with non-leguminous crops to form a synergistic association intended for nitrogen fixation (Bhattacharjee et al., 2008; Saravanan et al., 2008; Mattos et al., 2008; Govindarajan et al., 2008; Oliveira et al., 2009). Plant growth enhancement may occur *via* many approaches that include plant hormone production, like gibberellins, IAA (indole-3-acetic acid), ethylene, and cytokinin regulation and activity. Many endophytes have shown to exhibit an activity of enzyme ACC (1-aminocyclopropane-1-carboxylate) deaminase to modulate physiology by reducing ethylene content (Hardoim et al., 2008; Barnawal et al., 2012) since ethylene in plant growth inhibitive hormone. In previous studies, *Burkholderia phytofirmans*, a plant growth-promoting endophytic strain, has been proven to enhance the yields of numerous crops (Lazarovits and Nowak, 1997; Sharma and Nowak, 1998; Sessitsch et al., 2005; Barka

10.3389/fpls.2022.985429

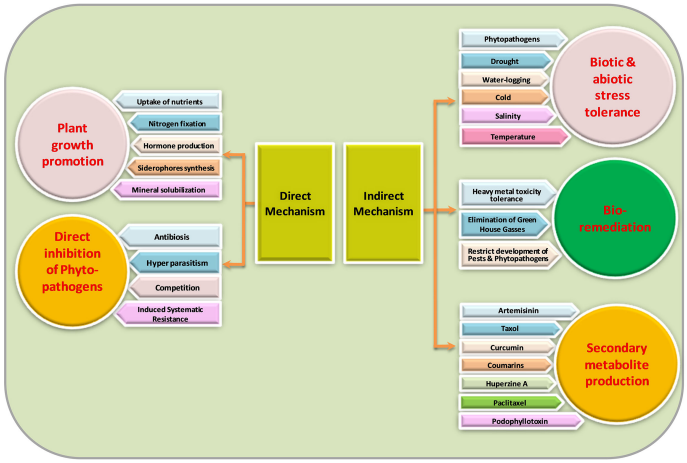

FIGURE 2
Mechanism of action of endophytic microorganisms.

et al., 2006). Similarly, Mattos et al. (2008) showed that *Burkholderia kururiensis*, an endophytic bacterium, enhances IAA hormone production. *Penicillium citrinum* strain generated a large amount of physiologically active gibberellins than *Gibberlla fujikuroi* (wild type), which offers to generate a biologically active source of gibberellic acid (GA3) (Khan et al., 2008). Various studies showed that a variety of fungal endophytes promoted height, biomass, and tiller number in numerous crops (Spiering et al., 2006; Zhang et al., 2007; Lowe et al., 2008). *Stagonospora* spp., a seed-borne endophytic fungus, increased the yield of *Phragmites australis* (Cav.) Trin. ex Steud. (Ernst et al., 2003), and endophytic fungus promoted growth in peppermint (Mucciarelli et al., 2003). Some examples of endophytic microbes' associated benefits in medicinal and aromatic plants are presented in Table 1.

Indirect beneficial mechanisms

Plants muddle through various unfavorable environmental conditions or abiotic stresses like cold, drought, hyper-salty situations, or pathogenesis. Endophytic microbes help the plant conquer such perturbations through some indirect mechanisms, which also promote the buildup of secondary metabolites (including drugs or important medicinal components) in plants.

The endophytic microbes support the host plants to defeat the before-mentioned stresses by some indirect mechanisms. They are also effective in bioremediation by various means, like they decrease heavy metal stress (Zhang et al., 2012), eliminating harmful greenhouse gases (Stępniewska and Kuźniar, 2013), and restricting the development of pests on plants (Azevedo et al., 2000). Endophytic microbes also support phytoremediation by reducing metal phytotoxicity. Simultaneously, for plants containing endophytes with requisite metabolic capabilities and degradation pathways for reducing phytotoxicity and magnifying degradation, the plant–endophyte relationships can be equipped to remediate wastelands and groundwater (Weyens et al., 2009). Rajkumar et al. (2009) reported that endophytic bacteria assist in promoting the extraction of heavy metals. Endophytes are also effective in the degradation of polyaromatic hydrocarbon (PAH). Radwan (2009) documented the phytoremediation of oily soils using rhizobacteria, which appears to be a cheap and environmentally friendly method of cleaning the environment.

Tolerance to biotic stresses

Endophytic microorganisms have the ability to enhance plant resistance systems against pathogen infestation through antagonistic activity (Miller et al., 2002; Gunatilaka, 2006). Many studies showed that endophytes have a crucial role in regulating the gene expression of the host, modulating physiological responses and plant defense-related pathways (Van Bael et al., 2012; Estrada et al., 2013; Salam et al., 2017). Khare et al. (2016) illustrated that jasmonic acid and salicylic acid could greatly contribute to plant stress responses against phytopathogens. Ren and Dai (2012) described that inoculation with *Gilmaniella* sp. AL12 induces jasmonic acid defense responses against pathogenic fungi in *Atractylodes lancea* (Thunb.) DC. The gibberellins produced by endophytes enhance insect and phytopathogens' resistance *via* salicylic and jasmonic acid pathways (Waqas et al., 2015a). An endophyte, *Fusarium solani*, elicits induced systemic resistance against a fungal pathogen, *Septoria lycopersici*, by stimulating gene expression

TABLE 1 Benefits conferred by endophytic microorganisms in medicinal and aromatic plants.

Endophytic microorganisms	Host plant	Associated benefits	References
Bacterial endophytes			
Pseudomonas putida BP25	*Piper nigrum* (L.)	Inhibition of phytopathogens	Sheoran et al., 2015
Bacillus licheniformi, B. subtilis, B. circulan, B. amyloliquefacien, B. licheniformi, Arthrobacter, Marmoricola sp., *Acinetobacte, Microbacterium, Kocuria* sp., *Janibacter*	*Papaver somniferum* (L.)	Plant productivity and alkaloid biosynthesis	Pandey et al., 2016a
Gordonea terrae	*Avicennia marina* (Forssk.) Vierh.	Plant growth promotion	Soldan et al., 2019
Pantoea, *Pseudomonas*, *Enterobacter*	*Eleusine coracana* (L.)	Plant growth promotion	Misganaw et al., 2019
Burkholderia phytofirmans strain PsJN	*Vitis vinifera* (L.)	Plant growth promotion, enhancement of chilling resistance	Barka et al., 2006
Bacillus subtilis LE24, Bacillus amyloliquefaciens LE109, Bacillus tequilensis PO80	*Citrus* (L.)	Biocontrol of pathogens	Daungfu et al., 2019
Enterobacter sp. SA187		Plant growth promotion and salinity stress tolerance	de Zélicourt et al., 2018
Burkholderia sp.	*Helianthus annuus* (L.)	Calcium and phosphate solubilization	Ambrosini et al., 2012
Fungal endophytes			
Mucor sp.	*Arabidopsis arenosa* (L.) Lawalrée	Metal toxicity tolerance	Domka et al., 2019
Colletotrichum tropicale	*Theobroma cacao* (L.)	Tolerance to *Phytophthora*	Mejia et al., 2008
Aspergillus fumigatus TS1, Fusarium proliferatum BRL1	*Oxalis corniculata* (L.)	Plant growth promotion	Bilal et al., 2018
Yarrowia lipolytica	*Euphorbia milii* Des Moul.	Plant growth promotion and salinity stress tolerance	Jan et al., 2019
Penicillium citrinum LWL4, Aspergillus terreus LWL5	*Helianthus annuus* (L.)	Plant growth promotion, disease resistance	Waqas et al., 2015b
Paecilomyces variotii, Penicillium purpurogenum	*Caralluma acutangula* (Decne.) N.E.Br.	Plant growth promotion	Ali et al., 2019
Sclerotium sp.	*Atracty lancea* (Thunb.) DC.	Increases cell protection from desiccationin and leaf metabolic capability of host	Chen et al., 2008
Epulorhiza sp.	*Anoectochillus formosanus* Hayata	Enhances enzyme activities	Tang et al., 2008
Epulorhiza sp., *Mycena anoectochila*	*Anoectochilus roxburghii* (Wall.) Lindl.	Enhances enzyme activities	Yu and Guo, 2000; Chen et al., 2005
Piriformospora indica	*Cymbidium aloifolium* (L.) Sw.	Plant growth promotion and abiotic stress tolerance	Shah et al., 2019a
Mycena orchdicola	*Cymbidium sinense* Willd.	Secretes phytohormones	Zhang et al., 1999
Fusarium sp.	*Dendrobium moniliforme* (L.) Sw.	Plant growth promotion	Shah et al., 2019b
Mycena dendrobii	*Dendrobium candidum* Wall. ex Lindl.	Secretes phytohormones	Zhang et al., 1999
Epulorhiza sp., *Mycena* sp., *Sebacinales, Cantharellales*	*Dendrobium nobile* Lindl., *D. chrysanthum* Wall.	Enhances the nutrient absorption in plants, promoting the seed germination of host	Chen and Guo, 2005
Aspergillus awamori W11	*Withania somnifera* (L.)	Plant growth promotion	Mehmood et al., 2019
Aspergillus terreus, *Penicillium oxalicum, Sarocladium kiliense*		Biosynthesis of withanolide	Kushwaha et al., 2019a
Aspergillus terreus, Penicillium oxalicum, Sarocladium kiliense		Plant growth promotion, enhances withanolide content	Kushwaha et al., 2019b

(Continued)

TABLE 1 Continued

Endophytic microorganisms	Host plant	Associated benefits	References
Mycena dendrobii, M. osmundicola, Mycena orchidicola, M. anoectochili	*Gastrodia elata* Blume	Secretes phytohormones, promoting seed germination	Guo and Wang, 2001
Epulorhiza sp., *Fusarium* sp.	*Pecteilis susannae* (L.) Raf.	Enhances NPK absorption plants promoting the seed germination of host	Chutima et al., 2011
Penicillium sp., *Aspergillus* sp.	*Monochoria vaginalis* (Burm.f.) C.Presl ex Kunth	Secretes gibberellins	Ahmad et al., 2010
Dark septate endophytic fungi (DSEF)	*Pedicularis* (L.)	Increases their nutrient utilization efficiency	Li and Guan, 2007
Ceratobasidium sp.	*Rehmannia glutinosa* Steud.	Secretes IAA	Chen et al., 2011a
Sebacina vermifera	*Nicotiana attenuata* Steud.	Enhances absorption of nutrient and promote the growth and fitness by inhibiting ethylene signaling	Barazani et al., 2007
Funneliformis mosseae, Rhizophagus intraradices,Claroideoglomus etunicatum	*Sesbania sesban* (L.) Merr.	Secretes phytohormones	Abd Allah et al., 2015
Chaetomium globosum, Aspergillus proliferans, Purpureocillium lilacinum	*Papaver somniferum* (L.)	Enhances plant productivity and benzylisoquinoline alkaloid (BIA) biosynthesis	Pandey et al., 2016a
Curvularia sp., *Choanephora infundibulifera*	*Catharanthus roseus* (L.)	Terpenoid indole alkaloid biosynthesis	Pandey et al., 2016b

linked to the pathogenesis (Kavroulakis et al., 2007). Foliar endophytic fungi, *Colletotrichum tropicale*, inoculated in *Theobroma cacao* (L.) enhance tolerance to *Phytophthora* (Mejía et al., 2008). The endophytic bacteria produce several antimicrobial compounds that can increase the resistance of the plants to various phytopathogenic fungi, bacteria, nematodes, etc. Endophytic *Pseudomonas putida* BP25 associated with black pepper inhibits a range of phytopathogens, viz., *Rhizoctonia solani, Phytophthora capsici, Gibberella moniliformis, Pythium myriotylum, Radopholus similis*, and *Colletotrichum gloeosporioides* by the production of several compounds (Sheoran et al., 2015). *Macrophomina phaseolina* causes charcoal rot disease in different crops and has been reported to be restricted by siderophore-producing *Rhizobium* (Arora et al., 2001). An endophyte, *Pseudomonas fluorescens*, having antagonistic effects against *Vertcillium* was isolated by Mercado-Blanco et al. (2004) from olive plant roots. Yong et al. (1994) established the role of endophyte *Fusarium* spp. in the enhancement of growth and terpenoid content in *Euphorbia pekinensis* Rupr.

The endophytic fungus *Phomopsis cassia* associated with *Cassia spectabilis* enhances tolerance against phytopathogenic fungi *Cadosporium sphaerospermum* and *C. cladosporioides* by producing cadinane sesquiterpenoids, which are toxic to pathogens (Silva et al., 2006). Similarly, Wang et al. (2012) reported that an endophyte, *Chaetomium globosum* L18, inhibits pathogenic fungi by synthesizing some toxic chemicals in *Curcuma wenyujin* Y. H. Chen & C. Ling. In another study, Cao et al. (2009) identified endophytic microbes *Choiromyces aboriginum, Stachybotrys elegans*, and *Cylindrocarpon* associated produces cell wall-degrading enzymes to kill pathogenic fungi in *Phragmites australis* (Cav.) Trin. ex Steud. Furthermore, an endophytic fungus, *Trichothecium roseum*, has a toxic chemical, "trichothecin", which enhances tolerance to pathogenic fungi in *Maytenus hookeri* Loes. (Zhang et al., 2010). Similarly, *Bacillus subtilis* and *Myxormia* sp. also enhance tolerance against pathogenic fungi *Fusarium oxysporum* and *F. solani* in *Angelica sinensis* (Oliv.) Diels (Yang et al., 2012).

Endophytic microbes *Chaetomium cochliodes, Cladosporium cladosporioides*, and *Trichoderma viride* enhance insect resistance in creeping thistle *via* producing some chemicals toxic to pathogens (Gange et al., 2012). Similarly, Sumarah et al. (2010) reported that fungal endophytes enhance resistance against *Choristoneura fumiferana* insect in red spruce (*Picea rubens* Sarg.). An endophyte, *Leucocoprinus gongylophorus*, increases insect resistance by synthesizing some chemicals antagonistic to ants' fungal symbiont (Bittleston et al., 2011). Furthermore, the endophyte *Chaetomium* Ch1001 associated with cucumber enhances tolerance against root-knot nematode by producing abscisic acid affecting the motility of the second-stage juveniles of insects (Yan et al., 2011). According to the study undertaken by Gómez-Vidal et al. (2009), endophytes *Beauveria bassiana, Lecanicillium dimorphum*, and *L.* cf. *Psalliotae* increase insect resistance to *Phoenix dactylifera* by modulating the expression of cell division-related proteins in the host plant. Strobel et al. (1999) reported that in thunder god vine (*Triptergyium wilfordii* Hook. f.), an endophye, *Cryptosporiopsis* cf. *quercina*, produces "cryptocin" and "cryptocandin" toxic to pathogenic fungi

Pyricularia oryzae in host plant. Daungfu et al. (2019) recently identified several endophytes, *Bacillus subtilis LE24*, *Bacillus amyloliquefaciens LE109*, and *Bacillus tequilensis PO80*, isolated from citrus plant having antagonistic effects against pathogens, which might be helpful in the biocontrol of pathogens. All these findings strongly confirm that the presence of endophytes in the host has the potential to increase their tolerance to pathogens through several mechanisms. Conversely, in resistance stimulation to disease facilitation, the process wherein endophytes invade plant tissues affects endophyte–pathogen interactions, perhaps producing facilitation (positive induction of pathogens), negatively strengthening host resistance, or having no effect at all (Suryanarayanan et al., 2009; Schmidt et al., 2014; Adame-Alvarez et al., 2014). These require further research for confirmation.

Tolerance to abiotic stresses

Abiotic stressful conditions, viz., drought, water-logging, salinity, cold, heat, and heavy metal toxicity, may cause adverse effects on soil and environmental health (Wang et al., 2003; Khare and Arora, 2015). Endophytes have a vital function in increasing tolerance against abiotic perturbations in plants (Wani et al., 2016). Waqas et al. (2012) reported that stomatal closure mediated by abscisic acid (ABA) might have a key function in the regulation of plant growth by reducing other abiotic stresses, including osmotic stress.

Under drought stress, an endophytic bacterium, *Sinorhizobium meliloti*, upregulated FeSOD and CU/ZnSOD, promoting drought tolerance in *Medicago sativa* (L.) (Naya et al., 2007). Similarly, *Arbuseular mycorrhiza* improves nutrient absorption and modifies Salvia's metabolic activities to boost drought tolerance (Meng and He, 2011). An endophytic microbe, *Trichoderma hamatum DIS 219b*, delayed drought-induced alterations in stomatal conductance and net photosynthesis, promoting drought tolerance in *Theobroma cacao* (L.) (Bae et al., 2009). According to Sziderics et al. (2007), a fungal endophyte, *Piriformospora indica*, enhances osmotic stress tolerance *via* encoding enzyme ACC oxidase and lipid transfer protein. Wang et al. (2009) reported that *Arbuseular mycorrhiza* and *Penicillium griseofulvum* reduce injury of water stress by increasing the activity of protective enzymes and osmotica contents, thereby enhancing tolerance against salt and drought stress in *Glycyrrhiza uralensis*. Liu et al. (2011) reported that soluble protein concentration and peroxidase activity (POD) are altered by *Chaetomium globosum and Botrytis* sp. Under salt stress in *Chrysanthemum morifolium* (Ramat.) Hemsl. A fungal endophyte, *Yarrowia lipolytica*, promotes salinity stress tolerance in *Euphorbia milii* Des Moul. (Jan et al., 2019).

Moreover, ABA-mediated signaling pathways and their biosynthesis during salinity stress are altered by several microbes in the plant endosphere and may help plant growth. *B. phytofirmans* (PsJN) altered gene expression for a cell surface signaling element, which passes signals to bacteria about the alteration in environmental conditions and consequently improves their metabolism (Sheibani-Tezerji et al., 2015). Fernandez et al. (2012) reported in PsJN bacterized grapevine that stress-induced gene expression in addition to metabolite levels improved over control at a lower temperature by balancing carbohydrate metabolism. Recently, de Zélicourt et al. (2018) reported that *Enterobacter* sp. (SA187), an endophyte, colonizes *Arabidopsis* root and shoot tissues and stimulates tolerance against salt stress by synthesizing KMBA (2-keto-4-methylthiobutyric acid). Márquez et al. (2007) reported that at high soil temperatures, *Curvularia protuberate*, an endophytic fungus, has been linked to *Dichanthelium lanuginosum* for its survival. Wan et al. (2012) reported that endophytes can also reduce the heavy metal-promoted oxidative injury. Earlier studies suggested endophytic bacteria's function in enhancing tolerance to metal toxicity through diverse mechanisms such as sequestration, intracellular accumulation, and extracellular precipitation or alteration of toxic metal ions to a minimum or non-toxic form (Ma et al., 2016; Mishra et al., 2017). Luo et al. (2012) discovered that a bacterial endophyte, *Bacillus* sp. *SLS18*, reduces heavy metal toxicity *via* root tillers and biomass accumulation in *Solanum nigrum* (L.) and *Phytolacca acinosa* Roxb. Recently, Domka et al. (2019) identified an endophytic fungus, *Mucor* sp., which enhances metal toxicity tolerance in *Arabidopsis arinosa* (L.) Lawalrée. Some examples of endophytes enhancing the tolerance of crop plants against abiotic and biotic stresses are presented in Table 2.

Endophytic microorganisms producing secondary metabolites/ bioactive compounds in the host plant

The diversity of bioactive compounds varies according to the habitats of the host plants; for example, in a tropical rain forest, limited resource availability leads to great competition among plants and their endophytes; thus, selection pressure is at the peak, resulting in the production of many novel molecules as compared to temperate forests (Reddell and Gordon, 2000). Isolation of indigenous microbes from different plant parts and their interaction with the host plant may divulge applicant microbes to promote plant growth and as biocontrol agents. Such microbial inoculants have the potential to provide resistance against environmental perturbations without affecting the indigenous microbial equilibrium (Palaniyandi et al., 2013).

TABLE 2 Host medicinal plants with enhanced defense responses conferred by endophytic microorganisms.

Endophytic microorganisms	Host plant	Type of stresses	Mechanism	References
Bacillus subtilis, Myxormia sp.	*Angelica sinensis* (Oliv.) Diels	Pathogenic fungi: Fusarium oxysporum and F. solani	Produce some chemicals toxic to pathogens	Yang et al., 2012
Gilmaniella sp. AL12.	*Atractylodes lancea* (Thunb.) DC.	Pathogenic fungi	Produce jasmonic acid inducing defense responses	Ren and Dai, 2012
P. indica	*Capsicum annum* (L.)	Osmotic stress	Encodes enzyme ACC oxidase, encodes a lipid transfer protein	Sziderics et al., 2007
Phomopsis cassia	*Cassia spectabilis* DC.	Pathogenic fungi: Cadosporium sphaerospermum, C. cladosporioides	Produce cadinane sesquiterpenoids toxic to pathogens	Silva et al., 2006
Chaetomium globosum, Botrytis sp.	*Chrysanthemum morifolium* (Ramat.) Hemsl.	Salt stress	Increase POD activity and soluble protein content	Liu et al., 2011
Chaetomium cochliodes, Cladosporium cladosporioides, Trichoderma viride	*Cirsium arvense* (L.) Scop.	Insect	Produce some chemicals toxic to pathogens	Gange et al., 2012
Leucocoprinus gongylophorus	*Cordia alliodora Cham.*	Insect	Produce some chemicals antagonistic to ants' fungal symbiont	Bittleston et al., 2011
Chaetomium Ch1001	*Cucumis sativus* (L.)	Insect: root-knot nematode Meloidogyne incognita	Produced abscisic acid affecting motility of the second stage juveniles of insects	Yan et al., 2011
Chaetomium globosum L18	*Curcuma wenyujin* Y.H. Chen & C. Ling	Pathogenic fungi	Produce some chemicals toxic to pathogens	Wang et al., 2012
Arbuseular mycorrhiza, Penicillium griseofulvum	*Glycyrrhiza uralensis* Fisch. ex DC.	Drought and salt stress	Reduce injury of water stress by increasing protective enzymes' activity and osmotica contents	Wang et al., 2009
Trichothecium roseum	*Maytenus hookeri* Loes.	Pathogenic fungi	Produce trichothecin toxic to pathogens	Zhang et al., 2010
Sinorhizobium meliloti	*Medicago sativa* (L.)	Drought stress	FeSOD and CU/ZnSOD are upregulated	Naya et al., 2007
Pseudomonas koreensis AGB-1	*Miscanthus sinensis* Andersson	Heavy metal toxicity (Zn, Cd, As, and Pb)	Through extracellular sequestration, increased catalase and SOD activities in plants	Babu et al., 2015
Beauveria bassiana, Lecanicillium dimorphum, L. cf. *Psalliotae*	*Phoenix dactylifera* (L.)	Insect	Modulate the expression of cell division-related proteins in host	Gómez-Vidal et al., 2009
Choiromyces aboriginum, Stachybotrys elegans, Cylindrocarpon	*Phragmites australis* (Cav.) Steud.	Pathogenic fungi	Produce cell wall-degrading enzymes to kill pathogenic fungi	Cao et al., 2009
150 foliar fungal endophytes	*Picea rubens* Sarg.	Insects: Choristoneura fumiferana	Produce some chemicals toxic to insects	Sumarah et al., 2010
Arbuseular mycorrhiza	*Salvia miltiorrhiza* Bunge	Drought stress	Increase the absorption of nutrient and alter metabolic activities in host	Meng and He, 2011
Bacillus sp. SLS18	*Solanum nigrum* (L.), Phytolacca acinosa Roxb.	Heavy metal toxicity (Mn and Cd)	Accumulation of root tillers and biomass	Luo et al., 2012
Trichoderma hamatum DIS 219b	*Theobroma cacao* (L.)	Drought stress	Delayed drought-induced changes in stomatal conductance and net photosynthesis	Bae et al., 2009
Cryptosporiopsis cf. *quercina*	*Triptergyium wilfordii* Hook.f.	Pathogenic fungi: Pyricularia oryzae	Produce cryptocin and cryptocandin toxic to pathogens	Strobel et al., 1999

Many endophytic microbes can synthesize a notable variety of secondary metabolites like antioxidant, anticancer, immunosuppressive, antidiabetic, antioomycete, antifungal, antibacterial, antiviral, and nematicidal agents (Gunatilaka, 2006; Zhang et al., 2006b; Verma et al., 2009; Aly et al., 2011). Shimizu (2011) reported that endophytic actinobacteria synthesize antibiotics, which is useful in plant growth promotion and improves the tolerance of plants to stress. Endophytes also have been in the limelight during the last decade or so because of their capability in producing several secondary metabolites that are bioactive (Tan and Zou, 2001; Schulz et al., 2002; Strobel, 2003; Prado et al., 2013). These compounds extracted from endophytes belong to the various chemical groups like xanthones, terpenoids, phenols, steroids, benzopyranones, isocoumarins, chinones, cytochalasins, tetralones, and enniatines (Schulz et al., 2002). Sometimes, these endophytic microbes may cause variation in well-known structural compounds like fungal steroids, ergosterol, or plant

hormone indole-3-acetic acid (Lu et al., 2000). Several endophytes can also be attributed to providing protection of plants against pests because of the compounds occurring in them (Poling et al., 2008).

There are many reports that have shown that host secondary metabolism can be induced by endophytes, but such interaction has not been much explored. Qawasmeh et al. (2012) reported that when endophytes (from the Clavicipitaceae family) interact with grasses, there is a production of phenolic compounds, which are mainly defense-related. However, secondary metabolites could remain unchanged or get reduced depending on which type of endophyte interacts with the host plant. A well-known example of a high-demanding anticancerous molecule is "taxol" isolated from *Taxomyces andreanae*, a taxol-producing fungal endophyte of *Taxus* species (Stierle et al., 1995). An example showed that bacterial endophytes have methanol dehydrogenase genes, which were known to express furanone biosynthesis and localized especially in vascular tissues of strawberry receptacles and plant achenes cells (Nasopoulou et al., 2014). Likewise, Koskimaki et al. (2009) have reported that fungal endophyte *Paraphaeosphaeria* sp. increased the accumulation and biosynthesis of flavan-3-ols phenolic acids and oligomeric proanthocyanidins in *Vaccinium myrtillus*. In *Artemisia annua* (L.), an endophytic bacterium, *Pseudonocardia* sp., has been reported to increase artemisinin synthesis by upregulating the cytochrome P450 monooxygenase (CYP71AVI) and cytochrome P450 oxidoreductase (CPR) genes, and this also activated a defense mechanism (Wang et al., 2006). It has also been found that endophytes may act as upregulators of the specific gene expression for tissue-specific roles, **e.g.,** foliar endophytes enhanced primary metabolites, crop yields could be increased by root endophytes, and endophytes isolated from the capsule could upregulate key genes of benzylisoquinoline alkaloid (BIA) biosynthesis in *Papaver somniferum* (L.) (Pandey et al., 2016a). Tiwari et al. (2010) found an improved content and yield of essential oils in holy basil. In the Chinese medicinal plant *Atractylodes lancea* (Thunb.) DC., the endophytic bacterium *P. fluorescens* could enhance the generation of ROS (reactive oxygen species), which resulted in an increase of sesquiterpenoids (Zhou et al., 2015). Endophytic bacteria *Aranicola proteolyticus, Bacillus cereus, B. thuringiensis, B. licheniformi*, and *Serratia liquefaciens* recovered from *Pinellia ternata* (Thunb.) Makino could produce inosine and guanosine alkaloids similar to their host plant in fermentation media (Liu et al., 2015). Tiwari et al. (2013) found that endophyte *Micrococcus* sp. and *Staphylococcus sciuri* inoculated plant had significantly higher amounts of ajmalicine, serpentine, and vindoline in *Catharanthus roseus* (L.) G. Don. Kumar et al. (2014) reported that the endophytic bacterium *Azotobactor chroococcum* could enhance the yield of curcumin in rhizomes of turmeric.

Endophytic microflora encompasses a high potential for the synthesis of an ample range of unidentified, undepicted novel secondary metabolites within or without host plants. It is needed to identify which type of mechanism or cryptic genes and what circumstances for the evolution of the genome are involved in the synthesis of novel compounds in endophytes as well as *in-planta*. Some examples of endophytes producing secondary metabolites in host plants are presented in Table 3.

Phytoremediation

Phytoremediation is the most efficient and eco-friendly system for restoring natural soil conditions when various environmental pollutants have contaminated it. In the past two decades, endophytes' usage in the phytoremediation of diverse environmental pollutants has received more attention (Sheng et al., 2008; McGuinness and Dowling, 2009; Weyens et al., 2009; Weyens et al., 2010; Hur et al., 2011; Segura and Ramos, 2013; Wei et al., 2014; Anyasi and Atagana, 2018). Such research has shown the potential of plant–microbe interaction in the restoration of polluted regions and may be helpful in designing efficient environmental pollutant removal systems. One of the reasons could be attributed to the complicated relationship between endophytes and their hosts. In contrast, the other reason has to do with the fact that it is practically impossible to comprehend the mechanisms of existence and situations of endophytes to be able to replicate them. It is impractical to exaggerate the role of endophytes in both management and harnessing the natural environment. Unfortunately, the holistic view of these taxa has been constrained by them. Such constraints include the fact that the process of isolation of endophyte relies on culture dependence, while several microorganisms exist that cannot be cultured. This emphasizes nonculture-dependent innovation as the barrier to understanding endophytes.

Agronomic practical application of endophytic microorganisms

The most frequently used inoculation technique in agriculture includes the use of endophytes; culture, facilitated by a carrier, is combined with the synthetically manufactured sticky seeds and sown. Moreover, several commercial formulations include liquid cultures directly applied or with the granular fertilizer or seed applications. Other techniques have also been used, including seed priming, seed coating, foliar spraying, root dipping, pelleting, and direct soil application (O'Callaghan, 2016). Given the presence of endophytic microbes, seed inoculation can accomplish this goal. Still, its effectiveness is constrained by the lengthy engaging period, subsequent physical abrasion, and competition with other soil microbes. Root dipping or seedlings treated with microbial

TABLE 3 Endophytic microorganisms producing plant secondary metabolites in host plants.

Endophytic microorganisms	Host plant	Plant secondary metabolite	Bioactivity of secondary metabolite	References
Bacterial endophytes				
Jishengella endophytica	*Xylocarpus granatum* J. Koenig	Perlolyrine	Antiviral effect	Wang et al., 2014
Streptomyces sp. *TP-A0569*	*Allium fistulosum* (L.)	Fistupyrone	Protection against pathogenic fungi	Bernardi et al., 2019
Streptomyces sp. *TP-A0556*	*Aucuba japonica* Thunb.	Coumarins TPU-0031-A and B	Antibiotic activity against Gram-positive and Gram-negative bacteria	Bernardi et al., 2019
Streptomyces hygroscopicus TP-A0451	*Pteridium aquilinum* (L.) Kuhn	Pteridic acids A and B, Pterocidin	Plant growth-promoting properties	Bernardi et al., 2019
Taxomyces andreanae	*Taxus brevifolia* Nutt.	Taxol	Anticancer	Strobel et al., 1993
Streptomyces griseus	*Kandelia candel* (L.) Druce	p-Aminoacetophenonic acids	Antimicrobial	Guan et al., 2005
Streptomyces NRRL 30562	*Kennedia nigricans* Lindl.	Munumbicins Munumbicin D	Antibiotic Antimalarial	Castillo et al., 2002
Serratia marcescens	*Rhyncholacis penicillata* Matthiesen	Oocydin A	Antifungal	Strobel et al., 2004
Pseudomonas fluorescens	*Atractylodes lancea* (Thunb.) DC.	Increases oxygenous sesquiterpenoid content	Triggers generation of ROS	Zhou et al., 2015
Azotobacter chroococcum	*Curcuma longa* (L.)	Curcumin	Anti-inflammatory, anti-tumor, and antioxidant	Kumar et al., 2014
Stenotrophomonas maltophilia	*Papaver somniferum* (L.)	Enhance alkaloid and morphine contents	Narcotic analgesics	Limón et al., 2015
Pseudonocardia sp.	*Artemisia annua* (L.)	Artemisinin	Antimalarial	Sato and Kumagai, 2013
Fungal endophytes				
Acremonium sp., *Shiraia* sp.	*Huperzia serrata* (Thunb.) Trevis.	Huperzine A	Anticholinesterase	Li et al., 2007
Alternaria sp.	*Phellodendron amurense* Rupr.	Berberine	Antibiotic	Duan et al., 2009
Alternaria sp.	*Sabina vulgaris* Antoine	Podophyllotoxin	Antitumor	Lu et al., 2006
Aspergillus fumigatus	*Podocarpus* sp. Pers.	Paclitaxel	Antitumor	Sun et al., 2008
Aspergillus nidulans, A. oryzae	*Ginkgo biloba* (L.)	Quercetin	Anti-inflammatory	Qiu et al., 2010
Blastomyces sp., *Botrytis* sp.	*Phlegmariurus cryptomerianus*	Huperzine A	Anticholinesterase	Ju et al., 2009
Botryodiplodia theobroma, Fusarium lateritium, Monochaetia sp., *Pestalotia bicilia*	*Taxus baccata* (L.)	Paclitaxel	Antitumor	Venkatachalam et al., 2008
Cephalosporium corda	*Fritillaria ussuriensis* (Maxim.)	Sipeimine	Antibechic and anti-ulcer	Yin and Chen, 2008
Cephalosporium sp., *Paecilomyces* sp.	*Paris polyphylla* var. *yunnanensis* (Franch.) Hand.-Mazz.	Diosgenin	Antitumor, anti-inflammatory, cardiovascular protection	Cao et al., 2007
Chaetomium globosum	*Hypericum perforatum* (L.)	Hypericin	Anti-depressant	Kusari et al., 2008
Cladosporium cladosporio	*Taxus media* Rehder	Paclitaxel	Antitumor	Zhang et al., 2009
Cochliobolus nisikadoi	*Cinnamomum camphora* chvar. *Borneol*	Borneol	Anti-inflammatory, antioxidant	Chen et al., 2011b
Colletotrichum gloeosporioides	*Piper nigrum* (L.)	Piperine	Antimicrobial, antidepressant, anti-inflammatory, and anticancer	Chithra et al., 2014
Entrophospora infrequens, Neurospora sp.	*Nothapodytes foetida* (Wight) Sleumer	Camptothecin	Antitumor	Amna et al., 2006; Rehman et al., 2008
Fusarium oxysporum	*Juniperus recurva* Buch.-Ham. ex D.Don	Podophyllotoxin	Antitumor	Kour et al., 2008

(Continued)

10.3389/fpls.2022.985429

TABLE 3 Continued

Endophytic microorganisms	Host plant	Plant secondary metabolite	Bioactivity of secondary metabolite	References
Fusarium oxysporum	*Ginkgo biloba* (L.)	Ginkgolide B	Antishock, anti-inflammatory, and antiallergic	Cui et al., 2012
Fusarium redolens	*Fritillaria wabuensis* S.Y. Teng & S.C. Yueh	Peimisine and imperialine-3β-D-glucoside	Get rid of sputum, cough, and antitumor	Pan et al., 2015
Fusarium solani	*Apodytes dimidiata* E.Mey. ex Arn.	Camptothecin	Antitumor	Shweta et al., 2010
Fusarium solani	*Camptotheca acuminata* Decne	Camptothecin	Antitumor	Kusari et al., 2009
Fusarium solani	*Taxus celebica* (Warb.) H.L. Li	Paclitaxel	Antitumor	Chakravarthi et al., 2008
Fusarium solani, Metarhizium anisopliae, Mucor rouxianus	*Taxus chinensis* Roxb.	Paclitaxel	Antitumor	Deng et al., 2009; Liu et al., 2009
Monilia sp., *Penicillium implication*	*Dysosma veitchii* (Hemsl. & E.H.Wilson) L.K.Fu ex T.S.Ying	Podophyllotoxin	Antitumor	Yang et al., 2003
Ozonium sp., *Alternaria alternata, Botrytis* sp., *Ectostroma* sp., *Fusarium mairei, Papulaspora* sp., Tubercularia sp.	*Taxus chinensis* var. *mairei* (Lemee & Levl.) W.C. Cheng & L.K. Fu	Paclitaxel	Antitumor	Zhou et al., 2007; Guo et al., 2009; Wu et al., 2013
Penicillium chrysogenum	*Lycopodium serratum* Thunb.	Huperzine A	Anticholinesterase	Zhou et al., 2009
Penicillium implicatum	*Diphylleia sinensis* H.L.Li	Podophyllotoxin	Antitumor	Zeng et al., 2004
Penicillium sp., *Phialocephala fortinii, Trametes hirsuta, Alternaria neesex*	*Sinopodophyllm hexandrum* (Royle) Ying	Podophyllotoxin	Antitumor	Li, 2007
Pestalotiopsis microspora, Sporormia minima, Trichothecium sp.	*Taxus wallachiana* Zucc.	Paclitaxel	Antitumor	Shrestha et al., 2001
Pestalotiopsis pauciseta	*Cardiospermum helicacabum* (L.)	Paclitaxel	Antitumor	Gangadevi et al., 2008
Pestalotiopsis terminaliae	*Terminalia arjuna* (Roxb. ex DC.) Wight & Arn.	Paclitaxel	Antitumor	Gangadevi and Muthumary, 2009
Phomopsis sp., *Diaporthe* sp., *Schizophyllum* sp., *Penicillium* sp., *Fomitopsis* sp., *Arthrinium* sp.	*Cinchona ledgeriana* Bern. Moens	Cinchona alkaloids: quinine, quinidine, cinchonidine, cinchonine	Antipyretic and antimalarial, analgesic and anti-inflammatory	Maehara et al., 2012
Phyllosticta citricarpa *Phyllosticta spinarum*	*Citrus medica* (L.) *Cupressus* (L.)	Paclitaxel	Antitumor	Kumaran et al., 2008
Phyllosticta dioscoreae	*Hibiscus rosa-sinensis* (L.)	Paclitaxel	Antitumor	Kumaran et al., 2009
Sordariomycete sp.	*Eucommia ulmoides* Oliv.	Chlorogenic acid	Antimicrobial and antitumor	Chen et al., 2010
Trichoderma atroviride D16	*Salvia miltiorrhiza* Bunge	Tanshinone IIA and tanshinone I	Antibacterial and anti-inflammatory	Ming et al., 2011

suspension are also susceptible to contamination and handling issues. The application of endophytes in bulk populations is made possible by pelleting or direct soil application. However, there is still an issue with the lack of homogeneity in the field and exposure to environmental perturbations. Despite using every conventional method, the microbes still need to endure for a few weeks before they may enter the plant after root hair emergence. Even while some endophytes' facultative character suggests the prospect of further colonization if they can endure in the rhizosphere, the ecological constraint exists. Seed priming with a predetermined duration can help the microbe's entrance during imbibitions. However, several scientific and technical difficulties are still associated with applying endophytes to seeds *via* coatings, sprays, granules, and capsules. Moreover, a seemingly simple procedure like plate counting also seems to have some technical problems, e.g., the "viable but not culturable" bacteria may not be detected by plate counting.

The formulation should facilitate the microorganism's penetration and colonization of the host while minimizing dosage and cost. It should also increase microbe establishment in the soil and close to or on the plant. The application of endophytes requires a thorough knowledge of the physicochemical and biological environment, including the phyllosphere, soil, seed surface, and rhizosphere, as well

as the cultivation and formulation of the biologicals to prolong shelf life. In the context of mycorrhiza, progress has been made in understanding the molecular plant–microbe interaction that needs to be integrated into novel formulation and application strategies. In other circumstances, such endophytic entomopathogenic fungi do not clearly understand how they invade and colonize. Basic research studies only use straightforward water-spore mixtures instead of more advanced and practical application methods.

Furthermore, designing formulations having high microbial inoculant concentration and survivability during storage is crucial for developing potent inoculants. Since it is impossible to test out every potential combination of parameters throughout the formulation process, it is challenging to determine the most critical variables. Nevertheless, it is challenging to maintain sterility throughout the formulation process for an extended period, which could lead to contamination. Even though we can find entomopathogenic fungi in nature in this form, their poor recovery rate from plants reveals that these organisms do not occur naturally.

Conclusion

Plant–microbe interactions benefit the all-embracing vicinity of agricultural applications. Microorganisms are abundantly present in nature and primarily colonized *in-planta*. Plant–endophyte interaction is mostly considered beneficial, having profound effects on the physiology of the host plant and the overall performance by promoting growth, development, and imparting fitness to the host plants against different biotic and abiotic stresses. They play a vital function in agricultural sustainability by providing eco-friendly inputs to enhance crop productivity and quality while minimizing harmful chemical fertilizers. The study of these plant–microbe interactions helps us acknowledge natural events that influence our daily lives and could benefit befalling in sustainable resources, a smaller influence on the atmosphere and surroundings, and control of environmental pollution. The benefits of using these interactions for biotechnological applications are huge. The utilization of the pre-existing plant–microbe interactions for the promotion of growth of the plant and biocontrol diminishes the use of unnatural synthetic pesticides and fertilizers, resulting in lowering input costs and, more importantly, reducing the influence of chemical nutrients and pesticides on existing useful fiora and fauna. Moreover, the production of beneficial compounds of industrial and pharmaceutical importance through plant–microbe symbiosis reduces the requirement to supply expensive catalysts and precursors and is energy-saving. In recent years, MAPs are being paid considerable attention worldwide due to their vast economic potential, primarily in the field of herbal medicine. Until the arrival of advanced medicines, an oversized population in emerging nations has traditionally relied upon the products obtained from plants. Furthermore, about 12.5% of the more than 422,000 plant species have been universally documented for medicinal properties; however, only a couple of hundreds are known to be in cultivation. There is a need to grow MAPs to maintain their steady supply and conservation amidst decreasing stocks from natural sources and rising global interest.

Limitations and further investigations

Endophytic microorganisms are tissue specific in nature; their establishment and functionality within the host are affected by several factors such as tissue type, host's genotype, and surrounding conditions. The lack of knowledge about the widespread presence of endophytic microorganisms' communities in plant tissues has been a hindrance in advancing research on endophytes in various fields. It should be noted that the development of successful endophyte application technologies would fully depend on improving our understanding of how they enter and colonize *in-planta*. Consequently, to guarantee reproducibility, reliable methods of endophytic inoculum delivery should be developed for better productivity of MAPs. Leveraging the relationship between plants and endophytes can be crucial for advancing sustainable development (Ryan et al., 2008); extensive research investigations are required to accept or refute this hypothesis. Therefore, in-depth future studies are needed to demonstrate an improved comprehension of the organism in its host to advance the viability of endophyte-assisted biological applications, especially in the field. The persistent reliance on the deployment of a generic method in their processing was inferred to be a hindrance to the capability to fully grasp the interaction between endophytes and their host concerning their utilization in biological activities. Since most organisms prefer to eschew them due to transformations, they cannot be recognized using those general techniques. Thus, using complex molecular processes in their processing will lead to a better understanding and enable the use of the endophytic application in agriculture/food processing, medicine, and environmental management.

Author contributions

AK and AT conceived and planned this review article. AT and PP wrote the original draft of the manuscript. ST helped in review and data collection. PP prepared the figures. All authors reviewed and agreed on the final version.

Acknowledgments

We are thankful to the Director of CSIR-Central Institute of Medicinal and Aromatic Plants for providing the necessary facilities to carry out the research work. AT is grateful to the Department of Science and Technology, India for the INSPIRE fellowship.

Conflict of interest

The authors declare that the research was conducted in the absence of any commercial or financial relationships that could be construed as a potential conflict of interest.

Publisher's note

All claims expressed in this article are solely those of the authors and do not necessarily represent those of their affiliated organizations, or those of the publisher, the editors and the reviewers. Any product that may be evaluated in this article, or claim that may be made by its manufacturer, is not guaranteed or endorsed by the publisher.

References

Abd Allah, E. F., Hashem, A., Alqarawi, A. A., Bahkali, A. H., and Alwhibi, M. S. (2015). Enhancing growth performance and systemic acquired resistance of medicinal plant sesbania sesban (L.) merr using arbuscular mycorrhizal fungi under salt stress. *Saudi J. Biol. Sci.* 22 (3), 274–283. doi: 10.1016/j.sjbs.2015.03.004

Adame-Alvarez, R. M., Mendiola-Soto, J., and Heil, M. (2014). Order of arrival shifts endophyte-pathogen interactions in bean from resistance induction to disease facilitation. *FEMS Microbiol. Lett.* 355, 100–107. doi: 10.1111/1574-6968.12454

Agarwal, S., and Shende, S. T. (1987). Tetrazolium reducing microorganisms inside the root of brassica species. *Curr. Sci.* 56, 187–188. Available at: https://www.currentscience.ac.in/Volumes/56/04/0187.pdf

Ahmad, N., Hamayun, M., Khan, S. A., Khan, A. L., Lee, I. J., and Shin, D. H. (2010). Gibberellin-producing endophytic fungi isolated from monochoria vaginalis. *J. Microbiol. Biotech.* 20 (12), 1744–1749. Available at: https://koreascience.kr/article/JAKO201018860405953.page

Ali, S., Charles, T. C., and Glick, B. R. (2014). Amelioration of high salinity stress damage by plant growth-promoting bacterial endophytes that contain ACC deaminase. *Plant Physiol. Biochem.* 80, 160–167. doi: 10.1016/j.plaphy.2014.04.003

Ali, S., Khan, S. A., Hamayun, M., Iqbal, A., Khan, A. L., Hussain, A., et al. (2019). Endophytic fungi from caralluma acutangula can secrete plant growth promoting enzymes. *Fresenius Environ. Bull.* 28, 2688–2696. Available at: https://www.cabdirect.org/cabdirect/abstract/20193515732

Alishahi, F., Alikhani, H. A., Khoshkholgh-Sima, N. A., and Etesami, H. (2020). Mining the roots of various species of the halophyte suaeda for halotolerant nitrogen-fixing endophytic bacteria with the potential for promoting plant growth. int. *J. Microbiol.* 23, 415–427. doi: 10.1007/s10123-019-00115-y

Aly, A. H., Debbab, A., and Proksch, P. (2011). Fungal endophytes: unique plant inhabitants with great promises. *Appl. Microbiol. Biotechnol.* 90 (6), 1829–1845. doi: 10.1007/s00253-011-3270-y

Ambrosini, A., Beneduzi, A., Stefanski, T., Pinheiro, F. G., Vargas, L. K., and Passaglia, L. M. (2012). Screening of plant growth promoting rhizobacteria isolated from sunflower (Helianthus annuus l.). *Plant Soil* 356 (1-2), 245–264. doi: 10.1007/s11104-011-1079-1

Amna, T., Puri, S. C., Verma, V., Sharma, J. P., Khajuria, R. K., Musarrat, J., et al. (2006). Bioreactor studies on the endophytic fungus entrophospora infrequens for the production of an anticancer alkaloid camptothecin. *Can. J. Microbiol.* 52 (3), 189–196. doi: 10.1139/w05-122

Anderson, T. A., Guthrie, E. A., and Walton, B. T. (1993). Bioremediation in the rhizosphere. *Environ. Sci. Technol.* 27 (13), 2630–2636. doi: 10.1021/es00049a001

Anyasi, R. O., and Atagana, H. I. (2018). Profiling of plants at petroleum contaminated site for phytoremediation. *Int. J. Phytorem.* 20, 352–361. doi: 10.1080/15226514.2017.1393386

Araújo, W. L., Maccheroni, W. C., Aguilar-Vildoso, C. I., Barroso, P. A., Saridakis, H. O., and Azevedo, J. L. (2001). Variability and interactions between endophytic bacteria and fungi isolated from leaf tissues of citrus rootstocks. *Can. J. Microbiol.* 47 (3), 229–236. doi: 10.1139/w00-146

Araujo, W. L., Marcon, J., Maccheroni, W., van Elsas, J. D., van Vuurde, J. W., and Azevedo, J. L. (2002). Diversity of endophytic bacterial populations and their interaction with xylella fastidiosa in citrus plants. *Appl. Environ. Microbiol.* 68 (10), 4906–4914. doi: 10.1128/AEM.68.10.4906-4914.2002

Arora, N. K., Kang, S. C., and Maheshwari, D. K. (2001). Isolation of siderophore-producing strains of rhizobium meliloti and their biocontrol potential against macrophomina phaseolina that causes charcoal rot of groundnut. *Curr. Sci.* 81, 673–677. Available at: https://www.currentscience.ac.in/Volumes/81/06/0673.pdf

Azevedo, J. L., Maccheroni, W.Jr., Pereira, J. O., and de Araújo, W. L. (2000). Endophytic microorganisms: a review on insect control and recent advances on tropical plants. *Electron. J. Biotechnol.* 3 (1), 15–16. doi: 10.2225/vol3-issue1-fulltext-4

Babu, A. G., Shea, P. J., Sudhakar, D., Jung, I. B., and Oh, B. T. (2015). Potential use of pseudomonas koreensis AGB-1 in association with miscanthus sinensis to remediate heavy metal (loid)-contaminated mining site soil. *J. Environ. Manage.* 151, 160–166. doi: 10.1016/j.jenvman.2014.12.045

Bacon, C. W., Glenn, A. E., and Hinton, D. M. (2002). "Isolation, in planta detection and culture of endophytic bacteria and fungi," in *Manual of environmental microbiology, 2nd edn.* Eds. C. J. Hurst, R. L. Crawford, M. J. McInerney, G. R. Knudsen and L. D. Stetzenbach (Washington DC: ASM Press).

Bacon, C. W., and White, J. (2000). *Microbial endophytes* (New York, Basel, Switzerland: CRC Press). doi: 10.1201/9781482277302

Badri, D. V., and Vivanco, J. M. (2009). Regulation and function of root exudates. *Plant Cell Environ.* 32, 666–681. doi: 10.1111/j.1365-3040.2009.01926.x

Badri, D. V., Weir, T. L., van der Lelie, D., and Vivanco, J. M. (2009). Rhizosphere chemical dialogues: plant–microbe interactions. *Curr. Opin. Biotechnol.* 20 (6), 642–650. doi: 10.1016/j.copbio.2009.09.014

Bae, H., Sicher, R. C., Kim, M. S., Kim, S. H., Strem, M. D., Melnick, R. L., et al. (2009). The beneficial endophyte trichoderma hamatum isolate DIS 219b promotes growth and delays the onset of the drought response in theobroma cacao. *J. Exp. Bot.* 60 (11), 3279–3295. doi: 10.1093/jxb/erp165

Barazani, O., von Dahl, C. C., and Baldwin, I. T. (2007). Sebacina vermifera promotes the growth and fitness of nicotiana attenuata by inhibiting ethylene signaling. *Plant Physiol.* 144 (2), 1223–1232. doi: 10.1104/pp.107.097543

Barka, E. A., Nowak, J., and Clément, C. (2006). Enhancement of chilling resistance of inoculated grapevine plantlets with a plant growth-promoting rhizobacterium, burkholderia phytofirmans strain PsJN. *Appl. Environ. Microbiol.* 72 (11), 7246–7252. doi: 10.1128/AEM.01047-06

Barnawal, D., Bharti, N., Maji, D., Chanotiya, C. S., and Kalra, A. (2012). 1-Aminocyclopropane-1-carboxylic acid (ACC) deaminase-containing rhizobacteria protect ocimum sanctum plants during waterlogging stress *via* reduced ethylene generation. *Plant Physiol. Biochem.* 58, 227–235. doi: 10.1016/j.plaphy.2012.07.008

Barnawal, D., Bharti, N., Maji, D., Chanotiya, C. S., and Kalra, A. (2014). ACC deaminase-containing arthrobacter protophormiae induces NaCl stress tolerance

through reduced ACC oxidase activity and ethylene production resulting in improved nodulation and mycorrhization in pisum sativum. *J. Plant Physiol.* 171 (11), 884–894. doi: 10.1016/j.jplph.2014.03.007

Bell, C. R., Dickie, G. A., Harvey, W. L. G., and Chan, J. W. Y. F. (1995). Endophytic bacteria in grapevine. *Can. J. Microbiol.* 41 (1), 46–53. doi: 10.1139/m95-006

Bernardi, D. I., das Chagas, F. O., Monteiro, A. F., dos Santos, G. F., and de Souza Berlinck, R. G. (2019). "Secondary metabolites of endophytic actinomycetes: Isolation, synthesis, biosynthesis, and biological activities," in *Progress in the chemistry of organic natural products*, vol. 108. (Springer Nature Switzerland AG: Springer, Cham), 207–296. doi: 10.1007/978-3-030-01099-7_3

Bhattacharjee, R. B., Singh, A., and Mukhopadhyay, S. N. (2008). Use of nitrogen-fixing bacteria as biofertiliser for non-legumes: prospects and challenges. *Appl. Microbiol. Biotechnol.* 80 (2), 199–209. doi: 10.1007/s00253-008-1567-2

Bhattacharya, D., and Medlin, A. L. (1998). Algal phylogeny and the origin of land plants. *Plant Physiol.* 116 (1), 9–15. doi: 10.1104/pp.116.1.9

Bilal, L., Asaf, S., Hamayun, M., Gul, H., Iqbal, A., Ullah, I., et al. (2018). Plant growth promoting endophytic fungi asprgillus fumigatus TS1 and fusarium proliferatum BRL1 produce gibberellins and regulates plant endogenous hormones. *Symbiosis* 76 (2), 117–127. doi: 10.1007/s13199-018-0545-4

Bittleston, L. S., Brockmann, F., Wcislo, W., and Van Bael, S. A. (2011). Endophytic fungi reduce leaf-cutting ant damage to seedlings. *Biol. Lett.* 7 (1), 30–32. doi: 10.1098/rsbl.2010.0456

Boddey, R. M., Urquiaga, S., Alves, B. J., and Reis, V. (2003). Endophytic nitrogen fixation in sugarcane: present knowledge and future applications. *Plant Soil* 252 (1), 139–149. doi: 10.1023/A:1024152126541

Cao, R., Liu, X., Gao, K., Mendgen, K., Kang, Z., Gao, J., et al. (2009). Mycoparasitism of endophytic fungi isolated from reed on soilborne phytopathogenic fungi and production of cell wall-degrading enzymes *in vitro*. *Curr. Microbiol.* 59 (6), 584–592. doi: 10.1007/s00284-009-9477-9

Cao, X., Li, J., and Zhou, L. (2007). Determination of diosgenin content of the endophytic fungi from Paris polyphylla var. yunnanensis by using an optimum ELISA. *Nat. Prod. Res.* 19, 1020–1023. doi: 10.3969/j.issn.1001-6880.2007.06.025

Casella, T. M., Eparvier, V., Mandavid, H., Bendelac, A., Odonne, G., Dayan, L., et al. (2013). Antimicrobial and cytotoxic secondary metabolites from tropical leaf endophytes: Isolation of antibacterial agent pyrrocidine c from lewia infectoria SNB-GTC2402. *Phytochemistry* 96, 370–377. doi: 10.1016/j.phytochem.2013.10.004

Castillo, U. F., Strobel, G. A., Ford, E. J., Hess, W. M., Porter, H., Jensen, J. B., et al. (2002). Munumbicins, wide-spectrum antibiotics produced by streptomyces NRRL 30562, endophytic on kennedia nigriscansaaThe GenBank accession number for the sequence determined in this work is AY127079. *Microbiology* 148 (9), 2675–2685. doi: 10.1099/00221287-148-9-2675

Chacón, M. R., Rodríguez-Galán, O., Benítez, T., Sousa, S., Rey, M., Llobell, A., et al. (2007). Microscopic and transcriptome analyses of early colonization of tomato roots by trichoderma harzianum. *Int. Microbiol.* 10 (1), 19–27. doi: 10.2436/20.1501.01.4

Chakravarthi, B. V. S. K., Das, P., Surendranath, K., Karande, A. A., and Jayabaskaran, C. (2008). Production of paclitaxel by fusarium solani isolated from taxus celebica. *J. Biosci.* 33 (2), 259–267. doi: 10.1007/s12038-008-0043-6

Chen, J. X., Dai, C. C., Li, X., Tian, L. S., and Xie, H. (2008). Endophytic fungi screening from atracty lancea and inoculating into the host plantlet. *Guihaia* 28 (2), 256–260. doi: 10.3969/j.issn.1000-3142.2008.02.022

Chen, X. M., and Guo, S. X. (2005). Effects of four species of endophytic fungi on the growth and polysaccharide and alkaloid contents of dendrobium nobile. *Zhongguo Zhong Yao Za Zhi* 30 (4), 253–257. doi: 10.3321/j.issn:1001-5302.2005.04.003

Chen, X. M., Guo, S. X., and Wang, C. L. (2005). Effects of four endophytic fungi on the growth and polysaccharide content of anoectochilus roxburghii (Wall.) lindl. *Chin. Pharm. J.* 40 (1), 13–16. doi: 10.3321/j.issn:1001-2494.2005.01.006

Chen, X., Sang, X., Li, S., Zhang, S., and Bai, L. (2010). Studies on a chlorogenic acid-producing endophytic fungi isolated from eucommia ulmoides oliver. j. Ind. microbiol. *Biotechnol* 37 (5), 447–454. doi: 10.1007/s10295-010-0690-0

Chen, B., Wang, M., Hu, Y., Lin, Z., Yu, R., and Huang, L. (2011a). Preliminary study on promoting effects of endophytic fungi to growth of rehmannia glutinosa. *Chin. J. Integr. Med.* 36, 1137–1140. doi: 10.4268/cjcmm20110906

Chen, M., Yang, L., Li, Q., Shen, Y., Shao, A., Lin, S., et al. (2011b). Volatile metabolites analysis and molecular identification of endophytic fungi bn12 from cinnamomum camphora chvar. *Borneol. Zhongguo Zhongyao Zazhi* 36 (23), 3217–3221. doi: 10.4268/cjcmm20112301

Chithra, S., Jasim, B., Sachidanandan, P., Jyothis, M., and Radhakrishnan, E. K. (2014). Piperine production by endophytic fungus colletotrichum gloeosporioides isolated from piper nigrum. *Phytomedicine* 21 (4), 534–540. doi: 10.1016/j.phymed.2013.10.020

Chutima, R., Dell, B., Vessabutr, S., Bussaban, B., and Lumyong, S. (2011). Endophytic fungi from pecteilis susannae (L.) rafin (Orchidaceae), a threatened terrestrial orchid in Thailand. *Mycorrhiza* 21 (3), 221–229. doi: 10.1007/s00572-010-0327-1

Costacurta, A., and Vanderleyden, J. (1995). Synthesis of phytohormones by plant-associated bacteria. *Crit. Rev. Microbiol.* 21 (1), 1–18. doi: 10.3109/10408419509113531

Cui, Y., Yi, D., Bai, X., Sun, B., Zhao, Y., and Zhang, Y. (2012). Ginkgolide b produced endophytic fungus (Fusarium oxysporum) isolated from ginkgo biloba. *Fitoterapia* 83 (5), 913–920. doi: 10.1016/j.fitote.2012.04.009

Daungfu, O., Youpensuk, S., and Lumyong, S. (2019). Endophytic bacteria isolated from citrus plants for biological control of citrus canker in lime plants. *Trop. Life Sci. Res.* 30 (1), 73. doi: 10.21315/tlsr2019.30.1.5

De Bary, A. (1879). "Die erscheinung der symbiose (Vol. 121)," in *Strassburg: Verlag von Karl J* (Strasbourg, France: Trübner). doi: 10.1515/9783111471839

Del Giudice, L., Massardo, D. R., Pontieri, P., Bertea, C. M., Mombello, D., Carata, E., et al. (2008). The microbial community of vetiver root and its involvement into essential oil biogenesis. *Environ. Microbiol.* 10 (10), 2824–2841. doi: 10.1111/j.1462-2920.2008.01703.x

Deng, B. W., Liu, K. H., Chen, W. Q., Ding, X. W., and Xie, X. C. (2009). Fusarium solani, tax-3, a new endophytic taxol-producing fungus from taxusá chinensis. *World J. Microbiol. Biotechnol.* 25 (1), 139. doi: 10.1007/s11274-008-9876-2

de Zélicourt, A., Synek, L., Saad, M. M., Alzubaidy, H., Jalal, R., Xie, Y., et al. (2018). Ethylene induced plant stress tolerance by enterobacter sp. SA187 is mediated by 2-keto-4-methylthiobutyric acid production. *PLoS. Genet.* 14 (3), e1007273. doi: 10.1371/journal.pgen.1007273

Domka, A., Rozpądek, P., Ważny, R., and Turnau, K. (2019). Mucor sp.–an endophyte of brassicaceae capable of surviving in toxic metal-rich sites. *J. Basic Microbiol.* 59 (1), 24–37. doi: 10.1002/jobm.201800406

Duan, L. I., Liwei, G., and Hong, Y. (2009). Isolation and identification of producing endophytic fungi of berberine from the plant phellodendron amurense. *J. Anhui. Agric. Sci.* 37 (22), 10340–10341, 10350. doi: 10.3969/j.issn.0517-6611.2009.22.007

Elmer, P. A. G., and Reglinski, T. (2006). Biosuppression of botrytis cinerea in grapes. *Plant Pathol.* 55 (2), 155–177. doi: 10.1111/j.1365-3059.2006.01348.x

Ernst, M., Mendgen, K. W., and Wirsel, S. G. (2003). Endophytic fungal mutualists: seed-borne stagonospora spp. enhance reed biomass production in axenic microcosms. *Mol. Plant Microbe Interact.* 16 (7), 580–587. doi: 10.1094/MPMI.2003.16.7.580

Estrada, G. A., Baldani, V. L. D., de Oliveira, D. M., Urquiaga, S., and Baldani, J. I. (2013). Selection of phosphate-solubilizing diazotrophic herbaspirillum and burkholderia strains and their effect on rice crop yield and nutrient uptake. *Plant Soil* 369 (1-2), 115–129. doi: 10.1007/s11104-012-1550-7

Fernandez, O., Theocharis, A., Bordiec, S., Feil, R., Jacquens, L., Clément, C., et al. (2012). Burkholderia phytofirmans PsJN acclimates grapevine to cold by modulating carbohydrate metabolism. *Mol. Plant Microbe Interact.* 25 (4), 496–504. doi: 10.1094/MPMI-09-11-0245

Frink, C. R., Waggoner, P. E., and Ausubel, J. H. (1999). Nitrogen fertilizer: retrospect and prospect. *Proc. Natl. Acad. Sci. U.S.A.* 96 (4), 1175–1180. doi: 10.1073/pnas.96.4.1175

Gagic, M., Faville, M. J., Zhang, W., Forester, N. T., Rolston, M. P., Johnson, R. D., et al. (2018). Seed transmission of epichloë endophytes in lolium perenne is heavily influenced by host genetics. *Front. Plant Sci.* 9, 1580. doi: 10.3389/fpls.2018.01580

Gagné, S., Richard, C., Rousseau, H., and Antoun, H. (1987). Xylem-residing bacteria in alfalfa roots. *Can. J. Microbiol.* 33 (11), 996–1000. doi: 10.1139/m87-175

Gangadevi, V., Murugan, M., and Muthumary, J. (2008). Taxol determination from pestalotiopsis pauciseta, a fungal endophyte of a medicinal plant. *Chin. J. Biotechnol.* 24 (8), 1433–1438. doi: 10.1016/S1872-2075(08)60065-5

Gangadevi, V., and Muthumary, J. (2009). Taxol production by pestalotiopsis terminaliae, an endophytic fungus of terminalia arjuna (arjun tree). biotechnol. *Appl. Biochem.* 52 (1), 9–15. doi: 10.1042/BA20070243

Gange, A. C., Eschen, R., Wearn, J. A., Thawer, A., and Sutton, B. C. (2012). Differential effects of foliar endophytic fungi on insect herbivores attacking a herbaceous plant. *Oecologia* 168 (4), 1023–1031. doi: 10.1007/s00442-011-2151-5

Germaine, K., Keogh, E., Garcia-Cabellos, G., Borremans, B., van der Lelie, D., Barac, T., et al. (2004). Colonisation of poplar trees by GFP expressing bacterial endophytes. *FEMS Microbiol. Ecol.* 48 (1), 109–118. doi: 10.1016/j.femsec.2003.12.009

Glick, B. R. (2005). Modulation of plant ethylene levels by the bacterial enzyme ACC deaminase. *FEMS Microbiol. Lett.* 251 (1), 1–7. doi: 10.1016/j.femsle.2005.07.030

Gómez-Vidal, S., Salinas, J., Tena, M., and Lopez-Llorca, L. V. (2009). Proteomic analysis of date palm (Phoenix dactylifera l.) responses to endophytic colonization

by entomopathogenic fungi. *Electrophoresis* 30 (17), 2996–3005. doi: 10.1002/elps.200900192

Govindarajan, M., Balandreau, J., Kwon, S. W., Weon, H. Y., and Lakshminarasimhan, C. (2008). Effects of the inoculation of burkholderia vietnamensis and related endophytic diazotrophic bacteria on grain yield of rice. *Microb. Ecol.* 55 (1), 21–37. doi: 10.1007/s00248-007-9247-9

Guan, S., Grabley, S., Groth, I., Lin, W., Christner, A., Guo, D., et al. (2005). Structure determination of germacrane-type sesquiterpene alcohols from an endophyte streptomyces griseus subsp. *Magn. Reson. Chem.* 43 (12), 1028–1031. doi: 10.1002/mrc.1710

Gunatilaka, A. L. (2006). Natural products from plant-associated microorganisms: distribution, structural diversity, bioactivity, and implications of their occurrence. *J. Natural Prod.* 69 (3), 509–526. doi: 10.1021/np058128n

Guo, S., and Wang, Q. (2001). Character and action of good strain on stimulating seed germination of gastrodia elata. *Jun Wu Xi Tong* 20 (3), 408–412. doi: 10.3969/j.issn.1672-6472.2001.03.023

Guo, D. D., Xu, C. X., Quan, J. S., Song, C. K., Jin, H., Kim, D. D., et al. (2009). Synergistic anti-tumor activity of paclitaxel-incorporated conjugated linoleic acid-coupled poloxamer thermosensitive hydrogel *in vitro* and *in vivo*. *Biomaterials* 30 (27), 4777–4785. doi: 10.1016/j.biomaterials.2009.05.051

Hallmann, Q. A., and Hallmann, J. (1997b). Bacterial endophytes in cotton: location and interaction with other plant-associated bacteria. *Can. J. Microbiol.* 43 (3), 254–259. doi: 10.1139/m97-035

Hallmann, J., Quadt-Hallmann, A., Mahaffee, W. F., and Kloepper, J. W. (1997a). Bacterial endophytes in agricultural crops. *Can. J. Microbiol.* 43 (10), 895–914. doi: 10.1139/m97-131

Hardoim, P. R., Van Overbeek, L. S., Berg, G., Pirttilä, A. M., Compant, S., Campisano, A., et al. (2015). The hidden world within plants: ecological and evolutionary considerations for defining functioning of microbial endophytes. *M. M. B. R.* 79 (3), 293–320. doi: 10.1128/MMBR.00050-14

Hardoim, P. R., van Overbeek, L. S., and van Elsas, J. D. (2008). Properties of bacterial endophytes and their proposed role in plant growth. *Trends Microbiol.* 16 (10), 463–471. doi: 10.1016/j.tim.2008.07.008

Hodgson, S., de Cates, C., Hodgson, J., Morley, N. J., Sutton, B. C., and Gange, A. C. (2014). Vertical transmission of fungal endophytes is widespread in forbs. *Ecol. Evol.* 4 (8), 1199–1208. doi: 10.1002/ece3.953

Hur, M., Kim, Y., Song, H. R., Kim, J. M., Choi, Y. I., and Yi, H. (2011). Effect of genetically modified poplars on soil microbial communities during the phytoremediation of waste mine tailings. *Appl. Environ. Microbiol.* 77, 7611–7619. doi: 10.1128/AEM.06102-11

Jacobs, M. J., Bugbee, W. M., and Gabrielson, D. A. (1985). Enumeration, location, and characterization of endophytic bacteria within sugar beet roots. *Can. J. Bot.* 63 (7), 1262–1265. doi: 10.1139/b85-174

Jan, F. G., Hamayun, M., Hussain, A., Jan, G., Iqbal, A., Khan, A., et al. (2019). An endophytic isolate of the fungus yarrowia lipolytica produces metabolites that ameliorate the negative impact of salt stress on the physiology of maize. *BMC Microbiol.* 19 (1), 1–10. doi: 10.1186/s12866-018-1374-6

Ju, Z., Wang, J., and Pan, S. L. (2009). Isolation and preliminary identification of the endophytic fungi which produce hupzine a from four species in hupziaceae and determination of huperzine a by HPLC. *Fudan Univ. J. Med. Sci.* 4, 017. doi: 10.3969/j.issn.1672-8467.2009.04.015

Kavroulakis, N., Ntougias, S., Zervakis, G. I., Ehaliotis, C., Haralampidis, K., and Papadopoulou, K. K. (2007). Role of ethylene in the protection of tomato plants against soil-borne fungal pathogens conferred by an endophytic fusarium solani strain. *J. Exp. Bot.* 58 (14), 3853–3864. doi: 10.1093/jxb/erm230

Khan, S. A., Hamayun, M., Yoon, H., Kim, H. Y., Suh, S. J., Hwang, S. K., et al. (2008). Plant growth promotion and penicillium citrinum. *BMC Microbiol.* 8 (1), 1–10. doi: 10.1186/1471-2180-8-231

Khare, E., and Arora, N. K. (2015). "Effects of soil environment on field efficacy of microbial inoculants," in *Plant microbes symbiosis: applied facets* (New Delhi: Springer), (pp. 353–381). doi: 10.1007/978-81-322-2068-8_19

Khare, E., Kim, K., and Lee, K. J. (2016). Rice OsPBL1 (ORYZA SATIVA ARABIDOPSIS PBS1-LIKE 1) enhanced defense of arabidopsis against pseudomonas syringae DC3000. *Eur. J. Plant Pathol.* 146 (4), 901–910. doi: 10.1007/s10658-016-0968-9

Koskimäki, J. J., Hokkanen, J., Jaakola, L., Suorsa, M., Tolonen, A., Mattila, S., et al. (2009). Flavonoid biosynthesis and degradation play a role in early defense responses of bilberry (Vaccinium myrtillus) against biotic stress. *Eur. J. Plant Pathol.* 125 (4), 629. doi: 10.1007/s10658-009-9511-6

Kour, A., Shawl, A. S., Rehman, S., Sultan, P., Qazi, P. H., and Suden, P. (2008). Isolation and identification of an endophytic strain of fusarium oxysporum producing podophyllotoxin from juniperus recurva. *World J. Microbiol. Biotechnol.* 24 (7), 1115–1121. doi: 10.1007/s11274-007-9582-5

Kumaran, R. S., Muthumary, J., and Hur, B. K. (2008). Taxol from phyllosticta citricarpa, a leaf spot fungus of the angiosperm citrus medica. *J. Biosci. Bioeng.* 106 (1), 103–106. doi: 10.1263/jbb.106.103

Kumaran, R. S., Muthumary, J., Kim, E. K., and Hur, B. K. (2009).). production of taxol from phyllosticta dioscoreae, a leaf spot fungus isolated from hibiscus rosa-sinensis. *Biotechnol. Bioprocess Eng.* 14 (1), 76–83. doi: 10.1007/s12257-008-0041-4

Kumar, A., Singh, R., Giri, D. D., Singh, P. K., and Pandey, K. D. (2014). Effect of azotobacter chroococcum CL13 inoculation on growth and curcumin content of turmeric (Curcuma longa l.). *Int. J. Curr. Microbiol. Appl. Sci.* 3 (9), 275–283.

Kusari, S., Lamshöft, M., Zühlke, S., and Spiteller, M. (2008). An endophytic fungus from hypericum perforatum that produces hypericin. *J. Natural Prod.* 71 (2), 159–162. doi: 10.1021/np070669k

Kusari, S., Zühlke, S., and Spiteller, M. (2011). An endophytic fungus from *Camptotheca acuminata* that produces camptothecin and analogues. *J. Nat. Prod.* 72 (1), 2–7. doi: 10.1021/np800455b

Kushwaha, R. K., Singh, S., Pandey, S. S., Kalra, A., and Babu, C. V. (2019a). Fungal endophytes attune withanolide biosynthesis in withania somnifera, prime to enhanced withanolide a content in leaves and roots. *World J. Microbiol. Biotechnol.* 35 (2), 20. doi: 10.1007/s11274-019-2593-1

Kushwaha, R. K., Singh, S., Pandey, S. S., Rao, D. V., Nagegowda, D. A., Kalra, A., et al. (2019b). Compatibility of inherent fungal endophytes of withania somnifera with trichoderma viride and its impact on plant growth and withanolide content. *J. Plant Growth Regul.* 38 (4), 1228–1242. doi: 10.1007/s00344-019-09928-7

Lata, R., Chowdhury, S., Gond, S. K., and White, J. F.Jr (2018). Induction of abiotic stress tolerance in plants by endophytic microbes. *Lett. Appl. Microbiol.* 66 (4), 268–276. doi: 10.1111/lam.12855

Lazarovits, G., and Nowak, J. (1997). Rhizobacteria for improvement of plant growth and establishment. *HortSci* 32 (2), 188–192. doi: 10.21273/HORTSCI.32.2.188

Leveau, J. H., and Lindow, S. E. (2001). Appetite of an epiphyte: quantitative monitoring of bacterial sugar consumption in the phyllosphere. *Proc. Natl. Acad. Sci.* 98 (6), 3446–3453. doi: 10.1073/pnas.061629598

Li, C. (2007). Fermentation conditions of sinopodophyllum hexandrum endophytic fungus on production of podophyllotoxin. *Food Ferment. Ind.* 33 (9), 28.

Li, A. R., and Guan, K. Y. (2007). Mycorrhizal and dark septate endophytic fungi of pedicularis species from northwest of yunnan province, China. *Mycorrhiza* 17 (2), 103–109. doi: 10.1007/s00572-006-0081-6

Limón, R. I., Peñas, E., Torino, M. I., Martínez-Villaluenga, C., Dueñas, M., and Frias, J. (2015). Fermentation enhances the content of bioactive compounds in kidney bean extracts. *Food Chem.* 172, 343–352. doi: 10.1016/j.foodchem.2014.09.084

Liu, K., Ding, X., Deng, B., and Chen, W. (2009). Isolation and characterization of endophytic taxol-producing fungi from taxus chinensis. *J. Ind. Microbiol. Biotechnol.* 36 (9), 1171. doi: 10.1007/s10295-009-0598-8

Liu, Y., Liu, W., and Liang, Z. (2015). Endophytic bacteria from pinellia ternata, a new source of purine alkaloids and bacterial manure. *Pharm. Biol.* 53 (10), 1545–1548. doi: 10.3109/13880209.2015.1016580

Liu, X., Song, W., Zhang, K., and Ye, Y. (2011). Effects of two kinds of endophytic fungi infection on water stress of seedlings of chrysanthemum morifolium. *Acta Hortic. Sin.* 38 (2), 335–342.

Li, W., Zhou, J., Lin, Z., and Hu, Z. (2007). Study on fermentation condition for production of huperzine a from endophytic fungus 2F09P03B of huperzia serrata. *Chin. Med. Biotechnol.* 2 (4), 254–259.

Lodewyckx, C., Vangronsveld, J., Porteous, F., Moore, E. R., Taghavi, S., Mezgeay, M., et al. (2002).). endophytic bacteria and their potential applications. *Crit. Rev. Plant Sci.* 21 (6), 583–606. doi: 10.1080/0735-260291044377

Lowe, K. F., Bowdler, T. M., Hume, D. E., Casey, N. D., and Tapper, B. A. (2008). The effect of endophyte on the performance of irrigated perennial ryegrasses in subtropical Australia. *Aust. J. Agric. Res.* 59 (6), 567–577. doi: 10.1071/AR08019

Lu, L., He, J., Yu, X., Li, G., and Zhang, X. (2006). Studies on isolation and identification of endophytic fungi strain SC13 from harmaceutical plant Sabina vulgaris ant. and metabolites. *Xi Bei Nong Ye Xue Bao* 15, 85–89. doi: 10.3969/j.issn.1004-1389.2006.05.021

Luo, S., Xu, T., Chen, L., Chen, J., Rao, C., Xiao, X., et al. (2012). Endophyte-assisted promotion of biomass production and metal-uptake of energy crop sweet sorghum by plant-growth-promoting endophyte bacillus sp. *SLS18. Appl. Microbiol. Biotechnol.* 93 (4), 1745–1753. doi: 10.1007/s00253-011-3483-0

Lu, H., Zou, W. X., Meng, J. C., Hu, J., and Tan, R. X. (2000). New bioactive metabolites produced by colletotrichum sp., an endophytic fungus in artemisia annua. *Plant Sci.* 151 (1), 67–73. doi: 10.1016/S0168-9452(99)00199-5

Maehara, S., Simanjuntak, P., Maetani, Y., Kitamura, C., Ohashi, K., and Shibuya, H. (2012). Ability of endophytic filamentous fungi associated with cinchona ledgeriana to produce cinchona alkaloids. *J. Nat. Med.* 67 (2), 421–423. doi: 10.1007/s11418-012-0701-8

Márquez, L. M., Redman, R. S., Rodriguez, R. J., and Roossinck, M. J. (2007). A virus in a fungus in a plant: three-way symbiosis required for thermal tolerance. *Science* 315 (5811), 513–515. doi: 10.1126/science.1136237

Marquez-Santacruz, H. A., Hernandez-Leon, R., Orozco-Mosqueda, M. D. C., Velazquez-Sepulveda, I., and Santoyo, G. (2010). Diversity of bacterial endophytes in roots of Mexican husk tomato plants (Physalisixocarpa) and their detection in the rhizosphere. *Genet. Mol. Res.* 9 (4), 2372–2380. doi: 10.4238/vol9-4gmr921

Mattos, K. A., Pádua, V. L., Romeiro, A., Hallack, L. F., Neves, B. C., Ulisses, T. M., et al. (2008). Endophytic colonization of rice (Oryza sativa l.) by the diazotrophic bacterium burkholderia kururiensis and its ability to enhance plant growth. *Anais Da Acad. Bras. Ciências* 80 (3), 477–493. doi: 10.1590/S0001-37652008000300009

Ma, Y., Zhang, C., Oliveira, R. S., Freitas, H., and Luo, Y. (2016). Bioaugmentation with endophytic bacterium E6S homologous to achromobacter piechaudii enhances metal rhizoaccumulation in host sedum plumbizincicola. *Front. Plant Sci.* 7, 75. doi: 10.3389/fpls.2016.00075

McGuinness, M., and Dowling, D. (2009). Plant-associated bacterial degradation of toxic organic compounds in soil. *Int. J. Environ. Res. Public Health* 6, 2226–2247. doi: 10.3390/ijerph6082226

Mehmood, A., Hussain, A., Irshad, M., Hamayun, M., Iqbal, A., and Khan, N. (2019). *In vitro* production of IAA by endophytic fungus aspergillus awamori and its growth promoting activities in zea mays. *Symbiosis* 77 (3), 225–235. doi: 10.1007/s13199-018-0583-y

Mejía, L. C., Rojas, E. I., Maynard, Z., Van Bael, S., Arnold, A. E., Hebbar, P., et al. (2008). Endophytic fungi as biocontrol agents of theobroma cacao pathogens. *Biol. Control* 46 (1), 4–14. doi: 10.1016/j.biocontrol.2008.01.012

Meng, J. J., and He, X. L. (2011). Effects of AM fungi on growth and nutritional contents of salvia miltiorrhiza bge. under drought stress. *J. Agricult. Univ. Hebei* 34 (1), 51–61. doi: 10.3969/j.issn.1000-1573.2011.01.011

Mercado-Blanco, J., Rodrıguez-Jurado, D., Hervás, A., and Jiménez-Dıaz, R. M. (2004). Suppression of verticillium wilt in olive planting stocks by root-associated fluorescent pseudomonas spp. *Biol. Control* 30 (2), 474–486. doi: 10.1016/j.biocontrol.2004.02.002

Miller, J. D., Mackenzie, S., Foto, M., Adams, G. W., and Findlay, J. A. (2002). Needles of white spruce inoculated with rugulosin-producing endophytes contain rugulosin reducing spruce budworm growth rate. *Myco. Res.* 106 (4), 471–479. doi: 10.1017/S0953756202005671

Ming, Q., Han, T., Li, W., Zhang, Q., Zhang, H., Zheng, C., et al. (2011). Tanshinone IIA and tanshinone I production by trichoderma atroviride D16, an endophytic fungus in salvia miltiorrhiza. *Phytomedicine* 19 (3-4), 330–333. doi: 10.1016/j.phymed.2011.09.076

Misganaw, G., Simachew, A., and Gessesse, A. (2019). Endophytes of finger millet (Eleusine coracana) seeds. *Symbiosis* 78 (3), 203–213. doi: 10.1007/s13199-019-00607-5

Mishra, J., Singh, R., and Arora, N. K. (2017). Alleviation of heavy metal stress in plants and remediation of soil by rhizosphere microorganisms. *Front. Microbiol.* 8, 1706. doi: 10.3389/fmicb.2017.01706

Mucciarelli, M., Scannerini, S., Bertea, C., and Maffei, M. (2003). *In vitro* and *in vivo* peppermint (Mentha piperita) growth promotion by nonmycorrhizal fungal colonization. *New Phytol.* 158 (3), 579–591. doi: 10.1046/j.1469-8137.2003.00762.x

Müller, J. L. (2015). Plants and endophytes: equal partners in secondary metabolite production? *Biotechnol. Let.* 37 (7), 1325–1334. doi: 10.1007/s10529-015-1814-4

Muthukumarasamy, R., Revathi, G., Seshadri, S., and Lakshminarasimhan, C. (2002). Gluconacetobacter diazotrophicus (syn. acetobacter diazotrophicus), a promising diazotrophic endophyte in tropics. *Curr. Sci.* 83, 137–145. Available at: https://www.currentscience.ac.in/Volumes/83/02/0137.pdf

Nasopoulou, C., Pohjanen, J., Koskimäki, J. J., Zabetakis, I., and Pirttilä, A. M. (2014). Localization of strawberry (Fragaria x ananassa) and methylobacterium extorquens genes of strawberry flavor biosynthesis in strawberry tissue by *in situ* hybridization. *J. Plant Physiol.* 171 (13), 1099–1105. doi: 10.1016/j.jplph.2014.03.018

Naya, L., Ladrera, R., Ramos, J., González, E. M., Arrese-Igor, C., Minchin, F. R., et al. (2007). The response of carbon metabolism and antioxidant defenses of alfalfa nodules to drought stress and to the subsequent recovery of plants. *Plant Physiol.* 144 (2), 1104–1114. doi: 10.1104/pp.107.099648

Ni, T., Yue, J., Sun, G., Zou, Y., Wen, J., and Huang, J. (2012). Ancient gene transfer from algae to animals: mechanisms and evolutionary significance. *BMC Evol. Biol.* 12 (1), 1–10. doi: 10.1186/1471-2148-12-83

Nogueira-Lopez, G., Greenwood, D. R., Middleditch, M., Winefield, C., Eaton, C., Steyaert, J. M., et al. (2018). The apoplastic secretome of trichoderma virens during interaction with maize roots shows an inhibition of plant defense and scavenging oxidative stress secreted proteins. *Front. Plant Sci.* 9, 409. doi: 10.3389/fpls.2018.00409

O'Callaghan, M. (2016). Microbial inoculation of seed for improved crop performance: issues and opportunities. *Appl. Microbiol. Biotechnol.* 100, 5729–5746. doi: 10.1007/s00253-016-7590-9

Oliveira, A. L. M., Stoffels, M., Schmid, M., Reis, V. M., Baldani, J. I., and Hartmann, A. (2009). Colonization of sugarcane plantlets by mixed inoculations with diazotrophic bacteria. *Eur. J. Soil Biol.* 45 (1), 106–113. doi: 10.1016/j.ejsobi.2008.09.004

Palaniyandi, S. A., Yang, S. H., Zhang, L., and Suh, J. W. (2013). Effects of actinobacteria on plant disease suppression and growth promotion. *Appl. Microbiol. Biotechnol.* 97 (22), 9621–9636. doi: 10.1007/s00253-013-5206-1

Palmer, J. D., Soltis, D. E., and Chase, M. W. (2004). The plant tree of life: an overview and some points of view. *Am. J. Bot.* 91 (10), 1437–1445. doi: 10.3732/ajb.91.10.1437

Pandey, S. S., Singh, S., Babu, C. V., Shanker, K., Srivastava, N. K., and Kalra, A. (2016a). Endophytes of opium poppy differentially modulate host plant productivity and genes for the biosynthetic pathway of benzylisoquinoline alkaloids. *Planta* 243 (5), 1097–1114. doi: 10.1007/s00425-016-2467-9

Pandey, S. S., Singh, S., Babu, C. V., Shanker, K., Srivastava, N. K., Shukla, A. K., et al. (2016b). Fungal endophytes of catharanthus roseus enhance vindoline content by modulating structural and regulatory genes related to terpenoid indole alkaloid biosynthesis. *Sci. Rep.* 6, 26583. doi: 10.1038/srep26583

Pan, X. W., Han, L., Zhang, Y. H., Chen, D. F., and Simonsen, H. T. (2015). Sclareol production in the moss physcomitrella patens and observations on growth and terpenoid biosynthesis. *Plant Biotechnol. Rep.* 9 (3), 149–159. doi: 10.1007/s11816-015-0353-8

Patriquin, D. G., and Dobereiner, J. (1978). Light microscopy observations of tetrazolium-reducing bacteria in the endorhizosphere of maize and other grasses in Brazil. *Can. J. Microbiol.* 24 (6), 734–742. doi: 10.1139/m78-122

Patten, C. L., and Glick, B. R. (2002). Role of pseudomonas putida indoleacetic acid in development of the host plant root system. *Appl. Environ. Microbiol.* 68 (8), 3795–3801. doi: 10.1128/AEM.68.8.3795-3801.2002

Penrose, D. M., Moffatt, B. A., and Glick, B. R. (2001). Determination of 1-aminocyclopropane-1-carboxylic acid (ACC) to assess the effects of ACC deaminase-containing bacteria on roots of canola seedlings. *Can. J. Microbiol.* 47 (1), 77–80. doi: 10.1139/w00-128

Poling, S. M., Wicklow, D. T., Rogers, K. D., and Gloer, J. B. (2008). Acremonium zeae, a protective endophyte of maize, produces dihydroresorcylide and 7-hydroxydihydroresorcylides. *J. Agricult. Food Chem.* 56 (9), 3006–3009. doi: 10.1021/jf073274f

Prado, R., Vendramim, J. D., Bicalho, K. U., dos Santos Andrade, M., Fernandes, J. B., de Andrade Moral, R., et al. (2013). Annona mucosa Jacq.(Annonaceae): a promising source of bioactive compounds against sitophilus zeamais Mots.(Coleoptera: Curculionidae). *J. Stored Prod. Res.* 55, 6–14. doi: 10.1016/j.jspr.2013.06.001

Preston, G. M., Bertrand, N., and Rainey, P. B. (2001). Type III secretion in plant growth-promoting pseudomonas fluorescens SBW25. *Mol. Microbiol.* 41 (5), 999–1014. doi: 10.1046/j.1365-2958.2001.02560.x

Qawasmeh, A., Obied, H. K., Raman, A., and Wheatley, W. (2012). Influence of fungal endophyte infection on phenolic content and antioxidant activity in grasses: interaction between lolium perenne and different strains of neotyphodium lolii. *J. Agricult. Food Chem.* 60 (13), 3381–3388. doi: 10.1021/jf204105k

Qiu, M., Xie, R. S., Shi, Y., Zhang, H., and Chen, H. M. (2010). Isolation and identification of two flavonoid-producing endophytic fungi from ginkgo biloba l. *Ann. Microbiol.* 60 (1), 143–150. doi: 10.1007/s13213-010-0016-5

Radwan, S. (2009). "Phytoremediation for oily desert soils," in *Advances in applied bioremediation* (Berlin, Heidelberg: Springer), (pp. 279–298). doi: 10.1007/978-3-540-89621-0_15

Rajkumar, M., Ae, N., and Freitas, H. (2009). Endophytic bacteria and their potential to enhance heavy metal phytoextraction. *Chemosphere* 77 (2), 153–160. doi: 10.1016/j.chemosphere.2009.06.047

Rashid, S., Charles, T. C., and Glick, B. R. (2012). Isolation and characterization of new plant growth-promoting bacterial endophytes. *Appl. Soil Ecol.* 61, 217–224. doi: 10.1016/j.apsoil.2011.09.011

Reddell, P., and Gordon, V. (2000). Lessons from nature': can ecology provide new leads in the search for novel bioactive chemicals from tropical rainforests?. in biodiversity: New leads for the pharmaceutical and agrochemical industries. *Proc Int Meeting Held 5-8 September 1999 Univ St Andrews UK*, 205–212. doi: 10.1039/9781847550231-00205

Rehman, S., Shawl, A. S., Kour, A., Andrabi, R., Sudan, P., Sultan, P., et al. (2008). An endophytic neurospora sp. from nothapodytes foetida producing camptothecin. *Appl. Biochem. Microbiol.* 44 (2), 203–209. doi: 10.1134/S0003683808020130

Ren, C. G., and Dai, C. C. (2012). Jasmonic acid is involved in the signaling pathway for fungal endophyte-induced volatile oil accumulation of atractylodes lancea plantlets. *BMC Plant Biol.* 12 (1), 128. doi: 10.1186/1471-2229-12-128

Rodriguez, R. J., White, J. F.Jr., Arnold, A. E., and Redman, A. R. A. (2009). Fungal endophytes: diversity and functional roles. *New Phytol.* 182 (2), 314–330. doi: 10.1111/j.1469-8137.2009.02773.x

Roos, I. M., and Hattingh, M. J. (1983). Scanning electron microscopy of pseudomonas syringae pv, morsprunorum on sweet cherry leaves. *J. Phytopathol.* 108 (1), 18–25. doi: 10.1111/j.1439-0434.1983.tb00559.x

Ryan, P. R., Germaine, K., Franks, A., Ryan, D. J., and Dowling, D. N. (2008). Bacterial endophytes: Recent developments and applications. FEMS microbiol. *Lett* 278, 1–9. doi: 10.1111/j.1574-6968.2007.00918.x

Sørensen, J., and Sessitsch, A. (2006). "Plant-associated bacteria lifestyle and molecular interactions," in *Modern soil microbiology*, *2nd edn*. Eds. J. D. Van Elsas, J. K. Jansson, J. T. Trevors and P. Nannipieri (Boca Raton: CRC press), 211–236.

Salam, N., Khieu, T. N., Liu, M. J., Vu, T. T., Chu-Ky, S., Quach, N. T., et al. (2017). Endophytic actinobacteria associated with dracaena cochinchinensis lour.: isolation, diversity, and their cytotoxic activities. *BioMed. Res. Int.* 2017, 1308563. doi: 10.1155/2017/1308563

Santoyo, G., Moreno-Hagelsieb, G., del Carmen Orozco-Mosqueda, M., and Glick, B. R. (2016). Plant growth-promoting bacterial endophytes. *Microbiol. Res.* 183, 92–99. doi: 10.1016/j.micres.2015.11.008

Saravanan, V. S., Madhaiyan, M., Osborne, J., Thangaraju, M., and Sa, T. M. (2008). Ecological occurrence of gluconacetobacter diazotrophicus and nitrogen-fixing acetobacteraceae members: their possible role in plant growth promotion. *Microb. Ecol.* 55 (1), 130–140. doi: 10.1007/s00248-007-9258-6

Sasse, J., Martinoia, E., and Northen, T. (2018). Feed your friends: do plant exudates shape the root microbiome? *Trends Plant Sci.* 23 (1), 25–41. doi: 10.1016/j.tplants.2017.09.003

Sato, F., and Kumagai, H. (2013). Microbial production of isoquinoline alkaloids as plant secondary metabolites based on metabolic engineering research. *Proc. Jpn. Acad. B.: Phys. Biol. Sci.* 89 (5), 165–182. doi: 10.2183/pjab.89.165

Schippmann, U., Leaman, D. J., and Cunningham, A. B. (2002). *Impact of cultivation and gathering of medicinal plants on biodiversity: Global trends and issues* (Rome, Italy: Inter-Department Working Group on Biology Diversity for Food and Agriculture, FAO). Available at: http://www.fao.org/3/aa010e/AA010E00.pdf.

Schmidt, R., Köberl, M., Mostafa, A., Ramadan, E. M., Monschein, M., Jensen, K. B., et al. (2014). Effects of bacterial inoculants on the indigenous microbiome and secondary metabolites of chamomile plants. *Front. Microbiol.* 5. doi: 10.3389/fmicb.2014.00064

Schulz, B., and Boyle, C. (2005). The endophytic continuum. *Mycol. Res.* 109 (6), 661–686. doi: 10.1017/S095375620500273X

Schulz, B., Boyle, C., Draeger, S., Römmert, A. K., and Krohn, K. (2002). Endophytic fungi: a source of novel biologically active secondary metabolites. *Mycol. Res.* 106 (9), 996–1004. doi: 10.1017/S0953756202006342

Schulz, B., Römmert, A. K., Dammann, U., Aust, H. J., and Strack, D. (1999). The endophyte-host interaction: a balanced antagonism? *Mycol. Res.* 103 (10), 1275–1283. doi: 10.1017/S0953756299008540

Scott, R. I., Chard, J. M., Hocart, M. J., Lennard, J. H., and Graham, D. C. (1996). Penetration of potato tuber lenticels by bacteria in relation to biological control of blackleg disease. *Potato Res.* 39 (3), 333–344. doi: 10.1007/BF02357937

Segura, A., and Ramos, J. L. (2013). Plant-bacteria interactions in the removal of pollutants. *Curr. Opin. Biotechnol.* 24, 467–473. doi: 10.1016/j.copbio.2012.09.011

Sessitsch, A., Coenye, T., Sturz, A. V., Vandamme, P., Barka, E. A., Salles, J. F., et al. (2005). Burkholderia phytofirmans sp. nov., a novel plant-associated bacterium with plant-beneficial properties. *Int. J. Syst. Evol. Microbiol.* 55 (3), 1187–1192. doi: 10.1099/ijs.0.63149-0

Shah, S., Shrestha, R., Maharjan, S., Selosse, M. A., and Pant, B. (2019b). Isolation and characterization of plant growth-promoting endophytic fungi from the roots of dendrobium moniliforme. *Plants* 8 (1), 5. doi: 10.3390/plants8010005

Shah, S., Thapa, B. B., Chand, K., Pradhan, S., Singh, A., Varma, A., et al. (2019a). Piriformospora indica promotes the growth of the in-vitro-raised cymbidium aloifolium plantlet and their acclimatization. *Plant Signal. Behav.* 14 (6), 1596716. doi: 10.1080/15592324.2019.1596716

Sharma, V. K., and Nowak, J. (1998). Enhancement of verticillium wilt resistance in tomato transplants by *in vitro* co-culture of seedlings with a plant growth promoting rhizobacterium (Pseudomonas sp. strain PsJN). *Can. J. Microbiol.* 44 (6), 528–536. doi: 10.1139/w98-017

Sheibani-Tezerji, R., Rattei, T., Sessitsch, A., Trognitz, F., and Mitter, B. (2015). Transcriptome profiling of the endophyte burkholderia phytofirmans PsJN indicates sensing of the plant environment and drought stress. *MBio* 6 (5), e00621–e00615. doi: 10.1128/mBio.00621-15

Sheng, X. F., Xia, J. J., Jiang, C. Y., He, L. Y., and Qian, M. (2008). Characterization of heavy metal-resistant endophytic bacteria from rape (Brassica napus) roots and their potential in promoting the growth and lead accumulation of rape. *Environ. pollut.* 156, 1164–1170. doi: 10.1016/j.envpol.2008.04.007

Sheoran, N., Nadakkakath, A. V., Munjal, V., Kundu, A., Subaharan, K., Venugopal, V., et al. (2015). Genetic analysis of plant endophytic pseudomonas putida BP25 and chemo-profiling of its antimicrobial volatile organic compounds. *Microbiol. Res.* 173, 66–78. doi: 10.1016/j.micres.2015.02.001

Shimizu, M. (2011). "Endophytic actinomycetes: biocontrol agents and growth promoters," in *Bacteria in agrobiology: Plant growth responses* (Springer), 201–220, Berlin, Heidelberg: Springer-Verlag. doi: 10.1007/978-3-642-20332-9_10

Shrestha, K., Strobel, G. A., Shrivastava, S. P., and Gewali, M. B. (2001). Evidence for paclitaxel from three new endophytic fungi of Himalayan yew of Nepal. *Planta Med.* 67 (04), 374–376. doi: 10.1055/s-2001-14307

Shweta, S., Zuehlke, S., Ramesha, B. T., Priti, V., Kumar, P. M., Ravikanth, G., et al. (2010). Endophytic fungal strains of fusarium solani, from apodytes dimidiata e. mey. ex arn (Icacinaceae) produce camptothecin, 10-hydroxycamptothecin and 9-methoxycamptothecin. *Phytochemistry* 71 (1), 117–122. doi: 10.1016/j.phytochem.2009.09.030

Silva, G. H., Teles, H. L., Zanardi, L. M., Young, M. C. M., Eberlin, M. N., Hadad, R., et al. (2006). Cadinane sesquiterpenoids of phomopsis cassiae, an endophytic fungus associated with cassia spectabilis (Leguminosae). *Phytochemistry* 67 (17), 1964–1969. doi: 10.1016/j.phytochem.2006.06.004

Soldan, R., Mapelli, F., Crotti, E., Schnell, S., Daffonchio, D., Marasco, R., et al. (2019). Bacterial endophytes of mangrove propagules elicit early establishment of the natural host and promote growth of cereal crops under salt stress. *Microbiol. Res.* 223, 33–43. doi: 10.1016/j.micres.2019.03.008

Spiering, M. J., Greer, D. H., and Schmid, J. A. N. (2006). Effects of the fungal endophyte, neotyphodium lolii, on net photosynthesis and growth rates of perennial ryegrass (Lolium perenne) are independent of in planta endophyte concentration. *Ann. Bot.* 98 (2), 379–387. doi: 10.1093/aob/mcl108

Sprent, J. I., and De Faria, S. M. (1989). "Mechanisms of infection of plants by nitrogen fixing organisms," in *Nitrogen fixation with non-legumes* (Dordrecht: Springer), (pp. 3–(pp11). doi: 10.1007/978-94-009-0889-5_1

Stępniewska, Z., and Kuźniar, A. (2013). Endophytic microorganisms–promising applications in bioremediation of greenhouse gases. *Appl. Microbiol. Biotechnol.* 97 (22), 9589–9596. doi: 10.1007/s00253-013-5235-9

Stacey, G., Libault, M., Brechenmacher, L., Wan, J., and May, G. D. (2006). Genetics and functional genomics of legume nodulation. *Curr. Opin. Plant Biol.* 9 (2), 110–121. doi: 10.1016/j.pbi.2006.01.005

Stierle, A., Strobel, G., Stierle, D., Grothaus, P., and Bignami, G. (1995). The search for a taxol-producing microorganism among the endophytic fungi of the pacific yew, taxus brevifolia. *J. Nat. Prod* 58 (9), 1315–1324. doi: 10.1021/np50123a002

Strobel, G. A. (2003). Endophytes as sources of bioactive products. *Microb. Inf.* 5 (6), 535–544. doi: 10.1016/S1286-4579(03)00073-X

Strobel, G., Daisy, B., Castillo, U., and Harper, J. (2004). Natural products from endophytic microorganisms. *J. Nat. Prod.* 67 (2), 257–268. doi: 10.1021/np030397v

Strobel, G. A., Miller, R. V., Martinez-Miller, C., Condron, M. M., Teplow, D. B., and Hess, W. M. (1999). Cryptocandin, a potent antimycotic from the endophytic fungus cryptosporiopsis cf. quercina. *Microbiology* 145 (8), 1919–1926. doi: 10.1099/13500872-145-8-1919

Strobel, G., Stierle, A., Stierle, D., and Hess, W. M. (1993). Taxomyces andreanae, a proposed new taxon for a bulbilliferous hyphomycete associated with pacific yew (Taxus brevifolia). *Mycotaxon* 47, 71–80. Available at: https://www.cabdirect.org/cabdirect/abstract/19932339243

Sumarah, M. W., Puniani, E., Sørensen, D., Blackwell, B. A., and Miller, J. D. (2010). Secondary metabolites from anti-insect extracts of endophytic fungi isolated from picea rubens. *Phytochemistry* 71 (7), 760–765. doi: 10.1016/j.phytochem.2010.01.015

Sun, Y., Cheng, Z., and Glick, B. R. (2009). The presence of a 1-aminocyclopropane-1-carboxylate (ACC) deaminase deletion mutation alters the physiology of the endophytic plant growth-promoting bacterium burkholderia phytofirmans PsJN. *FEMS Microbiol. Lett.* 296 (1), 131–136. doi: 10.1111/j.1574-6968.2009.01625.x

Sun, D., Ran, X., and Wang, J. (2008). Isolation and identification of a taxol-producing endophytic fungus from podocarpus. *Wei Sheng Wu Xue Bao* 48 (5), 589. doi: 10.3321/j.issn:0001-6209.2008.05.005

Suryanarayanan, T. S., Thirunavukkarasu, N., Govindarajulu, M. B., and Gopalan, V. (2012). Fungal endophytes: an untapped source of biocatalysts. *Fungal Div.* 54 (1), 19–30. doi: 10.1007/s13225-012-0168-7

Suryanarayanan, T. S., Thirunavukkarasu, N., Govindarajulu, M. B., Sasse, F., Jansen, R., and Murali, T. S. (2009). Fungal endophytes and bioprospecting. *Fungal Biol. Rev.* 23, 9–19. doi: 10.1016/j.fbr.2009.07.001

Sziderics, A. H., Rasche, F., Trognitz, F., Sessitsch, A., and Wilhelm, E. (2007). Bacterial endophytes contribute to abiotic stress adaptation in pepper plants (Capsicum annuum l.). *Can. J. Microbiol.* 53 (11), 1195–1202. doi: 10.1139/W07-082

Tanaka, A., Tapper, B. A., Popay, A., Parker, E. J., and Scott, B. (2005). A symbiosis expressed non-ribosomal peptide synthetase from a mutualistic fungal endophyte of perennial ryegrass confers protection to the symbiotum from insect herbivory. *Mol. Microbiol.* 57 (4), 1036–1050. doi: 10.1111/j.1365-2958.2005.04747.x

Tang, M. J., Meng, Z. X., Guo, S. X., Chen, X. M., and Xiao, P. G. (2008). Effects of endophytic fungi on the culture and four enzyme activities of anoectochilus roxburghii. *Chin. Pharm. J.* 43, 890–893. doi: 10.3321/j.issn:1001-2494.2008.12.003

Tan, R. X., and Zou, W. X. (2001). Endophytes: a rich source of functional metabolites. *Nat. Prod. Rep.* 18 (4), 448–459. doi: 10.1039/b100918o

Tilman, D. (1998). The greening of the green revolution. *Nature* 396 (6708), 211–212. doi: 10.1038/24254

Ting, A. S. Y., Meon, S., Kadir, J., Radu, S., and Singh, G. (2009). Induced host resistance by non-pathogenic fusarium endophyte as a potential defense mechanism in fusarium wilt management of banana. *Pest Technol.* 3 (1), 67–72.

Tiwari, R., Awasthi, A., Mall, M., Shukla, A. K., Srinivas, K. S., Syamasundar, K. V., et al. (2013). Bacterial endophyte-mediated enhancement of in planta content of key terpenoid indole alkaloids and growth parameters of catharanthus roseus. *Ind. Crops Prod.* 43, 306–310. doi: 10.1016/j.indcrop.2012.07.045

Tiwari, R., Kalra, A., Darokar, M. P., Chandra, M., Aggarwal, N., Singh, A. K., et al. (2010). Endophytic bacteria from ocimum sanctum and their yield enhancing capabilities. *Curr. Microbiol.* 60 (3), 167–171. doi: 10.1007/s00284-009-9520-x

Truyens, S., Jambon, I., Croes, S., Janssen, J., Weyens, N., Mench, M., et al. (2014). The effect of long-term cd and Ni exposure on seed endophytes of agrostis capillaris and their potential application in phytoremediation of metal-contaminated soils. *Int. J. Phytoremed.* 16 (7-8), 643–659. doi: 10.1080/15226514.2013.837027

Van Bael, S. A., Seid, M. A., and Wcislo, W. T. (2012). Endophytic fungi increase the processing rate of leaves by leaf-cutting ants (Atta). *Ecol. Entomol.* 37 (4), 318–321. doi: 10.1111/j.1365-2311.2012.01364.x

Vanessa, M. C., and Christopher, M. M. F. (2004). Analysis of the endophytic actinobacterial population in the roots of wheat (Triticum aestivum l.) by terminal restriction fragment length polymorphism and sequencing of 16S rRNA clones. *Appl. Environ. Microbiol.* 70 (3), 1787–1794. doi: 10.1128/AEM.70.3.1787-1794.2004

Vega, F. E., Posada, F., Aime, M. C., Pava-Ripoll, M., Infante, F., and Rehner, S. A. (2008). Entomopathogenic fungal endophytes. *Biol. Control* 46 (1), 72–82. doi: 10.1016/j.biocontrol.2008.01.008

Venkatachalam, R., Subban, K., and Paul, M. (2008). Taxol from botryodiplodia theobromae (BT 115)-an endophytic fungus of taxus baccata. *J. Biotechnol.* 136, S189–S190. doi: 10.1016/j.jbiotec.2008.07.1823

Verma, V. C., Gond, S. K., Kumar, A., Mishra, A., Kharwar, R. N., and Gange, A. C. (2009). Endophytic actinomycetes from azadirachta indica a. juss.: isolation, diversity, and anti-microbial activity. *Microb. Ecol.* 57 (4), 749–756. doi: 10.1007/s00248-008-9450-3

Verma, S. C., Ladha, J. K., and Tripathi, A. K. (2001). Evaluation of plant growth promoting and colonization ability of endophytic diazotrophs from deep water rice. *J. Biotechnol.* 91 (2-3), 127–141. doi: 10.1016/S0168-1656(01)00333-9

Villacieros, M., Power, B., Sánchez-Contreras, M., Lloret, J., Oruezabal, R. I., Martín, M., et al. (2003). Colonization behaviour of pseudomonas fluorescens and sinorhizobium meliloti in the alfalfa (Medicago sativa) rhizosphere. *Plant Soil* 251 (1), 47–54. doi: 10.1023/A:1022943708794

Viterbo, A. D. A., and Chet, I. (2006). TasHyd1, a new hydrophobin gene from the biocontrol agent trichoderma asperellum, is involved in plant root colonization. *Mol. Plant Pathol.* 7 (4), 249–258. doi: 10.1111/j.1364-3703.2006.00335.x

Vitousek, P. M., Mooney, H. A., Lubchenco, J., and Melillo, J. M. (1997). Human domination of earth's ecosystems. *Science* 277 (5325), 494–499. doi: 10.1126/science.277.5325.494

Wang, W. X., Barak, T., Vinocur, B., Shoseyov, O., and Altman, A. (2003). "Abiotic resistance and chaperones: possible physiological role of SP1, a stable and stabilizing protein from populus," in *Plant biotechnology 2002 and beyond* (Dordrecht: Springer), (pp. 439–443). doi: 10.1007/978-94-017-2679-5_91

Wang, P., Kong, F., Wei, J., Wang, Y., Wang, W., Hong, K., et al. (2014). Alkaloids from the mangrove-derived actinomycete jishengella endophytica 161111. *Mar. Drugs* 12 (1), 477–490. doi: 10.3390/md12010477

Wang, L., Liu, L., and Han, S. Z. (2009). Screening and identification of antimicrobe activity of endophytic fungus in glycyrrhiza uralensis. *Biotechnol. Bull.* 6, 034.

Wang, Y., Xu, L., Ren, W., Zhao, D., Zhu, Y., and Wu, X. (2012). Bioactive metabolites from chaetomium globosum L18, an endophytic fungus in the medicinal plant curcuma wenyujin. *Phytomedicine* 19 (3-4), 364–368. doi: 10.1016/j.phymed.2011.10.011

Wang, J. W., Zheng, L. P., and Tan, R. X. (2006). The preparation of an elicitor from a fungal endophyte to enhance artemisinin production in hairy root cultures of artemisia annua l. *Sheng Wu Gong Cheng Xue Bao* 22 (5), 829–834. doi: 10.3321/j.issn:1000-3061.2006.05.023

Wani, S. H., Kumar, V., Shriram, V., and Sah, S. K. (2016). Phytohormones and their metabolic engineering for abiotic stress tolerance in crop plants. *Crop J.* 4 (3), 162–176. doi: 10.1016/j.cj.2016.01.010

Wan, Y., Luo, S., Chen, J., Xiao, X., Chen, L., Zeng, G., et al. (2012). Effect of endophyte-infection on growth parameters and cd-induced phytotoxicity of cd-hyperaccumulator solanum nigrum l. *Chemosphere* 89 (6), 743–750. doi: 10.1016/j.chemosphere.2012.07.005

Waqas, M., Khan, A. L., Hamayun, M., Shahzad, R., Kang, S. M., Kim, J. G., et al. (2015a). Endophytic fungi promote plant growth and mitigate the adverse effects of stem rot: an example of penicillium citrinum and aspergillus terreus. *J. Plant Interact.* 10 (1), 280–287. doi: 10.1080/17429145.2015.1079743

Waqas, M., Khan, A. L., Hamayun, M., Shahzad, R., Kim, Y. H., Choi, K. S., et al. (2015b). Endophytic infection alleviates biotic stress in sunflower through regulation of defense hormones, antioxidants and functional amino acids. *Eur. J. Plant Pathol.* 141 (4), 803–824. doi: 10.1007/s10658-014-0581-8

Waqas, M., Khan, A. L., Kamran, M., Hamayun, M., Kang, S. M., Kim, Y. H., et al. (2012). Endophytic fungi produce gibberellins and indoleacetic acid and promotes host-plant growth during stress. *Mol. (Basel)* 17 (9), 10754–10773. doi: 10.3390/molecules170910754

Wei, J., Liu, X., Wang, Q., Wang, C., Chen, X., and Li, H. (2014). Effect of rhizodeposition on pyrene bioaccessibility and microbial structure in pyrene and pyrene-lead polluted soil. *Chemosphere* 97, 92–97. doi: 10.1016/j.chemosphere.2013.09.105

Weyens, N., Cross, S., Dupae, J., Newman, L., van der Lelie, D., Carleer, R., et al. (2010). Endophytic bacteria improve phytoremediation of Ni and TCE co-contamination. *Environ. pollut.* 158, 2422–2427. doi: 10.1016/j.envpol.2010.04.004

Weyens, N., van der Lelie, D., Taghavi, S., and Vangronsveld, J. (2009). Phytoremediation: plant–endophyte partnerships take the challenge. *Curr. Opin. Biotechnol.* 20 (2), 248–254. doi: 10.1016/j.copbio.2009.02.012

Whipps, J., and Gerhardson, B. (2007). Biological pesticides for control of seed- and soil-borne plant pathogens. *Modern Soil Microbiol. CRC Press Boca Raton* pp, 479–501. Available at: https://cir.nii.ac.jp/crid/1570854175613702528

Wiewiora, B., Żurek, G., and Pańka, D. (2015). Is the vertical transmission of neotyphodium lolii in perennial ryegrass the only possible way to the spread of endophytes? *PloS One* 10 (2), e0117231. doi: 10.1371/journal.pone.0117231

Williams, T. A., Foster, P. G., Cox, C. J., and Embley, T. M. (2013). An archaeal origin of eukaryotes supports only two primary domains of life. *Nature* 504 (7479), 231–236. doi: 10.1038/nature12779

Wu, C. H., Bernard, S. M., Andersen, G. L., and Chen, W. (2009). Developing microbe–plant interactions for applications in plant-growth promotion and disease control, production of useful compounds, remediation and carbon sequestration. *Microb. Biotechnol.* 2 (4), 428–440. doi: 10.1111/j.1751-7915.2009.00109.x

Wu, L., Han, T., Li, W., Jia, M., Xue, L., Rahman, K., et al. (2013). Geographic and tissue influences on endophytic fungal communities of taxus chinensis var. mairei in China. *Curr. Microbiol.* 66 (1), 40–48. doi: 10.1007/s00284-012-0235-z

Wu, J. Y., Ng, J., Shi, M., and Wu, S. J. (2007). Enhanced secondary metabolite (tanshinone) production of salvia miltiorrhiza hairy roots in a novel root–bacteria coculture process. *Appl. Microbiol. Biotechnol.* 77 (3), 543–550. doi: 10.1007/s00253-007-1192-5

Yang, N. Y., Jiang, S., Shang, E. X., Tang, Y. P., and Duan, J. A. (2012). A new phenylpentanamine alkaloid produced by an endophyte bacillus subtilis isolated from angelica sinensis. *J. Chem. Res.* 36 (11), 647–647. doi: 10.3184/174751912X13469254685262

Yang, X., Shiping, G., Lingqi, Z., and Hua, S. (2003). Select of producing podophyllotoxin endophytic fungi from podophyllin plant. *Nat. Prod. Res. Devel.* 15 (5), 419–422. doi: 10.3969/j.issn.1001-6880.2003.05.012

Yan, X. N., Sikora, R. A., and Zheng, J. W. (2011). Potential use of cucumber (Cucumis sativus l.) endophytic fungi as seed treatment agents against root-knot nematode meloidogyne incognita. *J. Zhejiang Univ. Sci.* 12 (3), 219–225. doi: 10.1631/jzus.B1000165

Yan, L., Zhu, J., Zhao, X., Shi, J., Jiang, C., and Shao, D. (2019). Beneficial effects of endophytic fungi colonization on plants. *Appl. Microbiol. Biotechnol.* 103 (8), 3327–3340. doi: 10.1007/s00253-019-09713-2

Yedidia, I., Benhamou, N., and Chet, I. (1999). Induction of defense responses in cucumber plants (Cucumis sativus l.) by the biocontrol agent trichoderma harzianum. *Appl. Environ. Microbiol.* 65 (3), 1061–1070. doi: 10.1128/AEM.65.3.1061-1070.1999

Yin, H., and Chen, J. L. (2008). Sipeimine-producing endophytic fungus isolated from: Fritillaria ussuriensis. *Z. Für Naturforschung C.* 63 (11-12), 789–793. doi: 10.1515/znc-2008-11-1202

Yong, Y., Dai, C., Gao, F., Yang, Q., and Zhao, M. (1994). Effects of endophytic fungi on growth and two kinds of terpenoids for euphorbia pekinensis. *Chin. Trad. Herbal. Drugs* 40, 18–22. Available at: https://pesquisa.bvsalud.org/portal/resource/pt/wpr-579810

Yu, X. M., and Guo, S. X. (2000). Establishment of symbiotic system for anoectochilus roxburghii (Wall.) lindl. and endophytic fungi. *Zhongguo Zhong Yao Za Zhi* 25 (2), 81–83. doi: 10.3321/j.issn:1001-5302.2000.02.006

Zeilinger, S., Gupta, V. K., Dahms, T. E., Silva, R. N., Singh, H. B., Upadhyay, R. S., et al. (2016). Friends or foes? emerging insights from fungal interactions with plants. *FEMS Microbiol. Rev.* 40 (2), 182–207. doi: 10.1093/femsre/fuv045

Zeng, S., Shao, H., and Zhang, L. (2004). An endophytic fungus producing a substance analogous to podophyllotoxin isolated from diphylleia sinensis. *J. Microbiol.* 24, 1–2. doi: 10.3969/j.issn.1005-7021.2004.04.001

Zhang, H., Bai, X., and Wu, B. (2012). Evaluation of antimicrobial activities of extracts of endophytic fungi from artemisia annua. *Bangladesh J. Pharmacol.* 7 (2), 120–123. doi: 10.3329/bjp.v7i2.10951

Zhang, X. X., George, A., Bailey, M. J., and Rainey, P. B. (2006b). The histidine utilization (hut) genes of pseudomonas fluorescens SBW25 are active on plant surfaces, but are not required for competitive colonization of sugar beet seedlings. *Microbiology* 152 (6), 1867–1875. doi: 10.1099/mic.0.28731-0

Zhang, X., Li, G., Ma, J., Zeng, Y., Ma, W., and Zhao, P. (2010). Endophytic fungus trichothecium roseum LZ93 antagonizing pathogenic fungi *in vitro* and its secondary metabolites. *J. Microbiol.* 48 (6), 784–790. doi: 10.1007/s12275-010-0173-z

Zhang, C. L., Liu, S. P., Lin, F. C., Kubicek, C. P., and Druzhinina, I. S. (2007). Trichoderma taxi sp. nov., an endophytic fungus from Chinese yew taxus mairei. *FEMS Microbiol. Lett.* 270 (1), 90–96. doi: 10.1111/j.1574-6968.2007.00659.x

Zhang, H. W., Song, Y. C., and Tan, R. X. (2006a). Biology and chemistry of endophytes. *Nat. Prod. Rep.* 23 (5), 753–771. doi: 10.1039/b609472b

Zhang, J., Wang, C., Guo, S., Chen, J., and Xiao, P. (1999). Studies on the plant hormones produced by 5 species of endophytic fungi isolated from medicinal plants (Orchidacea). *Zhongguo Yi Xue Ke Xue Yuan Xue Bao* 21 (6), 460–465.

Zhang, P., Zhou, P. P., and Yu, L. J. (2009). An endophytic taxol-producing fungus from taxus media, cladosporium cladosporioides MD2. *Curr. Microbiol.* 59 (3), 227. doi: 10.1007/s00284-008-9270-1

Zhou, X., Wang, Z., Jiang, K., Wei, Y., Lin, J., Sun, X., et al. (2007). Screening of taxol-producing endophytic fungi from taxus chinensis var. mairei. *Appl. Biochem. Microbiol.* 43 (4), 439–443. doi: 10.1134/S000368380704014X

Zhou, S. L., Yang, F., Lan, S. L., Xu, N., and Hong, Y. H. (2009). Huperzine a producing conditions from endophytic fungus in SHB huperzia serrata. *J. Microbiol.* 3, 32–36. doi: 10.3969/j.issn.1005-7021.2009.03.006

Zhou, J. Y., Yuan, J., Li, X., Ning, Y. F., and Dai, C. C. (2015). Endophytic bacterium-triggered reactive oxygen species directly increase oxygenous sesquiterpenoid content and diversity in atractylodes lancea. *Appl. Environ. Microbiol.* 82 (5), 1577–1585. doi: 10.1128/AEM.03434-15

frontiers | Frontiers in Plant Science

TYPE Original Research
PUBLISHED 06 October 2022
DOI 10.3389/fpls.2022.1028101

OPEN ACCESS

EDITED BY
Maurizio Ruzzi,
University of Tuscia, Italy

REVIEWED BY
RISHIKESH SINGH,
Panjab University, India
Zhenyu Wang,
Jiangnan University, China

*CORRESPONDENCE
Martin Brtnicky
martin.brtnicky@seznam.cz
Adnan Mustafa
adnanmustafa780@gmail.com

SPECIALTY SECTION
This article was submitted to Plant Nutrition, a section of the journal Frontiers in Plant Science

RECEIVED 25 August 2022
ACCEPTED 15 September 2022
PUBLISHED 06 October 2022

CITATION
Mustafa A, Brtnicky M, Hammerschmiedt T, Kucerik J, Kintl A, Chorazy T, Naveed M, Skarpa P, Baltazar T, Malicek O and Holatko J (2022) Food and agricultural wastes-derived biochars in combination with mineral fertilizer as sustainable soil amendments to enhance soil microbiological activity, nutrient cycling and crop production. *Front. Plant Sci.* 13:1028101. doi: 10.3389/fpls.2022.1028101

Food and agricultural wastes-derived biochars in combination with mineral fertilizer as sustainable soil amendments to enhance soil microbiological activity, nutrient cycling and crop production

Adnan Mustafa[1,2,3]*, Martin Brtnicky[1,2]*, Tereza Hammerschmiedt[1], Jiri Kucerik[2], Antonin Kintl[1,4], Tomas Chorazy[5], Muhammad Naveed[6], Petr Skarpa[1], Tivadar Baltazar[1], Ondrej Malicek[1] and Jiri Holatko[1,7]

[1]Department of Agrochemistry, Soil Science, Microbiology and Plant Nutrition, Faculty of AgriSciences, Mendel University in Brno, Brno, Czechia, [2]Institute of Chemistry and Technology of Environmental Protection, Faculty of Chemistry, Brno University of Technology, Brno, Czechia, [3]Institute for Environmental Studies, Faculty of Science, Charles University in Prague, Praha, Czechia, [4]Agricultural Research, Ltd., Troubsko, Czechia, [5]AdMaS Research Centre, Faculty of Civil Engineering, Brno University of Technology, Brno, Czechia, [6]Institute of Soil and Environmental Science, University of Agriculture Faisalabad, Faisalabad, Pakistan, [7]Agrovyzkum Rapotin, Ltd., Rapotin, Czechia

The ever-increasing human population associated with high rate of waste generation may pose serious threats to soil ecosystem. Nevertheless, conversion of agricultural and food wastes to biochar has been shown as a beneficial approach in sustainable soil management. However, our understanding on how integration of biochar obtained from different wastes and mineral fertilizers impact soil microbiological indicators is limited. Therefore, in the present study the effects of agricultural (AB) and food waste derived (FWB) biochars with and without mineral fertilizer (MF) on crop growth and soil health indicators were compared in a pot experiment. In particular, the impacts of applied amendments on soil microbiological health indicators those related to microbial extracellular (C, N and P acquiring) enzymes, soil basal as well as different substrate induced respirations along with crop's agronomic performance were explored. The results showed that compared to the control, the amendment with AB combined with MF enhanced the crop growth as revealed by higher above and below ground biomass accumulation. Moreover, both the biochars (FWB and AB) modified soil chemical properties (pH and electric conductivity) in the presence or absence of MF as compared to control. However, with the sole application of MF was most influential strategy to improve soil basal and arginin-induced respiration as well as most of the soil extracellular enzymes, those related to C, N and P cycling. Use of FWB resulted

in enhanced urease activity. This suggested the role of MF and FWB in nutrient cycling and plant nutrition. Thus, integration of biochar and mineral fertilizers is recommended as an efficient and climate smart package for sustainable soil management and crop production.

KEYWORDS

nutrient cycling, sustainable crop production, waste recycling, food security, agriculture

Introduction

The world's population has been increasing exponentially and is expected to turn up to 9.6 billion until 2050 (Tripathi et al., 2019) and is projected to be linked with a 60% increase in food demand (Boretti and Rosa, 2019). This overwhelming pace of human population, high food consumption and agricultural waste production will put pressure on the global agriculture which may outcome in negative environmental and socio-economic aspects. In fact, the higher food production and waste generation due to human consumption are concomitantly linked and approximately 1/3rd of the food produced is annually wasted around the globe (Kibler et al., 2018; Ishangulyyev et al., 2019). It has been estimated that the annual amount of this food waste is approximately 1.3 billion tons globally (Gustavsson et al., 2011). A big part of this amount (56%) is produced by developed world while the rest (44%) is being generated by the less developed countries (Bond et al., 2013; Lipinski et al., 2013). However, a big part of the wasted food material is lost, incinerated or buried in the landfills, causing soil and water pollution which is another of the main global concerns (Parry et al., 2007; Abiad and Meho, 2018). In this way, only in USA, around US$90 billion–US$100 billion a year is lost (Lundqvist et al., 2008). Therefore, the situation demands for the safer utilization of food and viable approaches to deal with the wasted materials to ensure the food security and environmental protection.

Several types of organic (including food and agricultural) wastes are generated worldwide with the potential to be utilized as soil amendments for enhancing soil health and crop production (Toscano et al., 2013; Sayara et al., 2020; Naveed et al., 2021). However, direct application of such wastes may cause risks to soil health, especially to soil chemical and microbiological characters (Urra et al., 2019). Therefore, bioconversion of agricultural and food wastes to non-hazardous and stable soil amendments is a viable alternative. This will not only reduce the risks associated with environmental burdens, but also ensures the safe disposal and utilization of end product as sustainable soil amendments (Sulok et al., 2021; Brtnicky et al., 2022). Conversion of agricultural and food wastes into biochar (a C rich) product produced by the pyrolysis is an effective way in this regard too. Biochar has been reported to enhance soil fertility, improve soil health and ultimately increasing crop yields (Ahmad et al., 2020; Karimi et al., 2020; Rasool et al., 2022). We took advantage of converting the collected food and agricultural wastes into biochars and utilized them for this study.

It has been recognized that intensive agricultural practices, injudicious use of chemical fertilizers, removal of crop straw and heavy tillage operations have resulted in the loss of soil fertility and degradation of arable lands (Sonmez et al., 2016). Currently, farmers heavily rely on the use of chemical fertilizers and crop protection chemicals to produce higher crop yields (Mustafa et al., 2019). This behavior of farmers has aggravates the soil degradation and its productive capacity as the higher use of chemicals and fertilizers deteriorate the environmental resources and cause soil salinity, eutrophication and heavy metal pollution in arable soils (Bouraoui and Grizzetti, 2014; Ali et al., 2019; Zulfiqar et al., 2022). To entail these challenges, researchers are focusing on developing alternative strategies, which ensure high crop yields without negative effects on the soil quality and water resources (Bais-Moleman et al., 2019; Tan et al., 2021; Kang et al., 2022; Wali et al., 2022). Nevertheless, chemical fertilizers have shown a potential to increase crop yields by modifying soil properties, the sole utilization of chemical fertilizers have been questioned in the face of climate change (Srivastav, 2020; Meena et al., 2020). In this respect, the combination of biochar together with mineral fertilizers could be an effective strategy to enhance soil health and crop biomass yields while keeping the mineral fertilizers at low levels. Previously many studies have shown the improvements in crop yields and soil fertility under the application of either chemical fertilizers or biochar (Atkinson et al., 2010; Khadem and Raiesi, 2017) or the combination of both (Singh et al., 2019a; Singh et al., 2019b). Most of these studies have shown the variable effects of biochar derived from various sources on soil properties (Prendergast-Miller et al., 2014; Hussain et al., 2017; Mohan et al., 2018) and agronomic and physiological responses of crops (Carter et al., 2013; Kuppusamy et al., 2016; Singh et al., 2020). Majority of these studies have only focused on soil physico-chemical properties

and the role of applied biochar amendments on soil microbiological attributes those elated to (soil extracellular enzymes and soil basal as well as substrate induced respirations) remained relatively unexplored till date. Moreover, the comparison of effects of biochars (derived from agricultural and food wastes) with and without mineral fertilizers on crop's photosynthetic efficiency remained neglected in the past. Therefore, we compared the effects of two types of biochars with and without mineral fertilizers on soil physico-chemical and microbiological properties and how they respond to crop growth and physiology. We considered the soil extracellular enzymes activity and microbial respiration as soil health indicators and crop's photosystem efficiency as agronomic performance respectively for evaluating the effects of applied biochars together with mineral fertilizer. The specific objectives of the present study were to (i) compare and analyze the effects of produced biochars with and without mineral fertilizer on soil basal and substrate induced respirations and extracellular enzymes, and (ii) assess the growth and physiological responses of crop under applied amendments.

Materials and methods

Procurement and preparation of biochars

For the purposes of pot experiment, the food waste biochar (FWB) was prepared in two steps. The first step involved the pre-treatment process, which consists of two consequent steps i.e., the dried food waste (dry matter approx. 90%) was mixed with 25% of spruce sawdust and subsequently the mixture was pelletized at a briquetting press for the production of pellets type JGE 260 with a matrix at a size of 6 mm of extrusion holes and a pellet length of 40 mm. The second step was the heat treatment of the samples, whereby thermal pyrolysis (TP) was performed in laboratory, small-scale conditions, in a small-scale TP unit working under 600°C. This unit works discontinuously, and the maximum capacity is around 5 kg·batch^{-1} of feedstock. The glass condenser attached to the pyrolyzer was used for the separation of gaseous products and the pyrolysis oil. The input weight of feedstock samples was 3 000 g·batch^{-1}. The feedstock was placed into the TP unit in a stainless-steel cylindrical reactor. During the experiments, the residence time was 340 - 410 minutes, and the temperature did not exceed 600°C.

Moreover, commercial biochar from agricultural waste was purchased from the manufacturer (Sonnenerde GmbH, Austria). This biochar was produced with a high-technology production unit Pyreg500 from grain husks, sunflower pods and pulp mud. The process temperature was set up at 650°C. The chemical composition of applied biochars is given in (Table 1).

Experimental design and treatments

The growth substrate used for the pot experiment was prepared by mixing a silty clay loam (USDA Textural Triangle) Haplic Luvisol (WRB soil classification) collected at field near the town Troubsko (Czech Rep., 49°10'28"N 16° 29'32"E) with a fine quartz sand (0.1–1.0 mm; ≥95% SiO_2) in a weight ratio of 1:1. The soil properties were as follows: total C 14.0 g·kg^{-1}, total N 1.60 g·kg^{-1}, available P 0.10 g·kg^{-1}, available S 0.15 g·kg^{-1}, available Ca 3.26 g·kg^{-1}, available Mg 0.24 g·kg^{-1}, available K 0.23 g·kg^{-1}; pH ($CaCl_2$) 7.3.

One kilogram of this growth substrate was mixed with 32 g (equivalent to 40 t.ha^{-1}) of a particular biochar (Table 1) and filled to experimental plastic pots (volume 1 L, top diameter 11 cm, bottom diameter 9 cm, height 13 cm). Control treatment was left without the addition of biochar. The mineral fertilizer (MF) NPK (16:16:16) was dissolved in demineralised water and applied on soil surface of specific variants in dose equal to 0.1 g N·kg^{-1} of soil. Following biochar treatments were applied in the presence and absence of mineral fertilizer; (i) control (no biochar) (ii) foodwaste biochar (FWB) with and without mineral fertilizer (hereinafter referred to as FWB+MF) and (iii) agricultural waste derived biochar (AB) with and without mineral fertilizer (hereinafter referred to as AB+MF). The experimental treatments are shown in (Table 2). Each treatment was carried out in 3 replicates (pots).

Pot experiment

The pot experiment with lettuce (*Lactuca sativa* L. var. *capitata*) took place in growth chamber Climacell EVO (BMT, Czech Rep.) under controlled conditions: full-spectrum LED lighting, light intensity 20,000 lux; photoperiod 12 h;

TABLE 1 Chemical composition of used biochars.

	TC[%]	ROC [%]	TIC [%]	TOC [%]	N[%]	H[%]	O[%]	C:N	H:C	O:C
AB	50.13± 0.02	0.45± 0.06	0.33± 0.00	49.80± 0.02	1.01± 0.06	1.60± 0.04	17.28± 0.21	49.67± 2.89	0.03± 0.00	0.34± 0.00
FWB	81.25± 0.03	0.28± 0.01	0.07± 0.00	81.18± 0.03	3.58± 0.05	3.04± 0.06	8.10± 0.25	22.71± 0.30	0.04± 0.00	0.10± 0.00

TC, total carbon; ROC, resistant organic carbon; TIC, total inorganic carbon; TOC, total organic carbon; N, nitrogen; H, hydrogen; O, oxygen.

10.3389/fpls.2022.1028101

TABLE 2 Description of experimental treatments.

Variant	FWB	AB	MF
Control	–	–	–
MF	–	–	✓
FWB	✓	–	–
FWB+MF	✓	–	✓
AB	–	✓	–
AB+MF	–	✓	✓

FWB, food waste derived biochar; AB, agricultural waste derived biochar; MF, mineral fertilizer. – means (not inculded) or (absent).✓ means (included) or (present).

temperature 18/22°C (night/day); relative humidity 70%. Lettuce seeds were sprouted on wet filter paper for two days and then five of them were sown to the depth of approximately 2 mm in each pot. After sowing, each pot was watered with 100 mL of distilled water. The 10-day-old seedlings were reduced to one plant per pot. Pot placement in the growth chamber was randomized. Soil humidity was controlled, and water content was maintained during the experiment at approximately 60% of water holding capacity. The pots were variably rotated once per week. The plants were harvested 8 weeks after sowing.

Plant biomass and photosynthesis characteristics measurements

At harvest time, determination of photochemical efficiency of photosystem II (PSII) of lettuce plants was carried out. The quantum yield of the PSII (Φ_{PSII}) was determined (at light intensity 2400 $\mu mol \cdot m^{-2} \cdot s^{-1}$) by the fluorometer PAR-FluorPen FP 110-LM/S (Photon Systems Instruments, Drásov, Czech Republic) and the software FluorPen 1.1 was used for the analysis of the measured data. Determination of normalized difference vegetation index (NDVI) was carried out too with PlantPen NDVI 310 (Photon System Instruments, Drásov, Czech Republic). The spectral reflectance of chlorophyll pigments, expressed as NDVI, is a measure of chlorophyll content (Garty et al., 2001) and its integrity (Castro and Sanchez-Azofeifa, 2008) and correlates with photosynthetic rate (Garty et al., 2001). Then, the lettuce shoots were cut at ground level, and the roots were gently cleaned of soil and washed with water. Fresh aboveground (AGB) and root biomass were estimated gravimetrically by weighing on the analytical scales.

Soil analysis for microbiological soil health indicators

A mixed soil sample was taken from each pot after harvesting the lettuce. Soil samples were homogenized by sieving through a sieve with mesh size 2 mm. Air dried samples were analyzed for pH (ISO 10390, 2005) and electric conductivity (EC) (Hardie et al., 2012). Freeze-dried samples were used for the analyses of enzymatic activities: β-glucosidase (GLU), phosphatase (PHOS), urease (URE) and N-acetyl-β-D-glucosaminidase (NAG) (ISO 20130, 2018). The samples stored at 4 °C were used for determination of dehydrogenase activity (DHA) using standard method based on triphenyltetrazolium chloride (TTC) (Małachowska-Jutsz and Matyja, 2019), soil basal respiration (BR) and substrate induced respirations (IR) – D-glucose (Glc-IR), L-alanine (Ala-IR) and L-arginine (Arg-IR) (Campbell et al., 2003) using MicroResp® device (The James Hutton Institute, Scotland).

Statistical analyses

The obtained data were statistically analyzed using the one-way analysis of variance (ANOVA), Treatment means were compared using Tukey HSD *post-hoc* test (at significance level $p = 0.05$).

To evaluate the effects of applied amendments, principal component analysis (PCA) was plotted for observed variables and observations using Rstudio.

Results

Plant growth and chlorophyll fluorescence

The application of biochars with and without mineral fertilizer (MF) differently affected the plant growth and photosynthetic parameters. The plant fresh above ground biomass (AGB-fresh) was significantly highest under AB+MF as compared to control and other treatments (Figure 1A). This trend was followed by MF alone and food waste biochar with mineral fertilizer (FWB+MF). The highest root fresh weight (Root-fresh) was observed under the application of AB+MF which was followed by FWB+MF relative to control (Figure 1B). The quantum yield of the electron transport of the PSII (Φ_{PSII}), which expresses the real capacity of the PSII for photochemical reactions, was relatively increased by MF application. There was no significant increase found for Φ_{PSII}, which acts as a measure of the overall efficiency of PSII reaction centers in light, under applied amendments (Figure 1C). The spectral reflectance of chlorophyll pigments, expressed as NDVI (Figure 1D) was correlated with Φ_{PSII} values (Figure 1C).

Soil chemical properties

The application of food waste biochar with and without mineral fertilization significantly enhanced the soil pH as compared to control (Figure 2A). The highest pH values were

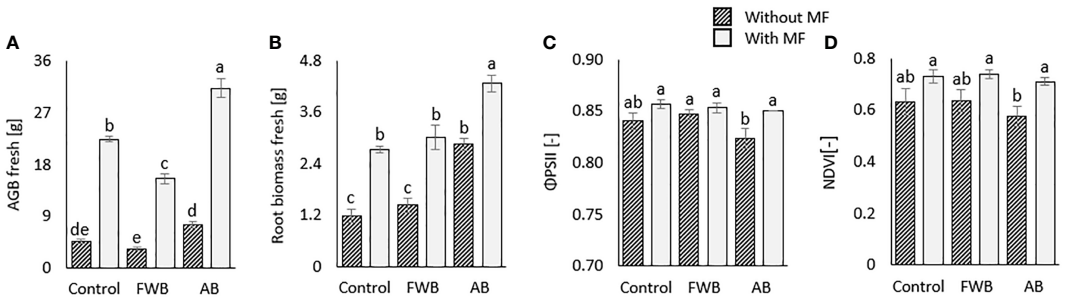

FIGURE 1
Comparative effects of applied food waste (FWB) and agricultural waste biochar (AB) with and without mineral fertilization (MF) on **(A)** above ground fresh biomass **(B)** root fresh biomass, quantum yield of the PSII **(C)** and NDVI **(D)**. Values are mean of three replicates. Different lowercase letters indicate statistical significance at $p<0.05$.

observed in soils receiving FWB, FWB+MF and AB, while the lowest was found under MF control which was statistically similar with the pH value under AB+MF application (Figure 2A). Remarkable variations were however observed for soil electrical conductivity (EC) under the applied biochars with and without MF. Specifically, the highest EC was observed under the application of FWB+MF and FWB without MF (Figure 2B) which were statistically significant as compared to other treatments and control.

Soil extracellular enzymes activities

The highest dehydrogenase activity (DHA) was observed under the sole application of MF (Figure 3A). All other amendments except AB significantly reduced DHA as compared to control (Figure 3A). Similar to DHA, the same treatment i.e., MF resulted in highest glucosidase (Glu) and phosphatase (PHOS) activities (Figures 3B, C). All other amendments resulted in reduced activities of Glu and PHOS as compared to control. Regarding urease, the significantly highest activity was recorded under the application of FWB and AB without MF as compared to control (Figure 3D). Moreover, the MF alone enhanced N-acetyl-glucosaminase (NAG) activity as compared to other treatments (Figure 3E), while no clear trend was observed for aryl sulphatase activity under applied treatments (Figure 3F).

Soil basal and substrate induced respiration

The application of food waste and agricultural biochars with and without mineral fertilization considerably affected the basal as well as substrate induced respirations (SIR). A significantly highest increase in soil basal respiration (BR) was observed under the sole application of MF and AB (Figure 4A) as compared to control and other treatments. The application of

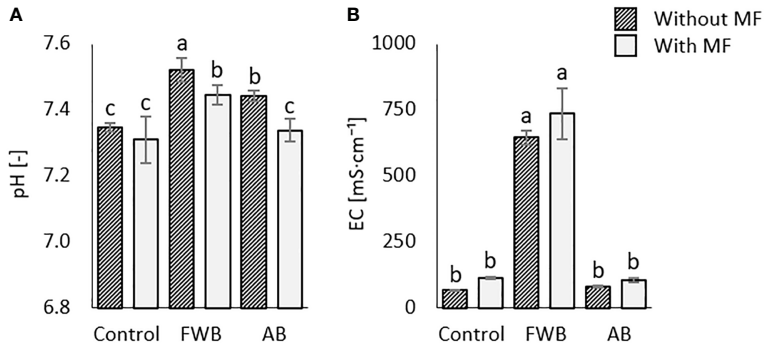

FIGURE 2
Comparative effects of applied food waste (FWB) and agricultural waste biochar (AB) with and without mineral fertilization (MF) on **(A)** soil pH and **(B)** soil electrical conductivity (EC). Values are mean of three replicates. Different lowercase letters indicate statistical significance at $p<0.05$.

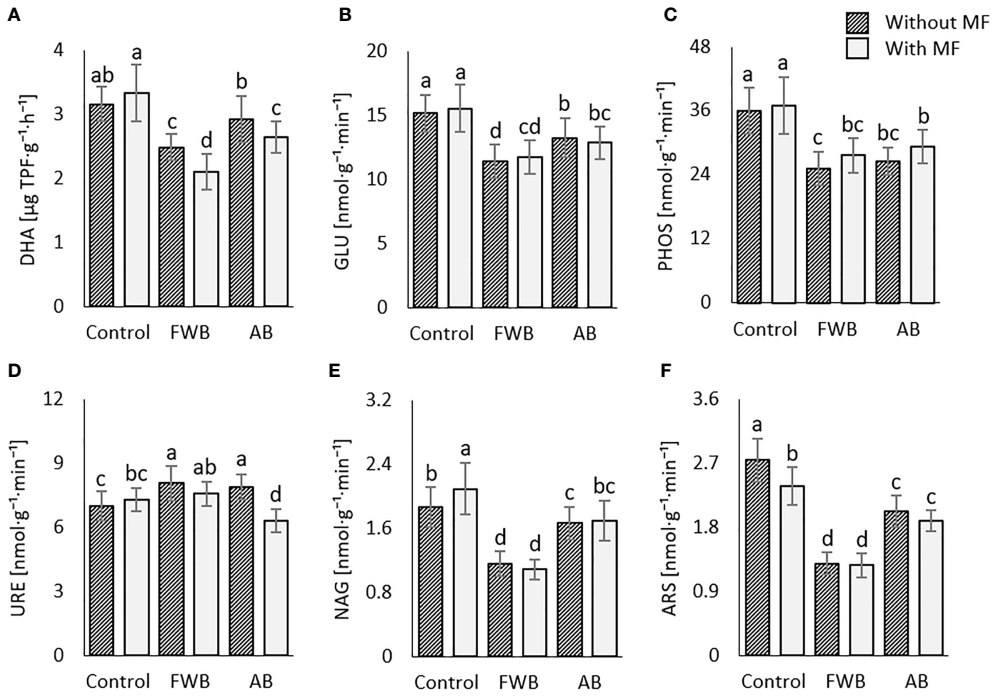

FIGURE 3
Comparative effects of applied food waste (FWB) and agricultural waste biochar (AB) with and without mineral fertilization (MF) on **(A)** dehydrogenase activity; **(B)** glucosidase activity; **(C)** phosphatase activity; **(D)** urease activity; **(E)** N-acetyl-glucosaminase activity and **(F)** aryl-sulphatase activity. Values are mean of three replicates. Different lowercase letters indicate statistical significance at $p<0.05$.

AB without MF resulted in significantly highest glucose-induced respiration (Glu-IR) and alanine-induced respiration (Ala-IR) respectively as compared to control (Figures 4B, C). This trend was followed by the application of MF alone. However, the sole application of MF enhanced the arginine-induced respiration (Arg-IR), which was significantly highest as compared to other treatments (Figure 4D).

Results from principal component analysis

The score and loading plots of principal component analysis (PCA) regarding the observed soil and plant characteristics are shown in (Figure 5). The extracted components (Dim1 and Dim 2) maximally (82.7%) accounted for the observed variations in the data set. The applied amendments were successfully separated by the principal components (as marked by different colors). This suggests the positive influence of applied amendments on the observed parameters. The treatments MF, AB and AB+MF were distributed in components 1 and FWB and FWB+MF were distributed in component 2 of the PCA (Figure 5). This clearly indicated the differential roles of applied amendments on the listed soil and plant parameters. As indicated by the PC1, the applied MF was found as the most influential treatment on most of the measured soil enzymes in the present study. While PC2 showed FWB and FWB+MF as most influential treatments regarding soil chemical properties (pH and EC). The most displaced parameters were soil pH, EC and plant chlorophyll fluorescence parameters Φ_{PSII} and NDVI, suggesting the differential effects of applied amendments on soil characteristics and plant growth and physiology.

Discussion

Agricultural and food wastes derived biochars have been regarded as alternative sources for enhancing soil chemical, physico-chemical and biological health and crop growth and development. However, the sole utilization of biochar does not always result in an increase in soil fertility and crop biomass. The present study, therefore, aimed to compare the effectiveness of agricultural and food wastes derived biochars with and without mineral fertilization for improving soil chemical, physico-chemical and biological properties related to microbial soil health indicators and crop growth. The results revealed that the application of agricultural biochar with mineral fertilization enhanced crop biomass (Figure 1). This enhancement might be

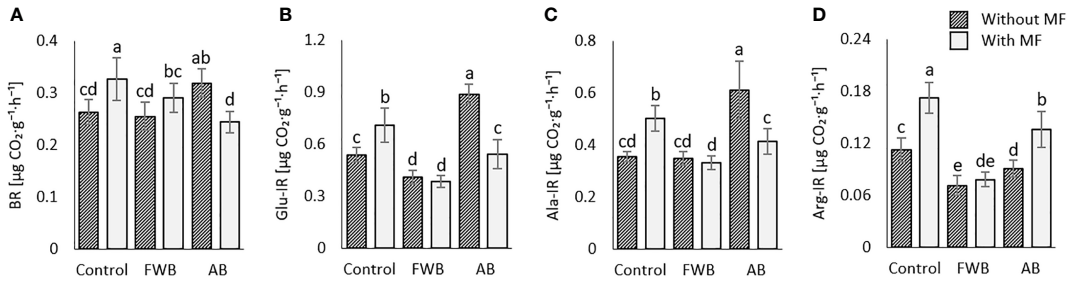

FIGURE 4
Comparative effects of applied food waste (FWB) and agricultural waste biochar (AB) with and without mineral fertilization (MF) on **(A)** soil basal respiration; **(B)** glucose-induced-respiration; **(C)** alanine-induced respiration; and **(D)** arginine-induced respiration. Values are mean of three replicates. Different lowercase letters indicate statistical significance at $p<0.05$.

associated with the increased acquisition of readily available plant nutrients under the applied biochar plus mineral fertilizer combination (Sadaf et al., 2017). Similarly, Jeffery et al. (2017), reported enhanced crop growth and yield. The authors stated that the enhancement of crop growth and yield is mainly related to enhanced soil nutrients under biochar application. These results are further substantiated by the findings of Lai et al. (2017) and Dong et al. (2015), who reported enhanced crop biomass and yield under applied biochar. In our work, the highest increase in biomass accumulation was observed under combined application of biochar with MF (Figures 1A, B), which agrees with the results of Ali et al. (2020), who reported higher crop biomass accumulation under combined application of biochar and nitrogenous fertilizers. This comparatively higher crop performance observed in the present study under AB+MF and FWB+MF revealed that integrated use of biochar and mineral fertilizers could be a suitable approach for enhancing crop production in a similar pattern observed by Singh et al. (2019a).

The higher crop growth might also be related to enhanced physiological parameters of crops under applied biochar and mineral fertilizer treatments (Qian et al., 2019; Ali et al., 2021).

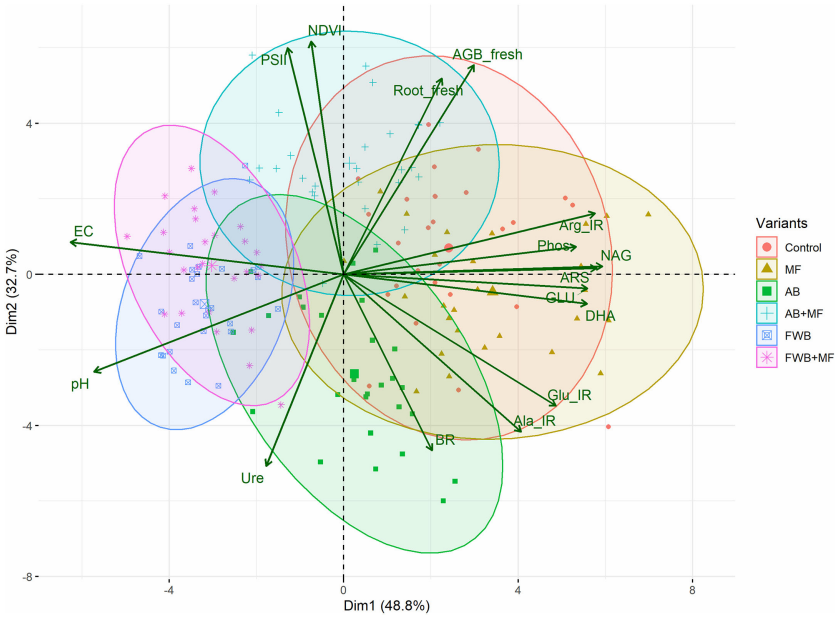

FIGURE 5
Principal component analysis of the observed microbiological and chemical soil health indicators and crop biomass and physiological parameters under the influence of applied food waste (FWB) and agricultural waste biochar (AB) with and without mineral fertilization (MF).

Despite the fact that we found no significant variations in the plant physiological parameters (ΦPSII, NDVI), their relative increase in MF fertilized treatments (Figures 1C, D) confirms the direct dependence of chlorophyll content and photosynthesis on nutrient availability, especially nitrogen (Huang et al., 2004; Mu and Chen, 2021). This shows that the applied biochars were unable to cast any additional benefit on crop's physiological parameters, however, their combination with mineral fertilizers shows the potential to increase plant growth, as demonstrated also by other studies (Kizito et al., 2019; Li et al., 2020; Ndoung et al., 2021; Liu et al., 2022). The improved crop performance under combined application of biochars and mineral fertilizers could be due to the improved crop nutrient and water availability coming from fertilizer and the mechanisms of biochar on retention and exchange of these nutrients on biochar surfaces which lead consistent supply of nutrients to crops (Agbna et al., 2017; Singh et al., 2019b; Faloye et al., 2019). On the other hand, the reduced or lower crop growth performance under sole application of biochar might be due to the clogging of micropores and reduced availability of crop nutrients (Singh et al., 2019b).

Soil chemical and physico-chemical properties are important determinants of soil quality. It has been shown that biochar application results in the modification of soil chemical properties mainly pH and electrical conductivity and soil nutrient status (Joseph et al., 2020; Holatko et al., 2022). We found enhanced soil pH under the application of food waste biochar (FWB) with and without MF (Figure 2A). This enhanced soil pH under biochar addition is related to the higher pH of the biochar itself and its liming effect as has been previously reported by many researchers (Ali et al., 2020; Hammerschmiedt et al., 2022). Moreover, the highest increase in EC under FWB+MF treatment than control (Figure 2B) might be the outcome of direct release of nutrients from MF which could be retained on the biochar surfaces and resulted in increased soluble salts in soil solution eventually showing higher EC. This is further supported by the results of PCA (Figure 5) suggesting FWB with and without MF as most influential treatments for soil chemical properties observed here. Moreover, higher pH and EC might be due to the higher porosity and surface area of biochar which together with applied fertilizers might have improved the soil physico-chemical properties through nutrient retention on biochar surfaces resulting in higher pH and EC (Jaafar et al., 2015). Our results are in line with Ali et al. (2021) who reported enhanced soil physico-chemical properties due to the application of biochar and N fertilizers.

Soil extracellular enzymes mediate the cycling of C, N and P in agroecosystems and are important determinants of soil organic matter decomposition (Bilen and Turan, 2022). We found differential responses of applied organic amendments with and without MF on various soil enzymes involved in C, N and P cycling (Figures 3A–F). In most of the cases, application of MF enhanced soil enzyme activities. Our findings agree with Tian et al. (2016) reporting enhanced soil enzyme activities under the application of mineral fertilization. Both mineral fertilization and biochar have been recognized to improve soil extracellular enzyme activities. The enhancement of enzyme activities under MF in the present study could be related to the increased availability of limiting nutrients to microbes as speculated by Zhang et al. (2014). Moreover, it has been acknowledged that the application of mineral fertilizers causes rapid mineralization of native soil organic matter (Foley et al., 2005; Liu et al., 2010), which is reflective in the findings obtained on enhanced activity of nutrient mineralizing enzymes under MF application in the present study (Figure 3). Moreover, Lehman et al. (2011) postulated that the alterations of soil pH due to biochar addition might affect the activities of enzymes especially phosphatases. Furthermore, in line with our findings, Song et al. (2020) in another study reported enhanced activity of C and N acquiring enzymes under the influence of mineral fertilization and biochar additions (Figure 3). Thus, the higher enzyme activities under applied amendments are suggestive for increased nutrients (C, N, P) mineralization in this study.

Soil respiration is one of the biological soil health indicators and is of significant concern in the face of climate change (Singh et al., 2019b). Considerable variations were observed for soil basal, and substrate induced respirations in soils subjected to various amendments (Figures 4A–D). The soil basal and SIR are considered active indicators of soil microbial biomass (Hassink, 1993). The sole application of MF yielded highest BR and Arg-IR while the amendment with AB without MF enhanced Glu-IR and Ala-IR in the present study (Figures 4A–C). We ascribe the higher BR and Arg-IR to increased utilization of nutrient sources by microbes and their proliferation under the application of MF and arginine (substrate). Moreover, the role of biochar in improving SIR has been well studied in many studies (Gul et al., 2015; Karimi et al., 2020). The enhanced SIR under AB in the present study might be related to an enhanced substrate availability and release of other biologically active compounds (Hermann et al., 2019). Moreover, biochar porosity provides the microbes with essential microenvironment, water and aeration, thereby enhancing their activity (Gul et al., 2015; Xu et al., 2016; Hermann et al., 2019). Generally, higher soil respiration is observed in biochar treated soils which further gets increased or decreased depending on biochar types and the amount of labile carbon present (Jones et al., 2012; Brunn et al., 2014; Mohan et al., 2018). The increase in Glu-IR and Ala-IR in the present study under applied AB treatment might reveal higher microbial activity due to the presence of more labile C (Hussain et al., 2017). Moreover, the higher variations observed for soil enzymes (Figure 3) and soil respiration (Figure 4) under applied

amendments might be associated with the large differences in C: N ratios of applied biochars (Table 1). This could have caused large variations in microbial growth and nutrient turnover and hence caused variations on observed microbial attributes.

Conclusion

Comparison and analysis of food and agricultural wastes derived biochar in combination/absence of mineral fertilizer revealed differential responses of soil microbial indicators and plant growth and physiological alteration. The study demonstrated that agricultural waste derived biochar enhanced crop growth and its combination with mineral fertilizers had the potential to improve its physiological attributes in terms of chlorophyll fluorescence indicators. This shows that the integration of biochar with mineral fertilizers could be a sustainable approach for enhancing crop production. The food waste derived biochar on the other hand, was found to enhance soil chemical properties owing to its alkaline nature and higher nutrient contents. Furthermore, the mineral fertilizer was most influential strategy in improving soil basal respiration and C, N and P cycling enzymes which suggests the role of fertilizers in nutrient cycling as indicated by the principal component analysis as well. It is thus concluded that, the application of food and agricultural waste derived biochars not only helps in waste recycling but also help in modification of soil bio-chemical properties together with mineral fertilizers. Based on findings, it can be concluded that a combination of biochar and mineral fertilizers is a viable approach for sustainable soil management and crop production in agro-ecosystems. However, further studies taking into account the functional groups characterization and surface chemistry of biochars derived from various wastes are required to deepen our understanding on the mechanisms by which biochar affects soil quality attributes and improve crop performance.

Data availability statement

The original contributions presented in the study are included in the article/supplementary material. Further inquiries can be directed to the corresponding authors.

Author contributions

AM, JH and MB: conceptualization. MB, TH, AK, OM: methodology. TH, TC, and TB: software. MN, JK, AK and JH: validation. MB and PS, TH: formal analysis. TC, AK, TB and OM: resources. TB and OM: data curation. AM: writing—original draft preparation. JK, AM, MB, TH, PS, MN and JH: writing— review and editing. MB, JK and TC: supervision. MB, JK, AK, TC and JH: project administration. MB, JK, AK and JH: funding acquisition. All authors have read and agreed to the published version of the manuscript.

Funding

The work was supported by the projects of Technology Agency of the Czech Republic TJ02000262 and TH03030319 and by the Ministry of Agriculture of the Czech Republic, institutional support MZE-RO1218, MZE-RO1722 and by Ministry of Education, Youth and Sports of the Czech Republic, grant number FCH-S-22-8001.

Conflict of interest

AK was employed by the company Agricultural Research, Ltd. and JH was employed by the company Agrovyzkum Rapotin, Ltd.

The remaining authors declare that the research was conducted in the absence of any commercial or financial relationships that could be construed as a potential conflict of interest.

Publisher's note

References

Abiad, M. G., and Meho, L. I. (2018). Food loss and food waste research in the Arab world: A systematic review. *Food Secur.* 10 (2), 1–12. doi: 10.1007/s12571-018-0782-7

Agbna, G.H., Dongli., S., Zhipeng., L., Elshaikh, N. A., Guangcheng, S., and Timm, L. C. (2017). Effects of deficit irrigation and biochar addition on the growth, yield, and quality of tomato. *Scientia Horticulturae.* 222, 90–101. doi: 10.1016/j.scienta.2017.05.004

Ahmad, M., Wang, X., Hilger, T. H., Luqman, M., Nazli, F., Hussain, A., et al. (2020). Evaluating biochar-microbe synergies for improved growth, yield of maize, and post- harvest soil characteristics in a semi-arid climate. *Agronomy* 10 (7), 1055. doi: 10.3390/agronomy10071055

Ali, H., Khan., E., and Ilahi., I. (2019). Environmental chemistry and ecotoxicology of hazardous heavy metals: Environmental persistence, toxicity, and bioaccumulation. *J. Chem.* 2019, 6730305. doi: 10.1155/2019/6730305

Ali, I., Ullah, S., He, L., Zhao, Q., Iqbal, A., Wei, S., et al. (2020). Combined application of biochar and nitrogen fertilizer improves rice yield, microbial activity and n-metabolism in a pot experiment. *PeerJ* 8, e10311. doi: 10.7717/peerj.10311

Ali, I., Zhao, Q., Wu, K., Ullah, S., Iqbal, A., Liang, H., et al. (2021). Biochar in combination with nitrogen fertilizer is a technique: to enhance physiological and morphological traits of rice (*Oryza sativa* l.) by improving soil physio-biochemical properties. *J. Plant Growth Regul.* 41, 1–15. doi: 10.1007/s00344-021-10454-8

Atkinson, C. J., Fitzgerald, J. D., and Hipps., N. A. (2010). Potential mechanisms for achieving agricultural benefits from biochar application to temperate soils: a review. *Plant Soil* 337 (1), pp.1–pp18. doi: 10.1007/s11104-010-0464-5

Bais-Moleman, A. L., Schulp., C. J. E., and Verburg., P. H. (2019). Assessing the environmental impacts of production- and consumption-side measures in sustainable agriculture intensification in the European union. *Geoderma* 338, 555–567. doi: 10.1016/j.geoderma.2018.11.042

Bilen, S., and Turan, V. (2022). "Enzymatic analyses in soils," in *Practical handbook on agricultural microbiology* (New York, NY: Humana), 377–385.

Bond, M., Meacham, T., Bhunnoo, R., and Benton, T. (2013). "Food waste within global food systems," in *Global food security* (Amsterdam, The Netherlands: Elsevier).

Boretti, A., and Rosa, L. (2019). Reassessing the projections of the world water development report. *NPJ Clean Water* 2, 15. doi: 10.1038/s41545-019-0039-9

Bouraoui, F., and Grizzetti, B. (2014). Modelling mitigation options to reduce diffuse nitrogen water pollution from agriculture. *Sci. Total Environ.* 468, 1267–1277. doi: 10.1016/j.scitotenv.2013.07.066

Brtnicky, M., Kintl, A., Holatko, J., Hammerschmiedt, T., Mustafa, A., Kucerik, J., et al. (2022). Effect of digestates derived from the fermentation of maize-legume intercropped culture and maize monoculture application on soil properties and plant biomass production. *Chem. Biol. Technol. Agric.* 9 (1), 1–24. doi: 10.1186/s40538-022-00310-6

Bruun, S., Clauson-Kaas, S., Bobulska, L., and Thomsen, I. K. (2014). Carbon dioxide emissions from biochar in soil: role of clay, microorganisms, and carbonates. *Eur. J. Soil Sci.* 65, 52–59. doi: 10.1111/ejss.12073

Campbell, C. D., Chapman, S. J., Cameron., C. M., Davidson., M. S., and Potts, J. M. (2003). "A rapid microtiter plate method to measure carbon dioxide evolved from carbon substrate amendments so as to determine the physiological profiles of soil microbial communities by using whole soil. *Appl. Environ. Microbiol.* 69 (6), 3593–3599. doi: 10.1128/AEM.69.6.3593-3599.2003

Carter, S., Shackley, S., Sohi, S., Suy, T. B., and Haefele, S. (2013). The impact of biochar application on soil properties and plant growth of pot grown lettuce (*Lactuca sativa*) and cabbage (*Brassica chinensis*). *Agronomy* 3, 404–418. doi: 10.3390/agronomy3020404

Castro, K. L., and Sanchez-Azofeifa, G. A. (2008). Changes in spectral properties, chlorophyll content and internal mesophyll structure of senescing populus balsamifera and populus tremuloides leaves. *Sensors* 8, 51–69. doi: 10.3390/s8010051

Dong, D., Feng, Q., Mcgrouther, K., Yang, M., Wang, H., and Wu, W. (2015). Effects of biochar amendment on rice growth and nitrogen retention in a waterlogged paddy field. *J. Soils Sediments* 15 (1), 153–162. doi: 10.1007/s11368-014-0984-3

Faloye, O. T., Alatise, M. O., Ajayi, A. E., and Ewulo, B. S. (2019). Efects of biochar and inorganic fertiliser applications on growth, yield and water use efficiency of maize under defcit irrigation. *Agric. Water Manage.* 217, 165–178. doi: 10.1016/j.agwat.2019.02.044

Foley, J. A., DeFries, R., Asner, G. P., Barford, C., Bonan, G., Carpenter, S. R., et al. (2005). Global consequences of land use. *Science*, 309 (5734), 570–574. doi: 10.1126/science.111177

Garty, J., Tamir, O., Hassid, I., Eshel, A., Cohen, Y., Karnieli, A., et al. (2001). Photosynthesis, chlorophyll integrity, and spectral reflectance in lichens exposed to air pollution. *J. Environ. Qual.* 30 (3), 884–893. doi: 10.2134/jeq2001.303884x

Gul, S., Whalen, J. K., Thomas, B. W., Sachdeva, V., and Deng, H. (2015). Physico-chemical properties and microbial responses in biochar-amended soils: mechanisms and future directions. *Agricul. Ecosyst. Environ.* 206, 46–59. doi: 10.1016/j.agee.2015.03.015

Gustavsson, J., Cederberg., C., Sonesson., U., van Otterdijk., R., and Meybeck., A. (2011). *Global food losses and food waste* (Rome, Italy: FAO).

Hammerschmiedt, T., Holatko, J., Kucerik, J., Mustafa, A., Radziemska, M., Kintl, A., et al. (2022). Manure maturation with biochar: Effects on plant biomass, manure quality and soil microbiological characteristics. *Agriculture* 12 (3), 314. doi: 10.3390/agriculture12030314

Hardie, M., Doyle, R., Shabala, S., and Cuin, T. A. (2012). "Measuring soil salinity," in *Plant salt tolerance: Methods and protocols, methods in molecular biology* (Totowa, NJ: Humana Press), 415–425. doi: 10.1007/978-1-61779-986-0_28

Hassink, J. (1993). Relationship between the amount and the activity of the microbial biomass in Dutch grassland soils: comparison of the fumigation-incubation method and the substrate- induced respiration method. *Soil Biol. Biochem.* 25 (5), 533–538. doi: 10.1016/0038-0717(93)90190-M

Herrmann, L., Lesueur, D., Robin, A., Robain, H., Wiriyakitnateekul, W., and Bräu, L. (2019). Impact of biochar application dose on soil microbial communities associated with rubber trees in north East Thailand. *Sci. Total Environ.* 689, 970–979. doi: 10.1016/j.scitotenv.2019.06.441

Holatko, J., Bielska, L., Hammerschmiedt, T., Kucerik, J., Mustafa, A., Radziemska, M., et al. (2022). Cattle manure fermented with biochar and humic substances improve the crop biomass, microbiological properties and nutrient status of soil. *Agronomy* 12 (2), 368. doi: 10.3390/agronomy12020368

Huang, Z. D., Jiang, Y., Yang, J., and Sun, S. J. (2004). Effects of nitrogen deficiency on gas exchange, chlorophyll fluorescence, and antioxidant enzymes in leaves of rice plants. *Photosynthetica* 42, 357–364. doi: 10.1023/B:PHOT.0000046153.08935.4c

Hussain, M., Farooq, M., Nawaz, A., Al-Sadi, A. M., Solaiman, Z. M., Alghamdi, S. S., et al. (2017). Biochar for crop production: potential benefits and risks. *J. Soils Sediments.* 17, 685–716. doi: 10.1007/s11368-016-1360-2

Ishangulyyev, R., Kim, S., and Lee, S. H. (2019). Understanding food loss and waste–why are we losing and wasting food? *Foods* 8, 297. doi: 10.3390/foods8080297

ISO_10390 (2005). *Soil quality - determination of ph* (Geneva, Switzerland: International Organization for Standardization).

ISO_20130 (2018). *Soil quality — measurement of enzyme activity patterns in soil samples using colorimetric substrates in micro-well plates* (Geneva, Switzerland: International Organization for Standardization).

Jaafar, N. M., Clode, P. L., and Abbott, L. K. (2015). Soil microbial responses to biochars varying in particle size, surface and pore properties. *Pedosphere* 25 (5), 770–780. doi: 10.1016/S1002-0160(15)30058-8

Jeffery, S., Abalos, D., Prodana, M., Bastos, A. C., Van Groenigen, J. W., Hungate, B. A., et al. (2017). Biochar boosts tropical but not temperate crop yields. *Environ. Res. Lett.* 12 (5), 053001. doi: 10.1088/1748-9326/aa67bd

Jones, D. L., Rousk., J., Edwards-Jones., G., DeLuca., T., and Murphy, D. V. (2012). Biochar-mediated changes in soil quality and plant growth in a three year field trial. *Soil Biol. Biochem.* 45, 113–124. doi: 10.1016/j.soilbio.2011.10.012

Joseph, S., Pow, D., Dawson, K., Rust, J., Munroe, P., Taherymoosavi, S., et al. (2020). Biochar increases soil organic carbon, avocado yields and economic return over 4 years of cultivation. *Sci. Total Environ.* 724, 138153. doi: 10.1016/j.scitotenv.2020.138153

Kang, S. M., Adhikari, A., Bhatta, D., Gam, H. J., Gim, M. J., Son, J. I., et al. (2022). Comparison of effects of chemical and food waste-derived fertilizers on the growth and nutrient content of lettuce (*Lactuca sativa* l.). *Resources* 11 (2), 21. doi: 10.3390/resources11020021

Karimi, A., Moezzi, A., Chorom, M., and Enayatizamir, N. (2020). Application of biochar changed the status of nutrients and biological activity in a calcareous soil. *J. Soil Sci. Plant Nutr.* 20 (2), 450–459. doi: 10.1007/s42729-019-00129-5

Khadem, A., and Raiesi, F. (2017). Responses of microbial performance and community to corn biochar in calcareous sandy and clayey soils. *Appl. Soil Ecol.* 114, 16–27. doi: 10.1016/j.apsoil.2017.02.018

Kibler, K. M., Reinhart., D., Hawkins., C., Motlagh., A. M., and Wright., J. (2018). Food waste and the food- energy-water nexus: A review of food waste management alternatives. *Waste Manage.* 74, 52–62. doi: 10.1016/j.wasman.2018.01.014

Kizito, S., Hongzhen, L., Jiaxin, L., Bah, H., Dong, R., and Wu, S. (2019). Role of nutrient-enriched biochar as a soil amendment during maize growth: exploring practical alternatives to recycle agricultural residuals and to reduce chemical fertilizer demand. *Sustainability* 11 p, 3211. doi: 10.3390/su11113211

Kuppusamy, S., Thavamani, P., Megharaj, M., Venkateswarlu, K., and Naidu, R. (2016). Agronomic and remedial benefits and risks of applying biochar to soil: Current knowledge and future research directions. *Environ. Int.* 87, 1–12. doi: 10.1016/j.envint.2015.10.018

Lai, L., Ismail, M. R., Muharam, F. M., Yusof, M. M., Ismail, R., and Jaafar, N. (2017). Effects of rice straw biochar and nitrogen fertilizer on rice growth and yield. *Asian J. Crop Sci.* 9 (4), 159–166. doi: 10.3923/ajcs.2017.159.166

Lehmann, J., Rillig, M. C., Thies, J., Masiello, C. A., Hockaday, W. C., and Crowley, D. (2011). Biochar effects on soil biota–a review. *Soil Biol. Biochem. 43(9)* pp.1812-, 1836. doi: 10.1016/j.soilbio.2011.04.022

Lipinski, B., Hanson, C., Waite, R., Searchinger, T., and Lomax, J. (2013). *Reducing food loss and waste*. Washington, DC: World Resources Institute. Available online at: http://www.worldresourcesreport.org.

Li, X., Shao, X. H., Ding, F., Yuan, Y., Li, R., Yang, X., et al. (2020). Effects of effective microorganisms biochar-based fertilizer on photosynthetic characteristics and chlorophyll content of flue-cured tobacco under water-saving irrigation strategies. *Chilean J. of Agric. Res.* 80 (3), 422–432. doi: 10.4067/S0718-58392020000300422

Liu, M., Linna, C., Ma, S., Ma, Q., Guo, J., Wang, F., et al. (2022). Effects of biochar with inorganic and organic fertilizers on agronomic traits and nutrient absorption of soybean and fertility and microbes in purple soil. *Front. Plant Science* 13. doi: 10.3389/fpls.2022.871021

Liu, E., Yan, C., Mei, X., He, W., Bing, S. H., Ding, L., et al. (2010). Long-term effect of chemical fertilizer, straw, and manure on soil chemical and biological properties in northwest China. *Geoderma* 158 (3-4), 173–180. doi: 10.1016/j.geoderma.2010.04.029

Lundqvist, J., de Fraiture, C., and Molden, D. (2008). *Saving water: From field to fork – curbing losses and wastage in the food chain. SIWI policy brief* (Sweden: Stockholm International Water Institute)2008. https://hdl.handle.net/10535/5088

Małachowska-Jutsz, A., and Matyja, K. (2019). Discussion on methods of soil dehydrogenase determination. *Int. J. Environ. Sci. Technol.* 16, 7777–7790. doi: 10.1007/s13762-019-02375-7

Meena, R. S., Kumar., S., Datta., R., Lal., R., Vijayakumar., V., Brtnicky, M., et al. (2020). Impact of agrochemicals on soil microbiota and management: A review. *Land* 9 (2), 34. doi: 10.3390/land9020034

Mohan, D., Abhishek, K., Sarswat, A., Patel, M., Singh, P., and Pittman, C. U. (2018). Biochar production and applications in soil fertility and carbon sequestration–a sustainable solution to crop-residue burning in India. *RSC Advances* 8, 508–520. doi: 10.1039/C7RA10353K

Mu, X. H., and Chen, Y. L. (2021). The physiological response of photosynthesis to nitrogen deficiency. *Plant Physiol. Biochem.* 158, 76–82. doi: 10.1016/j.plaphy.2020.11.019

Mustafa, A., Naveed, M., Saeed, Q., Ashraf, M. N., Hussain, A., Abbas, T., et al. (2019). Application potentials of plant growth promoting rhizobacteria and fungi as an alternative to conventional weed control methods. *Sustain. Crop Production.* 10, 247–60. doi: 10.5772/intechopen.86339

Naveed, M., Tanvir, B., Xiukang, W., Brtnicky, M., Ditta, A., Kucerik, J., et al. (2021). Co-Composted biochar enhances growth, physiological, and phytostabilization efficiency of brassica napus and reduces associated health risks under chromium stress. *Front. Plant Sci.* 12. doi: 10.3389/fpls.2021.775785

Ndoung, O. C. N., de Figueiredo, C. C., and Ramos, M. L. G. (2021). Ramos a scoping review on biochar- based fertilizers: enrichment techniques and agro-environmental application. *Heliyon* 7 (12), e08473. doi: 10.1016/j.heliyon.2021.e08473

Parry, M., Parry, M. L., Canziani, O., Palutikof, J., van der Linden, P., and Hanson, C. (2007). "Climate Change (2007). -Impacts,Adaptation and vulnerability," in *Working group II contribution to the fourth assessment report of the IPCC*, vol. Volume 4. (Cambridge, UK: Cambridge University Press).

Prendergast-Miller, M. T., Duvalla, M., and Sohi, S. P. (2014). Biochar – root interactions are mediated by biochar nutrient content and impacts on soil nutrient availability. *Eur. J. Soil Science* 65, 173–185. doi: 10.1111/ejss.12079

Qian, Z. H. U., Kong, L. J., Shan, Y. Z., Yao, X. D., Zhang, H. J., Xie, F. T., et al. (2019). Effect of biochar on grain yield and leaf photosynthetic physiology of soybean cultivars with different phosphorus efficiencies. *J. Integr. Agric.* 18 (10), 2242–2254. doi: 10.1016/S2095-3119(19)62563-3

Rasool, B., Mahmood-ur-Rahman,, and Zubair, M. (2022). Synergetic efficacy of amending Pb-polluted soil with p-loaded jujube (*Ziziphus mauritiana*) twigs biochar and foliar chitosan application for reducing Pb distribution in moringa leaf extract and improving its anti-cancer potential. *Water Air Soil Pollut.* 233, 344. doi: 10.1007/s11270-022-05807-2

Sadaf, J., Shah, G. A., Shahzad, K., Ali, N., Shahid, M., Ali, S., et al. (2017). Improvements in wheat productivity and soil quality can accomplish by co-application of biochars and chemical fertilizers. *Sci. Total Environ.* 607, 715–724. doi: 10.1016/j.scitotenv.2017.06.178

Sayara, T., Basheer-Salimia, R., Hawamde, F., and Sánchez, A. (2020). Recycling of organic wastes through composting: Process performance and compost application in agriculture. *Agronomy* 10, 1838. doi: 10.3390/agronomy10111838

Singh, R., Singh, P., Singh, H., and Raghubanshi, A. S. (2019a). Impact of sole and combined application of biochar, organic and chemical fertilizers on wheat crop yield and water productivity in a dry tropical agro-ecosystem. *Biochar* 1 (2), pp.229–pp.235. doi: 10.1007/s42773-019-00013-6

Singh, R., Srivastava, P., Bhadouria, R., Yadav, A., Singh, H., and Raghubanshi, A. S. (2020). Combined application of biochar and farmyard manure reduces wheat crop eco- physiological performance in a tropical dryland agro-ecosystem. *Energy Ecol. Environ.* 5 (3), pp.171–pp.183. doi: 10.1007/s40974-020-00159-1

Singh, R., Srivastava, P., Singh, P., Sharma, A. K., Singh, H., and Raghubanshi, A. S. (2019b). Impact of rice-husk ash on the soil biophysical and agronomic parameters of wheat crop under a dry tropical ecosystem. *Ecol. Indic.* 105, 505–515. doi: 10.1016/j.ecolind.2018.04.043

Song, D., Chen, L., Zhang, S., Zheng, Q., Ullah, S., Zhou, W., et al. (2020). Combined biochar and nitrogen fertilizer change soil enzyme and microbial activities in a 2-year field trial. *Eur. J. Soil Biol.* 99, 103212. doi: 10.1016/j.ejsobi.2020.103212

Sönmez, O.S.M.A.N., Turan, V., and Kaya, C. (2016). The effects of sulfur, cattle, and poultry manure addition on soil phosphorus. *Turkish J. Agric. Forestry* 40 (4), 536–541. doi: 10.3906/tar-1601-41

Srivastav, A. L. (2020). "Chemicalfertilizers and pesticides: role in groundwater contamination," in *Agrochemicals detection, treatment and remediation* (Oxford, United Kingdom: Butterworth-Heinemann), 143–159.

Sulok, K. M. T., Ahmed, O. H., Khew, C. Y., Zehnder, J. A. M., Jalloh, M. B., Musah, A. A., et al. (2021). Chemical and biological characteristics of organic amendments produced from selected agro-wastes with potential for sustaining soil health: A laboratory assessment. *Sustainability* 13 (9), 4919. doi: 10.3390/su13094919

Tan, J. K. N., Lee, J. T. E., Chiam, Z., Song, S., Arora, S., Tong, Y. W., et al. (2021). Applications of food waste-derived black soldier fly larval frass as incorporated compost, side-dress fertilizer and frass-tea drench for soilless cultivation of leafy vegetables in biochar-based growing media. *Waste Manage.* 130, 155–166. doi: 10.1016/j.wasman.2021.05.025

Tian, J., Wang, J., Dippold, M., Gao, Y., Blagodatskaya, E., and Kuzyakov, Y. (2016). Biochar affects soil organic matter cycling and microbial functions but does not alter microbial community structure in a paddy soil. *Sci. Total Environ.* 556, 89–97. doi: 10.1016/j.scitotenv.2016.03.010

Toscano, P., Casacchia, T., Diacono, M., and Montemurro, F. (2013). Composted olive mill by-products: Compost characterization and application on olive orchards. *J. Agric. Sci. Technol.* 15, 627–638.

Tripathi, A. D., Mishra, R., Maurya, K. K., Singh, R. B., and Wilson, D. W. (2019). "Chapter 1— estimates for world population and global food availability for global health," in *In the role of functional food security in global health*. Eds. R. B. Singh, R. R. Watson and T. Takahashi (Cambridge, MA, USA: Academic Press), 3–24.

Urra, J., Alkorta, I., and Garbisu, C. (2019). Urra potential benefits and risks for soil health derived from the use of organic amendments in agriculture. *Agronomy* 9, 542. doi: 10.3390/agronomy9090542

Wali, F., Sardar, S., Naveed, M., Asif, M., Nezhad, M., T., K., et al. (2022). Effect of consecutive application of phosphorus-enriched biochar with different levels of p on growth performance of maize for two successive growing seasons. *Sustainability* 14 (4), p.1987. doi: 10.3390/su14041987

Xu, N., Tan, G., Wang, H., and Gai, X. (2016). Effect of biochar additions to soil on nitrogen leaching, microbial biomass and bacterial community structure. *Eur. J. Soil Biol.* 74, 1–8. doi: 10.1016/j.ejsobi.2016.02.004

Zhang, L., Sun, X.-Y., Tian, Y., and Gong, X.-Q. (2014). Biochar and humic acid amendments improve the quality of composted green waste as a growth medium for the ornamental plant calathea insignis. *Scientia Hortic.* 176, 70–78. doi: 10.1016/j.scienta.2014.06.021

Zulfiqar, U., Jiang, W., Xiukang, W., Hussain, S., Ahmad, M., Maqsood, M. F., et al. (2022). Cadmium phytotoxicity, tolerance, and advanced remediation approaches in agricultural soils; a comprehensive review. *Front. Plant Sci.* 13. doi: 10.3389/fpls.2022.773815

frontiers | Frontiers in Plant Science

TYPE Review
PUBLISHED 18 October 2022
DOI 10.3389/fpls.2022.932311

OPEN ACCESS

EDITED BY
Youssef Rouphael,
University of Naples Federico II, Italy

REVIEWED BY
Marco Nuti,
Sant'Anna School of Advanced Studies, Italy
Serenella Nardi,
University of Padua, Italy
Daniela Minerdi,
University of Turin, Italy

*CORRESPONDENCE
Germán Tortosa
german.tortosa@eez.csic.es

SPECIALTY SECTION
This article was submitted to Plant Symbiotic Interactions, a section of the journal Frontiers in Plant Science

RECEIVED 29 April 2022
ACCEPTED 05 September 2022
PUBLISHED 18 October 2022

CITATION
Jindo K, Goron TL, Pizarro-Tobías P, Sánchez-Monedero MA, Audette Y, Deolu-Ajayi AO, van der Werf A, Teklu MG, Shenker M, Pombo Sudré C, Busato JG, Ochoa-Hueso R, Nocentini M, Rippen J, Aroca R, Mesa S, Delgado MJ and Tortosa G (2022) Application of biostimulant products and biological control agents in sustainable viticulture: A review. *Front. Plant Sci.* 13:932311. doi: 10.3389/fpls.2022.932311

Application of biostimulant products and biological control agents in sustainable viticulture: A review

Keiji Jindo[1], Travis L. Goron[2], Paloma Pizarro-Tobías[3], Miguel Ángel Sánchez-Monedero[4], Yuki Audette[5,6], Ayodeji O. Deolu-Ajayi[1], Adrie van der Werf[1], Misghina Goitom Teklu[1], Moshe Shenker[7], Cláudia Pombo Sudré[8], Jader Galba Busato[9], Raúl Ochoa-Hueso[10,11], Marco Nocentini[12], Johan Rippen[13], Ricardo Aroca[14], Socorro Mesa[14], María J. Delgado[14] and Germán Tortosa[14]*

[1]Agrosystems Research, Wageningen University and Research, Wageningen, Netherlands, [2]Department of Plant Agriculture, University of Guelph, Guelph, ON, Canada, [3]Faculty of Computer Sciences, Multimedia and Telecommunication, Universitat Oberta de Catalunya (UOC), Barcelona, Spain, [4]Department of Soil and Water Conservation and Organic Waste Management, Centro de Edafología y Biología Aplicada del Segura (CEBAS), Agencia Estatal CSIC, Murcia, Spain, [5]School of Environmental Sciences, University of Guelph, Guelph, ON, Canada, [6]Chitose Laboratory Corp., Kawasaki, Japan, [7]The Robert H. Smith Faculty of Agriculture, Food and Environment, Rehovot, Israel, [8]Laboratório de Melhoramento Genético Vegetal, Universidade Estadual do Norte Fluminense Darcy Ribeiro, UENF, Campos dos Goytacazes, Brazil, [9]Faculdade de Agronomia e Medicina Veterinária, Campus Universitário Darcy Ribeiro, Universidade de Brasília, Brasília, DF, Brazil, [10]Department of Biology, IVAGRO, Agroalimentario, Campus del Rio San Pedro, University of Cádiz, Cádiz, Spain, [11]Department of Terrestrial Ecology, Netherlands Institute of Ecology (NIOO-KNAW), Wageningen, Netherlands, [12]Dipartimento di Scienze e Tecnologie Agrarie, Alimentari, Ambientali e Forestali (DAGRI), Università degli Studi Firenze, Firenze, Italy, [13]Wijngaard El Placer, Lelystad, Netherlands, [14]Department of Soil Microbiology and Symbiotic Systems, Estación Experimental del Zaidín (EEZ), Agencia Estatal CSIC, Granada, Spain

Current and continuing climate change in the Anthropocene epoch requires sustainable agricultural practices. Additionally, due to changing consumer preferences, organic approaches to cultivation are gaining popularity. The global market for organic grapes, grape products, and wine is growing. Biostimulant and biocontrol products are often applied in organic vineyards and can reduce the synthetic fertilizer, pesticide, and fungicide requirements of a vineyard. Plant growth promotion following application is also observed under a variety of challenging conditions associated with global warming. This paper reviews different groups of biostimulants and their effects on viticulture, including microorganisms, protein hydrolysates, humic acids, pyrogenic materials, and seaweed extracts. Of special interest are biostimulants with utility in protecting plants against the effects of climate change, including drought and heat stress. While many beneficial effects have been reported following the application of these materials, most studies lack a mechanistic explanation, and important parameters are often undefined (e.g.,

soil characteristics and nutrient availability). We recommend an increased study of the underlying mechanisms of these products to enable the selection of proper biostimulants, application methods, and dosage in viticulture. A detailed understanding of processes dictating beneficial effects in vineyards following application may allow for biostimulants with increased efficacy, uptake, and sustainability.

KEYWORDS

biological agents, biostimulants, grapevine, organic, vineyard, viticulture, wine

Introduction

Grape (*Vitis vinifera*) production has increased globally over the last decade from 65 million to 77.8 million tons. The world's vineyards totaled 7.4 million hectares in 2018, of which ~4.5% were cultivated with organic approaches (i.e., refraining from pesticides and chemical fertilizer use and promoting sustainable cultivation practices). About 88% of organic vineyards are located in Europe, primarily in France, Italy, and Spain. There is a need, and increasing demand, for more ecologically-sustainable agricultural products as outlined by the United Nations Sustainable Development Goals (SDGs). For production to support demand despite current anthropogenic climate change (Roka, 2022), more research on sustainable food systems is urgently needed.

Higher yields are necessary for sustainable food security on a finite land basis (Godfray et al., 2010; Foley et al., 2011). According to Renaud-Gentié (Seufert et al., 2012), the yield ratio between organic and conventional agricultural production per unit area is 0.75. To close this yield gap while simultaneously satisfying consumer preference for organic products, improved techniques for organic grape farming are required.

Additionally, grape varieties often require specific environmental conditions, historically located in very narrow latitudinal zones (30–50°N and 30–40°S) with minimal temperature extremes (Nesbitt et al., 2018). Due to the high environmental sensitivity of *Vitis vinifera*, a strong correlation between meteorological conditions propelled by global warming (e.g., heat waves, extreme precipitation, droughts, hailstorms, and windstorms) and low grape yield and wine quality has been reported (Santos et al., 2020).

Biostimulants are substances or microorganisms applied to plants, which enhance nutrition use efficiency, abiotic stress tolerance, and crop quality traits, using mechanisms that do not directly add fertility to the soil (du Jardin, 2015), and in the EU the marketing of biostimulants is regulated by specific provisions (Regulation EU 1009, 2019). Initially, these technologies were primarily utilized in organic farming, with later uptake in both conventional and integrated systems (Rouphael and Colla, 2020). The application of biostimulant technologies is now a well-known tool, though poorly-researched strategy to enhance plant growth and prevent pests and diseases (Gutiérrez-Gamboa et al., 2019; Cataldo et al., 2022; Monteiro et al., 2022; Olavarrieta et al., 2022).

Biocontrol agents (BCAs) are organisms antagonistic to crop pests. Synthetic pesticides, mainly fungicides, are widely used in viticulture. However, pesticide residue contamination of grapes and grape products (raisins, juices, and wines) is widely studied and may be detrimental to consumer health (Walorczyk et al., 2011). An EU report (EFSA, 2021) has shown increased pesticide residue levels in primary commodity food products since 2016. Table grape products are of particular concern, in which 66% of products were contaminated, and 14.3% of products tested contained more than five different pesticide residues. In a sample of dried vine fruits, 28 pesticides were detected (Cabrera and Pastor, 2021). When testing grape leaves, 37.9% had residues above the allowed maximum residue levels (MRL). Gava et al. (2021) highlighted the importance of tracing contamination from the originating vineyard to the wine. Of additional concern is that these residues can affect alcoholic fermentation, change product flavor, and pose a toxicological risk to the consumer as well as those involved in the production chain.

This review presents a series of different biostimulant materials and biological control agents utilized in sustainable vineyards (their main effects on *Vitis vinifera* are summarized in Figure 1). Additionally, the origin of the materials, the application methods, and the underpinning functions/mechanisms of each material are described. The limitations of current practices and alternative approaches to aid future studies of the interaction between viticulture and global climate change are also addressed.

Biostimulant materials

Protein hydrolysates

Protein hydrolysates (PHs) refer to mixtures of polypeptides, oligopeptides, and amino acids that are manufactured from

10.3389/fpls.2022.932311

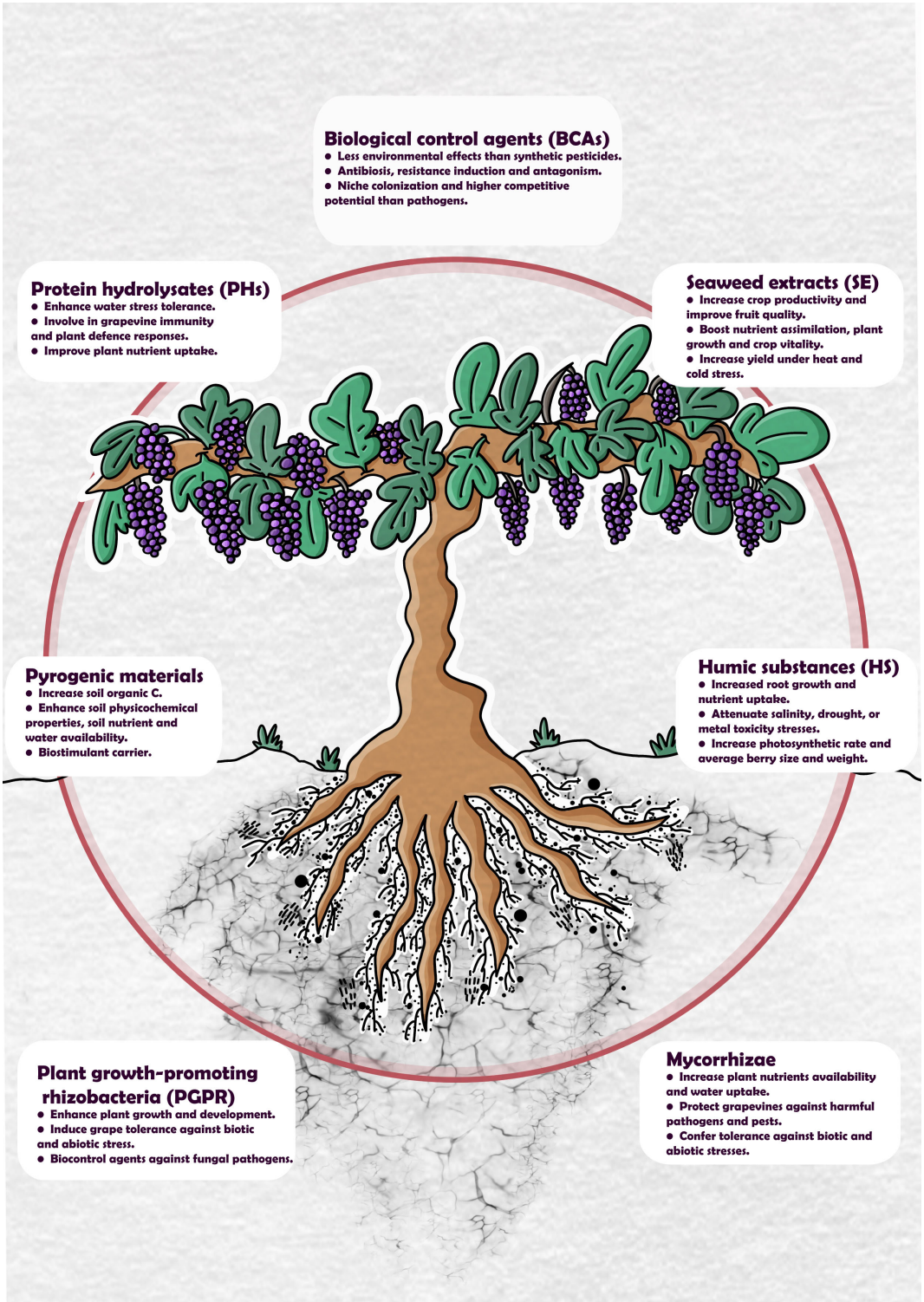

FIGURE 1
An overview of the main effects of biological control agents (BCAs), protein hydrolysates (PHs), seaweed extracts (SE), pyrogenic materials, humic substances (HS), plant growth-promoting rhizobacteria (PGPR), and mycorrhizae applied in viticulture.

protein sources using partial hydrolysis (Schaafsma, 2009). They are produced by either acid and/or alkaline hydrolysis (Schaafsma, 2009), enzymatic hydrolysis (Colla et al., 2015), or from by-products of plant or animal origins (Meggio et al., 2020). In horticulture, more than 90% of PH utilized is derived from animal origin, while plant-derived PHs are relatively novel (Colla et al., 2015). Animal-derived PHs often contain higher amounts of total amino acids compared to plant-derived PHs (Ertani et al., 2009). Plant-derived PHs contain carbohydrates and phenols, which enhance plant oxidative stress defenses, as well as aid in energy metabolism (Colla et al., 2015). PHs can be further subdivided into two categories: (1) protein fractions with a relatively high content of specific amino acids, such as glutamine peptides and cysteine/glycine and tryptophan peptides; and (2) bioactive peptides with specific amino-acid sequences (i.e., 3 to 20 amino acids), which are usually hydrophobic (Schaafsma, 2009). In general, the effects of PHs on plant physiology are closely related to the stimulation of carbon and nitrogen metabolism, hormone activity, and nutrient supply and uptake by plants (Figure 1). Moreover, it has been demonstrated that PHs can stimulate the plant microbiome which can promote plant growth and development by enhancing water and nutrient uptake as well as their adaptation to biotic and abiotic stresses (Colla et al., 2017, and sources reviewed within).

The effects of PHs on grapevine growth are reviewed in Table 1. PHs are known to regulate gene expression involved in the transport of nutrients, and the signaling and metabolism of reactive oxygen species, thereby enhancing plant stress tolerance (Meggio et al., 2020). For example, PHs can effectively improve grapevine tolerance to water deficit (Boselli et al., 2019; Meggio et al., 2020). A study by Boselli et al. (2019) showed that PH-treated grapevines contain higher levels of anthocyanins, often observed under water stress conditions (Castellarin et al., 2007). Therefore, PHs may be able to mimic water stress conditions in grapevine and reduce water loss due to evapotranspiration (Boselli et al., 2019).

In addition, PHs act as signal compounds to trigger plant defense responses (Boller, 1995). Grapevine is highly susceptible to various pathogens (Lachhab et al., 2014). In particular, downy mildew (*Plasmopara viticola*) and powdery mildew (*Erysiphe necator*) are the most widespread and devastating grapevine diseases worldwide (Gauthier et al., 2014; Nesler et al., 2015). Frequent fungicide applications (i.e., every 7-10 days in season) are often required to control these diseases, a practice which not only dramatically increases production costs but also negatively impacts the environment and human health (Jones et al., 2014). Plant defense by-products may be an attractive alternative to chemical pesticides (van Aubel et al., 2014). Elicitors including PHs are not toxic to plants and are recognized by plant membrane receptors, meaning they are often freely able to mobilize an array of plant defenses (Boller and Felix, 2009). PHs contain a large variety of bioactive peptides, which may act as plant growth regulators, antioxidants, and biostimulants (Colla et al., 2014), as well as directly influence numerous biological processes evoking hormonal and immunological responses (Ito et al., 2006; Phelan et al., 2009). Therefore, PHs can trigger signaling events involved in grapevine immunity (Gauthier et al., 2014). Some studies (Gauthier et al., 2014; Lachhab et al., 2014) report reduced symptoms of downy mildew and gray mold (*Botrytis cinerea*) on grapevine following applications of PHs derived from soybean and casein. PHs may improve plant nutrient uptake through modification of root architecture, by complexation of nutrients such as Zn (Ertani et al., 2018), or stimulation of microbial and enzymatic activities (Colla et al., 2015) – e.g., increased activity of N_2-fixing, P-solubilizing, and indoleacetic acid-producing bacteria was observed in lettuce (Colla et al., 2015) and tomato (Colla et al., 2014) after application of PHs. The application of PHs also increases the activity of both nitrate reductase and glutamine synthetase in roots and leaves (Ertani et al., 2009). Nitrate reductase reduces nitrate to ammonia, and glutamine synthetase catalyzes the ATP-dependent amination of glutamate to produce glutamine, thereby facilitating assimilation or re-assimilation of nitrogenous sources originating from a wide variety of anabolic or catabolic processes (Ertani et al., 2009). Applications of different PHs have been observed to increase grapevine yield, correlated with PH organic N content (Bosselli et al., 2019).

Further research on the effects of PHs on viticulture should be explored, especially the impact on microbial communities living in the rhizosphere or phyllosphere (aboveground plant surfaces inhabited by microbes), which has received little study (Colla et al., 2015 and Colla et al., 2017).

Seaweed extracts

Biostimulants can also be produced from marine macroalgae (i.e. seaweed extracts; SEs). In the last decade, the application of SEs in agriculture has gained traction and several seaweed species (such as brown seaweeds *Ascophyllum nosdosum*, *Ecklonia maxima*, and *Laminaria* spp, and red seaweeds *Kappaphycus alvarezii*, and *Gracilaria edulis*) are currently used in commercial production of biostimulants (Yakhin et al., 2017; El Boukhari et al., 2020). SEs have been successfully explored in arable cropping, including viticulture (Table 2). The most common method of applying SEs in vineyards is foliar spraying, although the extracts can be applied directly to the soil (Mancuso et al., 2006; de Carvalho et al., 2019). Like most biostimulants, SEs may increase crop productivity and improve fruit quality in both stressed and non-stressed conditions (Deolu-Ajayi et al., 2022). The vegetative shoot growth stage of the crop is frequently targeted for SE application to stimulate growth and boost crop vitality by modulating underlying biochemical processes, which are also

TABLE 1 An overview of the main effects of protein hydrolysates (PHs) applied in viticulture.

Crop variety	Applied material and properties	Dosage, the form of application, and stage of plant development	Experimental condition	Effects	Reference
Table grape inoculated with either B. cinerea (100 conidia/wound) or natural infections.	- PH derived from soybean. - PH derived from casein.	- 20 µL in the wound (3 x 3 mm) 24 h before inoculation. - Spraying at preharvest (0.8 and 1.6 g L^{-1} on vines every 15 d) or a combination of a pre- (0.8 g L^{-1}) and postharvest treatment (200 mL).	-Organic vineyard cultivation during the 2012/2013 season, planted in 1998 in Fumane, Valpolicella, Verona, Italy.	- Significant reduction of gray mold incidence by 67% (soybean PH) and 54% (casein PH) at a low application dose (0.8 g L^{-1}). - In the field, PH derived from either soybean or casein reduced gray mold incidence by 65 and 92% respectively compared to water control.	Lachhab et al. (2016).
Grapevine plantlets (*Vitis. Vinifera cv* Marselan) inoculated with *Plasmopara. viticola.*	- PH derived from soybean. - PH derived from casein.	- 10 mL of each PH per plant was sprayed on 8-week-old grapevine plantlets.	-Greenhouse conditions.	- Application of PH derived from either soybean or casein reduced downy mildew infected leaf surface by 76% and 63% as compared to the control, respectively. - Both PHs acted as elicitors to enhance grapevine immunity against pathogen attack.	Lachhab et al. (2014).
Grape cultivar *(Vitis Vinifera L., cv* Corvina).	- PH derived from soybean. - PH derived from casein. - PH derived from lupin.	-Spraying at two concentrations; 1.6 and 6.4 g L^{-1} at every 10 d three times, from fruit-set to bunch closure.	- Field experiments were carried out over 5 growing seasons (2012 to 2016) in an organically managed vineyard of *Vitis vinifera L.* cv. Corvina, 24-year-old vines located in the Valpolicella area, Italy.	- All treatments significantly ameliorated the total anthocyanin content of berries compared to the control. - The greatest effect was obtained by soybean-derived PH. - All PHs reduced plant water loss.	Boselli et al. (2019).
Grapevine *(Vitis Vinifera L., cv Sauvignon Blanc).*	- A novel PH biostimulant (APR).	-A concentration of 0.5 g L^{-1} PH was added to the soil or pot as a soil drench.	-Pot experiment approximating field-conditions in a tunnel at the "L. Toniolo" Experimental Farm of the University of Padua in Legnaro, NE Italy in 2018.	- Application of PHs to roots before imposing water deprivation mitigated consequences of stress by sustaining the growth of younger vegetative organs, and limiting the extent of cell dehydration.	Meggio et al. (2020).
Grapevine (*Vitis Vinifera* cv. Marselan) inoculated with *Plasmopara viticola.*	- Laminarin (Lam), a ß-1,3 glucan polymer from the algae *Laminaria digitata* - The chemically sulfated form of Lam, PS3.	-Lam and PS3 solution (5 g L^{-1}) were sprayed on upper and lower leaf faces until the run-off point.	-Greenhouse pot experiment	- PS3 triggered a long-lasting plasma membrane depolarization of grapevine cells. - PS3 and Lam shared a common stress-responsive transcriptome profile, which resulted in induced resistance against *P. viticola.*	Gauthier et al. (2014).
Grapevine (*Vitis vinifera L.*).	- nutrient broth PH – a natural derivative from peptone *via* meat (1.9 g L^{-1}) and yeast extract (0.7 g L^{-1}).	- 5.0 (2010), 3.0 (2011), and 3.0 g L^{-1} (2013) of PH -Treatment was applied weekly with a motorized backpack mist blower.	-Field trials were carried out in 2010, 2011, and 2013 at S. Michele all'Adige (Italy) in a vineyard planted in 1997.	-PH controlled powdery mildew on grapevine across seasons (comparable to standard fungicide treatments) both on leaves and bunches across three different years.	Nesler et al. (2015).

important at the reproductive stage (Figure 1). SEs may also enhance microbial biodiversity, but information about this effect on the plant microbiome is scarce (El Boukhari et al., 2020).

Physiologically, SEs boost nutrient assimilation and plant growth under non-stressed conditions. Spraying wine grapevines with any of three commercial SEs (Maxicrop, Proton, and Algipower) increased both macro- and micro-nutrient uptake from the soil (Turan and Köse, 2004; Table 2). Similar mineral uptake induction in wine grapevines was reported by Mancuso et al. (2006) and de Carvalho et al. (2019) when SEs were applied, resulting in a subsequent increase of dry weight by ~ 27% and fruit yield by ~ 24% (Table 2). Foliar application of either an *Ascophyllum*-derived seaweed extract or the commercially available extract "SUNRED" improved fruit quality and shortened the ripening time of wine grape (Frioni et al., 2018; Table 2) and table grape (Deng et al., 2019; Table 2) cultivars. The enhancement in fruit quality may be linked to an accumulation of anthocyanins and phenolic compounds, especially in the berry skin, which was also observed (Frioni et al., 2018; Deng et al., 2019).

During drought stress and water deprivation in controlled greenhouse experiments, foliar application of a seaweed indole-

TABLE 2 An overview of seaweed-based (SEs) biostimulants applied in viticulture.

Crop variety	Product details and seaweed species	Bioactive substance	Experimental conditions	Application and dosage	Physiological effects	References
Vitis vinifera L. cv. Karaerik	Commercial biostimulant "Maxicorp" containing *Ascophyllum nodosum*. Commercial biostimulant "Proton" (seaweed species not specified). Commercial biostimulant "Algipower" (seaweed species not specified).	Not Specified.	Greenhouse experiment with 1-year-old grapevine saplings grown in 20 cm diameter pots. Four increasing fertilization levels, including a control without any nutritional element, were used.	Foliar spray of seaweed biostimulants at individual concentrations of 0.5, 1, and 2 g L^{-1}. A total of 4 applications occurring every 15 days were performed. The initial treatment was applied to 2-week-old plants.	Increased macro- (nitrogen, phosphorus, potassium, calcium, and magnesium) and micronutrient (iron, zinc, magnesium, and copper) plant uptake.	Turan and Köse (2004).
Vitis vinifera L. cv. Sangiovese.	Not specified.	IPA (Indole-3- propionic acid) extract.	Greenhouse experiment with 1-year-old *V. vinifera* cv. Sangiovese grafted onto *V. berlandieri* x *riparia* '420A' in 25 cm^2 pots. Water stress was introduced by stopping irrigation for 6 days and restoring it after the dry period.	Biostimulant was applied at a rate of 10 g L^{-1}, with foliar sprays occurring 2 times weekly for the duration of the experiment. *A fertilizer NPK 9-5-4 was combined with the biostimulant treatment.	Significant increase in nitrogen, phosphorus, potassium, and magnesium uptake, and also in total dry weight. In water deficit conditions, plants showed faster recovery of their leaf water potential.	Mancuso et al. (2006).
Vitis vinifera L. cv. Niágara Rosada.	Commercial biostimulant "Acadian LSC" containing *A. nodosum*.	Not Specified	A field trial in an established vineyard in Lavras, Brazil. The vineyard was cultivated with the espalier method and has clayey soil.	Foliar application of the biostimulants at 6 g L^{-1}. Each biostimulant was applied 4 times: 20 days after dormancy, at blooming, fruit set, and veraison.	Significant increase in potassium, boron, and zinc; as well as an estimated yield increase of 24.15% (equivalent to 2.72 t ha^{-1}) compared to the control.	de Carvalho et al. (2019).
	Hypnea musciformis.				Significant increase in magnesium and zinc, but no significant increase in crop yield.	
	Lithothamnium sp.				Significant increase in boron only, and a 13.17% yield increase equivalent to 1.46 t ha^{-1}.	
	Sargassum vulgare.				Significant increase in magnesium, but no significant increase in crop yield.	
Vitis vinifera L. cv. Sangiovese.	A commercial biostimulant "Acadian marine plant extract powder" containing *A. nodosum*.	Not specified.	Field trial (2013) in Umbria, Italy growing only the Sangiovese cultivar. The vineyard has a vertical shoot-positioned trellis cultivation system, and loamy soil.	- Foliar application for all 3 cultivars at 1500 g ha^{-1}, 5 times during the growing season, beginning 2 weeks before grape veraison and occurring every 10-14 days.	Improved fruit color of the Sangiovese cultivar.	Frioni et al. (2018).
Vitis vinifera L. cv. Pinot Noir.			Field trial (2014) in an established vineyard with both Pinot Noir	- An additional treatment with 3000 g/	Increased vegetative parameters of both	

(Continued)

TABLE 2 Continued

Crop variety	Product details and seaweed species	Bioactive substance	Experimental conditions	Application and dosage	Physiological effects	References
Vitis vinifera L. cv. Cabernet Franc.			and Cabernet Franc, located in Benton Harbour, Michigan, USA. The vineyard has a vertical shoot-positioned trellis cultivation system, and sandy loam soil.	ha of the biostimulant was performed on only the Sangiovese cultivar.	grape cultivars. Shortened ripening time in only Pinot Noir.	
Vitis vinifera L. cv. Red globe.	Application of commercial biostimulant "SUNRED" containing an unspecified seaweed extract.	Not specified.	Field trial (2015/2016) in Pengshan county, Meishan, China. The cultivation method and soil were not specified.	Foliar biostimulant treatments of 0.6, 0.8, and 10 g L^{-1} were each applied twice: at the start of veraison and 5 days later.	Improved grape color at the different biostimulant concentrations.	Deng et al. (2019).
Vitis vinifera L. cv. Chardonnay.	Commercial biostimulant "Seasol" containing brown seaweeds *Durvillaea potatorum* and *A. nodosum*.	Not specified.	Field trials (2012/2013 and 2013/2014) near Kenley, Australia. The vineyard uses a double-wire cordon trellis system of cultivation and has calcareous loamy sandy soil.	Drip irrigation of 10 L ha^{-1} of biostimulant per application, with 8 and 4 applications at the 1st and 2nd field trials respectively. Biostimulant was first applied at the woolly bud and budburst growth stages respectively, and treatments occurred every 20-30 days.	Significant increase in grape yield by 13.8% (equivalent to 1.6 t/ha) compared to the control.	Arioli et al. (2021).
Vitis vinifera L. cv. Semillon.			Field trials (2012/2013 and 2013/2014) near Balranald, Australia. The vineyard uses a double-wire cordon trellis system, and has calcareous loamy sandy soil.	Drip irrigation of 5 L ha^{-1} of the biostimulant with 3 applications in both field trials. Treatments were applied at the budburst, flowering, and fruit set growth stages.	The yield increased by 10% (equivalent to 1.3 t/ha) compared to the control.	
Vitis vinifera L. cv. Merlot.			Field trial (2013/2014) near Loxton, Australia. The vineyard uses a double-wire cordon trellis system and its soil type is calcareous loamy sand.	Drip irrigation of 5 L ha^{-1} of the biostimulant with 3 applications. Treatments were applied at the budburst, flowering and fruit set growth stages.	The yield increased by 17.6% (equivalent to 1.8 t ha^{-1}) compared to the control.	
Vitis vinifera L. cv. Merlot.			Field trial (2014/2015) at Tharbogang, Australia. The vineyard uses a single-wire cordon trellis system and has duplex soils ranging from loamy sand to clay loam.	Drip irrigation of 10 L ha^{-1} of the biostimulant with 4 applications. Treatments were applied at the budburst, flowering, fruit set, and veraison growth stages.	The yield increased by 11% (equivalent to 0.5 t ha^{-1}) compared to the control.	
Vitis vinifera L. cv. Cabernet Sauvignon.			Field trial in (2016/2017) at Tharbogang, Australia. The vineyard uses a double-wire cordon trellis system and has duplex soils ranging from loamy sand to clay loam.	Drip irrigation of 10 L ha^{-1} of the biostimulant with 3 applications. Treatments were applied at 4-cm growth, flowering, and fruit set.	The yield increased by 10.7% (equivalent to 0.7 t ha^{-1}) compared to its control.	
Vitis vinifera L. cv. Montepulciano.	Not specified.	Laminarin.	Field trials (2012 and 2013) at Camerano, Italy grown according to the Guyot trellis system. Biostimulant treatment started at the inflorescence growth stage.	Foliar spraying with 1 L ha^{-1} of commercial biostimulant "Frontiere" in each of the 11 treatments, and treatments occurred weekly.	The biostimulant had no significant reduction of grapevine downy mildew.	Romanazzi et al. (2016).
Vitis vinifera L. cv. Moscato.	Not specified.	Laminarin.	Greenhouse conditions with ~ 60-day old transplanted grape plants in 4 L pots. Plants were inoculated twice with powdery mildew pathogen (*Erysiphe necator*).	- Treatment with 2 g L^{-1} of a commercial biostimulant "Vacciplant" per timepoint. Biostimulants were applied at 6 time points occurring every 7-9 days: 2 treatments occurred prior to 1st pathogen inoculation, another 2 before 2nd pathogen inoculation, and 2 last treatments after the 2nd pathogen inoculation.	Reduction in Powdery mildew disease severity in the grape plants.	Pugliese et al. (2018).

(Continued)

TABLE 2 Continued

Crop variety	Product details and seaweed species	Bioactive substance	Experimental conditions	Application and dosage	Physiological effects	References
				- A fungicide methiram was simultaneously used on the plants.		
			Field trials (2016 and 2017) at Piedmont, Italy, in an established vineyard with an espalier cultivation method and "Guyot" pruning.	Treatment with 2000 g/ha per timepoint. Biostimulant treatment was applied at 9 individual time points, occurring every 8-10 days. - A fungicide methiram was simultaneously used on the plants.		

3-propionic acid (IPA)-derived extract induced faster recovery of leaf water potential and stomatal kinetics (Mancuso et al., 2006). Different wine grape cultivars treated with a commercial seaweed biostimulant "Seasol" *via* soil fertigation, showed an average fruit yield increase of 14.7% across five locations with varying environmental conditions (Arioli et al., 2021; Table 2). Yield increase occurred irrespective of heat and/or cold stress in a single growing season (Arioli et al., 2021). The performance of the field experiments suggests an essential soil-crop interaction for increased productivity (Arioli et al., 2021). Unfortunately, analyses of the soils and the applied extracts were not reported and therefore, cannot support this hypothesis. Moreover, variations in the SE dosage in different fields in this study prevent further conclusions regarding the direct effect soil type (and properties) may have on SE, as well as the overall impact on crop productivity in the presence of the biostimulant.

Although SEs reduce the effects of crop diseases (Shukla et al., 2019) and non-seaweed-derived biostimulants also contribute to disease prevention in viticulture (reviewed in Gutiérrez-Gamboa et al., 2019), the specific use of SEs to mitigate diseases of grapevine has not been extensively studied. Treatment with a commercial seaweed-derived biostimulant "Vacciplant" caused a reduction in the effects of powdery mildew disease in both greenhouse experiments and field trials (Table 2). Grapevine disease severity was reduced by ~ 65% and 52% in greenhouse and field experiments, respectively (Pugliese et al., 2018). Thus, there is still potential for the application of seaweed-derived biostimulants in viticulture for disease control, especially considering the need for reduced agrochemical reliance in the coming decades.

Bioactive compounds have biological activity in plants, some of which result in increased crop productivity and resilience to stress. While the presence of bioactive compounds in seaweed has long been suspected of having stimulatory effects on plants, including complex polysaccharides (absent in arable crops, e.g. alginate, laminarin, and fucoidan), phytohormones, sterols, and osmolytes (Yakhin et al., 2017), speculations remain regarding underlying mechanisms. This is perhaps due to current research focusing on growth promotion, rather than also investigating and linking the role of these bioactive compounds to specific mechanisms. Further research is needed, and will also provide essential information for biostimulant optimization. Of note is that changes in mineral concentration due to foliar application of SEs do not always enhance crop productivity. Only two of four SEs tested caused a significant increase in grapevine yield (de Carvalho et al., 2019; Table 2), indicating that SEs must be tested independently to establish their benefits. Conflicting observations may be explained by variations in biochemical composition among seaweed species and their derived extracts, linked to the environmental conditions of the cultivation sites as well as harvesting times (Khairy and El-Shafay, 2013). Overall, the application of SE is beneficial for crops in both stressed and non-stressed conditions and thus may be attractive for wider adoption in viticulture.

Humic substances

Humic substances (HS) are an important carbon compartment present in soils, waters, and sediments. Although researchers are not in complete agreement as to how HS are formed and structured, a growing body of evidence indicates they may serve as biostimulants of plant growth. HS biostimulants are available commercially in the form of products based on humic acids (HA), fulvic acids (FA), or a mixture of both (HA+FA). Efficacy is related to the product's chemical composition, the form of extraction and application, the applied concentration, and the stage of development of the crop (Canellas et al., 2009; Zandonadi et al., 2013; Olivares et al., 2017; Jindo et al., 2020). Effects of HS application in plants often include the activation of plasma membrane H^+-ATPase and the alteration of the primary and secondary metabolism, generally resulting in increased root growth, nutrient uptake, rate of photosynthesis, and attenuation of stress associated with salinity, drought, or metal toxicity (Zandonadi et al., 2007; Dobbss et al., 2018; Jindo et al., 2020) (Figure 1). It is suggested that some biostimulant effects of HS originate from their impact on structural and physiological modifications in

roots and shoots related to nutrient assimilation and soil distribution (Canellas et al., 2015). Also, HS can simultaneously regulate the transcription and activity of some plant hormones following addition to the rhizosphere (Souza et al., 2022). Recently, it has been demonstrated that HS can alter the plant microbiome by favoring the recruitment of beneficial microorganisms after application (da Silva et al., 2021).

Despite a limited number of studies involving the specific use of HS in grape cultivation, several effects are consistently observed (Table 3). These include increases in photosynthetic rate, total soluble solids, total chlorophyll, and average berry size and weight (Ferrara and Brunetti, 2008 and Ferrara and Brunetti, 2010; Ibrahim and Ali, 2016; Popescu and Popescu, 2018; Irani et al., 2021). For example, Popescu and Popescu (2018) noted increased photosynthetic rate and total soluble fruit solids in cultivars 'Feteasca Regala' and 'Riesling Italian' planted in Romania, following foliar application of HA (40 and 50 mL L^{-1}) previously extracted from vermicompost. The increase was attributed to a higher concentration of carotenoids in the leaves. Ferrara and Brunetti (2010) reported an improvement of parameters associated with fruit quality (e.g. increase in total soluble solids, [°Brix], and the °Brix/titratable acidity ratio, and a decrease in tartaric acid) due to the application of HA (100 mg L^{-1}, extracted from the soil in Apulia, Italy) at full-bloom. In the cultivar 'Italy', six applications of HA (derived from different origins) increased chlorophyll content, °Brix value, and berry size (Ferrara and Brunetti, 2008). The authors attributed these effects to the presence of 6% nitrogen in the humic matrix. However, the increase in berry size might also be the result of the hormone-like activity of HA (i.e., auxin, gibberellin- and cytokinin-like activity), which is useful for organic seedless table grape production where the application of synthetic hormones is not permitted. In Egypt, Ibrahim and Ali (2016) applied HA (Greenhum Company, Italy) in both February and March to the cultivar 'Superior Seedless'. Chlorophyll content, berry weight, and total fruit volume significantly increased after HA was respectively applied to leaves (5.0 g L^{-1}) or to the soil (5 and 7.5 g L^{-1}, 2.5 g L^{-1}). In Spain, Sánchez-Sánchez et al. (2006) reported increased iron and phosphorus levels and reduced sodium in the leaves of cultivar 'Italy' following treatment with solutions containing HA+FA. Recently in Iran, Irani et al. (2021) applied FA (0.5%) *via* leaf spray or HA (20 g $plant^{-1}$) *via* irrigation, and observed the alleviation of drought stress, increased nutrient absorption, and concentration of proline (an important stress signaling molecule), carbohydrates, and soluble proteins. Additionally, HA and FA application resulted in greater berry weight, productivity, and concentration of total soluble solids (Irani et al., 2021).

Protocols outlining best practices in terms of vineyard HS application practices and optimal concentrations are yet to be developed, and research regarding potential negative structure-activity interactions has yet to be conducted. Despite these shortcomings, the beneficial effects of HS on grapevines are evident, generally resulting in increased production, increased fruit quality, and an expansion of the plant's ability to tolerate environmental stresses.

Pyrogenic materials

Pyrogenic materials are obtained by pyrolysis of plant biomass, a thermal decomposition process occurring at relatively high temperatures in the absence of oxygen. These materials represent a sustainable source of biostimulants with a long tradition in agriculture (Ogawa and Okimori, 2010). Pyrogenic materials include biochar (solid C-rich residue of pyrolysis), and pyroligneous acid (also known as wood vinegar, the aqueous fraction obtained from the condensation of pyrolysis vapors). Biochar is highly aromatic, porous, and possesses a chemically recalcitrant structure. It is generally used as a soil amendment, due to potential agronomic and environmental benefits associated with enhanced soil fertility and long-term soil C sequestration (Woolf et al., 2010; Lehmann et al., 2011). Pyroligneous acid consists of a mixture of a large number of oxygenated organic compounds (including acids, alcohols, ketones, phenols, furans, and ethers) and hydrocarbons with antioxidant and antimicrobial properties. Pyroligneous acid has potential as a plant growth and germination biostimulant, antioxidant and free-radical scavenger, pesticide, and antimicrobial agent (Mungkunkamchao et al., 2013; Grewal et al., 2018).

Biochar is more commonly used than pyroligneous acid in vineyards, either alone or in combination with compost (Figure 1 and Table 4). There is contrasting information in the literature regarding biochar's impact on vineyard productivity. A recent meta-analysis by Payen et al. (2021) showed that biochar application increased soil organic C, at a rate of 8.96 Mg CO_2-eq ha^{-1} yr^{-1}. The authors also postulated biochar application might lead to enhanced vineyard productivity, but additional long-term investigations are needed to support this statement. Several authors (Baronti et al., 2014; Genesio et al., 2015; Maienza et al., 2017) have reported increased productivity in biochar-amended vineyards, associated with enhanced physicochemical properties of the amended soils, increased soil water availability, and growth of fine root biomass (Amendola et al., 2017). However, there were no significant differences in grape quality. Conversely, other reports indicate only minor effects on soil physicochemical properties following biochar application over a three-year period, which did not significantly affect vineyard fertility (Schmidt et al., 2014; Sánchez-Monedero et al., 2019). Although these authors did observe benefits following the addition of biochar-blended compost to the soil, effects were similar to those in control vineyards amended with conventional compost without biochar.

Biochar may also act as a biostimulant when used as a carrier of inoculum for microorganisms (Hale et al., 2015; Głodowska

TABLE 3 An overview of the main effects of humic substances (HS) applied in viticulture.

Crop variety	Applied material and properties	Dosage, the form of application, and stage of plant development	Experimental condition	Effects	Reference
Vitis vinifera cv. Italia.	HA+FA commercial (Mol). Functional groups (with Nuclear Magnetic Resonance ^{13}C): 90.7% of fulvic acids with three main portions that consisted of 10% aliphatic C, 73% aromatic C and 16.9% carboxylic C.	Two applications were carried out on the soil, in mid and late March.	Field cultivation. Twelve-year-old plants; drip-irrigated.	An increase in Fe and P absorption, as well as a decrease in Na absorption; Increased berry weight.	Sánchez-Sánchez et al. (2006).
Vitis vinifera cv. Italia. Grapevines were grafted onto 1103 P (*V. berlandieri* x *V. rupestris*).	HA was extracted from soil or organic compost. 54.91% of C; 4.91% of H; 6.73% of N; 32.67% of O; C/N ratio of 9,52; Total acidity of 5.0 meq g^{-1} of C; Phenolic acidity of 2.2 meq g^{-1} of C and carboxyl 2.7 meq g^{-1} of C	5 and 20 mg L^{-1}, *via* leaf spray. Six applications with a 21-day interval.	Field cultivation. Forty-five-year-old plants; drip-irrigated.	Increased berry size and reduction in titrable acidity; Increase in N content, total chlorophyll content, yield, and soluble solids (°Brix).	Ferrara and Brunetti (2008).
Vitis vinifera cv. Feteasca Regala (henceforth RF) and cv. Riesling Italian (henceforth RI). Grapevines were grafted on rootstock hybrid Kober 5 BB (*Vitis berlandieri* x *Vitis riparia*).	Commercial HA (BioHumusSol Company Ltd.). 14.5 g humic substances L^{-1}, 19 ppm nitrate nitrogen (NO_3-N), 104 ppm ammonium nitrate (NH_4-N), 22.5 ppm P, 132 ppm K, 39 ppm Ca, 75 ppm Mg, 75 ppm Na	30, 40, and 50 mL L^{-1}, *via* leaf spray, one application at the pre-bloom and fruit set the phenological stage.	Field cultivation. Non-irrigated.	Increase in the total leaf area, yield, and total soluble solids (50 mL L^{-1}); Increase in photosynthesis rate, chlorophyll a and b, and carotenoids (40 e 50 mL L^{-1})	Popescu and Popescu (2018).
Vitis vinifera cv. Italia. Grapevines were grafted onto 1103 P (*V. berlandieri* x *V. rupestris*).	HA extracted from soil. 52.46% of C; 5.77% of H; 5.4% of N; 35.66% of O; C/N ratio of 11.33; Total acidity of 5.0 meq/g of C; Phenolic acidity of 2.2 meq/g of C and carboxyl 2.7 meq/g of C	100 mg L^{-1} *via* spray foliar.	Field cultivation. Drip-irrigated.	Increased berry weight; Increase in total soluble solids (°Brix); decrease of tartaric acid.	Ferrara and Brunetti (2010).
Vitis vinifera cv. Superior seedless.	Commercial HA (Humatic 8500).	One, two, or three applications.	Field cultivation. Eleven-year-old plants; drip-irrigated.	Increase in total soluble solids, yield, and fruit quality with four HA applications.	Ibrahim and Ali (2016).
Vitis vinifera cv. Yaghouti'.	HA (K_2O 10%; HA 55%; FA 15%) or FA Total nitrogen 3%; K_2O 10%; FA 50%; chlorine 4.3%.	Application of HA with irrigation water at a concentration of 20 g per vine, two times (bud swell and millet-sized berry). Application of FA as a foliar spray at a concentration of 0.5% two times (millet-sized berry and 2 weeks later).	Field cultivation. Ten years old (plants); drip-irrigated.	Increase in berry weight, yield, total soluble solids, proline, and soluble carbohydrates (both HA and FA; under water stress conditions or not). Increase in N, P, K, Zn, and Fe content (leaf). In the plants with and without water stress, only the N content was not increased.	Irani et al. (2021).

et al., 2016; Hardy and Knight, 2021), as a suppressor of plant disease (Graber et al., 2010; Debode et al., 2020), and as a coating for novel biochar-fertilizer composites (Joseph et al., 2013) or slow-release fertilizers (An et al., 2020). However, these applications have not been fully explored in vineyards. Hale et al. (2015) demonstrated in a soil incubation experiment that biochar might support high population densities of the plant growth-promoting rhizobacteria (PGPR) *Enterobacter cloacae*.

TABLE 4 An overview of the main effects of pyrogenic materials in viticulture.

Crop variety	Pyrogenic material	Properties	Application and dosage	Experimental condition	Effects	Reference
Vitis vinifera L. (cv. Pinot Noir).	Biochar from 80% various hardwoods and 20% various coniferous wood chips at 750°C.	Soil organic amendment.	8 t ha^{-1} of biochar (d.w.).63.2 t ha^{-1} biochar-compost (d.w.), biochar added at 20% before composting process.	Field trial (3 years),rainfed vineyard (25-35 years old).	No relevant effects on plant growth parameters of vine or vine health are caused by biochar and biochar-compost.Minor effects on grape quality only in the first year of trial.	Schmidt et al. (2014).
Vitis vinifera L. (cv. Merlot, clone 181; rootstock 3309 Couderc).	Biochar from orchard pruning at 500°C.	Soil organic amendment.	16.5 t ha^{-1} of biochar (d.w.) applied in two consecutive years.	Field trial,rainfed vineyard (20 years old).	After 3 years: Increased soil water holding capacity and plant available water content.	Baronti et al. (2014).
					After 5 years: Increased vineyard production with no detrimental effects on grape quality.	Genesio et al. (2015).
					After 5 years: No negative impact on soil microbial community, and no retention of toxic compounds (PAH and heavy metals).	Maienza et al. (2017)
					After 7 years: Biochar is effective in restoring degraded soil functionality. The effects persist after 7 years of following a one-time application.	Giagnoni et al. (2019).
Vitis vinifera L. (cv. Grenache).	Biochar from grapevine trunks at 550°C.	Soil organic amendment.	5 t C ha^{-1} of biochar.5 t C ha^{-1} biochar-compost.	Field trial (2 years),rainfed vineyard (20 years old).	Improvement in the N nutrient status of vines after application of 'compost' and 'compost x biochar' treatments in year two.	Ubalde et al. (2014).
Vitis vinifera L. (cv. Pinot Blanc).*Vitis vinifera* L. (cv. Ribolla Gialla).*Vitis vinifera* L. (cv. Sauvignon).	Biochar from oak at 650°C.	Soil organic amendment.	10.9 t C ha^{-1} of biochar (d.w.).10.9 t C ha^{-1} of biochar: compost (d.w.), biochar added at 10% before composting process.	Field trial (3 years),3 rainfed vineyards.	Biochar enhanced soil water availability, but had no significant effects on soil nutrient availability, grape yield, or must quality.Biochar-blended compost had a similar effect as conventional compost.	Sánchez-Monedero et al. (2019).
Vitis vinifera L. (cv. Shiraz)	Not available.	Soil organic amendment.	8.5 t ha^{-1} of biochar.	Field trial (4 years),rainfed vineyard	No significant effect on yield and vegetative growth	Botelho et al. (2020)
Vitis vinifera ssp. *vinifera.*	Biochar from maize corn cob rachis at 450 -500°C.	Soil organic amendment.	5 t C ha^{-1} of biochar.	Field trial (2 years),rainfed vineyard (25 years old).	Reduced soil microbial biomass for at least two years after application.No significant effects on the community composition of soil microbes or microarthropods.	Andrés et al. (2019).
Vitis vinifera L. (cv. Montepulciano).	Biochar from orchard pruning at 500°C.	Soil organic amendment.	10 t ha^{-1} of biochar (d.w.).	Field trial (1 year), rainfed vineyard (15 years old).	Increased organic carbon, available water content, and formation of a large fraction of macro aggregates.Increased fine root biomass with no significant effect on the production of arbuscular mycorrhizal fungi.	Amendola et al. (2017).
Vitis vinifera L. (cv. Chardonnay).	Biochar from orchard pruning at 500°C.	Soil organic amendment.	30 t ha^{-1} biochar (fresh weight).	Rhizobox.	Enhanced soil physicochemical soil properties and increased soil water content during the harsh summer period.Promoted earlier root production and lowered the number of fibrous roots.	Montagnoli et al. (2021).
Vitis rotundifolia L. (Muscadine grape cv. Alachua).	Biochar from southern yellow pine at 400°C.	Soil organic amendment.	0, 5%, 10%, 15%, and 20% of biochar (d.w.).	Greenhouse study in pots.	Enhanced soil water and nutrient status, and improved plant P and Mg uptake, with no significant differences in plant physiological performance.	Chang et al. (2021a).
					Improved soil physical properties and stimulation of fine root development.	Chang et al. (2021b).
Vitis vinifera L.	Biochar from dairy manure at 400°C.	Soil organic amendment.	2 g and 5 g of biochar kg^{-1} soil.	Pot experiment (2 months).	Enhanced plant growth and soil properties under water stress conditions.	Kanwal et al. (2018).
Vitis vinifera L. (cv. Pinot noir).	Not available.	Soil organic amendment.	2% of biochar (d.w.).	Pot experiment.	Enhanced soil water availability under water shortage.No significant impact on soil N availability.	Petrillo et al. (2020).

(Continued)

TABLE 4 Continued

Crop variety	Pyrogenic material	Properties	Application and dosage	Experimental condition	Effects	Reference
Vitis vinifera L.	Biochar from gasification of vineyard pruning at 900-950°C.	Growing media component for nursery grapevine production.	0, 10%, 20%, 40% vol. of biochar.	Greenhouse study in pots.	BC applied at 10% enhanced plant-growth response, particularly expressed at the shoot stage.	Ronga et al. (2019).
Vitis vinifera L. (cv. Grüner Veltliner).	Biochar from softwood chips and cereal husk.at 480°C.	Remediation of Cu-polluted soils.	1 to 6 kg m^{-2} of biochar (d.w.).	Greenhouse study in soil columns.	Biochar enhanced Cu mobilization in a neutral vineyard soil but reduced the ecotoxicologically relevant Cu^{2+} fraction.	Soja et al. (2018).
Vitis vinifera L. (cv. Chardonnay).	Biochar from poultry litter at 550°C.	Fungal-disease suppression and control of nematode population.	6.9 t ha^{-1} of biochar (d.w.).	Field trial (3 years),vineyard (5 years old).	Decreased plant-parasitic nematode population, andincreased free-living (non-plant-parasitic) nematode population.Possible role of biochar porous structure protecting bacteria and fungi from predators.	Rahman et al. (2014).
Vitis vinifera L. (Red Globe).	Bamboo biochar.	Microbial inoculum (*Pseudomonas putida*).	250 – 500 g biochar per tree (d.w.).12.5 g biochar mL^{-1} inoculum.	Field trial (1 year), vineyard (8 years old).	Inoculated biochar improved the yield and quality of the grapefruit.Enhanced soil properties and altered soil microbial community structure.	Wei et al. (2020).
Vitis vinifera L. (Red Globe).	Wood vinegar from a hardy rubber tree at 550°C.	Inhibition of grey mold infection (*Botrytis cinerea)* during grape storage.	Grapes soaked in wood vinegar diluted 600, 400, and 200 times for 15 s and left to air-dry.	Laboratory conditions.	Inhibitory effect on the disease *Botrytis cinerea* during grape storage by stimulation of antioxidant defense-related enzymes.	Chen et al. (2020).

d.w., dry weight.

Interestingly, chemical properties of the biochar (particularly pH and N content) affected initial inoculum survival, but physical properties (surface area and porosity) were mainly associated with later survival after soil application (Hale et al., 2015). Biochar did not negatively affect rhizobacterium activity, which may occur due to bacterial signaling compounds or bacteria-derived plant growth hormones binding to the biochar surface. Depending on feedstock and pyrolysis conditions, certain biochars with large surface area or high pH can adsorb or hydrolyze signaling molecules, disrupting soil microbe cell-to-cell communication (Gao et al., 2016).

Similarly, Zhu et al. (2017) reported that biochar could modify communication between rhizosphere microbial communities and plant roots, affecting plant response to soil-borne pathogens (Harel et al., 2012; Akhter et al., 2015). Graber et al. (2010) proposed that induced resistance against pathogens observed in both tomato and pepper following biochar application may be due either to a shift in soil microbial populations following biochar addition, or to the release of chemicals from biochar toxic to pathogens. The utilization of beneficial microorganisms as biostimulants is discussed in greater detail below, and other mechanisms by which biochar can act as a disease-suppressing agent have been previously summarized by Bonanomi et al. (2015) and Graber et al. (2014).

Pyroligneous acid is often applied as a foliar spray or soil drench (Mungkunkamchao et al., 2013), or in combination with biochar (Zhang et al., 2020). Zhang et al. (2020) demonstrated the benefit of applying biochar and pyroligneous acid for increased blueberry yield and nutritional quality, by enhancing soil organic matter and nutrient availability. In terms of vineyard pest management, Chen et al. (2020) studied the ability of pyroligneous acid to inhibit grey mold (*Botrytis cinerea*) infection of table grape cultivar 'Red Globe'. The application of diluted pyroligneous acids (200- and 400-fold dilution) improved grape resistance to grey mold, likely through stimulation of antioxidant defense-related enzyme activities, including those of superoxide dismutase, peroxidase, and ascorbate peroxidase. However, other investigations of pyroligneous acid use in vineyards are lacking.

The application of biostimulants from pyrogenic materials may help vineyards adapt to climate change, especially in a scenario of water shortage which may be particularly detrimental to viticulture (Maienza et al., 2017). Fascinatingly, the positive impacts of biochar on vineyard soil fertility are maintained in the long term (7 years), even after a single application (Giagnoni et al., 2019). This benefit has also been identified for improving the growth and symbiotic performance of other plants (lupin, *Lupinus angustifolius*) under drought stress conditions (Egamberdieva et al., 2017).

Microorganisms as biostimulants

Plant growth-promoting rhizobacteria

Certain prokaryotic soil microorganisms can establish beneficial relationships with plants. Coined 'plant growth-promoting rhizobacteria' (PGPR) (Kloepper and Schroth, 1979), these microbes can enhance plant growth and development through several direct and indirect processes, performed at different plant growth stages (Vorholt, 2012; Ruzzi and Aroca, 2015; Castellano-Hinojosa and Bedmar, 2017). According to Chauhan et al. (2015), the main PGPR traits are biofertilization and phytostimulation (through the excretion of phytohormones such as indole-3-acetic acid [IAA], cytokinins, and gibberellins), tolerance to biotic and abiotic stress (via 1-aminocyclopropane-1-carboxylate [ACC] deaminase activity), and biopesticide and biocontrol activity (production of antibiotics, lytic enzymes, hydrogen cyanide [HCN], and volatile organic compounds [VOCs], among others) (Chauhan et al., 2015; Kumar-Jha and Saraf, 2015; Goswami et al., 2016; Oleńska et al., 2020). Additionally, PGPRs can have synergistic interactions with the endophytic grape microbiome (Vandana et al., 2021).

Bacteria must first be isolated and cultured prior to their utilization as PGPRs. For use in viticulture, several authors have isolated viable PGPRs from the microbiome of *Vitis vinifera* L., which may then be re-applied as biostimulants in vineyards (Compant et al., 2011; Pinto and Gomes, 2016; Rezgui et al., 2016; Pacifico et al., 2019). The effectiveness of these PGPRs depends on several factors including environmental conditions, soil characteristics, and even crop variety (Pacifico et al., 2019). Nevertheless, PGPRs are a feasible tool for use in vineyards to effectively promote plant growth and protection (Figure 1).

Most studies of PGPRs in viticulture are focused on the initial stages of crop development in specific vine cultivars. Additionally, few studies testing strains at a field scale can be found (Table 5). Under *in vitro* and/or greenhouse conditions, Muganu et al. (2015); Köse et al. (2015), and Velásquez et al. (2020a) noted a wide variety of PGPR strains (*Ensifer, Burkholderia, Pseudomonas*, and *Bacillus*) were able to promote growth and root callusing percentage in four different *V. vinifera* cultivars: 'Beyaz Çavus', 'Italia', 'Cabernet Sauvignon', and 'Chardonnay'. Köse et al. (2003) observed *Bacillus* strains BAI6 and OSU142 increased rooting in 41B (a hardy cross between old-word *V. vinifera* and new-world *V. berlandieri*) rootstocks. Similarly, Sabir (2013) and Sabir et al. (2017) applied *P. putida* BA-8 and B. simplex T7 to 41B hybrids and recorded a promotion of graft callusing, scion shoot growth, nursery survival rate, and fruitfulness. Salomon et al. (2016) tested a combination of strains *B. licheniformis* and *P. fluorescens* in order to improve the growth of *V. vinifera* cultivar 'Malbec' in greenhouse conditions. Also in a greenhouse, the cytokinin and auxin-producing *B. megaterium* M3 was applied in combination with *Agrobacterium rubi* A18 and *Alcaligenes eutrophus* Ca-639 to *V. vinifera*, grafted onto 41 rootstocks. Growth enhancement and increased grapevine pruning residue weight were noted (Salomon et al., 2017).

In a rare field-scale experiment, Rolli et al. (2017) applied several bacteria from the genera *Paenibacillus, Pseudomona, Bacillus, Delftia*, and *Achromobacter*, to *V. vinifera* cultivars 'Syrah' and 'Sauvignon'. Increased plant growth, number of grape brunches, and grape production were recorded. Veliksar et al. (2017) applied strains of *Azotobacter*, *Pseudomonas*, and *Bacillus* to two *V. vinifera cultivars* in Moldova, and observed improved photosynthetic activity, as well as reduced mineral fertilizer requirements. Erdogan et al. (2018) achieved similar improvements with combinations of a wide range of PGPR strains in grafted rootstocks of *V. berlandieri* and *V. riparia* in Turkey. In China, Lu et al. (2020) observed enhanced growth and final grape quality, following the application of *P. putida* Rs-198 to a perennial variety.

In addition to general growth and quality enhancement, inoculation with PGPRs may also induce grape tolerance against biotic and abiotic stresses. For example, the application of phosphate-solubilizing bacteria isolated from the *Vitis* rhizosphere resulted in improved plant development when grown in saline-alkaline soils (Liu et al., 2016). Salomon et al. (2014) observed both drought alleviation and production of defense compounds in the grape cultivar 'Malbec'. Barka et al. (2006) found that *Burkholderia phytofirmans* PsJN could effectively protect Chardonnay grapes against cold stress.

Other studies focus on using PGPR strains to alleviate heavy metal stress. Funes-Pinter et al. (2018) identified *B. licheniformis, Micrococcus luteus*, and *P. fluorescens* as effective species for elevating growth and fruit yield in plants when grown in the presence of arsenic (As III). Veliksar et al. (2019) used strains of *Agrobacterium radiobacter, P. putida*, and *B. subtilis* to increase resistance against high soil concentrations of copper, and reduce the amount of mineral fertilizer needed.

Microorganisms may also be used as biocontrol agents against fungal pathogens in vineyard soils. For example, several studies have applied bacterial strains in order to protect vineyards from the common vine pest grey mold (*Botrytis cinerea*). Miotto-Vilanova et al. (2016) and Verhagen et al. (2010) found that several strains belonging to he *Pseudomonas*, *Burkholderia*, *Microbacterium*, *Kocuria*, and *Terribacillus* genera harbored plant growth and phytopathogen-control traits against *B. cinerea*. Andreolli et al. (2016) and Rezgui et al. (2016) also tested strains of *P. protegens* and *B. subtilis* against fungal pathogens, with the latter obtaining good results in field trial conditions. These studies show that a vast myriad of bacterial-borne traits can be effective for biocontrol, including the production of antibiotics, terpenes, pigments, and proteases, as well as inducing resistance against biotic stresses. As an indication of the high potential for PGPRs to combat plant biological stress, Asghari et al. (2020) applied *Pseudomonas* and

TABLE 5 An overview of the main effects of plant-growth-promoting rhizobacteria (PGPR) applied in viticulture.

Crop variety	PGPR strains	Properties	Application and dosage	Experimental condition	Effects	Reference
Vitis vinifera L. cv. Cabernet Sauvignon.	*Bacillus aryabhattai* JY17. *Bacillus aryabhattai*JY22.	Phosphate solubilization.IAA.Siderophore.ACC deaminase.Chitinase.HCN (JY22).	Inoculation with 50 mL (10^8 CFU mL^{-1}) into the middle part of the seedling roots.	Greenhouse, transplanted after 3-4 leaves had grown on the seedlings, 28 L pots.	Increased plant height, stem thickness, root and shoot dry weight.	Liu et al. (2016).
Vitis berlandieri hybrids (41B and 1103P).	*Pseudomonas putida* BA-8. *Bacillus simplex* T7.	Cytokinin synthesizer. Auxin synthesizer.	Scion node dipped into bacterial suspension (10^9 CFU mL^{-1}) for 1h.	Controlled greenhouse, and rootstocks.	Increased graft callusing, scion shoot growth, cane hardening, and nursery survival rate and fruitfulness	Sabir (2013).
Vitis vinifera L. (Malvasia bianca lunga).	*Burkholderia* spp. strain IF25.	Biostimulation.Phosphate solubilization.Siderophores.IAA production.	Bi-nodal shoots dipped into 50 µL of bacterial inoculum.	*In vitro.*	Induced advanced rooting and high rooting percentage.	Muganu et al. (2015).
Vitis vinifera cv. Beyaz Çavus and Italia.	*Pseudomonas* BA8. *Bacillus* BA16. *Bacillus* OSU142.	Auxin production.	Rootstocks dipped into bacterial suspension (10^9 CFU mL^{-1}).	*In vitro.*	Increased success and improvement of callusing rate, callusing degree, and full callusing rate in all rootstock-scion combinations.	Köse et al. (2015).
Vitis vinifera cv. Cabernet Sauvignon	*Ensifer meliloti* TSA41.	Phosphate solubilization.Phytase.IAA production.	Plants inoculated at sowing with 10^6 CFU g^{-1}.	*In vitro.*	Enhancement of plant growth.	Velásquez et al. (2020a).
Vitis rupestris and 41B (*Vitis vinifera* x *Vitis berlandieri*).	*Bacillus* BAI6. *Bacillus* OSU142.	Plant-growth promotion.	Rootstocks dipped in bacterial solution (10^9 CFU mL^{-1}).	Mist chamber.	The two strains combined increased rooting in 41B.	Köse et al. (2003).
Vitis vinifera cv. Malbec.	*Pseudomonas fluorescens.* *Bacillus licheniformis.*	Enhancement of growth.Decrease of water loss rate by increasing ABA concentrations in leaves, inducing systemic responses.	Cuttings were submerged in bacterial suspension (10^6 CFU mL^{-1}).	Greenhouse.	Growth improvement and increased defense mechanisms to cope with biotic and abiotic stresses.	Salomon et al. (2016).
Vitis berlandieri hybrids (41B and 1103P).	*Bacillus licheniformis* Rt4M10. *Pseudomonas fluorescens* Rt6M10.	Production of phytohormones.	Emerging roots of 15 days-old *in vitro* plants into bacterial culture (10^6 CFU mL^{-1}).	*In vitro.* Greenhouse.	Increased shoot and root length, and leaf area. Induction of terpenes and ABA synthesis. Alleviation of drought and production of defense compounds.	Salomon et al. (2014).
Vitis vinifera L. cv. Alphonse	*Bacillus megaterium* M3.	Auxin and cytokinin producing.N-fixing.$Ca(HCO_3)_2$ solubilizing.	Watering the plants with bacterial	Soilless growth system under	Enhanced shoot thickness and pruning residue	Sabir et al. (2017)

(Continued)

TABLE 5 Continued

Crop variety	PGPR strains	Properties	Application and dosage	Experimental condition	Effects	Reference
Lavallée) plants grafted on 41 (*V. vinifera* cv. Chasselas ×*V. berlandieri*) rootstock.	*Agrobacterium rubi* A18.	Auxin and cytokinin producing.$Ca(HCO_3)_2$ solubilizing.	solutions (10^9 CFU mL^{-1}) one week after bud break.	controlled glasshouse conditions.	weight of grapevines.	
	Alcaligenes eutrophus Ca-637.	Auxin producing.$Ca(HCO_3)_2$ solubilizing.				
Vitis champini (Ramsey).	Lactic acid bacteria: *Lactobacillus fermentum, L. Indolebutyric plantarum, L. Rhamnous, L. Delbrueckii.*	Plant-growth promotion.	EM•A (EM AGRITON) was applied to cuttings with different methods at different times and doses.	Greenhouse.	Increased rooting.	İşçı et al. (2019).
	Yeast: *Saccharomyces cerevisiae.*					
	Phototrophic bacteria: *Rhodopseudomonas palustrisBacillus subtilis.*					
Vitis vinifera L. cv. Chardonnay.	*Burkholderia phytofirmans* strain PsJN.	Endophyte.Enhancement of chilling resistance.	Nodal explants, immersed in the inoculum (10^6 CFU mL^{-1}).	Growth chamber.	Stimulation of growth and improvement of resistance to cold stress.	Barka et al. (2006).
Vitis vinifera L. cv. Malbec.	*Bacillus licheniformis.*	Plant-growth promotion.Protection against As(III).	Stem-base inoculation with 50 mL of bacterial suspensions (10^6 CFU mL^{-1}).	Greenhouse, two-year-old plant sprouts, 10 L pots, 50 mM $NaAsO_2$.	Stimulated growth and fruit yield, reducing AsIII toxicity indicators.	Funes-Pinter et al. (2018).
	Micrococcus luteus					
	Pseudomonas fluorescens.					
Vitis vinifera L. cv Victoria/ *Vitis vinifera* L. cv Viorica.	*Agrobacterium radiobacter.*	Plant-growth promotion.Protection against Cu.	Bacterial suspensions were applied into the soil during the planting of rooted cuttings (10^7CFU mL^{-1}).	Growing platform.	Enhancement of the resistance of grape seedlings to Cu excess in soil.Decreased need for mineral fertilizer.	Veliksar et al. (2019).
	Pseudomonas putida X.					
	Bacillus subtilis L.		Foliar fertilization.			
Vitis vinifera cv. Syrah*Vitis vinifera* cv. Sauvignon.	*Paenibacillus illinoisensis.*	IAA production.ACC deaminase.Phosphate solubilization.Nitrogen fixation.	The bacterial suspension (10^8 CFU mL^{-1}) was applied by root soaking and irrigation.	Field experiment. One-year-old Syrah plantlets were grafted onto 1103P rootstock, one-year-old Sauvignon plantlets grafted on SO4 rootstock, and 17-year-old Syrah plants grafted onto Fercal rootstock.	Increased plant growth, number of grape brunches, and grape production.	Rolli et al. (2017).
	Pseudomonas putida.	IAA.ACC deaminase.P solubilization.Siderophores.Ammonia production.				
	Bacillus subtilis.	ACC deaminase.Exopolysaccharides.Siderophores.N fixation.Protease synthesis.				
	Delfia tsuruhatensis.	IAA.ACC deaminase.P solubilization.Exopolysaccharides.				
	Pseudomonas fluorescens.	IAA.ACC deaminase.P solubilization.Siderophores.N fixation.				
	Pseudomonas rhodesiae.	IAA.ACC deaminase.P solubilization.Siderophores.				
	Achromobacter xylosoxidans.	ACC deaminase.Siderophores.				

(Continued)

TABLE 5 Continued

Crop variety	PGPR strains	Properties	Application and dosage	Experimental condition	Effects	Reference
Vitis vinifera cv. Codrinskii/ *Vitis vinifera* cv. Presentable.	*Azotobacter chroococcum.*	Plant-growth promotion.	Inoculation of rooted cuttings in 11L Plastic pots (10^7 CFU mL^{-1})	Growing platform.	Decreased need for mineral fertilizer and improvement of photosynthetic activity and plant growth.	Veliksar et al. (2017).
	Bacillus subtilis. *Pseudomonas fluorescens.*		Spray with bacterial metabolites.	Vine nursery.		
Italian grape species grafted on 5BB rootstock (*Vitis berlandieri*×*V. riparia*).	*Bacillus megaterium* RC07. *Pseudomonas putida* RC06. *Bacillus subtilis* RC11. *Pseudomonas putida* FA19d. *Pseudomonas fluorescens* RC77. *Bacillus subtilis* RC63. *Serratia marcescens* K2f.	Plant-growth promotion.	Inoculation of seedlings(10^8 CFU mL^{-1}).	Field trial.	Triple inoculation and single inoculation improved plant-growth parameters.	Erdogan et al. (2018).
Vitis vinifera (Red Globe).	*Pseudomonas putida* Rs-198.	Plant-growth promotion.	Bacterial suspension (1.8 10^{13} CFU mL^{-1}) at different doses. Application at dich around (close to 10 cm from each stem) old plants.	Field experiments. Old plants. One-season field experiment in the perennial vine.	Promoted alkaline phosphatase and invertase activity, increased the amount of available phosphorus and enhanced the growth and quality of the grape.	Lu et al. (2020).
Rootstock Kober 5BB clone ISV1 (*Vitis berlandieri* x *Vitis riparia*).	*Pseudomonas protegens* MP12.	IAA.Phosphate solubilization.ACC Deaminase.Ammonia production.	Bacterial suspension (10^8 CFU mL^{-1}).	*In vitro.*	Biocontrol agent and *in vitro* antimicrobial activity against several fungal pathogens.	Andreolli et al. (2016).
Vitis vinifera cv. Chardonnay.	*Burkholderia phytofirmans* PsJN.	Endophyte.Induction of plant resistance to biotic and abiotic stress.	Spray bacterial suspension (10^6 CFU mL^{-1}) on 4-week-old grapevine leaves of plantlets.	*In vitro*-plantlets, growth chamber.	Protection against *Botrytis cinerea.*	Miotto-Vilanova et al. (2016).
Vitis vinifera cv. Malbec.	*Microbacterium imperiale* Rz19M10. *Kocuria erythromyxa* Rt5M10. *Terribacillus saccharophilus* Rt17M10.	Stimulation of the synthesis of terpenes.	0.25 mL of Bacterial inoculum (10^6 CFU mL^{-1}).	*In vitro.*	Reduction of lesion diameter provoked by *Botrytis cinerea*, systemic response induction, and increased terpene production.	Salomon et al. (2016).

(Continued)

TABLE 5 Continued

Crop variety	PGPR strains	Properties	Application and dosage	Experimental condition	Effects	Reference
Vitis vinifera cv. Chardonnay 7535.	*Pseudomonas fluorescens* CHA0. *Pseudomonas aeruginosa* 7NSK2.	Induction of systemic resistance2;4-diacetylphloroglucinol.Pyoluteorin.Pyrrolnitrin.AprA, exoprotease.HCN. Induction of systemic resistance.Pyoverdin.Pyochelin.Pyocyanin.Salicylic acid.	Dipping the root system in a 20 mL bacterial suspension (10^7 CFU mL^{-1}).	*In vitro*, four-week-old grapevine plantlets.	Induced resistance in grapevine against *Botrytis cinerea*.	Verhagen et al. (2010).
Vitis vinifera cv. Muscat d'Italie.	*Bacillus subtilis* B6.	Antibiotic production.	Bacterial suspension (10^8 –10^9 CFU mL^{-1}) application in stem cutting.	*In vitro* and vineyard.	Protection against Grapevine Trunk Diseases (GTDs) and fungi antagonists.	Rezgui et al. (2016).
Vitis vinifera 'Chardonnay' (clone 7535).	*Pseudomonas* sp. Sn48. *Pantoea* sp. Sa14.	Endophytic.Reduced gall formation by *Agrobacterium tumefaciens*.	Root dipping in bacterial suspensions (10^8 CFU mL^{-1}) for 1–2 min.	*In vitro* and growth chamber.	Induction of defenses against *Agrobacterium tumefaciens*.	Asghari et al. (2020).

Pantoea sp. and noted lowered gall formation produced by *Agrobacterium tumefaciens*.

As shown above, PGPRs have so far primarily been researched *in vitro*, and in greenhouse trials. Few studies exist at the field scale and any practical yield benefit from these microorganisms has yet to be quantified (Bashan et al., 2014). Other optimizations must be performed before any selected consortia can be developed into commercial products. The survivability and persistence of the applied strains must be quantified not only in the soil along with any competitive/negative effects from the native rhizosphere microbiome but also in stable storage conditions. European legislation restricting the application of chemical substances to crops has been passed relatively recently (Regulation EC 1107 (2009). It is therefore alarming that only a single reviewed study concerned the development of commercial bioinoculants; İşçı et al. (2009) applied consortium EM·A (comprised of lactic acid, phototropic bacteria, and yeasts; EM AGRITON Ltd., Belgium) to *V. champini*, and recorded improved rooting.

Mycorrhizae

More than 400 MYA, the presence of mycorrhiza in soil was essential for the colonization of terrestrial environments by plants due to their ability to provide stress tolerance and soil resources *via* symbiosis (Heckman et al., 2001). This adaptation continues in the majority of plants on Earth, including grapevines (Trouvelot et al., 2015). Roots of grapevines form a particular type of mycorrhizal symbiosis called arbuscular mycorrhizae, characterized by the penetration and internal colonization of plant root cells by fungal hyphae (Trouvelot et al., 2015). Arbuscules form within the plant roots and serve as the exchange site for various metabolites (Trouvelot et al., 2015). Arbuscular mycorrhizal fungi (AMF) are widely known for being able to enhance the uptake of P in the host roots, a nutrient that is typically limiting in cropping systems like vineyards (Smith et al., 2011; Van Geel et al., 2017). However, they also provide increased plant uptake of N and other limiting elements including trace metals Fe, Mn, Cu, and Zn (Clark and Zeto, 2000), which are also critical to plant health (Figure 1). This is accomplished by greatly extending the root system's exploration and exploitation area (Smith and Read, 2008; Trouvelot et al., 2015), simultaneously increasing plant access to water sources that would be otherwise inaccessible (Al-Karaki and Clark, 1998). This feature may be particularly advantageous in rain-fed vineyards growing in nutrient-poor soils, which are widespread in most traditionally wine-producing regions such as the Mediterranean, Middle East, and Caucasian regions (Table 6).

In addition to their role in plant water and nutrient uptake, AMF contributes to the biosynthesis of a wide range of molecules such as vitamins and hormones needed to support the metabolism and health of plants (Strzelczyk et al., 1991), although this is poorly investigated in the context of vineyards. Arbuscular mycorrhizal fungi can also protect grapevines against harmful pathogens and pests, including the root-knot forming nematode *Meloidogyne incognita*, through the induction of a defense response involving enzymes like chitinases (Li et al., 2006). Moreover, AMF contributes to the development of a healthy rhizosphere community (i.e., a microbially diverse community that is functionally linked to the plant), which in turn may confer tolerance/resistance against a range of biotic and abiotic stresses (reviewed above), including heat, drought, salinity, pathogenic infection, and pests (Fitter

TABLE 6 An overview of the main effects of mycorrhizal inoculants applied in viticulture.

Crop variety	Applied material and properties	Dosage, the form of application, and stage of plant development	Experimental condition	Effects	Reference
Vitis vinifera cv. Pinot noir.	Mixed inoculum of 3 AMF isolated from a vineyard and recultured with *Sorghum bicolor*: *Scutellospora calospora* INVAM# OR219, *G. mosseae* INVAM# OR218, and *Glomus* sp. INVAM#215.	A mixture of soil with AM fungal spores, hyphae, and colonized root fragments. 20 g of inoculum plant^{-1}.	Potted plants in a greenhouse.	Vine growth was dependent on AMF in one soil, but inoculated and non-inoculated vines grew equally well in another soil. Increase in plant dry mass with AMF due to enhanced P uptake (833% increase). The uptake of most other nutrients was also enhanced by AMF in the first soil.	Schreiner (2007).
Vitis vinifera cv. Pusa Navrang.	Six single strains and a mixture of AMF (*G. manihotis*, *Glomus mosseae*, and *G. gigantean*) recultured with *Chloris guyana*: *Acaulospora laevis*, *A. scrobiculata*, *Entrophospora colombiana*, *Gigaspora gigantea*, *Glomus manihotis*, and *Scutellospora heterogama*.	A mixture of soil with AM fungal spores, hyphae, and colonized root fragments. 20 g of inoculum plant^{-1}.	Micropropagated plantlets in a greenhouse.	Enhanced survival and improved tolerance against stresses. Improved physiological and nutritional status and higher relative water content and photosynthetic rate. Higher concentrations of N, P, Mg, and Fe. Better hardening.	Krishna et al. (2005).
Vitis vinifera cv. Tempranillo.	GLOMYGEL Vid, Olivo, Frutales (Mycovitro S.L., Pinos Puente, Spain): Culture of AMF *Rhizophagus intraradices*.	8 mL of diluted mycorrhizal inoculum plant^{-1} (equivalent to 2000 propagules).	Cuttings are planted in 6.5-L plastic pots.	AMF inoculation improved parameters linked to phenolic maturity such as anthocyanin content and increased antioxidant activity under elevated temperature.	Torres et al. (2016).
Vitis vinifera cv. Sangiovese.	*Funneliformis mosseae* IMA1.	A mixture of soil with AM fungal spores, hyphae, and colonized root fragments and autoclaved peat in a proportion of 1:4 v/v + 2 mL of *F. mosseae* IMA1 inoculum filtrate.	Explants were cultivated in 150 mL sanitized pots.	Greater emission of volatiles related to plant defense and water stress.	Velásquez et al. (2020b).
Vitis vinifera cv. Viosinho.	*Funneliformis mosseae* inoculum (isolate BEG95, Symbiom®, Czech Republic).	10 g of inoculum plant^{-1} buried in ditches and mixed with soil and rye seeds.	Field experiment.	Greater establishment of new mycorrhizal taxa in vine roots. Greater photosynthetic efficiency after a heat wave. Compensation for water competition with cover crops.	Nogales et al. (2021).
Vitis vinifera cv. Cabernet Sauvignon.	Commercial inoculum Mykoflor (Mykoflor, Polland).	20 mL of suspension under the vine roots (~2000 propagules).	Field experiment.	Improved leaf gas exchange.Higher yield and number of clusters. Greater polyphenols and anthocyanins.	Karoglan et al. (2021).

and Garbaye, 1994; Gryndler, 2000; Jeffries et al., 2003; Gupta et al., 2018). Given their importance in vine nutrition and pathogen response, AMF are a critical pillar of healthy, functioning vineyards (Trouvelot et al., 2015), especially in the current context of widespread environmental degradation and climate change. In addition to direct benefits to plant health, mycorrhizae may also provide important ecosystem services, including increasing potential carbon sequestration of vineyard soils and reducing erosion (Trouvelot et al., 2015).

Despite these benefits, mycorrhizal symbiosis is frequently disrupted in croplands due to intensive management, including excessive tilling, which breaks the orderly structure of soil aggregates and fungal networks (Gosling et al., 2006; Bowles et al., 2017; Porter and Sachs, 2020), although this has been poorly investigated in vineyards (Winter et al., 2018). Biocides can also negatively affect mycorrhizal fungi, with deleterious consequences on the establishment of symbiosis (Gosling et al., 2006; Zaller et al., 2018), while synthetic fertilizers disrupt the mycorrhizal association due to the ablation of nutritional constraints, such as N and P (Gosling et al., 2006; Van Geel et al., 2017). Regenerating proper vine-mycorrhizal balance and function in degraded vineyards is thus a priority, which may yield many benefits to both growers and the wider society.

Regeneration of the vine-AMF interaction can take place through various means, which should be considered holistically in terms of impact on total vineyard management. One such strategy is the inoculation of grapevines with one or more strains of mycorrhizal fungi previously selected for their ability to colonize vine roots (Linderman and Davis, 2001; Trouvelot et al., 2015). One aspect in which inoculation with mycorrhizal biostimulants might be particularly important is to minimize the growing threat of trunk diseases (Petit and Gubler, 2006; Holland et al., 2019), which may be linked to widespread alteration of plant-microbial associations. It has been recently suggested that declines observed in woody plants are related to microbiome modifications or imbalances (i.e., dysbiosis) (Porter and Sachs, 2020). Arbuscular mycorrhizal fungi known to help re-establish symbiosis include various strains of *Glomus intraradices*, such as *G. intraradices* BEG72 (Nogales et al., 2008) and INVAM CA501 (Petit and Gubler, 2006).

Proper timing may be critical when inoculating plants with mycorrhizal biostimulants (Sohn et al., 2003), but there is little information for vineyards. It is suggested that rootstocks be submerged in an AMF spore solution before planting, but variable success is reported. For example, a study was carried out on *Vitis rupestris* cv. St. George using *G. intraradices* and reported that pre-inoculated plants were less susceptible to black foot disease (Petit and Gubler, 2006), while (Holland et al., 2019) observed no difference between inoculated and uninoculated plants. Some studies have also reported clear effects in the greenhouse, but not under realistic field conditions (Rosa et al., 2020). Other ways to add AMF to vineyards include the direct spraying of commercial biofertilizers on adult plants, through the addition of granules containing spores, and potentially also the translocation of whole soil inoculants from previously selected locations particularly diverse in terms of AMF such as forests. This latter approach is underexplored in vineyards. Perhaps contributing to variability in inoculation success is the difficulty in altering the pre-established microbiome of adult plants. Moreover, the mixed positive and neutral effects of inoculating vines with AMF, together with the fact that some (but not all) mycorrhizal fungi show a certain degree of host specificity (Campos et al., 2018), suggest the importance of screening AMF strains against potential compatible host vine cultivars/rootstocks prior to inoculum development (Schreiner, 2007). Finally, the vine-AMF symbiosis is context dependent and may be linked to factors critical for productive vineyards including soil fertility and other properties (e.g., soil organic matter content, pH, and texture) (Trouvelot et al., 2015). For example, the presence of a well-developed community of cover crops in vineyard inter-rows may favor inoculated AMF establishment, by providing an additional host crop and continuous reservoir for supplying adjacent grapevines (Winter et al., 2018).

Biological control agents

Climate change simulations predict that the fitness of crop insect pests will increase beyond 30° latitude North and South of the equator (Santos et al., 2020). Indeed, a three-decade study observed shifts in the phenology of grape berry moths (*Eupoecilia ambiguella*, *E. viteana*, and *Lobesia botrana*), distribution ranges of leafhoppers (*Scaphoideus titanus* Ball, a common vector of grapevine diseases), and range expansion of grapevine mealybugs (*Planococcus ficus*) (Reineke and Thiéry, 2016).

The effective control of crop pests is a continuous process. For native and newly introduced pests, the adoption of novel biological control agents (BCAs) is needed for sustainable alternative pest management (Figure 1). BCAs are living organisms antagonistic against pests. By definition, biological control must involve: 1) a biocontrol agent, 2) a pest to be controlled, and 3) a farmer or a stakeholder benefitting from the pest control (Stenberg et al., 2021). Organisms such as insects or mites, bacteria, fungi, and nematodes are used to control weeds or pests and diseases of cultivated plants (Ehlers, 2011). Viruses are not living entities, but contain structural biological components such as nucleic acids and proteins and are therefore also considered BCAs (Stenberg et al., 2021). Semiochemicals (chemical molecules produced by organisms that modify the behavior of other living beings, i.e., bio-communication) and plant extracts that can act directly on a pathogen or pest are other options for BCAs (Ehlers, 2011). Biological control is an interaction between at least two organisms, and success is therefore influenced by many factors including climate, reproduction mode and rate, food availability, and others. Holistically considering the total impact of all dynamic factors together when designing a balanced pest management plan is referred to as integrated pest management (IPM). BCAs are a main component of IPM, and together, are becoming increasingly utilized in agriculture.

Biocontrol agents may be naturally present in the agroecosystem (e.g. a native population of soil microbes antagonistic to plant-parasitic nematodes), or first grown *in vitro* and then released (Sharma et al., 2009; Stenberg et al., 2021). Grapevine is a perennial crop and harbors a large microbiome in both the rhizosphere and stem tissues. Additional microorganisms which act to balance the microbiota are also found in the phyllosphere and fructosphere (Ranade et al., 2021). Many of these microorganisms act as BCAs and are a promising ecological strategy for disease control (Carro-Huerga et al., 2021).

The cropping system (e.g. conventional vs. organic farming) also influences the potential number of biocontrol agents which may be isolated for application. Cordero-Bueso et al. (2017) evaluated the biocontrol potential of 230 grape yeast isolates from different cultivation systems. The fractions with the most candidates were isolated from wild vines (62.7%) and biodynamic vineyards (17.7%). The least number of candidates were isolated from organic (6.2%) and conventional systems (7.2%). Wild vine species may therefore serve as a valuable resource for bioprospecting future BCAs. Additional potential sources of candidates include other plants, insects, animal intestinal tracts, soils, and marine and freshwater environments (Kurtzman et al., 2011).

BCAs can have several mechanisms of action against pathogens. During resource limitation, BCAs may outcompete detrimental microbes in terms of space (niches), nutrients, water, and/or light (Wang et al., 2018; Almeida et al., 2020). Other mechanisms include iron depletion (Sipiczki, 2006; Cordero-Bueso et al., 2017); production of lytic enzymes (Cordero-Bueso et al., 2017; Cabañas et al., 2020); production of volatile organic and semio-compounds antagonistic against pests (Cabañas et al., 2020; Don et al., 2021); resistance induction of the host plant (Arras, 1996; Jeandet et al., 2002; Maachia et al.,

2015; Haidar et al., 2016); direct parasitism; tolerance of reactive oxygen species (ROS) (Aziz et al., 2003; Jamalizadeh et al., 2011); biofilm formation (Cabañas et al., 2020); synthesis of pathogenesis-related proteins (Chan and Tian, 2006); and antibiotic production (Maachia et al., 2015; Cordero-Bueso et al., 2017).

Production of extracellular mucilage produced by microbial antagonists throughout host cells may be linked to cell adhesion, and contain biochemical elicitors to signal defense responses (El-Ghaouth et al., 1998). Fragments of yeast cell wall oligosaccharides have also been noted to possess elicitor potential.

In viticulture, most BCAs are applied to control fungal diseases and pests associated with insect and mite vectors. However, other biological controls have also been researched and suggested for other pests. For example, harmful mollusks (snails) in vineyards in cool and wet climates may be effectively controlled by the nematode *Phasmarhabditis hermaphrodite* (Schneider), as there are restrictions on the use of synthetic molluscicides (Egleton et al., 2021). BCAs are also being developed for the control of weed species prevalent in vineyards (Samad et al., 2017).

In a grapevine host, antibiosis and resistance induction were observed, attributed to the antagonism of *Bacillus subtilis* B29 against *Uncinula necator* (powdery mildew) and *Botrytis cinerea* (grey mold) (Maachia et al., 2015). An n-hexane extraction of the cell-free supernatant of *B. subtilis* B29 revealed the presence of 17 fractions through HPLC. Two fractions were considered antibiotics against *M. ramannianus* and *M. luteus*, based on their antimicrobial activity (Sihem et al., 2011). *B. subtilis* B29 and B27 have also been described as inducing host resistance through the high production of phenolic compounds, with a significant increase in hydroxycinnamic acid (Maachia et al., 2015).

Antagonism against pests alone does not necessarily make an organism a BCA. The applied fungi, yeasts, and bacteria must possess other characteristics to allow for practical use in the field. For example, a BCA with greater adaptability than the pest may allow for widespread niche colonization and higher competitive potential (El-Ghaouth et al., 2004). Additionally, prior to application, the BCA candidate should be extensively screened for the production of metabolites harmful to non-pest organisms, especially humans. In the specific case of biological control of molds on grapes following harvest, the BCA should not leave residue on the berries. After identifying the mechanism of antagonism, and confirming BCA adaptability and safety, appropriate tests following the guidelines of national regulatory bodies must be conducted before registration as a commercial inoculant.

The use of BCAs in agriculture began in the second half of the 20th century, and several candidates have been identified. Although many researchers have since evaluated their pest control potential, few inoculants reach commercialization. *Bacillus subtilis* is one of the most widely applied fungicidal BCAs (Garrido and Botton, 2020). During the 2020/2021 harvest in Brazil, 182 commercial brands of synthetic fungicides were available for application to vineyards, compared to 28 biological fungicides (Table 7). Only two genera were represented, *Bacillus* and *Paecilomyces*, with a predominance of *Bacillus* (mostly *B. subtilis*). Other species of *Bacillus* were *B. amyloliquefaciens*; *B. licheniformis*; *B. methylotrophicus*; and *B. pumilus*. *Paecilomyces lilacinus* has been cited as an active ingredient in seven commercial brands. Most are composed of a single species and strain.

Esca is caused by the association of the fungi *Phaeoacremonium minimum* and *Phaeomoniella chlamydospore* and is one of the main Grapevine trunk diseases (GTDs). Control of Esca is achieved mainly through BCAs, in which common biological agents are *Trichoderma* fungi (Chervin et al., 2022). *Trichoderma* atroviride-based products (CS1 by Vintec® - Belchim Crop Production and I-1237 by Esquive® - Agrauxine by Lesaffre) are often effective because they have multiple mechanisms of action: substrate competition, antibiosis, and mycoparasitism (Pertot et al., 2015; Belchim, 2022). For the control of powdery mildew (*Uncinula necator*), AQ10® (*Ampelomyces quisqualis*) is used commercially (Benuzzi and Baldoni, 2000). Another biologically-controlled disease is downy mildew (*Plasmopara viticola*). *Trichoderma harzianum* (known as Trichodex®), acts against the oomycete by increasing lignin, callose, and hydrogen peroxide, in addition to upregulating the defense enzymes phenylalanine ammonia-lyase, peroxidase, and 1,3-glucanase (Kamble et al., 2021).

The choice of BCA is of paramount importance. Simultaneous with disease control, some BCAs can influence grape productivity and quality with variable effects on acidity, soluble solids content, and berry size. Malviya et al. (2022) cite significant differences in the acidity of vine fruits treated with three BCAs ranging from 3.7 to 4.2 and 4° Brix in the SST. Production per plant doubled when treated with BCAs and almost tripled when combined with BCA + sulfur.

As for insecticides and acaricides, 55 synthetic products and 38 biological commercial products have been authorized for grapevines. Twenty-six contain *Beauveria bassiana* as an active ingredient and three with *B. thuringiensis*. For the control of insects and mites, recommendations for predatory insects (one *Orius insidiosus* and one sterile male pupil of *Ceratitis capitata*), predatory mites (four *Neoselulus californicus* and two *Phytoselulus macropilis* with AcMNPV virus), and one viral compound (AcMNPV virus, ChinNPV Virus, HearNPV Virus, SfMNPV Virus) are available.

Many antagonists with BCA potential are studied with increasingly efficient and cost-effective techniques. In addition to bioprospecting for biopesticides, valuable antibiotics may also be obtained from these organisms. Decreased BCA production costs and improved management techniques that increase and prolong BCA effects will allow for scaling their use in viticulture. Thus, biological products with multiple benefits (controlling

TABLE 7 Principal biological control agents (BCAs) applied in viticulture in Brazil.

Trade (and company) names	BCA	Concentration	Dosage	Target pathogens	Application
NO-NEMA® (Biovalens Biotecnologia)	*Bacillus amyloliquefaciens*	42 (3 x10^9 UFC mL^{-1})	0.5 - 4.0 L ha^{-1}	Nematodes (several species)	Soil/Seed
DURÁVEL® (BASF)	*Bacillus amyloliquefaciens MBI600*	110 (5.5 x 10^{10}UFC g^{-1})	0.5 - 1.0 kg ha^{-1}	*Botrytis cinerea*	Soil/Aerial
ECO-SHOT® (IHARA)	*Bacillus amyloliquefaciens* cepa D-747	250 (5 x 10^{10} UFC g^{-1})	1.0 - 4.0 kg ha^{-1}	*Sclerotinia sclerotiorum, Colletotrichum gloeosporioides*	Foliar/fruit immersion
NEMA III	*Bacillus amyloliquefaciens*	42 (3 x10^9 UFC mL^{-1})	0.5 - 4.0 L ha^{-1}	Nematodes (several species)	Soil
NEMACONTROL® (Simbiose®)	*Bacillus amyloliquefaciens*	30 (5 x 10^9 UFC mL^{-1})	0.5 - 1.0 L ha^{-1}	*Pratylenchus brachyurus*	Seed
PFC-CONTROL	*Bacillus amyloliquefaciens*	30 (5 x 10^9 UFC mL^{-1})	0.5 - 1.0 L ha^{-1}	*Pratylenchus brachyurus*	Seed
QUARTZ SC	*Bacillus amyloliquefaciens*	1,5 (3 x 10^9 UFC mL^{-1})	1.0 - 2.0 L ha^{-1}	*Botrytis cinerea*	Soil
PROFIX® (Bula)	*Bacillus licheniformis, B. subtilis, Paecilomyces lilacinus*	200 + 200 + 200 (10^{10} UFC g^{-1})	50 - 70 g ha^{-1}	*Meloidogyne incognita, Pratylenchus brachyurus*	Soil/Seed
ONIX® (Lallemand)	*Bacillus methylotrophicus*	15 (10^9 UFC mL^{-1})	6.0 L ha^{-1}	*Meloidogyne javanica, Pratylenchus brachyurus*	Soil/Seed
ONIXog® (Lallemand)	*Bacillus methylotrophicus*	15 (10^9 UFC mL^{-1})	6.0 L ha^{-1}	*Meloidogyne javanica, Pratylenchus brachyurus*	Soil/Seed
SONATA® (Bayer CropScience)	*Bacillus pumilus* QST 2808	14.35 (10^9 UFC g^{-1})	2.0 - 4.0 L ha^{-1}	*Uncinula necator, Botrytis cinerea*	Aerial
BIO-IMUNE® (Vittia Grupo)	*Bacillus subtilis* BV02	42 (3 x10^9 UFC mL^{-1})	2.0 - 8.0 L ha^{-1}	*Uncinula necator*	Foliar
BIOBACI/BIOBACI III® (Biovalens Biotecnologia)	*Bacillus subtilis* BV09	7 (10^8 UFC g^{-1})	1.5 - 6.0 L ha^{-1}	*Meloidogyne* spp. *Fusarium oxysporum*	Soil
PRESENCE	*Bacillus subtilis* FMCH002, *Bacillus licheniformis* FMCH001	200 + 200 (10^{11} UFC g^{-1})	100 - 150 g 100 kg^{-1}	*Meloidogyne javanica, Pratylenchus brachyurus*	Seed
SERENADE® (Bayer CropScience)	*Bacillus subtilis* QST 713	13.68 (10^9 UFC g^{-1})	2.0 - 4.0 L ha^{-1}	*Botrytis cinerea, Colletotrichum gloeosporioides*	Soil/Aerial
RIZOS OG® (Lallemand Soluções Agrobiológicas Ltda)	*Bacillus subtilis* UFPDA 764	3 (3x10^9 UFC mL^{-1})	4.0 - 8.0 L ha^{-1}	*Meloidogyne javanica, Pratylenchus brachyurus*	Seed
BIOBAC® (Vital Brasil Chemical Indústria e Comércio de Produtos Químicos Ltda – ME)	*Bacillus subtilis* Y1336	500 (10^9 UFC g^{-1})	0.8 - 1.0 kg 100 L^{-1}	*Botrytis cinerea*	Aerial
QUATZO® (FMC Química do Brasil Ltda)	*Bacillus subtilis, Bacillus licheniformis*	200 + 200 (10^{11}UFC g^{-1})	130 - 300 g ha^{-1}	Nematodes (several species)	Soil
BN 40.001/19 (Ballagro)	*Paecilomyces lilacinus*	300 (7.5 x 10^9UFC g^{-1})	1.92 kg ha^{-1}	*Meloidogyne incognita*	Soil
MNG-02/14 (Agrobiológica Sustentabilidade)	*Paecilomyces lilacinus*	7 (10^5 UFC g^{-1})	1.0 - 4.0 kg ha^{-1}	*Meloidogyne incognita*	Soil
NEMAKILL® (Grupo Clínica Agrícola)	*Paecilomyces lilacinus*	7 (10^5 UFC g^{-1})	1.0 - 4.0 kg ha^{-1}	*Meloidogyne incognita*	Soil

(Continued)

TABLE 7 Continued

Trade (and company) names	BCA	Concentration	Dosage	Target pathogens	Application
NEMAT® (Agroindustrial Limsa)	*Paecilomyces lilacinus*	300 (7.5 x 10^9 UFC g^{-1})	0.1 - 0.25 kg ha^{-1}	*Meloidogyne incognita, Pratylenchus brachyurus*	Soil/Seed
NETTUS® (Ballagro Agro Tecnologia Ltda)	*Paecilomyces lilacinus*	300 (7.5 x 10^9 UFC g^{-1})	1.28 - 1.92 kg ha^{-1}	*Meloidogyne incognita*	Soil
Purpureonyd Fr25 (TZ Biotec)	*Paecilomyces lilacinus*	200(6.5 x 10^7 UFC g^{-1})	1 kg 15 ha^{-1}	*Meloidogyne incognita*	Soil/Aerial
VINTEC (Belchim Crop Production)	*Trichoderma atroviride*	1 x 10^{13} UFC g^{-1}	200 g. ha^{-1}	Esca, *Phaeomoniella chlamydospora*, *Togninia minima* (*Phaeoacremonium aleophilum*), *Eutypa lata, Botrytis fuckeliana, B. cinerea Fomitiporia mediterranea, Podosphaera xanthii, Armillaria mellea*, and *A. gallica*	Aerial (pulverization) or scion wood immersion

disease(s), promoting plant growth, and increasing grape quality) are compliant with the sustainable development objectives of the 2030 agenda of the United Nations (UN). The reduction of synthetic chemical inputs in this manner can simultaneously reduce contamination throughout the production chain and ecosystem.

Future studies should investigate other applications of BCAs, such as the use of parasitic nematodes (*Phasmarhabditis hermaphrodita*) or earthworms (*Lumbricidae*) for pest control against snails and slugs in vineyards.

Conclusions and future prospects for investigation

The application of biostimulants and BCAs may allow for improved sustainable viticulture and may serve as alternatives for chemically synthesized agronomic inputs, thereby reducing the negative environmental impact of pesticides and fungicides. The positive effects on plant growth are summarized in Figure 1 and vary widely depending on the type of biostimulant applied to the crop. The optimization of these materials is necessary for a successful application, by considering biostimulant concentration and dosage effects, plant developmental stage, climatic/environmental conditions, and experimental setup.

Therefore, the main limitations and areas for further investigation for future biostimulant and BCA optimization in sustainable viticulture are listed below:

A) Manufacturing and commercialization
- Harmonization of legislation and lack of regulations on product quality
- Competitive commercialization costs
- Availability of raw materials used for their manufacturing, especially the lack of quality material (i.e. heterogeneous composition)
- Storage and effectivity duration (especially for biological products)

B) Application
- Lack of information at field-scale, and very few reports on the application in uncontrolled realistic conditions with positive results
- Effect variability on the unknown plant microbiome
- Effect variability on plant growth, depending on product dosage (concentration and number of applications)
- Effect variability depending on the mode of product application (foliar spraying, or *via* soil irrigation/fertigation)
- Effect variability depending on the stage of crop development
- Speculation remains as to underlying mechanisms associated with the biostimulant
- Comparative studies with agrochemicals as control
- Synergetic effects with other products and potential negative effects
- Lack of standard protocols depending on grape cultivar

C) Environmental and practical issues
- Soil management
- Environmental and practical issues
- Soil management for effect optimization
- Integration with agronomical management (e.g. avoiding tillage for AMF)
- Short and long-term environmental impact (e.g. contamination of soil and watersheds)

Author contributions

KJ: Conceptualization, Methodology, Writing - Original Draft; TLG: Writing - Review and Editing; PP-T, MS-M, YA, AD-A, AW, MG, MS, CP, JB, RO-H, MN, JR, and RA: Writing - Original Draft; SM and MD: Funding acquisition; GT: Writing -

Original Draft, Writing - Review and Editing, Supervision and Funding acquisition. All authors approved the manuscript.

Funding

KJ wishes to acknowledge financial support (3710473400); MS-M thanks to RTI2018-099417-B-I00 (Spanish Ministry of Science, Innovation and Universities cofunded with EU FEDER funds); JB wish to acknowledge the Conselho Nacional de Desenvolvimento Científico e Tecnológico/Brasil (CNPQ process number 309477/2021-2); RO-H is supported by the Ramón y Cajal program from the MICINN (RYC-2017 22032), PAIDI 2020 (Ref. 20_00323), AEI GGOO 2020 (GOPC-CA-20-0001), "José Castillejo" program from the "Ministerio de Universidades" (CAS21/00125) and PID2019-106004RA-I00/AEI/10.13039/501100011033. SM and GT thanks to Ministerio de Ciencia e Innovación (grant PID2020-114330GB-100). PAIDI2020 from Junta de Andalucía, grant P18-RT-1401 to SM, MD, and GT is also acknowledged. GT acknowledge the support of the publication fee by the CSIC Open Access Publication Support Initiative through its Unit of Information Resources for Research (URICI).

Conflict of interest

Author YA was employed by Chitose Laboratory Corp.

The remaining authors declare that the research was conducted in the absence of any commercial or financial relationships that could be construed as a potential conflict of interest.

Publisher's note

References

Akhter, A., Hage-Ahmed, K., Soja, G., and Steinkellner, S. (2015). Compost and biochar alter mycorrhization, tomato root exudation, and development of *Fusarium oxysporum* f. sp. *lycopersici*. *Front. Plant Sci.* 6. doi: 10.3389/fpls.2015.00529

Al-Karaki, G. N., and Clark, R. B. (1998). Growth, mineral acquisition, and water use by mycorrhizal wheat grown under water stress. *J. Plant Nutr.* 21 (2), 263–276. doi: 10.1080/01904169809365401

Almeida, A. B. D., Concas, J., Campos, M. D., Materatski, P., Varanda, C., Patanita, M., et al. (2020). Endophytic fungi as potential biological control agents against grapevine trunk diseases in Alentejo region. *Biology* 9 (12), 420. doi: 10.3390/biology9120420

Amendola, C., Montagnoli, A., Terzaghi, M., Trupiano, D., Oliva, F., Baronti, S., et al. (2017). Short-term effects of biochar on grapevine fine root dynamics and arbuscular mycorrhizae production. *Agric. Ecosyst. Environ.* 239 236–245. doi: 10.1016/j.agee.2017.01.025

Andreolli, M., Lampis, S., Zapparoli, G., Angelini, E., and Vallini, G. (2016). Diversity of bacterial endophytes in 3 and 15 year-old grapevines of *Vitis vinifera* cv. corvina and their potential for plant growth promotion and phytopathogen control. *Microbiol. Res.* 183, 42–52. doi: 10.1016/j.micres.2015.11.009

Andrés, P., Rosell-Melé, A., Colomer-Ventura, F., Denef, K., Cotrufo, M. F., Riba, M., et al. (2019). Belowground biota responses to maize biochar addition to the soil of a Mediterranean vineyard. *Sci. Total Environ.* 660, 1522–1532. doi: 10.1016/j.scitotenv.2019.01.101

An, X., Wu, Z., Yu, J., Cravotto, G., Liu, X., Li, Q., et al. (2020). Copyrolysis of biomass, bentonite, and nutrients as a new strategy for the synthesis of improved biochar-based slow-release fertilizers. *ACS Sustain. Chem. Eng.* 8 (8), 3181–3190. doi: 10.1021/acssuschemeng.9b06483

Arioli, T., Mattner, S. W., Hepworth, G., McClintock, D., and McClinock, R. (2021). Effect of seaweed extract application on wine grape yield in Australia. *J. Appl. Phycol.* 33, 1883–1891. doi: 10.1007/s10811-021-02423-1

Arras, G. (1996). Mode of action of an isolate of *Candida famata* in biological control of *Penicillium digitatum* in orange fruits. *Postharvest Biol. Tec.* 8 (3), 191–198. doi: 10.1016/0925-5214(95)00071-2

Asghari, S., Harighi, B., Ashengroph, M., Clement, C., Aziz, A., Esmaeel, Q., et al. (2020). Induction of systemic resistance to *Agrobacterium tumefaciens* by endophytic bacteria in grapevine. *Plant Pathol.* 69 (5), 827–837. doi: 10.1111/ppa.13175

Aziz, A., Poinssot, B., Daire, X., Adrian, M., Bézier, A., Lambert, B., et al. (2003). Laminarin elicits defense responses in grapevine and induces protection against *Botrytis cinerea* and *Plasmopara viticola*. *Mol. Plant-Microbe Interact.* 16 (12), 1118–1128. doi: 10.1094/MPMI.2003.16.12.1118

Barka, E., Nowak, J., and Clément, C. (2006). Enhancement of chilling resistance of inoculated grapevine plantlets with a plant growth-promoting rhizobacterium, *Burkholderia phytofirmans* strain PsJN. *Appl. Environ. Microb.* 72 (11), 7246–7252. doi: 10.1128/AEM.01047-06

Baronti, S., Vaccari, F. P., Miglietta, F., Calzolari, C., Lugato, E., Orlandini, S., et al. (2014). Impact of biochar application on plant water relations in *Vitis vinifera* (L.). *Eur. J. Agron.* 53, 38–44. doi: 10.1016/j.eja.2013.11.003

Bashan, Y., de-Bashan, L. E., Prabhu, S. R., and Hernández, J. P. (2014). Advances in plant growth-promoting bacterial inoculant technology: Formulations and practical perspectives, (1998–2013). *Plant Soil* 378, 1–33. doi: 10.1007/s11104-013-1956-x

Belchim (2022) *Vintec: A natureza trabalhando por si.* Available at: https://belchim.pt/producten/vintec/ (Accessed July 30, 2022).

Benuzzi, M., and Baldoni, G. (2000). AQ 10, a new biofungicide based on *Ampelomyces quisqualis* for powdery mildew control on grapes. *Informatore Fitopatologico* 50 (5), 33–36.

Boller, T. (1995). Chemoperception of microbial signals in plant cells. *Annu Rev. Physical. Plant Mol. Biol.* 46, 189–214. doi: 10.1146/annurev.pp.46.060195.001201

Boller, T., and Felix, G. (2009). A ranaissance of elicitors: peception of microbe-associated molecular patterns and danger signals by pattern-recognition receptors. *Annu. Rev. Plant Biol.* 60 379–406. doi: 10.1146/annurev.arplant.57.032905.105346

Bonanomi, G., Ippolito, F., and Scala, F. (2015). A "black" future for plant pathology? Biochar as a new soil amendment for controlling plant diseases. *J. Plant Pathol.* 97, 223–234. doi: 10.4454/jpp.v97i2.3381

Boselli, M., Bahouaoui, M. A., Lachhab, N., Sanzani, S. M., Ferrara, G., and Ippolito, A. (2019). Protein hydrolysates effects on grapevine (*Vitis vinifera* L., cv. corvina) performance and water stress tolerance. *Sci. Hortic-Amsterdam* 258, 108784. doi: 10.1016/j.scienta.2019.108784

Botelho, M., Cruz, A., Ricardo- Da-Silva, J., De Castro, R., and Ribeiro, H. (2020). Mechanical pruning and soil fertilization with distinct organic amendments in vineyards of syrah: Effects on vegetative and reproductive growth. *Agronomy* 10 (8), 10081090. doi: 10.3390/agronomy10081090

Bowles, T. M., Jackson, L. E., Loeher, M., and Cavagnaro, T. R. (2017). Ecological intensification and arbuscular mycorrhizas: A meta-analysis of tillage and cover crop effects. *J. Appl. Ecol.* 54 (6), 1785–1793. doi: 10.1111/1365-2664.12815

Cabañas, C. M., Hernández, A., Martínez, A., Tejero, P., Vázquez-Hernández, M., Martín, A., et al. (2020). Control of *Penicillium glabrum* by indigenous antagonistic yeast from vineyards. *Foods* 9 (12), 1864. doi: 10.3390/foods9121864

Cabrera, L. C., and Pastor, P. M. (2021). The 2019 European union report on pesticide residues in food. *EFSA J.* 19 (4), 6491. doi: 10.2903/j.efsa.2021.6491

Campos, C., Carvalho, M., Brígido, C., Goss, M. J., and Nobre, T. (2018). Symbiosis specificity of the preceding host plant can dominate but not obliterate the association between wheat and its arbuscular mycorrhizal fungal partners. *Front. Microbiol.* 9 2920. doi: 10.3389/fmicb.2018.02920

Canellas, L. P., Olivares, F. L., Aguiar, N. O., Jones, D. L., Nebbioso, A., and Mazzei, P. (2015). Humic and fulvic acids as biostimulants in horticulture. *Sci. Hortic.* 196, 15–27. doi: 10.1016/j.scienta.2015.09.013

Canellas, L. P., Spaccini, R., Piccolo, A., Dobbss, L. B., Okorokova-Façanha, A. L., and Santos, G. A. (2009). Relationships between chemical characteristics and root growth promotion of humic acids isolated from Brazilian oxisols. *Soil Sci.* 174, 611–620. doi: 10.1097/SS.0b013e3181bf1e03

Carro-Huerga, G., Mayo-Prieto, S., Rodríguez-González, Á., González-López, Ó., Gutiérrez, S., and Casquero, P. A. (2021). Influence of fungicide application and vine age on *Trichoderma* diversity as source of biological control agents. *Agronomy* 11 (3), 446. doi: 10.3390/agronomy11030446

Castellano-Hinojosa, A., and Bedmar, E. J. (2017). "Methods for evaluating plant growth-promoting rhizobacteria traits", in *Advances in PGPR research*. Eds. B. Harikesh, Birinchi Singh, K. Sarma and K. Chetan (CABI, USA), ISBN: 978-1-78639-032-5. ePDF.

Castellarin, S. D., Pfeiffer, A., Sivilotti, P., Degan, M., Peterlunger, E., and Gaspero, G. (2007). Transcriptional regulation of anthocyanin biosynthesis in ripening fruits of grapevine under seasonal water deficit. *Plant Cell Environ.* 30 (11), 1381–1399. doi: 10.1111/j.1365-3040.2007.01716.x

Cataldo, E., Fucile, M., and Mattii, G. B. (2022). Biostimulants in viticulture: A sustainable approach against biotic and abiotic stresses. *Plants* 11 (2), 162. doi: 10.3390/plants11020162

Chang, Y., Rossi, L., Zotarelli, L., Gao, B., and Sarkhosh, A. (2021a). Greenhouse evaluation of pinewood biochar effects on nutrient status and physiological performance in muscadine grape (*Vitis rotundifolia* L.). *HortScience* 56 (2), 277–285. doi: 10.21273/HORTSCI15428-20

Chang, Y., Rossi, L., Zotarelli, L., Gao, B., Shahid, M. A., and Sarkhosh, A. (2021b). Biochar improves soil physical characteristics and strengthens root architecture in muscadine grape (*Vitis rotundifolia* L.). *Chem. Biol. Technol. Agric.* 8, 7. doi: 10.1186/s40538-020-00204-5

Chan, Z., and Tian, S. (2006). Induction of H_2O_2-metabolizing enzymes and total protein synthesis by antagonistic yeast and salicylic acid in harvested sweet cherry fruit. *Postharvest Biol. Tec.* 39 (3), 314–320. doi: 10.1016/j.postharvbio.2005.10.009

Chauhan, H., Bagyaraj, D. J., Selvakumar, G., and Sundaram, S. P. (2015). Novel plant growth promoting rhizobacteria: Prospects and potential. *Appl. Soil Ecol.* 95, 38–53. doi: 10.1016/j.apsoil.2015.05.011

Chen, Y. H., Li, Y. F., Wei, H., Li, X. X., Zheng, H. T., Dong, X. Y., et al. (2020). Inhibition efficiency of wood vinegar on grey mould of table grapes. *Food Biosci.* 38, 100755. doi: 10.1016/j.fbio.2020.100755

Chervin, J., Romeo-Oliván, A., Fournier, S., Puech-Pages, V., Dumas, B., Jacques, A., et al. (2022). Modification of early response of *Vitis vinifera* to pathogens relating to esca disease and biocontrol agent Vintec® revealed by untargeted metabolomics on woody tissues. *Front. Microbiol.* 2. doi: 10.3389/fmicb.2022.835463

Clark, R. B., and Zeto, S. K. (2000). Mineral acquisition by arbuscular mycorrhizal plants. *J. Plant Nutr.* 23 (7), 867–902. doi: 10.1080/01904160009382068

Colla, G., Hoagland, L., Ruzzi, M., Cardarelli, M., Bonini, P., Canaguier, R., et al. (2017). Biostimulant action of protein hydrolysates: Unraveling their effects on plant physiology and microbiome. *Front. Plant Sci.* 8. doi: 10.3389/fpls.2017.02202

Colla, G., Nardi, S., Cardarelli, M., Ertani, A., Lucini, L., Canaguier, R., et al. (2015). Protein hydrolysates as biostimulants in horticulture. *Sci. Hortic-Amsterdam* 196, 28–38. doi: 10.1016/j.scienta.2015.08.037

Colla, G., Rouphael, Y., Canaguier, R., Svecova, E., and Cardarelli., M. (2014). Biostimulant action of a plant-derived protein hydrolysate produced through enzymatic hydrolysis. *Front. Plant Sci.*, 5, 448. doi: 10.3389/fpls.2014.00448

Compant, S., Mitter, B., Colli-Mull, J., Gangl, H., and Sessitsch, A. (2011). Endophytes of grapevine flowers, berries, and seeds: Identification of cultivable bacteria, comparison with other plant parts, and visualization of niches of colonization. *Microb. Ecol.* 62, 188–197. doi: 10.1007/s00248-011-9883-y

Cordero-Bueso, G., Mangieri, N., Maghradze, D., Foschino, R., Valdetara, F., Cantoral, J. M., et al. (2017). Wild grape-associated yeasts as promising biocontrol agents against *Vitis vinifera* fungal pathogens. *Front. Microbiol.* 8. doi: 10.3389/fmicb.2017.02025

da Silva, M. S. R. A., Huertas Tavares, O. C., Gonçalves Ribeiro, T., da Silva, C. S. R. A., da Silva, C. S. R. A., García-Mina, J. M., et al. (2021). Humic acids enrich the plant microbiota with bacterial candidates for the suppression of pathogens. *Appl. Soil Ecol.* 168, 104146. doi: 10.1016/j.apsoil.2021.104146

Debode, J., Ebrahimi, N., D'Hose, T., Cremelie, P., Viaene, N., and Vandecasteele, B. (2020). Has compost with biochar added during the process added value over biochar or compost to increase disease suppression? *Appl. Soil Ecol.* 153, 103571. doi: 10.1016/j.apsoil.2020.103571

de Carvalho, R. P., Pasqual, M., de Oliveira Silveira, H. R., de Melo, P. C., Bispo, D. F. A., Laredo, R. R., et al. (2019). "Niágara rosada" table grape cultivated with seaweed extracts: Physiological, nutritional, and yielding behavior. *J. Appl. Phycol.* 31, 2053–2064. doi: 10.1007/s10811-018-1724-7

Deng, Q., Xia, H., Lin, L., Wang, J., Yuan, L., Li, K., et al. (2019). SUNRED, a natural extract-based biostimulant, application stimulates anthocyanin production in the skins of grapes. *Sci. Rep.* 9, 2590. doi: 10.1038/s41598-019-39455-0

Deolu-Ajayi, A. O., van der Meer, I. M., van der Werf, A., and Karlova, R. (2022). The power of seaweeds as plant biostimulants to boost crop production under abiotic stress. *Plant Cell Environ.* 45, 2537–2553. doi: 10.1111/pce.14391

Dobbss, L. B., Santos, T. C., Pittarello, M., Souza, S. B., Ramos, A. C., and Busato, J. G. (2018). Alleviation of iron toxicity in *Schinus terebinthifolius* raddi (Anacardiaceae) by humic substances. *Environ. Sci. Poll. Res.* 25, 9416–9425. doi: 10.1007/s11356-018-1193-1

Don, S. M. Y., Schmidtke, L. M., Gambetta, J. M., and Steel, C. C. (2021). Volatile organic compounds produced by *Aureobasidium pullulans* induce electrolyte loss and oxidative stress in *Botrytis cinerea* and *Alternaria alternata*. *Res. Microbiol.* 172 (1), 103788. doi: 10.1016/j.resmic.2020.10.003

du Jardin, P. (2015). Plant biostimulants: Definition, concept, main categories and regulation. *Sci. Horti-Amsterdam* 196, 3–14. doi: 10.1016/j.scienta.2015.09.021

EFSA (2021). *Consolidated Annual Activity Report 2021*. European Food Safety Authority (EFSA). Available in: https://www.efsa.europa.eu/sites/default/files/2022-03/ar2021.pdf (last access in 29 09 22).

Egamberdieva, D., Reckling, M., and Wirth, S. (2017). Biochar-based *Bradyrhizobium* inoculum improves growth of lupin (*Lupinus angustifolius* L.) under drought stress. *Eu. J. Soil Biol.* 78, 38–42. doi: 10.1016/j.ejsobi.2016.11.007

Egleton, M., Erdos, Z., Raymond, B., and Matthews, A. C. (2021). Relative efficacy of biological control and cultural management for control of mollusc pests in cool climate vineyards. *Biocontrol Sci. Techn.* 31 (7), 725–738. doi: 10.1080/09583157.2021.1882387

Ehlers, R. U. (2011). "Regulation of biological control agents and the EU policy support action REBECA", in *Regulation of biological control agents* (Dordrecht: Springer), 3–23. doi: 10.1007/978-90-481-3664-3

El Boukhari, M. E. M., Barakate, M., Bouhia, Y., and Lyamlouli, K. (2020). Trends in seaweed extract based biostimulants: Manufacturing process and beneficial effect on soil-plant systems. *Plants* 9, 359. doi: 10.3390/plants9030359

El-Ghaouth, A., Wilson, C. L., and Wisniewski, M. (1998). Ultrastructural and cytochemical aspects of the biological control of *Botrytis cinerea* by *Candida saitoana* in apple fruit. *Phytopathology* 88 (4), 282–291. doi: 10.1094/PHYTO.1998.88.4.282

El-Ghaouth, A., Wilson, C., and Wisniewski, M. (2004). "Biologically-based alternatives to synthetic fungicides for the control of postharvest diseases of fruit and vegetables", in *Diseases of fruits and vegetables: Volume II* (Dordrecht: Springer), 511–535.

Erdogan, U., Turan, M., Ates, F., Kotan, R., Çakmakçi, R., Erdogan, Y., et al. (2018). Effects of root plant growth promoting rhizobacteria inoculations on the growth and nutrient content of grapevine. *Commun. Soil Sci. Plan.* 49 (14), 1731–1738. doi: 10.1080/00103624.2018.1474910

Ertani, A., Cavani, L., Pizzeghello, D., Brandellero, E., Altissimo, A., Ciavatta, C., et al. (2009). Biostimulant activity of two protein hydrolyzates in the growth and nitrogen metabolism of maize seedlings. *J. Plant Nutr. Soil Sci.* 172, 237–244. doi: 10.1002/jpln.200800174

Ertani, A., Francisco, O., Ferrari, E., Schiavon, M., and Nardi, S. (2018). Spectroscopic-chemical fingerprint and biostimulant activity of a protein-based product in solid form. *Molecules* 23, 1031. doi: 10.3390/molecules23051031

Ferrara, G., and Brunetti, G. (2008). Influence of foliar applications of humic acids in *Vitis vinifera* L. cv italia. *J. Int. Sci. Vigne Vin* 42, 79–87. doi: 10.20870/oeno-one.2008.42.2.822

Ferrara, G., and Brunetti, G. (2010). Effects of the times of application of a soil humic acid on berry quality of table grape (*Vitis vinifera* L.) cv italia. *Spa. J. Agric. Res.* 8, 817–822. doi: 10.5424/1283

Fitter, A. H., and Garbaye, J. (1994). Interactions between mycorrhizal fungi and other soil organisms. *Plant Soil* 159 (1), 123–132. doi: 10.1007/BF00000101

Foley, J., Ramankutty, N., Brauman, K., Cassidy, E. S., Gerber, J. S., Johnston, M., et al. (2011). Solutions for a cultivated planet. *Nature* 478, 337–342. doi: 10.1038/nature10452

Frioni, T., Sabbatini, P., Tombesi, S., Norrie, J., Poni, S., Gatti, M., et al. (2018). Effects of a biostimulant derived from the brown seaweed *Ascophyllum nodosum* on ripening dynamics and fruit quality of grapevines. *Sci. Hortic-Amsterdam* 232, 97–106. doi: 10.1016/j.scienta.2017.12.054

Funes-Pinter, M. I., Salomon, M. V., Berli, F., Gil, R., Bottini, R., and Piccoli, P. (2018). Plant growth promoting rhizobacteria alleviate stress by AsIII in grapevine. *Agr. Ecosyst. Environ.* 267, 100–108. doi: 10.1016/j.agee.2018.08.015

Gao, X., Cheng, H. Y., Del Valle, I., Liu, S., Masiello, C. A., and Silberg, J. J. (2016). Charcoal disrupts soil microbial communication through a combination of signal sorption and hydrolysis. *ACS Omega* 1, 226–233. doi: 10.1021/acsomega.6b00085

Garrido, L. D. R., and Botton, M. (2020). *Agrotóxicos registrados para a cultura da Videira-Safra 945 2020/21. Embrapa Uva e Vinho-Comunicado Técnico (INFOTECA-E)*. Available at: https://www.embrapa.br/busca-de-publicacoes/-/publicacao/1124869/agrotoxicos-registrados-para-a-cultura-da-videira—safra-202021.

Gauthier, A., Trouvelot, S., Kelloniemi, J., Grettinger, P., Wendehenne, D., Daire, X., et al. (2014). The sulfated laminarin triggers a stress transcriptome before priming the SA- and ROS-dependent defenses during grapevine's induced resistance against *Plasmppara viticola*. *PLoS One* 9, e88145. doi: 10.1371/journal.pone.0194327

Gava, A., Emer, C. D., Ficagna, E., Fernandes de Andrade, S., and Fuentefria, A. M. (2021). Occurrence and impact of fungicides residues on fermentation during wine production–a review. *Food Addit. Contam*, 38(6), 1–19. doi: 10.1080/19440049.2021.1894357

Genesio, L., Miglietta, F., Baronti, S., and Vaccari, F. P. (2015). Biochar increases vineyard productivity without affecting grape quality: Results from a four years field experiment in Tuscany. *Agric. Ecosyst. Environ.* 201, 20–25. doi: 10.1016/j.agee.2014.11.021

Giagnoni, L., Maienza, A., Baronti, S., Vaccari, F. P., Genesio, L., Taiti, C., et al. (2019). Long-term soil biological fertility, volatile organic compounds and chemical properties in a vineyard soil after biochar amendment. *Geoderma* 344, 127–136. doi: 10.1016/j.geoderma.2019.03.011

Głodowska, M., Husk, B., Schwinghamer, T., and Smith, D. (2016). Biochar is a growth-promoting alternative to peat moss for the inoculation of corn with a pseudomonad. *Agron. Sustain. Dev.* 36 (1), 1–10. doi: 10.1007/s13593-016-0356-z

Godfray, H. C., Beddington, J. R., Crute, I. R., Haddad, L., Lawrence, D., Muir, J. F., et al. (2010). Food security: the challenge of feeding 9 billion people. *Science* 327 (5967), 812–818. doi: 10.1126/science.1185383

Gosling, P., Hodge, A., Goodlass, G., and Bending, G. D. (2006). Arbuscular mycorrhizal fungi and organic farming. *Agr. Ecosyst. Environ.* 113 (1), 17–35. doi: 10.1016/j.agee.2005.09.009

Goswami, D., Thakker, J. N., and Dhandhukia, P. C. (2016). Portraying mechanics of plant growth promoting rhizobacteria (PGPR): A review. *Cogent Food Agric.* 2, 1127500. doi: 10.1080/23311932.2015.1127500

Graber, E. R., Frenkel, O., Jaiswal, A. K., and Elad, Y. (2014). How may biochar influence severity of diseases caused by soilborne pathogens? *Carbon Manage.* 5 (2), 169–183. doi: 10.1080/17583004.2014.913360

Graber, E. R., Harel, Y. M., Kolton, M., Cytryn, E., Silber, A., David, D. R., et al. (2010). Biochar impact on development and productivity of pepper and tomato grown in fertigated soilless media. *Plant Soil* 337, 481–496. doi: 10.1007/s11104-010-0544-6

Grewal, A., Abbey, L. E., and Gunupuru, L. R. (2018). Production, prospects and potential application of pyroligneous acid in agriculture. *J. Ana. Appl. Pyrol.* 135, 152–159. doi: 10.1016/j.jaap.2018.09.008

Gryndler, M. (2000). *Interactions of arbuscular mycorrhizal fungi with other soil organisms BT - arbuscular mycorrhizas: Physiology and function*. Springer (USA) Eds. Y. Kapulnik and D. D. Douds doi: 10.1007/978-94-017-0776-3_11

Gupta, M. M., Aggarwal, A., and Asha, (2018). *From mycorrhizosphere to rhizosphere microbiome: The paradigm shift BT- root biology*. Springer (USA) Eds. R. Giri, Prasad, and A. Varma doi: 10.1007/978-3-319-75910-4_20enta.2017.12.054

Gutiérrez-Gamboa, G., Romanazzi, G., Garde-Cerdán, T., and Pérez-Álvarez, E. P. (2019). A review of the use of biostimulants in the vineyard for improved grape and wine quality: Effects on prevention of grapevine diseases. *J. Sci. Food Agric.* 99, 1001–1009. doi: 10.1002/jsfa.9353

Haidar, R., Fermaud, M., Calvo-Garrido, C., Roudet, J., and Deschamps, A. (2016). Modes of action for biological control of *Botrytis cinerea* by antagonistic bacteria. *Phytopathol. Mediterr*, 55(3), 301–322. doi: 10.14601/Phytopathol_Mediterr-18079

Hale, L., Luth, M., and Crowley, D. (2015). Biochar characteristics relate to its utility as an alternative soil inoculum carrier to peat and vermiculite. *Soil Biol. Biochem.* 81, 228–235. doi: 10.1016/j.soilbio.2014.11.023

Hardy, K., and Knight, J. D. (2021). Evaluation of biochars as carriers for *Rhizobium leguminosarum*. *Can. J. Microbiol.* 67 (1), 53–63. doi: 10.1139/cjm-2020-0416

Harel, Y. M., Elad, Y., Rav-David, D., Borenstein, M., Shulchani, R., Lew, B., et al. (2012). Biochar mediates systemic response of strawberry to foliar fungal pathogens. *Plant Soil* 357, 245–257. doi: 10.1007/s11104-012-1129-3

Heckman, D. S., Geiser, D. M., Eidell, B. R., Stauffer, R. L., Kardos, N. L., and Hedges, S. B. (2001). Molecular evidence for the early colonization of land by fungi and plants. *Science* 293 (5532), 1129–1133. doi: 10.1126/science.1061457

Holland, T., Bowen, P., Kokkoris, V., Urbez-Torres, J. R., and Hart, M. (2019). Does inoculation with arbuscular mycorrhizal fungi reduce trunk disease in grapevine rootstocks? *Horticulturae* 5 (3), 61. doi: 10.3390/horticulturae5030061

Ibrahim, M. M., and Ali, A. A. (2016). Effect of humic acid on productivity and quality of superior seedless grape cultivar. *Middle East J. Agric. Res.* 5, 239–246.

Irani, H., Kaji, B. V., and Naeini, M. R. (2021). Biostimulant-induced drought tolerance in grapevine is associated with physiological and biochemical changes. *Chem. Biol. Technol. Agric.* 8, 5. doi: 10.1186/s40538-020-00200-9

İşçı, B., Kacar, E., and Altindışlı, A. (2019). Effects of IBA and plant growth-promoting rhizobacteria (PGPR) on rooting of ramsey American grapevine rootstock. *Appl. Ecol. Environ. Res.* 17 (2), 4693–4705. doi: 10.15666/aeer/1702_46934705

Ito, Y., Nakanomyo, I., Motose, H., Iwamoto, K., Sawa, S., Dohmae, N., et al. (2006). Dodeca-CLE peptides as suppressors of plant stem cell differentiation. *Science 313* 313(5788), 842–845. doi: 10.1126/science.1128436

Jamalizadeh, M., Etebarian, H. R., Aminian, H., and Alizadeh, A. (2011). A review of mechanisms of action of biological control organisms against post harvest fruit spoilage. *Eppo Bull.* 41 (1), 65–71. doi: 10.1111/j.1365-2338.2011.02438.x

Jeandet, P., Douillet-Breuil, A. C., Bessis, R., Debord, S., Sbaghi, M., and Adrian, M. (2002). Phytoalexins from the vitaceae: Biosynthesis, phytoalexin gene expression in transgenic plants, antifungal activity, and metabolism. *J. Agr. Food Chem.* 50 (10), 2731–2741. doi: 10.1021/jf011429s

Jeffries, P., Gianinazzi, S., Perotto, S., Turnau, K., and Barea, J. M. (2003). The contribution of arbuscular mycorrhizal fungi in sustainable maintenance of plant health and soil fertility. *Biol. Fert. Soils* 37 (1), 1–16. doi: 10.1007/s00374-002-0546-5

Jindo, K., Olivares, F. L., Malcher, D. J. P., Sánchez-Monedero, M. A., Kempenaar, C., and Canellas, L. P. (2020). From lab to field: Role of humic substances under open-field and greenhouse conditions as biostimulant and biocontrol agent. *Front. Plant Sci.* 11. doi: 10.3389/fpls.2020.00426

Jones, L., Riaz, S., Morales-Cruz, A., Amrine, K. C. H., McGuire, B., Gubler, W. D., et al. (2014). Adaptive genomic structlural variation in the grape powdery mildew pathogen, *Erysiphe necator*. *BMC Genomics* 15 1081. doi: 10.1186/1471-2164-15-1081

Joseph, S., Graber, E. R., Chia, C., Munroe, P., Donne, S., Thomas, T., et al. (2013). Shifting paradigms: Development of high-efficiency biochar fertilizers based on nano-structures and soluble components. *Carbon Manage.* 4 (3), 323–343. doi: 10.4155/cmt.13.23

Kamble, M. V., Joshi, S. M., Hadimani, S., and Jogaiah, S. (2021). O Biopriming com *Trichoderma harzianum* da rizosfera promove proteção contra o míldio da videira, desencadeando respostas de defesa histopatológicas e bioquímicas. *Rhizosphere* 19, 100398. doi: 10.1016/j.rhisph.2021.100398

Kanwal, S., Batool, A., Ghufran, M. A., and Khalid, A. (2018). Effect of dairy manure derived biochar on microbial biomass carbon, soil carbon and *Vitis vinifera* under water stress conditions. *Pak. J. Bot.* 50 (5), 1713–1718.

Karoglan, M., Radić, T., Anić, M., Andabaka, Ž., Stupić, D., Tomaz, I., et al. (2021). Mycorrhizal fungi enhance yield and berry chemical composition of in field grown "Cabernet Sauvignon" grapevines (*V. vinifera* L.). *Agriculture* 11 (7), 615. doi: 10.3390/agriculture11070615

Khairy, H. M., and El-Shafay, S. M. (2013). Seasonal variations in the biochemical composition of some common seaweed species from the coast of Abu qir bay, Alexandria, Egypt. *Oceanologia* 55, 435–452. doi: 10.5697/oc.55-2.435

Kloepper, J. W., and Schroth, M. N. (1979). Plant growth promoting rhizobacteria: evidence that the mode of action involves root microflora interactions. *Phytophatology* 69, 1034.

Köse, C., Güleryüz, M., Şahin, F., and Demirtaş, I. (2003). Effects of some plant growth promoting rhizobacteria (PGPR) on rooting of grapevine rootstocks. *Acta Agrobot.* 56 (1-2), 47–52. doi: 10.5586/aa.2003.005

Köse, C., Güleryüz, M., Şahin, F., and Demirtaş, I. (2015). Effects of some plant growth promoting rhizobacteria (PGPR) on graft union of grapevine. *J. Sustain. Agr.* 26 (2), 139–147. doi: 10.1300/J064v26n02_10

Krishna, H., Singh, S. K., Sharma, R. R., Khawale, R. N., Grover, M., and Patel, V. B. (2005). Biochemical changes in micropropagated grape (*Vitis vinifera* L.)

plantlets due to arbuscular-mycorrhizal fungi (AMF) inoculation during *ex vitro* acclimatization. *Sci. Hortic-Amsterdam* 106, 554–567. doi: 10.1016/j.scienta.2005.05.009

Kumar Jha, C., and Saraf, M. (2015). Plant growth promoting rhizobacteria (PGPR): a review. *E3 J. Agric. Res. Dev.* 5 (2), 0108–0119. doi: 10.13140/RG.2.1.5171.2164

Kurtzman, C. P., Fell, J. W., and Boekhout, T. (2011). *The yeasts: A taxonomic study. Burlington: Elsevier science*. Elsevier, Amsterdam, Nederland.

Lachhab, N., Sanzani, S. M., Adrian, M., Chiltz, A., Balacey, S., Boselli, M., et al. (2014). Soybean and casein hydrolysates induce grapevine immune responses and resistance against *Plasmopara viticola*. *Front. Plant Sci. 5* 716. doi: 10.3389/fpls.2014.00716

Lachhab, N., Sanzani, S. M., Bahouaoui, M. A., Boselli, M., and Ippolito, A. (2016). Effect of some protein hydrolysates against gray mould of table and wine grapes. *Eur. J. Plant Pathol.* 144 (4), 821–830. doi: 10.1007/s10658-015-0749-x

Lehmann, J., Rillig, M. C., Thies, J., Masiello, C. A., Hockaday, W. C., and Crowley, D. (2011). Biochar effects on soil biota - a review. *Soil Biol. Biochem.* 43 (9), 1812–1836. doi: 10.1016/j.soilbio.2011.04.022

Linderman, R. G., and Davis, E. A. (2001). Comparative response of selected grapevine rootstocks and cultivars to inoculation with different mycorrhizal fungi. *Am. J. Enol. Viticult.* 52 (1), 8–11.

Liu, M., Liu, X., Cheng, B., Ma, X. L., Lyu, X. T., Zhao, X. F., et al. (2016). Selection and evaluation of phosphate-solubilizing bacteria from grapevine rhizospheres for use as biofertilizers. *Span. J. Agric. Res.* 14 (4), e1106. doi: 10.5424/sjar/2016144-9714

Li, H. Y., Yang, G. D., Shu, H. R., Yang, Y. T., Ye, B. X., Nishida, I., et al. (2006). Colonization by the arbuscular mycorrhizal fungus *Glomus versiforme* induces a defense response against the root-knot nematode *Meloidogyne incognita* in the grapevine (*Vitis amurensis* rupr.), which includes transcriptional activation of the class III chitin. *Plant Cell Physiol.* 47 (1), 154–163. doi: 10.1093/pcp/pci231

Lu, H., Wu, Z., Wang, W., Xu, X., and Liu, X. (2020). Rs-198 liquid biofertilizers affect microbial community diversity and enzyme activities and promote *Vitis vinifera* L. growth. *BioMed. Res. Int.*, 8321462. doi: 10.1155/2020/8321462

Maachia, B. S., Rafik, E., Chérif, M., Nandal, P., Mohapatra, T., and Bernard, P. (2015). Biological control of the grapevine diseases 'grey mold'and 'powdery mildew'by *Bacillus* B27 and B29 strains. *Indian J. Exp. Biol.* 53 (2), 109–115.

Maienza, A., Baronti, S., Cincinelli, A., Martellini, T., Grisolia, A., Miglietta, F., et al. (2017). Biochar improves the fertility of a Mediterranean vineyard without toxic impact on the microbial community. *Agron. Sustain. Dev.* 37, 47. doi: 10.1007/s13593-017-0458-2

Malviya, D., Thosar, R., Kokare, N., Pawar, S., Singh, U. B., Saha, S., et al. (2022). A comparative analysis of microbe-based technologies developed at ICAR-NBAIM against *Erysiphe necator* causing powdery mildew disease in grapes (*Vitis vinifera* l.). *Front. Microbiol.* 13, 871901. doi: 10.1400/53262

Mancuso, S., Azzarello, E., Mugnai, S., and Briand, X.. (2006). Marine bioactive substances (IPA extract) improve foliar ion uptake and water stress tolerance in potted Vitis vinifera plants. *Adv. Hortic. Sci.* 20, 156–161. doi: 10.1400/53262

Meggio, F., Trevisan, S., Manoli, A., Ruperti, B., and Quaggiotti, S. (2020). Systematic investigation of the effects of a novel protein hydrolysate on the growth, physiological parameters, fruit development and yield of grapevine (*Vitis vinifera* L., cv Sauvignon Blanc) under water stress conditions. *Agronomy* 10, 1785. doi: 10.3390/agronomy10111785

Miotto-Vilanova, L., Jacquard, C., Courteaux, B., Wortham, L., Michel, J., Clément, C., et al. (2016). *Burkholderia phytofirmans* PsJN confers grapevine resistance against *Botrytis cinerea via* a direct antimicrobial effect combined with a better resource mobilization. *Front. Plant Sci.* 7. doi: 10.3389/fpls.2016.01236

Montagnoli, A., Baronti, S., Alberto, D., Chiatante, D., Scippa, G. S., and Terzaghi, M. (2021). Pioneer and fibrous root seasonal dynamics of *Vitis vinifera* L. are affected by biochar application to a low fertility soil: A rhizobox approach. *Sci. Total Environ.* 751, 141455. doi: 10.1016/j.scitotenv.2020.141455

Monteiro, E., Gonçalves, B., Cortez, I., and Castro, I. (2022). The role of biostimulants as alleviators of biotic and abiotic stresses in grapevine: A review. *Plants* 31, 11(3):396. doi: 10.3390/plants11030396

Muganu, M., Paolocci, M., Bignami, C., and Di Mattia, E. (2015). Enhancement of adventitious root differentiation and growth of *in vitro* grapevine shoots inoculated with plant growth promoting rhizobacteria. *Vitis* 54, 73–77. doi: 10.5073/vitis.2015.54.73-77

Mungkunkamchao, T., Kesmala, T., Pimratch, S., Toomsan, B., and Jothityangkoon, D. (2013). Wood vinegar and fermented bioextracts: Natural products to enhance growth and yield of tomato (*Solanum lycopersicum* L.). *Sci. Horti-Amsterdam* 154, 66–72. doi: 10.1016/j.scienta.2013.02.020

Nesbitt, A., Dorling, S., and Lovett, A. (2018). A suitability model for viticulture in England and Wales: Opportunities for investment, sector growth and increased climate resilience. *J. Land Use Sci.*, 13(4), 414–438. doi: 10.1080/1747423X.2018.1537312

Nesler, A., Perazzolli, M., Puopolo, G., Giovannini, O., Elad, Y., and Pertot, I. (2015). A complex protein derivative acts as biogenic elicitor of grapevine resistance against powdery mildew under filed conditions. *Front. Plant Sci.* 6. doi: 10.3389/fpls.2015.00715

Nogales, A., Aguirreolea, J., Santa María, E., Camprubí, A., and Calvet, C. (2008). Response of mycorrhizal grapevine to *Armillaria mellea* inoculation: Disease development and polyamines. *Plant Soil* 317 (1), 177. doi: 10.1007/s11104-008-9799-6

Nogales, A., Rottier, E., Campos, C., Victorino, G., Costa, J. M., Coito, J. L., et al. (2021). The effects of field inoculation of arbuscular mycorrhizal fungi through rye donor plants on grapevine performance and soil properties. *Agric. Ecosyst. Environ.* 313, 107369. doi: 10.1016/j.agee.2021.107369

Ogawa, M., and Okimori, Y. (2010). Pioneering works in biochar research, Japan. *Aust. J. Soil Res.* 48 (6-7), 489–500. doi: 10.1071/SR10006

Olavarrieta, C. E., Sampedro, M. C., Vallejom, A., Štefelovám, N., Barriom, R. J., and De Diego, N. (2022). Biostimulants as an alternative to improve the wine quality from *Vitis vinifera* (cv. tempranillo) in La Rioja. *Plants* 11 (12), 1594. doi: 10.3390/plants11121594

Oleńska, E., Małek, W., Wójcik, M., Swiecicka, I., Thijs, S., and Vangronsveld, J. (2020). Beneficial features of plant growth-promoting rhizobacteria for improving plant growth and health in challenging conditions: A methodical review. *Sci. Total Environ.* 743, 140682. doi: 10.1016/j.scitotenv.2020.140682

Olivares, F. L., Busato, J. G., de Paula, A. M., Silva, L. L., Aguiar, N. O., and Canellas, L. P. (2017). Plant growth promoting bacteria and humic substances: Crop promotion and mechanisms of action. *Chem. Biol. Technol. Agric.* 4, 30. doi: 10.1186/s40538-017-0112-x

Pacifico, D., Squartini, A., Crucitti, D., Barizza, E., Lo Schiavo, F., Muresu, R., et al. (2019). The role of the endophytic microbiome in the grapevine response to environmental triggers. *Front. Plant Sci.* 10. doi: 10.3389/fpls.2019.01256

Payen, F. T., Sykes, A., Aitkenhead, M., Alexander, P., Moran, D., and MacLeod, M. (2021). Soil organic carbon sequestration rates in vineyard agroecosystems under different soil management practices: A meta-analysis. *J. Clea. Prod.* 290, 125736. doi: 10.1016/j.jclepro.2020.125736

Pertot, I., Longa, C. M. O., Savazzini, F., Prodorutti, D., and Michelon, L. (2015). *Trichoderma atroviride* SC1 for biocontrol of fungal diseases in plants, International Patent Application US 8,431,120B2.

Petit, E., and Gubler, W. D. (2006). Influence of *Glomus intraradices* on black foot disease caused by *Cylindrocarpon macrodidymum* on *Vitis rupestris* under controlled conditions. *Plant Dis.* 90 (12), 1481–1484. doi: 10.1094/PD-90-1481

Petrillo, M., Zanotelli, D., Lucchetta, V., Aguzzoni, A., Tagliavini, M., and Andreotti, C. (2020). The use of biochar as soil amendment: Effects on nitrogen and water availability for potted grapevines. *Italus Hortus* 27 (2), 28–40. doi: 10.26353/j.itahort/2020.2.2840

Phelan, M., Aherne, A., FitzGerald, R. J., and O'Brien, N. M. (2009). Casein-derived bioactive peptides: Biological effects, industrial uses, safety aspects and regulatroy status. *Int. Dairy J.* 19, 643–654. doi: 10.1016/j.idairyj.2009.06.001

Pinto, C., and Gomes, A. C. (2016). *Vitis vinifera* microbiome: from basic research to technological development. *BioControl* 61, 243–256. doi: 10.1007/s10526-016-9725-4

Popescu, G. G. C., and Popescu, M. (2018). Yield, berry quality and physiological response of grapevine to foliar humic acid application. *Bragantia* 77, 273–282. doi: 10.1590/1678-4499.2017030

Porter, S. S., and Sachs, J. L. (2020). Agriculture and the disruption of plant–microbial symbiosis. *Trends Ecol. Evol.* 35 (5), 426–439. doi: 10.1016/j.tree.2020.01.006

Pugliese, M., Monchiero, M., Gullino, M. L., and Garibaldi, A. (2018). Application of laminarin and calcium oxide for the control of grape powdery mildew on *Vitis vinifera* cv. moscato. *J. Plant Dis. Prot.* 125, 477–482. doi: 10.1007/s41348-018-0162-8

Rahman, L., Whitelaw-Weckert, M. A., and Orchard, B. (2014). Impact of organic soil amendments, including poultry-litter biochar, on nematodes in a riverina, new south Wales, vineyard. *Soil Res.* 52 (6), 604–619. doi: 10.1071/SR14041

Ranade, Y., Sawant, I., Saha, S., Chandrashekar, M., and Pathak, P. (2021). Epiphytic microbial diversity of *Vitis vinifera* fructosphere: Present status and potential applications. *Curr. Microbiol.*, 78, 1–13. doi: 10.1007/s00284-021-02385-0

Regulation EC 1107 (2009) *Regulation (EC) no 1107/2009 of the European parliament and of the council of 21 October 2009 concerning the placing of plant protection products on the market and repealing council directives 79/117/EEC and 91/414/EEC.* Available at: https://eur-lex.europa.eu/legal-content/EN/ALL/?uri=CELEX:32009R1107.

Regulation EU 1009 (2019) *Regulation EU 2019/1009 of the European parliament and of the council of 5 June 2019 laying down rules on the making available on the market of EU fertilising products and amending regulations (EC) no 1069/2009 and (EC) no 1107/2009 and repealing regulation (EC) no 2003/2003.*

Available at: https://eur-lex.europa.eu/legal-content/EN/TXT/HTML/?uri=CELEX:32019R1009&from=ES.

Reineke, A., and Thiéry, D. (2016). Grapevine insect pests and their natural enemies in the age of global warming. *J. Pest Sci.* 89 (2), 313–328. doi: 10.1007/s10340-016-0761-8

Rezgui, A., Ben Ghnaya-Chakroun, A., Vallance, J., Bruez, E., Hajlaoui, M. R., Sadfi-Zouaoui, N., et al. (2016). Endophytic bacteria with antagonistic traits inhabit the wood tissues of grapevines from Tunisian vineyards. *Biol. Control* 99, 28–37. doi: 10.1016/j.biocontrol.2016.04.005

Roka, K. (2022). "Anthropocene and climate change," in *Climate action, encyclopedia of the UN sustainable development goals*. Ed. W. Leal Filho, et al (Nature Switzerland: Springer), 2020. doi: 10.1007/978-3-319-95885-9

Rolli, E., Marasco, R., Saderi, S., Corretto, E., Mapelli, F., Cherif, A., et al. (2017). Root-associated bacteria promote grapevine growth: from the laboratory to the field. *Plant Soil* 410 (1–2), 369–382. doi: 10.1007/s11104-016-3019-6

Romanazzi, G., Mancini, V., Feliziani, E., Andrea, S., Endeshaw, S., and Neri, D. (2016). Impact of alternative fungicides on grape downy mildew control and vine growth and development. *Plant Dis.* 100 (4), 739–748. doi: 10.1094/PDIS-05-15-0564-RE

Ronga, D., Francia, E., Allesina, G., Pedrazzi, S., Zaccardelli, M., Pane, C., et al. (2019). Valorization of vineyard by-products to obtain composted digestate and biochar suitable for nursery grapevine (*Vitis vinifera* L.) production. *Agronomy* 9 (8), 420. doi: 10.3390/agronomy9080420

Rosa, D., Pogiatzis, A., Bowen, P., Kokkoris, V., Richards, A., Holland, T., et al. (2020). Performance and establishment of a commercial mycorrhizal inoculant in viticulture. *Agriculture* 10 (11), 539. doi: 10.3390/agriculture10110539

Rouphael, Y., and Colla, G. (2020). Editorial: Biostimulants in agriculture. *Front. Plant Sci.* 11. doi: 10.3389/fpls.2020.00040

Ruzzi, M., and Aroca, R. (2015). Plant growth-promoting rhizobacteria act as biostimulants in horticulture. *Sci. Hortic-Amsterdam* 196, 124–134. doi: 10.1016/j.scienta.2015.08.042

Sabir, A. (2013). Improvement of grafting efficiency in hard grafting grape berlandieri hybrid rootstocks by plant growth-promoting rhizobacteria (PGPR). *Sci. Hortic-Amsterdam* 164, 24–29. doi: 10.1016/j.scienta.2013.08.035

Sabir, A., Karaca, U., Yazar, K., Sabir, F. K., Yazici, M. A., Dogan, O., et al. (2017). Vine growth and yield response of alphonse lavallée (*V. vinifera* L.) grapevines to plant growth promoting rhizobacteria under alkaline condition in soilless culture. *Acta Sci. Pol-Hortoru.* 16 (4), 25–32. doi: 10.24326/asphc.2017.4.3

Salomon, M. V., Bottini, R., de Souza Filho, G. A., Cohen, A. C., Moreno, D., Gil, M., et al. (2014). Bacteria isolated from roots and rhizosphere of *Vitis vinifera* retard water losses, induce abscisic acid accumulation and synthesis of defense-related terpenes in *in vitro* cultured grapevine. *Physiol. Plantarum* 151 (4), 359–374. doi: 10.1111/ppl.12117

Salomon, M. V., Piccoli, P., Funes-Pinter, I., Stirk, W. A., Kulkarni, M., van Staden, J., et al. (2017). Bacteria and smoke-water extract improve growth and induce the synthesis of volatile defense mechanisms in *Vitis vinifera* l. *Plant Physiol. Biochem.* 120, 1–9. doi: 10.1016/j.plaphy.2017.09.013

Salomon, M. V., Purpora, R., Bottini, R., and Piccoli, P. (2016). Rhizosphere associated bacteria trigger accumulation of terpenes in leaves of Vitis vinifera L. cv. Malbec that protect cells against reactive oxygen species. *Plant Physiol. Biochem.* 106, 295–304. doi: 10.1016/j.plaphy.2016.05.007

Samad, A., Antonielli, L., Sessitsch, A., Compant, S., and Trognitz, F. (2017). Comparative genome analysis of the vineyard weed endophyte *Pseudomonas viridiflava* CDRTc14 showing selective herbicidal activity. *Sci. Rep.* 7 (1), 1–15. doi: 10.1038/s41598-017-16495-y

Sánchez-Monedero, M. A., Cayuela, M. L., Sánchez-García, M., Vandecasteele, B., D'Hose, T., López, G., et al. (2019). Agronomic evaluation of biochar, compost and biochar-blended compost across different cropping systems: Perspective from the European project FERTIPLUS. *Agronomy* 9 (5), 225. doi: 10.3390/agronomy9050225

Sánchez-Sánchez, A., Sánchez-Andreu, J., Juárez, M., Jordá, J., and Bermúdez, D. (2006). Improvement of iron uptake in table grape by addition of humic substances. *J. Plant Nutr.* 29, 259–272. doi: 10.1080/01904160500476087

Santos, J. A., Fraga, H., Malheiro, A. C., Moutinho-Pereira, J., Dinis, L. T., Correia, C., et al. (2020). A review of the potential climate change impacts and adaptation options for European viticulture. *App. Sci.* 10 (9), 3092. doi: 10.3390/app10093092

Schaafsma, G. (2009). Safety of protein hydrolysates, fractions thereof and bioactive peptides in human nutrition. *Eur. J. Clin. Nutr.* 63, 1161–1168. doi: 10.1038/ejcn.2009.56

Schmidt, H. P., Kammann, C., Niggli, C., Evangelou, M. W. H., Mackie, K. A., and Abiven, S. (2014). Biochar and biochar-compost as soil amendments to a vineyard soil influences on plant growth, nutrient uptake, plant health and grape quality. *Agric. Ecosyst. Environ.* 191, 117–123. doi: 10.1016/j.agee.2014.04.001

Schreiner, P. R. (2007). Effects of native and nonnative arbuscular mycorrhizal fungi on growth and nutrient uptake of 'Pinot noir' (*Vitis vinifera* l.) in two soils with contrasting levels of phosphorus. *Appl. Soil Ecol.* 36, 205–215. doi: 10.1016/j.apsoil.2007.03.002

Seufert, V., Ramankutty, N., and Foley, J. (2012). Comparing the yields of organic and conventional agriculture. *Nature* 485, 229–232. doi: 10.1038/nature11069

Sharma, R. R., Singh, D., and Singh, R. (2009). Biological control of postharvest diseases of fruits and vegetables by microbial antagonists: A review. *Biol. Control* 50 (3), 205–221. doi: 10.1016/j.biocontrol.2009.05.001

Shukla, P. S., Mantin, E. G., Adil, M., Bajpai, S., Critchley, A. T., and Prithiviraj, B. (2019). *Ascophyllum nodosum*-based biostimulants: Sustainable applications in agriculture for the stimulation of plant growth, stress tolerance, and disease management. *Front. Plant Sci.* 10. doi: 10.3389/fpls.2019.00655

Sihem, B. M., Rafik, E., Florence, M., Mohamed, C., and Ahmed, L. (2011). Identification and partial characterization of antifungal and antibacterial activities of two *Bacillus* sp. strains isolated from salt soil in Tunisia. *Afr. J. Microbiol. Res.* 5 (13), 1599–1608. doi: 10.5897/AJMR11.0

Sipiczki, M. (2006). *Metschnikowia* strains isolated from botrytized grapes antagonize fungal and bacterial growth by iron depletion. *App. Environ. Microbiol.* 72 (10), 6716–6724. doi: 10.1128/AEM.01275-06

Smith, S. E., Jakobsen, I., Grønlund, M., and Smith, F. A. (2011). Roles of arbuscular mycorrhizas in plant phosphorus nutrition: Interactions between pathways of phosphorus uptake in arbuscular mycorrhizal roots have important implications for understanding and manipulating plant phosphorus acquisition. *Plant Physiol.* 156 (3), 1050–1057. doi: 10.1104/pp.111.174581

Smith, S. E., and Read, D. (2008). *Mycorrhizal symbiosis. 3rd ed.* (Academic Press, Elsevier, Amsterdam, Neterland). doi: 10.1016/B978-0-12-370526-6.X5001-6

Sohn, B. K., Kim, K. Y., Chung, S. J., Kim, W. S., Park, S. M., Kang, J. G., et al. (2003). Effect of the different timing of AMF inoculation on plant growth and flower quality of chrysanthemum. *Sci. Hortic.Amsterdam* 98 (2), 173–183. doi: 10.1016/S0304-4238(02)00210-8

Soja, G., Wimmer, B., Rosner, F., Faber, F., Dersch, G., von Chamier, J., et al. (2018). Compost and biochar interactions with copper immobilisation in copper-enriched vineyard soils. *App. Geochem.* 88, 40–48. doi: 10.1016/j.apgeochem.2017.06.004

Souza, A. C., Olivares, F. L., Peres, L. E. P., Piccolo, A., and Canellas, L. P. (2022). Plant hormone crosstalk mediated by humic acids. *Chem. Biol. Technol. Agric.* 9, 29. doi: 10.1186/s40538-022-00295-2

Stenberg, J. A., Sundh, I., Becher, P. G., Björkman, C., Dubey, M., Egan, P. A., et al. (2021). When is it biological control? A framework of definitions, mechanisms, and classifications. *J. Pest Sci.* 94 (3), 665–676. doi: 10.1007/s10340-021-01354-7

Strzelczyk, E., Dahm, H., and Pachlewski, R. (1991). B-group vitamins production by mycorrhizal fungi in response to pH (*in vitro* studies). *Plant Soil* 137 (2), 237–241. doi: 10.1007/BF00011202

Torres, N., Goicoechea, N., Morales, F., and Antolín, M. C. (2016). Berry quality and antioxidant properties in *Vitis vinifera* cv. tempranillo as affected by clonal variability, mycorrhizal inoculation and temperature. *Crop Pasture Sci.* 67, 961–977. doi: 10.1071/CP16038

Trouvelot, S., Bonneau, L., Redecker, D., van Tuinen, D., Adrian, M., and Wipf, D. (2015). Arbuscular mycorrhiza symbiosis in viticulture: A review. *Agron. Sustain. Dev.* 35 (4), 1449–1467. doi: 10.1007/s13593-015-0329-7

Turan, M., and Köse, C. (2004). Seaweed extracts improve copper uptake of grapevine. *Acta Agric. Scand. Sect. B Soil Plant Sci.* 54, 213–220. doi: 10.1080/09064710410030311

Ubalde, J. M., Payan, E., Sort, X., Rosas, J. G., and Gómez, N. (2014). Application of biochar amendments to Mediterranean soils Effects on vine growth and grape quality. *Geophys Res. Abstr.* 16, 440000.

van Aubel, G., Buonatesta, R., and Van Cutsem, P. (2014). COS-OGA: A novel oligosaccharidic elicitor that protects grapes and cucumbers against powdery mildew. *Crop Prot.* 65, 129–137. doi: 10.1016/j.cropro.2014.07.015

Vandana, U. K., Rajkumari, J., Singha, L. P., Satish, L., Alavilli, H., Sudheer, P. D. V. N., et al. (2021). The endophytic microbiome as a hotspot of synergistic interactions, with prospects of plant growth promotion. *Biology* 10, 101. doi: 10.3390/biology10020101h

Van Geel, M., Verbruggen, E., De Beenhouwer, M., van Rennes, G., Lievens, B., and Honnay, O. (2017). High soil phosphorus levels overrule the potential benefits of organic farming on arbuscular mycorrhizal diversity in northern vineyards. *Agr. Ecosyst. Environ.* 248, 144–152. doi: 10.1016/j.agee.2017.07.017

Velásquez, A., Valenzuela, M., Carvajal, M., Fiaschi, G., Avio, L., Giovannetti, M., et al. (2020b). The arbuscular mycorrhizal fungus *Funneliformis mosseae* induces changes and increases the concentration of volatile organic compounds in *Vitis vinifera* cv. sangiovese leaf tissue. *Plant Physiol. Biochem.* 155, 437–443. doi: 10.1016/j.plaphy.2020.06.048

Velásquez, A., Vega-Celedón, P., Fiaschi, G., Agnolucci, M., Avio, L., Giovannetti, M., et al. (2020a). Responses of *Vitis vinifera* cv. Cabernet Sauvignon roots to the arbuscular mycorrhizal fungus *Funneliformis mosseae* and the plant growth-promoting rhizobacterium *Ensifer meliloti* include changes in volatile organic compounds. *Mycorrhiza* 30 (1), 161–170. doi: 10.1007/s00572-020-00933-3

Veliksar, S., Lemanova, N., Bratco, D., and Gladei, M. (2017). The influence of trace elements and PGPR on growth and photosynthetic activity of grape seedlings. *Lucrări ştiinţifice seria horticultură* 60 (1), 109–114.

Veliksar, S., Lemanova, N., Gladei, M., and Tatiana, D. (2022a). The impact of trace elements applied with PGPB on the *Vitis vinifera* L seedlings resistance to the copper excess in soil. *SSRG Int. J. Agric. Environ. Sci. (SSRG-IJAES)* 6 (4), 43–47.

Verhagen, B. W. M., Trotel-Aziz, P., Couderchet, M., Höfte, M., and Aziz, A. (2010). *Pseudomonas* spp.-induced systemic resistance to *Botrytis cinerea* is associated with induction and priming of defence responses in grapevine. *J. Exp. Bot.* 61 (1), 249–260. doi: 10.1093/jxb/erp295

Vorholt, J. (2012). Microbial life in the phyllosphere. *Nat. Rev. Microbiol.* 10, 828–840. doi: 10.1038/nrmicro2910

Walorczyk, S., Drożdżyński, D., and Gnusowski, B. (2011). Multiresidue determination of 160 pesticides in wines employing mixed-mode dispersive-solid phase extraction and gas chromatography-tandem mass spectrometry. *Talanta* 85 (4), 1856–1870. doi: 10.1016/j.talanta.2011.07.029

Wang, X., Glawe, D. A., Kramer, E., Weller, D., and Okubara, P. A. (2018). Biological control of *Botrytis cinerea*: Interactions with native vineyard yeasts from Washington state. *Phytopathology* 108 (6), 691–701. doi: 10.1094/PHYTO-09-17-0306-R

Wei, M., Liu, X., He, Y., Xu, X., Wu, Z., Yu, K., et al. (2020). Biochar inoculated with *Pseudomonas putida* improves grape (*Vitis vinifera* L.) fruit quality and alters bacterial diversity. *Rhizosphere* 16, 100261. doi: 10.1016/j.rhisph.2020.100261

Winter, S., Bauer, T., Strauss, P., Kratschmer, S., Paredes, D., Popescu, D., et al. (2018). Effects of vegetation management intensity on biodiversity and ecosystem services in vineyards: A meta-analysis. *J. App. Ecol.* 55 (5), 2484–2495. doi: 10.1111/1365-2664.13124

Woolf, D., Amonette, J. E., Street-Perrott, F. A., Lehmann, J., and Joseph, S. (2010). Sustainable biochar to mitigate global climate change. *Nat. Commun.* 1 (5), 56. doi: 10.1038/ncomms1053

Yakhin, O. I., Lubyanov, A. A., Yakhin, I. A., and Brown, P. H. (2017). Biostimulants in plant science: A global perspective. *Front. Plant Sci.* 7. doi: 10.3389/fpls.2016.02049

Zaller, J. G., Cantelmo, C., Dos Santos, G., Muther, S., Gruber, E., Pallua, P., et al. (2018). Herbicides in vineyards reduce grapevine root mycorrhization and alter soil microorganisms and the nutrient composition in grapevine roots, leaves, xylem sap and grape juice. *Environ. Sci. Pollut. Res. Int.* 25 (23), 23215–23226. doi: 10.1007/s11356-018-2422-3

Zandonadi, D. B., Canellas, L. P., and Façanha, A. R. (2007). Indolacetic and humic acids induce lateral root development through a concerted plasmalemma and tonoplast H^+ pumps activation. *Planta* 225, 1583–1595. doi: 10.1007/s00425-006-0454-452

Zandonadi, D. B., Santos, M. P., Busato, J. G., Peres, L. E. P., and Façanha, A. R. (2013). Plant physiology as affected by humified organic matter. *Theor. Exp. Plant Physiol.* 25, 13–25. doi: 10.1590/s2197-002520130001000

Zhang, Y., Wang, X., Liu, B., Liu, Q., Zheng, H., You, X., et al. (2020). Comparative study of individual and co-application of biochar and wood vinegar on blueberry fruit yield and nutritional quality. *Chemosphere* 246, 125699. doi: 10.1016/j.chemosphere.2019.125699

Zhu, X., Chen, B., Zhu, L., and Xing, B. (2017). Effects and mechanisms of biochar-microbe interactions in soil improvement and pollution remediation: A review. *Environ. pollut.* 227, 98–115. doi: 10.1016/j.envpol.2017.04.032

frontiers | Frontiers in Microbiology

TYPE Original Research
PUBLISHED 27 October 2022
DOI 10.3389/fmicb.2022.996054

OPEN ACCESS

EDITED BY
Maurizio Ruzzi,
University of Tuscia,
Italy

REVIEWED BY
Muhammad Shahid,
University of the Punjab, Pakistan
Paola Ganugi,
Catholic University of the Sacred Heart,
Italy

*CORRESPONDENCE
Mohamed Tarroum
mtarroum@ksu.edu.sa
Afif Hassairi
afif.hassairi@gmail.com

SPECIALTY SECTION
This article was submitted to Microbe and Virus Interactions With Plants, a section of the journal Frontiers in Microbiology

RECEIVED 17 July 2022
ACCEPTED 05 October 2022
PUBLISHED 27 October 2022

CITATION
Tarroum M, Romdhane WB, Al-Qurainy F, Ali AAM, Al-Doss A, Fki L and Hassairi A (2022) A novel PGPF *Penicillium olsonii* isolated from the rhizosphere of *Aeluropus littoralis* promotes plant growth, enhances salt stress tolerance, and reduces chemical fertilizers inputs in hydroponic system.
Front. Microbiol. 13:996054.
doi: 10.3389/fmicb.2022.996054

A novel PGPF *Penicillium olsonii* isolated from the rhizosphere of *Aeluropus littoralis* promotes plant growth, enhances salt stress tolerance, and reduces chemical fertilizers inputs in hydroponic system

Mohamed Tarroum[1]*, Walid Ben Romdhane[2], Fahad Al-Qurainy[1], Ahmed Abdelrahim Mohamed Ali[2], Abdullah Al-Doss[2], Lotfi Fki[3] and Afif Hassairi[2,4]*

[1]Department of Botany and Microbiology, College of Science, King Saud University, Riyadh, Saudi Arabia, [2]Department of Plant Production, College of Food and Agricultural Science, King Saud University, Riyadh, Saudi Arabia, [3]Laboratory of Plant Biotechnology Applied to Crop Improvement, Faculty of Sciences of Sfax, University of Sfax, Sfax, Tunisia, [4]Centre of Biotechnology of Sfax, University of Sfax, Sfax, Tunisia

The hydroponic farming significantly enhances the yield and enables multiple cropping per year. These advantages can be improved by using plant growth-promoting fungi (PGPF) either under normal or stress conditions. In this study, the fungal strain (A3) isolated from the rhizosphere of the halophyte plant *Aeluropus littoralis* was identified as *Penicillium olsonii* based on sequence homology of its ITS region. The A3 fungus was shown to be halotolerant (up to 1M NaCl) and its optimal growth was at 27°C, but inhibited at 40°C. In liquid culture medium, the A3 produced indole acetic acid (IAA) especially in the presence of L-tryptophan. Tobacco plants grown under hydroponic farming system were used to evaluate the promoting activity of the direct effect of A3 mycelium (DE) and the indirect effect (IDE) of its cell-free culture filtrate (A3CFF). The results showed that for the two conditions (DE or IDE) the tobacco seedlings exhibited significant increase in their height, leaf area, dry weight, and total chlorophyll content. Interestingly, the A3CFF (added to the MS liquid medium or to nutrient solution (NS), prepared from commercial fertilizers) induced significantly the growth parameters, the proline concentration, the catalase (CAT) and the superoxide dismutase (SOD) activities of tobacco plants. The A3CFF maintained its activity even after extended storage at 4°C for 1year. Since the A3 is a halotolerant fungus, we tested its ability to alleviate salt stress effects. Indeed, when added at 1:50 dilution factor to NS in the presence of 250mM NaCl, the A3CFF enhanced the plant salt tolerance by increasing the levels of total chlorophyll, proline, CAT, and SOD activities. In addition, the treated plants accumulated less Na^+ in their roots but more K^+ in their leaves. The A3CFF was also found to induce the expression of five salt stress related genes (NtSOS1, NtNHX1, NtHKT1, NtSOD, and NtCAT1).

Finally, we proved that the A3CFF can reduce by half the chemical fertilizers inputs. Indeed, the tobacco plants grown in a hydroponic system using 0.5xNS supplemented with A3CFF (1:50) exhibited significantly higher growth than those grown in 0.5xNS or 1xNS. In an attempt to explain this mechanism, the expression profile of some growth related genes (nitrogen metabolism (NR1, NRT1), auxin (TRYP1, YUCCA6-like), and brassinosteroid (DET2, DWF4) biosynthesis) was performed. The results showed that all these genes were up-regulated following plant treatment with A3CFF. In summary the results revealed that the halotolerant fungus *P. olsonii* can stimulates tobacco plant growth, enhances its salt tolerance, and reduces by half the required chemical fertilizer inputs in a hydroponic farming system.

KEYWORDS

***Penicillium olsonii*, halophilic PGPF, cell-free culture filtrate, salt stress, plant growth promotion, sustainable agriculture**

Introduction

Plants live in unstable environments that often inhibit growth and development. Unfavorable environmental conditions include biotic and abiotic stresses, such as drought, salt, and low or high temperatures, which greatly reduce plant productivity and threaten food security (Jamil et al., 2011; Zhu, 2016). Improving agricultural sustainability requires efficient management of soil fertility, fertilizer input, water use, and crop rotations, which help maintain proper soil equilibrium and high crop productivity. Biological processes in the soil play important roles in the cycling of essential elements for plant growth, including carbon, nitrogen, phosphorus, and sulfur (Drobek et al., 2019). In 2012, more than 6.2 million hectares in European countries were treated with biostimulants (Calvo et al., 2014; Colla and Rouphael, 2015). The use of microorganisms in improving nutrient availability for plants is an important strategy to protect biodiversity, and meet the increasing food demands of the global population (Vimal et al., 2017). It is well known that plant growth and health benefit from the presence of certain bacteria and fungi that live both within and around their tissues. In particular, soil fungi have long been known as a key element of soil fertility, plant nutrient turnover, and plant growth promotion (Haro and Benito, 2019). The plant growth-promoting fungi (PGPFs) can influence germination, seedling vigor, shoot growth, root growth, photosynthetic efficiency, flowering, and yield (López-Bucio et al., 2015; Hossain and Sultana, 2020b). Moreover, previous studies have revealed that PGPFs also improve systemic tolerance of abiotic stress in various crop plants (Khan et al., 2011; Zhang et al., 2016; Chandra and Singh, 2020). PGPFs include species of the genera *Aspergillus*, *Fusarium*, *Trichoderma*, *Penicillium*, *Piriformospora*, *Phoma*, and *Rhizoctonia* (Hossain et al., 2007, 2014, 2017; Shoresh et al., 2010). *Aspergillus*, *Fusarium*, *Penicillium*, *Piriformospora*, *Phoma*, and *Trichoderma* are specifically involved in abiotic stress tolerance (Chandra and Singh, 2020). The specific selection of halotolerant fungi that promote salt tolerance and plant growth could thus significantly enhance plant productivity either under normal or salt stress conditions, representing a promising approach for increasing nutrient bioavailability and helping advance saline soil-based agriculture.

The soil microorganisms play a fundamental role in regulating organic matter decomposition and the mobilization of nutrients for plants, thus promoting their growth and productivity (Yarzábal and Chica, 2017). PGPFs represent roughly 44.2% of rhizosphere fungal isolates (Hossain and Sultana, 2020a). However, their frequency of occurrence in the rhizosphere varies with host plant species (Schmid et al., 2018; Hakim et al., 2021). These beneficial fungi have a crucial role in physiological processes such as photosynthesis, phytohormone biosynthesis, and responses to salinity, drought, heat, cold and heavy metal stresses (Ansari et al., 2013). *Trichoderma virens* has been used to enhance biomass production and stimulate lateral root development in Arabidopsis seedlings (Contreras-Cornejo et al., 2009). A bushy root phenotype and strong stimulation of root hair development were observed in Chinese cabbage (*Brassica rapa*) seedlings treated with *Piriformospora indica* (Lee et al., 2011). Similarly, multiple species of PGPFs have been described that enhance cucumber (*Cucumis sativus*) plant growth *via* different mechanisms (Chandanie et al., 2009; Saldajeno and Hyakumachi, 2011; Hossain et al., 2014; Islam et al., 2014; Babu et al., 2015). Spinach (*Basella alba*) seedlings inoculated with the rhizosphere fungus *Fusarium* spp. showed more vegetative growth and both higher germination percentages and vigor indices compared to non-treated plants (Islam et al., 2014). Auxin and cytokinin phytohormones are involved in interactions between plant roots and soil microorganisms like bacteria and fungi (Boivin et al., 2016). The effectiveness of *Penicillium menonorum* on cucumber (*C. sativus*) growth is attributed to the secretion of indole acetic

acid (IAA), which potentially represents the main mechanism for plant growth stimulation (Babu et al., 2015). Additionally, Arabidopsis seedlings showed characteristic auxin-related phenotypes, including lateral root development and biomass increases, when inoculated with *Trichoderma virens* (Contreras-Cornejo et al., 2009). Salas-Marina et al. (2011) also noted that the *Aspergillus ustus* promotes growth in *Arabidopsis thaliana* through auxin synthesis in liquid cultures.

Besides observing the direct effects on plant growth from mycelium, potential effects of fungal culture filtrates have also been studied. Treatments with *Fusarium tricinctum* RSF-41 and *Alternaria alternata* RSF-61 culture filtrates have been found to improve growth of rice (*Oryza sativa*) seedlings *via* IAA secreted into culture media (Khan et al., 2015). Autoclaved and filter-sterilized culture filtrates of *P. indica* enhance hairy root growth and lignin production of *Linum album* (Kumar et al., 2012). Furthermore, *in vitro* co-cultivation with *P. indica* culture filtrate alters callus production, organogenesis, and photosynthetic pigment content in *Artemisia* annua (Baishya et al., 2015). Khan et al. (2015) suggested that fungi secrete plant hormone-like compounds into culture media that help re-program and regulate endogenous phytohormone levels of the host plant. The *Penicillium* genus, which is widely distributed in soil habitats of cultivated, forest, desert, beach, and marine regions, has several species that are known PGPFs that can produce phytohormones and enhance mineral solubilization (Babu et al., 2015). Results from previous studies conducted with *Penicillium* sp. showed effective enhancement of plant growth and improvement of biotic and abiotic stress tolerance in multiple plant species (Hossain et al., 2007; Khan et al., 2008; Khan and Lee, 2013; Hossain et al., 2014; Radhakrishnan et al., 2014; Khan et al., 2015), and in one such study it was demonstrated that isolated *Penicillium* sp. cultures promote growth of rice seedlings and *Suada japonica* (You et al., 2012).

Hydroponics systems usually require lower nutrients and water use and, thus promote environmental protection and agricultural sustainability, especially when combined with plant growth promoting microorganisms (PGPMs) (Bartelme et al., 2018). In the current study, our main objective was to mine the rhizosphere of the halophyte plants for the presence of beneficial microorganisms that can help plants to grow under normal as well as under stress conditions. For this, a fungus (A3) belonging to the *Penicillium* genus was isolated from the rhizosphere of the halophyte plant *A. littoralis* as first step of this work. We secondly tested the effect of A3 mycelium on plant growth in either solid or liquid media. Next, the ability of A3 cell-free culture filtrate (A3CFF) to promote the growth and to alleviate salinity stress in tobacco plants grown in a hydroponic system was evaluated. We then determined the potential of A3CFF to decrease the quantity of chemical fertilizers required in nutrient solution (NS) in a hydroponic growing system. Finally, in order to understand the possible mechanisms by which A3CFF can promote plant growth and enhance salinity stress tolerance, the expression profiles of certain growth- and salt stress-related genes were monitored using semi-quantitative and quantitative RT-PCR.

Materials and methods

Fungi isolation and qualitative evaluation of growth-promoting activity

Following the method described by Tarroum et al. (2021), the fungi were isolated from the soil surrounding the roots of *A. littoralis*, plants that dominate the salty soil at a location called "Salboukh" (north of Riyadh, Saudi Arabia: 25°04′48.6" N 46°20′27.7″ E). Following repeated sub-culturings on PDA plates of isolated mycelia, pure colonies were obtained and stored in 30% glycerol at −80°C for further study.

To evaluate the growth-promoting activity of the isolated fungus (referred as A3), tobacco seeds were soaked in 10% (v/v) bleach for 15 min, then rinsed with sterilized water four times and finally they were germinated on solid Murashige and Skoog medium (MS). The square petri plates (17 × 17 cm) containing seeds were incubated vertically in the growth chamber for 10 days at 25°C ± 2°C. Then, the isolated fungus (5 µl of a liquid culture) was inoculated at the bottom of treated petri dishes and for control ones 5 µl of sterilized water were added. One month after sowing, the plates were photographed and growth stimulation was evaluated qualitatively basing on root length and leaf surface.

Microscopic observation and fungal identification

Microscopic observation of A3 was performed as described by Tarroum et al. (2021). In brief, solid PDA medium was cut into small squares, and then transferred to new petri plates containing a wet filter paper. Using sterile needles, the four edges of each PDA block were then inoculated with isolated A3 fungus. Following incubation of plates for 72 h at 27°C, the coverslips were gently removed and transferred to microscope slides with a drop of lactophenol cotton blue stain. The slides were examined and photographed using a Nikon microscope.

Five-day-old mycelium was collected from PDA plate and ground in liquid nitrogen to a fine powder using a mortar and pestle. Genomic DNA was then extracted using a DNeasy Plant Mini Kit (Qiagen) according to the manufacturer's instructions. The isolated DNA was used for PCR amplification of a nuclear ribosomal internal transcribed spacer (ITS) region which was amplified by universal primers ITS1 (forward) and ITS4 (reverse) as listed in (White et al., 1990). PCR amplification was carried out in a 30 µl reaction volume as described by Tarroum et al. (2021). After running the amplified fragments on 1.5% agarose gels, they were purified and cloned into pGEM®-T Easy vectors (Promega) then sequenced by Macrogen Inc., (Seoul Korea). The resulting

sequences were used in BLAST searched using NCBI databases to identify the isolated fungus.

Temperature and salinity effects on A3 growth

To assess the effect of temperature on A3 growth, the mycelium was inoculated on PDA and incubated at 27°C or 40°C (three replicates each). The effect of salinity on fungal growth was tested on MS medium at five NaCl concentrations (100, 200, 400, 800, and 1,000 mM NaCl) with three replicates each. The isolated fungus was sub cultured at the center of 9 cm petri dishes each containing 20 ml medium and incubated at 27°C. The diameter of mycelium growth was measured every 2 days during 15 days.

Quantification of IAA in A3 filtrate

IAA production was measured according to Gordon and Weber (1951). In brief, the fungus was inoculated in liquid MS medium with or without L-tryptophan (1 mg/ml) and incubated at 27°C for 7, 14, 21, or 28 days. After incubation, each culture was centrifuged at 10,000 rpm during 15 min. The supernatant (1 ml) was mixed with 1 ml of Salkowski reagent (1 ml 0.5 M FeCl3, 30 ml concentrated H_2SO_4, and 50 ml distilled H_2O) and incubated in the dark at room temperature during 20 min. The optical density at 530 nm was measured and the amount of IAA produced was calculated using a standard curve.

Quantitative evaluation of growth-promoting activity by A3 fungus

To quantitatively evaluate the effects of A3 fungus on plant growth, two vertical plastic boxes were assembled, with the top box containing 15 holes and filled with sterilized vermiculite and fixed to a lower box containing sterilized MS liquid medium. Five sterilized tobacco seeds as described above were germinated into the vermiculite-containing box. Ten days later, five microliters of liquid culture containing isolated A3 fungus added to the MS medium. After three additional weeks of inoculation, plants were harvested and plant height, leaf area, dry weight, and total chlorophyll content were recorded.

Growth-promoting activity evaluation of A3 cell-free filtrate (CFF)

In MS liquid medium

To prepare A3CFF, a mycelium disc of 5 mm in diameter was picked from a 7-day-old culture grown on solid PDA medium then inoculated into a 250 ml Erlenmeyer flask containing 100 ml of MS medium. Cultures were then incubated at 27°C with shaking at 150 rpm for 30 days, vacuum filtered (0.22 µm), and the resulting A3CFF stored at 4°C for further use.

Growth containers were made consisting of two assembled and autoclaved boxes, with the top box containing nine holes into which plants can be inserted and the bottom box filled with 1.5 l of MS liquid media and covered with aluminum foil to avoid algal contamination. Sterilized tobacco seeds were sown in sterile 1.5 ml Eppendorf tubes that were perforated at the bottom and filled with vermiculite. One week after germination, seedlings of similar sizes were selected and transferred to growth containers containing one of three different dilutions of A3CFF (1:500, 1:1000, and 1:2000). Growth containers were then kept in a temperature and humidity-controlled growth chamber. Plants were harvested 1 month later and shoot length, root length; fresh and dry shoot weights, leaf number, and leaf area were recorded. The total chlorophyll and proline content as well as catalase (CAT) and superoxide dismutase (SOD) activity levels were also quantified.

The stability of A3CFF stored for 1 year at 4°C, was evaluated in liquid MS media using the growth containers described above. One week old seedlings were transferred to growth containers supplemented with 1:500 dilutions of fresh or stored A3CFF. The two parts of the growth container were carefully sealed and placed in growth chamber with controlled conditions. One month later, the shoot and root length, dry and fresh weight, leaf number, and leaf area was recorded.

In NS

In order to examine the potential use of A3CFF in hydroponic growing systems, its ability to promote plant growth when added to a NS in place of chemical fertilizers was evaluated. Full-strength NS was prepared by mixing the following in a total of 1 l water then adjusting the pH to 6.2: 600 mg Chem-GroTM fertilizer 8-15-36, 600 mg $CaNO_3$, 373 mg $MgSO_4$. Following procedures described above, germinated tobacco seeds were transferred to growth containers in which the bottom part was filled with NS and supplemented with a 1:50 or 1:500 dilution of A3CFF. One month later, morphological parameters such as shoot and root length, fresh/dry weight, leaf number, and leaf area were measured.

Evaluation of salt stress alleviation of A3CFF

Tobacco seeds were sterilized (as described above) then placed in sterile 1.5 ml Eppendorf tubes (perforated from the bottom) containing vermiculite. The tubes were fixed in a small plastic cups with a hole in the bottom and then kept in a sterile box for germination. Germinated seeds were then transferred to a hydroponic system consisting of two autoclaved boxes, with the top box containing nine holes for plant placement and the bottom box filled with 1.5 l of NS and covered with aluminum

foil to avoid algal contamination. After 2 weeks of growth, plants were subjected to one of four treatments: (1) growth in a hydroponic system containing only NS (control), (2) growth in NS supplemented with A3CFF at 1:50 dilution, (3) growth in NS and 250 mM NaCl, (4) growth in NS with 250 mM NaCl and a 1:50 dilution of A3CFF. The boxes containing the plants were kept for 6 weeks in a growth chamber (16 h light, 8 h dark, 25°C ± 2, relative humidity 60–70%). Plants were then harvested, growth parameters listed above recorded, and the samples immediately frozen in liquid nitrogen and kept at −80°C until further use.

Evaluation of fertilizer input substitution by A3CFF

Sterilized tobacco seeds were placed in sterile 1.5 ml Eppendorf tubes (perforated from the bottom) containing vermiculite. Following 10 days of germination, seedlings were transplanted to a hydroponic growing system (as described above) containing either full (NS) or half (0.5NS) NS. For the treated plants, 1 week after transplantation, the 0.5NS was supplemented with A3CFF at a dilution of 1:50. Plants were grown in a growth chamber (16 h light, 8 h dark, 25°C ± 2, relative humidity 60–70%) and plant growth parameters were measured after 1 month.

Estimation of physiological and biochemical parameters

Chlorophyll

Total chlorophyll was extracted in 80% acetone for 24 h at 4°C in the dark. Absorbance at 645 nm and 663 nm was determined with an Amersham spectrophotometer and used to calculate total leaf chlorophyll content according to the following equation: Total chlorophyll (μg/ml) = 20.2 (A645) + 8.02 (A663) (Liang et al., 2017).

Proline

Proline was extracted following the protocol described by Ábrahám et al. (2010). Liquid nitrogen was used to grind 0.5 g of fresh leaf tissue and the resulting powder incubated in 10 ml of 3% aqueous sulfosalicylic acid. The mixture was centrifuged at 10,000 rpm and 2 ml of supernatant added to 2 ml ninhydrin plus 2 ml glacial acetic acid. The mixture was then boiled at 100°C for 1 h and the reaction stopped by transferring the tubes to an ice bath for 5 min. Next, 6 ml of toluene was added, mixed vigorously for 15 s, and the absorbance of the upper phase read at 520 nm. The proline content was expressed in μg/g fresh weight.

CAT and SOD activity

Enzymes were isolated as described by Jogeswar et al. (2006). Fresh tissue (100 mg) was ground in liquid nitrogen then incubated in 0.1 M of phosphate buffer (pH 7.4) containing 0.1 mM EDTA, 1% (w/v) PVP, and 0.5% (v/v) Triton-X 100. The homogenate was centrifuged at 14,000 rpm for 20 min at 4°C, and the supernatant was used to estimate CAT and SOD activities.

CAT activity was measured following the method described by Claiborne (1985) and modified by Jogeswar et al. (2006). The reaction mixture consisted of 1 ml 0.06 M H_2O_2, 0.1 M sodium phosphate buffer (pH 7.4), 1.9 ml distilled water, and 100 μ enzyme extract. Catalytic activity was recorded by spectrophotomer using the decline in absorbance at 240 nm owing to degradation of H_2O_2 and was expressed as units/g protein.

SOD activity was measured following the method described by Chandrakar et al. (2016) with minor modifications. The reaction mixture (3 ml) contained 50 mM of Tris–HCl buffer (pH 8.2), 1 mM EDTA, 100 μl enzyme extract, 0.4 mM pyrogallol, and H_2O up to 3 ml. SOD activity (U/g protein) was defined as the amount of enzyme required to inhibit 50% of pyrogallol oxidation based on absorbance at 420 nm.

Determination of K^+ and Na^+ content

The concentrations of Na^+ and K^+ were estimated in root and leaf. Dried tissues were incubated in 0.5% HNO_3 for 7 days (Ben-Romdhane et al., 2018). The supernatant was filtered and the concentration of Na^+ and K^+ was then estimated using an atomic absorption spectrometer (Thermo Scientific™, United Kingdom) and reported as mg/g dry weight.

RNA extraction and genes expression profiling

Total RNA was extracted following plant treatment with A3CFF at three times (0, 24, and 72 h) using the QiagenRNAeasy Plant Mini Kit following the manufacturer's instructions. After quantification, total RNA was treated with DNaseI (RQ1, Promega, United States). The cDNAs were synthesized as follow: 5 μg of total RNA was reverse transcribed with random hexamer and oligo-(dT18) primers using SuperScript™ III reverse transcriptase (Invitrogen), as described in the manufacturer's instructions. The cDNA was used for RT-qPCR reactions, which were carried out using 480 SYBER Green I Master Mix (Roche, Switzerland) as described in the manufacturer's manual. The PCR cycling conditions were as follow: 95°C for 3 min, followed by 40 cycles of 95°C for 20 s, 60°C for 30 s, and 72°C for 1 min. To create a melting curve and check primer specificity, the extension temperature was increased from 72°C to 95°C after 40 cycles of amplification. Actin (380 bp, ACT-F and ACT-R) was selected as a reference gene. Primers targeting salt stress-related genes (NtSOS1, NtNHX1, NtHKT1, NtSOD, and NtCAT1) or those implicated in in nitrogen metabolism (NR1, NRT1), auxin biosynthesis (TRYP1, YUCCA6-like), and brassinosteroid biosynthesis (DET2, DWF4) selected for this study (Supplementary Table S1) were designed *via* primer 3

software.[1] Target gene expression was quantified and expressed relative to actin expression using either the ΔΔCT comparative method (Ben-Romdhane et al., 2018), ΔΔCt = (Ct target gene - Ct actin) treated plant - (Ct target gene - Ct actin) control or by the semi-quantitative PCR products analyzed using a 1.5% agarose gel. To ensure reproducibility, two biological and three technical replicates were performed for this experiment.

Statistical analysis

Data were analyzed using one-way ANOVA followed by Duncan's test *via* SPSS software version 25. Each value presented is the mean of five replicates for all growth parameters and three replicates for qPCR. Different letters on bar charts are used to indicate means that differ significantly at $p \leq 0.05$.

The identification of isolated fungus was performed by the use of NCBI-BLAST search and the phylogenetic tree was constructed using neighbor-joining method by bootstrapping 1000 times in MEGA X software.

Results

Isolation, identification, and qualitative evaluation of fungi growth-promoting activity

As a first step, 20 soil samples were collected from the rhizosphere of the halophyte grass *A. littoralis* growing in the sebkha of Salboukh. From these samples, 18 fungi (designed A1 to A18) were identified based on visual differences in their morphology when grown on PDA medium. The 18 isolated fungi were evaluated qualitatively for their ability to promote growth of tobacco seedlings cultivated on MS medium. The results showed that out of 18 tested fungi, only seven strains were able to clearly stimulate root and leaf growth of tobacco seedlings (data not shown). For further detailed investigations, the A3 fungus was chosen as it had the greatest effect on plant growth (Figure 1). Morphologically, on PDA media after 1 week of incubation at 27°C, the A3 colonies had moderate growth, with a green color on one side and pale yellow on the reverse side. Microscopic analysis revealed that the A3 strain has a septate hypha terminating in a complex conidiophore. Moreover, chlamydospore was clearly visible at 40x magnification (Supplementary Figure S1a). The growth of A3 showed maximum growth after 12 days of incubation at 27°C. However, at 40°C, total inhibition of A3 growth was observed (Supplementary Figure S1b). Since A3 was isolated from the rhizosphere of the halophyte grass *A. littoralis* its tolerance to NaCl in the culture media was also investigated.

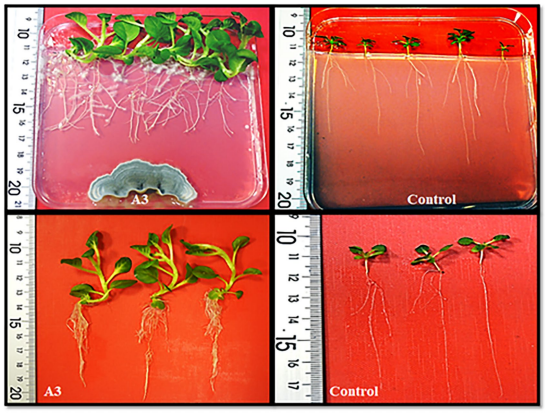

FIGURE 1
Evaluation of the qualitative growth promoting activity effect of tobacco seedlings cultivated on MS solid medium in the presence of the isolated A3 fungus.

Based on mycelial growth levels, the A3 fungus was able to grow in up to 1 M NaCl. Interestingly, the A3 fungus showed the largest colony diameter at 200 mM NaCl, while the growth rate of A3 mycelia was inhibited at NaCl concentrations above 200 mM (Supplementary Figure S1c). Finally, using Salkowski's reagent, IAA was detected in growth medium containing L-tryptophan at 0.93 ppm after 28 days of incubation. In a medium without L-tryptophan IAA was detected at 0.20, 0.22, 0.24, and 0.26 ppm after 7, 14, 20, and 28 days of incubation, respectively. This confirmed that the addition of L-tryptophan to growth media and extended incubation times are required for maximum auxin production by the A3 fungus (Supplementary Figure S2).

The ITS region was chosen as it is the barcode with the highest probability of correct identifying a huge number of sampled fungi (Raja et al., 2017). The isolated ITS sequence fragment was BLAST searched against the NCBI GenBank and showed 93.4% identity to the one of *Penicillium olsonii* (Supplementary Figure S3). Basing on these results the A3 is likely *P. olsonii*.

Quantitative evaluation of the A3 growth promoting activity

The direct effect of A3 mycelium (DE) on plant growth promotion in liquid MS medium was quantitatively evaluated using plastic boxes as described in Materials and Methods (Figure 2A). When compared to control plants, A3 fungus-treated plants showed significantly higher shoot length, leaf area, dry weight, and total chlorophyll content (2, 3, 5, and 1.5 times higher, respectively (Figures 2B–E). These results confirm that the A3 fungus positively enhances growth of tobacco seedlings cultivated in hydroponic systems when added to liquid MS medium and thus A3 is potentially a PGPF.

1 http://bioinfo.ut.ee/primer3-0.4.0/

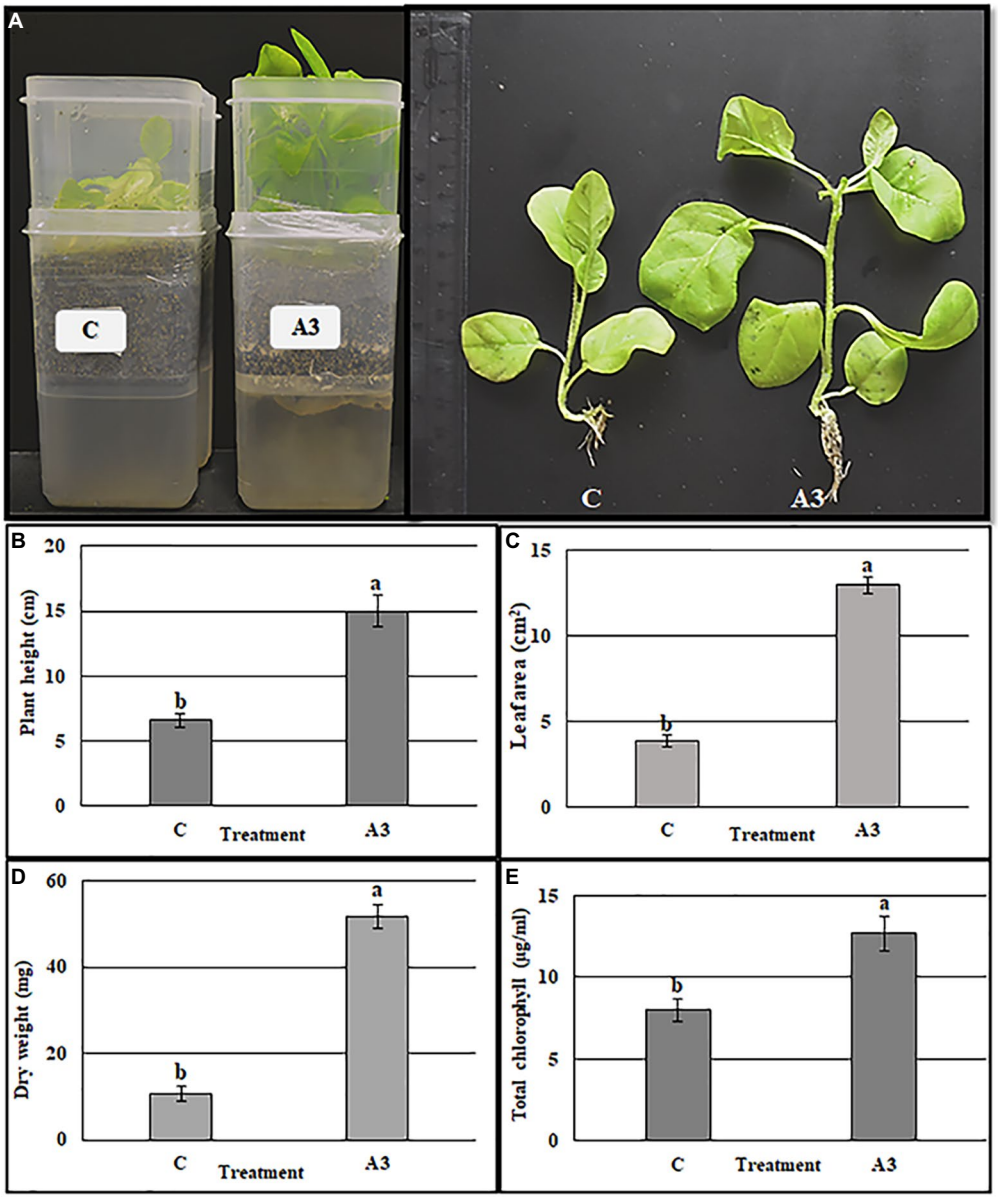

FIGURE 2
Quantification of A3 growth stimulation activity on tobacco seedling grown in MS liquid medium. Seeds of tobacco were cultivated in the two boxes hydroponic system, vermiculite in the top and MS liquid medium in the bottom. The treatment was performed by adding 5µl of A3 liquid culture in MS medium after 10days of sowing seeds. Plant morphology **(A)**, plant height **(B)**, leaf area **(C)**, plant dry weight **(D)**, and total chlorophyll **(E)**: Data are the means of five replicates±standard deviation; different letters on bars represent the significant values according to Duncan's test ($p<0.05$).

Quantitative evaluation of the A3CFF growth promoting activity

In MS liquid medium

The ability of cell-free culture filtrate from A3 culture (A3CFF) to stimulate growth of tobacco plants in a hydroponic system was determined. MS liquid medium was used as the growing media and was supplemented with one of three dilutions of A3CFF (1:500, 1:1000, or 1:2000). After 1 month of treatment with A3CFF, net improvements in growth (Figure 3A), physiological (Figures 3B–G), and biochemical (Figure 4) parameters were observed for all three tested dilutions. Each dilution significantly promoted shoot/root length, fresh/dry shoot weight, and leaf area (Figures 3B–G). In addition, the highest values of total chlorophyll (27.7 µg/ml), proline accumulation (159 µg/g FW), as well as CAT (8.1 U/g proteins), and SOD (19.8 U/mg proteins) activities were detected in plants treated with an A3CFF dilution of 1:500 (Figure 4). These increases in proline synthesis and CAT/SOD activities in A3CFF-treated plants suggest that A3 fungus can

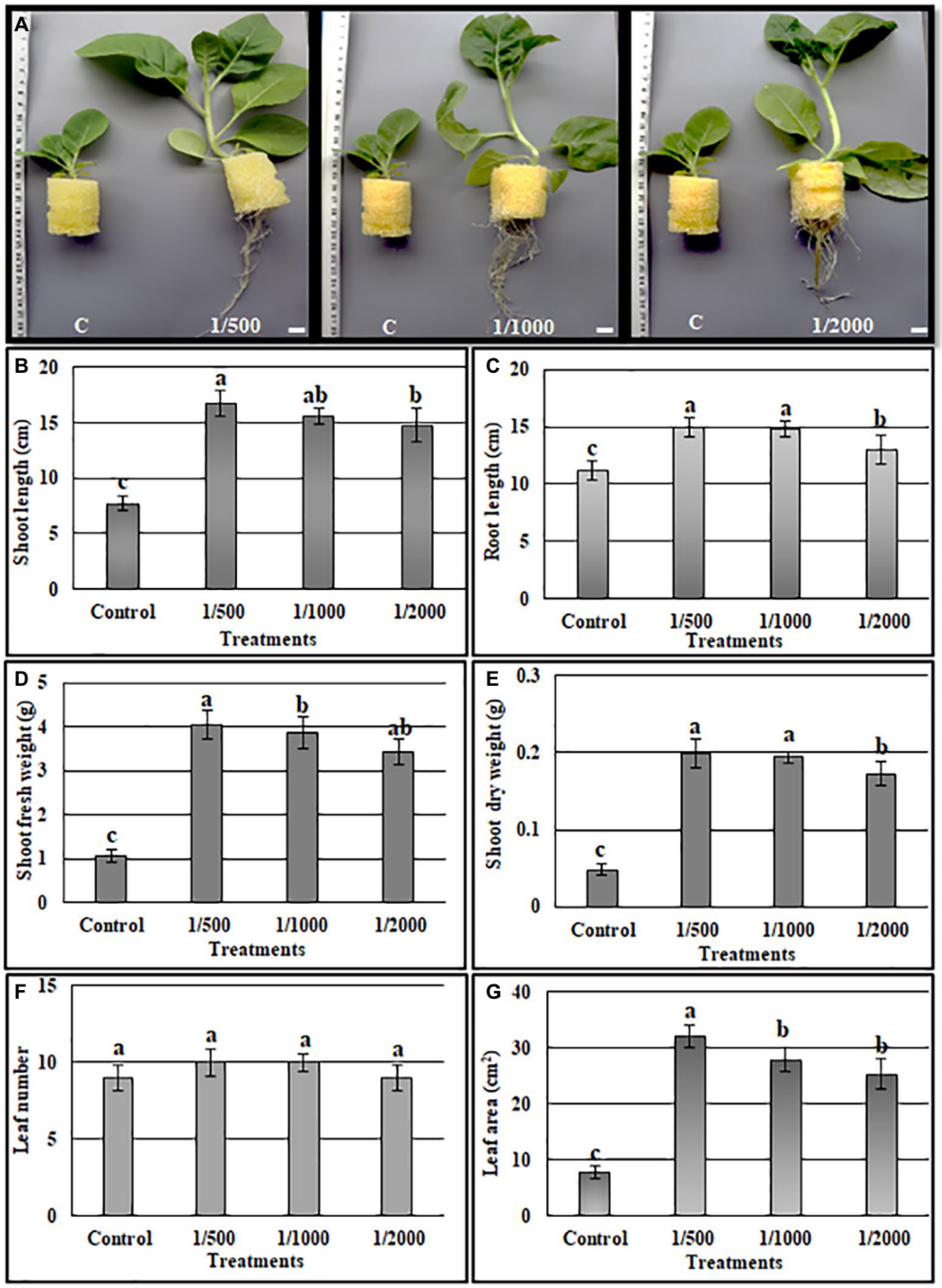

FIGURE 3
Quantification of A3 cell-free filtrate culture (CFF) growth stimulation activity on tobacco seedling grown in MS liquid medium. The MS liquid medium was supplemented with 1:500, 1:1000 and 1:2000 CFF dilutions. **(A)** Phenotype of plants after 1month, the shoot length **(B)**, root length **(C)**, shoot fresh weight **(D)**, shoot dry weight **(E)**, leaf number **(F)**, leaf area **(G)**. Data are the means of five replicates±standard deviation; different letters on bars represent the significant values according to Duncan's test (p<0.05).

alleviate salt stress. Finally, we tested the stability of A3CFF by growing tobacco seedlings in liquid MS medium containing a 1:500 dilution of fresh A3CFF or A3CFF stored at 4°C for 1 year (Supplementary Figure S4a). The results demonstrated that the positive effects on plant growth of A3CFF were preserved after 1 year of storage at 4°C (Supplementary Figures S4b–g).

In nutritive solution (NS)

The above results show that A3CFF stimulated plant growth when added to liquid MS medium in the absence of fungal mycelia. One of our goals from this work was to investigate the effects of PGPF application on hydroponically grown vegetable plants in conditions of reduced fertilization. We thus evaluated the

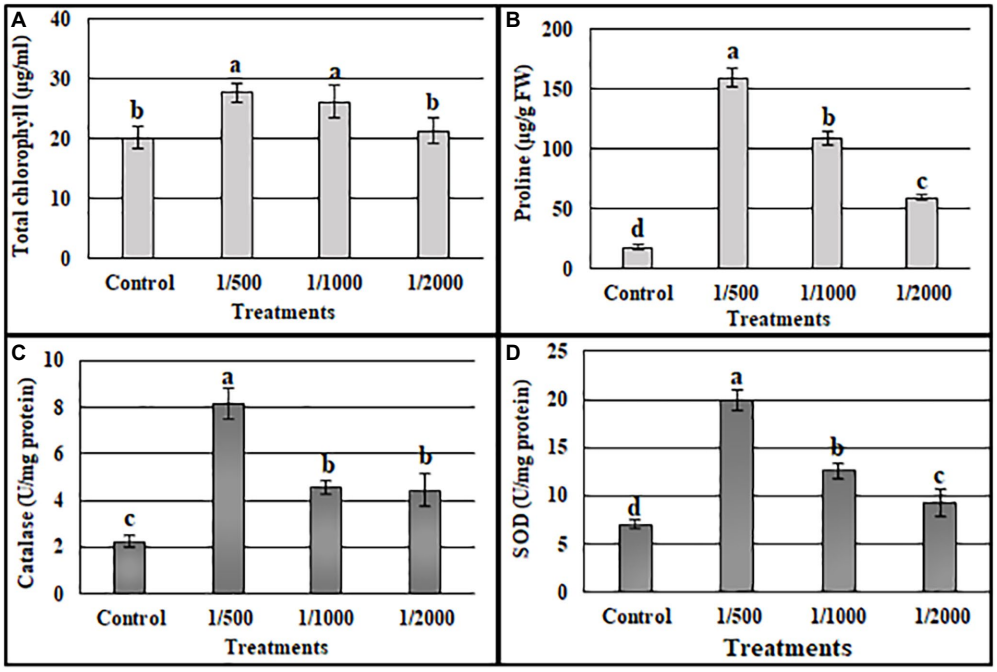

FIGURE 4
Effects of A3 CFFs at different dilutions (1:500, 1:1000 and 1:2000) on total chlorophyll **(A)**, proline **(B)**, catalase **(C)**, and SOD **(D)** activities in tobacco plants: Data are the means of five replicates ± standard deviation. Different letters on bars represent the significant values according to Duncan's test (p<0.05).

effectiveness of A3CFF in stimulating plant growth when mixed with commercial fertilizers in NS and used in hydroponic system. The two A3CFF dilutions, 1:500 or 1:50, when applied to tobacco seedlings grown in NS significantly stimulated growth (Figure 5A). Interestingly, the A3CFF dilution of 1:50 promoted the highest growth by increasing the shoot/root length, the shoot/root dry weight, and the leaf area by factors of 198, 174, 211, 319, and 200%, respectively (Figures 5B–F).

In The presence of salt stress

Tobacco plants treated with an A3CFF dilution of 1:500 and grown in MS liquid medium produced both higher CAT and SOD activities and proline levels compared to untreated plants (Figure 4). In addition, A3CFF in NS at a dilution factor of 1:50 induced more plant growth. Based on these results, we investigated the ability of A3CFF to alleviate salt stress. The addition of A3CFF to NS at a dilution of 1:50 in the presence or absence of 250 mM NaCl enhanced tobacco plant growth compared to control plants (Figure 6A). The presence of 250 mM NaCl in NS significantly reduced the biomass production shoot/root length, weight, and leaf area of tobacco plants compared to those in NS alone. This growth inhibition due to salt stress was decreased following the addition of A3CFF (1:50) to NS containing 250 mM NaCl and (Figures 6B–F). Additionally, the root lengths of the co-treated plants were significantly larger than that of control plants grown in NS only (Figures 6A,C). Moreover, after 1 month without NaCl, A3CFF increased shoot and root length by factors of 1.4 and 1.5, respectively, compared to control plants.

We also measured additional parameters to further assess the effects of A3CCF on salinity stress responses. Levels of total chlorophyll under salt stress were significantly lower than in control conditions. However, the application of the A3CCF in conjunction with salt stress restored total chlorophyll content to levels comparable to those of control plants under normal conditions (Figure 7A). In addition, the highest value of total chlorophyll, 14.05 µg/ml, was observed in plants grown with A3CCF without NaCl stress (Figure 7A). For proline accumulation, a significant difference was noted between inoculated and non-inoculated plants under salinity stress (Figure 7B). SOD and CAT activities during salt stress were also significantly higher in A3CFF-treated plants compared to non-treated plants (Figures 7C,D).

One of the most important mechanisms for coping with saline toxicity is the reduction of Na^+ uptake, which is accompanied by the increased K^+ retention in order to counter balance the Na^+ entry. Plants treated with 250 mM NaCl showed a significant increase in Na^+ levels in both roots and shoots compared to the control plants (Figure 7E). The addition of A3CFF to salt-stressed plants decreased Na^+ accumulation by 14.8% in roots and 6% in shoots compared to control ones. In contrast, in the absence of NaCl, no significant difference in the Na^+ levels in tissues was detected between inoculated and non-inoculated plants (Figure 7E). Unlike for the Na^+ levels, salt treatment inhibited the

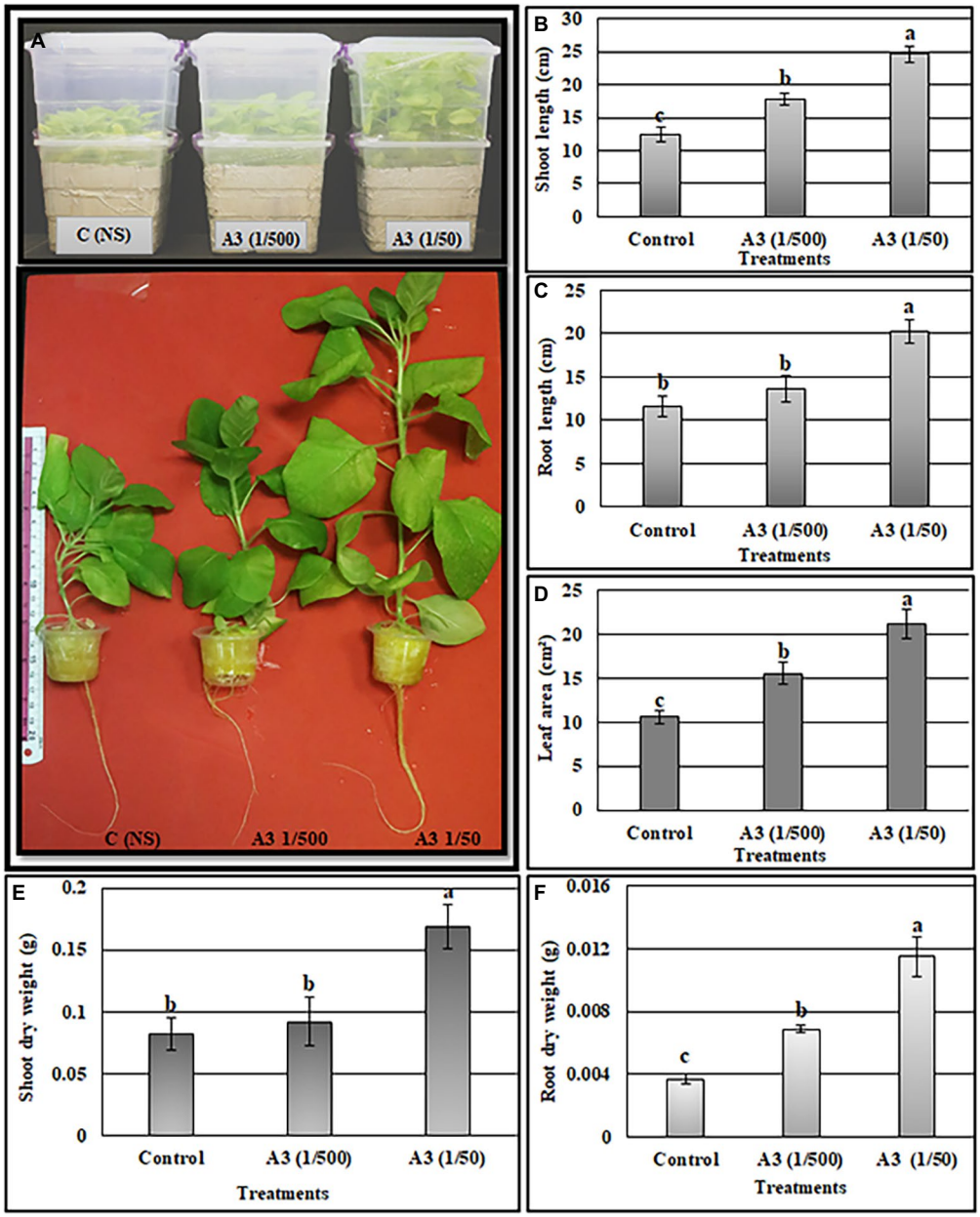

FIGURE 5
Effects of A3 CFF when added at dilutions of 1/50 and 1/500 to nutrient solution (NS) on promoting tobacco seedlings growth cultivated in hydroponics system. Plant morphology **(A)**, shoot length **(B)**, root length **(C)**, leaf area **(D)**, shoot dry weight **(E)**, root dry weight **(F)**. Different letters on bars represent the significant values according to Duncan's test ($p<0.05$).

K^+ uptake in shoots and roots (Figure 7F). Nevertheless, plants inoculated with A3CFF contained significantly more K^+ compared to non-inoculated plants under both control and salt stress conditions (Figure 7F). Thus these results demonstrated that the A3CFF treatments of plants cultivated in NS with 250 mM NaCl had no effect on Na^+ and K^+ concentrations in shoots and roots, respectively. On the other hand, it decreased Na^+ in roots but increased K^+ in shoots (Figures 7E,F).

In an attempt to understand the mechanisms by which A3CFF helps plants to cope with high salinity, the expression profiles of multiple salt stress genes (NtHKT1, NtNHX1, NtSOS1, NtSOD, and NtCAT1) were investigated in plants treated with A3CFF and 250 mM NaCl. Adding A3CFF to NS with or without 250 mM NaCl resulted in clear and significant upregulation in both roots and leaves of NtSOD and NtCAT1, which are implicated in the antioxidative mechanisms (Figures 8D,E). The highest expression levels of these two genes were recorded in the leaves and roots 72 h after the addition of A3CFF to NS with 250 mM NaCl. The other three salt stress-associated genes examined, NtHKT1, NtNHX1, and NtSOS1, are the key determinants of Na^+ and K^+ homeostasis in plant cells

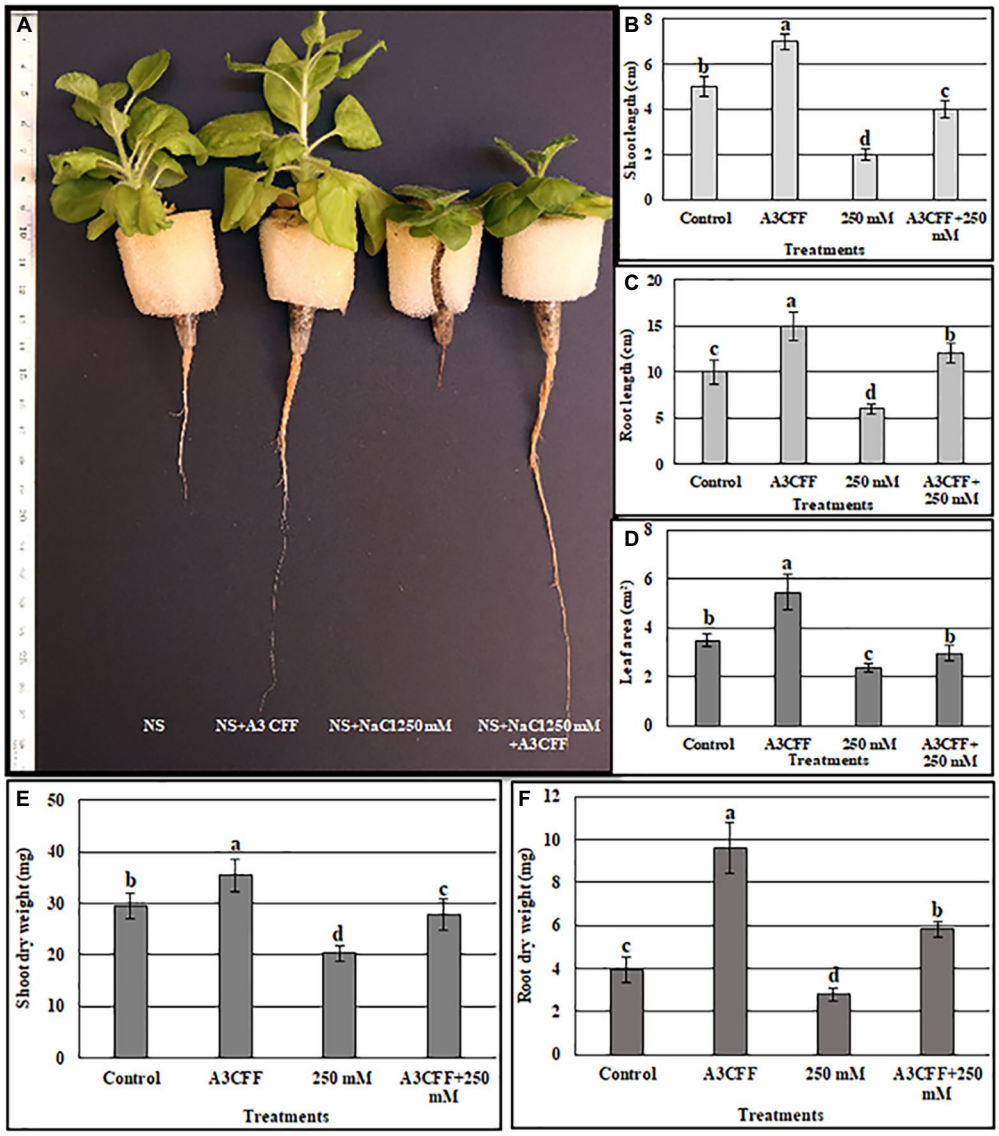

FIGURE 6
Evaluation the ability of A3 CFF to alleviate salt stress when added at 1:50 dilution to NS. **(A)** plant morphology photographed after 1month of treatment, Shoot length **(B)**, Root length **(C)**, Leaf area **(D)**, Shoot dry weight **(E)**, and Root dry weight **(F)** of tobacco seedlings grown in NS (control), in NS with CFF (A3CFF), with NaCl (250mM), with 250mM NaCl and CFF (A3CFF+250mM). Different letters on bars represent the significant values according to Duncan's test ($p < 0.05$).

and were upregulated following A3CFF treatment (Figures 8A–C). The Na^+/H^+antiporters (NtNHX1 and NtSOS1), which help plants to avoid Na^+ build-up in shoots were significantly upregulated in A3CFF-treated plants grown in NS with 250 mM NaCl compared to those cultivated only in the presence of salt stress. Moreover, this accumulation was higher in roots compared to leaves (Figures 8B,C).

Evaluation of A3CFF on chemical fertilizer inputs

The effectiveness of A3CFF in decreasing chemical fertilizer inputs without affecting plant growth was investigated by growing plants in 0.5NS supplemented with 1:50 dilution of A3CFF, 0.5NS alone, or full-strength NS (Figure 9A). Plants cultivated in 0.5NS and 1:50 A3CFF showed significantly enhanced growth parameters compared to plants cultivated only in NS or 0.5NS. Specifically, shoot/root length, dry weight, leaf number, and leaf area of plants grown in 0.5NS with 1:50 A3CFF were 160, 225, 209, 123,142, and 180%, respectively, of those values for plants grown in full NS (Figures 9B–G). These results revealed that A3CFF was able to compensate for the decrease in NS to half strength, suggesting that A3CFF can minimize the chemical fertilizers required for hydroponic systems without harming plant growth.

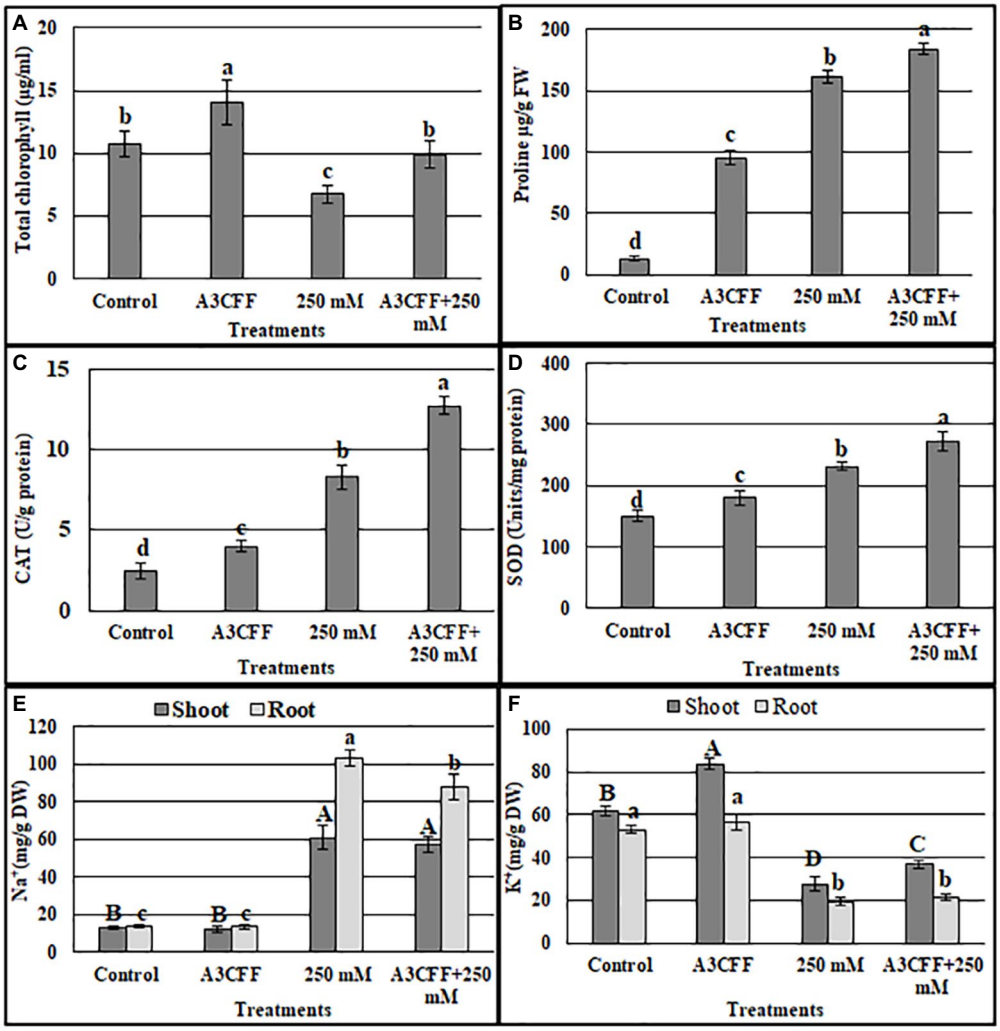

FIGURE 7
Estimation of total chlorophyll content **(A)**, proline accumulation **(B)**, catalase **(C)**, and SOD **(D)** activities, sodium **(E)** and potassium **(F)** contents in the tobacco seedlings grown in: NS (control), NS with A3 CFF, NS with 250mM NaCl (250mM), NS with 250mM NaCl and A3 CFF (A3CFF+250mM). Values are the mean of five replicates±SD. Different letters on bars represent the significant values according to Duncan's test (p<0.05).

The effects of the A3CFF on expression levels of several genes involved in plant growth, including DET, DWF4 (brassinosteroid biosynthesis), YUCCA6-like, TRYP1 (auxin biosynthesis), and NR1 and NRT1 (nitrogen-use efficiency) were examined in tobacco leaves and roots. Transcripts of all six genes were upregulated in both leaves and roots after A3CFF application (Supplementary Figure S5). The greatest transcript accumulation was observed for the YUCCA6-like and NR1 genes, which were most upregulated after 48 h and 72 h of treatment. Based on our results, we propose that A3CFF can induce the expression of growth-regulating DET2, DWF4, YUCCA6-like, and TRYP1 genes, likely explaining the observed plant growth stimulation. Moreover, accumulation of transcripts for the nitrogen-use efficiency-related genes NR1 and NRT may explain the compensation of A3CFF for decreased fertilizer levels in 0.5NS media.

Discussion

The main goals of smart agriculture are to assure both the quality and quantity of crops 'yield by developing organic and sustainable production systems. For this, the development of hydroponic systems ensures the reduction of fertilizer inputs and water consumption. Also, biostimulants are used in combination with conventional fertilizers to improve nutrient use efficiency and/or quality of crops (Halpern et al., 2015). The plant rhizosphere constitutes a valuable source of beneficial microorganisms that play important roles in shoot and root growth enhancement. PGPFs directly and indirectly influence both growth and productivity of a wide range of host plants with one study estimating that approximately 44% of rhizosphere fungal isolates are PGPFs (Hossain et al., 2017). In our study, a fungus designated *P. olsonii* was isolated from the

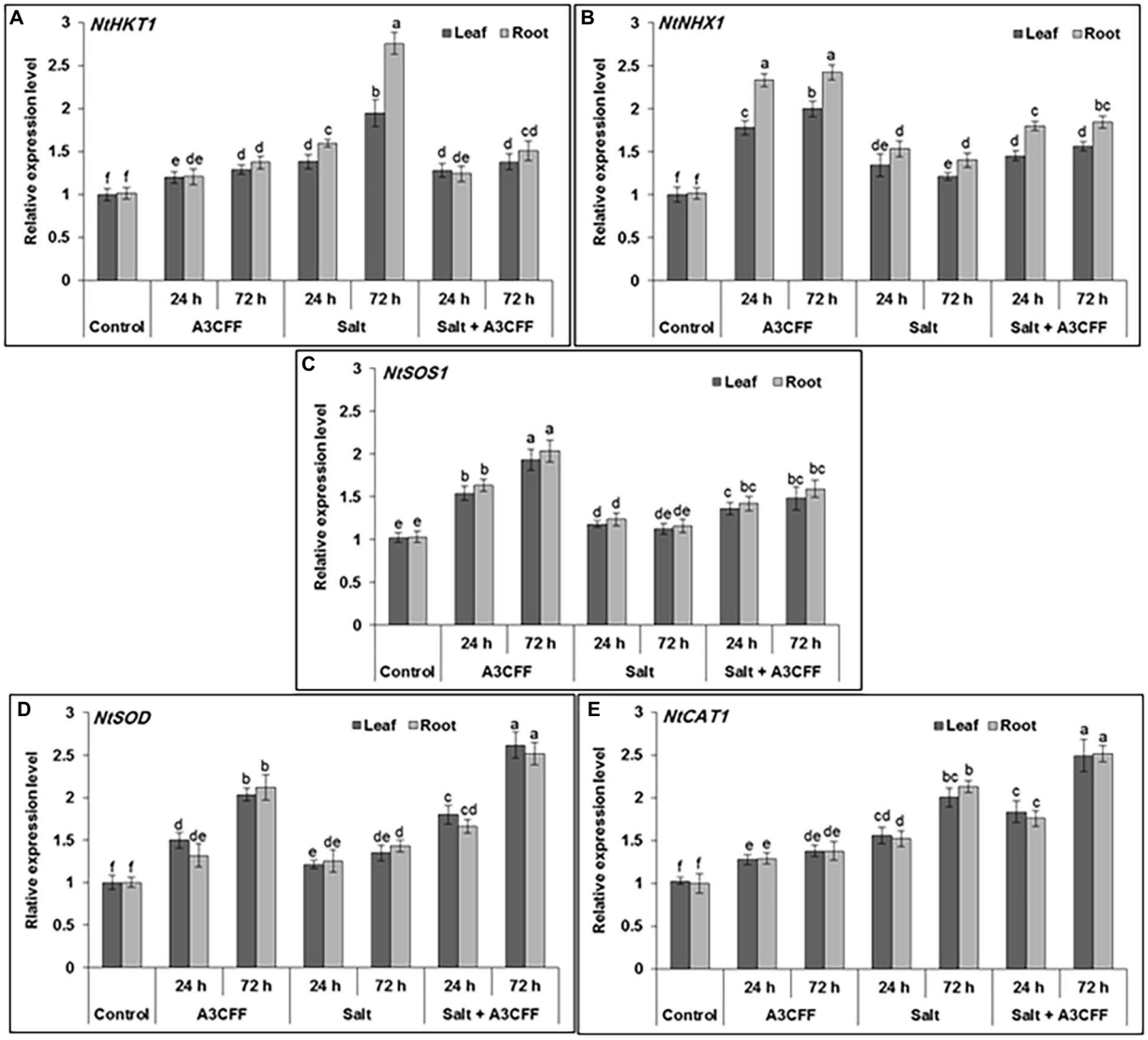

FIGURE 8
Quantitative RT-PCR analysis showing the effect of A3 CFF on gene expression levels of ROS-related and stress-responsive: HKT1 (XM_015785756), NHX1 (XM_015206776), SOS1 (KY752550), SOD (XM_019401370) and CAT (XM_009795943). The qRT-PCR was performed using RNA extracted from leaf and root at 0, 24, and 72h of salt (250mM of NaCl) application. Actin gene was used as reference.

rhizosphere of the extremophile plant *A. littoralis*. This fungus was found to significantly promote plant growth in solid or liquid culture media. Based on morphological and microscopic observations, the A3 fungus was identified as a *Penicillium* species, the morphological characteristics were in agreement with *Penicillium* description reported by Frisvad and Samson (2004). The ITS region has previously been shown to be an efficient tool for identifying huge numbers of fungal species and can help accommodate barcode gaps between inter and intra specific variation (Schoch et al., 2012). Furthermore, within the genus *Penicillium*, ITS marker has been noted to work well for providing species information (Visagie et al., 2014). Basing on the ITS sequences, the A3 fungus was identified as *P. olsonii*.

Our results showed that the optimum growth of A3 fungus is at 27°C but completely inhibited at 40°C. This finding is consistent with Diaz et al. (2002), who reported that *P. olsonii* grows at temperatures between 10°C and 25°C. In addition, the growth of *Penicillium marneffei* is dramatically inhibited at 40°C (Cao et al., 2007). As the A3 was isolated from salty soil we investigated its tolerance to the presence of NaCl in growth media. The results showed that A3 fungus tolerated up to 1,000 mM NaCl and it is an obligate halophile strain since its greatest growth was observed in the presence of 200 mM NaCl. This result is consistent with previous reports, as the growth of *P. olsonii* isolated from a sausage was enhanced by adding 3% NaCl to the media (Diaz et al., 2002). Moreover, previous research demonstrated that *P. spathulatum* grows in medium containing 5% NaCl (Frisvad et al., 2013).

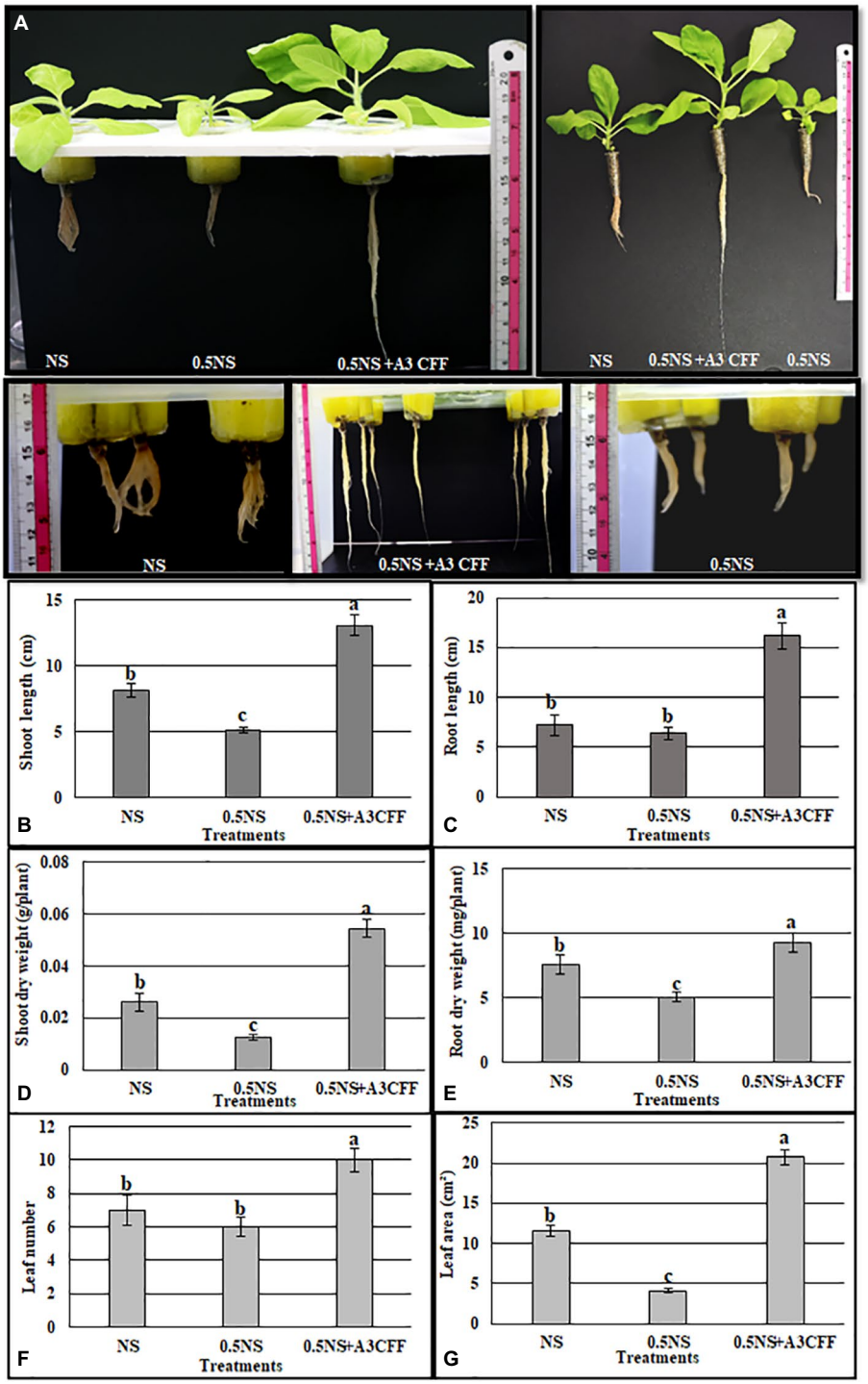

FIGURE 9
Effect of A3 CFF on tobacco plant growth cultivated in hydroponic system and in the presence of half strength NS (0.5NS). **(A)** Phenotypes of tobacco seedlings grown hydroponically in full NS, in 0.5 NS, in half NS supplemented with 1:50 dilution of A3 CFF (0.5NS+1:50CFF). The photos were taken after 1month following treatments. Shoot length **(B)**, root length **(C)**, shoot dry weight **(D)**, root dry weight **(E)**, leaf number **(F)**, and leaf area **(G)** in tobacco seedlings grown in 0.5 NS. Values are the mean of five replicates ± SD. Different letters on bars represent the significant values according to Duncan's test ($p<0.05$).

Fungal culture filtrates can contain metabolites, which are chemicals produced by fungi *via* multi-step enzymatic pathways. These metabolites include amino acids, mycotoxins, cyclic aromatic peptides, phenols, terpenoids, and plant growth regulators (Ogórek, 2016). In this study, we demonstrated that the A3 fungus secreted auxin, especially when the culture media

was enriched with L-tryptophan. Several fungal species that interact with plants have been revealed to produce and secrete auxin (Chanclud and Morel, 2016). The endophyte *Penicillium* sp. isolated form the Halophyte plants was reported to produce IAA (Kondrasheva et al., 2022). Similarly, *Phoma glomerata* and *Penicillium menonorum* can synthesize IAA, which may cause the significant growth increases detected in cucumber plants cultivated with both species (Babu et al., 2015; Waqas et al., 2015).

The quantitative evaluation of plant growth promotion by the A3 fungus was initially performed by directly applying A3 mycelia to liquid MS culture media. The most important value reflecting the growth-promoting activity of A3 fungus is the dry biomass production, which is 4.8 times higher compared to control plants. Similarly, *Penicillium menonorum*, *Penicillium citrinum*, and *Penicillium simplicissimum* were reported to increase the growth of cucumber, sunflower, and *A. thaliana* plants, respectively (Hossain et al., 2007; Babu et al., 2015; Waqas et al., 2015).

Cell-free culture filtrates produced by PGPFs have been found to effectively stimulate plant growth (Hossain et al., 2017), therefore we examined effects of A3CFF from cultures on plant growth. All tested dilutions (1:500, 1:1000, 1:2000) in MS liquid medium, resulted in significant increases of tobacco seedling growth parameters. Moreover, biochemical analyses of plants grown in all A3CFF dilutions revealed high levels of chlorophyll, proline, high SOD and CAT activities. The highest growth effects were observed by using a dilution factor of 1:500 of A3CFF. Moreover, it was demonstrated that the A3CFF activity was conserved even following storage at 4°C for 1 year. To our knowledge, this represents a novel investigation of CFF characteristics. This is very important result for applied practices to integrate the A3CFF into nutritive solutions for hydroponics system. Based on these results, the effects of two concentrations of A3CFF (1:50, 1:500) on plant growth in NS were examined. Only the 1:50 dilution of A3CFF significantly enhanced all growth parameters of tobacco seedlings. Similarly, the CFF from *Penicillium citrinum* cultures induces growth stimulation when applied to *Atriplex gemelinii* seedlings cultivated in solid agar medium, this was attributed to the secondary metabolites secreted by this fungus (Khan et al., 2008). In addition, the application of filtrate from *Penicillium simplicissimum* GP17-2 cultures was as effective as living *Penicillium* in promoting the growth of Arabidopsis. In contrast, while direct application of *Penicillium* sp. GP16-2 promoted plant growth, CFFs from *Penicillium* sp. GP16-2 cultures failed to enhance growth (Hossain et al., 2007, 2008). Besides improving plant growth, it was found that the cell-free culture filtrate from the PGPF *P. indica* cultures increased callus growth and induced lignin production (Kumar et al., 2012; Baishya et al., 2015).

As described above, A3CFF diluted in NS enhanced proline synthesis as well as SOD and CAT activities in tobacco seedlings grown in MS liquid medium. Several studies have demonstrated that proline is involved in osmotic homeostasis adjustments and that antioxidant enzymes such as SOD and CAT are important components of salt tolerance mechanisms in plant (Kumar et al., 2018; Ghosh et al., 2022). Basing on these findings, we tested the ability of A3CFF to alleviate salt stress in tobacco seedlings. Effects of salt stress were evident for tobacco plants grown in NS containing 250 mM NaCl, however, the addition of a 1:50 dilution of A3CCF increased all growth parameters relative to control plants. These results could be explained by the presence of IAA in the A3CFF and the significant increases in activities of SOD, CAT and levels of proline biosynthesis in treated plants. To develop sustainable approaches for salt stress alleviation, many beneficial microorganisms have been used that are efficient, low-cost, and readily adaptable (Fan et al., 2016). The harmful effects of excess salt not only disturbs ionic homeostasis and water uptake, but also causes inadequate oxidative stress responses and imbalances of growth-regulating hormones (Khalid and Aftab, 2020). The auxin secreted by cultured fungi may thus play a major role in adjusting the hormonal balance of stressed plants, contributing to stress alleviation. The application of *Phoma glomerata* and *Penicillium* sp. cultures containing IAA to cucumber plants significantly increased biomass and related growth parameters during NaCl and polyethylene glycol stresses (Waqas et al., 2012). On a related note, the IAA-producing fungus *Aspergillus aculeatus* accelerates the growth of bermudagrass under salt stress (Xie et al., 2017). It has also been reported that the endophytic fungus *Yarrowia lipolytica* promotes the growth of salt-stressed maize plants by controlling plant metabolism and hormonal (IAA and ABA) secretions (Jan et al., 2019). Likewise, application of the PGPFs *Trichoderma longibrachiatum*, *Trichoderma harzianum*, and *Paecilomyces formosus* promoted the growth of wheat, *Suaeda salsa* L, and cucumber plants, respectively, under high salinity conditions (Khan et al., 2012; Chen et al., 2016; Zhang et al., 2016).

Environmental stresses often reduce the chlorophyll content of plants, while chlorophyll accumulation is considered a potential indicator of salinity tolerance (Shah et al., 2017). In the present study, it was determined that the A3CFF significantly increased the chlorophyll content of tobacco seedlings under both normal and salinity stress conditions. Under salt stress conditions, Khan et al. (2011) observed that the growth, chlorophyll content, and photosynthesis rates were significantly higher in plants treated with *Penicillium funiculosum* LHL06 than in untreated plants. In the same way, the chlorophyll content was found to be higher in salt-stressed maize seedlings that had been inoculated with *Yarrowia lipolytica* than in uninoculated plants (Jan et al., 2019). Proline is a low molecular weight amino acid that is a well-known as osmoregulator and ROS scavenger for the salt stressed plants(Bhuyan et al., 2019; Tisarum et al., 2020). Treatment with *Trichoderma*

longibrachiatum and *Trichoderma harzianum* has been found to significantly increase the proline levels in salt-stressed wheat and *Brassica juncea* L plants, respectively (Ahmad et al., 2015; Zhang et al., 2016). In our study, under control conditions, the A3CFF was observed to exert no effect on the Na^+ accumulation in plants (shoots and roots), although it significantly increased the K^+ content of leaves. However, under salinity stress conditions, the A3CFF significantly decreased the Na^+ content of roots and increased the K^+ accumulation in leaves. It has previously shown that endophytic symbiotic fungi can both improve nutrient assimilation and assist in ionic homeostasis maintenance in saline-stressed plants (Gupta et al., 2020). For instance, the colonization of *A. thaliana* with *P. indica* under salt stress has been found to lower the Na^+/K^+ ratio (Abdelaziz et al., 2017). Similarly, the saline stress of *Suaeda salsa* L was determined to be counteracted by *Trichoderma harzianum* T83 colonization, thereby resulting in a higher K^+ uptake (Chen et al., 2016).

In the experiments conducted in this study, it was demonstrated that theA3CFF induced the growth of roots under salt stress, a finding that may be explained by the low Na^+/K^+ ratio observed in such plants. The analysis of the expression profiles of NtCAT1 and NtSOD confirmed the biochemical experimental results describing the CAT and SOD activity levels. Indeed, the A3CFF induced the upregulation of NtCAT1 and NtSOD in both the presence and absence of NaCl. Moreover, the genes encoding the key Na^+ transporters (NtSOS1, NtNHX1, and NtHKT1) involved in salt tolerance were also shown to be upregulated by the A3CFF treatment. Based on these results, it is likely that the enhanced salt tolerance observed in the presence of A3CFF at 250 mM NaCl occurred *via* the regulation of Na^+ homeostasis by the Na^+ transport system control at the whole-plant level. In addition, the enhancement of the antioxidant activities (CAT and SOD) may also have helped the plants to endure salinity stress.

It has been reported that plant growth-promoting microorganisms are able to increase the nutrient use efficiency of plants. This effect allows for crop production without yield loss in NS with 50% lower fertilizer inputs compared to in full NS (Da Costa et al., 2013). Our work revealed that reducing NS strength by 50% did not decrease plant growth when the NS was supplemented with a 1:50 dilution of A3CFF. Compared to plants grown in full NS, plants grown in 0.5NS showed significantly reduced shoot length, shoot dry weight, and root dry weight, and leaf area, while the addition of A3CFF significantly increased these parameters. In order to ultimately develop sustainable agricultural practices, several studies have been performed that use PGPFs to decrease the chemical inputs required for maximal yield (Xia et al., 2019). In one such study, tomatoes cultivated in pots or in field trials that were treated with 25% of typical commercial fertilizer levels plus *Trichoderma*-enriched bioorganic fertilizer produced yields equivalent to tomato plants treated with normal amounts of chemical fertilizer (Ye et al., 2020).

In an attempt to explain the mechanisms underlying the promotion of plant growth by A3CFF, the effects of the A3CFF treatment on the accumulation of transcripts for six genes related to growth, brassinosteroid biosynthesis (DET2, DWF4), auxin biosynthesis (YUCCA6-like, TRYP1), and nitrogen-use efficiency (NR, NRT1) were examined. All six genes were found to be upregulated in both roots and leaves following the addition of the A3CFF to the growth media. To our knowledge, there have been no previous reports showing a role for *P. olsonii* activation of genes related to plant growth. However, other species of PGPFs have been shown to influence growth-related gene expression, as *P. indica* was able to stimulate the expression of auxin-responsive genes and nitrate reductase-encoding genes in Arabidopsis and tobacco seedlings (Sherameti et al., 2005; Meents et al., 2019). Similarly, inoculation with *Trichoderma* increased accumulation of auxin-regulated gene transcripts in Arabidopsis and triggered ethylene/indole-3-acetic acid signaling in tomato plants (Contreras-Cornejo et al., 2009; De Palma et al., 2019). However, our study is the first report demonstrating the effect of A3CFF on genes involved in brassinosteroid biosynthesis.

Conclusion

In conclusion, this study isolated a fungus (A3) from the rhizosphere of the halophyte grass *A. littoralis*, identified as *P. olsonii*, and for the first time, described its role as a PGPF. This strain was determined to significantly promote tobacco plant growth in MS and NS, both directly *via* the application of A3 mycelium and through the application of its CFF. In addition, the A3CFF appeared stable following storage at 4°C for 1 year. The application of the A3CFF decreased the chemical fertilizer levels in NS by 50% and also significantly increased plant growth when compared with the control conditions. Finally, the A3CFF was found to mitigate salinity stress by inducing morphological, biochemical, and molecular changes in salt-stressed plants. Thus, the A3CFF could be used in hydroponics as a promising biotechnological tool for enabling the reduction of expensive chemical fertilizer inputs without compromising the yield, thereby improving agriculture and sustainability.

Data availability statement

The original contributions presented in the study are publicly available. This data can be found at: NCBI, OP680782.

Author contributions

MT, LF, and AH: conceptualization, methodology, writing—review and editing. MT, WR, and AH: formal analysis. AA, FA-Q, and AA-D: investigation. MT: writing—original draft preparation. AH: visualization. LF and AH: supervision. All authors have read and agreed to the published version of the manuscript criteria.

Funding

This research was funded by (RSP-2021/73) at King Saud University, Riyadh, Saudi Arabia.

Acknowledgments

The authors extend their appreciation to researchers supporting project number (RSP-2021/73) at King Saud University, Riyadh, Saudi Arabia.

Conflict of interest

The authors declare that the research was conducted in the absence of any commercial or financial relationships that could be construed as a potential conflict of interest.

Publisher's note

All claims expressed in this article are solely those of the authors and do not necessarily represent those of their affiliated organizations, or those of the publisher, the editors and the reviewers. Any product that may be evaluated in this article, or claim that may be made by its manufacturer, is not guaranteed or endorsed by the publisher.

Supplementary material

The Supplementary material for this article can be found online at: https://www.frontiersin.org/articles/10.3389/fmicb.2022.996054/full#supplementary-material

References

Abdelaziz, M. E., Kim, D., Ali, S., Fedoroff, N. V., and Al-Babili, S. (2017). The endophytic fungus *Piriformospora indica* enhances *Arabidopsis thaliana* growth and modulates Na+/K+ homeostasis under salt stress conditions. *Plant Sci.* 263, 107–115. doi: 10.1016/j.plantsci.2017.07.006

Ábrahám, E., Hourton-Cabassa, C., Erdei, L., and Szabados, L. (2010). "Methods for determination of proline in plants," in *Plant Stress Tolerance*. ed. R. Sunkar (New York, NY; Dordrecht; Heidelberg; London: Springer), 317–331.

Ahmad, P., Hashem, A., Abd-Allah, E. F., Alqarawi, A., John, R., Egamberdieva, D., et al. (2015). Role of *Trichoderma harzianum* in mitigating NaCl stress in Indian mustard (*Brassica juncea* L) through antioxidative defense system. *Front. Plant Sci.* 6:868. doi: 10.3389/fpls.2015.00868

Ansari, M. W., Trivedi, D. K., Sahoo, R. K., Gill, S. S., and Tuteja, N. (2013). A critical review on fungi mediated plant responses with special emphasis to *Piriformospora indica* on improved production and protection of crops. *Plant Physiol. Biochem.* 70, 403–410. doi: 10.1016/j.plaphy.2013.06.005

Babu, A. G., Kim, S. W., Yadav, D. R., Hyum, U., Adhikari, M., and Lee, Y. S. (2015). *Penicillium menonorum*: a novel fungus to promote growth and nutrient management in cucumber plants. *Mycobiology* 43, 49–56. doi: 10.5941/MYCO.2015.43.1.49

Baishya, D., Deka, P., and Kalita, M. C. (2015). In vitro co-cultivation of *Piriformospora indica* filtrate for improve biomass productivity in *Artemisia annua* (L.). *Symbiosis* 66, 37–46. doi: 10.1007/s13199-015-0331-5

Bartelme, R. P., Oyserman, B. O., Blom, J. E., Sepulveda-Villet, O. J., and Newton, R. J. (2018). Stripping away the soil: plant growth promoting microbiology opportunities in aquaponics. *Front. Microbiol.* 9:8. doi: 10.3389/fmicb.2018.00008

Ben-Romdhane, W., Ben-Saad, R., Meynard, D., Zouari, N., Mahjoub, A., Fki, L., et al. (2018). Overexpression of AlTMP2 gene from the halophyte grass *Aeluropus littoralis* in transgenic tobacco enhances tolerance to different abiotic stresses by improving membrane stability and deregulating some stress-related genes. *Protoplasma* 255, 1161–1177. doi: 10.1007/s00709-018-1223-3

Bhuyan, M. B., Hasanuzzaman, M., Nahar, K., Al Mahmud, J., Parvin, K., Bhuiyan, T. F., et al. (2019). "Plants behavior under soil acidity stress: insight into morphophysiological, biochemical, and molecular responses," in *Plant Abiotic Stress Tolerance*. eds. M. Hasanuzzaman, K. Rehman Hakeem, K. Nahar and h. F. Alharby (Switzerland AG: Springer), 35–82.

Boivin, S., Fonouni-Farde, C., and Frugier, F. (2016). How auxin and cytokinin phytohormones modulate root microbe interactions. *Front. Plant Sci.* 7:1240. doi: 10.3389/fpls.2016.01240

Calvo, P., Nelson, L., and Kloepper, J. W. (2014). Agricultural uses of plant biostimulants. *Plant Soil* 383, 3–41. doi: 10.1007/s11104-014-2131-8

Cao, C., Li, R., Wan, Z., Liu, W., Wang, X., Qiao, J., et al. (2007). The effects of temperature, pH, and salinity on the growth and dimorphism of *Penicillium marneffei*. *Sabouraudia* 45, 401–407. doi: 10.1080/13693780701358600

Chanclud, E., and Morel, J. B. (2016). Plant hormones: a fungal point of view. *Mol. Plant Pathol.* 17, 1289–1297. doi: 10.1111/mpp.12393

Chandanie, W., Kubota, M., and Hyakumachi, M. (2009). Interactions between the arbuscular mycorrhizal fungus Glomus mosseae and plant growth-promoting fungi and their significance for enhancing plant growth and suppressing damping-off of cucumber (*Cucumis sativus* L.). *Appl. Soil Ecol.* 41, 336–341. doi: 10.1016/j.apsoil.2008.12.006

Chandra, P., and Singh, R. (2020). "Soil salinity and its alleviation using plant growth–promoting fungi," in *Agriculturally Important Fungi for Sustainable Agriculture*. eds. A. Yadav, S. Mishra, D. Kour, N. Yadav and A. Kumar (Cham: Springer), 101–148.

Chandrakar, V., Dubey, A., and Keshavkant, S. (2016). Modulation of antioxidant enzymes by salicylic acid in arsenic exposed *Glycine max* L. *J. Soil Sci. Plant Nutr.* 16, 662–676. doi: 10.4067/S0718-95162016005000048

Chen, L.-H., Zheng, J.-H., Shao, X.-H., Shen, S.-S., Yu, Z.-H., Mao, X.-Y., et al. (2016). Effects of *Trichoderma harzianum* T83 on *Suaeda salsa* L. in coastal saline soil. *Ecol. Eng.* 91, 58–64. doi: 10.1016/j.ecoleng.2016.01.007

Claiborne, A. (1985). *Handbook of Methods for Oxygen Radical Research*. Florida: CRC Press, Boca Raton.

Colla, G., and Rouphael, Y. (2015). Biostimulants in horticulture. *Sci. Hortic.* 196, 1–2. doi: 10.1016/j.scienta.2015.10.044

Contreras-Cornejo, H. A., Macías-Rodríguez, L., Cortés-Penagos, C., and López-Bucio, J. (2009). *Trichoderma virens*, a plant beneficial fungus, enhances biomass production and promotes lateral root growth through an auxin-dependent mechanism in *Arabidopsis*. *Plant Physiol.* 149, 1579–1592. doi: 10.1104/pp.108.130369

Da Costa, P. B., Beneduzi, A., De Souza, R., Schoenfeld, R., Vargas, L. K., and Passaglia, L. M. (2013). The effects of different fertilization conditions on bacterial plant growth promoting traits: guidelines for directed bacterial prospection and testing. *Plant Soil* 368, 267–280. doi: 10.1007/s11104-012-1513-z

De Palma, M., Salzano, M., Villano, C., Aversano, R., Lorito, M., Ruocco, M., et al. (2019). Transcriptome reprogramming, epigenetic modifications and alternative

splicing orchestrate the tomato root response to the beneficial fungus *Trichoderma harzianum*. *Horticult. Res.* 6, 1–15. doi: 10.1038/s41438-018-0079-1

Diaz, T. L., González, C., Moreno, B., and Otero, A. (2002). Effect of temperature, water activity, pH and some antimicrobials on the growth of *Penicillium olsonii* isolated from the surface of Spanish fermented meat sausage. *Food Microbiol.* 19, 1–7. doi: 10.1006/fmic.2001.0440

Drobek, M., Frąc, M., and Cybulska, J. (2019). Plant biostimulants: importance of the quality and yield of horticultural crops and the improvement of plant tolerance to abiotic stress — a review. *Agronomy* 9:335. doi: 10.3390/agronomy9060335

Fan, P., Chen, D., He, Y., Zhou, Q., Tian, Y., and Gao, L. (2016). Alleviating salt stress in tomato seedlings using *Arthrobacter* and *Bacillus megaterium* isolated from the rhizosphere of wild plants grown on saline–alkaline lands. *Int. J. Phytoremediation* 18, 1113–1121. doi: 10.1080/15226514.2016.1183583

Frisvad, J. C., Houbraken, J., Popma, S., and Samson, R. A. (2013). Two new *Penicillium* species *Penicillium buchwaldii* and *Penicillium spathulatum*, producing the anticancer compound asperphenamate. *FEMS Microbiol. Lett.* 339, 77–92. doi: 10.1111/1574-6968.12054

Frisvad, J. C., and Samson, R. A. (2004). Polyphasic taxonomy of *Penicillium* subgenus *Penicillium*. A guide to identification of food and air-borne terverticillate *Penicillia* and their mycotoxins. *Stud. Mycol.* 49:174.

Ghosh, U., Islam, M., Siddiqui, M., Cao, X., and Khan, M. (2022). Proline, a multifaceted signalling molecule in plant responses to abiotic stress: understanding the physiological mechanisms. *Plant Biol.* 24, 227–239. doi: 10.1111/plb.13363

Gordon, S. A., and Weber, R. P. (1951). Colorimetric estimation of indoleacetic acid. *Plant Physiol.* 26, 192–195. doi: 10.1104/pp.26.1.192

Gupta, S., Schillaci, M., Walker, R., Smith, P. M., Watt, M., and Roessner, U. (2020). Alleviation of salinity stress in plants by endophytic plant-fungal symbiosis: current knowledge, perspectives and future directions. *Plant Soil* 461, 219–244. doi: 10.1007/s11104-020-04618-w

Hakim, S., Naqqash, T., Nawaz, M. S., Laraib, I., Siddique, M. J., Zia, R., et al. (2021). Rhizosphere engineering with plant growth-promoting microorganisms for agriculture and ecological sustainability. *Front. Sustain. Food Syst.* 5:617157. doi: 10.3389/fsufs.2021.617157

Halpern, M., Bar-Tal, A., Ofek, M., Minz, D., Muller, T., and Yermiyahu, U. (2015). The use of biostimulants for enhancing nutrient uptake. *Adv. Agron.* 130, 141–174. doi: 10.1016/bs.agron.2014.10.001

Haro, R., and Benito, B. (2019). The role of soil fungi in K+ plant nutrition. *Int. J. Mol. Sci.* 20:3169. doi: 10.3390/ijms20133169

Hossain, M. M., and Sultana, F. (2020a). Application and mechanisms of plant growth promoting fungi (PGPF) for phytostimulation. *Org. Agric.* 1–31. doi: 10.5772/intechopen.92338

Hossain, M. M., and Sultana, F. (2020b). "Application and mechanisms of plant growth promoting fungi (PGPF) for phytostimulation," in *Organic Agriculture*. ed. S. K. Das (London: IntechOpen).

Hossain, M. M., Sultana, F., and Islam, S. (2017). "Plant growth-promoting fungi (PGPF): phytostimulation and induced systemic resistance," in *Plant-Microbe Interactions in Agro-Ecological Perspectives*. eds. D. P. Singh, H. B. Singh and R. Prabha (Singapore: Springer), 135–191.

Hossain, M. M., Sultana, F., Kubota, M., and Hyakumachi, M. (2008). Differential inducible defense mechanisms against bacterial speck pathogen in *Arabidopsis thaliana* by plant-growth-promoting-fungus *Penicillium* sp. GP16-2 and its cell free filtrate. *Plant Soil* 304, 227–239. doi: 10.1007/s11104-008-9542-3

Hossain, M. M., Sultana, F., Kubota, M., Koyama, H., and Hyakumachi, M. (2007). The plant growth-promoting fungus *Penicillium simplicissimum* GP17-2 induces resistance in *Arabidopsis thaliana* by activation of multiple defense signals. *Plant Cell Physiol.* 48, 1724–1736. doi: 10.1093/pcp/pcm144

Hossain, M. M., Sultana, F., Miyazawa, M., and Hyakumachi, M. (2014). The plant growth-promoting fungus *Penicillium* spp. GP15-1 enhances growth and confers protection against damping-off and anthracnose in the cucumber. *J. Oleo Sci.* 63, 391–400. doi: 10.5650/jos.ess13143

Islam, S., Akanda, A. M., Sultana, F., and Hossain, M. M. (2014). Chilli rhizosphere fungus *Aspergillus* spp. PPA1 promotes vegetative growth of cucumber (*Cucumis sativus*) plants upon root colonisation. *Arch. Phytopathol. Plant Protect.* 47, 1231–1238. doi: 10.1080/03235408.2013.837633

Jamil, A., Riaz, S., Ashraf, M., and Foolad, M. R. (2011). Gene expression profiling of plants under salt stress. *Crit. Rev. Plant Sci.* 30, 435–458. doi: 10.1080/07352689.2011.605739

Jan, F. G., Hamayun, M., Hussain, A., Jan, G., Iqbal, A., Khan, A., et al. (2019). An endophytic isolate of the fungus Yarrowia lipolytica produces metabolites that ameliorate the negative impact of salt stress on the physiology of maize. *BMC Microbiol.* 19, 1–10. doi: 10.1186/s12866-018-1374-6

Jogeswar, G., Pallela, R., Jakka, N., Reddy, P., Rao, J. V., Sreenivasulu, N., et al. (2006). Antioxidative response in different sorghum species under short-term salinity stress. *Acta Physiol. Plant.* 28, 465–475. doi: 10.1007/BF02706630

Khalid, A., and Aftab, F. (2020). Effect of exogenous application of IAA and GA 3 on growth, protein content, and antioxidant enzymes of *Solanum tuberosum* L. grown in vitro under salt stress. *In Vitro Cell. Dev. Biol. Plant* 56, 377–389. doi: 10.1007/s11627-019-10047-x

Khan, A. L., Hamayun, M., Kang, S.-M., Kim, Y.-H., Jung, H.-Y., Lee, J.-H., et al. (2012). Endophytic fungal association via gibberellins and indole acetic acid can improve plant growth under abiotic stress: an example of *Paecilomyces formosus* LHL10. *BMC Microbiol.* 12:3. doi: 10.1186/1471-2180-12-3

Khan, A. L., Hamayun, M., Kim, Y.-H., Kang, S.-M., and Lee, I.-J. (2011). Ameliorative symbiosis of endophyte (*Penicillium funiculosum* LHL06) under salt stress elevated plant growth of *Glycine max* L. *Plant Physiol. Biochem.* 49, 852–861. doi: 10.1016/j.plaphy.2011.03.005

Khan, S. A., Hamayun, M., Yoon, H., Kim, H.-Y., Suh, S.-J., Hwang, S.-K., et al. (2008). Plant growth promotion and *Penicillium citrinum*. *BMC Microbiol.* 8, 1–10. doi: 10.1186/1471-2180-8-231

Khan, A. L., and Lee, I.-J. (2013). Endophytic *Penicillium funiculosum* LHL06 secretes gibberellin that reprograms *Glycine max* L. growth during copper stress. *BMC Plant Biol.* 13:86. doi: 10.1186/1471-2229-13-86

Khan, A. L., Waqas, M., and Lee, I.-J. (2015). Resilience of *Penicillium resedanum* LK6 and exogenous gibberellin in improving Capsicum annuum growth under abiotic stresses. *J. Plant Res.* 128, 259–268. doi: 10.1007/s10265-014-0688-1

Kondrasheva, K., Egamberdiev, F., Suyarova, R., Ruzieva, D., Nasmetova, S., Abdulmyanova, L., et al. (2022). "Production of indole-3-acetic acid by endophytic fungi of halophyte plants under salt stress," in *IOP Conference Series: Earth and Environmental science* (IOP Publishing), 012040.

Kumar, M., Kumar, R., Jain, V., and Jain, S. (2018). Differential behavior of the antioxidant system in response to salinity induced oxidative stress in salt-tolerant and salt-sensitive cultivars of *Brassica juncea* L. *Biocatal. Agric. Biotechnol.* 13, 12–19. doi: 10.1016/j.bcab.2017.11.003

Kumar, V., Rajauria, G., Sahai, V., and Bisaria, V. (2012). Culture filtrate of root endophytic fungus *Piriformospora indica* promotes the growth and lignan production of *Linum album* hairy root cultures. *Process Biochem.* 47, 901–907. doi: 10.1016/j.procbio.2011.06.012

Lee, Y.-C., Johnson, J. M., Chien, C.-T., Sun, C., Cai, D., Lou, B., et al. (2011). Growth promotion of Chinese cabbage and *Arabidopsis* by *Piriformospora indica* is not stimulated by mycelium-synthesized auxin. *Mol. Plant-Microbe Interact.* 24, 421–431. doi: 10.1094/MPMI-05-10-0110

Liang, Y., Urano, D., Liao, K.-L., Hedrick, T. L., Gao, Y., and Jones, A. M. (2017). A nondestructive method to estimate the chlorophyll content of *Arabidopsis* seedlings. *Plant Methods* 13, 1–10. doi: 10.1186/s13007-017-0174-6

López-Bucio, J., Pelagio-Flores, R., and Herrera-Estrella, A. (2015). *Trichoderma* as biostimulant: exploiting the multilevel properties of a plant beneficial fungus. *Sci. Hortic.* 196, 109–123. doi: 10.1016/j.scienta.2015.08.043

Meents, A. K., Furch, A. C., Almeida-Trapp, M., Özyürek, S., Scholz, S., Kirbis, A., et al. (2019). Beneficial and pathogenic Arabidopsis root-interacting fungi differently affect auxin levels and responsive genes during early infection. *Front. Microbiol.* 10:380. doi: 10.3389/fmicb.2019.00380

Ogórek, R. (2016). Enzymatic activity of potential fungal plant pathogens and the effect of their culture filtrates on seed germination and seedling growth of garden cress (*Lepidium sativum* L.). *Eur. J. Plant Pathol.* 145, 469–481. doi: 10.1007/s10658-016-0860-7

Radhakrishnan, R., Kang, S.-M., Baek, I.-Y., and Lee, I.-J. (2014). Characterization of plant growth-promoting traits of *Penicillium* species against the effects of high soil salinity and root disease. *J. Plant Interact.* 9, 754–762. doi: 10.1080/17429145.2014.930524

Raja, H. A., Miller, A. N., Pearce, C. J., and Oberlies, N. H. (2017). Fungal identification using molecular tools: a primer for the natural products research community. *J. Nat. Prod.* 80, 756–770. doi: 10.1021/acs.jnatprod.6b01085

Salas-Marina, M. A., Silva-Flores, M. A., Cervantes-Badillo, M. G., Rosales-Saavedra, M. T., Islas-Osuna, M. A., and Casas-Flores, S. (2011). The plant growth-promoting fungus *Aspergillus ustus* promotes growth and induces resistance against different lifestyle pathogens in *Arabidopsis thaliana*. *J. Microbiol. Biotechnol.* 21, 686–696. doi: 10.4014/jmb.1101.01012

Saldajeno, M., and Hyakumachi, M. (2011). The plant growth-promoting fungus *Fusarium* equiseti and the arbuscular mycorrhizal fungus Glomus mosseae stimulate plant growth and reduce severity of anthracnose and damping-off diseases in cucumber (*Cucumis sativus*) seedlings. *Ann. Appl. Biol.* 159, 28–40. doi: 10.1111/j.1744-7348.2011.00471.x

Schmid, M. W., Hahl, T., Van Moorsel, S. J., Wagg, C., De Deyn, G. B., and Schmid, B. (2018). Rhizosphere bacterial community composition depends on plant diversity legacy in soil and plant species identity. *BioRxiv*:287235. doi: 10.1101/287235

Schoch, C. L., Seifert, K. A., Huhndorf, S., Robert, V., Spouge, J. L., Levesque, C. A., et al. (2012). Nuclear ribosomal internal transcribed spacer (ITS) region as a universal DNA barcode marker for fungi. *Proc. Natl. Acad. Sci.* 109, 6241–6246. doi: 10.1073/pnas.1117018109

Shah, S. H., Houborg, R., and Mccabe, M. F. (2017). Response of chlorophyll, carotenoid and SPAD-502 measurement to salinity and nutrient stress in wheat (*Triticum aestivum* L.). *Agronomy* 7:61. doi: 10.3390/agronomy7030061

Sherameti, I., Shahollari, B., Venus, Y., Altschmied, L., Varma, A., and Oelmüller, R. (2005). The endophytic fungus *Piriformospora indica* stimulates the expression of nitrate reductase and the starch-degrading enzyme glucan-water dikinase in tobacco and Arabidopsis roots through a homeodomain transcription factor that binds to a conserved motif in their promoters. *J. Biol. Chem.* 280, 26241–26247. doi: 10.1074/jbc.M500447200

Shoresh, M., Harman, G. E., and Mastouri, F. (2010). Induced systemic resistance and plant responses to fungal biocontrol agents. *Annu. Rev. Phytopathol.* 48, 21–43. doi: 10.1146/annurev-phyto-073009-114450

Tarroum, M., Ben Romdhane, W., Ali, A. A. M., Al-Qurainy, F., Al-Doss, A., Fki, L., et al. (2021). Harnessing the Rhizosphere of the halophyte grass *Aeluropus littoralis* for Halophilic plant-growth-promoting fungi and evaluation of their biostimulant activities. *Plan. Theory* 10:784. doi: 10.3390/plants10040784

Tisarum, R., Theerawitaya, C., Samphumphuang, T., Polispitak, K., Thongpoem, P., Singh, H. P., et al. (2020). Alleviation of salt stress in upland Rice (*Oryza sativa* L. ssp. *indica* cv. Leum Pua) using arbuscular mycorrhizal fungi inoculation. *Front. Plant Sci.* 11:348. doi: 10.3389/fpls.2020.00348

Vimal, S. R., Singh, J. S., Arora, N. K., and Singh, S. (2017). Soil-plant-microbe interactions in stressed agriculture management: a review. *Pedosphere* 27, 177–192. doi: 10.1016/S1002-0160(17)60309-6

Visagie, C., Houbraken, J., Frisvad, J. C., Hong, S.-B., Klaassen, C., Perrone, G., et al. (2014). Identification and nomenclature of the genus *Penicillium*. *Stud. Mycol.* 78, 343–371. doi: 10.1016/j.simyco.2014.09.001

Waqas, M., Khan, A. L., Hamayun, M., Shahzad, R., Kang, S.-M., Kim, J.-G., et al. (2015). Endophytic fungi promote plant growth and mitigate the adverse effects of stem rot: an example of *Penicillium citrinum* and *Aspergillus terreus*. *J. Plant Interact.* 10, 280–287. doi: 10.1080/17429145.2015.1079743

Waqas, M., Khan, A. L., Kamran, M., Hamayun, M., Kang, S.-M., Kim, Y.-H., et al. (2012). Endophytic fungi produce gibberellins and indoleacetic acid and promotes host-plant growth during stress. *Molecules* 17, 10754–10773. doi: 10.3390/molecules170910754

White, T. J., Bruns, T., Lee, S., and Taylor, J. (1990). Amplification and direct sequencing of fungal ribosomal RNA genes for phylogenetics. *PCR Prot. Guide Methods Appl.* 18, 315–322. doi: 10.1016/B978-0-12-372180-8.50042-1

Xia, Y., Sahib, M. R., Amna, A., Opiyo, S. O., Zhao, Z., and Gao, Y. G. (2019). Culturable endophytic fungal communities associated with plants in organic and conventional farming systems and their effects on plant growth. *Sci. Rep.* 9, 1–10. doi: 10.1038/s41598-018-38230-x

Xie, Y., Han, S., Li, X., Amombo, E., and Fu, J. (2017). Amelioration of salt stress on bermudagrass by the fungus *Aspergillus aculeatus*. *Mol. Plant-Microbe Interact.* 30, 245–254. doi: 10.1094/MPMI-12-16-0263-R

Yarzábal, L. A., and Chica, E. J. (2017). "Potential for developing low-input sustainable agriculture in the tropical Andes by making use of native microbial resources" in *Plant-Microbe Interactions in Agro-Ecological Perspectives*. eds. D. P. Singh, H. B. Singh and R. Prabha (Singapore: Springer), 29–54.

Ye, L., Zhao, X., Bao, E., Li, J., Zou, Z., and Cao, K. (2020). Bio-organic fertilizer with reduced rates of chemical fertilization improves soil fertility and enhances tomato yield and quality. *Sci. Rep.* 10, 1–11. doi: 10.1038/s41598-019-56954-2

You, Y.-H., Yoon, H., Kang, S.-M., Shin, J.-H., Choo, Y.-S., Lee, I.-J., et al. (2012). Fungal diversity and plant growth promotion of endophytic fungi from six halophytes in Suncheon Bay. *J. Microbiol. Biotechnol.* 22, 1549–1556. doi: 10.4014/jmb.1205.05010

Zhang, S., Gan, Y., and Xu, B. (2016). Application of plant-growth-promoting fungi *Trichoderma longibrachiatum* T6 enhances tolerance of wheat to salt stress through improvement of antioxidative defense system and gene expression. *Front. Plant Sci.* 7:1405. doi: 10.3389/fpls.2016.01405

Zhu, J.-K. (2016). Abiotic stress signaling and responses in plants. *Cells* 167, 313–324. doi: 10.1016/j.cell.2016.08.029

frontiers | Frontiers in Plant Science

TYPE Original Research
PUBLISHED 31 October 2022
DOI 10.3389/fpls.2022.1017048

OPEN ACCESS

EDITED BY
Maurizio Ruzzi,
University of Tuscia, Italy

REVIEWED BY
Xiangnan Li,
Northeast Institute of Geography and Agroecology (CAS), China
Mrinalini Manna,
National Institute of Plant Genome Research (NIPGR), India

*CORRESPONDENCE
Ranjan Swarup
ranjan.swarup@nottingham.ac.uk

SPECIALTY SECTION
This article was submitted to Crop and Product Physiology, a section of the journal Frontiers in Plant Science

RECEIVED 11 August 2022
ACCEPTED 06 October 2022
PUBLISHED 31 October 2022

CITATION
Mohammed U, Davis J, Rossall S, Swarup K, Czyzewicz N, Bhosale R, Foulkes J, Murchie EH and Swarup R (2022) Phosphite treatment can improve root biomass and nutrition use efficiency in wheat. *Front. Plant Sci.* 13:1017048. doi: 10.3389/fpls.2022.1017048

Phosphite treatment can improve root biomass and nutrition use efficiency in wheat

Umar Mohammed[1], Jayne Davis[1], Steve Rossall[1], Kamal Swarup[1], Nathan Czyzewicz[1,2], Rahul Bhosale[1,3], John Foulkes[1], Erik H. Murchie[1] and Ranjan Swarup[1,4]*

[1]Division of Plant and Crop Science, School of Biosciences, University of Nottingham, Nottingham, United Kingdom, [2]Mars Petcare, Melton Mowbray United Kingdom, [3]Future Food Beacon of Excellence, University of Nottingham, Nottingham, United Kingdom, [4]Centre for Plant Integrative Biology, University of Nottingham, Nottingham, United Kingdom

Phosphite represents a reduced form of phosphate that belongs to a class of crop growth-promoting chemicals termed biostimulants. Previous research has shown that phosphite application can enhance root growth, but its underlying mechanism, especially during environmental stresses, remains elusive. To uncover this, we undertook a series of morphological and physiological analyses under nutrient, water and heat stresses following a foliar application in wheat. Non-invasive 3D imaging of root system architecture directly in soil using X-ray Computed Tomography revealed that phosphite treatment improves root architectural traits and increased root biomass. Biochemical and physiological assays identified that phosphite treatment significantly increases Nitrate Reductase (NR) activity, leaf photosynthesis and stomatal conductance, suggesting improved Nitrogen and Carbon assimilation, respectively. These differences were more pronounced under heat or drought treatment (photosynthesis and photosystem II stability) and nutrient deficiency (root traits and NR). Overall our results suggest that phosphite treatment improves the ability of plants to tolerate abiotic stresses through improved Nitrogen and Carbon assimilation, combined with improved root growth which may improve biomass and yield.

KEYWORDS

phosphite, biostimulants, wheat, oilseed rape, resource use efficiency, nutrition use efficiency, nitrate reductase

Introduction

Global food security is a key challenge facing world agriculture (IAASTD report, 2009; Royal Society, 2009; Godfray et al., 2010; Wheeler and von Braun, 2013; Myers et al., 2017). The world population is estimated to reach ~8.3 Bn by 2030 with the majority of that increase occurring in the developing world (IAASTD report, 2009; Royal

Society, 2009). The need to feed this growing population sustainably and against the significant threats to food crop harvests arising from climate change could not be more pressing (Hirabayashi et al., 2013; Ray et al., 2013; Ray et al., 2015). With no more agricultural land available, increases in food production of between 40-50% must be achieved through a sustainable intensification of agriculture to meet the future food demand (Wheeler and von Braun, 2013). This includes both improving and developing more diverse agricultural systems for low input agriculture against a backdrop of increasing climate unpredictability that can severely affect crop production (Wheeler and von Braun, 2013). There have been several studies and reports that suggest that improvement in root architecture can have profound impact in improving crop productivity and resource use efficiency (Lynch, 2011; Lynch, 2013; Lynch et al., 2014; Lynch, 2015; Lagunas et al., 2019; York et al., 2013)

Biostimulants are a class of biologically active chemicals that are added to plants during growth or to seeds before sowing that have been shown to have beneficial effects on growth and development (Brown and Saa, 2015; Yakhin et al., 2017; Xu and Geelen, 2018). Widely used biostimulants are typically derived from seaweed extracts and both crude extracts and more refined components rich in amino acids and peptides and polysaccharides are used. Seaweed based biostimulants have been shown to improve plant tolerance to abiotic stresses and have also been implicated in improving nutrient uptake (Khan et al., 2009; Conrath, 2011; Nair et al., 2012; Savvides et al., 2016; Rouphael and Colla, 2020). Similarly, protein hydrolysate based biostimulants have been reported to improve germination rate, plant growth and productivity in a range of crops (Colla et al., 2017). The biostimulant market is a multi-billion-dollar industry (Sible et al., 2021): based on Market date forecast, Market and Markets and Dunham Trimmer European Biostimulants Industry Council (EBIC) estimate biostimulants market in EU alone to be in the range of 1.5- 2 billion USD in 2022 with a compound annual growth rate (CAGR) of 10-12% emphasizing its major importance in agriculture (EBIC, 2022).

Biostimulants are not nutrients, nor fertilizers, or pesticides and can affect plant growth and development in a variety of ways throughout the life cycle of the crop, from seed germination to plant maturity (Yakhin et al., 2017; Fleming et al., 2019). They have been shown to improve crop quality, yield and tolerance to abiotic influences (Conrath, 2011; Savvides et al., 2016) and therefore can become a key component in integrated sustainable crop production playing an important role in securing yields and increasing efficiency (Brown and Saa, 2015; Yakhin et al., 2017; Xu and Geelen, 2018). If we understood how they function we may be able to develop new traits and mechanisms to enhance yield, however this information is lacking.

Here, we focused our attention on phosphite based biostimulants. Phosphite (Phi) is a reduced form of phosphate (Pi) and has been shown to have growth promoting properties in nutrient-replete conditions in oranges, celery, satsuma, wheat, oilseed rape and several other plants (Albrigo, 1999; Lovatt and Mikkelsen, 2006; Thao and Yamakawa, 2009; Rossall et al., 2016) but not in all cases (Carswell et al., 1996; Carswell et al., 1997; Forster et al., 1998; Ticconi et al., 2001; Varadarajan et al., 2002; Thao and Yamakawa, 2009). Phosphites cannot be used as a sole source of phosphorous as phosphites cannot replace phosphate in biological reactions (Thao and Yamakawa, 2009). There is no evidence that phosphite can replace phosphate whereas phosphite to phosphate conversion by the soil micro bacteria is too slow to provide any growth benefits (Thao and Yamakawa, 2009).

The mode of action of phosphite is still unclear, however, there is some evidence that it is root-specific, and not related to any role as pesticide or fertilizer. In a glasshouse study, carried out in axenic culture, using wheat, oilseed rape, sugar beet and ryegrass Rossall et al. (2016) showed that phosphites improved root biomass by about 30% and seemed to be acting as a specific biostimulant of root growth. Roots provide the means of capturing nutrients and water required to generate a productive photosynthetic canopy. Root anatomical properties such as root length, density, depth, root front velocity and angle could also be utilized to improve resilience in resource-poor conditions to enhance capture of water and mineral elements (Ahmadi et al., 2014). Therefore, phosphites provide scope to increase arable resilience and sustainability by potentially reducing the dependence on expensive nutrient inputs (Panda et al., 2012).

Bread wheat (*Triticum aestivum* L.) provides 20% of the calorific and protein intake in the human diet (Shiferaw et al., 2013). In the UK, grain yields typically reach between 40-95% of their yield potentials (Gobbett et al., 2017) causing large yield-gaps. Here we provide a substantial understanding of physiological mechanisms by which phosphite improves root growth in the UK winter wheat. We also show that improvement of root traits correlates with improvement in both nitrogen (N) and shoot carbon assimilation. We show that phosphite treatment increases the activity of Nitrate Reductase, which is a key enzyme in N assimilation. We propose that phosphite treatment improves plant tolerance of abiotic stresses through improved N and C assimilation which is in turn associated with improved root growth.

Materials and methods

Plant materials and growing conditions

KWS Siskin was used for most experiments including nutrient strength, water and heat temperature and X-ray micro CT imaging experiments to its versatility allowing it to grow in a diversity of sites in the UK. It is a high yield cultivar with a disease resistance rating of 6.5 for *Septoria tritici* and a

high rating for mildew and yellow rust resistance on the UK recommended list (AHDB, 2019). In addition, seven elite UK winter wheat varieties; Evolution, Diego, Leeds, Revolution, Solstice, Siskin and Skyfall were used for initial 2D root phenotyping studies.

Seeds were sieved through a calibrated graduated sieve (Scientific Laboratory Supplies Ltd. Hessle, UK) and a fraction of 2.8-3.35 mm was selected for experiments. Selected seeds were surfaced sterilized using 75% ethanol (1 min) and 30% sodium hypochlorite (10 min) and washed thoroughly using sterile water.

Germination paper assays

Sterilized seeds were germinated on a moist filter paper (Whatman) for 5-7 days at 4°C and 2 days in a controlled environment room set at 16/8h photoperiod (20/15°C). The uniformly germinated seeds (~0.5 cm radicle root) were transferred on to the blue paper germination pouches soaked in 1/6th strength Hoagland's 2.0 (Sigma) (Hoagland and Arnon, 1950) hydroponic media (pH 6.0).

4-5 days old seedlings were treated with a potassium phosphite based formulation (1 L ha-1 + 0.1% NA 13 wetting agent) as a foliar spray, using a calibrated, hand-held spray gun in a volume of water equivalent to 200 L ha^{-}1. Control plants were sprayed with 0.1% NA13 wetting agent only. The root impression underneath the black sheet revealed the position of each seminal root and was marked using a blue permanent marker to indicate the position of the root at the time of the foliar application.

A randomized block design was used with a minimum of 24 replicates per treatment. After 9 days (two-leaf stage), another mark was made on the new position of the roots as well as marking the newly developed roots based on the impression. The pouches were imaged on both the black sheet and the blue paper using a Nikon D600 DSLR camera as described by Atkinson et al. (2015).

Root images were processed using RootNav software as described in Pound et al. (2013) and ImageJ software (NeuronJ) for analyzing the changes in the root development after phosphite application.

X-ray micro CT imaging experiment

Seeds were surfaced sterilized (above) and stratified at 4°C in a square petri-dish containing moist filter paper for 3 days with each seed facing down. After 3 days, they were moved to a 22°C growth chamber and the petri-dish was wrapped in aluminum foil and placed at a 65° angle to allow the root radicle to grow towards gravity.

Soil (sandy loam) was collected from a field under winter wheat at the University of Nottingham experimental farm, Sutton Bonington campus. The soil was air-dried and sieved to <2 mm before being uniformly packed into columns (7.5 cm diameter and 17 cm height). A small yellow pipette tip was placed in the middle top of the soil to 0.5 cm depth before the soil was soaked. This prevents compaction during seed transplanting. The soil moisture was saturated at field capacity 24 hr before the wheat was transplanted. Once the root radicle emerged and was 0.2 cm long, the yellow tip in the middle of the column was removed and the germinating seed was replaced in the soil with roots directly facing downward. Soil of ~1 cm thick was placed over the top to bury the seeds. A completely randomized design was used with a minimum of 10 replicates per treatment. At 4 days after transplanting, the emerging leaves were treated with a potassium phosphite based formulation (1 L ha^{-1} + 0.1% NA 13 wetting agent) as a foliar spray, using a calibrated, hand-held spray gun in a volume of water equivalent to 200 L ha^{-1}. Control plants were sprayed with 0.1% NA13 wetting agent only. Ten biological replicates were made each and the columns were X-ray scanned at day 0, 6 and 12 after phosphite treatment using a Phoenix Nanotom (GE Measurement and Control Solutions, Wunstorf, Germany) micro CT scanner.

Image processing and analysis of the root system were segmented from the grey-scale micro CT images using the Volume Graphic Studio Max (VG StudioMax) software described by Tracy et al. (2013). The root volume and surface area were all extracted from the VG StudioMax while the root branching and root count were analyzed using semi-automated ROOTh imaging software.

Growth and phosphite application experiments in controlled conditions

For all phosphite treatments hereon, a potassium phosphite based formulation 0-28-19 (O-Phyte) (Omex Ltd.) containing 31.15% PO_3 was used. The 0-28-19 was diluted with water (5mL/L and mixed with 0.1% solution of the wetting agent NA13 (Omex Ltd). This solution containing 0.15% PO_3 was used as foliar spray at the rate of 1L per m^2. Control plants were sprayed with 0.1% NA13 wetting agent only.

The sterilized seeds were pre-germinated on a moist filter paper in Petri-dishes in the dark at 21°C for 3 days. Uniform-sized seeds with a root radicle of ~0.5 cm were sown in germinating plugs containing compost (John Inness, Norwich UK) and were grown in a glasshouse for 7-10 days until GS12 (Zadoks et al., 1974). Plants were then vernalized at 6°C for 4-5 weeks with a 16/8h photoperiod. Plants were then transferred into a glasshouse with 21°C/15°C day and night temperature and 16/8 h photoperiod for 7 days.

At 7 days post vernalization, plants were transplanted into deep, plastic pots filled with ~0.6-10 mm washed expanded clay pellets (Hydroleca) and maintained in this semi-hydroponic system by daily irrigation as described previously (Rossall et al., 2016). After a week in this semi-hydroponic system, phosphite and control treatments were applied as mentioned above. Root and shoots were harvested at different time points after treatment and dried at 70^0C for three days before dry weight calculations.

Nutrient strength experiment

Three different hydroponic media were used in the semi-hydroponic system described above. Two were commercially available media from Omex and Hortimix with a composition of NPK: 20-8-20 + Mg and S with trace elements and NPK: 15-7-30 with trace elements respectively. While the third hydroponic media was a modified laboratory formulated Hoagland's solution with EDTA as the iron chelator. The composition (g/L) of nitrate and phosphate was reduced by half; $(NH_4)_3PO_4$, 0.058g; $Ca(NO_3)_2$, 0.66g; $MgSO_4$, 1.01g; KNO_3, 0.304g; H_3BO_3, 0.114g; Cu_2SO_4, 0.3g; $MnCl_2(H_2O)_4$, 0.04g; MoO_3, 0.0008g; $ZnSO_4$, 0.0092g; FeHEDTA, 0.11g. The solution was adjusted to pH 6.0.

For the nutrient strength response experiment, the required amount of the two commercial hydroponic media was diluted with water to make up either ¾ or ½ or ¼ strength.

Mild drought experiment

At 7 days post vernalisation, plants were transplanted into a 1 m PVC constructed column containing ~0.6 – 10 mm hydroleca and irrigated with the full complement of nutrients using automated irrigation drips. 10 days after transplanting into the 1 m column, the plants were treated with a potassium phosphite based formulation as a foliar spray. The plants were set to a randomized complete block design. A week after the phosphite treatment, the irrigation was restricted and as the hydroleca is inert and does not hold water, the automated irrigator supplied 75 ml of water every 6 h to achieve a moderate drought. The plants were allowed to grow in this condition until they reached Growth Stage 65-69 i.e., mid to late anthesis before the plants were harvested for the shoot and root sampling.

Heat stress experiment

At 7 days post vernalisation, the wheat seedlings were transferred into a pot containing a mixture of soil and compost (John Innes No.3). All other environmental conditions are the same as above with the exception of the heat treatment. After 14 days at 21°C, they were sprayed with phosphite and were immediately subjected to heat stress of 35°C for 30 days in a controlled environment chamber (Conviron, Winnpeg) followed by an increased temperature of 38°C for 5 days before reducing the temperature back to 22°C for the remainder of the experiment.

Leaf gas exchange measurements and chlorophyll fluorescence

All leaf gas exchange measurements were taken on the uppermost, fully expanded leaf using an infra-red gas analyser (IRGA), Licor 6400XT or 6800 (Licor inc, Illinois, Nebraska). The same IRGA model was used within each experiment. Three types of measurements were made: single time point measurements of photosynthesis at light-saturation (A_{max}), Photosynthesis versus intercellular CO_2 concentration (*Ci*, A/*Ci*) analysis and light response curves as described previously by Webster et al. (2016). The photosynthetic model of Farquhar et al. (1980) was fitted using the bilinear method of the 'fitacis' function from the R package PLANTECOPHYS (Duursma, 2015). Except where noted, measurements were made under light-saturated conditions (1500 µmol m^{-2} s^{-1}). The block temperature was maintained at 22°C, the flow rate 500 ml min^{-1} and 60-65% humidity. The CO_2 concentration used was 400 µmol mol^{-1} (except where noted). All measurements took between 2 and 3 minutes to achieve stability. The leaf water instantaneous water use efficiency (IWUE) and intrinsic water use efficiency values (iWUE) were obtained from the ratio of photosynthetic CO_2 assimilation (A) to stomatal conductance (g_s), and A_n to leaf transpiration (E) respectively.

Chlorophyll fluorescence

From 5 days after phosphite application, between 11:00 am and 12:00 pm; the top and fully developed leaf was wrapped with a ~3 cm x 3 cm aluminium foil around the upper middle part of the leaf. The leaf was left to dark adapt for 30 mins and the light of the growth chamber was turned off before the measurement started. Handheld FluorPen FP 100 (Photon Systems Instruments, Brno) was used to measure the maximum quantum yield (F_v/F_m) of the dark-adapted leaf from ten biological replicates.

For disruptive analysis, the F_v/F_m was measured from excised leaf segment of 10 biological replicates of phosphite treated and untreated under two contrasting temperatures (Ferguson et al, 2020). The leaf segments were placed on a damp filter paper and the paper was encased between glass

plates. The plates were placed inside a closed 800C FluorCam chlorophyll fluorescence imager (Photon Systems Instrument, Brno) to dark adapt for 1 h before the standard F_v/F_m protocol was run as described by Mcausland et al. (2019).

Spectroradiometer

Hyperspectral reflectance was measured between 11:00 am and 2:00 pm using the ASD Field Spec 4 (ASD Field Spec ® 4, Boulder, CO, USA) with a spectral range from 350 – 2500 nm. The reflectance measurement was made using the leaf clip in two different leaves of the top fully expanded leaf as described by Robles-Zazueta et al. (2021). The measurements were taken in ten biological replicates. Chlorophyll content was measured on the two top fully expanded leaves using the SPAD meter (SPAD-502 meter, Konika Minolta, Japan).

Nitrate reductase assay

Nitrate reductase assay was done as described previously (Kim and Seo, 2018). A root or shoot tissue (500 mg) was ground using liquid nitrogen and suspended in 750µl of chilled extraction buffer (250 mM Tris-HCl, pH8, 1 mM EDTA, 1 µM Na_2MoO_4, 5 µM FAD, 3 mM DTT, 1% BSA, 12 mM 2-mercaptoethanol, 250 µM PMSF) and centrifuged at 17,000 g for 5 min. 150 µl of supernatant was added to 850 µl of reaction buffer (40 mM $NaNO_3$, 80 mM Na_2HPO_4, 20 mM NaH_2PO_4, 0.2 mM NADH) and incubated for 2 h at room temperature. 200 µl of 1% sulfanilamide and 200 µl of 0.05% N-(1-naphthyl) ethylenediamine were added to each reaction and incubated at room temperature for another 15 mins and absorbance measured at 540 nm. Protein contents were measured using the Bradford assay (Bradford, 1976) and NR activity was expressed as specific activity (units/mg protein).

Statistical analysis

Statistical analysis was performed within the R software environment (R Core Team, 2014) and GraphPad Prism 9.01 for Windows (La Jolla, CA, USA) for figures. Student T-tests were used in comparisons between two samples. Analysis of variance (ANOVA, one-way and two-way) with posthoc Tukey's multiple comparison procedure was used except where indicated otherwise. Pearson's product-moment correlation coefficient was performed for all pairwise traits interactions using the 'rcorr' correlation analysis from the R package HMISC, using the 'corrplot' function (Mckenna et al, 2015).

Results

Phosphite treatment improves root growth in wheat

Initially we tested the effect of phosphite on young seedlings in six commercial winter wheat varieties Diego, Evolution, Leeds, Revolution, Siskin and Skyfall. Early seedling stage root phenotyping was done using 2D high throughput root phenotyping system (Atkinson et al., 2015). Four out of six commercial winter wheat varieties; Diego, Leeds, Siskin and Skyfall showed a significant increase (Tukey's HSD P<0.05 and lower) in the seminal root length (Supplementary Figure 1A. The mean of the seminal root count in Diego was significantly (P<0.05) increased by 18% while its lateral root counts significantly (P<0.05) increased by 38% and Leeds by 58%). Interestingly, Evolution and Revelation did not respond to phosphite treatment indicating a varietal difference in their response to phosphite treatment.

In addition to its response to phosphite, winter wheat cultivar Siskin is more resistant to powdery mildew infection and hence was sub-selected for further experiments under reduced nutrient strength. Using the early-stage root phenotyping set up described above, Siskin plants were grown under reduced nutrient strength with and without phosphite treatment. Figure 1A shows superimposed 2D images of young Siskin seedlings showing improvement in seminal and nodal root length at 7 days post phosphite treatment and reveals an increase in the length and number of the nodal and seminal roots (Figure 1B).

X-ray CT imaging reveals that phosphite treatment improves root architectural traits

To test the impact of phosphite on root growth in soil, pre-germinated wheat (variety Siskin) seeds (~1cm radicle roots) were sown into sandy loam soil in small columns (7.5 x 17cm). 4d old seedlings were treated with a potassium phosphite based formulation through the foliar spray and X-RAY CT imaging was performed at 0, 6 and 12 d post-application (Figure 2)

The result was computed based on the changes between time points. The differences between day 6 and day 0 of treatment are referred to as Δ(D6-D0), similarly between day 12 and 6 and between day 12 and 0 as Δ(D12-D6) and Δ(D12-D0), respectively. The CT results revealed that at 6 d post-application Δ(D6-D0) there was a significant increase in the root volume (P=0.027) and the surface area of the root (P= 0.036) by 28% and 27%, respectively. The increase in both the

root volume and the surface area in response to the phosphite application can also be seen at the later time points but the increase was not significant (Figures 2G, H). There was also a significant increase in seminal and nodal root length (P=0.042) by 22% and lateral root count (P=0.002) by 39% (Figures 2I, K) 6 days after the phosphite treatment. We also found a significant positive correlation between the root biomass and lateral root count at 12 days post treatment; root surface area and root volume after 6 days post treatment (r=0.42, *r*=0.43 and *r*=0.60 respectively; Supplementary Figure 2). The shoot biomass also showed positive correlation with the root volume (r=0.55).

Phosphite treatment improves root biomass under nutrient deficiency

Roots are crucial for nutrient and water uptake from the soil. To test if improved root growth can lead to improvement in nutrient uptake, the plants were grown under three different nutrient strength solutions: full strength (100%), ¾ strength (75%) or ½ strength (50%). 10-day post transfer to the hydroponic set up, plants were subjected to foliar phosphite application. The growth was monitored through detailed physiological measurements and destructive root and shoot biomass analysis (30- and 45-days post treatment).

As shown in Figure 3A, phosphite treated plants showed a significant increase in root biomass at all three nutrient strengths compared to the control treatment. Phosphite treated plants at 75% nutrient strength solution showed the highest increase in root dry weight (51%) compared to control (P=0.0258); whereas there was a 34% increase in root dry weight at 100% strength nutrient solution (p=.0476); and 40% increase at 50% strength nutrient solution (p=0.0128) compared to control treatments. Moreover, phosphite treated plants grown in reduced nutrient strength solutions (75% and 50%) outperformed the full strength non-treated plants. All three nutrient concentrations also showed an increasing trend (17%, 22% and 25% respectively) in shoot biomass in phosphite treated plants compared to control treated plants.

To further validate these findings, we designed another experiment where plants were grown under formulated Hoaglands solution with half strength N and P and growth measurements were done at 2, 4 and 8 weeks post treatment. At all the three time points, phosphite treated plants had significantly longer (27, 20 and 39%, respectively) roots compared to the untreated control (Supplementary Figure 3). Results also show a significant increase in root dry weight by 28% (P=.045) in phosphite treated plants 2 weeks post application further confirming the observation (Figure 2) that phosphite treatment improves root growth and may help promote seedling establishment. In addition, a significant positive correlation was also seen in the root dry weight and maximum root length in both week 2 and 4 after treatment (r=0.6 and r=0.53, respectively).

Despite improvement in root growth and root dry weight, we did not detect any differences in the shoot dry weight between treated and untreated plants (Supplementary Figure 3Biii).

Phosphite treatment improves root length under limited water condition

Roots can establish at depths much greater than the pots commonly used in controlled environments. To measure root

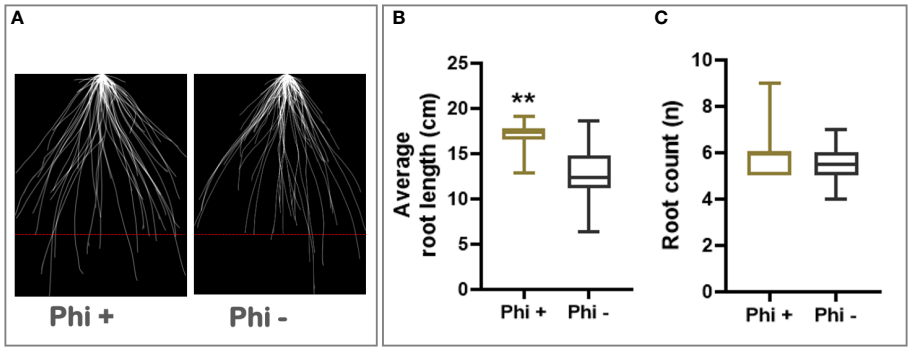

FIGURE 1
Phosphite promotes root growth in wheat seedling. **(A)** Superimposed 2D root images of young seedlings grown in low strength hydroponic media showing improvement in seminal and nodal root length at 7 days post phosphite treatment. **(B)** Seminal root length **(C)** seminal root count. All values are means ± SE (n= 25); ** indicates signifcant difference (P ≤0.01).

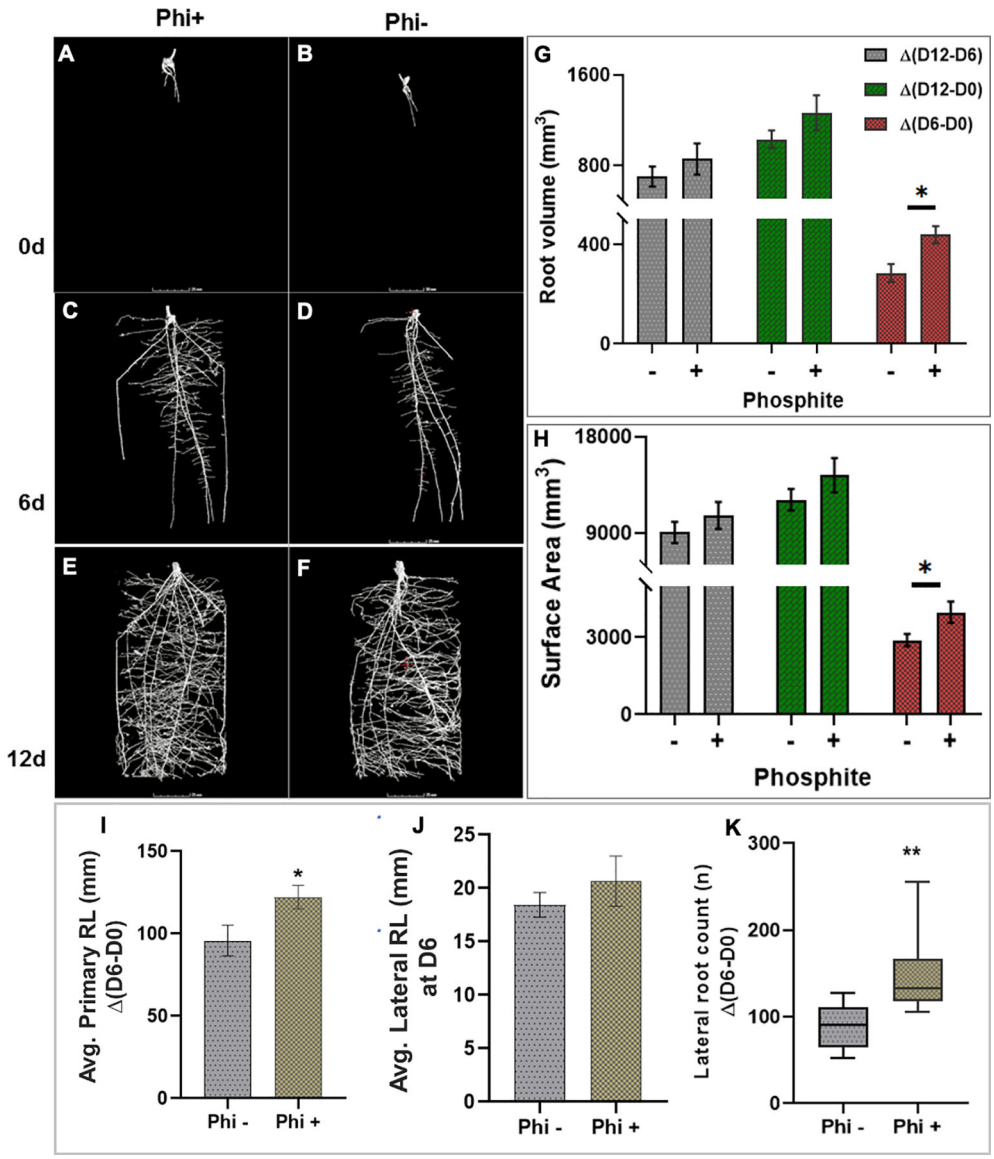

FIGURE 2
X-ray CT imaging in wheat revealed that phosphite improves root architectural traits. **(A–H)**. Time course X-ray CT imaging at 0, 6 and 12 d post treatment **(A–F)** reveals that phosphite treatment results in increase in root volume **(G)** and root surface area **(H)**. **(I–K)**. Average primary root length **(I)** average lateral root length **(J)** and lateral root count **(K)**. Wheat seedlings grown in sandy loam soil in small columns (7.5 x 17cm). 4 day old seedlings were treated with a potassium phosphite based formulation and X-RAY CT imaging performed at 0, 6 and 12 d post application. Student t test was used to compare between treatment and untreated control (*indicates significant difference *P ≤ 0.05 and **P ≤0.01). All values are means ± SE (n= 10).

depth in a restricted water experiment, seedlings were transferred to 1 m long columns containing expanded clay beads fitted with an automated drip irrigation system. Foliar phosphite treatment was done 5 days post transfer of the seedlings to these columns and water restriction was imposed a week later. Root growth assessment at 45 days after the treatment showed that phosphite treated plants have longer roots under restricted water regime (Figure 3B).

Phosphite treatment improves carbon assimilation under mild water and nutrient stress conditions

The observed alterations in root traits may have consequences for the plant capacity to supply the shoot with nutrients for synthesis of photosynthetic components and water for leaf gas exchange. To investigate this, we utilised infra-red

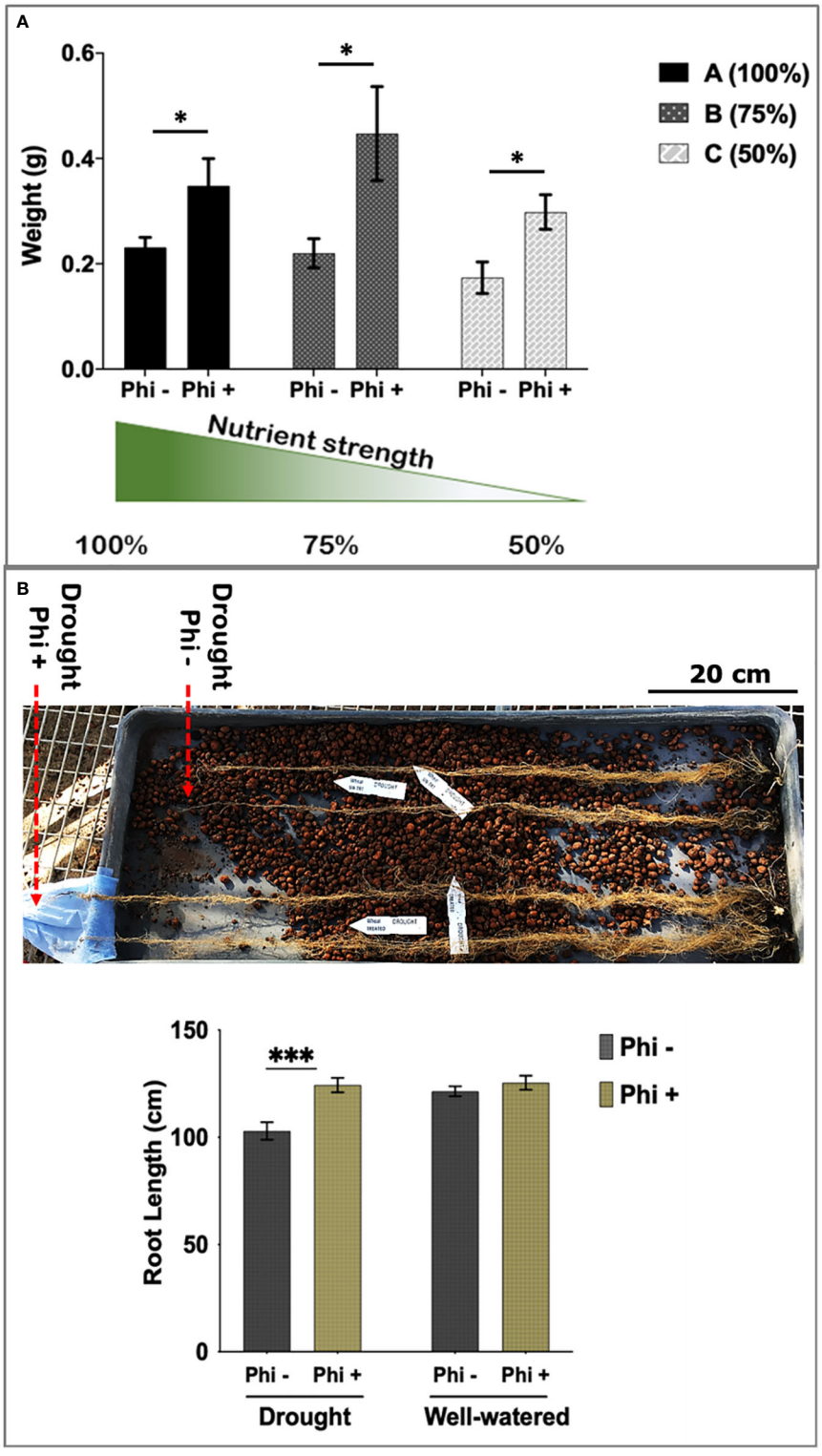

FIGURE 3
Phosphite treated plants show improved root development. **(A)** Root dry weight of Phosphite treated plants in pots under different nutrient strength of a commercial soluble fertilizer (NPK: 20-8-20) compared to untreated plants. *indicates significant difference (student's t test $P \leq 0.05$). **(B)** Deep columns were used to show an increase in maximum root length under mild drought compared to untreated plants. Arrowheads indicate end of root tips. Growth assessment 10-45 days after phosphite treatment. All values are means $\pm$ SE (n= 10-15); *indicates significant difference (*$P \leq 0.05$ and ***$P \leq 0.001$). Scale bar=20cm.

gas analysis. We observed enhanced photosynthesis as a common trend in phosphite treated plants. At both high (100%) and moderate (50%) nutrient strength, photosynthetic capacity (A_{max}) increased significantly by 12 and 21% respectively, after 28 days of phosphite treatment (P=0.027 and 0.001)(Figure 4A). Stomatal conductance (gs) and the transpiration rate at moderate nutrient strength (50%) were higher in the phosphite treated plants compared to untreated control plants (P=0.045 and 0.015 respectively; student's t test) (Figures 4B, C). Intrinsic leaf water use efficiency WUE (calculated as A/g_s) of phosphite treated plants in full nutrient complement also improved significantly (P=0.0004; Figure 4D).

Carbon assimilation and gas exchange rates were measured at 4 different time points within the first 15 days of mild water restriction (Supplementary Figure 4). Although not significant, the A_{max}, the stomatal conductance (g_s) and the transpiration rate (E) of phosphite treated were all numerically higher at all the 4-time points compared to non-treated under mild water stress with no alteration in WUE.

A-Ci analysis was used to separate biochemical components of photosynthesis such as the maximum rate of carboxylation by Rubisco (V_{cmax}) and the maximum rate of electron transport for ribulose-1-5-bisphosphonate (RuBP) regeneration (J_{max}) at 10 days of water restriction. For both the V_{cmax} and J_{max} effects were not significant comparing phosphite treatment under mild water stress to the untreated control (Supplementary Figure 4D).

Phosphite treatment improves responses to heat stress

During the heat stress period, the response of the maximum quantum efficiency of photosystem II (F_v/F_m) was measured every day in the first 5 days, followed by measurements at 5 days intervals. At 24 h after heat stress, F_v/F_m of the untreated plants was significantly lower than treated (P<0.05) Figure 5D). When the temperature was again increased at day 30 to 38°C, there was a trend for a sharp and substantial decline in F_v/F_m for the untreated plants but not treated (P=0.081). This suggests that phosphite treatment plays a role in helping to prevent photoinhibition, likely caused by damage to the PSII complex during heat stress.

To investigate this further, ACi analysis was performed during the heat stress treatment at 5-day intervals. On day 1 and 4 of the heat treatment, there was a substantial reduction in V_{cmax} (P=0.0169, Figures 5A, B) in untreated plants which mirrored the reduction in *Fv/Fm* but J_{max} was not significant (Figure 5C). Additionally, to determine if phosphite treatment

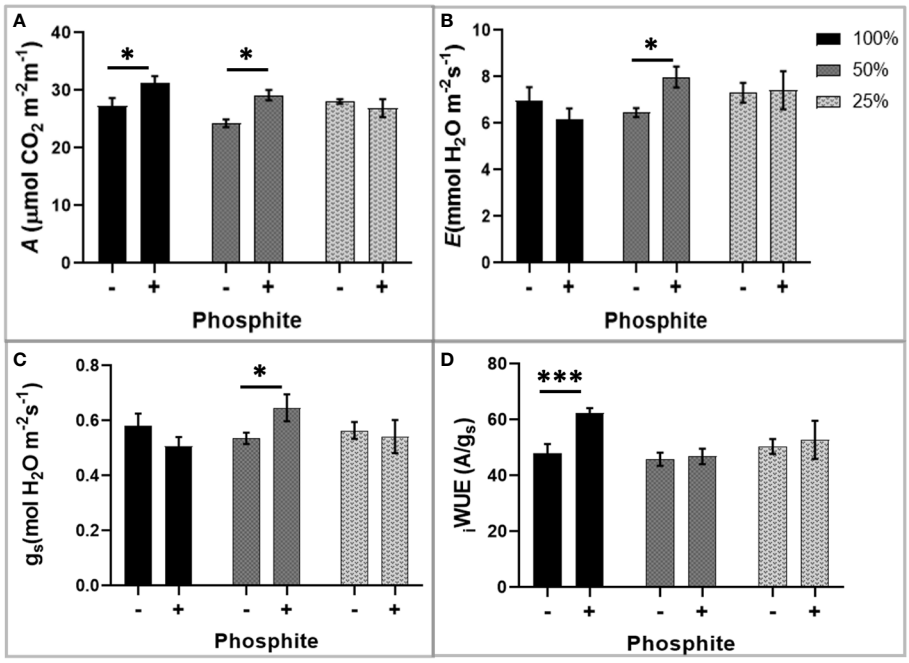

FIGURE 4
Phosphite treatment improves carbon assimilation under mild nutrient stress. Photosynthetic response of phosphite treated (+) and untreated **(-)** wheat plants grown under different nutrient strength of a commercial soluble fertilizer (NPK: 20-8-20). **(A)** Net carbon assimilation rate **(B)** Transpiration rate **(C)** Stomatal conductance **(D)** Intrinsic water use efficiency from a ratio of net photosynthesis to stomatal conductance. All values are means ± SE (n=6); *indicates significant difference (student's t test P ≤ 0.05). ***P ≤ 0.001.

has any role to play in leaf senescence under heat stress, we measured the whole plant senescence: Structural Insensitive Pigment Index (SIPI; Figure 5E) using the vegetative index calculated from hyperspectral reflectance at day 0 and 5 of heat stress.

Phosphite treatment increases nitrate reductase activity

It has recently been reported that phosphite application results in an increase in nitrate reductase activity.

To test the effect of phosphite treatment on nitrate reductase, nitrate reductase enzyme activity (NRA) was measured in phosphite treated and untreated plants grown in different growth mediums (soil columns; field condition and hydroponics) and different growth conditions (varying nutrients and water levels).

The nitrate reductase activity was measured on wheat shoots grown in ½ strength hydroponic media (Figure 6A). There was a significant increase in nitrate reductase activity 6 and 9d post application.

We next tested the nitrate reductase activity in field grown wheat plants. Plants were treated with phosphite in autumn, spring or both in autumn and spring. We detected a significant increase (51%) in nitrate reductase activity in dual phosphite application (autumn and spring; Figure 6B).

To test if the phosphite-influenced increase in nitrate reductase is only common to wheat, we measured the nitrate reductase

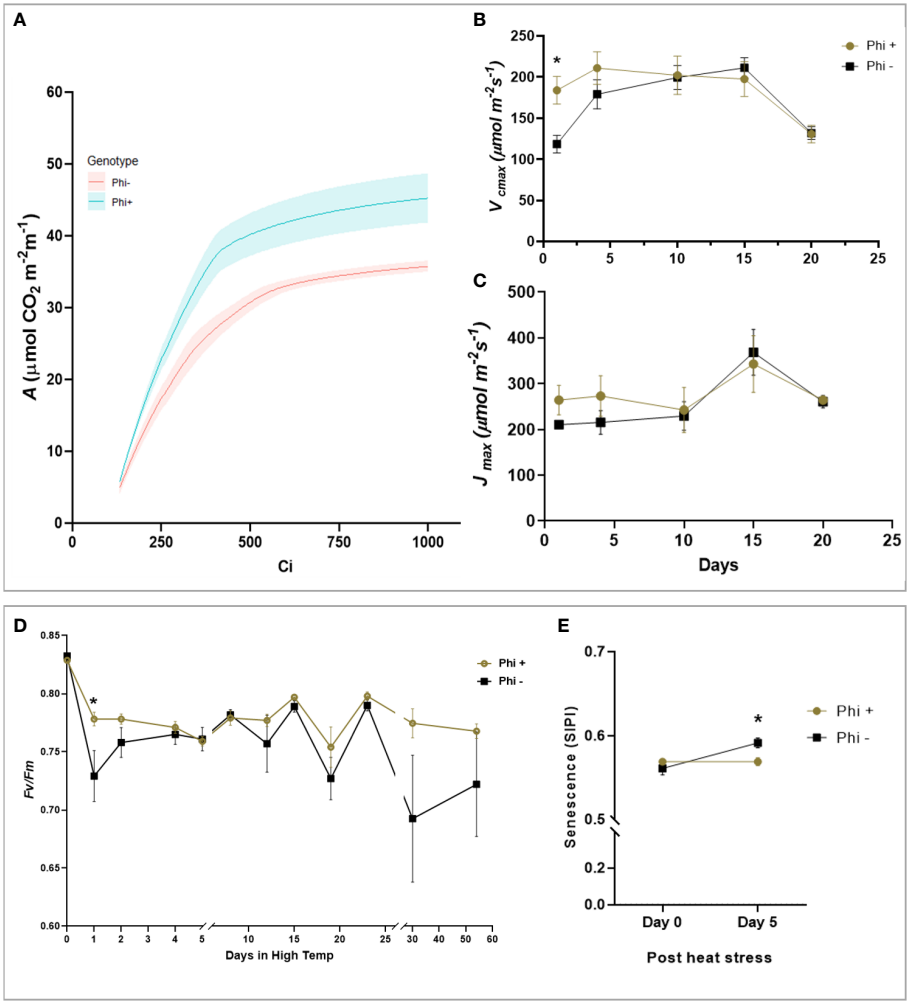

FIGURE 5
Phosphite treatment shows improve tolerance to heat treatment. **(A)**. *A* versus Ci response curve at 24hr of heat treatment. For visual clarity the lines are fitted through mean values and the shaded region show limits to the standard error of mean. **(B)**. Maximum rate of carboxylation of Rubisco (V_{cmax}) **(C)**. Maximum rate of RuBS regeneration/electron transport (J_{max}) **(D)**. Maximum efficiency of photosystem II after dark adaptation. **(E)** Canopy senescence (SIPI). All points are means ± SE (n= 5 - 10); (* represent significant differences between phosphite treated and untreated of the same time point ($P \leq 0.05$).

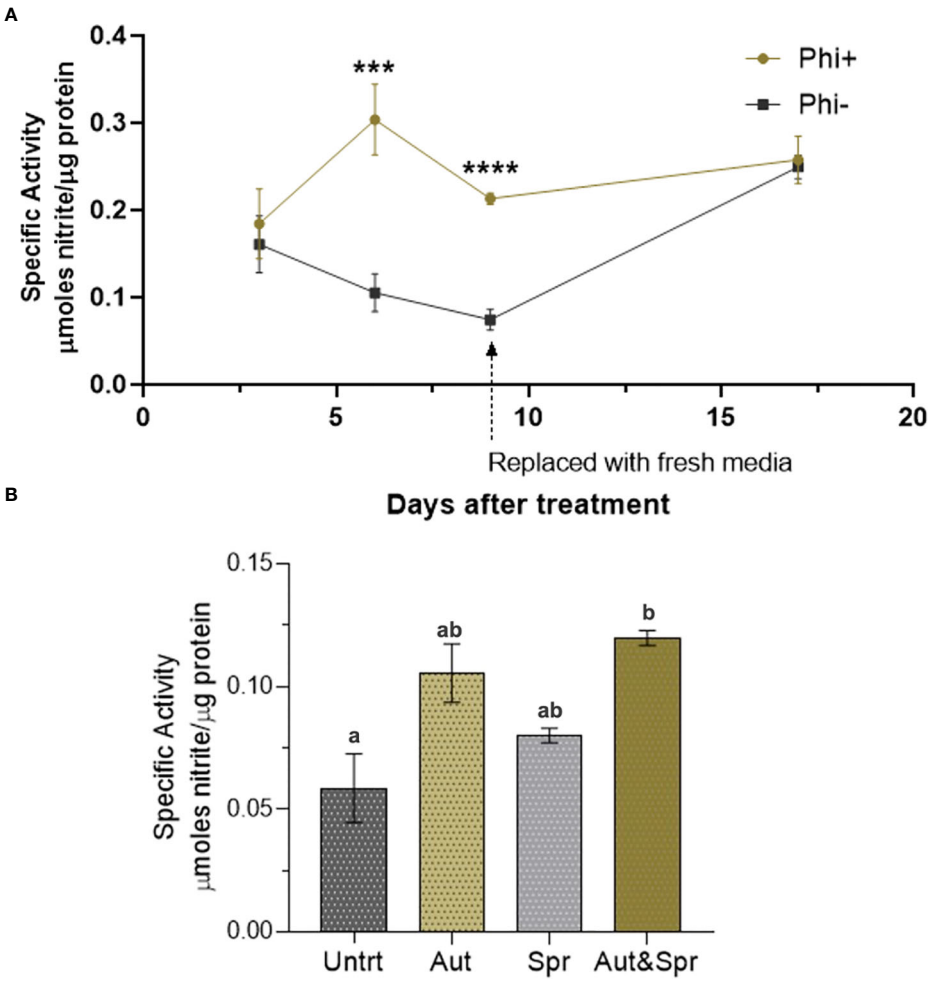

FIGURE 6
Phosphite enhances Nitrate Reductase activity. **(A)** Time-course assessment of NR activity of wheat plants grown under reduced nutrient (50% strength) from 3 days to 19 days post treatment. *indicates significant difference. (***P ≤0.001 and ****P ≤ 0.0001; student's t test) **(B)**. Wheat plants grown in the field with different times of phosphite application. Effect of phosphite on nitrate reductase activity is commonly observed under mild stress. All values are means ± SE (n= 5 - 25); Different letters denote statistical significance (P ≤ 0.05; one-way analysis of variances. All values are means ± SE (n= 5 - 25) for both **(A, B)**.

activity of winter brassica (dicot crop) using the same cultivation methodologies. In line with wheat experiments we used ½ strength of commercial NPK 20-8-20 hydroponic media as described in the methods. Our results show that 9 days after phosphite application, there was a significant increase (44%) in the nitrate reductase activity (Supplementary Figure 5A). We also tested the nitrate reductase activity of seedlings growing in soil column under restricted water conditions. *Brassica napus* (var Anastasia) and *B. rapa* (var Skye) seedlings were treated with phosphite and 5 days after phosphite application, water was restricted and nitrate reductase activity was measured 12-day post treatment. Our results show both varieties (Skye and Anastasia) have a significant increase in the nitrate reductase activity by 67% and 60% respectively (Supplementary Figure 5A).

Discussion

Biostimulants are emerging as a class of chemicals that promote crop growth. They also have been reported to improve plant fitness and performance under stress conditions (Ziosi et al, 2013; Brown and Saa, 2015; Bulgari et al, 2015; Bulgari et al, 2019). With increasing incidents of adverse growing conditions, the use of biostimulants to enhance crop establishment and growth is becoming more important and could be crucial for meeting future food demands.

Phosphite represents a reduced form of phosphate that has been shown to act as a biostimulant (Albrigo, 1999; Lovatt and Mikkelsen, 2006). Previous studies in wheat have shown that foliar application of phosphite enhances root growth and

development in a range of plant species, typically increasing biomass by around 30% (Rossall et al., 2016) but mechanisms of action are unclear.

Here we have carried out more detailed studies on the effect of phosphite on root growth and its impact on nutrient use efficiency and above ground physiology. In early seedling stage root studies, we tested the impact of phosphite in six commercial winter wheat varieties. Four of these varieties (Diego, Leeds, Siskin and Skyfall) responded to phosphite treatment and resulted in increase in the length and number of the nodal and seminal roots (Figure 1). Interestingly, Evolution and Revelation did not respond to phosphite treatment indicating a varietal difference in their response to phosphite treatment. Currently it is not clear why some varieties respond to phosphite treatment and others don't. Phosphite cannot be used as a source of P nutrition (Carswell et al., 1996; Forster et al., 1998; Schroetter et al., 2006). Phosphite can be taken up by the phosphate transporters but cannot replace Pi in most biological reactions but suppress the Pi starvation response (McDonald et al., 2001; Varadarajan et al., 2002). There is not much evidence either to suggest that phosphite can be converted to phosphate *in planta* (Thao and Yamakawa, 2009). However, there are some reports that suggest that phosphite can be converted to Pi by soil microbacteria but the conversion is very slow to account for any nutritional benefits (McDonald et al., 2001). Besides, the doses used here are very small and typically one application of phosphite is needed to promote root growth. Therefore, we rule out the possibility of phosphite as a source of P nutrition. However, it is possible that the varieties like Evolution and Revelation that do not respond to phosphite treatment, may lack components in phosphite perception and/or signal transmission.

We also tested the impact of phosphite on root growth in soil by X-ray CT imaging. X-ray CT is a non-invasive method that generates a sequence of images through a soil column and allows the root architecture of plants to be visualised in 3D in their natural environment. We find that at 6 d post-application Δ(D6-D0) there was a significant increase in the root volume and the surface area of the root. There was also a significant increase in seminal and nodal root length and lateral root count six days post phosphite treatment. These results indicate a clear impact of phosphite treatment on early root growth that is likely to improve seedling establishment.

Root system architecture (RSA) determines the distribution of root surface area within the soil profile and so the plant's capacity to capture nutrients and water (Ho et al., 2004; Hochholdinger & Tuberosa, 2009; Coudert et al., 2010; Gewin, 2010; Bhosale et al., 2018; Giri et al., 2018; Meng et al., 2019). These traits therefore have a direct bearing on crop productivity, particularly under conditions of low resource availability (Lynch, 2011; Lynch, 2013; Lynch et al., 2014; Lynch, 2015). Our nutrition use efficiency experiment further supports this view where we show that phosphite treated plants show a significant increase in root biomass compared to untreated plants when grown under reduced nutrient strength solutions and phosphite treated plants grown in 75% strength nutrient solution outperformed the full strength untreated plants (Figure 3).

Improved root traits may also have consequences for synthesis of photosynthesis components and water for leaf gas exchange and thus can explain an increase in photosynthetic capacity, transpiration rate, stomatal conductance and intrinsic leaf water use efficiency WUE of phosphite treated plants (Figure 4).

Effects of enhanced photosynthesis can be difficult to interpret due to interactions between enhancement of development in terms of plant size and increased photosynthesis per unit leaf area. We hypothesize that enhanced root morphology can provide greater opportunity to extract water for transpiration, lowering leaf resistance to CO_2 diffusion and to take up more nutrients to construct greater amounts of photosynthetic components per unit leaf area. Under conditions where resources are restricted these effects could amplify and we see some evidence of this. The difference shown in Figure 3A (moderate nutrient depletion) between control and Phi treated plants could be attributed to an increased ability to extract nutrients from the soil. However, the results we saw are not consistent: we would also expect the 25% treatment to also show a difference in A_{max}. Similarly, we would anticipate an improvement in iWUE would be expected under all treatments.

Our heat stress experiments showed improvements in *Fv/Fm* (an indicator of photoinactivated photosystem II (PSII)) and V_{cmax} (the maximum carboxylation rate of the enzyme Rubisco at key points following the heat treatment in phosphite treated plants. These are important findings because both of these processes are heat sensitive and represent a loss of activity in these two key photosynthetic components, PSII and Rubisco. An increased transpiration capacity that could form as a result of an enhanced root system might provide extra leaf cooling and reduce the impact of higher leaf temperatures in the initial phase of the heat treatment. To support this, we observed a significantly higher Gs in the phosphite treated plants compared to untreated at the first time point after the heat was applied. In addition, SIPI measurments revealed reduced senescence in phosphite treated plants (Figure 5E). Chlorophyll degradation can occur in cereals under high temperature stress and it is likely that phosphite treatment inhibits high temperature mediated chlorophyll degradation. However, we also cannot rule out an as yet unknown effect of phosphite on stress signalling pathways in the plant.

We find that phosphites regulate the activity of Nitrate reductase which is a key enzyme in N metabolism and catalyses nitrate to nitrite conversion (Figure 7) (Campbell,

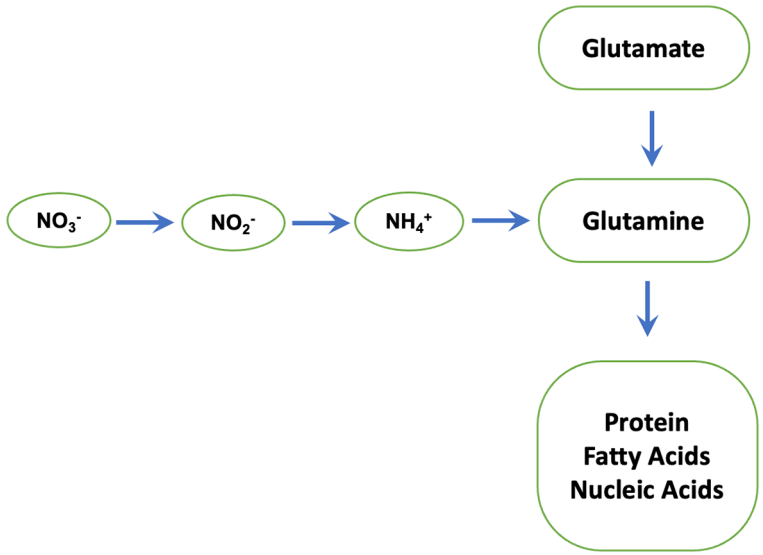

FIGURE 7
Nitrate reductase: a key enzyme in N metabolism. Nitrate reductase catalyses nitrate to nitrite conversion. The nitrite formed is reduced by the enzyme nitrite reductase to ammonium, which then reacts with glutamate to form glutamine by glutamine synthetase. The latter serves as the amino group donor for the synthesis of amino acids, proteins and Nucleic acids.

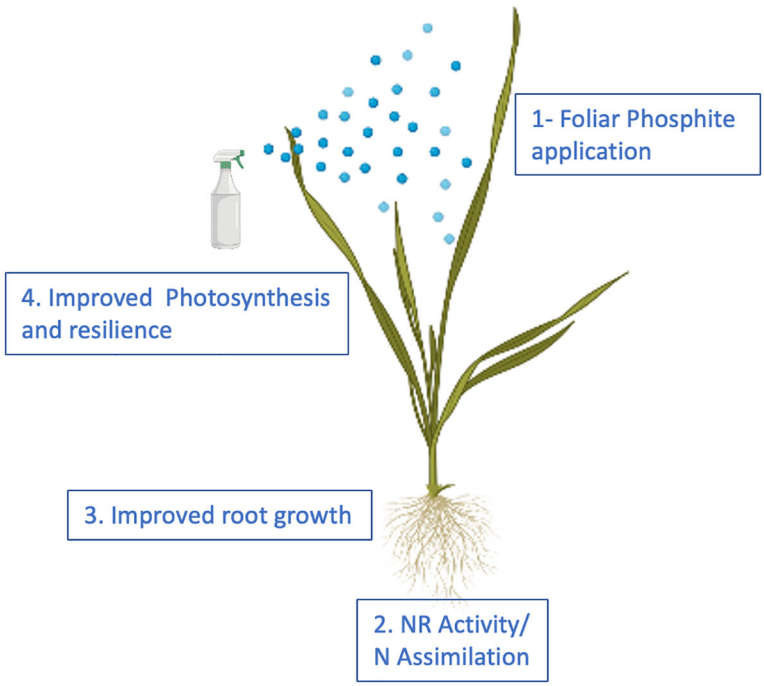

FIGURE 8
Proposed model for phosphite action. The model provides a temporal framework for impact of phosphite on root growth. Phosphite treatment results in the induction of NAS gene expression and Fe homeostasis to regulate NR activity and root growth.

1996). The nitrite formed is reduced by the enzyme nitrite reductase to ammonium, which then reacts with glutamate to form glutamine. The latter serves as the amino group donor for the synthesis of amino acids. The total nitrogen flux from nitrate to the amino acids is limited by the activity of the first enzyme nitrate reductase. In plants, the enzyme nitrate reductase therefore has an essential role in providing reduced, metabolizable nitrogen for growth and development and a decisive influence on the increased availability of nitrogen compounds in the plant. Accordingly, an increased nitrate reductase activity leads to increased assimilation of inorganic N to build up plant organs (root, stalk/stem, leaf, and grain/seed) and activity levels have been used as an indicator of plant N content.

Though currently it is not clear how phosphites regulate Nitrate reductase activity. There is some suggestion in the literature between possible link between ion homeostasis and Nitrogen metabolism (Zhao et al., 2019). It was shown that two of wheat Nicotianamine Synthase genes *TaNAS1* and *TaNAS2* are up regulated by increased N application (Zhao et al., 2019). Nicotianamine Synthases are key genes involved in the synthesis of non-proteinogenic amino acid Nicotianamine (Nozoye, 2018; Li et al., 2020). Nicotianamine is known to chelate many metal ions including Iron, Zinc, Copper and Manganese and is involved in internal metal transport (Nozoye, 2018). Crucially, Nicotianamine is involved in acquisition, transport and homeostasis (van Wiren et al., 1999; Pich et al., 2001) of iron, which is required for many of the enzymes involved in Nitrogen assimilation including Nitrate- and Nitrite-reductases (Wang et al., 2003). It has been reported that rice *NAS3* knock outs have reduced shoot and root growth further supporting a link between Nicotianamine Synthases and growth (Aung et al., 2019). In addition, over expression of *NAS* genes has been shown to increase Nicotianamine Synthase levels in several crop plants and confers tolerance to iron deficiency stress (Aung et al., 2019; Nozoye, 2018). Thus, it is possible that phosphite treatment increases Nitrate reductase activity through improved iron homeostasis.

Conclusions

Our results show that phosphite promotes root growth and improves nutrition use efficiency (root biomass per unit nutrient supply). We also present evidence for improved gas exchange capabilities under conditions of nutrient and water limitation and for enhanced abiotic stress tolerance.

We propose that phosphite treatment improves plant growth and the ability to survive abiotic stresses through improved Nitrogen and Carbon assimilation thus facilitating improved root growth that in turn improves root biomass, nutrition and water use efficiency (Figure 8).

In recent years, there has been a focus towards improving root architecture to enhance crop resource use efficiency. World food production has to increase to meet the demands of growing population and further understanding of the phosphite mediated growth promotion could provide a promising addition to agriculture management practices.

Data availability statement

The original contributions presented in the study are included in the article/Supplementary Material, further inquiries can be directed to the corresponding author/s.

Author contributions

UM, JD, SR, KS, NC, RB and RS performed experiments and contributed experimental data. UM, JD, JF, EM and RS designed experiments and analysed data. UM, JD, JF, EM, RB and RS wrote the manuscript. All authors contributed to the article and approved the submitted version.

Acknowledgments

This work was supported by the awards from the Biotechnology and Biological Sciences Research Council [grant number BB/P010520/1]. This work was also supported by funds from Industrial Partners- Biolchim S.p.A.; Brian Lewis AgricultureT/a Intracrop; Headland Amenity; OMEX Agriculture Ltd; Trade Corporation International SAU; Verdesian Life Sciences Europe Ltd. RB thanks Future Food Beacon Nottingham Research and BBSRC Discovery Fellowship (BB/S011102/1). We also thank Xin for helping in one of the experiments.

Conflict of interest

The authors declare that the research was conducted in the absence of any commercial or financial relationships that could be constructed as a potential conflict of interest.

This study received funding from Biolchim S.p.A., Brian Lewis Agriculture/Intracrop, Headland Amenity, OMEX Agriculture Ltd, Trade Corporation International SAU and Verdesian Life Sciences Europe Ltd. Except OMEX Agriculture Ltd, no other funders were involved in the study design, collection, analysis, interpretation of data, the writing of this article or the decision to submit it for publication. OMEX Agriculture Ltd. had only the following involvement with the study: They provided plots for field trials, but they were not involved in sample collection, enzyme assays and

data analysis presented in Figure 6B and this was all done by Nottingham.

Publisher's note

Supplementary material

The Supplementary Material for this article can be found online at: https://www.frontiersin.org/articles/10.3389/fpls.2022.1017048/full#supplementary-material

References

AHDB. (2019). Available at: https://projectblue.blob.core.windows.net/media/Default/Imported%20Publication%20Docs/AHDB%20Cereals%20&%20Oilseeds/Varieties/RL2019-20/Table%201.%20Winter%20wheat%20Recommended%20List%202019-20-1.pdf.

Ahmadi, N., Audebert, A., Bennett, M. J., Bishopp, A., Costa de Oliveira, A., Courtois, B., et al. (2014). The roots of future rice harvests. *Rice* 7, 29. doi: 10.1186/s12284-014-0029-y

Albrigo, L. G. (1999). Effects of foliar applications of urea or nutriphite on flowering and yields of Valencia orange trees. *Proc. Fla State Hort Soc.* 112, 1–4.

Atkinson, J. A., Wingen, L. U., Griffiths, M., Pound, M. P., Gaju, O., Foulkes, M., et al. (2015). Phenotyping pipeline reveals major seedling root growth QTL in hexaploid wheat. *J. Exp. Bot.* 66, 2283–2292. doi: 10.1093/jxb/erv006

Aung, M. S., Masuda, H., Nozoye, T., Kobayashi, T., Jeon, J.-S., An, G., et al. (2019). Nicotianamine synthesis by OsNAS3 is important for mitigating iron excess stress in rice. *Front. Plant Sci.* 10, 660.

Bhosale, R., Giri, J., Pandey, B. K., Giehl, R.F.H., Hartmann, A., Traini, R., et al. (2018). A mechanistic framework for auxin dependent arabidopsis root hair elongation to low external phosphate. *Nat. Comms* 9, 1409. doi: 10.1038/s41467-018-04281-x

Bradford, M. M. (1976). A rapid and sensitive method for the quantitation of microgram quantities of protein utilizing the principle of protein-dye binding. *Anal. Biochem.* 72, 248–254. doi: 10.1016/0003-2697(76)90527-3

Bulgari, R., Cocetta, G., Trivellini, A., Vernieri, P., and Ferrante, A. (2015). Biostimulants and crop responses: a review. *Biol. Agric. Horticulture* 31 (1), 1–17.

Bulgari, R., Giulia, F., and Antonio, F. (2019). Biostimulants Application in Horticultural Crops under Abiotic Stress Conditions. *Agronomy* 9, 306.

Brown, P., and Saa, S. (2015). Biostimulants in agriculture. *Front. Plant Sci.* 27, 6:671.

Campbell, W. (1996). Nitrate Reductase Biochemistry comes of age. *Plant Physiol.* 111, 355–361.

Carswell, M. C., Grant, B. R., and Plaxton, W. C. (1997). Disruption of the phosphate-starvation response of oilseed rape suspension cells by the fungicide phosphonate. *Planta* 203, 67–74. doi: 10.1007/s00050166

Carswell, M. C., Grant, B. R., Theodorou, M. E., Harris, J., Niere, J. O., and Plaxton, W. C. (1996). The fungicide phosphonate disrupts the phosphate-starvation response in brassica nigra seedlings. *Plant Physiol.* 110, 105–110. doi: 10.1104/pp.110.1.105

Colla, G., Hoagland, L., Ruzzi, M., Cardarelli, M., Bonini, P., Canaguier, R., et al. (2017). Biostimulant action of protein hydrolysates: Unraveling their effects on plant physiology and microbiome. *Front. Plant Sci.* 8, 2202. doi: 10.3389/fpls.2017.02202

Conrath, U. (2011). Molecular aspects of defence priming. *Trends Plant Sci.* 16 (10), 524–531. doi: 10.1016/j.tplants.2011.06.004

Coudert, Y., Périn, C., Courtois, B., Khong, N. G., and Gantet, P. (2010). Genetic control of root development in rice, the model cereal. *Trends Plant Sci.* 15, 219–226. doi: 10.1016/j.tplants.2010.01.008

Duursma, R. A. (2015). Plantecophys - an r package for analysing and modelling leaf gas exchange data. *PloS One* 10, e0143346. doi: 10.1371/journal.pone.0143346

EBIC. (2022) *Economic Overview of the European Biostimulants Market*. Available at: https://biostimulants.eu/highlights/economic-overview-of-the-european-biostimulants-market/.

Farquhar, G. D., Von Caemmerer, S., and BERRY, J. A. (1980). A biochemical model of photosynthetic CO2 assimilation in leaves of C3 species. *Planta* 149, 78–90. doi: 10.1007/BF00386231

Ferguson, J. N., McAusland, L., Smith, K. E., Price, A. H., Wilson, Z. A., and Murchie, E. H. (2020). Rapid temperature responses of photosystem II efficiency forecast genotypic variation in rice vegetative heat tolerance. *Plant J.* 104, 839–855. doi: 10.1111/tpj.14956

Fleming, T. R., Fleming, C. C., Levy, C. C. B., Repiso, C., Hennequart, F., Nolasco, J. B., et al. (2019). Biostimulants enhance growth and drought tolerance in *Arabidopsis thaliana* and exhibit chemical priming action. *Ann. Appl. Biol.* 174, 153–165. doi: 10.1111/aab.12482

Forster, H., Adaskaveg, J. E., Kim, D. H., and Stanghellini, M. E. (1998). Effect of phosphite on tomato and pepper plants and on susceptibility of peppers to phytophthora root and crown rot in hydroponic culture. *Plant Dis.* 82, 1165–1170. doi: 10.1094/PDIS.1998.82.10.1165

Gewin, V. (2010). An underground revolution: plant breeders are turning their attention to roots to increase yields without causing environmental damage. Virginia gewin unearths some promising subterranean strategies. *Nature* 466, 552–554. doi: 10.1038/466552a

Giri, J., Bhosale, R., Huang, G., Pandey, B. K., Parker, H., Zappala, S., Yang, J., et al. (2018). Rice auxin influx carrier *OsAUX1* facilitates root hair elongation in response to low external phosphate. *Nat. Comms* 9, 1408. doi: 10.1038/s41467-018-04280-y

Gobbett, D. L., Hochman, Z., Horan, H., Garcia, J. N., Grassini, P., and Cassman, K. G. (2017). Yield gap analysis of rainfed wheat demonstrates local to global relevance J. *Agric. Sci.* 155, 282–299. doi: 10.1017/S0021859616000381

Godfray, H. C., Beddington, J. R., Crute, I. R., Haddad, L., Lawrence, D., Muir, J. F., et al. (2010). Food security: the challenge of feeding 9 billion people. *Science* 327 (5967), 812–818.

Hirabayashi, Y., Mehendran, R., Koirala, S., Konoshima, L., Yamazaki, D., Watanabe, S., et al. (2013). Global flood risk under climate change. *Nat. Climate Change* 3, 816–821. doi: 10.1038/nclimate1911

Hoagland, D. R., and Arnon, D. I. (1950). The water-culture method for growing plants without soil. *Circular. California Agric. experiment Station* 347.

Hochholdinger, F., and Tuberosa, R. (2009). Genetic and genomic dissection of maize root development and architecture. *Curr. Opin. Plant Biol.* 12, 172–177. doi: 10.1016/j.pbi.2008.12.002

Ho, M., McCannon, B., and Lynch, J. (2004). Optimization modeling of plant root architecture for water and phosphorus acquisition. *J. Theo Biol.* 226, 331. doi: 10.1016/j.jtbi.2003.09.011

IAASTD report (2009). *Agriculture at a crossroads* Island Press.

Khan, W., Rayirath, U. P., Subramanian, S., Jithesh, M. N., Rayorath, P. D., Hodges, M., et al. (2009). Seaweed extracts as biostimulants of plant growth and development. *J. Plant Growth Regul.* 28, 386–399. doi: 10.1007/s00344-009-9103-x

Kim, J. Y., and Seo, H. S. (2018). Nitrate reductase activity assay from *Arabidopsis* crude extracts. *Bio-Protocol* 8, 7, e2785. doi: 10.21769/BioProtoc.2785

Lagunas, B., Dodd, I. C., and Gifford, M. L. (2019). A 'nodemap' to sustainable maize roots: linking nitrogen and water uptake improvements. *J. Exp. Bot.* 70 (19), 5036–5039. doi: 10.1093/jxb/erz315

Li, Q., Chen, L., and Yang, A. (2020). The molecular mechanisms underlying iron deficiency responses in rice. *Int. J. Mol. Sci.* 21, 43.

Lovatt, C. J., and Mikkelsen, R. L. (2006). Phosphite fertilizers: What are they? can you use them? what can they do? *Better Crops* 90, 11–13.

Lynch, J. P. (2011). Root phenes for enhanced soil exploration and phosphorus acquisition: tools for future crops. *Plant Physiol.* 156, 1041–1049.

Lynch, J. P. (2013). Steep, cheap and deep: an ideotype to optimize water and n acquisition by maize root systems. *Ann. Bot.* 112, 347–357.

Lynch, J. P. (2015). Root phenes that reduce the metabolic costs of soil exploration: opportunities for 21st century agriculture. *Plant Cell Environ.* 38, 1775–1784.

Lynch, J. P., Chimungu, J. G., and Brown, K. M. (2014). Root anatomical phenes associated with water acquisition from drying soil: targets for crop improvement. *J. Exp. Bot.* 65 (21), 6155–6166. doi: 10.1093/jxb/eru162

Mcausland, L., Atkinson, J. A., Lawson, T., and Murchie, E. H. (2019). High throughput procedure utilising chlorophyll fluorescence imaging to phenotype dynamic photosynthesis and photoprotection in leaves under controlled gaseous conditions. *Plant Methods* 15. doi: 10.1186/s13007-019-0485-x

McDonald, A. E., Grant, B. R., and Plaxton, W. C. (2001). Phosphite (phosphorous acid): its relevance in the environment and agriculture, and influence on the plant phosphate starvation response. *J. Plant Nutr.* 24, 1505–1519. doi: 10.1081/PLN-100106017

McKenna, S., Meyer, M., Gregg, C., and Gerber, S. (2016). s-CorrPlot: an interactive scatterplot for exploring correlation. *J. Comput. Graphical Stat* 25 (2), 445–463.

Myers, S. S., Smith, M. R., Guth, S., Golden, C. D., Vaitla, B., Mueller, N. D., et al. (2017). Climate change and global food systems: Potential impacts on food security and undernutrition. *Annu. Rev. Public Health* 38, 259–277. doi: 10.1146/annurev-publhealth-031816-044356

Nair, P., Kandasamy, S., Zhang, J., Ji, X., Kirby, C., Benkel, B., et al. (2012). Transcriptional and metabolomic analysis of ascophyllum nodosum mediated freezing tolerance in arabidopsis thali- ana. *BioMed. Cent. Genomics* 13, 643.

Nozoye, T. (2018). The nicotianamine synthase gene is a useful candidate for improving the nutritional qualities and fe-deficiency tolerance of various crops. *Front. Plant Sci.* 9, 340. doi: 10.3389/fpls.2018.00340

Panda, D., Pramanik, K., and Nayak, B. R. (2012). Use of seaweed extracts as plant growth regulators for sustainable agriculture. *Int. J. BioResour. Stress Manage.* 3, 404–411.

Pich, A., Manteuffel, R., Hillmer, S., Scholz, G., and Schmidt, W. (2001). Fe homeosta- sis in plant cells: does nicotianamine play multiple roles in the regulation of cytoplasmic fe concentration? *Planta* 213, 967–976. doi: 10.1007/s004250100573

Pound, M. P., French, A. P., Atkinson, J. A., Wells, D. M., Bennett, M. J., and Pridmore, T. (2013). RootNav: navigating images of complex root architectures. *Plant Physiol.* 162, 1802–1814. doi: 10.1104/pp.113.221531

R Core Team. (2014). R: A language and environment for statistical computing. *R Foundation Stat. Computing* (Vienna, Austria).

Ray, D. K., Gerber, J. S., Macdonald, G. K., and West, P. C. (2015). Climate variation explains a third of global crop yield variability. *Nat. Commun.* 6, 1–9. doi: 10.1038/ncomms6989

Ray, D. K., Mueller, D., West, P., and Foley, J. (2013). Yield trends are insufficient to double global crop production by 2050. *PloS One* 8, e66428. doi: 10.1371/journal.pone.0066428

Robles-Zazueta, C. A., Molero, G., PInto, F., Foulkes, M. J., Reynolds, M. P., and Murchie, E. H. (2021). Field-based remote sensing models predict radiation use efficiency in wheat. *J. Exp. Bot.* 72, 3756–3773. doi: 10.1093/jxb/erab115

Rossall, S., Qing, C., Paneri, M., Bennett, M., and Swarup, R. (2016). A 'growing' role for phosphites in promoting plant growth and development. *Acta Hortic.* 1148, 61–67. doi: 10.17660/ActaHortic.2016.1148.7

Rouphael, Y., and Colla, G. (2020). Editorial: Biostimulants in agriculture. *Front. Plant Sci.* 11, 40. doi: 10.3389/fpls.2020.00040

Royal Society (2009). 978-0-85403-784-1.

Savvides, A., Ali, S., Tester, M., and Fotopoulos, V. (2016). Chemical priming of plants against multiple abiotic stresses: Mission possible? *Trends Plant Sci.* 21 (4), 329–340.

Shiferaw, B., Smale, M., Braun, H., Duveiller, E., Reynolds, M., and Muricho, G. (2013). Crops that feed the world 10. Past successes and future challenges to the role played by wheat in global food security. *Food Secur.* 5, 291–317.

Schroetter, S., Angeles-Wedler, D., Kreuzig, R., and Schnug, E. (2006). Effects of phosphite on phosphorus supply and growth of corn (Zea mays). *Landbauforschu Volk.* 56, 87–99.

Sible, C. N., Seebauer, J. R., and Below, F. E. (2021). Plant biostimulants: A categorical review, their implications for row crop production, and relation to soil health indicators. *Agronomy* 11, 1297. doi: 10.3390/agronomy11071297

Thao, H. T. B., and Yamakawa, T. (2009). Phosphite (phosphorous acid): Fungicide, fertilizer or bio-stimulator? *Soil Sci. Plant Nutr.* 55, 228–234. doi: 10.1111/j.1747-0765.2009.00365.x

Ticconi, C. A., Delatorre, C. A., and Abel, S. (2001). Attenuation of phosphate starvation responses by phosphite in arabidopsis. *Plant Physiol.* 127, 963–972. doi: 10.1104/pp.010396

Tracy, S. R., Black, C. R., Roberts, J. A., and Mooney, S. J. (2013). Exploring the interacting effect of soil texture and bulk density on root system development in tomato (Solanum lycopersicum l.). *Environ. Exp. Bot.* 91, 38–47. doi: 10.1016/j.envexpbot.2013.03.003

van Wiren, N., Klair, S., Bansal, S., Briat, J. F., Khodr, H., Shioiri, T., et al. (1999). Nicotianamine chelates both fe-III and fe-II: implications for metal transport in plants. *Plant Physiol.* 119, 1107–1114. doi: 10.1104/pp.119.3.1107

Varadarajan, D. K., Karthikeyan, A. S., Matilda, P. D., and Raghothama, K. G. (2002). Phosphite, an analog of phosphate, suppresses the coordinated expression of genes under phosphate starvation. *Plant Physiol.* 129, 1232–1240. doi: 10.1104/pp.010835

Wang, R., Okamoto, M., Xing, X., and Crawford, N. M. (2003). Microarray analysis of the nitrate response in arabidopsis roots and shoots reveals over 1,000 rapidly responding genes and new linkages to glucose, trehalose-6-phosphate, iron, and sulfate metabolism. *Plant Physiol.* 132, 556–567. doi: 10.1104/pp.103.021253

Webster, R. J., Driever, S. M., Kromdijk, J., Mcgrath, J., Leakey, A. D., Siebke, K., et al. (2016). High C3 photosynthetic capacity and high intrinsic water use efficiency underlies the high productivity of the bioenergy grass arundo donax. *Sci. Rep.* 6, 20694. doi: 10.1038/srep20694

Wheeler, T., and von Braun, J. (2013). Climate change impacts on global food security. *Science* 341 (6145), 508–513.

Xu, L., and Geelen, D. (2018). Developing biostimulants from agro-food and industrial by-products. *Front. Plant Sci.* 9, 1567. doi: 10.3389/fpls.2018.01567

Yakhin, O. I., Lubyanov, A. A., Yakhin, I. A., and Brown, P. H. (2017). Biostimulants in plant science: A global perspective. *Front. Plant Sci.* 7, 2049. doi: 10.3389/fpls.2016.02049

York, L. M., Nord, E. A., and Lynch, J. P. (2013). Integration of root phenes for soil resource acquisition. *Front. Plant Sci.* 12, 4:355.

Zadoks, J. C., Chang, T. T., and Konzak, C. F. (1974). A decimal code for the growth stages of cereals. *Weed Res.* 14, 415–421. doi: 10.1111/j.1365-3180.1974.tb01084.x

Zhao, R.-R., Qu, B.-Y., Tong, Y.-P., and Zou, C.-Q. (2019). Iron and zinc accumulation in winter wheat regulated by NICOTIANAMINE SYNTHASE responded to increasing nitrogen levels. *J. Plant Nutr.* 42, 1624–1636.

Ziosi, V., Zandoli, R., Di Nardo, A., Biondi, S., Antognoni, F., and Calandriello, F. (2013). Biological activity of different botanical extracts as evaluated by means of an array of *in vitro* and *in vivo* bioassays. *Acta Hortic.* 1009, 69–66.

frontiers | Frontiers in Plant Science

TYPE Review
PUBLISHED 16 November 2022
DOI 10.3389/fpls.2022.1027390

OPEN ACCESS

EDITED BY
Youssef Rouphael,
University of Naples Federico II, Italy

REVIEWED BY
Youry Pii,
Free University of Bozen-Bolzano, Italy
Laith Khalil Tawfeeq Al-Ani,
Universiti Sains Malaysia, Malaysia

*CORRESPONDENCE
Jianjun Chen
jjchen@ufl.edu
Chunying Zhang
zhangchunying@shbg.org

SPECIALTY SECTION
This article was submitted to Crop and Product Physiology, a section of the journal Frontiers in Plant Science

RECEIVED 24 August 2022
ACCEPTED 27 October 2022
PUBLISHED 16 November 2022

CITATION
Wei X, Zhang W, Zulfiqar F, Zhang C and Chen J (2022) Ericoid mycorrhizal fungi as biostimulants for improving propagation and production of ericaceous plants.
Front. Plant Sci. 13:1027390.
doi: 10.3389/fpls.2022.1027390

Ericoid mycorrhizal fungi as biostimulants for improving propagation and production of ericaceous plants

Xiangying Wei[1], Wenbing Zhang[1], Faisal Zulfiqar[2], Chunying Zhang[3]* and Jianjun Chen[4]*

[1]Fujian Key Laboratory on Conservation and Sustainable Utilization of Marine Biodiversity, Fuzhou Institute of Oceanography, College of Geography and Oceanography, Minjiang University, Fuzhou, China, [2]Department of Horticultural Sciences, Faculty of Agriculture and Environment, The Islamia University of Bahawalpur, Bahawalpur, Pakistan, [3]Shanghai Engineering Research Center of Sustainable Plant Innovation, Shanghai Botanical Garden, Shanghai, China, [4]Mid-Florida Research and Education Center, Department of Environmental Horticulture, Institute of Food and Agricultural Sciences, University of Florida, Apopka, FL, United States

The mutualistic relationship between mycorrhizal fungi and plant roots is a widespread terrestrial symbiosis. The symbiosis enables plants to better adapt to adverse soil conditions, enhances plant tolerance to abiotic and biotic stresses, and improves plant establishment and growth. Thus, mycorrhizal fungi are considered biostimulants. Among the four most common types of mycorrhizae, arbuscular mycorrhiza (AM) and ectomycorrhiza (EcM) have been more intensively studied than ericoid mycorrhiza (ErM) and orchidaceous mycorrhiza (OrM). ErM fungi can form symbiotic relationships with plants in the family Ericaceae. Economically important plants in this family include blueberry, bilberry, cranberry, and rhododendron. ErM fungi are versatile as they are both saprotrophic and biotrophic. Increasing reports have shown that they can degrade soil organic matter, resulting in the bioavailability of nutrients for plants and microbes. ErM fungi can synthesize hormones to improve fungal establishment and plant root initiation and growth. ErM colonization enables plants to effective acquisition of mineral nutrients. Colonized plants are able to tolerate different abiotic stresses, including drought, heavy metals, and soil salinity as well as biotic stresses, such as pathogen infections. This article is intended to briefly introduce ErM fungi and document their beneficial effects on ericaceous plants. It is anticipated that the exploration of this special group of fungi will further improve our understanding of their value of symbiosis to ericaceous plants and ultimately result in the application of valuable species or strains for improving the establishment and growth of ericaceous plants.

KEYWORDS

biostimulants, blueberry, ericaceous plants, ericoid mycorrhiza, *Oidiodendron maius*, rhododendron

Introduction

Plant biostimulants are referred to as natural-occurring or synthetic substances, which when applied to soil, seeds, and/or plants, can promote plant growth. There are several definitions for plant biostimulants. du Jardin (2015) defined "a plant biostimulant is any substance or microorganism applied to plants with the aim to enhance nutrition efficiency, abiotic stress tolerance and/or crop quality traits, regardless of its nutrient content". Yakhin et al. (2017) proposed that a biostimulant is "a formulated product of biological origin that improves plant productivity as a consequence of the novel or emergent properties of the complex of constituents, and not as a sole consequence of the presence of known essential plant nutrients, plant growth regulators, or plant protective compounds." Under the new regulation of the European Union (EU, 2019), "a plant biostimulant shall be an EU fertilizing product, the function of which is to stimulate plant nutrition processes independently of the product's nutrient content with the sole aim of improving one or more of the following characteristics of the plant or the plant rhizosphere: (1) nutrient use efficiency, (2) tolerance to abiotic stress, (3) quality traits, or (4) availability of confined nutrients in the soil or rhizosphere". To be more explicit, plant biostimulants are products that can improve plant growth.

Biostimulants are derived from a wide range of biological and inorganic materials (Calvo et al., 2014) and have been classified into seven categories (du Jardin, 2015): (1) humic and fulvic acids or humic substances, which are a group of heterogeneous, highly acidic compounds resulting from the decomposition of soil animal, microbial, and plant residues; (2) protein hydrolysate and other nitrogen (N)-containing compounds, referring to a mixture of amino acids and peptides obtained through enzymatic and chemical hydrolyses of animal wastes and plant residues; (3) seaweed extracts and botanicals, which are derived from seaweed or plants with biostimulant activities; (4) chitosan and other biopolymers, this includes biodegradable and biocompatible poly- and oligomers produced from natural produces; (5) inorganic compounds, mainly referring to beneficial elements, such as silicon, titanium, sodium, selenium, iodine, and aluminum (Al); (6) beneficial fungi, which include those either associated, endophytic or symbiotic with plants that possess biostimulant activities; and (7) beneficial bacteria, also referring to associated, endophytic, or symbiotic bacteria promoting plant growth. Based on the above classifications, biostimulants could be broadly divided into non-microbial and microbial plant biostimulants (Rouphael and Colla, 2020). It was estimated that biostimulant products could grow to $2 billion in sales in 2018 (Calvo et al., 2014). More than 700 scientific papers on biostimulants had been published from 2009 to 2019 (Rouphael and Colla, 2020), indicating an increasing awareness of their importance to crop production.

Beneficial fungi include *Trichoderma* species, mycorrhizal fungi, yeasts, endophytes, and avirulent/hypovirulent strains of some pathogens (Ghorbanpour et al., 2018). Mycorrhizal fungi are a heterogeneous group of taxa that can establish symbiotic relationships with roots of most terrestrial plants, promoting plant acquisition of nutrients in exchange for carbon sources derived from photosynthesis (Addy et al., 2005; Bonfante and Genre, 2010; Leopold, 2016). Mycorrhizas are traditionally grouped into arbuscular mycorrhiza (AM), ericoid mycorrhiza (ErM), ectomycorrhiza (EcM), and orchidaceous mycorrhiza (OrM) (Pandey et al., 2019; Miyauchi et al., 2020). AMs are considered the most widespread symbiotic association as 80-90% of terrestrial plants can be colonized by this group of fungi (Gianinazzi et al., 2010). The beneficial effects of AMs on plants are known to be most noticeable when symbiotic relationships are established at the earliest stage of plant growth (Niemi et al., 2004). AM fungi have been reported as biostimulants (Xavier and Boyetchko, 2002; Rouphael et al., 2015), natural biofertilizers (Berruti et al., 2016), and plant growth regulators (Begum et al., 2019). However, ErM fungi as biostimulants have not been reported. An ErM is referred to as a symbiotic complex of plant roots and fungal components. ErM fungi represent a unique group of fungi that can symbolize with plants in the family Ericaceae or heather family and play vital roles for plants in adapting harsh growing environments (Read, 1996); however, ErM has been the least studied, and the least understood mycorrhizal symbiosis (Vohník, 2020).

This article is intended to briefly introduce ErM fungi and review available literature related to ErM fungi in biosynthesizing bioactive compounds, promoting plant growth, and improving plant tolerance and resilience to abiotic and biotic stresses. Our review indicates that ErM fungi are valuable biostimulants that can synthesize bioactive compounds, including plant growth regulators, promote seed germination and rooting of cuttings, improve plant tolerance to heavy metals, drought, and soil salinity, and resistance to plant diseases, and enhance the growth of ericaceous plants (Figure 1).

Ericoid mycorrhizal fungi

Ericoid mycorrhizal fungi largely belong to Ascomyceta and Basidiomycota (Perotto et al., 2018; Fehrer et al., 2019; Vohník, 2020). The most important ErM fungi in Ascomyceta include the *Hyaloscypha hepaticicola* aggregate, formerly known as the *Rhizoscyphus ericae* aggregate or *Hymenoscyphus ericae* aggregate (Fehrer et al., 2019), which include *H. hepaticicola*, possibly *Hyaloscypha variabilis* (syn. *Meliniomyces variabilis*) as well as *Oidiodendon maius* and *Leohumicola* spp (Vohník, 2020). *H. hepaticicola* was actually the first experimentally confirmed ErM species (Pearson and Read, 1973). *O. maius* was initially isolated by Barron (1962) from peat soils collected in Canada and subsequently from ericaceous plant roots in

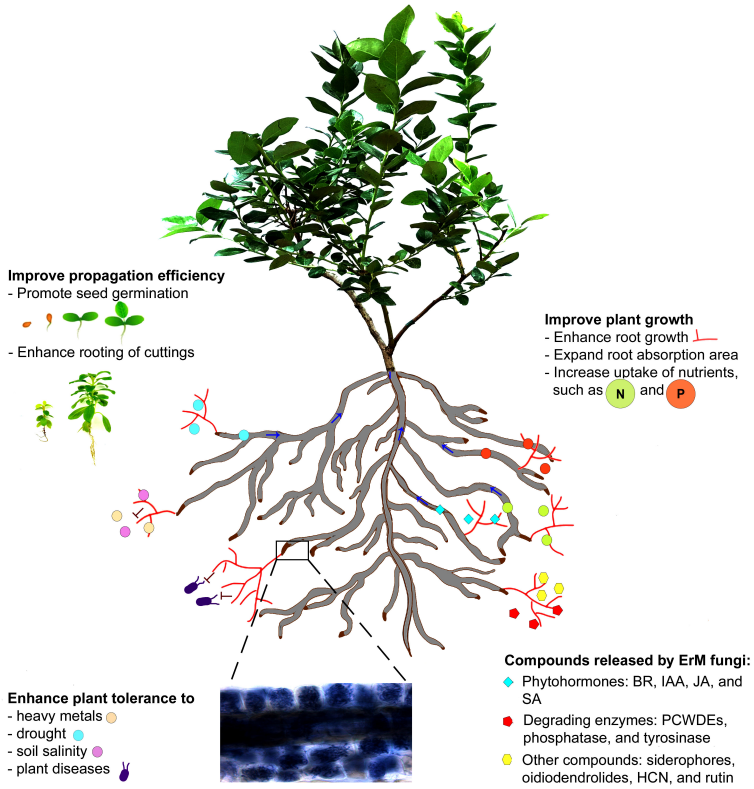

FIGURE 1
A schematic illustration of ericoid mycorrhizal fungi in establishment of the symbiotic relationship with an ericaceous plant (blueberry) and production bioactive compounds, which result in the improved seed germination and rooting of cuttings, and the symbiosis also enhances plant tolerance to different abiotic stresses and resistance to pathogen infections and promotes plant growth.

Japan (Tokumasu, 1973). Later, *O. maius* was identified from other plant roots and decayed organic materials, peat, and acidic soils (Rice and Currah, 2005; Rice and Currah, 2006). *Leohumicola* species are another group of ErM fungi, which have a remarkable tolerance to high temperatures (Adeoyo et al., 2018; Adeoyo et al., 2019).

The basidiomycetous ErM fungi are composed of sebacinoid fungi from Serendipitaceae (Vohník et al., 2016) and non-sebacinoid fungi (Kolařík and Vohník, 2018) as well as those from the *Kurtia argillacea* species complex (syn. *Hyphodontia argillaceum*, *Hyphoderma argillaceum*) (Vohník, 2020). With increasing exploitation of ErM fungi worldwide, more ericoid mycorrhizal fungi have been reported. For instance, two ascomycetous genera: *Cairneyella* (Midgley et al., 2016) and *Gamarada* (Midgley et al., 2018) were found to be ErM fungi in Australia.

Ericoid mycorrhizal fungi are able to colonize roots of ericaceous plants. The fungi initially grow on the surface of hair roots, establishing loose hyphal networks. Hyphae then penetrate cortical cell walls to form intracellular densely packed individual cells, which is known as coils (Vohník et al., 2012). Thus, ericoid mycorrhiza has structurally well-defined endomycorrhiza that are distinctly different from the other mycorrhizae due to the formation of fine compact intracellular hyphal coils in the rhizodermal cells of hair roots. The coil is the site for transferring nutrients absorbed by ErM fungi from the soil to root cells and carbohydrates fixed by plant photosynthesis to fungi. The hyphal sheaths or mantles around healthy hair roots are somewhat similar to those occurring in some EcM (Vohník, 2020). It was observed that both cell-to-cell (between neighboring rhizodermal cells) and single cell (from soil to individual rhizodermal cells) hyphal colonization happened in the rhizodermis of ErM-colonized hair roots (Massicotte et al., 2005; Vohník, 2020).

Interestingly, a recent study showed that ErM fungi, specifically those in the genus *Hyaloscypha* can colonize not only roots, but also stems, leaves, and flowers of *Vaccinium myrtillus* (Daghino et al., 2022). The colonization of the above-ground organs is explained by the evolutionary closeness between the genus *Hyaloscypha* and non-mycorrhizal fungal endophytes based on the genomic similarity. However, it is unknown at present what role *Hyaloscypha* plays in the aerial plant organs of ericaceous plants.

Ericaceous plants and their growing conditions

The family Ericaceae has about 4,500 species across 125 genera, which are either herbs, dwarf shrubs, shrubs, or trees that are distributed in tundra, heathland, and understory of boreal forests in the Northern Hemisphere (Luteyn, 2002; Grelet et al., 2009). Economically important ericaceous plants include *Rhododendron* L., blueberry (*Vaccinium* sect. *Cyanococcus* Rydb. spp.), bilberry (*Vaccinium myrtillus* L.), cranberry (*Vaccinium* subg. *Oxycoccus* (Hill) A. Gray spp.), and huckleberry (*Vaccinium parvifolium* sm.). Plants in the genus *Rododendron* are popular ornamental plants. There are more than 28,000 cultivars of *Rhododendron* (12,989 azaleas, 14,298 rhododendron, and 108 azaleodendrons hybrids) in the International Rhododendron Registry held by the Royal Horticultural Society (Leslie, 2002). Additionally, rhododendron plants are important ethnopharmacological and toxicological plants (Popescu and Kopp, 2013; Wei et al., 2018). On the other hand, the berries, such as blueberry and cranberry have high nutraceutical and pharmaceutical value and are considered super fruit (Whyte and Williams, 2015; Vendrame et al., 2016). Blueberry varieties include lowbush, southern highbush, northern highbush, half-high, and rabbiteye. Among them, the production of highbush varieties increased substantially from 58,400 ha in 2007 to 110,800 ha in 2014. North America accounted for more than 50% of the production area, representing about 60% of highbush blueberry production in the world in 2014 (Qiu et al., 2018).

Ericaceous plants have some unique characteristics: (1) Roots are fibrous, very fine multicellular roots ranging from 100 to 750 μm in diameter, and cortical cells never form root hairs. Instead, roots of ericaceous plants are known as hair roots (Watkinson, 2016). Roots are mainly distributed in the upper 5 cm of soil depth, representing more than 50% of new roots produced during a growing season (Atucha et al., 2020). Root growth of cranberry exhibited a unimodal curve with one significant flush at bloom and a peak at the end of fruit maturation. (2) They are able to grow in soils low in pH (4 to 5) and poor in nutrient availability. Under such a pH range, nitrification could be largely negligible due to its detrimental effect on the nitrifying bacteria (Paul and Clark, 1989). It was proposed that ericaceous plants grown in the low pH soil might lose their ability to take up nitrate (NO_3^-). (3) Roots are colonized by mycorrhizal fungi, mainly ErM fungi (Xiao and Berch, 1992; Usuki et al., 2003; Vohník et al., 2007; Tian et al., 2011). Root cortex and epidermis could be fully filled with mycorrhizal hyphal coils (Atucha et al., 2020). The colonization plays a critical role for ericaceous plants to absorb nutrients including NO_3^-. Cranberry roots inoculated with *R. ericae* were able to absorb NO_3^- under a low pH regime (Kosola et al., 2007). Accumulating evidence has indicated that the symbiosis established between roots and ErM fungi is essential for ericaceous plants to absorb nutrients and to survive and grow in the harsh environment (Read, 1996; Cairney and Meharg, 2003; Zhang et al., 2009; Perotto et al., 2012).

Ericoid mycorrhizal fungi promote seed germination and rooting of cuttings

Ericoid mycorrhizal fungi have been shown to improve seed germination and rooting of microcuttings or stem cuttings of ericaceous plants (Table 1). Seeds of ericaceous plants are small with an average length of 1.5 mm and a mean width of 0.5 mm, and they generally have a poor germination rate due to the limited supply of nutrition from the endosperm. In a mesocosm study conducted for determining if novel ErM communities could assist or hamper the shift of northward species of

TABLE 1 Ericoid mycorrhizal fungi improve seed germination and rooting of cuttings.

Fungal species	Host plant species	Observed responses	References
Hymenoscyphus ericae and *Pezizella ericae*	*Rhododendron minus* and *Rhododendron chapmanii*	Increased survival rates and subsequent growth	Barnes and Johnson, 1986
Hymenoscyphus ericae	*Vaccinium corymbosum* and *Calluna vulgaris*	Increased plantlet growth	Berta and Gianinazzi-Pearson, 1986
Hymenoscyphus ericae	*Pieris floribunda*	Stimulated microcutting growth *in vitro*	Starrett et al., 2001
Oidiodendron griseum and *Hymenoscyphus ericae*	*Leucothoe fontanesiana*	Increased root initiation and root growth of cuttings	Scagel, 2005b
Oidiodendron maius	*Vaccinium virgatum*	Two strains differentially altered root morphology cuttings	Baba et al., 2021a
Oidiodendron maius	*Vaccinium oldhamii*	Increased the length and branching of pioneer roots of seedlings	Baba et al., 2021b
Oidiodendron maius	*Rhododendron fortunei*	Enhanced rooting and root growth of microcuttings	Wei et al., 2020
Unspecified ericoid mycorrhizal fungi	*Rhododendron catawbiense* and *R. maximum*	Increased seed germination rates	Mueller et al., 2022

Rhododendron, Mueller et al. (2022) reported that germination rates of *R. catawbiense* and *R. maximum* after inoculation with novel soils containing ErM fungi were significantly greater than those of controls (without mycorrhizal fungi) or inoculated with conspecific soils, 75.2% vs. 54.5% for *R. catawbiense* and 65.7% vs. 54.4% for *R. maximum*. The increased germination rates were attributed to the occurrence in ErM fungi, but the authors did not provide the underlying mechanisms. In addition to seed germination, ErM has been documented to promote seedling growth of *Rhododendron*. An ErM fungus known as *O. maius* Om19 inoculated in a peat-based substrate substantially enhanced seedling growth of *R. fortunei* Lindl. because root growth including root length, root numbers, root fresh weight as well as shoot growth, including shoot overall height and shoot fresh weight of Om19 colonized seedlings were doubled compared to the uninoculated control seedlings (Wei et al., 2016a). Additionally, overall fresh and dry weights of *R. fortunei* seedlings inoculated with Om19 were 81% and 84% higher than those of the control, respectively. Furthermore, genes related to N uptake and metabolism were analyzed by qRT-PCR, and results showed that the expression of an *ammonium transporter* (*AMT*), two *nitrate transporters* (*NRT1*-1 and *NRT1-2*), glutamate synthase (*GOGAT*), and glutamine synthetase (*GS*) were highly upregulated in plants inoculated with Om19, ranging from 2 to 9 folds greater than the uninoculated plants (Wei et al., 2016a).

Ericoid mycorrhizal fungi can substantially improve rooting of stem cuttings as well as microcuttings derived from tissue culture (Eccher et al., 2010; Wei et al., 2020). Stem cuttings of blueberry plants inoculated with ErM fungi rooted more successfully and were followed by enhanced plant growth (Scagel et al., 2005a; Scagel et al., 2005b). Root initiation and root growth of dog hobble (*Leucothoe fontanesiana*) (Scagel, 2005b) and *Vaccinium meridionale*, a Colombian blueberry (Ávila Díaz-Granados et al., 2009) also increased with the inoculation of ErM fungi. Recently, micropropagation, shoot culture in particular, has been increasingly used for propagation of important ericaceous plants, such as rhododendron, cranberry, and blueberry (Fan et al., 2017; Wei et al., 2018). An interesting phenomenon observed during the rooting of microcuttings is that *in vitro* rooting is more difficult than *ex vitro* rooting (Gorecka, 1979; Fan et al., 2017; Qiu et al., 2018; Wei et al., 2018). To explore the underlying mechanisms behind this phenomenon, Wei et al. (2020) developed an *in vitro* culture system for *R. fortunei* and investigated the adventitious root (AR) formation in microcuttings inoculated with or without *O. maius* Om19. Key phytohormones and precursors involved in the pathway of indole-3-acetic acid (IAA) biosynthesis were analyzed in Om19 mycelium. Om19 was able to synthesize tryptophan (Trp), indole-3-pyruvate (IPA), and IAA, of which Trp concentration was greater than 4,000 mg/kg. The occurrence in Trp, IPA, and IAA indicated that Om19 biosynthesis of IAA is through the Trp-dependent pathway (Mano and Nemoto, 2012). Other hormones synthesized by Om19 include brassinolides (BRs), jasmonic acid (JA), and salicylic acid (SA). BRs were reported to positively impact the symbiosis of either tomato or tobacco roots with an AM fungus (von Sivers et al., 2019). JAs are known as a wound signal in AR formation because wounding quickly induces JA accumulation in plant tissues (Zhang et al., 2019). Increased JA concentrations have been shown to promote AR formation in cuttings by IAA accumulation in the base of stem cuttings towards AR source cells (Druege and Franken, 2019). SA is known for triggering systemic-acquired resistance (SAR) in plants (Chen et al., 1996). Low concentrations of SA was reported to promote AR formation and change the root apical meristem architecture, but high SA concentrations suppressed the root growth process (Pasternak et al., 2019). After Om19 inoculation, ARs rapidly appeared from microcuttings. Meanwhile, genes related the symbiosis including *SymRK* and *DMI* were activated in ARs, resulting in Om19 colonization of the roots. Furthermore, *YUC3*, a key gene controlling IAA biosynthesis in plants (Cheng et al., 2007; Won et al., 2011), genes encoding N absorption (*AMT* and *NRT*) and N metabolism (*GOGAT* and *GS*) as well as phosphate transporter (*PHT*) in Om19-inoculated plants were upregulated by 3 to 7 folds compared to control plants without Om19 inoculation. As a result, inoculated plants were able to take up significantly higher quantities of nutrients including N, P, K, Ca, Mg, and S, and plant growth substantially increased compared to the control plants. A working model for the Om19-mediated AR formation was proposed. The rapid AR formation on the one hand was induced by IAA produced by Om19 and on the other hand by IAA biosynthesized by plants. The high concentration of Trp synthesized by Om19 could be readily used by plant as the precursor to synthesis of IAA. The formation ARs, in turn, provided Om19 with host for colonization. This study for the first time documented the ability of Om19 to biosynthesize several hormones, of which IAA plays an important role in inducing AR formation.

This model also provides explanations as to why *ex vitro* rooting of microcuttings is more effective than *in vitro* rooting. A major component of commercial substrates is peat moss, ranging from 30% to 75% based on volume (Chen et al., 2005). As mentioned before, *O. maius* was initially isolated from peat soils by Barron (1962). Commercial substrates rich in peat moss might have ErM mycorrhizal fungi. Gorman and Starrett (2003) screened ErM occurrence in commercial substrates and found that the majority of the peat and peat-based substrates used in the U.S. and Canada contained ErM fungi. ErR fungi were reported to naturally colonize roots of blueberry plants during nursery production (Scagel, 2005a). Thus, the ErM fungi in the substrates could act similar to Om19 in biosynthesis of phytohormones including IAA for inducing AR formation of ericaceous plant cuttings. Those ErM may also synthesize a large amount of Trp for plants to produce endogenous IAA. In general, endogenous hormones are

more effective than exogenous application. Ismail et al. (2021) reported that bacterial and fungal endophytic metabolites significantly enhanced plant growth compared to exogenous applied hormones. IAA biosynthesized inside plants by either plants or ErM could be considered endogenous and thus could be more effective for inducing AR formation than exogenous applied auxin during *in vitro* rooting.

Ericoid mycorrhizal fungi also produce other bioactive compounds (Table 2). Some can increase bioavailability of soil mineral elements, such as siderophore for chelating soil Fe (Ahmed and Holmström, 2014). Some are enzymes, including cell-wall-degrading enzymes (PCWDEs) that can degrade soil organic matter (SOM) (Kohler et al., 2015; Martino et al., 2018). Others have antimicrobial activities (Hosoe et al., 1999; Ouyang, 2021), and still others are antioxidants, such as rutin (Lin et al., 2021).

Ericoid mycorrhizal fungi enhance plant growth

Ericoid mycorrhizal fungi have been well documented for promoting the growth of ericaceous crops. ErM fungi are able to establish symbiotic relationships with plant roots. The established symbiosis enables plants to better adapt to acidic soils with low pH values and low nutrient status and improve root acquisition of nutrients, thus, enhancing plant growth. The growth enhancement is attributed to several factors: (1) The ability of ErM to biodegrade SOM resulting in the bioavailability of nutrients for plants; (2) the symbiosis-resultant expansion of nutrient acquisition surface area for capturing more mineral elements; and (3) the upregulation of gene expression, such as those associated with symbiosis and N and P uptake and metabolism, leading to the increased N and P absorption and metabolism and enhanced plant growth.

ErM fungi mediated degradation of soil organic matter

A unique characteristic of ErM fungi is their capability to biodegrade SOM (Martino et al., 2018). SOM is the organic fraction of the soil consisting of animal and plant residues and microorganisms at different stages of decomposition and contributes significantly to soil fertility and productivity (Myers and Leake, 1996; Biswas and Kole, 2017). Ericaceous plants are native to acidic soils, low in nutrients but high in recalcitrant organic materials, which results in a low bioavailability of mineral

TABLE 2 Bioactive compounds released by ericoid mycorrhizal fungi.

Fungal species	Bioactive compounds	Role of the compound	References
Cryptosporiopsis sp.	Rutin	Antioxidative activity	Lin et al., 2021
Hymenoscyphus ericae and *Oidiodendron griseum*	Hydroxamate siderophore	A chelator product for improving iron bioavailability in soils	Schuler and Haselwandter, 1988
Hymenoscyphus ericae	Phenol-oxidation and extracellular o-polyphenol oxidase (tyrosinase)	Degraded lignin or soluble phenolic compounds	Bending and Read, 1997
Hymenoscyphus ericae	Chitinase	Involved in chitin degradation	Kerley and Read, 1997; Bougoure and Cairney, 2006
Leohumicola incrustata	Amyloglucosidase	Hydrolyzed individual glucose units from the non-reducing ends of starch chains	Adeoyo et al., 2018
Oidiodendron cf. truncatum	Four new tetranorditerpenoids, oidiodendrolides A, B, and C, and oidiodendronic acid	Antibiotic activity against pathogenic yeast	Hosoe et al., 1999
Oidiodendron maius	Plant cell wall-degrading enzymes, PCWDEs	Degraded plant cell wall	Kohler et al., 2015
Oidiodendron maius	Mucilage and soluble and wall-bound pigments	Chelated heavy metal ions	Martino et al., 2000b
Oidiodendron maius	Tryptophan, indole-3-pyruvate, indole-3-acetic acid (IAA), brassinolides (BRs), jasmonic acid (JA), and salicylic acid (SA)	Precursor for IAA biosynthesis. IAA, BRs, JA, and SA are plant growth regulators	Wei et al., 2020
Oidiodendron flavum	Harzianic acid	Antimicrobial activity	Ouyang, 2021
Oidiodendron truncatum	Fourteen norditerpene and three anthraquinone metabolites.	Antifungal activity	Rusman et al., 2020
Ericoid mycorrhizal fungi	Indole-3-acetic acid (IAA), hydrogen cyanide (HCN), siderophores, and phosphatase	IAA is plant growth regulator; HCN is a co-product of ethylene biosynthesis; siderophores improve nutrient bioavailability; and phosphatase solubilizes insoluble forms of phosphorus	Hamim et al., 2019

elements, particularly N and P (Cairney and Meharg, 2003). ErM fungi can degrade SOM, leading to the release of nutrients for host plants. Among the ErMs, *R. ericae* and *O. maius* were found to degrade cellulose, tannic acid, pectin, and chitin (Rice and Currah, 2001; Thormann et al., 2002; Rice and Currah, 2005). A wide range of enzymes were released from the two ErM fungi for degrading fungal and plant cell wall polymers, complex aliphatic compounds, and organic phosphorus (Smith and Read, 2008). Kohler et al. (2015) sequenced 13 EcM, ErM, and OrM species as well as five saprotrophs and found that EcM fungi have reduced numbers of genes for PCWDEs compared to their ancestral wood decayers. Later, Martino et al. (2018) sequenced genomes of ErM fungi *R. ericae*, *Meliniomyces bicolor*, *M. variablilis*, and *O. maius* and compared their gene repertoires with EcM, OrM, and six pathogenic or saprotrophic Leotimycetes and 50 other Basidiomycetes and Ascomycetes. The authors found that ErM fungi possessed lipases, polysaccharide-degrading enzymes, proteases, and enzymes in secondary metabolism that were comparable to those of pathogens and saprotrophs but higher than those of EcM fungi, suggesting the ErM fungi are unique due to their dual saprotrophic and biotrophic lifestyle. Additionally, RNA-Seq analysis showed that highly upregulated genes in ErM fungi were those involved in lipases, cell wall-degrading enzymes (CWDEs), transporters, proteases, and mycorrhizal-induced small-secreted proteins (MiSSPs). Thus, ErM fungi represent a unique group of fungi in degradation of SOM, which explains in part as to why ericaceous plants can survive and grow in the acidic and low nutrient soils.

Soil organic nitrogen (ON) is a fraction of SOM, including intracellular and cell-wall bound proteins and nucleic acids of plant and microbial origin (Nemeth et al., 1987; Abuarghub and Read, 1988). The main groups of soil ON compounds are aliphatic-N, including polysaccharide N and amino-N as well as aromatic N, such as those present in soil humus (Chen and Xu, 2006; Talbot and Treseder, 2010). These large molecules can be degraded by enzymes of ErM fungi into monomers, such as oligomer, small peptides, and amino acids (Talbot and Treseder, 2010) which are small enough for soil microbes and plants to take up or further mineralize and incorporate as ammonium and nitrate (Séneca et al., 2021). Studies have shown that mycorrhizal fungi and plant roots can take up amino acids. ErM fungi *R. ericae* were able to use all 20 common amino acids except glycine (Leake and Read, 1990; Cairney et al., 2000; Midgley et al., 2006), while *O.* spp. can use alanine, glutamic acid, arginine, lysine, proline, asparagine, glutamine, histidine, and cysteine (Whittaker and Cairney, 2001). Furthermore, ErM fungi have the capacity to use proteins, peptides or even chitin as a sole N source (Leake and Read, 1990; Read, 1996). Lin et al. (2011) evaluated three ErM isolates, Rf9 and Rf32 belonging to the genus *Cryptosporiopsis* and Rf28, a member of *Phialocephala* in decomposition SOM. Both Rf28 and Rf32 possessed the highest decomposition rates, up to 10.4% in 70 days, but Rf9 had a decomposition rate of 6.8%. Enzymatic assay showed that Rf28 and Rf 32 secreted cellulase, laccase, peroxidase, and tyrosinase, but Rf9 mainly released peroxidase and tyrosinase. Seedlings of *R. formosanum* Hemsl. grown in substrate without ErM inoculation showed chlorotic symptoms and limited root growth, while those inoculated with ErM exhibited much stronger growth vigor than those of the control. This study implies that ErM-mediated decomposition of soil ON provides seedlings with nutrients, particularly N.

Enhanced growth of plants through symbiosis

Inoculation of ErM fungi can substantially enhance the growth of ericaceous plants. In general, ericaceous plants can be naturally colonized by ErM fungi (Hambleton and Currah, 1997; Gorman and Starrett, 2003), but the colonization rates are low, less than 15%. Inoculation of ErM fungi can increase colonization rates, up to 30% (Scagel, 2005a), and the colonization promoted growth in blueberry cultivars. Table 3 lists growth enhancement of ErM fungi on ericaceous plants. Inoculation of ErM fungi affected acclimatization and growth of microcuttings of *Pieris floribunda* (Starrett et al., 2001). Container-grown *R. indica* inoculated with *O. maius* Om19 had more abundant roots and a larger above ground canopy than those uninoculated (Wei et al., 2016a). Plant height, root, shoot, and total fresh weights of seedlings of *R. kanehirae* inoculated with two ErM strains significantly increased when ammonium was used as a N source (Lin et al., 2021). ErM fungi in nature Finnish peat moss promoted rooting of rabbiteye blueberry (*V. virgatum* Ait.) and vegetative growth (Li et al., 2021). Dry weights of shoots, leaves, and roots of rooted cuttings were 2.37, 4.51, and 4.34 g, respectively compared to 0.47, 0.90, and 0.67 g of those grown in sterilized peat moss. Furthermore, root P and Mg concentrations and shoot K content increased in plants grown in unsterilized peat moss. A recent study also showed that single inoculation of *V. corymbosum* with *O. maius* or *Phialocephala fortinii* significantly increased plant dry weight (Wazny et al., 2022).

The increased growth of plants is largely attributed to the following factors: (1) The bioavailability of small ON compounds degraded by ErM fungi mentioned above. (2) The symbiosis results in the establishment of root and hyphal networks that greatly expand root surface areas for capturing more mineral nutrients. Atucha et al. (2020) studied the phenology of roots, root anatomy and morphology in terms of root orders in cranberry (*V. macrocarpon* Ait). More than 50% of new roots produced during the growing season were vertically distributed in the upper 5 cm of soil depth, and mycorrhizal fungi were able to colonize the intact cortex and epidermis of the first three root orders. It is known that large root systems generally have a larger root surface areas and concomitantly shorter average half distance between root axes in the soil or

TABLE 3 Ericoid mycorrhizal fungi improve rooting of propagules and enhance plant growth.

Fungal species	Host plant species	Observed responses	References
Cryptosporiopsis sp	*Rhododendron pseudochrysanthum*	Enhanced seedling growth as total fresh weight of inoculated seedlings was higher than the control seedlings	Lin et al., 2021
Hymenoscyphus ericae	*Pieris floribunda*	Increased survival rate of micropropagated plants during *ex vitro* acclimatization.	Starrett et al., 2001
Hymenoscyphus ericae, *Oidiodendron griseum*, and *Pezizella ericae*,	Seven highbush blueberry cultivars (*Vaccinium corymbosum*)	Improved plant growth as inoculants increased plant growth; but root/shoot biomass ratios decreased due to the application of organic or inorganic fertilizers	Scagel, 2005a; Scagel, 2005b
Hymenoscyphus ericae and *Oidiodendron griseum*	*Vaccinium corymbosum*	Improved plant growth as inoculated plants produced significantly larger floral displays, more fruits per inflorescence, and heavier fruits with lower sugar content, than uninoculated control plants.	Brody et al., 2019
Meliniomyces variabilis, *Oidiodendron maius*, *O. or Rhizoscyphus ericae*	*Vaccinium virgatum* 'Rabbiteye blueberry Ait.	Promoted vegetative growth including more leaves and shoots, greater total leaf area and shoot length than those grown in sterilized substrate	Li et al., 2021
Oidiodendron maius and *Hymenoscyphus* sp.	*Vaccinium corymbosum*	Improved plant growth and vitality and increased biomass accumulation	Wazny et al., 2022
Oidiodendron maius	*Rhododendron* cv. Azurro	Increased root biomass and plant phosphorus concentrations	Vohník et al., 2005
Oidiodendron maius	*Rhododendron fortunei*	Enhanced plant growth evidenced by larger canopies and root systems of seedlings, and genes related to plant uptake of N and N metabolism were highly upregulated	Wei et al., 2016a; Wei et al., 2016b
Oidiodendron maius	*Arabidopsis thaliana*	Increased shoot and root biomass, shortened the primary root and increased the lateral root length and number of seedlings	Casarrubia et al., 2016
Oidiodendron maius	*Rhododendron kanehirae*	Promoted plant growth since plant height, roots, shoots, and total fresh weight significantly increased when ammonium was used as a N source	Lin et al., 2020
Oidiodendron maius	*Rhododendron fortunei*	Enhanced microcutting growth and increased N and P contents of plants	Wei et al., 2020
Oidiodendron maius	*Vaccinium virgatum* Ait 'Tifblue'	Altered the length and branching of pioneer and/or fibrous roots of rooted cuttings	Baba et al., 2021a

substrate for more effectively capturing nutrient elements (Chen and Gabelman, 2000). Thus, absorption of N, P, and other mineral nutrients was markedly increased in ErM colonized plants. (3) ErM fungi are able to biosynthesize and release hormones for stimulating root growth, such as IAA, BR, JA, and SA, which can stimulate plant growth and improve plant stress tolerance. (4) ErM-colonization results in the increased expression of a large number of genes. To gain insight into the intimate relationships of ErM fungi with ericaceous plants and the mechanism underlying growth stimulation, Wei et al. (2016b) analyzed transcripts induced by the symbiosis between ErM Om19 and *R. fortunei* using RNA-Seq. The symbiosis induced 16,892 upregulated genes in Om19-coloinzed roots. Homologous to symbiosis related genes, such as *SymRK*, *CCaMK*, *DM1*, *NORK*, genes involved in N uptake including *AMT3*, *NRT1-1*, *NRT1-2*, as well as N metabolism, such as *GS-1* and *GS-2* and *GOGAT-1* and *GOGAT-2* were highly upregulated in roots inoculated with Om19, suggesting that ErM fungi might share the same strategy as AM fungi in the establishment of symbiotic relationships with ericaceous plants. The increased expression of the genes in N uptake and metabolism corresponded to the increased N absorption and metabolism as well as plant growth. Thus, the ability of ericaceous plants to survive and grow in acidic and low nutrient soils is largely associated with their symbiotic relationship with ErM fungi (Cairney and Meharg, 2003).

It is worthy of note that different strains within an ErM species may perform differently in regulation of N uptake in ericaceous plants. Five strains isolated from *Calluna vulgaris* had different capacities to use organic and mineral N sources (Grelet et al., 2005). Different isolates of epacrid root endophytes differed in the use of amino acids (Whittaker and Cairney, 2001). Using ^{15}N tracing, Grelet et al. (2009) found that the rates of appearance of ^{15}N in shoots of cranberry after roots were inoculated with three strains of Helotiales were low and not different from the control (no ErM inoculation) when nitrate was used as a N source. However, differences occurred among strains when glutamine was used as a N source. When NH_4 was used a N source, two strains had the highest rates compared to the other strains. Thus, for practical application of ErM fungi as biostimulants, appropriate species or strains should be chosen.

Improve plant tolerance to abiotic and biotic stresses

Plants as sessile organisms and permanently stay in their established sites. In addition to harsh environmental conditions,

ericaceous plants often encounter other stressful factors, such as salt, drought, heavy metals as well as plant pathogens. Evidence has shown that in addition to growth promotion, symbiotic ErM fungi can substantially improve plant tolerance to abiotic and biotic stresses (Table 4). The enhanced stress tolerance in turn can improve plant productivity compared to those without symbiotic establishment.

Resistance to heavy metals

Another distinct characteristic of ErM fungi is their adaptability to heavy metal stress (Meharg and Cairney, 2000). *C. vulgaris* is a dominant plant in mine spoil sites as it can tolerate Cu^{2+} and Zn^{2+}. Such a tolerance is attributed to its symbiotic relationship with ErM fungi. In the early 1980s, Bradley et al. (1981) reported that resistance of *C. vulgaris* to Cu^{2+} and Zn^{2+} was constitutive even in those mycorrhizal endophyte plants collected from sites without metal contamination (Bradley et al., 1981; Bradley et al., 1982). Martino et al. (2000b) reported that two isolates of *O. maius* from metal contaminated soils showed enhanced tolerance to Zn^{2+} *in vitro*, and later they reported that the mechanism behind the tolerance was due to the production of extracellular compounds, such as malate and citrate either to solubilize or chelate heavy metal ions (Martino et al., 2003). Subsequently, the ErM metal tolerant isolate known as *Oidiodendron maius* Zn has been used as model for studying the molecular basis underlying ErM-mediated metal tolerance (Daghino et al., 2016). Its genome was sequenced (Kohler et al., 2015). A recent report showed that a homeostatic mechanism at the cellular level mediated by transport proteins may play an important role (Ruytinx et al., 2020). Blueberry plants colonized by ErM fungi were also found to be able to tolerate high concentrations of Fe and Mn (Hashem, 1995a; Hashem, 1995b) as well as Al (Yang and Goulart, 2000). In addition to tolerance to Cu^{2+}, Cd^{2+}, and Zn^{2+}, ErM fungi are particularly resistant to arsenate (AsO_4^{3-}). Sharples et al. (2001) compared As resistance between isolates of *Hymenoscyphus ericae* derived from *C. vulgaris* in soils contaminated with AsO_4^{3-} and natural heathland soils and found that *H. ericae* isolated from the mine sites sustained significant growth at AsO_4^{3-} concentration up to 4.67 mol m^{-3}; however, the growth of the isolates from the heathland soils were almost completely inhibited. All isolates regardless of their origins had an identical response to Cu^{2+}. These results suggest that *H. ericae* response to As is adaptive but their response to Cu^{2+} is constitutive.

Although some progress on the tolerance of ErM fungi to heavy metals has been made, our understanding on how ErM colonization can improve plant tolerance to heavy metal stress remains incomplete. Sharples et al. (2001) reported that *C. vulgaris* tolerance to As in the mine sites was due to the colonization of *H. ericae*, which allows the host to maintain an adequate supply of PO_3^{3-} to limit the level of AsO_4^{3-} in the

TABLE 4 Ericoid mycorrhizal fungi improve plant tolerance to abiotic stresses.

Fungal species	Host plant species	Observed responses	References
Hymenoscyphus ericae	*Calluna vulgaris* and *Vaccinium macrocarpon*	Improved plant tolerance to Fe by limiting its transport to shoots	Shaw et al., 1990
Hymenoscyphys ericae	*Vaccinium macrocarpon*	Reduced Fe and Mn in leaves of mycorrhizal plants and increased Fe and Mn in root tissues, protected shoots from metal stress on the basis of exclusion rather than accumulation	Hashem, 1995a; Hashem, 1995b
Hymenoscyphus ericae	*Vaccinium mocrocarpon*	Provided plants with organic and inorganic P	Myers and Leake, 1996
Hymenoscyphus ericae	*Calluna vulgaris*	Enhanced plant tolerance to arsenate	Sharples et al., 2000a; Sharples et al., 2000b
Hymenoscyphus complex	*Woollsia pungens*	Improved plant tolerance to drought	Chen et al., 2003
Meliniomyces variabilis and *Oidiodendron maius*	*Rhododendron groenlandicum*, *Vaccinium myrtilloides*, and *Vaccinium vitisidaea*	Increased plants tolerance to salt stress	Fadaei et al., 2020
Oidiodendron maius	*Vaccinium corymbosum*	Improved plant tolerance to Al by restriction of Al in roots	Yang and Goulart, 2000
Oidiodendron maius	*Vaccinium myrtillus*	Enhanced plant tolerance to Zn by producing extracellular compounds to chelate Zn	Martino et al., 2000a; Martino et al., 2000b
Oidiodendron maius	*Rhododendron fortunei*	Increased N bioavailability to seedlings and induced the expression of genes related to N uptake and metabolism	Wei et al., 2016b
Pezoloma ericae	*Vaccinium macrocarpon*	Increased the ability of plant to utilize NO_3--N	Kosola et al., 2007

cytosol, i.e., an ErM-mediated avoidance mechanism in *C. vulgaris*. To address ErM fungal colonization modulated plant tolerance to heavy metals, Casarrubia et al. (2020) studied *O. maius* mediated Cd tolerance in *V. myrtillus* and found that ErM colonized roots exposed to Cd had a reduced level of Cd compared to those uninoculated. Transcriptomic analysis showed that GSH metabolism was involved in the Cd tolerance as phytochelatins are biosynthesized from GSH, which can bind Cd to reduce toxicity (Chen and Goldsbrough, 1994; Chen et al., 1997). Some plant metal transporters were also regulated during the symbiosis and may be responsible for the reduced Cd content observed in mycorrhizal roots exposed to this metal.

Tolerance to salt and drought stress

Several recent studies showed that ErM fungi can effectively improve ericaceous plant tolerance to salt stress. A recent study showed that velvetleaf blueberry (*V. myrtilloides*), labrador tea (*R. groenlandicum*), and lingonberry (*V. vitisidaea*) plants inoculated with *M. variabilis* had increased dry weights of roots when imposed on NaCl-treatment. Inoculation of *O. maius* increased root dry weight accumulation in lingonberry plants treated with NaCl at 30 mM (Fadaei et al., 2020). Salt stress generally disrupts plant water relations by adversely affecting water uptake and osmotic balance as well as root hydraulic conductivity in plants (Sutka et al., 2011), which then lead to the decrease in cell turgor and stomatal opening and the inhibition of cell elongation. As a result, transpiration rates and net photosynthetic rates decreased, and plant growth was suppressed (Vaziriyeganeh et al., 2018). In the report of Fadaei et al. (2020), transpiration and net photosynthetic rates of three ericaceous plant species treated with 30 mM NaCl were drastically reduced when grown in a substrate without ErM inoculation, but such detrimental effects were either completely or partially reversed by the inoculation of *O. maius* and *M. variabillis*. It was reported that EcM and AM colonization of roots increased the expression level of root aquaporins, resulting in the substantial improvement of root hydraulic conductivity (Xu et al., 2015). The authors believed that ErM fungi may act similar to AM in the alleviation of plant salt stress.

The ErM colonization also enhances drought tolerance of ericaceous plants. Mu et al. (2021) studied responses of lowland and upland blueberry seedlings to drought stress. Seedlings were grown in sterilized soil under controlled environmental conditions and inoculated with *M. variabilis*, *O. maius*, *P. ericae*, and *Pezoloma ericae*. All plants were imposed on three cycles of drought stress through withdrawing watering. Uninoculated, well-watered upland plants after three weeks of drought treatments produced higher dry weights compared to the uninoculated lowland plants. This difference, however, was offset after the plants were inoculated with ErM fungi, indicating that ErM addition significantly improved drought tolerance of the lowland and upland plants. Among the four ErM species, *Pezicula ericae* was found to be the most effective in enhancing drought resistance in lowland and upland seedlings as its inoculation maintained a higher water potential in plant shoots and higher net photosynthetic and transpiration rates, thus increased dry weight production.

Responses to biotic stress

Information regarding ErM fungi improving ericaceous plant resistance to pathogens is rather limited. In a study conducted to test if ErM fungi could suppress the infection of soil-borne pathogens on mycorrhizal roots of *C. vulgaris* and *R. hirsutum*, Grunewaldt-Stöcker et al. (2013) inoculated *Pythium* spp. and *Phytophthora cinnamomic*, respectively to roots. The establishment of mycorrhizae, pathogen infections, and disease development in plants were examined microscopically. Results showed that ErM fungi suppressed the growth of external pathogenic mycelium and reduced pathogen infections. A complete reduction was observed at higher ErM colonization levels. However, pathogen infection occurred in those with low ErM colonization. These results showed that ErM colonization played a role in the direct suppression of oomycete pathogens from infection of ericaceous plants.

Systemic acquired resistance (SAR) is an immune response of plants against pathogen infection. It has been reported that some mycorrhizal fungi and plant growth promoting bacteria can induce SAR against a wide range of plant pathogens (Pieterse et al., 2014; Backer et al., 2018). However, SAR induction by ErM fungi has not been reported in ericaceous crops. Considering the fact that SA can effectively induce SAR in plants (Chen et al., 1996; Metraux, 2001) and *O. maius* can biosynthesize SA (Wei et al., 2020), it is likely that ErM fungi, *O. maius* in particular, should be able to induce SAR in plants, providing plants with long-lasting resistance to some plant pathogens. Further studies are warranted to test this hypothesis.

Conclusion and future perspectives

Ericoid mycorrhizal fungi have saprotrophic and biotrophic lifestyles and are able to biodegrade SOM and establish symbiotic relationships with plants in the family Ericaceae. The degradation of SOM results in the bioavailability of nutrients to themselves and plants. The symbiosis extends their life cycle and also enhances seed germination, rooting of cuttings, plant growth as well as tolerance to abiotic and biotic stresses. This review documents that the improved plant growth is related to hormones produced by ErM fungi and also colonization-resultant expression of genes in N and P absorption and metabolisms. Thus, ErM fungi is considered biostimulants for promoting the establishment and growth of

ericaceous plants. Considering some species in the family Ericaceae are economically important crops, it is expected that some ErM fungi could be developed as biofertilizers for improve plant propagation and production.

Our understanding of the ErM-mediated biostimulating effects on ericaceous plants, however, is largely incomplete. Further research is warranted to (1) identify and isolate key genes from ErM fungi in biodegradation of SOM, particularly ON and explore the genes for improving soil fertility, (2) evaluate important ErM species or strains in biosynthesis of hormones and isolate those for increased production of hormones through bioreactor and utilize the isolates for improving plant propagation and production, (3) analyze heavy metal tolerant species or strains of ErM through omics to identify the mechanism underlying metal tolerance and use the isolates for phytoremediation of metal-contaminated soils, and (4) develop ErM biofertilizers by combining different species or strains, each with specific biostimulating effects on propagation, growth promotion, and/or stress tolerance for improving the productivity of ericaceous plants.

Author contributions

JC, XW, CZ, and FZ conceived the idea, WZ conducted literature search and prepared the tables and figures. JC and XW wrote the initial draft. All authors edited, refined the manuscript, and approved for its submission.

Funding

This work was supported in part by the Natural Science Foundation of Fujian Province to XW (General program, Grant No. 2020J01867).

Acknowledgments

The authors would like to thank Ms. Terri A. Mellich for critical review of this manuscript.

Conflict of interest

The authors declare that the research was conducted in the absence of any commercial or financial relationships that could be construed as a potential conflict of interest.

Publisher's note

References

Abuarghub, S. M., and Read, D. J. (1988). The biology of mycorrhiza in the ericaceae. 11. the distribution of nitrogen in soil of a typical upland callunetum with special reference to the free amino acids. *N. Phytol.* 108, 425–431. doi: 10.1111/j.1469-8137.1988.tb04183.x

Addy, H. D., Piercey, M. M., and Currah, R. S. (2005). Microfungal endophytes in roots. *Can. J. Bot.* 83, 1–13. doi: 10.1139/b04-171

Adeoyo, O. R., Pletschke, B. I., and Dames, J. F. (2018). Purification and characterization of an amyloglucosidase from an ericoid mycorrhizal fungus (*Leohumicola incrustata*). *AMB Expr* 8, 154. doi: 10.1186/s13568-018-0685-1

Adeoyo, O. R., Pletschke, B. I., and Dames, J. F. (2019). Molecular identification and antibacterial properties of an ericoid associated mycorrhizal fungus. *BMC Microbiol.* 19, 178. doi: 10.1186/s12866-019-1555-y

Ahmed, E., and Holmström, S. J. (2014). Siderophores in environmental research: roles and applications. *Microb. Biotechnol.* 7, 196–208. doi: 10.1111/1751-7915.12117

Atucha, A., Workmaster, B. A., and Bolivar-Medina, J. (2020). Root growth phenology, anatomy, and morphology among root orders in *Vaccinium macrocarpon ait*. *Botany* 99, 209–219. doi: 10.1139/cjb-2020-0129

Ávila Díaz-Granados, R. A., Orozco Silva, O. J., Ligarreto Moreno, G. A., Magnitskiy, S., and Rodríguez, A. (2009). Influence of mycorrhizal fungi on the rooting of stem and stolon cuttings of the Colombian blueberry (*Vaccinium meridionale* Swartz). *Intl. J. Fruit Sci.* 9, 372–384. doi: 10.1080/15538360903378575

Baba, T., Hirose, D., and Ban, T. (2021b). *In vitro* inoculation effects and colonization pattern of *Leohumicola verrucosa*, *Oidiodendron maius*, and *Leptobacillium leptobactrum* on fibrous and pioneer roots of *Vaccinium oldhamii* hypocotyl cuttings. *Plant Root* 15, 1–9. doi: 10.3117/plantroot.15.1

Baba, T., Hirose, D., Noma, S., and Ban, T. (2021a). Inoculation with two oidiodendron maius strains differentially alters the morphological characteristics of fibrous and pioneer roots of *Vaccinium virgatum* 'Tifblue' cuttings. *Sci. Hortic.* 281, 109948. doi: 10.1016/j.scienta.2021.109948

Backer, R., Rokem, J. S., Ilangumaran, G., Lamont, J., Praslickova, D., Ricci, E., et al. (2018). Plant growth-promoting rhizobacteria: context, mechanisms of action, and roadmap to commercialization of biostimulants for sustainable agriculture. *Front. Plant Sci.* 9. doi: 10.3389/fpls.2018.01473

Barnes, L. R., and Johnson, C. R. (1986). Evaluation of ericoid mycorrhizae and media on establishment of micropropagated *Rhododendron chapmanii*, Gray. *J. Environ. Hortic.* 4, 109–111. doi: 10.24266/0738-2898-4.4.109

Barron, G. L. (1962). New species and new records of *Oidiodendron*. *Can. J. Bot.* 40, 589–607. doi: 10.1139/b62-055

Begum, N., Qin, C., Ahanger, M. A., Raza, S., Khan, M. I., Ashraf, M., et al. (2019). Role of arbuscular mycorrhizal fungi in plant growth regulation: Implications in abiotic stress tolerance. *Front. Plant Sci.* 10, 1068. doi: 10.3389/fpls.2019.01068

Bending, G. D., and Read, D. J. (1997). Lignin and soluble phenolic degradation by ectomycorrhizal and ericoid mycorrhizal fungi. *Mycol. Res.* 101, 1348–1354. doi: 10.1017/S0953756297004140

Berruti, A., Lumini, E., Balestrini, R., and Bianciotto, V. (2016). Arbuscular mycorrhizal fungi as natural biofertilizers: Let's benefit from past successes. *Front. Microbiol.* 6, 1559. doi: 10.3389/fmicb.2015.01559

Berta, G., and Gianinazzi-Pearson, V. (1986). "Influence of mycorrhizal infection on root development in calluna vulgaris (L.) Hull seedlings," in *Physiological and genetical aspects of mycorrhizae*. Eds. V. Gianinazzi Pearson and S. Gianinazzi(Dijon, France: Institut National de la Recherche Agronomique), 673–676.

Biswas, T., and Kole, S. C. (2017). "Soil organic matter and microbial role in plant productivity and soil fertility," in *Advances in soil microbiology: Recent trends*

and future prospects. Eds. T. Adhya, B. Mishra, K. Annapurna, D. Verma and U. Kumar (Singapore: Springer), 219–238. doi: 10.1007/978-981-10-7380-9_10

Bonfante, P., and Genre, A. (2010). Mechanisms underlying beneficial plant–fungus interactions in mycorrhizal symbiosis. *Nat. Commun.* 1, 48. doi: 10.1038/ncomms1046

Bougoure, D., and Cairney, J. W. G. (2006). Chitinolytic activities of ericoid mycorrhizal and other root-associated fungi from *Epacris pulchella* (Ericaceae). *Mycol. Res.* 110, 328–334. doi: 10.1016/j.mycres.2005.09.015

Bradley, R., Burt, A. J., and Read, D. J. (1981). Mycorrhizal infection and resistance to heavy metal toxicity in *Calluna vulgaris*. *Nature* 292, 335–337. doi: 10.1038/292335a0

Bradley, R., Burt, A. J., and Read, D. J. (1982). The biology of mycorrhiza in the ericaceae. VIII. the role of mycorrhizal infection in heavy metal resistance. *New Phytol.* 91, 197–209. doi: 10.1111/j.1469-8137.1982.tb03306.x

Brody, A. K., Waterman, B., Ricketts, T. H., Degrassi, A. L., Gonzalez, J. B., Harris, J. M., et al. (2019). Genotype-specific effects of ericoid mycorrhizae on floral traits and reproduction in *Vaccinium corymbosum*. *Am. J. Bot.* 106, 1412–1422. doi: 10.1002/ajb2.1372

Cairney, J. W. G., and Meharg, A. A. (2003). Ericoid mycorrhiza: a partnership that exploits harsh edaphic conditions. *Eur. J. Soil Sci.* 54, 735–740. doi: 10.1046/j.1351-0754.2003.0555.x

Cairney, J. W. G., Sawyer, N. A., Sharples, J. M., and Meharg, A. A. (2000). Intraspecific variation in nitrogen source utilization by isolates of the ericoid mycorrhizal fungus *Hymenoscyphus ericae* (Read) KorfandKernan. *Soil. Biol. Biochem.* 32, 1319–1322. doi: 10.1016/S0038-0717(00)00025-0

Calvo, P., Nelson, L., and Kloepper, J. W. (2014). Agricultural uses of plant biostimulants. *Plant Soil* 383, 3–41. doi: 10.1007/s11104-014-2131-8

Casarrubia, S., Martino, E., Daghino, S., Kohler, A., Morin, E., Khouja, H. R., et al. (2020). Modulation of plant and fungal gene expression upon cd exposure and symbiosis in ericoid mycorrhizal *Vaccinium myrtillus*. *Front. Microbiol.* 11, 341. doi: 10.3389/fmicb.2020.00341

Casarrubia, S., Sapienza, S., Fritz, H., Daghino, S., Rosenkranz, M., Schnitzler, J. P., et al. (2016). Ecologically different fungi affect *Arabidopsis* development: Contribution of soluble and volatile compounds. *PLoS One* 11, e0168236. doi: 10.1371/journal.pone.0168236

Chen, J., and Gabelman, W. H. (2000). Morphological and physiological characteristics of tomato roots associated with potassium-acquisition efficiency. *Sci. Hortic.* 83, 213–225. doi: 10.1016/S0304-4238(99)00079-5

Cheng, Y., Dai, X., and Zhao, Y. (2007). Auxin synthesized by the YUCCA flavin monooxygenases is essential for embryogenesis and leaf formation in *Arabidopsis*. *Plant Cell* 19, 2430–2439. doi: 10.1105/tpc.107.053009

Chen, J., and Goldsbrough, P. B. (1994). Increased activity of γ-glutamylcysteine synthetase in tomato cells selected for cadmium tolerance. *Plant Physiol.* 106, 233–239. doi: 10.1104/pp.106.1.233

Chen, J., Jacobson, L., Handelsman, J., and Goodman, R. M. (1996). Compatibility of systemic acquired resistance and microbial biocontrol for suppression of plant diseases. *Mol. Ecol.* 5, 73–80. doi: 10.1111/j.1365-294X.1996.tb00292.x

Chen, D. M., Khalili, K., and Cairney, J. W. G. (2003). Influence of water stress on biomass production by isolates of an ericoid mycorrhizal endophyte of *Woollsia pungens* and *Epacris microphylla* (Ericaceae). *Mycorrhiza* 13, 173–176. doi: 10.1007/s00572-003-0228-7

Chen, J., McConnell, D. B., Norman, D. J., and Henny, R. J. (2005). "The foliage plant industry," in *Horticultural reviews*. Ed. J. Janick (Hoboken, NJ: John Wiley and Sons, Inc), 45–110.

Chen, C. R., and Xu, ,. Z. H. (2006). On the nature and ecological functions of soil soluble organic nitrogen (SON) in forest ecosystems. *J. Soils Sediments.* 6, 63–66. doi: 10.1065/jss2006.06.159

Chen, J., Zhou, J., and Goldsbrough, P. B. (1997). Characterization of phytochelatin synthase from tomato. *Plant Physiol.* 101, 165–172. doi: 10.1111/j.1399-3054.1997.tb01833.x

Daghino, S., Martino, E., and Perotto, S. (2016). Model system to unravel the molecular mechanisms of heavy metal tolerance in the ericoid mycorrhizal symbiosis. *Mycorrhiza* 26, 263–274. doi: 10.1007/s00572-015-0675-y

Daghino, S., Martino, E., Voyron, S., and Perotto, S. (2022). Metabarcoding of fungal assemblages in *Vaccinium myrtillus* endosphere suggests colonization of above-ground organs by some ericoid mycorrhizal and DSE fungi. *Sci. Reps.* 12, 1–11. doi: 10.1038/s41598-022-15154-1

Druege, U., and Franken, P. (2019). *Petunia* as model for elucidating adventitious root formation and mycorrhizal symbiosis: At the nexus of physiology, genetics, microbiology and horticulture. *Physiol. Plant* 165, 58–72. doi: 10.1111/ppl.12762

du Jardin, P. (2015). Plant biostimulants: Definition, concept, main categories and regulation. *Sci. Hortic.* 196, 3–14. doi: 10.1016/j.scienta.2015.09.021

Eccher, T., Piagnani, M. C., and Zordan, C. (2010). Influence of thirteen different strains of ericoid endomycorrhizae on rooting and growth of micropropagated *Azalea mollis*. *Acta Hortic.* 865, 321–326. doi: 10.17660/ActaHortic.2010.865.44

EU (2019). Regulation of the European parliament and of the council laying down rules on the making available on the market of EU fertilising products and amending regulations (EC) no 1069/2009 and (EC) no 1107/2009 and repealing regulation (EC) no 2003/2003. Available at: https://eur-lex.europa.eu/eli/reg/2019/1009/oj (accessed August 10, 2022).

Fadaei, S., Vaziriyeganeh, M., Young, M., Sherr, I., and Zwiazek, J. J. (2020). *Regulation of the European parliament and of the council laying down rules on the making available on the market of EU fertilising products and amending Regulations (EC) No 1069/2009 and (EC) No 1107/2009 and repealing Regulation (EC) No 2003/2003*. Available at: https://eur-lex.europa.eu/eli/reg/2019/1009/oj (August 10, 2022)

Fan, S., Jian, D., Wei, X., Chen, J., Beeson, R. C., Zhou, Z., et al. (2017). Micropropagation of blueberry 'Bluejay'and 'Pink lemonade'through *in vitro* shoot culture. *Sci. Hortic.* 226, 277–284. doi: 10.1016/j.scienta.2017.08.052

Fehrer, J., Réblová, M., Bambasová, V., and Vohník, M. (2019). The root-symbiotic *Rhizoscyphus ericae* aggregate and *Hyaloscypha* (*Leotiomycetes*) are congeneric: Phylogenetic and experimental evidence. *Stud. Mycol.* 92, 195–225. doi: 10.1016/j.simyco.2018.10.004

Ghorbanpour, M., Omidvari, M., Abbaszadeh-Dahaji, P., Omidvar, R., and Kariman, K. (2018).). mechanisms underlying the protective effects of beneficial fungi against plant diseases. *Biol. Cont.* 117, 147–157. doi: 10.1016/j.biocontrol.2017.11.006

Gianinazzi, S., Gollotte, A., Binet, M. N., van Tuinen, D., Redecker, D., and Wipf, D. (2010). Agroecology: the key role of arbuscular mycorrhizas in ecosystem services. *Mycorrhiza* 20, 519–530. doi: 10.1007/s00572-010-0333-3

Gorecka, K. (1979). The effect of growth regulators on rooting of ericaceae plants. *Acta Hortic.* 91, 483–489. doi: 10.17660/ActaHortic.1979.91.59

Gorman, N. R., and Starrett, M. C. (2003). Screening commercial peat and peat-based products for the presence of ericoid mycorrhizae. *J. Environ. Hortic.* 21, 30–33. doi: 10.24266/0738-2898-21.1.30

Grelet, G. A., Meharg, A. A., and Alexander, I. J. (2005). Carbon availability affects nitrogen source utilisation by *Hymenoscyphus ericae*. *Mycol. Res.* 109, 469–477. doi: 10.1017/S0953756204002138

Grelet, G. A., Meharg, A. A., Duff, E. I., Anderson, I. C., and Alexander, I. J. (2009). Small genetic differences between ericoid mycorrhizal fungi affect nitrogen uptake by *Vaccinium*. *New Phytol.* 181, 708–718. doi: 10.1111/j.1469-8137.2008.02678.x

Grunewaldt-Stöcker, G., von den Berg, C., Knopp, J., and von Alten, H. (2013). Interactions of ericoid mycorrhizal fungi and root pathogens in *Rhododendron: in vitro* tests with plantlets in sterile liquid culture. *Plant Root* 7, 33–48. doi: 10.3117/plantroot.7.33

Hambleton, S., and Currah, R. S. (1997). Fungal endophytes from the roots of alpine and boreal ericaceae. *Can. J. Bot.* 75, 1570–1581. doi: 10.1139/b97-869

Hamim, A., Boukeskasse, A., Ouhdouch, Y., Farrouki, A., Barrijal, S., Miché, L., et al. (2019). Phosphate solubilizing and PGR activities of ericaceous shrubs microorganisms isolated from Mediterranean forest soil. *Biocatal. Agric. Biotechnol.* 19, 101128. doi: 10.1016/j.bcab.2019.101128

Hashem, A. R. (1995a). The role of mycorrhizal infection in the resistance of *Vaccinium macrocarpon* to manganese. *Mycorrhiza* 5, 289–291. doi: 10.1007/BF00204964

Hashem, A. R. (1995b). The role of mycorrhizal infection in the resistance of *Vaccinium macrocarpon* to iron. *Mycorrhiza* 5, 451–454. doi: 10.1007/BF00213447

Hosoe, T., Nozawa, K., Lumley, T. C., Currah, R. S., Fukushima, K., Takizawa, K., et al. (1999). Tetranorditerpene lactones, potent antifungal antibiotics for human pathogenic yeasts, from a unique species of oidiodendron. *Chem. Pharm. Bull.* 47, 1591–1597. doi: 10.1248/cpb.47.1591

Ismail, M. A., Amin, M. A., Eid, A. M., Hassan, S. E. D., Mahgoub, H. A., Lashin, I., et al. (2021). Comparative study between exogenously applied plant growth hormones versus metabolites of microbial endophytes as plant growth promoting for *Phaseolus vulgaris* l. *Cells* 10, 1059. doi: 10.3390/cells10051059

Kerley, S. J., and Read, D. J. (1997). The biology of mycorrhiza in the ericaceae XIX. fungal mycelium as a nitrogen source for the ericoid mycorrhizal fungus *Hymenoscyphus ericae* (Read) korf & kernan and its host plants. *New Phytol.* 136, 691–701. doi: 10.1046/j.1469-8137.1997.00778.x

Kohler, A., Kuo, A., Nagy, L. G., Morin, E., Barry, K. W., Buscot, F., et al. (2015). Convergent losses of decay mechanisms and rapid turnover of symbiosis genes in mycorrhizal mutualists. *Nat. Genet.* 47, 410–415. doi: 10.1038/ng.3223

Kolařík, M., and Vohník, M. (2018). When the ribosomal DNA does not tell the truth: The case of the taxonomic position of *Kurtia argillacea*, an ericoid mycorrhizal fungus residing among hymenochaetales. *Fungal Biol.* 122, 1–18. doi: 10.1016/j.funbio.2017.09.006

Kosola, K. R., Workmaster, B. A. A., and Spada, P. A. (2007). Inoculation of cranberry (*Vaccinium macrocarpon*) with the ericoid mycorrhizal fungus *Rhizoscyphus ericae* increases nitrate influx. *New Phytol.* 176, 184–196. doi: 10.1111/j.1469-8137.2007.02149.x

Leake, J. R., and Read, D. J. (1990). Proteinase activity in mycorrhizal fungi. 2. the effects of mineral and organic nitrogen sources on induction of extracellular proteinase in *Hymenoscyphus ericae* (Read) korf and kernan. *New Phytol.* 116, 123–128. doi: 10.1111/j.1469-8137.1990.tb00517.x

Leopold, D. R. (2016). Ericoid fungal diversity: challenges and opportunities for mycorrhizal research. *Fungal Ecol.* 24, 114–123. doi: 10.1016/j.funeco.2016.07.004

Leslie, A. C. (2002). *The international rhododendron register and checklist. 2nd ed* (Edinburgh, U.K: Royal Botanic Garden Edinburgh).

Li, Y. C., Chen, S. J., and Li, K. T. (2021). Symbiotic fungi in nature Finnish peat moss promote vegetative growth in rabbiteye blueberry cuttings. *Hortic. Environ. Biotechnol.* 62, 191–198. doi: 10.1007/s13580-020-00313-y

Lin, L. C., Lee, M. J., and Chen, J. L. (2011). Decomposition of organic matter by the ericoid mycorrhizal endophytes of Formosan rhododendron (*Rhododendron formosanum* hemsl.). *Mycorrhiza* 21, 331–339. doi: 10.1007/s00572-010-0342-2

Lin, L. C., Lin, W. R., Hsu, Y. C., and Pan, H. Y. (2020). Influences of three *Oidiodendron maius* isolates and two inorganic nitrogen sources on the growth of *Rhododendron kanehirae*. *Hortic. Sci. Technol.* 38, 742–753. doi: 10.7235/HORT.20200067

Lin, L. C., Lin, C. Y., Lin, W. R., Tung, Y. T., and Wu, J. H. (2021). Effects of ericoid mycorrhizal fungi or dark septate endophytic fungi on the secondary metabolite of *Rhododendron pseudochrysanthum* (R. morii) seedlings. *Appl. Ecol. Environ. Res.* 19, 1221–1232. doi: 10.15666/aeer/1902_12211232

Luteyn, J. L. (2002). Diversity, adaptation, and endemism in neotropical ericaceae: biogeographical patterns in the *Vaccinieae*. *Bot. Rev.* 68, 55–87. doi: 10.1663/0006-8101(2002)068[0055:DAAEIN]2.0.CO;2

Mano, Y., and Nemoto, K. (2012). The pathway of auxin biosynthesis in plants. *J. Exp. Bot.* 63, 2853–2872. doi: 10.1093/jxb/ers091

Martino, E., Morin, E., Grelet, G., Kuo, A., Kohler, A., Daghino, S., et al. (2018). Comparative genomics and transcriptomics depict ericoid mycorrhizal fungi as versatile saprotrophs and plant mutualists. *New Phytol.* 217, 1213–1229. doi: 10.1111/nph.14974

Martino, E., Perotto, S., Parsons, R., and Gadd, G. M. (2003). Solubilization of insoluble inorganic zinc compounds by ericoid mycorrhizal fungi derived from heavy metal polluted sites. *Soil Biol. Biochem.* 34, 133–141. doi: 10.1016/S0038-0717(02)00247-X

Martino, E., Coisson, J.D., Lacourt, I., Favaron, F., Bonfante, P., and Perotto, S. (2000a). Influence of heavy metals on production and activity of pectinolytic enzymes in ericoid mycorrhizal fungi. *Mycol. Res.* 104, 825–833.

Martino, E., Turnau, K., Girlanda, M., Bonfante, P., and and Perotto, S. (2000b). Ericoid mycorrhizal fungi from heavy metal polluted soils: their identification and growth in the presence of zinc ions. *Mycol. Res.* 104, 338–344.

Massicotte, H. B., Melville, L. H., and Peterson, R. L. (2005). Structural characteristics of root-fungal interactions for five ericaceous species in eastern Canada. *Can. J. Bot.* 83, 1057–1064. doi: 10.1139/b05-046

Meharg, A. A., and Cairney, J. W. G. (2000). Co-Evolution of mycorrhizal symbionts and their hosts to metal contaminated environments. *Adv. Ecol. Res.* 30, 69–112. doi: 10.1016/S0065-2504(08)60017-3

Metraux, J. P. (2001). Systemic acquired resistance and salicylic acid: current state of knowledge. *Eur. J. Plant Path.* 107, 13–18. doi: 10.1023/A:1008763817367

Midgley, D. J., Jordan, L. A., Saleeba, J. A., and McGee, P. A. (2006). Utilisation of carbon substrates by orchid and ericoid mycorrhizal fungi from Australian dry sclerophyll forests. *Mycorrhiza* 16, 175–182. doi: 10.1007/s00572-005-0029-2

Midgley, D. J., Rosewarne, C. P., Greenfield, P., Li, D., Cassandra, J., Vockler, C. J., et al. (2016). Genomic insights into the carbohydrate catabolism of *Cairneyella variabilis* gen. nov. sp. nov., the first reports from a genome of an ericoid mycorrhizal fungus from the southern hemisphere. *Mycorrhiza* 26, 345–352. doi: 10.1007/s00572-016-0683-6

Midgley, D. J., Sutcliffe, B., Greenfield, P., and Tran-Dinh, N. (2018). *Gamarada debralockiae* gen. nov. sp. nov.–the genome of the most widespread Australian ericoid mycorrhizal fungus. *Mycorrhiza* 28, 379–389. doi: 10.1007/s00572-018-0835-y

Miyauchi, S., Kiss, E., Kuo, A., Drula, E., Kohler, A., Sanchez-Garcıa, M., et al. (2020). Large-Scale genome sequencing of mycorrhizal fungi provides insights into the early evolution of symbiotic traits. *Nat. Commun.* 11, 1–17. doi: 10.1038/s41467-020-18795-w

Mu, D., Du, N., and Zwiazek, J. J. (2021). Inoculation with ericoid mycorrhizal associations alleviates drought stress in lowland and upland velvetleaf blueberry (*Vaccinium myrtilloides*) seedlings. *Plants* 10, 2786. doi: 10.3390/plants10122786

Mueller, T. L., Karlsen-Ayala, E., Moeller, D. A., and Bellemare, J. (2022). Of mutualism and migration: will interactions with novel ericoid mycorrhizal communities help or hinder northward *Rhododendron* range shifts? *Oecologia* 198, 839–852. doi: 10.1007/s00442-021-05081-9

Myers, M. D., and Leake, J. R. (1996). Phosphodiesters as mycorrhizal p sources. II. ericoid mycorrhiza and the utilization of nuclei as a phosphorus and nitrogen source by *Vaccinium macrocarpon*. *New Phytol.* 132, 445–451. doi: 10.1111/j.1469-8137.1996.tb01864.x

Nemeth, K., Bartels, H., Heuer, C., and Maier, J. (1987). Determination by means of EUF of the inorganic and organic soil-nitrogen available to plants. *Zuckerindustrie* 112, 223–226.

Niemi, K., Scagel, C., and Haggman, H. (2004). Application of ectomycorrhizal fungi in vegetative propagation of conifers. *Plant Cell Tissue Org. Cult.* 78, 83–91. doi: 10.1023/B:TICU.0000020379.52514.72

Ouyang, X. (2021) *Witnessing the process of bacterial cell death: novel antimicrobials and their mechanisms of action*. Available at: https://hdl.handle.net/1887/3244017.

Pandey, D., Kehri, H. K., Zoomi, I., Akhtar, O., and Singh, A. K. (2019). "Recent advancement in white biotechnology through fungi," in *Deversity and enzymes perspectives*, vol. 1 . Eds. A. N. Yadav, S. Mishra, S. Singh and A. Gupta (Cham, Switzerland: Springer Nature Switzeland AG).

Pasternak, T., Groot, E. P., Kazantsev, F. V., Teale, W., Omelyanchuk, N., Kovrizhnykh, V., et al. (2019). Salicylic acid affects root meristem patterning *via* auxin distribution in a concentration-dependent manner. *Plant Physiol.* 180, 1725–1739. doi: 10.1104/pp.19.00130

Paul, E. A., and Clark, ,. F. E. (1989). *Soil MicrobiologyandBiochemistry* (SanDiego, CA: Academic Press).

Pearson, V., and Read, D. J. (1973). The biology of mycorrhiza in the ericaceae. II. the transport of carbon and phosphorus by the endophyte and the mycorrhiza. *New Phytol.* 72, 1325–1331. doi: 10.1111/j.1469-8137.1973.tb02110.x

Perotto, S., Daghino, S., and Martino, E. (2018). Ericoid mycorrhizal fungi and their genomes: another side to the mycorrhizal symbiosis? *New Phytol.* 220, 1141–1147. doi: 10.1111/nph.15218

Perotto, S., Martino, E., Abba, S., and Vallino, M. (2012). "Genetic diversity and functional aspects of ericoid mycorrhizal fungi," in *Fungal associations, 2nd ed*. Ed. B. Hock (Berlin Heidelberg: Springer-Verlag).

Pieterse, C. M., Zamioudis, C., Berendsen, R. L., Weller, D. M., Van Wees, S. C., and Bakker, P. A. (2014). Induced systemic resistance by beneficial microbes. *Annu. Rev. Phytopathol.* 52, 347–375. doi: 10.1146/annurev-phyto-082712-102340

Popescu, R., and Kopp, B. (2013). The genus *Rhododendron*: An ethnopharmacological and toxicological review. *J. Ethnopharmacol.* 147, 42–62. doi: 10.1016/j.jep.2013.02.022

Qiu, D., Wei, X., Fan, S., Jian, D., and Chen, J. (2018). Regeneration of blueberry cultivars through indirect shoot organogenesis. *HortScience* 53, 1045–1049. doi: 10.21273/HORTSCI13059-18

Read, D. J. (1996). The structure and function of the ericoid mycorrhizal root. *Ann. Bot.* 77, 365–374. doi: 10.1006/anbo.1996.0044

Rice, A. V., and Currah, R. S. (2001). Physiological and morphological variation in *Oidiodendron maius*. *Mycotaxon* 79, 383–396.

Rice, A. V., and Currah, R. S. (2005). *Oidiodendron*: a survey of the named species and related anamorphs of *Myxotrichum*. *Stud. Mycol.* 53, 83–120. doi: 10.3114/sim.53.1.83

Rice, A. V., and Currah, R. S. (2006). "Oidiodendron maius: Saprobe in sphagnum peat, mutualist in ericaceous roots?," in *Microbial roots endophytes*. Eds. B. J. E. Shulz, C. J. C. Boyle and T. B. Sieber (Berlin Heidelberg, Germany: Springer-Verlag), 227–246.

Rouphael, Y., and Colla, G. (2020). Editorial: Biostimulants in agriculture. *Front. Plant Sci.* 11, 1–7. doi: 10.3389/fpls.2020.00040

Rouphael, Y., Franken, P., Schneider, C., Schwarz, D., Giovannetti, M., and Agnolucci, M. (2015). Arbuscular mycorrhizal fungi act as bio-stimulants in horticultural crops. *Sci. Hortic.* 196, 91–108. doi: 10.1016/j.scienta.2015.09.002

Rusman, Y., Wilson, M. B., Williams, J. M., Held, B. W., Blanchette, R. A., Anderson, B. N., et al. (2020). Antifungal norditerpene oidiolactones from the fungus *Oidiodendron truncatum*, a potential biocontrol agent for white-nose syndrome in bats. *J. Nat. Prod.* 83, 344–353. doi: 10.1021/acs.jnatprod.9b00789

Ruytinx, J., Kafle, A., Usman, M., Coninx, L., Zimmermann, S. D., and Garcia, K. (2020). Micronutrient transport in mycorrhizal symbiosis; zinc steals the show. *Fungal Biol. Rev.* 34, 1–9. doi: 10.1016/j.fbr.2019.09.001

Scagel, C. F. (2005a). Inoculation with ericoid mycorrhizal fungi alters fertilizer use of highbush blueberry cultivars. *HortScience* 40, 786–794. doi: 10.21273/HORTSCI.40.3.786

Scagel, C. F. (2005b). Isolate-specific rooting responses of leucothoe fontanesiana cuttings to inoculation with ericoid mycorrhizal fungi. *J. Hortic. Sci. Biotechnol.* 80, 254–262. doi: 10.1080/14620316.2005.11511926

Scagel, C. F., Wagner, A., and Winiarski, P. (2005a). Frequency and intensity of root colonization by ericoid mycorrhizal fungi in nursery production of blueberry plants. *Small Fruits Rev.* 4, 95–112.

Scagel, C. F., Wagner, A., and Winiarski, P. (2005b). Inoculation with ericoid mycorrhizal fungi alters root colonization and growth in nursery production of blueberry plants from tissue culture and cuttings. *Small Fruits Rev.* 4, 113–135.

Schuler, R., and Haselwandter, K. (1988). Hydroxymate siderophore production by ericoid mycorrhizal fungi. *J. Plant Nutr.* 11, 907–913. doi: 10.1080/01904168809363855

Séneca, J., Söllinger, A., Herbold, C. W., Pjevac, P., Prommer, J., Verbruggen, E., et al. (2021). Increased microbial expression of organic nitrogen cycling genes in long-term warmed grassland soils. *ISME Commun.* 1, 1–9. doi: 10.1038/s43705-021-00073-5

Sharples, J. M., Meharg, A. A., Chambers, S. M., and Cairney, J. W. G. (2000a). Mechanism of arsenate resistance in the ericoid mycorrhizal fungus *Hymenoscyphus ericae*. *Plant Physiol.* 124, 1327–1334. doi: 10.1104/pp.124.3.1327

Sharples, J. M., Meharg, A. A., Chambers, S. M., and Cairney, J. W. G. (2000b). Symbiotic solution to arsenic contamination. *Nature* 404, 951–952. doi: 10.1038/35010193

Sharples, J. M., Meharg, A. A., Chambers, S. M., and Cairney, J. W. G. (2001). Arsenate resistance in the ericoid mycorrhizal fungus *Hymenoscyphus ericae*. *New Phytol.* 151, 265–270. doi: 10.1046/j.1469-8137.2001.00146.x

Shaw, G., Leake, J. R., Baker, A. J. M., and Read, D. J. (1990). The biology of mycorrhiza in the ericaceae. XVII. the role of mycorrhizal infection in the regulation of iron uptake by ericaceous plants. *New Phytol.* 115, 251–258. doi: 10.1111/j.1469-8137.1990.tb00450.x

Smith, S. E., and Read, D. (2008). "Ericoid mycorrhizas," in *Mycorrhizal symbiosis*, *3rd ed* (New York, NY, USA: Academic Press), 389–418.

Starrett, M. C., Blazich, F. A., Shafer, S. R., and Grand, L. F. (2001). *In vitro* colonization of micropropagated *Pieris floribunda* by ericoid mycorrhizae. II. effects on acclimatization and growth. *HortScience* 36, 357–359. doi: 10.21273/HORTSCI.36.2.357

Sutka, M., Li, G. W., Boudet, J., Boursiac, Y., Doumas, P., and Maurel, C. (2011). Natural variation of root hydraulics grown in normal and saltstressed conditions. *Plant Physiol.* 155, 1264–1276. doi: 10.1104/pp.110.163113

Talbot, J. M., and Treseder, K. K. (2010). Controls over mycorrhizal uptake of organic nitrogent. *Pedobiologia* 53, 169–179. doi: 10.1016/j.pedobi.2009.12.001

Thormann, M. N., Currah, R. S., and Bayley, S. E. (2002). The relative ability of fungi from *Sphagnum fuscum* to decompose selected carbon substrates. *Can. J. Microbiol.* 48, 204–211. doi: 10.1139/w02-010

Tian, W., Zhang, C. Q., Qiao, P., and Milne, R. (2011). Diversity of culturable ericoid mycorrhizal fungi of *Rhododendron decorum* in yunnan, China. *Mycologia* 103, 703–709. doi: 10.3852/10-296

Tokumasu, S. (1973). Notes on Japanese *Oidiodendron* (Japanese microscopic fungi II). *Trans. Mycol. Soc Jpn.* 14, 246–255.

Usuki, F., Abe, J. P., and Kakishima, M. (2003). Diversity of ericoid mycorrhizal fungi isolated from hair roots of *Rhododendron obtusum* var. *Kaempferi* in a Japanese red pine forest. *Mycoscience* 44, 97–102. doi: 10.1007/S10267-002-0086-8

Vaziriyeganeh, M., Lee, S. H., and Zwiazek, J. J. (2018). Water transport properties of root cells contribute to salt tolerance in halophytic grasses *Poa juncifolia* and *Puccinellia nuttalliana*. *Plant Sci.* 276, 54–62. doi: 10.1016/j.plantsci.2018.08.001

Vendrame, S., Del Bo, C., Ciappellano, S., Riso, P., and Klimis-Zacas, D. (2016). Berry fruit consumption and metabolic syndrome. *Antioxidants* 5, 34. doi: 10.3390/antiox5040034

Vohník, M. (2020). Ericoid mycorrhizal symbiosis: theoretical background and methods for its comprehensive investigation. *Mycorrhiza* 30, 671–695. doi: 10.1007/s00572-020-00989-1

Vohník, M., Albrechtová, J., and Vosátka, M. (2005). The inoculation with *Oidiodendron maius* and *Phialocephala fortinii* alters phosphorus and nitrogen uptake, foliar C:N ratio and root biomass distribution in *Rhododendron* cv. azurro. *Symbiosis* 40, 87–96.

Vohník, M., Fendrych, M., Albrechtová, J., and Vosátka, M. (2007). Intracellular colonization of *Rhododendron* and *Vaccinium* roots by *Cenococcum geophilum*, *Geomyces pannorum* and *Meliniomyces variabilis*. *Folia Microbiol.* 52, 407–414. doi: 10.1007/BF02932096

Vohník, M., Pánek, M., Fehrer, J., and Selosse, M. A. (2016). Experimental evidence of ericoid mycorrhizal potential within serendipitaceae (Sebacinales). *Mycorrhiza* 26, 831–846. doi: 10.1007/s00572-016-0717-0

Vohník, M., Sadowsky, J. J., Kohout, P., Lhotáková, Z., Nestby, R., and Kolaøík, M. (2012). Novel root-fungus symbiosis in ericaceae: sheathed ericoid mycorrhiza formed by a hitherto undescribed basidiomycete with affinities to trechisporales. *PLoS One* 7, e39524. doi: 10.1371/journal.pone.0039524

von Sivers, L., Jaspar, H., Johst, B., Roese, M., Bitterlich, M., Franken, P., et al. (2019). Brassinosteroids affect the symbiosis between the AM fungus *Rhizoglomus irregularis* and solanaceous host plants. *Front. Plant Sci.* 10, 571. doi: 10.3389/fpls.2019.00571

Watkinson, S. C. (2016). "Mutualistic symbiosis between fungi and autotrophs," in *The fungi*, *3rd Edition*. Eds. S. C. Watkinson, L. Boddy and N. P. Money (Boston: Academic Press), 205–243. doi: 10.1016/B978-0-12-382034-1.00007-4

Wazny, R., Jedrzejczyk, R. J., Rozpadek, P., Domka, A., and Turnau, K. (2022). Biotization of highbush blueberry with erioid mycorrhizal and endophytic fungi improves plant growth and vitality. *Environ. Biotechnol.* 106, 4775–4786. doi: 10.1007/s00253-022-12019-5

Wei, X., Chen, J., Zhang, C., Liu, H., Zheng, X., and Mu, J. (2020). Ericoid mycorrhizal fungus enhances microcutting rooting of rhododendron fortunei and subsequent growth. *Hortic. Res.* 7, 140. doi: 10.1038/s41438-020-00361-6

Wei, X., Chen, J., Zhang, C., and Pan, D. (2016a). A new *Oidiodendron maius* strain isolated from *Rhododendron fortunei* and its effects on nitrogen uptake and plant growth. *Front. Microbiol.* 7, 1327. doi: 10.3389/fmicb.2016.01327

Wei, X., Chen, J., Zhang, C., and Pan, D. (2016b). Differential gene expression in *Rhododendron fortunei* roots colonized by an ericoid mycorrhizal fungus and increased nitrogen absorption and plant growth. *Front. Plant Sci.* 7, 1594. doi: 10.3389/fpls.2016.01594

Wei, X., Chen, J., Zhang, C., and Wang, Z. (2018). *In vitro* shoot culture of *Rhododendron fortunei*: An important plant for bioactive phytochemicals. *Ind. Crops Prod.* 126, 459–465. doi: 10.1016/j.indcrop.2018.10.037

Whittaker, S. P., and Cairney, J. W. G. (2001). Influence of amino acids on biomass production by ericoid mycorrhizal endophytes from *Woollsia pungens* (Epacridaceae). *Mycol. Res.* 105, 105–111. doi: 10.1017/S0953756200002811

Whyte, A. R., and Williams, C. M. (2015). Effects of a single dose of a flavonoid-rich blueberry drink on memory in 8 to 10 y old children. *Nutrition* 31, 531–534. doi: 10.1016/j.nut.2014.09.013

Won, C., Shen, X., Mashiguchi, K., Zheng, Z., Dai, X., Cheng, Y., et al. (2011). Conversion of tryptophan to indole-3-acetic acid by TRYPTOPHAN AMINOTRANSFERASES OF ARABIDOPSIS and YUCCAs in *Arabidopsis*. *Proc. Natl. Acad. Sci. U.S.A.* 108, 18518–18523. doi: 10.1073/pnas.1108436108

Xavier, I. J., and Boyetchko, S. M. (2002). "Arbuscualr mycorhizal fungi as biostimulants and bioprotectants of crops," in *Applied mycology and biotechnology*, vol. 2 . Eds. G. G. Khachatouriand and D. K. Arora (Amsterdam: Elsevier), 311–330.

Xiao, G., and Berch, S. M. (1992). Ericoid mycorrhizal fungi of *Gaultheria shallon*. *Mycologia* 84, 470–471. doi: 10.1080/00275514.1992.12026162

Xu, H., Kemppainen, M., Kayal, W. E., Lee, S. H., Pardo, A. G., Cooke, J. E. K., et al. (2015). Overexpression of laccaria bicolor aquaporin JQ585595 alters root water transport properties in ectomycorrhizal white spruce (*Picea glauca*) seedlings. *New Phytol.* 205, 757–770. doi: 10.1111/nph.13098

Yakhin, O. I., Lubyanov, A. A., Yakhin, I. A., and Brown, P. H. (2017). Biostimulants in plant science: A global perspective. *Front. Plant Sci.* 7 2049. doi: 10.3389/fpls.2016.02049

Yang, W. Q., and Goulart, B. L. (2000). Mycorrhizal infection reduces short-term aluminum uptake and increases root cation exchange capacity of highbush blueberry plants. *HortScience* 35, 1083–1086. doi: 10.21273/HORTSCI.35.6.1083

Zhang, C., Yin, L., and Dai, S. (2009). Diversity of root-associated fungal endophytes in *Rhododendron fortunei* in subtropical forests of China. *Mycorrhiza* 19, 417–423. doi: 10.1007/s00572-009-0246-1

Zhang, G. F., Zhao, F., Chen, L. Q., Pan, Y., Sun, L. J., Bao, N., et al. (2019). Jasmonate-mediated wound signaling promotes plant regeneration. *Nat. Plants* 5, 491–497. doi: 10.1038/s41477-019-0408-x

frontiers | Frontiers in Microbiology

TYPE Original Research
PUBLISHED 29 November 2022
DOI 10.3389/fmicb.2022.1060554

OPEN ACCESS

EDITED BY
Maurizio Ruzzi,
University of Tuscia, Italy

REVIEWED BY
Kalpana Bhatt,
Purdue University, United States
Sajid Ali,
Yeungnam University, South Korea

*CORRESPONDENCE
Md. Azizul Haque
helalbmb2016@hstu.ac.bd
Kye Man Cho
kmcho@gnu.ac.kr

SPECIALTY SECTION
This article was submitted to Microbe and Virus Interactions with Plants, a section of the journal Frontiers in Microbiology

RECEIVED 03 October 2022
ACCEPTED 07 November 2022
PUBLISHED 29 November 2022

CITATION
Haque MA, Hossain MS, Ahmad I, Akbor MA, Rahman A, Manir MS, Patel HM and Cho KM (2022) Unveiling chlorpyrifos mineralizing and tomato plant-growth activities of *Enterobacter* sp. strain HSTU-ASh6 using biochemical tests, field experiments, genomics, and *in silico* analyses.
Front. Microbiol. 13:1060554.
doi: 10.3389/fmicb.2022.1060554

Unveiling chlorpyrifos mineralizing and tomato plant-growth activities of *Enterobacter* sp. strain HSTU-ASh6 using biochemical tests, field experiments, genomics, and *in silico* analyses

Md. Azizul Haque[1]*, Md. Shohorab Hossain[1], Iqrar Ahmad[2], Md. Ahedul Akbor[3], Aminur Rahman[4], Md. Serajum Manir[5], Harun M. Patel[2] and Kye Man Cho[6]*

[1]Department of Biochemistry and Molecular Biology, Hajee Mohammad Danesh Science & Technology University, Dinajpur, Bangladesh, [2]Division of Computer Aided Drug Design, Department of Pharmaceutical Chemistry, R. C. Patel Institute of Pharmaceutical Education and Research, Shirpur, India, [3]Institute of National Analytical Research and Services, Bangladesh Council of Scientific and Industrial Research, Dhaka, Bangladesh, [4]Department of Biomedical Sciences, College of Clinical Pharmacy, King Faisal University, Al Hofuf, Saudi Arabia, [5]Institute of Radiation and Polymer Technology, Bangladesh Atomic Energy Research Establishment, Dhaka, Bangladesh, [6]Department of GreenBio Science and Agri-Food Bio Convergence Institute, Gyeongsang National University, Jinju, South Korea

The chlorpyrifos-mineralizing rice root endophyte *Enterobacter* sp. HSTU-ASh6 strain was identified, which enormously enhanced the growth of tomato plant under epiphytic conditions. The strain solubilizes phosphate and grew in nitrogen-free Jensen's medium. It secreted indole acetic acid (IAA; 4.8 mg/mL) and ACC deaminase (0.0076 μg/mL/h) and hydrolyzed chlorpyrifos phosphodiester bonds into 3,5,6-trichloro-2-pyridinol and diethyl methyl-monophosphate, which was confirmed by Gas Chromatography – Tandem Mass Spectrometry (GC–MS/MS) analysis. *In vitro* and *in silico* (ANI, DDH, housekeeping genes and whole genome phylogenetic tree, and genome comparison) analyses confirmed that the strain belonged to a new species of *Enterobacter*. The annotated genome of strain HSTU-ASh6 revealed a sets of nitrogen-fixing, siderophore, *acd*S, and IAA producing, stress tolerance, phosphate metabolizing, and pesticide-degrading genes. The 3D structure of 28 potential model proteins that can degrade pesticides was validated, and virtual screening using 105 different pesticides revealed that the proteins exhibit strong catalytic interaction with organophosphorus pesticides. Selected docked complexes such as α/β hydrolase–crotoxyphos, carboxylesterase–coumaphos, α/β hydrolase–cypermethrin, α/β hydrolase–diazinon, and amidohydrolase–chlorpyrifos meet their catalytic triads in visualization, which showed stability in molecular dynamics simulation up to

100 ns. The foliar application of *Enterobacter* sp. strain HSTU-ASh6 on tomato plants significantly improved their growth and development at vegetative and reproductive stages in fields, resulting in fresh weight and dry weight was 1.8–2.0-fold and 1.3–1.6-fold higher in where urea application was cut by 70%, respectively. Therefore, the newly discovered chlorpyrifos-degrading species *Enterobacter* sp. HSTU-ASh6 could be used as a smart biofertilizer component for sustainable tomato cultivation.

KEYWORDS

chlorpyrifos mineralization, *Enterobacter* sp., tomato growth and yield, GC–MS/MS, MD simulation, *in silico* analysis, organophosphate pesticides (OPPs)

Introduction

Several strategies have been implemented in the agricultural sector to increase the production of crops/foods, such as the application of biofertilizers, chemical fertilizers, and pesticides, among which synthetic pesticides effectively improve the productivity of food and other agricultural commodities (Popp et al., 2013). Organophosphate (OP) pesticides are highly toxic chemicals that demonstrate extensive activity against pests and comprise approximately 38% of the all pesticides used on crops globally (Zhang et al., 2009). Excessive and inappropriate use of agrochemicals such as pesticides, herbicides, and fertilizers causes severe environmental and health issues (Dar et al., 2019).

To maintain sustainable food production, environmentally protected approaches, biofertilizers are urgently needed to improve crop growth, nitrogen fixation, and decrease yield loss under diverse stress conditions. The utilization of plant growth-promoting (PGP) endophytic bacteria is an efficient approach for stabilizing and improving crop yield. Due to their direct contact to plants, endophytic bacteria may exhibit greater ecological advantages than rhizospheric and epiphytic bacteria (James, 2000). The growth promotion of crop plants is regulated by endophytes by providing plant growth regulators, N fixation, phosphate solubilization, and ACC deaminase activity and improving tolerance against plant biotic and abiotic stresses (Carvalho et al., 2014). The application of PGP rhizobacteria (PPGPR) with plant growth-promoting traits is wanted due to its pragmatic, sustainable, and ecofriendly characteristics (Ali et al., 2022; Moon and Ali, 2022). In fact, a lot of ACC deaminase enzyme secreting PGPR was reported to improve crop plants' growth and development under various abiotic stress conditions (Moon and Ali, 2022). The PGPR can provide nutrients to non-leguminous plants even though they lack nodules, a process known as "associative nitrogen fixation" (Carvalho et al., 2014).

Furthermore, microorganisms play an important role in the detoxification of synthetic chemicals in soil (Bhatt et al., 2020; Rojas-Sánchez et al., 2022) and in the adaptation and defense of host plants by secreting bioactive compounds (Narayanan and Glick, 2022). They consume almost all-natural and synthetic compounds as their source of carbon and energy. Moreover, a significant number of genes such as *opd* (organophosphate degrading), carboxylesterase, *mpd* (methyl parathion degrading), and amidohydrolase, α/β hydrolase and several enzymes are known to be involved in degrading certain organophosphate pesticides (Yang et al., 2006; Parakhia et al., 2014; Lee et al., 2021; Das et al., 2022).

The endophyte *Enterobacter cloacae* have been reported to promote the growth of crop plants, such as rice, groundnut, black gram, and *Brassica napus* (Panigrahi et al., 2020). It has also been shown to establish nutrient transfer symbiosis with banana plants and protect them against the black sigatoka pathogen (Macedo-Raygoza et al., 2019) and exhibit antagonistic activity against *Pythium* damping-off of cucumber (Kazerooni et al., 2020). However, the effects of *E. cloacae* on tomato plants under epiphytic conditions have not been reported. Tomato plants are susceptible to diseases such as *Fusarium* and *Verticillium* wilt, early and late blight, bacterial speck, and anthracnose. Therefore, several agrochemicals and pesticides are being applied in tropical countries such as Bangladesh to prevent the frequent attacks of pests, insects, and pathogens, which has resulted in the contamination of tomato fruit bodies with excessive pesticide residues that can be ingested through diet and cause health hazards.

Endophytic effects on tomato plant growth and development with *Enterobacter* sp. were not thoroughly investigated. Endophytic effects on tomato plant growth and development with *Enterobacter* sp. were not thoroughly investigated yet. However, several studies have been conducted with other endophytes, such as indole acetic acid (IAA)-secreting *Bacillus subtilis* (Khan et al., 2016), ACC (1-aminocyclopropane-1-carboxylate) deaminase producing *Burkholderia* species (Onofre-Lemus et al., 2009), as well as *Ampelomyces* sp. and *Penicillium* sp. (Morsy et al., 2020), which improved tomato plant growth and promotion. Because tomato plants are non-leguminous, nitrogen fixation is not possible as it is in other leguminous plants. We chose an endophytic

bacterium from a non-leguminous rice plant for this purpose. A selective powerful strain namely *Enterobacter* sp. HSTU-ASh6 expressing higher plant growth promoting (PGP) traits such as germination induction, root and shoot development, IAA, ACC-deaminase producing activity, and chlorpyrifos pesticide degrading capability was assessed as biofertilizer components in fields at epiphytic conditions. With the application of this strain in fields, tomato plants demonstrated its resistance against pathogens and pests. Therefore, no additional agrochemicals were used in the fields, resulting in survival of the plants against biotic stress and saving the tomato plant from being impregnated with pesticides. The results of this study will be highly significant for the production of agrochemical-free edible crops with higher yields at a lower cost.

Materials and methods

Isolation and biochemical characterization of endophytic strain

The endophytic strain HSTU-ASh6 was isolated from healthy fresh rice plant roots. Two months old rice plants were collected from farmers' fields near Basherhat (25° 37′ 59.88″ N; 88° 39′ 0.00″ E), Sadar, Dinajpur, Bangladesh. The roots of rice plants were separated from whole plants. To get rid of soil and dust, the root samples were gently washed in distilled water. Following this, twenty root samples were then surface sterilized with 75% ethanol for 3 min and shaken in a 2.5% (w/v) NaOCl solution for 10 min at 120 rpm, which was adopted from Khan et al. (2016) and Das et al. (2022). The root samples underwent additional washings with autoclaved distilled water while they were agitated for 20 min. The roots were rolled on nutrient agar plates, and a 0.1 mL aliquot from the final wash was inoculated into 10 mL of nutrient broth for sterility testing. Samples were discarded if any growth of bacteria was detected in the sterility check (Das et al., 2022). Finally, sterilized rice plant roots were ground using a mortar and pestle and placed in a sterilized test tube (Haque et al., 2015). The squeezed roots were cultured in chlorpyrifos-enriched minimal nutrient media to isolate the chlorpyrifos mineralizing endophytic bacteria, as described (Das et al., 2022). Selected bacteria with prompt growth potentialities were sub-cultured in the same medium to obtain pure colonies, as described previously (Das et al., 2022). The isolate was preserved in 80% (v/v) glycerol at −20°C for further analysis. Biochemical tests, including methyl red, Voges–Proskauer, catalase, KOH string, oxidase, triple sugar iron, citrate utilization, motility indole urease, and urease, and individual sugar fermentation tests such as dextrose, lactose, maltose, and sucrose utilization (Adedayo et al., 2004; Das et al., 2022), were performed to facilitate the identification of the bacterium. In addition, the activities of extracellular cellulase, amylase, protease, and xylanase were determined as described elsewhere (Abdullah-Al-Mamun et al., 2022; Das et al., 2022).

Plant growth promoting activity tests

Indole acetic acid test

The quantification method for IAA of *Enterobacter* sp. HSTU-ASh6 was adopted as previous described (Ullah et al., 2013). Briefly, the bacterial suspension was cultured in 7 mL of modified Luria Bertani broth containing 0.01% tryptophan (L-Trp) separately and combined at 37°C for 7 days in a shaking incubator at 120 rpm. Then, 1 mL of each culture was transferred to 1.5-mL Eppendorf tubes and centrifuged at 10,000 rpm. The supernatant was transferred to glass test tubes to which 2 mL of Salkowski reagent (1 mL of 0.5 mL $FeCl_3$ to 50 mL of 35% $HClO_4$) was added. Then, the mixture was placed in the dark for 120 min. The resultant reddish-colored spectrum was read using spectrophotometer (UV-VIS spectrophotometer) at 530 nm. Finally, the strain HSTU-ASh6 secreted quantity of IAA was calculated using the standard calibration curve equation of pure IAA (Sigma-Aldrich Ltd, St. Louis, MO, USA) prepared separately.

1-Aminocyclopropane-1-carboxylate deaminase activity assay

The ACC deaminase activity of the bacterium was determined according to the modified methods of Shaharoona et al. (2006) and Belimov et al. (2015), which measures the amount of α-ketobutyrate produced upon the hydrolysis of ACC. The endophytic bacterium strain *Enterobacter* sp. strain HSTU-ASh6 was grown in Tryptic Soy Broth medium (TSB) for 18 h at 28°C to determine ACC deaminase activity. The cells were then harvested by centrifugation, washed with 0.1 M Tris–HCl (pH 7.5), and incubated for another 18 h in minimal medium containing 3 mM ACC as the sole source of nitrogen. The bacterial cells were collected by centrifugation and suspended in 5 mL of 0.1 moL L^{-1} of Tris–HCl, pH 7.6, and transferred to microcentrifuge tube. The contents of the tubes were centrifuged at 16,000 rpm for 5 min, and supernatant was removed. The pellets were suspended in 2 mL of 0.1 moL L^{-1} Tris HCl, pH 8.5. Next, 30 μL of toluene was added to the cell suspension and vortexed for 30 s. After 200 μL of the toluenized cells were placed in a fresh microcentrifuge tube, 20 μL of 0.5 moL L^{-1} ACC was added to the suspension, vortexed, and then incubated at 30°C for 15 min. Following the addition of 1 mL of 0.56 moL L^{-1} HCl, the mixture was vortexed and centrifuged for 5 min at 13,000 rpm at room temperature. Two mL of the supernatant was vortexed together with 1 mL of 0.56 moL

L^{-1} HCl. Thereupon, 2 mL of the 2, 4-dinitrophenylhydrazine reagent (0.2% 2, 4-dinitrophenylhydrazine in 2 moL L^{-1} HCl) was added to the glass tube, and the contents were vortexed and then incubated at 30°C for 30 min. Following the addition and mixing of 2 mL of 2 moL L^{-1} of NaOH, the absorbance of the mixture was measured by using a spectrophotometer at 540 nm. The cell suspension without ACC was used as a negative control and with $(NH_4)_2SO_4$ (0.2% w/v) as the positive control. The number of μmol of α-ketobutyrate produced by this reaction was determined by comparing the absorbance at 540 nm of a sample to a standard curve of α-ketobutyrate ranging between 10 and 200 μmoL (Honma and Shimomura, 1978; Shaharoona et al., 2006; Belimov et al., 2015).

Phosphate solubilization test

The phosphate solubilization ability of the isolate was determined qualitatively by streaking a strain on PVK agar media in a Petri plate. The plate was placed at 30°C for 72 h under aerobic conditions. The colonies that could grow and create a zone on the insoluble phosphate media were selected as the phosphate-solubilizing bacteria (Madhusmita et al., 2017).

Nitrogen fixation test

The nitrogen fixation capability of the endophytic strain HSTU-ASh6 was determined by streaking the strain on completely nitrogen-free Jensen's media (Sulistiyani and Meliah, 2017). The strain was grown for 5–7 days at 37°C in an incubator under aerobic conditions.

DNA extraction, amplification, sequencing, and analysis

The genomic content of the isolate was extracted using a commercial Quick-DNATM Miniprep Kit specific for bacteria (Zymo Research, Irvine, CA, USA), according to the manufacturer's specification. The 16S rRNA gene was amplified from the extracted DNA by polymerase chain reaction. The bacterial-specific universal forward primer 27F 5′-AGAGTTTGATCCTGGCTCAG-3′ and reverse primer 1492R 5′-TACGGTTACCTTGTTACGACTT-3′ were used in the PCR mixture. The master mix was prepared by adding Taq buffer, dNTPs, $MgCl_2$, and nuclease-free water in a PCR tube. The forward and reverse primers, $MgCl_2$, template DNA, and Taq DNA polymerase enzyme were added just before loading the sample in the PCR system (Haque et al., 2020; Das et al., 2022). After 36 cycles of PCR steps, the amplicon was stored at –20°C for further analysis. The amplified PCR products were visualized by agarose gel electrophoresis. DNA purification, cycle sequencing, and DNA sequencing of PCR amplicons were performed using a BDT v3 Cycle sequencing kit in a genetic analyzer 3130 (Haque et al., 2015, 2020). Finally, the 16S rRNA sequence was submitted to GenBank on the NCBI online server.

Effect of *Enterobacter* sp. strain HSTU-ASh6 on tomato plant growth promotion

The *Enterobacter* sp. HSTU-ASh6 effect on tomato plant growth promotion was assessed in two different ways. Firstly, its effect at seed germination stage was performed in laboratory conditions. Secondly, its effect on tomato plant seedlings development to vegetative and reproductive stages was investigated in fields at epiphytic conditions.

Effect of strain HSTU-ASh6 on tomato seeds germination

Seed sterilization and preparation

The tomato seeds were collected from Bangladesh Agricultural Development Corporation nursery. Firstly, the seeds were allowed to sundry. Then seeds were sterilized with 70% ethanol for 1 min and washed several times with sterilized water.

Seed bacterization

The sterilized seeds were placed in two sets of sterilized Eppendorf tubes. The first set of tubes contained seeds in 1 mL of bacterial suspension, and the second set contained seeds in 1 mL of distilled water without the strain (control). All tubes were placed in a dark environment for 8 h. After that the seeds were ready for germination.

Seed inoculation onto petri dishes

The seeds were sown for germination on Whatman filter paper in Petri dishes. The petri dishes were arranged in a Completely Randomized Design (CRD) with three replications. After 7 days of seed germination, 0.25 mL of bacterial suspension was applied in each petri dish. After 15 days of seed plantation, the following parameters of tomato plants with and without the strain were recorded.

Germination percentage

Germination percentage was calculated using the formula GP = Total germinated seeds/Total number of seeds × 100 (Ashraf and Foolad, 2005).

Root length and shoot length

Root length and shoot length were measured using a graduated ruler.

Vigor index

The vigor index was calculated using the formula Seedling length × germination percentage.

Effect of HSTU-ASh6 strain on tomato seedlings in field conditions

Tomato seedlings aged 32 days were collected from a local nursery and planted in the research field using a randomized complete block design method. The experiment was divided into the following five treatments to observe the effect of using different concentrations (30–100%) of urea doses and bacterial strains: T1 (30% urea with bacterium), T2 (70% urea with bacterium), T3 (100% urea with bacterium), Tc (100% urea without bacterium), and T0 (no urea and no bacterium/control). The experimental unit area (plot) was 1.80 m^2 and consisted of four rows measuring 1.32 m in width and 1.37 m in length, and the seedlings were planted using a hand drill method, maintaining a row-to-row distance of 40 cm and a plant-to-plant distance of 10 cm in a line. The plants were irrigated regularly according to requirement. The treatments were applied to the plants after 10, 20, 30, and 40 days of plantation. The root length, shoot length, leaf size, fresh weight, and dry weight were measured two times after 30 and 45 days of plantation.

Pesticide degradation analysis using GC–MS/MS

Firstly, the growth of the strain was checked in chlorpyrifos-enriched minimal salt broth media, in which chlorpyrifos (1 g/L) was the sole source of carbon (Lee et al., 2021; Das et al., 2022). Next, 5 μL of the stock bacterium was inoculated into the medium and kept for 14 days, after which 5 mL of chlorpyrifos-containing MSM was transferred into a separating funnel. Secondly, 25 mL of distilled water and 5 mL of *n*-hexane were added to the funnel and shaken vigorously for 5–10 min. The desired solvents in the n-hexane layer appeared on the top layer, whereas the unwanted layer remained on the bottom layer. The bottom layer was separated and kept in a bottle. Finally, to examine the biodegradation of chlorpyrifos, the n-hexane with appropriate solvent-containing layer solution was run on Gas Chromatography – Tandem Mass Spectrometry (GC–MS/MS) (Shimadzu QP2010, Japan). The GC–MS/MS instrumentation was set up according to Al Mansur et al. (2018), and following examination of each compound's mass spectrum were determined using the NIST11 library (Zaman et al., 2021).

Genomic DNA extraction, library preparation, whole genome sequencing

The preparation of the genomic library of *Enterobacter* sp. HSTU-ASh6 and the sequencing of the complete genome were performed using the Illumina MiniSeq System (Illumina, Inc., San Diego, CA, USA), as described previously (Abdullah-Al-Mamun et al., 2022; Das et al., 2022). After complete genome sequencing, the quality test was conducted using the fast QC analysis and Illumina Base Space sequence analysis Hub. SPAdes assembler version 3.5 was used to assemble the complete genome of *Enterobacter* sp. HSTU-ASh6, and the resulting assembled genome was annotated and analyzed using NCBI Prokaryotic Genome Annotation Pipeline (PGAP) version 4.5, Prokka. The circular genome map of *Enterobacter* sp. HSTU-ASh6 was prepared using CGView Comparison Tool. Next, different types of genes, e.g., those responsible for plant growth promotion (nitrogen fixation, phosphate solubilization, IAA production, ACC deaminase production, and sulfur assimilation), biofilm formation, root colonization (chemotaxis and mortality), pesticide degradation, and stress tolerance (heat shock and cold shock), were predicted from the PGAP file.

Strain classification

Phylogenetic tree construction

A comparative phylogenetic analysis of housekeeping genes, e.g., 16S rRNA, *gyr*B, *rec*A, *rpo*B, and *ton*B of different closely related *Enterobacter* sp. sequences, was performed using the NCBI database. The phylogenetic tree of HSTU-ASh6 whole genome sequence was constructed along with 29 nearest homologs genebank files accumulated from the NCBI database. The REALPHY 1.12 online server was used to construct the complete genome phylogenetic tree, which was modified using the MEGA-X.0 program. Finally, the phylogenetic trees of the housekeeping genes were constructed by the neighbor-joining method using Molecular Evolutionary Genetics Analysis (MEGA-X).

Average nucleotide identity and DNA–DNA hybridization

Average nucleotide identity (ANI) and digital DNA–DNA hybridization (DDH) analyses were performed using the JSpecies WS, Type Strain Genome Server (TYGS) and GGDC web server, respectively (Abdullah-Al-Mamun et al., 2022). A total of 15 types of nearest homolog complete genome sequences were utilized for the ANI analysis. For the DDH analysis, 15 different types of genomes were aligned with the HSTU-ASh6 genome.

Genome comparison

Multiple genome sequence alignment and pangenomic analysis

To determine the genetic diversity and similarities of *Enterobacter* sp. HSTU-ASh6, its genome sequence was compared with the genome sequences of six most closely related species, viz., *E. asburiae* (CP007546), *E. bugandensis* 220 (CP039453), *E. chengduensis* (CP043318), *E. cloacae* A1137 (CP021851), *E. roggenkampii* RHBSTW 00695 (CP056168), and *E. sichuanensis* SGAir0282 (CP027986), by pangenomic analysis using GView Server. The genome of *Enterobacter* sp. HSTU-ASh6 was further compared with four recently published nearest homologs, viz., *E. cloacae* A1137 (NZ_CP021851), *E. sichuanensis* SGAir0282 (NZ_CP027986), *E. roggenkampii* Ecl 20 981 (CP048650), and *E. asburiae* ATCC 35953 (CP011863), by multiple genomic analysis using the progressive Mauve software[1].

Insecticide degradation demonstrated by enzyme catalytic reaction

Homology modeling, protein preparation, and validation

The homology modeling of the protein was performed using the Iterative Threading ASSEmbly Refinement (I-TASSER) Server. Next, the model was subjected to energy minimization using the steepest descent and conjugate gradient techniques to eliminate lower quality contacts among protein atoms. Computations were performed *in vacuo* with GROMOS 96 43B1 parameters set using the Swiss-PDB Viewer. The 3D structures of the protein were saved in .pdb format. The SAVES v6.0 online server was used to check the validation and evaluate the quality of the minimized protein[2].

Small molecule/ligand collection and optimization

A total of 105 various types of organophosphorus pesticides, weed killers, and nerve agent small molecules were collected from the PubChem database[3]. After ordering, the ligands were optimized and minimized using the mmff94 force field and the steepest descent algorithm in the PyRx software environment. The 3D structures of small molecules were stored in a file in .sdf format.

1 http://darlinglab.org/mauve/mauve.html
2 https://saves.mbi.ucla.edu/
3 https://pubchem.ncbi.nlm.nih.gov/

Virtual screening, molecular docking, and visualization

A total of 105 pesticides (small molecules) with 28 valid protein structures were used individually and screened with 105 ligands for virtual screening. Virtual screening and molecular docking were performed using the PyRx software (Dallakyan and Olson, 2015). Protein–ligand complexes were constructed using the Chimera software, and 2D and 3D structure visualization was performed using Discover Studio 2021 Client. The results of virtual screening were displayed by boxplot analysis performed using the Origin Pro 8.0 software. Furthermore, protein and ligand non-bonded interactions were recognized using Discovery Studio 2021 Client. At the time of virtual screening, the grid box sizes were fixed at 61.6411, 61.6072, and 61.8787, which was the maximum size of the grid box, respectively for X, Y, and Z. However, in the case of molecular docking, the grid box sizes were not fixed, and they were dissimilar as for (i) α/β fold hydrolase (GM298_18675) with crotoxyphos, (ii) carboxylesterase with coumaphos, (iii) α/β fold hydrolase (GM298_08590) with cypermethrin, (iv) α/β fold hydrolase (GM298_00815) protein with diazinon, (v) amidohydrolase family protein (GM298_20245) with chlorpyrifos, and the X, Y, and Z sizes were 61.6411, 61.6072, and 61.8787, respectively. The binding affinity of protein with ligands was calculated in kcal/mole for a negative score.

Molecular dynamics simulation

To determine the potential pesticide-degrading stability of proteins with pesticides, a molecular dynamics simulation was run using the Desmond program (Schrodinger) that has an explicit solvent MD package linked to the OPLS 2005 force field. The protein preparation wizard was used to create the protein-ligand complexes, and the system builder panel was solvated them using the orthorhombic simple point-charge water model. The counter ions Na+ or Cl^{-} were added as necessary to charge and neutralize the solvated system. In order to relax the system to the lowest local energy, minimization tasks were carried out. Next, this model system was run to MD simulation steps using the OPLS 2005 force field parameter (Lee et al., 2021; Patel et al., 2021). The MD simulation was performed up to 100 ns using the NPT ensemble (isothermal-isobaric ensemble, constant temperature, constant pressure, and constant number of particles) at 300 K temperature and 1.013 bar pressure (Jorgensen et al., 1996; Lee et al., 2021). For controlling temperature and pressure, the Noose-Hover chain thermostat algorithm and the Martyna-Tobias-Klein barostat algorithm were employed, respectively. The particle mesh Ewald method was used to measure long-range electrostatic interactions, while

the other parameters were left at their default values (Patel et al., 2021). The behavior and interactions between the ligands and protein were examined using the Simulation Interaction Diagram tool. The output.cms file was imported, and root mean square deviation (RMSD) and root mean square fluctuation (RMSF) was chosen to produce the revealed plots.

Results

Isolation and biochemical characterization

The biochemical characterization of HSTU-ASh6 is summarized in **Supplementary Figure 1**. The strain was gram-negative; KOH dissolves the thin peptidoglycan layer of the cell wall of gram-negative bacteria, and they showed viscously and stuck in the loop within 30 s after the addition of KOH to the bacteria cultured for 24 h. Conversely, the isolate demonstrated positive results in the Voges–Proskauer, catalase, triple sugar iron, citrate utilization, motility indole urease, urease, dextrose, lactose, maltose, and sucrose utilization tests. However, the strain showed negative results in the indole, MR, and oxidase tests. It also exhibited mild activities of cellulase, amylase, and xylanase but a vigorous protease activity in the plate assay.

P solubilization, N fixation, indole acetic acid production, 1-aminocyclopropane-1-carboxylate deaminase activity

The results of phosphate solubilization, nitrogen fixation, and IAA production are summarized in **Supplementary Figure 2**. The phosphate solubilization test was positive because growth was detected and a hollow zone appeared in the PVK plate. The nitrogen fixation test was also positive based on the detection of the growth of HSTU-ASh6 in Jensen's medium. Moreover, the strain was capable of producing IAA as demonstrated by the reddish pink color, which amounted to 4.8 mg/mL compared to that in the control. In addition, the ACC deaminase activity of the strain was 0.0076 μ g/mL/h.

Growth promotion

Seed germination effect on tomato seeds

The HSTU-ASh6 suspension was applied three times to the tomato seeds sown on a filter paper in a Petri dish. After 9 days, the germination percentage, root length, shoot length, seedling length, and vigor index were recorded as 92%, 6.09, 5.39, 12.02 cm, and 1109.57 in the treated plants, respectively. In the control (seeds not treated with the bacterial strain), the respective values were 69%, 3.50, 5.34, 8.84 cm, and 611.99 (**Table 1**).

Tomato plant growth at vegetative and reproductive stages

The root length, shoot length, leaf length, fresh weight, and dry weight of tomato plants measured after 30 and 45 days of plantation are shown in **Table 2**. The highest root length, shoot length, leaf length, fresh weight, and dry weight were observed in T3 treatment. In particular, the fresh and dry weights of tomato plants were significantly higher in T3 treatment than in T2 and other treatments. The fresh and dry weights were 1.33–2.93-fold and 1.8–2.43-fold higher in T3 treatment, 1.95–2.3-fold and 1.41–2.17-fold higher in T2 treatment, 1.8–2.0-fold and 1.3–1.6-fold higher in T1 treatment, respectively, than in Tc treatment after 30–45 days of plantation. These results suggest that the inoculation of *Enterobacter* sp. strain HSTU-ASh6 significantly improved tomato plants' growth and development in fields at epiphytic conditions where the amount of urea fertilizer application was cut by 30–70% (**Table 2** and **Supplementary Figure 3**).

Chlorpyrifos biodegradation analysis using GC–MS

The GC–MS/MS analysis spectra revealed the presence of phorate sulfoxide, phorate sulfone, chlorpyrifos methyl, carbophenothion sulfoxide, oxydisulfoton, carbonochloridic acid, 2,4,5-trichlorophenyl ester, thionodemeton sulfone, 3-(2-thienyl)-DL-alanine, chlorpyrifos oxon, diethyl methanephosphonate (DEMP), and 3,5,6-trichloro-2-pyridinol (TCP), etc. (**Table 3**). On the basis of GC–MS/MS results, a pathway of chlorpyrifos biodegradation by HSTU-ASh6 was proposed as illustrated in **Figure 1**. Chlorpyrifos was initially degraded by hydrolysis to generate chlorpyrifos oxon that was further broken down to generate TCP and DEMP (spectrum = 8). Subsequently, TCP was again degraded by ring breakage, resulting in its complete detoxification.

Genomic features of *Enterobacter* sp. HSTU-ASh6

The genome size of *Enterobacter* sp. HSTU-ASh6 was 4,857,424 bp with 55.1% GC, 4478 protein-coding sequences (CDS), and 72 tRNAs. The subsystem of the RAST annotation is shown in **Supplementary Figure 4**. All proteins of *Enterobacter* sp. HSTU-ASh6 were revealed by CGview analysis in a proper genomic map (**Figure 2**).

TABLE 1 Germination percentage, root length, shoot length, seedling length, and vigor index of tomato plant with the strain at 9 days of seed plantation.

Name of isolate	Germination percentage	Root length (cm)	Shoot length (cm)	Seedling length (cm)	Vigor index
Control	69.23 ± 0.0^{b}	3.50 ± 0.58^{b}	5.34 ± 0.11^{ab}	8.84 ± 0.53^{b}	611.99 ± 36.71^{b}
HSTU-ASh6 (P7)	92.31 ± 0.0^{a}	6.09 ± 0.26^{a}	5.39 ± 0.13^{a}	12.02 ± 0.28^{a}	1109.57 ± 25.58^{a}

Different lowercase letters indicate significant difference at the 5% level.

TABLE 2 Effect of bacterium and fertilizer in different time period among different treatment group.

Data collection time	Treatments	Root length (cm)	Shoot length (cm)	Leaf length (cm)	Fresh weight (gm)	Dry weight (gm)
After 30 days of plantation	T1	22.33 ± 1.86^{ab}	32.67 ± 2.84^{a}	20.33 ± 0.88^{ab}	150 ± 1.16^{c}	78 ± 1.16^{c}
	T2	24.33 ± 0.33^{a}	34 ± 0.58^{a}	21 ± 0.58^{a}	162.67 ± 1.45^{b}	85.33 ± 0.88^{b}
	T3	25.33 ± 0.67^{a}	35 ± 0.58^{a}	21.33 ± 0.67^{a}	180 ± 1.15^{a}	90.33 ± 1.20^{a}
	Tc	15.33 ± 0.88^{c}	27 ± 0.58^{b}	18 ± 0.58^{c}	83.33 ± 2.01^{d}	60.33 ± 1.45^{d}
	To	10.67 ± 0.67^{d}	22.33 ± 0.88^{c}	16 ± 0.58^{d}	69.33 ± 1.20^{e}	41 ± 1.53^{e}
After 45 days of plantation	T1	26.33 ± 1.45^{a}	36.67 ± 2.88^{a}	22 ± 0.58^{ab}	190 ± 1.73^{c}	124.67 ± 2.60^{c}
	T2	28 ± 1^{a}	38 ± 1.53^{a}	23.33 ± 0.88^{a}	221 ± 2.08^{b}	168 ± 1.53^{b}
	T3	29 ± 3.06^{a}	40.33 ± 0.88^{a}	23.67 ± 0.33^{a}	278.33 ± 2.12^{a}	187.33 ± 1.45^{a}
	Tc	17.67 ± 0.67^{b}	30.67 ± 2.12^{b}	20.67 ± 1.45^{c}	95 ± 1.16^{d}	77.33 ± 1.45^{d}
	To	12 ± 0.58^{c}	25 ± 1.15^{c}	17.33 ± 0.33^{d}	83.67 ± 0.88^{e}	56.67 ± 1.20^{e}

T1, 30% urea treatment + strain HSTU-ASh6 treatment; T2, 70% urea treatment + HSTU-ASh6 treatment; T3, 100% urea treatment + HSTU-ASh6 treatment; T0, 0% urea treatment; Tc, 100% urea treatment. Different lowercase letters indicate significant difference at the 5% level.

The genomic map of proteins from *Enterobacter* sp. HSTU-ASh6 was created successfully, where GC-skew positivity indicates the presence of CDS downstream and GC-skew negativity shows the presence of CDS upstream. Although GC-skew is predominantly introduced by RNA synthesis in local genomic areas, it was first used to estimate the *ori* and *ter* positions computationally by looking at known genome sequences.

Taxonomic classification

Phylogenetic tree

Phylogenetic tree of housekeeping genes

The 16S rRNA phylogenetic tree demonstrated that HSTU-ASh6 positioned in the same sister taxa (with 45% similarity) with *E. sichuanensis* WCHECL1597 (Figure 3A). According to *gyr*B (Figure 3B) and *rpo*B (Figure 3C) alignment tree, HSTU-ASh6 was located in the same sister taxa with *E. cloacae* A1137 with 62% and 35% similarities, respectively. Moreover, *rec*A (Figure 3D) tree showed that HSTU-ASh6 was located in a different clade with *E. cloacae* A1137 and *E. sichuanensis* WCHECL1597. Moreover, *tonB* (Figure 3E) phylogenetic tree showed that HSTU-ASh6 was placed with *E. cloacae* A1137 and *E. sichuanensis* WCHECL1597 in the different taxa of the same node. In particular, HSTU-ASh6 was placed in the same node and was more close to *E. cloacae* A1137 in the whole genome sequence phylogenetic tree (Figure 3F).

Genome comparison

The pairwise ANI blast (ANIb) value observed between HSTU-ASh6 and *E. cloacae* A1137 was 98.89%. In fact, *E. sichuanensis* SGAir0282, *E. roggenkampii* RHBSTW, *E. asburiae* RHBSTW-01009, and *E. roggenkampii* Ecl 20 981 showed 98.12, 91.12, 91.02, and 91.06% ANIb values, respectively, where other *Enterobacter* species showed ANIb values < 91% (Supplementary Table 1). The DNA–DNA hybridization analysis of HSTU-ASh6 with its nearest homolog *E. cloacae* A1137 showed 92.6% DDH, whereas all other *Enterobacter* strains showed 38.9–45.6% DDH, except *E. sichuanensis* SGAir0282 that showed 85.6% DDH (Table 4).

The locally collinear block (LCB) of HSTU-ASh6 genome did not completely match with the LCBs of genomes included for genomic comparison. Therefore, there was a rearrangement of genomic regions between the two genomes in terms of collinearity. As shown in Figure 4A, HSTU-ASh6 shared the highest homologous region with A1137. It also shared almost similar LCBs as those of A1137 strain with SGAir0282. We performed a pangenomic analysis of HSTU-ASh6 with six nearest homologs to further investigate the genomic variance. In the circular plot, the pink color slot is identified as the pangenome, and the white space indicates a region missing in the specified genome (Figure 4B). The circular plot clearly indicates that several portions of the genome sequence of HSTU-ASh6 were not similar compared with the other six closest strains.

10.3389/fmicb.2022.1060554

TABLE 3 Spectrum, molecular form and chemical structure of chlorpyrifos (1 gm/100 mL) biodegradation observed using GC–MS/MS analysis.

Similarity of hit	Search Spectrum	Soft ionization (SI)	Spectrum	Molecular weight (Da)	Molecular form	Chemical structure
1	77	2921	88	2	Chlorpyrifos	
7	60	2588	3	6	Phorate sulfoxide	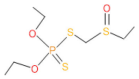
8	59	2588	4	7	Phorate sulfone	
12	56	2598	13	0	Chlorpyrifos-methyl	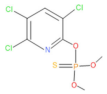
14	55	6515	38	4	2-Hydroxy-3,5,6-trichloropyridine/**3,5,6-Trichloro-2-pyridinol (TCP)**	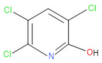
17	54	17297	40	4	Carbofenothion sulfoxide	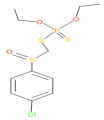
19	53	2497	7	6	Oxydisulfoton	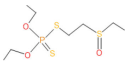
20	53	16947	69	6	Carbonochloridic acid, 2,4,5-trichlorophenyl ester	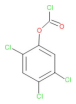
21	52	4891	54	7	Thionodemeton sulfone	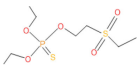
22	52	2021	58	1	3-(2-Thienyl)-dl-alanine	
23	51	5598	15	2	Phosphoric acid, diethyl 3,5,6-trichloro-2-pyridyl ester/**Chlorpyrifos oxon**	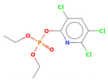
24	51	683	8	9	Diethyl methanephosphonate	

Plant growth-promoting and stress-tolerating genes

The genome of *Enterobacter* sp. HSTU-ASh6 harbors various types of PGP genes, namely those encoding nitrogen fixation (*isc*U, *nif* J, *isc*A, *isc*R, *isc*S, *isc*X, *suf* ABCDES, and *fdx*), nitrosative stress (*ntr*B, *nor*R, *nor*V, *nsr*R, and *gln*K), nitrogen metabolism regulation (*gln*D, *gln*B, and *pts*N), ammonia assimilation (*glt*B), ACC deaminase (*dcy*D and *rim*M), siderophore enterobactin (*fes*, *ent*FSD, *fhu*ABCD, and *tonB*), IAA production (*trp*CFBDS and *ipd*C), phosphate metabolism (*pit*A, *pst*ABCS, *phoU*, *ugpABE*, *pho*ABERHQ, and *pnt*AB), biofilm formation (*tom*B, *luxS*, *efp*, *flg*ABCDGHIJKLMN, *mot*AB, and *hfq*), sulfur assimilation (*cys*ACHIJKMNTWZ), sulfur metabolism (*fdx*H and *cys*ACDEHIJKMNQSWZ), root colonization (*che*ZYBRWA, *malE*, *rbsB*, *fli*ZDSTFZGHIJKMPQR, *hof* C, *pga*ABCD, *mot*AB, and *mur*J), superoxide dismutase

(*sod*ABC), and trehalose metabolism (*treBCR*, *ots*AB, and *lamb*) (Table 5). Furthermore, numerous types of genes associated with stress tolerance e.g., heat shock (*smp*B, *ibp*AB, *hsp*Q, *dna*JK, *rpo*H, *lep*A, and *grp*E), cold shock (*csp*ADE), and drought resistance (*nha*A, *cha*AB, *pro*ABQVWXPS, *bet*ABT, *trk*AH, and *kdp*ABCF) were detected in the HSTU-ASh6 genome (Table 5). These genes are essential for the plant to survive and grow in a harsh environment.

Pesticide-degrading protein model validation and evaluation

A significant number of genes whose products were responsible for pesticide degradation (*amp*D, *glp*ABQ, *pde*HR, *pep*ABDQ, *phn*FDGHJKLMOP, *paaC*, *hpx*KW, amidohydrolase, and alpha/beta fold hydrolase) were identified in the genome of HSTU-ASh6 (Supplementary Table 2).

For model validation, 39 modeled proteins were analyzed using the SAVESv6.0-structure validation server, among which 28 were validated according to VERIFY (3D-1D score), with their score recorded as 80.05–97.97%. Among these, alpha/beta fold hydrolase family protein (GM298_09990) had the maximum ERRAT quality score of 97.35 (Table 6). The individual protein average TM score, RMSD, IDEN, and Cov were 0.95, 0.75, 0.51, and 0.97, respectively, based on the I-TASSER result (Table 6). Moreover, the Ramachandran plot regions, including the most favored regions (A, B, L), additional allowed regions (a, b, l, p), generously allowed regions (~, ~b, ~l, ~p), and disallowed regions of the model proteins, are presented in Table 6. Consequently, the 28 validated model proteins were selected for virtual screening with 105 small molecules.

A total of 105 different pesticides, including weed killers and organophosphorus nerve agents, were screened with the 28 validated model proteins of *Enterobacter* sp. HSTU-ASh6 (Figure 5). The score ranged from −8.8 to −3.1 (kcal/mol). The highest negative score was recorded for cypermethrin with phnL (−8.8 kcal/mol), and the lowest negative score was found for demephion-O with amidohydrolase (GM298_10355) (−3.1 kcal/mol). The box plot analysis revealed that each box with the bold line represents median values, and the square sign indicates mean values. Moreover, the upper and lower lines in the box plots represent minimum and maximum values, respectively. Interestingly, most values were found between the 25th and 75th percentile. The 25th and 75th percentile quartile differences indicated the interquartile range. Surprisingly, in this dataset, some outlier data were observed, indicating the presence of some small molecules possessing an excellent binding affinity with respective proteins. It was also observed that the nine proteins' outlier binding affinities values were outside of IQR1.5.

Catalytic interactions of model proteins with selective pesticides

As shown in Figure 6, the alpha/beta fold hydrolase (GM298_18675) of *Enterobacter* sp. HSTU-ASh6 anchored with crotoxyphos and formed a potential catalytic triad in the binding pocket region with residues Ser153-His277-Asp152. Ser153 and Gly81 specifically mediated the attractive charge connection with the +P-atom of crotoxyphos and the typical H-bond contact with the O atom (Figure 6A). Besides other interactions, Val201 and Phe14 directly interacted with the phosphodiester bond of crotoxyphos via π-sigma and π-π stacked interaction. The interaction distances among the residues of the catalytic site were recorded within < 3 Å, except for Asp152, which was 5.36 Å.

Surprisingly, the residues Ser195, His400, and Glu194 constituted a putative catalytic triad in the binding pocket region of the *Enterobacter* sp. HSTU-ASh6 carboxylesterase. Ser195 and Arg199 interacted with the O atom to form the traditional H-bond, and Glu194 interacted with the +P atom to form phosphodiester bonds and the H atom to interact with the carbon-hydrogen bond of coumaphos (Figure 6B). Moreover, the π-π stacked bond was formed by the His400 residue of carboxylesterase with coumaphos ligand, and it directly interacted with the phosphodiester bond of ligand. The interaction distances among the residues of the catalytic site were recorded within <4 Å.

The alpha/beta fold hydrolase (GM298_08590) formed a potential catalytic triad Ser157-His279-Asp156 in the binding pocket region with cypermethrin (Figure 6C). The interaction distances among the catalytic site residues were recorded within <5.25 Å. Furthermore, the alpha/beta fold hydrolase (GM298_00815) protein–diazinon docked complex demonstrated interaction with multiple residues (Figure 6D). In particular, conventional H-bonds were made by Ser99, His231 with the O atom of the diazinon compound. In addition, the amidohydrolase family protein (GM298_20245) anchored with chlorpyrifos and showed a significant interaction (Figure 6E). For instance, Arg408 interacted with the O atom of chlorpyrifos by a conventional hydrogen bond. Moreover, alkyl and pi-alkyl bonds were made by Val547, Arg408, Ala550, Lys549, His250, His467, and Tyr545 with chlorpyrifos, respectively. Interestingly, all of them were observed with two bonds, except His467 and Tyr545. Only one amino acid made the attractive charge and was interconnected with +P-atom. His250 made pi-sulfur and pi-alkyl bond at a time.

Molecular dynamics simulation

The RMSD plot of the α/β hydrolase (GM298_18675)–crotoxyphos complex was sharply increased from 0 to 4 ns (Figure 7Aa), and it continued up to 30 ns with an

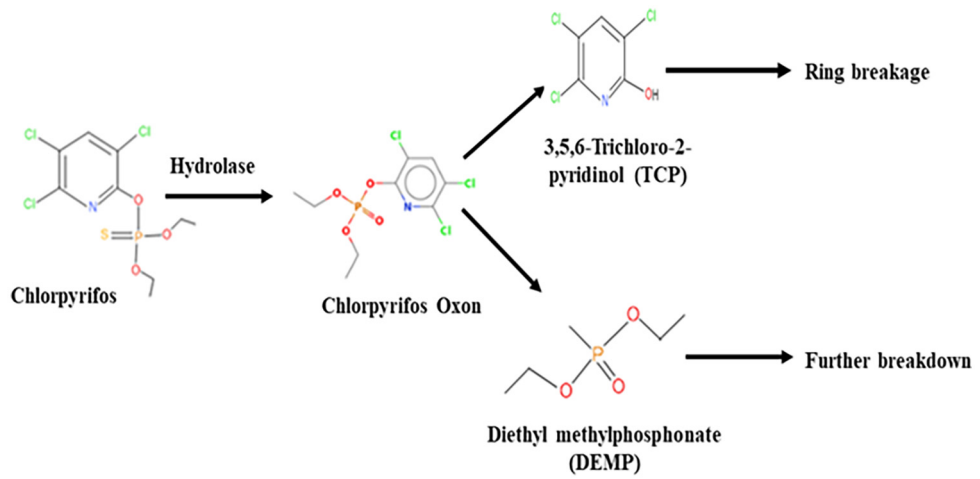

FIGURE 1
A proposed pathway of chlorpyrifos metabolism by the strain *Enterobacter* sp. HSTU-ASh6.

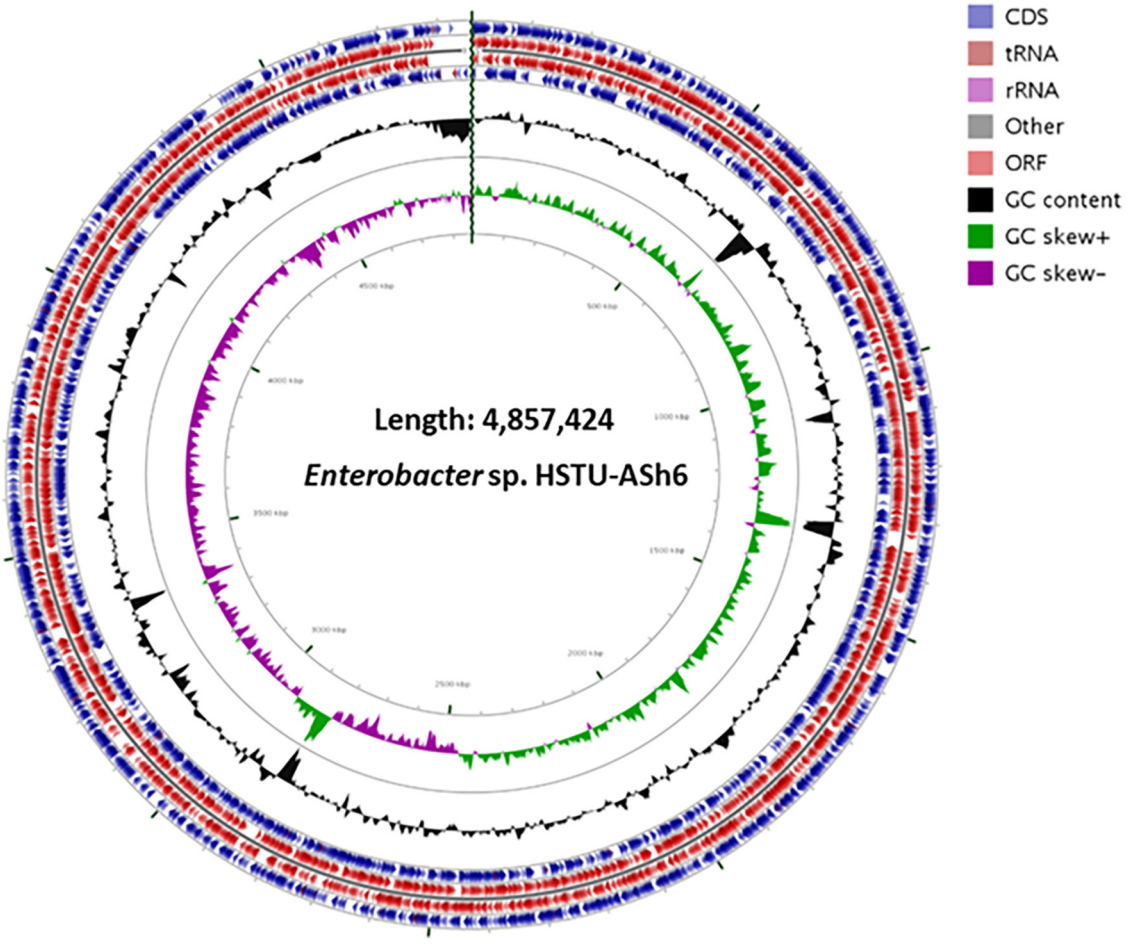

FIGURE 2
CDS map of the annotated genome of *Enterobacter* sp. HSTU-ASh6.

RMSD ranging from 2.6 to 3.45 Å. After a slight decrease in the RMSD of the protein, at 35 ns, an increasing parallel trend continued up to 100 ns, with an RMSD ranging from 2.5 to 3.35 Å, except a slight decrease at 83–86 ns of the ligand. In the RMSF plot of the alpha/beta hydrolase (GM298_18675)–crotoxyphos complex (Figure 7Ab), the favorable residues of alpha/beta hydrolase (GM298_18675) with crotoxyphos were observed at Leu10 (0.93 Å), Phe14 (1.161 Å), Lys19 (2.806 Å), Ser21 (3.243 Å), Ser22 (3.639 Å), Arg30 (0.798 Å), Gly33 (0.714 Å), Thr34 (0.636 Å), Ser37 (0.842 Å), Leu40 (0.975 Å), Gly81 (0.43 Å), Cys82 (0.416 Å), Ser85 (0.449 Å), Asp152 (0.378 Å), Tyr181 (0.425 Å), Val201 (0.70 Å), Ile202 (0.659 Å), Thr206 (0.644 Å), Leu207 (0.51 Å), Ile276 (0.542 Å), His277 (0.493 Å), Gly278 (0.456 Å), Gln281 (0.452 Å), Leu282 (0.539 Å), and Ile285 (1.005 Å). The Rg of the α/β hydrolase (GM298_18675)–crotoxyphos complex fluctuated throughout the simulation, with an average value of 3.960 Å. The MolSA, solvent-accessible surface area (SASA), and PSA of the alpha/beta hydrolase (GM298_18675)–crotoxyphos complex insignificantly varied throughout the simulation period. The average MolSA, SASA, and PSA were 310.304, 56.5454, and 81.3709 Å^2, respectively (Figure 7Ac).

The RMSD plot (Figure 7Ba) of the carboxylesterase–coumaphos complex was sharply increased from 0 to 3 ns, and it continued up to 23 ns, with an RMSD ranging from 2.3 to 3.45 Å. After a slight decrease in the RMSD of the protein, at 35 ns, a parallel increasing trend continued up to

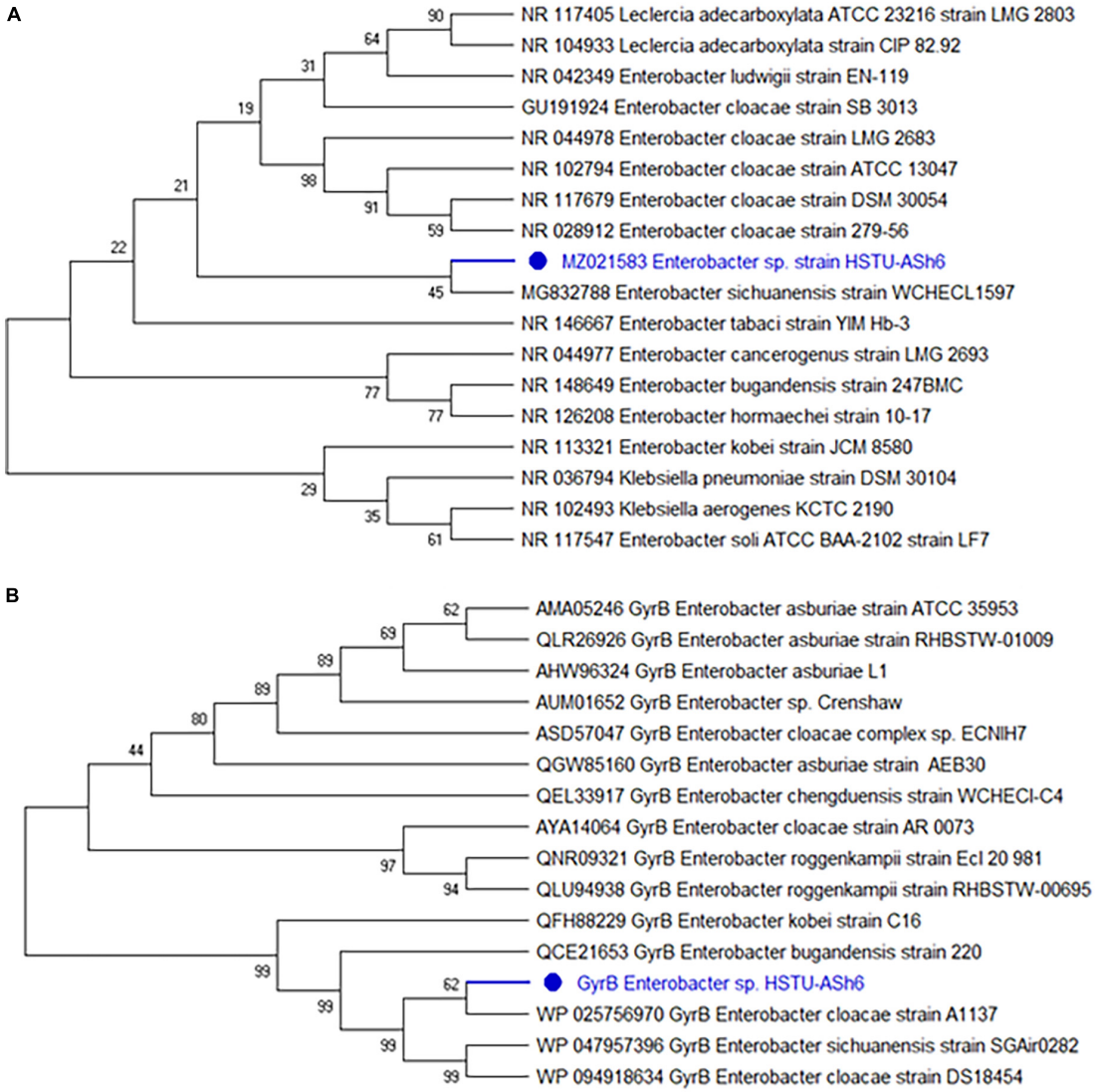

FIGURE 3
(Continued)

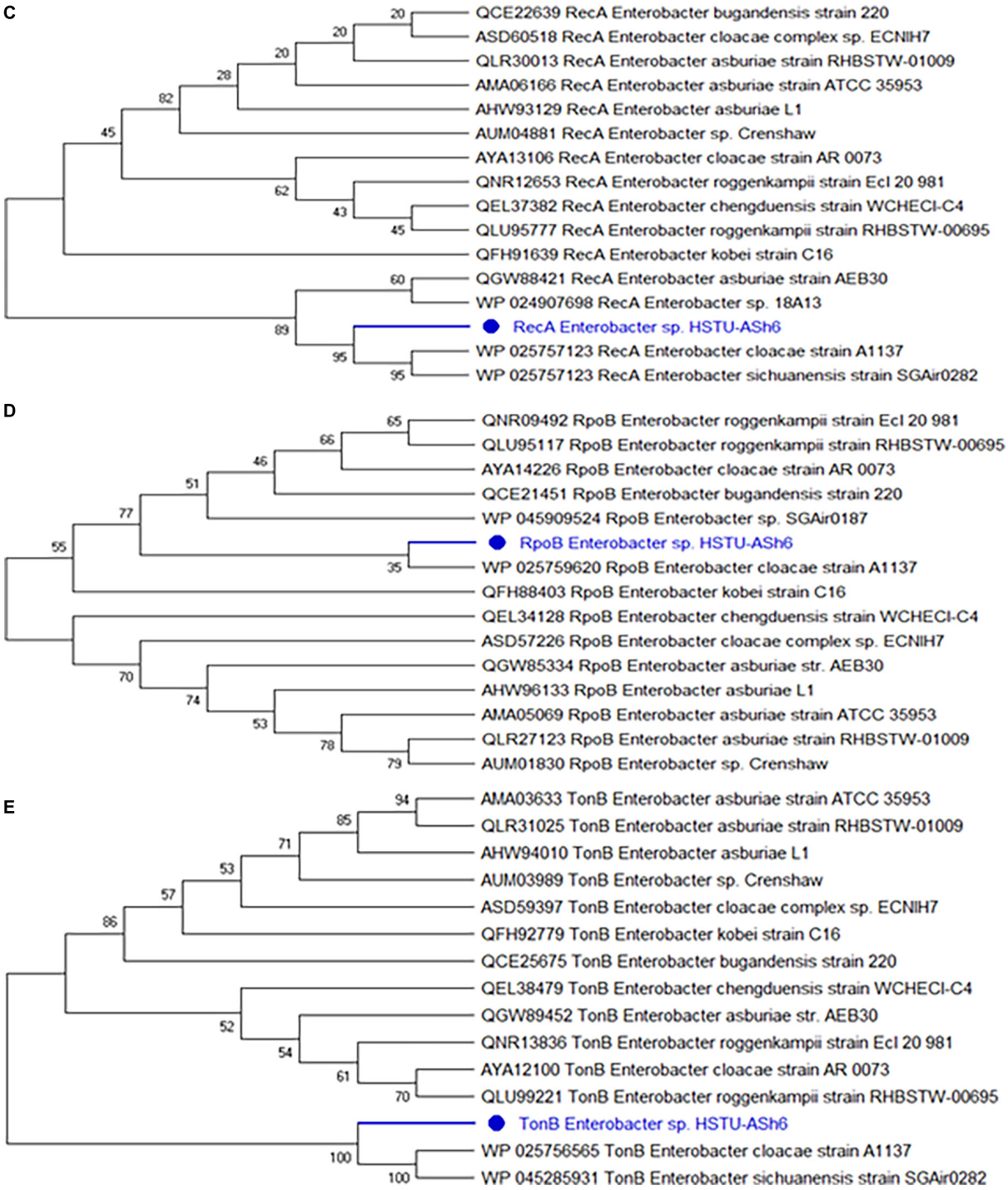

FIGURE 3
(Continued)

100 ns, with an RMSD ranging from 2.5 to 3.80 Å, except a slight decrease at 83–86 ns of the ligand. In the RMSF plot of the carboxylesterase–coumaphos complex (Figure 7Bb), the favorable residues of carboxylesterase with coumaphos were observed at Glu69 (1.491 Å), Thr73 (1.723 Å), Gly75 (1.948 Å), Gly76 (1.807 Å), Trp106 (0.456 Å), His108 (0.787 Å), Ile114 (0.918 Å), Leu119 (0.923 Å), Pro121 (0.736 Å), Tyr122 (0.66 Å), Phe192 (0.437 Å), Ser195 (0.64 Å), Ala196 (0.829 Å), Arg199 (0.71 Å), Ser221 (0.717 Å), Thr224 (2.112 Å), Leu225 (1.79 Å), Glu308 (0.59 Å), Val311 (0.716 Å), Met312 (0.884 Å), Val314

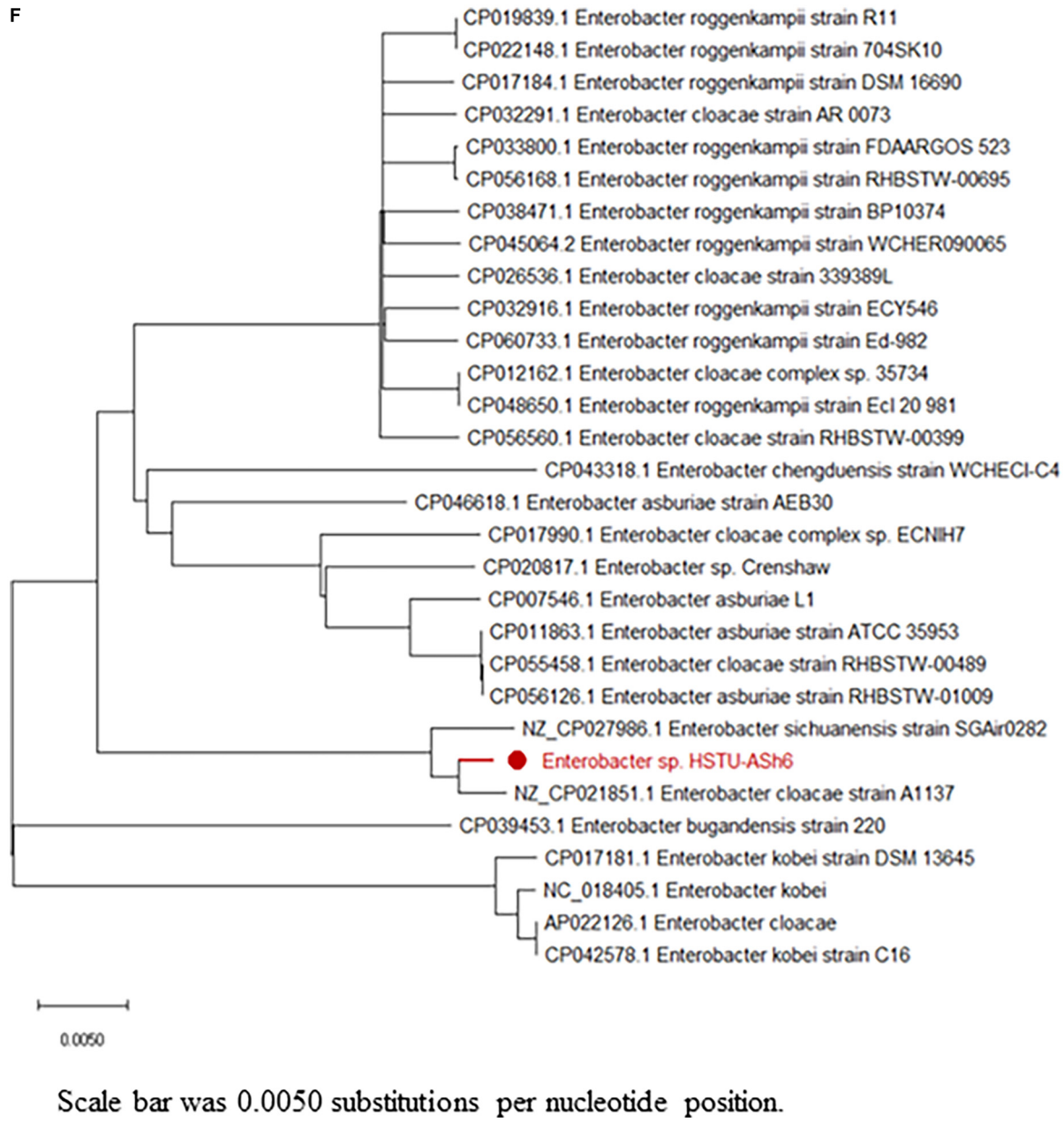

FIGURE 3
Phylogenetic tree constructed using the housekeeping genes of HSTU-ASh6. **(A)** 16S rRNA, **(B)** gyrase B, **(C)** RecA, **(D)** rpoB, **(E)** tonB, and **(F)** whole genome phylogenetic tree of *Enterobacter* sp. HSTU-ASh6.

(1.919 Å), Phe315 (1.881 Å), Ile317 (1.698 Å), Ala359 (0.803 Å), Phe360 (0.643 Å), His391 (1.243 Å), Trp399 (0.976 Å), His400 (0.734 Å), and Val404 (0.761 Å). The Rg of the carboxylesterase–coumaphos complex fluctuated throughout the simulation, with an average value of 4.147 Å. The MolSA, SASA, and PSA of the carboxylesterase–coumaphos complex insignificantly varied throughout the simulation period. The average MolSA, SASA, and PSA were 317.102, 38.885, and 82.488 $Å^2$, respectively (Figure 7Bc).

The RMSD plot of the α/β hydrolase (GM298_08590)–cypermethrin complex was sharply increased from 0 to 3 ns (Figure 7Ca), and it continued up to 100 ns with the exception of a few irregularities. The overall RMSD difference ranged from 3.5 to 4.01 Å. In the RMSF plot of the alpha/beta hydrolase (GM298_08590)–cypermethrin complex (Figure 7Cb), the favorable residues of alpha/beta hydrolase (GM298_08590) with cypermethrin were observed at Ala17 (3.112 Å), Pro18 (2.65 Å), Leu26 (0.956 Å), Ala29 (1.522 Å), Thr30 (1.435 Å), Leu34

10.3389/fmicb.2022.1060554

TABLE 4 Digital DNA–DNA hybridization (dDDH) for species determination of *Enterobacter* sp. HSTU-ASh6 depends on whole genome sequences.

Subject strain	dDDH (d0, in %)	C.I. (d0, in%	DDH (d4, in%)	C.I. (d4, in%)	dDDH (d6, in %)	C.I. (d6, in%)	G + C content difference (in %)
Enterobacter sichuanensis WCHECL1597	85.8	[82.1–88.8]	85.8	[83.2–88.1]	88.7	[85.8–91.0]	0.12
Enterobacter roggenkampii DSM16690	74.1	[70.1–77.7]	45.4	[42.9–48.0]	69.1	[65.7–72.3]	0.92
Enterobacter asburiae ATCC 35953	67.8	[63.9–71.5]	45.1	[42.5–47.7]	63.9	[60.6–67.1	0.34
Enterobacter quasiroggenkampii WCHECL1060 T	75.5	[71.5–79.1]	44.6	[42.1–47.2]	69.9	[66.4–73.1	0.56
Enterobacter vonholyi E13T	76.3	[72.3–79.9]	44.1	[41.6–46.7]	70.3	[66.9–73.6]	0.45
Enterobacter dykesii E1T	75.5	[71.5–79.0]	44.0	[41.5–46.6]	69.6	[66.2–72.9]	0.72
Enterobacter chengduensis WCHECl-C4	67.2	[63.3–70.8]	42.5	[40.0–45.1]	62.4	[59.1–65.6]	0.61
Enterobacter bugandensis EB-247	75.7	[71.7–79.3]	39.8	[37.4–42.2]	68.0	[64.5–71.2]	0.87
Enterobacter chuandaensis 090028T	73.6	[69.6–77.2]	39.7	[37.2–42.2]	66.2	[62.8–69.5]	0.56
Enterobacter kobei DSM 13645	65.5	[61.7–69.2]	39.2	[36.7–41.7]	59.8	[56.5–62.9	0.22
Enterobacter quasimori 090044	71.0	[67.1–74.7]	36.4	[34.0–38.9]	62.6	[59.3–65.8]	0.64
Enterobacter ludwigii DSM 16688	70.1	[66.2–73.8]	36.6	[32.2–37.2]	61.0	[57.8–64.2]	0.53
Enterobacter cancerogenus ATCC33241	56.6	[53.0–60.1]	31.2	[28.8–33.7]	49.5	[46.4–52.5	0.56
Leclercia adecarboxylata NBRC102595	44.0	[40.7–47.5	25.8	[23.5–28.3]	38.2	[35.2–41.2	0.44
Enterobacter kobei ATCC BAA-260	33.2	[29.8–36.7]	22.5	[20.2–25.0]	29.4	[26.5–32.5]	0.33

The strain comparison was done in type strain genome server (TYGS).

(1.069 Å), Leu37 (1.135 Å), His83 (0.858 Å), Gly85 (1.275 Å), Gly86 (1.409 Å), Trp87 (1.15 Å), Cys88 (1.027 Å), Leu89 (0.969 Å), Asp156 (0.639 Å), Ser157 (0.688 Å), Ala158 (0.771 Å), Gly159 (0.63 Å), Tyr185 (0.628 Å), Ala187 (0.845 Å), Phe205 (0.93 Å), Leu206 (1.228 Å), Asp209 (0.995 Å), Ala210 (0.974 Å), Met211 (0.878 Å), Phe213 (0.867 Å), Cys214 (0.883 Å), Thr215 (0.929 Å), Leu251 (0.61 Å), His279 (0.561 Å), Ala280 (0.652 Å), and His283 (0.856 Å). The Rg of the alpha/beta hydrolase (GM298_08590)–cypermethrin complex fluctuated throughout the simulation, with an average value of 4.512 Å. The MolSA, SASA, and PSA of the alpha/beta hydrolase (GM298_08590)–cypermethrin complex insignificantly varied throughout the simulation period. The average MolSA, SASA, and PSA were 378.775, 26.194, and 93.0372 $Å^2$, respectively (Figure 7Cc).

The RMSD plot of the α/β hydrolase (GM298_00815)–diazinon complex was sharply increased from 0 to 17 ns (Figure 7Da), and it continued up to 75 ns. Next, a slight parallel downward trend appeared from 75 to 100 ns. The overall RMSD difference ranged from 1.2 to 1.7 Å. In the RMSF plot of the alpha/beta fold hydrolase (GM298_00815)–diazinon complex (Figure 7Db), the favorable residues of alpha/beta fold hydrolase (GM298_00815) with diazinon were observed at Gly30 (0.689 Å), Leu31 (0.553 Å), Gly32 (0.767 Å), Cys33 (0.934 Å), Ala34 (0.947 Å), Ala35 (1.37 Å), Ser99 (0.656 Å), Met100 (0.76 Å), Ser103 (0.906 Å), Glu123 (0.66 Å), Pro124 (0.801 Å), Asn125 (1.033 Å), His127 (1.774 Å), Met132 (1.439 Å), Phe 133 (1.301 Å), Ser136 (1.316 Å), Ile137 (0.994 Å), Phe145 (1.217 Å), Gln148 (1.277 Å), Gly149 (1.105 Å), Asp151 (1.429 Å), Met153 (1.143 Å), Val181 (0.822Å), Val184 (0.792 Å), Ser207 (1.098 Å), Leu208 (1.684 Å), and His231 (1.028 Å). The Rg of the alpha/beta fold hydrolase (GM298_00815)–diazinon complex fluctuated throughout the simulation, with an average value of 3.29 Å. The MolSA, SASA, and PSA of the alpha/beta fold hydrolase (GM298_00815)–diazinon complex insignificantly varied throughout the simulation period. The average MolSA, SASA, and PSA were 304.144, 88.6872, and 33.733 $Å^2$, respectively (Figure 7Dc).

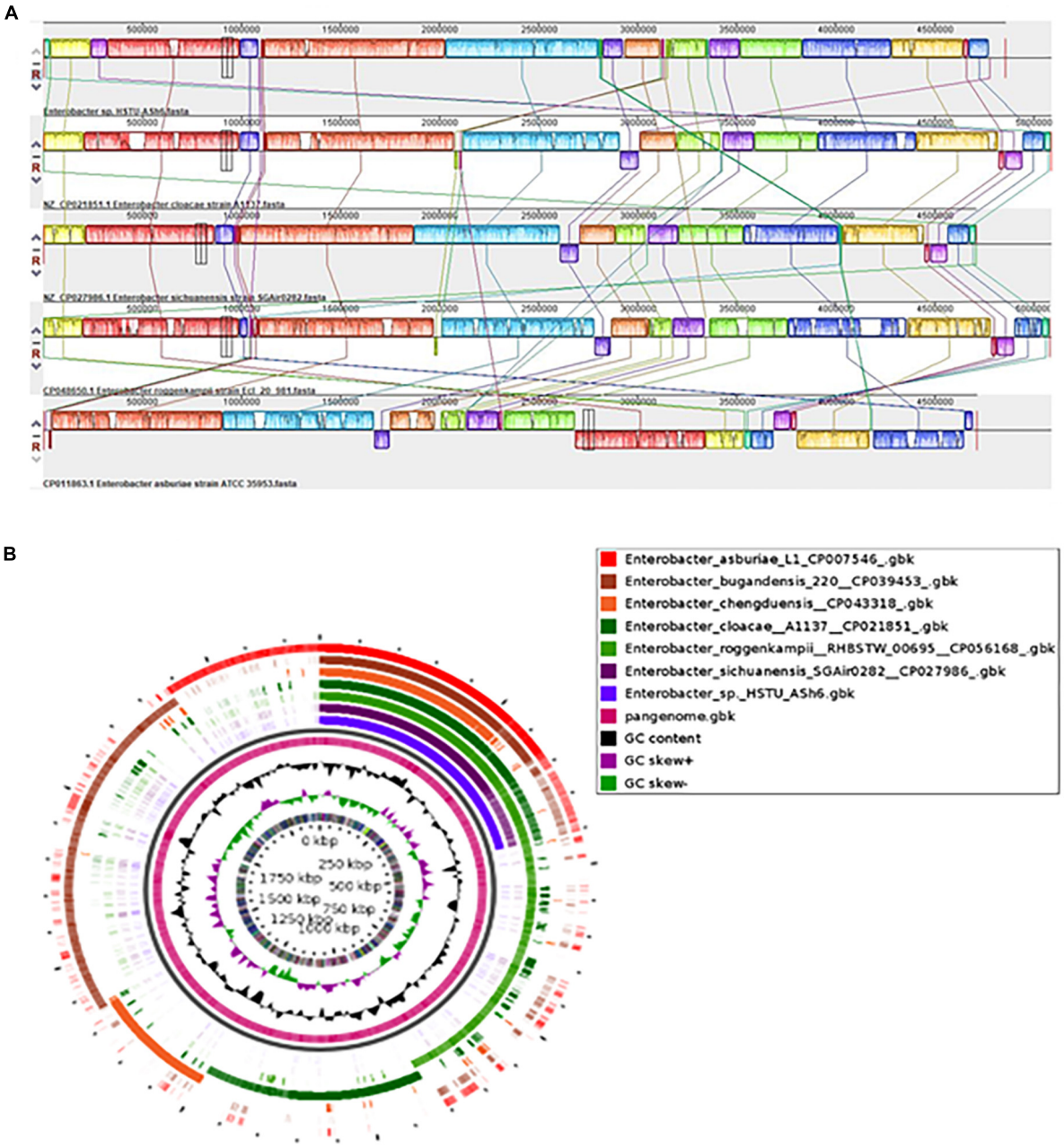

FIGURE 4
(A) Synteny analysis of *Enterobacter* sp. HSTU-ASh6 strain with other close related strains. **(B)** Pangenomic comparison map of *Enterobacter* sp. HSTU-ASh6 with nearest homologs. Multiple genome sequence analysis of *Enterobacter* sp. HSTU-ASh6 with other closely related strains. The same color module represents the homologs region. Good homology of *Enterobacter* sp. HSTU-ASh6 and other *E. cloacae* strains is shown.

The RMSD plot of the amidohydrolase (GM298_20245)–chlorpyrifos complex (Figure 7Ea) showed an increasing trend for the ligand protein from 0 to 14 ns. After 17 ns, an increasing parallel trend continued up to 44 ns, with an RMSD ranging from 2.5 to 3.5 Å. Next, a steady and stable RMSD remained up to 80 ns. Then, the RMSD difference was below ~1.2 Å up to 93 ns, which indicated the stable protein–ligand complex. In the RMSF plot of the amidohydrolase–chlorpyrifos complex (Figure 7Eb), the favorable residues of amidohydrolase with chlorpyrifos were observed at His81 (0.826 Å), Ser84 (0.99 Å), His109 (0.872 Å), Glu110 (0.888 Å), Glu174 (0.906 Å), Met176 (1.848 Å), Arg207 (1.4 Å), Asp276 (1.373 Å), Asp277 (1.118 Å), Ala407 (1.276 Å), Arg408 (1.631 Å), Tyr465 (0.683 Å), Ser466 (1.006 Å), His467 (1.215 Å), Asp468 (0.95 Å), Lys549 (1.393 Å), Ala550 (1.131 Å), Glu552

10.3389/fmicb.2022.1060554

TABLE 5 Genes involved in plant growth promoting, stress tolerating, and pesticide degrading activity.

PGP activities description	Gene name	Locus tag	CDS	Product	E.C. number
Nitrogen fixation	*isc*U	GM298_14895	87842.88228	Fe–S cluster assembly scaffold *IscU*	–
	nif J	GM298_00740	154364.157888	Pyruvate: ferredoxin (flavodoxin) oxidoreductase	–
	*isc*A	GM298_14890	87505.87828	Iron–sulfur cluster assembly protein IscA	–
	*isc*R	GM298_14905	89587.90078	Fe–S cluster assembly transcriptional regulator IscR	–
	*isc*S	GM298_14900	88253.89467	IscS subfamily cysteine desulfurase	2.8.1.7
	suf A	GM298_13615	3786.4154	Fe–S cluster assembly scaffold SufA	–
	suf B	GM298_13620	4163.5653	Fe–S cluster assembly protein SufB	–
	suf C	GM298_13625	5663.6409	Fe–S cluster assembly ATPase SufC	–
	suf D	GM298_13630	6384.7655	Fe–S cluster assembly protein SufD	–
	suf S	GM298_13635	7652.8872	Cysteine desulfurase SufS	2.8.1.7
	suf E	GM298_13640	8887.9303	Cysteine desulfuration protein SufE	–
	fdx	GM298_14875	84707.85042	ISC system 2Fe–2S type ferredoxin	–
	*isc*X	GM298_14870	84505.84705	Fe–S cluster assembly protein IscX	–
	*hsc*A	GM298_14880	85044.86894	Fe–S protein assembly chaperone HscA	–
	*hsc*B	GM298_14885	GM298_14885	Co-chaperone HscB	–
Nitrosative stress	*ntr*B	GM298_17410	55851.56729	Nitrate ABC transporter permease	–
	*nor*R	GM298_06640	225394.226908	Nitric oxide reductase transcriptional regulator *NorR*	–
	*nor*V	GM298_06635	223761.225206	Anaerobic nitric oxide reductase flavorubredoxin	–
	*nsr*R	GM298_16725	41824.42249	Nitric oxide-sensing transcriptional repressor NsrR	–
	*gln*K	GM298_11020	192488.192826	P-II family nitrogen regulator	–
Nitrogen metabolism regulatory protein	*gln*D	GM298_21660	33792.36467	Bifunctional uridylyltransferase GlnD	2.7.7.59
	*gln*B	GM298_14955	99618.99956	Nitrogen regulatory protein P-II	–
	*pts*N	GM298_07545	78409.78900	PTS IIA-like nitrogen regulatory protein PtsN	–
Ammonia assimilation	*glt*B	GM298_07465	54616.59076	Glutamate synthase large subunit	1.4.1.13
ACC deaminase	*dcy*D	GM298_02800	122850.123836	D-cysteine desulfhydrase	4.4.1.15
	*rim*M	GM298_07110	315522.316061	Ribosome maturation factor *RimM*	–
Siderophore					
Siderophore enterobactin	*fes*	GM298_16460	106085.107284	Enterochelin esterase	3.1.1.-
	*ent*F	GM298_16470	107504.111361	Enterobactin non-ribosomal peptide synthetase *EntF*	6.3.2.14
	*ent*S	GM298_16490	114337.115584	Enterobactin transporter EntS	–
	*ent*D	GM298_16450	102997.103638	Enterobactin synthase subunit *EntD*	6.3.2.14
	*fhu*A	GM298_08850	13884.16133	FerrichromeporinFhuA	–
	*fhu*B	GM298_08835	10167.12149	Fe (3+)-hydroxamate ABC transporter permease *FhuB*	–
	*fhu*C	GM298_08845	13036.13833	Fe3+ -hydroxamate ABC transporter ATP-binding protein *FhuC*	–
	*fhu*D	GM298_08840	12146.13036	Fe(3 +)-hydroxamate ABC transporter substrate-binding protein *FhuD*	-
	*ton*B	GM298_00165	26191.26913	TonB system transport protein *TonB*	–
	*fep*B	GM298_20350	112.1071	Fe2 + -enterobactin ABC transporter substrate-binding protein	–
	*fep*G	GM298_16480	112235.113224	Iron-enterobactin ABC transporter permease	–
	*exb*B	GM298_08520	272764.273495	Tol-pal system-associated acyl-CoA thioesterase	–
Plant hormones					
IAA production	*trp*CF	GM298_00215	33816.35174	Bifunctional indole-3-glycerol-phosphate synthase TrpC/phosphoribosylanthranilate isomerase TrpF	4.1.1.48/5.3.1.24
	*trp*S	GM298_19565	34038.35042	Tryptophan–tRNA ligase	6.1.1.2
	*trp*B	GM298_00210	32612.33805	Tryptophan synthase subunit beta	4.2.1.20

(Continued)

TABLE 5 (Continued)

PGP activities description	Gene name	Locus tag	CDS	Product	E.C. number
	*trp*D	GM298_00220	35178.36773	Bifunctional anthranilate synthase glutamate amidotransferase component TrpG/anthranilate phosphoribosyltransferaseTrpD	2.4.2.18/4.1.3.27
	*ipd*C	GM298_13340	183015.184673	Indolepyruvate decarboxylase	4.1.1.74
Phosphate metabolism	*pit*A	GM298_20710	16363.17862	Inorganic phosphate transporter PitA	–
	*pst*S	GM298_11455	21647.22687	Phosphate ABC transporter substrate-binding protein PstS	–
	*pst*C	GM298_11460	22816.23775	Phosphate ABC transporter permease PstC	–
	*pst*A	GM298_11465	23775.24665	Phosphate ABC transporter permease PstA	–
	*pst*B	GM298_11470	24713.25486	Phosphate ABC transporter ATP-binding protein PstB	–
	*pho*U	GM298_11475	25513.26238	Phosphate signaling complex protein PhoU	3.5.2.6
	*ugp*A	GM298_18020	82211.83098	sn-glycerol-3-phosphate ABC transporter permease UgpA	–
	*ugp*B	GM298_18025	83268.84584	sn-glycerol-3-phosphate ABC transporter substrate-binding protein UgpB	–
	*ugp*E	GM298_18015	81369.82214	sn-glycerol-3-phosphate ABC transporter permeaseugpE	–
	*pho*A	GM298_10665	117286.118701	Alkaline phosphatase	–
	*pho*E	GM298_10440	67233.68285	PhosphoporinPhoE	–
	*pho*B	GM298_10730	130482.131171	Phosphate response regulator transcription factor PhoB	–
	*pho*R	GM298_10735	131193.132488	Phosphate regulon sensor histidine kinase PhoR	2.7.13.3
	*pho*H	GM298_15155	2924.3988	Phosphate starvation-inducible protein PhoH	–
	*pnt*A	GM298_14045	87292.88821	Re/Si-specific NAD(P)(+) transhydrogenase subunit alpha	1.6.1.2
	*pnt*B	GM298_14050	88832.90220	Re/Si-specific NAD(P)(+) transhydrogenase subunit beta	–
	*pho*Q	GM298_15690	106230.107693	Two-component system sensor histidine kina se PhoQ	2.7.13.3
Biofilm formation	*tom*B	GM298_11140	213029.213403	Hha toxicity modulator TomB	–
	*lux*S	GM298_06765	245170.245685	*S*-ribosylhomocysteinelyase	4.4.1.21
	efp	GM298_16560	11964.12530	Elongation factor P	–
	*flg*A	GM298_02415	43673.44368	Flagellar basal body P-ring formation protein FlgA	–
	*flg*B	GM298_02420	44617.45027	Flagellar basal body rod protein FlgB	–
	*flg*C	GM298_02425	45034.45438	Flagellar basal body rod protein FlgC	–
	*flg*D	GM298_15380	39257.39967	Flagellar hook assembly protein FlgD	–
	*flg*G	GM298_15395	42032.42814	Flagellar basal-body rod protein FlgG	–
	*flg*H	GM298_15400	42872.43570	Flagellar basal body L-ring protein FlgH	–
	*flg*I	GM298_15405	43583.44680	Flagellar basal body P-ring protein FlgI	–
	*flg*J	GM298_15410	44680.45633	Flagellar assembly peptidoglycan hydrolase FlgJ	3.2.1.-
	*flg*K	GM298_15415	45709.47349	Flagellar hook-associated protein FlgK	–
	*flg*L	GM298_15420	47364.48317	Flagellar hook-filament junction protein FlgL	–
	*flg*N	GM298_15355	36787.37212	Flagella biosynthesis chaperone FlgN	–
	*flg*M	GM298_15360	37217.37510	Anti-sigma-28 factor FlgM	–
	*mot*A	GM298_02495	58314.59210	Flagellar motor stator protein MotA	–
	*mot*B	GM298_02500	59207.60112	Flagellar motor protein MotB	–
	hfq	GM298_16695	35967.36278	RNA chaperone Hfq	–
Sulfur assimilation	*cys*Z	GM298_13450	201004.201765	Sulfate transporter CysZ	–
	*cys*K	GM298_13455	201929.202900	Cysteine synthase A	2.5.1.47
	*cys*M	GM298_13480	206684.207595	Cysteine synthase CysM	2.5.1.47

(Continued)

TABLE 5 (Continued)

PGP activities description	Gene name	Locus tag	CDS	Product	E.C. number
	*cys*A	GM298_13485	207714.208808	Sulfate/thiosulfate ABC transporter ATP-binding protein CysA	–
	*cys*W	GM298_13490	208798.209673	Sulfate/thiosulfate ABC transporter permease CysW	–
	*cys*C	GM298_06350	167077.167682	Adenylyl-sulfate kinase	2.7.1.25
	*cys*N	GM298_06345	165653.167077	Sulfate adenylyltransferase subunit CysN	2.7.7.4
	*cys*D	GM298_06340	164735.165643	Sulfate adenylyltransferase subunit CysD	2.7.7.4
	*cys*H	GM298_06325	161245.161979	Phosphoadenosinephosphosulfate reductase	1.8.4.8
	*cys*I	GM298_06320	159433.161145	Assimilatory sulfite reductase (NADP) hemoprotein subunit	1.8.1.2
	*cys*J	GM298_06315	157628.159433	NADPH-dependent assimilatory sulfite reductase flavoprotein subunit	1.8.1.2
	*cys*T	GM298_13495	209673.210506	Sulfate/thiosulfate ABC transporter permease CysT	–
Sulfur metabolism	*cys*C	GM298_06350	167077.167682	Adenylyl-sulfate kinase	2.7.1.25
	*cys*N	GM298_06345	165653.167077	Sulfate adenylyltransferase subunit CysN	2.7.7.4
	*cys*D	GM298_06340	164735.165643	Sulfate adenylyltransferase subunit CysD	2.7.7.4
	*cys*H	GM298_06325	161245.161979	Phosphoadenosinephosphosulfate reductase	1.8.4.8
	*cys*I	GM298_06320	159433.161145	Assimilatory sulfite reductase (NADPH) hemoprotein subunit	1.8.1.2
	*cys*J	GM298_06315	157628.159433	NADPH-dependent assimilatory sulfite reductase flavoprotein subunit	1.8.1.2
	*cys*E	GM298_12115	152433.153254	Serine *O*-acetyltransferase	2.3.1.30
	*cys*Q	GM298_16885	72750.73490	3′(2′),5′′-bisphosphate nucleotidase CysQ	3.1.3.7
	*cys*K	GM298_13455	201929.202900	Cysteine synthase A	2.5.1.47
	*cys*S	GM298_11355	260870.262255	Cysteine–tRNA ligase	6.1.1.16
	*cys*Z	GM298_13450	201004.201765	Sulfate transporter CysZ	–
	*cys*M	GM298_13480	206684.207595	Cysteine synthase CysM	2.5.1.47
	*cys*A	GM298_13485	207714.208808	Sulfate/thiosulfate ABC transporter ATP-binding protein CysA	–
	*cys*W	GM298_13490	208798.209673	Sulfate/thiosulfate ABC transporter permease *CysW*	–
	*fdx*H	GM298_01155	243317.244198	Formate dehydrogenase subunit beta	–
Antimicrobial peptide	*pag*P	GM298_20535	36991.37608	Lipid IV(A) palmitoyltransferase PagP	2.3.1.251
	*sap*B	GM298_00400	75872.76837	Peptide ABC transporter permease *SapB*	–
Root colonization					
Chemotaxis	*che*Z	GM298_02265	17971.18609	Protein phosphatase CheZ	3.6.1.-
	*che*Y	GM298_02270	18615.19001	Chemotaxis protein CheY	-
	*che*B	GM298_02275	18991.20070	Chemotaxis-specific protein-glutamate methyltransferase *CheB*	3.1.1.61
	*che*R	GM298_03355	215588.216454	Protein-glutamate *O*-methyltransferase CheR	2.1.1.80
	*che*W	GM298_03310	204215.204718	Chemotaxis protein CheW	–
	*che*A	GM298_02505	60099.62018	Chemotaxis protein CheA	–
	*mal*E	GM298_21870	9111.10301	Maltose/maltodextrin ABC transporter substrate-binding protein MalE	–
	*rbs*B	GM298_22990	3204.4094	Ribose ABC transporter substrate-binding protein RbsB	–
Motility	*fli*Z	GM298_02790	121304.121855	Flagella biosynthesis regulatory protein FliZ	–
	*Fli*D	GM298_02755	111757.113181	PRJNA591446:GM298_02755	–
	*fli*S	GM298_02750	111331.111735	Flagellar export chaperone FliS	–
	*fli*T	GM298_02745	110951.111325	Flagella biosynthesis regulatory protein FliT	–
	*fli*F	GM298_02290	21526.23208	Flagellar basal body M-ring protein FliF	–
	*fli*E	GM298_02730	108072.108386	Flagellar hook-basal body complex protein FliE	–

(Continued)

TABLE 5 (Continued)

PGP activities description	Gene name	Locus tag	CDS	Product	E.C. number
	*fli*G	GM298_02720	105176.106174	Flagellar motor switch protein FliG	–
	*fli*H	GM298_02715	104476.105183	Flagellar assembly protein FliH	–
	*fli*I	GM298_02710	103106.104476	Flagellum-specific ATP synthase FliI	–
	*Fli*J	GM298_02705	102641.103084	Flagella biosynthesis chaperone FliJ	–
	*fli*K	GM298_02700	101409.102644	Flagellar hook length control protein FliK	–
	*fli*M	GM298_02325	28414.29406	Flagellar motor switch protein FliM	–
	*fli*P	GM298_02675	98299.99036	Flagellar type III secretion system pore protein FliP	–
	*fli*Q	GM298_02670	98020.98289	Flagellar biosynthesis protein FliQ"	–
	*fli*R	GM298_02665	97227.98012	Flagellar type III secretion system protein FliR	–
Adhesive structure	*hof*C	GM298_09075	69182.70366	Protein transport protein HofC	–
Adhesin production	*pga*A	GM298_08655	298669.301107	Poly-beta-1,6-*N*-acetyl-D-glucosamine export porin PgaA	–
	*pga*B	GM298_08650	296723.298660	Poly-beta-1,6-*N*-acetyl-D-glucosamine *N*-deacetylase PgaB	–
	*pga*C	GM298_08645	295399.296730	Poly-beta-1,6-*N*-acetyl-D-glucosamine synthase	–
	*pga*D	GM298_08640	294968.295402	Poly-beta-1,6-*N*-acetyl-D-glucosamine biosynthesis protein PgaD	–
Flageller protein	*fli*P	GM298_02675	98299.99036	Flagellar type III secretion system pore protein FliP	–
	*mot*A	GM298_02495	58314.59210	Flagellar motor stator protein MotA	–
	*mot*B	GM298_03300	201225.202154	Flagellar motor stator protein MotB	–
	*mur*J	GM298_15350	35192.36727	Murein biosynthesis integral membrane protein murJ	–
Superoxide dismutase	*sod*A	GM298_18770	40834.41454	Superoxide dismutase [Mn]	1.15.1.1
	*sod*B	GM298_13795	37254.37835	Superoxide dismutase [Fe]	1.15.1.1
	*sod*C	GM298_13845	45550.46068	Superoxide dismutase [Cu–Zn] SodC2	1.15.1.1
Trehalose metabolism	*tre*B	GM298_21730	11825.13243	PTS trehalose transporter subunit IIBC	2.7.1.201
	*tre*C	GM298_21725	10130.11773	Alpha, alpha-phosphotrehalase	3.2.1.93
	*tre*R	GM298_21735	13371.14318	HTH-type transcriptional regulator TreR	–
	*ots*A	GM298_03275	196622.198046	Alpha, alpha-trehalose-phosphate synthase	2.4.1.15
	*ots*B	GM298_03270	195844.196647	Trehalose-phosphatase	3.1.3.12
	*lam*B	GM298_21860	6246.7559	Maltoporin LamB	–
Abiotic stressDescription					
Cold Shock protein	*csp*A	GM298_12370	210631.210843	RNA chaperone/antiterminator CspA	–
	*csp*E	GM298_03640	272300.272509	Transcription antiterminator/RNA stability regulator CspE	–
	*csp*D	GM298_04675	137542.137763	Cold shock-like protein CspD	–
Heat Shock protein	*smp*B	GM298_07055	306189.306671	SsrA-binding protein SmpB	–
	*ibp*A	GM298_11605	52643.53053	Heat shock chaperone IbpA	–
	*ibp*B	GM298_11610	53190.53618	Heat shock chaperone IbpB	–
	*hsp*Q	GM298_05075	238055.238372	Heat shock protein HspQ	–
	*dna*J	GM298_09430	154155.155300	Molecular chaperone DnaJ	–
	*dna*K	GM298_09435	155388.157301	Molecular chaperone DnaK	–
	*rpo*H	GM298_18075	93268.94125	RNA polymerase sigma factor RpoH	–
	*lep*A	GM298_15045	119042.120841	Elongation factor 4	3.6.5.n1
	*grp*E	GM298_07085	310871.311464	Nucleotide exchange factor GrpE	–
Drought resistance	*nha*A	GM298_09425	152809.153984	Na+/H+ antiporter NhaA	–
	*cha*A	GM298_17370	47913.49013	Sodium-potassium/proton antiporter ChaA	–
	*cha*B	GM298_17375	49284.49514	Putative cation transport regulator ChaB	–
	*pro*A	GM298_10450	69705.70958	Glutamate-5-semialdehyde dehydrogenase	1.2.1.41

(Continued)

TABLE 5 (Continued)

PGP activities description	Gene name	Locus tag	CDS	Product	E.C. number
	*pro*B	GM298_10445	68590.69693	Glutamate 5-kinase	2.7.2.11
	*pro*Q	GM298_03590	263405.264091	RNA chaperone ProQ	–
	*pro*V	GM298_06810	255441.256652	Glycine betaine/L-proline ABC transporter ATP-binding protein ProV	–
	*pro*W	GM298_06805	254393.255457	Glycine betaine/L-proline ABC transporter permease ProW	–
	*pro*X	GM298_06800	253388.254383	Glycine betaine/L-proline ABC transporter substrate-binding protein ProX	–
	*pro*P	GM298_17635	1491.2993	Glycine betaine/L-proline transporter ProP	
	*pro*S	GM298_2152	4993.6711	Proline–tRNA ligase	6.1.1.15
	*bet*A	GM298_16415	95458.97122	Choline dehydrogenase	1.1.99.1
	*bet*B	GM298_16420	97136.98608	Betaine-aldehyde dehydrogenase	1.2.1.8
	*bet*T	GM298_16430	99338.101371	Choline BCCT transporter BetT	
	*trk*A	GM298_22580	7764.9140	Trk system potassium transporter TrkA	
	*trk*H	GM298_19395	80799.82250	Trk system potassium transporter TrkH	–
	*kdp*A	GM298_19955	40526.42205	Potassium-transporting ATPase subunit KdpA	–
	*kdp*B	GM298_19950	38459.40507	Potassium-transporting ATPase subunit Kdp	
	*kdp*C	GM298_19945	37871.38446	Potassium-transporting ATPase subunit KdpC	
	*kdp*F	GM298_19935	34509.35186	Two-component system response regulator KdpE	–

(1.336 Å), Gly553 (1.338 Å), and Leu556 (1.327 Å). The Rg of the amidohydrolase–chlorpyrifos complex fluctuated throughout the simulation, with an average value of 3.48 Å. The MolSA, SASA, and PSA of the amidohydrolase–chlorpyrifos complex insignificantly varied throughout the simulation period. The average MolSA, SASA, and PSA were 278.25, 156.69, and 37.03 $Å^2$, respectively (**Figure 7E**c).

Discussion

Endophytes play an important role in the agricultural sector by enhancing crop production, pathogen resistance, and pesticide detoxification. These characteristic endophytic bacteria can be used as biofertilizers for sustainable agriculture. In the present study, we extensively investigated a newly isolated rice root endophyte strain that might have mineralized chlorpyrifos as its carbon source and demonstrated the tomato PGP activities at germination, vegetative, and reproductive stages. In particular, the strain classification revealed that it newly evolved in Bangladesh and deviated far away from its nearest homologs.

The gram-negative bacterium HSTU-ASh6 showed positive results in the VP test, indicating its capability to produce acetoin in the growth media. It also showed a positive result in the catalase test. Several studies reported that endophytic strain showed catalase positive test (Son et al., 2006; Das et al., 2022). Catalase helps bacteria avoid cellular toxicity. The positive triple sugar iron test indicated that the isolate could ferment three sugars, including lactose, sucrose, and glucose, and iron. As the strain produced gas and exhibited motility properties, it was confirmed to be motility indole urease (MIU)–positive. The strain was also urease-positive, which is important for endophytic bacteria. Urease is an enzyme that splits urea into simple forms of nitrogen that the plants can readily absorb to promote growth. A previous study also demonstrated the occurrence and distribution of urease-positive endophytic bacteria in a legume community (Kumaresan and Suryanarayanan, 2001).

Previous reports have shown that several endophytic bacteria, including *Pseudomonas*, *Serratia*, and *Bacillus* species, can synthesize IAA that is involved in plant root regulation and growth control (Sgroy et al., 2009; Liu et al., 2010). Moreover, endophytes such as *Pantoea*, *Pseudomonas*, *and Serratia* have the ability to fix nitrogen in some plants (Loiret et al., 2004; Das et al., 2022). The present study assumed that the strain HSTU-ASh6 could fix nitrogen in Jensen's medium. Phosphate-solubilizing bacteria can dissolve insoluble phosphate and increase soil fertility and plant growth (Loiret et al., 2004; Das et al., 2022), which was also demonstrated by the strain HSTU-ASh6. Moreover, the strain enhanced the germination rate and increased tomato plant growth at vegetative and reproductive stages when using 70 and 30% reduced doses of urea. These results indicated that the strain could fix nitrogen in the tomato plant and assist its growth by providing phosphate solubilization, IAA, and ACC deaminase activities. In particular, a massive growth of tomato plants was observed in 100% urea + HSTU-ASh6 strain treatment

TABLE 6 Pesticide degrading model proteins quality assessment of *Enterobacter* sp. HSTU-ASh6 strain.

Model protein	Best PDB hit	TM-score, RMSD, IDEN, Cov	α –helix, β strand, η –coil, disordered	ERRAT (quality score)	VERIFY (3D-1D score)%	Ramachandran plot (core, allow, gener, disallow)
AmpD	1j3gA	0.994, 0.41, 0.809, 1.00	22, 15, 61, 2	83.33	89.62	61.2, 27.6, 9.2, 2.0
GlpA	2qcuB	0.877, 1.00, 0.241, 0.889	35, 19, 44, 4	94.19	78.97	72.5, 18.6, 6.4, 2.5
GlpB	6uziA	0.761, 1.89, 0.145, 0.802	26, 19, 54, 0	64.23	62.47	51.5, 34.8, 8.8, 5.0
GlpQ	1ydyA	0.927, 0.33, 0.857, 0.929	28, 13, 57, 7	85.79	90.93	76.1, 18.7, 3.5, 1.6
PdeH	4rnfA	0.957, 1.25, 0.185, 0.988	39, 18, 41, 6	91.96	74.32	85.0, 12.4, 1.3, 1.3
PdeR	5xgbA	0.810, 0.74, 0.256, 0.815	41, 25, 33, 1	81.52	71.95	72.9, 21.0, 5.1, 1.0
PepA	1gytL	0.999, 0.24, 0.972, 1.000	33, 20, 46, 1	94.30	97.61	85.2, 12.5, 2.1, 0.2
PepB	6cxdA	0.968, 0.27, 0.783, 0.970	34, 20, 45, 1	94.76	93.69	77.7, 18.3, 2.4, 1.6
PepD	3mruA	0.999, 0.27, 0.631, 1.000	26, 25, 48, 3	94.33	95.67	80.5, 16.1, 2.7, 0.7
pepQ	4qr8A	0.995, 0.23, 0.898, 0.996	27, 17, 55, 1	93.07	92.33	80.3, 17.6, 1.0, 1.0
PhnD	3p7iA	0.884, 0.44, 0.897, 0.888	43, 17, 39, 1	84.54	72.22	79.5, 14.2, 4.6, 1.7
PhnF	2wv0D	0.980, 0.51, 0.193, 0.988	28, 32, 39, 4	88.36	83.82	74.3, 21.6, 4.1, 0.0
PhnG	4xb6A	0.941, 0.69, 0.750, 0.960	44, 26, 29, 5	95.03	66.67	85.1, 13.4, 1.5, 0.0
PhnH	2fsuA	0.852, 0.67, 0.850, 0.861	24, 21, 54, 3	89.24	88.66	70.4, 23.7, 5.3, 0.6
PhnJ	4xb6D	0.984, 0.23, 0.957, 0.986	22, 19, 57, 4	85.34	85.05	78.0, 17.8, 3.3, 0.8
PhnK	4fwiB	0.980, 0.80, 0.320, 0.992	37, 23, 39, 2	93.41	90.44	80.2, 16.5, 1.4, 1.9
PhnL	5nikJ	0.929, 1.05, 0.290, 0.960	34, 24, 41, 0	93.57	89.38	78.4, 18.6, 2.0, 1.0
PhnM	1k1dA	0.890, 2.18, 0.169, 0.955	32, 22, 45, 0	78.10	75.93	61.9, 28.7, 5.7, 3.6
PhnO	1s5kA	0.914, 1.93, 0.168, 0.993	35, 33, 31, 2	97.05	80.56	74.6, 19.2, 3.8, 2.3
PhnP	3g1pB	0.989, 0.31, 0.768, 0.992	12, 28, 58, 0	84.23	98.41	70.1, 24.3, 2.3, 3.3
Carboxylesterase	1maaD	0.951, 1.38, 0.292, 0.976	30, 13, 55, 1	80.98	83.63	71.4, 21.4, 3.9, 2.9
PaaC	1otkA	0.978, 0.26, 0.802, 0.980	47, 12, 40, 1	95.83	89.92	91.3, 7.3, 0.90, 0.5
HpxK	5i4mA	0.906, 2.25, 0.321, 0.985	32, 22, 44, 1	88.22	94.65	78.4, 17.3, 2.0, 2.3
HpxW	4y23A	0.954, 1.63, 0.242, 0.981	33, 15, 51, 1	86.12	97.72	73.6, 22.1, 2.8, 1.6
Amidohydrolase (GM298_10355)	2e11A	0.984, 0.72, 0.467, 0.996	25, 32, 42, 1	84.55	87.50	75.9, 21.0, 1.3, 1.8
Amidohydrolase (GM298_00905)	4ewtA	0.989, 0.56, 0.334, 0.995	31, 24, 44, 0	89.04	95.17	78.1, 17.2, 2.8, 1.9
AHFP (GM298_01650)	4l5pA	0.936, 1.04, 0.271, 0.954	43, 11, 45, 0	93.15	90.70	78.2, 17.7, 1.4, 2.7
AHFP (GM298_06905)	2qt3B	0.842, 1.26, 0.213, 0.861	31, 16, 52, 11	89.357	74.51	67.0, 23.6, 6.7, 2.7
AHFP (GM298_20245)	3nqbA	0.954, 0.42, 0.507, 0.956	25, 26, 47, 2	83.90	97.97	75.8, 18.7, 2.9, 2.6
Amidohydrolase (GM298_14085)	4ewtA	0.870, 0.67, 0.254, 0.876	34, 20, 45, 0	85.545	85.78	71.9, 23.5, 3.2, 1.3
Amidohydrolase (GM298_21680)	2icsA	0.935, 0.92, 0.453, 0.950	26, 22, 51, 3	82.92	92.31	75.4, 20.1, 2.4, 2.1
GM298_09975AHFP	3ighX	0.758, 0.78, 0.204, 0.764	28, 16, 54, 10	75.12	88.60	80.5, 15.7, 2.8, 1.0
GM298_00815_ABFH	4lxgA	0.944, 1.60, 0.184, 0.996	36, 17, 45, 1	87.65	94.42	75.7, 19.0, 3.3, 1.9
GM298_08590_ABH	4ypvA	0.983, 0.66, 0.393, 0.993	31, 20, 47, 1	95.89	94.33	80.4, 15.3, 3.9, 0.4
GM298_09990_ABFH	1va4A	0.989, 0.36, 0.742, 0.993	39, 15, 45, 0	97.35	96.70	82.8, 14.6, 2.1, 0.4
GM298_18675_ABH	4ypvA	0.992, 0.58, 0.348, 1.000	38, 16, 45, 1	88.17	89.80	89.0, 9.5, 1.1, 0.4
GM298_01305_ABFH	3fvr	0.579, 2.12, 0.171, 0.607	31, 16, 51, 9	61.64	72.62	55.0, 30.4, 10.4, 4.2

compared with the control. The multi-branched bushy structure of bacterium-treated tomato plants was due to the secretion of the auxin (**Supplementary Figures 3A,B**), which is agreed to the Khan et al. (2016). Based on these results, it was confirmed that the bacterium exerted robust growth-promoting effects on tomato plants.

HSTU-ASh6 completely degraded 1 g L^{-1} of chlorpyrifos within 14 days of incubation in the minimal salt medium. A previous study reported that *Enterobacter* sp. B-14 rapidly degraded chlorpyrifos in MSM, and this strain used chlorpyrifos as the only source of carbon and phosphorus (Singh et al., 2004). Das et al. (2022) reported that HSTU strains degraded 42–100% of chlorpyrifos in broth media. Li et al. (2007) showed that *Sphingomonas* sp. DSP2 degraded 100% of chlorpyrifos (100 mg L^{-1}) in 24 h. It has also been shown that chlorpyrifos degradation results in the generation of several byproducts such as chlorpyrifos oxon, 3,5,6-trichloro-2-methoxypyridine, and 2-chloro-6-hydroxypyridine (Singh et al., 2004). A significant

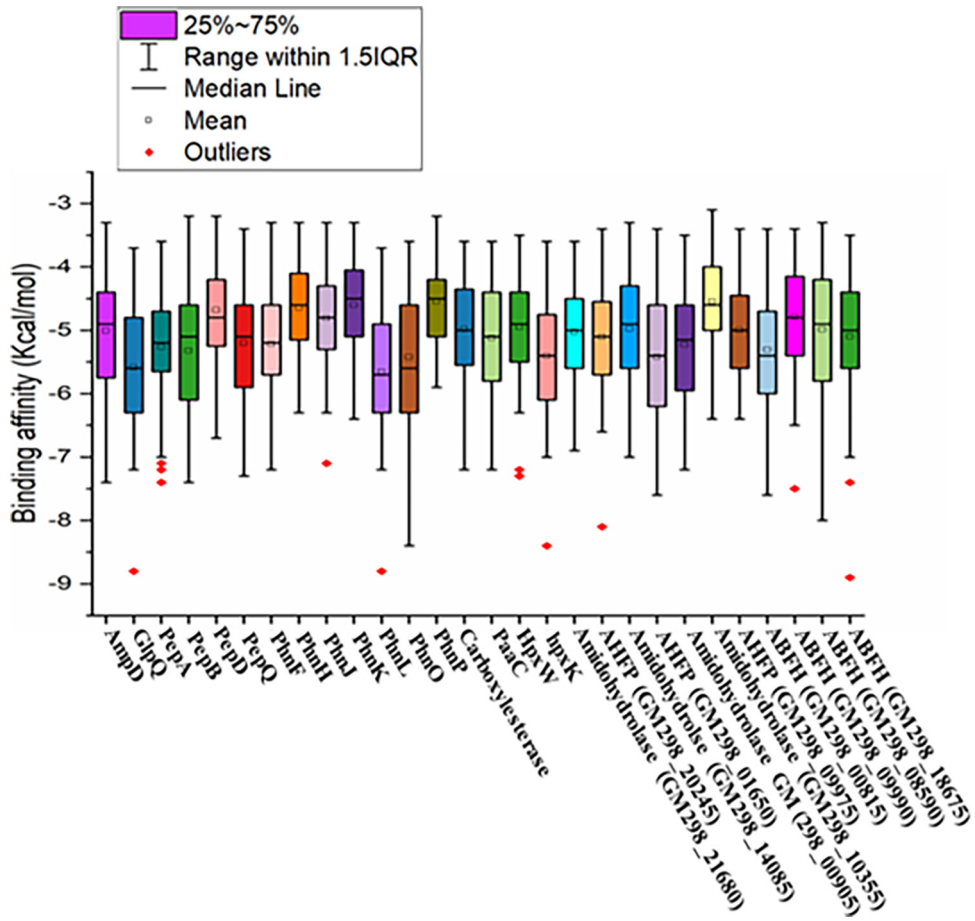

FIGURE 5
Graphical representation of virtual screening results of pesticide-degrading validated model proteins with 105 different organophosphorus pesticides and other common pesticides applied in fields.

number of spinoff products were observed, for instance, chlorodihydro-2-pyridone, dihydroxy pyridine, tetrahydro-2-pyridone, maleamide semialdehyde, maleamic acid, and pyruvic acid. It was reported that chlorpyrifos and TCP can be broken down to produce 1,3-bis (1,1-dimethylethyl) and benzene (Abraham and Silambarasan, 2013). Chlorpyrifos oxon, TCP, and DEMP are the metabolic byproducts generated by the breakdown of chlorpyrifos organophosphorus insecticide (Lovecka et al., 2015). In this study, the products generated after chlorpyrifos degradation were phorate sulfoxide, phorate sulfone, chlorpyrifos methyl, TCP, carbophenothion sulfoxide, oxydisulfoton, carbonochloridic acid, 2,4,5-trichlorophenyl ester, thionodemeton sulfone, 3-(2-thienyl)-DL-alanine, chlorpyrifos oxon, diethyl methanephosphonate, which were confirmed through GC–MS/MS analysis (**Table 3**). To the best of our knowledge, this is the first report describing that diethyl methanephosphonate (DEMP) is a chlorpyrifos metabolic byproduct.

The quality of the genome sequence was predicted according to the GC% of strain DNA. A good-quality sequence is ensured by its GC%, and at least 40–70% of GC% is accepted in research (Abdullah-Al-Mamun et al., 2022). The strain investigated in this study exhibited 55.1% GC% after fast QC analysis, and the sequence quality was confirmed to be excellent.

According to the phylogenetic tree analysis of 16S rRNA genes, *Enterobacter* sp. HSTU-ASh6 was placed with *E. sichuanensis* WCHECL1597 (MG832788) in the sister taxa. They were 45% similar to each other and identified as *E. sichuanensis*. However, depending only on 16S rRNA and the polyphyletic nature of the genus *Enterobacter* make its identification and categorization extremely difficult. Therefore, we further confirmed our result using three housekeeping genes (*recA*, *gyrB*, and *rpoB*), and a complete genome phylogenetic tree was constructed and analyzed separately. The constructed tree revealed that HSTU-ASh6 was appeared as *E. cloacae* A1137. Based on 16S rRNA, *Enterobacter* sp. HSTU-ASh6 was specified as *E. sichuanensis*. However, after the analysis

10.3389/fmicb.2022.1060554

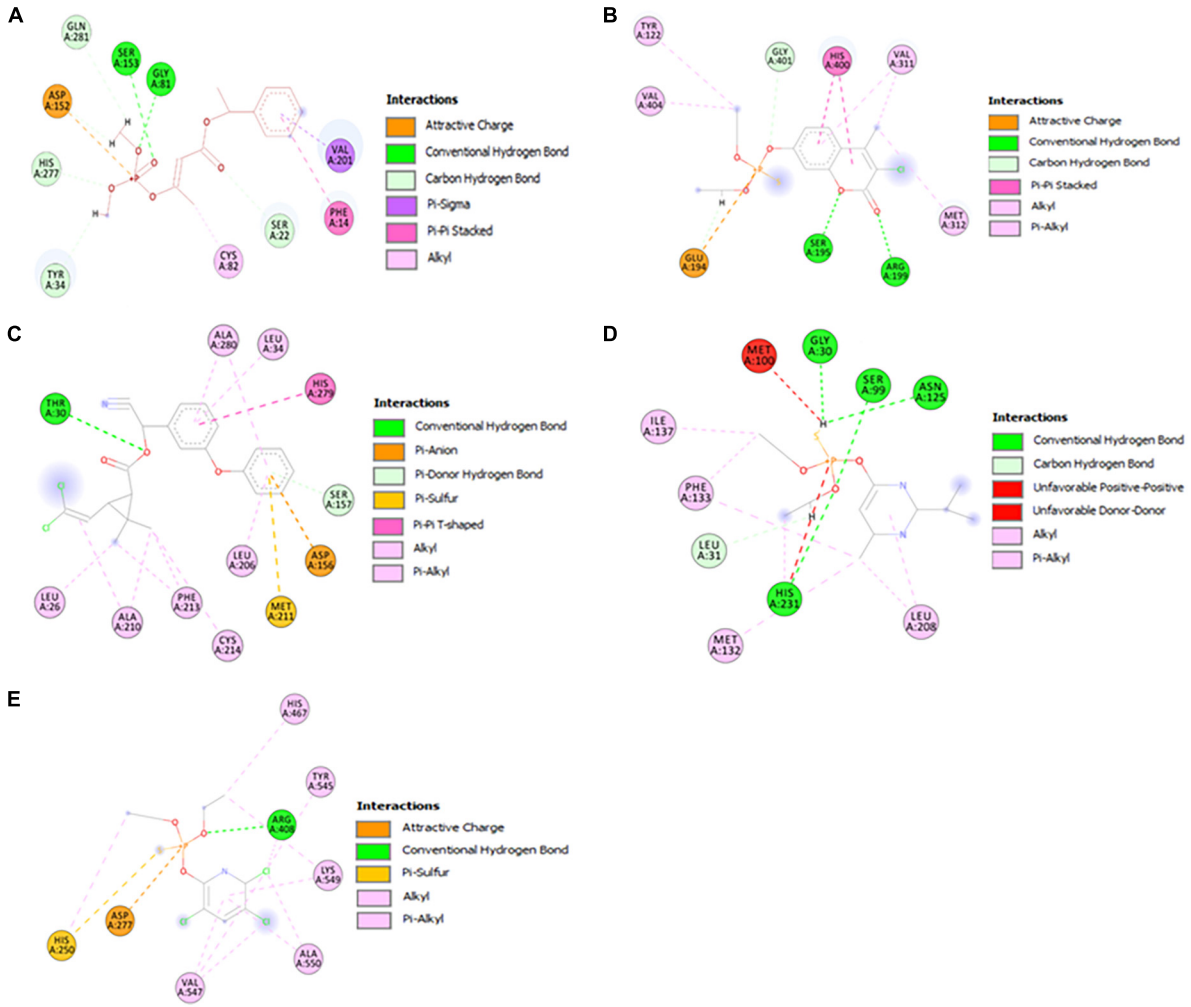

FIGURE 6
Visualization of the catalytic interactions of potential model proteins with pesticides. **(A)** α/β hydrolase (GM298_18675) with crotoxyphos, **(B)** carboxylesterase with coumaphos, **(C)** alpha/beta fold hydrolase (GM298_08590) with cypermethrin, **(D)** alpha/beta fold hydrolase (GM298_00815) protein with diazinon, **(E)** amidohydrolase family protein (GM298_20245) with chlorpyrifos.

of another three housekeeping genes and complete genome phylogenetic tree analyses, it was identified as *E. cloacae*. However, in the case of *rec*A tree, both *E. cloacae* A1137 and *E. sichuanensis* WCHECL1597 were placed in a different clade with *Enterobacter* sp. HSTU-ASh6, where *E. cloacae* A1137 was located in the first node. According to GGDC web server, a DDH value of >70% indicates that the strain belongs to the same species and >79% based on the formula: 2 indicates that the strain belongs to the same subspecies. In another analysis, an ANI cut-off of > 96% was observed for species declaration. Consequently, our study results suggested that the strain HSTU-ASh6 belonged to *Enterobacter* species because both DDH and ANI values exceeded the cut-off. After progressive Mauve and pangenomic analysis, it was concluded that *Enterobacter* sp. HSTU-ASh6 was completely diversified from its closest strains, which indicates its evolutionary properties. Therefore, *Enterobacter* sp. HSTU-ASh6 might be a new member of the *Enterobacter* species.

Escherichia coli and closely related *Enterobacteria* possess both Isc and Suf systems, encoded by the *isc*RSUA-hscBA-fdx-iscX operon and sufABCDSE operon, respectively (Ayala-Castro et al., 2008). In general, the endophytic bacterial genome contains *nif* and *fix* gene clusters for nitrogen fixation. However, a few endophytic bacteria contain other types of gene clusters, namely, Isc and Suf systems, which are responsible for nitrogen fixation in critical situations (Ayala-Castro et al., 2008). The present study showed that the genome of *Enterobacter* sp. HSTU-ASh6 harbors both Isc and Suf systems for biological nitrogen fixation, and the genome machinery also indicated that both Isc and Suf operons were present. To summarize, the PGP mechanism is encoded by genes that are directly linked to the generation of IAA and ACC deaminase and siderophore in

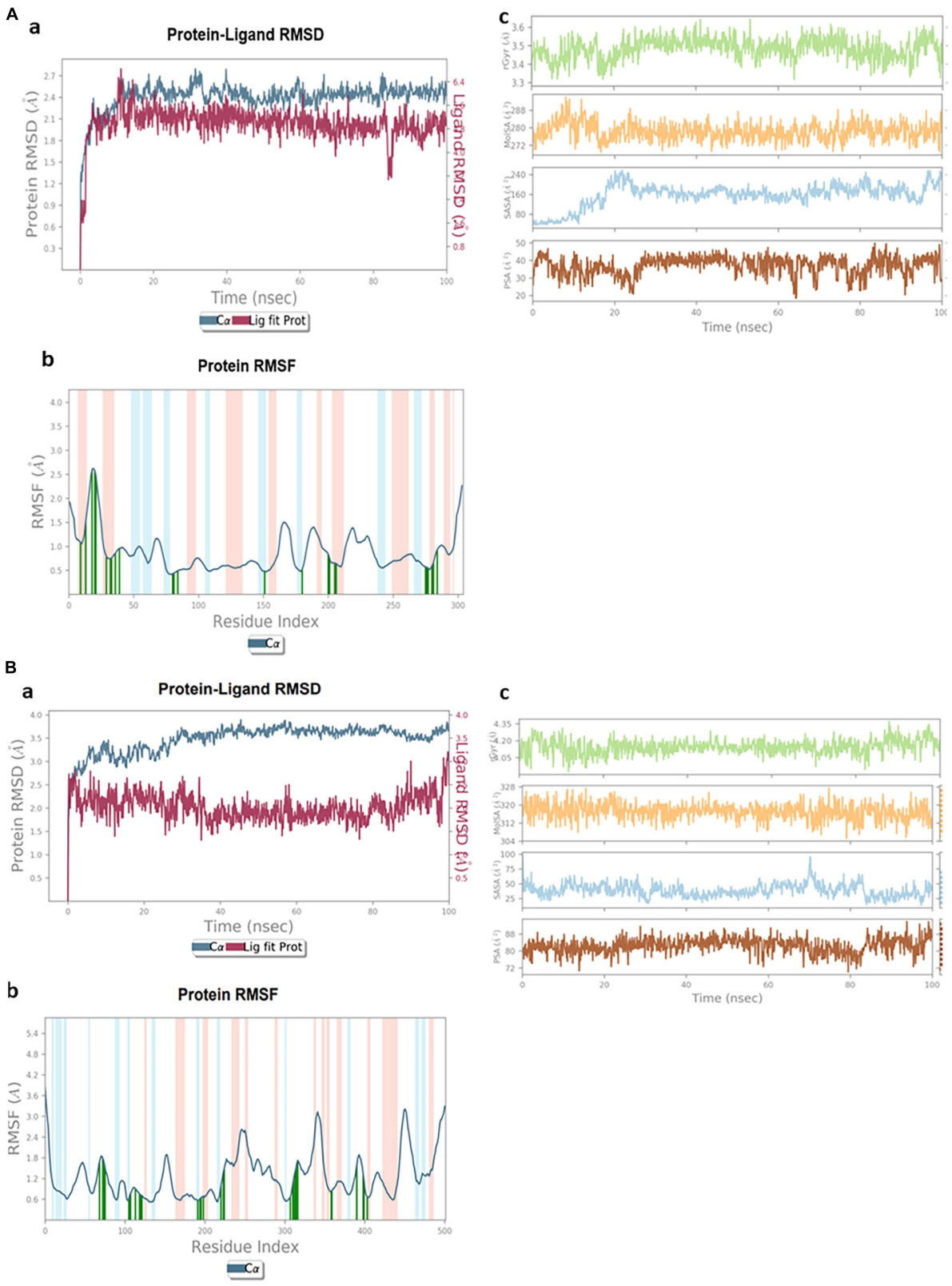

FIGURE 7
(Continued)

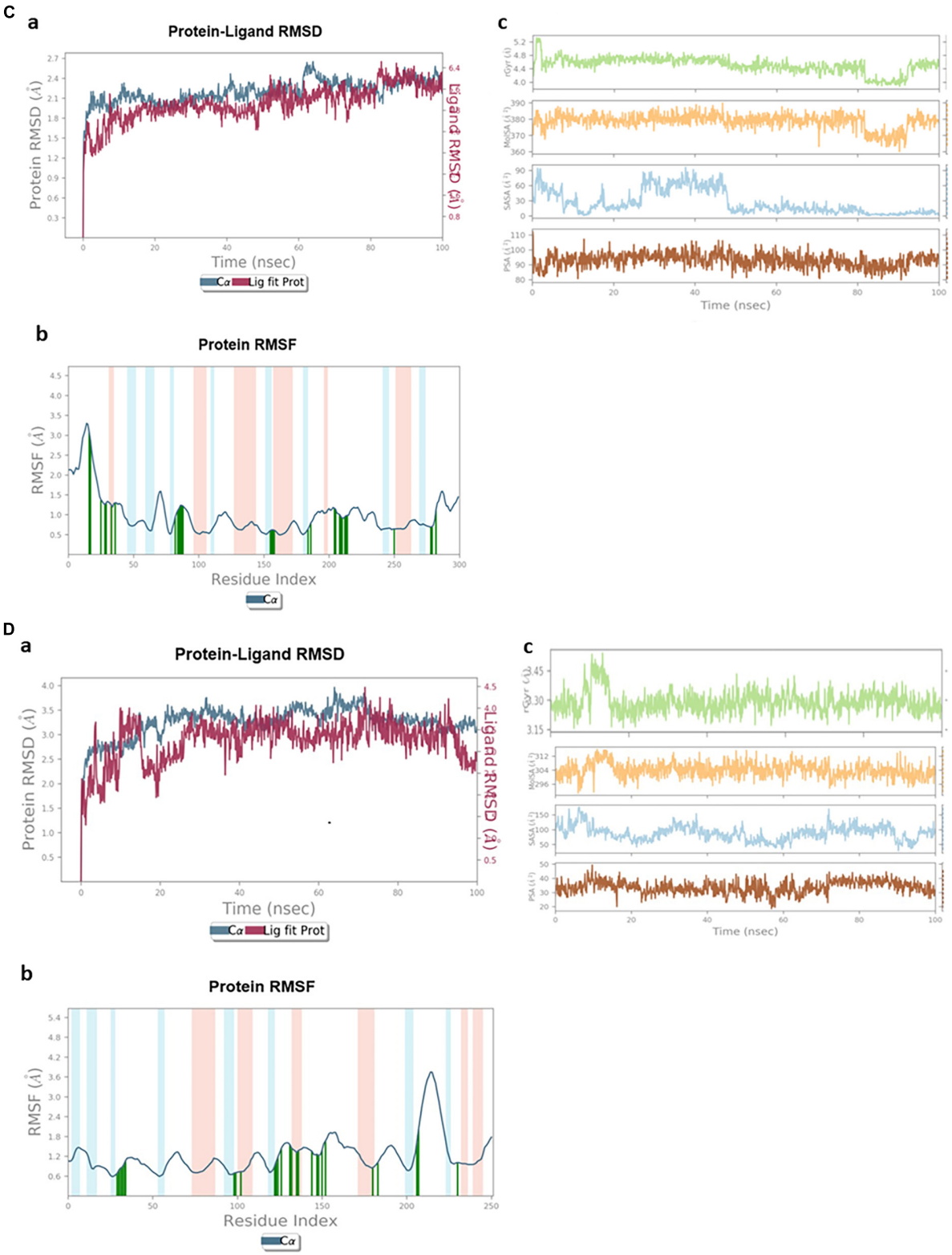

FIGURE 7
(Continued)

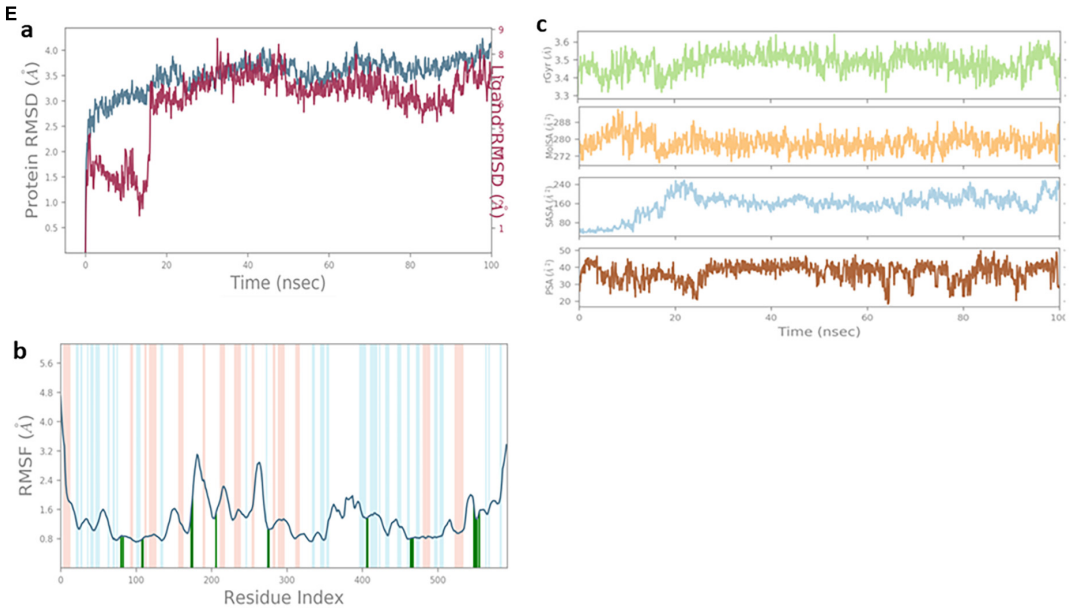

FIGURE 7
Stability of protein and pesticide interactions. **(A)** Molecular dynamics simulation of α/β hydrolase (GM298_18675)–crotoxyphos complex, (a) protein–ligand RMSD, (b) protein RMSF, and (c) Rg, MolSA, SASA, and PSA. **(B)** Carboxylesterase–coumaphos complex, (a) Protein–ligand RMSD, (b) protein RMSF, and (c) Rg, MolSA, SASA, and PSA. **(C)** α/β hydrolase (GM298_08590)–cypermethrin complex, (a) Protein–ligand RMSD, (b) protein RMSF, and (c) Rg, MolSA, SASA, and PSA. **(D)** α/β hydrolase (GM298_00815)–diazinon complex, (a) Protein–ligand RMSD, (b) protein RMSF, and (c) Rg, MolSA, SASA, and PSA. **(E)** Amidohydrolase (GM298_20245)–chlorpyrifos complex, (a) protein–ligand RMSD, (b) protein RMSF, and (c) Rg, MolSA, SASA, and PSA.

Enterobacter sp. HSTU-ASh6. In the same way, genes like *nha*A, *cha*AB, *pro*ABpqvwsx, *bet*ABT, *trk*AH, *kdp*ABCEF, and *kdb*D that help the plant deal with drought stress have been found in the genomes, indicating their involvement in drought tolerance by the plant (Das et al., 2022).

The conserved pentapeptide motif G-X-S-X-G is commonly observed in bacterial genome sequences (Schloss and Handelsman, 2003). The genome of *Enterobacter* sp. HSTU-ASh6 encodes proteins such as alpha/beta fold hydrolase (GM298_18675), alpha/beta fold hydrolase (GM298_08590), alpha/beta fold hydrolase (GM298_00815), and carboxylesterase sequences carrying the conserved pentapeptide G-X-S-X-G motif. The hydrolase-encoding genes, for instance, *opd* (McDaniel et al., 1988), *mpd* (Lu et al., 2013), and *ophc*2 (Ningfeng et al., 2004; Shen et al., 2010), are also crucial for the breakdown of pesticides. Das et al. (2022) reported that carboxylesterase and phosphotriesterase are directly involved in the breakdown of organophosphorus insecticides. Haque et al. (2018, 2020) also reported that several *opd* genes (*opd*A, *opd*E, and *opd*D) can degrade a range of organophosphorus insecticides. These results suggested that the genome of *Enterobacter* sp. HSTU-ASh6 retains pesticide-mineralizing genes. In addition, several hydrolases, esterase, and some hypothetical proteins may have catalytic interactions with organophosphorus insecticides, which is beyond the scope of this study.

The molecular docking investigations of pesticide-degrading enzymes with pesticides were subjected with a validity score. The RMSD of model protein indicates its acceptance when compared to a typical protein model. Since a smaller RMSD suggests fewer errors, it is always preferred. The 28 modeled proteins' average RMSD was 1.0, indicating that the analyses were valid. According to reports, protein models with RMSDs between 0.35 and 2.36 and their nearby homologs are acceptable (Dadheech et al., 2019). Depending on the molecular docking analysis, all five proteins (alpha/beta fold hydrolase (GM298_18675), alpha/beta fold hydrolase (GM298_08590), alpha/beta fold hydrolase (GM298_00815), amidohydrolase family protein (GM298_20245), and carboxyl esterase) with important amino acid residues for catalysis were found within 1.5–5.5 Å, which suggested its involvement in the degradation of organophosphate pesticides. Haque et al. (2018) reported that carboxylesterase provides Ser-His-Glu catalytic triad. The present study indicated that carboxylesterase docked with coumaphos and provided a similar type of Ser-His-Glu catalytic triad. Consequently, the alpha/beta fold hydrolase (GM298_18675) of *Enterobacter* sp. HSTU-ASh6 originated as a potential catalytic triad Ser-His-Asp (Hosokawa, 2008). Therefore, the α/β fold hydrolase (GM298_08590) was docked with cypermethrin and provided Ser-His-Asp catalytic triad (Hosokawa, 2008). Kubiak et al. (2001) detected the Arg-Asp-His catalytic triad in the enzymatic cleavage of

the phosphodiester bond. A similar triad (Arg-Asp-His) was observed in the present study, where amidohydrolase docked with chlorpyrifos insecticide. A recent study indicated that the Ser-His-Glu catalytic triad is predominant in long PepEs, and the Ser-His-Asn "catalytic triad" is predominant in short PepEs (Yadav et al., 2019). Interestingly, alpha/beta fold hydrolase (GM298_00815) bonded with diazinon pesticide and formed a new possible catalytic triad Ser-His-Asn.

Five different proteins with five different pesticides complex were subjected to MD simulation for 100 ns. The stability of the protein-ligand complex was determined (Patel et al., 2021) by comparing the RMSD and RMSF values of the unbound protein structure. In MD simulations, the RMSD parameter is used to evaluate the coherence and flexibility of proteins as well as to keep track of the separation between their atoms and backbones (Sargsyan et al., 2017). While a greater RMSD value signifies relatively less stability of the protein-ligand complex, a lower RMSD value throughout the simulation shows higher stability of the protein-ligand complex. It was shown that the enzyme-substrate complexes are stable for the biodegradation of pesticides by a slight fluctuation with lower smaller RMSD (Lee et al., 2021). The results showed that the MD simulations were stable at 100 ns for the insecticides chlorpyrifos, diazinon, crotoxyphos, cypermethrin, and coumaphos complex with pesticides degrading potential proteins (**Figures 7A–E**). The RMSF number reflects how each protein's amino acid moved and changed throughout the simulation. More flexibility during the simulation is implied by higher RMSF values, whilst superior stability is indicated by lower RMSF values. In this study, the RMSF values were different for the chlorpyrifos–amidohydrolase protein family (GM298_20245), diazinon–α/β fold hydrolase (GM298_00815), crotoxyphos–α/β fold hydrolase (GM298_18675), cypermethrin–alpha/beta fold hydrolase (GM298_08590), and coumaphos–carboxylesterase complexes, suggesting that the RMSF of these complexes was stable during the catalytic reactions. Previously, researchers have used RMSF to examine enzyme-pesticide complexes (Lee et al., 2021). The microbial enzymes are responsible for the biodegradation of pollutants like pesticides and they are interconnected (Joshi et al., 2021; Bhatt and Maheshwari, 2022). The changes in compactness of an enzyme-substrate complex are described using the radius of gyration (Rg). It refers to the folding and unfolding of proteins during MD simulations. Enzyme folding indicates Rg stability, whereas fluctuations in Rg signify enzyme unfolding (Adams et al., 2008). The results of Rg and PSA revealed that every enzyme-substrate complex displayed stable compactness in five instances of protein-ligand complexes, indicating that these are superiorly superimposed on each other and perfectly overlaid. SASA stands for solvent-assisted structure-activity relationship. It foresees the structural alterations that take place during interactions. All five protein-ligand complexes' SASA values during the 100-ns MD simulations of the enzyme-substrate complexes were significantly stable, indicating that the protein structure remained unchanged.

Conclusion

The endophytic and pesticide-degrading strain *Enterobacter* sp. HSTU-ASh6 isolated from rice roots significantly affected plant growth and pesticide detoxification. Housekeeping gene and whole genome phylogenetic tree, ANI, and DDH genomic analysis confirmed that *Enterobacter* sp. HSTU-ASh6 is a new species of *Enterobacter* strain. Whole genome sequencing also confirmed the presence of genes involved in plant growth, stress tolerance, and pesticide degradation. Therefore, the utilization of this remarkably versatile PGPB may be an essential eco-friendly alternative to improve crop growth and pesticide detoxification.

Nucleotide sequence accession number

The whole Genome sequence of the *Enterobacter* sp. HSTU-ASh6 strains was deposited at NCBI GenBank under the BioProject PRJNA591446, BioSample SAMN13387920 and accession number: WSPD00000000. In addition, the 16S rRNA gene sequence of the strain was deposited in the NCBI with accession number: MZ021583.

Data availability statement

The datasets presented in this study can be found in online repositories. The names of the repository/repositories and accession number(s) can be found below: BioProject: PRJNA591446, BioSample: SAMN13387920, and accession number: WSPD00000000.

Author contributions

MAH: conceptualization, private funding, experimentation, data analysis, and write the manuscript. MSH: experimentation, data analysis, and write first draft of the manuscript. MA: analyze GCŰMS/MS. IA and HP: conduct MD simulation. AR: critical revision and partial writing. KC: conceptualization, resource, critical reviewing, editing, proofreading, and fund acquisition. All authors contributed to the article and approved the submitted version.

Funding

This research was supported by the National Research Foundation (NRF), South Korea. This study was carried out with the Basic Science Research Program through the

National Research Foundation (NRF) funded by the Ministry of Education (Grant number: 2016R1D1A1B01009898), South Korea and the Bio & Medical Technology Development Program through the National Research Foundation (NRF) funded by the Ministry of Science & ICT (Grant number: 2020M3A9I3038560), South Korea.

Acknowledgments

We thank Ministry of Science and Technology (MOST), Bangladesh for providing NST student fellowship for MS student to MSH.

Conflict of interest

The authors declare that the research was conducted in the absence of any commercial or financial relationships that could be construed as a potential conflict of interest.

Publisher's note

All claims expressed in this article are solely those of the authors and do not necessarily represent those of their affiliated organizations, or those of the publisher, the editors and the reviewers. Any product that may be evaluated in this article, or claim that may be made by its manufacturer, is not guaranteed or endorsed by the publisher.

Supplementary material

The Supplementary Material for this article can be found online at: https://www.frontiersin.org/articles/10.3389/fmicb.2022.1060554/full#supplementary-material

References

Abdullah-Al-Mamun, M., Hossain, M., Debnath, G. C., Sultana, S., Rahman, A., Hasan, Z., et al. (2022). Unveiling lignocellulolytic trait of a goat omasum inhabitant *Klebsiella variicola* strain HSTU-AAM51 in light of biochemical and genome analyses. *Braz. J. Microbiol.* 53, 99–130. doi: 10.1007/s42770-021-00660-7

Abraham, J., and Silambarasan, S. (2013). Biodegradation of chlorpyrifos and its hydrolyzing metabolite 3, 5, 6-trichloro-2-pyridinol by *Sphingobacterium* sp. JAS3. *Process Biochem.* 48, 1559–1564. doi: 10.1016/j.procbio.2013.06.034

Adams, M. A., Luo, Y., Hove-Jensen, B., He, S. M., van Staalduinen, L. M., Zechel, D. L., et al. (2008). Crystal structure of PhnH: An essential component of carbon-phosphorus lyase in *Escherichia coli*. *J. Bacteriol.* 190, 1072–1083. doi: 10.1128/JB.01274-07

Adedayo, O., Javadpour, S., Taylor, C., Anderson, W. A., and Moo-Young, M. (2004). Decolourization and detoxification of methyl red by aerobic bacteria from a wastewater treatment plant. *World J. Microbiol. Biotechnol.* 20, 545–550. doi: 10.1023/B:WIBI.0000043150.37318.5f

Al Mansur, M. A., Siddiqi, M. M. A., Akbor, M. A., and Saha, K. (2018). Phytochemical screening and GC-MS chemical profiling of ethyl acetate extract of seed and stem of *Anethum sowa* Linn. *Dhaka Univ. J. Pharm. Sci.* 16, 187–194. doi: 10.3329/dujps.v16i2.35256

Ali, A., Moon, Y. S., Hamayun, M., Khan, M. A., Bibib, K., and Lee, I. J. (2022). Pragmatic role of microbial plant biostimulants in abiotic stress relief in crop plants. *J. Plant Interact.* 17, 705–718. doi: 10.1080/17429145.2022.2091801

Ashraf, M., and Foolad, M. R. (2005). Pre-sowing seed treatment—A shotgun approach to improve germination, plant growth, and crop yield under saline and non-saline conditions. *Adv. Agron.* 88, 223–271. doi: 10.1016/S0065-2113(05)88006-X

Ayala-Castro, C., Saini, A., and Outten, F. W. (2008). Fe-S cluster assembly pathways in bacteria. *Microbiol. Mol. Biol. Rev.* 72, 110–125. doi: 10.1128/MMBR.00034-07

Belimov, A. A., Dodd, I. C., Safronova, V. I., Shaposhnikov, A. I., Azarova, T. S., Makarova, N. M., et al. (2015). Rhizobacteria that produce auxins and contain 1-amino-cyclopropane-1- carboxylic acid deaminase decrease amino acid concentrations in the rhizosphere and improve growth and yield of well-watered and water-limited potato (*Solanum tuberosum*). *Ann. Appl. Biol.* 167, 11–25. doi: 10.1111/aab.12203

Bhatt, K., and Maheshwari, D. K. (2022). Insights into zinc-sensing metalloregulator 'Zur'deciphering mechanism of zinc transportation in *Bacillus* spp. by modeling, simulation and molecular docking. *J. Biomol. Struct. Dyn.* 40, 764–779. doi: 10.1080/07391102.2020.1818625

Bhatt, P., Huang, Y., Rene, E. R., Kumar, A. J., and Chen, S. (2020). Mechanism of allethrin biodegradation by a newly isolated *Sphingomonas trueperi* strain CW3 from wastewater sludge. *Bioresour. Technol.* 305:123074.

Carvalho, T. L. G., Balsemão-Pires, E., Saraiva, R. M., Ferreira, P. C. G., and Hemerly, A. S. (2014). Nitrogen signalling in plant interactions with associative and endophytic diazotrophic bacteria. *J. Exp. Bot.* 65, 5631–5642. doi: 10.1093/jxb/eru319

Dadheech, T., Jakhesara, S., Chauhan, P. S., Pandit, R., Hinsu, A., Kunjadiya, A., et al. (2019). Draft genome analysis of lignocellulolytic enzymes producing *Aspergillus terreus* with structural insight of β-glucosidases through molecular docking approach. *Int. J. Biol. Macromol.* 125, 181–190.

Dallakyan, S., and Olson, A. J. (2015). "Small-molecule library screening by docking with PyRx," in *Chemical Biology*, eds J. Hempel, C. Williams and C. Hong (New York, NY: Humana Press), 243–250.

Dar, M. A., Kaushik, G., and Villarreal-Chiu, J. F. (2019). Pollution status and bioremediation of chlorpyrifos in environmental matrices by the application of bacterial communities: A review. *J. Environ. Manage.* 239, 124–136. doi: 10.1016/j.jenvman.2019.03.048

Das, S. R., Haque, M. A., Akbor, M. A., Abdullah-Al-Mamun, M., Debnath, G. C., Hossain, M., et al. (2022). Organophosphorus insecticides mineralizing endophytic and rhizospheric soil bacterial consortium influence eggplant growth-promotion. *Arch. Microbiol.* 204:199. doi: 10.1007/s00203-022-02809-w

Haque, M. A., Hong, S. Y., Hwang, C. E., Kim, S. C., and Cho, K. M. (2018). Cloning of an organophosphorus hydrolase (*opd*D) gene of *Lactobacillus sakei* WCP904 isolated from chlorpyrifos-impregnated kimchi and hydrolysis activities of its gene product for organophosphorus pesticides. *Appl. Biol. Chem.* 61, 643–651. doi: 10.1007/s13765-018-0397-x

Haque, M. A., Hwang, C. E., Kim, S. C., Cho, D. Y., Lee, H. Y., Cho, K. M., et al. (2020). Biodegradation of organophosphorus insecticides by two organophosphorus hydrolase genes (*opd*A and *opd*E) from isolated *Leuconostoc mesenteroides* WCP307 of kimchi origin. *Process Biochem.* 94, 340–348. doi: 10.1016/j.procbio.2020.04.026

Haque, M. A., Lee, J. H., and Cho, K. M. (2015). Endophytic bacterial diversity in Korean kimchi made of Chinese cabbage leaves and their antimicrobial activity against pathogens. *Food Control.* 56, 24–33. doi: 10.1016/j.foodcont.2015.03.006

Honma, M., and Shimomura, T. (1978). Metabolism of 1-aminocyclopropane-1-carboxylic acid. *Agric. Biol. Chem.* 42, 1825–1831. doi: 10.1080/00021369.1978.10863261

Hosokawa, M. (2008). Structure and catalytic properties of carboxylesterase isozymes involved in metabolic activation of prodrugs. *Molecules* 13, 412–431. doi: 10.3390/molecules13020412

James, E. K. (2000). Nitrogen fixation in endophytic and associative symbiosis. *Field Crops Res.* 65, 197–209. doi: 10.1016/S0378-4290(99)00087-8

Jorgensen, W. L., Maxwell, D. S., and Tirado-Rives, J. (1996). Development and testing of the OPLS all-atom force field on conformational energetics and properties of organic liquids. *J. Am. Chem. Soc.* 118, 11225–11236. doi: 10.1021/ja9621760

Joshi, T., Joshi, T., Sharma, P., Chandra, S., and Pande, V. (2021). Molecular docking and molecular dynamics simulation approach to screen natural compounds for inhibition of *Xanthomonas oryzae* pv. *Oryzae* by targeting peptide deformylase. *J. Biomol. Struct. Dyn.* 39, 823–840. doi: 10.1080/07391102.2020.1719200

Kazerooni, E. A., Al-Shibli, H., Nasehi, A., and Al-Sadi, A. M. (2020). Endophytic *Enterobacter cloacae* exhibits antagonistic activity against pythium damping-off of cucumber. *Ciência Rural* 50:e20191035. doi: 10.1590/0103-8478cr20191035

Khan, A. L., Halo, B. A., Elyassi, A., Ali, S., Al-Hosni, K., Hussain, J., et al. (2016). Indole acetic acid and ACC deaminase from endophytic bacteria improves the growth of *Solanum lycopersicum*. *Electron. J. Biotechnol.* 21, 58–64. doi: 10.1016/j.ejbt.2016.02.001

Kubiak, R. J., Yue, X., Hondal, R. J., Mihai, C., Tsai, M. D., and Bruzik, K. S. (2001). Involvement of the Arg-Asp-His catalytic triad in enzymatic cleavage of the phosphodiester bond. *Biochemistry* 40, 5422–5432. doi: 10.1021/bi002371y

Kumaresan, V., and Suryanarayanan, T. S. (2001). Occurrence and distribution of endophytic fungi in a mangrove community. *Mycol. Res.* 105, 1388–1391. doi: 10.1017/S0953756201004841

Lee, H. Y., Cho, D. Y., Ahmad, I., Patel, H. M., Kim, M. J., Jung, J. G., et al. (2021). Mining of a novel esterase (est3S) gene from a cow rumen metagenomic library with organosphosphorus insecticides degrading capability: Catalytic insights by site directed mutations, docking, and molecular dynamic simulations. *Int. J. Biol. Macromol.* 190, 441–455. doi: 10.1016/j.ijbiomac.2021.08.224

Li, X., He, J., and Li, S. (2007). Isolation of a chlorpyrifos-degrading bacterium, *Sphingomonas* sp. strain Dsp-2, and cloning of the *mpd* gene. *Res. Microbiol.* 158, 143–149. doi: 10.1016/j.resmic.2006.11.007

Liu, X., Jia, J., Atkinson, S., Cámara, M., Gao, K., Li, H., et al. (2010). Biocontrol potential of an endophytic *Serratia* sp. G3 and its mode of action. *World J. Microbiol. Biotechnol.* 26, 1465–1471. doi: 10.1007/s11274-010-0321-y

Loiret, F. G., Ortega, E., Kleiner, D., Ortega-Rodés, P., Rodes, R., and Dong, Z. (2004). A putative new endophytic nitrogen-fixing bacterium *Pantoea* sp. from sugarcane. *J. Appl. Microbiol.* 97, 504–511. doi: 10.1111/j.1365-2672.2004.02329.x

Lovecka, P., Pacovska, I., Stursa, P., Vrchotova, B., Kochankova, L., and Demnerova, K. (2015). Organochlorinated pesticide degrading microorganisms isolated from contaminated soil. *N. Biotechnol.* 32, 26–31. doi: 10.1016/j.nbt.2014.07.003

Lu, P., Li, Q., Liu, H., Feng, Z., Yan, X., Hong, Q., et al. (2013). Biodegradation of chlorpyrifos and 3, 5, 6-trichloro-2-pyridinol by *Cupriavidus* sp. DT-1. *Bioresour. Technol.* 127, 337–342. doi: 10.1016/j.biortech.2012.09.116

Macedo-Raygoza, G. M., Valdez-Salas, B., Prado, F. M., Prieto, K. R., Yamaguchi, L. F., Kato, M. J., et al. (2019). *Enterobacter cloacae*, an endophyte that establishes a nutrient-transfer symbiosis with banana plants and protects against the black Sigatoka pathogen. *Front. Microbiol.* 10:804. doi: 10.3389/fmicb.2019.00804

Madhusmita, B., Pompi, D., Susanta, S. P., Robin, C. B., and Madhumita, B. (2017). Phosphate solubilization by endophytic bacteria isolated from *Oryza sativa*. *Int. J. Curr. Microb. App. Sci.* 6, 2713–2721. doi: 10.20546/ijcmas.2017.610.319

McDaniel, C. S., Harper, L. L., and Wild, J. R. (1988). Cloning and sequencing of a plasmid borne gene (*opd*) encoding a phosphotriesterase. *J. Bacteriol.* 170, 2306–2311. doi: 10.1128/jb.170.5.2306-2311.1988

Moon, Y. S., and Ali, S. (2022). Possible mechanisms for the equilibrium of ACC and role of ACC deaminase-producing bacteria. *Appl. Microbiol. Biotechnol.* 106, 877–887. doi: 10.1007/s00253-022-11772-x

Morsy, M., Cleckler, B., and Armuelles-Millican, H. (2020). Fungal endophytes promote tomato growth and enhance drought and salt tolerance. *Plants* 9:877. doi: 10.3390/plants9070877

Narayanan, Z., and Glick, B. R. (2022). Secondary metabolites produced by plant growth-promoting bacterial endophytes. *Microorganisms* 10:2008. doi: 10.3390/microorganisms10102008

Ningfeng, W., Minjie, D., Guoyi, L., Xiaoyu, C., Bin, Y., and Yunliu, F. (2004). Cloning and expression of *ophc*2, a new organphosphorus hydrolase gene. *Chin. Sci. Bull.* 49, 1245–1249. doi: 10.1360/04wc0146

Onofre-Lemus, J., Hernández-Lucas, I., Girard, L., and Caballero-Mellado, J. (2009). ACC (1-aminocyclopropane-1-carboxylate) deaminase activity, a widespread trait in *Burkholderia* species, and its growth-promoting effect on tomato plants. *Appl. Environ. Microbiol.* 75, 6581–6590. doi: 10.1128/AEM.01240-09

Panigrahi, S., Mohanty, S., and Rath, C. C. (2020). Characterization of endophytic bacteria *Enterobacter cloacae* MG00145 isolated from *Ocimum sanctum* with indole acetic acid (IAA) production and plant growth promoting capabilities against selected crops. *S. Afr. J. Bot.* 134, 17–26. doi: 10.1016/j.sajb.2019.09.017

Parakhia, M. V., Tomar, R. S., Malaviya, B. J., Dhingani, R. M., Rathod, V. M., Thakkar, J. R., et al. (2014). Draft genome sequence of the endophytic bacterium *Enterobacter* spp. MR1, isolated from drought tolerant plant (*Butea monosperma*). *Indian J. Microbiol.* 54, 118–119. doi: 10.1007/s12088-013-0429-5

Patel, H. M., Shaikh, M., Ahmad, I., Lokwani, D., and Surana, S. J. (2021). BREED based de novo hybridization approach: Generating novel T790M/C797S-EGFR tyrosine kinase inhibitors to overcome the problem of mutation and resistance in non-small cell lung cancer (NSCLC). *J. Biomol. Struct. Dyn.* 39, 2838–2856. doi: 10.1080/07391102.2020.1754918

Popp, J., Pető, K., and Nagy, J. (2013). Pesticide productivity and food security. A review. *Agron. Sustain. Dev.* 33, 243–255. doi: 10.1007/s13593-012-0105-x

Rojas-Sánchez, B., GuzmánGuzmán, P., Morales-Cedeño, L. R., Orozco-Mosqueda, M. D. C., SaucedoMartínez, B. C., Sánchez-Yáñez, J. M., et al. (2022). Bioencapsulation of microbial inoculants: Mechanisms, formulation types and application techniques. *Appl. Biosci.* 1, 198–220. doi: 10.3390/applbiosci1020013

Sargsyan, K., Grauffel, C., and Lim, C. (2017). How molecular size impacts RMSD applications in molecular dynamics simulations. *J. Chem. Theory Comput.* 13, 1518–1524. doi: 10.1021/acs.jctc.7b00028

Schloss, PD., and Handelsman, J. (2003). Biotechnological prospects from metagenomics. *Curr. Opin. Biotechnol.* 14, 303–310. doi: 10.1016/s0958-1669(03)00067-3

Sgroy, V., Cassán, F., Masciarelli, O., Del Papa, M. F., Lagares, A., and Luna, V. (2009). Isolation and characterization of endophytic plant growth-promoting (PGPB) or stress homeostasis-regulating (PSHB) bacteria associated to the halophyte *Prosopis strombulifera*. *Appl. Microbiol. Biotechnol.* 85, 371–381. doi: 10.1007/s00253-009-2116-3

Shaharoona, B., Riffat, B., Muhammad, A., Zahir, Z., and Ul-Hassan, Z. (2006). 1-Aminocylopropane-1- carboxylate (ACC)-deaminase rhizobacteria extenuates acc-induced classical triple response in etiolated pea seedlings. *Pak. J. Bot.* 38, 1491–1499.

Shen, Y. J., Lu, P., Mei, H., Yu, H. J., Hong, Q., and Li, S. P. (2010). Isolation of a methyl parathion-degrading strain *Stenotrophomonas* sp. SMSP-1 and cloning of the *ophc*2 gene. *Biodegradation.* 21, 785–792. doi: 10.1007/s10532-010-9343-2

Singh, B. K., Walker, A., Morgan, J. A. W., and Wright, D. J. (2004). Biodegradation of chlorpyrifos by *Enterobacter* strain B-14 and its use in bioremediation of contaminated soils. *Appl. Environ. Microbiol.* 70, 4855–4863. doi: 10.1128/AEM.70.8.4855-4863.2004

Son, H. J., Park, G. T., Cha, M. S., and Heo, M. S. (2006). Solubilization of insoluble inorganic phosphates by a novel salt-and pH-tolerant *Pantoea agglomerans* R-42 isolated from soybean rhizosphere. *Bioresour. Technol.* 97, 204–210. doi: 10.1016/j.biortech.2005.02.021

Sulistiyani, T. R., and Meliah, S. (2017). "Isolation and characterization of nitrogen fixing endophytic bacteria associated with sweet sorghum (*Sorghum bicolor*)," in *Proceedings of the SATREPS conference*, Vol. 1, Jawa Barat, 110–117.

Ullah, I., Khan, A. R., Park, G. S., Lim, J. H., Waqas, M., Lee, I. J., et al. (2013). Analysis of phytohormones and phosphate solubilization in *Photorhabdus* spp. *Food Sci. Biotechnol.* 22, 25–31. doi: 10.1007/s10068-013-0044-6

Yadav, P., Goyal, V. D., Chandravanshi, K., Kumar, A., Gokhale, S. M., Jamdar, S. N., et al. (2019). Catalytic triad heterogeneity in S51 peptidase family: Structural basis for functional variability. *Proteins* 87, 679–692. doi: 10.1002/prot.25693

Yang, C., Liu, N., Guo, X., and Qiao, C. (2006). Cloning of *mpd* gene from a chlorpyrifos-degrading bacterium and use of this strain in bioremediation of contaminated soil. *FEMS Microbiol. Lett.* 265, 118–125. doi: 10.1111/j.1574-6968.2006.00478.x

Zaman, N. R., Chowdhury, U. F., Reza, R. N., Chowdhury, F. T., Sarker, M., Hossain, M. M., et al. (2021). Plant growth promoting endophyte *Burkholderia contaminans* NZ antagonizes phytopathogen *Macrophomina phaseolina* through melanin synthesis and pyrrolnitrin inhibition. *PLoS One* 16:e0257863. doi: 10.1371/journal.pone.0257863

Zhang, H., Yang, C., Zhao, Q., and Qiao, C. (2009). Development of an autofluorescent organophosphates-degrading *Stenotrophomonas* sp. with dehalogenase activity for the biodegradation of hexachlorocyclohexane (HCH). *Bioresour. Technol.* 100, 3199–3204. doi: 10.1016/j.biortech.2009.02.008

frontiers | Frontiers in Plant Science

TYPE Original Research
PUBLISHED 13 December 2022
DOI 10.3389/fpls.2022.1017925

OPEN ACCESS

EDITED BY
Youssef Rouphael,
University of Naples Federico II, Italy

REVIEWED BY
Izabela Michalak,
Wrocław University of Science and Technology, Poland
Maria Giordano,
University of Naples Federico II, Italy

*CORRESPONDENCE
Silvia Valverde
silvia.valverde@uva.es

SPECIALTY SECTION
This article was submitted to Plant Nutrition, a section of the journal Frontiers in Plant Science

RECEIVED 12 August 2022
ACCEPTED 14 November 2022
PUBLISHED 13 December 2022

CITATION
Valverde S, Williams PL, Mayans B, Lucena JJ and Hernández-Apaolaza L (2022) Comparative study of the chemical composition and antifungal activity of commercial brown seaweed extracts. *Front. Plant Sci.* 13:1017925. doi: 10.3389/fpls.2022.1017925

Comparative study of the chemical composition and antifungal activity of commercial brown seaweed extracts

Silvia Valverde*, Paul Luis Williams, Begoña Mayans, Juan J. Lucena and Lourdes Hernández-Apaolaza

Department of Agricultural Chemistry and Food Science, Universidad Autónoma de Madrid, Madrid, Spain

Introduction: A sustainable agriculture and the great increase in consumers of organic products in the last years make the use of natural products one of the main challenges of modern agriculture. This is the reason that the use of products based on seaweed extracts has increased exponentially, specifically brown seaweeds, including Ascophyllum nodosum and Ecklonia maxima.

Methods: In this study, the chemical composition of 20 commercial seaweed extract products used as biostimulants and their antifungal activity against two common postharvest pathogens (Botrytis cinerea and Penicillium digitatum) from fruits were evaluated. Data were processed using chemometric techniques based on linear and non-linear models.

Results and discussion: The results showed that the algae species and the percentage of seaweed had a significant effect on the final composition of the products. In addition, great disparity was observed between formulations with similar labeling and antifungal effect of most of the analyzed products against some of the tested pathogens. These findings indicate the need for further research.

KEYWORDS

brown seaweed extracts, biostimulants, chemical composition, antifungal activity, chemometrics

Abbreviations: AA, alginic acid; *AN*, *Ascophyllum nodosum*; *EM*, *Ecklonia maxima*; IAA, indole-3-acetic acid; Lam, laminarin; Man-ol, mannitol; TAC, total antioxidant capacity; TCC, total carotenoid content; TFC, total flavonoid content; TTC, total tannin condensed capacity; TPC, total phenolic content; SA, salicylic acid; SWEs, seaweed extracts.

1 Introduction

The great challenge of food production is to use sustainable practices that increase the harvestable yield and quality of crops with minimal impact on the environment. It is well-known that chemical fertilizers have led to the deterioration of agricultural systems (Biau et al., 2012). In recent years, environment-friendly and economic alternatives have been sought that can reduce the use of traditional fertilizers (Trivedi et al., 2018), such as seaweed extracts (SWEs). Recently, a growing interest has been observed for the use of this type of products because they are natural and biostimulant substances that improve the crop growth and quality of fruits (Tabbara et al., 2018). Despite the fact that SWEs are traditionally used as biostimulants, supplementary fertilizers, or soil quality improvers, their use has also been reported as animal feed supplement, human nutritional supplement, and cosmetic products (Pereira et al., 2020).

The most widely used macroalgae in agriculture are brown seaweeds, including *Ascophyllum nodosum* (*AN*), *Ecklonia maxima (EM)*, *Fucus vesiculosus*, *Laminaria digitata*, *Sargassum* spp., and *Turbinarias* spp. (Khan et al., 2009), being the most commercialized extracts of the first two species. Their biochemical composition depends on their location and the conditions of the place where they grow. In this way, the content of active ingredients will be modified between each species and within the same species in relation to the availability of nutrients, light, salinity, depth, presence of organic contaminants, or content of heavy metals (Kumar and Sharma, 2021) with potential human risk associated, among others. *A. nodosum* grows on the coasts of the North Atlantic, mainly on the northwestern coast of Europe and North America. Unlike other species of brown algae, it supports periods of marine immersion and periods of exposure to the elements, depending on the tidal cycle. This fact of physiological adaptation provides a characteristic biochemical composition that is very useful for their use in agriculture (Hurtado et al., 2021). Meanwhile, *E. maxima*, an endemic South African seaweed, always grows submerged in water and did not emerge at times of low tide; thus, it is considered a potential source of beneficial bioactive compounds. After seaweed recollection, the active ingredients contained in algae are extracted from the cells and transferred to a liquid medium to obtain a commercial product using different extraction processes. Depending on the process used, the final composition of the product can be significantly altered (Povero et al., 2016). The most widespread extraction processes are traditional extraction based on the use of chemical agents and cold extraction. Chemical extraction uses strong acids or alkalis (KOH), and the product obtained is dark due to the high oxidation of its active components leading to denaturation of active ingredients that results in a drastic loss of properties (Calvo et al., 2014). Cold extraction has gained popularity because algae are subjected to a micronized process under high pressure without loss of active ingredients and pH is kept at its physiological level of 4.5 (Crampon et al., 2011). These products have a characteristic marine aroma and color that ranges from green to light brown.

SWEs contain a multitude of active components (Khan et al., 2009), although it is considered that the following are the main active ingredients: alginic acid, which is present in the cell walls and confers flexibility and adaptation to stress phenomena; mannitol, which blocks reactive species and prevents metabolic damage; reserve polysaccharides (laminarin and fucoidan) that are not found in terrestrial plants; polyphenols and tannins with high antioxidant power, which stabilizes and strengthens cell walls against pathogen attacks and minerals, among others. All these components have a synergistic effect in the crops, providing a strong root system, promoting plant growth, and improving leaf development and flowering (Mukherjee and Patel, 2019). In addition, the quality of the fruit and vegetables has been reported in numerous studies, not only providing physiological and nutritional benefits but also improving the organoleptic properties by the consumer (Kocira et al., 2018; Meng et al., 2022). The antifungal activity of SWE has also been studied in several research as preventive treatment to postharvest pathogens (De Corato et al., 2017; Lahbib et al., 2022). This is because marine organisms have developed an antimicrobial defense strategy based on the production of bioactive metabolites (Cortés et al., 2014) with antioxidant character.

According to the growing organic production expansion and efforts to reduce the use of chemical fungicides and fertilizers, SWEs may play a greater role in crop protection than was previously realized. In fact, many products containing SWEs are commercially available for application to various horticultural crops under different trade names. In most of the products, there is no homogeneity in the labeling, and a detailed description of the composition is not usual, making it difficult to understand its mode of action and its influence on the plant growth, fruit quality, and antifungal activity.

Hence, this study was conducted to investigate the chemical composition and *in vitro* antifungal assays against two common pathogens on four different fresh fruits of 20 representative commercial seaweed extracts and to further treat data by multivariate statistical analysis. To the authors' knowledge, this is the first time that such a detailed study of several brown seaweed extracts has been carried out. The contribution of this study is expected to provide a reference for the knowledge of these products and the ability of chemometrics multivariate methods to know the production factors that influence their composition and their relationship with antifungal activity.

2 Materials and methods

2.1 Samples

Several representative seaweed commercial products were selected in this study according to the species (*A. nodosum* and

E. maxima), method of extraction (basic media-KOH, acid media, or cold), pH (from 3.20 to 10.8), the way in which they are marketed—liquid products (LP, n=16) or solid products (SP, n=4)—and percentage of algae in the product—low (10%–30%) and high (100%). Products with high percentage (100%) are those that consist only of algae extract, while those that have low percentage are mixtures of algae extracts with other components such as amino acids or sugars, among others. The percentage indicates the amount of seaweed in the product and is usually specified on the labeling. All the samples were kindly provided by different fertilizer companies (n=18) and by Laboratorio Arbitral (Spain's Ministry of Agriculture, Fisheries and Food; MAPA) (n=2). Table 1 summarizes the main characteristics of the seaweed products selected in this study.

2.2 Sample preparation

Formulated liquid samples were previously freeze-dried and then pulverized with a mortar for all tests except for polysaccharides content (alginic acid, mannitol, and laminarin) and antifungal *in vitro* assays. Solid samples were previously homogenized with a mortar. All measurements were performed in triplicate.

2.2.1 Determination of chemical composition

2.2.1.1 Polysaccharides content

To estimate the alginic acid (AA), mannitol (Man-ol, polyol), and laminarin (Lam) content, the method of Valverde et al. (2022) was used. Briefly, 40 mg of liquid product (LP) or 20 mg of solid product (SP) was diluted in 100 ml (LP) or 250 ml (SP) of ultrapure water. For SP, a previous step was necessary based on crushing with a grind and passing it through a 40-mesh screen to obtain a homogenous sample. Then, the mixture was shaken in a vortex for 1 min and centrifuged for 5 min at 3,000 rpm. The samples were filtered through 0.45-µm nylon filter before analysis by high-performance liquid chromatography refractive index detector (HPLC-RID) system (1260 Infinity model Agilent Technologies, Waldbronn, Germany). A Bio-Rad Aminex HPX-87 H column (300 × 7.8 mm, 9 µm) was used, protected by a guard column from Phenomenex (Torrance, CA, USA). Analysis conditions were set as follows: the mobile phase was a 0.05% acetic acid, the flow rate was 0.5 ml/min, the injection volume was 50 µl, the column temperature was set at 65°C, and the temperature of the refractive index detector was at 50°C in positive polarity mode. Quantification was achieved using glycerol as internal standard (IS) calibration, employing glycerol in order to reduce analysis error (n=6) and fluctuations on the signal.

2.2.1.2 Sugar content

Sugar analysis (arabinose, fucose, glucose, glucuronic acid, rhamnose, sucrose, and xylose) was carried out using the reported methods with slight modifications (Sluiter et al., 2012; Manns et al., 2014; Badmus et al., 2019): A total of 150 mg of the sample was hydrolysed with 200 µl of sulphuric acid 72% w/w at 30°C for 1 h; the reaction mixture was then diluted

TABLE 1 Description of the seaweed products selected for this study according to criteria described in *Section 2.1*.

Sample code	Formulated	Species	Algae percentage (%)	Extraction method	pH ± SD	EC (mS cm^{-1}) ± SD
1	Liquid	AN	Low (25)	Cold	4.59 ± 0.01	5.34 ± 0.07
2		AN	Low (27)	Cold	4.26 ± 0.02	8.71 ± 0.1
3		AN	High (100)	Acid	3.35 ± 0.01	3.75 ± 0.02
4		AN	High (100)	Cold	4.40 ± 0.02	8.04 ± 0.09
5		AN	Low (27)	Cold	5.33 ± 0.03	20.1 ± 0.1
6		EM	Low (16)	Cold	5.20 ± 0.02	2.96 ± 0.01
7		EM	Low (15)	Cold	4.50 ± 0.01	2.17 ± 0.01
8		AN	Low (27)	KOH	10.0 ± 0.01	42.7 ± 0.2
9		AN	Low (30)	Acid	3.81 ± 0.01	10.2 ± 0.09
10		EM	Low (30)	Acid	3.79 ± 0.02	14.9 ± 0.1
11		AN	High (100)	Cold	4.70 ± 0.01	11.5 ± 0.09
12		AN	Low (20)	Cold	4.46 ± 0.01	8.33 ± 0.07
13		EM	High (100)	Cold	4.42 ± 0.01	13.1 ± 0.09
14		AN	High (100)	Cold	4.82 ± 0.02	9.01 ± 0.07
15		AN	High (100)	Cold	4.76 ± 0.01	5.55 ± 0.02
16		AN	High (100)	KOH	8.50 ± 0.01	13.2 ± 0.1
17	Solid	AN	High (100)	KOH	9.82 ± 0.03	12.1 ± 0.1
18		AN	High (100)	KOH	10.6 ± 0.02	20.4 ± 0.1
19		AN	High (100)	KOH	10.3 ± 0.03	20.2 ± 0.1
20		AN	High (100)	KOH	11.0 ± 0.03	21.0 ± 0.1

with 3.6 ml of ultrapure water reacting for 40 min at 100°C. After cooling, samples were centrifuged for 10 min at 5,000 rpm; ultrapure water was added, taking the supernatant up to 5 ml, and it was filtered through a 0.45-µm nylon filter before analysis by HPLC-RID system. A Bio-Rad Aminex HPX-87 H column (300 × 7.8 mm, 9 µm) was selected with 4 mM H_2SO_4 solution as the mobile phase at a flow rate of 0.6 ml/min; the injection volume was 50 µl, and the column temperature was set at 60°C.

2.2.1.3 Mineral content

Mineral profiling was obtained through digestion of 50 mg of powdered seaweed weighed into an Erlenmeyer flask and addition of 5 ml of concentrated trace metal grade nitric acid (67% assay) and 5 ml of hydrogen peroxide (30% assay). The mixture was left to react for an hour at room temperature and then heated at 80°C for 30 min with a plate digestion. After cooling, samples were filtered and made up to 25 ml with Milli-Q water. The certified reference material (CRM) NCS DC73350 (leaves of poplar) was prepared in the same manner to validate the accuracy of the analysis. The samples were analyzed by inductively coupled plasma–optical emission spectrometry (ICP-OES) (iCAP-PRO XDuo Spectrometer, Thermo Scientific, UK). Fourteen minerals were measured: calcium (Ca), magnesium (Mg), potassium (K), aluminium (Al), phosphorous (P), iron (Fe), copper (Cu), manganese (Mn), zinc (Zn), nickel (Ni), arsenic (As), cadmium (Cd), chromium (Cr), and lead (Pb). The optimal instrumental conditions of ICP-OES, along with the selected wavelengths and IS, are presented in Supplementary Table S1. In order to avoid ion signal fluctuations caused by the matrix, a diluted internal standard (IS) solution (10mg/L of ^{89}Y) was used. This solution was distributed in all solutions (blank, standard solutions, and unknown samples) using a second channel of the peristaltic pump.

2.2.1.4 Hormonal composition

Plant hormones (abscisic acid, indole-3-acetic acid, indole butyric acid, gibberellic acid, and salicylic acid) were analyzed using reported validated analytical methodologies (Jiang et al., 2006; Górka and Wieczorek, 2017). Briefly, 50 mg of powdered samples were extracted with 0.5 ml methanol 70% (v/v) and remained overnight at 4°C. The supernatant was concentrated under N_2 stream and dissolved in 1 ml Na_2HPO_4 at pH 9.0. The solution was extracted three times with ethyl acetate and adjusted to pH=2.5. Finally, the organic phases were dried with a gentle stream of N_2, dissolved in 1 ml of methanol 70% (v/v), and filtered through 0.45-µm nylon filter before analysis by HPLC with a diode-array detector (DAD) (HPLC-DAD) system. Chromatographic conditions were set as follows: analytical column Luna C_{18} (2) (150 × 4.6 mm, 3 µm), mobile phase consisted of (A) acetonitrile (0.1% formic acid) and (B) 0.1% formic acid in gradient elution mode; 0–10 min A:B, 25:75 (v/v); 11–17 min A:B, 50:50 (v/v); and 18–30 min A:B, 25:75 (v/v). Flow rate was 0.5 ml/min, injection volume was 10 µl, and the temperature of the column was maintained at 25°C. Detection was carried out at a wavelength of λ=214 nm.

2.2.1.5 Total phenol content

Methanolic SWE were obtained according to Badmus et al. (2019). Briefly, 250 mg of SWE and 5 ml of methanol was sonicated for 30 min and shaken for 4 h in an orbital shaker. Then, extracts were centrifuged for 10 min at 2,500 rpm. To estimate the total phenolic content (TPC), the modified Folin–Ciocalteu method was used with minor modifications. A total of 20 µl of the extract was combined with 100 µl of Folin–Ciocalteu reagent (1:10 v/v) and 80 µl of 7.5% sodium carbonate. The mixture was shaken for 30 s and allowed to stand for 2 h at room temperature in darkness. Standards (gallic acid) and blanks (methanol) were prepared and processed using the same method as for SWE. The absorbance was measured at 765 nm using a microtiter plate (SPECTROstar Nano, BMG Labtech Germany). Gallic acid was used as standard, and blanks (methanol) were prepared following the same method as for seaweed samples. Results were expressed as mg gallic acid equivalents/g dry extract.

2.2.1.6 Total flavonoid content

Seaweed ethanolic extracts were obtained previously as described in the previous section. Total flavonoid content was determined as described by Chang et al. (2002). Briefly, 15 µl of the sample was mixed with 307 µl of 10% aluminium chloride, 307 µl of 1M potassium acetate, and 200 µl of Milli-Q water. After incubation for 30 min in the dark at room temperature, the absorbance was measured at 510 nm (SPECTROstar Nano, BMG Labtech Germany), using quercetin as standard.

2.2.1.7 Total condensed tannin

The total condensed tannin content was performed by the vanillin–HCl method (Cox et al. (2010). Seaweed methanol extract (25 µl), obtained as in *Section 2.2.1.5*, was mixed with 150 µl of vanillin 4% and 75 µl of HCl concentrated. The solution was shaken and left at room temperature for 20 min of protected light. The absorbance of samples, standards ((+) catechin), and blanks (methanol) were recorded using a microtiter plate (SPECTROstar Nano, BMG Labtech Germany) at 500 nm.

2.2.1.8 Total carotenoid content

Carotenoids were determined according to the methodology of Kumar et al. (2009), with slight modifications. Briefly, 1 g of powdered samples was incubated with 10 ml of 80% acetone for 90 min at 20°C. Then, the mixture was centrifuged for 15 min at 3,000 rpm and filtered using a filter paper (Whatman No. 1). A standard curve was prepared using β-carotene, and results were obtained by measuring the absorbance at 480 nm (SPECTROstar Nano, BMG Labtech Germany).

2.2.1.9 Total antioxidant capacity

Total antioxidant capacity (TAC) was assessed according to a previous method (Costa et al., 2011). Seaweed methanolic extract (100 µl), obtained as previously described, was mixed with 1 ml of a solution containing 0.6 M sulphuric acid, 28 mM sodium phosphate dibasic and 4 mM ammonium molybdate (4:2:4 v/v/v). The mixture was incubated for 90 min at 95°C and cooled at room temperature. Then, the absorbance of standards (ascorbic acid), blanks (methanol), and samples were measured at 695 nm (SPECTROstar Nano, BMG Labtech Germany).

2.2.1.10 DPPH radical scavenging activity

The DPPH radical scavenging activity was determined using the method of Zhang et al. (2008) and Yang et al. (2008). Seaweed methanol extract (100 µl) and 0.16 mM 2,2-diphenyl-1-picrylhydrazyl hydrate (DPPH) (100 µl) in methanol were mixed. The mixture was shaken for 30 s and left in darkness at room temperature for 30 min. The absorbance was read in a microtiter plate (SPECTROstar Nano, BMG Labtech Germany) at 517 nm. The scavenging effect was calculated as an inhibition percentage using **Eq. (1)** as follows:

$$DPPH\ \ inhibition(\%) = \left(\frac{A_c - A_s}{A_c}\right) \times 100$$

where A_c is the absorbance of the control (100 µl of methanol solvent with 100 µl of the DPPH solution), and A_s is the absorbance of the sample.

2.2.2 *In vitro* antifungal activity assays

Previously, the products under study were tested to verify that they were free of microorganisms. For that purpose, the products were prepared at recommended dose by the manufacturer, and 500 µl was incubated on Petri dishes with a general culture medium, potato dextrose agar (PDA), to check the presence of any kind of microorganism. All the samples were done in triplicate. They were incubated at 26°C in the dark in a growth chamber for a week.

Pathogen fungi were isolated from the selected rotten fruits: *Penicillium digitatum* from orange, *Botrytis cinerea* from strawberry, blueberry, and tomato in PDA. Petri dishes were incubated in a growth chamber at 26°C in the dark. Once grown, 5-mm fungal plugs were inoculated in PDA plates, and the correspondent product was poured at a recommended dose by manufacturer, all in triplicate. They were grown in the same conditions for 22 days. The growth inhibition halo was evaluated.

2.3 Statistical analysis

IBM SPSS Statistics 26.0 software (SPSS Inc., Chicago, IL, USA) was used for multivariate analysis of covariance (MANCOVA), principal component analysis (PCA), hierarchical cluster analysis (HCA), and artificial neural network analysis (ANN).

3 Results

3.1 Chemical composition

The results of the analysis of characteristic and bioactive compounds, including the mean (and standard deviation), minimum, and maximum values of the products evaluated, are shown in Table 2. The selected products presented a wide range of pH from 3.9 to 10.7. This variety is mainly due to the extraction method used and the algae percentage in the product. The EC provides the value of the soluble salts present in the SWEs. The strong differences observed among the products can be attributed to the way in which the algae are extracted, e.g., alkaline media provide high concentrations of potassium, and/or the area where they have been collected (mainly *AN* grows in the Atlantic Ocean and *EM* in South Africa). It is recommended that a fertilizer has a low EC value to facilitate fertilization and avoid crop phytotoxicity. The variations in AA, Man-ol, and Lam were attributed to intrinsic botanical differences of the species. It was observed that *AN* products presented higher contents for these three components than *EM*. These results agreed with those reported in previous studies and can also be attributed to the different growing conditions of the source material and possible variations in the processing methods (Pereira et al., 2020; Valverde et al., 2022). Sugar profile was similar for both species, following the trend: glucose≃ glucuronic acid>sucrose≃ fucose>xylose. Although the concentration of sugars was higher for *AN*, all the products presented a variety of sugars that will facilitate the assimilation of nutrients and their transport by the plant, as they reduce the osmotic pressure, thus improving vegetative development. The mineral composition for *AN* product (Table 2) followed the trend, K>Mg>Ca>Al>P>Fe>Mn>Zn>Cu, whereas *EM* followed the trend, K>Mg>Ca>P>Al>Fe>Zn>Mn>Cu. Potassium, Mg, and Ca were the most abundant plant macronutrients in the studied products, highlighting that the higher concentrations of K may be due to the accumulation in the tissues of the algae and extraction methodology employed. Variations in microelements are attributed to the species of algae, the season in which they were collected, and the algae percentage of the product. Heavy metals were analyzed because seaweeds are known to accumulate pollutants. The results revealed the presence of Cr and Ni in most of the products, which can affect both the nutrition of the plants and their productive quality. *A. nodosum* products presented the higher concentrations (Ni, 0.15 ± 0.002 mg/kg; Cr, 0.19 ± 0.001 mg/kg) although within the established limits by European Commission under Regulation (UE) 2019/1009 about fertilizer products (Ni= 50 mg/kg and Cr=2 mg/kg dry matter). These results are in relation to those previously reported, indicating that *AN* is used as a biomonitor of metal concentration in coastal habitats (Morrison et al., 2008). The results of the hormonal analysis

10.3389/fpls.2022.1017925

TABLE 2 Summary of the compounds analyzed in seaweed extracts under study.

Variables		Min.	Max.	Mean.	SD
pH (1:5)[a], (1:25)[b]	pH	3.79	10.7	7.38	0.04
Electric conductivity (mS cm^{-1})	EC	2.17	42.7	22.4	0.1
Characteristic compounds					
Alginic acid (%)	AA	0.61	18.0	9.21	0.2
Mannitol (%)	Man-ol	<LOD[c]	5.84	2.92	0.05
Laminarin (%)	Lam	<LOD[c]	4.73	2.37	0.2
Potassium (g/kg)	K	5.04	180	92.5	1.5
Calcium (g/kg)	Ca	0.40	11.6	6.00	0.5
Magnesium (g/kg)	Mg	0.11	10.3	5.13	0.2
Aluminum (g/kg)	Al	0.20	2.10	1.15	0.05
Phosphorus (g/kg)	P	0.16	2.82	1.50	0.1
Iron (g/kg)	Fe	0.046	1.26	0.65	0.1
Copper (g/kg)	Cu	<LOD[c]	0.50	0.25	0.01
Manganase (g/kg)	Mn	<LOD[c]	0.75	0.38	0.05
Zinc (g/kg)	Zn	0.033	1.51	0.77	0.07
Chromium (mg/kg)	Cr	<LOD[c]	0.19	0.096	0.001
Nickel (mg/kg)	Ni	<LOD[c]	0.15	0.045	0.002
Sucrose (mg/kg)		<LOD[c]	70.0	34.9	0.84
Glucuronic acid (g/kg)		<LOD[c]	81.3	40.6	1.2
Glucose (g/kg)		5.10	31.1	18.1	0.7
Xylose (g/kg)		<LOD[c]	32.6	16.3	0.3
Rhamnose (g/kg)		<LOD[c]	5.16	2.58	0.4
Arabinose (g/kg)		<LOD[c]	5.40	2.69	0.2
Fucose (g/kg)		<LOD[c]	69.6	34.8	1.9
Σ%Sugars		0.20	14.5	7.30	0.2
Indole-3-acetic acid (g/kg)	IAA	<LOD[c]	16.6	8.27	0.8
Salicylic acid (mg/kg)	SA	<LOD[c]	54.3	27.1	2.1
Bioactive compounds					
Total phenol content (g/kg)	TPC	1.80	107	54.6	1.9
Total flavonoid content (g/kg)	TFC	1.90	274	138	2.0
Total tannin condensed content (μg/kg)	TTC	0.01	0.65	0.30	0.05
Total carotenoid content (g/kg)	TCC	0.30	14.6	7.50	0.9
Total antioxidant capacity (g/kg)	TAC	0.82	24.2	12.5	0.3
DPPH radical scavenging activity (%)	DPPH	0.00	87.3	43.7	1.3

Mean (n=20) values.
[a]pH dilution (1:5) for liquid products.
[b]pH dilution (1:25) for solid products.
[c]The measurement was under the detection limit (LOD).

were conditioned by the instrumental analysis technique used (HPLC-DAD) because these analytes are expected in low concentrations. Despite this, the most remarkable results, as expected, were for indole-3-acetic acid (IAA), the major hormone. It is the main auxin in plants and controls several physiological processes such as cell elongation and division. It was detected in products of both species; however, it was not detected in the solid formulations. This fact has not been previously reported in any studies, which suggests that the type of formulation may influence in some way the final hormonal composition of the product. The analysis of bioactive compounds revealed that the concentration of TFC (274 ± 2.0 g/kg) was higher than that of TPC (107 ± 1.9 g/kg) in all the products tested, *AN* being the products with the highest concentration. Notable concentrations of TCC (14.6 ± 0.87 g/kg), associated with the characteristic brownish color, were also detected with the same trend described above. Most of the samples presented tannins although at very low concentrations. It should be noted that the presence and abundance of these compounds depend on the species, the habitat, the seasonal influence, the stage of the life cycle, the environmental conditions, and the extraction method. All the products tested presented high concentrations of bioactive components as described in previous

studies (Agregán et al., 2017; Kocira et al., 2018; Habeebullah et al., 2021). The presence of these compounds will benefit the productive development of the plant and the quality of the fruit, providing them high added value. The antioxidant activity was evaluated by TAC and DPPH assays. According to the parameters studied previously, it was observed that the TAC was higher for *AN* (24.4 ± 0.32 g/kg) than for *EM* (0.84 ± 0.32 g/kg). These results are related to the presence of antioxidant compounds, which agree with the results obtained previously. DPPH assay has been used extensively as a free radical to evaluate the antioxidant potentials in plant extracts (Duan et al., 2006; Farasat et al., 2014). SWEs contain numerous antioxidant molecules that are able to reduce the DPPH free radicals by attacking the molecules to add hydrogen atom to it or donate an electron to it, providing a color change from purple to yellow in the DPPH solution (Devi et al., 2011). The average values for scavenging DPPH radical were always higher than 40% for most products, with a trend similar to that observed in TAC assay. Previous studies reported that brown seaweeds are rich in bioactive compounds compared with red and green seaweeds, so %DPPH reduction is greater (Cox et al., 2010; Leelavathi & Prasad, 2014).

3.2 Antifungal activity

All products under study were evaluated to elucidate if they could have any effect on the most common pathogen fungi of orange, strawberry, blueberry, and tomato. The presence of inhibition haloes was considered positive, as the products used in crops could inhibit the growth of these undesirable pathogens. Some of the tested products inhibited the fungal growth, as is shown in Table 3 with a (+) sign at 48 h, although the cultures were incubated for 22 days to know if the effect persisted. The initial microbiological test showed that at recommended doses, products 8 and 12 promoted in themselves the growth of some kind of microorganisms. The plates with product 8 seemed to grow fungi; meanwhile, product 12 showed a bacterial growth, but specialized research was required to properly describe them (see Supplementary Figure S1). Thus, their use might not be recommended, as the effect on soil microbiota and on fruits is not known and should be evaluated in further research. It should be noted that both products correspond to *AN* with low algae percentage. The results showed the products that inhibited both fungal growth at 48 h and continued with the effect for 22 days. *Botrytis cinerea* in tomato was inhibited in 65% (4,6,8–14,16–20) of the products studied, while in strawberry and blueberry, there were fewer products that presented action, 25% (6,10–13) and 35% (4,6,8–9, 16–17,20), respectively. Noteworthy, most of the products that showed inhibition in strawberry corresponded to *EM*. *Penicillium digitatum* was inhibited in 25% of the products studied (5,8–9,13,17). The products that inhibited the growth in more fruits were the following: product 6 against *B. cinerea* in all of the fruits studied; products 8, 9, and 17 showed a positive effect on tomato, blueberry, and orange; and product 13 against pathogens in tomato, blueberry, and orange. In Supplementary Figure S2, the Petri dishes of tomato and strawberry with product 13 (*EM*, 100%) are shown; the inhibition halo can be clearly seen especially in strawberry at 48 h (Supplementary Figure S2E), and the effect remains for 22 days (Supplementary Figure S2F).

These facts indicate that products of both species (*AN* and *EM*) showed inhibition halo and products of different percentage and type of formulation. Table 4 shows the most relevant previous works where the efficacy of SWE against different pathogens was evaluated. Only one previous study was found in which the effectiveness of *EM* was evaluated (Righini et al., 2020). In this research, *EM* did not present antifungal activity; it should be noted that both the pathogen and the fruit studied were different (*P. xanthii* in cucumber). Our study showed promising results for *EM* extracts especially in strawberry. Furthermore, previous studies also found a positive activity of *AN* against the pathogen *B. cinerea* in carrot, cucumber, and pear (Jayaraj et al., 2008; Jayaraj et al., 2011; Lutz et al., 2022) and similar results in *L. digitata* (common brown seaweed used in agriculture) in strawberry (De Corato et al., 2017). The antifungal effect of those products was related to polysaccharide content, carbohydrate content, or bioactive molecules of the algae such as polyphenols or pigments like carotene (see Table 4). In these studies, the SWE used presented 12%–18% alginic acid, 5%–6% Man-ol, and 10%–15%

TABLE 3 Results of antifungal activity *in vitro* after 48 h of application of the SWEs.

Sample code	Tomato	Blueberry	Strawberry	Orange
1	–	+	–	–
2	–	–	–	–
3	–	–	–	–
4	+	+	–	–
5	–	–	–	+
6	+	+	+	–
7	–	–	–	–
8	+	+	–	+
9	+	+	–	+
10	+	–	+	–
11	+	–	+	–
12	+	–	+	–
13	+	–	+	+
14	+	–	–	–
15	–	–	–	–
15	+	+	–	–
17	+	+	–	+
18	+	–	–	–
19	+	–	–	–
20	–	+	–	–

Symbol (-) represented the absence of effect of SWEs on the studied pathogens. Symbol (+) was associated with the positive effect of SWEs with the inhibition haloes on the studied pathogens.

TABLE 4 Antifungal activity of SWEs reported in published studies.

Algae	Species	SWE (n°)	SWE composition	Pathogen	Fruit/vegetables	*In vitro*	*In vivo*	Compounds involved	Ref.
Brown	*AN*	1	PS and CH	*Alternaria radicina*, *B. cinerea*	Carrot	No	Yes	CH and laminarin	Jayaraj et al., 2008
Brown	*AN*	1	PS and CH	*Alternaria cucumerinum*, *Fusarium oxysporum*, *B. cinerea*	Cucumber	No	Yes	CH, laminarin and carragen	Jayaraj et al., 2011
Brown and red	*L. digitata, U. pinnatifida, P. umbilicalis, E. denticulatum, G. pusillum*	5	Lipids, fatty acids, PS, and TPC	*B. cinerea, Monilinia laxa, P. digitatum*	Strawberry, peach and citrus lemon	Yes	Yes	Phenolic compounds, PS and lipids	De Corato et al., 2017
Brown and red	*EM* and *J. adhaerens*	2	Proteins, chlorophylls, carotenoids and antioxidant activity	*Podosphaera xanthii*	Cucumber	Yes	No	Proteins and carotenes	Righini et al., 2020
Red	*Gracilaropsis persica*	1	Bioactive compounds	*B. cinerea*, *Pyricularia oryzae, Aspergillus niger*, and *Penicillium. expansum*	Fungi collection (laboratory)	Yes	No	Phenolic compounds and tannin	Pourakbar et al., 2021
Brown	*AN*	1	NS	*B. cinerea*, *A. alternata*, and *Alternaria* spp.	Pear	Yes	Yes	NS	Lutz et al., 2022
Brown, red and green	*U. fasciata, (Rhodophyceae) B. bifurcata, (Chlorophyceae)*	4	TPC, TFC, and antioxidant activity	*P.digitatum*, *Penicillium expansum*, and *Penicillium italicum*	Fungi collection (laboratory)	No	Yes	Phenolic compounds and fatty acids	Lahbib et al., 2022
Brown	*AN* and *EM*	20	PS, mineral profile, CH content, hormonal composition, TPC, TFC, TCC, TTC, and antioxidant activity	*B. cinerea* and *P. digitatum*	Tomato, blueberry, strawberry and orange	Yes	No	PS, CH content and bioactive compounds	Present study

PS, polysaccharide content; CH, carbohydrate content; NS, not specified.

carbohydrate content, comparable to the solid products of this study (17–20), which showed activity against *B. cinerea* in different fruits. *Penicillium digitatum* was evaluated to a lesser extent; only two recent studies were found in brown algae. One of them evaluated the species *L. digitata* in citrus lemon (De Corato et al., 2017), and its positive effect was related to the content of polysaccharides (23%) and TPC (2.3%). In general, this content was higher than in the products of this study that presented positive activity against *P. digitatum*, but a relationship between two products was found: product 17 presented 19% polysaccharides content and product 5 a 2.5% TPC. Lahbib et al. (2022) related the fungicidal activity with TPC (14.26 mg/g) and TFC (9.16 mg/g). The products of this study present TPC values between 7–17 mg/g but much higher for TFC (30–240 mg/g). All these suggest that the antifungal activity may be due to the combined action of different compounds. Although it is true that previous works have evaluated other types of algae (red and green), brown algae are the ones that presented the highest fungicidal capacity (De Corato et al., 2017; Righini et al., 2020; Lahbib et al., 2022). This study evaluated for the first time the action of *AN* and *EM* against *P. digitatum*. Promising results were found for tomato (65% of the products showed positive action) and *EM* in strawberry. It should be noted that no previous studies on blueberries were found. In addition, 20 SWEs were evaluated compared to 5 in other studies, being the maximum number of products studied in previous research and providing a much more detailed information on the chemical composition. Moreover, this study lasted for 22 days to check the long-term fungicidal effect, while previously reported studies did not indicate this effect. However, in those pathogens, more research should be done, since the application of algae extract to fertilize the crops could have a positive effect on inhibiting pathogens, providing added value to these products. These promising results indicate that these products could be an alternative to use in to treat fruits and vegetables postharvest to minimize the damage caused by the attack of microorganisms.

These findings revealed that market SWEs have a great variety in their composition, thus justifying this study and the need to continue with this line of research carrying out tests *in vivo*.

3.3 Chemometric analysis

3.3.1 Multivariate generalized linear model

MANCOVA analysis was used to evaluate the effect of algae species and algae percentage on the final composition of the products studied. It was conducted to test the influence of several

independent variables in structural (AA, Man-ol, Lam, metal profile, IAA, SA, and sugar content) and bioactive compounds (TPC, TFC, TCC, TTC, TAC, and DPPH) of products studied. In order to make a preliminary determination of algae species, the percentage of SWE in the product and the extraction process were used as fixed factor and the formulation type as covariate. To evaluate the statistical significance of the model, Wilks's lambda, F-value, and p-values for main and interaction effects were employed. Levene's test of equality of error variances was given for all measured parameters. The level of significance was set at $p<0.05$. The results showed that the strongest explanatory variables were the percentage of SWE in the product (Wilks's $\lambda=0.02$, $F=4.045$, $p=0.028$) and algae species (Wilks's $\lambda=0.01$, $F=190.9$, $p=0.047$); meanwhile, the extraction process (Wilks's $\lambda=0.01$, $F=3.080$, $p=0.164$) had no significant effect, so we omitted this variable in the final MANCOVA model. The formulation type did not interact with fixed factors and had no significant effect (Wilks's $\lambda=0.02$, $F=81.98$, $p=0.085$), indicating that this covariate was selected correctly. The reported tests showed that for these variables—species and SWE percentage—the null hypothesis is rejected, so they significantly influence on the final composition of the products. These findings contribute to understanding the role of variables related to the production process on the final composition of SWE.

3.3.2 Principal component analysis

PCA was made using the raw data obtained from the composition analysis of SWE. To examine the suitability of these data, the Kaiser–Meyer–Olkin (KMO) test was performed. The KMO test measures the sampling adequacy and indicates the proportion of variance. The KMO result was 0.82 (≥0.5), indicating that PCA could be useful in providing significant reductions in the dimensionality of the raw data. Major components were extracted with eigenvalues >1.0. In this model, PC1 explains 35% of the accumulative variance; PC2, 60%; PC3, 69%; PC4, 75%; PC5, 84%; PC6, 87%; PC7, 91%; PC8, 92%; and PC9, 99%. The component plot rotated space generated from the first two PCs explained the variations in the seaweed products in relation to their composition (Figure 1A). PC1 had a medium positive loading (loading values, 0.50–0.70) of Ca, Mg, Al, TCC, and TTC and strong negative loading (loading values, 0.7–1.00) for Man-ol, TAC, and pH. Most of the samples showed a positive relation with PC1. On the other hand, a high negative relationship was observed corresponding to the solid formulations (see in Figure 1B) due to their low concentration of Ca, Mg, and Al and high levels of Man-ol, pH, and TAC. PC2 showed a medium positive loading (loading value, 0.50–0.70) of TPC, Ni, glucuronic acid, SA, TFC, TCC, and TTC and a medium negative loading of rhamnose, Mn, and Zn. As can be seen in Figure 1B, the product that presented the greatest negative relationship corresponded to sample number 13 and product 14 and showed a positive relationship with PC2. Product 13 is related to species EM and products with the highest algae percentage content. Hence, it has the lowest values for these variables and the highest value for rhamnose, which is specific for *EM*. Product 14 was related to *AN*, had 100% algae percentage, and had the highest values for these variables, especially Ni (0.15 ± 0.002 mg/kg) and no rhamnose levels. *AN*, hence, is found at a higher relationship with PC2 than EM. Overall, these findings are in accordance with the MANCOVA and concluded that composition profiling was influenced by species and percentage of seaweed in the formulation. In this way, it can be concluded that PCA satisfactorily highlighted the differences between the products based on the species and percentage of algae (Figure 1C).

3.3.3 Hierarchical cluster analysis

HCA allows to classify the products studied according to their similarities in chemical composition. It was performed using Ward's method with squared Euclidean distances to examine station similarities. Ward's method uses ANOVA to calculate the distance between groups to minimize the sum of squares of two possible groups at each step. Figure 2A shows the dendrogram of the products based on the analysis of polysaccharide's composition. Three well-defined main clusters were observed. Cluster 1 was clearly discernible and constituted by low algae percentage products mainly obtained through cold extraction and acid media. Clusters 2 and 3 were explained by algae percentage of products (100%) and the type of formulation; all solid products were grouped in these clusters and represented the products with the high polysaccharide content, between 8% and 12%. HCA results for the mineral profile is shown in Figure 2B. Two clusters with great similarities were observed, which is in good agreement with the previously described results. Most of the products follow the same trend in the mineral profile with the exception of products 6 and 16. These products showed large Euclidean distance, which indicated dissimilarity between the other products. Figure 2C represents the dendrogram of the sugar content. Clusters 1 and 2 are established by the products with the highest sugar content. They correspond to *AN* products, and most of them are in solid formulation. Clusters 3 and 4 are formed by the samples that have 3%–5% sugar content. The products with the highest sucrose content were grouped in cluster 3, while cluster 4 was formed by those with the highest glucose content. All the products of EM under the study were in cluster 4. Sample numbers 11 and 14 were the most different and had more than 15% sugar content. Figure 2D shows **3** main clusters for bioactive compounds and antioxidant activity. Cluster 1 grouped 13 products with the highest DPPH percentage (products 7, 8, 10, 11). This cluster was defined by high percentage SWE products, both *AN* and EM, and all solid products were in this

10.3389/fpls.2022.1017925

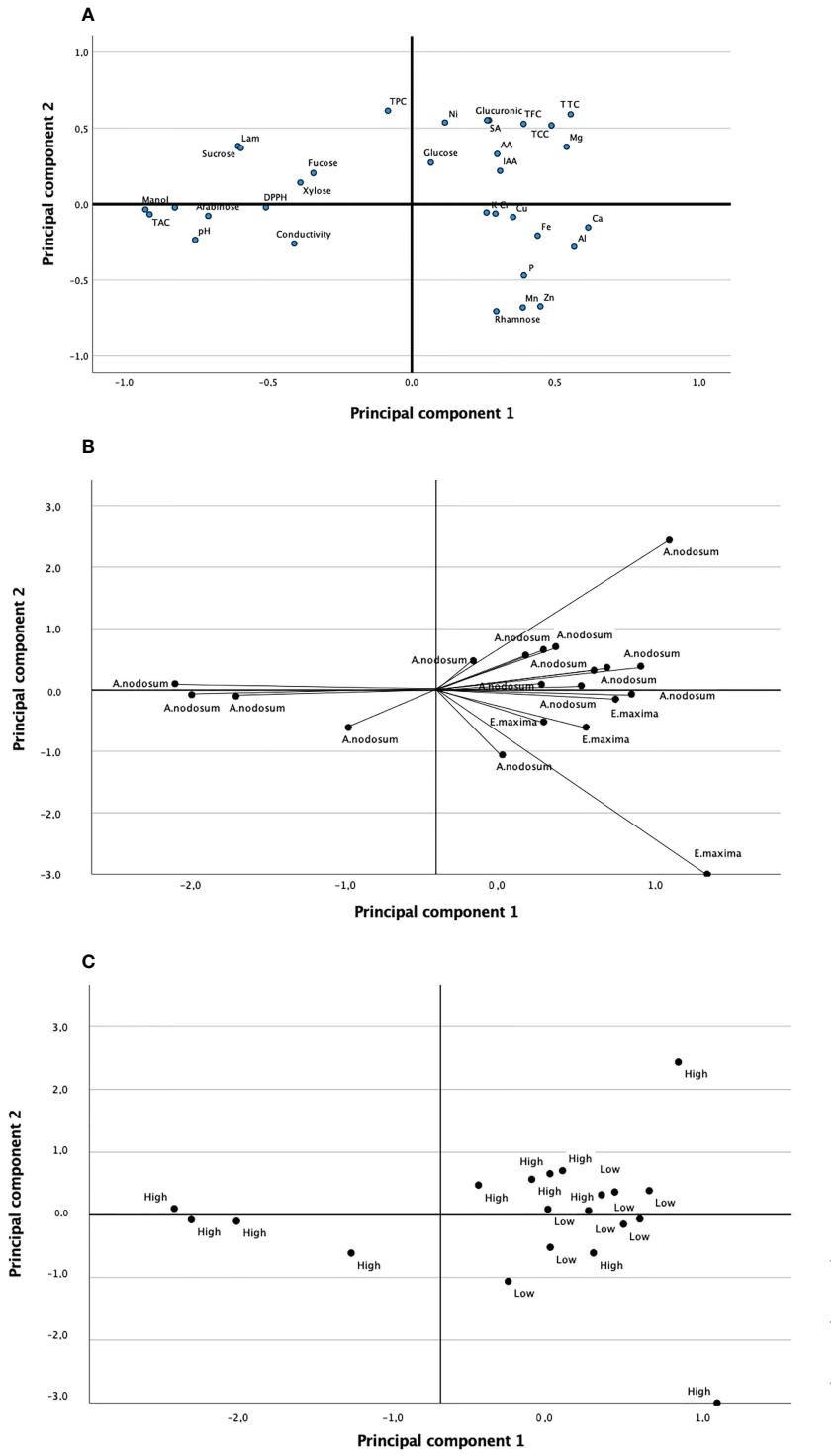

FIGURE 1
(A) Principal components plot in rotated space of variances of seaweed extracts based on chemical composition; **(B)** PCA based on algae species (*AN* and *EM*); **(C)** PCA based on algae percentage in products studied (low and high).

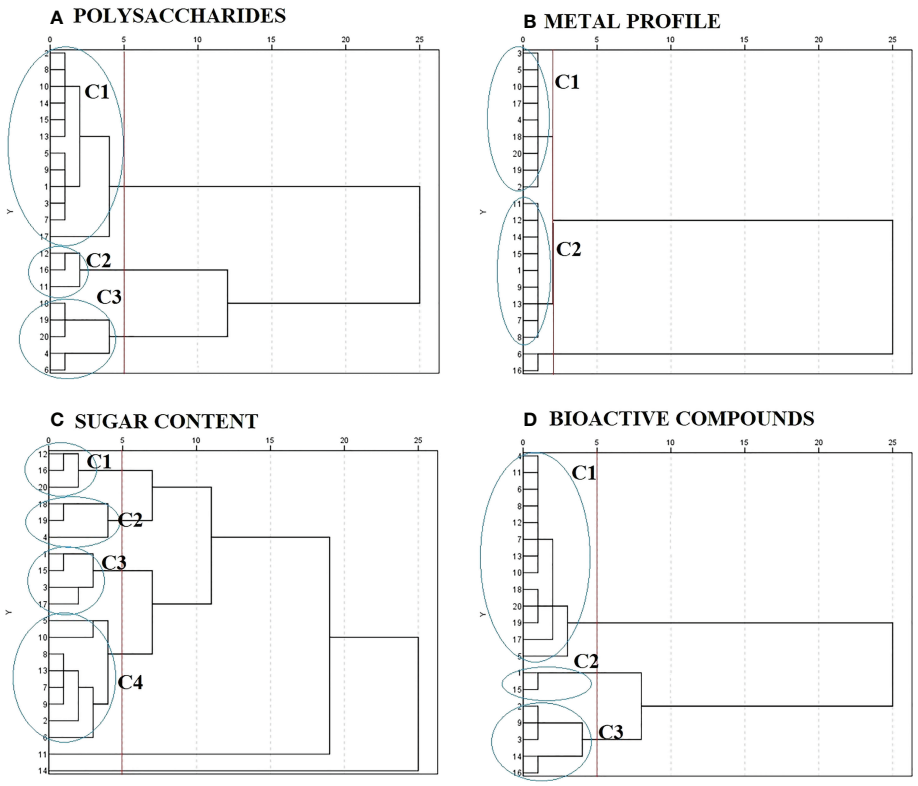

FIGURE 2
Dendrogram of hierarchical cluster analysis of seaweed extracts based on: **(A)** polysaccharides composition, **(B)** metal profile, **(C)** sugar content, and **(D)** bioactive compounds.

group. Cluster 2 was composed of the products with the highest TPC and cluster 3 with those that had the highest TFC. Both clusters presented similarities in terms of being formed by the products that correspond to mixtures (low algae percentage). This fact suggests that the products are mixed with some components that could enhance the presence of phenolic compounds. HCA has given a clear view of the composition pattern of SWE of the respective species and algae percentage. These results are in very good agreement with those observed in MANCOVA and PCA.

On the other hand, it is well-known that antifungal activity is related to the presence of multiple compounds, and HCA can be a useful tool to relate it. The products that presented action against *P. digitatum* (5, 8, 9, 13, and 17) were grouped in the same polysaccharide cluster (cluster 1), and for carbohydrates, four of them were grouped in cluster 4 and the other one in cluster 3. The characteristics of these clusters have been discussed previously; however, it should be noted that sucrose was not detected in these products. Sucrose is used by pathogens as a carbon source; possibly, its absence has inhibited their growth. In the case of tomato, the products of interest were grouped in cluster 1 (4, 6, 8, 10–13, 17–20) and cluster 3 (9, 14, 16) for bioactive components. The products that presented action on strawberry (6,10–13) were grouped in cluster 1 of bioactive components and that on blueberry were grouped in cluster 1 (4, 6, 8, 17, 20) and cluster 3 (9, 16). As can be seen, the fungicidal effect on *B. cinerea* was associated with polyphenolic compounds as described in other works (Table 4), while for *P. digatum*, it was associated with polysaccharide and carbohydrate content.

3.3.4 Artificial neural network analysis

ANN have gained popularity in recent years for modeling methodologies for food quality and food processing (Bhagya Raj and Kshirod, 2022). This methodology has numerous advantages such as flexibility, mapping ability, and high-speed information processing ability, and the ability to solve non-linear complex analysis even if the exact nature of the non-linear relationship between the input and output neurons is unknown (Abiodun et al., 2018). A multilayer perceptron (MLP) based on back propagation (BP) was applied for modeling the composition of the seaweed products. The best model analysis conditions were as follows: the activation function and the number of hidden layers were hyperbolic tangent and four

layers, respectively. The output layer activation function was Softmax, and the training type was batch training. Under this condition, the correct rate of model training and testing was 97.3% and 91.7%, respectively. The results showed that the SWE can be distinguished according to the components analyzed. Under this model, the components that made the greatest contribution to classification and their normalized importance were Zn (100%), EC (95%), K (91%), glucuronic acid (86%), TCC (77%), and Mn (72%).

4 Conclusions

This study has contributed to the knowledge about commercial SWEs used in agriculture. The composition of 20 commercial products with relevant characteristics and their antifungal potential against the usual fungi of certain fruits were analyzed. These results revealed important information about them and can contribute to improved labeling, whose problem is latent. Chemometric techniques were applied using linear and non-linear models in order to establish how the variables related to the production of the extracts influence the chemical composition of the products. MANCOVA allowed to determine the variable species and algae percentage in products as the most influential (p-value and Wilk's lambda test). Principal component analysis and hierarchical cluster analysis discriminated the dependent variables according to species and algae percentage. PCA revealed that rhamnose was a characteristic in *E. maxima* with 100% seaweed in its composition; this parameter could be used to control fraud in these products. In addition, a characteristic composition was observed in the solid products, defined by low concentrations of Ca, Mg, and Al and high concentrations of mannitol, total antioxidant content, and high pH values. HCA showed that the highest concentration of bioactive components was grouped in the same cluster corresponding to low algae percentage. This fact suggests that some component has been added to the products. In addition, HCA was used to relate the antifungal capacity of SWE to their composition. These results revealed that the fungal capacity against *B. cinerea* was related to the bioactive components, while that against *P. digitatum* was related to the polysaccharides and carbohydrates content. Moreover, ANN allowed to establish the influence of other variables (K, glucuronic acid, laminarin, and total carotenoid content) that were not revealed by the linear methods. The overall results could help to better understand the mode of action of these products through their composition and the importance of chemometric techniques to discern the most significant variables in the production process and their relationship with their fungal capacity. Future research on other products available on the market is recommended to deepen the investigation related to postharvest treatments due to their action against common pathogens in fruits.

Data availability statement

The original contributions presented in the study are included in the article/Supplementary Material. Further inquiries can be directed to the corresponding author.

Author contributions

SV, JJL and LHA designed the experiments. SV and PLW performed the analysis of chemical composition of SWEs. SV, PLW and BM performed the microbiological assays. SV and PLW acquiered and analyzed of data; BM, JJL and LHA hepled perform the analysis of data with constructive disscussions. SV, PLW and LHA wrote the manuscript. All authors revised the manuscript and approved the submitted version.

Funding

The authors gratefully acknowledge the financial support of Spain's Ministry of Economy and Competitiveness project no. RTI2018-096268-B-I00 and the Comunidad de Madrid (Spain) and Structural Funds 2014–2020 (ERDF and ESF) project AGRISOST-CM S2018/BAA-4330.

Acknowledgments

The authors are grateful to the fertilizer companies and Laboratorio Arbitral (Spain's Ministry of Agriculture, Fisheries and Food) for kindly donating samples for this investigation.

Conflict of interest

The authors declare that the research was conducted in the absence of any commercial or financial relationships that could be construed as a potential conflict of interest.

Publisher's note

Supplementary material

The Supplementary Material for this article can be found online at: https://www.frontiersin.org/articles/10.3389/fpls.2022.1017925/full#supplementary-material

References

Abiodun, O. I., Jantan, A., Omalara, A. E., Dada, K. V., Mohamed, N. A., and Arshad, H. (2018). State of the art in artificial neural network applications: A survey. *Helyon* 4, e00938. doi: 10.1016/j.heliyon.2018.e00938

Agregán, R., Munekata, P. E. S., Franco, D., Dominguez, R., Carballo, J., and Lorenzo, J. M. (2017). Phenolic compounds from three brown seaweed species using LC-DAD-ESI-MS/MS. *Food Res. Int.* 99, 979–985. doi: 10.1016/j.foodres.2017.03.043

Badmus, U., Taggart, M., and Boyd, K. G. (2019). The effect of different drying methods on certain nutritionally important chemical constituents in edible brown seaweeds. *J. Appl. Phycol.* 31, 3883–3897. doi: 10.1007/s10811-019-01846-1

Bhagya Raj, G. V. S., and Kshirod, K. D. (2022). Comprehensive study on applications of artificial neural network in food process modeling. *Crit. Rev. Food Sci. Nutr.* 62, 2756–2783. doi: 10.1080/10408398.2020.1858398

Biau, A., Santiveri, F., Mijangos, I., and Lloveras, J. (2012). The impact of organic and mineral fertilizers on soil quality parameters and the productivity of irrigated maize crops in semiarid regions. *Eur. J. Soil Biol.* 53, 56–61. doi: 10.1016/j.ejsobi.2012.08.008

Calvo, P., Nelson, L., and Kloepper, J. W. (2014). Agricultural uses of plant biostimulants. *Plant Soil* 383, 3–41. doi: 10.1007/s11104-014-2131-8

Chang, C. C., Yang, M. H., Wen, H. M., and Chern, J. C. (2002). Estimation of total flavonoid content in propolis by two complementary colorimetric methods. *J. Food. Drug Anal.* 10, 178–182. doi: 10.38212/2224-6614.2748

Cortés, Y., Hormanzábal, E., Leal, H., Urzúa, A., Mutis, A., Parra, L., et al. (2014). Novel antimicrobial activity of a dichloromethane extract obtained from red seaweed ceramium rubrum (Hudson) (Rhodophyta: Floridephycea) against yersinia ruckeri and saprolegnia parasitica, agents that cause diseases in salmonids. *Electron. J. Biotechnol.* 17, 126–131. doi: 10.1016/j.ejbt.2014.04.005

Costa, L. S., Fidelis, G. P., Silva Telles, C. B., Dantas-Santos, N., Camara, R. B. G., Cordeiro, S. L., et al. (2011). Antioxidant and antiproliferative activities of heterofucans from the seaweed sargassum filipendula. *Mar. Drugs* 9, 952–966. doi: 10.3390/md9060952

Cox, S., Abu-Ghannam, N., and Gupta, S. (2010). An assessment of the antioxidant and antimicrobial activity of six species of edible Irish seaweeds. *Int. Food Res. J.* 17, 205–220.

Crampon, C., Boutin, O., and Badens, E. (2011). Supercritical carbon dioxide extraction of molecules of interest from microalgae and seaweeds. *Ind. Eng. Chem. Res.* 50, 8941–8953. doi: 10.1021/ie102297d

De Corato, U., Salimbeni, R., De Pretis, A., Avella, N., and Patruno, G. (2017). Antifungal activity of crude extracts from brown and red seaweeds by a supercritical carbon dioxide technique against fruit postharvest fungal diseases. *Postharvest Biol. Technol.* 131, 16–30. doi: 10.1016/j.postharvbio.2017.04.011

Devi, G. K., Manivannan, K., Thirumaran, G., Rajathi, F. A., and Anantharaman, P. (2011). *In vitro* antioxidant activities of selected seaweeds from southeast coast of India. *Asian Pac. J. Trop. Med.* 4, 205–211. doi: 10.1016/S1995-7645(11)60070-9

Duan, X. J., Zhang, W. W., Li, X. M., and Wang, B. G. (2006). Evaluation of antioxidant property of extract and fractions obtained from a red alga, polysiphonia urceolata. *Food Chem.* 95, 37–43. doi: 10.1016/j.foodchem.2004.12.015

Farasat, M., Khavari-Nejad, R. A., Nabavi, S. M. B., and Namjooyan, F. (2014). Antioxidant activity, total phenolics and flavonoid contents of some edible green seaweeds from northern coasts of the Persian gulf. *Iran J.Pharm.Res.* 13, 163–170.

Górka, B., and Wieczorek, P. P. (2017). Simultaneous determination of nine phytohormones in seaweed and algae extracts by HPLC-PDA. *J. Chromatogr B Analyt Technol. BioMed. Life Sci.* 1057, 32–39. doi: 10.1016/j.jchromb.2017.04.048

Habeebullah, S. F. K., Alagarsamy, S., Arnous, A., and Jacobsen, C. (2021). Enzymatic extraction of antioxidant ingredients from Danish seaweed and characterization of active principles. *Algal Res.* 56, 102292. doi: 10.1016/j.algal.2021.102292

Hurtado, A. Q., Neish, I. C., Ali, M. K. M., Norrie, J., Pereira, L., Shukla, I. M. P. S., et al. (2021). "Extracts of seaweeds used as biostimulants on land and sea crops an efficacious, phyconomic, circular blue economy: with special reference to ascophyllum (brown) and kappaphycus (red) seaweeds," in *Biostimulants for crops from seed germination to plant development*. Eds. S. Gupta and J. Van Staden (Cambridge, Massachusetts: Academic Press), 263–288.

Jayaraj, J., Norrie, J., and Punja, Z. (2011). Commercial extract from the brown seaweed ascophyllum nodosum reduces fungal diseases in greenhouse cucumber. *J. Appl. Phycol.* 23, 353–361. doi: 10.1007/s10811-010-9547-1

Jayaraj, J., Wan, A., Rhaman, M., and Punja, Z. K. (2008). Seaweed extracts reduces foliar fungal diseases on carrot. *Crop Prot.* 27, 1360–1366. doi: 10.1016/j.cropro.2008.05.005

Jiang, T. F., Lv, Z. H., Wang, Y. H., and Yue, M. E. (2006). Separation of plant hormones from biofertilizer by capillary electrophoresis using a capillary coated dynamically with polycationic polymers. *Analytical Sci.* 22, 811–814. doi: 10.2116/analsci.22.811

Khan, W., Rayirath, U. P., Subramanian, S., Jithesh, M. N., Rayorath, P., Hodges, D. M., et al. (2009). Seaweed extracts as biostimulants of plant growth and development. *J. Plant Growth Regul.* 28, 386–399. doi: 10.1007/s00344-009-9103-x

Kocira, A., Świeca, M., Kocira, S., Złotek, U., and Jakubczykb, A. (2018). Enhancement of yield, nutritional and nutraceutical properties of two common bean cultivars following the application of seaweed extract (*Ecklonia maxima*). *Saudi J. Biol. Sci.* 25, 563–571. doi: 10.1016/j.sjbs.2016.01.039

Kumar, J. I. N., Kumar, R. N., Bora, A., Amb, M. K., and Chakraborthy, (2009). An evaluation of the pigment composition of eighteen marine macroalgae collected from okha cost, gulf of kutch, India. *Our Nat.* 7, 48–55. doi: 10.3126/on.v7i1.2553

Kumar, M. S., and Sharma, S. A. (2021). Toxicological effects of marine seaweeds: a cautions insight for human consumption. *Crit. Rev. Food Sci. Nutr.* 61, 500–521. doi: 10.1080/10408398.2020.1738334

Lahbib, F., Askarne, L., Boufous, E. H., Cherifi, O., and Cherifi, K. (2022). Antioxidant and antifungal activity of some Moroccan seaweeds against three postharvest fungal pathogens. *Asian J. Plant Sci.* 21, 328–338. doi: 10.3923/ajps.2022.328.338

Leelavathi, M. S., and Prasad, M. P. (2014). Evaluation of antioxidant properties of marine seaweed samples by DPPH method. *Int. J. Pure Appl. Biosci.* 2, 132–137.

Lutz, M. C., Colodner, A., Tudela, M. A., Carmona, M. A., and Sosa, M. C. (2022). Antifungal effects of low environmental risk compounds on development of pear postharvest diseases: Orchard and postharvest applications. *Sci. Hortic.* 295, 110862. doi: 10.1016/j.scienta.2021.110862

Manns, D., Deutschle, A. L., Saake, B., and Meyer, A. S. (2014). Methodology for quantitative determination of the carbohydrate composition of brown seaweeds. *RSC Adv.* 4, 25736–25746. doi: 10.1039/C4RA03537B

Meng, C., Gu, X., Liang, H., Wu, M., Wu, Q., Yang, L., et al. (2022). Optimized preparation and high-efficient application of seaweed fertilizer on peanut. *J. Agric. Res.* 7, 100275. doi: 10.1016/j.jafr.2022.100275

Morrison, L., Baumman, H. A., and Stengel, D. B. (2008). An assessment of metal contamination along the Irish coast using the seaweed ascophyllum nodosum (*Fucales, phaeophyceae*). *Environ. pollut.* 152, 293–303. doi: 10.1016/j.envpol.2007.06.052

Mukherjee, A., and Patel, J. S. (2019). Seaweed extract: bioestimulator of plant defense and plant productivity. *IJEST* 17, 553–558. doi: 10.1007/s13762-019-02442-z

Pereira, L., Morrison, L., Shukla, P. S., and Critchley, A. T. (2020). A concise review of the brown macroalga acophyllum nodosum (Linnaeous) le jolis. *J. Appl. Phycol.* 32, 3561–3584. doi: 10.1007/s10811-020-02246-6

Pourakbar, L., Moghaddam, S. S., Enshasy, H. A. E., and Sayyed, R. Z. (2021). Antifungal activity of the extract of a macroalgae, gracilariopsis persica, against four plant pathogenic fungi. *Plants* 26, 1781. doi: 10.3390/plants10091781

Povero, G., Mejia, J. F., Di Tommaso, D., Piaggesi, A., and Warrior, P. (2016). A systematic approach to discover and characterize natural plant biostimulants. *Front. Plant Sci.* 7, 435. doi: 10.3389/fpls.2016.00435

Righini, H., Somma, A., Cetrullo, S., D'Adamo, S., Flamigni, F., Quintana, A. M., et al. (2020). Inhibitory activity of aqueous extracts from anabaena minutissima, ecklonia maxima and jania adhaerens on the cucumber powdery mildew pathogen *in vitro* and *in vivo*. *J. Appl. Phycol.* 32, 3363–3375. doi: 10.1007/s10811-020-02160-x

Sluiter, A., Hames, B., Ruiz, R., Scarlata, C., Sluiter, J., Templeton, D., et al. (2012). *Determination of structural carbohydrates and lignin in biomass* (Colorado: Laboratory Analytical Procedure). Available at: http://www.nrel.gov/biomass/analytical_procedures.html.

Tabbara, L. I., Abdel-Hameid, N., and Bondok, A. (2018). Using of some environmentally safe treatments to improve the storability of navel orange (*Citrus sinensis l.)* fruits. *J. Agric. Sci.* 26, 519–526. doi: 10.21608/ajs.2018.15705

Trivedi, K., Vijay Anand, K. G., Pradip, V., and Ghosh, A. (2018). Differential growth, yield and biochemical responses of maize to the exogenous application of kappaphycus alvarezii seaweed extract, at grain filling stage under normal and drought conditions. *Algal Res.* 35, 236–244. doi: 10.1016/j.algal.2018.08.027

Valverde, S., Hernández-Apaolaza, L., and Lucena, J. J. (2022). A simple analytical method to determine alginic acid, laminarin and mannitol in seaweed extracts fertilisers. *J. Chromatogr. Sep. Tech.* 13, 470. doi: 10.35248/2329-9096-22.13.470

Yang, J., Guo, J., and Yuan, J. (2008). *In vitro* antioxidant properties of rutin. *LWT-Food Sci. Technol.* 41, 1060–1066. doi: 10.1016/j.lwt.2007.06.010

Zhang, H. C., Dong, J., Ren, X., and Qin, J. (2008). Antioxidant activities of ethanol extracts from ten kinds of bee pollens. *Food Sci.* 10, 75–79.

frontiers | Frontiers in Plant Science

TYPE Original Research
PUBLISHED 13 December 2022
DOI 10.3389/fpls.2022.1017191

OPEN ACCESS

EDITED BY
Maurizio Ruzzi,
University of Tuscia, Italy

REVIEWED BY
Marcin Debowski,
University of Warmia and Mazury in Olsztyn, Poland
Georg Carlsson,
Swedish University of Agricultural Sciences, Sweden

*CORRESPONDENCE
Adnan Mustafa
adnanmustafa780@gmail.com
Martin Brtnicky
martin.brtnicky@seznam.cz

SPECIALTY SECTION
This article was submitted to Plant Nutrition, a section of the journal Frontiers in Plant Science

RECEIVED 11 August 2022
ACCEPTED 31 October 2022
PUBLISHED 13 December 2022

CITATION
Hammerschmiedt T, Kintl A, Holatko J, Mustafa A, Vitez T, Malicek O, Baltazar T, Elbl J and Brtnicky M (2022) Assessment of digestates prepared from maize, legumes, and their mixed culture as soil amendments: Effects on plant biomass and soil properties. *Front. Plant Sci.* 13:1017191. doi: 10.3389/fpls.2022.1017191

Assessment of digestates prepared from maize, legumes, and their mixed culture as soil amendments: Effects on plant biomass and soil properties

Tereza Hammerschmiedt[1], Antonín Kintl[1,2], Jiri Holatko[1,3], Adnan Mustafa[1,4,5]*, Tomas Vitez[6,7], Ondrej Malicek[1], Tivadar Baltazar[1], Jakub Elbl[2,8] and Martin Brtnicky[1,4]*

[1]Department of Agrochemistry, Soil Science, Microbiology and Plant Nutrition, Faculty of AgriSciences, Mendel University in Brno, Brno, Czechia, [2]Agricultural Research, Ltd., Troubsko, Czechia, [3]Agrovyzkum Rapotin, Ltd., Rapotin, Czechia, [4]Institute of Chemistry and Technology of Environmental Protection, Faculty of Chemistry, Brno University of Technology, Brno, Czechia, [5]Institute for Environmental Studies, Faculty of Science, Charles University in Prague, Praha, Czechia, [6]Department of Agricultural, Food and Environmental Engineering, Faculty of AgriSciences, Mendel University in Brno, Brno, Czechia, [7]Department of Experimental Biology, Section of Microbiology, Faculty of Science, Masaryk University, Brno, Czechia, [8]Department of Agrosystems and Bioclimatology, Faculty of AgriSciences, Mendel University in Brno, Brno, Czechia

Digestate prepared from anaerobic digestion can be used as a fertilizer, as it contains ample amounts of plant nutrients, mainly nitrogen, phosphorous, and potassium. In this regard, digestates produced from mixed intercropped cereal and legume biomass have the potential to enrich soil and plants with nutrients more efficiently than monoculture-based digestates. The objective of this study was to determine the impact of different types of digestates applied at a rate of 40 t·ha^{-1} of fresh matter on soil properties and crop yield in a pot experiment with lettuce (*Lactuca sativa*) as a test crop. Anaerobic digestion of silages was prepared from the following monocultures and mixed cultures: broad bean, maize, maize and broad bean, maize and white sweet clover, and white sweet clover. Anaerobic digestion was performed in an automatic custom-made system and applied to the soil. Results revealed that fresh and dry aboveground biomass as well as the amount of nitrogen in plants significantly increased in all digestate-amended variants in comparison to control. The highest content of soil total nitrogen (+11% compared to the control) and urease (+3% compared to control) were observed for maize digestate amendment. Broad bean digestate mediated the highest oxidizable carbon (+48%), basal respiration (+46%), and N-acetyl-β-D-glucosamine-, L-alanine-, and L-lysine-induced respiration (+22%, +35%, +22%) compared to control. Moreover, maize and broad bean digestate resulted in the highest values of N-acetyl-β-D-glucosaminidase and β -glucosidase (+35% and +39%), and maize and white sweet clover digestate revealed the highest value of arylsulfatase (+32%). The observed differences in results suggest different effects of applied digestates. We thus concluded that legume-containing digestates possibly stimulate microbial activity (as found in increased

respiration rates), and might lead to increased nitrogen losses if the more quickly mineralized nitrogen is not taken up by the plants.

KEYWORDS

waste management, agriculture, organic fertilizer, microbial activity, nutrient cycling

Introduction

Anaerobic digestion (AD) is a microbially-controlled process of biomethanization. Originally it was used for processing of biodegradable waste from agriculture, industry, or households (Angelidaki et al., 2003). Due to increasing threat of climate change and limited fossil energy sources, the bioenergy obtained from biogas has become essential in climate change mitigation, energy security, resourcing, and sustainable agriculture development (Shakoor et al., 2020). Research on the processing of liquid animal manure and plant raw material by AD has been promoted and expanded across the world (Aravani et al., 2022). Especially in Europe, biogas production from energy crops has developed considerably, and maize (*Zea mays* L.) used to be the most common and preferred source crop (Weiland, 2010) until recently. The advantages of maize biomass as substrate are high yield performance and established crop management technology (Gissén et al., 2014; Purdy et al., 2017; Theuerl et al., 2019). However, scientists have recently been looking for possible new substrates (Dębowski et al., 2022), mainly because of the negative environmental impacts and economic balance associated with maize cultivation (von Cossel et al., 2021; Herman et al., 2022).

Apart from the main product's renewable energy (biogas), AD converts plant biomass to the second useful by-product—digestate. The resultant digestate has been characterized as having high amounts of plant-available nutrients and can act as a soil conditioner (Liedl et al., 2004; Arthurson, 2009; Brtnicky et al., 2022) or can be used as substrate for microalgae cultivation (Bauer et al., 2021; Kisielewska et al., 2021). Compared to the raw feedstock, the digestate obtains beneficial properties during AD, e.g., the increased availability of nitrogen mainly in NH_4^+ form (Gutser et al., 2005), potassium (Slepetiene et al., 2020) and phosphorus (Barłóg et al., 2020) for plants. The composition of digestate also depends on the raw materials being used as AD feedstock; for example, pig slurry contains more potassium (Zhan et al., 2020), whereas co-digested cattle slurry increased the content of phosphorus (Bachmann et al., 2011). Therefore, digestate (as an organo-mineral fertilizer) can provide comparably or almost as rich a nutrient supply as either mineral (Riva et al., 2016; Šimon et al., 2016) or organic fertilizers such as manure (Alburquerque et al., 2012; Bougnom et al., 2012).

So far, only a few studies have been focused on the quality of final digestate that are further governed by the type of feedstock (Risberg et al., 2017; Ehmann et al., 2018; Szymanska et al., 2018). However, substitutional crops are promising alternatives to biogas and digestate production from maize monocultures (Lebuhn et al., 2008; Oslaj et al., 2010; Sigurnjak et al., 2017; Gissén et al., 2014). Substitutional crops can be used either as co-substrates only (Meyer et al., 2015; Nurk et al., 2016; Fahlbusch et al., 2018; von Cossel et al., 2020) or blended biomass harvested from mixed cultures, such as maize and intercropped sunflower (Karpenstein-Machan 2005; Nassab et al., 2011), sorghum (Schittenhelm 2010; Samarappuli and Berti 2018), or legume (Gatta et al., 2013; Kintl et al., 2019). Alternatively, maize could be fully replaced by another bioenergy crop of a common type (e.g. sugar beet, wheat, hemp) (Nges et al., 2012; González-García et al., 2013; Gissén et al., 2014). Moreover, the intercropping of energy crops with legumes represents a promising approach. The main advantage is the contribution of leguminous species to the nitrogen nutrition of non-leguminous species (Råberg et al., 2017). Legume biomass itself tends to have higher nitrogen content and lower C:N ratio than non-leguminous material (Peoples et al., 1995). A low C:N ratio changes the stability and consumption of available N nutrients, leading to slower nitrogen utilization, followed by higher alkalinity, *via* ammonia metabolism (Muhayodin et al., 2021). The higher content of ammonium from legumes in the intercrop biomass could inhibit the production of methane in biogas during AD (Wahid et al., 2018, Kintl et al., 2022). According to Hutnan et al. (2010), the process of anaerobic digestion is unstable at low N content in maize silage, and they recommend the addition of a substrate with higher nitrogen content for stabilization. Nevertheless, down-shifted AD performance and efficiency is compensated by higher residual nitrogen in the final digestate. The significantly negative correlation between cumulative nitrogen mineralization and the C:N ratio in digestate (Tambone and Adani 2017) is indicative of improved digestate-derived nitrogen availability for plants in the amended soil (Barłóg et al., 2020), which is expected to further increase with increasing nitrogen content in

the digestate (Andruschkewitsch et al., 2013). Another study indicated that reallocation of processed plant biomass (crop residues and cover crops) in the form of digestate can increase the crop dry matter yield, as well as nitrogen content in soil over a long term (Stinner et al., 2008). We assume that the use of digestate from cereal-legume mixed substrate as fertilizer could keep the subsequent crop biomass productivity consistently enhanced, as discussed by Råberg et al. (2017). Such an agro-system could become the future direction of sustainable agriculture and management of renewable sources (Kettl et al., 2010; Lamei Hervani 2013).

The main objective of this study was thus to determine the impact of different types of digestates on soil properties and crop yield in a pot experiment with lettuce (*Lactuca sativa*). The feedstock used for digestate preparation was the biomass of either mixed crop (cereal-legume) cultures or monocultures (legumes, maize) varying in their chemical composition. We hypothesized that the soil amended with different digestates would contrast in: (I) final nutrient content (nitrogen, organic carbon) in soil, (II) the biomass yield of tested crop, and (III) soil microbial activities in relation to nutrient content in the digestates.

Materials and methods

Experimental field, plant biomass, and preparation of silages

The plants used for preparing digestates were grown at the Experimental Station for Fodder Crops in Vatin, Czech Republic (49°31'6"N 15°58'10"E). The station is located in a moderately warm area of the Bohemian-Moravian Highlands with a long-term average annual temperature of 7°C and a year-round long-term average rainfall of 658.6 mm; the values correspond to climate standards between 1981 and 2010 (Kintl et al., 2022). The soil of this site is characterized as sandy loam cambisol. The following variants were grown: a) monoculture of maize (*Zea mays* L.; BAYER, Ltd, Czech Republic); b) monoculture of broad bean (*Vicia faba* L. Amiga variety; Selgen a.s., Czech Republic); c) monoculture of white sweet clover (*Melilotus albus* MED., Meba variety - Research Institute for Fodder Crops, Ltd, Czech Republic); d) mixed culture of maize and broad bean; and e) mixed culture of maize and white sweet clover. The single crops as well as combination of maize and legume plants were sown by using the Kinze 3500 (Kinze Manufacturing, Williamsburg, IA, USA) "interplant system" seeding machine in a single operation (Kintl et al., 2019). Sowing was performed by alternating two rows of maize with two rows of legumes (Figure 1) to achieve a mixed culture system. The combination of maize and legume plants was sown at a rate of 150 thousand seeds per hectare, with maize and legume at the same rate of 75 thousand each. The monocultures were planted in half this sowing density at 75 thousand seeds per hectare with same row spacing (37.5 cm) as shown in Figure 1.

DASA fertilizer (300 $kg{\cdot}ha^{-1}$; DASA® 26/13 Fertilizer CE, produced by Duslo corp., Slovakia; 18.5% w/w N-NH_4, 7.5% w/w N-NO_3, 13% w/w soluble S) was applied to all variants before sowing, in a dose that was sufficient to cover the nutritional requirements of maize and not limit the growth of legumes at the same time. The plant biomass was harvested at DM 35% (BBCH stage 77 – 83), determined on maize crop.

Sampling of plant biomass was performed manually at a height of 18 cm above the ground. Subsequently, a 15-20 mm cut was carried out using the Deutz-Fahr MH 6505 cutter (Deutz-Fahr, Lauingen, Germany). The cut was used to prepare model micro-silages in triplicate; see Table 1. The preparation of micro-silages was the same for all variants. Cut biomass (8 kg) was placed in a micro-silage container (Ø150 mm x 1000 mm) with inoculant (Silo Solve EF, CHr. Hansen, Denmark; *Lactococcus lactis*, *L. plantarum*, *Enterococcus faecium* - dose $6.25{\cdot}10^5$ CFU per g of plant biomass), which equalled a dosage of 5 $g{\cdot}t^{-1}$ (of inoculant matter) + 3.5 $L{\cdot}t^{-1}$ H_2O. The prepared inoculated cut biomass was compacted in

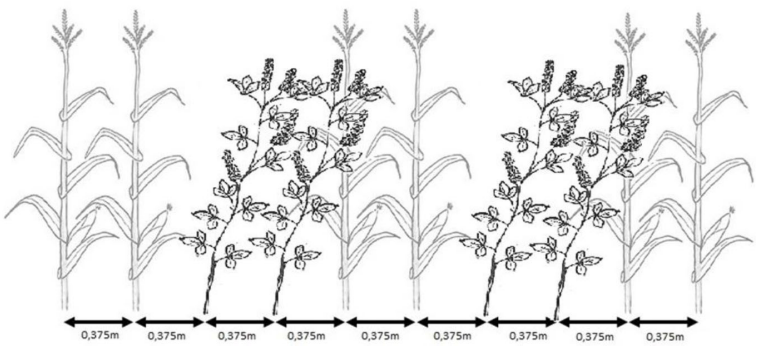

FIGURE 1
Scheme of sowing mixed culture of maize and selected legumes (Kintl et al., 2022).

TABLE 1 Prepared model silages.

Abbrev.	Variant	Weight content ofmaize fresh matter (%)	Weight content ofbroad bean fresh matter (%)	Weight content ofwhite sweet clover fresh matter (%)	Ratio
M	Maize	100	0	0	1
BB	Broad bean	0	100	0	1
WSC	White sweet clover	0	0	100	1
M+BB	M+BB	78.9	21.1	0	3.75:1
M+WSC	M+WSC	92.6	0	7.4	12.50:1

micro-silage containers using a pneumatic press with a force of 6 $N{\cdot}m^{-2}$. Subsequently, the micro-silage container was sealed and placed in an incubation room without access to light at a constant temperature of 28°C ± 1°C for 90 days. At the end of the incubation period, the micro-silage containers were opened, silage was extracted and homogenized. Frozen samples of silages were transported to the laboratory to perform chemical analysis and fermentation tests.

Production of digestate

Anaerobic digestion of prepared silages was performed using fermentation batch tests in an automatic custom-made system consisting of 5 L glass fermenters placed in a heated water bath with adjustable temperature of 42°C ± 0.1°C. Each sample was fermented in triplicate. On the first day of the experiment, the fermenters were filled with 3 L of filtered (3 mm) inoculum obtained from agricultural biogas plant-processing maize silage and slurry (80/20, w/w%), operated at mesophilic conditions, with a hydraulic retention time of 80–90 days. The basic parameters of inoculum were as follows: total solids content 3.8%, volatile solids content 73%, pH 7.2, FOS 1452 $mg{\cdot}L^{-1}$, TAC 4330 $mg{\cdot}L^{-1}$, and FOS : TAC 0.34.

Initial organic loading rate was 5.5 g volatile solids of introduced substrate per L. The fermentation test was carried out until the daily biogas production in three consecutive days was < 1% of the total biogas production as stated in VDI 4630 (2016). This led to a retention time of 21 days. The digestate produced was subsequently analyzed to determine the following parameters. The dry matter was determined gravimetrically by desiccation at a temperature of 105°C ± 3.5°C to constant weight according to standard CSN EN 15934. TN (total nitrogen) and TC (total carbon) were measured using the Vario Macro Cube (Elementar Analysensysteme GmbH, Langenselbold, Germany). The content of total organic (TOC) and total inorganic (TIC) carbon was measured using Soli TOC® Cube (Elementar Analysensysteme GmbH, Langenselbold, Germany). Basic nutrients (P, K) were extracted using the Mehlich III reagent and then analyzed using atomic emission spectroscopy (The Agilant55B AA, Agilent, CA, USA).

Pot experiment

The following pot experiment investigated the effect of prepared digestates (Table 2) amendment on the soil properties and the growth of lettuce (*Lactuca sativa*). The experimental pots of volume 1 L were filled with 1 kg of experimental soil, which was prepared from silty clay loam (Haplic Luvisol) collected from a depth of 0-10 cm, sieved through a grid size of 2.0 mm to remove all roots and coarse particles, and mixed with fine quartz sand 0.1–1.0 mm (1:1 each, w/w). The content of nutrients in the topsoil used was as follows: total carbon (TC) 7.0 $g{\cdot}kg^{-1}$, total nitrogen (TN) 800 $mg{\cdot}kg^{-1}$, available phosphorus (P) 485 $mg{\cdot}kg^{-1}$, and available potassium (K) 0.115 $mg{\cdot}kg^{-1}$. The detailed properties of the soil used can be found elsewhere (Holatko et al., 2020; Brtnicky et al., 2021).

TABLE 2 Properties of digestates, dosage of nitrogen in 40 tons of the digestates per hectare.

Variant	Dry matter [%]	N [$g{\cdot}kg^{-1}$ d.m.]	P [$g{\cdot}kg^{-1}$ d.m.]	K [$g{\cdot}kg^{-1}$ d.m.]	TOC [% d.m.]	TIC [% d.m.]	N dose [$kg{\cdot}ha^{-1}$]
M*	2.76 ± 0.06 ^{ab}	152.17 ± 7.54 ^{b}	22.01 ± 0.56 ^{c}	6.52 ± 0.21 ^{bc}	29.25 ± 0.01 ^{d}	0.08 ± 0.00 ^{c}	168.0 ± 11.8
BB*	2.49 ± 0.06 ^{bc}	180.72 ± 8.36 ^{ab}	23.29 ± 0.61 ^{c}	8.83 ± 0.40 ^{a}	28.80 ± 0.06 ^{e}	0.10 ± 0.00 ^{b}	180.0 ± 11.8
WSC	2.98 ± 0.14 ^{a}	146.60 ± 9.10 ^{b}	21.76 ± 0.65 ^{c}	6.32 ± 0.26 ^{c}	29.93 ± 0.05 ^{b}	0.10 ± 0.00 ^{b}	176.0 ± 11.8
M+BB*	2.94 ± 0.08 ^{a}	159.86 ± 5.89 ^{b}	31.63 ± 0.86 ^{a}	7.82 ± 0.34 ^{ab}	29.54 ± 0.05 ^{c}	0.10 ± 0.01 ^{b}	188.0 ± 9.8
M+WSC	2.23 ± 0.07 ^{c}	205.70 ± 12.66 ^{a}	28.18 ± 1.23 ^{b}	8.50 ± 0.32 ^{a}	30.21 ± 0.04 ^{a}	0.13 ± 0.00 ^{a}	184.0 ± 11.8

DM., dry matter; N, P, K, total nutrient (nitrogen, phosphorus, potassium) content; TOC, total organic carbon; TIC, total inorganic carbon. Different superscript letters indicate statistically significant differences between displayed values at the significance level $p \leq 0.05$.
*, that the respective variants were presented in our previous paper Brtnicky et al. (2022).

The control variant was unamended, whereas digestates were applied to the other variants at a dose corresponding to 40 t·ha^{-1}; see Table 2. A total of 6 variants (control and 5 digestate variants) were made in 3 repetitions each.

Five sprouted seeds of lettuce (*Lactuca sativa*) were planted into each of the filled pots. Seedlings were reduced to one in each pot after 14 days. The pot experiment was conducted for 6 weeks under controlled conditions in a growth chamber Climacell Evo (BMT, Czech Republic) under the following conditions: 12-hour photoperiod, white illumination, light intensity 20,000 lx, day/night temperature 22/18°C, and relative atmospheric humidity 70%. Soil moisture was maintained at 65% water-holding capacity throughout the experiment. Pots were placed in the growth chamber using a randomized scheme and rotated weekly to ensure homogeneity of growing conditions.

Plant and soil measurements and data collection

At the end of the experiment, the aboveground biomass (AGB) of individual seedlings was harvested, and the weight of fresh and subsequently dry (drying at 60°C) biomass was determined. Nitrogen content in harvested lettuce (Plant N) was measured using the Vario Macro Cube (Elementar Analysensysteme GmbH, Langenselbold, Germany). Nitrogen uptake by plants (N uptake) was calculated from dry weight of the plant and the nitrogen content in biomass. After harvest, a mixed soil sample from each pot was taken, homogenized, sieved (≤ 2mm), and air-dried for measuring pH, total nitrogen (TN), and oxidizable carbon (C_{ox}); cooled to 4°C for respiration measurement; and freeze-dried for enzyme activity estimation. The TN was determined according to ISO_13878 1998 and C_{ox} according to ISO_14235 1998. Basal respiration (BR) and substrate-induced respirations (SIRs) were measured using a MicroResp (The James Hutton Institute, Scotland) device according to the method (Campbell et al., 2003). Substrate-induced respiration was measured after adding specific energy sources to the substrate: N-acetyl-β-D-glucosamine (NAG-SIR), L-alanine (Ala-SIR), L-lysine (Lys-SIR), and L-arginine (Arg-SIR). Enzymatic activities of β-glucosidase (GLU), N-acetyl-β-D-glucosaminidase (NAG), arylsulfatase (ARS), phosphatase (Phos), and urease (Ure) were measured according to ISO_20130 2018.

Statistical analysis

Data processing and statistical analysis were carried out with the help of the statistical program R version 3.6.3. (R_CORE_TEAM 2020) together with the additional packages "ggplot2" (Wickham, 2016). Multivariate analysis of variance (MANOVA) and principal component analysis (PCA) with dependence of different treatments were used for modelling the relation between the soil properties and selected treatments with help of the additional packages "factoextra" (Kassambara and Mundt 2017) and "FactoMineR" (Lê et al., 2008). One-way analysis of variance (ANOVA) and Tukey's Honest Significant Difference (HSD) from package "agricolae" (Mendiburu 2020) at the significance level of 0.05 were used to detect the difference among the treatments. The factor level means calculation (with 95% confidence interval – CI) was carried out by using "treatment contrast". Partial eta-squared (ηp2) from package "BaylorEdPsych" (Beaujean, 2012) was used to measure the effect size, and the Pearson correlation coefficient was applied to determine the linear dependence among soil properties.

Results

Soil chemical properties and aboveground biomass

All the digestate-amended soils showed insignificantly different pH values compared to each other; the lowest average value of M+BB was 7.09; see Figure 2A. Also M, WSC, and M +BB digestates reduced soil pH significantly in comparison to the control. An antagonism was apparent between pH and Arg-SIR as well as NAG; see Figure 3. Further, pH was synergistic with Ure activity. The pH demonstrated significant ($p \leq 0.01$) but low negative correlation with C_{ox} ($r = -0.44$); see Figure 4A.

The highest soil TN (0.089%, in average) was detected in the M variant. On the other hand, BB variant showed the lowest TN value (0.07%). M, M+WSC, and WSC showed insignificantly different TN values (Figure 2B); all were significantly more TN abundant compared to the BB variant. TN correlated negatively and significantly ($p \leq 0.001$) with Ala-SIR ($r = -0.53$, Figure 4A) and showed an antagonism with other amino acid-induced respirations (Ala-SIR, Lys-SIR, NAG-SIR); see Figure 3.

The highest average C_{ox} was calculated in the WSC variant, but no statistical differences in values were found in any digestate-amended variants, which were significantly increased compared to the control; see Figure 2C. C_{ox} correlated positively and significantly with fresh AGB ($p \leq 0.001$, $r = 0.73$) and with dry AGB ($p \leq 0.01$, $r = 0.70$); see Figure 4A. Moreover, a significant ($p \leq 0.01$) positive correlation was found with BR ($r = 0.51$) and Arg-SIR ($r = 0.52$). C_{ox} showed synergism with all mentioned traits and Phos, and an antagonism with pH and Ure.

Both fresh and dry AGB were significantly increased in all digestate-amended variants compared to the control. However, the differences between the amended variants were insignificant; see Figures 2D, E. The highest average fresh and dry AGB were achieved by fertilization with BB digestate, despite having the lowest value of TN and only the third highest C_{ox} content in the respective soil. Concurrently with lowest TN, nitrogen uptake by plant (N uptake) was on average (insignificantly) the highest in

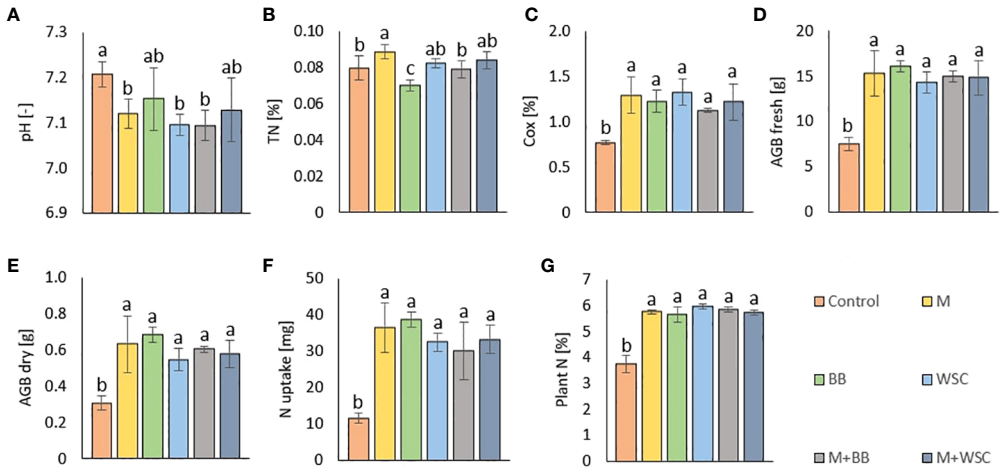

FIGURE 2
(A) Soil pH (n=6); **(B)** total nitrogen, TN (n=6); **(C)** total oxidizable carbon, C_{ox} (n=6); **(D)** fresh aboveground plant biomass, AGB fresh (n=3); **(E)** dry aboveground plant biomass, AGB dry (n=3); **(F)** nitrogen uptake by plant (n=3); **(G)** nitrogen content in plant biomass (n=9) of the control (no digestate) and all variants amended with digestates made from single crop and mixed cultures. Mean ± standard error of mean (error bars); different letters indicate statistically significant differences at the significance level $p \leq 0.05$.

the BB variant (Figure 2F). Nevertheless, neither N uptake nor nitrogen content in dry AGB (Plant N) showed any significant differences between the digestate-amended variants; only the unamended control significantly had the lowest values of both properties; see Figures 2F, G. Fresh and dry AGB correlated significantly ($p \leq 0.001$) positively and highly (r were 0.99 and 0.98) with N uptake; see Figure 4B. Both fresh and dry AGB correlated significantly ($p \leq 0.05$) positively with enzyme activities, namely ARS (r was 0.59 and 0.58, respectively), Phos (r was 0.53 and 0.47, respectively), and GLU (r was 0.57 and 0.54,

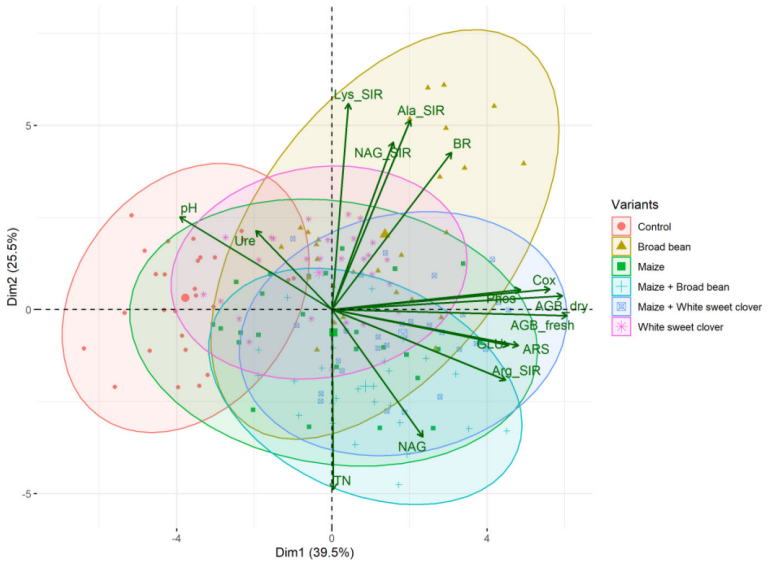

FIGURE 3
PCA biplot of relationships between soil and plant properties of all variants. Fresh (AGB_fresh) and dry (AGB_dry) aboveground plant biomass, soil pH, total nitrogen (TN), total oxidizable carbon (Cox), basal (BR), and substrate-induced respirations - N-acetyl-β-D-glucosamine (NAG_SIR), L-alanine (Ala_SIR), L-lysine (Lys_SIR), and L-arginine (Arg_SIR); enzyme activities - urease (Ure), arylsulfatase (ARS), N-acetyl-β-D-glucosaminidase (NAG), β-glucosidase (GLU), and phosphatase (Phos).

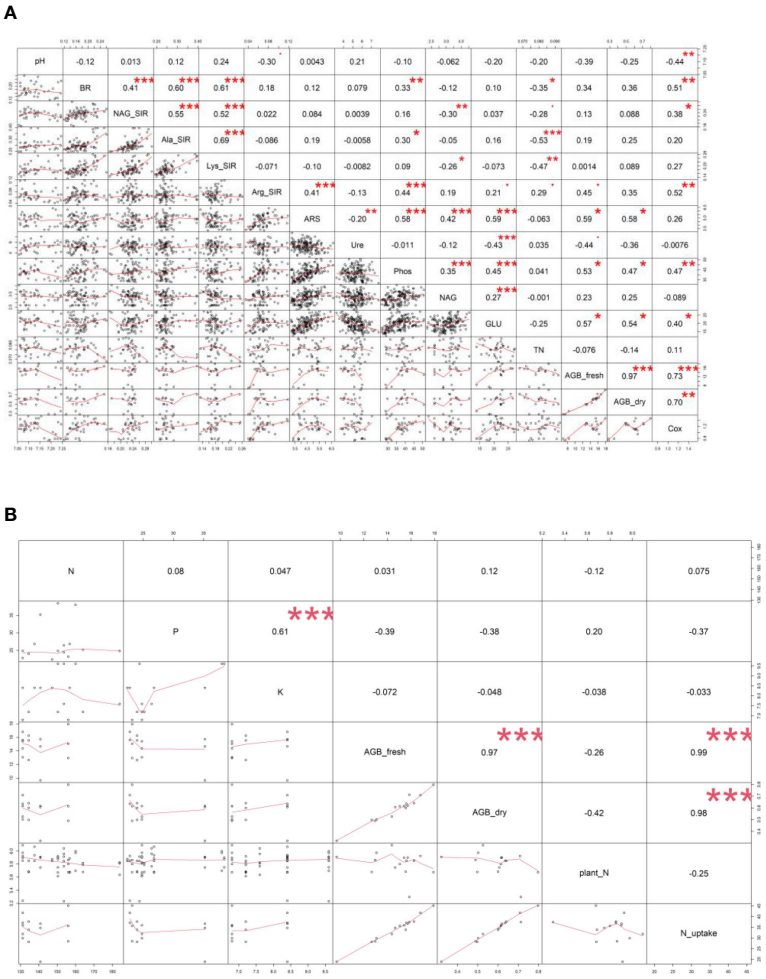

FIGURE 4
Pearson's correlation analysis – values of correlation coefficient (r) between **(A)** soil and plant properties, **(B)** digestate (N, P, K content) and plant properties of all variants. Displayed correlation coefficients (r) were calculated on the statistical level of significance: * $p \leq 0.05$, ** $p \leq 0.01$, *** $p \leq 0.001$. Fresh (AGB_fresh) and dry (AGB_dry) aboveground plant biomass, soil pH, total nitrogen (TN), total oxidizable carbon (Cox), basal (BR) and substrate-induced respirations - N-acetyl-β-D-glucosamine (NAG_SIR), L-alanine (Ala_SIR), L-lysine (Lys_SIR) and L-arginine (Arg_SIR), enzyme activities - urease (Ure), arylsulfatase (ARS), N-acetyl-β-D-glucosaminidase (NAG), β-glucosidase (GLU), phosphatase (Phos).

respectively); see Figure 3. Both fresh and dry AGB showed a strong synergism with these mentioned traits; see Figure 3.

Soil respiration and enzymatic activities

Soil BR was significantly increased (compared to the control) only in two variants: BB (the highest average value, 219 μg $CO_2 \cdot g^{-1} \cdot h^{-1}$) and M+WSC; see Figure 5A. On the other hand, the soil fertilized with M+BB digestate and control exerted the significantly lowest BR. BR showed significant ($p \leq 0.001$) positive correlation with NAG-SIR, Ala-SIR, and Lys-SIR (r was 0.41, 0.60, and 0.61, respectively); see Figure 4A. We revealed apparent synergism for four soil-respiration traits (BR, NAG-SIR, Ala-SIR, Lys-SIR); see Figure 3. NAG-SIR correlated significantly ($p \leq 0.001$) and positively with Ala-SIR and Lys-SIR (r was 0.55 and 0.52, respectively); see Figure 4A.

BB was only variant which exerted significantly increased NAG-, Ala-, and Lys-SIR in comparison to the control; see Figures 5B–D. We detected comparable values of these SIR for all other variants. Mutual correlation between NAG- and Ala-SIR, NAG- and Lys-SIR, and Ala- and Lys-SIR was significant ($p \leq 0.001$) and positive (r was 0.55, 0.52, and 0.69, respectively); see Figure 4A. Contrary to the other respiration traits, Arg-SIR was increased in all digestate-amended variants compared to the control; see Figure 5E. The amendment of M+WSC digestate showed the highest Arg-SIR. Arg-SIR correlated significantly ($p \leq 0.001$) and positively with ARS ($r = 0.41$) and Phos ($r = 0.44$); see Figure 4A.

We detected the unaltered Ure activity (compared to the control) only in two variants amended with digestate: BB and M; see Figure 6A. The M variant showed significantly increased Ure activity in comparison to WSC, M+WSC, and M+BB (the lowest Ure value). A significant ($p \leq 0.001$) negative correlation was found between Ure and GLU activity (r = - 0.43); see Figure 4A. PCA biplot showed antagonism with GLU, ARS, NAG activity, and Arg-SIR; see Figure 3.

Soil amended with M+WSC digestate exerted the significantly highest ARS activity, whereas amendment of WSC digestate resulted in comparably low ARS as detected in the control; see Figure 6B. ARS correlated highly significantly ($p \leq 0.001$) and positively with GLU, Phos, and NAG activity (r was 0.59, 0.58, and 0.42, respectively); less significant ($p \leq 0.05$) was the correlation of ARS and fresh AGB and dry AGB (r was 0.59 and 0.58, respectively); see Figure 4A. PCA biplot showed antagonism with GLU, ARS, NAG activity, and Arg-SIR; see Figure 3. The WSC variant revealed both the lowest ARS and lowest NAG from all digestate-amended variants; its NAG was significantly lower compared to the control; see Figure 6C. All other variants showed significantly increased NAG compared to the control, and M+BB variant had the significantly highest NAG.

The GLU and Phos activities of the control were significantly lowest compared to all other variants. GLU values of M and WSC variants were significantly lower in comparison to the highest M+BB variant; see Figure 6D. The highest Phos was revealed in the BB variant, which was significantly increased compared to the M+BB and WSC variants; see Figure 6E. GLU correlated significantly positively ($p \leq 0.001$) with Phos (r = 0.45) and less significantly ($p \leq 0.05$) with fresh AGB, dry AGB, and C_{ox} (r was 0.57, 0.54, and 0.40, respectively). Phos correlated significantly ($p \leq 0.05$) with fresh AGB and dry AGB (r was 0.53 and 0.47, respectively) and ($p \leq 0.01$) with C_{ox} (r = 0.47); see Figure 4A.

Discussion

Soil chemical properties and aboveground biomass

We discovered that adjustment of all digestates prepared from M, WSC, and M+BB decreased the average values of soil pH compared to the control's unamended soil; see Figure 2. The respective digestates (M, WSC, and M+BB) exerted lower nitrogen content (on average 152.17, 146.60, and 159.86 $g \cdot kg^{-1}$ d.m., respectively) and potassium content compared to other two digestate types (Table 2). These digestate properties might have contributed to the observed differences in soil pH values.

The highest TN (0.09%) content in soil was detected under treatment with M-derived digestate, which was the only significantly increased value in comparison to the control. This

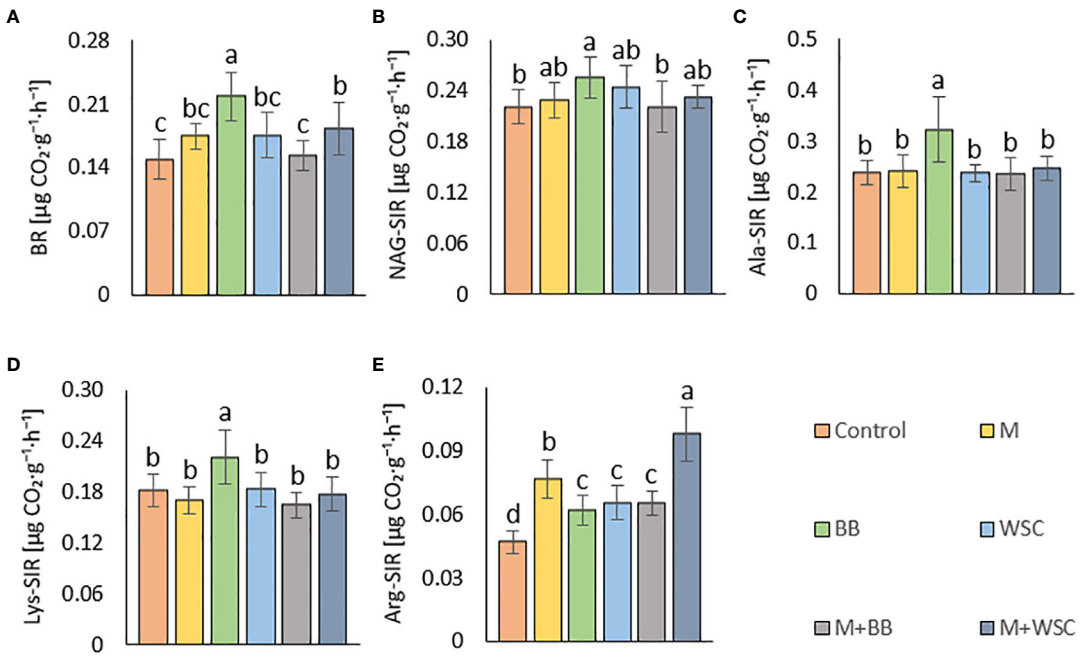

FIGURE 5
(A) Soil basal, BR and substrate-induced respirations - **(B)** N-acetyl- β -D-glucosamine, NAG-SIR; **(C)** L-alanine, Ala-SIR; **(D)** L-lysine, Lys-SIR; and **(E)** L-arginine, Arg-SIR; of the control (no digestate) and all variants amended with digestates made from single crop and mixed cultures, n=12. Mean ± standard error of mean (error bars); different letters indicate statistically significant differences at the significance level $p \leq 0.05$.

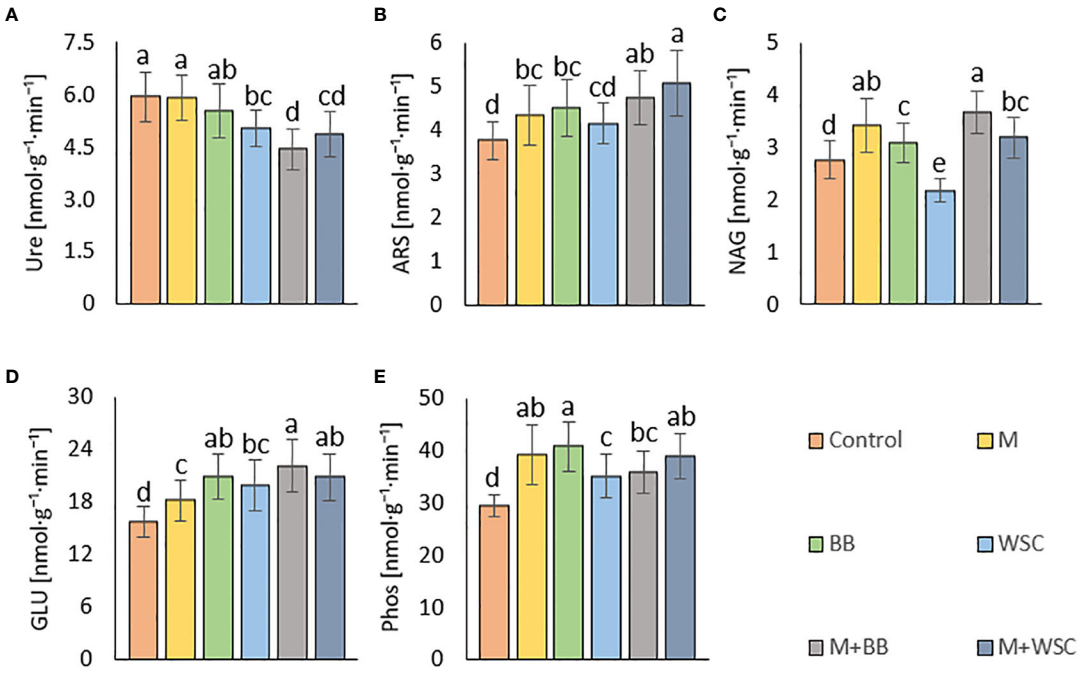

FIGURE 6
Soil enzyme activities - **(A)** urease, Ure; **(B)** arylsulfatase, ARS; **(C)** N-acetyl-β-D-glucosaminidase, NAG; **(D)** β-glucosidase, GLU; **(E)** phosphatase, Phos; of the control (no digestate) and all variants amended with digestates made from single crop and mixed cultures, n=27. Mean ± standard error of mean (error bars); different letters indicate statistically significant differences at the significance level $p \leq 0.05$.

finding did not correspond to the nitrogen doses applied to the soil with digestates. The M variant received a lower nitrogen dose compared to the nitrogen in BB and M+BB variants; see Table 2; however, these variants showed decreased TN in soil compared to the M digestate-amended soil. Because the nitrogen input did not correlate with N uptake by plants (Figure 4B), a possible explanation for this could be the lowered losses of nitrogen: lower pH putatively mediated reduction of ammonium to non-volatile cation form, and its volatilization was further mitigated due to enhanced nitrogen transformation and mineralization activities. A study done with slurry digestate showed that NH_3 emissions were lower when it was acidified (Covali et al., 2021). Decreased TN content in the M+BB variant could have been coupled with decreased nitrogen mineralization, determined by urease (Ure) activity (compared to other legume-based digestate variants); see Figure 6A. Ure was comparable to the control only in M variant, in which the Ure value was significantly increased compared to WSC, M+BB, and M+WSC. A ratio of soil C:N (C_{ox} : TN) was also slightly different from the most favorable value, 20:1, which presented an assimilation:mineralization equilibrium value as 14.6:1 in M variant, which was lower in comparison to 17.6:1 in BB and 16.2:1 in WSC variants, indicating an M digestate-mediated higher nitrogen mineralization, as discussed by Brust (2019). We ascertained from these findings a higher nitrification rate in soil treated with M digestate, which was evidenced by high Ure value and significantly increased Arg-SIR compared to control; see Figure 5E. These assumptions were further corroborated by negative correlation between TN content and Ala-SIR (r = -0.53, Figure 4A) and antagonism with Ala-SIR, Lys-SIR, and NAG-SIR, as displayed in PCA biplot; see Figure 3.

N-acetyl-β-D-glucosaminidase (NAG) was significantly increased in soil treated with M+BB variant compared to all other digestate variants; see Figure 6C. High NAG together with the (average) highest β-glucosidase (GLU) activity indicated enhanced turnover of soil fungal necromass and coupled nitrogen transformation, which could be also ascertained from the second lowest C_{ox} : TN ratio (14.3:1) of M+BB variant (Hu et al., 2015). With the enhanced turnover of putatively more abundant fungal biomass in the soil amended with the most phosphorus-rich digestate M+BB (31.63 ± 1.21 $g \cdot kg^{-1}$, Table 2), it was assumed that increment in fungal biomass was coupled with the respective digestate-derived improvement of phosphorus content in soil, as referred to by Du et al. (2019). On the other hand, a similar contributing effect to fungal biomass *via* higher access of phosphorus in soil could also be achieved by its mineral source, due to the fungal-derived improvement of phosphorus solubilization (Ceci et al., 2018).

All digestate-amended variants exerted significantly increased soil C_{ox} in comparison to the control variant. As C_{ox}

represents a sub-pool of labile SOC, we expected that C_{ox} could correspond to a dose of TOC applied in the digestate to the respective variants. However, disproportions between C_{ox} and the applied dose of TOC were detected; see Table 2 and Figure 2C. Although WSC showed the highest soil C_{ox} and the second highest TOC content in digestate, M+WSC reached the second lowest soil C_{ox} and concurrently the highest content of TOC in the respective digestate. The significant differences might have been caused by varied assimilation rate of carbon and nitrogen among the tested variants and could also be attributed to the digestibility of the organic carbon in the respective digestates, with higher lability of organic carbon in the fertilizer obtained from mono-substrate BB and WSC, M digestion. This assumption was based on the observed significantly longer lag in biogas production of the mixed culture feedstock compared to the monoculture corn feedstock (Kintl et al., 2022). We assumed vastly pre-digested, partially consumed (and therefore decreased to lower TOC values), and more easily available recalcitrant compounds in TOC of monoculture digestate, whereas the mixed culture digestate likely preserved a higher portion of moderately recalcitrant carbon. This might cause C_{ox} values to affect the respiratory and enzymatic activities in soil differently and incoherently with the carbon inputs derived by the various digestate variants. The efficiency of utilizing the digestate-derived external organic matter in the form of oxidizable carbon could be expressed as a ratio between TOC values of all digestate variants and C_{ox} values of respective amended variants used to treat soil. These ratios, calculated from Table 2 and the values in Figure 2C, were also the lowest for WSC (22.5:1), M (22.6:1), and BB (23.4:1), compared to values of M+WSC (24.7:1) and M+BB (26.2:1). The microbial community amended with mixed culture digestate putatively oxidized such partially digested recalcitrant carbon more slowly and likely led to the significantly lowered respiration (BR, NAG-SIR, Ala-SIR, Lys-SIR) values in M+BB compared to BB variant; see Figure 5. The observed higher soil catabolic activity (BR, SIRs, GLU, NAG) in the respective monoculture digestate variants, namely BB, corroborates this presumption of higher organic matter decomposition in the monoculture digestate-amended variants. A contradictory significant positive correlation between C_{ox} and both fresh and dry AGB (r was 0.73 and 0.70, respectively) could also be explained by this hypothesis and the mutual synergy of these properties on the PCA biplot; Figures 3, 4. An active pool of TOC could be also affected by the land use systems (Sahoo et al., 2019), but in this experiment the carbon sources in soil were much more affected by the addition of external organic matter of variable quality than by the changes in complexity of intrinsic SOM. Because C_{ox} correlated significantly and positively with BR ($r = 0.51$, $p \leq 0.01$), we presumed that higher digestibility of digestate amendment enhanced organic matter aerobic decomposition. Moreover, TN content was coupled with increased respiration, evidenced by the significant negative correlation of TN and Ala-SIR and Lys-SIR (r were - 0.53 and – 0.47, $p \leq 0.001$ and ≤ 0.01, respectively), and antagonism on PCA biplot; Figures 3, 4. Therefore, a strong dependence between a decrease in nitrogen content in soil and the co-decomposition of nitrogen sources together with carbon sources and their mineralization was ascertained from these relations. Nevertheless, all digestate-amended variants significantly increased fresh and dry AGB in comparison to the control, and their effects remained similar to each other (Figures 2D, E). The highest average fresh and dry AGB value was achieved in BB digestate-treated variant despite the lowest value of TN and the third highest C_{ox} content in soil. It was reported that digestates have a higher potential over a short- to mid-term use period to positively affect plant biomass yield in comparison to synthetic nitrogen fertilizer under favorable climatic conditions (Doyeni et al., 2021). However, we discovered that plant nitrogen content (%) in plant dry biomass did not correspond to the amount of nitrogen amended with the respective digestate doses to the experimental variants. Nevertheless, we found a very high significant correlation of N uptake and fresh and dry AGB (Figure 4B), despite the differences between variants not being significant. Thus, soil nitrogen losses and N uptake at the end of the experiment are balanced through nitrogen access (provided by amended digestate) and acquisition by the plant. However, we can ascribe the rate of nitrogen efflux from soil to higher incorporation of nitrogen into plant biomass, as revealed in the BB variant, which showed the lowest soil TN and the highest average N uptake by plants.

Soil respiration and enzymatic activities

Tested digestates consisting of M, M+BB, and WSC did not enhance the soil BR compared to the control; see Figure 5. Nevertheless, BR values of M,WSC, and M+WSC were comparable. We ascribed this finding to observation that the remaining organic fraction after AD was more recalcitrant than the feedstocks (Möller 2015), thus the readily available carbon for aerobic catabolism was limited. The highest BR in BB-treated soil corresponded to the significantly lower content of stable (left intact after AD decomposition) carbonaceous compounds (hemicellulose, neutral detergent fiber) in legume-based digestate than in *Poales*-based digestate (Slepetiene et al., 2016). This was putatively caused by the reported higher (by +62%) inhibition of plant cell wall digestion by lignin in grasses than in legumes (Buxton and Russell, 1988). The significantly highest NAG-SIR in the BB variant was thought to be caused by higher degradable organic matter (fungal necromass) and other labile SOM-associated organic nitrogen supplied *via* respective legume-digestate amendment. Nitrogen scarcity anticipated the level of Ure activity as well, which was significantly increased in the variant BB (with the lowest TN) compared to all other

legume-based variants (except WSC); see Figures 2B, 6A. The soil treated with variants M+BB, M+WSC, and WSC with TN was comparable to the control value, and the C_{ox} : TN ratio was significantly lower (from 14.5:1 to 16.2:1) compared to the BB (17.6:1) soil; significantly decreased Ure compared to the control and M was also found. Retarded organic matter deamination in M +BB variant was again putatively caused by higher recalcitrance of external organic matter of digestate and indicated by low C_{ox}:N ratio. Positive correlation between Ure activity and C:N ratio value was already reported (Gao et al., 2019; Pan et al., 2021).

It is generally known that fodder legumes are relatively less abundant in sulfur amino acids (Witten et al., 2015) compared to cereals such as maize. Thus, it was expected that the digestate made of single cropped BB and WSC might be deficient in sulfur. This assumption explained lower ARS (the enzyme involved in mineralization of organo-sulphates) in the WSC variant; see Figure 6B. The low ARS value in the M digestate-treated variant was less expected and comparable to the effect of BB digestate.

NAG is an enzyme involved in decomposition of fungal cell wall polysaccharide (chitin). Mycorrhizal fungi in the tested soil might have significantly affected the final fungal biomass and its turnover. Increment in fungal biomass was presumably coupled with the respective digestate-derived improvement of phosphorus content in soil, as discussed Du et al. (2019). The study by Yu et al. (2020) evidenced a negative correlation between N:P ratio and arbuscular mycorrhizal abundance and vesicle formation after root infection. This means that phosphorus supplementation by M+BB digestate with significantly lower N:P ratio (5.1:1) compared to other digestates (with N:P ratios demonstrably higher - from 6.7:1 to 7.8:1) may cause an increment in NAG values; see Figure 6C. On the other hand, WSC digestate dose exerted a higher N:P ratio of 6.7:1, which might partially explain the revealed lowest NAG although it was in contrast with the result of NAG-SIR determination. Our findings that NAG and ARS activity was related to the availability of nutrients in soil are further supported by the positive correlation of both enzyme activities with fresh and dry AGB.

The GLU enzyme catalyzes the hydrolysis of β-1→4-bonds in the cellulose and oligosaccharide molecules of soil organic matter (SOM) or digestate, especially its organic carbon fraction. Therefore, the significantly highest level of GLU in the M+BB variant corresponded to the highest dose of TOC in the respective applied digestate (372 $kg{\cdot}ha^{-1}$). Moreover, we assumed that digestates made of mixed cultures and monocultures of legumes contained more decomposition products of cellulose (hemicellulose) compounds due to the already mentioned digestion inhibition of cell wall compounds by lignin in grasses (Buxton and Russell, 1988) and thus induced higher GLU activity in comparison to the M digestate-amended variant.

We revealed the highest Phos activity in the BB variant, which was supplied with the lowest amount of available phosphorus (23 $kg{\cdot}ha^{-1}$) within the amended digestate dose in comparison to all other digestate variants; see Table 2. We assume that the increased demand for phosphorus of lettuce seedlings exerting the highest fresh and dry AGB in the BB variant induced the enhanced phosphate-solubilizing activity in soil, catalyzed by the Phos enzyme. We discovered that the enhanced Phos activity was related to the increase in GLU values, and this was in the line with coupled carbon- and phosphorus-cycling enzyme activities (Loeppmann et al., 2020). On the other hand, the significantly lowest Phos in WSC was indirectly related to the highest TOC:P ratio (13.8:1) in the respective amended digestate calculated from Table 2. This finding agreed with a negative correlation of C:P ratio to phosphate solubilization efficiency as reported by Zhan et al. (2021).

Conclusions

This study verified an apparently variable effect of digestates made from different feedstocks on soil properties. Fresh and dry aboveground biomass was significantly increased in the digestate-amended variants in comparison to the control but comparable after application of all five digestate types. The demonstrably highest content of total nitrogen and urease, and very high content of oxidizable carbon were observed for maize digestate amendment. However, the highest induction of respiration and enzyme activities occurred with the addition of digestates made of either legume monoculture or mixed cultures. We ascribe these observed differences to the effect of presumably increased soil degradability of legume-derived digestate organic matter and joint increased availability of nutrients after application, which might also lead to increased risks of nitrogen loss. Therefore, further investigation in this area could focus on the different ratios between maize and legume biomass in feedstock to achieve a better balance between the availability and recalcitrance of the digestate organic matter.

Data availability statement

The original contributions presented in the study are included in the article/supplementary material. Further inquiries can be directed to the corresponding authors.

Author contributions

Conceptualization, MB and TH; methodology, TH, AK, and AM; software, TB; validation, TB, JE, OM, and JH; formal analysis, JE and TH; investigation, AM; resources, JH and OM; data curation, TH, AM, and AK; writing - original draft preparation, TH, JH, AM, and MB; writing - review and editing, AK, AM, TV, and MB; visualization, TB and AM; supervision, MB, and TH; project administration, MB and AK; funding acquisition, JH, AK, and MB. All authors have read and agreed to the published version of the manuscript.

Funding

The work was supported by the project of Technology Agency of the Czech Republic TH04030132, by the Ministry of Agriculture of the Czech Republic institutional support MZE-RO1722 and MZE-RO1218 and by the project of Ministry of Education, Youth and Sports of the Czech Republic, grant number FCH-S-22-8001.

Conflict of interest

The authors JH and AK are employed by Agrovyzkum Rapotin, Ltd., Vyzkumniku 267, 788 13 Rapotin, Czech Republic and Agricultural Research, Ltd., Troubsko, Czech Republic.

The remaining authors declare that the research was conducted in the absence of any commercial or financial relationships that could be construed as a potential conflict of interest.

Publisher's note

References

Alburquerque, J. A., de la Fuente, C., Campoy, M., Carrasco, L., Nájera, I., Baixauli, C., et al. (2012). Agricultural use of digestate for horticultural crop production and improvement of soil properties. *Eur. J. Agron.* 43, 119–128. doi: 10.1016/j.eja.2012.06.001

Andruschkewitsch, M., Wachendorf, C., and Wachendorf, M. (2013). Effects of digestates from different biogas production systems on above and belowground grass growth and the nitrogen status of the plant-soil-system. *Grassland. Sci.* 59 (4), 183–195. doi: 10.1111/grs.12028

Angelidaki, I., Ellegaard, L., and Ahring, B. K. (2003). "Applications of the anaerobic digestion process," in *Biomethanation ii*. Eds. B. K. Ahring, B. K. Ahring, I. Angelidaki, J. Dolfing, L. EUegaard, H. N. Gavala, et al (Berlin, Heidelberg: Springer Berlin Heidelberg), 1–33. doi: 10.1007/3-540-45838-7_1

Aravani, V. P., Sun, H. Y., Yang, Z. Y., Liu, G. Q., Wang, W., Anagnostopoulos, G., et al. (2022). Agricultural and livestock sector's residues in Greece & China: Comparative qualitative and quantitative characterization for assessing their potential for biogas production. *Renew. Sust. Energ. Rev.* 154 (16), 111821. doi: 10.1016/j.rser.2021.111821

Arthurson, V. (2009). Closing the global energy and nutrient cycles through application of biogas residue to agricultural land – potential benefits and drawback. *Energies* 2 (2), 226–242. doi: 10.3390/en20200226

Bachmann, S., Wentzel, S., and Eichler-Lobermann, B. (2011). Codigested dairy slurry as a phosphorus and nitrogen source for zea mays l. and amaranthus cruentus l. *J. Plant Nutr. Soil Sci.* 174 (6), 908–915. doi: 10.1002/jpln.201000383

Barłóg, P., Hlisnikovský, L., and Kunzová, E. (2020) "Effect of digestate on soil organic carbon and plant-available nutrient content compared to cattle slurry and mineral fertilization." *Agronomy* 10 (3), 379 doi: 10.3390/agronomy10030379

Bauer, L., Ranglová, K., Masojídek, J., Drosg, B., and Meixner, K. (2021) "Digestate as sustainable nutrient source for microalgae–challenges and prospects." *Appl Sci* 11 (3), 1056 doi: 10.3390/app11031056

Beaujean, A. A. (2012). *R package for Baylor University educational psychology quantitative courses, BaylorEdPsych*. Available at: https://rdrr.io/cran/BaylorEdPsych/.

Bougnom, B. P., Niederkofler, C., Knapp, B. A., Stimpfl, E., and Insam, H. (2012). Residues from renewable energy production: Their value for fertilizing pastures. *Biomass Bioenergy* 39, 290–295. doi: 10.1016/j.biombioe.2012.01.017

Brtnicky, M., Hammerschmiedt, T., Elbl, J., Kintl, A., Skulcova, L., Radziemska, M., et al (2021). "The potential of biochar made from agricultural residues to increase soil fertility and microbial activity: Impacts on soils with varying sand content." *Agronomy* 11 (6), 1174. doi: 10.3390/agronomy11061174

Brtnicky, M., Kintl, A., Holatko, J., Hammerschmiedt, T., Mustafa, A., Kucerik, J., et al. (2022). EFFECT of digestates derived from the fermentation of maize-legume intercropped culture and maize monoculture application on soil properties and plant biomass production. *Chem. Biol. Technol. Agric.* 9 (1), p.1–p24. doi: 10.1186/s40538-022-00310-6

Brust, G. E. (2019). *Management strategies for organic vegetable fertility. safety and practice for organic food*. Eds. D. Biswas and S. A. Micallef (Amsterdam: Academic Press), 193–212. doi: 10.1016/b978-0-12-812060-6.00009-x

Buxton, D. R., and Russell, J. R. (1988). Lignin constituents and cell-wall digestibility of grass and legume stems. *Crop Sci.* 28 (3), 553–558. doi: 10.2135/cropsci1988.0011183X002800030026x

Campbell, C. D., Chapman, S. J., Cameron, C. M., Davidson, M. S., and Potts, J. M. (2003). A rapid microtiter plate method to measure carbon dioxide evolved from carbon substrate amendments so as to determine the physiological profiles of soil microbial communities by using whole soil. *Appl. Environ. Microbiol.* 69 (6), 3593–3599. doi: 10.1128/AEM.69.6.3593-3599.2003

Ceci, A., Pinzari, F., Russo, F., Maggi, O., and Persiani, A. M. (2018). Saprotrophic soil fungi to improve phosphorus solubilisation and release: *In vitro* abilities of several species. *Ambio* 47 (Suppl 1), 30–40. doi: 10.1007/s13280-017-0972-0

Covali, P., Raave, H., Escuer-Gatius, J., Kaasik, A., Tonutare, T., and Astover, A. (2021). The effect of untreated and acidified biochar on nh3-n emissions from slurry digestate. *Sustainability* 13 (2), 19. doi: 10.3390/su13020837

ČSN EN 15934 (2013) *Kaly, upravený bioodpad, půdy a odpady - výpočet podílu sušiny po stanovení zbytku po sušení nebo obsahu vody* (Prague: Česká agentura pro standardizaci). Available at: https://www.technicke-normy-csn.cz/csn-en-15934-838125-231751.html (Accessed 02-05-2022).

Dębowski, M., Kazimierowicz, J., Zieliński, M., and Bartkowska, I. (2022). Co-Fermentation of microalgae biomass and *Miscanthus* × *giganteus* silage–assessment of the substrate, biogas production and digestate characteristics. *Appl. Sci.* 12 (14), 7291. doi: 10.3390/app12147291

Doyeni, M. O., Stulpinaite, U., Baksinskaite, A., Suproniene, S., and Tilvikiene, V. (2021). The effectiveness of digestate use for fertilization in an agricultural cropping system. *Plants* 10 (8), 1734. doi: 10.3390/plants10081734

Du, Y., Wu, J. N., Anane, P. S., Wu, Y. S., Wang, C. Y., and Liu, S. X. (2019). Effects of different biochars on physicochemical properties and fungal communities of black soil. *Pol. J. Environ. Stud.* 28, 3125–3132. doi: 10.15244/pjoes/94816

Ehmann, A., Thumm, U., and Lewandowski, I. (2018). Fertilizing potential of separated biogas digestates in annual and perennial biomass production systems. *Front. Sustain. Food Syst.* 2. doi: 10.3389/fsufs.2018.00012

Fahlbusch, W., Hey, K., Sauer, B., and Ruppert, H. (2018). Trace element delivery for biogas production enhanced by alternative energy crops: Results from two-year field trials. *Energy Sustainability Soc.* 8 (1), 11. doi: 10.1186/s13705-018-0180-1

Gatta, G., Gagliardi, A., Soldo, P., and Monteleone, M. (2013). Grasses and legumes in mixture: An energy intercropping system intended for anaerobic digestion. *Ital. J. Agron.* 8 (1), 47–57. doi: 10.4081/ija.2013.e7

Gao, Y., Huang, H., Zhao, H., Xia, H., Sun, M., Li, P., et al. (2019). "Phosphorus affects enzymatic activity and chemical properties of cotton soil.". *Plant Soil Environ.* 65 (7), 361–368. doi: 10.17221/296/2019-pse

Gissén, C., Prade, T., Kreuger, E., Nges, I. A., Rosenqvist, H., Svensson, S.-E., et al. (2014). Comparing energy crops for biogas production – yields, energy input and costs in cultivation using digestate and mineral fertilisation. *Biomass Bioenergy* 64, 199–210. doi: 10.1016/j.biombioe.2014.03.061

González-García, S., Bacenetti, J., Negri, M., Fiala, M., and Arroja, L. (2013). Comparative environmental performance of three different annual energy crops for biogas production in northern italy. *J. Cleaner Production* 43, 71–83. doi: 10.1016/j.jclepro.2012.12.017

Gutser, R., Ebertseder, T., Weber, A., Schraml, M., and Schmidhalter, U. (2005). Short-term and residual availability of nitrogen after long-term application of organic fertilizers on arable land. *J. Plant Nutr. Soil Sci.* 168 (4), 439–446. doi: 10.1002/jpln.200520510

Herman, T., Nungesser, E., Miller, K. E., and Davis, S. C. (2022). Comparative Fuel Yield from Anaerobic Digestion of Emerging Waste in Food and Brewery Systems. *Energies* 15, 1538. doi: 10.3390/en15041538

Holatko, J., Hammerschmiedt, T., Datta, R., Baltazar, T., Kintl, A., Latal, O., et al. (2020). Humic acid mitigates the negative effects of high rates of biochar application on microbial activity. *Sustainability* 12 (22). doi: 10.3390/su12229524

Hu, H. W., Chen, D., and He, J. Z. (2015). Microbial regulation of terrestrial nitrous oxide formation: Understanding the biological pathways for prediction of emission rates. *FEMS Microbiol. Rev.* 39 (5), 729–749. doi: 10.1093/femsre/fuv021

Hutnan, M., Špalková, V., Bodík, I., Kolesarova, N., and Lazor, M. (2010). Biogas production from maize grains and maize silage. *Polish J. Environ. Stud.* 19, 323–329.

Karpenstein-Machan, M. (2005). *Energiepflanzenbau für biogasanlagenbetreiber* (Germany, DLG Verlag: Frankfurt am Main).

Kassambara, A., and Mundt, F. (2020). Factoextra: Extract and visualize the results of multivariate data analyses. *R Package Version 1.0.7.*. https://CRAN.R-project.org/package=factoextr.

Kettl, K.-H., Niemetz, N., Sandor, N., Eder, M., and Narodoslawsky, M. (2010). Ecological evaluation of biogas feedstock from intercrops. *Chem. Eng. Trans*, 433–438. doi: 10.3303/CET10210

Kintl, A., Elbl, J., Vítěz, T., Brtnický, M., Skládanka, J., Hammerschmiedt, T., et al. (2020). Possibilities of using white sweetclover grown in mixture with maize for biomethane production. *Agronomy* 10 (9), 1407. doi: 10.3390/agronomy10091407

Kintl, A., Huňady, I., Holátko, J., Vítěz, T., Hammerschmiedt, T., Brtnický, M., et al. (2022). Using the Mixed Culture of Fodder Mallow (Malva verticillata L.) and White Sweet Clover (Melilotus albus Medik.) for Methane Production. *Fermentation* 8, 94. doi: 10.3390/fermentation8030094

Kintl, A., Vítěz, T., Elbl, J., Vítězová, M., Dokulilová, T., Nedělník, J., et al. (2019). Mixed culture of corn and white lupine as an alternative to silage made from corn monoculture intended for biogas production. *Bioenergy Res.* 12 (3), 694–702. doi: 10.1007/s12155-019-10003-y

Kisielewska, M., Dębowski, M., Zieliński, M., Kazimierowicz, J., Quattrocelli, P., and Bordiean, A. (2021). Effects of Liquid Digestate Treatment on Sustainable Microalgae Biomass Production. *Bioenergy Res.* 15, 357–370. doi: 10.1007/s12155-021-10251-x

Lamei Hervani, J. (2013). Assessment of dry forage and crude protein yeilds, competition and advantage indices in mixed cropping of annual forage legume crops with barley in rainfed comditions of zanjan province in iran. *Seed And Plant Production J.* 29-2 (2), 169–183.

Liedl, B. E., Bombardiere, J, Williams, M. L., Stowers, A., Postalwait, C., Chatfield, J. M, et al (2004). Solid Effluent from Thermophilic Anaerobic Digestion of Poultry Litter as a Potential Fertilizer. *Hortscience* 39 (4), 877–877. doi: 10.21273/HORTSCI.39.4.877B

Lê, S., Josse, J., and Husson, F. (2008). "Factominer: Anrpackage for multivariate analysis.". *J. Stat. Software* 25 (1), 1–18. doi: 10.18637/jss.v025.i01

Lebuhn, M., Liu, F., Heuwinkel, H., and Gronauer, A. (2008). Biogas production from mono-digestion of maize silage-long-term process stability and requirements. *Water Sci. Technol.* 58 (8), 1645–1651. doi: 10.2166/wst.2008.495

Loeppmann, S., Breidenbach, A., Spielvogel, S., Dippold, M. A., and Blagodatskaya, E. (2020). "Organic nutrients induced coupled c- and p-cycling enzyme activities during microbial growth in forest soils.". *Front. Forests Global Change* 3 (100). doi: 10.3389/ffgc.2020.00100

Meyer, A. K. P., Schleier, C., Piorr, H.-P., and Holm-Nielsen, J. B. (2015). The potential of surplus grass production as co-substrate for anaerobic digestion: A case study in the region of southern denmark. *Renewable Agric. Food Syst.* 31 (4), 330–349. doi: 10.1017/s1742170515000277

Möller, K. (2015). "Effects of anaerobic digestion on soil carbon and nitrogen turnover, n emissions, and soil biological activity. a review.". *Agron. Sustain. Dev.* 35 (3), 1021–1041. doi: 10.1007/s13593-015-0284-3

Muhayodin, F., Fritze, A., and Rotter, V. S. (2021). Mass balance of c, nutrients, and mineralization of nitrogen during anaerobic co-digestion of rice straw with cow manure. *Sustainability* 13 (21), 11568. doi: 10.3390/su132111568

Nassab, A. D. M., Amon, T., and Kaul, H. P. (2011). Competition and yield in intercrops of maize and sunflower for biogas. *Ind. Crops Products* 34 (1), 1203–1211. doi: 10.1016/j.indcrop.2011.04.015

Nges, I. A., Bjorn, A., and Bjornsson, L. (2012). Stable operation during pilot-scale anaerobic digestion of nutrient-supplemented maize/sugar beet silage. *Bioresour Technol.* 118, 445–454. doi: 10.1016/j.biortech.2012.05.096

Nurk, L., Graβ, R., Pekrun, C., and Wachendorf, M. (2016). Methane yield and feed quality parameters of mixed silages from maize (zea mays l.) and common bean (phaseolus vulgaris l.). *Bioenergy Res.* 10 (1), 64–73. doi: 10.1007/s12155-016-9779-2

Oslaj, M., Mursec, B., and Vindis, P. (2010). Biogas production from maize hybrids. *Biomass Bioenergy* 34 (11), 1538–1545. doi: 10.1016/j.biombioe.2010.04.016

Pan, J., Guo, Q., Li, H., Luo, S., Zhang, Y., Yao, S., et al. (2021). "Dynamics of soil nutrients, microbial community structure, enzymatic activity, and their relationships along a chronosequence of pinus massoniana plantations.". *Forests* 12 (3). doi: 10.3390/f12030376

Peoples, M. B., Herridge, D. F., and Ladha, J. K. (1995). Biological nitrogen fixation: An efficient source of nitrogen for sustainable agricultural production? *Plant Soil* 174 (1/2), 3–28. doi: 10.1007/BF00032239

Purdy, S. J., Maddison, A. L., Nunn, C. P., Winters, A., Timms-Taravella, E., Jones, C. M., et al. (2017). Could Miscanthus replace maize as the preferred substrate for anaerobic digestion in the United Kingdom? Future breeding strategies. *Global Change Biol. Bioenergy* 9, 1122–1139. doi: 10.1111/gcbb.12419

Råberg, T. M., Carlsson, G., and Jensen, E. S. (2017). Productivity in an arable and stockless organic cropping system may be enhanced by strategic recycling of biomass. *Renewable Agric. Food Syst.* 34 (1), 20–32. doi: 10.1017/s1742170517000242

Risberg, K., Cederlund, H., Pell, M., Arthurson, V., and Schnurer, A. (2017). Comparative characterization of digestate versus pig slurry and cow manure - chemical composition and effects on soil microbial activity. *Waste Manag* 61, 529–538. doi: 10.1016/j.wasman.2016.12.016

Riva, C., Orzi, V., Carozzi, M., Acutis, M., Boccasile, G., Lonati, S., et al. (2016). Short-term experiments in using digestate products as substitutes for mineral (n) fertilizer: Agronomic performance, odours, and ammonia emission impacts. *Sci. Total Environ.* 547, 206–214. doi: 10.1016/j.scitotenv.2015.12.156

Sahoo, U. K., Singh, S. L., Gogoi, A., Kenye, A., and Sahoo, S. S. (2019). Active and passive soil organic carbon pools as affected by different land use types in mizoram, northeast India. *PloS One* 14 (7), e0219969. doi: 10.1371/journal.pone.0219969

Samarappuli, D., and Berti, M. T. (2018). Intercropping forage sorghum with maize is a promising alternative to maize silage for biogas production. *J. Cleaner Production* 194, 515–524. doi: 10.1016/j.jclepro.2018.05.083

Schittenhelm, S. (2010). Effect of drought stress on yield and quality of maize/sunflower and maize/sorghum intercrops for biogas production. *J. Agron. Crop Sci.* 196 (4), 253–261. doi: 10.1111/j.1439-037X.2010.00418.x

Shakoor, A., Ashraf, F., Shakoor, S., Mustafa, A., Rehman, A., and Altaf, M. M. (2020). Biogeochemical transformation of greenhouse gas emissions from terrestrial to atmospheric environment and potential feedback to climate forcing. *Environ. Sci. pollut. Res.* 27 (31), 38513–38536. doi: 10.1007/s11356-020-10151-1

Sigurnjak, I., Vaneeckhaute, C., Michels, E., Ryckaert, B., Ghekiere, G., Tack, F. M. G., et al. (2017). Fertilizer performance of liquid fraction of digestate as synthetic nitrogen substitute in silage maize cultivation for three consecutive years. *Sci. Total Environ.* 599-600, 1885–1894. doi: 10.1016/j.scitotenv.2017.05.120

Šimon, T., Kunzová, E., and Friedlová, M. (2016). The effect of digestate, cattle slurry and mineral fertilization on the winter wheat yield and soil quality parameters. *Plant Soil Environ.* 61 (No. 11), 522–527. doi: 10.17221/530/2015-pse

Slepetiene, A., et al. (2020). The potential of digestate as a biofertilizer in eroded soils of Lithuania. *Waste Manag* 102, 441–451. doi: 10.1016/j.wasman.2019.11.008

Slepetiene, A., Slepetys, J., Tilvikiene, V., Amaleviciute, K., Liaudanskiene, I., Ceseviciene, J., et al. (2016). Evaluation of chemical composition and biogas production from legumes and perennial grasses in anaerobic digestion using the oxitop system. *Fresenius Environ. Bull.* 25, 1342–1347.

Stinner, W., Möller, K., and Leithold, G. (2008). Effects of biogas digestion of clover/grass-leys, cover crops and crop residues on nitrogen cycle and crop yield in organic stockless farming systems. *Eur. J. Agron.* 29 (2-3), 125–134. doi: 10.1016/j.eja.2008.04.006

Szymanska, M., Szara, E., Sosulski, T., Stepien, W., Pilarski, K., and Pilarska, A. A. (2018). Chemical properties and fertilizer value of ten different anaerobic digestates. *Fresenius Environ. Bull.* 27 (5A), 3425–3432.

Tambone, F., and Adani, F. (2017). Nitrogen mineralization from digestate in comparison to sewage sludge, compost and urea in a laboratory incubated soil experiment. *J. Plant Nutr. Soil Sci.* 180 (3), 355–365. doi: 10.1002/jpln.201600241

Theuerl, S., Herrmann, C., Heiermann, M., Grundmann, P., Landwehr, N., Kreidenweis, U., et al. (2019). The future agricultural biogas plant in Germany: A vision. *Energies* 12 (3), 396. doi: 10.3390/en12030396

VDI 4630 (2016). *Fermentation of organic substances – substrate characterisation, sampling, data collection, fermentation tests* (Düsseldorf: Beuth Verlag).

von Cossel, M., Amarysti, C., Wilhelm, H., Priya, N., Winkler, B., and Hoerner, L. (2020) "The replacement of maize (zea mays l.) by cup plant (silphium perfoliatum l.) as biogas substrate and its implications for the energy and material flows of a large biogas plant." *Biofuels. Bioproducts. Biorefining* 14 (2), 152–179. doi: 10.1002/bbb.2084

von Cossel, M., Pereira, L. A., and Lewandowski, I. (2021). Deciphering substrate-specific methane yields of perennial herbaceous wild plant species. *Agronomy* 11 (3), 451. doi: 10.3390/agronomy11030451

Wahid, R., Feng, L., Cong, W.-F., Ward, A. J., Møller, H. B., and Eriksen, J. (2018). Anaerobic mono-digestion of lucerne, grass and forbs – influence of species and cutting frequency. *Biomass Bioenergy* 109, 199–208. doi: 10.1016/j.biombioe.2017.12.029

Weiland, P. (2010). Biogas production: Current state and perspectives. *Appl. Microbiol. Biotechnol.* 85 (4), 849–860. doi: 10.1007/s00253-009-2246-7

Wickham, H. (2016). *Ggplot2: Elegant graphics for data analysis* (New York: Springer-Verlag).

Witten, S., Böhm, H., and Aulrich, K. (2015). Effect of variety and environment on the contents of crude nutrients, lysine, methionine and cysteine in organically produced field peas (pisum sativum l) and field beans (vicia faba l). *Appl. Agric. Forestry Res.* 65, 205–216. doi: 10.3220/LBF1447765843000

Yu, M., Wang, Q., Tao, W., Liu, G., Liu, W., Wang, L., et al. (2020). Interactions between arbuscular mycorrhizal fungi and soil properties jointly influence plant c, n, and p stoichiometry in west lake, hangzhou. *RSC. Adv.* 10 (65), 39943–39953. doi: 10.1039/d0ra08185j

Zhan, Y. H., Yin, F. B., Yue, C. D., Zhu, J., Zhu, Z. P., Zou, M. Y., et al. (2020). Effect of pretreatment on hydraulic performance of the integrated membrane process for concentrating nutrient in biogas digestate from swine manure. *Membranes* 10 (10), 13. doi: 10.3390/membranes10100249

Zhan, Y., Zhang, Z., Ma, T., Zhang, X., Wang, R., Liu, Y., et al (2021) Phosphorus excess changes rock phosphate solubilization level and bacterial community mediating phosphorus fractions mobilization during composting." *Bioresour Technol* 337, 125433 doi: 10.1016/j.biortech.2021.125433

frontiers | Frontiers in Plant Science

TYPE Original Research
PUBLISHED 23 December 2022
DOI 10.3389/fpls.2022.1079180

OPEN ACCESS

EDITED BY
Maurizio Ruzzi,
University of Tuscia, Italy

REVIEWED BY
Prachi Pandey,
National Institute of Plant Genome Research (NIPGR), India
Rupesh Tayade,
Kyungpook National University, South Korea
Sławomir Kocira,
University of Life Sciences of Lublin, Poland

*CORRESPONDENCE
Donald L. Smith
donald.smith@mcgill.ca

SPECIALTY SECTION
This article was submitted to Crop and Product Physiology, a section of the journal Frontiers in Plant Science

RECEIVED 25 October 2022
ACCEPTED 01 December 2022
PUBLISHED 23 December 2022

CITATION
Nazari M, Yaghoubian I and Smith DL (2022) The stimulatory effect of Thuricin 17, a PGPR-produced bacteriocin, on canola (*Brassica, napus* L.) germination and vegetative growth under stressful temperatures. *Front. Plant Sci.* 13:1079180. doi: 10.3389/fpls.2022.1079180

The stimulatory effect of Thuricin 17, a PGPR-produced bacteriocin, on canola (*Brassica, napus* L.) germination and vegetative growth under stressful temperatures

Mahtab Nazari, Iraj Yaghoubian and Donald L. Smith*

Department of Plant Science, McGill University, Montreal, QC, Canada

Exposure to unfavorable conditions is becoming more frequent for plants due to climate change, posing a threat to global food security. Stressful temperature, as a major environmental factor, adversely affects plant growth and development, and consequently agricultural production. Hence, development of sustainable approaches to assist plants in dealing with environmental challenges is of great importance. Compatible plant-microbe interactions and signal molecules produced within these interactions, such as bacteriocins, could be promising approaches to managing the impacts of abiotic stresses on crops. Although the use of bacteriocins in food preservation is widespread, only a small number of studies have examined their potential in agriculture. Therefore, we studied the effect of three concentrations of Thuricin17 (Th17), a plant growth-promoting rhizobacterial signal molecule produced by *Bacillus thuringiensis*, on germination and vegetative growth of canola (*Brassica napus* L.) under stressful temperatures. Canola responded positively to treatment with the bacterial signal molecule under stressful temperatures. Treatment with 10^{-9} M Th17 (Thu2) was found to significantly enhance germination rate, seed vigor index, radical and shoot length and seedling fresh weight under low temperature, and this treatment reduced germination time which would be an asset for higher latitude, short growing season climates. Likewise, Thu2 was able to alleviate the adverse effects of high temperature on germination and seed vigor. Regarding vegetative growth, interestingly, moderate high temperature with the assistance of the compound caused more growth and development than the control conditions. Conversely, low temperature negatively affected plant growth, and Th17 did not help overcome this effect. Specifically, the application of 10^{-9} (Thu2) and 10^{-11} M (Thu3) Th17 had a stimulatory effect on height, leaf area and biomass accumulation under above-optimal conditions, which could be attributed to modifications of below-ground structures, including root length, root surface, root volume and root diameter, as well as photosynthetic rate. However, no significant effects were observed under optimal conditions for almost all measured variables.

Therefore, the signal compound tends to have a stimulatory impact at stressful temperatures but not under optimal conditions. Hence, supplementation with Th17 would have the potential as a plant growth promoter under stressed circumstances.

KEYWORDS

Brassica napus, bacteriocin, stressful temperatures, germination, vegetative growth

Introduction

Germination and vegetative growth are fundamentals of crop production. Rapid, uniform germination and emergence under various climatic conditions play a pivotal role in global food security. Abiotic and biotic factors including extreme temperature, moisture, light, nutrient availability, soil-borne pests and non-pathogen organisms, influence seed germination and establishment (Wang et al., 2016; Lamichhane et al., 2017). Among these, temperature is one of the major environmental factors influencing various plant functions, including seed dormancy and germination. Previous studies have emphasized the role of temperature in the regulatory network of seed germination (Xia et al., 2018; Zhou et al., 2018; Suriyasak et al., 2020; Xue et al., 2021). Temperature controls metabolic and cellular mechanisms, including phytohormone contents, mostly gibberellins and abscisic acid, and determines germination capability and rate (Oracz and Karpiński, 2016; Urbanova and Leubner-Metzger, 2016; Wang et al., 2018b). Some plant seeds germinate across a wide range of temperatures, while others germinate only at a narrow range of temperatures. Canola *(Brassica napus [L.])* has been widely cultivated and is one of the most important oilseeds and biodiesel fuel crops. However, cool spring temperatures slow germination and emergence of spring-sown *B. napus*, which delays flowering in mid-summer. Hence, strategies that improve early germination impact canola yield in cooler (higher latitude and altitude) climates. After seed germination, sufficient vegetative growth is required for the development of roots to uptake water and nutrients, shoots to support aboveground stems, and leaves for photosynthesis and biomass accumulation. However, climate change significantly increases the occurrence of abiotic stresses that adversely affect vegetative growth and development, and ultimately crop production. In such cases, sustainable practices and adopting environmentally friendly approaches can enhance resource efficiency and crop production under stressful conditions. Application of plant-associated microbes, or signal compounds produced by them, such as bacteriocins, can increase plant resistance through direct and indirect mechanisms, including nutrient acquisition, phytohormone production, siderophore production, biocontrol and induced systematic resistance to biotic stressful conditions (Khan et al., 2019; Xia et al., 2020; Antar et al., 2021; Lyu et al., 2021; Shah et al., 2021). Often, plant-microbe interaction signals positively influence plant growth at nearly all stages, from germination to seedling establishment, flowering, seed development and maturity (Gautam et al., 2016; Schwinghamer et al., 2016; Arunachalam et al., 2018). One of the well-known signal molecules is lipo-chitooligosaccharide (LCO) which specifies host-symbiont crosstalk communication and mediates rhizobia-legume associations (Oldroyd et al., 2011; Zipfel and Oldroyd, 2017). In addition, bacteriocins, a specific type of signal molecule with potential positive impacts on agriculture, are yet less known. They can control microbial population dynamics by excretion of versatile compounds known as bacteriocins acting as either a "a never ending arms race" (Riley, 1998) against competitors or, in some cases, signalling compounds are involved in plant colonization and plant growth stimulation. Bacteriocins are antimicrobial peptides produced by bacterial ribosomes and secreted by the bacteria (Arnison et al., 2013). They differ from antibiotics in that they hinder organisms that are closely related to the producer strains, and are active at extremely low concentrations (Mak, 2018). Bacteriocins can sometimes be efficient biocontrol agents in the food and pharmaceutical industries while less attention has been paid to their potential in agriculture. The capacity for bacteriocin production by plant growth-promoting rhizobacteria (PGPR) has been reported in some limited studies, such as bacteriocin exertion by *Pseudomonas fluorescens SF39a*, isolated from the wheat rhizosphere, which suppresses the growth of the phytopathogenic *Pseudomonas* and *Xanthomonas* strains (Godino et al., 2016). Bacteriocins synthesized by rhizobia have been named "Rhizobiocins" (Schwinghamer, 1975). For instance bacteriocin-substances have been isolated by *Bradyrhizobium japonicum* (Gross and Vidaver, 1978; Mojgani, 2017) and *Rhizobium leguminosarum* related strains (Hirsch, 1979; Hafeez et al., 2005). Among rhizosphere microbiome, *Bacillus* species were one of the first groups studied for production of diverse bacteriocins. So far, there have been reports of the synthesis of 18 bacteriocins from *B. thuringiensis* (Mojgani, 2017). Yet, bacteriocin excretion by *Bacillus* PGPR is poorly understood,

and none have been examined as thoroughly as Th17 for plant growth promotion; Th17 was discovered in our laboratory and is produced by *B. thuringiensis* non-*Bradyrhizobium* Endophytic Bacterium 17 (BtNEB17), an endophytic bacterium isolated from soybean root nodules [patent by Smith et al. (2008)]. Th17 is highly resistant to heat, stable across a pH range of 1.0–9.25 and is a low molecular weight peptide of 3.162 kDa with anti-microbial activity and plant growth promotion ability, particularly under stressful conditions (Jung et al., 2011; Prudent et al., 2015; Schwinghamer et al., 2015; Subramanian et al., 2016; Schwinghamer et al., 2016; Nazari and Smith, 2020). Interestingly, this bacteriocin could alter physiological and biochemical attributes of plants including increases in photosynthetic rate and antioxidant enzymes contents of plants under normal and stressed conditions (He, 2009; Jung et al., 2011) We should note that more recent characterization of Th17 has shown sufficient differences from our original understanding of its composition that we are considering renaming it to Bacillin 20. Although studies on the efficacy of plant-microbe interactions are abundant, there is a lack of studies around the agricultural potential of bacteriocins. We, therefore, conducted a series of experiments to examine the stimulatory effect of Th17, a plant growth promoting rhizobacteria signal molecule, on germination and vegetative growth of canola under contrasting temperature conditions. The aim is to develop an environmentally friendly approach to stimulation of plant growth and development in a constantly changing environment.

Materials and methods

Isolation and purification of Th17

BtNEB17 was grown in King's medium B as previously described (Gray et al., 2006). Cells for the initial broth inoculum were taken from plated material and cultivated in 250 mL flasks with 50 mL medium. For 48 h, the bacterium was cultivated at 28 ± 2 °C on an orbital shaker rotating at 150 rev min $^{-1}$. For the initial culture, 5 mL of subculture was inoculated into 2000 mL of broth, and the culture was grown under the same conditions. Bacterial populations were assessed by an Ultrospec 4050 Pro UV/Visible Spectrophotometer at 600 nm 96 h after initiation. A cell-free supernatant (CFS) containing BtNEB17 was obtained through centrifuging the bacterial culture at 13,000 g for 10 min, followed by analytical-HPLC identification. For partial purification, 800 mL of butanol was added to 2000 mL of bacterial culture for 12 h then the collected upper layer was extracted under vacuum in rotary evaporator. The viscose extract was collected with 12 mL of 30% Acetonitrile and centrifuged at 13,000 g for 13 min, and the supernatant was collected for chromatography (Gray et al., 2006). Th17 was selected based on peaks and retention times. After being lyophilized, the samples were kept at 20 °C for dilution to the required concentrations. For all experiments, 10^{-7} (Thu1), 10^{-9} (Thu2) and 10^{-11} (Thu3) M of Th17 were prepared based on the molecular weight of Th17.

Germination experiments

Canola seeds (cultivar L233P) were disinfected with 20% sodium hypochlorite and rinsed with distilled water before applying treatments. Twenty-five sterilized seeds were placed on petri plates (100 x 15 mm) lined with filter paper (QualitativeP8). The plates were randomly treated with 10 mL of Thu1, Thu2, Thu3 solution and distilled water. Petri dishes were then sealed with parafilm to prevent water loss and arranged in a completely randomized design, with four replications for each treatment, in growth chambers. Growth chambers were set to low (5 °C), optimal (20 °C), high (30 °C) temperatures, 70% humidity, and zero illumination. The total number of germinated seeds were counted at 24 h intervals, for 72 h at optimum and high temperature and 7 days for low temperature. Radical and shoot length were measured for all experiments after 7 days, and seedlings were weighted. Each experiment was repeated twice, and the data was pooled for analysis.

Plant growth experiments

Th17 was applied as a pre-planting seed treatment, seeds were soaked in 10 mL Thu1, Thu2, Thu3 solution and distilled water, and root irrigation after the stress induction time. Canola seeds (5 seeds per pot) were placed in 10 cm pots filled with AGRO MIX® G10 media, which was a mix of peat, limestone, balanced nutrient materials, with micronutrients, gypsum and wetting agent. This growth medium was chosen based on root application of Th17 and the ability of peat to gradually release water and/or the compound. The pots were placed in a growth chamber (Conviron R, Canada) at 22/18 °C day/night, with a photoperiod of 14/10 h light/darkness cycle, 60-70% relative humidity and photosynthetic irradiance of 350–400 μmol m^{-2} s^{-1} (Figure 1A). After a week, the seedlings were counted, and the plants were thinned to one seedling per pot. Plants were regularly watered with half strength Hoagland's solution and grown in the growth chamber until the end of the third week (Figure 1B). Then, 3-week-old seedlings (Figure 2) were randomly selected to transfer to the low (10/5 °C), optimum (22/18 °C) and high temperature (30/25 °C) chambers to determine the effect of stressful temperatures on the vegetative growth of canola. Plants were watered semi-weekly with 250 mL of either water (for controls) or Th17 (for Th17-treated plants). Following the start of the temperature treatment, the plants in each case were allowed to develop for 4 weeks before being sampled for data collection. A LI-COR 6400 portable photosynthesis metre (LI-COR Lincoln, NE), was used to measure the photosynthetic rate, transpiration rate,

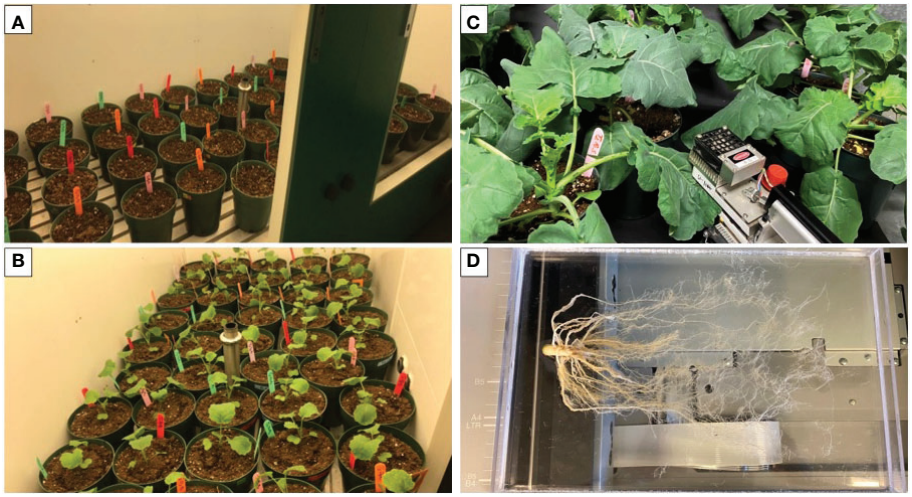

FIGURE 1
(A) Canola pots after seeding in the growth chamber (22/18 °C), **(B)** 3-week-old canola plants grown under optimal conditions (before starting temperature stress), **(C)** Physiological measurements with Licor from 7-week-old canola plants, **(D)** 7-week-old canola roots after removing soil particles.

stomatal conductance and CO_2 concentration inside the leaves. Readings were taken on a weekly basis (4, 5, 6, 7 weeks) after the 3-week-old seedling stage. An upper-most fully expanded leaf was used for determination of physiological variables between 10:00 and 14:00 h (Figure 1C). Plants were sampled at the end of the experiment for the following variables: plant height, leaf area, fresh weight, dry weight and root variables. After harvesting plants and measuring morphological traits, roots were coarsely shaken off to remove soil (destructive methods). Roots were then washed with water and adhering soil particles removed with

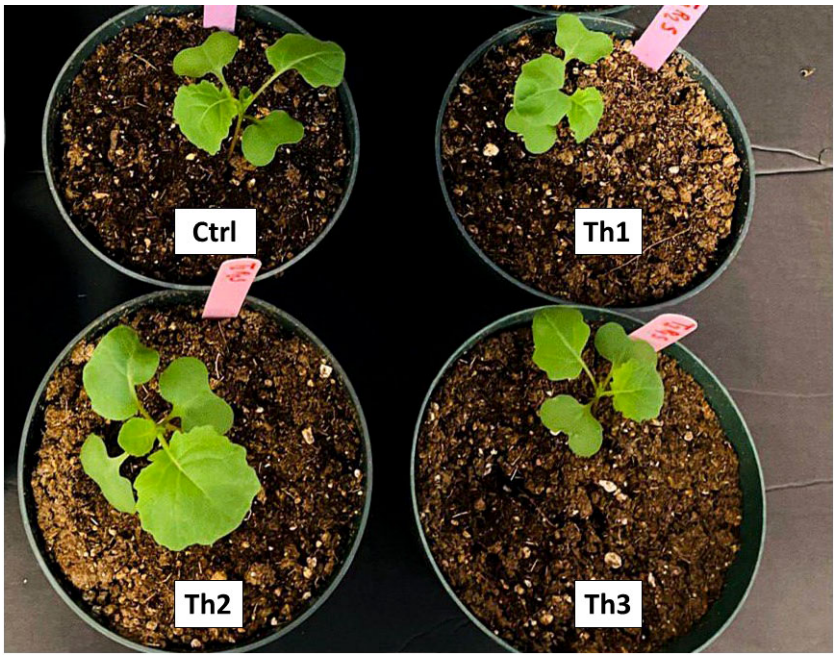

FIGURE 2
3-week-old canola plants grown under optimal conditions. Ctrl: seeds treated with distilled water, Th1: seeds treated with 10^{-7} M Th17, Th2: seeds treated with 10^{-9} M Th17, Th3: seeds treated with 10^{-11} M Th17.

brushes (Figure 1D). Total roots were scanned using EPSON-Expression 11000XL then root length, root volume, total root surface and root diameter were analyzed by WinRHIZO^{TM} Pro software. Each experiment described above was repeated twice with four replicates, and data were pooled for analysis.

Data analysis

Data from the experiments were analyzed, based on a completely randomized factorial design, using the SAS Statistical Package 9.3 (SAS Institute Inc., Cary, NC, USA). For germination data, observed values were analysed similarly to other variables and a non-linear regression model was fitted to predict the probability of germination, in Figure 3 (Piegorsch and Bailer, 2005; Schwinghamer et al., 2015). Duncan's multiple comparison test was used when there was a significant difference at the 95% confidence level.

Results

Germination

There were no significant differences in germination rate under optimal conditions (20 °C) (Figure 3B). The control had the highest germination rate, which did not differ significantly from Th17-treated seeds. The lowest germination rate under optimal conditions was for seeds treated with the lowest concentration, Thu3. With increasing temperature to 30 °C Figure 3C, germination decreased although applying Th17 helped alleviate the negative effect of high temperature on germination; in particular Thu2 treatment increased germination significantly. Cold stress strongly affected germination (Figure 3A); about 100 h were required to start germination, and it increased slowly after that. In marked contrast, the first germination was recorded approximately 12 h after onset of the experiment at 20 °C. Under cold stress conditions, the interaction of temperature and the compound application was significant ($p < 0.002$), and application of Th17 significantly influenced germination, mainly mid-range concentration (Thu2) maximized germination rate.

Germination time

Germination time, one of the main indicators of germination process, was altered by Th17 application and temperature (Figure 4). In general, temperature caused a decrease or increase in germination time whereas the application of different Th17 levels minimized germination time under low temperature, except for Thu1, which showed a maximum time of 7.54 days. Thu2 treatment caused the shortest germination time at 5 °C, at 7.23 days while this time was 1.84 and 1.66 days for control and Thu1 at 20 and 30 °C, respectively.

Length of radical and shoot

It is clear from data that radical and shoot length significantly responded to the interaction of Th17 and temperatures ($p < 0.001$ and $p < 0.002$, respectively) (Figure 5). The greatest radical length was for Thu1 treatment, 9.38 cm, at optimal temperature; however, it was not significantly different from the control. Although increasing the temperature reduced the radical length, using Th17 at low concentrations (Thu3) increased length and reduced the harmful effects of high temperature. Under low temperature, the longest and shortest radical were observed for Thu2 treated seedlings (7.6 cm) and the control (4.5 cm), respectively

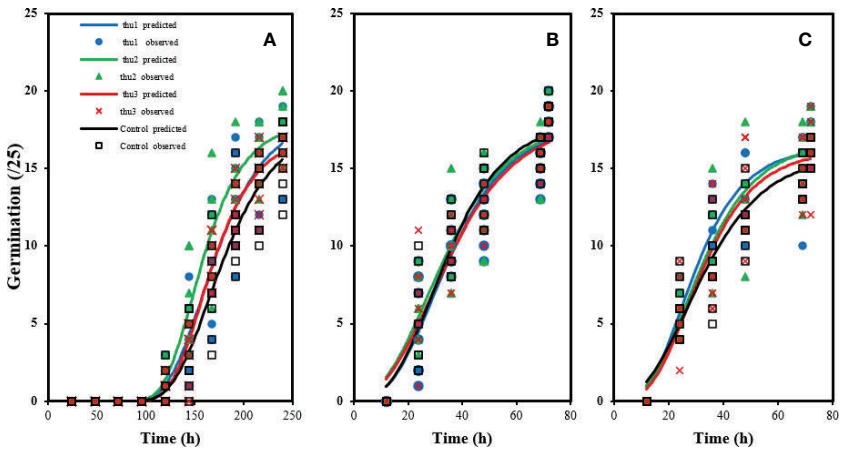

FIGURE 3
Effects of temperature and Th17 concentrations on germination rate at 5 °C **(A)**, 20 °C **(B)**, 30 °C **(C)**. thu1: 10^{-7} M Th17, thu2: 10^{-9} M Th17, thu3: 10^{-11} M Th17. Points and lines represent observed and predicted values, respectively.

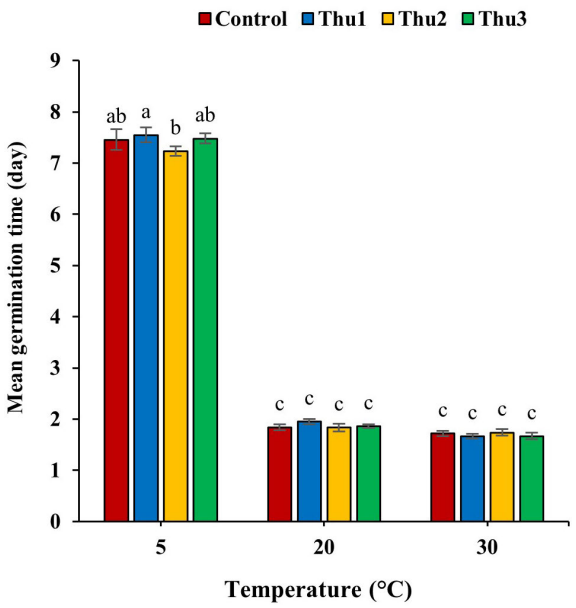

FIGURE 4
Effects of temperature and Th17 concentrations on mean germination time. Thu1: 10 $^{-7}$ M Th17, Thu2: 10 $^{-9}$ M Th17, Thu3: 10^{-11} M Th17. Each bar represents mean ± standard error (n=8). Means with the same letters are not significantly different ($p < 0.05$).

(Figure 5A). For shoot length, the tallest shoots (3.6 cm) were from Thu2 treated plants at 30 °C, which were about 0.5 cm longer than the control (Figure 5B). Likewise, shoot length increased at low temperature from 1.84 for the control (the shortest across all temperatures) to 2.9 cm for Thu2 seedlings. Surprisingly, Th17 application could not significantly affect shoot length compared to untreated seeds under optimal temperature conditions.

Seedling weight and length

The interaction of temperature and Th17 concentrations on radical ($p < 0.001$), shoot ($p < 0.001$) and seedling weight ($p < 0.001$) was significant. Cold stress caused a sharp decrease in the fresh weight of radicals, shoots and seedlings; however, Th17 enhanced seedling fresh weight, from 0.54 mg for control to 0.66 mg for Thu2. Conversely, under optimal conditions, radical, shoot and seedlings of untreated seeds were heavier, 0.38, 0.64 and 1.02 g, respectively, than Th17 treatments. At high temperature, similar to the optimum temperature, the highest fresh weight of radical and shoot was for control seeds. In addition, there were no significant effects of treatment on seedling length at 20 °C; however, the greatest level was for Thu1 treated seedlings (12.58 cm); the shortest seedling was that of the control under low temperature conditions (Table 1).

Seed vigor

Data in Figure 6 reveals the adverse effects of high and low temperatures on seed vigor; Th17 application significantly mitigated detrimental impacts of stressful temperatures ($p < 0.001$) while seed vigor decreased significantly by 33.99 and 56.18% for control seeds in response to high and low temperatures, respectively.

Plant growth and development

Plant height

Treating seeds with Th17 increased plant height, specifically Thu2 (Figure 7); the compound enhanced height by 25, 22.75 and 8.25% over control, at low, optimal and high temperatures, respectively.

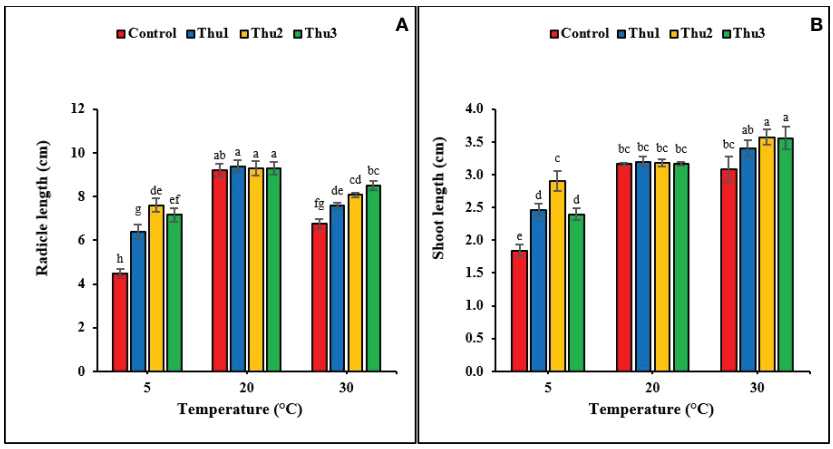

FIGURE 5
Effects of temperature and Th17 concentrations on radical **(A)** and shoot length **(B)**. Thu1: 10 $^{-7}$ M Th17, Thu2: 10 $^{-9}$ M Th17, Thu3: 10^{-11} M Th17. Each bar represents mean ± standard error (n=8). Means with the same letters are not significantly different ($p < 0.05$).

TABLE 1 Effects of temperature and Th17 concentrations on radicle, shoot and seedling fresh weight and length.

Temperature (°C)	Th17 Treatments	Radicle fresh weight (g)	Shoot fresh weight (g)	Seedling fresh weight (g)	Seedling length (cm)
5	**Control**	0.17 ± 0.03 e	0.36 ± 0.02 e	0.54 ± 0.04 d	6.33 ± 0.57 g
	Thu1	0.19 ± 0.05 de	0.40 ± 0.04 e	0.60 ± 0.8 cd	8.85 ± 1.15 f
	Thu2	0.21 ± 0.04 de	0.45 ± 0.02 de	0.66 ± 0.05 c	10.5 ± 1.34 cd
	Thu3	0.18 ± 0.02 e	0.38 ± 0.04 e	0.57 ± 0.05 cd	9.56 ± 1.11 ef
20	**Control**	0.38 ± 0.09 a	0.64 ± 0.11 ab	1.02 ± 0.12 a	12.37 ± 0.97 a
	Thu1	0.28 ± 0.06 b	0.53 ± 0.06 cd	0.81 ± 0.08 b	12.58 ± 0.85 a
	Thu2	0.28 ± 0.05 b	0.50 ± 0.06 cd	0.78 ± 0.06 b	12.47 ± 1.12 a
	Thu3	0.24 ± 0.03 bcd	0.51 ± 0.05 cd	0.75 ± 0.06 b	12.47 ± 0.85 a
30	**Control**	0.27 ± 0.06 bc	0.69 ± 0.2 a	0.63 ± 0.18 cd	9.82 ± 1.12 de
	Thu1	0.23 ± 0.05 cde	0.57 ± 0.11 bc	0.79 ± 0.14 b	10.99 ± 0.53 bc
	Thu2	0.24 ± 0.05 bcd	0.56 ± 0.06 c	0.80 ± 0.08 b	11.65 ± 0.49 ab
	Thu3	0.22 ± 0.03 cde	0.57 ± 0.09 bc	0.79 ± 0.11 b	12.06 ± 0.96 a

Thu1: 10^{-7} M Th17, Thu2: 10^{-9} M Th17, Thu3: 10^{-11} M Th17. Each value represents mean ± standard error (n=8). Means with the same letters are not significantly different ($p < 0.05$).

Leaf area

Leaf area responded strongly to Th17 at stressful temperatures (Figure 8). It decreased by 6.19 and 43.11% for the controls at high and low temperatures, respectively. Under optimal conditions, no stimulatory effect of Th17 was observed, except for Thu3, whereas positive responses occurred at stressful temperatures, particularly for Thu2 plants where leaf area increased by 39 and 30%, at 10 and 30 °C temperatures, respectively, compared to the control.

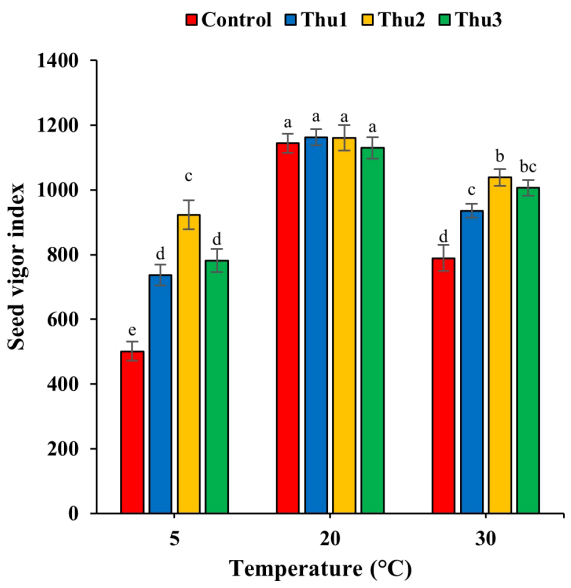

FIGURE 6
Effects of temperature and Th17 concentrations on seed vigor index. Thu1: 10^{-7} M Th17, Thu2: 10^{-9} M Th17, Thu3: 10^{-11} M Th17. Each bar represents mean ± standard error (n=8). Means with the same letters are not significantly different ($p < 0.05$).

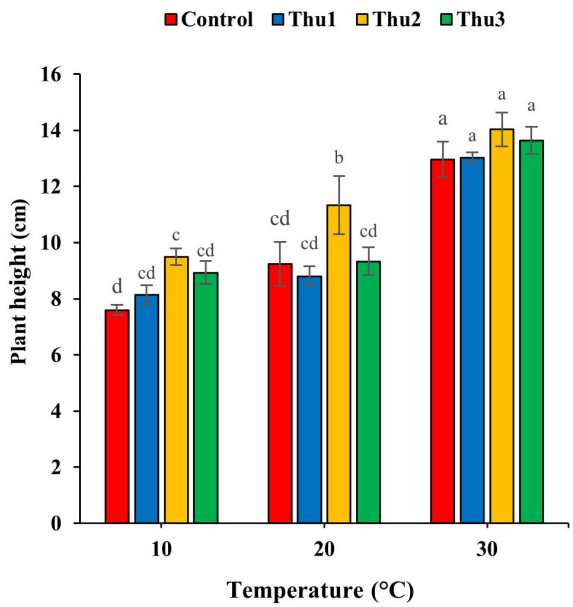

FIGURE 7
Effects of temperature and Th17 concentrations on canola height. Thu1: 10^{-7} M Th17, Thu2: 10^{-9} M Th17, Thu3: 10^{-11} M Th17. Each bar represents mean ± standard error (n=8). Means with the same letters are not significantly different ($p < 0.05$).

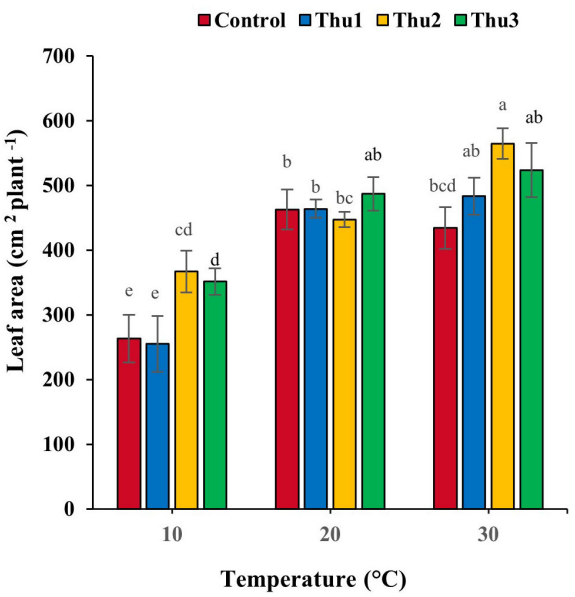

FIGURE 8
Effects of temperature and Th17 concentrations on canola leaf area. Thu1: 10 $^{-7}$ M Th17, Thu2: 10 $^{-9}$ M Th17, Thu3: 10^{-11} M Th17. Each bar represents mean ± standard error (n=8). Means with the same letters are not significantly different ($p < 0.05$).

Biomass

Plants grown at 30 °C had the highest fresh biomass accumulation (Figures 9, 10), particularly those treated with Thu2, with 38.33 g. Conversely, much less biomass accumulated under low temperature conditions although it increased by 25% when plants treated with Thu2 (Figure 9A). Our data clearly demonstrated that dry biomass significantly declined under stressful temperatures; however, Th17 application showed positive effects, with dry biomass increasing by 20.16 and 43.49% for Thu2 compared to the control at 30 and 10 °C, respectively. Similarly, dry biomass accumulation increased from 5.24 g for control to 5.56 g for Thu3 under optimal conditions (Figure 9B).

Root variables

Table 2 presents the root dry weight, length and root surface data and shows that they were negatively affected by stressful temperatures. Root dry weight ranged from 0.31 g for the control at 10 °C to 0.74 g for Thu3 under optimal conditions. Watering plants with Thu3 enhanced root length and surface across all temperatures (Figure 11). Conversely, the highest values for root diameter and volume were detected from Thu2 and Thu3 plants, respectively, at 30 °C.

Physiological variables

Photosynthetic rate was affected by temperature and Th17 as indicated in Figure 12; changes either below or above optimal temperature led to photosynthesis decline. As we expected, plants grown in a cold growth chamber manifested a steady decrease over time, and maximum photosynthesis was observed from Thu2-treated plants in the first week of measurement. Conversely, all treatments had an upward trend under optimal conditions during measurement times, and followed the same general pattern. The trend for 30 °C was increasing until the third measurement then control and Thu1 showed a decrease whereas Thu2 and Thu3 continued to increase; photosynthesis of Thu2 plants was approximately 40% higher than the control in the final measurement.

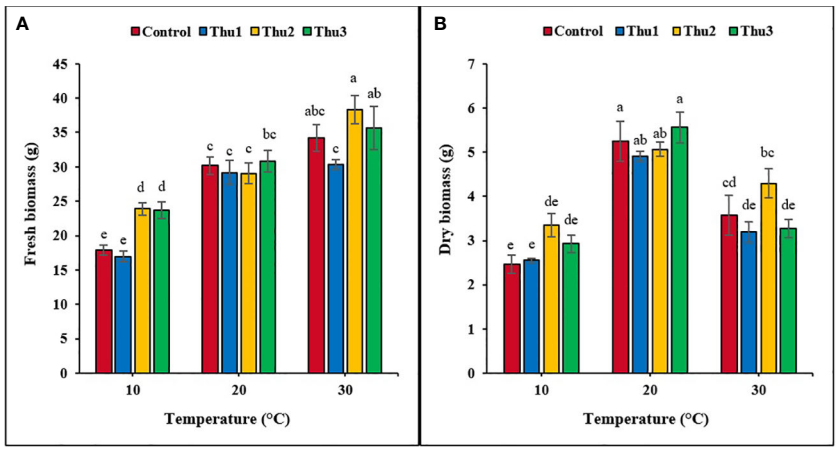

FIGURE 9
Effects of temperature and Th17 concentrations on canola fresh **(A)** and dry **(B)** biomass. Thu1: 10 $^{-7}$ M Th17, Thu2: 10 $^{-9}$ M Th17, Thu3: 10^{-11} M Th17. Each bar represents mean ± standard error (n=8). Means with the same letters are not significantly different ($p < 0.05$).

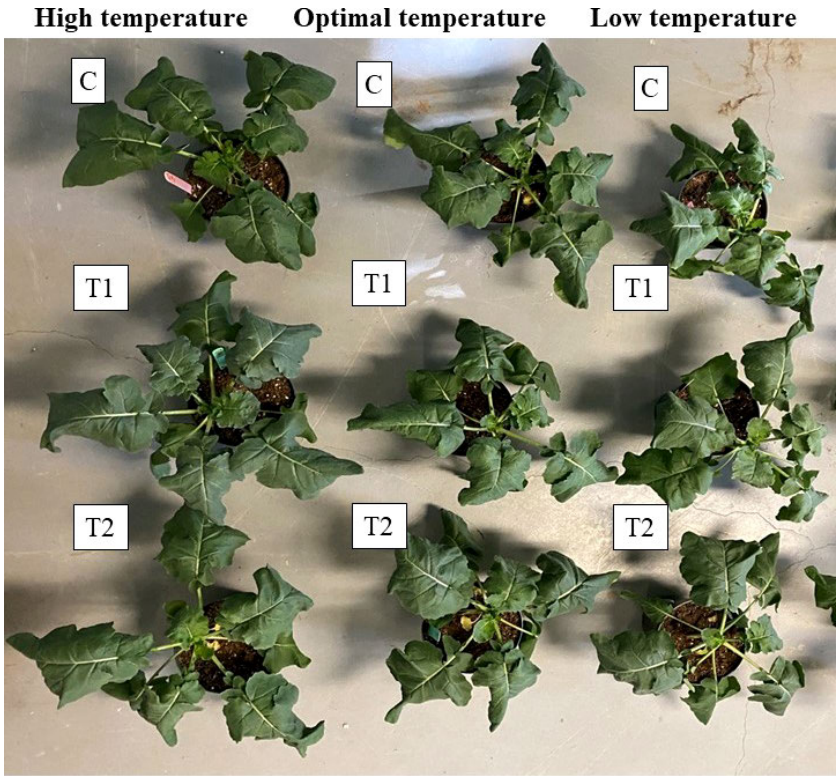

FIGURE 10
The effect of different temperatures and two of the best Th17 concentrations on canola growth and development. 7-week-old canola plants grown under high (30/25 °C, the first column of plants), optimal (22/18 °C, the second column of plants) and low (10/5 °C, the third column of plants) temperatures. C: seeds treated with distilled water and plants watered with water during temperature stress, T1: 10^{-9} M Th17 applied as seed treatment before sowing and root irrigation during temperature stress induction, T2: 10^{-11} M Th17 applied as seed treatment before sowing and root irrigation during temperature stress induction.

TABLE 2 Effects of temperature and Th17 concentrations on canola root variables.

Temperature °C	Treatment	Root length (cm)	Root surface (cm^2)	Root diameter (mm)	Root volume (cm^3)	Root dry weight (g)
10	**Control**	2077.1 ± 193.2 de	220.9± 46.2 c	0.21 ± 0.01 de	1.17 ± 0.12 c	0.31 ± 0.06 g
	Thu1	1841.1 ± 447.2 e	228.5 ± 32.7 bc	0.20 ± 0.02 e	1.01 ± 0.16 c	0.30 ± 0.08 g
	Thu2	2352.8 ± 99.8 de	258.5 ± 09.8 abc	0.25 ± 0.01 abc	1.27 ± 0.19 c	0.42 ± 0.04 f
	Thu3	3139.3 ± 67.2 bc	278.2 ± 27.6 abc	0.24 ± 0.01 cde	1.77 ± 0.36 ab	0.46 ± 0.04 ef
20	**Control**	3640.2 ± 563.8 abc	307.7 ± 62.8 ab	0.26 ± 0.02 abc	2.06 ± 0.30 a	0.66 ± 0.13 abc
	Thu1	3304.8 ± 213.7 abc	278.0 ± 60.6 abc	0.24 ± 0.04 cde	1.84 ± 0.21 ab	0.64 ± 0.03 bcd
	Thu2	3945.4 ± 861.2 ab	303.5 ± 37.1 abc	0.25 ± 0.02 bcd	1.89 ± 0.32 ab	0.70 ± 0.07 a
	Thu3	4178.5 ± 688.2 a	329.3 ± 22.3 a	0.25 ± 0.03 bcd	2.06 ± 0.17 a	0.74 ± 0.04 a
30	**Control**	2875.8 ± 543.7 cd	247.9 ± 42.5 abc	0.27 ± 0.01 ab	2.08 ± 0.11 a	0.55 ± 0.06 cde
	Thu1	2781.6 ± 618.7 cd	251.4 ± 52.6 abc	0.28 ± 0.01 abc	1.92 ± 0.19 ab	0.56 ± 0.06 cde
	Thu2	3552.8 ± 99.7 abc	254.9 ± 54.1 abc	0.29 ± 0.01 a	1.95 ± 0.18 ab	0.53 ± 0.02 def
	Thu3	3620.2 ± 456.7 abc	306.7 ± 34.4 ab	0.28 ± 0.02 ab	2.10 ± 0.14 a	0.68 ± 0.01 ab

Thu1: 10^{-7} M Th17, Thu2: 10^{-9} M Th17, Thu3: 10^{-11} M Th17. Each value represents mean ± standard error (n=8). Means with the same letters are not significantly different ($p < 0.05$).

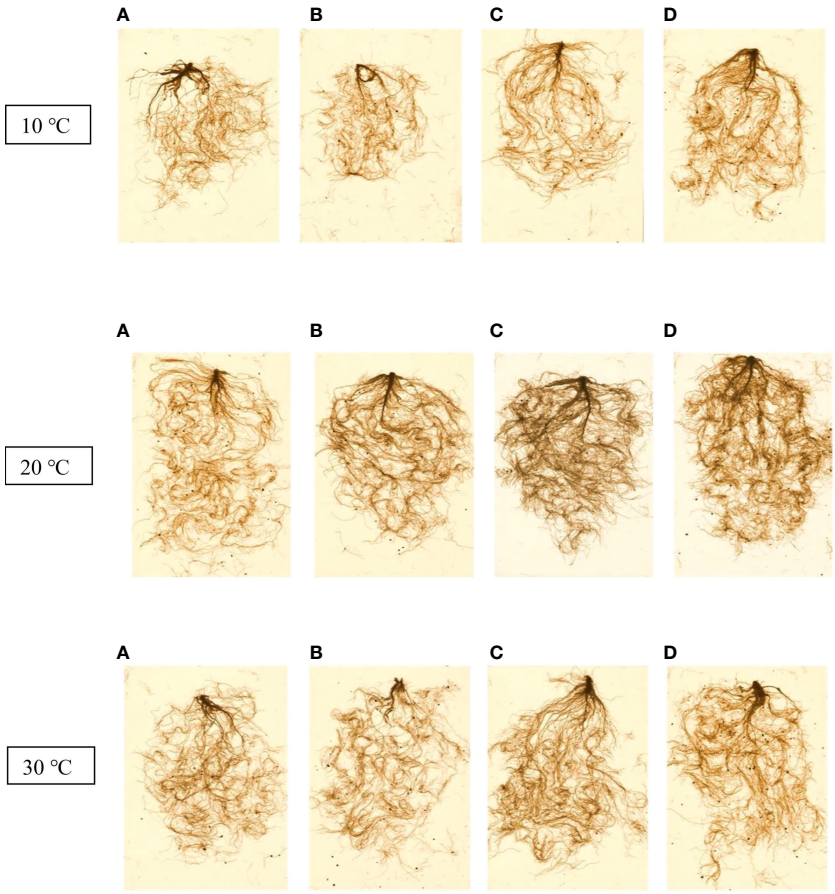

FIGURE 11
7-week-old canola root images for 10, 20 and 30 °C, respectively. **(A)** Control, **(B)** Thu1 (10^{-7} M Th17), **(C)** Thu2 (10^{-9} M Th17), **(D)**: Thu3 (10^{-11} M Th17).

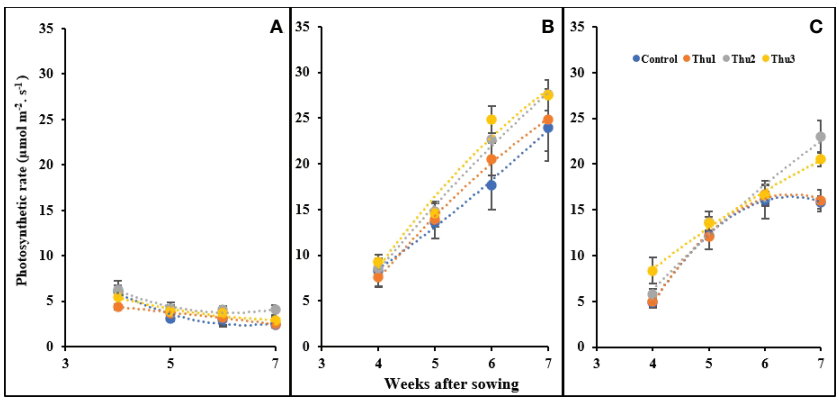

FIGURE 12
Changes in the photosynthetic rate under application of Th17 at low **(A)**, optimum **(B)** and high **(C)** temperature at 4, 5, 6 and 7 weeks after sowing. Thu1: 10^{-7} M Th17, Thu2: 10^{-9} M Th17, Thu3: 10^{-11} M Th17. Each point represents mean ± standard error (n=8).

Stomatal conductance

As indicated in Figure 13, stomatal conductance responded strongly to temperature and concentration of Th17. With rising temperature, conductivity increased; Thu2 treated plants indicated a sharp increase and had the highest conductivity, at 0.345 mol m^{-2} s^{-1}, as opposed to control with a gradual downward trend at 30 °C. Under cold temperature, conductivity drastically dropped for all plants; Thu2 plants could maintain their highest capacity for gas transport through the stomata. In clear contrast, a consistent enhancement occurred under optimal conditions, and this upward trend was similar for all treatments.

Intercellular CO_2

There were significant changes in intercellular CO_2 in response to temperature and Th17 levels (Figure 14). Our measurements indicated that the highest levels of intercellular CO_2 occurred at 20 °C, ranging from 225 μmol mol^{-1} for the control at the first measurement, to 380 μmol mol^{-1} for Thu2 at the last reading. Stressful temperatures both had a downward trend in which control plants absorbed more CO_2 than treated ones.

Transpiration

Transpiration rate was enhanced by increasing temperature; control plants grown at 10 °C had the lowest transpiration (1.21 mol m^{-2} s^{-1}) whereas the highest level was for Thu2 treatment (4.95 mol m^{-2} s^{-1}) at 30 °C. Interestingly, plants under high stress conditions showed an increase until 6 weeks after sowing, after which transpiration changed only slightly and/or decreased. Conversely, plants maintained a constant upward transpiration

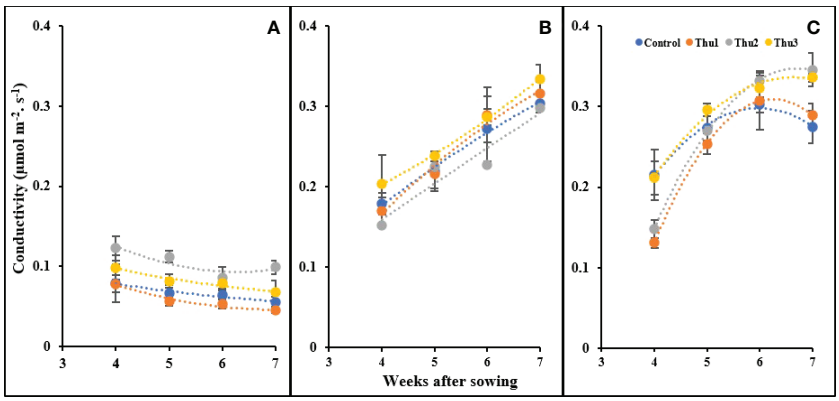

FIGURE 13
Changes in stomatal conductivity under application of Th17 at low **(A)**, optimum **(B)** and high **(C)** temperature at 4, 5, 6 and 7 weeks after sowing. Thu1: 10 $^{-7}$ M Th17, Thu2: 10 $^{-9}$ M Th17, Thu3: 10^{-11} M Th17. Each point represents mean ± standard error (n=8).

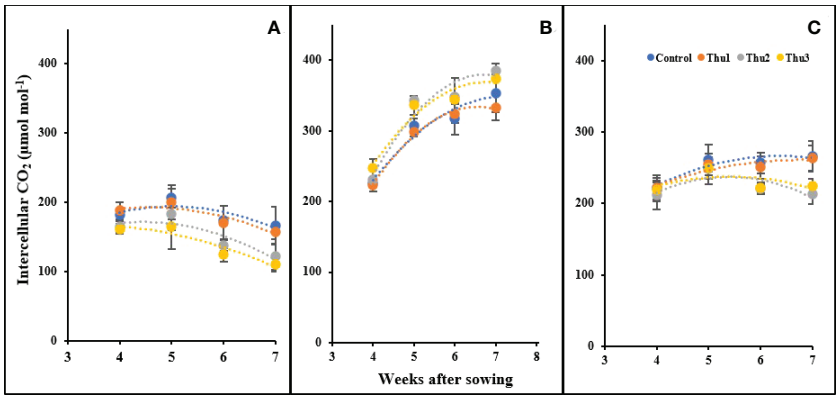

FIGURE 14
Changes in the intercellular CO_2 under application of Th17 at low **(A)**, optimum **(B)** and high **(C)** temperature at 4, 5, 6 and 7 weeks after sowing. Thu1: 10 $^{-7}$ M Th17, Thu2: 10 $^{-9}$ M Th17, Thu3: 10^{-11} M Th17. Each point represents mean ± standard error (n=8).

over time at optimal temperature. Predictably, at 10 °C, the transpiration rate was very low and slightly changed; Thu2 and Thu3 caused a marginal increase while transpiration for Thu1 and the control treatments showed a negligible decrease Figure 15).

Discussion

Germination

Seed germination is a very important stage in the life cycle of a plant and one that is very sensitive to both the intrinsic and extrinsic factors (Rifna et al., 2019). Among them, temperature is a major environmental factor determining seed germination (Finch-Savage and Leubner-Metzger, 2006). Early germination is an essential element that impacts the production of canola (*B. napus* [L.]). The optimal temperature for canola germination is 22°C (Nykiforuk and Johnson-Flanagan, 1994; Tasseva et al., 2004). Any temperature either below or above optimal induces uneven germination and, in the field, poor stand establishment, restricting the crop potential to produce yield. In this study, we found that germination and seedling growth indices were negatively affected by both low and high temperatures. Germination was delayed under low temperature conditions, which could have arisen from slowed water uptake, slower enzyme kinetics, higher levels of late embryogenesis-abundant proteins, induction of nuclear stress-responsive proteins and imbalanced amount of inhibitor and promoter phytohormones (Achard et al., 2008; Copeland and McDonald, 2012; Abdul Aziz et al., 2021). However, faster germination occurred at a higher temperature than optimal conditions, which could be due to a thermal effect, related to number of heat units required for germination. These results are consistent with previous studies that found stressfully high and low temperatures hindered final germination percentage of five cultivars of canola between 10 to 20 percent (Schwinghamer et al., 2015). Seedling growth was also impeded by both high and low temperatures, resulting in lower fresh weight and seedling vigor indices than optimum conditions (Zhang et al., 2015). Hence, discovery of technologies that improve seed germination and seedling establishment are of importance in agriculture. Here, the application of a bacteriocin could enhance canola germination percentage, radical and shoot length, seedling fresh weight and seed vigor compared to the controls under both low and high temperature stress conditions. To be more precise, among three levels of the compound, Thu2 considerably ameliorated negative effects of stress and showed high stimulatory impacts on both seeds and seedlings. This result is in line with findings of Gautam et al. (2016), which highlighted the response of soybean to 10^{-9} M and 10^{-11} M Th17 during germination and seedling development under low temperature. A similar conclusion was reached by He (2009) for Th17 treated corn seeds under a combination of stresses, including low temperature, salinity and drought stress under both controlled environment conditions and a cool spring climate in the field. In another study, the effect of LCO, a compound produced by *B. japonicum* 532C, Th17 and chitopentaose were tested on high oil content cultivars of canola. Treatment with 10^{-6} M LCO accelerated germination at 10 °C while seeds treated with 10^{-9} M Th17 had more even and uniform germination (Schwinghamer et al., 2015). LCO has been shown to be a stimulant for seed germination and seedling establishment as illustrated in a large body of published research, whereas Th17 has not been well studied (Kidaj et al., 2012; Suganya et al., 2016; Nandhini et al., 2018). The underlying mechanism of LCO and Th17 in soybean germination under stressful conditions was studied through proteomic approaches. The results indicated that energy, carbon and nitrogen metabolic pathways were influenced by signal compounds under stressful

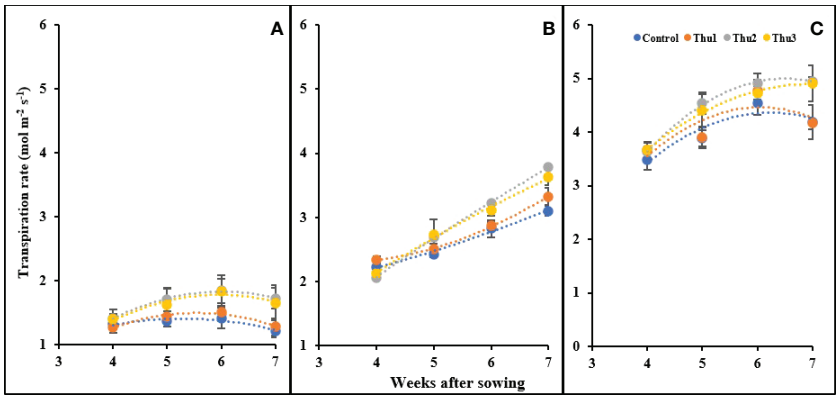

FIGURE 15
Changes in the transpiration rate under application of Th17 at low **(A)**, optimum **(B)** and high **(C)** temperature at 4, 5, 6 and 7 weeks after sowing. Thu1: 10^{-7} M Th17, Thu2: 10^{-9} M Th17, Thu3: 10^{-11} M Th17. Each point represents mean ± standard error (n=8).

environments. Some notable stress-related proteins, including PEP carboxylase, rubisco oxygenase large subunit, pyruvate kinase and other proteins are up regulated in response to LCO and Th17 treatments under stressful conditions (Subramanian et al., 2016). Similar results were observed where over 600 genes, mostly related to stress and defense, were up regulated in LCO treated soybean leaf tissue under stressful conditions (Wang et al., 2012). These findings highlight that signal molecules can alter metabolism and physiology to assist in alleviating sub-optimal conditions and improve germination and early growth.

Th17 effects on canola aboveground growth

Unfavourable temperature, as a major environmental factor, considerably affects plant growth and development. Some plants adapt themselves by altering their morphology, while others adjust their physiology or exhibit changes in gene expression, which modifies how they grow, survive and tolerate stresses (Raza et al., 2020; Gupta et al., 2020). However, susceptibility or tolerance is directly associated with plant lifecycle stage. We hypothesized that during vegetative growth of canola, different levels of Th17 would assist in tolerating stressful temperatures and enhance growth variables. The exposure of canola to cold conditions in northern climates like western Canada is unavoidable in early spring because early spring sowing is required to ensure that the crop matures without suffering yield losses due to summer heat stress. Canola, as a cold-acclimated crop, has the capacity to develop cold stress tolerance, known as cold acclimation, once exposed to chilling but not freezing temperature, although its growth might be slowed. Furthermore, the likelihood of high temperature occurrence during mid to end of canola vegetative growth is relatively high, as we experienced during May-June of the 2020 and 2021 canola field seasons in eastern Canada (unpublished data). In this study, plant height, leaf area and biomass accumulations were negatively altered, in contrast to optimal temperature, after 3 weeks of growing in the 10/5°C temperature range, but surprisingly application of the signal molecule efficiently acted as an alleviator and effective plant growth regulator. In contrast, canola showed positive responses to 30/25 °C temperature, suggesting acclimation ability to moderately high temperature. This could arise from thermomorphogensis, a group of morphological and architectural alterations caused by higher ambient temperatures, below the heat-stress level (Quint et al., 2016; Casal and Balasubramanian, 2019; Ludwig et al., 2021). Based on this, canola height was significantly enhanced across all treatments at moderately high temperature, which may indicate that the plant shifted from vegetative stage to flowering by stem elongation; leaf area and fresh biomass were also increased while irrigation with Thu2 and Thu3 resulted in higher levels of these variables than the control and Thu1 treatments. In contrast to many previous studies, which indicated heat as a growth inhibitor, in our experiment canola growth and development continued well at higher temperature, implying that heat acclimation ability, with assistance of the signal compound, could be quite high. However, stress-induction stage, duration of stress and combination with other stressors play a significant role in response to heat. A body of research has taken shaped around the effects of high temperature on crops, but only a few studies have examined the interaction of microbial signal molecules and high temperature on plants (Kilasi et al., 2018; Hussain et al., 2019; Anwar and Kim, 2020; Ayub et al., 2021; Lohani et al., 2021; Ahmad et al., 2021). Our findings fit well with previous studies that reported the interaction of 10^{-6} M LCO irrigation with relatively high temperature (30/30 °C), resulting in 1 more leaf per canola plant, as apposed to the 25/20 °C water-treated controls, which were unifoliate. Similarly, Th17 treatment increased the dry biomass of canola cultivar 04C111, by approximately 70 mg under saline (0.1 M NaCl) and moderately high (30/30 °C) temperature conditions (Schwinghamer et al., 2016). In this study, we observed that two concentrations, Thu2 and Thu3, had considerable positive impacts whereas the higher concentration level, Thu1, showed no significant stimulatory effect compared to the control. It is not surprising that such results were reported because most of the microbially produced substances are signalling molecules which are similar to phytohormones in that their presence, at very low concentrations, has long been recognised to either promote or inhibit plant growth (Backer et al., 2018; Antar et al., 2021). More than this, there are some other factors that highlight the effect of concentrations, including plant species, stage of life, growth conditions, method of application and so on. While certain chemicals can significantly improve plant growth at extremely low concentrations, others must be used at relatively high levels to have a positive impact.

Effects of Th17 on root architecture

Root growth relies on cell production within the root meristem, cell expansion and differentiation in which environmental factors play a vital role as stimuli. The root system possesses spatial architecture by which it can dynamically adapt itself to changes in the environment, such as shifts in temperature (Bardgett et al., 2014; Onwuka and Mang, 2018). It is worth noting that unlike the broad optimum temperature ranges for the development of aerial parts of various species, optimum root temperature (12-20 °C) is quite similar for almost all species except for tundra plants (Bell and Bliss, 1978). When plants are exposed to low and high temperatures, changes in the root system occur (Alsajri et al., 2019; Fonseca de Lima et al., 2021). In this study, root system growth was inhibited by low temperature, which is in line with previous

studies (Rymen et al., 2007; Shibasaki et al., 2009; Zhou et al., 2021). This could be explained by the fact that low temperature hinders cell cycle progression and cell division in root meristems. In addition, lower carbohydrate assimilation under chilling conditions impedes nutrient allocation to the underground system. Interestingly, the interaction of temperature and Th17 was significant; root system architecture was positively modified by irrigation with the compound, particularly Thu3-treated roots, which produced the highest length, surface area, volume, and dry weight across all temperatures. This might be associated with the role of Th17 in phytohormones modifications. In this regard, Prudent et al. (2015) reported that abscisic acid (ABA) was the first plant hormone to be considerably increased in soybean leaves and roots after the application of Th17. This phytohormone facilitates root elongation by restricting ethylene production, suggesting that a reason for changes in root architecture could be a shift in the balance of plant hormones (originating at the roots). As such, Th17 treatment could cause plants to modify their ABA content, which may have resulted in maximal root growth. However, to ascertain the mode of action of Th17 in canola roots, precise phytohormone measurements would be required in future studies.

Th17 and physiology characteristics

Most physiological functions of plants, including photosynthesis and transpiration are impacted by temperature. Stomatal conductance controls both carbon assimilation, and transpiration, and they mutually influence one another. Hence, temperature affects stomata indirectly by alterations in plant water status and vapor pressure deficit. We determined that photosynthesis increased linearly with time and was maximum under optimal temperature conditions whereas a considerable decline was seen across all physiology variables at low temperature. In accordance with our results, many studies have demonstrated a significant reduction of carbon assimilation rate and stomatal conductance at low temperatures, which is partly explained by disruption of chloroplast structure, thylakoid membrane damage, reductions in enzyme activities, decreased chlorophyll levels, reductions in expression and resulting concentrations of photosynthesis proteins, and reduced electron transport (Liu et al., 2012; Paredes and Quiles, 2015; Li et al., 2018; Khan et al., 2019; Zhao et al., 2020). Regarding high temperature, in line with many studies, carbon assimilation rate decreased with increasing temperature although in our study, the Th17 application could mitigate the reduction. In this regard, Thu2 and Thu3 enhanced photosynthesis rate compared to the control. Increasing conductivity with time under optimal conditions, coupled with more diffusion of CO_2, resulting in greater assimilation rates, whereas it caused higher transpiration rates which could lead to reduced leaf water potential at high temperatures. These results agree with those studies that reported stomata opening and increased transpiration at higher temperatures (Lu et al., 2000; Mott and Peak, 2010; Xu et al., 2016; Urban et al., 2017), while our findings are in contrast with some experiments that observed no significant changes of conductivity and/or closure of stomata (von Caemmerer and Evans, 2015; Abdulmajeed et al., 2017; Hlaváčová et al., 2018). It is worth noting that higher leaf temperature causes reduction in protein translation, chlorophyll breakdown, rubisco inactivation, photosystem II activity, electron transport chain activity and increased damage to photosynthetic apparatus (Kang et al., 2017; Wang et al., 2018a; Balfagón et al., 2019; Hu et al., 2020). As such, lowering leaf temperature by transpiration would be an approach to compensate for assimilation reduction which could be beneficial, even if, to some extent, water loss was not constrained. We observed greater transpiration rates in Th2 and Th3 treated plants which meant enhanced photosynthesis came at the cost of losing more water; however, it would assist in cooling leaves when water is not a limiting factor; therefore, photosynthesis systems could function more efficiently. This might be one of the explanations for continued increase of photosynthesis in Thu2 and Thu3 plants despite lower intercellular CO_2 amounts than the control. Lee et al. (2009) demonstrated that application of 10^{-9} and 10^{-11} M Th17, either through root irrigation or leaf spray enhanced soybean photosynthetic rate and leaf greenness. Our finding partly ties with a conclusion reached by Prudent et al. (2015); they demonstrated the positive effects of Th17 treatment on improving carbon assimilation in water-stressed soybean plants, but this was associated with an increased level of ABA, resulting in stomatal closure and reduced transpiration which is opposite to our findings.

Conclusions

Our results demonstrated that the Thu2 solution interacted with stressful temperatures to affect canola germination and seedling development. Notably, germination time was significantly reduced when seeds were treated with Thu2 under low temperature conditions, which would be a solution for slow germination of spring-sown canola. The moderately high temperature along with Thu2 and Thu3 treatments could produce taller plants with more leaf area and fresh biomass accumulation than control plants grown under optimal conditions. Watering plants with the bacterial compound promoted root growth and development, including root length, root volume and root diameter, which could facilitate

the uptake of water and nutrients. Interestingly, two levels of Th17 had stimulatory effects on photosynthetic rate although the mechanism underlying this is not yet clear. Considering these findings, it seems likely that this signal molecule had stimulatory effects, particularly under stressful temperatures, but we remain inconclusive regarding its mode of action.

Data availability statement

The original contributions presented in the study are included in the article/supplementary material. Further inquiries can be directed to the corresponding author.

Author contributions

MN designed the experiment, collected data and wrote the manuscript. IY assisted in data analysis. DS advised on scientific approach and provided editorial input and intellectual context as well as funding. All authors contributed to the article and approved the submitted version.

Funding

This study was funded through a grant from Eastern Canadian Oilseeds Alliance (ECODA).

Conflict of interest

The authors declare that the research was conducted in the absence of any commercial or financial relationships that could be construed as a potential conflict of interest.

Publisher's note

All claims expressed in this article are solely those of the authors and do not necessarily represent those of their affiliated organizations, or those of the publisher, the editors and the reviewers. Any product that may be evaluated in this article, or claim that may be made by its manufacturer, is not guaranteed or endorsed by the publisher.

References

Abdul Aziz, M., Sabeem, M., Mullath, S. K., Brini, F., and Masmoudi, K. (2021). Plant group II LEA proteins: intrinsically disordered structure for multiple functions in response to environmental stresses. *Biomolecules* 11, 1662. doi: 10.3390/biom11111662

Abdulmajeed, A. M., Derby, S. R., Strickland, S. K., and Qaderi, M. M. (2017). Interactive effects of temperature and UVB radiation on methane emissions from different organs of pea plants grown in hydroponic system. *J. Photochem. Photobiol. B: Biol.* 166, 193–201. doi: 10.1016/j.jphotobiol.2016.11.019

Achard, P., Gong, F., Cheminant, S., Alioua, M., Hedden, P., and Genschik, P. (2008). The cold-inducible CBF1 factor–dependent signaling pathway modulates the accumulation of the growth-repressing DELLA proteins *via* its effect on gibberellin metabolism. *Plant Cell* 20, 2117–2129. doi: 10.1105/tpc.108.058941

Ahmad, M., Waraich, E. A., Skalicky, M., Hussain, S., Zulfiqar, U., Anjum, M. Z., et al. (2021). Adaptation strategies to improve the resistance of oilseed crops to heat stress under a changing climate: An overview. *Front. Plant Sci.* 12. doi: 10.3389/fpls.2021.767150

Alsajri, F. A., Singh, B., Wijewardana, C., Irby, J. T., Gao, W., and Reddy, K. R. (2019). Evaluating soybean cultivars for low-and high-temperature tolerance during the seedling growth stage. *Agronomy* 9, 13. doi: 10.3390/agronomy9010013

Antar, M., Gopal, P., Msimbira, L. A., Naamala, J., Nazari, M., Overbeek, W., et al. (2021). "Inter-organismal signaling in the rhizosphere," in *Rhizosphere biology: Interactions between microbes and plants* (Singapore: Springer).

Anwar, A., and Kim, J.-K. (2020). Transgenic breeding approaches for improving abiotic stress tolerance: Recent progress and future perspectives. *Int. J. Mol. Sci.* 21, 2695. doi: 10.3390/ijms21082695

Arnison, P. G., Bibb, M. J., Bierbaum, G., Bowers, A. A., Bugni, T. S., Bulaj, G., et al. (2013). Ribosomally synthesized and post-translationally modified peptide natural products: Overview and recommendations for a universal nomenclature. *Natural product Rep.* 30, 108–160. doi: 10.1039/C2NP20085F

Arunachalam, S., Schwinghamer, T., Dutilleul, P., and Smith, D. L. (2018). Multi-year effects of biochar, lipo-chitooligosaccharide, thuricin 17, and experimental bio-fertilizer for switchgrass. *Agron. J.* 110, 77–84. doi: 10.2134/agronj2017.05.0278

Ayub, M., Ashraf, M. Y., Kausar, A., Saleem, S., Anwar, S., Altay, V., et al. (2021). Growth and physio-biochemical responses of maize (Zea mays l.) to drought and heat stresses. *Plant Biosystems-An Int. J. Dealing all Aspects Plant Biol.* 155, 535–542. doi: 10.1080/11263504.2020.1762785

Backer, R., Rokem, J. S., Ilangumaran, G., Lamont, J., Praslickova, D., Ricci, E., et al. (2018). Plant growth-promoting rhizobacteria: Context, mechanisms of action, and roadmap to commercialization of biostimulants for sustainable agriculture. *Front. Plant Sci.*, 1473. doi: 10.3389/fpls.2018.01473

Balfagón, D., Sengupta, S., Gómez-Cadenas, A., Fritschi, F. B., Azad, R. K., Mittler, R., et al. (2019). Jasmonic acid is required for plant acclimation to a combination of high light and heat stress. *Plant Physiol.* 181, 1668–1682. doi: 10.1104/pp.19.00956

Bardgett, R. D., Mommer, L., and De Vries, F. T. (2014). Going underground: Root traits as drivers of ecosystem processes. *Trends Ecol. Evol.* 29, 692–699. doi: 10.1016/j.tree.2014.10.006

Bell, K. L., and Bliss, L. (1978). Root growth in a polar semidesert environment. *Can. J. Bot.* 56, 2470–2490. doi: 10.1139/b78-299

Casal, J. J., and Balasubramanian, S. (2019). Thermomorphogenesis. *Annu. Rev. Plant Biol.* 70, 321–346. doi: 10.1146/annurev-arplant-050718-095919

Copeland, L. O., and McDonald, M. F. (2012). *Principles of seed science and technology* (Springer Science & Business Media).

Finch-Savage, W. E., and Leubner-Metzger, G. (2006). Seed dormancy and the control of germination. *New Phytol.* 171, 501–523. doi: 10.1111/j.1469-8137.2006.01787.x

Fonseca De Lima, C. F., Kleine-Vehn, J., De Smet, I., and Feraru, E. (2021). Getting to the root of belowground high temperature responses in plants. *J. Exp. Bot.* 72, 7404–7413. doi: 10.1093/jxb/erab202

Gautam, K., Schwinghamer, T. D., and Smith, D. L. (2016). The response of soybean to nod factors and a bacteriocin. *Plant Signaling Behav.* 11, e1241934. doi: 10.1080/15592324.2016.1241934

Godino, A., Príncipe, A., and Fischer, S. (2016). A ptsP deficiency in PGPR pseudomonas fluorescens SF39a affects bacteriocin production and bacterial fitness in the wheat rhizosphere. *Res. Microbiol.* 167, 178–189. doi: 10.1016/j.resmic.2015.12.003

Gray, E., Lee, K., Souleimanov, A., Di Falco, M., Zhou, X., Ly, A., et al. (2006). A novel bacteriocin, thuricin 17, produced by plant growth promoting rhizobacteria strain bacillus thuringiensis NEB17: isolation and classification. *J. Appl. Microbiol.* 100, 545–554. doi: 10.1111/j.1365-2672.2006.02822.x

Gross, D., and Vidaver, A. (1978). Bacteriocin-like substances produced by rhizobium japonicum and other slow-growing rhizobia. *Appl. Environ. Microbiol.* 36, 936–943. doi: 10.1128/aem.36.6.936-943.1978

Gupta, D., Gupta, A., Yadav, K., and Ranjan, R. (2020). "Molecular mechanism of plant adaptation and tolerance to cold stress," in *Plant ecophysiology and adaptation under climate change: Mechanisms and perspectives II* (Singapore: Springer).

Hafeez, F. Y., Naeem, F. I., Naeem, R., Zaidi, A. H., and Malik, K. A. (2005). Symbiotic effectiveness and bacteriocin production by rhizobium leguminosarum bv. viciae isolated from agriculture soils in faisalabad. *Environ. Exp. Bot.* 54, 142–147. doi: 10.1016/j.envexpbot.2004.06.008

He, X. (2009). *Effect of class IId bacteriocins: Thuricin 17 and bacthuricin F4 on crops growth under optimal and abiotic stress conditions* (QC, Canada: Master of Science, McGill).

Hirsch, P. R. (1979). Plasmid-determined bacteriocin production by rhizobium leguminosarum. *Microbiology* 113, 219–228. doi: 10.1099/00221287-113-2-219

Hlaváčová, M., Klem, K., Rapantová, B., Novotná, K., Urban, O., Hlavinka, P., et al. (2018). Interactive effects of high temperature and drought stress during stem elongation, anthesis and early grain filling on the yield formation and photosynthesis of winter wheat. *Field Crops Res.* 221, 182–195. doi: 10.1016/j.fcr.2018.02.022

Hu, S., Ding, Y., and Zhu, C. (2020). Sensitivity and responses of chloroplasts to heat stress in plants. *Front. Plant Sci.* 11, 375. doi: 10.3389/fpls.2020.00375

Hussain, H. A., Men, S., Hussain, S., Chen, Y., Ali, S., Zhang, S., et al. (2019). Interactive effects of drought and heat stresses on morpho-physiological attributes, yield, nutrient uptake and oxidative status in maize hybrids. *Sci. Rep.* 9, 1–12. doi: 10.1038/s41598-019-40362-7

Jung, W.-J., Mabood, F., Souleimanov, A., and Smith, D. L. (2011). Induction of defense-related enzymes in soybean leaves by class IId bacteriocins (thuricin 17 and bacthuricin F4) purified from bacillus strains. *Microbiological Res.* 167, 14–19. doi: 10.1016/j.micres.2011.02.004

Kang, L., Kim, H. S., Kwon, Y. S., Ke, Q., Ji, C. Y., Park, S.-C., et al. (2017). IbOr regulates photosynthesis under heat stress by stabilizing IbPsbP in sweetpotato. *Front. Plant Sci.* 8, 989. doi: 10.3389/fpls.2017.00989

Khan, T. A., Yusuf, M., Ahmad, A., Bashir, Z., Saeed, T., Fariduddin, Q., et al. (2019). Proteomic and physiological assessment of stress sensitive and tolerant variety of tomato treated with brassinosteroids and hydrogen peroxide under low-temperature stress. *Food Chem.* 289, 500–511. doi: 10.1016/j.foodchem.2019.03.029

Kidaj, D., Wielbo, J., and Skorupska, A. (2012). Nod factors stimulate seed germination and promote growth and nodulation of pea and vetch under competitive conditions. *Microbiological Res.* 167, 144–150. doi: 10.1016/j.micres.2011.06.001

Kilasi, N. L., Singh, J., Vallejos, C. E., Ye, C., Jagadish, S. K., Kusolwa, P., et al. (2018). Heat stress tolerance in rice (Oryza sativa l.): Identification of quantitative trait loci and candidate genes for seedling growth under heat stress. *Front. Plant Sci.* 9, 1578. doi: 10.3389/fpls.2018.01578

Lamichhane, J. R., Dürr, C., Schwanck, A. A., Robin, M.-H., Sarthou, J.-P., Cellier, V., et al. (2017). Integrated management of damping-off diseases. a review. *Agron. Sustain. Dev.* 37, 1–25. doi: 10.1007/s13593-017-0417-y

Lee, K. D., Gray, E. J., Mabood, F., Jung, W.-J., Charles, T., Clark, S. R., et al. (2009). The class IId bacteriocin thuricin-17 increases plant growth. *Planta* 229, 747–755. doi: 10.1007/s00425-008-0870-6

Li, S.-L., Li, Z.-G., Yang, L.-T., Li, Y.-R., and He, Z.-L. (2018). Differential effects of cold stress on chloroplasts structures and photosynthetic characteristics in cold-sensitive and cold-tolerant cultivars of sugarcane. *Sugar Tech* 20, 11–20. doi: 10.1007/s12355-017-0527-5

Liu, X. G., Xu, H., Zhang, J. Y., Liang, G. W., Liu, Y. T., and Guo, A. G. (2012). Effect of low temperature on chlorophyll biosynthesis in albinism line of wheat (Triticum aestivum) FA85. *Physiologia plantarum* 145, 384–394. doi: 10.1111/j.1399-3054.2012.01604.x

Lohani, N., Singh, M. B., Bhalla, P. L., and Science, C. (2021). Short-term heat stress during flowering results in a decline in canola seed productivity. *J. Agronomy* 208, 486–496. doi: 10.1111/jac.12534s

Ludwig, W., Hayes, S., Trenner, J., Delker, C., and Quint, M. (2021). On the evolution of plant thermomorphogenesis. *J. Exp. Bot.* 72, 7345–7358. doi: 10.1093/jxb/erab310

Lu, Z., Quiñones, M. A., and Zeiger, E. (2000). Temperature dependence of guard cell respiration and stomatal conductance co-segregate in an F2 population of pima cotton. *Funct. Plant Biol.* 27, 457–462. doi: 10.1071/PP98128

Lyu, D., Msimbira, L. A., Nazari, M., Antar, M., Pagé, A., Shah, A., et al. (2021). The coevolution of plants and microbes underpins sustainable agriculture. *Microorganisms* 9, 1036. doi: 10.3390/microorganisms9051036

Mak, P. (2018). *Pet-to-man travelling staphylococci: A world in progress*. Ed. V. Savini, (The Netherlands, Amsterdam: Elsevier, Academic Press) 161–171.

Mojgani, N. (2017). "Bacteriocin-producing rhizosphere bacteria and their potential as a biocontrol agent," in *Rhizotrophs: Plant growth promotion to bioremediation* (Singapore: Springer).

Mott, K. A., and Peak, D. (2010). Stomatal responses to humidity and temperature in darkness. *Plant Cell Environ.* 33, 1084–1090. doi: 10.1111/j.1365-3040.2010.02129.x

Nandhini, D. U., Somasundaram, E., and Amanullah, M. M. (2018). Effect of rhizobial nod factors (lipochitooligosaccharide) on seedling growth of blackgram under salt stress. *Legume Res. Int. J.* 41, 159–162. doi: 10.18805/LR-3597

Nazari, M., and Smith, D. L. (2020). A PGPR-produced bacteriocin for sustainable agriculture: A review of thuricin 17 characteristics and applications. *Front. Plant Sci.* 11. doi: 10.3389/fpls.2020.00916

Nykiforuk, C. L., and Johnson-Flanagan, A. M. (1994). Germination and early seedling development under low temperature in canola. *Crop Sci.* 34, 1047–1054. doi: 10.2135/cropsci1994.0011183X003400040039x

Oldroyd, G. E., Murray, J. D., Poole, P. S., and Downie, J. A. (2011). The rules of engagement in the legume-rhizobial symbiosis. *Annu. Rev. Genet.* 45, 119–144. doi: 10.1146/annurev-genet-110410-132549

Onwuka, B., and Mang, B. (2018). Effects of soil temperature on some soil properties and plant growth. advances in plants and agricultural research, 8 (1), 34–37. *Adv. Plants Agric. Res.* 8 (1), 34–37. doi: 10.15406/apar.2018.08.00288

Oracz, K., and Karpiński, S. (2016). Phytohormones signaling pathways and ROS involvement in seed germination. *Front. Plant Sci.* 7, 864. doi: 10.3389/fpls.2016.00864

Paredes, M., and Quiles, M. J. (2015). The effects of cold stress on photosynthesis in hibiscus plants. *PloS One* 10, e0137472. doi: 10.1371/journal.pone.0137472

Piegorsch, W. W., and Bailer, A. J. (2005). *Analyzing environmental data* (John Wiley & Sons).

Prudent, M., Salon, C., Souleimanov, A., Emery, R., and Smith, D. L. (2015). Soybean is less impacted by water stress using bradyrhizobium japonicum and thuricin-17 from bacillus thuringiensis. *Agron. Sustain. Dev.* 35, 749–757. doi: 10.1007/s13593-014-0256-z

Quint, M., Delker, C., Franklin, K. A., Wigge, P. A., Halliday, K. J., and Van Zanten, M. (2016). Molecular and genetic control of plant thermomorphogenesis. *Nat. Plants* 2, 1–9. doi: 10.1038/nplants.2015.190

Raza, A., Ashraf, F., Zou, X., Zhang, X., and Tosif, H. (2020). "Plant adaptation and tolerance to environmental stresses: Mechanisms and perspectives," in *Plant ecophysiology and adaptation under climate change: Mechanisms and perspectives I* (Singapore: Springer).

Rifna, E., Ramanan, K. R., and Mahendran, R. (2019). Emerging technology applications for improving seed germination. *Trends Food Sci. Technol.* 86, 95–108. doi: 10.1016/j.tifs.2019.02.029

Riley, M. A. (1998). Molecular mechanisms of bacteriocin evolution. *Annu. Rev. Genet.* 32, 255–278. doi: 10.1146/annurev.genet.32.1.255

Rymen, B., Fiorani, F., Kartal, F., Vandepoele, K., Inzé, D., and Beemster, G. T. (2007). Cold nights impair leaf growth and cell cycle progression in maize through transcriptional changes of cell cycle genes. *Plant Physiol.* 143, 1429–1438. doi: 10.1104/pp.106.093948

Schwinghamer, E. (1975). Properties of some bacteriocins produced by rhizobium trifolii. *Microbiology* 91, 403–413. doi: 10.1099/00221287-91-2-403

Schwinghamer, T., Souleimanov, A., Dutilleul, P., and Smith, D. (2015). The plant growth regulator lipo-chitooligosaccharide (LCO) enhances the germination of canola (Brassica napus [L.]). *J. Plant Growth Regul.* 34, 183–195. doi: 10.1007/s00344-014-9456-7

Schwinghamer, T., Souleimanov, A., Dutilleul, P., and Smith, D. (2016). Supplementation with solutions of lipo-chitooligosacharide nod bj V (C18: 1, MeFuc) and thuricin 17 regulates leaf arrangement, biomass, and root development of canola (Brassica napus [L.]). *Plant Growth Regul.* 78, 31–41. doi: 10.1007/s10725-015-0072-8

Shah, A., Nazari, M., Antar, M., Msimbira, L. A., Naamala, J., Lyu, D., et al. (2021). PGPR in agriculture: A sustainable approach to increasing climate change resilience 211. doi: 10.3389/fsufs.2021.667546

Shibasaki, K., Uemura, M., Tsurumi, S., and Rahman, A. (2009). Auxin response in arabidopsis under cold stress: Underlying molecular mechanisms. *Plant Cell* 21, 3823–3838. doi: 10.1105/tpc.109.069906

Smith, D., Lee, K. D., Gray, E., Souleimanov, A., and And Zhou, X. (2008). PCTACA2OO6.

Subramanian, S., Ricci, E., Souleimanov, A., and Smith, D. L. (2016). A proteomic approach to lipo-chitooligosaccharide and thuricin 17 effects on soybean germinationunstressed and salt stress. *PloS One* 11, e0160660. doi: 10.1371/journal.pone.0160660

Suganya, V., Velu, G., and Jeyakumar, P. (2016). Effect of lipo-chitooligosaccharides on seed germination, growth, vigour and biochemical changes in soybean seedling. *Int. J. Plant Sci.* 11, 244–248. doi: 10.15740/HAS/IJPS/11.2/244-248

Suriyasak, C., Oyama, Y., Ishida, T., Mashiguchi, K., Yamaguchi, S., Hamaoka, N., et al. (2020). Mechanism of delayed seed germination caused by high temperature during grain filling in rice (Oryza sativa l.). *Sci. Rep.* 10, 1–11. doi: 10.1038/s41598-020-74281-9

Tasseva, G., De Virville, J. D., Cantrel, C., Moreau, F., and Zachowski, A. (2004). Changes in the endoplasmic reticulum lipid properties in response to low temperature in brassica napus. *Plant Physiol. Biochem.* 42, 811–822. doi: 10.1016/j.plaphy.2004.10.001

Urban, J., Ingwers, M., Mcguire, M. A., and Teskey, R. (2017). Stomatal conductance increases with rising temperature. *Plant Signaling Behav.* 12, e1356534. doi: 10.1080/15592324.2017.1356534

Urbanova, T., and Leubner-Metzger, G. (2016). Gibberellins and seed germination. *Annu. Plant Rev.* 49, 253–284. doi: 10.1002/9781119210436.ch9

Von Caemmerer, S., and Evans, J. R. (2015). Temperature responses of mesophyll conductance differ greatly between species. *Plant Cell Environ.* 38, 629–637. doi: 10.1111/pce.12449

Wang, Q.-L., Chen, J.-H., He, N.-Y., and Guo, F.-Q. (2018a). Metabolic reprogramming in chloroplasts under heat stress in plants. *Int. J. Mol. Sci.* 19, 849. doi: 10.3390/ijms19030849

Wang, Y., Cui, Y., Hu, G., Wang, X., Chen, H., Shi, Q., et al. (2018b). Reduced bioactive gibberellin content in rice seeds under low temperature leads to decreased sugar consumption and low seed germination rates. *Plant Physiol. Biochem.* 133, 1–10. doi: 10.1016/j.plaphy.2018.10.020

Wang, N., Khan, W., and Smith, D. L. (2012). Changes in soybean global gene expression after application of lipo-chitooligosaccharide from bradyrhizobium japonicum under sub-optimal temperature. *PloS One* 7, e31571. doi: 10.1371/journal.pone.0031571

Wang, P., Mo, B., Long, Z., Fan, S., Wang, H., and Wang, L. (2016). Factors affecting seed germination and emergence of sophora davidii. *Ind. Crops* 87, 261–265. doi: 10.1016/j.indcrop.2016.04.053

Xia, Y., Farooq, M. A., Javed, M. T., Kamran, M. A., Mukhtar, T., Ali, J., et al. (2020). Multi-stress tolerant PGPR bacillus xiamenensis PM14 activating sugarcane (Saccharum officinarum l.) red rot disease resistance. *Plant Physiol. Biochem.* 151, 640–649. doi: 10.1016/j.plaphy.2020.04.016

Xia, Q., Ponnaiah, M., Cueff, G., Rajjou, L., Prodhomme, D., Gibon, Y., et al. (2018). Integrating proteomics and enzymatic profiling to decipher seed metabolism affected by temperature in seed dormancy and germination. *Plant Sci.* 269, 118–125. doi: 10.1016/j.plantsci.2018.01.014

Xue, X., Du, S., Jiao, F., Xi, M., Wang, A., Xu, H., et al. (2021). The regulatory network behind maize seed germination: Effects of temperature, water, phytohormones, and nutrients. *Crop J.* 9, 718–724. doi: 10.1016/j.cj.2020.11.005

Xu, G., Singh, S. K., Reddy, V. R., Barnaby, J. Y., Sicher, R. C., and Li, T. (2016). Soybean grown under elevated CO2 benefits more under low temperature than high temperature stress: Varying response of photosynthetic limitations, leaf metabolites, growth, and seed yield. *J. Plant Physiol.* 205, 20–32. doi: 10.1016/j.jplph.2016.08.003

Zhang, J., Jiang, F., Yang, P., Li, J., Yan, G., and Hu, L. (2015). Responses of canola (Brassica napus l.) cultivars under contrasting temperature regimes during early seedling growth stage as revealed by multiple physiological criteria. *Acta Physiologiae Plantarum* 37, 1–10. doi: 10.1007/s11738-014-1748-9

Zhao, Y., Han, Q., Ding, C., Huang, Y., Liao, J., Chen, T., et al. (2020). Effect of low temperature on chlorophyll biosynthesis and chloroplast biogenesis of rice seedlings during greening. *Int. J. Mol. Sci.* 21, 1390. doi: 10.3390/ijms21041390

Zhou, Y., Sommer, M. L., and Hochholdinger, F. (2021). Cold response and tolerance in cereal roots. *J. Exp. Bot.* 72, 7474–7481. doi: 10.1093/jxb/erab334

Zhou, Z.-H., Wang, Y., YE, X.-Y., and Li, Z.-G. (2018). Signaling molecule hydrogen sulfide improves seed germination and seedling growth of maize (Zea mays l.) under high temperature by inducing antioxidant system and osmolyte biosynthesis. *Front. Plant Sci.*, 1288. doi: 10.3389/fpls.2018.01288

Zipfel, C., and Oldroyd, G. E. (2017). Plant signalling in symbiosis and immunity. *Nature* 543, 328–336. doi: 10.1038/nature22009

frontiers | Frontiers in Microbiology

TYPE Original Research
PUBLISHED 10 January 2023
DOI 10.3389/fmicb.2022.1075633

OPEN ACCESS

EDITED BY
Maurizio Ruzzi,
University of Tuscia,
Italy

REVIEWED BY
Marika Pellegrini,
University of L'Aquila, Italy
Elizabeth Temitope Alori,
Landmark University,
Nigeria
Sushil K. Sharma,
National Institute of Biotic Stress
Management, India

*CORRESPONDENCE
Donald L. Smith
✉ donald.smith@mcgill.ca

SPECIALTY SECTION
This article was submitted to
Microbe and Virus Interactions With Plants,
a section of the journal
Frontiers in Microbiology

RECEIVED 20 October 2022
ACCEPTED 12 December 2022
PUBLISHED 10 January 2023

CITATION
Naamala J, Msimbira LA,
Subramanian S and Smith DL (2023)
Lactobacillus helveticus EL2006H cell-free
supernatant enhances growth variables in
Zea mays (maize), *Glycine max* L. Merill
(soybean) and *Solanum tuberosum* (potato)
exposed to NaCl stress.
Front. Microbiol. 13:1075633.
doi: 10.3389/fmicb.2022.1075633

Lactobacillus helveticus EL2006H cell-free supernatant enhances growth variables in *Zea mays* (maize), *Glycine max* L. Merill (soybean) and *Solanum tuberosum* (potato) exposed to NaCl stress

Judith Naamala, Levini A. Msimbira,
Sowmyalakshmi Subramanian and Donald L. Smith*

Department of Plant Science, McGill University, Montreal, QC, Canada

Plant growth promoting microorganisms and their derived compounds, such as cell-free supernatant (CFS), enhance plant growth under stressed and non stressed conditions. Such technology is sustainable and environmentally friendly, which is desirable amidst the climate change threat. The current study evaluated the effect of CFS obtained from *Lactobacillus helveticus* EL2006H on its ability to enhance mean percentage germination and mean radicle length of corn and soybean, as well as growth parameters of potato, using treatment formulations that consisted of 0.2 and 1.0% [v/v] *L. helveticus* EL2006H CFS concentrations and 100mM NaCl and 150mM NaCl levels. Results show that treatment with 100mM NaCl lowered percentage germination of corn by 52.63%, at 72h, and soybean by 50%, at 48h. Treatment with 100 NaCl +0.2% EL2006H enhanced percentage germination of soybean by 44.37%, at 48h, in comparison to that of the 100mM NaCl control. One hundred mM NaCl lowered radicle length of corn and soybean by 38.58 and 36.43%, respectively. Treatment with 100Mm NaCl +1.0% EL2006H significantly increased radicle length of corn by 23.04%. Treatment with 100mM NaCl +0.2% EL2006H significantly increased photosynthetic rate, leaf greenness and fresh weight of potato. Increasing NaCl concentration to 150 NaCl lowered the effectiveness of the 0.2% EL2006H CFS on the same growth variables of potato. In general, the lower CFS concentration of 0.2% was more efficient at enhancing germination in soybean while the higher concentration of 1.0% was more efficient at enhancing radicle length of corn. There was an observed variation in the effectiveness of *L. helveticus* EL2006H CFS across the different CFS concentrations, NaCl levels and crop species studied. In conclusion, based on findings of this study, CFS obtained from *L. helveticus* can be used as a bio stimulant to enhance growth of corn, soybean and potato. However, further studies need to be conducted, for validation, especially under field conditions, for commercial application.

KEYWORDS

cell-free supernatant, *Lactobacillus helveticus*, salinity stress, germination, radicle length, plant growth

1. Introduction

Plant growth promoting microorganisms (PGPM) live in close association with their host plants, forming a holobiont (Hartmann et al., 2014; Lyu et al., 2021); these relationships have existed for at least half a billion years (Knack et al., 2015). A plant's exudates into its surroundings are a major determinant of the phytomicrobiome composition in its rhizosphere (Zhang et al., 2017). The association between PGPM and their host plants can enhance the latter's growth and development, through mechanisms such as biostimulation, mitigation of abiotic stress effects, bioremediation and biocontrol (Glick, 2012; Ahemad and Kibret, 2014; Backer et al., 2018; Naamala and Smith, 2020), in a sustainable and environmentally friendly manner (Naamala and Smith, 2021a,b). PGPM and their derived compounds can be utilised in singular or consortium forms, results varying in such a way that some strains may be more effective when applied as single cells while others, in a consortium (Giassi et al., 2016; Subramanian et al., 2016a,b; Shah et al., 2022). *Lactobacillus helveticus* is a gram positive facultative anaerobic lactic acid bacterium (LAB) that is mostly known for its role in the food processing industry. Use of *L. helveticus* in plant agriculture, especially as biostimulants is not widely documented although the use of members of the genera *Lactobacillus* in crop production, as biostimulants and biocontrol agents, among other uses, has been practiced (Hamed et al., 2011). Members of the genus *Lactobacillus* are endophytic to a variety of plants species (Baffoni et al., 2015; Minervini et al., 2015; Lamont et al., 2017) while others have been isolated from the rhizosphere of plants. Examples of LAB species that have been used in plant agriculture include *Lactobacillus acidophilus*, *Lactobacillus plantarum*, *Lactobacillus rhamnosus* and *L. helveticus* (Hamed et al., 2011; Caballero et al., 2020; Msimbira et al., 2022). LAB play an important role in fermentation of organic matter to form organic fertilisers used in crop production (Lamont et al., 2017; Caballero et al., 2020). Lactic acid, a by-product of LAB has been reported to enhance plant growth (Rodríguez-Morgado et al., 2017). LAB strains have been reported to solubilise phosphate, produce siderophores (Shrestha et al., 2014; Giassi et al., 2016), produce antimicrobial compounds (Stoyanova et al., 2012), produce phytohormones such as indole −3- acetic acid [IAA] (Shrestha et al., 2014; Giassi et al., 2016) and enhance systemic acquired resistance (Hamed et al., 2011), all of which are desirable characteristics of PGPM.

Microbes, such as bacteria and fungi, exude into their growth environment, secondary metabolites such as hormones, enzymes, organic acids, bacteriocins, oligopolysaccharides and siderophores, among others (Piechulla et al., 2017; Schulz-Bohm et al., 2017; Lemfack et al., 2018). In laboratory-based experiments, such metabolites are exuded into the microbe's growth medium. Recent studies have focused on the possibility that such metabolite rich media, also known as cell-free supernatant (CFS) can enhance plant growth without the presence of microbial cells. Experimentation with CFSs has previously yielded interesting results, showing that such CFSs can enhance the growth of different crop species, such as corn, soybean, canola and tomato, at germination and seedling stages (Msimbira et al., 2022; Naamala et al., 2022, Shah et al., 2022). Earlier studies went further and extracted bioactive compounds from the CFS, resulting in the discovery of compounds such as lipo-chitooligosaccharide (LCO) from *Bradyrhizobium japonicum* CFS and thuricin17 from *Bacillus thuringiensis* NEB17 CFS (Prithiviraj et al., 2003; Gray et al., 2006a,b; Lee et al., 2009), which are already on the market as plant growth promoting biostimulants. Both compounds have shown efficacy in enhancing plant growth under growth chamber and field conditions (Subramanian et al., 2016a,b; Arunachalam et al., 2018). They were reported to enhance plant growth under normal and salt-stress conditions (Subramanian et al., 2016a,b). It has been reported that the nature of metabolites exuded vary with varying conditions of growth media in which the microbe is growing (Subramanian et al., 2021). For instance, the metabolic profile of CFS of a microbe grown under ideal conditions may significantly vary from that of the same microbe exposed to some level of stress, such as low pH or high salinity levels. Not all metabolites exuded in growth media enhance plant growth, although some are the bioactive ingredients that do so. The effectiveness of a bioactive metabolite/CFS also varies across plant species, concentration of the compound, level of stress to which a plant is exposed and growth stage of the plant (Msimbira et al., 2022; Naamala et al., 2022; Shah et al., 2022). This, in a sense, complicates the process of discovering novel microbe derived plant growth promoting compounds as it may require trials on several crop species under different growth conditions, at different concentrations, before bioactivity may be detected. The seemingly long and possibly complicated process is however potentially worth the effort since microbial derived compounds can overcome some issues associated with using microbial cells as inoculants if they are produced in fairly large quantities and are economical to isolate for application. For instance, compounds are less prone to diminished effects under harsh field conditions, are generally required in low concentrations and are easier to store compared to live microbial cells (Naamala and Smith, 2021a).

Salinity stress is a major abiotic stress of agricultural crops, resulting in decreased yield quantity and quality which subsequently causes economic losses estimated at US$ 12 billion

per year (FAO, 2020). It affects leaf area, chlorophyll content, plant vigour, plant height, rootlength, plant dry matter, nutrient, metabolite and protein contents, can delay plant development and at severe stress levels may lead to plant death (Bistgani et al., 2019; Garcia et al., 2019). Unfortunately, with current climate change projections, reduced rainfall, excess and improper application of inorganic fertilisers and other chemicals, arable land affected by salinity stress is projected to increase by 50% by 2050 (Jamil et al., 2011). PGPM and their derived compounds can mitigate the effect of salt stress on plants, hence, allowing better growth, yield quality and yield quantity, in salt affected fields (Naamala and Smith, 2021b). The aim of this study therefore was to elucidate the ability of *L. helveticus* EL2006H CFS to enhance germination and radicle length of corn and soybean, and growth parameters of potato, under saline conditions. Results of the study will be a baseline for further studies, with a possibility of isolating and identifying bioactive compounds. This study is part of a broader study that is studying CFSs of the EVL Inc., consortium strains, which comprises *L. helveticus* EL2006H and four other microbial species, in an effort to improve the product and or come up with new product combinations.

2. Materials and methods

2.1. Obtaining microbial CFS

L. helveticus EL2006H was cultured in De man, Rogosa and Sharpe (MRS) medium at pH 7.0, and incubated for 48 h, at 120 rpm and 37°C. At 48 h, the microbial culture was centrifuged for 10 min, at 10,000 rpm and 4°C, to pellet the microbial cells and separate them from the CFS (Gray et al., 2006a,b; Subramanian et al., 2021). The CFS was further filtered using 0.22 µm nylon filters to remove any microbial cells that could have remained after centrifugation. The obtained CFS was then used in the formulation of treatments used in the study.

2.2. Formulation of treatments

Treatments were formulated by mixing known quantities of distilled water, NaCl and CFS. Two NaCl levels, (100 mM NaCl and 150 mM NaCl) and two CFS levels (1.0 and 0.20% [v/v]) were used in the mixtures to formulate treatments. The two CFS concentrations were chosen because they exhibited positive results with *Bacillus amyloliquefaciens* EB2003 CFS, in our previous study (Naamala et al., 2022). 0, 100 and 150 mM NaCl, with no addition of CFS were used as negative controls. In addition, for each microbial CFS concentration, a similar concentration of microbial growth medium (not inoculated with microbe), was used to formulate positive controls. A treatment name ending in MRS or EL2006H implies that MRS medium and *L. helveticus* EL2006H CFSs were used, respectively.

2.3. Set up of germination and radicle length experiments

The germination experiments were carried out in a phytorium located at the Macdonald Campus of McGill University, Sainte Anne de Bellevue, Quebec, Canada. Soybean (cultivar P0962X) and corn (Hybrid 25 M75) were used for the study. The two crop species were chosen because they are widely consumed in Canada and the world over. In our previous study, the two species' germination and radicle lengths were stimulated by *B. amyloliquefaciens* CFS. The following treatments were used for the study: 0 mM NaCl (control), 100 mM NaCl (control), 100 mM NaCl +0.2% MRS (control), 100 mM NaCl +0.2% EL2006H, 100 mM NaCl +1.0% MRS (control) and 100 mM NaCl +1.0% EL2006H. Treatments with 0.2% EL2006H and 1.0% EL2006H, with their corresponding controls, were studied separately. It should also be noted that each crop was studied separately. Therefore, because each treatment, within each crop species, was studied in a separate experiment and the data obtained analysed separately, a completely randomised design (CRD) was used for each experiment, to randomly apply experimental units to treatments. For each experiment, ten seeds of the crop species under study were surface sterilized using 2% sodium hypochlorite, for 2 min, rinsed with 5 changes of sterilized distilled water and placed on petri-plates (Cat. no. 431760, sterile 100 × 15 mm polystyrene Petri dish, Fisher Scientific Co., Whitby, ON, Canada), lined with filter paper (09-795D, QualitativeP8, porosity coarse, Fisher Scientific Co., Pittsburg, PA, United States). Petri plates with seeds then randomly received the treatments with ten replicates per treatment, hence, 40 samples per experiment. The Petri plates were then sealed with parafilm and incubated for 7 days in the dark, at 25°C. Total number of germinated seeds per plate was recorded at 24 h intervals, for 72 h, as a percentage of the total number of seeds in the plate. i.e., (x/10)∗100, where X is the total number of germinated seeds per petri plate. After 7 days, radicle length was measured, in centimeters (cm). For each replicate, radicle length for all the germinated seeds, was summed, to obtain total radicle length of germinated seeds per plate. Each experiment was repeated twice. Percentage germination data for each time interval (24, 48, and 72 h) were analyzed separately.

2.4. Set up of greenhouse experiment

Potato cultivar goldrush was used for the study. Potato is grown and widely consumed in Canada, with a sizable fresh market area of production in Quebec. EVL Inc., the source of the bacterial strains in collaboration with SynAgri, focus on cultivation of potato cultivars. Hence this part of the study was focused on potato's response to treatment with the CFS, under greenhouse conditions. Treatments used for this experiment

were: 0 mM NaCl (control), 100 mM NaCl (control), 100 mM NaCl +0.2% MRS (control), 100 mM NaCl +0.2% EL2006H, 150 mM NaCl (control), 150 mM NaCl +0.2% MRS (control) and 150 mM NaCl +0.2% EL2006H. Twelve L pots were filled with G7 growth medium were used for plant growth. The rooting medium in each pot was fully saturated with water before sowing one potato seed per pot. At emergence, pots were allocated to treatments following a CRD, with four replicates per treatment, hence, a total of 28 samples. The experiment was repeated twice. A number of excess pots were sown with seed so that on the day of treatment application, only pots with seeds that emerged on the same day were applied to treatments, to minimize initial variation. Two L of treatment were applied twice a week, per pot, for 4 weeks after emergence, at which time harvesting was conducted. Data on variables: greenness, photosynthetic rate, leaf area, plant height and plant fresh weight were taken. Leaf greenness was measured in SPAD units, using a SPAD-502 chlorophyll meter at 3 weeks after treatment application. Greenness of ten leaves was randomly measured and average greenness recorded. Photosynthetic rate was measured in µmol CO_2 m^{-2} S^{-1} using a LI-COR 6400 portable photosynthesis meter (Lincoln, NE, United States), and recorded, 3 weeks after treatment application. Plant height was measured using a meter ruler, first, at emergence, just before the first application of treatments and 3 weeks after emergence. The difference in height was then recorded. Fresh weight was measured in grams, using a weighing scale balance (ME4001E, CH), 4 weeks after emergence. Leaf area was measured in cm^2, using a leaf area meter (LI-3100 C, Lincoln, NE, United States), 4 weeks after emergence.

2.5. Data analysis

Data obtained from all samples were analyzed using PROC GLM (SAS 9.4 software). Type III tests were used to determine effects of treatments on seed germination while differences between the treatments were assessed using a student t-test with the least square means (LSMEANS) statement, with Tukey's adjustment for multiple comparisons. Differences were considered significant at $p \leq 0.05$.

3. Results

3.1. Mean radicle length

3.1.1. Corn

3.1.1.1. 100mM NaCl +1.0% EL2006H

There was a significant effect of *L. helveticus* CFS on radicle length of corn, as shown in Figure 1. One hundred mM NaCl significantly lowered radicle length of corn by 38.58% ($p < 0.0001$) in comparison to the 0 mM NaCl control. Treatment with 100 mM NaCl +1.0% EL2006H significantly increased mean radicle length of corn by 23.04% ($p < 0.0001$). The greatest radicle length was for the 0 mM control (55.38 cm) while the smallest was for the 100 mM NaCl control (35.205 cm), which was also not significantly different from the 100 mM NaCl +1.0% MRS control (36.735 cm).

There was no significant effect of the 0.2% *L. helveticus* CFS on radicle length of corn.

3.1.2. Soybean

There was no significant effect of *L. helveticus* CFS on radicle length of soybean at both 0.2 and 1.0% concentrations, as shown in Table 1. Figure 2 shows the effect of treatments on radicle length of corn (1) and soybean (2).

3.2. Mean percentage germination

3.2.1. Soybean

3.2.1.1. 100mM NaCl +0.2% EL2006

At 24 h, there was a significant effect of *L. helveticus* EL2006H CFS on soybean germination. At 48 h, CFS significantly

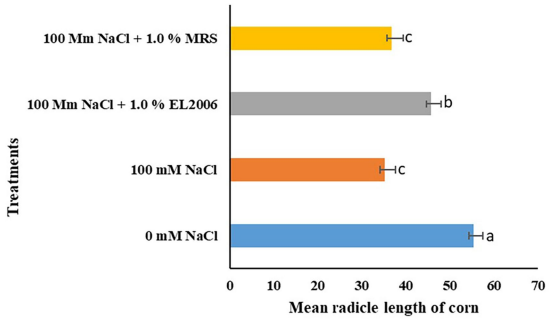

FIGURE 1
Effect of treatments on radicle length of corn at 1.0% [v/v]. Data represents the mean±SE (n=80); different letters indicate values determined by Tukey's multiple mean comparison significantly different at p<0.05. Values with the same letters are not significantly different at p<0.05.

TABLE 1 Effect of treatments on mean radicle length of soybean and corn.

Treatment	Mean radicle length of soybean (cm)	Mean radicle length of corn (cm)
0 mM NaCl	57.98 ± 2.636^a	49.81 ± 1.879^a
100 mM NaCl	37.43 ± 1.766^b	35.15 ± 1.232^b
100 Mm NaCl +0.2% EL2006	38.05 ± 1.773^b	38.76 ± 1.193^b
100 Mm NaCl +0.2% MRS	37.12 ± 2.088^b	40.26 ± 1.705^b
0 mM NaCl	63.355 ± 4. 230^a	55.38 ± 2.084^a
100 mM NaCl	38.910 ± 2.213^b	35.205 ± 2.491^c
100 Mm NaCl +1.0% EL2006	41.195 ± 2.393^b	45.745 ± 2.233^b
100 Mm NaCl +1.0% MRS	44.445 ± 3.600^b	36.735 ± 2.66^c

Data represents the mean ± SE (n = 80); in a column, different letters indicate values determined by Tukey's multiple mean comparison significantly different at $p < 0.05$. Values with the same letters are not significantly different at $p < 0.05$.

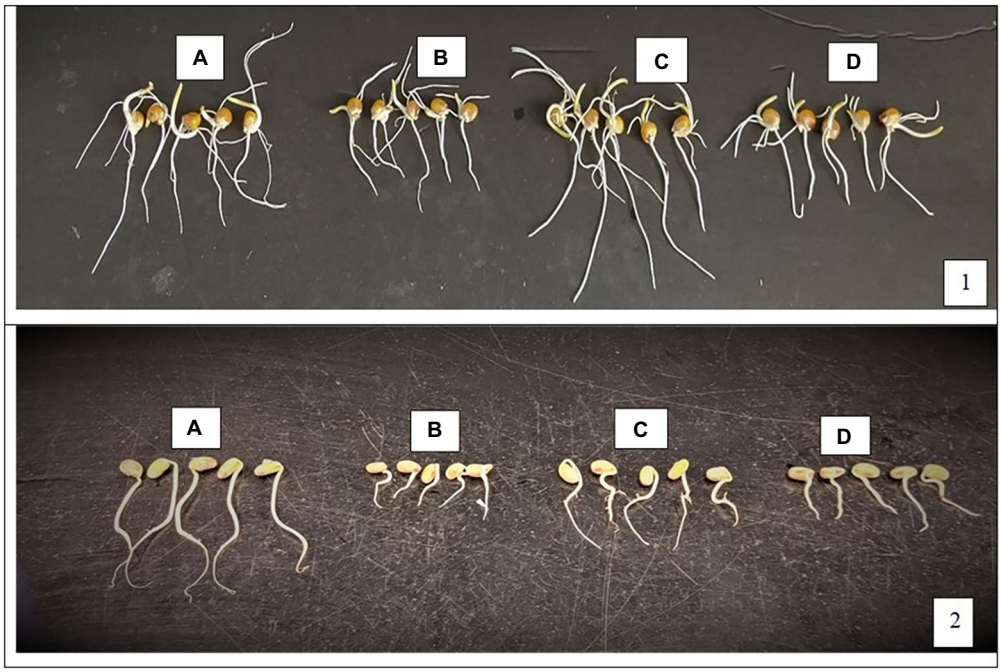

FIGURE 2
Effect of treatments on germination and radicle length of corn (1) and soybean (2). From left to right: 0mM NaCl **(A)**, 100mM NaCl **(B)**, 100mM NaCl +0.2% EL2006H **(C)** and 100mM NaCl +0.2% MRS **(D)**.

enhanced percentage germination of soybean. Treatment with 100 mM NaCl lowered percentage germination by 50% in comparison to the 0 mM NaCl control. The highest percentage germination was observed in the 0 mM NaCl control (84%) while the lowest was observed in soybean treated with 100 mM NaCl (42%). Percentage germination of soybean treated with 100 mM NaCl +0.2% EL2006H and 100 mM NaCl +0.2% MRS were 75.5 and 67.5%, respectively. The two were significantly higher than that observed for the 100 Mm NaCl control ($p < 0.0001$). In fact, the percentage germination of soybean treated with 100 mM NaCl +0.2% EL2006H CFS was significantly higher than that of the 100 mM NaCl control, by 44.37% ($p < 0.0001$) when treated with CFS and not different from that of the 0 mM NaCl control.

At 72 h, treatment with microbial CFS did not result in significant differences in the germination of soybean, when compared to the 100 mM NaCl control. However, treatments 100 mM NaCl +0.2% EL2006H increased percentage germination by 16.1, to a percentage not significantly different from the 0 mM NaCl control. Table 2 show the effect of treatments on percentage germination of soybean (Figure 3).

3.2.1.2. 100mM NaCl +1.0% EL2006

At 24 h, microbial CFS has not significant effect on germination of soybean. At 48 h, soybean treated with 100 mM NaCl +1.0% EL2006H and 100 mM NaCl +1.0% MRS exhibited percentages of 70.5 and 74%, respectively; both values were not significantly different from that of the 0 mM control, and higher, though not significantly different from the percentage germination observed for the 100 mM NaCl control. At 72 h there was no observed significant difference among the percentage germination of the different treatments.

3.2.2. Corn

There was no significant effect of *L. helveticus* CFS on germination percentage of corn at both 0.2 and 1.0% concentrations, as shown in Tables 3, 4.

3.2.3. Greenhouse experiment

While the above germination experiments were to establish the effects of *L. helveticus* CFS on seed/tuber germination as a possible positive plant growth promoter, the greenhouse experiment with potato was to add more value to the commercial application of the CFS, which is one of the goals of SynAgri/EVL's mandate and the crop of importance. Hence, experiments were carried out using potato variety goldrush (as per company's recommendation), to elucidate the effect of *L. helveticus* EL2006H CFS on the growth variables of potato. Results regarding variables varied between treatments.

3.2.3.1. Mean leaf greenness

The effect of treatments on mean leaf greenness was significantly different among treatments. Treatment with 100 mM and 150 mM NaCl resulted in 27.014 and 19.88% decreases in mean leaf greenness, respectively, in comparison to the 0 mM NaCl control, the two becoming significantly lower than the later

TABLE 2 Effect of treatments on mean percentage germination of soybean, at 72, 48 and 24h, respectively.

Treatment	Mean percentage germination at 72h	Mean percentage germination at 48h	Mean percentage germination at 24h
0 mM NaCl	89.5 ± 1.697a	86.0 ± 1.835^{a}	34.5 ± 2.563^{b}
100 mM NaCl	82.5 ± 3.898^{a}	66.0 ± 4.834^{b}	1.00 ± 0.688^{a}
100 mM NaCl +1.0% EL2006	88.5 ± 3.647^{a}	70.5 ± 5.452^{ab}	0.50 ± 0.500^{a}
100 mM NaCl +1.0% MRS	85.0 ± 3.591^{a}	74 ± 4.995^{ab}	1.00 ± 0.688^{a}

Data represents the mean ± SE ($n = 80$); in a column, different letters indicate values determined by Tukey's multiple mean comparison significantly different at $p < 0.05$. Values with the same letters are not significantly different at $p < 0.05$.

TABLE 3 Effect of treatments on mean percentage germination of corn at 72, 48 and 24h, respectively.

Treatment	Mean percentage germination at 72h±SEM	Mean percentage germination at 48h±SEM	Mean percentage germination at 24h±SEM
0 mM NaCl	57.0 ± 3.332^{a}	16.0 ± 2.938^{a}	0.00 ± 0.000^{a}
100 mM NaCl	27.0 ± 4.110^{b}	3.5 ± 1.817^{b}	0.00 ± 0.000^{a}
100 mM NaCl +0.2% EL2006	28.5 ± 3.789^{b}	4.0 ± 1.338^{b}	0.00 ± 0.000^{a}
100 mM NaCl +0.2% MRS	32.0 ± 3.742^{b}	0.00 ± 0^{b}	0.00 ± 0.000^{a}

Data represents the mean ± SE ($n = 80$); in a column, different letters indicate values determined by Tukey's multiple mean comparison significantly different at $p < 0.05$. Values with the same letters are not significantly different at $p < 0.05$.

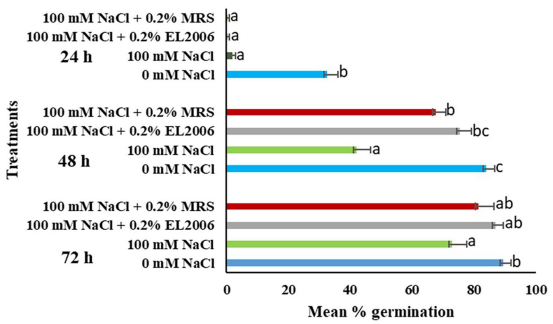

FIGURE 3
Effect of treatments on mean percentage germination of soybean. Data represents mean±SE (n=80); different letters indicate values determined by Tukey's multiple mean comparison significantly different at p<0.05. Values with the same letters are not significantly different at p<0.05.

($p < 0.0001$). Treatment with 100 mM NaCl +0.2% EL2006 resulted in leaf greenness significantly higher than the 100 mM NaCl control by 13.56% ($p < 0.0001$) and not significantly different from the 0 mM NaCl control, as shown in Figure 4. Although not significantly different, it was also higher than the 100 mM NaCl +0.2% MRS control. There was no significant difference between treatment 150 mM NaCl +0.2% EL2006 and its corresponding controls 150 mM NaCl and 150 mM NaCl +0.2% MRS. *L. helveticus* EL2006H CFS enhanced leaf greenness in potato treated with 100 mM NaCl but not 150 mM NaCl.

3.2.3.2. Mean photosynthetic rate

There was a significant effect of *L. helveticus* CFS on mean photosynthetic rate. as shown in Figure 4. Treatment with 100 and 150 mM NaCl resulted in 13.76 and 26.6% decreases in photosynthetic rate, respectively, in comparison to the 0 mM NaCl control. Treatment with 100 mM NaCl +0.2% EL2006 resulted in the highest photosynthetic rate (21.00 µmol CO_2 m^{-2} S^{-1}), significantly higher than that of the 100 mM NaCl control, by 17.97% ($p < 0.0001$), and higher but not significantly different from the 0 mM NaCl control, as shown in Figure 4. The lowest photosynthetic rate was observed in potato treated with 150 mM NaCl (14.863 µmol CO_2 m^{-2} S^{-1}).

3.2.3.3. Mean fresh weight

There was a significant effect of *L. helveticus* CFS on fresh weight of potato. One hundred mM NaCl and 150 mM NaCl lowered fresh weight of potato by 19.62 and 23.61%, respectively, in comparison to the fresh weight observed for the 0 mM NaCl control. Treatment with 100 mM NaCl +0.2% EL2006 resulted in potato with fresh weight higher but not significantly different from the 0 mM control. It was also significantly higher than the fresh weight of potato treated with 100 mM NaCl +0.2% MRS control (Figure 5).

There was no significant effect of *L. helveticus* CFS on leaf area and plant height of potato, as shown in Table 5.

4. Discussion

There is a continuous need to increase food production to quantities sufficient to feed the growing human population, without compromising quality, using sustainable and environmentally friendly approaches such as plant growth promoting microorganisms (PGPM) and their derived compounds (Lyu et al., 2020; Shah et al., 2021). NaCl stress is a

TABLE 4 Effect of treatments on mean percentage germination of corn at 72, 48 and 24h, respectively.

Treatment	Mean percentage germination at 72h±SEM	Mean percentage germination at 48h±SEM	Mean percentage germination at 24h±SEM
0 mM NaCl	71.5 ± 5.144[a]	15.5 ± 1.846[a]	0.00 ± 0.000[a]
100 mM NaCl	30.0 ± 3.770[b]	1.0 ± 0.688[b]	0.00 ± 0.000[a]
100 mM NaCl +1.0% EL2006	34.5 ± 3.515[b]	1.5 ± 0.819[b]	0.00 ± 0.000[a]
100 mM NaCl +1.0% MRS	26.5 ± 3.185[b]	2.0 ± 0.918[b]	0.00 ± 0.000[a]

Data represents the mean ± SE ($n = 80$); in a column, different letters indicate values determined by Tukey's multiple mean comparison significantly different at $p < 0.05$. Values with the same letters are not significantly different at $p < 0.05$.

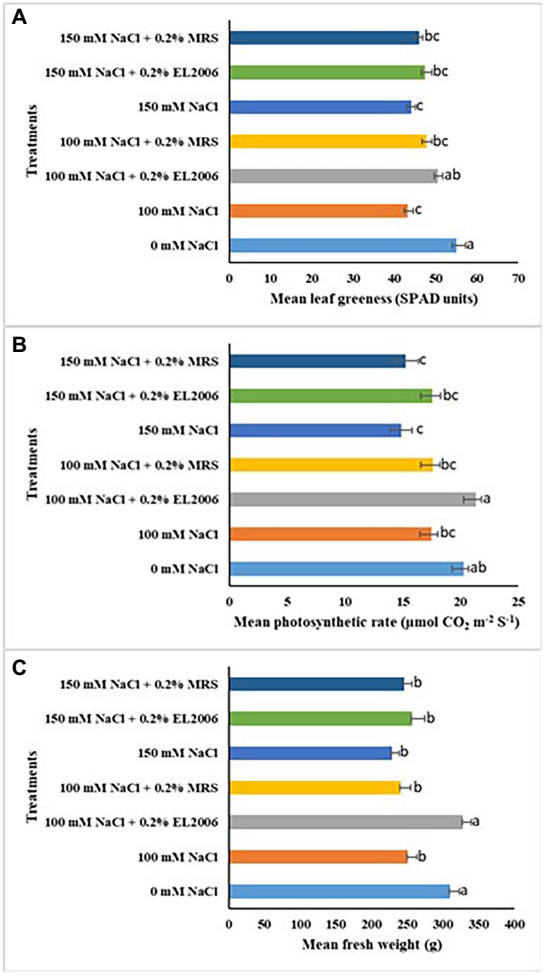

FIGURE 4
Effect of treatments on leaf greenness **(A)**, photosynthetic rate **(B)** and fresh weight **(C)** of potato. Data represents the mean±SE (n=48); different letters indicate values determined by Tukey's multiple mean comparison significantly different at p<0.05. Values with the same letters are not significantly different at p<0.05.

major global constraint to food production (Naamala and Smith, 2021b). Plant growth promoting microorganisms (PGPM), or their derived compounds have been reported to enhance plant growth under saline conditions (Schwinghamer et al., 2016; Subramanian et al., 2016a,b; Ilangumaran et al., 2021; Naamala et al., 2022). However, use of microbial CFS as plant growth biostimulants is less explored, with just a handful of publications available (Tewari et al., 2020; Naamala et al., 2022; Shah et al., 2022). It is possibile that CFS could enhance plant growth because microbes exude metabolites into their growth media in response to various signals, such as those related to biotic or abiotic stress (Subramanian et al., 2021). Among the exuded metabolites are some that possess phyto-stimulation properties, such as IAA, LCO and thuricin17 (Prithiviraj et al., 2003; Mohite, 2013; Subramanian et al., 2016a,b; Antar et al., 2021). In the laboratory setting, such signals/metabolites are exuded into the microbe's growth medium, which when filtered of microbial cells, will still contain the metabolites that can then enhance plant growth (Gray et al., 2006a). Consequently, the possible modes of action through CFS could enhance plant growth include presence of phytohormones such as jasmonic acid; presence of enzymes such as ACC deaminase; presence of osmoprotectants such as proline and presence of volatile organic compounds and exopolysaccharides, all of which may function to mitigate osmotic, oxidative and ionic stress associated with salinity (Forni et al., 2017; Khan et al., 2019; Cappellari and Banchio, 2020; Kumar et al., 2020; Fincheira et al., 2021; Lopes et al., 2021). There is limited publication on the role of members of the genus *Lactobacillus* and/or their CFS as plant growth biostimulants (Hamed et al., 2011; Lamont et al., 2017; Msimbira et al., 2022). The modes of action through which members of the genus *Lactobacillus* and their CFSs enhance plant growth are not fully understood (Lamont et al., 2017). However, plant growth promotion by LAB species has been attributed to production of metabolites such as IAA and siderophores (Omer et al., 2010; Mohite, 2013; Shrestha et al., 2014; Limanska N.V. et al., 2015; Limanska N. et al., 2015), and solubilisation of phosphorus (Shrestha et al., 2014), among other mechanisms. In general, PGPM and or their derived compounds can mitigate salinity stress by employing one or more of the following mechanisms: Production of antioxidants, production of enzymes such as *ACC* deaminase, production of exopolysaccharides, inducing systemic resistance in plants (Shrivastava and Kumar, 2015; Amna et al., 2019) and production of microbe-to-plant signal compounds (Backer et al., 2018).

The current study focused on the ability of CFS obtained from *L. helveticus* EL2006H to enhance growth of three crop species: corn, soybean and potato, exposed to NaCl stress, under

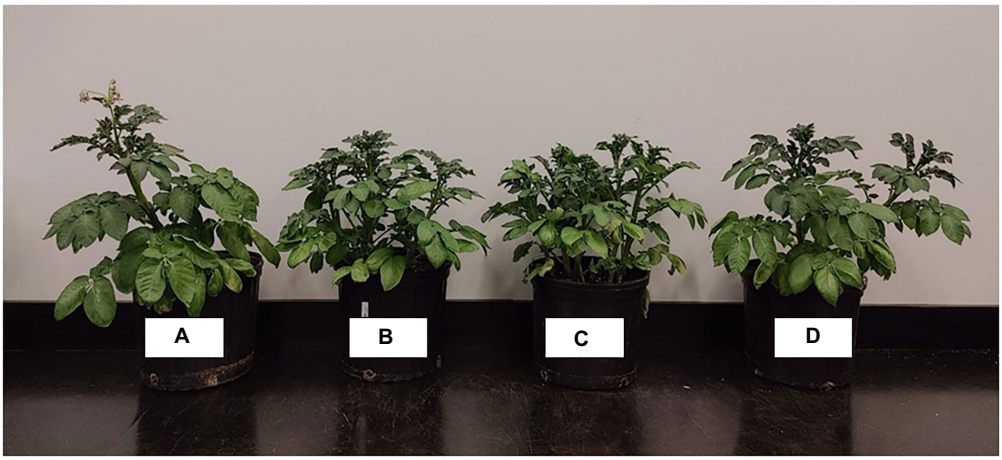

FIGURE 5
Potato treated with 0mM NaCl **(A)**, 100mM NaCl **(B)**, 100mM NaCl +0.2% MRS **(C)** and 100mM NaCl +0.2% EL2006H **(D)**.

TABLE 5 Effect of treatments on selected growth variables of potato.

Treatment	Height gain (cm)	Leaf area (cm^2)
0 mM NaCl	37.275 ± 7.531[a]	2851.261 ± 158.736[a]
100 mM NaCl	32.263 ± 5.739[a]	2951.652 ± 180.931[a]
100 mM NaCl +0.2% EL2006	34.838 ± 6.937[a]	3358.082 ± 156.557[a]
100 mM NaCl +0.2% MRS	33.113 ± 6.129[a]	2943.797 ± 234.763[a]
150 mM NaCl	38.9 ± 2.282[a]	3045.75 ± 157.209[a]
150 mM NaCl +0.2% EL2006	40.825 ± 1.723[a]	2960.841 ± 87.894[a]
150 mM NaCl +0.2% MRS	40.063 ± 2.233[a]	3076.615 ± 211.951[a]

Data represents the mean ± SE ($n = 48$); in a column, different letters indicate values determined by Tukey's multiple mean comparison significantly different at $p < 0.05$. Values with the same letters are not significantly different at $p < 0.05$.

controlled conditions. Results of the study highlight the role CFS concentration, NaCl level, crop species and growth level play in the effectiveness and efficacy of CFS as plant growth biostimulants.

The effect of CFS on mean radicle length varied among crop species, concentration of the CFS, and level of NaCl in the treatment. For instance, treatment with 100 mM NaCl +1.0% EL2006H resulted in a significant increase in corn radicle length but not soybean, suggesting crop specific responses. Although some PGPM, such as some *Rhizobium* species, can be promiscuous, enhancing growth in a wide range of crop species, others are host specific, enhancing growth of just one or two crop species (Lyu et al., 2020). PGPM and their host plants communicate through signals, which vary depending on the host plant needs (Antar et al., 2021). Sometimes, such signals will limit the host range of a particular PGPM. However, such PGPM can produce metabolites that enhance growth in a wide range of crops. For instance, LCO, can enhance growth of non-legumes although it is produced by *B. japonicum*, and plays a major role in nodulation of soybean. It is such advantages that make CFS and plant derived compounds relevant in PGPM technology (Naamala and Smith, 2020). Even then, there is not yet a single microbial derived compound or PGPM that enhances growth of all crop species. It is possible that the varied responses to CFS observed in corn, soybean and potato are in part due to variation in ways through which the three crops perceive and respond to the bioactive signals in the CFS. In another study, we also observed variation in soybean and corn responses to *B. amyloliquefaciens* CFS (Naamala et al., 2022). The *B. japonicum* derived LCO also exhibited variation in its effect on corn and soybean (Souleimanov et al., 2002). At a lower concentration, variations were observed in the response of canola varieties treated with LCO (Schwinghamer et al., 2015).

Lowering CFS concentration from 1.0% (v/v) to 0.2% EL2006H CFS resulted in no significant effect on both corn and soybean mean radicle length. This seems to suggest that the concentration and quantity of CFS applied to a plant is vital in determining efficacy and effectiveness of the applied CFS in enhancing plant growth. In this case, especially for corn, higher concentrations resulting in more effective results than lesser concentrations. The same cannot be said about soybean. Its possible that in soybean, perhaps minute quantities of the supernatant were enough to enhance growth. For example, Msimbira et al. (2022) observed variation in germination of corn, in response to *Bacillus subtilis* CFS, where a concentration of 0.1% (v/v) yielded better results than higher concentrations of 0.2, 0.4 and 1.0%. It should also be noted that high concentrations may sometimes inhibit growth of the crop in question (Naamala et al., 2021b), although there is no universal description of how much is sufficient and this could vary among crop species. Published studies on *L. helveticus* CFS as a plant biostimulant are currently limited to a study by Msimbira et al. (2022). In our previous study on *B. amyloliquefaciens* EB2003 CFS, we observed the effect of CFS concentration on its effectiveness in enhancing germination and radicle length of corn and soybean (Naamala et al., 2022). Studies on other members of the genus *Lactobacillus* have also

reported concentration as a major determinant of effectiveness and efficacy in plant growth promotion. For instance, radish plants responded differently to varying concentrations of *L. plantarum* (Higa and Kinjo, 1991).

Results on mean percentage germination varied between corn and soybean at the two CFS concentrations and three different time frames studied. For instance, in soybean, following treatment with 100 mM NaCl +0.2% EL2006H, greatest significance was observed at 48 h, where percentage germination of soybean was not only significantly higher than that of the 100 mM NaCl control, but was also not significantly different from that of the unstressed 0 mM NaCl control. At 24 h, there was no observed difference among the effects of treatments for percentage germination. It is however possible that the CFS was already working on the physio-chemical properties of the seed to mitigate the effect of NaCl on the plant, hence the higher percentage germination observed at 48 h. The plant also naturally attempts to put in place a defence against stress, but can be slower, which could explain why at 72 h, there was no significant difference in the percentage germination of all the treatments on soybean. Therefore, it seems likely that at 48 h, CFS mitigated delays in germination due to 100 mM stress, resulting in percentage germination levels higher than the stressed control and not significantly different from the unstressed control, which is desirable because slow germination exposes seed to attack by pathogens in the soil, among other disadvantages. Similar results were obtained by Msimbira et al. (2022) who observed variation in the effect of EL2006H CFS on germination of corn and tomato across time. Naamala et al. (2022) also observed variation in effect of *B. amyloliquefaciens* CFS among 24, 48 and 72 h sampling times. In corn however, there was no significant effect of the EL2006H CFS on mean percentage germination at all time intervals. The mean percentage germination of corn was significantly lower than the unstressed control at both 48 and 72 h. This again takes us back to the effect of crop species on effectiveness of the CFS. The effect of PGPM CFS and other PGPM derived compounds on seed germination has been reported by other researchers (Tallapragada et al., 2015; Subramanian et al., 2016a,b; Shah et al., 2022). *Devosia* sp. CFS enhanced germination of canola and soybean under NaCl stressed and optimal conditions (Shah et al., 2022).

Increasing concentration from 0.2 to 1.0% of CFS yielded less desirable results in soybean as there was no significant difference between mean percentage germination of soybean treated with 100 mM NaCl +0.2% EL2006H and 100 mM NaCl, at all measurement times, although the percentage germination of the latter was not significantly different from that observed in the 0 mM control at 48 h. Results seem to suggest that when it comes to mean percentage germination, lesser quantities of the CFS are required to mitigate the effect of NaCl stress on germination of soybean. In corn, CFS had no significant effect on mean percentage germination, with the unstressed control still significantly higher at both 48 and 72 h. Shah et al. also observed variations in the germination of canola and soybean treated with a range of concentrations of *Devosia* sp. CFS (Shah et al., 2022).

In the potato experiment, results exhibited effects of stress level on effectiveness of EL2006H CFS. The supernatant enhanced some growth variables but not all. Specifically, CFS enhanced fresh weight, photosynthetic rate and leaf greenness but not leaf area and plant height. Among the variables enhanced, levels varied across NaCl levels. Better results of the CFS were observed in potato treated with 100 mM NaCl than 150 mM NaCl. This implies that increasing NaCl level by 50 mM reduced effectiveness of the CFS. This is not surprising as its possible that the potential bioactive substance was less effective at 150 mM NaCl so that it/they could not function as efficiently as they would at lower concentrations, or, at 150 mM NaCl, potato plant cell components could have been damaged (Ilangumaran et al., 2021) to a point where even the CFS could not fully mitigate these effects on growth. The effect of NaCl level on the effectiveness of CFS was also observed by Naamala et al., (2022) on percentage germination and radicle length of soybean and corn treated with different concentrations of NaCl. The CFS enhanced radicle length in soybean not stressed with NaCl but not in soybean exposed to NaCl while the reverse was true for corn (Naamala et al., 2022). Subramanian et al. (2016a) also observed that LCO enhanced germination of soybean exposed to 100 mM NaCl but not higher NaCl concentrations of 150 mM NaCl and 175 mM NaCl. Shah et al. observed significant increases in germination of canola and soybean treated with *Devosia* sp. CFS (Shah et al., 2022).

The ability of PGPM, LAB included, to enhance plant growth can be affected by plant growth stage and growth variables, in which case a microbial strain or its CFS can enhance plant growth at a certain plant growth stage and not at another or enhance growth of one variable but not the other. For instance, under field conditions, Shrestha et al. (2014) observed an increase in growth of pepper plants treated with each of the three LAB they were studying, 1 week after transplanting. However, after that stage, only one strain of the three was able to enhance plant height. This, in a way, points out the complexity of depending on the plant-microbe interactions for plant growth stimulation.

Published research on *L. helveticus* as a plant growth biostimulant remains minimal. However, other members of the genus have been reported to enhance plant growth. For example, *L. plantarum* exhibited antimicrobial activity against *Fusarium* spp. in agar plate assays and a consortium consisting of the same and *B. amyloliquefaciens* reduced severity of *Fusarium* spp. in wheat (Baffoni et al., 2015). *L. plantarum* ONU 12 expressed antimicrobial properties in carrot, kalanchoe and grapes exposed to *Agrobacterium tumefaciens*, protection ranging from 72.7 to 100% of wounded kalanchoe tissues, depending on mode of application (Limanska N. et al., 2015). LAB species KLF01, KLC02 and KPD03 had antagonistic effects against *Xanthomonas campestris pv. vesicatoria* (Shrestha et al., 2014) while strains LB-1, LB-2 and LB-3 increased total fresh weight of tomato plants by 348, 260, and 390%, respectively (Hamed et al., 2011). LAB species identified as KLF01, KLC02 and KPD03 were reported to enhance chlorophyll content in pepper (Shrestha et al., 2014). The same strains, except KLC02, were reported to enhance shoot length in

pepper (Shrestha et al., 2014). Recently, research on PGPM has extended to their CFSs, attempting to elucidate whether it can enhance plant growth in the absence of the microbial cell. The ability of *L. helveticus* CFS at varying pH levels to enhance plant growth was recently reported (Msimbira et al., 2022). The effectiveness and efficacy of PGPM or their CFS, including LAB is dependent on several soil, plant and microbe factors, such soil conditions and plant species. A PGPM can enhance growth of one crop species but not another or enhance growth under certain soil conditions, such as under stressed conditions but not under optimal conditions.

At this stage we do not know whether the effect of CFS on the different variables is from a single bioactive compound or more than one; both scenarios are possible. As mentioned earlier, knowledge on the mechanisms employed by members of the genus *Lactobacillus* and or their CFSs to enhance plant growth remain poorly understood.

5. Conclusion

Based on the results of this study, it seems likely that *L. helveticus* EL2006H exudes into its growth media substances which enhance radicle length in corn, mean percentage germination in soybean and photosynthetic rate, greenness and mean fresh weight in potato. However, the effect varies depending on crop species, concentration of CFS and level of NaCl stress. *L. helveticus* CFS concentration of 0.2 and 1.0% were more effective at enhancing radicle length in corn and percentage germination in soybean, respectively. One hundred and fifty mM NaCl lowered the effectiveness of the 0.2% concentration in enhancing leaf greenness, mean photosynthetic rate and mean fresh weight of potato. Findings of this study can be used as a basis to further study of *Lactobacillus* CFSs and possibly identify the bioactive substances therein. Findings of this study are promising in the field of microbial inoculants where new ways of improving efficacy and effectiveness of the technology, especially under field conditions, are constantly sought. However, further studies need to be done, especially under field conditions, with trials on different crop species and varying soil conditions.

Data availability statement

The original contributions presented in the study are included in the article/supplementary material, further inquiries can be directed to the corresponding author.

Author contributions

JN set up the experiment and wrote the manuscript. LM helped with data collection and experimental set up. SS advised on scientific approach and provided background knowledge. DS provided funding, the intellectual context, and extensive editorial input and guided in scientific knowledge. All authors contributed to the article and approved the submitted version.

Funding

This work was funded through a grant from Consortium de recherche et innovations en bioprocédés industriels au Québec, number CRIBIQ 2017-034-C30, with support from synagri and EVL inc.

Conflict of interest

The authors declare that the research was conducted in the absence of any commercial or financial relationships that could be construed as a potential conflict of interest.

Publisher's note

References

Ahemad, M., and Kibret, M. (2014). Mechanisms and applications of plant growth promoting rhizobacteria: current perspective. *J. King Saud Univ. Sci.* 26, 1–20. doi: 10.1016/j.jksus.2013.05.001

Amna, D. B. U., Sarfraz, S., Xia, Y., Kamran, M. A., Javed, M. T., Sultan, T., et al. (2019). Mechanistic elucidation of germination potential and growth of wheat inoculated with exopolysaccharide and *ACC- deaminase* producing *bacillus* strains under induced salinity stress. *Ecotoxicol. Environ. Safety* 183:109466. doi: 10.1016/j.ecoenv.2019.109466

Antar, M., Gopal, P., Msimbira, L. A., Naamala, J., Nazari, M., Overbeek, W., et al. (2021). *Inter-Organismal Signaling in the Rhizosphere. Rhizosphere Biology: Interactions Between Microbes and Plants*. Singapore: Springer.

Arunachalam, S., Schwinghamer, T., Dutilleul, P., and Smith, D. L. (2018). Multiyear effects of biochar, lipo-chitooligosaccharide, thuricin 17, and experimental bio-fertilizer for switchgrass. *Agron. J.* 110, 77–84. doi: 10.2134/agronj2017.05.0278

Backer, R., Rokem, J. S., Ilangumaran, G., Lamont, J., Praslickova, D., Ricci, E., et al. (2018). Plant growth-promoting rhizobacteria: context, mechanisms of action, and roadmap to commercialization of bio stimulants for sustainable agriculture. *Front. Plant Sci.* 9:1473. doi: 10.3389/fpls.2018.01473

Baffoni, L., Gaggia, F., Dalanaj, N., Prodi, A., Nipoti, P., Pisi, A., et al. (2015). Microbial inoculants for the biocontrol of *Fusarium* spp. in durum wheat. *BMC Microbiol.* 15:242. doi: 10.1186/s12866-015-0573-7

Bistgani, Z. E., Hashemi, M., DaCosta, M., Craker, L., Maggi, F., and Morshedloo, M. R. (2019). Effect of salinity stress on the physiological characteristics, phenolic compounds and antioxidant activity of *Thymus vulgaris* L. and thymus daenensis Celak. *Ind. Crop. Prod.* 135, 311–320. doi: 10.1016/j.indcrop.2019.04.055

Caballero, P., Rodríguez-Morgado, B., Macías, S., Tejada, M., and Parrado, J. (2020). Obtaining plant and soil biostimulants by waste whey fermentation. *Waste Biomass Valoriz.* 11, 3281–3292. doi: 10.1007/s12649-019-00660-7

Cappellari, L. R., and Banchio, E. (2020). Microbial volatile organic compounds produced by *Bacillus amyloliquefaciens* GB03 ameliorate the effects of salt stress in Mentha piperita principally through acetoin emission. *J. Plant Growth Reg.* 39, 764–775. doi: 10.1007/s00344-019-10020-3

FAO (2020). *Salt-Affected Soils [Online 2021/07/13]*. Rome: FAO.

Fincheira, P., Quiroz, A., Tortella, G., Diez, M. C., and Rubilar, O. (2021). Current advances in plant-microbe communication via volatile organic compounds as an innovative strategy to improve plant growth. *Microbiol. Res.* 247:126726. doi: 10.1016/j.micres.2021.126726

Forni, C., Duca, D., and Glick, B. R. (2017). Mechanisms of plant response to salt and drought stress and their alteration by rhizobacteria. *Plant Soil* 410, 335–356. doi: 10.1007/s11104-016-3007-x

Garcia, C. L., Dattamudi, S., Chanda, S., and Jayachandran, K. (2019). Effect of salinity stress and microbial inoculations on glomalin production and plant growth parameters of snap bean (Phaseolus vulgaris). *Agronomy* 9:545. doi: 10.3390/agronomy9090545

Giassi, V., Kiritani, C., and Kupper, K. C. (2016). Bacteria as growth-promoting agents for citrus rootstocks. *Microbiol. Res.* 190, 46–54. doi: 10.1016/j.micres.2015.12.006

Glick, B. R. (2012). Plant growth-promoting bacteria: mechanisms and applications. *Scientifica (Cairo)* 2012:963401. doi: 10.6064/2012/963401

Gray, E. J., Di Falco, M. R., Souleimanov, A., and Smith, D. L. (2006b). Proteomic analysis of the bacteriocin thuricin 17 produced by *Bacillus thuringiensis* NEB17. *FEMS Microbiol. Lett.* 255, 27–32. doi: 10.1111/j.1574-6968.2005.00054.x

Gray, E. J., Lee, K. D., Souleimanov, A. M., Di Falco, M. R., Zhou, X., Ly, A., et al. (2006a). A novel bacteriocin, thuricin 17, produced by plant growth promoting rhizobacteria strain *Bacillus thuringiensis* NEB17: isolation and classification. *J. Appl. Microbiol.* 100, 545–554. doi: 10.1111/j.1365-2672.2006.02822.x

Hamed, H. A., Moustafa, Y. A., and Abdel-Aziz, S. M. (2011). *In vivo* efficacy of lactic acid bacteria in biological control against *Fusarium oxysporum* for protection of tomato plant. *Life Sci. J.* 8, 462–468.

Hartmann, A., Rothballer, M., Hense, B. A., and Peter, S. (2014). Bacterial quorum sensing compounds are important modulators of microbe-plant interactions. *Front. Plant Sci.* 5:131. doi: 10.3389/fpls.2014.00131

Higa, T., and Kinjo, S. (1991). "Effect of lactic acid fermentation bacteria on plant growth and soil humus formation" in *Proceedings of the First International Conference on Kyusei Nature Farming*. eds. J. F. Parr, S. B. Hornick and C. E. Whitman (Washington, DC: US Department of Agriculture), 140–147.

Ilangumaran, G., Schwinghamer, T. D., and Smith, D. L. (2021). Rhizobacteria from root nodules of an indigenous legume enhance salinity stress tolerance in soybean. *Front. Sustain. Food Syst.* 4:617978. doi: 10.3389/fsufs.2020.617978

Jamil, A., Riaz, S., Ashraf, M., and Foolad, M. R. (2011). Gene expression profiling of plants under salt stress. *Crit. Rev. Plant Sci.* 30, 435–458. doi: 10.1080/07352689.2011.605739

Khan, M. A., Asaf, S., Khan, A. L., Ullah, I., Ali, S., Kang, S., et al. (2019). Alleviation of salt stress response in soybean plants with the endophytic bacterial isolate *Curtobacterium* sp. SAK1. *Ann. Microbiol.* 69, 797–808. doi: 10.1007/s13213-019-01470-x

Knack, J. J., Wilcox, L. W., Delaux, P. M., Ané, J. M., Piotrowski, M. J., Cook, M. E., et al. (2015). Microbiomes of streptophyte algae and bryophytes suggest that a functional suite of microbiota fostered plant colonization of land. *Int. J. Plant Sci.* 176, 405–420. doi: 10.1086/681161

Kumar, A., Singh, S., Gaurav, A. K., Srivastava, S., and Verma, J. P. (2020). Plant growth-promoting bacteria: biological tools for the mitigation of salinity stress in plants. *Front. Microbiol.* 11:1216. doi: 10.3389/fmicb.2020.01216

Lamont, J. R., Wilkins, O., Bywater-Ekegärd, M., and Smith, D. L. (2017). From yogurt to yield: potential applications of lactic acid bacteria in plant production. *Soil Biol. Biochem.* 111, 1, 1–9. doi: 10.1016/j.soilbio.2017.03.015

Lee, K. D., Gray, E. J., Mabood, F., Jung, W. J., Charles, T., Clark, S. R. D., et al. (2009). The class IId bacteriocin thuricin 17 increases plant growth. *Planta* 229, 747–755. doi: 10.1007/s00425-008-0870-6

Lemfack, M. C., Gohlke, B. O., Toguem, S. M. T., Preissner, S., Piechulla, B., and Preissner, R. (2018). mVOC 2.0: a database of microbial volatiles. *Nucleic Acids Res.* 46, D1261–D1265. doi: 10.1093/nar/gkx1016

Limanska, N. V., Babenko, D. O., Yamborko, G. V., and Ivanytsia, V. O. (2015). Detection of plantaricin genes in strains of *Lactobacillus plantarum* antagonists of phytopathogenic bacteria. *Мікробіологія і Біотехнологія* 2, 27–33. doi: 10.18524/2307-4663.2015.2(30).48071

Limanska, N., Korotaeva, N., Biscola, V., Ivanytsia, T., Merlich, A., Franco, B. D. G. M., et al. (2015). Study of the potential application of lactic acid bacteria in the control of infection caused by *Agrobacterium tumefaciens*. *J. Plant Pathol. Microbiol.* 6:292. doi: 10.4172/2157-7471.1000292

Lopes, M. J. S., Dias-Filho, M. B., and Gurgel, E. S. C. (2021). Successful plant growth-promoting microbes: inoculation methods and abiotic factors. *Front. Sustain. Food Syst.* 5:606454. doi: 10.3389/fsufs.2021.606454

Lyu, D., Backer, R., Subramanian, S., and Smith, D. L. (2020). Phytomicrobiome coordination signals hold potential for climate change-resilient agriculture. *Front. Plant Sci.* 11:634. doi: 10.3389/fpls.2020.00634

Lyu, D., Zajonc, J., Pagé, A., Tanney, C. A., Shah, A., Monjezi, N., et al. (2021). Plant holobiont theory: the phytomicrobiome plays a central role in evolution and success. *Microorganisms* 9:675. doi: 10.3390/microorganisms9040675

Minervini, F., Celano, G., Lattanzi, A., Tedone, L., De Mastro, G., Gobbetti, M., et al. (2015). Lactic acid bacteria in durum wheat flour are endophytic components of the plant during its entire life cycle. *Applied Environ. Microbiol.* 81, 6736–6748. doi: 10.1128/AEM.01852-15

Mohite, B. (2013). Isolation and characterization of indole acetic acid (IAA) producing bacteria from rhizospheric soil and its effect on plant growth. *J. Soil Sci. Plant* 13, 638–649. doi: 10.4067/S0718-95162013005000051

Msimbira, L. A., Naamala, J., Antar, M., Subramanian, S., and Smith, D. L. (2022). Effect of microbial cell-free supernatants extracted from a range of pH levels on corn (*Zea mays* L.) and tomato (*Solanum lycopersicum* L.) seed germination and seedling growth. *Front. Sustain. Food Syst.* 6:789335. doi: 10.3389/fsufs

Naamala, J., and Smith, D. (2020). Relevance of plant growth promoting microorganisms and their derived compounds, in the face of climate change. *Agronomy* 10:1179. doi: 10.3390/agronomy10081179

Naamala, J., and Smith, D. L. (2021a). Microbial derived compounds, a step toward enhancing microbial inoculants technology for sustainable agriculture. *Front. Microbiol.* 12:634807. doi: 10.3389/fmicb.2021.634807

Naamala, J., and Smith, D. L. (2021b). Microbial derived compounds are a promising approach to mitigating salinity stress in agricultural crops. *Front. Microbiol.* 12:765320. doi: 10.3389/fmicb.2021.765320

Naamala, J., Msimbira, L. A., Antar, M., Subramanian, S., and Smith, D. L. (2022). Cell-Free Supernatant Obtained From a Salt Tolerant Bacillus amyloliquefaciens Strain Enhances Germination and Radicle Length Under NaCl Stressed and Optimal Conditions. *Front. Sustain. Food Syst.* 6:788939. doi: 10.3389/fsufs.2022.788939

Omer, Z. S., Jacobsson, K., Eberhard, T. H., and Johansson, L. K. H. (2010). Bacteria considered as biocontrol agents to control growth of white clover on golf courses. *Acta Agric. Scand. Sect. Besoil Plant Sci.* 60, 193–198. doi: 10.1080/09064710902773637

Piechulla, B., Lemfack, M. C., and Kai, M. (2017). Effects of discrete bioactive microbial volatiles on plants and fungi. *Plant Cell Environ.* 40, 2042–2067. doi: 10.1111/pce.13011

Prithiviraj, B., Zhou, X., Souleimanov, A., Khan, W. K., and Smith, D. L. (2003). A host specific bacteria-to-plant signal molecule (nod factor) enhances germination and early growth of diverse crop plants. *Planta* 216, 437–445. doi: 10.1007/s00425-002-0928-9

Rodríguez-Morgado, B., Jiménez, P., Moral, M., and Rubio, J. (2017). Effect of lactic acid from whey wastes on enzyme activities and bacterial diversity of soil. *Biol. Fertility Soils* 53, 389–396. doi: 10.1007/s00374-017-1187-z

Schulz-Bohm, K., Martín-Sánchez, L., and Garbeva, P. (2017). Microbial volatiles: small molecules with an important role in intra and inter-kingdom interactions. *Front. Microbiol.* 8:2484. doi: 10.3389/fmicb.2017.02484

Schwinghamer, T., Souleimanov, A., Dutilleul, P., and Smith, D. L. (2015). The plant growth regulator lipo-chitooligosaccharide (LCO) enhances the germination of canola (*Brassica napus* [L.]). *J. Plant Growth Regul.* 34, 183–195. doi: 10.1007/s00344-014-9456-7

Schwinghamer, T., Souleimanov, A., Dutilleul, P., and Smith, D. L. (2016). Supplementation with solutions of lipo-chitooligosacharide nod Bj V (C18:1, MeFuc) and thuricin 17 regulates leaf arrangement, biomass, and root development of canola (*Brassica napus* [L.]). *Plant Growth Regul.* 78, 31–41. doi: 10.1007/s10725-015-0072-8

Shah, A., Nazari, M., Antar, M., Msimbira, L. A., Naamala, J., Lyu, D., et al. (2021). PGPR in agriculture: a sustainable approach to increasing climate change resilience. *Front. Sustain. Food Syst.* 5:667546. doi: 10.3389/fsufs.2021.667546

Shah, A., Subramanian, S., and Smith, D. L. (2022). Seed priming with *Devosia* sp. cell-free supernatant (CFS) and citrus bioflavonoids enhance canola and soybean seed germination. *Molecules* 27:3410. doi: 10.3390/molecules27113410

Shrestha, A., Kim, S. K., and Park, D. H. (2014). Biological control of bacterial spot disease and plant growth-promoting effects of lactic acid bacteria on pepper. *Biocontrol Sci. Tech.* 24, 763–779. doi: 10.1080/09583157.2014.894495

Shrivastava, P., and Kumar, R. (2015). Soil salinity: a serious environmental issue and plant growth promoting bacteria as one of the tools for its alleviation. *Saudi J. Biol. Sci.* 22, 123–131. doi: 10.1016/j.sjbs.2014.12.001

Souleimanov, A., Prithiviraj, B., and Smith, D. L. (2002). The major nod factor of *Bradyrhizobium japonicum* promotes early growth of soybean and corn. *J. Exp. Bot.* 53, 1929–1934. doi: 10.1093/jxb/erf034

Stoyanova, L. G., Ustyugova, E. A., and Netrusov, A. I. (2012). Antibacterial metabolites of lactic acid bacteria: their diversity and properties. *Appl. Biochem. Microbiol.* 48, 229–243. doi: 10.1134/S0003683812030143

Subramanian, S., Ricci, E., Souleimanov, A., and Smith, D. L. (2016b). A proteomic approach to lipochitooligosaccharide and thuricin 17 effects on soybean germination unstressed and salt stress. *PLoS One* 11:e0160660. doi: 10.1371/journal.pone.0160660

Subramanian, S., Souleimanov, A., and Smith, D. L. (2016a). Proteomic studies on the effects of lipo-chitooligosaccharide and thuricin 17 under unstressed and salt stressed conditions in *Arabidopsis thaliana*. *Front. Plant Sci.* 7:1314. doi: 10.3389/fpls.2016.01314

Subramanian, S., Souleimanov, A., and Smith, D. L. (2021). Thuricin17 production and proteome differences in *Bacillus thuringiensis* NEB17 cell-free supernatant under NaCl stress. *Front. Sustain. Food Syst.* 5:630628. doi: 10.3389/fsufs.2021.630628

Tallapragada, P., Dikshit, R., and Seshagiri, S. (2015). Isolation and optimization of IAA producing *Burkholderia seminalis* and its effect on seedlings of tomato. *Songklanakar. J. Sci. Technol.* 37, 553–559.

Tewari, S., Pooniya, V., and Sharma, S. (2020). Next generation bioformulation prepared by amalgamating *Bradyrhizobium*, cell free culture supernatant, and exopolysaccharides enhances the indigenous rhizospheric rhizobial population, nodulation, and productivity of pigeon pea. *Appl. Soil Ecol.* 147:103363. doi: 10.1016/j.apsoil.2019.103363

Zhang, R., Vivanco, J. M., and Shen, Q. (2017). The unseen rhizosphere root-soil-microbe interactions for crop production. *Curr. Opin. Microbiol.* 37, 8–14. doi: 10.1016/j.mib.2017.03.008

frontiers | Frontiers in Plant Science

TYPE Original Research
PUBLISHED 15 February 2023
DOI 10.3389/fpls.2023.1077140

OPEN ACCESS

EDITED BY
Aliki Kapazoglou,
Hellenic Agricultural Organization (ELGO)-DIMITRA, Greece

REVIEWED BY
Abbu Zaid,
Govt. Degree College Doda, India
Sophia Letsiou,
University of West Attica, Greece

*CORRESPONDENCE
Monica Yorlady Alzate Zuluaga
monicayorlady.alzatezuluaga@unibz.it
Youry Pii
youry.pii@unibz.it

SPECIALTY SECTION
This article was submitted to Crop and Product Physiology, a section of the journal Frontiers in Plant Science

RECEIVED 22 October 2022
ACCEPTED 03 February 2023
PUBLISHED 15 February 2023

CITATION
Zuluaga MYA, Monterisi S, Rouphael Y, Colla G, Lucini L, Cesco S and Pii Y (2023) Different vegetal protein hydrolysates distinctively alleviate salinity stress in vegetable crops: A case study on tomato and lettuce.
Front. Plant Sci. 14:1077140.
doi: 10.3389/fpls.2023.1077140

Different vegetal protein hydrolysates distinctively alleviate salinity stress in vegetable crops: A case study on tomato and lettuce

Monica Yorlady Alzate Zuluaga[1]*, Sonia Monterisi[1], Youssef Rouphael[2], Giuseppe Colla[3], Luigi Lucini[4], Stefano Cesco[1] and Youry Pii[1]*

[1]Faculty of Science and Technology, Free University of Bozen/Bolzano, Bolzano, Italy, [2]Department of Agricultural Sciences, University of Naples Federico II, Portici, Italy, [3]Department of Agriculture and Forest Sciences, University of Tuscia, Viterbo, Italy, [4]Department for Sustainable Food Process, Research Centre for Nutrigenomics and Proteomics, Università Cattolica del Sacro Cuore, Piacenza, Italy

Plants have evolved diverse plant-species specific tolerance mechanisms to cope with salt stress. However, these adaptive strategies often inefficiently mitigate the stress related to increasing salinity. In this respect, plant-based biostimulants have gained increasing popularity since they can alleviate deleterious effects of salinity. Hence, this study aimed to evaluate the sensitivity of tomato and lettuce plants grown under high salinity and the possible protective effects of four biostimulants based on vegetal protein hydrolysates. Plants were set in a 2 × 5 factorial experimental design completely randomized with two salt conditions, no salt (0 mM) and high salt (120 mM for tomato or 80 mM for lettuce), and five biostimulant treatments (C: *Malvaceae*-derived, P: *Poaceae*-derived, D: Legume-derived commercial 'Trainer®', H: Legume-derived commercial 'Vegamin®', and Control: distilled water). Our results showed that both salinity and biostimulant treatments affected the biomass accumulation in the two plant species, albeit to different extents. The salinity stress induced a higher activity of antioxidant enzymes (e.g., catalase, ascorbate peroxidase, guaiacol peroxidase and superoxide dismutase) and the overaccumulation of osmolyte proline in both lettuce and tomato plants. Interestingly, salt-stressed lettuce plants showed a higher accumulation of proline as compared to tomato plants. On the other hand, the treatment with biostimulants in salt-stressed plants caused a differential induction of enzymatic activity depending on the plant and the biostimulant considered. Overall, our results suggest that tomato plants were constitutively more tolerant to salinity than lettuce plants. As a consequence, the effectiveness of biostimulants in alleviating high salt concentrations was more evident in lettuce. Among the four biostimulants tested, P and D showed to be the most promising for the amelioration of salt stress in both the plant species, thereby suggesting their possible application in the agricultural practice.

KEYWORDS

abiotic stress, antioxidant defense system, proline, salt-tolerant crop, salt-sensitive crop

Introduction

It is well known that plants, being sessile organisms, must exhibit a certain adaptive plasticity to survive when unfavorable or stressful factors are present in their growing environment (Zhu, 2016). Therefore, to efficiently express the adaptive responses to specific abiotic stresses, the quick reaction to environmental changes appears to be crucial (Nguyen et al., 2016). Among these stresses, salinity is certainly one of the most devastating, causing severe damage to plant growth and productivity and threatening food security. Around 20% of the world's cultivable lands (about 300 Mha) are impaired by high salinity, with an estimated annual global loss of 12 billion USD (Behera et al., 2022).

Vegetable crops are particularly susceptible to salinity stress compared to other agricultural crops (Machado and Serralheiro, 2017). In fact, the majority of vegetable crops have a low salinity threshold (EC_t) that ranges from 1.0 to 2.5 dS m^{-1} in saturated soil. However, it should be noted that the severity of salinity effects is variable among different plant species (Abiala et al., 2018). For instance, onion and carrot are considered salt-sensitive vegetable crops ($EC_t < 1.2$), potato, tomato and lettuce are moderately sensitive ($1.7 < EC_t < 2.5$), while asparagus has been classified as the most salt-tolerant vegetable crop ($EC_t > 4.0$) (Machado and Serralheiro, 2017). As concerns the plant effects, salinity can negatively alter morpho-physiological and biochemical functions at extents that are plant species-specific, thus resulting in nutritional and ion imbalance, oxidative and osmotic stress, damage to the cell membranes, proteins and photosynthetic machinery, and a decrease in plant growth and yield (Hasanuzzaman and Fujita, 2022).

To face salt stress and its effects, plants have developed different adaptive mechanisms, including the production of enzymes (*e.g.*, ascorbate peroxidase - APX, catalase - CAT, superoxide dismutase - SOD, monodehydroascorbate reductase - MDHAR) and molecules (*e.g.*, ascorbic acid, phenolic compounds, alkaloids, α-tocopherols) with antioxidant activity, and compatible osmolytes (*e.g.*, proline, glycine, betaine) (Ismail et al., 2014; Zaid and Wani, 2019; Behera et al., 2022). In addition, the modulation of the levels of endogenous phytohormones (*e.g.*, auxins, abscisic acid, salicylic acid, jasmonic acid, brassinosteroids) and the downstream changes in roots, leaves and cellular structures are also important response mechanisms (Fariduddin et al., 2019; Sadiq et al., 2020; Zaid et al., 2021; Behera et al., 2022). However, these adaptive strategies might not be enough to efficiently overcome the limitations imposed by salt stress. Therefore, the acquisition of new knowledge appears crucial for the development of agronomic approaches/practices that can strengthen the adaptive response of plants to salt stress. In this respect and in a framework of increasingly sustainable agriculture, different approaches based on the use of natural products have been developed.

Among these products, the class of plant biostimulants (PBs) encompasses a wide variety of effectors, including organic or inorganic substances and/or microorganisms, and they have recently emerged as potential and eco-friendly tools to improve plant growth, productivity and alleviate the negative effects of abiotic stresses (Bulgari et al., 2019). Vegetal-derived protein hydrolysates (PHs) are a particular category of PBs, formed by a mixture of soluble peptides and free amino acids with potential bioactive effects aimed at enhancing plant growth and nutrition as well as at improving tolerance to salt stress following leaves or roots application (Colla et al., 2017). The mechanisms underlying the protective action of PHs in the salinity stress mitigation may include: i) regulation of key enzymes involved in the TCA-cycle and N-assimilation pathway (Colla et al., 2017); ii) increased photosynthetic metabolism by the elicitation of hormone-like activities (Di Mola et al., 2021); iii) modulation of the phenylpropanoids metabolism (Bavaresco et al., 2020); iv) changes in the gene expression of certain stress-inducible proteins (Vaseva et al., 2022).

Considering the potential role of PHs in mitigating the harmful effects of abiotic stresses, their use in vegetable species, which are more prone to salinity stress, represents a feasible strategy to encounter the negative impact of high salt concentrations. Among vegetable crops, tomato constitutes one of the most important fruiting vegetable crop in the world (Behera et al., 2022), whereas lettuce is one of the most consumed leafy vegetables (Shin et al., 2020). However, for both the negative effect of salt stress on the growth, biomass accumulation and yield are well described (Rouphael et al., 2017; Alam et al., 2021).

Based on the premises previously reported, and also considering the increasing global concerns about salinity as well as the economic and nutritional importance of vegetable crops, this work aims at investigating i) the different sensitivity of tomato and lettuce plants to salinity stress, ii) the constitutive biochemical mechanisms (*i.e.*, activation of antioxidant enzymes, osmolyte accumulation) underpinning the different plant response to salinity in the short-term and iii) the effects of four PHs, obtained from different vegetal sources, in eliciting protective mechanisms (*i.e.*, osmolyte accumulation, antioxidant defense system, modulation of key genes and ion homeostasis) in tomato and lettuce grown under optimal and salt-stress conditions. Considering that PHs have been described as plant species-specific and origin-specific (Paradiković et al., 2019), we hypothesize that the effects observed on one particular PH-plant species combination could not be directly generalized to other PHs or other vegetable crops. For these reasons, we adopted a fully randomized experimental design based on two plant species, two salinity levels and five different treatments (four biostimulants and a negative control), focusing our investigations on biochemical and molecular parameters in a short-term experiment.

Materials and methods

Vegetal-derived biostimulants

Four protein hydrolysates (PHs) plus a control (consisting only of distilled water) were used in this experiment. Two of the biostimulants were commercial products resulting from enzymatic hydrolysis of legume-derived proteins: Trainer® (D) and Vegamin® (H) commercialized by Hello Nature USA Inc. (Anderson, IN 46016, US). The other two were provided by the Department of Agriculture and Forest Sciences (University of Tuscia, Italy) which were obtained by enzymatic hydrolysis of *Malvaceae* (C) and *Poaceae* (P) biomass, as previously described (Ceccarelli et al., 2021; Sorrentino et al., 2021).

The biostimulants were prepared at a concentration of 3 mL L^{-1} of water solution and then evaluated through foliar application. Plants were exposed to the biostimulants once a week until the harvest (Figure 1A).

Plant growth conditions and experimental design

Tomato (*Solanum. lycopersicum* L. cv MicroTom) and lettuce (*Lactuca. sativa* L. cv Aquino) plants were grown in 200 mL pots filled with 150 g of a substrate obtained by mixing sand and sieved peat (Substrate 2, Klasmann-Deilmann GmbH, Germany) in a proportion of 1:1 (*w/w*) ratio. Two hours before sowing, pots were irrigated with 40 mL of distilled water and afterwards two seeds were sown at a depth of 1 cm into each pot and placed into a climatic chamber (conditions: 14/10-h light/dark period, 24/19 °C, 250 µmol m^{-2} s^{-1} light intensity, and 70% relative humidity). After germination, seedlings were thinned to one plant per pot and irrigated twice a week with 40 mL of a modified Hoagland's solution (NS) composed as follows: 0.36 g L^{-1} Ca $(NO_3)_2$, 0.1 g L^{-1} KH_2PO_4, 0.80 g L^{-1} KNO_3, 0.04 g L^{-1} NH_4NO_3, 0.13 g L^{-1} $MgSO_4$, and 0.01 mg L^{-1} of Mikron fertilizer (Cifo Srl, Italy) (Figure 1A). At ten days after germination (DAG), when seedlings have reached the 2-true-leaf stage, salinity condition was imposed by irrigating plants with NS supplemented with NaCl at the final concentration of 120 mM for tomato plants or 80 mM for lettuce plants, as described by Sorrentino et al. (2022). Plants were subjected twice a week to salt application, resulting in a total of five applications throughout the whole experimental period (Figure 1A). Starting from 12 DAG, biostimulants were applied through foliar spraying once a week as described by (Zuluaga et al., 2022). A total of three foliar applications of PHs were done throughout the experiment (Figure 1A). Summarizing, plants were set in a 2 × 5 factorial experimental design completely randomized with two salt conditions: no salt (0 mM) and high salt (120 mM for tomato or 80 mM for lettuce); and four biostimulant treatments with the PHs (C, D, H and P) plus a Control treatment with distilled water (Figure 1B). Three biological replicates with two plants per replicate were performed for each treatment. At 28 DAG, plants were harvested: one plant of each biological was dried to a constant weight at 65°C following the determination of root dry weight (RDW) and shoot dry weight (SDW), while leaves from the remaining plant were immediately frozen in liquid nitrogen, then stored at -80°C until use.

Sodium and potassium content

Leaf tissues dried at 65°C were ground to a fine powder using Tissue Lyser II. Approximately 0.2–0.3 g of sample was weighed and acid digested with 69% ultrapure HNO_3 (Carlo Erba, Milano, Italy) in a single reaction chamber microwave digestion system (UltraWAVE, Milestone, Shelton, CT, USA). The digested samples were diluted to 2% HNO_3 with ultrapure grade water (18.2 MΩ·cm at 25°C), and then the concentration of Na and K was determined using an inductively coupled plasma–mass spectrometer (ICP-MS, iCAP™ RQ, Thermo Scientific). Element quantification was carried out using certified multi-element standards (CPI International, https://cpiinternational.com). NIST standard reference materials 1573a (tomato leaves) and 1570a

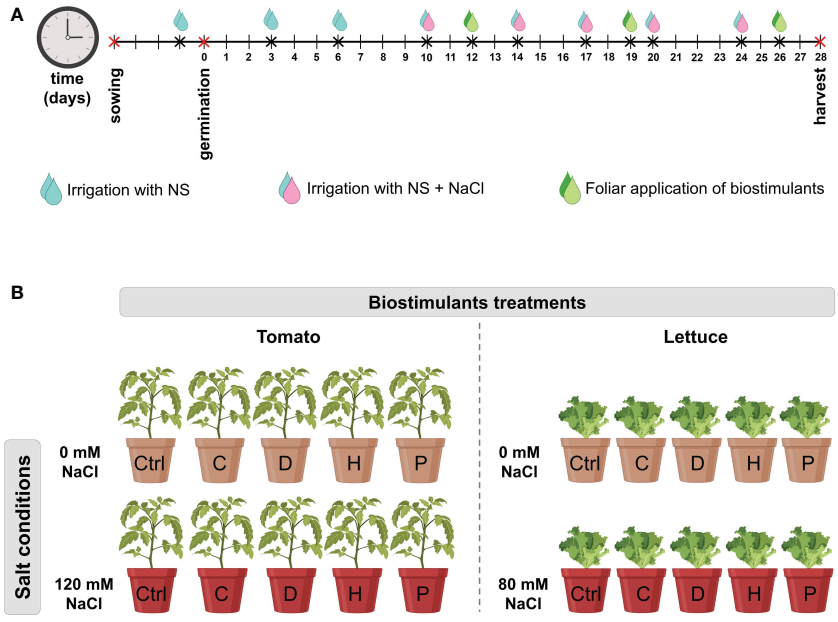

FIGURE 1
(A) Timeline of plant cultivation and treatments. Tomato and lettuce seeds were germinated for 5 days. After germination, seedlings were irrigated twice a week with 40 mL of NS. At 10 DAG, salinity condition was imposed by irrigating plants with NS supplemented with NaCl (120 mM for tomato and 80 mM for lettuce plants). Salt treatment was repeated twice a week. Starting from 12 DAG, biostimulants were foliarly applied once a week. Sampling was carried out at 28 DAG. **(B)** The experimental design of the present study. Plants were set in a 2 × 5 factorial experimental design completely randomized with two salt conditions: no salt (0 mM) and high salt (120 mM for tomato or 80 mM for lettuce); and four biostimulant treatments with the PHs (C, D, H and P) plus a Control (Ctrl) treatment with distilled water.

(spinach leaves) were used as external certified references, which were digested and analyzed the same way as the samples.

Proline content

Free proline content was determined *via* reaction with ninhydrin according to the method described by Bates et al. (1973). Briefly, 0.5 g of leaf samples frozen in liquid nitrogen were homogenized in 10 mL of 3% sulfosalicylic acid and centrifuged at 3000 x *g* at 4°C for 10 min. Two milliliters of supernatant were reacted with 2 mL of freshly prepared acid-ninhydrin reagent for 1 h at 90°C. The reaction was then stopped by an ice bath. The chromophore was extracted using 4 mL of toluene and the absorbance at 520 nm was recorded. The proline concentration was estimated through a calibration curve and data were expressed as μg proline per g fresh weight (μg g^{-1} FW).

Antioxidant enzyme activity

The enzymatic extract was prepared by grinding 0.5 g of frozen leaves in 5 mL of extraction buffer (100 mM potassium phosphate buffer, pH 7.5, containing 0.5 mM EDTA). The homogenate was centrifuged at 10,000 x *g* and 4°C for 10 min. The enzymatic extract was collected and subsequently used to determine APX, GPX, CAT, SOD and the total protein content determined by the Lowry method (Lowry et al., 1951) with bovine serum albumin as a standard curve.

Ascorbate peroxidase (EC 1.11.1.11) was assessed by following the consumption of ascorbate at 290 nm (Nakano and Asada, 1981). The APX activity was estimated based on the molar extinction coefficient of 2.8 mM^{-1} cm^{-1} and expressed in μmol ascorbate mg^{-1} protein min^{-1}. Guaiacol peroxidase (GPX, EC 1.11.1.7) activity was estimated by measuring the formation of tetraguaiacol at 470 nm (Castillo et al., 1984). The activity of the enzyme was calculated using the molar extinction coefficient of 26.6 mM^{-1} cm^{-1} and expressed in μmol tetraguaicol mg^{-1} protein min^{-1}. Catalase (CAT, EC 1.11.1.6) activity was determined by following the consumption of H_2O_2 at 240 nm (Aebi, 1984). The enzyme activity was calculated based on the molar extinction coefficient of 39.4 mM^{-1} cm^{-1} and expressed in μmol H_2O_2 mg^{-1} protein min^{-1}. Superoxide dismutase (SOD, EC 1.15.1.1) activity was measured at 560 nm using the photochemical reduction of nitroblue tetrazolium, NBT (Dhindsa et al., 1981). SOD activity was expressed on protein basis as units mg^{-1} protein. All the determinations have been performed on three independent biological replicates, whereby each biological replicate was formed by a pool of two plants.

Gene expression analysis

Leaf tissues frozen in liquid nitrogen were ground to a fine powder. Total RNA was extracted from 100 mg of ground leaves using the Spectrum Plant Total RNA Kit (Sigma- Aldrich, St. Louis, MO, USA) according to the manufacturer's instructions. The total RNA (1 μg) was treated with 10U of DNAse RQ1 to degrade possible DNA contamination, and cDNA was synthesized using the ImProm-II Reverse Transcription System (Promega, Madison, WI, USA) following the manufacturer's instructions. Gene-specific primers were designed for the target gene, as well as for the housekeeping gene, the elongation factor 1α (Supplementary Table 1). Quantitative real-time reverse transcription PCR (qRT-PCR) was carried out in triplicate with the following conditions: 5 min at 95°C, followed by 40 cycles at 95°C for 30 s and 55°C for 30 s. The housekeeping transcript was used to calculate the mean normalized expression value (MNE; (Simon, 2003)) for each sample and the relative expression ratio values were calculated by the $2^{-\Delta\Delta Ct}$ method according to Livak and Schmittgen (2001).

Statistical analysis

All the experimental data for both plant species (*S. lycopersicum* and *L. sativa*) were statistically subjected to two-way ANOVA using R software (version 4.0.3). The mean values were separated according to Tukey's HSD test with $p < 0.05$, and salinity levels effects were compared using the t-test. The following R packages were used for data visualization and statistical analyses: ggplot2, agricolae and ggpbur.

Results

Plant biomass

The biomass accumulation of both plant species was strongly influenced by salt stress. The results showed that dry matter accumulation in lettuce was more affected by salinity than in tomato plants. Moreover, the root system underwent a more pronounced decrease than the aerial parts, in both plant species. For instance, the root dry weight (RDW) of tomato under saline conditions, independently of the treatment applied, was significantly decreased by 58-65%, whilst in lettuce, the drop ranged between 47-72% compared to the no-salt condition (Table 1). On the other hand, the shoot dry weight (SDW) of tomato was reduced by about 28-42% under high salinity, whilst a decrement of 17-58% was observed in lettuce plants (Table 1). However, the application of PHs induced differential effects in each plant species, and they were dependent on the nature of the biostimulant applied and the salinity conditions. In the specific case of lettuce plants, all PHs applied stimulated the biomass accumulation in roots and shoots under high salinity compared to the saline control. Yet, biostimulant P induced the most remarkable effects enhancing RDW and SDW by more than 130%. Nonetheless, under no salt conditions, only biostimulant P induced the most significant effects in increasing lettuce biomass when compared to the untreated control (Table 1). Regarding tomato plants growing under salinity stress, only the application of PHs D and P significantly enhanced RDW (by 22% and 32%, respectively). At the same time, no significant effects were induced by the PHs on the SDW. However, under no-salt conditions, PHs D and P were also efficient in increasing RDW of tomato plants by about 20%. In contrast, C, H and P enhanced the accumulation of SDW by more than 15% compared to control plants (Table 1). In addition, as high

10.3389/fpls.2023.1077140

TABLE 1 Root dry weight (RDW), shoot dry weight (SDW) and root to shoot (R/S) ratio of tomato and lettuce grown under salinity stress and protein hydrolysates application.

Parameters	Salt levels	Tomato					Lettuce				
		Biostimulant treatment					Biostimulant treatment				
		Control	C	D	H	P	Control	C	D	H	P
RDW	No salt	0.099 Ab	0.110 Aab	0.119 Aa	0.106 Aab	0.120 Aa	0.047 Acd	0.040 Ad	0.055 Ab	0.051 Abc	0.073 Aa
	High salt	0.037 Bc	0.038 Bbc	0.045 Bab	0.044 Babc	0.049 Ba	0.013 Bd	0.021 Bbc	0.024 Bb	0.019 Bc	0.033 Ba
SDW	No salt	0.400 Ac	0.465 Aa	0.403 Abc	0.492 Aa	0.458 Aab	0.377 Ab	0.370 Ab	0.401 Ab	0.408 Ab	0.522 Aa
	High salt	0.287 B	0.289 B	0.266 B	0.286 B	0.291 B	0.159 Bd	0.307 Bb	0.292 Bb	0.237 Bc	0.365 Ba
R/S Ratio	No salt	0.248 Abc	0.236 Abc	0.295 Aa	0.216 Ac	0.263 Aab	0.124 Aab	0.109 Ab	0.138 Aa	0.133 Aa	0.139 Aa
	High salt	0.128 Bb	0.130 Bab	0.170 Ba	0.153 Bab	0.168 Bab	0.072 Bb	0.069 Bb	0.083 Bab	0.082 Bab	0.092 Ba

Differences between biostimulant treatments were determined using Tukey's HSD test, and significant differences ($p < 0.05$) are indicated by different lowercase letters when comparing means in rows. Salt level effects were compared using Student's t-test, and significant differences ($p < 0.05$) are indicated by different capital letters when comparing means in columns. No significant differences are indicated by omitting notation letters.

salt concentrations inhibited root growth more than shoot growth, the expected reduction of root-to-shoot ratio (R/S) was also observed in both plant species (Table 1). Nevertheless, tomato plants treated with biostimulant D presented a higher R/S ratio under both salinity conditions, whilst biostimulant P was notably better for lettuce plants.

Ion homeostasis

To investigate whether PHs application could mitigate salt stress in both plant species, we measured leaves' Na^+ and K^+ content. The salt stress significantly increased Na^+ content (ranging from 46% to 129%) and decreased K^+ content (ranging from 16% to 26%) in tomato under all treatments (Figures 2A, B). However, when PHs H and P were applied to NaCl-stressed tomato plants, there was a significant decrease in Na^+ content (by 12% and 25%, respectively) when compared to high salt control plants (Figure 2A), yet no remarkable differences were observed for K^+ concentration (Figure 2B).

On the other hand, in control lettuce plants, salt stress induced an increase of 246% in the Na^+ concentration compared to no salt plants; when considering the application of PHs, the most remarkable effect was produced by P, which reduced Na^+ concentration by about 21% compared to P-treated non-stressed plants (Figure 2D). Considering the data obtained in lettuce plants subjected to high salt stress, differential effects were triggered by the PHs application. In fact, PHs P and D reduced Na^+ concentration by about 69%, H by 56% and C by 34% compared to salt-stressed control plants (Figure 2D). In addition, under high salt conditions, K^+ concentration decreased by 15% in untreated-control plants and by 11% in P-treated plants (Figure 2E), whilst the application of C increased K^+ concentration by 28%, and no significant differences were observed for D and H, when compared to the same treatments under no-salt conditions (Figure 2E).

As a consequence of the changes in both elements induced by the use of different PHs, the Na^+/K^+ ratio of salt-stressed tomato plants significantly decreased in tomato plants treated with PHs H and P (by 12% and 23%, respectively) (Figure 2C), whereas for salt-stressed lettuce plants all PHs decreased the Na^+/K^+ ratio by 73% (D), 65% (P and H) and 45% (C), compared to NaCl-control plants (Figure 2F).

Osmolytes and antioxidative enzyme activities in leaves

The concentration of the osmolyte proline increased in the leaf tissue of both plant species when exposed to salinity stress (Figure 3). In salt-stressed tomato plants, proline concentration increased by about 100%, compared to non-stressed plants, independently of the PH applied (Figure 3A). On the other hand, in lettuce plants, salt stress induced an increase in the accumulation of proline by about 25-fold in untreated plants. However, the highest proline concentration was detected in salt-stressed lettuce treated with PHs D and P (increased by 200-fold and 90-fold, respectively) (Figure 3B). Interestingly, under non-saline conditions, the constitutive accumulation of proline in tomato plants was notably higher than in lettuce plants (by 80-fold). Moreover, the treatment of salt-stressed tomato plants with PHs did not induce significant effects in the accumulation of proline, while under no-salt conditions PHs C, D and H significantly increased this osmolyte compared to the corresponding control plants (Figure 3A). In salt-stressed lettuce plants, all PHs induced a significant increase of this osmolyte (ranging from 19-44%) compared to NaCl-control plants, whilst under normal conditions, only PHs C and H enhanced proline content (Figure 3B).

High salinity also stimulated the activity of antioxidant enzymes (CAT, APX, GPX and SOD) in leaves of both plant species, but APX and GPX were more enhanced in tomato, whereas CAT and APX were the most induced in lettuce (Table 2). In addition, the use of biostimulants promoted differential responses that were dependent on the plant species and the nature of the PHs applied. For instance, in lettuce plants grown under salinity stress, the use of PHs P and H significantly increased the activity of most of the antioxidant enzymes compared to untreated-control plants (Table 2), whereas in stressed-tomato plants each PH was efficient in enhancing the activity of a given enzyme.

PAL gene expression in leaves

Since phenylalanine ammonia lyase (PAL; EC 4.3.1.5) is a key upstream enzyme in synthesizing the majority of polyphenolic compounds involved in plant response to stresses (Hoffmann et al.,

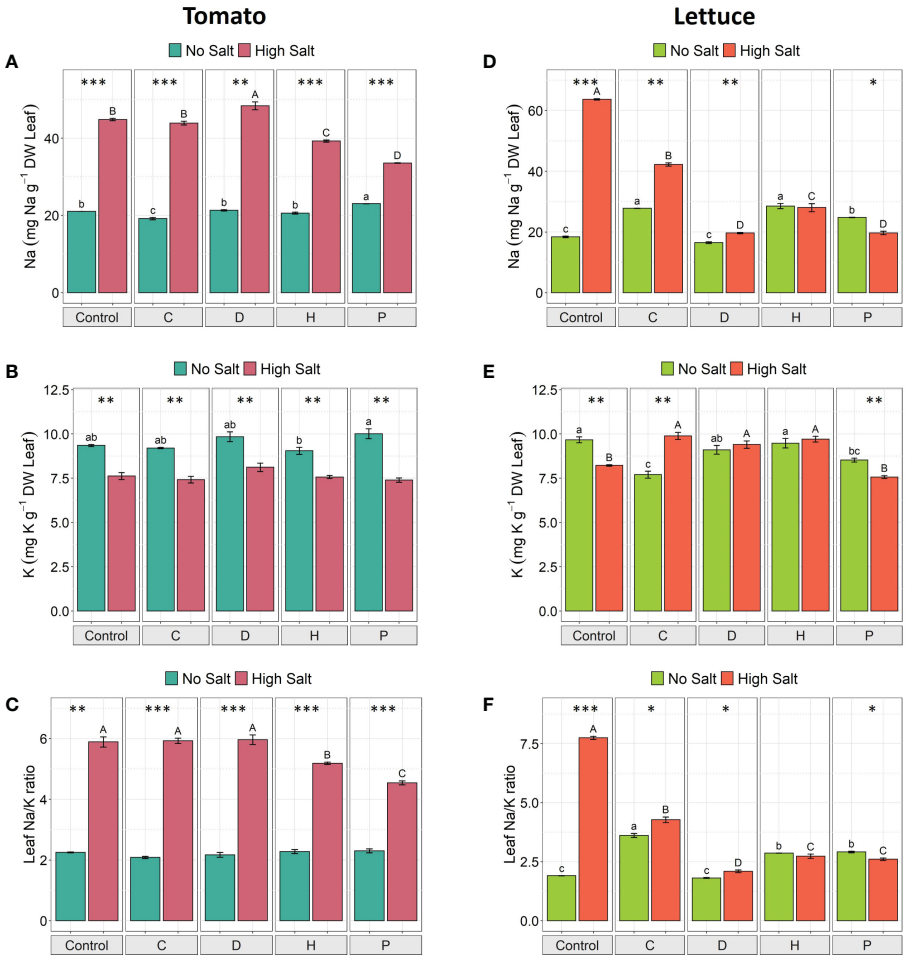

FIGURE 2
The concentration of Na^+, K^+ and Na^+/K^+ ratio in leaves of tomato **(A–C)** and lettuce **(D–F)** grown under salinity stress and protein hydrolysates application. Values are means ± SE. Lowercase letters compare treatments under no salt, and capital letters compare treatments under high salt. Equal letters correspond to average values that do not differ according to Tukey's HSD test ($p < 0.05$). Asterisks indicate significant differences between high and no salt, according to Student's *t*-test (*$p < 0.05$, **$p < 0.01$, ***$p < 0.001$).

2021), its transcriptional modulation was studied in order to shed light on its role in plant tolerance to high salinity conditions. The application of PHs influenced the *PAL* gene expression in both plant species subjected to either optimal or high salt conditions (Figure 4). In tomato plants grown under high NaCl, PHs C and D induced a slightly higher expression of the *PAL6* gene (1.3-fold) compared to control plants, albeit not significantly. However, under non-saline conditions, the biostimulant P was the only one to induce a higher

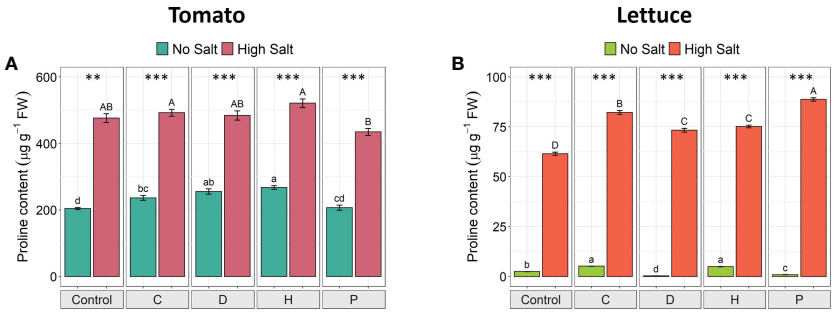

FIGURE 3
Effect of salinity and protein hydrolysates in the proline accumulation of tomato **(A)** and lettuce **(B)** plants. Values are means ± SE. Lowercase letters compare treatments under no salt, and capital letters compare treatments under high salt. Equal letters correspond to average values that do not differ according to Tukey's HSD test ($p < 0.05$). Asterisks indicate significant differences between high and no salt, according to Student's *t*-test (**$p < 0.01$, ***$p < 0.001$).

10.3389/fpls.2023.1077140

TABLE 2 Effects of salinity stress and protein hydrolysates application on antioxidant enzyme system in tomato and lettuce plants.

Antioxidant enzymes	Salt levels	Tomato					Lettuce				
		Biostimulant treatment					Biostimulant treatment				
		Control	C	D	H	P	Control	C	D	H	P
CAT	Low salt	5.52 Bb	5.92 Bb	8.86 Ba	6.72 Bb	8.73 Ba	4.28 Be	5.57 Bd	8.49 Bb	14.45 Ba	7.57 Bc
	High salt	18.35 Abc	22.17 Aa	19.77 Aab	16.53 Ac	22.05 Aa	28.52 Ab	31.48 Aab	32.30 Aa	32.69 Aa	32.13 Aa
APX	Low salt	194.67 Bb	216.95 Bab	259.11 Ba	195.55 Bb	252.89 Ba	177.33 B	176.19 B	179.51 B	198.28 B	197.06 B
	High salt	719.09 A	761.05 A	790.78 A	712.90 A	720.04 A	427.01 Ab	338.28 Ad	415.85 Abc	382.55 Ac	523.44 Aa
GPX	Low salt	171.16 Bb	191.76 Bab	211.38 Ba	140.08 Bc	167.69 Bbc	3.74 Bc	3.30 Bcd	2.85 Ba	6.46 Bd	5.26 Bb
	High salt	546.16 Ab	667.07 Aa	699.91 Aa	629.89 Aa	490.64 Ab	13.57 Ad	17.09 Ac	13.16 Ad	30.78 Aa	20.43 Ab
SOD	Low salt	1.31 Bb	1.36 Bb	1.63 Ba	1.05 Bc	1.70 Ba	0.71 Bb	0.64 Bb	0.66 Bb	1.10 Ba	1.13 Ba
	High salt	4.87 Aabc	4.83 Abc	5.20 Aab	5.47 Aa	4.55 Ac	2.60 Ab	2.11 Ac	3.27 Aa	3.43 Aa	3.16 Aa

Differences between biostimulant treatments were determined using Tukey's HSD test, and significant differences ($p < 0.05$) are indicated by different lowercase letters when comparing means in rows. Salt level effects were compared using Student's t-test and significant differences ($p < 0.05$) are indicated by different capital letters when comparing means in columns. No significant differences are indicated by omitting notation letter.

gene expression (1.4-fold) (Figure 4A). On the other hand, the application of P induced significant over-expression of *PAL2* in salt-stressed lettuce plants (1.7-fold), yet C and H also enhanced its expression (by ~1.4-fold), even though not significant when compared to the saline control. Under no salt conditions, all PHs downregulated the *PAL2* expression in lettuce leaves compared to the untreated control (Figure 4B).

PCA of plant responses to PHs application and salt stress

In order to better understand the influence of the single parameters recorded on the overall performance of plants subjected to the different treatments, a principal component analysis (PCA) considering both the agronomical and biochemical data was performed for each plant species. PCA confirmed that salt stress was the prevalent factor influencing the behavior of tomato and lettuce plants (Supplementary Figure S1). In this sense, to better understand the possible positive effects of PHs application, separated PCA have been carried out for the two plant species, keeping high salt and no salt conditions separated (Figure 5).

In tomato plants subjected to high salinity, the scatterplot obtained by combining the two principal components (PC1 and PC2) accounted for about 61% of the total variance and clearly showed the separation of the plants treated with PHs P and D along the PC1, with respect to a cluster formed by all the other samples (Figure 5A). For biostimulant P, the main drivers of the separation were the growth parameters and the CAT activity. At the same time, proline, GPX, Na^+/K^+ ratio (PC1) and K (PC2) were important to discriminate biostimulant D. Considering tomato grown under no-salt conditions (Figure 5B), the two principal components explained together about 70% of the total variance, showing that PHs D and P presented a similar effect on tomato plants mainly discriminated by the antioxidant enzymes, RDW, R/S ratio and K^+ content along PC1 axis. On the other hand, C and H biostimulants clustered very close to control samples, suggesting a milder effect on plants compared to the other PHs (Figure 5B).

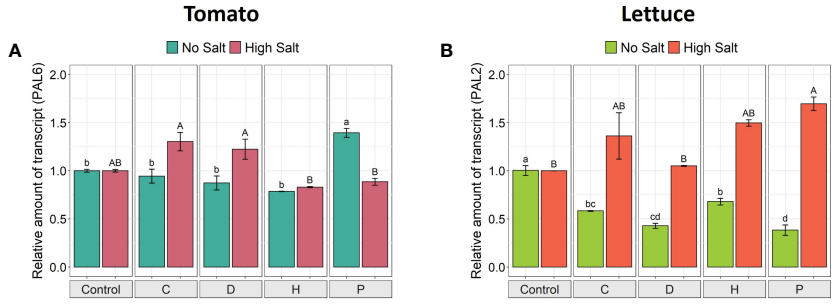

FIGURE 4
Gene expression analysis of *PAL6* in leaves of tomato **(A)** and *PAL2* in leaves of lettuce **(B)** grown under salinity stress and protein hydrolysates application. The expression levels of *PAL6* and *PAL2* genes were normalized to the expression levels of the elongation factor isoform 1-alpha (EF-1a) and the adenosine phosphoribosyl transferase (APT1), respectively. The relative expression ratios were calculated using the control treatment in each salinity condition as a calibrator sample. Values are means ± SE; n = 3. Lowercase letters compare treatments under no salt, and capital letters compare treatments under high salt. Equal letters correspond to average values that do not differ according to Tukey's HSD test ($p < 0.05$).

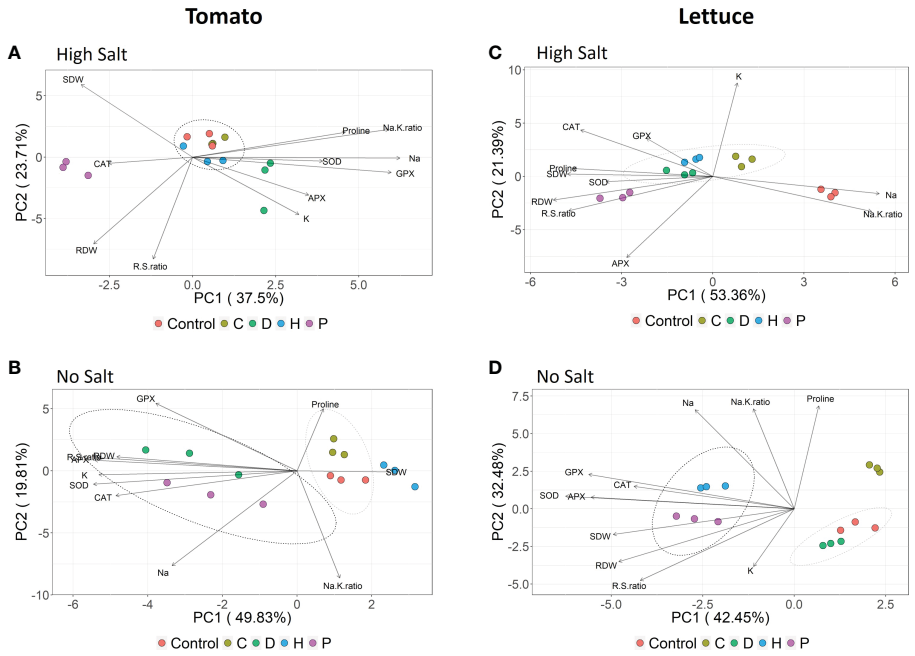

FIGURE 5
Principal component analysis (PCA) of major traits measured for tomato **(A, B)** and lettuce **(C, D)** summarizing the responses to vegetal-derived protein hydrolysates application (Control, C, D, H and P) under each salinity condition (no salt: 0 mM NaCl or high salt: 120 mM NaCl and 80 mM NaCl for tomato and lettuce, respectively).

In salt-stressed lettuce plants, the PCA produced a model in which the first two principal components, PC1 and PC2, accounted for about 53% and 21% of data variance, respectively (Figure 5C). Under this salinity condition, untreated-control plants were clearly separated along the PC1 from the PHs mainly due to Na^+ concentration and Na^+/K^+ ratio, whereas biostimulant P presented the most distinctive effect when compared to the other three PHs, mainly driven by the growth parameters and proline, as well as the antioxidant enzymes CAT and APX. Regarding the lettuce plants grown under no-salt conditions (Figure 5D), 75% of the total variance was explained by combining PC1 and PC2. The PHs P and H presented similar effects on lettuce plants under no saline conditions, strongly driven by the growth parameters and all antioxidant enzymes along the PC1 axis.

Discussion

Results here presented show that salinity stress shrank biomass accumulation of both vegetable species. However, this effect was particularly pronounced in lettuce. From a general point of view, it is well demonstrated that high salt concentrations within the plant tissues compromise the development of roots and leaves in most crops (Robin et al., 2016). Nevertheless, the severity of symptoms induced by salinity stress depends upon many factors, including species, genotype, phenological stage, salt concentration, and time span of plant exposure to the stress (Giordano et al., 2021). It is interesting to note that in this work the use of protein hydrolysates (PHs) induced a differential response in the plant growth according to the vegetable species, the salinity levels, and the origin of the PHs. In this respect, it should be noted that the bioactive potential of PHs in relation to root growth and leaf biomass is often ascribed to the stimulation of cell proliferation associated with the amino acids and peptides composing the PHs, which work as signaling molecules involved in the N metabolism (Caruso et al., 2019). All the four PHs supplied in the present work efficiently enhanced the growth of both root and shoot of salt-stressed lettuce plants, albeit the *Poaceae*-derived PH (P) induced more remarkable effect. On the other hand, none of the four tested PHs induced significant effects on leaves of salt-stressed tomato, whilst only D (Trainer®) and P improved root growth. Under abiotic stresses, PHs have been described to trigger several physiological and metabolic mechanisms, including plant hormone regulation, chlorophyll-related metabolism and stress-related metabolism (Lucini et al., 2015; Rouphael et al., 2017; Sorrentino et al., 2022). However, due to the variable composition of PHs, many crop systems respond differently to the biostimulant applied (Parađiković et al., 2019).

Previous studies have demonstrated that salt-tolerant species differ from more sensitive ones in preventing the accumulation of toxic salt levels in leaves (Munns, 2002). In the present work, both crop species showed an elevated Na^+ ion concentration in leaves, which led to ionic imbalance and decreased the concentration of K^+ ions. However, this effect was more marked in lettuce plants. Tomato and lettuce, featuring an EC_t of 2.5 and 2.0 dS m^{-1}, respectively, are considered moderately sensitive to salinity and show adaptive mechanisms to this abiotic stressor (Machado and Serralheiro, 2017). Nonetheless, variation in salt sensitivity is found between species and genotypes, mainly due to the ability to store Na^+ ions in leaves (Munns et al., 2016). Interestingly, all PHs reduced the concentration of Na^+ and Na^+/K^+ ratio in leaves of lettuce grown under high salinity, whereas only the PHs H and P produced the same effect in tomato. Indeed, maintaining the Na^+/K^+ ratio to minimal

values in leaves is an important indicator of salinity tolerance (Assaha et al., 2017), clearly suggesting active and differential roles of PHs in modulating ion homeostasis. In this sense, it has been previously reported that applying a plant-based biostimulant to chili pepper plant significantly alleviated the negative effects of salinity stress by rebalancing ions content and modulating phytohormones concentrations (Abou-Sreea et al., 2021).

Under salinity stress, plants can accumulate compatible solutes, such as proline, which play protective roles as an osmoprotectant, scavenging reactive oxygen species (ROS), stabilizing cellular structures and enzymes, and providing cellular redox balance (Meena et al., 2019). Although proline accumulation can be considered a general response to salinity in many plant species, its role in salinity tolerance can be ambiguous and strongly dependent on plant species (Arteaga et al., 2020). In this work, proline content in tomato plants grown under optimal conditions was constitutively higher than lettuce plants. However, under salinity stress, lettuce plants presented a higher accumulation, in terms of fold-change, of this osmolyte over tomato. Depending on the species involved and the severity and duration of the stress, proline content can be accumulated at significantly levels compared to non-stress conditions (Kavi Kishor and Sreenivasulu, 2014). In this context, it has been reported that salt-tolerant species are more efficient in maintaining cell osmolarity under saline conditions, whereas salt-sensitive species need to synthesize higher levels of proline to balance the intracellular osmotic potential (Chen et al., 2007; Kozminska et al., 2018). Therefore, our results suggest that lettuce is more sensitive to salt stress than tomato plants, albeit previous data consider them equally sensitive to salinity (Machado and Serralheiro, 2017). Furthermore, in salt-stressed tomato plants, the foliar application of PHs did not enhance the levels of proline, whereas in salt-stressed lettuce all PHs increased this osmolyte, indicating a correlation between salt-sensitivity and the beneficial effect of PHs. More precisely, the more salt-sensitive is a vegetable species, the higher is the ability of PHs to counteract the adverse effects of salinity.

It is well documented that, to deal with the oxidative damage induced by salinity stress, plants can activate the enzymatic antioxidant defense system represented by enzymes such as catalase (CAT), ascorbate peroxidase (APX), guaiacol peroxidase (GPX), and superoxide dismutase (SOD). In fact, they are all crucial in regulating and/or detoxifying harmful levels of reactive oxygen species (*i.e.*, H_2O_2, $O2^{\bullet-}$, $HO_2^{\bullet}$, $RO^{\bullet}$, $^{\bullet}OH$) (Hasanuzzaman et al., 2020) as a consequence of the stress. Results here presented show that the activities of the four enzymes were increased under high salinity and showed responses both plant species-specific and PH-related. It has been reported that an enhanced antioxidant defense system induced using biostimulants is directly involved in ROS scavenging and oxidative stress reduction in plants under salinity (Hasanuzzaman et al., 2021). Noteworthy, the specific use of PHs P (*Poaceae*-derived) and H (Vegamin®) showed greater potential in eliciting the antioxidant system in lettuce plants, whereas none of the tested PHs could contemporarily upregulate the activities of all the antioxidant enzymes in tomato plants. The fact that a specific PH induces a plant species-specific response in terms of enhanced activity of enzymatic antioxidants may be ascribable, at least in part, to the peptide components in the PH, acting as signal molecules in regulating physiological processes.

Overexpression of specific *PAL* gene isoforms has been reported to improve plant tolerance to several environmental stresses (Olsen et al., 2008; Kim and Hwang, 2014; Zhang et al., 2018). In the present work, when high salinity stress was imposed, some PHs up-regulated the expression of *PAL6* and *PAL2* in tomato and lettuce plants, respectively, but these responses were dependent on the vegetable species and the nature of the biostimulant applied. These results agree with other studies, which have also reported that using plant-based biostimulants can enhance the transcription of a set of stress-related genes, including *PAL* isoforms (Ertani et al., 2011; Ertani et al., 2013; Trevisan et al., 2019). Increased *PAL* activity is generally correlated with the increased production of phenylpropanoids and flavonoids (Vogt, 2010), which are believed to play a key role in plant stress protection by regulating the antioxidant system, photosynthetic system, plasma membrane integrity, and gene expression levels (Yaqoob et al., 2022).

The multivariate statistical analyses further demonstrated the variability observed in the response of the individual vegetable species to biostimulants application under a given salinity condition. All four tested PHs prompted the amelioration of NaCl-induced toxicity in lettuce plants. Yet, the *Poaceae*-derived biostimulant (P) showed the most remarkable effect associated with multiple mechanisms, including enhanced biomass accumulation, improved antioxidant defense machinery, and balanced ionic content. Under non-stress conditions, only P and H (Vegamin®) presented promising effects in enhancing lettuce growth and health. On the other hand, applying P and D (Trainer®) allowed tomato plants to cope with the adverse effects of salinity through different ways of action: while P stimulated plant growth, D activated the antioxidant system and ion homeostasis. The same two PHs also contributed to plant growth and the general fitness of tomato under no-salt conditions. Indeed, the differential effectiveness of plant-derived PHs can be ascribed to either synergistic or antagonistic effects of several bioactive molecules that are inherently present in the mixtures used (Bulgari et al., 2019). Therefore, the biostimulant properties of protein hydrolysates under normal or saline conditions seem to be strongly correlated to their origin and, thus, their composition, as reported in previous comparative studies using plant-derived biostimulants (Abdel Latef et al., 2017; Abou-Sreea et al., 2021).

Yet, it is very important to further highlight the demonstrated role of PHs in mitigating the harmful effects of abiotic stresses, which are predicted to threaten the agricultural production in the next years. Indeed, the regular application of these natural substances obtained by the valorization of waste biomass could represent on one side a virtuous example of circular economy and, on the other hand, they might constitute an innovative and sustainable agricultural approach.

Conclusions

The findings provided by this study demonstrate that foliar application of vegetal-derived protein hydrolysates to two different plant species grown under contrasting saline conditions effectively attenuated salinity stress damage to different extents. Our results demonstrated that, albeit being previously assessed as equally

sensitive, lettuce plants showed less tolerance to salt stress with respect to tomato plants. In addition, the effectiveness of PHs in counteracting the toxic effects of salinity was more evident in lettuce plants, *i.e.*, the most sensitive of the two vegetables used in this study. Nonetheless, we also demonstrated that both the botanical origin and the composition of PHs play a major role in the biostimulants effects on plant growth and stress amelioration. Yet, the *Poaceae*-derived (P) and Trainer® (D) were revealed as the most promising PHs for the amelioration of salt stress in both vegetable species. Overall, the evidence gathered strongly suggests that, to completely exploit the biostimulant potential of PHs in the context of specific abiotic stresses, the correct combination of plant species and PHs needs to be carefully considered. To this purpose, a deeper understanding of the mechanisms underlying the PHs effects on crops represents a fundamental step also for a more focused, efficient, and large-scale use of these natural products in a context of a continuously more sustainable and resilient agriculture.

Data availability statement

The original contributions presented in the study are included in the article/Supplementary Material. Further inquiries can be directed to the corresponding authors.

Author contributions

MYAZ, SC, and YP conceived the work and designed the experiment. MYAZ and SM carried out the experiments and generated the data. MYAZ and YP analyzed the data. MYAZ wrote the first draft of the manuscript, which was intensively edited by all authors. MYAZ, LL, YR, GC, SC, and YP reviewed the manuscript and carried out the English edition. All authors contributed to the article and approved the submitted version.

Funding

This work was financially supported by the Italian Ministry of Education, University and Research (MIUR) through the project PHOBOS coded 2017FYBLPP and by the Open Access Publishing Fund of the Free University of Bozen-Bolzano.

Conflict of interest

The authors declare that the research was conducted in the absence of any commercial or financial relationships that could be construed as a potential conflict of interest.

Publisher's note

All claims expressed in this article are solely those of the authors and do not necessarily represent those of their affiliated organizations, or those of the publisher, the editors and the reviewers. Any product that may be evaluated in this article, or claim that may be made by its manufacturer, is not guaranteed or endorsed by the publisher.

Supplementary material

The Supplementary Material for this article can be found online at: https://www.frontiersin.org/articles/10.3389/fpls.2023.1077140/full#supplementary-material

References

Abdel Latef, A. A. H., Srivastava, A. K., Saber, H., Alwaleed, E. A., and Tran, L. S. P. (2017). Sargassum muticum and jania rubens regulate amino acid metabolism to improve growth and alleviate salinity in chickpea. *Sci. Rep.* 7, 1–12. doi: 10.1038/s41598-017-07692-w

Abiala, M. A., Abdelrahman, M., Burritt, D. J., and Tran, L. S. P. (2018). Salt stress tolerance mechanisms and potential applications of legumes for sustainable reclamation of salt-degraded soils. *L. Degrad. Dev.* 29, 3812–3822. doi: 10.1002/ldr.3095

Abou-Sreea, A. I. B., Azzam, C. R., Al-Taweel, S. K., Abdel-Aziz, R. M., Belal, H. E. E., Rady, M. M., et al. (2021). Natural biostimulant attenuates salinity stress effects in chili pepper by remodeling antioxidant, ion, and phytohormone balances, and augments gene expression. *Plants* 10, 1–24. doi: 10.3390/plants10112316

Aebi, H. (1984). [13] catalase in vitro. *Methods Enzymol.* 105, 121–126. doi: 10.1016/S0076-6879(84)05016-3

Alam, M. S., Tester, M., Fiene, G., and Mousa, M. A. A. (2021). Early growth stage characterization and the biochemical responses for salinity stress in tomato. *Plants* 10, 1–20. doi: 10.3390/plants10040712

Arteaga, S., Yabor, L., Díez, M. J., Prohens, J., Boscaiu, M., and Vicente, O. (2020). The use of proline in screening for tolerance to drought and salinity in common bean (Phaseolus vulgaris l.) genotypes. *Agronomy* 10, 1–16. doi: 10.3390/agronomy10060817

Assaha, D. V. M., Ueda, A., Saneoka, H., Al-Yahyai, R., and Yaish, M. W. (2017). The role of na+ and k+ transporters in salt stress adaptation in glycophytes. *Front. Physiol.* 8. doi: 10.3389/fphys.2017.00509

Bates, L., Waldren, R., and Teare, I. (1973). Rapid determination of free proline for water-stress studies. *Plant Soil* 39, 205–207.

Bavaresco, L., Lucini, L., Squeri, C., Zamboni, M., and Frioni, T. (2020). Protein hydrolysates modulate leaf proteome and metabolome in water-stressed grapevines. *Sci. Hortic. (Amsterdam).* 270, 109413. doi: 10.1016/j.scienta.2020.109413

Behera, T. K., Krishna, R., Ansari, W. A., Aamir, M., Kumar, P., Kashyap, S. P., et al. (2022). Approaches involved in the vegetable crops salt stress tolerance improvement: Present status and way ahead. *Front. Plant Sci.* 12. doi: 10.3389/fpls.2021.787292

Bulgari, R., Franzoni, G., and Ferrante, A. (2019). Biostimulants application in horticultural crops under abiotic stress conditions. *Agronomy* 9, 1–30. doi: 10.3390/agronomy9060306

Caruso, G., De Pascale, S., Cozzolino, E., Giordano, M., El-Nakhel, C., Cuciniello, A., et al. (2019). Protein hydrolysate or plant extract-based biostimulants enhanced yield and quality performances of greenhouse perennial wall rocket grown in different seasons. *Plants* 8, 1–18. doi: 10.3390/plants8070208

Castillo, F. J., Penel, C., and Greppin, H. (1984). Peroxidase release induced by ozone in sedum album leaves. involvement of Ca2+. *Plant Physiol.* 74, 846–851. doi: 10.1104/pp.74.4.846

Ceccarelli, A. V., Miras-moreno, B., Buffagni, V., Senizza, B., Pii, Y., Cardarelli, M., et al. (2021). Foliar application of different vegetal-derived protein hydrolysates distinctively modulates tomato root development and metabolism. *Plants* 10, 1–14. doi: 10.3390/plants10020326

Chen, Z., Cuin, T. A., Zhou, M., Twomey, A., Naidu, B. P., and Shabala, S. (2007). Compatible solute accumulation and stress-mitigating effects in barley genotypes contrasting in their salt tolerance. *J. Exp. Bot.* 58, 4245–4255. doi: 10.1093/jxb/erm284

Colla, G., Hoagland, L., Ruzzi, M., Cardarelli, M., Bonini, P., Canaguier, R., et al. (2017). Biostimulant action of protein hydrolysates: unraveling their effects on plant physiology and microbiome. *Front. Plant Sci.* 8. doi: 10.3389/fpls.2017.02202

Dhindsa, R. S., Plumb-dhindsa, P., and Thorpe, T. A. (1981). Leaf senescence: correlated with increased levels of membrane permeability and lipid peroxidation, and

decreased levels of superoxide dismutase and catalase. *J. Exp. Bot.* 32, 93–101. doi: 10.1093/jxb/32.1.93

Di Mola, I., Conti, S., Cozzolino, E., Melchionna, G., Ottaiano, L., Testa, A., et al. (2021). Plant-based protein hydrolysate improves salinity tolerance in hemp: agronomical and physiological aspects. *Agronomy* 11, 1–18. doi: 10.3390/agronomy11020342

Ertani, A., Schiavon, M., Altissimo, A., Franceschi, C., and Nardi, S. (2011). Phenol-containing organic substances stimulate phenylpropanoid metabolism in zea mays. *J. Plant Nutr. Soil Sci.* 174, 496–503. doi: 10.1002/jpln.201000075

Ertani, A., Schiavon, M., Muscolo, A., and Nardi, S. (2013). Alfalfa plant-derived biostimulant stimulate short-term growth of salt stressed *Zea mays* l. plants. *Plant Soil* 364, 145–158. doi: 10.1007/s11104-012-1335-z

Fariduddin, Q., Zaid, A., and Mohammad, F. (2019). "Plant growth regulators and salt stress: mechanism of tolerance trade-off," in *Salt stress, microbes, and plant interactions: causes and solution*. Ed. M. S. Akhtar (Singapore: Springer Nature), 91–110. doi: 10.1007/978-981-13-8801-9

Giordano, M., Petropoulos, S. A., and Rouphael, Y. (2021). Response and defence mechanisms of vegetable crops against drought, heat and salinity stress. *Agric* 11, 1–30. doi: 10.3390/agriculture11050463

Hasanuzzaman, M., and Fujita, M. (2022). Plant responses and tolerance to salt stress: Physiological and molecular interventions. *Int. J. Mol. Sci.* 23, 1–6. doi: 10.3390/ijms23094810

Hasanuzzaman, M., Bhuyan, M. H. M. B., Zulfiqar, F., Raza, A., Mohsin, S. M., Al Mahmud, J., et al. (2020). Reactive oxygen species and antioxidant defense in plants under abiotic stress: Revisiting the crucial role of a universal defense regulator. *Antioxidants* 9, 1–52. doi: 10.3390/antiox9080681

Hasanuzzaman, M., Parvin, K., Bardhan, K., Nahar, K., Anee, T. I., Masud, A. A. C., et al. (2021). Biostimulants for the regulation of reactive oxygen species metabolism in plants under abiotic stress. *Cells* 10, 1–29. doi: 10.3390/cells10102537

Hoffmann, J., Berni, R., Sutera, F., Gutsch, A., Hausman, J., Saffie-siebert, S., et al. (2021). The effects of salinity on the anatomy and gene expression patterns in leaflets of tomato cv. micro-tom. *Genes (Basel).* 12, 1/17. doi: 10.3390/genes12081165

Ismail, A., Takeda, S., and Nick, P. (2014). Life and death under salt stress: Same players, different timing? *J. Exp. Bot.* 65, 2963–2979. doi: 10.1093/jxb/eru159

Kavi Kishor, P. B., and Sreenivasulu, N. (2014). Is proline accumulation per se correlated with stress tolerance or is proline homeostasis a more critical issue? *Plant Cell Environ.* 37, 300–311. doi: 10.1111/pce.12157

Kim, D. S., and Hwang, B. K. (2014). An important role of the pepper phenylalanine ammonia-lyase gene (PAL1) in salicylic acid-dependent signalling of the defence response to microbial pathogens. *J. Exp. Bot.* 65, 2295–2306. doi: 10.1093/jxb/eru109

Kozminska, A., Al Hassan, M., Hanus-Fajerska, E., Naranjo, M. A., Boscaiu, M., and Vicente, O. (2018). Comparative analysis of water deficit and salt tolerance mechanisms in silene. *South Afr. J. Bot.* 117, 193–206. doi: 10.1016/j.sajb.2018.05.022

Livak, K. J., and Schmittgen, T. D. (2001). Analysis of relative gene expression data using real-time quantitative PCR and the 2-ΔΔCT method. *Methods* 25, 402–408. doi: 10.1006/meth.2001.1262

Lowry, O. H., Rosebrough, N. J., Farr, A. L., and Randall, R. J. (1951). Protein measurement with the folin phenol reagent. *J. Biol. Chem.* 193, 265–275. doi: 10.1016/s0021-9258(19)52451-6

Lucini, L., Rouphael, Y., Cardarelli, M., Canaguier, R., Kumar, P., and Colla, G. (2015). The effect of a plant-derived biostimulant on metabolic profiling and crop performance of lettuce grown under saline conditions. *Sci. Hortic. (Amsterdam).* 182, 124–133. doi: 10.1016/j.scienta.2014.11.022

Machado, R. M. A., and Serralheiro, R. P. (2017). Soil salinity: Effect on vegetable crop growth. management practices to prevent and mitigate soil salinization. *Horticulturae* 3, 1–13. doi: 10.3390/horticulturae3020030

Meena, M., Divyanshu, K., Kumar, S., Swapnil, P., Zehra, A., Shukla, V., et al. (2019). Regulation of l-proline biosynthesis, signal transduction, transport, accumulation and its vital role in plants during variable environmental conditions. *Heliyon* 5, e02952. doi: 10.1016/j.heliyon.2019.e02952

Munns, R. (2002). Comparative physiology of salt and water stress. *Plant Cell Environ.* 25, 239–250. doi: 10.1046/j.0016-8025.2001.00808.x

Munns, R., James, R. A., Gilliham, M., Flowers, T. J., and and Colmer, T. D. (2016). Tissue tolerance: an essential but elusive trait for salt-tolerant crops. *Funct. Plant Biol.* 43, 1103–1113. doi: 10.1071/FP16187

Nakano, Y., and Asada, K. (1981). Hydrogen peroxide is scavenged by ascorbate-specific peroxidase in spinach chloroplasts. *Plant Cell Physiol.* 22, 867–880. doi: 10.1093/oxfordjournals.pcp.a076232

Nguyen, D., Rieu, I., Mariani, C., and van Dam, N. M. (2016). How plants handle multiple stresses: hormonal interactions underlying responses to abiotic stress and insect herbivory. *Plant Mol. Biol.* 91, 727–740. doi: 10.1007/s11103-016-0481-8

Olsen, K. M., Lea, U. S., Slimestad, R., Verheul, M., and Lillo, C. (2008). Differential expression of four *Arabidopsis PAL* genes; *PAL1* and *PAL2* have functional specialization in abiotic environmental-triggered flavonoid synthesis. *J. Plant Physiol.* 165, 1491–1499. doi: 10.1016/j.jplph.2007.11.005

Parađiković, N., Teklić, T., Zeljković, S., Lisjak, M., and Špoljarević, M. (2019). Biostimulants research in some horticultural plant species–a review. *Food Energy Secur.* 8, 1–17. doi: 10.1002/fes3.162

Robin, A. H. K., Matthew, C., Uddin, M. J., and Bayazid, K. N. (2016). Salinity-induced reduction in root surface area and changes in major root and shoot traits at the phytomer level in wheat. *J. Exp. Bot.* 67, 3719–3729. doi: 10.1093/jxb/erw064

Rouphael, Y., Cardarelli, M., Bonini, P., and Colla, G. (2017). Synergistic action of a microbial-based biostimulant and a plant derived-protein hydrolysate enhances lettuce tolerance to alkalinity and salinity. *Front. Plant Sci.* 8. doi: 10.3389/fpls.2017.00131

Sadiq, Y., Zaid, A., and Khan, M. A. (2020). "Adaptive physiological responses of plants under abiotic stresses: role of phytohormones," in *Plant ecophysiology and adaptation under climate change: mechanisms and perspectives I*. Ed. M. Hasanuzzaman (Singapore: Springer Nature), 797–824. doi: 10.1007/978-981-15-2156-0

Shin, Y. K., Bhandari, S. R., Jo, J. S., Song, J. W., Cho, M. C., Yang, E. Y., et al. (2020). Response to salt stress in lettuce: Changes in chlorophyll fluorescence parameters, phytochemical contents, and antioxidant activities. *Agronomy* 10, 1–16. doi: 10.3390/agronomy10111627

Simon, P. (2003). Q-gene: processing quantitative real-time RT-PCR data. *Bioinformatics* 19, 1439–1440. doi: 10.1093/bioinformatics/btg157

Sorrentino, M., De Diego, N., Ugena, L., Spíchal, L., Lucini, L., Miras-Moreno, B., et al. (2021). Seed priming with protein hydrolysates improves *Arabidopsis* growth and stress tolerance to abiotic stresses. *Front. Plant Sci.* 12. doi: 10.3389/fpls.2021.626301

Sorrentino, M., Panzarová, K., Spyroglou, I., Spíchal, L., Buffagni, V., Ganugi, P., et al. (2022). Integration of phenomics and metabolomics datasets reveals different mode of action of biostimulants based on protein hydrolysates in *Lactuca sativa* l. and *Solanum lycopersicum* l. under salinity. *Front. Plant Sci.* 12. doi: 10.3389/fpls.2021.808711

Trevisan, S., Manoli, A., and Quaggiotti, S. (2019). A novel biostimulant, belonging to protein hydrolysates, mitigates abiotic stress effects on maize seedlings grown in hydroponics. *Agronomy* 9, 1–16. doi: 10.3390/agronomy9010028

Vaseva, I. I., Simova-Stoilova, L., Kostadinova, A., Yuperlieva-Mateeva, B., Karakicheva, T., and Vassileva, V. (2022). Heat-Stress-Mitigating effects of a protein-Hydrolysate-Based biostimulant are linked to changes in protease, DHN, and HSP gene expression in maize. *Agronomy* 12, 1–20. doi: 10.3390/agronomy12051127

Vogt, T. (2010). Phenylpropanoid biosynthesis. *Mol. Plant* 3, 2–20. doi: 10.1093/mp/ssp106

Yaqoob, U., Jan, N., Raman, P. V., Siddique, K. H. M., and John, R. (2022). Crosstalk between brassinosteroid signaling, ROS signaling and phenylpropanoid pathway during abiotic stress in plants: Does it exist? *Plant Stress* 4, 100075. doi: 10.1016/j.stress.2022.100075

Zaid, A., and Wani, S. H. (2019). "Reactive oxygen species generation, scavenging and signaling in plant defense responses," in *Bioactive molecules in plant defense: signaling in growth and stress*. Eds. S. Jogaiah and M. Abdelrahman (Switzerland: Springer Nature), 111–132. doi: 10.1007/978-3-030-27165-7

Zaid, A., Mushtaq, M., and Wani, S. H. (2021). "Interactions of phytohormones with abiotic stress factors under changing climate," in *Frontiers in plant-soil interaction*. Eds. T. Aftab and K. R. Hakeem (Elsevier Inc), 221–236. doi: 10.1016/b978-0-323-90943-3.00010-9

Zhang, J., Zeng, L., Chen, S., Sun, H., and Ma, S. (2018). Transcription profile analysis of *Lycopersicum esculentum* leaves, unravels volatile emissions and gene expression under salinity stress. *Plant Physiol. Biochem.* 126, 11–21. doi: 10.1016/j.plaphy.2018.02.016

Zhu, J. K. (2016). Abiotic stress signaling and responses in plants. *Cell* 167, 313–324. doi: 10.1016/j.cell.2016.08.029.Abiotic

Zuluaga, M. Y. A., Miras-Moreno, B., Monterisi, S., Rouphael, Y., Colla, G., Lucini, L., et al. (2022). Integrated metabolomics and morpho-biochemical analyses reveal a better performance of *Azospirillum brasilense* over plant-derived biostimulants in counteracting salt stress in tomato. *Int. J. Mol. Sci.* 23, 1–19. doi: 10.3390/ijms232214216

frontiers | Frontiers in Microbiology

TYPE Original Research
PUBLISHED 24 February 2023
DOI 10.3389/fmicb.2023.1129042

OPEN ACCESS

EDITED BY
Maurizio Ruzzi,
University of Tuscia,
Italy

REVIEWED BY
César Marín,
Santo Tomás University,
Chile
Sara Fareed Mohamed Wahdan,
Suez Canal University,
Egypt
Marta Gallart,
Commonwealth Scientific and Industrial Research Organisation (CSIRO), Australia

*CORRESPONDENCE
Hong Li
✉ lih5176@126.com

SPECIALTY SECTION
This article was submitted to Microbe and Virus Interactions with Plants, a section of the journal Frontiers in Microbiology

RECEIVED 21 December 2022
ACCEPTED 06 February 2023
PUBLISHED 24 February 2023

CITATION
Sun N, Zhang W, Liao S and Li H (2023) Is foliar spectrum predictive of belowground bacterial diversity? A case study in a peach orchard. *Front. Microbiol.* 14:1129042. doi: 10.3389/fmicb.2023.1129042

Is foliar spectrum predictive of belowground bacterial diversity? A case study in a peach orchard

Na Sun[1], Weiwei Zhang[2], Shangqiang Liao[1] and Hong Li[1]*

[1]Institute of Plant Nutrition, Resources and Environment, Beijing Academy of Agriculture and Forestry Sciences, Beijing, China, [2]Institute of Grassland, Flowers and Ecology, Beijing Academy of Agriculture and Forestry Sciences, Beijing, China

Rhizosphere bacteria can have wide-ranging effects on their host plants, influencing plant biochemical and structural characteristics, and overall productivity. The implications of plant-microbe interactions provides an opportunity to interfere agriculture ecosystem with exogenous regulation of soil microbial community. Therefore, how to efficiently predict soil bacterial community at low cost is becoming a practical demand. Here, we hypothesize that foliar spectral traits can predict the diversity of bacterial community in orchard ecosystem. We tested this hypothesis by studying the ecological linkages between foliar spectral traits and soil bacterial community in a peach orchard in Yanqing, Beijing in 2020. Foliar spectral indexes were strongly correlated with alpha bacterial diversity and abundant genera that can promote soil nutrient conversion and utilization, such as *Blastococcus*, *Solirubrobacter,* and *Sphingomonas* at fruit mature stage. Certain unidentified or relative abundance <1% genera were also associated with foliar spectral traits. We selected specific indicators (photochemical reflectance index, normalized difference vegetable index, greenness index, and optimized soil-adjusted vegetation index) of foliar spectral indexes, alpha and beta diversities of bacterial community, and quantified the relations between foliar spectral traits and belowground bacterial community *via* SEM. The results of this study indicated that foliar spectral traits could powerfully predict belowground bacterial diversity. Characterizing plant attributes with easy-accessed foliar spectral indexes provides a new thinking in untangling the complex plant-microbe relationship, which could better cope with the decreased functional attributes (physiological, ecological, and productive traits) in orchard ecosystem.

KEYWORDS

foliar spectral traits, plant productivity, fruit quality, bacterial diversity, soil conditioner

1. Introduction

1.1. The interaction between plant and soil microbial community

Plants, microorganisms, and soils interact with each other and unite biotic and abiotic factors into a living complexity *via* material cycling and energy flow in the terrestrial ecosystem (Wardle et al., 2004; Bardgett et al., 2006; Bardgett and Van der Putten, 2014). The interactions between plants and soil biota exert influences on ecosystem functioning and plant community (Fierer et al., 2009; Sul et al., 2013; Tedersoo et al., 2014; Kaiser et al., 2016), in undescribed and diverse ways that were poorly understood to date (Sul et al., 2013). This has induced great

enthusiasm of researchers into interactions between aboveground plant productivity and belowground ecological functioning (Bardgett and Van der Putten, 2014; Leff et al., 2018; Cavender-Bares et al., 2022). Individual plant species can greatly impact soil microbial communities (Bardgett et al., 1999; Berg, 2009). Growing evidence showed discrepancies in soil bacterial and fungal communities that were linked to plant community composition at landscape (Grayston et al., 2001; de Vries et al., 2012) and global scales (Prober et al., 2015) in recent decades. Moreover, strong correlations between individual plant species and soil fungal (Lekberg and Waller, 2006), bacterial (Berg, 2009), and nematode (Bezemer et al., 2010) communities were observed in previous studies. However, it remains unclear that whether these correlations were driven by shared environmental preferences or by the direct influence from locally dominant plant species. Furthermore, plants affect soil microbial community in numerous ways, and it is not clear whether and what plant attributes could be used to predict soil microbial community (Leff et al., 2018; Cavender-Bares et al., 2022).

1.2. Plant traits characterize soil microbial community

The difficulty in understanding what controls co-distribution of plants and soil microbes is that plants exert influences on while subjecting to impacts from soil microbial community. The complex interactions pose an obstacle in understanding the co-distribution of plants and soil microbes. For instance, plants were reported associated with a nonrandom subset of soil microbes within distinct ecosystems (Gottel et al., 2011; Lundberg et al., 2012; Sul et al., 2013; Shi et al., 2015), while soil microbes can be differentiated within co-occurring plant species (Ishida et al., 2007; Bonito et al., 2014; Burns et al., 2015) or even different individuals within the same species (Massenssini et al., 2015; Gehring et al., 2016; Wagner et al., 2016). It has been observed that soil biota was more responsive to key functional traits of plants than to plant diversity. Foliar traits, such as biochemical and structural characteristics (Violle et al., 2007), were indicative for plant strategies (Wright et al., 2004), plant responses to environmental pressures (Garnier et al., 2007), and ecosystem processes and services (Díaz and Cabido, 2001; Lavorel and Garnier, 2002; Lavorel et al., 2011). Therefore, ecosystem management and studies are increasingly using foliar traits (Kokaly et al., 2003; Douma et al., 2012). However, the conditional acquisition of essential foliar traits is costly, time-consuming, and notoriously difficult to acquire, especially in remote areas (Schweiger et al., 2017).

1.3. Foliar spectral traits and their applications

The distinct spectral responses of vegetation are determined by biochemical and structural traits of plant tissues, and the three-dimensional structure of the canopy, which could be predicted by imaging spectroscopy that captures the spectral response in narrow, spectrally contiguous bands (Schaepman, 2007; Sul et al., 2013; Asner et al., 2017). Certain spectral bands were proved sensitive to biochemical and structural traits of plant tissues (Curran, 1989). For instance, foliar trait could influence its spectral properties: reflectance, transmittance, and absorbance of light (Ustin et al., 2009; Sul et al., 2013; Schneider et al., 2017; Schweiger et al., 2018). Hence, by measuring foliar spectral properties using, for example, spectroscopy (many adjacent spectral bands with high spectral resolution), foliar traits may be approximated easily and low-cost (Sul et al., 2013). Foliar spectral properties determined by a field spectrometer or airborne remote sensing have been widely used for individual sunlit top of canopy leaves in forest ecosystem (Asner et al., 2011; Doughty et al., 2017), and aboveground biomass of prairie ecosystems (Cavender-Bares et al., 2021). Little is known about the spectral properties in orchard ecosystem (Liu, 2022), which harbor a diverse microbial community that can be affected by tillage, microbicide application, soil fumigation, and fertilization (Peck et al., 2011; Sul et al., 2013; Wang et al., 2017; Liang et al., 2018). Monitoring plant (community) attributes has dramatically improved in recent decades with advances in fine-grain mapping of canopy structure and chemistry (Cavender-Bares et al., 2022), which could benefit the investigation of plant-microbe relationship in the orchard ecosystem.

Considering the feedback process between orchard ecosystem productivity and belowground bacterial composition and diversity, we hypothesized that plant productivity of orchard ecosystem would be detectable with field spectrometer and could be used to predict belowground bacterial diversity. To test this hypothesis, we adopted root-zone ecological restoration practices (RERP) with soil conditioner or organic fertilizer at the end of growing season to realize differentiated soil bacterial communities in a peach orchard in Beijing. Our previous results demonstrated that RERP increased bacterial diversity and altered bacterial taxonomy and metabolic functions *via* improved soil properties (balanced nutrients, decreased bulk density, and increased water holding capacity) at soil depth of 20–40 cm (Sun et al., 2022). In this study, soil bacterial diversity (0–20 cm and 20–40 cm), plant productivity, and the parallel foliar spectral profiles were obtained at fruit mature stage of the following growing season after treatment, with objectives as follows: (1) clarify which foliar spectral indexes could represent peach productivity; (2) test whether aboveground plant productivity, as detected from foliar spectral indexes, could predict soil bacterial processes and community composition; and (3) determine to what extent of belowground soil bacterial alpha and beta diversity processes could be inferred by foliar spectral indexes. Quantified linkage between foliar spectral indexes with soil bacterial diversity attributes could provide an easy access to belowground bacterial community for better coping with the decreased functional attributes (physiological, ecological, and productive traits) in degraded orchard ecosystem.

2. Materials and methods

The experimental peach orchard (20 ha) was established in 2008 on meadow cinnamon soil in Yanqing District, Beijing (115.99E, 40.53 N), with a warm, temperate, continental monsoon climate. The experimental location has an average annual temperature of 8.5°C and an average annual precipitation of 443 mm. Planted on a flat terrain, the test peach trees all received the same environmental conditions, such as sunlight and precipitation. An early-maturing cultivar named Chunxue has been planted since 2012 in the orchard, with a row

spacing of 4 m and a line spacing of 3 m. See pre-treatment soil properties of the orchard in 2020 in Supplementary Table S1.

2.1. Experimental treatments

A self-invented soil restoration practice-RERP (patent application No. 2021115124384) was employed in the experimental peach orchard (Sun et al., 2022). RERP can increase the productivity of the peach orchard (reflecting in fruit yield and quality) by improving soil physical, chemical, and microbial properties in the root zone. In order to implement RERP, a trench (12 m long, 0.8 m wide, and 0.6 m deep) that was 1.2 m apart from the west side of the trees were dug out in October 2020. The dug-out soil was placed in three piles and filled back to the trench according to soil depths (0–20 cm, 20–40 cm, and 40–60 cm). There were three treatments that applied on a total of 45 trees, with three replications for each treatment. Border rows were arranged around test trees. Treatment 1 (T1) was RERP with soil conditioner (3 t ha^{-1}), organic fertilizer (15 t ha^{-1} DW), and mineral fertilizer (N:P_2O_5:K_2O = 15:5:10, 900 kg ha^{-1}) and evenly applied at soil depths of 20, 40, and 60 cm in the trench. Treatment 2 (T2) was RERP with organic fertilizer. Application materials and methods of T2 was the same as T1, only without the application of 3 t ha^{-1} soil conditioner. Conventional practice (CK) in the orchard was considered as control, receiving 650 kg ha^{-1} of urea (46%), 600 kg ha^{-1} of calcium superphosphate, and 310 kg ha^{-1} potassium sulfate each year (applied on May and November). Pest control and regular management were conducted as required, following the local practices for all treatments.

2.2. Foliar spectral traits and fruit attributes determination

Foliar spectral traits were measured at mature fruit stage (July 19, 2021) on a sunny day during 10:00–11:00 am, with no irrigation or rainfall 1 week earlier. Normalized difference vegetable index (NDVI), greenness index (GI), optimized soil-adjusted vegetation index (OSAVI), photochemical reflectance index (PRI), normalized pigment chlorophyll index (NPCI), modified chlorophyll absorption ratio index (MCARI), and structure insensitive pigment index (SIPI) were measured on the 7th or 8th functional leaves on both south and north sides of each tree, using a potable plant reflectance spectrometer (PolyPen RP-410, Photon System Instruments, Drasov, CZ). Foliar spectral indexes were averaged over six reads from three trees (in one block) for each replication. Equations for calculation of these indexes are listed in Supplementary Table S2. Computed data of these indexes were downloaded from the reflectance spectrometer *via* SpectraPen software 1.1.0.14 (Photon System Instruments, Drasov, CZ).

For each treatment, a total of 18 mature fruits were taken on south and north sides of three trees for the determination of fruit attributes on 19 July 2021. Fruit attributes of each replication were determined and averaged over six fruits from three trees in one block. Fruit thinning was evenly performed on all test trees, with the same level of fruit numbers on each tree. Thereby, it is assumed that single fruit weight could represent yield. Fruit transverse diameter and vertical diameter were determined by a Vernier caliper. Total soluble solid content was determined using a refractometer (RHBO-90, Link Co. Ltd., Taiwan, China). Soluble sugar content was determined with anthrone-sulfuric colorimetric method (Dreywood, 1946). The contents of titratable acid, vitamin C, and nitrate were determined following national standards of GB 12293–90 (SBQTS 1990), GB 5009.86–2016 (NHFPC 2016), and GB 5009.33–2016 (NHFPC and FDA 2016), respectively.

2.3. DNA extraction, PCR amplification, and high-throughput sequencing

Soil samples (separately in two depths, 0–20 cm and 20–40 cm) were taken at six spots in root zone that were 1.5 m away from west side of three trees (in one block) and mixed together as one replication of each treatment on July 19, 2021. The collected samples were then transported to the lab in a box with ice packs, sieved (2 mm) and sent to Majorbio Bio-Pharm Technology Co. Ltd. with dry ice. Total bacterial community genomic DNA was extracted from 0.5 g fresh soil samples of surface (0–20 cm) and subsurface soils (20–40 cm). A pair of primers 338F (5'-ACTCCTACGGGAGGCAGCAG-3′) and 806R (5'-GGACTACHVGGGTWTCTAAT-3′) was used for bacterial 16S rDNA gene amplification in the hypervariable V3-V4 region. The polymerase chain reaction (PCR) was conducted with an ABI GeneAmp® 9,700 PCR thermocycler (ABI, CA, United States), with amplification conditions and PCR reaction mixture that can be found in Sun et al. (2022). PCR products were quantified using Quantus™ Fluorometer (Promega, United States) after purification. Purified amplicons were pooled in equimolar and paired-end sequenced on an Illumina MiSeq PE300 platform (Illumina, San Diego, United States) according to the standard protocols by Majorbio Bio-Pharm Technology Co. Ltd. (Shanghai, China). The obtained gene sequences from Illumina platform are deposited in the National Center for Biotechnology Information (NCBI) Sequence Read Archive with the accession number PRJNA835607.

The sequencing data were trimmed for barcodes and primers. Low-quality reads less than Q20 were removed (Magoč and Salzberg, 2011). The 18 test samples had a total number of 958,788 effective sequences with an average length of 417 bp. High-quality sequences were clustered into operational taxonomic units (OTUs) with a 97% similarity using UPARSE ([1]version 7.1). RDP classifier ([2]version 2.2) was used for comparison of the representative sequence of each OUT to the database Silva (Release115[3]) with a confidence threshold of 0.7 (Wang et al., 2007).

2.4. Data analysis

Analysis of variance (ANOVA) was conducted for foliar spectral traits (NDVI, GI, OSAVI, PRI, NPCI, MCARI, and SIPI), fruit attributes (single fruit weight, transverse diameter, vertical diameter, nitrate content, vitamin C, soluble sugar, titratable acid, and total soluble solid), and alpha diversity estimates (Sobs, Shannon, Simpson, ACE, and Chao1) as a function of three treatments at different soil depths using the PROC ANOVA procedure in the SAS statistical

1 http://drive5.com/uparse/
2 http://rdp.cme.msu.edu/
3 http://www.arb-silva.de

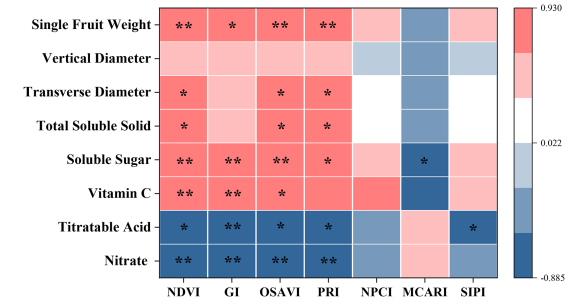

FIGURE 1
Spearman correlation analysis between foliar spectral indexes and fruit attributes. * indicates significant correlation (p<0.05), while ** indicates extremely significant correlation (p<0.01).

software package (SAS Institute Inc., Cary NC. United States). Shannon and Simpson estimate bacterial community diversity while ACE and Chao1 estimate bacterial community richness. Alpha-diversity metrics were assessed using Mothur ([4]version 1.31.2). Means were compared using the least significant difference test at the 5% probability level. The 30 most abundant genera at both soil depths of all treatments were compared *via* phyla stacked column diagram analysis in Origin 2021 (OriginLab Corporation, Northampton, MA, United States).

Bacterial genera in this study were firstly divided in identified or unidentified genera. The identified genera were then defined as abundant (>1%) or rare (<1%) genera. Beta-diversity of all treatments was calculated with the Bray–Curtis dissimilarity metric and visualized in a Principal Coordinates Analysis (PCoA) plot using R version 3.3.1 (Linux-GNU). Spearman correlation analysis was conducted between alpha diversity estimates (fruit attributes) and foliar spectral indexes and demonstrated in a heatmap *via* OriginLab. A redundancy analysis (RDA) was performed for relationships between foliar spectral indexes and fruit attributes in CANOCO 5.0. The manual forward-selection procedure was used to determine significance of soil characteristic variables ($p < 0.05$) using a Monte Carlo test with 499 permutations. Linear regression model was conducted to analyze the relations between foliar spectral indexes and alpha diversity estimates in OriginLab. Clustered heatmap analysis of the relations between foliar spectral indexes and the 30 most abundant genera were conducted using the pheatmap package in R (version 3.3.1, Linux-GNU).

Independent structural equation models (SEMs) were constructed at both soil depths, based on known effects and relationships among the drivers of plant productivity. Since some of the variables introduced were not normally distributed, the probability of a path coefficient differs from zero was tested using bootstrap resampling. Thus, data are randomly sampled with replacement to arrive at estimates of standard errors that are empirically associated with the distribution of the data found in the samples (Grace et al., 2010). For the structural model, we used the acceptable fit by Hair et al. (2019): Collinearity Statistics (VIF ≥ 5, probable critical collinearity; 5 > VIF ≥ 3, possible collinearity; VIF < 3, ideally show). The best fit SEM was accomplished *via* T Statistics (T > 1.96), p values ($p < 0.05$), root mean square error of approximation (SRMR; SRMR <0.08), and Comparative fit index (d_ULS < 0.95 and d_G < 0.95) (Hair et al., 2019). All the SEM analyses were used SmartPLS ([5] version 3.0).

3. Results and discussion

3.1. Linkage between foliar spectral traits and plant productivity characteristics

A previous study reported that spectral functional diversity of plant community explained 51% of the total variation of plant productivity ($r^2 = 0.51$, $p < 0.001$, Schweiger et al., 2018). This linkage between foliar spectral traits, functional, and evolutionary divergence provides the rationale for using spectral profiles in estimating biodiversity (Maherali and Klironomos, 2007; Cadotte et al., 2008; Hector et al., 2010). However, it is still challenging to choose spectral functional diversity indexes to capture the productivity of plant community that is location and time specific (Schweiger et al., 2018). Ultimately, the effects of biodiversity on plant community are a result of individual variation (Bolnick et al., 2011; Violle et al., 2012). Considering foliar spectral traits can be acquired relatively rapid on a regular basis than traditional protocols, we proposed to employ foliar spectral traits as indicators for plant productivity in orchard ecosystem.

In this study, RERP had positive effects on foliar spectral traits, fruit yield and quality ($p < 0.05$), with T1 a more efficient approach than T2 (Supplementary Tables S3, S4). Spearman correlation analysis revealed that selected spectral indexes of NDVI, GI, OSAVI, and PRI were significantly correlated to yield (single fruit weight) and quality (nitrate titratable acid, Vc, soluble sugar, and total soluble solid contents) as shown in Figure 1. Previous studies reported similar results of foliar spectral traits in assessing plant attributes (productivity) in other semi-arid ecosystems. Vegetation indexes, such as NDVI, GI, and OSAVI, reflected information of leaf area index and chlorophyll content, and were often used in inversion of vegetation coverage and growth status (Li et al., 2009; Ferna et al., 2018; Yang et al., 2020). NDVI and OSAVI estimated green biomass and vegetative coverage in grass ecosystem (Ferna et al., 2018), while PRI estimates instant light use efficiency at leaf scale, which was used to track changes of photoprotective pigment pools and capture eco-hydrologic sensitivity of a mixed conifer forest (Yang et al., 2020). Daily PRI measurements could be used to track changes of photoprotective pigment pools as plants respond to seasonal environment change. OSAVI introduced the factor of bare land in the calculation, which was in accordance with the increased bare land area from agricultural practices (such as weeding and pruning) for better growing conditions and higher yield in the orchard (Shu, 2003). Meanwhile, these agricultural practices affected fruit availability of photosynthetically active radiation, and consequently fruit sensorial and nutritional quality (Gullo et al., 2014).

RDA analysis further revealed a relationship between spectral traits and plant productivity (Figure 2). T1 was distinct from CK and T2, indicating a profound effect of RERP with soil conditioner

4 http://www.mothur.org/

5 http://www.smartpls.com

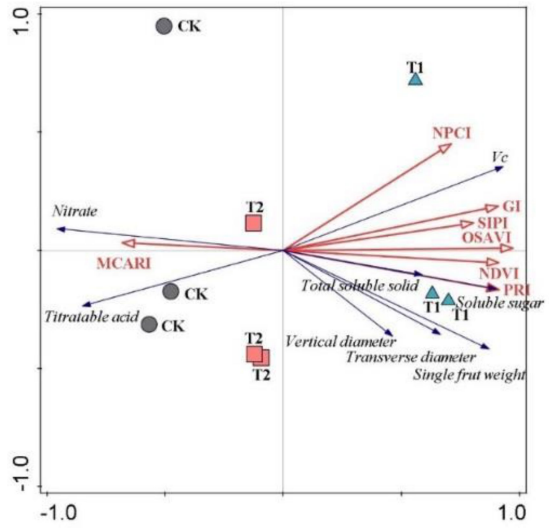

FIGURE 2
Redundancy analysis of relationships between foliar spectral indexes and fruit attributes.

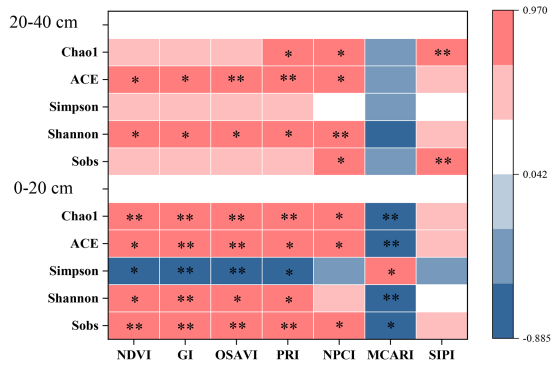

FIGURE 3
Spearman correlation analysis between spectral indexes and alpha diversity of bacterial community in surface and subsurface soils. * indicates significant correlation (p<0.05), while ** indicates extremely significant correlation (p<0.01).

(T1) on fruit yield and quality (Figure 3). The seven spectral indexes accounted for 94.3% in the first two constrained axes (axis 1 and 2 explained 83.15 and 11.15% of the variance, respectively). OSAVI was the only index that greatly contributed to the total variance (78.8%, $p = 0.002$). Spectral reflectance profiles are continuous representations of the interaction between electromagnetic radiation and matter across a range of wavelengths. In visible spectrum (400-700 nm), light is predominantly absorbed by leaf pigments (Ustin et al., 2009; Sul et al., 2013). Schweiger et al. (2018) also proved that spectral diversity (400–900 nm) was as predictive of ecosystem function as functional, phylogenetic or taxonomic diversity. Foliar spectral indexes were therefore used to assess biochemical traits that are significant in understanding plant growth and physiological status (Díaz and Cabido, 2001; Lavorel and Garnier, 2002; Wright et al., 2004; Asner et al., 2011; Lavorel et al., 2011). The results above suggested that plant productivity embodied in fruit yield and quality in orchard ecosystem could reflect in foliar traits and be predicted by foliar spectral indexes.

3.2. Linkage between foliar spectral traits and soil bacterial alpha diversity

Individuals with distinct ecological phenotypes within a plant community may influence soil microbial community (Scheibe et al., 2015; Gehring et al., 2016). In fact, plant ecological phenotype was not only displayed as distinct physical structures (plant organ, tissue, and cell), but also reflected in the quantizable phenotypic parameters related to plant physiology and biochemistry (Ustin et al., 2009; Ustin, 2013; Scheres and Van Der Putten, 2017), such as foliar spectral traits (Schweiger et al., 2018). Although leaf and canopy optical data from imaging spectroscopy were incorporate into ecological studies (Asner et al., 2011; Doughty et al., 2017), foliar spectral traits were seldomly studied in association with belowground microbial diversity.

In the present study, RERP (T1 in particular) had positive effects on bacterial alpha diversity that were soil depth dependent (Supplementary Table S5). T1 significantly increased bacterial diversity (Shannon) and richness (ACE and Chao1) in both surface and subsurface soils, mainly due to increased nutrient availability (N, K, Ca, Mg, and Zn), soil organic matter content, water holding capacity, soil porosity, and decreased soil bulk density (Sun et al., 2022). Stronger correlations between foliar spectral indexes and bacterial alpha diversity were observed in surface soil than in subsurface soil (Figure 3). Each foliar spectral index was significantly correlated to at least one bacterial diversity and richness estimates. NDVI, GI, and OSAVI were significantly correlated to all bacterial diversity and richness estimates in surface soil, but only to ACE and Shannon in subsurface soil. OSAVI had the highest correlation coefficients with alpha diversity estimate, such as Sobs, ACE, and Chao1 in surface soil and ACE and Shannon in subsurface soil. PRI and NPCI, relevant to leaf photosynthesis were correlated to both diversity and richness estimates at both soil depths. Although MCARI and SIPI were pertinent to foliar pigments, MCARI was only significantly correlated to alpha diversity in surface soil, while SIPI was better indicative of Sobs and Chao1 in subsurface soil.

Correlation analysis revealed that bacterial alpha diversity estimates were correlated with foliar spectral indexes to different extents. It is not clear whether the relations could be quantified by reliable models for prediction of bacterial diversity. Linear regression model was then employed to quantify the association between soil bacterial diversity and foliar spectral indexes (Figures 4A,B). Regression analysis results suggested that foliar spectral indexes could be adopted to predict bacterial alpha diversity. The relationships between foliar spectral indexes and bacterial diversity estimates varied by soil depths and the specific index (estimate). OSAVI, GI, and MCARI in surface soil, and OSAVI, PRI, GI, and SIPI in subsurface soil could directly explain 53–92% variance of bacterial alpha diversity. Foliar spectral indexes were more indicative of bacterial richness estimates than diversity estimates in general. Similarly, Cavender-Bares et al. (2021) reported remotely sensed vegetation cover was positively correlated with Simpson in prairie ecosystem with high productivity in Wood River, while Aji et al. (2021) reported a weak correlation between a large scale NDVI and soil microbial biomass

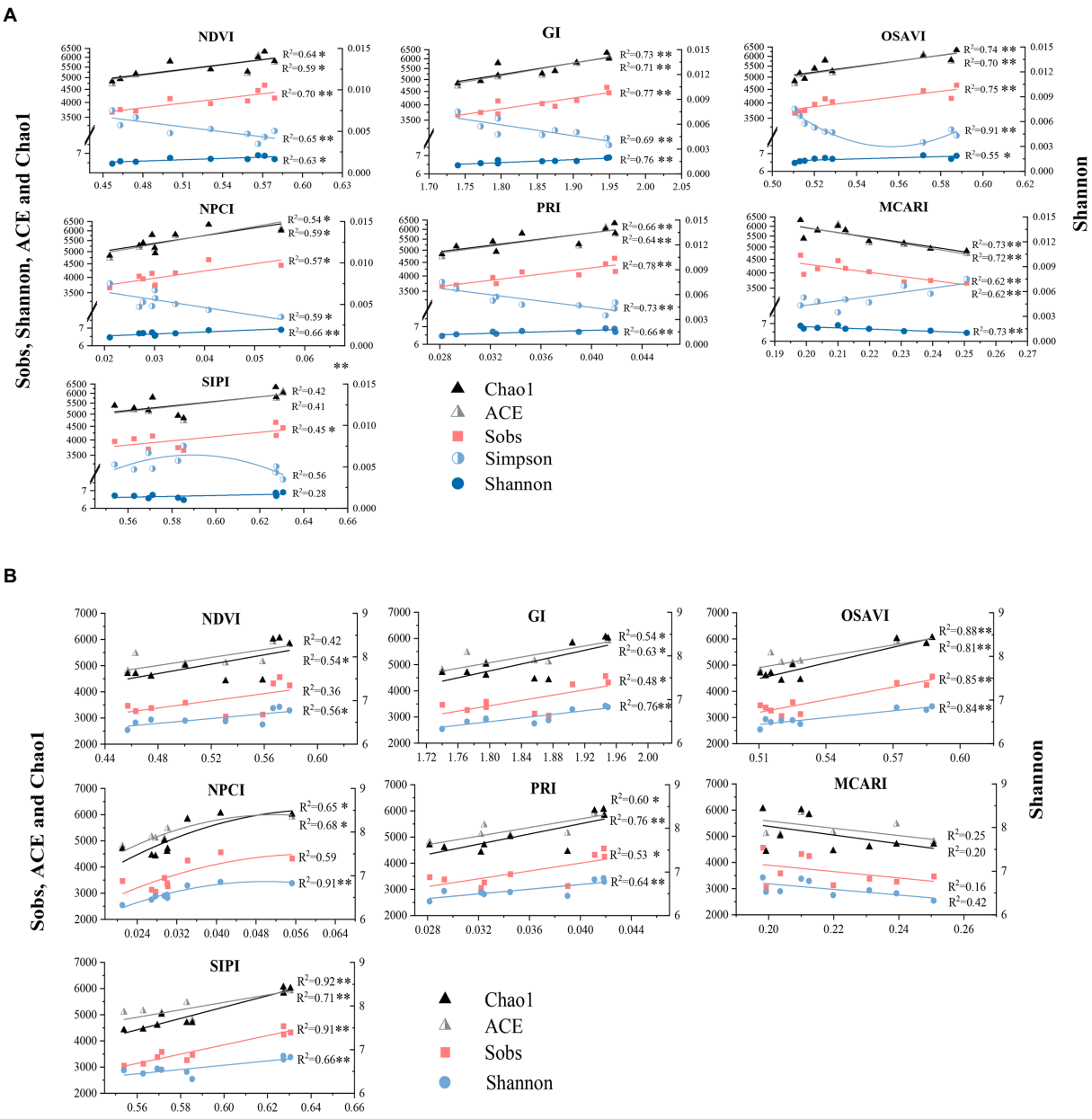

FIGURE 4
Linear regression analysis between foliar spectral indexes and alpha diversity estimates of bacterial community in surface **(A)** and subsurface **(B)** soils. * indicates significant correlation ($p<0.05$), while ** indicates extremely significant correlation ($p<0.01$).

in natural ecosystems (including lake area and protested forests) with minimum human disturbance. Generally, spectral indexes were more indicative of bacterial richness estimates than diversity estimates, and in subsurface soil than surface soil for all bacterial diversity estimates, except for Simpson. To date, few studies have been conducted on the association between specific spectral index and bacterial alpha diversity. In last decades, plant productivity was affected by declined microbial diversity from human activities and climate changes. This has triggered concerns of soil microbial diversity loss may impair key ecosystem functions with potential consequences on plant productivity (Cadotte, 2017; Schweiger et al., 2018; Chen et al., 2019). Therefore, avoiding or alleviating the loss of soil microbial diversity is critical in ecosystem (Chen Q. et al., 2020).

In this study, we draw the above conclusions based on the experimental orchard at the sampling time. Due to seasonal shifts in alpha diversity of soil bacterial community (Shi et al., 2015; Wagner et al., 2016), and in foliar spectral traits of deciduous trees in temperate arid and semiarid regions (Pederson et al., 2014), it is too early to decide if this quantified relations between foliar spectral traits and bacterial diversity can be applied at other growing stages of orchard ecosystem or to other ecosystems with the same spectral indexes at the same soil depths. Deeper understanding of specialized spectral indexes for further investigation of bacterial community variation is needed.

3.3. Linkage between foliar spectral traits and soil bacterial beta diversity

Soil bacterial assembly plays a more important role in driving soil bacterial and ecological functioning than bacterial alpha diversity (Bever et al., 2012; Bardgett and Van der Putten, 2014; Leff et al., 2018), which drove us into exploring whether and which foliar spectral traits could be employed as indicators of certain bacterial genera. RERP (both T1 and T2) significantly affected the bacterial composition on genus level in surface soil and subsurface soil (Supplementary Figure S1). Improved soil properties from RERP enriched certain genera (such as *Blastococcus*, *Bacillus*, *Sphingomonas*, and *Solirubrobacter*) in relation to increased soil nutrient content, organic matter, porosity, and water content (Sun et al., 2022). PCoA revealed larger discrepancy of bacterial community of three treatments in subsurface soil than in surface soil on genus level (Supplementary Figures S2A,B). In subsurface soil, 76.73% of the total variance was explained by the first two components. Samples of T1 were grouped together and distinct from samples of CK and T2. According to spearman correlation analysis (Figures 5A,B), more genera were in significant correlations with foliar spectral indexes in subsurface soil than in surface soil, possibly due to the frequent agricultural practices that have reduced differences between treatments in the orchard, or the more bacterial functional redundancy in surface soil. *MND1* in surface soil, and nine genera in subsurface soil (*Bacillus*, *Gaiella*, *Nocardioides*, *Sphingomonas*, *Microvirga*, *Blastococcus*, *Solirubrobacter*, *Rubrobacter*, and *RB41*) were significantly correlated to at least one foliar spectral index (NDVI, GI, OSAVI, and PRI in particular). Furthermore, correlations between the same foliar spectral indexes and soil bacteria genera were interacted with soil depth. Some genera were only in significant relations with certain foliar spectral indexes in one soil layer, such as *MND1* in surface soil (absolute value of correlation coefficient: 0.72–0.90, $p < 0.05$), and *Gaiella*, *Nocardioides,* and *Rubrobacter* in subsurface soil (absolute value of correlation coefficient: 0.67–0.82, $p < 0.05$).Some genera had opposite and enhanced relations with foliar spectral indexes at these two soil layers. For instance, *Bacillus* was in positive relation with SIPI in surface soil (correlation coefficient: 0.80, $p < 0.05$), but in negative relations with NDVI, GI, PRI, and OSAVI in subsurface soil (correlation coefficient: −0.7 to −0.82, $p < 0.05$). *Blastococcus* was in negative correlation with OSAVI (correlation coefficient: −0.67, $p < 0.05$), but in positive relations with NDVI, GI, and NPCI (correlation coefficient: 0.68 to 0.75, $p < 0.05$). *Gaiella* (reduce nitrate to nitrite) were involved in N cycle, which could affect soil N content and plant growth that further reflect on foliar spectral characteristics (Asner et al., 2011; Sul et al., 2013; Sebin et al., 2014). MND1 and *Nocardioides* were relevant to C and N nutrient cycling (Sul et al., 2013; Zhang et al., 2022) while *Solirubrobacter* were reported to affect sulfur availability for peach plants (Liu et al., 2022). *Microvirga* belong to α-proteobacterial that favored for nutritious soil (Sul et al., 2013). *Blastococcus* degrade organic material through proteolysis (Chen et al., 2016; Duan et al., 2019). *Sphingomonas* have been reported as plant growth promoting bacteria (Asaf et al., 2020; Chen L. et al., 2020) and was active in the biocontrol of pathogenic bacteria (Innerebner et al., 2011). According to previous studies, these bacterial genera in strong correlation with foliar spectral traits were those promoted soil nutrients (such as C, N, P, K, and S) cycling and uptake. This was supported by previous conclusion that foliar spectral profiles can reflect plant traits (including leaf structure, and the contents of pigments, nutrients and water) that were key to resource acquisition and stress tolerance (Sebin et al., 2014; Schweiger et al., 2018). Among these bacteria, genera with greater abundance discrepancy between treatments were in stronger correlations with foliar spectral indexes, indicating that leaf and canopy optical data were responsive to structural variance of bacterial community. It was speculated that these genera might have greater impact on aboveground plant.

However, we only investigated the 30 most abundant genera with relative abundances >1%. Certain unidentified or abundances <1% genera may have played an over-proportional role in biological processes, and being the major drive for bacterial community multifunctionality (Chen L. et al., 2020). Incomplete knowledge of these bacteria hindered further illustration of their function and contribution to plant productivity. Functional redundancy may have covered the distinction of soil microbial community, and compensated ecological functioning and plant productivity of the orchard ecosystem, which could have interfered the investigation on the relations between bacterial components and foliar spectral traits. Under the assumption that these genera in significant correlation with foliar spectral traits were key to ecosystem functioning, further investigation is in need on if exogenous addition of these bacteria in

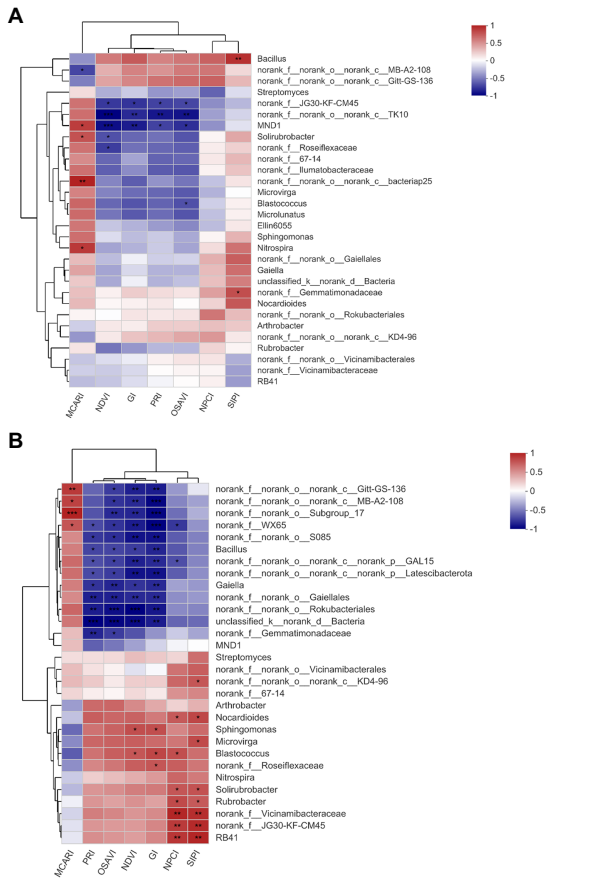

FIGURE 5
Clustered heat map analysis of the relationships between foliar spectral indexes and the 30 most abundant genera in surface **(A)** and subsurface **(B)** soils. * indicates significant correlation ($p<0.05$), while ** indicates extremely significant correlation ($p<0.01$).

bio-organic fertilizer could improve plant productivity and ecological functioning in fruit orchards (Gottel et al., 2011; Lundberg et al., 2012; Wagner et al., 2016).

3.4. Structural equation models between foliar spectral traits and soil bacterial community

Structural equation modeling (SEM) analyzes the complex networks of causal relationships among multiple variables, which has been increasingly adopted in ecological sciences in the last decade (Grace et al., 2010; Eisenhauer et al., 2015). Four similar latent variables were employed in both soil layers, with three of them (bacterial diversity, abundant genera and unidentified or < 1% genera) had soil-depth dependent indicators (Figures 6A,B). NDVI, PRI, GI, and OSAVI were best indicators of foliar spectral traits to detect bacterial diversity. Similarly, Delgado-Baquerizo et al. (2017) used NDVI as indicator of plant productivity, while Ferna et al. (2018) suggested NDVI and OSAVI as indicators of green biomass and coverage in a semi-arid rangeland. All variables were explained with different proportion of variance by the selected indicators. Generally, variables had higher R2 value in surface soil than in subsurface soil. This is possible due to the interference from frequent agricultural practices which resulted in a less effective approach of RERP in topsoil. Meanwhile, correlation coefficients between indicators and variables were higher in surface soil, which was in accordance with the higher bacterial diversity in surface soil (Delgado-Baquerizo et al., 2017). Foliar spectral traits were in negative association with unidentified or < 1% genera, and in positive associations with all other

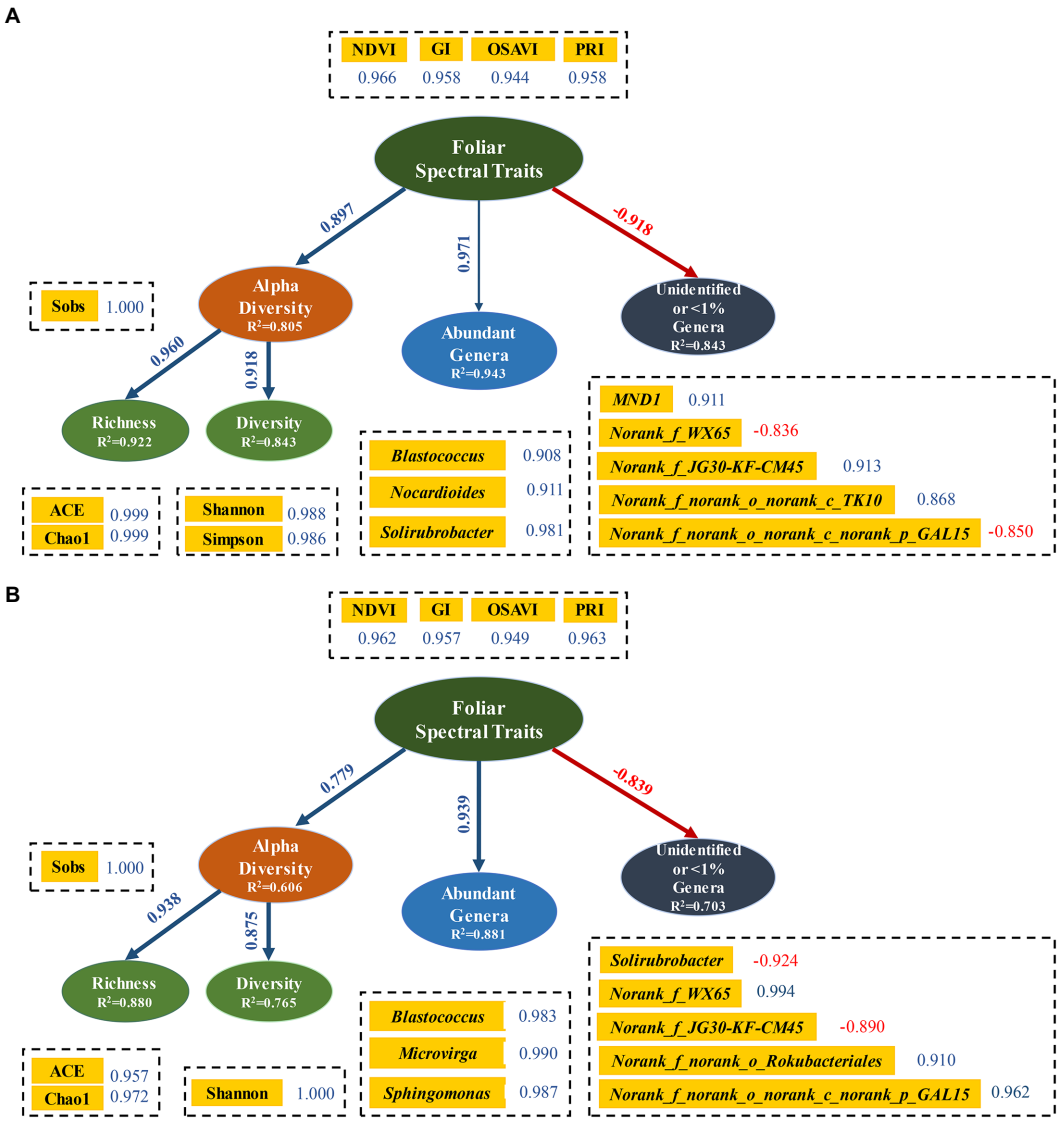

FIGURE 6
Structural equation models of relationships among foliar spectral traits, alpha diversity, abundant genera and rare genera in surface **(A)** and subsurface **(B)** soils. Blue lines indicate positive correlations. Red lines and numbers indicate negative correlations. Rare genera were with relative abundances <1%. Relationship between foliar spectral traits and abundant genera was not significant (p=0.086), indicating with a thin line, while all other relations were significant (p<0.05) with thicker lines.

variables. Furthermore, all path coefficients were extremely significant, except for association between abundant genera and foliar spectral traits in surface soil. This is likely due to the non-significant impacts of abundant genus in topsoil on plant growth, or functional redundancy from enriched abundant genera in topsoil, or the limited soil samples taken from the orchard.

Although experimental and observational databases in ecological studies are often complex, non-randomly distributed, and have spatial and temporal constraints (i.e., potential autocorrelations), SEM in this study indicated that foliar spectral traits (measured for peach productivity) were effective in predicting soil bacterial diversity and key genera. Latent variables, indicators and pathway coefficient of SEM in semi-arid peach orchard lay groundwork for further forecasting of bacterial diversity and structure in surface and subsurface soils. Environment, climate, and soil properties would all affect bacterial community and foliar spectral traits on a large scale. In this study, we focused on using foliar spectral traits to predict bacterial diversity at low cost, by using RERP to alter soil properties and obtain differentiated soil bacterial community (Sun et al., 2022). Since we conducted the field experiment in a peach orchard, the environmental and climatic factors were the same among treatments in this small scale. Although foliar spectral traits and soil microorganisms have obvious temporal dynamics, we selected the maturity period of experimental peach (July) as the critical timing for foliar spectral traits to represent productivity, since peach trees bear fruit only once a year in Beijing and the productivity of fruit trees is mainly reflected by fruit yield and quality. Spectral traits of typical leaves could then be used to characterize bacterial diversity and taxonomy. Of course, sampling on large scale with temporal dynamic are needed in order to obtain the general relationships between foliar spectra traits and soil bacteria community.

Generally, soil microbes were constrained by abiotic factors at large temporal and spatial scales, and by biotic factors at regional scale (Wang et al., 2015; Zhang et al., 2020). Ji et al. (2011) reported that cultivar, rather than tree age, played an important role in dominant bacteria community of rhizosphere soil in peach orchards in Shanghai. This has led us to the question: if the quantified linkage between foliar spectral indexes and soil bacterial community is applicable to other peach cultivar or to the same cultivar at different tree ages. Furthermore, can the quantified linkage be applied to other orchard ecosystems? Shao et al. (2020) reported eight deciduous fruit trees with different levels of metabolism and functional diversity of the soil bacterial community. Schweiger et al. (2017) also argued that spectral detectability of plant life/growth forms was dependent on the studied ecosystem and plant community. If this linkage can be extended to other fruit orchards, we could provide new insights into the mechanisms of optimizing plant productivity and maintaining plant community structure.

Hyperspectral measurements acquired from the method of airborne hyperspectral imaging in combination with high precision GNSS/IMU have improved spatial and spectral resolution to a centimeter level accuracy, which revealed messages that could not recognized by RGB or multi-spectral imaging. Recently, plant functional diversity was reported better indicated by spectral indexes in red edge, near infrared, shortwave infrared regions and other hyperspectral images, rather than in visible region (Asner et al., 2017; Schneider et al., 2017; Schweiger et al., 2018; Ma et al., 2019; Cavender-Bares et al., 2021, 2022). In future research, foliar spectral characteristics in near and far infrared region could be further looked into for the elucidation of broadened ecological linkages between foliar spectral characteristics and soil bacterial community in orchard ecosystem.

4. Conclusion

Foliar spectral traits are indicative of plant productivity and could be used to predict soil bacterial diversity in peach orchard. NDVI, GI, PRI, and in particularly OSAVI were selected as appropriate indicators of plant productivity. SEM revealed quantified linkages between foliar spectral indexes and bacterial richness, bacterial diversity, abundant genera, and unidentified or < 1% genera in both surface and subsurface soils. The results of this study enabled deeper understanding of the mechanisms in responses and adaptations of fruit trees to agricultural practices in the orchard ecosystem. Foliar spectral indexes could efficiently monitor soil bacterial diversity and functionality at low cost, with an ultimate goal of regulating plant physiological function by adjusting agricultural practices and the consequent microbial community accordingly.

However, additional information is in need on if the reliability of foliar spectral traits in predicting soil microbial community would be affected by plant species, environmental conditions and agricultural practices. A new concept of adopting foliar spectral traits as plant traits has simplified the research in exploring the associations between aboveground plant traits and belowground biodiversity at the scale of orchard ecosystem. With the scalability and repeatability of valid spectral indexes, this research could be scaled up to community, field, regional, and even terrestrial levels, to better realize the forecasting and regulating of aboveground and underground functionality in agricultural system, and further trade-ones of ecological and economical function in agroecological system.

Data availability statement

The datasets presented in this study can be found in online repositories. The names of the repository/repositories and accession number(s) can be found in the article/Supplementary material.

Author contributions

NS: data curation, formal analysis, funding acquisition, writing-original draft, and writing-review and editing. WZ: conceptualization, data curation, and writing-review and editing. SL: writing-review and editing. HL: conceptualization, data curation, formal analysis, methodology, funding acquisition, writing-original draft, and writing-review and editing. All authors contributed to the article and approved the submitted version.

Funding

This work was supported by Beijing Science and Technology Project of Beijing Municipal & Technology Commission (Z191100004019001), and Youth Research Fund of Beijing Academy of Agriculture and Forestry Sciences (QNJJ202202), and Beijing Leisure Agriculture Innovation Consortium (BJLA-G09).

Conflict of interest

The authors declare that the research was conducted in the absence of any commercial or financial relationships that could be construed as a potential conflict of interest.

Publisher's note

All claims expressed in this article are solely those of the authors and do not necessarily represent those of their affiliated organizations, or those of the publisher, the editors and the reviewers. Any product that may be evaluated in this article, or claim that may be made by its manufacturer, is not guaranteed or endorsed by the publisher.

Supplementary material

The Supplementary material for this article can be found online at: https://www.frontiersin.org/articles/10.3389/fmicb.2023.1129042/full#supplementary-material

References

Aji, A., Iryanthony, S. B., Sidiq, W. A. B. N., and Trihatmoko, E. (2021). Relationship between NDVI and the microbial content of soil in detecting fertility level at Semarang regency, Jawa Tengah Indonesia. *Nat. Environ. Poll. Technol.* 20, 425–432. doi: 10.46488/NEPT.2021.v20i01.051

Asaf, S., Numan, M., Khan, A. L., and Al-Harrasi, A. (2020). Sphingomonas: from diversity and genomics to functional role in environmental remediation and plant growth. *Crit. Rev. Biotechnol.* 40, 138–152. doi: 10.1080/07388551.2019.1709793

Asner, G. P., Martin, R. E., Anderson, C. B., Kryston, K., Vaughn, N., Knapp, D. E., et al. (2017). Scale dependence of canopy trait distributions along a tropical forest elevation gradient. *New Phytol.* 214, 973–988. doi: 10.1111/nph.14068

Asner, G. P., Martin, R. E., Knapp, D. E., Tupayachi, R., Anderson, C., Carranza, L., et al. (2011). Spectroscopy of canopy chemicals in humid tropical forests. *Remote Sens. Environ.* 115, 3587–3598. doi: 10.1016/j.rse.2011.08.020

Bardgett, R. D., Mawdsley, J. L., Edwards, S., Hobbs, P. J., Rodwell, J. S., and Davies, W. J. (1999). Plant species and nitrogen effects on soil biological properties of temperate upland grasslands. *Funct. Ecol.* 13, 650–660. doi: 10.1046/j.1365-2435.1999.00362.x

Bardgett, R. D., Smith, R. S., Shiel, R. S., Peacock, S., Simkin, J. M., and Quirk, H. (2006). Parasitic plants indirectly regulate belowground properties in grassland ecosystem. *Nature* 439, 969–972. doi: 10.1038/nature04197

Bardgett, R. D., and Van der Putten, W. H. (2014). Belowground biodiversity and ecosystem functioning. *Nature* 515, 505–511. doi: 10.1038/nature13855

Bates, S. T., Clemente, J. C., Flores, G. E., Walters, W. A., Parfrey, L. W., Knight, R., et al. (2013). Global biogeography of highly diverse protistan communities in soil. *ISME J.* 7, 652–659. doi: 10.1038/ismej.2012.147

Berg, G. (2009). Plant-microbe interactions promoting plant growth and health: perspectives for controlled use of microorganisms in agriculture. *Appl. Microbiol. Biotechnol.* 84, 11–18. doi: 10.1007/s00253-009-2092-7

Bever, J. D., Platt, T. G., and Morton, E. R. (2012). Microbial population and community dynamics on plant roots and their feedbacks on plant communities. *Annu. Rev. Microbiol.* 66, 265–283. doi: 10.1146/annurev-micro-092611-150107

Bezemer, T. M., Fountain, M. T., Barea, J. M., Christensen, S., Dekker, S. C., Duyts, H., et al. (2010). Divergent composition but similar function of soil food webs beneath individual plants: plant species and community effects. *Ecology* 91, 3027–3036. doi: 10.1890/09-2198.1

Bolnick, D. I., Amarasekare, P., Araujo, M. S., Burger, R., Levine, J. M., Novak, M., et al. (2011). Why intraspecifc trait variation matters in community ecology. *Trends Ecol. Evol.* 26, 183–192. doi: 10.1016/j.tree.2011.01.009

Bonito, G., Reynolds, H., Robeson, M. S., Nelson, J., Hodkinson, B. P., Tuskan, G., et al. (2014). Plant host and soil origin influence fungal and bacterial assemblages in the roots of woody plants. *Mol. Ecol.* 23, 3356–3370. doi: 10.1111/mec.12821

Burns, J. H., Anacker, B. L., Strauss, S. Y., and Burke, D. J. (2015). Soil microbial community variation correlates most strongly with plant species identity, followed by soil chemistry, spatial location and plant genus. *AoB Plants* 7:plv030. doi: 10.1093/aobpla/plv030

Cadotte, M. W. (2017). Functional traits explain ecosystem function through opposing mechanisms. *Ecol. Lett.* 20, 989–996. doi: 10.1111/ele.12796

Cadotte, M. W., Cardinale, B. J., and Oakley, T. H. (2008). Evolutionary history and the effect of biodiversity on plant productivity. *Proc. Natl. Acad. Sci. U. S. A.* 105, 17012–17017. doi: 10.1073/pnas.0805962105

Cavender-Bares, J., Schneider, F. D., Santos, M. J., Armstrong, A., Carnaval, A., Dahlin, K. M., et al. (2022). Integrating remote sensing with ecology and evolution to advance biodiversity conservation. *Nat. Ecol. Evol.* 6, 506–519. doi: 10.1038/s41559-022-01702-5

Cavender-Bares, J., Schweiger, A. K., Gamon, J. A., Gholizadeh, H., Helzer, K., Lapadat, C., et al. (2021). Remotely detected aboveground plant function predicts below ground processes in two prairie diversity experiments. *Ecol. Monogr.* 92:e01488. doi: 10.1002/ecm.1488

Chen, L., Brookes, P. C., Xu, J., Zhang, J., Zhang, C., Zhou, X., et al. (2016). Structural and functional differentiation of the root-associated bacterial microbiomes of perennial ryegrass. *Soil Biol. Biochem.* 98, 1–10. doi: 10.1016/j.soilbio.2016.04.004

Chen, C., Chen, H., Chen, X., and Huang, Z. (2019). Meta-analysis shows positive effects of plant diversity on microbial biomass and respiration. *Nat. Commun.* 10:1332. doi: 10.1038/s41467-019-09258-y

Chen, Q., Ding, J., Zhu, Y., He, J., and Hu, H. (2020). Soil bacterial taxonomic diversity is critical to maintaining the plant productivity. *Environ. Int.* 140:105766. doi: 10.1016/j.envint.2020.105766

Chen, L., Hao, Z., Li, K., Sha, Y., Wang, E., Sui, X., et al. (2020). Effects of growth-promoting rhizobacteria on maize growth and rhizosphere microbial community under conservation tillage in Northeast China. *Microb. Biotechnol.* 0, 1–16. doi: 10.1111/1751-7915.13693

Curran, P. J. (1989). Remote sensing of foliar chemistry. *Remote Sens. Environ.* 30, 271–278. doi: 10.1016/0034-4257(89)90069-2

de Vries, F. T., Manning, P., Tallowin, J. R. B., Mortimer, S. R., Pilgrim, E. S., Harrison, K. A., et al. (2012). Abiotic drivers and plant traits explain landscape-scale patterns in soil microbial communities. *Ecol. Lett.* 15, 1230–1239. doi: 10.1111/j.1461-0248.2012.01844.x

Delgado-Baquerizo, M., Powell, J. R., Hamonts, K., Reith, F., Mele, P., Brown, M. V., et al. (2017). Circular linkages between soil biodiversity, fertility and plant productivity are limited to topsoil at the continental scale. *New Phytol.* 215, 1186–1196. doi: 10.1111/nph.14634

Díaz, S., and Cabido, M. (2001). Vive la difference: plant functional diversity matters to ecosystem processes. *Trends Ecol. Evol.* 16, 646–655. doi: 10.1016/S0169-5347(01)02283-2

Doughty, C. E., Santos-Andrade, P. E., Goldsmith, G. R., Blonder, B., Shenkin, A., Bentley, L. P., et al. (2017). Can leaf spectroscopy predict leaf and Forest traits along a Peruvian tropical Forest elevation gradient? *J. Geophys. Res-Biogeo.* 122, 2952–2965. doi: 10.1002/2017JG003883

Douma, J., Aerts, R., Witte, J., Bekker, R., Kunzmann, D., Metselaar, K., et al. (2012). A combination of functionally different plant traits provides a means to quantitatively predict a broad range of species assemblages in NW Europe. *Ecography* 35, 364–373. doi: 10.1111/j.1600-0587.2011.07068.x

Dreywood, R. (1946). Qualitative test for carbohydrate material. *Ind. Eng. Chem. Anal. Ed.* 18:499. doi: 10.1021/i560156a015

Duan, Y., Awasthi, S. K., Liu, T., Verma, S., Wang, Q., Chen, H., et al. (2019). Positive impact of biochar alone and combined with bacterial consortium amendment on improvement of bacterial community during cow manure composting. *Bioresour. Technol.* 280, 79–87. doi: 10.1016/j.biortech.2019.02.026

Eisenhauer, N., Bowker, M. A., Grace, J. B., and Powell, J. R. (2015). From patterns to causal understanding: structural equation modeling (SEM) in soil ecology. *Pedobiologia* 58, 65–72. doi: 10.1016/j.pedobi.2015.03.002

Ferna, R. R., Foxleya, E. A., Brunob, A., and Morrisona, M. L. (2018). Suitability of NDVI and OSAVI as estimators of green biomass and coverage in a semi-arid rangeland. *Ecol. Indic.* 94, 16–21. doi: 10.1016/j.ecolind.2018.06.029

Fierer, N., Strickland, M. S., Liptzin, D., Bradford, M., and Cleveland, C. C. (2009). Global patterns in belowground communities. *Ecol. Lett.* 12, 1238–1249. doi: 10.1111/j.1461-0248.2009.01360.x

Garnier, E., Lavorel, S., Ansquer, P., Castro, H., Cruz, P., Dolezal, J., et al. (2007). Assessing the effects of land-use change on plant traits, communities and ecosystem functioning in grasslands: a standardized methodology and lessons from an application to 11 European sites. *Ann. Bot.* 99, 967–985. doi: 10.1093/aob/mcl215

Gehring, C. A., Sthultz, C. M., Flores-Renteria, L., Whipple, A. V., and Whitham, T. G. (2016). Tree genetics defines fungal partner communities that may confer drought tolerance. *PNAS* 114, 11169–11174. doi: 10.1073/pnas.1704022114

Gottel, N. R., Castro, H. F., Kerley, M., Yang, Z., Pelletier, D. A., Podar, M., et al. (2011). Distinct microbial communities within the endosphere and rhizosphere of populus deltoides roots across contrasting soil types. *Appl. Environ. Microb.* 77, 5934–5944. doi: 10.1128/AEM.05255-11

Grace, J. B., Anderson, T. M., Olff, H., and Scheiner, S. M. (2010). On the specification of structural equation models for ecological systems. *Ecol. Monogr.* 80, 67–87. doi: 10.1890/09-0464.1

Grayston, S. J., Griffith, G. S., Mawdsley, J. L., Campbell, C. D., and Bardgett, R. D. (2001). Accounting for variability in soil microbial communities of temperate upland grassland ecosystems. *Soil Biol. Biochem.* 33, 533–551. doi: 10.1016/S0038-0717(00)00194-2

Gullo, G., Motisi, A., Zappia, R., Dattola, A., Diamanti, J., and Mezzetti, B. (2014). Rootstock and fruit canopy position affect peach (Prunus persica (L.) Batsch) (cv. Rich may) plant productivity and fruit sensorial and nutritional quality. *Food Chem.* 153, 234–242. doi: 10.1016/j.foodchem.2013.12.056

Hair, J. F., Risher, J. J., Sarstedt, M., and Ringle, C. M. (2019). When to use and how to report the results of PLS-SEM. *Eur. Bus. Rev.* 31, 2–24. doi: 10.1108/EBR-11-2018-0203

Hector, A., Hautier, Y., Saner, P., Wacker, L., Bagchi, R., Joshi, J., et al. (2010). General stabilizing effects of plant diversity on grassland productivity through population asynchrony and overyielding. *Ecology* 91, 2213–2220. doi: 10.1890/09-1162.1

Homolova, L., Malenovsky, Z., Clevers, J. G., Garcıa-Santos, G., and Schaepman, M. E. (2013). Review of optical-based remote sensing for plant trait mapping. *Ecol Comp.* 15, 1–16. doi: 10.1016/j.ecocom.2013.06.003

Innerebner, G., Knief, C., and Vorholt, J. (2011). Protection of Arabidopsis thaliana against leaf-pathogenic pseudomonas syringae by Sphingomonas strains in a controlled model system. *Appl. Environ. Microb.* 77, 3202–3210. doi: 10.1128/AEM.00133-11

Ishida, T. A., Nara, K., and Hogetsu, T. (2007). Host effects on ectomycorrhizal fungal communities: insight from eight host species in mixed conifer–broadleaf forests. *New Phytol.* 174, 430–440. doi: 10.1111/j.1469-8137.2007.02016.x

Ji, L., Yang, W., Wang, Y., Liu, H., and Guo, J. (2011). Analysis of the Rhizosphere bacterial community collected from different orchards in Shanghai. *J. Agric. For.* 3, 55–59. doi: 10.3969/j.issn.1007-7774.2011.01.012

Kaiser, K., Wemheuer, B., Korolkow, V., Wemheuer, F., Nacke, H., Schöning, I., et al. (2016). Driving forces of soil bacterial community structure, diversity, and function in temperate grasslands and forests. *Sci. Rep.* 6:33696. doi: 10.1038/srep33696

Kokaly, R. F., Despain, D. G., Clark, R. N., and Livo, K. E. (2003). Mapping vegetation in Yellowstone National Park using spectral feature analysis of AVIRIS data. *Remote Sens. Environ.* 84, 437–456. doi: 10.1016/S0034-4257(02)00133-5

Lavorel, S., and Garnier, E. (2002). Predicting changes in community composition and ecosystem functioning from plant traits: revisiting the holy grail. *Funct. Ecol.* 16, 545–556. doi: 10.1046/j.1365-2435.2002.00664.x

Lavorel, S., Grigulis, K., Lamarque, P., Colace, M. P., Garden, D., Girel, J., et al. (2011). Using plant functional traits to understand the landscape distribution of multiple ecosystem services. *J. Ecol.* 99, 135–147. doi: 10.1111/j.1365-2745.2010.01753.x

Leff, J. W., Bardgett, R. D., Wilkinson, A., Jackson, B. G., Pritchard, W. J., De Long, J. R., et al. (2018). Predicting the structure of soil communities from plant community taxonomy, phylogeny, and traits. *ISME J.* 12, 1794–1805. doi: 10.1038/s41396-018-0089-x

Lekberg, Y., and Waller, L. P. (2006). What drives differences in arbuscular mycorrhizal fungal communities among plant species? *Fungal Ecol.* 24, 135–138. doi: 10.1016/j.funeco.2016.05.012

Li, S., Li, H., Sun, D., and Zhou, L. (2009). Estimation of regional leaf area index by remote sensing inversion of PROSAIL canopy spectral model. *Spectrosc. Spect. Anal.* 29, 2725–2729.

Liang, B., Ma, C., Fan, L., Wang, Y., and Yuan, Y. (2018). Soil amendment alters soil physicochemical properties and bacterial community structure of a replanted apple orchard. *Microbiol. Res.* 216, 1–11. doi: 10.1016/j.micres.2018.07.010

Liu, M. (2022). Remote sensing mapping of fruit tree planting age and evaluation of environmental risk and effect of orchard planting. Doctoral dissertation of China Agricultural University.

Liu, Y., Fang, B., Gao, L., Li, L., Wang, S., Jiang, H., et al. (2022). Community structure and ecological functions of soil microorganisms in the degraded area of Barkol Lake. *Acta Microbiol Sin.* 62, 2053–2073. doi: 10.13343/j.cnki.wsxb.20220269

Lundberg, D. S., Lebeis, S. L., Paredes, S. H., Yourstone, S., Gehring, J., Malfatti, S., et al. (2012). Defining the core Arabidopsis thaliana root microbiome. *Nature* 488, 86–90. doi: 10.1038/nature11237

Ma, X., Mahechab, M. D., Migliavaccab, M., van der Plasc, F., Benavidesd, R., Ratcliffee, S., et al. (2019). Inferring plant functional diversity from space: the potential of Sentinel-2. *Remote Sens. Environ.* 233:111368. doi: 10.1016/j.rse.2019.111368

Magoč, T., and Salzberg, S. L. (2011). FLASH: fast length adjustment of short reads to improve genome assemblies. *Bioinformatics* 27, 2957–2963. doi: 10.1093/bioinformatics/btr507

Maherali, H., and Klironomos, J. N. (2007). Influence of phylogeny on fungal community assembly and ecosystem functioning. *Science* 316, 1746–1748. doi: 10.1126/science.1143082

Massenssini, A. M., Bonduki, V. H. A., Melo, C. A. D., Totola, M. R., Ferreira, F. A., and Costa, M. D. (2015). Relative importance of soil physico-chemical characteristics and plant species identity to the determination of soil microbial community structure. *Appl. Soil Ecol.* 91, 8–15. doi: 10.1016/j.apsoil.2015.02.009

Peck, G. M., Merwin, I. A., Thies, J. E., Schindelbeck, R. R., and Brown, G. B. (2011). Soil properties change during the transition to integrated and organic apple production in a New York orchard. *Appl. Soil Ecol.* 48, 18–30. doi: 10.1016/j.apsoil.2011.02.008

Pederson, N., Dyer, J. M., McEwan, R. W., Hessl, A. E., Mock, C. J., Orwig, D. A., et al. (2014). The legacy of episodic climatic events in shaping temperate, broadleaf forests. *Ecol. Monogr.* 84, 599–620. doi: 10.1890/13-1025.1

Prober, S. M., Leff, J. W., Bates, S. T., Borer, E. T., Firn, J., Harpole, W. S., et al. (2015). Plant diversity predicts beta but not alpha diversity of soil microbes across grasslands worldwide. *Ecol. Lett.* 18, 85–95. doi: 10.1111/ele.12381

Schaepman, M. E. (2007). Spectrodirectional remote sensing: from pixels to processes. *Int. J. Appl. Earth Obs.* 9, 204–223. doi: 10.1016/j.jag.2006.09.003

Scheibe, A., Steffens, C., Seven, J., Jacob, A., Hertel, D., Leuschner, C., et al. (2015). Effects of tree identity dominate over tree diversity on the soil microbial community structure. *Soil Biol. Biochem.* 81, 219–227. doi: 10.1016/j.soilbio.2014.11.020

Scheres, B., and Van Der Putten, W. H. (2017). The plant perceptron connects environment to development. *Nature* 543, 337–345. doi: 10.1038/nature22010

Schneider, F. D., Morsdorf, F., Schmid, B., Petchey, O. L., Hueni, A., Schimel, D. S., et al. (2017). Mapping functional diversity from remotely sensed morphological and physiological forest traits. *Nat. Commun.* 8:1441. doi: 10.1038/s41467-017-01530-3

Schweiger, A. K., Cavender-Bares, J., Townsend, P. A., Hobbie, S. E., Madritch, M. D., Wang, R., et al. (2018). Plant spectral diversity integrates functional and phylogenetic components of biodiversity and predicts ecosystem function. *Nat. Ecol. Evol.* 2, 976–982. doi: 10.1038/s41559-018-0551-1

Schweiger, A. K., Schutz, M., Risch, A. C., Kneubuhler, M., Haller, R., and Schaepman, M. E. (2017). How to predict plant functional types using imaging spectroscopy: linking vegetation community traits, plant functional types and spectral response. *Methods Ecol. Evol.* 8, 86–95. doi: 10.1111/2041-210X.12642

Sebin, S. P., Singh, A., McNeil, B. E., Kingdon, C. C., and Townsend, P. A. (2014). Spectroscopic determination of leaf morphological and biochemical traits for northern temperate and boreal tree species. *Eco. Appl.* 24, 1651–1669. doi: 10.1890/13-2110.1

Shao, W., Yu, H., Zhang, P., Xu, G., Qiao, X., Gao, D., et al. (2020). Differences in metabolism and composition of microbial communities in rhizosphere soils with different deciduous fruit trees. *J. Fruit Sci.* 37, 1371–1383. doi: 10.13925/j.cnki.gsxb.20200081

Shi, S., Nuccio, E., Herman, D. J., Rijkers, R., Estera, K., Li, J., et al. (2015). Successional trajectories of rhizosphere bacterial communities over consecutive seasons. *MBio* 6:e00746. doi: 10.1128/mBio.00746-15

Shu, H. (2003). Development status of fruit industry in China and several problems to be studied. *Eng. Sci.* 5, 45–48.

Sul, W. J., Asuming-Brempong, S., Wang, Q., Tourlousse, D. M., Penton, C. R., Deng, Y., et al. (2013). Asuming-Brempong, S, Wang, Q, et al.Tropical agricultural land management influences on soil microbial communities through its effect on soil organic carbon. *Soil Biol. Biochem.* 65, 33–38, doi: 10.1016/j.soilbio.2013.05.007.

Sun, N., Zhang, W., Liao, S., and Li, H. (2022). Divergent changes in bacterial functionality as affected by root-zone ecological restoration in an aged peach orchard. *Microorganisms* 10:2127. doi: 10.3390/microorganisms10112127

Tedersoo, L., Bahram, M., Polme, S., Koljalg, U., Yorou, N. S., Wijesundera, R., et al. (2014). Global diversity and geography of soil fungi. *Science* 346:1256688. doi: 10.1126/science.1256688

Ustin, S. L. (2013). Remote sensing of canopy chemistry. *Proc. Natl. Acad. Sci.* 110, 804–805. doi: 10.1073/pnas.1219393110

Ustin, S. L., Gitelson, A. A., Jacquemond, S., Schaepman, M., and Asner, G. P. (2009). Retrieval of foliar information about plant pigment systems from high resolution spectroscopy. *Remote Sens. Environ.* 113, S67–S77. doi: 10.1016/j.rse.2008.10.019

Van der Putten, W. H., Bardgett, R. D., Bever, J. D., Bezemer, T. M., Casper, B. B., Fukami, T., et al. (2013). Plant-soil feedbacks: the past, the present and future challenges. *J. Ecol.* 101, 265–276. doi: 10.1111/1365-2745.12054

Violle, C., Enquist, B. J., McGill, B. J., Jiang, L., Albert, C. H., Hulshof, C., et al. (2012). The return of the variance: intraspecifc variability in community ecology. *Trends Ecol. Evol.* 27, 244–252. doi: 10.1016/j.tree.2011.11.014

Violle, C., Navas, M. L., Vile, D., Kazakou, E., Fortunel, C., Hummel, I., et al. (2007). Let the concept of trait be functional! *Oikos* 116, 882–892. doi: 10.1111/j.0030-1299.2007.15559.x

Wagner, M. R., Lundberg, D. S., del Rio, T. G., Tringe, S. G., Dangl, J. L., and Mitchell-Olds, T. (2016). Host genotype and age shape the leaf and root

microbiomes of a wild perennial plant. *Nat. Commun.* 7:12151. doi: 10.1038/ncomms12151

Wang, J., Chapman, S. J., and Yao, H. (2015). The effect of storage on microbial activity and bacterial community structure of drained and flooded paddy soil. *J. Soil Sedim.* 15, 880–889. doi: 10.1007/s11368-014-1053-7

Wang, Q., Garrity, G. M., Tiedje, J. M., and Cole, J. R. (2007). Naive Bayesian classifier for rapid assignment of rRNA sequences into the new bacterial taxonomy. *Appl. Environ. Microb.* 73, 5261–5267. doi: 10.1128/AEM.00062-07

Wang, L., Li, J., Yang, F., Raza, W., Huang, Q., and Shen, Q. (2017). Application of bioorganic fertilizer significantly increased apple yields and shaped bacterial community structure in orchard soil. *Microb. Ecol.* 73:404-416. doi: 10.1007/s00248-016-0849-y

Wardle, D. A., Bardgett, R. D., Klironomos, J. N., Setala, H., van der Putten, W. H., and Wall, D. H. (2004). Ecological linkages between aboveground and belowground biota. *Science* 304, 1629–1633. doi: 10.1126/science.1094875

Wright, I. J., Reich, P. B., Westoby, M., Ackerly, D. D., Baruch, Z., Bongers, F., et al. (2004). The worldwide leaf economics spectrum. *Nature* 428, 821–827. doi: 10.1038/nature02403

Yang, J. C., Magney, T. S., Yan, D., Knowles, J. F., Smith, W. K., Scott, R. L., et al. (2020). The photochemical reflectance index (PRI) captures the ecohydrologic sensitivity of a semiarid mixed conifer forest. *J. Geophys. Res-Biogeo.* 125:e2019jG005624. doi: 10.1029/2019JG005624

Yim, B., Smalla, K., and Winkelmann, T. (2013). Evaluation of apple replant problems based on different soil disinfection treatments—links to soil microbial community structure? *Plant Soil* 366, 617–631. doi: 10.1007/s11104-012-1454-6

Zhang, X., Ji, Z., Shao, Y., Guo, C., Zhou, H., Liu, L., et al. (2020). Seasonal variations of soil bacterial communities in Suaeda wetland of Shuangtaizi River estuary, Northeast China. *J. Environ. Sci.* 97, 45–53. doi: 10.1016/j.jes.2020.04.012

Zhang, D., Li, J., Huang, Y., Gao, S., and Zhang, J. (2022). Root-soil facilitation in mixed Eucalyptus grandis plantations including nitrogen-fixing species. *Forest Ecol. Manag.* 516:120215. doi: 10.1016/j.foreco.2022.120215

frontiers | Frontiers in Microbiology

TYPE Original Research
PUBLISHED 08 March 2023
DOI 10.3389/fmicb.2023.1022248

OPEN ACCESS

EDITED BY
Bernardo González,
Adolfo Ibáñez University,
Chile

REVIEWED BY
Dharmendra Kumar,
Central Potato Research Institute (ICAR),
India
Manoj Kumar Solanki,
University of Silesia in Katowice, Poland

*CORRESPONDENCE
Francesca Luziatelli
✉ f.luziatelli@unitus.it
Maurizio Ruzzi
✉ ruzzi@unitus.it

SPECIALTY SECTION
This article was submitted to Microbe and Virus Interactions with Plants, a section of the journal Frontiers in Microbiology

RECEIVED 18 August 2022
ACCEPTED 17 February 2023
PUBLISHED 08 March 2023

CITATION
Melini F, Luziatelli F, Bonini P, Ficca AG, Melini V and Ruzzi M (2023) Optimization of the growth conditions through response surface methodology and metabolomics for maximizing the auxin production by *Pantoea agglomerans* C1.
Front. Microbiol. 14:1022248.
doi: 10.3389/fmicb.2023.1022248

Optimization of the growth conditions through response surface methodology and metabolomics for maximizing the auxin production by *Pantoea agglomerans* C1

Francesca Melini[1,2], Francesca Luziatelli[1]*, Paolo Bonini[3], Anna Grazia Ficca[1], Valentina Melini[2] and Maurizio Ruzzi[1]*

[1]Department for Innovation in Biological, Agrofood and Forest Systems, University of Tuscia, Viterbo, Italy, [2]CREA Research Centre for Food and Nutrition, Rome, Italy, [3]OloBion–OMICS LIFE LAB, Barcelona, Spain

Introduction: The fermentative production of auxin/indole 3-acetate (IAA) using selected *Pantoea agglomerans* strains can be a promising approach to developing novel plant biostimulants for agriculture use.

Methods: By integrating metabolomics and fermentation technologies, this study aimed to define the optimal culture conditions to obtain auxin/IAA-enriched plant postbiotics using *P. agglomerans* strain C1. Metabolomics analysis allowed us to demonstrate that the production of a selected.

Results and discussion: Array of compounds with plant growth-promoting- (IAA and hypoxanthine) and biocontrol activity (NS-5, cyclohexanone, homo-L-arginine, methyl hexadecenoic acid, and indole-3-carbinol) can be stimulated by cultivating this strain on minimal saline medium amended with sucrose as a carbon source. We applied a three-level-two-factor central composite design (CCD) based response surface methodology (RSM) to explore the impact of the independent variables (rotation speed and medium liquid-to-flask volume ratio) on the production of IAA and IAA precursors. The ANOVA component of the CCD indicated that all the process-independent variables investigated significantly impacted the auxin/IAA production by *P. agglomerans* strain C1. The optimum values of variables were a rotation speed of 180 rpm and a medium liquid-to-flask volume ratio of 1:10. Using the CCD-RSM method, we obtained a maximum indole auxin production of 208.3±0.4 mg IAA_{equ}/L, which was a 40% increase compared to the growth conditions used in previous studies. Targeted metabolomics allowed us to demonstrate that the IAA product selectivity and the accumulation of the IAA precursor indole-3-pyruvic acid were significantly affected by the increase in the rotation speed and the aeration efficiency.

KEYWORDS

***Pantoea agglomerans*, metabolomics, response surface methodology, postbiotics, plant growth-promoting rhizobacteria, auxin**

Introduction

World population growth (UN, 2017), the effect of climate change on the global food systems (Myers et al., 2017), the COVID-19 pandemic (Mardones et al., 2020), and the impact of the war in Ukraine on the global energy market, the grains supply, and the food prices (Toffelson, 2022) are critical challenges for today's agriculture. Within this framework, the use of plant biostimulants has generated significant interest, and, among biostimulants, plant growth-promoting (rhizo)bacteria (PGPR or PGPB) look very promising to develop more efficient and sustainable production methods (Calvo et al., 2014; Ruzzi and Aroca, 2015; Rouphael and Colla, 2018).

PGPB are a heterogeneous group of endophytic and epiphytic bacteria associated with plant tissues and plant surfaces which can positively affect the health and growth of plants (Glick, 2012; de Souza et al., 2015). They can increase crop tolerance against abiotic stresses and improve nutrient use efficiency, plant health, productivity, and yield at different stages (Bulgari et al., 2015; Toscano et al., 2018). They exert beneficial effects on plants through direct and indirect mechanisms, which range from changes in hormonal content to the production of volatile organic compounds, the increase in nutrient availability, or the enhancement of abiotic stress tolerance (Ruzzi and Aroca, 2015; Oleńska et al., 2020).

So far, the European Union Regulation (EU) (2019)/1009 authorizes, as "microbial biostimulants," the use of bacteria belonging to only three taxonomic groups, namely, *Azotobacter*, *Azospirillum*, and *Rhizobium* [European Union Regulation (EU), 2019/1009]. These constraints preclude and limit the development of novel biostimulants that contain PGPR belonging to different taxonomic groups. A microorganism belonging to Risk Group I, according to the European Parliament Directive 2000/54/EC, is unlikely to cause disease in humans, animals, or plants, which does not mean that its presence could not affect the microbial biodiversity or, under critical life circumstances (e.g., an impaired health status), the health of a higher organism.

In many cases, in both humans and plants, health-promoting traits are associated with the production of soluble and volatile metabolites secreted in the culture medium. Recently, in the human sector, it has been introduced a new class of dietary biotics, the postbiotics or metabiotics. In 2021, the panel of experts designated by the International Association of Probiotics and Prebiotics (ISAPP) defined these products as a "preparation of inanimate microorganisms and/or their components that confer a health benefit on the host" containing "inactivated microbial cells or cell components, with or without metabolites, that contribute to observed health benefits" (Salminen et al., 2021). Bioactive compounds generated by fermentation using PGPR can represent a valuable approach to developing a novel class of biostimulants with higher safety and a lower environmental impact and studying the host plant response to PGPR's metabolites at the molecular level.

Regarding the production and activation of phytohormones by which plant growth is prompted, indole-3-acetic acid (IAA) is the primary auxin endogenously synthesized by PGPR with an essential effect on plant growth and development processes, such as cell elongation and organogenesis, and tropic responses (Woodward and Bartel, 2005; Teale et al., 2006; Halliday et al., 2009). Auxin contributes to root initiation, helps loosen plant cell walls to release exudates, stimulates root hair overproduction, increases lateral root formation, acts as a signaling molecule to both the plant and bacteria, aids in root elongation (Kasahara, 2016), and in the developmental response to stress (Bielach et al., 2017) and other environmental stimuli (Zwiewka et al., 2019). In plant tissues, the auxin responses are concentration-dependent, and different cells respond very differently to exogenous auxins (Paponov et al., 2008).

Indole auxin production by microbial isolates changes among different species and strains of the same species and is influenced by culture conditions, growth stage, and substrate availability (Duca et al., 2014). The presence of tryptophan, vitamins, salt, pH, temperature, carbon source, nitrogen source, and growth phase contribute to regulating auxin/IAA biosynthesis (Ryu and Patten, 2008; Swain and Ray, 2008; Apine and Jadhav, 2011; Bharucha et al., 2013; Peng et al., 2014; Luziatelli et al., 2020a). Plant exudates or specific compounds present in the rhizosphere are among the factors influencing bacterial auxin/IAA biosynthesis. Therefore, the mechanisms involved in the control of biosynthesis of IAA and indole-related compounds require a complete understanding.

Various IAA biosynthetic pathways have been proposed in plant-associated bacteria (Spaepen and Vanderleyden, 2011; McClerklin et al., 2018). Tryptophan is a major effector of IAA biosynthesis, considering most IAA biosynthesis pathways begin with tryptophan. Tryptophan-dependent pathways comprise the indole-3-acetamide (IAM), indole-3-pyruvic acid (IPyA), indole-3-acetonitrile (IAN), tryptamine (TAM), and tryptophan side-chain oxidase (TSO) pathways (Duca et al., 2014; Di et al., 2016). Organic nitrogen sources have been observed to promote auxin/IAA production more than inorganic nitrogen sources, and this may be due to the increased availability of tryptophan from proteins.

The application of the genus *Pantoea* as a biocontrol agent has been increasingly investigated, and exciting results have been obtained. Strains belonging to *Pantoea agglomerans* species are frequently found in association with plant hosts (Walterson and Stavrinides, 2015). These microorganisms are agronomically relevant for their plant-growth-promoting (PGP) features, biocontrol activity, and involvement in plant disease management (Dutkiewicz et al., 2016).

The PGP activities of *P. agglomerans* strains have been investigated through different application modes and under diverse experimental conditions (e.g., glasshouse, field, pots, greenhouse, etc.; Nunes et al., 2002; Feng et al., 2006; Venkadesaperumal et al., 2014; Moustaine et al., 2016; Paredes-Páliz et al., 2016; Kamran et al., 2017; Ozaktan et al., 2017; Xie et al., 2017; Saia et al., 2020; Luziatelli et al., 2020a,b).

Recently, we demonstrated by comparative genomic analysis high levels of conservation within genes of the IPyA pathway in this species. Independently from the natural environment from which the strain was isolated, in most of the sequenced genomes of isolates belonging to *P. agglomerans* species (45 out of 50), the genes encoding enzymes of the IPyA pathway share an identity higher than 95% over the full length of the sequence (Luziatelli et al., 2020a). This high sequence conservation has never been reported for IAA genes belonging to other species underlining that the production of auxin/IAA plays an important role in the interaction between *P. agglomerans* and host plants (Luziatelli et al., 2020a).

Optimizing the physical and chemical environmental factors that affect a fermentation process (such as temperature, pH,

aeration, and medium composition) is crucial for maximizing the yield of a specific bioproduct (Schmidt, 2005; Singh et al., 2017). Several optimization approaches can be used for this purpose, but the most common is the one-factor-at-a-time (OFAT). This approach offers the advantage of measuring whether a factor has any effect on the microbial production of the desired product and affects the metabolic traits of the producing strain (Singh et al., 2011). For the same reason, classical studies on comparative metabolomics mainly focus on the metabolic changes associated with the variation of an environmental factor only (Putri et al., 2013). The major downside of using OFAT is that it requires many experimental runs and is time-consuming and expensive, particularly in fermentation processes (Panda et al., 2007) and metabolomics analysis. Moreover, OFAT is not adequate for investigating the interaction between different variables. This limitation can be overcome using a statistical approach such as Response Surface Methodology (RSM). The latter is a useful multivariate statistical tool that allows one to design experiments, construct models, evaluate the combined effect of two or more parameters, and search for optimum conditions for desirable responses (Bezerra et al., 2008; Breig and Luti, 2021). RSM has been widely exploited to optimize fermentation processes, but surprisingly it has not been used in combination with metabolomics. This is probably because metabolomics (particularly untargeted metabolomics) is used when no *a priori* metabolic hypothesis is available (Gertsman and Barshop, 2018). At the same time, a proper selection of the factors ranges for designing the experimental matrix needs prior knowledge of the genetics and physiology of the microorganism (Breig and Luti, 2021).

Few studies are available on the process optimization of indole auxin production in *P. agglomerans* and other PGPB (Apine and Jadhav, 2011; Chaiharn and Lumyong, 2011; Balaji et al., 2012; Bharucha et al., 2013; Tallapragada et al., 2015; Bhutani et al., 2018; Myo et al., 2019; Luziatelli et al., 2021). Furthermore, there are no reports on the effect of the medium aeration on the *in vitro* production of indole auxin and, except for Luziatelli et al. (2020a), none of the above-mentioned studies has evaluated the impact of the culture conditions stimulating IAA synthesis on the production of other metabolites involved in pathways associated with PGP traits. *In vitro* studies carried out on *Pyrus communis* shoots demonstrated that *P. agglomerans* strain C1 produces metabolites that act in synergy with auxin, accelerating the adventitious roots (AR) formation when auxins are present, increasing the number and length of AR primordia that develop from stems, and modifying the response of the pear plant to exogenous auxins (Luziatelli et al., 2020c). These data suggest that in the development of an auxin-enriched plant postbiotic, the auxin/IAA concentration is not the unique parameter that should be considered.

The main goal of the present study was to optimize the auxin production in *P. agglomerans* strain C1 and evaluate the effect of the optimum conditions on the metabolites secreted in combination with auxin. To this aim, we investigated, by central composite design (CCD) combined with RSM, the effect of aeration efficiency and medium composition on auxin production. In combination with RSM-CCD, we also used a targeted and untargeted metabolomics approach to evaluate the effect of the growth conditions on the auxins profile and the production of metabolites potentially involved in the plant-microbe interaction.

Materials and methods

Bacterial strain and culture media

Pantoea agglomerans strain C1 was previously isolated from the phyllosphere of lettuce (*Lactuca sativa* L.) plants treated with vegetal-derived protein hydrolysates (Luziatelli et al., 2016, 2019a). Working cultures were routinely grown at 25°C on Lennox broth (LB; composition per liter: tryptone 10 g, yeast extract 5 g, NaCl 5 g; Lennox, 1955); and stored at −80°C as stock cultures, using glycerol (20% w/w) as a cryoprotectant. For auxin production, the strain was cultivated in a medium amended with 4 mM tryptophan (Trp), using either LB or a saline M9-sucrose broth (YES; composition per liter: M9 minimal salts 1× yeast extract 5 g, and sucrose 5 g). Tryptophan was prepared as 40 mM stock solution in mildly alkaline water, filter sterilized (0.22 µm), and stored in the dark at 4°C. All culture mediums were sterilized by autoclaving at 121°C for 20 min. Tryptone and yeast extract were purchased from BD Difco (Thermo Fisher Scientific, MA, United States), and sucrose and chemicals were procured from Sigma-Aldrich (Merck KGaA, Darmstadt, Germany).

Culture conditions

Pre-cultures were prepared by inoculating 50 mL of LB with 500 µL of a frozen (−80°C) stock culture. Cells were grown at 25°C in agitation (150 rpm) until the late exponential phase of growth (10^8 CFU/mL) using an INFORS HT Multitron incubator (Infors AG, Bottmingen, Switzerland). Aliquots of the pre-culture were transferred into 250 mL Erlenmeyer flasks containing YES medium broth amended with Trp to obtain an initial OD_{600} of 0.1 and were incubated at 25°C for 24 h. The total medium volume (mL) per flask and the agitation speed (rpm) were varied according to the experimental design described below (Table 1). To avoid any interference due to the flask geometry and type of closure, all experiments were carried out using (i) 500 mL Erlenmeyer flasks for strain pre-activation experiments, (ii) certified 250 mL narrow-neck Erlenmeyer flasks corresponding to the ISO 1773:1997 specifications (external diameter of bottom and neck of 85 ± 2 and 34 ± 1.5 mm, respectively), and (iii) T-32 silicon plugs with bubble sponge, for optimization of auxin/IAA production. Culture volume and vessels affect physiological responses and genetic stability in several microorganisms, such as *Escherichia coli* (Kram and Finkel, 2014; Gross et al., 2020).

TABLE 1 Range and levels of experimental variables of the two sets of experiments.

Factor	Experimental design no. 1			Experimental design no. 2		
	Actual levels of coded factors			*Actual levels of coded factors*		
	−1	0	+1	−1	0	+1
Rotation speed (rpm)	100	140	180	160	180	200
Medium volume (mL)	25	62.5	100	10	25	40

Factorial design for cell growth

The experimental design was established by using the DOE software package MODDE ver. 12 (Sartorius, Göttingen, Germany) as reported elsewhere (Luziatelli et al., 2019b). The Response Surface Methodology (RSM) method was used to determine the optimum level of each variable, and the combination thereof allowed the maximum productivity of auxin. Rotation speed (rpm) and liquid medium volume (mL) were set as factors. Cell biomass (OD_{600}) and auxin production (mg/L) were set as responses. Figure 1 shows the procedure used to develop the RSM design matrix and find optimum values for the input process parameters.

In the first experimental design, two ranges of values were set for the relevant factors (i.e., rotation speed and medium volume), as shown in Table 1. Each independent variable was tested at three levels, indicated as −1 (low level), 0 (central level), and + 1 (high level).

According to the first Central Composite Design (CCD1), 20 experimental runs were executed, with four center value replications, and the observations were fitted to the following second-order polynomial model:

$$Y = \beta_0 + \beta_1(X_1) + \beta_2(X_2) + \beta_{11}(X_1^2) + \beta_{22}(X_2^2) + \beta_{12}(X_1X_2).$$

Where: Y is the dependent variable (indole auxins production); X_1 and X_2 are the coded independent variables (rotation speed and medium volume); β_0 is the regression coefficient at the center point; β_1 and β_2 are the linear coefficients; β_{11} and β_{22} are the quadratic coefficients; β_{12} is the second-order interaction coefficient. The developed regression model was evaluated by analysis of variance (ANOVA) and p- and F-values. The quality of the fit of the polynomial model equation was expressed by the coefficient of determination, R^2. The significance of all terms in the polynomial was judged statistically by computing the F value at a probability (p) of 0.05. The regression coefficients were used to make statistical calculations to generate response surface curves from the regression models. To test the model accuracy, R^2 and adjusted R^2 were estimated.

Based on the results of the first round of experiments, a second experimental design was set by MODDE ver. 12 by centering on the agitation speed of 180 rpm and the volume of 25 mL. The RSM-CDD (CDD2) comprised a total of 18 experimental runs. The two ranges of value for the relevant factors set in the second experimental design are shown in Table 1.

All experiments were carried out in duplicate in the standard conditions previously defined: growth in YES-Trp medium for 24 h; cultivation in a rotary shaker at 25°C using 250 mL narrow-neck Erlenmeyer flasks with T-32 silicon plugs.

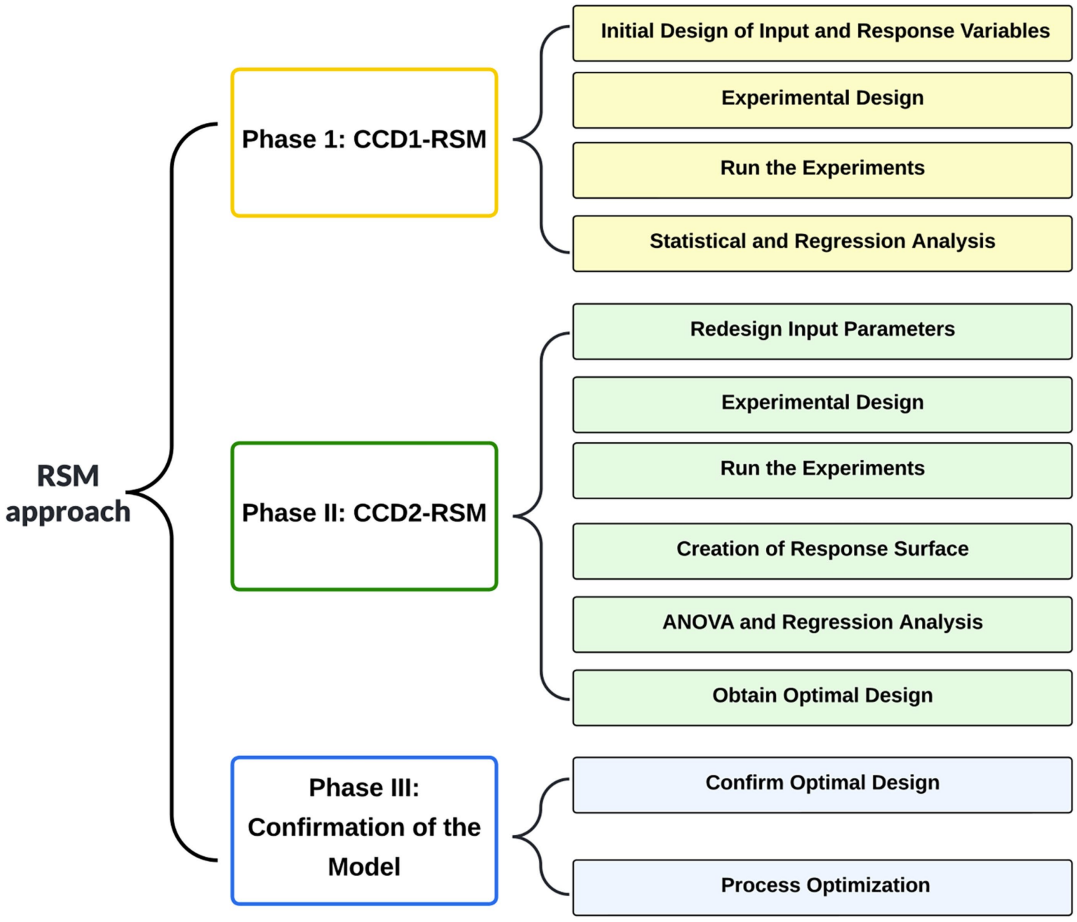

FIGURE 1
Flowchart of the Response Surface Methodology (RSM) modeling approach.

Spectrophotometric estimation of indole auxins

Auxin production was measured in the cell-free spent medium using a colorimetric assay with Salkowski's reagent (Patten and Glick, 2002). Briefly, cell culture was centrifuged at 10000 rpm for 10 min in a multispeed centrifuge (Thermo Fisher Scientific, Waltham, MA, USA), and the supernatant was recovered and filter-sterilized (0.22 µm). An aliquot (1 mL) of the supernatant, diluted as needed, was mixed vigorously with 2 mL of Salkowski's reagent (0.5 M $FeCl_3$, 35% v/v $HClO_4$), and the mixture was incubated at room temperature for 20 min in the dark. The developed pink color was read at 530 nm. Total indole auxins were quantified by using a calibration curve of pure indole-3-acetic-acid (Sigma–Aldrich, Milan, Italy) as a standard. Data were expressed as µg IAA equivalents (IAA_{equ}) per mL of liquid culture. No reaction product was determined using not inoculated medium amended with tryptophan as a control.

Footprinting of extracellular metabolites

The effect of the growth medium on the extracellular metabolites was tested by cultivating *P. agglomerans* strain C1, at optimal growth temperature (30°C), on LB and YES medium supplemented with Trp (4 mM). Exhausted liquid broth samples (1 mL) were extracted in 5 mL of cold (−20°C) acidified (0.1% HCOOH) 80:20 methanol:water using an Ultra-Turrax (Ika T-25, Staufen, Germany), centrifuged at 1,200 rpm and filtered through a 0.2 µm cellulose membrane. The analysis was carried out on an Agilent 6550 Q-TOF with ESI source (Agilent Technologies, Santa Clara, CA, United States), coupled with an Agilent 1290 UHPLC, as reported elsewhere (Luziatelli et al., 2020a). 2 µL of each sample were injected on a reversed-phase Acquity ethylene-bridged hybrid (BEH) HILIC C18 column (100 mm × 2.1 mm, 1.7 µm, Waters, Milford, MA, USA). A pooled quality control was obtained by mixing 10 µL of each sample and acquired in tandem mass spectroscopy mode using iterative function five consecutive times to increase the number of compounds with associate MS2 spectra.

The raw data were processed with the procedure described by Blaženović et al. (2019). Compounds identification was based on accurate mass and isotopic patterns and expressed as an overall identification score. Chemical Similarity Enrichment Analysis (ChemRICH) was performed, as described by Barupal and Fiehn (2017), and statistical significance *p*-values were obtained by self-contained Kolmogorov–Smirnov tests.

Auxin profiling

In targeted metabolomics, chromatographic separation, MS, and MS/MS acquisition parameters were carried out following the FiehnLab HILIC protocol, as previously described (Blaženović et al., 2018; Teleki and Takors, 2019). The injection volume was 2 µL, whereas Q-TOF was operated in positive SCAN mode (100–1,700 m/z + range) and extended dynamic range mode. All samples were injected in three biological replicates with three technical replicates each (total 9 injections/sample). Deconvolution, mass and retention time alignment, normalization, blank filtering, and identification were carried out using the Agilent Mass Hunter Quantitative Analysis software for Q-TOF version B.09. Standards for quantification and identification of Trp, IAA, and IPyA were purchased from Sigma-Aldrich. Three dilutions were prepared in duplicate with a concentration of 10, 100, 500, and 1,000 ppm from each standard to calculate the calibration curve, reaching an R^2 of 0.999 in all compounds.

Statistical analysis

Differences between treatment groups were compared using the One-way analysis of variance (ANOVA) test, followed by Tukey's honestly significant difference (HSD) test with significance set at $p < 0.05$.

Results

Effect of growth medium composition on exometabolome

As demonstrated in previous work (Luziatelli et al., 2020a), the production of IAA by *P. agglomerans* strain C1 is affected by the carbon source and the incubation temperature. Higher auxin levels were obtained by growing C1 strain on an M9 saline medium with sucrose (YES) as a carbon source under suboptimal temperature conditions (25°C; Luziatelli et al., 2020a). In this work, we comprehensively characterized strain C1 exometabolome of cultures grown on a medium amended with tryptophan as an auxin/IAA precursor. UHPLC-ESI-Q-TOF-MS analysis of the exhausted growth medium revealed a total of 204 features: 16 were more than two-fold higher, and 54 were more than two-fold lower, changing the cultivation medium from LB + Trp to YES+Trp (Figure 2; Supplementary Table S1). Comparing the metabolomic datasets of cultures grown on LB and YES medium by Chemical Similarity Enrichment Analysis (ChemRICH), we observed a significant increase in IAA (5.4 folds), indole-3-carbinol (3.9 folds), quinoline (2.8 folds), cyclohexane derivatives shifting from LB to YES (Supplementary Table S1). Under the same conditions, a significant decrease of IAA precursors (i.e., indole-3-acrylic acid, indole acetaldehyde, indole-3-acetamide, and indole-3-carboxylic acid) was observed (Supplementary Table S2). Growth in the YES medium also determined a significant variation in the hypoxanthine/xanthine ratio due to a 4.8-fold increase in hypoxanthine concentration and a 105-fold decrease in xanthine. Other metabolites, whose production was stimulated on YES medium, included compounds with antimicrobial activity such as the β-lactam antibiotics NS-5 and 2-hydroxyethylclavam, the cyclohexanone, the homo-L-arginine, and the methyl hexadecanoic acid.

Effect of oxygen availability on biomass and auxin yield

The effect of oxygen availability on cell biomass and auxin production was evaluated on YES medium using a shake-flask methodology by varying medium liquid-to-flask volume ratio

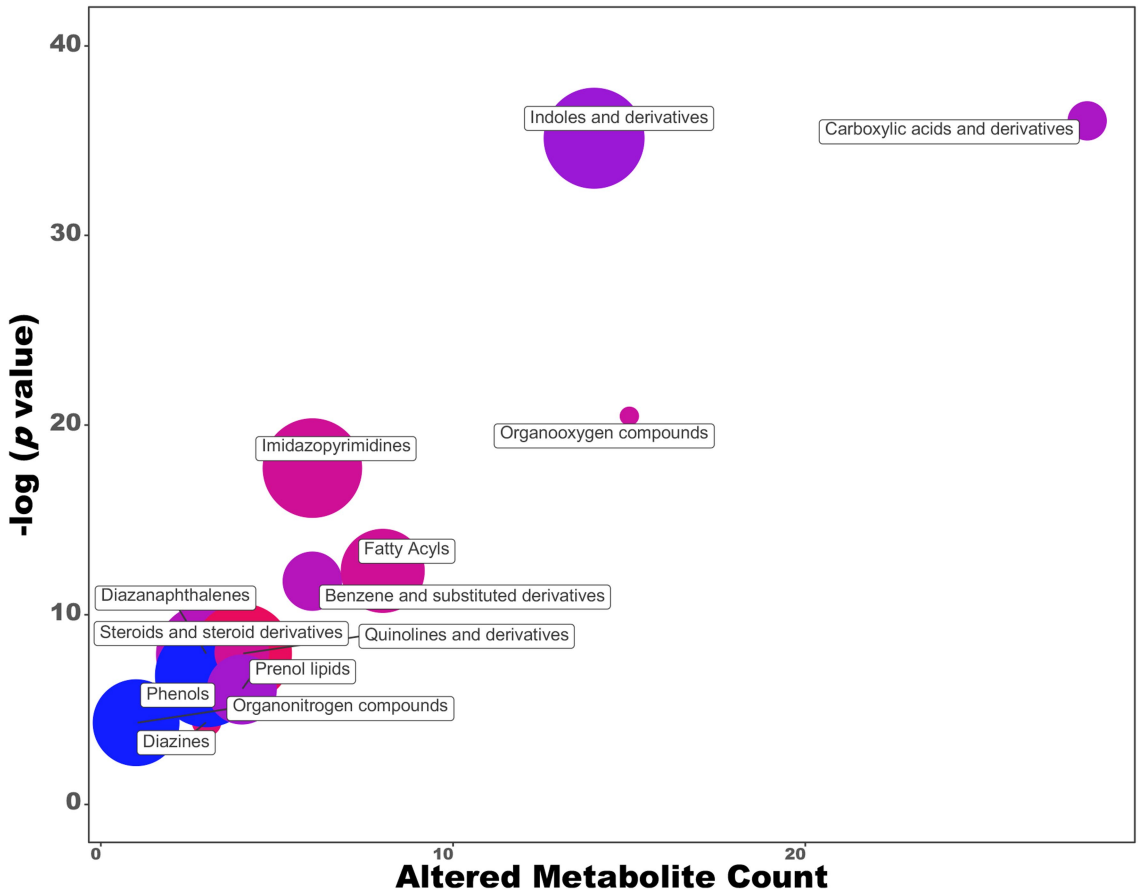

FIGURE 2
ChemRich analysis of exometabolome of *Pantoea agglomerans* C1 grown on YES vs. LB medium. Red clusters are associated with higher outcomes, and the blue ones are associated with lower outcomes.

(V_m/V_f) and rotation speed (rpm). Data reported in Figure 3A indicated that an increase in the biomass yield (OD_{600}) occurred upon increasing the gas–liquid interfacial area by either changing the V_m/V_f ratio (from 1:2.5 to 1:10) or the rotation speed (from 100 to 180 rpm). OD_{600} varied between 3.4 ± 0.0 and 6.4 ± 0.1, and the highest biomass production (OD_{600} = 6.45) was achieved at 180 rpm and V_m/V_f ratio of 1:10 (Table 2, run 4). At all V_m/V_f ratio values, no significant change in the OD_{600} was measured by increasing the rotation speed from 100 to 140 rpm. As expected, at 180 rpm, the increase in the biomass yield was more marked (OD_{600} from 4.2 ± 0.0 and 6.4 ± 0.1) by increasing the V_m/V_f ratio from 1:2.5 to 1:10 (Figure 3A).

Data reported in Figure 3B indicated that the aeration efficiency of the culture medium, dependent upon the rotation speed and liquid-to-flask volume ratio, also affected the extracellular concentration and specific productivity of auxin. When the oxygen availability was lower (lower rotation speed and higher medium liquid-to-flask volume ratio), a lower amount of auxin was obtained. At all agitation regimes, higher auxin values were achieved using a 1:10 medium liquid-to-flask volume ratio (Figure 3B). The highest auxin titer (208.0 ± 2.0 mg of IAA_{equ}/L) and specific productivity (32.6 ± 0.1 mg of IAA_{equ}/L/OD_{600}) mean values were obtained at 180 rpm with 25 mL of liquid culture in a 250 mL flask (run 4 and 20; Table 2).

Optimization of auxins production by RSM

To evaluate more precisely the effect of oxygen availability on auxin yield, a second experimental design centered on the agitation speed of 180 rpm and the liquid-to-flask volume ratio of 1:10 was performed. Predicted and observed data of CCD No. 2 for biomass (OD_{600}) and auxins production (mg/L) are reported in Table 3.

The results obtained with the experiments scheduled in the CCD2 confirmed that the highest auxin values (208.0 ± 0.2 mg of IAA_{equ}/L) were achieved when the C1 strain was grown at 180 rpm with 25 mL of liquid culture (1:10 medium liquid-to-flask volume ratio) in a 250 mL flask (run 9 and 18; Table 3).

The experimental results were fitted to a second-order polynomial quadratic equation. A multiple correlation analysis was done, and the following equation was thus obtained:

$$Y = 206.94 - 6.85\,X_1 - 6.31\,X_2 - 16.44\,X_1^2 - 26.76\,X_2^2 + 3.53\,X_1X_2$$

where Y was the predicted auxin concentration, and X_1 and X_2 were the coded values for medium volume and rotation speed, respectively.

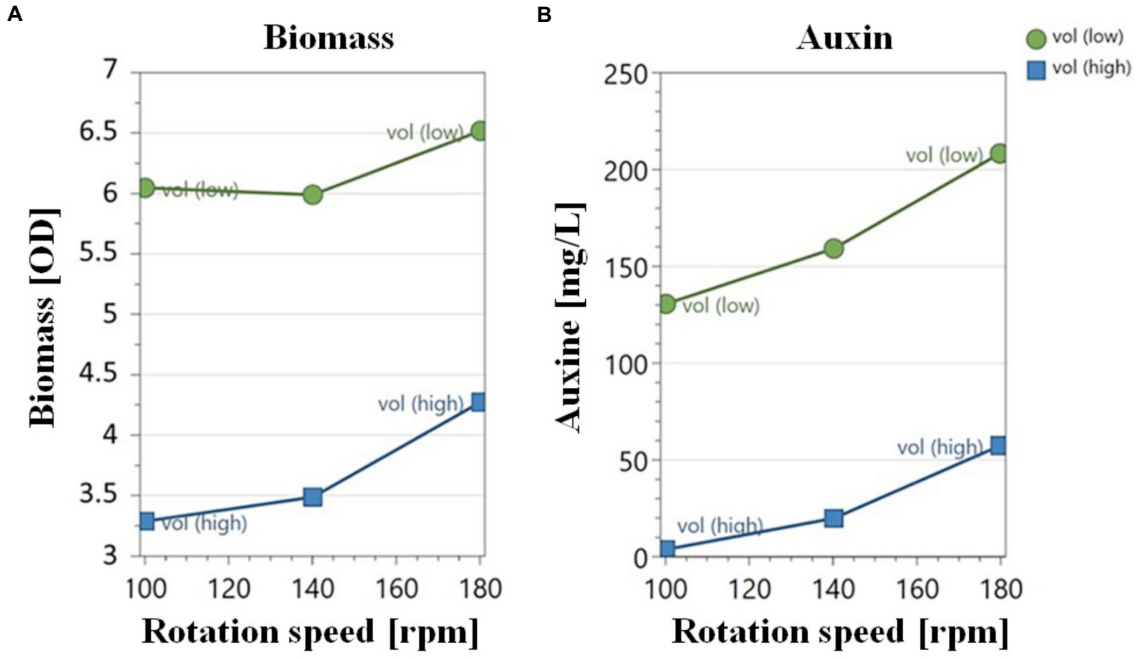

FIGURE 3
Effect of the rotation speed on biomass **(A)** and auxin yield **(B)** by *Pantoea agglomerans* strain C1 in shake-flask cultivation experiments carried out at a liquid-to flask V_m/V_f ratio of 1:2.5 (low) and 1:10 (high).

Statistical analysis results, including the regression coefficient and *p*-values for linear, quadratic, and interaction effects, are shown in Table 4.

The multiple regression analysis of auxin production showed that the model was significant ($p < 0.05$) and did not present a lack of fit ($p = 0.04$). The regression-based determination of R^2 was evaluated to test the model equation's fit. The R^2 value, which always ranges between 0 and 1, provided a measure of how the experimental factors and their interactions can explain much variability in the observed response values. In this study, the multiple coefficients of determination (R^2) for auxin production were 0.974, which means that the model can account for 97.4% of the variability in the response. The adjusted R^2 of 0.964 corrects the R^2 value for the sample size and the number of terms in the model. The Q^2 value, which provides a qualitative measure of consistency between the predicted and original data, was equal to 0.943, indicating that the model has good predictive relevance.

A response surface was also produced to determine each variable's optimum level for maximum productivity response and the combined effect of rotation speed and medium-to-flask volume ratio on auxin production (Figure 4). The graphical representation was a useful method to visualize the relationship between the response and the experimental levels of each variable and the type of interaction between test variables to deduce the optimum conditions. Response surface and contour plots showed that the highest auxin production (>205 mg IAA_{equ}/L) occurred when rotation speed ranges between 165 and 186 rpm and volume ranges from 17.25 to 29.25 mL. Above and below the ranges specified for rotation speed and volume, auxin production decreased, and lower values were obtained.

The objective of the application of RSM to C1 strain growth was to determine the levels of experimental factors which would allow obtaining the highest auxin production. The model allowed the prediction of an auxin production of 207.3 mg IAA_{equ}/L when optimal growth conditions, that is, 176 rpm and 24 mL medium volume, were applied. To validate the predicted model, five experiments were thus conducted at these optimum growth conditions, and the results showed a close match (208.3 ± 0.4 mg IAA_{equ}/L).

Effect of cultivation conditions on auxin profile

Targeted metabolomics provided insights into the effect of the culture conditions on the levels of IAA and its main precursor, indole-3-pyruvic acid (IPyA; Figure 5). After 24 of growth at 180 rpm, IPyA accumulated in the culture medium at a concentration between 0.12 ± 0.0 mM (and V_m/V_f ratio of 1:2.5) and 0.5 ± 0.0 mM (V_m/V_f ratio of 1:10; Figure 5A).

At a V_m/V_f ratio of 1:10, we observed an increase in the IPyA concentration (from 0.2 ± 0.0 to 0.5 ± 0.0 mM; Figure 5B) and a decrease in the IAA/IPyA ratio (from 5.2 ± 0.1 to 1.8 ± 0.1; Table 5) by increasing the agitation speed from 160 to 200 rpm.

At constant agitation speed (180 rpm), we observed that the accumulation of IAA and IPyA were inversely correlated to the culture volume. The IAA/IPyA ratio increased (from 1.5 ± 0.0 to 3.0 ± 0.1) by decreasing the culture volume from 100 (V_m/V_f = 1:2.5) to 25 (V_m/V_f = 1:10; Table 5).

10.3389/fmicb.2023.1022248

TABLE 2 Experimental design No. 1 and results of CCD1-RSM.

Run	Factor		Volume ratio	Observed response		Predicted response		Auxin spec. productivity (mg IAA_{equ} /L/ OD_{600})
	Rotation speed (rpm)	*Medium volume (mL)*	V_m/V_f	Biomass (OD_{600})	Auxin (mg IAA_{equ}/L)	Biomass (OD_{600})	Auxin (mg IAA_{equ}/L)	
1	(0) 140	(−1) 25.0	1:10	6.11	163.21	5.99	158.97	26.71
2	(−1) 100	(−1) 25.0	1:10	6.12	133.31	6.05	130.30	21.78
3	(+1) 180	(+1) 100.0	1:2.5	4.24	61.05	4.27	56.95	14.40
4	(+1) 180	(−1) 25.0	1:10	6.45	209.82	6.52	208.21	32.53
5	(−1) 100	(−1) 25.0	1:10	6.04	125.33	6.05	130.30	20.75
6	(+1) 180	(0) 62.5	1:4	5.37	98.73	5.10	103.92	18.39
7	(0) 140	(0) 62.5	1:4	4.18	47.73	4.45	60.93	11.42
8	(−1) 100	(+1) 100.0	1:2.5	3.37	3.43	3.29	4.04	1.02
9	(0) 140	(+1) 100.0	1:2.5	3.42	3.13	3.29	4.04	0.92
10	(+1) 180	(+1) 100.0	1:2.5	4.18	52.77	4.27	56.95	12.62
11	(−1) 100	(−1) 25.0	1:10	6.10	157.22	5.99	158.97	25.77
12	(0) 140	(0) 62.5	1:4	4.76	76.92	4.45	60.93	16.16
13	(−1) 100	(0) 62.5	1:4	4.34	48.98	4.38	38.51	11.29
14	(+1) 180	(0) 62.5	1:4	5.25	109.76	5.10	103.92	20.91
15	(−1) 140	(0) 62.5	1:4	4.54	53.71	4.45	60.93	11.83
16	(−1) 140	(0) 62.5	1:4	4.17	61.28	4.45	60.93	14.70
17	(0) 140	(+1) 100.0	1:2.5	3.50	21.44	3.49	20.21	6.13
18	(−1) 100	(0) 62.5	1:4	4.15	31.50	4.38	38.51	7.59
19	(0) 140	(+1) 100.0	1:2.5	3.39	20.57	3.49	20.21	6.07
20	(+1) 180	(−1) 25.0	1:10	6.31	206.08	6.52	208.21	32.66

Coded (in parentheses) and real values are shown.

The sum of IAA and IPyA concentrations was affected by both parameters. It was maximal (1.5 ± 0.1) at a working volume of 25 mL in a 250 mL flask (V_m/V_f = 1:10) and an agitation speed of 180 rpm (Figure 5).

The change in tryptophan (Trp) concentration (the precursor of IPyA and IAA; Table 5) was not consistent with the total content of IAA + IPyA (Figure 5). In almost all culture conditions, the moles of products (IAA + IPyA) obtained per moles of the substrate (Trp) were not equal to 1. Notably, at V_m/V_f = 1:10 (25 mL) and 160 rpm, only part of the consumed Trp was converted to IAA and IPyA (Table 5). In contrast, increasing the agitation speed up to 180 or 200 rpm, the final concentration of Trp after 24 h of growth was higher or equal to that of the not inoculated broths (Table 5), indicating that higher agitation speeds (up to 180 rpm) promote the biosynthesis of both IAA (Table 4) and Trp (Table 5).

Discussion

The production of phytohormones such as auxin is one of the central mechanisms beneficial bacteria use to enhance plant growth. Selection of the culture medium and optimization of the culture parameters that affect the biosynthesis of these compounds is thus pivotal to obtaining plant postbiotics based on auxin and plant growth-promoting molecules produced by PGPR. We previously demonstrated that selected *P. agglomerans* strains secrete a combination of metabolites that can act in synergy with auxins to induce adventitious root formation (Luziatelli et al., 2020c). Using *Pyrus communis* as a model system, we demonstrated that, in contrast to the synthetic hormone indole-3-butyric acid (IBA), the metabolites secreted by *P. agglomerans* C1 strain have an unusual auxin-like activity that could determine direct shoot regeneration without callus formation and earlier emergence of roots from stem tissues (Luziatelli et al., 2020c).

One of the major goals of this work was to analyze how to rationally develop plant biostimulants that fit within the definition of postbiotics ("*preparation of inanimate microorganisms and/or their components*") and make the most of the biosynthetic capabilities of a selected PGPR strain integrating metabolomics and fermentation technologies. For this purpose, we first identified, by untargeted metabolomics, the culture medium that better stimulates the production of a more comprehensive array of metabolites with plant-promoting or biocontrol activity, including auxin/IAA. We then used a three-level-two-factor response surface methodology based on the central composite design (RSM-CCD) to optimize the auxin/IAA production on the selected medium. For this purpose, we set two parameters (rotation speed and medium liquid-to-flask volume ratio) that affect the aeration efficiency in

10.3389/fmicb.2023.1022248

TABLE 3 Experimental design No. 2 and results of CCD2-RSM.

Run	Factor		Liquid-to-flask volume ratio	Observed Response	Predicted Response
	Rotation speed (rpm)	*Medium volume (mL)*	V_m/V_f	Auxin (mg IAA_{equ}/L)	Auxin (mg IAA_{equ}/L)
1	(−1) 160	(−1) 10	1:25	181.91	180.43
2	(+1) 200	(−1) 10	1:25	156.81	159.67
3	(−1) 160	(+1) 40	1:6.25	161.41	160.75
4	(+1) 200	(+1) 40	1:6.25	155.21	154.13
5	(−1) 160	(0) 25	1:10	192.42	197.35
6	(+1) 200	(0) 25	1:10	186.33	183.66
7	(0) 180	(−1) 10	1:25	190.51	186.49
8	(0) 180	(+1) 40	1:6.25	168.78	173.88
9	(0) 180	(0) 25	1:10	208.11	206.94
10	(−1) 160	(−1) 10	1:25	179.63	180.43
11	(+1) 200	(−1) 10	1:25	157.45	159.67
12	(−1) 160	(+1) 40	1:6.25	166.20	160.75
13	(+1) 200	(+1) 40	1:6.25	153.38	154.13
14	(−1) 160	(0) 25	1:10	195.51	197.35
15	(+1) 200	(0) 25	1:10	185.74	183.66
16	(0) 180	(−1) 10	1:25	186.89	186.49
17	(0) 180	(+1) 40	1:6.25	172.54	173.88
18	(0) 180	(0) 25	1:10	207.79	206.94

Coded (in parentheses) and real values are shown.

TABLE 4 Regression analysis of the full second-order polynomial model for optimization of auxins.

Model term	Coefficient estimated	Std. Errors	*p*-value	Confidence intervals (±)
Intercept	206.941	1.756	9.316 E-20	3.83
X_1	−6.847	0.962	1.213 E-05	2.10
X_2	−6.307	0.962	2.695 E-05	2.10
X_1^2	−16.437	1.665	4.129 E-09	3.63
X_2^2	−26.757	1.665	1.769 E-09	3.63
$X_1 X_2$	3.532	1.178	0.011	2.57

$R^2 = 0.974$, adj-$R^2 = 0.964$.

shake-flask conditions as response factors. Moreover, to better understand the interaction between these two parameters, we used an iterative RSM-CCD approach to define the correct ranges of the factors. Finally, by targeted metabolomics, we analyzed the effect of the aeration efficiency of the culture medium on the IAA product selectivity and the metabolic flux of Trp to IAA through IPyA.

Results reported in Figure 1 indicated that, in the production of a plant postbiotic, the culture medium has a central role in the balance between the target compound (indole auxins) and other metabolites secreted by the microorganism. A PGPR can produce and release in the culture medium a wide array of compounds that can enhance or modulate the plant's response to the exogenous auxins (Duca et al., 2014) or promote plant growth through different mechanisms (Olanrewaju et al., 2017). In this respect, the possibility of modifying the hypoxanthine/xanthine ratio shifting from LB to YES medium can be particularly interesting since these molecules interplay with the plant's response to auxin, environmental stresses, and, in the case of hypoxanthine, purine savage (Ashihara et al., 2018).

Untargeted metabolomics also indicated that the shift from LB to YES had a positive effect on the accumulation of some *P. agglomerans* metabolites with antimicrobial activity that can indirectly affect the promotion of plant growth, preventing the development of plant pathogens (Glick, 1995). Among these compounds, we found: NS-5, a β-lactam antibiotic active against Gram-positive and Gram-negative bacteria (Papp-Wallace et al., 2011); methyl hexadecanoic acid, a fatty acid methyl ester (FAME) with antibacterial activity against Gram-negative (Thormar, 2010); indole-3-carbinol, a compound toxic to herbivores, insects and pathogens (Kim and Jander, 2007; Figure 2; Supplementary Table S1).

In summary, the metabolomics analysis indicated that the use of plant postbiotics, in alternative to IBA or other synthetic hormones, gives the advantage of obtaining a selected array of compounds with plant-promoting or biocontrol activity whose synthesis pattern in the natural environment is unpredictable and whose importance in plant-microbe interaction could not be easily recognized using conventional systems. At the same time, the use of microbial metabolites by PGP bacteria or fungi not included in the list of microbial biostimulants approved by the EU legislation 2019/1009 can offer an interesting opportunity for scientists and entrepreneurs to develop novel bio-based biostimulants with a well-defined composition and well-characterized activities.

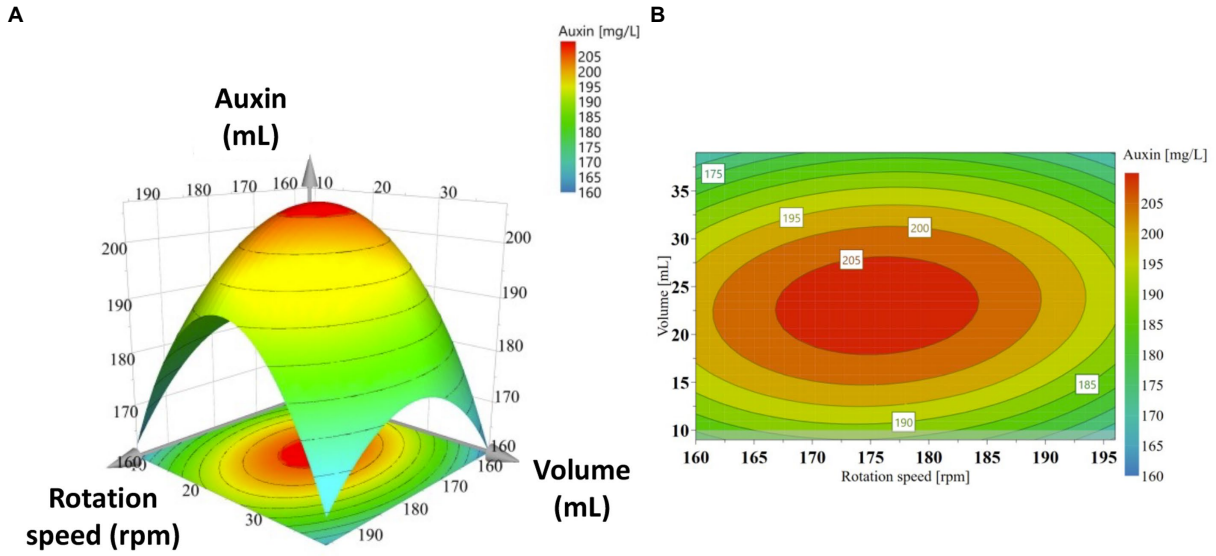

FIGURE 4
Response surface plots (3D, **A**) and contour plots (2D, **B**) of auxin production as a function of significant interactions between factors: rotation speed (X_1) and medium volume (X_2).

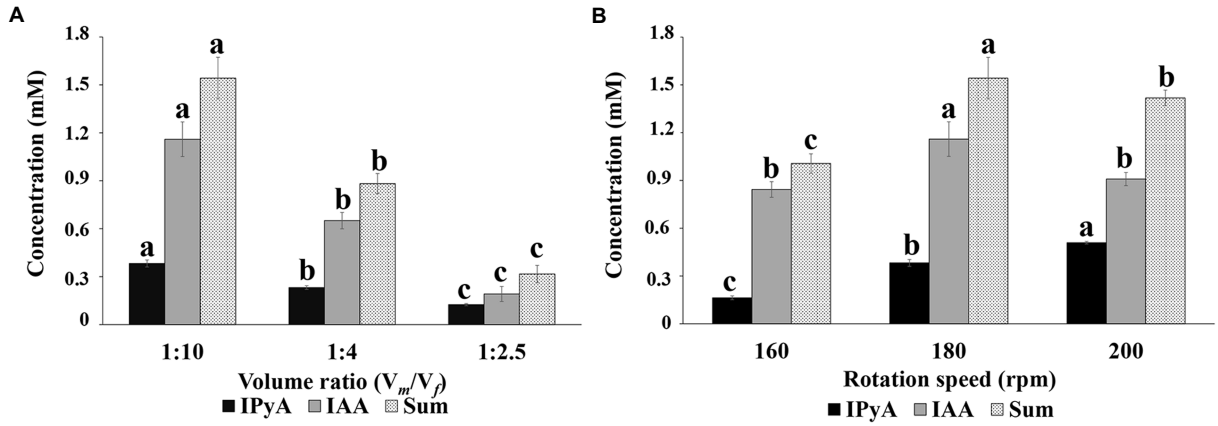

FIGURE 5
Results of the HPLC-MS analysis showing the effect of liquid-to-flask volume ratio **(A)** and rotation speed **(B)** on the conversion of tryptophan (Trp) to indole-3-acetic acid (IAA) *via* the indole-3-pyruvic acid (IPyA) pathway. All cultures were grown in YES + Trp medium at 25°C for 24h. Data are means ± standard error and refer to cultures grown at 180rpm **(A)** and a medium-to-flask volume ratio (V_m/V_f) of 1:10 **(B)**. The graphs show the molar concentration of the single compounds and the IAA+IPyA sum. Bars with no letter in common significantly differ at $p \leq 0.05$ (Tukey HSD test).

Results reported in Figure 1 also indicated that the shift from the rich (LB) to the saline (YES) medium determined a reduction in the formation of indolic secondary metabolites, including indole-3-acetaldehyde and indole-3-carboxylic acid (Supplementary Table S2). The latter compound can play an important role in pathogen defense (Böttcher et al., 2014) but can interfere with auxin-signaling (Kumar et al., 2021). Comparative metabolomics indicated that, if the primary goal is the production of postbiotics with higher auxin/IAA levels, the YES medium can provide better results regarding IAA titer and product selectivity. With *P. agglomerans* strain C1, shifting from LB to YES medium, most of the Trp-derived indoles, 11 out of 14 compounds belonging to the indoles and derivatives cluster, decreased, and a 5.4-fold IAA titer increase occurred (Supplementary Table S2). These differences can be dependent on differences in the composition of the growth media in terms of carbon and nitrogen source (peptides in LB and sucrose and NH_4^+ ions in YES) and Mg^{2+} ion concentration (30–40 μM in LB and 1 mM in YES; Papp-Wallace and Maguire, 2008). Magnesium ions, in combination with thiamine pyrophosphate (ThDP), are an essential cofactor of IPDC, the key enzyme involved in IAA biosynthesis *via* the tryptophan-dependent IPyA pathway. Koga et al. (1992) demonstrated that, in the absence of ThDP and Mg^{2+}, the active IPDC tetramers dissociate into inactive monomers and dimers. It can be postulated that the differences in the Mg^{2+} ion concentration can differentially modulate the IPCD activity and play a role in the

TABLE 5 Effect of medium-to flask volume ratio (V_m/V_f) and rotation speed (rpm) on the product selectivity (IAA/IPyA) and substrate consumption rate (final-to-initial Trp ratio).

Factor	Condition	Relative molar ratio	
		IAA/IPyA	Trp_f/Trp_i
Volume ratio (V_m/V_f)	1:10	3.0 ± 0.1^{a}	1.1 ± 0.1^{b}
	1:4	2.8 ± 0.1^{b}	1.3 ± 0.1^{a}
	1:2.5	1.5 ± 0.0^{c}	1.2 ± 0.1^{ab}
Rotation speed (rpm)	160	5.2 ± 0.1^{A}	0.6 ± 0.0^{C}
	180	3.0 ± 0.1^{B}	1.1 ± 0.1^{A}
	200	1.8 ± 0.1^{C}	1.0 ± 0.1^{B}

The superscript letters indicate similarities or significant differences between the values. Values with no letter in common significantly differ at $p \leq 0.05$ (Tukey HSD test).

differential accumulation of the Trp-derived indoles. The scientific literature provides extensive evidence that the magnesium availability in the fermentation media significantly affects the growth and metabolism of microbial cells (Walker, 1994). Our results showed that a culture medium with a higher Mg^{2+} content could be valuable for the microbial production of auxin/IAA through the IPyA pathway.

Many reports indicate that, in bacteria, auxin/IAA production is affected by several parameters, including medium components, growth temperature, incubation time, and medium pH (Apine and Jadhav, 2011; Balaji et al., 2012; Peng et al., 2014; Bhutani et al., 2018; Srisuk et al., 2018; Myo et al., 2019; Baliyan et al., 2021). Notably, none of these studies reported a detailed metabolomics analysis of the effect of these parameters on the production of other auxin-related compounds. On the other hand, no information is available on the effect of aeration efficiency on the microbial production of phytohormones such as auxin, whereas oxygen plays a crucial role in the growth and metabolism of aerobic and facultative anaerobic bacteria (Garcia-Ochoa et al., 2010; Seidel et al., 2021).

In this work, we demonstrated that the statistical optimization of the growth conditions was a powerful tool to optimize the auxin production by *P. agglomerans* strain C1 (Figure 4; Tables 2, 3). To the best of our knowledge, this is the first study investigating the effect of aeration efficiency on auxin production by plant growth-promoting bacteria. The statistical optimization of aeration efficiency, performed by varying the medium liquid-to-flask volume ratio (V_m/V_f) and rotation speed (rpm; Table 1), provided valuable insights into the effect of oxygen availability on IAA production by the *P. agglomerans* strain C1 (Tables 2, 3). From an agroecological perspective, this result also highlights the importance of oxygen availability on the plant-microbe's interaction in the rhizosphere, phyllosphere, and endosphere.

Our results indicated that the parameters that directly affect aeration efficiency in shake flask conditions (rotation speed and liquid-to-flask volume ratio) play an essential role in auxin/IAA production, which was improved from 3.1 mg IAA_{equ}/L (CCD1, rotation speed 140 rpm, 1:2.5 V_m/V_f) to 208.1 mg IAA_{equ}/L (CCD2, rotation speed 180 rpm, 1:10 V_m/V_f; Table 2; Figure 3). In agreement with this observation, higher IAA values were achieved using a 1:10 liquid-to-flask volume ratio at all agitation regimes (Table 2; Figure 3B). A higher amount of auxin/IAA was obtained when the oxygen availability was higher because of higher rotation speed and lower medium liquid-to-flask volume ratio (Tables 2, 3). However, data showed low tolerance of strain C1 to mechanical stress: IAA concentration decreased when the rotation speed was higher than 180 rpm (Table 3).

The polynomial equation indicated that the two independent variables, rotation speed (X_1 and X_1^2) and medium volume (X_2 and X_2^2), had a negative effect on the response (Table 4). In contrast, the interactive effect of these variables (X_1X_2) positively affected the auxin production (Table 4). The equation also indicated that the coefficient of the quadratic X_2 was larger than that of X_1^2, which means that the medium volume, and therefore the medium volume-to-flask ratio, had a greater effect on the auxin production than the rotation speed. This information was corroborated by the curvature of the 3D response surface that was more pronounced on the "Medium Volume" axis (Figure 4A). Similar evidence was also obtained by the 2D contour plot in which the contours around the stationary point were elliptical and elongated on the rotation speed axis (Figure 4B). Both plots indicated that: (1) at the extreme values of both variables, auxin/IAA concentration was low; (2) a slight change of the response value required a more significant move along the rotation speed axis than on the medium volume axis.

Validation carried out to verify the accuracy of the model showed that the predicted value (207.3 mg IAA_{equ}/L) agreed well with the experimental value (208.3 ± 0.4 mg IAA_{equ}/L). The application of the RSM through CCD allowed us to obtain the maximum auxin concentration at a medium liquid-to-flask volume ratio of 1:10 and a rotation speed of 176 rpm. The auxin concentration obtained under optimized conditions (208.3 ± 0.4 mg IAA_{equ}/L) was about 40% higher compared to the growth conditions previously described (Luziatelli et al., 2020b).

Targeted metabolomics highlighted some features of the *P. agglomerans*' IAA biosynthetic metabolism, which were not addressed by the RSM analysis underlining the importance of integrating the two methodologies. Data in Table 5 indicated that the culture conditions affected the flux of Trp to IAA through IPyA. At a rotary speed of 180 rpm, the product selectivity (IAA/IPyA molar ratio) had a 2-fold increase reducing the medium-to-flask volume ratio from 1:2.5 to 1:10 (higher aeration efficiency; Table 5). Surprisingly, at the lower medium-to-flask volume ratio (1:10), the product selectivity decreased about 2.9-fold when the rotation speed was increased from 160 to 200 rpm (Table 5). Thus, independently from the final concentration of IAA, it was evident that the mechanical and oxidative stresses associated with the increase in the rotary speed affected the conversion of Trp to IAA.

Results of targeted metabolomics indicated that an increase in the rotation speed determined an accumulation of IPyA in the culture medium (Figure 5B) and a decrease in the IAA product selectivity (Table 5, column IAA/IPyA). The increased difference between IAA and IAA + IPyA (Figure 5B) also indicated that the moles of IPyA converted to IAA decreased with the increase in the rotation speed from 180 to 200 rpm. Since no significant difference in the IAA level was observed between rotation speeds 160 and 200 rpm, the variation in the total amount of IAA + IPyA was strictly related to a difference in the accumulation of IPyA (Figure 5B). The higher flux of Trp in the IAA biosynthetic pathway and the lower conversion rate of IPyA to IAA occurring when the rotation speed was increased from 160 to 180 rpm could be due to a difference in the availability of the cofactors of the key enzyme of the IPyA pathway: pyridoxal-5-phosphate (PLP) for L-tryptophan/aromatic

amino acid aminotransferase (AAT); thiamin diphosphate for indole-3-pyruvate decarboxylase (IPDC); $NAD(H)^+$ for indole-3-acetaldehyde (IAAld) dehydrogenase/oxidase (AAO). Based on the literature (Lakaye et al., 2004; Taboada et al., 2008; Tramonti et al., 2021; Yuan et al., 2021), we expected, also in *P. agglomerans*, that the levels of these cofactors could be higher when the dissolved oxygen is not a limiting factor and its replenishment satisfies metabolic oxygen demands. However, the availability of these cofactors for the enzymes involved in the IAA synthesis depends upon the number of competitive reactions that consume the same cofactors and are active under the same growth conditions. In future research, we intend to combine metabolomics and RSM analysis to explore the correlation between IAA product selectivity and cofactors availability and improve the fermentation strategies focusing on both IAA yield and product selectivity.

Whereas in all *P. agglomerans* strains described so far (including strain C1), the production of high levels of IAA is dependent upon the addition of Trp to the culture medium, our data indicated that, under our experimental conditions, strain C1 synthetized Trp and released part of it in the culture medium (Table 5, column Trp_f/Trp_i). Interestingly, the highest IAA product selectivity was obtained when the residual Trp level was lower (Table 5, rotation speed of 160 rpm). Considering that the first step of the major pathways of Trp degradation involves PLP-dependent enzymes (Cellini et al., 2020), it can be postulated that the flux of Trp versus IPyA is modulated by the affinity of the AAT versus the substrate (Trp) and the cofactor (PLP) and the intracellular concentration of both. The highest IAA product selectivity obtained when the Trp biosynthesis is limited (Table 5, rotation speed of 160 rpm) can indicate that redirecting the Trp metabolic flux is pivotal, either in laboratory conditions or in natural environments, to modulate the IAA production by PGPRs.

The levels of auxin/IAA obtained in this study are lower than those reported for *P. agglomerans* PVM (Apine and Jadhav, 2011), *Klebsiella* SN 1.1 (Chaiharn and Lumyong, 2011), *Enterobacter* sp. DMKU-rp206 strain (Srisuk et al., 2018) and *Enterobacter* sp. P-36 (Luziatelli et al., 2021), but are indeed higher than those obtained upon optimization of IAA production by *Bacillus* strains isolated from *Vigna radiata* (Bhutani et al., 2018), *Streptomyces* sp. VSMGT1014 (Harikrishnan et al., 2014), *Burkholderia seminalis* S52 (Tallapragada et al., 2015), or *Pseudomonas putida* sp. Rs-198 strain (Peng et al., 2014). For *P. agglomerans* strain PVM (Apine and Jadhav, 2011), the higher levels of IAA were produced on a medium containing animal-derived ingredients (meat), which are not compliant with EU rules on fertilizing products.

Conclusion

Integration of RSM with metabolomics, which provides comprehensive information on the cellular response to external stimuli, can be valuable for optimizing various microbial products. In this study, we provided evidence that, in developing auxin-enriched plant postbiotics, the combined use of RSM and untargeted and targeted metabolomics can help discover new properties of PGPBs and take advantage of their metabolic capabilities. Postbiotics allow the rational design of cocktails of metabolites associated with PGP traits. The separate production of metabolites can be a valuable strategy in synthesizing molecules whose biosynthetic pathways compete in the cell for ATP, cofactors (auxins and gibberellins), or precursors (auxins and phenylpropanoids). Metabolites synthesized under different growing conditions or from different PGPBs can be produced separately and appropriately mixed to obtain tailor-made products for different crops and growing conditions. This study provides guidance for the sustainable development and optimization of postbiotics for agriculture.

Data availability statement

The original contributions presented in the study are included in the article/Supplementary material, further inquiries can be directed to the corresponding authors.

Author contributions

FM, FL, and MR contributed to the conception and design of the study, wrote the first draft of the manuscript, and wrote and edited the final version of the manuscript. FM, FL, PB, AF, VM, and MR contributed to defining the methodology and investigation. FM, FL, PB, and MR contributed to software analysis and data validation. All authors contributed to the article and approved the submitted version.

Funding

This study was carried out within the Agritech National Research Center and received funding from the European Union Next-GenerationEU [Piano Nazionale di Ripresa e Resilienza (PNRR)—Missione 4 Componente 2, Investimento 1.4—D.D. 1032 17/06/2022 and CN00000022].

Acknowledgments

We are grateful to the NGA Laboratory (Spain) for helping us with the metabolomics analysis and metabolite annotation.

Conflict of interest

The authors declare that the research was conducted in the absence of any commercial or financial relationships that could be construed as a potential conflict of interest.

Publisher's note

Author disclaimer

This manuscript reflects only the authors' views and opinions, neither the European Union nor the European Commission can be considered responsible for them.

Supplementary material

The Supplementary material for this article can be found online at: https://www.frontiersin.org/articles/10.3389/fmicb.2023.1022248/full#supplementary-material

References

Apine, O. A., and Jadhav, J. P. (2011). Optimization of medium for indole-3-acetic acid production using *Pantoea agglomerans* strain PVM. *J. Appl. Microbiol.* 110, 1235–1244. doi: 10.1111/j.1365-2672.2011.04976.x

Ashihara, H., Stasolla, C., Fujimura, T., and Crozier, A. (2018). Purine salvage in plants. *Phytochemistry* 147, 89–124. doi: 10.1016/j.phytochem.2017.12.008

Balaji, N., Lavanya, S. S., Muthamizhselvi, S., and Tamilarasan, K. (2012). Optimization of fermentation condition for indole acetic acid production by *pseudomonas* species. *Int. J. Adv. Biotechnol. Res.* 3, 797–803. doi: 10.1007/s12010-021-03558-0

Baliyan, N., Dhiman, S., Dheeman, S., Kumar, S., and Maheshwari, D. K. (2021). Optimization of indole-3-acetic acid using response surface methodology and its effect on vegetative growth of chickpea. *Rhizosphere* 17:100321. doi: 10.1016/j.rhisph.2021.100321

Barupal, D. K., and Fiehn, O. (2017). Chemical similarity enrichment analysis (ChemRICH) as alternative to biochemical pathway mapping for metabolomic datasets. *Sci. Rep.* 7, 14567–14511. doi: 10.1038/s41598-017-15231-w

Bezerra, M. A., Santelli, R. E., Oliveira, E. P., Villar, L. S., and Escaleira, L. A. (2008). Response surface methodology (RSM) as a tool for optimization in analytical chemistry. *Talanta* 76, 965–977. doi: 10.1016/j.talanta.2008.05.019

Bharucha, U., Patel, K., and Trivedi, U. B. (2013). Optimization of indole acetic acid production by *pseudomonas putida* UB1 and its effect as plant growth-promoting rhizobacteria on mustard (*Brassica nigra*). *Agric. Res.* 2, 215–221. doi: 10.1007/s40003-013-0065-7

Bhutani, N., Maheshwari, R., Negi, M., and Suneja, P. (2018). Optimization of IAA production by endophytic *bacillus* spp. from *Vigna radiata* for their potential use as plant growth promoters. *Isr. J. Plant Sci.* 65, 83–96. doi: 10.1163/22238980-00001025

Bielach, A., Hrtyan, M., and Tognetti, V. B. (2017). Plants under stress: involvement of auxin and cytokinin. *Int. J. Mol. Sci.* 18:1427. doi: 10.3390/ijms18071427

Blaženović, I., Kind, T., Ji, J., and Fiehn, O. (2018). Software tools and approaches for compound identification of LC-MS/MS data in metabolomics. *Meta* 8:31. doi: 10.3390/metabo8020031

Blaženović, I., Kind, T., Sa, M. R., Ji, J., Vaniya, A., Wancewicz, B., et al. (2019). Structure annotation of all mass spectra in untargeted metabolomics. *Anal. Chem.* 91, 2155–2162. doi: 10.1021/acs.analchem.8b04698

Böttcher, C., Chapman, A., Fellermeier, F., Choudhary, M., Scheel, D., and Glawischnig, E. (2014). The biosynthetic pathway of indole-3-carbaldehyde and indole-3-carboxylic acid derivatives in *Arabidopsis*. *Plant Physiol.* 165, 841–853. doi: 10.1104/PP.114.235630

Breig, S. J. M., and Luti, K. J. K. (2021). Response surface methodology: a review on its applications and challenges in microbial cultures. *Mater. Today Proc.* 42, 2277–2284. doi: 10.1016/j.matpr.2020.12.316

Bulgari, R., Cocetta, G., Trivellini, A., Vernieri, P., and Ferrante, A. (2015). Biostimulants and crop responses: a review. *Biol. Agric. Hortic.* 31, 1–17. doi: 10.1080/01448765.2014.964649

Calvo, P., Nelson, L., and Kloepper, J. W. (2014). Agricultural uses of plant biostimulants. *Plant and Soil* 383, 3–41. doi: 10.1007/s11104-014-2131-8

Cellini, B., Zelante, T., Dindo, M., Bellet, M. M., Renga, G., Romani, L., et al. (2020). Pyridoxal 5'-phosphate-dependent enzymes at the crossroads of host-microbe tryptophan metabolism. *Int. J. Mol. Sci.* 21:5823. doi: 10.3390/ijms21165823

Chaiharn, M., and Lumyong, S. (2011). Screening and optimization of indole-3-acetic acid production and phosphate solubilization from rhizobacteria aimed at improving plant growth. *Curr. Microbiol.* 62, 173–181. doi: 10.1007/s00284-010-9674-6

de Souza, R., Ambrosini, A., and Passaglia, L. M. (2015). Plant growth-promoting bacteria as inoculants in agricultural soils. *Genet. Mol. Biol.* 38, 401–419. doi: 10.1590/S1415-475738420150053

Di, D.-W., Wu, L., Zhang, L., An, C. -W., Zhang, T. -Z., Luo, P., et al. (2016). Functional roles of *Arabidopsis* CKRC2/YUCCA8 gene and the involvement of PIF4 in the regulation of auxin biosynthesis by cytokinin *Sci. Sci. Rep.* 6:36866. doi: 10.1038/srep36866

Duca, D., Lorv, J., Patten, C. L., Rose, D., and Glick, B. R. (2014). Indole-3-acetic acid in plant-microbe interactions. *Antonie Van Leeuwenhoek* 106, 85–125. doi: 10.1007/s10482-013-0095-y

Dutkiewicz, J., Mackiewicz, B., Lemieszek, M. K., Golec, M., and Milanowski, J. (2016). *Pantoea agglomerans*: a mysterious bacterium of evil and good. Part III. Deleterious effects: infections of humans, animals, and plants. *Ann. Agric. Environ. Med.* 23, 197–205. doi: 10.5604/12321966.1203878

European Union Regulation (EU) 2019/1009 of the European Parliament and of the council of 5 June 2019 laying down rules on the making available on the market of EU fertilising products and amending regulations (EC) no 1069/2009 and (EC) no 1107/2009 and repealing Regula. Off. J. Eur. Union (2019), 1–114.

Feng, Y., Shen, D., and Song, W. (2006). Rice endophyte *Pantoea agglomerans* YS19 promotes host plant growth and affects allocations of host photosynthates. *J. Appl. Microbiol.* 100, 938–945. doi: 10.1111/j.1365-2672.2006.02843.x

Garcia-Ochoa, F., Gomez, E., Santos, V. E., and Merchuk, J. C. (2010). Oxygen uptake rate in microbial processes: An overview. *Biochem. Eng. J.* 49, 289–307. doi: 10.1016/J.BEJ.2010.01.011

Gertsman, I., and Barshop, B. A. (2018). Promises and pitfalls of untargeted metabolomics. *J. Inherit. Metab. Dis.* 41, 355–366. doi: 10.1007/s10545-017-0130-7

Glick, B. R. (1995). The enhancement of plant growth by free-living bacteria. *Can. J. Microbiol.* 41, 109–117. doi: 10.1139/m95-015

Glick, B. R. (2012). Plant growth-promoting bacteria: mechanisms and applications. *Scientifica* 2012:963401. doi: 10.6064/2012/963401

Gross, J., Avrani, S., Katz, S., Hilau, S., and Hershberg, R. (2020). Culture volume influences the dynamics of adaptation under long-term stationary phase. *Genome Biol. Evol.* 12, 2292–2301. doi: 10.1093/GBE/EVAA210

Halliday, K. J., Martínez-García, J. F., and Josse, E. M. (2009). Integration of light and auxin signaling. *Cold Spring Harb. Perspect. Biol.* 1:a001586. doi: 10.1101/cshperspect.a001586

Harikrishnan, H., Shanmugaiah, V., and Balasubramanian, N. (2014). Optimization for production of indole acetic acid (IAA) by plant growth promoting *Streptomyces* sp. VSMGT1014 isolated from rice rhizosphere. *Int. J. Curr. Microbiol. App. Sci.* 3, 158–171.

Kamran, S., Shahid, I., Baig, D. N., Rizwan, M., Malik, K. A., and Mehnaz, S. (2017). Contribution of zinc solubilizing bacteria in growth promotion and zinc content of wheat. *Front. Microbiol.* 8:2593. doi: 10.3389/fmicb.2017.02593

Kasahara, H. (2016). Current aspects of auxin biosynthesis in plants. *Biosci. Biotechnol. Biochem.* 80, 34–42. doi: 10.1080/09168451.2015.1086259

Kim, J. H., and Jander, G. (2007). *Myzus persicae* (green peach aphid) feeding on *Arabidopsis* induces the formation of a deterrent indole glucosinolate. *Plant J.* 49, 1008–1019. doi: 10.1111/j.1365-313X.2006.03019.x

Koga, J., Adachi, T., and Hidaka, H. (1992). Purification and characterization of indolepyruvate decarboxylase. A novel enzyme for indole-3-acetic acid biosynthesis in *Enterobacter cloacae*. *J. Biol. Chem.* 267, 15823–15828. doi: 10.1016/S0021-9258(19)49609-9

Kram, K. E., and Finkel, S. E. (2014). Culture volume and vessel affect long-term survival, mutation frequency, and oxidative stress of *Escherichia coli*. *Appl. Environ. Microbiol.* 80, 1732–1738. doi: 10.1128/AEM.03150-13

Kumar, P., Lee, J. H., and Lee, J. (2021). Diverse roles of microbial indole compounds in eukaryotic systems. *Biol. Rev. Camb. Philos. Soc.* 96, 2522–2545. doi: 10.1111/BRV.12765

Lakaye, B., Wirtzfeld, B., Wins, P., Grisar, T., and Bettendorff, L. (2004). Thiamine triphosphate, a new signal required for optimal growth of *Escherichia coli* during amino acid starvation. *J. Biol. Chem.* 279, 17142–17147. doi: 10.1074/jbc.M313569200

Lennox, E. S. (1955). Transduction of linked genetic characters of the host by bacteriophage P1. *Virology* 1, 190–206. doi: 10.1016/0042-6822(55)90016-7

Luziatelli, F., Brunetti, L., Ficca, A. G., and Ruzzi, M. (2019a). Maximizing the efficiency of vanillin production by biocatalyst enhancement and process optimization. *Front. Bioeng. Biotechnol.* 7:279. doi: 10.3389/fbioe.2019.00279

Luziatelli, F., Ficca, A. G., Bonini, P., Muleo, R., Gatti, L., Meneghini, M., et al. (2020a). A genetic and metabolomic perspective on the production of indole-3-acetic acid by *Pantoea agglomerans* and use of their metabolites as biostimulants in plant nurseries. *Front. Microbiol.* 11:1475. doi: 10.3389/fmicb.2020.01475

Luziatelli, F., Ficca, A. G., Cardarelli, M., Melini, F., Cavalieri, A., and Ruzzi, M. (2020b). Genome sequencing of *Pantoea agglomerans* C1 provides insights into molecular and genetic mechanisms of plant growth-promotion and tolerance to heavy metals. *Microorganisms* 8:153. doi: 10.3390/microorganisms8020153

Luziatelli, F., Ficca, A. G., Colla, G., Baldassarre Švecová, E., and Ruzzi, M. (2019b). Foliar application of vegetal-derived bioactive compounds stimulates the growth of beneficial bacteria and enhances microbiome biodiversity in lettuce. *Front. Plant Sci.* 10:60. doi: 10.3389/fpls.2019.00060

Luziatelli, F., Ficca, A. G., Colla, G., Svecova, E., and Ruzzi, M. (2016). Effects of a protein hydrolysate-based biostimulant and two micronutrient-based fertilizers on plant growth and epiphytic bacterial population of lettuce. *Acta Hortic.* 1148, 43–48. doi: 10.17660/ActaHortic.2016.1148.5

Luziatelli, F., Gatti, L., Ficca, A. G., Medori, G., Silvestri, C., Melini, F., et al. (2020c). Metabolites secreted by a plant-growth-promoting *Pantoea agglomerans* strain improved rooting of *Pyrus communis* L. cv Dar Gazi cuttings. *Front. Microbiol.* 11:539359. doi: 10.3389/fmicb.2020.539359

Luziatelli, F., Melini, F., Bonini, P., Melini, V., Cirino, V., and Ruzzi, M. (2021). Production of indole auxins by *Enterobacter* sp. strain P-36 under submerged conditions. *Ferment.* 7:138. doi: 10.3390/FERMENTATION7030138

Mardones, F. O., Rich, K. M., Boden, L. A., Moreno-Switt, A. I., Caipo, M. L., Zimin-Veselkoff, N., et al. (2020). The COVID-19 pandemic and global food security. *Front. Vet. Sci.* 7:928. doi: 10.3389/fvets.2020.578508

McClerklin, S. A., Lee, S. G., Harper, C. P., Nwumeh, R., Jez, J. M., and Kunkel, B. N. (2018). Indole-3-acetaldehyde dehydrogenase-dependent auxin synthesis contributes to virulence of *pseudomonas syringae* strain DC3000. *PLoS Pathog.* 14:e1006811. doi: 10.1371/journal.ppat.1006811

Moustaine, M., Kahkahi, R.El, Benbouazza, A., Benkirane, R., El, A., and Achbani, H. (2016). The role of plant growth-promoting rhizobacteria (PGPR) in stimulating the growth of wheat (*Triticum aestivum* L.) in Meknes region. *Morocco. Plant Cell Biot. Mol. Biol.* 17, 363–373.

Myers, S. S., Smith, M. R., Guth, S., Golden, C. D., Vaitla, B., Mueller, N. D., et al. (2017). Climate change and global food systems: potential impacts on food security and undernutrition. *Annu. Rev. Public Health* 38, 259–277. doi: 10.1146/annurev-publhealth-031816-044356

Myo, E. M., Ge, B., Ma, J., Cui, H., Liu, B., Shi, L., et al. (2019). Indole-3-acetic acid production by *Streptomyces fradiae* NKZ-259 and its formulation to enhance plant growth. *BMC Microbiol.* 19:155. doi: 10.1186/s12866-019-1528-1

Nunes, C., Usall, J., Teixidó, N., Fons, E., and Viñ, I. (2002). Post-harvest biological control by *Pantoea agglomerans* (CPA-2) on Golden delicious apples. *J. Appl. Microbiol.* 92, 247–255. doi: 10.1046/j.1365-2672.2002.01524.x

Olanrewaju, O. S., Glick, B. R., and Babalola, O. O. (2017). Mechanisms of action of plant growth promoting bacteria. *World J. Microbiol. Biotechnol.* 33, 197–116. doi: 10.1007/S11274-017-2364-9

Oleńska, E., Małek, W., Wójcik, M., Swiecicka, I., Thijs, S., and Vangronsveld, J. (2020). Beneficial features of plant growth-promoting rhizobacteria for improving plant growth and health in challenging conditions: a methodical review. *Sci. Total Environ.* 743:140682. doi: 10.1016/J.SCITOTENV.2020.140682

Ozaktan, H., Malkoclu, M. C., Tüzel, Y., Oztekin, G. B., and Yolageldi, L. (2017). Effects of plant growth-promoting rhizobacteria on organic tomato seedling production. *Acta Hortic.* 1164, 63–68. doi: 10.17660/ActaHortic.2017.1164.8

Panda, B. P., Ali, M., and Javed, S. (2007). Fermentation process optimization. *Res. J. Microbiol.* 2, 201–208. doi: 10.3923/JM.2007.201.208

Paponov, I. A., Paponov, M., Teale, W., Menges, M., Chakrabortee, S., Murray, J. A., et al. (2008). Comprehensive transcriptome analysis of auxin responses in *Arabidopsis*. *Mol. Plant* 1, 321–337. doi: 10.1093/mp/ssm021

Papp-Wallace, K. M., Endimiani, A., Taracila, M. A., and Bonomo, R. A. (2011). Carbapenems: past, present, and future. *Antimicrob. Agents Chemother.* 55, 4943–4960. doi: 10.1128/AAC.00296-11

Papp-Wallace, K. M., and Maguire, M. E. (2008). Magnesium transport and magnesium homeostasis. *EcoSal Plus* 3. doi: 10.1128/ecosalplus.5.4.4.2

Paredes-Páliz, K. I., Pajuelo, E., Doukkali, B., Caviedes, M. Á., Rodríguez-Llorente, I. D., and Mateos-Naranjo, E. (2016). Bacterial inoculants for enhanced seed germination of *Spartina densiflora*: implications for restoration of metal polluted areas. *Mar. Pollut. Bull.* 110, 396–400. doi: 10.1016/j.marpolbul.2016.06.036

Patten, C. L., and Glick, B. R. (2002). Role of *pseudomonas putida* indoleacetic acid in development of the host plant root system. *Appl. Environ. Microbiol.* 68, 3795–3801. doi: 10.1128/AEM.68.8.3795-3801.2002

Peng, Y., He, Y., Wu, Z., Lu, J., and Li, C. (2014). Screening and optimization of low-cost medium for *pseudomonas putida* Rs-198 culture using RSM. *Braz. J. Microbiol.* 45, 1229–1237. doi: 10.1590/S1517-83822014000400013

Putri, S. P., Nakayama, Y., Matsuda, F., Uchikata, T., Kobayashi, S., Matsubara, A., et al. (2013). Current metabolomics: practical applications. *J. Biosci. Bioeng.* 115, 579–589. doi: 10.1016/j.jbiosc.2012.12.007

Rouphael, Y., and Colla, G. (2018). Synergistic biostimulatory action: designing the next generation of plant biostimulants for sustainable agriculture. *Front. Plant Sci.* 9:1655. doi: 10.3389/fpls.2018.01655

Ruzzi, M., and Aroca, R. (2015). Plant growth-promoting rhizobacteria act as biostimulants in horticulture. *Sci. Hortic.* 196, 124–134. doi: 10.1016/j.scienta.2015.08.042

Ryu, R. J., and Patten, C. L. (2008). Aromatic amino acid-dependent expression of indole-3-pyruvate decarboxylase is regulated by TyrR in *Enterobacter cloacae* UW5. *J. Bacteriol.* 190, 7200–7208. doi: 10.1128/JB.00804-08

Saia, S., Aissa, E., Luziatelli, F., Ruzzi, M., Colla, G., Ficca, A. G., et al. (2020). Growth-promoting bacteria and arbuscular mycorrhizal fungi differentially benefit tomato and corn depending upon the supplied form of phosphorus. *Mycorrhiza* 30, 133–147. doi: 10.1007/s00572-019-00927-w

Salminen, S., Collado, M. C., Endo, A., Hill, C., Lebeer, S., Quigley, E. M. M., et al. (2021). The international scientific Association of Probiotics and Prebiotics (ISAPP) consensus statement on the definition and scope of postbiotics. *Nat. Rev. Gastroenterol. Hepatol.* 18, 649–667. doi: 10.1038/s41575-021-00440-6

Schmidt, F. R. (2005). Optimization and scale up of industrial fermentation processes. *Appl. Microbiol. Biotechnol.* 68, 425–435. doi: 10.1007/s00253-005-0003-0

Seidel, S., Maschke, R. W., Werner, S., Jossen, V., and Eibl, D. (2021). Oxygen mass transfer in biopharmaceutical processes: numerical and experimental approaches. *Chem. Ing. Tech.* 93, 42–61. doi: 10.1002/CITE.202000179

Singh, V., Haque, S., Niwas, R., Srivastava, A., Pasupuleti, M., and Tripathi, C. (2017). Strategies for fermentation medium optimization: an in-depth review. *Front. Microbiol.* 7:2087. doi: 10.3389/fmicb.2016.02087

Singh, S. K., Singh, S. K., Tripathi, V. R., Khare, S. K., and Garg, S. K. (2011). Comparative one-factor-at-a-time, response surface (statistical) and bench-scale bioreactor level optimization of thermoalkaline protease production from a psychrotrophic *pseudomonas putida* SKG-1 isolate. *Microb. Cell Fact.* 10:114. doi: 10.1186/1475-2859-10-114

Spaepen, S., and Vanderleyden, J. (2011). Auxin and plant-microbe interactions. *Cold Spring Harb. Perspect. Biol.* 3:a001438. doi: 10.1101/cshperspect.a001438

Srisuk, N., Sakpuntoon, V., and Nutaratat, P. (2018). Production of indole-3-acetic acid by *Enterobacter* sp. DMKU-rp206 using sweet whey as a low-cost feed stock. *J. Microbiol. Biotechnol.* 28, 1511–1516. doi: 10.4014/jmb.1805.04043

Swain, M. R., and Ray, R. C. (2008). Optimization of cultural conditions and their statistical interpretation for production of in-dole-3-acetic acid by *Bacillus subtilis* CM5 using cassava fibrous residue. *J. Sci. Ind. Res.* 67, 622–628.

Taboada, H., Encarnación, S., Vargas Mdel, C., Mora, Y., Miranda-Ríos, J., Soberón, M., et al. (2008). Thiamine limitation determines the transition from aerobic to fermentative-like metabolism in *rhizobium etli* CE3. *FEMS Microbiol. Lett.* 279, 48–55. doi: 10.1111/j.1574-6968.2007.01006.x

Tallapragada, P., Dikshit, R., and Seshagiri, S. (2015). Isolation and optimization of IAA producing *Burkholderia seminalis* and its effect on seedlings of tomato. *Songklanakarin J. Sci. Technol.* 37, 553–559.

Teale, W. D., Paponov, I. A., and Palme, K. (2006). Auxin in action: signalling, transport and the control of plant growth and development. *Nat. Rev. Mol. Cell Biol.* 7, 847–859. doi: 10.1038/nrm2020

Teleki, A., and Takors, R. (2019). Quantitative profiling of endogenous metabolites using hydrophilic interaction liquid chromatography-tandem mass spectrometry (HILIC-MS/MS). *Methods Mol. Biol.* 1859, 185–207. doi: 10.1007/978-1-4939-8757-3_10

Thormar, H. (2010) Antimicrobial Lipids and Innate Immunity. in *Lipids and Essential Oils as Antimicrobial Agents*. ed. H. Thormar (John Wiley & Sons, Ltd), 123–150. doi: 10.1002/9780470976623.CH6

Toffelson, J. (2022). What the war in Ukraine means for energy, climate and food. *Nature* 604, 232–233. doi: 10.1038/d41586-022-00969-9

Toscano, S., Romano, D., Massa, D., Bulgari, R., Franzoni, G., and Ferrante, A. (2018). Biostimulant applications in low input horticultural cultivation systems. *Italus Hortus* 25, 27–36. doi: 10.26353/J.ITAHORT/2018.1.2736

Tramonti, A., Nardella, C., di Salvo, M. L., Barile, A., D'Alessio, F., de Crécy-Lagard, V., et al. (2021). Knowns and unknowns of vitamin B_6 metabolism in *Escherichia coli*. *EcoSal Plus* 9. doi: 10.1128/ecosalplus.ESP-0004-2021

UN. (2017). World population prospects: The 2017 revision. Multimedia library—United Nations Department of Economic and Social Affairs. Available at: https://www.un.org/development/desa/publications/world-population-prospects-the-2017-revision.html.

Venkadesaperumal, G., Amaresan, N., and Kumar, K. (2014). Plant growth promoting capability and genetic diversity of bacteria isolated from mud volcano and lime cave of Andaman and Nicobar Islands. *Braz. J. Microbiol.* 45, 1271–1281. doi: 10.1590/S1517-83822014000400018

Walker, G. M. (1994). The roles of magnesium in biotechnology. *Crit. Rev. Biotechnol.* 14, 311–354. doi: 10.3109/07388559409063643

Walterson, A. M., and Stavrinides, J. (2015). *Pantoea*: insights into a highly versatile and diverse genus within the Enterobacteriaceae. *FEMS Microbiol. Rev.* 39, 968–984. doi: 10.1093/femsre/fuv027

Woodward, A. W., and Bartel, B. (2005). Auxin: regulation, action, and interaction. *Ann. Bot.* 95, 707–735. doi: 10.1093/aob/mci083

Xie, J., Shu, P., Strobel, G., Chen, J., Wei, J., Xiang, Z., et al. (2017). *Pantoea agglomerans* SWg2 colonizes mulberry tissues, promotes disease protection and seedling growth. *Biol. Control* 113, 9–17. doi: 10.1016/j.biocontrol.2017.06.010

Yuan, X., McGhee, G. C., Slack, S. M., and Sundin, G. W. (2021). A novel signaling pathway connects thiamine biosynthesis, bacterial respiration, and production of the exopolysaccharide amylovoran in *Erwinia amylovora*. *Mol. Plant Microbe Interact.* 34, 1193–1208. doi: 10.1094/MPMI-04-21-0095-R

Zwiewka, M., Bilanovičová, V., Seifu, Y. W., and Nodzyński, T. (2019). The nuts and bolts of PIN auxin efflux carriers. *Front. Plant Sci.* 10:985. doi: 10.3389/fpls.2019.00985

frontiers | Frontiers in Plant Science

TYPE Original Research
PUBLISHED 22 May 2023
DOI 10.3389/fpls.2023.1122621

OPEN ACCESS

EDITED BY
Youssef Rouphael,
University of Naples Federico II, Italy

REVIEWED BY
Muhammad Ahsan Asghar,
Centre for Agricultural Research, Hungary
Oskars Purmalis,
University of Latvia, Latvia
Serenella Nardi,
University of Padua, Italy

*CORRESPONDENCE
Youlu Bai
baiyoulu@caas.cn

RECEIVED 13 December 2022
ACCEPTED 18 April 2023
PUBLISHED 22 May 2023

CITATION
Wang Y, Lu Y, Wang L, Song G, Ni L, Xu M, Nie C, Li B and Bai Y (2023) Analysis of the molecular composition of humic substances and their effects on physiological metabolism in maize based on untargeted metabolomics. *Front. Plant Sci.* 14:1122621. doi: 10.3389/fpls.2023.1122621

Analysis of the molecular composition of humic substances and their effects on physiological metabolism in maize based on untargeted metabolomics

Yuhong Wang[1,2], Yanli Lu[1], Lei Wang[1], Guipei Song[1], Lu Ni[1], Mengze Xu[1], Caie Nie[1], Baoguo Li[2] and Youlu Bai[1]*

[1]State Key Laboratory of Efficient Utilization of Arid and Semi-arid Arable Land in Northern China/Key Laboratory of Plant Nutrition and Fertilizer, Ministry of Agriculture and Rural Affairs/Institute of Agricultural Resources and Regional Planning, Chinese Academy of Agricultural Sciences, Beijing, China, [2]College of Land Science and Technology, China Agricultural University, Beijing, China

Introduction: Humic substances (HSs), components of plant biostimulants, are known to influence plant physiological processes, nutrient uptake and plant growth, thereby increasing crop yield. However, few studies have focused on the impact of HS on overall plant metabolism, and there is still debate over the connection between HS' structural characteristics and their stimulatory actions.

Methods: In this study, two different HSs (AHA, Aojia humic acid and SHA, Shandong humic acid) screened in a previous experiment were chosen for foliar spraying, and plant samples were collected on the tenth day after spraying (62 days after germination) to investigate the effects of different HSs on photosynthesis, dry matter accumulation, carbon and nitrogen metabolism and overall metabolism in maize leaf.

Results and discussion: The results showed different molecular compositions for AHA and SHA and a total of 510 small molecules with significant differences were screened using an ESI-OPLC-MS techno. AHA and SHA exerted different effects on maize growth, with the AHA inducing more effective stimulation than the SHA doing. Untargeted metabolomic analysis revealed that the phospholipid components of maize leaves treated by SHA generally increased significantly than that in the AHA and control treatments. Additionally, both HS-treated maize leaves exhibited different levels of accumulation of trans-zeatin, but SHA treatment significantly decreased the accumulation of zeatin riboside. Compared to CK treatment, AHA treatment resulted in the reorganization of four metabolic pathways: starch and sucrose metabolism, TCA cycle, stilbenes, diarylheptanes, and curcumin biosynthesis, and ABC transport, SHA treatment modified starch and sucrose metabolism and unsaturated fatty acid biosynthesis. These results demonstrate that HSs exert their function through a multifaceted mechanism of action, partially connected to their hormone-like activity but also involving hormoneindependent signaling pathways.

KEYWORDS

humic substances, metabolomics, hormone-like activity, starch and sucrose metabolism, chemical structures

1 Introduction

An inventive approach to the problems facing sustainable agriculture is the use of natural plant biostimulants. Humic substances (HSs), one type of plant biostimulants, has received increasing attention from researchers and farmers. Numerous studies have shown that plants grown in soils with sufficient HSs or exposed to foliar sprays composed of HSs are healthier because these plants are well adapted to and resistant to stressful conditions and show increased yield through increasing nutrient uptake (Quaggiotti et al., 2004; Mora et al., 2010).

For many years, soil scientists have been working to determine the chemical characteristics and molecular structure of HSs and to study how they regulate plant growth and development. Several studies have proposed the hypothesis that HSs may act on plants through two different mechanisms: (1) indirectly, by enhancing the chemical, physical and biological qualities of the soil; and (2) directly, by regulating growth processes, nutrient transport systems and primary and secondary metabolism through HSs active components (Canellas and Olivares, 2014; Nardi et al., 2016; Nunes et al., 2019; Pizzeghello et al., 2020). For example, HSs stimulate the synthesis of plasma membrane H^+-ATPase. Through the combination of ATP hydrolysis and H^+ transfer across the cell membrane, this enzyme promotes root growth by acidifying the plasma outer body, loosening the cell wall, and lengthening the cell (Zandonadi et al., 2007; Canellas and Olivares, 2014; De Azevedo et al., 2019). Activation of plasma membrane H^+-ATPase also improves plant nutrition by increasing the electrochemical proton gradient that drives ion transport across the cell membrane (Canellas et al., 2002). Earthworm-like HSs induce changes in the metabolism of reactive oxygen species (ROS) in plants after root application (García et al., 2012; García et al., 2014). ROS have been categorized as signal transduction molecules that participate in transduction mechanisms regulating metabolic activities, including plant growth and development, although they are mainly considered as hazardous compounds resulting from aerobic metabolism (Mittler et al., 2011; Mittler, 2017). In this context, ROS has been proposed as a possible target for the action of HSs in plants (Garcia et al., 2016; Roomi et al., 2018). Additionally, Zandonadi et al. (2010) showed that HSs induce nitric oxide (NO) production at the site of lateral root emergence. Both primary and secondary metabolism have been documented to be altered by HSs. For example, Nardi et al. (2007) observed the upregulation of glycolysis and the tricarboxylic acid cycle (TCA) enzymes in maize plants treated with 1 mg C L^{-1} HS, which also increased nitrogen uptake/assimilation and nitrogen metabolism. Furthermore, HS treatment was able to lower the pH of the root surface, promote H^+/NO_3^- symport and stimulate nitrate uptake, transport and nitrogen metabolism enzyme activity. In addition, HS treatment exerted a positive effect on phenylpropane metabolism and enzymes associated with cytoprotection (Garcia et al., 2016). Taken together, these findings illustrate the complexity of the relationship between HSs and plant physiology and emphasize the value of molecular approaches in understanding the nature of this interaction.

In the last decade, new molecular "omics" techniques (genomics, transcriptomics, proteomics and metabolism) have been applied to evaluate the effects of HSs on plant metabolism (Carletti et al., 2008; Nephali et al., 2020). Recent studies have described the impeccable ability and potential of omics techniques to reveal the mechanisms describing the interaction of biostimulants with plants. Trevisan et al. (2011) performed a transcriptomic analysis and Gene Ontology classification on *Arabidopsis* after three days of treatment and observed a widespread but slight modulation of the transcriptional activity involving the plant's main metabolic functions: respiration and photosynthesis, general cellular metabolism, fatty acids, nitrogen/sulfur, plant hormones, plant development, senescence, stress response, ion and water transport. Nunes et al. (2019) used a label-free quantitative proteomic approach to analyze the effect of humic acid on the soluble protein fraction of maize seedling roots, and differences were detected in root proteins relation to energy metabolism, the cytoskeleton, cellular trafficking, protein conformation and degradation, and DNA replication. However, few studies have investigated the effects of HSs on plant metabolism via metabolomics analysis. Metabolomics is a multidisciplinary omics science that provides unique opportunities to predict the mode of action of biostimulants on crops and to identify markers of biostimulatory effects (Nephali et al., 2020). In one of the very few cases when metabolomics techniques were utilized in HS response research, Marino et al. (2013) showed that HS-treated pears and papaya calli produced more asparagine than controls using ^{1}H HR-MAS NMR analysis.

Numerous studies have highlighted how HSs might improve plant responses and growth metrics, but the new challenge is to determine which parts or specific components of HSs are most likely to induce a positive response. For this analysis, the structure and composition of humic substances must be examined and characterized. In general, the characterization of HSs is divided into elemental, functional group and molecular weight categories, but these characterizations do not provide information at the molecular level. In 2001, Piccolo (2001) redefined fulvic acid (FA) as a hydrophilic small molecule conjugate with sufficient acid functional groups to allow its dispersion in solution at any pH. At neutral or alkaline pH, HSs are not stable polymers but supramolecular associations of relatively small heterogeneous molecules (polymethylenic chains, fatty acids and steroid compounds) held together by weak dispersion forces, such as van der Waals, π-π, CH-π, and interactions. As intermolecular hydrogen bonds are gradually formed at lower pH values, their conformation gradually increases until flocculation, and the concept of "humeomics" was thus introduced (Piccolo, 2001; Nebbioso and Piccolo, 2011). Furthermore, researchers have speculated that the progressive breakdown of the intra- and intermolecular interactions that support complex superstructures may reduce the complexity of humic supramolecules, releasing individual humic substances molecules that enter the plant or engage with receptors that interact with plant cells. These molecules are separated and identified by combining advanced analytical techniques (Nebbioso and Piccolo, 2011; Drosos et al., 2017). Further studies have noted that the main molecular components of HSs are fatty acids, ethers,

esters, alcohols, aromatic lignified fragments, polysaccharides and peptides (Scaglia et al., 2016; Drosos et al., 2017).

The complexity of the HS structure and its associated biological activity in plants has been extensively described. Despite the fact that several approaches have been employed in research on this topic, the direct relationship between the chemical structures of HSs and their effects on plant metabolism has not yet been fully elucidated so far. Initially, the molecule size, hydrophilicity, and particular functional groups of HSs were proposed to be closely associated with their activity. According to Nardi et al. (2007), the size exclusion chromatography fraction of HSs with the lowest molecular weight is the most effective in promoting plant metabolism, the most hydrophilic, and contains more sugars and less lignin-derived materials. Similarly, the effects of different molecular size fractions of HSs on root growth have been explored (Dobbss et al., 2010; Canellas et al., 2012). While all HS induced root growth in *Arabidopsis* and maize seedlings, the intensity of their effects varied depending on HS molecular size and plant species. Further analysis revealed that the hydrophobicity index (HB/HI) of HSs obtained using NMR parameters correlates with the appearance of lateral root hairs, but that the hydrophobic carbon content correlates negatively with the induction of lateral roots (Canellas et al., 2012). Other studies have also discovered a connection between hydrophobicity and plant responses, whereby more hydrophobic humic acids showed the greatest activity in stimulating plant responses, with certain HSs lengthening roots and others increasing root density. According to Scaglia et al. (2016), the hormone-like activity of HSs extracted from compost prepared from cow manure and leather waste varies depending on the maturity stage, and the molecules correlating with growth hormone-like activity were identified as carboxylic acids and amino acids.

The combination of a fine chemical analysis of HS molecules and overall metabolic studies of their effects on plants provides a new opportunity to expand knowledge of both the detailed chemistry and use management aspects of HSs. Based on this hypothesis, we sought to analyze the molecular composition of HSs through UHPLC-QTOF-MS technology, we employed a method based on UPHLC-QTOF-MS non-target metabolome to study the overall effect on HSs on maize metabolism. The mains aim of this study were as follows: i) assaying differences in chemical composition and biological activity from two different reservoirs; ii) appraising differential effects of these HSs on altering maize growth and metabolism over a long period; iii) attempt to analyze the molecular compositions of HSs, and explore the mechanism of promoting growth from the perspective of metabolomics in maize.

2 Materials and methods

2.1 Materials

The two HSs selected for this investigation were those that had been screened in earlier corn field trials and displayed the greatest variation in effects (data not shown). One of the humic substances (AHA, Aojia humic acid) was supplied by Beijing Aojia Fertilizer Co., Ltd. (Beijing, China), using Heilongjiang lignite as the raw material, and the other (SHA, Shangdong humic acid) was supplied by Shandong Nongda Fertilizer Technology Co., Ltd. (Jinan, China), also using Inner Mongolia lignite as the raw material.

The experiment was conducted in a glass greenhouse of the Institute of Agricultural Resources and Regional Planning, Chinese Academy of Agricultural Sciences. Both plant groups were grown in pots containing a mixture of perlite/vermiculite (1:1, v/v) in glass house. The composition of the Hoagland nutrient solution is as follows: 2 mM $MgSO_4$, 1 mM NH_4NO_3, 5 mM KNO_3,1 mM KH_2PO_4, 0.005 mM KI, 5.76 mM $Ca(NO_3)_2$, 0.1 mM H_3BO_3, 0.15 mM $MnSO_4$, 0.05 mM $ZnSO_4$, 0.00016 mM $CuSO_4$, 0.0019 mM $CoCl_2$, 0.1 mM NaFe-EDTA. The initial pH was adjusted to 5.8 ± 0.1.

Maize seeds (*Zea mays L.*, hybrid Zhengdan 958) were soaked in 0.5% NaClO for 30 min, then rinsed and soaked in water for 12 h for surface sterilization. Afterward, the seeds were sown in vermiculite-filled seedling trays and allowed to germinate in an incubator with 14 h of light at 28°C and 10 h of darkness at 20°C. The seedlings with the same growth vigor were selected and placed in pots after 7 days. During the rejuvenation period, Hoagland nutrient solution with a half-ionic strength was used. After 7 days, it was replaced with complete nutrient solution, and 1L of nutrient solution was applied every week.

2.2 Determination of molecular composition of HSs

HS molecular composition was determined using UHPLC-QTOF-MS as described below.

2.2.1 Sample preparation

The metabolites were extracted by adding 1 mL of pre-chilled extraction solution (2:2:1, (v/v/v) methanol: acetonitrile: water solvent mixture) to 80 mg of the samples. The sample was vortexed and mixed, sonicated at low temperature for 30 min, and then centrifuged at 14000×g for 20 min at 4°C. The supernatant was dried in a vacuum centrifuge, 100 µL of aqueous acetonitrile (1:1, (v/v) acetonitrile: water) was added before the LC-MS analysis, vortexed and centrifuged at 14000×g for 15 min at 4°C, and the supernatant was collect as the sample for analysis. In addition, pooled quality control (QC) samples were prepared by combining of equal amounts of the samples.

2.2.2 Liquid phase parameters

All samples were analyzed using the UHPLC (1290 Infinity LC, Agilent Technologies) system. An ACQUITY UPLC BEH HILIC column (100 mm × 2.1 mm, 1.7 µm, Waters, Ireland) was used for separation at a column oven temperature maintained at 25°C. The flow rate was set to 0.5 mL/min, while the mobile phase comprised solvent A (water, 25 mM ammonium acetate and 25 mM ammonium hydroxide) and solvent B (Acetonitrile),. Gradient elution conditions were set as follows: 0–0.5 min, 95% B; 0.5–7 min, 95–65% B; 7–8 min, 65–40% B; 8–9 min, 40% B; 9–9.1 min, 40–95% B; and 9.1–12 min, 95% B. The injection volume for each

sample was 42 µL. A random order was used for continuous analysis of the samples to avoid fluctuations detection signal in the instrument. QC samples were inserted in the sample queue for monitoring and evaluating the stability of the system and the reliability of the experimental data.

2.2.3 Mass spectrometry parameters

Samples eluted from the column were detected using a TripleTOF6600 high-resolution tandem mass spectrometer with Q-TOF operated in both positive and negative ion modes. The Ion spray voltage floating was wet to 5500 and -5500 V for the positive and negative ion modes, respectively. Mass spectrometry data were acquired on the information dependent acquisition IDA mode, with a TOF mass range set from 25 to 1000 Da, and the accumulation time for product ion scan was set to 0.05 s/spectra.

2.2.4 Data processing

The raw MS data were converted to MzXML files by ProteoWizard MSConvert, and then peak alignment and integration were conducted using XCMS software. The parameters of XCMS were as follows: mass range 25–1000 m/z, mass tolerance 10 ppm, retention time (RT) range 0.5–12.0 min, and RT width threshold 0.2 min. In the extracted ion features, only the variables with more than 50% of the nonzero measurement values in at least one group were retained. Compound identification of metabolites was performed by comparing of accuracy m/z value (<10 ppm), and MS/MS spectra with an in-house database established with available authentic standards.

After data normalization, the processed data matrix was submitted to R package (ropls) for multivariate statistical analysis. Principal component analysis (PCA) was conducted to observe the clustering pattern of all samples and the repeatability of the intra-group samples. Orthogonal partial least squares discriminant analysis (OPLS-DA) was further applied to filter out the noise irrelevant to the classification information and improve the parsing ability and effectiveness of the model. Variables with variable importance for the projection (VIP) values from the OPLS-DA analysis larger than 1.0 were considered as potential biomarkers since they can discriminate between two compared groups.

2.3 Experimental design

The experiment was arranged in randomized blocks using three treatments and ten replicates. The treatments were as follows: 1) foliar application of pure water, (CK), 2) foliar application of AHA (AHA), 3) foliar application of SHA (SHA). HSs was sprayed at a concentration of 0.5%, which was selected based on supplier recommendations and preliminary experiments assessing the effects of HS spraying on maize growth. Plants underwent foliar spraying around 16:00 using a portable sprayer, with which the upper and the lower surface of leaves were treated. The first spraying was conducted at 14 days after transplantation, and the remaining foliar sprays were applied at 10-day intervals for 5 total applications. The sampling point for plant samples was 10 days after the last spraying. For non-target metabolome analysis, the tip, middle, and base of the latest fully expanded leaves of six plants were collected and mixed, and immediately frozen in liquid nitrogen and stored at -80°C for subsequent analysis. For the biochemical analysis and to measure the fresh and dry weight of each plant's leaf, stem, and root, four samples were collected. Then, the different parts of the maize plant were oven-dried at 105°C for 30 min and maintained at 75°C for 48 h to obtain a stable dry weight. Dry matter was analyzed for total nitrogen, phosphorus and potassium percentages. Total nutrition absorption per plant was calculated based on the tissue nutrition content and dry weight.

2.4 Phenotypic analysis

A ruler was used to measure plant height from the stem base to the tip of the latest fully expanded leaf. Plant stem diameter was measured with caliper. Expanded leaves area was estimated non-destructively using the Yanxin-1242 portable leaf area meter of each leaf with ligule emergence. Vegetative developmental stage was based on the number of leaves with an emerged ligule and the number of visible leaves at harvest.

2.5 Parameters for measuring photosynthesis

The photosynthetic rates were measured between 9:00 and 11:00 using a portable photosynthesis system (Li-6400, LICOR Biosciences, Lincoln, USA). The air temperature, CO_2 concentration and photosynthetic photon flux density in the leaf chamber were set to 28°C, 500 µmol·mol^{-1}, 1500 µmol m^{-2} s^{-1}, respectively. Three biological repeats were included per data point. The instantaneous WUE was calculated as WUE = Pn/Tr (Chen et al., 2018).

Relative chlorophyll concentration in leaves was recorded using a portable SPAD meter (SPAD-502 Plus, KONICA MINOLTA, Japan) with 10 reading data. Both of these values were detected using the youngest leaf with ligule emergence.

2.6 Measurement of physiological parameters

Fresh leaf samples, which were previously stored at −80°C, were ground to a homogenous powder with liquid nitrogen. The protein concentration was determined using the Bradford method and a UV/Vis spectrophotometer at 595 nm wavelength. The protein concentration was reported as mg of protein per g of fresh leaf. The soluble sugar concentration was calculated using the sulfuric acid-anthrone colorimetric method. The free amino acid content was determined using the ninhydrin method with leucine as the standard.

Phenylalanine ammonia-lyase (PAL) was extracted by homogenizing frozen tissue into pre-cooled sodium borate buffer (100 mM, pH 8.7) at a ratio of 1:9 (w/v). After centrifugation at 10,000 rpm/min for 10 min at 4°C, the supernatant was collected for the enzyme assay using a previously described method (Assis et al., 2001). One unit

(U) of PAL activity was defined as the amount of enzyme extract producing an increase in the optical density of 0.1 per min, which was measured at 290 nm by using UV/Vis spectrophotometer. Sucrose synthase (SS) and nitrate reductase (NR) activities were measured using the corresponding assay kits according to the manufacturer's instructions (Beijing Solarbio Technology Co., Ltd., Beijing, China). Briefly, 0.1 g leaf sample was added to 1 mL extraction solution, followed by the ice bath homogenization, and the mixture was centrifuged at 8000 g for 10 min at 4°C, supernatant was collected for further analysis. The absorbance at 480 nm was used for the calculation of SS activity and one unit of SS activity was defined as 1 μg of sucrose per g of tissue catalyzed per minute. For NR activity, 0.1 g leaf samples were extracted in 1 ml extraction solution and the mixture was centrifuged at 4000 g for 10 min. The resulting supernatant was collected for further analysis. The absorbance at 340 nm was used for the calculation of NR activity, one unit (U) of NR activity was defined as the amount of 1 μmol NADH consumed per hour per g of sample.

2.7 Metabolomics analysis of maize leaf

2.7.1 Sample preparation

The maize leaf samples were quickly frozen in liquid nitrogen and grounded with a homogenizer. The metabolites were extracted by adding 1 mL of pre-chilled extraction solution (2:2:1, (v/v/v) methanol: acetonitrile: water-water solvent mixture) to 80 mg (fresh weight) of the samples. The sample was vortexed and mixed, sonicated at low temperature for 30 min, and then centrifuged at 14000×g for 20 min at 4°C. The supernatant was dried in vacuum centrifuge, and 100 μL of aqueous acetonitrile (1:1, (v/v) acetonitrile: water) were added before the LC-MS analysis. The samples were vortexed and centrifuged at 14000×g for 15 min at 4° C, and the supernatant was collected as the sample for analysis.

2.7.2 Liquid phase parameters

The samples were separated using a UHPLC (1290 Infinity LC, Agilent Technologies) system with a C-18 column. The column temperature was 40°C. The flow rate was set to 0.4 mL/min; and the injection volume was 2 μL. The mobile phase A consisted of 25 mM ammonium acetate and 0.5% formic acid in water, mobile phase B was methanol. Gradient elution conditions were set as follows: 0–0.5 min, 5% B; 0.5–10 min, 5–100% B; 10–12 min, 100% B; 12–12.1 min, 100–5% B; 12.1–16 min, 5% B. During the whole analysis, the sample was placed in an automatic sampler at 4°C.

The mass spectrometry parameters and data processing were the same as the determination of the HS molecular composition described in Section 2.2.

2.8 Data analysis

Analysis of variance (one-way ANOVA) was performed using the SPSS 23 (IBM Corp) software with type of treatment as factor followed by a pairwise *post hoc* analyses (Duncan test) to determine which means differed significantly at $p < 0.05$.

3 Results

3.1 The molecular composition of HSs

An untargeted metabolomics approach based on UHPLC-QTOF-MS was used to obtain the molecular composition profiles of these two HSs, and 1320 small molecules were detected, of which 754 were detected in positive ion mode and 566 were detected in negative ion mode. The principal component analysis (PCA) explained 59.43%, 69.55% of the overall variance in molecules detected in positive and negative ion mode, respectively (Figure 1). The PCA score plots (Figure 1) showed two main clusters accounting for the AHA and SHA, respectively. Within each cluster, the molecular composition profiles did not overlap, thus indicating distinct molecular signatures.

The 1320 small molecules classified into eighteen categories according to their chemical properties (Figure 2). The six categories that accounted for a higher percentage were benzenes, organic heterocyclic compounds, organic acids and derivatives, lipids and lipid-like molecules, organic oxygen compounds, phenylpropanoids and polyketides.

As PCA is an unsupervised data analysis method, orthogonal partial least squares discriminant analysis (OPLS-DA) was further employed to filter out the noise unrelated to the classification information and improve the parsing ability and effectiveness of the model. The OPLS-DA plot (Figure S1) of the two samples showed a clear separation. The OPLS-DA model was also used to obtain the variable weight values (VIP) and measure the intensity and explanatory power of the effect of each small-molecule substance on the classification discrimination of the AHA and SHA groups. Thereafter, multivariate analysis of OPLS-DA and univariate analysis of *t*-test were used to identify differential accumulated component ions. The use of VIP≥1 and $p \leq 0.05$ as cutoff thresholds revealed 357 differentially expressed positive ions, of which 234 and 123 shown FC (fold change, AHA/SHA) >1 and FC<1, respectively (Support Material 1, Figure S2).

Among the 510 small molecules with significant differences, 17 were attributed to hormones and their derivatives (Table 1). With exception of Trans-zeatin and Forchlorfenuron, two plant and hormone-like substances with an ionic strength FC<1, the remaining 15 bioactive substances showed FC>1, especially 5-methoxytryptophan, Gibberellin a4 and gamma.-hydroxybutyric acid, whose FC were 486.10, 263.50 and 109.57, respectively. Notably, we also found that AHA and SHA contain a variety of substances with bacteriostatic and anthelmintic effects, such as fludioxonil, vanillic acid, triadimefon, Penthiopyrad, dinex, dichlormid, etc (Support Material 1).

3.2 Phenotype changes in maize

Foliar applications of AHA and SHA exerted differing effects on maize growth. In plant treated with AHA, a greater number of expanded leaves, plant height, leaf area and leaf dry weight was observed (+4.72%, 6.12%, 12.87% and 13.29%, respectively) compared to CK treatment ($p<0.05$), but root growth was not

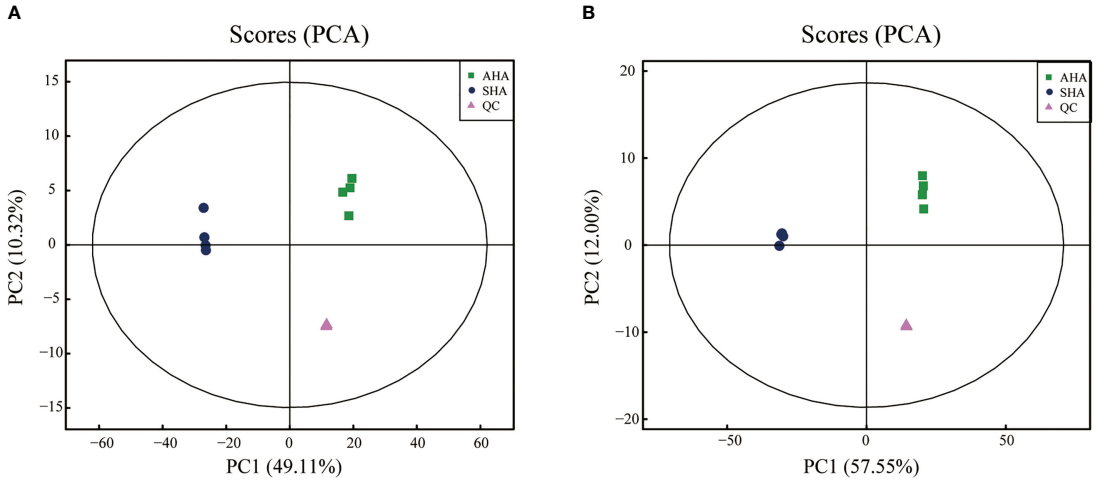

FIGURE 1
PCA score plots of the molecules profiles in positive ions mode **(A)** and negative ions mode **(B)**.

modified (Table 2). Meanwhile, SHA treatment did not induce any significant changes in these parameters (except for the number of expanded leaves) compared to CK treatment. The increment in shoot leaf area after treatment with AHA was due to a small increment in total leaf number per shoot and a significant increment in average leaf size compared to SHA and CK treatments. In particular, compared with SHA and CK, the leaf area of AHA treatment group increased by 12.87% and 18.91%, respectively, and the leaf dry weight increased by 13.29% and 11.69%, respectively. Based on these results, AHA inducing more effective stimulation than the SHA.

3.3 Nutrient absorption

Both foliar spray treatments increased the P concentration in the leaves, stems and roots of maize plants (Figure 3A). The AHA and SHA treatments increased the stem N concentration by 6.4% and 13.04%, respectively, compared with the control treatment, but only the SHA group was declared to be significantly different from control plants ($p<0.05$). The K concentrations in maize were not affected by the tested biostimulants (Figure 3A). In contrast to stem N concentration, the N content in the plant following the AHA treatment increased by 43.52%, 20.62% compared with that observed after SHA and control treatments, respectively, due to the higher stem dry weight (Figure 3B). Similarly, the AHA treatment significantly increased the N, P and K content of the whole plant than that in SHA treatment plant ($p<0.05$, Figure 3B).

3.4 Photosynthetic parameters

A positive effect of HSs was also been observed on the photosynthesis in maize leaves (Figure 4). Compared to the control treatment, plants subjected to the AHA foliar spraying treatment exhibited a significantly increased relative chlorophyll content (SPAD value) and C and subsequently displayed an increase in net photosynthesis; whereas there was a slight increase in SPAD values of SHA-treated leaves, their C and Pn were similarly significantly increased. There was no statistical

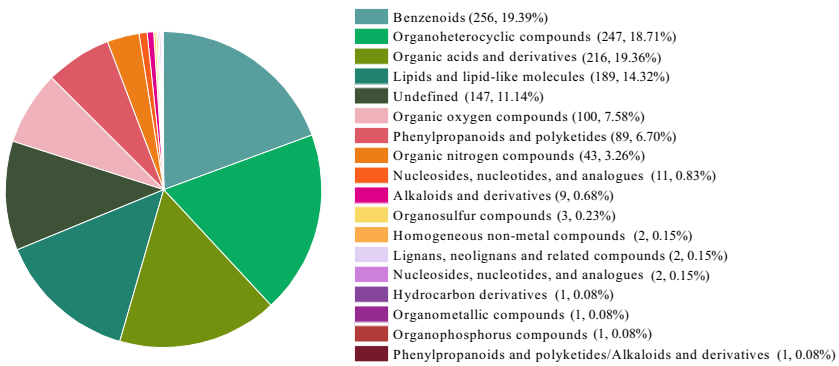

FIGURE 2
The classification of small molecules of AHA and SHA. The numbers in parentheses represent the amount of small molecule in each category and their proportion to the total number small molecules identified.

TABLE 1 Analysis of differentially abundant phytohormones and its derived small molecules.

Components	VIP	Fold Change	p-value	m/z	rt(s)
Gibberellin a4	2.04	263.50	7.92E-06	297.14446	351.356
Jasmonic acid	4.23	98.18	4.67E-05	193.09733	196.536
Dopamine	2.24	91.95	0.0017	137.05984	196.68
Melatonin	1.82	44.66	3.11E-07	255.11309	66.3665
Indolelactic acid	2.08	18.89	0.0005	206.08133	110.1555
(+)-.Alpha.-tocopherol	1.35	16.12	0.0027	165.09113	268.667
1 H-indole-3-carboxylic acid, 1-[2-(2,5-dimethylphenoxy)ethyl]	1.95	13.17	0.0025	292.11777	357.409
6-hydroxymelatonin	1.06	7.95	1.38E-10	232.09689	108.6255
5-methoxytryptophan	4.77	486.10	1.63E-11	233.08499	66.7377
N-phthalyl-l-tryptophan	1.08	52.47	0.0002	333.0663	239.1855
Indole-3-acetamide	1.19	15.78	0.0020	173.08133	255.88
Gamma-hydroxybutyric acid	1.41	109.57	1.16E-08	103.03909	332.3425
Aldosterone	1.01	12.50	0.0004	359.19024	239.082
3-bromo-5-phenylsalicylic acid	1.11	70.97	6.97E-08	246.95881	378.625
Trans-zeatin	2.21	0.19	9.63E-09	220.1121	60.8938
Forchlorfenuron	3.56	0.11	0.0027	248.07057	272.306

The VIP value is the value of variable weights obtained using the OPLS-DA model; Fold Change is the fold change of ionic strength of the substance in AHA and SHA; m/z is the mass-to-charge ratio of the substance; rt(s) is the retention time of the substance.

difference in leaf SPAD, C and Pn between the humic acid treatments (Figure 4).

3.5 Carbon and nitrogen metabolism-related enzymes and substances

Compared to the control group, plants subjected to the AHA foliar spraying treatment presented higher levels of soluble carbohydrates and free amino acid content, but did not exhibit a change in the leaf protein concentration (Figure 5). SHA treatment did not exert any significant effect on leaf soluble carbohydrate concentrations but induced a slight reduction in free amino acid concentration when compared to CK treatment. SS, NR and PAL activities in maize leaves were significantly increased by AHA treatment than that in SHA and CK treatments plant ($p \leq 0.05$, Figure 5).

3.6 Metabolomic profile

3.6.1 Effects of different treatments on overall metabolic profile

An untargeted metabolomics approach based on UPLC-QTOF-MS was used to obtain the metabolite profiles of maize leaves. Notably, 1373 characteristic peaks were detected and 1272 metabolites were identified. The PCA score plot (Figure 6) showed that the positive and negative ion modes explained 45.09% and 43.15% of the total variance, respectively. All groups in the positive ion mode were separated along PC2, and in the

TABLE 2 Results of phenotypic analyses of maize subjected to different treatments.

Treatment	Number of visible leaves	Number of expanded leaves	Plant height (cm)	Stem diameter (mm)	Leaf area (cm^2)	Leaf dry weight (g per plant)	Stem dry weight ($g \cdot plant^{-1}$)	Root dry weight ($g \cdot plant^{-1}$)
AHA	15.00 ± 0.47	11.10 ± 0.32 a	187.33 ± 7.47a	18.47 ± 1.23	3143.70 ± 237.72a	15.77 ± 1.21 a	13.38 ± 2.70	6.83 ± 1.77
SHA	14.60 ± 0.52	11.00 ± 0 a	183.25 ± 3.5ab	17.78 ± 1.52	2785.16 ± 296.09b	13.92 ± 1.67 b	11.62 ± 2.54	5.36 ± 1.14
CK	14.60 ± 0.52	10.60 ± 0.52 b	176.53 ± 9.46b	18.32 ± 1.39	2643.73 ± 311.57b	14.12 ± 1.08 b	13.28 ± 1.97	6.95 ± 0.28

Values are presented as the means ± standard errors (n = 4). Different letters in the same group indicate statistically significant differences at $p \leq 0.05$.

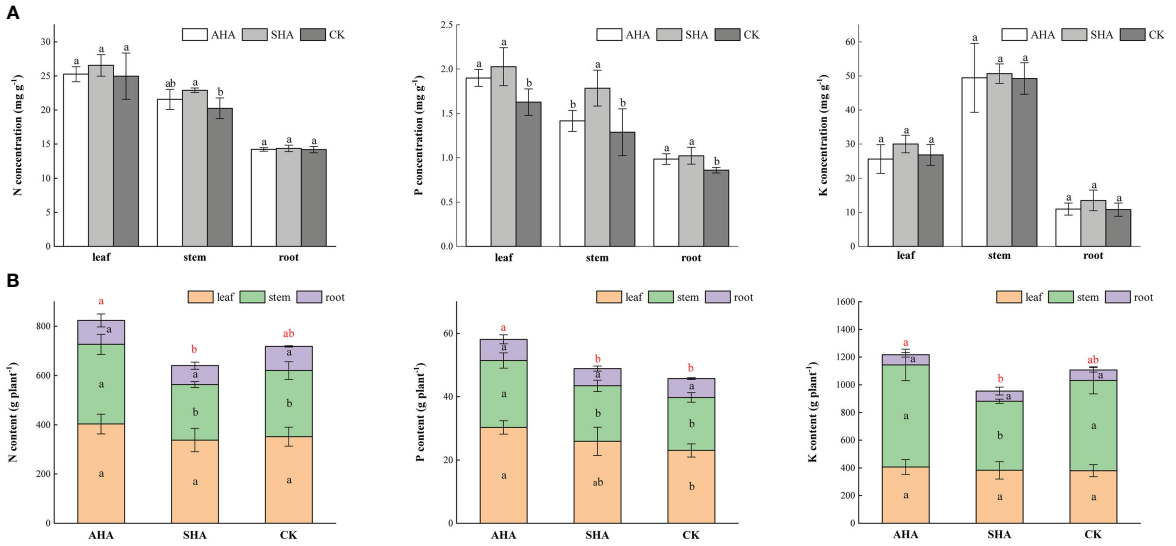

FIGURE 3
Different portions of maize subjected to various treatments differ in their nutrient concentration **(A)** and content **(B)**. Different letters indicate statistically significant differences at $p \leq 0.05$. Different red letters indicate statistically significant differences of whole plant nutrient content at $p \leq 0.05$. Vertical bars indicate means ± standard errors (n=4).

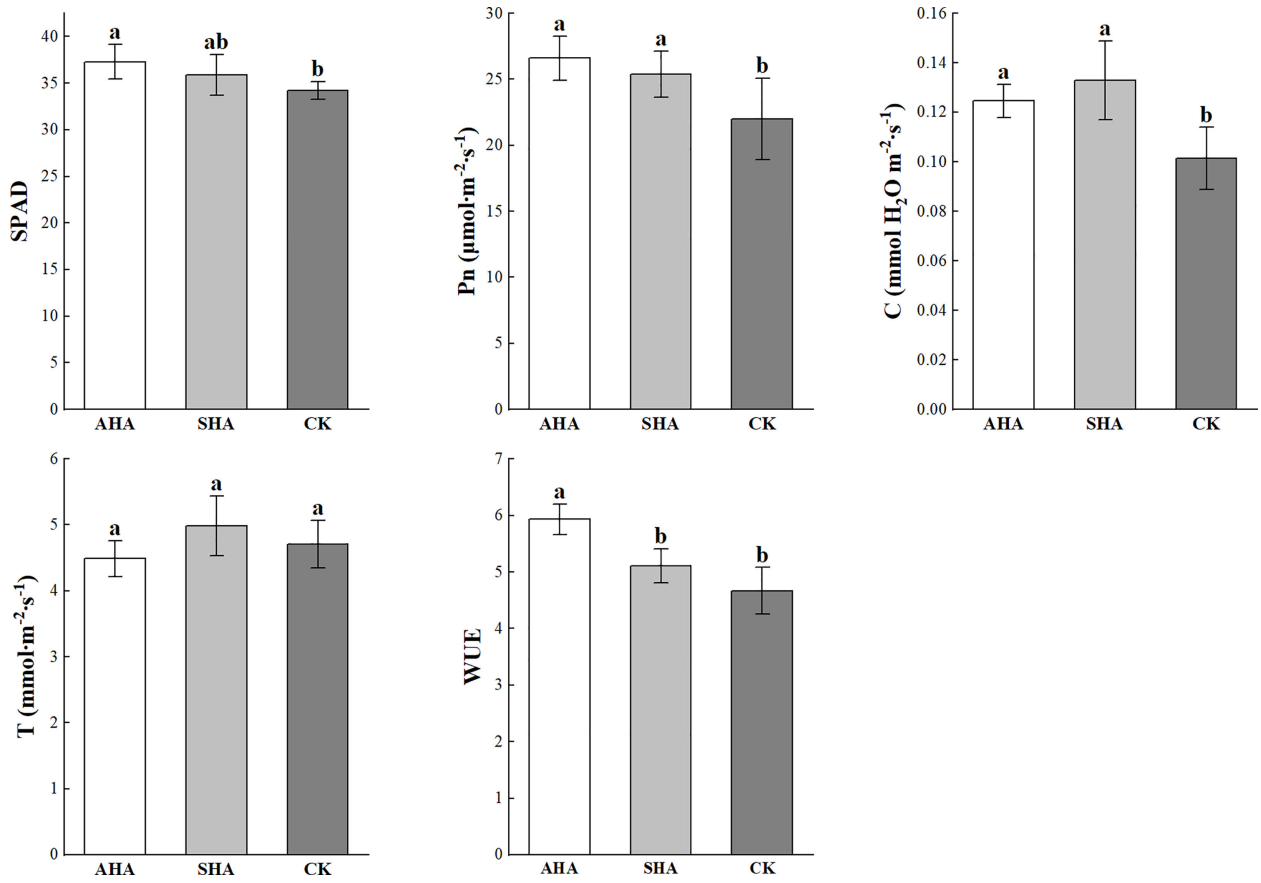

FIGURE 4
Effects of different treatments on photosynthesis. Different letters indicate statistically significant differences at $p \leq 0.05$. Vertical bars indicate means ± standard errors (n=4). SPAD, relative chlorophyll content measured portable SPAD meter; Pn, net photosynthetic rate; C, stomal conductance; T, transpiration rate; WUE, instantaneous water use efficiency.

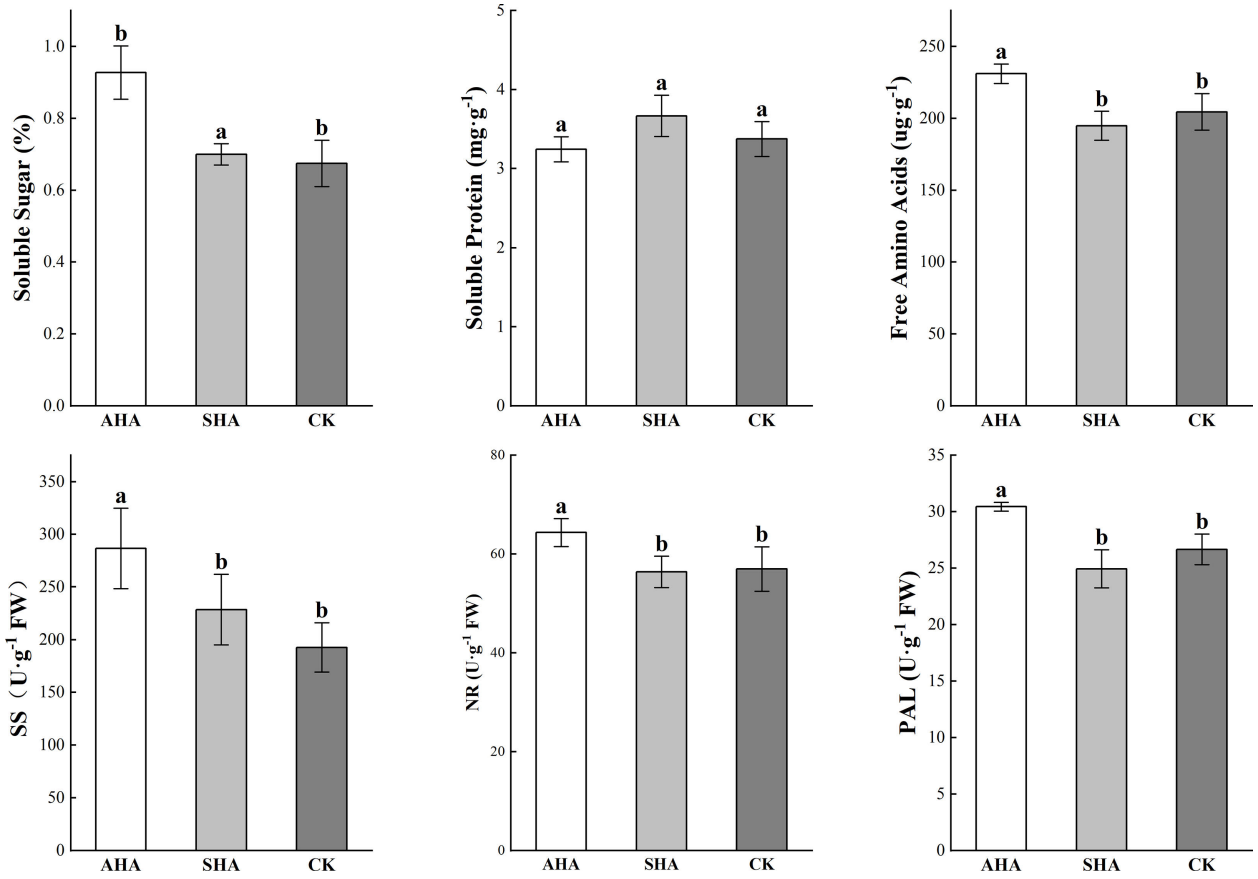

FIGURE 5
Carbon and nitrogen metabolites and their related enzyme activities in maize leaves subjected to different treatments. Different letters indicate statistically significant differences at $p \leq 0.05$. Vertical bars indicate means ± standard errors (n=4). SS, sucrose synthase; NR, nitrate reductase; PAL, phenylalanine ammonia-lyase.

negative ion mode the treatment groups and CK were separated along PC2 and between treatment groups along PC1, reflecting the differences in their metabolic profiles. Metabolomics data were compared between the three treatment groups using OPLS-DA for a two-by-two comparison to maximize intragroup separation. The OPLS-DA scores for metabolomic profiles off the various treatment groups indicated a definite distinction between the groups (Figure 7).

3.6.2 Identification of the discriminatory metabolites

Based on the VIP threshold (VIP>1) in OPLS-DA combined with $p<0.05$ from the univariate statistical analysis, 145 differentially abundant metabolites were screened. The identification of metabolites associated with the effects of humic acid spraying contributes to the understanding of the mechanism of action of HS. A Venn diagram (Figure 8A) was constructed to depict the differences and shared differentially abundant metabolites between the AHA treatment and CK groups, between the SHA treatment and CK groups, and between the AHA treatment and SHA treatment. Six shared differentially abundant metabolites were identified in all pairwise comparisons (trehalose, palatinose, diadinochrome A, fecosterol murrayone and 5-O-feruloylquinic acid). Compared to the CK treatment, there were 15 specific differentially abundant metabolites were observed in the AHA treatment group (including HDMBOA-Glc and Hirsuteine) and 42 specific differentially abundant metabolites were observed in the SHA treatment (such as jasmonic acid, linolenic acid and diosmin).

The 145 differentially abundant metabolites were classified into six categories according to their chemical properties (Figure 8B). Among which 80 metabolites (55.17% of the differentially abundant metabolites) were classified as lipids and lipid-like molecules, which are integral cellular components of the organism and play a key role in regulating normal cellular physiology and function, indicating that the different treatments significantly interfered with lipid metabolism in maize leaves. Phospholipids are a large class of lipids and lipid-like molecules and essential components of plant cell membranes and cellular signal transduction cascade reactions. In this study, 13 classes of phospholipid molecules and 53 species were identified. Eleven differentially abundant phospholipid molecules were screened in the comparison of SHA and CK treated maize leaves, of which 10 differentially abundant phospholipid molecules had an FC>1 (Table S1). Ten differentially abundant phospholipid molecules were screened in the comparison of AHA and SHA treated maize leaves, of which

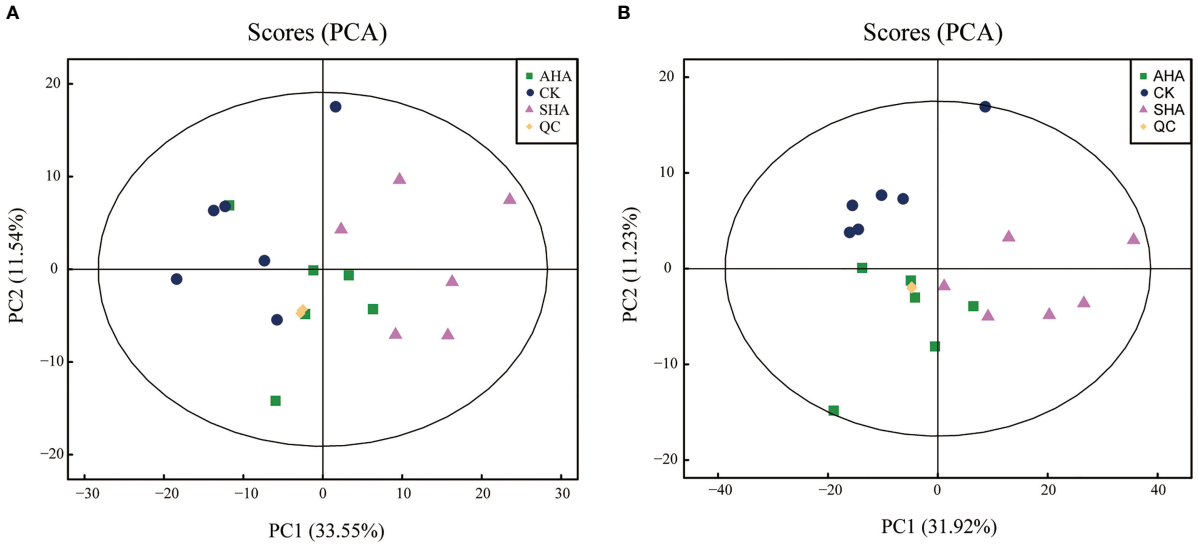

FIGURE 6
PCA score plots of metabolite profiles data obtained for maize leaf in in positive ions mode **(A)** and negative ions mode **(B)** (n=6).

9 differentially abundant phospholipid molecules had an FC>1 (Table S1). In summary, a generally significant increase in phospholipid composition was observed in SHA treated maize leaves, suggesting a disorder of lipid metabolism.

Nine of the nineteen organic oxygen compounds were carbohydrates and carbohydrate conjugates (Figures 8B, 9A), which are the energy carriers and the building blocks of primary and secondary metabolism in plants and play an important role in plant growth. Therefore, changes in carbohydrate response suggest that carbon redistribution and mobilization are important features of maize leaves subjected to different treatments.

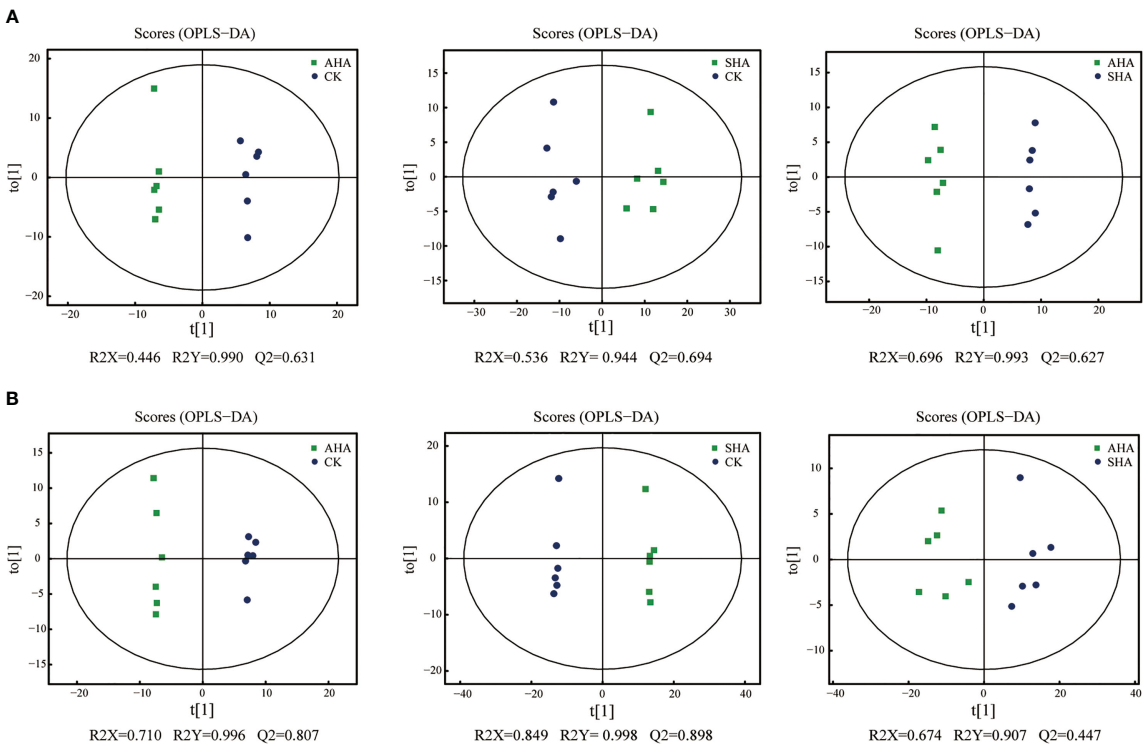

FIGURE 7
OPLS-DA score plots of maize leaf metabolome in positive ions mode **(A)** and negative ions mode **(B)**. The values at the bottom of the figure show the parameters evaluated in the model that were obtained after 7-fold cross-validation.

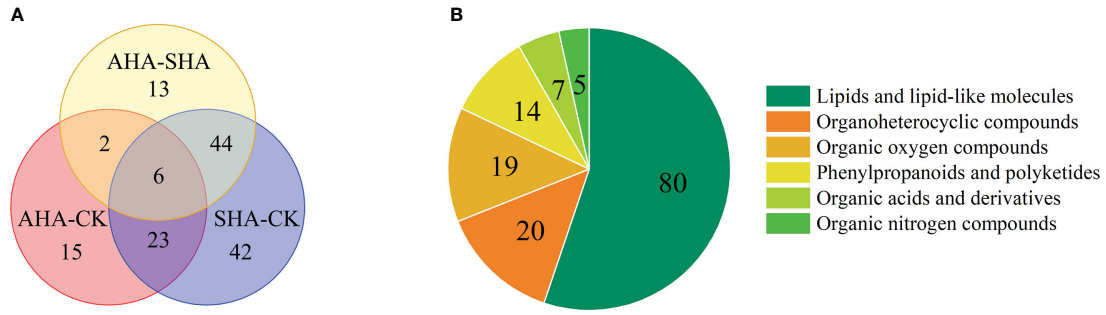

FIGURE 8
(A) Venn diagram of differentially abundant metabolites in maize leaves from different treatments groups. **(B)** the classification of differentially abundant metabolites in maize leaf.

Among other metabolites, the response of benzoxazinone-glucoside (Bxs-Glc) differed among the different treatment (Figure 9B), and the relative abundance values of DIMBOA-Glc and HMBOA-Glc were significantly lower in the leaves of both groups subjected to humic acid spray treatments than in the CK treated leaves, while HDMBOA-Glc was a specific differentially abundant metabolite detected in the AHA treated leaves.

3.6.3 Alterations in metabolic pathways in maize leaves in response to different treatments

Changes in the abundance of metabolites reflect the inhibition or activation of specific metabolic pathways, which also represent the regulation of metabolism. Annotation of the identified metabolites yielded 19 metabolic pathways, including starch and sucrose metabolism; the citrate cycle (TCA cycle); stilbenoid, diarylheptanoid and gingerol biosynthesis; ABC transporters; biosynthesis of unsaturated fatty acids; alpha-linolenic acid metabolism; tryptophan metabolism and carotenoid biosynthesis, among others (Table S1). The present study identified 21 differentially abundant metabolites produced by various metabolic pathways, including trehalose, sucrose, phenmetrazine, trimethoprim, meperidine, nandrolone, 2,5-Dihydroxybenzoic acid, 3-p-coumaroylquinic acid, stearic acid, trimethoprim, nostoxanthin, antheraxanthin, 9s,13r-12-oxophytodienoic acid, jasmonic acid, linolenic acid, safranal, cyromazine, cinobufagin, cholestenone, tryptophol, peonidin-3,5-O-di-beta-glucopyranoside, phenmetrazine, pergolide.

An enrichment analysis of metabolic pathways was subsequently performed to identify significantly affected metabolic and signal transduction pathways (Figure 10). Compared to the CK treatment, AHA treatment resulted in the reorganization of four metabolic pathways: starch and sucrose metabolism, TCA cycle, stilbenes, diarylheptanes, and curcumin biosynthesis, and ABC transport (Figure 10A). Of these, starch and sucrose metabolism,

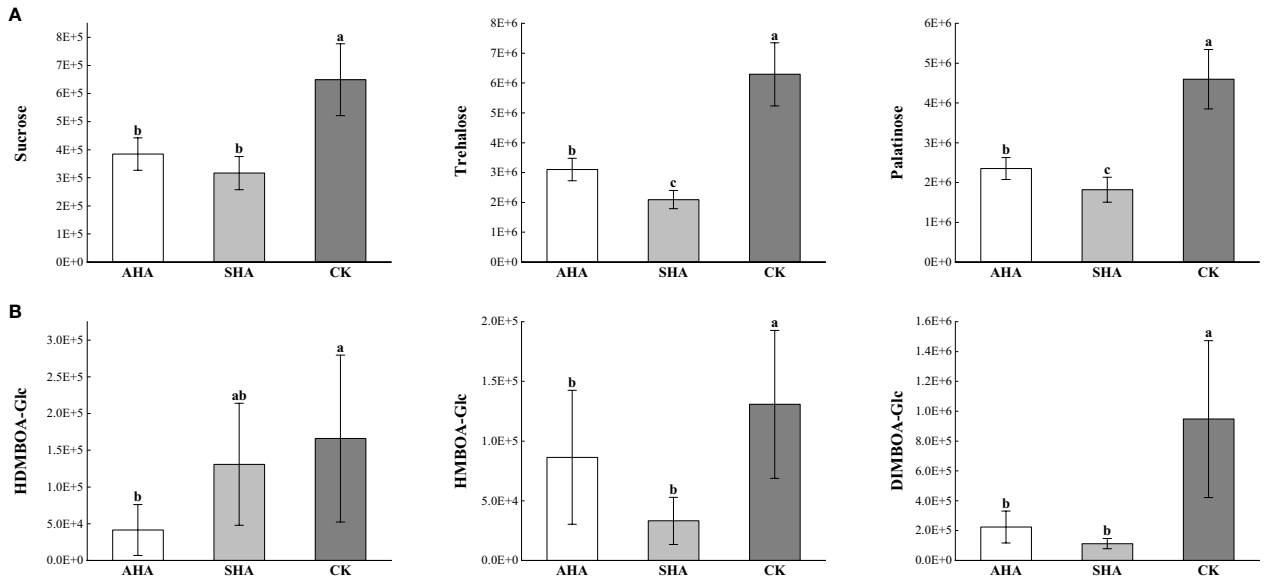

FIGURE 9
Relative abundance of differential metabolites in Maize leaf in different treatments. **(A)** relative abundance of carbohydrates; **(B)** relative abundance of Benzoxazinones (Bxs).

the TCA cycle is central to carbohydrate metabolism. Two metabolic pathways-starch and sucrose metabolism and unsaturated fatty acid biosynthesis-were modified by SHA therapy (Figure 10B). Only one metabolic pathway, starch and sucrose metabolism, was enriched when comparing the metabolic enrichment status of leaves treated with AHA and SHA (Figure 10C). One biological pathway, starch and sucrose metabolism, was altered in the comparisons of all treatment groups when they were compared, indicating that this pathway is sensitive in leaf tissue.

However, considering the effects of interconnected networks of metabolic pathways leads to a more thorough understanding. A more detailed sketch map of the metabolite network modifications in the main metabolic biosynthetic pathway which includes glycolysis, the TCA cycle, abscisic acid biosynthesis, and jasmonic acid biosynthesis, was shown in Figure 11. Regarding phytohormones, nostoxanthin and antheraxanthin, which are intermediates in the abscisic acid biosynthesis pathway, were down-regulated by both humic acid spray treatments when compared to CK treatment (Figure 11; Table S1), which may have led to a reduction in abscisic acid synthesis. Compared to the CK treatment, the accumulation of linolenic acid, jasmonic acid, and methyl jasmonate was decreased by SHA treatment in terms of the biosynthesis of jasmonic acid; AHA treatment only reduced the accumulation of methyl jasmonate, it had no effect on the accumulation of α-linolenic acid, 12-OPDA, or jasmonic acid (Figure 11; Table S1). Additionally, different treatments exerted distinct effects on the cytokinin production pathway. Compared to the CK treatment, SHA treatment increased trans-zeatin accumulation (VIP=0.18, $p<0.05$), while AHA treatment increased trans-zeatin accumulation (VIP=0.20, $p<0.05$), but substantially decreased zeatin nucleoside accumulation (VIP=0.44, $p<0.05$).

4 Discussion

HSs increase plant growth, root system development (Canellas et al., 2002; Zandonadi et al., 2007; Trevisan et al., 2010), and several physiological processes (Mora et al., 2010; Conselvan et al., 2017). HSs may be applied directly to the soil or sprayed over leaves. Both applications are commonly utilized in agricultural practices, the majority of the documented effects of HSs on plant growth are derived from studies of short-term HSs application to roots in the greenhouse, whether in hydroponics or soil. However, other studies have highlighted the ability of HSs to promote plant growth when applied as a foliar spray. The effects of root-applied HSs are typically distinguished by two different mechanisms: one is indirect and involves enhancing the chemical, physical, and biological qualities of soil; the other is a direct result of the effects of the active ingredients on the controlling of growth processes, nutrient transport mechanisms, and primary and secondary metabolism. HSs applied to the leaves have little impact on the soil or rhizosphere, but there are major responses and interactions that take place between the soil and the roots that boost nutrient absorption. In this case, the mode of action of HSs seems to involve unique plant nutritional, metabolic and physiological responses.

De Hita et al. (2020) designed experiments to distinguish the mechanisms of action of foliar treatment of sedimentary humic acid on plant development compared with root application. Both application strategies promoted the growth of aboveground parts and roots. The potential of sedimentary humic acid to increase cytokinin concentration in aboveground tissues and indole-3-acetic acid concentrations in roots was shared by its foliar and root applications. Although foliar-applied sedimentary humic acid significantly increased shoot and root growth, it had no effect on the levels of nutrients in the leaves. Kishor et al. (2021) and Hernandez et al. (2014) found that foliar application of humic acid improved significantly the plant growth, yield and physiological processes in coffee and lettuce. The results presented here reveal various effects of two HSs from distinct origins on plant growth and highlight the challenge of research involving complex mixtures of poorly characterized components. Previous studies have observed the full range of plant responses to HSs, ranging from an inhibitory effect to a stimulatory effect (Rose et al., 2014; Canellas et al., 2015). In this study, foliar-applied AHA produced a larger biomass, plant height, leaf area, relative chlorophyll content and net photosynthesis, all of which indicated rapid resource utilization and subsequent rapid growth. However, AHA treatment did not cause any change in plant nutrient concentrations (except for the leaf P concentration, Figure 3). In combination with the findings of De Hita et al. (2020), this result may be attributed to the lack of an increase in H^+-ATPase activity in the root plasma membrane following foliar spraying. The diluting effect may also account for the comparability of N and

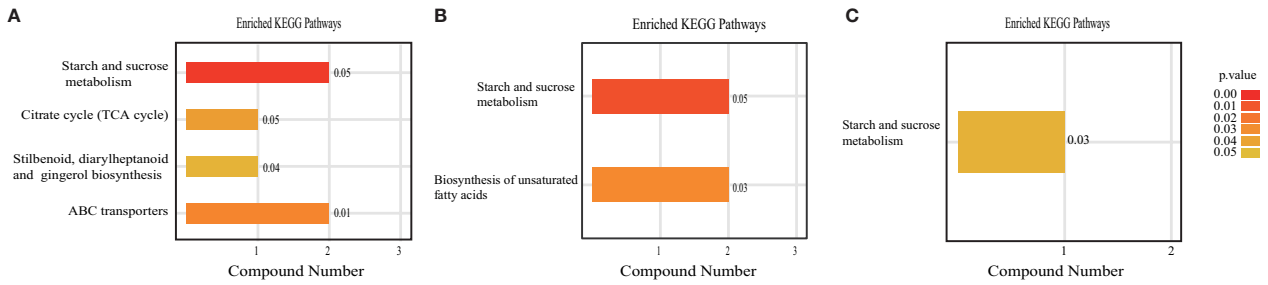

FIGURE 10
KEGG enrichment analyze of differentially expressed metabolites in maize leaf. The values after bars indicate enrichment factor. **(A)** AHA vs CK, **(B)** SHA vs CK, **(C)** AHA vs SHA.

10.3389/fpls.2023.1122621

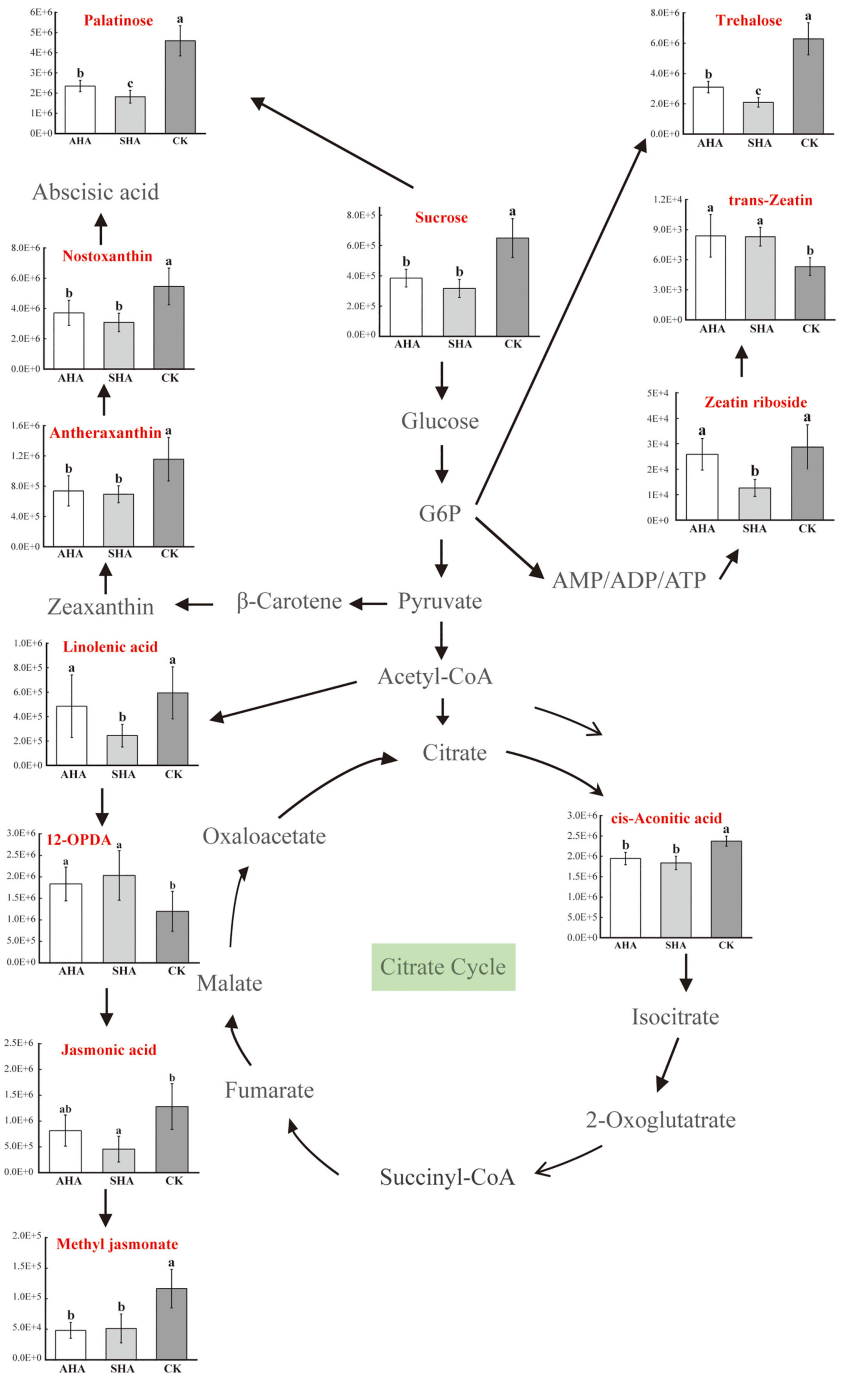

FIGURE 11
Simplified metabolic pathways of maize leaves exposed to different treatments. G6P, glucose-6-phosphate; AMP/ADP/ATP, adenosine monophosphate/adenosine diphosphate/adenosine triphosphate.

K concentrations in the AHA-treated plants to the control plants due to the relatively large plant size (Figure 3; Table 2). Furthermore, the AHA treatment significantly increased leaf dry matter while having no effect on plant root growth (Table 2). A possible explanation for this phenomenon is that AHA treatment reduces root redundancy in maize plants, which is highly energy intensive and has significant constraints on the formation of economic yield. It has long been accepted wisdom that the larger the root system, the more water and nutrients the plant obtains, and the greater the output. However, excessive root growth will unavoidably result in redundancy, which will have an effect on aboveground growth (Hu et al., 2011). In addition, the application of AHA to maize leaves significantly enhanced photosynthesis, which in turn increased the amount of soluble sugar in the leaves. Meanwhile, AHA treatment also raised sucrose synthase activity, therefore, promoting the conversion and utilization of sugars in leaves, leading to an increase in the aboveground biomass.

Despite the considerable amount of data concerning the physiological and biochemical effects of these compounds on specific metabolic pathways, little information is available on the global effects exerted by HS on metabolism. As stated above, HSs appears to influence plant physiology through a cascade mechanism targeting multiple metabolic steps. Their hormone-like activity may have a role in this process, but other unidentified signaling networks may also contribute. A comprehensive study of the plant response to these substances might significantly contribute to improving our understanding of the molecular mode of action of these substances. Thus, we employed metabolomics to perform a large-scale investigation into the overall metabolic effects of HSs on maize. In this study, an untargeted metabolomics approach based on UPLC-QTOF-MS was used to obtain metabolite profiles of maize leaves, and PCA revealed differences in the metabolic profiles between the two humic acid treatment groups and CK group, as well as between the two humic acid treatment groups, which verified the different effects of these two humic acids on maize growth. Integration of KEGG enrichment analysis of differential metabolites revealed that compared to the CK group, AHA treatment reshaped four metabolic pathways: starch and sucrose metabolism, the TCA cycle, stilbenes, diarylheptanes and curcumin biosynthesis and ABC transport, of which starch and sucrose metabolism and the TCA cycle are the core of carbohydrate and energy metabolism.

Sugar is an energy source for plants and can act as a signaling molecule during plant growth. Previous studies have shown that changes in the amount of free sugars in maize modulate the expression of growth regulatory genes (Gibson, 2005). In this study, the relative sucrose content in maize leaves treated with CK was higher than that in AHA treatment group, and the stomatal conductance of leaves was also observed to be lower than that in AHA treatment group, resulting in a significant reduction in leaf photosynthesis. Several research papers have documented an effect of HSs on carbohydrate metabolism, modifying the level and distribution of sugars in treated plants. As an illustration, Conselvan et al. (2018) suggested that the lower sucrose concentration in HS-treated *Arabidopsis* roots and leaves may be responsible for higher glycolytic activity to support HS-stimulated metabolic activities and hence boost plant growth. This result is supported by the discovery of increased sucrose synthase activity in the AHA-treated leaves in the current study (Figure 5). A logical assumption is that rapidly growing plants have an increased demand for source leaf (fully expanded leaves) photoassimilates after spraying with AHA. Therefore, the sucrose export rate from the source leaf should be higher, with less sucrose accumulated during the daytime. As anticipated, the sucrose concentration was lower than that in parallel control leaves, but the photosynthesis and soluble sugar contents of the AHA-treated source leaves were higher than those of parallel control leaves (Figures 4, 5). Furthermore, excess sucrose may act as a signaling molecule to induce stomatal closure and reduce CO_2 uptake in guard cell. The surplus sucrose is delivered toward the stomata by the transpiration stream and triggers stomatal closure via hexokinase when the rate of sucrose production exceeds the rate at which sucrose is loaded into the phloem (Kelly et al., 2013). Regarding trehalose, which is a typical stress metabolite, the larger amount of trehalose in CK treatment leaves may suggest the onset of a state of stress in plants. Indeed, plants typically contain little trehalose, as environmental stress increases, trehalose production starts to increase (Iordachescu and Imai, 2008; Wang et al., 2020).

Membrane lipids are also involved in the HS-induced modulation of plant signaling molecules. Phospholipids, which are plasma membrane component, are crucial for cell signaling, membrane trafficking, and apoptosis (Xue et al., 2009). The HS-based biostimulant treatment changed the phospholipids profile. The SHA treatment altered the levels of 11 foliar metabolites compared to CK, and 10 foliar metabolites compared to the AHA treatment. Therefore, maize leaves exposed to SHA may exhibit abnormalities in lipid metabolism, which exert a negative effect on the fluidity and integrity of cell membranes, thereby inhibiting maize growth and development.

Furthermore, we particularly noted that the content of benzoxazinones (BXs, such as BIMBOA-Glc, HDMBOA-Glc and HMBOA-Glc) was significantly lower in the leaves of maize sprayed with HSs than that in CK treatment. Benzoxazinoids (BXs) are regarded as a class of secondary metabolites involved in general defense in gramineae. Generally, BXs exist stably in plants in the form of glucosides, which are degraded into the corresponding glycosides and sugars to play a defensive role when the plant is attacked (Du Fall and Solomon, 2011). A general threshold for the induction of BXs production exists in plants upon pest and disease infestation and insect feeding, indicating that the plant mobilizes BXs for defense only after a certain level of damage by pathogens and insects occurs, which reduces the metabolic burden (Gianoli and Niemeyer, 1997). Furthermore, fulvic acid fractions have been shown to be effective in controlling several plant diseases, which were characterized by their capacity to induce host resistance towards a wide range of diseases or by directly acting as an antibacterial agent (Abdel-Monaim et al., 2011; Kamel et al., 2014). This also explained that the relative abundance of HDMBOA-Glc, HMBOA-Glc and DIMBOA-Glc in maize leaves sprayed with AHA and SHA in this study was generally lower than that in CK group, which may imply that maize leaves in the CK treatment group may consume more energy for defense.

The modulation of the phytohormone network contributed to the responses of plants to HS spray treatment. Nostoxanthin and antheraxanthin are two important intermediates in the synthetic pathway of the phytohormone abscisic acid (ABA). ABA is generally considered as the main phytohormone for plant resistance to abiotic stress, and ABA levels in plants increase when they are exposed to drought, salt, low temperature, high temperature, and injury. Therefore, ABA is also known as the adversity hormone (Klingler et al., 2010). Both HSs spray treatments significantly decreased the accumulation of these two metabolites, which may inhibit ABA synthesis. In addition, in this experiment, we observed that the stomatal conductance of CK-treated maize leaves was significantly lower than that of the humic acid spray treatment (Figure 4), which may also imply that the ABA content of humic acid-treated maize leaves was lower than that of the CK treatment, considering the relationship between stomatal conductance and ABA (Wang et al., 1994).

In the present study, SHA treatment decreased the accumulation of linolenic acid, a precursor in the jasmonic acid biosynthetic pathway, and the accumulation of jasmonic acid (JA) and methyl jasmonate (MeJA). Similarly, AHA treatment also decreased linolenic acid, JA and MeJA levels, but only the accumulation of MeJA was significantly different (Figure 10; Table S1). Since plant defense is an energy-intensive operation, JA is a stress hormone that controls how plants adapt to biotic and abiotic stress, forcing plants to stop active development (Ghorbel et al., 2021). In respect to cytokinins (CTK), both HSs treated maize leaves exhibited different levels of accumulation of tran-zeatin (tZ), but SHA treatment significantly decreased the accumulation of zeatin riboside when compared to CK treatment (Figure 11). The decreased accumulation of zeatin riboside, the main transport form of CTK, indicated that the CTK reserve in leaves treated with SHA was lower than that in leaves treated with CK and AHA (Figure 11). CTK negatively regulates the expression of chlorophyll-degrading enzyme-related genes, and induces the degradation of chlorophyll-degrading enzymes, resulting in an increase in the chlorophyll content, maintaining the normal photosynthetic capacity of leaves and the structure and function of the photosynthetic system, and extending the valid period of photosynthesis and the supply of photosynthetic compounds, it is the only known plant hormone that can delay leaf senescence (Talla et al., 2016). In the present study, the order of SPAD of maize leaves was AHA>SHA>CK, and the order of net photosynthesis was AHA, SHA>CK (Figure 4), consistent with the trend for tZ accumulation in leaves. In combination with the above discussion, the application of humic acid AHA increased the accumulation of tZ and down-regulated the relative levels of JA, MeJA and BXs in maize compared to CK, suggesting that there is a trade-off between growth and defense in plants sprayed with AHA and that this trade-off results in stimulation of plant growth.

Overall, although attributing the stimulation of the plant to few/some specific compounds is difficult, we speculate that the altered balance of phytohormones may have played a pivotal role in plant growth. Indeed, plant growth and development have consistently been shown to be tightly connected to hormone profile. Comparatively, much less is understood about the signaling pathways related to membrane lipids and the elicitation of secondary metabolism by HSs in terms of biotic stress induced systemic response to data, and further studies on this topic are advised.

For many years, soil scientists have endeavored to define the chemical characteristics and molecular structure of HSs and clarify how they can affect the growth and development of plants. Previous studies have observed that the complexity, chemical structure characteristics and biological activity of HSs determine their roles as plant growth biostimulators. Nardi et al. (2007) reported that low molecular weight HSs with high content of hydrophilic compounds significantly increased nitrogen uptake, the glycolytic pathway and the Krebs cycle in maize seedlings. The experimental results reported by Conselvan et al. (2018) revealed different response between plants treated with IAA and HS, emphasizing that responses evidenced by changes carbohydrate and amino acid concentrations were only partially attributed to the effects of IAA on HS substrates. The presence of other molecules present in the HS matrix can be used to determine their biostimulatory effect.

Most commercial products currently available for agronomic purposes are obtained from nonrenewable coal substrates such as peat, weathered coal coals and lignite, which raises the question of whether key structural aspects related to plant stimulation are also present in coal-related HSs. The opposite consequences of coal-derived HS on crop productivity (i.e., promoted or diminished effects) may be reinterpreted in light of the different structures of these materials. In the present study, the differences in plant growth and nutrient content between the AHA and SHA treatment groups (Table 2; Figure 3) suggested that the response of maize plant to HSs depends on its molecular composition. The positive effects of AHA on maize growth, even under well-watered and fertilized conditions, suggest a direct effect of compounds present in AHA on the plant. These two HSs have different elemental and molecular structural compositions (Table 2; Figure 1; Support Material 1). Combining the molecular structural features of the two HSs, we deduced that growth-promoting effect observed following AHA application was mainly attributed to GA4, JA, dopamine, and cross talk with the other hormones present at lower concentrations. Gibberellin plays an important role in regulating the growth and size of various organs during the period of plant nutritional growth, including hypocotyl growth, leaf extension, plant height regulation and root development. Its regulation of plant nutritional organ growth and development is mainly reflected in the promotion of cell elongation and promotion of cell division.

3,5-dichlorosalicylic acid is a chemical inducer of systemic acquired resistance of plants to a wide range of pathogens (Basson and Dubery, 2007) with an FC value of 404.91 in both HS-treated groups (Support Material 1). In addition, we found that the two HSs contained different levels of small molecules with fungicidal and insecticidal properties, including methamidophos, dichlormid, drazoxolon, triadimefon, penthiopyrad, pyrimethanil, perillaldehyde isocarbamid, mepanipyrim, moxamide, diethofencarb, triflumuron, bixafen, flusilazole, omethoate, spirodiclofen, fludioxonil, vanillic acid chlorogenic acid, quinolin-2-ol. These molecules may partly be responsible for the decreased activity of pathways regulating the biosynthesis of JA and ABA were in the HS-sprayed maize plants.

5 Conclusions

In this study, the molecular structures of two humic acids were characterized by ESI-UPLC-MS technique, and it was discovered that the molecular compositions of different sources of humic acids were similar with different relative abundances, and a total of 510 small molecules with significant differences were screened by combining multivariate statistical analysis. Pot spraying trials showed different effects of the two humic acids on maize growth and development: higher biomass, plant height, leaf area, chlorophyll content, and net photosynthesis were all observed in maize plants treated with AHA; the SHA treatment did not induce any significant changes in maize growth. Metabolomics revealed

that a total of 145 metabolites were significantly altered between the different spray treatments. Further analysis revealed that leaf lipid metabolism, starch and sucrose metabolism and some phytohormone-related biological pathways were regulated by the humic acid spray treatments. Among them, there was a generally significant increase in phospholipid composition of SHA treated maize leaves compared to CK and AHA treatments. Regarding phytohormones, nostoxanthin and antheraxanthin, which are intermediates in the abscisic acid biosynthesis pathway, were down-regulated by both spray treatments. In addition, both humic acid treatments stimulated the accumulation of tZ, SHA treatment significantly down-regulated the accumulation of zeatin nucleosides when compared to CK treatment.

Data availability statement

The original contributions presented in the study are publicly available. This data can be found here: MetaboLights, accession MTBLS7849.

Author contributions

YW, YB designed the research. YW, GS, MX and CN performed the research. YW wrote the paper. YW, YB, BL, YL, LW and LN edited the paper. All authors contributed to the article and approved the submitted version.

Funding

This study was funded by National Key Research and Development Program of China (2021YFD1700900).

Conflict of interest

The authors declare that the research was conducted in the absence of any commercial or financial relationships that could be construed as a potential conflict of interest.

Publisher's note

Supplementary material

The Supplementary Material for this article can be found online at: https://www.frontiersin.org/articles/10.3389/fpls.2023.1122621/full#supplementary-material

References

Abdel-Monaim, M. F., Ismail, M. E., and Morsy, K. M. (2011). Induction of systemic resistance of benzothiadiazole and humic acid in soybean plants against fusarium wilt disease. *Mycobiology* 39, 290–298. doi: 10.5941/MYCO.2011.39.4.290

Assis, J. S., Maldonado, R., Muñoz, T., Escribano, M. A. I., and Merodio, C. (2001). Effect of high carbon dioxide concentration on PAL activity and phenolic contents in ripening cherimoya fruit. *Postharvest Biol. Technol.* 23, 33–39. doi: 10.1016/S0925-5214(01)00100-4

Basson, A. E., and Dubery, I. A. (2007). Identification of a cytochrome P450 cDNA (CYP98A5) from *Phaseolus vulgaris*, inducible by 3,5-dichlorosalicylic acid and 2,6-dichloro isonicotinic acid. *J. Plant Physiol.* 164, 421–428. doi: 10.1016/j.jplph.2006.02.006

Canellas, L. P., Dobbss, L. B., Oliveira, A. L., Chagas, J. G., Aguiar, N. O., Rumjanek, V. M., et al. (2012). Chemical properties of humic matter as related to induction of plant lateral roots. *Eur. J. Soil Sci.* 63, 315–324. doi: 10.1111/j.1365-2389.2012.01439.x

Canellas, L. P., and Olivares, F. L. (2014). Physiological responses to humic substances as plant growth promoter. *Chem. Biol. Technol. Agric.* 1. doi: 10.1186/2196-5641-1-3

Canellas, L. P., Olivares, F. L., Aguiar, N. O., Jones, D. L., Nebbioso, A., Mazzei, P., et al. (2015). Humic and fulvic acids as biostimulants in horticulture. *Sci. Hortic.* 196, 15–27. doi: 10.1016/j.scienta.2015.09.013

Canellas, L. P., Olivares, F. L., Okorokova-Facanha, A. L., and Facanha, A. R. (2002). Humic acids isolated from earthworm compost enhance root elongation, lateral root emergence, and plasma membrane H^+-ATPase activity in maize roots. *Plant Physiol.* 130, 1951–1957. doi: 10.1104/pp.007088

Carletti, P., Masi, A., Spolaore, B., Polverino De Laureto, P., De Zorzi, M., Turetta, L., et al. (2008). Protein expression changes in maize roots in response to humic substances. *J. Chem. Ecol.* 34, 804–818. doi: 10.1007/s10886-008-9477-4

Chen, Z., Wang, Z., Yang, Y., Li, M., and Xu, B. (2018). Abscisic acid and brassinolide combined application synergistically enhances drought tolerance and photosynthesis of tall fescue under water stress. *Sci. Hortic.* 228, 1–9. doi: 10.1016/j.scienta.2017.10.004

Conselvan, G. B., Fuentes, D., Merchant, A., Peggion, C., Francioso, O., and Carletti, P. (2018). Effects of humic substances and indole-3-acetic acid on *arabidopsis* sugar and amino acid metabolic profile. *Plant Soi.* 426, 17–32. doi: 10.1007/s11104-018-3608-7

Conselvan, G. B., Pizzeghello, D., Francioso, O., Di Foggia, M., and S.and Carletti, P. (2017). Biostimulant activity of humic substances extracted from leonardites. *Plant Soil* 420, 119–134. doi: 10.1007/s11104-017-3373-z

De Azevedo, I. G., Olivares, F. L., Ramos, A. C., Bertolazi, A. A., and Canellas, L. P. (2019). Humic acids and herbaspirillum seropedicae change the extracellular H^+ flux and gene expression in maize roots seedlings. *Chem. Biol. Technol. Agric.* 6. doi: 10.1186/s40538-019-0149-0

De Hita, D., Fuentes, M., Fernandez, V., Zamarreno, A. M., Olaetxea, M., and Garcia-Mina, J. M. (2020). Discriminating the short-term action of root and foliar application of humic acids on plant growth: emerging role of jasmonic acid. *Front. Plant Sci.* 11. doi: 10.3389/fpls.2020.00493

Dobbss, L. B., Pasqualoto Canellas, L., Lopes Olivares, F., Oliveira Aguiar, N., Peres, L. E. P., Azevedo, M., et al. (2010). Bioactivity of chemically transformed humic matter from vermicompost on plant root growth. *J. Agric. Food Chem.* 58, 3681–3688. doi: 10.1021/jf904385c

Drosos, M., Nebbioso, A., Mazzei, P., Vinci, G., Spaccini, R., and Piccolo, A. (2017). A molecular zoom into soil humeome by a direct sequential chemical fractionation of soil. *Sci. Total Environ.* 586, 807–816. doi: 10.1016/j.scitotenv.2017.02.059

Du Fall, L. A., and Solomon, P. S. (2011). Role of cereal secondary metabolites involved in mediating the outcome of plant-pathogen interactions. *Metabolites* 1, 64–78. doi: 10.3390/metabo1010064

Garcia, A. C., Olaetxea, M., Santos, L. A., Mora, V., Baigorri, R., Fuentes, M., et al. (2016). Involvement of hormone- and ROS-signaling pathways in the beneficial action of humic substances on plants growing under normal and stressing conditions. *BioMed. Res. Int.* 2016, 3747501–3747513. doi: 10.1155/2016/3747501

García, A. C., Santos, L. A., Izquierdo, F. G., Rumjanek, V. M., Castro, R. N., Dos Santos, F. S., et al. (2014). Potentialities of vermicompost humic acids to alleviate water stress in rice plants *(Oryza sativa* L.). *J. Geochem. Explor.* 136, 48–54. doi: 10.1016/j.gexplo.2013.10.005

García, A. C., Santos, L. A., Izquierdo, F. G., Sperandio, M. V. L., Castro, R.N., and Berbara, R. L. L. (2012). Vermicompost humic acids as an ecological pathway to protect rice plant against oxidative stress. *Ecol. Eng.* 47, 203–208. doi: 10.1016/j.ecoleng.2012.06.011

Ghorbel, M., Brini, F., Sharma, A., and Landi, M. (2021). Role of jasmonic acid in plants: the molecular point of view. *Plant Cell Rep.* 40, 1471–1494. doi: 10.1007/s00299-021-02687-4

Gianoli, E., and Niemeyer, H. (1997). Characteristics of hydroxamic acid induction in wheat triggered by aphid infestation. *J. Chem. Ecol.* 23, 2695–2705. doi: 10.1023/A:1022554708782

Gibson, S. I. (2005). Control of plant development and gene expression by sugar signaling. *Curr. Opin. Plant Biol.* 8, 93–102. doi: 10.1016/j.pbi.2004.11.003

Hernandez, O. L., Calderín, A., Huelva, R., Martínez-Balmori, D., Guridi, F., Aguiar, N. O., et al. (2014). Humic substances from vermicompost enhance urban lettuce production. *Agron. Sustain. Dev.* 35, 225–232. doi: 10.1007/s13593-014-0221-x

Hu, Y., Zhang, X., Mao, Z., Shen, X., Guo, L., and Shu, H. R. (2011). Fertility level affects apple rootstock structure and Root:Shoot ratio. *Acta Hortic.* 903, 909–913. doi: 10.17660/ActaHortic.2011.903.127

Iordachescu, M., and Imai, R. (2008). Trehalose biosynthesis in response to abiotic stresses. *J. Integr. Plant Biol.* 50, 1223–1229. doi: 10.1111/j.1744-7909.2008.00736.x

Kamel, S. M., Afifi, M. M. I., El-Shoraky, F. S., and El-Sawy, M. M. (2014). Fulvic acid: a tool for controlling powdery and downy mildews in cucumber plants. *Int. J. Phytopathol.* 03, 101–108. doi: 10.33687/phytopath.003.02.0866

Kelly, G., Moshelion, M., David-Schwartz, R., Halperin, O., Wallach, R., Attia, Z., et al. (2013). Hexokinase mediates stomatal closure. *Plant J.* 75, 977–988. doi: 10.1111/tpj.12258

Kishor, M., Jayakumar, M., Gokavi, N., Mukharib, D. S., Raghuramulu, Y., and Udayar Pillai, S. (2021). Humic acid as foliar and soil application improve the growth, yield and quality of coffee (cv. c x r) in Western ghats of India. *J. Sci. Food Agric.* 101, 2273–2283. doi: 10.1002/jsfa.10848

Klingler, J. P., Batelli, G., and Zhu, J. K. (2010). ABA receptors: the START of a new paradigm in phytohormone signalling. *J. Exp. Bot.* 61, 3199–3210. doi: 10.1093/jxb/erq151

Marino, G., Righi, V., Simoni, A., Schenetti, L., Mucci, A., Tugnoli, V., et al. (2013). Effect of a peat humic acid on morphogenesis in leaf explants of *Pyrus communis* and *Cydonia oblonga* . metabolomic analysis at an early stage of regeneration. *J. Agric. Food Chem.* 61, 4979–4987. doi: 10.1021/jf4004785

Mittler, R. (2017). ROS are good. *Trends Plant Sci.* 22, 11–19. doi: 10.1016/j.tplants.2016.08.002

Mittler, R., Vanderauwera, S., Suzuki, N., Miller, G., Tognetti, V. B., Vandepoele, K., et al. (2011). ROS signaling: the new wave? *Trends Plant Sci.* 16, 300–309. doi: 10.1016/j.tplants.2011.03.007

Mora, V., Bacaicoa, E., Zamarreno, A. M., Aguirre, E., Garnica, M., Fuentes, M., et al. (2010). Action of humic acid on promotion of cucumber shoot growth involves nitrate-related changes associated with the root-to-shoot distribution of cytokinins, polyamines and mineral nutrients. *J. Plant Physiol.* 167, 633–642. doi: 10.1016/j.jplph.2009.11.018

Nardi, S., Ertani, A., and Francioso, O. (2016). Soil–root cross-talking: the role of humic substances. *J. Plant Nutr. Soil Sci.* 180, 5–13. doi: 10.1002/jpln.201600348

Nardi, S., Muscolo, A., Vaccaro, S., Baiano, S., Spaccini, R., and Piccolo, A. (2007). Relationship between molecular characteristics of soil humic fractions and glycolytic pathway and krebs cycle in maize seedlings. *Soil Biol. Biochem.* 39, 3138–3146. doi: 10.1016/j.soilbio.2007.07.006

Nebbioso, A., and Piccolo, A. (2011). Basis of a humeomics science: chemical fractionation and molecular characterization of humic biosuprastructures. *Biomacromolecules* 12, 1187–1199. doi: 10.1021/bm101488e

Nephali, L., Piater, L. A., Dubery, I. A., Patterson, V., Huyser, J., Burgess, K., et al. (2020). Biostimulants for plant growth and mitigation of abiotic stresses: a metabolomics perspective. *Metabolites* 10 (12), 505. doi: 10.3390/metabo10120505

Nunes, R. O., Domiciano, G. A., Alves, W. S., Melo, A. C. A., Nogueira, F. C. S., Canellas, L. P., et al. (2019). Evaluation of the effects of humic acids on maize root architecture by label-free proteomics analysis. *Sci. Rep.* 9, 12019. doi: 10.1038/s41598-019-48509-2

Piccolo, A. (2001). The supramolecular structure of humic substance. *Soil Sci.* 166, 810–832. doi: 10.1016/S0065-2113(02)75003-7

Pizzeghello, D., Schiavon, M., Francioso, O., Dalla Vecchia, F. A., and Nardi, S. (2020). Bioactivity of size-fractionated and unfractionated humic substances from two forest soils and comparative effects on n and s metabolism, nutrition, and root anatomy of *Allium sativum* L. *Front. Plant Sci.* 11, 1203. doi: 10.3389/fpls.2020.01203

Quaggiotti, S., Ruperti, B., Pizzeghello, D., Francioso, O., Tugnoli, V., and Nardi, S. (2004). Effect of low molecular size humic substances on nitrate uptake and expression of genes involved in nitrate transport in maize *(Zea mays* L.). *J. Exp. Bot.* 55, 803–813. doi: 10.1093/jxb/erh085

Roomi, S., Masi, A., Conselvan, G. B., Trevisan, S., Quaggiotti, S., Pivato, M., et al. (2018). Protein profiling of *Arabidopsis* roots treated with humic substances: insights into the metabolic and interactome networks. *Front. Plant Sci.* 9. doi: 10.3389/fpls.2018.01812

Rose, M. T., Patti, A. F., Little, K. R., Brown, A. L., Jackson, W. R., and Cavagnaro, T. R. (2014). A meta-analysis and review of plant-growth response to humic substances. *Adv. Agron.* 124, 37–89. doi: 10.1016/b978-0-12-800138-7.00002-4

Scaglia, B., Nunes, R. R., Rezende, M. O. O., Tambone, F., and Adani, F. (2016). Investigating organic molecules responsible of auxin-like activity of humic acid fraction extracted from vermicompost. *Sci. Total Environ.* 562, 289–295. doi: 10.1016/j.scitotenv.2016.03.212

Talla, S. K., Panigrahy, M., Kappara, S., Nirosha, P., Neelamraju, S., and Ramanan, R. (2016). Cytokinin delays dark-induced senescence in rice by maintaining the chlorophyll cycle and photosynthetic complexes. *J. Exp. Bot.* 67, 1839–1851. doi: 10.1093/jxb/erv575

Trevisan, S., Botton, A., Vaccaro, S., Vezzaro, A., Quaggiotti, S., and Nardi, S. (2011). Humic substances affect *Arabidopsis* physiology by altering the expression of genes involved in primary metabolism, growth and development. *Environ. Exp. Bot.* 74, 45–55. doi: 10.1016/j.envexpbot.2011.04.017

Trevisan, S., Pizzeghello, D., Ruperti, B., Francioso, O., Sassi, A., Palme, K., et al. (2010). Humic substances induce lateral root formation and expression of the early auxin-responsive IAA19 gene and DR5 synthetic element in *Arabidopsis*. *Plant Biol.* 12, 604–614. doi: 10.1111/j.1438-8677.2009.00248.x

Wang, W., Chen, Q., Xu, S., Liu, W. C., Zhu, X., and Song, C. P. (2020). Trehalose-6-phosphate phosphatase e modulates ABA-controlled root growth and stomatal movement in *Arabidopsis*. *J. Integr. Plant Biol.* 62, 1518–1534. doi: 10.1111/jipb.12925

Wang, Y. Y., Zhou, R., and Zhou, X. (1994). Endogenous levels of ABA and cytokinins and their relation to stomatal behavior in dayflower *(Commelina communis* L.). *J. Plant Physiol.* 144, 45–48. doi: 10.1016/S0176-1617(11)80990-9

Xue, H. W., Chen, X., and Mei, Y. (2009). Function and regulation of phospholipid signalling in plants. *Biochem. J.* 421, 145–156. doi: 10.1042/BJ20090300

Zandonadi, D. B., Canellas, L. P., and Facanha, A. R. (2007). Indolacetic and humic acids induce lateral root development through a concerted plasmalemma and tonoplast H^+ pumps activation. *Planta* 225, 1583–1595. doi: 10.1007/s00425-006-0454-2

Zandonadi, D. B., Santos, M. P., Dobbss, L. B., Olivares, F. L., Canellas, L. P., Binzel, M. L., et al. (2010). Nitric oxide mediates humic acids-induced root development and plasma membrane H^+-ATPase activation. *Planta* 231, 1025–1036. doi: 10.1007/s00425-010-1106-0

Frontiers in Plant Science

Cultivates the science of plant biology and its applications

The most cited plant science journal, which advances our understanding of plant biology for sustainable food security, functional ecosystems and human health.

Discover the latest Research Topics

See more →

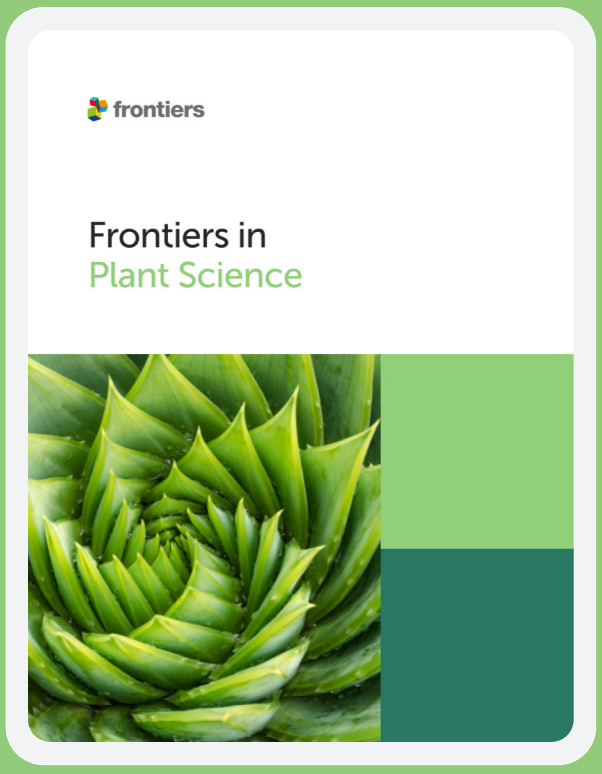

Frontiers

Avenue du Tribunal-Fédéral 34
1005 Lausanne, Switzerland
frontiersin.org

Contact us

+41 (0)21 510 17 00
frontiersin.org/about/contact